24

VOLUME 24 / NUMBER 1
JANUARY 8, 1986
ACC. NOS. N86-10001 TO N86-11144

STAR

AN ABSTRACT JOURNAL

S & T REFERENCE
LD C U.S. DOCUMENTS
NEWARK PUBLIC LIBRARY

Scientific and Technical Aerospace Reports

PRODUCED BY THE
SCIENTIFIC AND TECHNICAL
INFORMATION
BRANCH

NASA

NAS 1.9/4

NATIONAL AERONAUTICS AND SPACE ADMINISTRATION

WHAT YOU CAN DO FOR *STAR*

All users of this abstract service are urged to forward reports to be considered for announcement in *STAR*. This will aid NASA in its efforts to provide the fullest possible coverage of all scientific and technical publications that might support aeronautics and space research and development. If you have prepared relevant reports (other than those that you will transmit to NASA, DoD, or DOE through the usual contract- or grant-reporting channels), please send them for consideration to the NASA Scientific and Technical Information Facility, P.O. Box 8757, B.W.I. Airport, Maryland 21240.

Reprints of journal articles, book chapters, and conference papers are also welcome. These will be considered for announcement in *STAR's* companion journal, *International Aerospace Abstracts*.

You may specify a particular source to be included in a report announcement if you wish; otherwise the report will be placed on public sale at the National Technical Information Service. Copyrighted publications will be announced but not distributed or sold.

PURCHASE OF *STAR*

The semimonthly issues are available for sale by the Superintendent of Documents, U.S. Government Printing Office, Washington, D.C. 20402.

PUBLISHED BY:

UNITED STATES GOVERNMENT
NATIONAL AERONAUTICS AND SPACE ADMINISTRATION
SCIENTIFIC AND TECHNICAL INFORMATION BRANCH

Scientific and Technical Aerospace Reports, Volume 24, is prepared by the NASA Scientific and Technical Information Facility operated for the National Aeronautics and Space Administration by RMS Associates.

The Administrator of the National Aeronautics and Space Administration has determined that the publication of this periodical is necessary in the transaction of the public business required by law of this Agency. Use of funds for printing this periodical has been approved by the Director of the Office of Management and Budget through March 22, 1988.

US ISSN 0036-8741

INTRODUCTION

Scientific and Technical Aerospace Reports (STAR) is a major component of a comprehensive National Aeronautics and Space Administration information system covering aeronautics, space, and supporting disciplines. *STAR* is issued on the 8th and 23rd of each month and announces current publications of the following types:

- NASA, NASA contractor, and NASA grantee reports
- Reports issued by other U.S. Government agencies, domestic and foreign institutions, universities, and private firms
- Translations in report form
- NASA-owned patents and patent applications
- Dissertations and theses

Cumulative index volumes are published annually.

Journal, book, and conference literature, cover-to-cover journal translations, and certain foreign dissertations are announced in a companion journal, *International Aerospace Abstracts (IAA)*, available on subscription from the American Institute of Aeronautics and Astronautics, Technical Information Service, 555 West 57th Street, 12th Floor, New York, New York 10019.

SUBJECT SCOPE

Subject scope of *STAR*, and *IAA* includes all aspects of aeronautics and space research and development, supporting basic and applied research, and applications. Aerospace aspects of earth resources, energy development, conservation, oceanography, environmental protection, urban transportation, and other topics of high national priority are also covered.

OTHER NASA PUBLICATIONS

Other NASA publications and information services are described in the publication, *The NASA Scientific and Technical Information System ... and How to Use It*, available without charge from the NASA Scientific and Technical Information Facility, P.O. Box 8757, B.W.I. Airport, Maryland 21240.

READEX FICHE best copy available

HOW TO USE *STAR* SUBJECT CATEGORIES

STAR is categorized by 10 major subject divisions divided into 74 specific subject categories and one general category/division. The major subject divisions are listed in the Table of Contents, together with a note for each that defines its scope and provides any cross-references. For example:

> **AERONAUTICS**
>
> Includes aeronautics (general); aerodynamics; air transportation and safety; aircraft communications and navigation; aircraft design, testing and performance; aircraft instrumentation; aircraft propulsion and power; aircraft stability and control; and research and support facilities (air).
>
> For related information see also *Astronautics*.

Each major division is further divided into as many as nine specific categories, which are identified by category numbers.

Abstracts in *STAR* are grouped by specific category, the categories appearing in sequential order. Category breaks in the abstract section are identified by the category number and title, and a scope note. Cross-references to other categories are provided as appropriate. For example:

> **02 AERODYNAMICS**
>
> Includes aerodynamics of bodies, combinations, wings, rotors, and control surfaces; and internal flow in ducts and turbomachinery.
>
> For related information see also *34 Fluid Mechanics and Heat Transfer*.

CROSS-REFERENCES

Individual *STAR* abstracts are not ordinarily cross-referenced, except for certain conference reports or book translations that have had separate abstracts written for their component papers or chapters. Citations and abstracts of the components follow immediately after those of the parent document. When the subject content of a component differs sufficiently from the general content of the parent, a cross-reference citation also is printed at the end of the category to which it normally would have been assigned if it were independent.

DOCUMENTS ON MICROFICHE

Documents on microfiche(1) are designated by a pound sign (#) following the accession number. The pound sign is used without regard to the source or quality of the microfiche.

AVAILABILITIES

One or more sources from which a document announced in *STAR* is available to the public is given in each citation. The most commonly indicated sources and their acronyms or abbreviations are listed below. If the publication is available from a source other than those listed, the publisher and his address will be displayed on the availability line or in combination with the corporate source line.

---

(1) A microfiche is a transparent sheet of film, 105 by 148 mm in size, containing as many as 60 to 98 pages of information reduced to micro images (not to exceed 26:1 reduction).

Avail: NTIS. Sold by the National Technical Information Service. Prices for hard copy (HC) and microfiche (MF) are indicated by a price code following the letters HC or MF in the *STAR* citation. Current values for the price codes are given in the tables on page vii.

Initially distributed microfiche under the NTIS SRIM (Selected Research in Microfiche) is available at greatly reduced unit prices. For this service and for information concerning subscription to NASA printed reports, consult the NTIS Subscription Section, Springfield, Va. 22161.

NOTE ON ORDERING DOCUMENTS: When ordering NASA publications (those followed by the * symbol), use the N accession number. NASA patent applications (only the specifications are offered) should be ordered by the US-Patent-Appl-SN number. Non-NASA publications (no asterisk) should be ordered by the AD, PB, or other *report* number shown on the last line of the citation, not by the N accession number. It is also advisable to cite the title and other bibliographic identification.

Avail: SOD (or GPO). Sold by the Superintendent of Documents, U.S. Government Printing Office, in hard copy. The current price and order number are given following the availability line. (NTIS will fill microfiche requests, as indicated above, for those documents identified by a # symbol.)

Avail: NASA Public Document Rooms. Documents so indicated may be examined at or purchased from the National Aeronautics and Space Adminstration, Public Documents Room (Room 126), 600 Independence Ave., S.W., Washington, D.C. 20546, or public document rooms located at each of the NASA research centers, the NASA Space Technology Laboratories, and the NASA Pasadena Office at the Jet Propulsion Laboratory.

Avail: DOE Depository Libraries. Organizations in U.S. cities and abroad that maintain collections of Department of Energy reports, usually in microfiche form, are listed in *Energy Research Abstracts*. Services available from the DOE and its depositories are described in a booklet, *DOE Technical Information Center - Its' Functions and Services* (TID-4660), which may be obtained without charge from the DOE Technical Information Center.

Avail: Univ. Microfilms. Documents so indicated are dissertations selected from *Dissertation Abstracts* and are sold by University Microfilms as xerographic copy (HC) and microfilm. All requests should cite the author and the Order Number as they appear in the citation.

Avail: USGS. Originals of many reports from the U.S. Geological Survey, which may contain color illustrations, or otherwise may not have the quality of illustrations preserved in the microfiche or facsimile reproduction, may be examined by the public at the libraries of the USGS field offices whose addresses are listed in this Introduction. The libraries may be queried concerning the availability of specific documents and the possible utilization of local copying services, such as color reproduction.

Avail: HMSO. Publications of Her Majesty's Stationery Office are sold in the U.S. by Pendragon House, Inc. (PHI), Redwood City, California. The U.S. price (including a service and mailing charge) is given, or a conversion table may be obtained from PHI.

Avail: BLL (formerly NLL): British Library Lending Division, Boston Spa, Wetherby, Yorkshire, England. Photocopies available from this organization at the price shown. (If none is given, inquiry should be addressed to the BLL.)

Avail: Fachinformationszentrum, Karlsruhe. Sold by the Fachinformationszentrum Energie, Physik, Mathematik GMBH, Eggenstein Leopoldshafen, Federal Republic of Germany, at the price shown in deutschmarks (DM).

Avail: Issuing Activity, or Corporate Author, or no indication of availability. Inquiries as to the availability of these documents should be addressed to the organization shown in the citation as the corporate author of the document.

Avail: U.S. Patent and Trademark Office. Sold by Commissioner of Patents and Trademarks, U.S. Patent and Trademark Office, at the standard price of 50 cents each, postage free. (See discussion of patents and patent applications below.)

Avail: ESDU. Pricing information on specific data, computer programs, and details on ESDU topic categories can be obtained from ESDU International Ltd. Requesters in North America should use the Virginia address while all other requesters should use the London address, both of which are on page vi.

NASA PATENTS AND PATENT APPLICATIONS

Patents and patent applications owned by NASA are announced in *STAR* under appropriate subject categories and are referenced in the *STAR* indexes. In the Report/Accession Number Index, patents are indexed by the NASA Case Number (which appears in lieu of the report number in other indexes), the U.S. Patent Number, the U.S. Patent Application Serial Number, and the U.S. Patent Class. Patent applications for which patents have not yet been issued are indexed by the NASA Case Number and the U.S. Patent Application Serial Number.

NASA *patent application specifications* are sold in paper copy by the National Technical Information Service at price code A02 ($9.95 domestic; $19.90 foreign). Microfiche are sold at price code A01 ($5.95 domestic; $11.90 foreign). The US-Patent-Appl-SN- number should be used in ordering either paper copy or microfiche from NTIS. Printed copies of *patents* (which are not microfiched) are available for purchase at 50 cents per copy from:

Commissioner of Patents and Trademarks
U.S. Patent and Trademark Office
Washington, D.C. 20231

When ordering patents, the U.S. Patent Number should be used, and payment must be remitted in advance, preferably by money order or check payable to the Commissioner of Patents and Trademarks. Prepaid purchase coupons for ordering are also available from the Patent and Trademark Office. The patents and patent applications announced in *STAR* are owned by NASA and are available for royalty-free licensing. Requests for licensing terms and further information should be addressed to:

Assistant General Counsel for Patent Matters/Code GP-1
National Aeronautics and Space Administration
Washington, D.C. 20546

ELIGIBILITY AND REGISTRATION FOR NASA INFORMATION PRODUCTS AND SERVICES

A variety of services is available to organizations of the following types that have registered with NASA to receive specific services or products:

1. NASA offices, research centers, contractors, subcontractors, grantees, and consultants;
2. Other U.S. Government agencies and their contractors;
3. Libraries in the United States that have arrangements with NASA to maintain collections of NASA documents for public reference;
4. Other organizations in the United States having a need for NASA documents in work related to aeronautics and space research;
5. Organizations abroad that have established reciprocal document exchange arrangements with NASA.

Only the central service points or central points of document acquisition and control within qualified organizations are eligible to register for NASA products and services. Domestic organizations that may be eligible to receive various classes of NASA publications and services should address their requests for registration or for further information to:

NASA Scientific and Technical Information Facility
ATTN: Registration Activity
P.O. Box 8757
B.W.I. Airport, Maryland 21240

Organizations abroad should direct requests to the same address, but to the attention of: International Exchange Program.

AVAILABILITY OF *STAR* ABSTRACTS ON MICROFICHE

Microfiche of the abstract sections of this issue and other issues of *STAR* are available on annual subscription from NTIS, Attn: Subscriptions, 5285 Port Royal Road, Springfield, Virginia 22161. Annual subscription rates are $60.00 North America; $120.00 foreign. Abstract sections for previous years retroactive to 1964 are available at the current rates. Microfiche for individual *STAR* issue abstract sections are not available.

PUBLIC COLLECTIONS OF NASA DOCUMENTS

DOMESTIC: NASA and NASA-sponsored documents and a large number of aerospace publications are available to the public for reference purposes at the library maintained by the American Institute of Aeronautics and Astronautics, Technical Information Service, 555 West 57th Street, 12th Floor, New York, New York 10019.

EUROPEAN: An extensive collection of NASA and NASA-sponsored publications is maintained by the British Library Lending Division, Boston Spa, Wetherby, Yorkshire, England for public access. The British Library Lending Division also has available many of the non-NASA publications cited in *STAR*. European requesters may purchase facsimile copy or microfiche of NASA and NASA-sponsored documents, those identified by both the symbols # and * from ESA - Information Retrieval Service European Space Agency, 8-10 rue Mario-Nikis, 75738 Paris CEDEX 15, France.

FEDERAL DEPOSITORY LIBRARY PROGRAM

In order to provide the general public with greater access to U.S. Government publications, Congress established the Federal Depository Library Program under the Government Printing Office (GPO), with 50 regional depositories responsible for permanent retention of material, inter-library loan, and reference services. Over 1,300 other depositories also exist. A list of the regional GPO libraries appears on the inside back cover of *STAR*.

ADDRESSES OF ORGANIZATIONS

American Institute of Aeronautics and
Astronautics
Technical Information Service
555 West 57th Street, 12th Floor
New York, New York 10019

British Library Lending Division,
Boston Spa, Wetherby, Yorkshire,
England

Commissioner of Patents and
Trademarks
U.S. Patent and Trademark Office
Washington, D.C. 20231

Department of Energy
Technical Information Center
P.O. Box 62
Oak Ridge, Tennessee 37830

ESA-Information Retrieval Service
ESRIN
Via Galileo Galilei
00044 Frascati (Rome) Italy

ESDU International, Ltd.
1495 Chain Bridge Road
McLean, Virginia 22101

ESDU International, Ltd.
251-259 Regent Street
London, W1R 7AD, England

Fachinformationszentrum Energie, Physik,
Mathematik GMBH
7514 Eggenstein Leopoldshafen
Federal Republic of Germany

Her Majesty's Stationery Office
P.O. Box 569, S.E. 1
London, England

NASA Scientific and Technical Information
Facility
P.O. Box 8757
B.W.I. Airport, Maryland 21240

National Aeronautics and Space
Administration
Scientific and Technical Information
Branch (NIT-1)
Washington, D.C. 20546

National Technical Information Service
5285 Port Royal Road
Springfield, Virginia 22161

Pendragon House, Inc.
899 Broadway Avenue
Redwood City, California 94063

Superintendent of Documents
U.S. Government Printing Office
Washington, D.C. 20402

University Microfilms
A Xerox Company
300 North Zeeb Road
Ann Arbor, Michigan 48106

University Microfilms, Ltd.
Tylers Green
London, England

U.S. Geological Survey Library
National Center – MS 950
12201 Sunrise Valley Drive
Reston, Virginia 22092

U.S. Geological Survey Library
2255 North Gemini Drive
Flagstaff, Arizona 86001

U.S. Geological Survey
345 Middlefield Road
Menlo Park, California 94025

U.S. Geological Survey Library
Box 25046
Denver Federal Center, MS 914
Denver, Colorado 80225

NTIS PRICE SCHEDULES

(Effective October 1, 1985)

Schedule A
STANDARD PRICE DOCUMENTS AND MICROFICHE

PRICE CODE	PAGE RANGE	NORTH AMERICAN PRICE	FOREIGN PRICE
A01	Microfiche	$ 5.95	$11.90
A02-A03	001-050	9.95	19.90
A04-A05	051-100	11.95	23.90
A06-A09	101-200	16.95	33.90
A10-A13	201-300	22.95	45.90
A14-A17	301-400	28.95	57.90
A18-A21	401-500	34.95	69.90
A22-A25	501-600	40.95	81.90
A99	601-up	*	*
NO1		$40.00	70.00
NO2		40.00	70.00

Schedule E
EXCEPTION PRICE DOCUMENTS AND MICROFICHE

PRICE CODE	NORTH AMERICAN PRICE	FOREIGN PRICE
E01	$ 7.50	15.00
E02	10.00	20.00
E03	11.00	22.00
E04	13.50	27.00
E05	15.50	31.00
E06	18.00	36.00
E07	20.50	41.00
E08	23.00	46.00
E09	25.50	51.00
E10	28.00	56.00
E11	30.50	61.00
E12	33.00	66.00
E13	35.50	71.00
E14	38.50	77.00
E15	42.00	84.00
E16	46.00	92.00
E17	50.00	100.00
E18	54.00	108.00
E19	60.00	120.00
E20	70.00	140.00
E99	*	*

*Contact NTIS for price quote.

IMPORTANT NOTICE

NTIS Shipping and Handling Charges (effective June 1, 1985)
U.S., Canada, Mexico — ADD $3.00 per TOTAL ORDER
All Other Countries — ADD $4.00 per TOTAL ORDER

Exceptions — Does NOT apply to:
ORDERS REQUESTING NTIS RUSH HANDLING
ORDERS FOR SUBSCRIPTION OR STANDING ORDER PRODUCTS *ONLY*

NOTE: Each additional delivery address on an order
requires a separate shipping and handling charge.

VOLUME 24 NUMBER 1 / JANUARY 8, 1986

TABLE OF CONTENTS

AERONAUTICS

Includes aeronautics (general); aerodynamics; air transportation and safety; aircraft communications and navigation; aircraft design, testing and performance; aircraft instrumentation; aircraft propulsion and power; aircraft stability and control; and research and support facilities (air).

For related information see also *Astronautics*.

01 AERONAUTICS (GENERAL) 1

02 AERODYNAMICS 3

Includes aerodynamics of bodies, combinations, wings, rotors, and control surfaces; and internal flow in ducts and turbomachinery.

For related information see also *34 Fluid Mechanics and Heat Transfer*

03 AIR TRANSPORTATION AND SAFETY 6

Includes passenger and cargo air transport operations; and aircraft accidents.

For related information see also *16 Space Transportation* and *85 Urban Technology and Transportation.*

04 AIRCRAFT COMMUNICATIONS AND NAVIGATION N.A.

Includes digital and voice communication with aircraft; air navigation systems (satellite and ground based); and air traffic control.

For related information see also *17 Spacecraft Communications, Command and Tracking* and *32 Communications.*

05 AIRCRAFT DESIGN, TESTING AND PERFORMANCE 6

Includes aircraft simulation technology.

For related information see also *18 Spacecraft Design, Testing and Performance* and *39 Structural Mechanics.*

06 AIRCRAFT INSTRUMENTATION N.A.

Includes cockpit and cabin display devices; and flight instruments.

For related information see also *19 Spacecraft Instrumentation* and *35 Instrumentation and Photography.*

07 AIRCRAFT PROPULSION AND POWER N.A.

Includes prime propulsion systems and systems components, e.g., gas turbine engines and compressors; and on-board auxiliary power plants for aircraft.

For related information see also *20 Spacecraft Propulsion and Power, 28 Propellants and Fuels,* and *44 Energy Production and Conversion.*

08 AIRCRAFT STABILITY AND CONTROL 8

Includes aircraft handling qualities; piloting; flight controls; and autopilots.

09 RESEARCH AND SUPPORT FACILITIES (AIR) 9

Includes airports, hangars and runways; aircraft repair and overhaul facilities; wind tunnels; shock tube facilities; and engine test blocks.

For related information see also *14 Ground Support Systems and Facilities (Space).*

ASTRONAUTICS

Includes astronautics (general); astrodynamics; ground support systems and facilities (space); launch vehicles and space vehicles; space transportation; spacecraft communications, command and tracking; spacecraft design, testing and performance; spacecraft instrumentation; and spacecraft propulsion and power.

For related information see also *Aeronautics*

12 ASTRONAUTICS (GENERAL) 9

For extraterrestrial exploration see *91 Lunar and Planetary Exploration.*

13 ASTRODYNAMICS 35

Includes powered and free-flight trajectories; and orbit and launching dynamics.

14 GROUND SUPPORT SYSTEMS AND FACILITIES (SPACE) 35

Includes launch complexes, research and production facilities; ground support equipment, e.g., mobile transporters; and simulators.

For related information see also *09 Research and Support Facilities (Air).*

15 LAUNCH VEHICLES AND SPACE VEHICLES 36

Includes boosters; manned orbital laboratories; reusable vehicles; and space stations.

16 SPACE TRANSPORTATION 36

Includes passenger and cargo space transportation, e.g., shuttle operations; and rescue techniques.

For related information see also *03 Air Transportation and Safety* and *85 Urban Technology and Transportation.*

17 SPACECRAFT COMMUNICATION, COMMAND AND TRACKING 46

Includes telemetry; space communications networks; astronavigation; and radio blackout.

For related information see also *04 Aircraft Communications and Navigation* and *32 Communications.*

18 SPACECRAFT DESIGN, TESTING AND PERFORMANCE 46

Includes spacecraft thermal and environmental control; and attitude control.

For life support systems see *54 Man/System Technology and Life Support.* For related information see also *05 Aircraft Design, Testing and Performance* and *39 Structural Mechanics.*

19 SPACECRAFT INSTRUMENTATION 48

For related information see also *06 Aircraft Instrumentation* and *35 Instrumentation and Photography.*

20 SPACECRAFT PROPULSION AND POWER 48

Includes main propulsion systems and components, e.g., rocket engines; and spacecraft auxiliary power sources.

For related information see also *07 Aircraft Propulsion and Power, 28 Propellants and Fuels,* and *44 Energy Production and Conversion.*

CHEMISTRY AND MATERIALS

Includes chemistry and materials (general); composite materials; inorganic and physical chemistry; metallic materials; nonmetallic materials; and propellants and fuels.

23 CHEMISTRY AND MATERIALS (GENERAL) 49

Includes biochemistry and organic chemistry.

24 COMPOSITE MATERIALS 49

Includes laminates.

25 INORGANIC AND PHYSICAL CHEMISTRY 51

Includes chemical analysis, e.g., chromatography; combustion theory; electrochemistry; and photochemistry.

For related information see also *77 Thermodynamics and Statistical Physics.*

26 METALLIC MATERIALS 53

Includes physical, chemical, and mechanical properties of metals, e.g., corrosion; and metallurgy.

27 NONMETALLIC MATERIALS 57

Includes physical, chemical, and mechanical properties of plastics, elastomers, lubricants, polymers, textiles, adhesives, and ceramic materials.

28 PROPELLANTS AND FUELS 60

Includes rocket propellants, igniters, and oxidizers; storage and handling; and aircraft fuels.

For related information see also *07 Aircraft Propulsion and Power, 20 Spacecraft Propulsion and Power,* and *44 Energy Production and Conversion.*

ENGINEERING

Includes engineering (general); communications; electronics and electrical engineering; fluid mechanics and heat transfer; instrumentation and photography; lasers and masers; mechanical engineering; quality assurance and reliability; and structural mechanics.

For related information see also *Physics.*

31 ENGINEERING (GENERAL) 61

Includes vacuum technology; control engineering; display engineering; and cryogenics.

32 COMMUNICATIONS 62

Includes land and global communications; communications theory; and optical communications.

For related information see also *04 Aircraft Communications and Navigation* and *17 Spacecraft Communications, Command and Tracking.*

33 ELECTRONICS AND ELECTRICAL ENGINEERING 69

Includes test equipment and maintainability; components, e.g., tunnel diodes and transistors; microminiaturization; and integrated circuity.

For related information see also *60 Computer Operations and Hardware* and *76 Solid-State Physics.*

34 FLUID MECHANICS AND HEAT TRANSFER 75

Includes boundary layers; hydrodynamics; fluidics; mass transfer; and ablation cooling.

For related information see also *02 Aerodynamics* and *77 Thermodynamics and Statistical Physics.*

35 INSTRUMENTATION AND PHOTOGRAPHY 80

Includes remote sensors; measuring instruments and gages; detectors; cameras and photographic supplies; and holography.

For aerial photography see *43 Earth Resources.* For related information see also *06 Aircraft Instrumentation* and *19 Spacecraft Instrumentation.*

36 LASERS AND MASERS 88

Includes parametric amplifiers.

37 MECHANICAL ENGINEERING 89

Includes auxiliary systems (non-power); machine elements and processes; and mechanical equipment.

38 QUALITY ASSURANCE AND RELIABILITY 92

Includes product sampling procedures and techniques; and quality control.

39 STRUCTURAL MECHANICS 92

Includes structural element design and weight analysis; fatigue; and thermal stress.

For applications see *05 Aircraft Design, Testing and Performance* and *18 Spacecraft Design, Testing and Performance.*

GEOSCIENCES

Includes geosciences (general); earth resources; energy production and conversion; environment pollution; geophysics; meteorology and climatology; and oceanography.

For related information see also *Space Sciences.*

42 GEOSCIENCES (GENERAL) N.A.

43 EARTH RESOURCES 97

Includes remote sensing of earth resources by aircraft and spacecraft; photogrammetry; and aerial photography.

For instrumentation see *35 Instrumentation and Photography.*

44 ENERGY PRODUCTION AND CONVERSION 105

Includes specific energy conversion systems, e.g., fuel cells and batteries; global sources of energy; fossil fuels; geophysical conversion; hydroelectric power; and wind power.

For related information see also *07 Aircraft Propulsion and Power, 20 Spacecraft Propulsion and Power, 28 Propellants and Fuels,* and *85 Urban Technology and Transportation.*

45 ENVIRONMENT POLLUTION 110

Includes air, noise, thermal and water pollution; environment monitoring; and contamination control.

46 GEOPHYSICS 112

Includes aeronomy; upper and lower atmosphere studies; ionospheric and magnetospheric physics; and geomagnetism.

For space radiation see *93 Space Radiation.*

47 METEOROLOGY AND CLIMATOLOGY 116

Includes weather forecasting and modification.

48 OCEANOGRAPHY 118

Includes biological, dynamic and physical oceanography; and marine resources.

LIFE SCIENCES

Includes sciences (general); aerospace medicine; behavioral sciences; man/system technology and life support; and planetary biology.

51 LIFE SCIENCES (GENERAL) 119

Includes genetics.

52 AEROSPACE MEDICINE 125

Includes physiological factors; biological effects of radiation; and weightlessness.

53 BEHAVIORAL SCIENCES 127

Includes psychological factors; individual and group behavior; crew training and evaluation; and psychiatric research.

54 MAN/SYSTEM TECHNOLOGY AND LIFE SUPPORT 129

Includes human engineering; biotechnology; and space suits and protective clothing.

55 PLANETARY BIOLOGY N.A.

Includes exobiology; and extraterrestrial life.

MATHEMATICAL AND COMPUTER SCIENCES

Includes mathematical and computer sciences (general); computer operations and hardware; computer programming and software; computer systems; cybernetics; numerical analysis; statistics and probability; systems analysis; and theoretical mathematics.

59 MATHEMATICAL AND COMPUTER SCIENCES (GENERAL) 130

60 COMPUTER OPERATIONS AND HARDWARE 130

Includes computer graphics and data processing.

For components see *33 Electronics and Electrical Engineering*

61 COMPUTER PROGRAMMING AND SOFTWARE 134

Includes computer programs, routines, and algorithms.

62 COMPUTER SYSTEMS 138

Includes computer networks.

63 CYBERNETICS 139

Includes feedback and control theory.

For related information see also *54 Man System Technology and Life Support.*

64 NUMERICAL ANALYSIS 139

Includes iteration, difference equations, and numerical approximation.

65 STATISTICS AND PROBABILITY 143

Includes data sampling and smoothing; Monte Carlo method; and stochastic processes.

66 SYSTEMS ANALYSIS 145

Includes mathematical modeling; network analysis; and operations research.

67 THEORETICAL MATHEMATICS 145

Includes topology and number theory.

PHYSICS

Includes physics (general); acoustics; atomic and molecular physics; nuclear and high-energy physics; optics; plasma physics; solid-state physics; and thermodynamics and statistical physics.

For related information see also *Engineering.*

70 PHYSICS (GENERAL) 146

For geophysics see *46 Geophysics.* For astrophysics see *90 Astrophysics.* For solar physics see *92 Solar Physics.*

71 ACOUSTICS 146

Includes sound generation, transmission, and attenuation.

For noise pollution see *45 Environment Pollution.*

72 ATOMIC AND MOLECULAR PHYSICS 148

Includes atomic structure and molecular spectra.

73 NUCLEAR AND HIGH-ENERGY PHYSICS 152

Includes elementary and nuclear particles; and reactor theory.

For space radiation see *93 Space Radiation.*

74 OPTICS 155

Includes light phenomena.

75 PLASMA PHYSICS 157

Includes magnetohydrodynamics and plasma fusion.

For ionospheric plasmas see *46 Geophysics.* For space plasmas see *90 Astrophysics.*

76 SOLID-STATE PHYSICS 166

Includes superconductivity.

For related information see also *33 Electronics and Electrical Engineering* and *36 Lasers and Masers.*

77 THERMODYNAMICS AND STATISTICAL PHYSICS 168

Includes quantum mechanics; and Bose and Fermi statistics.

For related information see also *25 Inorganic and Physical Chemistry* and *34 Fluid Mechanics and Heat Transfer.*

SOCIAL SCIENCES

Includes social sciences (general); administration and management; documentation and information science; economics and cost analysis; law and political science; and urban technology and transportation.

80 SOCIAL SCIENCES (GENERAL) 169

Includes educational matters.

81 ADMINISTRATION AND MANAGEMENT 170

Includes management planning and research.

82 DOCUMENTATION AND INFORMATION SCIENCE 171

Includes information storage and retrieval technology; micrography; and library science.

For computer documentation see *61 Computer Programming and Software.*

83 ECONOMICS AND COST ANALYSIS N.A.

Includes cost effectiveness studies.

84 LAW AND POLITICAL SCIENCE N.A.

Includes space law; international law; international cooperation; and patent policy.

85 URBAN TECHNOLOGY AND TRANSPORTATION 172

Includes applications of space technology to urban problems; technology transfer; technology assessment; and surface and mass transportation.

For related information see *03 Air Transportation and Safety, 16 Space Transportation,* and *44 Energy Production and Conversion.*

SPACE SCIENCES

Includes space sciences (general); astronomy; astrophysics; lunar and planetary exploration; solar physics; and space radiation.

For related information see also *Geosciences.*

88 SPACE SCIENCES (GENERAL) N.A.

89 ASTRONOMY 174

Includes radio and gamma-ray astronomy; celestial mechanics; and astrometry.

90 ASTROPHYSICS 178

Includes cosmology; and interstellar and interplanetary gases and dust.

91 LUNAR AND PLANETARY EXPLORATION 180

Includes planetology; and manned and unmanned flights.

For spacecraft design see *18 Spacecraft Design, Testing and Performance.* For space stations see *15 Launch Vehicles and Space Vehicles.*

92 SOLAR PHYSICS 180

Includes solar activity, solar flares, solar radiation and sunspots.

93 SPACE RADIATION 181

Includes cosmic radiation; and inner and outer earth's radiation belts.

For biological effects of radiation see *52 Aerospace Medicine.* For theory see *73 Nuclear and High-Energy Physics.*

GENERAL

99 GENERAL N.A.

Note: N.A. means that no abstracts were assigned to this category for this issue.

SUBJECT INDEX I-1
PERSONAL AUTHOR INDEX I-69
CORPORATE SOURCE INDEX I-77
CONTRACT NUMBER INDEX I-91
REPORT/ACCESSION NUMBER INDEX I-95

TYPICAL CITATION AND ABSTRACT

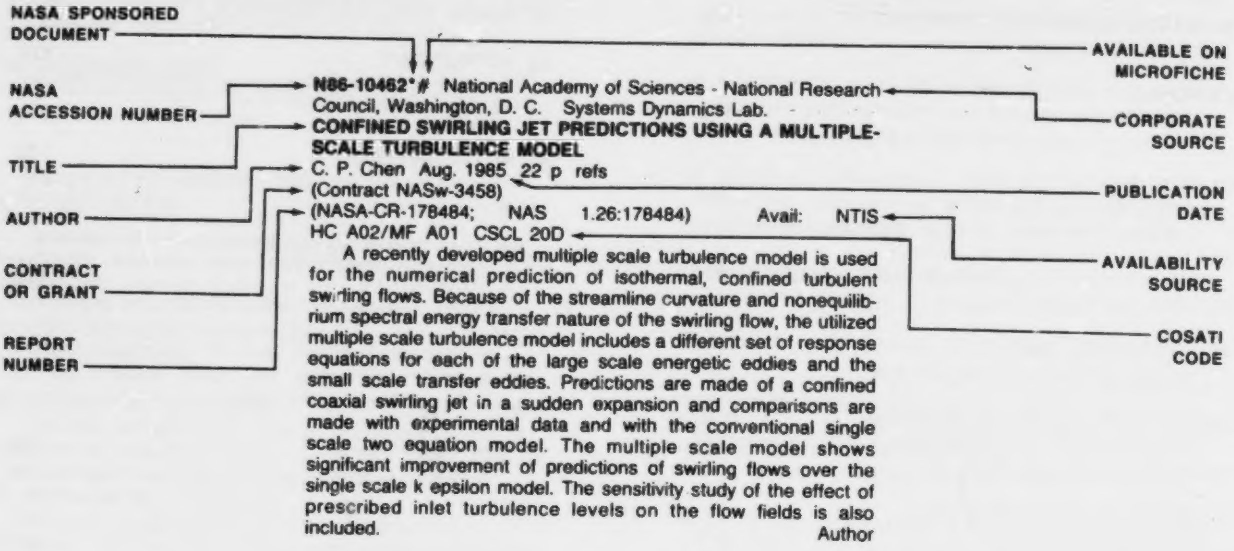
NASA SPONSORED DOCUMENT
AVAILABLE ON MICROFICHE
NASA ACCESSION NUMBER
CORPORATE SOURCE
TITLE
AUTHOR
PUBLICATION DATE
CONTRACT OR GRANT
AVAILABILITY SOURCE
REPORT NUMBER
COSATI CODE

N86-10462*# National Academy of Sciences - National Research Council, Washington, D. C. Systems Dynamics Lab.
CONFINED SWIRLING JET PREDICTIONS USING A MULTIPLE-SCALE TURBULENCE MODEL
C. P. Chen Aug. 1985 22 p refs
(Contract NASw-3458)
(NASA-CR-178484; NAS 1.26:178484) Avail: NTIS HC A02/MF A01 CSCL 20D

A recently developed multiple scale turbulence model is used for the numerical prediction of isothermal, confined turbulent swirling flows. Because of the streamline curvature and nonequilibrium spectral energy transfer nature of the swirling flow, the utilized multiple scale turbulence model includes a different set of response equations for each of the large scale energetic eddies and the small scale transfer eddies. Predictions are made of a confined coaxial swirling jet in a sudden expansion and comparisons are made with experimental data and with the conventional single scale two equation model. The multiple scale model shows significant improvement of predictions of swirling flows over the single scale k epsilon model. The sensitivity study of the effect of prescribed inlet turbulence levels on the flow fields is also included. Author

VOLUME 24 NUMBER 1 / JANUARY 8, 1986

Scientific and Technical Aerospace Reports

A Semimonthly Publication of the National Aeronautics and Space Administration

01 AERONAUTICS (GENERAL)

N86-10001# Air Force Systems Command, Wright-Patterson AFB, Ohio. Foreign Technology Div.
ACTA AERONAUTICA ET ASTRONAUTICA SINICA (SELECTED ARTICLES)
4 Oct. 1984 64 p refs Transl. into ENGLISH from Hangkong Xuebao (China), v. 4, no. 4, 1983 p 1-19, 11-19; 39-47; 101-104 (AD-A147304; FTD-ID(RS)T-1120-84) Avail: NTIS HC A04/MF A01 CSCL 01/2

Research in aeronautics and astronautics in China is discussed. Some areas of research are: (1) approximation method for transonic flow over swept wings; (2) shock turbulent interaction over a compression corner for supersonic flow; (3) optimum design of an aircraft wing; and (4) a simple estimation method for two phase flow in a nozzle of rocket ramjet engine. For individual titles, see N86-10002 through N86-10005.

N86-10002# Air Force Systems Command, Wright-Patterson AFB, Ohio. Foreign Technology Div.
SECOND ORDER APPROXIMATION METHOD FOR TRANSONIC FLOWS OVER SWEPT WINGS **c02**
Shen Keyang (Shanghai Aviation Industry Corp.) *In its* Acta Aeron. and Astronautica Sinica (FTD-ID(RS)T-1120-84) 4 Oct. 1984 p 1-17 refs Transl. into ENGLISH from Hangkong Xuebao (China), v. 4, no. 4, 1983 p 1-10 (For primary document see N86-10001 01-01)
Avail: NTIS HC A04/MF A01 CSCL 01/1

The TSDH equation is used to calculate the transonic flows over three dimensional swept wings. It considers the leading edge boundary conditions and leading edge velocity potential equation suitable for the blunt leading edge of wings. The expanded form of the Jameson scheme is used in the unequal step length grid for the discretization of the TSDH equation into a set of finite difference equations. A rarefied grid was arranged in the calculation space, then a dense grid was arranged near the wing and alternate iteration of the rarefied and dense meshes was carried out so as to accelerate convergence and raise calculation precision. Calculations of the supercritical without shock wave and with shock wave conditions of the ONERA M6 wing show that there is good agreement between the TSDH solution and the FVP solution and wind tunnel tests. Author

N86-10003# Air Force Systems Command, Wright-Patterson AFB, Ohio. Foreign Technology Div.
A NUMERICAL SOLUTION OF THE SHOCK-TURBULENT INTERACTION OVER A COMPRESSION CORNER FOR SUPERSONIC FLOW **c02**
Cao Qipeng (Nanjing Aeronautical Inst.) *In its* Acta Aeron. et Astronautica Sinica (FTD-ID(RS)T-1120-84) 4 Oct. 1985 p 18-33 refs Transl. into ENGLISH from Hangkong Xuebao (China), v. 4, no. 4, 1983 p 11-19 (For primary document see N86-10001 01-01)
Avail: NTIS HC A04/MF A01 CSCL 01/1

The shock turbulent boundary layer interaction over a compression corner for supersonic flow is calculated. The calculations use the Cebeci-Kellet box method; the turbulence model uses the algebraic eddy viscosity model; the pressure strength distribution uses the unified hypersonic and supersonic formulas of flowing over a wedge. Iteration correction is carried out of the shock turbulent boundary layer disturbance. The calculations predict the wall pressure distribution as well as the initial rise point location of the pressure. Author

N86-10004# Air Force Systems Command, Wright-Patterson AFB, Ohio. Foreign Technology Div.
OPTIMUM DESIGN OF AN AIRCRAFT WING STRUCTURE WITH MULTIPLE CONSTRAINTS BY THE DIRECT-VISION CRITERIA METHOD **c05**
Li Linang (Shenyang Aircraft Corp.) *In its* Acta Aeron. et Astronautica Sinica (FTD-ID(RS)T-1120-84) 4 Oct. 1984 p 34-52 refs Transl. into ENGLISH from Hangkong Xuebao (China), v. 4, no. 4, 1983 p 39-47 (For primary document see N86-10001 01-01)
Avail: NTIS HC A04/MF A01 CSCL 01/1

An optimized computer program (SAFDOP) is introduced which uses the direct vision criteria method for a wing surface structure with multiple constraints. This program can separately carry out analysis, optimization and synthetic optimization calculations of stress, displacement, flutter and static aeroelasticity. The alternate constraint method was used for synthetic optimization calculations. Aside from the stress constraints using the full stress method, each of the other constraints used the uniform derivative criteria. For practical purposes, the element linking weight was used as an independent design variable, in the optimum design the automatic sieve selection design variable and other methods were used and the automatic generation of initial numerical data was considered. This program was used to calculate a typical fighter wing and it proved to be feasible. Author

N86-10005# Air Force Systems Command, Wright-Patterson AFB, Ohio. Foreign Technology Div.
THEORETICAL SPECIFIC IMPULSE FOR TWO-PHASE FLOW IN NOZZLE OF ROCKET-RAMJET ENGINE: A SIMPLE ESTIMATION METHOD **c20**
Bi Shiguan (China Precision Machinery Co.) *In its* Acta Aeron. et Astronautica Sinica (FTD-ID(RS)T-1120-84) 4 Oct. 1984 p 53-60 refs Transl. into ENGLISH from Hangkong Xuebao (China), v. 4, no. 4, 1984 p 101-104 (For primary document see N86-10001 01-01)
Avail: NTIS HC A04/MF A01 CSCL 21/8

A theoretical specific impulse formula is derived for two phase flow in nozzle rocket ramjet engine on the basis of similarity to that used for rocket engines. Theoretically, it is proved that the properties of two phase flow in nozzle for these two types of engines can be analyzed with a common combined parameter which is equivalent to the exhaust velocity. A simple estimation method is introduced for specific impulse losses of two phase flow with variable lag. An approximate solution is proposed to deal with the problem of singularity. Author

N86-10006# Information Spectrum, Inc., Arlington, Va.
F-16X MSIP (MULTI-NATIONAL STAGED IMPROVEMENT PROGRAM) CASE EXAMPLE: OPERATING AND SUPPORT COST ESTIMATION USING VAMOSC (VISIBILITY AND MANAGEMENT OF OPERATING AND SUPPORT COSTS) Final Technical Report
W. C. Redeen 17 Aug. 1984 71 p
(Contract F33600-82-C-0543)
(AD-A156893; ISI-V-4859-02) Avail: NTIS HC A04/MF A01 CSCL 05/1

This case example of a hypothetical F-16X MSIP (Multi-National Staged Improvement Program) Operating and Support (O&S) cost estimate, sponsored by AFLC/MM (VAMOSC), has been prepared to demonstrate and test the capability of the Air Force Visibility and Management of Operating and Support Costs (VAMOSC) system to provide unique and detailed experience data suitable for credible and explicit O&S cost estimation for advanced Air Force aircraft systems and subsystems. The specific objective of this effort is: To produce a case example of VAMOSC applicability to O&S cost estimation which conforms to the following conditions: Is compatible with OSD/CAIG and USAF costing guidance. Is linkable to reported experience data for existing aircraft. Provided a VAMOSC-Supported Methodology which can be utilized to predict the impact of configuration changes on system O&S costs. Depicts a methodology which is applicable to O&S costing for any aircraft system in advanced conceptual development. Provides estimates which are verifiable by tests. Identifies areas of VAMOSC requiring enhancement or modification to improve system integrity and applicability. GRA

N86-10007# Air Force Systems Command, Wright-Patterson AFB, Ohio. Foreign Technology Div.
THREE ARTICLES ON NEW CALCULATION METHODS IN AERONAUTICS (SELECTED ARTICLES)
17 Aug. 1984 55 p refs Transl. into ENGLISH from Hangkong Xuebao (China), v. 4, no. 3, Sep. 1983 p 1-18, 56-62, and 102-104
(AD-A145745; FTD-ID(RS)T-0910-84) Avail: NTIS HC A04/MF A01 CSCL 01/2

Selected research topics are investigated in search of new calculation methods for aeronautics. Numerical solutions are sought for calculating hypersonic flow and unsteady supersonic aerodynamic forces. Methods for determining aerodynamic coefficients are discussed. Selected highlights of the third conference of the Aeronautical Society of China are also discussed. Shear layer effects on the stability of an axisymmetrical external compression air intake are investigated. For individual titles, see N86-10008 through N86-10011.

N86-10008# Air Force Systems Command, Wright-Patterson AFB, Ohio. Foreign Technology Div.
NUMERICAL SOLUTION OF HYPERSONIC FLOW NEAR LEADING EDGE OF A FLAT PLATE c02
Dexun Fu *In its* Three Articles on New Calculation Methods in Aeron. (Selected Articles) (FTD-ID(RS)T-0910-84) 17 Aug. 1984 p 1-14 refs Transl. into ENGLISH from Hangkong Xuebao (China), v. 4, no. 3, Sep. 1983 p 1-8 Original language document announced in IAA as A84-23903 (For primary document see N86-10007 01-01)
Avail: NTIS HC A04/MF A01 CSCL 01/2

A one-step difference scheme for solving two-dimensional steady state Navier-Stokes equations is proposed to handle supersonic and hypersonic viscous interaction problems near the leading edge of a flat plate. The scheme is considered and analyzed with a model equation. It has second-order accuracy in space for steady state problems and its stability condition is improved. The scheme is much simpler, compared to the commonly used two-step predictor-corrector difference scheme for N-S equations and also is convenient for programming. Two viscous interaction problems are solved with the proposed scheme; the solutions are valid throughout the boundary layer, shock-wave structure, and inviscid core. The results show good agreement with experimental data. The numerical solutions show that the nonslip conditions can be used for weak viscous interaction. C.D. (IAA)

N86-10009# Air Force Systems Command, Wright-Patterson AFB, Ohio. Foreign Technology Div.
A NEW METHOD FOR CALCULATING UNSTEADY SUPERSONIC AERODYNAMIC FORCES AND ITS APPLICATION c02
Xianxin Wang *In its* Three Articles on New Calculation Methods in Aeron. (Selected Articles) (FTD-ID(RS)T-0910-84) 17 Aug. 1984 p 15-31 refs Transl. into ENGLISH from Hangkong Xuebao (China), v. 4, no. 3, Sep. 1983 p 9-18 (For primary document see N86-10007 01-01)
Avail: NTIS HC A04/MF A01 CSCL 01/2

This paper proposes a new method for calculating supersonic unsteady aerodynamic forces. It combines the piston theory for unsteady supersonic flow with the conical flow theory for steady flow so that the interaction between points on a wing neglected in the piston theory is approximated by the conical flow theory. This method was used in this paper for flutter calculations of 29 cases for wings with 10 different types of plane forms. The results were compared with flutter test results obtained in wind tunnels and they were in satisfactory agreement. It was especially the case that the accuracy of flutter analysis improved by this method was noticeably higher than that obtained by the piston theory. This shows that this method is reliable and feasible for supersonic flutter analysis. It possesses the advantages of being a more succinct method and having higher calculation accuracy, less computing time and easier programming. Author

N86-10010# Air Force Systems Command, Wright-Patterson AFB, Ohio. Foreign Technology Div.
EFFECT OF A SHEAR LAYER ON THE STABILITY OF AN AXISYMMETRICAL EXTERNAL COMPRESSION AIR INTAKE c02
Kunyuan Zhang, Shaozhi Yu, and Chengyi Peng *In its* Three Articles on New Calculation Methods in Aeron. (Selected Articles) (FTD-ID(RS)T-0910-84) 17 Aug. 1984 p 32-42 refs Transl. into ENGLISH from Hangkong Xuebao (China), v. 4, no. 3, Sep. 1983 p 56-62 (For primary document see N86-10007 01-01)
Avail: NTIS HC A04/MF A01 CSCL 01/2

The influence of shear layers of various strengths on the stability of an axisymmetric compression supersonic air intake is studied. Strength is defined as the ratio of total pressure difference between the two sides of a shear layer to the total pressure of the incoming flow. Six central bodies with different cone angles were used to produce shear layers with strengths ranging from 5 to 11 percent of the total pressure of upstream flow inside a free stream wind tunnel with a fixed Mach number of 1.72. Shear layers with less than 10 percent strength were strong enough to cause separation of the boundary layer from the inside surface of the cowl. Shear layers of strength less than 11 percent failed to induce buzz in the axisymmetric intake. The influence of a shear layer depended on its distance from the lip of the cowl, and was most noticeable at a distance of 10 to 18 percent of the cowl radius. C.D. (IAA)

N86-10011# Air Force Systems Command, Wright-Patterson AFB, Ohio. Foreign Technology Div.
COMMENT ON DETERMINATION OF AERODYNAMIC COEFFICIENTS FOR A REENTRY BODY BY MEANS OF THE KALMAN FILTER METHOD c02
Jinshi Cai *In its* Three Articles on New Calculation Methods in Aeron. (Selected Articles) (FTD-ID(RS)T-0910-84) 17 Aug. 1984 p 43-46 Transl. into ENGLISH from Hangkong Xuebao (China), v. 4, no. 3, Sep. 1983 p 102-104 (For primary document see N86-10007 01-01)
Avail: NTIS HC A04/MF A01 CSCL 01/2

Research emphatically indicates that a mathematical model for aerodynamic parameter identification of a reentry body bases only on the data of angular rates and accelerations onboard but not on trajectory observation data. It can only determine the ratio between aerodynamic coefficients of the reentry body but can't determine the aerodynamic coefficients directly. B.W.

02 AERODYNAMICS

Includes aerodynamics of bodies, combinations, wings, rotors, and control surfaces; and internal flow in ducts and turbomachinery.

For related information see also *34 Fluid Mechanics and Heat Transfer.*

N86-10012 Georgia Inst. of Tech., Atlanta.
A STUDY OF THE AERODYNAMIC PERFORMANCE OF WEIS-FOGH WINGS Ph.D. Thesis
Hsun Hu Chen 1985 145 p
Avail: Univ. Microfilms Order No. DA8510956

A general theory of aerodynamics developed on the basis of viscous flow equations, is utilized in an investigation of the Weis-Fogh problem. The general theory is ideally suited for nonlinear unsteady aerodynamic problems. It is also shown that the general theory permits the important flow elements dominating the aerodynamics of nonlinear unsteady flows to be identified and their contributions evaluated individually. The Weis-Fogh problem is a well known biofluiddynamics problem involving articulate lifting bodies. The present study has yielded useful results for the lift and drag acting on a wing undergoing the fling and the clap phases of the Weis-Fogh motion. Closed form expressions have been obtained for the unsteady aerodynamic forces and the power expenditure of the Weis-Fogh wing. These results have led to the identification of major contributions to aerodynamic performance of the Weis-Fogh wings and to an assessment of the relative importance of these contributions. Dissert. Abstr.

N86-10013 Princeton Univ., N. J.
ON THE DESIGN OF AIRFOILS IN TRANSONIC FLOW USING THE EULER EQUATIONS Ph.D. Thesis
John Foster Fay 1985 83 p
Avail: Univ. Microfilms Order No. DA8509636

This work falls naturally into two parts. One part describes a computer program that designs airfoils using the Lighthill method of conformal mappings. This program involves the use of the Euler equations to solve for the flow past a given initial shape, and also around intermediate shapes. The other part is a derivation of an extension of the Lighthill method to compressible flows with the assumptions of potential flow and small disturbances of the free stream. The description of the program speaks to its various aspects, namely the Euler solution formulation and the actual process of design. Several other topics are also mentioned; these include several factors affecting the rate of convergence of the design process, the importance of equaling the lift coefficients of the initial and final shapes; and the effect of using the same design velocity distribution at different freestream Mach numbers. There is a short appendix giving a plausible argument indicating that the interaction for small disturbance and arbitrary subsonic Mach number will converge to a desired shape. Dissert. Abstr.

N86-10014*# Vanderbilt Univ., Nashville, Tenn. Dept. of Mechanical and Materials Engineering.
THE ROLE OF FREESTREAM TURBULENCE SCALE IN SUBSONIC FLOW SEPARATION Interim Progress Report, 1 Jan. - 30 Jun. 1985
J. Leith Potter, W. R. Seebaugh, Carl E. Fisher, R. Joel Barnett, and Rajiv B. Gokhale 30 Jun. 1985 56 p
(Grant NAG1-483)
(NASA-CR-176237; NAS 1.26:176237; IPR-2) Avail: NTIS HC A04/MF A01 CSCL 01A

The clarification of the role of freestream turbulence scale in determining the location of boundary layer separation is discussed. Modifications to the test facility were completed. Wind tunnel flow characteristics, including turbulence parameters, were determined with two turbulence generating grids, as well as no grid. These results are summarized. Initial results on the role of scale on turbulent boundary layer separation on the upper surface of an airfoil model are also discussed. Author

N86-10015*# National Aeronautics and Space Administration. Ames Research Center, Moffett Field, Calif.
EVALUATION OF AN AERODYNAMIC-LOAD PREDICTION METHOD ON A STOL FIGHTER CONFIGURATION
Joseph Katz Aug. 1985 33 p refs Previously announced as N85-33121
(NASA-TM-86762; Rept-85358; NAS 1.15:86762) Avail: NTIS HC A03/MF A01 CSCL 01A

A three-dimensional panel method was used to compute the aerodynamic loads on a large-scale, powered wind tunnel model. The size of the computation grid was selected such that turnaround times, on present computers remained satisfactory. With this constraint, the STOL aircraft configuration was modeled and the capabilities and limitations of the prediction method were investigated. After this study, a similar numerical model was established for a forward-swept-wing aircraft configuration which is planned for large-scale, low-speed testing. The resulting aerodynamic-load predictions are discussed and will be utilized, together with the future experimental results, to obtain a broader validation of this method as well as to reduce the necessary size of the matrix of the test parameters. Author

N86-10016*# National Aeronautics and Space Administration. Langley Research Center, Hampton, Va.
OPERATING CHARACTERISTICS OF THE MULTIPLE CRITICAL VENTURI SYSTEM AND SECONDARY CALIBRATION NOZZLES USED FOR WEIGHT-FLOW MEASUREMENTS IN THE LANGLEY 16-FOOT TRANSONIC TUNNEL
Bobby L. Berrier, Laurence D. Leavitt, and Linda S. Bangert Sep. 1985 74 p refs
(NASA-TM-86405; L-15960; NAS 1.15:86405) Avail: NTIS HC A04/MF A01 CSCL 01A

An investigation has been conducted in the Langley 16 Foot Transonic Tunnel to determine the weight flow measurement characteristics of a multiple critical Venturi system and the nozzle discharge coefficient characteristics of a series of convergent calibration nozzles. The effects on model discharge coefficient of nozzle throat area, model choke plate open area, nozzle pressure ratio, jet total temperature, and number and combination of operating Venturis were investigated. Tests were conducted at static conditions (tunnel wind off) at nozzle pressure ratios from 1.3 to 7.0. Author

N86-10017*# National Aeronautics and Space Administration. Lewis Research Center, Cleveland, Ohio.
THREE-DIMENSIONAL INVISCID ANALYSIS OF RADIAL TURBINE FLOW AND A LIMITED COMPARISON WITH EXPERIMENTAL DATA
Y. K. Choo and K. C. Civinskas (Army Aviation Research and Technology Activity) [1985] 28 p refs To be presented at the ASME Winter Ann. Meeting, 3-Dimensional Flow Phenomena in Fluid Machinery Symp., Miami, Fla., 17-22 Nov. 1985
(NASA-TM-87091; E-2679; NAS 1.15:87091; USAAVSCOM-TR-85-C-12) Avail: NTIS HC A03/MF A01 CSCL 01A

The three-dimensional inviscid DENTON code is used to analyze flow through a radial-inflow turbine rotor. Experimental data from the rotor are compared with analytical results obtained by using the code. The experimental data available for comparison are the radial distributions of circumferentially averaged values of absolute flow angle and total pressure downstream of the rotor exit. The computed rotor-exit flow angles are generally underturned relative to the experimental values, which reflect the boundary-layer separation at the trailing edge and the development of wakes downstream of the rotor. The experimental rotor is designed for a higher-than-optimum work factor of 1.126 resulting in a nonoptimum positive incidence and causing a region of rapid flow adjustment and large velocity gradients. For this experimental rotor, the computed radial distribution of rotor-exit to turbine-inlet total pressure ratios are underpredicted due to the errors in the finite-difference approximations in the regions of rapid flow adjustment, and due to using the relatively coarser grids in the middle of the blade region where the flow passage is highly three-dimensional. Additional results obtained from the three-dimensional inviscid computation are also presented, but without comparison due to the lack of experimental data. These include quasi-secondary velocity vectors on cross-channel surfaces, velocity components on the meridional and blade-to-blade surfaces, and blade surface loading diagrams. Computed results show the evolution of a passage vortex and large streamline deviations from the computational streamwise grid lines. Experience gained from applying the code to a radial turbine geometry is also discussed.

Author

N86-10018*# National Aeronautics and Space Administration. Johnson (Lyndon B.) Space Center,

NUMERICAL PROCEDURE FOR THREE-DIMENSIONAL HYPERSONIC VISCOUS FLOW OVER AEROBRAKE CONFIGURATION

Chien-peng Li Aug. 1985 17 p refs
(NASA-TM-58269; S-549; NAS 1.15:58269) Avail: NTIS HC A02/MF A01 CSCL 01A

A numerical method, which is simpler and more efficient than others currently in use, is proposed for the computation of the full viscous flow over an aerobrake body in hypersonic stream at high altitude. It treats the shock layer surrounding the blunt forebody and the near wake behind the base simultaneously by formulating the Navier-Stokes equations in conformal and azimuthal-angle coordinates. The computational domain is confined by the body wall, outflow surface and the shock, which is adjusted along the coordinate normal to the wall in the course of iterations. Because of the optimal grid and a well developed alternating direction implicit factorization technique for the governing equations, reasonably accurate results can be obtained with a 28 x 36 x 7 grid and 400 time-marching iterations. Excellent agreement of shock location is found between the present result and the schlieren photograph. Details of the base flow and shear layer impingement on the cylindrical aft body are presented for an adiabatic wall case.

Author

N86-10019*# National Aeronautics and Space Administration. Lewis Research Center, Cleveland, Ohio.

FORCED RESPONSE ANALYSIS OF AN AERODYNAMICALLY DETUNED SUPERSONIC TURBOMACHINE ROTOR

Daniel Hoyniak and Sanford Fleeter (Purdue Univ., West Lafayette, Ind.) 1985 24 p refs Presented at 10th Bien. Design Eng. Div. Conf. and Exhibit on Mech. Vibration and Noise, Cincinnati, 10-13 Sep. 1985; sponsored by ASME
(NASA-TM-87093; E-2685; NAS 1.15:87093) Avail: NTIS HC A02/MF A01 CSCL 01A

High performance aircraft-engine fan and compressor blades are vulnerable to aerodynamically forced vibrations generated by inlet flow distortions due to wakes from upstream blade and vane rows, atmospheric gusts, and maldistributions in inlet ducts. In this report, an analysis is developed to predict the flow-induced forced response of an aerodynamically detuned rotor operating in a supersonic flow with a subsonic axial component. The aerodynamic detuning is achieved by alternating the circumferential spacing of adjacent rotor blades. The total unsteady aerodynamic loading acting on the blading, as a result of the convection of the transverse gust past the airfoil cascade and the resulting motion of the cascade, is developed in terms of influence coefficients. This analysis is used to investigate the effect of aerodynamic detuning on the forced response of a 12-blade rotor, with Verdon's Cascade B flow geometry as a uniformly spaced baseline configuration. The results of this study indicate that, for forward traveling wave gust excitations, aerodynamic detuning is very beneficial, resulting in significantly decreased maximum-amplitude blade responses for many interblade phase angles.

Author

N86-10020# Department of the Air Force, Washington, D.C.

SUBMERGED RAM AIR INLETS FOR ECM (ELECTRONIC COUNTERMEASURES) PODS Patent Application

Foxwell, inventor (to Air Force) Filed 27 Jun. 1985 15 p
(AD-D011801; US-Patent-Appl-SN-749333) Avail: NTIS HC A02/MF A01 CSCL 21/5

The present invention utilizes a substantially pear-shaped submerged air inlet duct in the surface of an electronic countermeasures (ECM) pod to provide cooling air for heat exchanger units which are utilized to cool electronic components in a ECM pod. The smaller opening is in the forward most position.

GRA

N86-10021# Sandia Labs., Albuquerque, N. Mex.

INVISCID FLOW FIELD ANALYSIS OF MANEUVERING HYPERSONIC VEHICLES USING THE SCM FORMULATION AND PARABOLIC GRID GENERATION

R. W. Noack 1985 13 p Presented at the 18th Fluid Dyn., Plasma Dyn. and Lasers, Cincinnati, 16 Jul. 1985
(Contract DE-AC04-76DP-00789)
(DE85-013950; SAND-84-2670C; CONF-850717-1) Avail: NTIS HC A02/MF A01

The split-coefficient matrix (SCM) form of the Euler equations for a cylindrical base coordinate system is extended to allow the use of a generalized three-dimensional grid generation scheme. A grid generation scheme based on a parabolic partial differential equation is developed. Grids are obtained without iteration by marching from the body to the shock with body and shock points specified. The SCM type body boundary condition has been found to underpredict surface pressure for geometries with small radii of curvature. An improved method of characteristic (MOC) type body boundary condition has been developed which uses SMC type differencing in the crossflow direction. The improved MOC boundary condition has been found to have the robustness of the SCM type scheme while having superior accuracy. Solutions using the SCM form of the Euler equations with the parabolic grid generator and the improved MOC body boundary condition have been obtained for a hypersonic six fin missile. Generally good agreement is found in comparisons of the inviscid predictions with experimental data.

DOE

N86-10022# Office National d'Etudes et de Recherches Aerospatiales, Paris (France). Direction Scientifique de la Resistance des Structures.

THEORETICAL STUDY OF THE UNSTEADY LINEAR PROBLEM FOR A RECTANGULAR WING WITH A PITCHING MOVEMENT Final Report [ETUDE THEORIQUE DU PROBLEME INSTATIONNAIRE LINEAIRE POUR UNE AILE RECTANGULAIRE ANIMEE D'UN MOUVEMENT DE TANGAGE]

C. Coneim Jun. 1984 35 p refs In FRENCH
(Contract DRET-83-34-135)
(ONERA-RT-17/1841-RY-010-R) Avail: NTIS HC A03/MF A01

The pressure distribution on a helicopter rectangular wing with a positive angle of attack and a harmonic pitching movement is computed. The flow separation is not taken in account as the incidence is assumed to be low. The treatment of the singularity is detailed. Results for relatively high frequencies and three profiles are presented. The three dimensional effects of the wing tip are shown.

Author (ESA)

N86-10023# Societe Nationale Industrielle Aerospatiale, Toulouse (France). Div. Avions.

AERODYNAMICS OF HYPERLIFT SYSTEMS [AERODYNAMIQUE DES SYSTEMES HYPERSUSTENTATEURS]

P. Capbern, J. Javelle, N. Larger, A. J. Paut, and C. Bonnet 23 Jan. 1985 97 p refs In FRENCH
(Contract DRET-83-34-051-00-470-75-01)
(SNIAS-443.501/85) Avail: NTIS HC A05/MF A01

A method to compute two dimensional noncompressible viscous flow on multiprofile configurations is described. The potential flow and the viscous layers are solved interactively. The potential flow is obtained by a singularities method. The boundary layers are treated by integral equations. Evaluation using the ATR 42 configuration (narrow slots, separated flow) shows the robustness of the method when treating difficult problems and a good prediction of separation and pressure distribution. The computer

program is adapted to industrial utilization on CRAY 1 computer.
Author (ESA)

N86-10024# Societe Nationale Industrielle Aerospatiale, Toulouse (France).
ANALYSIS OF HYPERLIFT SYSTEMS. STUDY OF A SINGULARITIES METHOD [ANALYSE DES SYSTEMES HYPERSUSTENATATEURS. ETUDE D'UNE METHODE DE SINGULARITES]
N. Larger 10 Sep. 1984 42 p In FRENCH
(SNIAS-443.529/84; SNIAS-443.501/85) Avail: NTIS HC A03/MF A01

Singularity models are tested to solve problems imposed by narrow airfoil profiles commonly found in industrial configurations. Solutions including computation phases, skeleton and thick profile, and the adoption of vortices for either the skeleton or the full profile are described. The results obtained are better than those from classic methods. Author (ESA)

N86-10025# Deutsche Forschungs- und Versuchsanstalt fuer Luft- und Raumfahrt, Goettingen (West Germany). Abt. Hochgeschwindigkeitsstroemungen.
INVESTIGATIONS ON A SUPERCRITICAL AIRFOIL WITH BOUNDARY LAYER SUCTION THROUGH A PERFORATED STRIP IN THE SHOCK REGION
Paul Krogmann Nov. 1984 56 p refs In GERMAN; ENGLISH summary Report will also be announced as translation (ESA-TT-940)
(DFVLR-FB-85-15; ISSN-0171-1342) Avail: NTIS HC A04/MF A01; DFVLR, Cologne DM 16.50

The effect of local boundary layer suction through a perforated strip on the flow development and aerodynamic characteristics of a transonic airfoil is investigated in a 1 m X 1 m transonic wind tunnel. In comparison with reference measurements on the same model with a solid surface, the results show that, aside from the improvements due to suction, the flow development in the non-suction case is most favorably affected by the arrangement of the perforated strip with a cavity underneath. Due to a secondary flow through the perforation and cavity, caused by the strong adverse pressure gradients occurring at higher angles of attack, the shock location as well as the flow field downstream of the shock are affected. Thus, considerable gain in maximum lift and drag reductions can be achieved. Author (ESA)

N86-10026# Deutsche Forschungs- und Versuchsanstalt fuer Luft- und Raumfahrt, Goettingen (West Germany). Forschungsbereich Stroemungsmechanik.
EXPERIMENTAL AND THEORETICAL INVESTIGATIONS OF THE FLOW AROUND AIRFOIL SYSTEMS WITH GROUND EFFECT
Dieter Steinbach Sep. 1984 63 p refs
(DFVLR-FB-85-17; ISSN-0171-1342) Avail: NTIS HC A04/MF A01; DFVLR, Cologne DM 21.50

For two rectangular wings with flaps (Q/R4 and NACA 4415) pressure distribution for plane flow and low flow velocities is measured. For ground simulation fixed ground boards adjustable in height are used. Reynolds and Mach numbers are 1.6 million and 0.15. For the NACA 4415 wing flow field measurements are carried out also. The surface singularity method with separation model used for the calculations is outlined. Agreement between experiment and theory is good to satisfactory, especially if flow separation is not too large. But even for large separated flow regions the separation model improves results. The presence of ground gives enlarged flow separation, higher pressure and base pressure values, and lower suction peaks. High-lift systems with positive camber line show considerable losses of lift near ground. A static instability of lift with respect to ground distance occurs. This effect becomes stronger as the angle of attack is increased.
Author (ESA)

N86-10027# Deutsche Forschungs- und Versuchsanstalt fuer Luft- und Raumfahrt, Goettingen (West Germany). Inst. fuer Experimentelle Stroemungsmechanik.
INVESTIGATION OF DENSITY GRADIENT FLUCTUATIONS IN A TURBULENT FREE JET BY MEANS OF THE LASER SCHLIEREN CROSSED-BEAM METHOD
Juergen Kompenhans, Hans R. Hoefer, and Sabine Rannenberg Dec. 1984 94 p refs In GERMAN; ENGLISH summay Report will also be announced as translation (ESA-TT-942)
(DFVLR-FB-85-19; ISSN-0171-1342) Avail: NTIS HC A05/MF A01; DFVLR, Cologne DM 25.50

Density gradient fluctuations within a round, turbulent jet were investigated at Mach numbers of 0.62 and 0.95 by laser schlieren photography. Cross spectral density, coherence function and phase velocity of the density gradient fluctuations were obtained using an arrangement of two crossed laser beams at various distances from the nozzle. Information on coherent structures in a jet was obtained, even at high Mach numbers. Author (ESA)

N86-10028# Max-Planck-Institut fuer Stroemungsforschung, Goettingen (West Germany).
OSCILLATIONS OF SUBSONIC FLOW IN AN ABRUPTLY EXPANDING CIRCULAR DUCT
W. C. Selerowicz, A. P. Szumowski, and G. E. A. Meier Sep. 1984 39 p refs
(MPIS-16/1984; ISSN-0436-1199) Avail: NTIS HC A03/MF A01; Fachinformationszentrum, Karlsruhe, West Germany DM 17

Subsonic flow in an abruptly expanding duct driven from a pressure reservoir, which shows self-excited oscillations of considerable amplitude was studied by visualization and acoustic pressure measurements. Depending on the pressure drop in the duct and its dimensions, three distinct types of flow oscillations are observed. These are characterized by symmetrical and antisymmetrical oscillations of the separated jet in the abruptly expanding section, and symmetrical oscillations of the jet periodically separating and reattaching to the wall. The oscillations are accompanied by intensive noise, with an intensity of 40 dB above the turbulence noise level. Author (ESA)

N86-10029# German-Dutch Wind Tunnel, North East Polder (Netherlands).
[ACTIVITIES REPORT OF THE GERMAN-DUTCH WIND TUNNEL] Annual Report, 1983
1984 18 p refs
Avail: NTIS HC A02/MF A01

Tests, maintenance, demonstrations, systems integration, and the 1983 accounts of the German-Dutch Wind tunnel are described. Installation of turbine powered simulators, and propeller simulation technology are outlined. Author (ESA)

N86-10002# Air Force Systems Command, Wright-Patterson AFB, Ohio. Foreign Technology Div.
SECOND ORDER APPROXIMATION METHOD FOR TRANSONIC FLOWS OVER SWEPT WINGS
Shen Keyang (Shanghai Aviation Industry Corp.) *In its* Acta Aeron. and Astronautica Sinica (FTD-ID(RS)T-1120-84) 4 Oct. 1984 p 1-17 refs Transl. into ENGLISH from Hangkong Xuebao (China), v. 4, no. 4, 1983 p 1-10 (For primary document see N86-10001 01-01)
Avail: NTIS HC A04/MF A01 CSCL 01/1

N86-10003# Air Force Systems Command, Wright-Patterson AFB, Ohio. Foreign Technology Div.
A NUMERICAL SOLUTION OF THE SHOCK-TURBULENT INTERACTION OVER A COMPRESSION CORNER FOR SUPERSONIC FLOW
Cao Qipeng (Nanjing Aeronautical Inst.) *In its* Acta Aeron. et Astronautica Sinica (FTD-ID(RS)T-1120-84) 4 Oct. 1985 p 18-33 refs Transl. into ENGLISH from Hangkong Xuebao (China), v. 4, no. 4, 1983 p 11-19 (For primary document see N86-10001 01-01)
Avail: NTIS HC A04/MF A01 CSCL 01/1

N86-10008# Air Force Systems Command, Wright-Patterson AFB, Ohio. Foreign Technology Div.
NUMERICAL SOLUTION OF HYPERSONIC FLOW NEAR LEADING EDGE OF A FLAT PLATE

Dexun Fu *In its* Three Articles on New Calculation Methods in Aeron. (Selected Articles) (FTD-ID(RS)T-0910-84) 17 Aug. 1984 p 1-14 refs Transl. into ENGLISH from Hangkong Xuebao (China), v. 4, no. 3, Sep. 1983 p 1-8 Original language document announced in IAA as A84-23903 (For primary document see N86-10007 01-01)
Avail: NTIS HC A04/MF A01 CSCL 01/2

N86-10009# Air Force Systems Command, Wright-Patterson AFB, Ohio. Foreign Technology Div.
A NEW METHOD FOR CALCULATING UNSTEADY SUPERSONIC AERODYNAMIC FORCES AND ITS APPLICATION
Xianxin Wang *In its* Three Articles on New Calculation Methods in Aeron. (Selected Articles) (FTD-ID(RS)T-0910-84) 17 Aug. 1984 p 15-31 refs Transl. into ENGLISH from Hangkong Xuebao (China), v. 4, no. 3, Sep. 1983 p 9-18 (For primary document see N86-10007 01-01)
Avail: NTIS HC A04/MF A01 CSCL 01/2

N86-10010# Air Force Systems Command, Wright-Patterson AFB, Ohio. Foreign Technology Div.
EFFECT OF A SHEAR LAYER ON THE STABILITY OF AN AXISYMMETRICAL EXTERNAL COMPRESSION AIR INTAKE
Kunyuan Zhang, Shaozhi Yu, and Chengyi Peng *In its* Three Articles on New Calculation Methods in Aeron. (Selected Articles) (FTD-ID(RS)T-0910-84) 17 Aug. 1984 p 32-42 refs Transl. into ENGLISH from Hangkong Xuebao (China), v. 4, no. 3, Sep. 1983 p 56-62 (For primary document see N86-10007 01-01)
Avail: NTIS HC A04/MF A01 CSCL 01/2

N86-10011# Air Force Systems Command, Wright-Patterson AFB, Ohio. Foreign Technology Div.
COMMENT ON DETERMINATION OF AERODYNAMIC COEFFICIENTS FOR A REENTRY BODY BY MEANS OF THE KALMAN FILTER METHOD
Jinshi Cai *In its* Three Articles on New Calculation Methods in Aeron. (Selected Articles) (FTD-ID(RS)T-0910-84) 17 Aug. 1984 p 43-46 Transl. into ENGLISH from Hangkong Xuebao (China), v. 4, no. 3, Sep. 1983 p 102-104 (For primary document see N86-10007 01-01)
Avail: NTIS HC A04/MF A01 CSCL 01/2

03 AIR TRANSPORTATION AND SAFETY

Includes passenger and cargo air transport operations; and aircraft accidents.

For related information see also *16 Space Transportation* and *85 Urban Technology and Transportation.*

N86-10030# Deutsche Forschungs- und Versuchsanstalt fuer Luft- und Raumfahrt, Cologne (West Germany). Hauptabt. Verkehrsforschung.
TENDENCIES TOWARD LIBERALIZATION IN EUROPEAN AIR TRAFFIC CONTROL
Rolf Juergen Haupt and Paul-Juergen Weber Mar. 1985 131 p refs In GERMAN; ENGLISH summary Report will also be announced as translation (ESA-TT-947)
(DFVLR-FB-85-23; ISSN-0171-1342) Avail: NTIS HC A07/MF A01; DFVLR, Cologne DM 37.50

Deregulation of European air transportation is discussed. Aim and content of proposed or decided regulations are considered, and proposals for the further development of the air transport system are offered. Aspects of competition, market entry and tariff regulations are presented and the fundamentals of air transport policy of Great Britain, Federal Republic of Germany and The Netherlands are described, indicating the points of view of the air transport managers (governments, airlines, and travel agencies) and of the users. Author (ESA)

N86-10031# Deutsche Forschungs- und Versuchsanstalt fuer Luft- und Raumfahrt, Cologne (West Germany). Haupabt. Verkehrsforschung.
THE AIR TRAFFIC DEMAND IN PASSENGER TRAVEL OF THE FEDERAL REPUBLIC OF GERMANY 1990 - 2000. UPDATE OF THE DFVLR AIR TRAFFIC FORECAST
Dieter Wilken and Klaus Bachmann Dec. 1984 125 p refs In GERMAN; ENGLISH summary
(DFVLR-Mitt-85-06; ISSN-0176-7739) Avail: NTIS HC A06/MF A01; DFVLR, Cologne DM 36

The future air transport demand for the Federal Republic of Germany was studied in order to update the demand part of the DFVLR air traffic forecast, with estimates of traffic at the German airports. The future demand volume was forecast with respect to trip purpose, region, and type of service. Reflecting a series of forecast hypotheses, especially regarding economic growth, demand for air travel is expected to grow from 16.3 million in 1982 to about 28 million air travellers in the year 2000. Primarily because of a strong growth of business travel, the demand for scheduled services will rise faster than the demand for charter services. Author (ESA)

04 AIRCRAFT COMMUNICATIONS AND NAVIGATION

Includes digital and voice communication with aircraft; air navigation systems (satellite and ground based); and air traffic control.

For related information see also *17 Spacecraft Communications, Command, and Tracking* and *32 Communications.*

No abstracts in this category.

05 AIRCRAFT DESIGN, TESTING AND PERFORMANCE

Includes aircraft simulation technology.

For related information see also *18 Spacecraft Design, Testing and Performance* and *39 Structural Mechanics.*

N86-10032 Department of the Air Force, Washington, D.C.
ATTACHMENT METHOD-CERAMIC RADOME TO METAL BODY Patent
J. S. Perry, inventor (to Air Force) Issued 28 May 1985 6 p Supersedes AD-D010270
(AD-D011778; US-Patent-4,520,364; US-Patent-Appl-SN-486603; US-Patent-Class-343-872) Avail: US Patent and Trademark Office CSCL 13/8

A radome assembly for an airframe and a method for attaching the assembly to an airframe are provided. The radome assembly comprises a ceramic shell with a polymeric transition section bonded thereto, which shell is adapted for mounting to a metal airframe. The transition section has a coefficient of thermal expansion intermediate between that of the ceramic shell and that of the metal airframe. The method of this invention comprises preloading the transition section in circumferential compression when the radome assembly is attached to the airframe. Author (GRA)

N86-10033*# Virginia Polytechnic Inst. and State Univ., Blacksburg. Dept. of Chemistry.
A FUNDAMENTAL STUDY OF THE STICKING OF INSECT RESIDUES TO AIRCRAFT WINGS Annual Technical Report
N. S. Eiss, Jr., J. P. Wightman, D. R. Gilliam, and E. J. Siochi Apr. 1985 191 p refs
(Grant NAG1-300)
(NASA-CR-176231; NAS 1.26:176231) Avail: NTIS HC A09/MF A01 CSCL 01C

The aircraft industry has long been concerned with the increase of drag on airplanes due to fouling of the wings by insects. The present research studied the effects of surface energy and surface roughness on the phenomenon of insect sticking. Aluminum plates of different roughnesses were coated with thin films of polymers with varying surface energies. The coated plates were attached to a custom jig and mounted on top of an automobile for insect collection. Contact angle measurements, X-ray photoelectron spectroscopy and specular reflectance infrared spectroscopy were used to characterize the surface before and after the insect impact experiments. Scanning electron microscopy showed the topography of insect residues on the exposed plates. Moments were calculated in order to find a correlation between the parameters studied and the amount of bugs collected on the plates. An effect of surface energy on the sticking of insect residues was demonstrated. Author

N86-10034# Air Command and Staff Coll., Maxwell AFB, Ala.
THE DIRIGIBLE: A CATALYST FOR RESOURCE EXPLOITATION IN REMOTE AREAS?
J. C. Murphy Apr. 1985 80 p
(AD-A156518; ACSC-85-1950) Avail: NTIS HC A05/MF A01 CSCL 01/3

Many developing nations have considerable wealth in natural resources, but are unable to exploit it. Located in remote areas, the countries simply cannot afford to invest the enormous amounts required to build roads, railroads, or airfields to access the regions. The dirigible--modern day blimp--offers a potentially inexpensive, flexible, and capable method of of transporting minerals, timber, or crops in areas without traditional transportation support. Even more important, they can stimulate agricultural or industrial development a significant distance from principal roads thereby unlocking the wealth of the land for a nation. The airship can be the catalyst for colonization at the same time it strengthens the economy. This study provides a cost/benefit model to evaluate the relative benefits of different transportation systems in the exploitation of resources. Author (GRA)

N86-10035# Naval Postgraduate School, Monterey, Calif.
CONSTRUCTION AND USE OF A RADIO CONTROLLED MODEL HELICOPTER FOR RESEARCH M.S. Thesis
C. J. Hintze Mar. 1985 67 p
(AD-A156547) Avail: NTIS HC A04/MF A01 CSCL 01/3

This thesis examines the relationship that exists between a radio controlled model helicopter and a full-size helicopter. The construction of a radio controlled model helicopter and flight training involved is discussed. Initial hover performance testing of a radio controlled helicopter is evaluated. Author (GRA)

N86-10036# Aeronautical Research Labs., Melbourne (Australia).
A REVIEW OF AUSTRALIAN INVESTIGATIONS ON AERONAUTICAL FATIGUE DURING THE PERIOD APRIL 1983 TO MARCH 1985
G. S. Jost Mar. 1985 93 p
(AD-A156602; ARL/STRUC-TM-399) Avail: NTIS HC A05/MF A01 CSCL 01/3

A summary is presented of the aircraft fatigue research and associated activities which form part of the programs of the Aeronautical Research Laboratories, the Department of Aviation and the Australian aircraft industry. The major topics discussed include the fatigue of both civil and military aircraft structures, fatigue damage detection, analysis and repair and fatigue life monitoring and assessment. Author (GRA)

N86-10037# Aeronautical Research Labs., Melbourne (Australia).
REPORT ON AN OVERSEAS VISIT
C. M. Scala Nov. 1984 33 p
(AD-A156603; ARL/MAT-TM-388) Avail: NTIS HC A03/MF A01 CSCL 14/2

A report is given on an overseas visit by Dr C.M. Scala of Australia to the USA, U.K. and Switzerland for a period of thirty-two days departing Australia on 7 July 1984. The principal purposes of the visit were to: (1) attend and present a paper at the Review of Progress in Quantitative NDE held at the University of California, San Diego; (2) undertake updating visits to laboratories in the USA and U.K. to review current research in nondestructive evaluation (NDE) and to determine useful directions for future NDE research; and (3) coordinate progress (in both the USA and Switzerland) on the DSTO contract with Battelle Pacific Northwest Laboratories to monitor fatigue crack growth in a Mirage aircraft using acoustic emission (AE). GRA

N86-10038# Air Command and Staff Coll., Maxwell AFB, Ala.
RETROFIT OF SAC EC-135C AND RC-135 AIRCRAFT WITH CFM-56 ENGINES
W. N. Stooke, Jr. Apr. 1985 42 p
(AD-A156688; ACSC-85-2630) Avail: NTIS HC A03/MF A01 CSCL 15/5

This report is an analysis of the advantages and disadvantages of retrofitting SAC's EC-135C and RC-135 fleet with the CFM-56 engine package being used to convert the KC-135As to KC-135Rs. It reviews selected components of the modification package and compares the performance capabilities of current and modified aircraft during takeoff, cruise, receiver aerial refueling, and landing. The projected fuel savings on the investment dollar are calculated in Af Regulation 173-13, USAF Cost and Planning Factors, and could pay for the retrofit of the 31 aircraft in 18 years. Finally, the advantage of logistics commonality among all three aircraft is assessed. GRA

N86-10039# Aeronautical Research Labs., Melbourne (Australia).
PROPOSED MODIFICATIONS FOR THE RAAF AIRTRAINER CT-4A COCKPIT
K. W. Anderson and K. C. Hendy Dec. 1984 23 p
(AD-A156808; ARL/SYS-TM-75) Avail: NTIS HC A02/MF A01 CSCL 01/3

The design of the CT-4A Airtrainer cockpit is known to breach numerous ergonomics principles and several ASCC Air Standards. As a result, pilots report problems such as inadequate reach envelopes and obstruction of the control column by the left pilot's left knee. Consequently, the RAAF asked ARL to study the cockpit design and recommend simple changes. An anthropometric model was developed and used to evaluate several patterns of seat adjustment. The best of these (a ramp at 40 degrees to the fuselage reference line) was evaluated in practical trials with an experimental seat in a CT-4A fuselage. For each of the thirty pilot subjects, a sitting position with acceptable view, reach and clearance was found with the experimental arrangement. The ARL recommendations for cockpit modifications include: a smaller left side throttle quadrant with external pushrods, a seat adjustable along a 40 degree ramp, improved instrument lighting, pedals moved forwards, control column modifications, lowered lap belt anchor points, dual fuel gauges and a center transponder location. Incorporation of these recommendations is expected to enhance training effectiveness and improve flying safety. GRA

N86-10040# Air Command and Staff Coll., Maxwell AFB, Ala.
THE QUEST FOR A HELICOPTER SUITABLE FOR COMBAT RESCUE, 1967 - 1983
T. O. Jahnke Apr. 1985 30 p
(AD-A156842; AD-E301723; ACSC-85-1330) Avail: NTIS HC A03/MF A01 CSCL 01/3

This paper provides a concise, historical perspective of the quest for a helicopter suitable for combat rescue. Concentrating on the period 1967 to 1983, this report looks at the historical development, roles and missions, and analyzes the selection process of four different combat rescue helicopters. The study concludes that the unique mission requirements of combat rescue require aircraft designed from the ground on as pure rescue helicopters. Author (GRA)

N86-10041# Naval Postgraduate School, Monterey, Calif.
A COMPARATIVE ANALYSIS OF A CV HELICOPTER AND A JVX (JOINT SERVICES ADVANCED VERTICAL LIFT) TILT-ROTOR AIRCRAFT IN AN AIRCRAFT CARRIER BASED ASW (ANTI-SUBMARINE WARFARE) M.S. Thesis
R. L. Wilde Mar. 1985 134 p

(AD-A156871) Avail: NTIS HC A07/MF A01 CSCL 01/3

This thesis analyzes the environmental compatibility and the potential performance capabilities of two proposed types of vertical flight capable aircraft in an aircraft carrier Anti-Submarine role. The aircraft compared are the CV Helicopter(SH-60F) and an ASW variant of the Joint Services Advanced Vertical Lift (JVX) tilt-rotor aircraft. This thesis compares their adaptability and relative expected mission effectiveness by analyzing their physical dimensions and characteristics and their projected flight performance parameters. Their expected performance in a specific scenario, an ASW pouncer mission employing active dipping sonar, is analyzed using a simulation model. GRA

N86-10042*# Texas Technological Univ., Lubbock. Dept. of Electrical Engineering.

ELECTROMAGNETIC RESONANCES OF CYLINDERS AND AIRCRAFT MODEL WITH RESISTIVE WIRES Final Report, Apr. 1983 - Apr. 1984

G. W. Wood and T. F. Trost Apr. 1985 61 p
(Contract NAG1-28; DA Proj. 376-3)
(NASA-CR-176250; NAS 1.26:176250; AD-A156960;
AFWL-TR-84-90) Avail: NTIS HC A04/MF A01 CSCL 01C

Laboratory experiments were done to determine the natural frequencies of the electromagnetic resonances of conducting bodies with attached wires. The bodies include two cylinders and an approximate scale model of the NASA F-106B aircraft. All are three feet in length. Time-domain waveforms of B-dot and D-dot were obtained from a sampling oscilloscope, and Prony analysis was used to extract the natural frequencies. This work is an extension of previous work, but smaller, more resistive wires have been used. The first four natural frequencies of the cylinders (and wires) were determined, and a comparison with calculated results of other investigators show reasonable agreement. Seven natural frequencies were determined for the F-106B model (wire wires), and these have been compared with results obtained by NASA in 1982 during direct lightning strikes to the aircraft. The agreement between the corresponding natural frequencies of the model and the aircraft is fairly good and is better than that obtained in the previous work using wires with less resistance. The frequencies lie between 6.5 MHz and 41 MHz, and all of the normalized damping rates are between 0.14 and 0.27. GRA

N86-10043# European Space Agency, Paris (France).

SYSTEM MODELING AND IDENTIFICATION OF EQUIVALENT SYSTEMS WITH AND WITHOUT COMPENSATING TIME DELAY FOR CONTROL-AUGMENTED AIRCRAFT

Jean Skudridakis Oct. 1985 104 p refs Transl. into ENGLISH of "Systemmodellierung und Identifizierung von aequivalenten' Systemen mit und ohne Ersatztotleit fuer reglergestuetzte Flugzeuge' Rept. DFVLR-FB-83-36, DFVLR, Brunswick, 1983 Original language document was previously announced as N84-24570
(ESA-TT-852; DFVLR-FB-83-36) Avail: NTIS HC A06/MF A01; original German version available from DFVLR, Cologne DM 34

The identification of the aerodynamic and equivalent derivatives in the longitudinal and lateral motions of modern fighter aircraft is described. Determination of handling qualities parameters through reduced evaluation methods in order to fulfill the requirements of the MIL-F-8785 C calculation is discussed. To accomplish that goal, the highly complex method of observing aircraft motion was reduced by goal-oriented simplifications to a lower order system. The mathematical modeling for various control inputs with and without compensating time-delay, their influence on the results, and their accuracy are outlined. Author (ESA)

N86-10044# Fraunhofer-Inst. fuer Betriebsfestigkeit, Darmstadt (West Germany).

REVIEW OF INVESTIGATIONS ON AERONAUTICAL FATIGUE IN THE FEDERAL REPUBLIC OF GERMANY Review Period, May 1983 - April 1985

O. Buxbaum and H. Huth 1985 86 p refs Presented at 19th Intern. Comm. on Aeron. Fatigue (ICAF) Conf., Pisa, 1985
(LBF-S-173; ISSN-0721-5320) Avail: NTIS HC A05/MF A01; Fachinformationszentrum, Karlsruhe, West Germany DM 95

Measurement and analysis of operational loads on aircraft; metal fatigue (notch strength, low cycle fatigue, crack propagation and fracture mechanics); composites (fatigue, environmental influences, damage mechanisms); joints; fatigue life prediction; and component and full scale tests are summarized. Author (ESA)

N86-10045# Technische Hogeschool, Delft (Netherlands). Dept. of Aerospace Engineering.

FATIGUE, STATIC TENSILE STRENGTH AND STRESS CORROSION OF AIRCRAFT MATERIALS AND STRUCTURES

J. Schijve Oct. 1982 203 p refs Presented at Summer School Course, Bandung, Indonesia, Aug. 1982 Sponsored by Netherlands and Indonesian Governments
(VTH-LR-360-Pt-1) Avail: NTIS HC A10/MF A01

Failure modes in aircraft structures; stress concentration at notches; plastic deformation and residual stress; stress intensity factors of cracks; failure in tension; stress corrosion; material fatigue; fatigue under constant and variable amplitude loading; joint fatigue; fatigue loads on aircraft structures; and fatigue of aircraft structures are discussed. Author (ESA)

N86-10004# Air Force Systems Command, Wright-Patterson AFB, Ohio. Foreign Technology Div.

OPTIMUM DESIGN OF AN AIRCRAFT WING STRUCTURE WITH MULTIPLE CONSTRAINTS BY THE DIRECT-VISION CRITERIA METHOD

Li Linang (Shenyang Aircraft Corp.) *In its* Acta Aeron. et Astronautica Sinica (FTD-ID(RS)T-1120-84) 4 Oct. 1984 p 34-52 refs Transl. into ENGLISH from Hangkong Xuebao (China), v. 4, no. 4, 1983 p 39-47 (For primary document see N86-10001 01-01)
Avail: NTIS HC A04/MF A01 CSCL 01/1

06 AIRCRAFT INSTRUMENTATION

Includes cockpit and cabin display devices; and flight instruments.

For related information see also *19 Spacecraft Instrumentation* and *35 Instrumentation and Photography.*

No abstracts in this category.

07 AIRCRAFT PROPULSION AND POWER

Includes prime propulsion systems and systems components, e.g., gas turbine engines and compressors; and on-board auxiliary power plants for aircraft.

For related information see also *20 Spacecraft Propulsion and Power, 28 Propellants and Fuels,* and *44 Energy Production and Conversion.*

No abstracts in this category.

08 AIRCRAFT STABILITY AND CONTROL

Includes aircraft handling qualities; piloting; flight controls; and autopilots.

N86-10046 Mississippi State Univ., State College.

GUIDANCE AND CONTROL OF A CABLE BASED PAYLOAD PICKUP SYSTEM Ph.D. Thesis

Young-whoon Jun 1984 130 p
Avail: Univ. Microfilms Order No. DA8507876

A payload capsule in a hostile environment can be retrieved by use of a cable attached to an aircraft. The free end of the cable may be guided to the payload capsule by a specially designed tug aircraft. To accomplish this mission successfully, a control law is needed to obtain the minimum miss-distance (less than .6 ft), optimal trajectory and minimum horizontal range which provides obstacle clearance for the tug. These objectives can be obtained by applying optimal control theory to a control system for the tug. A computer simulation study has been made to obtain the control law giving the minimum clearance range and optimal trajectory of the cable pickup system. The simulated tug has a sensor package which provides precise measurement information. With this information, the control can be generated to allow a hook engagement for a small target. Dissert. Abstr.

N86-10047# Deutsche Forschungs- und Versuchsanstalt fuer Luft- und Raumfahrt, Brunswick (West Germany). Abt. Flaechenflugzeuge.
CONTROL CONCEPTS FOR IN-FLIGHT SIMULATION INCLUDING ACTUATOR NONLINEARITIES AND TIME DELAYS
Frohmut Henschel Mar. 1985 69 p refs In GERMAN; ENGLISH summary Report will also be announced as translation (ESA-TT-948)
(DFVLR-FB-85-24; ISSN-0171-1342) Avail: NTIS HC A04/MF A01; DFVLR, Cologne DM 23.50

A model-following system was developed to study the dynamic behavior of transport aircraft with reduced longitudinal stability. The system is divided into two parts. The first consists of feedforward branches. If a linear description of the model and the basic aircraft is assumed an exact model-following is achieved by this part. For the control matrices algebraic expressions are derived. In the equations the influence of actuator dynamics is considered. A set of formulas in which all variables are assumed to be discretized for processing on a digital computer is developed. By the second subsystem an error suppression is achieved. The application of a cost vector method is demonstrated for one example. It is shown that nonlinearities and time lags can be included in the calculation of the feedback gains. Author (ESA)

09 RESEARCH AND SUPPORT FACILITIES (AIR)

Includes airports, hangars and runways; aircraft repair and overhaul facilities; wind tunnels; shock tube facilities; and engine test blocks.

For related information see also *14 Ground Support Systems and Facilities (Space).*

N86-10048*# National Aeronautics and Space Administration. Ames Research Center, Moffett Field, Calif.
MANNED FLIGHT SIMULATION: CHALLENGE AND RESPONSE
John C. Dusterberry Sep. 1985 10 p refs
(NASA-TM-86827; Rept-85392; NAS 1.15:86827) Avail: NTIS HC A02/MF A01 CSCL 14B

Early AGARD papers on manned flight simulation describe the status of an emerging test technique and then offer suggestions of problems that should be solved to advance the technique and predictions of the results that will be obtained by its use. Later AGARD literature is examined to determine how these challenges have been met, both in ground-based and in-flight simulation and how AGARD has played an important role in advancing the technique so that it is now an integral part of the aerospace vehicle design process. Author

N86-10049# Sandia Labs., Albuquerque, N. Mex.
SIMULATED DIRECT-STRIKE LIGHTNING TESTING AT SANDIA NATIONAL LABORATORIES
G. L. Maxam 1985 10 p Presented at the Intern. Symp. on Electromagnetic Compatibility, Wakefield, Miss., 20 Aug. 1985
(Contract DE-AC04-76DP-00789)
(DE85-012033; SAND-85-0063C; CONF-850884-1) Avail: NTIS HC A02/MF A01

The design of the Sandia Lightning Simulator is described and its capabilities are summarized. The approach generally used in testing components and systems including the instrumentation used for test item diagnostics and for data acquisition is also described. Several applications of the simulator test capabilities are examined including Sandia systems, Navy aircraft and an ALCM missile. Some future directions now envisioned are discussed. DOE

N86-10050# Eidgenoessisches Flugzeugwerk, Emmen (Switzerland).
INVESTIGATIONS TO IMPROVE THE SLOTTED-WALL TEST SECTION OF THE F+W TRANSONIC WIND TUNNEL
Gerard Capitaine Nov. 1984 29 p refs Presented at European Mech. Colloq. No. 137 on Adaptive Wall Wind Tunnels and Wall Interferences Correction Methods, Goettingen, West Germany, 15-17 Oct. 1984
(Grant LFP-955147)
(F+W-FO-1752) Avail: NTIS HC A03/MF A01

Efficiency of a slotted wind tunnel wall is improved; wall and wall interferences of the selected wall configuration for three dimensional models are estimated. The influence of the opening of the ventilated wall on the aerodynamic coefficients of tested models is investigated. The cross-flow characteristics of the ventilated wall are determined. Due to the particular test section design (deep slots, small plenum chamber) and the natural mass outflow removal, the precise determination of the wall characteristics is difficult. In order to assess the mass flow through the wall, direct measurements and an indirect method were used. The latter method is based on the simple one-dimensional channel flow equation, taking into account the boundary layer development along the test section walls. Direct and indirect method results agree. Author (ESA)

N86-10051# Deutsche Forschungs- und Versuchsanstalt fuer Luft- und Raumfahrt, Goettingen (West Germany). Abt. Hochgeschwindigkeitsstroemungen.
THE RUBBER TUBE TEST SECTION OF THE DFVLR IN GOETTINGEN, WEST GERMANY
Erich Wedemeyer and Alfred Heddergott Jul. 1984 45 p refs
(DFVLR-FB-85-18; ISSN-0171-1342) Avail: NTIS HC A03/MF A01; DFVLR, Cologne DM 13.50

To realize three-dimensional adaptative wind tunnel walls a test section is constructed from a thick walled rubber tube. Test section length = 240 cm, and circular cross section = 80 cm. It is installed in a high speed wind tunnel. The cylindrical walls of the test section can be adapted to interference free boundary conditions by a set of 64 jacks driven by stepping motors. The measurement and evaluation of wall pressures, the computation of the interference free wall contour, and the wall adaptation by the 64 jacks are computer-controlled and performed automatically. Model tests demonstrate the achievement of interference free flow. Author (ESA)

N86-10052# German-Dutch Wind Tunnel, North East Polder (Netherlands).
[ACTIVITIES REPORT OF THE GERMAN-DUTCH WIND TUNNEL] Annual Report, 1982
1983 18 p refs
Avail: NTIS HC A02/MF A01

Testing, calibrating, demonstrations and systems integration of a large, low speed wind tunnel are outlined. Rotor noise and automobile tests are described. Author (ESA)

12 ASTRONAUTICS (GENERAL)

For extraterrestrial exploration see *91 Lunar and Planetary Exploration.*

N86-10053*# National Aeronautics and Space Administration, Washington, D.C.

MICROGRAVITY SCIENCE AND APPLICATIONS PROGRAM TASKS

Elizabeth Pentecost, comp. May 1985 224 p refs
(NASA-TM-87568; NAS 1.15:87568) Avail: NTIS HC A10/MF A01 CSCL 22A

This report is a compilation of the active research tasks as of the end of the fiscal year 1984 of the Microgravity Science and Applications Program, NASA-Office of Space Science and Applications, involving several NASA centers and other organizations. The purpose of the document is to provide an overview of the program scope for managers and scientists in industry, university, and government communities. The report is structured to include an introductory description of the program, strategy and overall goal; identification of the organizational structures and people involved; and a description of each research task, together with a list of recent publications. The tasks are grouped into six categories: (1) electronic materials; (2) solidification of metals, alloys, and composites; (3) fluid dynamics and transports; (4) biotechnology; (5) glasses and ceramics; and (6) combustion. For individual titles, see N86-10054 through N86-10178.

N86-10054*# North Carolina State Univ., Raleigh.

PROCESSING OF COMPLEX COMPOUND SEMICONDUCTORS IN SPACE Abstract Only

Klaus Bachmann *In* NASA, Washington Microgravity Sci. and Appl. Program Tasks May 1985 p 7 (For primary document see N86-10053 01-12)
(Grant NAG1-354)
Avail: NTIS HC A10/MF A01 CSCL 22A

The purpose of this first year ground based research effort was to develop growth and characterization facilities for bulk single crystals of compound semiconductor alloys. As a system of 2-6 alloy crystal growth, C sub x Mn sub (1-x)Te was chosen since it has a relatively narrow solidus-liquidus separation serving as a suitable first model for zone melting and solution growth. Also, it allows, in principle, perfect lattice matching to Cd sub x Hg sub(1-x)Te that needs to be studied as a model for the investigation of heteroepitaxial growth from Te-solutions. A vertical zone melting furnace was built and used in the synthesis of Cd sub x Mn sub(1-x)Te from the elements and crystal growth in carbon coated fused silica crucibles of Bridgman growth geometry. Photoluminescence spectra of the crystals reveal band to band recombination at energies that agree with the reported literature data. In addition, deep luminescence is present at energies corresponding to proportional shifts from the 1.4 eV deep emission observed for bulk single crystals of CdTe. Author

N86-10055*# Massachusetts Inst. of Tech., Cambridge.

FLUID FLOW IN CRYSTAL GROWTH: ANALYSIS OF THE VERTICLE BRIDGMAN AND FLOATING ZONE PROCESS

Robert A. Brown *In* NASA, Washington Microgravity Sci. and Appl. Program Tasks May 1985 p 8-10 refs (For primary document see N86-10053 01-12)
(Grant NsG-7645)
Avail: NTIS HC A10/MF A01 CSCL 22A

Research is aimed at the fundamental understanding of the interactions of heat and mass transport and fluid mechanics in crystal growth from the melt, especially in how it pertains to experiments supported by the Microgravity Science and Applications program. Emphasis has been on studies of the vertical Bridgman system, on small-scale floating zone systems proposed for space flight, and on quantitative prediction of nonlinear transitions in melt/solid interface morphologies leading to the formation of dendrites in directional solidification. The analysis of vertical Bridgman growth has lead to the complete numerical analysis of transport phenomena in directional solidification and to a detailed comparison of calculations to the GaGe growth experiments of Wang and Witt. Calculations show the central role of the ampoule material in determining the radial temperature gradients in the melt and thus, the intensity of convection. Results indicate that diffusion-controlled growth can not be achieved on Earth with conventional growth systems, but are feasible in microgravity B.W.

N86-10056*# Massachusetts Inst. of Tech., Cambridge. Dept. of Materials Sciences and Engineering.

SOLUTAL CONVECTION AND ITS EFFECTS ON CRYSTAL GROWTH AND SEGREGATION IN BINARY AND PSEUDO-BINARY SYSTEM WITH LARGE LIQUIDUS-SOLIDUS SEPARATION

Robert A. Brown and August F. Witt *In* NASA, Washington Microgravity Sci. and Appl. Program Tasks May 1985 p 11 (For primary document see N86-10053 01-12)
(Grant NsG-7645)
Avail: NTIS HC A10/MF A01 CSCL 22A

This research program is composed of theoretical and experimental studies of solutal convection and its effects on crystal growth and segregation in binary and pseudo-binary systems with large liquidus-solidus separation. The theoretical program has resulted in the development of a transient simulation of the growth of concentrated alloys in microgravity and has been used to study the dynamics of GeSi, PbSnTe, HgCdTe growth. Finite element analysis has also been developed for studying the interactions of buoyancy-driven convection in the melt caused by temperature and concentration variations with melt-solid interface morphology and alloy segregation in the grown crystal. These calculations are being compared directly to experimental measurements of segregation and interface shape for GeSi growth and GaGe growth. The results for SiGe indicate that careful design of the thermal system can result in almost diffusion-controlled growth on Earth because of the stabilizing influence of the concentration gradient ahead of the solidification front. B.W.

N86-10057*# National Aeronautics and Space Administration. Langley Research Center, Hampton, Va.

CRYSTAL GROWTH RESEARCH IN SPACE

R. K. Crouch and A. L. Fripp *In* NASA, Washington Microgravity Sci. and Appl. Program Tasks May 1985 p 12-13 refs (For primary document see N86-10053 01-12)
Avail: NTIS HC A10/MF A01 CSCL 22A

The objectives of this work are to develop growth techniques and theory leading to improved bulk growth of semiconductor single crystals. Ground based experiments will be complemented by experiments carried out in the low-g environment provided by the space shuttle. Analytical studies and laboratory investigations are being conducted to better define the causes of crystalline defects and inhomogeneities. The compound semiconductor lead-tin-telluride is being used as the modeling material. Theoretical techniques are being developed to predict the thermal and solutal fields which are present during bulk growth from a melt. Techniques for measuring the thermophysical properties of semiconductors at high temperatures have been developed. During the past year electrochemical etching techniques have been developed for delineation of inhomogeneous regions in crystals. Thermal diffusivity measurements have been completed for the solid and liquid phases of PbTe and PbSnTe. Preliminary results have been obtained on the effects on crystal morphology of gravity, interface shape and interaction between the melt and the container. B.W.

N86-10058*# National Aeronautics and Space Administration. Marshall Space Flight Center, Huntsville, Ala.

GROWTH OF ORGANIC CRYSTALS BY OSTWALD RIPENING Abstract Only

William Egbert (Minnesota Mining and Manufacturing Co.), Christopher Podsiadly (Minnesota Mining and Manufacturing Co.), and Robert Naumann *In* NASA, Washington Microgravity Sci. and Appl. Program Tasks May 1985 p 14 (For primary document see N86-10053 01-12)
Avail: NTIS HC A10/MF A01 CSCL 22A

The objective of this investigation is to evaluate the growth of various organic crystals by chemical precipitation and Ostwald ripening. Six precipitation reactors were flown on STS-51A. Five of the reactors contained proprietary materials. The sixth contained urea dissolved in ethanol with toluene as the precipitating agent. The size distribution will be analyzed and compared with a similar model being developed. B.W.

N86-10059*# Stanford Univ., Calif. Center for Materials Research.

THE INFLUENCE OF LOW FREQUENCY MECHANICAL VIBRATIONS ON THE GROWTH OF SINGLE CRYSTALS

Robert S. Feigelson and Dennis Elwell *In* NASA, Washington Microgravity Sci. and Appl. Program Tasks May 1985 p 15 (For primary document see N86-10053 01-12)
(Contract NAS8-34872)
Avail: NTIS HC A10/MF A01 CSCL 22A

The optimum conditions for crystal growth are usually achieved either by suppressing convective fluid flows (e.g., by the use of a low-gravity environment) or by over-riding thermal and solutal convection by the use of a strong stirring action. A novel stirring technique has been developed which involves subjecting a vertical crucible to a circle in a horizontal plane (without rotation). Use of an amplitude of 3 mm at a frequency of approx 6 Hz produced complete mixing of a non-uniform aqueous liquid in a few seconds. The mixing action involved the downward flow of liquid in the outer annulus of the liquid, driven by surface waves. When the downward flowing liquid reaches the bottom of the crucible, it is reflected in a central, upward flowing spiral. This flow pattern should be beneficial for crystal growth by the Bridgman method since it will sweep impurities away from the walls and produce a more convex solid-liquid interface. Initial attempts to apply the new stirring technique to CdTe crystal growth did not show significant improvement in the number of crystals nucleated, but the interface shape appeared to be close to that predicted. B.W.

N86-10060*# Science Applications, Inc., Huntsville, Ala.

THE CONTROL OF FLOAT ZONE INTERFACES BY THE USE OF SELECTED BOUNDARY CONDITIONS

Larry M. Foster *In* NASA, Washington Microgravity Sci. and Appl. Program Tasks May 1985 p 16 (For primary document see N86-10053 01-12)
(Contract NAS8-35108)
Avail: NTIS HC A10/MF A01 CSCL 22A

Since the float zone process involves two solid-melt interfaces, possible gas interfaces, heat and mass transfers, various driving forces and complex heating sources, an analysis of the entire process would be very complex. For an initial investigation, a more feasible approach is to examine each component of the process separately. The three principal components are: (1) the shapes of the melt and solid-melt interfaces, (2) the heat and mass transfers, and (3) the heating and cooling sources. This study combined facets of all three components. The purpose of this effort was to study and compute the surface boundary conditions required to give flat (float zone) FZ solid-melt interfaces. This study was undertaken in two phases. The first phase was to investigate the solid zones surface boundary conditions required for flat solid-melt interfaces when given the melt zone surface boundary conditions. The second phase complemented the first and was to investigate the melt zone surface boundary conditions required for flat solid-melt interfaces if given the solid zones surface boundary conditions. Dual integral transform methods were used in both phases; in addition, the use of various numerical methods for differential equations and linear systems of equations were required. B.W.

N86-10061*# Massachusetts Inst. of Tech., Cambridge.

CRYSTAL GROWTH OF DEVICE QUALITY GaAs IN SPACE

Harry C. Gatos *In* NASA, Washington Microgravity Sci. and Appl. Program Tasks May 1985 p 17-18 refs (For primary document see N86-10053 01-12)
(Grant NsG-7331)
Avail: NTIS HC A10/MF A01 CSCL 22A

The GaAs research evolves about these key thrust areas. The overall program combines: (1) studies of crystal growth on novel approaches to engineering of semiconductor material (i.e., GaAs and related compounds); (2) investigation and correlation of materials properties and electronic characteristics on a macro- and microscale; and (3) investigation of electronic properties and phenomena controlling device applications and device performance. This effort is aimed at the essential ground-based program which would insure successful experimentation with and eventually processing of GaAs in near zero gravity environment. It is believed that this program addresses in a unique way materials engineering aspects which bear directly on the future exploitation of the potential of GaAs and related materials in device and systems applications. Author

N86-10062*# Massachusetts Inst. of Tech., Cambridge.

CRYSTAL MELTS UNDER REDUCED GRAVITY

Harvey P. Greenspan *In* NASA, Washington Microgravity Sci. and Appl. Program Tasks May 1985 p 19 (For primary document see N86-10053 01-12)
(Contract NAS8-35412)
Avail: NTIS HC A10/MF A01 CSCL 22A

To date, fluid motion due to thermocapillary convection and centrifugal buoyancy has been studied theoretically and numerically, by adapting specialized programs for rotating viscous fluids. It has been shown that by rotating the crystal melt, thermocapillary flow can be confined to a thin layer at the melt-gas interface even when the interfacial velocity is large enough for non-linear effects to be important. Theoretical analysis of the basic processes proceeds, but a much larger effort is now being devoted to the numerical simulation of the actual motion in a rotating crystal melt. A numerical program is under development for the study of the fully nonlinear problem. Although the flow is viewed, to start, as one of rapid rotation (in order that certain boundary layer simplifications can be invoked), a more general approach will allow consideration of the situations and conditions of real practical interest B.W.

N86-10063*# Westech Systems, Inc., Phoenix, Ariz.

MICROGRAVITY SILICON ZONING INVESTIGATION

E. L. Kern *In* NASA, Washington Microgravity Sci. and Appl. Program Tasks May 1985 p 20 (For primary document see N86-10053 01-12)
(Contract NAS8-34920)
Avail: NTIS HC A10/MF A01 CSCL 22A

This research program is directed toward the understanding of the float zone crystal growth process, the melt interactions which lead to crystal inhomogeneities, and the influence of microgravity on reducing these inhomogeneities. Silicon was selected as the model crystal because its inhomogeneities lead to known variations in device performance, and because the mechanisms involved in its growth are understood better than for other high temperature crystals. The objective of the program is to understand the growth mechanisms in float zone growth and thereby determine the feasibility and advantages of float zone growth of silicon under microgravity conditions. This will be done by characterizing the growth at g = 1, projecting the changes in melt flows due to microgravity, observing these in space growth and determining the effects on defective inhomogeneities. A Thin Rod Zoner was constructed as a laboratory prototype for flight growth of 5 mm diameter silicon crystals, which can be done within the power and cooling capabilities of shuttle flights. A new method of zoning silicon, using resistance heating, has resulted in melting 5 mm diameter ingots. B.W.

N86-10064*# Alabama A & M Univ., Normal. Dept. of Physics and Mathematics.

SOLUTION GROWTH OF CRYSTALS IN ZERO-GRAVITY

R. B. Lal and R. L. Kroes *In* NASA, Washington Microgravity Sci. and Appl. Program Tasks May 1985 p 21-22 refs (For primary document see N86-10053 01-12)
(Contract NAS8-32945)
Avail: NTIS HC A10/MF A01 CSCL 22A

In a low-g environment, buoyancy driven convection effects in solution crystal growth are greatly reduced and, thus, one can study diffusion mass transport which in 1-g is masked by convective phenomena. Crystals of triglycine sulfate (TGS) will be grown aboard the Spacelab 3 mission, using a specially developed Fluids Experiments System (FES). The objectives of the experiment are: (1) to develop a technique for solution crystal growth in a low-g environment, (2) to characterize the growth environment provided by an orbiting spacecraft and to determine the influence of the environment on the growth behavior, and (3) to determine how gravity in a low-gravity environment influences the properties of a resulting TGS crystal. Single crystals of TGS have been grown using conventional low-temperature solution crystal growth method and the growth process has been extensively characterized. Various physical properties of TGS solution have been measured. Also, a unique technique of growing solution growth crystals by extracting heat at a programmed rate from the crystal through a semi-insulating sting has been developed and tested in 1-g environment. B.W.

N86-10065*# National Aeronautics and Space Administration. Marshall Space Flight Center, Huntsville, Ala.

GROWTH OF SOLID SOLUTION CRYSTALS

S. L. Lehoczky, F. R. Szofran, and L. R. Holland (Wyle Labs., Inc., Huntsville, Ala.) *In* NASA, Washington Microgravity Sci. and Appl. Program Tasks May 1985 p 23-25 refs (For primary document see N86-10053 01-12)
Avail: NTIS HC A10/MF A01 CSCL 22A

The major objective of this program is to determine the conditions under which single crystals of solid solutions can be grown from the melt in a Bridgman configuration with a high degree of chemical homogeneity. The central aim is to assess the role of gravity in the growth process and to explore the possible advantages for growth in the absence of gravity. The alloy system being investigated is the solid solution semiconductor with x-values appropriate for infrared detector applications in Hg sub (1-x) Cd sub x Te the 8 to 14 micro m wavelength region. Both melt and Te-solvent growth are being considered. The study consists of an extensive ground-based experimental and theoretical research effort followed by flight experimentation where appropriate. Experimental facilities have been established for the purification, casting, and crystal growth of the alloy system. Facilities have been also established for the metallurgical, compositional, electric and optical characterization of the alloys. Crystals are being grown by the Bridgman-Stockbarger method and are analyzed by various experimental techniques to evaluate the effects of growth conditions on the longitudinal and radial compositional variations and defect densities in the crystals. B.W.

N86-10066*# Edgerton, Germeshausen and Grier, Inc., Goleta, Calif.

HgI SUB 2 CRYSTAL GROWTH FOR NUCLEAR DETECTORS

W. F. Schnepple and L. VandenBerg *In* NASA, Washington Microgravity Sci. and Appl. Program Tasks May 1985 p 26-27 refs (For primary document see N86-10053 01-12)
(NASA Order H-73830-B)
Avail: NTIS HC A10/MF A01 CSCL 22A

The objectives of this program are to obtain a benchmark quality sample grown at low-g conditions and to study vapor growth phenomena under space conditions. Ground-based crystals show a defect structure which impairs their performance as nuclear radiation detectors. These defects may be caused by the gravitational force acting on the crystal in its weakended state at the elevated growth temperature and by irregular convection patterns in the vapor during growth. Mechanical strength measurements have been performed (uniaxial compression tests) which show that the crystals exhibit slip parallel to the c-planes at stresses as low as 1/2 psi. Preliminary calculations using a simple linearized model indicate the oscillating instabilities in the convection part of the vapor transport system are unlikely, even at 1-g, provided that the utmost care is taken in the preparation of the crystal growth source material. Author

N86-10067*# Ames Lab., Iowa.

FLOAT ZONE EXPERIMENTS IN SPACE

John D. Verhoeven *In* NASA, Washington Microgravity Sci. and Appl. Program Tasks May 1985 p 28-29 refs (For primary document see N86-10053 01-12)
(NASA Order H-34328-B)
Avail: NTIS HC A10/MF A01 CSCL 22A

The objective of this work has been to evaluate whether or not Marangoni flow could be suppressed in molten metals by the presence of very thin oxide films. Experimental work has been carried out on molten Sn under UHV conditions. A disk floating zone arrangement was developed to allow in situ Auger examination of molten surfaces. An electron energy loss technique was developed which allows detection of continuous tin oxide films of 6 A or greater. Experiments were planned to detect the effects of oxide formation upon Marangoni flow by measuring: (1) temperature profiles, (2) solid liquid interface shapes, (3) macrosegregation, and (4) the onset of oscillatory Marangoni flow by detecting oscillating temperature variations. Work on (4) showed that oscillatory temperature variations of frequency < or = 10 Hz were not present in the disk float zone geometry under conditions of Ma = 4300 with an oxide free molten surface. The disk float zone geometry was modeled with a finite element analysis and temperature and velocity profiles were determined. B.W.

N86-10068*# Rensselaer Polytechnic Inst., Troy, N. Y. Dept. of Chemistry.

FLUID DYNAMICS AND THERMODYNAMICS OF VAPOR PHASE CRYSTAL GROWTH

H. Wiedemeier *In* NASA, Washington Microgravity Sci. and Appl. Program Tasks May 1985 p 30-31 refs (For primary document see N86-10053 01-12)
(Contract NAS8-33562)
Avail: NTIS HC A10/MF A01 CSCL 22A

The ground-based research effort under this program is concerned with systematic studies of the effects of variations: (1) of the relative importance of buoyancy-driven convection, and (2) of diffusion and viscosity conditions on crystal properties. These experimental studies are supported by thermodynamic characterizations of the systems, based on which fluid dynamic parameters can be determined. The specific materials under investigation include: the GeSe-GeI4, Ge-GeI4, HgTe-HgI2, and Hg sub (1-x)Cd sub (x) Te-HgI2 systems. Mass transport rate studies of the GeSe-GeI system as a function of orientation of the density gradient relative to the gravity vector demonstrated the validity of flux anomalies observed in earlier space experiments. The investigation of the effects of inert gases on mass flux yielded the first experimental evidence for the existence of a boundary layer in closed ampoules. Combined with a thorough thermodynamic analysis, a transport model for diffusive flow including chemical vapor transport, sublimation, and Stefan flow was developed. B.W.

N86-10069*# Rensselaer Polytechnic Inst., Troy, N. Y. Dept. of Chemistry.

VAPOR GROWTH OF ALLOY-TYPE SEMICONDUCTOR CRYSTALS

H. Wiedemeier *In* NASA, Washington Microgravity Sci. and Appl. Program Tasks May 1985 p 32-33 refs (For primary document see N86-10053 01-12)
(Contract NAS8-32936)
Avail: NTIS HC A10/MF A01 CSCL 22A

The present effort is part of a continuing research program directed towards the investigation of basic vapor transport phenomena and of crystal growth properties of electronic materials. The primary purpose of ground-based studies is the development and definition of optimum experimental parameters for flight experiments. The ground-based effort includes the investigation of gravity-driven convection effects on mass transport rates and on crystal morphology for different orientations of the density gradient with respect to the gravity vector, and as a function of pressure and of temperature. In addition to the experimental tasks, theoretical efforts involve the quantitative thermodynamic analysis of the systems under investigation, the computation of fluid dynamic parameters, and the consideration of other possible effects on fluid flow under vertical, stabilizing and microgravity conditions. The specific experiments to be performed in a microgravity environment include the investigation of vapor transport and crystal growth phenomena of the GeSe-Xenon system and of the mass flux and growth of bulk and layer-type crystals of Hg sub (1-x) Cd sub x Te using HgI as a transport agent. B.W.

N86-10070*# Clarkson Coll. of Technology, Potsdam, N.Y. Dept. of Chemical Engineering.

STUDY OF EUTECTIC FORMATION

W. R. Wilcox *In* NASA, Washington Microgravity Sci. and Appl. Program Tasks May 1985 p 34-35 refs (For primary document see N86-10053 01-12)
(Contract NAS8-34887)
Avail: NTIS HC A10/MF A01 CSCL 22A

The objectives of this program are to determine the influence of convection on the microstructure of eutectics and to develop a technique for revealing the longitudinal microstructure of the MnBi-Bi eutectic. Both objectives aim at trying to explain the observed influence of space processing on the microstructure of MnBi-Bi. A computer program was developed and used to determine the concentration field in front of a growing lamellar eutectic. From this the deviation of the interfacial concentration from the eutectic composition was calculated as a function of eutectic composition, freezing rate, convection, and lamellar spacing. B.W.

N86-10071*# Clarkson Coll. of Technology, Potsdam, N.Y. Dept. of Chemical Engineering.

MODELING DIRECTIONAL SOLIDIFICATION

W. R. Wilcox and T. Paptheodorou *In* NASA, Washington Microgravity Sci. and Appl. Program Tasks May 1985 p 36-37 ref (For primary document see N86-10053 01-12)
(Contract NAS8-34891)
Avail: NTIS HC A10/MF A01 CSCL 22A

The objective of the research is to develop tools of use in explaining the results of directional solidification experiments in space. These tools consist of mathematical and experimental models. Experiments are also being flown at low-g to validate the ground-based results. Many metals and semiconductors directionally solidified in space had a diameter less than that of the containing ampoule. In fact this occurred whenever the ampoule contained a gas space. This phenomenon has been attributed in a vague way to lack of wetting of the ampoule wall by the melt. The actual liquid behavior by use of low temperature analogs is being observed aboard the KC-135. In the first flight, water was placed in plastic ampoules (not wet) with ceramic end plugs which were wet by the water to simulate a solid-liquid interface. Unfortunately during storage prior to the flight the water began to wet the ampoule wall. Discrete bubbles formed down the axis of the ampoules. New ampoule materials are being used now, with testing for stability prior to the next flight. A theoretical model has also been developed for this phenomenon. B.W.

N86-10072*# Massachusetts Inst. of Tech., Cambridge.

HEAT FLOW AND SEGREGATION IN DIRECTIONAL SOLIDIFICATION

August F. Witt *In* NASA, Washington Microgravity Sci. and Appl. Program Tasks May 1985 p 38-39 refs (For primary document see N86-10053 01-12)
(Grant NsG-7645)
Avail: NTIS HC A10/MF A01 CSCL 22A

This research is composed of three major components: (1) development of interface morphology control for automated Bridgman growth of semiconductor systems; (2) comparative analysis of segregation during crystal growth in a reduced gravity environment and in the presence of magnetic fields; and (3) consequences of seeding by meltback in Bridgman growth under reduced gravity conditions. In attempts to optimize furnace design for crystal growth in a reduced gravity environment, an analytical approach to heat transfer was developed. It was thus found that charge confining crucibles diminish the ability to control the growth interface morphology through its position within the gradient zone. A heat pipe hot zone system for Bridgman growth, in reduced gravity environment, of crystal with diameters up to 16 mm was developed. For growth of Ga-doped germanium in the multipurpose (ASTP) furnace, it was found that the application of transverse magnetic fields (up to 36 kg) does not substantially increase the effective distribution coefficient; i.e., diffusion-controlled segregation observed in reduced gravity environment cannot be reached nor approached by magnetic field induced melt stabilization. B.W.

N86-10073*# Vanderbilt Univ., Nashville, Tenn. Dept. of Mechanical and Materials Engineering.

EFFECT OF UNDERCOOLING IN A LOW-GRAVITY CONTAINERLESS ENVIRONMENT ON THE STRUCTURE AND PROPERTIES OF ALLOYS

Robert J. Bayuzick *In* NASA, Washington Microgravity Sci. and Appl. Program Tasks May 1985 p 43-44 refs (For primary document see N86-10053 01-12)
(Contract NAS8-34676)
Avail: NTIS HC A10/MF A01 CSCL 22A

The 30 meter and 100 meter drop tubes at the Marshall Space Flight Center offer a unique opportunity to study solidification in a containerless, microgravity environment. Samples are melted in a furnace at the top of the drop tube and solidify during a 4.5 second free fall in the 100 meter drop tube or a 2.6 second free fall in the 30 meter drop tube. The cooling rate obtained in the drop tubes is lower than cooling rates in atomization and splat-quenching processes. Decoupling the rapid solidification process allows the study of the effects of undercooling and recalescence on alloy morphologies. The research therefore has a three-fold purpose. The first is examination of the limits of undercooling of niobium and niobium-base alloys in the drop tube. The second purpose is the observation of microstructures resulting from the solidification of samples at large undercoolings and moderate cooling rates. The third purpose is the observation of metastable phase formation in highly undercooled samples. B.W.

N86-10074*# National Bureau of Standards, Washington, D.C.

MEASUREMENT OF HIGH TEMPERATURE THERMOPHYSICAL PROPERTIES

D. W. Bonnell *In* NASA, Washington Microgravity Sci. and Appl. Program Tasks May 1985 p 45-46 refs (For primary document see N86-10053 01-12)
(NASA Order H-27954-B)
Avail: NTIS HC A10/MF A01 CSCL 22A

Technique development and the application of electromagnetic levitation to thermophysical property measurement, including determining heats of fusion, heat capacities, and enthalpy increment functions for extremely refractory materials are discussed. Tungsten properties and the development of an apparatus employing electromagnetic levitation and electron beam heating capable of melting levitating tungsten high temperature heat content measurements by drop calorimetry are emphasized. The development of a prototype microcomputer data acquisition system suitable for controlling the ground based system, with consequent improvement in system handling, which can serve as a model for the system needed for flight experiments is described, which include the development of techniques for imaging pyrometry at temperatures above 3500 K, a semiautomatic calorimeter system capable of handling liquid tungsten, and development of a two color imaging pyrometer system. E.A.K.

N86-10075*# Houston Univ., Tex. Dept. of Physics.

EFFECT OF UNDERCOOLING AND MODIFIED MICROSTRUCTURE ON THE PHYSICAL PROPERTIES OF MATERIAL SYNTHESIZED IN THE DROP TUBE AND DROP TOWER

C. W. Chu *In* NASA, Washington Microgravity Sci. and Appl. Program Tasks May 1985 p 47-48 refs (For primary document see N86-10053 01-12)
(Contract NAS8-35161)
Avail: NTIS HC A10/MF A01 CSCL 22A

The effects of undercooling and modified microstructure on the physical properties of synthesized materials were investigated. The objectives of this program are: (1) to determine the possible existence of metastable phases and novel physical processes on material prepared in a microgravity environment; and (2) to investigate the feasibility of fabricating advanced electronic devices using material with microstructures obtainable in a microgravity environment. The specific alloys and compounds under study are Au-Ge and immiscible alloys Nb-Ge compounds, and Ga-Bi immiscible alloys, and Ba-Pb-Bi-O. The superconducting and normal state transport properties of the materials under different pressures and in different magnetic fields were determined. The simultaneous study on the physical properties and the microstructure of material will provide information about the potential applications of materials processed in a microgravity environment. E.A.K.

N86-10076*# Battelle Memorial Inst., Columbus, Ohio.
THE INFLUENCE OF CONTAINERLESS UNDERCOOLING AND RAPID SOLID-STATE QUENCHING ON THE SUPERCONDUCTIVE AND MAGNETIC PROPERTIES OF SOME CLUSTERING ALLOY SYSTEMS
E. W. Collings *In* NASA, Washington Microgravity Sci. and Appl. Program Tasks May 1985 p 49-50 refs (For primary document see N86-10053 01-12)
(Contract NAS8-35145)
Avail: NTIS HC A10/MF A01 CSCL 22A

The potential of the 100-meter drop-tube for producing materials with new and important properties by their rapid solidification containerless undercooling was investigated. Materials produced exhibit evidence of very rapid quenching. The importance of rapid quenching in producing materials of considerable scientific and technological interest is emphasized. It is indicated that containerless undercooling, using at first a drop tube and eventually a space-shuttle-serviced orbiting laboratory, will provide another powerful approach for rapid quenching. A special advantage of the drop tube is that the microgravity condition is imposed ballistically; it is therefore possible to obtain either spherical samples by allowing solidification to take place in flight, or splats by allowing the sample material while still in undercooled liquid form to impact a stationary quench plate. E.A.K.

N86-10077*# National Bureau of Standards, Washington, D.C.
CONVECTION DURING UNIDIRECTIONAL SOLIDIFICATION
S. R. Coriell, R. J. Schaefer, and G. B. McFadden *In* NASA, Washington Microgravity Sci. and Appl. Program Tasks May 1985 p 51-52 refs (For primary document see N86-10053 01-12)
(NASA Order H-27954-B)
Avail: NTIS HC A10/MF A01 CSCL 22A

The fluid flow and solute segregation which occur during directional solidification, including effects of gravity and microgravity were studied. The nature of the fluid flow, its effects on the shape of the crystal-metal interface and the resulting distribution of solutes are examined. During solidification of a binary alloy at constant velocity vertically upwards, thermosolutal convection occurs if the solute rejection or preferential incorporation at the crystal-melt interface decreases the density of the melt. Numerical calculations of the solute, temperature, and flow fields are carried out by using previously developed algorithms for Schmidt numbers Sc = 1, 10, 81. The time periodic flow, which occurs over a narrow range of parameters, is investigated. E.A.K.

N86-10078*# Massachusetts Inst. of Tech., Cambridge. Dept. of Materials Science and Engineering.
SIGNAL ANALYSIS OF GAS TUNGSTEN ARC WELDS
T. W. Eagar *In* NASA, Washington Microgravity Sci. and Appl. Program Tasks May 1985 p 53 (For primary document see N86-10053 01-12)
(Grant NsG-7645)
Avail: NTIS HC A10/MF A01 CSCL 22A

Gas tungsten arc welding is a process in which the input parameters such as current, voltage and travel speed, can be easily controlled and/or monitored. However, weld quality is not solely a function of these parameters. An adaptive method of observing weld quality is desired to improve weld quality assurance. The use of dynamic electrical properties of the welding arc as a weld quality monitor was studied. The electrical properties of the arc are characterized by the current voltage transfer function. The hardware and software necessary to collect the data at a maximum rate of 45 kHz and to allow the off-line processing of this data are tested. The optimum input current waveform is determined. Bead-on-plate welds to observe such characteristics of the weld as the fundamental frequency of the puddle are studied. Future work is planned to observe changes of the arc response with changes in joint geometry, base metal chemistry, and shielding gas composition are discussed. E.A.K.

N86-10079*# Commissariat a l'Energie Atomique, Grenoble (France). Center for Nuclear Studies.
MEPHISTO: INTERFACIAL DESTABILIZATION IN METAL ALLOYS
J. J. Favier and Y. Malmejac *In* NASA, Washington Microgravity Sci. and Appl. Program Tasks May 1985 p 54 (For primary document see N86-10053 01-12)
Avail: NTIS HC A10/MF A01 CSCL 22A

The destabilizing mechanisms at a solidification interface were studied to obtain information on the kinetics and morphologies in the transient and steady state, and to separate the influences of liquid phase instabilities from interfacial instabilities. A differential seebeck voltage measurements technique was developed to provide a continuous record of the solid-liquid interface temperature as the solidification rate is varied to determine the kinetic coefficients. Signal processing and noise suppression techniques allow nonovolt precision which corresponds to mK accuracy for the interfacial temperature. E.A.K.

N86-10080*# Massachusetts Inst. of Tech., Cambridge. Materials Processing Center.
UNDERCOOLING, REMELTING, AND COARSENING
Merton C. Flemings and Y. Shiohara *In* NASA, Washington Microgravity Sci. and Appl. Program Tasks May 1985 p 55-56 refs (For primary document see N86-10053 01-12)
(Grant NsG-7645)
Avail: NTIS HC A10/MF A01 CSCL 22A

Solidification of metal alloys with initial high undercoolings occurs with rapid recalescence due to rapid heat release of the latent heat of fusion. The recalescence temperature is usually higher than the solidus and/or the thermodynamic T sub o temperature of the alloy, depending on the initial undercooling and alloy composition. The rapid heating during recalescence alters the initially solidified structures, in ways that must include partial remelting, ripening, coarsening, and decomposition of the rapidly solidified primary metastable or supersaturated phases. New ways to study the solidification and remelting phenomena associated with the rapid heating during recalescence of undercooled alloys were developed. The phenomena are studied by using: (1) emulsions of iron and nickel base alloys in viscous liquid carriers; and (2) rapid heating of metal samples by electric discharge, using a technique similar to the exploding wire process (EWP), except with less power input. Experimental results are combined with theoretical analyses to better understand the solidification of levitated metal droplets with high undercooling, which relates to the solidification process. E.A.K.

N86-10081*# Gelles (S. H.) Associates, Columbus, Ohio.
LIQUID PHASE MISCIBILITY GAP MATERIALS
S. H. Gelles and A. J. Markworth (Battelle Columbus Lab.) *In* NASA, Washington Microgravity Sci. and Appl. Program Tasks May 1985 p 57-58 ref (For primary document see N86-10053 01-12)
(Contract NAS8-32952)
Avail: NTIS HC A10/MF A01 CSCL 22A

The manner in which the microstructural features of liquid-phase miscibility gap alloys develop was determined. This will allow control of the microstructures and the resultant properties of these alloys. The long-duration low gravity afforded by the shuttle will allow experiments supporting this research to be conducted with minimal interference from buoyancy effects and gravitationally driven convection currents. Ground base studies were conducted on Al-In, Cu-Pb, and Te-Tl alloys to determine the effect of cooling rate, composition, and interfacial energies on the phase separation and solidification processes that influence the development of microstructure in these alloys. Isothermal and directional cooling experiments and simulations are conducted. The ground based activities are used as a technological base from which flight experiments formulated and to which these flight experiments are compared. E.A.K.

N86-10082*# Rensselaer Polytechnic Inst., Troy, N. Y.
DENDRITIC GROWTH IN UNDERCOOLED MELTS
Martin E. Glicksman *In* NASA, Washington Microgravity Sci. and Appl. Program Tasks May 1985 p 59 (For primary document see N86-10053 01-12)
Avail: NTIS HC A10/MF A01 CSCL 22A

The kinetic and morphological behavior of systems solidifying at small undercooling were investigated with emphasis on the role of convective and diffusive transport and the influence of gravity. A data base was established for pure succinonitrile which permits a comprehensive check on diffusional dendrite growth theory and the development of scaling laws to extend the theory to other material systems. A departure from diffusional-controlled growth was observed which becomes more significant at smaller undercoolings. A shuttle experiment is prepared to test the theory at the low undercoolings where convective effects begin to dominate. E.A.K.

N86-10083*# Rensselaer Polytechnic Inst., Troy, N. Y.
INFLUENCE OF MELT CONVECTION ON SOLID-LIQUID INTERFACE UNDER TERRESTRIAL AND REDUCED GRAVITY ENVIRONMENTS
Martin E. Glicksman *In* NASA, Washington Microgravity Sci. and Appl. Program Tasks May 1985 p 60-62 refs (For primary document see N86-10053 01-12)
(Grant NAG3-333)
Avail: NTIS HC A10/MF A01 CSCL 22A

Solidification and crystal growth processes involve thermal and solutal gradients within a molten phase. In the presence of gravity, such gradients result in convective flows which interact with diffusion fields at the solid-liquid interface. Dendritic growth kinetics was studied in transparent model systems which freeze similarily to most metals. Succinonitrile shows a strong influence of convection at supercoolings below about 1K. Fluid flows adjacent to solid-liquid interfaces and the behavior of shear flows in vertical annular geometries are studied. Novel low-frequency eigenstates were discovered and classified as coupled modes, for their involvement with interfacial deformation coupled to the fluid flow, and are unknown in systems without deformable interfaces. The dependence of coupled convection modes on interfacial geometry, gravity, fluid properties, and transformation characteristics studied for several annual flow arrangements with nominally pure solid-liquid systems. E.A.K.

N86-10084*# Deere and Co., Moline, Ill.
CONTROL OF CAST IRON MICROSTRUCTURE
James Graham, Norman Lillybeck, Nick Franco, and Doru M. Stefanescu *In* NASA, Washington Microgravity Sci. and Appl. Program Tasks May 1985 p 63 (For primary document see N86-10053 01-12)
Avail: NTIS HC A10/MF A01 CSCL 22A

The use of microgravity for industrial research in the processing of cast iron was investigated. Solidification experiments were conducted using the KC-135 and F-104 aircraft, and an experiment plan was developed for follow-on experiments using the Shuttle. Three areas of interest are identified: (1) measurement of thermophysical properties in the melt; (2) understanding of the relative roles of homogeneous nucleation, grain multiplication, and innocultants in forming the microstructure; and (3) exploring the possibility of obtaining an aligned graphite structure in hypereutectic Fe, Ni, and Co. E.A.K.

N86-10085*# Massachusetts Inst. of Tech., Cambridge.
THE ROLE OF ENTRAINED SURFACE OXIDES IN RS-PM ALUMINUM ALLOYS ON RESULTANT STRUCTURES AND PROPERTIES
N. J. Grant *In* NASA, Washington Microgravity Sci. and Appl. Program Tasks May 1985 p 64 refs (For primary document see N86-10053 01-12)
(Grant NsG-7645)
Avail: NTIS HC A10/MF A01 CSCL 22A

The RS-PM aluminum alloys which show less than anticipated toughness properties were studied. After eliminating negative variables such as sodium and potassium in lithium containing alloys, hydrogen in all Al alloys, and trapped impurities from the atomization processing the data pointed to fine oxides, as the primary cause of poor toughness properties. The oxide content of aluminum powders increases with: decreasing powder size, deviations from spherical powder shapes, exposure to moist atmospheres either during atomization or in subsequent powder handling, and alloy compositions which contain significant amounts of lithium, magnesium, cerium, and other reactive elements. E.A.K.

N86-10086*# Michigan Technological Univ., Houghton. Dept. of Metallurgical Engineering.
THE DEVELOPMENT AND PREVENTION OF CHANNEL SEGREGATION DURING ALLOY SOLIDIFICATION
Angus Hellawell *In* NASA, Washington Microgravity Sci. and Appl. Program Tasks May 1985 p 65-66 refs (For primary document see N86-10053 01-12)
(Grant NAG3-560)
Avail: NTIS HC A10/MF A01 CSCL 22A

During alloy solidification, interdendritic microsegregation causes density differences between entrapped liquid and bulk liquid which provides a driving force for convection. One of the consequences of this effect is the formation of long, nearly vertical liquid channels, rich in solute, flowing through the solid-liquid mushy zone somewhat as a river and tributary system. In ingot castings where the heat flow is vertically downwards and the solute less dense than the solute the convective flow is antiparallel with the flow caused by contraction on freezing. Identification of the mechanisms involved in these two problems is discussed. It is known that certain types of bulk liquid movements can inhibit channel development and the mechanism by which they do so are examined. E.A.K.

N86-10087*# National Aeronautics and Space Administration. Marshall Space Flight Center, Huntsville, Ala.
STUDY OF THE REACTIVE-ELEMENT EFFECT IN OXIDATION OF Fe-Cr ALLOYS USING TRANSVERSE SECTION ANALYTICAL ELECTRON MICROSCOPY
Wayne E. King (Argonne National Lab.) and Edwin C. Ethridge *In* NASA, Washington Microgravity Sci. and Appl. Program Tasks May 1985 p 67-68 (For primary document see N86-10053 01-12)
Avail: NTIS HC A10/MF A01 CSCL 22A

The role of trace additions of reactive elements like Y, Ce, Th, or Hf to Cr bearing alloys was studied by applying a new developed technique of transverse section analytical electron microscopy. This reactive-element effect improves the high temperature oxidation resistance of alloys by strongly reducing the high temperature oxidation rate and enhancing the adhesion of the oxide scale, however, the mechanisms for this important effect remain largely unknown. It is indicated that the presence of yttrium affects the oxidation of Fe-Cr-Y alloys in at least two ways. The reactive element alters the growth mechanism of the oxide scale as evidenced by the marked influence of the reactive element on the oxide scale microstructure. The present results also suggest that reactive-element intermetallic compounds, which internally oxidize in the metal during oxidation, act as sinks for excess vacancies thus inhibiting vacancy condensation at the scale-metal interface and possibly enhancing scale adhesion. E.A.K.

N86-10088*# California Univ., Santa Barbara.
THEORETICAL PROBLEMS IN MATERIALS SCIENCE Inst. for Theoretical Physics.
J. S. Langer and M. E. Glicksman *In* NASA, Washington Microgravity Sci. and Appl. Program Tasks May 1985 p 69 (For primary document see N86-10053 01-12)
(Grant NSF PHY-77-27084)
Avail: NTIS HC A10/MF A01 CSCL 22A

interactions between theoretical physics and material sciences to identify problems of common interest in which some of the powerful theoretical approaches developed for other branches of physics may be applied to problems in materials science are presented. A unique structure was identified in rapidly quenched Al-14% Mn. The material has long-range directed bonds with icosahedral symmetry which does not form a regular structure but instead forms an amorphous-like quasiperiodic structure. Finite volume fractions of second phase material is advanced and is coupled with nucleation theory to describe the formation and structure of precipitating phases in alloys. Application of the theory of pattern formation to the problem of dendrite formation is studied E.A.K.

N86-10089*# Grumman Aerospace Corp., Bethpage, N.Y. Materials and Structural Mechanics Research.
ORBITAL PROCESSING OF ALIGNED MAGNETIC COMPOSITES
David J. Larson *In* NASA, Washington Microgravity Sci. and Appl. Program Tasks May 1985 p 70-71 (For primary document see N86-10053 01-12)
(Contract NAS8-35483)
Avail: NTIS HC A10/MF A01 CSCL 22A

Experiments will be conducted on the space shuttle in which aligned, two-phase magnetic composites will be grown by plane front directional solidification. The objectives are to: (1) identify and quantitatively evaluate the influences of gravitationally driven thermo-solutal convection on contained plane front solidification of binary, eutectic, off-eutectic, and peritectic magnetic composites; (2) to evaluate the effectiveness of micro-g processing as a means of damping convection; and (3) to evaluate the uniqueness of micro-g processing relative to the best of terrestrial convection damping. E.A.K.

N86-10090*# Case Western Reserve Univ., Cleveland, Ohio. Dept. of Metallurgy and Materials Science.
SOLIDIFICATION FUNDAMENTALS
V. Laxmanan and J. F. Wallace *In* NASA, Washington Microgravity Sci. and Appl. Program Tasks May 1985 p 72-73 refs (For primary document see N86-10053 01-12)
(Grant NAG3-417)
Avail: NTIS HC A10/MF A01 CSCL 22A

The fundamental aspects of a variety of solidification phenomena were studied, taking advantage of the unique opportunities offered by the microgravity environment of space. Containerless processing and an understanding of the role of fluids induced by gravitational effects are the two major objectives justifying an experimental program in reduced gravity. The solidification phenomena which are likely to benefit are: macro and microsegregation, columnar-equiaxed transition, pore formation, and undercooling. E.A.K.

N86-10091*# Rice Univ., Houston, Tex. Dept. of Chemistry.
MEASUREMENT OF THE PROPERTIES OF TUNGSTEN AT HIGH TEMPERATURES
John L. Margrave *In* NASA, Washington Microgravity Sci. and Appl. Program Tasks May 1985 p 74 (For primary document see N86-10053 01-12)
(Contract NAS8-33199)
Avail: NTIS HC A10/MF A01 CSCL 22A

The thermophysical properties of tungsten and other materials were measured using containerless techniques. Levitation of liquid silver, gallium and tungsten were studied. The studies of liquid aluminum are almost complete and are expected to derive new, reliable properties for liquid aluminum. E.A.K.

N86-10092*# Midwest Research Inst., Kansas City, Mo.
CONTAINERLESS HIGH TEMPERATURE PROPERTY MEASUREMENTS BY ATOMIC FLUORESCENCE
Paul C. Nordine *In* NASA, Washington Microgravity Sci. and Appl. Program Tasks May 1985 p 75 refs (For primary document see N86-10053 01-12)
Avail: NTIS HC A10/MF A01 CSCL 22A

Laser induced fluorescence (LIF) provides a noncontact method for measuring high temperature properties. It is used with aerodynamic and/or electromagnetic levitation, and electromagnetic and/or CW CO2 laser heating to develop new methods for containerless high temperature property measurements and process control. The capabilities and limitations of Earth-based experiments are demonstrated and the information necessary to design improved experiments in space is obtained. The LIF methods were developed to measure temperature and component activities, which will be applied to containerless property measurements on liquids and to process control in synthesis experiments. Component activities will be obtained from relative LIF intensities over a compound and its components at the same temperature. Author

N86-10093*# Wisconsin Univ., Madison. Dept. of Metallurgical and Mineral Engineering.
CONTAINERLESS PROCESSING OF UNDERCOOLED MELTS
John H. Perepezko *In* NASA, Washington Microgravity Sci. and Appl. Program Tasks May 1985 p 76 (For primary document see N86-10053 01-12)
(Grant NAG3-436)
Avail: NTIS HC A10/MF A01 CSCL 22A

The physical mechanisms controlling liquid undercooling were studied for application to solidification processing methods. The undercooling potential of containerless processing was assessed on droplet samples of high melting temperature metals drop tube and drop tower facilities and in a laboratory-scale apparatus. New insight into nucleation and crystal growth will be obtained in undercooled liquids of high melting temperature iron and nickel-base systems. The processing parameters include melt superheat, droplet size and particle statistics and droplet surface coating. The solidification behavior is determined by thermal analysis and by structural and metallographic characterization. E.A.K.

N86-10094*# Grumman Aerospace Corp., Bethpage, N.Y.
THERMAL AND SOLUTAL CONVECTION DAMPING USING AN APPLIED MAGNETIC FIELD
R. G. Pirich and J. L. DeCarlo *In* NASA, Washington Microgravity Sci. and Appl. Program Tasks May 1985 p 77-78 refs (For primary document see N86-10053 01-12)
Avail: NTIS HC A10/MF A01 CSCL 22A

Samples of eutectic Bi/Mn alloy were directionally solidified in the presence of a transverse magnetic field to determine if gravity-induced convection effects could be reduced or eliminated. The microstructure of Bi/MnBi is characterized by a regular, aligned-rod eutectic morphology that is sensitive to growth conditions. This, combined with ferromagnetism of one of the components, MnBi, can be used to eliminate whether convection effects are significant enough to be effected by the presence of a static, homogeneous, magnetic field. E.A.K.

N86-10095*# Johns Hopkins Univ., Baltimore, Md.
METALLIC FOAMS
Robert B. Pond *In* NASA, Washington Microgravity Sci. and Appl. Program Tasks May 1985 p 79 (For primary document see N86-10053 01-12)
(Contract NAS8-33021)
Avail: NTIS HC A10/MF A01 CSCL 22A

The formation of metallic foams by use of a blowing agent in the melt was investigated. It was attempted to produce a metallic foam by melting a mixture of Cu powder and graphite in a SPAR rocket. The graphite combines with the oxide on the copper to form Co and acts as a blowing agent. No foam was formed, and it could not be determined whether the foam fails to form, forms but was lost to surface tension instabilities, or is destroyed by incomplete solidification before reentry. E.A.K.

N86-10096*# Johns Hopkins Univ., Baltimore, Md.
DIFFUSION IN IMMISCIBLE MELTS
Robert B. Pond *In* NASA, Washington Microgravity Sci. and Appl. Program Tasks May 1985 p 80 (For primary document see N86-10053 01-12)
(Contract NAS8-35620)

Avail: NTIS HC A10/MF A01 CSCL 22A

The objective of this program is to measure the diffusion coefficients for molten Pb in Zn in the immiscible liquid-phase region. Diffusion couples of pure Pb and Zn were prepared using a shear cell. These have been placed in graphite crucibles and encapsulated in stainless steel cartridges and are awaiting the next Materials Experiment Assembly (MEA) flight opportunity. In flight, one couple will be soaked for 40 minutes at 440 deg C (just above the monotectic temperature) and the second couple will be soaked for 40 minutes 820 deg C (just above the consolute temperature). After the soak both samples will be rapidly quenched by flowing He to minimize redistribution of the immiscible phases. Post flight compositional analysis will be accomplished using X-ray fluorescence in the scanning electron microscopy. Author

N86-10097*# Commissariat a l'Energie Atomique, Grenoble (France). Centre d'Etudes Nucleaires.

DIRECTIONAL SOLIDIFICATION OF MONOTECTIC AND HYPERMONOTECTIC ALUMINUM-INDIUM ALLOYS UNDER MICRON-G

Claude Potard *In* NASA, Washington Microgravity Sci. and Appl. Program Tasks May 1985 p 81-82 (For primary document see N86-10053 01-12)

Avail: NTIS HC A10/MF A01 CSCL 22A

The objective of this program is to analyze the mechanisms involved in the composite solid structure formation obtained from a miscibility gap alloy under microgravity. The metallic system aluminum-indium was chosen for its low critical temperature, broad miscibility gap, and rather well-known thermodynamic properties. The experiment was performed aboard the Salyut-7 spacecraft. The theories of capture of particulates by an advancing front were not able to explain the observations made on SPAR and Salyut-7 experiments. A new model was developed based on the filtration theory considering the globules population: the solid/liquid interface is like a filter of negligible thickness for the globules and its efficiency is limited by a pressure barrier measured for Al-In alloys by ground based experiments. The Materials Experiment Assembly (MEA)-3 experiment was consequently adjusted to take into account the new model. The behavior of the globules in an interacting population on the solid front is, of course, an essential factor in the theory. The theory is at present being completed by results obtained by the Laboratoire d'Aerothermique of Meudon. The hydrodynamic and thermal interactions between pairs of globules placed in a temperature gradient have been calculated showing a large reduction of the Marangoni effect compared to the isolated globule. Physico-chemical properties of metallic liquid interface are currently being investigated. R.J.F.

N86-10098*# Massachusetts Inst. of Tech., Cambridge. Materials Processing Center.

METALS ELECTROPROCESSING IN MOLTEN SALTS

D. R. Sadoway *In* NASA, Washington Microgravity Sci. and Appl. Program Tasks May 1985 p 83 (For primary document see N86-10053 01-12)

(Grant NsG-7645)

Avail: NTIS HC A10/MF A01 CSCL 22A

The present study seeks to explain the poor quality of solid electrodeposits in molten salts through a consideration of the effects of fluid flow of the electrolyte. Transparent cells allow observation of electrolyte circulation by a laser schlieren optical technique during the electrodeposition of solid zinc from the molten salt electrolyte, ZnCl2 - LiCl-KCl. Experimental variables are current, density, electrolyte composition, and cell geometry. Based on the results of earlier electrodeposition studies as well as reports in the literature, these parameters are identified as having the primary influence on cell performance and deposit quality. Experiments are conducted to measure the fluid flow patterns and the electrochemical cell characteristics, and to correlate this information with the morphology of the solid electrodeposit produced. Specifically, cell voltage, cell current, characteristic time for dendrite evolution, and dendrite growth directions are noted. Their relationship to electrolyte flow patterns and the morphology of the resulting electrodeposit are derived. Results to date indicate that laser schlieren imaging is capable of revealing fluid flow patterns in a molten salt electrolyte. R.J.F.

N86-10099*# Syracuse Univ., N. Y. Dept. of Chemical Engineering and Materials Science.

ENVIRONMENTAL DEGRADATION OF MATERIALS: SURFACE CHEMISTRY RELATED TO STRESS CORROSION CRACKING

James A. Schwarz *In* NASA, Washington Microgravity Sci. and Appl. Program Tasks May 1985 p 84 (For primary document see N86-10053 01-12)

(Grant NAGw-466)

Avail: NTIS HC A10/MF A01 CSCL 22A

Parallel experiments have been performed in order to develop a comprehensive model for stress cracking (SCC) in structural materials. The central objective is to determine the relationship between the activity and selectivity of the microstructure of structural materials to their dissolution kinetics and experimentally measured SCC kinetics. Zinc was chosen as a prototype metal system. The SCC behavior of two oriented single-crystal disks of zinc in a chromic oxide/sodium sulfate solution (Palmerton solution) were determined. It was found that: (1) the dissolution rate is strongly (hkil)-dependent and proportional to the exposure time in the aggressive environment; and (2) a specific slip system is selectively active to dissolution under applied stress and this slip line controls crack initiation and propagation. As a precursor to potential microgrvity experiments, electrophoretic mobility measurements of zinc particles were obtained in solutions of sodium sulfate (0.0033 M) with concentrations of dissolved oxygen from 2 to 8 ppm. The equilibrium distribution of exposed oriented planes as well as their correlation will determine the particle mobility. Author

N86-10100*# Alabama Univ., Huntsville. College of Engineering.

GRAPHITE FORMATION IN CAST IRON

D. M. Stefanescu *In* NASA, Washington Microgravity Sci. and Appl. Program Tasks May 1985 p 85 (For primary document see N86-10053 01-12)

(Grant NAGw-469)

Avail: NTIS HC A10/MF A01 CSCL 22A

In the first phase of the project it was proven that by changing the ratio between the thermal gradient and the growth rate for commercial cast iron samples solidifying in a Bridgman type furnace, it is possible to produce all types of graphite structures, from flake to spheroidal, and all types of matrices, from ferritic to white at a certain given level of cerium. KC-135 flight experiments have shown that in a low-gravity environment, no flotation occurs even in spheroidal graphite cast irons with carbon equivalent as high as 5%, while extensive graphite flotation occurred in both flake and spheroidal graphite cast irons, in high carbon samples solidified in a high gravity environment. This opens the way for production of iron-carbon composite materials, with high carbon content (e.g., 10%) in a low gravity environment. By using KC-135 flights, the influence of some basic elements on the solidification of cast iron will be studied. The mechanism of flake to spheroidal graphite transition will be studied, by using quenching experiments at both low and one gravity for different G/R ratios. R.J.F.

N86-10101*# Ohio State Univ., Columbus. Dept. of Physics.

THEORETICAL STUDIES OF THE SURFACE TENSION OF LIQUID METAL SYSTEM Report, Jul. 1984 - Jul. 1987

David G. Stroud and Wei-Heng Shih *In* NASA, Washington Microgravity Sci. and Appl. Program Tasks May 1985 p 86-87 (For primary document see N86-10053 01-12)

(Grant NAG-483)

Avail: NTIS HC A10/MF A01 CSCL 22A

A major goal of this project is to understand the surface tension and other thermophysical properties of liquid metals and alloys from a fundamental viewpoint. The approach is to calculate these quantities by a first principles technique which combines the statistical-mechanical theory of the liquid state with an electronic pseudopotential theory of electrons in metals. The inhomogeneity of the surface is treated using an ionic-density-functional formalism developed with the support of NASA. Of particular interest are the variation of surface tension with temperature and impurity concentration: such variations strongly influence the types of convection which make take place in a low-gravity environment. Some progress has already been achieved in computing the reduction of surface tension due to the presence of low-surface-tension impurities, and the corresponding surface segregation of such impurities. In the coming year, it is planned to concentrate on the surface properties of materials of particular interest to the MSA program: Si, Ga and GaSn alloys. An additional goal is to gain some theoretical understanding of the high temperature thermophysical properties of liquid metals, particularly high melting point materials which have not been studied extensively from a theoretical viewpoint. Author

N86-10102*# Jet Propulsion Lab., California Inst. of Tech., Pasadena.
CONTAINERLESS STUDIES OF NUCLEATION AND UNDERCOOLING Abstract Only
Eugene H. Trinh *In* NASA, Washington Microgravity Sci. and Appl. Program Tasks May 1985 p 88 (For primary document see N86-10053 01-12)
(Contract NAS7-918)
Avail: NTIS HC A10/MF A01 CSCL 22A

The long term research goals are to perform experiments to determine the achievable limits of undercooling, the characteristics of heterogeneous nucleation, and the physical properties of significantly undercooled melts. The techniques used are based on the newly developed containerless manipulation methods afforded by acoustic levitation. Ground based investigations involved 0.1 to 2 mm specimens of pure metals and alloys (In, Ga, Sn, Ga-In, ...) as well as glass-forming organic compounds (O-Terphenyl). A currently operating ultrasonic high temperature apparatus has allowed the ground-based levitation of 1 to 2 mm samples of solid aluminum at 550 deg C in an argon atmosphere. Present work is concentrating on the undercooling of pure metal samples (In, Sn), and on the measurements of surface tension and viscosity of the undercooled melts via shape oscillation techniques monitored through optical detection methods. The sound velocity of undercooled O-Terphenyl is being measured in an immiscible liquid levitation cells. R.J.F.

N86-10103*# National Aeronautics and Space Administration. Marshall Space Flight Center, Huntsville, Ala.
CLOUD MICROPHYSICS BY THERMAL WAVE METHODS
B. Jeffrey Anderson, David A. Bowdle (Universities Space Research Association), and Michael Reischel (Universities Space Research Association) *In* NASA, Washington Microgravity Sci. and Appl. Program Tasks May 1985 p 91-92 (For primary document see N86-10053 01-12)
Avail: NTIS HC A10/MF A01 CSCL 22A

This experiments series is the first application of a low-gravity experimental technique to the study of cloud microphysics. The low-gravity environment is provided by the parabolic maneuver of NASA's KC-135 aircraft. The primary objective is to compare experimental observations of cloud droplet growth and evaporation in a convection free environment with a numerical model of the process. Beyond that, the work also involves the development and testing of low-gravity research techniques. In particular, passive methods of thermal control have been devised and used effectively. The study to date has shown that the method is particularly suitable for looking at interactions between adjoining portions of the cloud drop field and interactions of the drop field with a solid interface. After final analysis of the data, it is expected the results will shed light on the development of cloud droplet size spectra in natural clouds as well as the performance of certain types of cloud physics instrumentation, particularly continuous flow diffusion chambers and loud condensation nuclei counters. R.J.F.

N86-10104*# National Aeronautics and Space Administration. Marshall Space Flight Center, Huntsville, Ala.
EXTENSION OF OSTWALD RIPENING THEORY
James Baird (Alabama Univ., Huntsville) and Robert Naumann *In* NASA, Washington Microgravity Sci. and Appl. Program Tasks May 1985 p 93 (For primary document see N86-10053 01-12)
Avail: NTIS HC A10/MF A01 CSCL 22A

The objective is to develop models based on the mean field approximation of Ostwald ripening to describe the growth of second phase droplets or crystallites. The models will include time variations in nucleation rate, control of saturation through addition of solute, precipitating agents, changes in temperature, and various surface kinetic effects. Numerical integration schemes have been developed and tested against the asymptotic solution of Liftshitz, Slyozov and Wagner (LSW). A second attractor (in addition to the LSW distribution) has been found and, contrary to the LSW theory, the final distribution is dependent on the initial distribution. A series of microgravity experiments is being planned to test this and other results from this work. Author

N86-10105*# Massachusetts Inst. of Tech., Cambridge. Dept. of Chemical Engineering.
MODELLING OF LASER-ENHANCED CHEMICAL VAPOR DEPOSITION
Robert A. Brown *In* NASA, Washington Microgravity Sci. and Appl. Program Tasks May 1985 p 94 (For primary document see N86-10053 01-12)
(Grant NsG-7645)
Avail: NTIS HC A10/MF A01 CSCL 22A

Research is directed at development of a detailed model of mass and heat transfer and chemical reaction in the pyrolysis of silane for the growth of thin amorphous silicon substrates incorporating laser heating of the gas phase above the film. The model will be the basis for evaluation of the relative importances of the decomposition of SiH4 in the vapor phase, mass transfer of the intermediate species, e.g., SiH2, and the evolution of hydrogen gas. Plans are also underway for developing a model for homogeneous nucleation of Si in the vapor phase to model the rate limitations observed at high gas-phase temperatures and high partial pressures of silane. Work was concentrated on an almost one-dimensional model for the coupling of the CO2 laser beam for heat transfer of the vapor phase with simple kinetic models for SiH4 decomposition and subsequent absorption of Si vapor on the substrate. Mass transfer in the vapor phase is assumed to be solely by diffusion. The role of convection in the vapor phase caused by the large changes in density in and around the center of the laser beam will be analyzed to evaluate the potential of microgravity experiments for increasing the uniformity of the film and the deposition rate. Author

N86-10106*# National Bureau of Standards, Washington, D.C.
DYNAMIC THERMOPHYSICAL MEASUREMENTS IN SPACE
Ared Cezairliyan, A. P. Miller, M. S. Morse, and L. A. Schmid *In* NASA, Washington Microgravity Sci. and Appl. Program Tasks May 1985 p 95 (For primary document see N86-10053 01-12)
(NASA Order H-27954-B) Avail: NTIS HC A10/MF A01 CSCL 22A

The objective is to develop techniques for the dynamic measurement of selected thermophysical properties (e.g., heat of fusion, heat capacity, electrical resistivity) of solids and liquids at temperatures above 2000 K in a near zero-gravity environment. The first phase involves establishing the stability (geometrical) limits of specimens when rapidly heated to temperatures beyond their melting point. A test equipment package was designed and constructed for this purpose, consisting of removable specimen cartridge cells, a battery-bank power supply, a high-speed framing camera, a single-wavelength pyrometer, and electronic switching and control equipment. The operation of the equipment package was tested in the laboratory in preparation for near zero-gravity experiments to be performed during a KC-135 flight in September, 1984. Author

N86-10107*# National Aeronautics and Space Administration. Lewis Research Center, Cleveland, Ohio.
TRANSPORT PROCESSES IN SOLUTION CRYSTAL GROWTH
A.-T. Chai *In* NASA, Washington Microgravity Sci. and Appl. Program Tasks May 1985 p 96 (For primary document see N86-10053 01-12)

Avail: NTIS HC A10/MF A01 CSCL 22A

The objective of this effort is to conduct fundamental research in reduced gravity on transport processes occurring during solution crystal growth. Experimental techniques will be developed to monitor and control key parameters at the interface between a growing crystal and the solution from which it grows. Techniques developed will lead to an in-space experiment in the Shuttle. The focus will be on non-incursive ground-based laboratory measurements of model systems and the definition of requirements for space experimentation. Initially, aqueous solutions will be used for easier control and instrumentation. Model systems with imposed steady flows and simplified boundary conditions will be studied for characterization. Various nonincursive measurement techniques are being investigated for proper applications in a newly built laboratory capable of flow visualization, laser Doppler velocimetry, Schlieren photography, specklegram, holographic interferometry, and Raman spectroscopy. Author

N86-10108*# California Univ., Berkeley.
FREE SURFACE PHENOMENA UNDER LOW- AND ZERO-GRAVITY CONDITIONS
Paul Concus, D. Coles (California Inst. of Tech.), R. Finn (Stanford Univ.), and L. Hesselink (Stanford Univ.) *In* NASA, Washington Microgravity Sci. and Appl. Program Tasks May 1985 p 97 (For primary document see N86-10053 01-12)
(Grant NAG3-147)
Avail: NTIS HC A10/MF A01 CSCL 22A

In a low- or zero-gravity environment the free surface of a liquid can behave in striking, unexpected ways. For example, in a partially filled container, a free surface that is well behaved under terrestrial conditions can rise to an arbitrarily large height or even fail to exist when gravity is absent. An answer is sought to the central mathematical questions: Under what conditions can free surfaces exist and what are their properties? -- and experimental questions of what means can be devised to observe and to measure the surfaces quantitatively. Current activity focuses on material selection and the design of optical diagnostic methods for in-space experiments. These experiments will test mathematical predictions of discontinuous transition from existence to nonexistence of capillary free surfaces in certain geometric configurations under zero gravity conditions. Liquids and container materials suitable for achieving the required contact-angle range and optical properties are being investigated, as well as the effects of contaminants and fluid motion on contact angle. The optical diagnostic technique investigation concerns laser-induced fluorescence, including emphasis on data on acquisition, sources and detectors, reliability, data management, and computer control. Author

N86-10109*# Northwestern Univ., Evanston, Ill. Dept. of Engineering Sciences and Applied Mathematics.
THERMOCAPILLARY FLOWS AND THEIR STABILITY: EFFECTS OF SURFACE LAYERS AND CONTAMINATION
S. H. Davis and G. M. Homsey (Stanford Univ.) *In* NASA, Washington Microgravity Sci. and Appl. Program Tasks May 1985 p 98-99 (For primary document see N86-10053 01-12)
(Contract NAS8-33881)
Avail: NTIS HC A10/MF A01 CSCL 22A

The objective is to study quantitatively thermocapillary flows in two-dimensional and axisymmetric geometries in order to learn the impact of such flows on float-zone refining configurations. The work begins with the analytical study of steady flows in slots and zones to obtain predictions of surface curvature, flow and heat transport. It then examines the instability of such flows. Three new instability mechanisms have been identified and the results show that thermocapillary flows of high Prandtl number fluid become convectively unstable while those of low Prandtl number fluid become hydrodynamically unstable. The work includes numerical simulations of steady, high Marangoni number flows in unit aspect ratio boxes and asymptotic solutions in large boxes. Furthermore, the effect of surface contamination on the steady thermocapillary flows was examined. This fundamental study focused on fluid dynamical systems used to understand events in the flow of melts in float-zone geometries both on Earth and in microgravity environments. Author

N86-10110*# Toledo Univ., Ohio.
MASS TRANSPORT PHENOMENA BETWEEN BUBBLES AND DISSOLVED GASES IN LIQUIDS UNDER REDUCED GRAVITY CONDITIONS
Kenneth J. DeWitt and J. L. Brockwell (Union Carbide Technical Center) *In* NASA, Washington Microgravity Sci. and Appl. Program Tasks May 1985 p 100-101 (For primary document see N86-10053 01-12)
(Grant NAG3-34)
Avail: NTIS HC A10/MF A01 CSCL 22A

The long term objective of the experiment is to observe the dissolution of isolated, immobile gas bubbles of specified size and composition in a solvent liquid of known concentration in the reduced gravity environment of earth orbit. Preliminary bubble dissolution experiment conducted both in the NASA Lewis 2.2 sec drop tower and in normal gravity using SO2 - Toluene system were not completely successful in their objective. The method of gas injection and lack of bubble interface stabiliy experienced due to the extreme solubility of SO in Toluene has the effects of changing the problem from that of bubble dissolution to one of bubble formation stability and subsequent dissolution in a liquid of unknown initial solute concentration. Current work involves further experimentation in order to refine the bubble injection system and to investigate the concept of having a bubble with a critical radius in a state of unstable equilibrium. R.J.F.

N86-10111*# George Washington Univ., Washington, D.C.
SUPPRESSION OF MARANGONI CONVECTION IN FLOAT ZONES
Robert F. Dressler *In* NASA, Washington Microgravity Sci. and Appl. Program Tasks May 1985 p 102-103 (For primary document see N86-10053 01-12)
Avail: NTIS HC A10/MF A01 CSCL 22A

The basic purpose of this program is to demonstrate by means of an Earth-based 1-g experiment that the undesirable Marangoni (surface tension) convection can be suppressed or significantly reduced by means of gas jets directed tangentially to the free surface of the liquid in a float zone. These jets will establish the tangential shear stress field over the surface which must be adjusted to equal the counter-stress resultant of the Marangoni shear stress which causes the convection. For proposed materials processing in space (o-g), particularly of important, highly reactive semiconductor materials, e.g., silicon, microgravity will virtually eliminate the unwanted thermal-buoyancy convection in the liquid silicon, but will have no effect in reducing the Marangoni convection. Unless this can be sufficiently suppressed by other means, there may be no significant advantages to the proposed space processing of reactive semiconductors. Although some inert gas such as argon must be used for the corrosive liquid silicon, the Earth-based experiment uses air jets and various transparent oils, since the basic principle involved is the same. The first float zone is enclosed in a very small rectangular box with a quasi-planar free surface. Stable Marangoni convection has been achieved and velocities measured photographically. The air jet system with variable velocity and temperature is under construction. Three independent parameters must be optimized to attain maximum suppression: the gas velocity, angle of attack, and gas temperature. R.J.F.

N86-10112*# National Aeronautics and Space Administration. Marshall Space Flight Center, Huntsville, Ala.
STUDIES OF MODEL IMMISCIBLE SYSTEMS
Donald O. Frazier, B. R. Facemire, W. K. Witherow, U. Fanning, and William F. Kaukler (Universities Space Research Association) *In* NASA, Washington Microgravity Sci. and Appl. Program Tasks May 1985 p 104-105 (For primary document see N86-10053 01-12)
Avail: NTIS HC A10/MF A01 CSCL 22A

The objectives are to use model transparent monotectics to obtain fundamental information applicable to two-phase systems in general, to apply this understanding to materials of interest in the Microgravity Science and Applications program, and to interpret results of flight experimental involving monotectic alloys. A number of model immiscible systems are in use to study various aspects of two-phase behavior within the miscibility gap and during solidification. Particle growth, coalescence and particle motions are under investigation using a holographic microscopy system. The system is capable of working with particle densities up to 10 to the 7th power particles/cubic centimeters through a 100 micron depth and can resolve particles of the order of 2 to 3 micron in diameter throughout the entire cell volume. Particle size, distribution changes with respect to time and temperature are observable from sequential holograms. Initial experiments using diethylene glycol/ethyl salicylate (DEG/ES) have demonstrated the usefulness of the technique. The thermal system controls temperature to at least plus or minus 0.001 K over the course of an experiment. A time-lapse film, made from holograms, of a succinonitrile/water solution shows particle size and number distribution changes with time under isothermal conditions. The observations are consistent with Ostwald ripening theory. Author

N86-10113*# Maryland Univ., College Park.
LIGHT SCATTERING TESTS OF FUNDAMENTAL THEORIES OF TRANSPORT PROPERTIES IN THE CRITICAL REGION
R. W. Gammon and M. R. Moldover (NBS, Washington, D.C.) *In* NASA, Washington Microgravity Sci. and Appl. Program Tasks May 1985 p 106 (For primary document see N86-10053 01-12)
(Grant NAG3-470)
Avail: NTIS HC A10/MF A01 CSCL 22A

The objective of this program is to measure the decay rates of critical density fluctuations in a simple fluid (xenon) very near its liquid-vapor critical point using laser light scattering and photon correlation spectroscopy. Such experiments have been severely limited on Earth by the presence of gravity which causes large density gradients in the sample when the compressibility diverges approaching the critical point. The goal is to measure decay rates deep in the critical region where the scaled wavevector is the order of 1000. This will require loading the sample to 0.01% of the critical density and taking data as close as 3 microKelvin to the critical temperature (Tc = 289.72 K). Other technical problems have to be addressed such as multiple scattering and the effect of wetting layers. The ability to avoid multiple scattering by using a thin sample (100 microns) was demonstrated, as well as a temperature history which can avoid wetting layers satisfactory temperature control and measurement, and accurate sample loading. Thus the questions of experimental art are solved leaving the important engineering tasks of mounting the experiment to maintain alignment during flight and automating the state-of-the-art temperature bridges for microcomputer control of the experiment. R.J.F.

N86-10114*# National Bureau of Standards, Boulder, Colo.
TRANSIENT HEAT TRANSFER IN ZERO GRAVITY ENVIRONMENT
P. G. Giarratano, Vincent D. Arp, and A. Kumakawa (National Aerospace Lab., Mijagi, Japan) *In* NASA, Washington Microgravity Sci. and Appl. Program Tasks May 1985 p 107 (For primary document see N86-10053 01-12)
(NASA Order H-27954B) Avail: NTIS HC A10/MF A01 CSCL 22A

The objective is to provide computer codes and/or correlations for application in the design of transient heat transfer systems. The mathematical models in the computer codes are being tested by experimental data obtained in the laboratory using optical techniques. The elimination of natural convection (buoyancy) in the experimental data obtained in zero-g (KC-135) facilitates the study of thermal expansion effects which is of interest in the development and testing of the mathematical models of the transient heat transfer. Initial flight in the KC 135 (June 1983) suggested some modifications to the experimental apparatus and the data acquisition technique (high speed video will replace high speed movies for recording optical records generated during the experiments). A series of KC-135 flights with this experiment on board are scheduled for summer/fall 1984. The acquisition of the aforementioned data using interferometry and beam deflection optical techniques is anticipated. The measurements provide time dependent temperature fields above a horizontal heater surface submerged in a static fluid (Freon 13). The heater surface is electrically heated for a time interval approximately < 0.100 sec. during which the data are optically recorded. Author

N86-10115*# National Bureau of Standards, Washington, D.C. Inst. for Materials Research.
SURFACE TENSIONS AND THEIR VARIATIONS WITH TEMPERATURE AND IMPURITIES
S. C. Hardy and J. Fine *In* NASA, Washington Microgravity Sci. and Appl. Program Tasks May 1985 p 108 (For primary document see N86-10053 01-12)
(NASA Order H-27954b) Avail: NTIS HC A10/MF A01 CSCL 22A

The surface tensions in this work were determined using the sessile drop technique. This method is based on a comparison of the profile of a liquid drop with the profile calculated by solving the Young-Laplace equation. The comparison can be made in several ways; the traditional Bashforth-Adams procedure was used in conjunction with recently calculated drop shape tables which virtually eliminate interpolation errors. Although previous study has found little difference in measurements with pure and oxygen doped silicon, there is other evidence suggesting that oxygen in dilute concentrations severely depresses the surface tension of silicon. The surface tension of liquid silicon in purified argon atmospheres was measured. A temperature coefficient near -0.28 mJ/square meters K was found. The experiments show a high sensitivity of the surface tension to what is believed are low concentrations of oxygen. Thus one cannot rule out some effect of low levels of oxygen in the results. However, the highest surface tension values obtained in conditions which minimized the residual oxygen pressure are in good agreement with a previous measurement in pure hydrogen. Therefore, depression of the surface tension by oxygen is insignificant in these measurements. R.J.F.

N86-10116*# Alabama Univ., Huntsville.
DIRECT OBSERVATION OF CRITICAL POINT WETTING IN MICROGRAVITY
William F. Kaukler *In* NASA, Washington Microgravity Sci. and Appl. Program Tasks May 1985 p 109 (For primary document see N86-10053 01-12)
Avail: NTIS HC A10/MF A01 CSCL 22A

The objective of this program is to observe the interface shape in single and multicomponent systems at the onset of critical wetting in microgravity using the MSFC drop tower and KC-135 aircraft. Test cells for the drop facility were built and tested up to critical point of CCl. Low temperature drops were conducted for two component systems near the critical consolute point. Contact angle seems to approach 90 deg near the critical consolute temperature contrary to expectations. It is suspected that since the interfacial energy becomes vanishingly small at the critical consolute temperature, the interface shape has not reached equilibrium in the available low-gravity time. Author

N86-10117*# National Aeronautics and Space Administration. Lewis Research Center, Cleveland, Ohio.
SURFACE TENSION INDUCED INSTABILITIES IN REDUCED GRAVITY: THE BENARD PROBLEM
E. Koschmieder (Texas Univ., Austin) and A.-T. Chai *In* NASA, Washington Microgravity Sci. and Appl. Program Tasks May 1985 p 110 (For primary document see N86-10053 01-12)
(Grant NAG3-303)
Avail: NTIS HC A10/MF A01 CSCL 22A

A Benard convection experiment has been set up, and the onset of convection in shallow layers of silicone oil two millimeters or less deep has been studied. The onset has been observed visually or has been determined by the break in the heat transfer curve which accompanies the onset of convection. The outcome of these experiments has been very surprising, from the point of view of theoretical expectations. The onset of convection at temperature differences far below the critical value for fluid depths smaller than 2mm was observed. The discrepancy between experiments and theory increases with decreasing fluid depth. According to theoretical considerations, the effects of surface tension become more important as the fluid depth is decreased. Actually, one observes that the onset of convection tales place in two stages. There is first an apparently surface tension driven instability, occuring at subcritical temperature differences according to conventional theory. If then the temperature difference is increased, a second instability occurs which transform the first pattern into conventional strong hexagonal Benard cells. The second instability is in agreement with the critical temperature gradients predicted by Nield. R.J.F.

N86-10118*# Stanford Univ., Calif. Dept. of Physics.
LAMBDA POINT EQUIPMENT
John A. Lipa and William M. Fairbank *In* NASA, Washington Microgravity Sci. and Appl. Program Tasks May 1985 p 111-112 (For primary document see N86-10053 01-12)
(Contract JPL-955057; Grant NAG2-62)
Avail: NTIS HC A10/MF A01 CSCL 22A

A compilation of the active research tasks as of the end of the fiscal year 1984 of the Microgravity Science and Applications Program, NASA-Office of Space Science and Applications, involving several NASA centers and other organizations is presented. The purpose is to provide an overview of the program scope for managers and scientists in industry, university, and government communities. An introductory description of the program, strategy and overall goal; identification of the organizational structures and people involved; and a description of each research task, together with a list of recent publications is presented. The tasks are grouped into six categories: Electronic Materials; Solidification of Metals, Alloys, and Composites; Fluid Dynamics and Transports; Biotechnology; Glasses and Ceramics; and Combustion. Author

N86-10119*# Duke Univ., Durham, N. C. Dept. of Physics.
CRITICAL TRANSPORT PHENOMENA IN FLUID HELIUM UNDER LOW GRAVITY
Horst Meyer and Robert P. Behringer *In* NASA, Washington Microgravity Sci. and Appl. Program Tasks May 1985 p 113 (For primary document see N86-10053 01-12)
(Grant NAG4-379)
Avail: NTIS HC A10/MF A01 CSCL 22A

The feasibility of carrying out measurements of certain critical transport properties of pure fluid under conditions of low gravity was studied. These properties are the thermal conductivity, kappa, the shear viscosity zeta and the diffusive relaxation time tau, which are predicted to diverge (tend to infinity) as the liquid-vapor critical point is approached. However, in this critical region, the Earth's gravity effect becomes very important. As the critical point is approached, the gravity effects increasingly distort the results. The reason for this is that the compressibility of the fluid also diverges and under the influence of gravity causes a vertical density gradient in the fluid, which is significant even when very thin fluid layers (typically 1 mm high) are being used. The result is that the temperature dependence of kappa, zeta, and tau tends to flatten off as T sub c is approached instead of continuing to increase, and therefore the predictions from the renormalization group and mode coupling theories cannot be subjected to a satisfactory test. G.L.C.

N86-10120*# National Bureau of Standards, Washington, D.C.
PRECISE VISCOSITY MEASUREMENTS VERY CLOSE TO CRITICAL POINTS
M. R. Moldover and B. Berg *In* NASA, Washington Microgravity Sci. and Appl. Program Tasks May 1985 p 114 (For primary document see N86-10053 01-12)
(NASA Order C-86129D) Avail: NTIS HC A10/MF A01 CSCL 22A

A torsion oscillator is being developed to measure the viscosity of fluids at moderate temperatures (0-100 C) and pressures (0-10 MPa) at very low frequencies (0.5 Hz) and very low shear rates (0.05/sec). These conditions are required to measure the shear viscosity of fluids extremely close to the critical point. The oscillator, thermostat, vacuum system, and instrumentation were assembled and are undergoing debugging. Preliminary measurements indicate that the system has a noise corresponding to 0.2% of the viscosity of methanol-cyclohexane mixtures near the consolute point. Author

N86-10121*# National Bureau of Standards, Washington, D.C.
EXPERIMENTAL AND THEORETICAL STUDIES OF WETTING AND MULTILAYER ADSORPTION
M. R. Moldover, J. W. Schmidt, J. W. Cahn, and R. F. Kayser *In* NASA, Washington Microgravity Sci. and Appl. Program Tasks May 1985 p 115 (For primary document see N86-10053 01-12)
(NASA Order H-27954B) Avail: NTIS HC A10/MF A01 CSCL 22A

The recent work with partially miscible binary liquid mixtures has established that the structure of the liquid-vapor interface can undergo a first-order phase transition from incomplete to complete wetting of the vapor as the temperature is raised. A discontinuity in the change of interfacial tension as a function of temperature at the phase transition has been predicted to occur in many systems and to play an important role in the growth of uniform composites from alloy melts at monotectic points. These measurements are the first to establish the order of the transition. Studies of capillary rise in SF6 in a unique interferometer have led to the first measurements of the thickness of wetting layers (or equivalently, multilayer adsorbed films) on a solid surface near a liquid-vapor critical point. Instabilities in wetting layers were observed. A theory for the instabilities is being developed and will be checked by both static and dynamic optical experiments. The effect of gravity on the apparent thickness of interfaces (as measured by ellipsometry) is under study. Author

N86-10122*# National Bureau of Standards, Washington, D.C. Thermophysics Div.
IMPURITY EXTRACTION BY DROPLETS
Graham Morrison and J. M. Kincaid *In* NASA, Washington Microgravity Sci. and Appl. Program Tasks May 1985 p 116-117 (For primary document see N86-10053 01-12)
Avail: NTIS HC A10/MF A01 CSCL 22A

The goals are to model and to measure the phase equilibrium properties of a finely divided fluid containing a large number of chemically similar species. The objective is to develop an accurate, usable model for such phenomena as pollutant extraction of rain clouds, industrial separation in spray towers, and separation in emulsions. The project was designed as a hierarchy of complementary theoretical and experimental steps. A theory was developed to describe the segregation of complex impurities at the interface of a solvent. This phenomenon is important in phase behavior when a large fraction of molecules in a material are near an interface, the situation in a finely divided material. The theory will be modified to account for the effect of surface curvature on the surface tension. The study of mixtures differs from pure fluids not only because of the surface effects but also because composition differences between the droplet and the surrounding vapor can stabilize a droplet with respect to a bulk phase. G.L.C.

N86-10123*# Arizona State Univ., Tempe. Dept. of Mechanical and Aerospace Engineering.
ENERGY STABILITY OF THERMOCAPILLARY CONVECTION IN MODELS OF THE FLOAT ZONE PROCESS Abstract Only
G. Paul Neitzel and Daniel F. Jankowski *In* NASA, Washington Microgravity Sci. and Appl. Program Tasks May 1985 p 118 (For primary document see N86-10053 01-12)
(Grant NAG3-568)
Avail: NTIS HC A10/MF A01 CSCL 22A

The energy-stability of thermocapillary convection in models of the float-zone, crystal-growing process was studied. Stability limits, as functions of pertinent parameters, that will identify conditions which will not allow the existence of an undesirable oscillatory flow instability were determined. Such instabilities may occur in the space processing of semiconductor materials. The determination of the stability limits will involve two sets of numerical computations: (1) solution of the nonlinear governing equations together with the appropriate boundary conditions to determine the basic state (in general, velocity, pressure and temperature fields and the displacement of free surfaces and interfaces); and (2) solution of a nonlinear Euler-Lagrange systems for the energy-stability limit. Both computations, while difficult, should be within the scope of available computer capability and available concepts in numerical analysis. Finite-element methods are attractive candidates for the numerical work. G.L.C.

N86-10124*# Case Western Reserve Univ., Cleveland, Ohio. Dept. of Mechanical and Aerospace Engineering.
SURFACE-TENSION DRIVEN CONVECTION
S. Ostrach and Y. Kamotani *In* NASA, Washington Microgravity Sci. and Appl. Program Tasks May 1985 p 119-120 (For primary document see N86-10053 01-12)
(Grant NAG3-570)
Avail: NTIS HC A10/MF A01 CSCL 22A

The present experiments are directed to examine surface-tension gradients. The surface-tension induced convection under reduced gravity it's comparison with normal gravity convection with all other identical conditions are studied. The intensities of such flows and their penetration depth below the free surface are also determined. In this way, the dominant role of a free surface in a reduced-gravity environment is indicated. The interface between two fluid phases can influence the motion of fluids when either the interface has finite curvature or when the interfacial tension varies from point to point. In both cases, forces appear in the interfacial region that can affect or generate fluid motions. G.L.C.

N86-10125*# National Aeronautics and Space Administration. Lewis Research Center, Cleveland, Ohio.
THERMOCAPILLARY MOTION RESEARCH
Todd T. Peterson and A.-T. Chai *In* NASA, Washington Microgravity Sci. and Appl. Program Tasks May 1985 p 121 (For primary document see N86-10053 01-12)
Avail: NTIS HC A10/MF A01 CSCL 22A

Fundamental microgravity research on interfacial surface tension driven motion by a linear temperature gradient was conducted. A vertical linear temperature gradient will be established within a test container filled with a host fluid. The thermal gradient will be positive in the upward vertical direction to avoid any free convective currents. With minimal disturbance, a single immisible fluid droplet will be introduced into the host fluid. As predicted by existing theory, the droplet will move in the direction of higher temperature due to tangential shear stresses created by surface tension variations along the periphery of the droplet. G.L.C.

N86-10126*# Utah Univ., Salt Lake City.
MORPHOLOGICAL STABILITY AND FLUID DYNAMICS OF VAPOR CRYSTAL GROWTH
Franz Rosenberger *In* NASA, Washington Microgravity Sci. and Appl. Program Tasks May 1985 p 122-124 (For primary document see N86-10053 01-12)
(Grant NsG-1534)
Avail: NTIS HC A10/MF A01 CSCL 22A

A fundamental understanding of the conditions under which crystals can retain morphological stability, i.e., shape stability of the advancing interface, during growth from vapors was studied. Morphological stability (MS) is a necessary condition for the growth of homogeneous single crystals required for numerous device applications. For crystallization from melts, the MS concepts are well developed and are essentially based on heat and mass transfer conditions about the advancing interface. For crystallization from vapors, the MS requirements are more complex and not well understood. The added complexity arises from the fact that anisotropies in interfacial kinetics are typically stronger in crystallization from vapors than from melts. These pronounced anisotropies root in the distinctly lower atomic roughness of most vapor-solid interfaces. G.L.C.

N86-10127*# Massachusetts Inst. of Tech., Cambridge. Materials Processing Center.
AUTOMATIC PROCESSING OF REACTIVE POLYMERS
David Roylance *In* NASA, Washington Microgravity Sci. and Appl. Program Tasks May 1985 p 125 (For primary document see N86-10053 01-12)
(Grant NsG-7645)
Avail: NTIS HC A10/MF A01 CSCL 22A

A series of process modeling computer codes were examined. The codes use finite element techniques to determine the time-dependent process parameters operative during nonisothermal reactive flows such as can occur in reaction injection molding or composites fabrication. The use of these analytical codes to perform experimental control functions is examined; since the models can determine the state of all variables everywhere in the system, they can be used in a manner similar to currently available experimental probes. A small but well instrumented reaction vessel in which fiber-reinforced plaques are cured using computer control and data acquisition was used. The finite element codes were also extended to treat this particular process. G.L.C.

N86-10128*# Colorado Univ., Boulder. Dept. of Chemical Engineering.
THERMOCAPILLARY AND DIFFUSOCAPILLARY MIGRATION OF A FLUID DROP
Robert L. Sani *In* NASA, Washington Microgravity Sci. and Appl. Program Tasks May 1985 p 126 (For primary document see N86-10053 01-12)
(Grant NAG3-493)
Avail: NTIS HC A10/MF A01 CSCL 22A

The migration of bubbles, or drops, plays an important role in many engineering science and space manufacturing problems. In material science processes as in the manufacturing of glasses, etc., gas bubbles can be formed from the by-products of chemical reactions or gas trapped in the interstices of the raw material. In the low-g environment of space, forces other than gravitational must be utilized as a bubble separation technique. It is well-known that gradients in interfacial tension on the bubbles' surface can promote droplet motion in the direction of decreasing interfacial tension and hence provide such a separation mechanism. Thus, the role of thermocapillary and diffusocapillary migration of a bubble, or drop, can be of paramount interest in materials processing in space. G.L.C.

N86-10129*# Princeton Univ., N. J. Dept. of Chemical Engineering.
TRANSPORT PROCESSES RESEARCH
Dudley A. Saville and W. B. Russel *In* NASA, Washington Microgravity Sci. and Appl. Program Tasks May 1985 p 127 (For primary document see N86-10053 01-12)
(Grant NAG3-447)
Avail: NTIS HC A10/MF A01 CSCL 22A

Fundamental research in reduced gravity on transport processes occurring during crystallization and/or during solidification processes was studied. The details of the transport processes in various materials processing modes will be systematically studied. A Shuttle experiment will be planned to provide a better understanding of the role of fluid motion on the formation of morphological patterns and roles of these patterns in solid composition. The approach to the research will involve theoretical modeling of transport processes, non-incursive ground-based laboratory measurements of model systems, and the definition of requirements for space experimentation. Author

N86-10130*# Princeton Univ., N. J. Dept. of Chemical Engineering.
ELECTROHYDRODYNAMICS
Dudley A. Saville *In* NASA, Washington Microgravity Sci. and Appl. Program Tasks May 1985 p 128 (For primary document see N86-10053 01-12)
(Grant NAG3-259)
Avail: NTIS HC A10/MF A01 CSCL 22A

Models of electrohydrodynamic processes involving liquids with poorly ionized solutes at high (applied) field strengths were developed and tested. Extant theories which account for the details of physico-chemical processes associated with charged interfaces deal mainly with low field strengths and fully ionized solutes. The model used to describe processes at high field strengths--the leaky dielectric--omits consideration of electric double-layers, adsorption at interfaces, and chemical processes involved in the dissociation and recombination of solute species. Thus, even though the model depicts some features associated with bulk fluid motion, it fails to give a comprehensive picture. One example of the shortcomings of both the classical model of eletrokinetics at low field strengths and the leaky-dielectric model for high field strengths is found in the field strength dependence of the mobility of small particles in apolar liquids. The research will provide a more general model of electrohydrodynamic phenomena capable of application in diverse circumstances. G.L.C.

N86-10131*# National Bureau of Standards, Washington, D.C. Thermophysics Div.
MISCIBILITY GAP SYSTEMS
L. A. Schmid *In* NASA, Washington Microgravity Sci. and Appl. Program Tasks May 1985 p 129 (For primary document see N86-10053 01-12)
(NASA Order H-27954B) Avail: NTIS HC A10/MF A01 CSCL 22A

Immiscible droplets embedded in a host fluid in which a temperature gradient exists migrate toward the hot end of the host fluid because of the temperature dependence of the interfacial energy of the droplet. This thermocapillary migration effect was exploited in the design of a controllable heat valve which is the thermal analog of the electronic vacuum triode. Studies have also been made of test cells that could use thermocapillary migration to facilitate the study of condensation and dissolution kinetics in miscibility-gap solutions. Author

N86-10132*# Aerodyne Research, Inc., Billerica, Mass.
EXPERIMENTAL AND THEORETICAL ANALYSIS OF CHEMICAL VAPOR DEPOSITION WITH PREDICTION OF GRAVITY EFFECTS
Charter D. Stinespring and Karl E. Spear (Pennsylvania State Univ.) *In* NASA, Washington Microgravity Sci. and Appl. Program Tasks May 1985 p 130 (For primary document see N86-10053 01-12)
(Contract NAS3-23934)
Avail: NTIS HC A10/MF A01 CSCL 22A

A combined experimental and theoretical study to characterize the effects of gravitationally-induced transport on atmospheric pressure silicon epitaxy by SiH_4 pyrolysis is planned. Experimentally, flow regimes in which free convective transport contributes to the Chemical Vapor Deposition (CVD) process will be identified, and, for these conditions, the flow and deposition process will be characterized. Specifically, this will include measurements of three dimensional temperature variations using in situ Rayleigh scattering, gas phase composition profiles using laser absorption and fluorescence techniques, and deposition rates and defect densities. Subsequently, the free convective transport contribution to the CVD process will be minimized and/or altered while leaving deposition chemistry unaltered, and the characterization will be repeated. Based on these analyses, the effects of gravitationally-induced transport on atmospheric pressure CVD will be assessed. G.L.C.

N86-10133*# Massachusetts Inst. of Tech., Cambridge.
ROLE OF CONVECTION IN GRAIN REFINING
Julian Szekely, Merton C. Flemings, N. El-Kaddah, and Y. Shiohara *In* NASA, Washington Microgravity Sci. and Appl. Program Tasks May 1985 p 131-132 (For primary document see N86-10053 01-12)
(Grant NsG-7645)
Avail: NTIS HC A10/MF A01 CSCL 22A

A quantitative representation of the heat and fluid flow fields in electromagnetically levitated (positioned) metallic specimens is examined. Experimental studies as well as modelling of those studies on undercooling and solidification of levitated metal droplets are also considered. Thermal measurements will be made of the undercooling and solidification of levitated metal droplets. Thermal measurements will be made of the undercooling and of the details of the ultra-rapid recalescence. This levitation technique combined with quenching will be used to aid in the development of coherent model for the solidification process related to structural studies, including thermodynamics and kinetics for nucleation and metastable solute partition, kinetics for solid/liquid interface velocity with high undercooling, and heat flow consideration. G.L.C.

N86-10134*# Michael Reese Research Foundation, Chicago, Ill.
BIOCHEMICAL ASSAYS OF CULTURED CELLS
Grant H. Barlow *In* NASA, Washington Microgravity Sci. and Appl. Program Tasks May 1985 p 135 (For primary document see N86-10053 01-12)
(Contract NAS9-16389)
Avail: NTIS HC A10/MF A01 CSCL 22A

Subpopulations of human embryonic kidney cells isolated from continuous flow electrophoresis experiments performed at McDonnell Douglas and on STS-8 have been analyzed. These analyses have included plasminogen activator assays involving indirect methodology on fibrin plated and direct methodology using chromogenic substrates. Immunological studies were performed and the conditioned media for erythropoietin activity and human granulocyte colony stimulating (HGCSF) activity was analyzed. G.L.C.

N86-10135*# Arizona Univ., Tucson. Dept. of Microbiology.
HORMONE PURIFICATION BY ISOELECTRIC FOCUSING
Milan Bier *In* NASA, Washington Microgravity Sci. and Appl. Program Tasks May 1985 p 136-137 (For primary document see N86-10053 01-12)
(Contract NAS8-32950)
Avail: NTIS HC A10/MF A01 CSCL 22A

Various ground-based research approaches are being applied to a more definitive evaluation of the natures and degrees of electroosmosis effects on the separation capabilities of the Isoelectric Focusing (IEF) process. A primary instrumental system for this work involves rotationally stabilized, horizontal electrophoretic columns specially adapted for the IEF process. Representative adaptations include segmentation, baffles/screens, and surface coatings. Comparative performance and development testing are pursued against the type of column or cell established as an engineering model. Previously developed computer simulation capabilities are used to predict low-gravity behavior patterns and performance for IEF apparatus geometries of direct project interest. Three existing mathematical models plus potential new routines for particular aspects of simulating instrument fluid patterns with varied wall electroosmosis influences are being exercised. G.L.C.

N86-10136*# Oregon Health Sciences Univ., Portland. Dept. of Neurology.
CELL PARTITION IN TWO POLYMER AQUEOUS PHASES
Donald E. Brooks *In* NASA, Washington Microgravity Sci. and Appl. Program Tasks May 1985 p 138-139 (For primary document see N86-10053 01-12)
(Contract NAS8-35333)
Avail: NTIS HC A10/MF A01 CSCL 22A

In a reduced gravity environment the two polymer phases will not separate via density driven settling in an acceptably short length of time. It is to be expected that a certain amount of phase separation will take place, however, driven by the reduction in free energy gained when the interfacial area is reduced. This stage of separation process will therefore depend directly on the magnitude of the interfacial tension between the phases. In order to induce complete phase separation in a short time, electric field-induced separation which occurs because the droplets of one phase in the other have high electrophoretic mobilities which increase with droplet size was investigated. These mobilities are significant only in the presence of certain salts, particularly phosphates. The presence of such salts, in turn has a strong effect on the cell partition behavior in dextran-poly (ethylene glycol) (PEG) systems. The addition of the salts necessary to produce phase drop mobilities has a large effect on the interfacial tensions in the systems. G.L.C.

N86-10137*# Sydney Univ. (Australia). Dept. of Medicine.

A STUDY OF BLOOD FLOW AND OF AGGREGATION OF BLOOD CELLS UNDER CONDITIONS OF ZERO GRAVITY: ITS RELEVANCE TO THE OCCLUSIVE DISEASES AND CANCER

Leopold Dintenfass *In* NASA, Washington Microgravity Sci. and Appl. Program Tasks May 1985 p 140 (For primary document see N86-10053 01-12)
Avail: NTIS HC A10/MF A01 CSCL 22A

The objectives of this program are: (1) to determine whether the size of red cell aggregates, kinetics and morphology of these aggregates are influenced by near-zero gravity; (2) whether viscosity, especially at low shear rate, is afflicted by near-zero gravity (the latter preventing sedimentation of red cells); (3) whether the actual shape of red cells changes; and (4) whether blood samples obtained from different donors (normal and patients suffering from different disorders) react in the same manner to near-zero gravity. G.L.C.

N86-10138*# Alabama Univ., Huntsville.

NEW INSTRUMENTATION FOR PHASE PARTITIONING

J. Milton Harris *In* NASA, Washington Microgravity Sci. and Appl. Program Tasks May 1985 p 141-142 (For primary document see N86-10053 01-12)
(Contract NAS8-35334)
Avail: NTIS HC A10/MF A01 CSCL 22A

Cells and molecules can be purified by partitioning between the two immiscible liquid phases formed by aqueous solutions of poly/ethylene glycol and dextran. Such purification can be more selective, higher yielding, and less destructive to sensitive biological materials than other available techniques. Earth's gravitational field is a hindering factor as it causes sedimentation of particles to be purified and shear-induced particle randomization. The present proposal is directed toward developing new instrumentation for performing phase partitioning both on Earth and in microgravity. G.L.C.

N86-10139*# Alabama Univ., Huntsville.

CELL PARTITION IN TWO POLYMER AQUEOUS PHASES

J. Milton Harris *In* NASA, Washington Microgravity Sci. and Appl. Program Tasks May 1985 p 143 (For primary document see N86-10053 01-12)
(Contract NAS8-35362)
Avail: NTIS HC A10/MF A01 CSCL 22A

Partition of biological cells in two phase aqueous polymer systems is recognized as a powerful separation technique which is limited by gravity. The synthesis of new, selective polymer ligand conjugates to be used in affinity partition separations is of interest. The two most commonly used polymers in two phase partitioning are dextran and polyethylene glycol. A thorough review of the chemistry of these polymers was begun, particularly in the area of protein attachment. Preliminary studies indicate the importance in affinity partitioning of minimizing gravity induced randomizing forces in the phase separation process. The PEG-protein conjugates that were prepared appear to be ideally suited for achieving high quality purifications in a microgravity environment. An interesting spin-off of this synthetic work was the observation of catalytic activity for certain of our polymer derivatives. Author

N86-10140*# National Aeronautics and Space Administration. Johnson (Lyndon B.) Space Center,

PURIFICATION AND CULTIVATION OF HUMAN PITUITARY GROWTH HORMONES SECRETING CELLS

Wesley C. Hymer (Pennsylvania State Univ., University Park), Paul Todd (Pennsylvania State Univ., University Park), Richard Grindeland (Pennsylvania State Univ., University Park), Wayne Lanham (Pennsylvania State Univ., University Park), and Dennis Morrison *In* NASA, Washington Microgravity Sci. and Appl. Program Tasks May 1985 p 144-145 refs (For primary document see N86-10053 01-12)
(Contract NAS9-15566)
Avail: NTIS HC A10/MF A01 CSCL 22A

The rat and human pituitary gland contains a mixture of hormone producing cell types. The separation of cells which make growth hormone (GH) is attempted for the purpose of understanding how the hormone molecule is made within the pituitary cell; what form(s) it takes within the cell; and what form(s) GH assumes as it leaves the cell. Since GH has a number of biological targets (e.g., muscle, liver, bone), the assessment of the activities of the intracellular/extracellular GH by new and sensitive bioassays. GH cells contained in the mixture was separated by free flow electrophoresis. These experiments show that GH cells have different electrophoretic mobilities. This is relevant to NASA since a lack of GH could be a prime causative factor in muscle atrophy. Further, GH has recently been implicated in the etiology of motion sickness in space. Continous flow electrophoresis experiment on STS-8 showed that GH cells could be partially separated in microgravity. However, definitive cell culture studies could not be done due to insufficient cell recoveries. Author

N86-10141*# National Aeronautics and Space Administration. Johnson (Lyndon B.) Space Center,

CELL SEPARATIONS IN MICROGRAVITY AND DEVELOPMENT OF A SPACE BIOREACTOR

Dennis R. Morrison *In* NASA, Washington Microgravity Sci. and Appl. Program Tasks May 1985 p 146-147 refs (For primary document see N86-10053 01-12)
Avail: NTIS HC A10/MF A01 CSCL 22A

A bioreactor optimized for operations in space is now being developed. The current research is focused on determining the optimum cell-bead ratios, medium content and proper maintenance conditions required to keep living cell specimens alive and healthy for the entire flight. The bioreactor development project has recently added a microprocessor/computer to the JSC prototype for control and data analysis. Appropriate new technology is being combined with the current bioreactor designs and tested to determine what specific features must be included in the fabrication of a bioreactor designed to operate for STS demonstration tests. Considerations include: (1) circulation and resupply of culture media; (2) sensors required to monitor temperature, cell growth, mass transport, and oxygen consumption; and (3) inflight control of shear stress on cells, gas transfer in microgravity, diffusion, and intracellular transport. These data and results from the JSC prototype bioreactor test will be used for the design and construction of a small space bioreactor for the Orbiter middeck. Author

N86-10142*# National Aeronautics and Space Administration. Johnson (Lyndon B.) Space Center,

CELL MAINTENANCE SYSTEMS

Dennis R. Morrison *In* NASA, Washington Microgravity Sci. and Appl. Program May 1985 p 148 (For primary document see N86-10053 01-12)
Avail: NTIS HC A10/MF A01 CSCL 22A

Living human cells require attachment to a suitable surface and special culture conditions in order to grow. These requirements are modified and amplified when cells are taken into a weightless environment. Special handling and maintenance systems are required for routine laboratory procedures conducted in the Orbiter and in the Spacelab. Methods were developed to maintain cells in special incubators designed for the Orbiter middeck, however, electrophoresis and other experiments require cells to be harvested off of the culture substrate before they can be processed or used. The cell transport assembly (CTA) was flown on STS-8, and results show that improvements are required to maintain adequate numbers of cells in this device longer than 48 hours. The life sciences middeck centrifuge probably can be used, but modifications will be required to transfer cells from the CTA and keep the cells sterile. Automated systems such as the Skylab SO-15 flight hardware and crew operated systems are being evaluated for use on the Space Shuttle, Spacelab, and Space Station research modules. Author

N86-10143*# National Aeronautics and Space Administration. Marshall Space Flight Center, Huntsville, Ala.

MATHEMATICAL MODELS OF CONTINUOUS FLOW ELECTROPHORESIS

D. A. Saville (Princeton Univ.) and R. S. Snyder *In* NASA,

Washington Microgravity Sci. and Appl. Program Tasks May 1985 p 149-150 refs (For primary document see N86-10053 01-12)
(Contract NAS8-32614)
Avail: NTIS HC A10/MF A01 CSCL 22A

Development of high resolution continuous flow electrophoresis devices ultimately requires comprehensive understanding of the ways various phenomena and processes facilitate or hinder separation. A comprehensive model of the actual three dimensional flow, temperature and electric fields was developed to provide guidance in the design of electrophoresis chambers for specific tasks and means of interpreting test data on a given chamber. Part of the process of model development includes experimental and theoretical studies of hydrodynamic stability. This is necessary to understand the origin of mixing flows observed with wide gap gravitational effects. To insure that the model accurately reflects the flow field and particle motion requires extensive experimental work. Another part of the investigation is concerned with the behavior of concentrated sample suspensions with regard to sample stream stability particle-particle interactions which might affect separation in an electric field, especially at high field strengths. Mathematical models will be developed and tested to establish the roles of the various interactions. Author

N86-10144*# National Aeronautics and Space Administration. Marshall Space Flight Center, Huntsville, Ala.
ELECTROPHORESIS TECHNOLOGY
R. S. Snyder *In* NASA, Washington Microgravity Sci. and Appl. Program Tasks May 1985 p 151-152 refs (For primary document see N86-10053 01-12)
Avail: NTIS HC A10/MF A01 CSCL 22A

A new high resolution apparatus designed for space was built as a laboratory prototype. Using a moving wall with a low zeta potential coating, the major sources of flow distortion for an electrophoretic sample stream are removed. Highly resolved fractions, however, will only be produced in space because of the sensitivity of this chamber to buoyancy-induced convection in the laboratory. The second and third flights of the McDonnell Douglas Astronautics Corporation continuous flow electrophoresis system carried samples developed at MSFC intended to evaluate the broad capabilities of free flow electrophoresis in a reduced gravity environment. Biological model materials, hemoglobin and polystyrene latex microspheres, were selected because of their past use as electrophoresis standards and as visible markers for fluid flow due to electroosmosis, spacecraft acceleration or other factors. The dependence of the separation resolution on the properties of the sample and its suspension solution was assessed. Author

N86-10145*# Pennsylvania State Univ., University Park.
KIDNEY CELL ELECTROPHORESIS
Paul Todd *In* NASA, Washington Microgravity Sci. and Appl. Program Tasks May 1985 p 153 (For primary document see N86-10053 01-12)
(Contract NAS9-15584)
Avail: NTIS HC A10/MF A01 CSCL 22A

Materials and procedures for microgravity electrophoresis of living human embryonic kidney cells were evaluated, ground support in the form of analytical cell electrophoresis and flow cytometry was provided and cells returned from space flight were analyzed. Preflight culture media, electrophoresis buffer, fraction collection media, temperature profiles, and urokinase assay procedures were tested prior to flight. Electrophoretic mobility distributions of aliquots of the cell population to be fractionated in flight were obtained. The protocol established and utilized is given. Author

N86-10146*# National Aeronautics and Space Administration. Marshall Space Flight Center, Huntsville, Ala.
PRODUCTION OF LARGE-PARTICLE-SIZE MONODISPERSE LATEXES IN MICROGRAVITY
J. W. Vanderhoff (Lehigh Univ.), F. J. Micale (Lehigh Univ.), M. S. El-Aasser (Lehigh Univ.), and M. Kornfeld *In* NASA, Washington Microgravity Sci. and Appl. Program Tasks May 1985 p 154-155 refs (For primary document see N86-10053 01-12)
(Contract NAS8-32951)
Avail: NTIS HC A10/MF A01 CSCL 22A

A latex is a suspension of very tiny (micrometer-size) plastic spheres in water, stabilized by emulsifiers. The growth of billions of these tiny plastic spheres to sizes larger than can be grown on Earth is attempted while keeping all of them exactly the same size and perfectly spherical. Thus far on several of the Monodisperse Latex Reactor (MLR) flights, the latex spheres have been returned to Earth with standard deviations of better than 1.4%. In microgravity the absence of buoyancy effects has allowed growth of the balls up to 30 micrometers in diameter thus far. The MLR has now flown 5 times on the Shuttle. The MLR has now produced the first commercial space product; that is the first commercial material ever manufactured in space and marketed on Earth. Once it is demonstrated that these large-size-monodisperse latexes can be routinely produced in quantity and quality, they can be marketed for many types of scientific applications. They can be used in biomedical research for such things as drug carriers and tracers in the body, human and animal blood flow studies, membrane and pore-sizing in the body, and medical diagnostic tests. Author

N86-10147*# Massachusetts Inst. of Tech., Cambridge.
COLLOIDAL OXIDE PROPERTIES AND KINETIC STUDIES
I-Wei Chen *In* NASA, Washington Microgravity Sci. and Appl. Program Tasks May 1985 p 159 (For primary document see N86-10053 01-12)
(Grant NSG-7645)
Avail: NTIS HC A10/MF A01 CSCL 22A

Silica based oxide particles prepared by various methods are compared in terms of their gellation kinetics, densification kinetics, and microable structural evolutions begin at very low temperature. Additional work reported in literature further suggested that the colloidal behaviors and the dried gel structures of the same oxide from different preparation techniques differ fundamentally. These differences significantly affect the densification kinetics and the product microstructure. Gravitational segregation of particles of different sizes in a gravitational field is modelled as a diffusion/segregation problem. A structural free volume model was used to describe the activation process of jump statistics. The sizes of the particles, the interstices, and their packing topology are accounted for in the estimation of the free volume. An attempt frequency is ascribed to particles to account for the vibrational rearrangement during powder packing. Author

N86-10148*# Missouri Univ., Rolla.
CONTAINERLESS PROCESSING OF GLASS FORMING MELTS IN SPACE
Delbert D. Day *In* NASA, Washington Microgravity Sci. and Appl. Program Tasks May 1985 p 160-161 refs (For primary document see N86-10053 01-12)
(Contract NAS8-34758)
Avail: NTIS HC A10/MF A01 CSCL 22A

The major objectives of this work are: (1) obtain quantitative evidence for the suppression of heterogeneous nucleation/crystallization in containerless melts in micro-g; (2) study melt homogenization in the absence of gravity driven convection; (3) develop the procedures for preparing precursor samples suitable for flight experiments; (4) perform comparative property analysis of glasses melted on Earth and in micro-g; (5) determine the feasibility of preparing glass shells in micro-g for use as laser fusion targets; and (6) assess the operational performance of the single axis acoustic levitator/furnace apparatus for processing multicomponent, glass forming melts in micro-g. Ways of obtaining these goals are discussed. Author

N86-10149*# Rensselaer Polytechnic Inst., Troy, N. Y.
CRYSTALLIZATION, OPTICAL AND CHEMICAL PROPERTIES OF FLUORIDE GLASSES
Robert H. Doremus *In* NASA, Washington Microgravity Sci. and Appl. Program Tasks May 1985 p 162 (For primary document see N86-10053 01-12)
(Contract JPL-955870)
Avail: NTIS HC A10/MF A01 CSCL 22A

Fluoride glasses have great promise as infrared optical components, especially fibers, because they are transparent to 8 micrometers and higher. In order to optimize properties, different glass compositions are needed. Some are hard to form in a container, and may possibly be formable in a containerless furnace. Understanding of crystallization with and without a container could lead to glasses with optimum properties. Chemical durability (attack by water) can limit or extend the applicability of fluoride glasses. Progress to date is given. Author

N86-10150*# KMS Fusion, Inc., Ann Arbor, Mich.

GEL PRECURSORS AS GLASS AND CERAMIC STARTING MATERIALS FOR SPACE PROCESSING APPLICATIONS RESEARCH

Raymond L. Downs and Wayne J. Miller *In* NASA, Washington Microgravity Sci. and Appl. Program Tasks May 1985 p 163 (For primary document see N86-10053 01-12)
(Contract NAS7-100)
Avail: NTIS HC A10/MF A01 CSCL 22A

The crystallization kinetics and glass forming ability of reluctant glass formers is investigated. This could ultimately aid the formation of bulk samples of unique glass compositions outside of normal glass forming regions allowing the optimization of certain properties of the glass. One important aspect of processing in space is the containerless undercooling of molten substances. Theoretically, the extent of undercooling can be greatly enhanced by solidifying in the absence of heterogeneous nucleation resulting from contact with crucibles or molds. Techniques were established for the measurement of crystallization kinetics and critical cooling rates. The glass formation ability and crystallization kinetics of Ga2O-43CaO and several Al2O3-CaO compositions were measured. An apparatus was set up to measure the temperature of spherical samples on a thermocouple at large cooling rates. The time and temperature of nucleation is recorded and the probability of nucleation at various cooling rates can be measured. Author

N86-10151*# National Aeronautics and Space Administration. Marshall Space Flight Center, Huntsville, Ala.

GLASS FORMATION IN RELUCTANT GLASS FORMERS

E. C. Ethridge *In* NASA, Washington Microgravity Sci. and Appl. Program Tasks May 1985 p 164-165 refs (For primary document see N86-10053 01-12)
Avail: NTIS HC A10/MF A01 CSCL 22A

The crystallization kinetics and glass forming ability of reluctant glass formers is investigated. This could ultimately aid the formation of bulk samples of unique glass compositions outside of normal glass forming regions allowing the optimization of certain properties of the glass. One important aspect of processing space is the containerless undercooling of molten substances. Theoretically, the extent of undercooling can be greatly enhanced by solidifying in the absence of heterogeneous nucleation resulting from contact with crucibles or molds. Techniques were established for the measurement of crystallization kinetics and critical cooling rates. The glass formation ability and crystallization kinetics of Ga2O-43CaO and several Al2O3-CaO compositions were measured. An apparatus was set up to measure the temperature of spherical samples on a thermocouple at large cooling rates. The time and temperature of nucleation is recorded and the probability of nucleation at various cooling rates can be measured. Author

N86-10152*# Massachusetts Inst. of Tech., Cambridge. Materials Processing Center.

RAPID SOLIDIFICATION OF MAGNETIC OXIDES

G. Kalonji and M. R. DeGuire *In* NASA, Washington Microgravity Sci. and Appl. Program Tasks May 1985 p 166 (For primary document see N86-10053 01-12)
(Grant NSG-7645)
Avail: NTIS HC A10/MF A01 CSCL 22A

The enhanced control over microstructural evolution inherent in rapid solidification processing techniques are exploited to create novel ceramic magnetic materials. The great sensitivity of magnetic properties to local structure provides a powerful probe both for the study of structure and of microscopic solidification mechanisms. The first system studied is the SrO-Fe2O3 binary, which contains the commercially important hard magnetic compound strontium hexaferrite. The products were analyzed by transmission electron microscopy, Mossbauer spectroscopy, magnetic measurements, and differential thermal analysis. As-quenched ribbons contain high concentrations of super-paramagnetic particles, 80 to 250 Angstroms in diameter, in a glassy matrix. This suggests the possibility of crystallizing monodomain strontium hexaferrite during subsequent heat treatment, with a resulting increase in coercivity over conventionally processed ferrite magnets. That magnetic properties can be controlled in solidification processing by varying the quench rate is demonstrated. Author

N86-10153*# Jet Propulsion Lab., California Inst. of Tech., Pasadena.

SOL-GEL GLASSES

S. P. Mukherjee *In* NASA. Washington Microgravity Sci. and Appl. Program Tasks May 1985 p 167-169 (For primary document see N86-10053 01-12)
Avail: NTIS HC A10/MF A01 CSCL 22A

Multicomponent homogeneous, ultrapure noncrystalline gels/gel derived glasses are promising batch materials for the containerless glass melting experiments in microgravity. Hence, ultrapure, homogeneous gel precursors could be used to: (1) investigate the effect of the container induced nucleation on the glass forming ability of marginally glass forming compositions; and (2) investigate the influence of gravity on the phase separation and coarsening behavior of gel derived glasses in the liquid-liquid immiscibility zone of the nonsilicate systems having a high density phase. The structure and crystallization behavior of gels in the SiO2-GeO2 as a function of gel chemistry and thermal treatment were investigated. As are the chemical principles involved in the distribution of a second network former in silica gel matrix being investigated. The procedures for synthesizing noncrystalline gels/gel-monoliths in the SiO2-GeO2, GeO2-PbO systems were developed. Preliminary investigations on the levitation and thermal treatment of germania silicate gel-monoliths in the Pressure Facility Acoustic Levitator were done. Author

N86-10154*# Harvard Univ., Cambridge, Mass.

BULK FORMATION OF METALLIC GLASSES AND AMORPHOUS SILICON FROM THE MELT

Frans Spaepen *In* NASA, Washington Microgravity Sci. and Appl. Program Tasks May 1985 p 170-171 refs (For primary document see N86-10053 01-12)
(Contract NAS8-35416)
Avail: NTIS HC A10/MF A01 CSCL 22A

By using metallic glass compositions with a high relative glass transition temperature, such as Pd40Ni40P20, homogeneous nucleation also becomes negligible. Large (5g) masses of this alloys were obtained using a molten B2O3 flux. Presently, bulk glass formation in iron based glasses is being investigated. It is expected that if an undercooling of about 250K can be achieved in a Ge or Si melt, formation of the amorphous semiconductor phase (rather than the crystal) may be kinetically favored. The volumetric behavior of undercooled liquid Ga droplet dispersion is investigated by dilatometry. A theoretical model (both analytical and numerical) was developed for transient nucleation in glass forming melts. The model, originally designed for isothermal conditions, was extended to continuous quenching. It is being applied to glass formation in various metallic and oxide systems. A further refinement will be the inclusion of diffusion controlled interfacial rearrangements governing the growth of the crystal embryos. Author

N86-10155*# Clarkson Coll. of Technology, Potsdam, N.Y. Dept. of Chemical Engineering.

PHYSICAL PHENOMENA IN CONTAINERLESS GLASS PROCESSING

R. S. Subramanian and Robert Cole *In* NASA, Washington Microgravity Sci. and Appl. Program Tasks May 1985 p 172-173 refs (For primary document see N86-10053 01-12)

Avail: NTIS HC A10/MF A01 CSCL 22A

An investigation into the various physical phenomena of importance in the space experiments is under way. Theoretical models of thermocapillary flow in drops, thermal migration of bubbles and droplets, the motion of bubbles inside drops, and the migration of bubbles in rotating liquid bodies are being developed. Experiments were conducted on the migration of bubbles and droplets to the axis of a rotating liquid body, and the rise of bubbles in molten glass. Also, experiments on thermocapillary motion in silicone oils as well as glass melts were performed. Experiments are currently being conducted on the migration of bubbles in a thermal gradient, and on their motion inside unconstrained liquid drops in a rotating liquid. Author

N86-10156*# Jet Propulsion Lab., California Inst. of Tech., Pasadena.

FUSION TARGET TECHNOLOGY

T. G. Wang *In* NASA, Washington Microgravity Sci. and Appl. Program Tasks May 1985 p 174 refs (For primary document see N86-10053 01-12)

Avail: NTIS HC A10/MF A01 CSCL 22A

In order to produce the high quality spherical shells that are required, three parameters must be controlled accurately: the shell dimensions, shell sphericity and concentricity, and the surface topology of the shell. Attempts to conduct experiments on the dynamics of liquid bubbles (molten shells) in laboratories are limited by a strong coupling among the three parameters, time, gravity, and temperature. These limitations are circumvented and detailed study of each of the important processes is carried out through the use of low gravity environments collectively available in drop towers, in KC-135 flights, in a neutrally buoyant immiscible system, and in an acoustic levitation system. Author

N86-10157*# Jet Propulsion Lab., California Inst. of Tech., Pasadena.

GLASS RESEARCH

Michael C. Weinberg *In* NASA, Washington Microgravity Sci. and Appl. Program Tasks May 1985 p 175-176 refs (For primary document see N86-10053 01-12)

Avail: NTIS HC A10/MF A01 CSCL 22A

Research efforts span three general areas of glass science: glass refining, gel-derived glasses, and nucleation and crystallization of glasses. Gas bubbles which are present in a glass product are defects which may render the glass totally useless for the end application. For example, optical glasses, laser host glasses, and a variety of other specialty glasses must be prepared virtually defect free to be employable. Since a major mechanism of bubble removal, buoyant rise, is virtually inoperative in microgravity, glass fining will be especially difficult in space. On the other hand, the suppression of buoyant rise and the ability to perform containerless melting experiments in space allows the opportunity to carry out several unique bubble experiments in space. Gas bubble dissolution studies may be performed at elevated temperatures for large bubbles with negligible bubble motion. Also, bubble nucleation studies may be performed without the disturbing feature of heterogeneous bubble nucleation at the platinum walls. Ground based research efforts are being performed in support of these potential flight experiments. Author

N86-10158*# Massachusetts Inst. of Tech., Cambridge. Materials Processing Center.

OXIDATION BEHAVIOR OF GLASSY ALLOYS

G. Yurek *In* NASA, Washington Microgravity Sci. and Appl. Program Tasks May 1985 p 177 (For primary document see N86-10053 01-12)

(Grant NSG-7645)

Avail: NTIS HC A10/MF A01 CSCL 22A

The oxidation behavior of high temperature glassy alloys produced by rapid solidification processing is investigated and the effects of processing and composition on oxidation behavior is studied. Glassy Ta-44.5at%Ir, Ta-40at%Ir-10at%B and Nb-45at%Ir oxidized rapidly at 700 to 800 C at an oxygen partial pressure of .001 atm. The alloys were embrittled during the oxidation process. No apparent oxidation or embrittlement of the Ta-Ir alloy occurred after oxidation for 4h at 500 C at an oxygen partial pressure of .001 atm. Embrittlement occurred, however, after 100h of exposure under the latter conditions. Alloy embrittlement is associated with the partial or full conversion of the metallic glass to a mixture of crystalline beta-Ta2O5 and metallic iridium. Hot compaction of glassy alloys of this type must be limited to relatively low temperatures (approx. 500 C) and short times at the low temperatures unless extremely low oxygen partial pressures can be achieved during the compaction process. Author

N86-10159*# Kentucky Univ., Lexington. Dept. of Mechanical Engineering.

SOLID SURFACE COMBUSTION AT REDUCED GRAVITY

Robert A. Altenkirch *In* NASA, Washington Microgravity Sci. and Appl. Program Tasks May 1985 p 181 refs (For primary document see N86-10053 01-12)

Avail: NTIS HC A10/MF A01 CSCL 22A

The spread of a flame in the gas over the surface of a solid combustible involves in an essential way the transfer of heat from the flame to the solid fuel immediately ahead of it. This heat transfer is affected by the character of the gas phase flame, and so the phenomenon of flame spreading under reduced gravity, in which the flow is generated by gasification of the solid combustible, is apt to be different from what occurs under the Earth's normal gravitational acceleration where the flow is largely buoyancy driven. An experiment is being designed for the Middeck of the Space Shuttle to aid us in understanding the process of flame spreading in the absence of a buoyancy driven flow. A chamber approximately 0.35 cu.m. in volume is to contain either a thin sample of a cellulosic material or a thick sample of polymethyl-methacrylate and an oxidizing environment of O2 and N2. Samples will be ignited at one end, and the ensuing flame spread will be filmed. The spread rate can be determined from the films, and surface and gas-phase temperatures just above the surface will also be recorded. These data will help to clarify the mechanism of forward heat transfer in the low gravity flames. Author

N86-10160*# California Univ., San Diego, La Jolla. Energy Center.

PARTICLE CLOUD COMBUSTION EXPERIMENT

A. L. Berlad *In* NASA, Washington Microgravity Sci. and Appl. Program Tasks May 1985 p 182 refs (For primary document see N86-10053 01-12)

(Grant NAG3-381)

Avail: NTIS HC A10/MF A01 CSCL 22A

Preparation of flight experiment designs is supported by experimental studies of acoustically induced mixing process, optical transmissivities of particle cloud distributions, wall saturation effects and their control through the use of electrically neutral flame tube materials and surfaces, and the pyrolysis-vaporization kinetics of selected organic particulates. Drop tower tests of stabilized particle cloud flames have allowed valuable comparison of $g = 0$ and $g = 1$ (upwards and downwards) stabilized flame propagation. These stabilized flame data will be valuable assists in dealing with the freely propagating particle cloud flame data anticipated through Space Shuttle experimentation. Supporting theoretical studies emphasize comprehensive flame propagation and extinction relations among premixed single phase (gaseous) flames and premixed particle cloud flames, for both stabilized and freely propagating flames. Author

N86-10161*# Science Applications, Inc., Chatsworth, Calif. Combustion Science and Advanced Technology Dept.

BUOYANCY EFFECTS UPON VAPOR FLAME AND EXPLOSION PROCESSES

Raymond B. Edelman and Phillip T. Harsha *In* NASA, Washington Microgravity Sci. and Appl. Program Tasks May 1985 p 183 ref (For primary document see N86-10053 01-12)

(Contract NAS3-22822)

Avail: NTIS HC A10/MF A01 CSCL 22A

The objective of this microgravity project is to develop an experimental and theoretical analyses critical to the understanding

of the coupling of buoyancy and turbulence generation and its effect on fuel-air mixing, flame intensity and flame propagation in jet diffusion flames. The experiment is designed to examine certain effects of buoyancy acting on a diffusion flame in which the flame is directed either upward or downward. This change from negative to positive g is observed to significantly alter the flame shape although all other operating conditions are the same for both configurations. However, to perform this experiment a significant coaxial secondary air flow is needed in order to prevent flow reversal when the flame is inverted. The theoretical analysis that has been developed handles the secondary air flow and the extreme change in gravity vector direction. Thus the data will provide a measure of credibility of the analysis which will then be used to assist in the design of the actual zero-g experiment.
F.M.R.

N86-10162*# California Univ., Berkeley.
A FUNDAMENTAL STUDY OF SMOLDERING WITH EMPHASIS ON EXPERIMENTAL DESIGN FOR ZERO-g
Patrick J. Pagni and A. Carlos Fernandez-Pello *In* NASA, Washington Microgravity Sci. and Appl. Program Tasks May 1985 p 184 (For primary document see N86-10053 01-12)
(Grant NAG3-443)
Avail: NTIS HC A10/MF A01 CSCL 22A

The objective of this section of the microgravity project is to identify key sets of low-gravity experiments which would critically compliment a larger set of more easily performed normal-gravity experiments to explain the phenomena found in smoldering combustion. It is planned to follow through on the conceptual design of these experiments by participating in the future in the fabrication of the refined apparatus and in the data collection and interpretation. Low-gravity experiments are appropriate for smoldering combustion because of the complexity of smoldering which requires every means possible to discriminate among the many chemical and physical mechanisms active in most smoldering combustion scenarios. Efforts will be primarily analytical, attempting to identify appropriate approximations and dominant dimensionless groups based on existing data and state-of-the-art combustion modelling. Transient stability questions such as ignition, extinction and the choices among charring, tarring, or flaming modes will be included.
F.M.R.

N86-10163*# Carnegie-Mellon Univ., Pittsburgh, Pa.
IGNITION AND FLAME SPREAD ABOVE LIQUID FUEL POOLS
William A. Sirignano *In* NASA, Washington Microgravity Sci. and Appl. Program Tasks May 1985 p 185 (For primary document see N86-10053 01-12)
(Grant NAG3-404)
Avail: NTIS HC A10/MF A01 CSCL 22A

Phenomena of ignition and flame spread above liquid fuel pools are studied and factors that can improve fire safety are determined. Dominant mechanisms for convective heat transfer and impact on ignition and flame spread above liquid fuel pools will be determined from these efforts. The approach is: (1) analytical and computational studies to evaluate scaling factors; (2) experimental design, development, and operation in laboratory at Earth's gravity; (3) experimental design for drop towers at NASA Lewis Research Center; (4) development and operation of drop tower experiments together with NASA Lewis Research personnel and; (5) develop recommendations for Lear Jet and/or Space Shuttle experiments. Through this research, a mathematical model of two-phase systems is formulated and is being coded for the computer.
F.M.R.

N86-10164*# Illinois Univ., Urbana.
FLAMMABILITY LIMITS OF GASES UNDER LOW GRAVITY CONDITIONS
Roger A. Strehlow *In* NASA, Washington Microgravity Sci. and Appl. Program Tasks May 1985 p 186-187 refs (For primary document see N86-10053 01-12)
(Contract NAS3-23770)
Avail: NTIS HC A10/MF A01 CSCL 22A

The purpose of this combustion science investigation is to determine the effect of zero, fractional, and super gravity on the flammability limits of a premixed methane air flame in a standard 51 mm diameter flammability tube and to determine, if possible, the fluid flow associated with flame passage under zero-g conditions and the density (and hence, temperature) profiles associated with the flame under conditions of incipient extinction. This is accomplished by constructing an appropriate apparatus for placement in NASA's Lewis Research Center Lear Jet facility and flying the prescribed g-trajectories while the experiment is being performed. Data is recorded photographically using the visible light of the flame. The data acquired is: (1) the shape and propagation velocity of the flame under various g-conditions for methane compositions that are inside the flammable limits, and (2) the effect of gravity on the limits. Real time accelerometer readings for the three orthogonal directions are displayed in full view of the cameras and the framing rate of the cameras is used to measure velocities.
F.M.R.

N86-10165*# Princeton Univ., N. J.
FUNDAMENTAL STUDIES OF DROPLET COMBUSTION AT REDUCED GRAVITY
Forman A. Williams *In* NASA, Washington Microgravity Sci. and Appl. Program Tasks May 1985 p 188 (For primary document see N86-10053 01-12)
(Grant NAG3-380)
Avail: NTIS HC A10/MF A01 CSCL 22A

Reduced gravity is used to carry out scientific investigations of droplet combustion. In earlier work a preliminary conceptual design had been developed for droplet burning experiments for Spacelab. Refinements of the earlier work with special consideration given to possible experiments for Mid-Deck Modules of the Space Shuttle is discussed. A re-evaluation of suitable experiments on droplet combustion is done to ascertain whether influences of reduced buoyancy on time-dependent processes of heat and mass transfer in the gas or in the liquid on extinction processes or on disruptive burning phenomena are best suited for further investigation. Components of the experimental apparatus, which include a droplet dispensing system, a droplet positioning system, a droplet ignition system and provision for recording, primarily photographically, the combustion of the individual droplet in a chamber having a controlled gas atmosphere, are studied to determine optimal approaches to the experimental design. Methods for data reduction and interpretation are being made more specific, particularly in the context of an objective to calculate overall gas-phase chemical-kinetic parameters for the combustion from observations of extinction conditions in different atmospheres.
F.M.R.

N86-10166*# National Aeronautics and Space Administration. Marshall Space Flight Center, Huntsville, Ala.
DEVELOPMENT OF MATERIALS PROCESSING SYSTEMS FOR USE IN SPACE ON LOW-g SIMULATION DEVICES
B. R. Aldrich and W. D. Whitt *In* NASA, Washington Microgravity Sci. and Appl. Program May 1985 p 191 (For primary document see N86-10053 01-12)
Avail: NTIS HC A10/MF A01 CSCL 22A

Advanced furnace systems are being developed for use in space. Systems are being tested for current experiment applications and modified for future experiment requirements. Future projects are: (1) fabrication and testing of the Advanced Automated Directional Solidification Furnace (AADSF) flight hardware; (2) development of a Heat Pipe Furnace (HPF) for use in space. Heat pipes will be tested for space flight qualification in conjunction with the furnace development. The HPF design will be based on the AADSF development and will be of modular design including capabilities of operating with or without heat pipes; and (3) the AADSF furnace will be modified and tested to operate at temperatures up to 1700 C in the heated cavity. This will be accomplished by developing a new hot end heating module and insulation package for the existing AADSF. Refurbishment of the Drop Tower Furnace (DTF) is under way. The DTF can operate at temperatures up to 1700 C. The sample size will be approximately 3/8 in. dia. x 5/8 in. long. Design improvements for the General Purpose

Rocket Furnace (GPFR) for use in the Material Experiment Assembly (MEA) are to be accomplished. F.M.R.

N86-10167*# Jet Propulsion Lab., California Inst. of Tech., Pasadena.
MULTIMODE ACOUSTIC RESEARCH
Martin Barmatz *In* NASA, Washington Microgravity Sci. and Appl. Program Tasks May 1985 p 192 refs (For primary document see N86-10053 01-12)
(Contract NAS7-918)
Avail: NTIS HC A10/MF A01 CSCL 22A

There is a need for high temperature containerless processing facilities that can efficiently position and manipulate molten samples in the reduced gravity environment of space. The goal of the research is to develop sophisticated high temperature manipulation capabilities such as selection of arbitrary axes rotation and rapid sample cooling. This program will investigate new classes of acoustic levitation in rectangular, cylindrical and spherical geometries. The program tasks include calculating theoretical expressions of the acoustic forces in these geometries for the excitation of up to three acoustic modes (multimodes). These calculations are used to: (1) determine those acoustic modes that produce stable levitation, (2) isolate the levitation and rotation capabilities to produce more than one axis of rotation, and (3) develop methods to translate samples down long tube cylindrical chambers. Experimental levitators will then be constructed to verify the stable levitation and rotation predictions of the models. F.M.R.

N86-10168*# Bjorksten Research Labs., Inc., Madison, Wis.
CONTINUOUS FIBERIZATION OF SILICON-CARBIDE-NITRIDE PRECURSOR RESIN
Stanley A. Dunn *In* NASA, Washington Microgravity Sci. and Appl. Program Tasks May 1985 p 193 (For primary document see N86-10053 01-12)
(Contract NAS8-34648)
Avail: NTIS HC A10/MF A01 CSCL 22A

The objective of this project is to design and build a laboratory scale extruder and with it to fiberize 5000 continuous feet of silicon-carbide-nitride precursor resin. Subsequently the objective is extended to include the cross-linking and pyrolysis of approximately 100 feet of the resin fiber. The extruder is designed to accommodate approximately 1 cubic centimeter samples at accurately controllable rates corresponding to take-up from a single orifice of a 25 micron fiber at speeds in the 1000 feet/minute region. Positive feed delivery is achieved with a cylinder and piston driven by a geared down electric motor. Gear reduction is achieved primarily with off-the-shelf parts. Over 5000 feet of fiber, 20 to 30 micron diameter, are spun from precursor resin samples. The formation of continuous silicon carbide/silicon nitride fiber appears to be feasible. F.M.R.

N86-10169*# Bjorksten Research Labs., Inc., Madison, Wis.
LEVITATING FURNANCE FOR CONTAINERLESS PROCESSING IN SPACE
Stanley A. Dunn *In* NASA, Washington Microgravity Sci. and Appl. Program Tasks May 1985 p 194 (For primary document see N86-10053 01-12)
(Contract NAS8-33513)
Avail: NTIS HC A10/MF A01 CSCL 22A

The purpose of this project is to design, construct and test a levitator which would function reliably in a radiant heated cold wall furnace in a reduced gravity environment. A prototype levitating/positioning device termed the Sonic Pump Levitator is designed, built and successfully tested in full gravity and in the reduced gravity of the parabolic flight regime of the KC-135. Positioning is achieved by timely and appropriate application of gas momentum from one or more of six sonic pumps. The sonic pumps, which are arranged orthogonally in opposed pairs about the levitation region, are activated by an electro-optical, computer controlled, feedback system. The Sonic Pump Levitator is a promising candidate for containerless processing in microgravity. Being a null point device, it imposes minimal perturbation on the levitated, or positioned, target. Functioning as it does by optical feedback controlled jets of air, it would be expected to be free from disturbance caused by high temperature. This expectation is now being examined experimentally. F.M.R.

N86-10170*# Bjorksten Research Labs., Inc., Madison, Wis.
ELECTRIC FIELD CONTAINERLESS PROCESSING TECHNOLOGY
D. D. Elleman and W. K. Rhim *In* NASA, Washington Microgravity Sci. and Appl. Program Tasks May 1985 p 195 refs (For primary document see N86-10053 01-12)
Avail: NTIS HC A10/MF A01 CSCL 22A

The objective of this task is to develop the science and technology base required to design and construct a high temperature electric field positioning module that could be used by materials scientists to conduct containerless science experiments in a low gravity environment. Containerless science modules that employ electric fields to position and manipulate samples offer several advantages over acoustic or electromagnetic systems. The electric field system will operate not only at atmospheric pressures but also in a vacuum, in contrast to the acoustic modules which can only operate in atmosphere where the acoustic forces are sufficient. The electric field technique puts minimum energy into the sample, whereas the electromagnetic system can deposit energy into the sample through eddy current heat as well as physical mixing in the sample. Two types of electric field modules have been constructed and tested to date. One employs a charged sample and uses electrostatic forces to position and control the sample. The second type of module induces electrical polarization of the sample and electric field gradients to position and control the sample. F.M.R.

N86-10171*# Stanford Univ., Calif. Lab. of Physics.
CRYOGENIC EQUIVALENCE PRINCIPLE EXPERIMENT
C. W. F. Everitt and Paul W. Worden *In* NASA, Washington Microgravity Sci. and Appl. Program Tasks May 1985 p 196-197 refs (For primary document see N86-10053 01-12)
Avail: NTIS HC A10/MF A01 CSCL 22A

The purpose of this project is to test the equivalence of inertial and passive gravitational mass in an Earth-orbiting satellite. A ground-based experiment is now well developed. It consists of comparing the motions of two cylindrical test masses suspended in precision superconducting magnetic bearings and free to move along the horizontal (axis) direction. The masses are made of niobium and lead-plated aluminum. A position detector based on a SQUID magnetometer measures the differential motion between the masses. The periods of the masses are matched by adjustment of the position detector until the system is insensitive to common mode signals, and so that the experiment is less sensitive to seismic vibration. The apparatus is contained in a twelve inch helium dewar suspended in a vibration isolation stand. The stand achieves 30 db isolation from horizontal motions between 0.1 and 60 Hz, by simulating the motion of a 200 meter long pendulum with an air bearing. With this attenuation of seismic noise and a common mode rejection ratio of 10 to the 5th power in the differential mode, the ground based apparatus should have a sensitivity to equivalence principle violations of one part in 10 to the 13th power; the satellite version might have a sensitivity of one part in 10 to the 17th power. F.M.R.

N86-10172*# General Electric Co., Philadelphia, Pa.
MODIFICATION OF THE ELECTROMAGNETIC LEVITATOR (EML) HARDWARE
R. T. Frost *In* NASA, Washington Microgravity Sci. and Appl. Program Tasks May 1985 p 198 (For primary document see N86-10053 01-12)
(Contract NAS8-34321)
Avail: NTIS HC A10/MF A01 CSCL 22A

The goals of this project are: (1) to study the upgrade requirements and approaches needed for incorporation of an Electromagnetic Levitator (EML) into the shuttle orbiter, (2) to work with members of the Electromagnetic Containerless Processing science working group (SWG) to define future experiments for the EML, and (3) to assist these investigators in further development of ground-based experiment techniques to the limits possible in the terrestrial gravitational environment. Present work is directed toward: (1) upgrading the EML flight apparatus to meet requirements of safety and integration interfaces with the MSL orbiter carrier, (2) development of new experiment components required to carry out approved experiments in undercooled solidification and associated fluid flow studies directed by MIT, and (3) construction, test, qualification and integration assistance for the EML MSL flight package. Author

N86-10173*# National Aeronautics and Space Administration. Lewis Research Center, Cleveland, Ohio.
MICROGRAVITY MATERIALS SCIENCE LABORATORY
S. J. Grisaffe *In* NASA, Washington Microgravity Sci. and Appl. Program Tasks May 1985 p 199 (For primary document see N86-10053 01-12)
Avail: NTIS HC A10/MF A01 CSCL 22A

A Microgravity Materials Science Laboratory (MMSL) has been planned, designed, and is being developed. This laboratory will support related efforts to define the requirements for the Microgravity and Materials Processing Laboratory (MMPF) and the MMPF Test Bed for the Space Station. The MMSL will serve as a check out and training facility for science mission specialists for STS, Spacelab and Space Station prior to the full operation of the MMPF Test Bed. The focus of the MMSL will be on experiments related to the understanding of metal/ceramic/glass solidification, high perfection crystal growth and fluid physics. This ground-based laboratory will be used by university/industry/government researchers to examine and become familiar with the potential of new microgravity materials science concepts and to conduct longer term studies aimed at fully developing a l-g understanding of materials and processing phenomena. Such research will help create new high quality concepts for space experiments and will provide the basis for modeling, theories, and hypotheses upon which key space experiments can be defined and developed. Author

N86-10174*# National Aeronautics and Space Administration. Marshall Space Flight Center, Huntsville, Ala.
ADVANCED OPTICAL MEASUREMENT TECHNIQUES
R. B. Owen, M. H. Johnston, and W. K. Witherow *In* NASA, Washington Microgravity Sci. and Appl. Program Tasks May 1985 p 200 (For primary document see N86-10053 01-12)
Avail: NTIS HC A10/MF A01 CSCL 22A

This research analyzes four areas: (1) Improved Techniques for Optical Measurement; (2) KC-135 Low Gravity Simulation Flight Preparation; (3) In-Line Holographic Microscopy; and (4) Holographic Optical Schlieren System (HOSS). The first task provides for laboratory breadboarding of advanced optical measurement techniques which appear promising for use in Material Processing System (MPS) flight experiments. A laboratory schlieren system has been constructed which simulates a similar optical system on the Fluids Experiment System (FES) which is to be flown on Spacelab 3. The second task allows improved optical systems and breadboards to be built for experiments and hardware tests on the KC-135 aircraft. A new, more stable Mach-Zehnder interferometer has been developed and components have been ordered. The third task is concerned with improvements on the optical system being used to study immiscible fluids. Experiments studying the dynamics of nucleation and the separation of immiscible fluids have been conducted. The four task involves building breadboard reconstruction systems for holograms taken in the HOSS. The HOSS is an early prototype of the Fluids Experiments System (FES) which is scheduled to fly on Spacelab 3. F.M.R.

N86-10175*# National Aeronautics and Space Administration. Marshall Space Flight Center, Huntsville, Ala.
DESIGN, FABRICATION AND TESTING OF AN EXPERIMENTAL APPARATUS FOR DETERMINING PARTICLE BEHAVIOR UNDER VERY LOW INTERGRANULAR STRESSES
Stein Sture and Nicholas Costes *In* NASA, Washington Microgravity Sci. and Appl. Program Tasks May 1985 p 201-202 (For primary document see N86-10053 01-12)
(Contract NAS8-35668)
Avail: NTIS HC A10/MF A01 CSCL 22A

Because the constitutive laws for soils are governed mainly by interparticle friction, all aspects of their mechanical behavior depend strongly on gravitational body forces. This fact poses serious limitations on the formulation of a materially objective soil constitutive theory, based on experimentation performed on Earth. In particular, the presence of the Earth's gravity prohibits the design of controlled experiments to properly simulate a variety of critical phenomena associated with the dynamic response of soils to seismic excitation in a very low effective confining stress field. For these reasons, laboratory-controlled experiments in the Space Shuttle, under essentially zero-gravity conditions, could offer invaluable opportunities for developing a quantitative understanding of fundamental aspects of soil behavior during or after an earthquake, which, in turn, could result in significant technological advances in geotechnical earthquake engineering. Author

N86-10176*# Jet Propulsion Lab., California Inst. of Tech., Pasadena.
ADVANCED CONTAINERLESS PROCESSING TECHNOLOGY
T. G. Wang *In* NASA, Washington Microgravity Sci. and Appl. Program Tasks May 1985 p 203 refs (For primary document see N86-10053 01-12)
Avail: NTIS HC A10/MF A01 CSCL 22A

Breadboards for high temperature containerless processing systems are to be developed, the principles of operation are to be studied, the performance is to be characterized, the limitations identified, and the influence of the acoustic field on the samples established. The subjects to be addressed are experimental and theoretical studies of: (1) acoustic positioning and manipulation capabilities in a high temperature gradient environment (from 26 C to 990 C); (2) acoustic waveforms, harmonic contents, power transfer, sample transport and stability associated with high temperature gradient system; (3) high temperature ground based levitation systems which will allow melting, processing, and solidifying samples without crucibles in the laboratory, (4) KC-135 and laboratory tests of various acoustic geometries which may have spherical applications in the Materials Processing in Space Program; and (5) provide technical information to Acoustics Containerless Experimental System (ACES) engineering team and establish the operation conditions for ACES. F.M.R.

N86-10177*# Intersonics, Inc., Northbrook, Ill.
ACOUSTIC LEVITATION CONTAINERLESS PROCESSING
R. R. Whymark and C. A. Rey *In* NASA, Washington Microgravity Sci. and Appl. Program Tasks May 1985 p 204 refs (For primary document see N86-10053 01-12)
(Contract NAS8-33742)
Avail: NTIS HC A10/MF A01 CSCL 22A

This research program consists of the development of acoustic containerless processing systems with applications in the areas of research in material sciences, as well as the production of new materials, solid forms with novel and unusual microstructures, fusion target spheres, and improved optical fibers. Efforts have been focused on the containerless processing at high temperatures for producing new kinds of glasses. Also, some development has occurred in the areas of containerlessly supporting liquids at room temperature, with applications in studies of fluid dynamics, potential undercooling of liquids, etc. The high temperature area holds the greatest promise for producing new kinds of glasses and ceramics, new alloys, and possibly unusual structural shapes, such as very uniform hollow glass shells for fusion target applications. High temperature acoustic levitation required for containerless processing has been demonstrated in low-g environments as well as in ground-based experiments. Future activities include continued development of the signals axis acoustic levitator. F.M.R.

N86-10178*# National Aeronautics and Space Administration. Johnson (Lyndon B.) Space Center,
HIGH-TEMPERATURE CONTROLLED REDOX CRYSTALLIZATION STUDIES

Richard J. Williams *In* NASA, Washington Microgravity Sci. and Appl. Program Tasks May 1985 p 205 (For primary document see N86-10053 01-12)
Avail: NTIS HC A10/MF A01 CSCL 22A

The crystallization of silicates containing redox sensitive ions (e.g., Fe, Ti, Ce) must be performed under controlled and known redox conditions in order to obtain the maximum scientific benefit from experimental study. Furthermore, many compositions crystallize dense phases which settle during ground-based experiments. This settling influences the texture and chemical evolution of the crystallizing system. The purpose of this investigation is to develop a test system in which controlled redox experiments can be performed in the microgravity environment. The system will use solid ceramic oxygen electrolyte cells for control, measurements, and production of the required redox conditions. A preliminary design for a prototype is developed, the electrolyte and furnace tested, and a tentative protocol for experiment developed. The control parameter is to be established and a laboratory prototype built. F.M.R.

N86-10179*# National Aeronautics and Space Administration, Washington, D. C.
PROJECT VESTA, EXPLORATORY MISSION TO THE ASTEROIDS: SCIENTIFIC OBJECTIVES AND TECHNICAL SPECIFICATIONS
Sep. 1985 13 p Transl. into ENGLISH of "Project VESTA, Interet Scientifique d'une Mission d'Exploration vers les Petits Corps" Paris, CNES, 1985 p 1-14 Transl. by The Corporate Word, Inc., Pittsburgh, Pa.
(Contract NASw-4006)
(NASA-TM-77669; NAS 1.15:77669) Avail: NTIS HC A02/MF A01 CSCL 22A

The VESTA project, a Franco-Soviet collaboration, is described. The VESTA probe will be launched and will pass through the asteroid belts before encountering comets. The probe will be an autonomous vehicle. The scientific objectives are to obtaining information on asteroids, comets, solar system formation, meteorites and other sources of extraterrestrial material. The surface morphology, mineral composition and internal structure of asteroids will be studied. E.A.K.

N86-10180# Bundesministerium fuer Forschung und Technologie, Bonn (West Germany).
SATELLITE USE FOR MEN [SATELLITENNUTZUNG FUER DEN MENSCHEN]
1985 39 p In GERMAN
Avail: NTIS HC A03/MF A01

Research satellites with German participation are listed. Satellite image maps for the Antartic region Neuschwaben land, for the Dodoma region in Tanzania, and for Upper Volta (Burkina) were made. Sondes to study trace gases in the atmosphere and the Earth radiation budget were developed. A modem for highly exact satellite position determination was developed. Large single protein crystals were grown in space. For individual titles, see N86-10181 through N86-10186.

N86-10181# Bundesministerium fuer Forschung und Technologie, Bonn (West Germany).
HOW ANTARCTICA WAS UNVEILED. MASTERPIECES OF FRANKFURT TOPOGRAPHIC SURVEYORS. A PART OF THE GERMAN ANTARCTICA RESEARCH PROGRAM [WIE DIE ANTARKTIS ENTSCHLEIERT WIRD. MEISTERSTUECKE FRANKFURTER ERDVERMESSER. EIN TEIL DES DEUTSCHEN ANTARKTIS-FORSCHUNGSPROGRAMMS] c43
Ruediger Jungbluth *In its* Satellite Use for Men 1985 p 5-10 In GERMAN (For primary document see N86-10180 01-12)
Avail: NTIS HC A03/MF A01

Satellite image maps for the Antartic region were produced, the most important of which is a 1:6 million map covering the Atlantic half of Antartic, made from NOAA and LANDSAT data. The way in which the digital satellite data were converted into analog representations is described. An optimal gray scale discrimination is obtained for the most important continental areas. Distortion effects are compensated by adding several pictures to a mosaic. Author (ESA)

N86-10182# Bundesministerium fuer Forschung und Technologie, Bonn (West Germany).
SATELLITE DATA EVEN FOR A POULTRY FARM. A DEVELOPMENT FOR TANZANIA. IMAGE EVALUATION FOLLOWING NEW WAYS [SATELLITENDATEN SELBST FUER EINE HUEHNERFARM. EIN ENTWICKLUNGSPROJEKT FUER TANSANIA. BILDAUSWERTUNG AUF NEUEN WEGEN] c43
Philip Erdoes *In its* Satellite Use for Men 1985 p 11-16 In GERMAN (For primary document see N86-10180 01-12)
Avail: NTIS HC A03/MF A01

Maps of the 11,000 sq km Dodoma region in Tanzania were made using LANDSAT-3 data. Multispectral scanner data were processed using Intensity-Saturation color theory. The intensity gives information about the relief. The ratio images give information about the type of soil and vegetation. A classification of 14 geographically homogeneous land units, and a ground water map were made. Author (ESA)

N86-10183# Bundesministerium fuer Forschung und Technologie, Bonn (West Germany).
WITH ARGUS EYES FROM SPACE. SATELLITE DIAGNOSIS FOR UPPER VOLTA. SEVEN MAPS WITHOUT MYSTERY [MIT ARGUSAUGEN AUS DEM ALL. SATELLITEN-DIAGNOSE FUER OBERVOLTA. SIEBEN KARTEN OHNE SIEBEN SIEGEL] c43
Uwe Andresen *In its* Satellite Use for Men 1985 p 17-21 In GERMAN (For primary document see N86-10180 01-12)
Avail: NTIS HC A03/MF A01

Maps of Upper Volta (Burkina) were made using LANDSAT images. It is shown that the interpretation of satellite data is by far superior to any other method if these interpretations are checked in situ by sampling tests. Maps giving information on geology, soil science, land use, and hydrogeology were made. A map which provides detailed information about settlement density, cultivation possibilities of the soil, and ground water expectations is discussed. The results show substantial perturbations of the vegetation structure due to extended livestock and agricultural methods such as overgrazing, uncontrolled deforestation, and burnt cleared land. Author (ESA)

N86-10184# Bundesministerium fuer Forschung und Technologie, Bonn (West Germany).
THE AIR OF LIFE OF THE BLUE PLANET. ATMOSPHERE RESEARCH FROM SPACE USING DATA AND FACTS AGAINST CLIMATE SPECULATIONS [DIE LEBENSLUFT DES BLAUEN PLANETEN. ATMOSPHAERENFORSCHUNG VOM WELTRAUM AUS DATEN UND FAKTEN GEGEN KLIMA-SPEKULATIONEN] c47
Dieter Schwab *In its* Satellite Use for Men 1984 p 22-25 In GERMAN (For primary document see N86-10180 01-12)
Avail: NTIS HC A03/MF A01

Three satellite-borne sondes to provide exact data on trace gases in the atmosphere between 20 and 100 km height, and on the Earth radiation budget are described. The sondes predict changes in the climate due to trace gases and the reduction of the ozone concentration. The Michelson Interferometer for Passive Atmospheric Sounding analyzes the light spectrum and is based on interference phenomena. The Microwave Atmospheric Sounder analyzes the characteristic electromagnetic waves emitted by trace gases. The Conical Scan Radiometer CSR measures the sunlight on Earth as well as the heat radiation from the Earth in several directions. Author (ESA)

N86-10185# Bundesministerium fuer Forschung und Technologie, Bonn (West Germany).
A NANOSECOND OR THIRTY CENTIMETERS: WHY ATOMIC CLOCKS HAVE TO BE SYNCHRONIZED. MITREX OPENS NEW

DIMENSIONS FOR MEASURING ACCURACY [EINE MILLIARDSTELSEKUNDE ODER 30 ZENTIMETER: WESHALB ATOMUHREN WELTWEIT GLEICHLAUFEN MUESSEN. MITREX OEFFENT NEUE DIMENSIONEN DER MESSGENAUIGKEIT] c35
Hans-Dieter Wolz *In its* Satellite Use for Men 1985 p 26-29 In GERMAN (For primary document see N86-10180 01-12)
Avail: NTIS HC A03/MF A01

Microwave Time and Ranging Experiment was developed to enable highly exact satellite position determination. The measurement is performed in ground stations. The portable system allows position measurements with an accuracy as high as 30 cm, and is planned to be long term tested in order to be introduced as a standard. The required signal strength is very low. The processing of the electromagnetic signals allows reliable statements about the time of flight and about perturbations. The application possibilities of the MITREX-system are presented. Author (ESA)

N86-10186# Bundesministerium fuer Forschung und Technologie, Bonn (West Germany).
GROWTH OF LARGER SINGLE CRYSTALS [ZUECHTUNG VON GROESSEREN EINKRISTALLEN] c76
Ruediger Jungbluth *In its* Satellite Use for Men 1985 p 30-32 In GERMAN (For primary document see N86-10180 01-12)
Avail: NTIS HC A03/MF A01

Large single protein crystals were grown during the Spacelab 1 flight in order to study metabolism phenomena. For X-ray structural analysis the single crystals have to be sufficiently large (about 1 mm in all 3 directions). The crystals grown under weightlessness conditions (excluding convection effects) in a few minutes are comparable to those grown on Earth after several days. Two model proteins were grown: the high-molecular enzyme beta-galactosidasis and the low-molecular enzyme lysozyme. The testing of a large number of protein species is necessary in order to allow a definitive prognosis about this technique. Author (ESA)

N86-10187# Deutsche Forschungs- und Versuchsanstalt fuer Luft- und Raumfahrt, Cologne (West Germany).
THE FIRST GERMAN SPACELAB MISSION D1 REPORTS Progress Report [ERSTE DEUTSCHE SPACELAB-MISSION D1-REPORT]
Oct. 1984 4 p In GERMAN
(PR-1) Avail: NTIS HC A02/MF A01

The Spacelab mission; Spacelab specifications and technical concept; Spacelab history, and scheduling from December 1984 to October 1985 are discussed. Author (ESA)

N86-10188# Deutsche Forschungs- und Versuchsanstalt fuer Luft- und Raumfahrt, Cologne (West Germany).
THE FIRST GERMAN SPACELAB MISSION D1 REPORTS Progress Report [ERSTE DEUTSCHE SPACELAB-MISSION D1-REPORT]
Dec. 1984 8 p In GERMAN
(PR-2) Avail: NTIS HC A02/MF A01

Spacelab D1 payload integration; aerospace medicine in weightlessness; process technology; NAVEX program: Earth observation, communication and navigation; project management; the environmental control and life support systems; the MEDEA, Biorack payloads; and the Mirror heating facility are discussed. Author (ESA)

N86-10189# Deutsche Forschungs- und Versuchsanstalt fuer Luft- und Raumfahrt, Cologne (West Germany).
THE FIRST GERMAN SPACELAB MISSION D1 REPORTS Progress Report [ERSTE DEUTSCHE SPACELAB-MISSION D1-REPORT]
Feb. 1985 7 p In GERMAN
(PR-3) Avail: NTIS HC A02/MF A01

Astronaut preparation with the Spacelab training simulator; project planning for the Columbus and Ariane 5 programs; the D1 - Transport platforms: a 4 m wide and 6.5 m long special container for integral payload transport; milestones of the European space programs since 1969; and opinions against manned space flights are discussed. Author (ESA)

N86-10209# Hamburg Univ. (West Germany).
INFLUENCES AFFECTING SEPARATION IN MONOTECTIC ALLOYS UNDER MICROGRAVITY
H. Ahlborn and K. Loehberg (Technische Univ., Berlin) *In* ESA Fifth European Symp. on Mater. Sci. under Microgravity. Results of Spacelab 1 Dec. 1984 p 55-61 refs (For primary document see N86-10200 01-16)
Avail: NTIS HC A21/MF A01

N86-10210# Max-Planck-Inst. fuer Metallforschung, Stuttgart (West Germany).
PARTICLE COARSENING IN IMMISCIBLE ZINC-LEAD ALLOYS UNDER MICROGRAVITY
A. Kneissel (Montanuniv. Leoban, Austria) and H. Fischmeister *In* ESA Fifth European Symp. on Mater. Sci. under Microgravity. Results of Spacelab 1 Dec. 1984 p 63-68 refs Sponsored by Austrian Ministry of Science and Research (For primary document see N86-10200 01-16)
Avail: NTIS HC A21/MF A01

N86-10211# Katholieke Universiteit te Leuven (Belgium). Dept. Metaalkunde und Toegepaste Materiaalkunde.
MELTING AND SOLIDIFICATION OF METAL MATRIX COMPOSITES UNDER MICROGRAVITY
L. Froyen and A. Deruyttere *In* ESA Fifth European Symp. on Mater. Sci. under Microgravity. Results of Spacelab 1 Dec. 1984 p 69-78 refs (For primary document see N86-10200 01-16)
Avail: NTIS HC A21/MF A01

N86-10212# Technische Hogeschool, Delft (Netherlands). Dept. of Metals Science.
UNIDIRECTIONAL SOLIDIFICATION OF CAST IRON: EXPERIMENT ES-325
H. Nieswaag, T. Luyendijk, and W. H. M. Alsem *In* ESA Fifth European Symp. on Mater. Sci. under Microgravity. Results of Spacelab 1 Dec. 1984 p 79-85 refs Sponsored by Netherlands State Department (For primary document see N86-10200 01-16)
Avail: NTIS HC A21/MF A01

N86-10213# Maschinenfabrik Augsburg-Nuernberg A.G., Munich (West Germany).
SKIN CASTING OF ALLOYS AND COMPOSITES: RESULTS OF SPACELAB (SL)-1 AND TEXUS EXPERIMENTS
H. Sprenger *In* ESA Fifth European Symp. on Mater. Sci. under Microgravity. Results of Spacelab 1 Dec. 1984 p 87-94 refs Sponsored by Bundesministerium fuer Forschung und Technologie (For primary document see N86-10200 01-16)
Avail: NTIS HC A21/MF A01

N86-10214# Technische Univ., Vienna (Austria).
VACUUM BRAZING UNDER MICROGRAVITY
K. Frieler, R. Stickler (Bundesanstalt fuer Materialpruefung.), and E. Siegfried *In* ESA Fifth European Symp. on Mater. Sci. under Microgravity. Results of Spacelab 1 Dec. 1984 p 95-99 refs (For primary document see N86-10200 01-16)
Avail: NTIS HC A21/MF A01

N86-10215# Bologna Univ. (Italy). Dipt. di Fisica.
MELTING AND SOLIDIFICATION IN 0-g OF SINTERED ALLOYS: EXPERIMENTS ES 311 A AND B BUBBLE REINFORCED MATERIALS
F. Barbier, C. Patuelli, P. Gonndi (Rome Univ.), and R. Montanari (Rome Univ.) *In* ESA Fifth European Symp. on Mater. Sci. under Microgravity. Results of Spacelab 1 Dec. 1984 p 101-107 refs (For primary document see N86-10200 01-16)
Avail: NTIS HC A21/MF A01

N86-10216# Technische Univ., Clausthal-Zellerfeld (West Germany). Arbeitsgruppe Glas.
INTERDIFFUSION IN THE GLASS MELT SYSTEM (Na2O+Rb2O) .3SIO2
M. Braedt, V. Braetsch, and G. H. Frischat *In* ESA Fifth European Symp. on Mater. Sci. under Microgravity. Results of Spacelab 1 Dec. 1984 p 109-112 refs Sponsored by Bundesministerium fuer Forschung und Technologie (For primary document see N86-10200 01-16)
Avail: NTIS HC A21/MF A01

N86-10218# Commissariat a l'Energie Atomique, Grenoble (France). Dept. de Metallurgie.
DIRECTIONAL SOLIDIFICATION OF AN ALUMINUM-ZINC VAPOR EMULSION IN MICROGRAVITY
C. Potard and P. Morgand *In* ESA Fifth European Symp. on Mater. Sci. under Microgravity. Results of Spacelab 1 Dec. 1984 p 121-125 (For primary document see N86-10200 01-16)
Avail: NTIS HC A21/MF A01

N86-10219# Commissariat a l'Energie Atomique, Grenoble (France). Dept. de Metallurgie.
DIRECTIONAL SOLIDIFICATION OF EUTECTIC ALLOYS
J. J. Favier and J. deGoer *In* ESA Fifth European Symp. on Mater. Sci. under Microgravity. Results of Spacelab 1 Dec. 1984 p 127-133 refs (For primary document see N86-10200 01-16)
Avail: NTIS HC A21/MF A01

N86-10220# Centre National de la Recherche Scientifique, Meudon-Bellevue (France). Equipe de Technologie de la Croissance Cristalline.
LEAD TELLURIDE CRYSTALS GROWN IN MICROGRAVITY: EXPERIMENT ES 318 [CRISTAUX DE TELLURURE DE PLOMB ELABORES EN MICROGRAVITE EXPERIENCE ES 318]
H. Rodot and O. Tottereau *In* ESA Fifth European Symp. on Mater. Sci. under Microgravity. Results of Spacelab 1 Dec. 1984 p 135-139 refs In FRENCH (For primary document see N86-10200 01-16)
Avail: NTIS HC A21/MF A01

N86-10221# Erlangen-Nuremberg Univ. (West Germany). Inst. fuer Werkstoffwissenschaften.
DIRECTIONAL SOLIDIFICATION OF InSb-NiSb EUTECTIC
G. Mueller and P. Kyr *In* ESA Fifth European Symp. on Mater. Sci. under Microgravity. Results of Spacelab 1 Dec. 1984 p 141-146 refs Sponsored by DFVLR and Bundesministerium fuer Forschung und Technologie (For primary document see N86-10200 01-16)
Avail: NTIS HC A21/MF A01

N86-10222# Commissariat a l'Energie Atomique, Grenoble (France). Dept. de Metallurgie.
THERMOMIGRATION OF COBALT IN LIQUID TIN: EXPERIMENT 1 ES 320
Y. Malmejac and J. P. Praizey *In* ESA Fifth European Symp. on Mater. Sci. under Microgravity. Results of Spacelab 1 Dec. 1984 p 147-152 refs (For primary document see N86-10200 01-16)
Avail: NTIS HC A21/MF A01

N86-10224# Stuttgart Univ. (West Germany). Inst. fuer Physikalisches.
GaSb-SEMICONDUCTOR CRYSTALS UNDER MICROGRAVITY: EXPERIMENT ES 323
K. W. Benz and G. Nagel *In* ESA Fifth European Symp. on Mater. Sci. under Microgravity. Results of Spacelab 1 Dec. 1984 p 157-161 refs (For primary document see N86-10200 01-16) (Contract DFVLR-01-QV-698)
Avail: NTIS HC A21/MF A01

N86-10225# Freiburg Univ. (West Germany). Inst. fuer Kristollographisches.
SOLUTION GROWTH OF CADMIUM TELLURIDE: EXPERIMENT ES 322
R. Schoenholz, R. Dian, and R. Nitsche *In* ESA Fifth European Symp. on Mater. Sci. under Microgravity. Results of Spacelab 1 Dec. 1984 p 163-167 refs Sponsored by Bundesministerium fuer Forschung und Technologie (For primary document see N86-10200 01-16)
Avail: NTIS HC A21/MF A01

N86-10226# Wacker-Chemie G.m.b.H. Burghausen (West Germany).
CRYSTALLIZATION OF A SILICON SPHERE
H. Koelker *In* ESA Fifth European Symp. on Mater. Sci. under Microgravity. Results of Spacelab 1 Dec. 1984 p 169-172 refs (For primary document see N86-10200 01-16)
Avail: NTIS HC A21/MF A01

N86-10227# Freiburg Univ. (West Germany). Inst. fuer Kristollographisches.
CRYSTAL GROWTH OF SILICON IN SPACELAB 1: EXPERIMENT ES-321
A. Eyer, H. Leiste, and R. Nitsche *In* ESA Fifth European Symp. on Mater. Sci. under Microgravity. Results of Spacelab 1 Dec. 1984 p 173-182 refs (For primary document see N86-10200 01-16)
Avail: NTIS HC A21/MF A01

N86-10228# Freiburg Univ. (West Germany). Chemisches Lab.
PROTEIN SINGLE CRYSTAL GROWTH UNDER MICROGRAVITY
W. Littke and C. John *In* ESA Fifth European Symp. on Mater. Sci. under Microgravity. Results of Spacelab 1 Dec. 1984 p 185-188 refs Original language document previously announced as A85-39084 Sponsored by Bundesministerium fuer Forschung und Technologie (For primary document see N86-10200 01-16)
Avail: NTIS HC A21/MF A01

N86-10229# Technical Univ. of Denmark, Lyngby. Physics Lab. 3.
CRYSTAL GROWTH FROM SOLUTION
G. Galster and K. F. Nielsen *In* ESA Fifth European Symp. on Mater. Sci. under Microgravity. Results of Spacelab Dec. 1984 p 189-191 refs Sponsored by Danish Space Board (For primary document see N86-10200 01-16)
Avail: NTIS HC A21/MF A01

N86-10230# Paris VI Univ. (France). Lab. de Mineralogie et Cristallographie.
GROWTH AND CHARACTERIZATION OF BRUSHITE AND LEAD MONETITE, SIMULATION AND RESULTS
M. C. Robert, F. Lefaucheux, and A. Authier *In* ESA Fifth European Symp. on Mater. Sci. under Microgravity. Results of Spacelab 1 Dec. 1984 p 193-199 refs Sponsored by CNES (For primary document see N86-10200 01-16)
Avail: NTIS HC A21/MF A01

N86-10231# Technische Univ., Berlin (West Germany). Inst. fuer Metallforschung.
SELF DIFFUSION OF Sn112 AND Sn124 IN LIQUID TIN
G. Frohberg, K.-H. Kraatz, and H. Wever *In* ESA Fifth European Symp. on Mater. Sci. under Microgravity. Results of Spacelab 1 Dec. 1984 p 201-205 refs (For primary document see N86-10200 01-16)
Avail: NTIS HC A21/MF A01

N86-10232# Politecnico di Milano (Italy).
ADHESION OF METALS: EXPERIMENT 1 ES-340
F. Rossitto and G. Ghersini (Centro Informazioni Studi Esperienze) *In* ESA Fifth European Symp. on Mater. Sci. under Microgravity. Results of Spacelab 1 Dec. 1984 p 207-217 refs Sponsored by CNR (For primary document see N86-10200 01-16)
Avail: NTIS HC A21/MF A01

N86-10233*# Harvard Univ., Cambridge, Mass. Div. of Applied Sciences.
CRYSTAL NUCLEATION AND GLASS FORMATION IN METALLIC ALLOY MELTS
F. Spaepen *In* ESA Fifth European Symp. on Mater. Sci. under Microgravity. Results of Spacelab 1 Dec. 1984 p 215-219 refs (For primary document see N86-10200 01-16)

(Contract NAS8-36516)
Avail: NTIS HC A21/MF A01

N86-10234*# Massachusetts Inst. of Tech., Cambridge.
CRYSTAL GROWTH OF GaAs IN SPACE
H. C. Gatos, J. Lagowski, L. M. Pawlowicz, F. Dabkowski, and C.-J. Li *In* ESA Fifth European Symp. on Mater. Sci. under Microgravity. Results of Spacelab 1 Dec. 1984 p 221-225 refs (For primary document see N86-10200 01-16)
Avail: NTIS HC A21/MF A01

N86-10236# Academy of Sciences (USSR), Moscow. Inst. for Problems in Mechanics.
MATHEMATICAL SIMULATION OF DISTURBING FORCES AND MATERIAL SCIENCE PROCESSES UNDER LOW GRAVITY
V. I. Polezhaev, A. P. Lebedev, and S. A. Nikitin *In* ESA Fifth European Symp. on Mater. Sci. under Microgravity. Results of Spacelab 1 Dec. 1984 p 237-243 refs (For primary document see N86-10200 01-16)
Avail: NTIS HC A21/MF A01

N86-10246*# National Aeronautics and Space Administration. Marshall Space Flight Center, Huntsville, Ala. Space Science Lab.
SEPARATION OF AQUEOUS TWO-PHASE POLYMER SYSTEMS IN MICROGRAVITY
J. M. VanAlstine, J. M. Harris (Alabama Univ., Huntsville), S. Synder, P. A. Curreri, S. B. Bamberger (Oregon Health Sciences Univ.), and D. E. Brooks (Oregon Health Sciences Uni.) *In* ESA Fifth European Symp. on Mater. Sci. under Microgravity. Results of Spacelab 1 Dec. 1984 p 309-312 refs Sponsored by Universities Space Research Association (For primary document see N86-10200 01-16)
(Contracts NAS8-35333; NAS8-35334; NAS8-35362)
Avail: NTIS HC A21/MF A01 CSCL 22A

N86-10247*# National Aeronautics and Space Administration. Marshall Space Flight Center, Huntsville, Ala. Dept. of Pathology and Chemistry.
RATIONALE FOR TWO PHASE POLYMER SYSTEM MICROGRAVITY SEPARATION EXPERIMENTS
D. E. Brooks (British Columbia Univ.), S. B. Bamberger (Oregon Health Sciences Univ.), J. M. Harris (Alabama Univ., Huntsville), and J. VanAlstine *In* ESA Fifth European Symp. on Mater. Sci. under Microgravity. Results of Spacelab 1 Dec. 1984 p 315-318 refs Sponsored in part by NASA (For primary document see N86-10200 01-16)
(Grant USPN-HL-23374)
Avail: NTIS HC A21/MF A01 CSCL 22A

N86-10248# Alabama Univ., Huntsville. Dept. of Chemistry.
APPLICATION OF THE THEORY OF OSTWALD RIPENING TO MICROGRAVITY PHASE SEPARATION EXPERIMENTS
J. K. Baird *In* ESA Fifth European Symp. on Mater. Sci. under Microgravity. Results of Spacelab 1 Dec. 1984 p 319-321 refs Sponsored by Alabama University (For primary document see N86-10200 01-16)
Avail: NTIS HC A21/MF A01

N86-10254# Technische Univ., Clausthal-Zellerfeld (West Germany). Inst. fuer Nichtmetallische Werkstoffe.
SHRINKING OF A GAS BUBBLE IN A GLASS MELT UNDER MICROGRAVITY CONDITIONS
V. Rosenkranz and G. H. Frischat *In* ESA Fifth European Symp. on Mater. Sci. under Microgravity. Results of Spacelab 1 Dec. 1984 p 353-357 refs Sponsored by Bundesministerium fuer Forschung und Technologie (For primary document see N86-10200 01-16)
Avail: NTIS HC A21/MF A01

N86-10255# Technische Univ., Munich (West Germany).
PHYSICAL AND CHEMICAL PROPERTIES OF A NICKEL CATALYST PROCESSED UNDER MICROGRAVITY
H. Riepl *In* ESA Fifth European Symp. on Mater. Sci. under Microgravity. Results of Spacelab 1 Dec. 1984 p 359-363 refs (For primary document see N86-10200 01-16)
Avail: NTIS HC A21/MF A01

N86-10256# Royal Inst. of Tech., Stockholm (Sweden). Dept. of Casting Metals.
A PRELIMINARY REPORT ON FLOATING ZONE EXPERIMENTS WITH GERMANIUM CRYSTALS IN A SOUNDING ROCKET
T. Carlberg *In* ESA Fifth European Symp. on Mater. Sci. under Microgravity. Results of Spacelab 1 Dec. 1984 p 367-373 refs (For primary document see N86-10200 01-16)
Avail: NTIS HC A21/MF A01

N86-10257# Deutsche Forschungs- und Versuchsanstalt fuer Luft- und Raumfahrt, Cologne (West Germany). Inst. for Space Simulation.
TRANSPORT PROCESSES IN DIRECTIONAL SOLIDIFICATION DURING SPACE SHUTTLE FLIGHT
H. Klein, R. Naehle, and K. Wanders *In* ESA Fifth European Symp. on Mater. Sci. under Microgravity. Results of Spacelab 1 Dec. 1984 p 375-378 refs (For primary document see N86-10200 01-16)
Avail: NTIS HC A21/MF A01

N86-10258# Deutsche Forschungs- und Versuchsanstalt fuer Luft- und Raumfahrt, Cologne (West Germany). Inst. for Space Simulation.
STABILITY OF METALLIC DISPERSIONS
H. Otto *In* ESA Fifth European Symp. on Mater. Sci. under Microgravity. Results of Spacelab 1 Dec. 1984 p 379-388 refs (For primary document see N86-10200 01-16)
Avail: NTIS HC A21/MF A01

N86-10259# Deutsche Forschungs- und Versuchsanstalt fuer Luft- und Raumfahrt, Cologne (West Germany). Inst. for Space Simulation.
UNDERCOOLING INVESTIGATIONS ON THE EASY GLASS FORMER Pd-Cu-Si
D. M. Herlach, R. Willnecker, and F. Gillessen *In* ESA Fifth European Symp. on Mater. Sci. under Microgravity. Results of Spacelab 1 Dec. 1984 p 389-397 refs (For primary document see N86-10200 01-16)
Avail: NTIS HC A21/MF A01

N86-10260# Deutsche Forschungs- und Versuchsanstalt fuer Luft- und Raumfahrt, Cologne (West Germany). Inst. for Space Simulation.
CONTAINERLESS UNDERCOOLING OF Ni
D. M. Herlach, R. Willnecker, and F. Gillessen *In* ESA Fifth European Symp. on Mater. Sci. under Microgravity. Results of Spacelab 1 Dec. 1984 p 399-402 refs (For primary document see N86-10200 01-16)
Avail: NTIS HC A21/MF A01

N86-10261*# National Aeronautics and Space Administration. Lewis Research Center, Cleveland, Ohio.
DENDRITIC SOLIDIFICATION IN A BINARY ALLOY MELT: STEADY-STATE VERSUS MORPHOLOGICAL STABILITY THEORIES
V. Laymanan *In* ESA Fifth European Symp. on Mater. Sci. under Microgravity. Results of Spacelab 1 Dec. 1984 p 403-407 refs Sponsored in part by NASA (For primary document see N86-10200 01-16)
Avail: NTIS HC A21/MF A01

N86-10262# Commissariat a l'Energie Atomique, Grenoble (France). Lab. d'Etude de la Solidification.
CELLULAR MORPHOLOGIES IN LEAD-THALLIUM ALLOYS
B. Billia (Faculte des Sciences St-Jerome, Marseille), H. Jamgotchian (Faculte des Sciences St.-Jerome, Marseille), J. J. Favier, and D. Camel *In* ESA Fifth European Symp. on Mater. Sci. under Microgravity. Results of Spacelab 1 Dec. 1984 p 409-412 refs Sponsored by CNES (For primary document see N86-10200 01-16)
Avail: NTIS HC A21/MF A01

N86-10264*# Gelles (S. H.) Associates, Columbus, Ohio.
SPACE SHUTTLE EXPERIMENTS ON Al-In LIQUID PHASE

MISCIBILITY GAP (LPMG) ALLOYS
S. H. Gelles and A. J. Markworth (Battelle Columbus Labs., Columbus) *In* ESA Fifth European Symp. on Mater. Sci. under Microgravity. Results of Spacelab 1 Dec. 1984 p 417-422 refs
(For primary document see N86-10200 01-16)
(Contract NAS8-32952)
Avail: NTIS HC A21/MF A01

N86-10267# Eidgenoessische Technische Hochschule, Zurich (Switzerland).
CRYSTAL GROWTH FROM SOLUTIONS AND NUCLEATION FROM THE VAPOR PHASE
E. Kaldis *In* ESA Fifth European Symp. on Mater. Sci. under Microgravity. Results of Spacelab 1 Dec. 1984 p 439-441 refs
(For primary document see N86-10200 01-16)
Avail: NTIS HC A21/MF A01

N86-10396*# Jet Propulsion Lab., California Inst. of Tech., Pasadena. TDA Planning Office.
A VLA EXPERIMENT: PLANNING FOR VOYAGER AT NEPTUNE
J. W. Layland, P. J. Napier (National Radio Astronomy Observatory), and A. R. Thompson (National Radio Astronomy Observatory) *In its* The Telecommun. and Data Acquisition Progr. Rept. 15 Aug. 1985 p 136-142 refs (For primary document see N86-10382 01-32)
Avail: NTIS HC A10/MF A01 CSCL 22A

13 ASTRODYNAMICS

Includes powered and free-flight trajectories; and orbit and launching dynamics.

N86-10190# Royal Aircraft Establishment, Farnborough (England).
LUMPED GEOPOTENTIAL HARMONICS OF ORDER 14, FROM THE ORBIT OF 1967-11G
D. G. King-Hele Jan. 1985 20 p
(AD-A156627; RAE-TR-85002; DRIC-BR-95198) Avail: NTIS HC A02/MF A01 CSCL 08/5

The satellite 1967-11G, which had an orbital inclination of 40 deg, passed through 14th-order resonance with the Earth's gravitational field in 1974. The changes in its orbital inclination at resonance were analyzed to obtain values for four lumped 14th-order harmonics in the geopotential, with accuracies equivalent to about 5 cm in geoid height. Analysis of the eccentricity was also attempted, but did not yield useful results. As no previous satellite analyzed at 14th-order resonance has had an inclination near 40 deg., the results have proved to be valuable in determining individual 14th-order harmonics in the geopotential. GRA

14 GROUND SUPPORT SYSTEMS AND FACILITIES (SPACE)

Includes launch complexes, research and production facilities; ground support equipment, e.g., mobile transporters; and simulators.

For related information see also *09 Research Support Facilities (Air).*

N86-10191# Armament Development and Test Center, Eglin AFB, Fla.
DYNAMIC ANALYSIS OF A SLED TRAVELING ALONG A ROUGH RAIL Final Report, Nov. 1983 - May 1985
G. L. Ferguson 15 May 1985 317 p
(AF Proj. TKSI)
(AD-A156589; AD-TR-85-39) Avail: NTIS HC A14/MF A01 CSCL 12/1

Rocket sleds are commonly used for simulation of special environments for testing purposes. The motion of a sled on the track induces large quasi-steady-state and dynamic forces on the sled. Design of sleds requires knowledge of these forces and of established techniques for application of measured and theoretical forcing functions to proven mathematical structural simulations. The prediction of the quasi-steady-state sled loads is relatively straight-forward and requires few specialized techniques. Dynamic force prediction on the other hand is somewhat of a black art. Several techniques have been theorized but the results have been extremely marginal at best. This research is intended to find a reliable force prediction tool that is not extremely cumbersome to use. GRA

N86-10192# Sandia Labs., Albuquerque, N. Mex.
LASER GENERATION AND TRANSPORT OF A RELATIVISTIC ELECTRON BEAM
S. L. Shope, C. A. Frost, G. T. Leifeste, C. E. Crist, P. D. Kiekel, J. W. Poukey, and B. B. Godfrey 1985 14 p Presented at the Particle Accelerator Conf., Vancouver, British Columbia, 13 May 1985 Prepared in cooperation with Mission Research Corp., Albuquerque, N. Mex.
(Contract DE-AC04-76DP-00789)
(DE85-011709; SAND-85-0042C; CONF-850504-30) Avail: NTIS HC A02/MF A01

A foilless diode usually requires an externally applied magnetic field to control expansion and transport of a relativistic electron beam. A new foilless diode was developed that does not require an external magnetic field. A low pressure organic gas is introduced into the diode and the transport region. A UV laser beam is injected through the transport region and is terminated at the cathode. The laser photoionizes the low pressure gas forming an ionized channel that captures the electron beam near the cathode. The electron beam is focused and guided by electrostatic attraction to the ionized channel. A 1.5-MeV, 20-kA electron beam was generated and transported 1 m using this technique. The laser is replaced by an 800 V, 250 ma, low energy electron beam which is used to guide the relativistic electron beam 4 m through a 90 bend. E.A.K.

N86-10193# Virginia Univ., Charlottesville. Dept. of Materials Science.
SIMULATING THE CTR ENVIRONMENT IN THE HVBM Final Report, 1 Sep. 1975 - 31 Aug. 1984
W. A. Jesser 1984 18 p
(Contract DE-AS05-76ET-52023)
(DE85-011745; DOE/ET-52023/34) Avail: NTIS HC A02/MF A01

The first high voltage electron microscope-ion accelerator facility in the world was established in 1976. Through use of this facility, helium embrittlement as revealed through intergranular fracture was shown to be independent of helium bubble content in the grain boundaries. This result is contrary to most current thinking and theories of helium embrittlement. The most likely mechanism of helium embrittlement is a plastic deformation assisted distribution of helium in finely dispersed helium-vacancy clusters. The key to overcoming helium embrittlement should lie in preventing the fine dispersion by providing benign sinks or treatments that agglomerate the helium. DOE

N86-10194# Kanner (Leo) Associates, Redwood City, Calif.
RFQ-FUNNELING
A. Schempp 1985 11 p Transl. into ENGLISH of rept. Int. Rep. 85-6 Inst. fuer Angewandte Physik der Univ. Frankfurt/Main, Feb. 1985 Prepared for LASL
(Contract W-7405-eng-36)
(DE85-012483; LA-tr-85-21) Avail: NTIS HC A02/MF A01

Funneling which is the joining of beams in a zipper arrangement while doubling the frequency to increase the beam current, to utilize the acceptance of the linear accelerator even at the higher frequency is discussed. Funneling is necessary to obtain higher current, higher brilliance. No experiments were conducted although it is one of the prerequisites for the realization of this high current accelerator. Several divergent ideas on funneling are compiled and presented. DOE

N86-10195# Sandia Labs., Albuquerque, N. Mex.
COMPACT, LOW JITTER, TRIGGERED SPARK GAP
W. K. Tucker, E. E. Jones, T. L. Franklin, I. F. Bennett, and G. Reber 10 Jun. 1985 4 p Presented at the 5th IEEE Pulsed Power Conf., Washington, D.C., 10 Jun. 1985
(Contract DE-AC04-76DP-00789)
(DE85-012812; SAND-84-2395C; CONF-850616-18) Avail: NTIS HC A02/MF A01

High energy particle accelerators using compact, high gradient cavities will require small, highly reliable, triggered spark gaps. This paper will discuss the design and development of V/N triggered spark gaps operating from 520 kV to 1280 kV. Spark gap jitter of < ns has been obtained with trigger voltages of 60 kV. Capacitively balancing the trigger blade electrode, coupled with a trigger voltage rise time of 10 ns, produces three or more arcs across the main electrode gaps. A 2.3 (UC OMEGA) injector using 12 parallel spark gaps operating at 1280 kV has been successfully tested. The total number of shots on this injector exceeds 700 without having to refurbish the gaps. A C.44 (UC OMEGA) accelerating cavity with 24 parallel spark gaps and operating at 520 kV charge voltage has also been tested. DOE

N86-10196# Department of Energy, Washington, D. C.
COUNTERPULSE RAILGUN ENERGY RECOVERY CIRCUIT Patent Application
E. M. Honig, inventor (to DOE (LASL) Filed 28 Sep. 1985 16 p
(DE85-011603; US-Patent-Appl-SN-655490) Avail: NTIS HC A02/MF A01

The invention presented relates to a high-power pulsing circuit and more particularly to a repetitive pulse inductive energy storage and transfer circuit for an electromagnetic launcher. In an electromagnetic launcher such as a railgun for propelling a projectile at high velocity, a counterpulse energy recovery circuit is employed to transfer stored inductive energy from a source inductor to the railgun inductance to propel the projectile down the railgun. Switching circuitry and an energy transfer capacitor are used to switch the energy back to the source inductor in readiness for a repetitive projectile propelling cycle. DOE

N86-10197# Department of Energy, Washington, D. C.
OVERPULSE RAILGUN ENERGY RECOVERY CIRCUIT Patent Application
E. M. Honig, inventor (to DOE) (LASL) Filed 28 Sep. 1984 17 p
(DE85-011607; US-Patent-Appl-SN-655593) Avail: NTIS HC A02/MF A01

A high power pulsing circuit is presented and more particularly a repetitive pulse inductive energy storage and transfer circuit for an electromagnetic launcher. In an electromagnetic launcher such as a railgun for propelling a projectile at high velocity, an overpulse energy recovery circuit is employed to transfer stored inductive energy from a source inductor to the railgun inductance to propel the projectile down the railgun. Switching circuitry and an energy transfer capacitor are used to switch the energy back to the source inductor in readiness for a repetitive projectile propelling cycle. DOE

N86-10394*# Jet Propulsion Lab., California Inst. of Tech., Pasadena. TDA Mission Support and DSN Operations Office.
JPL EMERGENCY SUPPORT OF TDRSS AND COMPATIBLE SATELLITES
N. A. Fanelli *In its* The Telecommun. and Data Acquisition Progr. Rept. 15 Aug. 1985 p 120-124 (For primary document see N86-10382 01-32)
Avail: NTIS HC A10/MF A01 CSCL 14B

N86-10395*# Jet Propulsion Lab., California Inst. of Tech., Pasadena. TDA Planning Office.
PLANNING FOR VLA/DSN ARRAYED SUPPORT TO THE VOYAGER AT NEPTUNE
J. W. Layland and D. W. Brown *In its* The Telecommun. and Data Acquisition Progr. Rept. 15 Aug. 1985 p 125-135 refs (For primary document see N86-10382 01-32)
Avail: NTIS HC A10/MF A01 CSCL 14B

N86-10399*# Jet Propulsion Lab., California Inst. of Tech., Pasadena. TDA Engineering Section.
THE GCF MARK 4 IMPLEMENTATION AND BEYOND
R. A. Crowe *In its* The Telecommun. and Data Acquisition Progr. Rept. 15 Aug. 1985 p 163-172 refs (For primary document see N86-10382 01-32)
Avail: NTIS HC A10/MF A01 CSCL 14B

15 LAUNCH VEHICLES AND SPACE VEHICLES

Includes boosters; manned orbital laboratories; reusable vehicles; and space stations.

N86-10198# Department of the Navy, Washington, D. C.
IMPROVED ARRESTING AND RECOVERY SYSTEM FOR TEST MISSILES Patent Application
R. E. Kennedy and J. D. Neef, inventors (to Navy) Filed 2 Aug. 1984 18 p
(AD-D011743; US-Patent-Appl-SN-637238) Avail: NTIS HC A02/MF A01 CSCL 16/1

A system for arresting and recovering test ballistic missiles is adaptable for use in an existing facility and with the existing arresting engine. A long loop of cable encircles a sheave on the nose-end of the test missile and is supported by sheaves mounted on the support structure. The ends of the cable loop are terminated on one side of a singletree device. The other side is connected by a single cable to the arresting engine. One end of the cable loop slidably engages with the singletree and has an end cap. As the test missile is launched the cable loop and singletree are drawn toward a ratchet mechanism which grasp the end cap. An intermittent pulling machine is disposed for anchoring one leg of the cable loop whereby the test missile may be later raised or lowered for recovery. The system effectively doubles the load carrying capacity of an existing arresting engine by providing mechanical advantage. GRA

N86-10199# Air Command and Staff Coll., Maxwell AFB, Ala.
AN ANTHOLOGY: RATIONALE FOR A US BALLISTIC MISSILE DEFENSE (1969 - 1984) Student Report
E. C. Tircuit Apr. 1985 122 p
(AD-A156761; ACSC-85-2715) Avail: NTIS HC A06/MF A01 CSCL 15/3

This anthology is a selection and short synopsis of representative articles on the rationale for a US ballistic missile defense (BMD). Unclassified articles and documents were reviewed and analyzed to identify and include nine representative articles in the anthology. The anthology reduces the search for quality material on the subject and documents the fundamental rationale for a BMD. The author concluded that the fundamental rationale for a US BMD is to deter nuclear war. In addition, specific rationale for a US BMD is provided in the anthology. Finally, an extensive bibliography is included in the anthology to enhance further research on the subject. GRA

16 SPACE TRANSPORTATION

Includes passenger and cargo space transportation, e.g., shuttle operations; and rescue techniques.

For related information see also *03 Air Transportation and Safety* and *85 Urban Technology and Transportation.*

N86-10200# European Space Agency, Paris (France).
FIFTH EUROPEAN SYMPOSIUM ON MATERIAL SCIENCES UNDER MICROGRAVITY. RESULTS OF SPACELAB 1
T. D. Guyenne, comp. and J. J. Hunt, comp. Dec. 1984 489 p refs Partly in ENGLISH and FRENCH Proc. held at Schloss Elmau, West Germany, 5-7 Nov. 1984; sponsored by DFVLR, ESA, Bundesministerium fuer Forschung und Technologie, Bonn, West

Germany, European Low-Gravity Research Association, CNES, Dornier-Werke GmbH, Friedrichshafen, West Germany, Erno GmbH, Bremen, West Germany, and Kodak Ltd., Harrow, England
(ESA-SP-222; ISSN-0379-6566) Avail: NTIS HC A21/MF A01

Spacelab Fluid Physics Module; isothermal furnace; gradient furnace; and mirror furnace experiments were discussed. The experiments include investigations of composite materials; metallurgy; melt and solution growth experiments involving semiconductors; nucleation from the vapor phase; and liquids and interfaces. For individual titles, see N86-10201 through N86-10268.

N86-10201# European Space Agency. European Space Research and Technology Center, ESTEC, Noordwijk (Netherlands).
THE FLUID PHYSICS MODULE: A TECHNICAL DESCRIPTION c34
A. Gonfalone *In its* Fifth European Symp. on Mater. Sci. under Microgravity. Results of Spacelab 1 Dec. 1984 p 3-7 refs (For primary document see N86-10200 01-16)
Avail: NTIS HC A21/MF A01

The Spacelab Fluid Physics Module (FPM) is a multipurpose facility for investigations on the behavior of fluids in a microgravitational environment. It can establish a floating zone between two parallel coaxial disks, allowing for disturbance to be applied to the liquid, whose behavior is filmed. The stimuli can be mechanical (rotation, vibration or lateral displacement) or thermal (heating). Experiments on fluid motions induced by differences in surface tension, bubble motions, and fluid dynamics can be performed. The FPM is mounted in the Material Science Double Rack.
Author (ESA)

N86-10202# Kodak Ltd., London (England).
CAPILLARY FORCES IN A LOW GRAVITY ENVIRONMENT c34
J. E. Padday *In* ESA Fifth European Symp. on Mater. Sci. under Microgravity. Results of Spacelab 1 Dec. 1984 p 9-14 refs Sponsored by Kodak Ltd. and England Department of Industry (For primary document see N86-10200 01-16)
Avail: NTIS HC A21/MF A01

The capillary properties of a liquid (silicone oil) attached to a large circular solid surface (titanium) and held in the form of an axisymmetric liquid zone by a second smaller solid disk were studied on Spacelab. The unperturbed shapes and stability properties of these (zero-g) axisymmetric zones were obtained from the Laplace capillary equation. The principle by which a Laplace shape may be distorted by external force fields is described and the features of the method by which solid-liquid disjoining pressure is measured, are given. Experimental methods, image recording, image processing and the antispread treatment are described. It is found that the antispread works nominally and that the electrical field shows no effects. Equilibrium is reached very quickly and zone breakage was recorded. Thirteen data points were obtained with capillary pressures in the range -0.4 to -0.009 N/sqcm. At the lower pressure, very thick liquid films form; at higher pressures the films are thin. Author (ESA)

N86-10203# Naples Univ. (Italy). Inst. of Aerodynamics Umberto Nobile.
SOME RESULTS OF THE MARANGONI FREE CONVECTION EXPERIMENT c34
L. G. Napolitano, R. Monti, and G. Russo *In* ESA Fifth European Symp. on Mater. Sci. under Microgravity. Results of Spacelab 1 Dec. 1984 p 15-22 refs (For primary document see N86-10200 01-16)
(Contract CNR-PSN-83-070)
Avail: NTIS HC A21/MF A01

Thermally induced Marangoni flows in a floating zone under a variety of imposed boundary conditions were investigated on Spacelab. Problems in measuring the velocity in the bulk fluid, and the implications of the values obtained that confirm the attainment of a Marangoni boundary layer regime are discussed. Heat transferred across the floating zone is considered. The method used to determine, from the measured temperature of the hot disk, the time evolution of the temperature of the cold disk and its steady state Nusselt number is given, and results obtained from one run are presented. Author (ESA)

N86-10204# Centre National de la Recherche Scientifique, Meudon-Bellevue (France). Equipe de Technologie de la Croissance Cristalline.
OSCILLATIONS OF SEMI-FREE LIQUIDS IN MICROGRAVITY: SPACELAB 1 EXPERIMENT ES 326 [OSCILLATIONS DE VOLUMES LIQUIDES SEMI-LIBRES EN MICROGRAVITE: EXPERIENCE ES 326 DANS SPACELAB 1] c34
H. Rodot and C. Bisch *In* ESA Fifth European Symp. on Mater. Sci. under Microgravity. Results of Spacelab 1 Dec. 1984 p 23-29 refs In FRENCH (For primary document see N86-10200 01-16)
Avail: NTIS HC A21/MF A01

The effects of axial vibration on semi-free liquid in microgravity were studied on Spacelab 1. Amplitude, resonant frequencies, and oscillation damping of the liquid spheres were determined, using silicone oil injected onto a vibrating plate. Results confirm theoretical models and show that the liquid is very sensitive to vibrations in the 0.2 to 2 Hz range. To prevent strong resonance, e.g., during crystal growth, a small support/sphere diameter ratio is recommended. It is difficult to evaluate wetting factors.
Author (ESA)

N86-10205# Universidad Politecnica de Madrid (Spain). Dept. of ETSI Aeronautics.
LIQUID COLUMN STABILITY: EXPERIMENT 1 ES-331 c34
T. Martinez *In* ESA Fifth European Symp. on Mater. Sci. under Microgravity. Results of Spacelab 1 Dec. 1984 p 31-36 refs Sponsored by Spanish Commission for Space Research (For primary document see N86-10200 01-16)
Avail: NTIS HC A21/MF A01

The Spacelab floating zone stability in zero gravity experiment to form a long cylindrical liquid bridge (10 cm), between 2 solid coaxial disks, to study the surface deformation and inner liquid motion resulting from the application of mechanical disturbances is described. The scheduled investigations were not accomplished due to the impossibility of holding the liquid interface anchored at the nominal disk edge, but considerable knowledge on experiment design, e.g., on the difficulty of getting a clean start, and on the role of inertia in bridge formation was acquired. Author (ESA)

N86-10206# National Aerospace Lab., Amsterdam (Netherlands).
AXISYMMETRIC FREE SURFACE BEHAVIOR OF MOVING LIQUID IN A CYLINDER IN MICROGRAVITY c34
J. P. B. Vreeburg *In* ESA Fifth European Symp. on Mater. Sci. under Microgravity. Results of Spacelab 1 Dec. 1984 p 37-42 refs (For primary document see N86-10200 01-16)
Avail: NTIS HC A21/MF A01

The behavior of silicone oil during spin-up and spin-down of the container, and liquid response to forced oscillations, in stationary and steadily rotating states were studied on Spacelab. Nonlinear growth and decay of the half subharmonic resonance of the free liquid surface were examined. A diagnostic method for the determination of free liquid surface shape is outlined. The free liquid surface is included as a reflecting or refracting optical surface by which an illuminated line is observed. Via ray tracing and analysis, shape parameters of the surface are determined from the images of this line. The extreme wetting behavior of the oil produces a bubble of the air in the container rather than the formation of a spherical meniscus with a defined contact line (with zero contact angle). The excitation of capillary surface resonances is difficult. Most easily generated is a zero order mode in which the undeformed bubble oscillates. Author (ESA)

N86-10207# Bristol Univ. (England). School of Chemistry.
KINETICS OF SPREADING OF LIQUIDS IN MICROGRAVITY: EXPERIMENT 1 ES 327 c34
J. M. Haynes *In* ESA Fifth European Symp. on Mater. Sci. under Microgravity. Results of Spacelab 1 Dec. 1984 p 43-46 refs (For primary document see N86-10200 01-16)
Avail: NTIS HC A21/MF A01

The phenomenology of spreading of a tethered liquid drop is reviewed, and compared with the data obtained in microgravity experiments conducted in the fluid physics module during the Spacelab 1 mission. Recommendations for conduct of experiments of this kind are made. Author (ESA)

N86-10208# Deutsche Forschungs- und Versuchsanstalt fuer Luft- und Raumfahrt, Cologne (West Germany). Inst. fuer Raumsimulation.
THE ISOTHERMAL HEATING FACILITY c18
K. Wittmann *In* ESA Fifth European Symp. on Mater. Sci. under Microgravity. Results of Spacelab 1 Dec. 1984 p 49-54 refs (For primary document see N86-10200 01-16)
Avail: NTIS HC A21/MF A01

The Spacelab Isothermal Heating Facility (IHF) is a resistance heated vacuum furnace integrated in the Material Science Double Rack (MSDR). In the first Spacelab Mission the IHF was used for heating (Tmax = 1500 c) and rapid cooling of a wide range of sample material enclosed in standard sample container in 12 experiments. Besides the isothermal mode with low temperature gradients within the sample, the IHF can establish time variable axial temperature gradients in special gradient samples. The IHF heating and cooling cycles are performed automatically, controlled by the central computer of the MSDR. Author (ESA)

N86-10209# Hamburg Univ. (West Germany).
INFLUENCES AFFECTING SEPARATION IN MONOTECTIC ALLOYS UNDER MICROGRAVITY c12
H. Ahlborn and K. Loehberg (Technische Univ., Berlin) *In* ESA Fifth European Symp. on Mater. Sci. under Microgravity. Results of Spacelab 1 Dec. 1984 p 55-61 refs (For primary document see N86-10200 01-16)
Avail: NTIS HC A21/MF A01

Specimens from the monotectic systems Zn-Bi, Zn-Pb, and Zn-Bi-Pb were cooled (30 K/min) through the miscibility gap in microgravity on Spacelab to study separation. Results are contradictory, and it is not possible to decide if the separation process in monotectic alloys under microgravity is determined by one or more processes, and which of these is the most efficient. To obtain a homogeneous distribution of small sized droplets of the minority phase in a liquid matrix, its volume portion should not exceed 5%, and a low interfacial energy between the droplets and the matrix, and a high viscosity of the matrix are required.
Author (ESA)

N86-10210# Max-Planck-Inst. fuer Metallforschung, Stuttgart (West Germany).
PARTICLE COARSENING IN IMMISCIBLE ZINC-LEAD ALLOYS UNDER MICROGRAVITY c12
A. Kneissel (Montanuniv. Leoben, Austria) and H. Fischmeister *In* ESA Fifth European Symp. on Mater. Sci. under Microgravity. Results of Spacelab 1 Dec. 1984 p 63-68 refs Sponsored by Austrian Ministry of Science and Research (For primary document see N86-10200 01-16)
Avail: NTIS HC A21/MF A01

Spacelab experiments on the liquid-liquid system Zn-Pb are described. Using alloys consisting of a low volume fraction of Pb-rich droplets in a Zn-rich matrix, it was demonstrated that a homogeneous dispersion of fine droplets can be maintained under microgravity and solidified into a homogeneous dispersion structure at the cooling rates available in the isothermal furnace of Spacelab. The particle coarsening which occurs during a hold in the two-liquid region is compatible with known data for the Pb-Zn system within the error limits of the measurements. Disturbance of the Ostwald process by Marangoni and residual g convection is unimportant.
Author (ESA)

N86-10211# Katholieke Universiteit te Leuven (Belgium). Dept. Metaalkunde und Toegepaste Materiaalkunde.
MELTING AND SOLIDIFICATION OF METAL MATRIX COMPOSITES UNDER MICROGRAVITY c12
L. Froyen and A. Deruyttere *In* ESA Fifth European Symp. on Mater. Sci. under Microgravity. Results of Spacelab 1 Dec. 1984 p 69-78 refs (For primary document see N86-10200 01-16)
Avail: NTIS HC A21/MF A01

Particulate composites with Al-matrix were melted, held during 40 min at 800C and solidified in the Spacelab Isothermal Heating Facility. Comparison with ground processed reference samples shows that the space processed samples are much more homogeneous, for coarse and fine dispersed particles. Higher homogeneity leads to an important increase of the uniformity of macro-Vickers hardness. The abrasive wear resistance of the Al-SiC composite after melting and solidification in space is as good as in samples prepared by powder metallurgy. The particle rearrangements in the 1 g-reference and micro g-samples can be explained by interfacial energy considerations, sedimentation, and convection.
Author (ESA)

N86-10212# Technische Hogeschool, Delft (Netherlands). Dept. of Metals Science.
UNIDIRECTIONAL SOLIDIFICATION OF CAST IRON: EXPERIMENT ES-325 c12
H. Nieswaag, T. Luyendijk, and W. H. M. Alsem *In* ESA Fifth European Symp. on Mater. Sci. under Microgravity. Results of Spacelab 1 Dec. 1984 p 79-85 refs Sponsored by Netherlands State Department (For primary document see N86-10200 01-16)
Avail: NTIS HC A21/MF A01

Eutectic cast iron with 3.9%C-1.5%Si-0.01%P-0.025%S was solidified unidirectionally in the Spacelab isothermal furnace at 4 growth rates between 0.1 and 1.0 mm/min to study graphite growth and the sulfur transport in the liquid during solidification under microgravity. From the sulfur concentration profile it is concluded that a stronger convection occurs in space. Transients in the sulfur concentration at changing solidification rate prove, however, that a narrow diffusive boundary layer must be present. The graphite flakes are not better aligned than at 1 g. The flight specimen is separated into two parts in a more pronounced way than observed under terrestrial conditions. Cavities are found in the micro g sample at the position where the solid-liquid interface stopped after melting. The plasma-sprayed alumina skin was rigid enough to keep the liquid specimen in its original shape, although cracks are observed. Author (ESA)

N86-10213# Maschinenfabrik Augsburg-Nuernberg A.G., Munich (West Germany).
SKIN CASTING OF ALLOYS AND COMPOSITES: RESULTS OF SPACELAB (SL)-1 AND TEXUS EXPERIMENTS c12
H. Sprenger *In* ESA Fifth European Symp. on Mater. Sci. under Microgravity. Results of Spacelab 1 Dec. 1984 p 87-94 refs Sponsored by Bundesministerium fuer Forschung und Technologie (For primary document see N86-10200 01-16)
Avail: NTIS HC A21/MF A01

Shape stability of alumina skin coated cast iron specimens during heat-up, melting, hold time, and directional solidification were studied in TEXUS sounding rocket and Spacelab experiments. It is shown that the main contributions to skin deformation come from the volume change during melting and from interfacial tension forces between melt and skin. In the Spacelab experiment, the cast iron sample shows unexpected behavior due to strong deviation of the experiment run from the intended time temperature profile. The appearance of pores and the separation of the melt into two parts, caused by gas formation, influences the resulting thermal gradient and solidification rate. There is evidence, however, that these parameters are also influenced by the strongly reduced convection during the directional solidification phase. Author (ESA)

N86-10214# Technische Univ., Vienna (Austria).
VACUUM BRAZING UNDER MICROGRAVITY c12
K. Frieler, R. Stickler (Bundesanstalt fuer Materialpruefung.), and E. Siegfried *In* ESA Fifth European Symp. on Mater. Sci. under Microgravity. Results of Spacelab 1 Dec. 1984 p 95-99 refs (For primary document see N86-10200 01-16)
Avail: NTIS HC A21/MF A01

Gravity dependent vacuum brazing process control parameters including thermal history, geometry of brazing gaps, and flow patterns were studied in the Spacelab Isothermal Heating Facility under microgravity. Gap filling, braze mixing, and microstructure as a function of joint hardness were examined. Only the liquid phase of the braze is gravity dependent. More pronounced mixing occurs for micro-g than for 1 g cases. While all the gaps of the 1 g specimen are filled to the degree indicated by the equilibrium of hydrostatic and capillary pressure, only the outer 200 micron gap of the micro-g sample is filled completely. Microgravity increases porosity. The segregation of CuNi dendrites and melt at 1100 K seen at 1 g is absent in micro-g. Author (ESA)

N86-10215# Bologna Univ. (Italy). Dipt. di Fisica.
MELTING AND SOLIDIFICATION IN O-g OF SINTERED ALLOYS: EXPERIMENTS ES 311 A AND B BUBBLE REINFORCED MATERIALS c12
F. Barbier, C. Patuelli, P. Gonndi (Rome Univ.), and R. Montanari (Rome Univ.) *In* ESA Fifth European Symp. on Mater. Sci. under Microgravity. Results of Spacelab 1 Dec. 1984 p 101-107 refs (For primary document see N86-10200 01-16)
Avail: NTIS HC A21/MF A01

The behavior after melting and solidification in O and 1 g of sintered Cu-Ag and Al alloys was compared in Spacelab experiments. Oxide films are efficient in maintaining the initial shape after melting and solidification in O g. After melting and solidification in O g the bubble distribution appears to be connected with sweeping phenomena, and to phase and grain boundaries, along the solidification front. The eutectics in O g present larger lamella spacings, depending on smaller solidification rates, larger diffusion coefficients, and/or smaller nucleation rates. The Al alloys show reduced coalescence in O g, leading to uniform distribution of aggregates of limited size, much smaller than the one of the aggregates forming in 1 g and depending on Brownian motion. No evidence for effects of convective motions depending on the surface tension gradients in these liquid metals with oxide film coating is found. Author (ESA)

N86-10216# Technische Univ., Clausthal-Zellerfeld (West Germany). Arbeitsgruppe Glas.
INTERDIFFUSION IN THE GLASS MELT SYSTEM (Na2O+Rb2O) .3SiO2 c12
M. Braedt, V. Braetsch, and G. H. Frischat *In* ESA Fifth European Symp. on Mater. Sci. under Microgravity. Results of Spacelab 1 Dec. 1984 p 109-112 refs Sponsored by Bundesministerium fuer Forschung und Technologie (For primary document see N86-10200 01-16)
Avail: NTIS HC A21/MF A01

An investigation of the interdiffusion between Na2O.3SiO2 and Rb2O.3SiO2 glass melts and the corrosion of SiO2 glass by alkalisilicate glass melts at 1200 C was planned for Spacelab. The temperature-time program, planned to maintain a 30 min period of constant temperature of 1200 C was quite different. Only the interdiffusion experiment can be evaluated for an effective temperature of 1180 C, with an effective time of 1730 sec. Despite the problems, the micro-g diffusion profiles result in a concentration-dependent interdiffusion coefficient with typical mixed-alkali effect behavior. For a composition of 0.5 Na2O.0.5 Rb2O.3SiO2 the D value approaches (1.1 + or - 0.3) 0.00001 sqcm/sec, and fits the order of data obtained earlier. The 1 g reference experiment was totally disturbed by convection effects. Author (ESA)

N86-10217# Centre National d'Etudes Spatiales, Toulouse (France).
GRADIENT HEATING FACILITY BEHAVIOR c18
G. Cambon, B. Castets, O. Boutemy, J. P. Gicquel, R. Aubron, M. Boddaert, and J. Benoit *In* ESA Fifth European Symp. on Mater. Sci. under Microgravity. Results of Spacelab 1 Dec. 1984 p 115-119 refs (For primary document see N86-10200 01-16)
Avail: NTIS HC A21/MF A01

The Spacelab Gradient Heating Facility (GHF) is a furnace with 3 heating zones with cooled heat sink permitting the control of unidirectional solidification without pulling device at temperatures up to 1250 C. The GHF can run three 0.7 gr cartridges simultaneously. The experiment and the furnace can be cooled together very rapidly after helium injection at low partial pressure. Flight data analysis shows that only a maximum of 50% of data are available. It is difficult to have a complete assurance of the correct working of the GHF plus Materials Science Double Rack and in particular, to understand the reasons for the oxydizing of GHF cartridges during the heating. Author (ESA)

N86-10218# Commissariat a l'Energie Atomique, Grenoble (France). Dept. de Metallurgie.
DIRECTIONAL SOLIDIFICATION OF AN ALUMINUM-ZINC VAPOR EMULSION IN MICROGRAVITY c12
C. Potard and P. Morgand *In* ESA Fifth European Symp. on Mater. Sci. under Microgravity. Results of Spacelab 1 Dec. 1984 p 121-125 (For primary document see N86-10200 01-16)
Avail: NTIS HC A21/MF A01

A Spacelab experiment tested a method of creating solid structures in which aluminum-zinc alloys are directionally solidified under controlled partial pressure of zinc and thermal conditions. Destabilization of interfacial liquid zone was expected to give rise to vapor phase nucleation growth and trapping by the advancing solid-liquid front. This was partially realized during the space processing of the specimens: bubble populations are present in the sample. This is due to a nonwetting effect in space not observed on the ground. The microstructures of samples processed in space and on the ground are compared. Author (ESA)

N86-10219# Commissariat a l'Energie Atomique, Grenoble (France). Dept. de Metallurgie.
DIRECTIONAL SOLIDIFICATION OF EUTECTIC ALLOYS c12
J. J. Favier and J. deGoer *In* ESA Fifth European Symp. on Mater. Sci. under Microgravity. Results of Spacelab 1 Dec. 1984 p 127-133 refs (For primary document see N86-10200 01-16)
Avail: NTIS HC A21/MF A01

Eutectic alloys Ag-Ge, Al3Ni-Al, Al2Cu-Al forming respectively, under ground conditions, irregular, fiberlike and lamelar structures were directionally solidified under well defined thermal conditions in the Spacelab Gradient Heating Facility. The microstructures are compared with those obtained under the same conditions on the ground. The major difference appears with the fiberlike Al-Ni system, for which the main spacing between the needles is larger in space than on Earth, confirming TEXUS results. An explanation taking into account off-eutectic considerations is proposed. Author (ESA)

N86-10220# Centre National de la Recherche Scientifique, Meudon-Bellevue (France). Equipe de Technologie de la Croissance Cristalline.
LEAD TELLURIDE CRYSTALS GROWN IN MICROGRAVITY: EXPERIMENT ES 318 [CRISTAUX DE TELLURURE DE PLOMB ELABORES EN MICROGRAVITE EXPERIENCE ES 318] c12
H. Rodot and O. Tottereau *In* ESA Fifth European Symp. on Mater. Sci. under Microgravity. Results of Spacelab 1 Dec. 1984 p 135-139 refs In FRENCH (For primary document see N86-10200 01-16)
Avail: NTIS HC A21/MF A01

Three lead telluride monocrystals grown in the Spacelab Gradient Heating Facility under microgravity (two from seeds, one without by the Bridgman method) were compared with crystals grown on the ground. Results show that it is possible to grow large (17 mm diameter) lead telluride crystals in space, with better quality than those on Earth, which have defects due to gravity induced convection. The rate and stability of acceleration are the main factors for successful crystal growth in space, and exclude manned vehicles or those with multiple payloads incompatible with these requirements. Author (ESA)

N86-10221# Erlangen-Nuremberg Univ. (West Germany). Inst. fuer Werkstoffwissenschaften.
DIRECTIONAL SOLIDIFICATION OF InSb-NiSb EUTECTIC c12
G. Mueller and P. Kyr *In* ESA Fifth European Symp. on Mater. Sci. under Microgravity. Results of Spacelab 1 Dec. 1984 p 141-146 refs Sponsored by DFVLR and Bundesministerium fuer Forschung und Technologie (For primary document see N86-10200 01-16)

Avail: NTIS HC A21/MF A01

The InSb-NiSb quasi binary eutectic was directionally solidified under microgravity and Earth-gravity conditions in the Spacelab Gradient Heating Facility by the power down technique. Comparison of space and Earth processed samples reveals a 30% decrease in the spacing of the SiSb fibers in the samples grown under microgravity. Author (ESA)

N86-10222# Commissariat a l'Energie Atomique, Grenoble (France). Dept. de Metallurgie.
THERMOMIGRATION OF COBALT IN LIQUID TIN: EXPERIMENT 1 ES 320 c12
Y. Malmejac and J. P. Praizey *In* ESA Fifth European Symp. on Mater. Sci. under Microgravity. Results of Spacelab 1 Dec. 1984 p 147-152 refs (For primary document see N86-10200 01-16)
Avail: NTIS HC A21/MF A01

Thermomigration of cobalt in liquid tin was studied on the spacelab by heating capillary samples of liquid tin containing 0.5% cobalt in a thermal gradient of 200 deg/cm. When chemical steady state is reached, the liquid alloy is sampled, and the cobalt concentration analyzed by activation. On Earth, a constant concentration profile is obtained. In microgravity relative concentration of cobalt varies from 0.7 at the cold end to 1.4 at the hot end. The heat of transport can be expressed by: Q cal/mole = - (3,72 + or - 0,08) T (K) for 593 to 933 K. Soret coefficient is 0.024/K at 773 K. Convection calculations explain why thermomigration effects are measurable in microgravity but not on Earth in the configuration considered. Author (ESA)

N86-10223# Freiburg Univ. (West Germany). Inst. fuer Kristallographisches.
THE MIRROR HEATING FACILITY: PERFORMANCE AND EXPERIENCES c18
R. Nitsche *In* ESA Fifth European Symp. on Mater. Sci. under Microgravity. Results of Spacelab 1 Dec. 1984 p 155-156 refs (For primary document see N86-10200 01-16)
Avail: NTIS HC A21/MF A01

The Spacelab Mirror Heating Facility (MHF) is a multiuser furnace of low thermal inertia, providing high local temperatures (up to 2000 deg C) at relatively low power consumption. The sample is radiation heated by two 400 W halogen lamps, situated in the foci of a double ellipsoid mirror. The mirror can be translated relative to the stationary, but rotatable, sample. This makes the MHF especially suited for crystal growth from the melt by the floating zone method and for solution growth by the traveling heater method. The MHF was part of the Materials Science Double Rack (MSDR). The MHF was activated eight times, with varying success, before breakdown of the MSDR cooling system crippled it. Author (ESA)

N86-10224# Stuttgart Univ. (West Germany). Inst. fuer Physikalisches.
GaSb-SEMICONDUCTOR CRYSTALS UNDER MICROGRAVITY: EXPERIMENT ES 323 c12
K. W. Benz and G. Nagel *In* ESA Fifth European Symp. on Mater. Sci. under Microgravity. Results of Spacelab 1 Dec. 1984 p 157-161 refs (For primary document see N86-10200 01-16) (Contract DFVLR-01-QV-698)
Avail: NTIS HC A21/MF A01

The Traveling-heater method was used to grow the III-V compound GaSb on Spacelab. Convective transport phenomena and the origins of dopant inhomogeneities under Earth and space conditions were studied. Earth grown crystals show strong dopant variations mainly due to convective flow phenomena. The Spacelab experiment reveals an increase of dopant homogeneity in the space grown crystal because of the absence of natural convection. Author (ESA)

N86-10225# Freiburg Univ. (West Germany). Inst. fuer Kristallographisches.
SOLUTION GROWTH OF CADMIUM TELLURIDE: EXPERIMENT ES 322 c12
R. Schoenholz, R. Dian, and R. Nitsche *In* ESA Fifth European Symp. on Mater. Sci. under Microgravity. Results of Spacelab 1 Dec. 1984 p 163-167 refs Sponsored by Bundesministerium fuer Forschung und Technologie (For primary document see N86-10200 01-16)
Avail: NTIS HC A21/MF A01

Microgravity growth of CdTe from Te solution by the traveling heater method was achieved on Spacelab. The experiment was terminated after 6 instead of 17 hr of growth, due to breakdown of the cooling system. The tiny layer of material grown in this time could not be analyzed satisfactorily. It was severely cracked by thermal stress since the slow cooling phase was not carried out. Author (ESA)

N86-10226# Wacker-Chemie G.m.b.H. Burghausen (West Germany).
CRYSTALLIZATION OF A SILICON SPHERE c12
H. Koelker *In* ESA Fifth European Symp. on Mater. Sci. under Microgravity. Results of Spacelab 1 Dec. 1984 p 169-172 refs (For primary document see N86-10200 01-16)
Avail: NTIS HC A21/MF A01

Directional solidification of silicon was investigated in the spacelab under zero gravity to see if surface driven flow exists in liquid silicon. After solidification, the Si-crystal was sliced, polished and etched, and the striation pattern studied with a microscope. The result clearly suggests the existence of time dependent surface driven flow. Author (ESA)

N86-10227# Freiburg Univ. (West Germany). Inst. fuer Kristallographisches.
CRYSTAL GROWTH OF SILICON IN SPACELAB 1: EXPERIMENT ES-321 c12
A. Eyer, H. Leiste, and R. Nitsche *In* ESA Fifth European Symp. on Mater. Sci. under Microgravity. Results of Spacelab 1 Dec. 1984 p 173-182 refs (For primary document see N86-10200 01-16)
Avail: NTIS HC A21/MF A01

A phosphorus doped silicon crystal of 10 mm diameter and 112 mm length was grown by the floating zone method at a rate of 5 mm/min aboard Spacelab 1. Zone forms and interface shapes of the microgravity and the terrestrial reference sample differ considerably, but the patterns of (nonrotational) striations are very similar. Thus, time dependent thermocapillary flows, driven by gravity independent surface tension gradients in the molten zone, appear to be the dominant cause for these dopant inhomogeneities in space as well as on Earth. Author (ESA)

N86-10228# Freiburg Univ. (West Germany). Chemisches Lab.
PROTEIN SINGLE CRYSTAL GROWTH UNDER MICROGRAVITY c12
W. Littke and C. John *In* ESA Fifth European Symp. on Mater. Sci. under Microgravity. Results of Spacelab 1 Dec. 1984 p 185-188 refs Original language document previously announced as A85-39084 Sponsored by Bundesministerium fuer Forschung und Technologie (For primary document see N86-10200 01-16)
Avail: NTIS HC A21/MF A01

Single crystals of Beta galactosidase and Lysozyme were grown in Spacelab for X-ray diffraction studies of three dimensional crystal structure. The Beta galactosidase shows a 27-fold, Lysozyme a 1000-fold increase in volume compared with crystals grown under terrestrial conditions. The crystalline material is well shaped and microscopic examinations under polarized light show good quality. Wide fronts of diffusion favor the formation of large crystals. Applying an increasing temperature gradient improves crystallization of galactosidase. Perfect habit is found with crystals grown free floating out of the solution without touching the wall. The equipment and procedures are described. Author (ESA)

N86-10229# Technical Univ. of Denmark, Lyngby. Physics Lab. 3.
CRYSTAL GROWTH FROM SOLUTION c12
G. Galster and K. F. Nielsen *In* ESA Fifth European Symp. on Mater. Sci. under Microgravity. Results of Spacelab Dec. 1984 p 189-191 refs Sponsored by Danish Space Board (For primary

document see N86-10200 01-16)
Avail: NTIS HC A21/MF A01

Experiments on crystal growth using the method of opposite oriented diffusion growth in Spacelab 1 are described. The growth of calcium-tartrate crystals demonstrates that filters between the three chambers of a growth reactor are necessary even in the low gravity environment of the Spacelab. Attempts to grow low-dimensional, electrically conducting crystals failed due to chemical disintegration during the prolonged waiting period prior to launch. Author (ESA)

N86-10230# Paris VI Univ. (France). Lab. de Mineralogie et Cristallographie.
GROWTH AND CHARACTERIZATION OF BRUSHITE AND LEAD MONETITE, SIMULATION AND RESULTS **c12**
M. C. Robert, F. Lefaucheux, and A. Authier *In* ESA Fifth European Symp. on Mater. Sci. under Microgravity. Results of Spacelab 1 Dec. 1984 p 193-199 refs Sponsored by CNES (For primary document see N86-10200 01-16)
Avail: NTIS HC A21/MF A01

Single crystals obtained in Spacelab experiments of solution growth by coprecipitation were characterized by optical and X-ray topographic techniques. It is shown how gel growth simulation experiments can be used to select the parameters for space experiments and to analyze the growth features of the crystals. Author (ESA)

N86-10231# Technische Univ., Berlin (West Germany). Inst. fuer Metallforschung.
SELF DIFFUSION OF Sn112 AND Sn124 IN LIQUID TIN **c12**
G. Frohberg, K.-H. Kraatz, and H. Wever *In* ESA Fifth European Symp. on Mater. Sci. under Microgravity. Results of Spacelab 1 Dec. 1984 p 201-205 refs (For primary document see N86-10200 01-16)
Avail: NTIS HC A21/MF A01

The temperature dependence of self diffusion and isotope effect in molten tin under micro-g and 1 g conditions were investigated on the Spacelab. Eight cartridges, 16 tin samples were isothermally annealed at 8 diffusion temperatures between 240 and 1250 C. The penetration profiles were analyzed. Significantly lower diffusion coefficients than under 1 g indicate the absence of gravity-driven microconvections. Accuracy is typically 0.5%. An isotope effect of 0.1 (400 C) and 0.9 (810 C) is reported. Author (ESA)

N86-10232# Politecnico di Milano (Italy).
ADHESION OF METALS: EXPERIMENT 1 ES-340 **c12**
F. Rossitto and G. Ghersini (Centro Informazioni Studi Esperienze) *In* ESA Fifth European Symp. on Mater. Sci. under Microgravity. Results of Spacelab 1 Dec. 1984 p 207-217 refs Sponsored by CNR (For primary document see N86-10200 01-16)
Avail: NTIS HC A21/MF A01

The characterization of stainless steel surface forces and interface energies at the contact between real surfaces, was studied in the Spacelab ultrahigh vacuum (UHV) chamber. In spite of the malfunctions during the experiment and in the output data, it can be affirmed that most of the objectives of the experiment are reached. The flight shows the nominal performance of the UHV Chamber, and single pulse analysis is able to explore the adhesion mechanisms, to characterize the interaction model between the colliding bodies, and to evaluate dynamically the interface energy. Author (ESA)

N86-10233*# Harvard Univ., Cambridge, Mass. Div. of Applied Sciences.
CRYSTAL NUCLEATION AND GLASS FORMATION IN METALLIC ALLOY MELTS **c12**
F. Spaepen *In* ESA Fifth European Symp. on Mater. Sci. under Microgravity. Results of Spacelab 1 Dec. 1984 p 215-219 refs (For primary document see N86-10200 01-16)
(Contract NAS8-36516)
Avail: NTIS HC A21/MF A01

Homogeneous nucleation, containerless solidification, and bulk formation of metallic glasses are discussed. Homogeneous nucleation is not a limiting factor for metallic glass formation at slow cooling rates if the reduced glass transition temperature is high enough. Such glasses can be made in bulk if heterogeneous nucleants are removed. Containerless processing eleminates potential sources of nucleants, but as drop tube experiments on the Pd-Si alloys show, the free surface may still be a very effective heterogeneous nucleant. Combination of etching and heating in vacuum or fluxing can be effective for cleaning fairly large ingots of nucleants. Reduced gravity processing has a potentially useful role in the fluxing technique, for example to keep large metallic ingots surrounded by a low density, low fluidity flux if this proved difficult under ground conditions. For systems where heterogeneous nucleants in the bulk of the ingot need gravity to segregate to the flux-metal interface, reduced gravity processing may not be appropriate for bulk glass formation. Author (ESA)

N86-10234*# Massachusetts Inst. of Tech., Cambridge.
CRYSTAL GROWTH OF GaAs IN SPACE **c12**
H. C. Gatos, J. Lagowski, L. M. Pawlowicz, F. Dabkowski, and C.-J. Li *In* ESA Fifth European Symp. on Mater. Sci. under Microgravity. Results of Spacelab 1 Dec. 1984 p 221-225 refs (For primary document see N86-10200 01-16)
Avail: NTIS HC A21/MF A01

It is shown that stoichiometry variations in the GaAs melt during growth constitute the most critical parameter regarding defect formations and their interactions; this defect structure determines all relevant characteristics of GaAs. Convection in the melt leads to stoichiometric variations. Growth in axial magnetic fields reduces convection and permits the study of defect structure. In order to control stoichiometry in space and to accommodate expansion during solidification, a partially confined configuration was developed. A triangular prism is employed to contain the growth melt. This configuration permits the presence of the desired vapor phase in contact with the melt for controlling the melt stoichiometry. Author (ESA)

N86-10235# Naples Univ. (Italy). Inst. of Aerodynamics Umberto Nobile.
THE TEXUS FLIGHT RESULTS ON CONVECTIVE FLOWS AND HEAT TRANSFER IN SIMULATED FLOATING ZONES **c34**
R. Monti, L. G. Napolitano, and G. Mannara *In* ESA Fifth European Symp. on Mater. Sci. under Microgravity. Results of Spacelab 1 Dec. 1984 p 229-236 refs (For primary document see N86-10200 01-16)
Avail: NTIS HC A21/MF A01

On TEXUS 9 sounding rocket flight, a cylindrical liquid bridge between 2 circular disks was created and 1 of the disks then heated with an assigned temperature time profile. The experiment collected data on the thermofluidynamic fields that prevail at high Peclet number and unsteady thermal conditions. Thermocouple failure caused problems in heat transfer data reduction, and in numerical correlation. Author (ESA)

N86-10236# Academy of Sciences (USSR), Moscow. Inst. for Problems in Mechanics.
MATHEMATICAL SIMULATION OF DISTURBING FORCES AND MATERIAL SCIENCE PROCESSES UNDER LOW GRAVITY **c12**
V. I. Polezhaev, A. P. Lebedev, and S. A. Nikitin *In* ESA Fifth European Symp. on Mater. Sci. under Microgravity. Results of Spacelab 1 Dec. 1984 p 237-243 refs (For primary document see N86-10200 01-16)
Avail: NTIS HC A21/MF A01

A model of microgravity aboard an unmanned Earth satellite is suggested. The results of microgravity calculation of unmanned spacecraft in gravity stabilized flight are presented. The thermal convection and impurity distribution in germanium melt in time-dependent microgravity cases on the base of Boussinesq equations mathematical models are studied. It is shown that in the cases of the low-frequencies microgravity oscillations when average microgravity is not zero, there is a sharply pronounced maximum in the macroinhomogeneity. It is also shown that high frequency convection has a small effect on impurity distribution in crystal, but low frequency convection results in striations like the ones in terrestrial conditions. Author (ESA)

N86-10237# Goettingen Univ. (West Germany). Inst. fuer Angewandte Mechanik und Stroemungsphysik.

THE INFLUENCE OF THERMOCAPILLARITY ON THE MIGRATION OF DROPLETS IN A LIQUID POSSESSING A UNIFORM TEMPERATURE GRADIENT c34

V. Delitzsch, H. Eckelmann, and W. Wuest (Deutsche Forshungs- und Versuchsanstalt fuer Luft- und Raumfahrt, Goettingen, West Germany) *In* ESA Fifth European Symp. on Mater. Sci. under Microgravity. Results of the Spacelab 1 Dec. 1984 p 245-249 refs (For primary document see N86-10200 01-16)

Avail: NTIS HC A21/MF A01

The influence of thermocapillarity on the migration of water droplets in butylbenzoate and fluorobenzene is investigated at low Reynolds and Marangoni numbers. The two components of both liquid systems are immiscible with one another and have the same density at 32 and 50 C respectively. At temperature gradients of 1 C/cm in stratified butylbenzoate and 4 C/cm in stratified fluorobenzene in equilibrium, gravity is reduced to a hundredth of the interfacial force. Water droplets injected into the test cell are sorted out in the gravity field dependent on their diameters. Under these conditions the smaller droplets migrate to higher temperature than the bigger ones. The final position of a droplet is determined by the balance of Marangoni and gravity forces both of which depend on droplet diameter. The positions of the droplets in the test cell are evaluated photographically. The interface tension gradients are 0.000001 N/cm for both systems. Author (ESA)

N86-10238# Naples Univ. (Italy). Inst. of Aerodynamics Umberto Nobile.

NUMERICAL SIMULATION OF UNSTEADY THERMAL MARANGONI FLOWS c34

L. G. Napolitano, C. Golia, and A. Viviani *In* ESA Fifth European Symp. on Mater. Sci. under Microgravity. Results of Spacelab 1 Dec. 1984 p 251-258 refs (For primary document see N86-10200 01-16)

(Contract CNR-PSN-83-070)

Avail: NTIS HC A21/MF A01

A two-dimensional numerical code for the analysis of unsteady thermal Marangoni flows which solves the full Navier-Stokes equation for natural, Marangoni, or combined free convection in plane and axisymmetric geometries and arbitrary variations of surface tension with temperature is developed. The equations are discretized using a semi-implicit finite difference scheme that preserves conservative and transport properties within cell mesh and allows the use of time-steps much larger than those relative to a purely explicit technique. Results pertain to a plane configuration with surface tension varying linearly with temperature. The time evolution of the velocity and temperature fields, and the assessement of the range of validity of the so-called shallow-cavity approximation for steady state are discussed. Author (ESA)

N86-10239# Canadian Astronautics Ltd., Ottawa (Ontario).

NUMERICAL SIMULATION OF CONVECTIONS IN THE MICROGRAVITY ENVIRONMENT c34

R. Boudreault *In* ESA Fifth European Symp. on Mater. Sci. under Microgravity. Results of Spacelab 1 Dec. 1984 p 259-264 refs (For primary document see N86-10200 01-16)

Avail: NTIS HC A21/MF A01

A numerical simulation program to study g-jitter and Marangoni convection in the liquid phase under microgravity were produced. The program solves the Navier-Stokes equations in the derived variable configuration. An alternative direction implicit method is used to solve the finite differences equations representing flow in the cavity. The resulting flow field and mixing characteristic are analyzed at different dimensionless times. Author (ESA)

N86-10240# Hochschule der Bundeswehr, Munich (West Germany). Inst. fuer Raumfahrttechnik.

OSCILLATIONS OF A VISCOELASTIC LIQUID DROP IN ZERO-GRAVITY c34

H. F. Bauer *In* ESA Fifth European Symp. on Mater. Sci. under Microgravity. Results of Spacelab 1 Dec. 1984 p 265-270 refs (For primary document see N86-10200 01-16)

Avail: NTIS HC A21/MF A01

The transcendental frequency equation for a viscoelastic spherical liquid drop is presented. For small viscoelasticity the viscous effect dominates, where the oscillation ceases to exist for small relaxation time, while for large viscoelasticity of the liquid the elastic effects dominate the vibrational behavior, producing oscillations again. A viscoelastic liquid drop subjected to a fluctuating temperature gradient also produces oscillations, which may disintegrate the system. The response of the drop with surface tension, viscosity and relaxation time as parameters is presented. Author (ESA)

N86-10241# Gesamthochschule, Essen (West Germany).

VERIFICATION OF TURBULENCE DEVELOPING FROM THE OSCILLATORY MARANGONI CONVECTION IN A LIQUID COLUMN c34

Ch.-H. Chun *In* ESA Fifth European Symp. on Mater. Sci. under Microgravity. Results of Spacelab 1 Dec. 1984 p 271-280 refs (For primary document see N86-10200 01-16)

Avail: NTIS HC A21/MF A01

A microgravity experiment during the TEXUS 7 rocket flight investigated whether the Marangoni convection of a liquid column at Marangoni numbers of 94,000 and 124,000 (far beyond the critical values for the first oscillatory instability) remains oscillatory or goes into the turbulent state, and studied the role of the aspect ratio of the liquid column on the instabilities. Oscillatory turbulent states are found. A physical model concept, criteria for the higher oscillation mode occurrence, and their development into turbulent nonperiodic structure are discussed. Author (ESA)

N86-10242# Giessen Univ. (West Germany). Inst. fuer Physkikalisches.

MEASUREMENTS OF THE CRITICAL MARANGONI NUMBER OF THE LAMINAR-OSCILLATORY TRANSITION OF THERMOCAPILLARY CONVECTION IN FLOATING ZONES c34

D. Schwabe and A. Scharmann *In* ESA Fifth European Symp. on Mater. Sci. under Microgravity. Results of Spacelab 1 Dec. 1984 p 281-289 refs (For primary document see N86-10200 01-16)

(Contract BMFT-01-QV-148-ZA-SN-SLN-7786)

Avail: NTIS HC A21/MF A01

The critical Marangoni number of the transition point from laminar to oscillatory thermocapillary convection in a liquid bridge with free cylindrical surface (floating zone) is measured under microgravity. The critical Marangoni numbers of NaNO3-zones with 6 mm diameter and length 4.00 and 4.79 mm are compared with measurements under normal Earth gravity. Data on the dependence of the oscillation frequency on the Marangoni number are given. Frequency jumps and beat frequencies are found in microgravity and normal gravity. Author (ESA)

N86-10243# Ishikawajima-Harima Heavy Industries Co. Ltd., Yokohama (Japan).

EXPERIMENTAL STUDY ON MARANGONI CONVECTION c34

J. Ochiai, K. Kuwahara, M. Morioka, S. Enya, K. Sezaki, T. Maekawa (Ioyo Univ., Japan), and I. Tanasawa (Tokyo Univ.) *In* ESA Fifth European Symp. on Mater. Sci. under Microgravity. Results of Spacelab 1 Dec. 1984 p 291-295 refs Sponsored by Japanese Science and Technology Agency (For primary document see N86-10200 01-16)

Avail: NTIS HC A21/MF A01

The natural convection in a rectangular container driven by surface tension gradient is investigated in the laboratory and the Marangoni effect under microgravity is estimated. The flow patterns are visualized and the velocity distributions are obtained under various thermal conditions and aspect ratios. The flow and the temperature fields of the Marangoni convection strongly depend on the coupled buoyant convection and the aspect ratio of the liquid layer. Thin wires placed on the free surface and the external magnetic field reduce the convective motion considerably and are expected to be effective means for obtaining desirable flow conditions. Author (ESA)

N86-10244# Universidad Politecnica de Madrid (Spain). Lab. de Aerodinâmica.

STABILITY OF LONG LIQUID COLUMNS c34

J. Meseguer *In* ESA Fifth European Symp. on Mater. Sci. under Microgravity. Results of Spacelab 1 Dec. 1984 p 297-300 refs (For primary document see N86-10200 01-16)
Avail: NTIS HC A21/MF A01

Analytical expressions for minimum volume stability limits of long liquid bridges having cylindrical volume are reviewed and compared with numerical results. These expressions show the dependence of stability limits on the length of the liquid column and the microgravity level. Unequal disk effects are added, and the resulting expression extended to the case of noncylindrical volume configurations through a linear analysis of interface equilibrium shapes. Author (ESA)

N86-10245# Mons Univ. (Belgium). Faculty of Sciences.

RAYLEIGH-BENARD INSTABILITY IN SYSTEMS PRESENTING A MINIMUM IN SURFACE TENSION c34

D. Villers and J. K. Platten *In* ESA Fifth European Symp. on Mater. Sci. under Microgravity. Results of Spacelab 1 Dec. 1984 p 301-305 refs (For primary document see N86-10200 01-16)
Avail: NTIS HC A21/MF A01

It is shown that in the Benard configuration, when the temperature of the upper surface is exactly Tmin, the Marangoni number is equal to zero and therefore Marangoni convection should be suppressed. The rest state (linearly stable) is unstable with respect to at least one particular type of perturbation, provided that the curvature of surface tension is important and, simultaneously, the initial temperature fluctuation exceeds a critical threshold. Author (ESA)

N86-10246*# National Aeronautics and Space Administration. Marshall Space Flight Center, Huntsville, Ala. Space Science Lab.

SEPARATION OF AQUEOUS TWO-PHASE POLYMER SYSTEMS IN MICROGRAVITY c12

J. M. VanAlstine, J. M. Harris (Alabama Univ., Huntsville), S. Synder, P. A. Curreri, S. B. Bamberger (Oregon Health Sciences Univ.), and D. E. Brooks (Oregon Health Sciences Uni.) *In* ESA Fifth European Symp. on Mater. Sci. under Microgravity. Results of Spacelab 1 Dec. 1984 p 309-312 refs Sponsored by Universities Space Research Association (For primary document see N86-10200 01-16)
(Contracts NAS8-35333; NAS8-35334; NAS8-35362)
Avail: NTIS HC A21/MF A01 CSCL 22A

Phase separation of polymer systems in microgravity is studied in aircraft flights to prepare shuttle experiments. Short duration (20 sec) experiments demonstrate that phase separation proceeds rapidly in low gravity despite appreciable phase viscosities and low liquid interfacial tensions (i.e., 50 cP, 10 micro N/m). Ostwald ripening does not appear to be a satisfactory model for the phase separation mechanism. Polymer coated surfaces are evaluated as a means to localize phases separated in low gravity. Contact angle measurements demonstrate that covalently coupling dextran or PEG to glass drastically alters the 1-g wall wetting behavior of the phases in dextran-PEG two phase systems. Author (ESA)

N86-10247*# National Aeronautics and Space Administration. Marshall Space Flight Center, Huntsville, Ala. Dept. of Pathology and Chemistry.

RATIONALE FOR TWO PHASE POLYMER SYSTEM MICROGRAVITY SEPARATION EXPERIMENTS c12

D. E. Brooks (British Columbia Univ.), S. B. Bamberger (Oregon Health Sciences Univ.), J. M. Harris (Alabama Univ., Huntsville), and J. VanAlstine *In* ESA Fifth European Symp. on Mater. Sci. under Microgravity. Results of Spacelab 1 Dec. 1984 p 315-318 refs Sponsored in part by NASA (For primary document see N86-10200 01-16)
(Grant USPN-HL-23374)
Avail: NTIS HC A21/MF A01 CSCL 22A

The two-phase systems that result when aqueous solutions of dextran and poly(ethylene glycol) are mixed at concentrations above a few percent are discussed. They provide useful media for the partition and isolation of macromolecules and cell subpopulations. By manipulating their composition, separations based on a variety of molecular and surface properties are achieved, including membrane hydrophobic properties, cell surface charge, and membrane antigenicity. Work on the mechanism of cell partition shows there is a randomizing, nonthermal energy present which reduces separation resolution. This stochastic energy is probably associated with hydrodynamic interactions present during separation. Because such factors should be markedly reduced in microgravity, a series of shuttle experiments to indicate approaches to increasing the resolution of the procedure are planned. Author (ESA)

N86-10248# Alabama Univ., Huntsville. Dept. of Chemistry.

APPLICATION OF THE THEORY OF OSTWALD RIPENING TO MICROGRAVITY PHASE SEPARATION EXPERIMENTS c12

J. K. Baird *In* ESA Fifth European Symp. on Mater. Sci. under Microgravity. Results of Spacelab 1 Dec. 1984 p 319-321 refs Sponsored by Alabama University (For primary document see N86-10200 01-16)
Avail: NTIS HC A21/MF A01

A heuristic derivation of the theory of Ostwald ripening which is correct up to constants of the order of unity is applied to the separation of aqueous solutions of dextran and polyethylene glycol, used in the phase partitioning of biological cells. In the absence of gravity, it is calculated that the suspension should be stable for > 1 yr. Author (ESA)

N86-10249# Deutsche Forschungs- und Versuchsanstalt fuer Luft- und Raumfahrt, Cologne (West Germany). Inst. for Space Simulation.

HOLOGRAPHIC INTERFEROMETRY NEAR GAS/LIQUID CRITICAL POINTS: GROUND-BASED STUDY OF A D1 EXPERIMENT c34

H. Klein and K. Wanders *In* ESA Fifth European Symp. on Mater. Sci. under Microgravity. Results of Spacelab 1 Dec. 1984 p 323-325 refs (For primary document see N86-10200 01-16)
Avail: NTIS HC A21/MF A01

Ground-based investigations for a Spacelab Holographic Optics Laboratory study of density distribution in three cells filled with SF6 at different near-critical densities cycled through the critical temperature are described. Results show that cooling is so fast that gravity-induced free convection can develop in the sample. As a result, temperature gradients are formed which, via thermal expansion coefficient, cause density gradients, like gravity via compressibility. At the critical point, thermal expansion coefficient and compressibility are singular; the density gradients caused by temperature gradients and gravity are large. For small cooling rates and gravitational effects, density distribution is greatly affected by temperature gradients produced from outside or by temperature gradients produced as a result of adiabatic mass rearrangements inside the sample. Author (ESA)

N86-10250# Technische Univ., Munich (West Germany). Lehrstuhl A fuer Thermodynamik.

NUCLEATE POOL BOILING IN SUBCOOLED LIQUID UNDER MICROGRAVITY: RESULTS OF TEXUS EXPERIMENTAL INVESTIGATIONS c34

M. Zell, J. Straub, and A. Weinzierl *In* ESA Fifth European Symp. on Mater. Sci. under Microgravity. Results of Spacelab 1 Dec. 1984 p 327-333 refs Sponsored by Bundesministerium fuer Forschung und Technologie (For primary document see N86-10200 01-16)
Avail: NTIS HC A21/MF A01

Experiments on subcooled nucleate pool boiling in microgravity were carried out to separate gravity driven effects on heat transfer within the boiling process. A ballistic trajectory by sounding rocket flight (TEXUS 5 and 10) achieved a gravity level of a/g = 0.0001 for 380 sec. For determination of geometrical effects on heat transport two different experimental configurations (platinum wire and flat plate) were employed. Boiling curves and bubble dynamics recorded by cinematography lead to gravity independent modelling of the boiling phenomena. The results ensure the applicability and high efficiency of nucleate pool boiling for heat exchangers in space laboratories. Author (ESA)

N86-10251# Technische Univ., Munich (West Germany). Lehrstuhl A fuer Thermodynamik.
ISOCHORIC SPECIFIC HEAT OF SULFUR HEXAFLUORIDE AT THE CRITICAL POINT. A SPACELAB EXPERIMENT FOR THE GERMAN D1-MISSION IN 1985 **c18**
K. Nitsche, J. Straub, and R. Lange *In* ESA Fifth European Symp. on Mater. Sci. under Microgravity. Results of Spacelab 1 Dec. 1984 p 335-340 refs Sponsored by Bundesministerium fuer Forschung und Technologie (For primary document see N86-10200 01-16)
Avail: NTIS HC A21/MF A01

The mechanical and functional concept of a space qualified scanning ratio calorimeter for measuring the isochoric specific heat of SF6 near the critical point is presented. The microgravity relevance of this experiment is discussed and underlined by laboratory measurements, the hydrostatic height of the specimen being varied. In 1-g reference experiments the critical exponent and parameters for cv are determined. Critical relaxation effects are taken into account by a functional time profile for the Spacelab experiment. Author (ESA)

N86-10252# Milan Univ. (Italy).
SURFACE FORCES IN CONTACTING SOLIDS **c26**
G. Poletti and D. Cambiaghi (Centrotecnica) *In* ESA Fifth European Symp. on Mater. Sci. under Microgravity. Results of Spacelab 1 Dec. 1984 p 341-346 refs (For primary document see N86-10200 01-16)
Avail: NTIS HC A21/MF A01

A dynamic experiment on surface forces in contacting solids to be performed within the TEXUS rocket program is discussed. It measures surface force and surface energy in the contact area between real bodies and assesses their dependence on mechanical, physical and geometrical parameters. A small metallic sphere impacts against a metal target and time behavior of contact force, contact time, and restitution coefficient are measured as a function of the incoming sphere velocity. Computer simulation of the experiment indicates that suitable conditions exist in which surface force effects can be measured. To fulfill these conditions the experiment must be carried out in microgravity under ultrahigh vacuum. The experimental device is discussed together with the value of the parameters chosen for the experiment. Author (ESA)

N86-10253# Lyon-1 Univ. (France).
SPACE EXPERIMENT ON THERMAL DIFFUSION. PREPARATION AND THEORETICAL ANALYSIS **c34**
J. Bert, D. Henry, P. Layani, G. Chuzeville, J. Dupuy, and B. Roux (Marseille Univ.) *In* ESA Fifth European Symp. on Mater. Sci. under Microgravity. Results of Spacelab 1 Dec. 1984 p 347-352 refs Sponsored by CNES (For primary document see N86-10200 01-16)
Avail: NTIS HC A21/MF A01

A spaceborne experiment on the Soret coefficient of a binary solution is suggested. Analysis of the experimental problems in measuring emf variations induced by thermal diffusion on a AgIxKI(1-x) system indicates a thermodiffusion cell design. A mathematical treatment of the convective problem in a case close to experimental conditions, and with two microgravity levels is outlined. The separations (normalized to 1 for pure Soret effect) are 0.46 and 0.98 for g = 0.001 and 0.0001, respectively, indicating that 0.0001 is a threshold for the separation regime (corresponding to an unperturbed separation). A cell size decrease to check the measurement validity is proposed. Author (ESA)

N86-10254# Technische Univ., Clausthal-Zellerfeld (West Germany). Inst. fuer Nichtmetallische Werkstoffe.
SHRINKING OF A GAS BUBBLE IN A GLASS MELT UNDER MICROGRAVITY CONDITIONS **c12**
V. Rosenkranz and G. H. Frischat *In* ESA Fifth European Symp. on Mater. Sci. under Microgravity. Results of Spacelab 1 Dec. 1984 p 353-357 refs Sponsored by Bundesministerium fuer Forschung und Technologie (For primary document see N86-10200 01-16)
Avail: NTIS HC A21/MF A01

Shrinking of a helium bubble in a glass melt at 1100 C was observed under microgravity for 93 min by taking photographs every minute. The diffusion coefficient was determined from the radius-time data. The bubble shrinks almost linearly with time to a residual volume of 10%, while its center remains stationary. No motion due to Marangoni convection or residual gravity is observed. The experiment ran fully automatically in a MAUS container during the STS-11 mission. Author (ESA)

N86-10255# Technische Univ., Munich (West Germany).
PHYSICAL AND CHEMICAL PROPERTIES OF A NICKEL CATALYST PROCESSED UNDER MICROGRAVITY **c12**
H. Riepl *In* ESA Fifth European Symp. on Mater. Sci. under Microgravity. Results of Spacelab 1 Dec. 1984 p 359-363 refs (For primary document see N86-10200 01-16)
Avail: NTIS HC A21/MF A01

A nickel catalyst processed under microgravity was compared with a reference sample produced on Earth. The examination methods are hydrogen peroxide decomposition, stereoselective hydrogenation with hydrazine, and physical methods. An abnormal thermal behavior of the microgravity processed catalyst is found. Kinetic data differ from normal. Electron microscopy and X-ray indicate analysis a different structure of the payload catalyst. Author (ESA)

N86-10256# Royal Inst. of Tech., Stockholm (Sweden). Dept. of Casting Metals.
A PRELIMINARY REPORT ON FLOATING ZONE EXPERIMENTS WITH GERMANIUM CRYSTALS IN A SOUNDING ROCKET **c12**
T. Carlberg *In* ESA Fifth European Symp. on Mater. Sci. under Microgravity. Results of Spacelab 1 Dec. 1984 p 367-373 refs (For primary document see N86-10200 01-16)
Avail: NTIS HC A21/MF A01

Dopant homogeneity was studied in floating zone experiments in a sounding rocket. It is found that convective mixing occurs in space and on Earth. Fluid dynamic analysis shows that Marangoni convection causes mixing in the space samples. Results from samples processed on Earth indicate stronger convection. Author (ESA)

N86-10257# Deutsche Forschungs- und Versuchsanstalt fuer Luft- und Raumfahrt, Cologne (West Germany). Inst. for Space Simulation.
TRANSPORT PROCESSES IN DIRECTIONAL SOLIDIFICATION DURING SPACE SHUTTLE FLIGHT **c12**
H. Klein, R. Naehle, and K. Wanders *In* ESA Fifth European Symp. on Mater. Sci. under Microgravity. Results of Spacelab 1 Dec. 1984 p 375-378 refs (For primary document see N86-10200 01-16)
Avail: NTIS HC A21/MF A01

The conditions for producing solid metallic dispersions from the melt under microgravity were studied during STS-7. The system CsCl with second phase inclusions (air bubbles and Pb drops) was selected as transparent model material for a solidifying metal. About 200 photographs were taken during melting and directional solidification of the CsCl matrix. Results confirm metal-like solidification of CsCl. Features identified in the photographs include solidification front distortions induced by Marangoni convection, air bubble and Pb drop motions caused by gravitationally driven convection, and particle pushing by the solidification front. Author (ESA)

N86-10258# Deutsche Forschungs- und Versuchsanstalt fuer Luft- und Raumfahrt, Cologne (West Germany). Inst. for Space Simulation.

STABILITY OF METALLIC DISPERSIONS c12

H. Otto *In* ESA Fifth European Symp. on Mater. Sci. under Microgravity. Results of Spacelab 1 Dec. 1984 p 379-388 refs (For primary document see N86-10200 01-16)

Avail: NTIS HC A21/MF A01

An experiment to investigate the stability of metallic dispersions was flown aboard STS-7 in 2 MAUS containers mounted on the carrier OSTA-2. The gallium-mercury with a miscibility gap in the liquid state was used to form the dispersed state in a sample under microgravity conditions. The sample was cooled into the miscibility gap with different cooling rates but no solidification was attempted. The appearance of the liquid/liquid dispersion of mercury droplets in a gallium matrix was recorded by X-ray transmission photography. About 100 X-ray photographs were obtained for evaluation of homogenization, precipitation, aging, and droplet growth. Author (ESA)

N86-10259# Deutsche Forschungs- und Versuchsanstalt fuer Luft- und Raumfahrt, Cologne (West Germany). Inst. for Space Simulation.

UNDERCOOLING INVESTIGATIONS ON THE EASY GLASS FORMER Pd-Cu-Si c12

D. M. Herlach, R. Willnecker, and F. Gillessen *In* ESA Fifth European Symp. on Mater. Sci. under Microgravity. Results of Spacelab 1 Dec. 1984 p 389-397 refs (For primary document see N86-10200 01-16)

Avail: NTIS HC A21/MF A01

The undercooling behavior of the easy glass former Pd77. 5Cu6Si16.5 was studied under high vacuum. Formation of the intermetallic phase Pd3Si initiates the solidification of the undercooled melt. Reducing this heterogeneous nucleation within the volume extends undercooling up to 310K enabling the formation of 2 distinct metastable phases both crystalline and nucleated at the surface. Transformation kinetics of heterogeneous nucleation is estimated and compared with homogeneous nucleation rates as determined within nucleation theory. Author (ESA)

N86-10260# Deutsche Forschungs- und Versuchsanstalt fuer Luft- und Raumfahrt, Cologne (West Germany). Inst. for Space Simulation.

CONTAINERLESS UNDERCOOLING OF Ni c12

D. M. Herlach, R. Willnecker, and F. Gillessen *In* ESA Fifth European Symp. on Mater. Sci. under Microgravity. Results of Spacelab 1 Dec. 1984 p 399-402 refs (For primary document see N86-10200 01-16)

Avail: NTIS HC A21/MF A01

An electromagnetic levitation apparatus for containerless melts and solidification of metallic systems is described. Undercooling experiments on Ni within an Al2O3 crucible and in containerless state show that eliminating heterogeneous nucleation due to container walls enables an enlargement of undercooling by a factor of 4. However, the electromagnetic levitation technique is limited to high melting point metals. A lower limit in attainable temperature of 1000K in the containerless process can be given due to the high power absorption necessary to levitate heavy samples as metals with densities of > several g/cc under 1 g conditions. The only possibility to overcome this limitation is the use of a reduced gravity environment. Author (ESA)

N86-10261*# National Aeronautics and Space Administration. Lewis Research Center, Cleveland, Ohio.

DENDRITIC SOLIDIFICATION IN A BINARY ALLOY MELT: STEADY-STATE VERSUS MORPHOLOGICAL STABILITY THEORIES c12

V. Laxmanan *In* ESA Fifth European Symp. on Mater. Sci. under Microgravity. Results of Spacelab 1 Dec. 1984 p 403-407 refs Sponsored in part by NASA (For primary document see N86-10200 01-16)

Avail: NTIS HC A21/MF A01

A model for dendritic growth in a binary alloy melt, in the presence of a positive temperature gradient in the liquid, is presented. The model describes satisfactorily the transition from a dendritic interface to a planar interface at very low and very large growth rates. A dendrite tip stability parameter is derived, strictly from steady state considerations, without resorting to a perturbation analysis. The estimates of the parameter agree with those obtained by models based on perturbation analyses. Author (ESA)

N86-10262# Commissariat a l'Energie Atomique, Grenoble (France). Lab. d'Etude de la Solidification.

CELLULAR MORPHOLOGIES IN LEAD-THALLIUM ALLOYS c12

B. Billia (Faculte des Sciences St-Jerome, Marseille), H. Jamgotchian (Faculte des Sciences St.-Jerome, Marseille), J. J. Favier, and D. Camel *In* ESA Fifth European Symp. on Mater. Sci. under Microgravity. Results of Spacelab 1 Dec. 1984 p 409-412 refs Sponsored by CNES (For primary document see N86-10200 01-16)

Avail: NTIS HC A21/MF A01

Unidirectionally grown lead-thallium alloys were chosen for a comparative study of the cellular strucutres obtained on Earth with cells solidified under microgravity during the Spacelab D1 mission. Results show that whatever the orientation of growth with respect to the gravity field, on Earth there is convection in the liquid phase. Thus only under reduced gravity is it possible to lower convection enough for transport in the melt to be essentially by diffusion. Author (ESA)

N86-10263# Ceskoslovenska Akademie Ved, Prague. Inst. of Physics.

EXPERIMENTAL FACILITY FOR MATERIALS RESEARCH IN SPACE (CSK-1) c18

C. Barta, A. Triska, J. Trinka, and L. L. Regel (Academy of Sciences, Moscow) *In* ESA Fifth European Symp. on Mater. Sci. under Microgravity. Results of Spacelab 1 Dec. 1984 p 413-415 (For primary document see N86-10200 01-16)

Avail: NTIS HC A21/MF A01

Equipment designed for studying material solidification and crystallization processes under zero-gravity conditions was developed. A series of 19 pre-programmed experiments can be performed without the direct presence of an operator. Each experiment has its own temperature and movement control and can be run in any sequence. The next series of experiments can be run after exchange of the chamber with specimens and of the cassette of the recorder tape where program and data of previous series of experiments are recorded. Author (ESA)

N86-10264*# Gelles (S. H.) Associates, Columbus, Ohio.

SPACE SHUTTLE EXPERIMENTS ON Al-In LIQUID PHASE MISCIBILITY GAP (LPMG) ALLOYS c12

S. H. Gelles and A. J. Markworth (Battelle Columbus Labs., Columbus) *In* ESA Fifth European Symp. on Mater. Sci. under Microgravity. Results of Spacelab 1 Dec. 1984 p 417-422 refs (For primary document see N86-10200 01-16)
(Contract NAS8-32952)

Avail: NTIS HC A21/MF A01

Massive phase separation observed at low-g was studied during the phase separation process while cooling through the miscibility gap under a controlled thermal gradient was investigated. The molten drops which form during the phase separation process appear to move in a direction opposite to that predicted by the theory of thermocapillary droplet motion. A second experiment utilized a plunger arrangement designed to eliminate the surface tension driven convection currents originating at a free surface. This experiment suggests that the free surface does contribute to the coalescence process but that there are other mechanisms which are more important. Author (ESA)

N86-10265# European Space Agency, Paris (France).

FIRST SPACELAB PAYLOAD (FSLP) EXPERIMENTS ON COMPOSITE MATERIALS c24

H. U. Walter *In its* Fifth European Symp. on Mater. Sci. under

Microgravity. Results of Spacelab 1 Dec. 1984 p 425-433 refs
(For primary document see N86-10200 01-16)
Avail: NTIS HC A21/MF A01

Liquid phase processing of composite materials in the First Spacelab Payload is summarized. It is shown that spinodal decomposition is not a feasible approach to produce homogeneous composites. Dispersions formed by solidifying heterogeneous mixtures prepared by mixing or formed by nucleation and growth of nuclei are only homogeneous at low volume fractions. Capillarity phenomena play a dominant role in determining the equilibrium configuration under microgravity conditions. Transport of inclusions due to Marangoni flow is observed in many systems; temperature gradients should be kept minimal during cooling and solidification. The influence of added impurities that lower interfacial tension and reduce Marangoni flow should be studied. Ostwald ripening can be studied under diffusion controlled conditions and the interaction of the solidification front with inclusions can be studied without the interference of sedimentation and buoyancy.
Author (ESA)

N86-10266# Commissariat a l'Energie Atomique, Grenoble (France). Lab. d'Etude de la Solidification.
FIRST SPACELAB PAYLOAD (FSLP) EXPERIMENTS IN METALLURGY c26
J. J. Favier *In* ESA Fifth European Symp. on Mater. Sci. under Microgravity. Results of Spacelab 1 Dec. 1984 p 435-436 (For primary document see N86-10200 01-16)
Avail: NTIS HC A21/MF A01

The First Spacelab Payload metallurgy experiments consisted of tests of metallurgical technologies in space for direct space application (e.g., vacuum brazing under microgravity); measurement of thermophysical and physical parameters in better conditions, and tests of theories; and elaboration of new or better materials (composites, emulsions, special crystals). The best results emerge from the first two groups of experiments, because the background resulting from ground-based studies is more developed in these cases.
Author (ESA)

N86-10267# Eidgenoessische Technische Hochschule, Zurich (Switzerland).
CRYSTAL GROWTH FROM SOLUTIONS AND NUCLEATION FROM THE VAPOR PHASE c12
E. Kaldis *In* ESA Fifth European Symp. on Mater. Sci. under Microgravity. Results of Spacelab 1 Dec. 1984 p 439-441 refs
(For primary document see N86-10200 01-16)
Avail: NTIS HC A21/MF A01

First Spacelab Payload studies of protein crystallization; growth of insoluble crystals by homogeneous nucleation via precipitation; and nucleation and growth experiments from the vapor phase with the model substance HgJ2 are summarized. Author (ESA)

N86-10268# Battelle Inst., Frankfurt am Main (West Germany).
LIQUIDS AND INTERFACES c34
D. Langbein *In* ESA Fifth European Symp. on Mater. Sci. under Microgravity. Results of Spacelab 1 Dec. 1984 p 443-447 (For primary document see N86-10200 01-16)
Avail: NTIS HC A21/MF A01

Spacelab Fluid Physics Module experiments are summarized. The experiments studied capillarity (menisci, drops, wetting, contact angle, coalescence); and interface convection, including bubble/drop migration and growth fronts. Author (ESA)

N86-10269# Weston Observatory, Mass.
VIBRO-ACOUSTIC FORECAST FOR SPACE SHUTTLE LAUNCHES AT VANDENBERG AFB: THE PAYLOAD CHANGEOUT ROOM AND THE ADMINISTRATION BUILDING
F. A. Crowley and E. B. Hartnett Hanscom AFB, Mass. AFGL 31 Oct. 1984 71 p
(Contract F19628-84-C-0011)
(AD-A156944; AFGL-TR-84-0322; SR-2) Avail: NTIS HC A04/MF A01 CSCL 22/4

The Payload Changeout Room and Administration Building vibro-acoustic environment is simulated for Shuttle launches at Vandenberg AFB using local responses and a source term founded on Kennedy Space Center launch pressures. Overpressure emanating from above the Launch Mount at VAFB is materially altered in form and level by site reverberations. Motion produced in simulations regularly approaches or exceeds velocity and acceleration thresholds cited for other launch support structures. Forecasts call for PCR roof displacements toward the PPR exceeding 2.0 cm for most launches. The expected maximum displacement after 5 launches is 3.5 cm. An exceedance of 5 cm can be anticipated over the facility life cycle (about 100 launches).
Author (GRA)

17 SPACECRAFT COMMUNICATIONS, COMMAND AND TRACKING

Includes telemetry; space communications networks; astronavigation; and radio blackout.

For related information see also *04 Aircraft Communications and Navigation* and *32 Communications.*

N86-10270# Technische Hogeschool, Eindhoven (Netherlands). Div. of Telecommunications.
DIGITAL TRANSMISSION EXPERIMENTS WITH THE ORBITAL TEST SATELLITE
J. Dijk, A. P. Verlijsdonk, and J. C. Arnbak Oct. 1984 50 p refs
(EUT-84-E-144; ISBN-90-6144-144-7; ISSN-0167-9708) Avail: NTIS HC A03/MF A01

Digital satellite communication experiments in the 11/14 GHz band were performed on a 115 km link by OTS (ESA). Equipment was developed and tested via a translator loop. For transmission and reception of RF signals, paraboloid antennas of 3 and 8 m diameter were used. Digital transmission tests were carried out via the OTS-A and OTS-B transponders. Spectra of the transmitted and received signals were measured for different QPSK modulation and demodulation strategies at bit rates of 4 and 8.448 Mbit/sec. Videophone and single channel per carrier digital telephony demonstrations in satellite loop operation were given. Bit error rate was measured for QPSK modulation at bitrates of 4 and 8.448 and 32 kbit/sec. Author (ESA)

18 SPACECRAFT DESIGN, TESTING AND PERFORMANCE

Includes spacecraft thermal and environmental control; and attitude control.

For life support systems see *54 Man/System Technology and Life Support.* For related information see also *05 Aircraft Design, Testing and Performance* and *39 Structural Mechanics.*

N86-10271*# Massachusetts Inst. of Tech., Cambridge. Space Systems Lab.
ROBUST FAILURE DETECTION FILTERS M.S. Thesis
Alejandro Miguel SanMartin 1 Jul. 1985 135 p refs
(Grant NAG1-126)
(NASA-CR-176232; NAS 1.26:176232; SSL-17-85) Avail: NTIS HC A07/MF A01 CSCL 22B

The robustness of detection filters applied to the detection of actuator failures on a free-free beam is analyzed. This analysis is based on computer simulation tests of the detection filters in the presence of different types of model mismatch, and on frequency response functions of the transfers corresponding to the model mismatch. The robustness of detection filters based on a model of the beam containing a large number of structural modes varied dramatically with the placement of some of the filter poles. The dynamics of these filters were very hard to analyze. The design of detection filters with a number of modes equal to the number of sensors was trivial. They can be configured to detect any number

of actuator failure events. The dynamics of these filters were very easy to analyze and their robustness properties were much improved. A change of the output transformation allowed the filter to perform satisfactorily with realistic levels of model mismatch.
Author

N86-10272*# University of Southern California, Los Angeles.
EVALUATION OF A PULSE CONTROL LAW FOR FLEXIBLE SPACECRAFT Final Technical Report, 1 Jun. 1984 - 31 May 1985
Jun. 1985 40 p
(Grant NAG1-471)
(NASA-CR-176233; NAS 1.26:176233) Avail: NTIS HC A03/MF A01 CSCL 22B

The following analytical and experimental studies were conducted: (1) A simple algorithm was developed to suppress the structural vibrations of 3-dimensional distributed parameter systems, subjected to interface motion and/or directly applied forces. The algorithm is designed to cope with structural oscillations superposed on top of rigid-body motion: a situation identical to that encountered by the SCOLE components. A significant feature of the method is that only local measurements of the structural displacements and velocities relative to the moving frame of reference are needed. (2) A numerical simulation study was conducted on a simple linear finite element model of a cantilevered plate which was subjected to test excitations consisting of impulsive base motion and of nonstationary wide-band random excitation applied at its root. In each situation, the aim was to suppress the vibrations of the plate relative to the moving base. (3) A small mechanical model resembling an aircraft wing was designed and fabricated to investigate the control algorithm under realistic laboratory conditions.
G.L.C.

N86-10273*# National Aeronautics and Space Administration, Washington, D. C.
X-RAY SATELLITE Status Report, second quarter 1985
Sep. 1985 44 p Transl. into ENGLISH of "Roentgen Satellit Statusbericht, 2. Quartal 1985" rept. DFVLR-WF2/8734 DFVLR, Cologne, 30 Jun. 1985 p 1-63 Transl. by The Corporate Word, Inc., Pittsburgh, Pa.
(Contract NASw-4006)
(NASA-TM-77923; NAS 1.15:77923; DFVLR-WF2/8734) Avail: NTIS HC A03/MF A01 CSCL 22B

An overview of the second quarter 1985 development of the X-ray satellite project is presented. It is shown that the project is proceeding according to plan and that the projected launch date of September 9, 1987 is on schedule. An overview of the work completed and underway on the systems, subsystems, payload, assembly, ground equipment and interfaces is presented. Problem areas shown include cost increases in the area of focal instrumentation, the star sensor light scattering requirements, and postponements in the data transmission subsystems.
Author

N86-10274*# Lockheed Missiles and Space Co., Palo Alto, Calif.
TEST AND EVALUATE PASSIVE ORBITAL DISCONNECT STRUTS (PODS 3)
R. T. Parmley, W. C. Henninger, S. A. Katz, and I. Spradley Aug. 1985 83 p refs
(Contract NAS2-11946)
(NASA-CR-177368; NAS 1.26:177368) Avail: NTIS HC A05/MF A01 CSCL 22B

The objectives of the Passive Orbital Disconnect Struts (PODS) test are to evaluate modal resonance of the PODS-III supports to obtain engineering data required for use of PODS-III on flight systems; determine possible performance improvements in large LO2/LH2 space applications. (1) Modal Vibration Tests. A modal resonance survey is performed on a set of six PODS-III struts assembled in a dewar simulator. The survey conditions simulate both launch and orbital loadings of the struts. The orbital load range spans a full to an empty tank. The frequencies surveyed cover the range consistent with Shuttle qualification requirements and the principal resonant modes of the strut system. (2) Benefit study. The benefit of using PODS-III supports on OTV and Space Station LO sub 2 and LH sub 2 reference tanks was compared to nondisconnect supports. Four LO sub 2 and LH sub 2 tanks were studied under various conditions: (1) holding the launch resonance at 35 Hz and varying the orbit resonance; (2) analyzing both full and emtpy tanks at launch; (3) varying orbit boundary temperaure; (4) varying the number of struts; (5) varying orbit times; and (6) using or not using vapor cooling.
Author

N86-10275# Air Force Inst. of Tech., Wright-Patterson AFB, Ohio.
NONLINEAR METHODS FOR SPACECRAFT ATTITUDE MANEUVERS Ph.D. Thesis
A. L. Batten 1985 152 p
(AD-A156956; AFIT/CI/NR-85-51D) Avail: NTIS HC A08/MF A01 CSCL 22/1

Spacecraft attitude control is described by a nonlinear dynamic mathematical model. When Euler parameters are used to define the orientation of a spacecraft with respect to an inertial frame, the model takes a certain form where the components of one factor are quadratic or higher order functions of the state vehicles. Large-angle maneuvers have traditionally been accomplished as a succession of small-angle rotations from a sequence of defined operating points about which the model is linearized. Alternatively, a sequence of single axis rotations are performed. These processes are computationally burdensome and are unable to produce fast multi-axial rotational maneuvers.
GRA

N86-10208# Deutsche Forschungs- und Versuchsanstalt fuer Luft- und Raumfahrt, Cologne (West Germany). Inst. fuer Raumsimulation.
THE ISOTHERMAL HEATING FACILITY
K. Wittmann *In* ESA Fifth European Symp. on Mater. Sci. under Microgravity. Results of Spacelab 1 Dec. 1984 p 49-54 refs
(For primary document see N86-10200 01-16)
Avail: NTIS HC A21/MF A01

N86-10217# Centre National d'Etudes Spatiales, Toulouse (France).
GRADIENT HEATING FACILITY BEHAVIOR
G. Cambon, B. Castets, O. Boutemy, J. P. Gicquel, R. Aubron, M. Boddaert, and J. Benoit *In* ESA Fifth European Symp. on Mater. Sci. under Microgravity. Results of Spacelab 1 Dec. 1984 p 115-119 refs (For primary document see N86-10200 01-16)
Avail: NTIS HC A21/MF A01

N86-10223# Freiburg Univ. (West Germany). Inst. fuer Kristallographisches.
THE MIRROR HEATING FACILITY: PERFORMANCE AND EXPERIENCES
R. Nitsche *In* ESA Fifth European Symp. on Mater. Sci. under Microgravity. Results of Spacelab 1 Dec. 1984 p 155-156 refs
(For primary document see N86-10200 01-16)
Avail: NTIS HC A21/MF A01

N86-10251# Technische Univ., Munich (West Germany). Lehrstuhl A fuer Thermodynamik.
ISOCHORIC SPECIFIC HEAT OF SULFUR HEXAFLUORIDE AT THE CRITICAL POINT. A SPACELAB EXPERIMENT FOR THE GERMAN D1-MISSION IN 1985
K. Nitsche, J. Straub, and R. Lange *In* ESA Fifth European Symp. on Mater. Sci. under Microgravity. Results of Spacelab 1 Dec. 1984 p 335-340 refs Sponsored by Bundesministerium fuer Forschung und Technologie (For primary document see N86-10200 01-16)
Avail: NTIS HC A21/MF A01

N86-10263# Ceskoslovenska Akademie Ved, Prague. Inst. of Physics.
EXPERIMENTAL FACILITY FOR MATERIALS RESEARCH IN SPACE (CSK-1)
C. Barta, A. Triska, J. Trinka, and L. L. Regel (Academy of Sciences, Moscow) *In* ESA Fifth European Symp. on Mater. Sci. under Microgravity. Results of Spacelab 1 Dec. 1984 p 413-415 (For primary document see N86-10200 01-16)
Avail: NTIS HC A21/MF A01

19 SPACECRAFT INSTRUMENTATION

For related information see also *06 Aircraft Instrumentation* and *35 Instrumentation and Photography.*

N86-10276# Defence Research Establishment, Ottawa. (Ontario).
SARSAT LUC (LOCAL USER TERMINAL) TO CMCC (CANADIAN MISSION CONTROL CENTRE) ALERT DATA INTERFACE: A CRITICAL REVIEW
W. R. McPherson and S. Y. Slinn Dec. 1984 47 p
(AD-A156881; DREO-TN-84-24) Avail: NTIS HC A03/MF A01 CSCL 17/2

The transfer of beacon alert data from the SARSAT Local User Terminal (LUT) to the Canadian Mission Control Center (CMCC) has shortcomings. On the one hand, the LUT provides alert data quality indicators which during the SARSAT Demonstration and Evaluation have been demonstrated to be inadequate, while on the other hand, it retains data descriptors which are required by operational personnel. The purpose of this report is to critically review data available at the LUT, determine its operational utility and outline a definition of transfer from the LUT to the CMCC. The potential impact of implementing this definition will be assessed with the aid of historical data. The subject work is documented in terms of the background to the problem, an outline of approach and analytical tools developed, validation of the approach, summary comments and recommendations. GRA

20 SPACECRAFT PROPULSION AND POWER

Includes main propulsion systems and components, e.g., rocket engines; and spacecraft auxiliary power sources.

For related information see also *07 Aircraft Propulsion, 28 Propellants and Fuels,* and *44 Energy Production and Conversion.*

N86-10277 Department of the Air Force, Washington, D.C.
SMALL CARTRIDGE HEATER Patent
F. L. Merritt and C. H. Taylor, inventors (to Air Force) Issued 9 Apr. 1985 5 p Supersedes AD-D010971
(AD-D011784; US-Patent-4,510,377; US-Patent-Appl-SN-577391) Avail: US Patent and Trademark Office CSCL 21/8

A cylindrical core of a ceramic such as alumina (Al2O3) has grooves in the form of a double lead thread. A coil of Nichrome V is placed in the grooves, starting in one lead of the thread and returning in the other. A coil of Nichrome V is placed in the grooves, starting in one lead of the thread and returning in the other. A split ring of a ceramic such as beryllia surrounds the core. The heater is enclosed in a housing of a metal such as Inconel 600. The entire cartridge is only one inch long and 3/16 inch diameter. It is used as a catalyst bed heater for a satellite thruster. GRA

N86-10278*# National Aeronautics and Space Administration. Marshall Space Flight Center, Huntsville, Ala.
ANALYTICAL INVESTIGATION OF SOLID ROCKET NOZZLE FAILURE
Kenneth E. McCoy and J. Hester Aug. 1985 24 p ref
(NASA-TM-86513; NAS 1.15:86513) Avail: NTIS HC A02/MF A01 CSCL 21H

On April 5, 1983, an Inertial Upper Stage (IUS) spacecraft experienced loss of control during the burn of the second of two solid rocket motors. The anomaly investigation showed the cause to be a malfunction of the solid rocket motor. This paper presents a description of the IUS system, a failure analysis summary, an account of the thermal testing and computer modeling done at Marshall Space Flight Center, a comparison of analysis results with thermal data obtained from motor static tests, and describes some of the design enhancement incorporated to prevent recurrence of the anomaly. Author

N86-10279*# National Aeronautics and Space Administration. Lewis Research Center, Cleveland, Ohio.
COMPATIBILITY OF GRAIN-STABILIZED PLATINUM WITH CANDIDATE PROPELLANTS FOR RESISTOJETS
Margaret V. Whalen and Stanley P. Grisnik [1985] 21 p refs Presented at the 18th Intern. Elec. Propulsion Conf., Alexandria, Va., 30 Sep. - 2 Oct. 1985; cosponsored by AIAA, DGLR and JSASS
(NASA-TM-87118; E-2725; NAS 1.15:87118; AIAA-85-2014) Avail: NTIS HC A02/MF A01 CSCL 21I

Resistojets are candidates for space station auxiliary propulsion, and should be characterized by both long life and multipropellant operations, requirements limited by available materials. Grain stabilized platinum is examined for use as a resistojet thruster material. Use of platinum in other applications indicates it can be used at moderately high temperatures for extended periods of time. Past results indicate that grain-stabilized platinum should be sufficiently inert in candidate propellant environments. Therefore, compatibility of platinum-yttria (P/Y2O3) and platinum-zirconia (Pt/ZrO2) with carbon dioxide, methane, hydrogen and ammonia is examined. A series of 1000 hr tests in CO2, H2, and NH3 is conducted at 1400 C and a series of 1000 hr tests in CH4 is conducted at about 500 C. Scanning electron microscopy, Auger electron spectroscopy and depth profiling analysis are then used to determine the effects of propellants on the material surface, to evaluate possible material contamination and to evaluate grain growth. The results indicate that there is carbon deposition on the surface of the Pt/Y2O3 and Pt/ZrO2 in both the CO2 and CH4 environments. In the H2 environment, the Pt/Y2O3 and Pt/ZrO2 specimen surfaces are roughened. After exposure to the NH3 environment, the Pt/Y2O3 and Pt/ZrO2 are roughened and pitted over the entire heated area with some pitted areas along the grain boundaries. SEM photos show grain growth in cross-sectional views of all the Pt/Y2O3 samples and the Pt/ZrO2 samples, except that tested in methane. Mass loss measurements indicate that Pt/Y2O3 and Pt/ZrO2 would last in excess of 200,000 hr in each propellant environment. However, in NH3 both Pt/Y2O3 and Pt/ZrO2 are severely pitted, with voids up to 50 percent into the material. Pt/Y2O3 and Pt/ZrO2 are not recommended for high temperature service in NH3. Author

N86-10280*# National Aeronautics and Space Administration. Lewis Research Center, Cleveland, Ohio.
RAPID EVALUATION OF ION THRUSTER LIFETIME USING OPTICAL EMISSION SPECTROSCOPY
Brian A. Rock (Arizona State Univ.), Maris A. Mantenieks (Arizona State Univ.), and Michael L. Parsons 1985 47 p refs Presented at the 18th Intern. Elec. Propulsion Conf., Alexandria, Va., 30 Sep. - 2 Oct. 1985; cosponsored by AIAA, JSASS, and DGLR
(NASA-TM-87103; E-2700; NAS 1.15:87103; AIAA-85-2011) Avail: NTIS HC A03/MF A01 CSCL 21H

A major life-limiting phenomenon of electric thrusters is the sputter erosion of discharge chamber components. Thrusters for space propulsion are required to operate for extended periods of time, usually in excess of 10,000 hr. Lengthy and very costly life-tests in high-vacuum facilities have been required in the past to determine the erosion rates of thruster components. Alternative methods for determining erosion rates which can be performed in relatively short periods of time at considerably lower costs are studied. An attempt to relate optical emission intensity from an ion bombarded surface (screen grid) to the sputtering rate of that surface is made. The model used a kinetic steady-state (KSS) approach, balancing the rates of population and depopulation of ten low-lying excited states of the sputtered molybdenum atom (MoI) with those of the ground state to relate the spectral intensities of the various transitions of the MoI to the population densities. Once this is accomplished, the population density can be related to the sputtering rate of the target. Radiative and collisional modes of excitation and decay are considered. Since actual data has not been published for MoI excitation rate and decay constants, semiempirical equations are used. The calculated sputtering rate and intensity is compared to the measured intensity and sputtering rates of the 8 and 30 cm ion thrusters. Author

N86-10281*# National Aeronautics and Space Administration. Lewis Research Center, Cleveland, Ohio.
EXPERIMENTAL PERFORMANCE OF A 1-KILOWATT ARCJET THRUSTER
Shigeo Nakanishi 1985 30 p refs
(NASA-TM-87131; E-2744; NAS 1.15:87131) Avail: NTIS HC A03/MF A01 CSCL 21C

A formerly unused cathode and anode/nozzle assembly from a flight model arcjet was tested with nitrogen, hydrogen, and nitrogen-hydrogen mixture simulating ammonia decomposition products at arc power levels from about 300 to 950 W. Two different power sources and two nozzle configurations were tested at low back-ground pressures to exclude facility effects. Increased nozzle expansion ratio improved cold flow nozzle efficiency from 0.8 to 0.9. Hydrogen thrust efficiency of 0.26 at 872 sec specific impulse matched some 1964 performance on a similar device. Simulated ammonia thrust efficiency was 0.31 at 422 sec. Spontaneously occurring voltage mode changes at constant arc current could be partially stabilized with appropriate power source characteristics. In the higher voltage mode specific impulse was higher, but thrust efficiency changed only slightly from that of the lower voltage mode. Sustained tests of up to 2 hr duration exhibited no apparent performance degradation with time. Author

N86-10005# Air Force Systems Command, Wright-Patterson AFB, Ohio. Foreign Technology Div.
THEORETICAL SPECIFIC IMPULSE FOR TWO-PHASE FLOW IN NOZZLE OF ROCKET-RAMJET ENGINE: A SIMPLE ESTIMATION METHOD
Bi Shiguan (China Precision Machinery Co.) *In its* Acta Aeron. et Astronautica Sinica (FTD-ID(RS)T-1120-84) 4 Oct. 1984 p 53-60 refs Transl. into ENGLISH from Hangkong Xuebao (China), v. 4, no. 4, 1984 p 101-104 (For primary document see N86-10001 01-01)
Avail: NTIS HC A04/MF A01 CSCL 21/8

23 CHEMISTRY AND MATERIALS (GENERAL)

Includes biochemistry and organic chemistry.

N86-10282 Department of the Army, Washington, D. C.
RECOVERY OF ALCOHOL FROM A FERMENTATION SOURCE BY SEPARATION RATHER THAN DISTILLATION Patent
D. C. Sayles, inventor (to Army) Issued 2 Apr. 1985 5 p
(AD-D011782; US-Patent-4,508,929; US-Patent-Appl-SN-455362; US-Patent-Class-568-923) Avail: US Patent and Trademark Office CSCL 07/3

Ethanol is recovered from fermentation products by a countercurrent extraction process which employs diethyl ether as the extraction process which employs diethyl ether as the extraction solvent to form a diethyl ether-ethanol mixture. The ethanol is salted out by adding calcium chloride to the mixture, and the diethyl ether layer is separated and recycled. The calcium chloride in ethanol solution is removed by adding sodium carbonate to form the solids calcium carbonate and sodium chloride which are removed by filtration. The ethanol is recovered as the filtrate. Author (GRA)

N86-10283# Columbia Univ., New York. Dept. of Chemistry.
A PROCEDURE IDENTIFYING A POLYACETYLENE INITIATOR OF OLEFIN METATHESIS. THE REACTIVITIES OF METAL-CARBENES TOWARD ALKENES AND ALKYNES
C. C. Han and T. J. Katz 10 Jul. 1985 63 p
(Contract N00014-79-C-0683)
(AD-A156997; AD-E950724; TR-11) Avail: NTIS HC A04/MF A01 CSCL 07/3

When phenylacetylene plus tungsten hexachloride initiate the metathesis of cyclopentene, poly(phenylacetylene) is found attached to the resulting polypentenamer chains. The average amount of this poly(phenylacetylene) does not vary as the growth of the polypentenamer chains is checked by added diphenylacetylene, showing it to be present as a block at their start. The implication is that the metathesis is initiated by the growning acetylene writing with the olefin, strong evidence for the hypothesis that the acetylene polymerizatrion is propagated by metal-carbenes. The variations that occur in the length of the chains and the amount of poly(phenylacetylene) attached to the average chain as the acetylene concentration is varied are analyzed for the underlying kinetic parameters. The stabilized metal-carbenes propagating the phenylacetylene polymerization react 3,000 times more quickly with phenylacetylene than with cyclopentene, whereas the less stabilized metal-carbenes propagating the cyclopentene, metathesis select 17-fold in the opposite direction. Diphenylacetylene is 26 times more effective than phenylacetylene in quenching the metathesis, and 2.4 times more effective than phenylmethylacetylene. The key to the experiments is the observation that diphenylacetylene in minute amounts quenches metathesis but does not initiate the reaction. GRA

24 COMPOSITE MATERIALS

Includes laminates.

N86-10284 Yale Univ., New Haven, Conn.
THE MECHANICS OF DELAMINATION IN COMPOSITE MATERIALS Ph.D. Thesis
William Joseph Bottega 1984 114 p
Avail: Univ. Microfilms Order No. DA8509687

A growth law is derived which governs the propagation of an arbitrary shaped delamination embedded in a layered plate, where the plate is of an arbitrary shape as well and is considered to be subjected to edge loading. The phenomenon of delamination buckling and growth is then analyzed to a compressively loaded two layer circular plate containing an initial penny shaped delamination and for a compressively loaded two layer rectangular plate containing an initial thru delamination. An asymptotic technique is used for the postbuckling analysis and the influence of imperfections is also examined. The dynamics of delamination growth in layered plates as a result of delamination buckling is studied in the context of the aforementioned circular plate problem. The interaction of delamination buckling and normal impact is modeled through the application of a uniform transverse tension pulse, simulating the effect of wave front passing through the layer interface, in conjunction with the radial loading. The interfacial response of multilayered plates subject to a time dependent normal point load is found by way of an eigenfunction expansion technique. Dissert. Abstr.

N86-10285 Delaware Univ., Newark.
MECHANICS OF COATED FIBER COMPOSITES Ph.D. Thesis
Yozo Mikata 1984 159 p
Avail: Univ. Microfilms Order No. DA8511217

The mechanics of coated fiber composites were studied. Two types of coated fiber composite are considered: coated short fiber composite, which is modeled as an infinite medium containing two confocal spheroidal inhomogeneities, and coated continuous fiber composite, which is modeled as an infinite medium containing three concentric long circular cylinders. Interaction of fibers is included in the formulation for coated continuous fiber composites, while it is not for coated short fiber composites. Stress fields are obtained for both types of coated fiber composites under thermomechanical loadings. A possibility of cracking in coating layer is discussed. Dissert. Abstr.

N86-10286 Illinois Univ., Chicago.
THREE-DIMENSIONAL STRESS SINGULARITIES IN ANISOTROPIC MATERIALS AND COMPOSITES Ph.D. Thesis
Nihal Somaratna 1985 96 p
Avail: Univ. Microfilms Order No. DA8511281

The simplified case of a transversely isotropic material bounded by one or two axisymmetric conical boundaries is studied analytically. Eigenequations for delta are obtained in terms of Legendre functions of the first and second kind. These results are subsequently used as benchmark tests for the more general numerical method proposed. A finite element scheme is developed for the more general case of a notch/inclusion of an arbitrary shape in a completely anisotropic material. The method is tested against some known results for the stress singularity at the tip of a quarter infinite crack in an isotropic half space and also against the results for the axisymmetric conical notch/inclusion in a transversely isotropic material obtained. Excellent agreement is evident. Then the finite element scheme is used to study the possible existence of stress singularities at 3-d corners in anisotropic materials and also at the free surface tip of a crack normal to the interface of a laminated composite. Dissert. Abstr.

N86-10287 Georgia Inst. of Tech., Atlanta.
THE EFFECT OF DEBOND GROWTH ON CRACK PROPAGATION IN COMPOSITE PLATES REINFORCED WITH ADHESIVELY BONDED COMPOSITE STRINGERS Ph.D. Thesis
Catherine Ann Bigelow 1984 153 p
Avail: Univ. Microfilms Order No. DA8510952

A general solution for the problem of the adhesively bonded stringer was developed. A fundamental analysis was used, assuming that the adherends were in a state of plane stress and the adhesive was in pure shear. Using Green's functions and the complex variable theory of elasticity developed by Lekhnitski, a set of integral equations were solved numerically to produce the shear stress distribution in the adhesive layer. Using these adhesive stresses, equations for the crack tip stress intensity factors were also found. The solution of the integral equations assuming a linear adhesive was presented. The most critical parameter for reducing the stress intensity factors was found to be the distance from the centerline of the crack to the edge of the stringer. The effect of debonding in the adhesive on the stress intensity factors was also examined. In the cases studied, adding a nonlinear adhesive to the debonding decreased the stress intensity factors relative to the linear solution and increased the stress levels necessary to cause debonding. Dissert. Abstr.

N86-10288 Case Western Reserve Univ., Cleveland, Ohio.
FUNDAMENTAL STUDIES OF LOW VELOCITY IMPACT RESISTANCE OF GRAPHITE FIBER REINFORCED POLYMER MATRIX COMPOSITES Ph.D. Thesis
Kenneth James Bowles 1985 255 p
Avail: Univ. Microfilms Order No. DA8510096

A study was conducted to relate the impact resistance of graphite fiber reinforced composites with matrix properties through gaining an understanding of the basic mechanics involved in the deformation and fracture process, and the effect of the polymer matrix structure on these mechanisms. It was found that the resin matrix structure influences the composite impact resistance in at least two ways. The integration of flexibilizers into the polymer chain structure tends to reduce the T sub g and the mechanical properties of the polymer. The reduction in the mechanical properties of the matrix does not enhance the composite impact resistance because it allows matrix controlled failure to initiate impact damage. It was found that when the instrumented drop-weight impact tester is used as a means for assessing resin toughness, the resin toughness is enhanced by the ability of the clamped specimen to deflect enough to produce sufficient membrane action to support a significant amount of the load. The results of this study indicate that crossplied composite impact resistance is very much dependent on the matrix mechanical properties. Dissert. Abstr.

N86-10289 Department of the Air Force, Washington, D.C.
EROSION-RESISTANT NOSETIP CONSTRUCTION Patent
A. R. Taverna and W. S. Thompson, inventors (to Air Force) Issued 7 May 1985 6 p Supersedes AD-D011346; N85-15797
(AD-D011787; US-Patent-4,515,847; US-Patent-Appl-SN-643140; US-Patent-Class-428-107) Avail: US Patent and Trademark Office CSCL 22/2

A pierced fabric carbon-carbon structure is selectively loaded with a particulate material to provide resistance to erosion. Author (GRA)

N86-10290*# National Aeronautics and Space Administration. Lewis Research Center, Cleveland, Ohio.
PROGRESSIVE DAMAGE, FRACTURE PREDICTIONS AND POST MORTEM CORRELATIONS FOR FIBER COMPOSITES
1985 21 p refs Presented at Intern. Conf.: Post Failure Anal. Tech. Fiber Reinforced Composites, Dayton, Ohio, 1-3 Jul. 1985; sponsored by Air Force
(NASA-TM-87101; E-2695; NAS 1.15:87101) Avail: NTIS HC A02/MF A01 CSCL 11D

Lewis Research Center is involved in the development of computational mechanics methods for predicting the structural behavior and response of composite structures. In conjunction with the analytical methods development, experimental programs including post failure examination are conducted to study various factors affecting composite fracture such as laminate thickness effects, ply configuration, and notch sensitivity. Results indicate that the analytical capabilities incorporated in the CODSTRAN computer code are effective in predicting the progressive damage and fracture of composite structures. In addition, the results being generated are establishing a data base which will aid in the characterization of composite fracture. Author

N86-10291# Michigan Univ., Ann Arbor. Dept. of Materials and Metallurgical Engineering.
PRELIMINARY REPORTS, MEMORANDA AND TECHNICAL NOTES OF THE MATERIALS RESEARCH COUNCIL SUMMER CONFERENCE, LA JOLLA, CALIFORNIA
M. J. Sinnott Jul. 1984 242 p Conf. held at La Jolla, Calif.
(Contract MDA903-84-K-0232; DARPA Order 4000)
(AD-A156776) Avail: NTIS HC A11/MF A01 CSCL 11/4

Papers provided for workshops on the following topics include: Bulk Crystal Growth of Electronic Materials - Strengthening and structure of semiconducting crystals, Formation of new phases from systems that are not in metastable Equilibrium, A mechanism for the reduction in dislocation Density in as-grown GaAs crystals by Indium additions, and Analysis of the potential of a reduced gravity environment for growth of electronic materials; Structure and Properties of Solid Interfaces Relevant to Electronic Materials - Electronic properties of interfaces, Organometallic chemical vapor deposition, Edge cracking of multilayer strained superlattices, Damage of strained superlattices by dislocation injection, and Epitaxial methods for preparing thin semiconducting layers; Integration of Solid State Electronics and Chemical and Biological Systems; Mitigation of Coupling and Shock Waves from Intense Single Pulse Lasers; Optical Interconnects in Computer Networks - Interconnections and VLSI; Fracture Toughness of Advanced Fibrous Composites -Metal matrix composites, Matrix cracking in ceramic-matrix composites, and Shear strength of brittle matrix fiber composites. GRA

N86-10292# Dayton Univ., Ohio.
PROCESS MODELS FOR 3D COMPOSITES Interim Technical Report, 1 Sep. 1981 - 1 Dec. 1983
S. R. Soni and N. J. Pagano Wright-Patterson AFB, Ohio AFWAL Mar. 1985 148 p
(Contract F33615-81-C-5056)
(AD-A156889; AFWAL-TR-85-4002) Avail: NTIS HC A07/MF A01 CSCL 11/4

This work deals with the process environment modeling of carbon-carbon composites. Capabilities of the process environment model (PEM) computer code developed by Science Application Incorporated, California, have been discussed. Users instructions for PEM code have been given. Illustrative examples for different phases of processing of carbon-carbon composites are presented. Close form analytical solutions for impregnation analysis have been derived. A comparison between close from solution results and PEM results has been given. The primary purpose of the PEM is to predict the pressure and temperature environment for the mechanical model. GRA

N86-10265# European Space Agency, Paris (France).
FIRST SPACELAB PAYLOAD (FSLP) EXPERIMENTS ON COMPOSITE MATERIALS
H. U. Walter *In its* Fifth European Symp. on Mater. Sci. under Microgravity. Results of Spacelab 1 Dec. 1984 p 425-433 refs (For primary document see N86-10200 01-16)
Avail: NTIS HC A21/MF A01

N86-10389*# Jet Propulsion Lab., California Inst. of Tech., Pasadena. Ground Antennas and Facilities Engineering Section.
LOAD-DEFLECTION TESTS AND COMPUTER ANALYSES OF A HIGH-PRECISION ADHESIVE-BONDED ANTENNA REFLECTOR PANEL
C. T. Chian and R. Levy *In its* The Telecommun. and Data Acquisition Progr. Rept. 15 Aug. 1985 p 68-81 (For primary document see N86-10382 01-32)
Avail: NTIS HC A10/MF A01 CSCL 11D

25 INORGANIC AND PHYSICAL CHEMISTRY

Includes chemical analysis, e.g., chromatography; combustion theory; electrochemistry; and photochemistry.

For related information see also *77 Thermodynamics and Statistical Physics.*

N86-10293*# National Aeronautics and Space Administration, Washington, D. C.
DETERMINATION OF THERMOPHYSICAL CHARACTERISTICS OF SOLID MATERIALS BY ELECTRICAL MODELLING OF THE SOLUTIONS TO THE INVERSE PROBLEMS IN NONSTEADY HEAT CONDUCTION
L. A. Kozdoba and F. A. Krivoshei Sep. 1985 7 p refs Transl. into ENGLISH from "Thermophysical Properties of Solid Materials" Moscow, Izdatelstvo Nauk, 1973 p 28-31 Original language document announced in IAA as A74-45335 Transl. by Kanner (Leo) Associates, Redwood City, Calif.
(Contract NASw-4005)
(NASA-TM-77907; NAS 1.15:77907) Avail: NTIS HC A02/MF A01 CSCL 07D

The solution of the inverse problem of nonsteady heat conduction is discussed, based on finding the coefficient of the heat conduction and the coefficient of specific volumetric heat capacity. These findings are included in the equation used for the electrical model of this phenomenon. IAA

N86-10294# Defence Research Establishment, Ottawa. (Ontario).
DESIGN AND CALIBRATION OF A FLAT-FLAME BURNER USING LINE REVERSAL TECHNIQUES
D. R. Snelling and M. Fischer Apr. 1985 40 p Original contains color illustrations
(AD-A156724; DREO-TN-85-4) Avail: NTIS HC A03/MF A01 CSCL 21/2

A premixed methane/air flat-flame burner is described. The burner was designed to have a central flame which can be seeded with sodium, and an annular guard flame which ensured a flat temperature profile in the seeded region. The burner produced a well behaved flat flame for linear gas velocities of 20 to 30 cm/s and air to fuel ratios within 15% of stoichiometric. The temperature distribution in the flame was measured for a range of operating conditions using the sodium line-reversal technique. The temperatures measured were within the range 2000 to 2100 K, slightly lower than the adiabatic methane/air flame temperature. This burner will be used as a calibration tool in the development of CARS (Coherent Antistokes Raman Spectroscopy). GRA

N86-10295# National Bureau of Standards, Boulder, Colo. Time and Frequency Div.
COOLED ION FREQUENCY STANDARD Annual Summary Report, FY 1985
D. J. Wineland 1 Jul. 1985 21 p
(Contract N00014-85-F-0004; RR0-1103)
(AD-A156813) Avail: NTIS HC A02/MF A01 CSCL 04/2

The purpose of this work is to develop techniques to overcome the fundamental limits of present frequency standards,the second and residual first-order Doppler shifts. To this end we study suitable frequency reference transitions in ions which are stored on electromagnetic traps and cooled by radiation pressure to > 1K. GRA

N86-10296# California Univ., Livermore. Lawrence Livermore Lab.
NEW DIRECTIONS IN CHEMICAL ANALYSIS
T. B. Hirschfeld May 1985 35 p Presented at the IUCCP Symp., College Station, Tex., 1 Apr. 1985
(Contract W-7405-eng-48)
(DE85-012930; UCRL-92731; CONF-8504138-1) Avail: NTIS HC A03/MF A01

The last twenty years have seen a steady increase in the work load of analytical chemistry. A number of procedures have evolved in the analytical laboratory to deal with this increase in work load. By far, the most important one of these is the preponderance of lab automation. Because of the entrance of computers in the laboratories, we can achieve productivity increases that would have been inconceivable without them. The second new procedure that has evolved in analytical chemistry to cope with the work load increase has been the incorporation of systems engineering as a part of the analytical laboratory practice. This paper discusses in depth the role of personal computers and systems engineering in analytical chemistry. DOE

N86-10297# Pacific Northwest Lab., Richland, Wash.
RAPID ANALYSIS USING CAPILLARY SUPERCRITICAL FLUID CHROMATOGRAPHY
B. W. Wright and R. D. Smith Mar. 1985 10 p Presented at the 6th Intern. Symp. on Capillary Chromatography, Riva del Garda, Italy, 16 May 1985
(Contract DE-AC06-76RL-01830)
(DE85-012460; PNL-SA-12698; CONF-8505151-1) Avail: NTIS HC A02/MF A01

Capillary supercritical fluid chromatography (SFC) is proving to be a viable and useful separation method for thermally labile and nonvolatile materials. As with other capillary chromatographic techniques, very fast separations can be accomplished by sacrificing total efficiency and optimizing the conditions for rapid analysis. This is achieved using short, small-bore capillary columns, increased mobile phase linear velocities and very fast pressure programming rates. These principles are demonstrated for the rapid separation of selected component systems. DOE

N86-10298# Sandia Labs., Albuquerque, N. Mex.
THEORETICAL COMPARISON OF CLASSICAL (K-MATRIX) AND INVERSE (P-MATRIX) LEAST-SQUARES METHODS FOR QUANTITATIVE INFRARED SPECTROSCOPY
D. M. Haaland 1985 9 p Presented at the Intern. Conf. on Fourier and Computerized Infrared Spectry., Ottawa, 24 Jun. 1985
(Contract DE-AC04-76DP-00789)
(DE85-012827; SAND-85-02980; CONF-8506118-1) Avail: NTIS HC A02/MF A01

Both classical and inverse least-squares methods have been applied to the quantitative IR spectra analysis of multicomponent samples. The two methods are presented and compared in this paper. The classical method is capable of higher precision and accuracy since it can use all of the data in a spectrum. Its ability to obtain full-spectrum residuals provides methods for identifying problems in the spectral data. The inverse method has the potential advantage that it can be applied even if only one component in the sample is known. DOE

N86-10299# Pacific Northwest Lab., Richland, Wash.
DETERMINING A PHYSICALLY APPROPRIATE NEUTRON SPECTRUM FROM MULTISPHERE DATA
R. I. Scherpelz and I. W. Brackenbush Apr. 1985 22 p Presented at the Health Phys. Soc. Ann. Meeting, Chicago, 26 May 1985

(Contract DE-AC06-76RL-01830)
(DE85-013045; PNL-SA-12888; CONF-8505103-3) Avail: NTIS HC A02/MF A01

The multisphere (or Bonner Sphere) spectrometer system is widely used for the characterization of neutron radiation fields due to its good sensitivity over a wide range of energies. The multisphere data must first be processed by an unfolding code to determine the neutron parameters, and this code must select the spectrum from an infinite number of mathematically correct possibilities. Recent studies heve shown that the neutron spectra determined by an unfolding code can be influenced by features of the code such as the choice of initial spectra or the method of smoothing. This study further explores the characteristics of a multisphere measurement and unfolding code that can influence the calculated spectrum and its approximation of a physical realistic neutron spectrum. The use of data from another spectrometer system for setting the initial spectrum is shown to be a very promising technique for generating physically meaningful results. Other factors discussed in this study include the detector response functions and the convergence criteria and duration of iteration. The study shows that the determination of a physically appropriate neutron spectrum can only be accomplished with proper attention to these factors. DOE

N86-10300# New Mexico Univ., Albuquerque.
CATALYTIC ACTIVITY OF SHOCK MODIFIED ZnO FOR CO OXIDATION AND METHANOL SYNTHESIS
F. L. Williams, Y. K. Lee, B. Morosin, and R. A. Graham 22 Jul. 1985 8 p refs Presented at Am. Phys. Soc. Topical Conf. on Shock Waves in Condensed Matter, Spokane, Wash., 22 Jul. 1985
(Contract DE-AC04-76DP-00789)
(DE85-014704; SAND-85-0721C; CONF-850736-19) Avail: NTIS HC A02/MF A01

Alteration of the catalytic activity of inorganic powders by dynamic shock compression has been reported in the literature. Previous work on the effect of shock compression on ZnO catalysis revealed an enhanced activity for CO oxidation that decreased during the rate measurements. Steady-state rate measurements of CO oxidation and methanol synthesis over shock compressed ZnO powers under reaction conditions believed to be transport limitation free is reported. The best explanation of the enhanced catalytic activity of ZnO powders is that shock compression modified the ability of the particle surface to form active centers under reaction conditions. The shock compression probably does not itself put long lived active centers at the surface or major changes in activation energies or selectivity would be observed. However, if local strain or defects were induced in the surface, it would be possible for atomic rearrangement of the surface to result in additional sites like those on unshocked ZnO. In that way, the catalytic chemistry of all the powders would only be different in the number of sites available for catalysis. The minima may then result from a surface distortion in the unshocked powder that is released by a relatively mild shock compression. DOE

N86-10301# Exxon Research and Engineering Co., Annandale, N.J.
LASER RAMAN SPECTROSCOPY STUDY OF THE ZINC AND BROMIDE ION COMPLEX EQUILIBRIUM IN ZINC/BROMINE BATTERY ELECTROLYTES
P. G. Grimes and J. A. Larrabee 1985 5 p Presented at the 168th Meeting of the Electrochem. Soc., Las Vegas, Nev., 13 Oct. 1985
(Contract DE-AC04-76DP-00789)
(DE85-011820; SAND-85-71960; CONF-851048-2) Avail: NTIS HC A02/MF A01

Laser Raman spectroscopy is used to study the zinc and bromide ion complex equilibrium in zinc bromine battery model electrolytes. Solutions of zinc bromide with added KBr, HBr and N-methyl, N-ethyl morpholinium (MEM) bromide are examined and compared. Solutions studied ranged from 1 to 3 molar in zinc and from 2.5 to 8 molar in bromide. A typical Raman spectrum of a zinc bromide solution is shown. Each of the zinc species is identified, Zn(++) (aq), ZnBr(+), ZnBr2 (aq), ZnBr3(-) and ZnBr4(2-). By the use of peak heights or deconvolution/integration along with published Raman cross sections, the amount of each zinc species could be quantitatively determined. The addition of bromide ions to the zinc bromide solutions will shift the equilibrium toward higher bromide complexes. The added cations will influence the shifts. It is noted that the conductivity of the electrolyte decreases when the quaternary ammonium ions are present compared to cations such as potassium or hydrogen. Significantly more free zinc is present in zinc bromide solutions with added KBr than with either MEMBr or HBr. Shifts are also noted with the other zinc ion containing species. It appears that the quaternary ammonium ions and possibly the pH could have a stabilizing effect on zinc bromide complex ion formation. DOE

N86-10302# National Bureau of Standards, Washington, D.C. Center for Fire Research.
SELF-HEATING TO IGNITION MEASUREMENTS AND COMPUTATION OF CRITICAL SIZE FOR SOLAR ENERGY COLLECTOR MATERIALS Final Report
J. J. Loftus Mar. 1985 37 p
(Contract DE-AT01-77DP-70032)
(DE85-011449; NBSIR-85-3122) Avail: NTIS HC A03/MF A01

Kinetic constants of the self-heating reaction are determined for plywood, a retardant treated plywood, and eight samples of polyurethane foam representing possibly two different kinds of foam materials. Under the assumption that self-heating follows a first order reaction, these constants are used to calculate the critical half thickness of slabs of these materials for surface temperatures likely to be experienced during long term use in solar energy collectors. Based on these calculations, estimates are provided on the self-heating or ignition hazards associated with the size and use of these materials in solar energy systems. DOE

N86-10303# Arizona Univ., Tucson. Dept. of Chemistry.
EXTRACTION OF LANTHANIDE IONS BY 2-METHYL-8-QUINOLINOL
S. Taguchi and H. Freiser 1985 14 p refs
(Contract DE-AC02-76ER-04073)
(DE85-014277; DOE/ER-04073/18) Avail: NTIS HC A02/MF A01

The equilibrium extraction behavior of a series of tervalent lanthanides (La, Pr, Eu, Ho, and Yb) with 2-methyl-8-quinolinol (HL) in chloroform has been studied. Although the sterically hindered extractant does not form neutral LnL3 complexes, ion pair complexes of intermediate chelates with either perchlorate or thiocyanate ions are extractable. The extraction constants of such species are smaller than those of other 8-quinolinols and closer together because the adverse steric influence of the 2-methyl group is greater on the heavier lanthanide ions. DOE

N86-10304# Sandia Labs., Albuquerque, N. Mex.
CHEMICAL KINETICS AND CELLULAR STRUCTURE OF DETONATIONS IN HYDROGEN SULPHIDE AND AIR
J. E. Shepherd, A. Sulmistras, A. J. Saber, and I. O. Moen 25 Feb. 1985 31 p refs Presented at the 10th Intern. Colloq. on Dyn. of Explosions and Reactive Systems, Berkeley, Calif., 4 Aug. 1985 Prepared in cooperation with Concordia Univ., Montreal, Quebec
(Contract DE-AC04-76DP-00789)
(DE85-009408; SAND-85-0256C; CONF-850830-2) Avail: NTIS HC A03/MF A01

Analyses of hydrogen sulphide oxidation have been used to characterize the reaction zone structure at temperatures and pressures typical of detonations in mixtures of hydrogen sulphide and air. Detonation reaction zone lengths are calculated for a wide range of compositions, and the variation of these lengths with initial pressure and water vapor dilution are calculated. Estimates of detonation cell size lambda are made based on scaling factors established for other fuel-air systems. These estimates are compared with results obtained in an experimental investigation of the detonability of mixtures of hydrogen sulphide and air. The predicted cell size of 10 cm at stoichiometric composition and standard initial conditions is in excellent agreement with the

experimental results. The predicted variation of cell size also agrees well with the experimental observations over a concentration range of 10 to 20% (by volume) hydrogen sulphide. Based on the d(sub c) = 12lambda estimate of critical tube diameter d(sub c), the minimun critical tube diameter (for a stoichiometric mixture) is 1.3 m. Mixtures of hydrogen sulphide and air are therefore slightly less sensitive to detonation than propane-air mixtures, which have a minimum critical tube diameter of 0.9 m.
DOE

N86-10305# Michigan Univ., Ann Arbor. Dept. of Aerospace Engineering.
EFFECTS OF CHEMISTRY AND SWIRL ON THE PRODUCTION OF TURBULENCE IN A FLAME Annual Report, Dec. 1983 - Nov. 1984
J. F. Driscoll Mar. 1985 29 p refs
(PB85-219632; GRI-85/0064) Avail: NTIS HC A03/MF A01 CSCL 13A

The goal of this project is to measure the gas velocity, temperature, and turbulence levels within a swirl stabilized flame while independently varying the swirl number and the air-fuel ratio. The measurements are used to identify how much turbulence and recirculation are needed to obtain a stable flame of a desired length; results are also used to improve current computer models of turbulent combustion so that they can better handle swirl and thus be more useful for the design of practical burners. The measurements are used to assess several computer models. Laser velocimetry and laser Rayleigh scattering diagnostics are used.
GRA

26 METALLIC MATERIALS

Includes physical, chemical, and mechanical properties of metals, e.g., corrosion; and metallurgy.

N86-10306 Metals Society, London (England).
MECHANISM OF THE FORMATION OF BORONISED LAYERS ON HIGH CARBON STEEL
A. Galibois, O. Boutenko, and B. Voyzelle Sep. 1984 19 p refs Transl. into ENGLISH from Acta Met., no. 28, 1980 p 1753-1763 Original language document announced in IAA as A81-15771
(BLL-BISI-Trans-23036-(9022.06)) Avail: British Library Lending Div., Boston Spa, Engl.: £13.00; overseas $30.00

The coating of steels and alloys by boronizing is used to improve their resistance to wear and corrosion. Several types of processes used, which differ according to the media, are solid, liquid, or gaseous. The solid medium is the most widespread for technological and economic reasons. Within the solid media, a choice is made between the technology of pastes or powders. The pastes obtain thicker layers for the same duration of treatment, and it is preferred to attain the principal objective, which is to study the composition of the different sections of boronized layers and the mechanism of their formation on the surface of industrial high-carbon steel.
E.A.K.

N86-10307 Metals Society, London (England).
BORONISING OF IRON AND STEEL BY IONIC BOMBARDMENT BY DIBORANE
P. Casadesus and C. Frantz Sep. 1984 17 p refs Transl. into ENGLISH from Mem. Sci. Rev. Met. (Paris), v. 75, no. 2, 1978 p 81-91 Original language document announced in IAA as A78-29273
(BLL-BISI-Trans-23034-(9022.06)) Avail: British Library Lending Div., Boston Spa, Engl.: £10.00; overseas $22.50

The possibilities of boronizing iron and steel by ionic bombardment with diborane are discussed. The influence of the principal parameters: composition of atmosphere, nature of substrate, temperature, and length of treatment on the composition and thickness of boronized layers and on their morphology and structure was studied. Various layer arrangements, characterized by different proportions of the borides of iron, FeB and Fe2B, are obtained. The suitability of various types of steel for boronizing over a wide temperature range is studied. The growth rate of the boronized layers, which are produced by the process of ionic bombardment is analyzed.
E.A.K.

N86-10308 Metals Society, London (England).
APPLICATION OF THE UNLOADING COMPLIANCE METHODS IN FRACTURE TOUGHNESS MEASUREMENTS OF A QUENCHED AND TEMPERED STEEL
J. Albrecht and C. Wuethrich Oct. 1984 17 p refs Transl. into ENGLISH from Z. Werkstofftech. (West Germany), no. 13, 1982 p 96-103
(BLL-BISI-Trans-21628-(9022.06)) Avail: British Library Lending Div., Boston Spa, Engl.: £13.00; overseas $30.00

The application of the J-integral leads to a considerable reduction of material needed for establishing toughness data. The number of specimens is further reduced by measuring the crack resistance curve in a single specimen. This requires monitoring the crack extension during the experiment. A comparison of several methods showed that the unloading compliance technique is particularly suitable for that purpose. This method was applied for measuring the toughness as a function of location in a large forging of a steel 25 NiCrMo 145. Good toughness values (about 200 MPam sup 1/2) with little scatter were found over the whole cross section of the forging.
Author

N86-10309 British Aerospace Aircraft Group, Bristol (England).
PRE-BOND TREATMENT FOR TITANIUM ALLOYS
A. Kennedy, comp. and R. Kohler, comp. 26 Jan. 1984 82 p refs
(Contract MIN-DEF-A93b/1034)
(BAe-AL/MAT/3864; BR91991) Avail: NTIS

Pre-bond surface preparations were investigated to optimize the initial strength and durability properties of 6A1 4V (BS TA10) and CP (BS TA6) titanium metal to metal adhesive joints exposed under conditions of heat, moisture and stress. Anodizing in sodium hydroxide solutions and in sodium hydroxide/hydrogen peroxide mixtures, and treatment in sodium hydroxide/hydrogen peroxide mixtures catalyzed by the additon of heavy metal ions were assessed. It is shown that 10V anodizing at ambient temperature for 30 min in 5M sodium hydroxide solution gives surfaces which form highly durable bonds with epoxy adhesives. This process presents very low operating and environmental hazards and is suitable for large scale continuous production use. The presence of hydrogen peroxide is not necessary and can reduce adhesive bond durability. Titanium/epoxy adhesive joints with acceptable durability can be produced by treating the titanium at ambient temperature in a mixture of 1M sodium hydroxide and 0.5M hydrogen peroxide catalyzed by the addition of 160 mg/l of manganese sulfate.
Author (ESA)

N86-10310*# Analytical Services and Materials, Inc., Tabb, Va.
A SIMPLE METHOD OF OBTAINING CONCENTRATION DEPTH-PROFILES FROM X-RAY DIFFRACTION
K. E. Wiedemann and J. Unnam Warrendale, Pa. Metallurgical Society of AIME 1984 13 p refs
(NASA-CR-176262; NAS 1.26:176262; TMS-Paper-F8415) Avail: NTIS HC A02/MF A01 CSCL 11F

The construction of composition profiles from X-ray intensity bands was investigated. The intensity band-to-composition profile transformation utilizes a solution which can be easily evaluated. The technique can be applied to thin films and thick speciments for which the variation of lattice parameters, linear absorption coefficient, and reflectivity with composition are known. A deconvolution scheme with corrections for the instrumental broadening and ak-alfadoublet is discussed.
E.A.K.

N86-10311*# National Aeronautics and Space Administration. Lewis Research Center, Cleveland, Ohio.
CREEP-FATIGUE BEHAVIOR OF NiCoCrAlY COATED PWA 1480 SUPERALLOY SINGLE CRYSTALS
Robert V. Miner, John Gayda, and Mohan G. Hebsur 1985 20 p refs Presented at the Symp. on Low-Cycle Fatigue Directions for the Future, Bolton Landing, N.Y., 30 Sep. - 4 Oct. 1985; sponsored

by American Society for Testing Materials
(NASA-TM-87110; E-2710; NAS 1.15:87110) Avail: NTIS HC A02/MF A01 CSCL 11F

Single crystal specimens of a Ni base superalloy, PWA 1480, with a low pressure plasma sprayed NiCoCrAlY coating were tested in various 0.1 Hz fatigue and creep fatigue cycles both at 1015 and 1050 C. Creep fatigue tests of the cp, pc, and cc types were conducted with various constant total strain ranges employing creep dwells at various constant stresses. Considerable cyclic softening occurred as was evidenced particularly by rapidly increasing creep rates in the creep fatigue tests. The cycle time in the creep fatigue tests typically decreased by more than 80 percent at 0.5 N sub f. Though cyclic life did correlate with delta epsilon sub in a better correlation existed with sub f for both the fatigue and creep fatigue tests, and poor correlations were observed with either sigma sub max or the average cycle time. A model containing both delta sigma and delta sigma (sub in), N sub f = alpha delta sigma (sub in) beta delta sigma gamma, with best fit values of sigma for each cycle type, but the same values of beta and gamam, was found to provide good correlations. Life lines were not greatly different among the cycle types, differing only by a factor of about three. The cp cycle life line was lowest for both test temperatures, however among the other three cycle types there was no consistent ranking. For all test types failure occurred predominately by multiple internal cracking originating at pores. The strong correlation of life with delta sigma may reflect a significant crack growth period in the life of the specimens. B.W.

N86-10312*# Spectrolab, Inc., Sylmar, Calif.
DEVELOPMENT OF METALLIZATION PROCESS Final Report
A. Garcia, III Apr. 1985 99 p
(Contracts NAS7-100; JPL-956205)
(NASA-CR-176209; DOE/JPL/956205-85/8; NAS 1.26:176209; DE85-013585; DRL-175) Avail: NTIS HC A05/MF A01 CSCL 11F

The object of this contract is the optimization, evaluation, and demonstration of a novel metallization applied by a screen printing process. A paste consisting of molybdenum, tin, and titanium hydride is selected as the promising composition. No satisfactory cells are made using any of the molybdenum/tin pastes used as a complete replacement for conventional silver pastes. The major problem is the inability to form a bond between the pastes and silicon that withstands soldering. This problem can be overcome by using a two step process where any interconnection to the cell is done at small pads of conventional screen printed silver. The most promising use of the molybdenum/tin metallization system would be this two step process with a silver paste serving as the soldering pad. The Mo/Sn system would compete with silver economically if silver prices rose and could serve as a backup process. The use of a heated stage SEM with reactive gases is a great help in elucidating problems and suggesting solutions. DOE

N86-10313# Department of the Navy, Washington, D. C.
RUSTY BOLT INTERMODULATION INTERFERENCE REDUCER Patent Application
R. Panayappan and J. C. Cooper, inventors (to Navy) Filed 12 Apr. 1985 13 p
(AD-D011748; US-Patent-Appl-SN-722579) Avail: NTIS HC A02/MF A01 CSCL 09/1

In the preferred embodiment of the invention about 20 percent by weight of copper-pyrrolidine-chloride, about 5 percent by weight of polyvinyl pyrrodlidinone, and about 75 percent by weight of ethylene gylcol are mixed to form a viscious green solution which can be applied to metal surfaces by any common means, preferably painting or spraying. The chelating functional groups in PVP and pyrrolidine incorporate the metal of the metal oxide into their structure thus removing the metal oxide from the MOM junction. The PVP is cross-linked by metal ions removed from the metal oxide thus producing a structurally strong, hard material that sets in place and remains there to provide structural integrity at the junction. The PVP is also a mild reducing agent which prevents future oxidative or electrolytic corrosion. GRA

N86-10314# Department of the Navy, Washington, D. C.
PASSIVATION OF STEEL WITH AQUEOUS AMINE SOLUTIONS Patent Application
P. J. Hearst, inventor (to Navy) Filed 3 May 1985 13 p
(AD-D011749; US-Patent-Appl-SN-729849) Avail: NTIS HC A02/MF A01 CSCL 11/6

This is a process that allows previously cleaned steel (which may have been cleaned in any of several different ways) to be passivated with a rinse of almost pure water, that is made slightly alkaline to inhibit corrosion, and flash rusting such that any small residue remaining of the steel surface after drying of the water will itself evaporate and in such a manner that any remaining residue will be incorporated into a subsequently applied non-aqueous protective coating without leaving any water-soluble or ionic residue on the surface of the steel that will cause corrosion or affect adhesion of the protective coating. GRA

N86-10315# Army Materials and Mechanics Research Center, Watertown, Mass.
DEVELOPMENT OF A SHEATH FOR SENSOR PROTECTION IN MOLTEN STEEL APPLICATIONS Final Report
G. G. Bryant, T. V. Hynes, and J. J. Swab May 1985 109 p
(AD-A156764; AMMRC-TR-85-9) Avail: NTIS HC A06/MF A01 CSCL 13/8

Studies were performed to select appropriate candidate materials for development of thermal sensor protective sheaths for liquid steel processing systems. Samples of refractory ceramics were tested in laboratory scale melts and the best ceramic, boron nitride (BN), was tested at industrial scale in a continuous casting tundish. Industrial tests were performed on a prototype sensor sheath system at 1565 + or - 40 C for six tests of approximately five hours each, beginning with cold immersion. The sensor sheath system performed as a temperature monitor and demonstrated a high survivability rate due to the chemical inertness, low wetability high thermal conductivity, and low thermal expansion of the boron nitride. Materials studies included development of representative laboratory test environments, evaluation of failure mechanisms of materials, measurement of erosion/corrosion and wetting/penetration, and compatibility of materials and sensor systems. Analyses included optical microscopy, X-ray diffraction of reaction interface materials, and electron probe detection of the penetration of iron. GRA

N86-10316# Department of the Air Force, Washington, D.C.
LIQUID CRYSTAL NON-DESTRUCTIVE INSPECTION OF METALS Patent Application
G. J. Pech, inventor (to Air Force) Filed 14 Jun. 1985 23 p
(AD-D011772; US-Patent-Appl-SN-744593) Avail: NTIS HC A02/MF A01 CSCL 14/2

This patent application pertains to a non-destructive visual inspection arrangement for ferrous and non-ferrous metallic workpieces. The inspection arrangement employs a liquid crystal indicator medium and electrical current flow through the workpiece to develop potential differences across work surface flaws that are to be detected. The concepts of direct application of the liquid crystal medium to the work area surface and containment of the liquid crystal medium within a viewing device are also included. Author (GRA)

N86-10317# California Univ., Livermore. Lawrence Livermore Lab.
HUGONIOT MEASUREMENTS IN ALUMINUM TO 420 GPa USING THE LLNL TWO-STAGE LIGHT-GAS GUN
G. R. Gathers and A. C. Mitchell Jun. 1985 6 p refs Presented at the Am. Phys. Soc. Topical Conf. on Shock Waves in Condensed Matter, Spokane, 22 Jul. 1985
(Contract W-7405-eng-48)
(DE85-013821; UCRL-92204; CONF-850736-4) Avail: NTIS HC A02/MF A01

Aluminum is a standard material for shock wave experiments.

The increased velocity of our two-stage light-gas gun has been used to extend the range of previous aluminum measurements in order to reduce the gap between laboratory data and the data obtained with the nuclear driven shock inpedance match methods. The experiments reported include direct collision Hugoniot measurements with tantalum impactors and reshock measurements using tantalum impactors and both platinum and copper anvils. DOE

N86-10318# McElroy (Ralph) Co., Austin, Tex.
NONLINEAR PROPAGATION OF ELASTOPLASTIC WAVES IN Ke PENETRATORS (EXCERPTS)
G. F. Kuscher May 1985 143 p Transl. into ENGLISH of "Nicht-Lineare Ausbreitung Elasto-Plastischer Wellen in Ke-Penetratoren" rept. 2/85 Ernst-Mach Inst., Freiburg, West Germany, Feb. 1985 Prepared for California Univ., Livermore, Lawrence Livermore Lab.
(Contract W-7405-eng-48)
(DE85-011450; UCRL-Trans-12061) Avail: NTIS HC A07/MF A01

The characteristic principles of the approximation models are discussed briefly. As a result of the present study, it has been possible for the first time to obtain experimental confirmation of the basic hypotheses of the theory of elastic as well as elastoplastic wave propagation and to obtain dynamic material data corresponding to the theoretical definitions. The one-dimensional elastic and elastoplastic theory of wave propagation is discussed in detail. In general, all authors assume a one-dimensional treatment of wave propagation as the basis for an experimental study of elastoplastic properties of materials in bars. Within the resent study, no experimental findings were obtained, such as boundary influences or dispersion of the elastic wave, which would not justify this type of analysis. DOE

N86-10319# Du Pont de Nemours (E. I.) and Co., Aiken, S.C. Savannah River Lab.
MULTIPURPOSE PAN DEVELOPMENT
G. C. Rodrigues 1985 14 p Presented at the 9th Ann. Actinide Separations Workshop, Richland, Wash., 22 May 1985
(Contract DE-AC09-76SR-00001)
(DE85-012326; DP-MS-85-57; CONF-8505139-2) Avail: NTIS HC A02/MF A01

Savannah River Plant presently uses separate pans for filtration and roasting PuF3 precipitates in the Pu metal finishing line. Savannah River Laboratory has developed a multipurpose pan which uses platinum filter media for filtration and roasting. DOE

N86-10320# Edgerton, Germeshausen and Grier, Inc., Idaho Falls, Idaho.
FRACTURE TOUGHNESS AND STRESS RELIEF RESPONSE OF IRRADIATED TYPE 347/348 STAINLESS STEEL
F. M. Haggag 1985 7 p refs Presented at 8th Intern. Conf. on Struct. Mech. in Reactor Technol., Brussels, 19 Aug. 1985
(Contract DE-AC07-76ID-01570)
Avail: NTIS HC A02/MF A01

A test program has experimentally determined: (1) The fracture toughness of Type 347/348 stainless steel (SS) specimens with high values of irradiation fluence (2.3 to 4.8 x 10 to the 22nd power n/sq. cm. (2), E > 1.0 MeV) and experiencing different levels of irradiation creep (0.0, 0.6, 1.1, 1.8%), (2) the effect of thermal stress relief on fracture toughness recovery for the highly irradiated material, and (3) the mechanisms associated with fracture toughness recovery due to thermal stress relief. The postirradiation fracture toughness tests and tensile tests were conducted at 427 C. DOE

N86-10321# California Univ., Berkeley. Lawrence Berkeley Lab.
ELECTRONIC AND MAGNETIC PROPERTIES OF NOBLE-METAL AND TRANSITION-METAL ALLOYS, INTERFACES AND OVERLAYERS
L. M. Falicov May 1985 12 p refs Presented at 114th AIME Ann. Meeting (includes Soc. of Mining Engr.), New York, 24 Feb. 1985
(Contract DE-AC03-76SF-00098)
(DE85-014532; LBL-19695; CONF-850211-10) Avail: NTIS HC A02/MF A01

The electronic and magnetic properties of noble-metal and transition-metal alloys, interfaces and overlayers are examined theoretically. In particular, results are reported on the electronic and magnetic structure of: (1) nickel-copper alloys; (2) cobalt-iron alloys; (3) nickel-copper interfaces; and (4) chromium, cobalt, nickel and copper overlayers on a variety of substrates. General trends are examined and qualitative rules derived. DOE

N86-10322# Argonne National Lab., Ill.
PORTEVIN-LE CHATELIER EFFECT. 1: MODEL FOR THE TYPE-E SERRATIONS
R. B. Schwarz Jan. 1985 7 p Presented at the 7th Intern. Conf. on the Strength of Met. and Alloys, Montreal, 12 Aug. 1985
(Contract W-31-109-eng-38)
(DE85-006879; CONF-850823-3) Avail: NTIS HC A02/MF A01

A model is advanced for the discontinuous propagation of a Pottevin-Le Chatelier deformation band in tensile tests. The glide resistance is assumed to be a superposition of a time-independent strain hardening component and a time-dependent solute hardening component. The amplitude of the stress serrations, the strain increment across the band, and the propagation of the band per serration are calculated as a function of the work-hardening parameter, and material and machine parameters. The predictions of the model are found in good agreement with measurements. DOE

N86-10323# California Univ., Livermore. Lawrence Livermore Lab.
WORK-HARDENING AND EFFECTIVE VISCOSITY IN SOLID BERYLIUM
D. Steinberg, D. Breithaupt, and C. Honodel Jun. 1985 9 p refs Presented at 10th High Pressure Conf. on Res. in High Pressure Sci. and Technol., Amsterdam, 8 Jul. 1985
(Contract W-7405-eng-48)
(DE85-013978; UCRL-91892; CONF-850759-2) Avail: NTIS HC A02/MF A01

Results from Hopkinson split-bar, plate-impact, and cylinder deceleration experiments on beryllium are compared with hydrodynamic computer code simulations. By substantially increasing the beryllium work-hardening in the Steinberg-Guinan constitutive model, excellent agreement between the experiments and the calculations is achieved. A model to estimate effective viscosity is also proposed and the resultant calculations are in reasonable agreement with those derived from another model advanced by Asay, Chhabildas and Wise. DOE

N86-10324# Sandia Labs., Albuquerque, N. Mex.
WELD METAL HOT-CRACKING OF HASTELLOY ALLOYS C-22 AND C-276: A STUDY BY ANALYTICAL ELECTRON MICROSCOPY
M. J. Cieslak, A. D. Romig, Jr., and T. J. Headley 1985 25 p Presented at the Joint Meeting of the Electron Microscopy Soc. of Am. and the Microbeam Anal. Soc., Lousiville, Ky., 5 Aug. 1985
(Contract DE-AC04-76DP-00789)
(DE85-009437; SAND-85-0098C; CONF-850840-2) Avail: NTIS HC A02/MF A01

Weld metal hot-cracking in multi-component alloys systems is often the result of the formation of small volume fractions of nonequilibrium constituents along solidification grain boundaries. These constituents arise as a result of the segregation phenomenon accompanying weld solidification and often serve to extend the solidification temperature range well below the equilibrium solidus. Purpose of this study is to identify and characterize (crystal structure and composition) by analytical electron microscopy (AFM) the phases associated with weld metal hot-cracking in Hastelloy alloys O-22 and O-276. DOE

N86-10325# Rockwell International Corp., Golden, Colo
METALLURGY AND METALLOGRAPHY OF BRAZE JOINTS

M. M. McDonald 1985 59 p Presented at the Intern. Metal. Soc. Conf., Denver, 21 Jul. 1985
(Contract DE-AC04-76DP-03533)
(DE85-014563; RFP-3848; CONF-850753-2) Avail: NTIS HC A04/MF A01

Metallographic examination of braze joints involves standard metallographic procedures with a need for special attention to some unique characteristics of braze joints. These unique characteristics include very thin joints and dissimilar metal combinations. The thin joint geometry sometimes requires special sectioning techniques. The dissimilar metal combinations, usually involving soft and hard metals, can result in problems during polishing and etching. Imperfections that one should be on the lookout for in the metallographic examination of braze joints include cracks, entrapped flux, porosity, intermetallics phases, incomplete joining, corrosion, and erosion. In investigating possible origins of failure of braze joints, nonmetallurgical factors should not be overlooked. Improper design, particularly those that result in poor distribution of stress or improper clearances are often responsible for failures of braze joints. Inadequate cleaning or protection of parts and incorrect choices of heating process, filler metal and flux may all lead to a poor braze joint. DOE

N86-10326# Battelle Columbus Labs., Ohio.
RESEARCH NEEDS FOR CORROSION CONTROL AND PREVENTION IN ENERGY CONSERVATION SYSTEMS
E. W. Brooman and J. W. Hurwitch Jun. 1985 107 p
(Contract DE-AC06-76RL-01830)
(DE85-014852; PNL-5457) Avail: NTIS HC A06/MF A01

A group of 28 electrochemists, materials scientists, and corrosion engineers is brought together to determine if the government could have a role as a focal point for corrosion R and D, discuss opportunities in fundamental research and solving corrosion problems, and develop a research agenda. Participants from government, industry and academia assembled into four technical discussion groups: localized corrosion, general corrosion, high temperature corrosion, and corrosion control and prevention. Research needs are identified, discussed, then assigned a figure of merit. Some 44 corrosion control and prevention topics are identified as having a high priority for consideration for funding. Another 35 topics are identified as having a medium priority for funding. When classified according to corrosion phenomenon, the areas which should receive the most attention are molten salt attack, crevice corrosion, stress-corrosion cracking, erosion-corrosion, pitting attack, intergranular attack and corrosion fatigue. When classified according to the sector or system involved, those which should receive the most attention are chemical processes, transportation, buildings and structures, electric power generation, and batteries and fuel cells. DOE

N86-10327# California Inst. of Tech., Pasadena. Lab. of Engineering Materials
FORMATION AND CHARACTERIZATION OF AMORPHOUS ERBIUM-BASED ALLOYS PREPARED BY NEAR-ISOTHERMAL COLD-ROLLING OF ELEMENTAL COMPOSITES
M. Atzmon, K. M. Unruh, and W. L. Johnson Jul. 1985 27 p
(Contract DE-AT03-81ER-10870)
(DE85-014853; DOE/ER-10870/156) Avail: NTIS HC A3/MF A01

The formation of bulk single phase amorphous Cu-Er and Ni-Er alloys by extensive cold rolling of elemental foils is reported. The reaction is driven by the negative enthalpies of mixing of the constituent elements and occurs near ambient temperature. The crystallization behavior of the alloys obtained is studied by means of differential scanning calorimetry and found to agree closely with that of the corresponding sputtered and liquid quenched alloys. Radial distribution functions are measured for sputtered and rolled Cu72Er28 and are found to be in good agreement. DOE

N86-10328# Nooter Corp., St. Louis, Mo.
FABRICATION AND METALLURGICAL PROPERTIES OF MODIFIED 9Cr-1 Mo STEEL
M. Jawad, V. K. Sikka, and P. Patriarca 1985 24 p refs Presented at the Am. Petroleum Inst. Midyear Refining Meeting, Kansas City, Mo., 14 May 1985 Prepared in cooperation with ORNL
(Contract DE-AC05-84CR-21400)
(DE85-012865; CONF-8505145-1) Avail: NTIS HC A02/MF A01

A newly developed modified 9 Cr-1 Mo steel has good potential as a replacement for 2 1/4 Cr-1 Mo steel because of its high strength and creep rupture properties at elevated temperatures. Melting, fabrication, mechanical properties, and operating experience in power plants are discussed. Cost comparisons between modified 9 Cr-1 Mo and 2 1/4 Cr-1 Mo steel are also presented. DOE

N86-10329# Oak Ridge National Lab., Tenn.
SWELLING AND TENSILE PROPERTIES OF EBR-2-IRRADIATED TANTALUM ALLOYS FOR SPACE REACTOR APPLICATIONS
M. I. Grossbeck and F. W. Wiffen 1985 34 p refs Presented at the 2nd Symp. on Space Nucl. Power Systems, Albuquerque, N. Mex., 14 Jan. 1985
(Contract DE-AC05-84OR-21400)
(DE85-012887; CONF-850103-10) Avail: NTIS HC A03/MF A01

The tantalum alloys T-111, ASTAR-811C, Ta-10 W, and unalloyed tantalum are examined following EBR-II irradiation to a fluence of 1.7 x 10(26) neutrons/m(2) ($E > 0.1$ MeV) at temperatures from 650 to 950 K. Swelling is found to be negligible for all alloys; only tantalum is found to exhibit swelling, 0.36%. Tensile testing reveals that irradiated T-111 and Ta-10 W are susceptible to plastic instability, but ASTAR-881C and tantalum are not. The tensile properties of ASTAR-811C appear adequate for current SP-100 space nuclear reactor designs. Irradiated, oxygen-doped T-111 exhibits no plastic deformation, and the abrupt failure is intergranular in nature. The absence of plastic instability in ASTAR-811C is encouraging for alloys containing carbide precipitates. These fine precipitates might prevent dislocation channeling, which leads to plastic instability in many bcc metals after irradiation. DOE

N86-10330# Oak Ridge Y-12 Plant, Tenn.
ALUMINUM ION PLATING FOR CORROSION PROTECTION OF URANIUM, REVISION 1
C. M. Egert 25 Apr. 1985 12 p Presented at the US Army Corps of Eng. Ion Plating Workshop, Champaign, Ill., 12 Dec. 1984
(Contract DE-AC05-84OS-21400)
(DE85-012419; Y/DV-404-Rev-1; CONF-841267-1) Avail: NTIS HC A02/MF A01

This report discusses the coating structure and corrosion resistance for two methods of ion plating aluminum on uranium subject to a 100 C temperature limit. The first method is an evaporative technique using aluminum on resistivity heated tungsten filaments. This technique is presented used in production at the Oak Ridge Y-12 Plant for uranium coating processes. Another technique, presently under development, is magnetron bias sputter deposition where a magnetron sputter source replaces the filaments as the source of aluminum. This new technique results in considerable improvement in coating structure and consequently the corrosion resistance. DOE

N86-10331# Sandia Labs., Albuquerque, N. Mex.
METASTABLE PHASE FORMATION IN NI-IMPLANTED Al: AN ANALYTICAL ELECTRON MICROSCOPE INVESTIGATION
D. M. Follstaedt and A. D. Romig, Jr. 1985 17 p Presented at the Joint Meeting of the Electron Microscopy Soc. of Am. and the Microbeam Anal. Soc., Louisville, Ky., 5 Aug. 1985
(Contract DE-AC04-76DP-00789)
(DE85-009105; SAND-85-0262C; CONF-850840-3) Avail: NTIS HC A02/MF A01

By athermally injecting ions with energies from a few keV up to several MeV, virtually any atomic species can be alloyed into any host metal, independently of many of the thermodynamic constraints which apply to thermal alloying processes. Implanted alloy microstructures are currently being extensively investigated in attempts to arrive at a more general understanding of the phases that are produced. The phase types include metastable solid solutions, amorphous phases and second crystalline phases. DOE

N86-10332# European Space Agency, Paris (France).
LOW TEMPERATURE PLASTIC DEFORMATION MECHANISMS OF ALPHA-TITANIUM SINGLE CRYSTALS
Shigehisa Naka Apr. 1985 226 p refs Transl. into ENGLISH of "Etude des Mechanisms de Deformation Plastique a Basse Temperature de Monocristaux de Titane Alpha" rept. ONERA-NT-1983-7 ONERA, Paris, 1983
(ESA-TT-871; ONERA-NT-1983-7) Avail: NTIS HC A11/MF A01

The importance of the Peierls mechanism in the plastic deformation behavior of titanium is emphasized, as is the case of BCC metals. A non-planar core structure of screw dislocations was proposed; the core is dissociated simultaneously in one prismatic plane (10 bar 10) and two 1st order pyramidal planes (10 bar 11) and (10 bar 1 bar 1). The model of the core structure permitted qualitative explanation of various experimental results associated with the movement of screw dislocations (macro yield stress) which needs a recombination of the partials lying out of the slip plane. The hardening effect of inertial impurities was explained by introducing a modification of the core structure by the presence of impurities in the form of clusters (chemical interaction). This modification makes the recombination of the core more difficult. The presence of stage 2 on the stress vs strain curve at 77 K was explained by the fact that the micro yield stress corresponding to the propagation of edge dislocations was relatively high. That seems to be a particularity of titanium, at least, within the purity range of the titanium used. Author (ESA)

N86-10252# Milan Univ. (Italy).
SURFACE FORCES IN CONTACTING SOLIDS
G. Poletti and D. Cambiaghi (Centrotecnica) *In* ESA Fifth European Symp. on Mater. Sci. under Microgravity. Results of Spacelab 1 Dec. 1984 p 341-346 refs (For primary document see N86-10200 01-16)
Avail: NTIS HC A21/MF A01

N86-10266# Commissariat a l'Energie Atomique, Grenoble (France). Lab. d'Etude de la Solidification.
FIRST SPACELAB PAYLOAD (FSLP) EXPERIMENTS IN METALLURGY
J. J. Favier *In* ESA Fifth European Symp. on Mater. Sci. under Microgravity. Results of Spacelab 1 Dec. 1984 p 435-436 (For primary document see N86-10200 01-16)
Avail: NTIS HC A21/MF A01

27 NONMETALLIC MATERIALS

Includes physical, chemical, and mechanical properties of plastics, elastomers, lubricants, polymers, textiles, adhesives, and ceramic materials.

N86-10333 Massachusetts Univ., Amherst.
ELECTRICALLY CONDUCTING POLYMERS Ph.D. Thesis
John Robert Reynolds 1985 237 p
Avail: Univ. Microfilms Order No. DA8509596

A thorough investigation of the electronic properties of perchlorate doped polyacetylene was carried out. The conductivity of the polymer changes from semiconducting to values greater than 10(-2)Scm(-1) with doping and shows a distinct semiconductor to metal transition $.0001 < y < .001$. The polyacetylene films were doped using either electrochemical oxidation or a novel oxidation by ferric perchlorate allowing comparison of the two techniques. The changes in the electronic properties of a variety of arylenevinlene compounds, including poly(phenylene vinylene) (PPV), were examined with oxidation by AsF5. Conductivities as high as 1 Scm(-1) were observed for heavily doped PPV. Specific electron paramagnetic resonance characteristics were closely studied and a possible mechanism for conduction proposed. To overcome some of the limitations of the doped conjugated organic polymers a series of poly(metal tetrathiooxalates) (MTTO) were synthesized for the first time. Dissert. Abstr.

N86-10334 Massachusetts Univ., Amherst.
POLYACETYLENE POLYMERIZATION, STRUCTURE, AND ELECTRICAL TRANSPORT PROPERTIES Ph.D. Thesis
Michael Alan Schen 1985 344 p
Avail: Univ. Microfilms Order No. DA8509602

The field of highly conducting polymeric charge transfer complexes has focused principally on conjugated polymers with polyacetylene [CH] sub x, receiving the greatest attention. From an electrical transport properties view, much is known about polyacetylene. However, due to its insolubility and intractability, some of the most fundamental polymeric aspects of polyacetylene have not been addressed. The aim of this dissertation has been to elucidate the interrelationships which exist between polyacetylene molecular weight and the observed structural and electrical transport properties. Polyacetylene was polymerized using the Ziegler-Natta catalyst T(OBu) sub 4/A(Et) sub 3. Using radioactive c-14 labeled carbon monoxide and carbon dioxide as specific labels and h3 labeled methanol as a nonspecific label, the polymerization kinetics were fully elucidated. Simultaneously, the number average molecular weight, M sub n, of [CH] sub x obtained under a wide range of reaction conditions have been determined. Dissert. Abstr.

N86-10335 Georgia Inst. of Tech., Atlanta.
STEADY STATE FRICTIONAL BEHAVIOR OF THIN FILM COATINGS Ph.D. Thesis
Yutaka Shimazaki 1985 255 p
Avail: Univ. Microfilms Order No. DA8510973

Steady state frictional behavior of thin film coatings were studied and the effect of the applied coating thickness was emphasized. Four coating materials are studied, of which three are solid lubricants and one is wear resistance material. Film thickness, substrate roughness, applied load and substrate hardness were studied. The effect of these parameters on the transition and steady state friction coefficients are evaluated. It is shown that the steady state friction coefficients of MoS2 WSe2 WSe2/In/Ga coatings vary with the applied coating thicknesses. With the thicker coatings the wear track is fully covered with deformed coating material and the friction coefficients become higher. The steady state friction coefficient of WSe2/In/Ga coatings are determined by the behavior of the debonded and resmeared coating material. The substrate hardness seems to play the most dominant role upon the behavior of the resmeared film.
Dissert. Abstr.

N86-10336 Rensselaer Polytechnic Inst., Troy, N. Y.
FUEL AND LUBRICANT BEHAVIOR IN BOUNDARY LAYERS ANALYZED BY INFRARED EMISSION FOURIER TRANSFORM SPECTROMETRY Ph.D. Thesis
Peter Vogel 1984 188 p
Avail: Univ. Microfilms Order No. DA8509671

Thin films on metal surfaces were analyzed by Fourier transform infrared emission microspectrophotometry. The theory of thin films on a reflector was further developed to explore the possibilities of determining molecular alignment, film thickness and temperature from the emission spectra. The mechanism of deposit formation seems to be a two-stage process. Lubricants, used on magnetic recording media to minimize damage in case of a head crash, were studied by infrared emission spectrophotometry. The spectra of very thin layers of the lubricant directly on a mirror finished metal surface were quite different compared to the spectra of the bulk fluid. It is possible to detect the lubricant on top of the magnetic coating, which has strong bands in the same spectral region as the lubricant. A linear relationship between spectral intensity and lubricant concentration is found. Infrared emission spectrophotometry is a powerful tool for characterizing the lubricant as well as determine its concentration in a noncontact nondestructive way. Dissert. Abstr.

N86-10337 Johns Hopkins Univ., Baltimore, Md.
ELASTIC PROPERTIES AND THERMAL STABILITY CHARACTERIZATION OF METALLIC GLASSES BY GUIDED WAVE TECHNIQUES Ph.D. Thesis
Carl Lee Friant 1985 113 p
Avail: Univ. Microfilms order No. DA8510413

This study utilizes guided wave techniques for the determination of the isotropic elastic moduli of several metallic glass alloys. In addition, structural relaxation in the amorphous state that occurs during annealing below the crystallization temperature was monitored through changes in the elastic moduli using these methods. Metallic glasses unlike their crystalline counterparts are thermodynamically nonequilibrium structures. Consequently, knowledge of their thermal stability is of great importance from both a scientific and commercial standpoint. Structural relaxation of the asquenched structure manifests itself in the form of elastic moduli and density changes at temperatures well below that required for crystallization. Traditional techniques for characterizing the crystallization of metallic glssses such as X-ray diffraction and differential scanning and calorimetry are not effective for monitoring changes that take place in the wholly amorphous condition.
Dissert. Abstr.

N86-10338 Department of the Air Force, Washington, D.C.
SYNTHESIS OF ARYLENE SILOXANYLENE POLYMERS AND COPOLYMERS Patent
H. Rosenberg and T. T. Tsai, inventors (to Air Force) Issued 21 May 1985 11 p Supersedes AD-D009359
(AD-D011780; US-Patent-4,518,759; US-Patent-Appl-SN-343032; US-Patent-Class-528-35) Avail: US Patent and Trademark Office CSCL 07/3

This invention is directed to the preparation of certain arylene bis-silanols in highly purified form and to the preparation of five new arylene bis-silanols in particular, along with a procedure for ploymerizing these and other arylene-type bis-silanols using phosgene as a polymerization promotor or catalyst, to obtain highly purified, high molecular weight arylenesiloxanylene polymers. Preferred polymers are those which, when laminated to polycarbonate sheets or glass maintain their transparency, stability and adherence to said substrates at temperatures of up to and including 400 F. Such polymers are useful for the formulation of high temperature interlayers for windshields and canopies for aircraft and related aerospace vehicles.
GRA

N86-10339 Imperial Metal Industries Ltd., Kidderminster (England).
[CARBON FIBER REINFORCED POLYMIDE FILAMENT WOUND TUBE MANUFACTURING] Quarterly Progress Report
M. W. Jones Jun. 1974 9 p
(Contract MIN-DEF-K80B/33)
(BR64172; QPR-6) Avail: Issuing Activity

Progress in the development of a manufacturing process for information surveys of holes, joints, sandwich and open pattern structures; a design study on preferred joint designs; the formulation of a mathematical analysis to predict buckling; and test programs using glass reinforced polymide, filament wound tubes to validate theoretical analyses covering the prediction of strain distributions and buckling is summarized. Tube testing of glass polymide tubes was completed. Practical and theoretical data show good correlation for the winding angles most likely to be required for structures designed on flexural type loadings although at other winding patterns agreement is poor. Test data show the previous design study assessment of glass reinforced polymide tubes to be conservative for ambient temperature.
Author (ESA)

N86-10340*# Martin Marietta Aerospace, Denver, Colo. Mechanical Materials Engineering Section.
EVALUATION AND PREDICTION OF LONG-TERM ENVIRONMENTAL EFFECTS ON NON METALLIC MATERIALS Final Report
Harold Papazian Jan. 1985 26 p refs Addendum to N85- 19137
(NASA-CR-178495; NAS 1.26:178495; MCR-85-506-Addn) Avail: NTIS HC A03/MF A01 CSCL 11G

Predictive modeling of environmental conditions on nonmetallic materials was studied. The in-flight data of the atomic oxygen reaction with carbon and osmium, the laboratory and in-flight data of the atomic oxygen reaction with polymeric films and the effect of electron irradiation on the rates of oxidation are discussed. No information is found that can be used to model such effects on composites. The effects of the space environment on thermal control coatings and its effect on the space station are examined.
Author

N86-10341*# National Aeronautics and Space Administration. Lewis Research Center, Cleveland, Ohio.
TRIBOLOGICAL PROPERTIES OF STRUCTURAL CERAMICS
Donald H. Buckley and Kazuhisa Miyoshi Sep. 1985 103 p refs Submitted for publication
(NASA-TM-87105; E-2649; NAS 1.15:87105) Avail: NTIS HC A06/MF A01 CSCL 11B

The tribological and lubricated behavior of both oxide and nonoxide ceramics are reviewed in this chapter. Ceramics are examined in contact with themselves, other harder materials and metals. Elastic, plastic and fracture behavior of ceramics in solid state contact is discussed. The contact load necessary to initiate fracture in ceramics is shown to be appreciably reduced with tangential motion. Both friction and wear of ceramics are anisotropic and relate to crystal structure as has been observed with metals. Grit size effects in two and three body abrasive wear are observed for ceramics. Both free energy of oxide formation and the d valence bond character of metals are related to the friction and wear characteristics for metals in contact with ceramics. Surface contaminants affect friction and adhesive wear. For example, carbon on silicon carbide and chlorine on aluminum oxide reduce friction while oxygen on metal surfaces in contact with ceramics increases friction. Lubrication increases the critical load necessary to initiate fracture of ceramics both in indentation and with sliding or rubbing. Ceramics compositions both as coatings and in composites are described for the high temperature lubrication of both alloys and ceramics.
Author

N86-10342# Plant Resources Inst., Salt Lake City, Utah.
WHOLE PLANT UTILIZATION OF SUNFLOWERS AS A RENEWABLE SOURCE OF STRATEGIC MATERIALS (RUBBER) Final Report, 1 May 1983 - 30 Apr. 1984
M. F. Balandrin, J. R. Martineau, and G. A. Stone 14 Apr. 1985 14 p
(Contract DAAG29-83-C-0016)
(AD-A155833; ARO-20679.1-MS-S) Avail: NTIS HC A02/MF A01 CSCL 06/3

In an attempt to discover and develop new domestic sources of natural rubber (NR), 143 population of 47 species of sunflowers were collected and analyzed for their content of NR. Yields of crude NR obtained ranged from traces to 2.15% of the dry weight of the plant material. These quantities of NR are significantly lower (by approximately one order of magnitude) than those obtainable from domestic guayule plants. In addition, samples of sunflower NR were examined using chromatographic and spectroscopic techniques and were found to have low molecular weight elastomeric properties unsuitable for use in traditional Hevea latex or guayule NR applications. Thus, because of low yields, low NR molecular weights and quality, and relatively narrow genetic diversity in sunflower NR production characteristics, it is highly unlikely that sunflowers could serve as a domestic source of NR in the foreseeable future.
GRA

N86-10343# Royal Aircraft Establishment, Farnborough (England).
CALCULATION OF THE GLASS TRANSITION TEMPERATURES OF LINEAR POLYMERS. PART 1: RULES FOR HIERARCHICAL ORDERING OF THE DATA SET
W. A. Lee Nov. 1984 17 p
(AD-A156584; RAE-TR-84109-Pt-1; DRIC-BR-94287-Pt-1) Avail: NTIS HC A02/MF A01 CSCL 07/3

The rational ordering of polymers in a large data set for the correlation of glass transition temperature (Tg) with structure requires the establishment of seniority criteria. An extension of polymer nomenclature rules published by the International Union of Pure and Applied Chemistry is proposed and applied, with examples, to the groups in a large polymer data set. The rules can be extended to cover new polymers without upsetting the original order. GRA

N86-10344# Naval Air Systems Command, Washington, D. C.
POLYMER ENGINEERING: POLYMERIC AND MOLECULAR ELECTRONIC, DIELECTRIC AND OPTICAL PROPERTIES FOR DEVICE APPLICATIONS
T. W. Barrett 1985 68 p
(AD-A156671) Avail: NTIS HC A04/MF A01 CSCL 09/3

In the first five chapters the theoretical physics and chemistry which underpin device function is introduced. Chapters six to nine address the problems of material organization. Chapters ten to fifteen address applications. An attempt has been made in these chapters to indicate the possibilities and opportunities in this emerging field, but, at the same time, to indicate the difficulties. Chapter headings include the following: Polymer Semiconductors; Physical Bases of Excitons; Soliton Physics and Quantum Engineering; Photon Molecular Switching; Properties of Bioconductors; Langmuir-Blodgett Films for Oriented Mono and Multilayers; Organization of Polymeric Conductors; Devices: Material Considerations; Polymer Interfaces; Applications; Application of Advanced Devices; Architectures; Other Applications including Advanced Sensors; Defense and Aerospace Applications; Defense and Aerospace Market Considerations. GRA

N86-10345# Lockheed Missiles and Space Co., Palo Alto, Calif.
BINDER-FILLER INTERACTION IN ENERGETIC POLYMERS Final Report, May 1983 - Dec. 1984
R. H. Martinson 31 Mar. 1985 88 p
(Contract N00014-83-C-0271)
(AD-A156752; LMSC/F035789) Avail: NTIS HC A05/MF A01 CSCL 07/3

The objective of this study was to measure the kinetics of the dewetting process in a variety of filled energetic polymers being studied as candidates for improved solid rocket and gun propellants in the Office of Naval Research ONR Power Program. By studying the dewetting process in detail, correlations between surface energetics and dewetting behavior would be obtained. Specific questions addressed in this document are: (1) What is the relation, if any, between the particle size of RDX and the voids created by dewetting? (2) Does the number density of voids caused by strain vary with solids loading in the same binder? (3) What is the influence of plasticizers on the size and number density of voids? (4) What is the relative number density of voids in compositions that fracture at different strains? The size? and (5) What do the growth curves of voids look like as functions of strain? By combining Small Angle X-Ray Scattering (SAXS) and ultrasonic wave scattering (UWS) data with existing theories of scattering, partial answers to these questions can be derived. GRA

N86-10346# Northwestern Univ., Evanston, Ill. Dept. of Civil Engineering.
FINITE DEFORMATION CRACK-LINE FIELDS IN A THIN ELASTO-PLASTIC SHEET Interim Report
N. Nishimura and J. D. Achenbach Feb. 1985 39 p
(Contract N00014-76-C-0063)
(AD-A156757; NU-SML-TR-85-2) Avail: NTIS HC A03/MF A01 CSCL 20/11

Finite deformation in the crack-tip zone of plastic deformation is investigated for Mode-1 opening of a crack in a thin sheet of elasto-plastic material. The materials obeys the Von Mises yield criterion in the true stresses, and the stretching tensor satisfies a flow law of the Prandtl-Reuss type. Incompressibility and a state of generalized plane stress are assumed. It is assumed that linearized elasticity applies outside the zone of plastic deformation. On the crack line between the crack tip and the elastic-plastic boundary, two distinct regions were recognized: the near tip zone and the intermediate region. In the near tip zone the fields are controlled by the radius of curvature of the blunted crack tip. Here the stress field was approximated by classical plane stress results. It was that the crack-line stresses may be taken as uniform in the intermediate region. In each region, deformation variables were determined by the use of the constitutive relations, and the results were matched to the corresponding quantities in the neighboring region(s). In this manner expressions were constructed for the deformation gradients on the crack line, in terms of the distance to the crack tip in the deformed configuration, the yield stress in shear and the stress-intensity factor of linear elastic fracture mechanics. GRA

N86-10347# Materials Research Labs., Ascot Vale (Australia).
AGE-LIFE PREDICTION OF NYLON 66 PARACHUTE MATERIALS. PART 2: CHANGES IN THE CHEMICAL AND PHYSICAL PROPERTIES OF MATERIALS ON AGING
G. T. Egglestone and G. A. George Jan. 1985 31 p
(AD-A156909; MRL-R-950-Pt-2) Avail: NTIS HC A03/MF A01 CSCL 11/5

Changes in the chemical properties of nylon 66 taffeta material and olive drab ripstop material on accelerated thermal aging are reported. The thermooxidative changes that occurred were used to measure rates and degree of polymer degradation. Relationships between tensile strength, molecular weight and other chemical changes were established and found to be applicable for in-service parachutes. The nylon 66 materials were also examined for photochemical degradation after outdoor exposure. No photoendering was found for the dyed material and the difference in the degradation rates was attributed to different stabilizers being used during fiber manufacture. GRA

N86-10348# Du Pont de Nemours (E. I.) and Co., Aiken, S.C.
RECIRCULATION WITHIN A GLASS MIXTURE SUBJECTED TO EXTERNAL AND RESISTIVE HEATING
D. W. Pepper 1985 15 p refs Presented at the 4th Intern. Conf. on Numerical Methods in Laminar and Turbulent Flow, Swansea, England, 8 Jul. 1985
(Contract DE-AC09-76SF-00001)
(DE85-010068; DP-MS-85-29; CONF-850745-8) Avail: NTIS HC A02/MF A01

Convective motion within a glass mixture undergoing external and resistive (joule) heating is numerically simulated. A time-split finite element technique and a pseudo-pressure formulation are used to solve the two and three-dimensional primitive equations of motion. The viscosity, thermal diffusivity, and electrical conductivity vary as a function of temperature; the temperature varies from ambient to 1150 C. DOE

N86-10349# Los Alamos National Lab., N. Mex.
MIXED-MODE FRACTURE OF CERAMICS
J. J. Petrovic 1985 10 p Presented at the 4th Intern. Symp. on the Fracture Mech. of Ceram., Blacksburg, Va., 18 Jun. 1985
(Contract W-7405-eng-36)
(DE85-014087; LA-UR-85-2195; CONF-8506128-2) Avail: NTIS HC A02/MF A01

The mixed-mode fracture behavior of ceramic materials is of importance for monolithic ceramics in order to predict the onset of fracture under generalized loading conditions and for ceramic composites to describe crack deflection toughening mechanisms. Experimental data on surface flaw mixed-mode fracture in various ceramics indicate that the flaw-plane normal stress at fracture decreases with increasing in-flaw-plane shear stress, although present data exhibit a fairly wide range in details f this sigma-tau relationship. Fracture from large cracks suggests that mode 2 has a greater effect on Mode 1 fracture than Mode 3. A comparison of surface flaw and large crack mixed-mode 1-2 fracture responses indicated that surface flaw behavior is influenced by shear resistance effects. DOE

N86-10350# Sandia Labs., Albuquerque, N. Mex.
ANALYSIS OF TRANSITIONS BETWEEN FERROELECTRIC AND ANTIFERROELECTRIC STATES UNDER CONDITIONING OF UNIAXIAL STRAIN
S. T. Montgomery 1985 11 p Presented at the Am. Phys. Soc. Topical Conf. on Shock Waves in Condensed Matter, Spokane,

22 Jul. 1985
(Contract DE-AC04-76DP-00789)
(DE85-014468; SAND-85-0554C; CONF-850736-14) Avail: NTIS HC A02/MF A01

The ferroelectric ceramic PZT 95/5, formed as a solid solution from the antiferroelectric, PbZrO3, and the ferroelectric PbTiO3, is known to transform to an antiferroelectric state under pressure. This transition can be used to convert mechanical energy to electrical energy under shock conditions. A mathematical model for this transformation has been developed for conditions of uniaxial strain. It uses two order parameters as internal state variables to reflect the microscopic state of the material. One order parameter corresponds to the spontaneous lattice polarization. The other represents the microscopic alignment of the spontaneous polarization within the lattice with parallel alignment corresponding to a ferroelectric state and anti-parallel alignment corresponding to an antiferroelectric state. A numerical method for solution is used to illustrate dynamic material response from the transition. DOE

N86-10351# Sandia Labs., Albuquerque, N. Mex.
THERMAL EXPANSION OF GLASSES IN THE SOLID AND LIQUID PHASES
W. D. Drotning 1985 18 p Presented at the 9th Symp. on Thermophys. Properties, Boulder, Colo., 24 Jun. 1985
(Contract DE-AC04-76DP-00789)
(DE85-013953; SAND-84-2342C; CONF-850617-1) Avail: NTIS HC A02/MF A01

The thermal expansion of a number of mixed oxide glasses is measured in the solid and liquid regions by gamma densitometry. Dead borate glasses are examined in the range 27 to 42 mol % PbO. The liquid phase volumetric thermal expansion coefficient is observed to decrease with increasing PbO content, in contrast to the solid phase linear thermal expansion coefficients, which displays some increase with increasing PbO composition. At 33.3 and 42 mol % PbO, these glasses display crystallization behavior during cooling from the melt, depending on the cooling rate. In soda-baria phosphate glasses (50 mol % P2O5), liquid phase volumetric expansion coefficients. For those phosphates with Na2O, crystallization is observed on cooling from the melt. Measurements on a lithia-aluminosilicate glass ceramic are obtained by this method to approximately 400 C above the limit of conventional dilatometry, thereby allowing the measurement of the thermal expansion of high temperature crystalline phases, as well as the liquid phase density. The gamma densitometry technique can yeild density, thermal expansion, T(sub g) and crystallization information, and quenching rate dependence data on glasses to temperatures in excess of 1500 C, and thus provides a means for high temperature characterization of glasses which complements conventional dilatometry, calorimetry, and thermal analysis. DOE

N86-10352# Karlsruhe Univ. (West Germany). Inst. fuer Werkstoffkunde 2.
HIGH TEMPERATURE PROPERTIES AND CHARACTERIZATION OF S3-N4 MATERIALS Final Report, Dec. 1983
Georg Grathwohl and Franz Porz Bonn Bundesministerium fuer Forschung und Technologie May 1985 145 p refs In GERMAN; ENGLISH summary Sponsored by Bundesministerium fuer Forschung und Technologie
(BMFT-FB-T-85-046; ISSN-0340-7608) Avail: NTIS HC A07/MF A01; Fachinformationszentrum, Karlsruhe, West Germany DM 30.50

The applicability of reaction-bonded silicon nitrides (RBSN) at high temperatures (up to 1,500 C) is studied by investigating their high temperature characteristics, creep strength and long term stability as well as their oxidation behavior depending on the size and distribution of the material pores. The variations in RBSN strength induced by static and cyclic oxidation treatment are measured. Failure at high temperatures and under lower stresses is due to creep rupture, slow crack growth, creep strain and creep damage explaining the differences in the lifetimes of silicon nitrides. Author (ESA)

N86-10353# Karlsruhe Univ. (West Germany). Inst. fuer Werkstoffkunde 2.
HIGH TEMPERATURE PROPERTIES OF SIC MATERIALS Final Report, Dec. 1983
Henri Cohrt, Rainer Hamminger, and Georg Grathwolh Bonn Bundesministerium fuer Forschung und Technologie May 1985 141 p refs In GERMAN; ENGLISH summary Sponsored by Bundesministerium fuer Forschung und Technologie
(BMFT-FB-T-85-047; ISSN-0340-7608) Avail: NTIS HC A07/MF A01; Fachinformationszentrum, Karlsruhe, West Germany DM 30

The oxidation and creep properties as well as the microstructural parameters and grain boundaries of several SiSiC and SSiC materials were studied to determine their applicability at high temperatures. Stress distributions in the bending specimens are calculated. Creep deformation occurs in a transient mode approaching zero creep in long term tests. Further improvement of SiSiC materials can be achieved by optimizing the microstructure of the green compact, that of SSiC materials by optimizing the processing and sintering techniques. Inclusions and segregations with high concentrations of impurities and additives were analyzed. Thin grain boundary films were studied with high resolution Auger electron spectroscopy. Author (ESA)

28 PROPELLANTS AND FUELS

Includes rocket propellants, igniters, and oxidizers; storage and handling; and aircraft fuels.

For related information see also *07 Aircraft Propulsion and Power, 20 Spacecraft Propulsion and Power,* and *44 Energy Production and Conversion.*

N86-10354# Army Armament Research and Development Command, Dover, N. J. Large Caliber Weapon Systems Lab.
EMACK RAILGUN FIRING TEST REPORT NUMBER 9 Final Technical Report, for period ending 20 Dec. 1983
A. E. Zielinski, J. A. Pappas, W. Williams, and G. Zsidisin Jun. 1985 44 p
(AD-A156661; AD-E401349; ARLCD-TR-85009; Test-9) Avail: NTIS HC A03/MF A01 CSCL 20/3

The test firing of the EMACK railgun test bed was successfully conducted on 20 December 1983 at a peak system current of 430 kiloamperes and 1.6 megajoules stored inertially in the homopolar generator. Current was successfully commutated into the launcher in 800 microseconds. The D1.1 projectile in-flight shadowgraphs were taken with a 150 KV Hewlett Packard flash X-ray system and a motion picture of the muzzle arc was taken with a 5000 frame-per-second high speed camera. The projectile weighed 566 grams and reached a velocity of 506 m/s in the 5 meter-long barrel. The improved armature design left the barrel intact and acceptable for EMACK shot no. 10. GRA

N86-10355# Department of the Air Force, Washington, D.C.
GAS GENERATOR FUEL FLOW THROTTLE CONTROL SYSTEM Patent Application
W. H. Miller, inventor (to Air Force) Filed 21 Mar. 1984 30 p
(AD-D011797; US-Patent-Appl-SN-591715) Avail: NTIS HC A03/MF A01 CSCL 21/8

In this patent application, a gas generator fuel flow throttle control system provides a fuel rich gas to a propellant grain of a small diameter rocket. An adaptive iterative gain technique allows the throttle to closely follow a commanded fuel flow rate as required by a missile processor. GRA

N86-10356# Los Alamos Scientific Lab., N. Mex.
DEVELOPMENT OF NEW AMMONIUM NITRATE COMPOSITE EXPLOSIVES Final Report, Oct. 1982 - Jan. 1984
K. Y. Lee Mar. 1985 10 p refs
(Contract W-7405-eng-36)
(DE85-014252; LA-10276) Avail: NTIS HC A02/MF A01

Studies of several ammonium nitrate (AN) based composite explosive systems were continued from earlier work. The critical temperature (T(sub c)) of AN/ANT, AN/ENT, and AN/DETN systems were measured and their thermal stabilities evaluated. We have also studied the effect of ENT on the melt temperature of EA (EDD/AN) and found that ENT forms a eutectic with EA. The eutectic temperature of the ternary system AN/EDD/ENT (AENT) is 89C. Results from an initial pahse-diagram study of the quaternary system AN/KN/EDD/DETN (DEAK) are also presented. DOE

N86-10357# Sandia Labs., Albuquerque, N. Mex.
EXPLOSIVE INITIATION BY VERY SMALL CONICAL SHAPED CHARGE JETS
M. G. Vigil 1985 11 p refs Presented at the 8th Intern. Symp. on Detonation, Albuquerque, N. Mex., 15 Jul. 1985
(Contract DE-AC04-76DP-00789)
(DE85-009443; SAND-84-18440; CONF-850706-9) Avail: NTIS HC A02/MF A01

Very small conical shaped charge (CSC) jets are used to initiate four different secondary explosives. The liner thicknesses vary between 0.076 and 0.17 mm. LX-13 (80% PETN and 20% SYLGARD) explosive is used to drive the conical liners to form the CSC jets. The CSC jet velocities vary between 3.6 and 6.5 mm/(MU)s. The jet tip diameters range from 0.041 and 1.10 mm. The explosive acceptor or target diameters vary between 1.90 19.1 mm. The lateral confinement of the acceptor explosives is minimal. Relationships for critical jet initiation energy and dimensionless explosive/jet parameter as a function of initiation parameters is developed. The jet initiation data from this investigation as well as previously published data are shown to be consistent with the developed relationships. The threshold initiation parameter (jet velocity squared times jet diameter) for LX-13, PETN, PBX-9407, and TETRYl were experimentally determined to be 0.011, 0.0130, 0.041, and 0.044 cucm/(MU)s(2), respectively, for copper jets impacting bare explosive acceptors. The lower values for the LX-13 and PETN indicate these two explosives are more sensitive to shock initiation than PBX-9407 and TETRYL explosives. Author

N86-10358# Heller (Jean), Los Alamos, N. Mex.
PROPERTIES OF PLASTIC-BONDED NITROGUANIDINE
H. Dong, Y. Tian, X. Chen, F. Meng, and Q. Wang 1985 14 p refs Transl. into ENGLISH from Baozha yu Chongji (China), no. 1, 1981 p 77-83
(Contract W-7405-eng-36)
(DE85-015316; LA-tr-85-30) Avail: NTIS HC A02/MF A01

The formuiation of bonded nitroguanidine used is Nq/TnT/PVB 97.5/1/1/5, which is designated as PB-NQ-1. Various properties of PB-NQ-1 were determined. Its detonation parameters were measured with 100-mm-diameter charges, initiated by a plane wave lens and a 100-mm-diameter by 10-mm-thick Comp. B booster. The detonation velocity is 8.159 mm/(MU)s, and the effective C-J detonation pressure is 26.2 GPa at rho0 = 1.676 g/cm(3). The energy of the one-dimensional plate push test is 65% that of PBX 9704. Experimental data show the performance of nitrogunaidine, insensitivity characteristics and stability under normal temperatures, are comparable to those of TATB. Hence nitroguanidine may be used as a cheaper substitute for the latter. DOE

N86-10359# California Univ., Livermore. Lawrence Livermore Lab.
COMPOSITE EXPLOSIVES FOR METAL ACCELERATION: THE EFFECT OF DETONATION TEMPERATURE
R. R. McGuire and M. Finger 10 Jun. 1985 9 p refs Presented at the 8th Intern. Symp. on Detonation, Albuquerque, N. Mex., 15 Jul. 1985
(Contract W-7405-eng-48)
(DE85-013982; UCRL-91482; CONF-850706-21) Avail: NTIS HC A02/MF A01

Previous work in the area of composite explosives has emphasized the necessity of small particle size and intimate contact between fuel and oxidizer in obtaining prompt performance from fuel/oxidizer mixtures. This work has provided a basis for the definition of a composite explosive as an explosive system that requires the transport, mixing and subsequent reaction of the initial decomposition products of the system components in order to achieve the predicted detonation performance. A general working model and present experimental evidence demonstrating the importance of detonation temperature in achieving performance from composite explosives in metal acceleration experiments is presented. DOE

N86-10360# Research Inst. of National Defence, Umea (Sweden). ABC Research Dept.
METHOD FOR DETERMINING ELEMENTAL SULFUR IN JET FUEL
Birgitta Olofsson and Roger Roffey Jan. 1985 38 p refs In SWEDISH; ENGLISH summary
(FOA-C-40211-B4; ISSN-0347-2124) Avail: NTIS HC A03/MF A01; Research Institute of National Defence, KR 50

A method to determine elemental sulfur in jet fuel, based on differential pulse polarography, which needs smaller sample size, and is more sensitive than older methods is developed. The detection limit is 0.1 mg/l and the analytical range tested 0.1 to 10 mg/l. The test can be reproduced with a precision better than 10% for samples above 1 mg/l, and 15% to 20% near the detection limit. Accuracy is > 5%. The influence on the polarographic peak of interferences is studied. Author (ESA)

31 ENGINEERING (GENERAL)

Includes vacuum technology; control engineering; display engineering; and cryogenics.

N86-10361 North Carolina State Univ., Raleigh.
FREEZER MODEL USING A POPULATION BALANCE APPROACH FOR STEADY-STATE, DIRECT-CONTACT, SECONDARY REFRIGERANT, FREEZE DESALINATION Ph.D. Thesis
Larry Wayne Byrd 1984 131 p
Avail: Univ. Microfilms Order No. DA8507355

A study of the secondary refrigerant, direct-contact, freeze desalination process is presented. In the study, a mathematical analysis of crystallization which occurs in the freezer is carried out and pilot plant data interpreted in light of the analytically implied behavior. The mathematical model assumes that refrigerant drop sizes are dispersed at any instant of time according to a scaled beta distribution. The inlet liquid refrigerant drops have a mondisperse size distribution while the ice crystal distribution has the form I sub c(r sub c) = (beta G)exp(-BETA r sub c/G) where BETA and G are empirical relations describing crystal nucleation and growth respectively. Agglomeration and breakage of droplets and crystals is included in the theory, although excluded in calculations. A number conservation equation, equations describing well-mixed behavior, a heat and mass balance, a salt balance, a volume constraint, and brine property relations are used to describe freezer operation. Author

N86-10362 Rensselaer Polytechnic Inst., Troy, N. Y.
MODELING AND CONTROL OF NONLINEAR SYSTEMS Ph.D. Thesis
Soleyman Mohseni 1984 125 p
Avail: Univ. Microfilms Order No. DA8509661

A method is presented for modeling a class of nonlinear systems by a linear combination of a library of differentiable, independent, and continuous functions that are possible suspects for inclusion in the model. While each possible model structure is represented by a node in a tree, it is shown that searching the tree for the optimal n-term model structure can be done in n stages using an algorithm based on conjungate direction ideas. The essential feature of the technique is that it generates a sequence of projection matrices such that the original vector-valued functions become conjugate directions. This leaves the original nonlinear terms intact and allows the structure for the optimal n-term model to be assembled in n selections from the library. It is also shown that if applied to the quadratic optimization problem, the method obtains the extremum of the quadratic objective function after n stages without any explicit line search and/or matrix inversion. Dissert. Abstr.

N86-10363# Office National d'Etudes et de Recherches Aerospatiales, Paris (France).
LA RECHERCHE AEROSPATIALE, BIMONTHLY BULLETIN, NO. 1984-5, SEPTEMBER-OCTOBER 1985
Claude Sevestre, ed. Paris ESA Apr. 1985 81 p refs Transl. into ENGLISH of 'La Rech. Aerospatiale, Bull. Bimensuel. No. 1984-5, Sep. - Oct. 1984" France, ONERA
(ESA-TT-899) Avail: NTIS HC A05/MF A01; print copy in ENGLISH available at ONERA, Paris FF 70; original report in FRENCH available at ONERA, Paris FF 70

A numerical optimization method for airfoil design; noncentered numerical schemes in two-dimensional gas dynamics; a chemical laser by oxygen-iodine excitation transfer; a model for quantitative X-ray microanalysis (application to in-depth analysis of heterogeneous samples); a multidimensional case of an etropic variational formulation of conservative hyperbolic systems; and a radar signature analysis facility are discussed. Author (ESA)

N86-10364# Research Inst. of National Defence, Stockholm (Sweden).
REPORT ON A VISIT TO ENGLAND
Gunilla Derefeldt and Ulf Berggrund Mar. 1985 46 p refs Partly in ENGLISH, SWEDISH, and FRENCH Proc. of Nato Workshop on Color Coded VS Monochrome Electron. Displays, Farnborough, England, 28 Feb. - 1 Mar. 1984
(FOA-C5-85-0006-H2; ISSN-0347-7665) Avail: NTIS HC A03/MF A01

Color and monochrome display cost and system effectiveness; color displays in aircraft cockpits; digitally generated maps for aircraft; subjective reactions to color displays; and raster graphics were discussed. Author (ESA)

N86-10365# Nationaal Inst. voor Kernfysica en Hoge Energiefysica, Amsterdam (Netherlands). Sectie-H.
[ACTIVITIES REPORT IN SAFETY] Annual Report, 1983 [VEILIGHEIDSJAARVERSLAG 1983]
1984 38 p In DUTCH
Avail: NTIS HC A03/MF A01

Conventional and radiation aspects of safety management, and safety programs at a nuclear research institute are presented. The design of the laboratory is described. The technical execution of the safety management is outlined. Author (ESA)

32 COMMUNICATIONS

Includes land and global communications; communications theory; and optical communications.

For related information see also *04 Aircraft Communications and Navigation* and *17 Spacecraft Communications, Command and Tracking.*

N86-10366 British Broadcasting Corp., Kingswood (England). Engineering Div.
AN EVALUATION OF THE USE OF MICROPHONE ARRAYS FOR STUDIO RECORDING
P. S. Gaskell, C. Eng, and K. A. Bradbury Aug. 1985 20 p refs
(BBC-RD-1985/8; PH-273) Avail: BBC, Kingswood Warren, Tadworth, Surrey, Engl.

The feasibility of using arrays of microphones as a studio recording technique in those situations where it is difficult to site the microphone close to the source was assessed.It was shown that the reverberant field, present in all studios, imposes severe demands on the performance of the array. It is estimated that the minimum number of microphones needed for a practical array is of the order of 100. The array would have to be constructed to stringent practical tolerances and would need considerable signal processing hardware for cophasing and beam steering. This technique therefore is unlikely to be appropriate for studio recording except in special circumstances. E.A.K.

N86-10367 Maryland Univ., College Park.
TOPICS IN NONLINEAR WAVE THEORY WITH APPLICATIONS Ph.D. Thesis
Eugene Raymond Tracy 1984 232 p
Avail: Univ. Microfilms Order No. DA8510466

Selected topics in nonlinear wave theory are discussed and applications to the study of modulational instabilities are presented. A historical survey is given of topics relating to solitons and modulational problems. A method is then presented for generating exact periodic and quasiperiodic solutions to several nonlinear wave equations which have important physical applications. The method is then specialized for the purposes of studying the modulated instability of a plane wave solution of the nonlinear Schrodinger equation, an equation with general applicability in one dimensional modulational problems. Some numerical results obtained in conjunction with the analytic study are presented. The analytic approach explains the recurrence phenomena seen in our numerical studies, and the numerical work of other authors. The method of solution (related to the Inverse Scattering Method) is then analyzed within the context of Hamiltonian dynamics. The construction of closed form solutions of these nonlinear wave equations, via the solution of Jacobi's Inversion Problem, is surveyed briefly. Dissert. Abstr.

N86-10368 Delaware Univ., Newark.
THE INTERPOLATION OF SIGNALS SAMPLED AT LESS THAN THE NYQUIST RATE Ph.D. Thesis
Khan Lutful Kabir 1984 126 p
Avail: Univ. Microfilms Order No. DA8511213

To obtain analog information by digitally processing uniformly spaced samples depends on the interpolation scheme. The constraints for the usual Shannon-Whittaker interpolation is to sample such signals at or above the Nyquist rate of twice the highest frequency present. This interpolation scheme produces poor reconstruction for signals with no highest frequency. In this dissertation, a new sampling theorem is developed based on the Newton-Gregory interpolation formula which is applicable to signals produced by stable physical systems with rational transfer functions. According to this theorem, such a signal is uniquely specified by its samples whenever the poles of the system transfer function all have frequencies less than one-sixth the sampling rate. A direct application of the Newton-Gregory interpolation scheme is made to numerically evaluate the spectra of poorly bandlimited signals at frequencies well above the sampling rate. Dissert. Abstr.

N86-10369 Case Western Reserve Univ., Cleveland, Ohio.
THEORETICAL AND NUMERICAL INVESTIGATION OF DIPOLE RADIATION OVER A FLAT EARTH Ph.D. Thesis
George Konstantin Karawas 1985 204 p
Avail: Univ. Microfilms Order No. DA8510121

The electromagnetic problem of dipole radiation in the presence of a conducting half-space is old and has been treated extensively in the literature. Various writers, including such prominent names as H. Weyl and B. van der Pol, have given different but equivalent presentations of the solution. A short derivation, similar to that of van der Pol, is given in an appendix for the field along the surface of the earth. It is then shown how this representation can be used to derive a new form of an asymptotic expansion, whose first term is identical with the one to be found in the literature. A recurrence relation is derived for calculating the higher order terms of the expansion and a tight bound is derived which permits an easy estimate of the truncation error. A discussion is presented about the numerical computation of the complementary error function which figures prominently in the present problem. Two methods are presented, one in form of the solution of a simple system of ordinary differential equations of the first order and another in form of continued fractions. Dissert. Abstr.

N86-10370 Georgia Inst. of Tech., Atlanta.
THE MEASUREMENT AND APPLICATION OF TRANSPORT

PROPERTIES OF ION SWARMS IN GASES Ph.D. Thesis
Franklin Benton Holleman 1984 179 p
Avail: Univ. Microfilms Order No. DA8510962

The drift velocities, mobilities, and longitudinal diffusion coefficients of the ion-gas combinations Tl + in He, Ne, Ar, and O2, Cl in N2 and NO + in N2 were measured at constant room temperature as a function of E/N, where E is the electric field strength and N is the number density of the neutral gas. T measured mobilities of Tl + in Ar were used to determine the ion-neutral interaction potential. The measured mobilities of Cl-in N2 were used to determine an effective ion-neutral interaction potential. Cross sections for momentum transfer were calculated as a function of ion-neutral collision energy in the center-of-mass frame from the directly determined ion-neutral interaction potentials for the Tl + in Ar and Cl-in N2 gas combinations. The data taken as a function of E/N were obtained in a low pressure drift tube mass spectrometer. For this study the Tl + ions were obtained by thermionic emission from a specially coated filament while the Cl- and NO+ ions were generated by electron bombardment of trace gases. Arrival time histograms were built up for the mass-selected ions. Dissert. Abstr.

N86-10371 Department of the Air Force, Washington, D.C.
ANGLE SET-ON APPARATUS Patent
R. R. Willmore, inventor (to Air Force) Issued 14 May 1985 6 p
Supersedes AD-D009406
(AD-D011766; US-Patent-4,517,568; US-Patent-Appl-SN-347749; US-Patent-Class-343-18) Avail: US Patent and Trademark Office CSCL 17/9

An angle set on apparatus for an electronic countermeasure system utilizing a single dual mode phased array antenna which is operated under receiver/processor control to serve as both a transmit and receive element thereby avoiding the need for a separate direction finding system and, since transmit and receive functions share the same antenna, eliminating the need for precision pointing accuracy. The receiver/processor unit would continue to identify emitters using the jamming unit's receive antenna element and, where appropriate, PRI trackers would be assigned. The time of arrival window would be assigned. The time of arrival window would then be used to blank the transmitter signal and to switch the phased array to the receive mode. During sequential time of arrival windows the receiver/processor would vary the pointing angle of the phase array until the emitter angle of arrival is determined and stored in memory. At periodic intervals in the future, the receiver/processor unit would be pointed to the stored angle of arrival value for high effective radiated power jamming. GRA

N86-10372 Department of the Air Force, Washington, D.C.
METHOD FOR TUNING A PHASED ARRAY ANTENNA Patent
R. P. Gray, Jr., inventor (to Air Force) Issued 14 May 1985 5 p
Supersedes AD-D010172
(AD-D011768; US-Patent-4,517,570; US-Patent-Appl-SN-471550; US-Patent-Class-343-372) Avail: US Patent and Trademark Office CSCL 09/6

During installation or maintenance of a phased array antenna system in which the transmission line to each element includes an adjustable phase shift device, it is required that the effective electrical lengths of the lines be adjusted to be equal, or alternatively that the phase errors be determined and stored as correction data for use during normal operation. One way of doing this is to phase modulate by + or - 90 deg the phase shift device of one element at a time, while applying a test signal to all elements. The signal is radiated by the array, received via a test antenna, and supplied to and envelope has different amplitudes at + 90 deg and - 90 deg of the modulation. The element is tuned by adjusting the length of its transmission line or line or the adjustment of its phase shift device to obtain a null at the amplitude detector. In an improved technique, to reduce certain errors, sum tuning is used, in which the + or 90 deg phase modulation is applied to all of the phase shift devices, except for that of the element being tuned. GRA

N86-10373 Department of the Air Force, Washington, D.C.
HIGH SENSITIVITY MILLIMETER-WAVE MEASUREMENT APPARATUS Patent
T. T. Mori, R. B. Dybdal, and R. D. Etcheverry, inventors (to Air Force) Issued 9 Apr. 1985 5 p Supersedes AD-D009697
(AD-D011786; US-Patent-4,510,622; US-Patent-Appl-SN-388327; US-Patent-Class-455-67) Avail: US Patent and Trademark Office CSCL 09/5

A millimeter wave measurement apparatus utilizing a phase-locked transmitter to generate a millimeter wave signal and a phase-locked local oscillator receiver to receive the transmitted millimeter wave signal. A conventional microwave receiver unit receives the IF signal from the millimeter wave receiver and downconverts the IF signal for detectiona and measurement. GRA

N86-10374 Department of the Air Force, Washington, D.C.
SAMPLE DATA PHASE LOCKED LOOP FOR ADAPTIVE DOPPLER TRACKER Patent
A. W. Roeder, inventor (to Air Force) Issued 23 Apr. 1985 9 p
Supersedes AD-D010534
(AD-D011788; US-Patent-4,513,429; US-Patent-Appl-SN-329558; US-Patent-Class-375-120) Avail: US Patent and Trademark Office CSCL 09/5

Precise phase acquisition and tracking of a data modulated pulse signal in order to recover the data in a low signal to noise ratio environment is achieved by a sample data phase locked loop that is adaptive, second order, and uses baseband polar coordinate processing. The circuit utilizes an adaptive second order loop where the loop bandwidth can be adjusted by a coherence measurement. This provides wide bandwidths during initial acquisition, medium bandwidths during acquisition/track transition and narrow bandwidth during tracking. GRA

N86-10375 Department of the Navy, Washington, D. C.
PHASE-CODED PULSE EXPANDER-COMPRESSOR Patent
B. L. Lewis, inventor (to Navy) Issued 2 Apr. 1985 11 p
Supersedes AD-D009914
(AD-D011812; US-Patent-4,509,051; US-Patent-Appl-SN-420209; US-Patent-Class-343-17.2PC) Avail: US Patent and Trademark Office CSCL 17/9

A pulse expansion and compression system, especially useful for radar ranging, comprising a pulse coder for expanding an input pulse and a pulse compressor of the matched-filter type. The coder consists of a plurality of delay stages into which the input pulse is fed, a discrete Fourier transform (DFT) circuit to which the output signals of the delay stages are fed by way of respective phase weights and for which every other frequency port is inverted prior to entry to a time-dispersion-means (TDM) comprising an arrangement of adders interconnected by delay stages for differently delaying the output signals from the DFT. The adders are connected in N/2-fold cyclically permutated order to the frequency ports, where N is the number of frequency ports if that number is even, and N is the number of frequency ports less one if that number is odd. The TDM output is fed to a phase modulator and then to the transmitter. The echo signals are conjugated, time-inverted, and passed through the same DFT as the input pulse signal by way of the phase weights. The outputs of the DFT are then inverted at every other frequency port and passed through the TDM, but this time in time-inverted order. The outputs of the TDM are fed through an envelope detector to provide a cross-correlated facsimile of the original input pulse. Author (GRA)

N86-10376 Department of the Navy, Washington, D. C.
PHASE CODED PULSE EXPANDER-COMPRESSOR Patent
B. L. Lewis, inventor (to Navy) Issued 18 Jun. 1985 8 p
Supersedes AD-D009614
(AD-D011817; US-Patent-4,524,362; US-Patent-Appl-SN-377107; US-Patent-Class-17.2-PC) Avail: US Patent and Trademark Office CSCL 17/9

A pulse expansion and compression system, especially useful for radar ranging, comprising a pulse coder for expanding an input pulse and a pulse compressor of the matched-filter type. The coder consists of a plurality of delay stages into which the input pulse is fed, a discrete Fourier transform (DFT) circuit to which the output signals of the delay stages are fed by way of respective phase weights and for which every other frequency port is inverted prior to entry to a time-dispersion means (TDM) comprising an arrangement of adders interconnected by delay stages for differently delaying the output signals from the DFT. The TDM output is fed to a phase modulator and then to the transmitter. The echo signals are conjugated, time-inverted, and passed through the same DFT as the input pulse signal by way of the phase weights. The outputs of the DFT are then inverted at every other frequency port and passed through the TDM, but this time in time-inverted order. The outputs of the TDM are fed through an envelope detector to provide a cross-correlated facsimile of the original input pulse. Author (GRA)

N86-10377*# Illinois Univ., Urbana. Electromagnetics Lab.
NUMERICAL METHODS FOR ANALYZING ELECTROMAGNETIC SCATTERING Seimannual Report, 25 Mar. - 24 Sep. 1985
S. W. Lee, Y. T. Lo, S. L. Chuang, and C. S. Lee 24 Sep. 1985 176 p refs
(Grant NAG3-475)
(NASA-CR-176141; NAS 1.26:176141) Avail: NTIS HC A09/MF A01 CSCL 20N

Attenuation properties of the normal modes in an overmoded waveguide coated with a lossy material were analyzed. It is found that the low-order modes, can be significantly attenuated even with a thin layer of coating if the coating material is not too lossy. A thinner layer of coating is required for large attenuation of the low-order modes if the coating material is magnetic rather than dielectric. The Radar Cross Section (RCS) from an uncoated circular guide terminated by a perfect electric conductor was calculated and compared with available experimental data. It is confirmed that the interior irradiation contributes to the RCS. The equivalent-current method based on the geometrical theory of diffraction (GTD) was chosen for the calculation of the contribution from the rim diffraction. The RCS reduction from a coated circular guide terminated by a PEC are planned schemes for the experiments are included. The waveguide coated with a lossy magnetic material is suggested as a substitute for the corrugated waveguide. E.A.K.

N86-10378*# National Aeronautics and Space Administration, Washington, D. C.
DISCUSSION ON THE PROGRESS AND FUTURE OF SATELLITE COMMUNICATION (JAPAN)
M. Ogata, H. Mizusawa, and K. Irie Sep. 1985 20 p refs Transl. into ENGLISH from Mitsubishi Gunki Giho (Japan), v. 59, no. 6, 1985 p 408-412 Transl. by The Corporate Word, Inc. Pittsburgh, Pa.
(Contract NASw-4006)
(NASA-TM-77672; NAS 1.15:77672) Avail: NTIS HC A02/MF A01 CSCL 17B

The current status of communications satellite development in Japan is presented. It is shown that beginning with research on satellite communucations in the late 1950's, progress was made in the areas of communications, remote sensing, and technology experimentation. The current status of communication satellites is presented, stressing development in the areas of CFRP construction elements, the use of LSI and MIC circuits, advanced multibeam antenna systems, Ku and Ka band transmission systems, and the shift to small-scale earth stations. Methods for reducing costs and increasing transmission efficiency are shown. The technical specifications of all satellite projects currently under development are given. Users of Japanese communications satellite are presented. E.A.K.

N86-10379*# National Aeronautics and Space Administration. Lewis Research Center, Cleveland, Ohio.
TEST RESULTS FOR 20-GHz GaAs FET SPACECRAFT POWER AMPLIFIER
Kurt A. Shalkhauser Aug. 1985 22 p refs
(NASA-TM-87072; E-2573; NAS 1.15:87072) Avail: NTIS HC A02/MF A01 CSCL 09C

Test were conducted to measure the performance of the 20-GHz solid state, proof-of-concept amplifier. The amplifier operates over the 17.7 to 20.2-GHz frequency range and uses high power gallium arsenide field effect transistors. The amplifier design and test methods are briefly described. NASA and contractor performance data are compared. Author

N86-10380*# National Aeronautics and Space Administration. Lewis Research Center, Cleveland, Ohio.
A DUAL FREQUENCY MICROSTRIP ANTENNA FOR Ka BAND
Richard Q. Lee and Maurice F. Baddour 1985 12 p refs Presented at 1985 Antenna Appl. Symp., 18-20 Sep. 1985; Sponsored by Illinois Univ. and RADC, Monticello, Ill.
(NASA-TM-87124; E-2737; NAS 1.15:87124) Avail: NTIS HC A02/MF A01 CSCL 20N

For fixed satellite communication systems at Ka band with downlink at 17.7 to 20.2 GHz and uplink at 27.5 to 30.0 GHz, the focused optics and the unfocused optics configurations with monolithic phased array feeds have often been used to provide multiple fixed and multiple scanning spot beam coverages. It appears that a dual frequency microstrip antenna capable of transmitting and receiving simultaneously is highly desirable as an array feed element. This paper describes some early efforts on the development and experimental testing of a dual frequency annular microstrip antenna. The antenna has potential application for use in conjunction with a monolithic microwave integrated circuit device as an active radiating element in a phased array of phased array feeds. The antenna is designed to resonate at TM sub 12 and TM sub 13 modes and tuned with a circumferential microstrip ring to vary the frequency ratio. Radiation characteristics at both the high and low frequencies are examined. Experimental results including radiating patterns and swept frequency measurements are presented. Author

N86-10381*# National Aeronautics and Space Administration. Lewis Research Center, Cleveland, Ohio.
A NUMERICAL METHOD FOR APPROXIMATING ANTENNA SURFACES DEFINED BY DISCRETE SURFACE POINTS
Richard Q. Lee and Roberto Acosta 1985 10 p refs Presented at 1985 Antenna Appl. Symp., 18-20 Sep. 1985; sponsored by Illinois Univ. and RADC, Monticello, Ill.
(NASA-TM-87125; E-2738; NAS 1.15:87125) Avail: NTIS HC A02/MF A01 CSCL 20N

A simple numerical method for the quadratic approximation of a discretely defined reflector surface is described. The numerical method was applied to interpolate the surface normal of a parabolic reflector surface from a grid of nine closest surface points to the point of incidence. After computing the surface normals, the geometrical optics and the aperture integration method using the discrete Fast Fourier Transform (FFT) were applied to compute the radiaton patterns for a symmetric and an offset antenna configurations. The computed patterns are compared to that of the analytic case and to the patterns generated from another numerical technique using the spline function approximation. In the paper, examples of computations are given. The accuracy of the numerical method is discussed. Author

N86-10382*# Jet Propulsion Lab., California Inst. of Tech., Pasadena.
THE TELECOMMUNICATIONS AND DATA ACQUISITION REPORT Progress Report, Apr. - Jun. 1985
E. C. Posner, ed. 15 Aug. 1985 218 p refs
(Contract NAS7-918)
(NASA-CR-176203; NAS 1.26:176203; TDA-PR-42-82) Avail: NTIS HC A10/MF A01 CSCL 17B

Deep Space Network (DSN) progress in flight project support, tracking and data acquisition research and technology, network engineering, hardware and software implementation, and operation is discussed. In addition, developments in Earth-based radio technology as applied to geodynamics, astrophysics and the radio search for extraterrestrial intelligence are reported. For individual titles, see N86-10383 through N86-10402.

N86-10383*# Jet Propulsion Lab., California Inst. of Tech., Pasadena. Tracking Systems and Applications Section.
A VLBI SURVEY AT 2.29 GHz
D. D. Morabito, R. A. Preston, J. G. Williams, J. Faulkner, D. L. Jauncey (CSIRO, Sydney, Australia), and G. D. Nicolson (Council for Scientific and Industrial Research, Johannesburg, South Africa) *In its* The Telecommun. and Data Acquisition Progr. Rept. 15 Aug. 1985 p 1-10 refs (For primary document see N86-10382 01-32)
Avail: NTIS HC A10/MF A01 CSCL 20N

The Deep Space Network (DSN) is establishing a high-accuracy VLBI celestial reference frame. The results of a search for suitable radio sources to be used in constructing this frame are given. The VLBI observations using DSN baselines at 2.29 GHz with fringe spacings of about 3 milliarcseconds have been performed on 1398 radio sources spread over the entire sky. Of those, 917 sources were detected including 93% of the identifed BL Lacertae objects, 86% of Quasars and 36% of galaxies. The resulting catalog of compact radio sources is also useful for various astrophysical studies and in the formation of VLBI celestial reference frames. Author

N86-10384*# Jet Propulsion Lab., California Inst. of Tech., Pasadena. Tracking Systems and Applications Section.
COMPARISON OF THE CALIBRATION OF IONOSPHERIC DELAY IN VLBI DATA BY THE METHODS OF DUAL FREQUENCY AND FARADAY ROTATION
J. A. Scheid *In its* The Telecommun. and Data Acquisition Progr. Rept. 15 Aug. 1985 p 11-23 refs (For primary document see N86-10382 01-32)
Avail: NTIS HC A10/MF A01 CSCL 20N

When both S-band and X-band data are recorded for a signal which has passed through the ionosphere, it is possible to calculate the ionospheric contribution to signal delay. In Very Long Baseline Interferometry (VLBI) this method is used to calibrate the ionosphere. In the absence of dual frequency data, the ionospheric content measured by Faraday rotation, using a signal from a geostationary satellite, is mapped to the VLBI observing direction. The purpose here is to compare the ionospheric delay obtained by these two methods. The principal conclusions are: (1) the correlation between delays obtained by these two methods is weak; (2) in mapping Faraday rotation measurements to the VLBI observing direction, a simple mapping algorithm which accounts only for changes in hour angle and elevation angle is better than a more elaborate algorithm which includes solar and geomagnetic effects; (3) fluctuations in the difference in total electron content as seen by two antennas defining a baseline limit the application of Faraday rotation data to VLBI. Author

N86-10385*# Jet Propulsion Lab., California Inst. of Tech., Pasadena. Ground Antennas and Facilities Engineering Section.
A NEW 70-METER ANTENNA QUADRIPOD WITH REDUCED RF BLOCKAGE
J. J. Cucchissi *In its* The Telecommun. and Data Acquisition Progr. Rept. 15 Aug. 1985 p 24-30 refs (For primary document see N86-10382 01-32)
Avail: NTIS HC A10/MF A01 CSCL 20N

The new subreflector mount (quadripod) for the 64-meter to 70-meter antenna extension project was the result of many trial designs aimed at reducing radio frequency spherical and plane wave blockage and minimizing structural weight while satisfying strength and natural frequency requirements. An optimum design emerged which has a gain improvement of 0.32 dB over the present 64-meter design. Some of the trial designs made and the final optimum configuration selected are described. Author

N86-10386*# Jet Propulsion Lab., California Inst. of Tech., Pasadena. Ground Antennas and Facilities Engineering Section.
SEISMIC ANALYSIS OF THE LARGE 70-METER ANTENNA, PART 1: EARTHQUAKE RESPONSE SPECTRA VERSUS FULL TRANSIENT ANALYSIS c46
K. Kiedron and C. T. Chian *In its* The Telecommun. and Data Acquisition Progr. Rept. 15 Aug. 1985 p 31-42 ref (For primary document see N86-10382 01-31)
Avail: NTIS HC A10/MF A01 CSCL 08K

As a check on structure safety aspects, two approaches in seismic analysis for the large 70-m antennas are presented. The first approach, commonly used by civil engineers, utilizes known recommended design response spectra. The second approach, which is the full transient analysis, is versatile and applicable not only to earthquake loading but also to other dynamic forcing functions. The results obtained at the fundamental structural frequency show that the two approaches are in good agreement with each other and both approaches show a safe design. The results also confirm past 64-m antenna seismic studies done by the Caltech Seismology Staff. Author

N86-10387*# Jet Propulsion Lab., California Inst. of Tech., Pasadena. Radio Frequency and Microwave Subsystems Section.
AN EXPERIMENTAL TE SUB 12 - TE SUB 11 CIRCULAR WAVEGUIDE MODE CONVERTER c33
D. Hoppe *In its* The Telecommun. and Data Acquisition Progr. Rept. 15 Aug. 1985 p 43-56 refs (For primary document see N86-10382 01-32)
Avail: NTIS HC A10/MF A01 CSCL 09C

Theoretical and experimental results for a prototype TE sub 12 to TE sub 11 circular waveguide mode converter are discussed. The system which requires such device, the high power Ka-Band transmitter is described briefly. A short review of coupled mode theory is given, and the theoretical performance of the final converter design is given. Experimental results for the fabricated converter are presented and compared with theory. A method of identifying the various circular waveguide modes in a multimode device is described. Given the close agreement between the theoretical predictions and experimental results, the computer code may be used with confidence in the design of future multimode tapers and mode converters. Author

N86-10388*# Jet Propulsion Lab., California Inst. of Tech., Pasadena. Radio Frequency and Microwave Subsystems Section.
PROPAGATION AND RADIATION CHARACTERISTICS OF A MULTIMODE CORRUGATED WAVEGUIDE FEEDHORN
D. Hoppe *In its* The Telecommun. and Data Acquisition Progr. Rept. 15 Aug. 1985 p 57-67 refs (For primary document see N86-10382 01-32)
Avail: NTIS HC A10/MF A01 CSCL 20N

A prototype of the multimode corrugated feedhorn which will be used in the 400 kW CW Ka-band radar system is described. A rough design is done using coupled mode theory and standard corrugated waveguide modes. A more exact analysis using mode matching techniques is then used which takes into account the effect of a finite number of corrugations per wavelength and determines the modes which are reflected from the device. A prototype feedhorn has been constructed and measured. These experimental results are then compared to the theoretical predictions which agree satisfactorily closely. Author

N86-10389*# Jet Propulsion Lab., California Inst. of Tech., Pasadena. Ground Antennas and Facilities Engineering Section.
LOAD-DEFLECTION TESTS AND COMPUTER ANALYSES OF A HIGH-PRECISION ADHESIVE-BONDED ANTENNA REFLECTOR PANEL c24
C. T. Chian and R. Levy *In its* The Telecommun. and Data Acquisition Progr. Rept. 15 Aug. 1985 p 68-81 (For primary document see N86-10382 01-32)
Avail: NTIS HC A10/MF A01 CSCL 11D

New adhesive-bonded panels are being investigated as a part of an effort to extend and upgrade the 64-m to a 70-m antenna network. Load-deflection tests were conducted on a sample high-precision adhesive-bonded panel for comparison with design criteria. Two computerized structural models were developed in order to predict the deformation patterns under different types of distributed and concentrated loadings. The main purpose was to obtain empirical stiffness factors for the slit beams and girders in the panel structure. With determination and use of the empirical stiffness factors, there is a good agreement between the theoretically predicted deflections and the test measurements. It was also found that the new bonded panels satisfy the stringent design specifications and surface tolerance bounds. Author

N86-10390*# Jet Propulsion Lab., California Inst. of Tech., Pasadena. Communications Systems Research Section.

A SEQUENTIAL DECODING PERFORMANCE ANALYSIS FOR INTERNATIONAL COMET EXPLORER c61

D. Divsalar *In its* The Telecommun. and Data Acquisition Progr. Rept. 15 Aug. 1985 p 82-91 refs (For primary document see N86-10382 01-32)

Avail: NTIS HC A10/MF A01 CSCL 09B

The effect of a noisy reference carrier on the performance of International Comet Explorer (ICE) Sequential decoder is analyzed. Ideal reference models for frame deletion probability are given for the Telemetry Processing Assembly (TPA) and the Linkabit (LS4815) sequential decoders. Based on these ideal reference models the deletion probability in the presence of noisy reference carrier is computed for both the high and the low data rate cases. A medium data rate performance model is then derived using an interpolation method. The derived medium rate performance model depends on the phase locked loop bandwidth-integration time product. Results are obtained for frame length 1024 bits, data bit rates of 1024 bps and 512 bps, modulation index of 60 deg, and threshold loop bandwidths of 10 Hz and 3 Hz. The medium rate model agrees with experimental data to within measurement uncertainty. For the 10 Hz loop bandwidth and modulation index of 60 deg at frame deletion rate of 0.0001, the required total received power to noise ratio is 36 dB. The analysis given is general and applicable to any sequential decoder, provided that the ideal reference model of the decoder is available. Author

N86-10391*# Jet Propulsion Lab., California Inst. of Tech., Pasadena. Communications System Research Section.

THE VLSI DESIGN OF ERROR-TRELLIS SYNDROME DECODING FOR CONVOLUTIONAL CODES c64

I. S. Reed (Univ. of Southern California, Los Angeles), J. M. Jensen (Univ. of Southern California, Los Angeles), T. K. Truong, and I. S. Hsu *In its* The Telecommun. and Data Acquisition Progr. Rept. 15 Aug. 1985 p 92-107 refs (For primary document see N86-10382 01-32)

Avail: NTIS HC A10/MF A01 CSCL 12A

A recursive algorithm using the error-trellis decoding technique is developed to decode convolutional codes (CCs). An example, illustrating the very large scale integration (VLSI) architecture of such a decode, is given for a dual-K CC. It is demonstrated that such a decoder can be realized readily on a single chip with metal-nitride-oxide-semiconductor technology. Author

N86-10392*# Jet Propulsion Lab., California Inst. of Tech., Pasadena. Communications Systems Research Section.

HIGH-RATE CONVOLUTIONAL CODE CONSTRUCTION WITH THE MINIMUM REQUIRED SNR CRITERION c64

P. J. Lee *In its* The Telecommun. and Data Acquisition Progr. Rept. 15 Aug. 1985 p 108-112 refs (For primary document see N86-10382 01-32)

Avail: NTIS HC A10/MF A01 CSCL 12A

New short constraint length, high-rate convolutional codes which minimize the required signal to noise ratios (SNR) are found and tabulated for rates 2/3, 3/4, and 4/5, and for constraint length K up to 10. When compared with previously reported codes, most of the new codes reduce the required SNR only slightly. However, there are some pairs of K and code rate for which the new codes require considerably less SNR. The most significant one is the new K = 8, ate 4/5 code which requires 1.2 dB less SNR than the known code with the same parameters, for a desired bit error rate of 0.000001. Author

N86-10393*# Jet Propulsion Lab., California Inst. of Tech., Pasadena. TDA Engineering Section.

DSN FREQUENCY AND TIMING SYSTEM, MARK 4-85

B. W. Falin *In its* The Telecommun. and Data Acquisition Progr. Rept. 15 Aug. 1985 p 113-119 (For primary document see N86-10382 01-32)

Avail: NTIS HC A10/MF A01 CSCL 20N

As part of the Deep Space Network (DSN) Mark IVA implementation program, the DSN frequency and timing system is currently undergoing changes. With the implementation of signal processing centers (SPC) at each deep space communications complex (DSCC), major changes to the frequency and timing distribution equipment were necessary. A functional description of the Mark IVA frequency and timing system (FTS) as it exists today and planned capabilities through 1988 is given. Author

N86-10394*# Jet Propulsion Lab., California Inst. of Tech., Pasadena. TDA Mission Support and DSN Operations Office.

JPL EMERGENCY SUPPORT OF TDRSS AND COMPATIBLE SATELLITES c14

N. A. Fanelli *In its* The Telecommun. and Data Acquisition Progr. Rept. 15 Aug. 1985 p 120-124 (For primary document see N86-10382 01-32)

Avail: NTIS HC A10/MF A01 CSCL 14B

The Tracking and Data Relay Satellite System (TDRSS) will consist of three identical satellites in geosynchronous orbits and a dedicated ground receiving station. The first two satellites (TDRS East and TDRS West) will form the operational TDRS service network providing near-global real-time user satellite coverage. The third TDRS satellite will act as an in-orbit spare. Since the TDRSS satellite are supported by a single ground station, a method of providing emergency support for TDRS and user satellites is needed. The support to be provided by JPL's Deep Space Network is described. Author

N86-10395*# Jet Propulsion Lab., California Inst. of Tech., Pasadena. TDA Planning Office.

PLANNING FOR VLA/DSN ARRAYED SUPPORT TO THE VOYAGER AT NEPTUNE c14

J. W. Layland and D. W. Brown *In its* The Telecommun. and Data Acquisition Progr. Rept. 15 Aug. 1985 p 125-135 refs (For primary document see N86-10382 01-32)

Avail: NTIS HC A10/MF A01 CSCL 14B

Preplanning for the use of the National Radio Astronomy Observatory's Very Large Array (VLA) in support of Voyager at Neptune has been underway since early 1982. When arrayed with the Deep Space Network (DSN) antennas at Goldstone, CA, the VLA more than doubles the potential data return over the American longitude for the 1989 Voyager encounter. The background, rationale and current status of planning for VLA-DSN Arrayed Support to the Voyager at Neptune are discussed. Author

N86-10396*# Jet Propulsion Lab., California Inst. of Tech., Pasadena. TDA Planning Office.

A VLA EXPERIMENT: PLANNING FOR VOYAGER AT NEPTUNE c12

J. W. Layland, P. J. Napier (National Radio Astronomy Observatory), and A. R. Thompson (National Radio Astronomy Observatory) *In its* The Telecommun. and Data Acquisition Progr. Rept. 15 Aug. 1985 p 136-142 refs (For primary document see N86-10382 01-32)

Avail: NTIS HC A10/MF A01 CSCL 22A

A very large array (VLA) engineering experiment was conducted on the night of July 22, 1983 to explore one aspect of the potential for the VLA to support Voyager at its Neptune encounter in August of 1989. Specifically, the experiment tested the ability of the VLA to self-calibrate on a natural radio source whose effective signal strength is the same as Voyager's will be at its Neptune encounter. The experiment was successful and supported the belief that the VLA would be able to be self-calibrated with Voyager's signal. Author

N86-10397*# Jet Propulsion Lab., California Inst. of Tech., Pasadena. Reliability Engineering Section.

PERIODIC BINARY SEQUENCES WITH VERY GOOD AUTOCORRELATION PROPERTIES c64

S. Tyler and J. Loftsson *In its* The Telecommun. and Data

Acquisition Progr. Rept. 15 Aug. 1985 p 143-158 refs (For primary document see N86-10382 01-32)
Avail: NTIS HC A10/MF A01 CSCL 12A

Computer searches were performed using both an 8086 microprocessor and a Cyber 750 mainframe to find repeated binary phase coded waveforms with very good matched and mismatched autocorrelation properties. The best results for every period up to 64 are given. Sequences with optimal peak sidelobes were discovered for each of these periods. These sequences have extensive applications in radar and communications, particularly in situations when there are very unfavorable signal-to-noise ratios. The best sequence of period 64 when processed using a mismatched filter giving no sidelobes has a reduction in the main lobe of less than 0.23 dB. Author

N86-10398*# Jet Propulsion Lab., California Inst. of Tech., Pasadena. Reliability Engineering Section.
A BINARY SEQUENCE OF PERIOD 60 WITH BETTER AUTOCORRELATION PROPERTIES THAN THE BARKER SEQUENCE OF PERIOD 13 c64
J. Watkins (TRW, Inc., Redondo Beach, Calif.), J. Loftsson, and S. Tyler *In its* The Telecommun. and Data Acquisition Progr. Rept. 15 Aug. 1985 p 159-162 refs (For primary document see N86-10382 01-32)
Avail: NTIS HC A10/MF A01 CSCL 12A

A binary sequence of period 60 has been discovered which in some respects has better autocorrelation properties than the Barker sequence of period 13. When both sequences are processed using appropriate sidelobe-eliminating mismatched filters, the Barker sequence's main lobe is reduced by a factor of 1.040 or 0.17 dB, while the new sequence's main lobe is reduced by a factor of only 1.035 or 0.15 dB. This sequence is the first counterexample known to the authors of the hypothesis that the autocorrelation properties of all sequences of periods greater than 13 are inferior to those of the Barker period-13 sequences. Sequences of this type are very useful in radar and deep space communications, especially in situations where there is an adverse signal to noise ratio. Author

N86-10399*# Jet Propulsion Lab., California Inst. of Tech., Pasadena. TDA Engineering Section.
THE GCF MARK 4 IMPLEMENTATION AND BEYOND c14
R. A. Crowe *In its* The Telecommun. and Data Acquisition Progr. Rept. 15 Aug. 1985 p 163-172 refs (For primary document see N86-10382 01-32)
Avail: NTIS HC A10/MF A01 CSCL 14B

A brief overview is given of the major subsystems that comprise the Mark IVA ground communication facility (GCF) along with key information on basic functionality that may be inadequately or imperfectly understood. The evolving GCF System as it is currently being designed is described. Author

N86-10400*# Jet Propulsion Lab., California Inst. of Tech., Pasadena. Communications Systems Research Section.
SETI RADIO SPECTRUM SURVEILLANCE SYSTEM
B. Crow, A. Lokshin, M. Marina, and L. Ching *In its* The Telecommun. and Data Acquisition Progr. Rept. 15 Aug. 1985 p 173-184 (For primary document see N86-10382 01-32)
Avail: NTIS HC A10/MF A01 CSCL 20N

The SETI Radio Spectrum Surveillance System (SRSSS) will provide a data base for assessing the radio frequency interference (RFI) environment for SETI and minimizing RFI disruptions during the search. The system's hardware and software are described and the sensitivity of the system is discussed. Author

N86-10401*# Jet Propulsion Lab., California Inst. of Tech., Pasadena. Tracking Systems and Applications Section.
MOBILE VLBI AND GPS MEASUREMENT OF VERTICAL CRUSTAL MOTION c46
P. M. Kroger, J. M. Davidson, and E. C. Gardner (Kalamazoo Coll.) *In its* The Telecommun. and Data Acquisition Progr. Rept. 15 Aug. 1985 p 185-198 refs (For primary document see N86-10382 01-32)
Avail: NTIS HC A10/MF A01 CSCL 08E

Mobile Very Long Base Interferometry (VLBI) and Global Positioning System (GPS) geodetic measurements have many error sources in common. Calibration of the effects of water vapor on signal transmission through the atmosphere, however, remains the primary limitation to the accuracy of vertical crustal motion measurements made by either technique. The two primary methods of water vapor calibration currently in use for mobile VLBI baseline measurements were evaluated: radiometric measurements of the sky brightness near the 22 GHz emission line of free water molecules and surface meteorological measurements used as input to an atmospheric model. Based upon a limited set of 9 baselines, it is shown that calibrating VLBI data with water vapor radiometer measurements provides a significantly better fit to the theoretical decay model than calibrating the same data with surface meteorological measurements. The effect of estimating a systematic error in the surface meteorological calibration is shown to improve the consistency of the vertical baseline components obtained by the two calibration methods. A detailed error model for the vertical baseline components obtained indicates current mobile VLBI technology should allow accuracies of order 3 cm with WVR calibration and 10 cm when surface meteorological calibration is used. Author

N86-10402*# Jet Propulsion Lab., California Inst. of Tech., Pasadena. Communications Systems Research Section.
IMPROVED MAPPING OF RADIO SOURCES FROM VLBI DATA BY LEAST-SQUARE FIT
E. R. Rodemich *In its* The Telecommun. and Data Acquisition Progr. Rept. 15 Aug. 1985 p 199-210 refs (For primary document see N86-10382 01-32)
Avail: NTIS HC A10/MF A01 CSCL 20N

A method is described for producing improved mapping of radio sources from Very Long Base Interferometry (VLBI) data. The method described is more direct than existing Fourier methods, is often more accurate, and runs at least as fast. The visibility data is modeled here, as in existing methods, as a function of the unknown brightness distribution and the unknown antenna gains and phases. These unknowns are chosen so that the resulting function values are as near as possible to the observed values. If researchers use the radio mapping source deviation to measure the closeness of this fit to the observed values, they are led to the problem of minimizing a certain function of all the unknown parameters. This minimization problem cannot be solved directly, but it can be attacked by iterative methods which we show converge automatically to the minimum with no user intervention. The resulting brightness distribution will furnish the best fit to the data among all brightness distributions of given resolution. Author

N86-10403# Weapons Systems Research Lab., Adelaide (Australia).
A SIMPLIFIED METHOD OF ESTIMATION OF THE SPECULAR COMPONENTS OF RADAR CROSS SECTION FOR SOME RE-ENTRANT CONDUCTORS
L. A. Nicholls Dec. 1984 34 p
(AD-A156573; WSRL-0389-TM) Avail: NTIS HC A03/MF A01 CSCL 17/9

Methods of ray optics are used to describe the wavefronts emerging from the specular lines or specular rings on three separate irradiated reentrant conductors for short radar wavelengths. The conductors are a biconical reflector, a hollow circular cylinder with a far flat termination, and a thin spherical shell with a circular hole. The associated far fields and hence their Radar Cross Section (RCS) components are then found from evaluation of the associated simple field integrals using Huygen's Principle. GRA

N86-10404# Naval Weapons Center, China Lake, Calif.
RADOME ANALYSIS AND DESIGN CAPABILITIES OF THE RF AND MICROWAVE TECHNOLOGY BRANCH Interim Report, Fiscal Year 1982 - 1984
P. L. Overfelt Apr. 1985 39 p
(AD-A156662; AD-E900475; NWC-TP-6636) Avail: NTIS

HC A03/MF A01 CSCL 17/9

A description of computer codes covering boresight error prediction, flat panel reflection and transmission properties, Von Karman geometry parameters, and spherical wave propagation for radomes is presented. The theoretical basis for each code is discussed, and examples of inputs and outputs are given. Comparison of theory with experimental data shows reasonable correlation. Thus, these codes can predict many interesting and useful properties needed for adequate initial radome design without resorting to expensive and time-consuming test procedures. GRA

N86-10405# Mission Research Corp., Santa Barbara, Calif.
ACOUSTIC GRAVITY WAVE CHEMISTRY MODEL FOR THE RAYTRACE CODE Technical Report, 30 Jun. 1983 - 31 Jul. 1984
T. E. Old 1 Mar. 1984 38 p
(Contract DNA001-80-C-0022)
(AD-A156850; AD-E301723; MRC-R-815; DNA-TR-84-127) Avail: NTIS HC A03/MF A01 CSCL 20/14

This report discusses the implementation of F-region electron chemistry in the acoustic gravity wave model of the code RAYTRACE. The chemistry consists of three dominant reactions that control electron depletion in an F-region parcel that is pushed down into the higher density E-region atmosphere by the passage of a large amplitude gravity wave. The effect of electron depletion on the propagation of high frequency radio waves is shown by comparison of RAYTRACE radio propagation calculations with and without chemistry. GRA

N86-10406# Naval Research Lab., Washington, D. C.
ON THE USE OF X-BAND CW NANOSECOND AIRBORNE RADAR FOR TERRAIN PROFILING Final Report, Oct. 1984 - Apr. 1985
D. T. Chen and E. A. Uliana 25 Jun. 1985 21 p
(DA Proj. W05-270)
(AD-A156886; NRL-MR-5599) Avail: NTIS HC A02/MF A01 CSCL 17/9

Terrain profile sensed by a 10 GHz X-band airborne nanosecond radar has been compared against the terrain profile sensed simultaneously by a pulse laser profilometer. Several facts can be observed from a series of inter-comparisons between these two profiles. First, under the condition of comparable sampling intervals, the terrain profile sensed by radar is almost the same as that sensed by the laser profilometer except radar sensed profile does not contain information of narrow and tall objects above the ground surface. Second, a radar range resolution finer than 4 nanoseconds and a better algorithm on return waveform analysis for identifying narrow and tall objects in addition to the ground surface are going to improve accuracy and precision of radar's capability in terrain profiling. Third, for a short flight track, the removal of the effects on radar range measurements due to aircraft motion can not be achieved with knowing three ground surface elevations whose locations are well separated along the flight track. Last, the limit at which radar range tracking circuitry loses its lock and, thus, its ability in resolving ranging is higher for aftside range slopes than for foreside range slopes. GRA

N86-10407# Politecnico di Torino (Italy). Dept. di Elettronica.
COMPUTATIONAL TECHNIQUES FOR THE ANALYSIS AND DESIGN OF DIGITAL COMMUNICATION SYSTEMS Final Technical Report, 28 Jan. 1982 - 28 Mar. 1985
E. Biglieri Mar. 1985 107 p
(Contract DAJA37-80-C-0011; DA Proj. 1L1-61102-BH-57)
(AD-A156945; AD-E750985) Avail: NTIS HC A06/MF A01 CSCL 12/1

In this report we introduce some computational techniques for the analysis and design of digital communication systems, possibly operating over a nonlinear channel (a typical example is a digital satellite system, with the transponder amplifier working at or near saturation for better efficiency). We first consider evaluation of error probabilities when the disturbances are only incompletely known. Then we describe a combined simulation-and-analytical technique to evaluate the power density spectrum of a digital signal passed through a nonlinear channel. Next, we consider the problem of designing and evaluating the performance of the optimum linear receiving filter for transmission over a nonlinear channel. Finally, we consider Ungerboeck codes; a new class of multidimensional codes is introduced, its applications discussed, and an important property concerning their power spectral densities is shown. GRA

N86-10408# Sandia Labs., Albuquerque, N. Mex.
METHODS FOR DEVELOPING JAM-RESISTANT SECURITY COMMUNICATIONS NETWORKS AT FIXED-SITE FACILITIES
D. J. Gangel, J. E. Heustess, and M. K. Snell 1985 5 p Presented at the 1st Ann. AFCEA Symp. and Exposition on Phys. and Electron. Security, Philadelphia, 19 Aug. 1985
(Contract DE-AC04-76DP-00789)
(DE85-012032; SAND-85-0200C; CONF-850885-1) Avail: NTIS HC A02/MF A01

Considerable work has been done identifying and developing equipment and procedures that can be used to improve the survivability of a security communications network during a jamming assault. Insight is given into alternate communications methods that can be used to develop resistance to jamming by supplementing existing radio communications. The spatial properties of jamming are then discussed and examples of how these properties can be explocited are examined. Also discussed are spread-spectrum radios that are highly resistant to jamming and the importance of jamming exercises. DOE

N86-10409# California Univ., Livermore. Lawrence Livermore Lab.
MICROWAVE EVALUATION OF MATERIALS
F. J. King and V. R. Latorre May 1985 14 p
(Contract W-7405-eng-48)
(DE85-013183; UCID-20437) Avail: NTIS HC A02/MF A01

Modern microwave tools and measurement techniques show considerable promise for evaluating the electrical and physical properties of materials. These techniques are particularly useful for measuring the dielectric and conductive properties in situ. From these measurements, it is possible to infer many physical parameters such as moisture content, porosity, state of cure or aging, the presence of surface cracks, surface roughness, fiber/filler ratio, bulk fiber orientation, and some constitutent parameters such as graphite. While the wavelength of microwaves (centimeters) limits the spatial resolution required to locate small flaws (deep cracks, voids, etc.), microwaves are ideally suited to measure small variations in density and semiconductive properties of nonmetals. This is best accomplished using coherent techniques which are highly sensitive and capable of measuring the phase as well as the amplitude of the microwave signals being coupled to the test material. Moreover, since microwaves are polarized vector fields, they are highly sensitive to the anisotropy of materials. DOE

N86-10410# Allied Bendix Aerospace, Kansas City, Mo.
MINIATURE RADAR PACKAGING Final Report
G. W. Andrews Jun. 1985 105 p
(Contract DE-AC04-76DP-00613)
(DE85-014598; BDX-613-3266) Avail: NTIS HC A06/MF A01

Several concepts of interconnections between coaxial cables and RF HMCs were evaluated resulting in two approaches that function well electrically and mechanically and that are easily processed. Methods of attaching various configurations of large ceramic substrates into assemblies were investigated, yielding a better understanding of why breakage occurs, and to find ways to reduce the occurrence of breakage. An evaluation of several materials for use as gaskets to shield against RF interference between RF circuit compartments resulted in two suitable possibilities. Resistive film and microwave absorber liners were evaluated on the inside of RF circuit compartment covers, with favorable results obtained from one that reduced the effect of the lid proximity on the circuit performance. DOE

N86-10411# Research Inst. of National Defence, Linkoeping (Sweden).

DIGITAL RADIO LINK: METHOD AND A MEASURING SYSTEM FOR STUDYING THE RADIO CHANNEL DURING FREQUENCY SELECTIVE FADING

Stefan Mattsson Mar. 1985 57 p refs In SWEDISH; ENGLISH summary
(FOA-C-30386-E2; ISSN-0347-3708) Avail: NTIS HC A04/MF A01; Research Institute of National Defence, Stockholm KR 50

Methods to calculate propagation parameters during multipath propagation on microwave line-of-sight paths are reviewed. Spectrum measurements to verify a channel model for Swedish conditions, in the 7 and 13 GHz frequency bands are described. The measurements are controlled, in the sense that received power spectra are recorded if the discrepancy from a reference exceeds a given threshold. The program is described, and methods based on the characteristic frequency dependent attenuation during frequency selective fading are outlined. Author (ESA)

N86-10412# Deutsche Forschungs- und Versuchsanstalt fuer Luft- und Raumfahrt, Oberpfaffenhofen (West Germany). Inst. fuer Hochfrequenztechnik.

DIRECT-COUPLED CAVITY FILTERS WITH IRISES OF ARBITRARY THICKNESS

Manfred Weisser and Karl Hans Waegel Jan. 1985 67 p refs In GERMAN; ENGLISH summary Report will also be announced as translation (ESA-TT-939)
(DFVLR-FB-85-14; ISSN-0171-1342) Avail: NTIS HC A04/MF A01; DFVLR, Cologne DM 21

The transmission characteristics of symmetrical waveguide filters are investigated. The thickness of the irises is taken into account. The calculations are based on an exact mode matching method. In the frequency range of the X-band one-, two-, three-, four-, and six-cavity filters are analyzed and parameters such as aperture, thickness of irises, and cavity length are changed. The results of the measurements are in good agreement with the computed transmission characteristics. Author (ESA)

N86-10413# Deutsche Forschungs- und Versuchsanstalt fuer Luft- und Raumfahrt, Oberpfaffenhofen (West Germany). Abteilung HF-Verfahren.

SAR IMAGE QUALITY: A REVIEW

Timonthy K. Pike Mar. 1985 41 p refs
(DFVLR-Mitt-85-07; ISSN-0176-7739) Avail: NTIS HC A03/MF A01; DFVLR, Cologne DM 14

The necessities and applications of Synthetic Aperture Radar (SAR) image quality measurement, and the common SAR image quality parameters including spatial resolution, radiometric resolution, radiometric accuracy, energy distribution, and geometric distortion are discussed. Measurement techniques are described and supplemented with examples from SAR campaigns. Author (ESA)

N86-10616*# Jet Propulsion Lab., California Inst. of Tech., Pasadena.

RADAR SYSTEM DESCRIPTION

D. N. Held and W. E. Brown *In its* NASA/JPL Aircraft SAR Workshop Proc. 15 Jun. 1985 p 5-12 Original contains color illustrations (For primary document see N86-10615 01-43)
Avail: NTIS HC A05/MF A01 CSCL 17I

N86-10617*# Jet Propulsion Lab., California Inst. of Tech., Pasadena.

CV-990 L-BAND SAR: A CALIBRATION EXPERIMENT

D. N. Held and C. Werner *In its* NASA/JPL Aircraft SAR Workshop Proc. 15 Jun. 1985 p 17-20 ref Original contains color illustrations (For primary document see N86-10615 01-43)
Avail: NTIS HC A05/MF A01 CSCL 17I

33 ELECTRONICS AND ELECTRICAL ENGINEERING

Includes test equipment and maintainability; components, e.g., tunnel diodes and transistors; microminiaturization; and integrated circuitry.

For related information see also *60 Computer Operations and Hardware* and *76 Solid-State Physics.*

N86-10414 Department of the Air Force, Washington, D.C.

PROTECTION CIRCUITRY FOR HIGH VOLTAGE DRIVERS Patent

G. H. Frank, inventor (to Air Force) Issued 14 May 1985 5 p Supersedes AD-D010559
(AD-D011781; US-Patent-4,517,618; US-Patent-Appl-SN-529412; US-Patent-Class-361-58) Avail: US Patent and Trademark Office CSCL 09/1

Protection circuitry interposed between a power source and a load is arranged to gradually apply high voltage has attained a predetermined percentage of its nominal value. In the event that the load current exceeds a prescribed maximum limit, or in the absence of additional load voltages, the high voltage supply is disconnected from the load. GRA

N86-10415 Department of the Navy, Washington, D. C.

AMPLITUDE AND PHASE MODULATION IN FIN-LINES ELECTRICAL TUNING Patent

C. Vittoria, inventor (to Navy) Issued 19 Mar. 1985 6 p
(AD-D011813; US-Patent-4,506,234; US-Patent-Appl-SN-505569; US-Patent-Class-332-16R) Avail: US Patent and Trademark Office CSCL 09/1

A fin-line waveguide device for modulating signals passing there through, was discussed. The device comprises a fin-line waveguide including two channel members longitudinally extending in the direction of signal propagation through the device. The channel members are physically and electrically separated by a ferrite dielectric slab which is oriented in a longitudinally extending plane parallel to the electric field lines of the signal passing through the device. A magnetic field is applied to the ferrite slab to magnetically bias the slab to ferromagnetic resonance. A voltage is applied across the ferrite slab to alter the ferromagnetic resonance characteristics of the slab. The phase and amplitude of the signal processing through the waveguide are modulated in response to the applied voltage. GRA

N86-10416 Department of the Navy, Washington, D. C.

P-N JUNCTION CONTROLLED FIELD EMITTER ARRAY CATHODE Patent

R. F. Greene and H. F. Gray, inventors (to Navy) Issued 23 Apr. 1985 11 p Supersedes AD-D009923
(AD-D011815; US-Patent-4,513,308; US-Patent-Appl-SN-421766; US-Patent-Class-357-55) Avail: US Patent and Trademark Office CSCL 09/1

A Field Emitter Array comprising a semiconductor substrate with an emitter surface formed thereon. A plurality of emitter pyramids is disposed on the emitter surface for emitting an electron current. The magnitude of the electron current emitted by each emitter pyramid 1 max, is controlled by a reverse-biased p-n junction associated with each emitter pyramid where 1 max = j sat X A p-n, j sat being the saturation current density and A p-n being the area of the reverse-biased p-n junction associated with each emitter pyramid. A grid, positively biased relative to the emitter surface and the emitter pyramids, is disposed above the emitter surface for creating a electric field that induces the emission of the electron current from the emitter tips. Author (GRA)

N86-10417 Department of the Navy, Washington, D. C.

PULSE COMPRESSION SYSTEM Patent

B. L. Lewis, inventor (to Navy) Issued 4 Jun. 1985 14 p Supersedes AD-D007318
(AD-D011833; US-Patent-4,521,779; US-Patent-Appl-SN-143399; US-Patent-Class-343-17.2PC) Avail: US Patent and Trademark

Office CSCL 09/4

This patent desribes a system for polyphase encoding transmitted pulses of energy and for decoding the received signals to enhance returns from the range interval being examined during a particular processing period and attenuate returns from contiguous range intervals (pulse compression). The system includes a decoding device which comprises a delay circuit having N distributed outputs including its input for producing a uniform delay between adjacent outputs corresponding to N inputted elements of received phase-coded signal of length N squared; a conjugator circuit coupled to the first N/2 successive outputs of the delay circuit; a first signal-combining circuit coupled to the conjugator circuit and to the last N/2 successive outputs of the delay circuit; a multiplier circuit coupled to the first signal-combining circuit; and a second signal-combining circuit coupled to the multiplier circuit. The decoding device provides a decoding phase shift to the signal elements of the phase-coded signal. GRA

N86-10418*# National Aeronautics and Space Administration, Washington, D. C.

DESIGN AND CONSTRUCTION OF A FARADAY CUP FOR MEASUREMENT OF SMALL ELECTRONIC CURRENTS

Andre Veyssiere Sep. 1985 35 p refs Transl. into ENGLISH of "Etudes et Realisation d'une Coupe de Faraday pour les Mesures de Faibles Courants Electroniques" Saclay, CEA, Oct. 1967 p 1-28 Original language document announced as N68-25321 Transl. by Scientific Translation Service, Santa Barbara, Calif. (Contract NASw-4004)
(NASA-TM-77915; NAS 1.15:77915; CEA-R-3276) Avail: NTIS HC A03/MF A01 CSCL 09A

The design of a device to measure and integrate very small currents generated by the impact of a charged particle beam upon a Faraday cut is described. The main component is a graphite block capable of stopping practically all the incident changes. The associated electronic apparatus required to measure better than 10/13 ampere with a precision of 10/0 is described. E.A.K.

N86-10419# Defence Research Establishment Valcartier (Quebec).

AN ACTIVE TRACKING BAND-PASS FILTER

A. Morin and P. Labbe May 1985 50 p
(AD-A156559; DREV-4347/85) Avail: NTIS HC A03/MF A01 CSCL 09/5

A frequency-agile tracking filter, which operates over a wide frequency range with a high immunity to noise and interference, has been designed. It consists of a second-order bandpass filter which is continuously tunable over the 5 to 140-kHz band. The resonant frequency of the filter is adjusted by means of a feedback loop to the frequency component of greatest amplitude in the input signal. The loop includes a fast AGC amplifier, a fast frequency-to-voltage converter and a low-pass filter. The components of the tracking filter are described and analyzed. Analysis of the tracking filter, as regards its immunity to noise and interference, its frequency agility and the stability of its control loop, is also presented to optimize system parameters. Finally, the performance of the processor is shown by experimental measurements. GRA

N86-10420# Washington Univ., St. Louis, Mo. Dept. of Electrical Engineering.

CRITERIA FOR THE DESIGN OR SELECTION OF A BIOELECTROMAGNETICS EXPERIMENT Final Technical Report, 1 Sep. 1984 - 31 May 1985

W. F. Pickard 28 Jun. 1985 15 p
(Contract N00014-84-K-0457)
(AD-A156575) Avail: NTIS HC A02/MF A01 CSCL 06/19

By athermal, one normally means an effect which: (1) has been explained explicitly and unambiguously in terms of mechanisms other than increased random molecular motion (i.e., heating), or (2) occurs at absorbed power levels so low that a thermal mechanism seems unlikely, or (3) displays so unexpected a dependence upon some experimental variable that it is hard to see how heating could lie behind it. The aim of this report is to discuss guidelines by which and experiment directed toward the discovery or elucidation of an athermal effect might be designed or evaluated. It will consist of three main sections. First, the great commandment of athermal bioelectromagnetics will be discussed; that any reported, putatively athermal bioeffect be robustly reproducible. Six criteria are propounded for judging the credibility of a reported experiment in athermal bioelectromagnetics. It is concluded that experimentation in athermal bioelectromagnetics would be markedly facilitated by the identification of the mechanisms underlying the observed effects. GRA

N86-10421# Department of the Navy, Washington, D. C.

CONSTANT RISE AGC (AUTOMATIC GAIN CONTROL) DEVICE Patent Application

R. A. Slack, inventor (to Navy) Filed 25 Mar. 1985 19 p
(AD-D011744; US-Patent-Appl-SN-715992) Avail: NTIS HC A02/MF A01 CSCL 09/5

The invented device provides automatic gain control (AGC) of incoming signals over a large dynamic range of input levels with a constant rise time. The constant rise AGC device includes a primary AGC loop for receiving the incoming or input signal and splitting the input signal to input and output components of the primary AGC loop. The input signal to the input component is processed within the primary AGC loop to control the gain of the input signal at the output component of the primary AGC loop. The primary AGC loop has a slow detector. A secondary AGC loop is provided within the primary AGC loop, and this secondary AGC loop includes the aforementioned input component and has its output connected to the slow detector. The secondary AGC loop has a fast detector for preventing self-imposed saturation. With this arrangement the secondary AGC loop can be utilized to provide a constant AGC buildup signal for any input signal which is greater than a predetermined dB range, and the remainder of the primary AGC loop, which receives the constant AGC buildup signal from the secondary AGC loop, can be optimized for desired rise and fall times so that the latter's output signal can be relatively unaffected by interference bursts, signal gaps, and fading in the input signal. Author (GRA)

N86-10422# Department of the Navy, Washington, D. C.

EXTENDED PRECISION IN VIDEO BANDWIDTH ANALOG TO DIGITAL CONVERTER USING OPTICAL TECHNIQUES Patent Application

H. F. Taylor, inventor (to Navy) Filed 28 Mar. 1985 19 p
(AD-D011745; US-Patent-Appl-SN-717365) Avail: NTIS HC A02/MF A01 CSCL 09/5

Two interferometric electro-optic modulators formed from single mode waveguides in a single crystal substrate of pockels (linear) electro-optic material is used in conjunction with optical sampling techniques and conventional Analog-to-Digital technology to convert analog signals to a binary representation. Author (GRA)

N86-10423# Department of the Navy, Washington, D. C.

HIGH OUTPUT PROGRAMMABLE SIGNAL CURRENT SOURCE FOR LOW OUTPUT IMPEDANCE APPLICATIONS Patent Application

D. G. Jablonski and R. W. Watkins, inventors (to Navy) Filed 10 May 1985 10 p
(AD-D011751; US-Patent-Appl-SN-732330) Avail: NTIS HC A02/MF A01 CSCL 09/5

The present invention relates to a high output programmable current source. Complementary output stages are connected between appropriate power supply polarities for driving a low impedance load which is connected to circuit ground. An operational amplifier is connected between the input and emitter of each of the complementary stages providing negative feedback for virtually eliminating in the input offset voltage of the respective output stage. A programmable function signal source is connected to the operational amplifiers for driving a programmable signal current to the extent possible through the load resistance from a limited voltage supply. Author (GRA)

N86-10424# Department of the Air Force, Washington, D.C.
TOTAL INTERNAL REFLECTION MODULATOR/DEFLECTOR Patent Application
Birnbaum, inventor (to Air Force) Filed 22 Apr. 1985 21 p
(AD-D011757; US-Patent-Appl-SN-726872) Avail: NTIS HC A02/MF A01 CSCL 20/3

This document refers to a total internal reflection modulator/deflector assembly for use with a focused beam of polarized incident laser light. The application of a low direct current voltage (e.g., less than 50 volts) to a pair of identical stacked crystals exhibiting the Pockel's effect produces an index of refraction difference at their interface. Since the index changes are small, the incidence angle of the impinging polarized laser light is large, e.g., 89 degrees. In the preferred embodiment, one crystal is rotated relative to the other, such that the applied electric field causes and index changes of +(delta)n in one crystal and of -(delta)n in the other crystal. As a result, the impinging polarized laser light is refraction into two portions, one of which is totally internal reflected, and transmitted in the desired modulated conditions. Two electrode members are used to apply the low direct current voltage to the interface of the crystals, with the electrodes arranged to face each other across the crystals, and also positioned such that the incident light need not traverse them. GRA

N86-10425# Department of the Air Force, Washington, D.C.
INSTANTANEOUS FREQUENCY MEASUREMENT RECEIVER WITH DIGITAL PROCESSING Patent Application
J. B. Y. Tsui, inventor (to Air Force) Filed 30 May 1985 13 p
(AD-D011759; US-Patent-Appl-SN-739413) Avail: NTIS HC A02/MF A01 CSCL 14/2

The receiver comprises a 90 deg hybrid and analog-to-digital converters between the RF section and digital processing: which makes it possible to eliminate a phase correlator, four diode detectors and two differential amplifiers used in previous IFM (Instantaneous Frequency Measurement) receivers to obtain the sine and cosine signal samples at an initial time and at a delayed time. GRA

N86-10426# Department of the Air Force, Washington, D.C.
PHOTOIONIZATION TECHNIQUE FOR GROWTH OF METALLIC FILMS Patent Application
J. G. Eden, inventor (to Air Force) Filed 29 May 1985 21 p
(AD-D011760; US-Patent-Appl-SN-738817) Avail: NTIS HC A02/MF A01 CSCL 13/8

A novel method and system for depositing films of selected metallic or semiconductor materials, and particularly of the group 3, 4, and 5 elements, is described which comprises heating a halide compound of the material to produce vapor within a substantially closed chamber, irradiating the vapor with light of preselected wavelength to dissociatively photoionize the vapor with light of preselected wavelength to dissociatively photoionize the vapor into the constituent positive ions of the material and negative halogen ions, and subjecting the photoionized vapor to an electric field to selectively remove the positive ions of the material for plating as a film. GRA

N86-10427# Department of the Air Force, Washington, D.C.
SIGNAL ANALYSIS RECEIVER WITH ACOUSTO-OPTIC DELAY LINES Patent Application
J. B. Y. Tsui, inventor (to Air Force) Filed 10 Jun. 1985 15 p
(AD-D011761; US-Patent-Appl-SN-742825) Avail: NTIS HC A02/MF A01 CSCL 09/1

The system makes use of an interferometric Bragg cell for the time delays needed by the multiple antenna inputs in an angle-of-arrival (AOA) measurement system, for accurate measurements over wide bandwidths. A signal Bragg cell is modulated with a selected band of the EW signal environment, using a separate transducer coupled to each quadrant antenna element. A reference Bragg cell is modulated with a chirp signal. Coherent light from a laser is split and directed to both the signal. Coherent light from a laser is split and directed to both the signal cell and the reference cell. The output light beams from the reference Bragg cell and signal Bragg cell are combined and focused onto photo detectors having a one-dimensional array for each quadrant antenna element. The reference and signals are heterodyned at the photodetectors, which results in a channelized spectral output with each channel at the same intermediate frequency (IF). The outputs of the photodetectors are used by a phase comparison unit, cued by a frequency measurement receiver to the correct detectors, to provide the AOA measurement. GRA

N86-10428# Electronics Research Lab., Adelaide (Australia).
A COMPACT BULK ACOUSTO-OPTIC TIME INTEGRATING CORRELATOR
D. A. B. Fogg Nov. 1984 48 p
(AD-A156608; ERL-0323-TR) Avail: NTIS HC A03/MF A01 CSCL 09/3

This report describes the design and testing of a prototype correlator using lead molybdate Bragg cells. It indicates the suitability of this design for cells made of materials with longer transition times, such as tellurium dioxide. Compactness and simplicity are achieved by the use of a specially designed prism. An analysis of the AO, TIC process and performance parameters is given. GRA

N86-10429# Stanford Univ., Calif. Electronics Lab.
INVESTIGATION OF METALLIC IMPURITIES INTRODUCED INTO SIO2 AND SILICON BY VARIOUS CANDIDATE VLSI METALLIZATION SYSTEMS: CHEMICAL REACTIONS, DIFFUSION, AND ELECTRICAL PROPERTIES Final Report
T. W. Sigmon and R. M. Swanson Apr. 1985 17 p
(Contract MDA903-82-K-0412; DARPA Order A04541)
(AD-A156609) Avail: NTIS HC A02/MF A01 CSCL 09/5

The main objectives of this project were to investigate the diffusion of various gate metals into SiO2 and the diffusion of metals into silicon from contact metallization. The bulk of the work was performed on SiO2, and experimental diffusion results were obtained for Ag, Cu, Pd, Au, Ta, and Ti. From these results, a model for interstitial diffusion in SiO2 was developed that predicts both the ionization state and activation energy for diffusion and solid solubility as a function of temperature. The work concluded that Pd, Au, Mo, Ta, W, Pt, Ti, and Al are suitable candidates for VLSI gate and interconnect metallizations, whereas Ag, Cu, Na, Ni, Mn, Fe, Mg, and Ga are not. This report covers work performed to detect and measure the diffusion of contact metals into crystalline Si. This effort encountered more experimental problems than the SiO2 case, partially because in VLSI technology there are both different types on contacts and varying junction depths present below the contacts. Realizing the importance of these points enabled us to choose a suitable mask set to take these parameters into account. The parameters on interest in this work are; junction depth, junction conductivity type; overlapped or enclosed junction geometry, and contact metallization. Junctions with different combinations of these parameters are subjected to Bias Current Temperature Stressing (BJTS) at elevated temperatures to simulate a long Dt diffusion. The various diodes are packaged to avoid direct probing, and to make sure the temperature is constant for all diodes undergoing BJTS. GRA

N86-10430# Weapons Systems Research Lab., Adelaide (Australia).
A COMPARISON OF SWEPT FREQUENCY AND FFT METHODS USED TO CALIBRATE ARRAY TEST MODULES
G. B. Gillman Oct. 1984 47 p
(AD-A156629; WSRL-0383-TR) Avail: NTIS HC A03/MF A01 CSCL 20/1

A description is given of swept frequency and Fast Fournier Transform (FFT) methods used to calibrate array test modules. The FFT method is shown to give sensitivity versus frequency plots with relative ease and known accuracy. The swept frequency method is capable of giving similar results but only after operator interpretation of the mean of fluctuating signals and calculations on a point to point basis. A digital filtering method is briefly described which can be used to process the signals obtained in swept frequency calibration obviating the need for operator interpretation. The accuracy of the FFT method is discussed and an overall accuracy figure is obtained for the derived sensitivity of the test array. A summary of the FFT method is given as a guide for future hydrophone calibration experiments. GRA

N86-10431# Virginia Polytechnic Inst., Blacksburg.
INTRINSIC MECHANISMS OF MULTILAYER CERAMIC CAPACITOR FAILURE Annual Report, 15 Mar. 1984 - 13 Mar. 1985
L. C. Burton Apr. 1985 53 p
(Contract N00014-83-K-0168)
(AD-A156638) Avail: NTIS HC A04/MF A01 CSCL 09/1

The possible role of grain boundaries (GB) in MLC capacitors, with respect to insulation resistance and its degradation, is reviewed. Activation energy (E sub A) can be related directly to GB barrier height, Phi sub B. The voltage dependent activation energies for poly-Si, ZnO varistors and PTC devices has been attributed directly to E sub A. Varistor and PTC device degradation is caused GB passivation. A similar voltage dependence is reported here for barrier layer and COG capacitor types where E sub A decreases from 0.91 to 0.44eV and from 1.61 to 0.90eV respectively, with concurrent super-ohmic increases in leakage current. Such a voltage dependent E sub A is not seen for X7R devices, even though the current is super-ohmic. Reasons to account for this are discussed. It is concluded that the GB potential barrier may offer a major source of impedance to leakage current for MLC capacitors, and its decrease may result in failure. It has been ascertained that E sub A decreases for degraded X7R devices, with an increase in the I-V slope. These results are consistent with our earlier reports on degraded devices, and with the space charge limited current model for emission from electrodes. X7R chips with no internal electrodes exhibit both ohmic and super-ohmic characteristics, with activation energies independent of voltage. A near-exponential rate of current increase with time, accompanied by a linear decrease in E sub A, was seen for both X7R and Z5U capacitors. GRA

N86-10432# Carnegie-Mellon Inst. of Research, Pittsburgh, Pa. Dept. of Computer Science.
IMPLEMENTATION ISSUES FOR ALGORITHMIC VLSI (VERY LARGE SCALE INTEGRATION) PROCESSOR ARRAYS Ph.D. Thesis
A. L. Fisher Oct. 1984 108 p
(Contracts F33615-81-K-1539; N00014-76-C-0370; N00014-80-C-0236)
(AD-A156699) Avail: NTIS HC A06/MF A01 CSCL 09/5

Advances in very large scale integration (VLSI) have led to a great deal of interest in highly parallel cellular architectures as high-performance solutions to computational bottlenecks. These architectures pose a number of novel implementation issues not encountered in traditional designs. This thesis investigates and resolves some of the most important of these issues, taking both practical and theoretical points of view. Chapter 2 considers the subject of programmability for arrays of processors. It describes some of the advantages and disadvantages of flexible implementations, and discusses processor design issues in light of the requirements of the array environment. In particular, it describes the design of PSC, a chip designed for systolic array implementations, which has been realized in nMOS. It also discusses alternative combinations of processors and memories for the implementation of systolic algorithms. Chapter 3 examines the question of synchronization in large arrays of processors. It gives asymptotic upper and lower bounds for the speed of clocked arrays of differing topologies under differing models of clock skew, and also makes some observations on practical issues of synchronization in large systems. Chapter 4 concentrates on implementations in which arithmetic is broken up into serial bit or subword steps; it shows how systolic serialized systems can be designed, and discusses some practical issues of cost and performance. Finally, Chapter 5 presents a case study of architectures for a family of information retrieval tasks. GRA

N86-10433# Reliability Analysis Center, Griffiss AFB, N. Y.
MICROCIRCUIT DEVICE RELIABILITY FIELD EXPERIENCE DATABASE. VOLUME 1. FIELD DATA. VOLUME 2. FAILURE EVENT/ANALYSIS DATA
D. J. Maher and M. J. Rossi 11 Feb. 1985 715 p
(Contract F30602-84-C-0162)
(AD-A156836; AD-E301723; MDR-21A-Vol-1/2) Avail: NTIS HC A99/MF A02 CSCL 09/5

MDR-21a is a Structured presentation of Field Experience Reliability Data which covers Digital, Linar, Interface, Memory and VLSI Device Types. GRA

N86-10434# Air Force Inst. of Tech., Wright-Patterson AFB, Ohio.
CONTACT EFFECTS IN LIGHT ACTIVATED GaAs SWITCHES M.S. Thesis
P. S. Durkin May 1985 41 p
(AD-A156957; AFIT/CI/NR-85-40T) Avail: NTIS HC A03/MF A01 CSCL 09/5

The purpose of this work was to examine the effects of various types of contacts on the switching behavior of a light-triggered power switch. The switch was constructed from a homogeneous wafer of chromium-doped gallium arsenide; the contacts were either ohmic, non-ohmic, or Schottky barriers. These were formed on the wafer in two geometries; both contacts on one side, and one contact spacings were used to permit the effects of the location of the existing laser pulse to be studied. A high voltage power supply (zero to 20 kV) was employed as the bias supply. A Nd:YAG laser, in the pulsed mode, was used to trigger the switch, which was mounted on a cold finger cooled to near liquid nitrogen temperature. Cooling reduced the dark current to manageable values (less than 1 micro A), and also reduced the avalanche breakdown voltage. The results of the measurements indicate that ohmic contacts produced more reliable switching than the non-ohmic or Schottky contacts, in as much as the shape of the output current pulse was better, and the number of pulses which the switches could sustain before the pulse shape deteriorated was greater, for the ohmic contacts. Surface discharge between the one-sided contacts obscured any differences in switching characteristics which might have depended on the location of the pulsed light excitation, so that no correlation between position and behavior could be obtained. GRA

N86-10435# Department of the Air Force, Washington, D.C.
APPARATUS FOR LOCATING PASSIVE INTERMODULATION INTERFERENCE SOURCES Patent Application
J. C. Mantovani, inventor (to Air Force) Filed 4 Apr. 1985 24 p
(AD-D011798; US-Patent-Appl-SN-719792) Avail: NTIS HC A02/MF A01 CSCL 20/1

An apparatus for locating passive interference sources by using a pair of different RF signals in conjunction with an acoustic signal to generate intermodulation products in metal-to-metal junctions. The acoustic tagging technique utilizes a focused, high power beam of acoustic energy to mechanically vibrate the suspected offending junction. This mechanical vibration causes the level of intermodulation products that are generated in the junction to become amplitude modulated at the frequency of the acoustic illumination. The detection of the AM sidebands with a low noise RF receiver that is tuned to a particular intermodulated component, permits the offending junction to be located. Author (GRA)

N86-10436# Department of the Air Force, Washington, D.C.
INTERDIGITAL SCHOTTKY BARRIER CAPACITOR APPARATUS Patent Application
Bierig, inventor (to Air Force) Filed 7 May 1985 19 p
(AD-D011799; US-Patent-Appl-SN-731223) Avail: NTIS HC A02/MF A01 CSCL 09/1

The present invention relates broadly to Schottky barrier capacitors, and in particular to an interdigital Schottky barrier capacitor apparatus: In the prior art, the Schottky barrier diode is rather well known. In general, a Schottky barrier device comprises a semiconductor substrate layer that is formed by a first layer of heavily doped materials and a second layer of lightly doped materials upon which a layer of barrier metal is deposited thereon. The maximum reverse bias voltage which can be appplied to the Schottky barrier device is determined by the thickness of the lightly doped layer of semiconductive material which is deposited upon the substrate layer. This is only one of the factors that determined the reverse bias voltage. When a guardring is diffused into the lightly doped layer of semiconductive substrate material, the thickness of the layer is reduced, and therefore, the reverse bias voltage that can be applied to the Schottky device is reduced. GRA

N86-10437# Department of the Air Force, Washington, D.C.
MULTI-ROW CONNECTOR WITH GROUND PLANE BOARD Patent Application
J. C. Cunningham, inventor (to Air Force) Filed 6 Mar. 1985 12 p
(AD-D011803; US-Patent-Appl-SN-708909) Avail: NTIS HC A02/MF A01 CSCL 09/1

The present invention relates to electrical connectors and particularly to a multi-row connector having a printed circuit ground plane board associated there with for grounding the outer shields of conductors at the connector. This patent application discloses a multi-row connector having a ground plane board mounted between rows of connector pins on the backside of the connector. Conductor shields of individual wires are soldered directly to conductor strips on the printed circuit ground plane board, and the strips are jumpered to a grounding pin on the connector. GRA

N86-10438# Brookhaven National Lab., Upton, N. Y. School of Chemical Engineering Practice.
STREAMING POTENTIALS IN CONDUCTIVE AND NONCONDUCTIVE TUBING
A. Fung, R. Conti, and J. Ruszkay Sep. 1984 73 p refs
(Contract DE-AC02-76CH-00016)
(DE85-012984; BNL-51875; MIT/BNL-84-4) Avail: NTIS HC A04/MF A01

The feasibility of using streaming potentials measured in blood flow for diagnostic purposes (electroarteriograms) was studied by flowing electrolyte solutions in both nonconductive and conductive tubings as model systems. Streaming potentials measured for 10 to the minus 4 power M and 10 to the minus 5 power M sodium chloride solutions in nonconductive polyethylene tubing obeyed the published theoretical relationships between potential and velocity. Under the same conditions, tubes constructed from conductive Nafion and a cationic exchange material which possessed the same ion-exchange group did not exhibit measurable streaming potentials while an apperent streaming potential was observed with an anionic exchange tubing. Electroarteriogram signals may not represent streaming potentials since blood electrolyte concentrations yield a conductivity that may be too high to cause a measurable effect. DOE

N86-10439# Sandia Labs., Albuquerque, N. Mex.
CALIBRATED FARADAY CURRENT AND MAGNETIC FIELD SENSOR
B. T. Neyer, J. Chang, G. J. Lockwood, and L. E. Ruggles 1985 10 p Presented at the 5th IEEE Pulsed Power Conf., Washington, D.C., 10 Jun. 1985
(Contract DE-AC04-76DP-00789)
(DE85-013438; SAND-84-2544C; CONF-850616-38) Avail: NTIS HC A02/MF A01

A calibrated optical fiber Faraday rotation current sensor is developed. This sensor has a gigahertz response, is immune to electromagnetic interference, and is constructed entirely of dielectric material. All of these advantages make the sensor ideal for pulsed power measurements. DOE

N86-10440# Washington Univ., St. Louis, Mo.
NON-EMPIRICAL INTERATOMIC POTENTIALS FOR TRANSITION METALS Progress Report
7 Jun. 1985 7 p
(Contract DE-FG02-84ER-45130)
(DE85-013448; DOE/ER-45130/T1) Avail: NTIS HC A02/MF A01

Research is reported in the study of metallic bonding and interatomic potential functions. Topics covered include many-atom interactions and the notion of an effective pair potential in a metal, interactions between transition metal ions in semiconductors and insulators, mathematical techniques for extrapolation from incomplete information about atomic distribution functions, and bonding and electronic structure of filled d-band tetrahedral compounds. DOE

N86-10441# Westinghouse Research and Development Center, Pittsburgh, Pa.
DELAY TIMES AND JITTER IN TRIGGERED VACUUM SPARK GAPS USING METAL VAPOR AND SURFACE FLASHOVER TYPES OF TRIGGERS
R. E. Voshall, D. Bhasavanich, J. G. Gorman, and M. T. Buttram (Sandia Labs., Albuquerque, N. Mex.) 1985 5 p refs Presented at 5th IEEE Pulsed Power Conf., Washington, D.C., 10 Jun. 1985
(Contract DE-AC04-76DP-00789)
(DE85-013966; CONF-850616-46) Avail: NTIS HC A02/MF A01

Triggered vacuum spark gap experiments were performed in a demountable arc chamber with a pressure of 10/2 to 10/4 m torr. Planar copper electrodes were used in which one electrode contained the trigger. Metal vapor spark triggers and surface flash-over types of triggers were explored. The delay time between the trigger breakdown and the conduction of the main gap, and the jitter in this time, were measured as a function of main gap voltage ranging from 3 to 20 kV and main gap separations of 13 to 19 mm. Main gap current following breakdown ranged from 3 to 15 kA. Using the metal vapor trigger, delay times as long as 500 ns were observed for a gap field of 500 V/mm while using the surface flashover type of triggers, delay times of 300 ns were observed for a similar main gap field strength. When the trigger was in the cathode electrode and the trigger was pulsed negatively, the operation of the gap was more consistent and the delay times were observed to increase with main gap voltage. The experimental data are interpreted on the basis of plasma expansion models. DOE

N86-10442# California Univ., Berkeley. Lawrence Berkeley Lab.
DEFECT IDENTIFICATION IN HIGH-ENERGY SEMICONDUCTORS
E. E. Haller May 1985 14 p Presented at the 2nd Spring Meeting of the Mater. Res. Soc., San Francisco, 15 Apr. 1985
(Contract DE-AC03-76SF-00098)
(DE85-014533; LBL-19218; CONF-850421-01) Avail: NTIS HC A02/MF A01

The elemental semiconductors silicon and germanium can be purified to electrically active impurity concentrations as low as approx. 10(10) cm(-3). Highly sensitive, energy dispersive analytical techniques have been developed to identify and measure the concentration of the residual elemental impurities. The application of these techniques to very pure materials has also resulted in the discovery of a large number of new levels which are due to impurity/defect complexes. Photothermal ionization spectroscopy using uniaxial stress or a magnetic field, electron paramagnetic resonance, and doping experiments using stable and radioactive elements have been used in combination to identify the composition and the structure of some of the new centers. DOE

N86-10443# Argonne National Lab., Ill.
SOUDAN 2 DATA ACQUISITION AND TRIGGER ELECTRONICS
J. Dawson, R. laird, E. May, N. Mondal, J. Schlereth, N. Solomey, J. Thron, and S. Heppelman 1985 5 p refs Presented at 4th Topical Conf. on Computerized Data Acquisition in Particle and Nucl. Phys., Chicago, 19 May 1985
(Contract W-31-109-eng-38)
(DE85-013864; CONF-850579-3) Avail: NTIS HC A02/MF A01

The 1.1 kton Soudan 2 detector is read out by 15 K anode wires and 3 2 K cathode strips. Preamps from each wire or strip are bussed together in groups of 8 to reduce the number of ADC channels. The resulting 6144 channels of ionization signals are flash-digitized every 150 ns and stored in RAM. The raw data hit patterns are continually compared with programmable trigger multiplicity and adjacency conditions. The data acquisition process is managed in a system of 24 parallel crates each containing an Intel 8086 microprocessor, which supervises a pipe-lined data compactor, and allows transfer of the compacted data via CAMAC to the host computer. The 8086's also manage the local trigger conditions and can perform some parallel processing of the data. Due to the scale of the system and multiplicity of identical channels, semi-custom gate array chips are used for much of the logic, utilizing 2.5 micron CMOS technology. DOE

N86-10444# Physical Sciences, Inc., Andover, Mass.
FUEL CELL TECHNOLOGY ASSESSMENT PROGRAM, WORK ELEMENT NO. 6 Final Report, 30 Sep. 1981 - 30 Sep. 1984
D. Bloomfield and H. Piperopoulou Sep. 1985 187 p
(Contract DE-AC21-81FE-15078)
(DE85-008228; DOE/FE-15078/6-1; PSI-TR-451) Avail: NTIS HC A09/MF A01

The Fuel Cell Technology Assessment Program (FCTAP) developed at Physical Sciences Inc. (PSI) is a set of four computer codes which may be used to determine the effect of advances in fuel cell technology on the distribution of energy in the United States. The four codes are written for use on IBM/PC microcomputers (or equivalent) and are summarized. DOE

N86-10445# Department of Energy, Washington, D. C.
ALUMINUM BATTERY ALLOYS Patent Application
D. S. Thompson, inventor (to DOE) (California Univ., Livermore, Lawrence Livermore Lab.) and D. H. Scott, inventor (to DOE) (California Univ., Livermore, Lawrence Livermore Lab.) Filed 28 Sep. 1984 25 p
(Contract W-7405-eng-48)
(DE85-011599; US-Patent-Appl-SN-655486) Avail: NTIS HC A02/MF A01

Aluminum alloys suitable for use as anode structures in electrochemical cells are disclosed. These alloys include iron levels higher than previously felt possible, due to the presence of controlled amounts of manganese, with possible additions of magnesium and controlled amounts of gallium. DOE

N86-10446# California Univ., Berkeley. Lawrence Berkeley Lab.
EFFECT OF H2S AND COS IN THE FUEL GAS ON THE PERFORMANCE OF AMBIENT PRESSURE PHOSPHORIC ACID FUEL CELLS
P. N. Ross, Jr. Apr. 1985 40 p refs
(Contract DE-AC03-76SF-00098)
(DE85-013913; LBL-18001) Avail: NTIS HC A03/MF A01

The objective of this project was to determine in laboratory cells the tolerance of phosphoric acid fuel cells (PAFC) to hydrogen sulfide and carbonyl sulphide impurities in the anode feed gas. The study was conducted in three phases: the first was testing in a small (1 sq cm) free electrolyte cell to examine the effect of electrode structure on cell tolerance and to determine the order of magnitude of sulfur causing failure in cells at zero utilization; the second was testing in standard 2' x 2' PAFC laboratory hardware at ambient pressure to examine the effect of hydrogen utilization on tolerance and the possible effect of fuel impurities on cathode performance; the final phase was testing with a 2' x 2' cell in a pressure vessel to determine the effect of pressurized operation on cell tolerance. The poisoning effect of hydrogen sulfide was characteristically different from the effects of carbon monoxide, in that it was not manifested by a marginal (e.g., 0 to 50 mV) increase in anode potential but either had no effect or caused catastrophic polarization. Critical levels were derived for hydrogen sulfide as related to cell operating conditions. DOE

N86-10447# Institute of Gas Technology, Chicago, Ill.
EFFECTS OF H2S ON MOLTEN CARBONATE FUEL CELLS Progress Report, 1 Jul. - 30 Sep. 1984
R. J. Remick Jun. 1985 41 p refs
(Contract DE-AC21-83MC-20212)
(DE85-014052; DOE/MC-20212/1850) Avail: NTIS HC A03/MF A01

Phase 2 work was directed toward determination of the impact of H2S contaminants upon the ability of nickel-10% chromium anodes to catalyze the steam reforming reaction. Small amounts of three hydrocarbons representative of three homologous series were added to the fuel. These series were the paraffin series with methane as its representative, the olefin series with ethylene and the aromatics with toluene. Results indicated that the nickel-10% chromium anode had little catalytic activity toward the steam reforming of methane, but the steam reform did have 70% of the ethylene and about 30% of the toluene. The addition of 5 ppM hydrogen sulfide to the fuel totally poisoned all steam reforming activity. Phase 3 work addressed the impact on cell performance of SO2 in the oxidant gases. The cell was operated for 200 hours on clean fuel and oxidant. After baseline data had been collected, the cell was switched to an oxidant supply that contained 2 ppM of SO2. After 170 hours of operation on contaminated oxidant, no SO2 could be detected in the oxidant exhaust although 200 ppM of H2S were present in the fuel exhaust steam. DOE

N86-10448# Tennessee Univ., Knoxville. Dept. of Chemical and Metallurgical Engineering.
THERMODYNAMIC CONSTRAINTS ON ION BEAM MIXING OF METALS ON INSULATORS
G. C. Farlow, B. R. Appleton, L. A. Boatner, C. J. McHargue, C. W. White, G. J. Clark, and J. E. F. Baglin 1985 10 p Presented at the 2nd Spring Meeting of the Mater. Res. Soc., San Francisco, 15 Apr. 1985 Prepared in cooperation with IBM Research Lab., Yorktown Heights, N.Y.
(Contract DE-AC05-84OR-21400)
(DE85-013628; CONF-850421-10) Avail: NTIS HC A02/MF A01

Several different insulating substrates are coated with various metal films and ion beams irradiated using either Xe or Kr ions. These are then examined by Rutherford backscattering spectroscopy and scanning electron microscopy to determine if interfacial mixing has taken place. These results are compared with the sign of the reaction enthalpy of the metal and substrate to test the proposition that metals mix on insulators if the reaction enthalpy is negative and do not mix if it is positive. The enthalpy rule is, in general, valid. Two exceptions are found: Cr on SiO2 and Zr on Al2O3; however, these exceptions contain ambiguous features. Irradiation with a light, reactive ion is found to produce no mixing. DOE

N86-10449# Messwandler-Bau G.m.b.H., Bamberg (West Germany).
HIGH VOLTAGE INSTRUMENT TRANSFORMERS FOR OUTDOOR SERVICE WITH AN INSULATION OF LOW PRESSURE SF6 GAS AND PLASTIC FOILS Final Report, Jul. 1984
Uwe Brand Bonn Bundesministerium fuer Forschung und Technologie Apr. 1985 40 p refs In GERMAN; ENGLISH summary Sponsored by Bundesministeriun fuer Forschung und Technologie
(BMFT-FB-T-85-034; ISSN-0340-7608) Avail: NTIS HC A03/MF A01; Fachinformationszentrum, Karlsruhe, West Germany DM 8.50

Gas-insulated failsafe high voltage instrument transformers with system voltages in the range of 123 to 420 kV for outdoor service were developed. The basic physics and high power tests performed on gas-filled instrument transformer housings are discussed. Construction and design of gas-insulated voltage transformers are explained. The insulation of the 123 kV model consists of low pressurized SF6 gas and plastic foils. The 245 kV unit has the same principal design; however, a higher SF6 pressure is used and the apparatus is fitted with a hollow composite insulator made of a fiber reinforced plastics tube and silicone casing. For the 420 kV model the same insulator type is used and a design for the voltage grading along the insulator is developed. The transformers show good performance in service; they are a safe and environment-protecting alternative to oil insulated equipment. Author (ESA)

N86-10450# Kernforschungsanlage, Juelich (West Germany). Inst. fuer Grenzflaechenforschung und Vakuumphysik.
DIELECTRIC PROPERTIES OF SILICON SURFACES AND SILVER THIN FILMS Thesis - Technische Hochchule, Aachen [DIELEKTRISCHE EIGENSCHAFTEN VON SILIZIUMOBERF-

LAECHEN UND DUENNEN SILBERFILMEN]
U. Backes Jan. 1985 85 p refs In GERMAN; ENGLISH summary
(JUEL-1968; D-82; ISSN-0366-0885) Avail: NTIS HC A05/MF A01

The metallic behavior of silicon (111) 7x7-surfaces with different misorientation angles is investigated. Its contribution to quasielastic peak broadening and to high background of inelastically scattered electrons is quantitatively shown using High Resolution Electric Energy Loss Spectroscopy (HREELS) by measuring the scattering cross sections for multiple plasmon excitation localized within a thin layer at the surface. The theoretical assumptions are confirmed by the spectra detected on the silver film-silicon substrate whose presence is explained by plasmon theory. Author (ESA)

N86-10451# Valvo Roehren- und Halbleiterwerke der Philips G.m.b.H., Hamburg (West Germany). Produktber. MOS-ICS.
INCREASE OF THE PACKAGING DENSITY OF VERY LARGE SCALE INTEGRATION (VLSI) CIRCUITS USING AUTOMATIC ALIGNMENT Final Report, Dec. 1983
Heino Fehling Bonn Bundesministerium fuer Forschung und Technologie Mar. 1985 104 p refs In GERMAN; ENGLISH summary Sponsored by Bundesministerium fuer Forschung und Technologie
(BMFT-FB-T-85-020; ISSN-0340-7608) Avail: NTIS HC A06/MF A01; Fachinformationszentrum, Karlsruhe, West Germany DM 22

Experiments in a production line were conducted to investigate the possible reduction of safety distances in VLSI circuits when an automatic alignment system is used. The test setup is described. With the very accurate alignment system of the Philips silicon repeater, the safety distance between a contact hole and a polysilicon-gate in a modified microcomputer circuit is reduced 0.7 micron without any yield loss. Design rules based on these experiments, and on lithography investigations were applied to redesign a 4 k static read-only memory. The area of a single memory cell in this redesign is 825 59 microns, compared to 1800 sq microns in the original version, and the final chip area is reduced to 8 sq mm compared to 13 sq mm. Author (ESA)

N86-10452# Nationaal Inst. voor Kernfysica en Hoge Energiefysica, Amsterdam (Netherlands). Sectie-K.
RENOVATED COOLING AT PIMU [VERNIEUWDE KOELING BY PIMU]
P. deGroen 18 Apr. 1985 27 p In DUTCH
(LINO-122) Avail: NTIS HC A03/MF A01

An electronic temperature control system for the cool water circuit at the PIMU section is described. The system consists of a temperature reader, control, offset and switch print, a programmable logic circuit (plc) and a motor speed control unit for the ventilators. From 21 to 6 C, with every 1.4 C temperature increase an extra cooling unit is switched on up to 30 C; every unit is switched off 1.4 C lower than its switching on temperature. Switching on a unit, an air value is opened and a ventilator starts on 10% of its maximum power and is regulated with the temperature increase within the 1.4 C step. Author (ESA)

N86-10453# National Bureau of Standards, Gaithersburg, Md. Electricity Div.
INVESTIGATION OF THE UNCERTAINTIES OF THE NBS (NATIONAL BUREAU OF STANDARDS) THERMAL VOLTAGE AND CURRENT CONVERTERS Final Report
F. L. Hermach Apr. 1985 124 p refs
(PB85-200178; NBSIR-84-2903) Avail: NTIS HC A06/MF A01 CSCL 14B

The uncertainties of the NBS reference and working standards for ac-dc current and voltage transfer measurements have been redetermined, to 50 and 100 kHz, respectively, by means of a set of multijunction thermal converters (MJTCs), an improved emf comparator, and extensive series of intercomparisons. As a result the accuracy of the NBS standards and the output of its calibration service for ac-dc current and voltage transfer are considered to be on a much firmer and better documented basis. Improvement by factors of two to five in the calibration accuracy for high-quality, single-range thermoelements and thermal voltage converters is possible for certain ranges of current, voltage, and frequency. For very special tests, such as international comparisons, accuracies approaching 1 ppm are within reach. GRA

N86-10387*# Jet Propulsion Lab., California Inst. of Tech., Pasadena. Radio Frequency and Microwave Subsystems Section.
AN EXPERIMENTAL TE SUB 12 - TE SUB 11 CIRCULAR WAVEGUIDE MODE CONVERTER
D. Hoppe *In its* The Telecommun. and Data Acquisition Progr. Rept. 15 Aug. 1985 p 43-56 refs (For primary document see N86-10382 01-32)
Avail: NTIS HC A10/MF A01 CSCL 09C

N86-10814# Joint Publications Research Service, Arlington, Va.
COMPACT, HIGH-SPEED ALGORITHM FOR LAYING OUT PRINTED CIRCUIT BOARD RUNS
D. Ye. Zapolotskiy *In its* USSR Rept.: Cybernetics, Computers and Automation Technol. (JPRS-UCC-85-006) 5 Sep. 1985 p 59-67 refs Transl. into ENGLISH from Upravlyayushchiye Sistemy i Mashiny (Kiev), no. 2, Mar. - Apr. 1985 p 33-37 (For primary document see N86-10809 01-60)
Avail: NTIS HC A08

34 FLUID MECHANICS AND HEAT TRANSFER

Includes boundary layers; hydrodynamics; fluidics; mass transfer; and ablation cooling.

For related information see also *02 Aerodynamics* and *77 Thermodynamics and Statistical Physics.*

N86-10454 Purdue Univ., Lafayette, Ind.
ON THE METHOD OF CHARACTERISTICS AND ITS APPLICATION TO THE CALCULATIONS OF ANNULAR NOZZLE FLOWFIELDS Ph.D. Thesis
Ber Nien Wang 1984 154 p
Avail: Univ. Microfilms Order No. DA8507772

A new, simple and effective approach to deriving the characteristic equations of gas dynamics is proposed. The compatibility equation is derived in vector form, which is valid for any coordinate system. The concepts of this derivation are clearer than previous derivations. A general form of the energy equation which contains the speed of sound directly is obtained. This form, which is valid for either ideal or real gases, is particularly useful for the method of characteristics. Coordinate transformation by algebraic methods is studied in detail. It is found that this method may be the only practical method for solving moving boundary problems, such as the free jet boundary problem. Using the basic concepts of coordinate transformations, all the viscous force terms and the dissipative terms in a curved coordinate system are obtained. Thus, the method of characteristics can be used to solve either real viscous flowfields or flowfields with artificial viscosity for smearing shock waves. Dissert. Abstr.

N86-10455 Arizona Univ., Tucson.
MEAN TURBULENCE STRUCTURE IN STRONGLY HEATING AIR FLOWS Ph.D. Thesis
Ahmed-Mohsen Tawfick Mohamed Shehata 1984 272 p
Avail: Univ. Microfilms Order No. DA8510896

Measurements of mean velocity and mean temperature fields and wall parameters for air flowing in a smooth, vertical tube at low entry Reynolds numbers are presented for heating with constant wall heat flux along the heated length. Two entry Reynolds numbers of approximately 6000 and 4000 were employed with three heating rates of approximately 0.0018, 0.0035 and 0.0045. The flow development was measured by obtaining internal profiles along the heated length at axial locations from x/D = 3.17 to x/D = 24.54. An adiabatic entry of 50 diameters preceded the heated region. The three heating rates caused slight, large and severe property variations of the air. The highest heating rate was found to cause significant buoyancy effects. The internal measurements were obtained using constant temperature hot wire anemometry and resistance thermometry for velocity and temperature, respectively, employing a single short wire probe. The measurements are compared to numerical predictions employing two simple versions of the van Driest mixing length turbulence model. Dissert. Abstr.

N86-10456 Maryland Univ., College Park.
ANALYSIS OF COMBINED NATURAL AND FORCED CONVECTION AROUND CYLINDERS AND SPHERES Ph.D. Thesis
Soung Hong Moon 1984 310 p
Avail: Univ. Microfilms Order No. DA8510267

Combined natural and forced convection around cylinders and spheres was numerically investigated using stream function, vorticity formulations with hybrid (central and upwind) differences and nonuniform grid spacing for gases having a Prandtl number of 0.7. A successive overrelaxation method was employed to solve the stream, vorticity and temperature equations. For recovery of the pressure distribution, the pressure Poisson's equation was solved after convergence of stream and vorticity solutions. Numerical results were found to be functions of Reynolds number, Grashof number and Froude number. Local and average Nusselt numbers were obtained at various Grashof numbers. The mixed convection boundaries were defined: (1) when the buoyancy force of natural convection is significant in forced convection, and (2) when forced convection is significant in natural convection. Temperature and velocity distributions around cylinders and spheres were obtained and the effects of Reynolds and Grashof numbers and the separation point, drag coefficient and pressure were found. Dissert. Abstr.

N86-10457 Virginia Polytechnic Inst. and State Univ., Blacksburg.
FINITE ELEMENT SOLUTION OF THE NAVIER-STOKES EQUATIONS FOR 3-D TURBULENT FREE SHEAR FLOWS Ph.D. Thesis
Dominique Henri Pelletier 1984 228 p
Avail: Univ. Microfilms Order No. DA8507209

A half-equation model of turbulence has been developed to describe three-dimensional turbulent free shear flows. The model is used in a general purpose finite element procedure using primitive variables. The penalty function method is used, in a generalized Galerkin weak formulation of the Navier-Stokes equations, to enforce the conservation of mass. In this procedure the pressure does not explicitly appear, thus significantly reducing the computation time when compared to the velocity-pressure approach. Numerical solutions are obtained for four problems: a round jet issuing from a wall into still surroundings, a three-dimensional square jet issuing from a wall into still surroundings, a uniform flow past a free running propeller, and a shear flow past a free running propeller. An actuator disk with variable radial distribution of thrust and torque is used to model the propeller. Very good agreement between prediction and experiments is observed for the jet problems. Dissert. Abstr.

N86-10458 Washington Univ., Seattle.
RADIATIVE HEAT TRANSFER IN NONISOTHERMAL COMBUSTION PRODUCTS Ph.D. Thesis
Mohammed Ahmed Hamdan 1985 166 p
Avail: Univ. Microfilms Order No. DA8510851

Radiative heat transfer plays a significant and sometimes dominant role within combustion systems. Heat flux measurements in such systems are sometimes economically disadvantaged and difficult, if not impractical to perform. To demonstrate a feasible alternative, a simplified numerical model using total transmittance data, TTNH, was developed for predicting the heat flux from nonisothermal combustion systems containing variable concentrations of water vapor, carbon dioxide, and methane. Total and spectral experimental measurements were carried out, to test the numerical model, using nonisothermal mixtures of water vapor/carbon dioxide and methane/ethene, and using isothermal mixtures of methane and ethene. In general, the TTNH model was found to be reliable to predict the total emitted energy by nonisothermal mixtures of carbon dioxide and water vapor within 10%. However, the model was found not reliable to predict the theoretical emittance of methane. Dissert. Abstr.

N86-10459 Dartmouth Coll., Hanover, N.H.
ANALYSIS OF ANNULAR TWO-PHASE FLOW WITH LIQUID ENTRAINMENT Ph.D. Thesis
Mohamed Abdelfatah Abolfadl 1985 195 p
Avail: Univ. Microfilms Order No. DA8509840

A differential model for adiabatic annular gas-liquid to phase flow with liquid entrainment was developed by postulating a mixing length distribution in the turbulent flow region, across both the liquid and the core phases. The model is based on a modified form of the single phase mixing length function to account for turbulence intensity attenuation due to the presence of entrained liquid droplets in the gas core and the presence of the core film interface. The shear stress velocity gradient relationships are integrated numerically by using the complete shear stress distribution to produce the velocity profile which in turn is integrated to obtain the flow rates of each phase. A nondimensional form of the model is used to handle different fluids and tube diameters. Predicted velocity profiles in the core region also compare well with data. The model includes a new treatment of the characteristic shear stress in the laminar wall layer that makes it possible to predict flow rates in vertical flow at the point of zero wall shear stress in agreement with limited experimental results.
Dissert. Abstr.

N86-10460*# Universities Space Research Association, Columbia, Md.
A ROOT-MEAN-SQUARE PRESSURE FLUCTUATIONS MODEL FOR INTERNAL FLOW APPLICATIONS
Y. S. Chen Washington NASA Sep. 1985 17 p refs
(Contract NAS8-35918)
(NASA-CR-3928; NAS 1.26:3928) Avail: NTIS HC A02/MF A01 CSCL 20D

A transport equation for the root-mean-square pressure fluctuations of turbulent flow is derived from the time-dependent momentum equation for incompressible flow. Approximate modeling of this transport equation is included to relate terms with higher order correlations to the mean quantities of turbulent flow. Three empirical constants are introduced in the model. Two of the empirical constants are estimated from homogeneous turbulence data and wall pressure fluctuations measurements. The third constant is determined by comparing the results of large eddy simulations for a plane channel flow and an annulus flow. Author

N86-10461*# Stanford Univ., Calif. Thermosciences Div.
FILM COOLING ON A CONVEX WALL: HEAT TRANSFER AND HYDRODYNAMIC MEASUREMENTS FOR FULL AND PARTIAL COVERAGE Final Report
K. Furuhama, R. J. Moffat, J. P. Johnston, and W. M. Kays Aug. 1985 170 p refs
(Grant NAG3-3)
(NASA-CR-174964; NAS 1.26:174964) Avail: NTIS HC A08/MF A01 CSCL 20D

Turbine-blade cooling is an important issue for high-efficiency turbine engines, and discrete-hole injection is widely used as a cooling method. In the present study, detailed measurements were made of the heat transfer and hydrodynamics of a film-cooled flow on a convex wall, both for full and partial coverage. Two important parameters were altered: the blowing ratio, m, and the number of rows of injection holes. Three values of m were tested: m = 0.2, 0.4, and 0.6. In the blown region, m = 0.4 results in the lowest Stanton numbers of the three blowing ratios tested. This indicates that the value of m = 0.4 is near optimum on the convex wall from the point of view of cooling effect by injection. In the recovery region, Stanton numbers gradually approach the no injection values. Although the heat-transfer behavior during recovery from injection looks relatively complicated, the behavior of Stanton number can be explained in terms of two mechanisms:

recovery from the thermal effect of injection and recovery from the turbulence augmentation. This interpretation of the data is supported by the hydrodynamic and temperture-profile measurements. For partial blowing cases, the data follow the full-coverage values inside the blown region. In the unblown region, both in the curved and in the flat plate, the effect of the number of blown rows is clearly seen. Hydrodynamic boundary-layer profiles were measured with the aid of a triple hot-water probe. Three mean-velocity components and six turbulence quantities were simultaneously measured, and inside the blown region strong three-dimensionality was observed. Author

N86-10462*# National Academy of Sciences - National Research Council, Washington, D. C. Systems Dynamics Lab.
CONFINED SWIRLING JET PREDICTIONS USING A MULTIPLE-SCALE TURBULENCE MODEL
C. P. Chen Aug. 1985 22 p refs
(Contract NASw-3458)
(NASA-CR-178484; NAS 1.26:178484) Avail: NTIS HC A02/MF A01 CSCL 20D

A recently developed multiple scale turbulence model is used for the numerical prediction of isothermal, confined turbulent swirling flows. Because of the streamline curvature and nonequilibrium spectral energy transfer nature of the swirling flow, the utilized multiple scale turbulence model includes a different set of response equations for each of the large scale energetic eddies and the small scale transfer eddies. Predictions are made of a confined coaxial swirling jet in a sudden expansion and comparisons are made with experimental data and with the conventional single scale two equation model. The multiple scale model shows significant improvement of predictions of swirling flows over the single scale k epsilon model. The sensitivity study of the effect of prescribed inlet turbulence levels on the flow fields is also included. Author

N86-10463*# National Aeronautics and Space Administration. Lewis Research Center, Cleveland, Ohio.
THEORETICAL MODELING OF THE VAPOR CAVITATION IN DYNAMICALLY LOADED JOURNAL BEARINGS
David E. Brewe [1985] 35 p refs Presented at the Tribology Conf., Atlanta, 8-10 Oct. 1985; cosponsored by Am. Soc. of Lubrication Engr., and ASME Sponsored in part by Army
(NASA-TM-87076; E-2651; USAAVSCOM-TR-85-C-15; NAS 1.15:87076) Avail: NTIS HC A03/MF A01 CSCL 13I

A theoretical investigation is made of the evolution of a vapor-bubble for a submerged journal bearing under dynamically loaded conditions using the Elrod algorithm. This method conserves mass throughout the computational domain. A comparison study is performed to determine some of the consequences of applying a nonconservative theory (pseudo-Gumbel BC) to a dynamic problem. A complete dynamic cycle of a journal whirling in a circular path is chosen for the basis of comparison. Significant differences are observed in the load components near the end of the cycle. Further, good agreement with experiment is found for stationary and nonstationary cavitation. Author

N86-10464*# National Aeronautics and Space Administration. Ames Research Center, Moffett Field, Calif.
LARGE EDDY INTERACTIONS IN A TURBULENT CHANNEL FLOW
S. K. Hong Sep. 1985 66 p refs
(NASA-TM-86757; Rept-85265; NAS 1.15:86757) Avail: NTIS HC A04/MF A01 CSCL 20D

The dynamic processes of large eddies in a turbulent channel flow have been examined by utilizing an orthogonal expansion of the velocity fluctuation, known in the literature as the Proper Orthogonal Decomposition Theorem. The mathematical form of these functions is unknown in contrast to the Fourier analysis. Attention is focused on the nonlinear, turbulence-turbulence interaction process in the dynamical equation for large eddies (the first term in the expansion). The nonlinear interactions of the components of the first mode are treated exactly, but influences of higher modes are modeled. This requires adjustment of both the skewness and the effective Reynolds number so that the energy equilibrium of the large eddies is ensured when the mean velocity distribution is assumed known for experiments. Computational results show that the first mode contributes significantly to turbulent intensities and possesses a structural and statistical character similar to that of the entire flow. Author

N86-10465# IBM Research Lab., San Jose, Calif.
CHARACTERIZATION OF VAPOR AND AEROSOL FLOWS BY PHOTOTHERMAL METHODS
H. Sontag and A. C. Tam 25 Jun. 1985 8 p
(Contract N00014-83-C-0170)
(AD-A156601; TR-19) Avail: NTIS HC A02/MF A01 CSCL 20/4

Pulsed laser heating is used to label aerosols or absorbing vapors which can be detected by optical means yielding flow and spectroscopic information. Author (GRA)

N86-10466# California Univ., Livermore. Lawrence Livermore Lab.
ANGLE OF INCIDENCE EFFECTS FOR UNDERWATER SHOCK USING GENERIC COMPUTATIONAL MODELS
C. E. Rosenkilde and J. H. Ginsberg Feb. 1985 23 p Presented at the 55th Shock and Vibration Symp., Dayton, Ohio, 23 Oct. 1984 Prepared in cooperation with Georgia Inst. of Tech. 2 Vol.
(Contract W-7405-eng-48)
(DE85-012936; UCRL-91078-2; CONF-8410159-2) Avail: NTIS HC A02/MF A01

The computer programs for three models which provide the ability to perform damage assessments, particularly regarding the significance of angle of incidence are described. Each computer code evaluates the temporal response of the structure for an explosive source situated at a specified angle relative to the axis. Responses are displayed as temporal histories of the velocity and acceleration components relative to a body fixed coordinate system. Such results are evaluated for the center of mass and points at each end of the cylindrical segment. When a sequence of heading angles covering a quarter circle are input, the magnitude of the instantaneous (vector) velocity and acceleration at each point is monitored for its maximum value. In conjunction with the evaluation of the structural motion, in TDEF, a simple model is used to correlate the shock severity of the structural motion to that experienced by a small piece of equipment. This model consists of a one-degree-of-freedom oscillator whose base motion is obtained from the motion arising from any of the aforementioned structural models. DOE

N86-10467# California Univ., Livermore. Lawrence Livermore Lab.
ANGLE OF INCIDENCE EFFECTS FOR UNDERWATER SHOCK USING GENERIC COMPUTATIONAL MODELS, REV. 1
C. E. Rosenkilde and J. H. Ginsberg Feb. 1985 33 p Presented at the 55th Shock and Vibration Symp., Dayton, Ohio, 23 Oct. 1984 Prepared in cooperation with Georgia Inst. of Tech. 2 Vol.
(Contract W-7405-eng-48)
(DE85-012921; UCRL-91078-Rev-1; CONF-8410159-2-Rev-1) Avail: NTIS HC A03/MF A01

The modeling techniques used to develop several generic models of the shock response of submarines are described. The result is three overlapping models: (1) CAPS, in which the directly arriving shock wave is applied to a rigid capped cylinder that contains a large spring supported mass; (2) REFLECT, in which a rigid cylinder capped by hemispheres is subjected to direct and reflected shock waves resulting from an explosive source at an arbitrary location; and (3) TDEF, in which the directly arriving shock wave drives a deformable capped cylinder that is modeled by a combination of rigid body modes, beam modes, and axisymmetric shell modes. How the computer programs for these models provide the ability to perform damage assessments, is described, particularly regarding the significance of angle of incidence. Each computer code evaluates the temporal response of the structure for an explosive source situated at a specified angle relative to the axis. Results are evaluated for the center of mass and points at each end of the cylindrical segment. When a sequence of heading angles covering a quarter circle is input, the magnitude of the instantaneous (vector) velocity and acceleration at each point is monitored for its maximum value. DOE

N86-10468# GA Technologies, Inc., San Diego, Calif.
HIGH EFFICIENCY HEAT TRANSPORT AND POWER CONVERSION SYSTEM FOR CASCADE
I. Maya, R. F. Borque, R. I. Creedon, and K. R. Schultz Feb. 1985 8 p Presented at the 6th Topical Meeting on the Technol. of Fusion Energy, San Francisco, 3 Mar. 1985
(Contract W-7405-eng-48)
(DE85-012959; UCRL-15640; CONF-850310-110) Avail: NTIS HC A02/MF A01

The cascade ICF reactor features a flowing blanket of solid BeO and LiAlO2 granules with very high temperature capability (up to approx. 2300 K). Presented here are the design of a high temperature granule transport and heat exchange system, and two options for high efficiency power conversion. The centrifugal throw transport system uses the peripheral speed imparted to the granules by the rotating chamber to effect granule transport and requires no additional equipment. The heat exchanger design is a vacuum heat transfer concept utilizing gravity induced flow of the granules over ceramic heat exchange surfaces. A reference Brayton power cycle is presented which achieves 55% net efficiency with 1300 K peak helium temperature. A modified Field steam cycle (a hybrid Rankine/Brayton cycle) is presented as an alternate which achieves 56% net efficiency. DOE

N86-10469# Los Alamos Scientific Lab., N. Mex.
KRAK: A COMPUTER PROGRAM FOR TWO-PHASE, TWO-COMPONENT POROUS FLOW AND FRACTURE PROPAGATION, REVISION
B. J. Travis, A. H. Davis, T. D. Kunkle, and R. G. Deupree Apr. 1985 96 p
(Contract W-7405-eng-36)
(DE85-014264; LA-9703-Rev) Avail: NTIS HC A05/MF A01

The KRAK code models the mass, momentum, and energy flow of steam liquid water, and a noncondensable gas in a porous medium. It can model the initiation and propagation of hydrofracture in this medium by any or all of the fluid components using finite difference techniques. The interaction of the flow and the cracking is self-consistently performed. Furthermore, flow in the crack is treated by a full-momentum equation, which allows rapid fracturing. The code has been used in studies of the underground containment of radioactive gases produced by nuclear explosions and of siting underground nuclear power reactors. The code could also be applied to a wide variety of geophysical situations such as geothermal energy extraction, geysers, convection in a fractured medium, and explosive well stimulation. The physical model includes heat transfer between the porous medium and the flowing fluid, an equation of state that allows fluid condensation and evaporation, a model for the viscosity of each fluid component and the composite viscosity, and a permeability model that successfully treats interfaces of greatly differing permeabilities (produced by either different materials or different states of the same material). Cracking is controlled by a simple fracture mechanics model. DOE

N86-10470# California Univ., Livermore. Lawrence Livermore Lab.
SPONTANEOUS RAMAN SPECTROSCOPY OF SHOCKED H2O
N. C. Holmes, W. J. Nellis, W. B. Graham, and G. E. Walrafen Jun. 1985 13 p refs Presented at 10th High Pressure Conf. on Res. in High Pressure Sci. and Technol., Amsterdam, 8 Jul. 1985
(Contract W-7405-eng-48)
(DE85-014557; UCRL-92895; CONF-850759-3) Avail: NTIS HC A02/MF A01

A new Raman spectroscopic system for recording spontaneous Raman spectra from shocked mater at high pressure and temperature during shock passage has been developed. This system is applied to the study of the OH-stretch band of water shocked to pressures between 7.5 and 25.7 GPa. The spectra indicate that strong intermolecular hydrogen-bonding persists to 12 GPa and decreases in strength at higher pressures. A two-component mixture model fits the data well under shock conditions. DOE

N86-10471# California Univ., Livermore. Lawrence Livermore Lab.
TIME-IMPLICITY SIMULATION OF PARTICLE-FLUID SYSTEMS
J. Denavit 17 Jan. 1985 20 p Presented at the 2nd Intern. School for Space Simulation, Honolulu, 3 Feb. 1985
(Contract W-7405-eng-48)
(DE85-012944; UCRL-91642; CONF-850266-6) Avail: NTIS HC A02/MF A01

One-dimensional particle-fluid hybrid simulations are presented in which the strongly collisional components of the plasma (e.g., ions and thermal electrons with nu(sub cf) (DELTA) t > 1) are treated as fluids and the weakly collisional components (e.g., energetic electrons with nu(sub cp) (DELTA) t < 1) are treated as particles. Here nu(sub cf) denotes the fluid ion and electron collision frequencies, nu(sub cp) is the energetic between particle and fluid components are treated by a Monte-Carlo method and mass transfers between the particle and fluid electron computed implicitly to allow time steps with (LC OMEGA) (sub p) (DELTA) t > 1 ((LC OMEGA) (sub p): plasma frequency). DOE

N86-10472# Oak Ridge National Lab., Tenn.
ENGINE-DRIVEN AND ABSORPTION HEAT PUMP PROGRAMS
G. T. Privon 1984 4 p Presented at the DOE/ORNL Heat Pump Conf., Washington, D.C., 10 Dec. 1984
(Contract DE-AC05-84OR-21400)
(DE85-013930; CONF-841231-21) Avail: NTIS HC A02/MF A01

The development of energy efficient, thermally activated heat pumps for heating and cooling is reported. A breadboard system with a 32.5%-BHP-efficient linear engine in the final phase of steady state was tested. The absorption heat pump advanced cycle program is in progress. Analysis confirms the level of potential and preferred cycles and fluids are selected. Reliability for the linear engine heat pump and long life of the shaft seal must be established. The advanced absorption systems each require high performance from an internal counterflow heat exchanger and the development of reliable, high performance fluid pumps. DOE

N86-10473# Oak Ridge National Lab., Tenn.
LABORATORY EXPERIMENTS OF HEAT PUMP DYNAMIC LOSSES
W. A. Miller 1985 6 p refs Presented at the DOE/ORNL Heat Pump Conf., Washington, D.C., 10 Dec. 1984
(Contract DE-AC05-84OR-21400)
(DE85-013931; CONF-841231-22) Avail: NTIS HC A02/MF A01

Air-source heat pump experiments at ORNL: (1) provide detailed system and component performance data usable in understanding dynamic loss phenomena, and (2) enable formulation and evaluation of methods that could reduce dynamic losses. Results presented herein are from a series of laboratory experiments performed at ORNL aimed at providing detailed characterization steady-state performance data. Continuous modulation heat pump experiments to observe dynamic loss trends under part-load heat pump operation will follow. DOE

N86-10474# Sandia Labs., Albuquerque, N. Mex.
EFFECTS OF SCALE AND GEOMETRY ON HYDROGEN-AIR DETONATIONS
M. Berman 1985 56 p refs Presented at the Natl. Heat Transfer Conf., Denver, 4 Aug. 1985
(Contract DE-AC04-76DP-00789)
(DE85-006762; SAND-85-0171C; CONF-850810-6) Avail: NTIS HC A04/MF A01

Recent experiments have investigated the influence of scale and geometry on the ability of a fuel-air mixture to propagate or sustain a detonation, and on the probability that a deflagration will undergo a transition to detonation. The data show that many past concepts concerning detonations need to be revised. In particular, the occurrence of detonations may not be as unlikely as previously considered, especially in large-scale industrial environments. This paper reviews some of the important recent experimental research, and provides some qualitative ideas concerning the interpretation of the experiments and their implications for improving safety. DOE

N86-10475# Kernforschungsanlage, Juelich (West Germany). Inst. fuer Reaktorbauelemente.
DUST DEPOSITION IN REGIONS OF SEPARATED FLOW [STAUBABLAGERUNG IN GEBIETEN ABGELOESTER STROEMUNG]
R. Griemert Mar. 1985 150 p refs In GERMAN; ENGLISH summary
(JUEL-1985; ISSN-0336-0885) Avail: NTIS HC A07/MF A01

A numerical assessment of the forces on dust grains in a closed duct is made as well as a measurement of the wall shear stress distribution and of fluid velocity and fluid fluctuations in the main flow direction at forward and backward facing steps. The deposition conditions were determined from photographs of copper, tin, and rubber dust to provide manufacturers of high temperature reactors with data on optimal hot gas pipe shapes and fluid dynamical data under determined pressure, temperature and geometrical conditions so that dust deposition in recirculation region can be avoided. Operating parameters can also be selected so that former dust deposition is not reentrained and does not fill the recirculation region. Author (ESA)

N86-10476# Stuttgart Univ. (West Germany). Inst. fuer Kernenergetik und Energiesysteme.
LAMINAR FILM CONDENSATION IN VERTICAL CLOSED TWO-PHASE THERMOSIPHONS Ph.D. Thesis [LAMINARE FILMKONDENSATION IM VERTIKALEN GESCHLOSSENEN SWEIPHASEN-THERMOSIPHON]
Thomas Spendel Feb. 1985 111 p refs In GERMAN; ENGLISH summary
(IKE-5-220; ISSN-0173-6892) Avail: NTIS HC A06/MF A01

The influence of the vapor flow on laminar film condensation heat transfer in closed two-phase thermosiphons is studied. The calculation of the vapor flow is based on the conservative equations for steady incompressible two-dimensional flow for which a finite difference method is applied to solve the system of equations. The influence of the vapor flow on heat transfer depends on the value of the Froude number. The influence of temperature-dependent material parameters and the condensation parameter on heat transfer are examined. Author (ESA)

N86-10477# Technische Hogeschool, Delft (Netherlands). Lab. of Fluid Mechanics.
EXPERIMENTS AND COMPUTATIONS ON UNSTEADY SEPARATING FLOW IN AN EXPANDING FLUME
G. S. Stelling (Netherlands Department of Transport and Public Works) and L.-X. Wang (Water Conservancy and Hydroelectric Power Research Institute, Beijing, China) 1984 62 p refs
(Rept-2-84) Avail: NTIS HC A04/MF A01

An unsteady, separating, flume flow with a free surface was investigated with a physical model and a numerical model. To simulate tidal flow, the prescribed flow rate at the inflow boundary was a half-period sine function of time. Velocities and wave heights were measured by a laser Doppler velocimeter and a wave-height meter in a straight open channel with a sudden widening and a nonreflective outlet. Distributions of depth-averaged velocities at different times were obtained. Numerical simulation of this flow was carried out using a computer program of second-order accuracy. The development of the recirculation region in course of time was well simulated, and the observed splitting of the main eddy in a later phase and the secondary eddy in the concave corner were reproduced. The computational results are markedly influenced by the boundary conditions at closed boundaries and the eddy viscosity applied. Author (ESA)

N86-10201# European Space Agency. European Space Research and Technology Center, ESTEC, Noordwijk (Netherlands).
THE FLUID PHYSICS MODULE: A TECHNICAL DESCRIPTION
A. Gonfalone *In its* Fifth European Symp. on Mater. Sci. under Microgravity. Results of Spacelab 1 Dec. 1984 p 3-7 refs (For primary document see N86-10200 01-16)
Avail: NTIS HC A21/MF A01

N86-10202# Kodak Ltd., London (England).
CAPILLARY FORCES IN A LOW GRAVITY ENVIRONMENT
J. E. Padday *In* ESA Fifth European Symp. on Mater. Sci. under Microgravity. Results of Spacelab 1 Dec. 1984 p 9-14 refs Sponsored by Kodak Ltd. and England Department of Industry (For primary document see N86-10200 01-16)
Avail: NTIS HC A21/MF A01

N86-10203# Naples Univ. (Italy). Inst. of Aerodynamics Umberto Nobile.
SOME RESULTS OF THE MARANGONI FREE CONVECTION EXPERIMENT
L. G. Napolitano, R. Monti, and G. Russo *In* ESA Fifth European Symp. on Mater. Sci. under Microgravity. Results of Spacelab 1 Dec. 1984 p 15-22 refs (For primary document see N86-10200 01-16)
(Contract CNR-PSN-83-070)
Avail: NTIS HC A21/MF A01

N86-10204# Centre National de la Recherche Scientifique, Meudon-Bellevue (France). Equipe de Technologie de la Croissance Cristalline.
OSCILLATIONS OF SEMI-FREE LIQUIDS IN MICROGRAVITY: SPACELAB 1 EXPERIMENT ES 326 [OSCILLATIONS DE VOLUMES LIQUIDES SEMI-LIBRES EN MICROGRAVITE: EXPERIENCE ES 326 DANS SPACELAB 1]
H. Rodot and C. Bisch *In* ESA Fifth European Symp. on Mater. Sci. under Microgravity. Results of Spacelab 1 Dec. 1984 p 23-29 refs In FRENCH (For primary document see N86-10200 01-16)
Avail: NTIS HC A21/MF A01

N86-10205# Universidad Politecnica de Madrid (Spain). Dept. of ETSI Aeronautics.
LIQUID COLUMN STABILITY: EXPERIMENT 1 ES-331
T. Martinez *In* ESA Fifth European Symp. on Mater. Sci. under Microgravity. Results of Spacelab 1 Dec. 1984 p 31-36 refs Sponsored by Spanish Commission for Space Research (For primary document see N86-10200 01-16)
Avail: NTIS HC A21/MF A01

N86-10206# National Aerospace Lab., Amsterdam (Netherlands).
AXISYMMETRIC FREE SURFACE BEHAVIOR OF MOVING LIQUID IN A CYLINDER IN MICROGRAVITY
J. P. B. Vreeburg *In* ESA Fifth European Symp. on Mater. Sci. under Microgravity. Results of Spacelab 1 Dec. 1984 p 37-42 refs (For primary document see N86-10200 01-16)
Avail: NTIS HC A21/MF A01

N86-10207# Bristol Univ. (England). School of Chemistry.
KINETICS OF SPREADING OF LIQUIDS IN MICROGRAVITY: EXPERIMENT 1 ES 327
J. M. Haynes *In* ESA Fifth European Symp. on Mater. Sci. under Microgravity. Results of Spacelab 1 Dec. 1984 p 43-46 refs (For primary document see N86-10200 01-16)
Avail: NTIS HC A21/MF A01

N86-10235# Naples Univ. (Italy). Inst. of Aerodynamics Umberto Nobile.
THE TEXUS FLIGHT RESULTS ON CONVECTIVE FLOWS AND HEAT TRANSFER IN SIMULATED FLOATING ZONES
R. Monti, L. G. Napolitano, and G. Mannara *In* ESA Fifth European Symp. on Mater. Sci. under Microgravity. Results of Spacelab 1 Dec. 1984 p 229-236 refs (For primary document see N86-10200 01-16)
Avail: NTIS HC A21/MF A01

N86-10237# Goettingen Univ. (West Germany). Inst. fuer Angewandte Mechanik und Stroemungsphysik.
THE INFLUENCE OF THERMOCAPILLARITY ON THE MIGRATION OF DROPLETS IN A LIQUID POSSESSING A UNIFORM

TEMPERATURE GRADIENT
V. Delitzsch, H. Eckelmann, and W. Wuest (Deutsche Forshungs- und Versuchsanstalt fuer Luft- und Raumfahrt, Goettingen, West Germany) *In* ESA Fifth European Symp. on Mater. Sci. under Microgravity. Results of the Spacelab 1 Dec. 1984 p 245-249 refs (For primary document see N86-10200 01-16)
Avail: NTIS HC A21/MF A01

N86-10238# Naples Univ. (Italy). Inst. of Aerodynamics Umberto Nobile.
NUMERICAL SIMULATION OF UNSTEADY THERMAL MARANGONI FLOWS
L. G. Napolitano, C. Golia, and A. Viviani *In* ESA Fifth European Symp. on Mater. Sci. under Microgravity. Results of Spacelab 1 Dec. 1984 p 251-258 refs (For primary document see N86-10200 01-16)
(Contract CNR-PSN-83-070)
Avail: NTIS HC A21/MF A01

N86-10239# Canadian Astronautics Ltd., Ottawa (Ontario).
NUMERICAL SIMULATION OF CONVECTIONS IN THE MICROGRAVITY ENVIRONMENT
R. Boudreault *In* ESA Fifth European Symp. on Mater. Sci. under Microgravity. Results of Spacelab 1 Dec. 1984 p 259-264 refs (For primary document see N86-10200 01-16)
Avail: NTIS HC A21/MF A01

N86-10240# Hochschule der Bundeswehr, Munich (West Germany). Inst. fuer Raumfahrttechnik.
OSCILLATIONS OF A VISCOELASTIC LIQUID DROP IN ZERO-GRAVITY
H. F. Bauer *In* ESA Fifth European Symp. on Mater. Sci. under Microgravity. Results of Spacelab 1 Dec. 1984 p 265-270 refs (For primary document see N86-10200 01-16)
Avail: NTIS HC A21/MF A01

N86-10241# Gesamthochschule, Essen (West Germany).
VERIFICATION OF TURBULENCE DEVELOPING FROM THE OSCILLATORY MARANGONI CONVECTION IN A LIQUID COLUMN
Ch.-H. Chun *In* ESA Fifth European Symp. on Mater. Sci. under Microgravity. Results of Spacelab 1 Dec. 1984 p 271-280 refs (For primary document see N86-10200 01-16)
Avail: NTIS HC A21/MF A01

N86-10242# Giessen Univ. (West Germany). Inst. fuer Physikalisches.
MEASUREMENTS OF THE CRITICAL MARANGONI NUMBER OF THE LAMINAR-OSCILLATORY TRANSITION OF THERMOCAPILLARY CONVECTION IN FLOATING ZONES
D. Schwabe and A. Scharmann *In* ESA Fifth European Symp. on Mater. Sci. under Microgravity. Results of Spacelab 1 Dec. 1984 p 281-289 refs (For primary document see N86-10200 01-16)
(Contract BMFT-01-QV-148-ZA-SN-SLN-7786)
Avail: NTIS HC A21/MF A01

N86-10243# Ishikawajima-Harima Heavy Industries Co. Ltd., Yokohama (Japan).
EXPERIMENTAL STUDY ON MARANGONI CONVECTION
J. Ochiai, K. Kuwahara, M. Morioka, S. Enya, K. Sezaki, T. Maekawa (Ioyo Univ., Japan), and I. Tanasawa (Tokyo Univ.) *In* ESA Fifth European Symp. on Mater. Sci. under Microgravity. Results of Spacelab 1 Dec. 1984 p 291-295 refs Sponsored by Japanese Science and Technology Agency (For primary document see N86-10200 01-16)
Avail: NTIS HC A21/MF A01

N86-10244# Universidad Politecnica de Madrid (Spain). Lab. de Aerodinamica.
STABILITY OF LONG LIQUID COLUMNS
J. Meseguer *In* ESA Fifth European Symp. on Mater. Sci. under Microgravity. Results of Spacelab 1 Dec. 1984 p 297-300 refs (For primary document see N86-10200 01-16)
Avail: NTIS HC A21/MF A01

N86-10245# Mons Univ. (Belgium). Faculty of Sciences.
RAYLEIGH-BENARD INSTABILITY IN SYSTEMS PRESENTING A MINIMUM IN SURFACE TENSION
D. Villers and J. K. Platten *In* ESA Fifth European Symp. on Mater. Sci. under Microgravity. Results of Spacelab 1 Dec. 1984 p 301-305 refs (For primary document see N86-10200 01-16)
Avail: NTIS HC A21/MF A01

N86-10249# Deutsche Forschungs- und Versuchsanstalt fuer Luft- und Raumfahrt, Cologne (West Germany). Inst. for Space Simulation.
HOLOGRAPHIC INTERFEROMETRY NEAR GAS/LIQUID CRITICAL POINTS: GROUND-BASED STUDY OF A D1 EXPERIMENT
H. Klein and K. Wanders *In* ESA Fifth European Symp. on Mater. Sci. under Microgravity. Results of Spacelab 1 Dec. 1984 p 323-325 refs (For primary document see N86-10200 01-16)
Avail: NTIS HC A21/MF A01

N86-10250# Technische Univ., Munich (West Germany). Lehrstuhl A fuer Thermodynamik.
NUCLEATE POOL BOILING IN SUBCOOLED LIQUID UNDER MICROGRAVITY: RESULTS OF TEXUS EXPERIMENTAL INVESTIGATIONS
M. Zell, J. Straub, and A. Weinzierl *In* ESA Fifth European Symp. on Mater. Sci. under Microgravity. Results of Spacelab 1 Dec. 1984 p 327-333 refs Sponsored by Bundesministerium fuer Forschung und Technologie (For primary document see N86-10200 01-16)
Avail: NTIS HC A21/MF A01

N86-10253# Lyon-1 Univ. (France).
SPACE EXPERIMENT ON THERMAL DIFFUSION. PREPARATION AND THEORETICAL ANALYSIS
J. Bert, D. Henry, P. Layani, G. Chuzeville, J. Dupuy, and B. Roux (Marseille Univ.) *In* ESA Fifth European Symp. on Mater. Sci. under Microgravity. Results of Spacelab 1 Dec. 1984 p 347-352 refs Sponsored by CNES (For primary document see N86-10200 01-16)
Avail: NTIS HC A21/MF A01

N86-10268# Battelle Inst., Frankfurt am Main (West Germany).
LIQUIDS AND INTERFACES
D. Langbein *In* ESA Fifth European Symp. on Mater. Sci. under Microgravity. Results of Spacelab 1 Dec. 1984 p 443-447 (For primary document see N86-10200 01-16)
Avail: NTIS HC A21/MF A01

35 INSTRUMENTATION AND PHOTOGRAPHY

Includes remote sensors; measuring instruments and gages; detectors; cameras and photographic supplies; and holography.

For aerial photography see *43 Earth Resources.* For related information see also *06 Aircraft Instrumentation,* and *19 Spacecraft Instrumentation.*

N86-10478 State Univ. of New York, Buffalo.
DIGITAL DECODING OF IN-LINE HOLOGRAMS Ph.D. Thesis
Levent Onural 1985 151 p
Avail: Univ. Microfilms Order No. DA8510353

In-line holography is a useful tool in the study of dynamic objects in three-dimensional space. A hologram is a specific non-linear coding which is recorded in the presence of coherent illumination. The physical reconstruction is done by reilluminating the hologram, and the resulting image is contaminated by the interfering twin-image. Here in this dissertation, a system of digital filters is presented, which is applied directly to the in-line hologram and maps the hologram into an image of the boundaries (edges) of the objects encoded in it, provided that the object distribution function is real. This technique bypasses physical reconstruction completely and gives a clear decoding of the objects. In the first stage of the system, the hologram is approximated as the dc shifted output of a linear system. An approximation inverse filter is used to obtain the desired object distribution from the hologram since the exact inverse is not realizable. The linear approximate inverse filter is a truncated series expansion of the inverse filter in the Fourier transform domain. Dissert. Abstr.

N86-10479 Texas Christian Univ., Fort Worth.
REAL-TIME HOLOGRAPHY BY STIMULATED RAMAN AND BRILLOUIN SCATTERING Ph.D. Thesis
Swati Roy 1984 99 p
Avail: Univ. Microfilms Order No. DA8510382

Experimental investigations on the quality of real image reconstruction by stimulated Brillouin scattering (SBS) and stimulated Raman scattering (SRS) are reported here. The quality of real image reconstruction under two separate experimental conditions was found to be highly dependent on: (1) the amplitude modulations of the laser radiation, (2) the input laser power and (3) the position of the lens-focus. The best quality of reconstruction was observed when the lens focus was in front of the cell and the real image of the object formed by the lens was located inside the nonlinear medium, within 3 cm of the entrance window of the cell. Also, this experimental condition reconstructed a smaller area of the illuminated object than the inside focus condition. According to existing theory, when the lens-focus is inside the nonlinear medium, the complex interference pattern near the entrance window of the cell plays the role of a real-time hologram. Dissert. Abstr.

N86-10480 Department of the Air Force, Washington, D.C.
SENSOR SYSTEM Patent
J. E. Heath and H. W. Swenson, inventors (to Air Force) Issued 14 May 1985 6 p Supersedes AD-D011242; N85-11828
(AD-D011767; US-Patent-4,517,464; US-Patent-Appl-SN-431866; US-Patent-Class-250-370) Avail: US Patent and Trademark Office CSCL 17/5

An infrared sensor system for use on satellites comprising dual arrays of mercury cadmium tellurice semiconductor elements is described. One array of conventional photovoltaic detectors is wired in parallel with a novel array of HdCdTe material in which the n-type region of each mesa and the resulting p-n junction is considerably smaller than that utilized in the conventional detector. As the cumulative dose of incident radiation is increased, type conversion in both arrays occurs resulting in degraded performance in the conventional array but an increase in performance caused by the now effective p-n junction area in the novel array. An electronic switching device, coupled with a dosimeter, alternately selects the conventional array or the novel array depending upon the total dose of radiation received. GRA

N86-10481 Department of the Air Force, Washington, D.C.
STEREOSCOPIC VIDEO IMAGERY GENERATION Patent
G. G. Kuperman and F. R. Bodine, inventors (to Air Force) Issued 9 Apr. 1985 5 p Supersedes AD-D009489
(AD-D011785; US-Patent-4,510,525; US-Patent-Appl-SN-361016; US-Patent-Class-358-88) Avail: US Patent and Trademark Office CSCL 14/5

Flying spot scanner technology is combined with stereo photography in motion to produce two channels of video imagery which can be optically combined to produce the perception of dynamic stereoscopic detail. The scanner generates alternate lines with lateral offset corresponding to the physical separation between stereo photographic pairs to provide two rasters. Author (GRA)

N86-10482 Department of the Air Force, Washington, D.C.
FALL VELOCITY INDICATOR/VIEWER Patent
R. O. Berthel, V. G. Plank, S. H. Jones, and A. J. Matthews, inventors (to Air Force) Issued 30 Apr. 1985 8 p Supersedes AD-D010045
(AD-D011789; US-Patent-4,514,758; US-Patent-Appl-SN-442496; US-Patent-Class-358-93) Avail: US Patent and Trademark Office CSCL 04/2

A fall velocity indicator/viewer having a sampling compartment, a camera system, and an elongated tunnel for interconnecting the camera system to the sampling compartment is described. The camera system includes a video camera for continuously monitoring snowflakes as they naturally fall through a viewing area in the sampling compartment. The snowflakes are illuminated by a pair of strobe lights directly and in combination with reflected light from a pair of mirrors. In addition, a mirror in the tunnel provides a reflected view from the top of the snowflakes. The video camera is capable of thereby monitoring multiple views of snowflakes in a single video frame and provide sufficient data to analyze the physical characteristics of the snowflakes as well as aid in making velocity determinations and other observations of naturally falling snowflakes. Author (GRA)

N86-10483 Department of the Navy, Washington, D. C.
PRECISE BEARING SUPPORT DITHERER WITH PIEZOELECTRIC DRIVE MEANS Patent
G. L. Assard and A. L. Moorcroft, inventors (to Navy) Issued 11 Jun. 1985 6 p
(AD-D011819; US-Patent-4,523,120; US-Patent-Appl-SN-617049; US-Patent-Class-310-323) Avail: US Patent and Trademark Office CSCL 13/9

A relatively solid mounting surface, which may be part of a leveling gimbal, supports a piezoelectric bearing mount which has the properties of an acoustic transducer. The transducer has electrodes thereon which are powered from multi-phase electrical sources causing the bearing mount, and a bearing jewel which is rigid therewith, to move so as to dither the jewel in a rotary or other preselected fashion, thereby reducing bearing friction. Bandwidth, level and phasing sequence of the power sources are adjustable permitting optimized average dynamic motion and corresponding increased readout accuracy. Author (GRA)

N86-10484*# Illinois Univ., Urbana-Champaign. Dept. of Electrical and Computer Engineering.
SEMICONDUCTOR SUPERLATTICE PHOTODETECTORS Semiannual Report, Jan. - 30 Jun. 1985
S. L. Chuang, K. Hess, J. J. Coleman, and J. P. Leburton Jun. 1985 23 p refs
(Grant NAG1-500)
(NASA-CR-176249; NAS 1.26:176249) Avail: NTIS HC A02/MF A01 CSCL 14B

Two novel types of superlattice photodetectors were studied. The first was a superlattice photomultiplier and the second a photodetector based on the real space transfer mechanism. A summary of the results is presented. G.L.C.

N86-10485# European Space Agency, Paris (France).
METRIC CAMERA WORKSHOP
T. D. Guyenne, ed. and J. J. Hunt, ed. Apr. 1985 210 p refs Workshop held in Oberpfaffenhofen, West Germany, 11-13 Feb. 1985; sponsored by DFVLR and ESA
(ESA-SP-209; ISSN-0379-6566) Avail: NTIS HC A10/MF A01

Photogrammetry, photomapping, geological surveys, and thematic mapping with the Spacelab metric camera were discussed. For individual titles, see N86-10486 through N86-10522.

N86-10486# Stuttgart Univ. (West Germany). Inst. of Photogrammetry.
DIGITAL ELEVATION MODEL FROM SPACELAB METRIC CAMERA PHOTOGRAPHS
F. Ackermann and E. Stark *In* ESA Metric Camera Workshop Apr. 1985 p 9-12 (For primary document see N86-10485 01-35)
Avail: NTIS HC A10/MF A01

In two different pairs of Spacelab metric camera photographs terrain elevations were measured in an area of fluvioglacial morphology. The derived digital terrain model and contour lines are compared with each other and absolutely checked against topographic maps. The results show that height accuracy is 20m, with 15m accuracy possible, giving a contour interval of 50m. A slower film and image motion compensation are recommended. Doubts about the suitability of metric camera photography for line mapping are expressed. Author (ESA)

N86-10487# Technische Univ., Hanover (West Germany). Inst. for Photogrammetry and Engineering Surveys.
ORTHOPHOTOMAPPING FROM METRIC CAMERA IMAGERY
H. Engel and G. Konecny *In* ESA Metric Camera Workshop Apr. 1985 p 13-18 refs (For primary document see N86-10485 01-35)
Avail: NTIS HC A10/MF A01

The advantages and techniques of orthophoto generation for topographic mapping from Spacelab metric camera imagery are outlined. The technique combines high efficiency and precision, minimized loss of information caused by the involved direct photographic process, independence of interpretation, and possible application of and common photogrammetric instruments. Preprocessing involves densification of control points and determination of the parameters of exterior orientation by aerotriangulation with bundle block adjustment, and generating digital terrain models for differential rectification. Author (ESA)

N86-10488# Technische Univ., Vienna (Austria). Inst. of Photogrammetry.
STEREO-ORTHOPHOTOS IN VARIOUS MAP PROJECTIONS
G. Fritze, J. Jansa, and K. Kraus *In* ESA Metric Camera Workshop Apr. 1985 p 19-24 refs (For primary document see N86-10485 01-35)
Avail: NTIS HC A10/MF A01

The production of stereo-orthophoto maps from aerial and spaceborne photographs is discussed. When making orthophotos from satellite images, Earth curvature and map projections have to be taken into account. There are also problems having control points all determined in one homogenous coordinate system. The terrain data of the large area belong to different systems, and have to be transformed to the map coordinate system in which the orthophoto is produced. With stereo-orthophotos, users are given additional information on terrain heights without having to apply complicated photogrammetric compilation techniques. Author (ESA)

N86-10489# Karlsruhe Univ. (West Germany). Inst. fuer Photogrammetrie und Topographie.
RESTITUTION OF SPACELAB PHOTOGRAPHY BY ANALOG STEREOPLOTTER
H. P. Baehr *In* ESA Metric Camera Workshop Apr. 1985 p 25-28 refs (For primary document see N86-10485 01-35)
Avail: NTIS HC A10/MF A01

Analog restitution of Spacelab metric camera photography using conventional instrumentation was chosen to meet the needs and capacities of Third World users. Absolute orientation of a whole stereomodel is not possible because of distortion between geocentric and geodetic coordinate systems. Limiting the restored area to 40 km x 30 km, height errors from system distortion stay below 15 m. Test results correspond to theory for single height points. On-line plotting of contour lines, however, seems critical, though analog orthophoto production is done without any problems for graphical presentation. Author (ESA)

N86-10490# Politecnico di Milano (Italy). Ist. di Topografia Fotogrammetria e Geofisica.
EVALUATION OF THE ACCURACY OF THE METRIC CAMERA IMAGES FOR THE PRODUCTION OF LINE MAPS AND ORTHOPHOTOS
G. Togliatti and A. Moriondo *In* ESA Metric Camera Workshop Apr. 1985 p 29-34 (For primary document see N86-10485 01-35)
Avail: NTIS HC A10/MF A01

The accuracy of Spacelab metric camera black and white images was analyzed on stereomodels. The heights of 1500 trigonometric vertices and the planimetric position of 150 points were measured. Pointing errors in planimetry and height were computed by a comparison with the coordinates of the national trigonometric grids. For selected areas repeated drawing of contours were checked against 1:25,000 scale maps. Accuracy is best in altimetry (20 m) and contours, good as expected in planimetry (N = 13 m, E = 12 m), poor in detail identification due to lack of illumination and of image motion compensator. The production of orthophotos on the scale 1:100,000 is completely successful. Accuracy evaluated on 50 photographic points is the same as obtained for line maps derived from stereomodels. Author (ESA)

N86-10491# Heidelberg Univ. (West Germany). Inst. fuer Geographie.
PHOTOMAPPING IN DIFFERENT CLIMATIC ZONES
K. P. Wiesner and F. E. Fezer *In* ESA Metric Camera Workshop Apr. 1985 p 37-41 ref (For primary document see N86-10485 01-35)
Avail: NTIS HC A10/MF A01

Use of Spacelab metric camera color infrared images for updating topographic maps and developing thematic maps was assessed. Test areas included the Alps, Brittany, Sudan, Zimbabwe, and Qinghai (China). Scales of 1:250,000 in all vegetation zones; and 1:100,000 in arid zones were used. For map revision urban growth; new roads, railways, mines, man-made lakes; cropped and wooded areas expanding or reducing were studied. For thematic maps landforms and vegetation were examined. Although photo quality is generally poor because of the weather, objects not represented on conventional maps show up well. Organic materials cannot be distinguished from scrub, and manmade patterns are difficult to find, but objects such as railroads can be identified. Author (ESA)

N86-10492# Mainz Univ. (West Germany).
A GEOLOGICAL STRUCTURAL ANALYSIS OF THE SOUTH-EASTERN ZAGROS (IRAN) RANGES BASED ON METRIC CAMERA PHOTOS
M. Fuerst *In* ESA Metric Camera Workshop Apr. 1985 p 43-46 refs (For primary document see N86-10485 01-35)
Avail: NTIS HC A10/MF A01

Spacelab metric photography was used to make a tetonic inventory of the southeastern Zagros Ranges on the Persian Gulf. Photogeological structural analysis shows that the fold mountains are cut by overthrust faults and by major faults. The latter strike at a right or an acute angle to the folds. They are inferred to be associated with the rigid competent basement and punch through the sedimentary cover. Active and inactive salt plugs together with collapse structures occur along these overthrust faults and along major faults, which represent intricate plate tectonic movement planes. The salt plugs are confined to the intersections of areas of pressure maximum and salt concentration with these tectonic elements. Author (ESA)

N86-10493# Ecole Polytechnique Federale de Lausanne (Switzerland). Inst. des Mensurations.
EROSION CONTROL AND WATERSHED MANAGEMENT BY SPACELAB PHOTOGRAPHY
O. Koelbl and P. dePury *In* ESA Metric Camera Workshop Apr. 1985 p 47-52 (For primary document see N86-10485 01-35)
Avail: NTIS HC A10/MF A01

The interpretability of false color Spacelab photographs for erosion control and water shed management was assessed using photos taken over Nepal and the Mount Everest Massif. The thematic interpretation was done by a geologist working in this region. Scale limitations, image reproduction, and filtering of the photographs are discussed. Results show that much information can be extracted using relatively simple means. Color infrared photography must be used since panchromatic imagery does not show enough detail. Author (ESA)

N86-10494# Geological Survey, Reston, Va.
HIGH-RESOLUTION IMAGE DATA FROM THE SPACE SHUTTLE
F. J. Doyle *In* ESA Metric Camera Workshop Apr. 1985 p 55-58

(For primary document see N86-10485 01-35)
Avail: NTIS HC A10/MF A01

Shuttle Mission STS-41G carried the Large Format Camera with its stellar Attitude Reference System, and the Shuttle Imaging Radar. Exceptional photographs which should permit compilation of 1:50,000 scale image and topographic maps were obtained. The photographs will be made available through the United States Geological Survey EORS data center. The radar, though plagued with operational problems, also produced images useful for Earth science and development of radar mapping procedures.
Author (ESA)

N86-10495# University Coll., London (England). School of Oriental and African Studies.
EVALUATION OF METRIC CAMERA IMAGES AT THE UNIVERSITY OF LONDON
I. J. Downman, A. Meneguette, and J. A. Allan *In* ESA Metric Camera Workshop Apr. 1985 p 59-64 ref (For primary document see N86-10485 01-35)
Avail: NTIS HC A10/MF A01

Methods to determine coordinates and produce maps using a stereo comparator and an analytical stereo plotter as the measuring devices, and interpretation and plotting of data for land use studies with Spacelab metric camera image are discussed. Photogrammetric procedures of space resection, orientation and plotting are outlined. Results which indicate the inherent precision of the data and the accuracy which may be obtained when carrying out mapping or map revision are given. The type of detail which may be correctly interpreted and land use interpretation in arid areas are considered.
Author (ESA)

N86-10496# Bonn Univ. (West Germany).
PARTIAL IN-FLIGHT CALIBRATION OF THE METRIC CAMERA Interim Report
G. Kupfer *In* ESA Metric Camera Workshop Apr. 1985 p 65-66 refs (For primary document see N86-10485 01-35)
Avail: NTIS HC A10/MF A01

Black and white, and color infrared photographs were used to assess whether in-flight calibration of the Spacelab metric camera is possible. Results suggest that it is feasible given sufficient geodetic control.
Author (ESA)

N86-10497# Institut Geographique National, Paris (France).
IDENTIFICATION OF PLANIMETRIC FEATURES FROM THE METRIC CAMERA
A. Baudoin *In* ESA Metric Camera Workshop Apr. 1985 p 69-73 refs (For primary document see N86-10485 01-35)
Avail: NTIS HC A10/MF A01

The Spacelab metric camera flight over the southeast of France where many maps and aerial photographs exist and where a strip of 1:60,000 aerial photos was acquired the same day of the Shuttle flight was studied. It was possible to measure the percentage of planimetric features visible on the Spacelab images. This percentage depends on the kind of features (road, railways, hedges, rivers etc.), on their size (width, surface) and on their contrast. The results show that these space images could be helpful to revise medium scale topographic maps (1:100,000 or 1:50,000).
Author (ESA)

N86-10498# Technische Univ., Munich (West Germany). Lehrstuhl fuer Geographie und Geographische Fernerkundung.
ANALYSIS OF METRIC CAMERA IMAGES FROM THE USA AND THEIR SUITABILITY FOR TOPOGRAPHIC AND THEMATIC MAPPING
K. R. Dietz *In* ESA Metric Camera Workshop Apr. 1985 p 75-80 refs (For primary document see N86-10485 01-35)
Avail: NTIS HC A10/MF A01

Spacelab metric camera images of the Black Hills and the Mississippi Valley were analyzed to assess their suitability for topographic and thematic mapping. Ground checks in the respective areas were carried out in 1982 and 1984. Although both selected photos permit the delimitation of larger natural units, they are only of restricted value for topographic and thematic mapping, as their information content is unevenly distributed. Due to the unfavorable illumination conditions during the data acquisition many details required for topographic mapping are lost, through shadow effects or lacking contrast. The illumination also negatively affects attempts at thematic mapping on the 1:100,000 scale.
Author (ESA)

N86-10499# Rennes Univ. (France). Equipe Aerogeographie.
LONG RANGE TRANSLOCATIONS ASHORE TO OFFSHORE USING SPACELAB-1 METRIC CAMERA IMAGERY IN THE PERSPECTIVE OF INTEGRATED GEOPHYSICAL SURVEYS
G. Galibert *In* ESA Metric Camera Workshop Apr. 1985 p 81-85 refs (For primary document see N86-10485 01-35)
Avail: NTIS HC A10/MF A01

It is shown that long range translocations ashore to offshore of points or objects are possible (up to 150,000 m, X and Y) using Spacelab metric camera imagery when conventional methods of positioning by triangulation, Doppler satellites or radio-electric hyperbolic systems are unusable. Experiments in the Saint Malo coastal area along the French side of the English Channel are described. Dimensional measurements of colored crystals give an accuracy of 8 to 20 m through analog or digital methods, X and Y, with a possible transfer on topographical maps or charts at scales of 1:25000 or 1:15560. Transfers of digitized images on helicopter head up displays (theoretical accuracy 1 m) is also possible to prepare airborne coastal surveys over shallow waters.
Author (ESA)

N86-10500# Deutsche Forschungs- und Versuchsanstalt fuer Luft- und Raumfahrt, Oberpfaffenhofen (West Germany). Inst. of Optoelectronics.
LINE MAPPING AND RESOLUTION TESTS WITH METRIC CAMERA DATA
M. Schroeder, W. Schuhr (Technische Univ., Hanover), and A. Schuering (Technische Univ., Hanover) *In* ESA Metric Camera Workshop Apr. 1985 p 87-90 refs (For primary document see N86-10485 01-35)
Avail: NTIS HC A10/MF A01

The utility of Spacelab metric camera imagery for topographic mapping was assessed. The edge gradient analysis applied to derive modulation transfer function curves is described. The resolution on the ground for a line pair is equivalent up to 20 m for high contrast. Samples for line map production and updating are shown for conventional medium scale maps by analytical plotters as well as for quasi-line maps by digital image processing.
Author (ESA)

N86-10501# United Nations Economic Commission for Africa, Addis Ababa (Ethiopia).
ROLE OF THE ECONOMIC COMMISSION FOR AFRICA AS A PRINCIPAL INVESTIGATOR IN THE METRIC CAMERA EXPERIMENT AND REPORTS OF THE RESULT OF THE ASSESSMENT FOR TOPOGRAPHIC AND REVISION OF MAPS IN POPULATED AND DEVELOPED AREAS OF THE WORLD
OluFunso Olujohungbe *In* ESA Metric Camera Workshop Apr. 1985 p 91-93 (For primary document see N86-10485 01-35)
Avail: NTIS HC A10/MF A01

Spacelab metric camera photographs of the irrigation areas of the Al Gezira region of Sudan were used to assess the feasibility of using the camera for map revision and making in Africa. Results confirm the high resolution of the images, particularly details registered in the infrared, favorable for observation and identification of features, and rapid stereoplotting from space photographs for topographic and small scale mapping.
Author (ESA)

N86-10502# Parma Univ. (Italy). Ist. di Geologia.
THE ROLE OF VERY SMALL SCALE METRIC IMAGES IN MODERN GEOLOGY
M. Sgavetti *In* ESA Metric Camera Workshop Apr. 1985 p 97-102 refs (For primary document see N86-10485 01-35)
Avail: NTIS HC A10/MF A01

The suitability of the Spacelab metric camera stratigraphic resolution for the construction of models for sedimentary basins and the structural analysis of tectonically complex areas was assessed. Metric camera images, large scale aerial photos, and seismic profiles are compared, in terms of resolution of physical surfaces (bed pattern). The Spacelab images give good results in structural analysis of tectonically complex areas. Author (ESA)

N86-10503# Technische Hochschule, Graz (Austria). Inst. of Image Processing and Computer Graphics.
GEOLOGICAL MAPPING OF REMOTE MOUNTAINOUS REGIONS USING METRIC CAMERA IMAGERY
M. F. Buchroithner *In* ESA Metric Camera Workshop Apr. 1985 p 103-108 refs (For primary document see N86-10485 01-35)
Avail: NTIS HC A10/MF A01

The applicability of colored infrared Spacelab metric camera photography for geological reconnaissance mapping and for more detailed studies up to scales larger than 1:100,000 is demonstrated with mountainous regions of different geological structure in Western Saudi Arabia, in the Afghan Hindu Kush, and in the East Nepalese Himalayas. Advantages and drawbacks for geological mapping in remote areas are discussed. Author (ESA)

N86-10504# Technische Univ., Munich (West Germany). Inst. fuer Geographie.
INTERPRETATION OF METRIC CAMERA CONCERNING HYDROLOGIC STRUCTURES OF THE RHONE DELTA
K. Halm *In* ESA Metric Camera Workshop Apr. 1985 p 109-114 (For primary document see N86-10485 01-35)
Avail: NTIS HC A10/MF A01

Hydrological maps are made visually using Spacelab metric camera (MC) imagery after contrast enhancement, edge enhancement, and enlargements 8 x and 16 x as transparencies and prints. Field-work is carried out simultaneously with the MC data acquisition time (landcover mapping, object recording, terrestrial photo documentation, sediment and water samples) to check MC mapping. Linear elements cannot be clearly classified (watercourses, roads, paths, field boundaries). In a lagoon zone, it is possible to differentiate 6 classes using the MC image. Water basins can be classified into five classes. It is impossible to differentiate agricultural acreage. This should be possible using a combined system of panchromatic and multispectral recording, as shown on example of the double exposure of MC and MSS-LANDSAT. Author (ESA)

N86-10505# Topographical Survey Branch, Kathmandu (Nepal). Survey Dept.
TEST ON MAPPING APPLICATION OF METRIC CAMERA IMAGERY
K. R. Adhikary *In* ESA Metric Camera Workshop Apr. 1985 p 115-118 refs (For primary document see N86-10485 01-35)
Avail: NTIS HC A10/MF A01

The accuracy reliability, production difficulties, and costs of Spacelab metric camera imagery for topographic mapping of the eastern Himalayas in Nepal are compared with existing maps. It appears possible to extract sufficient cartographic details from Spacelab imagery for mapping at the scale of 1:100,000, however, an extensive field completion is required for all the hidden details due to very small original negative scale of the imagery. This costs more time and money than conventional topographic mapping. Using identifiable points in existing maps (1 in = 1 mile) as control, accuracy of planimetric details is 50 m, a little larger than the map accuracy standard for 1:100,000 of 34 m. Proper identification and post-pointing of geodetic control is possible to meet the accuracy standard of topographic mapping. Author (ESA)

N86-10506# Deutsche Forschungs- und Versuchsanstalt fuer Luft- und Raumfahrt, Cologne (West Germany). Bereich fuer Projekttraegerschaften.
STATUS OF PREPARATION ACTIVITIES FOR METRIC CAMERA REFLIGHT ON EOM-1/2
A. Langner *In* ESA Metric Camera Workshop Apr. 1985 p 121-123 (For primary document see N86-10485 01-35)
Avail: NTIS HC A10/MF A01

In autumn 1986 the Metric Camera will be reflown in the Earth Observation Shuttle Mission. The implementation of a forward motion compensation mechanism and the use of high resolution films will increase ground resolution by a factor of 2. Hardware refurbishment and modifications are nearly completed and the system is ready for integration into the FOM-1/2 payload. Mission objective is to demonstrate the mapping capability of high resolution space photography for compiling topographic and thematic maps for unpopulated or less developed regions of the world, and updating and revising topographic and thematic maps in populated and developed areas of the world. Images will be taken with 60% or 80% overlap for stereoscopic evaluation. Author (ESA)

N86-10507# University Coll., London (England).
OEEPE PARTICIPATION IN TESTING METRIC CAMERA PHOTOGRAPHY
I. J. Downman *In* ESA Metric Camera Workshop Apr. 1985 p 125-126 (For primary document see N86-10485 01-35)
Avail: NTIS HC A10/MF A01

A test program for the Spacelab metric camera is outlined. Image content, image accuracy, map compilation and revision, orthophoto production, and aerial triangulation are tested. Position on photograph, mode of viewing (monoscopic or stereoscopic), amount of overlap for stereo viewing, and emulsion (color infrared or panchromatic) are investigated. Author (ESA)

N86-10508# Technische Univ., Berlin (West Germany). Dept. of Photogrammetry and Cartography.
TOPOGRAPHIC INTERPRETATION OF METRIC CAMERA IMAGES: AN EXAMPLE IN SOMALIA
J. Albertz and A. A. Gulaid *In* ESA Metric Camera Workshop Apr. 1985 p 129-133 refs (For primary document see N86-10485 01-35)
Avail: NTIS HC A10/MF A01

An extremely arid area of Somalia was used to test the Spacelab metric camera's ability to distinguish topographic map elements such as landforms, drainage, planimetric elements and vegetation. Landforms (except small valleys and ridges) the sea, wadis, and watersheds are identified well. Vegetation, small streams, paths, and settlements are hard or impossible to distinguish. Identification strongly depends on contrast, object size, and their relative arrangement. Interpretation experience gained in other regions cannot simply be transferred to arid zones. Author (ESA)

N86-10509# Institut Geographique National, Paris (France).
THEMATIC INVESTIGATIONS IN FRANCE BASED ON METRIC CAMERA IMAGERY
P.-Y. Lecordix *In* ESA Metric Camera Workshop Apr. 1985 p 135-137 In FRENCH; ENGLISH summary (For primary document see N86-10485 01-35)
Avail: NTIS HC A10/MF A01

Spacelab metric camera images were used to study geological features, land use, and forestry, and were compared with other data sources used in cartography. For geological surveys, the metric camera is comparable to SPOT satellite, and better than LANDSAT. For land use, Spacelab images are unsatisfactory in urban areas; woodland and scrub is over-represented due to shadow effects and inclusion of water covered with aquatic plants; forest distribution is well reproduced; sandy features are well identified. For forest inventories, results are surprisingly good, e.g., only 4% error in distinguishing resinous and leafy trees. Author (ESA)

N86-10510# Technische Univ., Munich (West Germany). Inst. fuer Geographie.
THEMATIC MAPPING OF METRIC CAMERA COLOR INFRARED AND BLACK AND WHITE PHOTOGRAPHS FOR LAND USE CLASSIFICATION
H. G. Gierloff-Emden *In* ESA Metric Camera Workshop Apr. 1985 p 139-145 (For primary document see N86-10485 01-35)
Avail: NTIS HC A10/MF A01

The use of Spacelab metric camera black and white, and color infrared photography for land use and thematic mapping was tested for a mountainous region, interspersed with very flat features in Mexico (black and white) and a coastal zone in France (color). Ground checks were carried out in both regions, though not during the time of the flight. Results show that black and white is superior concerning line detection and minimum visibility. Both images could serve as auxiliary means for thematic mapping on scales of 1:100,000. Author (ESA)

N86-10511# Technische Univ., Hanover (West Germany). Inst. fuer Photogrammetrie und Ingenieurvermessungen.
DIGITAL IMAGE PROCESSING OF METRIC CAMERA IMAGERY
P. Lohmann *In* ESA Metric Camera Workshop Apr. 1985 p 147-152 refs (For primary document see N86-10485 01-35)
Avail: NTIS HC A10/MF A01

The use of digitized Spacelab metric camera imagery for map updating is demonstrated for an area of Germany featuring agricultural and industrial areas, and a region of the White Nile. LANDSAT and Spacelab images were combined, and digital image processing techniques used for image enhancement. Updating was achieved by semiautomatic techniques, but for many applications manual editing may be feasible. Author (ESA)

N86-10512# Silsoe Coll., Bedford (England).
LAND EVALUATION SUCCESSES WITH THE METRIC CAMERA
M. A. Keech *In* ESA Metric Camera Workshop Apr. 1985 p 153-156 refs (For primary document see N86-10485 01-35)
Avail: NTIS HC A10/MF A01

The Spacelab metric camera as a data source for land resource planning was demonstrated using stereophotographs of Oman (after cloud covered most of the proposed areas in Brazil and the Andes). The photographs show drainage patterns, vegetation patterns, roads, and settlements. The scale variation is small, the resolution is adequate for all but the most detailed survey work, and for geologist, agriculturalist, or forest planner the images provide the most useful synoptic view of an area, which the human eye and brain can interpret without further image processing. Author (ESA)

N86-10513# Freiburg Univ. (West Germany). Abteilung Luftbildmessung und Fernerkundung.
REQUIREMENTS AND POSSIBILITIES OF SPACELAB METRIC CAMERA PHOTOS USAGE FOR INVENTORIES OF LARGE AREAS OF EXTENSIVELY MANAGED FORESTS
W. Forstreuter *In* ESA Metric Camera Workshop Apr. 1985 p 157-160 (For primary document see N86-10485 01-35)
Avail: NTIS HC A10/MF A01

LANDSAT MSS and Spacelab metric camera coverage, spectral and geometric resolution, data handling, and results for forest are compared. Discrimination of vegetation types is poor for both sensors in a test area of wet forest. Mapping of a very small stream was very difficult, and it could not even be seen in LANDSAT images. Author (ESA)

N86-10514# Technische Univ., Munich (West Germany). Inst. fuer Geographie.
TOPOGRAPHIC AND THEMATIC MAPPING: ANALYSIS OF METRIC CAMERA BLACK AND WHITE PHOTOGRAPHS OF THE RHONE DELTA
W. Stolz *In* ESA Metric Camera Workshop Apr. 1985 p 161-166 refs (For primary document see N86-10485 01-35)
Avail: NTIS HC A10/MF A01

A Spacelab Metric Camera (MC) black and white photograph of the Rhone Delta was analyzed concerning the information content of the image for topographic and thematic mapping. Ground check was carried out at the same time of the flight. The interpretation shows that the image meets the standards of medium scale topographic maps with limitations. For thematic mapping the image could serve as auxiliary means in scales around 1:100,000. Comparison with aerial photographs demonstrates the information loss caused by enlargement of the MC-image. Author (ESA)

N86-10515# Zurich Univ. (Switzerland). Dept. of Geography.
EVALUATION OF METRIC CAMERA PHOTOS
H. Haefner and F. Hugentobler *In* ESA Metric Camera Workshop Apr. 1985 p 169-171 (For primary document see N86-10485 01-35)
Avail: NTIS HC A10/MF A01

The resolution of linear features, and the mapping of the transient snowline and the snow cover on Spacelab metric camera photographs of the Alps were investigated. Forest, shrubland, settlements and roads can be identified. Snowlines on glaciers cannot be identified, but the transient snow line is clear. Small features, including moraines and crevasses can be seen. Shadow and vegetation cover can cause problems in identifying snowfree areas. The main advantage of the photos is the synoptic view of large areas and the possibility to determine correlations between various features and/or regions. Single features may be recognized and mapped in great detail. The resolution capability, and the density and variety of the information for studies of larger areas is unmatched by other remote sensing systems, including LANDSAT MSS. Author (ESA)

N86-10516# Indian Space Research Organization, Ahmedabad. Space Applications Center.
CREATION OF GROUND CONTROL POINTS (GCP) LIBRARY USING ESA SPACELAB METRIC CAMERA IMAGERY
P. K. Srivastava, S. N. Jha, P. M. Udani, A. K. S. Gopalan, and D. S. Kamat *In* ESA Metric Camera Workshop Apr. 1985 p 173-174 ref (For primary document see N86-10485 01-35)
Avail: NTIS HC A10/MF A01

Using standard software for aerial triangulation and coordinates of ground control from 1:250,000 scale maps, the ground coordinates of ground control points for precision processing of remote sensing data were obtained. With 10 points for control, coordinates of test points are found to be off by as much as 200 m. A digital image restitution model is presented. It is hoped to obtain 30 to 40 m accuracy. Author (ESA)

N86-10517# Technische Univ., Munich (West Germany). Inst. fuer Geographie.
UPDATING OF TOPOGRAPHIC MAPS BY MEANS OF METRIC CAMERA PHOTOS EXAMPLE: HALLERTAU (BAVARIA)
P. Kammerer *In* ESA Metric Camera Workshop Apr. 1985 p 175-180 refs (For primary document see N86-10485 01-35)
Avail: NTIS HC A10/MF A01

The environmental changes (land use, settlements, roads) in a Spacelab metric camera test region are described and the suitability of metric camera photos for the updating of topographic maps is analyzed. The photos allow updating of forest on the scale 1:100,000 in combination with ground truth. Because of the snow cover and the low Sun elevation, the possibilities for the mapping of settlements and roads are limited. Author (ESA)

N86-10518# Technische Univ., Munich (West Germany).
INTERPRETATION OF SPACELAB-1 PHOTOGRAPHS FOR THE GENERATION OF 1:200000 TOPOGRAPHIC MAP
R. Finsterwalder *In* ESA Metric Camera Workshop Apr. 1985 p 181-182 (For primary document see N86-10485 01-35)
Avail: NTIS HC A10/MF A01

The interpretation of Spacelab metric camera photographs for the generation of a 1:200 000 topographic map was assessed for an area of 1,100 sq km, in a densely populated area. Forests, water, roads, and settlements were mapped from photographic enlargements (diapositives) 1:100,000, partly with the help of stereoscopic viewing. The reliability of the interpretation was examined by comparing with the official topographic map (1:200,000). The semantic information of the Spacelab photographs is not sufficient to produce a topographic map from a densely populated region which corresponds to the quality of the official map. Author (ESA)

N86-10519# Technische Univ., Munich (West Germany). Inst. fuer Geographie.
METRIC CAMERA IMAGE OF MUNICH AS ADDITIONAL MEANS FOR URBAN CARTOGRAPHY

F. W. Strathmann *In* ESA Metric Camera Workshop Apr. 1985 p 183-189 refs (For primary document see N86-10485 01-35)
Avail: NTIS HC A10/MF A01

The utilization of Spacelab metric camera (MC) image photointerpretation for urban mapping was tested in a snow covered townscape. Because of information gaps in areas with little contrast, small-scale urban maps (overview maps/basic maps) cannot be produced by MC-images, nor can they be updated completely in a revision interval. Because the gray tone combinations often allow several interpretations of the urban land use, an extensive mapping of real land use without evaluation of maps and aerial photos and/or additional ground truth is not feasible. In the quality of the first MC mission the image detail for the city can only be a limited help for further data acquisition.
Author (ESA)

N86-10520# Hosei Univ., Tokyo (Japan). Coll. of Engineering.
AN EXAMPLE OF SINGLE MODEL ORIENTATION OF METRIC CAMERA STEREOPHOTOGRAPHS
T. Oshima, K. Miyashita, M. Yoshimura, S. Tanaka (Remote Sensing Technology Center of Japan), and T. Sugiura (Remote Sensing Technology Center of Japan) *In* ESA Metric Camera Workshop Apr. 1985 p 191-192 (For primary document see N86-10485 01-35)
Avail: NTIS HC A10/MF A01

Accuracy of the model orientation of Spacelab metric camera photographs was evaluated. Control points on the map were read using the map scale 1:200,000 giving a distinguishable limit of the naked eye is of 20 m in actual size. The results are within the permissible range of errors and the results of height errors are also effective for actual use. Mean square errors are: mx = + or - 39.9 m; my = + or -37.2 m; mz = + or - 29.6 m. Author (ESA)

N86-10521# Technische Univ., Munich (West Germany). Arbeitsgruppe Geowissenschaftliche.
TECTONIC ANALYSIS OF TYPICAL FOLD STRUCTURES IN THE ZAGROS MOUNTAINS (IRAN) BY THE APPLICATION OF QUANTITATIVE PHOTOGRAMMETRIC METHODS ON METRIC CAMERA DATA
J. Bodechtel, M. Kley, and U. Muenzer *In* ESA Metric Camera Workshop Apr. 1985 p 193-197 refs (For primary document see N86-10485 01-35)
Avail: NTIS HC A10/MF A01

Photometric methods were applied on 1:850,000 scale metric camera data for the evaluation of tectonic values on typical fold structures in arid selective eroded Zagros ridges in Iran. The black and white photographs clearly reveal a frequent bending of anticlinal structures, and improve qualitative interpretation. Author (ESA)

N86-10522# Mapping and Charting Establishment, Ottawa (Ontario).
TEST RESULTS USING METRIC CAMERA PHOTOGRAPHY FOR 1:250,000 MAPPING
G. G. Dalgity and E. A. Fleming *In* ESA Metric Camera Workshop Apr. 1985 p 199-206 (For primary document see N86-10485 01-35)
Avail: NTIS HC A10/MF A01

Spacelab metric camera photography over a region in southern Alberta, Canada was used to compile a map at the scale of 1:250,000. Culture, drainage and contours were drawn using an analytical plotter. Map accuracy tests were applied and content was compared with that of the published 1:250,000 map of the area. Notwithstanding the faults of the photography, a map accuracy classification of NATO B-1 is achieved. Map content is not as great as that of the published map. Author (ESA)

N86-10523# Advanced Engineering Lab., Adelaide (Australia).
SPECIFICATION FOR THE PERFORMANCE, DESIGN, DEVELOPMENT AND TEST REQUIREMENTS FOR A SEVERE ENVIRONMENT CARTRIDGE RECORDER. ISSUE 4
S. J. Caldecott and N. J. Phillis 20 Nov. 1984 17 p
(AD-A156637; AEL-0125-SD) Avail: NTIS HC A02/MF A01 CSCL 14/3

This specification establishes the performance, design, development and test requirements for a Severe Environment Cartridge Recorder (SECR). The SECR shall consist of a magnetic tape cartridge recorder intended for recording analog or digital data in high vibration, high acceleration and wide temperature range environments. The SECR shall comprise a single assembly in which shall be housed an electric motor, a means of securing and driving a magnetic tape cartridge, electronic speed control circuitry and a four-track magnetic recording tape head. No signal-conditioning electronics shall be contained within the SECR. Replay of magnetic tape cartridges shall be accomplished with the Cartridge Replay Machine (CRM).
GRA

N86-10524# Science Applications International Corp., McLean, Va.
HIGH FLUX CALORIMETRY
M. McDonnell, N. Olson, and S. Woods 5 May 1984 147 p
(Contract DNA001-82-C-0185)
(AD-A156852; AD-E301731; SAIC-84/1104; DNA-TR-84-183)
Avail: NTIS HC A07/MF A01 CSCL 14/2

Four basic radiant energy sensing concepts were examined for applicability to high flux calorimetry measurement. Calorimeters were cross calibrated using five radiant energy sources. Commercial availability was an important criterion. A commercial calorimeter with a specially designed and fabricated adapter appears to be an acceptable calorimeter for High Flux Measurements. GRA

N86-10525# Department of the Air Force, Washington, D.C.
CAPTIVE VOLUME DEVICE AS A SAFE LIFE MONITOR Patent Application
Borgardt, inventor (to Air Force) Filed 27 Jun. 1985 15 p
(AD-D011802; US-Patent-Appl-SN-749335) Avail: NTIS HC A02/MF A01 CSCL 21/9

The present invention utilizes a closed chamber or structure to enclose a small of amount of a solid propellant whose useful life is to be measured or sensed. The closed chamber forms a captive volume device in which there is included a detecting means. The useful life detecting means may comprise either colorimetric material which change color or a differential pressure device which changes its position in relationship to the useful life of the solid propellant material. A visual viewing port is provided in the captive volume device to allow the state of the detecting means to be observed.
GRA

N86-10526# Oak Ridge National Lab., Tenn.
AUTOMATED ANALYSIS OF DIGITAL IMAGES GENERATED BY TWO-DIMENSIONAL GEL ELECTROPHORESIS
R. C. Mann, B. K. Mansfield, and J. K. Selkirk 1985 11 p refs
Presented at the 2nd Intern. Congr. of Appl. Pattern Recognition, Amsterdam, 19 Jun. 1985
(Contract DE-AC05-84OR-21400)
(DE85-011906; CONF-8506115-1) Avail: NTIS HC A02/MF A01

Two-dimensional gel electrophoresis is a method to separate proteins according to their molecular weights and mobilities in an electric field at a certain pH value. The presence of a radioactively or fluorescently labeled protein in a preparation is indicated by a spot that is produced on a film with the intensity of the spot indicative of the amount of protein. This article presents algorithms that accomplish automated quantitative analysis of digitized gel images. The limits of currently available analysis systems are discussed. The methods are implemented by software on a commercially available digital image processor that uses a minicomputer host.
DOE

N86-10527# Pacific Northwest Lab., Richland, Wash.
ELCAP INSTRUMENTATION
G. J. Schuster and S. D. Tomich Apr. 1985 7 p Presented at the EPRI End-Use Metering Workshop, Seattle, 15 Jan. 1985
(Contracts DE-AC06-76RL-01830; DE-AC79-83BP-13795)
(DE85-013042; PNL-SA-12863; CONF-850175-1) Avail: NTIS HC A02/MF A01

Over the past few years Pacific Northwest Laboratory has developed a series of data loggers. The most recently completed logger, designed to meet these requirements, is currently being deployed in the End-Use Load and Conservation Assessment

Program (ELCAP), an end-use metering study of 1000 residential and commercial structures in BPA's service territory. This document provides a functional description of the data logger, describing both the main hardware components and the system's software. Application of the logger to power measurements and meteorological and interior condition measurements is discussed along with experience on field performance. A table is provided showing approximate data logger, sensor, and installation costs as experienced in this study. DOE

N86-10528# Edgerton, Germeshausen and Grier, Inc., Goleta, Calif.

PARALLEL PULSE PROCESSING FOR MERCURIC IODIDE GAMMA-RAY DETECTORS

A. Beyerle, V. Gerrish, and K. Hull 1985 19 p Presented at the 8th Symp. on X- and Gamma-Ray Sources and Appl., Ann Arbor, Mich., 21 May 1985
(Contract DE-AC08-83NV-10282)
(DE85-013391; EGG/10282-2055; CONF-850533-9) Avail: NTIS HC A02/MF A01

Mercuric iodide (HgI2) is a semiconductor material of interest for use as a gamma ray detector because of its wide band-gap and high atomic number. The current work is with detectors of intermediate thickness (2 to 5mm), to be used to get good energy resolution with some reasonable gamma ray efficiency. The work reported covers the parallel pulse processing to obtain interaction depth information which is used to extend the usable thickness through resolution enhancements, and to obtain better detector performance from selected portions of the thicker detectors through pulse rejection techniques. A sample spectrum from a 2.5-mm-thick detector is shown. Resolution is about 10% and peak-to-valley ratio about 4:1. After taking advantage of the enhancement techniques described, resolution of 5% and peak-to-valley ratios of 8:1 are common. Poor hole mobility has been used to advantage to obtain interaction depth information. Two techniques are demonstrated for extracting conventional energy spectra from two-parameter spectra - the spectral enhancement technique which corrects for hole losses in every interaction in the detector and increases the number which fall under the full energy peak, and the pulse rejection technique which selects only those pulses which need no correction. DOE

N86-10529# Heller (Jean), Los Alamos, N. Mex.

TYPE OF NEW CHINESE-PRODUCED HIGH-SPEED CAMERA AND ITS UTILIZATION IN DETONATION PHYSICS EXPERIMENTS

Y. Sang 1985 7 p Transl. into ENGLISH from Baozha yu Chongji (China), no. 2, 1981 p 113-115
(Contract W-7405-eng-36)
(DE85-015191; LA-tr-85-31) Avail: NTIS HC A02/MF A01

This paper introduces the technological capability and special features of the new, domestically produced, Type SJZ-15 high-speed rotating mirror scanning camera and its utilization in detonation physics experiments. The camera uses an axial flow gas turbine and a two-stage internal blower for cooling. The turbine and blower use the same group of nozzles. The structure is simple, has good axial balance, and improves the cooling capability of the driving bearing housing. The two ends of the rotating mirror use three elastic bearing supporters. The axial bearings have 0-type elastic rubber balls, which are automatically centered and absorb vibration very well. The rotating mirror does not use an axial vacuum system, but the picture quality is excellent. The first objective lens Fujica type and permits use as a split-range camera. The operation handles are located on the same side of the camera. The operation handles for the rotating mirror and the main objective lens are not as convenient as the micrometer adjustment. Detonation experimental tests, technology evaluations, and actual usage prove the operation is simple and reliable, the quality of optical image formation is excellent, the light strength is appropriate, and it is an instrument of comparatively great potential. DOE

N86-10530# Edgerton, Germeshausen and Grier, Inc., Idaho Falls, Idaho.

VELOCITIES OF GAS AND PLASMAS FROM REAL TIME HOLOGRAPHIC INTEROGRAMS

V. A. Deason, L. D. Reynolds, and M. E. McIlwain 1985 9 p refs Presented at Soc. of Photo-Opt. Instr. Engr. Symp., Los Angeles, Calif., 21 Jan. 1985
(Contract DE-AC07-76ID-01570)
(DE85-014618; EGG-M-27084; CONF-850137-4) Avail: NTIS HC A02/MF A01

A truly noninvasive measurement technique for plasma velocity has not been demonstrated. Plasma velocities have been inferred using laser Doppler anemometry or photographic analysis of the position of smoke or small particles. An alternate method based on the refractive index change created in a plasma by a gaseous probe material injected into the plasma is described. This disturbance of the refractive index can be monitored using interferometry. A multipass real time holographic interferometry system is used to follow the changes of the interferometric pattern, and the data is recorded using high speed cinematography. A transparent model of an industrial plasma torch is employed in these studies, and a number of different types of trace gas materials are used to track the plasma flow. Using a combination of multipass interferometry and a laser line absorbing gas, sufficient interferometric sensitivity is obtained to determine plasma velocities in the 100 m/s range. Based on these results, a working plasma torch is constructed. Further studies are planned using this torch and actual plasmas. DOE

N86-10531# Sandia Labs., Albuquerque, N. Mex.

GEOTHERMAL LOST CIRCULATION ZONE MAPPING TOOL

T. J. Bauman 1985 7 p refs Presented at the Intern. Symp. on Geothermal Energy, Kailua Kona, Hawaii, 26 Aug. 1985
(Contract DE-AC04-76DP-00789)
(DE85-008696; CONF-850801-7) Avail: NTIS HC A02/MF A01

Lost circulation is an expensive and often encountered problem when drilling into geothermal formations. A method is needed to more accurately describe loss zones encountered during geothermal drilling to allow for more realistic testing since present testing techniques are inadequate. A Lost Circulation Zone Mapping Tool (LCZMT) is being developed that will quickly locate a loss zone and then provide a visual image of this zone as it interesects the wellbore. A modified Sandia high temperature Acoustic Borehole Televiewer should allow modeling of geothermal loss zones, which would in turn lead to testing that can be performed to evaluate lost circulation materials under simulated downhole conditions. DOE

N86-10532# California Univ., Livermore. Lawrence Livermore Lab.

IMPROVED PARTICLE-VELOCITY TRANSDUCER FOR EQUATION-OF-STATE EXPERIMENTS

S. J. Spataro 30 May 1985 21 p Presented at the 13th Transducer Workshop, Monterey, Calif., 4 Jun. 1985
(Contract W-7405-eng-48)
(DE85-013204; UCRL-92648; CONF-8506131-1) Avail: NTIS HC A02/MF A01

An improved particle velocity transducer was developed for use in equation of state experiments in the low(sub-kilobar) stock region. In low amplitude shock experiments, the standard one turn transducer generated voltages so low that signal to noise problems limited the resolution. By using multiple turns in the new transducer, an increase in signal proportional to the number of turns, with no apparent increase in noise. The complete experiment system consists of passive, multiple turn current loop transducers, a Helmholtz pair of electromagnets, a firing and timing system, a data recording system, the material under study, and a small explosive charge. Each current loop is actually a narrow linear strip of very thin copper foil, which is embedded in the test material. The shock wave from the emplaced explosive charge moves the element across an orthogonal magnetic field causing, for a brief period, a voltage output proportional to the velocity of the element. The theory and design of a new three turn transducer, its advantages, its error sources, and some typical test results are presented. The magnetic field generator, the data recording system, and data processing are also described. DOE

N86-10533# Societe Crouzet, Valence (France).
ELASTIC WAVE GYROMETER. EXPERIMENTS WITH A PARAMETRIC WAVE DEVICE [GYROMETRE A ONDES ELASTIQUES. EXPERIMENTATION D'UN DISPOSITIF A ONDES PARAMETRIQUES]
21 Feb. 1985 15 p In FRENCH
(Contract DRET-83-056)
(Rept-26/5005/HF/AR) Avail: NTIS HC A02/MF A01

The sensitivity of a parameter wave generator to detect Coriolis acceleration is tested. The generator is built using a quartz crystal with metal electrodes and two high frequency quartz generators. A rotating table is used in experiments at angular velocities of + or - 300 deg/sec. Electronic circuits and filters, a phase meter with 0.1 deg sensitivity, and an HP 85 minicomputer are used. The results are negative, showing that the sensitivity of the device is inferior to the phase meter resolution. Author (ESA)

N86-10534# Technische Hogeschool, Eindhoven (Netherlands). Vakgroep Meten en Regelen.
MEASUREMENT OF WORKPIECE TEMPERATURE DURING WELDING FOR WELDING ROBOT CONTROL Progress Report, Mar. 1982 - Mar. 1983 [HET METEN VAN WERKSTUKTEMPERATUREN BIJ HET LASSEN OM EEN LASROBOT TE STUREN]
P. F. A. Illegrams 1983 98 p refs In DUTCH
Avail: NTIS HC A05/MF A01

MIG/MAG welding robot seam tracking system based on a symetrically noncontact temperature measurement is presented. Using literature in formation on temperature distribution during welding, a model for the prediction of the behavior of a pyrometer twin is constructed. The temperature difference between the measuring points constitutes the signal for a position control of the twin holding welding torch. As temperature measurement is made impossible by radiation originating from the welding arc, this is done during intermittent welding in time intervals in which the welding arc is switched off. Author (ESA)

N86-10185# Bundesministerium fuer Forschung und Technologie, Bonn (West Germany).
A NANOSECOND OR THIRTY CENTIMETERS: WHY ATOMIC CLOCKS HAVE TO BE SYNCHRONIZED. MITREX OPENS NEW DIMENSIONS FOR MEASURING ACCURACY [EINE MILLIARDSTELSEKUNDE ODER 30 ZENTIMETER: WESHALB ATOMUHREN WELTWEIT GLEICHLAUFEN MUESSEN. MITREX OEFFENT NEUE DIMENSIONEN DER MESSGENAUIGKEIT]
Hans-Dieter Wolz *In its* Satellite Use for Men 1985 p 26-29 In GERMAN (For primary document see N86-10180 01-12)
Avail: NTIS HC A03/MF A01

36 LASERS AND MASERS

Includes parametric amplifiers.

N86-10535 Tennessee Univ., Knoxville.
DETERMINATION OF OPTICAL PROPERTIES BY THIRD-HARMONIC GENERATION IN NOBLE GASES IN UNFOCUSED LASER BEAMS Ph.D. Thesis
Wanda Randall Ferrell 1985 124 p
Avail: Univ. Microfilms Order No. DA8511381

A new laser technique involving phase-matched third-harmonic generation in unfocused laser beams has been used to determine vacuum ultraviolet (VUV) oscillator strengths in xenon, VUV indices of refraction for the buffer gas (krypton or argon), and the VUV absorption coefficients were determined through total ionization measurements in the frequency regions of phase matching resulting from the interaction of unfocused linearly polarized light with mixtures of xenon and positively dispersive buffer gases. Since the multiphoton ionization mechanism is sharply dominated by the dimer absorption of third-harmonic photons, the ionization signal provides an excellent probe for determination of these optical parameters. Absolute ionization measurements were made through the use of a proportional counter which was calibrated by the ionization resulting from an internal Fe-55 source. Dissert. Abstr.

N86-10536 Department of the Air Force, Washington, D.C.
LASER TARGET SPECKLE ELIMINATOR Patent
C. N. Scully, inventor (to Air Force) Issued 16 Apr. 1985 5 p Supersedes AD-D010049
(AD-D011775; US-Patent-4,511,220; US-Patent-Appl-SN-452601; US-Patent-Class-350-403) Avail: US Patent and Trademark Office CSCL 20/6

An apparatus for eliminating the phenomenon of speckle with regard to laser light reflected from a distant target whose roughness exceeds the wavelength of the laser light. The apparatus includes a half plate wave member, a first polarizing beam splitter member, a totally reflecting right angle prism, and a second polarizing beam splitter member, all of which are in serial optical alignment, that are used in combination to convert a linearly (i.e., vertically) polarized light beam, which is emitted by a laser having a known coherence length, into two coincident, orthogonally polarized, beams that are not coherent with each other, and that have an optical path difference which exceeds the known coherence length of the emitting laser, to eliminate the speckle. Author (GRA)

N86-10537 Department of the Navy, Washington, D. C.
DEVICE FOR CRYOGENICALLY FABRICATING SOURCE MATERIAL FOR PLASMA X-RAY LASERS Patent
R. C. Elton, R. H. Dixon, and J. L. Ford, inventors (to Navy) Issued 2 Apr. 1985 6 p Supersedes AD-D010383
(AD-D011814; US-Patent-4,508,055; US-Patent-Appl-SN-500725; US-Patent-Class-118-724) Avail: US Patent and Trademark Office CSCL 20/5

This patent describes a device for fabricating a target of a lasing material and a pump material for lasing at X-ray wavelengths wherein one of the materials occurs naturally as a gas. A substrate of the other material is cooled below the freezing point of the one material occuring naturally as a gas. Then a gaseous atmosphere of the latter material is supplied to the cooled substrate so that a frozen layer of the latter material condenses onto the substrate to form the target. GRA

N86-10538 Department of the Navy, Washington, D. C.
W-SHAPED DIFFUSED STRIPE GaAs/AlGaAs LASER Patent
Y. Z. Liu, C. S. Hong, and D. Dapkus, inventors (to Navy) Issued 4 Jun. 1985 7 p Supersedes AD-D009849
(AD-D011818; US-Patent-4,521,887; US-Patent-Appl-SN-415639; US-Patent-Class-372-45) Avail: US Patent and Trademark Office CSCL 20/5

This patent describes a w-shaped diffused stripe GaAs/AlGaAs laser and a method for making the same. A double heterostructure layered structure includes a p-type GaAs active layer in contact with a p-type AlGaAss current blocking layer. These layers are sandwiched between two N-type AlGaAs confinement layers. A p-type zinc diffused stripe region having a w-shaped diffusion front extends longtudinally between two reflective surfaces located on respective ends of the device and extends vertically from the surface of the upper confinement layer and through a portion of the lower confinement layer and through portions of the various intervening layers. In a method of forming the device, the various layers are formed by epitaxial growth or by metalorganic chemical vapor deposition. The stripe region is formed by diffusing zinc into the device from a source through a pair of parallel slots in a diffusion mask. The zinc diffused into the device is further driven-in by heating the device on the absence of the zinc source. GRA

N86-10539*# Florida Univ., Gainesville. Dept. of Nuclear Engineering Sciences.
RESEARCH ON SOLAR PUMPED LIQUID LASERS Final Report
John D. Cox, Ulrich H. Kurzweg, Neil H. Weinstein, and Richard T. Schneider Apr. 1985 67 p refs
(Grant NAG1-135)
(NASA-CR-176235; NAS 1.26:176235) Avail: NTIS

HC A04/MF A01 CSCL 20E

A solar pumped liquid laser that can be scaled up to high power (10 mW CW) for space applications was developed. Liquid lasers have the advantage over gases in that they provide much higher lasant densities and thus high-power densities. Liquids also have advantages over solids in that they have much higher damage thresholds and are much cheaper to produce for large scale applications. Among the liquid laser media that are potential candidates for solar pumping, the POC13: Nd sup 3+:ZrC14 liquid was chosen for its high intrinsic efficiency and its relatively good stability against decomposition due to protic contamination. The development of a manufacturing procedure and performance testing of the laser, liquid and the development of an inexpensive large solar concentrator to pump the laser are examined. E.A.K.

N86-10540*# Washington Univ., Seattle. Aerospace and Energetics Research Program.
SCALING STUDIES OF SOLAR PUMPED LASERS Semiannual Progress Report, 1 Jan. - 30 Jun. 1985
W. H. Christiansen and J. Chang Aug. 1985 8 p refs
(Grant NAG1-176)
(NASA-CR-176240; NAS 1.26:176240) Avail: NTIS
HC A02/MF A01 CSCL 20E

A progress report of scaling studies of solar pumped lasers is presented. Conversion of blackbody radiation into laser light has been demonstrated in this study. Parametric studies of the variation of laser mixture composition and laser gas temperature were carried out for CO2 and N2O gases. Theoretical analysis and modeling of the system have been performed. Reasonable agreement between predictions in the parameter variation and the experimental results have been obtained. Almost 200 mW of laser output at 10.6 micron was achieved by placing a small sapphire laser tube inside an oven at 1500 K the tube was filled with CO2 laser gas mixture and cooled by longitudinal nitrogen gas flow. B.W.

N86-10541# IBM Research Lab., San Jose, Calif.
TIME RESOLVED FLOW VELOCITY AND CONCENTRATION MEASUREMENTS USING A TRAVELLING THERMAL LENS
H. Sontag and A. C. Tam 25 Jun. 1985 17 p
(Contract N00014-83-C-0170)
(AD-A156706; TR-18) Avail: NTIS HC A02/MF A01 CSCL 05/9

The travelling thermal lens technique is a new all optical method for probing concentration and velocity patterns in flowing media. A thermal lens created by absorption of a short laser pulse moves with the flow and can be probed by a CW laser beam further downstream as a deflection signal. This technique enables optical measurements of the flow velocity component perpendicular to the probe laser at high spatial resolution. Its application requires no seeding with particulates as needed in most other optical techniques. GRA

N86-10542# RAND Corp., Santa Monica, Calif.
SOVIET FREE-ELECTRON LASER RESEARCH Interim Report
S. Kassel May 1985 92 p
(Contract MDA903-85-C-0030)
(AD-A156898; RAND/R-3259-ARPA) Avail: NTIS
HC A05/MF A01 CSCL 20/5

The purpose of this report is to evaluate free-electron laser (FEL) research and development in the Soviet Union and to compare it with the corresponding activity in the U.S. In presenting this material, the intention is to acquaint U.S. researchers with the objectives, techniques, and results of their Soviet counterparts, as well as to provide the broad context of this area of Soviet R&D that consists of the organization, facilities, personalities, and leadership involved. The U.S. Soviet comparison has focused on the experimental programs, the most important area of this new technology. Section 2 compares individual experiments conducted by the USSR and the United States. In Section 3 the history of the theoretical development of FEL is presented, providing an insight into the conceptual issues that shaped FEL research in both countries. The remainder of the report is devoted primarily to the Soviet side of FEL research. Section 4 describes the organizational features of this research in terms of the performer institutes and leadership, focusing on the role of the Academy of Sciences, USSR. Section 5 analyzes the scientific objectives of Soviet FEL research, for the most part as discussed by Soviet reviewers of their research program. Section 6 presents conclusions. GRA

N86-10543# Spectra Technology, Inc., Bellevue, Wash.
DESIGN, FABRICATE AND TEST A 1.06(MU) REPETITIVELY PULSED LASER Final Report
J. M. Eggleston and E. A. Crawford 28 Jun. 1985 71 p
(Contract DE-AC06-83FR-53157)
(DE85-014439; DOE/ER-53157/T1) Avail: NTIS
HC A04/MF A01

The results of a program to develop the Thomson scattering diagnostic laser are described. Background material and technical justification for the design approach are given. Principal results of the developmental program were the construction of a rep rated slab glass amplifier, and the accumulation of the design knowledge necessary to build such amplifiers for maximum performance. Significant advances are made in reducing second order optical distortions. DOE

N86-10544# Deutsche Forschungs- und Versuchsanstalt fuer Luft- und Raumfahrt, Oberpfaffenhofen (West Germany). Abt. Lasertechnik.
EXPERIMENTAL INVESTIGATIONS OF PULSE-PULSE INTERFERENCE IN HETERODYNE DETECTION
Friedrich Malota May 1984 25 p refs In GERMAN; ENGLISH summary Report will also be announced as translation (ESA-TT-949)
(DFVLR-FB-85-26; ISSN-0171-1342) Avail: NTIS
HC A02/MF A01; DFVLR, Cologne DM 10

The interference of two laser pulses originating from the same source and thus having a constant frequency difference was investigated. The calculation of the heterodyne currents in the interference of two pulses is described. It is shown that a coherent pulse-pulse interference is possible in a pulse heterodyne system. Experimental data are in good agreement with theoretical predictions, especially the determination of the intermediate frequency. Author (ESA)

37 MECHANICAL ENGINEERING

Includes auxiliary systems (non-power); machine elements and processes; and mechanical equipment.

N86-10545 Purdue Univ., Lafayette, Ind.
DYNAMIC ANALYSIS OF ROBOTIC MANIPULATIONS WITH FLEXIBLE LINKS Ph.D. Thesis
Liang-Wey Chang 1984 189 p
Avail: Univ. Microfilms Order No. DA8507666

The development dynamic model for flexible manipulator systems and a solution method to solve the equations of motion efficiently is discussed. The model describes the global motion of the flexible manipulators as a large motion and a small motion. The large motion is represented by the Equivalent Rigid Link System (ERLS) which is kinematically equivalent to the real rigid link system. The small motion represents deformations of the system relative to the ERLS. A sequential integration method is applied to integrate the equations of motion numerically to obtain significant improvement in computation efficiency. The sequential integration method is particularly efficient for solving the equations of motion of the manipulator system which possesses a wide range of frequencies of which only the lower frequencies are excited. Robotic dynamics of the flexible mannipulator is useful in the design and the control areas. Procedures are proposed to solve the robotic dynamics. A planar manipulator is used as an example to demonstrate the simulation results. Dissert. Abstr.

N86-10546 United Kingdom Atomic Energy Authority, Risley (England).

THE INFLUENCE OF THE SUBSTRATE ON THE PRACTICAL MACHINING APPLICATIONS OF CUTTING EDGES COATED WITH DIFFERENT MATERIALS

K.-E. Klemme 25 Nov. 1984 11 p refs Transl. into ENGLISH from Werkstatt und Betrieb (West Germany), v. 114, no. 5, 1981 p 291-293
(BLL-Risley-TR-5039-(9091.9F)) Copyright. Avail: British Library Lending Div., Boston Spa, Engl.

Coated cutting edges were employed to extend tool life and to increase the volume of the material. The coatings are applied to the hardmetal substrate very largely using the Chemical Vapor Deposition (CVD) method. The application of these coatings from the gasous phase is no problems. The influence of the substrate, irrespective of the coating, on the service life attained by a cutting edge is studied. The manner in which the machining character of a cutting edge is altered is examined. E.A.K.

N86-10547 Johns Hopkins Univ., Baltimore, Md.

STIFFENED AND PRESTRESSED COMPOSITE OVERWRAPPED PRESSURE VESSELS Ph.D. Thesis

Mostefa Djamel Boussouf 1985 246 p
Avail: Univ. Microfilms Order No. DA8510402

A structural analysis of a stiffened inner metal layer strengthened by two unidirectional composite overwrapped layers in which the fibers have a ring winding. One layer covers the structure completely and provides reinforcement in the axial direction, while another covers the cylindrical part only with a circumferential composite overwrap. Methods are developed for deriving equivalent flexural rigidity, and interaction influence stiffness. Analytical solutions and numerical results for vessels with and without edge stiffeners are presented. This study is confined to the isotropic/orthotropic thin shell theory and uses load sharing liners, it also assumes that there is no adhesive between layers, thus no shear coupling. The analysis takes into consideration the variation in the radii of individual layers. It is assumed that fiber winding of the composite layers are coincident with the principal directions of the structure, that is the axial and circumferential for the cylinder and only meridional for the spherical cap. Dissert. Abstr.

N86-10548 Ohio State Univ., Columbus.

DIGITAL CONTROL OF THE HYDRAULIC ACTUATORS OF AN ADAPTIVE SUSPENSION VEHICLE Ph.D. Thesis

Joseph Alan Dworak 1985 498 p
Avail: Univ. Microfilms Order No. DA8510565

A series-bypass hydraulic power circuit is evaluated for use on a six-legged walking vehicle. This vehicle will be totally autonomous and have the capability to carry a man and 500 lbs. payloads. This hydraulic circuit is part of a closed loop feedback system which uses microprocessors to control the vehicle trajectory. The series-bypass circuit combines features of pump and valve controlled hydraulic circuits to achieve high energy efficiency and maximize the closed loop bandwidth. The circuit is mathematically modeled and analyzed using linearized symbolic and frequency response transfer functions and a nonlinear time domain simulation. These methods are used to select and test controller designs. The control architecture is primarily designed by using classical transfer function methods. Due to the nature of the series-bypass circuit and performance objectives, it is also necessary to employ multivariable techniques in designing and analyzing the closed loop systems. Based on the simulation and linearized studies, controller designs are experimentally evaluated on a microprocessor controlled prototype series-bypass circuit. Dissert. Abstr.

N86-10549 Ohio State Univ., Columbus.

COMPUTER CONTROL OF AN ELECTRIC HYDRAULIC ROBOT LEG WITH PROXIMITY RANGING SYSTEM Ph.D. Thesis

Chi-Keng Tsai 1985 286 p
Avail: Univ. Microfilms Order No. DA8510647

Real-time control was implemented using an Intel 8086 microprocessor-based microcomputer. State Feedback Control with a simplified Inverse Plant feedforward term was implemented to improve the joint servo performance of high speed leg motion and to solve the highly underdampled system problem. In particular, filtered pressure feedback is used to speed up the response and improve the damping characteristics. The new approaches based on the Jacobian were implemented as the basis for finding the joint positions associated with a constrained foot position. Two proximity sensors mounted on the Prototype Leg were successfully used for the purpose of stepping over an object during the leg transfer phase. The control algorithm developed is of general form so as to be appropriate for other tasks and configurations of sensors. Dissert. Abstr.

N86-10550 Westland Helicopters Ltd., Yeovil (England).

TRIALS ON THE ASPERITY COUNTING MONITORING SYSTEM Final Report

R. Wordsworth (Imperial Coll. of Science and Technology) and P. B. MacPherson May 1984 32 p refs
(Contract A12/1347)
(Res-Paper-670; BR93962) Avail: Issuing Activity

A monitoring system, based on asperity contacts within a loaded and lubricated pair of metal surfaces, was evaluated in a mini disk machine. Results confirm the sensitivity of the system to changes in surface topography. With additional storage capacity available in microcomputers, a tool for laboratory test running normally undertaken in a mechanical research laboratory is available. The monitor could also be applied in a gearbox test rig for studying the performance of a specific bearing or gear set. Although interest in grease as a gearbox lubricant waned an effective system for routine monitoring of helicopter tail and intermediate gearboxes is feasible. Author (ESA)

N86-10551*# National Aeronautics and Space Administration. Lewis Research Center, Cleveland, Ohio.

MEASUREMENT OF THE DENSITY OF BASE FLUIDS AT PRESSURES 0.422 TO 2.20 GPa

Bernard J. Hamrock, Bo O. Jacobson (Lulea Univ.), and Sten-Ivar Bergstroem (Lulea Univ.) [1985] 22 p refs Presented at the Ann. Meeting of the Am. Soc. of Lubrication Engrs., Toronto, 12-15 May 1986
(NASA-TM-87114; E-2650; NAS 1.15:87114) Avail: NTIS HC A02/MF A01 CSCL 20D

The influence of pressure on the density of six base fluids is experimentally studied for a range of pressures from 0.422 to 2.20 GPa. An important parameter used to describe the results is the change in relative volume with change in pressure dv sub r/dp. For pressures less than the solidification pressure ($p < ps$) a small change in pressure results in a large change in dv sub r/ps. For pressures greater than the solidification pressure ($p > ps$) there is no change in dv sub r/dp with changing pressure. The solidification pressures of the base fluids varies considerably, as do the slopes that the experimental data assumes for $p < ps$. A new formula is developed that describes the effect of pressure on density in terms of four constants. These constants vary for the different base fluids tested. Author

N86-10552*# National Aeronautics and Space Administration. Lewis Research Center, Cleveland, Ohio.

THE MECHANISM OF EROSION OF METALLIC MATERIALS UNDER CAVITATION ATTACK

B. C. S. Rao (Case Western Reserve Univ.) and D. H. Buckley 1985 18 p refs Proposed for presentation at the Intern. Symp. on Cavitation, Sendai, 16-19 Apr. 1986; sponsored by Japan Society of Mechanical Engineers, ASME, Institution of Mechnanical Engineers (British), JSCE and International Association for Hydraulic Research
(NASA-TM-87133; E-2684; NAS 1.15:87133) Avail: NTIS HC A02/MF A01 CSCL 11F

The mean depth of penetration rates (MDPRs) of eight polycrystalline metallic materials, Al 6061-T6, Cu, brass, phosphor bronze, Ni, Fe, Mo, and Ti-5Al-2.5Sn exposed to cavitation attack in a viscous mineral oil with a 20 kHz ultrasonic oscillator vibrating at 50 micron amplitude are reported. The titanium alloy followed by molybdenum have large incubation periods and small MDPRs.

The incubation periods correlate linearly with the inverse of hardness and the average MDPRs correlate linearly with the inverse of tensile strength of materials. The linear relationships yield better statistical parameters than geometric and exponential relationships. The surface roughness and the ratio of pit depth to pit width (h/a) increase with the duration of cavitation attack. The ratio h/a varies from 0.1 to 0.8 for different materials. Recent investigations (20) using scanning electron microscopy to study deformation and pit formation features are briefly reviewed. Investigations with single crystals indicate that the geometry of pits and erosion are dependent on their orientation. Author

N86-10553# Admiralty Marine Technology Establishment, Teddington (England).
THE GENERATION AND TRANSMISSION OF VIBRATION IN PLAIN CYLINDRICAL BEARINGS. PART 2. EXPERIMENT
L. V. Embling, C. J. Jenkins, and P. Meyer Sep. 1984 67 p
(AD-A156577; AMTE(N)/R84009-Pt-2; DRIC-BR-95691-Pt-2) Avail: NTIS HC A04/MF A01 CSCL 13/9

The vibration transmission characteristics of hydrodynamic bearings have been investigated at frequencies well above the out of balance frequency. Part 1 of this report developed theories to predict the linear transfer functions of bearings and to examine the effects of nonlinearities in modulating the response to external forces. This part of the report describes an experimental investigation on a bearing test rig aimed at validating the theories. It is concluded that: (1) bearings are not always rigid to vibration, the frequency range over which the rigidity applies being determined by the bearing parameters; (2) transfer functions across the bearing in the direction of the applied force are reciprocal; and (3) the bearing can introduce modulation in the response to a single-frequency force. GRA

N86-10554# Department of the Navy, Washington, D. C.
AIRBOC (AIR RAPID BLOOM OFFBOARD CHAFF) CHAFF DEPLOYMENT SYSTEM Patent Application
W. Humphries, J. Bryant, R. C. Eklund, D. C. Hayes, and P. Ferko, inventors (to Navy) Filed 1 Apr. 1985 14 p
(AD-D011746; US-Patent-Appl-SN-718399) Avail: NTIS HC A02/MF A01 CSCL 17/4

An AIRBOC (Air Rapid Bloom Offboard Chaff) chaff deployment apparatus comprising a canister with a wind flap attached externally to the canister and connected to a drogue chute that is housed inside the canister. The drogue chute is situated atop a main chute that is atop a release mechanism, which is atop a fuze and that is atop a chaff payload, all of which is housed inside the canister. When the AIRBOC is dropped from a plane, the wind flap extends, pulling out the drogue chute. The drogue chute in turn activates the release mechanism which frees the drogue chute to pull out the main chute to which the drogue chute is connected. The deployment of the main chute causes a force greater than 40 lbs to be applied to the release mechanism, resulting in the chaff payload being released from the canister and the fuze being activated, consequently detonating the released chaff payload. GRA

N86-10555# Department of the Navy, Washington, D. C.
MARGINAL-TERRAIN STRADDLE-LIFT CONTAINER HANDLER Patent Application
C. I. Skaalen, H. G. Lange, and P. S. Springston, inventors (to Navy) Filed 11 Apr. 1985 29 p
(AD-D011752; US-Patent-Appl-SN-718762) Avail: NTIS HC A03/MF A01 CSCL 13/6

A highly maneuverable straddle carrier vehicle structure is provided for handling various sizes of containers and outsized loads over rough, unleveled, weak and unprepared soils to meet austere requirements which are beyond the capability of commercial straddle lifts that normally operate on prepared surfaces within specific boundaries of yards and docks. Features include high flotation tires capable of operation over marginal terrain, fording capability, all wheel 360 degree steering and offset wheel yokes which permits automatic changing of wheelbase dimensions for rugged sloping terrain operations and wheel positioning for optimum mobility including lateral and oblique movement and vehicle rotation within its own length for a variety of close quarters operations. Load stabilization devices permit container securing during transit and hinged transverse members operate to reduce torsion and bending moments on the vehicle structure over severe terrain. GRA

N86-10556# Department of the Air Force, Washington, D.C.
OVER-CENTER TOGGLE LATCH Patent Application
F. T. Hinds, inventor (to Air Force) Filed 14 Aug. 1984 12 p
(AD-D011753; US-Patent-Appl-SN-640623) Avail: NTIS HC A02/MF A01 CSCL 13/5

This patent application discloses an improved low profile over-center toggle latch arm with an internally threaded latch barrel nut for adjustable cooperation with a threaded latched draw bolt. The bolt is pivotally coupled to a latch handle assembly. The latter comprises projecting sidewalls and a grip end. The latch handle assembly is mounted by means of integral flanges cooperating with journals defined in a mounting stirrup, the latter being mounted on the container body. GRA

N86-10557# Air Force Inst. of Tech., Wright-Patterson AFB, Ohio.
A TRANSFORMATION METHOD FOR THE EVALUATION OF THE RESPONSE MOMENTS OF ELASTIC STRUCTURES WITH RANDOM PROPERTIES Ph.D. Thesis
R. H. Bennett Apr. 1985 169 p
(AD-A156882; AFIT/CI/NR-85-46D) Avail: NTIS HC A08/MF A01 CSCL 20/11

In this investigation a new method for computing the first and second moments of the displacement response of linear elastic structures with random stiffness and damping is developed. The method accurately computes the mean and variance of the displacement of a dynamically loaded structure as functions of time. The probability that the displacement will be greater than a specified value is also computed. The results of the transformation method are compared to exact solutions for a number of cases. The influence of the randomness in the underlying parameters on the randomness of the response is discussed. Author (GRA)

N86-10558# Department of the Air Force, Washington, D.C.
TERMINATION LOAD CARRYING DEVICE Patent Application
J. N. Tervo, inventor (to Air Force) Filed 19 Jun. 1985 11 p
(AD-D011800; US-Patent-Appl-SN-746617) Avail: NTIS HC A02/MF A01 CSCL 13/9

A follower nut assembly is attached to a load carrying nut all of which is threaded onto a ball screw of a drive actuator. The actuator drive causes a load attached to said load carrying nut to be translated to a fully extended position. At about the fully extended position, a run-off end without threads of the ball screw is positioned in the load carrying nut. This causes the translating force to be fully applied to a follower nut which is normally shear pinned to the load carrying nut. Because of the inertia of the load, the follower nut shears the pin and then rotates within a cage of the follower nut assembly. The translation of the load stops when the shear pin is broken. A thrust bearing is positioned between the follower nut and the load carrying nut to provide the necessary support when the load is fully extended. Author (GRA)

N86-10559# Princeton Univ., N. J. Dept. of Mechanical and Aerospace Engineering.
MODELING OF ENGINE SPRAYS
F. V. Bracco 1985 24 p
(Contract DE-AC04-81AL-16338)
(DE85-010020; DOE/AL-16338/T1) Avail: NTIS HC A02/MF A01

Atomization and full-cone sprays from single cylindrical orifices were considered. The following subjects are reviewed: the structure of the breakup region; the structure of the far field; modern models that, given the outcome of the breakup process, compute the steady and transient of sprays; some comparison with detailed measurements; and some practical applications. It is concluded that the spray breakup and the development regions are the most relevant in engine applications, the inner structure of the breakup region is still largely unknown, two and three-dimensional spray models are available, but remain mostly untested, particularly in their vaporization and combustion components, in part because of a lack of accurate measurements in controlled engine-type environments, engine applications of such models are recommended for learning, interpretative, and exploratory studies, but not for predictions. DOE

N86-10560# Deutsche Gold- und Silber-Scheideanstalt, Frankfurt am Main (West Germany). Fertigungstechnik Metall.
REDUCTION OF NOBLE METAL STOCK AND NOBLE METAL LOSS DURING WIRE PRODUCTION WITH THE CONFORM EXTRUSION PROCESS Final Report, Dec. 1983
Wolfgang Diem Bonn Bundesministerium fuer Forschung und Technologie May 1985 34 p refs In GERMAN; ENGLISH summary Sponsored by Bundesministerium fuer Forschung und Technologie
(BMFT-FB-T-85-049; ISSN-0340-7608) Avail: NTIS HC A03/MF A01; Fachinformationszentrum, Karlsruhe, West Germany DM 7

The conform continuous extrusion process used in wire production was tested to optimize the process and facilities and to determine its economical use in copper and silver hard solder production taking into account a reduction of the noble metal stock and noble metal loss during production. The Conform extrusion process allows a reduction in the amount of noble metals recycled and in the material loss during production resulting from a reduction in the number of production steps and thus in the mean production time. However, the Conform process cannot be economically used in copper and silver hard solder production because of quality control and tool durability problems.
Author (ESA)

N86-10587# Indian Inst. of Science, Bangalore. Dept. of Mechanical Engineering.
RECENT ADVANCES IN THE ANALYSIS OF EXHAUST MUFFLERS
M. L. Munjal *In* Shock and Vibration Information Center The Shock and Vibration Digest, Vol. 17, No. 3 Mar. 1985 p 3-16 refs (For primary document see N86-10585 01-39)
Avail: SVIC, Code 5804, Naval Research Lab., Washington, D.C. 20375 CSCL 13/9

38 QUALITY ASSURANCE AND RELIABILITY

Includes product sampling procedures and techniques; and quality control.

N86-10561*# National Aeronautics and Space Administration. Lewis Research Center, Cleveland, Ohio.
ULTRASONIC EVALUATION OF MECHANICAL PROPERTIES OF THICK, MULTILAYERED, FILAMENT WOUND COMPOSITES
Harold E. Kautz Sep. 1985 36 p refs
(MASA-TM-87088; E-2676; NAS 1.15:87088) Avail: NTIS HC A03/MF A01 CSCL 14D

A preliminary investigation is conducted to define capabilities and limitations of ultrasonic and acousto-ultrasonic measurements related to mechanical properties of filament wound graphite/epoxy composite structures. The structures studied are segments of filament wound cylinders formed of multiple layers of hoop and helical windings. The segments consist of 24 to 35 layers and range from 3.02 to 3.34 cm in wall thickness. The resultant structures are anisotropic, heterogeneous, porous, and highly attenuating to ultrasonic frequencies greater than 1 MHz. The segments represent structures to be used for space shuttle booster cases. Ultrasonic velocity and acousto-ultrasonic stress wave factor measurement approaches are discussed. Correlations among velocity, density, and porosity, and between the acousto-ultrasonic stress wave factor and interlaminar shear strength are presented.
Author

N86-10562# Laboratorio de Acustica e Sonica, Sao Paulo (Brazil).
ULTRASONIC INSPECTION OF WELDMENTS IN LARGE SIZE SPIRAL BOX FOR HYDROELECTRIC PLANT
L. X. Nepomuceno and A. Vendetti 19 Jul. 1985 51 p In PORTUGUESE; ENGLISH summary
(AS-701/85) Avail: NTIS HC A04/MF A01

The adopted procedures, the criteria established for acceptance of the inspected weldments and the observed results are described. The detected discontinuities are corrected, the weld is reinspected and applied to the acceptance criteria. E.A.K.

N86-10563# Army Test and Evaluation Command, Aberdeen Proving Ground, Md.
TEST, MEASUREMENT, AND DIAGNOSTIC EQUIPMENT (SYSTEM PECULIAR) Final Report
30 May 1985 15 p Supersedes report dated 7 May 1974, AD-781946
(AD-A156669; TOP-6-2-335) Avail: NTIS HC A02/MF A01 CSCL 14/2

This Test Operations Procedure (TOP) provides guidance for planning tests of system-peculiar test, measurement, and diagnostic equipment (TMDE) including Test Program Sets (TPS) needed to support a system, to ensure its conformance with requirements documents, Acquisition Plan (AP), Test Program Set Management Plan (TPSMP), and Item Integrated Logistics Support Plan (ILSP). Subtests to satisfy the requirements for the particular TMDE and test type (DT 2 and 3) can be selected or supplemented from those listed in the test procedures. GRA

N86-10564# Societe Nationale Industrielle Aerospatiale, Suresnes (France). Lab. Central.
NONDESTRUCTIVE CONTROL OF THICK STRUCTURES MADE WITHOUT DISASSEMBLING [CONTROLE NON DESTRUCTIF D'ASSEMBLAGE DE FORTES EPAISSEURS SANS DEMONTAGE DES FIXATIONS, PROCES VERBAL 43-954/F/3]
D. Lecuru 21 Jan. 1985 43 p refs In FRENCH
(Contract STPA-82-96-006)
(PV-43-954/F/3) Avail: NTIS HC A03/MF A01

Ultrasonic and Foucault current methods to inspect aircraft structures in places were plate superposition gives a total thickness > 5 to 7 mm were studied. The feasibility of the ultrasonic is demonstrated for external plates, while that of the Foucault current method is shown for the inner plates up to 20 mm thickness.
Author (ESA)

39 STRUCTURAL MECHANICS

Includes structural element design and weight analysis; fatigue; and thermal stress.

For applications see *05 Aircraft Design, Testing and Performance* and *18 Spacecraft Design, Testing and Performance.*

N86-10565 Iowa Univ., Iowa City.
DESIGN SENSITIVITY ANALYSIS AND OPTIMIZATION OF BUILT-UP STRUCTURES Ph.D. Thesis
Hee Gag Lee 1984 184 p
Avail: Univ. Microfilms Order No. DA8507953

Design sensitivity analysis and optimization of built-up structures are formulated, analyzed, and solved numerically. A variational approach is used to incorporate both finite dimensional and distributed state and design variables in the same energy equation. Kinematic and natural boundary conditions at the interfaces between structural components of built-up structures are defined. Variation of the energy equation with the material derivative idea from continuum mechanics and introduction of an adjoint variational equation yield design sensitivity vectors and functions with respect to conventional and shape design variables. A unified method of shape design sensitivity analysis for static and eigenvalue problems, to complement the finite element method of structural analysis is developed. Standard shape design sensitivity forms are derived for structural components and may be applied to various kinds of built-up structures to obtain design sensitivity forms at the interfaces between structural components of built-up structures. This method provides potential for shape optimization of complex built-up structures. Dissert. Abstr.

N86-10566 Clemson Univ., S.C.
AN ANALYTICAL AND NUMERICAL STUDY OF THE BUCKLING BEHAVIOR OF FIBER-REINFORCED BEAMS Ph.D. Thesis
Hossam Nasser Mohamed-Aly 1984 189 p
Avail: Univ. Microfilms Order No. DA8507587

A nonlinear theory suitable for determining bifurcation loads, or limit point loads, for straight beams with thin-walled open cross sections that are made from midplane symmetric, fiber-reinforced laminates is presented. A computer code is developed that computes requisite section properties for six different cross-sectional shapes. It can be used to compute bifurcation or limit point loads for three different loading conditions under a variety of boundary conditions and any midplane symmetrical, angle ply fiber pattern. The nonlinear equilibrium equations and boundary conditions associated with limit point buckling, or bifurcation buckling, are solved iteratively using Newton's method. First order finite-difference formulas are used to obtain a numerical analogue for the system of lienar correctional equations obtained by the Newton method. This system of equations is solved using Potter's algorithm. An interval halfing procedure is used to refine the accuracy of a buckling load so that a sign change in the buckling determinant occurs between load levels for which the load increment is less than one percent. Dissert. Abstr.

N86-10567 Florida Univ., Gainesville.
ANALYTICAL AND EXPERIMENTAL STUDY OF CRACKS EMANATING FROM AN ELLIPTICAL HOLE IN UNIDIRECTIONAL COMPOSITE MATERIAL Ph.D. Thesis
Said Abdel-Maaboud Khalil 1984 214 p
Avail: Univ. Microfilms Order No. DA8509948

A fundamental study of stress fields around an elliptical hole, with and without cracks emanating from it, in unidirectional composite materials is presented. The first part deals with stress concentration factors. The second part discusses stress intensity factors and energy release rate. The fracture mechanics part starts with a discussion of the application of different energy principles to the finite element technique. This discussion is followed by the introduction of a new mathematical formulation of a finite element model. This model is based on the modified complementary energy principle in conjunction with the anisotropic elasticity and complex variable techniques. Calculations of stress intensity factors for single mode and mixed mode fractures are included. Analytical and experimental evaluations of the strain energy release rate are determined. Analytical evaluation of the energy release rate is based on the finite element solution. The experimental part of this evaluation is based on the compliance calibration technique. Dissert. Abstr.

N86-10568 Yale Univ., New Haven, Conn.
STRENGTH OF SHELLS UNDER LOCAL TRANSVERSE LOADS Ph.D. Thesis
Mandayam Anandanpillai Srinivasan 1984 293 p
Avail: Univ. Microfilms Order No. DA8509786

This thesis is concerned with the estimation of the limit load of thin shells composed of ductile materials and subjected to local transverse loads which are quasi-static and monotonically increasing. Two problems are considered: an axisymmetric spherical dome with a cutout and a cylindrical shell under a rigid punch. Application of the theorems of limit analysis to the suitably nondimensionalized governing equations supplied by shell theory lead to constrained optimization problems in the presence of two parameters measuring the load size and the thickness of the shell, where the latter is very small. One of the main purposes is to devise systematic analytical procedures that take advantage of the presence of this small parameter in obtaining close bounds to the optimum, the limit load. The spherical dome is loaded radially along the circumference of the circular cut-out. The complete solution (i.e., the limit load and the associated velocity and stress resultant fields) of the problem covering a wide range of parameter values is obtained. Dissert. Abstr.

N86-10569 Akron Univ., Ohio.
FINITE ELEMENT ANALYSIS OF METALS AT ELEVATED TEMPERATURE USING UNIFIED CONSTITUTIVE THEORIES Ph.D. Thesis
Jium-Pang Chang 1985 242 p
Avail: Univ. Microfilms Order No. DA8511183

The present study is aimed at the finite element formulation of a family of viscoplastic models intended for inelastic analysis of structures deformed at elevated temperatures. The constitutive theories considered in this dissertation represent the state of the art approach in high-temperature applications. That is, the inelastic strains are treated as unified quantities (no distinction between creep and plastic strains), which are the functions of stress, temperature and state variables. The approach is capable of representing creep, stress relaxation, plasticity, cyclic behavior, and creep-plasticity interaction of metals. In order to effectively investigate the uniaxial responses of various viscoplastic models, an interactive computerized procedure with extensive graphic display features has been developed. Its applications include the predictions of cyclic stress-strain response, creep, stress relaxation, and thermomechanical fatigue loop. It also serves as a tool for the parametric study of a given material model and the evaluation of numerical integration schemes. Dissert. Abstr.

N86-10570 Johns Hopkins Univ., Baltimore, Md.
LOAD SPACE FORMULATION OF RELIABILITY FOR NONLINEAR RANDOM STRUCTURAL SYSTEMS Ph.D. Thesis
Tzyy Shan Lin 1985 216 p
Avail: Univ. Microfilms Order No. DA8510428

A technique is proposed for determining the reliability of redundant ductile framed structures. A nonlinear structural analysis program and incremental load procedure are used to find the limit state function in load space for fixed structural properties. The failure probability of this deterministic structure is then computed by integrating the joint distribution function of loads over the failure region in load space. The procedure is extended to include randomness in the strength of the structure by introducing a random resistance variable unique to each load path. The statistics of this variable can be found by relating magnitudes of the load vector to successive component failure. The load space formulation of system reliability appears applicable to realistic structures of reasonable complexity. Dissert. Abstr.

N86-10571 Case Western Reserve Univ., Cleveland, Ohio.
FINITE ELEMENT ANALYSIS OF STATICS AND DYNAMIC STRUCTURAL ENGINEERING PROBLEMS USING SEMI-EXPLICIT METHODS Ph.D. Thesis
Rupasiri Purasinghe 1985 116 p
Avail: Univ. Microfilms Order No. DA8510102

Improved semi-explicit methods to solve static and dynamic structural engineering problems are presented which have computer implementation advantages in large and small systems. In solving structural dynamic problems in large systems an unsymmetric splitting method of the stiffness matrix is presented. This technique has the advantage of an explicit method that no matrix factorization of the effective stiffness matrix is necessary at each time step. Besides this method has the advantage of an implicit method that a large time step, larger than that provided in a classical explicit formulation is achieved. In solving static and dynamic problems on small systems, improved iterative techniques which have less storage requirements are presented. These improved iterative techniques are based on a projection of the residuals using a partial Choleski decomposition of the global stiffness matrix. A use of line search to accelerate convergence is included. Dissert. Abstr.

N86-10572 Illinois Univ., Chicago.
OPTIMAL DESIGN OF PORTAL FRAMES AGAINST BUCKLING Ph.D. Thesis

Naser Rezaie-Keyvan 1985 100 p
Avail: Univ. Microfilms Order No. DA8511278

The application of standard stationarity conductions to the optimal design of a structure against buckling may actually lead to a reduction of its real strength in the sense that the optimized structure has been weakened with respect to higher modes to the extent that these have now become fundamental. In this case, a true optimum occurs when the magnitudes of several eigenvalues coalesce, and the corresponding optimality condition is then no longer stationary, but singular. The relevant equations are developed, and an analytical solution is obtained for the case of a symmetric portal frame under symmetric loading for various height-to-span ratios. As expected, and in conformity with the know solution to the fixed-fixed column problem, The correct optimal design exhibits no hinges. Unlike the column problem, however, the value of the associated optimal load parameter is appreciably below the one corresponding to a single-mode solution.
Dissert. Abstr.

N86-10573 Florida Univ., Gainesville.
INELASTIC ANALYSIS OF FRAME STRUCTURES INCLUDING MEMBER AND JOINT SHEARS Ph.D. Thesis
Vinayagamoorthy Balachandran 1984 435 p
Avail: Univ. Microfilms Order No. DA8509902

A computer program, FRAME82, is developed to perform inelastic static and dynamic analyses of plane frame structures including member and joint shear deformations. The effects of parameters such as inelastic material properties and member and joint supports, nonlinear geometry, cyclic loading, mass dependent viscous damping, etc., are also included in the program, FRAME82 utilizes a newly developed Discrete (Finite) Element Shear Model to incorporate the effects of member shear, in addition to the Discrete Element Flexural Model that considers only flexural and axial deformations. Joint shear panels are assumed to have only shear deformations, and flexural and axial deformations are ignored. Besides the three regular degrees of freedom, namely, horizontal, vertical, and rotational displacement, the program requires an additional rotational degree of freedom, namely, horizontal, vertical, and rotational displacement, the program requires an additional rotational degree of freedom for each joint to include the joint shear deformation effects. The structure stiffness is formulated from the stress-stain level and several inelastic models including Masing are incorporated. The program updates the structure stiffness after each iteration within each time step and adds any unbalance in dynamic equilibrium as a corrective load at the beginning of the subsequent iteration. Dissert. Abstr.

N86-10574 Georgia Inst. of Tech., Atlanta.
THE USE OF NEW PATH INDEPEDENT INTEGRALS IN ELASTIC-PLASTIC AND CREEP FRACTURE Ph.D. Thesis
Frederick William Brust, Jr. 1984 262 p
Avail: Univ. Microfilms Order No. DA8510953

A new path independent integral referred to as T* is presented and critically examined with respect to its ability to characterize nonlinear fracture mechanics. T* can characterize nonlinear fracture since it is equivalent to the currently established parameters, which are theoretically valid under limited circumstances. The application of T* to nonlinear fracture includes elastic-plastic stable crack growth, creep fracture, low cycle fatigue situations, and even in a situation where time dependent and time independent material behavior prevail. Experimental data on elastic-plastic stable crack growth in steel is modeled via the finite element method. The ability of T* to characterize the fracture process under these circumstances, and the corresponding inability of the currently established plastic fracture parameters is established. Finite element analyses were performed to evaluate the effectiveness of the T* parameter under creep conditions. This is done, in part, by modeling experimental data of creep crack growth.
Dissert. Abstr.

N86-10575 Testwell Ltd., Daventry (England).
FRACTURE TOUGHNESS TESTING OF CENTRIFUGALLY CAST NICKEL ALUMINIUM BRONZE
May 1984 43 p
(Contract AMTE-NSM42D/1611)
(Rept-MAT/720; BR94518) Avail: NTIS

Fracture toughness of a large centrifugally cast component was assessed by testing 49 specimens from various locations of the component. The AC-PD technique was used to detect the initiation of ductile tearing and show stable crack growth. Metallographic examination was carried out on five specimens, one from each of the test locations, in order to investigate any correlation of grain size with the initiation of ductile tearing. A J resistance curve for each location was determined with a minimum of five specimens in each case; J IC was evaluated by extrapolation of the resistance curve to a blunting line. The J initiation was estimated from the AC-PD measurements and J resistance curves were derived.
Author (ESA)

N86-10576 Sussex Univ., Brighton (England). School of Chemistry and Molecular Sciences.
THE PREPARATION AND TESTING OF TITANIUM AND ZIRCONIUM COUPLING AGENTS Final Report
Rowena Lalanandham, Paul D. Calvert, and David R. M. Walton
Feb. 1984 47 p refs
(Contract MIN-DEF-ERC/9/4/2120/034)
(SJ70; BR91279) Avail: NTIS

A series of titanium and zirconium-based coupling agents containing isopropoxy and epoxy or amine-functional carboxylate groups selected so as to promote bonding between epoxy resins and aluminum or iron oxide surfaces were prepared. Infrared spectral studies show that titanium and zirconium alkoxides form strong water-stable bonds with aluminum, iron, and silica surfaces. Carboxylates carrying epoxide or amino functions can bond to epoxy resins. Titanium and zirconium isopropoxy tricarboxylates were tested as coupling agents on epoxy-aluminum bonds exposed to water. Only small strength improvements result, but fracture is found to be in the oxide layer rather than interfacial. Author (ESA)

N86-10577*# Old Dominion Univ., Norfolk, Va. Dept. of Civil Engineering.
PASSIVE DAMPING CONCEPTS FOR SLENDER COLUMNS IN SPACE STRUCTURES Progress Report, 1 Feb. - 1 Jul. 1985
Zia Razzaq and Rajendra K. Ekhelikar May 1985 137 p refs
(Grant NAG1-336)
(NASA-CR-176234; NAS 1.26:176234) Avail: NTIS HC A07/MF A01 CSCL 20K

An experimental and theoretical study of three different passive damping concepts is conducted for a slender member with partial rotational end restraints. Over a hundred full-scale natural vibration experiments were conducted to evaluate the effectiveness of mass-string, polyethylene tubing, and chain damping concepts. The damping properties obtained from the experiments were used in the approximate analyses based on the partial differential equation of motion for the problem. The comparison of the experimental and the theoretical deflection-time relations shows that the velocity-dependent damping model used in the theory is adequate. From the experimental results, the effect of end connection friction and induced axial forces on damping is identified. The definition of an efficiency index is proposed based on the damping ratio and the mass of a given passive damping device. Using this definition, the efficiencies of the three damping devices are compared. The polyethylene tubing concept resulted into a low damping efficiency.
B.W.

N86-10578*# College of William and Mary, Williamsburg, Va.
STUDY OF STATIS AND DYNAMIC STRESS EFFECTS IN NONLINEAR SOLIDS Semiannual Progress Report, 15 Dec. 1984 - 15 Jun. 1985
Min Namkung 15 Jun. 1985 19 p refs
(Grant NCC1-75)
(NASA-CR-176236; NAS 1.26:176236) Avail: NTIS HC A02/MF A01 CSCL 20K

As the basic physical principles behind the low-field magnetoacoustic interactions have been unfolded, a new step in the present research had to be taken. First, the stress measurements began in samples obtained in real railroad wheel and rail materials. Second, the effect of texture, which is the prime obstacle of conventional NDE techniques, has been investigated. The first stage shows experimental results on these subjects again confirmed that the present technique is most suited for nondestructive stress characterization in steel components. The stress effects on the magnetoacoustic interaction obtained in a sample made from railroad rail which were very similar to those obtained previously in 1045 steel. These results being somewhat different from the results with low (1020) and high (1095) carbon steels, there seemed to be certain range of medium carbon steels having the same characteristics. Also, as expected from the model, the stress information obtained by this technique has been confirmed to be least affected by the presence of texture. Author

N86-10579*# National Aeronautics and Space Administration. Lewis Research Center, Cleveland, Ohio.

JOINT RESEARCH EFFORT ON VIBRATIONS OF TWISTED PLATES, PHASE 1: FINAL RESULTS

Robert E. Kielb, Arthur W. Leissa, James C. MacBain, and Kelly S. Carney Washington Sep. 1985 100 p refs
(NASA-RP-1150; E-2576; NAS 1.61:1150) Avail: NTIS HC A05/MF A01 CSCL 20K

The complete theoretical and experimental results of the first phase of a joint government/industry/university research study on the vibration characteristics of twisted cantilever plates are given. The study is conducted to generate an experimental data base and to compare many different theoretical methods with each other and with the experimental results. Plates with aspect ratios, thickness ratios, and twist angles representative of current gas turbine engine blading are investigated. The theoretical results are generated by numerous finite element, shell, and beam analysis methods. The experimental results are obtained by precision matching a set of twisted plates and testing them at two laboratories. The second and final phase of the study will concern the effects of rotation. Author

N86-10580*# National Aeronautics and Space Administration. Langley Research Center, Hampton, Va.

THREE-DIMENSIONAL VIBRATION ANALYSIS OF A UNIFORM BEAM WITH OFFSET INERTIAL MASSES AT THE ENDS

Daniel K. Robertson (Cincinnati Univ.) Sep. 1985 71 p refs
(NASA-TM-86393; NAS 1.15:86393) Avail: NTIS HC A04/MF A01 CSCL 20K

Analysis of a flexible beam with displaced end-located inertial masses is presented. The resulting three-dimensional mode shape is shown to consist of two one-plane bending modes and one torsional mode. These three components of the mode shapes are shown to be linear combinations of trigonometric and hyperbolic sine and cosine functions. Boundary conditions are derived to obtain nonlinear algebraic equations through kinematic coupling of the general solutions of the three governing partial differential equations. A method of solution which takes these boundary conditions into account is also presented. A computer program has been written to obtain unique solutions to the resulting nonlinear algebraic equations. This program, which calculates natural frequencies and three-dimensional mode shapes for any number of modes, is presented and discussed. Author

N86-10581*# National Aeronautics and Space Administration. Langley Research Center, Hampton, Va.

FATIGUE OF GRAPHITE/EPOXY BUFFER STRIP PANELS WITH CENTER CRACKS

C. A. Bigelow Aug. 1985 32 p refs
(NASA-TM-87595; NAS 1.15:87595) Avail: NTIS HC A03/MF A01 CSCL 20K

The effects of fatigue loading on the behavior of graphite/epoxy panels with either S-Glass or Kevlar-49 buffer strips is studied. Buffer strip panels are fatigued and tested in tension to measure their residual strength with crack-like damage. Panels are made with [45/0/-45/90] sub 2s layup with either S-Glass or Kevlar-49 buffer strip material. The buffer strips are parallel to the loading direction and made by replacing narrow strips of the 0-degree graphite plies with strips of either 0-degree S-Glass/epoxy or Kevlar-49/epoxy on a one-for-one basis. The panels are subjected to a fatigue loading spectrum MINITWIST, the shortened version of the standardized load program for the wing lower surface of a transport aircraft. Two levels of maximum strain are used in the spectrum with three durations of the fatigue spectrum. One group of panels is preloaded prior to the application of the fatigue cycling. The preload consists of statistically loading the spectrum in tension until the crack-tip damage zone reaches the ajacent buffer strips. After fatigue loading, all specimens are statistically loaded in tension to failure to determine their residual strengths. Author

N86-10582*# National Aeronautics and Space Administration. Lewis Research Center, Cleveland, Ohio.

IMPROVED STUD CONFIGURATIONS FOR ATTACHING LAMINATED WOOD WIND TURBINE BLADES Final Report

James R. Fadoul Sep. 1985 29 p refs
(Contract DE-AI01-76ET-20320)
(NASA-TM-87109; DOE/NASA/20320-66; E-2709; NAS 1.15:87109) Avail: NTIS HC A03/MF A01

A series of bonded stud design configurations was screened on the basis of tension-tension cyclic tests to determine the structural capability of each configuration for joining a laminated wood structure (wind turbine blade) to a steel flange (wind turbine hub). Design parameters which affected the joint strength (ultimate and fatigue) were systematically varied and evaluated through appropriate testing. Two designs showing the most promise were used to fabricate addiate testing. Two designs showing the most promise were used to fabricate additional test specimens to determine ultimate strength and fatigue curves. Test results for the bonded stud designs demonstrated that joint strengths approaching the 10,000 to 12,000 psi ultimate strength and 5000 psi high cycle fatigue strength of the wood epoxy composite could be achieved. Author

N86-10583# Technion - Israel Inst. of Tech., Haifa. Dept. of Aeronautical Engineering.

EFFECT OF SEQUENCE OF LOADING ON INTERACTION CURVES FOR BUCKLING OF STIFFENED SHELLS

T. Weller and H. Abramovich Sep. 1984 89 p refs Sponsored in part by DFG in cooperation with RWTH Aachen
(TAE-536) Avail: NTIS HC A05/MF A01

The effect of order of loading on the behavior of stringer-stiffened circular cylindrical shells, on the way to and at buckling under combined axial compression and external pressure was studied. The feasibility of deriving more realistic interaction buckling curves for repeatedly buckled shells by use of the nondestructive vibration correlation technique for definition of boundary conditions was demonstrated. It was shown that the method is feasible, provided that the shell is subjected to an appropriate sequence of loading-constant axial compression first and the external pressure is increased until buckling occurs. Reversing the order of loading, and applying a constant external pressure first, reduced the axial load carrying capacity of the shell. E.A.K.

N86-10584# Technion - Israel Inst. of Tech., Haifa. Dept. of Aeronautical Engineering.

CORRELATION BETWEEN VIBRATIONS AND BUCKLING OF CYLINDRICAL SHELLS STIFFENED BY SPOT-WELDED AND RIVETED STRINGERS

T. Weller, H. Abramovich, and J. Singer Jan. 1985 81 p refs Sponsored in part by DFG in cooperation with RWTH Aachen
(TAE-537) Avail: NTIS HC A05/MF A01

The Vibration Correlation Techniques (VCT) was successfully applied, as a nondestructive tool for definition of actual boundary conditions and better prediction of buckling loads, to shells with spot-welded and riveted stringer stiffeners. It was demonstrated that the effective boundary conditions of the shells are fairly well by this technique, and that the lumping effects of the initial imperfection in the definition of the equivalent restraints are relatively small. Measurements of initial geometrical imperfections were conducted prior to testing of each shell. It is shown that calculation of their degrading effect on the buckling load serves as a complementary tool for improved predictions of actual buckling loads. When combined with the more precisely defined boundary conditions, yielded by the VCT, the agreement between predictions and tests is significantly improved. E.A.K.

N86-10585# Shock and Vibration Information Center (Defense), Washington, D. C.
THE SHOCK AND VIBRATION DIGEST, VOLUME 17, NO. 3 Monthly Report
Judith Nagle-Eshleman, ed. Mar. 1985 105 p refs
(AD-A154144) Avail: SVIC, Code 5804, Naval Research Lab., Washington, D.C. 20375 CSCL 20/11

Abstracts, book reviews, current news, and literature reviews concerning themselves with shock and vibration are presented. The featured articles is on the analysis of exhaust mufflers and vibration problems in jet engines. For individual titles, see N86-10586 through N86-10587.

N86-10586# Shock and Vibration Information Center (Defense), Washington, D. C.
EDITORS RATTLE SPACE **c85**
Ronald E. Eshleman, ed. *In its* The Shock and Vibration Digest, Vol. 17, No. 3 Mar. 1985 p 2 (For primary document see N86-10585 01-39)
Avail: SVIC, Code 5804, Naval Research Lab., Washington, D.C. 20375 CSCL 05/2

The technology transfer process has developed rapidly during the past ten years to provide more knowledge to engineers at a faster rate. However, the distillation of the literature into handbooks and monographs has lagged the progress on information retrieval and short course performance. Up to now there is no magical, fast way to transform specialized technology from journals and reports into handbooks, tables, and computer data bases. The problem always arises on who will organize and pay for it. It is obvious that it requires joint efforts with the cost spread out over many companies. Today, no good means has been found to accomplish this process on a large scale basis. Author

N86-10587# Indian Inst. of Science, Bangalore. Dept. of Mechanical Engineering.
RECENT ADVANCES IN THE ANALYSIS OF EXHAUST MUFFLERS **c37**
M. L. Munjal *In* Shock and Vibration Information Center The Shock and Vibration Digest, Vol. 17, No. 3 Mar. 1985 p 3-16 refs (For primary document see N86-10585 01-39)
Avail: SVIC, Code 5804, Naval Research Lab., Washington, D.C. 20375 CSCL 13/9

Recent advances are reviewed in three major approaches to the analysis of exhaust mufflers: aeroacoustic, finite element, and finite wave. Contributions in the last four years are assessed in the context of earlier work as well as contemporary work. Emphasis is on application and usefulness in design of exhaust mufflers. Author

N86-10588*# Georgia Inst. of Tech., Atlanta.
ANALYSIS OF LARGE, NON-ISOTHERMAL ELASTIC-VISCOPLASTIC DEFORMATIONS
R. Riff, R. L. Carlson, and G. J. Simitses [1984] 4 p refs
(Grant NAG3-534)
(NASA-CR-176220; NAS 1.26:176220) Avail: NTIS HC A02/MF A01 CSCL 20K

The development of a general mathematical model and solutions of test problems to analyze large nonisothermal elasto-visco-plastic deformatisms of structures is discussed. Geometric and material type nonlinearities of higher order are present in the development of the mathematical model and in the developed solution methodology. DOE

N86-10589*# Southwest Research Inst., San Antonio, Tex.
CONSTITUTIVE MODELING FOR ISOTROPIC MATERIALS (HOST) Annual Status Report
U. S. Lindholm, K. S. Chan, S. R. Bodner, R. M. Weber, K. P. Walker, and B. N. Cassenti 20 Aug. 1985 185 p refs
(Contract NAS3-23925)
(NASA-CR-174980; NAS 1.26:174980; SwRI-7576/30; ASR-2)
Avail: NTIS HC A09/MF A01 CSCL 20K

This report presents the results of the second year of work on a problem which is part of the NASA HOST Program. Its goals are: (1) to develop and validate unified constitutive models for isotropic materials, and (2) to demonstrate their usefulness for structural analyses of hot section components of gas turbine engines. The unified models selected for development and evaluation are that of Bodner-Partom and Walker. For model evaluation purposes, a large constitutive data base is generated for a B1900 + Hf alloy by performing uniaxial tensile, creep, cyclic, stress relation, and thermomechanical fatigue (TMF) tests as well as biaxial (tension/torsion) tests under proportional and nonproportional loading over a wide range of strain rates and temperatures. Systematic approaches for evaluating material constants from a small subset of the data base are developed. Correlations of the uniaxial and biaxial tests data with the theories of Bodner-Partom and Walker are performed to establish the accuracy, range of applicability, and integability of the models. Both models are implemented in the MARC finite element computer code and used for TMF analyses. Benchmark notch round experiments are conducted and the results compared with finite-element analyses using the MARC code and the Walker model. Author

N86-10590# Southwest Research Inst., San Antonio, Tex.
CHARACTERIZATION OF MECHANICAL DAMAGE MECHANISMS IN CERAMIC COMPOSITE MATERIALS Interim Technical Report, 24 May 1984 - 23 May 1985
J. Lankford Jun. 1985 68 p
(Contract N00014-84-C-0123)
(AD-A156574) Avail: NTIS HC A04/MF A01 CSCL 11/4

This report summarizes research performed on two distinctly different ceramic composite materials. One was SiC-fiber reinforced LAS glass, while the other was an yttrium partially-stabilized, tetragonal-cubic phase zirconia. Silicon carbide fiber reinforced glass-ceramic matrix composite material has been tested in compression over a wide range in temperature. Both unidirectionally and multiaxially reinforced composites were tested. Compressive strength was measured, and pre-failure damage mechanisms characterized using acoustic emission and optical and scanning electron microscopy. Results are contrasted with corresponding tensile failure modes, and interpreted in terms of matrix microfracture, fiber kinking, and fiber orientation. Deformation and failure mechanisms are characterized for fully and partially yttria-stabilized single crystals tested in compression from 23 C to 1150 C. It is found that both types of material exhibit extensive plastic flow with increasing temperature. Tetragonal to monoclinic transformation-induced plasticity is not observed; rather, plastic flow is related solely to dislocation activity. Evidence is found for apparent cubic to rhombohedral transformation during polishing, and reverse rhombohedral to cubic transformation during imposed compressive stress. GRA

N86-10591# California Univ., Los Angeles. School of Engineering and Applied Science.
HIGH TEMPERATURE MECHANICAL TESTING OF A CYLINDRICAL WEAVE CARBON-CARBON COMPOSITE
S. Mack and G. Sines 1 Jul. 1985 84 p
(Contract N00014-77-C-0505)
(AD-A156639; UCLA-ENG-85-20) Avail: NTIS HC A05/MF A01 CSCL 11/4

The goal is to provide the material property information that is needed to decide whether radial bundles can reduce the stress in the circumferential bundles during the thermal processing of billets. Testing consisted of bundle pull-out experiments at room temperature, 1000 C, and 1500 C on coupons excised from as billet and of rupture and creep experiments on bundles processed to different degrees. The pull-out specimens showed increasing shear strength with temperature and the data showed a decrease in the coefficient of variation with temperature. The average bundle-matrix bond strength at 1500 C had a value of 1940 ksi with a coefficient variation of 4.9%. The tests at 1000 C and room temperature had a coefficient variation of 7.9% and 19.2 % respectively. The tensile strengths of the bundles were relatively insensitive to processing and varied from 190 to 260 ksi. No creep was observed at the maximum available temperature of 1800 C. Author (GRA)

N86-10592# Naval Weapons Center, China Lake, Calif.
FRACTURE TOUGHNESS OF HYDROGEN-EMBRITTLED PRECIPITATION-HARDENED STAINLESS STEELS Final Report, 1982 - 1983
K. F. Hayes Apr. 1985 25 p
(AD-A156664; AD-E900472; NWC-TP-6488) Avail: NTIS HC A02/MF A01 CSCL 11/6

The chevron-notched specimen method was used to determine the fracture toughness of precipitation-hardened (PH) stainless steels possessing a range of microstructures. The specimens were tested while immersed in various aggressive environments (air, salt water, acidified salt water, or after cathodic polarization). GRA

N86-10593# Northwestern Univ., Evanston, Ill. Structural Mechanics Lab.
RESISTANCE CURVES FOR CRACK GROWTH UNDER PLANE-STRESS CONDITIONS IN AN ELASTIC PERFECTLY-PLASTIC MATERIAL Interim Report
J. D. Achenbach and Z. L. Li Jan. 1985 15 p
(Contract N00014-76-C-0063)
(AD-A156778; NU-SML-TR-85-1) Avail: NTIS HC A02/MF A01 CSCL 20/11

A recently developed solution for a plastic strain on the crack line is used in conjunction with a critical strain criterion to construct curves for K sub R (a) versus a, where a is the increase in crack length. Resistance curves have been computed for various values of the critical plastic strain. They show a monotonic increase of K sub R (a) with increase in crack length, to a constant steady-state value. Author (GRA)

N86-10594# Societe Nationale Industrielle Aerospatiale, Suresnes (France). Lab. Central.
NONDESTRUCTIVE CORROSION TEST OF ALUMINUM ALLOY STRUCTURES [CONTROLE NON DESTRUCTIF DE LA CORROSION DANS LES ASSEMBLAGES EN ALLIAGES D'ALUMINIUM, PROCES VERBAL PV 43-954/F2]
D. Lecuru 21 Jan. 1985 63 p refs In FRENCH
(Contract STPA-82-96006)
(PV-43-954/F/2) Avail: NTIS HC A04/MF A01

In order to avoid maintenance cost penalties, aluminum aircraft structure nondestructive test methods are studied, including ultrasonics, radiography, neutronography and Foucault currents. The results show that pitting corrosion is easy to detect, but intergranular corrosion is better detected by ultrasonics or neutronography. The best solution to inspect real aircraft structures is a method based on multiparameter analysis of ultrasonic signals. Author (ESA)

N86-10595# Kernforschungsanlage, Juelich (West Germany). Dept. for Reactor Materials.
EXPERIMENTS WITH TUBULAR PROBES MADE OF INCOLOY 800 H UNDER UNIAXIAL AND MULTIAXIAL STRAIN
M. Roedig, H. J. Penkalla, K. Franzke, F. Schubert, and H. Nickel Feb. 1985 65 p refs In GERMAN; ENGLISH summary
(JUEL-1979; ISSN-0366-0885) Avail: NTIS HC A04/MF A01

The transferability of material data and constitutive equations in the high temperature region is verified by performing uniaxial and multiaxial creep tests on heat exchanger tubes made of INCOLOY 800 H from the same master heat and exposed to various combinations of tension, internal pressure, and torsion at 950 C. Under strain combinations with the same deviatoric stress the different tube lifetimes measured can be explained by constitutive equations. Their deformation under multiaxial strain cannot be predicted exactly with the mathematical model. The tubes under superposed strain conditions failed by leak formation or fracture but never spontaneously. The transfer methods may be improved with the application of extensometers for expansion measures. Author (ESA)

N86-10596# Fraunhofer Inst. fuer Werkstoffmechanik, Freiburg (West Germany).
NUMERICAL SIMULATION OF CRACK ARREST EXPERIMENTS ON ARALDITE B USING THE FINITE DIFFERENCE METHOD
H. Stoeckl Dec. 1982 52 p refs In GERMAN; ENGLISH summary Sponsored by Bundesministerium fuer Forschung und Technologie
(Rept-W-9/82) Avail: NTIS HC A04/MF A01

A program based on the finite difference method was developed on an HP 1000 computer to simulate crack arrest experiments on rectangular double cantilever beam specimens made of Araldite B. The program solves the equations of motion for linear elastic plane models by explicit time integration. The values of the stress intensity factor influencing crack propagation are calculated from a path integral corrected for dynamic effects. The values are compared with experimental values determined with the shadow optical method. The results confirm the experimental method. The numerical method can be applied for dynamic propagation with at most small plastic fracture mechanisms. Author (ESA)

42 GEOSCIENCES (GENERAL)

No abstracts in this category.

43 EARTH RESOURCES

Includes remote sensing of earth resources by aircraft and spacecraft; photogrammetry; and aerial photography.

For instrumentation see *35 Instrumentation and Photography.*

N86-10597* Pacific Northwest Lab., Richland, Wash.
LANDSAT TM IMAGE DATA QUALITY ANALYSIS FOR ENERGY-RELATED APPLICATIONS Final Report
G. E. Wukelic, H. P. Foote, G. M. Petrie, J. C. Barnard, and J. R. Eliason Aug. 1985 21 p refs Original contains color imagery, Original photography may be purchased from the EROS Data Center, Sioux Falls, S.D. 57198 ERTS
(NASA Order S-12402-C)
(E85-10109; NASA-CR-176268; NAS 1.26:176268; PNL-5572) Avail: NTIS HC A02 CSCL 08G

This project represented a no-cost agreement between National Aeronautic Space Administration Goddard Space Flight Center (NASA GSFC) and the Pacific Northwest Laboratory, a Department of Energy (DOE) national laboratory. The objective of the investigation was to evaluate LANDSAT's thematic mapper (TM) data quality and utility characteristics from an energy research and technological perspective. Of main interest was the extent to which repetitive TM data might support DOE efforts relating to siting, developing, and monitoring energy-related facilities, and to basic geoscientific research. The investigation involved: (1) both LANDSAT 4 and 5 TM data, (2) qualitative and quantitative use consideration, and (3) NASA P (corrected) and A (uncorrected) CCT analysis for a variety of sites of DOE interest. All results substantiate the consistent performance of the LANDSAT TM system, and the added application value associated with the increased spectral and spatial capabilities of the TM. Such data are being incorporated into several DOE programs involving continental scientific drilling, acid rain, wind energy, contaminant transport, geologic studies, and environmental/ecological research. Author

N86-10598 Yale Univ., New Haven, Conn.
MODELING GROUNDWATER FLOW INTO LAKES Ph.D. Thesis

John F. Dowo 1984 338 p
Avail: Univ. Microfilms Order No. DA8509696

Groundwater flow into a lake was investigated for conditions similar to those found is a deep kettle hole pond in glacial outwash material. Steady state conditions were used, based upon observed and extrapolated lake elevations and piezometer observations for annual and seasonal averaging times. The finite element procedure operated in a transformed space using smooth basis functions that were formed as one-dimensional cubic B-splines. The effects of anisotropy, but not heterogeneity, of hydraulic conductivity were investigated. Both constant head and noflow were used for boundary conditions on the watertable. The nonlinear problem, where the watertable location was found as part of the solution, was also examined. The flux decreases rapidly with distance from the lake margin, although this decrease was less rapid for anisotropic conditions. For most cases, the integrated least squares exponential fit to the model solution was similar to the direct integration of the finite element results using Gauss-Legendre quadrature. Numerical instability was increased when the aquifer domain boundary and lake boundary were relatively close to the lake margin. The finite element procedure provides an efficient method for obtaining groundwater flux along a lake bottom. Integration of these fluxes provides a useful estimate of average groundwater contributions to a lake. Dissert. Abst.

N86-10599*# Jet Propulsion Lab., California Inst. of Tech., Pasadena.

REPORT OF THE WORKSHOP ON GEOLOGIC APPLICATIONS OF REMOTE SENSING TO THE STUDY OF SEDIMENTARY BASINS

Harold R. Lang, ed. 1 Aug. 1985 81 p refs Workshop held in Lakewood, Colo., 10-11 Jan. 1985 ERTS
(Contract NAS7-918)
(E86-10002; NASA-CR-176211; JPL-Pub-85-44; NAS 1.26:176211) Avail: NTIS HC A05/MF A01 CSCL 08G

The Workshop on Geologic Applications of Remote Sensing to the Study of Sedimentary Basins, held January 10 to 11, 1985 in Lakewood, Colorado, involved 43 geologists from industry, government, and academia. Disciplines represented ranged from vertebrate paleontology to geophysical modeling of continents. Deliberations focused on geologic problems related to the formation, stratigraphy, structure, and evolution of foreland basins in general, and to the Wind River/Bighorn Basin area of Wyoming in particular. Geological problems in the Wind River/Bighorn basin area that should be studied using state-of-the-art remote sensing methods were identified. These include: (1) establishing the stratigraphic sequence and mapping, correlating, and analyzing lithofacies of basin-filling strata in order to refine the chronology of basin sedimentation, and (2) mapping volcanic units, fracture patterns in basement rocks, and Tertiary-Holocene landforms in searches for surface manifestations of concealed structures in order to refine models of basin tectonics. Conventional geologic, topographic, geophysical, and borehole data should be utilized in these studies. Remote sensing methods developed in the Wind River/Bighorn Basin area should be applied in other basins. For individual titles, see N86-10600 through N86-10609.

N86-10600*# Geological Survey, Sioux Falls, S. Dak. EROS Data Center.

SOME OPINIONS ON REMOTE SENSING AND GEOLOGIC STUDIES c46

G. Bryan Bailey *In* JPL Rept. of the Workshop on Geol. Appl. of Remote Sensing to the Study of Sedimentary Basins 1 Aug. 1985 p 29-30 ERTS (For primary document see N86-10599 01-43)
Avail: NTIS HC A05/MF A01 CSCL 08G

The principal role of remote sensing data in geologic studies is as a source of geologic information from which meaningful geologic interpretations can be made. Remote sensing data are important in sedimentary basin analysis and other geologic studies as independent and sometimes unique sources of important lithologic and structural information; however, their greatest benefit to exploration-oriented investigations may come when these data are used with other relevant data in a digital database approach to exploration. Modern computer technology facilitates the rapid integration and synthesis of satellite, topographic, gravity, aeromagnetic, geochemical, and other data collected from a given region. Once such data are geometrically registered, they can be digitally processed, within the constraints of defined geologic models, to rapidly identify, and focus further exploration efforts on, target areas that have the greatest potential for success. R.J.F.

N86-10601*# Hawaii Univ., Honolulu. Planetary Geosciences Div.

POSITION PAPER: WORKSHOP ON GEOLOGIC APPLICATIONS OF REMOTE SENSING TO THE STUDY OF SEDIMENTARY BASINS c46

Pamela L. Blake, Robert B. Singer, and Eileen Bruckenthal *In* JPL Rept. of the Workshop on Geol. Appl. of Remote Sensing to the Study of Sedimentary Basins 1 Aug. 1985 p 31-32 ERTS (For primary document see N86-10599 01-43)
Avail: NTIS HC A05/MF A01 CSCL 08G

The utility of LANDSAT Multispectral Scanner (MSS) and Thematic Mapper (TM) data for providing regional coverage has been demonstrated. Information derived from LANDSAT spectral data is varied, but has primarily been used for distinguishing materials in a scene. Because of the limited number and width of the MSS and TM bands, LANDSAT data has only limited utility for actual identification of materials. The new advanced sensors (currently airborne, but eventually shuttle-based) have more limited areal extent than LANDSAT, but greater spatial and spectral resolution. The Airborne Imaging Spectrometer (AIS) has spectral resolution of about .01 microns and, typically, has 10m/pixel spatial resolution. This improved spectral resolution means that diagnostic spectral features may now be identified, which in turn means that actual identification of mineral phases present can be addressed (of either monomineralic or composite materials). Another new sensor, the Thermal Infrared Multispectral Scanners (TMS), obtains data in the 8 to 12 micron range. The information from the various sensors (e.g., LANDSAT, AIS, and TIMS) is complementary, covering different wavelength regions and consequently sensitive to different materials or physical properties of materials. In addition, the new sensors also produce a higher volume of data, which must be cleverly and efficiently handled. R.J.F.

N86-10602*# University of Southern California, Los Angeles. Dept. of Geological Sciences.

CHRONOLOGIC ANALYSIS OF TERRESTRIAL SEDIMENTS AND BASIN EVOLUTION c46

Douglas Burbank *In* JPL Rept. of the Workshop on Geol. Appl. of Remote Sensing to the Study of Sedimentary Basins 1 Aug. 1985 p 33-36 ERTS (For primary document see N86-10599 01-43)
Avail: NTIS HC A05/MF A01 CSCL 08G

The use of magnetic-polarity stratigraphy to provide detailed chronologies of numerous areas within a sedimentary basin is discussed. Sediments suitable for magnetostratigraphic studies are identified. Sets of figures intended to illustrate some of the applications of magnetic-polarity stratigraphy to various aspects of basin analysis are given. Most of the examples are drawn from the Himalayan molasse (Indo-Gangetic foredeep) in northern Pakistan and northwestern India. Each of the figures illustrates an example of how detailed chronologies can be utilized in enhancing and refining models of basin analysis and tectonic deformation. R.J.F.

N86-10603*# Jet Propulsion Lab., California Inst. of Tech., Pasadena.

TERTIARY AND QUATERNARY RESEARCH WITH REMOTE SENSING METHODS c46

James E. Conel *In its* Rept. of the Workshop on Geol. Appl. of Remote Sensing to the Study of Sedimentary Basins 1 Aug. 1985 p 37-40 refs ERTS (For primary document see N86-10599 01-43)
Avail: NTIS HC A05/MF A01 CSCL 08G

Problems encountered in mapping the Quaternary section of the Wind River Region using remote sensing methods are discussed. Analysis of the stratigraphic section is a fundamental aspect of the geologic study of sedimentary basins. Stratigraphic analysis of post-Cretaceous rocks in the Wind River Basin encounters problems of a distinctly different character from those involved in studying the pre-Cretaceous section. The interior of the basin is predominantly covered by Tertiary and Quaternary sediments. These rocks, except on the basin margin to the north, are mostly flat lying or gently dipping. The Tertiary section consists of sandstones, siltstones, and tuffaceous sediments, some variegated, but in general poorly bedded and of great lithologic similarity. The Quaternary sediments consist of terrace, fan, and debris tongue deposits, unconsolidated alluvium occupying the bottoms of modern watercourses, deposits of eolian origin and tufa. Terrace and fan deposits are compositionally diverse and reflect the lithologic diversity of the source terranes. R.J.F.

N86-10604*# Jet Propulsion Lab., California Inst. of Tech., Pasadena.
MULTISENSOR DATA INTEGRATION TECHNIQUES
Diane L. Evans, Pamela L. Blake (Hawaii Univ., Honolulu), James E. Conel, Harold R. Lang, Thomas L. Logan, Barbara A. McGuffie, Ernest D. Paylor, Robert B. Singer (Hawaii Univ., Honolulu), and Leslie R. Schenck *In its* Rept. of the Workshop on Geol. Appl. of Remote Sensing to the Study of Sedimentary Basins 1 Aug. 1985 p 41 ERTS (For primary document see N86-10599 01-43)
Avail: NTIS HC A05/MF A01 CSCL 05B

The availability of data from sensors operating in several different wavelength regions had led to the development of new techniques and strategies for both data management and image analysis. Work is ongoing to develop computer techniques for analysis of integrated data sets. These techniques include coregistration of multisensor images, rectification of radar images in areas of topographic relief to ensure pixel to pixel registration with planimetric data sets, calibration of data so that signatures can be applied to remote areas, normalization of data acquired with disparate sensors and determination of extended spectral signatures of surface units. In addition, software is being developed to analyze coregistrated digital terrain and image data so that automated stratigraphic and structural analyses can be performed. These software procedures include: strike and dip determination, terrain profile generation, stratigraphic column generation, stratigraphic thickness measurements, structural cross-section generation, and creation of 3-D block diagrams. These techniques were applied to coregistered LANDSAT 4 Thematic Mapper (TM), Thermal Infrared Multispectral Scanner (TIMS), and multipolarization synthetic aperture radar (SAR) data of the Wind River Basin in Wyoming. R.J.F.

N86-10605*# Washington Univ., St. Louis, Mo. McDonnell Center for the Space Sciences.
[ANALYSIS OF REMOTE SENSING DATA] c46
E. A. Guiness, M. Sultan, and R. E. Arvidson *In* JPL Rept. of the Workshop on Geol. Appl. of Remote Sensing to the Study of Sedimentary Basins 1 Aug. 1985 p 45-46 ERTS (For primary document see N86-10599 01-43)
Avail: NTIS HC A05/MF A01 CSCL 08G

A brief assessment of remote sensing applied to geological studies is given. An analysis of thematic mapping data on oak-hickory forests in southern Missouri is discussed. It was found that there is a control on the infrared reflectance (bands 4, 5, and 7 of the Thematic Mapper (TM) of the forests that correlates with rock and soil types. During the growing season, soils with low water retention capacities correlate with high infrared (band 4, lesser with band 5 and 7) signatures. A metamorphic core complex called the Meatiq located in the Eastern Desert of Egypt was studied. The dome provides exposure of most of the rock units of the Arabian-Nubian Precambrian Shield. The dome bears many resemblances to Cordilleran metamorphic complexes. LANDSAT TM data was used to improve on reconnaissance maps of the dome. The remote sensing data was interpreted in the context of field observations, petrographic, and chemical analysis of rock units in the dome, in order to map similar domes in the Eastern Desert from TM data. Mapping projects such as the one just described will help constrain the geologic evolution of the Arabian-Nubian Shield. Two particular hypotheses that researchers hope to test for the development of the shield are: (1) closure of a proto-Red Sea; and (2) accretion of a primitive island arc system onto the shield. R.J.F.

N86-10606*# Jet Propulsion Lab., California Inst. of Tech., Pasadena.
REMOTE STRATIGRAPHIC AND STRUCTURAL ANALYSIS: MULTISENSOR RESULTS IN THE WIND RIVER/BIGHORN BASIN AREA, WYOMING c46
Harold R. Lang, Earnest D. Paylor, and James E. Conel *In its* Rept. of the Workshop on Geol. Appl. of Remote Sensing to the Study of Sedimentary Basins 1 Aug. 1985 p 51-52 ERTS (For primary document see N86-10599 01-43)
Avail: NTIS HC A05/MF A01 CSCL 08G

A brief survey is given of research on the San Juan Basin located in northwest New Mexico and Southern Colorado. Seismic, LANDSAT multispectral scanner and geologic data will be examined in order to understand the changing structural configuration of the basin. Several questions concerned with the discrimination of lithology using LANDSAT multispectral scanner data are posed. R.J.F.

N86-10607*# Lamont-Doherty Geological Observatory, Palisades, N. Y.
STRUCTURAL MAPPING OF FOLDED SEDIMENTARY ENVIRONMENTS FROM SATELLITE IMAGES: AN EXAMPLE FROM CENTRAL ASIA c46
William Leith *In* JPL Rept. of the Workshop on Geol. Appl. of Remote Sensing to the Study of Sedimentary Basins 1 Aug. 1985 p 53-54 refs ERTS (For primary document see N86-10599 01-43)
Avail: NTIS HC A05/MF A01 CSCL 08G

In the Tadjik Depression, in Soviet Central Asia, in the absence of existing geologic or topographic maps, an enhanced LANDSAT multispectral scanner image was used in combination with field data to produce a 1:250000 geologic map of the Vakhsh fold-and-thrust belt and adjacent autochthon. Several structural conclusions are reached as a result of this mapping. Deformation of the Cretaceous and Tertiary strata of the fold-and-thrust belt is, in the central Tadjik Depression, conspicuously absent north of a buried basement fault that marks the hinge-zone of the Late Mesozoic passive margin. But, in the eastern half of the depression, thrusting has moved coherent sheets northward, over the block fault, these sheets now lie flat atop the autochthon to the north. The crustal structure inherited from the Mesozoic extensional phase has strongly influenced the Late Cenozoic pattern of deformation, producing the fold-and-thrust belt that is markedly asymmetric. The development of the thrust system has included the progressive overlapping of thrust: the later thrusts apparently formed internal to the older thrusts, and subsequently overrode them. R.J.F.

N86-10608*# Jet Propulsion Lab., California Inst. of Tech., Pasadena.
FORELAND BASIN STRUCTURES AND REMOTE SENSING c46
Earnest D. Paylor *In its* Rept. of the Workshop on Geol. Appl. of Remote Sensing to the Study of Sedimentary Basins 1 Aug. 1985 p 55-56 ERTS (For primary document see N86-10599 01-43)
Avail: NTIS HC A05/MF A01 CSCL 08G

Rocky Mountain foreland basins are somewhat unique in that the basins may exhibit a variety of structural styles. It is generally agreed that shortening has occurred in the foreland basement but the cause is controversial: vertical vs compressional horizontal tectonics. Even when shortening is attributed to compression, the attitude (dip) of the fault plane and whether the horizontal or vertical component of movement is dominant is unconstrained. The controversy is difficult to resolve from surface data alone due to the variety of possible interpretations. Detailed surface mapping and geologic modeling are needed to constrain subsurface interpretations. In many areas of the Wind River and Bighorn basins detailed geologic maps do not exist. State-of-the-art remote sensing data could potentially provide an efficient means of mapping surface geology. State-of-the-art remote sensing systems now provide geometrically correct data at 30 meter pixel size and increased spectral coverage, capable of more detailed geologic analyses. These data can be photographically enlarged to 1:24, 000 scale and combined with 7 1/2' uses topographic quads to provide an excellent base map for geologic interpretations. R.J.F.

N86-10609*# Carnegie Museum of Natural History, Pittsburgh, Pa. Section of Vertebrate Fossils.
PALEOGENE VERTEBRATE PALEONTOLOGY, GEOLOGY AND REMOTE SENSING IN THE WIND RIVER BASIN c46
Richard K. Stucky and Leonard Krishtalka *In* JPL Rept. of the Workshop on Geol. Appl. of Remote Sensing to the Study of Sedimentary Basins 1 Aug. 1985 p 59-60 refs ERTS (For primary document see N86-10599 01-43)
Avail: NTIS HC A05/MF A01 CSCL 08G

Biostratigraphic and lithostratigraphic studies were used to correlate different events in the geologic evolution of the northeastern part of the Wind River Basin and have suggested several conclusions. Laterally equivalent exposures of the Lysite member from Cedar Ridge to Bridger Creek show a gradation in lithology from interbedded boulder conglomerates and sandstones to interbedded lenticular sandstones and mudstones to interbedded carbonaceous shales, coals and tabular sandstones. This gradation suggests a shift from alluvial fan to braided stream to paludal or lacustrine sedimentary environments during the late early Eocene. The Lysite and Lost Cabin members of the Wind River Formation are in fault contact in the Bridger Creek area and may intertongue to the east along Cedar Ridge. Ways in which remote sensing could be used in these studies are discussed. R.J.F.

N86-10610*# Purdue Univ., Lafayette, Ind. Lab. for Applications of Remote Sensing.
VEGETATION AND SOILS FIELD RESEARCH DATA BASE: EXPERIMENT SUMMARIES
L. L. Biehl, C. S. T. Daughtry, and M. E. Bauer Dec. 1984 24 p refs Revised ERTS
(Contract NAS9-16528)
(E85-10110; NASA-CR-171894; NAS 1.26:171894; LARS-TR-042382) Avail: NTIS HC A02/MF a01 CSCL 05B

Understanding of the relationships between the optical spectral characteristics and important biological-physical parameters of earth-surface features can best be obtained by carefully controlled studies over fields and plots where complete data describing the condition of targets are attainable and where frequent, timely spectral measurement can be obtained. Development of a vegetation and soils field research data base was initiated in 1972 at Purdue University's Laboratory for Applications of Remote Sensing and expanded in the fall of 1974 by NASA as part of LACIE. Since, then over 250,000 truck-mounted and helicopter-borne spectrometer/multiband radiometer observations have been obtained of more than 250 soil series and 20 species of crops, grasses, and trees. These data are supplemented by an extensive set of biophysical and meteorological data acquired during each mission. Experiment summaries are given in table form. In addition, separate tables are presented which include specifications of the spectroradiometers and multiband radiometers used for obtaining the spectral data, and the vegetation for which data have been acquired. M.G.

N86-10611*# National Aeronautics and Space Administration, Washington, D. C.
MAXIMUM WATER RESERVES IN THE SNOW COVER IN THE EUROPEAN TERRITORY OF THE USSR ACCORDING TO DATA FOR 1892-1960
V. D. Komarov and Ye. S. Sinegub Aug. 1985 18 p refs Transl. into ENGLISH from Trudy Psi. (USSR), no. 148, 1966 p 150-160 Transl. by Kanner (Leo) Associates, Redwood City, Calif.
(Contract NASw-4005)
(NASA-TM-77901; NAS 1.15:77901) Avail: NTIS HC A02/MF A01 CSCL 08H

The snow cover of the European territory of the U.S.S.R. is examined. Maps of the average greatest and least magnitudes of the maximum water reserves are given, as well as a map of the coefficient of variation of the maximum reserve. E.A.K.

N86-10612*# National Aeronautics and Space Administration, Washington, D. C.
REPRESENTATION OF THE DISTRIBUTION OF THE SNOW COVER ON THE SURFACE OF THE EARTH'S DRY LAND
G. D. Rikhter and L. A. Petrova Aug. 1985 6 p Transl. into ENGLISH from "Geografia Snezhnogo Pokrova" Moscow, Academy of Sciences of the Soviet Union Press, 1960 p 5-7 Transl. by Kanner (Leo) Associates, Redwood City, Calif.
(Contract NASw-4005)
(NASA-TM-77909; NAS 1.15:77909) Avail: NTIS HC A02/MF A01 CSCL 08L

The distribution of the snow cover on the surface of the Earth's dry land, is discussed. The general laws of this distribution and the influencing factors are determined. E.A.K.

N86-10613*# National Aeronautics and Space Administration, Washington, D. C.
OBSERVATIONS OF THE SNOW COVER IN THE SOUTHERN PART OF THE BURYAT AUTONOMOUS SOVIET SOCIALIST REPUBLIC
Ye. A. Nefedeva Aug. 1985 16 p refs Transl. into ENGLISH from "Geografia Snezhnogo Pokrova" Moscow, Academy of Sciences of the Soviet Union Press, 1960 p 37-44 Transl. by Kanner (Leo) Associates, Redwood City, Calif.
(Contract NASw-4005)
(NASA-TM-77910; NAS 1.15:77910) Avail: NTIS HC A02/MF A01 CSCL 08L

The characteristics of the snow cover, as a function of various natural factors, in sectors of the southern part of the Buryat Autonomous Soviet Socialist Republic were examined. The thawing process is also discussed. E.A.K.

N86-10614*# National Aeronautics and Space Administration, Washington, D. C.
LAWS OF DISTRIBUTION OF THE SNOW COVER ON THE GREATER CAUCASUS (SOVIET UNION)
Ye. Ye. Gurtovaya, G. K. Sulakvelidze, and A. V. Yashina Aug. 1985 24 p refs Transl. from "Geografia Snezhnogo Pokrova" Moscow, Academy of Sciences of the Soviet Union Press, 1960 p 7-20 Transl. by Kanner (Leo) Associates, Redwood City, Calif.
(Contract NASw-4005)
(NASA-TM-77911; NAS 1.15:77911) Avail: NTIS HC A02/MF A01 CSCL 08L

The laws of the distribution of the snow cover on the mountains of the greater Caucasus are discussed. It is shown that an extremely unequal distribution of the snow cover is caused by the complex orography of this territory, the diversity of climatic conditions and by the difference in altitude. Regions of constant, variable and unstable snow cover are distinguished because of the clearly marked division into altitude layers, each of which is characterized by climatic differences in the nature of the snow accumulation. E.A.K.

N86-10615*# Jet Propulsion Lab., California Inst. of Tech., Pasadena.
NASA/JPL AIRCRAFT SAR WORKSHOP PROCEEDINGS
N. Donovan, ed., D. L. Evans, ed., and D. N. Held, ed. 15 Jun. 1985 82 p refs Workshop held in Pasadena, Calif., 4-5 Feb. 1985 Original contains color illustrations
(Contract NAS7-918)
(NASA-CR-176204; NAS 1.26:176204; JPL-Pub-85-39) Avail: NTIS HC A05/MF A01 CSCL 17I

Speaker-supplied summaries of the talks given at the NASA/JPL Aircraft SAR Workshop on February 4 and 5, 1985, are provided. These talks dealt mostly with composite quadpolarization imagery from a geologic or ecologic prespective. An overview and summary of the system characteristics of the L-band synthetic aperture radar (SAR) flown on the NASA CV-990 aircraft are included as supplementary information. Other topics ranging from phase imagery and interferometric techniques classifications of specific areas, and the potentials and limitations of SAR imagery in various applications are discussed. For individual titles, see N86-10616 through N86-10629.

N86-10616*# Jet Propulsion Lab., California Inst. of Tech., Pasadena.
RADAR SYSTEM DESCRIPTION **c32**
D. N. Held and W. E. Brown *In its* NASA/JPL Aircraft SAR Workshop Proc. 15 Jun. 1985 p 5-12 Original contains color illustrations (For primary document see N86-10615 01-43)
Avail: NTIS HC A05/MF A01 CSCL 17I

A brief overview is given of the hardware and software utilized to generate the CV-990 synthetic aperture radar's image products. The on-board hardware is described, then the operational processing software, and finally the image products that are routinely available. Author

N86-10617*# Jet Propulsion Lab., California Inst. of Tech., Pasadena.
CV-990 L-BAND SAR: A CALIBRATION EXPERIMENT **c32**
D. N. Held and C. Werner *In its* NASA/JPL Aircraft SAR Workshop Proc. 15 Jun. 1985 p 17-20 ref Original contains color illustrations (For primary document see N86-10615 01-43)
Avail: NTIS HC A05/MF A01 CSCL 17I

Calibrated image data is required by most users of synthetic aperture radar (SAR) data particularly those attempting to classify targets based upon their radar backscatter signature as a function of frequency polarization or incidence angle. In this experiment, the backscatter derived by calibrating the NASA/JPL CV-990 L-band SAR, and the backscatter reported from a pass of the NASA/JSC C-130 scatterometer as the two instruments flew over the same site at different times are compared. Author

N86-10618*# Jet Propulsion Lab., California Inst. of Tech., Pasadena.
NEOGENE COMPRESSIONAL DEFORMATION AND POSSIBLE THRUST FAULTING IN SOUTHWEST DOMINICAN REPUBLIC Abstract Only
M. P. Golombek, P. Goreau, and T. H. Dixon *In its* NASA/JPL Aircraft SAR Workshop Proc. 15 Jun. 1985 p 21 (For primary document see N86-10615 01-43)
Avail: NTIS HC A05/MF A01 CSCL 08B

Analysis of regional and high resolution remote sensing data coupled with detailed field investigations indicates Neogene compressional deformation in the southwest Dominican Republic. Airborne synthetic aperture radar data and high resolution near infrared photography show folds in Tertiary sediments and possible thrust fault scarps implying NE to SW compression in the region. Large road cuts through the scarps allow study of otherwise poorly accessible, heavily vegetated karst terrain. Deformation increases toward scrap fronts where small bedding-plane thrust faults become more numerous. Analysis of mesoscopic faults with slickensides indicates compression oriented between N to S and E to W. The lowermost scarp has highly sheared fault breccia and undeformed frontal talus breccias implying it is the basal thrust into which the higher thrust faults sole. Thus, the scarps probably formed in a regional NE to SW compressional stress regime and are the toes of thrust sheets. Previous workers have suggested that these scarps are ancient shorelines. However, the gross morphology of the scarps differs substantially from well known erosional terraces on the north coast. Author

N86-10619*# National Aeronautics and Space Administration. Goddard Space Flight Center, Greenbelt, Md.
THE EFFECT OF VEGETATION TYPE, MICRORELIEF, AND INCIDENCE ANGLE ON RADAR BACKSCATTER
Manfred Owe, Peggy E. ONeill, Thomas J. Jackson, and Thomas J. Schmugge *In* JPL NASA/JPL Aircraft SAR Workshop Proc. 15 Jun. 1985 p 25-29 Original contains color illustrations (For primary document see N86-10615 01-43)
Avail: NTIS HC A05/MF A01 CSCL 17E

The NASA/JPL Synthetic Aperture Radar (SAR) was flown over a 20 x 110 km test site in the Texas High Plains regions north of Lubbock during February/March 1984. The effect of incidence angle was investigated by comparing the pixel values of the calibrated and uncalibrated images. Ten-pixel-wide transects along the entire azimuth were averaged in each of the two scenes, and plotted against the calculated incidence angle of the center of each range increment. It is evident from the graphs that both the magnitudes and patterns exhibited by the corresponding transect means of the two images are highly dissimilar. For each of the cross-poles, the uncalibrated image displayed very distinct and systematic positive trends through the entire range of incidence angles. The two like-poles, however, exhibited relatively constant returns. In the calibrated image, the cross-poles exhibited a constant return, while the like-poles demonstrated a strong negative trend across the range of look-angles, as might be expected. Author

N86-10620*# Jet Propulsion Lab., California Inst. of Tech., Pasadena.
AGE-DATING VOLCANIC AND ALLUVIAL SURFACES WITH MULTIPOLARIZATION DATA **c46**
Tom G. Farr *In its* NASA/JPL Aircraft SAR Workshop Proc. 15 Jun. 1985 p 31-36 refs Original contains color illustrations (For primary document see N86-10615 01-43)
Avail: NTIS HC A05/MF A01 CSCL 08G

A false-color multipolarization version of one of the images of Owens Valley area acquired by the JPL Synthetic Aperture Radar (SAR) is given. A geologic map of the alluvial fans there (Gillespie, 1982) is also given for comparison. In general, brightness in the multipolarization images can be seen to be inversely proportional to the age of the surfaces. A more detailed investigation of the relationship between backscatter and age of the surfaces was undertaken with calibrated aircraft SAR data. The quantitative relationship between backscatter coefficient and age for the three polarizations is shown. The straight lines connecting the measured data points imply a steady-state process, although the process or processes leading to this relationship may have operated at rates that varied with climate fluctuations, such as the glacial ages. It is expected that the relationship between radar brightness and age is a consistent one, and that with the wider availability of calibrated radar backscatter data, these relationships can be less well-known areas. The effect of variable such as past climate fluctuations, tectonic disturbance, and rock type must be understood before extension beyond the Mojave Desert region can be attempted. R.J.F.

N86-10621*# National Aeronautics and Space Administration. Goddard Space Flight Center, Greenbelt, Md.
THE EFFECTS OF MERGING TM AND A/C RADAR ON WETLAND CLASSIFICATION
James P. Ormsby and Patricia J. Mulligan *In* JPL NASA/JPL Aircraft SAR Workshop Proc. 15 Jun. 1985 p 37-38 refs (For primary document see N86-10615 01-43)
Avail: NTIS HC A05/MF A01 CSCL 08B

While radar does not provide detailed begetation discrimination, it provide the means to separate areas of different moisture conditions. Thus, the use of LANDSAT Thematic Mapper (TM) in conjunction with the microwave data was attempted. If successful, information on shoreline cover, emergent wetland vegetation and extent, and submerged grassbeds would provide much needed data for planning and maintenance of wetlands. Originally, the goal was to determine the accuracy with which one could categorize various types of vegetation and land use within an inland wetland using LANDSAT TM data. First, a Level 1/2 supervised classification was performed. Following a more detailed ground trust survey, a Level 3 classification was done. Aircraft L-band radar data were received and the decision was made to merge the TM and L-band data and assess whether vegetation catagories within the wetland areas could be better defined. Preliminary results indicate vegetation delineation is improved for open agricultural areas and water, but other features are more confused. R.J.F.

N86-10622*# Jet Propulsion Lab., California Inst. of Tech., Pasadena.

TOPOGRAPHIC MAPPING FROM INTERFEROMETRIC SYNTHETIC APERTURE RADAR OBSERVATIONS

Howard A. Zebker and Richard M. Goldstein *In its* NASA/JPL Aircraft SAR Workshop Proc. 15 Jun. 1985 p 41-44 refs Original contains color illustrations (For primary document see N86-10615 01-43)

Avail: NTIS HC A05/MF A01 CSCL 08B

The production of high-resolution topographic maps derived from interferometric synthetic aperture radar observations of the Earth is reported. Topographic maps are typically determined from stereo-pair optical photographs. Vertical relief causes the same terrain to appear in a slightly different projection for differing look angles, and this shift in appearance is interpreted in terms of the height of the terrain. The radar interferometric approach is related to the stereo technique in that the terrain is viewed at two different angles; however, in this case, the angular separation of the antennas is extremely small, on the order of a milliradian or less, as compared to tens of degrees for the optical case. Thus, the geometrical distortion and subsequent rectification correction algorithms are much less severe in the reduction of interferometric data. R.J.F.

N86-10623*# Washington Univ., Seattle.

STRATEGIES FOR ANALYZING MIXED PIXELS IN REMOTELY SENSED IMAGERY

Milton Smith and John Adams *In* JPL NASA/JPL Aircraft SAR Workshop Proc. 15 Jun. 1985 p 47-48 (For primary document see N86-10615 01-43)

Avail: NTIS HC A05/MF A01 CSCL 05B

Two uncalibrated synthetic aperture radar (SAR) scenes from Death Valley, California, and two uncalibrated scenes from Owens Valley, California, were used to test a technique to identify and separate the primary factors associated with multipolarized radar image sets. Unique to the technique is the concept that varied types of radar polarization signatures are a result of the interaction of a few physical factors (e.g., roughness, volume scattering, and dielectric constant). Thus, the varied signatures observed in an image reflect the interaction between these factors. The objectives are to first separate the interaction of factors directly influencing the measurement and to attempt to identify these factors. Interpretation of the SAR image sets proceeds by testing models that hypothesize the cause and effect relations between those factors directly affecting the radar measurement and those features of interest to the interpreter. The results of our analysis indicated two consistent endmember types over all four image scenes. These types are defined by a high flat polarized signature near a level of 255 DN and a low level flat signature near 0 DN for all polarizations. Four other endmember types were also isolated. The spatial distribution of these endmember types indicates possible correspondence to surface volume scattering and changes in surface dielectric. However, the shapes of these endmember types were different from scene to scene. R.J.F.

N86-10624*# Jet Propulsion Lab., California Inst. of Tech., Pasadena.

LITHOLOGIC MAPPING IN A SEDIMENTARY ENVIRONMENT USING MULTIPOLARIZATION SAR IMAGES

Diane L. Evans and Leslie R. Schenck *In its* NASA/JPL Aircraft SAR Workshop Proc. 15 Jun. 1985 p 49-50 refs Original contains color illustrations (For primary document see N86-10615 01-43)

Avail: NTIS HC A05/MF A01 CSCL 08B

Multipolarization Synthetic Aperture Radar (SAR) data from the NASA/JPL aircraft SAR were used in conjunction with LANDSAT Thematic Mapper (TM), Thermal Infrared Multispectral Scanner (TIMS), and Airborne Imaging Spectrometer (AIS) data as part of a three-year research program to evaluate the utility of remote sensing measurements for analysis of sedimentary basins. The purpose of this research effort is to construct stratigraphic columns, map variations in the lithology, geometry, and structure of sedimentary rocks in the Wind River/Bighorn Basin area, Wyoming, and to integrate remote sensing data with conventional rain models of basin formation and evolution. Author

N86-10625*# Jet Propulsion Lab., California Inst. of Tech., Pasadena.

MAPPING DIVERSE FOREST COVER WITH MULTIPOLARIZATION AIRBORNE RADAR

J. P. Ford, D. E. Wickland, and R. R. Sharitz (Dupont de Nemours (E. I.) and Co., Aiken, S.C.) *In its* NASA/JPL Aircraft SAR Workshop Proc. 15 Jun. 1985 p 53-54 ref Original contains color illustrations (For primary document see N86-10615 01-43)

Avail: NTIS HC A05/MF A01 CSCL 02F

Imaging radar backscatter in continuously forested areas contains information about the forest canopy; it also contains data about topography, landforms, and terrain texture. For purposes of radar image interpretation and geologic mapping researchers were interested in identifying and separating forest canopy effects from geologic or geomorphic effects on radar images. The objectives of this investigation was to evaluate forest canopy variables in multipolarization radar images under conditions where geologic and topographic variables are at a minimum. A subsidiary objective was to compare the discriminatory capabilities of the radar images with corresponding optical images of similar spatial resolution. It appears that the multipolarization images discriminate variation in tree density, but no evidence was found for discrimination between evergreen and deciduous forest types. R.J.F.

N86-10626*# National Aeronautics and Space Administration. National Space Technology Labs., Bay Saint Louis, Miss.

POTENTIAL APPLICATIONS OF MULTIPOLARIZATION SAR FOR PINE PLANTATION BIOMASS ESTIMATION

S. T. Wu *In* JPL NASA/JPL Aircraft SAR Workshop Proc. 15 Jun. 1985 p 59-61 (For primary document see N86-10615 01-43)

Avail: NTIS HC A05/MF A01 CSCL 02F

This study was conducted as a part of the research tasks under the Radar Land Cover Analysis Program. The Radar Land Cover Analysis objective is, through utilization of multisensor data, to gain a basic understanding of the measurements and data characteristics in the visible-IR-microwave regions of the electromagnetic spectrum associated with specific surface features and cover types. Since the results of analysis of data acquired by Shuttle Imaging Radar (SIR-A) and LANDSAT Thematic Mapper (TM) over the study area were reported (NSTL/ERL Report No. 228, December 1984), this study focused on the analysis and evaluation of the L-band multipolarization airborne SAR data acquired over a southeastern pine forest scene. The data acquisition mission was flown on September 8 and 9, 1983. The HH, HV polarizations and the VV, VH polarizations were used on the first and the second day, respectively. Due to instrumentation difficulties, the digital recorder recorded only the second day's data. Because of this, only the VV and VH polarization data were used in this analysis. However, the HH and HV polarization images were available for visual comparison. It appears that SAR digital numbers correlate with the index of green biomass. Author

N86-10627*# Jet Propulsion Lab., California Inst. of Tech., Pasadena.

ON THE USE OF L-BAND MULTIPOLARIZATION AIRBORNE SAR FOR SURVEYS OF CROPS, VINEYARDS, AND ORCHARDS IN A CALIFORNIA IRRIGATED AGRICULTURAL REGION

Jack F. Paris *In its* NASA/JPL Aircraft SAR Workshop Proc. 15 Jun. 1985 p 63 Original contains color illustrations (For primary document see N86-10615 01-43)

Avail: NTIS HC A05/MF A01 CSCL 02C

The airborne L-band synthetic aperture radar (SAR) collected multipolarization calibrated image data over an irrigated agricultural test site near Fresno, CA, on March 6, 1984. The conclusions of the study are as follows: (1) the effects of incidence angle on the measured backscattering coefficients could be removed by using a correction factor equal to the secant of the angle raised to the

1.4 power, (2) for this scene and time of year, the various polarization channels were highly correlated such that the use of more than one polarization added little to the ability of the radar to discriminate vegetation type or condition; the exception was barley which separated from vineyards only when a combination of like and cross polarization data were used (polarization was very useful for corn identification in fall crops), (3) an excellent separation between herbaceous vegetation (alfalfa, barley, and oats) or bare fields and trees in orchards existed in brightness was well correlated to alfalfa height or biomass, especially for the HH polarization combination, (5) vineyards exhibited a narrow range of brightnesses with no systematic effects of type or number of stakes nor of number of wires in the trellises nor of the size of the vines, (6) within the orchard classes, areal biomass [characterized by basal area] differences caused radar image brightness differences for small to medium trees but not for medium to large trees. Author

N86-10628*# Jet Propulsion Lab., California Inst. of Tech., Pasadena.

VEGETATION CANOPY DISCRIMINATION AND BIOMASS ASSESSMENT USING MULTIPOLARIZED AIRBORNE SAR

F. T. Ulaby (Michigan Univ.), M. C. Dobson (Michigan Univ.), and D. N. Held *In its* NASA/JPL Aircraft SAR Workshop Proc. 15 Jun. 1985 p 67-75 Original contains color illustrations (For primary document see N86-10615 01-43)

Avail: NTIS HC A05/MF A01 CSCL 02C

Multipolarized airborne Synthetic Aperture Radar (SAR) data were acquired over a largely agricultural test site near Macomb, Illinois, in conjunction with the Shuttle Imaging Radar (SIR-B) experiment in October 1984. The NASA/JPL L-band SAR operating at 1.225 GHz made a series of daily overflights with azimuth view angles both parallel and orthogonal to those of SIR-B. The SAR data was digitally recorded in the quadpolarization configuration. An extensive set of ground measurements were obtained throughout the test site and include biophysical and soil measurements of approximately 400 agricultural fields. Preliminary evaluation of some of the airborne SAR imagery indicates a great potential for crop discrimination and assessment of canopy condition. False color composites constructed from the combination of three linear polarizations (HH, VV, and HV) were found to be clearly superior to any single polarization for purposes of crop classification. In addition, an image constructed using the HH return to modulate intensity and the phase difference between HH and VV returns to modulate chroma indicates a clear capability for assessment of canopy height and/or biomass. In particular, corn fields heavily damaged by infestations of corn borer are readily distinguished from noninfested fields. Author

N86-10629*# Jet Propulsion Lab., California Inst. of Tech., Pasadena.

MODELLING OF VEGETATION VOLUMES

Jakob J. vanZyl (California Inst. of Tech.), Charles H. Papas (California Inst. of Tech.), Nader Engheta, and Charles Elachi *In its* NASA/JPL Aircraft SAR Workshop Proc. 15 Jun. 1985 p 77-79 (For primary document see N86-10615 01-43)

Avail: NTIS HC A05/MF A01 CSCL 02C

The purpose is to describe work that is being done to find theoretical models to describe radar backscatter from vegetation layers. The geometry of the problem is shown. The information that one would like to find through the application of the results of these models would include: the thickness of the layer; the absorption in the layer (i.e., density, moisture content, and biomass); the geometry of the scatterers (i.e., shape and orientation); how much of the received power is due to volume scattering only; and a way to enhance the ratio of scattering that has some interaction with the ground surface. The proposed ways to find this information are discussed. R.J.F.

N86-10630# Army Engineer Topographic Labs., Fort Belvoir, Va.

ANALYSIS OF EDGE DETECTION ALGORITHMS ON DIAL (DIGITAL IMAGE ANALYSIS LABORATORY)

J. M. Brown Jan. 1985 38 p

(DA Proj. 4A7-62707-A-855)

(AD-A156735; ETL-0371) Avail: NTIS HC A03/MF A01 CSCL 12/1

As part of an effort to deliver to the Defense Mapping Agency in FY85 a semiautomated feature extraction system, the Engineer Topographic Laboratories is conducting a feature extraction study. One of the objectives of this study is to determine whether selected edge-finding algorithms can be used to find such lineal features as roads and boundaries. The purpose of this document is to report on progress to date on an analysis of several edge-detection algorithms that exist on ETL's Digital Image Analysis Laboratory image-processing facility. In addition to evaluating the algorithms, this study investigated the possibilities of integrating the algorithms' resultant edges with other feature classification algorithms. Three fundamental edge-detection methods were compare: (1) a nonlinear edge-enhancement operator; (2) a directional edge operator; and (3) an extraction of the zero-crossings from filtering an image with the Laplacian of a symmertric Gaussian function. GRA

N86-10631# Pacific Northwest Lab., Richland, Wash.

ENERGY BALANCE IN A DEEP COLORADO VALLEY: ASCOT 84

J. R. Simpson, L. J. Fritschen, C. D. Whiteman, and M. M. Orgill Jan. 1985 5 p refs Presented at the 17th Conf. on Agr. and Forest Meteorol., Phoenix, Ariz., 20 May 1985 Prepared in cooperation with Washington Univ., Seattle

(Contract DE-AC06-76RL-01830)

(DE85-012441; PNL-SA-12990; CONF-850581-3) Avail: NTIS HC A02/MF A01

Five portable, battery-operated energy balance stations were installed and operated in the deep, semiarid Brush Creek Valley of western Colorado for 22 days. Surface energy budget data from these stations are presented for the clear day of September 29, 1984. DOE

N86-10632# California Univ., Livermore. Lawrence Livermore Lab.

APPLICATION OF THE RUTHENIUM AND TECHNETIUM THERMODYNAMIC DATA BASES USED IN THE EQ3/6 GEOCHEMICAL CODES

D. Isherwood Apr. 1985 63 p

(Contract W-7405-eng-48)

(DE85-013766; UCRL-53594) Avail: NTIS HC A04/MF A01

Based on a critical review of the available thermodynamic data, computerized data bases for technetium and ruthenium were created for use with the EQ3/6 geochemical computer codes. The technetium data base contains thermodynamic data for 8 aqueous species and 15 solids; 26 aqueous species and 9 solids were included in the ruthenium data base. The EQ3NR code was used to calculate solubility limits for ruthenium (8 x 10(-16) M) in ground water from Yucca Mountain, a potential nuclear waste repository site near the Nevada Test Site (NTS). The code confirmed the essentially unlimited solubility of technetium in oxidizing conditions, such as those that are believed to exist in the unsaturated zone at Yucca Mountain and the Cambric Nuclear event site at the NITS. Ruthenium migration observed from the Cambric site was evaluated. The solubility limit for ruthenium (as the aqueous species RuO4(-)) when constrained by BuO2 is approximately equal to the concentration of ruthenium found in the cavity ground water (i.e., 2.1 x 10(-11) vs 4.5 x 10(-11) M). Differences in ruthenium solubility limits between Yucca Mountain and Cambric are primarily due to differences in ground-water pH. Technetium solubility (3 x 10(-8) M) for moderately reducing conditions (Eh = -0.1 V) using the metastable oxide, TcO2.2H2O, as the solubility constraint is within the range of experimental values. DOE

N86-10633# Rockwell International Corp., Richland, Wash.

TIME-TERM ANALYSIS OF UPPER CRUSTAL STRUCTURE IN THE COLUMBIA BASIN, WASHINGTON

A. C. Rohay, D. W. Glover, and S. D. Malone Apr. 1985 24 p Presented at the Seismological Soc. of Am. Conf., Austin, Tex.,

14 Apr. 1985
(Contract DE-AC06-77RL-01030)
(DE85-012390; RHO-BW-SA-435P; CONF-8504151-1) Avail: NTIS HC A02/MF A01

Arrival time data from existing permanent networks and supplementary portable stations were collected during the US Geological Survey (USGS) refraction program in August 1984. Reduced travel time plots of these data and USGS record sections were used to select data from two branches of the travel time curve. Sixty-six arrival times selected in the distance range 3 to 63 km were fit to a velocity of 5.16 km/s (plus or minus 0.02 km/s). Time terms determined at 31 stations range from -0.10 to +0.15 s (plus or minus 0.05 s) and show correlations with elevation and near-surface geology. The four intercept times range from 0.15 to 0.22 s (plus or minus 0.05 s), implying an average depth of 0.5 km to the 5.16-km/s refracting horizon within the basalt. Eighty-three arrival times selected in the distance range 50 to 145 km were fit to a velocity of 6.16 km/s (plus or minus 0.02 km/s). Time terms calculated at 40 stations range from -0.6 to +0.6 s (plus or minus 0.1 s), with the four intercept times ranging from 1.4 to 2.0 s (plus or minus 0.1 s). These show a systematic regional pattern consistent with previous studies (Malone and Rohay 1983) but extended by portable-station coverage. Conversion of the time terms to basement depth is dependent upon the lateral extent of an inferred low-velocity layer beneath the basalts, which is suggested by deep-borehole logs and magnetotelluric data. DOE

N86-10634# Western Research Inst., Laramie, Wyo.
GEOLOGIC EVALUATION AND RESERVOIR PROPERTIES OF THE PR SPRING TAR SAND DEPOSIT, UINTAH AND GRAND COUNTIES, UTAH
D. J. Sinks Jan. 1985 197 p refs
(Contract DE-FC21-83FE-60177)
(DE85-013248; DOE/FE-60177/1883) Avail: NTIS HC A09/MF A01

A seven-corehole drilling program at the PR Spring tar sand deposit, southeastern Uinta Basin, Utah was completed. The data were integrated with other resource information to complete lithologic correlations, to evaluate general reservoir property trends for each major tar sand zone, and to identify areas of potential in situ processing. Five distinct arkoses (sandstones) of lacustrine origin have definable areal extents and are variable saturated with bitumen. Two newly recognized zones stratigraphically lower than the other five, were tentatively identified in one core from the southeast portion of the deposit. Core descriptions and analytical data were used to generate computerized maps to identify general areal trends in resource parameters for the five major zones. Two pairs of zones exhibit similar areal trends, indicating similar depositional conditions. Insufficient data for zone E inhibited the identification of any resemblance to other zones. Direction of increase for some reservoir properties were noted for all zones. Portions of all five zones are suitable for surface mining. DOE

N86-10635# Argonne National Lab., Ill.
APPROACHES TO CUMULATIVE IMPACT ASSESSMENT
G. W. Witmer 1985 15 p refs Presented at the Natl. Wetland Assessment Symp., Portland, Oreg., 17 Jun. 1985
(Contract W-31-109-eng-38)
(DE85-013891; CONF-8506146-1) Avail: NTIS HC A02/MF A01

The quantity and quality of North American wetlands were reduced this century. Growing concern over the social and ecological effects lead to studies of wetlands ecology and efforts to classify, monitor, and predict impacts to wetlands. Assessing and predicting land use and developmental activity impacts particularly cumulative impacts to wetlands is difficult because of their diverse, complex, and dynamic nature. The methods allow for multiple projects or land uses, an extended time frame, the aggregation of impacts, a flexibility in geographic boundaries, and adaptability to new techniques and sources of information. Nine categories of existing methods are reviewed. It is probable that a combination of these methods can be used for cumulative impact assessment. To do so effectively, some additional concepts must be incorporated. DOE

N86-10636# Deutsche Forschungs- und Versuchsanstalt fuer Luft- und Raumfahrt, Oberpfaffenhofen (West Germany). Abt. Fernerkundung.
CALIBRATION OF THE MULTISPECTRAL SCANNER (MSS) SATELLITE DATA TO EVALUATE CHANGE IN THE REFLECTION OF CONIFEROUS STOCKS Ph.D. Thesis - Technische Univ., Berlin
Gerd-Peter Fehlert Sep. 1984 184 p refs In GERMAN; ENGLISH summary Report will also be announced as translation (ESA-TT-938) Original contains color illustrations
(DFVLR-FB-84-44; ISSN-0171-1342) Avail: NTIS HC A09/MF A01; DFVLR, Cologne DM 71

A relative calibration is performed in order to allow a comparative, multitemporal analysis of MSS satellite data and hence the detection of reflectory changes with regard to selected object classes. By applying the method to the class wood, the age of a coniferous stock can be determined, and during the stage of growth distinct age groups show locally differing reflectory properties. The latter suggests disorders of the proliferation of young sprouts. This method can be an early indicator for the detection of damaged forest areas. The atmospheric influence on satellite data is determined by a multilayer atmospheric model. Author (ESA)

N86-10637# Delft Hydraulics Lab. (Netherlands).
THE RHINE-MEUSE ESTUARY HYDRAULIC SCALE MODEL. EXPERIENCES WITH COMPUTER CONFIGURATION AND SOFTWARE
W. Scholten Feb. 1985 8 p refs Presented at 21st Intern. Assoc. for Hydraulic Res. Congr., Melbourne, 19-23 Aug. 1985
(Publ-335) Avail: NTIS HC A02/MF A01

The hardware and software configurations of the Rhine-Meuse estuary hydraulic model are described. The system for real time processing consists of a PDP 11/24 computer and a FOX digital control system. A PDP 11/44 performs offline processing. The RSX-11M system is used. Programs to simulate tidal movements, acquire measurement data, prepare boundary conditions, administer measurements, and process measurements were created. Adjustment of tidal flows at sea boundaries takes 1 day; salinity measurements are free from initial conditions after 3 hr. Programming is time consuming because of the relatively limited free space available (48 kbytes). Author (ESA)

N86-10638# Instituut voor Cultuurtechniek en Waterhuishouding, Wageningen (Netherlands).
REMOTE SENSING
G. J. A. Nieuwenhuis and J. M. M. Bouwmans (Landinrichtingsdienst) May 1984 46 p, In DUTCH
(NOTA-1535) Avail: NTIS HC A03/MF A01

Electromagnetic radiation, and remote sensors are introduced. Color and false color, multispectral and stereophotography, multispectral and infrared line scanning, and microwave techniques are described. The impact of wave length, and the way the images are obtained and compiled on the resulting image content is discussed. Interpretation and analog and digital procedures are surveyed. Applications such as crop identification and meteorological research are reviewed. Author (ESA)

N86-10639# Instituut voor Cultuurtechniek en Waterhuishouding, Wageningen (Netherlands).
REMOTE SENSING STUDY PROJECT EAST GELDERLAND (NETHERLANDS). PART 2: REMOTE SENSING FLIGHTS IN 1982 AND 1983; ORGANIZATION ASPECTS [REMOTE SENSING STUDIEPROJECT OOST-GELDERLAND. DEELRAPPORT 2: REMOTE SENSING VLUCHTEN IN 1982 EN 1983: ORGANISATORISCHE ASPECTEN]
G. J. A. Nieuwenhuis Jun. 1983 30 p refs In DUTCH
Avail: NTIS HC A03/MF A01

Photographs of 2 strips of peatland of 8 x 40 km at 5000 m altitude and detailed studies at 800 to 2000 m were made under different weather conditions with visibility from 5 to 15 km. As infrared photography is visibility and cloud independent and quality can be improved by repeating a trajectory and processing afterwards, it is concluded that flights should go on even under bad navigation circumstances. Author (ESA)

N86-10640# Haskoning, Consulting Engineers, Nijmegen (Netherlands).
UTILIZATION OF SATELLITE REMOTE SENSING FOR THE MONITORING OF OIL POLLUTION AND MARINE ECOSYSTEMS IN INDONESIA. A TROPICAL EARTH RESOURCES SATELLITE PROGRAM (TERS) CASE STUDY IMPLEMENTED FOR THE NLR, DELFT
Nov. 1983 67 p refs
Avail: NTIS HC A04/MF A01

The suitability of a remote sensing satellite for environmental monitoring in tropical zones with considerable cloud cover was assessed in a case study of the impact of an oil refinery extension on coastal and mangrove swamp ecology. It is concluded that the Tropical Earth Resources Satellite (TERS) program panchromatic and spectral bands in the wavelength interval between 40 to 1000 nm are suitable for the detection of the mangrove zone, dead tree zones, the location and drift of oil spills, and the location of sources of pollution-like drilling and production platforms, tanker traffic, and pipeline traces. The TERS system can be used as a first stage waring system, with follow-up by aerial and ground surveys. Author (ESA)

N86-10641# Texas Dept. of Water Resources, Austin.
EVALUATING THE GROUND-WATER RESOURCES OF THE HIGH PLAINS OF TEXAS, VOLUME 4
T. Knowles, P. Nordstrom, and W. B. Klemt Dec. 1984 393 p
(PB85-191625; TDWR/R-288-Vol-4) Avail: NTIS HC A17/MF A01; also avail: in set of 4 reports HC E99 as PB85-191583 CSCL 08H

This report is prepared in four volumes. Volume 4 contains the basic data for the counties in the southern third of the study area as shown on the accompanying map. GRA

N86-10181# Bundesministerium fuer Forschung und Technologie, Bonn (West Germany).
HOW ANTARCTICA WAS UNVEILED. MASTERPIECES OF FRANKFURT TOPOGRAPHIC SURVEYORS. A PART OF THE GERMAN ANTARCTICA RESEARCH PROGRAM [WIE DIE ANTARKTIS ENTSCHLEIERT WIRD. MEISTERSTUECKE FRANKFURTER ERDVERMESSER. EIN TEIL DES DEUTSCHEN ANTARKTIS-FORSCHUNGSPROGRAMMS]
Ruediger Jungbluth *In its* Satellite Use for Men 1985 p 5-10 In GERMAN (For primary document see N86-10180 01-12)
Avail: NTIS HC A03/MF A01

N86-10182# Bundesministerium fuer Forschung und Technologie, Bonn (West Germany).
SATELLITE DATA EVEN FOR A POULTRY FARM. A DEVELOPMENT FOR TANZANIA. IMAGE EVALUATION FOLLOWING NEW WAYS [SATELLITENDATEN SELBST FUER EINE HUEHNERFARM. EIN ENTWICKLUNGSPROJEKT FUER TANSANIA. BILDAUSWERTUNG AUF NEUEN WEGEN]
Philip Erdoes *In its* Satellite Use for Men 1985 p 11-16 In GERMAN (For primary document see N86-10180 01-12)
Avail: NTIS HC A03/MF A01

N86-10183# Bundesministerium fuer Forschung und Technologie, Bonn (West Germany).
WITH ARGUS EYES FROM SPACE. SATELLITE DIAGNOSIS FOR UPPER VOLTA. SEVEN MAPS WITHOUT MYSTERY [MIT ARGUSAUGEN AUS DEM ALL. SATELLITEN-DIAGNOSE FUER OBERVOLTA. SIEBEN KARTEN OHNE SIEBEN SIEGEL]
Uwe Andresen *In its* Satellite Use for Men 1985 p 17-21 In GERMAN (For primary document see N86-10180 01-12)
Avail: NTIS HC A03/MF A01

44 ENERGY PRODUCTION AND CONVERSION

Includes specific energy conversion systems, e.g., fuel cells and batteries; global sources of energy; fossil fuels; geophysical conversion; hydroelectric power; and wind power.

For related information see also *07 Aircraft Propulsion and Power, 20 Spacecraft Propulsion and Power, 28 Propellants and Fuels,* and *85 Urban Technology and Transportation.*

N86-10642 Department of the Air Force, Washington, D.C.
NICKEL-CADMIUM BATTERY CONDITIONER AND TESTER APPARATUS Patent
D. C. Kinney, inventor (to Air Force) Issued 14 May 1985 5 p
Supersedes AD-D009945
(AD-D011770; US-Patent-4,517,517; US-Patent-Appl-SN-431434; US-Patent-Class-324-433) Avail: US Patent and Trademark Office CSCL 14/2

This provides a battery test apparatus for determining the state of quality of a nickel-cadmium battery. The battery test apparatus provides a battery discharge circuit that discharges the battery under test until a specified terminal voltage level is reached wherein the discharge cycle is automatically terminated. Since a visual indication is provided at the initiation of the discharge cycle and visual indication is provided at the end of the test cycle, the elapsed time for the discharge test is accurately measured. If the time required to discharge the battery to the predetermined level exceeds a certain value, such as 48 minutes the level exceeds a certain value, such as 48 minutes the quality of the battery is acceptable. The battery test apparatus also includes a reconditioning switch for recharging acceptable batteries to full charge capacity. GRA

N86-10643*# National Aeronautics and Space Administration. Lewis Research Center, Cleveland, Ohio.
PHOTOVOLTAIC SYSTEMS IN REMOTE LOCATIONS: AN EXPERIENCE SUMMARY Final Report
A. F. Ratajczak [1985] 19 p refs Presented at the Solar Appl. in Remote Locations Workshop, Las Cruces, N. Mex., 11-14 Mar. 1985
(Contract DE-AI01-79ET-20485)
(NASA-TM-87106; E-2703; DOE/NASA/20485-20; NAS 1.15:87106) Avail: NTIS HC A02/MF A01 CSCL 10A

Since 1979, the NASA Lewis Research Center has been responsible for the design, installation and operational support of 58 photovoltaic systems located in 27 countries. Together these systems contain 77.1 kW of photovoltaic modules and provide power for a variety of loads ranging from single low-power street light systems to a utility type power system for a village of over 150 people. Systems installation, reliability, operation, maintenance and repair experience is given and major problem areas are listed. Experience indicates that photovoltaic system technology is a proven technology, but that developing countries need to better posture themselves to acquire and utilize the technology. Recommendations are given. Author

N86-10644# Sandia Labs., Albuquerque, N. Mex.
CHARACTERIZATION OF CATHODIC CORROSION PRODUCTS IN THE Ca/CaCrO4 THERMAL BATTERY
R. A. Guidott, F. W. Reinhardt, E. L. Venturini, J. W. Rogers, Jr., and W. N. Cathey May 1985 35 p Prepared in cooperation with Nevada Univ., Reno
(Contract DE-AC04-76DP-00789)
(DE85-013442; SAND-84-1098) Avail: NTIS HC A03/MF A01

Using thermal analysis techniques, the corrosion process resulting from the reaction of iron, nickel, and stainless steel (used as current collectors in Ca/CaCrO4 thermal batteries) with CaCrO4 dissolved in LiCl-KCl eutectic was investigated. The reaction product for iron was synthesized in bulk external to the battery and was characterized by chemical analysis, X-ray diffraction, Moessbauer spectroscopy, X-ray photoelectron spectroscopy, static magnetization, and electrical conductivity. This characterization provides a better understanding of the cathodic corrosion processes that occur in the Ca/CaCrO4 thermal battery, and how the properties of the reaction layer at the catholyte-current collector interface influence battery performance. DOE

N86-10645# Midwest Research Inst., Golden, Colo. Solar Energy Research Inst.
IDENTIFICATION OF CHEMICAL AND PHYSICAL PHENOMENA AFFECTING THE DURABILITY OF SILVERED POLYMER (PMMA) MIRRORS
P. Schissel, H. H. Neidlinger, and A. W. Czanderna May 1985 42 p
(Contract DE-AC02-83CH-10093)
(DE85-012131; SERI/PR-255-2493) Avail: NTIS HC A03/MF A01

Mirrors are the device of choice in concentrating solar radiation for solar thermal applications. Efficiency requirements and economic factors dictate that the mirrors maintain high reflectance for many years. The mirrors must have such surface perfection that they can deliver all their reflected energy into an angle of 1 to 5 milliradians (mrad). Other design factors such as weight, flexibility, and cost make silvered polymer films highly desirable for solar thermal use. Factors that affect the durability and performance of silvered polymer films in outdoor exposure are reported. The results presented are based on laboratory analyses of various polymers silvered by various processes. The crucial role in degradation played by ultraviolet (UV) light is shown. The screens in the polymer improve weatherability and inconel uv blockers improve adhesive performance. Weather-Ohmeter studies comparing exposures with and without UV radiation show more rapid degradation due to UV. Fourier transform infrareds (FT-IR) show synergistic effects with UV, Chlorine, and silver. DOE

N86-10646# Conservation and Renewable Energy Inquiry and Referral Service, Silver Spring, Md.
GEOTHERMAL ENERGY TECHNOLOGY PROGRAM SUMMARY
May 1985 4 p
(Contract DE-AC01-83CE-30780)
(DE85-013101; DOE/CE-0111) Avail: NTIS HC A02/MF A01

The progress to date of the geothermal energy program of the US Department of Energy is briefly summarized. Federal/industry cooperation, program focus, and a budget are discussed. DOE

N86-10647# Oak Ridge National Lab., Tenn.
SIMPLIFIED ANALYSIS OF STIRLING ENGINES AND HEAT PUMPS
N. C. J. Chen, F. P. Griffin, and C. D. West 12 Dec. 1984 9 p
Presented at the DOE/ORNL Heat Pump Conf., Washington, D.C., 10 Dec. 1984
(Contract DE-AC05-84OR-21400)
(DE85-005366; CONF-841231-5) Avail: NTIS HC A02/MF A01

Because most of the parameters describing the instantaneous state of the working fluid in a Stirling engine (i.e., the pressure, mass and temperature of the gas in the various parts of the engine) are time dependent, the mass and energy conservation equations must be expressed as differential equations. Generally, the equations are nonlinear and can only be solved by numerical approximations. Such solutions are plagued by both instabilities and by numerical artifacts, although given sufficient computer time and programming effort, satisfactory results can usually be obtained. There is, however, a simpler approach that is not only much more economical but also more revealing. In the new method all of the relevant quantities are represented by linear combinations of sine and cosine terms. Because the differentials of harmonic functions are also harmonic functions (the sine and cosine are the only periodic functions for which this is true), when they are substituted into the differential equations, the equations become simple algebraic ones. DOE

N86-10648# Conservation and Renewable Energy Inquiry and Referral Service, Silver Spring, Md.
PASSIVE AND HYBRID SOLAR TECHNOLOGIES PROGRAM SUMMARY
May 1985 3 p
(Contract DE-AC01-83CE-30780)
(DE85-013100; DOE/CE-0109) Avail: NTIS HC A02/MF A01

The goal of the national energy policy is to foster an adequate supply of energy at reasonable prices. This policy recognizes that adequate supply requires flexibility, with no undue reliance on any single source of supply. The goal of reasonable prices suggests economic efficiency so that consumers, individuals, commercial and industrial users alike, are not penalized by government regulation or subside. The strategies for achieving this energy policy goal are: (1) to minimize federal regulation in energy pricing while maintaining public health and safety and environmental quality, and (2) to promote a balanced and mixed energy resource system through research and development. One of the keys to energy sufficiently is the scientific application of passive solar energy techniques. DOE

N86-10649# Brookhaven National Lab., Upton, N. Y.
IMPROVED BLUE RESPONSE AND EFFICIENCY OF A-SI:H SOLAR CELLS DEPOSITED FROM DISILANE USING A DUAL-CHAMBER PLASMA SYSTEM
G. Rajeswaran, P. E. Vanier, R. R. Corderman, and F. J. Kampas 1985 10 p Presented at the 18th IEEE Photovoltaic Spec. Conf., Las Vegas, Nev., 21 Oct. 1985
(Contract DE-AC02-76CH-00016)
(DE85-013289; BNL-36577; CONF-851043-1) Avail: NTIS HC A01/MF A01

Thin film amorphous silicon solar cells with glass/SnO2/p/i/n/A1 structures and 6 to 7% AM1 conversion efficiencies were fabricated at rapid deposition rates in a dual-chamber glow discharge deposition system. Parameters such as electrode spacing, Si2H6 partial pressure and flow rate were optimized to produce uniform deposition over large areas. Identical solar cells were deposited in either the single-chamber mode or the dual-chamber mode for comparison. Single-chamber mode cells perform poorly over the visible wavelengths and hence produce low short circuit currents. The dual-chamber mode cells show a significant improvement in blue response and a factor of two increase in short circuit current over the single-chamber mode cells. Under short circuit conditions, 15 mA sq cm was generated from rapidly deposited cells from disilane and 18 MA/sq cm was generated from rapidly deposited cells from disilane and 18 MA/sq cm from low deposition rate monosilane cells. DOE

N86-10650# Tennessee Univ., Knoxville.
GROUND-COUPLED HEAT PUMP RESEARCH AT THE UNIVERSITY OF TENNESSEE WASHINGTON, D.C., 10 DEC. 1984
W. S. Johnson, B. A. McGraw, R. N. Baugh, and W. A. Griffith 1984 10 p refs Presented at DOE/ORNL Heat Pump Conf.,
(Contract DE-AC05-84OR-21400)
(DE85-005357; CONF-841231-7) Avail: NTIS HC A02/MF A01

The seasonal performance of a horizontal-coil ground-coupled heat pump system in both the heating and cooling mode was evaluated to determine its potential for use in the Knoxville, TN area. The effects of the significant parameters on performance were determined with the required data to develop an optimized system. The ground-coupled heat pump system was installed in TECH House I. The following conclusions are presented: (1) the data indicate that the ground coil heat exchanger is undersized for summer operation, operation during the winter season was acceptable with an overall seasonal performance factor of 2.6 which is higher than a typical air-air heat pump; (2) an undersized ground coil in a ground-coupled heat pump system will produce a significant performance penalty; (3) backfilling with clay must be carefully done to avoid having air pockets in the ground due to the tendency of clay to agglomerate; (4) backfilling with sand around the ground coil produced improved performance of the system during the initial summer of operation; (5) during winter operation, no electric resistance backup heating is required;

(6) a ground-coupled heat pump in this area of the country must be sized based on the cooling peak which will normally result in an overdesign for the winter season, such as overdesign maybe, desirable because of reduced need for backup resistance heat. DOE

N86-10651# United Technologies Corp., South Windsor, Conn. Power Systems Div.
PHOSPHORIC AND ELECTRIC UTILITY FUEL TECHNOLOGY DEVELOPMENT Technical Progress Report, quarter ending Dec. 1984
R. D. Breault, T. A. Briggs, J. V. Congdon, R. L. Geltig, G. J. Goller, W. L. Luoma, M. W. McCloske, A. P. Mientek, J. J. OBrien, and S. A. Randall 1985 69 p refs
(Contract DE-AC21-83FE-60338)
(DE85-014741; FCR-6948P; TPR-20) Avail: NTIS HC A04/MF A01

Seventeen hundred hours and 11 thermal cycles were accumulated on the second 10 sq ft short stack at 120 psia and 405 F. A subscale cell out from 10 sq ft electrodes in the same batch used for the second 10 sq ft short stack accumulated over 4100 hours with performance conforming close to the E-line goal at 120 psia and 400 F. Over 14,870 hours and 42 thermal cycles were accumulated on the 3.7 sq ft, 30-cell short stack at 120 psia and 405 F. A subscale cell with GSB-18 catalyst completed over 10,000 hours of operation at 120 psia, 400 F. The full-size, 10 sq ft stack containment vessel and reactant gas manifolds were observed. The improved edge seal decreased leakage by more than 50% from the conventional edge seal. Cross-pressure tolerance also improved. Continuous automatic operation of the substrate forming machine was demonstrated by producing substrates at a 50% faster rate with high yields and low material loss. The cooler bonding cycle was significantly reduced by using a cold press in conjunction with the hot press. A lower cost stainless steel tubing is identified that could reduce cooler array cost by up to 50%. Assembly of the automated cell fill and assembly machine is initiated. DOE

N86-10652# United Technologies Corp., South Windsor, Conn. Power Systems Div.
PHOSPHORIC AND ELECTRIC UTILITY FUEL CELL TECHNOLOGY DEVELOPMENT Technical Progress Report, Jan. 1985
R. D. Breault, T. A. Briggs, J. V. Congdon, R. L. Gelting, G. J. Goller, W. L. Luoma, M. W. McCloskey, A. P. Mientek, J. J. OBrien, S. A. Randall et al Jan. 1985 35 p refs
(Contract DE-AC21-83FE-60338)
(DE85-014552; FCR-6956P; TPR-21) Avail: NTIS HC A03/MF A01

A subscale cell containing GSB-18, dry mix catalyst has accumulated over 6500 hours with performance 10 mV above E-line at 120 psia and 400 F. Over 150 thick separator plates were molded for use in cooler assemblies. The full-size 10-ft, 460 cell structural work-up is completed. All repeat components for the next 10-ft short stack are formed and processed. DOE

N86-10653# Oak Ridge National Lab., Tenn.
COMPARATIVE ANALYSIS OF SINGLE AND CONTINUOUSLY VARIABLE-CAPACITY HEAT PUMP CONCEPTS
C. K. Rice and S. K. Fischer 1984 9 p refs Presented at the DOE/ORNL Heat Pump Conf., Washington,D. C., 10 Dec. 1984
(Contract DE-AC05-84OR-21400)
(DE85-004089; CONF-841231-23) Avail: NTIS HC A02/MF A01

An initial assessment is given of the potential benefits of continuous-capacity-modulation in electric-driven, air to air heat pumps for residential application. The purpose was to provide a quantitative estimate of the possible annual performance gains of advanced continuously modulating heat pumps relative to single-speed designs at comparable levels of development. Seasonal (heating and cooling) and annual performance factor (APF) analysis capability was added to earlier design work to allow direct evaluation of annual energy use from heat pump performance data generated by the ORNL heat pump model. A modulating version of the heat pump model was developed to provide a means for simulating the steady state performance of continuously variable-speed (CVS) systems. With these tools, the APFs of both single and continuously variable-capacity (CVC) concepts could be studied as basic heat pump design variables were varied. DOE

N86-10654# Carrier Corp., Syracuse, N.Y.
ADVANCED ABSORPTION HEAT PUMP CYCLES
R. C. Reimann 1984 3 p ref Presented at the DOE/ORNL Heat Pump Conf., Washington, D.C., 10 Dec. 1984
(Contract DE-AC05-84OR-21400)
(DE85-003914; CONF-841231-20) Avail: NTIS HC A02/MF A01

The main goal is the development of significantly improved absorption machinery. This was to be directed specifically towards the development of a direct natural gas-fired absorption heat pump with both heating and cooling efficiencies advanced beyond current commercial offerings. These were to be accomplished through the use of novel and superior cycles, or by improved component performance. To keep the focus on machinery, the stipulation was agreed that candidate absorbent-refrigerant combinations were to be selected from among those whose properties were adequately known to permit cycle calculations and preliminary machine layouts. DOE

N86-10655# Purdue Univ., Lafayette, Ind. School of Electrical Engineering.
THEORY OF ADVANCED, HIGH-EFFICIENCE CONCENTRATOR CELLS Final Report
M. S. Lundstrom, R. J. Schwartz, C. M. Maziar, and P. D. DeMoulin 1985 195 p
(Contract DE-AC02-83CH-10093)
(DE85-008821; SERI/STR-211-2687) Avail: NTIS HC A09/MF A01

The goal of this project was to begin developing accurate, and ultimately predictive, device models for 3-V concentrator cells. The project consisted of extending a one-dimensional numerical device model previously developed at Purdue to 3-V solar cells. The accuracy of the code was verified by comparing computed and measured solar cell characteristics. Gallium arsenide was selected because it is the most mature 3-V technology and because GaAs solar cells have demonstrated high conversion efficiency. Materials models for GaAs solar cells were compiled, evaluated, and in some cases extended. These materials models were then implemented into the numerical device model. The device mode as also extended to analyze optical absorption and reflection from bare and anti-reflection (AR) coated cells. To test the GaAs cell model, its predictions were compared to measured results for an N(+)P cell (the shallow homojunction cell reported by Fan and co-workers) and a P(+)N cell (fabricated by Borrego and co-workers). In general, good agreement between theory and experiment was obtained for both concentrated and unconcentrated conditions. DOE

N86-10656# Bonneville Power Administration, Portland, Oreg. Solar Utilization Network.
PASSIVE SOLAR DESIGN HANDBOOK
M. S. Baker Apr. 1985 28 p
(DE85-014263; DOE/BP-2) Avail: NTIS HC A03/MF A01

A basic introduction to solar energy is provided in this manual. The most common passive solar heating designs are described very briefly. The designs presented fall under three passive heating classifications: direct gain, indirect gain, and isolated gain. Design considerations for buildings are included along with considerations for: thermal storage walls, thermal storage roofs, attached sunspaces, and convectiv loops. A glossary of solar energy related terms is included. DOE

N86-10657# Midwest Research Inst., Golden, Colo.
SOLAR THERMAL TECHNICAL INFORMATION GUIDE
May 1985 180 p
(Contract DE-AC02-83CH-10093)
(DE85-002941; SERI/SP-271-2511) Avail: NTIS HC A09/MF A01

This guide is designed to help investigators search for information in the solar thermal technology field. The information ranges from history and technology basics to the latest in research and develoment. It is written to help several audiences, including engineers and scientists who may be unfamiliar with a particular aspect of solar thermal energy, university researchers who are interested in the field, manufacturers needing to learn more about specific topics, and librarians who provide information to their clientele. The guide is divided into ten chapters, with Chapters 1 to 8 providing background on solar thermal energy development (including its history and current status) by topic. Within each topic, an overview is provided with references to relevant publications or information sources. Chapters 9 and 10 contain directories listing research centers and major technical information sources, respectively. DOE

N86-10658# Midwest Research Inst., Golden, Colo.
PHOTOVOLTAICS: REPORT, 1984 Annual Progress Report, 1984
Jun. 1985 39 p refs
(Contract DE-AC02-83CH-10093)
(DE85-014713; DOE/CE-0128) Avail: NTIS HC A03/MF A01

Progress on the research and development of photovoltaics in 1984 is summarized. Some of the achievements in materials, collector, and systems research are presented. The major materials research activity in 1984 was the single junction thin films research which received over 12 million dollars in funding. The Flat Plate Solar Array Project was yet another major recipient of research funding with just over seven million dollars. Other research achievements are briefly discussed and include: multijunction and innovative concepts, silicon materials, concentrator collectors, module reliability, and balance of system developments. DOE

N86-10659# Argonne National Lab., Ill.
ADVANCED FUEL CELL DEVELOPMENT Progress Report, Jul. - Sep. 1984
R. D. Pierce, N. Q. Minh, J. L. Smith, G. H. Kucera, F. C. Mrazek, J. R. Stapay, J. Moreschi, R. Herceq, R. B. Poeppel, and J. Routhort
Jun. 1985 31 p ref
(Contract W-31-109-eng-38)
(DE85-014550; ANL-85-7) Avail: NTIS HC A03/MF A01

Fuel cell research and development activities at Argonne National Laboratory (ANL) during the period July through September 1984 are discussed. These efforts were directed toward seeking alternative cathode materials to NiO for molten carbonate fuel cells. Particular emphasis was placed on studying the relationship of synthesis and sintering conditions on the resistivity of doped and undoped LiFeO2 and Li2MnO3 and on achieving a better understanding of the crystalline defect structures of phases that are thermodynamically stable at 1- and 10-atm pressure. To this end, several experimental assemblies (including synthesis, solubility, and sintering vessels and a high-pressure thermogravimetric analyzer) were constructed to permit 10-atm operation. Methods to improve the corrosion resistance of stainless steel components in ion-migration test cells are under assessment. A study to provide improved understanding of anode creep and densification occuring under fuel cell conditions is under way. DOE

N86-10660# Los Alamos Scientific Lab., N. Mex.
GENERAL-PURPOSE HEAT SOURCE DEVELOPMENT: SAFETY VERIFICATION TEST PROGRAM. BULLET/FRAGMENT TEST SERIES
T. G. George, R. E. Tate, and K. M. Axler May 1985 38 p
(Contract W-7405-eng-36)
(DE85-014262; LA-10364-MS) Avail: NTIS HC A03/MF A01

The radioisotope thermoelectric generator (RTG) that will provide power or space missions contains 18 General-Purpose Heat Source (GPHS) modules. Each module contains four (238) PuO2-fueled clads and generates 250 W sub (t). Because a launch-pad or post-launch explosion is always possible, the ability of GPHS fueled clads within a module to survive fragment impact needs to be determined. The bullet/fragment test series, part of the Safety Verification Test Plan, was designed to provide information on clad response to impact by a compact, high-energy, aluminum-alloy fragment and to eestablish a threshold value of fragment energy required to breach the iridium cladding. Test results show that a velocity of 555 m/s (1820 ft/s) with an 18-g bullet is at or near the threshold value of fragment velocity that will cause a clad breach. Results also show that an exothermic Ir/Al reaction occurs if aluminum and hot iridium are in contact, a contact that is possible and most damaging to the clad within a narrow velocity range. The observed reactions between the iridium and the aluminum were studied in the laboratory and are reported. DOE

N86-10661# Oak Ridge National Lab., Tenn.
STIRLING-ENGINE-DRIVEN HEAT PUMP PROGRAM OVERVIEW
F. C. Chen 1984 5 p Presented at the DOE/ORNL Heat Pump Conf., Washington, D.C., 10 Dec. 1984
(Contract DE-AC05-84OR-21400)
(DE85-004796; CONF-841231-10) Avail: NTIS HC A02/MF A01

A brief summary is given of the Stirling-engine-driven heat pump project being carried out by Oak Ridge National Laboratory (ORNL) for the Department of Energy. The Objective and approach, early development effort, current status and accomplishments, and future technology options are discussed. DOE

N86-10662# Midwest Research Inst., Golden, Colo. Solar Energy Research Inst.
SOME ASPECTS OF LONG-RANGE, HIGH-RISK PHOTOVOLTAIC RESEARCH AT SERI
S. K. Deb Jul. 1985 13 p Presented at the SPIE Tech. Symp. East '85, Arlington, Va., 8 Apr. 1985
(Contract DE-AC02-83CH-100983)
(DE85-012144; SERI/TP-212-2749; CONF-8504109-2) Avail: NTIS HC A02/MF A01

The work described includes some aspects of the long-range, high-risk research being conducted at the Solid State Photovoltaic Research Branch at SERI. The areas covered include: amorphous silicon, high efficiency, multijunction solar cells, CdS/CuInSe2 thin films, crystal growth research and solid state theory. In each of these areas specific research projects which have long-range implications are highlighted. DOE

N86-10663# Los Alamos Scientific Lab., N. Mex.
RECENT DEVELOPMENT IN THE HOT DRY ROCK GEOTHERMAL ENERGY PROGRAM
P. R. Franke and G. J. Nunz 1985 5 p Presented at the Intern. Symp. on Geothermal Theory, Kailua Kona, Hawaii, 26 Aug. 1985
(Contract W-7405-eng-36)
(DE85-009562; LA-UR-85-934; CONF-850801-24) Avail: NTIS HC A02/MF A01

The hot dry rock programs effort has focused on the extraction technology development effort. The pair of approximately 400 m wells for the phase 2 engineering system of the Fenton Hill Project were completed. Hydraulic fracture operations were carried out to develop the geothermal reservoir. Advances were made in fracture identification techniques and instrumentation. To develop a satisfactory interwellbore flow connection the next step is to redrill the lower section of one of the wells into the fractured region. Chemically reactive tracer techniques are developed to determine the effective size of the reservoir area. Hot dry rock resource are estimated based upon geothermal gradiant data. DOE

N86-10664# Phillips Engineering Co., St. Joseph, Mich.
ANALYSIS OF ADVANCED RESIDENTIAL ABSORPTION HEAT PUMP CYCLES
B. A. Phillips 1985 22 p Presented at the DOE/ORNL Heat Pump Conf., Washington, D.C., 10 Dec. 1984
(Contract DE-AC05-84OR-21400)
(DE85-005244; CONF-841231-17) Avail: NTIS HC A02/MF A01

The development and proof testing of advanced absorption refrigeration cycle concepts is reported. The purpose is to develop a gas fired absorption heat pump for residential and small commercial applications that will produce a coefficient of performance of at least 1.6 Btu heating and .7 Btu of cooling per Btu of gas input. The goals refer to air-to-air heat pump operation at the rating conditions of 47 F outdoor ambient in heating mode and 95 F ambient in cooling mode. For year-round residential and small commerical use other requirements were added. One was that the heat pump itself will provide all the heating and cooling required by the building over the majority of temperatures experienced in the United States (from -10 F to 110 F) without resource to supplemental heat. The means of making major improvements in gas fired absorption systems include the following categories: higher efficiency cycles, better fluids, and higher flues efficiencies. High efficiency absorption cycles were evaluated and the cycle and working fluid combination preferred for development of an advanced absorption test unit of residential size is selected. DOE

N86-10665# Sandia Labs., Albuquerque, N. Mex.
PHOTOVOLTAIC CONCENTRATOR ARRAY EVALUATION
A. B. Maish 1985 5 p Presented at INTERSOL '85 Solar Energy: The Diverse Solution, Montreal, 23 Jun. 1985
(DE85-013789; SAND-84-1775C; CONF-850604-6) Avail: NTIS HC A02/MF A01

Photovoltaic (PV) concentrator arrays are tested at the Sandia PV test facility in order to characterize the performance of the array subsystems during baseline tests and to evaluate array performance during extended operation. Array testing is designed to evaluate the complete array system (modules, structure, drives, and tracking controls) following module development and qualification testing and preceding full field tests. The major baseline tests characterize array electrical and thermal efficiency, sensitivity to tracking errors, full day tracking accuracy and array power requirements. DOE

N86-10666# Pacific Northwest Lab., Richland, Wash.
OVERVIEW OF WIND TURBINE SITING RESEARCH: PROSPECTING TO MICROSITING
L. L. Wendell May 1985 9 p Presented at the Delphi Workshop of Wind Energy Appl., Delphi, Greece, 20 May 1985
(Contract DE-AC06-76RL-01830)
(DE85-013496; PNL-SA-13032; CONF-8505171-1) Avail: NTIS HC A02/MF A01

The Federal Wind Energy Program of the United States' Department of Energy has directed research in wind behavior relevant to the economic extraction of power from the wind. The variability of the wind in time and space is important in this process. Topics of research related to wind turbine siting have included resource assessment, siting techniques, and techniques for documenting the variability of wind over space and time and the impact of this variability on energy capture. Siting techniques were developed to select areas most promising for wind energy development. The evaluation of candidate sites within these areas included a period of direct wind measurement so that long-term and hourly or subhourly time variability of the wind could be analyzed. In the study of spatial wind variability, turbine placement strategy has sought to minimize adverse effects of terrain or upwind machine wakes. Modeling techniques were developed to examine the variability of the wind over time and space and to correlate wind variability with turbine power output. Developments in terrain digitization and visual depiction and refined numerical flow modeling show promise of becoming operational tools that can be used in arrangement of turbines in clusters for maximum energy capture in complex terrain. DOE

N86-10667# Argonne National Lab., Ill.
CHEMICAL/HYDROGEN ENERGY SYSTEMS Annual Report, 1 Jan. - 31 Dec. 1984
May 1985 126 p
(Contract DE-AC02-76CH-00016)
(DE85-012742; BNL-51865) Avail: NTIS HC A07/MF A01

Activities conducted in 1984 within the Chemical/Hydrogen Energy Systems Program are described. Progress made is summarized for work in electrolytic hydrogen production, hydrogen storage materials, and transport systems. During 1984 the development of a technology base for hydrogen which would be used for coupling the abundant/renewable energy resources to the demand sector uses in the far term is emphasized. Hydrogen generation via water vapor electrolysis, three novel hydrogen storage concepts, hydrogen embrittlement of pipeline steels, and operational testing of advanced hydrogen systems in the hydrogen technology evaluation center (HTEC) are reported. Related International Energy Agency cooperative efforts and plans and major activities scheduled for 1985 are summarized. DOE

N86-10668# Chronar Corp., Princeton, N.J.
PHOTOVOLTAIC DEVICES USING A Si:H FROM HIGHER ORDER SILANES Final Subcontract Report, 1 Sep. 1983 - 31 Aug. 1984
A. E. Delahoy Mar. 1985 59 p
(Contract DE-AC02-83CH-10093)
(DE85-008804; SERI/STR-211-2637) Avail: NTIS HC A04/MF A01

The preparation of hydrogenated amorphous silicon (a-Si:H) films and photovoltaic devices by chemical vapor deposition (CVD) from higher silanes, and the properties of such films and devices are described. The motivation for this research is the prospect of preparing by a new technique a-Si:H having electronic properties similar to material prepared by the well-known glow discharge technique. Possible advantages of thermal CVD are the absence of ion bombardment, high deposition rates, efficient utilization of feedstock gases, lower levels of impurity incorporation, absence of pinholes, and greater material stability. Photochemical vapor deposition of a-Si:H from disilane is described and yield higher efficiency solar cells than thermal CVD. DOE

N86-10669# Centronic Ltd., Croydon (England).
MAKING THE RIGHT CHOICE
J. O. Miller 1985 5 p
Avail: NTIS HC A02/MF A01

Performance and cost criteria for choosing silicon photodiodes are given. Spectral response, response time, minimum detectable power, diode configuration, temperature effects, and operating circuits are discussed. Author (ESA)

N86-10670# Fachhochschule, Giessen (West Germany). Labor fuer Elektrische Messtechnik.
CONTRIBUTION OF WIND ENERGY TO THE ENERGY BALANCE OF A COMBINED SOLAR AND WIND ENERGY SYSTEM. PART 1: SYSTEM DESCRIPTION, DATA ACQUISITION AND SYSTEM PERFORMANCE Final Report, Jun. 1984
Rainer Ferger and Uwe Machens Bonn Bundesministerium fuer Forschung und Technologie May 1985 95 p refs In GERMAN; ENGLISH summary Sponsored by Bundesministerium fuer Forschung und Technologie 2 Vol.
(BMFT-FB-T-85-051-Vol-1; ISSN-0340-7608) Avail: NTIS HC A05/MF A01; Fachinformationszentrum, Karlsruhe, West Germany DM 20

A one-family house was equipped with a combined solar and wind energy system plus a night storage heater to measure the seasonal complementary contribution of wind and solar energy to energy demand. Project implementation, problems encountered and modifications to the initial system are described. Meteorological and operational data and house consumption data were recorded on computer-based measuring system. Data on the combined effects of and interdependence between solar collector and wind energy converter are discussed. Author (ESA)

N86-10671# Kernforschungsanlage, Juelich (West Germany). Programmgruppe.
CONTRIBUTION OF WIND ENERGY TO THE ENERGY BALANCE OF A COMBINED SOLAR AND WIND ENERGY SYSTEM. PART 2: COMPUTER-ASSISTED INVESTIGATIONS Final Report, Jun. 1984
Peter Wilhelm Wensierski Bonn Bundesministerium fuer Forschung und Technologie May 1985 141 p refs In GERMAN; ENGLISH summary Sponsored by Bundesministerium fuer Forschung und Technologie 2 Vol.
(BMFT-FB-T-85-052-Vol-2; ISSN-0340-7608) Avail: NTIS

HC A07/MF A01; Fachinformationszentrum, Karlsruhe, West Germany DM 29.50

A mathematical simulation model of the combined solar and wind energy system was used to determine the weak points of a wind-solar energy domestic system and to analyze the thermodynamic behavior of its different components and regulation functions. The simulation results are compared with the measured data to collect data for the optimization of the system for economical use and for determining the optimal complementarity of both energy sources. Different system configurations are studied for a better supply utilization according to regional climatology. Recommendations to improve the system performance are given taking into account an unchanged and a modified system configuration and the selection of the wind energy system. Author (ESA)

N86-10672# Groningen Rijksuniversiteit (Netherlands). Vrije Studierichting Scheikunde.
WIND ENERGY IN AGRICULTURE, A PROMISE [WINDENERGIE IN DE LANDBROUW, EEN BELOFTE]
Johan Koops Aug. 1982 43 p refs In DUTCH
(SS-45; B8476135) Avail: NTIS HC A03/MF A01

The investment possibilities of windpowered generators on dairy-farms in the northern Netherlands are investigated. Data concerning the energy consumption of five farms are statistically correlated with wind velocity distributions and the characteristics of a 10 kWh windmill. Using the buying and selling energy prices of the local power stations and the investment costs, the feasibility is estimated. The attitude of 105 farmers is assessed. Unless special energy storage provisions are made, the investment will not pay within 10 years, so is not interesting enough. Author (ESA)

N86-10673# Groningen Rijksuniversiteit (Netherlands). Vrije-Studierichting Scheikunde.
WIND ENERGY, A FEASIBILITY INVESTIGATION FOR WIND MILLS IN AGRICULTURE [WINDENERGIE EEN HAALBAARHEIDSONDERZOEK NAAR WINDMOLLENS IN DE LANDBOUW]
Johan Koops Jan. 1982 33 p refs In DUTCH
(SS-45A; B8475856) Avail: NTIS HC A03/MF A01

The investment possibilities of windpowered generators on dairy-farms in the northern Netherlands are investigated. Data concerning the energy consumption of four farms are statistically correlated with wind velocity distribution data and the characteristics of a 10 kWh windmill. Using the buying and selling energy prices of the local power stations and the investment costs, the feasibility is estimated. Unless special energy storage provisions are made, the investment will not pay within 10 years. Author (ESA)

45 ENVIRONMENT POLLUTION

Includes air, noise, thermal and water pollution; environment monitoring; and contamination control.

N86-10674 Department of the Air Force, Washington, D.C.
MULTIPLE SITE LASER EXCITED POLLUTION MONITORING SYSTEM Patent
J. A. Gelbwachs, inventor (to Air Force) Issued 14 May 1985 6 p Supersedes AD-D009407
(AD-D011769; US-Patent-4,516,858; US-Patent-Appl-SN-347391; US-Patent-Class-356-437) Avail: US Patent and Trademark Office CSCL 13/2

A multiple site laser excited pollution monitoring system having a single laser located at a central location capable of providing a laser output beam, deflected in timed sequence, in a plurality of distinct different directions. Transmitting means, preferably in the form of a plurality of optical fibers, transmit the laser output beam in timed sequence to a plurality of remotely located laser excited pollution detectors (photoacoustic detector heads). Signals from the pollution detectors are transmitted to a signal processor and display unit also located at the central location. As a consequence thereof, a single laser can provide power for a plurality of laser excited detectors at a multiplicity of remote sites and thereby greatly reduce the expense involved in detecting the presence of pollutants at each of the plurality remote locations. Author (GRA)

N86-10675# California Univ., Irvine, Dayton, Ohio.
EVALUATION OF THE 90-DAY INHALATION TOXICITY OF PETROLEUM AND OIL SHALE JP-5 JET FUEL Technical Report, Jul. 1977 - Jul. 1983
C. L. Gaworski, J. D. MacEwen, E. H. Vernot, C. C. Haun, and H. F. Leahy Wright-Patterson AFB, Ohio AFAMRL Apr. 1985 40 p Prepared in cooperation with Naval Medical Research Inst.
(Contract F33615-80-C-0512)
(AD-A156815; AFAMRL-TR-85-035) Avail: NTIS HC A03/MF A01 CSCL 06/20

Subchronic 90-day inhalation studies were conducted to compare the toxicity of Petroleum and Oil Shale derived JP-5 jet fuel. Beagle dogs, Fischer 344 rats, and C57BL/6 mice were continuously exposed to JP-5 at concentrations of 150 mg/m cum and 750 mg/cum 3. Unexposed control groups were also maintained. All dogs and a portion of each rodent group were sacrificed and examined at exposure termination. Remaining rodents were held for observation up to 21 months postexposure. The most significant exposure related effect occurred in male rats, where JP-5 produced nephropathy characterized by hyaline droplets, necrosis, and intratubular casts. Accentuated tubular degeneration and medullary mineralization were noted in exposed rats held for long-term postexposure observation. Female rats were free of significant JP-5 related renal damage. Consistent with the pathologic changes in male rats exposed to 750 mg/cu m 3 were increased kidney weight and increased serum creatinine and BUN levels. Reduced body weight gains also occurred in male rats exposed to JP-5. No pathologic lesions were observed in dogs exposed to JP-5. Hepatocellular vacuolization and fatty change occurred in mice exposed to JP-5 from either source and in rats exposed to Shale JP-5. The results of this study suggest that there are no substantial differences between Petroleum and Shale JP-5. GRA

N86-10676# Argonne National Lab., Ill. Energy and Environmental Systems Div.
DEVELOPMENT OF THE MULTI-ATTRIBUTE HAZARD ASSESSMENT SYSTEM (MAHAS) AND ITS APPLICATION TO ENERGY-RELATED WASTE STREAMS
Donald J. Fingleton, Loren J. Habegger, Shen-Yann Chiu, Susan G. Barisas, and Ray H. Petersen (Illinois Inst. of Tech., Chicago) Apr. 1985 12 p refs Presented at the Air Pollution Control Assoc. Ann. Meeting and Exhibition, Detroit, 16 Jun. 1985
(Contract W-31-109-eng-38)
(DE85-010278; CONF-850612-2) Avail: NTIS HC A02/MF A01

The Multi-Attribute Hazard Assessment System (MAHAS), which determines the relative health risk associated with various waste streams, is described. The degree of hazard for several waste streams is presented. DOE

N86-10677# Oak Ridge National Lab., Tenn.
EXAMPLES OF REGIONAL ENVIRONMENTAL ASSESSMENT USING ACID DEPOSITION DATA
R. J. Olson, R. S. Turner, and L. J. Allison 1985 27 p refs Presented at the Natl. Conf. on Hazardous Wastes and Environ. Emergencies, Cincinnati, 14 May 1985
(Contract DE-AC05-84OR-21400)
(DE85-012903; CONF-8505149-1) Avail: NTIS HC A03/MF A01

Integrated assessments of acid deposition impacts require data on pollutant emissions, pollutant deposition, air quality, aquatic resources, crops, forests, and manmade materials. These data must have common spatial and temporal attributes that can be readily accessed for statistical analysis, modeling, and display purposes. The Acid Deposition Assessment Staff of Task Group I established the Acid Deposition Data Network (ADDNET) at Oak Ridge National Laboratory to provide accurate and reliable data to conduct assessment and policy analysis for the National Acid Precipitation Assessment Program (NAPAP). Two applications of the ADDNET Data Base to assessment activities are described: estimation of the extent of sensitive lakes at risk to high atmospheric deposition and the mapping of regional soil properties according to hypothesized sensitivity criteria. Both examples cover New York and the New England states and show the integration of data from diverse sources for analyses. DOE

N86-10678# Oak Ridge National Lab., Tenn.
NATIONAL PERSPECTIVE ON ENVIRONMENTAL CONSTRAINTS TO HYDROELECTRIC DEVELOPMENT
S. G. Hildebrand, M. J. Sale, G. F. Cada, and J. M. Loar 1985 12 p Presented at the Natl. Conf. on Perspectives on Nonpoint Source Pollution, Kansas City, Mo., 19 May 1985
(Contract DE-AC05-84OR-21400)
(DE85-013111; CONF-8505148-1) Avail: NTIS HC A02/MF A01

Two issues are analyzed relative to problems associated with the concentration of dissolved oxygen in tailwaters below dams and instream flow requirements for fisheries. The need for and technical challenges related to assessment of the environmental effects of multiple-project development in river basins are discussed. Although the focus of the DOE program is on small-scale hydroelectric development, the issues discussed here are applicable to large-scale facilities as well. DOE

N86-10679# Oak Ridge National Lab., Tenn.
DEVELOPMENT AND EVALUATION OF MULTISPECIES TEST PROTOCOLS FOR ASSESSING CHEMICAL TOXICITY
C. T. Garten, Jr., ed., G. W. Suter, Jr., ed., and B. G. Blaylock, ed. Jun. 1985 158 p refs
(Contract DE-AC05-84OR-21400)
(DE85-013526; ORNL/TM-9225; Environ-Sci-Div-2354) Avail: NTIS HC A08/MF A01

Toxicity testing is a tool to assist in evaluating the hazards of chemicals to individual biological species. Multispecies toxicity tests are well developed. Three test systems were examined: the legume-Rhizobium symbiosis for N-fixation, soil microbial populations, and algal multispecies interactions. Test protocols were developed and tested using several different chemicals. Test protocols for the legume-Rhizobium and soil microorganisms systems were developed and are presented. DOE

N86-10680# Tennessee Valley Authority, Knoxville. Office of Natural Resources and Economic Development.
SEDIMENT CHARACTERIZATION. TASK 2: INSTREAM CONTAMINANT STUDY. VOLUME 2: APPENDICES
Apr. 1985 453 p
(Contract DE-AI05-84CR-21444)
(DE85-013503; DOE/OR-21444/T2-Vol-2) Avail: NTIS HC A20/MF A01

Data are appended for mercury concentration and particle size, and for Cesium 137 radionuclide concentrations. Quality control and sampling procedures are detailed. DOE

N86-10681# Department of Energy, Pittsburgh, Pa. Energy Technology Center.
MICROCOMPUTER AIDED CALCULATIONS OF PARAMETERS FOR SPRAY DRYER OPERATION
J. T. Yeh, D. F. Gyorke, H. W. Pennline, and C. J. Drummond 1985 31 p Presented at the Air Pollution Control Assoc. Ann. Meeting and Exhibition, Detroit, 16 Jun. 1985
(DE85-013468; CONF-850612-4) Avail: NTIS HC A03/MF A01

This paper provides a series of practical microcomputer programs that can be used as a tool by engineers and researchers working with spray dryers for combustion process effluent control. The microcomputer programs calculate flue gas composition (CO2, N2, O2, H2O, and SO2) from the composition of the fuel. The residence time of the flue gas in a spray dryer can be estimated, and using values provided by the user for the flow of water and absorbent slurry in the spray dryer, the program recalculates the flue gas composition and heat capacity at the exit of the spray dryer without accounting for any SO2 removal that could occur in the spray dryer. From these values and the system pressure, the dew point and flue gas temperature at the spray dryer exit are calculated, providing the approach to saturation resulting from this choice of operating parameters. This computer code would enable a process engineer to quickly evaluate effects of important process parameters, such as flue gas temperature at the inlet to the spray dryer, atomizer water feed rate, and absorbent slurry concentration and feed rate, on the operation of a spray dryer. DOE

N86-10682# Membrane Technology and Research, Inc., Menlo Park, Calif.
MEMBRANE RESEARCH IN ENERGY AND SOLVENT RECOVERY FROM INDUSTRIAL EFFLUENT STREAMS Annual Report, 5 Nov. 1983 - 31 Jan. 1985
R. W. Baker 1985 46 p
(Contract DE-AC07-83ID-12379)
(DE85-014583; DOE/ID-12379/T2) Avail: NTIS HC A03/MF A01

The overall feasibility of using membranes to separate organic vapors from effluent air streams was demonstrated. High-performance, ultrathin composite membranes were prepared and incorporated into small spiral wound membrane modules. The modules were evaluated on a series of organic solvent-air mixtures. Typical solvent fluxes with silicone rubber membranes were 2 to 10 litres sq. m day. An economic analysis of the process based on these fluxes and using reasonable values for the costs of the membrane modules and pump and system components shows that a process using these membranes would be economical with a number of effluent air streams. Process payback times vary from 4 to 10 months. Particularly suitable feed streams are those containing 0.5 to 2% of high value solvents that can be reused in the plant producing the stream. DOE

N86-10683# Tennessee Valley Authority, Knoxville. Office of Natural Resources and Economic Development.
SEDIMENT CHARACTERIZATION. TASK 2: INSTREAM CONTAMINANT STUDY, VOLUME 1
Apr. 1985 87 p refs
(DE85-013502; DOE/OR-21444/T2-Vol-1) Avail: NTIS HC A05/MF A01

The instream contaminant study is presented. The results of laboratory analyses of sediment samples collected downstream of the DOE facilities are analyzed. The samples were collected from June through November 1984. The sediment data and the procedures for the collecting, handling, and analyzing the samples are reported. Results are summarized in graphs and tables that include available criteria, standards, and background levels. The procedures and data are discussed but not evaluated. DOE

N86-10684# Pacific Northwest Lab., Richland, Wash.
RADIONUCLIDE COMPLEXATION IN XYLEM EXUDATES OF PLANTS
D. A. Cataldo, D. M. McFadden, T. R. Garland, and R. R. Wildung Apr. 1985 14 p refs Presented at the Seminar on the Speciation of Fission Prod. in the Environ., Oxford, England, 16 Apr. 1985
(Contract DE-AC06-76RL-01830)
(DE85-013446; PNL-SA-12549; CONF-850473-3) Avail: NTIS HC A02/MF A01

The plant xylem is the primary avenue for transport of nutrient and pollutant elements from the roots of aerial portions of the plant. It is proposed that the transport of reactive or hydrolyzable ions is facilitated by the formation of stable/soluble complexes with organic metabolites. The xylem exudates of soybean were characterized as to their inorganic and organic components, complexation patterns for radionuclides, both in vivo and in vitro, and for class fractions of exudates using thin-layer electrophoresis. The radionuclides Pu-238 and Fe-59 were found primarily as organic acid complexes, while Ni-63 and Cd-109 were associated primarily with components of the amono acid fraction. Technetium-99 was found to be uncomplexed and transported as the pertechnetate ion. It was not possible to duplicate fully complexes formed in vivo by back reaction with whole exudates or class fractions, indicating the possible importance of plant induction processes, reaction kinetics and/or the formation of mixed ligand complexes. DOE

N86-10685# Deutsche Forschungs- und Versuchsanstalt fuer Luft- und Raumfahrt, Oberpfaffenhofen (West Germany). Inst. fuer Physik der Atmosphaere.
AIRBORNE MEASUREMENTS OF THE BORDER-CROSSING AIR POLLUTION IN THE AREA BETWEEN WEIDEN AND HOF/BAVARIA
Dieter Paffrath Feb. 1985 79 p refs In GERMAN; ENGLISH summary
(DFVLR-FB-85-25; ISSN-0171-1342) Avail: NTIS
HC A05/MF A01; DFVLR, Cologne DM 19.50

An airborne measuring system was used under various weather conditions to determine the air pollution in an area of the German-Czechoslovakian frontier where pollution is particularly high due to exhaust gases produced by Czechoslovakian sources. Mass fluxes of SO2, NOx and NO were determined by airborne measurements of horizontal and vertical distributions of concentrations, and by wind profile measurements. The results show that the mass fluxes vary to a large extent depending on the fluctuating emission rate, on the weather situation, and on the season of the year. Author (ESA)

N86-10686# Radian Corp., Morrisville, N.C.
PROCEEDINGS: FIRST ANNUAL ACID DEPOSITION EMISSIONS INVENTORY SYMPOSIUM Report, Sep. 1984 - Apr. 1985
James B. Homolya, comp. May 1985 147 p refs Symp. held at Raleigh, N. Car., 3-4 Dec. 1984
(Contract EPA-68-02-3994)
(PB85-200004; EPA-600/9-85-015) Avail: NTIS
HC A07/MF A01 CSCL 13B

The proceedings document a 2-day symposium on the progress in implementing the National Acid Precipitation Assessement Program (NAPAP) Task Group B's emission inventory programs. Topics included the development of emission factors for a wide range of pollutant emissions and the use of detailed emission inventories for atmospheric transport, transformation, and deposition modeling. The meeting:(1) provided detailed presentation and information transfer of the NAPAP emission inventory program; (2) illustrated and strengthened the relationship between the emission inventory data base and its users; and (3) compared and contrasted the NAPAP emission inventory with other on-going emission inventory development programs. GRA

N86-10687# Environmental Protection Agency, Research Triangle Park, N.C. Environmental Monitoring Systems Lab.
VOLATILE ORGANIC COMPOUNDS IN INDOOR AIR: A SURVEY OF VARIOUS STRUCTURES
J. D. Pleil, K. Oliver, and W. A. McClenny 1985 15 p refs Prepared in cooperation with Northrop Services, Inc.
(PB85-198356; EPA-600/D-85-100) Avail: NTIS
HC A02/MF A01 CSCL 07D

Co-workers collected indoor air samples in their homes in SUMMA polished canisters. The whole air samples were analyzed for volatile organic compounds (VOCs) using cryogenic sample preconcentration and subsequent capillary column chromatography. Simultaneous flame ionization and electron capture detection yielded quantitative concentration data in a range 0.1 to 10 ppbv for 19 calibration compounds, vinyl chloride, vinylidene chloride. Freon 113, chloroform, 1,2-dichloroethane, methyl chloroform, benzene, carbon tetrachlonide, trichloroethylene, cis-1,3-dichloropropene, trans-1,3-dichloropropene, toluene, 1,2-dibromoethane, tetrachloroethylene, chlorobenzene, b-xylene, benzyl chloride and hexachlorobutadiene. These data are presented in three sample groups: summer indoor samples, winter indoor samples, and combined summer and winter outdoor samples. GRA

N86-10688# Engineering-Science, Inc., Fairfax, Va.
EMISSIONS OF NOx, SOx AND VOC FROM ANTROPOGENIC SOURCES
D. A. Toothman and J. D. Mobley 1985 9 p refs
(Contract EPA-68-02-3996)
(PB85-193530; EPA-600/D-85-106) Avail: NTIS
HC A02/MF A01 CSCL 05B

A 1980 emisssions inventory for use in the National Acid Precipitation Assessment Program (NAPAP) is discussed. The current inventory contains point source data for 50,200 plants with more than 201,000 emission points and area source data for the 3,069 counties in the 48 contiguous States and the District of Columbia. Emissions of SO2, NOx, VOC, sulfates, ammonia, CO, and particulates are included in the inventory, but the paper focuses on SO2, NOx, and VOC which are of primary interest for acid deposition research. NAPAP Version 4.0 emissions of SO2, NOx, and VOC are 27.1, 23.7 and 23.3 million tons per year, respectively. The NAPAP report represents the best detailed inventory of emissions on a national scale that has been developed to date. Nevertheless, additional improvements are planned, focusing on major point sources. GRA

N86-10689# Battelle Columbus Labs., Ohio.
EVALUATION OF PASSIVE SAMPLING DEVICES (PSDS)
R. W. Coutant Apr. 1985 74 p refs
(Contract EPA-68-02-3487)
(PB85-196418; EPA-600/4-85-034) Avail: NTIS
HC A04/MF A01 CSCL 14B

This study is to evaluate the performance of the EPA passive sampling device (PSD) for ambient level volatile organic compounds (VOC's); to develop an understanding of the mechanics of passive sampling using reversible adsorption; and to apply this understanding to development of an improved PSO that is usable for sampling of VOC's over periods of 8 to 24 hours. Laboratory and limited field evaluations of the standard and modified RSD's were conducted and a model relating sorbent properties and device design to samplining rates was developed. The results show the standard PSD's to be useful for sampling of VOC's having large retention volumes. Modified PSD's having greatly reduced sampling rates show promise for sampling compounds having retention volumes as low as 5 to 10 L/g over 8 to 24 hour sampling periods. GRA

46 GEOPHYSICS

Includes aeronomy; upper and lower atmosphere studies; ionospheric and magnetospheric physics; and geomagnetism.

For space radiation see *93 Space Radiation.*

N86-10690 North Carolina Univ., Chapel Hill.
CRETACEOUS AND CENOZOIC STRATIGRAPHY OF THE UPPER AND MIDDLE COASTAL PLAIN, HARNETT COUNTY AREA, NORTH CAROLINA Ph.D. Thesis
Suellen Cabe 1984 121 p
Avail: Univ. Microfilms Order No. DA8508571

Criteria for differenting and correlating Cretaceous sediments and younger surficial deposits were determined. The results indicate that each of the units can be distinguished by a particular set of grain size and clay mineral characteristics. The Cretaceous units in the study area are the Cape Fear and Middendorf Formations. The Cape Fear Formation is characterized by smectite in the < 0.002 mm fraction and by finer sand size and higher percentages of silt and clay than the Middendorf Formation, which contains no smectite and is dominated by kaolinite in the clay fraction. Dissert. Abstr.

N86-10691 Iowa Univ., Iowa City.
STRATIGRAPHY, PETROLOGY, DEPOSITIONAL AND POST-DEPOSITIONAL HISTORIES AND THEIR EFFECTS UPON RESERVOIR PROPERTIES OF THE PARKMAN FORMATION OF THE MESA VERDE GROUP, POWDER RIVER BASIN, WYOMING Ph.D. Thesis
Ahmet Umran Dogan 1984 282 p
Avail: Univ. Microfilms Order No. DA8507934

The depositional system within which deposition of the Upper Cretaceous Parkman Formation (= Parkman Sandstone Member of the Mesaverde Formation) in the Wyoming portion of the Powder River Basin took place, was delineated using a combination of data from outcrops, subsurface cores, and geophysical well logs. The post-depositional history of these rocks was determined, semi-quantitative compositional analyses of authigenic components were made, and paragenetic sequences were established with the aid of scanning electron microscope and transmission electron microscope both equipped with energy dispersive X-ray microanalyzer. Dissert. Abstr.

N86-10692 California Univ., Santa Barbara.

PALEONTOLOGY AND STRATIGRAPHY OF LOWER CAMBRIAN AND UPPER PROTEROZOIC SEDIMENTS, CABORCA REGION, NORTHWESTERN SONORA, MEXICO Ph.D. Thesis

Mark Allan Schulte McMenamin 1984 229 p

Avail: Univ. Microfilms Order No. DA8509445

Shelly fossils from a homoclinal sequence of sediments spanning the Precambrian-Cambrian transition in the Caborca region of northwestern Sonora, Mexico, are among the oldest in North America. These fossils, together with new finds of Lower Cambrian trilobites and trace fossils, permit correlations between the Caborca sequence and Lower Cambrian sediments of Nevada and eastern California (USA). The Lower Cambrian Nevadella and Fallotaspis zones of Fritz (1972) can now be recognized in the La Cienega and Puerto Blanco Formations of the Caborca sequence. Because of the abundant fossils, the stratigraphic interval between the top of the Nevadella zone and the lowest shelly fossils can be subdivided into six new assemblages (in ascending stratigraphic order): the (1) Sinotubulites, (2) Monomorphichnus multilineatus, (3) Fallotaspis cf. F. tazemmourtensis, (4) Fallotaspis-Judomia, (5) Nevadia, and (6) Nevadella assemblages. Dissert. Abstr.

N86-10693 Pittsburgh Univ., Pa.

DYNAMIC LITHOSTRATIGRAPHY AND PALEECOLOGY OF UPPER MISSISSIPPI (CHESTERIAN) STRATA OF THE NORTH-CENTRAL APPALACHIAN BASIN Ph.D. Thesis

David Kevin Brezinski 1984 132 p

Avail: Univ. Microfilms Order No. DA8504406

Chesterian strata of the northcentral Appalachians consist of intertonguing marine carbonates and paralic to terrestrial clastics. The basal unit, the Loyalhanna, rests unconformably upon lower Mississippian Pocono sandstones and accumulated under conditions of episodic sea level transgression. The Loyalhanna, in most places is a festoon cross-bedded, sandy lime grainstone, but a nearshore interbedded carbonate-shale facies is also recognized. Minor oscillations in sea level resulted in a vertical repetition of marine and nonmarine rocks after which a major episodic marine transgression began which resulted in the deposition of the Wymps Gap Limestone. Two facies of the Wymps Gap developed; a calcareous sandstone and thinly interbedded wackestone and shale. Topographic relief created by a thick lobe of underlying clastics resulted in the formation of a local carbonate platform along the edge of which developed a carbonate sand shoal, containing grainstone. Dissert. Abstr.

N86-10694 Ohio State Univ., Columbus.

A NUMERICAL MODEL FOR THE ESTIMATION OF SOLAR RADIATION ON RUGGED TERRAIN Ph.D. Thesis

Evelyn Carole Anderson 1985 252 p

Avail: Univ. Microfilms Order No. DA8510545

A physically-based numerical model has been developed to estimate the receipt of solar radiation for high-altitude, rugged terrain. Previously, similar models have been developed and tested for locations with surface elevations well below 1000 m, and their usefulness has not before been shown for higher elevations. The model was employed to estimate the daily receipt of solar radiation on a horizontal surface for three high-altitude stations: Albuquerque, NM; El Paso, TX; and Great Falls, MT. The results of this simulation indicate that, for both clear and cloudy conditions, the model produced results as accurate as those which have been obtained using a similar algorithm for low-altitude locations. The use of the model for non-horizontal terrain was demonstrated using several idealized surfaces including a valley with a north-south axis and a bowl-shaped depression. Dissert. Abstr.

N86-10695 Wisconsin Univ., Milwaukee.

ALTITUDINAL DISTRIBUTION OF GRANITIC LANDFORMS IN THE SOUTH CENTRAL SIERRA NEVADA, CALIFORNIA Ph.D. Thesis

Mark F. Windsor 1984 498 p

Avail: Univ. Microfilms Order No. DA8509271

The study verifies three hypotheses relating weathered and exhumed granitic landforms to altitude in the Sierra Nevada. (1) Granitic landform types are distributed in distinctive patterns related to altitude. (2) Assemblages of these landform types are regionalized by altitude. (3) These landform distributions reflect the altitudinally differentiated morphogenetic environments. The study focuses on unglaciated granitic landform distributions in three sample transects on the western slope; theories of origins and ages of landforms and paleo-morphogenetic environments provide supportive evidence for interpretation of the distributions. Three regions of wheatered granitic landform assemblages are identified; the Grusified Corestone - Tor Region at low altitudes, the Tor and Dome region at intermediate altitudes and the Felsburg - Felsenmeer Highland Region at high altitudes. Dissert. Abstr.

N86-10696 Johns Hopkins Univ., Baltimore, Md.

ULTRAVIOLET SPECTROSCOPY OF THE EARTH'S DAYGLOW AND MAGNETOSPHERE CLEFT Ph.D. Thesis

Richard Wayne Eastes 1985 230 p

Avail: Univ. Microfilms Order No. DA8510411

Separate observations, made from sounding rockets, of the ultraviolet photon spectrum emitted by the Earth's dayglow and the magnetospheric cleft are described. The two sets of observations are complementary. In the dayglow, excitation is by photoelectron impact and ultraviolet solar photons, while in the cleft, excitation by energetic particle impact dominates. The different excitation mechanisms and energy spectra of the exciting particles results in significantly different spectra. These differences lead to a better understanding of the excitation mechanisms responsible for emissions in the Earth's atmosphere. The dayglow spectra are at higher resolution than any previous observations over a broad range of ultraviolet wavelengths. The observation of the cleft's emissions are the first sounding rocket measurements of the ultraviolet emissions from this regional of the atmosphere. Dissert. Abstr.

N86-10697 State Univ. Coll. of New York, Buffalo.

GEOTHERMAL INFLUENCES ON THE LONG-TERM THICKNESS OF THE MECHANICAL LITHOSPHERE DURING FLEXURE Ph.D. Thesis

Robert F. DeRito 1985 111 p

Avail: Univ. Microfilms Order No. DA8510323

The fundamental relationship between temperature and the thickness of the mechanical lithosphere may be demonstrated by combining realsistic rock rheology with a simple flexure model. The temperature dependent, nonlinear Maxwell law is the simplest rheology capable of reconciling experimental creep data with the apparently elastic behavior of the lithosphere in the long term. The Maxwell model attains effective thicknesses that are consistent with those obtained empirically using elastic flexure models, since the former reaches a quasi-steady state in the long term. Rheological zones develop in the model lithosphere due to the increase of temperature with depth. An upper, predominantly elastic or lithospheric zone yields to a lower, predominantly viscous, or asthenospheric zone through a narrow vicoelastic transition zone. The initial thickness of the lithospheric plate is relatively unimportant during the long term. Dissert. Abstr.

N86-10698 Columbia Univ., New York.

FUNDAMENTAL STUDY OF THE CLOSURE PROPERTY OF JOINTS Ph.D. Thesis

Stephen Ray Brown 1984 242 p

Avail: Univ. Microfilms Order No. DA8511484

In three papers, the results of a fundamental study of joint closure are presented. Considering the joint surfaces to have random topography, which remains elastic during deformation, paper 1 presents a derivation of the constitutive law relating the joint closure to the applied normal stress. The theory shows that the joint closure depends as much on the topography of the contacting surfaces as on the elastic properties of the material. Paper 2 also discusses the application of the theory to mated joints, where the surfaces are highly correlated. The results of papers 1 and 2 show that the elastic joint closure depends only on a limited band of topographic features, which is defined by the correlation between the surfaces and the onset of plastic flow. Paper 3 presents the results of a general study of the topography of natural rock surfaces, including surfaces of tension fractures, a frictional wear surface, and a bedding pine surface.Dissert. Abstr.

N86-10699 California Univ., Santa Barbara.
STRUCTURAL DISCONTINUITY WITHIN THE SOUTHERN CALIFORNIA CONTINENTAL MARGIN: SEISMIC AND GRAVITY MODELS OF THE WESTERN TRANSVERSE RANGES Ph.D. Thesis
Barry Ruland Keller 1984 108 p
Avail: Univ. Microfilms Order No. DA8509435

Crustal models of P wave velocity structure and bulk density along a north-south profile across the western Transverse Ranges of California are based on published seismic reflection profiles, a seismic refraction experiment using shots at sea to receivers on land and at sea, Pn and teleseismic arrivals at permanent seismic stations, and published gravity data on land and at sea. The seismic ray trace model is further constrained by two intersecting east-west crustal refraction profiles. The density model is constrained by an auxiliary profile tying the outer Borderland to oceanic lithosphere. A range of density models is evaluated based on the range of densities reported for particular P wave velocities and the preferred model is selected by regional seismic criteria. Lateral variations in the crust are resolved to greater than 10 km depth. Variations observed in teleseismic arrival times are substantially accounted for by the crustal velocity model. The western Transverse Ranges are not in isostatic balance, the south side being heavier than the north side. Dissert. Abstr.

N86-10700 Texas Univ., El Paso.
CRUSTAL STRUCTURE OF THE SOUTHERN RIO GRANDE RIFT DETERMINED FROM SEISMIC REFRACTION, SURFACE WAVE DISPERSION, AND GRAVITY DATA Ph.D. Thesis
Yehia Ahmed Sinno 1984 195 p
Avail: Univ. Microfilms Order No. DA8509026

A series of seismic refraction profiles have been recorded in south central New Mexico with the goal of determining the crustal structure in the southern Rio Grande rift. These lines consist of three regional profiles a reversed E-W line across the rift, an unreversed N-S axial line, and an unreversed NW-SE line. The reversed E-W line shows no significant dip along the Moho (approx. 32 km thick crust) and 7.7 km/sec Pn velocity. Results from the N-S axial line and the NW-SE line indicate an apparent Pn velocity of 7.95 km/sec and significant dip along the Moho in the south and southeast directions, respectively. When interpreted together, these data indicate a crustal thinning in the southern rift of 4 to 6 km with respect to the northern rift and the adjacent Basin and Range province. The regional Pn velocity is approximately 7.7 km/sec. An analysis of regional Bouguer gravity anomalies in the area is consistent with these seismic results and indicate the crust is thinnest (approx. 26 km) within a oval N-S trending area near El Paso, Texas. Dissert. Abstr.

N86-10701 Hawaii Univ., Honolulu.
A BOUNDARY LAYER FLOW MODEL FOR AREAS OF COMPLEX TERRAIN Ph.D. Thesis
David Andre Eramus 1984 153 p
Avail: Univ. Microfilms Order No. DA8508776

In areas of complex terrain, the topography affects the boundary layer wind field. When the basic flow is at least of moderate strength, mechanical effect will dominate thermal effects in determining the topographically modified wind field. A boundary layer flow model is developed for application under these conditions. The model is applied to a complex terrain area on the island of Oahu, Hawaii. Objective and subjective analyses of the observed and modeled winds are performed to evaluate the model. These analyses show that the model is able to simulate the topographically modified wind field successfully when conditions for which the model is developed prevail. The results also suggest that the model may be applied successfully in other complex terrain areas with wind regimes similar to that in the experimental area. Dissert. Abstr.

N86-10702 Tennessee Univ., Knoxville.
THE EFFECTS OF OROGRAPHY ON LAND-ATMOSPHERE TURBULENT EXCHANGE PROCESSES Ph.D. Thesis
John Speridon Theon 1985 232 p
Avail: Univ. Microfilms Order No. DA8511404

An experimental investigation of the effects of orography on the boundary layer was conducted in February 1984 in the vicinity of Boulder, Colorado. Wind and thermodynamic data were acquired principally by the NASA B-57B aircraft but also with rawinsondes, the Boulder Atmospheric Observatory meteorological tower, the PROFS Mesonet surface stations, the radar wind profiler network, and the Boulder wind network. The aircraft, which was instrumented to measure 3-axis mean winds and turbulence fluctuations as well as temperature and moisture information, was flown in a box-like pattern at multiple levels from approximately 305m (1000 ft) to 3140m (10,300 ft) above the surface. These data provided a three-dimensional view of the flow in the lee of the Rocky Mountains, including the front range, the Flat Irons. Separation of the flow from the sharp edges of orographic features was detected. Indication of flow reattachment and even reverse flows on the plain downstream of the mountain range was evident. Dissert. Abstr.

N86-10703 Instituut TNO voor Bouwmaterialen en Bouwconstructies, Delft (Netherlands).
SIMULATION OF THE ATMOSPHERIC BOUNDARY LAYER IN THE LARGE WIND TUNNEL OF THE TNO INSTITUTE FOR BUILDING MATERIALS AND CONSTRUCTIONS (IBBC). PART 1: THEORY [SIMULATIE VAN DE ATMOSFERISCHE GRENSLAAG IN DE GROTE WINDTUNNEL VAN HET IBBC. DEEL 1: THEORIE]
P. Vermeulen 1983 80 p refs In DUTCH
(BI-76-39/08.7.23100-Pt-1) Avail: Issuing Activity

The turbulence structures describing of wind tunnel simulated and real atmospheric boundary layers (ABL) were compared, to determine the flow around and dynamic load on buildings. A 1 m thick wind tunnel boundary layer was formed on a rough foreground of 17 m length. The scale value between prototype and wind tunnel model was determined. Author (ESA)

N86-10704 Instituut TNO voor Bouwmaterialen en Bouwconstructies, Delft (Netherlands).
SIMULATION OF THE ATMOSPHERIC BOUNDARY LAYER IN THE LARGE WIND TUNNEL OF THE TNO INSTITUTE FOR BUILDING MATERIALS AND CONSTRUCTION (IBBC). PART 2: EXPERIMENTS [SIMULATIE VAN DE ATMOSFERISCHE GRENSLAAG IN DE GROTE WINDTUNNEL VAN HET IBBC. DEEL 2: EXPERIMENTEN]
P. Vermeulen 1983 60 p ref In DUTCH 2 Vol.
(BI-76-39/08.7.23100-Pt-2) Avail: Issuing Activity

Experiments to create a workable simulation of the atmospheric boundary layer and to verify the derived relation between the power law exponent and roughness height were performed. Using a power law exponent x = 0.26, a foreground consisting of 3.75 x 2.5 x 2.5 cm cubes with a 0.17 density and 1.5 slenderness, and a scale value of 1:300, it is shown that turbulence intensity, energy spectra, longitudinal integral length scales and coherences are in quantitatively and qualitatively well simulated. Author (ESA)

N86-10705*# Roberts Associates, Inc., Vienna, Va.
COMPUTATION OF FLOW REGIMES IN PARAMETER SPACE FOR THE AGCE Final Report, 13 Sep. 1984 - 13 Jul. 1985

Glyn O. Roberts 27 Jul. 1985 20 p refs
(NASA Order H-78181-B)
(NASA-CR-178480; NAS 1.26:178480; RAI-84-AG-4) Avail: NTIS HC A02/MF A01 CSCL 04A

This report describes the results of a small study program in support of the design studies for NASA's proposed Atmospheric General Circulation Experiment (AGCE). The proposed experiment will model the atmosphere using a hemispherical layer of a dielectric fluid such as silicone oil, heated at the equator, and with a large radial AC electric field producing a temperature-dependent radial body force similar to radial gravity. The effect of terrestrial gravity on the experiment can be eliminated by doing the experiment in space flight. The author developed a series of three computer models to support these design studies. The first two calculate axisymmetric solutions and their stability to small non-axisymmetric perturbations. The third computes three-dimensional solutions. These codes allow the option of solving problems in a cylindrical geometry as well as a rather generally defined spherical layer.
B.W.

N86-10706# Universite des Sciences et Techniques du Languedoc, Montpellier (France). Dept. de Physique Mathematique.
FORMATION OF WAVES BY GROUND MOTION
Pierre C. Sabatier [1984] 102 p refs Submitted for publication
(PM/84/09) Avail: NTIS HC A06/MF A01

Models devised for understanding the formation of water waves by ground motion were surveyed. The models which are used to understand the formation of water waves by ground motion are described. Theoretical models, real events, and a survey of secondary effects are presented.
EAK

N86-10707*# Jet Propulsion Lab., California Inst. of Tech., Pasadena.
CHEMICAL KINETICS AND PHOTOCHEMICAL DATA FOR USE IN STRATOSPHERIC MODELING
W. B. DeMore, J. J. Margitan, M. J. Molina, R. T. Watson, D. M. Golden, R. F. Hampson, M. J. Kurylo, C. J. Howard, and A. R. Ravishankara 1 Jul. 1985 226 p refs
(Contract NAS7-918)
(NASA-CR-176198; NAS 1.26:176198; JPL-Pub-85-37) Avail: NTIS HC A11/MF A01 CSCL 04A

Rate constants and photochemical cross sections are presented. The primary application of the data is for modeling of the stratospheric processes, with particular emphasis on the ozone layer and its possible perturbation by anthropogenic and natural phenomena.
E.A.K.

N86-10708# Aerospace Corp., El Segundo, Calif. Space Sciences Lab.
POTENTIAL STRUCTURES AND PARTICLE ACCELERATION ON AURORAL FIELD LINES
D. J. Gorney 1 May 1985 31 p
(Contract F04701-83-C-0084)
(AD-A156694; TR-0084A(5940-05)-6; SD-TR-85-12) Avail: NTIS HC A03/MF A01 CSCL 04/1

In the 1970's major advances in the understanding of auroral processes were brought about by observations of plasmas and electric fields within the regions of space responsible for auroral particle acceleration. The major contribution of these observations was the verification of the existence of electric fields with components parallel to the magnetic field over large regions of altitude (1000 to 20000 kilometers). These electric fields constitute potential drops of several kilovolts, accelerating magnetospheric electrons downward to form the aurora and ionospheric ions upward, where they contribute significantly to the magnetospheric hot ion population. Perpendicular spatial scales of about 100 kilometers are most common, although finer scales have been observed embedded, and individual small amplitude double layers occur on much smaller parallel spatial scales. More recently, the same data sets have revealed the existance of about 100 V electric potential drops directed downward in return current regions. Downward electric fields are in a direction to accelerate electrons out of the ionsphere and tend to retard the propagation of ions upward. An association between upflowing electron beams and transversely heated ions at low altitude has been noted, and a casual relationship between downward electric fields and ion conics is suggested.
GRA

N86-10709# Kiruna Geophysical Inst. (Sweden).
[ACTIVITIES REPORT IN GEOPHYSICS] Annual Report, 1984
1984 53 p refs Sponsored by Swedish Governement and Swedish Board for Space Activities
(KGI-188; ISSN-0347-6405) Avail: NTIS HC A04/MF A01

Acceleration mechanisms for auroral particles; magnetospheric wave-particle interactions as observed primarily in the particle populations; composition measurements in the hot magnetospheric plasma; convection electric field effects on magnetospheric particle populations; and EISCAT related research are discussed. Rocket and satellite sounding are described.
Author (ESA)

N86-10710# Systems Applications, Inc., San Rafael, Calif.
TECHNICAL CONSIDERATIONS IN REGIONAL AEROSOL MODELING
C. Seigneur and H. M. Barnes 1985 39 p refs
(Contract EPA-68-02-4076)
(PB85-193027; EPA-600/D-85-083) Avail: NTIS HC A03/MF A01 CSCL 04A

This work addresses the theoretical aspects of the behavior of aerosol particles in the atmosphere. In particular, it focuses on mathematical modeling of atmospheric aerosols at the regional scale (3001000 km). The paper discusses the evolution of the model in a stepwise fashion. First is considered the mathematical formulation of the transport mechanisms used. Second is a synopsis of the physical processes that affect aerosol dynamics of the aerosol population. Then a review of the pertinent chemistry of atmospheric aerosols is given. Various mathematical models of aerosol dynamics and chemistry and the formulation of the complete aerosol model are discussed. Concluding remarks include suggestions for future work such as the treatment of aerosols in clouds and model evaluation with data.
Author (GRA)

N86-10386*# Jet Propulsion Lab., California Inst. of Tech., Pasadena. Ground Antennas and Facilities Engineering Section.
SEISMIC ANALYSIS OF THE LARGE 70-METER ANTENNA, PART 1: EARTHQUAKE RESPONSE SPECTRA VERSUS FULL TRANSIENT ANALYSIS
K. Kiedron and C. T. Chian *In its* The Telecommun. and Data Acquisition Progr. Rept. 15 Aug. 1985 p 31-42 ref (For primary document see N86-10382 01-31)
Avail: NTIS HC A10/MF A01 CSCL 08K

N86-10401*# Jet Propulsion Lab., California Inst. of Tech., Pasadena. Tracking Systems and Applications Section.
MOBILE VLBI AND GPS MEASUREMENT OF VERTICAL CRUSTAL MOTION
P. M. Kroger, J. M. Davidson, and E. C. Gardner (Kalamazoo Coll.) *In its* The Telecommun. and Data Acquisition Progr. Rept. 15 Aug. 1985 p 185-198 refs (For primary document see N86-10382 01-32)
Avail: NTIS HC A10/MF A01 CSCL 08E

N86-10600*# Geological Survey, Sioux Falls, S. Dak. EROS Data Center.
SOME OPINIONS ON REMOTE SENSING AND GEOLOGIC STUDIES
G. Bryan Bailey *In* JPL Rept. of the Workshop on Geol. Appl. of Remote Sensing to the Study of Sedimentary Basins 1 Aug. 1985 p 29-30 ERTS (For primary document see N86-10599 01-43)
Avail: NTIS HC A05/MF A01 CSCL 08G

N86-10601*# Hawaii Univ., Honolulu. Planetary Geosciences Div.
POSITION PAPER: WORKSHOP ON GEOLOGIC APPLICATIONS

OF REMOTE SENSING TO THE STUDY OF SEDIMENTARY BASINS
Pamela L. Blake, Robert B. Singer, and Eileen Bruckenthal *In* JPL Rept. of the Workshop on Geol. Appl. of Remote Sensing to the Study of Sedimentary Basins 1 Aug. 1985 p 31-32 ERTS (For primary document see N86-10599 01-43)
Avail: NTIS HC A05/MF A01 CSCL 08G

N86-10602*# University of Southern California, Los Angeles. Dept. of Geological Sciences.
CHRONOLOGIC ANALYSIS OF TERRESTRIAL SEDIMENTS AND BASIN EVOLUTION
Douglas Burbank *In* JPL Rept. of the Workshop on Geol. Appl. of Remote Sensing to the Study of Sedimentary Basins 1 Aug. 1985 p 33-36 ERTS (For primary document see N86-10599 01-43)
Avail: NTIS HC A05/MF A01 CSCL 08G

N86-10603*# Jet Propulsion Lab., California Inst. of Tech., Pasadena.
TERTIARY AND QUATERNARY RESEARCH WITH REMOTE SENSING METHODS
James E. Conel *In its* Rept. of the Workshop on Geol. Appl. of Remote Sensing to the Study of Sedimentary Basins 1 Aug. 1985 p 37-40 refs ERTS (For primary document see N86-10599 01-43)
Avail: NTIS HC A05/MF A01 CSCL 08G

N86-10605*# Washington Univ., St. Louis, Mo. McDonnell Center for the Space Sciences.
[ANALYSIS OF REMOTE SENSING DATA]
E. A. Guiness, M. Sultan, and R. E. Arvidson *In* JPL Rept. of the Workshop on Geol. Appl. of Remote Sensing to the Study of Sedimentary Basins 1 Aug. 1985 p 45-46 ERTS (For primary document see N86-10599 01-43)
Avail: NTIS HC A05/MF A01 CSCL 08G

N86-10606*# Jet Propulsion Lab., California Inst. of Tech., Pasadena.
REMOTE STRATIGRAPHIC AND STRUCTURAL ANALYSIS: MULTISENSOR RESULTS IN THE WIND RIVER/BIGHORN BASIN AREA, WYOMING
Harold R. Lang, Earnest D. Paylor, and James E. Conel *In its* Rept. of the Workshop on Geol. Appl. of Remote Sensing to the Study of Sedimentary Basins 1 Aug. 1985 p 51-52 ERTS (For primary document see N86-10599 01-43)
Avail: NTIS HC A05/MF A01 CSCL 08G

N86-10607*# Lamont-Doherty Geological Observatory, Palisades, N. Y.
STRUCTURAL MAPPING OF FOLDED SEDIMENTARY ENVIRONMENTS FROM SATELLITE IMAGES: AN EXAMPLE FROM CENTRAL ASIA
William Leith *In* JPL Rept. of the Workshop on Geol. Appl. of Remote Sensing to the Study of Sedimentary Basins 1 Aug. 1985 p 53-54 refs ERTS (For primary document see N86-10599 01-43)
Avail: NTIS HC A05/MF A01 CSCL 08G

N86-10608*# Jet Propulsion Lab., California Inst. of Tech., Pasadena.
FORELAND BASIN STRUCTURES AND REMOTE SENSING
Earnest D. Paylor *In its* Rept. of the Workshop on Geol. Appl. of Remote Sensing to the Study of Sedimentary Basins 1 Aug. 1985 p 55-56 ERTS (For primary document see N86-10599 01-43)
Avail: NTIS HC A05/MF A01 CSCL 08G

N86-10609*# Carnegie Museum of Natural History, Pittsburgh, Pa. Section of Vertebrate Fossils.
PALEOGENE VERTEBRATE PALEONTOLOGY, GEOLOGY AND REMOTE SENSING IN THE WIND RIVER BASIN
Richard K. Stucky and Leonard Krishtalka *In* JPL Rept. of the Workshop on Geol. Appl. of Remote Sensing to the Study of Sedimentary Basins 1 Aug. 1985 p 59-60 refs ERTS (For primary document see N86-10599 01-43)
Avail: NTIS HC A05/MF A01 CSCL 08G

N86-10620*# Jet Propulsion Lab., California Inst. of Tech., Pasadena.
AGE-DATING VOLCANIC AND ALLUVIAL SURFACES WITH MULTIPOLARIZATION DATA
Tom G. Farr *In its* NASA/JPL Aircraft SAR Workshop Proc. 15 Jun. 1985 p 31-36 refs Original contains color illustrations (For primary document see N86-10615 01-43)
Avail: NTIS HC A05/MF A01 CSCL 08G

47 METEOROLOGY AND CLIMATOLOGY

Includes weather forecasting and modification.

N86-10711 Royal Netherlands Meteorological Inst., De Bilt. Werkgroep Grenslag.
LIST OF PUBLICATIONS ON THE 200 m METEOROLOGICAL MAST AT CABAUW, THE NETHERLANDS
A. G. M. Driedonks Feb. 1985 16 p refs
(KNMI-FM-85-6) Avail: Issuing Activity

About 120 publications on the site and installation, and impact of a 200 m tower used to study atmospheric boundary layer phenomena are listed. Author (ESA)

N86-10712# Naval Weapons Center, China Lake, Calif.
SURFACE WINDS AT NWC (NAVAL WEAPONS CENTER): 1964 - 1982 Final Report
A. R. Kelso and R. W. Evert Feb. 1985 75 p
(AD-A156660; AD-E900456; NWC-TP-6572) Avail: NTIS HC A04/MF A01 CSCL 04/2

This report contains surface wind data for the China Lake Complex of the Naval Weapons Center (NWC), China Lake, California. The data, collected from 1964 through 1982, are presented in graphs and tables. These illustrations depict monthly as well as daily time segment compilations of wind directional frequencies and average speeds. This information will be useful to Center personnel in planning, scheduling, and evaluating mission-related tests. GRA

N86-10713# Air Command and Staff Coll., Maxwell AFB, Ala.
ROTARY-WING OPERATIONS IN A MICROBURST ENVIRONMENT
E. E. Mace Apr. 1985 43 p
(AD-A156695; ACSC-85-1670) Avail: NTIS HC A03/MF A01 CSCL 04/2

Microburst wind shear has been directly or indirectly involved in 28 aircraft incidents or accidents since 1964. Following the last major aircraft accident attributed to microburst wind shear in 1982, a major effort was undertaken to study the hazard. The majority of the work that has been accomplished deals with the publicity of the phenomenon to the aviation community and with acceptable methods of detecting it before it occurs. This study explores the background, detection systems and special considerations of helicopter operations in relation to microburst induced wind shear. Included are subjective hazards, aircraft response and recommended pilot actions to successfully penetrate the wind shear if inadvertently encountered. The study recommends that it be used as an interim measure to supplement existing microburst wind shear information and that additional helicopter microburst testing be conducted. Author (GRA)

N86-10714# Naval Research Lab., Washington, D. C.
THE LIU, KATSAROS, AND BUSINGER (1979) BULK ATMOSPHERIC FLUX COMPUTATIONAL ITERATION PROGRAM IN FORTRAN AND BASIC
W. T. Liu and T. V. Blanc 8 May 1984 19 p
(RR0-3302)
(AD-A156736; NRL-MR-5291) Avail: NTIS HC A02/MF A01 CSCL 04/2

The computer program described by Liu, Katsaros, and

Businger (1979) for calculating the bulk-derived atmospheric fluxes, stability, and roughness is presented in both the FORTRAN and BASIC versions. The results of 12 test calculations are presented to ensure that the program has been properly encoded. The program requires seven input parameters: (1) wind speed; (2) air temperature; (3) specific humidity; (4) water temperature at the surface; (5) altitude of the wind-speed measurement; (6) altitude of the air-temperature measurement; and (7) altitude of the humidity measurement. GRA

N86-10715# Air Force Inst. of Tech., Wright-Patterson AFB, Ohio.
A COMPOSITE CLIMATOLOGICAL STUDY OF THE FREQUENCY AND DISTRIBUTION OF SEVERE WEATHER ASSOCIATED WITH SPRING SEASON COLORADO CYCLOGENESIS M.S. Thesis
J. H. Peters 1985 95 p
(AD-A156981; AD-E950724; AFIT/CI/NR-85-52T) Avail: NTIS HC A05/MF A01 CSCL 04/2

A composite approach is used to investigate the evolution and distribution of severe weather events for 39 cases of spring season Colorado cyclogenesis. The study also examined the incidence of severe weather during a jet streak subsample of 15 cases, based on the presence of a 300 mb wind maximum over the New Mexico-Texas area on the day of cyclogenesis, and a complement subsample of the cyclogenetic cases not included in the jet streak subsample. Composites were constructed of the normalized frequency of: (1) tornadoes, (2) high winds, (3) large hail, (4) funnel clouds and (5) total severe weather events for the total sample of 39 cases and the two subsamples for three 24 hour intervals with the first interval coinciding with the day of cyclogenesis. Distribution and frequency of severe weather for the three days was consistent with the mean synoptic features as the composite cyclone developed and moved away from its lee side development site in the southern Rockies. The area where severe weather occurred significantly broadened and moved northeastward on the two days following cyclogenesis. For each of the three samples, the maximum frequency of total severe storm events was highest on the day after cyclogenesis. GRA

N86-10716# Sandia Labs., Albuquerque, N. Mex.
ESTIMATING WIND SPEED AS A FUNCTION OF HEIGHT ABOVE GROUND: AN ANALYSIS OF DATA OBTAINED AT THE SOUTHWEST RESIDENTIAL EXPERIMENT STATION, LAS CRUCES, NEW MEXICO
D. F. Menicucci and I. J. Hall May 1985 24 p
(Contract DE-AC04-76DP-00789)
(DE85-013262; SAND-84-2530) Avail: NTIS HC A02/MF A01

Thermel modelling of photovoltaic arrays requires accurate estimates of wind speed at the level of the arrays. Wind speed data are normally recorded by an anemometer at the 30-foot level. To estimate the relationship between wind speed and height, wind speed data were acquired at various heights in the range of 10 to 30 feet and a nonlinear regression analysis was performed. This analysis shows that, over the range of conditions covered by the present data, the predictive relationship given by the Mechanical Engineer's Handbook is quite accurate; wind velocity can generally be estimated to within plus or minus 1.5 mph. DOE

N86-10717# California Univ., Livermore. Lawrence Livermore Lab.
SMOKE INPUTS TO CLIMATE MODELS: OPTICAL PROPERTIES AND HEIGHT DISTRIBUTION FOR NUCLEAR WINTER STUDIES
J. E. Penner and I. C. Haselman, Jr. Apr. 1985 27 p refs Presented at the Intern. Conf. on Nucl. War, Erice, Sicily, 19 Aug. 1984
(Contract W-7405-eng-48)
(DE85-011363; UCRI-92523; CONF-8408122-3) Avail: NTIS HC A03/MF A01

Smoke from fires produced in the aftermath of a major nuclear exchange has been predicted to cause large decreases in land surface temperatures. The extent of the decrease and even the sign of the temperature change depend on the optical characteristics of the smoke and how it is distributed with altitude. The height distribution of smoke over a fire is determined by the amount of buoyant energy produced by the fire and the amount of energy released by the latent heat of condensation of water vapor. The optical properties of the smoke depend on the size distribution of smoke particles which changes due to coagulation within the lofted plume. Calculations are presented demonstrating these processes and estimate their importance for the smoke source term input for climate models. For high initial smoke densities and for absorbing smoke ($m = 1.75 - 0.3i$), coagulation of smoke particles within the smoke plume is predicted to first increase, then decrease, the size-integrated extinction cross section. DOE

N86-10718# California Univ., Livermore. Lawrence Livermore Lab.
MICROPHYSICAL/MESOSCALE ASPECTS OF NUCLEAR WINTER AND NEW DIRECTIONS IN ASSESSMENTS
J. B. Knox Jun. 1985 13 p refs Presented at the 4th Intern. Conf. on Nucl. War, Erice, Italy, 19 Aug. 1984
(Contract W-7405-eng-48)
(DE85-013479; UCRL-91359; CONF-8408122-5) Avail: NTIS HC A02/MF A01

Recent results of model studies and sensitivity tests have shown the degree to which the intensity and duration of nuclear winter depends on the mass of soot and dust suspended, its optical properties, its vertical distribution in the atmosphere, and the residence time. The soot from urban fires is viewed as evolving during its dispersion from the early fire induced plumes, to cloud scale systems, to the mesoscale and large systems. Micro-physical processes are perceived as operating within these systems in a manner to enhance removal from the troposphere, and to alter the vertical distribution of the soot or its subsequent, aging or evolving aerosol. Relevant observations and studies of these processes are presented and discussed. Critical inputs to the climate simulation models may well be altered significant by these process effects, many of which are in need of better definition. Appropriate research needs to be initiated to address and better define these microphysical/mesoscale processes of potential importance in the altered atmospheric system after a major nuclear exchange. DOE

N85-10719# Brookhaven National Lab., Upton, N. Y.
SEASONAL VARIATIONS IN ATMOSPHERIC CHEMISTRY IN THE ADIRONDACKS
T. J. Kelly, R. L. Tanner, S. E. McLaren, and M. V. DuBois Mar. 1985 11 p refs Presented at the Air Pollution Control Assoc. Ann. Meeting and Exhibition, Detroit, 16 Jun. 1985 Prepared in cooperation with the State Univ. of New York, Albany
(Contract DE-AC02-76CH-00016)
(DE85-014227; BNL-36671; CONF-850612-5) Avail: NTIS HC A02/MF A01

The results of continuous real-time measurements of aerosol composition, HNO3, and SO2, performed at the summit of Whiteface Mountain, New York, during 1984 are reported. The purpose was to shed light on the seasonal variation in atmospheric acidity in this ecologically sensitive area. DOE

N86-10720# Deutsche Forschungs- und Versuchsanstalt fuer Luft- und Raumfahrt, Oberpfaffenhofen (West Germany). Abt. fuer Physik der Atmosphaere.
COMPARATIVE FLIGHT MEASUREMENT OF ICING PARAMETERS FOR THE PROPELLER AIRCRAFT Do-28D2 OF THE TEST STATION 61 OF THE DFVLR AND FOR THE DFVLR AIRCRAFT FALON 20e IN STRATUS CLOUDS
Klaus-Peter Schickel and Kurt Uwira (Bundesamt fuer Wehrtechnik und Beschaffung, Landsberg/Lech, West Germany) Dec. 1984 52 p refs In GERMAN; ENGLISH summary Report will also be announced as translation (ESA-TT-941)
(DFVLR-FB-85-16; ISSN-0171-1342) Avail: NTIS HC A04/MF A01; DFVLR, Cologne DM 15.50

Two aircraft of different types and instrumentation were compared during a flight operation in icing stratus clouds. The results of the measurements are comparable. It is established that differences between icing and nonicing stratus clouds can be detected in infrared satellite pictures; possible causes of these differences are given. The improvement of forecasts of icing stratus clouds is planned. Author (ESA)

N86-10721# Deutsche Forschungs- und Versuchsanstalt fuer Luft- und Raumfahrt, Oberpfaffenhofen (West Germany). Abteilung Wolkenphysik.
USER MANUAL FOR THE FALCON SYSTEM
Feb. 1985 134 p refs In GERMAN; ENGLISH summary Report will also be announced as translation (ESA-TT-936)
(DFVLR-Mitt-85-08; ISSN-0176-7739) Avail: NTIS HC A07/MF A01; DFVLR, Cologne DM 36.50

The user manual for the meteorological research aircraft Falcon E, operated by DFVLR, is presented. The system and its technical data are described. The meteorological mission possibilities are discussed, and measuring campaigns are reviewed. Basic and special equipment is described. The onboard data acquisition system and the operational data evaluation programs are discussed. Author (ESA)

N86-10722# GKSS-Forschungszentrum Geesthacht (West Germany). Inst. fuer Physik.
THE BOUNDARY CONDITION IN A NUMERICAL MODEL OF ATMOSPHERIC FLOWS OVER FIXED INTERFACES [DIE UNTERE RANDBEDINGUNG IN EINEM NUMERISCHEN MODELL ATMOSPHAERISCHER STROEMUNGEN UEBER UNBEWEGTEN GRENZFLAECHEN]
M. Claussen 1985 35 p refs In GERMAN; ENGLISH summary
(GKSS-85-E-10; ISSN-0344-9629) Avail: NTIS HC A03/MF A01

The boundary conditions of wind velocity, temperature and humidity are formulated in a numerical model of atmospheric flows to calculated wind velocity taking into account the roughness length. Different models of surface temperature and humidity taking into account surface energy balance, heat and water transfer within the soil are compared with each other. Strongly simplified models are inappropriate for medium range temperature forecasts. For short range forecasts soil moisture prediction can be omitted if the surface humidity is properly diagnosed from synoptic parameters. The calculation of a boundary value of the wind velocity is reduced to the determination of a roughness length and the problems related to that reduction are discussed. Author (ESA)

N86-10723# National Oceanic and Atmospheric Administration, Boulder, Colo. Atmospheric Observatory.
FIELD COMPARISON OF IN SITU METEOROLOGICAL SENSORS
J. C. Kaimal, J. E. Gaynor, P. L. Finkelstein (EPA, Research Triangle Park, N. C.), M. E. Graves (Northrup Services, Inc., Research Triangle Park, N. C.), and T. J. Lockhart (Meteorology Research, Inc., Altadena, Calif.) Dec. 1984 105 p refs Sponsored in part by EPA
(PB85-196988; BAO-6) Avail: NTIS HC A06/MF A01 CSCL 04B

Measurements of wind speed, wind direction, and the vertical wind component from five conventional in situ meteorological systems were compared with similar measurements from a fast response sonic anemometer. The systems tested were an orthogonal three axis propeller anomometer, a light bivane and cup anemometer, a bivane propeller anemometer, a light cup and vane with a vertical propeller, and a vane mounted propeller anemometer with a vertical propeller. Computed accuracy and field precision variables measured by each system are presented. GRA

N86-10724# National Weather Service, Washington, D.C. Climate Analysis Center.
MONTHLY AND SEASONAL WEATHER OUTLOOK FOR MID-APRIL TO MID-MAY 1985, VOLUME 39, NUMBER 8
13 Apr. 1985 11 p
(PB85-195345) Avail: NTIS HC A02/MF A01 CSCL 04B

The report gives the precipitation and temperature weather outlook for periodic and seasonal variations for North America. GRA

N86-10184# Bundesministerium fuer Forschung und Technologie, Bonn (West Germany).
THE AIR OF LIFE OF THE BLUE PLANET. ATMOSPHERE RESEARCH FROM SPACE USING DATA AND FACTS AGAINST CLIMATE SPECULATIONS [DIE LEBENSLUFT DES BLAUEN PLANETEN. ATMOSPHAERENFORSCHUNG VOM WELTRAUM AUS DATEN UND FAKTEN GEGEN KLIMA-SPEKULATIONEN]
Dieter Schwab *In its* Satellite Use for Men 1984 p 22-25 In GERMAN (For primary document see N86-10180 01-12)
Avail: NTIS HC A03/MF A01

48 OCEANOGRAPHY

Includes biological, dynamic and physical oceanography; and marine resources.

N86-10725 Columbia Univ., New York.
IN-SITU GEOPHYSICAL INVESTIGATIONS INTO THE NATURE OF THE OCEANIC CRUST Ph.D. Thesis
Robin L. Newmark 1985 236 p
Avail: Univ. Microfilms Order No. DA8511536

The layered structure of the oceanic crust is characterized by changes in geophysical gradients. Correlation of geophysical logs and cores recovered from DSDP Hole 504B provides some insight into the physical properties which control these gradient changes. Physical characteristics of crustal layers 2A, 2B and 2C such as the detailed sonic velocity and lithostratigraphic structure and variations of porosity with depth are obtained through analysis of the sonic, borehold televiewer, electrical resistivity and other logs. Several well logs which are sensitive to the presence of fractures and open porosity in the formation indicate many zones of fracturing. Interpretation of these observations suggests that there may be a fundamental pattern of cooling-induced structure in the oceanic crust. Synthetic seismograms in the tau-p domain, constructed using a detailed velocity model derived from the sonic logs run in Hole 504B are used to examine the evidence of narrow low-velocity channels in the shallow crust at seismic wavelengths. Dissert. Abstr.

N86-10726 Columbia Univ., New York.
A QUANTITATIVE METHOD FOR ANALYZING THE ROUGHNESS OF THE SEAFLOOR Ph.D. Thesis
Christopher Gene Fox 1985 233 p
Avail: Univ. Microfilms Order No. DA8511501

A method has been developed which allows a valid statistical model of the variability of oceanic depths to be derived from digital bathymetric soundings. Existing bathymetric contour charts represent low-frequency, deterministic models of the seafloor. To describe the higher frequency variability, or roughness, of the seafloor requires the development of a valid stochastic model. The statistical model of seafloor roughness is also a valuable tool for predicting acoustic scattering and in addition contains a wealth of geological information for interpreting deep-sea processes. To allow the variability of depths to be described as a function of scale (spatial frequency), the amplitude spectrum is employed as the fundamental statistic underlying the model. Since the validity of the amplitude spectrum depends upon the assumption of a statistically stationary sample space, a computer algorithm operating in the spatial domain was developed which delineates geographic provinces of limited statistical heterogeneity. Dissert. Abstr.

N86-10727# Polar Research Lab., Inc., Carpinteria, Calif.
LONG TERM STATISTICAL MEASUREMENTS OF ENVIRONMENTAL ACOUSTICS PARAMETERS IN THE ARCTIC. AEAS REPORT NUMBER 2. LOW FREQUENCY TRANSMISSION LOSS MEASUREMENTS IN THE CENTRAL ARCTIC OCEAN
B. M. Buck 15 Jan. 1985 105 p
(Contract N00014-84-C-0394)
(AD-A156576; PRL-TR-55; AEAS-2) Avail: NTIS HC A06/MF A01 CSCL 20/1

Propagation loss data were taken using manned ice camps and aircraft and ambient noise levels were measured using arctic data buoys that operated through the NIMBUS 6 and NOAA series satellites. The present report of the series addresses propagation loss in deep water (i.e., over 1000 m) of the Central Arctic Ocean at low frequencies (10 - 500 Hz). The data were taken primaily for underwater shots, although some CW data are included, at source depths between 18.3 m and 243.8 m. Receiving hydrophones were at depths between 18.3 m and 243.8 m. Receiving hydrophones were at depths between 9 and 91 m. Other data in the tabulations include for the source: station name, type, depth below sea level and below the ice, nominal TNT yield, measured yield, latitude and longitude, water depth, and source energy at the analysis frequencies. For the receiver: station name, hydrophone depth below sea level and below the ice, nominal TNT yield, measured yield, latitude and longitude, water depth, and source energy at the analysis frequencies. For the receiver: station name, hydrophone depth below sea level and below the ice, latitude and longitude, water depth, and received signal energy at the analysis frequencies. For the path: range, bottomside ice roughness, % of path less than 1000 m deep, % of path over an abyssal plain, mean path depth, and minimum depth in the path. GRA

N86-10728# Coastal Engineering Research Center, Vicksburg, Miss.
APPLICATION OF THE DUTCH METHOD FOR ESTIMATING STORM-INDUCED DUNE EROSION Final Report
F. E. Sargent and W. A. Birkemeier May 1985 46 p
(AD-A156717; CERC-IR-85-2) Avail: NTIS HC A03/MF A01 CSCL 08/3

The Delft Hydraulics Laboratory of the Netherlands has developed a reasonable and simple method for estimating dune and beach erosion caused by severe storms. The method requires knowledge of the sediment size, wave height, and surge level. Major assumptions are that the expected shape of the poststorm beach profile can be predicted by the incident deepwater wave height and sediment size, and that the amount of material eroded will equal the deposition (i.e., cross-shore transport). The method has been verified for the Dutch coast based on both field measurements and laboratory experiments. An evaluation using a limited amount of data for the Atlantic and Gulf coasts of the United States found quantitative agreement with the method, justifying its application to storm conditions in the United States. This report discusses the method and identifies its inherent limitations. The procedure may be solved graphically or by using the included FORTRAN computer program. GRA

N86-10729# Naval Postgraduate School, Monterey, Calif.
EVALUATION OF SURFACE EXCHANGE COEFFICIENTS FROM MILDEX OCEAN/ATMOSPHERE MIXED LAYER DATA M.S. Thesis
H. S. Rosner Mar. 1985 75 p
(AD-A156765) Avail: NTIS HC A04/MF A01 CSCL 08/3

This thesis evaluates a coupled oceanic-atmospheric boundary (ABL/OBL) model which provides single-station prediction capability relative to wind stress and oceanic mixed layer depth observations. The model is initialized and verified using data obtained during the 1983 Mixed Layer Dynamics Experiment (MILDEX). Model computation of friction velocity and oceanic mixed layer depth are compared with observations from both atmospheric frontal and non-frontal synoptic situations. Favorable results of model predictions are achieved although in some cases they are slightly higher than observed turbulence values. Mixed layer predictions are very close to the observed except in frontal regions. Proper ABL/OBL model initialization of boundary layer values is critical in order to achieve favorable results. GRA

N86-10730# Naval Research Lab., Washington, D. C.
A PROCESSOR FOR THE STUDY OF OCEAN FINE-SCALE PATCHES
L. J. Rosenblum, G. O. Marmorino, and J. P. Dugan 17 Jul. 1985 48 p
(AD-A157019; NRL-MR-5573) Avail: NTIS HC A03/MF A01 CSCL 08/10

When a vertical array of temperature sensors is towed through the upper thermocline, patches of high temperature variance of considerable horizontal length can be observed. The Ocean Dynamics Branch at NRL has developed a towed thermistor array system which is extremely useful in obtaining finely detailed data on the horizontal/vertical structure of small-scale temperature fluctuations in the upper ocean. This report documents an algorithm for using towed thermistor array data to study these patches. Briefly, the algorithm detrends the temperature data and computes the FFT of the windowed data for 16 second data blocks. An estimate of the temperature variance is thus obtained within a user-selected band, typically 1 to 3 m. A normalization is generally performed to remove the effects of a changing vertical temperature gradient. Shades of gray plots are then used to display the patch structure. The algorithm is applied to data from a 1981 Atlantic Ocean experiment near the Sargasso Sea. Many examples of patch processor output are shown, along with other results. It will be seen that the patch processor algorithm provides an effective medium for the portrayal of high variance of ocean fine structure. GRA

N86-10731# Conservation and Renewable Energy Inquiry and Referral Service, Silver Spring, Md.
OCEAN ENERGY TECHNOLOGY PROGRAM SUMMARY
May 1985 4 p
(Contract DE-AC01-83CE-30780)
(DE85-013102; DOE/CE-0114) Avail: NTIS HC A02/MF A01

One of the possible ways to achieve national energy sufficiency is to recycle the solar energy stored within the world's oceans in the form of thermal energy, waves and currents. The Department of Energy's (DOE) Ocean Energy Technology (OET) Program was instituted in 1978 to develop technologies which could exploit these resources in an economically viable and environmentally acceptable manner. Presently, the OET Program is investigating Ocean Thermal Energy Conversion (OTEC) Pneumatic Wave Energy Conversion (PWEC), and Hybrid Geothermal1/OTEC (GEOTEC) technologies. DOE

N86-10732# Royal Netherlands Meteorological Inst., De Bilt. Div. of Oceanographic Research.
MONTHLY BULLETIN NORTH SEA: VOLUME 2, JANUARY 1985
F. B. Koek, ed., C. G. Korevaar, ed., and R. A. vanMoerkerken, ed. Jan. 1985 25 p
(KNMI-167-Vol-2; ISSN-0168-8332) Avail: NTIS HC A02/MF A01

Weather charts and graphs of the North Sea in January 1985 covering visibility; height of cloud base; dewpoint temperature; air temperature; sea surface temperature; wind direction; wind speed; and wave height are some discussion areas presented. Author (ESA)

51 LIFE SCIENCES (GENERAL)

Includes genetics.

N86-10733# Committee on Energy and Commerce (U. S. House).
BIOTECHNOLOGY REGULATION
Washington GPO 1985 186 p Hearing before the Subcomm. on Oversight and Invest. of the Comm. on Energy and Com., 98th Congr., 2nd Sess., 11 Dec. 1984
(GPO-43-778) Avail: Subcommittee on Oversight and Investigations

Testimony and hearings in support of biotechnology regulation. Before The Subcommittee On Oversight And Investigations Of The Committee On Energy And Commerce House Of Representatives are presented. Special consideration is given to the regulation of genetic engineering. B.W.

N86-10734*# National Aeronautics and Space Administration. Ames Research Center, Moffett Field, Calif.
LIFE SCIENCES RESEARCH ON THE SPACE STATION: AN INTRODUCTION
Sep. 1985 18 p refs
(NASA-TM-86836; Rept-85408; NAS 1.15:86836) Avail: NTIS HC A02/MF A01 CSCL 06B

The Space Station will provide an orbiting, low gravity, permanently manned facility for scientific research, starting in the 1990s. The facilities for life sciences research are being designed to allow scientific investigators to perform research in Space Medicine and Space Biology, to study the consequences of long-term exposure to space conditions, and to allow for the permanent presence of humans in space. This research, using humans, animals, and plants, will provide an understanding of the effects of the space environment on the basic processes of life. In addition, facilities are being planned for remote observations to study biologically important elements and compounds in space and on other planets (exobiology), and Earth observations to study global ecology. The life sciences community is encouraged to plan for participation in scientific research that will be made possible by the Space Station research facility. Author

N86-10735# Federation of American Societies for Experimental Biology, Bethesda, Md.
[LSRO/ONR AD HOC REVIEW PROCESS] Annual Progress Report, 1 May 1984 - 30 Apr. 1985
13 Jun. 1985 14 p
(Contract N00014-83-C-0196)
(AD-A156590) Avail: NTIS HC A02/MF A01 CSCL 06/1

This annual progress report covers the ad hoc review process. Efforts are continuing to increase the number of peer reviewers who are experienced in the LSRO/ONR review process. The LSRO/FASEB Proposal Rating Form, the form used for the ad hoc peer review evaluation activity, has been reorganized so that it can, if required, be used by all programs of the Biological Sciences Division. The LSRO Oversight Panel on the Office of Naval Research Molecular Biology Program has continued to function with further refinement. In performing evaluations of certain aspects of the Molecular Biology Program, selected members of the LSRO Oversight Panel attended a meeting with selected contractors of the Molecular Biology Program whose research focuses on biotechnology and protein engineering. Non-contract Activities; Contract Problems Encountered and Resolved; Review Process Time; Contract Modifications; LSRO Oversight Panel Reorganization are discussed. GRA

N86-10736# Edgerton, Germeshausen and Grier, Inc., Idaho Falls, Idaho.
KINETICS OF BIOLOGICAL FERROUS IRON OXIDATION
P. I. Wichlacz and H. Olem 1985 15 p refs Presented at the 114th AIME Ann. Meeting, New York, 24 Feb. 1985; sponsored in cooperation with Society of Mining Engineers Prepared in cooperation with Tennessee Valley Authority, Chattanooga
(Contract DE-AC07-76ID-01570)
(DE85-014616; EGG-M-27484; CONF-850211-12) Avail: NTIS HC A02/MF A01

A mathematical model of growth and ferrous iron oxidation for attached bacteria was applied to rotating biological contactor (RBC) units treating acidic mine drainage. The model describes attached bacterial growth as a saturation function, where the rate of substrate utilization is determined by a maximum substrate oxidation rate constant, a half saturation constant, and the concentration of substrate within the RBC. The maximum oxidation rate constant was proportional to flow rate and the substrate concentration in the reactor varied with influent substrate concentration. The model was tested at three separate sites and with three different size RBC units. The ability of the model to predict the rate of iron oxidation under all test conditions was significant. The accuracy of the model was found to be affected by unit size and vary with specific test site. DOE

N86-10737# California Univ., Livermore. Lawrence Livermore Lab.
SOMATIC CELL AND MOLECULAR GENETICS APPROACH TO DNA REPAIR AND MUTAGENESIS
L. H. Thompson 14 Jun. 1985 10 p Presented at the 4th Intern. Conf. on Environ. Mutagens, Stockholm, 24 Jun. 1985
(Contract W-7405-eng-48)
(DE85-014181; UCRL-92834; CONF-8506137-4) Avail: NTIS HC A02/MF A01

In the CHO cell line, UV-sensitive mutants representing five genetic complementation groups were identified. Mutants from each of these groups were shown to be defective in performing the incision step of repair after exposure to UV. It is questioned whether the large number of complementation groups of xeroderma pigmentosa mutations of these groups all correspond to single gene loci. The same issue applies to the five groups of UV-sensitive CHO mutants. The human karyotype of the genes that complement the defects in the CHO mutants were localized. By marking CHO/human cell hybrids under the appropriate selective conditions, each of the complementing human genes are mapped. The mutation in strain UV20 (Group 2) was complemented by human chromosome 19. Preliminary evidence suggests that UV5 may also be complemented by human chromosome 19 while each of the other 3 groups involves a different human chromosome. Mutant EM9 is also complemented by a gene on chromosome 19. DOE

N86-10738# Joint Publications Research Service, Arlington, Va.
USSR REPORT: LIFE SCIENCES. BIOMEDICAL AND BEHAVIORAL SCIENCES
18 Sep. 1985 103 p Transl. into ENGLISH from various Russian articles
(JPRS-UBB-85-023) Avail: NTIS HC A06

Progress in research in the life sciences, with emphasis on biomedical and behavioral sciences is reported. Topics discussed include: aerospace medicine, biotechnology; military medicine, nonionizing electromagnetic radiation effects, and physiology. For individual titles, see N86-10739 through N86-10767.

N86-10739# Joint Publications Research Service, Arlington, Va.
HEMODYNAMICS DURING GRAVITATIONAL OVERLOADS (MATHEMATICAL MODELING) Abstract Only c52
B. L. Palets, A. A. Popov, M. A. Tikhonov, and D. Yu. Arkhangelskiy *In its* USSR Rept.: Life Sci. Biomed. and Behavioral Sci. (JPRS-UBB-85-023) 18 Sep. 1985 p 1 Transl. into ENGLISH from Fiziol. Cheloveka (Moscow), v. 11, no. 2, Mar. - Apr. 1985 p 185-191 Original language document announced in IAA as A85-33952 (For primary document see N86-10738 01-51)
Avail: NTIS HC A06

A mathematical model is developed for the regulation of human blood circulation under +Gz acceleration in the head-pelvis direction. A digital-computer study of the model shows that it is adequate to experimental data with respect to indices of systemic hemodynamics in the entire +Gz acceleration range up to the tolerance limit. Regulatory processes detemining changes in the central blood volume are shown to play an important role in the pattern of circulation response to +Gz acceleration; the role of active venomotor responses is relatively small. B.J. (IAA)

N86-10740# Joint Publications Research Service, Arlington, Va.
STUDY OF HYPOKINESIA AND ACCELERATION EFFECTS ON HUMAN CHROMOSOMES Abstract Only c52
N. N. Bobkova *In its* USSR Rept.: Life Sci. Biomed. and Behavioral Sci. (JPRS-UBB-85-023) 18 Sep. 1985 p 1 Transl. into ENGLISH from Fiziol. Cheloveka (Moscow), v. 11, no. 2, Mar. - Apr. 1985 p 300-302 (For primary document see N86-10738 01-51)
Avail: NTIS HC A06

A thirty-day antiorthostatic hypokinesia with an -8 deg angle to horizontal position followed by laterally-directed 8 g accelerations for 40 s did not lead to any chromosomal damage in peripheral blood lymphocytes of adult subjects with arthereosclerosis and vegetative vascular dystonia. E.A.K.

N86-10741# Joint Publications Research Service, Arlington, Va.
ROMANIAN PLANT PRODUCES PROTEIN CONCENTRATE FROM PARAFFIN-NOURISHED YEASTS
In its USSR Rept.: Life Sci. Biomed. and Behavioral Sci. (JPRS-UBB-85-023) 18 Sep. 1985 p 17-18 Transl. into ENGLISH from Nauka i Tekhn. (Riga), no. 6, May 1985 p 28-29 (For primary document see N86-10738 01-51)
Avail: NTIS HC A06

Protein concentrate production from paraffin nourished yeasts is reported. Abioprotein plant converts candida type yeasts microorganisms into flour which contains protein concentrate used on cattle and animal feed. The culture growth medium contains sulfates and phosphates. Paraffin supplies the carbon essential to the microorganisms' viability. The development of a technology to produce proteins from methanol is considered. E.A.K.

N86-10742# Joint Publications Research Service, Arlington, Va.
BIOTECHNOLOGY: SCIENCE AND PRACTICE
A. Ilyaletdinov *In its* USSR Rept.: Life Sci. Biomed. and Behavioral Sci. (JPRS-UBB-85-023) 18 Sep. 1985 p 19-21 Transl. into ENGLISH from Kazakhstansk. Pravda (Alma-Ata), Jun. 1985 p 3 (For primary document see N86-10738 01-51)
Avail: NTIS HC A06

The development of scientific research and the introduction of biotechnology's achievements into production are discussed. The development of an antibiotics industry, based upon the use of pure microorganism cultures under sterile conditions, and a microbiological industry, producing feed protein for animal husbandry and microbiological means for fighting agricultural pests is outlined. Industrial microbiology is related. A technology for culturing feed yeasts directly in feed shops by using media containing starch preliminary subjected to fermentation with the malt of germinated grain--barley or other cereal grains is proposed. The method of fermenting starch-containing stock with malt amylase, is turned into feed production. Special species of yeast, produced by our staff members, are used to obtain the feed protein. The contributions of microbiology and virology to the development of biological Science and Scientific and technical progress are outlined. E.A.K.

N86-10743# Joint Publications Research Service, Arlington, Va.
DYNAMICS OF CHANGES OF STATISTICAL INDICATORS OF HEART RHYTHM OF PERSONS WITH DIFFERENT DEGREE OF MOTION SICKNESS Abstract Only c52
S. S. Markaryan, A. V. Igrevskiy, and Yu. A. Korotkov *In its* USSR Rept.: Life Sci. Biomed. and Behavioral Sci. (JPRS-UBB-85-023) 18 Sep. 1985 p 46 Transl. into ENGLISH from Fiziol. Cheloveka (Moscow), v. 11, no. 1, Jan. - Feb. 1985 p 157-158 (For primary document see N86-10738 01-51)
Avail: NTIS HC A06

The possibility of using variation pulsometry to reveal latent forms of motion sickness, in seamen who participate in long voyages was studied. It was shown that this procedure could detect latent motion sickness in seamen. It is found that there are definite differences of adaptation to motion sickness in persons with different levels of resistance of Coriolis acceleration. Subjects resistant to vestibular effects revealed only a slight tendency toward insignificant changes of heart rhythm. E.A.K.

N86-10744# Joint Publications Research Service, Arlington, Va.
EFFECT OF SINGLE ACTIONS OF WEAK ELECTROMAGNETIC FIELDS OF ULTRALOW FREQUENCY ON INDICES OF ENDOCRINE SYSTEM Abstract Only c52
Ye. A. Zagorskaya *In its* USSR Rept.: Life Sci. Biomed. and Behavioral Sci. (JPRS-UBB-85-023) 18 Sep. 1985 p 50 Transl. into ENGLISH from Fiziol. Cheloveka (Moscow), v. 11, no. 2, Mar. - Apr. 1985 p 293-299 (For primary document see N86-10738 01-51)
Avail: NTIS HC A06

Functions of the human endocrine system was studied after a single exposure to weak electromagnetic field of ultralow frequency with a tension close to the real geomagnetic background and one approaching the alpha rhythm of human EEG. A single 5 hr exposure of healthy male subjects led to decreased activity of hypophysis-adrenal system manifested by lower levels of urinary 17-keto steroids, lower plasma cortisol and corticosterone and increased ACTH levels, accompanied by increased levels of circulating blood testosterone which in some cases exceeded the normal physiological range. Increased levels of TSH and free and total thyroxin in blood was noted in some subjects. The findings represent adaptable compensatory reactions of the regulatory systems showing that this system is highly sensitive to the effect of a magnetic field. E.A.K.

N86-10745# Joint Publications Research Service, Arlington, Va.
EFFECT OF EMOTIONAL STRESS ON HEMOSTASIS SYSTEM OF HEALTHY PERSONS Abstract Only c53
Ye. I. Sokolov, T. P. Khovanskaya, I. V. Novikov, and M. V. Baluda *In its* USSR Rept.: Life Sci. Biomed. and Behavioral Sci. (JPRS-UBB-85-023) 18 Sep. 1985 p 62 Transl. into ENGLISH from Fiziol. Cheloveka (Moscow), v. 11, no. 1, Jan. - Feb. 1985 p 79-82 (For primary document see N86-10738 01-51)
Avail: NTIS HC A06

The effect of emotional stress on activity of the sympathoadrenal system and of some indicators of the system of thrombocytic-vascular and plasma links of hemostasis was studied. Emotional stress of the subjects caused increase of catecholamines in the blood and increases of excretion of them in the urine and activation of the anticoagulation system and increase of the blood heparin level while the fibrinolytic activity increased and the fibrogen concentration in the blood decreased. Thromboelastograms recorded in the first phase of coagulation showed a tendency toward hypocoagulation in the subjects, under emotional stress. Emotional stress shows a tendency toward the increase of heparin tolerance of the plasma but does not change the ADP-induced aggregation of thrombocytes. E.A.K.

N86-10746# Joint Publications Research Service, Arlington, Va.
ASSESSMENT OF STATE OF CHRONOTROPIC AND INOTROPIC HEART FUNCTION AT DIFFERENT DEGREES OF PHYSICAL FITNESS Abstract Only c52
V. V. Aksenov and I. G. Tazetdinov *In its* USSR Rept.: Life Sci. Biomed. and Behavioral Sci. (JPRS-UBB-85-023) 18 Sep. 1985 p 62-63 Transl. into ENGLISH from Fiziol. Cheloveka (Moscow), v. 11, no. 1, Jan. - Feb. 1985 p 96-101 Original language document announced in IAA as A85-27781 (For primary document see N86-10738 01-51)
Avail: NTIS HC A06

An approach to the mathematical analysis of cardiosignals is developed which makes it possible to quantitatively evaluate the chronotropic and inotropic functions of the heart from a systems point of view. Combining statistical, cross-correlation, and frequency analyses, this approach makes it possible to assess physical-training level in aerospace and sports medicine. As an example, cardiosignals from the flight commanders and engineers on the Salyut-5 and Salyut-6 orbital stations were analyzed. It is concluded that the mathematical analysis of cardiosignals recorded in conditions of rest makes it possible to evlauate physical-training level as the potential readiness of regulatory systems to provide for the required high level of body functioning under physical loads. B.J. (IAA)

N86-10747# Joint Publications Research Service, Arlington, Va.
CAPACITY FOR WORK AND HEMODYNAMICS IN MALES RESIDING AT MIDDLE AND HIGH LATITUDES Abstract Only c52
L. N. Matveyev *In its* USSR Rept.: Life Sci. Biomed. and Behavioral Sci. (JPRS-UBB-85-023) 18 Sep. 1985 p 63 Transl. into ENGLISH from Fiziol. Cheloveka (Moscow), v. 11, no. 1, Jan. - Feb. 1985 p 113-120 (For primary document see N86-10738 01-51)
Avail: NTIS HC A06

The reaction of the cardiovascular system to physical exertion of various intensity was studied. Fitness for physical work of nonindigenous population of the Northeast is closely associated with length of stay in the North. Performance of work analogous to that performed by men from Moscow produces a significant hyperenergic reaction of the cardovascular system. Persons staying in the North for up to 5 years have adequate metabolic requirements from hyper-dynamia which provides adequate capacity for physical work and rapid recovery rates but a stay of more than 5 years gives lesser capacity for phyiscal work and slowing of recovery rates, due to an approach to the limits of adaptational capacities of the cardiovascular system. Men born in the North have some limitation on their capacity for physical work but have rather rapid recovery rates, indicating a whole complex of adaptational changes. E.A.K.

N86-10748# Joint Publications Research Service, Arlington, Va.

INDIVIDUAL TYPOLOGICAL FEATURES OF AUTONOMIC REACTIONS DURING AUTOGENIC TRAINING IN POLAR EXPEDITION MEMBERS IN PERIOD OF WINTERING IN ANTARCTICA Abstract Only c52

Yu. A. Sidorov *In its* USSR Rept.: Life Sci. Biomed. and Behavioral Sci. (JPRS-UBB-85-023) 18 Sep. 1985 p 64 Transl. into ENGLISH from Fiziol. Cheloveka (Moscow), v. 11, no. 1, Jan. - Feb. 1985 p 121-128 (For primary document see N86-10738 01-51)

Avail: NTIS HC A06

Subjects at a coastal Antarctic station underwent autotraining sesions in individual rooms, seated in a comfortable position. Autotraining sessions to achieve relaxation were most effectiv in the expedition members with average or low level of adaptive plasticity, beginning in the second half of wintering at the station. Intersystem inter-relationships of central and peripheral links for providing adaptive reconstructions during autotraining of the expedition members depended on individual parameters of cerebral neurodynamics. Autotraining proved to be an adequate nonmedical method for preventing and correcting disadaptational disturbances in the expedition members during their stay in Antarctica. Individual differences in the plasticity of neurodynamic processes determine the nature of autonomic reactions of the body to autotraining. E.A.K.

N86-10749# Joint Publications Research Service, Arlington, Va.

EFFECT OF INCLUSION OF SUPPLEMENTARY ASCORBIC ACID IN DAILY DIET ON DEGREE OF VITAMIN SATURATION OF BODY AND THERMORESISTANCE OF ERYTHROCYTES WHILE WORKING IN ARID ZONE Abstract Only c52

I. M. Mommadov, V. A. Grafova, and G. A. Tupikova *In its* USSR Rept.: Life Sci. Biomed. and Behavioral Sci. (JPRS-UBB-85-023) 18 Sep. 1985 p 64-65 Transl. into ENGLISH from Fiziol. Cheloveka (Moscow), v. 11, no. 1, Jan. - Feb. 1985 p 129-133 Original language document announced in IAA as A85-27786 (For primary document see N86-10738 01-51)

Avail: NTIS HC A06

The physiological needs for ascorbic acid and of the effect of vitamin C supplements at the rate of 150 mg/day on human resistance to heat in arid zones were studied. Ascorbic acid sufficiency was determined by its level in the fasting morning urine. Subjects ate a dragee containing 50 mg of ascorbic acid 3 times a day immediately after meals which increased the vitamin C level in the morning urine. The 150 mg/day dosage normalized the studies ascorbic acid level. The vitamin C supplement increases erythrocytes resistance to heat when working in high temperatures with high insolation. E.A.K.

N86-10750# Joint Publications Research Service, Arlington, Va.

EFFECT OF VARIOUS DOSES OF SOME VITAMINS ON NONSPECIFIC MECHANISMS OF ADAPTATION OF MAN Abstract Only c52

V. S. Novikov and V. N. Bortnovskiy *In its* USSR Rept.: Life Sci. Biomed. and Behavioral Sci. (JPRS-UBB-85-023) 18 Sep. 1985 p 65 Transl. into ENGLISH from Fiziol. Cheloveka (Moscow), v. 11, no. 1, Jan. - Feb. 1985 p 134-137 Original language document announced in IAA as A85-27787 (For primary document see N86-10738 01-51)

Avail: NTIS HC A06

An experimental study was conducted to investigate the effect of vitamin additions on the state of the vascular system in the nonspecific resistance of the body in persons working in unfavorable environmental conditions. Thirty operators 19 to 23 years of age were studied whose work was characterized by high work strain, hypokinesia, and environmental discomfort (e.g., high air temperature). One group of 10 subjects received the following vitamins daily: retinol acetate (0.00172 g), thiamine bromide (0.0026 g), riboflavin (0.002 g), nicotinamide (.015 g) pyridoxin hydrochloride (0.002 g), and ascorbic acid (0.07 g). A second group of 10 subjects received a double dose of the same vitamins, while a third group (the control) received placebos. Administration of the vitamins in a double dose was found to prevent the development of deadaptive changes. It is concluded that vitamin additions can prevent a reduction in the nonspecific resistance of the body under extreme environmental conditions. E.A.K.

N86-10751# Joint Publications Research Service, Arlington Va

ADAPTATION OF MAN TO EXTREME CONDITIONS OF ANTARCTICA Abstract Only c52

S. I. Soroko, A. L. Matusov, and Yu. A. Sidorov *In its* USSR Rept.: Life Sci. Biomed. and Behavioral Sci. (JPRS-UBB-85-023) 18 Sep. 1985 p 66 Transl. into ENGLISH from Fiziol. Cheloveka (Moscow), v. 10, no. 6, Nov. - Dec. 1984 p 907-920 (For primary document see N86-10738 01-51)

Avail: NTIS HC A06

An effort is made to clarify the problem of human adaptation to Antarctic conditions on the basic of multiyear complex ecological-physiological studies. These studies include the investigation of: (1) the ecological factors (natural and anthropogenic) of Antarctica; (2) individual features of the adaptive plasticity of central and vegetative mechanisms of regulation under various factors of the winter stay; (3) the dynamics of analyzer systems; (4) the work capacity of polar workers; (5) the psychoneural status of workers; and (6) the health of expedition members. It is concluded that the complex of extreme factors of Antarctica makes severe demands on the nervous, vegetative, and psychoemotional elements of human beings, calling forth all the reserve capacities of the body. B.J. (IAA)

N86-10752# Joint Publications Research Service, Arlington, Va.

INDIVIDUAL TYPOLOGICAL SELF-REGULATION OF CARDIOVASCULAR SYSTEM Abstract Only c52

Ye. G. Vashchillo, M. A. Konstantinov, and D. N. Menitskiy *In its* USSR Rept.: Life Sci. Biomed. and Behavioral Sci. (JPRS-UBB-85-023) 18 Sep. 1985 p 67 Transl. into ENGLISH from Fiziol. Cheloveka (Moscow), v. 10, no. 6, Nov. - Dec. 1984 p 929-936 Original language document announced in IAA as A85-19936 (For primary document see N86-10738 01-51)

Avail: NTIS HC A06

New data are reported pertaining to individual expological differences in the guided self-regulation of heart rate (HR) and arterial pressure (AP) in a visual feedback tracking study. Particular attention is given to individual differences in the latency of effects from baroreceptors at different levels of CNS regulation, these differences being manifested in differences in the amplitude-phase characteristics of guided oscillations of HR and AP rhythms with respect to a sinusoidal control signal. It is concluded that the proposed technique can be used as a training tool in alternating-load exercise and to study the possibility of destabilizing a regulation system with the aim of changing its state. Author

N86-10753# Joint Publications Research Service, Arlington, Va.

CONDITIONING POTENTIALITIES OF RESPIRATORY APPARATUS Abstract Only c52

F. T. Agarkov *In its* USSR Rept.: Life Sci. Biomed. and Behavioral Sci. (JPRS-UBB-85-023) 18 Sep. 1985 p 69 Transl. into ENGLISH from Fiziol. Cheloveka (Moscow), v. 10, no. 6, Nov. - Dec. 1984 p 981-987 (For primary document see N86-10738 01-51)

Avail: NTIS HC A06

The temperature of expired alveolar air sublingual, axillary and rectal temperature with temperature of the environment at -30 up to +30 C +50, +60 and +70 C in a heat chamber. Temperature of expired alveolar air at the height of maximally deep exhalation has the same value. Heat or cold, disturbing the isothermy, caused destabilization and an increasing change of the temperature of exhaled alveolar air. Exogenous heat effects disturb isothermy of the organism and destabilize the temperature of the alveolar air. Factors which limit the conditionaing potentials of the respiratory apparatus in the presence of intense heat include the air temperature, the air humidity and developing hypothermia, the degree of pronouncement of which determines the degree of increase of temperature of the alveolar air, to the greatest extent. It is assumed that the respiratory apparatus is not an ideal conditioner and the existing idea about the constancy and the conformity of the temperature of the alveolar air to the temperature of the core of the body is reconsidered. E.A.K.

N86-10754# Joint Publications Research Service, Arlington, Va.
SHORT TERM HEAT EFFECT ON ADRENO- AND CHOLINO-SENSITIVITY OF RAT'S SMALL INTESTINE Abstract Only
Kh. A. Mezidova, B. N. Manukhin, and F. F. Sultanov *In its* USSR Rept.: Life Sci. Biomed. and Behavioral Sci. (JPRS-UBB-85-023) 18 Sep. 1985 p 70 Transl. into ENGLISH from Fiziol. Zh. SSSR Im. I. M. Sechenov (Leningrad), v. 71, no. 2, Feb. 1985 p 195-199 (For primary document see N86-10738 01-51)
Avail: NTIS HC A06

The dynamics of adreno and choline sensitivity of the smooth muscles of rat's small intestine were studied at various times after exposure to 45 C for 30 or 60 minutes. The body temperature of test animals increased rapidly under the influence of the external temperature. Sensitivity of the intestine to noradrenaline also increased under conditions of hyperthermia, following the pattern of body temperature. Sensitivity of acetylcholine was less initial heating resulted in a slight decrease followed by an increase after a 1 hr exposure; after termination of the experiment, the sensitivity remained below that of control values for about 5 days. It is shown that changes in adrenoreceptor sensitivity could be controlled by the altering of environmental temperature. E.A.K.

N86-10755# Joint Publications Research Service, Arlington, Va.
CLASSIFICATION OF CHANGES IN ELECTROCARDIOGRAM DURING MUSCULAR EXERTION OF HEALTHY INDIVIDUALS Abstract Only
c52
A. I. Zavyalov *In its* USSR Rept.: Life Sci. Biomed. and Behavioral Sci. (JPRS-UBB-85-023) 18 Sep. 1985 p 73 Transl. into ENGLISH from Fiziol. Cheloveka (Moscow), v. 11, no. 2., Mar. - Apr. 1985 p 201-207 (For primary document see N86-10738 01-51)
Avail: NTIS HC A06

The determination of human endurance during physical stress is one of the most important tasks in aviation, space, work and in sport physiology. Bodily fuctioning depends on the cardio-respiratory system and evaluation of the myocardium during exertion is achieved by study of the electric activity of the heart. The dynamics of EKG were studied on subjects while applying various stress loads. Advanced athletes and sedentary individuals were examined during exercise and in rest periods. Telemetric and conductive EKG seismography, photoplethysmography and arterial pressure were studied. The data statistically leading to comparative analysis was analyzed. Appearance of overstress signals on EKG was accompanied by decreased frequency of heart contractions, a drop in systolic arterial pressure, lowered blood supply, decreased amplitude of seismocardiac signals and of the photoplethysmography wave, indicating a disorder in the contractural function of the myocardium. E.A.K.

N86-10756# Joint Publications Research Service, Arlington, Va.
EYE-MOVEMENT ACTIVITY AS INDEX OF FUNCTIONAL STATE OF BRAIN Abstract Only
c52
Ye. D. Khomskaya and I. V. Yefimova *In its* USSR Rept.: Life Sci. Biomed. and Behavioral Sci. (JPRS-UBB-85-023) 18 Sep. 1985 p 73 Transl. into ENGLISH from Fiziol. Cheloveka (Moscow), v. 11, no. 2., Mar. - Apr. 1985 p 235-240 (For primary document see N86-10738 01-51)
Avail: NTIS HC A06

Two types of eye movements slow or tracing movements and fast, saccadic movements with different control mechanisms were studied. Rhythmic saccadic eye movements were studied in relationship to mental fatigue which develops during the day and the characteristics of eye movements in individuals with varying degree of motor activity. A definite correlation between the parameters of eye movement reactions and general motor activity of the subjects with their functional state was found. Fatigue and emotional stress resulted in increased frequency of eye movements especially in the more sedentary individuals. It is suggested that eye movement reactions could be used as diagnostic tools in determining the functioning state of the brain. E.A.K.

N86-10757# Joint Publications Research Service, Arlington Va
MECHANISM OF ADAPTOGENIC ACTION OF PRICKLY ELEUTHEROCOCCUS ON MAN DURING HEAT STRESS Abstract Only
c52
G. N. Novozhilov and K. K. Silchenko *In its* USSR Rept.: Life Sci. Biomed. and Behavioral Sci. (JPRS-UBB-85-023) 18 Sep. 1985 p 74 Transl. into ENGLISH from Fiziol. Cheloveka (Moscow), v. 11, no. 2., Mar. - Apr. 1985 p 303-306 Original language document announced in IAA as A85-33964 (For primary document see N86-10738 01-51)
Avail: NTIS HC A06

The application of eleutherococcus extract in the course of 10 days prior to applied heat stress was found to have a favorable effect on body thermoregulation; body temperature was 0.73 C lower in test subjects than in the control group. However, a high biological cost for the heat adaptation was observed, expressed in two effects: (1) a significantly higher energy cost of enhanced thermal stability under eleutherococcus administration than in the control group; and (2) a more pronounced mobilization of proteins, manifested in the growth of the fraction of protein consumed in the energy metabolism and in a higher level of excretion of nitrogen compounds in the sweat and urine. Author

N86-10758# Joint Publications Research Service, Arlington, Va.
VESTIBULAR RESISTANCE AND BLOOD CIRCULATION CHANGES IN ORTHOSTATIC POSITION DURING HYPERTHERMIA Abstract Only
c52
V. I. Sobolevskiy *In its* USSR Rept.: Life Sci. Biomed. and Behavioral Sci. (JPRS-UBB-85-023) 18 Sep. 1985 p 74-75 Transl. into ENGLISH from Fiziol. Cheloveka (Moscow), v. 11, no. 2., Mar. - Apr. 1985 p 327-330 (For primary document see N86-10738 01-51)
Avail: NTIS HC A06

Vestibular and orthostatic stability of the body under various environmental conditions in applied human physiology especially under conditions of progressive exogenic hyperthermia was studied. Thermogenic changes of arterial pressure, volume of circulating blood and peripheral resistance were studied in gravitational and vestibular loads. It was shown that with limited internal hyperthermia the vestibular and orthostatic stabilities of men are unaffected. The principal mechanism of lowering resistance to vestibular and gravitational irritants is the disturbance in the blood circulating system and in cardiac activity. E.A.K.

N86-10759# Joint Publications Research Service, Arlington, Va.
HEAT TRANSFER MECHANISM IN HUMAN EXTREMITIES Abstract Only
c52
T. G. Raygorodskaya, V. N. Koshelev, and O. L. Pertsov *In its* USSR Rept.: Life Sci. Biomed. and Behavioral Sci. (JPRS-UBB-85-023) 18 Sep. 1985 p 75 Transl. into ENGLISH from Fiziol. Cheloveka (Moscow), v. 11, no. 2., Mar. - Apr. 1985 p 336-338 (For primary document see N86-10738 01-51)
Avail: NTIS HC A06

The possible effects of conductive and convective forms of heat transfer on the formation of the skin temperature field in the lower extremities during exercise of the muscles are assessed by a comparison of experimental data with numerical results obtained on the basis of the mathematical model of Koshelev and Pertsov (1978). Results indicate that the role of heat conduction in the transfer of heat from deep muscles to extremity surfaces is insignificant, while most of the heat dissipation in the tissues and heat transfer to the surfaces occurs convectively. B.J. (IAA)

N86-10760# Joint Publications Research Service, Arlington, Va.
REACTION OF RABBIT RESPIRATION SYSTEM TO HYPOXIC STIMULUS IN NITROGEN-OXYGEN MEDIUM AT ELEVATED PRESSURE Abstract Only
Zh. A. Donina *In its* USSR Rept.: Life Sci. Biomed. and Behavioral Sci. (JPRS-UBB-85-023) 18 Sep. 1985 p 75 Transl. into ENGLISH from Fiziol. Zh. SSSR Im. I. M. Sechenov (Leningrad), v. 71, no. 3, Mar. 1985 p 316-319 Original language document announced in IAA as A85-33968 (For primary document see N86-10738 01-51)
Avail: NTIS HC A06

Respiratory changes in exposed animals to increasing hypoxia was investigated on rabbits under normal conditions and in nitrogen-oxygen mixture at elevated pressure. While remaining at atmospheric pressure in air, the oxygen pressure in arterial blood dropped gradually during recycled breathing from a bag, resulting in hyperventilation. The largest increase in respiratory volume is observed when oxygen pressure in blood drops to 44.9 mm Hg; this occurred while the respiration becomes deeper and more frequent. During hyperbaria, the requency of breathing decreases while the depth of the respiration increases. The increase in respiratory volume and lung ventilation is accompanied by increased pressure in the lungs and by more labored breathing. E.A.K.

N86-10761# Joint Publications Research Service, Arlington, Va.
INDICES OF BLOOD OXYGEN TRANSPORTING PROPERTIES AND ERYTHROPOIESIS IN RATS AFTER PROLONGED STAY IN NITROGEN-OXYGEN MIXTURE AT ELEVATED PRESSURE Abstract Only
A. M. Volzhskaya, G. V. Troshikhin, and T. Ye. Shumilova *In its* USSR Rept.: Life Sci. Biomed. and Behavioral Sci. (JPRS-UBB-85-023) 18 Sep. 1985 p 76 Transl. into ENGLISH from Fiziol. Zh. SSSR Im. I. M. Sechenov (Leningrad), v. 71, no. 3, Mar. 1985 p 320-323 (For primary document see N86-10738 01-51)
Avail: NTIS HC A06

Principal blood indices determining the oxygen transport properties and the intensity of erythropoiesis in rats exposed for different times to elevated pressure in a mixed nitrogen-oxygen atmosphere were investigated. After decompression, the animals showed increased concentration of hemoglobin, elevated levels of hematocrit and higher quantities of erythrocytes, which persisted for 4 hrs; after 24 hrs the values returned to normal. The concentration of 2,3-diphosphoglycerate in erythrocytes increased and remained that way for 72 hrs. The erythropoietic activity was intensified through the 72 hrs. Mechanisms aimed at improving delivery of oxygen to the tissue and representing compensatory reactions to hypoxia are indicated. E.A.K.

N86-10762# Joint Publications Research Service, Arlington, Va.
HOMOCARNOSIN IN RAT BRAIN DURING ADAPTATION TO COLD Abstract Only
T. I. Bondarenko, A. A. Krichevskaya, and G. N. Koshchiy *In its* USSR Rept.: Life Sci. Biomed. and Behavioral Sci. (JPRS-UBB-85-023) 18 Sep. 1985 p 76 Transl. into ENGLISH from Fiziol. Zh. SSSR Im. I. M. Sechenov (Leningrad), v. 71, no. 3, Mar. 1985 p 333-336 (For primary document see N86-10738 01-51)
Avail: NTIS HC A06

Homocarnosin (gamma-aminobutyryl-1-histidine) is a peptide neuromediator of the central nervous system; its content in white rate brain was studied during cold adaptation process lasting from 1 to 45 days. It was shown that the homocarnosin level dropped progressively with exposure to this temperature. During the stress period, peroxide oxidation intensified and the hemoglobin in serum was elevated. Stimulation of the peroxide oxidation damaged some enzymes and the structure of the membranes and some of their properties were altered. Adaptation time to the cold varied in different animals. At that time the level of homocarnosin in cold-adapted animals was 56% lower than controls. The exposure to low temperature led to decrease in homocarnosin-carnosynthetase activity which explained the lower levels of homocarnosin in cold adapted animals. E.A.K.

N86-10763# Joint Publications Research Service, Arlington, Va.
EFFICIENCY OF MUSCULAR WORK IN WHITE RATS DURING ADAPTATION TO COLD Abstract Only
Ye. Ya. Tkachenko and M. A. Yakimenko *In its* USSR Rept.: Life Sci. Biomed. and Behavioral Sci. (JPRS-UBB-85-023) 18 Sep. 1985 p 77 Transl. into ENGLISH from Fiziol. Zh. SSSR Im. I. M. Sechenov (Leningrad), v. 71, no. 3, Mar. 1985 p 337-341 (For primary document see N86-10738 01-51)
Avail: NTIS HC A06

The relationship between heat production and muscle work performed under various work loads by adult rats adapted to a cold medium was investigated to determine the maximum of work ability and its energetic optimum. Temperature increase in the contracting muscle per unit work (delta/A) was plotted as a function of the magnitude of completed work by cold-adapted and control rats. It is shown that work effectiveness changed with adaptation in cold: optimum performance was achieved by cold adapted animals with loads of 200 to 250 g as compared to controls which showed a 320 to 380 g loads. E.A.K.

N86-10764# Joint Publications Research Service, Arlington, Va.
INTRADIURNIAL ORGANIZATION OF WAKEFULNESS-SLEEP SEQUENCE AND ENERGY METABOLISM IN RATS EXPOSED TO LOW AMBIENT TEMPERATURE Abstract Only
V. S. Sazonov and Yu. F. Pastukhov *In its* USSR Rept.: Life Sci. Biomed. and Behavioral Sci. (JPRS-UBB-85-023) 18 Sep. 1985 p 77 Transl. into ENGLISH from Fiziol. Zh. SSSR Im. I. M. Sechenov (Leningrad), v. 71, no. 3, Mar. 1985 p 342-347 Original language document announced in IAA as A85-36311 (For primary document see N86-10738 01-51)
Avail: NTIS HC A06

Sleep characteristics were studied as a function of energy exchange under conditions of acute and chronic exposure to low ambient temperature. Two sleep phases were identified in all animals regardless of the temperature; (1) slow wave sleep, further subdivided into surface and deep subgroups; and (2) paradoxial sleep. Three control rats were used and five cold-adapted ones. At low ambient temperature, controls had a lighter, shorter and often interrupted sleep. After cold adaptation daily sleeping period increased both at low and ambient temperatures. It is assumed that after prolonged cold the sleep initiation mechanisms continue to be active, while those of the sleep development arrested. E.A.K.

N86-10765# Joint Publications Research Service, Arlington, Va.
TV MONITORING CONTROL SYSTEM IN ELECTROPHYSIOLOGICAL STUDIES Abstract Only c52
Yu. G. Kratin, Ye. P. Popechitelev, A. N. Solovyev, and Yu. I. Buch *In its* USSR Rept.: Life Sci. Biomed. and Behavioral Sci. (JPRS-UBB-85-023) 18 Sep. 1985 p 78 Transl. into ENGLISH from Fiziol. Zh. SSSR Im. I. M. Sechenov (Leningrad), v. 71, no. 3, Mar. 1985 p 381-383 (For primary document see N86-10738 01-51)
Avail: NTIS HC A06

In electrophysiological experiments and during determination of EEG curves, the flow of formation must be filtered to isolate most important indices to be able to follow the functional state of the brain. A special monitor was constructed which consists of a TV camera, video-control unit and an image synthesizer consisting of synchronous impulse selector, round figure contructor and a coloring block. The degree of brain activity is converted to the background color scheme, to study the subject concurrently with the observation of brain activation. This apparatus can be modified for other clinical applications. E.A.K.

N86-10766# Joint Publications Research Service, Arlington, Va.
EFFECT OF COLD ON BRAIN SEROTONIN SYSTEM AND PLASMA CORTICOSTEROID LEVEL IN DIFFERENT STRAINS OF MICE Abstract Only
L. A. Koryakina, A. V. Kulikov, M. Yu. Figurova, and N. K. Popova *In its* USSR Rept.: Life Sci. Biomed. and Behavioral Sci. (JPRS-UBB-85-023) 18 Sep. 1985 p 78-79 Transl. into ENGLISH from Fiziol. Zh. SSSR Im. I. M. Sechenov (Leningrad), v. 71, no. 3,

Mar. 1985 p 422-427 (For primary document see N86-10738 01-51)
Avail: NTIS HC A06

The activity of tryptophan hydroxylase in brain and was evaluated the plasma corticosteroid levels in male mice while exposed to +4 C for 1 or 6 hrs. It is shown that the activity of tryptophan hydroxylase dropped during the cooling process, and it is assumed that the activity of the entire serotonin system in brain lowered. Decreased synthesis of serotonin supported temperature homeostasis and increased the resistance of animals to cold. The changes in the serotonin system were of an adaptive nature. No linear relationship is noted between the degree of activation of hypothalamo-hypophyseal-adrenal systems and the drop in body temperature of the experimental animals. It is assumed that the observed changes in the synthesis of biogenic amine represent a specific reaction of the body to the cooling process and are caused by participation of brain serotonin in central thermoregulation. E.A.K.

N86-10767# Joint Publications Research Service, Arlington, Va.
DYNAMICS OF GENERAL RESISTANCE OF RATS DURING READAPTATION PERIOD AFTER TRAINING IN ALTERED GAS ENVIRONMENT Abstract Only
Ye. Ye. Zverkova *In its* USSR Rept.: Life Sci. Biomed. and Behavioral Sci. (JPRS-UBB-85-023) 18 Sep. 1985 p 79 Transl. into ENGLISH from Fiziol. Zh. SSSR Im. I. M. Sechenov (Leningrad), v. 71, no. 4, Apr. 1985 p 523-526 (For primary document see N86-10738 01-51)
Avail: NTIS HC A06

The duration of retained resistance of animals to external conditions was studied on 330 white rats as a function of adaptive training and specific conditions of altered gas medium. The adaptation training to combined hypoxia and hypercapnia or to pure hypoxia lasted 15 and 30 days for each modality. It was shown that a 15-day training by either of above methods had an insignificant effect on high altutide resistance. The animals exposed to 30 day treatment showed significant increase in resistance to acute hypoxia. The high altitude resistance was higher at all times in the groups exposed to a combination of hypoxia and hypercapnia training. This type of resistance lasted for up to 60 days after thre readaptation period. E.A.K.

52 AEROSPACE MEDICINE

Includes physiological factors; biological effects of radiation; and weightlessness.

N86-10768* National Aeronautics and Space Administration, Washington, D. C.
AEROSPACE MEDICINE AND BIOLOGY: A CONTINUING BIBLIOGRAPHY WITH INDEXES (SUPPLEMENT 275)
Sep. 1985 99 p
(NASA-SP-7011(275); NAS 1.21:7011(275)) Avail: NTIS HC $7.00 (special price) CSCL 06E

This bibliography lists 321 reports, articles, and other documents introduced into the NASA scientific and technical information system in August 1985. E.A.K.

N86-10769 Maryland Univ., College Park.
DETERMINATION OF SYMMETRY AND PHASE IN HUMAN VISUAL RESPONSE FUNCTIONS: THEORY AND EXPERIMENTS Ph.D. Thesis
David Geoffrey Stork 1984 189 p
Avail: Univ. Microfilms Order DA8510459

Several mathematical and experimental techniques to deduce the temporal impulse response and static line spread function of the human visual system were employed. The problem of linearity in the visual system near threshold is recieved and the mathematical foundations of different experimental approaches are discussed. It is found that the method of constant (threshold) output avoids certain difficulties associated with other methods. The use of harmonic stimuli in vision, and the inherent phase or symmetry ambiguities associated with it are described. Physiological data on cat responses are analyzed. It is demonstrated that a spatially antisymmetric line spread function explains this data better that a spatially symmetric one. A novel stimulus segconverging and diverging stimuli is introduced and show how it can be used to probe spatial symmetry of the line spread function.It is demonstrated that the sensitivity to converging and diverging stimuli are equal. It is shown that adaptation to velocity stimuli at one retinal position can affect (reduce) sensitivity at spatially separated positions. Dissert. Abstr.

N86-10770*# Pennsylvania Univ., Philadelphia. Dept. of Computer and Information Service.
STRENGTH MODELING REPORT
Norman I. Badler, Philip Lee, and Sui Wong 30 May 1985 79 p refs
(Contract NAS9-16634)
(NASA-CR-171896; NAS 1.26:171896) Avail: NTIS HC A05/MF A01 CSCL 06P

Strength modeling is a complex and multi-dimensional issue. There are numerous parameters to the problem of characterizing human strength, most notably: (1) position and orientation of body joints; (2) isometric versus dynamic strength; (3) effector force versus joint torque; (4) instantaneous versus steady force; (5) active force versus reactive force; (6) presence or absence of gravity; (7) body somatotype and composition; (8) body (segment) masses; (9) muscle group envolvement; (10) muscle size; (11) fatigue; and (12) practice (training) or familiarity. In surveying the available literature on strength measurement and modeling an attempt was made to examine as many of these parameters as possible. The conclusions reached at this point toward the feasibility of implementing computationally reasonable human strength models. The assessment of accuracy of any model against a specific individual, however, will probably not be possible on any realistic scale. Taken statistically, strength modeling may be an effective tool for general questions of task feasibility and strength requirements. G.L.C.

N86-10771# Federal Aviation Administration, Washington, D.C. Office of Aviation Medicine.
THE EFFECTS OF AGE, SLEEP DEPRIVATION, AND ALTITUDE ON COMPLEX PERFORMANCE
H. W. Mertens and W. E. Collins May 1985 22 p
(AD-A156987; AD-E950724; FAA-AM-85-3) Avail: NTIS HC A02/MF A01 CSCL 06/19

Little research has been concerned with the combined effects on performance of age, sleep deprivation, and altitude. This study examined their potential interaction with laboratory tasks measuring aviation-related psychological functions. Healthy men in two age groups, 30-39 yr (N=16) and 60-69 yr (N=14), were evaluated for complex (time-shared) performance in the four possible combinations of two altitudes (ground level vs. 3,810 m (12,500 ft)) and two sleep conditions (sleep permitted vs. sleep deprived). Following training, performance was evaluated during 3-h test sessions in the morning and afternoon of each of 4 test days. Complex performance, measured by the Multiple Task Performance Battery (MTPB), included: monitoring of warning lights and meters, mental arithmetic, problem solving, target identification, and tracking. Workload was varied within each hour by varying the tasks performed simultaneously. Performance was significantly lower in the older subjects, but age did not interact significantly with sleep deprivation or altitude. When subjects were rested, altitude had no effect. When subjects were sleep deprived, performance was significantly lower in general, and the greatest decrement in performance occurred at altitude. Increasing workload enhanced the interaction of sleep deprivation and altitude. The performance of older subjects tended to be more affected by increases in workload, but decrements induced by sleep deprivation and altitude did not appear to interact with age. These findings provide empirical evidence in support of warnings in the aeromedical literature concerning greater effects of sleep deprivation as altitude increases within the general aviation range. GRA

N86-10772# Pacific Northwest Lab., Richland, Wash.
APPROACHES TO QUANTITATIVE EXPRESSION OF DOSE RESPONSE
E. S. Gilbert Apr. 1985 16 p refs Presented at the Symp. on Epidemiol. and Health Risk Assessment, Columbia, Md., 14 May 1985
(Contract DE-AC06-76RL-01830)
(DE85-013498; PNL-SA-13193; CONF-850577-1) Avail: NTIS HC A02/MF A01

Quantifying risks experienced by populations been exposed to relatively low levels of harmful agents for substances are discussed. DOE

N86-10773# Hauptverband der Gewerblichen Berufsgenossenschaften, e. V., Bonn (West Germany).
REPORT ON THE RESEARCH ACTIVITIES ON WHOLE-BODY VIBRATIONS. HUMAN STRAIN DUE TO MECHANICAL VIBRATIONS [BEANSPRUCHUNG DES MENSCHEN DURCH MECHANISCHE SCHWINGUNGEN. KENNTNISSTAND ZUR WIRKUNG VON GANZ-KOERPER-SCHWINGUNGEN]
H. Dupuis (Mainz Univ., West Germany) and G. Zerlett (Rheinische Braunkohlenwerke AG) May 1984 148 p refs In GERMAN
(ISBN-3-88383-107-7) Avail: NTIS HC A07/MF A01

Knowledge of whole-body vibration effects on man was surveyed to give authorities a guide for decision-making and judgement regarding occupational problems. The acute effects of mechanical vibrations on man's organism and physiological functions are reported as well as the chronic effects of whole-body vibrations and the influence of specific strain factors. Prevention measures are listed together with West German legislation and guidelines regarding the protection against mechanical vibrations at work. Author (ESA)

N86-10774# Amsterdam Univ. (Netherlands). Lab. voor Medischefysica.
VARIABILITY ANALYSIS OF VISUALLY INDUCED RESPONSES IN THE MIDST OF NOISE Ph.D. Thesis [VARIABILITEITS ANALYSE VAN VISUEEL OPGEWEKTE RESPONSIES TE MIDDEN VAN RUIS]
M. F. vanLoon Apr. 1984 91 p refs In DUTCH
(B8564052) Avail: NTIS HC A05/MF A01

The variability of EEG responses to visual stimuli, and possible relations between variations in latency and amplitude are investigated. A matched filter to detect and estimate the magnitude of variabilities on series of recordings until a 20% signal to noise ratio is reached was applied to responses of two subjects. Measurements show that in case of variability no relation exists between stimulus and the magnitude of the variability in latency or amplitude. Variability seems mainly to depend on the condition of the subject. Author (ESA)

N86-10739# Joint Publications Research Service, Arlington, Va.
HEMODYNAMICS DURING GRAVITATIONAL OVERLOADS (MATHEMATICAL MODELING) Abstract Only
B. L. Palets, A. A. Popov, M. A. Tikhonov, and D. Yu. Arkhangelskiy *In its* USSR Rept.: Life Sci. Biomed. and Behavioral Sci. (JPRS-UBB-85-023) 18 Sep. 1985 p 1 Transl. into ENGLISH from Fiziol. Cheloveka (Moscow), v. 11, no. 2, Mar. - Apr. 1985 p 185-191 Original language document announced in IAA as A85-33952 (For primary document see N86-10738 01-51)
Avail: NTIS HC A06

N86-10740# Joint Publications Research Service, Arlington, Va.
STUDY OF HYPOKINESIA AND ACCELERATION EFFECTS ON HUMAN CHROMOSOMES Abstract Only
N. N. Bobkova *In its* USSR Rept.: Life Sci. Biomed. and Behavioral Sci. (JPRS-UBB-85-023) 18 Sep. 1985 p 1 Transl. into ENGLISH from Fiziol. Cheloveka (Moscow), v. 11, no. 2, Mar. - Apr. 1985 p 300-302 (For primary document see N86-10738 01-51)
Avail: NTIS HC A06

N86-10743# Joint Publications Research Service, Arlington, Va.
DYNAMICS OF CHANGES OF STATISTICAL INDICATORS OF HEART RHYTHM OF PERSONS WITH DIFFERENT DEGREE OF MOTION SICKNESS Abstract Only
S. S. Markaryan, A. V. Igrevskiy, and Yu. A. Korotkov *In its* USSR Rept.: Life Sci. Biomed. and Behavioral Sci. (JPRS-UBB-85-023) 18 Sep. 1985 p 46 Transl. into ENGLISH from Fiziol. Cheloveka (Moscow), v. 11, no. 1, Jan. - Feb. 1985 p 157-158 (For primary document see N86-10738 01-51)
Avail: NTIS HC A06

N86-10744# Joint Publications Research Service, Arlington, Va.
EFFECT OF SINGLE ACTIONS OF WEAK ELECTROMAGNETIC FIELDS OF ULTRALOW FREQUENCY ON INDICES OF ENDOCRINE SYSTEM Abstract Only
Ye. A. Zagorskaya *In its* USSR Rept.: Life Sci. Biomed. and Behavioral Sci. (JPRS-UBB-85-023) 18 Sep. 1985 p 50 Transl. into ENGLISH from Fiziol. Cheloveka (Moscow), v. 11, no. 2, Mar. - Apr. 1985 p 293-299 (For primary document see N86-10738 01-51)
Avail: NTIS HC A06

N86-10746# Joint Publications Research Service, Arlington, Va.
ASSESSMENT OF STATE OF CHRONCTROPIC AND INOTROPIC HEART FUNCTION AT DIFFERENT DEGREES OF PHYSICAL FITNESS Abstract Only
V. V. Aksenov and I. G. Tazetdinov *In its* USSR Rept.: Life Sci. Biomed. and Behavioral Sci. (JPRS-UBB-85-023) 18 Sep. 1985 p 62-63 Transl. into ENGLISH from Fiziol. Cheloveka (Moscow), v. 11, no. 1, Jan. - Feb. 1985 p 96-101 Original language document announced in IAA as A85-27781 (For primary document see N86-10738 01-51)
Avail: NTIS HC A06

N86-10747# Joint Publications Research Service, Arlington, Va.
CAPACITY FOR WORK AND HEMODYNAMICS IN MALES RESIDING AT MIDDLE AND HIGH LATITUDES Abstract Only
L. N. Matveyev *In its* USSR Rept.: Life Sci. Biomed. and Behavioral Sci. (JPRS-UBB-85-023) 18 Sep. 1985 p 63 Transl. into ENGLISH from Fiziol. Cheloveka (Moscow), v. 11, no. 1, Jan. - Feb. 1985 p 113-120 (For primary document see N86-10738 01-51)
Avail: NTIS HC A06

N86-10748# Joint Publications Research Service, Arlington, Va.
INDIVIDUAL TYPOLOGICAL FEATURES OF AUTONOMIC REACTIONS DURING AUTOGENIC TRAINING IN POLAR EXPEDITION MEMBERS IN PERIOD OF WINTERING IN ANTARCTICA Abstract Only
Yu. A. Sidorov *In its* USSR Rept.: Life Sci. Biomed. and Behavioral Sci. (JPRS-UBB-85-023) 18 Sep. 1985 p 64 Transl. into ENGLISH from Fiziol. Cheloveka (Moscow), v. 11, no. 1, Jan. - Feb. 1985 p 121-128 (For primary document see N86-10738 01-51)
Avail: NTIS HC A06

N86-10749# Joint Publications Research Service, Arlington, Va.
EFFECT OF INCLUSION OF SUPPLEMENTARY ASCORBIC ACID IN DAILY DIET ON DEGREE OF VITAMIN SATURATION OF BODY AND THERMORESISTANCE OF ERYTHROCYTES WHILE WORKING IN ARID ZONE Abstract Only
I. M. Mommadov, V. A. Grafova, and G. A. Tupikova *In its* USSR Rept.: Life Sci. Biomed. and Behavioral Sci. (JPRS-UBB-85-023) 18 Sep. 1985 p 64-65 Transl. into ENGLISH from Fiziol. Cheloveka (Moscow), v. 11, no. 1, Jan. - Feb. 1985 p 129-133 Original language document announced in IAA as A85-27786 (For primary document see N86-10738 01-51)
Avail: NTIS HC A06

N86-10750# Joint Publications Research Service, Arlington, Va.
EFFECT OF VARIOUS DOSES OF SOME VITAMINS ON NONSPECIFIC MECHANISMS OF ADAPTATION OF MAN Abstract Only
V. S. Novikov and V. N. Bortnovskiy *In its* USSR Rept.: Life Sci. Biomed. and Behavioral Sci. (JPRS-UBB-85-023) 18 Sep. 1985 p 65 Transl. into ENGLISH from Fiziol. Cheloveka (Moscow), v. 11, no. 1, Jan. - Feb. 1985 p 134-137 Original language

document announced in IAA as A85-27787 (For primary document see N86-10738 01-51)
Avail: NTIS HC A06

N86-10751# Joint Publications Research Service, Arlington, Va.
ADAPTATION OF MAN TO EXTREME CONDITIONS OF ANTARCTICA Abstract Only
S. I. Soroko, A. L. Matusov, and Yu. A. Sidorov *In its* USSR Rept.: Life Sci. Biomed. and Behavioral Sci. (JPRS-UBB-85-023) 18 Sep. 1985 p 66 Transl. into ENGLISH from Fiziol. Cheloveka (Moscow), v. 10, no. 6, Nov. - Dec. 1984 p 907-920 (For primary document see N86-10738 01-51)
Avail: NTIS HC A06

N86-10752# Joint Publications Research Service, Arlington, Va.
INDIVIDUAL TYPOLOGICAL SELF-REGULATION OF CARDIOVASCULAR SYSTEM Abstract Only
Ye. G. Vashchillo, M. A. Konstantinov, and D. N. Menitskiy *In its* USSR Rept.: Life Sci. Biomed. and Behavioral Sci. (JPRS-UBB-85-023) 18 Sep. 1985 p 67 Transl. into ENGLISH from Fiziol. Cheloveka (Moscow), v. 10, no. 6, Nov. - Dec. 1984 p 929-936 Original language document announced in IAA as A85-19936 (For primary document see N86-10738 01-51)
Avail: NTIS HC A06

N86-10753# Joint Publications Research Service, Arlington, Va.
CONDITIONING POTENTIALITIES OF RESPIRATORY APPARATUS Abstract Only
F. T. Agarkov *In its* USSR Rept.: Life Sci. Biomed. and Behavioral Sci. (JPRS-UBB-85-023) 18 Sep. 1985 p 69 Transl. into ENGLISH from Fiziol. Cheloveka (Moscow), v. 10, no. 6, Nov. - Dec. 1984 p 981-987 (For primary document see N86-10738 01-51)
Avail: NTIS HC A06

N86-10755# Joint Publications Research Service, Arlington, Va.
CLASSIFICATION OF CHANGES IN ELECTROCARDIOGRAM DURING MUSCULAR EXERTION OF HEALTHY INDIVIDUALS Abstract Only
A. I. Zavyalov *In its* USSR Rept.: Life Sci. Biomed. and Behavioral Sci. (JPRS-UBB-85-023) 18 Sep. 1985 p 73 Transl. into ENGLISH from Fiziol. Cheloveka (Moscow), v. 11, no. 2., Mar. - Apr. 1985 p 201-207 (For primary document see N86-10738 01-51)
Avail: NTIS HC A06

N86-10756# Joint Publications Research Service, Arlington, Va.
EYE-MOVEMENT ACTIVITY AS INDEX OF FUNCTIONAL STATE OF BRAIN Abstract Only
Ye. D. Khomskaya and I. V. Yefimova *In its* USSR Rept.: Life Sci. Biomed. and Behavioral Sci. (JPRS-UBB-85-023) 18 Sep. 1985 p 73 Transl. into ENGLISH from Fiziol. Cheloveka (Moscow), v. 11, no. 2., Mar. - Apr. 1985 p 235-240 (For primary document see N86-10738 01-51)
Avail: NTIS HC A06

N86-10757# Joint Publications Research Service, Arlington, Va.
MECHANISM OF ADAPTOGENIC ACTION OF PRICKLY ELEUTHEROCOCCUS ON MAN DURING HEAT STRESS Abstract Only
G. N. Novozhilov and K. K. Silchenko *In its* USSR Rept.: Life Sci. Biomed. and Behavioral Sci. (JPRS-UBB-85-023) 18 Sep. 1985 p 74 Transl. into ENGLISH from Fiziol. Cheloveka (Moscow), v. 11, no. 2., Mar. - Apr. 1985 p 303-306 Original language document announced in IAA as A85-33964 (For primary document see N86-10738 01-51)
Avail: NTIS HC A06

N86-10758# Joint Publications Research Service, Arlington, Va.
VESTIBULAR RESISTANCE AND BLOOD CIRCULATION CHANGES IN ORTHOSTATIC POSITION DURING HYPERTHERMIA Abstract Only
V. I. Sobolevskiy *In its* USSR Rept.: Life Sci. Biomed. and Behavioral Sci. (JPRS-UBB-85-023) 18 Sep. 1985 p 74-75 Transl. into ENGLISH from Fiziol. Cheloveka (Moscow), v. 11, no. 2., Mar. - Apr. 1985 p 327-330 (For primary document see N86-10738 01-51)
Avail: NTIS HC A06

N86-10759# Joint Publications Research Service, Arlington, Va.
HEAT TRANSFER MECHANISM IN HUMAN EXTREMITIES Abstract Only
T. G. Raygorodskaya, V. N. Koshelev, and O. L. Pertsov *In its* USSR Rept.: Life Sci. Biomed. and Behavioral Sci. (JPRS-UBB-85-023) 18 Sep. 1985 p 75 Transl. into ENGLISH from Fiziol. Cheloveka (Moscow), v. 11, no. 2., Mar. - Apr. 1985 p 336-338 (For primary document see N86-10738 01-51)
Avail: NTIS HC A06

N86-10765# Joint Publications Research Service, Arlington, Va.
TV MONITORING CONTROL SYSTEM IN ELECTROPHYSIOLOGICAL STUDIES Abstract Only
Yu. G. Kratin, Ye. P. Popechitelev, A. N. Solovyev, and Yu. I. Buch *In its* USSR Rept.: Life Sci. Biomed. and Behavioral Sci. (JPRS-UBB-85-023) 18 Sep. 1985 p 78 Transl. into ENGLISH from Fiziol. Zh. SSSR Im. I. M. Sechenov (Leningrad), v. 71, no. 3, Mar. 1985 p 381-383 (For primary document see N86-10738 01-51)
Avail: NTIS HC A06

53 BEHAVIORAL SCIENCES

Includes psychological factors; individual and group behavior; crew training and evaluation; and psychiatric research.

N86-10775 Institute for Perception RVO-TNO, Soesterberg (Netherlands).
STUDIES ON HUMAN VEHICLE CONTROL
Hans Godthelp 1984 159 p refs
(B8563352) Avail: Issuing Activity

The accuracy of closed and open loop steering were measured in a reproduction task. Precognitive control aspects of open and closed loop steering in a lane change maneuver were studied. Preview control in open and closed loop steering on entering a bend was investigated. Straight lane keeping compensatory control and the limits of error neglecting in lane keeping were examined. For closed loop conditions, amplitude accuracy is linearly dependent on movement velocity, illustrating the validity of Fitts/ law for continuous, closed loop movements. However, for open loop conditions the results indicate the amplitude accuracy to depend only on movement amplitude and not on velocity. Driver's self-chosen occlusion times correspond closely with time of lane crossing. Author (ESA)

N86-10776 Institute for Perception RVO-TNO, Soesterberg (Netherlands).
CAR DRIVING AS A SUPERVISORY CONTROL TASK
Gerard Jan Blaauw 1984 139 p refs
(B8563351) Avail: Issuing Activity

Car driving was analyzed using a supervisory driver model. The driver is assumed to supervise single tasks like lateral and longitudinal vehicle control, each of which is assumed to be autonomously controlled. The driver only intervenes when the conditions of a single task force him to. An integral description of multitask performance in driving is possible. An observation/ prediction block, a control block and a decision-making block are distinguished. Results suggest that lateral control does not need continuous foveal visual information. In conditions creating a minimum level of attention for lateral control, skilled and unskilled drivers show an acceptable stay within their lane, although variations in lateral control are larger than in other conditions. Performance during occlusion is not much affected in relation to multitask or deteriorated driving conditions. However, skilled drivers choose longer occlusion times than the unskilled drivers for comparable levels of driving performance. Author (ESA)

N86-10777*# National Aeronautics and Space Administration. Ames Research Center, Moffett Field, Calif.
THE SYNTHESIS AND ANALYSIS OF COLOR IMAGES
Brian A. Wandell Sep. 1985 37 p refs
(NASA-TM-86844; Rept-85419; NAS 1.15:86844) Avail: NTIS HC A03/MF A01 CSCL 05I

A method is described for performing the synthesis and analysis of digital color images. The method is based on two principles. First, image data are represented with respect to the separate physical factors, surface reflectance and the spectral power distribution of the ambient light, that give rise to the perceived color of an object. Second, the encoding is made efficient by using a basis expansion for the surface spectral reflectance and spectral power distribution of the ambient light that takes advantage of the high degree of correlation across the visible wavelengths normally found in such functions. Within this framework, the same basic methods can be used to synthesize image data for color display monitors and printed materials, and to analyze image data into estimates of the spectral power distribution and surface spectral reflectances. The method can be applied to a variety of tasks. Examples of applications include the color balancing of color images, and the identification of material surface spectral reflectance when the lighting cannot be completely controlled. Author

N86-10778# Department of the Air Force, Washington, D.C.
VISION TEST CHART AND METHOD USING GAUSSIANS Patent Application
H. L. Task, inventor (to Air Force) Filed 23 Jan. 1985 19 p
(AD-D011756; US-Patent-Appl-SN-693927) Avail: NTIS HC A02/MF A01 CSCL 06/12

A novel vision test device and method for measuring the ability of a subject to perceive contrasts is described, which comprises a chart for display to the subject having a plurality of visual test shapes systematically organized thereover in a predetermined array on a background of preselected luminance or reflectance level, each test shape having a preselected luminance level providing maximum contrast relative to background at its center and substantially zero contrast relative to background at its edges, the luminance (or reflectance) level of each test shape varying radially from its preselected distribution factor. GRA

N86-10779# Office of Naval Research, Arlington, Va. Psychological Sciences Div.
PSYCHOLOGICAL SCIENCES DIVISION 1984 PROGRAMS Annual Report, 1 Jan. - 1 Dec. 1984
M. A. Tolcott 1 Dec. 1984 184 p
(AD-A156631; Rept-442-4) Avail: NTIS HC A09/MF A01 CSCL 05/10

This booklet describes research carried out under the Psychological Sciences Division of ONR during Fiscal Year 1984. The booklet is divided into three programmatic research area: Engineering Psychology; Personnel and Training; and Organizational Effectiveness - the last area will be re-named Group Psychology in Fiscal Year 1985. Specific study areas are: Man-Machine System Interfaces, Perception, Decision Making, Distributed Tactical Decision Making, Special Projects. Man-Machine Systems Technology, Defense Small Business Advanced Technology Program, Effective Heterogeneous Groups, personnel Turnover and Retention, Productivity in Organizations, Manpower R&D Programs, Theory-Based Personnel Assessment, Information-Processing Abilities, Attention and Action, Instructional Theory and Methods, Cognitive Processes. Each report within these sections gives specific objectives, approach, progress, potential applications. GRA

N86-10780# Deutsche Forschungs- und Versuchsanstalt fuer Luft- und Raumfahrt, Hamburg (West Germany). Abt. Flugphysiologie und Psychologie.
EXTENDED ANALYSIS OF THE STRUCTURE OF ERROR SCORES IN PSYCHOLOGICAL APTITUDE TESTS
Klaus-Martin Goeters Mar. 1985 50 p refs In GERMAN; ENGLISH summary Report will also be announced as translation (ESA-TT-943)
(DFVLR-FB-85-20; ISSN-0171-1342) Avail: NTIS HC A03/MF A01; DFVLR, Cologne DM 16.50

A series of psychological aptitude tests was analyzed with respect to human performance and reliability. A factor analysis of the test scores reveals five components of performance. Three independent error components are extracted: errors in quick visual detection of targets; difficulties in mental processing of numbers and symbols; and erroneous actions under performance stress. All three factors are the expression of a deficient control of performance. They are discussed as functional aspects of decision making and human information processing. Author (ESA)

N86-10781# Deutsche Forschungs- und Versuchsanstalt fuer Luft- und Raumfahrt, Hamburg (West Germany). Abt. Flugphysiologie und Psychologie.
SPEED OF WORK AND ERROR RATE: ANALYSES OF INDIVIDUAL DIFFERENCES IN A CHOICE REACTION SERIES WITH A COGNITIVE COMPONENT
Klaus-Martin Goeters Mar. 1985 27 p refs In GERMAN; ENGLISH summary Report will also be announced as translation (ESA-TT-944)
(DFVLR-FB-85-21; ISSN-0171-1342) Avail: NTIS HC A03/MF A01; DFVLR, Cologne DM 10.50

A visual choice reaction test with a cognitive component was introduced to measure response processes in more detail than is possible with summarizing scoring of paper pencil tests. For each reaction the following information was registered: stimulus (light), reaction (right/wrong), reaction time, and omission (yes/no). Each subject had to react on 320 successive signals without pause. From the reaction protocol of each subject indices for speed of work, oscillation of performance, error disposition, and reaction inhibition were computed. The main result is that in this reaction test speed of work and error disposition are not coupled. Errors are not a consequence of quick reactions. The observed errors seem to be the expression of an increased variation in performance. The results are discussed with a view to a psychophysiological model of activation. Author (ESA)

N86-10782# Institute for Perception RVO-TNO, Soesterberg (Netherlands). Afd. Psychologie.
STANDARDIZATION OF TASKS: APPROACH PLANNING
A. W. K. Gaillard and L. C. Boer Jul. 1984 19 p In DUTCH; ENGLISH summary
(Contract A83/K/045)
(IZF-1984-19; TDCK-79518) Avail: NTIS HC A02/MF A01

Ten information processing tasks were grouped on a microcomputer for use in, e.g., personnel selection, the registration of pyschological fitness (combat readiness) and assessing mental workload. Testing areas are: reaction time, (continuing) memory searching, selective attention, pursuit-tracking, serial memory, word classification, logical arguing, and response-conflict situations. The program is developped to be administered by personnel with 1 week training. Author (ESA)

N86-10783# Institute for Perception RVO-TNO, Soesterberg (Netherlands). Traffic Behavior Group.
PATH ERROR-NEGLECTION IN STRAIGHT LANE DRIVING
J. Godthelp Oct. 1984 21 p refs
(IZF-1984-32; TDCK-79696) Avail: NTIS HC A02/MF A01

Decision rules, describing how drivers switch from error-neglection to error-correction when approaching the edge of a lane, were derived for a straight lane keeping task. Drivers were instructed to neglect the vehicle path error and to switch over to error-correction only at that moment. The vehicle motion still could comfortably be corrected to prevent a crossing of the lane boundary. The results show that the lateral distance from the lance boundary at which drivers switch to error-correction increases linearly with the lateral approach speed. This mechanism results in a constant time to lane crossing distance at this decision moment, this result being consistant for a broad range of speeds. Author (ESA)

N86-10745# Joint Publications Research Service, Arlington, Va.
EFFECT OF EMOTIONAL STRESS ON HEMOSTASIS SYSTEM OF HEALTHY PERSONS Abstract Only
Ye. I. Sokolov, T. P. Khovanskaya, I. V. Novikov, and M. V. Baluda *In its* USSR Rept.: Life Sci. Biomed. and Behavioral Sci. (JPRS-UBB-85-023) 18 Sep. 1985 p 62 Transl. into ENGLISH from Fiziol. Cheloveka (Moscow), v. 11, no. 1, Jan. - Feb. 1985 p 79-82 (For primary document see N86-10738 01-51)
Avail: NTIS HC A06

54 MAN/SYSTEM TECHNOLOGY AND LIFE SUPPORT

Includes human engineering; biotechnology; and space suits and protective clothing.

N86-10784 Ohio State Univ., Columbus.
THE INFLUENCE OF TACTUAL SEAT-MOTION CUES ON TRAINING AND PERFORMANCE IN A ROLL-AXIS COMPENSATORY TRACKING TASK SETTING Ph.D. Thesis
Edward Albert Martin 1985 327 p
Avail: Univ. Microfilms Order No. DA8510600

A considerable body of knowledge exists regarding the influence of whole-body motion on the control behavior and task performance of a vehicle operator required to compensate for the effects of unexpected external disturbances. The research described was conducted to determine whether similar effects would be observed if the motion information were tactually displayed through the seat pan, rather than in a whole-body motion environment. The experiment was designed such that the transfer of training from a tactual dynamic seat display to a whole-body motion environment could also be evaluated. The environmental task required subjects to regulate for a random-appearing, roll-axis disturbance in a simulated vehicle having aircraft-like dynamics. A centrally located compensatory display, subtending about nine degrees, provided visual roll error information. Control inputs were made via a right side-arm isometric controller. The two-phase experiment included a training phase and a criterion phase. The data clearly demonstrate that a dynamic sea pan can effectively impart motion information. Dissert. Abstr.

N86-10785*# Pennsylvania Univ., Philadelphia. Dept. of Computer and Information Science.
TEMPUS: SIMULATING PERSONNEL AND TASKS IN A 3-D ENVIRONMENT Final Report
Norman I. Badler and Jon D. Korein 31 May 1985 18 p
(Contract NAS9-16634)
(NASA-CR-171901; NAS 1.26:171901) Avail: NTIS HC A02/MF A01 CSCL 05H

The latest TEMPUS installation occurred in March, 1985. Another update is slated for early June, 1985. An updated User's Manual is in preparation and will be delivered approximately mid-June, 1985. NASA JSC has full source code listings and internal documentation for installed software. NASA JSC staff has received instruction in the use of TEMPUS. Telephone consultations have augmented on-site instruction. G.L.C.

N86-10786# Defence Research Establishment, Ottawa. (Ontario).
EFFECT OF INCREASED BODY CLOTHING INSULATION ON HAND TEMPERATURE IN A COLD ENVIRONMENT
S. D. Livingstone, R. W. Nolan, and S. W. Cattroll Dec. 1984 17 p
(AD-A156597; DREO-TN-84-26) Avail: NTIS HC A02/MF A01 CSCL 06/17

Thermal protection of personnel who must remain relatively inactive while performing tasks outdoors in the cold is a continuing problem. Provision of comfort and allowing for mobility are design difficulties experienced by persons working in the cold at tasks for which manual dexterity is required is In such situations only very light handwear can be worn and often, mitts or gloves must be removed in order to perform the task. A particular example of such a task exists at the CF Satellite Tracking and Identification Unit at St. Margaret's, New Brunswick. The telescope which is used for tracking satellites is located outdoors when operational. To minimize optical interference, the area around the telescope cannot be heated in winter. During the course of the tracking sequence, which takes about 30 minutes, the operator must be in contact with the large metal mass of the telescope. In addition, the operation of the steering control button requires that if any handwear is worn, it must be very thin. Operating temperatures as low as -20 C are often experienced. It was found that, as predicted, if additional insulation was applied to the whole body of the man, the temperature of his hands could be maintained for a longer period of time. GRA

N86-10787# Air Force Inst. of Tech., Wright-Patterson AFB, Ohio.
MILD HYPOXIA AND VISUAL PERFORMANCE WITH NIGHT VISION GOGGLES M.S. Thesis
L. L. Leber May 1985 57 p
(AD-A156969; AD-E950724; AFIT/CI/NR-85-35T) Avail: NTIS HC A04/MF A01 CSCL 06/5

Pilots have frequently reported an apparent darkening of the visual field while flying at high altitude without supplemental oxygen, and subsequent exposure to oxygen resulted in marked increases in the brightness of lights. Likewise, at low light intensities visual acuity is greatly decreased during oxygen deprivation. In contrast, at high light intensities, the effect of moderate oxygen deprivation on visual acuity is slight. Even though the Night Vision Goggles (NVGs) amplify low night illumination, the interaction between amplified illumination and high altitude effects may provide to be important factors in visual performance. The objective of this research was to investigate the effects of mild hypoxid aon monocular visual performance with NVGs. This study revealed that mild oxygen deprivation significantly affects unaided square-0wave grating visual acuity but does not significantly affect NVG-augmented performance. Large differences between visual sensitivities at different spatial frequencies were not differentially affected by mild hypoxia. Supplemental oxygen did significantly improve naked-eye but not NVG-augmented night resolution acuity up to an altitude of 13,000 feet (3,692 m) above sea level (ASL). GRA

N86-10788# Aeronautical Research Labs., Melbourne (Australia).
A GRAPHIC ANTHROPOMETRIC AID FOR SEATING AND WORKPLACE DESIGN
K. C. Hendy, K. W. Anderson, and D. M. Drumm Apr. 1984 60 p
(AD-A156988; AD-E950724; ARL/SYS-R-29) Avail: NTIS HC A04/MF A01 CSCL 06/14

In recent workplace design projects at ARL, a procedure for the use of anthropometric information has be developed which relies on the use of sets of anthropometric data from individuals rather than the conventionally used pooled data. This report describes a graphic anthropometric design aid which has been devised to assist in the implementation of this procedure. The aid predicts the positions, in side elevation, of certain cardinal points which are considered to be important to the design process, viz, the eye, thumb tip reach, knee point, seat reference point and heel point. This report also contains details of the design aid's validation, the concept of the aid's use and the fidelity of the aid within the design process. GRA

N86-10789# Institute for Perception RVO-TNO, Soesterberg (Netherlands). Afd. Thermofysiologie.
THE WEARING COMFORT OF THE PVC: COMBAT BACK PACK
F. J. G. vanderlinde and H. VanMiddendorp Nov. 1984 24 p In DUTCH; ENGLISH summary
(Contract A79/KL/097)
(IZF-1984-34; TDCK-79782) Avail: NTIS HC A02/MF A01

A PVC coated back pack was compared to canvas ones. Wearing comfort, particularly with regard to sweat build-up, body temperatures, and thermal sensation were studied. Data from two subjects walking on a treadmill in a climate chamber were obtained. The PVC prototype scores slighthy better the canvas rucksack. Author (ESA)

55 PLANETARY BIOLOGY

Includes exobiology; and extraterrestrial life.

No abstracts in this category.

59 MATHEMATICAL AND COMPUTER SCIENCES (GENERAL)

N86-10790# IIT Research Inst., Rome, N.Y.
CATALOG OF RESOURCES FOR EDUCATION IN Ada (TRADEMARK) AND SOFTWARE ENGINEERING (CREASE). VERSION 3.0
May 1985 334 p
(Contract MDA903-83-C-0306)
(AD-A156687) Avail: NTIS HC A15/MF A01 CSCL 05/9

Over the last twenty-five years, software technology has made enormous strides. The Ada program serves as a focal point for the consolidation of state-of-the-art thinking about this technology. Proper use of the technology can contribute significantly to controlling the cost and improving the quality of software. However, this is a sophisticated technology, and its proper use depends upon sophisticated education and training for the people applying it. The effectiveness of the Ada programming language will be determined by the degree to which people are able to use it to implement software engineering practices in applications programming. A carefully planned education and training program, which teaches both fundamental software engineering concepts and the effective use of the Ada language, is therefore essential. This publication is intended to serve as a source of information about resources available to those who are planning such programs, with the hope that it will not only serve as a ready reference, but will also increase awareness of the many aspects of education in Ada and Software Engineering. GRA

60 COMPUTER OPERATIONS AND HARDWARE

Includes computer graphics and data processing.
For components see *33 Electronics and Electrical Engineering.*

N86-10791# Naval Postgraduate School, Monterey, Calif.
COMPUTER-BASED TRAINING FOR THE US COAST GUARD STANDARD TERMINAL MICROCOMPUTER: A BASIS FOR IMPLEMENTATION UTILIZING THE ELABORATION THEORY OF INSTRUCTIONAL DESIGN M.S. Thesis
S. E. Johnson Mar. 1985 81 p
(AD-A156548) Avail: NTIS HC A05/MF A01 CSCL 09/2

Various factors concerning the U.S. Coast Guard Standard Terminal microcomputer, including the large number of installation sites, steady turnover of user personnel, and conflicting demands of operational commitments indicate that computer-based training is a desirable approach for indoctrinating new users of the computer system. Any such instructional computer program developed for this purpose should consider the characteristics of the trainee audience, particularly the varied levels of procedural detail desired and constraints on time available for training. The elaboration theory of instructional design provides an excellent framework for creating a viable computer-based course of instruction. A Pascal computer program and demonstration lesson modules utilize the macro-strategy components of Elaboration Theory in an introductory course on computer procedures. Course presentation is controlled by special characters imbedded in the lesson text files and interpreted by the program. Author (GRA)

N86-10792# Department of the Navy, Washington, D. C.
PARALLEL LOCAL INTERFACE BUS Patent Application
G. J. Palatucci, C. M. Nowicki, and R. Whitsel, inventors (to Navy)
Filed 29 Nov. 1984 20 p
(AD-D011742; US-Patent-Appl-SN-677136) Avail: NTIS HC A02/MF A01 CSCL 09/2

A modular parallel local interface bus provides a two-way interface between a microprocessor and a plurality of distributed signal processing units which are controlled by the microprocessor. Likewise, the microprocessor is enabled to read operational parameter data from sensors in the signal processing units. In this way, a plurality of discrete signal processing units may be controlled to perform required RF transmit-receive functions. The units may also be monitored for any operational problems which could develop. Author (GRA)

N86-10793# Royal Signals and Radar Establishment, Malvern (England).
SPECIAL PURPOSE HARDWARE ARCHITECTURES FOR LANGUAGE RECOGNITION
R. A. Evans and J. D. Morison Mar. 1985 22 p
(AD-A156634; RSRE-Memo-3806; DRIC-BR-95704) Avail: NTIS HC A02/MF A01 CSCL 09/2

Two distinct chip architectures for language recognition are presented. THe first allows a recogniser for any regular expression to be constructed by simply assembling predefined cells linto a linear array. The cells correspond to the symbols which can occur in a regular expression, and the appropriate cells are placed in a line in the same order as the expression. The recogniser is then correct by construction, and all inter-cell connections are made automatically. The second architecture can be programmed to recognize any LL(1) context-free language by loading it with the appropriate grammar rules. The grammar rules are embodied within and array of identical cells, which, in conjunction with a standard LIFO stack, form the recognition hardware. Author (GRA)

N86-10794# Yale Univ., New Haven, Conn. Dept. of Computer Science.
ALTERNATING DIRECTION METHODS ON MULTIPROCESSORS: AN EXTENDED ABSTRACT
Y. Saad and M. H. Schultz Apr. 1985 7 p
(Contract N00014-82-K-0184)
(AD-A156722; Yaleu/DCS/RR-381) Avail: NTIS HC A02/MF A01 CSCL 09/2

We propose a few implementations of the Alternating Direction Method for solving parabolic partial differential equations on multiprocessors. A careful complexity analysis of these implementations shows that, contrary to what is generally believed, the method can be made highly efficient on parallel architectures by using pipelining and variations of the classical Gaussian elimination algorithm for solving tridiagonal systems. GRA

N86-10795# Yale Univ., New Haven, Conn. Dept. of Computer Science.
EFFICIENT SYSTOLIC ARRAYS FOR THE SOLUTION OF TOEPLITZ SYSTEMS: AN ILLUSTRATION OF A METHODOLOGY FOR THE CONSTRUCTION OF SYSTOLIC ARCHITECTURES IN VLSI (VERY LARGE SYSTEMS INTEGRATION)
J. M. Delosme and I. C. F. Ipsen Jun. 1985 25 p
(Contracts N00014-82-K-0184; N00014-84-K-0092)
(AD-A156767; Yaleu/DCS/RR-370) Avail: NTIS HC A02/MF A01 CSCL 09/2

Advanced high resolution methods for real-time signal processing require fast multiprocessor architectures, realized as Very Large Scale Integrated systems, for their implementation. A class of parallel structures, systolic arrays, fulfills the demands of signal processing and at the same time conforms to the limitations of

VLSI technology. The design of efficient systems of systolic arrays is an iterative process in which the information gathered from mapping algorithms onto hardware is influential in the development of the algorithms. Presently, the absence of mapping tools makes it extremely difficult to find good systolic implementations for many important problems. Often, one cannot do better than implementing structurally simple but numerically inferior algorithms, which is undesirable for most signal processing tasks. A methodology is proposed that automates the mapping of recurrence equations to processor arrays. Two aspects distinguish our methodology from extant work: (1) complex coupled systems of recurrence equations can be systematically treated, and (2) the resulting systolic systems are optimal. The methodology takes as input recurrence equations describing the algorithm, along with certain desirable hardware features. GRA

N86-10796# Naval Postgraduate School, Monterey, Calif.
INITIAL DESIGN OF A RELATIONAL DATABASE SYSTEM FOR NPS COMPUTER ASSET IDENTIFICATION AND VALUATION FOR RISK ASSESSMENT M.S. Thesis
F. W. Thompson Mar. 1985 124 p
(AD-A156847; AD-E301723) Avail: NTIS HC A06/MF A01 CSCL 09/2

Relational database technology is examined as a means to support computer Risk Assessment at the Naval Postgraduate School. The current methodology for conducting computer Risk Assessment within the Department of the Navy is used to construct an initial design for a relational database system. The initial design focuses on computer asset identification and valuation as the first step of the computer Risk Assessment process. GRA

N86-10797# Naval Postgraduate School, Monterey, Calif.
DEVELOPMENT OF IS2100: AN INFORMATION SYSTEMS LABORATORY M.S. Thesis
C. S. D. Witten Mar. 1985 41 p
(AD-A156848; AD-E301723) Avail. NTIS HC A03/MF A01 CSCL 09/2

On the premise that fundamental concepts and uses of microcomputers can be better taught in a hands-on environment, the Administrative Science Department Instructional Laboratory was established. IS 2100, an Information Systems Laboratory uses these facilities to reinforce material taught in the first two quarters of the Computer System Management Curriculum. Its purpose and objective is to develop computer literacy and introduce the student to microcomputers and the facilities of the developing laboratory. This thesis is the report of the development of IS 2100 as first taught during Winter 1985. GRA

N86-10798# Air Force Inst. of Tech., Wright-Patterson AFB, Ohio.
APPLICATIONS FOR THREE-DIMENSIONAL COMPUTER GRAPHIC CLOUD REPRESENTATIONS PRODUCED FROM SATELLITE IMAGERY M.S. Thesis
A. C. Meade 1985 112 p
(AD-A156903; AFIT/CI/NR-85-50T) Avail: NTIS HC A06/MF A01 CSCL 04/2

In this research process, two-dimensional satellite topographic images are used to produce 3-D, mathematically defined, cloud-topography models. This research focuses on applications for three-dimensional cloud representations which are displayed above a topographic surface. The computer graphic cloud-topography displays are produced using actual GOES satellite data, Defense Mapping Agency topography data, and rawinsonde upper air data. Data from these three sources is used to generate three-dimensional models which mathematically define cloud cover and topography for a given area. By applying computer graphics techniques, these three-dimensional models can be displayed as continuous tone images or perspective line drawings. Satellite data and topography data, displayed in this manner, produces a realistic depiction of cloud cover displayed above a topographic surface. As for applications, these displays can be used for cloud studies, briefing aids, and flight simulations. GRA

N86-10799# Department of the Air Force, Washington, D.C.
HARMONIC DISTORTION REDUCTION TECHNIQUE FOR DATA ACQUISITION Patent Application
W. P. Evans, inventor (to Air Force) Filed 12 Jun. 1985 18 p
(AD-D011771; US-Patent-Appl-SN-743853) Avail: NTIS HC A02/MF A01 CSCL 09/2

An analog to digital converter (ADC) is presented which uses a calibration technique to reduce harmonic distortion in data acquisition systems. This mechanization also allows faster conversion rates than previously possible for high resolution analog-to-digital converters. This converter makes use of a subrange or half Flash architecture where the subrange digital-to-analog converter (DAC) is augmented with a software calibrated DAC which removes system nonlinearities. The advantage of this system is that it allows the building of higher speed data acquisition systems with higher spurious free dynamic range than would be possible with conventional techniques. By adding the correction to the input of the subrange ADC, correction resolution can be a fraction of a quanta. A second approach using the same mathematics places at the output of the ADC a RAM or ROM look up table which linearizes the transfer function. Author (GRA)

N86-10800# Department of the Air Force, Washington, D.C.
ARITHMETIC PIPELINE FOR IMAGE PROCESSING Patent Application
W. R. Steiner, inventor (to Air Force) Filed 6 Jun. 1985 77 p
(AD-D011773; US-Patent-Appl-SN-741644) Avail: NTIS HC A05/MF A01 CSCL 09/2

The arithmetic pipeline processor (which is used for computer graphics such as a flight simulator) is a group of boards capable of solving an equation of a certain form. It includes a digital logarithmic calculator using shifters and stored tables to perform arithmetic functions such as multiplication, division, squares, square roots, and fourth roots. It comprises two imput ports each capable of receiving digital data N bits wide. Included are a log transform unit, a log sum or difference unit and an antilog unit. Following these is an M-bit Ariithmetic Logic Unit and circuitry for converting between fixed point and floating numbers. It uses piece wise linear approximation in conjunction with stored slope information in tables to do the transform calculation of logarithms and antilogarithms. The M-bit arithmetic unit performs accumulation of up to k terms. In a specific embodiment, N=32, M-36, and K=128. Note that a pipeline processor has no central processing unit or software in itself, but it may interface with a computer for inputs and outputs including control information. GRA

N86-10801# Stanford Linear Accelerator Center, Calif.
DISSECTING THE COW
E. Linstadt Apr. 1985 3 p Presented at the Particle Accelerator Conf., Vancouver, British Columbia, 13 May 1985
(Contract DE-AC03-76SF-00515)
(DE85-013369; SU-SLAC-PUB-3638; CONF-850504-69) Avail: NTIS HC A02/MF A01

The COW, or Console On Wheels, is the primary operator interface to the Stanford Linear Collider (SLC) accelerator control system. A hardware and oftware description of the COW, a microcomputer based system with a color graphics display output and touch-panel and knob inputs, is given. The ease of development and expandability, due to both the modular nature of the hardware and the multitasking, interrupt driven software running in the COW, are described. Integration of the COW into the SLCNET communications network and SLC Control system is detailed. DOE

N86-10802# Technische Hogeschool, Eindhoven (Netherlands). Digital Systems Group.
DESIGN OF A MULTIFUNCTION INPUT-OUTPUT (I/O) CONTROLLER
M. P. J. Stevens and M. P. M. vanLoon Aug. 1984 63 p refs In FRENCH; ENGLISH summary
(EUT-84-E-143; ISBN-90-6144-143-9; ISSN-0167-9708) Avail: NTIS HC A04/MF A01

A multifunction I/O-controller used for the exchange of data between a microcomputer and a peripheral was designed. Design strategies for the realization of (V)LSI-circuits are discussed. By partitioning the controller into subsystems and carefully defining the interaction between these subsystems, the design can be implemented in a number of technologies like custom designed NMOS or gate-arrays. The controller can be used with many Intel and Motorola processors and it has four programmable modes: direct I/O, handshake I/O, three wire I/O and bidirectional I/O. Author (ESA)

N86-10803# Technische Hogeschool, Eindhoven (Netherlands). Digital Systems Group.
MINIMIZATION OF PROGRAMMABLE LOGIC ARRAYS
M. J. M. vanWeert Nov. 1984 48 p refs In DUTCH; ENGLISH summary
(EUT-84-E-145; ISBN-90-6144-145-5; ISSN-0167-9708) Avail: NTIS HC A03/MF A01

The efforts undertaken to minimize four programmable logic arrays (PLA) and so to define part of the control section of a multifunction I/O controller, are described. The silicon area occupied by the minimized PLA is equal to 65% of the original area. It is shown that searching for and recognizing terms as don't care terms, and inverting one or more output functions contribute a lot to the final result. The functional behavior of the PLA was simulated before and after minimization, and is found to be correct. Author (ESA)

N86-10804# Technische Hogeschool, Eindhoven (Netherlands). Digital Systems Group.
REALIZATION OF A MULTIFUNCTION INPUT/OUTPUT (I/O) CONTROLLER BY MEANS OF A GATE ARRAY
L. T. Rozendaal, M. P. J. Stevens, and P. M. C. M. vandenEijnden Jan. 1985 110 p refs In DUTCH; ENGLISH summary
(EUT-85-E-147; ISBN-90-6144-147-1; ISSN-0167-9708) Avail: NTIS HC A06/MF A01

The implementation process of a multifunction I/O controller using a gate consisting of Schottky TTL gates is described. This process is straightforward if during the logic design (analysis) of the chip, care is given to a modular construction and when the logic in the chip is defined using regular structures like programmable logic arrays instead of so-called wild logic. The software package used to define, simulate, and test the design of the I/O controller, is described. Author (ESA)

N86-10805# Technische Hogeschool, Eindhoven (Netherlands). Digital Systems Group.
A COURSE ON FIELD PROGRAMMABLE LOGIC
P. M. C. M. vandenEijnden Apr. 1985 122 p refs
(EUT-85-E-148; ISBN-90-6144-148-X; ISSN-0167-9708) Avail: NTIS HC A06/MF A01

Programmable logic components that can be used to realize both combinational and sequential logic circuits are reviewed. A general structure for these components starting with boolean equations and state diagrams is determined. The considerations with respect to optimization and decomposition of a circuit, important in designs with these components, are discussed. Commercially available products are included. Author (ESA)

N86-10806# Technische Hogeschool, Delft (Netherlands). Lab. voor Schakeltechniek en Techniek van de Informatieverwerkende Machines.
THE LOCAL DISK CONTROLLER
G. E. Houtekamer 7 Feb. 1985 20 p refs
(Rept-1-68430-44(1985)01) Avail: NTIS HC A02/MF A01

The performance of the input/output (I/O) subsystem in the the IBM 370-XA architecture was increased considerably by a modified of the new channel subsystem, as compared to the System/370. The emphasis in the 370-XA architecture is on reducing the CPU load associated with I/0, and on reducing the contention in multi-CPU, shared systems, by redesigning the channel system. It is shown that a reallocation of the control unit logic may triple channel subsytem capacity, while still using the same disk drives. The performance gain is achieved by adding intelligence and local buffer memory to each disk drive, creating a local disk controller. The proposed system remains fully software compatible with the 370-XA architecture. Author (ESA)

N86-10807# Technische Hogeschool, Delft (Netherlands). Lab. voor Schakeltechniek en Techniek van de Informatieverwerkende Machines.
PERFORMANCE ANALYSIS OF THE IBM DIRECT ACCESS STORAGE DEVICE (DASD) SUBSYSTEM, AND SOME SUGGESTIONS FOR IMPROVED SYSTEMS
G. E. Houtekamer 7 Feb. 1985 19 p refs
(Rept-1-68430-44(1985)02) Avail: NTIS HC A02/MF A01

The IBM 370-XA input/output (I/O) architecture is described. The I/O response time consists of several components, such as the seek and rotational delay. All access time components are analyzed, and suggestions to improve the system are given. The buffered disk system and local disk controller system are discussed. After modifications to the hardware of the 370-XA I/O subsystem they provide a much better performance. The local disk controller system allows access rate of the order of 60 SIOs per disk per second. The performance improvements achievable with caching for the control unit based system, and for the local disk controller system are investigated. Author (ESA)

N86-10808# Technische Hogeschool, Delft (Netherlands). Lab. voor Schakeltechniek en Techniek van de Informatieverwerkende Machines.
AN INTELLIGENT LOCAL DISK CONTROL SYSTEM
G. E. Houtekamer 1 May 1984 131 p refs
(Rept-051560-28(1984)08) Avail: NTIS HC A07/MF A01

A disk input/output (I/O) system for IBM 30xx series main frames was developed. The system is based on the utilization of an intelligent local control for each disk pack. The disks are connected to the central computer via a high-speed bus (32 MB/sec). Every disk is equipped with an Intel iAPx 286 microprocessor, which controls the disk hardware and executes the I/O programs. The system is designed so that the most expensive components of the I/O system; the top model from the IBM disk-series (3380); and the present software (IBM/MUS operating system) can be used without adaptation. Author (ESA)

N86-10809# Joint Publications Research Service, Arlington, Va.
USSR REPORT: CYBERNETICS, COMPUTERS AND AUTOMATION TECHNOLOGY
5 Sep. 1985 153 p refs Transl. into ENGLISH from various Russian articles
(JPRS-UCC-85-006) Avail: NTIS HC A08

Progress is reported in U.S.S.R. cybernetics, computers and automation technology. Topics discussed include: (1) general automation technology; (2) hardware; (3) software; (4) computer applications; (5) computer networks; (6) computation theory; (7) education; and (8) automation organizations. For individual titles, see N86-10810 through N86-10818.

N86-10810# Joint Publications Research Service, Arlington, Va.
PROSPECTS FOR CREATION OF OPTICAL DIGITAL HIGH-PERFORMANCE COMPUTERS
V. M. Yegorov and E. G. Kostsov *In its* USSR Rept.: Cybernetics, Computers and Automation Technol. (JPRS-UCC-85-006) 5 Sep. 1985 p 22-36 refs Transl. into ENGLISH from Avtometriya (Novosibirsk), no. 1, Jan. - Feb. 1985 p 114-126 (For primary document see N86-10809 01-60)
Avail: NTIS HC A08

The technological feasibility of creating optical digital high-performance computers is investigated. The need for increased computer productivity in solving large-scale problems in space research and mathematical physics is established. General advances in microelectronic technology are discussed in the area of optical data processing. Specifically, the possibility of fabricating a thin film electrooptic light modulator is explored. B.W.

N86-10811# Joint Publications Research Service, Arlington, Va.
ELEKTRONIKA MS 1603 HIGH-SPEED PERIPHERAL PROCESSOR

V. A. Dyboy, V. V. Kashtanov, V. O. Lazarev, and A. A. Fokin *In its* USSR Rept.: Cybernetics, Computers and Automation Technol. (JPRS-UCC-85-006) 5 Sep. 1985 p 39-43 Transl. into ENGLISH from Avtometriya (Novosibirsk), no. 2, Mar. - Apr. 1985 p 88-90 (For primary document see N86-10809 01-60)
Avail: NTIS HC A08

High-speed peripheral processors, with their high computation speed, high reliability, compact design and low power requirement, have found wide application in recent years. An example of such a system is the Elektronika MT-70 high-speed peripheral processor, series-produced by domestic industry for many years. The Elektronika MS 1603 was developed on the basis of operational experience with the MT-70 and is compatible with the latter at the application program level. The Elektronika MSS 1603 high-speed peripheral processor can be used in conjunction with any computer having a common-bus type parallel bus interface between modules. Its primary purpose in operation with an Elektronia 60 computer system is the execution of a large number of vector multiplication and addition operations. The technical specifications of the Elektronika MS 1603 high-speed peripheral processor are given. B.W.

N86-10812# Joint Publications Research Service, Arlington, Va.
DIAGNOSTICS OF PERIPHERAL PROCESSORS AND CONTROLLERS
V. A. Dyboy, O. S. Semenova, and A. A. Fokin *In its* USSR Rept.: Cybernetics, Computers and Automation Technol. (JPRS-UCC-85-006) 5 Sep. 1985 p 48-53 Transl. into ENGLISH from Avtometriya (Novosibirsk), no. 2, Mar. - Apr. 1985 p 90-93 (For primary document see N86-10809 01-60)
Avail: NTIS HC A08

One of the problems facing computer system manufacturers and users is that of calibration and maintenance. The problem is caused by the increasing complexity of equipment combined with the inflexible nature of the methods of testing employed. These methods are based on component troubleshooting (the location and correction of failed components) according to indirect signs generated as the result of operational monitoring. Under these conditions, the introduction of more progressive and higher quality (and more complex) equipment is inefficient due to the concomitant need for hiring or training highly qualified specialists to calibrate (during production) or repair (during operation) this equipment. A diagnostic method using built-in diagnostic hardware is described which allows a significant increase in the scope of troubleshooting. B.W.

N86-10813# Joint Publications Research Service, Arlington, Va.
AN APPROACH TO IMPLEMENTING CAMAC MICROPROCESSOR MODULES
Ye. M. Bazarnyy, A. N. Vystavkin, L. Z. Pososhenko, V. P. Reztsov, and A. B. Furshchik *In its* USSR Rept.: Cybernetics, Computers and Automation Technol. (JPRS-UCC-85-006) 5 Sep. 1985 p 54-58 refs Transl. into ENGLISH from Upravlyayushchiye Sistemy i Mashiny (Kiev), no. 2, Mar. - Apr. 1985 p 106-108 (For primary document see N86-10809 01-60)
Avail: NTIS HC A08

CAMAC (computer automated measurement and control) hardware is widely used in the creation of systems for automating scientific research. The use of microprocessors in CAMAC hardware allows substantial improvement in functional characteristics and increases in system efficiency. In addition to the design of multicontroller microprocessor systems, a generation of smart modules needs to be developed to enable preliminary data processing directly in the control subprogram execution module and to perform a number of auxiliary tasks (automonitoring, parameter correction, etc.). This article discusses one possible architecture for a new generation of CAMAC modules based on microprocessor components and points out the superior properties of these modules. Author

N86-10814# Joint Publications Research Service, Arlington, Va.
COMPACT, HIGH-SPEED ALGORITHM FOR LAYING OUT PRINTED CIRCUIT BOARD RUNS c33
D. Ye. Zapolotskiy *In its* USSR Rept.: Cybernetics, Computers and Automation Technol. (JPRS-UCC-85-006) 5 Sep. 1985 p 59-67 refs Transl. into ENGLISH from Upravlyayushchiye Sistemy i Mashiny (Kiev), no. 2, Mar. - Apr. 1985 p 33-37 (For primary document see N86-10809 01-60)
Avail: NTIS HC A08

A high speed printed circuit connection layout algorithm is described which was developed within the framework of an interactive system for designing two-sided printed circuit broads. For this reason, algorithm speed was considered, a priori, as a requirement equally as important as the inherent demand for minimizing circuit run lengths and the number of junction openings. This resulted from the fact that, in order to provide psychological man/machine compatibility in the design process, real-time dialog during the layout phase is possible only within limited time frames (on the order of several seconds) for each circuit run. The work was carried out for use on an ARM-R automated work site complex based on an SM-4 minicomputer with a 32K-word memory. This limited memory capacity heightened the demand for algorithm speed and also tightened data file structure and size requirements. The layout algorithm's design logic is analyzed. The structure and organization of the data files are described. B.W.

N86-10815# Joint Publications Research Service, Arlington, Va.
CLASSIFICATION OF REAL-TIME PROGRAM TESTING TASKS AND METHODS c61
I. N. Dolganyuk and Ye. Ya. Karpovskiy *In its* USSR Rept.: Cybernetics, Computers and Automation Technol. (JPRS-UCC-85-006) 5 Sep. 1985 p 70-83 refs Transl. into ENGLISH from Upravlyayushchiye Sistemy i Mashiny (Kiev), no. 2, Mar. - Apr. 1985 p 57-62 (For primary document see N86-10809 01-60)
Avail: NTIS HC A08

The testing of real-time programs, one of the most important steps in program debugging, is a critical problem in modern programming theory. Usually debugging is understood as the group of activities involved in detecting (identifying) and correcting errors in programs. These activities are grouped in stages: establishing the presence of an error, identifying the error and, finally, correcting the error. In the course of debugging programs, developers are faced with a number of questions involving the determination of current test method capabilities and suitability. An understanding of the nature of the testing process is essential in classifying the methods and tasks involved in seeking errors in programs. The research suggests that the presence of an error in a program is detected by means of the following sequence of actions: (1) test objective definition, (2) tactical goal assignment; (3) criteria selection; (4) test design and generation; (5) test introduction and program execution; (6) program result processing to determine the existence of errors; and (7) testing cutoff point determination. B.W.

N86-10816# Joint Publications Research Service, Arlington, Va.
DBS/R DATABASE CONTROL SYSTEM
Yu. Sharr *In its* USSR Rept.: Cybernetics, Computers and Automation Technol. (JPRS-UCC-85-006) 5 Sep. 1985 p 84-92 Transl. into ENGLISH from Upravlyayushchiye Sistemy i Mashiny (Kiev), no. 2, Mar. - Apr. 1985 p 97-101 (For primary document see N86-10809 01-60)
Avail: NTIS HC A08

The Robotron combine (GDR) is producing YeS- and SM-series computers and developing a wide assortment of system and application software. This paper highlights the database software developed at the Robotron combine which includes database management systems (DBMS) and information retrieval system. One system in particular is examined, the DBS/R Data Base Management System. The general features, functions and languages; applications, and economic effects of the DBS/R are discussed in detail. B.W.

N86-10817# Joint Publications Research Service, Arlington, Va.
COLLECTIVE USE COMPUTER SYSTEM FOR THE ACADEMY OF SCIENCES KaSSR
U. M. Sultangazin, I. T. Pak, M. A. Bulakh, G. T. Manabayev, and

V. A. Tsay *In its* USSR Rept.: Cybernetics, Computers and Automation Technol. (JPRS-UCC-85-006) 5 Sep. 1985 p 105-111 refs Transl. into ENGLISH from Upravlyayushchiye Sistemy i Mashiny (Kiev), no. 2, Mar. - Apr. 1985 p 108-111 (For primary document see N86-10809 01-60)
Avail: NTIS HC A08

At this time electronic computer technology is penetrating many branches of industry at various levels and is solving increasing complex problems. A number of automated control systems for production and engineering processes have been created and are being developed to solve these types of problems. The role and place of the computer in automated control systems has quite definitely grown because of this. A particularly promising field for computer application are automated systems for scientific research which are oriented toward automating labor-intensive processes and which facilitate the establishment of principles behind the phenomena studied. The critical need for computer technology in scientific research has been clearly pointed out in this research. A computer network known as VSKP is described which is intended to increase scientific research efficiency at the Academy of Sciences KaSSR. B.W.

N86-10818# Joint Publications Research Service, Arlington, Va.
DIGITAL PROCESSING OF IMAGES IN TRACKING A MOVING OBJECT **c61**
B. A. Alpatov, A. A. Selyayev, and A. I. Stapashkin *In its* USSR Rept.: Cybernetics, Computers and Automation Technol. (JPRS-UCC-85-006) 5 Sep. 1985 p 123-127 refs Transl. into ENGLISH from Proborostr. (Leningrad), no. 2, Feb. 1985 p 39-43 (For primary document see N86-10809 01-60)
Avail: NTIS HC A08

A digital algorithm for digital processing images in tracking a moving object is proposed. The results of computer simulation are given which confirm the expediency of using the preliminary smoothing of images to increase the precision of evaluating coordinates. Author

61 COMPUTER PROGRAMMING AND SOFTWARE

Includes computer programs, routines, and algorithms.

N86-10819*# Informatics, Inc., Palo Alto, Calif.
LANES 1 USERS' GUIDE
Joe Jordan Feb. 1985 21 p
(Contract NAS2-11555)
(NASA-CR-177334; NAS 1.26:177334; TN-84-7104-925-46) Avail: NTIS HC A02/MF A01 CSCL 09B

This document is intended for users of the Local Area Network Extensible Simulator, version I. This simulator models the performance of a Fiber Optic network under a variety of loading conditions and network characteristics. The options available to the user for defining the network conditions are described in this document. Computer hardware and software requirements are also defined. Author

N86-10820*# Pennsylvania Univ., Philadelphia. Dept. of Computer and Information Science.
USER INTERFACE ENHANCEMENT REPORT
Norman I. Badler, Jeffrey Gangel, Gwen Shields, and Glenn Fala 31 May 1985 50 p refs
(Contract NAS9-16634)
(NASA-CR-171898; NAS 1.26:171898) Avail: NTIS HC A03/MF A01 CSCL 09B

The existing user interfaces to TEMPUS, Plaid, and other systems in the OSDS are fundamentally based on only two modes of communication: alphanumeric commands or data input and grapical interaction. The latter are especially suited to the types of interaction necessary for creating workstation objects with BUILD and with performing body positioning in TEMPUS. Looking toward the future application of TEMPUS, however, the long-term goals of OSDS will include the analysis of extensive tasks in space involving one or more individuals working in concert over a period of time. In this context, the TEMPUS body positioning capability, though extremely useful in creating and validating a small number of particular body positions, will become somewhat tedious to use. The macro facility helps somewhat, since frequently used positions may be easily applied by executing a stored macro. The difference between body positioning and task execution, though subtle, is important. In the case of task execution, the important information at the user's level is what actions are to be performed rather than how the actions are performed. Viewed slightly differently, the what is constant over a set of individuals though the how may vary. G.L.C.

N86-10821*# Pennsylvania Univ., Philadelphia. Dept. of Computer and Information Science.
SYSTEM INTEGRATION REPORT
Norman I. Badler, Jon D. Korein, Craig Meyer, Kamran Manoochehri, Jane Rovins, Jeffrey Beale, and Brian Barr 31 May 1985 42 p refs
(Contract NAS9-16634)
(NASA-CR-171900; NAS 1.26:171900) Avail: NTIS HC A03/MF A01 CSCL 09B

Several areas that arise from the system integration issue were examined. Intersystem analysis is discussed as it relates to software development, shared data bases and interfaces between TEMPUS and PLAID, shaded graphics rendering systems, object design (BUILD), the TEMPUS animation system, anthropometric lab integration, ongoing TEMPUS support and maintenance, and the impact of UNIX and local workstations on the OSDS environment. E.A.K.

N86-10822*# New Orleans Univ., La. Dept. of Physics.
STUDY OF ONE- AND TWO-DIMENSIONAL FILTERING AND DECONVOLUTION ALGORITHMS FOR A STREAMING ARRAY COMPUTER Final Report
George E. Ioup [1985] 6 p
(Grant NsG-1648)
(NASA-CR-176221; NAS 1.26:176221) Avail: NTIS HC A02/MF A01 CSCL 09B

The development of vector processing computers of the streaming array architectures has made possible a dramatic decrease in the time required for the solution of problems, i.e., for those algorithms which readily lend themselves to sequential operations on long vectors. There has concurrently been rapid growth in the applications of the techniques generally known as mathematical digital filtering, also called signal analysis, digital signal processing, time series analysis, and digital image processing. The best known applications of these techniques is to seismic data and two-dimensional images, data types consisting of very large collections of numbers. A major limitation for these cases is the size and speed of the computer available. Therefore, a move to the streaming array architecture can result in marked improvement in the data analysis techniques which may be employed. Author

N86-10823*# New Orleans Univ., La. Dept. of Physics.
A STUDY OF MORRISON'S ITERATIVE NOISE REMOVAL METHOD Final Report M. S. Thesis
George E. Ioup and Karin Ann Ringer Wright Oct. 1985 165 p refs
(Grant NsG-1648)
(NASA-CR-176222; NAS 1.26:176222) Avail: NTIS HC A08/MF A01 CSCL 09B

Morrison's iterative noise removal method is studied by characterizing its effect upon systems of differing noise level and response function. The nature of data acquired from a linear shift invariant instrument is discussed so as to define the relationship between the input signal, the instrument response function, and the output signal. Fourier analysis is introduced, along with several pertinent theorems, as a tool to more thorough understanding of the nature of and difficulties with deconvolution. In relation to such difficulties the necessity of a noise removal process is discussed. Morrison's iterative noise removal method and the restrictions upon its application are developed. The nature of permissible response functions is discussed, as is the choice of the response functions used. Author

N86-10824*# New Orleans Univ., La. Dept. of Physics.
ALWAYS-CONVERGENT ITERATIVE NOISE REMOVAL AND DECONVOLUTION FOR IMAGE DATA Final Report
M.S. Thesis
George E. Ioup and Mark A. Whitehorn Dec. 1981 143 p refs
(Contract NsG-1648)
(NASA-CR-176223; NAS 1.26:176223) Avail: NTIS HC A07/MF A01 CSCL 09B

Linear filtering techniques currently used for the restoration of noisy, blurred or otherwise degraded image data are discussed and new techniques related to the iterative techniques of Morrison and van Cittert are developed and implemented. Programs written for the implementation are discussed in the appendices. It is shown that the new techniques are convergent for any system response function, and they are applied to the task of restoring a severely blurred image. Author

N86-10825*# New Orleans Univ., La. Dept. of Physics.
A STUDY OF DERIVATIVE FILTERS USING THE DISCRETE FOURIER TRANSFORM Final Report M. S. Thesis
George E. Ioup May 1980 105 p refs
(Grant NsG-1648)
(NASA-CR-176224; NAS 1.26:176224) Avail: NTIS HC A06/MF A01 CSCL 09B

Important properties of derivative (difference) filters using the discrete Fourier transform are investigated. The filters are designed using the derivative theorem of Fourier analysis. Because physical data are generally degraded by noise, the derivative filter is modified to diminish the effects of the noise, especially the noise amplification which normally occurs while differencing. The basis for these modifications is the reduction of those Fourier components for which the noise most dominates the data. The various filters are tested by applying them to find differences of two-dimensional data to which various amounts of signal dependent noise, as measured by a root mean square value, have been added. The modifications, circular and square ideal low-pass filters and a cut-off pyramid filter, are all found to reduce noise in the derivative without significantly degrading the result. Author

N86-10826*# New Orleans Univ., La. Dept. of Physics.
COORDINATE AXES, LOCATION OF ORIGIN, AND REDUNDANCY FOR THE ONE AND TWO-DIMENSIONAL DISCRETE FOURIER TRANSFORM Final Report
George E. Ioup and Juliette W. Ioup [1985] 24 p refs
(Grant NsG-1648)
(NASA-CR-176225; NAS 1.26:176225) Avail: NTIS HC A02/MF A01 CSCL 09B

Appendix 4 of the Study of One- and Two-Dimensional Filtering and Deconvolution Algorithms for a Streaming Array Computer discusses coordinate axes, location of origin, and redundancy for the one- and two-dimensional Fourier transform for complex and real data. F.M.R.

N86-10827*# New Orleans Univ., La. Dept. of Physics.
STUDY OF ONE- AND TWO-DIMENSIONAL FILTERING AND DECONVOLUTION ALGORITHMS FOR A STREAMING ARRAY COMPUTER Final Report
George E. Ioup [1985] 10 p refs
(Grant NsG-1468)
(NASA-CR-176226; NAS 1.26:176226) Avail: NTIS HC A02/MF A01 CSCL 09B

Appendix 5 of the Study of One- and Two-Dimensional Filtering and Deconvolution Algorithms for a Streaming Array Computer includes a resume of the professional background of the Principal Investigator on the project, lists of this publications and research papers, graduate thesis supervised, and grants received. F.M.R.

N86-10828*# National Aeronautics and Space Administration. Langley Research Center, Hampton, Va.
USER'S GUIDE FOR LANGLEY RESEARCH CENTER ORBITAL LIFETIME PROGRAM
Lynne H. Orr Sep. 1985 65 p refs
(NASA-TM-87587; NAS 1.15:87587) Avail: NTIS HC A04/MF A01 CSCL 09B

A FORTRAN program used by Langley Research Center for analyzing orbital lifetimes of spacecraft is described. Calculations can, at the user's option, take into account perturbations in the orbit due to atmospheric drag, solar radiation pressure, and gravitation effects of the Sun, the Moon, and Earth oblateness. Instructions are provided for access and use of the program, and several sample cases are included with detailed descriptions of their associated input and output. Author

N86-10829# Institute for Defense Analyses, Alexandria, Va.
Ada (TRADEMARK) PROGRAMMING SUPPORT ENVIRONMENT (APSE) EVALUATION AND VALIDATION (E AND V) WORKSHOP REPORT HELD AT AIRLIE, VIRGINIA ON 2-6 APRIL 1984 Final Report
V. L. Castor, C. M. Anderson, T. E. Lindquist, and J. F. Kramer, Jr. Dec. 1984 128 p Workshop held at Airlie, Va., 2-6 Apr. 1984
(Contract MDA903-84-C-0031)
(AD-A156667; AD-E500721; IDA-M-34; IDA/HQ-84-29295) Avail: NTIS HC A07/MF A01 CSCL 09/2

The Evaluation & Validation (E&V) Task has been established by the AJPO to develop technology necessary to assess the quality of software tools that will be included in an Ada Programming Support Environment (APSE). An E&V Workshop convened April 2 to 6, 1984, consisted of government and industry representatives who developed draft documents in three E&V subject areas--Task Recommendations, Task Requirements, and the APSE Evaluation Reference Manual. This report contains an account of the plenary sessions and the papers that address the three subject areas under discussion during this workshop. GRA

N86-10830# Geological Survey, Reston, Va. Water Resources Div.
SUTRA (SATURATED-UNSATURATED TRANSPORT). A FINITE-ELEMENT SIMULATION MODEL FOR SATURATED-UNSATURATED, FLUID-DENSITY-DEPENDENT GROUND-WATER FLOW WITH ENERGY TRANSPORT OR CHEMICALLY-REACTIVE SINGLE-SPECIES SOLUTE TRANSPORT Final Report, 29 Dec. 1982 - 30 Jan. 1985
C. I. Voss 30 Dec. 1984 427 p
(Contract MIPR-N-83-18; AF Proj. 2103)
(AD-A156779; USGS/WRI/84-4369; AFESC/ESL-TR-85-10) Avail: NTIS HC A19/MF A01 CSCL 09/2

SUTRA (Saturated-Unsaturated Transport) is a computer program which simulates fluid movement and the transport of either energy or dissolved substances in a subsurface environment. The mathematical model employs a two-dimensional hybrid finite-element and integrated-finite-difference method to approximate the governing equations that describe the two interdependent processes that are simulated by SUTRA: (1) fluid density-dependent saturated or unsaturated ground-water flow, and either; (2a) transport of a solute in the ground water, in which the solute may be subject to: equilibrium adsorption on the porous matrix, and both first-order and zero-order production or decay, or, (2b) transport of thermal energy in the ground water and solid matrix of the aquifer. SUTRA provides, as the primary calculated result, fluid pressures and either solute concentrations or temperatures, as they vary with time, everywhere in the simulated subsurface system. SUTRA may also be used to simulate simpler subsets of the above process. Author (GRA)

N86-10831# Air Command and Staff Coll., Maxwell AFB, Ala.
LET'S GET SERIOUS ABOUT SOFTWARE
J. R. Hegland Apr. 1985 47 p
(AD-A156819; ACSC-85-1130) Avail: NTIS HC A03/MF A01 CSCL 09/2

This guide translates applicable Air Force and TAC data processing requirements into language and examples fighter crews can relate to and understand. It provides information on methods of programming, documenting, and submitting software to TAC. It is designed to help get fighter squadron software into TAC-wide distribution and prevent wasted efforts. Author (GRA)

N86-10832# Army Military Personnel Center, Alexandria, Va.
SUPERVISORY CONTROL OF THE RIGHT ARM OF THE BEAM ASSEMBLY TELEOPERATOR Final Report
A. J. Manganiello 10 May 1985 173 p
(AD-A156856) Avail: NTIS HC A08/MF A01 CSCL 13/9

This thesis develops a method of supervisory control of the five-degree-of-freedom dexterous right arm of the Beam Assembly Teleoperator (BAT). The thesis imposes a constraint that the end effector of the right arm or manipulator must move in a straight line. The joint angles are used to transform the position of the end effector into cylindrical coordinates. With the initial and final position known, an equation for a straight line is obtained and the cylindrical coordinates of the end effector for each point on the straight line are found. The cylindrical coordinates are then transformed back into joint angles for each point and the joint angles are used to control the BAT's right arm. The method of moving the end effector in a straight line is implemented in two ways. The first implementation uses an unknown starting position and moves to a known finish point. Here the previously developed BAT software is used to input the starting position of the arm. Then the straight line path method uses this starting point and drives the arm to the known finish point. In the second implementation, a method is developed in which a set of points is remembered by the BAT and the straight line path method is used to drive the arm from any start point, through all the stored points and return to the original point. Further extensions using this method are discussed. GRA

N86-10833# Yale Univ., New Haven, Conn. Dept. of Computer Science.
THE DUCK MANUAL
D. McDermott Jun. 1985 95 p
(Contract N00014-83-K-0281; Grant NSF DCR-84-07077)
(AD-A156936; YALEU/DCS/RR-399) Avail: NTIS HC A05/MF A01 CSCL 09/2

Duck is deductive database designed to work as an adjunct to Artificial-Intelligence application programs written in Lisp. It provides the following features: Backward chaining logic interpreter; Forward chaining; Data dependencies and reason maintenance; Integration of deduction with Lisp computation; Multiple databases; Syntax checking for deductive rules; Trace package; Interactive examination of successful and failed deductions; and Generation of quasi-English versions of rules. Author (GRA)

N86-10834# Colorado Univ., Boulder. Dept. of Computer Science.
COMPLEXITY OF HIGHER-ORDER PROGRAMS
J. Shultis Jan. 1985 31 p refs
(Contract DE-FG02-84ER-13283)
(DE85-012776; DOE/ER-13283/2) Avail: NTIS HC A03/MF A01

A logic for analyzing the time complexity of programs using higher-order functions is presented. A simple functional language with static binding and call-by-value as its only parameter discipline was studied. The language is defined by denotational semantics that model both the functionality and cost of programs. The logic is derived from the semantic model, and tested against an implementation of the language based directly on the semantics. The use of the logic is demonstrated for a number of examples including data structure omparison and higher-order recursive functions. DOE

N86-10835# Los Alamos Scientific Lab., N. Mex.
NEW PROBABILISTIC MODELING AND SIMULATION METHODS FOR COMPLEX TIME-DEPENDENT SYSTEMS
R. J. Bartholomew 1985 13 p Presented at the 7th Intern. System Safety Conf., San Jose, Calif., 25 Jul. 1985
(Contract W-7405-eng-36)
(DE85-009575; LA-UR-85-828; CONF-850723-2) Avail: NTIS HC A02/MF A01

This paper is a tutorial that presents a new method of modeling the probabilistic description of failure mechanisms in complex, time-dependent systems. The method of modeling employs a state vector differential equation representation of cumulative failure probabilities derived from Markov models associated with certain generic fault trees, and the method automatically includes common cause/common mode statistical dependences, as well as time-related dependencies not considered in the literature previously. Simulations of these models employ a population dynamics representation of a probability space involving probability particle transitions among the Markov disjoint states. The particle transitions are governed by a random, Monte Carlo selection process. DOE

N86-10836# Stanford Linear Accelerator Center, Calif.
KLYSTRON CONTROL SOFTWARE IN THE SIC
R. K. Jobe, K. Thompson, and N. Phinney May 1985 3 p Presented at the Particle Accelerator Conf., Vancouver, British Columbia, 13 May 1985
(Contract DE-AC03-76SF-00515)
(DE85-013068; SU-SLAC-PUB-3667; CONF-850504-79) Avail: NTIS HC A02/MF A01

Triggering, control, and monitoring of 240 high-power klystrons will be supported by the Stanford Linear Collider (SLC) control system. The control software is distributed among a VAX host computer, a local microprocessor cluster, and a dedicated intelligent CAMAC module. The functions performed by these three components and the algorithms used are discussed. DOE

N86-10837# Los Alamos National Lab., N. Mex.
REVISION OF AND DOCUMENTATION FOR THE STANDARD VERSION OF THE POISSON-GROUP CODES
J. L. Warren, G. P. Boicourt, M. T. Menzel, G. W. Rodenz, and M. C. Vasquez 1985 4 p Presented at the Particle Accelerator Conf., Vancouver, British Columbia, 13 May 1985
(Contract W-7405-eng-36)
(DE85-012659; LA-UR-85-1618; CONF-850504-62) Avail: NTIS HC A02/MF A01

The main applications are in the design of electromagnets (POISSON and PANDIRA) and RF cavities (SUPERFISH). Other applications include electrostatics heat transport, and finding mathematical surfaces of minimum area. The standard version was revised and corrected and a comprehensive manual containing many examples and a summary of the theory behind the codes is written. Some of the capabilities of the codes are illustrated and the manual is summarized. DOE

N86-10838# Department of Energy, Oak Ridge, Tenn. Office of Scientific and Technical Information.
COMPUTER CODES: A BIBLIOGRAPHY, SUPPLEMENT 1
G. H. Thoeming, ed. Jun. 1985 987 p
(DE85-008721; DOE/TIC-3386-Suppl-1) Avail: NTIS HC A99/MF E04

Included are 3964 citations to literature on computer codes contained in the DOE Energy Data Base for the period March 1981 through January 1985. The citations represent all Energy Data Base subject categories and include reports, journal articles, books, conference papers, and monographs. Corporate, personal Author, Subject, and Report Number Indexes are provided. DOE

N86-10839# Los Alamos Scientific Lab., N. Mex.
GUIDELINES FOR A THERMOCHEMICAL KINETICS COMPUTER PROGRAM
J. I. Janney May 1985 11 p
(Contract W-7405-eng-36)
(DE85-014266; LA-10361-MS) Avail: NTIS HC A02/MF A01

Guidelines are given for an interactive computer program that will analyze thermochemical decomposition rate data obtained by isothermal differential-scanning calorimetry. Data from any portion of the rate curve may be analyzed, and either normal or autocatalytic rate laws may be used. The computer calculates and displays normalized data listings, rate curves, order plots, and autocatalytic rate law plots. It calculates rate constants by linear regression treatment of data from curve segments chosen by the user. Many options are available, and many forms of the rate laws may be selected. This program was designed primarily for research rather than routine use. DOE

N86-10840# Oak Ridge National Lab., Tenn.
BOX METHOD FOR FINDING INTERSECTIONS OF A TRAJECTORY WITH AXISYMMETRIC FLUX SURFACES
S. E. Attenberger and W. A. Houlberg May 1985 43 p
(Contract DE-AC05-84OR-21400)
(DE85-013525; ORNL/TM-9483) Avail: NTIS HC A03/MF A01

Computer routines were developed for handling a difficult geometry problem which frequently occurs in the analysis of toroidal plasmas. It is assumed that the plasma may be described in terms of a set of nested toroidal magnetic flux surfaces. Presented here is a set of algorithms that determine the intersections of a given trajectory with a given set of flux surfaces. DOE

N86-10841# Los Alamos Scientific Lab., N. Mex.
FRAMEWORK FOR GENERATING EXPERT SYSTEMS TO PERFORM COMPUTER SECURITY RISK ANALYSIS
S. T. Smith and J. J. Lim 1985 8 p Presented at the 1st Ann. AFCEA Symp. and Exposition on Phys. and Electron. Security, Philadelphia, 19 Aug. 1985
(Contract W-7405-eng-36)
(DE85-014134; LA-UR-85-1933; CONF-850885-2) Avail: NTIS HC A02/MF A01

A framework to generate knowledge based expert systems for performing automated risk analyses upon a subject system was developed. The expert system is a computer program that models experts' knowledge about A topic, including facts, assumptions, insights, and decision rationale. The subject system is a member of the class of systems with three identifying characteristics: (1) a set of desirable assets (or targets); (2) a set of adversaries (or threats) desiring to obtain or to do harm to the assets; and (3) a set of protective mechanisms to safeguard the assets from the adversaries. Risk analysis evaluates both vulnerability to and the impact of successful threats against the targets by determining the overall effectiveness of the subject system safeguards, identifying vulnerabilities in that set of safeguards, and determining cost effective improvements to the safeguards. The inherent vulnerabilities and risks in a system of computer security safeguards are evaluated. The method considers safeguards protecting four generic targets. The automated procedure to assess the effectiveness of computer security safeguards differs from traditional risk analysis methods. DOE

N86-10842# Allied Bendix Aerospace, Kansas City, Mo.
SOFTWARE FOR AN AUTOMATED GAGING SYSTEM Final Report
R. E. Hines May 1985 100 p
(Contract DE-AC04-76DP-00613)
(DE85-013322; BDX-613-3268) Avail: NTIS HC A05/MF A01

Gaging software was developed for an automated gaging system. The system acquires and processes dimensional data from product that is inspected on multi-probe rotary gages. Speed and flexibility are major advantages of the gaging system. For example, it collects 60 readings each from 40 probes on a part, analyzes the data for 90 characteristics, compares against tolerance limits, and prints a detailed report in 8 minutes. This would take over 8 hours to do with manual methods. The software and hardware are general purpose, which allows the system to be easily re-programmed for different gaging applications. The system is currently operating at Bendix Kansas City with seven different gages. The software, which is programmed in both FORTRAN (about 80%) and assembly anguages, is to read, interpret, and process the keyword commands from user-defined control files. Routines are available for 12 varieties of feature analysis: contour, radius, wall thickness, diameter, dimension, position, concentricity, perpendicularity, runout, parallelism, surface angle, and the difference between two probes. The results from the feature analysis routines can then be compared to either product, guardband, or monitor unit limit files. DOE

N86-10843# Oak Ridge Gaseous Diffusion Plant, Tenn.
HALFBREED: AN EXTENDED CAPABILITY VERSION OF THE YAQUI CODE
J. E. Park Jun. 1985 21 p
(Contract DE-AC05-84CT-21400)
(DE85-014237; K/CSD/INF-85/4) Avail: NTIS HC A02/MF A01

Several special modifications to the ICE-ALE computer code, UAQUI, are described. The modified code was dudded HALFBREED. DOE

N86-10844# Technische Hogeschool, Eindhoven (Netherlands). Dept. of Electrical Engineering.
THE IDENTIFICATION PACKAGE SATER
A. J. W. vandenBoom and R. Bollen 1983 7 p refs
(ER-83/08) Avail: NTIS HC A02/MF A01

Structure and identification methods of an interactive program package for identification of linear single-input systems are described. The computer package is meant for inexperienced users of (application of) identification methods and for students. Interaction is very user friendly. The package contains parameter estimation routines, order testing routines, a program for converting discrete models into continuous models, simulation and test signal generation modules, facilities for preprocessing measured signals, as well as modules for analyzing continuous systems based on Nyquist, Bode and root-locus diagrams. Author (ESA)

N86-10845# Technische Hogeschool, Eindhoven (Netherlands). Vakgroep Automatischen Systeemontwerpen.
COMPACT: COMPACTION OF HIERARCHICAL CHIP LAYOUTS BASED ON A CONSTRAINT GRAPH METHOD WITH DOUBLE-SIDED CONSTRAINTS Progress Report, Jun. 1982-May 1983
X. I. M. Timmermans 1983 45 p refs
Avail: NTIS HC A03/MF A01

The compaction program COMPACT used in interactive computer aided design of integrated circuit layouts is described. The compaction method is based on a constraint graph. Compaction is achieved in one or more subsequent steps by grouping the layout elements into features and then shifting these features together in horizontal or vertical direction. The nodes and edges of the graph represent the features and the constraints between the features. The compaction algorithm can handle one-sided and two-sided constraints. The two-sided constraints are resolved by backtracking. Constraints on the shift of layout elements which overlap each other are determined with a linear method. For determination of constraints of nonoverlapping elements, windowing and shadowing techniques are used to reduce computation time. Author (ESA)

N86-10846# Technische Hogeschool, Eindhoven (Netherlands). Digital Systems Group.
STATE ASSIGNMENT IN SEQUENTIAL CIRCUITS
Jan. 1985 22 p refs In DUTCH; ENGLISH summary
(EUT-85-E-146; ISBN-90-6144-146-3; ISSN-0167-9708) Avail: NTIS HC A02/MF A01

An algorithm for optimizing the code assignement in sequential digital circuits is described. Source for this algorithm are three heuristic rules. These rules aim to find the largest block of 1-s in a Karnaugh-diagram. The algorithm starts with a state table and ends with the excitation tables. During the code assignement the user is asked to choose between several alternatives, after which the excitation tables are settled. Author (ESA)

N86-10847# National Bureau of Standards, Gaithersburg, Md.
NBSGSC: A FORTRAN PROGRAM FOR QUANTITATIVE X-RAY FLUORESCENCE ANALYSIS Final Technical Note
G. Y. Tao, P. A. Pella, and R. M. Rousseau Apr. 1985 124 p
Prepared in cooperation with Geological Survey of Canada
(PB85-206068; NBS/TN-1213) Avail: NTIS HC A06/MF A01; also Avail: SOD as SN003-003-02653-1 CSCL 07D

A FORTRAN program (NBSGSC) is developed for performing quantitative analysis of bulk specimens by X-ray fluorescence spectrometry. This program corrects for X-ray absorption/enhancement phenomena using the comprehensive alpha coefficient algorithm proposed by Lachance (COLA). Part one of the program (CALCO) performs the calculation of theoretical alpha coefficients, and part two (CALCOMP) computes the composition of the analyte specimens. The analysis of alloys, pressed minerals, and fused specimens can currently be treated by the program. In addition to using measured X-ray tube spectral distributions, spectra from seven commonly used X-ray tube targets could also be calculated with an NBS algorithm included in the program.
GRA

N86-10390*# Jet Propulsion Lab., California Inst. of Tech., Pasadena. Communications Systems Research Section.
A SEQUENTIAL DECODING PERFORMANCE ANALYSIS FOR INTERNATIONAL COMET EXPLORER
D. Divsalar *In its* The Telecommun. and Data Acquisition Progr. Rept. 15 Aug. 1985 p 82-91 refs (For primary document see N86-10382 01-32)
Avail: NTIS HC A10/MF A01 CSCL 09B

N86-10815# Joint Publications Research Service, Arlington, Va.
CLASSIFICATION OF REAL-TIME PROGRAM TESTING TASKS AND METHODS
I. N. Dolganyuk and Ye. Ya. Karpovskiy *In its* USSR Rept.: Cybernetics, Computers and Automation Technol. (JPRS-UCC-85-006) 5 Sep. 1985 p 70-83 refs Transl. into ENGLISH from Upravlyayushchiye Sistemy i Mashiny (Kiev), no. 2, Mar. - Apr. 1985 p 57-62 (For primary document see N86-10809 01-60)
Avail: NTIS HC A08

N86-10818# Joint Publications Research Service, Arlington, Va.
DIGITAL PROCESSING OF IMAGES IN TRACKING A MOVING OBJECT
B. A. Alpatov, A. A. Selyayev, and A. I. Stapashkin *In its* USSR Rept.: Cybernetics, Computers and Automation Technol. (JPRS-UCC-85-006) 5 Sep. 1985 p 123-127 refs Transl. into ENGLISH from Proborostr. (Leningrad), no. 2, Feb. 1985 p 39-43 (For primary document see N86-10809 01-60)
Avail: NTIS HC A08

62 COMPUTER SYSTEMS

Includes computer networks.

N86-10848*# Carnegie-Mellon Univ., Pittsburgh, Pa.
FAULT-FREE BEHAVIOR OF RELIABLE MULTIPROCESSOR SYSTEMS: FTMP EXPERIMENTS IN AIRLAB
Ed Clune, Zary Segall, and Daniel Siewiorek Aug. 1985 33 p refs
(Grant NAG1-190)
(NASA-CR-177967; NAS 1.26:177967) Avail: NTIS HC A03/MF A01 CSCL 09B

This report describes a set of experiments which were implemented on the Fault tolerant Multi-Processor (FTMP) at NASA/Langley's AIRLAB facility. These experiments are part of an effort to formulate and evaluate validation methodologies for fault-tolerant computers. This report deals with the measurement of single parameters (baselines) of a fault free system. The initial set of baseline experiments lead to the following conclusions: (1) The system clock is constant and independent of workload in the tested cases; (2) the instruction execution times are constant; (3) the R4 frame size is 40mS with some variation; (4) the frame stretching mechanism has some flaws in its implementation that allow the possibility of an infinite stretching of frame duration. Future experiments are planned. Some will broaden the results of these initial experiments. Others will measure the system more dynamically. The implementation of a synthetic workload generation mechanism for FTMP is planned to enhance the experimental environment of the system.
Author

N86-10849# Naval Postgraduate School, Monterey, Calif.
SHIPBOARD NON-TACTICAL COMPUTER SYSTEMS OF THE US NAVY M.S. Thesis
W. J. McMican and J. J. Richards Mar. 1985 129 p
(AD-A156769) Avail: NTIS HC A07/MF A01 CSCL 09/2

This thesis reviews the development and application of current non-tactical shipboard ADP systems in the U.S. Navy, and provides an analysis of each systems' strengths and weaknesses. The primary focus of this review includes Perq/ZOG, WANG installations, and SNAP II. The methodologies of procurement, development and implementation vary as widely as the scope and complexity of the various systems. This analysis provides insight into some primary management issues, limitations, and constrait encountered in providing non-tactical automatic data processing to the fleet.
Author (GRA)

N86-10850# Yale Univ., New Haven, Conn. Dept. of Computer Science.
TOPOLOGICAL PROPERTIES OF HYPERCUBES
Y. Saad and M. H. Schultz Jun. 1985 19 p
(Contract N00014-82-K-0184)
(AD-A156777; Yaleu/DCS/RR-389) Avail: NTIS HC A02/MF A01 CSCL 12/1

The n-dimensional hypercube or n-cube is a highly concurrent multiprocessor architecture consisting of 2 to the nth nodes each connected or n neighbors. Such machines have been advocated as ideal ensemble architectures because of their powerful interconnection. In this paper we examine the hypercube architecture from the graph theory point of view and we consider those features which make the hypercube interconnection so appealing. Among other things, we propose a theoretical characterization of the hypercube as a graph and show how to map various other architectures into a hypercube. The hypercube is a loosely coupled parallel multiprocessor based on a binary n-cube network and introduced under different names (for example, cosmic cube, n-cube, binary n-cube, and boolean n-cube). A few machines based on the hypercube topology have been implemented by several groups, see (7) for references, and others are now being built. An n-cube parallel multiprocessor consists of (2) identical processors, each provided with its own sizable memory, and connected to n neighbors in the form of a binary n-cube network. There are essentially two broad classes of MIMD parallel multiprocessor processor designs with large number of processors. The first type of architecture consists of a large number of identical processors connected to one another according to some convenient pattern. In these machines there is no shared memory and no global synchronization. The second important class of parallel multiprocessors consists of those systems with N identical processors connected via a large switching network to N memories.
GRA

N86-10851# Technische Hogeschool, Eindhoven (Netherlands). Computing Center.
STOCK-TAKING OF DATA BASE MANAGEMENT SYSTEMS CHOICE CONSIDERATIONS FOR THE EINDHOVEN TECHNICAL UNIVERSITY COMPUTING CENTER (THE-RC) [INVENTARISATIE VAN DATA BASE MANAGEMENT SYSTEMEN EN KEUZEOVERWEGINGEN VOOR HET THE-RC]
Th. H. Bruning Dec. 1983 38 p In DUTCH
(Comp-Cent-Note-18; B8562872) Avail: NTIS HC A03/MF A01

Nine data base management systems, namely: DMS II (Burroughs), SQL/DS (IBM), IDMS (Cullinane), ORACLE (Relational Software), RAPPORT (Logica), TOTAL (Cincom Systems), ADABAS (Software AG), BASIS (Batelle), and MIMER (Savant) are examined. Systems for administrative purposes are distinguished from technico scientific systems, and aspects such as data base structure, integration of the functions, transfer possibilities, user friendliness, facilities, and costs are discussed. A definitive selection is not made.
Author (ESA)

63 CYBERNETICS

Includes feedback and control theory.
For related information see also *54 Man/System Technology and Life Support.*

N86-10852 Wyoming Univ., Laramie.
SPILLOVER MINIMIZATION IN SELF-ADJOINT DISTRIBUTED-PARAMETER SYSTEMS WITH DIRECT OUTPUT FEEDBACK Ph.D. Thesis
David Steven Barker 1984 142 p
Avail: Univ. Microfilms Order No. DA8508862

Control of a high-dimensional system by a low-dimensional controller is intriguing problem. High-dimensional systems (distributed-parameter systems) and low-dimensional controllers (lumped-parameter controllers) are mismatched due to their different dimensionality. The question which is addressed here is whether a low-dimensional controller can be designed for a high-dimensional system. Several control strategies exist and none is simpler than direct output feedback which multiplies sensor outputs by constants and adds the results to form the actuator inputs. Optimum sensor and actuator placement schemes for a direct output feedback controller which gives significant damping to a few modes of oscillation and minimally interacts with the higher modes of oscillation is discussed. Unwanted interaction among modes of oscillation which occurs through the controller is commonly referred to as spillover. The results for the Euler-Bernoulli beam (a self-adjoint distributed parameter system) will provide bench marks for other controllers. Dissert. Abstr.

N86-10853 Case Western Reserve Univ., Cleveland, Ohio.
OPTIMAL CONTROL MODELING OF LOWER EXTREMITY MUSCULOSKELETAL MOTION Ph.D. Thesis
Musa Latangrang Audu 1985 233 p
Avail: Univ. Microfilms Order No. DA8510114

The application of optimal control theory in the study of musculoskeletal motion was investigated. The research includes a comparative study of muscle models of varying complexity. Four such models ranging in complexity from simple input-output models to very sophisticated phenomenological models were examined. A model was developed which was able to strike a compromise between model complexity and practicability in musculoskeletal motion applications. Dissert. Abstr.

N86-10854# Oxford Univ. (England). Dept. of Engineering Science.
IDENTIFICATION OF A PLANT'S WEIGHTING SEQUENCE
D. W. Clarke 1984 40 p refs
(OUEL-1534/84) Avail: NTIS HC A03/MF A01

The mathematical foundation of the weighting sequence model and a set of algorithms which can estimate its parameters are described. It is shown how a multi-input single-output plant (e.g., a single loop with known load-disturbances) can be modelled. The algorithms are designed to cope with offsets, noise, and drift of the plant output, and provide compromises between rapid estimation and possible effects of noisy data on the results. The UDU implementation of recursive least squares which is the optimal method but which involves considerable computations, and the recursive learning method as used by the IDCOM controller design which is simple but which can be sensitive to noise are recommended. Author (ESA)

64 NUMERICAL ANALYSIS

Includes iteration, difference equations, and numerical approximation.

N86-10855 State Univ. of New York, Buffalo.
ADVANCED DEVELOPMENT OF BEM FOR TWO AND THREE DIMENSIONAL NONLINEAR ANALYSIS Ph.D. Thesis
S. T. Raveendra 1985 149 p
Avail: Univ. Microfilms Order No. DA8510358

Application of the boundary element method are applied to solve nonlinear problems. The material behavior is idealized by elastoplastic and viscoplastic models. The boundary element method formulation of the governing equations of elastoplasticity developed makes use of an initial stress approach in which the incremental solutions are modified by the presence of initial stresses. The viscoplastic model which describes the time-dependent inelastic deformation of solids is used to solve creep problems as well as elastoplastic problems since steady state viscoplasticity can be conceived as an alternative description of elastoplastic behavior. The iterative procedure is accelerated by extrapolating the past plastic history which reduces the computing time substantially. A new formulation to solve problems in elastoplasticity is developed by exploiting some of the characteristics of the constitutive relationships. This approach is equivalent to the variable stiffness method employed in finite element algorithms in which no iterative procedure is necessary. Dissert. Abstr.

N86-10856# Tata Inst. of Fundamental Research, Bombay (India).
PRINCIPAL BUNDLES ON THE AFFINE LINE
M. S. Raghunathan and A. Ramanthan 20 Feb. 1985 16 p refs
Avail: NTIS HC A02/MF A01

Assume that G is connected and reductive. Let B be an element of A be a principal G-bundle on A such that B sub(Spec k) x Spec k subs is trivial over Spec k subs [T] where k subs is the separable closure of k. Then there is a principal G-bundle B sub 0 over Spec k such that B is K-isomorphic to the pull back of B sub 0 by the structure morphism A be an element of Spec k. If k is algebraically closed it follows from a theorem of Steinberg that all G-bundles on A, with G connected, are trivial. Thus if k is perfect (in particular if the characteristic of k is zero) the assumption of triviality over k sub s is always satisfied. On the other hand Knus, Ojanguren and Saltman have shown that for separably closed non-perfect fields k there exist non-trivial PGL(n)-bundles on A. However it seems likely that for simply connected groups G such a phenomenon does not occur. G.L.C.

N86-10857# Tata Inst. of Fundamental Research, Bombay (India). School of Mathematics.
COINCIDENCE DENSITIES AND SPECTRA OF A CLASS OF SUBSTITUTION MINIMAL SETS
S. Muralidharan 17 May 1985 24 p refs
Avail: NTIS HC A02/MF A01

For any primitive substitution theta on (0,1) such that the theta-matrix is singular, we show that the coincidence density D(theta) exists and is rational. We also prove that the associated minimal dynamical system has discrete spectrum if and only if D(theta) = 1; this verifies a conjecture of Michel for the class of substitutions as above. Author

N86-10858# Universite des Sciences et Techniques du Languedoc, Montpellier (France). Lab. de Physique Mathematique.
WELL-POSED QUESTIONS AND EXPLORATION OF THE SPACE OF PARAMETERS IN LINEAR AND NONLINEAR INVERSION
Pierre C. Sabatier [1984] 22 p refs Sponsored in part by CNRS
(PN-84/13) Avail: NTIS HC A02/MF A01

Solving inverse problems is defining convenient routes, in the space of parameters, towards those called solutions of the problem. Thus methods for solving inverse problems are primarily related to the existence of routes in a space rather than to statistical, algebraic, or other considerations. After a brief survey of the local routes which yield for instance least square inversion, global routes obtained by using geometric transforms are dealt with. One shows on examples how to construct these routes, how to use them, what questions can be answered which escape the range of local routes. These methods apply at least to all inverse problems related with exact solutions of nonlinear partial differential equations, and in particular to the inverse problems of wave equations. They yield efficient algorithms. The case in which localization of the desired solutions is only obtained through some extreme points of a domain is then reviewed. In this method of analysis, one replaces the ill-posed problem of finding solutions that correspond to actual measurements by a set of well-posed questions whose answers are inequalities on theoretical measurements of the set of solutions and enable decision in applied problems. Several applications in engineering and geophysical research were given in the last few years. Author

N86-10859# Universite des Sciences et Techniques du Languedoc, Montpellier (France). Lab. de Physique Mathematique.
A MODIFIED MODIFIED KORTEWEG-DEVRIES EQUATION
F. Calogero (Rome Univ.) and A. Degasperis (Rome Univ.) Dec. 1984 18 p refs Sponsored in part by Italian Ministry of Education Submitted for publication
(PN-84/27) Avail: NTIS HC A02/MF A01

The solution of the Cauchy problem, an infinite set of conserved quantities, a variational formulation, the auto-Backlund transformations and the soliton phenomenology (featuring singly and doubly humped solitons, as well as breathers) are tersely surveyed, for the integrable nonlinear evolution partial differential equation known as the modified-modified Kortwege-deVries equation. Author

N86-10860*# Georgia Inst. of Tech., Atlanta. School of Engineering Science and Mechanics.
BOUNDING SOLUTIONS OF GEOMETRICALLY NONLINEAR VISCOELASTIC PROBLEMS
John M. Stubstad and George J. Simitses [1985] 3 p refs
(Grant NAG3-534)
(NASA-CR-176219; NAS 1.26:176219) Avail: NTIS HC A02/MF A01 CSCL 12A

Integral transform techniques, such as the Laplace transform, provide simple and direct methods for solving viscoelastic problems formulated within a context of linear material response and using linear measures for deformation. Application of the transform operator reduces the governing linear integro-differential equations to a set of algebraic relations between the transforms of the unknown functions, the viscoelastic operators, and the initial and boundary conditions. Inversion either directly or through the use of the appropriate convolution theorem, provides the time domain response once the unknown functions have been expressed in terms of sums, products or ratios of known transforms. When exact inversion is not possible approximate techniques may provide accurate results. The overall problem becomes substantially more complex when nonlinear effects must be included. Situations where a linear material constitutive law can still be productively employed but where the magnitude of the resulting time dependent deformations warrants the use of a nonlinear kinematic analysis are considered. The governing equations will be nonlinear integro-differential equations for this class of problems. Thus traditional as well as approximate techniques, such as cited above, cannot be employed since the transform of a nonlinear function is not explicitly expressible. Author

N86-10861# Carnegie-Mellon Univ., Pittsburgh, Pa. Management Sciences Research Group.
TWO ALGORITHMS FOR WEIGHTED MATROID INTERSECTION
C. Brezovec, G. Cornuejols, and F. Glover Mar. 1985 26 p
(Contract N00014-82-K-0329; Grant NSF ECS-82-05425)
(AD-A156525; MSRR-517; WP-29-84-85) Avail: NTIS HC A03/MF A01 CSCL 12/1

Consider a finite set E, a weight function w:E approaches R, and two matroids M1 and M2 defined on E. The weighted matroid intersection problem consists of finding a set of E, independent in both matroids, that maximizes sigma E w(e): e in 1. This improves the complexity of earlier algorithms by a factor r, when c < or = O(n), and by a factor n when max(c, log n) < or = O(r). A related problem is to find a maximum weight set, independent in both matroids, and of given cardinality k (if one exists). Our algorithm also solves this problem. In addition, we present a second algorithm which, given a feasible solution of cardinality k, finds an optimal one of the same cardinality. A sensitivity analysis on the weights is easy to perform using this approach. GRA

N86-10862# Maryland Univ., College Park. Lab. for Numerical Analysis.
THE h, p AND h-p VERSIONS OF THE FINITE ELEMENT METHOD IN DIMENSION. PART 1: THE ERROR ANALYSIS OF THE p-VERSION Final Report
W. Gui and I. Babuska Apr. 1985 60 p
(Contract N00014-85-K-0169; Grant NSF DMS-83-15216)
(AD-A156600; BN-1036) Avail: NTIS HC A04/MF A01 CSCL 12/1

This paper is the first one in the series of three which are addressing in detail the properties of the three basic versions of the finite element method in the one dimensional setting. The main emphasis is placed on the analysis when the (exact) solution has singularity of x sub alpha type. The first part analyzes the p-version, the second the h-version and general h-p version and the final third part addresses the problems of the adaptive h-p version. Author (GRA)

N86-10863# Naval Underwater Systems Center, New London, Conn.
AN IMPROVED FFT (FAST FOURIER TRANSFORM) FOR A FOUR PARALLEL PIPE SIMD ARITHMETIC PROCESSOR Progress Report
T. T. Tylaska and T. C. Choinski 1 May 1985 35 p
(S14-40)
(AD-A156625; NUSC-TR-7363) Avail: NTIS HC A03/MF A01 CSCL 12/1

An algorithm is derived that reduces the execution time of a fast Fourier transform (FFT) by a factor of 4 utilizing a loosely coupled four parallel pipe processor that a single instruction, multiple data (SIMD) stream architecture. This algorithm distributes the FFT computations among the four parallel pipes for the radix-4 and the mixed radix-2/-4 cases. The algorithm is demonstrated specifically for both a 16- and 32-point FFT. In addition, the radix-4 FFT algorithm is derived in detail, along with formulas for the execution times and a method that computes the inverse FFT. The necessity for prescrambling the input data is explained and a simple hardware implementation is given. Author (GRA)

N86-10864# Maryland Univ., College Park. Lab. for Numerical Analysis.
THE h, p AND h-p VERSIONS OF THE FINITE ELEMENT METHOD IN 1 DIMENSION. PART 3. THE ADAPTIVE h-p VERSION Final Report
W. Gui and I. Babuska Jun. 1985 50 p
(Contract N00014-85-K-0169; Grant NSF DMS-83-15216)
(AD-A156626; BN-1038) Avail: NTIS HC A03/MF A01 CSCL 12/1

The paper is the third and final part in the series of three devoted to the detailed analysis of the three basic versions of the finite element method in one dimension. The first part analyzed the p-version, and the second part concentrated on the h and h-p version. This paper analyzes a theoretical frame of the adaptive h-p version and based on it the authors provide a concrete algorithm for the one dimensional problem. It is proven that in the case that the solution has x sub alpha-type singularity, the adaptive algorithm give an exponential rate of convergence, very close to the optimal one analyzed in the second part of the paper. GRA

N86-10865# Defence Research Establishment Valcartier (Quebec).
ACCELERATION-INVARIANT APPROXIMATION METHOD FOR RECURSIVE DIGITAL FILTERS
A. Morin and P. Labbe May 1985 23 p
(AD-A156655; DREV-4371/85) Avail: NTIS HC A02/MF A01 CSCL 12/1

This document describes a procedure for designing recursive digital filters from continuous-time filters when the ratio of the sampling frequency to the pole frequency is small. The discrete-time transfer function of digital filters obtained by this method, called the acceleration-invariant transformation, has been derived from the partial fraction expansion of the continuous-time transfer function. An error function between the digital and analog transfer

functions has also been deduced. Finally, the performance of the proposed method is demonstrated by plotting the frequency response of high-order Butterworth and elliptic filters.
Author (GRA)

N86-10866# Rensselaer Polytechnic Inst., Troy, N. Y.
A MESH MOVING TECHNIQUE FOR TIME DEPENDENT PARTIAL DIFFERENTIAL EQUATIONS IN TWO SPACE DIMENSIONS Final Technical Report
D. C. Arney and J. E. Flaherty Jun. 1985 41 p Presented at 2nd Army Conf. on Appl. Math and Computing (2nd), 22-24 May 1984, Troy, NY
(Contract DAAG29-82-K-0197; Grant AF-AFOSR-0192-80)
(AD-A156663; AD-E440287; ARLCB-TR-85016) Avail: NTIS HC A03/MF A01 CSCL 12/1

We discuss an adaptive mesh moving technique that can be used with a finite difference or finite element scheme to solve initial-boundary value problems for vector systems or partial differential equations in two space dimensions and time. The mesh moving technique is based on an algebraic node movement function determined from the propagation of significant error regions. The algorithm is designed to be flexible, so that it can be used with many existing finite difference and finite element methods. To test the algorithm, we implemented the mesh mover in a system code along with an initial mesh generator and a MacCormack finite volume integrator on quadralateral cells to solve hyperbolic vector systems. Results are presented for several computational examples. This moving mesh reduces dispersion errors near shocks and wave fronts and thereby reduces the grid requirements necessary to compute accurate solutions while increasing efficiency.
GRA

N86-10867# Yale Univ. Observatory, New Haven, Conn. Dept. of Computer Science.
PARTIAL EIGENSOLUTIONS OF LARGE NONSYMMETRIC MATRICES
Y. Saad Jun. 1985 28 p
(Contract N00014-82-K-0184)
(AD-A156711; Yaleu/DCS/RR-397) Avail: NTIS HC A03/MF A01 CSCL 12/1

We propose several methods based on combinations of deflation techniques and polynomial iteration methods, for computing small invariant subspaces of large matrices, associated with the eigenvalues with largest (or smallest) real parts. We consider both Chebyshev polynomials and least-squares polynomials for the acceleration scheme and we propose a deflation technique which is a variant of Wielandt's deflation that does not require the left eigenvectors of the matrix. As an application we compare our methods on an example issued from a bifurcation problem and show their efficiency when the number of eigenvalues required is small.
GRA

N86-10868# Yale Univ. Observatory, New Haven, Conn. Dept. of Computer Science.
ON THE LANCZOS METHOD FOR SOLVING SYMMETRIC LINEAR SYSTEMS WITH SEVERAL RIGHT-HAND-SIDES
Y. Saad 13 Jun. 1985 14 p
(Contracts N00014-82-K-0184; DE-AC02-81ER-10996; Grant AF-AFOSR-0193-81)
(AD-A156816; Yaleu/DCS/RR-396) Avail: NTIS HC A02/MF A01 CSCL 12/1

This paper analyses two methods based on the Lanczos algorithm for solving large sparse symmetric linear systems with several right hand sides. The methods examined are suitable for the case where the right sides are not too different from one another as is often the case in time dependent or parameter dependent problems. We will show in particular that a modified Lanczos algorithm, introduced by Parlett is in some sense equivalent to the block Lanczos algorithm.
Author (GRA)

N86-10869# Maryland Univ., College Park. Lab. for Numerical Analysis.
THE h, p AND h-p VERSIONS OF THE FINITE ELEMENT METHOD IN 1 DIMENSION. PART 2. THE ERROR ANALYSIS OF THE H AND h-p VERSIONS Final Report
W. Gui and I. Babuska 1 May 1985 77 p
(Contract N00014-85-K-0169; Grant NSF DMS-83-15216)
(AD-A156835; AD-E301723; BN-1037-Pt-2) Avail: NTIS HC A05/MF A01 CSCL 12/1

This paper is the second part in a series of three parts which address in detail the properties and performance of the h, p and h--p versions of the finite element method in one dimensional setting. In general the h-version of FEM has the degree of elements fixed and the convergence is achieved by the refinement of the mesh. The p-version fixes the mesh and increases the degree of elements. The h-p version combines both approaches. This part investigates the h and h-p version.
GRA

N86-10870# Michigan Univ., Ann Arbor.
TEST OF A MULTILEVEL COMPUTATIONAL THEORY OF STEREOSCOPIC VISUAL IMAGE PROCESSING Final Report, 1 Dec. 1984 - 31 May 1985
W. R. Uttal 1 Jun. 1985 16 p
(Contract N00014-85-K-0131; RR0-4209)
(AD-A157011; PERLAB-6) Avail: NTIS HC A02/MF A01 CSCL 12/1

The scientific objective of this contract was to develop and test a computational model of human detection, discrimination, recognition, and reconstruction of dotted forms. Both computer programming and psychophysical research efforts were necessary to fulfill this goal. The dotted form continues to be a powerful vehicle with which to study visual perception by human observes as well as by computer image processors. Several experiments comparing detection, discrimination, and recognition are reported and the current status of the mathematical model describing these visual processes is presented.
GRA

N86-10871# Argonne National Lab., Ill.
COMPUTING THE STRUCTURAL INDEX
I. S. Duff and C. W. Gear Mar. 1985 13 p
(Contract W-31-109-eng-38)
(DE85-014370; ANL/MCS-TM-50) Avail: NTIS HC A02/MF A01

The index of many differential/algebraic equations is determined by the tructure of the system, that is, by the pattern of nonzero entries in the Jacobians. It is important to be able to determine if the index is two or less because such problems can be solved numerically. An algorithm that determines if the index is one, two, or greater, based only on the sturcture is presented. The algorithm can be exponential in its execution time. However, in many practical problems, this algorithm will execute in polynomial time.
DOE

N86-10872# Chalmers Univ. of Technology, Goteborg (Sweden). Dept. of Mathematics.
ERROR ESTIMATES AND AUTOMATIC TIME STEP CONTROL FOR NUMERICAL METHODS FOR STIFF ORDINARY DIFFERENTIAL EQUATIONS
Claes Johnson 1984 45 p refs
(CTH-Math-1984-27; ISSN-0347-2809) Avail: NTIS HC A03/MF A01

Numerical methods for initial value problems for stiff ordinary differential equations (ODE) are considered. Runge-Kutta methods (RKM) resulting from discretizing in time of a discontinuous Galerkin method (DGM) are studied. A special class of RKM given satisfactory error estimates for monotone ODE, is discussed. This technique is suggested as the basis for rational methods for automatic time step control. This error estimate can be extended to nonlinear ODE when linear autonomous parabolic problems of DGM are analyzed.
Author (ESA)

N86-10873# Chalmers Univ. of Technology, Goteborg (Sweden). Dept. of Mathematics.
ON THE ABSOLUTE CONTINUITY OF ELLIPTIC MEASURES
Bjoern E. J. Dahlberg 1984 27 p refs
(CTH-Math-1984-28; ISSN-0347-2809) Avail: NTIS HC A03/MF A01

The Dirichlet for elliptic equations in divergence form with bounded measurable coefficients into n-dimensional space, is studied. It is proven that conditions on the coefficients of partial differential elliptic operators imply the existence of elliptic measures which are absolutely continuous. Author (ESA)

N86-10874# Chalmers Univ. of Technology, Goteborg (Sweden). Dept. of Mathematics.
ESTIMATES FOR MAXIMAL FUNCTIONS ALONG HYPERSURFACES
Hasse Carlsson and Peter Joergen 1984 25 p refs
(CTH-Math-1984-29; ISSN-0347-2809) Avail: NTIS HC A02/MF A01

Maximal function operator (MFO) of a surface in the n-dimensional real space, is considered. The fact that boundaries and regularity conditions of the Hessian at origin on the surface gives an MFO bounded, in the sense of L supp function space, is proven. Author (ESA)

N86-10875# Chalmers Univ. of Technology, Goteborg (Sweden). Dept. of Mathematics.
ON MAXIMAL AND DISTRIBUTIONAL COUPLING
Hermann Thorisson 1984 8 p refs
(CTH-Math-1984-30; ISSN-0347-2809) Avail: NTIS HC A02/MF A01

A method for the construction of maximal coupling (MC) of discrete time stochastic processes, is given. This method does not consider topological restriction on state space. Maximal coupling is given by way of a distributional coupling concept. The MC of continuous time stochastic processes is considered. Author (ESA)

N86-10876# Chalmers Univ. of Technology, Goteborg (Sweden). Dept. of Mathematics.
POISSON SEMIGROUPS AND SINGULAR INTEGRALS
Bjoern E. J. Dahlberg 1985 15 p refs
(CTH-Math-1985-05; ISSN-0347-2809) Avail: NTIS HC A02/MF A01

The Dirichlet problem of the Laplace operator in Lipschitz domain (LD) is discussed. Properties on L sq-function space of the solution operator that corresponds to Dirichlet Problem in LD are given. Author (ESA)

N86-10877# Chalmers Univ. of Technology, Goteborg (Sweden). Dept. of Mathematics.
BRAUER-SEVERI SCHEMES OF ORDERS
Juliusz Brzezinski 1985 36 p refs
(CTH-Math-1985-06; ISSN-0347-2809) Avail: NTIS HC A03/MF A01

Algebraic properties of orders over a Dedekind ring in a central simple algebra over its quotient field and geometric properties of its Brauer-Severi Scheme (BS) are discussed. Explicit description of the BS schemes for orders in quaternion algebra is given. Gorenstein orders (Bass and hereditary properties) are equivalent to BS integral schemes (Normal and Regular properties). It is proved that the singularites of normal BS schemes are rational double points (quaternion case). Author (ESA)

N86-10878# Centre d'Etudes Aerodynamiques et Thermiques, Poitiers (France). Lab. d'Etudes Aerodynamiques.
SPECTRAL METHODS IN ADAPTED CURVED GRIDS Final Report [METHODES SPECTRALES EN MAILLAGE CURVILIGNE ADAPTE]
T. Alziary deRoquefort and A. Farcy Dec. 1984 70 p refs In FRENCH
(Contract DRET-81-668)
Avail: NTIS HC A04/MF A01

Two dimensional problems are studied using single domain transformations based on Chebyshev polynomials developed in two directions. Grid generation and the possibility of creating orthogonal grids are examined. The transformation of partial differential equations and the calculation of the derivatives in the transformed plans are analyzed. The Poisson equation with Dirichlet limit conditions is developed. The solution confirms method efficiency. Author (ESA)

N86-10879# Technische Hogeschool, Eindhoven (Netherlands). Dept. of Electrical Engineering.
MULTIVARIABLE PARTIAL REALIZATION AND THE ASPECT OF UNIQUENESS
Paul VandenHof, Ad Damen, and Andrzej Hajdasinski (Tilburg Univ., Netherlands) 1983 7 p refs
(ER-83/09) Avail: NTIS HC A02/MF A01

The realization of a finite sequence of Markov parameters is handled by exact and approximate realization. For the partial realization problem, a necessary and sufficient condition for the existence of a unique realization which can always be evaluated using the Ho-Kalman algorithm is introduced. A class of finite generic sequences containing sequences constructed from noisy data is defined. When such a sequence is considered, the criterion for uniqueness of a minimal partial realization takes a very simple form. A straightforward algebraic test on the length of the available sequence shows uniqueness or nonuniqueness of the extension sequence. This unique extension is important when trying to find an approximate realization of prescribed low dimension, which fits the original sequence as well as possible. The problem of approximate partial realization is defined, and it is shown how a unique solution to this problem may be obtained. Author (ESA)

N86-10880# Technische Hogeschool, Eindhoven (Netherlands). Dept. of Electrical Engineering.
NAIVE APPROXIMATE REALIZATION OF NOISY DATA
Andrzej Hajdasinski (Tilburg Univ.), Paul VandenHof, and Ad Damen 1983 7 p refs
(ER-83/10) Avail: NTIS HC A02/MF A01

Suboptimal solutions to the problem of approximate partial realization: given a multivariable formal power series of finite length, a state space description has to be constructed with limited dimension, in such a way that it approximates the available matrix sequence with respect to a criterion are presented. Methods based on the Ho-Kalman algorithm and employing a Hankel matrix or an alternative to it, a Page matrix, fail theoretically but appear to be practically quite useful. Results of the simulations allow cases in which the Hankel or Page matrix approach is more appropriate to be determined. Author (ESA)

N86-10881# Groningen Rijksuniversiteit (Netherlands). Dept. of Mathematics.
A MODIFIED SUCCESSIVE OVER-RELAXATION (SOR) METHOD FOR THE POISSON EQUATION IN UNSTEADY FREE-SURFACE FLOW CALCULATIONS
Eugen F. F. Botta and Marcel H. M. Ellenbroek 1985 27 p refs
(TW-264) Avail: NTIS HC A03/MF A01

Convergence difficulties that occur if the successive over relaxation (SOR) method is applied to the Poisson equation on a region with irregular free boundaries are analyzed. It is shown that these difficulties are related to the treatment of the free boundaries and caused by the appearance of complex eigenvalues in the system of discrete equations, when standard centered differences are used. After a modification of this system of equations such that the complex eigenvalues become small, a modified SOR method where two relaxation factors are used alternately is presented. The method leads to fast convergence without requiring specific information about the complex eigenvalues. Author (ESA)

N86-10882# Nationaal Inst. voor Kernfysica en Hoge Energiefysica, Amsterdam (Netherlands). Sectie-H.
ON THE ANALYTICAL EVALUATION OF THE PARTITION FUNCTION FOR UNIT HYPERCUBES IN FOUR DIMENSIONS
N. D. Hari Dass Oct. 1984 34 p refs
(NIKHEF-H/84-12) Avail: NTIS HC A03/MF A01

The group integrations required for the analytic evaluation of the partition function for unit hypercubes in four dimensions are carried out. Modifications of the graphical rules for SU(2) group integrations are developed. A complete classification of all surfaces that can be embedded in the unit hypercube is given and their individual contribution to the partition function worked out. Applications are discussed. Author (ESA)

N86-10883# Nationaal Inst. voor Kernfysica en Hoge Energiefysica, Amsterdam (Netherlands). Sectie-H.
VARIATIONAL ESTIMATES FOR THE MASS GAP OF SU(2) EUCLIDEAN LATTICE GAUGE THEORY
N. D. Hari Dass Oct. 1984 14 p refs
(NIKHEF-H/84-13; B8561677) Avail: NTIS HC A02/MF A01

The application of variational techniques to the Euclidean SU(2) lattice gauge theories is reviewed. Variational results based on the single plaquette ansatz augmented with larger Wilson loops as glueball creation operators support many of the qualitative features of the Monte Carlo studies of SU(2) glueball mass. The most salient of these are the relative unimportance of the plaquettes in higher representations; the importance of the extended operators; and the trend for the mass gap to start increasing again immediately after the crossover region. The improvement of the mass gap estimates with the effective dimensionality has a simple interpretation; when the effective dimensionality is lower the glueball is squeezed more, resulting in a higher mass. Author (ESA)

N86-10884# Center for Mathematics and Computer Science, Amsterdam (Netherlands). Department of Computer Science.
PARTIAL EVOLUTION AND OMEGA COMPLETENESS OF ALGEBRAIC SPECIFICATIONS
J. Heering Jan. 1985 17 p refs Submitted for publication
(CWI-CS-R8501) Avail: NTIS HC A02/MF A01

The concept of partial evaluation (or mixed computation) is introduced. Suppose P(x,y) is a program with two arguments, whose first argument has a known value c, but whose second argument is not yet known. Partial evaluation of P(c,y) should result in a specialized residual program Pc(y) in which as much as possible is computed on the basis of c. This is expressed by saying that partial evaluation amounts to making maximal use of incomplete information. A precise meaning is given to this notion in the context of initial algebra specifications and term rewriting systems. It turns out that, if maximal propagation of incomplete information is to be achieved, as a first step it is necessary to add equations to the algebraic specification in question until it is omega-complete (if ever). The basic properties of omega-complete specifications are discussed, and examples of omega-complete specifications and specifications that do not have a finite omega-complete enrichment are given. Author (ESA)

N86-10391*# Jet Propulsion Lab., California Inst. of Tech., Pasadena. Communications System Research Section.
THE VLSI DESIGN OF ERROR-TRELLIS SYNDROME DECODING FOR CONVOLUTIONAL CODES
I. S. Reed (Univ. of Southern California, Los Angeles), J. M. Jensen (Univ. of Southern California, Los Angeles), T. K. Truong, and I. S. Hsu *In its* The Telecommun. and Data Acquisition Progr. Rept. 15 Aug. 1985 p 92-107 refs (For primary document see N86-10382 01-32)
Avail: NTIS HC A10/MF A01 CSCL 12A

N86-10392*# Jet Propulsion Lab., California Inst. of Tech., Pasadena. Communications Systems Research Section.
HIGH-RATE CONVOLUTIONAL CODE CONSTRUCTION WITH THE MINIMUM REQUIRED SNR CRITERION
P. J. Lee *In its* The Telecommun. and Data Acquisition Progr. Rept. 15 Aug. 1985 p 108-112 refs (For primary document see N86-10382 01-32)
Avail: NTIS HC A10/MF A01 CSCL 12A

N86-10397*# Jet Propulsion Lab., California Inst. of Tech., Pasadena. Reliability Engineering Section.
PERIODIC BINARY SEQUENCES WITH VERY GOOD AUTOCORRELATION PROPERTIES
S. Tyler and J. Loftsson *In its* The Telecommun. and Data Acquisition Progr. Rept. 15 Aug. 1985 p 143-158 refs (For primary document see N86-10382 01-32)
Avail: NTIS HC A10/MF A01 CSCL 12A

N86-10398*# Jet Propulsion Lab., California Inst. of Tech., Pasadena. Reliability Engineering Section.
A BINARY SEQUENCE OF PERIOD 60 WITH BETTER AUTOCORRELATION PROPERTIES THAN THE BARKER SEQUENCE OF PERIOD 13
J. Watkins (TRW, Inc., Redondo Beach, Calif.), J. Loftsson, and S. Tyler *In its* The Telecommun. and Data Acquisition Progr. Rept. 15 Aug. 1985 p 159-162 refs (For primary document see N86-10382 01-32)
Avail: NTIS HC A10/MF A01 CSCL 12A

65 STATISTICS AND PROBABILITY

Includes data sampling and smoothing; Monte Carlo method; and stochastic processes.

N86-10885# Maryland Univ., College Park. Dept. of Management Sciences and Statistics.
A MODIFIED REPAIR STRATEGY FOR TWO-COMPONENT SYSTEMS WITH REVEALED AND UNREVEALED FAULTS Technical Report, Feb. - May 1985
N. L. Johnson and S. Kotz May 1985 15 p
(Contract N00014-84-K-0301)
(AD-A156715; UMD-DMSS-85/5) Avail: NTIS HC A02/MF A01 CSCL 12/1

Some consequences of a modified repair system for Phillips' model for a two component system are discussed. In the original model, both components are repaired whenever a revealed fault occurs; in the modified model only faulty components are repaired. Specifically: (1) the distribution of time from the initial state up to discovery of an unrevealed fault, (2) the expected propagation of the time during which there exists an unrepaired fault, and (3) the distribution of number of revealed faults up to and including the one which leads to a discovery of an unrevealed fault, are obtained. The theory is illustrated by examples, based on specific distributions for the times between repairs and occurrences of the two types of faults. A characterization of the exponential distribution is indicated. GRA

N86-10886# Maryland Univ., College Park. Dept. of Management Sciences and Statistics.
ESTIMATION BY MOMENTS IN A MODEL OF FAULTY INSPECTION Technical Report, Mar. - Jun. 1985
M. Shisong, S. Kotz, and N. L. Johnson Jun. 1985 9 p
(Contract N00014-84-K-0301)
(AD-A156754; UMD-DMSS-85/6) Avail: NTIS HC A02/MF A01 CSCL 12/1

Methodology developed by Blischke is applied to estimate the parameters in a model of faulty inspection, and to obtain approximate formulae for the variances of these estimators. GRA

N86-10887# Yale Univ., New Haven, Conn. Dept. of Computer Science.
RANK REVEALING QR-FACTORIZATIONS
T. F. Chan Jun. 1985 13 p
(Contracts N00014-82-K-0184; DAAG29-83-K-0177; DE-AC02-81ER-10996)
(AD-A156756; Yaleu/DCS/RR-398) Avail: NTIS HC A02/MF A01 CSCL 12/1

An algorithm is presented for computing a column permutation Pi and a QR-factorization (A)(Pi) = QR of an m by n (m > or = n) matrix A such that a possible rank deficiency of A will be revealed in the triangular factor R having a small lower right block. For low rank deficient matrices, the algorithm is guaranteed to reveal the rank of A and the cost is only slightly more than the cost of one regular QR-factorization. A posteriori upper and lower bounds on the singular values of A are derived and can be used to infer the numerical rank of A. GRA

N86-10888# Technische Hogeschool, Eindhoven (Netherlands). Computing Center.

ADAPTIVE DISTRIBUTION-FREE TEST FOR THE K RANDOM SAMPLING PROBLEM, PART 1 [ADAPTIEVE VERDELINGSVRIJE TOETS VOOR HET K-STEEKPROEVENPROBLEEM]

T. Smeulders, R. Doornbos, and J. B. Dijkstra Jan. 1983 25 p refs In DUTCH 2 Vol.
(Comp-Cent-Note-14-Pt-1; THE-RC-51408-Pt-1) Avail: NTIS HC A02/MF A01

A rank test adapted to random sample data distributions is developed. Knowing that for the double-exponential and normal distributions the median and Van der Waerden tests have a bigger power and using the Hogg compartimentator to estimate the distribution, the test is derived. In case of a small random sample the Kruskal and Wallis test is used. However, results show that the distinguishing power of the adaptive test is not greater than that of Kruskal and Wallis. Author (ESA)

N86-10889# Technische Hogeschool, Eindhoven (Netherlands). Computing Center.

ADAPTIVE DISTRIBUTION FREE TEST FOR THE K RANDOM SAMPLING PROBLEM, PART 2 [ADAPTIEVE VERDELINGSVRIJE TOETS VOOR HET K-STEEKPROEVENPROBLEEM, DEEL 2]

R. V. H. Rooijakkers, R. Doornbos, and J. B. Dijkstra Feb. 1983 18 p refs In DUTCH 2 Vol.
(Comp-Cent-Note-15-Pt-2; THE-RC-52082-Pt-2) Avail: NTIS HC A02/MF A01

The power of an adaptive distribution-free test is compared with the power of each of the three distribution-free tests, from which it is derived. (Van der Waerden, Kruskal Wallis and Mood Brown test). Starting from 4 random samples of the same size at 15, 300 samplings are taken for certain sample shiftings. This is done on normal, log and double-exponential distributions. For each test the number of rejections of the null hypothesis is calculated. Next this is done for the value of 40. Results show that the Kruskal Wallis test is the most powerful. Author (ESA)

N86-10890# Technische Hogeschool, Eindhoven (Netherlands). Computing Center.

ROBUSTNESS OF MULTIPLE COMPARISONS AGAINST VARIANCE HETEROGENEITY

Jan B. Dijkstra 1983 15 p refs Presented at Conf. on Robustness of Statistical Methods and Nonparametric Statistics, Schwerin, East Germany, 29 May - 4 Jun. 1983
(Comp-Cent-Note-17; B8562871) Avail: NTIS HC A02/MF A01

The source of differences when the null hypothesis mu1 = ... muk is rejected for normal populations with classical one way analysis of variance is discussed. If the population variances are equal, the: (1) least significant difference test, (2) multiple range test for equal sample sizes, (3) an adaptation for unequal sample sizes (4) multiple F-test, or (5) multiple Comparisons test can be considered. For all these methods (including the one way analysis of variance) alternatives that are robust against variance heterogeneity exist. A modification of (3) has unattractive properties if the variances and the sample sizes differ greatly. The adaptations for unequal variances of (4) and (5) seem better than (1) for cases with many samples. Test (2) is rather robust in itself if the variances are not too different. Modifications that allow slight unequalities in the sample sizes exist. Author (ESA)

N86-10891# Technische Hogeschool, Eindhoven (Netherlands). Computing Center.

NONPARAMETRIC COMPARISON OF SEVERAL MEAN VALUES WITH MILD ADAPTATION TO SOME SAMPLE CHARACTERISTICS

Jan B. Dijkstra 1984 16 p refs Presented at Computation Statistics (COMPSTAT) Conf., Prague, 27-31 Aug. 1984
(Comp-Cent-Note-20; B8562873) Avail: NTIS HC A02/MF A01

Criteria for choosing between rank tests for log, double exponential, and normal distributions are considered. For certain criteria, the principle of taking the combined sample and ignoring the origin of individual values is seriously violated, so that the resulting tests do not remain permutation tests. A simulation study to find out how much this violation affects control over the chosen size is performed. Powers are estimated for various alternatives, also by using simulation techniques. It is concluded that mild adaptation is possible in this situation without serious harm in the sense of size-control. Extra power can be gained by it, though not for small samples. Author (ESA)

N86-10892# Groningen Rijksuniversiteit (Netherlands). Dept. of Mathematics.

ON THE NUMERICAL DETERMINATION OF THE DIMENSION OF AN ATTRACTOR

F. Takens 1985 11 p refs
(ZW-8415) Avail: NTIS HC A02/MF A01

The convergence of an algorithm to estimate the correlation dimension from experimental data (i.e., errors to be expected when using a finite part of the data sequence) is discussed. The method consists of reconstruction of the phase space in IRn and second the determination of the correlation dimension of a bounded subset in IRn with a probability measure. Using ideas from mathematical statistics, particularly Fischer's maximum likelihood rule, the algorithm is extended to minimize errors. Author (ESA)

N86-10893# Tilburg Univ. (Netherlands). Dept. of Business and Economics.

SUPEREFFICIENT ESTIMATION OF POWER FUNCTIONS IN SIMULATION EXPERIMENTS

J. P. C. Kleijnen 1985 16 p refs
(B8562445) Avail: NTIS HC A02/MF A01

A superefficient procedure that computes the extreme parameter value that would still be accepted under the null hypothesis, given the sample outcome is outlined. This transforms the estimation of the power function into the estimation of a distribution function. Comparing power functions becomes straightforward. The power function is contrasted with Schruben's (1980) coverage function. Author (ESA)

N86-10894# Tilburg Univ. (Netherlands). Dept. of Business and Economics.

THE POWER OF WEIGHTED AND ORDINARY LEAST SQUARES WITH ESTIMATED UNEQUAL VARIANCES IN EXPERIMENTAL DESIGN

J. P. C. Kleijnen, P. Cremers, and F. vanBelle 1985 21 p refs
(B8562446) Avail: NTIS HC A02/MF A01

Response variances are estimated using replications for each experimental condition. The resulting estimated variances can be used to derive the correct variances of the Ordinary Least Squares (OLS) estimators. The estimates can also be used to compute the Estimated Least Squares (EWLS) estimators. The asymptotic covariance formula for EWLS might be used to test the EWLS estimators. The type 1 and 7 errors of this test procedure are compared with those for the OLS estimations. If the variances are constant, EWLS should not be used, but with strong heterogeneity EWLS is more efficient if the variance can be estimated from more than two observations. Author (ESA)

N86-10895# Tilburg Univ. (Netherlands). Dept. of Business and Economics.

REGRESSION ANALYSIS: ASSUMPTIONS, ALTERNATIVES, APPLICATIONS

J. P. C. Kleijnen 1985 51 p refs
Avail: NTIS HC A04/MF A01

The use of a regression model to summarize the reaction of the output of a simulation program to changes in the input is considered. The applicability, testing, and alternatives to six assumptions are discussed: a non-singular matrix of independent variables; a regression model with linear parameters; responses with constant variances; independent responses; normally distributed responses; and a valid or correctly specified regression model. Author (ESA)

66 SYSTEMS ANALYSIS

Includes mathematical modeling; network analysis; and operations research.

N86-10896*# Pennsylvania Univ., Philadelphia. Dept. of Computer and Information Science.
MOTION ANALYSIS REPORT
Norman I. Badler 31 May 1985 33 p refs
(Contract NAS9-16634)
(NASA-CR-171897; NAS 1.26:171897) Avail: NTIS HC A03/MF A01 CSCL 12B

Human motion analysis is the task of converting actual human movements into computer readable data. Such movement information may be obtained though active or passive sensing methods. Active methods include physical measuring devices such as goniometers on joints of the body, force plates, and manually operated sensors such as a Cybex dynamometer. Passive sensing de-couples the position measuring device from actual human contact. Passive sensors include Selspot scanning systems (since there is no mechanical connection between the subject's attached LEDs and the infrared sensing cameras), sonic (spark-based) three-dimensional digitizers, Polhemus six-dimensional tracking systems, and image processing systems based on multiple views and photogrammetric calculations. G.L.C.

N86-10897*# Pennsylvania Univ., Philadelphia. Dept. of Computer and Information Science.
ZERO-GRAVITY MOVEMENT STUDIES
Norman I. Badler, Paul Fishwick, Nina Taft, and Mukul Agrawala 31 May 1985 113 p refs
(Contract NAS9-16634)
(NASA-CR-171899; NAS 1.26:171899) Avail: NTIS HC A06/MF A01 CSCL 12B

The use of computer graphics to simulate the movement of articulated animals and mechanisms has a number of uses ranging over many fields. Human motion simulation systems can be useful in education, medicine, anatomy, physiology, and dance. In biomechanics, computer displays help to understand and analyze performance. Simulations can be used to help understand the effect of external or internal forces. Similarly, zero-gravity simulation systems should provide a means of designing and exploring the capabilities of hypothetical zero-gravity situations before actually carrying out such actions. The advantage of using a simulation of the motion is that one can experiment with variations of a maneuver before attempting to teach it to an individual. The zero-gravity motion simulation problem can be divided into two broad areas: human movement and behavior in zero-gravity, and simulation of articulated mechanisms. G.L.C.

N86-10898# Massachusetts Inst. of Tech., Cambridge. Lab. for Computer Science.
REACHING APPROXIMATE AGREEMENT IN THE PRESENCE OF FAULTS Interim Research Report
D. Dolev, N. A. Lynch, S. S. Pinter, E. W. Stark, and W. E. Weihl Mar. 1985 27 p
(Contract N00014-83-K-0125)
(AD-A156541; MIT/LCS/TM-276) Avail: NTIS HC A03/MF A01 CSCL 12/1

This paper considers a variant on the Byzantine Generals problem, in which processes start with arbitrary real values rather than Boolean values or values from some bounded range, and in which approximate, rather than exact, agreement is the desired goal. Algorithms are presented to reach approximate agreement in asynchronous, as well as synchronous systems. The asynchronous agreement algorithm is an interesting contrast to a result of Fischer, Lynch, and Patterson, who show that exact agreement in not attainable in an asynchronous system with a provable convergence rate that depends on the ratio between the number of faults and the number of processes. Lower bounds on the convergence rate for algorithms of this form are proven, and the algorithms presented are shown to be optimal. GRA

N86-10899# Carnegie-Mellon Univ., Pittsburgh, Pa. Dept. of Computer Science.
DERIVATIONAL ANALOGY: A THEORY OF RECONSTRUCTIVE PROBLEM SOLVING AND EXPERTISE ACQUISITION
J. G. Carbonell 5 Mar. 1985 26 p
(Contracts N00014-79-C-0661; N00014-82-C-5076)
(AD-A156817; CMU-CS-85-115) Avail: NTIS HC A03/MF A01 CSCL 05/10

Derivational analogy, a method of solving problems based on the transfer of past experience to new problem situations, is discussed in the context of other general approaches to problem solving. The experience transfer process consists of recreating lines of reasoning, including decision sequences and accompanying justifications, that proved effective in solving particular problems requiring similar initial analysis. The role of derivational analogy in case-based reasoning and in automated expertise acquisition is discussed. Author (GRA)

N86-10900# Air Force Inst. of Tech., Wright-Patterson AFB, Ohio.
GENERATION OF FLIGHT PATHS USING HIERARCHICAL PLANNING M.S. Thesis
K. B. Kline 1985 265 p
(AD-A156905; AFIT/CI/NR-85-37T) Avail: NTIS HC A12/MF A01 CSCL 12/2

This thesis examines the use of an artificial intelligence technique, hierarchical planning, to solve the problem of generating an aircraft route and finding a path through various hostile environments. A route or path is evaluated by the number and type of threats the aircraft encounters on the route and the route length. An algorithm using hierarchical planning is presented and tested against several hostile environments. Specifically, the algorithms will divide the problem space or grid into smaller spaces or boxes. These boxes are then assigned values based upon the input hostile environment. Block paths are then constructed and evaluated based on the values in the boxes. An exhaustive search is performed on the two best block paths to find a flight path for the aircraft. Test results are compared to previous results obtained using heuristic search and indicate an improvement in solution quality. Although specific plans are incorporated into the algorithm to obtain test results, many other plans within the realm of hierarchical planning certainly exist and could be used to solve this problem. GRA

N86-10901# Technische Hogeschool, Eindhoven (Netherlands). Dept. of Industrial Engineering.
OPERATIONS RESEARCH APPLICATIONS [OPERATIONS-RESEARCH TOEPASSINGEN]
C. B. Tilanus Mar. 1983 27 p refs In DUTCH Submitted for publication
(ARW-03-THE-BDK/ORS/83-08) Avail: NTIS HC A03/MF A01

The essentials of operations research (OR) are illustrated. The term OR, and similarities and differences with related terms are elucidated. The OR applications in the Netherlands are classified by economic sector, problem area, methods and computer languages. As an example of the long way from mathematical methods, via standardized programs to the utilization in concerns and other organizations, vice versa, linear programming is treated and standard programs are presented. Author (ESA)

67 THEORETICAL MATHEMATICS

Includes topology and number theory.

N86-10902# Chalmers Univ. of Technology, Goteborg (Sweden). Dept. of Mathematics.
SOME REMARKS ABOUT CUSP FORMS: HOLOMORPHIC AND NON-HOLOMORPHIC
Dennis A. Hejhal 1984 35 p refs
(CTH-Math-1984-26; ISSN-0347-2809) Avail: NTIS HC A03/MF A01

Cusp forms on a modular group and its congruence subgroups are considered. It is proven that estimations and properties of Fourier coefficients of nonholomorphic cusp forms depending on the norm of the fundamental region, the level, and other constants can be handled by the Kloosterman-Estermann (KE) approach. The KE approach is an analog of the Ramanujan-Peterson conjecture. Author (ESA)

N86-10903# Chalmers Univ. of Technology, Goteborg (Sweden). Dept. of Mathematics.
ON CLASS GROUPS OF LATTICES
Juliusz Brzezinski 1985 22 p refs
(CTH-Math-1985-08; ISSN-0347-2809) Avail: NTIS HC A03/MF A01

General formulas for spinor class groups of orders are given. The formulas are analogous to the formulas for the locally free class groups of a subring of a central simple algebra over the quotient of a Dedekind ring. Author (ESA)

N86-10904# Chalmers Univ. of Technology, Goteborg (Sweden). Dept. of Mathematics.
GALOIS DESCENT AND CLASS GROUPS OF ORDERS
Per Salberger 1985 19 p refs
(CTH-Math-1985-09; ISSN-0347-2809) Avail: NTIS HC A02/MF A01

It is proved that class groups are finite for maximal order over polynomial rings with coefficients in the field of finite transcendence degree over its prime fields, in a central simple K(t) algebras over the algebra of rational functions. The Galois descent method is used. The best-results are obtained for number fields K. Author (ESA)

N86-10905# Groningen Rijksuniversiteit (Netherlands). Dept. of Mathematics.
A NOTE ON THE DIFFERENCIABILITY OF CENTER MANIFOLDS
Floris Takens 1985 7 p refs
(ZW-8414) Avail: NTIS HC A02/MF A01

Center manifold theorem is discussed. An example of a center manifold that cannot be smoothed by restricting it to a small neighborhood of the origin is studied. An explicit construction on four dimensional space is given. Author (ESA)

70 PHYSICS (GENERAL)

For geophysics see *46 Geophysics*. For astrophysics see *90 Astrophysics*. For solar physics see *92 Solar physics*.

N86-10906 Department of the Air Force, Washington, D.C.
INFRARED SYSTEM WITH COMPUTERIZED IMAGE DISPLAY Patent
R. P. Walker, J. D. Rex, and J. H. Schummers, inventors (to Air Force) Issued 28 May 1985 15 p Supersedes AD-D009774
(AD-D011777; US-Patent-4,520,504; US-Patent-Appl-SN-403246; US-Patent-Class-382-1) Avail: US Patent and Trademark Office CSCL 17/5

An object of this invention is to provide a system in which detected signals from an infrared scanner can be used to provide a calibrated display, and by which the data can be stored for later use. In the system according to the invention, image signals originating from an infrared scanner are transformed into a digitized form for storage in a computer and manipulated to produce a calibrated display. This transforms the merely qualitative utility of such a scanner into a quantitative capability allowing analysis of heat energy losses from structures of interest with only modest investments in capital equipment. GRA

N86-10907# California Univ., Livermore. Lawrence Livermore Lab.
NEW APPROACH TO MULTIPHASE EQUILIBRIA: APPLICATION TO HIGH-PRESSURE PHYSICS PROBLEMS
F. H. Ree Jun. 1985 19 p refs Presented at 10th High Pressure Conf. on Res. in High Pressure Sci. and Technol., Amsterdam, 8 Jul. 1985
(Contract W-7405-eng-48)
(DE85-013820; UCRL-92121; CONF-850759-1) Avail: NTIS HC A02/MF A01

A multiphase, multicomponent equation-of-state (EOS) model based on first principles of statistical mechanics is described. The model was used to study fluid-fluid phase separations in binary (H2-He, Ar-Ne, Xe-He, and N2-H20) and ternary or more complex systems involving species with C, H, N, and O atoms. Results of these calculations and a brief description of a new theory which can simultaneously describe both solid and fluid EOS properties are given. DOE

N86-10908# California Univ., Livermore. Lawrence Livermore Lab.
CRYOGENIC STRUCTURAL MATERIALS FOR SUPERCONDUCTING MAGNETS
E. N. C. Dalder and J. W. Morris, Jr. 22 Feb. 1985 19 p Presented at the 8th Intern. Conf. on Struct. Mech. in Reactor Technol., Brussels, 19 Aug. 1985
(Contract W-7405-eng-48)
(DE85-008026; UCRL-92161; CONF-850809-19) Avail: NTIS HC A02/MF A01

Research in the United States and Japan on structural materials for high-field superconducting magnets is reviewed. Superconducting magnets are used for magnetic fusion energy devices and for accelerators that are used in particle-physics research. The cryogenic structural materials that were reviewed are used for magnet cases and support structures. Increased materials requirements are expected in the future. DOE

71 ACOUSTICS

Includes sound generation, transmission and attenuation. For noise pollution see *45 Environment Pollution*.

N86-10909 ESDU International Ltd., London (England).
SUMMARY OF WORK ON JET NOISE PREDICTION
R. F. Lambert Apr. 1985 38 p refs
(ESDU-BR-62636; ESDU-AN-36B) Copyright. Avail: ESDU

Design data for aircraft noise, which include the estimation of subsonic far-field jet mixing noise are presented. It is proposed to extend the existing far field jet mixing noise to supersonic jet velocity conditions. The theories which form the basis for jet exhaust noise prediction are summarized. Measured and predicted overall and spectrum noise levels are compared. The existing data item, the theoretical basis for extending the item into the supersonic jet velocity region, and comparison with jet noise predictions are assessed. E.A.K.

N86-10910 North Carolina State Univ., Raleigh.
SOUND RADIATION FROM REPETITIVE TRANSIENT VIBRATIONS USING MULTI-CHANNEL DIGITAL SIGNAL PROCESSING WITH APPLICATION TO IMPACT MACHINERY Ph.D. Thesis
Ronald Bruce Coleman 1984 242 p
Avail: Univ. Microfilms Order No. DA8507359

Sound radiation from repetitive transient vibrations has been investigated both experimentally and analytically to determine techniques capable of ranking acoustic sources on transient impact machinery. Several of the difficulties encountered in analyzing transient impact noise have been overcome through advanced digital signal processing techniques. These digital signal processing techniques indicated for the first time that traditional multiple input/single output modes of the sound radiation froeXcomplex machinery, characterized by omnidirectional energy flow and/or high spatial coherence throughout the structure, will fail to accurately rank acoustic sources. The utility of cepstral analysis in deconvolving contaminated pressure signals from repetitive transient machinery tested under semi-anechoic conditions, and acoustic intensity measurements in the near- and far-field have also been demonstrated. Approximate and analytical models of repetitive transient vibrations and sound radiation have been investigated. Dissert. Abstr.

N86-10911 Johns Hopkins Univ., Baltimore, Md.
PHYSICAL ACOUSTICS: INVESTIGATION OF CHEMICAL KINETIC AND THERMODYNAMIC PROPERTIES OF FLUIDS Ph.D. Thesis
Timothy Scott Margulies 1984 146 p
Avail: Univ. Microfilms Order No. DA8501663

Measurement of the absorption and dispersion of forced acoustic waves propagating in fluids in equilibrium have been used to determine thermostatic properties and the kinetics of reactions. A theoretical treatment of this problem using the linearized (or first-order) balance equations of mass, linear momentum, energy and chemical kinetics is presented. General results are obtained in the form of a characteristic equation for the complex propagation variable x= - (alpha + i omega/c) where alpha is the attenuation coefficient, c is the phase speed for the progressive wave, and omega = 2 pi F is the angular frequency. Dissert. Abstr.

N86-10912*# Purdue Univ., Lafayette, Ind.
A STUDY OF METHODS TO PREDICT AND MEASURE THE TRANSMISSION OF SOUND THROUGH THE WALLS OF LIGHT AIRCRAFT. INTEGRATION OF CERTAIN SINGULAR BOUNDARY ELEMENT INTEGRALS FOR APPLICATIONS IN LINEAR ACOUSTICS
Dan Zimmerle and Robert J. Bernhard Jul. 1985 40 p
(Grant NAG1-58)
(NASA-CR-176229; NAS 1.26:176229; HL-85-21; Rept-0226-16)
Avail: NTIS HC A03/MF A01 CSCL 20A

An alternative method for performing singular boundary element integrals for applications in linear acoustics is discussed. The method separates the integral of the characteristic solution into a singular and nonsingular part. The singular portion is integrated with a combination of analytic and numerical techniques while the nonsingular portion is integrated with standard Gaussian quadrature. The method may be generalized to many types of subparametric elements. The integrals over elements containing the root node are considered, and the characteristic solution for linear acoustic problems are examined. The method may be generalized to most characteristic solutions. E.A.K.

N86-10913*# National Aeronautics and Space Administration. Langley Research Center, Hampton, Va.
INVESTIGATION OF COMPOSITE MATERIALS PROPERTY REQUIREMENTS FOR SONIC FATIGUE RESEARCH
Howard V. L. Patrick (Embry-Riddle Aeronautical Univ.) Aug. 1985 37 p refs
(NASA-TM-87601; NAS 1.15:87601) Avail: NTIS HC A03/MF A01 CSCL 20A

Experimental techniques for determining the extensional and bending stiffness characteristics for symmetric laminates are presented. Vibrational test techniques for determining the dynamic modulus and material damping are also discussed. Partial extensional stiffness results intially indicate that the laminate theory used for predicting stiffness is accurate. It is clearly shown that the laminate theory can only be as accurate as the physical characteristics describing the lamina, which may vary significantly. It is recommended that all of the stiffness characteristics in both extension and bending be experimentally determined to fully verify the laminate theory. Dynamic modulus should be experimentally evaluated to determine if static data adequately predicts dynamic behavior. Material damping should also be ascertained because laminate damping is an order of magnitude greater than found in common metals and can significantly effect the displacement response of composite panels. Author

N86-10914# Naval Postgraduate School, Monterey, Calif.
FIBER OPTIC GRADIENT HYDROPHONE CONSTRUCTION AND CALIBRATION FOR SEA TRIAL M.S. Thesis
G. E. MacDonald Mar. 1985 125 p
(AD-A156469) Avail: NTIS HC A06/MF A01 CSCL 17/1

A Mach-Zehnder interferometric fiber optic gradient hydrophone, for operation at 632.8 nm wavelength, was designed and constructed for testing in the laboratory. Two individual fiber optic hydrophone sensing coils with 10 m of fiber each were wound and potted on an epoxy mandrel and their respective sensitivities were obtained. They then were mounted on a rigid bar, separated by 10 cm, to form a gradient hydrophone. The sensitivity of this arrangement then was obtained in a calibrator which allowed the coil pair to be rotated 360 deg. Since the laboratory interferometric system was too large to be used in the sea trial tests, a second interferometric system, operating at 830 nm wavelength, using diode lasers was designed and constructed. This was mounted in an experimental apparatus designed and constructed for sea trial. A sea trial of a standard Navy type DIFAR hydrophone was conducted to test the effectiveness of the experimental apparatus. The results of the laboratory tests are summarized and discussed and recommendations for further studies are presented. GRA

N86-10915# Department of the Air Force, Washington, D.C.
TUNABLE ACOUSTO-OPTIC FILTER WITH IMPROVED SPECTRAL RESOLUTION AND INCREASED APERTURE Patent Application
I. C. Chang, inventor (to Air Force) Filed 26 Apr. 1985 21 p
(AD-D011758; US-Patent-Appl-SN-727507) Avail: NTIS HC A02/MF A01 CSCL 09/5

This document refers to a transverse configuration, electronically tunable acousto-optic filter assembly with improved spectral resolution and increased aperture. The crystal prism member is made of TeO(2) and has a large prism angle (i.e., close to 90 degrees). An acoustic prism coupler member made of material with low acoustic velocity (such as TeO(2), AsS(3), or GeAsSe), to avoid total internal reflection of the interface, is bonded in optical contact with a face of the crystal prism member which defines one extreme of the large prism angle, and which is not traversed by a polarized light beam that is transmitted through the crystal prism member and that interacts with a generated, perpendicularly directed, acoustic wave. The use of the acoustic prism couple member, together with the use of a large prism angle in the crystal prism member, result in high spectral resolution and large aperture of the filter assembly and its desired usability in the infrared region. GRA

N86-10916# Southwest Research Inst., San Antonio, Tex.
EXPLORATORY DEVELOPMENT FOR A HIGH RELIABILITY FLAW CHARACTERIZATION MODULE Final Report, 31 Aug. 1981 - 31 Jan. 1985
G. J. Gruber, G. J. Hendrix, and T. A. Mueller Wright-Patterson AFB, Ohio AFWAL Mar. 1985 155 p
(Contract F33615-81-C-5066)
(AD-A156632; AFWAL-TR-84-4172) Avail: NTIS HC A08/MF A01 CSCL 14/2

Two sets of ultrasonic characterization procedures were applied under blind test conditions to 42 manufacturing flaws (inclusions and voids) embedded in titanium and IN100 alloy specimens. The Born inversion procedures (BIP) resulted in size estimates that were independent of not only flaw composition, but also shape, size, and orientation. Instead, the Born diameters were determined to be directly related to the period of the incident wave. For this reason, the BIP results could not be reproduced with different transducers. The Born inversion algorithm correctly treats the first half-cycle of the impulse response of a volumetric flaw as the front-surface echo, but mistakes its third half-cycle for a back-surface (internal satellite pulse) or a creeping-wave return (external satellite pulse). The characterization procedures based on the satellite-pulse observation technique (SPOT) proved to be insensitive to the period of the employed high-frequency transducers and, as expected, the practically constant separation between the front-surface echo and the satellite pulse was found to be directly related to flaw size. Semiautomated satellite analysis procedures (SSAP) that waive the requirement for a highly trained ultrasonic examiner were developed and qualified on 32 test flaws. GRA

N86-10917# Human Engineering Labs., Aberdeen Proving Ground, Md.

PROPOSED AURAL NONDETECTABILITY LIMITS FOR ARMY MATERIEL Final Report
G. R. Garinther, J. T. Kalb, D. C. Hodge, and G. R. Price Mar. 1985 61 p
(AD-A156704; HEL-TM-3-85) Avail: NTIS HC A04/MF A01 CSCL 20/1

The parameters which affect the propagation and detectability of sound are discussed and assessed for the purpose of revising the aural nondetectability limits of MIL-STD-1474 (1979). The factors considered are geometric spreading, atmospheric absorption, ground effect, atmospheric turbulence, refraction due to wind and temperature gradients, barriers, foliage, threshold of hearing, psychoacoustic factors, and background noise at the listener's location. Examples are given of the effect on sound propagation of varying the parameters, and several suggestions are offered for field expedient measures to control or detect sound. Standard conditions for sound propagation and detectability are proposed, along with two assumed background noise levels. These conditions and background noise levels form the basis for two proposed nondetectability limits. These limits, expressed in 1/3-octave bands, are provided for critical and typical military scenarios and a rationale for selecting between them is developed. Measurement procedures for determining conformance with the limits and an explanation of the methods and rationale used in computing the limits are also presented. The proposed limits are intended to provide nondetectability under most conditions likely to be encountered. However sound propagation conditions are identified which might allow materiel meeting the limits to be detected. Author (GRA)

N86-10918# Mississippi Univ., University. Physical Acoustics Research Lab.
ACOUSTIC CAVITATION AND BUBBLE DYNAMICS
A. A. Atchley and L. A. Crum 15 Jun. 1985 126 p
(Contract N00014-84-C-0193)
(AD-A156888; TR-2-85) Avail: NTIS HC A07/MF A01 CSCL 20/1

The topic of this chapter, acoustic cavitation, is but one of several possible mechanisms through which ultrasound can interact with a liquid medium. Acoustic cavitation can affect a liquid through two possible avenues. The first is the bubble itself. The liquid is disrupted by the inhomogeneous presence of the bubble. The second avenue through which bubbles affect a fluid is through bubble dynamics. The bubble's interior and the liquid immediately surrounding the bubble are regions which undergo continual change. The bubble-liquid interface continually changes shape and size; liquid molecules diffuse into and out of the bubble; the concentration of gas in the surrounding liquid varies; acoustic streaming occurs in the liquid in the vicinity of the bubble often resulting in severe shear stresses; the interior pressure and temperature fluctuate rapidly; the bubble radiates acoustic energy as it oscillates; thermal and viscous damping hinder the bubble oscillations. GRA

N86-10919# Royal Aircraft Establishment, Farnborough (England).
MEASUREMENTS OF THE ACOUSTIC INTERFERENCE BETWEEN ADJACENT MICROPHONES
R. W. Copplestone Aug. 1984 26 p
(AD-A156892; RAE-TM-P-1030; DRIC-BR-94556) Avail: NTIS HC A03/MF A01 CSCL 20/1

An experimental technique is described to determine the disturbance to the response of one microphone due to the presence of a second identical microphone. The measurements were carried out in a free field environment using plane waves incident normally onto the microphones and protection grids were used. The microphone diaphragms were coplanar and the spacing between the microphone centers was varied from one to sixteen microphone diameters. Amplitude deviations up to 1 dB and phase deviations up to 7 degrees have been measured. The magnitudes of the disturbances have been found to be in good agreement with theory. Author (GRA)

N86-10920# Sandia Labs., Albuquerque, N. Mex.
UNDERSTANDING AND IMPROVING ACOUSTIC TO SEISMIC COUPLING AS IT PERTAINS TO SANDIA'S HELICOPTER DETECTOR
G. Elliott and R. J. Fogler 18 Mar. 1985 22 p
(Contract DE-AC04-76DP-00789)
(DE85-009440; SAND-85-0841C) Avail: NTIS HC A02/MF A01

The basic physics of the acoustic-to-seismic coupling phenomenon involved in the operation of a helicopter detector under development are reported. A series of tests were conducted near Albuquerque, New Mexico, investigating the coupling phenomenon using an impulsive noise source and two different helicopters. Results of the tests including the evaluation of a new microphone windscreen design are presented. DOE

72 ATOMIC AND MOLECULAR PHYSICS

Includes atomic structure and molecular spectra.

N86-10921 Maryland Univ., College Park.
MATTER-ANTIMATTER TRANSITION OPERATORS: A MANUAL FOR MODELING Ph.D. Thesis
Janko Milutinovic 1984 171 p
Avail: Univ. Microfilms order No. DA8510265

With the advent of grand unified theories of strong and electroweak interactions, some previously sacred principles, like baryon and lepton number conservation, have had to be abandoned. New interactions have rendered possible several processes which violate these conservation laws. The two most important and most extensively discussed such processes are proton decay and neutron-antineutron (NN) oscillations. Dissert. Abstr.

N86-10922 Pittsburgh Univ., Pa.
CHARGE EXCHANGE IN SLOW COLLISIONS OF ATOMS AND MOLECULES Ph.D. Thesis
Pradip Kumar Gangopadhyay 1984 90 p
Avail: Univ. Microfilms Order No. DA8511041

The cross section for symmetric charge transfer in ion-atom collisions is usually determined by the adiabatic theory. In this work the adiabatic theory is extended to very low energies taking into account the curvature of the nuclear motion due to polarization forces. At the very high energy end the Demkov-Ostrovskii theory is used to compare with the experimental results. The Coulomb force is incorporated into the standard adiabatic theory to determine the cross section for charge transfer between multiply charged ions. The results obtained are in very good agreement with the experimental results. The slight discrepancy between the modified asymptotic theory and the quantum result, in the case of HE*-He+, is studied numerically. Ion-molecule charge transfer is studied numerically. Ion-molecule charge transfer is studied using the close-coupling method. The relative importance of short and long range electron transfer mechanism is studied. The merits and demerits of a surface crossing model are discussed. The importance of including the strong electronic-vibrational coupling in any theory dealing with molecular charge transfer is emphasized. Dissert. Abstr.

N86-10923# National Bureau of Standards, Gaithersburg, Md. Office of Standard Reference Data.
SELECTED TABLES OF ATOMIC SPECTRA. ATOMIC ENERGY LEVELS AND MULTIPLET TABLE O3
Charlotte E. Moore Jul. 1985 35 p refs Prepared in cooperation with NRL
(NBS/NSRDS-3/11; LC-64-60074) Avail: NTIS HC A03/MF A01

The present publication is the eleventh section of a series being prepared in response to the need for a current revision of two sets of the author's tables containing data on atomic spectra as derived from analyses of optical spectra. As in the previous Sections, Part A contains the atomic energy levels and Part B the multiplet tables. Section 11 includes these data for O3. Author

N86-10924# Naval Research Lab., Washington, D. C.
ELECTRON MOMENTUM TRANSFER COLLISION FREQUENCY

IN N(2), O(2) AND AIR Interim Report, 1984 - 1985
S. Slinker and A. W. Ali 26 Jul. 1985 30 p
(ARPA Order 4395)
(AD-A157030; NRL-MR-5614) Avail: NTIS HC A03/MF A01 CSCL 20/8

The electron momentum transfer collision frequencies in N2, O2 and air are calculated for a Maxwellian electron velocity distribution using several definitions of nu sub m (the momentum transfer collision frequency).
Author (GRA)

N86-10925# Rochester Univ., N. Y. Dept. of Chemistry.
COOPERATIVE EMISSION BY TWO DIFFERENT ATOMS INTO SURFACE PLASMONS Interim Report
K. C. Liu and T. F. George Jul. 1985 36 p Prepared in cooperation with State Univ. of New York, Buffalo
(Contract N00014-80-C-0472)
(AD-A157033; URochester/DC/85/TR-68) Avail: NTIS HC A03/MF A01 CSCL 07/4

The interaction between surface plasmons and two atoms with different electronic transition frequencies near a metal or doped semiconductor surface is considered. The atom-atom and atom-surface separations are assumed to be smaller than the corresponding mean resonance wavelength. The time evolution of the emission rate of such an atomic pair into surface plasmon modes is calculated in a fully quantum-mechanical manner. Explicit results are given for various initial states of the diatomic system. As the frequency difference Delta < or = gamma, where gamma is the mean half-width of the atomic resonance lines, the emission behaves as if there are two identical atoms. On the other hand, when Delta > gamma, oscillations are found in the emission rate as a function of time in all cases as a manifestation of beating. The oscillations are especially pronounced when the diatomic system is initially in a coherent state. For the form of the particular state corresponding to complete photon trapping in the case of two identical atoms, a pair of two different atoms exhibits oscillating emission into the superadiant region before eventual decay to zero.
Author (GRA)

N86-10926# Oak Ridge National Lab., Tenn. Physics Div.
THE 1984 BIBLIOGRAPHY OF ATOMIC AND MOLECULAR PROCESSES
C. F. Barnett, comp., H. B. Gilbody, comp. (Queen's Univ., Belfast), D. C. Gregory, comp., P. M. Griffin, comp., C. C. Havener, comp., A. M. Howard, comp., M. I. Kirkpatrick, comp., E. W. McDaniel, comp. (Georgia Tech. Research Inst.), F. W. Meyer, comp., T. J. Morgan, comp. (Wesleyan Univ.) et al Apr. 1985 209 p
(Contract DE-AC05-84OR-21400)
(DE85-010583; ORNL-6157) Avail: NTIS HC A10/MF A01

This annotated bibliography includes papers on atomic and molecular processes published during 1984. Sources include scientific journals, conference proceedings, and books. Each entry is designated by one or more of the 114 categories of atomic and molecular processes used by the Controlled Fusion Atomic Data Center, Oak Ridge National Laboratory to classify data. Also indicated is whether the work was experimental or theoretical, what energy range was covered, what reactants were investigated, and the country of origin of the first author. Following the bibliographical listing, the entries are indexed according to the categories and according to reactants within each subcategory.
DOE

N86-10927# Los Alamos National Lab., N. Mex.
THEORY OF DENSE MOLECULAR FLUID EQUATIONS OF STATE WITH APPLICATION TO DETONATION PRODUCTS
M. S. Shaw, J. D. Johnson, and B. L. Holian 1984 4 p Presented at the 8th Intern. Symp. on Detonation, Albuquerque, N. Mex., 15 Jul. 1985
(Contract W-7405-eng-36)
(DE84-016822; LA-UR-84-2753; CONF-850706-1) Avail: NTIS HC A02/MF A01

Because of the uncertainty in using spherical potentials, a series of benchmark calculations was made using molecular dynamics with realistic anisotropic potentials. The configurational part of the Helmholtz free energy for an anisotropic molecular system can be obtained by using an equivalent spherical potential. Such potentials were obtained for N2, O2, NO, CO, and CO2.
DOE

N86-10928# Sandia Labs., Albuquerque, N. Mex.
PROVIDING AUTOMATED CONTROL FOR PBFA-2
V. M. Italiano 1985 10 p Presented at the 5th IEEE Pulsed Power Conf., Washington, D.C., 10 Jun. 1985
(Contract DE-AC04-76DP-00789)
(DE85-012867; SAND-84-2434C; CONF-850616-1D) Avail: NTIS HC A02/MF A01

Four levels of control which are available to the operator in the particle beam fusion accelerator 2 (PBFA-2) control/monitor system are discussed. At the lowest control level, remote manual, the operator is responsible for all accelerator control and coordination and for interpreting sensor and actuator values to determine the state of the accelerator. At the highest control level, autostaging, the computer integrates the sensor and actuator values into reports. The operator controls several accelerator subsystems with single autostaging commands which the control/monitor system interprets into sequences of integrated functions. The control system is implemented from the bottom up, from remote manual to autostaging. Control action tasks are integrated with no major changes to the control/monitor design. Once the control action tasks are completely implemented no more changes are expected in the design. The control/monitor system is reviewed. DOE

N86-10929# Los Alamos National Lab., N. Mex.
HIGH-BRIGHTNESS PHOTOEMITTER INJECTOR FOR ELECTRON ACCELERATORS
J. S. Fraser, R. L. Sheffield, E. R. Gray, and G. W. Rodenz 1985 4 p refs Presented at the Particle Accelerator Conf., Vancouver, British Columbia, 13 May 1985
(Contract W-7405-eng-36)
(DE85-012673; LA-UR-85-1532; CONF-850504-96) Avail: NTIS HC A02/MF A01

A free-electron laser (FEL) oscillator, driven by an RF linac, requires a train of electron bunches delivered to an undulator. The electron-beam brightness requirement exceeds that available from a conventional buncher. The demonstrated high peak brightness of laser-illuminated photoemitters indicates that the conventional buncher system might be eliminated entirely without the usual large loss in beam brightness that occurs in bunchers. A photoemitter with a current density of about 200 A/cm (2) is located on an end wall of an RF cavity to accelerate a 60-ps bunch of electrons to 1 MeV as rapidly as possible. Preliminary experimental work and simulation calculations are presented. DOE

N86-10930# Los Alamos National Lab., N. Mex.
MEASUREMENT AND RESULTING FIRST AND SECOND ORDER APPROXIMATIONS FOR A 9 DEG BENDING MAGNET IN LAMPF'S 750-keV TRANSPORT
J. W. Hurd 1985 4 p Presented at the Particle Accelerator Conf., Vancouver, British Columbia, 13 May 1985
(Contract W-7405-eng-36)
(DE85-012691; LA-UR-85-1528; CONF-850504-118) Avail: NTIS HC A02/MF A01

The three Cartesian components of magnetic field are measured for a 9 degree bending magnet. Measurement errors are corrected and the data is fit to a polynomial which satisfies Maxwell's equations. Particle paths through the magnet are calculated by numerical integration and the corresponding first and second order particle transformation matrices are generated. A parameterization for the first order transformation matrix is developed and the resulting approximations for predicting particle motion in the magnet are compared to the results of the numerical integration.
DOE

N86-10931# Brookhaven National Lab., Upton, N. Y.
METHOD FOR DETERMINING THE POSITION, ANGLE AND OTHER INJECTION PARAMETERS OF A SHORT PULSED BEAM IN THE BROOKHAVEN AGS

C. Gardner and L. Ahrens 1985 4 p Presented at the Particle Accelerator Conf., Vancouver, British Columbia, 13 May 1985
(Contract DE-AC02-76CH-00016)
(DE85-012523; BNL-36490; CONF-850504-135) Avail: NTIS HC A02/MF A01

As part of the effort to improve the monitoring of the injection process at the Brookhaven Alternating Gradient Synchrotron (AGS), a beam diagnostics package has been developed which processes the signals from the plates of a pick-up electrode (PUE) located near the injection region of the AGS and provides measurements of the position and angle (with respect to the equilibrium orbit) of the injected beam at the stripping foil where the incident H(-) beam is converted into protons. In addition the package provides measurements of the tune and chromaticity of the AGS at injection, and a measurement of the momentum spread of the injected beam. The diagnostics package is referred to as PIP which stands for Pulsed Injection Parameters. DOE

N86-10932# North Carolina Univ., Charlotte.
INITIAL INCREASE, PEAKING EFFECT, IN THE INTERNAL FRICTION OF COPPER FOLLOWING PULSED NEUTRON AND ELECTRON IRRADIATION
H. M. Simpson, D. M. Parkin, J. A. Goldstone, and J. W. Hemsky 1985 6 p Presented at the Conf. on Internal Friction and Ultrasonic Attenuation in Solids, Urbana, Ill., 3 Jun. 1985 Prepared in cooperation with LASL and Wright State Univ., Dayton, Ohio
(Contract W-7405-eng-36)
(DE85-012767; LA-UR-85-1829; CONF-8506125-2) Avail: NTIS HC A02/MF A01

Under certain experimental conditions the internal friction in metals can first increase and following prolonged irradiation decrease. Many models have been proposed to account for this peaking effect; however, in many of the cases, no effort is made to distinguish between the influence of interstitials and/or vacancies. To determine the nature of the point defect responsible for the peaking effect in high purity copper, a series of pulsed irradiations using neutrons and electrons were performed. In all of the experiments an initial very rapid rise in the internal friction and Young's modulus was observed. These data show that a fast diffusing defect is responsible for the peaking effect: i.e., the interstitial. DOE

N86-10933# Brookhaven National Lab., Upton, N. Y.
METHOD FOR COMPENSATING BELLOWS PRESSURE LOADS WHILE ACCOMMODATING THERMAL DEFORMATIONS
M. H. Woodle 1985 3 p Presented at the Particle Accelerator Conf., Vancouver, British Columbia, 13 May 1985
(Contract DE-AC02-76CH-00016)
(DE85-013306; BNL-36572; CONF-850504-144) Avail: NTIS HC A02/MF A01

Many metal bellows are used on storage ring vacuum chambers. They allow the ring to accommodate deformations with alignment, mechanical assembly and thermal expansion. The national synchrotron light source (NSLS) has two such electron storage rings, the VUV ring and the X-ray ring. Both rings utilize a number of welded metal bellows within the ring and at every beam port. There are provisions for 16 beam ports on the VUV and 28 ports in the X-ray ring. At each of these locations the bellows are acted on by an external pressure of 1 atmosphere, which causes a 520 lb reaction at the vacuum chamber beam port and at the beamline flange downstream of the bellows. The use of rigid tie rods across the bellows flanges to support this load is troublesome because most storage ring vacuum chambers are baked in situ to achieve high internal vacuum. Significant forces can develop on components if thermal deformation is restrained and damage could occur. DOE

N86-10934# Argonne National Lab., Ill.
USE OF THE MURA TRANSFORMATION TO GENERATE THE FIELDS AND CALCULATE THE MOTION OF PROTONS IN THE DESIGNED ARGONNE MINI-ASPUN FFAG SPIRAL SECTOR ACCELERATOR
E. A. Crosbie 13 May 1985 3 p refs Presented at the Particle Accelerator Conf., Vancouver, British Columbia, 13 May 1985
(Contract W-31-109-eng-38)
(DE85-011477; ANL-HEP-CP-85-34) Avail: NTIS HC A02/MF A01

As a long range goal for the production of high intensity neutrons, Argonne National Laboratory has proposed the construction of a 1.5 GeV FFAG Spiral Sector Accelerator called ASPUN. The 500-MeV injector for this proposed accelerator is a smaller FFAG Spiral Sector Accelerator named Mini-ASPUN. Until such a time as the larger machine could be built, it was planned that Mini-ASPUN would replace the present RCS now being used for the IPNS program at Argonne. In order to obtain an accurate estimation of the orbits and betatron oscillations in such a machine, it is necessary that realistic field values be used in the equations of motion. Obtaining these fields from 3-dimensional relaxation calculations is both time consuming and costly. However, because of the required scaling of the machine, the field-generating potential of three variables can be separated into a known function of the radius and a function of two variables. The second order differential equation satisfied by this function can be solved by ordinary relaxation methods. The fields generated from a mesh of values for this function will be accurate except for the extreme inside and outside orbits, which will be affected by the necessary termination of the inside and outside ends of the magnet. DOE

N86-10935# Brookhaven National Lab., Upton, N. Y.
AGS POLARIZED H(-) SOURCE
A. Kponcu, J. G. Alessi, and T. Sluyters 1985 7 p Presented at the Particle Accelerator Conf., Vancouver, British Columbia, 13 May 1985
(Contract DE-AC02-76CH-00016)
(DE85-013296; BNL-36486; CONF-850504-142) Avail: NTIS HC A02/MF A01

The AGS polarized H(-) source is now operational. During a month-long experimental physics run in July 1984, pulses equivalent to 15 (MU)A x 300 (MU)s (approx. 3 x 10 the 10 protons) were injected into the RFQ preaccelerator. Beam polarization, measured at 200 MeV, was approx. 75%. After the run, a program to increase the H(-) yield of the source was begun and significant progress was made. The H(-) current is now frequently 20 to 30 (MU)A. DOE

N86-10936# Oak Ridge National Lab., Tenn.
EXPERIMENTAL X-RAY SCATTERING CROSS SECTIONS FOR H2 AND RARE ATOMIC GASES
G. E. Ice 1985 23 p Presented at the New Directions in X-ray Scattering Workshop, Asilomar, Calif., 3 Apr. 1985
(Contract DE-AC05-84OR-21400)
(DE85-011572; CONF-8504136-1) Avail: NTIS HC A02/MF A01

Slides are presented for a talk on X-ray scattering from rare gases as an unambiquous test of ab initio wave functions and theoretical X-ray scattering cross sections. DOE

N86-10937# Brookhaven National Lab., Upton, N. Y.
METHANE-BUBBLE FORMATION IN HYDROGEN-CHARGED Fe-30 ppM C
C. L. Snead, Jr., K. G. Lynn, and M. Suenaga 1985 4 p refs Presented at the 7th Intern. Conf. on Positron Annihilation, New Delhi, 6 Jan. 1985
(Contract DE-AC02-76CH-00016)
(DE85-012526; BNL-36414; CONF-850169-13) Avail: NTIS HC A02/MF A01

Positrons were used as a probe of the early-stage growth of methane bubbles in hydrogen-charged polycrystalline Fe. Ferrovac E (30 ppM C) was charged at 900 psi of H2 at 475(0)C for various times to generate the methane internally. It is known that this process generates methane bubbles. Results show that, even at very early bubble-growth stages, dislocations are generated. A lifetime definitely associated with trapping at bubbles is not observed, due either to trapping by dislocations that are generated and which can screen the bubbles, or by passivation of the bubbles as positron traps by the presence of hydrogen or methane in them. DOE

N86-10938# Pacific Northwest Lab., Richland, Wash.

SECONDARY STANDARDS LABORATORIES FOR IONIZING RADIATION CALIBRATIONS: THE NATIONAL LABORATORY INTERESTS

P. I. Roberson and G. W. Campbell Nov. 1984 8 p ref Presented at the Workshop on Radiation Survey Instruments and Calibrations, Gaithersburg, Md., 10 Jul. 1985 Prepared in cooperation with Rockwell International Corp.
(Contract DE-AC06-76RL-01830)
(DE85-007046; PNL-SA-12423; CONF-850726-1) Avail: NTIS HC A02/MF A01

The national laboratories are probable candidates to serve as secondary standards laboratories for the federal sector. Representatives of the major Department of Energy laboratories were polled concerning attitudes toward a secondary laboratory structure. Generally, the need for secondary laboratories was recognized and the development of such a program was encouraged. The secondary laboratories should be reviewed and inspected by the National Bureau of Standards. They should offer all of the essential, and preferably additional, calibration services in the field of radiological health protection. The selection of secondary laboratories should be based on economic and geographic criteria and/or be voluntary. DOE

N86-10939# Atlanta Univ., Ga.

THEORETICAL INVESTIGATION OF ELECTRON-POSITIVE ION-ATOM INTERACTIONS Progress Report, 1 Jul. 1984 - 20 Mar. 1985

A. Z. Msezane 1985 6 p
(Contract DE-FG05-84FR-13266)
(DE85-013019; DOE/ER-13266/T1) Avail: NTIS HC A02/MF A01

Research involved investigations of e-positive ion/atom collisions and photoionization of excited atomic states. The latter is useful in determining appropriate wave functions for use in weakly bound systems which characterize excited states. Accurate differential cross sections for ZnII, MgII and Cu, integral cross sections for MgII, CdII, and Cu, and innershell excitation cross sections for Ti(3+) by electron impact were obtained. The close-coupling approximation was used with accurate configuration interaction wave functions. Also, photoionization cross sections for excited Na 3p, Na 4d and Ag 5d subshells are obtained in Hartree-Fock approximation using accurate wave functions. The purpose was to provide benchmark results to guide measurements. Differential cross section measurements for ions are very difficult owing to low target ion densities. Multi-minima in photoionization of excited states were not observed experimentally because of the lack of reliable predictions. DOE

N86-10940# Sandia Labs., Albuquerque, N. Mex.

PHOTONIC DIAGNOSTICS AND PULSED POWER RESEARCH

J. Chang, G. Allen, W. F. Filter, G. J. Lockwood, and B. T. Neyer 10 Jun. 1985 9 p Presented at the 5th IEEE Pulsed Power Conf., Washington, D.C., 10 Jun. 1985
(Contract DE-AC04-76DP-00789)
(DE85-013752; SAND-84-2500C; CONF-850616-44) Avail: NTIS HC A02/MF A01

Photonic methods offer a powerful approach to pulsed power diagnostics. The use of photon analog signals rather than the conventional electrical analog signals to make pulsed power measurements is a fundamental change that promises to evolutionize pulsed power research. This new approach uses inherently broadband optical components, and a picosecond streak camera to perform high speed measurements. We have developed sensors that use photonics principles to monitor voltages and currents, methods of using optical fibers to transmit the photon analog signals, and a High Speed Multi-Channel Data Recorder to economically record them. This system not only offers economy, compactness, high bandwidth, and EMI resistance, but it also accesses high field regions previously impossible to reach with metallic electrical monitors. The Photonic system will greatly reduce the complexity of pulsed power diagnostics. DOE

N86-10941# Argonne National Lab., Ill.

THE 20 keV UNDULATORS FOR A 6-GeV STORAGE RING

S. H. Kim and Y. Cho 1985 4 p refs Presented at the Particle Accelerator Conf., Vancouver, British Columbia, 13 May 1985
(Contract W-31-109-eng-38)
(DE85-013867; CONF-850504-177) Avail: NTIS HC A02/MF A01

The main goal of the future 6-GeV electron storage ring is to provide 20-keV fundamental harmonic radiations from insertion devices. Parameter restrictions of REC-Vanadium permendur hybrid undulators were examined. The critical factor is the achievable minimum gap of the undulator. Variations of the spectral brilliance for different beam parameters are also shown. DOE

N86-10942# Argonne National Lab., Ill.

NEW PARTICLE SEARCHES

M. Derrick 1985 39 p Presented at the PEP High Luminosity Workshop, Stanford, Calif., 5 Apr. 1985
(Contract W-31-109-eng-38)
(DE85-014073; ANL-HEP-CP-85-44; CONF-8504155-2) Avail: NTIS HC A03/MF A01

The Standard Model is a remarkable result of decades of work in particle physics, but it is clearly an incomplete representation of the world. Exploring possibilities beyond the Standard Model is a major preoccupation of both theorists and experimentalists. Despite the many suggestions that are extant about the missing links within the Standard Model as well as extensions beyond it, no hard experimental evidence exists. In particular, in more than five years of experimentation both at PETRA and PEP no new particles have been found that would indicate new physics. Several reasons are possible for these negative results: the particles may be too heavy; the experiments may not be looking in the proper way; the cross sections may be too small or finally the particles may not exist. A continuing PEP program, at high luminosity will ensure that the second and third reason continue to be addressed. The higher energy e(+)e(-) storage rings such as TRISTAN and LEP will extend the mass limits. High mass particles can also be produced at the CERN collider and soon with the Tevatron collider. A concise summary of the mass limits from the PETRA experiments was given in a recent Mark J publication. The results shown provide a convenient yardstick against which to measure future search experiments. DOE

N86-10943# Los Alamos Scientific Lab., N. Mex.

ANGULAR DISTRIBUTION OF NEUTRAL HYDROGEN FOLLOWING COLLISIONAL ELECTRON DETACHMENT FROM H(-)

J. D. Moses, D. Holtkamp, J. D. King, P. W. Lisowski, and J. E. Simmons Mar. 1985 16 p
(Contract W-7405-eng-36)
(DE85-014258; LA-10326-ML) Avail: NTIS HC A02/MF A01

The angular distribution of neutral hydrogen following electron detachment from H(-) was measured for H(-) on nitrogen and hydrogen gas, both for neutral atoms left in the 2S state, and for all neutrals independent of the state of excitation. The results are essentially in agreement with calculations based on the Born approximation, although there is some disagreement in detail. DOE

N86-10944# Los Alamos Scientific Lab., N. Mex.

PRELIMINARY INVESTIGATION OF CHANGES IN X-RAY MULTILAYER OPTICS SUBJECTED TO HIGH RADIATION FLUX

M. P. Hockaday, R. L. Blake, J. S. Grosso, M. M. Selph, M. M. Klein, W. Matuska, Jr., M. A. Palmer, and R. J. Liefeld 1985 9 p refs Presented at the SPIE Intern. Tech. Symp. on Optical and Electro-Optical Eng., San Diego, Calif., 18 Aug. 1985 Prepared in cooperation with Sandia National Labs., Albuquerque, N. Mex. and New Mexico State Univ., Las Cruces
(Contract W-7405-eng-36)
(DE85-014074; LA-UR-85-2265; CONF-850887-4) Avail: NTIS HC A02/MF A01

A variety of metal multilayers was exposed to high X-ray flux using Sandia National Laboratories' PROTO II machine in the gas puff mode. Fluxes incident on the multilayers above 700 MW/sq.cm. in total radiation, in nominal 20 ns pulses, were realized. The neon hydrogen- and helium-like resonance lines were used to probe the X-ray reflectivity properties of the multilayers as they underwent change of state during the heating pulse. A fluorescer-fiber optic-streak camera system was used to monitor the changes in X-ray reflectivity as a function of time and irradiance. Preliminary results are presented for a W/C multilayer. DOE

N86-10945# Texas Univ., Austin.
NATURE OF PHOTOEMISSION INTO DIELECTRIC FLUIDS Progress Report
Dec. 1984 29 p
(Contract DE-FG05-84ER-45064)
(DE85-013017; DOE/ER-40561/1) Avail: NTIS HC A03/MF A01

The photoyield was measured in pure ammonia using a pulsed technique. It has been measured as a function of bias, temperature, and photon energy, in order to study the density of electron states in NH3 and the photo-injection process into the ammonia. The photoyield versus reference potential shows a much greater range of response than previous CW techniques. A strong temperature dependence was observed in the yield and a two slope behavior in the yield, observations which are consistent with our idea that there is a significant tail of localized states just below the conduction band in polar fluids. A systematic variation was found in the decay mode of the injected current as a function of reference potential, temperature, and impurity concentration giving us a new tool with which to examine the photo-injection process. DOE

N86-10946# Fermi National Accelerator Lab., Batavia, Ill.
HYPERON POLARIZATION: AN UNRESOLVED PROBLEM
J. Lach 10 Mar. 1985 7 p Presented at the 20th Recontre de Moriond, Les Arcs, France, 10 Mar. 1985
(Contract DE-AC02-76CH-03000)
(DE85-012296; FNAL/C-85/65; CONF-850375-1) Avail: NTIS HC A02/MF A01

Hyperons produced in high energy collisions have polarizations as large as 20%. These polarizations allowed high precision measurements of most hyperon magnetic moments and a confirmation of the Cabibbo theory involving semileptonic hyperon decays. However, a satisfactory quantitative explanation of hyperon polarization is still lacking. The question of whether the omega(-) is produced with significant polarization is crucial to the measurement of its magnetic moment. Present data are inconclusive as to whether the omega(-) is produced polarized. Phenomenological models and data on antihyperon production may not be useful guides in predicting the omega(-) polarization. DOE

N86-10947# Brookhaven National Lab., Upton, N. Y.
BEAM PROFILE MONITOR FOR THE NSLS VUV RING EMPLOYING LINEAR PHOTODIODE ARRAYS
R. J. Nawrocky, J. Galayda, L. H. Yu, and D. M. Shu 1985 4 p Presented at the Particle Accelerator Conf., Vancouver, British Columbia, 13 May 1985
(Contract DE-AC02-76CH-00016)
(DE85-012184; BNL-36497; CONF-850504-172) Avail: NTIS HC A02/MF A01

Among the most important parameters of a storage accelerator are the position and size of the particle beam. In an electron machine, these parameters can be derived from measurements of the emitted synchroton radiation. A system which monitors the two-dimensional profile of the synchrotron light in the NSLS VUV ring commercially available high-resolution linear photosensitive diode arrays is discussed. The optical system was designed to match the size of the image space to the dimensions of the diode sensor area. The scanning rate is automatically adjusted to hold the peaks of the profiles constant over a wide range of beam intensity variations. Video signals from the diode sensors can be readily interfaced to a computer for beam diagnostic purposes. Optics and factors determining the overall resolution of the system are discussed. Preliminary results of beam observations are presented. DOE

N86-10948# Brookhaven National Lab., Upton, N. Y.
SURFACE CONDITIONING OF SYNCHROTRON RADIATION SOURCE TO IMPROVE BEAM LIFETIME
T. S. Chou 1985 3 p Presented at the Particle Accelerator Conf., Vancouver, British Columbia, 13 May 1985
(Contract DE-AC02-76CH-00016)
(DE84-012185; BNL-36546; CONF-850504-170) Avail: NTIS HC A02/MF A01

Surface cleanliness is of prime importance to achieve the desirable vacuum condition for long beam lifetime in all synchrotron radiation sources. The Photon Factory at KEK resolved the severe gas load from synchrotron radiation by in-situ Ar glow discharging the whole storage ring. Sufficient experience was gained in the past two years operation on the synchrotron radiation source, especially on the VUV ring of the National Synchrotron Light Source (NSLS), to allow a decision to glow discharge the VUV ring. In hoping to obtain higher circulating current and to reveal the cause of lifetime limitation, a better understanding of the beam loss mechanism is needed. Photo desorption is the major gas load in all existing electron (position) storage rings. It is generally believed that these photodesorbed species (neutral and charged) provide the major loss mechanism to lessen the beam lifetime. The interaction of these species to the beam give rise to the various loss mechanisms, such as multiple Coulomb scattering, single scattering, bremsstrahlung and ion trapping. All these mechanisms were under intense study at NSLS. The result of surface condition and beam lifetime are described. DOE

N86-10949# Oak Ridge National Lab., Tenn.
EXPERIMENTAL STUDIES OF TRANSITION RADIATION AND OPTICAL BREMSSTRAHLUNG
E. T. Arakawa 1985 19 p refs Presented at the Penetration Phenomena Workshop, Oak Ridge, Tenn., 14 Apr. 1985
(Contract DE-AC05-84OR-21400)
(DE85-0135637; CONF-850464-1) Avail: NTIS HC A02/MF A01

Research on the optical emission from thin films and bulk metals bombarded by 25 to 120 keV electrons carried out at Oak Ridge National Laboratory is presented. Measurements were carried out on the dependence of the emitted spectra on angle of observation, polarization, sample thickness, surface roughness, surface contamination, and incident electron energy. DOE

N86-10950# Los Alamos National Lab., N. Mex.
WIDE DYNAMIC RANGE BEAM PROFILE MONITOR
D. M. Lee, D. Brown, R. A. Hardekopf, J. R. Bilskie, and O. B. V. vanDyck 1985 4 p Presented at the Particle Accelerator Conf., Vancouver, British Columbia, 13 May 1985
(Contract W-7405-eng-36)
(DE85-012709; LA-UR-85-1651; CONF-850504-134) Avail: NTIS HC A02/MF A01

An economical harp multiplexer system was developed to achieve a wide dynamic range. The harp system incorporates a pneumatically actuated harp detector with ceramic boards and carbon wires; a high-sensitivity multiplexer packaged in a double-wide NIM module; and flat, shielded ribbon cable consisting of individual twisted pairs. The system multiplexes 30 wires in each of the x and y planes simultaneously and operates with or without computer control. The system has operated in beams of 100 nA to 1 mA, 1- to 120-Hz repetition rate, with a signal-to-noise ratio of greater than 10/1. DOE

73 NUCLEAR AND HIGH-ENERGY PHYSICS

Includes elementary and nuclear particles; and reactor theory.

For space radiation see *93 Space Radiation.*

N86-10951# Army Military Personnel Center, Alexandria, Va.
THE DEVELOPMENT OF A NEUTRON EVAPORATION THEORY CODE FOR THE THERMAL FISSION OF URANIUM-235 Final

Report. M.S. Thesis
T. J. Rosener 3 May 1985 116 p
(AD-A156593) Avail: NTIS HC A06/MF A01 CSCL 20/8

The thermal fission of Uranium-235 has been studied by developing a computer code that used evaporation theory based on the Weisskopf model for neutron emission from individual fission fragments. This computer code calculates a prompt neutron spectrum for the thermal fission of Uranium-235, calculates the total gamma ray energy for the fission of Uranium-235, and calculates the average prompt neutron kinetic energy. Until now, evaporation theory codes used average values of mass and energy in determining prompt neutron spectra, and this code was developed to use all possible fission fragment combinations in order to eliminate this averaging. This approach is necessary to compute certain measured data such as the probability that 0,1,2,... neutrons are emitted per fission. This code uses subroutines to calculate rest masses, to correct the calculated rest mass to agree with experiment, and to determine the emitted neutron kinetic energies. Evaporation theory codes have predicted low total gamma energy release in fission, but agree quite favorably with experiments in predicting the average prompt neutron kinetic energy. The prompt neutron spectrum obtained in this code has a high tail region, that is, below 0.5 MeV. The average kinetic energy of the neutrons agree very well with experiment, and the total gamma energy is lower than experiment, as previous evaporation theory codes have been. GRA

N86-10952# Argonne National Lab., Ill.
SCOPING STUDIES OF VAPOR BEHAVIOR DURING A SEVERE ACCIDENT IN A METAL-FUELING REACTOR
B. W. Spencer and J. F. Marchaterre 15 Apr. 1985 17 p refs Presented at ANS/ENS Fast Reactor Safety Meeting, Knoxville, Tenn., 21 Apr. 1985
(Contract W-31-109-eng-38)
(DE85-011474; CONF-850410-47) Avail: NTIS HC A02/MF A01

The consequences of fuel melting and pin failures for a reactivity-insertion type accident in a sodium-cooled, pool-type reactor fueled with a metal alloy fuel were examined. The principal gas and vapor species released are shown to be Xe, Cs, and bond sodium contained within the fuel porosity. Condensation of sodium vapor as it expands into the upper sodium pool in a jet mixing regime may occur as rapidly as the vapor emerges from the disrupted core. If the predictions of rapid direct-contact condensation can be verified experimentally for the sodium system, the ability of vapor expansion to perform appreciable work on the system and the ability of an expanding vapor bubble to transport fuel and fission produce species to the cover gas region where they may be released to the containment are largely eliminated. The radionuclide species except for fission gas are largely retained within the core and sodium pool. DOE

N86-10953# Department of Energy, Argonne, Ill.
EVALUATION OF THE INTERNATIONAL ATOMIC ENERGY AGENCY (IAEA) SAFEGUARDS ANALYTICAL LABORATORY QUALITY ASSURANCE PROGRAM
C. E. Pietri and J. T. Bracey Feb. 1985 58 p refs Prepared in cooperation with Martin Marietta Energy Systems, Paducah, Ky.
(Contract DE-AC05-84OU-21400)
(DE85-012078; NBL-312; ISPO-232) Avail: NTIS HC A04/MF A01

Destructive analysis is used to verify the inventory of nuclear materials at nuclear facilities. The reliability and quality of these measurements must be assured in a systematic manner. The development and implementation for the quality assurance measures for the analytical procedures used in the destructive analysis of these safeguards samples are discussed. The procedures used for the destructive analysis of safeguards samples and the statistical evaluation of the resulting measurement data are evaluated. The procedures include analytical methods, quality control measures, and the treatment of data from these activities. Modifications to the system, which would provide routine assurance to management that these procedures are functioning properly to achieve safeguards objectives are recommended. The sample handling procedures, measurement control activities, analytical methods, reference materials, calibration procedures, statistical analysis of data, and data management system are evaluated. The degree to which laboratory quality assurance is achieved is assessed by comparing it to accepted standards of quality assurance. DOE

N86-10954# Idaho National Engineering Lab., Idaho Falls.
ON-LINE GAMMA-RAY DATA ACQUISITION AT THE POWER BURST FACILITY
J. K. Hartwell and E. W. Killian 1985 16 p refs Presented at the 6th Symp. on X- and Gamma-Ray Sources and Appl., Ann Arbor, Mich., 21 May 1985
(Contract DE-AC07-76ID-01570)
(DE85-011957; EGG-M-08985; CONF-850533-5) Avail: NTIS HC A02/MF A01

The PBF (Power Burst Facility) Fission Product Detection System (FPDS) incorporates four on-line gamma ray spectrometers controlled by operators one kilometer distant. The FPDS is uniquely designed to monitor the high fission product concentrations generated when reactor fuel rods are severely damaged. Through the use of variable collimators, fast analog electronics, a pulser subsystem, and a carefully designed shield, this system has monitored samples with dose rate readings greater than 900 R/h. The spectral data acquired by the FPDS have provided fission product release and transport behavior information not previously available from off-line or gross radiation monitoring methods. DOE

N86-10955# Los Alamos Scientific Lab., N. Mex.
POLARIZATION TRANSFER IN INELASTIC SCATTERING AND PIONIC MODELS OF THE EMC EFFECT
J. M. Moss 1985 13 p refs Presented at the Conf. on Antinucleon and Nucleon-Nucleus Interactions, Tessuride, Colo., 18 Mar. 1985
(Contract W-7503-eng-36)
(DE85-010738; LA-UR-85-1450; CONF-850315-2) Avail: NTIS HC A02/MF A01

A measurement of the sigma vector . q vector or spin-longitudinal nuclear response function was discussed. A LAMPF experiment was proposed. The European Muon Collaboration (EMC) effect, and the possibility that this ultrahigh-energy physics result may be related to nuclear pions and, the isovector sigma vector . q vector nuclear response function was investigated. The EMC effect and its interpretation in terms of excess nuclear pions is discussed. This model establishes a connection between the vastly different scales of the EMC experiment and the Los Alamos experiment. The Los Alamos experiment and its interpretation in terms of excess nuclear pions is described. Quark effects in nuclei based on the EMC and Los Alamos experimental results are analyzed. DOE

N86-10956# California Univ., Livermore. Lawrence Livermore Lab.
MEAN LIFE OF THE 2p(4)((1)S)3s (2)S STATE IN FLUORINE
K. T. Cheng and M. H. Chen 17 May 1985 5 p refs Presented at the Workshop on Autoionization of Atoms and Small Molecules, Argonne, Ill., 2 May 1985
(Contract W-7405-eng-48)
(DE85-012929; UCRL-92713; CONF-850560-5) Avail: NTIS HC A02/MF A01

The radiationless as well as the radiative decay rates for the 2p(4)((1)S)3s (2)S state are calculated. For comparison purposes similar calculations for the 2p(4)((1)D)4s (2)D state were also made. Calculations are based on the multi-configuration Dirac-Fock (MCDF) method. As spin-orbit interaction is built in, this method is capable of studying LS forbidden Auger transitions. Details of the Auger transition calculations have been given before. DOE

N86-10957# Georgia Inst. of Tech., Atlanta. School of Mechanical Engineering.
DEVELOPMENT AND APPLICATION OF THE ELECTROCHEMICAL ETCHING TECHNIQUE
M. E. Sanders Jul. 1984 119 p
(Contract DE-AS05-76FV-04814)

(DE85-010302; DOE/EV-04814/T2) Avail: NTIS HC A06/MF A01

The advances achieved in the development and application of several etched damage track plastic dosimeters that can be used to measure dose-equivalent from neutrons with energies from thermal to 20 MeV are discussed. The project was initiated with the design of a rem-responding dosimeter that measured fast (> 1 Mev) neutron dose-equivalent as a function of the damage track density directly induced within the volume of polycarbonate foils amplified by electrochemical etching. The thermal neutron dosimeter was composed of an external radiator tablet made of (7)LiF in contact with a polycarbonate foil and utilized the thermal neutron-induced (6) Li(n, (Alpha)) (3)H reaction to give a dose-equivalent response as a function of alpha track density registered in the detector foil. An intermediate (1 eV-1 MeV) neutron dosimeter was developed and was shown to give an approximately dose-equivalent response to neutrons with energies from 1 eV to 17 MeV. The intermediate neutron dosimeter consists of (6)LiF-Teflon/CR-3-9 Polymer foil assembly which is enclosed by a (Cd + In) neutron filter. The neutron dose-equivalent is measured as a variable function of these damage track density registered in the CR-39 detector foil to alpha particles from the 1/v dependent (6)Li(n, (ALPHA))(3)H reaction, recoil H, C, O nuclei from neutron-induced elastic scattering within the foil volume, and protons from the (6)Li(n, p) reaction for neutron energies above 2 MeV. DOE

N86-10958# Oak Ridge National Lab., Tenn.

ORR CORE RE-CONFIGURATION MEASUREMENTS TO INCREASE THE FAST NEUTRON FLUX IN THE MAGNETIC FUSION ENERGY (MFE) EXPERIMENTS

R. W. Hobbs, R. M. Stinnett, and T. M. Sims Jun. 1985 73 p
(Contract DE-AC05-84OR-21400)
(DE85-013520; ORNL/TM-9615) Avail: NTIS HC A04/MF A01

The relative increases obtainable in the fast neutron flux in the Magnetic Fusion Energy (MFE) experiment positions were studied by reconfiguring the current ORR core. The percentage increase possible in the current displacement per atom (dpa) rate was examined. The principle methods to increase the fast flux, consisted of reducing the current core size (number of fuel elements), to increase the core average power density and arrangement of the fuel elements in the reduced-size core to tilt the core power distribution towards the MFE positions were investigated. It is concluded that fast fluxes in the E-3 core position can be increased by approximately 15 to 20% over current values and in E-5 by approximately 45 to 55%. DOE

N86-10959# California Univ., Livermore. Lawrence Livermore Lab.

IMPACT OF LONG-LIVED RADIONUCLIDES ON WASTE CLASSIFICATION FOR FUSION

R. C. Maninger 10 May 1985 13 p Presented at the Ann. Meeting of the Am. Nucl. Soc., Boston, 9 Jun. 1985
(Contract W-7405-eng-48)
(DE85-013205; UCRL-91885; CONF-850610-30) Avail: NTIS HC A02/MF A01

A major goal for commercial applications of fusion reactors is to minimize radioactive wastes and to dispose of them by near surface burial. There currently are no regulations specifically applicable to fusion wastes but those in force for fission wastes furnish a framework for expected fusion regulations. It is recommended that all nuclides with half lives greater than five years be assigned concentration limits as done in 10CFR61 for fission wastes. Approximate limits for all the significant long half life sources of gamma radiation in the currently known periodic table are given. In the absence of working fusion reactors, computer models must be used to estimate the expected actual concentrations of radioactive nuclides. These estimates are needed to guide design parameters to achieve minimum radioactivity in fusion reactors. It is believed that the computer models and nuclear libraries must be much more comprehensive than ordinarily used today to do activation calculations. DOE

N86-10960# Oak Ridge National Lab., Tenn.

EVOLUTION OF THE FUSION POWER DEMONSTRATION TANDEM MIRROR REACTOR CONFIGURATION

J. A. OToole and D. C. Lousteau 1985 6 p Presented at the 6th Top. Meeting on the Technol. of Fusion Energy, San Francisco, 3 Mar. 1985
(Contract DE-AC05-84OR-21400)
(DE85-012889; CONF-850310-109) Avail: NTIS HC A02/MF A01

A presentation of the evolution of configurations proposed for tandem mirror Fusion Power Demonstration (FPD) machines is presented. The FPD study was undertaken to scope the mission as well as the technical and design requirements of the next tandem mirror device. Three configurations, entitled FPD I, II, and III were studied. During this process new systems were conceived and integrated into the design, resulting in a significantly changed overall machine configuration. The machine can be divided into two areas. A new center cell configuration, minimizing magnetic field ripple and thus maximizing center cell fusion power, features a semicontinuous solenoid. A new end cell has evolved which maintains the required thermal barrier in a significantly reduced axial length. The reduced end cell effective length leads to a shorter central cell length being required to obtain minimum ignition conditions. Introduced is the concept of an electron mantle stabilized octopole arrangement. The engineering features of the new end cell and maintenance concepts developed are influenced to a great extent by the octopole-based design. The new ideas introduced during the FPD study have brought forth a new perspective of the size, design, and maintenance of tandem mirror reactors, making them more attractive as commercial power sources. DOE

N86-10961# Argonne National Lab., Ill.

INFORMATION ON CONTINUUM STATES FROM FEEDING TIMES AND TOTAL (GAMMA) SPECTRA MEASURED WITH BGO SUPPRESSED DETECTORS

T. L. Khoo, I. Ahmad, P. Chowdhury, D. Frekers, R. Holzmann, R. V. F. Janssens, D. C. Radford, N. Azqui, H. Emling, and M. W. Drigert [1985] 14 p Prepared in cooperation with Gesellschaft fuer Schwerionenforschung m.b.H., Notre Dame Univ., Lappeenrannan Teknillinen and Purdue Univ., Lafayette, Ind.
(Contract W-31-109-eng-38)
(DE85-013868; DOE/NBM-5013868) Avail: NTIS HC A02/MF A01

The shape of nuclei is influenced by the occupation of Nilsson-orbitals, which changes with nucleon number, spin and temperature. The shape variation with neutron (or proton) number and spin in the N = 90 transitional region is now well understood for the cold yrast line. In contrast, the structural evolution with increasing temperature above the yrast line remains an open problem. To probe this evolution, to establish the link between yrast and continuum states, and to identify the collective modes built on high-spin aligned particle states, we have measured: (1) the feeding times of yrast states in /sup 152, 154/Dy (N = 86,88), and (2) the total GAMMA spectrum in Ho-153 (N = 86) with Compton-suppressed Ge detectors. Author

N86-10962# California Univ., Berkeley. Lawrence Berkeley Lab.

REPORT ON THE ENGINEERING TEST OF THE LBL 30 SECOND NEUTRAL BEAM SOURCE FOR THE MFTF-B PROJECT

M. C. Vella, P. A. Pincosy, C. A. Hauck, and R. V. Pyle Aug. 1985 58 p
(Contract DE-AC03-76SF-00098)
(DE85-013317; LBL-17550) Avail: NTIS HC A04/MF A01

Positive ion based neutral beam development has centered on the long pulse, advanced positive ion source (APIS). The APIS focused on development of 30 second sources for MFTF-B. The engineering test was part of competitive testing of the LBL and ORNL long pulse sources carried out for the NFTF-E Project. The test consisted of 500 beam shots with 80kV, 30 second deuterium. The results of LBL testing, in which the LBL APIS demonstrated that it would meet the requirements for MFTF-B 30 second sources are summarized. The LBL design was found to be suitable as the baseline for a common long pulse source design for MFTF-B, TFTR, and doublet upgrade. DOE

N86-10963# Los Alamos Scientific Lab., N. Mex.
DIRECT MASS MEASUREMENTS IN THE LIGHT NEUTRON-RICH REGION USING A COMBINED ENERGY AND TIME-OF-FLIGHT TECHNIQUE
C. Pillai, I. W. Swenson, D. J. Vieira, G. W. Butler, J. M. Woutes, S. H. Rokni, K. Vaziri, and I. P. Remsberg 1985 6 p Presented at the Intern. Conf. on Nucl. Data for Basic and Appl. Sci., Santa Fe, N. Mex., 13 May 1985 Prepared in cooperation with Oregon State Univ., Corvallis
(Contract W-7405-eng-36)
(DE85-012758; LA-UR-85-1923; CONF-850507-40) Avail: NTIS HC A02/MF A01

This experiment has demonstrated that direct mass measurements can be performed (albeit of low precision in this first attempt) using the M proportional to ET(2) method. This technique has the advantage that many particle-bound nuclei, produced in fragmentation reactions can be measured simultaneously, independent of their N or Z. The main disadvantage of this approach is that both energy and time-of-flight must be measured precisely on an absolute scale. Although some mass walk with N and Z was observed in this experiment, these uncertainties were largely removed by extrapolating the smooth dependence observed for known nuclei which lie closer to the valley of (BETA)-stability. Mass measurements for several neutron-rich light nuclei ranging from C-17 to NE-26 have been performed. In all cases these measurements agree with the latest mass compilation of Wapstra and Audi. The masses of N-20 N and F-24 have been determined for the first time. DOE

N86-10964# Stanford Linear Accelerator Center, Calif.
PARASITIC MODE LOSSES VERSUS SIGNAL SENSITIVITY IN BEAM POSITION MONITORS
J. C. Denard, K. L. Bane, J. Bijleveld, A. M. Hutton, J. I. Pellegrin, L. Rivkin, P. Wang, and J. N. Weaver Apr. 1985 4 p Presented at the Particle Accelerator Conf., Vancouver, British Columbia, 13 May 1985
(Contract DE-AC03-76SF-00515)
(DE85-014367; SU-SLAC-PUB-3654; CONF-850504-190) Avail: NTIS HC A02/MF A01

A beam position monitor (BPM) for a storage or damping ring may be subject to heating problems due to the parasitic mode (PM) losses, beam interception and synchrotron radiation interception. In addition, high PM losses can cause beam instabilities under some conditions. Recessing and/or masking the BPM may increase the PM losses in the process of solving the latter two problems. Three complementary methods for estimating the PM losses and for improving the design of a stripline directional coupler type of BPM: bench measurements, computer modeling (TBCI), and an equivalent circuit representation are presented. These methods lead to a decrease in PM losses without significant reduction in output signal for the north Stanford Linear Collider (SLC) damping ring BPMs. DOE

N86-10965# Stanford Linear Accelerator Center, Calif.
BEAM-BEAM DEFLECTIONS TO MEASURE SIZE SPOT AND OFFSET AT SLC IP
P. Bambade 10 Jun. 1985 17 p
(Contract DE-AC03-76SF-00515)
(DE85-014285; SU-SLAC-CN-303) Avail: NTIS HC A02/MF A01

As soon as two SLC beams make it to the intersection region, both transverse offsets, spot sizes and shapes can be extracted from the pattern of angular deflections produced by the electromagnetic interaction of the two beams, as one is scanned across the other. These deflections, measured in two high resolution Beam Position Monitors (BPM) mounted symmetrically on both sides of the intersection point, will produce detectable signals allowing spot sizes to be tuned, even with the very low luminosities expected at turn on. They will also furnish a good signal to monitor beam centering and will therefore become an important part of the FFS feedback system. Summarized are the formulae which will allow us to correlate BPM offset readings with the properties of the two beams, and described are the range and limitations of the technique in the case of SLC. DOE

N86-10966# Rice Univ., Houston, Tex.
SUPERSONIC METAL CLUSTER BEAMS Technical Progress Report, 15 Mar. 1984 - 1 Apr. 1985
R. E. Smalley 1985 15 p
(Contract DE-AS05-78ER-06035)
(DE85-014321; DOE/ER-06035/7) Avail: NTIS HC A02/MF A01

Four major areas of bare metal cluster beams were studied: neutral cluster, chemical reactivity, cold cluster ion source development (both positive and negative), bare cluster ion ICR (ion cyclotron resonance) development, and photofragmentation studies of bare metal cluster ions. DOE

N86-10967# Nationaal Inst. voor Kernfysica en Hoge Energiefysica, Amsterdam (Netherlands). Sectie-K.
REPORT ON A VISIT TO CERN IN FEBRUARY 1985. NOTES ON BUNCH MONITORS, HIGH-FREQUENCY SYSTEMS, LINACS, KICKERS, MAGNETS, VACUUM AND BUNCH EXTRACTION [VERSLAG CERN BEZOEK FEBRUARI 1985. NOTITIES OVER BUNDELMONITOREN, HOOGFREQUENTSYSTEMEN, LINACS, KICKERS, MAGNETEN, VACUUM- EN BUNDELEXTRACTIE]
E. B. Kroes, G. Luijckx, R. Maas, and J. Noomen 1985 16 p ref In DUTCH
(LINO-119) Avail: NTIS HC A02/MF A01

The CERN Super Proton Synchrotor (SPS) vacuum installation, the development of magnets, and lamped element kickers with resonance built-in pulse generators are discussed. High resonance frequencies, computer programs, transmitters, cavities and construction aspects of linear accelerators are reported. The SPS monitors, Q-meter methods, and a stochastic extraction method are presented. Author (ESA)

N86-10968# Nationaal Inst. voor Kernfysica en Hoge Energiefysica, Amsterdam (Netherlands). Sectie-K.
THE MEA VACUUM SYSTEM [MEA VAKUUM SYSTEEM]
R. Stroo, H. Schwebeke, and E. Heine 31 Dec. 1984 18 p refs In DUTCH
(LINO-120) Avail: NTIS HC A02/MF A01

The leak security system and multiple pump unit with turbomolecular pump of the MEA vacuum system, consisting of a klystron system with diode pump and a bunch-conducting system with triode pump, is described. The triode pump has better pump capacities for rare gases but as it only works from 0.0001 Torr the pump unit has to be used. To replace the klystrons the two systems are coupled by two windows with nitrogen in between for high frequencies. To safeguard the system, slow isolation valves with Pirani gages, fast valves with ionization gages, and residual gas analyzers are installed. Hand valves and residual gas analyzer heads are used for the pump unit. The vacuum level is better than 0.0000001 Torr. Author (ESA)

N86-10969# Nationaal Inst. voor Kernfysica en Hoge Energiefysica, Amsterdam (Netherlands).
THE NETHERLANDS INSTITUTE FOR NUCLEAR AND HIGH ENERGY PHYSICS (NIKHEF) TRAVELING WAVE MONITOR USER GUIDE
I. Sluijk 27 Nov. 1984 15 p
(LINO-121) Avail: NTIS HC A02/MF A01

Instructions for operating a traveling wave monitor to measure beam displacement are given. Author (ESA)

74 OPTICS

Includes light phenomena.

N86-10970 Maryland Univ., College Park.
LIE ALGEBRAIC METHODS FOR CHARGED PARTICLE BEAMS AND LIGHT OPTICS Ph.D. Thesis
Joseph Cham Eugene Patrice Etienne Forest 1984 334 p

Avail: Univ. Microfilms Order No. DA8509163

The motion of a charged particle or the propagation of a ray in an optical system can be described in many cases by a Hamiltonian. One is often interested in deviation from a certain ideal trajectory. For this problem, the Lie algebraic methods are ideal tools. It has been shown that the Lie operators offer a very efficient parameterization of Hamiltonian maps. Along these lines, the parameterization of optical interaces is examined. It is shown that their Lie algebraic polynomials aere made of irreducible representations of the symplectic group. Our methods are also ideally suited for tracking particles in small and large rings. A complete theory of the computation of Lie algebraic maps is presented. Dissert. Abstr.

N86-10971 Arizona Univ., Tucson.

OPTICAL TESTING OF LARGE TELESCOPES USING MULTIPLE SUBAPERTURES Ph.D. Thesis

Tilman Werner Stuhlinger 1984 218 p

Avail: Univ. Microfilms Order No. DA8504134

The construction of telescope systems with large apertures (approx. 10 meters) is currently being planned. These entire telescope systems should be optically tested in a double-pass configuration. The high cost of manufacturing optical flats large enough to test a large telescope has stimulated research on a new type of testing in which several smaller flats, or subapertures, are distributed over the telescope aperture. The problem is to combine the partial data obtained only over the subapertures in order to obtain the wavefront over the entire aperture. The question of the necessity of phasing the subapertures relative to each other was specifically addressed in the experiment. Dissert. Abstr.

N86-10972 Department of the Air Force, Washington, D.C.

KALMAN FILTER PREPROCESSOR Patent

M. K. Giles and R. B. Rogers, inventors (to Air Force) Issued 16 Apr. 1985 7 p Supersedes AD-D009695

(AD-D011774; US-Patent-4,511,219; US-Patent-Appl-SN-388574; US-Patent-Class-350-388) Avail: US Patent and Trademark Office CSCL 09/2

This document describes an optical signal preprocessor for computing the input functions required to utilize an extended Kalman filter algorithm. An incoming stream of time-varying images is integrated to form a reference image, which is then subtracted from each subsequently sampled image. The result is digitized for use with the extended Kalman filter algorithm. The reference image is also fed through a spatial filter and then put into two light valve image subtraction systems to produce difference image approximations of two partial derivatives. These derivative functions are then digitized and utilized as inputs to the extended Kalman filter algorithm. Author (GRA)

N86-10973 Department of the Air Force, Washington, D.C.

MEASUREMENT OF VISUAL CONTRAST SENSITIVITY Patent

H. E. VonGierke and A. R. Marko, inventors (to Air Force) Issued 16 Apr. 1985 10 p Supersedes AD-D010599

(AD-D011776; US-Patent-4,511,228; US-Patent-Appl-SN-403247; US-Patent-Class-351-243) Avail: US Patent and Trademark Office CSCL 06/16

This invention involves measurement of the visual contrast sensitivity (modulation transfer) function of a human subject by means of linear or circular spatial frequency pattern on a cathode ray tube whose contrast is automatically decreasing or increasing depending on the subject pressing or releasing a hand-switch button. The threshold of detection of the pattern modulation is found by the subject by adjusting the contrast to values which vary about the subject's threshold thereby determining the threshold and also providing by the magnitude of the contrast fluctuations between reversals some estimate of the variability of the subject's absolute threshold. The invention also involves the slow automatic sweeping of the spatial frequency of the pattern over the spatial frequencies after preset time intervals or after threshold has been defined at each frequency by a selected number of subject-determined threshold crossings; i.e., contrast reversals. Author (GRA)

N86-10974 Department of the Air Force, Washington, D.C.

OPTICAL DISC TRANSPORT SYSTEM Patent

A. P. Gilson, inventor (to Air Force) Issued 21 May 1985 7 p Supersedes AD-D010276

(AD-D011779; US-Patent-4,519,055; US-Patent-Appl-SN-486477; US-Patent-Class-369-37) Avail: US Patent and Trademark Office CSCL 14/3

A carrousel disc transport system has a donut shaped cartridge storage module, a changer and a record/read station. The changer is centrally located in said donut shaped module and selectively removes or replaces selected cartridges. A carrier of the changer has a carriage that is translated along a ball screw to be positioned over the storage module. A pair of transporting arms connected to drive means engages the selected cartridge in the module. The driving means of the ball screw transfer the carriage with the arms to move the cartridge to a transfer location where a second transporting means moves the cartridge to the record/read station. The reverse is required to replace the selected cartridge in the module. GRA

N86-10975 Department of the Navy, Washington, D. C.

SPATIAL FREQUENCY MULTIPLEXED COHERENT OPTICAL PROCESSOR FOR CALCULATING GENERALIZED MOMENTS Patent

J. A. Blodgett, H. H. Szu, C. L. Giles, and R. Athale, inventors (to Navy) Issued 19 Mar. 1985 6 p Supersedes AD-D010312

(AD-D011816; US-Patent-4,505,544; US-Patent-Appl-SN-387133; US-Patent-Class-350-162.13) Avail: US Patent and Trademark Office CSCL 20/6

An optical processor that can compute the moments of a two-dimensional image in parallel is discussed. The image is placed at the plane of a holographic mask which is diposed in the front focal plane of a Fourier-transforming lens and each of the desired moments is found at a respective one of a plurality of photodetectors arrayed in the back focal plane of the lens. Author (GRA)

N86-10976 Department of the Navy, Washington, D. C.

FIBER OPTIC SYSTEM FOR MEASURING ELECTRIC FIELDS Patent

L. C. Bobb, inventor (to Navy) Issued 18 Jun. 1985 5 p Supersedes AD-D010483

(AD-D011830; US-Patent-4,524,322; US-Patent-Appl-SN-442497; US-Patent-Class-324-72) Avail: US Patent and Trademark Office CSCL 14/2

A fiber optic sensor system and associated technique is disclosed for measuring an electric field wherein a sensor arm of optical fiber cable is wound about a core member of piezoelectric material. A reference arm of optical fiber cable substantially equal in optical path length to the sensor arm is isolated and connected in parallel to the sensor arm so that coherent light generated by a single model laser source may be split through the fiber-optic arms and recombined after passage there through for phase comparison. When subjected to a local electric field, the core member of piezoelectric material varies in dimensions and thereby causes a change in the strain in the optical fiber cable of the sensor arm. Relative phase changes in the coherent light caused by the resulting optical path length change of the strained homodyne demodulator and deterministic of the value of the local electric field. A vane-type shield is adapted to be rotated about the core member for periodically reducing the local electric field to near zero thereby providing a reference level for field measurement. GRA

N86-10977# IBM Research Lab., San Jose, Calif.

OPTICAL DETECTION OF PHOTOACOUSTIC PULSES IN THIN SILICON WAFERS

H. Sontag and A. C. Tam 25 Jun. 1985 11 p

(Contract N00014-83-C-0170)

(AD-A156705; TR-20) Avail: NTIS HC A02/MF A01 CSCL 20/6

A probe beam deflection method is used to study the propagation of photoacoustic longitudinal waves and plate modes in silicon wafers. Nanosecond acoustic pulses are produced in thin silicon wafers by absorption of weak nitrogen laser pulses causing no sample ablation. A HeNe probe laser is tightly focused on the same or on the opposite side of the wafer. Deflections of this probe beam are monitored by a photodiode located in the Gaussian wing of the reflected, diverging beam. The transient deflection signal can be observed on a Tektronix Mod. 7104 oscilloscope in a single shot mode at nanosecond time resolution. The absorption of the pump laser pulse causes a permanent surface distortion, which is the source of longitudinal and shear wave pulses propagating into the sample. In conclusion, the probe beam deflection technique is shown to be a fast and simple method for measuring acoustic pulse propagation in solids. It does not require elaborate servo mechanisms as the interferometric detection scheme while offering similar sensitivity. GRA

N86-10978# California Univ., Berkeley. Lawrence Berkeley Lab.
INTEGRATING SPHERE MEASUREMENTS OF DIRECTIONAL-HEMISPHERICAL TRANSMITTANCE OF WINDOW SYSTEMS
J. Kessel and S. Selkowitz 5 Aug. 1984 23 p refs Presented at Illuminating Eng. Soc. Ann. Conf., St. Louis, 5 Aug. 1984
(Contract DE-AC03-76SF-00098)
(DE85-013926; LBL-17284; CONF-840817-3; EEB-W-84-22) Avail: NTIS HC A02/MF A01

Equations are presented that express the directional-hemispherical transmittance of window systems in terms of the experimental parameters of an integrating sphere. The construction and operation of a 2-meter-diameter sphere is described. Experimental results are given for both conventional and novel window systems. DOE

N86-10979# Argonne National Lab., Ill.
BEAM STABILITY IN A 6 GeV SYNCHROTRON LIGHT SOURCE
J. Norem, M. Knott, and A. Rauchas 1985 4 p Presented at the Particle Accelerator Conf., Vancouver, British Columbia, 13 May 1985
(Contract W-31-109-eng-38)
(DE85-013850; CONF-850504-175) Avail: NTIS HC A02/MF A01

Future synchrotron radiation sources designed to produce low emittance electron beams for wigglers and undulators will present beam position control problems essentially similar to those encountered by users of existing accelerators, however tolerances will be tighter due to: (1) the small emittence (7 x 10 to the 9th mrad) proposed for the electron beam and the correspondingly small emittences (sizes) of secondary photon beams, (2) the sensitivity of the electron beam closed orbit to quadrupole motion and dipole roll, (3) the high power levels associated with undulator and wiggler beams which will permit (and probably require) high precision and stability of the photon beam position measurements, in addition, (4) the large number of users on the roughly sixty beam lines will demand beams capable of producing the best experimental results. The effects of motion of beam components (quads, RF cavities and dipoles) on the beam is described and the properties of a compensation system from the perspective of users is considered. The system departs from standard particle in considering active perturbation of the electron beam to verify beam corrections. The effects of local closed orbit perturbations to direct undulator beams at different experimental setups are also considered. DOE

N86-10980# Research Inst. of National Defence, Linkoeping (Sweden).
INFORMATION TECHNIQUE 1985: OPTICAL TECHNOLOGY AND ELECTRO-OPTICS, A DEFENSE TECHNICAL COMPONENT REVIEW
Lars Bohman, Olof Engstroem, Ingmar Renhorn, and Soeren Svensson May 1985 62 p refs In SWEDISH; ENGLISH summary
(FOA-A-30037-E; ISSN-0281-0212) Avail: NTIS HC A04/MF A01; Research Institute of National Defence, Stockholm KR 50

Microelectronic image sensors for visible radiation and for IR wavelengths; laser applications, e.g., high energy lasers, lasers with a weapon effect, investigation lasers, excimer lasers, Q-switched lasers, copper vapor lasers, diode lasers; adaptive optics; optical information retrieval; optical data storage, e.g., storage of large quantities of information; electro-optical crystals; and optical fibers, e.g., IR fiber techniques, fluoride fibers, and optical fiber sensors. Author (ESA)

N86-10981# Deutsche Forschungs- und Versuchsanstalt fuer Luft- und Raumfahrt, Oberpfaffenhofen (West Germany).
SCATTERING BY COMPLICATED STRUCTURES: CALCULATION OF THE RADAR PROPERTIES OF METALLIC TARGETS BY MEANS OF PHYSICAL OPTICS
Dieter Klement Mar. 1985 55 p refs In GERMAN; ENGLISH summary Report will also be announced as translation (ESA-TT-946)
(DFVLR-FB-85-22; ISSN-0171-1342) Avail: NTIS HC A04/MF A01; DFVLR, Cologne DM 19.50

Theory and computer program for the determination of the radar cross section of metallic targets are described. The geometry of complicated targets is represented by plane quadrangles. The calculation of the radar cross section is carried out by the method of physical optics. Computer results of simple targets are compared with rigorous solutions, approximations and measurements. The influence of surface shaping is demonstrated. Author (ESA)

75 PLASMA PHYSICS

Includes magnetohydrodynamics and plasma fusion.
For ionospheric plasmas see *46 Geophysics*. For space plasmas see *90 Astrophysics*.

N86-10982# State Univ. of New York at Buffalo, Amherst. Dept. of Physics.
TWO-DIMENSIONAL ELECTRONS Annual Report, 1 Jun. 1984 - 31 May 1985
A. Isihara 31 May 1985 3 p
(Contract N00014-84-K-0387)
(AD-A156894) Avail: NTIS HC A02/MF A01 CSCL 20/8

Papers Submitted: Two-Dimensional Electrons in Strong Magnetic Field, Low-temperature Properties of Two-Dimensional Electrons. Effects of Level Broadening on the Magnetothermal Oscillations in Two-Dimensional Electron Systems; Magnetothermal Oscillations in a Two-Dimensional Electron System; Elementary Excitations and Energy Dispersion in TTF-TCNQ, Magnetoconductivity of 2D Conductors; Memory Function for Cyclotron Resonance of Two-Dimensional Electron Systems; and Quantum Oscillations of 2D Electron Systems. GRA

N86-10983# Naval Research Lab., Washington, D. C.
DYNAMICS OF IMPLODING NEON GAS PUFF PLASMAS. 1 Memorandum Report, Oct. 1984 - Oct. 1985
R. W. Clark and J. Davis 19 Jul. 1985 40 p
(T99-QMXL)
(AD-A156916; NRL-MR-5613) Avail: NTIS HC A03/MF A01 CSCL 20/9

The implosion of a cylindrical neon puff-gas plasma on a low density central core is investigated using a 1D non-LTE radiation-hydrodynamic model. Radiation transports energy into the core plasma and produces heating deep within the puff-gas. The implosion very efficiently converts kinetic energy into soft X-rays; about two-thirds of the initial plasma energy is radiated away. Comparison is made with a neon puff-gas implosion without a central core and with pure hydrodynamic calculations. For each case, detailed self-consistent emission spectra and energy partitioning are discussed. Author (GRA)

N86-10984# California Univ., Livermore. Lawrence Livermore Lab.
THEORETICAL ASPECTS OF MAGNETIC HELICITY
J. H. Hammer 15 Apr. 1985 12 p refs Presented at IAEA Tech. Comm. Meeting on Advan. in Compact Toroid Res., Sydney, 4 Mar. 1985

(Contract W-7405-eng-48)
(DE85-011846; UCRL-92538; CONF-8503137-1) Avail: NTIS HC A02/MF A01

Magnetic helicity, a function of the vector potential and the magnetic field, measures the topological linkage of magnetic fluxes. It also manifests itself in the twistedness and knottedness of flux tubes. The significance of helicity in plasma physics is that it is an ideal MHD invariant -- the linkage of a flux tube with all other flux tubes is preserved when the tubes are filled with infinitely conducting plasma. Even when finite resistivity and magnetic reconnection are allowed, one finds that the global magnetic helicity (accounting for all linkages) is still approximately preserved on the reconnection time scale. Local topological changes (tearing, etc.) that destroy local helicity invariance are allowed as long as the global linkage is preserved. F.M.R.

N86-10985# Los Alamos Scientific Lab., N. Mex.
BEAM LINE WINDOWS AT LAMPF
R. D. Brown, D. L. Grisham, and J. E. Lambert 1985 4 p refs Presented at Particle Accelerator Conf., Vancouver, British Columbia, 13 May 1985
(Contract W-7405-eng-26)
(DE85-012723; LA-UR-85-1737; CONF-850504-113) Avail: NTIS HC A02/MF A01

The A-6 main beam-line window at LAMPF separates the vacuum of the main beam line from the isotope production station, proton irradiation ports, and the beam stop, which operate in air. This window must withstand the design beam current of 1 mA at 800 MeV for periods of at least 3000 hours without failure. The window is water cooled and must be strong enough to withstand the 2.1 MPa (300 psig) cooling water pressure, as well as beam-induced thermal stresses. Two designs have been used to meet these goals, a stepped-plate window and a hemispherical window, both made from a precipitation-hardened nickel base alloy, Alloy 718. Calculations of the temperatures and stresses in each of these windows are presented. DOE

N86-10986# Los Alamos Scientific Lab., N. Mex.
PROPOSED BUNCHING SCHEME FOR A POLARIZED H(-) INJECTOR
G. R. Swain and A. A. Browman 1985 4 p Presented at the Particle Accelerator Conf., Vancouver, British Columbia, 13 May 1985
(Contract W-7405-eng-36)
(DE85-012648; LA-UR-85-1640; CONF-850504-48) Avail: NTIS HC A02/MF A01

Improvements to the polarized H(-) injector at LAMPF which will include a two-stage buncher and beam chopper are discussed. The buncher scheme will permit the compression of a major part of the current in 20 RF cycles of the drift-tube linac (100 nsec) into a single RF cycle (5 nsec), making possible time-of-flight experiments with the polarized H(-) beam. A proposed first buncher stage would use a ramp drive waveform; the second stage, a sinusoidal waveform. Design and sensitivity calculations are summarized, including beam energy considerations, buncher and chopper drive requirements, and longitudinal and transverse beam dynamics. It is indicated that about 70% of the beam from the source may be bunched in the 1-nsec acceptance region of the linac, with less than 0.1% of the beam in neighboring RF cycles. DOE

N86-10987# Los Alamos Scientific Lab., N. Mex.
BEAM-CAVITY INTERACTION MEASUREMENTS IN A DAW STRUCTURE
Y. Iwashita, S. O. Schriber, J. M. Potter, D. A. Swenson, and G. S. Mavrogenes 1985 4 p refs Presented at the Particle Accelerator Conf., Vancouver, British Columbia, 13 May 1985
(Contract W-7405-eng-36)
(DE85-012660; LA-74-85-1617; CONF-850504-56) Avail: NTIS HC A02/MF A01

Mode excitations induced by relativistic electron beams have been measured in a disk and washer (DAW) structure. The structure had three washers, each with four radial support stems, and half disk end terminations. The design DAW operating frequency was 1300 MHz, the same as that used to accelerate the electron beam. Both short pulse (35-ps, 800-Hz, 17-nC/pulse) and long pulse (10-(MU)s, 2-A average) conditions were used in the beam excitation experiments. Mode spectra were measured and identified using low power techniques employed after the high power beam measurements. Mode frequency calculations for the complete three washer geometry were performed using URMEL for up to m = 7. Calculated results are compared with data determined from low power and beam driven excitation of the DAW structure. DOE

N86-10988# Los Alamos Scientific Lab., N. Mex.
INCREASED PARTICLE CONFINEMENT WITH THE USE OF EXTERNAL dc BIAS FIELD IN THE CTX SPHEROMAK
C. W. Barnes, H. W. Hoida, I. Henins, J. C. Fernandez, T. R. Jarboe, and G. J. Marklin 1985 6 p Presented at the 7th US Symp. on Compact Toroid Res., Santa Fe, N. Mex., 21 May 1985
(Contract W-7405-eng-36)
(DE85-012744; LA-UR-85-1789; CONF-8505100-5) Avail: NTIS HC A02/MF A01

Spheromaks are formed in a mesh flux conserver in the presence of an external dc bias field. The spheromaks remain stable to tilt instabilities with ratios of bias to spheromak flux of up to 47 + or - 7%. Normally applied bias flux puts the spheromak separatrix inside the metal mesh and improves the particle confinement. DOE

N86-10989# Brookhaven National Lab., Upton, N. Y.
SEPARATED K(-) BEAMS (10 GeV AND ABOVE)
G. M. Bunce 1985 4 p refs Presented at the Intern. Conf. on Hadron Spectroscopy, College Park, Md., 20 Apr. 1985
(Contract DE-AC02-76CH-00016)
(DE85-012527; BNL-36450; CONF-8504133-2) Avail: NTIS HC A02/MF A01

Separated kaon beams with intensity similar to present pion beams are, in fact, possible to build now, with the potential of even high kaon flux in the future. It is particularly attractive to work with a kaon minus beam due to the large number of final state combinations which would be available, due to the strange quark. Cason and Donoghue showed that a kaon beam combined with a complete spectrometer capable of observing both neutral and charged particles would increase the available states for spectroscopy for masses from 1 to 3 GeV by a factor of 10. They urged a complete mapping of states, using a sky survey as an analogy. The present capability is similar to scans of the sky made only in the optical range. They also point out that the specific subject of confinement - whether there can be combinations of quarks and gluons not yet seen - is an exciting topic which is beginning to get theoretical guidance from QCD calculations on a lattice. This confluence of technical advance (intensity) and physics interest (confinement) makes a separated kaon beam particularly compelling. DOE

N86-10990# Los Alamos Scientific Lab., N. Mex.
TREATMENT PLANNING WITH ION BEAMS
M. H. Foss 1985 4 p Presented at the Particle Accelerator Conf., Vancouver, British Columbia, 13 May 1985
(Contract W-7405-eng-36)
(DE85-012661; LA-UR-85-1616; CONF-850504-54) Avail: NTIS HC A02/MF A01

Ions have higher linear energy transfer (LET) near the end of their range and lower LET away from the end of their range. Mixing radiations of different LET complicates treatment planning because radiation kills cells in two statistically independent ways. In some cases, cells are killed by a single-particle, which causes a linear decrease in log survival at low dosage. When the linear decrease is subtracted from the log survival curve, the remaining curve has zero slope at zero dosage. This curve is the log survival curves for cells that are killed only by two or more particles. These two mechanisms are statistically independent. To calculate survival these two kinds of doses must be accumulated separately. The effect of each accumulated dosage must be read from its survival curve, and the logarithms of the two effects added to get the log survival. Treatment plans for doses of protons, He(3) ions, and He(4) ions suggest that these ions will be useful therapeutic modalites. DOE

N86-10991# Argonne National Lab., Ill.
PERFORMANCE OF THE H(-) ION SOURCE FOR THE INTENSE PULSED NEUTRON SOURCE
V. Stipp and A. DeWitt 1985 3 p Presented at the Particle Accelerator Conf., Vancouver, British Columbia, 13 May 1985
(Contract W-31-109-eng-38)
(DE85-012368; CONF-850504-117) Avail: NTIS HC A02/MF A01

In January of 1983, a magnetron type H(-) ion source was installed in the intense Pulse Neutron Source (IPNS) at Argonne National Laboratory. The higher available H(-) current has helped enable the weekly average intensity of the Rapid Cycling Synchrotron (RCS) to be increased from 8 (MU)A to over 12 (MU)A. After two years of operation, the reliability of the source producing 40 mA of H(-) ions at a 30 Hz repetition rate continues to be excellent. DOE

N86-10992# Los Alamos Scientific Lab., N. Mex.
NONINTERCEPTIVE TECHNIQUES FOR THE MEASUREMENT OF LONGITUDINAL PARAMETERS FOR INTENSE H(-) BEAMS
W. B. Cottingame, G. P. Boicourt, J. H. Cortez, W. W. Higgins, O. R. Sander, and D. P. Sandoval 1985 4 p refs Presented at the Particle Accelerator Conf., Vancouver, British Columbia, 13 May 1985
(Contract W-7405-eng-36)
(DE85-012662; LA-UR-85-1615; CONF-850504-53) Avail: NTIS HC A02/MF A01

With increasing brightness, beam diagnostic techniques requiring interception of the beam become impractical. For H(-) particle beams, solutions for this problem based on the phenomenon of photodissociation are currently under investigation at the Los Alamos National Laboratory accelerator test stand (ATS). A laser can be used to selectively neutralize portions of the beam that can be characterized after the charged particles have been swept away. This technique has been used for the measurement of current density versus longitudinal phase and the longitudinal phase-space distribution at the output of the ATS radio frequency quadrupole (RFQ). The results of our measurement are compared with the predictions of the particle-dynamics code, PARMTEQ. DOE

N86-10993# Los Alamos Scientific Lab., N. Mex.
HIGH-POWER RF CONTROLS FOR THE NBS-LOS ALAMOS RACETRACK MICROTRON
I. M. Young and R. S. Biddle 1985 4 p refs Presented at the Particle Accelerator Conf., Vancouver, British Columbia, 13 May 1985
(Contract W-7405-eng-36)
(DE85-012658; LA-UR-85-1619; CONF-850504-61) Avail: NTIS HC A02/MF A01

The high power RF system for the National Bureau of Standards (NBS) Los Alamos racetrack microtron (RTM) uses waveguide power splitters and waveguide phase shifters to distribute RF power from a single 500-kW CW klystron to four side-coupled accelerating structures. The amplitude and phase of each structure is controlled by a feedback system that uses the waveguide variable power splitters, waveguide phase shifters, and klystron drive as the active control elements. A block diagram of this system is shown, as is a subset of the complete system on which the measurements reported in this paper were performed. The feedback controls on the capture section use low level RF amplitude and phase controls on the RF drive to the klystron. These controls are very fast with an open loop gain bandwidth of approximately 40 kHz. DOE

N86-10994# Stanford Linear Accelerator Center, Calif.
APPLICATIONS OF THE SECOND-ORDER ACHROMAT CONCEPT TO THE DESIGN OF PARTICLE ACCELERATORS
K. L. Brown and R. V. Servranckx May 1985 3 p Presented at the Particle Accelerator Conf., Vancouver, British Columbia, 13 May 1985 Prepared in cooperation with European Organization for Nuclear Research, Geneva, and Saskatchewan Univ.
(Contract DE-AC03-76SF-00515)
(DE85-013072; SU-SLAC-PUB-3675; CONF-850504-77) Avail: NTIS HC A02/MF A01

A property of the second-order achromat, whereby dipole and sextupole families may be inserted into a lattice for chromatic corrections without introducing second-order geometrical (on momentum) optical distortions, has been incorporated in several new particle accelerator designs. These include the SLC at SLAC, LEP at CERN, the EROS pulse stretcher ring at Saskatoon, the CEBAF ring at SURA, and the MIT ring. DOE

N86-10995# Stanford Linear Accelerator Center, Calif.
SUPERCONVERGENT TRACKING AND INVARIANT SURFACES IN PHASE SPACE
R. D. Ruth, T. Raubenheimer, and R. L. Warnock Apr. 1985 4 p Presented at the Particle Accelerator Conf., Vancouver, British Columbia, 13 May 1985 Prepared in cooperation with California Univ., Berkeley, Lawrence Berkeley Lab.
(Contracts DE-AC03-76SF-00515; DE-AC03-76SF-00098)
(DE85-013051; SU-SLAC-PUB-3660; CONF-850504-75) Avail: NTIS HC A02/MF A01

Long term beam stability in very large storage rings presents an extraordinary challenge in nonlinear dynamics. Current computational methods seem less than adequate on the long time scales involved, and several methods that either are new or have not yet tried in accelerator problems heretofore were evaluated. The methods we investigate fall into two categories: (1) iteration of maps describing concatenated machine elements, for tracking of single particles; and (2) infinite-time methods for direct computation of invariant surfaces in phase space. DOE

N86-10996# Los Alamos National Lab., N. Mex.
FERRITE KICKER MAGNET FOR THE IAMPF SWITCHYARD UPGRADE
R. A. Hardekopf, E. F. Higgins, and J. S. Lunsford 1985 4 p refs Presented at the Particle Accelerator Conf., Vancouver, British Columbia, 13 May 1985
(Contract W-7405-eng-36)
(DE85-012657; IA-UR-85-1620; CONF-850504-60) Avail: NTIS HC A02/MF A01

The IAMPF switchyard requires a kicker magnet as the first element in the transport line leading to the proton storage ring (PSR). The magnet must produce 1-ms-long pulses with 40-(MU)s rise time and < 0.3% flat-top regulation to deflect the 800-MeV H(-) beam by 1.2(0). Two 1-m-long, single-turn ferrite magnets, each powered by a modulator supplying up to 2400 A at a maximum rate of 24 Hz were constructed. The modulators use a transistor amplifier/regulator, a dual pulse-forming-network (PFN), and a compensating circuit driven by a function generator to achieve a total 0.1% current variation in the pulse. The system also produces an alternate kicking mode consisting of 150-(MU)s-long pulses at a maximum rate of 120 Hz; the two modes can be multiplexed within the charging power-supply limitations. DOE

N86-10997# Fermi National Accelerator Lab., Batavia, Ill.
FIELD-INDEPENDENT NORMALIZATION OF SSC COLLIDER RING COSTS
T. E. Toohig 25 Mar. 1985 3 p
(Contract DE-AC02-76CH-03000)
(DE85-012425; FNAL-TM-1306) Avail: NTIS HC A02/MF A01

The SSC Collider Ring represents the dominating cost element of the SSC project. The number of variables involved in optimizing the facility is very large so it is helpful to try to parameterize them in a way that allows a straightforward comparison of primary options. Cost information was drawn from the Reference Designs Study. Various studies indicate that a 9' to 10' tunnel seems optimal from a construction and operation viewpoint and is adequate for installation. According to both studies cited a tunnel of this size in reasonable geology will cost approximately $800 per linear foot. For the purposes of this analysis this is adopted as the standard tunnel. DOE

N86-10998# Los Alamos National Lab., N. Mex.
LOCAL DRIFT PARAMETER, J/N SUB E AND RESISTIVITY ANOMALY MEASUREMENTS IN CTX SPHEROMAKS
H. W. Hoida, C. W. Barnes, I. Henins, T. R. Jarboe, C. J. Buchenauer, and G. J. Marklin 1985 7 p Presented at the 7th U.S. Symp. on Compact Toroid Res., Santa Fe, N. Mex., 21 May 1985
(Contract W-7405-eng-36)
(DE85-012740; LA-UR-85-1791; CONF-8505100-12) Avail: NTIS HC A02/MF A01

The ratio of the electron drift velocity to the electron thermal velocity, also known as the drift parameter (streaming parameter), and j/n sub e (approx. V sub d) have been measured locally at the magnetic axis in CTX spheromaks at Los Alamos. The drift parameter and j/n sub e appear to be correlated with local measurements of the resistivity anomaly (eta/eta sub Spitz) at the magnetic axis. The drift parameter and j/n sub e are varied by changing the background fill pressure. Data is presented for three cases: high density (6 mT fill), medium density (4mT fill) and low density (0 mT fill). DOE

N86-10999# Los Alamos National Lab., N. Mex.
INTRODUCTION TO THE M = 1 HELICITY SOURCE
D. A. Platts, T. R. Jarboe, and B. L. Wright 1985 6 p Presented at the 7th U.S. Symp. on Compact Toroid Res., Santa Fe, N. Mex., 21 May 1985
(Contract W-7405-eng-36)
(DE85-012771; LA-UR-85-1820; CONF-8505100-11) Avail: NTIS HC A02/MF A01

The m = 1 Helicity Source, formerly called the Kinked 2-pinch, was developed as part of the Electrode Studies program at Los Alamos. The Electrode Studies program was initiated to study the control of electrode erosion in long discharge duration spheromak sources. Erosion control is necessary to reduce plasma impurities and to obtain adequate electrode lifetimes. The first task of the Electrode Studies program is to determine, from among a variety of configurations including the coaxial one, a helicity source geometry with good prospects for erosion control. The more efficient the helicity source the easier it will be to control erosion, but the source must also be easy to diagnose and modify if it is to be a useful test bed. The various erosion control techniques which were proposed will require extensive experimentation to evaluate and optimize. Proposed techniques include, using refractory metals, profiling of the electrodes and magnetic fields, and various gas injection schemes including porous electrodes. It is considered necessary to do these experiments on an optimized helicity source so that the electrode geometries and plasma properties will be relevant. Therefore the present Electrode Studies program is aimed at developing an improved helicity source design. DOE

N86-11000# Massachusetts Inst. of Tech., Cambridge. Plasma Fusion Center.
US SUPERCONDUCTING MAGNET DATA BASE ASSESSMENT FOR INTOR
J. H. Schultz and D. B. Montgomery 10 Dec. 1984 20 p
(Contract DE-AC02-78ET-51013)
(DE85-013648; PFC/RR-84-19; DOE/ET-51013/139) Avail: NTIS HC A02/MF A01

Because of its size, performance requirements and exposure to neutron and gamma irradiation, the superconducting magnet system for INTOR would represent a significant advance in superconducting magnet technology. US programs such as LCP, MFTF-B and others provide a significant data base for the INTOR application. The assessment of the adequacy of the US data base for the INTOR magnets is largely generic, and applies to the superconducting magnet systems for other magnetic confinement fusion reactors. Assessments of the data base generated by other national magnet technology programs are being prepared by the other INTOR participants. DOE

N86-11001# Los Alamos National Lab., N. Mex.
BEGINNINGS OF REMOTE HANDLING AT THE RAL SPALLATION NEUTRON SOURCE
D. J. Liska and J. Hirst 1985 4 p Presented at the Particle Accelerator Conf., Vancouver, British Columbia, 13 May 1985
(Contract W-7405-eng-36)
(DE85-012681; LA-UR-85-1585; CONF-850504-109) Avail: NTIS HC A02/MF A01

Expenditure of funds and resources for remote maintenance systems traditionally are delayed until late in an accelerator's development. However, simple remote-surveillance equipment can be included early in facility planning to set the stage for future remote-handling needs and to identify appropriate personnel. Some basic equipment that serves this function and was used to monitor beam loss during commissioning is described. A photograph of this equipment, positioned over the extractor septum magnet, is shown. This method can serve as a pattern approach to the problem of initiating remote-handling activities in other facilities. DOE

N86-11002# Los Alamos National Lab., N. Mex.
ANALYTIC EVALUATION OF LAMPF 2 BOOSTER CAVITY DESIGN
C. C. Friedrichs 1985 4 p Presented at the Particle Accelerator Conf., Vancouver, British Columbia, 13 May 1985
(Contract W-7405-eng-36)
(DE85-012680; LA-UR-85-1586; CONF-850504-108) Avail: NTIS HC A02/MF A01

Through the past few decades, a great deal of sophistication has evolved in the numeric codes used to evaluate electromagnetically resonant structures. The numeric methods are extremely precise, even for complicated geometries, whereas analytic methods require a simple uniform geometry and a simple, known mode configuration if the same precision is to be obtained. The code SUPERFISH, which is near the present state of the art of numeric methods, does have the following limitations: No circumferential geometry variations are permissible; there are no provisions for magnetic or dielectric losses; and finally, it is impractical (because of the complexity of the code) to modify it to extract particular bits of data one might want that are not provided by the code as written. SUPERFISH was used as an aid in derivating an analytic model of the Los Alamos Meson Physics Facility (LAMPF) II Booster Cavity. One a satisfactory model was derived, simple FORTRAN codes were generated to provide whatever data was required. The analytic model is made up of TEM and radial mode transmission line sections, as well as lumped elements where appropriate. Radial transmission line equations, which include losses, were not found in any literature, and the extension of the lossless equations to include magnetic and dielectric losses are included. DOE

N86-11003# Los Alamos Scientific Lab., N. Mex.
ENERGY EFFICIENCY OF THE CTX MAGNETIZED COAXIAL PLASMA SOURCE
J. C. Fernandez, C. W. Barnes, T. R. Jarboe, S. O. Knox, D. A. Platts, and K. F. McKenna 1985 5 p Presented at the 7th US Symp. on Compact Toroid Res., Santa Fe, N. Mex., 21 May 1985
(Contract W-7405-eng-36)
(DE85-012735; LA-UR-85-1818; CONF-8505100-2) Avail: NTIS HC A02/MF A01

The energy efficiency of the CTX coaxial plasma source in creating spheromaks is determined experimentally to be in agreement with the theoretical prediction of lambda sub sp/lambda g, where del x B = lambda sub sp B in the spheromak, and lambda sub g identical with (MU) 0I sub g// phi sub g with I sub g the source current and phi sub g the magnetic flux through either source electrode. This is shown to be equivalent to magnetic helicity conservation. The spheromak impurity radiation was measured using an absolutely calibrated single chord bolometer system. The theoretical efficiency is within the experimental uncertainty of the ratio of spheromak radiated energy to source input energy in a group of dirty discharges. The radiation measurement uncertainty is too large to determine whether a substantial part of the excess source energy not used in the production of spheromak magnetic energy is radiated from the spheromak volume. DOE

N86-11004# Stanford Linear Accelerator Center, Calif.
ELECTRON WIND IN STRONG WAVE GUIDE FIELDS
F. Krienen Mar. 1985 4 p Presented at the Particle Accelerator Conf., Vancouver, British Columbia, 13 May 1985
(Contract DE-AC03-76SF-00515)
(DE85-013062; SU-SLAC-PUB-3616; CONF-850504-110) Avail: NTIS HC A02/MF A01

The X-ray activity observed near highly powered waveguide structures is usually caused by local electric discharges originating from discontinuities such as couplers, tuners or bends. In traveling waves electrons move in the direction of the power flow. Seed electrons can multipactor in a traveling wave, the moving charge pattern is different from the multipactor in a resonant structure and is self-extinguishing. The charge density in the wave guide will modify impedance and propagation constant of the wave guide. The radiation level inside the output wave guide of the SLAC, 50 MW, S-band, klystron is estimated. Possible contributions of radiation to window failure are discussed. DOE

N86-11005# Sandia Labs., Albuquerque, N. Mex.
RADIATION FIELD RESULTS FROM THE SPEED TRIAXIODE, A LARGE AREA, HIGH DOSE RATE, SHORT PULSE 1MV BREMSSTRAHLUNG SOURCE
M. A. Hedemann, A. L. Pregenzer, L. D. Posey, D. C. Evans, and P. W. Spence 1985 5 p refs Presented at the 22nd Ann. Conf. on Nucl. and Space Radiation Effects, Monterey, Calif., 22 Jul. 1985 Prepared in cooperation with Pulse Sciences, Inc., San Leandro, Calif.
(Contract DE-AC04-76DP-00789)
(DE85-009438; SAND-85-0459C; CONF-850711-7) Avail: NTIS HC A02/MF A01

Measurements and calculations were performed which characterize a short pulse-width (10 to 18 ns) fast rise-time (12 ns) source which provides more than 5 x 10 to the 11) Rad(Si)/sec over an area larger than 150 sq.cm. DOE

N86-11006# Kanner (Leo) Associates, Redwood City, Calif.
ION SOURCES FOR HIGH-FREQUENCY ACCELERATORS
R. Keller 1985 45 p refs Transl. into ENGLISH of "Ionenquellen fuer Hochfrequenzbeschleuniger" rept. VDI-Bildungswerk 41-18-02 Gesellschaft fuer Schweionenforschung m.b.H, Darmstadt, West Germany, 3 May 1982
(Contract W-7405-eng-36)
(DE85-012992; LA-tr-85-16) Avail: NTIS HC A03/MF A01

Ion sources are being applied increasingly in many areas of physics and technology, from basic research in nuclear and atomic physics to energy research, isotope separation, implantation technology, surface processing and analysis all the way to biomedicine. The function and problems of the types important for high-frequency accelerators are explained using a few individual examples in order to stimulate a basic understanding for this technically sophisticated and little-known equipment. The sources discussed here supply single or multiple positively charged ions. DOE

N86-11007# GA Technologies, Inc., San Diego, Calif.
GA THEORY NEWS, JANUARY-MARCH 1985
B. Harvey, ed. May 1985 12 p
(Contract DE-AT03-84ER-53158)
(DE85-012572; GA-A-17995) Avail: NTIS HC A02/MF A01

GA Theory News is a quarterly publication presenting condensed versions of recent research reports printed by the Fusion Theory Group at GA Technologies. This issue contains the following three summaries: (1) neoclassical transport in tokamaks with divertors, (2) how a swing behaves, and (3) subcritical MHD turbulence. DOE

N86-11008# California Univ., Berkeley. Lawrence Berkeley Lab.
PROCEEDINGS OF A WORKSHOP ON ELECTROWEAK SYMMETRY BREAKING
I. Hinchliffe Oct. 1984 87 p Proc. held at Berkeley, Calif., 4-22 Jun. 1984
(Contract DE-AC03-76SF-00098; Grant NSF PHY-84-01063)
(DE85-004444; LBL-18571; CONF-8406190) Avail: NTIS HC A05/MF A01

A theoretical workshop on electroweak symmetry breaking at the Superconducting Supercollider was held at Lawrence Berkeley Laboratory, June 4-22, 1984. The purpose of the workshop was to focus theoretical attention on the ways in which experimentation at the SSC could reveal manifestations of the phenomenon responsible for electroweak symmetry breaking. This issue represents, at present, the most compelling scientific argument for the need to explore the energy region to be made accessible by the SSC, and a major aim of the workshop was to involve a broad cross section of particle theoretists in the ongoing process of sharpening the requirements for both accelerator and detector design that will ensure detection and identification of meaningful signals, whatever form the electroweak symmetry breaking phenomenon should actually take. DOE

N86-11009# Stanford Linear Accelerator Center, Calif.
EFFECTS OF SLOTS/HOLES IN DISKS ON FREQUENCIES OF TM01 AND EH11 WAVES IN THE DISK-LOADED WAVEGUIDE
C. G. Yao Mar. 1985 4 p Presented at the Particle Accelerator Conf., Vancouver, British Columbia, 13 May 1985 Prepared in cooperation with Nanjing Univ.
(Contract DE-AC03-76SF-00515)
(DE85-013376; SU-SLAC-PUB-3599; CONF-850504-150) Avail: NTIS HC A02/MF A01

The increase in the BBU threshold current is very important for the high and medium energy electron linacs because of the larger operating current attainable or a smaller emittance available at certain operating current. For this purpose, many means can be used, among which the improvement in the accelerating structure itself is always fundamental. SLAC's three-meter long section is unique with truly constant gradient performance. The theoretical analyses and operating experiences at SLAC have indicated that detuning the Nos. 3, 4 and 5 cavities of some sections by 2 or 4 MHz for TM01 wave had considerably raised the BBU threshold current. A method of opening four holes symmetrically distributed on disks as described in detail will get the benefits in improvement of BBU threshold current. DOE

N86-11010# Brookhaven National Lab., Upton, N. Y.
MICROWAVE INSTABILITY ACROSS THE TRANSITION ENERGY
S. Y. Lee and J. M. Wang 1985 4 p Presented at the Particle Accelerator Conf., Vancouver, British Columbia, 13 May 1985
(Contract DE-AC02-76CH-00016)
(DE85-013304; BNL-36564; CONF-850504-146) Avail: NTIS HC A02/MF A01

It is well known that during the acceleration of hadrons in a storage ring, the beam always goes above the microwave instability threshold near the transition energy (GAMMA)sub t. The reason is that the longitudinal revolution frequency spread of the beam which otherwise provides landau damping vanishes at the transition energy. The amount of the beam dilution near the transition energy is determined by tau sub th, the length of time when the beam stays unstable, and the growth rate of the instability. It is pointed out that tau sub th is proportional to the fourth power of (GAMMA) sub t, and thus the choice of a large (GAMMA) sub t is not desirable from this point of view. An analysis is also given of the microwave instability induced heat dilution for the proposed Relativistic Heavy Ion Collider at Brookhaven National Laboratory. DOE

N86-11011# Sandia Labs., Albuquerque, N. Mex.
ADVANCES IN DATA ACQUISITION SYSTEM TECHNOLOGY FOR PBFA 2
W. B. Boyer, F. A. Bouchier, T. F. Ezell, C. B. Mattson, and C. C. Newcom 1985 14 p Presented at the 5th IEEE Pulsed Power Conf., Washington, D.C., 10 Jun. 1985
(Contract DE-AC04-76DP-00789)

(DE85-012860; SAND-8402519C; CONF-850616-30) Avail: NTIS HC A02/MF A01

The data acquisition system being built for particle beam fusion accelerator (PBFA) II incorporates several new advanced technology features. The system will have 80 new waveform recorders with a 1.35 GHz sampling rate, 250 MHz bandwidth and 10,000 sample record length. A fast analog multiplexer will be used to enable recording multiple signals on each recorder. The accelerator performance monitor system will use time interval digitizers with a time window of + or - 8 msec. This long window and the pretrigger feature will provide data for a thorough analysis of accelerator prefires. The calibration system will automatically route precision dc levels, sine waves and fast rise pulses to the waveform recorders. The waveform recording system is being characterized using special multichannel, high level simultaneous pulse generators. The system computer has a 32 bit CPU, 350 Mbytes of disc storage and a virtual memory operating system. All software is being written in FORTRAN 77. DOE

N86-11012# Stanford Linear Accelerator Center, Calif.

HIGH-RESOLUTION PHOSPHOR SCREEN BEAM PROFILE MONITOR

S. Yencho and D. R. Walz May 1985 4 p refs Presented at the Particle Accelerator Conf., Vancouver, British Columbia, 13 May 1985

(Contract DE-AC03-76SF-00515)

(DE85-013074; SU-SLAC-PUB-3671; CONF-850504-83) Avail: NTIS HC A02/MF A01

A high resolution luminescent screen beam profile monitor was developed to allow viewing of both conventional large diameter SLAC e(+)/e(-) beams, and also collider RF bunches having small transverse spatial extent, with one instrument. The principal features of the monitor are described. They include the two power magnification system offering magnifications of 12 and 78X, respectively; the reticle grid which is optically superimposed on the screen image by a cube beam splitter; selection of a suitable camera; and the Al2O3(Cr) phosphor screen. A simplified version of the monitor for viewing of only micron sized beams for applications in the collider arcs and final focus regions and achieving a magnification of approx. 40X, coupled with a resolution of approx. 20(MU)m is also presented. DOE

N86-11013# Sandia Labs., Albuquerque, N. Mex.

ENGINEERING HIGH RELIABILITY, LOW-JITTER MARX GENERATORS

L. X. Schneider and G. J. Lockwood 1985 4 p refs Presented at 5th IEEE Pulsed Power Conf., Washington, D.C., 10 Jun. 1985

(Contract DE-AC04-76DP-00789)

(DE85-012811; SAND-84-2499C) Avail: NTIS HC A02/MF A01

Multimodule pulsed power accelerators typically require high module reliability and nanosecond simultaneity between modules. Energy storage using bipolar Marx generators can meet these requirements. Experience gained from computer simulations and the development of the DEMON II Marx generator led to a fundamental understanding of the operation of these multistage devices. As a result of this research, significant improvements in erection time jitter and reliability were realized in multistage, bipolar Marx generators. Erection time jitter was measured as low as 2.5 nanoseconds for the 3.2 MV, 16-stage PBFA I Marx and 3.5 nanoseconds for the 6.0 MV, 30-stage PBFA II (DEMON II) Marx, while maintaining exceptionally low prefire rates. Performance data are presented from the DEMON II Marx research program, as well as discussions on the use of computer simulations in designing low-jitter Marx generators. DOE

N86-11014# Stanford Linear Accelerator Center, Calif.

SLC POSITRON DAMPING RING OPTICS DESIGN

J. P. Delahaye and I. Rivkin Apr. 1985 4 p refs Presented at Particle Accelerator Conf., Vancouver, British Columbia, 13 May 1985

(Contracts DE-AC03-76SF-00515; DE-AC03-81ER-40050)

(DE85-013054; SU-SLAC-Pub-3649; CONF-850504-99) Avail: NTIS HC A02/MF A01

The basic SLAC Linear Collider operation scheme assumes the use of two damping rings, one for the e(-), one for the e(+), in order to reduce the colliding beam normalized emittances to 30 (PI) radm hence raising the corresponding luminosity by a factor 170. The e(-) damping ring optics, designed by H. Wiedemann, were extensively studied and modelled since it's completion at the end of 1982. The e(+) damping ring being built will be based on the same design except for some modifications resulting from the studies on the e(-) damping ring which clearly pointed out two major weak points as far as the optics is concerned. Basic modifications of the ring lattice and main equipment positions in order to improve the situation in the Positron Damping Ring are described. DOE

N86-11015# Stanford Univ., Calif.

COMPUTER CONTROL OF RF AT SLAC

H. D. Schwarz Mar. 1985 6 p refs Presented at Particle Accelerator Conf., ancouver, British Columbia, 13 May 1985

(Contract DE-AC03-76SF-00515)

(DE85-013065; ; SU-SLAC-PUB-3600) Avail: NTIS HC A02/MF A01

The Stanford Linear Accelerator is upgrading for the SLAC Linear Collider project. The energy will be increased from approximately 31 GeV to 50 GeV. Two electron beams and one positron beam will be accelerated with high demands on the quality of the beams. The beam specifications are shown. To meet these specifications, all parameters influencing the beams have to be under tight control and continuous surveillance. This task is accomplished by a new computer system implemented at SLAC which has, among other functions, control over RF accelerating fields. DOE

N86-11016# California Univ., Livermore. Lawrence Livermore Lab.

COMPACT TORUS COMPRESSION OF MICROWAVES

D. W. Hewett and A. B. Langdon 17 May 1985 6 p refs Presented at 7th Symp. on Compact Toroid Res., Santa Fe, N.Y., 21 May 1985

(Contract W-7405-eng-48)

(DE85-012919; UCRL-92690; CONF-8505100-6) Avail: NTIS HC A02/MF A01

The possibility that a compact torus (CT) might be accelerated to large velocities was suggested by Hartman and Hammer. If this is feasible one application of these moving CTs might be to compress microwaves. The proposed mechanism is that a coaxial vacuum region in front of a CT is prefilled with a number of normal electromagnetic modes on which the CT impinges. A crucial assumption of this proposal is that the CT excludes the microwaves and therefore compresses them. Should the microwaves penetrate the CT, compression efficiency is diminished and significant CT heating results. MFE applications in the same parameters regime have found electromagnetic radiation capable of penetrating, heating, and driving currents. DOE

N86-11017# California Univ., Livermore. Lawrence Livermore Lab.

APPLICATION OF STRUCTURAL-MECHANICS METHODS TO THE DESIGN OF LARGE TANDEM-MIRROR FUSION DEVICES (MFTF-B)

V. N. Karpenko and D. S. Ng 4 Mar. 1985 14 p Presented at the 8th Intern. Conf. on Struct. Mech. in Reactor Technol., Brussels, 19 Aug. 1985

(Contract W-7405-eng-48)

(DE85-008960; UCRL-92246; CONF-850809-29) Avail: NTIS HC A02/MF A01

The Mirror Fusion Test Facility (MFTF-B) at Lawrence Livermore National Laboratory requires state-of-the-art structural-mechanics methods to deal with access constraints for plasma heating and diagnostics, alignment requirements, and load complexity and variety. Large interactive structures required an integrated analytical approach to achieve a reasonable level of overall system optimization. The Tandem Magnet Generator (TMG) creates a magnet configuration for the EFFI calculation of electromagnetic-field forces that, coupled with other loads, form the input loading to magnet and vessel finite-element models. The analytical results provide the data base for detailed design of magnet, vessel, foundation, and interaction effects. DOE

N86-11018# Brookhaven National Lab., Upton, N. Y.
THEORY OF NON-PLANAR ORBITS
A. Anitilon and M. Month 1985 4 p refs Presented at the Particle Accelerator Conf., Vancouver, British Columbia, 13 May 1985
(Contract DE-AC02-76CH-00016)
(DE85-013284; BNL-36495; CONF-850504-160) Avail: NTIS HC A02/MF A01

The basic dynamics of a planar accelerator is extended to the non-planar case. This is one using the geometrical concept of torsion and extending the Hamiltonian formalism. A generalized non-planar reference orbit is adopted which introduces torsion in appropriately chosen drift spaces. The parameters of the reference orbit are associated with uncoupled and coupled betatron parameters currently in use. DOE

N86-11019# Sandia Labs., Albuquerque, N. Mex.
PHOTOACTIVATION OF PBFA-2
T. N. Simmons and J. B. Mashburn 1985 5 p Presented at the 5th IEEE Pulsed Power Conf., Washington, D.C., 10 Jun. 1985
(Contract DE-AC04-76DP-00789)
(DE85-013439; SAND-84-2576C; CONF-850616-35) Avail: NTIS HC A02/MF A01

A 30 MV peak output voltage will be produced. A substantial portion of the output energy will be lost as free electrons which produce hard X-rays. Many X-rays will have energies within the photoneutron giant resonance. A PBFA-2 shot will produce about 5 x 10 E14 photoneutrons. These photoneutron reactions will induce radioactivity in and about PBFA-2. Activation structural components in the center section will be limited by substituting aluminum for stainless steel in regions of high X-ray intensity. Air will be activated above and below the center section after shots; however, X-ray shielding will limit initial concentrations to five times health guidelines. The short half-lives of air radioactivity will permit reentry following simple decay without ventilation. Some radioactive material will be eroded by arcing, but the resulting contamination whould be small. Miniscule concentrations of radioactivity will be produced in the water surrounding the center section. DOE

N86-11020# Massachusetts Inst. of Tech., Cambridge. Plasma Fusion Center.
CONDUCTING WALL AND PRESSURE PROFILE EFFECT ON MHD STABILIZATION OF AXISYMMETRIC MIRROR
X. Z. Li, J. Kesner, and B. Lane 1985 37 p
(Contract DE-AC02-78ET-51013)
(DE85-013647; DOE/ET-51013/135; PFC/RR-84-15) Avail: NTIS HC A03/MF A01

The MHD Energy Princple is used to examine the stabilization effect of a conducting wall located near to the plasma surface. The stabilization effect is maximized when the normal components of the perturbed magnetic field approaches zero (Q sub n = 0) at the plasma surface. Under this boundary condition, the eigen-equation of the plasma displacement is solved for a two-step flat pressure profile model, which can include both the non-hollow and a hollow pressure profile. Only the rigid m-1 mode is considered due to the FLR effect. For an isotropic pressure component it is found that a hollow profile has better stability than a uniform pressure when the integral of the radial pressure profile is fixed. The implication for plasma experiments and fusion reactors is discussed. DOE

N86-11021# Brookhaven National Lab., Upton, N. Y.
THERMAL AND STRUCTURAL ANALYSIS OF RING COMPONENTS BY THE FINITE ELEMENT METHOD
R. Alforque and S. Sharma 1985 4 p Presented at the Particle Accelerator Conf., Vancouver, British Columbia, 13 May 1985
(Contract DE-AC02-76CH-00016)
(DE85-013305; BNL-36573; CONF-850504-145) Avail: NTIS HC A02/MF A01

In a previous report, a thermal study was made in order to determine the effects of a shift in the electron vertical orbital plane, and the resulting displacement of the wiggler photon beam striking the inner surface of the vacuum chamber. Since then, due to some changes in the physical parameters of the vacuum chamber, a new design has been developed. The new geometry is quite different from the one described earlier, due primarily to an increase in the chamber vertical aperture which was opened to 23 mm. from an initial opening of 6 mm. A new study is conducted for this new chamber design that includes a structural analysis in order to determine the stresses and deflections of the vacuum chamber due to the combined thermal and mechanical loading. It should be noted that various geometrical models are analyzed before the final geometry is decided. This report describes in detail the results of the thermal and structural analysis of the final geometry using the finite element code. DOE

N86-11022# Brookhaven National Lab., Upton, N. Y.
UNICELL STRUCTURE FOR SUPERCONDUCTING STORAGE RINGS
G. Danby, B. DeVito, J. Jackson, G. Keohane, Y. Y. Lee, R. Phillips, S. Plate, L. Repeta, J. Skaritka, and L. Smith 1985 4 p Presented at the Particle Accelerator Conf., Vancouver, British Columbia, 13 May 1985
(Contract DE-AC02-76CH-00016)
(DE85-013303; BNL-36559; CONF-850504-147) Avail: NTIS HC A02/MF A01

Mechanically integrated, magnetically decoupled storage rings were designed for a heavy ion collider for 100 GeV/amu Au, at B - 2.7T. New concepts were developed, including detailed engineering design and cost estimates. A unicell contains a half-cell of both rings within a single He vessel. The unicell design is optimized for economical mass production. Survey pads welded to the laminations provide external fiducials to locate the magnet cores. Roller bearing self aligning supports accommodate cool-down shrinkage. The design tolerates relative motion of components resulting from longitudinal shrinkage in the approx. 15 m long unicell without affecting performance. Magnetic and physical lengths are the same, eliminating waste space. Archomatic quadrupoles with sextupoles at both ends are located on a common precision beam tube which aligns and supports a pick-up electrode. The unicell accommodates longer dipoles compared to conventional designs, reducing B sub max, stored energy, and the volume of iron and superconductor. DOE

N86-11023# Brookhaven National Lab., Upton, N. Y.
TRACKING STUDIES ON THE EFFECTS OF MAGNET MULTIPOLES ON THE APERTURE OF THE RHIC HEAVY ION COLLIDER
G. F. Dell and G. Parzen 13 May 1985 4 p refs Presented at the Particle Accelerator Conf., Vancouver, British Columbia, 13 May 1985
(Contract DE-AC02-76CH-00016)
(DE85-013282; BNL-36566; CONF-850504-157) Avail: NTIS HC A02/MF A01

Tracking studies including the effects of random multipoles resulting from construction errors have been made for Relativistic Heavy Ion collider (RHIC) at Brookhaven National Laboratory (NHIC) with two independent tracking programs at three different tunes. The studies were made using ten different sets of random errors for each of the programs. The aperture was defined as the worst case, and the results of the two programs are in good agreement. A second set of studies was made for which the number of dipoles was doubled to determine whether doubling the number of independent random errors results in a reduction of the effects or random multipoles. The results for the two cases, one dipole per half cell and two dipoles per half cell, indicate there is little difference in dynamic aperture. DOE

N86-11024# Stanford Linear Accelerator Center, Calif.
TIMING SYSTEM CONTROL SOFTWARE IN THE SLC
K. Thompson and N. Phinney Apr. 1985 3 p Presented at the

Particle Accelerator Conf., Vancouver, British Columbia, 13 May 1985
(Contract DE-AC03-76SF-00515)
(DE85-013380; SU-SLAC-PUB-3651; CONF-850504-87) Avail: NTIS HC A02/MF A01

A new timing system that allows precision (approx. 1 to 2 ns) control of the trigger times of klystrons, beam position monitors, and other devices on a pulse-to-pulse basis at up to 360 Hz is in operation in the first third of the SLAC linear accelerator. The control software is divided between a central host VAX and local Intel 8086-based microprocessor clusters. Facilities exist to set up and adjust the timing of devices or groups of devices independently for beam pulses having different destinations and purposes, which are run in an interlaced fashion during normal machine operation. Upgrading of the system is currently underway, using a new version of the Programmable Delay Unit CAMAC module to allow pipelining of timing information for three machine pulses. An overview of the current state of the system is presented with an emphasis on software control. DOE

N86-11025# Stanford Linear Accelerator Center, Calif.
BEAM STEERING IN THE SLC LINAC
J. C. Sheppard, M. J. Lee, M. C. Ross, J. T. Seeman, R. F. Stiening, and M. D. Woodley Feb. 1985 3 p Presented at the Particle Accelerator Conf., Vancouver, British Columbia, 13 May 1985
(Contract DE-AC03-76SF-00515)
(DE85-013370; SU-SLAC-PUB-3583; CONF-850504-70) Avail: NTIS HC A02/MF A01

In order to control emittance growth due to transverse wakefields it will be necessary to transport electrons and positrons through the Stanford Linear Collider (SLC) linac to within a hundred (MU)m of the centers of the linac irises. Beam centering will be accomplished using computer routines to read stripline beam position monitors and in turn correct the orbits with dipole magnets. Several different steering algorithms have been investigated using electrons in the first third of the SLC linac lattice. The most promising scheme is a cascade of modified three-bumps in conjunction with long spanning harmonic corrections. General features of the orbit correcting software are discussed along with the mathematical recipes for correction. Experimental results and a discussion of future plans are presented. DOE

N86-11026# Brookhaven National Lab., Upton, N. Y.
RHIC LATTICE
S. Y. Lee, J. Claus, E. D. Courant, H. Hahn, and G. Parzen 1985 4 p refs Presented at the Particle Accelerator Conf., Vancouver, British Columbia, 13 May 1985
(Contract DE-AC02-76CH-00016)
(DE85-013289) Avail: NTIS HC A02/MF A01

An antisymmetric lattice for the proposed Relativistic Heavy Ion Collider at Brookhaven National Laboratory is presented, which was designed to have (1) an energy range from 7 GeV/amu up to 100 GeV/amu; (2) a good tunability of (BETA) and betatron tune; (3) freedom in the choice of crossing angle between beams; and (4) capability of operating unequal species, for example, proton on gold. Suppression of structure resonances is achieved by a proper choice of the phase advances across the insertion and the arc cells. DOE

N86-11027# Los Alamos Scientific Lab., N. Mex.
GENERALIZED HELICITY AND ITS TIME DERIVATIVE
T. R. Jarboe and G. J. Marklin 1985 8 p Presented at the 7th US Symp. on Compact Toroid Res., Santa Fe, N. Mex., 21 May 1985
(Contract W-7405-eng-36)
(DE85-012770; LA-UR-85-1821; CONF-8505100-15) Avail: NTIS HC A02/MF A01

Spheromaks can be sustained against resistive decay by helicity injection because they tend to obey the minimum energy principle. A plasma-laden magnetic configuration will relax to a state of minimum energy subject to the constraint that the magnetic helicity is conserved. Use of helicity as a constraint on the minimization of energy was proposed in connection with astrophysical phenomena. Helicity does decay on the resistive diffusion time. However, if helicity is created and made to flow continuously into a confinement geometry, these additional linked fluxes can relax and sustain the configuration indefinitely against the resistive decay. An extension of the definition of helicity to include systems where B vector can penetrate the boundary and the penetration can be varying in time is presented. The sustainment of RFPs and spheromaks in terms of helicity injection is discussed. DOE

N86-11028# Los Alamos Scientific Lab., N. Mex.
RECENT HELICITY SOURCE AND POWER SUPPLY IMPROVEMENTS IN CTX
I. Henins, S. O. Knox, T. R. Jarboe, and C. W. Barnes 1985 6 p Presented at the 7th US Symp. on Compact Toroid Res., Santa Fe, N. Mex., 21 May 1985
(Contract W-7405-eng-36)
(DE85-012741; LA-UR-1790; CONF-8505100-4) Avail: NTIS HC A02/MF A01

Since the last CT Symposium, two major changes in CTX have been the introduction of pulse forming networks (PFNs) to drive the coaxial electrode helicity source, and the very recent installation of a larger source with electrode diameters about twice the previous ones. The power supplies used for CTX have ranged from the simple connection of the capacitor bank across the electrode collector plates (slow mode) to the more sophisticated PFNs, described here, which optimize the energy transfer from the capacitor bank to the magnetic fields of the spheromak. Using the PFNs, the formation and sustainment phase to peak toroidal plasma current lasts longer (approx. = 0.7 ms) than in the slow mode (approx. = 0.05 ms), thus lowering the peak current that must flow through the electrode surfaces. Also, by supplying the source electrodes with both a square pulse current waveform and a quasi-steady source flux, phi sub g, one can generate helicity at a constant source lambda sub g parameter. The use of a larger diameter helicity source will improve the energy efficiency of helicity injection and allow higher source current for the same surface current density because of the larger electrode surface area. DOE

N86-11029# Los Alamos Scientific Lab., N. Mex.
EQUILIBRIUM OF THE KINK SOURCE EXPERIMENT
G. Marklin 1985 5 p Presented at the 7th US Symp. on Compact Toroid Res., Santa Fe, N. Mex., 21 May 1985
(Contract W-7405-eng-36)
(DE85-012764; LA-UR-85-1837; CONF-8505100-14) Avail: NTIS HC A02/MF A01

The kink source experiment (KSX) was conceived of as a method of injecting helicity into a spheromak making special use of the m = 1 helical Taylor state. It has a Z pinch as a helicity generating source, connected to a flux conserver through an entrance region. Since the entrance region is a long (length > diameter) cyclinder, the magnetic field should be close to the helical Taylor state, which is the minimum energy configuration of a magnetized plasma in an infinite cylinder with no net flux. Modeling the actual fields in the entrance region of the KSX using zer-beta ideal MHD equilibrium theory is described. DOE

N86-11030# California Univ., Livermore. Lawrence Livermore Lab.
LIQUID TO GAS LEAK RATIOS WITH LIQUID NITROGEN AND LIQUID HELIUM
T. H. Batzer and W. R. Call 26 Feb. 1985 4 p Presented at the 6th Topical Meeting on the Technol. of Fusion Energy, San Francisco, 3 Mar. 1985
(Contract W-7405-eng-48)
(DE85-012950; UCRL-91953; CONF-850310-112) Avail: NTIS HC A02/MF A01

To predict the leak rates of liquid helium and liquid nitrogen containers at operating conditions we need to know how small leaks 10 to the -8 to 10 to the -5 atm cc air/sec, measured at standard conditions, behave when flooded with these cryogens. Two small leaks were measured at ambient conditions (approx. 750 Torr and 295 K), at the normal boiling points of LN2 and

LHe, and at elevated pressures above the liquids. The ratios of the leak rates of the liquids at ambient pressure to the gases (G) at ambient pressure and room temperature were: GN2(1), LN2(18), GHe(1), and LHe(172). The leak rate ratio of LN2 at elevated pressure was linear with pressure. The leak rate ratio of LHe at elevated pressure was also linear with pressure. DOE

N86-11031# Los Alamos Scientific Lab., N. Mex.
ALTERNATIVE FUSION CONCEPTS AND THE PROSPECTS FOR IMPROVED REACTORS
R. A. Krakowski 1985 9 p Presented at the 20th Intersoc. Energy Conversion Eng. Conf., Miami Beach, Fla., 18 Aug. 1985
(Contract W-7405-eng-36)
(DE85-009622; LA-UR-85-1035; CONF-850808-3) Avail: NTIS HC A02/MF A01

Past trends, present status, and future directions in the search for an improved fusion reactor are reviewed, and promising options available to both the principle tokamak and other supporting concept are summarized. DOE

N86-11032# TRW Space Technology Labs., Redondo Beach, Calif. Energy Div.
SYMMETRIC TANDEM MIRROR PROGRAM Annual Progress Report
1985 56 p
(Contract DE-AC03-79ET-51017)
(DE85-012352; DOE/ET-51017/T2) Avail: NTIS HC A04/MF A01

The overall objective was to examine confinement of high-(BETA) plasmas in an axisymmetric mirror configuration which is stabilized by the presence of a plasma produced, annular magnetic well (ELMO-ring). To accomplish this objective, the high-(BETA) mirror-confined plasmas were generated by ICRH. The annular wells result from diamagnetism of hot electrons generated by ECRH. The development of techniques for controlling the spatial and energy distributions of these electrons was an esential ingredient in the program. The culmination of this work is the successful generation of hot-ion plasmas by ICRH with anti n approx. 1 x to the 13th/cc and T sub i approx. 300 eV corresponding to anti (BETA) approx. = 5%. DOE

N86-11033# Stanford Linear Accelerator Center, Calif.
PROGRAMMABLE DELAY UNIT INCORPORATING A SEMI-CUSTOM INTEGRATED CIRCUIT
E. Linstadt Apr. 1985 3 p Presented at the Particle Acclerator Conf., Vancouver, British Columbia, 13 May 1985
(Contract DE-AC03-76SF-00515)
(DE85-013379; SU-SLAC-PUB-3637; CONF-850504-72) Avail: NTIS HC A02/MF A01

The synchronization of Stanford Linear Collider (SLC) accelerator control and monitoring functions is realized by a CAMAC module, the PDU II (Programmable Delay Unit II, SLAC 253-002), which includes a semi-custom gate array integrated circuit. The PDU II distributes 16 channels of independently programmable delayed pulses to other modules within the same CAMAC crate. The delays are programmable in increments of 8.4 ns. Functional descriptions of both the module and the semi-custom integrated circuit used to generate the output pulses are given. Author

N86-11034# Los Alamos Scientific Lab., N. Mex.
HEATING AND GENERATION OF SUPRATHERMAL PARTICLES AT COLLISIONLESS SHOCKS
M. F. Thomsen 1985 28 p refs Presented at the Am. Inst. of Phys. Conf., Taos, N. Mex., 6 Aug. 1984
(Contract W-7405-eng-36)
(DE85-014114; LA-UR-85-2073; CONF-8408121-4) Avail: NTIS HC A03/MF A01

Collisionless plasma shocks are different from ordinary collisional fluid shocks in several important respects. They do not in general heat the electrons and ions equally, nor do they produce Maxwellian velocity distributions downstream. Furthermore, they commonly generate suprathermal particles which propagate into the upstream region, giving advance warning of the presence of the shock and providing a seed population for further acceleration to high energies. Recent space observations and theory have revealed a great deal about the heating mechanisms which occur in collisionless shocks and about the origin of the various suprathermal particle populations which are found in association with them. An overview of the present understanding of these subjects is presented. DOE

N86-11035# Stanford Linear Accelerator Center, Calif.
SEARCH FOR HEAVY NEUTRINES PRODUCED IN e(+)e(-) ANNIHILATION
G. J. Feldman May 1985 6 p refs Presented at the 20th Recontre de Moriond, Les Arcs, France, 10 Mar. 1985
(Contract DE-AC03-76SF-00515)
(DE85-013372; SU-SLAC-PUB-3684; CONF-850375-4) Avail: NTIS HC A02/MF A01

A search for long-lived heavy neutrinos produced by the neutral weak current in e(+)e(-) annihilation at 29 GeV at PEP was conducted. Data from the Mark II detector are examined for evidence of events with one or more separated vertices in the radial range of 2 mm to 10 cm. No events were found that were consistent with the hypothesis of heavy neutrino production, eliminating the possibility of heavy neutrinos with decay lengths of 1 to 20 cm in mass range 1 to 13 GeV/c(2). DOE

N86-11036# Argonne National Lab., Ill.
EXPERIMENTAL INVESTIGATIONS OF THERMAL RADIATION FROM POTASSIUM ATOMS AND DESIGN APPLICATIONS
C. S. Wang and L. S. H. Chow 1985 8 p refs Presented at the Natl. Heat Transfer Conf., Denver, 4 Aug. 1985
(Contract W-31-109-eng-38)
(DE85-004086; CONF-850810-3) Avail: NTIS HC A02/MF A01

Theoretical models of thermal radiation from potassium-laden combustion gases show that thermal radiation from potassium atoms can contribute significantly to the radiant heat flux in radiant furnaces of steam generating systems. The potassium radiation is being investigated experimentally at Argonne National Laboratory. Experimental data were interpreted by a radiant heat transfer model that calculates the total gas emissivity and absorptivity from the spectral properties of CO2, H2O, and potassium atoms. The model was applied to provide design data for radiant furnaces of coal-fired magnetohydrodynamic (MHD) power generation systems, where considerable amount of potassium atoms would be present. DOE

N86-11037# Oak Ridge National Lab., Tenn.
HOT CELL FACILITY DESIGN FOR LARGE FUSION DEVICES
R. J. Barrett and G. T. Bussell 1985 6 p Presented at the 6th Topical Meeting on the Technol. of Fusion Energy, San Francisco, 3 Mar. 1985 Prepared in cooperation with Burns and Roe, Inc., Oradell, N.J. and Stone and Webster Engineering Corp., Boston, Mass.
(Contract DE-AC05-84OR-21400)
(DE85-012893; CONF-850310-104) Avail: NTIS HC A02/MF A01

Large hot cell facilities will be necessary to support the operation of large fusion devices. The supporting hot cells will be needed to serve a variety of different functions and tasks, which include reactor component maintenance, tool and maintenance equipment repair, and preparation of radioactive material for shipment and disposal. This paper discusses hot cell facility functions, requirements, and design issues and techniques. Suggested solutions and examples are given. DOE

N86-11038# Nationaal Inst. voor Kernfysica en Hoge Energiefysica, Amsterdam (Netherlands). Sectie-H.
TWO-LOOP LARGE HIGGS MASS CORRECTIONS TO VECTOR BOSON SELF-COUPLINGS
J. J. vanderBij Oct. 1984 20 p refs
(NIKHEF-H/84-15; B8561680) Avail: NTIS HC A02/MF A01

The two-loop corrections to the three-vector boson vertices are calculated in the limit of large Higgs mass. Corrections growing quadratically with the Higgs mass appear in the anomalous magnetic moment of the charged vector boson and the corresponding WOW+W- coupling. The weak coupling constant in the WOW+W- vertex receives a correction compared to the coupling in mu-decay. The results suggest a breakdown of perturbation theory for a Higgs mass of 3.4 TeV and larger. Author (ESA)

N86-11039# FOM-Inst. voor Plasmafysica, Rijnhuizen, Jutphaas (Netherlands).
[ACTIVITIES REPORT IN PLASMA PHYSICS] Annual Status Report, 31 Dec. 1984
Apr. 1985 140 p refs Sponsored by Euratom and Nederlandse Organisatie voor, Zuiver-Wetenschappelijk Onderzoek (ZWO)
Avail: NTIS HC A07/MF A01

Some areas of study were plasma pinches, turbulent heating in TORTUR tokamak and diagnostical studies, numerical calculations on cold plasma blankets, and electron cyclotron resonance heating. Plasma diagnostics, fusion reactor technology, magnetohydrodynamics, wave dynamics, and transport problems were also studied. Author (ESA)

76 SOLID-STATE PHYSICS

Includes superconductivity.

For related information, see also *33 Electronics and Electrical Engineering* and *36 Lasers and Masers.*

N86-11040 Rutgers - The State Univ., New Brunswick, N. J.
AN INVESTIGATION OF VORTEX DYNAMICS IN 2-DIMENSIONAL SUPERFLUID FILMS OF HELIUM-4 Ph.D. Thesis
Mokyang Kim 1985 198 p
Avail: Univ. Microfilms Order No. DA8510811

Recently the superfluidity in 2-dimensional helium film has been actively investigated theoretically and experimentally. By measuring the third sound damping associated with the amplitude of the oscillation and/or with the externally driven rotation, the vortex dynamics in 2-dimensional superfluid films of helium-4 was systematically investigated. Firstly, the effective vortex density when the present pair-breakings of bound pairs was measured for the both situations when the net vorticity of the system is zero and nonzero. The measured effective vortex density for the former case was compared with the theoretical predictions and that for the latter case was used to determine an empirical relation between the effective density of rotation-induced vortices from pair breaking. Secondly, the effective diffusion constant was measured and fitted experimentally. Thirdly, the decay of persistent current was measured in an open geometry when vortices leave the film and enter the film. Dissert. Abstr.

N86-11041 Columbia Univ., New York.
A SUPERCONDUCTING TUNNEL JUNCTION RECEIVER FOR MILLIMETER-WAVE ASTRONOMY Ph.D. Thesis
Shing-Kuo Pan 1984 245 p
Avail: Univ. Microfilms Order No. DA8511539

The development and construction of an ultra-low noise heterodyne receiver for millimeter wavelength ratio astronomy, and its use for spectral line observations of the 115.3 GHz rotational transition of interstellar CO is described. The receiver uses a Superconductor - Insulator - Superconductor (SIS) quasiparticle tunnel junction mixer to convert the millimeter wavelength signal to a microwave intermediate frequency. Experiments aimed at quantitative verification of J. R. Tucker's newly published quantum mixer theory are described. Experimental results were in excellent agreement with theory, assuming the 3-frequency approximation. Infinite available gain and negative output resistance were observed for the first time. Using this SIS receiver on the Columbia-GISS 4-ft telescope, 7 well separated large molecular clouds were observed at velocities between -80 and -20 km/sec towards the Cygnus-X region. The kinematic distances of these clouds lie between 6.5 and 12.7 kpc corresponding to galactocentric radii of 11 to 14.7 kpc. The total mass of these clouds is about 2 x 10 to the 6th power solar mass. Dissert. Abstr.

N86-11042 Illinois Inst. of Tech., Chicago.
FREE CARRIER ABSORPTION FROM ELECTRONS IN CONFINED SYSTEMS Ph.D. Thesis
Halina Adamska 1984 82 p
Avail: Univ. Microfilms Order No. DA8510285

A calculation of the free carrier absorption for two-dimensional quantum well structures and ultrathin wires fabricated from III-V semiconducting materials, where the carriers are scattered either by polar optical phonons or acoustic phonons is presented. The free carrier absorption coefficient is found to be an oscillatory function of the photon frequency when the carriers are confined in quasi-low-dimensional structures such as superlattice heterostructures, quantum wells or thin wires. The absorption in quasi-low-dimensional structures is enhanced by going to layers of decreasing widths or to wires of decreasing widths or to wires of smaller transverse dimensions over its value in the bulk III-V semiconducting materials. In addition, it was found that in quasi-low-dimensional structures made from these materials the electron - polar optical phonon interaction gives greater contribution to the absorption than the electron - acoustic phonon interaction. Dissert. Abstr.

N86-11043 Yale Univ., New Haven, Conn.
ELECTRON TUNNELING IN METAL/TUNNEL-OXIDE/DEGENERATE SILICON JUNCTIONS Ph.D. Thesis
Izak Bencuya 1984 176 p
Avail: Univ. Microfilms Order No. DA8509683

Electron tunneling through very thin oxides (approx. 20 angstroms) on degenerate silicon was studied at room, liquid nitrogen and liquid helium temperatures. Metal, silicon and silicon dioxide vibrational modes were identified by the method of inelastic tunneling spectroscopy at liquid helium temperatures. Variations of the tunneling conductance and location of the silicon phonon peaks with orientation and carrier type of the semiconductor, and the shape of the lead superconducting gap in the tunneling conductance, centered about zero bias, show that the current flow is predominantly by direct, band-to-band, momentum-conserving tunneling. Dissert. Abstr.

N86-11044 Maryland Univ., College Park.
ADSORPTION OF OXYGEN ON SINGLE CRYSTAL TIN AT LIQUID HELIUM TEMPERATURES Ph.D. Thesis
John Michael Cavallo 1984 132 p
Avail: Univ. Microfilms Order No. 8509150

The initial stages of oxygen adsorption on single crystal tin surfaces were studied at liquid helium temperatures. The low temperatures slowed the reaction of the oxygen with the tin so that stages, which pass quickly at room temperature, could be studied. The reactions were studied by monitoring changes in the work function and in low energy electron transmission spectra. Dissert. Abstr.

N86-11045 Harvard Univ., Cambridge, Mass.
TOPICS IN THE ELECTRONIC THEORY OF DISORDERED SEMICONDUCTORS Ph.D. Thesis
Kenneth Charles Hass 1984 305 p
Avail: Univ. Microfilms, Order No. DA8503535

Two topics in the electronic theory of disordered semiconductors are discussed. First various aspects of the electronic theory of zincblende pseudobinary alloys are developed. The effects of chemical and bond-length disorder are modeled using the empirical tight binding method (ETBM). The choice of parameters is given special emphasis. A relativistic ETEM-CPA formalism is developed for systems with pure substitutional disorder. Its implementation is simplified through the development of a novel computational scheme (based on analytic continuation) which is also applicable in other types of green's function calculations. Secondly, the theory of interband optical absorption is discussed. A new method is presented for testing models of the electronic structure and chemical bonding in amorphous semiconductors based on a comparative analysis of moments of e2 in amorphous materials and related crystals. An application to published data is shown to provide insight into (1) bonding differences between various classes of amorphous semiconductors and (2) the validity of the independent band model. Dissert. Abstr.

N86-11046 Maryland Univ., College Park.
CRITICAL DYNAMICS IN SUPERFLUID HELIUM Ph.D. Thesis
Michael Steven Korth 1984 222 p
Avail: Univ. Microfilms Order No. DA8510254

The properties of liquid He-4 were very extensively studied and are, consequently, fairly well characterized. This, together with the capability of approaching the lambda-temperature (T sub lambda) closely and making high-precision measurements, accounts for the superiority of this system as a proving ground for any theory of critical phenomena. Thus when recent experiments on the thermal conductivity and the light-scattering spectrum near T sub lambda both manifested clear deviations from the predictions of dynamic scaling theory, the theory was seriously questioned. A mode-coupling type approach was used to calculate these two quantities. Non-critical background terms are included in a natural way. In the first three-term epsilon-expansion in critical dynamics, the asymptotic region (in which dynamic scaling ideas apply) is found to be very small--beyond the range of current experiments. Proper inclusion of these two effects (the non-critical and the non-asymptotic) are shown to be the key to reconciling the theory and experiments. Dissert. Abstr.

N86-11047*# Eloret Corp., Sunnyvale, Calif.
THE INTERACTION OF SMALL METAL PARTICLES WITH REFRACTORY OXIDE SUPPORTS Final Technical Report
Ch. Park and Klaus Heinemann 4 Mar. 1985 85 p refs
(NASA Order R05-030-001; Grant NCC2-248)
(NASA-CR-176228; NAS 1.26:176228) Avail: NTIS HC A05/MF A01 CSCL 20L

Islands and continuous layers of Pd were grown in UHV on Mo and MoO subtrates. As-deposited Pd islands and layers exhibited bulk Pd adsorption properties for CO when the Pd had been deposited at RT and at thicknesses exceeding 3 ML. However, CO adsorption was drastically reduced upon annealing. This deactivation was interpreted in terms of substrate/support interaction involving the diffusion of substrate species toward the Pd surface, using AES, TPD, and work function measurement techniques. A study of the growth and annealing behavior of Pd on Mo(110) was made for thicknesses up to 12 monolayers and substrate temperatures up to 1300K, using AES, XPS, LEED, and work function measurements. At low tempertures Pd formed a monolayer without alloying. In thick layers (12 ML) annealed about 700 K, Mo diffusion into the Pd layer and alloying were noted. Such layers remained continuous up to 1100 K. Thinner Pd layers were less stable and started coalescing upon annealing to as little as 550 K. Significant changes in Pd Auger peak shape, as well as shifts of Pd core levels, were observed during layer growth and annealing. Author

N86-11048*# National Aeronautics and Space Administration. Lewis Research Center, Cleveland, Ohio.
ION BEAM SPUTTER DEPOSITED ZINC TELLURIDE FILMS
Daniel A. Gulino 1985 19 p refs Proposed for presentation at 32nd Natl. Symp. of the Am. Vacuum Soc., Houston, Tex., 18-22 1985
(NASA-TM-87119; E-2726; NAS 1.15:87119) Avail: NTIS HC A02/MF A01 CSCL 20L

Zinc telluride is of interest as a potential electronic device material, particularly as one component in an amorphous superlattice, which is a new class of interesting and potentially useful materials. Some structural and electronic properties of ZnTe films deposited by argon ion beam sputter depoairion are described. Films (up to 3000 angstroms thick) were deposited from a ZnTe target. A beam energy of 1000 eV and a current density of 4 mA/sq. cm. resulted in deposition rates of approximately 70 angstroms/min. The optical band gap was found to be approximately 1.1 eV, indicating an amorphous structure, as compared to a literature value of 2.26 eV for crystalline material. Intrinsic stress measurements showed a thickness dependence, varying from tensile for thicknesses below 850 angstroms to compressive for larger thicknesses. Room temperature conductivity measurement also showed a thickness dependence, with values ranging from 1.86 x to to the -6/ohm. cm. for 300 angstrom film to 2.56 x 10 to the -1/ohm. cm. for a 2600 angstrom film. Measurement of the temperature dependence of the conductivity for these films showed complicated behavior which was thickness dependent. Thinner films showed at least two distinct temperature dependent conductivity mechanisms, as described by a Mott-type model. Thicker films showed only one principal conductivity mechanism, similar to what might be expected for a material with more crystalline character. Author

N86-11049# Naval Research Lab., Washington, D. C.
RENORMALIZATION OF AN INVERSE SCATTERING THEORY FOR INHOMOGENEOUS DIELECTRICS Memorandum Report
H. D. Ladouceur and A. K. Jordan Apr. 1985 28 p
(DA Proj. RR0-3302)
(AD-A156636) Avail: NTIS HC A03/MF A01 CSCL 20/3

Renormalized solutions are obtained for an inverse scattering problem that are equivalent to the second-order regular perturbation approximations for the exact theory (Gelfand-Levitan-Marchenko). We have developed an inversion method for reconstructing the permitivity profiles of inhomogeneous dielectric slabs from reflection coefficient data. Solutions with increased radii of convergence are obtained. Numerical examples are demonstrated for simulated scattering data from Gaussian, homogeneous slab and parabolic profiles. GRA

N86-11050# Oregon Graduate Center for Study and Research, Beaverton.
TRANSIENT VELOCITY ASSESSMENT IN GALLIUM ARSENIDE, AND OF OTHER GaAs CHARACTERISTICS RELATED TO DEVICE FUNCTIONS Semiannual Technical Report, Aug. 1984 - Feb. 1985
J. S. Blakemore and R. E. Kremer 10 Jun. 1985 41 p
(Contract MDA903-84-K-0374; ARPA Order 5020)
(AD-A156983; AD-E950724; Rept-71-521-SA-1) Avail: NTIS HC A03/MF A01 CSCL 20/12

Reports on the first six months of the program, with four tasks in two general areas. Concerning submicron GaAs devices and the possibility of high speed operation by velocity overshoot or ballistic mechanisms, tasks were to assemble the pertinent literature (now essentially done), and evaluate this - on which an interim evaluation is provided in the report to the effect that newly recognized scattering mechanisms make ballistic transport unlikely unless electron transit distances can be made less than some 100nm. This looks more feasible with vertically-oriented devices. The other two tasks were an assessment of literature and information concerning EL2 and other significant defect states in GaAs (for which a substantial data base has been assembled), and participation in collaborative activities directed towards optimization of evaluation techniques for GaAs wafers to be used for FET and related integrated circuit purposes. Work to date indicates that the local population of the EL2 midgap donor is likely to have a direct effect on FET properties. GRA

N86-11051# Stanford Linear Accelerator Center, Calif.
SUPERCONDUCTORS FOR PULSED RF ACCELERATORS
I. E. Campisi and Z. D. Parkas Apr. 1985 4 p Presented at the Particle Accelerator Conf., Vancouver, British Columbia, 13 May 1985
(Contract DE-AC03-76SF-00515)
(DE85-013378; SU-SLAC-PUB-3617; CONF-850504-67) Avail: NTIS HC A02/MF A01

The choice of superconducting materials for accelerator RF cavities has been determined in the past only in part by basic properties of the superconductors, such as the critical field, and to a larger extent by criteria which include fabrication processes, surface conditions, heat transfer capabilities and so on. For CW operated cavities the trend has been toward choosing materials with higher critical temperatures and lower surface resistance, from lead to niobium, from niobium to Nb3Sn. This trend has been dictated by the specific needs of storage ring CW system and by the relatively low fields which could be reached without breakdown. The work performed on superconducting cavities using microsecond long high power RF pulses has shown that in Pb, Nb, and Nb3Sn, fields close to the critical magnetic fields can be reached without magnetic breakdown. DOE

N86-11052# Argonne National Lab., Ill.
FERMI SURFACE STUDY OF CeSb IN THE FERROMAGNETIC AND ANTIFERROMAGNETIC PHASES
H. Aoki, G. W. Crabtree, W. Joss, and F. Hulliger Feb. 1985 12 p Presented at the 5th Intern. Conf. on Crystalline Field Effects in f-Electron Systems: ICCF5
(Contract W-31-109-eng-38)
(DE85-012122; CONF-8504115-4) Avail: NTIS HC A02/MF A01

A de Haas-van Alphen effect study of CeSb in the intermediate field antiferromagnetic phase and in the high field ferromagnetic phase is reported. The results are discussed in the light of the p-f mixing model and a new weak coupling model based on a band structure calculation with localized f-orbitals. DOE

N86-11053# City Univ. of New York, N.Y.
MAGNETIC PROPERTIES OF DOPED SEMICONDUCTORS Progress Report, 1 Aug. 1984 - 31 Jul. 1985
M. P. Sarachik 1985 5 p
(Contract DE-FG02-84ER-45153)
(DE85-012090; DOE/ER-45153/1) Avail: NTIS HC A02/MF A01

The susceptibility of a series of boron-doped silicon samples with concentrations spanning the metal-nonmetal transition has been measured between 1.25K and 300K, and the magnetization has been measured to 50 kG. The magnetization of an insulating phosphorus-doped silicon sample is investigated, and the results are analyzed using the scaling theory of Bhatt and Lee. The assembly and testing of a Faraday balance is planned, as well as measurements of the Hall effect and magnetoresistance in pumped helium 4, and studies of thermoelectric power at low temperatures. DOE

N86-11054# Sandia Labs., Albuquerque, N. Mex.
SHOCK LOADING AND RELEASE BEHAVIOR OF X-CUT QUARTZ
L. C. Chabildas 1985 5 p refs Presented at Am. Phys. Soc. Topical Conf. on Shock Waves in Condensed Matter, Spokane, Wash., 22 Jul. 1985
(Contract DE-AC04-76DP-00789)
(DE85-013954; SAND-85-0149C; CONF-850736-6) Avail: NTIS HC A02/MF A01

Results of release-adiabat measurements are reported for shock-loaded x-cut quartz over the stress range of 15 GPa to 110 GPa. Release paths determined from a shock stress of 15 GPa indicate a return to the original density, while measurements of release adiabats from shock stresses over 50 GPa suggest release to be occurring primarily from and in the high density phase. Significant hysteretic effects are observed upon release and a retransformation to a low density phase is observed at lower stresses. Measurements of wave speeds in shocked quartz at stresses over 50 GPa indicate a decrease in wave speeds over the stress regime 71 to 108 GPa. DOE

N86-11055# Sandia Labs., Albuquerque, N. Mex.
HIGH-PRESSURE RELEASE-WAVE MEASUREMENTS AND PHASE TRANSFORMATION IN CaCO3
D. E. Grady 1985 13 p refs Presented at the Am. Phys. Soc. Topical Conf. on Shock Waves in Condensed Matter, Spokane, 22 Jul. 1985
(Contract DE-AC04-76DP-00789)
(DE85-012592; SAND-85-0148C; CONF-850736-2) Avail: NTIS HC A02/MF A01

Release-wave measurements on theoretical-density single crystal calcium carbonate from Hugoniot states of 11.5-, 17.0- and 26.5-GPa shock pressure were performed using time-resolved laser velocity interferometry diagnostics. Samples were subjected to planar impact with metal discs accelerated to high velocity using a powder gun facility. Motion was measured at a diffusely reflecting interface between the sample and lithium fluoride window material. Evidence for a high-pressure phase transformation between 12 and 14 GPa was provided from the 17.0- and 26.5-GPa experiments in terms of a well-defined rarefaction shock wave. The new phase may be a further metastable phase of calcite or identical to the high pressure state of argonite. DOE

N86-11056# Argonne National Lab., Ill.
ANELASTIC RELAXATION IN IRRADIATED Cu-Be
L. E. Rehn, H. Wiedersich, and A. V. Granato May 1985 5 p Presented at the Internal Friction and Ultrasonic Attenuation in Solids Conf., Urbana, Ill., 3 Jun. 1985 Prepared in cooperation with Illinois Univ., Urbana
(Contract W-31-109-eng-38)
(DE85-013893; CONF-8506125-3) Avail: NTIS HC A02/MF A01

Ultrasonic velocity measurements were made after thermal neutron irradiation of single-crystal Cu specimens containing 700 or 3700 appM Be. Ultrasonic attenuation was measured in similar specimens after 3 MeV electron irradiation. Three inelastic relaxation processes due to self-interstitial-Be complexes were observed. Cu-Be 1 was found to occur near liquid helium temperature; the temperature dependence of the velocity change suggests that reorientation of the Cu-Be 1 complex may involve quantum mechanical tunneling. Cu-Be produced an attenuation peak at approx. 2.5 K at a frequency of 10 MHz. Cu-Be 3 appeared simultaneously with 2 as a shoulder on the high temperature side of the 2.5 K attenuation peak. DOE

N86-11057# California Univ., Berkeley. Lawrence Berkeley Lab.
SURFACE SCIENCE AND CATALYSIS
G. A. Somorjai Feb. 1985 46 p refs Presented at the Royal Soc. Discussion Meeting, London, 28 Feb. 1985
(Contract DE-AC03-76SF-00098)
(DE85-013922; LBL-19139; CONF-850286-1) Avail: NTIS HC A03/MF A01

Modern surface science studies have explored a large number of metal catalyst systems. Three classes of catalytic reactions can be identified: (1) those that occur over the metal surface; (2) reactions that take place on top of a strongly adsorbed overlayer and (3) reactions that occur on co-adsorbate modified surfaces. Case histories for each class are presented. DOE

N86-10186# Bundesministerium fuer Forschung und Technologie, Bonn (West Germany).
GROWTH OF LARGER SINGLE CRYSTALS [ZUECHTUNG VON GROESSEREN EINKRISTALLEN]
Ruediger Jungbluth *In its* Satellite Use for Men 1985 p 30-32 In GERMAN (For primary document see N86-10180 01-12)
Avail: NTIS HC A03/MF A01

77 THERMODYNAMICS AND STATISTICAL PHYSICS

Includes quantum mechanics; and Bose and Fermi statistics.

For related information see also *25 Inorganic and Physical Chemistry* and *34 Fluid Mechanics and Heat Transfer.*

N86-11058 Rensselaer Polytechnic Inst., Troy, N. Y.
HEAT TRANSFER IN CONDENSING AND EVAPORATING TWO-COMPONENT, TWO-PHASE FLOW INSIDE A HORIZONTAL TUBE Ph.D. Thesis
Walter M. B. Duval 1984 111 p
Avail: Univ. Microfilms Order No. DA8509649

The effect of adding a small amount of oil to condensing and evaporation refrigerant R-12 following inside a horizontal tube is investigated both experimentally and analytically. Analytically, the problem is addressed assuming annular flow inside the tube. The analysis is based on the momentum and energy equations with the heat transfer in the liquid film determined using the Reynolds analogy between turbulent heat and momentum transfer. Two separate methods are developed for extending this model to include the effects of the two-component nature of the flow. Experimentally, two-phase local heat transfer measurements and flow pattern visualization are made for both condensation and evaporation. From the measurements, correlations are developed to predict two-phase heat transfer for the range of 0%, 2% and 5% oil fraction by mass flow. Dissert. Abstr.

N86-11059*# Virginia Univ., Charlottesville. Dept. of Materials Science.
A STUDY OF THE APPLICABILITY OF NUCLEATION THEORY TO QUASI-THERMODYNAMIC TRANSITIONS OF SECOND AND HIGHER EHRENFEST-ORDER Annual Report
R. E. Barker, Jr. and K. W. Campbell Jul. 1985 75 p refs
(Grant NAG1-419)
(NASA-CR-176238; NAS 1.26:176238; UVA/528230/MS86/101)
Avail: NTIS HC A04/MF A01 CSCL 20M

The applicability of classical nucleation theory to second (and higher) order thermodynamic transitions in the Ehrenfest sense has been investigated and expressions have been derived upon which the qualitative and quantitative success of the basic approach must ultimately depend. The expressions describe the effect of temperature undercooling, hydrostatic pressure, and tensile stress upon the critical parameters, the critical nucleus size, and critical free energy barrier, for nucleation in a thermodynamic transition of any general order. These expressions are then specialized for the case of first and second order transitions. The expressions for the case of undercooling are then used in conjunction with literature data to estimate values for the critical quantities in a system undergoing a pseudo-second order transition (the glass transition in polystyrene). Methods of estimating the interfacial energy gamma in systems undergoing a first and second order transition are also discussed. Author

N86-11060*# Virginia Univ., Charlottesville. Dept. of Materials Science.
A STUDY OF THE APPLICABILITY OF NUCLEATION THEORY TO QUASI-THERMODYNAMIC TRANSFORMATIONS OF SECOND AND HIGHER EHRENFEST-ORDER Status Report, 15 Dec. 1984 - 14 Jun. 1985
R. E. Barker, Jr. 14 Jun. 1985 31 p refs
(Grants NAG1-419; AF-AFOSR-0290-82)
(NASA-CR-176230; NAS 1.26:176230; UVA/5-28230; SAPR-2)
Avail: NTIS HC A03/MF A01 CSCL 20M

Transient and steady-state phenomena in temperature, stress, and electric, field intensity in ferroelectric polymers were investigated. The application and extension of the theory in the primary stage to the polarization domain nucleation and growth in ferroelectric polymers were developed. The kinetics of this growth were investigated. Expressions describing nucleation under the influence of an electric field were found through the expansion of the Gibbs' free energy in a Maclaurin series. The series was expanded in the electric field strength rather than the degree of undercooling. The resulting expressions were manipulated and applied to the case of nucleation of polarized domains in ferroelectric polymers. The kinetics of the nucleation and growth of polarized domains are also investigated. This was accomplished through the modification of the Johnson-Mehl-Avrami treatment of crystallization kinetics to be applicable to the growth of polarization domains in ferroelectric materials. E.A.K.

N86-11061# Johns Hopkins Univ., Baltimore, Md. Dept. of Chemical Engineering.
THERMODYNAMICS OF POLYMER-SUPERCRITICAL SOLVENT MIXTURES Final Technical Report, Jul. 1983 - Jun. 1985
M. A. McHugh 3 Jul. 1985 6 p
(Contract N00014-83-K-0613)
(AD-A157038) Avail: NTIS HC A02/MF A01 CSCL 07/4

The objectives of this research are to experimentally investigate the high pressure fluid phase behavior of polymer solutions and to characterize the resultant phase behavior using contemporary polymer solution theories. The polymer solutions of interest are of three types: (1) a binary mixture of polymer and organic solvent; (2) a binary mixture of polymer and supercritical fluid (SCF) solvent; and (3) a ternary mixture of polymer, organic solvent, and SCF solvent. There are three goals of the experimental phase of this project. The first goal is to determine the effect of high pressure on the lower critical solution temperature (LCST) of the polymer-organic solvent mixture at conditions close to the critical point of the organic solvent. The second goal is to study the phase behavior of polymer - SCF solvent mixtures. The final experimental goal is to study the high pressure phase behavior of tenary mixtures consisting of a polymer, an organic solvent, and an SCF solvent. GRA

N86-11062# Massachusetts Univ., Amherst. Dept. of Physics and Astronomy.
RELATIVISTIC WAVEFUNCTION AT THE ORIGIN AND THE PION DECAY CONSTANT
E. Hagg and H. Suura [1985] 13 p Prepared in cooperation with Minnesota Univ., Minneapolis
(Contract DE-AC02-83ER-40105)
(DE85-012392; DOE/ER-40105/T3; COO-1764-408) Avail: NTIS HC A02/MF A01

A hybrid Breit-Salpeter amplitude related to f sub (PI) is finite at the origin if the full relativistic equation is solved. This leads to an unambiguous calculation of f sub (PI). It is shown that this finiteness of the wavefunction is due to a suppression of the Coulomb potential whereby the 1/r singularity at the origin is reduced to a logarithmic one. DOE

N86-11063# Texas Univ., Austin. Inst. for Fusion Studies.
LOCAL CONSERVATION LAWS FOR THE MAXWELL-VLASOV AND COLLISIONLESS KINETIC GUIDING CENTER THEORIES
D. Pfirsch and P. J. Morrison Apr. 1985 17 p
(Contract DE-FG05-80ET-53088)
(DE85-013122; DOE/ET-53088/177; IFSR-177) Avail: NTIS HC A02/MF A01

Using one of the recent variational formulations of the Maxwell-Vlasov and guiding center theories, the energy momentum and angular momentum tensors for such theories are derived and the corresponding local conservation laws are proven. The energy momentum tensor is shown to be symmetric in its spatial components while the angular momentum density is naturally antisymmetric. DOE

80 SOCIAL SCIENCES (GENERAL)

Includes educational matters.

N86-11064*# Old Dominion Univ., Norfolk, Va.
NASA/AMERICAN SOCIETY FOR ENGINEERING EDUCATION (ASEE) SUMMER FACULTY FELLOWSHIP PROGRAM, 1985
G. Goglia, comp. Sep. 1985 156 p refs
(Grant NGT-47-003-029)
(NASA-CR-177972; NAS 1.26:177972) Avail: NTIS HC A08/MF A01 CSCL 05I

Since 1964, the National Aeronautics and Space Administration (NASA) has supported a program of summer faculty fellowships for engineering and science educators. In a series of collaborations between NASA research and development centers and nearby universities, engineering faculty members spend 10 weeks working with professional peers on research. The Summer Faculty Program Committee of the American Society for Engineering Education supervises the programs. The objectives of this program are: (1) to further the professional knowledge of qualified engineering and science faculty members; (2) to simulate and exchange ideas between participants and NASA; (3) to enrich and refresh the research and teaching activities of participants institutions; and (4) to contribute to the research objectives of the NASA center. College or university faculty members will be appointed as research fellows to spend 10 weeks in cooperative research and study at the NASA Langley Research Center. The fellows will devote

approximately 90 percent of the time to a research problem and the remaining time to a study program. The study program will consist of lectures and seminars on topics of general interest or that are directly relevant to the fellows' research project. The lecturers and seminar leaders will be distinguished scientists and engineers from NASA, the educational community, or industry.
Author

N86-11065# George Mason Univ., Fairfax, Va. Dept. of Psychology.
AN ANNOTATED BIBLIOGRAPHY OF ABSTRACTS ON THE USE OF SIMULATORS IN TECHNICAL TRAINING
A. Ayres, R. T. Hays, M. J. Singer, and m. Heinicke Oct. 1984 555 p
(Contract MDA903-83-M-2646)
(AD-A156792; ARI-RP-84-21) Avail: NTIS HC A24/MF A01 CSCL 05/9

This document contains annotated abstracts of 149 selected papers from the literature on simulator training devices and programs. The abstracts are organized into two sections: abstracts of 83 empirical articles and abstracts of 66 theoretical articles. Each abstract is organized according to a standardized format, with the following headings: Authors; Title; Source; Topic keywords; Short summary; Device; Institution; Type of article. The purpose of these annotated abstracts is to effectively summarize, and not merely to describe or identify, the contents of the papers under review. The abstract will be entered into a computerized data base for future analyses.
GRA

N86-11066# Amsterdam Univ. (Netherlands). Research Group for Science Dynamics.
MISSION ORIENTATION IN SCIENCE
W. vandenDaele May 1984 155 p refs Sponsored by Netherlands Ministry of Education and Sciences
Avail: NTIS HC A08/MF A01

A program to study social orientation and political direction of scientific development particularly in chemistry and ecology is outlined. Projects include adjustment of technological potentials to social priorities; technology development within universities; mission orientation in ecology; polyunsaturated fats; hybrid forms in the development of chemical toxicology; the conception of nature in ecosystems; and the concept of normative science.
Author (ESA)

81 ADMINISTRATION AND MANAGEMENT

Includes management planning and research.

N86-11067# Bundesministerium fuer Forschung und Technologie, Bonn (West Germany).
SPACE UTILIZATION [NUTZUNG DES WELTRAUMS]
Jan. 1985 64 p refs In GERMAN
Avail: NTIS HC A04/MF A01

The perspectives of the commercial utilization of space sciences are discussed. The scientific-technical user requirements in the field of astronautics till the end of the century are considered. The expenses of the Federal Ministry of Research and Technology (BMFT) in the field of space sciences are reviewed for the period 1983-1985. For individual titles, see N86-11068 through N86-11070.

N86-11068# Bundesministerium fuer Forschung und Technologie, Bonn (West Germany).
SPACE SCIENCES: PERSPECTIVES OF COMMERCIAL UTILIZATION FOR THE GERMAN INDUSTRY [WELTRAUMFORSCHUNG: PERSPEKTIVEN DER KOMMERZIELLEN NUTZUNG FUER DIE DEUTSCHE INDUSTRIE]
H. L. Jordan *In its* Space Utilization Jan. 1985 p 2-16 In GERMAN Presented at BDI Ausschuss fuer Forsch.- u. Wissenschaftspolitik, Bonn, 19 Oct. 1984 (For primary document see N86-11067 01-81)
Avail: NTIS HC A04/MF A01

Space sciences and their possible utilization by industry are presented. The development of astronautics and applications in observation techniques, communication, and navigation are reviewed. Utilization of reduced gravitational force effects: diffusion phenomena, crystal growth, production process for metals and composite materials, biochemistry, biotechnology, and biosciences are considered.
Author (ESA)

N86-11069# Bundesministerium fuer Forschung und Technologie, Bonn (West Germany).
DFVLR, STRATEGIC STUDY OF ASTRONAUTICS 1984, USER REQUIREMENTS [DFVLR: STRATEGIESTUDIE RAUMFAHRT 1984, NUTZERBEDARF]
In its Space Utilization Jan. 1985 p 17-50 In GERMAN (For primary document see N86-11067 01-81)
Avail: NTIS HC A04/MF A01

In order to determine the scientific-technical requirements in the field of astronautics till the end of the century the disciplines which are used or are going to use astronautics are considered: extraterrestrial research, Earth observation, biosciences, materials sciences, telecommunication, navigation, and new applications. Astronomy, astrophysics, solar terrestrial relations, Sun and solar system, planets, and comets are discussed. Atmospheric physics and climate, meteorology, cartography and land use, oceans and ice geodesy, and reconnaissance are treated. Human physiology and medicine, space biology, gravity, radiology, exobiology, and biotechnology (bioprocessing) are discussed. Materials research and its applications; and the commercial market and technology program for telecommunication and navigation are presented. Solar energy utilization in orbit, waste treatment, orbital flow test stand, orbital laboratory for planet surface, and quarantine station for planet materials are discussed.
Author (ESA)

N86-11070# Bundesministerium fuer Forschung und Technologie, Bonn (West Germany).
SPACE RESEARCH EXPENSES OF THE FEDERAL MINISTRY OF RESEARCH AND TECHNOLOGY (BMFT) IN THE PERIOD 1983-1985 [WELTRAUMFORSCHUNGSAUSGABEN DES BMFT IN 1983-1985]
In its Space Utilization Jan. 1985 p 51-62 In GERMAN (For primary document see N86-11067 01-81)
Avail: NTIS HC A04/MF A01

The expenses of the BMFT in space flight techniques, utilization of space laboratories and satellites, royalties for space transport, extraterrestrial basic research, operation of test stands, contribution to ESA, development of communication satellites, and DFVLR research are shown.
Author (ESA)

N86-11071# Institute for Defense Analyses, Alexandria, Va.
REPORT OF THE AD HOC COMMITTEE TO REVIEW THE PROGRAM OF THE SDI DIRECTORATE ON INNOVATIVE SCIENCE AND TECHNOLOGY (IST) Final Report, Feb. - Apr. 1985
B. Balko Apr. 1985 16 p
(Contract MDA903-84-C-0031)
(AD-A156668; AD-E500720; IDA-M-83; IDA/HQ-85-29861) Avail: NTIS HC A02/MF A01 CSCL 15/3

Deliberations and conclusions are summarized of an ad hoc Committee to review the Innovative Science and Technology (IST) Directorate. Areas for programmatic emphasis, proposal selection, funding for individuals and consortia, and desirable budgetary levels are discussed.
GRA

N86-11072# Research Inst. of National Defence, Stockholm (Sweden).
MANAGEMENT OF ORGANIZATIONAL OPERATIONS IN DYNAMIC ENVIRONMENTS TOWARDS A FRAME OF REFERENCE
Roger Hagafors and Robert Allard Feb. 1985 25 p refs
(FOA-C5-85-0003-H2; ISSN-0347-7665) Avail: NTIS HC A02/MF A01

The premises, the structure and the process of managing organizations are discussed. The organization is regarded as an open system and a dynamic environment model is assumed. The implications of the assumptions are described, and a frame of reference for analyzing the management situation is put forward. The hierarchical structure of organizations, the dimension of time in the management process, and the role of the management task, are discussed. Author (ESA)

N86-11073# Technische Hogeschool, Eindhoven (Netherlands). Dept. of Industrial Engineering.
ON THE STRUCTURE OF MANPOWER PLANNING, A CONTRIBUTION OF SIMULATION EXPERIMENTS WITH DECOMPOSITION METHODS
J. D. vanderBij, J. Wessels, and J. Wijngaard Aug. 1983 19 p refs
(Manpower-Planning-28) Avail: NTIS HC A02/MF A01

Manpower planning in a personnel system consisting of one personnel group, located in different organizational units is considered. The ease with which personnel availability can be matched to personnel requirement, when the flexibility within the personnel group is used is analyzed. This is done by comparing the performance of integrated planning, coordinated planning, and decomposed planning. Results are derived by simulation experiments. Author (ESA)

N86-11074# Technische Hogeschool, Eindhoven (Netherlands). Dept. of Industrial Engineering.
ASPECTS OF MANPOWER PLANNING AT A DUTCH UNIVERSITY, AN EXAMPLE OF AGGREGATION AND DECOMPOSITION METHODS IN MANPOWER PLANNING
N. Aerts, J. D. vanderBij, and J. Wessels Dec. 1983 41 p refs
(Manpower-Planning-29) Avail: NTIS HC A03/MF A01

The choice of the categories for the medium term manpower planning in an organization is considered in a system with a simple personnel structure, consisting of two function groups on different hierarchical levels. An example of such a system is the research and teaching staff of a university, when only the two lowest function groups are considered. In this system the question can be posed whether two or more categories have to be distinguished for the medium term manpower planning or whether it is sufficient to distinguish one aggregate category. If two or more categories are distinguished, another question is which relationships between the categories are important for the medium term manpower planning. Simulation experiments with aggregation and decomposition methods show that model choice depends on costs. Author (ESA)

N86-11075# Technische Hogeschool, Eindhoven (Netherlands). Dept. of Industrial Engineering.
ON THE STRUCTURE OF MANPOWER PLANNING, A CONTRIBUTION OF SIMULATION EXPERIMENTS WITH AGGREGATION METHODS
J. D. vanderBij, J. Wessels, and J. Wijngaard Aug. 1983 24 p refs
(Manpower-Planning-30) Avail: NTIS HC A02/MF A01

Two ways to estimate the possibilities of matching manpower availability to manpower requirement in the organization activity plan of a task oriented unit of an organization are considered. One estimation procedure is based on detailed information about the personnel groups which are located in the task oriented unit. The other procedure is based on aggregate information about total availability and total personnel requirement in the whole unit. A situation for the case that steps are taken on the basis of detailed information and for the case that steps are taken on the basis of aggregate information was analyzed. Results show that use of aggregate information in drawing up personnel plans causes no extra problems if the maximum potential mobility is high or if future manpower requirements in personnel groups is highly correlated. Author (ESA)

N86-11076# Technische Hogeschool, Eindhoven (Netherlands). Dept. of Industrial Engineering.
FAILURES AND SUCCESSES OF QUANTITATIVE METHODS IN MANAGEMENT
C. B. Tilanus May 1984 18 p refs Presented at ORSA/TIMS Joint Natl. Meeting, San Diego, CA., 25-27 Oct. 1982, 15th Operational Res. Soc. of India Ann. Conv., Kharagpur, India, 9-11 Dec. 1982, and Netherlands Soc. of Statistics and Operations Res. Ann. Conf., Eindhoven, Netherlands, 31 Mar. 1983 Revised
(ARW-03-THE-BDK/ORS/83-06) Avail: NTIS HC A02/MF A01

About 60 cases of failures and successes of quantitative methods in management, collected in industry, business and government are analyzed for features determining failure or success. Author (ESA)

N86-11077# Institute for Perception RVO-TNO, Soesterberg (Netherlands). Experimental Psychology Group.
RISK PROPENSITY, ACTION READINESS AND THE ROLES OF SOCIETAL AND INDIVIDUAL DECISION MAKERS
S. Lichtenstein, W. A. Wagenfar, G. B. Keren, and T. W. vanderSchaaf Aug. 1984 21 p refs Sponsored by Central Organization TNO
(IZF-1984-27; TDCK-79524) Avail: NTIS HC A02/MF A01

Decision making by public officials and citizens was compared by eliminating different socio-economic backgrounds and different available information; to investigate the effects of adopting one role or the other (societal vs individual). Dependent measures were the willingness to choose a risky option vs a sure outcome, and the readiness to take explicit action or not. A total of 478 student subjects read the same cover story which deals with the decision problem of how to limit the number of victims of an epidemic. The results (choices and reasons) show that societal decision makers are less likely than individuals to take explicit action. Taking action is more often preferred when associated with the risky option than with the sure outcome. The large majority of subjects justify their choice on the basis of the number of victims. Results are discussed in terms of framing. Author (ESA)

82 DOCUMENTATION AND INFORMATION SCIENCE

Includes information storage and retrieval technology; micrography; and library science.

For computer documentation see *61 Computer Programming and Software.*

N86-11078# R-K Research and System Design, Malibu, Calif.
ANNOTATED BIBLIOGRAPHY OF PUBLICATIONS DEALING WITH OCCUPATIONAL HEALTH AND MEDICAL INFORMATION SYSTEMS, COST ANALYSIS PROCEDURES, EVALUATION METHODOLOGY AND RELATED LEGAL ISSUES
1984 43 p
(Contract N00014-84-C-0601)
(AD-A156650) Avail: NTIS HC A03/MF A01 CSCL 06/10

The purpose of this selective bibliography is to provide a sense of the scope of the literature relevant to the subject matter of interest in this project to test and evaluate the Navy Occupational Health Information Management System (NOHIMS). The intent has been to describe the contents of each reference in sufficient detail so that a decision could be made whether or not to obtain a copy of the complete article. Articles are taken from journals such as The New England Journal of Medicine, Proceedings of the Fifth Annual Symposium on Computer Applications in Medical Care, Journal of Occupational Medicine, Navy Lifeline and Science. Topics cover a variety of topics such as liability for personal injuries caused by defective medical computer programs, computers in medical care, mental health information systems, COSTAR, Environmental Health Systems, and Medical surveillance requirements. GRA

N86-11079# Naval Postgraduate School, Monterey, Calif.
A SYSTEMS DEVELOPMENT LIFE CYCLE STUDY OF THE INFORMATION CENTER M.S. Thesis
M. L. Lechleitner Mar. 1985 133 p

(AD-A156977; AD-E950724) Avail: NTIS HC A07/MF A01 CSCL 05/2

End user computing has penetrated most large organizations in an uncontrolled fashion. The newness of the technology, the lack of management expertise, and the inability to gain corporate-wide control under the traditional organizational structure have often resulted in inefficiency, incompatibility, and missed opportunities. One solution to this situation is the Information Center (IC). ICs are centralized coordination centers for end user computing and offer end user computer expertise. ICs may be any combination of consulting services, training services, mainframe computer terminals, or microcomputers. This thesis examines the IC concept from the viewpoint of the manager tasked with implementation and provides a methodology, the Systems Development Life Cycle, to evaluate and implement an IC. Each phase of the methodology is explained and some innovative ideas on IC implementation and operation are provided. Examples of past successes and mistakes are also presented. GRA

N86-11080# California Univ., Livermore. Lawrence Livermore Lab.
WRITER/EDITOR AND THE COMPUTER
B. R. Smith Apr. 1985 7 p Presented at Forum 85, Helsingor, Denmark, 26 Aug. 1985
(Contract W-7405-eng-48)
(DE85-011843; UCRL-92525; CONF-850864-1) Avail: NTIS HC A02/MF A01

Computer development in the publications process is discussed. Authors and editors of scientific and engineering documents felt the impact in adverse and beneficial ways. When the computer entered the scene, the writer/editor had to learn different hardware systems to try to keep up with the software explosion. An innate flexibility and specialized knowledge of how to get a document into the best form for its specific audience quaranteed the writer/editor's survival. The experiences of writer/editors in one scientific laboratory are reviewed. The experiences typify challenges the forward-moving manager of a technical document production system can expect to encounter. DOE

N86-11081# Technische Hogeschool, Delft (Netherlands). Afd. der Scheikundige Technologie.
ACQUAINTANCE WITH ON LINE LITERATURE RESEARCH. AN INTRODUCTION FOR EDUCATION AT THE CHEMICAL TECHNOLOGY SECTION [KENNISMAKING MET ONLINE LITERATUUR-ONDERZOEK. EEN INLEIDING BIJ HET ONDERWIJS AAN DE AFDELING PER SCHEIKUNDIGE TECHNOLOGIE]
L. Maat, C. A. G. Konings, and M. VandenHondel Feb. 1985 39 p In DUTCH
Avail: NTIS HC A03/MF A01

A manual for automated information retrieval in international (bio-) chemical data banks is presented. The indexing elements (keywords, classification systems), searching language and search profile are discussed and explained. Accessible databanks (Chemical- and Biological Abstracts, Science Citation Index) are surveyed. Author (ESA)

N86-11082# Executive Office of the President, Washington, D.C.
PUBLICATION OF THE EXECUTIVE OFFICE OF THE PRESIDENT, JANUARY 20, 1981 - DECEMBER 31, 1984
1985 7 p
(PB85-187110) Avail: NTIS HC A02/MF A01 CSCL 05B

The bibliography lists the documents issued by the components of the Executive Office of the President, and are available for sale to the public. GRA

83 ECONOMICS AND COST ANALYSIS

Includes cost effectiveness studies.

No abstracts in this category.

84 LAW AND POLITICAL SCIENCE

Includes space law; international law; international cooperation; and patent policy.

No abstracts in this category.

85 URBAN TECHNOLOGY AND TRANSPORTATION

Includes applications of space technology to urban problems; technology transfer; technology assessment; and surface and mass transportation.

For related information see *03 Air Transportation and Safety, 16 Space Transportation,* and *44 Energy Production and Conversion.*

N86-11083*# Jet Propulsion Lab., California Inst. of Tech., Pasadena.
ADVANCED VEHICLE SYSTEMS ASSESSMENT. VOLUME 2: SUBSYSTEMS ASSESSMENT
K. Hardy Mar. 1985 167 p refs For Volume 1, see N85-28887 5 Vol.
(Contract NAS7-918; JPL Proj. 5030-573; Contract DE-AI01-78CS-54209)
(NASA-CR-176205; JPL-5030-573-Vol-2; JPL-Pub-84-79-Vol-2; NAS 1.26:176205; DOE/CS-54209/22-Vol-2) Avail: NTIS HC A08/MF A01 CSCL 13F

Volume 2 (Subsystems Assessment) is part of a five-volume report entitled Advanced Vehicle Systems Assessment. Volume 2 presents the projected performance capabilities and cost characteristics of applicable subsystems, considering an additional decade of development. Subsystems of interest include energy storage and conversion devices as well as the necessary powertrain components and vehicle subsystems. Volume 2 also includes updated battery information based on the assessment of an independent battery review board (with the aid of subcontractor reports on advanced battery characteristics). Author

N86-11084*# Jet Propulsion Lab., California Inst. of Tech., Pasadena.
ADVANCED VEHICLE SYSTEMS ASSESSMENT. VOLUME 3: SYSTEMS ASSESSMENT
K. Hardy Mar. 1985 292 p refs For Volume 1, see N85-28887 5 Vol.
(Contract NAS7-918; JPL Proj. 5030-573; Contract DE-AI01-78CS-54209)
(NASA-CR-176206; JPL-5030-573-Vol-3; JPL-Pub-84-79-Vol-3; NAS 1.26:176206; DOE/CS-54209/22-Vol-3) Avail: NTIS HC A08/MF A01 CSCL 13F

The systems analyses integrate the advanced component and vehicle characteristics into conceptual vehicles with identical performance (for a given application) and evaluates the vehicles in typical use patterns. Initial and life-cycle costs are estimated and compared to conventional reference vehicles with comparable technological advances, assuming the vehicles will be in competition in the early 1990s. Electric vans, commuter vehicles, and full-size vehicles, in addition to electric/heat-engine hybrid and fuel-cell powered vehicles, are addressed in terms of performance and economics. System and subsystem recommendations for vans and two-passenger commuter vehicles are based on the economic analyses in this volume. Author

N86-11085*# Jet Propulsion Lab., California Inst. of Tech., Pasadena.
ADVANCED VEHICLE SYSTEMS ASSESSMENT. VOLUME 4: SUPPORTING ANALYSES
K. Hardy Mar. 1985 125 p refs For Volume 1, see N85-28887 5 Vol.
(Contract NAS7-918; JPL Proj. 5030-573; Contract DE-AI01-78CS-54209)
(NASA-CR-176207; JPL-5030-573-Vol-4; JPL-Pub-84-79-Vol-4; NAS 1.26:176207; DOE/CS-54209/22-Vol-4) Avail: NTIS HC A08/MF A01 CSCL 13F

Volume 4 (Supporting Analyses) is part of a five-volume report, Advanced Vehicle Systems Assessment. Thirty-nine individuals, knowledgeable in advanced technology, were interviewed to obtain their preferences. Rankings were calculated for the eight groups they represented, using multiplicative and additive utility models. The four topics for consideration were: (1) preferred range for various battery technologies; (2) preferred battery technology for each of a variety of travel ranges; (3) most promising battery technology, vehicle range combination; and (4) comparison of the most preferred electric vehicle with the methanol-fueled, spark-ignition engine vehicle and with the most preferred of the hybrid vehicles. G.L.C.

N86-11086*# Jet Propulsion Lab., California Inst. of Tech., Pasadena.
ADVANCED VEHICLE SYSTEMS ASSESSMENT. VOLUME 5: APPENDICES
K. Hardy Mar. 1985 615 p For Volume 1, see N85-28887 5 Vol.
(Contract NAS7-918; JPL Proj. 5030-573; Contract DE-AI01-78CS-54209)
(NASA-CR-176208; JPL-5030-573-Vol-5; JPL-Pub-84-79-Vol-5; NAS 1.26:176208; DOE/CS-54209/22-Vol-5) Avail: NTIS HC A08/MF A01 CSCL 13F

An appendix to the systems assessment for the electric hybrid vehicle project is presented. Included are battery design, battery cost, aluminum vehicle construction, IBM PC computer programs and battery discharge models. G.L.C.

N86-11087*# Garrett Mfg. Ltd., Rexdale (Ontario).
ADVANCED GAS TURBINE (AGT) POWERTRAIN SYSTEM DEVELOPMENT FOR AUTOMOTIVE APPLICATIONS REPORT Semiannual Progress Report, Jan. - Jun. 1984
Dec. 1984 112 p refs
(NASA-CR-174886; DOE/NASA/0167-9; NAS 1.26:174886; Rept-31-3725(9); SAPR-9) Avail: NTIS HC A06/MF A01 CSCL 13F

This report describes progress and work performed during January through June 1984 to develop technology for an Advanced Gas Turbine (AGT) engine for automotive applications. Work performed during the first eight periods initiated design and analysis, ceramic development, component testing, and test bed evaluation. Project effort conducted under this contract is part of the DOE Gas Turbine Highway Vehicle System Program. This program is oriented at providing the United States automotive industry the high-risk long-range techology necessary to produce gas turbine engines for automobiles with reduced fuel consumption and reduced environmental impact. Technology resulting from this program is intended to reach the marketplace by the early 1990s. B.W.

N86-11088# Westat Research, Inc., Rockville, Md.
ACADEMIC RESEARCH EQUIPMENT IN SELECTED SCIENCE-ENGINEERING FIELDS, 1982-83. AN ANALYSIS OF FINDINGS FROM THE BASELINE NATIONAL SURVEY OF ACADEMIC RESEARCH INSTRUMENTS AND INSTRUMENTATION NEEDS
Kenneth Burgdorf and Howard J. Hausman Aug. 1985 221 p refs
(Grant NSF SRS-80-17873)
Avail: NTIS HC A10/MF A01

This report presents information from the two-phase baseline cycle of the National Science Foundation's (NSF's) National Survey of Academic Research Instruments and Instrumentation Needs. Phase 1, conducted in early 1983 with reference to instrumentation existing on December 31, 1982, involved collection of instrument-related data from physical and computer science and engineering departments at a stratified probability sample of 43 universities. The following year, in phase 2 data pertaining to 1983 instrumentation were collected for the agricultural, biological and environmental sciences at the same 43 universities. Phase 2 also included biological science departments (not clinical departments) at a stratified probability sample of 24 medical schools. In each phase, (1) department and facility administrators were surveyed to ascertain their equipment-related activities, needs and priorities, and (2) samples of existing research equipment were selected and the responsible faculty investigators were asked to provide information about each item's age, condition, cost, usage, etc. The resulting data bases contain questionnaire responses from over 900 department and facility heads and for over 10,000 individual items of research equipment. B.W.

N86-11089# National Aerospace Lab., Amsterdam (Netherlands).
AEROSPACE RESEARCH AT NLR
1984 39 p Original contains color illustrations
Avail: NTIS HC A03/MF A01

The NLR fluid dynamics, flight, structures and materials, space, and engineering and technical services divisions activities are presented. Research covers wind tunnel tests, computational aerodynamics, unsteady aerodynamics, aeroacoustics, propulsion systems, flight tests, aircraft performance assessment, human factors engineering, aircraft structures, aircraft loads, fatigue and corrosion, engine tests, satellite attitude control and ground operations, microgravity effects, robotics, and signal processing. Author (ESA)

N86-11090# National Aerospace Lab., Amsterdam (Netherlands). Ruimtevaartlab.
[ACTIVITIES REPORT OF THE SPACE FLIGHT LABORATORY] Annual Report, 1982 [VERSLAG OVER HET JAAR]
1983 127 p refs In DUTCH; ENGLISH summary Original contains color illustrations
Avail: NTIS HC A07/MF A01

Aerodynamics, flight, structures and materials, spaceflight technology, computer, remote sensing, and environment and energy supply research is summarized. Wind tunnel model investigations with turbo-powered simulators and remote sensing data processing are described. Activities in the German Dutch Windtunnel, European Transonic Windtunnel, the Group for Aeronautical Research and Technology in Europe, and cooperation with Indonesia are discussed. Author (ESA)

N86-11091# National Aerospace Lab., Amsterdam (Netherlands). Ruimtevaartlab.
[ACTIVITIES REPORT OF THE SPACE FLIGHT LABORATORY] Annual Report, 1983 [VERSLAG OVER HET JAAR 1983]
1984 126 p refs In DUTCH; ENGLISH summary Original contains color illustrations
Avail: NTIS HC A07/MF A01

Aerodynamics, flight, structures and materials, spaceflight and remote sensing, applied informatics, and environment and energy supply research is summarized. Helicopter-ship qualification testing, and design and manufacture of large wind-tunnel models are described. Activities of the Netherlands Agency of Aerospace Programs, and international cooperation such as the Advisory Group for Aerospace Research and Development, the German Dutch Windtunnel, European Transonic Windtunnel, the Group for Aeronautical Research and Technology in Europe and cooperation with Indonesia are discussed. Author (ESA)

N86-10586# Shock and Vibration Information Center (Defense), Washington, D. C.

EDITORS RATTLE SPACE
Ronald E. Eshleman, ed. *In its* The Shock and Vibration Digest, Vol. 17, No. 3 Mar. 1985 p 2 (For primary document see N86-10565 01-39)
Avail: SVIC, Code 5804, Naval Research Lab., Washington, D.C. 20375 CSCL 05/2

88 SPACE SCIENCES (GENERAL)

No abstracts in this category.

89 ASTRONOMY

Includes radio and gamma-ray astronomy; celestial mechanics; and astrometry.

N86-11092 Wyoming Univ., Laramie.
THE TWO MICRON SPECTRUM OF R SCUTI Ph.D. Thesis
David Mozurkewich 1984 195 p
Avail: Univ. Microfilms Order No. DA8508874

High-resolution two micron spectrograms of R Scuti, the brightest RV Tauri variable, were obtained to study the mass loss rate and the kinematics of the star's circumstellar material. These observations include atomic lines as well as molecular bands of CO, H2O and OH. There are four major results of this research. (1) The atomic velocities execute a continuous velocity curve with a period of 145 days, twice the period of the discontinuous velocity curve determined from the visible spectrum. (2) The star is surrounded by two circumstellar layers. One is at a temperature of 2200K and is falling toward the star at 13 Km/s. The second is at 1000K and is stationary. The mass of the infalling layer is about 10 to the -5 power solar mass. The stationary shell is a factor of ten larger. (3) Atomic and molecular emission are visible in most of the spectra, apparently originating in an extended envelope surrounding the star. This envelope is at approximately 3000K and contains 3 x 10 to the -7 power solar mass. (4) There are occasional outbursts during which material is expelled from the star at less than escape velocity. This material presumably fuels both the infalling layer of CO and the circumstellar emission.
Dissert. Abstr.

N86-11093 Brandeis Univ., Waltham, Mass.
RADIO STUDIES OF A COMPLETE SAMPLE OF QUASARS Ph.D. Thesis
Robert Ira Potash 1985 195 p
Avail: Univ. Microfilms Order No. DA8509832

Fifty-seven quasars were observed with the NRAO 3 element interferometer. Fifty-two of the quasars comprise a complete radio/optical sample, consisting of all quasars in a particular area of sky with radio and optical flux denities above specified limits (Schmidt 1976). Radio structures were determined at lambda 3.7 and 11.1 cm. These data were combined with data from other complete samples to perform statistical studies of quasar linear sizes. The correlation between size and redshift is demonstrated. The quasar distribution is assumed separable into a space density function, optical, and radio (color) distributions. These distributions are derived for different linear size ranges. The results favor but do not prove an underlying size-radio luminosity relation.
Dissert. Abstr.

N86-11094# Royal Observatory, Edinburgh (Scotland).
OPTICAL/IR TELESCOPE ARRAYS: A STUDY OF THEIR POTENTIAL FOR SATISFYING OBSERVATIONAL REQUIREMENTS IN ASTRONOMY FOR A LARGE APERTURE SYSTEM IN THE 1990s AND BEYOND
C. M. Humphries, D. J. Walshaw, V. C. Reddish, and A. H. Greenaway 1984 140 p refs
(Rept-15; ISSN-0309-099X) Avail: NTIS HC A07/MF A01

The diffuse light received from the sky background and the angular proximity of resolved faint sources both act as constraints against which astronomical observations are made. Existing ground-based optical telescopes operate successfully at source faintness levels where at visible wavelengths the signal to be extracted is only about one per cent of that due to the sky background. At infrared wavelengths, where sky background levels are much higher, sky-chopping allows this ratio to be extended to approx. 10 to 3d power - 10 to the 6th power. The rate at which such information can be obtained is determined almost entirely by telescope aperture and it is unlikely that telescopes being used today will continue to satisfy observational needs. Large aperture optical telescopes improve angular resolution. The sensitivity (i.e., limiting magnitude) at which ground-based interferometric measurements are made, is also dependent on telescope aperture, whereas angular resolution is determined by the length of the baseline between separate phased apertures. With an array (or multiple-mirror) telescope, the aperture synthesis technique used routinely in radioastronomy becomes a possibility also at optical and infrared wavelengths.
F.M.R.

N86-11095*# Alabama Univ., Birmingham. Dept. of Physics.
THEORETICAL ANALYSIS OF WOLTER/LSM X-RAY TELESCOPE SYSTEMS Final Report, 1 Oct. 1984 - 26 May 1985
D. L. Shealy and S. Chao 26 May 1985 57 p refs
(NASA Order H-78183-B)
(NASA-CR-176244; NAS 1.26:176244) Avail: NTIS HC A04/MF A01 CSCL 03A

A ray tracing analysis has been performed for the spectral slicing zoom X-ray telescope for configurations in which a convex layered synthetic microstructure (LSM) optic is placed in front of the prime focus or a concave LSM optic is placed behind the prime focus. The analysis has considered the geometrical shape of the LSM optic to be either a hyperboloid, sphere, ellipsoid or constant optical path aspheric element for two configurations of the glancing incidence X-ray telescope: the ATM Experimental S-056 Wolter I system and the Stanford/MSFC Wolter-Schwarzchild nested system. For the different systems the RMS blur circle radii, the point spread function (PSF), the full width half maximum (FWHM) of the PSF have been evaluated as a function of field angle and magnification of the secondary to determine resoluton of the system. The effects of decentration and tilt of the selected LSM element on the performance of the system have been studied to determine mounting and alignment tolerances.
B.W.

N86-11096# European Space Agency, Paris (France).
COLLOQUIUM ON KILOMETRIC OPTICAL ARRAYS IN SPACE
N. Longdon, ed. and O. Melita, ed. Apr. 1985 196 p refs Proc. held at Cargese, Corsica, 23-25 Oct. 1984; sponsored by ESA and Centre d'Etudes et de Recherches Geodynamiques et Astronomiques
(ESA-SP-226; ISSN-0379-6566) Avail: NTIS HC A09/MF A01

The use of configurations of two or three satellites to constitute a kilometric optical array in space was discussed. Scientific goals, image reconstruction, aperture synthesis, and lessons from radio astronomy were considered. For individual titles, see N86-11097 through N86-11126.

N86-11097# Centre d'Etudes et de Recherches Geodynamiques et Astronomiques, St. Vallier de Thiey (France).
RESULTS AND LIMITATIONS OF GROUND-BASED OPTICAL ARRAYS
A. Labeyrie *In* ESA Colloq. on Kilometric Opt. Arrays in Space Apr. 1985 p 1-6 refs (For primary document see N86-11096 01-89)
Avail: NTIS HC A09/MF A01

The usefulness and limits of ground based interferometers for astronomy are discussed, and current and planned systems are described. While optical arrays do work on the ground, and can probably reach baselines on the order of 300 m, their observing efficiency and limiting magnitude are greatly affected by the turbulent atmosphere, as well as their capability to generate reconstructed images. At a cost comparable to the planned VLT array, floating arrays of two or more small apertures in space can reach higher limiting magnitudes and produce more results in a given time. With large component apertures, and many of them, floating arrays are bound to enormously increase optical penetration into the universe. The wider spectral window in space is also of interest in image reconstruction. Author (ESA)

N86-11098# Padua Univ. (Italy). Ist. di Astronomia.
EXTRAGALACTIC OBSERVATIONS WITH OPTICAL SPACE ARRAYS
E. Bertola *In* ESA Colloq. on Kilometric Opt. Arrays in Space Apr. 1985 p 7-9 refs (For primary document see N86-11096 01-89)
Avail: NTIS HC A09/MF A01

Results achievable by optical arrays in space with resolution of 0.000001 arcsec are assessed from theoretical models predicting small scale features, and VLBI radio domain results. Extragalactic topics which could be investigated by a space interferometer allowing, in addition to high resolution imaging, the possibility of precise measurements of proper motions and parallaxes in nearby galaxies, are reviewed. Objects such as HII regions and supernovae in external galaxies, as well as the broad line region in Seyfert's and QSO's are good candidates for interferometric observations, while interesting effects caused by gravitational lenses can be detected. Author (ESA)

N86-11099# Cambridge Univ. (England). Inst. of Astronomy.
ASTRONOMICAL CRITERIA FOR INTERFEROMETRIC ARRAYS
Edward Kibblewhite *In* ESA Colloq. on Kilometric Opt. Arrays in Space Apr. 1985 p 13-16 (For primary document see N86-11096 01-89)
Avail: NTIS HC A09/MF A01

The effect of Michelson stellar interferometric arrays on spacecraft design is discussed. Almost all sources that can be resolved by kilometer baseline interferometers are bright. Most active galaxies and QSO's contain a compact object which enables the amplitude and phase of features in weak spectral lines to be measured to a few per cent even with the simplest spacecraft. Many of the most interesting stars and binary systems need at least kilometer baselines to obtain adequate spatial resolution across their disks but also rotate with periods of hours or days. This greatly complicates the design of the spacecraft and means two telescope interferometers may only have limited usefulness in obtaining star spot pictures. However, accurate diameters can be measured in a few hours and the spacecraft could obtain submicroarcsecond astrometry on certain classes of object. Other considerations dictate the use of high orbits and relatively long observation times for first generation interferometers in space. Author (ESA)

N86-11100# Paris VII Univ. (France).
HIGH ANGULAR RESOLUTION IN THE INFRARED: PROSPECTS FOR SPACE OBSERVATIONS
P. Lena *In* ESA Colloq. on Kilometric Opt. Arrays in Space Apr. 1985 p 17-21 refs (For primary document see N86-11096 01-89)
Avail: NTIS HC A09/MF A01

The growth of high angular resolution (sub arc second) programs in infrared astronomy (from 1 to 1000 microns) is discussed. Ground based programs (speckle or two-telescope interferometry) are reviewed. It is shown that interferometry in space will improve the sensitivity, extend the wavelength coverage, and open a new field in astrophysics, even with current detector and system performances, and with only a 50 m baseline. Author (ESA)

N86-11101# Centre d'Etudes et de Recherches Geodynamiques et Astronomiques, St. Vallier de Thiey (France).
STRATEGY FOR THE DEVELOPMENT OF SPACE ARRAYS
A. Labeyrie *In* ESA Colloq. on Kilometric Opt. Arrays in Space Apr. 1985 p 23-25 refs (For primary document see N86-11096 01-89)
Avail: NTIS HC A09/MF A01

The development of large telescopes in space is discussed. Rigid and floating arrays are attractive. For a modest price increase, a four aperture floating array is much faster, more reliable, and considerably facilitates image reconstruction. Rather than waiting for support from the space agencies, a World Agency for Space Observatories should be created and provided with funds for developing space arrays. Technology tests should start as soon as possible aboard shuttle flights. Author (ESA)

N86-11102# Centre d'Etudes et de Recherches Geodynamiques et Astronomiques, St. Vallier de Thiey (France).
TRIO: A KILOMETRIC ARRAY STABILIZED BY SOLAR SAILS
A. Labeyrie, B. Authier, Th. Degraauw, E. Kibblewhite, and G. Weigelt *In* ESA Colloq. on Kilometric Opt. Arrays in Space Apr. 1985 p 27-33 refs (For primary document see N86-11096 01-89)
Avail: NTIS HC A09/MF A01

A spaceborne optical array (TRIO) consisting of 2 to 4 telescopes spaced up to 1000 m apart, at Lagrange point 5 of the Earth-Moon trajectory is described. For kilometric baselines and variable aperture patterns allowing image reconstructions, TRIO has free flying telescopes and a focal station. Small solar sails point and stabilize the system. Electrostatic mounts support the telescopes. Many apertures can be utilized in later versions. Author (ESA)

N86-11103*# National Aeronautics and Space Administration. Goddard Space Flight Center, Greenbelt, Md.
SAMSI: AN ORBITING SPATIAL INTERFEROMETER FOR MICRO-ARC SECOND ASTRONOMICAL OBSERVATIONS
R. V. Stachnik (Harvard Smithsonian Center for Astrophysics, Cambridge, Mass.) and D. Y. Gezari *In* ESA Colloq. on Kilometric Opt. Arrays in Space Apr. 1985 p 35-42 refs (For primary document see N86-11096 01-89)
(Contract NASw-3755; Grant NsG-7176)
Avail: NTIS HC A09/MF A01 CSCL 03A

The concept and performance of (SAMSI) Spacecraft Array for Michelson Spatial Interferometry, an orbiting spatial interferometer comprised of three free-flying spacecraft, two collector telescopes and a central mixing station are described. In the one-dimensional interferometry mode orbits exist which provide natural scanning of the baseline. These orbits place extremely small demands on thrusters and fuel consumption. Resolution of 0.00001 arcsecond and magnitude limits of mv = 15 to 20 are achievable in a single orbit. In the imaging mode, SAMSI could synthesize images equivalent to those produced by equal diameter filled apertures in space, making use of the fuel resupply capability of a space station. Simulations indicate that image reconstruction can be performed with milliarcsecond resolution to a visual magnitude 12 in 12 hr of spiral scanning integration time. Author (ESA)

N86-11104*# Harvard-Smithsonian Center for Astrophysics, Cambridge, Mass.
COSMIC: A HIGH RESOLUTION, LARGE COLLECTING AREA TELESCOPE
W. A. Traub and N. P. Carleton *In* ESA Colloq. on Kilometric Opt. Arrays in Space Apr. 1985 p 43-48 refs (For primary document see N86-11096 01-89)
(Grant NsG-7176)
Avail: NTIS HC A09/MF A01 CSCL 03A

The spaceborne Coherent Optical System of Modular Imaging Collectors (COSMIC) is presented. It has high angular resolution and can produce images of complex, low-surface-brightness objects such as distant galaxies. If configured as a 36 m filled linear array, COSMIC can have 15 times better angular resolution and 10 times greater collecting area than the Space Telescope. Alternatively, if the collecting area is spread out to create an unfilled two-dimensional array, there is the additional advantage of not needing to rotate the array in order to build up a reconstructed image. Considerations which led to the design concept, scientific goals, and the potentially useful role of a space station for assembly are discussed. Author (ESA)

N86-11105# Centre National de la Recherche Scientifique, Verrieres-Le Buisson (France). Service d'Aeronomie.
A FIBER-LINKED VERSION OF PROJECT TRIO
P. Connes, Cl. Froehly (Limoges University, France), and P. Facq (Limoges University, France) *In* ESA Colloq. on Kilometric Opt. Arrays in Space Apr. 1985 p 49-61 refs (For primary document see N86-11096 01-89)
Avail: NTIS HC A09/MF A01

It is shown that the TRIO spaceborne telescope array can be simplified by using two equal-length single-mode fibers to connect the two telescopes to the central station. The price to be paid is mostly a reduction of base-length at the short wavelength end of the spectrum. The number of parameters to be accurately controlled is much reduced: one merely has to guide telescopes and null path-difference. All motions of the central station become irrelevant. Star acquisition is performed in a docked configuration of all three elements. The necessary cables may also be used to feed power to the two telescopes; hence these require neither power generating nor propulsion devices. Possible base line scanning methods either in high orbits (e.g., at the Lagrange points) or in low orbits are discussed. Author (ESA)

N86-11106# Royal Greenwich Observatory, Herstmonceux (England).
OASIS: OPTICAL APERTURE SYNTHESIS IN SPACE
J. E. Noordam, P. D. Atherton (Groningen University, Netherlands), and A. H. Greenaway (Royal Signals and Radar Establishment, Malvern, UK) *In* ESA Colloq. on Kilometric Opt. Arrays in Space Apr. 1985 p 63-69 (For primary document see N86-11096 01-89)
Avail: NTIS HC A09/MF A01

Techniques necessary to accomplish optical aperture synthesis in space (OASIS) are described. The purpose of OASIS is to obtain reliable, high resolution images of astronomical sources, in emission lines, absorption lines, and the continuum, with high dynamic range. Redundant spacing calibration allows the identification of phase and amplitude errors associated with a particular telescope in an array. This requires the separate availability of the visibility phase and amplitude for all interferometers (telescope pairs). Issues which determine the design and feasibility of the technique are discussed. Author (ESA)

N86-11107# Perkin-Elmer Corp., Danbury, Conn.
FUTURE SPACE TELESCOPE DESIGN CONCEPTS
Alan N. Bunner *In* ESA Colloq. on Kilometric Opt. Arrays in Space Apr. 1985 p 71-76 refs (For primary document see N86-11096 01-89)
Avail: NTIS HC A09/MF A01

Five generically-different approaches to a high resolution, high sensitivity space telescope covering the options of focal and afocal collectors, filled apertures and dilute apertures and one-dimensional and two-dimensional arrays are described. These concepts are compared, given equal collecting area and equal observing time, on the basis of angular resolution and sensitivity to faint point sources and extended sources in the presence of photon statistics, zodical background light, and other sources in the field. Technology development issues involved in the realization of advanced telescopes are listed. Author (ESA)

N86-11108# Centre National de la Recherche Scientifique, Marseilles (France). Lab. d'Astronomie Spatiale.
TRIO OPTICS
B. Authier, P. Rabout, and A. Labeyrie *In* ESA Colloq. on Kilometric Opt. Arrays in Space Apr. 1985 p 79-84 refs (For primary document see N86-11096 01-89)
Avail: NTIS HC A09/MF A01

The optical train of the TRIO spaceborne stellar interferometer is discussed. Thermal variation and their effect on the Cassegrain telescopes are calculated. Designs for the beam recombiner in the central station are considered. The main difficulty is to utilize efficiently the wide spectral range available, with a 2-D formatting of the fringe information versus wavelength, using as few pixels as possible. Stray light in the coude beams, generated by structure lighting rather than by meteoritic dust, may affect the limiting magnitude if it is not efficiently baffled. Author (ESA)

N86-11109# Centre National de la Recherche Scientifique, Marseilles (France).
SOLAR PROPULSION FOR THE TRIO INTERFEROMETER [PROPULSION SOLAIRE POUR L'INTERFEROMETRE TRIO]
J. L. Boit *In* ESA Colloq. on Kilometric Opt. Arrays in Space Apr. 1985 p 85-90 refs In FRENCH; ENGLISH summary (For primary document see N86-11096 01-89)
Avail: NTIS HC A09/MF A01

A solar sailing device was designed to cope with the large displacement and high accuracy positioning of each of the three satellites of the TRIO interferometer, which require a long-service-life, clean, modulated propulsion system. The six Euler movements must be uncoupled. An articulated link between the solar sail and the satellite is necessary, and electrostatic devices are proposed. Problems related to mechanics, thermal behavior, celestial mechanics, attitude correction strategy, and positioning error detection, are discussed. Author (ESA)

N86-11110# European Space Agency. European Space Research and Technology Center, ESTEC, Noordwijk (Netherlands). Mathematical Support Div.
PRELIMINARY STUDIES OF A SPINNING TETHER-CONNECTED TRIO CONCEPT
E. B. Crellin *In* ESA Colloq. on Kilometric Opt. Arrays in Space Apr. 1985 p 91-94 refs (For primary document see N86-11096 01-89)
Avail: NTIS HC A09/MF A01

Use of a slowly spinning interferometer configuration with the telescopes attached to the central station using tethers of equal length, including tether configuration, mass and storage is discussed. Slow rotation allows measurements of each source at different baseline angles. When the maximum baseline length is reached, the tethers can be retracted (stopping at intermediate lengths for further measurements, if required) and the telescopes recaptured by the central station. The attitude change to another source can be performed with the rigid configuration. Author (ESA)

N86-11111# Centre National de la Recherche Scientifique, Marseilles (France). Lab. d'Astronomie Spatiale.
TRIO INTERFEROMETER POSITIONING
B. Authier *In* ESA Colloq. on Kilometric Opt. Arrays in Space Apr. 1985 p 95-97 refs (For primary document see N86-11096 01-89)
Avail: NTIS HC A09/MF A01

The high accuracy positioning of each of the three satellites of the TRIO interferometer, with respect to the others and to the reference stars, is discussed. Based on ground interferometer experience, strategy guidelines are presented with related recommendations for spacecraft design. After star pointing, the two telescopes are aligned with respect to the central station so that the star images are within the central station field of view while optical path difference is smaller than the coherence length. Fine guidance is obtained from image superimposition on the central station focal plane, and from fringe contrast measurement. Author (ESA)

N86-11112# Centre d'Etudes et de Recherches Geodynamiques et Astronomiques, St. Vallier de Thiey (France). Observation de Calern.
FRINGE DRIFT COMPENSATION IN COMPUTER MEMORY
L. Koechlin *In* ESA Colloq. on Kilometric Opt. Arrays in Space Apr. 1985 p 99-105 refs (For primary document see N86-11096 01-89)
Avail: NTIS HC A09/MF A01

Fringe detection and contrast measurement techniques used on a groundbased 6 to 67m baseline Michelson interferometer are described. Very faint object interferometric observation with spacecraft such as TRIO is proposed. Author (ESA)

N86-11113# Centre d'Etudes et de Recherches Geodynamiques et Astronomiques, St. Vallier de Thiey (France). Synthese d'Ouverture Optique.

TRIANGLE: A DIFFERENT DESIGN FOR A THREE SATELLITE INTERFEROMETER IN SPACE

Farrokh Vakili *In* ESA Colloq. on Kilometric Opt. Arrays in Space Apr. 1985 p 107-111 (For primary document see N86-11096 01-89)

Avail: NTIS HC A09/MF A01

A design for the optical and geometrical arrangement of a TRIO-type array made up of three spacecraft is proposed. Instead of having two telescopes and a central station, TRIANGLE consists of three identical satellites, each acting as a telescope and a central station. The satellites are maintained on the summits of an equilateral triangle and provide a triple baseline interferometer. The configuration of the system is presented. Problems concerning the optics, imaging efficiency, and stabilization are discussed. Author (ESA)

N86-11114# European Space Agency. European Space Operations Center, Darmstadt (West Germany).

MISSION ANALYSIS ASPECTS

E. A. Roth *In* ESA Colloq. on Kilometric Opt. Arrays in Space Apr. 1985 p 113-116 refs (For primary document see N86-11096 01-89)

Avail: NTIS HC A09/MF A01

Astrodynamical problems associated with projects where the baseline of the interferometer is represented by two (or more) free-flying satellites are considered. High terrestrial orbits, quasi-periodic orbits around the triangular libration points (L4, L5) in the Earth-Moon system, or orbits near these points in the Earth-Sun system are considered. It is shown that constraints imposed on the baseline and on the attitude control of the satellites require considerably more detailed investigations before the feasibility of the project can be assessed. The number of problems is multiplied if the number of satellites is increased for optical arrays in space. Author (ESA)

N86-11115# Centre d'Etudes et de Recherches Geodynamiques et Astronomiques, St. Vallier de Thiey (France).

PROBLEMS IN IMAGE RECONSTRUCTION WITH OPTICAL ARRAYS

A. Labeyrie *In* ESA Colloq. on Kilometric Opt. Arrays in Space Apr. 1985 p 117-119 refs (For primary document see N86-11096 01-89)

Avail: NTIS HC A09/MF A01

Ways of reconstructing images with space arrays are discussed. With 2 apertures, the 0.1' field makes it difficult to obtain phase information, but the readily available multicolor phases can help phaseless reconstruction algorithms. With three or more apertures, phases are obtained through phase-closure algorithms. A four aperture system for a first generation optical array in space is recommended to reduce observation time. Author (ESA)

N86-11116# Harvard-Smithsonian Center for Astrophysics, Cambridge, Mass.

NUMERICAL EXPERIMENTS IN IMAGE RECONSTRUCTION

M. Faucherre, R. V. Stachnik, and S. Aram (Wellesley College, MA.) *In* ESA Colloq. on Kilometric Opt. Arrays in Space Apr. 1985 p 121-127 refs Sponsored in part by ESA (For primary document see N86-11096 01-89)

Avail: NTIS HC A09/MF A01

An approach to Fourier transform phase recovery which can work for two-element interferometers and does not require a reference star is described. It depends on the fact that, for many small, bounded, realistic sources, the Fourier transform amplitude and phase structure is dominated by the edges. Numerical experiments which illustrate the Fourier amplitude and phase structure associated with realistic sources; produce reconstructions by simple Fourier inversion for sources of varying brightness; simulate degradation in the recovered image due to reference phase errors; and show the consequence of invoking the simplest of a number of more sophisticated image recovery algorithms, phase array relaxation are presented. Author (ESA)

N86-11117# Mullard Radio Astronomy Observatory, Cambridge (England). Cavendish Lab.

RADIO ASTRONOMY EXPERIENCE IN IMAGE RECONSTRUCTION. A HISTORY LESSON FOR OPTICAL ASTRONOMERS

P. J. Warner *In* ESA Colloq. on Kilometric Opt. Arrays in Space Apr. 1985 p 129-131 refs (For primary document see N86-11096 01-89)

Avail: NTIS HC A09/MF A01

The difficulties faced by radio astronomers in reconstructing images without phase information are reviewed. Very long baseline interferometry investigations of the Sun and radio sources show that mistakes can arise if assumptions about brightness distribution are inaccurate. If baselines are not small enough to include all the flux density, objects can be missed. There appear to be fundamental difficulties in reconstructing images of complicated objects without phase. Author (ESA)

N86-11118# Harvard-Smithsonian Center for Astrophysics, Cambridge, Mass.

COSMIC IMAGE RECONSTRUCTION

M. G. Lacasse and W. A. Traub *In* ESA Colloq. on Kilometric Opt. Arrays in Space Apr. 1985 p 133-140 refs (For primary document see N86-11096 01-89)

(Grant NsG-7176)

Avail: NTIS HC A09/MF A01 CSCL 03A

Numerical methods of image reconstruction for use with an orbiting array of optical telescopes in which a rotating rectangular aperture mimics a large circular aperture are discussed. Numerical simulations to test the robustness of algorithms in the presence of photon noise are described. Measures of the quality of the reconstructed image as a function of total photon count are presented. Results of laboratory simulations using relatively bright, complex images and broad band optical filters are also presented. Good quality images are readily reconstructed from the numerical and laboratory simulations. Author (ESA)

N86-11119# Groningen Rijksuniversiteit (Netherlands).

THE OASIS CORRELATOR

P. D. Atherton, A. H. Greenaway (Royal Signals and Radar Establishment, Malvern, UK), and J. E. Noordam (Royal Greenwich Observatory, Hertsmonceux, UK) *In* ESA Colloq. on Kilometric Opt. Arrays in Space Apr. 1985 p 141-144 (For primary document see N86-11096 01-89)

Avail: NTIS HC A09/MF A01

The principle of nonredundant recombination of a redundant array of telescopes is described. The design of the Optical Aperture Synthesis in Space correlator is presented. Advantages of pupil plane over image plane interference are summarized. Author (ESA)

N86-11120# Erlangen-Nuremberg Univ. (West Germany). Inst. fuer Physik.

IMAGING SPECKLE INTERFEROMETER IN SPACE: DIGITAL SIMULATIONS OF IMAGE RECONSTRUCTION AND PHOTON NOISE

K.-H. Hofmann and G. Weigelt *In* ESA Colloq. on Kilometric Opt. Arrays in Space Apr. 1985 p 145-151 refs (For primary document see N86-11096 01-89)

Avail: NTIS HC A09/MF A01

Image reconstruction for the Imaging Speckle Interferometer (ISI) a space-based multiple mirror interferometer which can produce high-resolution images is discussed. At short UV wavelengths a multiple mirror interferometer produces speckle interferograms caused by aberrations of the interferometer. From the speckle interferograms true images can easily be reconstructed with the speckle masking method. In speckle masking no point source is required near the object. Digital simulations of image reconstruction from ISI data, in which various multiple mirror pupil functions and various amounts of photon noise (1000 to 10 photons per pixel) were simulated are shown. Speckle spectroscopy with ISI, and image reconstruction from 2-telescope interferograms are considered. Author (ESA)

N86-11121# Centre d'Etudes et de Recherches Geodynamiques et Astronomiques, St. Vallier de Thiey (France). Observatoire du Calern.

ON LINE ASTRONOMICAL IMAGE PROCESSING USING MICROCOMPUTERS

C. Thom *In* ESA Colloq. on Kilometric Opt. Arrays in Space Apr. 1985 p 153-154 refs (For primary document see N86-11096 01-89)

Avail: NTIS HC A09/MF A01

A microprocessor based system for reducing images on a large astronomical interferometer was built for use as an autocorrelator. It consists of three standard VME boards (two CPU boards and a graphic visualization controller) and a board built for image acquisition. The CPU 1 is a 128 kbyte, MC 68000 with 8 MHz clock. It does photon centroiding and image cleaning; CPU 2 is a 512 kbyte, MC 68000 with 10 MHz clock. It does image autocorrelation and integration, but can be adapted to user needs. The graphic controller is 256 x 256 pixels in 16 colors. Images are stored in two fast flip-flop RAMs to allow the processor to work on the last image without interference with acquisition of the next one.

Author (ESA)

N86-11122# Centre d'Etudes et de Recherches Geodynamiques et Astronomiques, St. Vallier de Thiey (France).

THE INTENSIFIED MULTI CCD CAMERA

A. Blazit *In* ESA Colloq. on Kilometric Opt. Arrays in Space Apr. 1985 p 155-156 (For primary document see N86-11096 01-89)

Avail: NTIS HC A09/MF A01

A photon counting 40 mm diameter TV camera for a space interferometer is described. It is an intensified mosaic of 4 CCD: CCD pixels are subdivided in 4 x 4 subpixels by a photon centroiding processor, yielding a total of 7,000,000 image elements. Its main advantage over a CCD camera is that it does not require perfect compensation of fringe drifts. Author (ESA)

N86-11123# Joint Inst. for Lab. Astrophysics, Boulder, Colo.

SPACE ANTENNA FOR GRAVITATIONAL WAVE ASTRONOMY

J. E. Faller, P. L. Bender, J. L. Hall, D. Hils, and M. A. Vincent *In* ESA Colloq. in Kilometric Opt. Arrays in Space Apr. 1985 p 157-163 refs Prepared in cooperation with National Bureau of Standards, Boulder, Colorado (For primary document see N86-11096 01-89)

Avail: NTIS HC A09/MF A01

Designs for a laser gravitational wave antenna in space using free test masses and heterodyne (interferometric) detection were investigated. Use of 1 million km baselines between three spacecraft in nearly circular 1 yr solar orbit is considered. With milliwatt-transmitted laser power levels and 50 cm diameter optics, a strain sensitivity of 10 to the minus 19th power per sq root Hz over at least the period range from 10 to 10,000 sec is feasible. The measurements observe gravitational radiation associated with present or past interactions of supermassive objects. Binary sources can also be studied. For periods <10 sec the sensitivity for a baseline length of 1 million km degrades as a result of multiple gravitational wavelengths being contained in the arm lengths. For longer periods, the main limitation is likely to come from spurious accelerations due to forces other than the gravitational attraction of the Sun and planetary bodies.

Author (ESA)

N86-11124# Centre National de la Recherche Scientifique, Toulouse (France).

APERTURE SYNTHESIS WITH OR WITHOUT PHASE INFORMATION FOR KILOMETRIC ARRAYS INTERPOLATION ALGORITHMS FOR STABILIZED IMAGE RECONSTRUCTION

A. Lannes *In* ESA Colloq. on Kilometric Opt. Arrays in Space Apr. 1985 p 165-169 refs (For primary document see N86-11096 01-89)

Avail: NTIS HC A09/MF A01

Reconstructing high resolution images from a sparsely sampled two dimensional frequency plane with synthetic aperture spaceborne interferometers is discussed. At the cost of compromise between resolution and robustness, the problem must be stated in terms of interpolation. Using the steepest descent method a very simple and powerful algorithm for interpolation with or without phase data is introduced. The constraint of nonnegativity on limited field is taken into consideration. The Fienup algorithm can be retrieved as a special case and improved by modifying its constraint operator and the implicit choice of its relaxation parameter.

Author (ESA)

N86-11125# Centre d'Etudes et de Recherches Geodynamiques et Astronomiques, St. Vallier de Thiey (France).

THE DUO: FAR INFRARED HETERODYNE CONCEPT FOR SPACE INTERFEROMETRY

J. Gay and Y. Rabbia *In* ESA Colloq. on Kilometric Opt. Arrays in Space Apr. 1985 p 171-176 refs (For primary document see N86-11096 01-89)

Avail: NTIS HC A09/MF A01

The direct Michelson technique and heterodyning are compared for spaceborne far infrared interferometer design. Constraints for space interferometry are recalled. The high spectral selectivity; diffraction-limited field of view; handling of electrical signals for correlation; low sensitivity to background radiation; and heavy and sophisticated equipment involved in heterodyning are discussed. The greatest advantage of heterodyning is the need for two satellites instead of three. Author (ESA)

N86-11126# California Inst. of Tech., Pasadena.

VLBI AT OPTICAL AND RADIO WAVELENGTHS: CONGRUENCES AND CONTRASTS

Bernard F. Burke *In* ESA Colloq. on Kilometric Opt. Arrays in Space Apr. 1985 p 177-183 refs (For primary document see N86-11096 01-89)

Avail: NTIS HC A09/MF A01

It is pointed out that conceptually there are few distinctions between aperture synthesis interferometry at radio, infrared, or optical wavelengths, and the experience and software developed in the radio domain should be largely applicable to the optical case. Coherence time is a vital consideration for radio and optical cases. Radio VLBI practice requires use of phase closure and amplitude closure relations; this may be the case for optical interferometric systems as well. This means that the optical aperture synthesis interferometer will consists of many elements. In the near term (10 to 20 yr) there will be orbiting devices; if a manned lunar base is established, an optical equivalent of the VLA might be constructed and operated on the Moon. Author (ESA)

90 ASTROPHYSICS

Includes cosmology; and interstellar and interplanetary gases and dust.

N86-11127 Texas Univ., Austin.

A METHOD FOR NUMERICAL RELATIVITY: SIMULATION OF AXISYMMETRIC GRAVITATIONAL COLLAPSE AND GRAVITATIONAL RADIATION GENERATION Ph.D. Thesis

Charles Ross Evans, II 1984 285 p

Avail: Univ. Microfilms Order No. DA8508264

A method is presented which allows fully self-consistent numerical simulation of asymptotically flat axisymmetric nonrotating general relativistic systems. These techniques have been developed to model and understand resulting relativistic effects in gravitational core collapse and gravitational radiation generation. Both vacuum (Brill) spacetimes and matter-filled configurations can be treated. The (3 + 1) decomposition of Arnowitt, Deser and Misner is used to write general relativity in a dynamical form. The conformal approach, including the transverse-traceless decomposition of extrinsic curvature due to York, is used to solve the initial value problem. In addition, these techniques are extended to provide a fully constrained evolution scheme. Several new boundary conditions, applied at large but finite radius, are derived for the elliptic constraint equations. This method uses a simplifying

three-gauge, placing the metric in quasi-isotropic form.
Dissert. Abstr.

N86-11128 Texas Univ., Austin.
INITIAL DATA FOR N BLACK HOLES Ph.D. Thesis
Anil Dattatray Kulkarni 1984 111 p
Avail: Univ. Microfilms Order No. DA8508294

The N-body problem in general relativity is of enormous difficulty, especially in the nonlinear regime where radiation is important. It is now possible to study this problem by treating it as a Cauchy problem and by using large-scale computers to develop numerical models. With this motivation, the Cauchy formulation of Einstein equations is described. It consists of the Hamiltonian and momentum constraint equations, and the evolution equations. The constraints are analyzed using the conformal technique. The first step in this approach is to set up initial data compatible with the constraints. The N-body data, in general, will depend on the stress-energy tensor of the bodies. Hence this issue is bypassed by considering the matter free representation of particles in terms of the geometries of certain non-Euclidean manifolds, such as the Einstein-Rosen manifold M sub n and the (N + 1)-sheeted manifold (sigma sub-n). Among these possibilities, the Einstein-Rosen manifold is of special interest because of its symmetry.
Dissert. Abstr.

N86-11129 Boston Univ., Mass.
GRAVITATIONAL COLLAPSE OF A SCALAR FIELD Ph.D. Thesis
Tara Maithreyan 1985 90 p
Avail: Univ. Microfilms Order No. DA8508916

A self-similar collapse of massless scalar waves is considered, and the Einstein field equations in classical general relativity are solved to obtain the metric for the collapse. These scalar waves satisfy the massless wave equation and the energy momentum tensor associated with them is derived from their Lagrangian density. The collapse begins at t = 0 before which spacetime is flat, empty spacetime described by the Minkowski metric. Self similarity assumes that a homothetic Killing vector exists for the collapse, which satisfies the corresponding homothetic Killing equation. The solution obtained contains a constant c2 whose value determines the nature of the collapse and the kind of singularity formed by the collapsing scalar waves. The three different cases are outlined and the corresponding Penrose diagrams are given. The apparent horizons, defined by Hawking as the limit of the trapped surfaces surrounding the singularity are calculated for each case.
Dissert. Abstr.

N86-11130 Washington Univ., Seattle.
PHYSICAL CONDITIONS IN GIANT EXTRAGALACTIC H2 REGIONS Ph.D. Thesis
Evan David Skillman 1984 223 p
Avail: Univ. Microfilms Order No. DA8508091

Giant Extragalactic H2 Regions (GEHRs) in nearby galaxies have been observed at both radio and optical wavelengths. Narrow band optical imaging, large and small aperture optical spectrophotometry, radio continuum imaging at lambda 6 cm and lambda 21 cm, and lambda 21 cm H1 spectral line mapping have been employed to investigate the point to point variations of the physical conditions within and surrounding the GEHRs. Measurement of reddening and extinction were found to be strongly dependent on resolution. Variations in extinction as measured by the optical method were not found to correlate with those measured with the optical-radio method. In at least one case this was due to the presence of a nonthermal radio continuum source. Significant differences in optical line strength ratios exist between different points in a single GEHR. These differences point to variations of the physical conditions within the GEHR.
Dissert. Abstr.

N86-11131 Princeton Univ., N. J.
THE DYNAMICS AND STELLAR CONTENT OF GLOBULAR STAR CLUSTERS Ph.D. Thesis
Robert Hugh Lupton 1985 175 p
Avail: Univ. Microfilms Order No. DA8509640

Models are rpesented of rotating globular clusters with an anisotropic velocity dispersion, based upon the assumption that the total angular momentum is a good integral even for systems with slightly flattened potentials. Such models are given of the cluster M13 and M29, using both photometry and stellar radial velocities to constrain the fits. It is shown that the data is satisfactorily represented by models with anisotropy radii of about 5 and 20 core radii respectively, and mass functions of Salpeter index about 2.25. These models predict mass segregation, with the lighter stars which contribute a negligible proportion of the light being found futher from the cluster center. A computer program is presented to do star counts in crowded fields complete to about 23.5th magnitude, and the conversion from the Gunn gri photometric system to mass for pop 2 main sequence stars, based on published infrared photometry. To within the errors in the star counts no evidence is found of mass segregation, which is consistent with the published models of M3 and the model presented for M13.
Dissert. Abstr.

N86-11132 Pittsburgh Univ., Pa.
ELECTRON-ION RECOMBINATION STUDIES OF PLANETARY IONOSPHERIC AND ASTROPHYSICAL IONS Ph.D. Thesis
Bishwajit Ganguli 1984 104 p
Avail: Univ. Microfilms Order No. DA8511040

The rates of rcombination of HCO +, H2CN + and H2CN + HCN ions with electrons were determined as a function of electron temperature T sub e using a microwave afterglow/mass spectrometer apparatus employing microwave electron heating. In addition, an investigation was carried out to obtain qualitatively the inelastic energy loss frequency Nu sub e sup' inel (T sub e) of electrons in dilute N2-Ne mixtures using microwave techniques.
Dissert. Abstr.

N86-11133*# Atmospheric and Environmental Research, Inc., Cambridge, Mass.
COMETARY ATMOSPHERES: MODELING THE SPATIAL DISTRIBUTION OF OBSERVED NEUTRAL RADICALS Interim Report, Jun. - Aug. 1985
Michael R. Combi Oct. 1985 8 p refs
(Contract NASw-3950)
(NASA-CR-176242; NAS 1.26:176242) Avail: NTIS HC A02/MF A01 CSCL 03B

The analysis of observed brightness profiles for the C2 radical in comets with Haser's model implies that the parent scale length varies as the square of the heliocentric distance. The use of new Haser scale lengths for C2 and CN determined under this project appears to explain the apparent drop in the C2-to-CN ratio with increasing heliocentric distance.
Author

N86-11134# California Univ., Livermore. Lawrence Livermore Lab.
STELLAR s-PROCESS DIAGNOSTICS
G. J. Mathews, R. A. Ward, K. Takahashi, and W. M. Howard May 1985 10 p Presented at the 20th Recontre de Moriond, Les Arcs, France, 10 Mar. 1985
(Contract W-7405-eng-48)
(DE85-012926; UCRL-92724; CONF-850375-5) Avail: NTIS HC A02/MF A01

The solar-system sigma-N curve is best understood if the s-process is largely produced by stars in the mass range of M approx. 2 to 4 M0. Observations were studied as indicators of the validity of this hypothesis. It is found that isotopic Zr abundances and elemental (Ba/Sr) vs (Ba/Nd) ratios are consistent with these conditions. It is found that the elemental (Tc/Nb) ratio is not an indicator of temperature as was suggested but rather a measure of the age of an AGB star in the third dredge-up phase.
DOE

N86-11135# European Southern Observatory, Munich (West Germany).
[ACTIVITIES REPORT OF THE EUROPEAN SOUTHERN OBSERVATORY] Annual Report, 1984
1985 86 p refs In ENGLISH, FRENCH, and GERMAN Original contains color illustrations

Avail: NTIS HC A05/MF A01

Observations of a ring around Neptune, Halley's comet, asteroids, stellar atmospheres, stellar chromospheres, stellar oscillations, binary stars, the interstellar medium, and galaxies are summarized. Gamma, X-ray, infrared, ultraviolet, and satellite-borne astronomy are discussed. Facilities at the European Southern Observatory are described. Author (ESA)

91 LUNAR AND PLANETARY EXPLORATION

Includes planetology; and manned and unmanned flights. For spacecraft design see *18 Spacecraft Design Testing, and Performance.* For space stations see *15 Launch Vehicles and Space Vehicles.*

N86-11136 Arizona State Univ., Tempe.
CONTEMPORARY AEOLIAN PROCESSES ON MARS: LOCAL DUST STORMS Ph.D. Thesis
Alan Richard Peterfreund 1985 263 p
Avail: Univ. Microfilms Order No. DA8510680

Local and major dust storms play a dominant role in contemporary aeolian processes on Mars. As a means of better documenting the role of dust storms on the surface, a record of their occurrence during the four years of the Viking Mission has been established using thermal infrared and visual observations. The dust storm record was then compared to observations of the Martian surface. Particle transport, source region characteristics, and effects of dust storms, proximal and distal to their source are considered for both the Earth and Mars. Basic elements necessary for a dust storm on Earth and Mars (i.e., adequate winds, sufficient sediment supply, and surface susceptible to erosion) are similar. The frequency, intensity, and geologic impact of dust storms, however, differ due to variations in these elements. On Mars, large temporal and spatial variations in atmospheric pressure and temperature are the primary control. On Earth, sediment supply and surface conditions appear to be the more variable factors. On both planets these conditions are related to climatic cycles. Dissert. Abstr.

N86-11137*# Jet Propulsion Lab., California Inst. of Tech., Pasadena.
GALILEO: EXPLORATION OF JUPITER'S SYSTEM
T. V. Johnson, C. M. Yeates, L. Colin (NASA. Ames Research Center), F. P. Fanale (Hawaii Univ.), L. Frank (Iowa Univ.), and D. M. Hunten (Arizona Univ.) Jun. 1985 179 p refs
(NASA-SP-479; NAS 1.12/6:479) Avail: NTIS HC A09/MF A01 CSCL 03B

The scientific objectives of the Galileo mission to the Jovian system is presented. Topics discussed include the history of the project, our current knowledge of the system, the objectives of interrelated experiments, mission design, spacecraft, and instruments. The management, scientists, and major contractors for the project are also given. Author

N86-11138*# National Aeronautics and Space Administration. Goddard Space Flight Center, Greenbelt, Md.
PHOTOGRAPHIC CATALOG OF SELECTED PLANETARY SIZE COMPARISONS
Stephen Paul Meszaros Sep. 1985 130 p refs
(NASA-TM-86207; Rept-85B0346; NAS 1.15:86207) Avail: NTIS HC A07/MF A01 CSCL 03B

Photographs taken by NASA spacecraft, and cartographic products based on these photos, are used to illustrate size comparisons of the planets and moons of the solar system. Global views and prominent geographical features are depicted at the same scale, allowing size relationships to be studied visually. Author

N86-11139*# Jet Propulsion Lab., California Inst. of Tech., Pasadena.
A MODELING ANALYSIS PROGRAM FOR THE JPL TABLE MOUNTAIN Io SODIUM CLOUD Interim Report, 1 Jun. - 31 Aug. 1985
William H. Smyth (Atmospheric and Environmental Research, Inc., Cambridge, Mass.) and Bruce A. Goldberg Dec. 1984 23 p refs
(Contract NASw-3949)
(NASA-CR-176241; NAS 1.26:176241) Avail: NTIS HC A02/MF A02 CSCL 03B

A data quality review for the entire set of the 1981 Region B/C images has been completed and is presented. The review indicates that almost all images are of sufficient quality to be valuable in our analysis of this data set. Five data-correlation studies for the same data set have also been completed and are useful in classifying and studying the sodium cloud morphology and its interactions with solar radiation pressure and the plasma torus. Additional progress in developing new image processing techniques and in improving the Io sodium cloud model is also discussed. Author

N86-11140# Technische Univ., Berlin (West Germany). Inst. fuer Luft- und Raumfahrt.
A LOGISTICS SCENARIO FOR AN EARLY LUNAR BASE
H. H. Koelle and B. Johenning 10 Dec. 1984 47 p refs
(ILR-Mitt-143) Avail: NTIS HC A03/MF A01

Mission, base, and logistics models were used to assess the feasibility of a lunar base. It is shown that a heavy lift launch vehicle (HLLV) using the present space shuttle main engine can serve as the backbone of such a lunar logistics system. A typical launch schedule reaching 24 flights in its 7th operational year is developed. This HLLV can carry 300 metric tons to the 530Km space station orbit or 70 metric tons directly to the lunar surface. The lunar base model suggests landing the first 20 people on the Moon in 1999 and reaches a level of 120 people on the lunar base, plus 20 people in lunar orbit in its 8th year of operation. The lunar base facilities have a total mass of 4000 metric tons in its 10th year. Author (ESA)

92 SOLAR PHYSICS

Includes solar activity, solar flares, solar radiation and sunspots.

N86-11141*# National Aeronautics and Space Administration. Goddard Space Flight Center, Greenbelt, Md.
DIRECTIONALITY OF BREMSSTRAHLUNG FROM RELATIVISTIC ELECTRONS IN SOLAR FLARES
Charles D. Dermer and Reuven Ramaty Sep. 1985 40 p refs
Submitted for publication
(NASA-TM-87509; NAS 1.15:87509) Avail: NTIS HC A03/MF A01 CSCL 03B

Angular and energy spectra of bremsstrahlung have been calculated from anisotropic electron distributions in solar flares. Results have been compared to observations of gamma-ray limb-brightening and to data on the variation of the gamma-ray spectrum with flare position on the sun. Author

N86-11142# Louisiana State Univ., Baton Rouge. Dept. of Physics and Astronomy.
SOLAR FLARES AND MAGNETOSPHERIC PARTICLES: INVESTIGATIONS BASED UPON THE ONR-602 EXPERIMENT Annual Letter Report, 1 Apr. 1984 - 30 Jun. 1985
J. P. Wefel 28 Jun. 1985 14 p
(Contract N00014-83-K-0365)
(AD-A156583) Avail: NTIS HC A02/MF A01 CSCL 03/2

The work performed during the past year can be divided into three areas: (1) data reduction/processing and instrument response; (2) solar flare studies, and (3) magnetospheric particles. Our analysis effort had been divided between obtaining an overview of the entire ONR-602 (Phenix 1) dataset, identifying data processing/analysis problems and locating scientifically interesting effects for additional study, and studying specific areas or fully understand the operation of the ONR-602 instrument in the space environment and the complicated particle flux variations over the spacecraft orbit. GRA

93 SPACE RADIATION

Includes cosmic radiation; and inner and outer Earth's radiation belts.

For biological effects of radiation see *52 Aerospace Medicine*. For theory see *73 Nuclear and High-Energy Physics*.

N86-11143 New Hampshire Univ., Durham.
SOLAR MODULATION OF GALACTIC COSMIC RAYS: TECHNIQUES AND APPLICATIONS Ph.D. Thesis
John Steven Perko 1984 78 p
Avail: Univ. Microfilms Order No. DA8510482

The time dependent, spherically symmetric, solar modulation of galactic cosmic rays is discussed. A numerical technique was introduced for the solution of this problem. A model for the solar cycle variation in cosmic ray intensity illustrated this method, using enhanced particle scattering regions. An attempt to explain recent observations which show that cosmic ray electrons are returning to higher intensities, characteristic of solar minimum, faster than cosmic ray protons of about the same energy, the reverse of the previous eleven year cycle is presented. The solar modulation of galactic antiprotons is explained. It appears that a recent low energy measurement of these particles has given cosmic ray theorists trouble devising an interstellar spectrum to fit the observations. A spherically symmetric, stead state calculation of the effects of a strong termination shock in the heliosphere is also presented. The overall effect of a shock on the near-Earth spectra seems negligible. Dissert. Abstr.

N86-11144 Rutgers - The State Univ., New Brunswick, N. J.
EXTRA-GALACTIC X-RAY SOURCES AND THE DIFFUSE X-RAY BACKGROUND Ph.D. Thesis
Chris R. Shrader 1985 170 p
Avail: Univ. Microfilms Order No. DA8510828

The source of the isotropic, diffuse X-ray background (DXRB) is considered in the context of observational data obtained by the HEAO-1 and HEAO-2 spacecraft. Attempts are made to determine the contribution to the DXRB by unresolved discrete sources. Several different approaches are followed. QSO optical and X-ray luminosities were correlated and optical luminosity functions were used to estimate faint X-ray counts. Results are consistent with those previously published. Dissert. Abstr.

99 GENERAL

No abstracts in this category.

SUBJECT INDEX

SCIENTIFIC AND TECHNICAL AEROSPACE REPORTS VOLUME 24 NUMBER 1

Typical Subject Index Listing

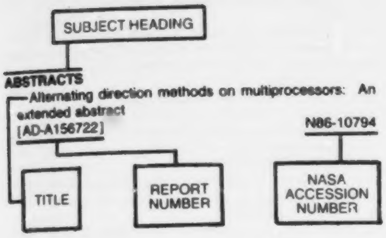

The subject heading is the key to the subject content of the document. Titles, report numbers, and accession numbers of pertinent documents are provided under each subject heading. When the title is insufficiently descriptive of the document content, a title extension has been added, separated from the title by three hyphens. The report number helps to indicate the type of document cited (e.g., NASA report, NASA translation, NASA contractor report). The NASA accession number is the number by which the document abstracts are arranged in this journal and by which the document is sold or requested. The titles, with title extensions if present, are arranged under each subject heading in ascending accession number order. The subject headings have been selected from the latest revision of the *NASA Thesaurus* (NASA SP-7051).

A

ABSORPTION

Engine-driven and absorption heat pump programs [DE85-013930] N86-10472

The interaction of small metal particles with refractory oxide supports [NASA-CR-176228] N86-11047

ABSORPTION COOLING

Analyses of advanced residential aborption heat pump cycles [DE85-005244] N86-10664

ABSTRACTS

Alternating direction methods on multiprocessors: An extended abstract [AD-A156722] N86-10794

An annotated bibliography of abstracts on the use of simulators in technical training [AD-A156792] N86-11065

ABUNDANCE

Physical conditions in giant extragalactic H2 regions N86-11130

ACCELERATION (PHYSICS)

Composite explosives for metal acceleration: The effect of detonation temperature [DE85-013982] N86-10359

ACCELERATION STRESSES (PHYSIOLOGY)

Hemodynamics during gravitational overloads (mathematical modeling) N86-10739

Study of hypokinesia and acceleration effects on human chromosomes N86-10740

Dynamics of changes of statistical indicators of heart rhythm of persons with different degree of motion sickness N86-10743

ACCELERATION TOLERANCE

Hemodynamics during gravitational overloads (mathematical modeling) N86-10739

ACCELERATORS

Simulating the CTR environment in the HVBM [DE85-011745] N86-10193

ACCIDENT PREVENTION

Activities report in safety N86-10365

ACCIDENTS

Scoping studies of vapor behavior during a severe accident in a metal-fueling reactor [DE85-011474] N86-10952

ACCURACY

A nanosecond or thirty centimeters: Why atomic clocks have to be synchronized. MITREX opens new dimensions for measuring accuracy N86-10185

A comparison of swept frequency and FFT methods used to calibrate array test modules [AD-A156629] N86-10430

Investigation of the uncertainties of the NBS (National Bureau of Standards) thermal voltage and current converters [PB85-200178] N86-10453

ACID RAIN

Examples of regional environmental assessment using acid deposition data [DE85-012903] N86-10677

Proceedings: First Annual Acid Deposition Emissions Inventory Symposium [PB85-200004] N86-10686

Emissions of NOx, SOx and VOC from Antropogenic sources [PB85-193530] N86-10688

Seasonal variations in atmospheric chemistry in the Adirondacks [DE85-014227] N86-10719

ACIDITY

Phosphoric and electric utility fuel technology development [DE85-014741] N86-10651

ACIDS

Kinetics of biological ferrous iron oxidation [DE85-014616] N86-10736

ACOUSTIC ATTENUATION

Physical acoustics: Investigation of chemical kinetic and thermodynamic properties of fluids N86-10911

ACOUSTIC EMISSION

Report on an overseas visit [AD-A156603] N86-10037

Multimode acoustic research N86-10167

ACOUSTIC LEVITATION

Containerless studies of nucleation and undercooling N86-10102

Multimode acoustic research N86-10167

Advanced containerless processing technology N86-10176

Acoustic levitation containerless processing N86-10177

ACOUSTIC MEASUREMENT

Long term statistical measurements of environmental acoustics parameters in the arctic. AEAS report number 2. Low frequency transmission loss measurements in the central arctic ocean [AD-A156576] N86-10727

Sound radiation from repetitive transient vibrations using multi-channel digital signal processing with application to impact machinery N86-10910

Understanding and improving acoustic to seismic coupling as it pertains to Sandia's helicopter detector [DE85-009440] N86-10920

ACOUSTIC SCATTERING

Exploratory development for a high reliability flaw characterization module [AD-A156632] N86-10916

ACOUSTIC VELOCITY

On the method of characteristics and its application to the calculations of annular nozzle flowfields N86-10454

Tunable acousto-optic filter with improved spectral resolution and increased aperture [AD-D011758] N86-10915

ACOUSTICS

Vibro-acoustic forecast for space shuttle launches at Vandenberg AFB: The payload changeout room and the administration building [AD-A156944] N86-10269

Ultrasonic inspection of weldments in large size spiral box for hydroelectric plant [AS-701/85] N86-10562

A study of methods to predict and measure the transmission of sound through the walls of light aircraft. Integration of certain singular boundary element integrals for applications in linear acoustics [NASA-CR-176229] N86-10912

Proposed aural nondetectability limits for Army materiel [AD-A156704] N86-10917

Measurements of the acoustic interference between adjacent microphones [AD-A156892] N86-10919

ACOUSTO-OPTICS

Signal analysis receiver with acousto-optic delay lines [AD-D011761] N86-10427

A compact bulk acousto-optic time integrating correlator [AD-A156606] N86-10428

Fiber optic gradient hydrophone construction and calibration for sea trial [AD-A156469] N86-10914

Tunable acousto-optic filter with improved spectral resolution and increased aperture [AD-D011758] N86-10915

ACQUISITION

Derivational analogy: A theory of reconstructive problem solving and expertise acquisition [AD-A156817] N86-10899

ACTIVATION

Contact effects in light activated GaAs switches [AD-A156957] N86-10[illegible]

ACTUATORS

Control concepts for in-flight simulation including actuator nonlinearities and time delays [DFVLR-FB-85-24] N86-10047

Robust failure detection filters [NASA-CR-176232] N86-10271

Soudan 2 data acquisition and trigger electronics [DE85-013864] N86-10443

Termination load carrying device [AD-D011800] N86-10558

ADA (PROGRAMMING LANGUAGE)

Ada (trademark) Programming Support Environment (APSE) Evaluation and Validation (E and V) workshop report held at Airlie, Virginia on 2-6 April 1984 [AD-A156667] N86-10829

ADAPTATION

The rubber tube test section of the DFVLR in Goettingen, West Germany --- wind tunnel walls [DFVLR-FB-85-18] N86-10051

Dynamics of changes of statistical indicators of heart rhythm of persons with different degree of motion sickness N86-10743

Dynamics of general resistance of rats during readaptation penod after training in altered gas environment N86-10767

ADAPTIVE CONTROL

Gas generator fuel flow throttle control system [AD-D011797] N86-10355

ADDITIVES

Magnetic properties of doped semiconductors [DE85-012090] N86-11053

ADHESION

Development of metallization process [NASA-CR-176209] N86-10312

Tribological properties of structural ceramics [NASA-TM-87105] N86-10341

ADHESION TESTS

Adhesion of metals: Experiment 1 ES-340 --- Spacelab N86-10232

ADHESIVE BONDING

The effect of debond growth on crack propagation in composite plates reinforced with adhesively bonded composite stringers N86-10287

Pre-bond treatment for titanium alloys [BAE-AL/MAT/3864] N86-10309

Load-deflection tests and computer analyses of a high-precision adhesive-bonded antenna reflector panel N86-10389

The preparation and testing of titanium and zirconium coupling agents [SJ70] N86-10576

ADIABATIC EQUATIONS
Charge exchange in slow collisions of atoms and molecules N86-10922
ADIRONDACK MOUNTAINS (NY)
Seasonal variations in atmospheric chemistry in the Adirondacks
[DE85-014227] N86-10719
ADSORPTION
Evaluation of Passive Sampling Devices (PSDs)
[PB85-196418] N86-10689
Adsorption of oxygen on single crystal tin at liquid helium temperatures N86-11044
AERIAL PHOTOGRAPHY
Remote sensing study project East Gelderland (Netherlands). Part 2: Remote sensing flights in 1982 and 1983; organization aspects N86-10639
AEROACOUSTICS
Recent advances in the analysis of exhaust mufflers N86-10587
AEROBRAKING
Numerical procedure for three-dimensional hypersonic viscous flow over aerobrake configuration
[NASA-TM-58269] N86-10018
AERODYNAMIC CHARACTERISTICS
Three articles on new calculation methods in aeronautics (selected articles)
[AD-A145745] N86-10007
Theoretical study of the unsteady linear problem for a rectangular wing with a pitching movement
[ONERA-RT-17/1841-RY-010-R] N86-10022
AERODYNAMIC COEFFICIENTS
Comment on Determination of Aerodynamic Coefficients for a Reentry Body by Means of the Kalman Filter Method N86-10011
AERODYNAMIC CONFIGURATIONS
Aerodynamics of hyperlift systems
[SNIAS-443.501/85] N86-10023
Analysis of hyperlift systems. Study of a singularities method
[SNIAS-443.529/84] N86-10024
AERODYNAMIC DRAG
A fundamental study of the sticking of insect residues to aircraft wings
[NASA-CR-176231] N86-10033
AERODYNAMIC FORCES
A new method for calculating unsteady supersonic aerodynamic forces and its application N86-10009
AERODYNAMIC INTERFERENCE
The rubber tube test section of the DFVLR in Goettingen, West Germany — wind tunnel walls
[DFVLR-FB-85-18] N86-10051
AEROELASTICITY
Forced response analysis of an aerodynamically detuned supersonic turbomachine rotor
[NASA-TM-87093] N86-10019
AERONAUTICAL ENGINEERING
A review of Australian investigations on aeronautical fatigue during the period April 1983 to March 1985
[AD-A156602] N86-10036
AEROSOLS
Characterization of vapor and aerosol flows by photothermal methods
[AD-A156601] N86-10465
Technical considerations in regional aerosol modeling
[PB85-193027] N86-10710
AEROSPACE ENGINEERING
Aerospace research at NLR N86-11089
Activities report of the Space Flight Laboratory N86-11090
Activities Report of the Space Flight Laboratory N86-11091
AEROSPACE ENVIRONMENTS
Influence of melt convection on solid-liquid interface under terrestrial and reduced gravity environments N86-10083
Control of cast iron microstructure N86-10084
Solidification fundamentals N86-10090
Life sciences research on the space station: An introduction
[NASA-TM-86836] N86-10734
AEROSPACE INDUSTRY
Space utilization N86-11067
Space sciences: Perspectives of commercial utilization for the German industry N86-11068
AEROSPACE MEDICINE
Aerospace medicine and biology: A continuing bibliography with indexes (supplement 275)
[NASA-SP-7011(275)] N86-10768
The effects of age, sleep deprivation, and altitude on complex performance
[AD-A156987] N86-10771
AEROSPACE SCIENCES
Space utilization N86-11067
Space sciences: Perspectives of commercial utilization for the German industry N86-11068
Space research expenses of the Federal Ministry of Research and Technology (BMFT) in the period 1983-1985 N86-11070
AEROSPACE SYSTEMS
Aerospace research at NLR N86-11089
AEROSPACE TECHNOLOGY TRANSFER
Activities Report of the Space Flight Laboratory N86-11091
AEROSPACE VEHICLES
Manned flight simulation: Challenge and response
[NASA-TM-86827] N86-10048
AFRICA
Role of the Economic Commission for Africa as a principal investigator in the metric camera experiment and reports of the result of the assessment for topographic and revision of maps in populated and developed areas of the world N86-10501
AGGLOMERATION
Cell partition in two polymer aqueous phases N86-10136
New instrumentation for phase partitioning N86-10138
AGING (BIOLOGY)
The effects of age, sleep deprivation, and altitude on complex performance
[AD-A156987] N86-10771
AGING (MATERIALS)
Age-life prediction of nylon 66 parachute materials. Part 2: Changes in the chemical and physical properties of materials on aging
[AD-A156909] N86-10347
Microwave evaluation of materials
[DE85-013183] N86-10409
AGRICULTURE
Wind energy in agriculture, a promise
[SS-45] N86-10672
Wind energy, a feasibility investigation for wind mills in agriculture
[SS-45A] N86-10673
AIR
Chemical kinetics and cellular structure of detonations in hydrogen sulphide and air
[DE85-009408] N86-10304
Effects of scale and geometry on hydrogen-air detonations
[DE85-006762] N86-10474
AIR COOLING
Submerged ram air inlets for ECM (electronic countermeasures) pods
[AD-D011801] N86-10020
AIR FLOW
Mean turbulence structure in strongly heating air flows N86-10455
AIR INTAKES
Three articles on new calculation methods in aeronautics (selected articles)
[AD-A145745] N86-10007
Effect of a shear layer on the stability of an axisymmetrical external compression air intake N86-10010
Submerged ram air inlets for ECM (electronic countermeasures) pods
[AD-D011801] N86-10020
AIR LAW
Tendencies toward liberalization in European air traffic control
[DFVLR-FB-85-23] N86-10030
AIR POLLUTION
Airborne measurements of the border-crossing air pollution in the area between Weiden and Hof/Bavaria
[DFVLR-FB-85-25] N86-10685
Proceedings: First Annual Acid Deposition Emissions Inventory Symposium
[PB85-200004] N86-10686
Evaluation of Passive Sampling Devices (PSDs)
[PB85-196418] N86-10689
AIR QUALITY
Proceedings: First Annual Acid Deposition Emissions Inventory Symposium
[PB85-200004] N86-10686
Emissions of NOx, SOx and VOC from Antropogenic sources
[PB85-193530] N86-10688
AIR SAMPLING
Emissions of NOx, SOx and VOC from Antropogenic sources
[PB85-193530] N86-10688
Evaluation of Passive Sampling Devices (PSDs)
[PB85-196418] N86-10689
AIR TRAFFIC
Tendencies toward liberalization in European air traffic control
[DFVLR-FB-85-23] N86-10030
The air traffic demand in passenger travel of the Federal Republic of Germany 1990 - 2000. Update of the DFVLR air traffic forecast
[DFVLR-MITT-85-06] N86-10031
AIR TRANSPORTATION
Tendencies toward liberalization in European air traffic control
[DFVLR-FB-85-23] N86-10030
The dirigible: A catalyst for resource exploitation in remote areas?
[AD-A156518] N86-10034
AIR WATER INTERACTIONS
The Liu, Katsaros, and Businger (1979) bulk atmospheric flux computational iteration program in FORTRAN and BASIC
[AD-A156736] N86-10714
Evaluation of surface exchange coefficients from mildex ocean/atmosphere mixed layer data
[AD-A156765] N86-10729
AIRBORNE EQUIPMENT
Airborne measurements of the border-crossing air pollution in the area between Weiden and Hof/Bavaria
[DFVLR-FB-85-25] N86-10685
AIRCRAFT ACCIDENTS
Rotary-wing operations in a microburst environment
[AD-A156695] N86-10713
AIRCRAFT CARRIERS
A comparative analysis of a CV helicopter and a JVX (Joint Services Advanced Vertical Lift) tilt-rotor aircraft in an aircraft carrier based ASW (Anti-Submarine Warfare)
[AD-A156871] N86-10041
AIRCRAFT CONSTRUCTION MATERIALS
Review of investigations on aeronautical fatigue in the Federal Republic of Germany
[LBF-S-173] N86-10044
Fatigue, static tensile strength and stress corrosion of aircraft materials and structures
[VTH-LR-360-PT-1] N86-10045
AIRCRAFT CONTROL
Control concepts for in-flight simulation including actuator nonlinearities and time delays
[DFVLR-FB-85-24] N86-10047
AIRCRAFT DESIGN
Acta Aeronautica et Astronautica Sinica (selected articles)
[AD-A147304] N86-10001
Optimum design of an aircraft wing structure with multiple constraints by the direct-vision criteria method N86-10004
Summary of work on jet noise prediction
[ESDU-BR-62636] N86-10909
AIRCRAFT ENGINES
Retrofit of SAC EC-135C and RC-135 aircraft with CFM-56 engines
[AD-A156688] N86-10038
AIRCRAFT HAZARDS
Electromagnetic resonances of cylinders and aircraft model with resistive wires
[NASA-CR-176250] N86-10042
AIRCRAFT MANEUVERS
System modeling and identification of equivalent systems with and without compensating time delay for control-augmented aircraft
[ESA-TT-852] N86-10043
AIRCRAFT MODELS
Evaluation of an aerodynamic-load prediction method on a STOL fighter configuration
[NASA-TM-86782] N86-10015
Electromagnetic resonances of cylinders and aircraft model with resistive wires
[NASA-CR-176250] N86-10042
System modeling and identification of equivalent systems with and without compensating time delay for control-augmented aircraft
[ESA-TT-852] N86-10043
AIRCRAFT RELIABILITY
A review of Australian investigations on aeronautical fatigue during the period April 1983 to March 1985
[AD-A156602] N86-10036
AIRCRAFT SAFETY
Proposed modifications for the RAAF Airtrainer CT-4A cockpit
[AD-A156808] N86-10039
Rotary-wing operations in a microburst environment
[AD-A156695] N86-10713
AIRCRAFT STRUCTURES
Review of investigations on aeronautical fatigue in the Federal Republic of Germany
[LBF-S-173] N86-10044
Fatigue, static tensile strength and stress corrosion of aircraft materials and structures
[VTH-LR-3R0-PT-1] N86-10045
Nondestructive control of thick structures made without disassembling
[PV-43-954/F/3] N86-10564

Nondestructive corrosion test of aluminum alloy structures
[PV-43-954/F/2] N86-10594

AIRFOIL PROFILES

Analysis of hyperlift systems. Study of a singularities method
[SNIAS-443.529/84] N86-10024

La Recherche Aerospatiale, bimonthly bulletin, no. 1984-5, September-October 1985
[ESA-TT-899] N86-10333

AIRFOILS

A new method for calculating unsteady supersonic aerodynamic forces and its application N86-10009

On the design of airfoils in transonic flow using the Euler equations N86-10013

A fundamental study of the sticking of insect residues to aircraft wings
[NASA-CR-176231] N86-10033

AIRFRAMES

Attachment method-ceramic radome to metal body
[AD-D011778] N86-10032

A review of Australian investigations on aeronautical fatigue during the period April 1983 to March 1985
[AD-A156602] N86-10036

AIRLINE OPERATIONS

Tendencies toward liberalization in European air traffic control
[DFVLR-FB-85-23] N86-10030

AIRSHIPS

The dirigible: A catalyst for resource exploitation in remote areas?
[AD-A156518] N86-10034

ALGAE

Development and evaluation of multispecies test protocols for assessing chemical toxicity
[DE85-013526] N86-10679

ALGEBRA

Computing the structural index
[DE85-014370] N86-10871

Brauer-Severi schemes of orders
[CTH-MATH-1985-06] N86-10877

ALGORITHMS

Automatic processing of reactive polymers
N86-10127

Modeling and control of nonlinear systems
N86-10362

The VLSI design of error-trellis syndrome decoding for convolutional codes N86-10391

Acoustic gravity wave chemistry model for the RAYTRACE code
[AD-A156850] N86-10405

Implementation issues for algorithmic VLSI (Very Large Scale Integration) processor arrays
[AD-A156699] N86-10432

Automated analysis of digital images generated by two-dimensional gel electrophoresis
[DE85-011906] N86-10526

Analysis of edge detection algorithms on DIAL (Digital Image Analysis Laboratory)
[AD-A156735] N86-10630

A processor for the study of ocean fine-scale patches
[AD-A157019] N86-10730

Alternating direction methods on multiprocessors: An extended abstract
[AD-A156722] N86-10794

Compact, high-speed algorithm for laying out printed circuit board runs N86-10814

Coordinate axes, location of origin, and redundancy for the one and two-dimensional discrete Fourier transform
[NASA-CR-176225] N86-10826

State assignment in sequential circuits
[EUT-85-E-146] N86-10846

Identification of a plant's weighting sequence — self-tuning control
[OUEL-1534/84] N86-10854

Two algorithms for weighted matroid intersection
[AD-A156525] N86-10861

An improved FFT (Fast fourier transform) for a four parallel pipe SIMD arithmetic processor
[AD-A156625] N86-10863

The h, p and h-p versions of the finite element method in 1 dimension. Part 3. The adaptive h-p version
[AD-A156626] N86-10864

A mesh moving technique for time dependent partial differential equations in two space dimensions
[AD-A156663] N86-10866

On the lanczos method for solving symmetric linear systems with several right-hand-sides
[AD-A156616] N86-10868

Error estimates and automatic time step control for numerical methods for stiff ordinary differential equations
[CTH-MATH-1984-27] N86-10872

Rank revealing QR-Factorizations
[AD-A156756] N86-10887

Generation of flight paths using hierarchical planning
[AD-A156905] N86-10900

Exploratory development for a high reliability flaw characterization module
[AD-A156632] N86-10916

ALIGNMENT

Parasitic mode losses versus signal sensitivity in beam position monitors
[DE85-014367] N86-10964

Beam steering in the SLC linac
[DE85-013370] N86-11025

ALKENES

A procedure identifying a polyacetylene initiator of olefin metathesis. The reactivities of metal-carbenes toward alkenes and alkynes
[AD-A156997] N86-10263

ALKYL COMPOUNDS

Synthesis of arylene siloxanylene polymers and copolymers
[AD-D011780] N86-10338

ALLOYS

Microgravity Science and Applications Program tasks
[NASA-TM-87568] N86-10053

The influence of containerless undercooling and rapid solid-state quenching on the superconductive and magnetic properties of some clustering alloy systems
N86-10076

Undercooling, remelting, and coarsening N86-10080

Liquid phase miscibility gap materials N86-10081

The development and prevention of channel segregation during alloy solidification N86-10086

Theoretical problems in materials science
N86-10088

Lambda point equipment N86-10118

Acoustic levitation containerless processing
N86-10177

Portevin-Le Chatelier effect. 1: Model for the type-E serrations
[DE85-006879] N86-10322

Weld metal hot-cracking of hastelloy alloys C-22 and C-276: A study by analytical electron microscopy
[DE85-009437] N86-10324

Constitutive modeling for isotropic materials (HOST)
[NASA-CR-174980] N86-10589

ALPHA PARTICLES

Development and application of the electrochemical etching technique
[DE85-010302] N86-10957

ALPS MOUNTAINS (EUROPE)

Evaluation of metric camera photos — Spacelab; alpine snow cover N86-10515

ALTERNATING CURRENT

Investigation of the uncertainties of the NBS (National Bureau of Standards) thermal voltage and current converters
[PB85-200178] N86-10453

ALTITUDE

Laws of distribution of the snow cover on the greater Caucasus (Soviet Union)
[NASA-TM-77911] N86-10614

Altitudinal distribution of granitic landforms in the south central Sierra Nevada, California N86-10695

The effects of age, sleep deprivation, and altitude on complex performance
[AD-A156967] N86-10771

ALTITUDE TOLERANCE

Dynamics of general resistance of rats during readaptation period after training in altered gas environment N86-10767

ALUMINUM

Theoretical problems in materials science
N86-10088

Containerless studies of nucleation and undercooling
N86-10102

Hugoniot measurements in aluminum to 420 GPa using the LLNL two-stage light-gas gun
[DE85-013821] N86-10317

Aluminum ion plating for corrosion protection of uranium, revision 1
[DE85-012419] N86-10330

Metastable phase formation in Ni-implanted Al: An analytical electron microscope investigation
[DE85-009105] N86-10331

The mechanism of erosion of metallic materials under cavitation attack
[NASA-TM-87130] N86-10552

An analytical and numerical study of the buckling behavior of fiber-reinforced beams N86-10566

ALUMINUM ALLOYS

The role of entrained surface oxides in RS-PM aluminum alloys on resultant structures and properties
N86-10085

Directional solidification of monotectic and hypermonotectic aluminum-indium alloys under micron-g
N86-10097

Space shuttle experiments on Al-in liquid phase miscibility gap (LPMG) alloys N86-10264

Metastable phase formation in Ni-implanted Al: An analytical electron microscope investigation
[DE85-009105] N86-10331

Aluminum battery alloys
[DE85-011599] N86-10445

Nondestructive corrosion test of aluminum alloy structures
[PV-43-954/F/2] N86-10594

ALUMINUM COMPOUNDS

Directional solidification of an aluminum-zinc vapor emulsion in microgravity — Spacelab N86-10218

ALUMINUM GALLIUM ARSENIDES

W-shaped diffused stripe GaAs/AlGaAs laser
[AD-D011816] N86-10538

ALUMINUM OXIDES

High efficiency heat transport and power conversion system for cascade
[DE85-012959] N86-10466

ALUMINUM SILICATES

Thermal expansion of glasses in the solid and liquid phases
[DE85-013953] N86-10351

ALVEOLAR AIR

Conditioning potentialities of respiratory apparatus
N86-10753

AMBIENCE

Evaluation of Passive Sampling Devices (PSDs)
[PB85-196416] N86-10669

AMINES

Passivation of steel with aqueous amine solutions
[AD-D011749] N86-10314

Development of new ammonium nitrate composite explosives
[DE85-014252] N86-10356

AMMETERS

Calibrated Faraday current and magnetic field sensor
[DE85-013438] N86-10439

AMMONIA

Nature of photoemission into dielectric fluids
[DE85-013017] N86-10945

AMMONIUM NITRATES

Development of new ammonium nitrate composite explosives
[DE85-014252] N86-10356

AMORPHOUS MATERIALS

Bulk formation of metallic glasses and amorphous silicon from the melt N86-10154

Formation and characterization of amorphous erbium-based alloys prepared by near-isothermal cold-rolling of elemental composites
[DE85-014853] N86-10327

Photovoltaic devices using a Si:H from higher order silanes
[DE85-008804] N86-10668

Ion beam sputter deposited zinc telluride films
[NASA-TM-87119] N86-11048

AMORPHOUS SEMICONDUCTORS

Topics in the electronic theory of disordered semiconductors N86-11045

AMPLIFIERS

Instantaneous frequency measurement receiver with digital processing
[AD-D011759] N86-10425

AMPLITUDE MODULATION

Amplitude and phase modulation in fin-lines electrical tuning
[AD-D011813] N86-10415

AMPLITUDES

Forced response analysis of an aerodynamically detuned supersonic turbomachine rotor
[NASA-TM-87093] N86-10019

Real-time holography by stimulated Raman and Brillouin scattering N86-10479

Measurements of the acoustic interference between adjacent microphones
[AD-A156892] N86-10919

ANALOG DATA

Restitution of Spacelab photography by analog stereoplotter N86-10489

ANALOG TO DIGITAL CONVERTERS

Extended precision in video bandwidth analog to digital converter using optical techniques
[AD-D011745] N86-10422

Instantaneous frequency measurement receiver with digital processing
[AD-D011759] N86-10425

Digital image processing of metric camera imagery — Spacelab N86-10511

Harmonic distortion reduction technique for data acquisition
[AD-D011771] N86-10799

ANALOGIES

Derivational analogy: A theory of reconstructive problem solving and expertise acquisition
[AD-A156817] N86-10899

ANALYSIS (MATHEMATICS)

Nonlinear methods for spacecraft attitude maneuvers [AD-A156956] N86-10275

Progressive damage, fracture predictions and post mortem correlations for fiber composites [NASA-TM-87101] N86-10290

Freezer model using a population balance approach for steady-state, direct-contact, secondary refrigerant, freeze desalination N86-10361

Analytical and experimental study of cracks emanating from an elliptical hole in unidirectional composite material N86-10567

A composite climatological study of the frequency and distribution of severe weather associated with spring season Colorado cyclogenesis [AD-A156981] N86-10715

ANALYSIS OF VARIANCE

Robustness of multiple comparisons against variance heterogeneity [COMP-CENT-NOTE-17] N86-10890

The power of weighted and ordinary least squares with estimated unequal variances in experimental design [B8562446] N86-10894

ANALYTIC FUNCTIONS

Some remarks about cusp forms: Holomorphic and non-holomorphic [CTH-MATH-1984-26] N86-10902

ANALYTIC GEOMETRY

Estimates for maximal functions along hypersurfaces [CTH-MATH-1984-29] N86-10874

ANALYTICAL CHEMISTRY

New directions in chemical analysis [DE85-012930] N86-10296

ANCHORS (FASTENERS)

Improved arresting and recovery system for test missiles [AD-D011743] N86-10198

ANEMOMETERS

Velocities of gas and plasmas from real time holographic interograms [DE85-014618] N86-10530

ANGLE OF ATTACK

Angle set-on apparatus [AD-D011766] N86-10371

ANGLES (GEOMETRY)

Total internal reflection modulator/deflector [AD-D011757] N86-10424

Angle of incidence effects for underwater shock using generic computational models [DE85-012936] N86-10466

Angle of incidence effects for underwater shock using generic computational models, rev. 1 [DE85-012921] N86-10467

The effect of vegetation type, microrelief, and incidence angle on radar backscatter N86-10619

ANGULAR DISTRIBUTION

Joint research effort on vibrations of twisted plates, phase 1: Final results [NASA-RP-1150] N86-10579

Angular distribution of neutral hydrogen following collisional electron detachment from H(-) [DE85-014258] N86-10943

ANGULAR MOMENTUM

Local conservation laws for the Maxwell-Vlasov and collisionless kinetic guiding center theories [DE85-013122] N86-11063

The dynamics and stellar content of globular star clusters N86-11131

ANGULAR RESOLUTION

Angle of incidence effects for underwater shock using generic computational models, rev. 1 [DE85-012921] N86-10467

Tunable acousto-optic filter with improved spectral resolution and increased aperture [AD-D011758] N86-10915

Optical/IR telescope arrays: A study of their potential for satisfying observational requirements in astronomy for a large aperture system in the 1990s and beyond [REPT-15] N86-11094

High angular resolution in the infrared: Prospects for space observations N86-11100

ANISOTROPIC MEDIA

Analytical and experimental study of cracks emanating from an elliptical hole in unidirectional composite material N86-10567

ANISOTROPIC SHELLS

Three-dimensional stress singularities in anisotropic materials and composites N86-10286

ANISOTROPY

Theory of dense molecular fluid equations of state with application to detonation products [DE84-016822] N86-10927

ANNEALING

The interaction of small metal particles with refractory oxide supports [NASA-CR-176228] N86-11047

ANNUAL VARIATIONS

Observations of the snow cover in the southern part of the Buryat Autonomous Soviet Socialist Republic [NASA-TM-77910] N86-10613

Seasonal variations in atmospheric chemistry in the Adirondacks [DE85-014227] N86-10719

ANNULAR DUCTS

Oscillations of subsonic flow in an abruptly expanding circular duct [MPIS-16/1984] N86-10028

ANNULAR FLOW

Analysis of annular two-phase flow with liquid entrainment N86-10459

ANNULAR NOZZLES

On the method of characteristics and its application to the calculations of annular nozzle flowfields N86-10454

ANODIC COATINGS

Chemical/hydrogen energy systems [DE85-012742] N86-10667

ANOMALIES

Local drift parameter, j/n sub e and resistivity anomaly measurements in CTX spheromaks [DE85-012740] N86-10998

ANTARCTIC REGIONS

How Antarctica was unveiled. Masterpieces of Frankfurt topographic surveyors. A part of the German Antarctica research program N86-10181

Individual typological features of autonomic reactions during autogenic training in polar expedition members in period of wintering in Antarctica N86-10748

Adaptation of man to extreme conditions of Antarctica N86-10751

ANTENNA ARRAYS

Angle set-on apparatus [AD-D011766] N86-10371

Method for tuning a phased array antenna [AD-D011768] N86-10372

A dual frequency microstrip antenna for Ka band [NASA-TM-87124] N86-10380

Planning for VLA/DSN arrayed support to the Voyager at Neptune N86-10395

A VLA experiment: Planning for Voyager at Neptune N86-10396

ANTENNA COMPONENTS

Signal analysis receiver with acousto-optic delay lines [AD-D011761] N86-10427

ANTENNA DESIGN

Space antenna for gravitational wave astronomy N86-11123

ANTENNA FEEDS

A dual frequency microstrip antenna for Ka band [NASA-TM-87124] N86-10380

ANTENNA RADIATION PATTERNS

A numerical method for approximating antenna surfaces defined by discrete surface points [NASA-TM-87125] N86-10381

ANTHROPOMETRY

A graphic anthropometric aid for seating and workplace design [AD-A156988] N86-10788

System integration report [NASA-CR-171900] N86-10821

ANTIFERROELECTRICITY

Analysis of transitions between ferroelectric and antiferroelectric states under conditioning of uniaxial strain [DE85-014468] N86-10350

ANTIFERROMAGNETISM

Fermi surface study of CeSb in the ferromagnetic and antiferromagnetic phases [DE85-012122] N86-11052

ANTIMISSILE DEFENSE

An anthology: Rationale for a US ballistic missile defense (1969 - 1984) [AD-A156781] N86-10199

Report of the ad hoc committee to review the program of the SDI Directorate on Innovative Science and Technology (IST) [AD-A156668] N86-11071

ANTIMONY ALLOYS

Fermi surface study of CeSb in the ferromagnetic and antiferromagnetic phases [DE85-012122] N86-11052

ANTIPARTICLES

Matter-antimatter transition operators: A manual for modeling N86-10921

ANTISUBMARINE WARFARE AIRCRAFT

A comparative analysis of a CV helicopter and a JVX (Joint Services Advanced Vertical Lift) tilt-rotor aircraft in an aircraft carrier based ASW (Anti-Submarine Warfare) [AD-A156871] N86-10041

APERTURES

Tunable acousto-optic filter with improved spectral resolution and increased aperture [AD-D011758] N86-10915

Optical testing of large telescopes using multiple subapertures N86-10971

Thermal and structural analysis of ring components by the finite element method [DE85-013305] N86-11021

Tracking studies on the effects of magnet multipoles on the aperture of the RHIC heavy ion collider [DE85-013282] N86-11023

Optical/IR telescope arrays: A study of their potential for satisfying observational requirements in astronomy for a large aperture system in the 1990s and beyond [REPT-15] N86-11094

APPALACHIAN MOUNTAINS (NORTH AMERICA)

Dynamic lithostratigraphy and paleecology of upper Mississippi (Chesterian) strata of the northcentral Appalachian Basin N86-10693

APPROXIMATION

Second order approximation method for transonic flows over swept wings N86-10002

A fundamental study of smoldering with emphasis on experimental design for zero-g N86-10162

A numerical method for approximating antenna surfaces defined by discrete surface points [NASA-TM-87125] N86-10381

Acceleration-invariant approximation method for recursive digital filters [AD-A156655] N86-10865

Naive approximate realization of noisy data [ER-83/10] N86-10880

Renormalization of an inverse scattering theory for inhomogeneous dielectrics [AD-A156636] N86-11049

A study of the applicability of nucleation theory to quasi-thermodynamic transformations of second and higher Ehrenfest-order [NASA-CR-176230] N86-11060

APTITUDE

Extended analysis of the structure of error scores in psychological aptitude tests [DFVLR-FB-85-20] N86-10780

AQUEOUS SOLUTIONS

Separation of aqueous two-phase polymer systems in microgravity N86-10246

Streaming potentials in conductive and nonconductive tubing [DE85-012984] N86-10438

AQUIFERS

Modeling groundwater flow into lakes N86-10598

Evaluating the ground-water resources of the high plains of Texas, Volume 4 [PB85-191625] N86-10641

ARC JET ENGINES

Experimental performance of a 1-kilowatt arcjet thruster [NASA-TM-87131] N86-10281

ARCHITECTURE

Implementation issues for algorithmic VLSI (Very Large Scale Integration) processor arrays [AD-A156699] N86-10432

ARCHITECTURE (COMPUTERS)

Special purpose hardware architectures for language recognition [AD-A156634] N86-10793

Alternating direction methods on multiprocessors: An extended abstract [AD-A156722] N86-10794

Efficient systolic arrays for the solution of toeplitz systems: An illustration of a methodology for the construction of systolic architectures in VLSI (Very Large Systems Integration) [AD-A156767] N86-10795

Design of a multifunction Input-Output (I/O) controller [EUT-84-E-143] N86-10802

The local disk controller [REPT-1-68430-44(1985)01] N86-10806

An intelligent local disk control system [REPT-051560-28(1984)08] N86-10808

USSR report: Cybernetics, computers and automation technology [JPRS-UCC-85-006] N86-10809

Prospects for creation of optical digital high-performance computers N86-10810

Elektronika MS 1603 high-speed peripheral processor N86-10811

Diagnostics of peripheral processors and controllers N86-10812

An approach to implementing CAMAC microprocessor modules N86-10813

Compact, high-speed algorithm for laying out printed circuit board runs N86-10814

Fault-free behavior of reliable multiprocessor systems: FTMP experiments in AIRLAB [NASA-CR-177967] N86-10848

Topological properties of hypercubes [AD-A156777] N86-10850

ARCTIC OCEAN
Long term statistical measurements of environmental acoustics parameters in the arctic. AEAS report number 2. Low frequency transmission loss measurements in the central arctic ocean
[AD-A156576] N86-10727
ARID LANDS
Topographic interpretation of metric camera images: An example in Somalia — Spacelab N86-10508
Representation of the distribution of the snow cover on the surface of the Earth's dry land
[NASA-TM-77909] N86-10612
Effect of inclusion of supplementary ascorbic acid in daily diet on degree of vitamin saturation of body and thermoresistance of erythrocytes while working in arid zone N86-10749
ARMED FORCES (UNITED STATES)
F-16X MSIP (Multi-national Staged Improvement Program) case example: Operating and support cost estimation using VAMOSC (Visibility And Management Of Operating and Support Costs)
[AD-A156893] N86-10006
Let's get serious about software
[AD-A156819] N86-10831
ARRAYS
An evaluation of the use of microphone arrays for studio recording
[BBC-RD-1985/8] N86-10366
P-N junction controlled field emitter array cathode
[AD-D011815] N86-10416
Signal analysis receiver with acousto-optic delay lines
[AD-D011761] N86-10427
Implementation issues for algorithmic VLSI (Very Large Scale Integration) processor arrays
[AD-A156699] N86-10432
Results and limitations of ground-based optical arrays — stellar interferometry N86-11097
ARRESTING GEAR
Improved arresting and recovery system for test missiles
[AD-D011743] N86-10198
ARRIVALS
Angle set-on apparatus
[AD-D011766] N86-10371
ARTIFICIAL INTELLIGENCE
USSR report: Cybernetics, computers and automation technology
[JPRS-UCC-85-006] N86-10809
The DUCK manual
[AD-A156936] N86-10833
Generation of flight paths using hierarchical planning
[AD-A156905] N86-10900
ARTIFICIAL SATELLITES
Cryogenic equivalence principle experiment
N86-10171
ASCORBIC ACID METABOLISM
Effect of inclusion of supplementary ascorbic acid in daily diet on degree of vitamin saturation of body and thermoresistance of erythrocytes while working in arid zone N86-10749
ASIA
Structural mapping of folded sedimentary environments from satellite images: An example from Central Asia
N86-10607
ASPECT RATIO
Joint research effort on vibrations of twisted plates, phase 1: Final results
[NASA-RP-1150] N86-10579
ASSESS PROGRAM
The first German Spacelab mission D1 reports — Spacelab payloads
[PR-2] N86-10188
ASSESSMENTS
Initial design of a relational database system for NPS computer asset identification and valuation for risk assessment
[AD-A156847] N86-10796
ASTEROID BELTS
Project VESTA, exploratory mission to the asteroids: Scientific objectives and technical specifications
[NASA-TM-77669] N86-10179
ASTEROID MISSIONS
Project VESTA, exploratory mission to the asteroids: Scientific objectives and technical specifications
[NASA-TM-77669] N86-10179
ASTRONAUT PERFORMANCE
The first German Spacelab mission D1 reports — Spacelab payloads
[PR-2] N86-10188
ASTRONAUT TRAINING
The first German Spacelab mission D1 reports — Spacelab payloads
[PR-3] N86-10189
ASTRONAUTICS
Space utilization N86-11067
DFVLR, strategic study of astronautics 1984, user requirements N86-11069
ASTRONOMICAL OBSERVATORIES
Activities report of the European Southern Observatory N86-11135
ASTRONOMICAL TELESCOPES
Planning for VLA/DSN arrayed support to the Voyager at Neptune N86-10395
Optical/IR telescope arrays: A study of their potential for satisfying observational requirements in astronomy for a large aperture system in the 1990s and beyond
[REPT-15] N86-11094
Results and limitations of ground-based optical arrays — stellar interferometry N86-11097
Extragalactic observations with optical space arrays
N86-11098
Strategy for the development of space arrays
N86-11101
TRIO: A kilometric array stabilized by solar sails — Spaceborne astronomy N86-11102
SAMSI: An orbiting spatial interferometer for micro-arc second astronomical observations — Spacecraft Array for Michelson Spatial Interferometry (SAMSI) N86-11103
COSMIC: A high resolution, large collecting area telescope — Coherent Optical System of Modular Imaging Collectors (COSMIC) N86-11104
A fiber-linked version of project TRIO — telescope array N86-11105
OASIS: Optical Aperture Synthesis in Space
N86-11106
Future space telescope design concepts N86-11107
TRIO optics — spaceborne optical interferometer (TRIO) N86-11108
On line astronomical image processing using microcomputers N86-11121
The intensified multi CCD camera — spaceborne interferometers N86-11122
Activities report of the European Southern Observatory N86-11135
ASTRONOMY
Activities report of the European Southern Observatory N86-11135
ASYMPTOTIC SERIES
The h, p and h-p versions of the finite element method in dimension. Part 1: The error analysis of the p-version
[AD-A156600] N86-10862
ATMOSPHERIC BOUNDARY LAYER
Simulation of the atmospheric boundary layer in the large wind tunnel of the TNO institute for Building materials and Constructions (IBBC). Part 1: Theory
[BI-76-39/08.7.23100-PT-1] N86-10703
Simulation of the atmospheric boundary layer in the large wind tunnel of the TNO Institute for Building Materials and Construction (IBBC). Part 2: Experiments
[BI-76-39/08.7.23100-PT-2] N86-10704
List of publications on the 200 m meteorological mast at Cabauw, the Netherlands
[KNMI-FM-85-6] N86-10711
ATMOSPHERIC CHEMISTRY
Acoustic gravity wave chemistry model for the RAYTRACE code
[AD-A156850] N86-10405
Technical considerations in regional aerosol modeling
[PB85-193027] N86-10710
Seasonal variations in atmospheric chemistry in the Adirondacks
[DE85-014227] N86-10719
ATMOSPHERIC CIRCULATION
Computation of flow regimes in parameter space for the AGCE
[NASA-CR-178480] N86-10705
The Liu, Katsaros, and Businger (1979) bulk atmospheric flux computational iteration program in FORTRAN and BASIC
[AD-A156736] N86-10714
A composite climatological study of the frequency and distribution of severe weather associated with spring season Colorado cyclogenesis
[AD-A156981] N86-10715
Microphysical/mesoscale aspects of nuclear winter and new directions in assessments
[DE85-013479] N86-10716
ATMOSPHERIC MODELS
Simulation of the atmospheric boundary layer in the large wind tunnel of the TNO Institute for Building materials and Constructions (IBBC). Part 1: Theory
[BI-76-39/08.7.23100-PT-1] N86-10703
Simulation of the atmospheric boundary layer in the large wind tunnel of the TNO Institute for Building Materials and Construction (IBBC). Part 2: Experiments
[BI-76-39/08.7.23100-PT-2] N86-10704
Computation of flow regimes in parameter space for the AGCE
[NASA-CR-178480] N86-10705
Technical considerations in regional aerosol modeling
[PB85-193027] N86-10710
Smoke inputs to climate models: Optical properties and height distribution for nuclear winter studies
[DE85-011363] N86-10717
ATMOSPHERIC PRESSURE
Chemical kinetics and cellular structure of detonations in hydrogen sulphide and air
[DE85-009408] N86-10304
Reaction of rabbit respiration system to hypoxic stimulus in nitrogen-oxygen medium at elevated pressure
N86-10760
ATMOSPHERIC SOUNDING
The air of life of the blue planet. Atmosphere research from space using data and facts against climate speculations N86-10184
ATMOSPHERIC TEMPERATURE
Monthly and Seasonal Weather Outlook for mid-April to mid-May 1985, Volume 39, Number 8
[PB85-195345] N86-10724
ATOMIC CLOCKS
A nanosecond or thirty centimeters: Why atomic clocks have to be synchronized. MITREX opens new dimensions for measuring accuracy N86-10185
ATOMIC ENERGY LEVELS
Theoretical investigation of electron-positive ion-atom interactions
[DE85-013019] N86-10939
ATOMIC EXCITATIONS
Theoretical investigation of electron-positive ion-atom interactions
[DE85-013019] N86-10939
ATOMIC INTERACTIONS
Evaluation and prediction of long-term environmental effects on non metallic materials
[NASA-CR-178495] N86-10340
ATOMIC PHYSICS
The 1984 bibliography of atomic and molecular processes
[DE85-010583] N86-10926
ATOMIC SPECTRA
Cooled ion frequency standard
[AD-A156813] N86-10295
Selected tables of atomic spectra. Atomic energy levels and multiplet table O3
[NBS/NSRDS-3/11] N86-10923
Cooperative emission by two different atoms into surface plasmons
[AD-A157033] N86-10925
The two micron spectrum of R Scuti N86-11092
ATOMIC STRUCTURE
Electronic and magnetic properties of noble-metal and transition-metal alloys, interfaces and overlayers
[DE85-014532] N86-10321
Non-empirical interatomic potentials for transition metals
[DE85-013448] N86-10440
ATOMIC WEIGHTS
Direct mass measurements in the light neutron-rich region using a combined energy and time-of-flight technique
[DE85-012758] N86-10963
ATOMIZING
The role of entrained surface oxides in RS-PM aluminum alloys on resultant structures and properties
N86-10085
Modeling of engine sprays
[DE85-010020] N86-10559
ATTENUATION
Ultrasonic evaluation of mechanical properties of thick, multilayered, filament wound composites
[MASA-TM-87088] N86-10561
AUDITORY SIGNALS
Apparatus for locating passive intermodulation interference sources
[AD-D011798] N86-10435
Measurements of the acoustic interference between adjacent microphones
[AD-A156892] N86-10919
AUGER EFFECT
Mean life of the 2p(4)((1)S)3s (2)S state in fluorine
[DE85-012929] N86-10956
AURORAS
Potential structures and particle acceleration on auroral field lines
[AD-A156694] N86-10708
Activities report in geophysics
[KGI-188] N86-10709
AUTOCORRELATION
Periodic binary sequences with very good autocorrelation properties N86-10397
A binary sequence of period 60 with better autocorrelation properties than the Barker sequence of period 13 N86-10398

AUTOMATIC CONTROL

New directions in chemical analysis [DE85-012930] N86-10296

Automated analysis of digital images generated by two-dimensional gel electrophoresis [DE85-011906] N86-10526

Computer control of an electric hydraulic robot leg with proximity ranging system N86-10549

Framework for generating expert systems to perform computer security risk analysis [DE85-014134] N86-10841

AUTOMATIC GAIN CONTROL

Constant rise AGC (Automatic Gain Control) device [AD-D011744] N86-10421

AUTOMATION

USSR report: Cybernetics, computers and automation technology [JPRS-UCC-85-006] N86-10809

An approach to implementing CAMAC microprocessor modules N86-10813

Compact, high-speed algorithm for laying out printed circuit board runs N86-10814

Collective use computer system for the Academy of Sciences KaSSR N86-10817

AUTOMOBILES

Studies on human vehicle control [B8563352] N86-10775

Car driving as a supervisory control task [B8563351] N86-10776

Path error-neglection in straight lane driving [IZF-1984-32] N86-10783

Advanced vehicle systems assessment. Volume 2: Subsystems assessment [NASA-CR-176205] N86-11083

Advanced vehicle systems assessment. Volume 3: Systems assessment [NASA-CR-176206] N86-11084

AUTONOMIC NERVOUS SYSTEM

Individual typological features of autonomic reactions during autogenic training in polar expedition members in period of wintering in Antarctica N86-10748

AUTONOMOUS NAVIGATION

Digital control of the hydraulic actuators of an adaptive suspension vehicle N86-10548

AXES OF ROTATION

Multimode acoustic research N86-10167

AXIAL COMPRESSION LOADS

Effect of sequence of loading on interaction curves for buckling of stiffened shells [TAE-536] N86-10583

AXIAL STRAIN

Analysis of transitions between ferroelectric and antiferroelectric states under conditioning of uniaxial strain [DE85-014468] N86-10350

Inelastic analysis of frame structures including member and joint shears N86-10573

Experiments with tubular probes made of INCOLOY 800 H under uniaxial and multiaxial strain [JUEL-1979] N86-10595

AXIAL STRESS

Defect identification in high-energy semiconductors [DE85-014533] N86-10442

AXISYMMETRIC BODIES

Strength of shells under local transverse loads N86-10568

AXISYMMETRIC FLOW

Effect of a shear layer on the stability of an axisymmetrical external compression air intake N86-10010

B

BACKGROUND NOISE

Proposed aural nondetectability limits for Army materiel [AD-A156704] N86-10917

BACKGROUND RADIATION

Extra-galactic X-ray sources and the diffuse X-ray background N86-11144

BACKSCATTERING

CV-990 L-band SAR: A calibration experiment N86-10617

The effect of vegetation type, microrelief, and incidence angle on radar backscatter N86-10619

Age-dating volcanic and alluvial surfaces with multipolarization data N86-10620

Mapping diverse forest cover with multipolarization airborne radar N86-10625

Modelling of vegetation volumes N86-10629

BACTERIA

Kinetics of biological ferrous iron oxidation [DE85-014616] N86-10736

BAGS

The wearing comfort of the PVC: Combat back pack [IZF-1984-34] N86-10789

BALLISTIC MISSILES

Improved arresting and recovery system for test missiles [AD-D011743] N86-10198

BALLISTICS

Transient velocity assessment in gallium arsenide, and of other GaAs characteristics related to device functions [AD-A156983] N86-11050

BANDPASS FILTERS

An active tracking band-pass filter [AD-A156559] N86-10419

BANDWIDTH

Phase-coded pulse expander-compressor [AD-D011812] N86-10375

Extended precision in video bandwidth analog to digital converter using optical techniques [AD-D011745] N86-10422

BARIUM COMPOUNDS

Thermal expansion of glasses in the solid and liquid phases [DE85-013953] N86-10351

BEACHES

Application of the dutch method for estimating storm-induced dune erosion [AD-A156717] N86-10728

BEAM CURRENTS

Laser generation and transport of a relativistic electron beam [DE85-011709] N86-10192

RFQ-funneling [DE85-012483] N86-10194

BEAM INJECTION

RFQ-funneling [DE85-012483] N86-10194

High-brightness photoemitter injector for electron accelerators [DE85-012673] N86-10929

Method for determining the position, angle and other injection parameters of a short pulsed beam in the Brookhaven AGS [DE85-012523] N86-10931

Proposed bunching scheme for a polarized H(-) injector [DE85-012648] N86-10986

Noninterceptive techniques for the measurement of longitudinal parameters for intense H(-) beams [DE85-012662] N86-10992

Effects of slots/holes in disks on frequencies of TM01 and EH11 waves in the disk-loaded waveguide [DE85-013376] N86-11009

Generalized helicity and its time derivative [DE85-012770] N86-11027

BEAM INTERACTIONS

Beam-beam deflections to measure size spot and offset at SLC IP [DE85-014285] N86-10965

SLC positron damping ring optics design [DE85-013054] N86-11014

RHIC lattice [DE85-013289] N86-11026

BEAM WAVEGUIDES

The Netherlands Institute for Nuclear and High Energy Physics (NIKHEF) traveling wave monitor user guide [LINO-121] N86-10969

Superconvergent tracking and invariant surfaces in phase space [DE85-013051] N86-10995

Effects of slots/holes in disks on frequencies of TM01 and EH11 waves in the disk-loaded waveguide [DE85-013376] N86-11009

BEAMS (RADIATION)

RFQ-funneling [DE85-012483] N86-10194

Surface conditioning of synchrotron radiation source to improve beam lifetime [DE84-012165] N86-10948

Wide dynamic range beam profile monitor [DE85-012709] N86-10950

Beam-beam deflections to measure size spot and offset at SLC IP [DE85-014285] N86-10965

Beam line windows at LAMPF [DE85-012723] N86-10985

Proposed bunching scheme for a polarized H(-) injector [DE85-012648] N86-10986

Applications of the second-order achromat concept to the design of particle accelerators [DE85-013072] N86-10994

Effects of slots/holes in disks on frequencies of TM01 and EH11 waves in the disk-loaded waveguide [DE85-013376] N86-11009

BEAMS (SUPPORTS)

Load-deflection tests and computer analyses of a high-precision adhesive-bonded antenna reflector panel N86-10389

An analytical and numerical study of the buckling behavior of fiber-reinforced beams N86-10566

Joint research effort on vibrations of twisted plates, phase 1: Final results [NASA-RP-1150] N86-10579

Three-dimensional vibration analysis of a uniform beam with offset inertial masses at the ends [NASA-TM-86393] N86-10580

BEARINGS

Precise bearing support ditherer with piezoelectric drive means [AD-D011819] N86-10483

The generation and transmission of vibration in plain cylindrical bearings. Part 2. Experiment [AD-A156577] N86-10553

BEHAVIOR

Contact effects in light activated GaAs switches [AD-A156957] N86-10434

USSR report: Life sciences. Biomedical and behavioral sciences [JPRS-UBB-85-023] N86-10736

BELLOWS

Method for compensating bellows pressure loads while accommodating thermal deformations [DE85-013306] N86-10933

BENARD CELLS

Rayleigh-Benard instability in systems presenting a minimum in surface tension N86-10245

BENDING

Measurement and resulting first and second order approximations for a 9 deg bending magnet in LAMPF's 750-keV transport [DE85-012691] N86-10930

BERYLLIUM

Work-hardening and effective viscosity in solid beryllium [DE85-013978] N86-10323

Anelastic relaxation in irradiated Cu-Be [DE85-013893] N86-11056

BERYLLIUM OXIDES

High efficiency heat transport and power conversion system for cascade [DE85-012959] N86-10469

BETA FACTOR

Freezer model using a population balance approach for steady-state, direct-contact, secondary refrigerant, freeze desalination N86-10361

BETATRONS

Use of the MURA transformation to generate the fields and calculate the motion of protons in the designed Argonne Mini-ASPUN FFAG spiral sector accelerator [DE85-011477] N86-10934

Theory of non-planar orbits [DE85-013284] N86-11018

BIBLIOGRAPHIES

An anthology: Rationale for a US ballistic missile defense (1969 - 1984) [AD-A156781] N86-10199

Aerospace medicine and biology: A continuing bibliography with indexes (supplement 275) [NASA-SP-7011(275)] N86-10768

Computer codes: A bibliography, supplement 1 [DE85-008721] N86-10838

The 1984 bibliography of atomic and molecular processes [DE85-010583] N86-10926

An annotated bibliography of abstracts on the use of simulators in technical training [AD-A156792] N86-11065

Annotated bibliography of publications dealing with occupational health and medical information systems, cost analysis procedures, evaluation methodology and related legal issues [AD-A156650] N86-11078

Publication of the Executive Office of the President, January 20, 1981 - December 31, 1984 [PB85-187110] N86-11082

BINARY ALLOYS

Stability of metallic dispersions — microgravity N86-10258

Dendritic solidification in a binary alloy melt: Steady-state versus morphological stability theories N86-10261

BINARY CODES

Periodic binary sequences with very good autocorrelation properties N86-10397

A binary sequence of period 60 with better autocorrelation properties than the Barker sequence of period 13 N86-10398

BINARY FLUIDS

Cell partition in two polymer aqueous phases N86-10139

BINARY MIXTURES
New approach to multiphase equilibria: Application to high-pressure physics problems
[DE85-013620] N86-10907

BINARY SYSTEMS (MATERIALS)
Solutal convection and its effects on crystal growth and segregation in binary and pseudo-binary system with large liquidus-solidus separation N86-10056
Separation of aqueous two-phase polymer systems in microgravity N86-10246
Rationale for two phase polymer system microgravity separation experiments N86-10247
Application of the theory of Ostwald ripening to microgravity phase separation experiments N86-10248
Thermodynamics of polymer-supercritical solvent mixtures
[AD-A157038] N86-11061

BINOMIALS
Estimation by moments in a model of faulty inspection
[AD-A156754] N86-10686

BIOASSAY
Development and evaluation of multispecies test protocols for assessing chemical toxicity
[DE85-013526] N86-10679

BIOCHEMISTRY
Biochemical assays of cultured cells N86-10134

BIOCONTROL SYSTEMS
Individual typological self-regulation of cardio-vascular system N86-10752

BIOCONVERSION
Romanian plant produces protein concentrate from paraffin-nourished yeasts N86-10741

BIODEGRADATION
Evaluation of the 90-day inhalation toxicity of petroleum and oil shale JP-5 jet fuel
[AD-A156815] N86-10675

BIOELECTRICITY
Criteria for the design or selection of a bioelectromagnetics experiment
[AD-A156575] N86-10420

BIOENGINEERING
LSRO/ONR ad hoc review process
[AD-A156590] N86-10735

BIOGRAPHY
Study of one- and two-dimensional filtering and deconvolution algorithms for a streaming array computer
[NASA-CR-176226] N86-10627

BIOLOGICAL EFFECTS
Aerospace medicine and biology: A continuing bibliography with indexes (supplement 275)
[NASA-SP-7011(275)] N86-10768

BIOLOGICAL MODELS (MATHEMATICS)
Mathematical models of continuous flow electrophoresis N86-10143
Hemodynamics during gravitational overloads (mathematical modeling) N86-10739

BIOMASS
Potential applications of multipolarization SAR for pine plantation biomass estimation N86-10626
Vegetation canopy discrimination and biomass assessment using multipolarized airborne SAR
N86-10628

BIOMEDICAL DATA
USSR report: Life sciences. Biomedical and behavioral sciences
[JPRS-UBB-85-023] N86-10738
Annotated bibliography of publications dealing with occupational health and medical information systems, cost analysis procedures, evaluation methodology and related legal issues
[AD-A156650] N86-11078

BIOMETRICS
Dynamics of changes of statistical indicators of heart rhythm of persons with different degree of motion sickness N86-10743

BIOREACTORS
Cell separations in microgravity and development of a space bioreactor N86-10141
Kinetics of biological ferrous iron oxidation
[DE85-014616] N86-10736

BIOTECHNOLOGY
Microgravity Science and Applications Program tasks
[NASA-TM-87568] N86-10053
Lambda point equipment N86-10118
Biotechnology regulation
[GPO-43-776] N86-10733
USSR report: Life sciences. Biomedical and behavioral sciences
[JPRS-UBB-85-023] N86-10738
Biotechnology: Science and practice N86-10742

BISMUTH
Study of eutectic formation N86-10070
Thermal and solutal convection damping using an applied magnetic field N86-10094

BLACK AND WHITE PHOTOGRAPHY
Thematic mapping of metric camera color infrared and black and white photographs for land use classification
N86-10510
Topographic and thematic mapping: Analysis of metric camera black and white photographs of the Rhone Delta
N86-10514

BLACK BODY RADIATION
Scaling studies of solar pumped lasers
[NASA-CR-176240] N86-10540
Initial data for N black holes N86-11126

BLAST LOADS
Angle of incidence effects for underwater shock using generic computational models
[DE85-012936] N86-10466
Angle of incidence effects for underwater shock using generic computational models, rev. 1
[DE85-012921] N86-10467

BLOOD
A study of blood flow and of aggregation of blood cells under conditions of zero gravity: Its relevance to the occlusive diseases and cancer N86-10137
Evaluation of the 90-day inhalation toxicity of petroleum and oil shale JP-5 jet fuel
[AD-A156815] N86-10675

BLOOD CIRCULATION
Vestibular resistance and blood circulation changes in orthostatic position during hyperthermia N86-10758
Reaction of rabbit respiration system to hypoxic stimulus in nitrogen-oxygen medium at elevated pressure
N86-10760
Indices of blood oxygen transporting properties and erythropoiesis in rats after prolonged stay in nitrogen-oxygen mixture at elevated pressure
N86-10761

BLOOD FLOW
Streaming potentials in conductive and nonconductive tubing
[DE85-012984] N86-10438

BLOOD PLASMA
Effect of emotional stress on hemostasis system of healthy persons N86-10745

BLOOD PRESSURE
Vestibular resistance and blood circulation changes in orthostatic position during hyperthermia N86-10758

BODY TEMPERATURE
Short term heat effect on adreno- and cholino-sensitivity of rat's small intestine N86-10754
Efficiency of muscular work in white rats during adaptation to cold N86-10763
Effect of increased body clothing insulation on hand temperature in a cold environment
[AD-A156597] N86-10786

BODY WEIGHT
Evaluation of the 90-day inhalation toxicity of petroleum and oil shale JP-5 jet fuel
[AD-A156815] N86-10675

BOLTS
Rusty bolt intermodulation interference reducer
[AD-D011748] N86-10313
Over-center toggle latch
[AD-D011753] N86-10556

BOLTZMANN-VLASOV EQUATION
Local conservation laws for the Maxwell-Vlasov and collisionless kinetic guiding center theories
[DE85-013122] N86-11063

BONDING
Properties of plastic-bonded nitroguanidine
[DE85-015316] N86-10358

BOOLEAN ALGEBRA
Partial evolution and omega completeness of algebraic specifications
[CWI-CS-R8501] N86-10884
Reaching approximate agreement in the presence of faults
[AD-A156541] N86-10898

BORANES
Boronising of iron and steel by ionic bombardment by diborane
[BLL-BISI-TRANS-23034-(9022.06)] N86-10307

BORATES
Thermal expansion of glasses in the solid and liquid phases
[DE85-013953] N86-10351

BOREHOLES
Geologic evaluation and reservoir properties of the PR Spring tar sand deposit, Uintah and Grand Counties, Utah
[DE85-013248] N86-10634

BORESIGHTS
Radome analysis and design capabilities of the RF and Microwave Technology Branch
[AD-A156662] N86-10404

BORIDES
Mechanism of the formation of boronised layers on high carbon steel
[BLL-BISI-TRANS-23036-(9022.06)] N86-10306

BORON
Magnetic properties of doped semiconductors
[DE85-012090] N86-11053

BORON NITRIDES
Development of a sheath for sensor protection in molten steel applications
[AD-A156764] N86-10315

BOROSILICATE GLASS
Recirculation within a glass mixture subjected to external and resistive heating
[DE85-010088] N86-10346

BOSON FIELDS
Polarization transfer in inelastic scattering and pionic models of the EMC effect
[DE85-010738] N86-10955

BOSONS
Proceedings of a Workshop on Electroweak Symmetry Breaking
[DE85-004444] N86-11008
Two-loop large Higgs mass corrections to vector boson self-couplings
[NIKHEF-H/84-15] N86-11038

BOUNDARIES
Correlation between vibrations and buckling of cylindrical shells stiffened by spot-welded and riveted stringers
[TAE-537] N86-10584
A study of methods to predict and measure the transmission of sound through the walls of light aircraft. Integration of certain singular boundary element integrals for applications in linear acoustics
[NASA-CR-176229] N86-10912

BOUNDARY ELEMENT METHOD
Advanced development of BEM for two and three dimensional nonlinear analysis N86-10855

BOUNDARY LAYER FLOW
Acta Aeronautica et Astronautica Sinica (selected articles)
[AD-A147304] N86-10001
Second order approximation method for transonic flows over swept wings N86-10002
Investigations on a supercritical airfoil with boundary layer suction through a perforated strip in the shock region
[DFVLR-FB-85-15] N86-10025
A boundary layer flow model for areas of complex terrain N86-10701
Simulation of the atmospheric boundary layer in the large wind tunnel of the TNO Institute for Building materials and Constructions (IBBC). Part 1: Theory
[BI-76-39/08.7.23100-PT-1] N86-10703
Simulation of the atmospheric boundary layer in the large wind tunnel of the TNO Institute for Building Materials and Construction (IBBC). Part 2: Experiments
[BI-76-39/08.7.23100-PT-2] N86-10704

BOUNDARY LAYER SEPARATION
The role of freestream turbulence scale in subsonic flow separation
[NASA-CR-176237] N86-10014
Three-dimensional inviscid analysis of radial turbine flow and a limited comparison with experimental data
[NASA-TM-87091] N86-10017

BOUNDARY LAYERS
Fuel and lubricant behavior in boundary layers analyzed by infrared emission Fourier transform spectrometry
N86-10336
The effects of orography on land-atmosphere turbulent exchange processes N86-10702

BOUNDARY VALUE PROBLEMS
A mesh moving technique for time dependent partial differential equations in two space dimensions
[AD-A156663] N86-10866
Error estimates and automatic time step control for numerical methods for stiff ordinary differential equations
[CTH-MATH-1984-27] N86-10872

BRAGG ANGLE
Signal analysis receiver with acousto-optic delay lines
[AD-D011761] N86-10427

BRAIN
TV monitoring control system in electrophysiological studies N86-10765

BRAYTON CYCLE
High efficiency heat transport and power conversion system for cascade
[DE85-012959] N86-10468

BRAZING
Vacuum brazing under microgravity --- Spacelab
N86-10214
Metallurgy and metallography of braze joints
[DE85-014563] N86-10325

BREADBOARD MODELS
Advanced optical measurement techniques
N86-10174

Advanced containerless processing technology
N86-10176

BREMSSTRAHLUNG

Radiation field results from the SPEED triaxiode, a large area, high dose rate, short pulse 1MV bremsstrahlung source
[DE85-009438] N86-11005

Directionality of bremsstrahlung from relativistic electrons in solar flares
[NASA-TM-87509] N86-11141

BRIDGMAN METHOD

Microgravity Science and Applications Program tasks
[NASA-TM-87568] N86-10053

Fluid flow in crystal growth: Analysis of the verticle Bridgman and floating zone process N86-10055

Growth of solid solution crystals N86-10065

Heat flow and segregation in directional solidification
N86-10072

Lead telluride crystals grown in microgravity: Experiment ES 318 — Spacelab N86-10220

BRIGHTNESS

Age-dating volcanic and alluvial surfaces with multipolarization data N86-10620

Mild hypoxia and visual performance with night vision goggles
[AD-A156969] N86-10787

High-brightness photoemitter injector for electron accelerators
[DE85-012673] N86-10929

BRIGHTNESS DISTRIBUTION

Improved mapping of radio sources from VLBI data by least-square fit N86-10402

Radio studies of a complete sample of quasars
N86-11093

Cometary atmospheres: Modeling the spatial distribution of observed neutral radicals
[NASA-CR-176242] N86-11133

BRILLOUIN EFFECT

Real-time holography by stimulated Raman and Brillouin scattering N86-10479

BROADCASTING

An evaluation of the use of microphone arrays for studio recording
[BBC-RD-1985/8] N86-10366

BROKEN SYMMETRY

Proceedings of a Workshop on Electroweak Symmetry Breaking
[DE85-004444] N86-11008

BROMIDES

Laser Raman spectroscopy study of the zinc and bromide ion complex equilibrium in zinc/bromine battery electrolytes
[DE85-011820] N86-10301

BROMINE

Laser Raman spectroscopy study of the zinc and bromide ion complex equilibrium in zinc/bromine battery electrolytes
[DE85-011820] N86-10301

BRONZES

The mechanism of erosion of metallic materials under cavitation attack
[NASA-TM-87133] N86-10552

Fracture toughness testing of centrifugally cast nickel aluminium bronze
[REPT-MAT/720] N86-10575

BUBBLE TECHNIQUE

Theoretical modeling of the vapor cavitation in dynamically loaded journal bearings
[NASA-TM-87076] N86-10463

BUBBLES

Mass transport phenomena between bubbles and dissolved gases in liquids under reduced gravity conditions N86-10110

Thermocapillary and diffusocapillary migration of a fluid drop N86-10128

Fusion target technology N86-10156

Shrinking of a gas bubble in a glass melt under microgravity conditions — STS-11 N86-10254

Acoustic cavitation and bubble dynamics
[AD-A156888] N86-10918

Methane-bubble formation in hydrogen-charged Fe-30 ppM C
[DE85-012526] N86-10937

BUCKLING

An analytical and numerical study of the buckling behavior of fiber-reinforced beams N86-10566

Optimal design of portal frames against buckling
N86-10572

Effect of sequence of loading on interaction curves for buckling of stiffened shells
[TAE-536] N86-10583

Correlation between vibrations and buckling of cylindrical shells stiffened by spot-welded and riveted stringers
[TAE-537] N86-10584

BUDGETS

Report of the ad hoc committee to review the program of the SDI Directorate on Innovative Science and Technology (IST)
[AD-A156568] N86-11071

BUILDINGS

Vibro-acoustic forecast for space shuttle launches at Vandenberg AFB: The payload changeout room and the administration building
[AD-A156944] N86-10269

Load space formulation of reliability for nonlinear random structural systems N86-10570

BUNCHING

Report on a visit to CERN in February 1985. Notes on bunch monitors, high-frequency systems, linacs, kickers, magnets, vacuum and bunch extraction
[LINO-119] N86-10967

Proposed bunching scheme for a polarized H(-) injector
[DE85-012648] N86-10986

BUOYANCY

Crystal melts under reduced gravity N86-10062

Float zone experiments in space N86-10067

Fluid dynamics and thermodynamics of vapor phase crystal growth N86-10069

Buoyancy effects upon vapor flame and explosion processes N86-10161

Fundamental studies of droplet combustion at reduced gravity N86-10165

BURKINA

With Argus eyes from space. Satellite Diagnosis for Upper Volta. Seven maps without mystery N86-10183

BURNERS

Design and calibration of a flat-flame burner using line reversal techniques
[AD-A156724] N86-10294

Effects of chemistry and swirl on the production of turbulence in a flame
[PB85-219632] N86-10305

BURNING RATE

A fundamental study of smoldering with emphasis on experimental design for zero-g N86-10162

BYPASSES

Digital control of the hydraulic actuators of an adaptive suspension vehicle N86-10548

C

CABLES (ROPES)

Guidance and control of a cable based payload pickup system N86-10046

CADMIUM TELLURIDES

Solution growth of cadmium telluride: Experiment ES 322 — Spacelab N86-10225

Sensor system
[AD-D011767] N86-10480

CALCIUM CARBONATES

High-pressure release-wave measurements and phase transformation in CaCO3
[DE85-012592] N86-11055

CALCIUM COMPOUNDS

Crystal growth from solution — Spacelab N86-10229

Characterization of cathodic corrosion products in the Ca/CaCrO4 thermal battery
[DE85-013442] N86-10644

CALCIUM PHOSPHATES

Growth and characterization of brushite and lead monetite, simulation and results — Spacelab
N86-10230

CALIBRATING

Operating characteristics of the multiple critical Venturi System and secondary calibration nozzles used for weight-flow measurements in the Langley 16-foot transonic tunnel
[NASA-TM-86405] N86-10016

Design and calibration of a flat-flame burner using line reversal techniques
[AD-A156724] N86-10294

Comparison of the calibration of ionospheric delay in VLBI data by the methods of dual frequency and Faraday rotation N86-10384

A VLA experiment: Planning for Voyager at Neptune
N86-10396

Mobile VLBI and GPS measurement of vertical crustal motion N86-10401

A comparison of swept frequency and FFT methods used to calibrate array test modules
[AD-A156629] N86-10430

Calibrated Faraday current and magnetic field sensor
[DE85-013438] N86-10439

Investigation of the uncertainties of the NBS (National Bureau of Standards) thermal voltage and current converters
[PB85-200178] N86-10453

Partial in-flight calibration of the metric camera — Spacelab N86-10496

High flux calorimetry
[AD-A156852] N86-10524

CV-990 L-band SAR: A calibration experiment
N86-10617

Calibration of the multispectral scanner (MSS) satellite data to evaluate change in the reflection of coniferous stocks
[DFVLR-FB-84-44] N86-10636

Harmonic distortion reduction technique for data acquisition
[AD-D011771] N86-10799

Fiber optic gradient hydrophone construction and calibration for sea trial
[AD-A156469] N86-10914

Secondary standards laboratories for ionizing radiation calibrations: The national laboratory interests
[DE85-007046] N86-10938

CALIFORNIA

Structural discontinuity within the southern California continental margin: Seismic and gravity models of the western Transverse Ranges N86-10699

Surface winds at NWC (Naval Weapons Center): 1964 - 1982
[AD-A156660] N86-10712

CALORIMETERS

High flux calorimetry
[AD-A156852] N86-10524

Guidelines for a thermochemical kinetics computer program
[DE85-014266] N86-10839

CAMERAS

Fall velocity indicator/viewer
[AD-D011789] N86-10482

OEEPE participation in testing metric camera photography — European Organization for Experimental Photogrammetric Investigations (OEEPE) N86-10507

Land evaluation successes with the metric camera — Spacelab N86-10512

Type of new Chinese-produced high-speed camera and its utilization in detonation physics experiments
[DE85-015191] N86-10529

CANOPIES (VEGETATION)

Mapping diverse forest cover with multipolarization airborne radar N86-10625

Vegetation canopy discrimination and biomass assessment using multipolarized airborne SAR
N86-10626

CANTILEVER PLATES

Joint research effort on vibrations of twisted plates, phase 1: Final results
[NASA-RP-1150] N86-10579

CAPACITORS

Intrinsic mechanisms of multilayer ceramic capacitor failure
[AD-A156638] N86-10431

Interdigital Schottky barrier capacitor apparatus
[AD-D011799] N86-10436

CAPILLARY FLOW

Thermocapillary flows and their stability: Effects of surface layers and contamination N86-10109

Energy stability of thermocapillary convection in models of the float zone process N86-10123

Thermocapillary and diffusocapillary migration of a fluid drop N86-10128

Miscibility gap systems
[NASA ORDER H-27954B] N86-10131

Capillary forces in a low gravity environment — Spacelab N86-10202

Liquid column stability: Experiment 1 ES-331 — Spacelab N86-10205

The influence of thermocapillarity on the migration of droplets in a liquid possessing a uniform temperature gradient N86-10237

Measurements of the critical Marangoni number of the laminar-oscillatory transition of thermocapillary convection in floating zones N86-10242

CAPILLARY TUBES

Rapid analysis using capillary supercritical fluid chromatography
[DE85-012460] N86-10297

CARBON

Cometary atmospheres: Modeling the spatial distribution of observed neutral radicals
[NASA-CR-176242] N86-11133

CARBON DIOXIDE

Rapid analysis using capillary supercritical fluid chromatography
[DE85-012460] N86-10297

A superconducting tunnel junction receiver for millimeter-wave astronomy N86-11041

CARBON FIBER REINFORCED PLASTICS

Carbon fiber reinforced polymide filament wound tube manufacturing
[BR64172] N86-10339

CARBON FIBERS
Continuous fiberization of silicon-carbide-nitride precursor resin N86-10168
CARBON MONOXIDE
Catalytic activity of shock modified ZnO for CO oxidation and methanol synthesis
[DE85-014704] N86-10300
Effect of H2S and COS in the fuel gas on the performance of ambient pressure phosphoric acid fuel cells
[DE85-013913] N86-10446
The two micron spectrum of R Scuti N86-11092
CARBON STEELS
Mechanism of the formation of boronised layers on high carbon steel
[BLL-BISI-TRANS-23036-(9022.06)] N86-10306
Boronising of iron and steel by ionic bombardment by diborane
[BLL-BISI-TRANS-23034-(9022.06)] N86-10307
Study of statis and dynamic stress effects in nonlinear solids
[NASA-CR-176236] N86-10578
CARBON-CARBON COMPOSITES
Erosion-resistant nosetip construction
[AD-D011787] N86-10289
Process models for 3D composites
[AD-A156889] N86-10292
High temperature mechanical testing of a cylindrical weave carbon-carbon composite
[AD-A156639] N86-10591
CARBONATES
Effects of H2S on molten carbonate fuel cells
[DE85-014052] N86-10447
CARDIOVASCULAR SYSTEM
Capacity for work and hemodynamics in males residing at middle and high latitudes N86-10747
Individual typological self-regulation of cardio-vascular system N86-10752
Classification of changes in electrocardiogram during muscular exertion of healthy individuals N86-10755
CARRIER MOBILITY
Free carrier absorption from electrons in confined systems N86-11042
CARTRIDGES
Small cartridge heater
[AD-D011784] N86-10277
Specification for the performance, design, development and test requirements for a severe environment cartridge recorder. Issue 4
[AD-A156637] N86-10523
Optical disc transport system
[AD-D011779] N86-10974
CASSEGRAIN OPTICS
TRIO optics --- spaceborne optical interferometer (TRIO) N86-11108
CAST ALLOYS
Unidirectional solidification of cast iron: Experiment ES-325 --- Spacelab N86-10212
CASTING
Skin casting of alloys and composites: Results of Spacelab (SL)-1 and TEXUS experiments N86-10213
CASTINGS
Control of cast iron microstructure N86-10084
Graphite formation in cast iron N86-10100
CATALOGS (PUBLICATIONS)
Catalog of Resources for Education in Ada (trademark) and Software Engineering (CREASE). Version 3.0
[AD-A156687] N86-10790
CATALYSIS
Surface science and catalysis
[DE85-013922] N86-11057
CATALYSTS
Physical and chemical properties of a nickel catalyst processed under microgravity --- STS-7 N86-10255
Effects of H2S on molten carbonate fuel cells
[DE85-014052] N86-10447
Phosphoric and electric utility fuel technology development
[DE85-014741] N86-10651
Phosphoric and electric utility fuel cell technology development
[DE85-014552] N86-10652
CATALYTIC ACTIVITY
Catalytic activity of shock modified ZnO for CO oxidation and methanol synthesis
[DE85-014704] N86-10300
CATHODE RAY TUBES
Measurement of visual contrast sensitivity
[AD-D011776] N86-10973
CATHODES
P-N junction controlled field emitter array cathode
[AD-D011815] N86-10416
Effects of H2S on molten carbonate fuel cells
[DE85-014052] N86-10447
Characterization of cathodic corrosion products in the Ca/CaCrO4 thermal battery
[DE85-013442] N86-10644
CATIONS
Report on the engineering test of the LBL 30 second neutral beam source for the MFTF-B project
[DE85-013317] N86-10962
CAUCASUS MOUNTAINS (U.S.S.R.)
Laws of distribution of the snow cover on the greater Caucasus (Soviet Union)
[NASA-TM-77911] N86-10614
CAUCHY PROBLEM
A modified modified Korteweg-deVries equation
[PN-84/27] N86-10859
Initial data for N black holes N86-11128
CAVITATION FLOW
Theoretical modeling of the vapor cavitation in dynamically loaded journal bearings
[NASA-TM-87076] N86-10463
The mechanism of erosion of metallic materials under cavitation attack
[NASA-TM-87133] N86-10552
Acoustic cavitation and bubble dynamics
[AD-A156888] N86-10918
CAVITIES
Development of materials processing systems for use in space on low-g simulation devices N86-10166
CAVITY RESONATORS
Compact, low jitter, triggered spark gap
[DE85-012812] N86-10195
An experimental TE sub 12 - TE sub 11 circular waveguide mode converter N86-10387
Direct-coupled cavity filters with irises of arbitrary thickness
[DFVLR-FB-85-14] N86-10412
Beam-cavity interaction measurements in a DAW structure
[DE85-012660] N86-10987
Analytic evaluation of LAMPF 2 Booster Cavity design
[DE85-012680] N86-11002
Superconductors for pulsed RF accelerators
[DE85-013378] N86-11051
CELESTIAL REFERENCE SYSTEMS
A VLBI survey at 2.29 GHz N86-10383
CELL CATHODES
Advanced fuel cell development
[DE85-014550] N86-10659
CELL DIVISION
Cell partition in two polymer aqueous phases N86-10139
Purification and cultivation of human pituitary growth hormones secreting cells N86-10140
Cell separations in microgravity and development of a space bioreactor N86-10141
CELLS (BIOLOGY)
Biochemical assays of cultured cells N86-10134
Cell partition in two polymer aqueous phases N86-10136
Purification and cultivation of human pituitary growth hormones secreting cells N86-10140
Cell separations in microgravity and development of a space bioreactor N86-10141
Cell maintenance systems N86-10142
Kidney cell electrophoresis N86-10145
Somatic cell and molecular genetics approach to DNA repair and mutagenesis
[DE85-014181] N86-10737
Treatment planning with ion beams
[DE85-012661] N86-10990
CENTRAL NERVOUS SYSTEM
Homocarnosin in rat brain during adaptation to cold N86-10762
CENTRAL PROCESSING UNITS
Arithmetic pipeline for image processing
[AD-D011773] N86-10800
CENTRIFUGAL CASTING
Fracture toughness testing of centrifugally cast nickel aluminium bronze
[REPT-MAT/720] N86-10575
CERAMICS
Attachment method-ceramic radome to metal body
[AD-D011778] N86-10032
Microgravity Science and Applications Program tasks
[NASA-TM-87568] N86-10053
Lambda point equipment N86-10118
Gel precursors as glass and ceramic starting materials for space processing applications research N86-10150
Rapid solidification of magnetic oxides N86-10152
Glass research N86-10157
Microgravity Materials Science Laboratory N86-10173
Acoustic levitation containerless processing N86-10177
High-temperature controlled redox crystallization studies N86-10178
Small cartridge heater
[AD-D011784] N86-10277
Tribological properties of structural ceramics
[NASA-TM-87105] N86-10341
Mixed-mode fracture of ceramics
[DE85-014087] N86-10349
High efficiency heat transport and power conversion system for cascade
[DE85-012959] N86-10468
Characterization of mechanical damage mechanisms in ceramic composite materials
[AD-A156574] N86-10590
Advanced Gas Turbine (AGT) powertrain system development for automotive applications report
[NASA-CR-174886] N86-11087
CERIUM COMPOUNDS
Fermi surface study of CeSb in the ferromagnetic and antiferromagnetic phases
[DE85-012122] N86-11052
CESIUM 137
Sediment characterization. Task 2: Instream contaminant study. Volume 2: Appendices
[DE85-013503] N86-10680
CHAFF
AIRBOC (air rapid bloom offboard chaff) chaff deployment system
[AD-D011746] N86-10554
CHANGE DETECTION
Calibration of the multispectral scanner (MSS) satellite data to evaluate change in the reflection of coniferous stocks
[DFVLR-FB-84-44] N86-10636
CHANNEL FLOW
The development and prevention of channel segregation during alloy solidification N86-10086
Large eddy interactions in a turbulent channel flow
[NASA-TM-86757] N86-10464
CHANNELS (DATA TRANSMISSION)
Parallel local interface bus
[AD-D011742] N86-10792
An intelligent local disk control system
[REPT-051560-28(1984)08] N86-10808
CHARGE COUPLED DEVICES
The intensified multi CCD camera --- spaceborne interferometers N86-11122
CHARGE EXCHANGE
Charge exchange in slow collisions of atoms and molecules N86-10922
CHARGE TRANSFER
Polyacetylene polymerization, structure, and electrical transport properties N86-10334
Charge exchange in slow collisions of atoms and molecules N86-10922
CHARGED PARTICLES
Design and construction of a Faraday cup for measurement of small electronic currents
[NASA-TM-77915] N86-10418
Hyperon polarization: An unresolved problem
[DE85-012298] N86-10946
Lie algebraic methods for charged particle beams and light optics N86-10970
CHARPY IMPACT TEST
Fabrication and metallurgical properties of modified 9Cr-1 Mo steel
[DE85-012885] N86-10328
CHARRING
A fundamental study of smoldering with emphasis on experimental design for zero-g N86-10162
CHARTS
Vision test chart and method using Gaussians
[AD-D011756] N86-10778
CHEBYSHEV APPROXIMATION
Partial eigensolutions of large nonsymmetric matrices
[AD-A156711] N86-10867
Spectral methods in adapted curved grids N86-10878
CHECKOUT
Classification of real-time program testing tasks and methods N86-10815
Collective use computer system for the Academy of Sciences KaSSR N86-10817
CHELATES
Extraction of lanthanide ions by 2-methyl-8-quinolinol
[DE85-014277] N86-10303
CHELATION
Rusty bolt intermodulation interference reducer
[AD-D011748] N86-10313
CHEMICAL ANALYSIS
Biochemical assays of cultured cells N86-10134
New directions in chemical analysis
[DE85-012930] N86-10296
Theoretical comparison of classical (K-matrix) and inverse (P-matrix) least-squares methods for quantitative infrared spectroscopy
[DE85-012827] N86-10298

Weld metal hot-cracking of hastelloy alloys C-22 and C-276: A study by analytical electron microscopy
[DE85-009437] N86-10324
Development and evaluation of multispecies test protocols for assessing chemical toxicity
[DE85-013526] N86-10679

CHEMICAL BONDS
A procedure identifying a polyacetylene initiator of olefin metathesis. The reactivities of metal-carbenes toward alkenes and alkynes
[AD-A156997] N86-10283
Non-empirical interatomic potentials for transition metals
[DE85-013448] N86-10440

CHEMICAL CLEANING
Passivation of steel with aqueous amine solutions
[AD-D011749] N86-10314

CHEMICAL COMPOSITION
Fabrication and metallurgical properties of modified 9Cr-1 Mo steel
[DE85-012885] N86-10328
Development of new ammonium nitrate composite explosives
[DE85-014252] N86-10356
Evaluation of the 90-day inhalation toxicity of petroleum and oil shale JP-5 jet fuel
[AD-A156815] N86-10675
Microcomputer aided calculations of parameters for spray dryer operation
[DE85-013408] N86-10681
Radionuclide complexation in xylem exudates of plants
[DE85-013446] N86-10684

CHEMICAL ELEMENTS
Study of the reactive-element effect in oxidation of Fe-Cr alloys using transverse section analytical electron microscopy N86-10087

CHEMICAL ENGINEERING
Research needs for corrosion control and prevention in energy conservation systems
[DE85-014852] N86-10326
Acquaintance with on line literature research. An introduction for education at the Chemical Technology Section N86-11081

CHEMICAL EQUILIBRIUM
Laser Raman spectroscopy study of the zinc and bromide ion complex equilibrium in zinc/bromine battery electrolytes
[DE85-011820] N86-10301

CHEMICAL EXPLOSIONS
Development of new ammonium nitrate composite explosives
[DE85-014252] N86-10356
Type of new Chinese-produced high-speed camera and its utilization in detonation physics experiments
[DE85-015191] N86-10529
Guidelines for a thermochemical kinetics computer program
[DE85-014266] N86-10839

CHEMICAL LASERS
La Recherche Aerospatiale, bimonthly bulletin, no. 1984-5, September-October 1985
[ESA-TT-899] N86-10363

CHEMICAL PROPERTIES
Colloidal oxide properties and kinetic studies N86-10147
Crystallization, optical and chemical properties of fluoride glasses N86-10149
Fundamental studies of droplet combustion at reduced gravity N86-10165
Age-life prediction of nylon 66 parachute materials. Part 2: Changes in the chemical and physical properties of materials on aging
[AD-A156909] N86-10347

CHEMICAL REACTIONS
A procedure identifying a polyacetylene initiator of olefin metathesis. The reactivities of metal-carbenes toward alkenes and alkynes
[AD-A156997] N86-10283
Chemical kinetics and cellular structure of detonations in hydrogen sulphide and air
[DE85-009408] N86-10304
Investigation of metallic impurities introduced into SiO2 and silicon by various candidate VLSI metallization systems: Chemical reactions, diffusion, and electrical properties
[AD-A156609] N86-10429
Chemical kinetics and photochemical data for use in stratospheric modeling
[NASA-CR-176198] N86-10707
Surface science and catalysis
[DE85-013922] N86-11057

CHIPS (ELECTRONICS)
The VLSI design of error-trellis syndrome decoding for convolutional codes N86-10391
Making the right choice — silicon photodiodes N86-10669
Prospects for creation of optical digital high-performance computers N86-10610

CHLORINE COMPOUNDS
Sediment characterization. Task 2: Instream contaminant study, volume 1
[DE85-013502] N86-10683

CHLOROFORM
Extraction of lanthanide ions by 2-methyl-8-quinolinol
[DE85-014277] N86-10303

CHOKES (FUEL SYSTEMS)
Operating characteristics of the multiple critical Venturi System and secondary calibration nozzles used for weight-flow measurements in the Langley 16-foot transonic tunnel
[NASA-TM-86406] N86-10016

CHOLINE
Short term heat effect on adreno- and cholino-sensitivity of rat's small intestine N86-10754

CHROMATES
Characterization of cathodic corrosion products in the Ca/CaCrO4 thermal battery
[DE85-013442] N86-10644

CHROMATOGRAPHY
New instrumentation for phase partitioning N86-10138
Rapid analysis using capillary supercritical fluid chromatography
[DE85-012480] N86-10297
Volatile organic compounds in indoor air: A survey of various structures
[PB85-198356] N86-10687
Applications of the second-order achromat concept to the design of particle accelerators
[DE85-013072] N86-10994

CHROMIUM
Environmental degradation of materials: Surface chemistry related to stress corrosion cracking N86-10099

CHROMIUM ALLOYS
Study of the reactive-element effect in oxidation of Fe-Cr alloys using transverse section analytical electron microscopy N86-10087
Electronic and magnetic properties of noble-metal and transition-metal alloys, interfaces and overlayers
[DE85-014532] N86-10321

CHROMIUM STEELS
Fabrication and metallurgical properties of modified 9Cr-1 Mo steel
[DE85-012885] N86-10328

CHROMOSOMES
Study of hypokinesia and acceleration effects on human chromosomes N86-10740

CIRCADIAN RHYTHMS
Intradiurnal organization of wakefulness-sleep sequence and energy metabolism in rats exposed to low ambient temperature N86-10764

CIRCUIT BOARDS
Multi-row connector with ground plane board
[AD-D011803] N86-10437

CIRCUITS
Miniature radar packaging
[DE85-014598] N86-10410

CIRCULATION
Effects of chemistry and swirl on the production of turbulence in a flame
[PB85-219632] N86-10305
Recirculation within a glass mixture subjected to external and resistive heating
[DE85-010068] N86-10348
Geothermal lost circulation zone mapping tool
[DE85-008696] N86-10531

CITIES
Metric camera image of Munich as additional means for urban cartography — Spacelab N86-10519

CIVIL AVIATION
A review of Australian investigations on aeronautical fatigue during the period April 1983 to March 1985
[AD-A156802] N86-10036

CLADDING
General-purpose heat source development: Safety Verification Test Program. Bullet/fragment test series
[DE85-014262] N86-10660

CLASSIFICATIONS
The effects of merging TM and A/C radar on wetland classification N86-10621
Classification of real-time program testing tasks and methods N86-10615

CLEANING
Impurity extraction by droplets N86-10122

CLIMATE
Observations of the snow cover in the southern part of the Buryat Autonomous Soviet Socialist Republic
[NASA-TM-77910] N86-10613
Smoke inputs to climate models: Optical properties and height distribution for nuclear winter studies
[DE85-011363] N86-10717
contemporary Aeolian processes on Mars: Local dust storms N86-11136

CLIMATOLOGY
The air of life of the blue planet. Atmosphere research from space using data and facts against climate speculations N86-10184
Laws of distribution of the snow cover on the greater Caucasus (Soviet Union)
[NASA-TM-77911] N86-10614
A composite climatological study of the frequency and distribution of severe weather associated with spring season Colorado cyclogenesis
[AD-A156961] N86-10715

CLINICAL MEDICINE
Annotated bibliography of publications dealing with occupational health and medical information systems, cost analysis procedures, evaluation methodology and related legal issues
[AD-A156650] N86-11078

CLOSED CIRCUIT TELEVISION
Geothermal lost circulation zone mapping tool
[DE85-008696] N86-10531

CLOSURES
Fundamental study of the closure property of joints N86-10696

CLOUD COVER
Applications for three-dimensional computer graphic cloud representations produced from satellite imagery
[AD-A156903] N86-10798

CLOUD GLACIATION
Comparative flight measurement of icing parameters for the propeller aircraft Do-28D2 of the test station 61 of the DFVLR and for the DFVLR aircraft Falon 20e in stratus clouds
[DFVLR-FB-85-16] N86-10720

CLOUD PHYSICS
Cloud microphysics by thermal wave methods N86-10103

CLOUDS
Cloud microphysics by thermal wave methods N86-10103
Particle cloud combustion experiment N86-10160
Applications for three-dimensional computer graphic cloud representations produced from satellite imagery
[AD-A156903] N86-10798
A modeling analysis program for the JPL table mountain In sodium cloud
[NASA-CR-176241] N86-11139

CLUMPS
Supersonic metal cluster beams
[DE85-014321] N86-10966

COARSENESS
Undercooling, remelting, and coarsening N86-10080

COASTAL ECOLOGY
Utilization of satellite remote sensing for the monitoring of oil pollution and marine ecosystems in Indonesia. A Tropical Earth Resources Satellite program (TERS) case study implemented for the NLR, Delft N86-10640

COASTAL PLAINS
Cretaceous and cenozoic stratigraphy of the upper and middle coastal plain, Harnett County area, North Carolina N86-10690

COASTAL WATER
Long range translocations ashore to offshore using Spacelab-1 metric camera imagery in the perspective of integrated geophysical surveys N86-10499

COATINGS
Mechanics of coated fiber composites N86-10265
Steady state frictional behavior of thin film coatings N86-10335
The influence of the substrate on the practical machining applications of cutting edges coated with different materials
[BLL-RISLEY-TR-5039-(9091.9F)] N86-10546

COAXIAL CABLES
Miniature radar packaging
[DE85-014598] N86-10410

COAXIAL FLOW
Buoyancy effects upon vapor flame and explosion processes N86-10161

COBALT
Thermomigration of cobalt in liquid tin: Experiment 1 ES 320 — Spacelab N86-10222

COBALT ALLOYS
Electronic and magnetic properties of noble-metal and transition-metal alloys, interfaces and overlayers
[DE85-014532] N86-10321

COCKPITS
Proposed modifications for the RAAF Airtrainer CT-4A cockpit
[AD-A156808] N86-10039

CODERS
Phase coded pulse expander-compressor
[AD-D011817] N86-10376
CODING
Progressive damage, fracture predictions and post mortem correlations for fiber composites
[NASA-TM-87101] N86-10290
Determining a physically appropriate neutron spectrum from multisphere data
[DE85-013045] N86-10299
High-rate convolutional code construction with the minimum required SNR criterion N86-10392
An analytical and numerical study of the buckling behavior of fiber-reinforced beams N86-10566
COGENERATION
Fuel Cell Technology Assessment Program, work element no. 6
[DE85-008228] N86-10444
COGNITION
Psychological Sciences Division 1984 programs
[AD-A156631] N86-10779
COGNITIVE PSYCHOLOGY
Risk propensity, action readiness and the roles of societal and individual decision makers
[IZF-1984-27] N86-11077
COHERENT LIGHT
Signal analysis receiver with acousto-optic delay lines
[AD-D011761] N86-10427
COSMIC: A high resolution, large collecting area telescope — Coherent Optical System of Modular Imaging Collectors (COSMIC) N86-11104
COLD ACCLIMATIZATION
Individual typological features of autonomic reactions during autogenic training in polar expedition members in period of wintering in Antarctica N86-10748
Adaptation of man to extreme conditions of Antarctica N86-10751
Homocarnosin in rat brain during adaptation to cold N86-10762
Efficiency of muscular work in white rats during adaptation to cold N86-10763
Intradiurnial organization of wakefulness-sleep sequence and energy metabolism in rats exposed to low ambient temperature N86-10764
COLD TOLERANCE
Effect of cold on brain serotonin system and plasma corticosteroid level in different strains of mice N86-10766
COLD WEATHER
Microphysical/mesoscale aspects of nuclear winter and new directions in assessments
[DE85-013479] N86-10718
COLD WORKING
Formation and characterization of amorphous erbium-based alloys prepared by near-isothermal cold-rolling of elemental composites
[DE85-014853] N86-10327
COLLIMATION
Beam-beam deflection: to measure size spot and offset at SLC IP
[DE85-014265] N86-10965
Tracking studies on the effects of magnet multipoles on the aperture of the RHIC heavy ion collider
[DE85-013282] N86-11023
COLLIMATORS
Applications of the second-order achromat concept to the design of particle accelerators
[DE85-013072] N86-10994
COLLISION PARAMETERS
Charge exchange in slow collisions of atoms and molecules N86-10922
COLLISION RATES
Rapid evaluation of ion thruster lifetime using optical emission spectroscopy
[NASA-TM-87103] N86-10280
COLLISIONAL PLASMAS
Time-implicity simulation of particle-fluid systems
[DE85-012944] N86-10471
COLLISIONLESS PLASMAS
Heating and generation of suprathermal particles at collisionless shocks
[DE85-014114] N86-11034
Local conservation laws for the Maxwell-Vlasov and collisionless kinetic guiding center theories
[DE85-013122] N86-11063
COLLISIONS
Hugoniot measurements in aluminum to 420 GPa using the LLNL two-stage light-gas gun
[DE85-013621] N86-10317
Electron momentum transfer collision frequency in N(2), O(2) and air
[AD-A157030] N86-10924
COLLOIDS
Colloidal oxide properties and kinetic studies N86-10147
COLOR
The synthesis and analysis of color images
[NASA-TM-86844] N86-10777
COLOR CENTERS
Defect identification in high-energy semiconductors
[DE85-014533] N86-10442
COLOR CODING
Report on a visit to England — color and monochrome displays
[FOA-C5-85-0006-H2] N86-10364
COLOR INFRARED PHOTOGRAPHY
Erosion control and watershed management by Spacelab photography N86-10493
Thematic mapping of metric camera color infrared and black and white photographs for land use classification N86-10510
Remote sensing study project East Gelderland (Netherlands). Part 2: Remote sensing flights in 1982 and 1983; organization aspects N86-10639
COLORADO
Report of the Workshop on Geologic Applications of Remote Sensing to the Study of Sedimentary Basins
[E86-10002] N86-10599
Position paper: Workshop on Geologic Applications of Remote Sensing to the Study of Sedimentary Basins N86-10601
Tertiary and quaternary research with remote sensing methods N86-10603
Remote stratigraphic and structural analysis: Multisensor results in the Wind River/Bighorn Basin area, Wyoming N86-10606
Foreland basin structures and remote sensing N86-10608
A composite climatological study of the frequency and distribution of severe weather associated with spring season Colorado cyclogenesis
[AD-A156981] N86-10715
COLORIMETRY
Captive volume device as a safe life monitor
[AD-D011802] N86-10525
COLUMNS (SUPPORTS)
Passive damping concepts for slender columns in space structures
[NASA-CR-176234] N86-10577
COMBAT
The quest for a helicopter suitable for combat rescue, 1967 - 1983
[AD-A156842] N86-10040
COMBINATORIAL ANALYSIS
State assignment in sequential circuits
[EUT-85-E-146] N86-10846
COMBINED STRESS
Three-dimensional stress singularities in anisotropic materials and composites N86-10286
COMBUSTION
Microgravity Science and Applications Program tasks
[NASA-TM-87568] N86-10053
Lambda point equipment N86-10118
Buoyancy effects upon vapor flame and explosion processes N86-10161
Fundamental studies of droplet combustion at reduced gravity N86-10165
Effects of scale and geometry on hydrogen-air detonations
[DE85-006762] N86-10474
Type of new Chinese-produced high-speed camera and its utilization in detonation physics experiments
[DE85-015191] N86-10529
COMBUSTION PHYSICS
Solid surface combustion at reduced gravity N86-10159
Particle cloud combustion experiment N86-10160
Experimental investigations of thermal radiation from potassium atoms and design applications
[DE85-004086] N86-11036
COMBUSTION PRODUCTS
Radiative heat transfer in nonisothermal combustion products N86-10458
COMBUSTION TEMPERATURE
A fundamental study of smoldering with emphasis on experimental design for zero-g N86-10162
COMETARY ATMOSPHERES
Cometary atmospheres: Modeling the spatial distribution of observed neutral radicals
[NASA-CR-176242] N86-11133
COMETS
A sequential decoding performance analysis for International Comet Explorer N86-10390
Cometary atmospheres: Modeling the spatial distribution of observed neutral radicals
[NASA-CR-176242] N86-11133
COMFORT
The wearing comfort of the PVC: Combat back pack
[IZF-1984-34] N86-10789
COMMERCE
Space utilization N86-11067
COMMUNICATION NETWORKS
Methods for developing jam-resistant security communications networks at fixed-site facilities
[DE85-012032] N86-10408
COMMUNICATION SATELLITES
Discussion on the progress and future of satellite communication (Japan)
[NASA-TM-77672] N86-10378
COMPACTING
COMPACT: Compaction of hierarchial chip layouts based on a constraint graph method with double-sided constraints N86-10845
COMPARATORS
Investigation of the uncertainties of the NBS (National Bureau of Standards) thermal voltage and current converters
[PB85-200178] N86-10453
Nickel-cadmium battery conditioner and tester apparatus
[AD-D011770] N86-10642
COMPARISON
Theoretical comparison of classical (K-matrix) and inverse (P-matrix) least-squares methods for quantitative infrared spectroscopy
[DE85-012827] N86-10298
Advanced vehicle systems assessment. Volume 3: Systems assessment
[NASA-CR-176206] N86-11084
Advanced vehicle systems assessment. Volume 4: Supporting analyses
[NASA-CR-176207] N86-11085
Photographic catalog of selected planetary size comparisons
[NASA-TM-86207] N86-11138
COMPENSATORY TRACKING
The influence of tactual seat-motion cues on training and performance in a roll-axis compensatory tracking task setting N86-10784
COMPLETENESS
Partial evolution and omega completeness of algebraic specifications
[CWI-CS-R8501] N86-10884
COMPLEX VARIABLES
Coordinate axes, location of origin, and redundancy for the one and two-dimensional discrete Fourier transform
[NASA-CR-176225] N86-10826
COMPOSITE MATERIALS
Microgravity Science and Applications Program tasks
[NASA-TM-87568] N86-10053
Lambda point equipment N86-10118
First Spacelab Payload (FSLP) experiments on composite materials N86-10265
The mechanics of delamination in composite materials N86-10284
Evaluation and prediction of long-term environmental effects on non metallic materials
[NASA-CR-178495] N86-10340
Development of new ammonium nitrate composite explosives
[DE85-014252] N86-10356
Composite explosives for metal acceleration: The effect of detonation temperature
[DE85-013982] N86-10359
Analytical and experimental study of cracks emanating from an elliptical hole in unidirectional composite material N86-10567
Characterization of mechanical damage mechanisms in ceramic composite materials
[AD-A156574] N86-10590
Investigation of composite materials property requirements for sonic fatigue research
[NASA-TM-87601] N86-10913
COMPOSITE STRUCTURES
A review of Australian investigations on aeronautical fatigue during the period April 1983 to March 1985
[AD-A156602] N86-10036
The effect of debond growth on crack propagation in composite plates reinforced with adhesively bonded composite stringers N86-10287
COMPOSITE WRAPPING
Stiffened and prestressed composite overwrapped pressure vessels N86-10547
COMPOSITION (PROPERTY)
Glass formation in reluctant glass formers N86-10151
Oxidation behavior of glassy alloys N86-10158
COMPRESSIBLE BOUNDARY LAYER
A numerical solution of the shock-turbulent interaction over a compression corner for supersonic flow N86-10003
COMPRESSION LOADS
Catalytic activity of shock modified ZnO for CO oxidation and methanol synthesis
[DE85-014704] N86-10300

COMPRESSION TESTS

Hugoniot measurements in aluminum to 420 GPa using the LLNL two-stage light-gas gun [DE85-013821] N86-10317

COMPRESSIVE STRENGTH

Characterization of mechanical damage mechanisms in ceramic composite materials [AD-A156574] N86-10590

COMPUTATION

Progressive damage, fracture predictions and post mortem correlations for fiber composites [NASA-TM-87101] N86-10290

Self-heating to ignition measurements and computation of critical size for solar energy collector materials [DE85-011449] N86-10302

Computational techniques for the analysis and design of digital communication systems [AD-A156945] N86-10407

New probabilistic modeling and simulation methods for complex time-dependent systems [DE85-009575] N86-10835

Revision of and documentation for the standard version of the Poisson-Group codes [DE85-012659] N86-10837

Guidelines for a thermochemical kinetics computer program [DE85-014266] N86-10839

Kalman filter preprocessor [AD-D011774] N86-10972

COMPUTATIONAL FLUID DYNAMICS

Numerical solution of hypersonic flow near leading edge of a flat plate N86-10008

Numerical simulation of unsteady thermal Marangoni flows N86-10236

Numerical simulation of convections in the microgravity environment N86-10239

Experiments and computations on unsteady separating flow in an expanding flume [REPT-2-84] N86-10477

Spectral methods in adapted curved grids N86-10878

COMPUTATIONAL GRIDS

Inviscid flow field analysis of maneuvering hypersonic vehicles using the SCM formulation and parabolic grid generation [DE85-013950] N86-10021

A mesh moving technique for time dependent partial differential equations in two space dimensions [AD-A156663] N86-10866

The h, p and h-p versions of the finite element method in 1 dimension. Part 2. The error analysis of the H and h-p versions [AD-A156835] N86-10869

Spectral methods in adapted curved grids N86-10878

COMPUTER AIDED DESIGN

COMPACT: Compaction of hierarchial chip layouts based on a constraint graph method with double-sided constraints N86-10845

COMPUTER ASSISTED INSTRUCTION

Catalog of Resources for Education in Ada (trademark) and Software Engineering (CREASE). Version 3.0 [AD-A156687] N86-10790

Computer-based training for the US Coast Guard standard terminal microcomputer: A basis for implementation utilizing the elaboration theory of instructional design [AD-A156548] N86-10791

Development of IS2100: An information systems laboratory [AD-A156846] N86-10797

COMPUTER COMPONENTS

A course on field programmable logic [EUT-85-E-148] N86-10805

COMPUTER GRAPHICS

TEMPUS: Simulating personnel and tasks in a 3-D environment [NASA-CR-171901] N86-10785

Applications for three-dimensional computer graphic cloud representations produced from satellite imagery [AD-A156903] N86-10798

Arithmetic pipeline for image processing [AD-D011773] N86-10800

USSR report: Cybernetics, computers and automation technology [JPRS-UCC-85-006] N86-10809

Zero-gravity movement studies [NASA-CR-171899] N86-10897

Infrared system with computerized image display [AD-D011777] N86-10906

COMPUTER INFORMATION SECURITY

Initial design of a relational database system for NPS computer asset identification and valuation for risk assessment [AD-A156847] N86-10796

Framework for generating expert systems to perform computer security risk analysis [DE85-014134] N86-10841

COMPUTER NETWORKS

Methods for developing jam-resistant security communications networks at fixed-site facilities [DE85-012032] N86-10408

COMPUTER PROGRAMMING

An analytical and numerical study of the buckling behavior of fiber-reinforced beams N86-10566

DBS/R database control system N86-10816

Let's get serious about software [AD-A156819] N86-10831

The DUCK manual [AD-A156936] N86-10833

NBSGSC: A FORTRAN program for quantitative X-ray fluorescence analysis [PB85-206068] N86-10847

Test of a multilevel computational theory of stereoscopic visual image processing [AD-A157011] N86-10870

COMPUTER PROGRAMS

Optimum design of an aircraft wing structure with multiple constraints by the direct-vision criteria method N86-10004

On the design of airfoils in transonic flow using the Euler equations N86-10013

Automatic processing of reactive polymers N86-10127

Progressive damage, fracture predictions and post mortem correlations for fiber composites [NASA-TM-87101] N86-10290

High-rate convolutional code construction with the minimum required SNR criterion N86-10392

Radome analysis and design capabilities of the RF and Microwave Technology Branch [AD-A156662] N86-10404

KRAK: A computer program for two-phase, two-component porous flow and fracture propagation, revision [DE85-014264] N86-10469

Finite element analysis of metals at elevated temperature using unified constitutive theories N86-10569

Radar system description N86-10616

Analysis of edge detection algorithms on DIAL (Digital Image Analysis Laboratory) [AD-A156735] N86-10630

Application of the ruthenium and technetium thermodynamic data bases used in the EQ3/6 geochemical codes [DE85-013766] N86-10632

The Liu, Katsaros, and Businger (1979) bulk atmospheric flux computational iteration program in FORTRAN and BASIC [AD-A156736] N86-10714

Application of the dutch method for estimating storm-induced dune erosion [AD-A156717] N86-10728

TEMPUS: Simulating personnel and tasks in a 3-D environment [NASA-CR-171901] N86-10785

Catalog of Resources for Education in Ada (trademark) and Software Engineering (CREASE). Version 3.0 [AD-A156687] N86-10790

Computer-based training for the US Coast Guard standard terminal microcomputer: A basis for implementation utilizing the elaboration theory of instructional design [AD-A156548] N86-10791

Special purpose hardware architectures for language recognition [AD-A156634] N86-10793

Dissecting the cow [DE85-013369] N86-10801

USSR report: Cybernetics, computers and automation technology [JPRS-UCC-85-006] N86-10809

Classification of real-time program testing tasks and methods N86-10815

System integration report [NASA-CR-171900] N86-10821

Supervisory control of the right arm of the beam assembly teleoperator [AD-A156856] N86-10832

Compexity of higher-order programs [DE85-012776] N86-10834

Klystron control software in the SIC [DE85-013068] N86-10836

Computer codes: A bibliography, supplement 1 [DE85-008721] N86-10838

Guidelines for a thermochemical kinetics computer program [DE85-014266] N86-10839

Box method for finding intersections of a trajectory with axisymmetric flux surfaces [DE85-013525] N86-10840

Software for an automated gaging system [DE85-013322] N86-10842

HALFBREED: An extended capability version of the YAQUI code [DE85-014237] N86-10843

Timing system control software in the SLC [DE85-013380] N86-11024

COMPUTER SYSTEMS DESIGN

Shipboard non-tactical computer systems of the US Navy [AD-A156769] N86-10849

On line astronomical image processing using microcomputers N86-11121

COMPUTER SYSTEMS PERFORMANCE

The Rhine-Meuse estuary hydraulic scale model. Experiences with computer configuration and software [PUBL-335] N86-10637

Performance analysis of the IBM Direct Access Storage Device (DASD) subsystem, and some suggestions for improved systems [REPT-1-66430-44(1985)02] N86-10807

Shipboard non-tactical computer systems of the US Navy [AD-A156769] N86-10849

COMPUTER SYSTEMS PROGRAMS

Numerical simulation of convections in the microgravity environment N86-10239

The identification package SATER [ER-83/08] N86-10844

COMPACT: Compaction of hierarchial chip layouts based on a constraint graph method with double-sided constraints N86-10845

Writer/editor and the computer [DE85-011643] N86-11080

COMPUTER TECHNIQUES

Periodic binary sequences with very good autocorrelation properties N86-10397

Multisensor data integration techniques N86-10604

Collective use computer system for the Academy of Sciences KaSSR N86-10817

Study of one- and two-dimensional filtering and deconvolution algorithms for a streaming array computer [NASA-CR-176221] N86-10822

Coordinate axes, location of origin, and redundancy for the one and two-dimensional discrete Fourier transform [NASA-CR-176225] N86-10826

Revision of and documentation for the standard version of the Poisson-Group codes [DE85-012659] N86-10837

An annotated bibliography of abstracts on the use of simulators in technical training [AD-A156792] N86-11065

Writer/editor and the computer [DE85-011643] N86-11080

COMPUTER VISION

Test of a multilevel computational theory of stereoscopic visual image processing [AD-A157011] N86-10870

COMPUTERIZED SIMULATION

Automatic processing of reactive polymers N86-10127

Hormone purification by isoelectric focusing N86-10135

Work-hardening and effective viscosity in solid berylium [DE85-013976] N86-10323

Acoustic gravity wave chemistry model for the RAYTRACE code [AD-A156850] N86-10405

Angle of incidence effects for underwater shock using generic computational models, rev. 1 [DE85-012921] N86-10467

KRAK: A computer program for two-phase, two-component porous flow and fracture propagation, revision [DE85-014264] N86-10469

Dynamic analysis of robotic manipulations with flexible links N86-10545

Numerical simulation of crack arrest experiments on Araldite B using the finite difference method [REPT-W-9/82] N86-10596

The Rhine-Meuse estuary hydraulic scale model. Experiences with computer configuration and software [PUBL-335] N86-10637

Contribution of wind energy to the energy balance of a combined solar and wind energy system. Part 2: Computer-assisted investigations [BMFT-FB-T-85-052-VOL-2] N86-10671

Strength modeling report [NASA-CR-171896] N86-10770

TEMPUS: Simulating personnel and tasks in a 3-D environment [NASA-CR-171901] N86-10785

Minimization of programmable logic arrays
[EUT-84-E-145] N86-10803
Digital processing of images in tracking a moving object N86-10818
LANES 1 Users' Guide
[NASA-CR-177334] N86-10819
User interface enhancement report
[NASA-CR-171898] N86-10820
SUTRA (Saturated-unsaturated transport). A finite-element simulation model for saturated-unsaturated, Fluid-Density-Dependent ground-water flow with energy transport or chemically-reactive single-species solute transport
[AD-A156779] N86-10830
New probabilistic modeling and simulation methods for complex time-dependent systems
[DE85-009575] N86-10835
Framework for generating expert systems to perform computer security risk analysis
[DE85-014134] N86-10841
Regression analysis: Assumptions, alternatives, applications N86-10895
Motion analysis report
[NASA-CR-171897] N86-10896
Zero-gravity movement studies
[NASA-CR-171899] N86-10897
Infrared system with computerized image display
[AD-D011777] N86-10906
Impact of long-lived radionuclides on waste classification for fusion
[DE85-013205] N86-10959
Analytic evaluation of LAMPF 2 Booster Cavity design
[DE85-012680] N86-11002
Engineering high reliability, low-jitter Marx generators
[DE85-012811] N86-11013

COMPUTERS
New directions in chemical analysis
[DE85-012930] N86-10296
Initial design of a relational database system for NPS computer asset identification and valuation for risk assessment
[AD-A156847] N86-10796
User interface enhancement report
[NASA-CR-171898] N86-10820
Computer control of rf at SLAC
[DE85-013065] N86-11015
Beam steering in the SLC linac
[DE85-013370] N86-11025

CONCENTRATION (COMPOSITION)
Evaluation of the 90-day inhalation toxicity of petroleum and oil shale JP-5 jet fuel
[AD-A156815] N86-10675

CONCENTRATORS
Research on solar pumped liquid lasers
[NASA-CR-176235] N86-10539
Time resolved flow velocity and concentration measurements using a travelling thermal lens
[AD-A156706] N86-10541
Identification of chemical and physical phenomena affecting the durability of silvered polymer (PMMA) mirrors
[DE85-012131] N86-10645
Theory of advanced, high-efficience concentrator cells
[DE85-008821] N86-10655
Photovoltaic concentrator array evaluation
[DE85-013789] N86-10665

CONCENTRIC CYLINDERS
Mechanics of coated fiber composites N86-10285

CONDITIONS
Analysis of transitions between ferroelectric and antiferroelectric states under conditioning of uniaxial strain
[DE85-014468] N86-10350

CONDUCTIVE HEAT TRANSFER
Determination of thermophysical characteristics of solid materials by electrical modelling of the solutions to the inverse problems in nonsteady heat conduction
[NASA-TM-77907] N86-10293

CONDUCTORS
Conducting wall and pressure profile effect on MHD stabilization of axisymmetric mirror
[DE85-013647] N86-11020

CONFERENCES
Fifth European symposium on Material Sciences under Microgravity. Results of Spacelab 1
[ESA-SP-222] N86-10200
Report on a visit to England — color and monochrome displays
[FOA-C5-85-0006-H2] N86-10364
Metric Camera Workshop — Spacelab
[ESA-SP-209] N86-10485
Report of the Workshop on Geologic Applications of Remote Sensing to the Study of Sedimentary Basins
[E86-10002] N86-10599
NASA/JPL Aircraft SAR Workshop Proceedings
[NASA-CR-176204] N86-10615
Proceedings: First Annual Acid Deposition Emissions Inventory Symposium
[PB85-200004] N86-10686
Ada (trademark) Programming Support Environment (APSE) Evaluation and Validation (E and V) workshop report held at Airlie, Virginia on 2-6 April 1984
[AD-A156667] N86-10829
Proceedings of a Workshop on Electroweak Symmetry Breaking
[DE85-004444] N86-11003
Colloquium on Kilometric Optical Arrays in Space
[ESA-SP-226] N86-11096

CONFORMAL MAPPING
On the design of airfoils in transonic flow using the Euler equations N86-10013

CONGRESSIONAL REPORTS
Biotechnology regulation
[GPO-43-778] N86-10733

CONICAL BODIES
Explosive initiation by very small conical shaped charge jets
[DE85-009443] N86-10357

CONIFERS
Potential applications of multipolarization SAR for pine plantation biomass estimation N86-10626
Calibration of the multispectral scanner (MSS) satellite data to evaluate change in the reflection of coniferous stocks
[DFVLR-FB-84-44] N86-10636

CONSERVATION EQUATIONS
Freezer model using a population balance approach for steady-state, direct-contact, secondary refrigerant, freeze desalination N86-10361
Laminar film condensation in vertical closed two-phase thermosiphons
[IKE-5-220] N86-10476

CONSERVATION LAWS
Local conservation laws for the Maxwell-Vlasov and collisionless kinetic guiding center theories
[DE85-013122] N86-11063

CONSTITUTIVE EQUATIONS
Finite element analysis of metals at elevated temperature using unified constitutive theories
N86-10569

CONSTRAINTS
Thermodynamic constraints on ion beam mixing of metals on insulators
[DE85-013628] N86-10448
National perspective on environmental constraints to hydroelectric development
[DE85-013111] N86-10678
Always-convergent iterative noise removal and deconvolution for image data
[NASA-CR-176223] N86-10824

CONSTRUCTION
Erosion-resistant nosetip construction
[AD-D011787] N86-10289

CONTAINERLESS MELTS
Fluid flow in crystal growth: Analysis of the verticle Bridgman and floating zone process N86-10055
Crystal growth research in space N86-10057
Crystal melts under reduced gravity N86-10062
Effect of undercooling in a low-gravity containerless environment on the structure and properties of alloys
N86-10073
Convection during unidirectional solidification
N86-10077
Solidification fundamentals N86-10090
Containerless high temperature property measurements by atomic fluorescence N86-10092
Containerless processing of undercooled melts
N86-10093
Containerless studies of nucleation and undercooling
N86-10102
Containerless processing of glass forming melts in space N86-10148
Gel precursors as glass and ceramic starting materials for space processing applications research N86-10150
Sol-gel glasses N86-10153
Physical phenomena in containerless glass processing
N86-10155
Levitating furnance for containerless processing in space N86-10169
Electric field containerless processing technology
N86-10170
Advanced containerless processing technology
N86-10176
Acoustic levitation containerless processing
N86-10177
Undercooling investigations on the easy glass former Pd-Cu-Si N86-10259
Containerless undercooling of Ni N86-10260

CONTAINERS
Marginal terrain straddle-lift container handler
[AD-D011752] N86-10555

CONTAMINANTS
Compatibility of grain-stabilized platinum with candidate propellants for resistojets
[NASA-TM-87118] N86-10279
Effects of H2S on molten carbonate fuel cells
[DE85-014052] N86-10447
Volatile organic compounds in indoor air: A survey of various structures
[PB85-198356] N86-10687
Emissions of NOx, SOx and VOC from Antropogenic sources
[PB85-193530] N86-10688
Evaluation of Passive Sampling Devices (PSDs)
[PB85-196418] N86-10689

CONTAMINATION
A fundamental study of the sticking of insect residues to aircraft wings
[NASA-CR-176231] N86-10033
Thermocapillary flows and their stability: Effects of surface layers and contamination N86-10109

CONTINUOUS WAVE RADAR
On the use of X-band CW nanosecond airborne radar for terrain profiling
[AD-A156886] N86-10406

CONTINUUM FLOW
Mathematical models of continuous flow electrophoresis N86-10143

CONTINUUM MODELING
Design sensitivity analysis and optimization of built-up structures N86-10565

CONTOURS
Evaluation of the accuracy of the metric camera images for the production of line maps and orthophotos
N86-10490
Line mapping and resolution tests with metric camera data — Spacelab N86-10500

CONTRACT MANAGEMENT
LSRO/ONR ad hoc review process
[AD-A156590] N86-10735

CONTRACTS
LSRO/ONR ad hoc review process
[AD-A156590] N86-10735

CONTRAST
Vision test chart and method using Gaussians
[AD-D011756] N86-10778
Measurement of visual contrast sensitivity
[AD-D011776] N86-10973

CONTROL
Collective use computer system for the Academy of Sciences KaSSR N86-10617

CONTROL EQUIPMENT
Dissecting the cow
[DE85-013369] N86-10801
Klystron control software in the SIC
[DE85-013068] N86-10836
Beam stability in a 6 GeV synchrotron light source
[DE85-013850] N86-10979
Computer control of rf at SLAC
[DE85-013065] N86-11015
Beam steering in the SLC linac
[DE85-013370] N86-11025
Programmable delay unit incorporating a semi-custom integrated circuit
[DE85-013379] N86-11033

CONTROL SIMULATION
Control concepts for in-flight simulation including actuator nonlinearities and time delays
[DFVLR-FB-85-24] N86-10047

CONTROL STICKS
Proposed modifications for the RAAF Airtrainer CT-4A cockpit
[AD-A156806] N86-10039

CONTROL SYSTEMS DESIGN
Modeling and control of nonlinear systems
N86-10362
Design of a multifunction Input-Output (I/O) controller
[EUT-84-E-143] N86-10802
The local disk controller
[REPT-1-68430-44(1985)01] N86-10806
An approach to implementing CAMAC microprocessor modules N86-10813
The identification package SATER
[ER-83/08] N86-10844

CONTROL THEORY
Guidance and control of a cable based payload pickup system N86-10046
Car driving as a supervisory control task
[B8563351] N86-10776
The influence of tactual seat-motion cues on training and performance in a roll-axis compensatory tracking task setting N86-10784
Spillover minimization in self-adjoint distributed-parameter systems with direct output feedback N86-10852
Optimal control modeling of lower extremity musculoskeletal motion N86-10853

Identification of a plant's weighting sequence — self-tuning control
[OUEL-1534/84] N86-10854

CONTROL UNITS (COMPUTERS)
Design of a multifunction Input-Output (I/O) controller
[EUT-84-E-143] N86-10802
Minimization of programmable logic arrays
[EUT-84-E-145] N86-10803
Realization of a multifunction Input/Output (I/O) controller by means of a gate array
[EUT-85-E-147] N86-10804
An intelligent local disk control system
[REPT-051560-28(1984)08] N86-10806

CONTROLLABILITY
System modeling and identification of equivalent systems with and without compensating time delay for control-augmented aircraft
[ESA-TT-852] N86-10043

CONTROLLED ATMOSPHERES
Dynamics of general resistance of rats during readaptation period after training in altered gas environment N86-10767

CONTROLLERS
Modeling and control of nonlinear systems N86-10362

CONVECTION
Solutal convection and its effects on crystal growth and segregation in binary and pseudo-binary system with large liquidus-solidus separation N86-10056
The influence of low frequency mechanical vibrations on the growth of single crystals N86-10059
Solution growth of crystals in zero-gravity N86-10064
Fluid dynamics and thermodynamics of vapor phase crystal growth N86-10068
Vapor growth of alloy-type semiconductor crystals N86-10069
Study of eutectic formation N86-10070
Suppression of Marangoni convection in float zones N86-10111
Surface tension induced instabilities in reduced gravity: The Benard problem N86-10117
Recirculation within a glass mixture subjected to external and resistive heating
[DE85-010068] N86-10348

CONVECTIVE FLOW
Convection during unidirectional solidification N86-10077
Thermal and solutal convection damping using an applied magnetic field N86-10094
Role of convection in grain refining N86-10133

CONVECTIVE HEAT TRANSFER
Ignition and flame spread above liquid fuel pools N86-10163
The TEXUS flight results on convective flows and heat transfer in simulated floating zones N86-10235
Nucleate pool boiling in subcooled liquid under microgravity: Results of TEXUS experimental investigations N86-10250

CONVERGENCE
Comment on Determination of Aerodynamic Coefficients for a Reentry Body by Means of the Kalman Filter Method N86-10011
Determining a physically appropriate neutron spectrum from multisphere data
[DE85-013045] N86-10299
A study of Morrison's iterative noise removal method
[NASA-CR-176222] N86-10823
Always-convergent iterative noise removal and deconvolution for image data
[NASA-CR-176223] N86-10824
A modified Successive Over-Relaxation (SOR) method for the Poisson equation in unsteady free-surface flow calculations
[TW-264] N86-10861
Superconvergent tracking and invariant surfaces in phase space
[DE85-013051] N86-10995

CONVERTERS
An experimental TE sub 12 - TE sub 11 circular waveguide mode converter N86-10387

CONVOLUTION INTEGRALS
A simple method of obtaining concentration depth-profiles from X-ray diffraction
[NASA-CR-176262] N86-10310
The VLSI design of error-trellis syndrome decoding for convolutional codes N86-10391
Study of one- and two-dimensional filtering and deconvolution algorithms for a streaming array computer
[NASA-CR-176221] N86-10822
A study of Morrison's iterative noise removal method
[NASA-CR-176222] N86-10823
Coordinate axes, location of origin, and redundancy for the one and two-dimensional discrete Fourier transform
[NASA-CR-176225] N86-10826

COOLING
Effect of undercooling in a low-gravity containerless environment on the structure and properties of alloys N86-10073
The influence of containerless undercooling and rapid solid-state quenching on the superconductive and magnetic properties of some clustering alloy systems N86-10076
Undercooling, remelting, and coarsening N86-10080
Liquid phase miscibility gap materials N86-10081
Dendritic growth in undercooled melts N86-10082
Containerless processing of undercooled melts N86-10093
Containerless studies of nucleation and undercooling N86-10102
Fusion target technology N86-10156
Acoustic levitation containerless processing N86-10177
Test and evaluate passive orbital disconnect struts (PODS 3)
[NASA-CR-177368] N86-10274
Beam line windows at LAMPF
[DE85-012723] N86-10985

COOLING SYSTEMS
High efficiency heat transport and power conversion system for cascade
[DE85-012959] N86-10468

COORDINATES
Coordinate axes, location of origin, and redundancy for the one and two-dimensional discrete Fourier transform
[NASA-CR-176225] N86-10826
Supervisory control of the right arm of the beam assembly teleoperator
[AD-A156856] N86-10832

COPOLYMERS
Synthesis of arylene siloxanylene polymers and copolymers
[AD-D011780] N86-10338

COPPER
The mechanism of erosion of metallic materials under cavitation attack
[NASA-TM-87133] N86-10552
Initial increase, peaking effect, in the internal friction of copper following pulsed neutron and electron irradiation
[DE85-012767] N86-10932

COPPER ALLOYS
Electronic and magnetic properties of noble-metal and transition-metal alloys, interfaces and overlayers
[DE85-014532] N86-10321
Anelastic relaxation in irradiated Cu-Be
[DE85-013893] N86-11056

COPPER CHLORIDES
Rusty bolt intermodulation interference reducer
[AD-D011748] N86-10313

COPPER OXIDES
Rusty bolt intermodulation interference reducer
[AD-D011748] N86-10313

CORIOLIS EFFECT
Elastic wave gyrometer. Experiments with a parametric wave device
[REPT-26/5005/HF/AR] N86-10533
Dynamics of changes of statistical indicators of heart rhythm of persons with different degree of motion sickness N86-10743

CORRECTION
Applications of the second-order achromat concept to the design of particle accelerators
[DE85-013072] N86-10994

CORRELATION
Correlation between vibrations and buckling of cylindrical shells stiffened by spot-welded and riveted stringers
[TAE-537] N86-10584

CORRELATORS
Instantaneous frequency measurement receiver with digital processing
[AD-D011759] N86-10425
A compact bulk acousto-optic time integrating correlator
[AD-A156608] N86-10428

CORROSION
Characterization of cathodic corrosion products in the Ca/CaCrO4 thermal battery
[DE85-013442] N86-10644

CORROSION PREVENTION
Rusty bolt intermodulation interference reducer
[AD-D011748] N86-10313
Passivation of steel with aqueous amine solutions
[AD-D011749] N86-10314
Research needs for corrosion control and prevention in energy conservation systems
[DE85-014852] N86-10326

CORROSION RESISTANCE
Mechanism of the formation of boronised layers on high carbon steel
[BLL-BISI-TRANS-23036-(9022.06)] N86-10306
Development of a sheath for sensor protection in molten steel applications
[AD-A156764] N86-10315
Aluminum ion plating for corrosion protection of uranium, revision 1
[DE85-012419] N86-10330

CORROSION TESTS
Nondestructive corrosion test of aluminum alloy structures
[PV-43-954/F/2] N86-10594

CORTICOSTEROIDS
Effect of cold on brain serotonin system and plasma corticosteroid level in different strains of mice N86-10766

COSMIC RAYS
Solar modulation of galactic cosmic rays: Techniques and applications N86-11143

COSMIC X RAYS
Extra-galactic X-ray sources and the diffuse X-ray background N86-11144

COST ANALYSIS
Field-independent normalization of SSC Collider Ring costs
[DE85-012425] N86-10997
Annotated bibliography of publications dealing with occupational health and medical information systems, cost analysis procedures, evaluation methodology and related legal issues
[AD-A156650] N86-11078
Advanced vehicle systems assessment. Volume 3: Systems assessment
[NASA-CR-176206] N86-11084

COST EFFECTIVENESS
Retrofit of SAC EC-135C and RC-135 aircraft with CFM-56 engines
[AD-A156688] N86-10038
Test on mapping application of metric camera imagery --- Spacelab N86-10505
Editors rattle space N86-10586
An annotated bibliography of abstracts on the use of simulators in technical training
[AD-A156792] N86-11065

COST ESTIMATES
F-16X MSIP (Multi-national Staged Improvement Program) case example: Operating and support cost estimation using VAMOSC (Visibility And Management Of Operating and Support Costs)
[AD-A156893] N86-10006

COST REDUCTION
Nondestructive corrosion test of aluminum alloy structures
[PV-43-954/F/2] N86-10594

COSTS
Report of the ad hoc committee to review the program of the SDI Directorate on Innovative Science and Technology (IST)
[AD-A156668] N86-11071

COULOMB POTENTIAL
Relativistic wavefunction at the origin and the pion decay constant
[DE85-012392] N86-11062

COUPLING COEFFICIENTS
Evaluation of surface exchange coefficients from mildex ocean/atmosphere mixed layer data
[AD-A156765] N86-10729

CRACK ARREST
Numerical simulation of crack arrest experiments on Araldite B using the finite difference method
[REPT-W-9/82] N86-10596

CRACK INITIATION
Fracture toughness testing of centrifugally cast nickel aluminium bronze
[REPT-MAT/720] N86-10575

CRACK PROPAGATION
A review of Australian investigations on aeronautical fatigue during the period April 1983 to March 1985
[AD-A156602] N86-10036
Report on an overseas visit
[AD-A156603] N86-10037
The effect of debond growth on crack propagation in composite plates reinforced with adhesively bonded composite stringers N86-10287
Creep-fatigue behavior of NiCoCrAlY coated PWA 1480 superalloy single crystals
[NASA-TM-87110] N86-10311
Fabrication and metallurgical properties of modified 9Cr-1 Mo steel
[DE85-012885] N86-10328
Finite deformation crack-line fields in a thin elasto-plastic sheet
[AD-A156757] N86-10346
Analytical and experimental study of cracks emanating from an elliptical hole in unidirectional composite material N86-10567
The use of new path indepedent integrals in elastic-plastic and creep fracture N86-10574

Fatigue of graphite/epoxy buffer strip panels with center cracks
[NASA-TM-87595] N86-10581
Resistance curves for crack growth under plane-stress conditions in an elastic perfectly-plastic material
[AD-A156778] N86-10593

CRACK TIPS
Fatigue of graphite/epoxy buffer strip panels with center cracks
[NASA-TM-87595] N86-10581

CRACKS
Metallurgy and metallography of braze joints
[DE85-014563] N86-10325
Mixed-mode fracture of ceramics
[DE85-014087] N86-10349
Microwave evaluation of materials
[DE85-013183] N86-10409

CREEP PROPERTIES
Creep-fatigue behavior of NiCoCrAlY coated PWA 1480 superalloy single crystals
[NASA-TM-87110] N86-10311

CREEP RUPTURE STRENGTH
Fabrication and metallurgical properties of modified 9Cr-1 Mo steel
[DE85-012685] N86-10328
High temperature properties of SiC materials
[BMFT-FB-T-85-047] N86-10353

CREEP STRENGTH
The use of new path indepedent integrals in elastic-plastic and creep fracture N86-10574

CREEP TESTS
Constitutive modeling for isotropic materials (HOST)
[NASA-CR-174980] N86-10589
Experiments with tubular probes made of INCOLOY 800 H under uniaxial and multiaxial strain
[JUEL-1979] N86-10595

CRITICAL MASS
Self-heating to ignition measurements and computation of critical size for solar energy collector materials
[DE85-011449] N86-10302

CRITICAL POINT
Critical transport phenomena in fluid helium under low gravity N86-10119
Precise viscosity measurements very close to critical points
[NASA ORDER C-86129D] N86-10120
Holographic interferometry near gas/liquid critical points: Ground-based study of a D1 experiment --- Spacelab N86-10249
Isochoric specific heat of sulfur hexafluoride at the critical point. A Spacelab experiment for the German D1-mission in 1985 N86-10251

CRITICAL TEMPERATURE
Self-heating to ignition measurements and computation of critical size for solar energy collector materials
[DE85-011449] N86-10302
Development of new ammonium nitrate composite explosives
[DE85-014252] N86-10356

CRITICAL VELOCITY
Transport processes in directional solidification during space shuttle flight N86-10257

CROP IDENTIFICATION
On the use of L-band multipolarization airborne SAR for surveys of crops, vineyards, and orchards in a California irrigated agricultural region N86-10627
Vegetation canopy discrimination and biomass assessment using multipolarized airborne SAR N86-10628

CRUDE OIL
Evaluation of the 90-day inhalation toxicity of petroleum and oil shale JP-5 jet fuel
[AD-A156815] N86-10675

CRUSTAL FRACTURES
Formation of waves by ground motion
[PM/84/09] N86-10706

CRYOGENIC FLUID STORAGE
Test and evaluate passive orbital disconnect struts (PODS 3)
[NASA-CR-177368] N86-10274

CRYOGENIC MAGNETS
Cryogenic equivalence principle experiment N86-10171
Cryogenic structural materials for superconducting magnets
[DE85-008026] N86-10908

CRYOGENICS
Volatile organic compounds in indoor air: A survey of various structures
[PB85-198356] N86-10687

CRYSTAL DEFECTS
The control of float zone interfaces by the use of selected boundary conditions N86-10060
Microgravity silicon zoning investigation N86-10063
HgI sub 2 crystal growth for nuclear detectors N86-10066
Defect identification in high-energy semiconductors
[DE85-014533] N86-10442

CRYSTAL DISLOCATIONS
Low temperature plastic deformation mechanisms of alpha-titanium single crystals
[ESA-TT-871] N86-10332

CRYSTAL GROWTH
Fluid flow in crystal growth: Analysis of the verticle Bridgman and floating zone process N86-10055
Solutal convection and its effects on crystal growth and segregation in binary and pseudo-binary system with large liquidus-solidus separation N86-10056
Crystal growth research in space N86-10057
Growth of organic crystals by Ostwald ripening N86-10058
The influence of low frequency mechanical vibrations on the growth of single crystals N86-10059
The control of float zone interfaces by the use of selected boundary conditions N86-10060
Crystal growth of device quality GaAs in space N86-10061
Crystal melts under reduced gravity N86-10062
Microgravity silicon zoning investigation N86-10063
Solution growth of crystals in zero-gravity N86-10064
HgI sub 2 crystal growth for nuclear detectors N86-10066
Fluid dynamics and thermodynamics of vapor phase crystal growth N86-10068
Vapor growth of alloy-type semiconductor crystals N86-10069
Study of eutectic formation N86-10070
Heat flow and segregation in directional solidification N86-10072
Dendritic growth in undercooled melts N86-10082
Orbital processing of aligned magnetic composites N86-10089
Thermal and solutal convection damping using an applied magnetic field N86-10094
Extension of Ostwald ripening theory N86-10104
Transport processes in solution crystal growth N86-10107
Surface tensions and their variations with temperature and impurities
[NASA ORDER H-27954B] N86-10115
Energy stability of thermocapillary convection in models of the float zone process N86-10123
Morphological stability and fluid dynamics of vapor crystal growth N86-10126
Experimental and theoretical analysis of chemical vapor deposition with prediction of gravity effects N86-10132
Glass formation in reluctant glass formers N86-10151
Microgravity Materials Science Laboratory N86-10173
High-temperature controlled redox crystallization studies N86-10178
Satellite use for men --- West German space program N86-10180
Growth of larger single crystals N86-10186
GaS-semiconductor crystals under microgravity: Experiment ES 323 --- Spacelab N86-10224
Solution growth of cadmium telluride: Experiment ES 322 --- Spacelab N86-10225
Crystal growth from solution --- Spacelab N86-10223
Crystal growth from solutions and nucleation from the vapor phase --- Spacelab N86-10267
Preliminary reports, memoranda and technical notes of the Materials Research Council Summer Conference, La Jolla, California
[AD-A156776] N86-10291
The interaction of small metal particles with refractory oxide supports
[NASA-CR-176228] N86-11047

CRYSTAL STRUCTURE
Crystal growth research in space N86-10057
High-temperature controlled redox crystallization studies N86-10178
Growth and characterization of brushite and lead monetite, simulation and results --- Spacelab N86-10230
A preliminary report on floating zone experiments with germanium crystals in a sounding rocket N86-10256
Cellular morphologies in lead-thallium alloys --- gravitational effects N86-10262

CRYSTALLITES
Extension of Ostwald ripening theory N86-10104

CRYSTALLIZATION
Convection during unidirectional solidification N86-10077
Crystallization, optical and chemical properties of fluoride glasses N86-10149
Glass formation in reluctant glass formers N86-10151
Glass research N86-10157
High-temperature controlled redox crystallization studies N86-10178
Crystal nucleation and glass formation in metallic alloy melts N86-10233
Experimental facility for materials research in space (CSK-1) N86-10263
Formation and characterization of amorphous erbium-based alloys prepared by near-isothermal cold-rolling of elemental composites
[DE85-014853] N86-10327
Elastic properties and thermal stability characterization of metallic glasses by guided wave techniques N86-10337
Thermal expansion of glasses in the solid and liquid phases
[DE85-013953] N86-10351
Freezer model using a population balance approach for steady-state, direct-contact, secondary refrigerant, freeze desalination N86-10361

CRYSTALLOGRAPHY
Protein single crystal growth under microgravity --- Spacelab N86-10228
Growth and characterization of brushite and lead monetite, simulation and results --- Spacelab N86-10230

CUBES (MATHEMATICS)
On the analytical evaluation of the partition function for unit hypercubes in four dimensions --- lattice theory
[NIKHEF-H/84-12] N86-10682

CULTURE TECHNIQUES
Purification and cultivation of human pituitary growth hormones secreting cells N86-10140
Cell separations in microgravity and development of a space bioreactor N86-10141
Cell maintenance systems N86-10142
Kidney cell electrophoresis N86-10145

CURRENT DENSITY
Improved blue response and efficiency of A-Si:H solar cells deposited from disilane using a dual-chamber plasma system
[DE85-013289] N86-10649
Noninterceptive techniques for the measurement of longitudinal parameters for intense H(-) beams
[DE85-012662] N86-10992

CURRENT REGULATORS
High output programmable signal current source for low output impedance applications
[AD-D011751] N86-10423

CURVATURE
Charge exchange in slow collisions of atoms and molecules N86-10922

CURVES
Resistance curves for crack growth under plane-stress conditions in an elastic perfectly-plastic material
[AD-A156778] N86-10593

CUSPS (MATHEMATICS)
Some remarks about cusp forms: Holomorphic and non-holomorphic
[CTH-MATH-1984-26] N86-10902

CUTTING
The influence of the substrate on the practical machining applications of cutting edges coated with different materials
[BLL-RISLEY-TR-5039-(9091.9F)] N86-10546

CYBERNETICS
USSR report: Cybernetics, computers and automation technology
[JPRS-UCC-85-006] N86-10809

CYCLES
Advanced absorption heat pump cycles
[DE85-003914] N86-10654

CYCLIC ACCELERATORS
Ion sources for high-frequency accelerators
[DE85-012992] N86-11006

CYCLIC HYDROCARBONS
A procedure identifying a polyacetylene initiator of olefin metathesis. The reactivities of metal-carbenes toward alkenes and alkynes
[AD-A156997] N86-10283

CYCLIC LOADS
Inelastic analysis of frame structures including member and joint shears N86-10573

CYCLOGENESIS
A composite climatological study of the frequency and distribution of severe weather associated with spring season Colorado cyclogenesis
[AD-A156981] N86-10715

CYCLONES
A composite climatological study of the frequency and distribution of severe weather associated with spring season Colorado cyclogenesis
[AD-A156981] N86-10715

CYCLOTRON RESONANCE
Two-dimensional electrons
[AD-A156894] N86-10982

CYCLOTRONS
Supersonic metal cluster beams
[DE85-014321] N86-10966

CYGNUS CONSTELLATION
A superconducting tunnel junction receiver for millimeter-wave astronomy N86-11041

CYLINDRICAL BODIES
Electromagnetic resonances of cylinders and aircraft model with resistive wires
[NASA-CR-176250] N86-10042
Analysis of combined natural and forced-convection around cylinders and spheres N86-10456
Stiffened and prestressed composite overwrapped pressure vessels N86-10547

CYLINDRICAL SHELLS
Strength of shells under local transverse loads
N86-10568
Effect of sequence of loading on interaction curves for buckling of stiffened shells
[TAE-536] N86-10583
Correlation between vibrations and buckling of cylindrical shells stiffened by spot-welded and riveted stringers
[TAE-537] N86-10584

D

DAMAGE
Progressive damage, fracture predictions and post mortem correlations for fiber composites
[NASA-TM-87101] N86-10290
Evaluation of the 90-day inhalation toxicity of petroleum and oil shale JP-5 jet fuel
[AD-A156815] N86-10675

DAMPING
Thermal and solutal convection damping using an applied magnetic field N86-10094
Passive damping concepts for slender columns in space structures
[NASA-CR-176234] N86-10577
SLC positron damping ring optics design
[DE85-013054] N86-11014

DATA ACQUISITION
Simulated direct-strike lightning testing at Sandia National Laboratories
[DE85-012033] N86-10049
Development of new ammonium nitrate composite explosives
[DE85-014252] N86-10356
The Telecommunications and Data Acquisition Report
[NASA-CR-176203] N86-10382
Soudan 2 data acquisition and trigger electronics
[DE85-013864] N86-10443
Laboratory experiments of heat pump dynamic losses
[DE85-013931] N86-10473
ELCAP instrumentation
[DE85-013042] N86-10527
Measurement of the density of base fluids at pressures 0.422 to 2.20 GPa
[NASA-TM-87114] N86-10551
Remote sensing
[NOTA-1535] N86-10638
Harmonic distortion reduction technique for data acquisition
[AD-D011771] N86-10799
Advances in data acquisition system technology for PBFA 2
[DE85-012860] N86-11011
Academic Research Equipment in selected science-engineering fields, 1982-83. An analysis of findings from the Baseline National Survey of academic research instruments and instrumentation needs
N86-11088

DATA BASE MANAGEMENT SYSTEMS
DBS/R database control system N86-10816
Stock-taking of data base management systems choice considerations for the Eindhoven Technical University Computing Center (THE-RC)
[COMP-CENT-NOTE-18] N86-10851

DATA BASES
SARSAT LUC (Local user terminal) to CMCC (Canadian Mission Control Centre) alert data interface: A critical review
[AD-A156661] N86-10276
Microcircuit device reliability field experience database. Volume 1. Field data. Volume 2. Failure Event/Analysis data
[AD-A156636] N86-10433
Vegetation and soils field research data base: Experiment summaries
[E85-10110] N86-10610
Application of the ruthenium and technetium thermodynamic data bases used in the EQ3/6 geochemical codes
[DE85-013766] N86-10632
Examples of regional environmental assessment using acid deposition data
[DE85-012903] N86-10677
Initial design of a relational database system for NPS computer asset identification and valuation for risk assessment
[AD-A156847] N86-10796
DBS/R database control system N86-10816
System integration report
[NASA-CR-171900] N86-10821
Ada (trademark) Programming Support Environment (APSE) Evaluation and Validation (E and V) workshop report held at Airlie, Virginia on 2-6 April 1984
[AD-A156667] N86-10829
The DUCK manual
[AD-A156936] N86-10833
Stock-taking of data base management systems choice considerations for the Eindhoven Technical University Computing Center (THE-RC)
[COMP-CENT-NOTE-18] N86-10851
US superconducting magnet data base assessment for INTOR
[DE85-013648] N86-11000
Acquaintance with on line literature research. An introduction for education at the Chemical Technology Section N86-11061
Academic Research Equipment in selected science-engineering fields, 1982-83. An analysis of findings from the Baseline National Survey of academic research instruments and instrumentation needs
N86-11088

DATA LINKS
LANES 1 Users' Guide
[NASA-CR-177334] N86-10819

DATA PROCESSING
Automated analysis of digital images generated by two-dimensional gel electrophoresis
[DE85-011906] N86-10526
Multisensor data integration techniques N86-10604
USSR report: Cybernetics, computers and automation technology
[JPRS-UCC-85-006] N86-10609
LANES 1 Users' Guide
[NASA-CR-177334] N86-10619
Solar flares and magnetospheric particles: Investigations based upon the ONR-602 experiment
[AD-A156583] N86-11142

DATA RECORDERS
Advances in data acquisition system technology for PBFA 2
[DE85-012860] N86-11011

DATA RECORDING
Simulated direct-strike lightning testing at Sandia National Laboratories
[DE85-012033] N86-10049

DATA REDUCTION
Harmonic distortion reduction technique for data acquisition
[AD-D011771] N86-10799

DATA SAMPLING
Sample data phase locked loop for adaptive Doppler tracker
[AD-D011788] N86-10374
Nonparametric comparison of several mean values with mild adaptation to some sample characteristics
[COMP-CENT-NOTE-20] N86-10891

DATA SMOOTHING
Determining a physically appropriate neutron spectrum from multisphere data
[DE85-013045] N86-10299

DATA SYSTEMS
Methods for developing jam-resistant security communications networks at fixed-site facilities
[DE85-012032] N86-10408

DATA TRANSMISSION
A sequential decoding performance analysis for International Comet Explorer N86-10390
The GCF Mark 4 implementation and beyond
N86-10399
Methods for developing jam-resistant security communications networks at fixed-site facilities
[DE85-012032] N86-10408

DAYGLOW
Ultraviolet spectroscopy of the Earth's dayglow and magnetosphere cleft N86-10696

DAYTIME
A composite climatological study of the frequency and distribution of severe weather associated with spring season Colorado cyclogenesis
[AD-A156961] N86-10715

DECAY
Matter-antimatter transition operators: A manual for modeling N86-10921
Mean life of the 2p(4)((1)S)3s (2)S state in fluorine
[DE85-012929] N86-10956

DECAY RATES
Rapid evaluation of ion thruster lifetime using optical emission spectroscopy
[NASA-TM-87103] N86-10280

DECISION MAKING
Psychological Sciences Division 1984 programs
[AD-A156631] N86-10779
Extended analysis of the structure of error scores in psychological aptitude tests
[DFVLR-FB-85-20] N86-10780
Path error-neglection in straight lane driving
[IZF-1984-32] N86-10783
Derivational analogy: A theory of reconstructive problem solving and expertise acquisition
[AD-A156817] N86-10899
Risk propensity, action readiness and the roles of societal and individual decision makers
[IZF-1984-27] N86-11077

DECODERS
A sequential decoding performance analysis for International Comet Explorer N86-10390
High-rate convolutional code construction with the minimum required SNR criterion N86-10392

DECODING
A sequential decoding performance analysis for International Comet Explorer N86-10390
The VLSI design of error-trellis syndrome decoding for convolutional codes N86-10391
High-rate convolutional code construction with the minimum required SNR criterion N86-10392
Digital decoding of in-line holograms N86-10478

DECOMPOSITION
Large eddy interactions in a turbulent channel flow
[NASA-TM-86757] N86-10464
Guidelines for a thermochemical kinetics computer program
[DE85-014266] N86-10839

DEEP SPACE NETWORK
The Telecommunications and Data Acquisition Report
[NASA-CR-176203] N86-10382
A VLBI survey at 2.29 GHz N86-10383
DSN frequency and timing system, Mark 4-85
N86-10393
JPL emergency support of TDRSS and compatible satellites N86-10394
Planning for VLA/DSN arrayed support to the Voyager at Neptune N86-10395
The GCF Mark 4 implementation and beyond
N86-10399

DEFECTS
Mixed-mode fracture of ceramics
[DE85-014087] N86-10349
Defect identification in high-energy semiconductors
[DE85-014533] N86-10442
Exploratory development for a high reliability flaw characterization module
[AD-A156632] N86-10916
ORR core re-configuration measurements to increase the fast neutron flux in the Magnetic Fusion Energy (MFE) experiments
[DE85-013520] N86-10958

DEFENSE PROGRAM
Report of the ad hoc committee to review the program of the SDI Directorate on Innovative Science and Technology (IST)
[AD-A156668] N86-11071

DEFLECTION
Beam-beam deflections to measure size spot and offset at SLC IP
[DE85-014285] N86-10965

DEFLECTORS
Total internal reflection modulator/deflector
[AD-D011757] N86-10424

DEFORMATION
Fundamental studies of low velocity impact resistance of graphite fiber reinforced polymer matrix composites
N86-10288
Binder-filler interaction in energetic polymers
[AD-A156752] N86-10345
Resistance curves for crack growth under plane-stress conditions in an elastic perfectly-plastic material
[AD-A156778] N86-10593
Neogene compressional deformation and possible thrust faulting in southwest Dominican Republic N86-10618
Bounding solutions of geometrically nonlinear viscoelastic problems
[NASA-CR-176219] N86-10860

DEFROSTING
Laboratory experiments of heat pump dynamic losses
[DE85-013931] N86-10473

DEGRADATION
Intrinsic mechanisms of multilayer ceramic capacitor failure
[AD-A156638] N86-10431

DELAMINATING
The mechanics of delamination in composite materials
N86-10284
The effect of debond growth on crack propagation in composite plates reinforced with adhesively bonded composite stringers N86-10287

DELAY
Comparison of the calibration of ionospheric delay in VLBI data by the methods of dual frequency and Faraday rotation N86-10384
DELAY CIRCUITS
Programmable delay unit incorporating a semi-custom integrated circuit
[DE85-013379] N86-11033
DELAY LINES
Signal analysis receiver with acousto-optic delay lines
[AD-D011761] N86-10427
DENDRITIC CRYSTALS
Dendritic growth in undercooled melts N86-10082
The development and prevention of channel segregation during alloy solidification N86-10086
Theoretical problems in materials science N86-10088
Dendritic solidification in a binary alloy melt: Steady-state versus morphological stability theories N86-10261
DENSITY
Computational techniques for the analysis and design of digital communication systems
[AD-A156945] N86-10407
DENSITY (MASS/VOLUME)
Light scattering tests of fundamental theories of transport properties in the critical region N86-10113
DENSITY DISTRIBUTION
Investigation of density gradient fluctuations in a turbulent free jet by means of the laser schlieren crossed-beam method
[DFVLR-FB-85-19] N86-10027
Flammability limits of gases under low gravity conditions N86-10164
DEOXYRIBONUCLEIC ACID
Somatic cell and molecular genetics approach to DNA repair and mutagenesis
[DE85-014181] N86-10737
DEPLOYMENT
AIRBOC (air rapid bloom offboard chaff) chaff deployment system
[AD-D011746] N86-10554
DEPOLARIZATION
Chemical/hydrogen energy systems
[DE85-012742] N86-10667
DEPOSITION
Dust deposition in regions of separated flow
[JUEL-1985] N86-10475
Examples of regional environmental assessment using acid deposition data
[DE85-012903] N86-10677
Application of the dutch method for estimating storm-induced dune erosion
[AD-A156717] N86-10728
DEPOSITS
Metals electroprocessing in molten salts N86-10098
DEPRIVATION
Mild hypoxia and visual performance with night vision goggles
[AD-A156969] N86-10787
DEPTH MEASUREMENT
A simple method of obtaining concentration depth-profiles from X-ray diffraction
[NASA-CR-176262] N86-10310
DERIVATION
A study of derivative filters using the discrete Fourier transform
[NASA-CR-176224] N86-10825
DESALINIZATION
Freezer model using a population balance approach for steady-state, direct-contact, secondary refrigerant, freeze desalination N86-10361
DESIGN
Collective use computer system for the Academy of Sciences KaSSR N86-10817
DESIGN ANALYSIS
Geothermal lost circulation zone mapping tool
[DE85-008696] N86-10531
Design sensitivity analysis and optimization of built-up structures N86-10565
Design of a multifunction Input-Output (I/O) controller
[EUT-84-E-143] N86-10802
Evolution of the fusion power demonstration tandem mirror reactor configuration
[DE85-012889] N86-10960
Advanced Gas Turbine (AGT) powertrain system development for automotive applications report
[NASA-CR-174886] N86-11067
DESORPTION
Surface conditioning of synchrotron radiation source to improve beam lifetime
[DE84-012185] N86-10948
DESTABILIZATION
Mephisto: Interfacial destabilization in metal alloys N86-10079
DESTRUCTIVE TESTS
Evaluation of the International Atomic Energy Agency (IAEA) Safeguards Analytical Laboratory quality assurance program
[DE85-012078] N86-10953
DETECTION
Robust failure detection filters
[NASA-CR-176232] N86-10271
Analysis of edge detection algorithms on DIAL (Digital Image Analysis Laboratory)
[AD-A156735] N86-10630
Volatile organic compounds in indoor air: A survey of various structures
[PB85-198356] N86-10687
Proposed aural nondetectability limits for Army materiel
[AD-A156704] N86-10917
Understanding and improving acoustic to seismic coupling as it pertains to Sandia's helicopter detector
[DE85-009440] N86-10920
New particle searches
[DE85-014073] N86-10942
Wide dynamic range beam profile monitor
[DE85-012709] N86-10950
Optical detection of photoacoustic pulses in thin silicon wafers
[AD-A156705] N86-10977
DETECTORS
Instantaneous frequency measurement receiver with digital processing
[AD-D011759] N86-10425
DETONATION
Chemical kinetics and cellular structure of detonations in hydrogen sulphide and air
[DE85-009408] N86-10304
Development of new ammonium nitrate composite explosives
[DE85-014252] N86-10356
Explosive initiation by very small conical shaped charge jets
[DE85-009443] N86-10357
Composite explosives for metal acceleration: The effect of detonation temperature
[DE85-013982] N86-10359
Effects of scale and geometry on hydrogen-air detonations
[DE85-006762] N86-10474
Type of new Chinese-produced high-speed camera and its utilization in detonation physics experiments
[DE85-015191] N86-10529
Theory of dense molecular fluid equations of state with application to detonation products
[DE84-016822] N86-10927
DEVELOPMENT
Collective use computer system for the Academy of Sciences KaSSR N86-10817
DEXTRANS
Separation of aqueous two-phase polymer systems in microgravity N86-10246
Application of the theory of Ostwald ripening to microgravity phase separation experiments N86-10248
DIAGNOSIS
Test, measurement, and diagnostic equipment (system peculiar)
[AD-A156669] N86-10563
DIATOMIC MOLECULES
Cooperative emission by two different atoms into surface plasmons
[AD-A157033] N86-10925
DIBORANE
Boronising of iron and steel by ionic bombardment by diborane
[BLL-BISI-TRANS-23034-(9022.06)] N86-10307
DIELECTRIC PROPERTIES
Polymer engineering: Polymeric and molecular electronic, dielectric and optical properties for device applications
[AD-A156671] N86-10344
Microwave evaluation of materials
[DE85-013163] N86-10409
DIELECTRICS
Thermodynamic constraints on ion beam mixing of metals on insulators
[DE85-013628] N86-10448
Renormalization of an inverse scattering theory for inhomogeneous dielectrics
[AD-A156636] N86-11049
DIFFERENCES
A study of derivative filters using the discrete Fourier transform
[NASA-CR-176224] N86-10825
DIFFERENTIAL EQUATIONS
Three-dimensional stress singularities in anisotropic materials and composites N86-10286
Theoretical and numerical investigation of dipole radiation over a flat earth N86-10369
Analysis of annular two-phase flow with liquid entrainment N86-10459
Computing the structural index
[DE85-014370] N86-10871
DIFFERENTIAL PRESSURE
Cryogenic equivalence principle experiment N86-10171
DIFFRACTION PATTERNS
A simple method of obtaining concentration depth-profiles from X-ray diffraction
[NASA-CR-176262] N86-10310
Fringe drift compensation in computer memory --- Michelson interferometry N86-11112
DIFFUSION
Colloidal oxide properties and kinetic studies N86-10147
Investigation of metallic impurities introduced into SiO2 and silicon by various candidate VLSI metallization systems: Chemical reactions, diffusion, and electrical properties
[AD-A156609] N86-10429
Smoke inputs to climate models: Optical properties and height distribution for nuclear winter studies
[DE85-011353] N86-10717
DIFFUSION COEFFICIENT
Diffusion in immiscible melts N86-10096
Interdiffusion in the glass melt system (Na2O+Rb2O).3SiO2 --- Spacelab N86-10216
Self diffusion of Sn112 and Sn124 in liquid tin N86-10231
Transport processes in directional solidification during space shuttle flight N86-10257
The measurement and application of transport properties of ion swarms in gases N86-10370
DIFFUSION FLAMES
Buoyancy effects upon vapor flame and explosion processes N86-10161
DIGITAL COMMAND SYSTEMS
Digital control of the hydraulic actuators of an adaptive suspension vehicle N86-10548
DIGITAL COMPUTERS
USSR report: Cybernetics, computers and automation technology
[JPRS-UCC-85-006] N86-10809
Prospects for creation of optical digital high-performance computers N86-10810
DIGITAL FILTERS
Digital decoding of in-line holograms N86-10478
Acceleration-invariant approximation method for recursive digital filters
[AD-A156655] N86-10865
DIGITAL SIMULATION
Evaluating the ground-water resources of the high plains of Texas, Volume 4
[PB85-191625] N86-10641
Imaging speckle interferometer in space: Digital simulations of image reconstruction and photon noise N86-11120
DIGITAL SPACECRAFT TELEVISION
Digital transmission experiments with the Orbital Test Satellite
[EUT-84-E-144] N86-10270
DIGITAL SYSTEMS
The interpolation of signals sampled at less than the Nyquist rate N86-10368
Specification for the performance, design, development and test requirements for a severe environment cartridge recorder. Issue 4
[AD-A156637] N86-10523
Automated analysis of digital images generated by two-dimensional gel electrophoresis
[DE85-011906] N86-10526
Digital processing of images in tracking a moving object N86-10818
Study of one- and two-dimensional filtering and deconvolution algorithms for a streaming array computer
[NASA-CR-176221] N86-10822
DIGITAL TECHNIQUES
The interpolation of signals sampled at less than the Nyquist rate N86-10368
Digital radio link: Method and a measuring system for studying the radio channel during frequency selective fading
[FOA-C-30386-E2] N86-10411
Extended precision in video bandwidth analog to digital converter using optical techniques
[AD-D011745] N86-10422
Sound radiation from repetitive transient vibrations using multi-channel digital signal processing with application to impact machinery N86-10910
DIMENSIONLESS NUMBERS
A fundamental study of smoldering with emphasis on experimental design for zero-g N86-10162
DIMENSIONS
Two-dimensional electrons
[AD-A156894] N86-10982

DIODES

Investigation of metallic impurities introduced into SiO2 and silicon by various candidate VLSI metallization systems: Chemical reactions, diffusion, and electrical properties
[AD-A156609] N86-10429

DIRECT CURRENT

Total internal reflection modulator/deflector
[AD-D011757] N86-10424

Investigation of the uncertainties of the NBS (National Bureau of Standards) thermal voltage and current converters
[PB85-200176] N86-10453

DIRECTIONAL SOLIDIFICATION (CRYSTALS)

Modeling directional solidification N86-10071

Effect of undercooling in a low-gravity containerless environment on the structure and properties of alloys N86-10073

Unidirectional solidification of cast iron: Experiment ES-325 — Spacelab N86-10212

Gradient heating facility behavior — Spacelab N86-10217

Directional solidification of an aluminum-zinc vapor emulsion in microgravity — Spacelab N86-10218

Directional solidification of eutectic alloys — Spacelab N86-10219

Crystallization of a silicon sphere — Spacelab N86-10226

Crystal growth of silicon in Spacelab 1: Experiment ES-321 N86-10227

Transport processes in directional solidification during space shuttle flight N86-10257

Stability of metallic dispersions — microgravity N86-10258

Dendritic solidification in a binary alloy melt: Steady-state versus morphological stability theories N86-10261

Cellular morphologies in lead-thallium alloys — gravitational effects N86-10262

DIRICHLET PROBLEM

On the absolute continuity of elliptic measures
[CTH-MATH-1984-26] N86-10873

Poisson semigroups and singular integrals
[CTH-MATH-1985-05] N86-10876

DISCONNECT DEVICES

AIRBOC (air rapid bloom offboard chaff) chaff deployment system
[AD-D011746] N86-10554

DISCRETE FUNCTIONS

Phase-coded pulse expander-compressor
[AD-D011812] N86-10375

Phase coded pulse expander-compressor
[AD-D011817] N86-10376

Acceleration-invariant approximation method for recursive digital filters
[AD-A156655] N86-10865

DISKS (SHAPES)

Effects of slots/holes in disks on frequencies of TM01 and EH11 waves in the disk-loaded waveguide
[DE85-013376] N86-11009

DISORDERS

Topics in the electronic theory of disordered semiconductors N86-11045

DISPERSIONS

Production of large-particle-size monodisperse latexes in microgravity N86-10146

DISPLAY DEVICES

Report on a visit to England — color and monochrome displays
[FOA-C5-85-0006-H2] N86-10364

Guidelines for a thermochemical kinetics computer program
[DE85-014266] N86-10839

Infrared system with computerized image display
[AD-D011777] N86-10906

DISSOLVED GASES

Mass transport phenomena between bubbles and dissolved gases in liquids under reduced gravity conditions N86-10110

DISTORTION

Harmonic distortion reduction technique for data acquisition
[AD-D011771] N86-10799

DISTRIBUTED PARAMETER SYSTEMS

Spillover minimization in self-adjoint distributed-parameter systems with direct output feedback N86-10852

DISTHIBUTED PROCESSING

Parallel local interface bus
[AD-D011742] N86-10792

DITHERS

Precise bearing support ditherer with piezoelectric drive means
[AD-D011819] N86-10483

DIURNAL VARIATIONS

Intradiurnial organization of wakefulness-sleep sequence and energy metabolism in rats exposed to low ambient temperature N86-10764

DIVERTERS

GA Theory News, January-March 1985
[DE85-012572] N86-11007

DOCUMENTATION

Let's get serious about software
[AD-A156819] N86-10831

DOCUMENTS

Study of one- and two-dimensional filtering and deconvolution algorithms for a streaming array computer
[NASA-CR-176226] N86-10827

DOGS

Evaluation of the 90-day inhalation toxicity of petroleum and oil shale JP-5 jet fuel
[AD-A156815] N86-10675

DOMAINS

Digital control of the hydraulic actuators of an adaptive suspension vehicle N86-10548

DOMESTIC ENERGY

Contribution of wind energy to the energy balance of a combined solar and wind energy system. Part 1: System description, data acquisition and system performance
[BMFT-FB-T-85-051-VOL-1] N86-10670

Contribution of wind energy to the energy balance of a combined solar and wind energy system. Part 2: Computer-assisted investigations
[BMFT-FB-T-85-052-VOL-2] N86-10671

DOPED CRYSTALS

A preliminary report on floating zone experiments with germanium crystals in a sounding rocket N86-10256

DOPPLER EFFECT

Cooled ion frequency standard
[AD-A156813] N86-10295

DOSAGE

Effect of various doses of some vitamins on non-specific mechanisms of adaptation of man N86-10750

DOSIMETERS

Development and application of the electrochemical etching technique
[DE85-010302] N86-10957

DRAG CHUTES

AIRBOC (air rapid bloom offboard chaff) chaff deployment system
[AD-D011746] N86-10554

DRAG REDUCTION

A study of the aerodynamic performance of Weis-Fogh wings N86-10012

DRAINAGE

Kinetics of biological ferrous iron oxidation
[DE85-014616] N86-10736

DRIFT RATE

Local drift parameter, j/n sub e and resistivity anomaly measurements in CTX spheromaks
[DE85-012740] N86-10996

DROP SIZE

Cloud microphysics by thermal wave methods N86-10103

Freezer model using a population balance approach for steady-state, direct-contact, secondary refrigerant, freeze desalination N86-10361

DROP TESTS

Ignition and flame spread above liquid fuel pools N86-10163

DROP TOWERS

Effect of undercooling in a low-gravity containerless environment on the structure and properties of alloys N86-10073

The influence of containerless undercooling and rapid solid-state quenching on the superconductive and magnetic properties of some clustering alloy systems N86-10076

Development of materials processing systems for use in space on low-g simulation devices N86-10166

DROPS (LIQUIDS)

Cloud microphysics by thermal wave methods N86-10103

Extension of Ostwald ripening theory N86-10104

Surface tensions and their variations with temperature and impurities
[NASA ORDER H-27954B] N86-10115

Fundamental studies of droplet combustion at reduced gravity N86-10165

Kinetics of spreading of liquids in microgravity: Experiment 1 ES 327 — Spacelab N86-10207

The influence of thermocapillarity on the migration of droplets in a liquid possessing a uniform temperature gradient N86-10237

Oscillations of a viscoelastic liquid drop in zero-gravity N86-10240

DRUGS

Mechanism of adaptogenic action of prickly eleuterococcus on man during heat stress N86-10757

DRYING APPARATUS

Microcomputer aided calculations of parameters for spray dryer operation
[DE85-013468] N86-10681

DUCTED FLOW

Oscillations of subsonic flow in an abruptly expanding circular duct
[MPIS-16/1984] N86-10028

Dust deposition in regions of separated flow
[JUEL-1965] N86-10475

DUCTILITY

Fabrication and metallurgical properties of modified 9Cr-1 Mo steel
[DE85-012685] N86-10328

Strength of shells under local transverse loads N86-10568

DUNES

Application of the dutch method for estimating storm-induced dune erosion
[AD-A156717] N86-10728

DUOPLASMATRONS

Ion sources for high-frequency accelerators
[DE85-012992] N86-11006

DURABILITY

Identification of chemical and physical phenomena affecting the durability of silvered polymer (PMMA) mirrors
[DE85-012131] N86-10645

DUST

Dust deposition in regions of separated flow
[JUEL-1985] N86-10475

DUST STORMS

contemporary Aeolian processes on Mars: Local dust storms N86-11136

DYNAMIC CHARACTERISTICS

Dynamic analysis of a sled traveling along a rough rail
[AD-A156589] N86-10191

Inelastic analysis of frame structures including member and joint shears N86-10573

Acoustic cavitation and bubble dynamics
[AD-A156888] N86-10918

DYNAMIC LOADS

Dynamic analysis of a sled traveling along a rough rail
[AD-A156589] N86-10191

Theoretical modeling of the vapor cavitation in dynamically loaded journal bearings
[NASA-TM-87076] N86-10463

DYNAMIC MODELS

Dynamic analysis of robotic manipulations with flexible links N86-10545

DYNAMIC RESPONSE

Design, fabrication and testing of an experimental apparatus for determining particle behavior under very low intergranular stresses N86-10175

Determination of symmetry and phase in human visual response functions: Theory and experiments N86-10769

DYNAMIC STRUCTURAL ANALYSIS

Acta Aeronautica et Astronautica Sinica (selected articles)
[AD-A147304] N86-10001

Optimum design of an aircraft wing structure with multiple constraints by the direct-vision criteria method N86-10004

Seismic analysis of the large 70-meter antenna, part 1: Earthquake response spectra versus full transient analysis N86-10386

Finite element analysis of statics and dynamic structural engineering problems using semi-explicit methods N86-10571

DYNAMICAL SYSTEMS

Large eddy interactions in a turbulent channel flow
[NASA-TM-86757] N86-10464

DYSPROSIUM ISOTOPES

Information on continuum states from feeding times and total (GAMMA) spectra measured with BGO suppressed detectors
[DE85-013868] N86-10961

E

E GLASS

Undercooling investigations on the easy glass former Pd-Cu-Si N86-10259

EARTH (PLANET)

Theoretical and numerical investigation of dipole radiation over a flat earth N86-10369

EARTH ATMOSPHERE

The air of life of the blue planet. Atmosphere research from space using data and facts against climate speculations N86-10184

EARTH CRUST

Mobile VLBI and GPS measurement of vertical crustal motion N86-10401

Time-term analysis of upper crustal structure in the Columbia Basin, Washington
[DE85-012390] N86-10633
Crustal structure of the southern Rio Grande rift determined from seismic refraction, surface wave dispersion, and gravity data N86-10700
In-situ geophysical investigations into the nature of the oceanic crust N86-10725

EARTH MOVEMENTS
Mobile VLBI and GPS measurement of vertical crustal motion N86-10401

EARTH ORBITS
User's guide for Langley Research Center Orbital Lifetime program
[NASA-TM-87587] N86-10828

EARTH RESOURCES
The dirigible: A catalyst for resource exploitation in remote areas?
[AD-A156518] N86-10034
Geologic evaluation and reservoir properties of the PR Spring tar sand deposit, Uintah and Grand Counties, Utah
[DE85-013248] N86-10634
Remote sensing
[NOTA-1535] N86-10638

EARTH SURFACE
Representation of the distribution of the snow cover on the surface of the Earth's dry land
[NASA-TM-77909] N86-10612

EARTHQUAKE RESISTANCE
Seismic analysis of the large 70-meter antenna, part 1: Earthquake response spectra versus full transient analysis N86-10386

EARTHQUAKE RESISTANT STRUCTURES
Seismic analysis of the large 70-meter antenna, part 1: Earthquake response spectra versus full transient analysis N86-10386

EARTHQUAKES
Design, fabrication and testing of an experimental apparatus for determining particle behavior under very low intergranular stresses N86-10175

ECCENTRICITY
Lumped geopotential harmonics of order 14, from the orbit of 1967-11G
[AD-A156627] N86-10190

ECOLOGY
Sediment characterization. Task 2: Instream contaminant study, volume 1
[DE85-013502] N86-10683
Adaptation of man to extreme conditions of Antarctica N86-10751
Mission orientation in science N86-11066

ECONOMIC ANALYSIS
Fuel Cell Technology Assessment Program, work element no. 6
[DE85-008228] N86-10444

EDGES
The influence of the substrate on the practical machining applications of cutting edges coated with different materials
[BLL-RISLEY-TR-5039-(9091.9F)] N86-10546

EDUCATION
Methods for developing jam-resistant security communications networks at fixed-site facilities
[DE85-012032] N86-10408
Catalog of Resources for Education in Ada (trademark) and Software Engineering (CREASE). Version 3.0
[AD-A156687] N86-10790
NASA/American Society for Engineering Education (ASEE) Summer Faculty Fellowship Program, 1985
[NASA-CR-177972] N86-11064

EFFICIENCY
Aluminum battery alloys
[DE85-011599] N86-10445
Analyses of advanced residential abosrption heat pump cycles
[DE85-005244] N86-10664
Photovoltaic concentrator array evaluation
[DE85-013789] N86-10665
Energy efficiency of the CTX magnetized coaxial plasma source
[DE85-012735] N86-11003

EFFLUENTS
Membrane research in energy and solvent recovery from industrial effluent streams
[DE85-014583] N86-10682

EGYPT
Report of the Workshop on Geologic Applications of Remote Sensing to the Study of Sedimentary Basins
[E86-10002] N86-10599
Analysis of remote sensing data N86-10605

EIGENVALUES
Design sensitivity analysis and optimization of built-up structures N86-10565
Optimal design of portal frames against buckling N86-10572
Partial eigensolutions of large nonsymmetric matrices
[AD-A156711] N86-10867
Conducting wall and pressure profile effect on MHD stabilization of axisymmetric mirror
[DE85-013647] N86-11020

EINSTEIN EQUATIONS
Initial data for N black holes N86-11128
Gravitational collapse of a scalar field N86-11129

ELASTIC DEFORMATION
Finite deformation crack-line fields in a thin elasto-plastic sheet
[AD-A156757] N86-10346
Analysis of large, non-isothermal elastic-visco-plastic deformations
[NASA-CR-176220] N86-10586

ELASTIC PROPERTIES
Elastic properties and thermal stability characterization of metallic glasses by guided wave techniques N86-10337
A transformation method for the evaluation of the response moments of elastic structures with random properties
[AD-A156882] N86-10557
Analytical and experimental study of cracks emanating from an elliptical hole in unidirectional composite material N86-10567

ELASTIC WAVES
Nonlinear propagation of elastoplastic waves in Ke penetrators (excerpts)
[DE85-011450] N86-10318
Elastic wave gyrometer. Experiments with a parametric wave device
[REPT-26/5005/HF/AR] N86-10533

ELASTOHYDRODYNAMICS
Measurement of the density of base fluids at pressures 0.422 to 2.20 GPa
[NASA-TM-87114] N86-10551

ELASTOPLASTICITY
Nonlinear propagation of elastoplastic waves in Ke penetrators (excerpts)
[DE85-011450] N86-10318
The use of new path indepedent integrals in elastic-plastic and creep fracture N86-10574
Advanced development of BEM for two and three dimensional nonlinear analysis N86-10855

ELECTRIC BATTERIES
Laser Raman spectroscopy study of the zinc and bromide ion complex equilibrium in zinc/bromine battery electrolytes
[DE85-011820] N86-10301
Aluminum battery alloys
[DE85-011599] N86-10445
Nickel-cadmium battery conditioner and tester apparatus
[AD-D011770] N86-10642
Phosphoric and electric utility fuel cell technology development
[DE85-014552] N86-10652
Advanced vehicle systems assessment. Volume 2: Subsystems assessment
[NASA-CR-176205] N86-11083
Advanced vehicle systems assessment. Volume 4: Supporting analyses
[NASA-CR-176207] N86-11085

ELECTRIC CONDUCTORS
Electrically conducting polymers N86-10333
Polymer engineering: Polymeric and molecular electronic, dielectric and optical properties for device applications
[AD-A156671] N86-10344

ELECTRIC CONNECTORS
Multi-row connector with ground plane board
[AD-D011803] N86-10437

ELECTRIC CONTACTS
Development of metallization process
[NASA-CR-176209] N86-10312
Contact effects in light activated GaAs switches
[AD-A156957] N86-10434

ELECTRIC CURRENT
Signal analysis of gas tungsten arc welds N86-10078
Protection circuitry for high voltage drivers
[AD-D011781] N86-10414

ELECTRIC DISCHARGES
Nickel-cadmium battery conditioner and tester apparatus
[AD-D011770] N86-10642

ELECTRIC EQUIPMENT
Photovoltaic systems in remote locations: An experience summary
[NASA-TM-87106] N86-10643

ELECTRIC FIELDS
Mathematical models of continuous flow electrophoresis N86-10143
Electric field containerless processing technology N86-10170
Amplitude and phase modulation in fin-lines electrical tuning
[AD-D011813] N86-10415
Total internal reflection modulator/deflector
[AD-D011757] N86-10424
Photoionization technique for growth of metallic films
[AD-D011760] N86-10426
Computation of flow regimes in parameter space for the AGCE
[NASA-CR-176480] N86-10705
Fiber optic system for measuring electric fields
[AD-D011830] N86-10976
Electron wind in strong wave guide fields
[DE85-013062] N86-11004
A study of the applicability of nucleation theory to quasi-thermodynamic transformations of second and higher Ehrenfest-order
[NASA-CR-176230] N86-11060

ELECTRIC FURNACES
Recirculation within a glass mixture subjected to external and resistive heating
[DE85-010068] N86-10348

ELECTRIC GENERATORS
Photovoltaic systems in remote locations: An experience summary
[NASA-TM-87106] N86-10643

ELECTRIC HYBRID VEHICLES
Advanced vehicle systems assessment. Volume 2: Subsystems assessment
[NASA-CR-176205] N86-11083
Advanced vehicle systems assessment. Volume 3: Systems assessment
[NASA-CR-176206] N86-11084
Advanced vehicle systems assessment. Volume 5: Appendices
[NASA-CR-176208] N86-11086

ELECTRIC MOTOR VEHICLES
Advanced vehicle systems assessment. Volume 4: Supporting analyses
[NASA-CR-176207] N86-11085

ELECTRIC POTENTIAL
Signal analysis of gas tungsten arc welds N86-10078
Intrinsic mechanisms of multilayer ceramic capacitor failure
[AD-A156638] N86-10431
Interdigital Schottky barrier capacitor apparatus
[AD-D011799] N86-10436
Increased particle confinement with the use of external dc bias field in the CTX spheromak
[DE85-012744] N86-10988

ELECTRIC PROPULSION
Experimental performance of a 1-kilowatt arcjet thruster
[NASA-TM-87131] N86-10281

ELECTRICAL ENGINEERING
Report on the engineering test of the LBL 30 second neutral beam source for the MFTF-B project
[DE85-013317] N86-10962

ELECTRICAL FAULTS
Contact effects in light activated GaAs switches
[AD-A156957] N86-10434

ELECTRICAL GROUNDING
Multi-row connector with ground plane board
[AD-D011803] N86-10437

ELECTRICAL IMPEDANCE
High output programmable signal current source for low output impedance applications
[AD-D011751] N86-10423

ELECTRICAL INSULATION
Numerical methods for analyzing electromagnetic scattering
[NASA-CR-176141] N86-10377
High voltage instrument transformers for outdoor service with an insulation of low pressure SF6 gas and plastic foils
[BMFT-FB-T-85-034] N86-10449

ELECTRICAL PROPERTIES
Miniature radar packaging
[DE85-014596] N86-10410

ELECTRICAL RESISTIVITY
Electrically conducting polymers N86-10333
A simplified method of estimation of the specular components of radar cross section for some re-entrant conductors
[AD-A156573] N86-10403
Theoretical aspects of magnetic helicity
[DE85-011846] N86-10984
Local drift parameter, j/n sub e and resistivity anomaly measurements in CTX spheromaks
[DE85-012740] N86-10998
Electron tunneling in metal/tunnel-oxide/degenerate silicon junctions N86-11043

ELECTRO-OPTICS
Levitating furnance for containerless processing in space N86-10169

Extended precision in video bandwidth analog to digital converter using optical techniques
[AD-D011745] N86-10422
Information technique 1985: Optical technology and electro-optics, a defense technical component review
[FOA-A-30037-E] N86-10980

ELECTROACOUSTIC TRANSDUCERS
Precise bearing support ditherer with piezoelectric drive means
[AD-D011819] N86-10483

ELECTROCARDIOGRAPHY
Assessment of state of chronotropic and inotropic heart function at different degrees of physical fitness
N86-10746
Individual typological self-regulation of cardio-vascular system N86-10752

ELECTROCHEMICAL CELLS
Metals electroprocessing in molten salts N86-10098
A compact bulk acousto-optic time integrating correlator
[AD-A156608] N86-10428
Aluminum battery alloys
[DE85-011599] N86-10445

ELECTRODEPOSITION
Metals electroprocessing in molten salts N86-10098

ELECTRODES
Phosphoric and electric utility fuel cell technology development
[DE85-014552] N86-10652
Introduction to the m = 1 helicity source
[DE85-012771] N86-10999

ELECTROENCEPHALOGRAPHY
TV monitoring control system in electrophysiological studies N86-10765
Variability analysis of visually induced responses in the midst of noise
[B8564052] N86-10774

ELECTROHYDRODYNAMICS
Electrohydrodynamics N86-10130

ELECTROLYSIS
Chemical/hydrogen energy systems
[DE85-012742] N86-10667

ELECTROLYTES
Laser Raman spectroscopy study of the zinc and bromide ion complex equilibrium in zinc/bromine battery electrolytes
[DE85-011820] N86-10301
Streaming potentials in conductive and nonconductive tubing
[DE85-012984] N86-10438
Phosphoric and electric utility fuel technology development
[DE85-014741] N86-10651

ELECTROMAGNETIC ABSORPTION
Free carrier absorption from electrons in confined systems N86-11042

ELECTROMAGNETIC FIELDS
Modification of the electromagnetic levitator (EML) hardware N86-10172
Criteria for the design or selection of a bioelectromagnetics experiment
[AD-A156575] N86-10420
Effect of single actions of weak electromagnetic fields of ultralow frequency on indices of endocrine system
N86-10744

ELECTROMAGNETIC INTERACTIONS
Proceedings of a Workshop on Electroweak Symmetry Breaking
[DE85-004444] N86-11008

ELECTROMAGNETIC INTERFERENCE
Apparatus for locating passive intermodulation interference sources
[AD-D011798] N86-10435
Experimental investigations of pulse-pulse interference in heterodyne detection
[DFVLR-FB-85-26] N86-10544
Measurements of the acoustic interference between adjacent microphones
[AD-A156892] N86-10919

ELECTROMAGNETIC PROPERTIES
Electromagnetic resonances of cylinders and aircraft model with resistive wires
[NASA-CR-176250] N86-10042

ELECTROMAGNETIC PROPULSION
Overpulse railgun energy recovery circuit
[DE85-011607] N86-10197

ELECTROMAGNETIC PULSES
Experimental investigations of pulse-pulse interference in heterodyne detection
[DFVLR-FB-85-26] N86-10544
Method for determining the position, angle and other injection parameters of a short pulsed beam in the Brookhaven AGS
[DE85-012523] N86-10931
Optical detection of photoacoustic pulses in thin silicon wafers
[AD-A156705] N86-10977
Beam-cavity interaction measurements in a DAW structure
[DE85-012680] N86-10987

ELECTROMAGNETIC RADIATION
Theoretical and numerical investigation of dipole radiation over a flat earth N86-10369
Remote sensing
[NOTA-1535] N86-10636
USSR report: Life sciences. Biomedical and behavioral sciences
[JPRS-UBB-85-023] N86-10738
Analytic evaluation of LAMPF 2 Booster Cavity design
[DE85-012680] N86-11002

ELECTROMAGNETIC SCATTERING
Numerical methods for analyzing electromagnetic scattering
[NASA-CR-176141] N86-10377

ELECTROMAGNETIC WAVE TRANSMISSION
Integrating sphere measurements of directional-hemispherical transmittance of window systems
[DE85-013926] N86-10973

ELECTROMAGNETISM
Measurement of high temperature thermophysical properties N86-10074

ELECTROMAGNETS
Revision of and documentation for the standard version of the Poisson-Group codes
[DE85-012659] N86-10837
Report on a visit to CERN in February 1985. Notes on bunch monitors, high-frequency systems, linacs, kickers, magnets, vacuum and bunch extraction
[LINO-119] N86-10967

ELECTROMECHANICAL DEVICES
Levitating furnance for containerless processing in space N86-10169

ELECTRON ACCELERATORS
High-brightness photoemitter injector for electron accelerators
[DE85-012673] N86-10929
The MEA vacuum system
[LINO-120] N86-10968

ELECTRON BEAMS
Compact, low jitter, triggered spark gap
[DE85-012812] N86-10195
An experimental TE sub 12 - TE sub 11 circular waveguide mode converter N86-10387
Potential structures and particle acceleration on auroral field lines
[AD-A156694] N86-10708
Initial increase, peaking effect, in the internal friction of copper following pulsed neutron and electron irradiation
[DE85-012767] N86-10932
Beam profile monitor for the NSLS VUV ring employing linear photodiode arrays
[DE85-012184] N86-10947
Beam stability in a 6 GeV synchrotron light source
[DE85-013850] N86-10979
Beam-cavity interaction measurements in a DAW structure
[DE85-012680] N86-10987
Effects of slots/holes in disks on frequencies of TM01 and EH11 waves in the disk-loaded waveguide
[DE85-013376] N86-11009
Computer control of rf at SLAC
[DE85-013065] N86-11015

ELECTRON BUNCHING
The MEA vacuum system
[LINO-120] N86-10968
High-resolution phosphor screen beam profile monitor
[DE85-013074] N86-11012

ELECTRON CAPTURE
Volatile organic compounds in indoor air: A survey of various structures
[PB85-198356] N86-10687

ELECTRON DISTRIBUTION
Electron momentum transfer collision frequency in N(2), O(2) and air
[AD-A157030] N86-10924
Electron wind in strong wave guide fields
[DE85-013062] N86-11004

ELECTRON EMISSION
Electron wind in strong wave guide fields
[DE85-013062] N86-11004

ELECTRON ENERGY
Angular distribution of neutral hydrogen following collisional electron detachment from H(-)
[DE85-014258] N86-10943
Electron-ion recombination studies of planetary ionospheric and astrophysical ions N86-11132

ELECTRON IMPACT
Ultraviolet spectroscopy of the Earth's dayglow and magnetosphere cleft N86-10696

ELECTRON IRRADIATION
Evaluation and prediction of long-term environmental effects on non metallic materials
[NASA-CR-178495] N86-10340
Experimental studies of transition radiation and optical bremsstrahlung
[DE85-0135637] N86-10949

ELECTRON MICROSCOPY
A fundamental study of the sticking of insect residues to aircraft wings
[NASA-CR-176231] N86-10033
Study of the reactive-element effect in oxidation of Fe-Cr alloys using transverse section analytical electron microscopy N86-10067
Simulating the CTR environment in the HVBM
[DE85-011745] N86-10193
Weld metal hot-cracking of hastelloy alloys C-22 and C-276: A study by analytical electron microscopy
[DE85-009437] N86-10324
Metastable phase formation in Ni-implanted Al: An analytical electron microscope investigation
[DE85-009105] N86-10331

ELECTRON OPTICS
Superconvergent tracking and invariant surfaces in phase space
[DE85-013051] N86-10995

ELECTRON RECOMBINATION
Electron-ion recombination studies of planetary ionospheric and astrophysical ions N86-11132

ELECTRON SCATTERING
Electron momentum transfer collision frequency in N(2), O(2) and air
[AD-A157030] N86-10924

ELECTRON TRANSFER
Electron momentum transfer collision frequency in N(2), O(2) and air
[AD-A157030] N86-10924

ELECTRON TRANSITIONS
Selected tables of atomic spectra. Atomic energy levels and multiplet table O3
[NBS/NSRDS-3/11] N86-10923
Cooperative emission by two different atoms into surface plasmons
[AD-A157033] N86-10925
Mean life of the 2p(4)((1)S)3s (2)S state in fluorine
[DE85-012929] N86-10956
A superconducting tunnel junction receiver for millimeter-wave astronomy N86-11041

ELECTRON TUNNELING
Electron tunneling in metal/tunnel-oxide/degenerate silicon junctions N86-11043

ELECTRONIC CONTROL
Renovated cooling at PIMU
[LINO-122] N86-10452

ELECTRONIC COUNTERMEASURES
Submerged ram air inlets for ECM (electronic countermeasures) pods
[AD-D011801] N86-10020
Angle set-on apparatus
[AD-D011766] N86-10371

ELECTRONIC EQUIPMENT
Simulated direct-strike lightning testing at Sandia National Laboratories
[DE85-012033] N86-10049
Soudan 2 data acquisition and trigger electronics
[DE85-013864] N86-10443

ELECTRONIC PACKAGING
Increase of the packaging density of Very Large Scale Integration (VLSI) circuits using automatic alignment
[BMFT-FB-T-85-020] N86-10451

ELECTRONIC TRANSDUCERS
Fiber optic system for measuring electric fields
[AD-D011830] N86-10976

ELECTRONS
Theoretical studies of the surface tension of liquid metal system N86-10101
Theoretical investigation of electron-positive ion-atom interactions
[DE85-013019] N86-10939
The 20 keV undulators for a 6-GeV storage ring
[DE85-013867] N86-10941
Two-dimensional electrons
[AD-A156894] N86-10962
Local drift parameter, j/n sub e and resistivity anomaly measurements in CTX spheromaks
[DE85-012740] N86-10998
SLC positron damping ring optics design
[DE85-013054] N86-11014
Beam steering in the SLC linac
[DE85-013370] N86-11025
Symmetric Tandem Mirror Program
[DE85-012352] N86-11032

Free carrier absorption from electrons in confined systems N86-11042

ELECTROPHORESIS
Mathematical models of continuous flow electrophoresis N86-10143
Electrophoresis technology N86-10144
Kidney cell electrophoresis N86-10145
Automated analysis of digital images generated by two-dimensional gel electrophoresis
[DE85-011906] N86-10526

ELECTROPHYSIOLOGY
TV monitoring control system in electrophysiological studies N86-10765

ELECTROSTATIC CHARGE
Design and construction of a Faraday cup for measurement of small electronic currents
[NASA-TM-77915] N86-10418

ELECTROSTATIC PROBES
Polymer engineering: Polymeric and molecular electronic, dielectric and optical properties for device applications
[AD-A156671] N86-10344

ELECTROSTATICS
Electric field containerless processing technology N86-10170

ELEMENTARY EXCITATIONS
A superconducting tunnel junction receiver for millimeter-wave astronomy N86-11041

ELEVATION
A graphic anthropometric aid for seating and workplace design
[AD-A156988] N86-10788

ELEVATION ANGLE
Guidance and control of a cable based payload pickup system N86-10046

ELLIPTIC FUNCTIONS
Acceleration-invariant approximation method for recursive digital filters
[AD-A156655] N86-10865

EMBRITTLEMENT
Simulating the CTR environment in the HVBM
[DE85-011745] N86-10193

EMISSION
Emissions of NOx, SOx and VOC from Antropogenic sources
[PB85-193530] N86-10688
Cooperative emission by two different atoms into surface plasmons
[AD-A157033] N86 10925

EMISSION SPECTRA
Selected tables of atomic spectra. Atomic energy levels and multiplet table O3
[NBS/NSRDS-3/11] N86-10923
Experimental studies of transition radiation and optical bremsstrahlung
[DE85-0135637] N86-10949
Mean life of the 2p(4)((1)S)3s (2)S state in fluorine
[DE85-012929] N86-10956
Dynamics of imploding neon gas puff plasmas. 1
[AD-A156916] N86-10983
Directionality of bremsstrahlung from relativistic electrons in solar flares
[NASA-TM-87509] N86-11141

EMITTERS
P-N junction controlled field emitter array cathode
[AD-D011815] N86-10416

ENDOCRINE SYSTEMS
Effect of single actions of weak electromagnetic fields of ultralow frequency on indices of endocrine system N86-10744

ENERGY ABSORPTION
Advanced absorption heat pump cycles
[DE85-003914] N86-10654

ENERGY BUDGETS
Energy balance in a deep Colorado valley: ASCOT 84
[DE85-012441] N86-10631

ENERGY CONSERVATION
Research needs for corrosion control and prevention in energy conservation systems
[DE85-014852] N86-10326

ENERGY CONSUMPTION
Laboratory experiments of heat pump dynamic losses
[DE85-013931] N86-10473

ENERGY CONVERSION
Membrane research in energy and solvent recovery from industrial effluent streams
[DE85-014583] N86-10682
Ocean energy technology program summary
[DE85-013102] N86-10731

ENERGY CONVERSION EFFICIENCY
Theory of advanced, high-efficience concentrator cells
[DE85-006821] N86-10655

ENERGY DISSIPATION
Float zone experiments in space N86-10067
Laboratory experiments of heat pump dynamic losses
[DE85-013931] N86-10473

Photoactivation of PBFA-2
[DE85-013439] N86-11019

ENERGY LEVELS
Selected tables of atomic spectra. Atomic energy levels and multiplet table O3
[NBS/NSRDS-3/11] N86-10923
Nature of photoemission into dielectric fluids
[DE85-013017] N86-10945
Fermi surface study of CeSb in the ferromagnetic and antiferromagnetic phases
[DE85-012122] N86-11052

ENERGY METHODS
On the method of characteristics and its application to the calculations of annular nozzle flowfields N86-10454

ENERGY POLICY
Contribution of wind energy to the energy balance of a combined solar and wind energy system. Part 1: System description, data acquisition and system performance
[BMFT-FB-T-85-051-VOL-1] N86-10670
Contribution of wind energy to the energy balance of a combined solar and wind energy system. Part 2: Computer-assisted investigations
[BMFT-FB-T-85-052-VOL-2] N86-10671
Wind energy in agriculture, a promise
[SS-45] N86-10672
Wind energy, a feasibility investigation for wind mills in agriculture
[SS-45A] N86-10673

ENERGY SPECTRA
Polarization transfer in inelastic scattering and pionic models of the EMC effect
[DE85-010738] N86-10955
Information on continuum states from feeding times and total (GAMMA) spectra measured with BGO suppressed detectors
[DE85-013868] N86-10961

ENERGY STORAGE
Counterpulse railgun energy recovery circuit
[DE85-011603] N86-10196
Overpulse railgun energy recovery circuit
[DE85-011607] N86-10197
Advanced vehicle systems assessment. Volume 2: Subsystems assessment
[NASA-CR-176205] N86-11083

ENERGY TECHNOLOGY
LANDSAT TM image data quality analysis for energy-related applications
[E85-10109] N86-10597
Ground-coupled heat pump research at the University of Tennessee Washington, D.C., 10 Dec. 1984
[DE85-005357] N86-10650
Phosphoric and electric utility fuel cell technology development
[DE85-014552] N86-10652
Chemical/hydrogen energy systems
[DE85-012742] N86-10667
Ocean energy technology program summary
[DE85-013102] N86-10731
Computer codes: A bibliography supplement 1
[DE85-006721] N86-10838

ENERGY TRANSFER
SUTRA (Saturated-unsaturated transport). A finite-element simulation model for saturated-unsaturated, Fluid-Density-Dependent ground-water flow with energy transport or chemically-reactive single-species solute transport
[AD-A156779] N86-10830
Recent helicity source and power supply improvements in CTX
[DE85-012741] N86-11028

ENGINE MONITORING INSTRUMENTS
Trials on the asperity counting monitoring system --- helicopter gearboxes
[RES-PAPER-670] N86-10550

ENGINEERING
NASA/American Society for Engineering Education (ASEE) Summer Faculty Fellowship Program, 1985
[NASA-CR-177972] N86-11064

ENGINES
Simplified analysis of Stirling engines and heat pumps
[DE85-005366] N86-10647
Stirling-engine-driven heat pump program overview
[DE85-004796] N86-10661

ENTHALPY
Thermodynamic constraints on ion beam mixing of metals on insulators
[DE85-013628] N86-10448

ENTRAINMENT
Analysis of annular two-phase flow with liquid entrainment N86-10459

ENVIRONMENT EFFECTS
Evaluation and prediction of long-term environmental effects on non metallic materials
[NASA-CR-178495] N86-10340
Approaches to cumulative impact assessment
[DE85-013891] N86-10635

Examples of regional environmental assessment using acid deposition data
[DE85-012903] N86-10677

ENVIRONMENT MANAGEMENT
Erosion control and watershed management by Spacelab photography N86 10493

ENVIRONMENT MODELS
Process models for 3D composites
[AD-A156889] N86-10292

ENVIRONMENT POLLUTION
Chemical kinetics and photochemical data for use in stratospheric modeling
[NASA-CR-176198] N86-10707

ENVIRONMENTAL CHEMISTRY
Preliminary reports, memoranda and technical notes of the Materials Research Council Summer Conference, La Jolla, California
[AD-A156776] N86-10291
Mission orientation in science N86-11066

ENVIRONMENTAL MONITORING
Specification for the performance, design, development and test requirements for a severe environment cartridge recorder. Issue 4
[AD-A156637] N86-10523
Utilization of satellite remote sensing for the monitoring of oil pollution and marine ecosystems in Indonesia. A Tropical Earth Resources Satellite program (TERS) case study implemented for the NLR, Delft N86-10640

ENVIRONMENTAL TESTS
Test, measurement, and diagnostic equipment (system peculiar)
[AD-A156869] N86-10563
Fracture toughness of hydrogen-embrittled precipitation-hardened stainless steels
[AD-A156664] N86-10592

ENVIRONMENTS
National perspective on environmental constraints to hydroelectric development
[DE85-013111] N86-10678

ENZYME ACTIVITY
Romanian plant produces protein concentrate from paraffin-nourished yeasts N86-10741
Biotechnology: Science and practice N86 10742

EOSS
Mathematical simulation of disturbing forces and material science processes under low gravity N86-10236

EPINEPHRINE
Short term heat effect on adreno- and cholino-sensitivity of rat's small intestine N86-10754

EPITAXY
W-shaped diffused stripe GaAs/AlGaAs laser
[AD-D011818] N86-10538

EPOXY COMPOUNDS
Investigation of composite materials property requirements for sonic fatigue research
[NASA-TM-87601] N86-10913

EPOXY RESINS
The preparation and testing of titanium and zirconium coupling agents
[SJ70] N86-10576

EQUATIONS OF MOTION
Theory of non-planar orbits
[DE85-013284] N86-11018

EQUATIONS OF STATE
Work-hardening and effective viscosity in solid berylium
[DE85-013978] N86-10323
KRAK: A computer program for two-phase, two-component porous flow and fracture propagation, revision
[DE85-014264] N86-10469
Improved particle-velocity transducer for equation-of-state experiments
[DE85-013204] N86-10532
New approach to multiphase equilibria: Application to high-pressure physics problems
[DE85-013820] N86-10907
Theory of dense molecular fluid equations of state with application to detonation products
[DE84-016822] N86-10927

EQUIVALENCE
Cryogenic equivalence principle experiment N86-10171

ERBIUM ALLOYS
Formation and characterization of amorphous erbium-based alloys prepared by near-isothermal cold-rolling of elemental composites
[DE85-014853] N86-10327

EROS (SATELLITES)
Utilization of satellite remote sensing for the monitoring of oil pollution and marine ecosystems in Indonesia. A Tropical Earth Resources Satellite program (TERS) case study implemented for the NLR, Delft N86-10640

EROSION
Rapid evaluation of ion thruster lifetime using optical emission spectroscopy
[NASA-TM-87103] N86-10280
Erosion-resistant nosetip construction
[AD-D011787] N86-10289
The mechanism of erosion of metallic materials under cavitation attack
[NASA-TM-87133] N86-10552
Introduction to the m = 1 helicity source
[DE85-012771] N86-10999
ERROR ANALYSIS
Extended analysis of the structure of error scores in psychological aptitude tests
[DFVLR-FB-85-20] N86-10780
Classification of real-time program testing tasks and methods N86-10815
A study of Morrison's iterative noise removal method
[NASA-CR-176222] N86-10823
Fault-free behavior of reliable multiprocessor systems: FTMP experiments in AIRLAB
[NASA-CR-177967] N86-10848
The h, p and h-p versions of the finite element method in dimension. Part 1: The error analysis of the p-version
[AD-A156600] N86-10862
The h, p and h-p versions of the finite element method in 1 dimension. Part 3. The adaptive h-p version
[AD-A156626] N86-10864
The h, p and h-p versions of the finite element method in 1 dimension. Part 2. The error analysis of the H and h-p versions
[AD-A156835] N86-10869
Error estimates and automatic time step control for numerical methods for stiff ordinary differential equations
[CTH-MATH-1984-27] N86-10872
On the numerical determination of the dimension of an attractor — strange attractors
[ZW-8415] N86-10882
ERROR FUNCTIONS
Acceleration-invariant approximation method for recursive digital filters
[AD-A156655] N86-10865
Superefficient estimation of power functions in simulation experiments
[B8562445] N86-10893
ERRORS
The VLSI design of error-trellis syndrome decoding for convolutional codes N86-10391
A mesh moving technique for time dependent partial differential equations in two space dimensions
[AD-A156663] N86-10866
ERYTHROCYTES
A study of blood flow and of aggregation of blood cells under conditions of zero gravity: Its relevance to the occlusive diseases and cancer N86-10137
Effect of inclusion of supplementary ascorbic acid in daily diet on degree of vitamin saturation of body and thermoresistance of erythrocytes while working in arid zone N86-10749
Indices of blood oxygen transporting properties and erythropoiesis in rats after prolonged stay in nitrogen-oxygen mixture at elevated pressure
N86-10761
ESCAPE VELOCITY
The two micron spectrum of R Scuti N86-11092
ESTIMATES
A numerical model for the estimation of solar radiation on rugged terrain N86-10694
Estimation by moments in a model of faulty inspection
[AD-A156754] N86-10886
ESTIMATING
Application of the dutch method for estimating storm-induced dune erosion
[AD-A156717] N86-10728
ESTUARIES
The Rhine-Meuse estuary hydraulic scale model. Experiences with computer configuration and software
[PUBL-335] N86-10637
ETHYL ALCOHOL
Recovery of alcohol from a fermentation source by separation rather than distillation
[AD-D011782] N86-10282
ETHYLENE COMPOUNDS
Rusty bolt intermodulation interference reducer
[AD-D011748] N86-10313
EULER EQUATIONS OF MOTION
On the design of airfoils in transonic flow using the Euler equations N86-10013
EUROPE
Tendencies toward liberalization in European air traffic control
[DFVLR-FB-85-23] N86-10030
Maximum water reserves in the snow cover in the European territory of the USSR according to data for 1892-1980
[NASA-TM-77901] N86-10611
EUROPEAN SPACE PROGRAMS
Satellite use for men — West German space program
N86-10180
EUROPIUM
Extraction of lanthanide ions by 2-methyl-8-quinolinol
[DE85-014277] N86-10303
EUTECTIC ALLOYS
Study of eutectic formation N86-10070
Thermal and solutal convection damping using an applied magnetic field N86-10094
Melting and solidification in O-g of sintered alloys: Experiments ES 311 A and B bubble reinforced materials — Spacelab N86-10215
Directional solidification of eutectic alloys — Spacelab
N86-10219
Directional solidification of InSb-NiSb eutectic — Spacelab N86-10221
EUTECTIC COMPOSITES
Orbital processing of aligned magnetic composites
N86-10089
EUTECTICS
Development of new ammonium nitrate composite explosives
[DE85-014252] N86-10356
EVALUATION
Test and evaluate passive orbital disconnect struts (PODS 3)
[NASA-CR-177368] N86-10274
Theoretical comparison of classical (K-matrix) and inverse (P-matrix) least-squares methods for quantitative infrared spectroscopy
[DE85-012627] N86-10298
Ultrasonic evaluation of mechanical properties of thick, multilayered, filament wound composites
[MASA-TM-87088] N86-10561
Photovoltaic concentrator array evaluation
[DE85-013789] N86-10665
EVAPORATION
Cloud microphysics by thermal wave methods
N86-10103
The development of a neutron evaporation theory code for the thermal fission of Uranium-235
[AD-A156593] N86-10951
EXCITATION
Rapid evaluation of ion thruster lifetime using optical emission spectroscopy
[NASA-TM-87103] N86-10280
EXHAUST GASES
Airborne measurements of the border-crossing air pollution in the area between Weiden and Hof/Bavaria
[DFVLR-FB-85-25] N86-10685
EXHAUST SYSTEMS
The Shock and Vibration Digest, volume 17, no. 3
[AD-A154144] N86-10585
Recent advances in the analysis of exhaust mufflers
N86-10587
EXHAUST VELOCITY
Acta Aeronautica et Astronautica Sinica (selected articles)
[AD-A147304] N86-10001
Theoretical specific impulse for two-phase flow in nozzle of rocket-ramjet engine: A simple estimation method
N86-10005
EXOBIOLOGY
Life sciences research on the space station: An introduction
[NASA-TM-86836] N86-10734
Aerospace medicine and biology: A continuing bibliography with indexes (supplement 275)
[NASA-SP-7011(275)] N86-10768
EXPERIMENT DESIGN
Ignition and flame spread above liquid fuel pools
N86-10163
Rationale for two phase polymer system microgravity separation experiments N86-10247
Space experiment on thermal diffusion. Preparation and theoretical analysis N86-10253
The power of weighted and ordinary least squares with estimated unequal variances in experimental design
[B8562446] N86-10894
EXPERIMENTAL BREEDER REACTOR 2
Swelling and tensile properties of EBR-2-irradiated tantalum alloys for space reactor applications
[DE85-012867] N86-10329
EXPERIMENTATION
Progressive damage, fracture predictions and post mortem correlations for fiber composites
[NASA-TM-87101] N86-10290
Laboratory experiments of heat pump dynamic losses
[DE85-013931] N86-10473
Measurement of the density of base fluids at pressures 0.422 to 2.20 GPa
[NASA-TM-87114] N86-10551
Analytical and experimental study of cracks emanating from an elliptical hole in unidirectional composite material N86-10567
Experimental X-ray scattering cross sections for H2 and rare atomic gases
[DE85-011572] N86-10936
EXPERT SYSTEMS
Framework for generating expert systems to perform computer security risk analysis
[DE85-014134] N86-10841
EXPIRED AIR
Conditioning potentialities of respiratory apparatus
N86-10753
EXPLOSIONS
Angle of incidence effects for underwater shock using generic computational models, rev. 1
[DE85-012921] N86-10467
EXPLOSIVES
Development of new ammonium nitrate composite explosives
[DE85-014252] N86-10356
Explosive initiation by very small conical shaped charge jets
[DE85-009443] N86-10357
Properties of plastic-bonded nitroguanidine
[DE85-015316] N86-10358
Composite explosives for metal acceleration: The effect of detonation temperature
[DE85-013982] N86-10359
Guidelines for a thermochemical kinetics computer program
[DE85-014266] N86-10839
EXPONENTIAL FUNCTIONS
A modified repair strategy for two-component systems with revealed and unrevealed faults
[AD-A156715] N86-10885
EXPOSURE
Approaches to quantitative expression of dose response
[DE85-013498] N86-10772
EXTINCTION
A fundamental study of smoldering with emphasis on experimental design for zero-g N86-10162
Flammability limits of gases under low gravity conditions N86-10164
Fundamental studies of droplet combustion at reduced gravity N86-10165
EXTRACTION
Recovery of alcohol from a fermentation source by separation rather than distillation
[AD-D011782] N86-10282
Beam line windows at LAMPF
[DE85-012723] N86-10985
EXTRAGALACTIC RADIO SOURCES
Physical conditions in giant extragalactic H2 regions
N86-11130
EXTRATERRESTRIAL INTELLIGENCE
SETI radio spectrum surveillance system N86-10400
EXTREMELY HIGH FREQUENCIES
An experimental TE sub 12 - TE sub 11 circular waveguide mode converter N86-10387
Propagation and radiation characteristics of a multimode corrugated waveguide feedhorn N86-10388
EXTRUDING
Continuous fiberization of silicon-carbide-nitride precursor resin N86-10168
Reduction of noble metal stock and noble metal loss during wire production with the Conform extrusion process
[BMFT-FB-T-85-049] N86-10560
EYE (ANATOMY)
A graphic anthropometric aid for seating and workplace design
[AD-A156988] N86-10788

F

F REGION
Acoustic gravity wave chemistry model for the RAYTRACE code
[AD-A156850] N86-10405
FABRICATION
Fabrication and metallurgical properties of modified 9Cr-1 Mo steel
[DE85-012865] N86-10328
Device for cryogenically fabricating source material for plasma X-ray lasers
[AD-D011814] N86-10537
FAILURE
Intrinsic mechanisms of multilayer ceramic capacitor failure
[AD-A156638] N86-10431

FAILURE ANALYSIS
Robust failure detection filters [NASA-CR-176232] N86-10271
Analytical investigation of solid rocket nozzle failure [NASA-TM-86513] N86-10278
Metallurgy and metallography of braze joints [DE85-014563] N86-10325
Load space formulation of reliability for nonlinear random structural systems N86-10570
New probabilistic modeling and simulation methods for complex time-dependent systems [DE85-009575] N86-10835
Investigation of composite materials property requirements for sonic fatigue research [NASA-TM-87601] N86-10913
Failures and successes of quantitative methods in management [ARW-03-THE-BDK/ORS/83-06] N86-11076

FAILURE MODES
New probabilistic modeling and simulation methods for complex time-dependent systems [DE85-009575] N86-10835
Investigation of composite materials property requirements for sonic fatigue research [NASA-TM-87601] N86-10913

FALLING SPHERES
Fall velocity indicator/viewer [AD-D011789] N86-10482

FAR FIELDS
Summary of work on jet noise prediction [ESDU-BR-62636] N86-10909

FAR INFRARED RADIATION
The DUO: Far infrared heterodyne concept for space interferometry N86-11125

FAR ULTRAVIOLET RADIATION
Determination of optical properties by third-harmonic generation in noble gases in unfocused laser beams N86-10535

FARADAY EFFECT
Comparison of the calibration of ionospheric delay in VLBI data by the methods of dual frequency and Faraday rotation N86-10384
Calibrated Faraday current and magnetic field sensor [DE85-013438] N86-10439

FARM CROPS
Vegetation and soils field research data base: Experiment summaries [E85-10110] N86-10610

FAST FOURIER TRANSFORMATIONS
A comparison of swept frequency and FFT methods used to calibrate array test modules [AD-A156629] N86-10430
An improved FFT (Fast fourier transform) for a four parallel pipe SIMD arithmetic processor [AD-A156625] N86-10863

FAST NEUTRONS
ORR core re-configuration measurements to increase the fast neutron flux in the Magnetic Fusion Energy (MFE) experiments [DE85-013520] N86-10958

FATIGUE (BIOLOGY)
Eye-movement activity as index of functional state of brain N86-10756

FATIGUE (MATERIALS)
A review of Australian investigations on aeronautical fatigue during the period April 1983 to March 1985 [AD-A156602] N86-10036
Report on an overseas visit [AD-A156603] N86-10037
Review of investigations on aeronautical fatigue in the Federal Republic of Germany [LBF-S-173] N86-10044
Fatigue, static tensile strength and stress corrosion of aircraft materials and structures [VTH-LR-360-PT-1] N86-10045
Fatigue of graphite/epoxy buffer strip panels with center cracks [NASA-TM-87595] N86-10581

FATIGUE LIFE
A review of Australian investigations on aeronautical fatigue during the period April 1983 to March 1985 [AD-A156602] N86-10036

FATIGUE TESTS
Creep-fatigue behavior of NiCoCrAlY coated PWA 1480 superalloy single crystals [NASA-TM-87110] N86-10311

FAULT TOLERANCE
Diagnostics of peripheral processors and controllers N86-10812
Fault-free behavior of reliable multiprocessor systems: FTMP experiments in AIRLAB [NASA-CR-177967] N86-10848
Reaching approximate agreement in the presence of faults [AD-A156541] N86-10898

FAULT TREES
New probabilistic modeling and simulation methods for complex time-dependent systems [DE85-009575] N86-10835

FAULTS
A modified repair strategy for two-component systems with revealed and unrevealed faults [AD-A156715] N86-10885

FEASIBILITY ANALYSIS
Wind energy in agriculture, a promise [SS-45] N86-10672
Wind energy, a feasibility investigation for wind mills in agriculture [SS-45A] N86-10673
A logistics scenario for an early lunar base [ILR-MITT-143] N86-11140

FEED SYSTEMS
Continuous fiberization of silicon-carbide-nitride precursor resin N86-10168

FEEDBACK
Levitating furnance for containerless processing in space N86-10169

FEEDBACK CONTROL
Digital control of the hydraulic actuators of an adaptive suspension vehicle N86-10548
Studies on human vehicle control [B8563352] N86-10775
Spillover minimization in self-adjoint distributed-parameter systems with direct output feedback N86-10852
Identification of a plant's weighting sequence --- self-tuning control [OUEL-1534/84] N86-10854
High-power rf controls for the NBS-Los Alamos racetrack microtron [DE85-012658] N86-10993

FEMALES
Evaluation of the 90-day inhalation toxicity of petroleum and oil shale JP-5 jet fuel [AD-A156815] N86-10675

FERMENTATION
Recovery of alcohol from a fermentation source by separation rather than distillation [AD-D011782] N86-10282
Biotechnology: Science and practice N86-10742

FERMI SURFACES
Fermi surface study of CeSb in the ferromagnetic and antiferromagnetic phases [DE85-012122] N86-11052

FERRITES
Amplitude and phase modulation in fin-lines electrical tuning [AD-D011813] N86-10415

FERROELECTRICITY
Analysis of transitions between ferroelectric and antiferroelectric states under conditioning of uniaxial strain [DE85-014468] N86-10350

FERROMAGNETIC RESONANCE
Amplitude and phase modulation in fin-lines electrical tuning [AD-D011813] N86-10415

FERROUS METALS
Liquid crystal non-destructive inspection of metals [AD-D011772] N86-10316

FIBER COMPOSITES
Directional solidification of InSb-NiSb eutectic --- Spacelab N86-10221
Mechanics of coated fiber composites N86-10285
Stiffened and prestressed composite overwrapped pressure vessels N86-10547

FIBER OPTICS
Acoustic levitation containerless processing N86-10177
Multiple site laser excited pollution monitoring system [AD-D011769] N86-10674
LANES 1 Users' Guide [NASA-CR-177334] N86-10819
Fiber optic gradient hydrophone construction and calibration for sea trial [AD-A156469] N86-10914
Fiber optic system for measuring electric fields [AD-D011830] N86-10976
A fiber-linked version of project TRIO --- telescope array N86-11105

FIBER REINFORCED COMPOSITES
Fundamental studies of low velocity impact resistance of graphite fiber reinforced polymer matrix composites N86-10288
Erosion-resistant nosetip construction [AD-D011787] N86-10289
An analytical and numerical study of the buckling behavior of fiber-reinforced beams N86-10566
Characterization of mechanical damage mechanisms in ceramic composite materials [AD-A156574] N86-10590

FIBERS
Continuous fiberization of silicon-carbide-nitride precursor resin N86-10168
Acoustic levitation containerless processing N86-10177

FIELD EFFECT TRANSISTORS
Test results for 20-GHz GaAs FET spacecraft power amplifier [NASA-TM-87072] N86-10379
Transient velocity assessment in gallium arsenide, and of other GaAs characteristics related to device functions [AD-A156983] N86-11050

FIELD STRENGTH
Electrohydrodynamics N86-10130

FIELD THEORY (PHYSICS)
Gravitational collapse of a scalar field N86-11129

FIGHTER AIRCRAFT
System modeling and identification of equivalent systems with and without compensating time delay for control-augmented aircraft [ESA-TT-852] N86-10043
Let's get serious about software [AD-A156819] N86-10831

FILAMENT WINDING
Carbon fiber reinforced polymide filament wound tube manufacturing [BR64172] N86-10339
Ultrasonic evaluation of mechanical properties of thick, multilayered, filament wound composites [MASA-TM-87088] N86-10561

FILE MAINTENANCE (COMPUTERS)
DBS/R database control system N86-10816

FILLERS
Binder-filler interaction in energetic polymers [AD-A156752] N86-10345

FILM CONDENSATION
Laminar film condensation in vertical closed two-phase thermosiphons [IKE-5-220] N86-10476

FILM COOLING
Film cooling on a convex wall: Heat transfer and hydrodynamic measurements for full and partial coverage [NASA-CR-174964] N86-10461

FILTERS
Robust failure detection filters [NASA-CR-176232] N86-10271

FILTRATION
Recovery of alcohol from a fermentation source by separation rather than distillation [AD-D011782] N86-10282
Multipurpose pan development [DE85-012326] N86-10319

FINANCIAL MANAGEMENT
Space research expenses of the Federal Ministry of Research and Technology (BMFT) in the period 1983-1985 N86-11070

FINITE DIFFERENCE THEORY
Second order approximation method for transonic flows over swept wings N86-10002
Numerical simulation of crack arrest experiments on Araldite B using the finite difference method [REPT-W-9/82] N86-10596
Arithmetic pipeline for image processing [AD-D011773] N86-10800
A mesh moving technique for time dependent partial differential equations in two space dimensions [AD-A156663] N86-10866

FINITE ELEMENT METHOD
Process models for 3D composites [AD-A156889] N86-10292
Finite element solution of the Navier-Stokes equations for 3-D turbulent free shear flows N86-10457
Finite element analysis of metals at elevated temperature using unified constitutive theories N86-10569
Finite element analysis of statics and dynamic structural engineering problems using semi-explicit methods N86-10571
Joint research effort on vibrations of twisted plates, phase 1: Final results [NASA-RP-1150] N86-10579
Recent advances in the analysis of exhaust mufflers N86-10587
Modeling groundwater flow into lakes N86-10598
SUTRA (Saturated-unsaturated transport). A finite-element simulation model for saturated-unsaturated, Fluid-Density-Dependent ground-water flow with energy transport or chemically-reactive single-species solute transport [AD-A156779] N86-10830
The h, p and h-p versions of the finite element method in dimension. Part 1: The error analysis of the p-version [AD-A156600] N86-10862

The h, p and h-p versions of the finite element method in 1 dimension. Part 3. The adaptive h-p version
[AD-A156626] N86-10664
A mesh moving technique for time dependent partial differential equations in two space dimensions
[AD-A156663] N86-10666
The h, p and h-p versions of the finite element method in 1 dimension. Part 2. The error analysis of the H and h-p versions
[AD-A156835] N86-10669
Thermal and structural analysis of ring components by the finite element method
[DE85-013305] N86-11021

FIRE PREVENTION
Ignition and flame spread above liquid fuel pools N86-10163
Self-heating to ignition measurements and computation of critical size for solar energy collector materials
[DE85-011449] N86-10302

FISHERIES
National perspective on environmental constraints to hydroelectric development
[DE85-013111] N86-10678

FISSION
The development of a neutron evaporation theory code for the thermal fission of Uranium-235
[AD-A156593] N86-10951

FISSION PRODUCTS
The development of a neutron evaporation theory code for the thermal fission of Uranium-235
[AD-A156593] N86-10951
Scoping studies of vapor behavior during a severe accident in a metal-fueling reactor
[DE85-011474] N86-10952
On-line gamma-ray data acquisition at the Power Burst facility
[DE85-011957] N86-10954

FLAME IONIZATION
Volatile organic compounds in indoor air: A survey of various structures
[PB85-198356] N86-10687

FLAME PROPAGATION
Particle cloud combustion experiment N86-10160
A fundamental study of smoldering with emphasis on experimental design for zero-g N86-10162
Ignition and flame spread above liquid fuel pools N86-10163
Flammability limits of gases under low gravity conditions N86-10164
Effects of scale and geometry on hydrogen-air detonations
[DE85-006762] N86-10474

FLAME STABILITY
Buoyancy effects upon vapor flame and explosion processes N86-10161
Flammability limits of gases under low gravity conditions N86-10164

FLAME TEMPERATURE
Design and calibration of a flat-flame burner using line reversal techniques
[AD-A156724] N86-10294

FLAMES
Effects of chemistry and swirl on the production of turbulence in a flame
[PB85-219632] N86-10305

FLAMMABILITY
Flammability limits of gases under low gravity conditions N86-10164

FLAMMABLE GASES
Flammability limits of gases under low gravity conditions N86-10164

FLANGES
Over-center toggle latch
[AD-D011753] N86-10556

FLAPS (CONTROL SURFACES)
AIRBOC (air rapid bloom offboard chaff) chaff deployment system
[AD-D011746] N86-10554

FLASHOVER
Delay times and jitter in triggered vacuum spark gaps using metal vapor and surface flashover types of triggers
[DE85-013966] N86-10441

FLAT PLATES
Three articles on new calculation methods in aeronautics (selected articles)
[AD-A145745] N86-10007
Numerical solution of hypersonic flow near leading edge of a flat plate N86-10008
Self-heating to ignition measurements and computation of critical size for solar energy collector materials
[DE85-011449] N86-10302

FLEXIBILITY
Dynamic analysis of robotic manipulations with flexible links N86-10545

FLEXIBLE SPACECRAFT
Evaluation of a pulse control law for flexible spacecraft
[NASA-CR-176233] N86-10272
Three-dimensional vibration analysis of a uniform beam with offset inertial masses at the ends
[NASA-TM-86393] N86-10580

FLEXING
Geothermal influences on the long-term thickness of the mechanical lithosphere during flexure N86-10697

FLIGHT ALTITUDE
Mild hypoxia and visual performance with night vision goggles
[AD-A156969] N86-10787

FLIGHT PATHS
Generation of flight paths using hierarchical planning
[AD-A156905] N86-10900

FLIGHT SIMULATION
Manned flight simulation: Challenge and response
[NASA-TM-86827] N86-10048

FLOAT ZONES
Microgravity Science and Applications Program tasks
[NASA-TM-87568] N86-10053
Fluid flow in crystal growth: Analysis of the verticle Bridgman and floating zone process N86-10055
The influence of low frequency mechanical vibrations on the growth of single crystals N86-10059
The control of float zone interfaces by the use of selected boundary conditions N86-10060
Microgravity silicon zoning investigation N86-10063
HgI sub 2 crystal growth for nuclear detectors N86-10066
Float zone experiments in space N86-10067
Thermocapillary flows and their stability: Effects of surface layers and contamination N86-10109
Suppression of Marangoni convection in float zones N86-10111
The TEXUS flight results on convective flows and heat transfer in simulated floating zones N86-10235
Measurements of the critical Marangoni number of the laminar-oscillatory transition of thermocapillary convection in floating zones N86-10242
A preliminary report on floating zone experiments with germanium crystals in a sounding rocket N86-10256

FLOORS
Modeling groundwater flow into lakes N86-10596

FLOW DISTRIBUTION
Inviscid flow field analysis of maneuvering hypersonic vehicles using the SCM formulation and parabolic grid generation
[DE85-013950] N86-10021
Experimental and theoretical investigations of the flow around airfoil systems with ground effect
[DFVLR-FB-85-17] N86-10026
On the method of characteristics and its application to the calculations of annular nozzle flowfields N86-10454

FLOW GEOMETRY
The rubber tube test section of the DFVLR in Goettingen, West Germany — wind tunnel walls
[DFVLR-FB-85-18] N86-10051

FLOW MEASUREMENT
Experiments and computations on unsteady separating flow in an expanding flume
[REPT-2-84] N86-10477

FLOW RESISTANCE
Precise viscosity measurements very close to critical points
[NASA ORDER C-86129D] N86-10120

FLOW VELOCITY
Mean turbulence structure in strongly heating air flows N86-10455
Time resolved flow velocity and concentration measurements using a travelling thermal lens
[AD-A156706] N86-10541
HALFBREED: An extended capability version of the YAQUI code
[DE85-014237] N86-10843

FLUE GASES
Microcomputer aided calculations of parameters for spray dryer operation
[DE85-013468] N86-10681

FLUID BOUNDARIES
Liquids and interfaces — Spacelab N86-10266
New approach to multiphase equilibria: Application to high-pressure physics problems
[DE85-013820] N86-10907

FLUID DYNAMICS
Microgravity Science and Applications Program tasks
[NASA-TM-87568] N86-10053
Fluid dynamics and thermodynamics of vapor phase crystal growth N86-10068
Surface tension induced instabilities in reduced gravity: The Benard problem N86-10117
Lambda point equipment N86-10118
Critical transport phenomena in fluid helium under low gravity N86-10119
Morphological stability and fluid dynamics of vapor crystal growth N86-10126
Miscibility gap systems
[NASA ORDER H-27954B] N86-10131
Experimental and theoretical analysis of chemical vapor deposition with prediction of gravity effects N86-10132
Measurement of the density of base fluids at pressures 0.422 to 2.20 GPa
[NASA-TM-87114] N86-10561

FLUID FLOW
Fluid flow in crystal growth: Analysis of the verticle Bridgman and floating zone process N86-10055
Convection during unidirectional solidification N86-10077
Metals electroprocessing in molten salts N86-10098
Transport processes in solution crystal growth N86-10107
Surface tensions and their variations with temperature and impurities
[NASA ORDER H-27954B] N86-10115
Surface-tension driven convection N86-10124
Role of convection in grain refining N86-10133
Electrophoresis technology N86-10144
Flammability limits of gases under low gravity conditions N86-10164
Modification of the electromagnetic levitator (EML) hardware N86-10172
Process models for 3D composites
[AD-A156889] N86-10292
KRAK: A computer program for two-phase, two-component porous flow and fracture propagation, revision
[DE85-014264] N86-10489
Time-implicity simulation of particle-fluid systems
[DE85-012944] N86-10471
Physical acoustics: Investigation of chemical kinetic and thermodynamic properties of fluids N86-10911

FLUID MECHANICS
Surface-tension driven convection N86-10124
Thermocapillary motion research N86-10125
Transport processes research N86-10129
The fluid physics module: A technical description — Spacelab N86-10201
HALFBREED: An extended capability version of the YAQUI code
[DE85-014237] N86-10843

FLUID PRESSURE
SUTRA (Saturated-unsaturated transport). A finite-element simulation model for saturated-unsaturated, Fluid-Density-Dependent ground-water flow with energy transport or chemically-reactive single-species solute transport
[AD-A156779] N86-10630

FLUORESCENCE
Containerless high temperature property measurements by atomic fluorescence N86-10092
Automated analysis of digital images generated by two-dimensional gel electrophoresis
[DE85-011906] N86-10526

FLUORIDES
Crystallization, optical and chemical properties of fluoride glasses N86-10149

FLUX (RATE)
ORR core re-configuration measurements to increase the fast neutron flux in the Magnetic Fusion Energy (MFE) experiments
[DE85-013520] N86-10958

FLUXES
Metallurgy and metallography of braze joints
[DE85-014563] N86-10325

FLYING SPOT SCANNERS
Stereoscopic video imagery generation
[AD-D011785] N86-10481

FOCUSING
Beam-beam deflections to measure size spot and offset at SLC IP
[DE85-014285] N86-10986
Applications of the second-order achromat concept to the design of particle accelerators
[DE85-013072] N86-10994

FOILS (MATERIALS)
Formation and characterization of amorphous erbium-based alloys prepared by near-isothermal cold-rolling of elemental composites
[DE85-014853] N86-10327
Development and application of the electrochemical etching technique
[DE85-010302] N86-10957

FOLDS (GEOLOGY)
Tectonic analysis of typical fold structures in the Zagros Mountains (Iran) by the application of quantitative photogrammetric methods on metric camera data — Spacelab N86-10521
Structural mapping of folded sedimentary environments from satellite images: An example from Central Asia N86-10607

FORBIDDEN TRANSITIONS
Mean life of the 2p(4)((1)S)3s (2)S state in fluorine
[DE85-012929] N86-10956
FORCED CONVECTION
Analysis of combined natural and forced convection around cylinders and spheres N86-10456
FORECASTING
The air traffic demand in passenger travel of the Federal Republic of Germany 1990 - 2000. Update of the DFVLR air traffic forecast
[DFVLR-MITT-85-06] N86-10031
FOREST MANAGEMENT
Requirements and possibilities of Spacelab metric camera photos usage for inventories of large areas of extensively managed forests N86-10513
FORESTS
Thematic investigations in France based on metric camera imagery --- Spacelab N86-10509
Analysis of remote sensing data N86-10605
Mapping diverse forest cover with multipolarization airborne radar N86-10625
Potential applications of multipolarization SAR for pine plantation biomass estimation N86-10626
FORMING TECHNIQUES
Formation and characterization of amorphous erbium-based alloys prepared by near-isothermal cold-rolling of elemental composites
[DE85-014853] N86-10327
FORMULAS (MATHEMATICS)
Estimation by moments in a model of faulty inspection
[AD-A156754] N86-10886
FORTRAN
User's guide for Langley Research Center Orbital Lifetime program
[NASA-TM-87567] N86-10828
SUTRA (Saturated-unsaturated transport). A finite-element simulation model for saturated-unsaturated, Fluid-Density-Dependent ground-water flow with energy transport or chemically-reactive single-species solute transport
[AD-A156779] N86-10830
NBSGSC: A FORTRAN program for quantitative X-ray fluorescence analysis
[PB85-206068] N86-10847
FOSSILS
Paleogene vertebrate paleontology, geology and remote sensing in the Wind River Basin N86-10609
Paleontology and stratigraphy of Lower Cambrian and upper Proterozoic sediments, Caborca region, northwestern Sonora, Mexico N86-10692
FOURIER ANALYSIS
A study of Morrison's iterative noise removal method
[NASA-CR-176222] N86-10823
FOURIER TRANSFORMATION
Process models for 3D composites
[AD-A156889] N86-10292
Fuel and lubricant behavior in boundary layers analyzed by infrared emission Fourier transform spectrometry
N86-10336
Phase-coded pulse expander-compressor
[AD-D011812] N86-10375
Phase coded pulse expander-compressor
[AD-D011817] N86-10376
A study of derivative filters using the discrete Fourier transform
[NASA-CR-176224] N86-10825
Coordinate axes, location of origin, and redundancy for the one and two-dimensional discrete Fourier transform
[NASA-CR-176225] N86-10826
Spatial frequency multiplexed coherent optical processor for calculating generalized moments
[AD-D011816] N86-10975
Numerical experiments in image reconstruction --- stellar interferometry N86-11116
FRACTURE MECHANICS
Progressive damage, fracture predictions and post mortem correlations for fiber composites
[NASA-TM-87101] N86-10290
Preliminary reports, memoranda and technical notes of the Materials Research Council Summer Conference, La Jolla, California
[AD-A156776] N86-10291
Fracture toughness and stress relief response of irradiated type 347/348 stainless steel N86-10320
Finite deformation crack-line fields in a thin elasto-plastic sheet
[AD-A156757] N86-10346
Fracture toughness testing of centrifugally cast nickel aluminium bronze
[REPT-MAT/720] N86-10575
Numerical simulation of crack arrest experiments on Araldite B using the finite difference method
[REPT-W-9/82] N86-10596
Recent development in the Hot Dry Rock Geothermal Energy Program
[DE85-009562] N86-10663
FRACTURE STRENGTH
Application of the unloading compliance methods in fracture toughness measurements of a quenched and tempered steel
[BLL-BISI-TRANS-21626-(9022.06)] N86-10308
Fracture toughness and stress relief response of irradiated type 347/348 stainless steel N86-10320
The use of new path indepedent integrals in elastic-plastic and creep fracture N86-10574
Fracture toughness testing of centrifugally cast nickel aluminium bronze
[REPT-MAT/720] N86-10575
Fatigue of graphite/epoxy buffer strip panels with center cracks
[NASA-TM-87595] N86-10581
Characterization of mechanical damage mechanisms in ceramic composite materials
[AD-A156574] N86-10590
Fracture toughness of hydrogen-embrittled precipitation-hardened stainless steels
[AD-A156664] N86-10592
FRACTURES (MATERIALS)
Fundamental studies of low velocity impact resistance of graphite fiber reinforced polymer matrix composites
N86-10288
Mixed-mode fracture of ceramics
[DE85-014087] N86-10349
FRACTURING
Progressive damage, fracture predictions and post mortem correlations for fiber composites
[NASA-TM-87101] N86-10290
FRAMES
Optimal design of portal frames against buckling
N86-10572
FREE BOUNDARIES
Free surface phenomena under low- and zero-gravity conditions N86-10108
Suppression of Marangoni convection in float zones
N86-10111
On the method of characteristics and its application to the calculations of annular nozzle flowfields N86-10454
FREE CONVECTION
Energy stability of thermocapillary convection in models of the float zone process N86-10123
Some results of the Marangoni free convection experiment --- Spacelab N86-10203
Analysis of combined natural and forced convection around cylinders and spheres N86-10456
FREE ELECTRON LASERS
Soviet free-electron laser research
[AD-A156898] N86-10542
High-brightness photoemitter injector for electron accelerators
[DE85-012673] N86-10929
FREE ELECTRONS
Photoactivation of PBFA-2
[DE85-013439] N86-11019
FREE FLOW
The role of freestream turbulence scale in subsonic flow separation
[NASA-CR-176237] N86-10014
FREE JETS
Investigation of density gradient fluctuations in a turbulent free jet by means of the laser schlieren crossed-beam method
[DFVLR-FB-85-19] N86-10027
FREEZING
Freezer model using a population balance approach for steady-state, direct-contact, secondary refrigerant, freeze desalination N86-10361
FREON
Transient heat transfer in zero gravity environment
[NASA ORDER H-27954B] N86-10114
FREQUENCY DISTRIBUTION
A composite climatological study of the frequency and distribution of severe weather associated with spring season Colorado cyclogenesis
[AD-A156981] N86-10715
FREQUENCY HOPPING
An active tracking band-pass filter
[AD-A156559] N86-10419
FREQUENCY STANDARDS
Cooled ion frequency standard
[AD-A156813] N86-10295
DSN frequency and timing system, Mark 4-85
N86-10393
FREQUENCY SYNCHRONIZATION
DSN frequency and timing system, Mark 4-85
N86-10393
FRICTION
Tribological properties of structural ceramics
[NASA-TM-87105] N86-10341
FROST
Laboratory experiments of heat pump dynamic losses
[DE85-013931] N86-10473
FROUDE NUMBER
Laminar film condensation in vertical closed two-phase thermosiphons
[IKE-5-220] N86-10476
FUEL CELL POWER PLANTS
Fuel Cell Technology Assessment Program, work element no. 6
[DE85-008228] N86-10444
FUEL CELLS
Fuel Cell Technology Assessment Program, work element no. 6
[DE85-008228] N86-10444
Effects of H2S on molten carbonate fuel cells
[DE85-014052] N86-10447
Phosphoric and electric utility fuel technology development
[DE85-014741] N86-10651
Phosphoric and electric utility fuel cell technology development
[DE85-014552] N86-10652
Advanced fuel cell development
[DE85-014550] N86-10659
FUEL CONTAMINATION
Method for determining elemental sulfur in jet fuel --- differential pulse polarography
[FOA-C-40211-B4] N86-10360
FUEL FLOW
Gas generator fuel flow throttle control system
[AD-D011797] N86-10355
FUEL INJECTION
Modeling of engine sprays
[DE85-010020] N86-10559
FUEL-AIR RATIO
Design and calibration of a flat-flame burner using line reversal techniques
[AD-A156724] N86-10294
Effects of chemistry and swirl on the production of turbulence in a flame
[PB85-219632] N86-10305
FUELS
Retrofit of SAC EC-135C and RC-135 aircraft with CFM-56 engines
[AD-A156688] N86-10038
Remote stratigraphic and structural analysis: Multisensor results in the Wind River/Bighorn Basin area, Wyoming N86-10606
FUNCTIONS (MATHEMATICS)
Arithmetic pipeline for image processing
[AD-D011773] N86-10800
FURNACES
Graphite formation in cast iron N86-10100
Development of materials processing systems for use in space on low-g simulation devices N86-10166
Levitating furnance for containerless processing in space N86-10169
High-temperature controlled redox crystallization studies N86-10178
FUSELAGES
Proposed modifications for the RAAF Airtrainer CT-4A cockpit
[AD-A156806] N86-10039
FUSION (MELTING)
Fusion target technology N86-10156
Revision of and documentation for the standard version of the Poisson-Group codes
[DE85-012659] N86-10837
Scoping studies of vapor behavior during a severe accident in a metal-fueling reactor
[DE85-011474] N86-10952
Photoactivation of PBFA-2
[DE85-013439] N86-11019
FUSION REACTORS
Providing automated control for PBFA-2
[DE85-012867] N86-10928
Impact of long-lived radionuclides on waste classification for fusion
[DE85-013205] N86-10959
Evolution of the fusion power demonstration tandem mirror reactor configuration
[DE85-012889] N86-10960
Alternative fusion concepts and the prospects for improved reactors
[DE85-009622] N86-11031
Hot cell facility design for large fusion devices
[DE85-012893] N86-11037

G

GALACTIC RADIATION
Solar modulation of galactic cosmic rays: Techniques and applications N86-11143
Extra-galactic X-ray sources and the diffuse X-ray background N86-11144

GALAXIES
A superconducting tunnel junction receiver for millimeter-wave astronomy N86-11041

GALERKIN METHOD
Error estimates and automatic time step control for numerical methods for stiff ordinary differential equations
[CTH-MATH-1984-27] N86-10872

GALILEO PROJECT
Galileo: Exploration of Jupiter's system
[NASA-SP-479] N86-11137

GALLIUM ANTIMONIDES
GaS-semiconductor crystals under microgravity: Experiment ES 323 — Spacelab N86-10224

GALLIUM ARSENIDE LASERS
W-shaped diffused stripe GaAs/AlGaAs laser
[AD-D011818] N86-10538

GALLIUM ARSENIDES
Crystal growth of device quality GaAs in space N86-10061
Crystal growth of GaAs in space N86-10234
Test results for 20-GHz GaAs FET spacecraft power amplifier
[NASA-TM-87072] N86-10379
Contact effects in light activated GaAs switches
[AD-A156957] N86-10434
Theory of advanced, high-efficience concentrator cells
[DE85-008821] N86-10655
Transient velocity assessment in gallium arsenide, and of other GaAs characteristics related to device functions
[AD-A156983] N86-11050

GAMMA RAY SPECTRA
Parallel pulse processing for mercuric iodide gamma-ray detectors
[DE85-013391] N86-10528
Directionality of bremsstrahlung from relativistic electrons in solar flares
[NASA-TM-87509] N86-11141

GAMMA RAYS
The development of a neutron evaporation theory code for the thermal fission of Uranium-235
[AD-A156593] N86-10951
Information on continuum states from feeding times and total (GAMMA) spectra measured with BGO suppressed detectors
[DE85-013868] N86-10961

GAPS
Liquid phase miscibility gap materials N86-10081

GAS DYNAMICS
La Recherche Aerospatiale, bimonthly bulletin, no. 1984-5, September-October 1985
[ESA-TT-899] N86-10383

GAS FLOW
Design and calibration of a flat-flame burner using line reversal techniques
[AD-A156724] N86-10294
Gas generator fuel flow throttle control system
[AD-D011797] N86-10355

GAS GENERATORS
Gas generator fuel flow throttle control system
[AD-D011797] N86-10355

GAS INJECTION
Mass transport phenomena between bubbles and dissolved gases in liquids under reduced gravity conditions N86-10110

GAS JETS
Suppression of Marangoni convection in float zones N86-10111

GAS MIXTURES
Scaling studies of solar pumped lasers
[NASA-CR-176240] N86-10540

GAS PRESSURE
Effect of H2S and COS in the fuel gas on the performance of ambient pressure phosphoric acid fuel cells
[DE85-013913] N86-10446

GAS TUNGSTEN ARC WELDING
Signal analysis of gas tungsten arc welds N86-10078
Measurement of workpiece temperature during welding for welding robot control N86-10534

GAS TURBINE ENGINES
Constitutive modeling for isotropic materials (HOST)
[NASA-CR-174980] N86-10589
Advanced Gas Turbine (AGT) powertrain system development for automotive applications report
[NASA-CR-174886] N86-11087

GASES
KRAK: A computer program for two-phase, two-component porous flow and fracture propagation, revision
[DE85-014264] N86-10469
Velocities of gas and plasmas from real time holographic interograms
[DE85-014618] N86-10530

GATES (CIRCUITS)
Investigation of metallic impurities introduced into SiO2 and silicon by various candidate VLSI metallization systems: Chemical reactions, diffusion, and electrical properties
[AD-A156809] N86-10429
Realization of a multifunction Input/Output (I/O) controller by means of a gate array
[EUT-85-E-147] N86-10804

GAUGE THEORY
On the analytical evaluation of the partition function for unit hypercubes in four dimensions — lattice theory
[NIKHEF-H/84-12] N86-10882
Variational estimates for the mass gap of SU(2) Euclidean lattice gauge theory
[NIKHEF-H/84-13] N86-10883

GAUSS EQUATION
A study of methods to predict and measure the transmission of sound through the walls of light aircraft. Integration of certain singular boundary element integrals for applications in linear acoustics
[NASA-CR-176229] N86-10912

GEARS
Trials on the asperity counting monitoring system — helicopter gearboxes
[RES-PAPER-670] N86-10550

GELS
Gel precursors as glass and ceramic starting materials for space processing applications research N86-10150
Sol-gel glasses N86-10153
Glass research N86-10157
Growth and characterization of brushite and lead monetite, simulation and results — Spacelab N86-10230
Automated analysis of digital images generated by two-dimensional gel electrophoresis
[DE85-011906] N86-10526

GENETIC ENGINEERING
Biotechnology regulation
[GPO-43-778] N86-10733
Somatic cell and molecular genetics approach to DNA repair and mutagenesis
[DE85-014181] N86-10737

GENETICS
Somatic cell and molecular genetics approach to DNA repair and mutagenesis
[DE85-014181] N86-10737

GEOCHEMISTRY
Application of the ruthenium and technetium thermodynamic data bases used in the EQ3/6 geochemical codes
[DE85-013766] N86-10632

GEOCHRONOLOGY
Report of the Workshop on Geologic Applications of Remote Sensing to the Study of Sedimentary Basins
[E86-10002] N86-10599
Chronologic analysis of terrestrial sediments and basin evolution N86-10602
Remote stratigraphic and structural analysis: Multisensor results in the Wind River/Bighorn Basin area, Wyoming N86-10606
Foreland basin structures and remote sensing N86-10608
Age-dating volcanic and alluvial surfaces with multipolarization data N86-10620

GEODESY
Mobile VLBI and GPS measurement of vertical crustal motion N86-10401

GEODETIC SURVEYS
How Antarctica was unveiled. Masterpieces of Frankfurt topographic surveyors. A part of the German Antarctica research program N86-10181

GEOLOGICAL FAULTS
Structural mapping of folded sedimentary environments from satellite images: An example from Central Asia N86-10607
Neogene compressional deformation and possible thrust faulting in southwest Dominican Republic N86-10618
Structural discontinuity within the southern California continental margin: Seismic and gravity models of the western Transverse Ranges N86-10699
Crustal structure of the southern Rio Grande rift determined from seismic refraction, surface wave dispersion, and gravity data N86-10700

GEOLOGICAL SURVEYS
Metric Camera Workshop — Spacelab
[ESA-SP-209] N86-10485
A geological structural analysis of the southeastern Zagros (Iran) ranges based on metric camera photos N86-10492
The role of very small scale metric images in modern geology — Spacelab metric camera N86-10502
Geological mapping of remote mountainous regions using metric camera imagery — Spacelab N86-10503
Thematic investigations in France based on metric camera imagery — Spacelab N86-10509
Time-term analysis of upper crustal structure in the Columbia Basin, Washington
[DE85-012390] N86-10633

GEOMETRICAL THEORY OF DIFFRACTION
Numerical methods for analyzing electromagnetic scattering
[NASA-CR-176141] N86-10377

GEOMETRY
Effects of scale and geometry on hydrogen-air detonations
[DE85-006762] N86-10474
Topological properties of hypercubes
[AD-A156777] N86-10850

GEOPHYSICAL OBSERVATORIES
Activities report in geophysics
[KGI-186] N86-10709

GEOPHYSICS
Report of the Workshop on Geologic Applications of Remote Sensing to the Study of Sedimentary Basins
[E86-10002] N86-10599
Formation of waves by ground motion
[PM/84/09] N86-10706
In-situ geophysical investigations into the nature of the oceanic crust N86-10725

GEOPOTENTIAL HEIGHT
Lumped geopotential harmonics of order 14, from the orbit of 1967-11G
[AD-A156827] N86-10190

GEOTEMPERATURE
Geothermal influences on the long-term thickness of the mechanical lithosphere during flexure N86-10697

GEOTHERMAL ENERGY EXTRACTION
Recent development in the Hot Dry Rock Geothermal Energy Program
[DE85-009562] N86-10663

GEOTHERMAL ENERGY UTILIZATION
Ocean energy technology program summary
[DE85-013102] N86-10731

GEOTHERMAL RESOURCES
Geothermal lost circulation zone mapping tool
[DE85-008896] N86-10531
Geothermal Energy Technology Program summary
[DE85-013101] N86-10646
Recent development in the Hot Dry Rock Geothermal Energy Program
[DE85-009562] N86-10663

GEOTHERMAL TECHNOLOGY
Geothermal Energy Technology Program summary
[DE85-013101] N86-10646

GERMANIUM
A preliminary report on floating zone experiments with germanium crystals in a sounding rocket N86-10256
Defect identification in high-energy semiconductors
[DE85-014533] N86-10442

GERMANIUM ALLOYS
Effect of undercooling and modified microstructure on the physical properties of material synthesized in the drop tube and drop tower N86-10075

GEYSERS
KRAK: A computer program for two-phase, two-component porous flow and fracture propagation, revision
[DE85-014264] N86-10469

GIANT STARS
Physical conditions in giant extragalactic H2 regions N86-11130

GIRDERS
Load-deflection tests and computer analyses of a high-precision adhesive-bonded antenna reflector panel N86-10389

GLASS
Lambda point equipment N86-10118
Containerless processing of glass forming melts in space N86-10148
Gel precursors as glass and ceramic starting materials for space processing applications research N86-10150
Glass formation in reluctant glass formers N86-10151
Sol-gel glasses N86-10153
Physical phenomena in containerless glass processing N86-10155
Glass research N86-10157
Microgravity Materials Science Laboratory N86-10173
Acoustic levitation containerless processing N86-10177
Shrinking of a gas bubble in a glass melt under microgravity conditions — STS-11 N86-10254
Calculation of the glass transition temperatures of linear polymers. Part 1: Rules for hierarchical ordering of the data set
[AD-A156584] N86-10343
Thermal expansion of glasses in the solid and liquid phases
[DE85-013953] N86-10351

Fatigue of graphite/epoxy buffer strip panels with center cracks
[NASA-TM-87595] N86-10581
Fundamental study of the closure property of joints
N86-10698
A study of the applicability of nucleation theory to quasi-thermodynamic transformations of second and higher Ehrenfest-order
[NASA-CR-176230] N86-11060

GLOBAL POSITIONING SYSTEM
Mobile VLBI and GPS measurement of vertical crustal motion N86-10401

GLOBULAR CLUSTERS
The dynamics and stellar content of globular star clusters N86-11131

GLOVES
Effect of increased body clothing insulation on hand temperature in a cold environment
[AD-A156597] N86-10786

GLOW DISCHARGES
Surface conditioning of synchrotron radiation source to improve beam lifetime
[DE84-012185] N86-10948

GLYCEROLS
Rapid analysis using capillary supercritical fluid chromatography
[DE85-012460] N86-10297

GLYCOLS
Separation of aqueous two-phase polymer systems in microgravity N86-10246
Application of the theory of Ostwald ripening to microgravity phase separation experiments N86-10248

GNOMONIC PROJECTION
Stereo-orthophotos in various map projections
N86-10488

GOLD ALLOYS
Effect of undercooling and modified microstructure on the physical properties of material synthesized in the drop tube and drop tower N86-10075

GOVERNMENT PROCUREMENT
F-16X MSIP (Multi-national Staged Improvement Program) case example: Operating and support cost estimation using VAMOSC (Visibility And Management Of Operating and Support Costs)
[AD-A156893] N86-10006

GRAIN BOUNDARIES
Design, fabrication and testing of an experimental apparatus for determining particle behavior under very low intergranular stresses N86-10175
Compatibility of grain-stabilized platinum with candidate propellants for resistojets
[NASA-TM-87118] N86-10279
Intrinsic mechanisms of multilayer ceramic capacitor failure
[AD-A156638] N86-10431

GRANITE
Altitudinal distribution of granitic landforms in the south central Sierra Nevada, California N86-10695

GRANTS
Study of one- and two-dimensional filtering and deconvolution algorithms for a streaming array computer
[NASA-CR-176226] N86-10827

GRANULAR MATERIALS
Compatibility of grain-stabilized platinum with candidate propellants for resistojets
[NASA-TM-87118] N86-10279
High efficiency heat transport and power conversion system for cascade
[DE85-012959] N86-10468

GRAPHIC ARTS
A graphic anthropometric aid for seating and workplace design
[AD-A156988] N86-10788

GRAPHITE
Graphite formation in cast iron N86-10100
Fundamental studies of low velocity impact resistance of graphite fiber reinforced polymer matrix composites
N86-10288
High temperature mechanical testing of a cylindrical weave carbon-carbon composite
[AD-A156639] N86-10591
Investigation of composite materials property requirements for sonic fatigue research
[NASA-TM-87601] N86-10913

GRAPHITE-EPOXY COMPOSITES
Progressive damage, fracture predictions and post mortem correlations for fiber composites
[NASA-TM-87101] N86-10290
Ultrasonic evaluation of mechanical properties of thick, multilayered, filament wound composites
[MASA-TM-87088] N86-10561
Fatigue of graphite/epoxy buffer strip panels with center cracks
[NASA-TM-87595] N86-10581

GRAVELS
Cretaceous and cenozoic stratigraphy of the upper and middle coastal plain, Harnett County area, North Carolina N86-10690

GRAVITATIONAL COLLAPSE
A method for numerical relativity: Simulation of axisymmetric gravitational collapse and gravitational radiation generation N86-11127
Gravitational collapse of a scalar field N86-11129

GRAVITATIONAL EFFECTS
Thermal and solutal convection damping using an applied magnetic field N86-10094
Metallic foams N86-10095
Cell partition in two polymer aqueous phases
N86-10139
Colloidal oxide properties and kinetic studies
N86-10147
Fusion target technology N86-10156
Cryogenic equivalence principle experiment
N86-10171
Design, fabrication and testing of an experimental apparatus for determining particle behavior under very low intergranular stresses N86-10175
Fifth European symposium on Material Sciences under Microgravity. Results of Spacelab 1
[ESA-SP-222] N86-10200
The fluid physics module: A technical description --- Spacelab N86-10201
Influences affecting separation in monotectic alloys under microgravity N86-10209
Melting and solidification of metal matrix composites under microgravity --- Spacelab N86-10211
Unidirectional solidification of cast iron: Experiment ES-325 --- Spacelab N86-10212
Vacuum brazing under microgravity --- Spacelab
N86-10214
Directional solidification of an aluminum-zinc vapor emulsion in microgravity --- Spacelab N86-10218
Crystal growth of silicon in Spacelab 1: Experiment ES-321 N86-10227
Mathematical simulation of disturbing forces and material science processes under low gravity
N86-10236
Experimental study on Marangoni convection
N86-10243
Rationale for two phase polymer system microgravity separation experiments N86-10247
Application of the theory of Ostwald ripening to microgravity phase separation experiments N86-10248
Nucleate pool boiling in subcooled liquid under microgravity: Results of TEXUS experimental investigations N86-10250
Shrinking of a gas bubble in a glass melt under microgravity conditions --- STS-11 N86-10254
Physical and chemical properties of a nickel catalyst processed under microgravity --- STS-7 N86-10255
A preliminary report on floating zone experiments with germanium crystals in a sounding rocket N86-10256
Cellular morphologies in lead-thallium alloys --- gravitational effects N86-10262
Computation of flow regimes in parameter space for the AGCE
[NASA-CR-178480] N86-10705
User's guide for Langley Research Center Orbital Lifetime program
[NASA-TM-87587] N86-10828
Space antenna for gravitational wave astronomy
N86-11123

GRAVITATIONAL FIELDS
Lumped geopotential harmonics of order 14, from the orbit of 1967-11G
[AD-A156627] N86-10190

GRAVITATIONAL WAVE ANTENNAS
Space antenna for gravitational wave astronomy
N86-11123

GRAVITATIONAL WAVES
A method for numerical relativity: Simulation of axisymmetric gravitational collapse and gravitational radiation generation N86-11127

GREAT PLAINS CORRIDOR (NORTH AMERICA)
Vegetation and soils field research data base: Experiment summaries
[E85-10110] N86-10610

GROUND BASED CONTROL
Construction and use of a radio controlled model helicopter for research
[AD-A156547] N86-10035
Optical/IR telescope arrays: A study of their potential for satisfying observational requirements in astronomy for a large aperture system in the 1990s and beyond
[REPT-15] N86-11094

GROUND EFFECT (AERODYNAMICS)
Experimental and theoretical investigations of the flow around airfoil systems with ground effect
[DFVLR-FB-85-17] N86-10026

GROUND STATIONS
JPL emergency support of TDRSS and compatible satellites N86-10394
The GCF Mark 4 implementation and beyond
N86-10399

GROUND TRUTH
Creation of Ground Control Points (GCP) library using ESA Spacelab metric camera imagery --- ground control point (gcp) N86-10516
Vegetation and soils field research data base: Experiment summaries
[E85-10110] N86-10610

GROUND WATER
Modeling groundwater flow into lakes N86-10598
Evaluating the ground-water resources of the high plains of Texas, Volume 4
[PB85-191625] N86-10641

GROUP THEORY
On class groups of lattices
[CTH-MATH-1985-08] N86-10903

GROWTH
Cell maintenance systems N86-10142

GUN PROPELLANTS
Binder-filler interaction in energetic polymers
[AD-A156752] N86-10345

GUSTS
Forced response analysis of an aerodynamically detuned supersonic turbomachine rotor
[NASA-TM-87093] N86-10019

GYROCOMPASSES
Elastic wave gyrometer. Experiments with a parametric wave device
[REPT-26/5005/HF/AR] N86-10533

H

HADRONS
Microwave instability across the transition energy
[DE85-013304] N86-11010

HALF LIFE
Information on continuum states from feeding times and total (GAMMA) spectra measured with BGO suppressed detectors
[DE85-013868] N86-10961
Relativistic wavefunction at the origin and the pion decay constant
[DE85-012392] N86-11062

HALIDES
Photoionization technique for growth of metallic films
[AD-D011760] N86-10426

HAMILTONIAN FUNCTIONS
Lie algebraic methods for charged particle beams and light optics N86-10970

HAND (ANATOMY)
Effect of increased body clothing insulation on hand temperature in a cold environment
[AD-A156597] N86-10786

HANDBOOKS
Solar thermal technical information guide
[DE85-002941] N86-10657

HARDNESS
Fabrication and metallurgical properties of modified 9Cr-1 Mo steel
[DE85-012885] N86-10328

HARMONIC GENERATIONS
Determination of optical properties by third-harmonic generation in noble gases in unfocused laser beams
N86-10535

HARMONIC MOTION
Theoretical study of the unsteady linear problem for a rectangular wing with a pitching movement
[ONERA-RT-17/1841-RY-010-R] N86-10022

HARMONIC RADIATION
The 20 keV undulators for a 6-GeV storage ring
[DE85-013867] N86-10941

HARMONICS
Harmonic distortion reduction technique for data acquisition
[AD-D011771] N86-10799

HASTELLOY (TRADEMARK)
Weld metal hot-cracking of hastelloy alloys C-22 and C-276: A study by analytical electron microscopy
[DE85-009437] N86-10324

HAZARDS
Development of the Multi-Attribute Hazard Assessment System (MAHAS) and its application to energy-related waste streams
[DE85-010278] N86-10676
Biotechnology regulation
[GPO-43-778] N86-10733

HEARING
Proposed aural nondetectability limits for Army materiel
[AD-A156704] N86-10917

HEART FUNCTION
Assessment of state of chronotropic and inotropic heart function at different degrees of physical fitness N86-10746

HEART RATE
Dynamics of changes of statistical indicators of heart rhythm of persons with different degree of motion sickness N86-10743
Assessment of state of chronotropic and inotropic heart function at different degrees of physical fitness N86-10746

HEAT
Advanced absorption heat pump cycles
[DE85-003914] N86-10654

HEAT ACCLIMATIZATION
Mechanism of adaptogenic action of prickly eleuterococcus on man during heat stress N86-10757

HEAT BALANCE
Freezer model using a population balance approach for steady-state, direct-contact, secondary refrigerant, freeze desalination N86-10361

HEAT EXCHANGERS
Submerged ram air inlets for ECM (electronic countermeasures) pods
[AD-D011801] N86-10020
High efficiency heat transport and power conversion system for cascade
[DE85-012959] N86-10468
Ground-coupled heat pump research at the University of Tennessee Washington, D.C., 10 Dec. 1984
[DE85-005357] N86-10650

HEAT FLUX
Nucleate pool boiling in subcooled liquid under microgravity: Results of TEXUS experimental investigations N86-10250
Radiative heat transfer in nonisothermal combustion products N86-10458
Energy balance in a deep Colorado valley: ASCOT 84
[DE85-012441] N86-10631

HEAT MEASUREMENT
Thermal expansion of glasses in the solid and liquid phases
[DE85-013953] N86-10351
High flux calorimetry
[AD-A156852] N86-10524

HEAT OF COMBUSTION
Guidelines for a thermochemical kinetics computer program
[DE85-014266] N86-10839

HEAT OF FUSION
Measurement of the properties of tungsten at high temperatures N86-10091

HEAT PIPES
Development of materials processing systems for use in space on low-g simulation devices N86-10166

HEAT PUMPS
Engine-driven and absorption heat pump programs
[DE85-013930] N86-10472
Laboratory experiments of heat pump dynamic losses
[DE85-013931] N86-10473
Simplified analysis of Stirling engines and heat pumps
[DE85-005366] N86-10647
Ground-coupled heat pump research at the University of Tennessee Washington, D.C., 10 Dec. 1984
[DE85-005357] N86-10650
Comparative analysis of single and continuously variable-capacity heat pump concepts
[DE85-004089] N86-10653
Advanced absorption heat pump cycles
[DE85-003914] N86-10654
Stirling-engine-driven heat pump program overview
[DE85-004796] N86-10661
Analyses of advanced residential abosrption heat pump cycles
[DE85-005244] N86-10664

HEAT RESISTANT ALLOYS
Oxidation behavior of glassy alloys N86-10158
Experiments with tubular probes made of INCOLOY 800 H under uniaxial and multiaxial strain
[JUEL-1979] N86-10595

HEAT SOURCES
General-purpose heat source development: Safety Verification Test Program. Bullet/fragment test series
[DE85-014262] N86-10660

HEAT STORAGE
Passive solar design handbook
[DE85-014263] N86-10656

HEAT TOLERANCE
Effect of inclusion of supplementary ascorbic acid in daily diet on degree of vitamin saturation of body and thermoresistance of erythrocytes while working in arid zone N86-10749

HEAT TRANSFER
Modelling of laser-enhanced chemical vapor deposition N86-10105
Transient heat transfer in zero gravity environment
[NASA ORDER H-27954B] N86-10114
Solid surface combustion at reduced gravity N86-10159
Fundamental studies of droplet combustion at reduced gravity N86-10165
Analytical investigation of solid rocket nozzle failure
[NASA-TM-86513] N86-10278
Film cooling on a convex wall: Heat transfer and hydrodynamic measurements for full and partial coverage
[NASA-CR-174964] N86-10461
High efficiency heat transport and power conversion system for cascade
[DE85-012959] N86-10468
KRAK: A computer program for two-phase, two-component porous flow and fracture propagation, revision
[DE85-014264] N86-10469
Laminar film condensation in vertical closed two-phase thermosiphons
[IKE-5-220] N86-10476
The boundary condition in a numerical model of atmospheric flows over fixed interfaces
[GKSS-85-E-10] N86-10722
Heat transfer mechanism in human extremities N86-10759
Physical acoustics: Investigation of chemical kinetic and thermodynamic properties of fluids N86-10911
Heat transfer in condensing and evaporating two-component, two-phase flow inside a horizontal tube N86-11058

HEAT TRANSFER COEFFICIENTS
Freezer model using a population balance approach for steady-state, direct-contact, secondary refrigerant, freeze desalination N86-10361

HEAT TRANSMISSION
The control of float zone interfaces by the use of selected boundary conditions N86-10060
Heat flow and segregation in directional solidification N86-10072

HEATERS
Small cartridge heater
[AD-D011784] N86-10277

HEATING
Efficiency of muscular work in white rats during adaptation to cold N86-10763

HEATING EQUIPMENT
Small cartridge heater
[AD-D011784] N86-10277

HEAVY IONS
Microwave instability across the transition energy
[DE85-013304] N86-11010
Unicell structure for superconducting storage rings
[DE85-013303] N86-11022
Tracking studies on the effects of magnet multipoles on the aperture of the RHIC heavy ion collider
[DE85-013282] N86-11023

HEIGHT
Digital elevation model from Spacelab metric camera photographs N86-10486

HELICAL FLOW
Theoretical aspects of magnetic helicity
[DE85-011846] N86-10984

HELICAL INDUCERS
Generalized helicity and its time derivative
[DE85-012770] N86-11027

HELICOPTERS
Construction and use of a radio controlled model helicopter for research
[AD-A156547] N86-10035
The quest for a helicopter suitable for combat rescue, 1967 - 1983
[AD-A156842] N86-10040
A comparative analysis of a CV helicopter and a JVX (Joint Services Advanced Vertical Lift) tilt-rotor aircraft in an aircraft carrier based ASW (Anti-Submarine Warfare)
[AD-A156871] N86-10041
Trials on the asperity counting monitoring system — helicopter gearboxes
[RES-PAPER-670] N86-10550
Understanding and improving acoustic to seismic coupling as it pertains to Sandia's helicopter detector
[DE85-009440] N86-10920

HELIUM
Cryogenic equivalence principle experiment N86-10171
Simulating the CTR environment in the HVBM
[DE85-011745] N86-10193
Experimental X-ray scattering cross sections for H2 and rare atomic gases
[DE85-011572] N86-10936
Magnetic properties of doped semiconductors
[DE85-012090] N86-11053

HELIUM ISOTOPES
An investigation of vortex dynamics in 2-dimensional superfluid films of helium-4 N86-11040

HEMATOPOIESIS
Indices of blood oxygen transporting properties and erythropoiesis in rats after prolonged stay in nitrogen-oxygen mixture at elevated pressure N86-10761

HEMODYNAMIC RESPONSES
Hemodynamics during gravitational overloads (mathematical modeling) N86-10739
Capacity for work and hemodynamics in males residing at middle and high latitudes N86-10747

HETERODYNING
A superconducting tunnel junction receiver for millimeter-wave astronomy N86-11041

HEURISTIC METHODS
State assignment in sequential circuits
[EUT-85-E-146] N86-10846

HIERARCHIES
Calculation of the glass transition temperatures of linear polymers. Part 1: Rules for hierarchical ordering of the data set
[AD-A156584] N86-10343
Generation of flight paths using hierarchical planning
[AD-A156905] N86-10900

HIGH ENERGY INTERACTIONS
Proceedings of a Workshop on Electroweak Symmetry Breaking
[DE85-004444] N86-11006
Search for heavy neutrines produced in e(+)e(-) annihilation
[DE85-013372] N86-11035

HIGH FREQUENCIES
Report on a visit to CERN in February 1985. Notes on bunch monitors, high-frequency systems, linacs, kickers, magnets, vacuum and bunch extraction
[LINO-119] N86-10967

HIGH PASS FILTERS
On the use of X-band CW nanosecond airborne radar for terrain profiling
[AD-A156886] N86-10406

HIGH PRESSURE
Spontaneous Raman spectroscopy of shocked H2O
[DE85-014557] N86-10470
Measurement of the density of base fluids at pressures 0.422 to 2.20 GPa
[NASA-TM-87114] N86-10551
Liquid to gas leak ratios with liquid nitrogen and liquid helium
[DE85-012950] N86-11030
High-pressure release-wave measurements and phase transformation in CaCO3
[DE85-012592] N86-11055
Thermodynamics of polymer-supercritical solvent mixtures
[AD-A157038] N86-11061

HIGH RESOLUTION
Cooled ion frequency standard
[AD-A156813] N86-10295

HIGH SPEED
Type of new Chinese-produced high-speed camera and its utilization in detonation physics experiments
[DE85-015191] N86-10529
Elektronika MS 1603 high-speed peripheral processor N86-10811
Diagnostics of peripheral processors and controllers N86-10812
Transient velocity assessment in gallium arsenide, and of other GaAs characteristics related to device functions
[AD-A156983] N86-11050

HIGH TEMPERATURE
Measurement of the properties of tungsten at high temperatures N86-10091
Containerless high temperature property measurements by atomic fluorescence N86-10092
Advanced containerless processing technology N86-10176
Acoustic levitation containerless processing N86-10177
High-temperature controlled redox crystallization studies N86-10178
Multipurpose pan development
[DE85-012326] N86-10318
Swelling and tensile properties of EBR-2-irradiated tantalum alloys for space reactor applications
[DE85-012887] N86-10329
Spontaneous Raman spectroscopy of shocked H2O
[DE85-014557] N86-10470
Dust deposition in regions of separated flow
[JUEL-1985] N86-10475
Finite element analysis of metals at elevated temperature using unified constitutive theories N86-10569
Constitutive modeling for isotropic materials (HOST)
[NASA-CR-174980] N86-10589

Liquid to gas leak ratios with liquid nitrogen and liquid helium [DE85-012950] N86-11030

HIGH TEMPERATURE ENVIRONMENTS

Dynamic thermophysical measurements in space [NASA ORDER H-27954-B] N86-10106

HIGH TEMPERATURE PLASMAS

Potential structures and particle acceleration on auroral field lines [AD-A156694] N86-10706

Symmetric Tandem Mirror Program [DE85-012352] N86-11032

HIGH TEMPERATURE RESEARCH

Measurement of high temperature thermophysical properties N86-10074

HIGH TEMPERATURE TESTS

High temperature properties and characterization of S3-N4 materials [BMFT-FB-T-85-046] N86-10352

High temperature properties of SiC materials [BMFT-FB-T-85-047] N86-10353

High temperature mechanical testing of a cylindrical weave carbon-carbon composite [AD-A156639] N86-10591

Experiments with tubular probes made of INCOLOY 800 H under uniaxial and multiaxial strain [JUEL-1979] N86-10595

HIGH VOLTAGES

Calibrated Faraday current and magnetic field sensor [DE85-013438] N86-10439

High voltage instrument transformers for outdoor service with an insulation of low pressure SF6 gas and plastic foils [BMFT-FB-T-85-034] N86-10449

HIMALAYAS

Test on mapping application of metric camera imagery — Spacelab N86-10505

Report of the Workshop on Geologic Applications of Remote Sensing to the Study of Sedimentary Basins [E86-10002] N86-10599

HOLE GEOMETRY (MECHANICS)

Analytical and experimental study of cracks emanating from an elliptical hole in unidirectional composite material N86-10567

HOLMIUM

Extraction of lanthanide ions by 2-methyl-8-quinolinol [DE85-014277] N86-10303

HOLMIUM ISOTOPES

Information on continuum states from feeding times and total (GAMMA) spectra measured with BGO suppressed detectors [DE85-013868] N86-10961

HOLOGRAPHIC INTERFEROMETRY

Holographic interferometry near gas/liquid critical points: Ground-based study of a D1 experiment — Spacelab N86-10249

HOLOGRAPHY

Advanced optical measurement techniques N86-10174

Digital decoding of in-line holograms N86-10478

Velocities of gas and plasmas from real time holographic interograms [DE85-014616] N86-10530

Spatial frequency multiplexed coherent optical processor for calculating generalized moments [AD-D011816] N86-10975

HOMEOSTASIS

Effect of emotional stress on hemostasis system of healthy persons N86-10745

HOMOLOGY

Galois descent and class groups of orders [CTH-MATH-1985-09] N86-10904

HORMONES

Hormone purification by isoelectric focusing N86-10135

Effect of single actions of weak electromagnetic fields of ultralow frequency on indices of endocrine system N86-10744

HORN ANTENNAS

Propagation and radiation characteristics of a multimode corrugated waveguide feedhorn N86-10386

HOT CORROSION

Weld metal hot-cracking of hastelloy alloys C-22 and C-276: A study by analytical electron microscopy [DE85-009437] N86-10324

HOT PRESSING

Containerless processing of glass forming melts in space N86-10148

HOUSINGS

Small cartridge heater [AD-D011784] N86-10277

HUGONIOT EQUATION OF STATE

Hugoniot measurements in aluminum to 420 GPa using the LLNL two-stage light-gas gun [DE85-013821] N86-10317

HUMAN BEHAVIOR

Individual typological features of autonomic reactions during autogenic training in polar expedition members in period of wintering in Antarctica N86-10748

HUMAN BODY

Motion analysis report [NASA-CR-171897] N86-10896

HUMAN FACTORS ENGINEERING

Proposed modifications for the RAAF Airtrainer CT-4A cockpit [AD-A156808] N86-10039

The synthesis and analysis of color images [NASA-TM-86844] N86-10777

LANES 1 Users' Guide [NASA-CR-177334] N86-10819

HUMAN PERFORMANCE

The effects of age, sleep deprivation, and altitude on complex performance [AD-A156987] N86-10771

Studies on human vehicle control [B8563352] N86-10775

Car driving as a supervisory control task [B8563351] N86-10776

Standardization of tasks: Approach planning — human performance assessment [IZF-1984-19] N86-10782

HUMAN TOLERANCES

Effect of various doses of some vitamins on non-specific mechanisms of adaptation of man N86-10750

HUMIDITY

Laboratory experiments of heat pump dynamic losses [DE85-013931] N86-10473

HUYGENS PRINCIPLE

A simplified method of estimation of the specular components of radar cross section for some re-entrant conductors [AD-A156573] N86-10403

HYDRAULIC CONTROL

Digital control of the hydraulic actuators of an adaptive suspension vehicle N86-10548

HYDRAULIC EQUIPMENT

Computer control of an electric hydraulic robot leg with proximity ranging system N86-10549

HYDRAULIC FLUIDS

The Rhine-Meuse estuary hydraulic scale model. Experiences with computer configuration and software [PUBL-335] N86-10637

HYDRIDES

Development of metallization process [NASA-CR-176209] N86-10312

HYDROBROMIC ACID

Laser Raman spectroscopy study of the zinc and bromide ion complex equilibrium in zinc/bromine battery electrolytes [DE85-011820] N86-10301

HYDRODYNAMICS

Streaming potentials in conductive and nonconductive tubing [DE85-012984] N86-10438

Time-implicity simulation of particle-fluid systems [DE85-012944] N86-10471

The generation and transmission of vibration in plain cylindrical bearings. Part 2. Experiment [AD-A156577] N86-10553

Dynamics of imploding neon gas puff plasmas. 1 [AD-A156916] N86-10983

HYDROELECTRIC POWER STATIONS

Ultrasonic inspection of weldments in large size spiral box for hydroelectric plant [AS-701/85] N86-10562

National perspective on environmental constraints to hydroelectric development [DE85-013111] N86-10678

HYDROELECTRICITY

National perspective on environmental constraints to hydroelectric development [DE85-013111] N86-10678

HYDROGEN

Effects of scale and geometry on hydrogen-air detonations [DE85-006762] N86-10474

Experimental X-ray scattering cross sections for H2 and rare atomic gases [DE85-011572] N86-10936

Angular distribution of neutral hydrogen following collisional electron detachment from H(-) [DE85-014258] N86-10943

Proposed bunching scheme for a polarized H(-) injector [DE85-012648] N86-10986

Noninterceptive techniques for the measurement of longitudinal parameters for intense H(-) beams [DE85-012662] N86-10992

HYDROGEN EMBRITTLEMENT

Fracture toughness of hydrogen-embrittled precipitation-hardened stainless steels [AD-A156684] N86-10592

Chemical/hydrogen energy systems [DE85-012742] N86-10667

Methane-bubble formation in hydrogen-charged Fe-30 ppM C [DE85-012526] N86-10937

HYDROGEN IONS

AGS polarized H(-) source [DE85-013296] N86-10935

Performance of the H(-) ion source for the intense pulsed neutron source [DE85-012368] N86-10991

HYDROGEN PRODUCTION

Chemical/hydrogen energy systems [DE85-012742] N86-10667

HYDROGEN SULFIDE

Chemical kinetics and cellular structure of detonations in hydrogen sulphide and air [DE85-009408] N86-10304

Method for determining elemental sulfur in jet fuel — differential pulse polarography [FOA-C-40211-B4] N86-10360

HYDROLOGY

Interpretation of metric camera concerning hydrologic structures of the Rhone Delta — Spacelab N86-10504

HYDROLOGY MODELS

Modeling groundwater flow into lakes N86-10598

HYDROMECHANICS

Recent development in the Hot Dry Rock Geothermal Energy Program [DE85-009562] N86-10663

HYDROPHONES

A comparison of swept frequency and FFT methods used to calibrate array test modules [AD-A156629] N86-10430

Fiber optic gradient hydrophone construction and calibration for sea trial [AD-A156469] N86-10914

HYDROTHERMAL SYSTEMS

Geothermal Energy Technology Program summary [DE85-013101] N86-10646

HYDROXYL COMPOUNDS

Extraction of lanthanide ions by 2-methyl-8-quinolinol [DE85-014277] N86-10303

HYDROXYL EMISSION

The two micron spectrum of R Scuti N86-11092

HYPERBOLIC FUNCTIONS

La Recherche Aerospatiale, bimonthly bulletin, no. 1984-5, September-October 1985 [ESA-TT-899] N86-10363

HYPERCAPNIA

Dynamics of general resistance of rats during readaptation period after training in altered gas environment N86-10767

HYPERONS

Hyperon polarization: An unresolved problem [DE85-012298] N86-10946

HYPERSONIC FLOW

Three articles on new calculation methods in aeronautics (selected articles) [AD-A145745] N86-10007

Numerical solution of hypersonic flow near leading edge of a flat plate N86-10008

Numerical procedure for three-dimensional hypersonic viscous flow over aerobrake configuration [NASA-TM-58269] N86-10018

Inviscid flow field analysis of maneuvering hypersonic vehicles using the SCM formulation and parabolic grid generation [DE85-013950] N86-10021

HYPERSONIC VEHICLES

Inviscid flow field analysis of maneuvering hypersonic vehicles using the SCM formulation and parabolic grid generation [DE85-013950] N86-10021

HYPERSONIC WAKES

Numerical procedure for three-dimensional hypersonic viscous flow over aerobrake configuration [NASA-TM-58269] N86-10018

HYPERSPACES

On the analytical evaluation of the partition function for unit hypercubes in four dimensions — lattice theory [NIKHEF-H/84-12] N86-10882

HYPERTHERMIA

Short term heat effect on adreno- and cholino-sensitivity of rat's small intestine N86-10754

Vestibular resistance and blood circulation changes in orthostatic position during hyperthermia N86-10758

HYPERVELOCITY GUNS

EMACK railgun firing test report number 9 [AD-A156661] N86-10354

HYPERVELOCITY LAUNCHERS
EMACK railgun firing test report number 9
[AD-A156661] N86-10354
HYPOKINESIA
Study of hypokinesia and acceleration effects on human chromosomes N86-10740
HYPOTHERMIA
Intradiurnial organization of wakefulness-sleep sequence and energy metabolism in rats exposed to low ambient temperature N86-10764
HYPOXIA
Reaction of rabbit respiration system to hypoxic stimulus in nitrogen-oxygen medium at elevated pressure
N86-10760
Indices of blood oxygen transporting properties and erythropoiesis in rats after prolonged stay in nitrogen-oxygen mixture at elevated pressure
N86-10761
Dynamics of general resistance of rats during readaptation period after training in altered gas environment N86-10767
Mild hypoxia and visual performance with night vision goggles
[AD-A156969] N86-10787

I

IBM 370 COMPUTER
The local disk controller
[REPT-1-68430-44(1985)01] N86-10806
Performance analysis of the IBM Direct Access Storage Device (DASD) subsystem, and some suggestions for improved systems
[REPT-1-68430-44(1985)02] N86-10807
An intelligent local disk control system
[REPT-051560-26(1984)08] N86-10808
IDEAL GAS
On the method of characteristics and its application to the calculations of annular nozzle flowfields N86-10454
IDENTIFYING
Defect identification in high-energy semiconductors
[DE85-014533] N86-10442
IGNITION
Solid surface combustion at reduced gravity
N86-10159
Ignition and flame spread above liquid fuel pools
N86-10163
Self-heating to ignition measurements and computation of critical size for solar energy collector materials
[DE85-011449] N86-10302
IGNITION SYSTEMS
Fundamental studies of droplet combustion at reduced gravity N86-10165
IGNITION TEMPERATURE
A fundamental study of smoldering with emphasis on experimental design for zero-g N86-10162
ILLUMINATING
Methods for developing jam-resistant security communications networks at fixed-site facilities
[DE85-012032] N86-10408
Passive and hybrid solar technologies program summary
[DE85-013100] N86-10648
IMAGE ANALYSIS
Satellite data even for a poultry farm. A development for Tanzania. Image evaluation following new ways
N86-10182
LANDSAT TM image data quality analysis for energy-related applications
[E85-10109] N86-10597
Multisensor data integration techniques N86-10604
Analysis of edge detection algorithms on DIAL (Digital Image Analysis Laboratory)
[AD-A156735] N86-10630
IMAGE CORRELATORS
The OASIS correlator — Optical Aperture Synthesis in Space (OASIS) N86-11119
On line astronomical image processing using microcomputers N86-11121
IMAGE FURNACES
The mirror heating facility: Performance and experiences — Spacelab N86-10223
IMAGE PROCESSING
Real-time holography by stimulated Raman and Brillouin scattering N86-10479
Evaluation of metric camera images at the University of London — Spacelab N86-10495
Digital image processing of metric camera imagery — Spacelab N86-10511
Creation of Ground Control Points (GCP) library using ESA Spacelab metric camera imagery — ground control point (gcp) N86-10516
Automated analysis of digital images generated by two-dimensional gel electrophoresis
[DE85-011906] N86-10526
Remote sensing
[NOTA-1535] N86-10636
Applications for three-dimensional computer graphic cloud representations produced from satellite imagery
[AD-A158903] N86-10798
Arithmetic pipeline for image processing
[AD-D011773] N86-10800
Digital processing of images in tracking a moving object N86-10818
Always-convergent iterative noise removal and deconvolution for image data
[NASA-CR-176223] N86-10824
Test of a multilevel computational theory of stereoscopic visual image processing
[AD-A157011] N86-10870
Kalman filter preprocessor
[AD-D011774] N86-10972
Spatial frequency multiplexed coherent optical processor for calculating generalized moments
[AD-D011816] N86-10975
Fringe drift compensation in computer memory — Michelson interferometry N86-11112
Numerical experiments in image reconstruction — stellar interferometry N86-11116
On line astronomical image processing using microcomputers N86-11121
A modeling analysis program for the JPL table mountain Io sodium cloud
[NASA-CR-176241] N86-11139
IMAGE RECONSTRUCTION
Digital decoding of in-line holograms N86-10478
Real-time holography by stimulated Raman and Brillouin scattering N86-10479
Restitution of Spacelab photography by analog stereoplotter N86-10489
Problems in image reconstruction with optical arrays — spaceborne astronomy N86-11115
Numerical experiments in image reconstruction — stellar interferometry N86-11116
Radio astronomy experience in image reconstruction. A history lesson for optical astronomers N86-11117
COSMIC image reconstruction — Coherent Optical System of Modular Imaging Collectors (COSMIC)
N86-11118
The OASIS correlator — Optical Aperture Synthesis in Space (OASIS) N86-11119
Imaging speckle interferometer in space: Digital simulations of image reconstruction and photon noise
N86-11120
Aperture synthesis with or without phase information for kilometric arrays interpolation algorithms for stabilized image reconstruction N86-11124
IMAGE RESOLUTION
SAR image quality: A review
[DFVLR-MITT-85-07] N86-10413
Line mapping and resolution tests with metric camera data — Spacelab N86-10500
IMAGERY
Stereoscopic video imagery generation
[AD-D011785] N86-10481
IMAGES
Radar system description N86-10616
IMAGING TECHNIQUES
Digital decoding of in-line holograms N86-10478
The synthesis and analysis of color images
[NASA-TM-86844] N86-10777
Information technique 1985: Optical technology and electro-optics, a defense technical component review
[FOA-A-30037-E] N86-10980
Physical conditions in giant extragalactic H2 regions
N86-11130
IMPACT LOADS
The mechanics of delamination in composite materials
N86-10284
Fundamental studies of low velocity impact resistance of graphite fiber reinforced polymer matrix composites
N86-10288
Explosive initiation by very small conical shaped charge jets
[DE85-009443] N86-10357
IMPACT RESISTANCE
Fundamental studies of low velocity impact resistance of graphite fiber reinforced polymer matrix composites
N86-10288
IMPACT STRENGTH
Fabrication and metallurgical properties of modified 9Cr-1 Mo steel
[DE85-012885] N86-10328
IMPLOSIONS
Preliminary investigation of changes in X-ray multilayer optics subjected to high radiation flux
[DE85-014074] N86-10944
IMPURITIES
Surface tensions and their variations with temperature and impurities
[NASA ORDER H-27954B] N86-10115
Impurity extraction by droplets N86-10122
Investigation of metallic impurities introduced into SiO2 and silicon by various candidate VLSI metallization systems: Chemical reactions, diffusion, and electrical properties
[AD-A156609] N86-10429
IN-FLIGHT MONITORING
Partial in-flight calibration of the metric camera — Spacelab N86-10498
INCIDENCE
Angle of incidence effects for underwater shock using generic computational models
[DE85-012936] N86-10456
Angle of incidence effects for underwater shock using generic computational models, rev. 1
[DE85-012921] N86-10457
The effect of vegetation type, microrelief, and incidence angle on radar backscatter N86-10619
INCLUSIONS
Three-dimensional stress singularities in anisotropic materials and composites N86-10296
INCOMPRESSIBLE FLOW
A root-mean-square pressure fluctuations model for internal flow applications
[NASA-CR-3929] N86-10460
INDEPENDENT VARIABLES
The Liu, Katsaros, and Businger (1979) bulk atmospheric flux computational iteration program in FORTRAN and BASIC
[AD-A156736] N86-10714
INDEXES (DOCUMENTATION)
The 1984 bibliography of atomic and molecular processes
[DE85-010583] N86-10926
Advanced vehicle systems assessment. Volume 5: Appendices
[NASA-CR-176208] N86-11086
INDIA
Report of the Workshop on Geologic Applications of Remote Sensing to the Study of Sedimentary Basins
[E86-10002] N86-10589
Chronologic analysis of terrestrial sediments and basin evolution N86-10602
INDIUM ALLOYS
Directional solidification of monotectic and hypermonotectic aluminum-indium alloys under micron-g
N86-10097
Space shuttle experiments on Al-In liquid phase miscibility gap (LPMG) alloys N86-10294
INDOOR AIR POLLUTION
Volatile organic compounds in indoor air: A survey of various structures
[PB85-198356] N86-10687
INDUCTANCE
Compact, low jitter, triggered spark gap
[DE85-012812] N86-10195
INDUCTORS
Overpulse railgun energy recovery circuit
[DE85-011607] N86-10197
INDUSTRIAL PLANTS
Identification of a plant's weighting sequence — self-tuning control
[OUEL-1534/84] N86-10854
INDUSTRIAL SAFETY
Effect of various doses of some vitamins on non-specific mechanisms of adaptation of man N86-10759
Report on the research activities on whole-body vibrations. Human strain due to mechanical vibrations
[ISBN-3-88383-107-7] N86-10773
Annotated bibliography of publications dealing with occupational health and medical information systems, cost analysis procedures, evaluation methodology and related legal issues
[AD-A156650] N86-11078
INDUSTRIAL WASTES
Membrane research in energy and solvent recovery from industrial effluent streams
[DE85-014583] N86-10652
INDUSTRIES
Research needs for corrosion control and prevention in energy conservation systems
[DE85-014852] N86-10328
Biotechnology: Science and practice N86-10742
INELASTIC SCATTERING
Polarization transfer in inelastic scattering and pionic models of the EMC effect
[DE85-010738] N86-10985
INELASTIC STRESS
Inelastic analysis of frame structures including member and joint shears N86-10573
Analysis of large, non-isothermal elastic-visco-plastic deformations
[NASA-CR-176220] N86-10580

INERTIAL CONFINEMENT FUSION
High efficiency heat transport and power conversion system for cascade
[DE85-012959] N86-10458
INERTIAL UPPER STAGE
Analytical investigation of solid rocket nozzle failure
[NASA-TM-86513] N86-10278
INFORMATION DISSEMINATION
Project VESTA, exploratory mission to the asteroids: Scientific objectives and technical specifications
[NASA-TM-77669] N86-10179
Solar thermal technical information guide
[DE85-002941] N86-10657
Publication of the Executive Office of the President, January 20, 1981 - December 31, 1984
[PB85-187110] N86-11082
INFORMATION FLOW
Editors rattle space N86-10586
INFORMATION RETRIEVAL
Publication of the Executive Office of the President, January 20, 1981 - December 31, 1984
[PB85-187110] N86-11082
INFORMATION SYSTEMS
Development of IS2100: An information systems laboratory
[AD-A156848] N86-10797
Annotated bibliography of publications dealing with occupational health and medical information systems, cost analysis procedures, evaluation methodology and related legal issues
[AD-A156650] N86-11078
Publication of the Executive Office of the President, January 20, 1981 - December 31, 1984
[PB85-187110] N86-11082
INFRARED ASTRONOMY
Optical/IR telescope arrays: A study of their potential for satisfying observational requirements in astronomy for a large aperture system in the 1990s and beyond
[REPT-15] N86-11094
High angular resolution in the infrared: Prospects for space observations N86-11100
The DUO: Far infrared heterodyne concept for space interferometry N86-11125
INFRARED DETECTORS
Sensor system
[AD-D011767] N86-10480
INFRARED IMAGERY
Infrared system with computerized image display
[AD-D011777] N86-10906
INFRARED PHOTOGRAPHY
Neogene compressional deformation and possible thrust faulting in southwest Dominican Republic N86-10618
INFRARED SCANNERS
Infrared system with computerized image display
[AD-D011777] N86-10906
INFRARED SPECTROPHOTOMETERS
Fuel and lubricant behavior in boundary layers analyzed by infrared emission Fourier transform spectrometry N86-10336
INFRARED SPECTROSCOPY
Theoretical comparison of classical (K-matrix) and inverse (P-matrix) least-squares methods for quantitative infrared spectroscopy
[DE85-012827] N86-10298
INHOMOGENEITY
Mechanics of coated fiber composites N86-10285
INITIATION
Explosive initiation by very small conical shaped charge jets
[DE85-009443] N86-10357
INLET PRESSURE
Effect of a shear layer on the stability of an axisymmetrical external compression air intake N86-10010
INPUT
Signal analysis of gas tungsten arc welds N86-10078
Phase-coded pulse expander-compressor
[AD-D011812] N86-10375
INPUT/OUTPUT ROUTINES
Design of a multifunction Input-Output (I/O) controller
[EUT-84-E-143] N86-10802
Realization of a multifunction Input/Output (I/O) controller by means of a gate array
[EUT-85-E-147] N86-10804
The local disk controller
[REPT-1-68430-44(1985)01] N86-10806
Performance analysis of the IBM Direct Access Storage Device (DASD) subsystem, and some suggestions for improved systems
[REPT-1-68430-44(1985)02] N86-10807
INSECTS
A fundamental study of the sticking of insect residues to aircraft wings
[NASA-CR-176231] N86-10033
INSPECTION
Nondestructive control of thick structures made without disassembling
[PV-43-954/F/3] N86-10564
INSTRUMENT TRANSFORMERS
High voltage instrument transformers for outdoor service with an insulation of low pressure SF6 gas and plastic foils
[BMFT-FB-T-85-034] N86-10449
INSULATION
Transient velocity assessment in gallium arsenide, and of other GaAs characteristics related to device functions
[AD-A156983] N86-11050
INSULATORS
Thermodynamic constraints on ion beam mixing of metals on insulators
[DE85-013628] N86-10448
INTEGRALS
The use of new path indepedent integrals in elastic-plastic and creep fracture N86-10574
A study of methods to predict and measure the transmission of sound through the walls of light aircraft. Integration of certain singular boundary element integrals for applications in linear acoustics
[NASA-CR-176229] N86-10912
INTEGRATED CIRCUITS
Investigation of metallic impurities introduced into SiO2 and silicon by various candidate VLSI metallization systems: Chemical reactions, diffusion, and electrical properties
[AD-A156809] N86-10429
Efficient systolic arrays for the solution of toeplitz systems: An illustration of a methodology for the construction of systolic architectures in VLSI (Very Large Systems Integration)
[AD-A156767] N86-10795
COMPACT: Compaction of hierarchial chip layouts based on a constraint graph method with double-sided constraints N86-10845
Transient velocity assessment in gallium arsenide, and of other GaAs characteristics related to device functions
[AD-A156983] N86-11050
INTERATOMIC FORCES
Non-empirical interatomic potentials for transition metals
[DE85-013448] N86-10440
INTERFACE STABILITY
Mephisto: Interfacial destabilization in metal alloys N86-10079
Dendritic solidification in a binary alloy melt: Steady-state versus morphological stability theories N86-10261
INTERFACES
Thermodynamic constraints on ion beam mixing of metals on insulators
[DE85-013628] N86-10448
Design sensitivity analysis and optimization of built-up structures N86-10565
Parallel local interface bus
[AD-D011742] N86-10792
LANES 1 Users' Guide
[NASA-CR-177334] N86-10819
User interface enhancement report
[NASA-CR-171898] N86-10820
System integration report
[NASA-CR-171900] N86-10821
INTERFACIAL TENSION
Theoretical studies of the surface tension of liquid metal system N86-10101
Suppression of Marangoni convection in float zones N86-10111
Surface tensions and their variations with temperature and impurities
[NASA ORDER H-27954B] N86-10115
Surface tension induced instabilities in reduced gravity: The Benard problem N86-10117
Surface-tension driven convection N86-10124
Thermocapillary motion research N86-10125
Thermocapillary and diffusocapillary migration of a fluid drop N86-10128
Cell partition in two polymer aqueous phases N86-10136
The influence of thermocapillarity on the migration of droplets in a liquid possessing a uniform temperature gradient N86-10237
Rayleigh-Benard instability in systems presenting a minimum in surface tension N86-10245
Surface forces in contacting solids — microgravity rocket experiment N86-10252
INTERFEROMETERS
Imaging speckle interferometer in space: Digital simulations of image reconstruction and photon noise N86-11120
INTERFEROMETRY
Experimental and theoretical studies of wetting and multilayer adsorption
[NASA ORDER H-27954B] N86-10121
Signal analysis receiver with acousto-optic delay lines
[AD-D011761] N86-10427
Velocities of gas and plasmas from real time holographic interograms
[DE85-014618] N86-10530
NASA/JPL Aircraft SAR Workshop Proceedings
[NASA-CR-176204] N86-10615
Topographic mapping from interferometric synthetic aperture radar observations N86-10622
Imaging speckle interferometer in space: Digital simulations of image reconstruction and photon noise N86-11120
INTERGALACTIC MEDIA
Extragalactic observations with optical space arrays N86-11098
INTERMETALLICS
Metallurgy and metallography of braze joints
[DE85-014563] N86-10325
INTERMODULATION
Rusty bolt intermodulation interference reducer
[AD-D011748] N86-10313
Apparatus for locating passive intermodulation interference sources
[AD-D011798] N86-10435
INTERNAL COMBUSTION ENGINES
Modeling of engine sprays
[DE85-010020] N86-10559
INTERNAL FRICTION
Initial increase, peaking effect, in the internal friction of copper following pulsed neutron and electron irradiation
[DE85-012767] N86-10932
INTERNAL PRESSURE
Acoustic cavitation and bubble dynamics
[AD-A156888] N86-10918
INTERNATIONAL COOPERATION
Project VESTA, exploratory mission to the asteroids: Scientific objectives and technical specifications
[NASA-TM-77669] N86-10179
INTERPOLATION
The interpolation of signals sampled at less than the Nyquist rate N86-10368
A numerical method for approximating antenna surfaces defined by discrete surface points
[NASA-TM-87125] N86-10381
A sequential decoding performance analysis for International Comet Explorer N86-10390
Aperture synthesis with or without phase information for kilometric arrays interpolation algorithms for stabilized image reconstruction N86-11124
INTERSTELLAR GAS
A superconducting tunnel junction receiver for millimeter-wave astronomy N86-11041
INVERSE SCATTERING
Renormalization of an inverse scattering theory for inhomogeneous dielectrics
[AD-A156636] N86-11049
INVERSIONS
Well-posed questions and exploration of the space of parameters in linear and non linear inversion
[PN-84/13] N86-10858
INVISCID FLOW
Three-dimensional inviscid analysis of radial turbine flow and a limited comparison with experimental data
[NASA-TM-87091] N86-10017
Inviscid flow field analysis of maneuvering hypersonic vehicles using the SCM formulation and parabolic grid generation
[DE85-013950] N86-10021
IO
A modeling analysis program for the JPL table mountain Io sodium cloud
[NASA-CR-176241] N86-11139
IODIDES
Parallel pulse processing for mercuric iodide gamma-ray detectors
[DE85-013391] N86-10528
ION ACCELERATORS
Microwave instability across the transition energy
[DE85-013304] N86-11010
Tracking studies on the effects of magnet multipoles on the aperture of the RHIC heavy ion collider
[DE85-013282] N86-11023
ION BEAMS
Simulating the CTR environment in the HVBM
[DE85-011745] N86-10193
RFQ-funneling
[DE85-012483] N86-10194
Thermodynamic constraints on ion beam mixing of metals on insulators
[DE85-013628] N86-10448

Supersonic metal cluster beams
[DE85-014321] N86-10966
Treatment planning with ion beams
[DE85-012661] N86-10990

ION IMPLANTATION
Metastable phase formation in Ni-implanted Al: An analytical electron microscope investigation
[DE85-009105] N86-10331

ION IRRADIATION
Boronising of iron and steel by ionic bombardment by diborane
[BLL-BISI-TRANS-23034-(9022.06)] N86-10307
Thermodynamic constraints on ion beam mixing of metals on insulators
[DE85-013628] N86-10448

ION MOTION
The measurement and application of transport properties of ion swarms in gases N86-10370

ION PROPULSION
Rapid evaluation of ion thruster lifetime using optical emission spectroscopy
[NASA-TM-87103] N86-10280

ION RECOMBINATION
Electron-ion recombination studies of planetary ionospheric and astrophysical ions N86-11132

ION SOURCES
AGS polarized H(-) source
[DE85-013296] N86-10935
Report on the engineering test of the LBL 30 second neutral beam source for the MFTF-B project
[DE85-013317] N86-10962
Performance of the H(-) ion source for the intense pulsed neutron source
[DE85-012368] N86-10991
Ion sources for high-frequency accelerators
[DE85-012992] N86-11006

ION STORAGE
Cooled ion frequency standard
[AD-A156813] N86-10295

IONIC COLLISIONS
The measurement and application of transport properties of ion swarms in gases N86-10370
Charge exchange in slow collisions of atoms and molecules N86-10922
Angular distribution of neutral hydrogen following collisional electron detachment from H(-)
[DE85-014258] N86-10943

IONIC MOBILITY
Electrohydrodynamics N86-10130
The measurement and application of transport properties of ion swarms in gases N86-10370

IONIZING RADIATION
Criteria for the design or selection of a bioelectromagnetics experiment
[AD-A156575] N86-10420

IONOSPHERE
Comparison of the calibration of ionospheric delay in VLBI data by the methods of dual frequency and Faraday rotation N86-10384
Potential structures and particle acceleration on auroral field lines
[AD-A156694] N86-10708
Activities report in geophysics
[KGI-188] N86-10709
Electron-ion recombination studies of planetary ionospheric and astrophysical ions N86-11132

IONS
Laser Raman spectroscopy study of the zinc and bromide ion complex equilibrium in zinc/bromine battery electrolytes
[DE85-011820] N86-10301
Extraction of lanthanide ions by 2-methyl-8-quinolinol
[DE85-014277] N86-10303
Potential structures and particle acceleration on auroral field lines
[AD-A156694] N86-10708
Theoretical investigation of electron-positive ion-atom interactions
[DE85-013019] N86-10939

IRAN
A geological structural analysis of the southeastern Zagros (Iran) ranges based on metric camera photos
N86-10492
Tectonic analysis of typical fold structures in the Zagros Mountains (Iran) by the application of quantitative photogrammetric methods on metric camera data --- Spacelab N86-10521

IRIDIUM
General-purpose heat source development: Safety Verification Test Program. Bullet/fragment test series
[DE85-014262] N86-10660

IRISES (MECHANICAL APERTURES)
Direct-coupled cavity filters with irises of arbitrary thickness
[DFVLR-FB-85-14] N86-10412

IRON
Control of cast iron microstructure N86-10084
Study of the reactive-element effect in oxidation of Fe-Cr alloys using transverse section analytical electron microscopy N86-10087
Graphite formation in cast iron N86-10100
The mechanism of erosion of metallic materials under cavitation attack
[NASA-TM-87133] N86-10552
Advanced fuel cell development
[DE85-014550] N86-10659
Kinetics of biological ferrous iron oxidation
[DE85-014616] N86-10736
Methane-bubble formation in hydrogen-charged Fe-30 ppM C
[DE85-012526] N86-10937

IRON ALLOYS
Unidirectional solidification of cast iron: Experiment ES-325 --- Spacelab N86-10212
Skin casting of alloys and composites: Results of Spacelab (SL)-1 and TEXUS experiments N86-10213
Electronic and magnetic properties of noble-metal and transition-metal alloys, interfaces and overlayers
[DE85-014532] N86-10321

IRRADIATION
Swelling and tensile properties of EBR-2-irradiated tantalum alloys for space reactor applications
[DE85-012867] N86-10329
Approaches to quantitative expression of dose response
[DE85-013498] N86-10772
Initial increase, peaking effect, in the internal friction of copper following pulsed neutron and electron irradiation
[DE85-012767] N86-10932

IRRIGATION
On the use of L-band multipolarization airborne SAR for surveys of crops, vineyards, and orchards in a California irrigated agricultural region N86-10627

ISLANDS
Analysis of remote sensing data N86-10605

ISOCHORIC PROCESSES
Isochoric specific heat of sulfur hexafluoride at the critical point. A Spacelab experiment for the German D1-mission in 1985 N86-10251

ISOTHERMAL PROCESSES
The isothermal heating facility --- Spacelab
N86-10208

ISOTOPE SEPARATION
Beam line windows at LAMPF
[DE85-012723] N86-10985

ISOTROPIC MEDIA
Stiffened and prestressed composite overwrapped pressure vessels N86-10547
Constitutive modeling for isotropic materials (HOST)
[NASA-CR-174980] N86-10589

ITERATION
Second order approximation method for transonic flows over swept wings N86-10002
Determining a physically appropriate neutron spectrum from multisphere data
[DE85-013045] N86-10299

ITERATIVE SOLUTION
Improved mapping of radio sources from VLBI data by least-square fit N86-10402
A study of Morrison's iterative noise removal method
[NASA-CR-176222] N86-10823
Always-convergent iterative noise removal and deconvolution for image data
[NASA-CR-176223] N86-10824

J

J INTEGRAL
Application of the unloading compliance methods in fracture toughness measurements of a quenched and tempered steel
[BLL-BISI-TRANS-21628-(9022.06)] N86-10308

JAMMING
Methods for developing jam-resistant security communications networks at fixed-site facilities
[DE85-012032] N86-10408

JET AIRCRAFT NOISE
Summary of work on jet noise prediction
[ESDU-BR-62636] N86-10909

JET BOUNDARIES
On the method of characteristics and its application to the calculations of annular nozzle flowfields N86-10454

JET ENGINE FUELS
Method for determining elemental sulfur in jet fuel --- differential pulse polarography
[FOA-C-40211-B4] N86-10360

JET ENGINES
Retrofit of SAC EC-135C and RC-135 aircraft with CFM-56 engines
[AD-A156688] N86-10038
The Shock and Vibration Digest, volume 17, no. 3
[AD-A154144] N86-10585

JET FLOW
Buoyancy effects upon vapor flame and explosion processes N86-10161
Confined swirling jet predictions using a multiple-scale turbulence model
[NASA-CR-178484] N86-10462

JET MIXING FLOW
Summary of work on jet noise prediction
[ESDU-BR-62636] N86-10909

JET THRUST
Experimental performance of a 1-kilowatt arcjet thruster
[NASA-TM-87131] N86-10281

JOINTS (JUNCTIONS)
Metallurgy and metallography of braze joints
[DE85-014563] N86-10325
Inelastic analysis of frame structures including member and joint shears N86-10573
Improved stud configurations for attaching laminated wood wind turbine blades
[NASA-TM-87109] N86-10582
Fundamental study of the closure property of joints
N86-10698

JOURNAL BEARINGS
Theoretical modeling of the vapor cavitation in dynamically loaded journal bearings
[NASA-TM-87076] N86-10463

JP-5 JET FUEL
Evaluation of the 90-day inhalation toxicity of petroleum and oil shale JP-5 jet fuel
[AD-A156815] N86-10675

JUPITER ATMOSPHERE
Galileo: Exploration of Jupiter's system
[NASA-SP-479] N86-11137

K

KALMAN FILTERS
Comment on Determination of Aerodynamic Coefficients for a Reentry Body by Means of the Kalman Filter Method N86-10011
SARSAT LUC (Local user terminal) to CMCC (Canadian Mission Control Centre) alert data interface: A critical review
[AD-A156881] N86-10276
Kalman filter preprocessor
[AD-D011774] N86-10972

KAONS
Separated K(-) beams (10 GeV and above)
[DE85-012527] N86-10989

KEVLAR (TRADEMARK)
Fatigue of graphite/epoxy buffer strip panels with center cracks
[NASA-TM-87595] N86-10581

KIDNEYS
Biochemical assays of cultured cells N86-10134
Kidney cell electrophoresis N86-10145

KINEMATICS
Design sensitivity analysis and optimization of built-up structures N86-10565
Analysis of large, non-isothermal elastic-visco-plastic deformations
[NASA-CR-176220] N86-10588
The two micron spectrum of R Scuti N86-11092

KINETIC ENERGY
The effects of orography on land-atmosphere turbulent exchange processes N86-10702
The development of a neutron evaporation theory code for the thermal fission of Uranium-235
[AD-A156593] N86-10951
Dynamics of imploding neon gas puff plasmas. 1
[AD-A156916] N86-10983

KINETIC FRICTION
Steady state frictional behavior of thin film coatings
N86-10335

KINETICS
Environmental degradation of materials: Surface chemistry related to stress corrosion cracking
N86-10099
Colloidal oxide properties and kinetic studies
N86-10147
Crystallization, optical and chemical properties of fluoride glasses N86-10149
Glass formation in reluctant glass formers
N86-10151
Kinetics of spreading of liquids in microgravity: Experiment 1 ES 327 --- Spacelab N86-10207

Rapid evaluation of ion thruster lifetime using optical emission spectroscopy
[NASA-TM-87103] N86-10280
Type of new Chinese-produced high-speed camera and its utilization in detonation physics experiments
[DE85-015191] N86-10529
Chemical kinetics and photochemical data for use in stratospheric modeling
[NASA-CR-176198] N86-10707

KLYSTRONS
An experimental TE sub 12 - TE sub 11 circular waveguide mode converter N86-10387
Klystron control software in the SIC
[DE85-013068] N86-10836
The MEA vacuum system
[LINO-120] N86-10968
High-power rf controls for the NBS-Los Alamos racetrack microtron
[DE85-012658] N86-10993

KNEE (ANATOMY)
A graphic anthropometric aid for seating and workplace design
[AD-A156988] N86-10788

KORTEWEG-DEVRIES EQUATION
A modified modified Korteweg-deVries equation
[PN-84/27] N86-10859

KRYPTON
Thermodynamic constraints on ion beam mixing of metals on insulators
[DE85-013628] N86-10448

L

LABORATORIES
Microgravity Materials Science Laboratory
N86-10173
Laboratory experiments of heat pump dynamic losses
[DE85-013931] N86-10473
Secondary standards laboratories for ionizing radiation calibrations: The national laboratory interests
[DE85-007046] N86-10938

LABORATORY EQUIPMENT
Continuous fiberization of silicon-carbide-nitride precursor resin N86-10168
The fluid physics module: A technical description — Spacelab N86-10201
The isothermal heating facility — Spacelab
N86-10208
The mirror heating facility: Performance and experiences — Spacelab N86-10223
Experimental facility for materials research in space (CSK-1) N86-10263

LAKES
Examples of regional environmental assessment using acid deposition data
[DE85-012903] N86-10677

LAMELLA (METALLURGY)
Study of eutectic formation N86-10070

LAMINAR FLOW
Measurements of the critical Marangoni number of the laminar-oscillatory transition of thermocapillary convection in floating zones N86-10242

LAMINATES
Three-dimensional stress singularities in anisotropic materials and composites N86-10286
Ultrasonic evaluation of mechanical properties of thick, multilayered, filament wound composites
[MASA-TM-87088] N86-10561

LAND
The effects of orography on land-atmosphere turbulent exchange processes N86-10702

LAND MANAGEMENT
Land evaluation successes with the metric camera — Spacelab N86-10512

LAND USE
Thematic investigations in France based on metric camera imagery — Spacelab N86-10509
Thematic mapping of metric camera color infrared and black and white photographs for land use classification
N86-10510
Approaches to cumulative impact assessment
[DE85-013691] N86-10635

LANDAU DAMPING
Microwave instability across the transition energy
[DE85-013304] N86-11010

LANDFORMS
Altitudinal distribution of granitic landforms in the south central Sierra Nevada, California N86-10695

LANDSAT SATELLITES
The effects of merging TM and A/C radar on wetland classification N86-10621
Lithologic mapping in a sedimentary environment using multipolarization SAR images N86-10624

LANGUAGES
Special purpose hardware architectures for language recognition
[AD-A156834] N86-10793

LANTHANUM
Extraction of lanthanide ions by 2-methyl-8-quinolinol
[DE85-014277] N86-10303

LARGE SPACE STRUCTURES
Passive damping concepts for slender columns in space structures
[NASA-CR-176234] N86-10577

LASER ANNEALING
W-shaped diffused stripe GaAs/AlGaAs laser
[AD-D011818] N86-10538

LASER APPLICATIONS
Containerless high temperature property measurements by atomic fluorescence N86-10092
Scaling studies of solar pumped lasers
[NASA-CR-176240] N86-10540
Information technique 1985: Optical technology and electro-optics, a defense technical component review
[FOA-A-30037-E] N86-10980

LASER DOPPLER VELOCIMETERS
Velocities of gas and plasmas from real time holographic interograms
[DE85-014618] N86-10530

LASER HEATING
Modelling of laser-enhanced chemical vapor deposition N86-10105
Characterization of vapor and aerosol flows by photothermal methods
[AD-A156601] N86-10465

LASER INTERFEROMETRY
Optical detection of photoacoustic pulses in thin silicon wafers
[AD-A156705] N86-10977

LASER MATERIALS
Device for cryogenically fabricating source material for plasma X-ray lasers
[AD-D011814] N86-10537

LASER OUTPUTS
Laser generation and transport of a relativistic electron beam
[DE85-011709] N86-10192
Laser Raman spectroscopy study of the zinc and bromide ion complex equilibrium in zinc/bromine battery electrolytes
[DE85-011820] N86-10301
Contact effects in light activated GaAs switches
[AD-A156957] N86-10434
Laser target speckle eliminator
[AD-D011775] N86-10536
Research on solar pumped liquid lasers
[NASA-CR-176235] N86-10539
Scaling studies of solar pumped lasers
[NASA-CR-176240] N86-10540
Multiple site laser excited pollution monitoring system
[AD-D011769] N86-10674

LASER PUMPING
Device for cryogenically fabricating source material for plasma X-ray lasers
[AD-D011814] N86-10537
Research on solar pumped liquid lasers
[NASA-CR-176235] N86-10539

LASER TARGET INTERACTIONS
Laser target speckle eliminator
[AD-D011775] N86-10536

LASING
Research on solar pumped liquid lasers
[NASA-CR-176235] N86-10539

LATCHES
Over-center toggle latch
[AD-D011753] N86-10556

LATERAL CONTROL
Car driving as a supervisory control task
[B8563351] N86-10776

LATEX
Production of large-particle-size monodisperse latexes in microgravity N86-10146

LATITUDE
Capacity for work and hemodynamics in males residing at middle and high latitudes N86-10747

LATTICES (MATHEMATICS)
On the analytical evaluation of the partition function for unit hypercubes in four dimensions — lattice theory
[NIKHEF-H/84-12] N86-10882
Variational estimates for the mass gap of SU(2) Euclidean lattice gauge theory
[NIKHEF-H/84-13] N86-10883

LAVA
Age-dating volcanic and alluvial surfaces with multipolarization data N86-10620

LAW (JURISPRUDENCE)
Annotated bibliography of publications dealing with occupational health and medical information systems, cost analysis procedures, evaluation methodology and related legal issues
[AD-A156650] N86-11078

LAYOUTS
COMPACT: Compaction of hierarchial chip layouts based on a constraint graph method with double-sided constraints N86-10845

LEAD (METAL)
Diffusion in immiscible melts N86-10096

LEAD ALLOYS
Particle coarsening in immiscible zinc-lead alloys under microgravity — Spacelab N86-10210
Cellular morphologies in lead-thallium alloys — gravitational effects N86-10262

LEAD OXIDES
Thermal expansion of glasses in the solid and liquid phases
[DE85-013953] N86-10351

LEAD TELLURIDES
Lead telluride crystals grown in microgravity: Experiment ES 318 — Spacelab N86-10220

LEADING EDGES
Three articles on new calculation methods in aeronautics (selected articles)
[AD-A145745] N86-10007
Numerical solution of hypersonic flow near leading edge of a flat plate N86-10008

LEAKAGE
Liquid to gas leak ratios with liquid nitrogen and liquid helium
[DE85-012950] N86-11030

LEARNING
NASA/American Society for Engineering Education (ASEE) Summer Faculty Fellowship Program, 1985
[NASA-CR-177972] N86-11064

LEAST SQUARES METHOD
Theoretical comparison of classical (K-matrix) and inverse (P-matrix) least-squares methods for quantitative infrared spectroscopy
[DE85-012827] N86-10298
Improved mapping of radio sources from VLBI data by least-square fit N86-10402
Radome analysis and design capabilities of the RF and Microwave Technology Branch
[AD-A156662] N86-10404
Rank revealing QR-Factorizations
[AD-A156756] N86-10887
The power of weighted and ordinary least squares with estimated unequal variances in experimental design
[B8562446] N86-10894
Regression analysis: Assumptions, alternatives, applications N86-10895

LEGENDRE FUNCTIONS
The h, p and h-p versions of the finite element method in dimension. Part 1: The error analysis of the p-version
[AD-A156600] N86-10882

LENSES
Time resolved flow velocity and concentration measurements using a travelling thermal lens
[AD-A156706] N86-10541

LEVITATION
Measurement of high temperature thermophysical properties N86-10074
Undercooling, remelting, and coarsening N86-10080
Role of convection in grain refining N86-10133
Modification of the electromagnetic levitator (EML) hardware N86-10172

LEVITATION MELTING
Multimode acoustic research N86-10167
Levitating furnance for containerless processing in space N86-10169
Containerless undercooling of Ni N86-10260

LIBRARIES
A systems development life cycle study of the information center
[AD-A156977] N86-11079

LIE GROUPS
Lie algebraic methods for charged particle beams and light optics N86-10970

LIFE (DURABILITY)
Compatibility of grain-stabilized platinum with candidate propellants for resistojets
[NASA-TM-87118] N86-10279
High temperature properties and characterization of S3-N4 materials
[BMFT-FB-T-85-046] N86-10352

LIFE CYCLE COSTS
Advanced vehicle systems assessment. Volume 3: Systems assessment
[NASA-CR-176206] N86-11084

LIFE SCIENCES

Life sciences research on the space station: An introduction
[NASA-TM-86836] N86-10734

USSR report: Life sciences. Biomedical and behavioral sciences
[JPRS-UBB-85-023] N86-10736

LIFT AUGMENTATION

Aerodynamics of hyperlift systems
[SNIAS-443.501/85] N86-10023

Analysis of hyperlift systems. Study of a singularities method
[SNIAS-443.529/84] N86-10024

LIFT DEVICES

Aerodynamics of hyperlift systems
[SNIAS-443.501/85] N86-10023

Analysis of hyperlift systems. Study of a singularities method
[SNIAS-443.529/84] N86-10024

LIGANDS

Cell partition in two polymer aqueous phases
N86-10139

LIGHT (VISIBLE RADIATION)

Optical/IR telescope arrays: A study of their potential for satisfying observational requirements in astronomy for a large aperture system in the 1990s and beyond
[REPT-15] N86-11094

LIGHT EMISSION

Photonic diagnostics and pulsed power research
[DE85-013752] N86-10940

LIGHT MODULATION

Extended precision in video bandwidth analog to digital converter using optical techniques
[AD-D011745] N86-10422

LIGHT SCATTERING

Light scattering tests of fundamental theories of transport properties in the critical region N86-10113

A study of the applicability of nucleation theory to quasi-thermodynamic transformations of second and higher Ehrenfest-order
[NASA-CR-176230] N86-11060

LIGHTNING

Electromagnetic resonances of cylinders and aircraft model with resistive wires
[NASA-CR-176250] N86-10042

Simulated direct-strike lightning testing at Sandia National Laboratories
[DE85-012033] N86-10049

LIMBS (ANATOMY)

Heat transfer mechanism in human extremities
N86-10759

LINE OF SIGHT

Mild hypoxia and visual performance with night vision goggles
[AD-A156969] N86-10787

LINEAR ACCELERATORS

RFQ-funneling
[DE85-012483] N86-10194

Klystron control software in the SIC
[DE85-013068] N86-10836

High-brightness photoemitter injector for electron accelerators
[DE85-012673] N86-10929

Beam-cavity interaction measurements in a DAW structure
[DE85-012660] N86-10987

Radiation field results from the SPEED triaxiode, a large area, high dose rate, short pulse 1MV bremsstrahlung source
[DE85-009438] N86-11005

High-resolution phosphor screen beam profile monitor
[DE85-013074] N86-11012

Beam steering in the SLC linac
[DE85-013370] N86-11025

Programmable delay unit incorporating a semi-custom integrated circuit
[DE85-013379] N86-11033

LINEAR EQUATIONS

Well-posed questions and exploration of the space of parameters in linear and non linear inversion
[PN-84/13] N86-10858

LINEAR FILTERS

Always-convergent iterative noise removal and deconvolution for image data
[NASA-CR-176223] N86-10824

LINEAR INTEGRATED CIRCUITS

Microcircuit device reliability field experience database. Volume 1. Field data. Volume 2. Failure Event/Analysis data
[AD-A156836] N86-10433

LINEAR SYSTEMS

Digital decoding of in-line holograms N86-10478

On the lanczos method for solving symmetric linear systems with several right-hand-sides
[AD-A156816] N86-10868

Multivariable partial realization and the aspect of uniqueness
[ER-83/09] N86-10879

Naive approximate realization of noisy data
[ER-83/10] N86-10880

LINEARITY

Finite deformation crack-line fields in a thin elasto-plastic sheet
[AD-A156757] N86-10346

Determination of symmetry and phase in human visual response functions: Theory and experiments
N86-10769

LINEARIZATION

A study of methods to predict and measure the transmission of sound through the walls of light aircraft. Integration of certain singular boundary element integrals for applications in linear acoustics
[NASA-CR-176229] N86-10912

LININGS

Explosive initiation by very small conical shaped charge jets
[DE85-009443] N86-10357

LIPSCHITZ CONDITION

Poisson semigroups and singular integrals
[CTH-MATH-1985-05] N86-10876

LIQUID COOLING

Renovated cooling at PIMU
[LINO-122] N86-10452

LIQUID CRYSTALS

Liquid crystal non-destructive inspection of metals
[AD-D011772] N86-10316

LIQUID FLOW

Capillary forces in a low gravity environment — Spacelab N86-10202

Some results of the Marangoni free convection experiment — Spacelab N86-10203

Oscillations of semi-free liquids in microgravity: Spacelab 1 experiment ES 326 N86-10204

Kinetics of spreading of liquids in microgravity: Experiment 1 ES 327 — Spacelab N86-10207

The influence of thermocapillarity on the migration of droplets in a liquid possessing a uniform temperature gradient N86-10237

Liquids and interfaces — Spacelab N86-10268

LIQUID FUELS

Ignition and flame spread above liquid fuel pools
N86-10163

LIQUID HELIUM

Liquid to gas leak ratios with liquid nitrogen and liquid helium
[DE85-012950] N86-11030

An investigation of vortex dynamics in 2-dimensional superfluid films of helium-4 N86-11040

Critical dynamics in superfluid helium N86-11046

LIQUID LASERS

Research on solar pumped liquid lasers
[NASA-CR-176235] N86-10539

LIQUID METAL FAST BREEDER REACTORS

Scoping studies of vapor behavior during a severe accident in a metal-fueling reactor
[DE85-011474] N86-10952

LIQUID METALS

Undercooling, remelting, and coarsening N86-10080

Measurement of the properties of tungsten at high temperatures N86-10091

Theoretical studies of the surface tension of liquid metal system N86-10101

Multimode acoustic research N86-10157

Development of a sheath for sensor protection in molten steel applications
[AD-A156764] N86-10315

LIQUID NITROGEN

Liquid to gas leak ratios with liquid nitrogen and liquid helium
[DE85-012950] N86-11030

LIQUID PHASE EPITAXY

Processing of complex compound semiconductors in space N86-10054

LIQUID PHASES

Mephisto: Interfacial destabilization in metal alloys
N86-10079

Liquid phase miscibility gap materials N86-10081

Diffusion in immiscible melts N86-10096

Verification of turbulence developing from the oscillatory Marangoni convection in a liquid column — rocket flight
N86-10241

Space shuttle experiments on Al-In liquid phase miscibility gap (LPMG) alloys N86-10264

First Spacelab Payload (FSLP) experiments on composite materials N86-10265

Thermal expansion of glasses in the solid and liquid phases
[DE85-013953] N86-10351

LIQUID SURFACES

Free surface phenomena under low- and zero-gravity conditions N86-10106

Suppression of Marangoni convection in float zones
N86-10111

Axisymmetric free surface behavior of moving liquid in a cylinder in microgravity — Spacelab N86-10206

LIQUID-LIQUID INTERFACES

The influence of thermocapillarity on the migration of droplets in a liquid possessing a uniform temperature gradient N86-10237

Rationale for two phase polymer system microgravity separation experiments N86-10247

Application of the theory of Ostwald ripening to microgravity phase separation experiments N86-10248

LIQUID-SOLID INTERFACES

Liquid phase miscibility gap materials N86-10081

Influence of melt convection on solid-liquid interface under terrestrial and reduced gravity environments
N86-10083

The development and prevention of channel segregation during alloy solidification N86-10086

Thermal and solutal convection damping using an applied magnetic field N86-10094

Liquid column stability: Experiment 1 ES-331 — Spacelab N86-10205

Stability of long liquid columns N86-10244

LIQUID-VAPOR INTERFACES

Experimental and theoretical studies of wetting and multilayer adsorption
[NASA ORDER H-27954B] N86-10121

Impurity extraction by droplets N86-10122

Holographic interferometry near gas/liquid critical points: Ground-based study of a D1 experiment — Spacelab
N86-10249

LIQUIDS

Dynamic thermophysical measurements in space
[NASA ORDER H-27954-B] N86-10106

Mass transport phenomena between bubbles and dissolved gases in liquids under reduced gravity conditions N86-10110

Light scattering tests of fundamental theories of transport properties in the critical region N86-10113

Surface tensions and their variations with temperature and impurities
[NASA ORDER H-27954B] N86-10115

Acoustic cavitation and bubble dynamics
[AD-A156888] N86-10916

LITHIUM

Advanced fuel cell development
[DE85-014550] N86-10659

LITHIUM OXIDES

Thermal expansion of glasses in the solid and liquid phases
[DE85-013953] N86-10351

High efficiency heat transport and power conversion system for cascade
[DE85-012959] N86-10468

LITHOLOGY

Remote stratigraphic and structural analysis: Multisensor results in the Wind River/Bighorn Basin area, Wyoming N86-10606

Lithologic mapping in a sedimentary environment using multipolarization SAR images N86-10624

Geologic evaluation and reservoir properties of the PR Spring tar sand deposit, Uintah and Grand Counties, Utah
[DE85-013248] N86-10634

LITHOSPHERE

Stratigraphy, petrology, depositional and post-depositional histories and their effects upon reservoir properties of the Parkman Formation of the Mesa Verde group, Powder River Basin, Wyoming N86-10691

Paleontology and stratigraphy of Lower Cambrian and upper Proterozoic sediments, Caborca region, northwestern Sonora, Mexico N86-10692

Geothermal influences on the long-term thickness of the mechanical lithosphere during flexure N86-10697

LOAD DISTRIBUTION (FORCES)

Stiffened and prestressed composite overwrapped pressure vessels N86-10547

LOADS (FORCES)

Mechanics of coated fiber composites N86-10285

Application of the unloading compliance methods in fracture toughness measurements of a quenched and tempered steel
[BLL-BISI-TRANS-21626-(9022.06)] N86-10306

Load-deflection tests and computer analyses of a high-precision adhesive-bonded antenna reflector panel
N86-10389

Termination load carrying device
[AD-D011800] N86-10556

Strength of shells under local transverse loads
N86-10566

Optimal design of portal frames against buckling
N86-10572

Effect of sequence of loading on interaction curves for buckling of stiffened shells
[TAE-536] N86-10583

LOGARITHMS
Arithmetic pipeline for image processing
[AD-D011773] N86-10800
LOGIC CIRCUITS
Minimization of programmable logic arrays
[EUT-84-E-145] N86-10803
A course on field programmable logic
[EUT-85-E-148] N86-10805
LOGIC DESIGN
Realization of a multifunction Input/Output (I/O) controller by means of a gate array
[EUT-85-E-147] N86-10804
A course on field programmable logic
[EUT-85-E-148] N86-10805
Compexity of higher-order programs
[DE85-012776] N86-10834
LOGIC PROGRAMMING
A course on field programmable logic
[EUT-85-E-148] N86-10805
LOGICAL ELEMENTS
Minimization of programmable logic arrays
[EUT-84-E-145] N86-10803
A course on field programmable logic
[EUT-85-E-148] N86-10805
LONG TERM EFFECTS
Evaluation and prediction of long-term environmental effects on non metallic materials
[NASA-CR-178495] N86-10340
LOOPS
Sample data phase locked loop for adaptive Doppler tracker
[AD-D011788] N86-10374
LOSSES
Geothermal lost circulation zone mapping tool
[DE85-008696] N86-10531
Surface conditioning of synchrotron radiation source to improve beam lifetime
[DE84-012185] N86-10948
Parasitic mode losses versus signal sensitivity in beam position monitors
[DE85-014367] N86-10964
The two micron spectrum of R Scuti N86-11092
LOW FREQUENCIES
The influence of low frequency mechanical vibrations on the growth of single crystals N86-10059
LOW GRAVITY MANUFACTURING
Effect of undercooling and modified microstructure on the physical properties of material synthesized in the drop tube and drop tower N86-10075
The influence of containerless undercooling and rapid solid-state quenching on the superconductive and magnetic properties of some clustering alloy systems
N86-10076
Liquid phase miscibility gap materials N86-10081
Orbital processing of aligned magnetic composites
N86-10089
Metallic foams N86-10095
Graphite formation in cast iron N86-10100
Containerless studies of nucleation and undercooling
N86-10102
Suppression of Marangoni convection in float zones
N86-10111
LOW PASS FILTERS
An active tracking band-pass filter
[AD-A156559] N86-10419
A study of derivative filters using the discrete Fourier transform
[NASA-CR-176224] N86-10825
LOW SPEED
Fundamental studies of low velocity impact resistance of graphite fiber reinforced polymer matrix composites
N86-10288
LOW SPEED WIND TUNNELS
Activities report of the German-Dutch wind tunnel
N86-10029
Activities report of the German-Dutch wind tunnel
N86-10052
LOW TEMPERATURE
Adsorption of oxygen on single crystal tin at liquid helium temperatures N86-11044
LOW TEMPERATURE ENVIRONMENTS
Effect of increased body clothing insulation on hand temperature in a cold environment
[AD-A156597] N86-10786
LOW VOLTAGE
Total internal reflection modulator/deflector
[AD-D011757] N86-10424
LUBRICANT TESTS
Trials on the asperity counting monitoring system --- helicopter gearboxes
[RES-PAPER-670] N86-10550
LUBRICANTS
Steady state frictional behavior of thin film coatings
N86-10335
LUBRICATION
Measurement of the density of base fluids at pressures 0.422 to 2.20 GPa
[NASA-TM-87114] N86-10551
LUMINANCE
Vision test chart and method using Gaussians
[AD-D011756] N86-10778
LUMINOSITY
Beam-beam deflections to measure size spot and offset at SLC IP
[DE85-014285] N86-10965
LUMINOUS INTENSITY
A simple method of obtaining concentration depth-profiles from X-ray diffraction
[NASA-CR-176262] N86-10310
Mild hypoxia and visual performance with night vision goggles
[AD-A156969] N86-10787
LUNAR BASES
A logistics scenario for an early lunar base
[ILR-MITT-143] N86-11140
LUNAR LOGISTICS
A logistics scenario for an early lunar base
[ILR-MITT-143] N86-11140
LYMPHOCYTES
Study of hypokinesia and acceleration effects on human chromosomes N86-10740

M

MACH-ZEHNDER INTERFEROMETERS
Advanced optical measurement techniques
N86-10174
Fiber optic gradient hydrophone construction and calibration for sea trial
[AD-A156469] N86-10914
MACHINERY
Sound radiation from repetitive transient vibrations using multi-channel digital signal processing with application to impact machinery N86-10910
MACHINING
The influence of the substrate on the practical machining applications of cutting edges coated with different materials
[BLL-RISLEY-TR-5039-(9091.9F)] N86-10546
MAGNET COILS
Improved particle-velocity transducer for equation-of-state experiments
[DE85-013204] N86-10532
MAGNETIC DIPOLES
Theoretical and numerical investigation of dipole radiation over a flat earth N86-10369
Tracking studies on the effects of magnet multipoles on the aperture of the RHIC heavy ion collider
[DE85-013282] N86-11023
MAGNETIC DISKS
The local disk controller
[REPT-1-68430-44(1985)01] N86-10806
Performance analysis of the IBM Direct Access Storage Device (DASD) subsystem, and some suggestions for improved systems
[REPT-1-68430-44(1985)02] N86-10807
An intelligent local disk control system
[REPT-051560-28(1984)08] N86-10808
MAGNETIC FIELD CONFIGURATIONS
Box method for finding intersections of a trajectory with axisymmetric flux surfaces
[DE85-013525] N86-10840
Evolution of the fusion power demonstration tandem mirror reactor configuration
[DE85-012889] N86-10960
Theoretical aspects of magnetic helicity
[DE85-011846] N86-10984
Increased particle confinement with the use of external dc bias field in the CTX spheromak
[DE85-012744] N86-10988
GA Theory News, January-March 1985
[DE85-012572] N86-11007
Generalized helicity and its time derivative
[DE85-012770] N86-11027
Equilibrium of the kink source experiment
[DE85-012764] N86-11029
MAGNETIC FIELD INVERSIONS
Theoretical aspects of magnetic helicity
[DE85-011846] N86-10984
MAGNETIC FIELDS
Thermal and solutal convection damping using an applied magnetic field N86-10094
Calibrated Faraday current and magnetic field sensor
[DE85-013438] N86-10439
Measurement and resulting first and second order approximations for a 9 deg bending magnet in LAMPF's 750-keV transport
[DE85-012891] N86-10930
Use of the MURA transformation to generate the fields and calculate the motion of protons in the designed Argonne Mini-ASPUN FFAG spiral sector accelerator
[DE85-011477] N86-10934
Two-dimensional electrons
[AD-A156894] N86-10982
US superconducting magnet data base assessment for INTOR
[DE85-013648] N86-11000
A study of the applicability of nucleation theory to quasi-thermodynamic transformations of second and higher Ehrenfest-order
[NASA-CR-176230] N86-11060
MAGNETIC FLUX
Box method for finding intersections of a trajectory with axisymmetric flux surfaces
[DE85-013525] N86-10840
Local drift parameter, j/n sub e and resistivity anomaly measurements in CTX spheromaks
[DE85-012740] N86-10998
MAGNETIC MATERIALS
Rapid solidification of magnetic oxides N86-10152
MAGNETIC MIRRORS
Conducting wall and pressure profile effect on MHD stabilization of axisymmetric mirror
[DE85-013647] N86-11020
Symmetric Tandem Mirror Program
[DE85-012352] N86-11032
MAGNETIC MOMENTS
Hyperon polarization: An unresolved problem
[DE85-012298] N86-10946
MAGNETIC PROPERTIES
Orbital processing of aligned magnetic composites
N86-10089
Electronic and magnetic properties of noble-metal and transition-metal alloys, interfaces and overlayers
[DE85-014532] N86-10321
Cryogenic structural materials for superconducting magnets
[DE85-008026] N86-10908
Topics in the electronic theory of disordered semiconductors N86-11045
Magnetic properties of doped semiconductors
[DE85-012090] N86-11053
MAGNETIC RECORDING
An evaluation of the use of microphone arrays for studio recording
[BBC-RD-1985/8] N86-10366
Specification for the performance, design, development and test requirements for a severe environment cartridge recorder. Issue 4
[AD-A156637] N86-10523
MAGNETIC SIGNALS
Amplitude and phase modulation in fin-lines electrical tuning
[AD-D011813] N86-10415
MAGNETOHYDRODYNAMIC FLOW
Velocities of gas and plasmas from real time holographic interograms
[DE85-014618] N86-10530
MAGNETOHYDRODYNAMICS
GA Theory News, January-March 1985
[DE85-012572] N86-11007
Conducting wall and pressure profile effect on MHD stabilization of axisymmetric mirror
[DE85-013647] N86-11020
MAGNETOMETERS
Calibrated Faraday current and magnetic field sensor
[DE85-013438] N86-10439
MAGNETORESISTIVITY
Two-dimensional electrons
[AD-A156894] N86-10982
MAGNETOSPHERE
Potential structures and particle acceleration on auroral field lines
[AD-A156694] N86-10708
Activities report in geophysics
[KGI-188] N86-10709
Solar flares and magnetospheric particles: Investigations based upon the ONR-602 experiment
[AD-A156583] N86-11142
MAGNETS
Ferrite kicker magnet for the IAMPF switchyard upgrade
[DE85-012657] N86-10896
MAINTENANCE
A modified repair strategy for two-component systems with revealed and unrevealed faults
[AD-A156715] N86-10835
MAN ENVIRONMENT INTERACTIONS
Adaptation of man to extreme conditions of Antarctica
N86-10751
Individual typological self-regulation of cardio-vascular system N86-10752

MANAGEMENT ANALYSIS
Management of organizational operations in dynamic environments. Towards a frame of reference.
[FOA-C5-85-0003-H2] N86-11072
MANAGEMENT METHODS
Management of organizational operations in dynamic environments. Towards a frame of reference.
[FOA-C5-85-0003-H2] N86-11072
Failures and successes of quantitative methods in management
[ARW-03-THE-BDK/ORS/83-06] N86-11076
MANAGEMENT PLANNING
Land evaluation successes with the metric camera — Spacelab N86-10512
Operations research applications
[ARW-03-THE-BDK/ORS/83-08] N86-10901
Management of organizational operations in dynamic environments. Towards a frame of reference.
[FOA-C5-85-0003-H2] N86-11072
On the structure of manpower planning, a contribution of simulation experiments with decomposition methods
[MANPOWER-PLANNING-28] N86-11073
Aspects of manpower planning at a Dutch university, an example of aggregation and decomposition methods in manpower planning
[MANPOWER-PLANNING-29] N86-11074
On the structure of manpower planning, a contribution of simulation experiments with aggregation methods
[MANPOWER-PLANNING-30] N86-11075
A systems development life cycle study of the information center
[AD-A156977] N86-11079
MANEUVERABILITY
Marginal terrain straddle-lift container handler
[AD-D011752] N86-10555
MANGANESE
Study of eutectic formation N86-10070
Theoretical problems in materials science N86-10088
Thermal and solutal convection damping using an applied magnetic field N86-10094
Advanced fuel cell development
[DE85-014550] N86-10659
MANIFOLDS (MATHEMATICS)
Estimates for maximal functions along hypersurfaces
[CTH-MATH-1984-29] N86-10874
A note on the differenciability of center manifolds
[ZW-8414] N86-10905
MANIPULATORS
Dynamic analysis of robotic manipulations with flexible links N86-10545
Supervisory control of the right arm of the beam assembly teleoperator
[AD-A156856] N86-10832
MANNED ORBITAL RESEARCH LABORATORIES
The first German Spacelab mission D1 reports — Spacelab payloads
[PR-3] N86-10189
The fluid physics module: A technical description — Spacelab N86-10201
MANNED SPACE FLIGHT
Manned flight simulation: Challenge and response
[NASA-TM-86827] N86-10048
A logistics scenario for an early lunar base
[ILR-MITT-143] N86-11140
MANPOWER
On the structure of manpower planning, a contribution of simulation experiments with decomposition methods
[MANPOWER-PLANNING-28] N86-11073
Aspects of manpower planning at a Dutch university, an example of aggregation and decomposition methods in manpower planning
[MANPOWER-PLANNING-29] N86-11074
On the structure of manpower planning, a contribution of simulation experiments with aggregation methods
[MANPOWER-PLANNING-30] N86-11075
MANUALS
User manual for the Falcon system — Falcon research aircraft
[DFVLR-MITT-85-08] N86-10721
The DUCK manual
[AD-A156936] N86-10833
The Netherlands Institute for Nuclear and High Energy Physics (NIKHEF) traveling wave monitor user guide
[LINO-121] N86-10969
MAPPING
Improved mapping of radio sources from VLBI data by least-square fit N86-10402
Maximum water reserves in the snow cover in the European territory of the USSR according to data for 1892-1960
[NASA-TM-77901] N86-10611
Geologic evaluation and reservoir properties of the PR Spring tar sand deposit, Uintah and Grand Counties, Utah
[DE85-013248] N86-10634
MARANGONI CONVECTION
Some results of the Marangoni free convection experiment — Spacelab N86-10203
Crystallization of a silicon sphere — Spacelab N86-10226
The TEXUS flight results on convective flows and heat transfer in simulated floating zones N86-10235
Numerical simulation of unsteady thermal Marangoni flows N86-10238
Numerical simulation of convections in the microgravity environment N86-10239
Verification of turbulence developing from the oscillatory Marangoni convection in a liquid column — rocket flight N86-10241
Measurements of the critical Marangoni number of the laminar-oscillatory transition of thermocapillary convection in floating zones N86-10242
Experimental study on Marangoni convection N86-10243
Rayleigh-Benard instability in systems presenting a minimum in surface tension N86-10245
MARINE ENVIRONMENTS
Evaluation of surface exchange coefficients from mildex ocean/atmosphere mixed layer data
[AD-A156765] N86-10729
MARINE TECHNOLOGY
LSRO/ONR ad hoc review process
[AD-A156590] N86-10735
MARKET RESEARCH
The air traffic demand in passenger travel of the Federal Republic of Germany 1990 - 2000. Update of the DFVLR air traffic forecast
[DFVLR-MITT-85-06] N86-10031
MARKOV PROCESSES
New probabilistic modeling and simulation methods for complex time-dependent systems
[DE85-009575] N86-10835
Multivariable partial realization and the aspect of uniqueness
[ER-83/09] N86-10879
Naive approximate realization of noisy data
[ER-83/10] N86-10880
MARS ATMOSPHERE
contemporary Aeolian processes on Mars: Local dust storms N86-11136
MASS DISTRIBUTION
Freezer model using a population balance approach for steady-state, direct-contact, secondary refrigerant, freeze desalination N86-10361
Representation of the distribution of the snow cover on the surface of the Earth's dry land
[NASA-TM-77909] N86-10612
Observations of the snow cover in the southern part of the Buryat Autonomous Soviet Socialist Republic
[NASA-TM-77910] N86-10613
Laws of distribution of the snow cover on the greater Caucasus (Soviet Union)
[NASA-TM-77911] N86-10614
MASS FLOW
The control of float zone interfaces by the use of selected boundary conditions N86-10060
The two micron spectrum of R Scuti N86-11092
MASS SPECTRA
Direct mass measurements in the light neutron-rich region using a combined energy and time-of-flight technique
[DE85-012758] N86-10963
Stellar s-process diagnostics
[DE85-012926] N86-11134
MASS TRANSFER
Solution growth of crystals in zero-gravity N86-10064
Modelling of laser-enhanced chemical vapor deposition N86-10105
Mass transport phenomena between bubbles and dissolved gases in liquids under reduced gravity conditions N86-10110
Fundamental studies of droplet combustion at reduced gravity N86-10165
Microphysical/mesoscale aspects of nuclear winter and new directions in assessments
[DE85-013479] N86-10718
MATERIALS HANDLING
Theoretical problems in materials science N86-10088
Development of materials processing systems for use in space on low-g simulation devices N86-10166
Microgravity Materials Science Laboratory N86-10173
Swelling and tensile properties of EBR-2-irradiated tantalum alloys for space reactor applications
[DE85-012887] N86-10329
Marginal terrain straddle-lift container handler
[AD-D011752] N86-10555
Hot cell facility design for large fusion devices
[DE85-012893] N86-11037
MATERIALS RECOVERY
Recovery of alcohol from a fermentation source by separation rather than distillation
[AD-D011782] N86-10282
MATHEMATICAL MODELS
Acta Aeronautica et Astronautica Sinica (selected articles)
[AD-A147304] N86-10001
A numerical solution of the shock-turbulent interaction over a compression corner for supersonic flow N86-10003
Impurity extraction by droplets N86-10122
Role of convection in grain refining N86-10133
Ignition and flame spread above liquid fuel pools N86-10163
Mathematical simulation of disturbing forces and material science processes under low gravity N86-10236
Dendritic solidification in a binary alloy melt: Steady-state versus morphological stability theories N86-10261
Nonlinear methods for spacecraft attitude maneuvers
[AD-A156956] N86-10275
The mechanics of delamination in composite materials N86-10284
Determination of thermophysical characteristics of solid materials by electrical modelling of the solutions to the inverse problems in nonsteady heat conduction
[NASA-TM-77907] N86-10293
Analysis of transitions between ferroelectric and antiferroelectric states under conditioning of uniaxial strain
[DE85-014468] N86-10350
Freezer model using a population balance approach for steady-state, direct-contact, secondary refrigerant, freeze desalination N86-10361
Radiative heat transfer in nonisothermal combustion products N86-10458
Analysis of annular two-phase flow with liquid entrainment N86-10459
Confined swirling jet predictions using a multiple-scale turbulence model
[NASA-CR-178484] N86-10462
Angle of incidence effects for underwater shock using generic computational models
[DE85-012936] N86-10466
Experiments with tubular probes made of INCOLOY 800 H under uniaxial and multiaxial strain
[JUEL-1979] N86-10595
Contribution of wind energy to the energy balance of a combined solar and wind energy system. Part 2: Computer-assisted investigations
[BMFT-FB-T-85-052-VOL-2] N86-10671
A numerical model for the estimation of solar radiation on rugged terrain N86-10694
Geothermal influences on the long-term thickness of the mechanical lithosphere during flexure N86-10697
Strength modeling report
[NASA-CR-171896] N86-10770
Applications for three-dimensional computer graphic cloud representations produced from satellite imagery
[AD-A156903] N86-10798
SUTRA (Saturated-unsaturated transport). A finite-element simulation model for saturated-unsaturated, Fluid-Density-Dependent ground-water flow with energy transport or chemically-reactive single-species solute transport
[AD-A156779] N86-10830
On maximal and distributional coupling
[CTH-MATH-1984-30] N86-10875
A modified repair strategy for two-component systems with revealed and unrevealed faults
[AD-A156715] N86-10885
Estimation by moments in a model of faulty inspection
[AD-A156754] N86-10886
Measurement and resulting first and second order approximations for a 9 deg bending magnet in LAMPF's 750-keV transport
[DE85-012691] N86-10930
Polarization transfer in inelastic scattering and pionic models of the EMC effect
[DE85-010738] N86-10955
Equilibrium of the kink source experiment
[DE85-012764] N86-11029
Experimental investigations of thermal radiation from potassium atoms and design applications
[DE85-004086] N86-11036
A method for numerical relativity: Simulation of axisymmetric gravitational collapse and gravitational radiation generation N86-11127
The dynamics and stellar content of globular star clusters N86-11131
Solar modulation of galactic cosmic rays: Techniques and applications N86-11143

MATHEMATICAL PROGRAMMING
Study of one- and two-dimensional filtering and deconvolution algorithms for a streaming array computer
[NASA-CR-176221] N86-10822
MATRICES (MATHEMATICS)
Theoretical comparison of classical (K-matrix) and inverse (P-matrix) least-squares methods for quantitative infrared spectroscopy
[DE85-012827] N86-10298
Coincidence densities and spectra of a class of substitution minimal sets N86-10857
Partial eigensolutions of large nonsymmetric matrices
[AD-A156711] N86-10867
Computing the structural index
[DE85-014370] N86-10871
Rank revealing QR-Factorizations
[AD-A156756] N86-10887
MATRIX THEORY
Variational estimates for the mass gap of SU(2) Euclidean lattice gauge theory
[NIKHEF-H/84-13] N86-10883
MAXIMUM LIKELIHOOD ESTIMATES
On the numerical determination of the dimension of an attractor — strange attractors
[ZW-8415] N86-10892
MAXWELL EQUATION
Geothermal influences on the long-term thickness of the mechanical lithosphere during flexure N86-10697
Electron momentum transfer collision frequency in N(2), O(2) and air
[AD-A157030] N86-10924
MEAN
Mean turbulence structure in strongly heating air flows N86-10455
Nonparametric comparison of several mean values with mild adaptation to some sample characteristics
[COMP-CENT-NOTE-20] N86-10891
MEASURE AND INTEGRATION
On the absolute continuity of elliptic measures
[CTH-MATH-1984-28] N86-10873
MEASURING INSTRUMENTS
High sensitivity millimeter-wave measurement apparatus
[AD-D011786] N86-10373
ELCAP instrumentation
[DE85-013042] N86-10527
Velocities of gas and plasmas from real time holographic interograms
[DE85-014618] N86-10530
Software for an automated gaging system
[DE85-013322] N86-10642
MECHANICAL DEVICES
Mathematical models of continuous flow electrophoresis N86-10143
MECHANICAL DRIVES
Termination load carrying device
[AD-D011800] N86-10558
MECHANICAL MEASUREMENT
Portevin-Le Chatelier effect. 1: Model for the type-E serrations
[DE85-006879] N86-10322
MECHANICAL PROPERTIES
Ultrasonic evaluation of mechanical properties of thick, multilayered, filament wound composites
[MASA-TM-87068] N86-10561
MECHANICAL SHOCK
The Shock and Vibration Digest, volume 17, no. 3
[AD-A154144] N86-10585
MEDICAL SCIENCE
USSR report: Life sciences. Biomedical and behavioral sciences
[JPRS-UBB-85-023] N86-10738
MEDICAL SERVICES
Annotated bibliography of publications dealing with occupational health and medical information systems, cost analysis procedures, evaluation methodology and related legal issues
[AD-A156650] N86-11078
MELTING
Undercooling, remelting, and coarsening N86-10080
Metallic foams N86-10095
Melting and solidification in O-g of sintered alloys: Experiments ES 311 A and B bubble reinforced materials — Spacelab N86-10215
Interdiffusion in the glass melt system (Na2O+Rb2O).3SiO2 — Spacelab N86-10216
Recirculation within a glass mixture subjected to external and resistive heating
[DE85-010068] N86-10348
Maximum water reserves in the snow cover in the European territory of the USSR according to data for 1892-1960
[NASA-TM-77901] N86-10611
MELTS (CRYSTAL GROWTH)
Growth of solid solution crystals N86-10065
Dendritic growth in undercooled melts N86-10082
Influence of melt convection on solid-liquid interface under terrestrial and reduced gravity environments N86-10083
Solidification fundamentals N86-10090
Containerless processing of undercooled melts N86-10093
Metallic foams N86-10095
Morphological stability and fluid dynamics of vapor crystal growth N86-10126
Bulk formation of metallic glasses and amorphous silicon from the melt N86-10154
Crystal growth of GaAs in space N86-10234
Dendritic solidification in a binary alloy melt: Steady-state versus morphological stability theories N86-10261
MEMBRANES
Streaming potentials in conductive and nonconductive tubing
[DE85-012984] N86-10438
Membrane research in energy and solvent recovery from industrial effluent streams
[DE85-014583] N86-10682
MEMORY (COMPUTERS)
Elektronika MS 1603 high-speed peripheral processor N86-10811
MENTAL PERFORMANCE
The effects of age, sleep deprivation, and altitude on complex performance
[AD-A156967] N86-10771
Derivational analogy: A theory of reconstructive problem solving and expertise acquisition
[AD-A156817] N86-10899
MERCURY (METAL)
Sediment characterization. Task 2: Instream contaminant study. Volume 2: Appendices
[DE85-013503] N86-10680
Sediment characterization. Task 2: Instream contaminant study, volume 1
[DE85-013502] N86-10683
MERCURY COMPOUNDS
Sensor system
[AD-D011767] N86-10480
Parallel pulse processing for mercuric iodide gamma-ray detectors
[DE85-013391] N86-10528
MESOSCALE PHENOMENA
The boundary condition in a numerical model of atmospheric flows over fixed interfaces
[GKSS-85-E-10] N86-10722
METABOLISM
Intradiurnial organization of wakefulness-sleep sequence and energy metabolism in rats exposed to low ambient temperature N86-10764
METAL BONDING
Metallurgy and metallography of braze joints
[DE85-014563] N86-10325
The preparation and testing of titanium and zirconium coupling agents
[SJ70] N86-10576
METAL COATINGS
The role of entrained surface oxides in RS-PM aluminum alloys on resultant structures and properties N86-10085
METAL CRYSTALS
Transport processes in directional solidification during space shuttle flight N86-10257
Stability of metallic dispersions — microgravity N86-10258
Surface science and catalysis
[DE85-013922] N86-11057
METAL FATIGUE
Fabrication and metallurgical properties of modified 9Cr-1 Mo steel
[DE85-012885] N86-10328
METAL FILMS
Photoionization technique for growth of metallic films
[AD-D011760] N86-10426
Thermodynamic constraints on ion beam mixing of metals on insulators
[DE85-013626] N86-10448
METAL FINISHING
Multipurpose pan development
[DE85-012326] N86-10319
METAL FOAMS
Metallic foams N86-10095
METAL MATRIX COMPOSITES
Melting and solidification of metal matrix composites under microgravity — Spacelab N86-10211
Preliminary reports, memoranda and technical notes of the Materials Research Council Summer Conference, La Jolla, California
[AD-A156776] N86-10291
METAL PARTICLES
Particle coarsening in immiscible zinc-lead alloys under microgravity — Spacelab N86-10210
METAL PLATES
Nondestructive control of thick structures made without disassembling
[PV-43-954/F/3] N86-10564
METAL PROPELLANTS
Compatibility of grain-stabilized platinum with candidate propellants for resistojets
[NASA-TM-87118] N86-10279
METAL SURFACES
Mechanism of the formation of boronised layers on high carbon steel
[BLL-BISI-TRANS-23036-(9022.06)] N86-10306
Boronising of iron and steel by ionic bombardment by diborane
[BLL-BISI-TRANS-23034-(9022.06)] N86-10307
Fuel and lubricant behavior in boundary layers analyzed by infrared emission Fourier transform spectrometry N86-10336
Surface science and catalysis
[DE85-013922] N86-11057
METAL-NITRIDE-OXIDE-SEMICONDUCTORS
The VLSI design of error-trellis syndrome decoding for convolutional codes N86-10391
METALLIC GLASSES
Crystallization, optical and chemical properties of fluoride glasses N86-10149
Bulk formation of metallic glasses and amorphous silicon from the melt N86-10154
Fusion target technology N86-10156
Oxidation behavior of glassy alloys N86-10158
Crystal nucleation and glass formation in metallic alloy melts N86-10233
Formation and characterization of amorphous erbium-based alloys prepared by near-isothermal cold-rolling of elemental composites
[DE85-014853] N86-10327
Elastic properties and thermal stability characterization of metallic glasses by guided wave techniques N86-10337
METALLIZING
Development of metallization process
[NASA-CR-176209] N86-10312
Investigation of metallic impurities introduced into SiO2 and silicon by various candidate VLSI metallization systems: Chemical reactions, diffusion, and electrical properties
[AD-A156609] N86-10429
The mechanism of erosion of metallic materials under cavitation attack
[NASA-TM-87133] N86-10552
METALLOGRAPHY
Fracture toughness of hydrogen-embrittled precipitation-hardened stainless steels
[AD-A156664] N86-10592
METALLURGY
First Spacelab Payload (FSLP) experiments in metallurgy N86-10266
Metallurgy and metallography of braze joints
[DE85-014563] N86-10325
METALS
Attachment method-ceramic radome to metal body
[AD-D011778] N86-10032
Microgravity Science and Applications Program tasks
[NASA-TM-87568] N86-10053
Undercooling, remelting, and coarsening N86-10080
Microgravity Materials Science Laboratory N86-10173
Weld metal hot-cracking of hastelloy alloys C-22 and C-276: A study by analytical electron microscopy
[DE85-009437] N86-10324
Research needs for corrosion control and prevention in energy conservation systems
[DE85-014852] N86-10326
Composite explosives for metal acceleration: The effect of detonation temperature
[DE85-013982] N86-10359
Thermodynamic constraints on ion beam mixing of metals on insulators
[DE85-013628] N86-10448
Finite element analysis of metals at elevated temperature using unified constitutive theories N86-10569
Preliminary investigation of changes in X-ray multilayer optics subjected to high radiation flux
[DE85-014074] N86-10944
Surface science and catalysis
[DE85-013922] N86-11057
METASTABLE STATE
High-pressure release-wave measurements and phase transformation in CaCO3
[DE85-012592] N86-11055
METEOROLOGICAL CHARTS
Monthly Bulletin North Sea: Volume 2, January 1985
[KNMI-167-VOL-2] N86-10732

METEOROLOGICAL FLIGHT

Comparative flight measurement of icing parameters for the propeller aircraft Do-28D2 of the test station 61 of the DFVLR and for the DFVLR aircraft Falon 20e in stratus clouds [DFVLR-FB-85-16] N86-10720

User manual for the Falcon system — Falcon research aircraft [DFVLR-MITT-85-08] N86-10721

METEOROLOGICAL INSTRUMENTS

Fall velocity indicator/viewer [AD-D011789] N86-10482

METEOROLOGICAL PARAMETERS

ELCAP instrumentation [DE85-013042] N86-10527

Surface winds at NWC (Naval Weapons Center): 1964 - 1982 [AD-A156660] N86-10712

Monthly Bulletin North Sea: Volume 2, January 1985 [KNMI-167-VOL-2] N86-10732

METEOROLOGICAL SERVICES

List of publications on the 200 m meteorological mast at Cabauw, the Netherlands [KNMI-FM-85-6] N86-10711

METHANE

Flammability limits of gases under low gravity conditions N86-10164

Design and calibration of a flat-flame burner using line reversal techniques [AD-A156724] N86-10294

Catalytic activity of shock modified ZnO for CO oxidation and methanol synthesis [DE85-014704] N86-10300

Methane-bubble formation in hydrogen-charged Fe-30 ppM C [DE85-012526] N86-10937

METHOD OF CHARACTERISTICS

On the method of characteristics and its application to the calculations of annular nozzle flowfields N86-10454

METHOD OF MOMENTS

A transformation method for the evaluation of the response moments of elastic structures with random properties [AD-A156882] N86-10557

METRIC PHOTOGRAPHY

Metric Camera Workshop — Spacelab [ESA-SP-209] N86-10485

Digital elevation model from Spacelab metric camera photographs N86-10486

Orthophotomapping from metric camera imagery — Spacelab N86-10487

Restitution of Spacelab photography by analog stereoplotter N86-10489

Evaluation of the accuracy of the metric camera images for the production of line maps and orthophotos N86-10490

Photomapping in different climatic zones — Spacelab metric camera N86-10491

A geological structural analysis of the southeastern Zagros (Iran) ranges based on metric camera photos N86-10492

Erosion control and watershed management by Spacelab photography N86-10493

High-resolution image data from the Space Shuttle N86-10494

Evaluation of metric camera images at the University of London — Spacelab N86-10495

Partial in-flight calibration of the metric camera — Spacelab N86-10496

Identification of planimetric features from the metric camera — Spacelab N86-10497

Analysis of metric camera images from the USA and their suitability for topographic and thematic mapping — Spacelab N86-10498

Long range translocations ashore to offshore using Spacelab-1 metric camera imagery in the perspective of integrated geophysical surveys N86-10499

Line mapping and resolution tests with metric camera data — Spacelab N86-10500

Role of the Economic Commission for Africa as a principal investigator in the metric camera experiment and reports of the result of the assessment for topographic and revision of maps in populated and developed areas of the world N86-10501

The role of very small scale metric images in modern geology — Spacelab metric camera N86-10502

Geological mapping of remote mountainous regions using metric camera imagery — Spacelab N86-10503

Interpretation of metric camera concerning hydrologic structures of the Rhone Delta — Spacelab N86-10504

Test on mapping application of metric camera imagery — Spacelab N86-10505

Status of preparation activities for metric camera reflight on EOM-1/2 N86-10506

OEEPE participation in testing metric camera photography — European Organization for Experimental Photogrammetric Investigations (OEEPE) N86-10507

Topographic interpretation of metric camera images: An example in Somalia — Spacelab N86-10508

Thematic investigations in France based on metric camera imagery — Spacelab N86-10509

Thematic mapping of metric camera color infrared and black and white photographs for land use classification N86-10510

Digital image processing of metric camera imagery — Spacelab N86-10511

Land evaluation successes with the metric camera — Spacelab N86-10512

Requirements and possibilities of Spacelab metric camera photos usage for inventories of large areas of extensively managed forests N86-10513

Evaluation of metric camera photos — Spacelab; alpine snow cover N86-10515

Creation of Ground Control Points (GCP) library using ESA Spacelab metric camera imagery — ground control point (gcp) N86-10516

Updating of topographic maps by means of metric camera photos example: Hallertau (Bavaria) N86-10517

Interpretation of Spacelab-1 photographs for the generation of 1:200000 topographic map N86-10518

Metric camera image of Munich as additional means for urban cartography — Spacelab N86-10519

An example of single model orientation of metric camera stereophotographs — Spacelab N86-10520

Tectonic analysis of typical fold structures in the Zagros Mountains (Iran) by the application of quantitative photogrammetric methods on metric camera data — Spacelab N86-10521

Test results using metric camera photography for 1:250,000 mapping — Spacelab N86-10522

METRIC SPACE

Gravitational collapse of a scalar field N86-11129

MICHELSON INTERFEROMETERS

Colloquium on Kilometric Optical Arrays in Space [ESA-SP-226] N86-11096

Results and limitations of ground-based optical arrays — stellar interferometry N86-11097

Extragalactic observations with optical space arrays N86-11098

Astronomical criteria for interferometric arrays — Spacecraft design N86-11099

TRIO: A kilometric array stabilized by solar sails — Spaceborne astronomy N86-11102

SAMSI: An orbiting spatial interferometer for micro-arc second astronomical observations — Spacecraft Array for Michelson Spatial Interferometry (SAMSI) N86-11103

COSMIC: A high resolution, large collecting area telescope — Coherent Optical System of Modular Imaging Collectors (COSMIC) N86-11104

TRIO optics — spaceborne optical interferometer (TRIO) N86-11106

Solar propulsion for the TRIO interferometer N86-11109

Preliminary studies of a spinning tether-connected TRIO concept — spaceborne interferometer (TRIO) N86-11110

TRIO interferometer positioning — spaceborne interferometers (TRIO) N86-11111

Fringe drift compensation in computer memory — Michelson interferometry N86-11112

TRIANGLE: A different design for a three satellite interferometer in space N86-11113

Mission analysis aspects — spaceborne interferometry N86-11114

Problems in image reconstruction with optical arrays — spaceborne astronomy N86-11115

Numerical experiments in image reconstruction — stellar interferometry N86-11116

On line astronomical image processing using microcomputers N86-11121

The DUO: Far infrared heterodyne concept for space interferometry N86-11125

VLBI at optical and radio wavelengths: Congruences and contrasts N86-11126

MICROBIOLOGY

Biotechnology: Science and practice N86-10742

MICROCOMPUTERS

Radar system description N86-10616

Microcomputer aided calculations of parameters for spray dryer operation [DE85-013468] N86-10681

Computer-based training for the US Coast Guard standard terminal microcomputer: A basis for implementation utilizing the elaboration theory of instructional design [AD-A156548] N86-10791

Development of IS2100: An information systems laboratory [AD-A156846] N86-10797

Dissecting the cow [DE85-013369] N86-10801

Klystron control software in the SIC [DE85-013068] N86-10836

Software for an automated gaging system [DE85-013322] N86-10842

A systems development life cycle study of the information center [AD-A156977] N86-11079

On line astronomical image processing using microcomputers N86-11121

MICROELECTRONICS

Microcircuit device reliability field experience database. Volume 1. Field data. Volume 2. Failure Event/Analysis data [AD-A156836] N86-10433

Prospects for creation of optical digital high-performance computers N86-10810

MICROORGANISMS

Development and evaluation of multispecies test protocols for assessing chemical toxicity [DE85-013526] N86-10679

Biotechnology: Science and practice N86-10742

MICROPHONES

An evaluation of the use of microphone arrays for studio recording [BBC-RD-1985/8] N86-10366

Measurements of the acoustic interference between adjacent microphones [AD-A156892] N86-10919

MICROPROCESSORS

Periodic binary sequences with very good autocorrelation properties N86-10397

Souden 2 data acquisition and trigger electronics [DE85-013664] N86-10443

ELCAP instrumentation [DE85-013042] N86-10527

Digital control of the hydraulic actuators of an adaptive suspension vehicle N86-10548

Parallel local interface bus [AD-D011742] N86-10792

USSR report: Cybernetics, computers and automation technology [JPRS-UCC-85-006] N86-10809

Elektronika MS 1603 high-speed peripheral processor N86-10811

Diagnostics of peripheral processors and controllers N86-10812

An approach to implementing CAMAC microprocessor modules N86-10813

MICROSCOPY

Advanced optical measurement techniques N86-10174

MICROSTRIP TRANSMISSION LINES

A dual frequency microstrip antenna for Ka band [NASA-TM-87124] N86-10380

MICROSTRUCTURE

Study of eutectic formation N86-10070

Modeling directional solidification N86-10071

Effect of undercooling and modified microstructure on the physical properties of material synthesized in the drop tube and drop tower N86-10075

The influence of containerless undercooling and rapid solid-state quenching on the superconductive and magnetic properties of some clustering alloy systems N86-10076

Liquid phase miscibility gap materials N86-10081

Control of cast iron microstructure N86-10084

The role of entrained surface oxides in RS-PM aluminum alloys on resultant structures and properties N86-10085

The development and prevention of channel segregation during alloy solidification N86-10086

Environmental degradation of materials: Surface chemistry related to stress corrosion cracking N86-10099

Rapid solidification of magnetic oxides N86-10152

Sol-gel glasses N86-10153

Acoustic levitation containerless processing N86-10177

Progressive damage, fracture predictions and post mortem correlations for fiber composites [NASA-TM-87101] N86-10290

Fabrication and metallurgical properties of modified 9Cr-1 Mo steel [DE85-012885] N86-10328

Aluminum ion plating for corrosion protection of uranium, revision 1 [DE85-012419] N86-10330

Theoretical analysis of Wolter/LSM X-ray telescope systems [NASA-CR-176244] N86-11095

MICROWAVE ANTENNAS

A new 70-meter antenna quadripod with reduced RF blockage N86-10365

MICROWAVE EQUIPMENT
Miniature radar packaging
[DE85-014596] N86-10410
MICROWAVE TRANSMISSION
Radome analysis and design capabilities of the RF and Microwave Technology Branch
[AD-A156662] N86-10404
MICROWAVES
Microwave evaluation of materials
[DE85-013183] N86-10409
Potential applications of multipolarization SAR for pine plantation biomass estimation N86-10626
Compact torus compression of microwaves
[DE85-012919] N86-11016
MIGRATION
The influence of thermocapillarity on the migration of droplets in a liquid possessing a uniform temperature gradient N86-10237
MILITARY PSYCHOLOGY
Standardization of tasks: Approach planning --- human performance assessment
[IZF-1984-19] N86-10782
MILITARY TECHNOLOGY
USSR report: Life sciences. Biomedical and behavioral sciences
[JPRS-UBB-85-023] N86-10738
Information technique 1985: Optical technology and electro-optics, a defense technical component review
[FOA-A-30037-E] N86-10960
MILLIMETER WAVES
High sensitivity millimeter-wave measurement apparatus
[AD-D011786] N86-10373
A superconducting tunnel junction receiver for millimeter-wave astronomy N86-11041
MINERAL DEPOSITS
Remote stratigraphic and structural analysis: Multisensor results in the Wind River/Bighorn Basin area, Wyoming N86-10606
MINERAL OILS
The mechanism of erosion of metallic materials under cavitation attack
[NASA-TM-87133] N86-10552
MINES (EXCAVATIONS)
Kinetics of biological ferrous iron oxidation
[DE85-014616] N86-10736
MINICOMPUTERS
Compact, high-speed algorithm for laying out printed circuit board runs N86-10814
MINKOWSKI SPACE
Gravitational collapse of a scalar field N86-11129
MIRAGE AIRCRAFT
Report on an overseas visit
[AD-A156603] N86-10037
MIRROR FUSION
Evolution of the fusion power demonstration tandem mirror reactor configuration
[DE85-012889] N86-10960
Application of structural-mechanics methods to the design of large tandem-mirror fusion devices (MFTF-B)
[DE85-008960] N86-11017
MIRRORS
Identification of chemical and physical phenomena affecting the durability of silvered polymer (PMMA) mirrors
[DE85-012131] N86-10645
Optical/IR telescope arrays: A study of their potential for satisfying observational requirements in astronomy for a large aperture system in the 1990s and beyond
[REPT-15] N86-11094
Theoretical analysis of Wolter/LSM X-ray telescope systems
[NASA-CR-176244] N86-11095
MISSION PLANNING
A comparative analysis of a CV helicopter and a JVX (Joint Services Advanced Vertical Lift) tilt-rotor aircraft in an aircraft carrier based ASW (Anti-Submarine Warfare)
[AD-A156871] N86-10041
The first German Spacelab mission D1 reports --- Spacelab payloads
[PR-1] N86-10187
Status of preparation activities for metric camera reflight on EOM-1/2 N86-10506
Mission analysis aspects --- spaceborne interferometry N86-11114
Galileo: Exploration of Jupiter's system
[NASA-SP-479] N86-11137
MISSOURI
Analysis of remote sensing data N86-10605
MIXING
The influence of low frequency mechanical vibrations on the growth of single crystals N86-10059
Particle cloud combustion experiment N86-10160
Recirculation within a glass mixture subjected to external and resistive heating
[DE85-010068] N86-10348
Thermodynamic constraints on ion beam mixing of metals on insulators
[DE85-013626] N86-10448
MIXTURES
Effects of scale and geometry on hydrogen-air detonations
[DE85-006762] N86-10474
MODELS
Thermocapillary motion research N86-10125
Electrohydrodynamics N86-10130
Experimental and theoretical analysis of chemical vapor deposition with prediction of gravity effects N86-10132
Theoretical modeling of the vapor cavitation in dynamically loaded journal bearings
[NASA-TM-87076] N86-10463
Constitutive modeling for isotropic materials (HOST)
[NASA-CR-174980] N86-10589
Evaluation of surface exchange coefficients from mildex ocean/atmosphere mixed layer data
[AD-A156765] N86-10729
TEMPUS: Simulating personnel and tasks in a 3-D environment
[NASA-CR-171901] N86-10785
Optimal control modeling of lower extremity musculoskeletal motion N86-10853
New approach to multiphase equilibria: Application to high-pressure physics problems
[DE85-013820] N86-10907
MODEMS
A nanosecond or thirty centimeters: Why atomic clocks have to be synchronized. MITREX opens new dimensions for measuring accuracy N86-10185
MODULARITY
Realization of a multifunction Input/Output (I/O) controller by means of a gate array
[EUT-85-E-147] N86-10804
MODULATION
Solar modulation of galactic cosmic rays: Techniques and applications N86-11143
MODULATORS
Total internal reflection modulator/deflector
[AD-D011757] N86-10424
MODULES
An approach to implementing CAMAC microprocessor modules N86-10813
MOISTURE CONTENT
Microwave evaluation of materials
[DE85-013183] N86-10409
MOLDING MATERIALS
Automatic processing of reactive polymers N86-10127
MOLECULAR BIOLOGY
LSRO/ONR ad hoc review process
[AD-A156590] N86-10735
MOLECULAR CLOUDS
A superconducting tunnel junction receiver for millimeter-wave astronomy N86-11041
MOLECULAR SPECTRA
The two micron spectrum of R Scuti N86-11092
MOLECULAR STRUCTURE
Synthesis of arylene siloxanylene polymers and copolymers
[AD-D011780] N86-10338
MOLECULAR WEIGHT
Polyacetylene polymerization, structure, and electrical transport properties N86-10334
Automated analysis of digital images generated by two-dimensional gel electrophoresis
[DE85-011906] N86-10526
MOLECULES
Theory of dense molecular fluid equations of state with application to detonation products
[DE84-016822] N86-10927
MOLTEN SALT ELECTROLYTES
Metals electroprocessing in molten salts N86-10098
MOLTEN SALTS
Crystal growth from solution --- Spacelab N86-10229
MOLYBDENUM
Rapid evaluation of ion thruster lifetime using optical emission spectroscopy
[NASA-TM-87103] N86-10280
Development of metallization process
[NASA-CR-176209] N86-10312
The mechanism of erosion of metallic materials under cavitation attack
[NASA-TM-87133] N86-10552
MOLYBDENUM ALLOYS
Fabrication and metallurgical properties of modified 9Cr-1 Mo steel
[DE85-012885] N86-10328
MOMENTUM TRANSFER
Electron momentum transfer collision frequency in N(2), O(2) and air
[AD-A157030] N86-10924
MONITORS
Specification for the performance, design, development and test requirements for a severe environment cartridge recorder. Issue 4
[AD-A156637] N86-10523
Captive volume device as a safe life monitor
[AD-D011802] N86-10525
TV monitoring control system in electrophysiological studies N86-10765
Providing automated control for PBFA-2
[DE85-012867] N86-10928
Wide dynamic range beam profile monitor
[DE85-012709] N86-10950
Advances in data acquisition system technology for PBFA 2
[DE85-012860] N86-11011
High-resolution phosphor screen beam profile monitor
[DE85-013074] N86-11012
MONOTECTIC ALLOYS
Studies of model immiscible systems N86-10112
Influences affecting separation in monotectic alloys under microgravity N86-10209
Particle coarsening in immiscible zinc-lead alloys under microgravity --- Spacelab N86-10210
MONOTONE FUNCTIONS
Strength of shells under local transverse loads N86-10568
MONTE CARLO METHOD
Time-implicity simulation of particle-fluid systems
[DE85-012944] N86-10471
New probabilistic modeling and simulation methods for complex time-dependent systems
[DE85-009575] N86-10835
Superefficient estimation of power functions in simulation experiments
[B8562445] N86-10893
MOON
Photographic catalog of selected planetary size comparisons
[NASA-TM-86207] N86-11138
MORPHOLOGY
Morphological stability and fluid dynamics of vapor crystal growth N86-10126
Dendritic solidification in a binary alloy melt: Steady-state versus morphological stability theories N86-10261
MOTION SICKNESS
Dynamics of changes of statistical indicators of heart rhythm of persons with different degree of motion sickness N86-10743
MOTION SIMULATORS
Motion analysis report
[NASA-CR-171897] N86-10896
Zero-gravity movement studies
[NASA-CR-171899] N86-10897
MOUNTAINS
A geological structural analysis of the southeastern Zagros (Iran) ranges based on metric camera photos N86-10492
Geological mapping of remote mountainous regions using metric camera imagery --- Spacelab N86-10503
Tectonic analysis of typical fold structures in the Zagros Mountains (Iran) by the application of quantitative photogrammetric methods on metric camera data --- Spacelab N86-10521
MUFFLERS
The Shock and Vibration Digest, volume 17, no. 3
[AD-A154144] N86-10585
Recent advances in the analysis of exhaust mufflers N86-10587
MULTIPLEXING
Wide dynamic range beam profile monitor
[DE85-012709] N86-10950
MULTIPROCESSING (COMPUTERS)
Alternating direction methods on multiprocessors: An extended abstract
[AD-A156722] N86-10794
Efficient systolic arrays for the solution of toeplitz systems: An illustration of a methodology for the construction of systolic architectures in VLSI (Very Large Systems Integration)
[AD-A156767] N86-10795
Fault-free behavior of reliable multiprocessor systems: FTMP experiments in AIRLAB
[NASA-CR-177967] N86-10848
Topological properties of hypercubes
[AD-A156777] N86-10850
MULTISPECTRAL BAND SCANNERS
Multisensor data integration techniques N86-10604
Lithologic mapping in a sedimentary environment using multipolarization SAR images N86-10624
Calibration of the multispectral scanner (MSS) satellite data to evaluate change in the reflection of coniferous stocks
[DFVLR-FB-84-44] N86-10636

MULTIVARIATE STATISTICAL ANALYSIS

Theoretical comparison of classical (K-matrix) and inverse (P-matrix) least-squares methods for quantitative infrared spectroscopy
[DE85-012827] N86-10298

MUON SPIN ROTATION

Polarization transfer in inelastic scattering and pionic models of the EMC effect
[DE85-010738] N86-10955

MUSCLES

Strength modeling report
[NASA-CR-171896] N86-10770

MUSCULAR FUNCTION

Assessment of state of chronotropic and inotropic heart function at different degrees of physical fitness
N86-10746

Heat transfer mechanism in human extremities
N86-10759

Strength modeling report
[NASA-CR-171896] N86-10770

MUSCULAR STRENGTH

Efficiency of muscular work in white rats during adaptation to cold N86-10763

Strength modeling report
[NASA-CR-171896] N86-10770

MUSCULOSKELETAL SYSTEM

Optimal control modeling of lower extremity musculoskeletal motion N86-10853

MUTAGENS

Somatic cell and molecular genetics approach to DNA repair and mutagenesis
[DE85-014181] N86-107[illegible]7

MYOCARDIUM

Classification of changes in electrocardiogram during muscular exertion of healthy individuals N86-10755

N

N-TYPE SEMICONDUCTORS

W-shaped diffused stripe GaAs/AlGaAs laser
[AD-D011818] N86-10538

NASA PROGRAMS

NASA/American Society for Engineering Education (ASEE) Summer Faculty Fellowship Program, 1985
[NASA-CR-177972] N86-11064

NATURAL GAS

Analyses of advanced residential aboerption heat pump cycles
[DE85-005244] N86-10664

NAVIER-STOKES EQUATION

Numerical solution of hypersonic flow near leading edge of a flat plate N86-10008

Numerical procedure for three-dimensional hypersonic viscous flow over aerobrake configuration
[NASA-TM-58269] N86-10018

Numerical simulation of unsteady thermal Marangoni flows N86-10238

Finite element solution of the Navier-Stokes equations for 3-D turbulent free shear flows N86-10457

NEODYMIUM

Research on solar pumped liquid lasers
[NASA-CR-176235] N86-10539

NEODYMIUM LASERS

Design, fabricate and test a 1.06(MU) repetitively pulsed laser
[DE85-014439] N86-10543

NEON

Dynamics of imploding neon gas puff plasmas. 1
[AD-A158916] N86-10983

NEON ISOTOPES

Direct mass measurements in the light neutron-rich region using a combined energy and time-of-flight technique
[DE85-012758] N86-10963

NEPTUNE (PLANET)

Planning for VLA/DSN arrayed support to the Voyager at Neptune N86-10395

A VLA experiment: Planning for Voyager at Neptune
N86-10396

NERVOUS SYSTEM

Eye-movement activity as index of functional state of brain N86-10756

NETHERLANDS

Wind energy in agriculture, a promise
[SS-45] N86-10672

Wind energy, a feasibility investigation for wind mills in agriculture
[SS-45A] N86-10673

Activities report of the Space Flight Laboratory
N86-11090

Activities Report of the Space Flight Laboratory
N86-11091

NETWORK ANALYSIS

LANES 1 Users' Guide
[NASA-CR-177334] N86-10819

NETWORK SYNTHESIS

Spectral methods in adapted curved grids
N86-10878

NEUTRAL BEAMS

Report on the engineering test of the LBL 30 second neutral beam source for the MFTF-B project
[DE85-013317] N86-10962

Noninterceptive techniques for the measurement of longitudinal parameters for intense H(-) beams
[DE85-012662] N86-10992

NEUTRAL GASES

Cometary atmospheres: Modeling the spatial distribution of observed neutral radicals
[NASA-CR-176242] N86-11133

NEUTRINOS

Matter-antimatter transition operators: A manual for modeling N86-10921

Search for heavy neutrines produced in e(+)e(-) annihilation
[DE85-013372] N86-11035

NEUTRON BEAMS

Initial increase, peaking effect, in the internal friction of copper following pulsed neutron and electron irradiation
[DE85-012767] N86-10932

NEUTRON IRRADIATION

Anelastic relaxation in irradiated Cu-Be
[DE85-013893] N86-11056

NEUTRON SOURCES

Use of the MURA transformation to generate the fields and calculate the motion of protons in the designed Argonne Mini-ASPUN FFAG spiral sector accelerator
[DE85-011477] N86-10934

Performance of the H(-) ion source for the intense pulsed neutron source
[DE85-012368] N86-10991

Beginnings of remote handling at the RAL Spallation Neutron Source
[DE85-012681] N86-11001

NEUTRON SPECTRA

Determining a physically appropriate neutron spectrum from multisphere data
[DE85-013045] N86-10299

The development of a neutron evaporation theory code for the thermal fission of Uranium-235
[AD-A156593] N86-10951

NEUTRON SPECTROMETERS

Determining a physically appropriate neutron spectrum from multisphere data
[DE85-013045] N86-10299

NEUTRONS

The development of a neutron evaporation theory code for the thermal fission of Uranium-235
[AD-A156593] N86-10951

Development and application of the electrochemical etching technique
[DE85-010302] N86-10957

Photoactivation of PBFA-2
[DE85-013439] N86-11019

NEW MEXICO

Remote stratigraphic and structural analysis: Multisensor results in the Wind River/Bighorn Basin area, Wyoming N86-10606

NICKEL

Physical and chemical properties of a nickel catalyst processed under microgravity — STS-7 N86-10255

Containerless undercooling of Ni N86-10260

NICKEL ALLOYS

Undercooling, remelting, and coarsening N86-10080

Small cartridge heater
[AD-D011784] N86-10277

Electronic and magnetic properties of noble-metal and transition-metal alloys, interfaces and overlayers
[DE85-014532] N86-10321

Formation and characterization of amorphous erbium-based alloys prepared by near-isothermal cold-rolling of elemental composites
[DE85-014853] N86-10327

Metastable phase formation in Ni-implanted Al: An analytical electron microscope investigation
[DE85-009105] N86-10331

NICKEL CADMIUM BATTERIES

Nickel-cadmium battery conditioner and tester apparatus
[AD-D011770] N86-10642

NIGHT VISION

Mild hypoxia and visual performance with night vision goggles
[AD-A156969] N86-10787

NITRIC OXIDE

Emissions of NOx, SOx and VOC from Antropogenic sources
[PB85-193530] N86-10688

NITRIDES

Continuous fiberization of silicon-carbide-nitride precursor resin N86-10168

NITRO COMPOUNDS

Development of new ammonium nitrate composite explosives
[DE85-014252] N86-10356

Composite explosives for metal acceleration: The effect of detonation temperature
[DE85-013982] N86-10359

NITROGEN

Membrane research in energy and solvent recovery from industrial effluent streams
[DE85-014583] N86-10682

NITROGUANIDINE

Properties of plastic-bonded nitroguanidine
[DE85-015316] N86-10358

NOISE POLLUTION

Recent advances in the analysis of exhaust mufflers
N86-10587

NOISE PREDICTION

Recent advances in the analysis of exhaust mufflers
N86-10587

NOISE PREDICTION (AIRCRAFT)

Summary of work on jet noise prediction
[ESDU-BR-62636] N86-10909

NOISE PROPAGATION

A study of derivative filters using the discrete Fourier transform
[NASA-CR-176224] N86-10825

NOISE REDUCTION

A study of Morrison's iterative noise removal method
[NASA-CR-176222] N86-10823

Always-convergent iterative noise removal and deconvolution for image data
[NASA-CR-176223] N86-10824

A study of derivative filters using the discrete Fourier transform
[NASA-CR-176224] N86-10825

A superconducting tunnel junction receiver for millimeter-wave astronomy N86-11041

NONDESTRUCTIVE TESTS

Report on an overseas visit
[AD-A156603] N86-10037

Liquid crystal non-destructive inspection of metals
[AD-D011772] N86-10316

Nondestructive control of thick structures made without disassembling
[PV-43-954/F/3] N86-10564

Study of statis and dynamic stress effects in nonlinear solids
[NASA-CR-176236] N86-10578

Nondestructive corrosion test of aluminum alloy structures
[PV-43-954/F/2] N86-10594

Exploratory development for a high reliability flaw characterization module
[AD-A156632] N86-10916

NONFERROUS METALS

Liquid crystal non-destructive inspection of metals
[AD-D011772] N86-10316

NONISOTHERMAL PROCESSES

Analysis of large, non-isothermal elastic-visco-plastic deformations
[NASA-CR-176220] N86-10588

NONLINEAR EQUATIONS

Topics in nonlinear wave theory with applications
N86-10367

Three-dimensional vibration analysis of a uniform beam with offset inertial masses at the ends
[NASA-TM-86393] N86-10580

Well-posed questions and exploration of the space of parameters in linear and non linear inversion
[PN-84/13] N86-10858

A modified modified Korteweg-deVries equation
[PN-84/27] N86-10859

NONLINEAR EVOLUTION EQUATIONS

On the absolute continuity of elliptic measures
[CTH-MATH-1984-28] N86-10673

NONLINEAR FILTERS

Computational techniques for the analysis and design of digital communication systems
[AD-A156945] N86-10407

NONLINEAR SYSTEMS

Control concepts for in-flight simulation including actuator nonlinearities and time delays
[DFVLR-FB-85-24] N86-10047

Modeling and control of nonlinear systems
N86-10362

Large eddy interactions in a turbulent channel flow
[NASA-TM-86757] N86-10464

Constitutive modeling for isotropic materials (HOST)
[NASA-CR-174980] N86-10589

Superconvergent tracking and invariant surfaces in phase space
[DE85-013051] N86-10995

NONLINEARITY

A study of the aerodynamic performance of Weis-Fogh wings N86-10012

Nonlinear methods for spacecraft attitude maneuvers
[AD-A156956] N86-10275

Nonlinear propagation of elastoplastic waves in Ke penetrators (excerpts)
[DE85-011450] N86-10318

Topics in nonlinear wave theory with applications
N86-10367

An analytical and numerical study of the buckling behavior of fiber-reinforced beams N86-10566

Load space formulation of reliability for nonlinear random structural systems N86-10570

Analysis of large, non-isothermal elastic-visco-plastic deformations
[NASA-CR-176220] N86-10588

Always-convergent iterative noise removal and deconvolution for image data
[NASA-CR-176223] N86-10824

Advanced development of BEM for two and three dimensional nonlinear analysis N86-10855

Bounding solutions of geometrically nonlinear viscoelastic problems
[NASA-CR-176219] N86-10860

NONSTABILIZED OSCILLATION

Oscillations of a viscoelastic liquid drop in zero-gravity
N86-10240

NORTH SEA

Monthly Bulletin North Sea: Volume 2, January 1985
[KNMI-167-VOL-2] N86-10732

NOSE TIPS

Erosion-resistant nosetip construction
[AD-D011787] N86-10289

NOTCH STRENGTH

Three-dimensional stress singularities in anisotropic materials and composites N86-10286

NOZZLE DESIGN

Operating characteristics of the multiple critical Venturi System and secondary calibration nozzles used for weight-flow measurements in the Langley 16-foot transonic tunnel
[NASA-TM-86405] N86-10016

NOZZLE EFFICIENCY

Experimental performance of a 1-kilowatt arcjet thruster
[NASA-TM-87131] N86-10281

NOZZLE FLOW

Theoretical specific impulse for two-phase flow in nozzle of rocket-ramjet engine: A simple estimation method
N86-10005

Operating characteristics of the multiple critical Venturi System and secondary calibration nozzles used for weight-flow measurements in the Langley 16-foot transonic tunnel
[NASA-TM-86405] N86-10016

NUCLEAR CHEMISTRY

Evaluation of the International Atomic Energy Agency (IAEA) Safeguards Analytical Laboratory quality assurance program
[DE85-012078] N86-10953

NUCLEAR EXPLOSION EFFECT

Microphysical/mesoscale aspects of nuclear winter and new directions in assessments
[DE85-013479] N86-10718

NUCLEAR EXPLOSIONS

Smoke inputs to climate models: Optical properties and height distribution for nuclear winter studies
[DE85-011363] N86-10717

Microphysical/mesoscale aspects of nuclear winter and new directions in assessments
[DE85-013479] N86-10718

NUCLEAR FUEL ELEMENTS

On-line gamma-ray data acquisition at the Power Burst facility
[DE85-011957] N86-10954

NUCLEAR FUSION

ORR core re-configuration measurements to increase the fast neutron flux in the Magnetic Fusion Energy (MFE) experiments
[DE85-013520] N86-10958

NUCLEAR PHYSICS

The 1984 bibliography of atomic and molecular processes
[DE85-010583] N86-10926

Report on the engineering test of the LBL 30 second neutral beam source for the MFTF-B project
[DE85-013317] N86-10962

NUCLEAR POWER PLANTS

Methods for developing jam-resistant security communications networks at fixed-site facilities
[DE85-012032] N86-10408

NUCLEAR RADIATION

HgI sub 2 crystal growth for nuclear detectors
N86-10066

NUCLEAR RESEARCH AND TEST REACTORS

Activities report in safety N86-10365

NUCLEAR SCATTERING

Charge exchange in slow collisions of atoms and molecules N86-10922

NUCLEAR WARFARE

An anthology: Rationale for a US ballistic missile defense (1969 - 1984)
[AD-A156781] N86-10199

NUCLEAR WEAPONS

Microphysical/mesoscale aspects of nuclear winter and new directions in assessments
[DE85-013479] N86-10718

NUCLEATE BOILING

Nucleate pool boiling in subcooled liquid under microgravity: Results of TEXUS experimental investigations N86-10250

NUCLEATION

Theoretical problems in materials science
N86-10088

Containerless studies of nucleation and undercooling
N86-10102

Extension of Ostwald ripening theory N86-10104

Bulk formation of metallic glasses and amorphous silicon from the melt N86-10154

Glass research N86-10157

Crystal nucleation and glass formation in metallic alloy melts N86-10233

Undercooling investigations on the easy glass former Pd-Cu-Si N86-10259

Crystal growth from solutions and nucleation from the vapor phase --- Spacelab N86-10267

A study of the applicability of nucleation theory to quasi-thermodynamic transitions of second and higher Ehrenfest-order
[NASA-CR-176238] N86-11059

A study of the applicability of nucleation theory to quasi-thermodynamic transformations of second and higher Ehrenfest-order
[NASA-CR-176230] N86-11060

NUCLEI (NUCLEAR PHYSICS)

Direct mass measurements in the light neutron-rich region using a combined energy and time-of-flight technique
[DE85-012758] N86-10963

NUCLEONICS

Information on continuum states from feeding times and total (GAMMA) spectra measured with BGO suppressed detectors
[DE85-013868] N86-10961

NUCLEONS

Soudan 2 data acquisition and trigger electronics
[DE85-013864] N86-10443

NULL HYPOTHESIS

Superefficient estimation of power functions in simulation experiments
[B8562445] N86-10893

NUMBER THEORY

Freezer model using a population balance approach for steady-state, direct-contact, secondary refrigerant, freeze desalination N86-10361

Some remarks about cusp forms: Holomorphic and non-holomorphic
[CTH-MATH-1984-26] N86-10902

Galois descent and class groups of orders
[CTH-MATH-1985-09] N86-10904

NUMERICAL ANALYSIS

Numerical procedure for three-dimensional hypersonic viscous flow over aerobrake configuration
[NASA-TM-58269] N86-10018

Analysis of transitions between ferroelectric and antiferroelectric states under conditioning of uniaxial strain
[DE85-014468] N86-10350

An analytical and numerical study of the buckling behavior of fiber-reinforced beams N86-10566

NUMERICAL CONTROL

Dissecting the cow
[DE85-013369] N86-10801

Providing automated control for PBFA-2
[DE85-012867] N86-10928

Timing system control software in the SLC
[DE85-013380] N86-11024

NUMERICAL WEATHER FORECASTING

The boundary condition in a numerical model of atmospheric flows over fixed interfaces
[GKSS-85-E-10] N86-10722

NUTS (FASTENERS)

Over-center toggle latch
[AD-D011753] N86-10556

Termination load carrying device
[AD-D011800] N86-10558

NYLON (TRADEMARK)

Age-life prediction of nylon 66 parachute materials. Part 2: Changes in the chemical and physical properties of materials on aging
[AD-A156909] N86-10347

NYQUIST FREQUENCIES

The interpolation of signals sampled at less than the Nyquist rate N86-10368

O

OCEAN BOTTOM

In-situ geophysical investigations into the nature of the oceanic crust N86-10725

A quantitative method for analyzing the roughness of the seafloor N86-10726

Long term statistical measurements of environmental acoustics parameters in the arctic. AEAS report number 2. Low frequency transmission loss measurements in the central arctic ocean
[AD-A156576] N86-10727

OCEAN CURRENTS

Ocean energy technology program summary
[DE85-013102] N86-10731

OCEAN DYNAMICS

Formation of waves by ground motion
[PM/84/09] N86-10706

A processor for the study of ocean fine-scale patches
[AD-A157019] N86-10730

OCEAN MODELS

Formation of waves by ground motion
[PM/84/09] N86-10706

OCEAN THERMAL ENERGY CONVERSION

Ocean energy technology program summary
[DE85-013102] N86-10731

OCEANOGRAPHIC PARAMETERS

A processor for the study of ocean fine-scale patches
[AD-A157019] N86-10730

Monthly Bulletin North Sea: Volume 2, January 1985
[KNMI-167-VOL-2] N86-10732

OCEANS

In-situ geophysical investigations into the nature of the oceanic crust N86-10725

OIL POLLUTION

Utilization of satellite remote sensing for the monitoring of oil pollution and marine ecosystems in Indonesia. A Tropical Earth Resources Satellite program (TERS) case study implemented for the NLR, Delft N86-10640

OILS

Surface tension induced instabilities in reduced gravity: The Benard problem N86-10117

Heat transfer in condensing and evaporating two-component, two-phase flow inside a horizontal tube
N86-11058

ON-LINE SYSTEMS

Acquaintance with on line literature research. An introduction for education at the Chemical Technology Section N86-11081

On line astronomical image processing using microcomputers N86-11121

ONE DIMENSIONAL FLOW

Time-implicity simulation of particle-fluid systems
[DE85-012944] N86-10471

OPEN CHANNEL FLOW

Experiments and computations on unsteady separating flow in an expanding flume
[REPT-2-84] N86-10477

OPENINGS

Optimal design of portal frames against buckling
N86-10572

OPERATING COSTS

F-16X MSIP (Multi-national Staged Improvement Program) case example: Operating and support cost estimation using VAMOSC (Visibility And Management Of Operating and Support Costs)
[AD-A156893] N86-10006

OPERATIONAL AMPLIFIERS

High output programmable signal current source for low output impedance applications
[AD-D011751] N86-10423

OPERATIONS RESEARCH

Operations research applications
[ARW-03-THE-BDK/ORS/83-08] N86-10901

Failures and successes of quantitative methods in management
[ARW-03-THE-BDK/ORS/83-06] N86-11076

OPERATOR PERFORMANCE

Effect of various doses of some vitamins on non-specific mechanisms of adaptation of man N86-10750

OPERATORS (MATHEMATICS)

Lie algebraic methods for charged particle beams and light optics N86-10970

OPTICAL COMPUTERS

Spatial frequency multiplexed coherent optical processor for calculating generalized moments
[AD-D011816] N86-10975

OPTICAL COUPLING

A fiber-linked version of project TRIO --- telescope array N86-11105

OPTICAL DATA PROCESSING
Prospects for creation of optical digital high-performance computers N86-10610

OPTICAL DISKS
Optical disc transport system [AD-D011779] N86-10974

OPTICAL EMISSION SPECTROSCOPY
Rapid evaluation of ion thruster lifetime using optical emission spectroscopy [NASA-TM-87103] N86-10260

OPTICAL EQUIPMENT
Always-convergent iterative noise removal and deconvolution for image data [NASA-CR-176223] N86-10824

OPTICAL HETERODYNING
Experimental investigations of pulse-pulse interference in heterodyne detection [DFVLR-FB-85-26] N86-10544
The DUO: Far infrared heterodyne concept for space interferometry N86-11125

OPTICAL MEASUREMENT
Advanced optical measurement techniques N86-10174
Time resolved flow velocity and concentration measurements using a travelling thermal lens [AD-A156706] N86-10541
Optical detection of photoacoustic pulses in thin silicon wafers [AD-A156705] N86-10977

OPTICAL MEASURING INSTRUMENTS
Photonic diagnostics and pulsed power research [DE85-013752] N86-10940

OPTICAL MEMORY (DATA STORAGE)
Optical disc transport system [AD-D011779] N86-10974

OPTICAL PROPERTIES
Crystallization, optical and chemical properties of fluoride glasses N86-10149
Polymer engineering: Polymeric and molecular electronic, dielectric and optical properties for device applications [AD-A156671] N86-10344
Determination of optical properties by third-harmonic generation in noble gases in unfocused laser beams N86-10535

OPTICAL PUMPING
Scaling studies of solar pumped lasers [NASA-CR-176240] N86-10540

OPTICAL TRANSFER FUNCTION
Always-convergent iterative noise removal and deconvolution for image data [NASA-CR-176223] N86-10824

OPTICAL WAVEGUIDES
Extended precision in video bandwidth analog to digital converter using optical techniques [AD-D011745] N86-10422
Fiber optic system for measuring electric fields [AD-D011830] N86-10976

OPTIMAL CONTROL
Optimal control modeling of lower extremity musculoskeletal motion N86-10853

OPTIMIZATION
Optimum design of an aircraft wing structure with multiple constraints by the direct-vision criteria method N86-10004
High temperature properties of SiC materials [BMFT-FB-T-85-047] N86-10353
Modeling and control of nonlinear systems N86-10362
Design sensitivity analysis and optimization of built-up structures N86-10565
Strength of shells under local transverse loads N86-10568
Harmonic distortion reduction technique for data acquisition [AD-D011771] N86-10799
Minimization of programmable logic arrays [EUT-84-E-145] N86-10803
State assignment in sequential circuits [EUT-85-E-146] N86-10846

OPTOMETRY
Measurement of visual contrast sensitivity [AD-D011776] N86-10973

ORBITAL ASSEMBLY
Test and evaluate passive orbital disconnect struts (PODS 3) [NASA-CR-177368] N86-10274

ORBITAL LIFETIME
User's guide for Langley Research Center Orbital Lifetime program [NASA-TM-87587] N86-10828

ORBITAL MECHANICS
User's guide for Langley Research Center Orbital Lifetime program [NASA-TM-87587] N86-10828

ORBITS
Lumped geopotential harmonics of order 14, from the orbit of 1967-11G [AD-A156627] N86-10190

ORCHARDS
On the use of L-band multipolarization airborne SAR for surveys of crops, vineyards, and orchards in a California irrigated agricultural region N86-10627

ORGANIC CHEMISTRY
Growth of organic crystals by Ostwald ripening N86-10058

ORGANIC COMPOUNDS
Volatile organic compounds in indoor air: A survey of various structures [PB85-198356] N86-10687
Emissions of NOx, SOx and VOC from Antropogenic sources [PB85-193530] N86-10688
Evaluation of Passive Sampling Devices (PSDs) [PB85-196418] N86-10689

ORGANIZING
Remote sensing study project East Gelderland (Netherlands). Part 2: Remote sensing flights in 1982 and 1983; organization aspects N86-10639

OROGRAPHY
Observations of the snow cover in the southern part of the Buryat Autonomous Soviet Socialist Republic [NASA-TM-77910] N86-10613
Laws of distribution of the snow cover on the greater Caucasus (Soviet Union) [NASA-TM-77911] N86-10614
The effects of orography on land-atmosphere turbulent exchange processes N86-10702

ORTHOGONAL FUNCTIONS
Large eddy interactions in a turbulent channel flow [NASA-TM-86757] N86-10464

ORTHOPHOTOGRAPHY
Orthophotomapping from metric camera imagery — Spacelab N86-10487
Stereo-orthophotos in various map projections N86-10488
Evaluation of the accuracy of the metric camera images for the production of line maps and orthophotos N86-10490

ORTHOSTATIC TOLERANCE
Study of hypokinesia and acceleration effects on human chromosomes N86-10740
Vestibular resistance and blood circulation changes in orthostatic position during hyperthermia N86-10758

ORTHOTROPIC SHELLS
Stiffened and prestressed composite overwrapped pressure vessels N86-10547

OSCILLATING FLOW
Oscillations of subsonic flow in an abruptly expanding circular duct [MPIS-16/1984] N86-10028
Measurements of the critical Marangoni number of the laminar-oscillatory transition of thermocapillary convection in floating zones N86-10242

OSCILLATIONS
Theory of non-planar orbits [DE85-013284] N86-11018

OTS (ESA)
Digital transmission experiments with the Orbital Test Satellite [EUT-84-E-144] N86-10270

OUTPUT
Phase-coded pulse expander-compressor [AD-D011812] N86-10375

OXIDATION
Study of the reactive-element effect in oxidation of Fe-Cr alloys using transverse section analytical electron microscopy N86-10087
Oxidation behavior of glassy alloys N86-10158
Catalytic activity of shock modified ZnO for CO oxidation and methanol synthesis [DE85-014704] N86-10300
Chemical kinetics and cellular structure of detonations in hydrogen sulphide and air [DE85-008406] N86-10304
Evaluation and prediction of long-term environmental effects on non metallic materials [NASA-CR-178495] N86-10340
Kinetics of biological ferrous iron oxidation [DE85-014616] N86-10736

OXIDATION RESISTANCE
High temperature properties and characterization of S3-N4 materials [BMFT-FB-T-85-046] N86-10352

OXIDES
The role of entrained surface oxides in RS-PM aluminum alloys on resultant structures and properties N86-10065
Environmental degradation of materials: Surface chemistry related to stress corrosion cracking N86-10099
Rapid solidification of magnetic oxides N86-10152

OXYGEN
High-temperature controlled redox crystallization studies N86-10178
Mild hypoxia and visual performance with night vision goggles [AD-A156969] N86-10787
Adsorption of oxygen on single crystal tin at liquid helium temperatures N86-11044

OXYGEN CONSUMPTION
Reaction of rabbit respiration system to hypoxic stimulus in nitrogen-oxygen medium at elevated pressure N86-10760

OXYGEN METABOLISM
Indices of blood oxygen transporting properties and erythropoiesis in rats after prolonged stay in nitrogen-oxygen mixture at elevated pressure N86-10761

OXYGEN SPECTRA
Selected tables of atomic spectra. Atomic energy levels and multiplet table O3 [NBS/NSRDS-3/11] N86-10923

OZONE
Chemical kinetics and photochemical data for use in stratospheric modeling [NASA-CR-176198] N86-10707

P

P WAVES
Structural discontinuity within the southern California continental margin: Seismic and gravity models of the western Transverse Ranges N86-10699

P-N JUNCTIONS
P-N junction controlled field emitter array cathode [AD-D011815] N86-10416

P-TYPE SEMICONDUCTORS
W-shaped diffused stripe GaAs/AlGaAs laser [AD-D011818] N86-10538

PACKAGING
Miniature radar packaging [DE85-014598] N86-10410

PAIR PRODUCTION
Search for heavy neutrines produced in e(+)e(-) annihilation [DE85-013372] N86-11035

PAKISTAN
Report of the Workshop on Geologic Applications of Remote Sensing to the Study of Sedimentary Basins [E86-10002] N86-10599
Chronologic analysis of terrestrial sediments and basin evolution N86-10602

PALEONTOLOGY
Paleogene vertebrate paleontology, geology and remote sensing in the Wind River Basin N86-10609
Paleontology and stratigraphy of Lower Cambrian and upper Proterozoic sediments, Caborca region, northwestern Sonora, Mexico N86-10692

PALLADIUM
The interaction of small metal particles with refractory oxide supports [NASA-CR-176228] N86-11047

PANELS
Load-deflection tests and computer analyses of a high-precision adhesive-bonded antenna reflector panel N86-10389
Inelastic analysis of frame structures including member and joint shears N86-10573
Fatigue of graphite/epoxy buffer strip panels with center cracks [NASA-TM-87595] N86-10581

PANT PROGRAM
Erosion-resistant nosetip construction [AD-D011787] N86-10289

PARABOLIC FLIGHT
Advanced optical measurement techniques N86-10174

PARACHUTE FABRICS
Age-life prediction of nylon 66 parachute materials. Part 2: Changes in the chemical and physical properties of materials on aging [AD-A156909] N86-10347

PARAFFINS
Romanian plant produces protein concentrate from paraffin-nourished yeasts N86-10741

PARALLEL PROCESSING (COMPUTERS)
An improved FFT (Fast fourier transform) for a four parallel pipe SIMD arithmetic processor [AD-A156625] N86-10863

PARALLEL PROGRAMMING
Soudan 2 data acquisition and trigger electronics [DE85-013864] N86-10443

PARAMETER IDENTIFICATION

Comment on Determination of Aerodynamic Coefficients for a Reentry Body by Means of the Kalman Filter Method N86-10011

System modeling and identification of equivalent systems with and without compensating time delay for control-augmented aircraft
[ESA-TT-852] N86-10043

Spillover minimization in self-adjoint distributed-parameter systems with direct output feedback N86-10652

Multivariable partial realization and the aspect of uniqueness
[ER-83/09] N86-10879

PARAMETERIZATION

Theoretical specific impulse for two-phase flow in nozzle of rocket-ramjet engine: A simple estimation method
N86-10005

Field-independent normalization of SSC Collider Ring costs
[DE85-012425] N86-10997

PARAMETRIC AMPLIFIERS

Elastic wave gyrometer. Experiments with a parametric wave device
[REPT-26/5005/HF/AR] N86-10533

PARTIAL DIFFERENTIAL EQUATIONS

Alternating direction methods on multiprocessors: An extended abstract
[AD-A156722] N86-10794

A modified modified Korteweg-deVries equation
[PN-84/27] N86-10859

A mesh moving technique for time dependent partial differential equations in two space dimensions
[AD-A156663] N86-10866

A note on the differenciability of center manifolds
[ZW-8414] N86-10905

PARTICLE ACCELERATION

Potential structures and particle acceleration on auroral field lines
[AD-A156694] N86-10708

PARTICLE ACCELERATORS

Revision of and documentation for the standard version of the Poisson-Group codes
[DE85-012659] N86-10837

Providing automated control for PBFA-2
[DE85-012667] N86-10928

AGS polarized H(-) source
[DE85-013296] N86-10935

New particle searches
[DE85-014073] N86-10942

Separated K(-) beams (10 GeV and above)
[DE85-012527] N86-10989

Beginnings of remote handling at the RAL Spallation Neutron Source
[DE85-012681] N86-11001

Proceedings of a Workshop on Electroweak Symmetry Breaking
[DE85-004444] N86-11008

Advances in data acquisition system technology for PBFA 2
[DE85-012660] N86-11011

Engineering high reliability, low-jitter Marx generators
[DE85-012811] N86-11013

SLC positron damping ring optics design
[DE85-013054] N86-11014

Computer control of rf at SLAC
[DE85-013065] N86-11015

Theory of non-planar orbits
[DE85-013264] N86-11018

Photoactivation of PBFA-2
[DE85-013439] N86-11019

Unicell structure for superconducting storage rings
[DE85-013303] N86-11022

Timing system control software in the SLC
[DE85-013380] N86-11024

RHIC lattice
[DE85-013289] N86-11026

PARTICLE BEAMS

Revision of and documentation for the standard version of the Poisson-Group codes
[DE85-012659] N86-10837

Providing automated control for PBFA-2
[DE85-012667] N86-10928

Parasitic mode losses versus signal sensitivity in beam position monitors
[DE85-014367] N86-10964

Separated K(-) beams (10 GeV and above)
[DE85-012527] N86-10989

Noninterceptive techniques for the measurement of longitudinal parameters for intense H(-) beams
[DE85-012662] N86-10992

Ferrite kicker magnet for the IAMPF switchyard upgrade
[DE85-012657] N86-10996

Advances in data acquisition system technology for PBFA 2
[DE85-012660] N86-11011

High-resolution phosphor screen beam profile monitor
[DE85-013074] N86-11012

Photoactivation of PBFA-2
[DE85-013439] N86-11019

RHIC lattice
[DE85-013289] N86-11026

PARTICLE EMISSION

Ultraviolet spectroscopy of the Earth's dayglow and magnetosphere cleft N86-10696

PARTICLE INTERACTIONS

Improved particle-velocity transducer for equation-of-state experiments
[DE85-013204] N86-10532

Cooperative emission by two different atoms into surface plasmons
[AD-A157033] N86-10925

Supersonic metal cluster beams
[DE85-014321] N86-10966

PARTICLE MASS

Variational estimates for the mass gap of SU(2) Euclidean lattice gauge theory
[NIKHEF-H/84-13] N86-10883

Two-loop large Higgs mass corrections to vector boson self-couplings
[NIKHEF-H/84-15] N86-11038

PARTICLE MOTION

Electrophoresis technology N86-10144

Measurement and resulting first and second order approximations for a 9 deg bending magnet in LAMPF's 750-keV transport
[DE85-012691] N86-10930

PARTICLE SIZE DISTRIBUTION

Production of large-particle-size monodisperse latexes in microgravity N86-10146

Binder-filler interaction in energetic polymers
[AD-A156752] N86-10345

PARTICLE TELESCOPES

The intensified multi CCD camera --- spaceborne interferometers N86-11122

PARTICLE TRACKS

Tracking studies on the effects of magnet multipoles on the aperture of the RHIC heavy ion collider
[DE85-013282] N86-11023

PARTICLE TRAJECTORIES

Lie algebraic methods for charged particle beams and light optics N86-10970

PARTICLES

Particle cloud combustion experiment N86-10160

New particle searches
[DE85-014073] N86-10942

Solar flares and magnetospheric particles: Investigations based upon the ONR-602 experiment
[AD-A156583] N86-11142

PARTITIONS (MATHEMATICS)

On the analytical evaluation of the partition function for unit hypercubes in four dimensions --- lattice theory
[NIKHEF-H/84-12] N86-10882

PASSENGERS

The air traffic demand in passenger travel of the Federal Republic of Germany 1990 - 2000. Update of the DFVLR air traffic forecast
[DFVLR-MITT-85-06] N86-10031

PASSIVITY

Passivation of steel with aqueous amine solutions
[AD-D011749] N86-10314

PATTERN RECOGNITION

Analysis of edge detection algorithms on DIAL (Digital Image Analysis Laboratory)
[AD-A156735] N86-10630

Special purpose hardware architectures for language recognition
[AD-A156634] N86-10793

PAYLOAD INTEGRATION PLAN

The first German Spacelab mission D1 reports --- Spacelab payloads
[PR-2] N86-10188

PAYLOADS

Guidance and control of a cable based payload pickup system N86-10046

PEPTIDES

Homocarnosin in rat brain during adaptation to cold
N86-10762

PERCHLORATES

Composite explosives for metal acceleration: The effect of detonation temperature
[DE85-013982] N86-10359

PERFORMANCE PREDICTION

A comparative analysis of a CV helicopter and a JVX (Joint Services Advanced Vertical Lift) tilt-rotor aircraft in an aircraft carrier based ASW (Anti-Submarine Warfare)
[AD-A156871] N86-10041

High temperature mechanical testing of a cylindrical weave carbon-carbon composite
[AD-A156639] N86-10591

Optical testing of large telescopes using multiple subapertures N86-10971

PERFORMANCE TESTS

Test and evaluate passive orbital disconnect struts (PODS 3)
[NASA-CR-177368] N86-10274

Explosive initiation by very small conical shaped charge jets
[DE85-009443] N86-10357

Test results for 20-GHz GaAs FET spacecraft power amplifier
[NASA-TM-87072] N86-10379

Implementation issues for algorithmic VLSI (Very Large Scale Integration) processor arrays
[AD-A156699] N86-10432

Type of new Chinese-produced high-speed camera and its utilization in detonation physics experiments
[DE85-015191] N86-10529

Advanced Gas Turbine (AGT) powertrain system development for automotive applications report
[NASA-CR-174886] N86-11087

PERIPHERAL EQUIPMENT (COMPUTERS)

Elektronika MS 1603 high-speed peripheral processor
N86-10811

Diagnostics of peripheral processors and controllers
N86-10812

Shipboard non-tactical computer systems of the US Navy
[AD-A156769] N86-10849

PERMEABILITY

KRAK: A computer program for two-phase, two-component porous flow and fracture propagation, revision
[DE85-014264] N86-10469

PERSIAN GULF

A geological structural analysis of the southeastern Zagros (Iran) ranges based on metric camera photos
N86-10492

PERSONNEL MANAGEMENT

Psychological Sciences Division 1984 programs
[AD-A156631] N86-10779

On the structure of manpower planning, a contribution of simulation experiments with decomposition methods
[MANPOWER-PLANNING-28] N86-11073

Aspects of manpower planning at a Dutch university, an example of aggregation and decomposition methods in manpower planning
[MANPOWER-PLANNING-29] N86-11074

On the structure of manpower planning, a contribution of simulation experiments with aggregation methods
[MANPOWER-PLANNING-30] N86-11075

PERSONNEL SELECTION

Standardization of tasks: Approach planning --- human performance assessment
[IZF-1984-19] N86-10782

PERTURBATION

Nonlinear methods for spacecraft attitude maneuvers
[AD-A156956] N86-10275

Computation of flow regimes in parameter space for the AGCE
[NASA-CR-178480] N86-10705

PETROLEUM PRODUCTS

Evaluation of the 90-day inhalation toxicity of petroleum and oil shale JP-5 jet fuel
[AD-A156815] N86-10675

PETROLOGY

Stratigraphy, petrology, depositional and post-depositional histories and their effects upon reservoir properties of the Parkman Formation of the Mesa Verde group, Powder River Basin, Wyoming N86-10691

PH

Hormone purification by isoelectric focusing
N86-10135

PH FACTOR

Hormone purification by isoelectric focusing
N86-10135

Automated analysis of digital images generated by two-dimensional gel electrophoresis
[DE85-011906] N86-10526

PHARMACOLOGY

Mechanism of adaptogenic action of prickly eleuterococcus on man during heat stress N86-10757

PHASE CHANGE MATERIALS

Metastable phase formation in Ni-implanted Al: An analytical electron microscope investigation
[DE85-009105] N86-10331

PHASE DEVIATION

Aperture synthesis with or without phase information for kilometric arrays interpolation algorithms for stabilized image reconstruction N86-11124

PHASE DIAGRAMS
Weld metal hot-cracking of hastelloy alloys C-22 and C-276: A study by analytical electron microscopy [DE85-009437] N86-10324
PHASE LOCKED SYSTEMS
High sensitivity millimeter-wave measurement apparatus [AD-D011786] N86-10373
Sample data phase locked loop for adaptive Doppler tracker [AD-D011788] N86-10374
PHASE MODULATION
Phase-coded pulse expander-compressor [AD-D011812] N86-10375
Phase coded pulse expander-compressor [AD-D011817] N86-10376
Amplitude and phase modulation in fin-lines electrical tuning [AD-D011813] N86-10415
PHASE SHIFT
Method for tuning a phased array antenna [AD-D011768] N86-10372
Determination of symmetry and phase in human visual response functions: Theory and experiments N86-10769
High-power rf controls for the NBS-Los Alamos racetrack microtron [DE85-012656] N86-10993
PHASE SHIFT CIRCUITS
Pulse compression system [AD-D011833] N86-10417
PHASE SWITCHING INTERFEROMETERS
Radio astronomy experience in image reconstruction. A history lesson for optical astronomers N86-11117
PHASE TRANSFORMATIONS
Experimental and theoretical studies of wetting and multilayer adsorption [NASA ORDER H-27954B] N86-10121
Impurity extraction by droplets N86-10122
Analysis of transitions between ferroelectric and antiferroelectric states under conditioning of uniaxial strain [DE85-014468] N86-10350
Measurement of the density of base fluids at pressures 0.422 to 2.20 GPa [NASA-TM-87114] N86-10551
New approach to multiphase equilibria: Application to high-pressure physics problems [DE85-013820] N86-10907
High-pressure release-wave measurements and phase transformation in CaCO3 [DE85-012592] N86-11055
PHASED ARRAYS
Angle set-on apperatus [AD-D011766] N86-10371
Method for tuning a phased array antenna [AD-D011768] N86-10372
Optical/IR telescope arrays: A study of their potential for satisfying observational requirements in astronomy for a large aperture system in the 1990s and beyond [REPT-15] N86-11094
PHENOLS
Sediment characterization. Task 2: Instream contaminent study, volume 1 [DE85-013502] N86-10683
PHOSPHATES
Thermal expansion of glasses in the solid and liquid phases [DE85-013953] N86-10351
PHOSPHORIC ACID FUEL CELLS
Effect of H2S and COS in the fuel gas on the performance of ambient pressure phosphoric acid fuel cells [DE85-013913] N86-10446
PHOSPHORUS
The mechanism of erosion of metallic materials under cavitation attack [NASA-TM-87133] N86-10552
Magnetic properties of doped semiconductors [DE85-012090] N86-11053
PHOTOACOUSTIC SPECTROSCOPY
Optical detection of photoacoustic pulses in thin silicon wafers [AD-A156705] N86-10877
PHOTOCHEMICAL REACTIONS
Chemical kinetics and photochemical data for use in stratospheric modeling [NASA-CR-176196] N86-10707
PHOTODECOMPOSITION
Age-life prediction of nylon 66 parachute materials. Part 2: Changes in the chemical and physical properties of materials on aging [AD-A156909] N86-10347
Photoionization technique for growth of metallic films [AD-D011760] N86-10426
PHOTODIODES
Making the right choice — silicon photodiodes N86-10669
PHOTOELECTRIC EMISSION
Nature of photoemission into dielectric fluids [DE85-013017] N86-10945
PHOTOELECTRIC MATERIALS
High-brightness photoemitter injector for electron accelerators [DE85-012673] N86-10929
PHOTOELECTRONS
Ultraviolet spectroscopy of the Earth's dayglow and magnetosphere cleft N86-10696
PHOTOGEOLOGY
LANDSAT TM image data quality analysis for energy-related applications [E85-10109] N86-10597
Report of the Workshop on Geologic Applications of Remote Sensing to the Study of Sedimentary Basins [E86-10002] N86-10599
Some opinions on remote sensing and geologic studies N86-10600
Position paper: Workshop on Geologic Applications of Remote Sensing to the Study of Sedimentary Basins N86-10601
Chronologic analysis of terrestrial sediments and basin evolution N86-10602
Tertiary and quaternary research with remote sensing methods N86-10603
Multisensor data integration techniques N86-10604
Foreland basin structures and remote sensing N86-10606
PHOTOGRAMMETRY
Metric Camera Workshop — Spacelab [ESA-SP-209] N86-10485
High-resolution image data from the Space Shuttle N86-10494
Evaluation of metric camera images at the University of London — Spacelab N86-10495
OEEPE participation in testing metric camera photography — European Organization for Experimental Photogrammetric Investigations (OEEPE) N86-10507
An example of single model orientation of metric camera stereophotographs — Spacelab N86-10520
Tectonic analysis of typical fold structures in the Zagros Mountains (Iran) by the application of quantitative photogrammetric methods on metric camera data — Spacelab N86-10521
PHOTOGRAPHY
Fundamental studies of droplet combustion at reduced gravity N86-10165
Type of new Chinese-produced high-speed camera and its utilization in detonation physics experiments [DE85-015191] N86-10529
PHOTOINTERPRETATION
Metric Camera Workshop — Spacelab [ESA-SP-209] N86-10485
Erosion control and watershed management by Spacelab photography N86-10493
Topographic interpretation of metric camera images: An example in Somalia — Spacelab N86-10508
Thematic investigations in France based on metric camera imagery — Spacelab N86-10509
Evaluation of metric camera photos — Spacelab; alpine snow cover N86-10515
Interpretation of Spacelab-1 photographs for the generation of 1:200000 topographic map N86-10518
The effect of vegetation type, microrelief, and incidence angle on radar backscatter N86-10619
Age-dating volcanic and alluvial surfaces with multipolarization data N86-10620
The effects of merging TM and A/C radar on wetland classification N86-10621
Strategies for analyzing mixed pixels in remotely sensed imagery N86-10623
Mapping diverse forest cover with multipolarization airborne radar N86-10625
Remote sensing [NOTA-1535] N86-10636
PHOTOIONIZATION
Photoionization technique for growth of metallic films [AD-D011760] N86-10426
Theoretical investigation of electron-positive ion-atom interactions [DE85-013019] N86-10939
Nature of photoemission into dielectric fluids [DE85-013017] N86-10945
PHOTOMAPPING
Satellite use for men — West German space program N86-10180
How Antarctica was unveiled. Masterpieces of Frankfurt topographic surveyors. A part of the German Antarctica research program N86-10181
Satellite data even for a poultry farm. A development for Tanzania. Image evaluation following new ways N86-10182
With Argus eyes from space. Satellite Diagnosis for Upper Volta. Seven maps without mystery N86-10183
Metric Camera Workshop — Spacelab [ESA-SP-209] N86-10485
Digital elevation model from Spacelab metric camera photographs N86-10486
Orthophotomapping from metric camera imagery — Spacelab N86-10487
Stereo-orthophotos in various map projections N86-10488
Restitution of Spacelab photography by analog stereoplotter N86-10489
Evaluation of the accuracy of the metric camera images for the production of line maps and orthophotos N86-10490
Photomapping in different climatic zones — Spacelab metric camera N86-10491
High-resolution image data from the Space Shuttle N86-10494
Evaluation of metric camera images at the University of London — Spacelab N86-10495
Identification of planimetric features from the metric camera — Spacelab N86-10497
Analysis of metric camera images from the USA and their suitability for topographic and thematic mapping — Spacelab N86-10498
Line mapping and resolution tests with metric camera data — Spacelab N86-10500
Role of the Economic Commission for Africa as a principal investigator in the metric camera experiment and reports of the result of the assessment for topographic and revision of maps in populated and developed areas of the world N86-10501
The role of very small scale metric images in modern geology — Spacelab metric camera N86-10502
Geological mapping of remote mountainous regions using metric camera imagery — Spacelab N86-10503
Interpretation of metric camera concerning hydrologic structures of the Rhone Delta — Spacelab N86-10504
Test on mapping application of metric camera imagery — Spacelab N86-10505
Status of preperation activities for metric camera reflight on EOM-1/2 N86-10506
Thematic mapping of metric camera color infrared and black and white photographs for land use classification N86-10510
Digital image processing of metric camera imagery — Spacelab N86-10511
Topographic and thematic mapping: Analysis of metric camera black and white photographs of the Rhone Delta N86-10514
Updating of topographic maps by means of metric camera photos example: Hallertau (Bavaria) N86-10517
Interpretation of Spacelab-1 photographs for the generation of 1:200000 topographic map N86-10518
Metric camera image of Munich as additional means for urban cartography — Spacelab N86-10519
Test results using metric camera photography for 1:250,000 mapping — Spacelab N86-10522
Report of the Workshop on Geologic Applications of Remote Sensing to the Study of Sedimentary Basins [E86-10002] N86-10599
Chronologic analysis of terrestrial sediments and basin evolution N86-10602
Tertiary and quaternary research with remote sensing methods N86-10603
Analysis of remote sensing data N86-10605
Structural mapping of folded sedimentary environments from satellite images: An example from Central Asia N86-10607
Foreland basin structures and remote sensing N86-10606
Topographic mapping from interferometric synthetic aperture radar observations N86-10622
Lithologic mapping in a sedimentary environment using multipolarization SAR images N86-10624
PHOTOMAPS
Structural mapping of folded sedimentary environments from satellite images: An example from Central Asia N86-10607
PHOTOMETERS
Signal analysis receiver with acousto-optic delay lines [AD-D011761] N86-10427
Semiconductor superlattic photodetectors [NASA-CR-176249] N86-10484
Making the right choice — silicon photodiodes N86-10669
PHOTOMULTIPLIER TUBES
Semiconductor superlattic photodetectors [NASA-CR-176249] N86-10484
PHOTON BEAMS
The 20 keV undulators for a 6-GeV storage ring [DE85-013867] N86-10941
Beam stability in a 6 GeV synchrotron light source [DE85-013850] N86-10979

Thermal and structural analysis of ring components by the finite element method
[DE85-013305] N86-11021

PHOTON DENSITY

The intensified multi CCD camera — spaceborne interferometers N86-11122

PHOTONICS

Photonic diagnostics and pulsed power research
[DE85-013752] N86-10940

PHOTONS

Ultraviolet spectroscopy of the Earth's dayglow and magnetosphere cleft N86-10696

Photonic diagnostics and pulsed power research
[DE85-013752] N86-10940

Surface conditioning of synchrotron radiation source to improve beam lifetime
[DE84-012165] N86-10945

PHOTONUCLEAR REACTIONS

Experimental X-ray scattering cross sections for H2 and rare atomic gases
[DE85-011572] N86-10936

PHOTOOXIDATION

Age-life prediction of nylon 66 parachute materials. Part 2: Changes in the chemical and physical properties of materials on aging
[AD-A156909] N86-10047

PHOTOTHERMAL CONVERSION

Time resolved flow velocity and concentration measurements using a travelling thermal lens
[AD-A156706] N86-10541

PHOTOVOLTAIC CELLS

Photovoltaic systems in remote locations: An experience summary
[NASA-TM-87106] N86-10643

Photovoltaic concentrator array evaluation
[DE85-013789] N86-10665

PHOTOVOLTAIC EFFECT

Sensor system
[AD-D011767] N86-10480

Photovoltaic systems in remote locations: An experience summary
[NASA-TM-87106] N86-10643

Some aspects of long-range, high-risk photovoltaic research at SERI
[DE85-012144] N86-10662

PHYSICAL EXERCISE

Assessment of state of chronotropic and inotropic heart function at different degrees of physical fitness
N86-10746

Classification of changes in electrocardiogram during muscular exertion of healthy individuals N86-10755

PHYSICAL FACTORS

Identification of chemical and physical phenomena affecting the durability of silvered polymer (PMMA) mirrors
[DE85-012131] N86-10645

PHYSICAL OPTICS

Scattering by complicated structures: Calculation of the radar properties of metallic targets by means of physical optics
[DFVLR-FB-85-22] N86-10961

PHYSICAL WORK

Efficiency of muscular work in white rats during adaptation to cold N86-10763

PHYSIOLOGICAL EFFECTS

Effect of emotional stress on hemostasis system of healthy persons N86-10745

Short term heat effect on adreno- and cholino-sensitivity of rat's small intestine N86-10754

Indices of blood oxygen transporting properties and erythropoiesis in rats after prolonged stay in nitrogen-oxygen mixture at elevated pressure
N86-10761

Homocarnosin in rat brain during adaptation to cold
N86-10762

The effects of age, sleep deprivation, and altitude on complex performance
[AD-A156967] N86-10771

Report on the research activities on whole-body vibrations. Human strain due to mechanical vibrations
[ISBN-3-88383-107-7] N86-10773

PHYSIOLOGICAL RESPONSES

Effect of single actions of weak electromagnetic fields of ultraslow frequency on indices of endocrine system
N86-10744

Individual typological features of autonomic reactions during autogenic training in polar expedition members in period of wintering in Antarctica N86-10748

Individual typological self-regulation of cardio-vascular system N86-10752

TV monitoring control system in electrophysiological studies N86-10765

Effect of cold on brain serotonin system and plasma corticosteroid level in different strains of mice
N86-10766

Variability analysis of visually induced responses in the midst of noise
[B8564052] N86-10774

PHYSIOLOGICAL TESTS

The wearing comfort of the PVC: Combat back pack
[IZF-1984-34] N86-10789

PHYSIOLOGY

USSR report: Life sciences. Biomedical and behavioral sciences
[JPRS-UBB-85-023] N86-10738

PIEZOELECTRIC TRANSDUCERS

Precise bearing support ditherer with piezoelectric drive means
[AD-D011819] N86-10483

PIEZOELECTRICITY

Precise bearing support ditherer with piezoelectric drive means
[AD-D011819] N86-10483

Fiber optic system for measuring electric fields
[AD-D011830] N86-10976

PIEZOMETERS

Modeling groundwater flow into lakes N86-10598

PILOT ERROR

Extended analysis of the structure of error scores in psychological aptitude tests
[DFVLR-FB-85-20] N86-10780

Speed of work and error rate: Analyses of individual differences in a choice reaction series with a cognitive component
[DFVLR-FB-85-21] N86-10781

PILOT PERFORMANCE

Mild hypoxia and visual performance with night vision goggles
[AD-A156969] N86-10787

PILOT TRAINING

Proposed modifications for the RAAF Airtrainer CT-4A cockpit
[AD-A156808] N86-10039

PIONS

Relativistic wavefunction at the origin and the pion decay constant
[DE85-012392] N86-11062

PIPELINING (COMPUTERS)

Arithmetic pipeline for image processing
[AD-D011773] N86-10600

PIPES (TUBES)

Carbon fiber reinforced polymide filament wound tube manufacturing
[BR64172] N86-10339

Streaming potentials in conductive and nonconductive tubing
[DE85-012964] N86-10438

PITCH (INCLINATION)

Theoretical study of the unsteady linear problem for a rectangular wing with a pitching movement
[ONERA-RT-17/1841-RY-010-R] N86-10022

PITUITARY HORMONES

Purification and cultivation of human pituitary growth hormones secreting cells N86-10140

PLAINS

Observations of the snow cover in the southern part of the Buryat Autonomous Soviet Socialist Republic
[NASA-TM-77910] N86-10613

PLANE WAVES

Topics in nonlinear wave theory with applications
N86-10367

Measurements of the acoustic interference between adjacent microphones
[AD-A156892] N86-10919

PLANETS

Photographic catalog of selected planetary size comparisons
[NASA-TM-86207] N86-11138

PLANNING

F-16X MSIP (Multi-national Staged Improvement Program) case example: Operating and support cost estimation using VAMOSC (Visibility And Management Of Operating and Support Costs)
[AD-A156893] N86-10006

Research needs for corrosion control and prevention in energy conservation systems
[DE85-014852] N86-10326

Generation of flight paths using hierarchical planning
[AD-A156905] N86-10900

Application of structural-mechanics methods to the design of large tandem-mirror fusion devices (MFTF-B)
[DE85-008960] N86-11017

PLANT ROOTS

Radionuclide complexation in xylem exudates of plants
[DE85-013446] N86-10684

PLANTS (BOTANY)

Radionuclide complexation in xylem exudates of plants
[DE85-013446] N86-10684

Romanian plant produces protein concentrate from paraffin-nourished yeasts N86-10741

PLASMA ACCELERATORS

Theoretical aspects of magnetic helicity
[DE85-011846] N86-10984

Introduction to the m = 1 helicity source
[DE85-012771] N86-10999

Energy efficiency of the CTX magnetized coaxial plasma source
[DE85-012735] N86-11003

PLASMA COMPRESSION

Compact torus compression of microwaves
[DE85-012919] N86-11016

PLASMA CONTROL

Increased particle confinement with the use of external dc bias field in the CTX spheromak
[DE85-012744] N86-10986

Compact torus compression of microwaves
[DE85-012919] N86-11016

Symmetric Tandem Mirror Program
[DE85-012352] N86-11032

PLASMA CURRENTS

Recent helicity source and power supply improvements in CTX
[DE85-012741] N86-11028

PLASMA DENSITY

Local drift parameter, j/n sub e and resistivity anomaly measurements in CTX spheromaks
[DE85-012740] N86-10998

PLASMA DIAGNOSTICS

Activities report in geophysics
[KGI-188] N86-10709

Activities report in plasma physics N86-11039

PLASMA DYNAMICS

Dynamics of imploding neon gas puff plasmas. 1
[AD-A156916] N86-10983

PLASMA EQUILIBRIUM

Conducting wall and pressure profile effect on MHD stabilization of axisymmetric mirror
[DE85-013647] N86-11020

PLASMA GUNS

Theoretical aspects of magnetic helicity
[DE85-011846] N86-10984

PLASMA HEATING

Heating and generation of suprathermal particles at collisionless shocks
[DE85-014114] N86-11034

PLASMA JETS

Velocities of gas and plasmas from real time holographic interograms
[DE85-014618] N86-10530

PLASMA PHYSICS

Activities report in plasma physics N86-11039

PLASMA PINCH

Introduction to the m = 1 helicity source
[DE85-012771] N86-10999

Activities report in plasma physics N86-11039

PLASMA SHEATHS

Generalized helicity and its time derivative
[DE85-012770] N86-11027

PLASMA SPRAYING

Creep-fatigue behavior of NiCoCrAlY coated PWA 1480 superalloy single crystals
[NASA-TM-87110] N86-10311

PLASMAS (PHYSICS)

Improved blue response and efficiency of A-Si:H solar cells deposited from disilane using a dual-chamber plasma system
[DE85-013289] N86-10649

Dynamics of imploding neon gas puff plasmas. 1
[AD-A156916] N86-10983

PLASMONS

Dielectric properties of silicon surfaces and silver thin films
[JUEL-1968] N86-10450

Cooperative emission by two different atoms into surface plasmons
[AD-A157033] N86-10925

PLASTIC DEFORMATION

Low temperature plastic deformation mechanisms of alpha-titanium single crystals
[ESA-TT-871] N86-10332

PLASTIC PROPERTIES

Nonlinear propagation of elastoplastic waves in Ke penetrators (excerpts)
[DE85-011450] N86-10318

Swelling and tensile properties of EBR-2-irradiated tantalum alloys for space reactor applications
[DE85-012887] N86-10329

Finite deformation crack-line fields in a thin elasto-plastic sheet
[AD-A156757] N86-10346

Resistance curves for crack growth under plane-stress conditions in an elastic perfectly-plastic material
[AD-A156778] N86-10593

PLASTICIZERS
Binder-filler interaction in energetic polymers
[AD-A156752] N86-10345
PLASTICS
Automatic processing of reactive polymers
N86-10127
Properties of plastic-bonded nitroguanidine
[DE85-015316] N86-10358
PLATINUM
Multipurpose pan development
[DE85-012326] N86-10319
PLATINUM COMPOUNDS
Compatibility of grain-stabilized platinum with candidate propellants for resistojets
[NASA-TM-87118] N86-10279
PLOTTERS
Restitution of Spacelab photography by analog stereoplotter N86-10489
PLUMES
Vibro-acoustic forecast for space shuttle launches at Vandenberg AFB: The payload changeout room and the administration building
[AD-A156944] N86-10269
PLUTONIUM FLUORIDES
Multipurpose pan development
[DE85-012326] N86-10319
PODS (EXTERNAL STORES)
Test and evaluate passive orbital disconnect struts (PODS 3)
[NASA-CR-177368] N86-10274
POISONING (REACTION INHIBITION)
Effect of H2S and COS in the fuel gas on the performance of ambient pressure phosphoric acid fuel cells
[DE85-013913] N86-10446
Effects of H2S on molten carbonate fuel cells
[DE85-014052] N86-10447
POISSON EQUATION
Analysis of combined natural and forced convection around cylinders and spheres N86-10456
Poisson semigroups and singular integrals
[CTH-MATH-1985-05] N86-10876
A modified Successive Over-Relaxation (SOR) method for the Poisson equation in unsteady free-surface flow calculations
[TW-264] N86-10881
POLARIZATION
Electric field containerless processing technology
N86-10170
POLARIZATION (CHARGE SEPARATION)
AGS polarized H(-) source
[DE85-013296] N86-10935
Beam steering in the SLC linac
[DE85-013370] N86-11025
POLARIZATION (WAVES)
Charge exchange in slow collisions of atoms and molecules N86-10922
POLARIZED RADIATION
Polarization transfer in inelastic scattering and pionic models of the EMC effect
[DE85-010738] N86-10955
Proposed bunching scheme for a polarized H(-) injector
[DE85-012648] N86-10986
POLAROGRAPHY
Method for determining elemental sulfur in jet fuel — differential pulse polarography
[FOA-C-40211-B4] N86-10360
POLICE
Methods for developing jam-resistant security communications networks at fixed-site facilities
[DE85-012032] N86-10408
POLICIES
Tendencies toward liberalization in European air traffic control
[DFVLR-FB-85-23] N86-10030
An anthology: Rationale for a US ballistic missile defense (1969 - 1984)
[AD-A156781] N86-10199
POLLUTION CONTROL
Proceedings: First Annual Acid Deposition Emissions Inventory Symposium
[PB85-200004] N86-10686
POLLUTION MONITORING
Utilization of satellite remote sensing for the monitoring of oil pollution and marine ecosystems in Indonesia. A Tropical Earth Resources Satellite program (TERS) case study implemented for the NLR, Delft N86-10640
Multiple site laser excited pollution monitoring system
[AD-D011769] N86-10674
POLLUTION TRANSPORT
Sediment characterization. Task 2: Instream contaminant study, volume 1
[DE85-013502] N86-10683
POLYACETYLENE
Electrically conducting polymers N86-10333
Polyacetylene polymerization, structure, and electrical transport properties N86-10334
POLYAMIDE RESINS
Age-life prediction of nylon 66 parachute materials. Part 2: Changes in the chemical and physical properties of materials on aging
[AD-A156909] N86-10347
POLYCRYSTALS
The mechanism of erosion of metallic materials under cavitation attack
[NASA-TM-87133] N86-10552
POLYETHYLENES
Cell partition in two polymer aqueous phases
N86-10139
Passive damping concepts for slender columns in space structures
[NASA-CR-176234] N86-10577
POLYIMIDES
Carbon fiber reinforced polymide filament wound tube manufacturing
[BR64172] N86-10339
POLYMER CHEMISTRY
Cell partition in two polymer aqueous phases
N86-10139
Calculation of the glass transition temperatures of linear polymers. Part 1: Rules for hierarchical ordering of the data set
[AD-A156584] N86-10343
Polymer engineering: Polymeric and molecular electronic, dielectric and optical properties for device applications
[AD-A156671] N86-10344
Thermodynamics of polymer-supercritical solvent mixtures
[AD-A157038] N86-11061
POLYMER PHYSICS
Polymer engineering: Polymeric and molecular electronic, dielectric and optical properties for device applications
[AD-A156671] N86-10344
POLYMERIC FILMS
Evaluation and prediction of long-term environmental effects on non metallic materials
[NASA-CR-178495] N86-10340
High voltage instrument transformers for outdoor service with an insulation of low pressure SF6 gas and plastic foils
[BMFT-FB-T-85-034] N86-10449
POLYMERIZATION
Polyacetylene polymerization, structure, and electrical transport properties N86-10334
Synthesis of arylene siloxanylene polymers and copolymers
[AD-D011780] N86-10338
POLYNOMIALS
Partial eigensolutions of large nonsymmetric matrices
[AD-A156711] N86-10867
POLYPHENYLS
Electrically conducting polymers N86-10333
POLYSTATION DOPPLER TRACKING SYSTEM
Sample data phase locked loop for adaptive Doppler tracker
[AD-D011788] N86-10374
POLYSTYRENE
Production of large-particle-size monodisperse latexes in microgravity N86-10146
POLYURETHANE FOAM
Self-heating to ignition measurements and computation of critical size for solar energy collector materials
[DE85-011449] N86-10302
POLYVINYL CHLORIDE
The wearing comfort of the PVC: Combat back pack
[IZF-1984-34] N86-10789
POROSITY
Metallurgy and metallography of braze joints
[DE85-014563] N86-10325
POROUS MATERIALS
KRAK: A computer program for two-phase, two-component porous flow and fracture propagation, revision
[DE85-014264] N86-10469
POSITION (LOCATION)
Long range translocations ashore to offshore using Spacelab-1 metric camera imagery in the perspective of integrated geophysical surveys N86-10499
Capacity for work and hemodynamics in males residing at middle and high latitudes N86-10747
Supervisory control of the right arm of the beam assembly teleoperator
[AD-A156856] N86-10832
POSITION ERRORS
Path error-neglection in straight lane driving
[IZF-1984-32] N86-10783
POSITIONING
User interface enhancement report
[NASA-CR-171898] N86-10820
Parasitic mode losses versus signal sensitivity in beam position monitors
[DE85-014367] N86-10984
Beam stability in a 6 GeV synchrotron light source
[DE85-013850] N86-10979
TRIO interferometer positioning — spaceborne interferometers (TRIO) N86-11111
POSITRON ANNIHILATION
Search for heavy neutrines produced in e(+)e(-) annihilation
[DE85-013372] N86-11035
POSITRONS
Methane-bubble formation in hydrogen-charged Fe-30 ppM C
[DE85-012526] N86-10937
SLC positron damping ring optics design
[DE85-013054] N86-11014
Computer control of rf at SLAC
[DE85-013065] N86-11015
Beam steering in the SLC linac
[DE85-013370] N86-11025
POTASSIUM
Experimental investigations of thermal radiation from potassium atoms and design applications
[DE85-004096] N86-11036
POTASSIUM NITRATES
Development of new ammonium nitrate composite explosives
[DE85-014252] N86-10356
POTENTIAL FIELDS
Potential structures and particle acceleration on auroral field lines
[AD-A156694] N86-10708
POWDER METALLURGY
The role of entrained surface oxides in RS-PM aluminum alloys on resultant structures and properties
N86-10085
Mechanism of the formation of boronised layers on high carbon steel
[BLL-BISI-TRANS-23036-(9022.06)] N86-10306
POWER AMPLIFIERS
Test results for 20-GHz GaAs FET spacecraft power amplifier
[NASA-TM-87072] N86-10379
POWER SERIES
Multivariable partial realization and the aspect of uniqueness
[ER-83/09] N86-10879
POWER SPECTRA
Computational techniques for the analysis and design of digital communication systems
[AD-A156945] N86-10407
POWER SUPPLY CIRCUITS
Protection circuitry for high voltage drivers
[AD-D011781] N86-10414
PRASEODYMIUM
Extraction of lanthanide ions by 2-methyl-8-quinolinol
[DE85-014277] N86-10303
PRECIPITATION (CHEMISTRY)
Growth of organic crystals by Ostwald ripening
N86-10058
Theoretical problems in materials science
N86-10088
Growth and characterization of brushite and lead monetite, simulation and results — Spacelab
N86-10230
PRECIPITATION (METEOROLOGY)
Observations of the snow cover in the southern part of the Buryat Autonomous Soviet Socialist Republic
[NASA-TM-77910] N86-10613
Monthly and Seasonal Weather Outlook for mid-April to mid-May 1985, Volume 39, Number 8
[PB85-195345] N86-10724
PRECIPITATION HARDENING
Fracture toughness of hydrogen-embrittled precipitation-hardened stainless steels
[AD-A156664] N86-10592
PREDICTION ANALYSIS TECHNIQUES
Evaluation of an aerodynamic-load prediction method on a STOL fighter configuration
[NASA-TM-86782] N86-10015
Dynamic analysis of a sled traveling along a rough rail
[AD-A156589] N86-10191
Process models for 3D composites
[AD-A156889] N86-10292
Approaches to cumulative impact assessment
[DE85-013891] N86-10635
Evaluation of surface exchange coefficients from mildex ocean/atmosphere mixed layer data
[AD-A156765] N86-10729
PREDICTIONS
Manned flight simulation: Challenge and response
[NASA-TM-86827] N86-10048
Progressive damage, fracture predictions and post mortem correlations for fiber composites
[NASA-TM-87101] N86-10290

Scaling studies of solar pumped lasers
[NASA-CR-176240] N86-10540

PREPROCESSING
Kalman filter preprocessor
[AD-D011774] N86-10972

PRESIDENTIAL REPORTS
Publication of the Executive Office of the President, January 20, 1981 - December 31, 1984
[PB85-187110] N86-11082

PRESSURE
Effect of sequence of loading on interaction curves for buckling of stiffened shells
[TAE-536] N86-10583

PRESSURE BREATHING
Reaction of rabbit respiration system to hypoxic stimulus in nitrogen-oxygen medium at elevated pressure
N86-10760

PRESSURE DEPENDENCE
Rapid analysis using capillary supercritical fluid chromatography
[DE85-012460] N86-10297
Chemical kinetics and cellular structure of detonations in hydrogen sulphide and air
[DE85-009408] N86-10304

PRESSURE DISTRIBUTION
Experimental and theoretical investigations of the flow around airfoil systems with ground effect
[DFVLR-FB-85-17] N86-10026

PRESSURE DROP
Effect of a shear layer on the stability of an axisymmetrical external compression air intake
N86-10010

PRESSURE EFFECTS
Conducting wall and pressure profile effect on MHD stabilization of axisymmetric mirror
[DE85-013647] N86-11020

PRESSURE GRADIENTS
A root-mean-square pressure fluctuations model for internal flow applications
[NASA-CR-3928] N86-10460

PRESSURE VESSELS
Stiffened and prestressed composite overwrapped pressure vessels N86-10547

PRESTRESSING
Stiffened and prestressed composite overwrapped pressure vessels N86-10547

PREVENTION
Report on the research activities on whole-body vibrations. Human strain due to mechanical vibrations
[ISBN-3-88383-107-7] N86-10773

PRINTED CIRCUITS
Multi-row connector with ground plane board
[AD-D011803] N86-10437
Soudan 2 data acquisition and trigger electronics
[DE85-013864] N86-10443
Increase of the packaging density of Very Large Scale Integration (VLSI) circuits using automatic alignment
[BMFT-FB-T-85-020] N86-10451
Compact, high-speed algorithm for laying out printed circuit board runs N86-10814

PRINTING
Development of metallization process
[NASA-CR-176209] N86-10312

PRISMS
Tunable acousto-optic filter with improved spectral resolution and increased aperture
[AD-D011758] N86-10915

PROBABILITY DISTRIBUTION FUNCTIONS
Superefficient estimation of power functions in simulation experiments
[B8562445] N86-10893

PROBABILITY THEORY
Computational techniques for the analysis and design of digital communication systems
[AD-A156945] N86-10407
New probabilistic modeling and simulation methods for complex time-dependent systems
[DE85-009575] N86-10835
On maximal and distributional coupling
[CTH-MATH-1984-30] N86-10875

PROBLEM SOLVING
The effects of age, sleep deprivation, and altitude on complex performance
[AD-A156987] N86-10771
Extended analysis of the structure of error scores in psychological aptitude tests
[DFVLR-FB-85-20] N86-10780
Well-posed questions and exploration of the space of parameters in linear and non linear inversion
[PN-84/13] N86-10858
On the lanczos method for solving symmetric linear systems with several right-hand-sides
[AD-A156816] N86-10868
Computing the structural index
[DE85-014370] N86-10871
Derivational analogy: A theory of reconstructive problem solving and expertise acquisition
[AD-A156817] N86-10899

PROCESS CONTROL (INDUSTRY)
Automatic processing of reactive polymers
N86-10127

PROCUREMENT POLICY
Making the right choice — silicon photodiodes
N86-10669

PRODUCT DEVELOPMENT
Carbon fiber reinforced polymide filament wound tube manufacturing
[BR64172] N86-10339
Phosphoric and electric utility fuel technology development
[DE85-014741] N86-10651
Strategy for the development of space arrays
N86-11101

PROFILOMETERS
On the use of X-band CW nanosecond airborne radar for terrain profiling
[AD-A156886] N86-10406

PROGRAMMING LANGUAGES
Catalog of Resources for Education in Ada (trademark) and Software Engineering (CREASE). Version 3.0
[AD-A156887] N86-10790
User interface enhancement report
[NASA-CR-171898] N86-10820
The DUCK manual
[AD-A156936] N86-10833
Compexity of higher-order programs
[DE85-012776] N86-10834

PROJECT PLANNING
The first German Spacelab mission D1 reports — Spacelab payloads
[PR-3] N86-10189

PROJECT SETI
SETI radio spectrum surveillance system N86-10400

PROJECTILES
Counterpulse railgun energy recovery circuit
[DE85-011603] N86-10196

PROJECTIVE GEOMETRY
Brauer-Severi schemes of orders
[CTH-MATH-1985-06] N86-10877
Some remarks about cusp forms: Holomorphic and non-holomorphic
[CTH-MATH-1984-26] N86-10902
Galois descent and class groups of orders
[CTH-MATH-1985-09] N86-10904

PROPAGATION (EXTENSION)
The mechanics of delamination in composite materials
N86-10284

PROPELLANT GRAINS
Gas generator fuel flow throttle control system
[AD-D011797] N86-10355

PROPORTIONAL COUNTERS
Soudan 2 data acquisition and trigger electronics
[DE85-013864] N86-10443

PROPULSION
Compatibility of grain-stabilized platinum with candidate propellants for resistojets
[NASA-TM-87118] N86-10279

PROPULSION SYSTEM PERFORMANCE
Experimental performance of a 1-kilowatt arcjet thruster
[NASA-TM-87131] N86-10281

PROTECTION
Development of a sheath for sensor protection in molten steel applications
[AD-A156764] N86-10315
Protection circuitry for high voltage drivers
[AD-D011781] N86-10414

PROTECTIVE COATINGS
Passivation of steel with aqueous amine solutions
[AD-D011749] N86-10314
Aluminum ion plating for corrosion protection of uranium, revision 1
[DE85-012419] N86-10330

PROTEIN METABOLISM
Growth of larger single crystals N86-10186

PROTEINS
Protein single crystal growth under microgravity — Spacelab N86-10228
Automated analysis of digital images generated by two-dimensional gel electrophoresis
[DE85-011906] N86-10526
Romanian plant produces protein concentrate from paraffin-nourished yeasts N86-10741
Biotechnology: Science and practice N86-10742

PROTON BEAMS
Use of the MURA transformation to generate the fields and calculate the motion of protons in the designed Argonne Mini-ASPUN FFAG spiral sector accelerator
[DE85-011477] N86-10934
Treatment planning with ion beams
[DE85-012661] N86-10990
Microwave instability across the transition energy
[DE85-013304] N86-11010

PROTON IRRADIATION
Beam line windows at LAMPF
[DE85-012723] N86-10985

PROTONS
Matter-antimatter transition operators: A manual for modeling N86-10921
Method for determining the position, angle and other injection parameters of a short pulsed beam in the Brookhaven AGS
[DE85-012523] N86-10931
Development and application of the electrochemical etching technique
[DE85-010302] N86-10957

PSYCHOACOUSTICS
Proposed aural nondetectability limits for Army materiel
[AD-A156704] N86-10917

PSYCHOLOGICAL EFFECTS
Report on the research activities on whole-body vibrations. Human strain due to mechanical vibrations
[ISBN-3-88383-107-7] N86-10773

PSYCHOLOGICAL FACTORS
Effect of emotional stress on hemostasis system of healthy persons N86-10745

PSYCHOLOGICAL TESTS
Extended analysis of the structure of error scores in psychological apitude tests
[DFVLR-FB-85-20] N86-10780
Speed of work and error rate: Analyses of individual differences in a choice reaction series with a cognitive component
[DFVLR-FB-85-21] N86-10781
Standardization of tasks: Approach planning — human performance assessment
[IZF-1984-19] N86-10782

PSYCHOLOGY
Psychological Sciences Division 1984 programs
[AD-A156631] N86-10779

PUBLIC HEALTH
Development of the Multi-Attribute Hazard Assessment System (MAHAS) and its application to energy-related waste streams
[DE85-010278] N86-10676
Biotechnology regulation
[GPO-43-778] N86-10733

PULLEYS
Improved arresting and recovery system for test missiles
[AD-D011743] N86-10198

PULSE AMPLITUDE MODULATION
Apparatus for locating passive intermodulation interference sources
[AD-D011798] N86-10435

PULSE CODE MODULATION
Phase coded pulse expander-compressor
[AD-D011817] N86-10376
Pulse compression system
[AD-D011833] N86-10417

PULSE COMMUNICATION
High-rate convolutional code construction with the minimum required SNR criterion N86-10392
The GCF Mark 4 implementation and beyond
N86-10399
Computational techniques for the analysis and design of digital communication systems
[AD-A156945] N86-10407

PULSE COMPRESSION
Phase-coded pulse expander-compressor
[AD-D011812] N86-10375
Pulse compression system
[AD-D011833] N86-10417

PULSE DURATION
Timing system control software in the SLC
[DE85-013380] N86-11024
Recent helicity source and power supply improvements in CTX
[DE85-012741] N86-11028

PULSE GENERATORS
Overpulse railgun energy recovery circuit
[DE85-011607] N86-10197
Calibrated Faraday current and magnetic field sensor
[DE85-013438] N86-10439
Ferrite kicker magnet for the IAMPF switchyard upgrade
[DE85-012657] N86-10996
Engineering high reliability, low-jitter Marx generators
[DE85-012811] N86-11013
Recent helicity source and power supply improvements in CTX
[DE85-012741] N86-11028
Programmable delay unit incorporating a semi-custom integrated circuit
[DE85-013379] N86-11033

PULSE RADAR
Topographic mapping from interferometric synthetic aperture radar observations N86-10622
PULSE RATE
Dynamics of changes of statistical indicators of heart rhythm of persons with different degree of motion sickness N86-10743
PULSE REPETITION RATE
Overpulse railgun energy recovery circuit
[DE85-011607] N86-10197
PULSED LASERS
Contact effects in light activated GaAs switches
[AD-A156957] N86-10434
Time resolved flow velocity and concentration measurements using a travelling thermal lens
[AD-A156706] N86-10541
Design, fabricate and test a 1.06(MU) repetitively pulsed laser
[DE85-014439] N86-10543
Optical detection of photoacoustic pulses in thin silicon wafers
[AD-A156705] N86-10977
PULSED RADIATION
Radiation field results from the SPEED triaxiode, a large area, high dose rate, short pulse 1MV bremsstrahlung source
[DE85-009436] N86-11005
PULSES
Parallel pulse processing for mercuric iodide gamma-ray detectors
[DE85-013391] N86-10528
PURIFICATION
New instrumentation for phase partitioning
N86-10138
Purification and cultivation of human pituitary growth hormones secreting cells N86-10140
PYROLYSIS
Modelling of laser-enhanced chemical vapor deposition N86-10105

Q

Q FACTORS
SAR image quality: A review
[DFVLR-MITT-85-07] N86-10413
Q SWITCHED LASERS
Characterization of vapor and aerosol flows by photothermal methods
[AD-A156601] N86-10465
QUADRATURES
A study of methods to predict and measure the transmission of sound through the walls of light aircraft. Integration of certain singular boundary element integrals for applications in linear acoustics
[NASA-CR-176229] N86-10912
QUADRUPOLE NETWORKS
RFQ-funneling
[DE85-012483] N86-10194
QUALITY CONTROL
Reduction of noble metal stock and noble metal loss during wire production with the Conform extrusion process
[BMFT-FB-T-85-049] N86-10560
Software for an automated gaging system
[DE85-013322] N86-10642
QUANTITATIVE ANALYSIS
Theoretical comparison of classical (K-matrix) and inverse (P-matrix) least-squares methods for quantitative infrared spectroscopy
[DE85-012827] N86-10298
QUANTUM EFFICIENCY
Improved blue response and efficiency of A-Si:H solar cells deposited from disilane using a dual-chamber plasma system
[DE85-013289] N86-10649
QUARTZ
Shock loading and release behavior of x-cut quartz
[DE85-013954] N86-11054
QUASARS
A VLBI survey at 2.29 GHz N86-10383
Radio studies of a complete sample of quasars
N86-11093
QUASI-STEADY STATES
Strength of shells under local transverse loads
N86-10568
QUATERNARY ALLOYS
Laser Raman spectroscopy study of the zinc and bromide ion complex equilibrium in zinc/bromine battery electrolytes
[DE85-011820] N86-10301
QUATERNIONS
Brauer-Severi schemes of orders
[CTH-MATH-1985-06] N86-10677
QUENCHING (COOLING)
Theoretical problems in materials science
N86-10088
Application of the unloading compliance methods in fracture toughness measurements of a quenched and tempered steel
[BLL-BISI-TRANS-21628-(9022.06)] N86-10308
QUINOLINE
Extraction of lanthanide ions by 2-methyl-8-quinolinol
[DE85-014277] N86-10303

R

RADAR
Periodic binary sequences with very good autocorrelation properties N86-10397
A binary sequence of period 60 with better autocorrelation properties than the Barker sequence of period 13 N86-10398
Miniature radar packaging
[DE85-014598] N86-10410
RADAR CROSS SECTIONS
A simplified method of estimation of the specular components of radar cross section for some re-entrant conductors
[AD-A156573] N86-10403
RADAR IMAGERY
SAR image quality: A review
[DFVLR-MITT-85-07] N86-10413
Multisensor data integration techniques N86-10604
NASA/JPL Aircraft SAR Workshop Proceedings
[NASA-CR-176204] N86-10615
Radar system description N86-10616
The effect of vegetation type, microrelief, and incidence angle on radar backscatter N86-10619
Age-dating volcanic and alluvial surfaces with multipolarization data N86-10620
Strategies for analyzing mixed pixels in remotely sensed imagery N86-10623
Mapping diverse forest cover with multipolarization airborne radar N86-10625
RADAR MAPS
High-resolution image data from the Space Shuttle
N86-10494
RADAR RANGE
Guidance and control of a cable based payload pickup system N86-10046
On the use of X-band CW nanosecond airborne radar for terrain profiling
[AD-A156886] N86-10406
RADAR RESOLUTION
SAR image quality: A review
[DFVLR-MITT-85-07] N86-10413
RADAR SCATTERING
Modelling of vegetation volumes N86-10629
Scattering by complicated structures: Calculation of the radar properties of metallic targets by means of physical optics
[DFVLR-FB-85-22] N86-10961
RADAR SIGNATURES
La Recherche Aerospatiale, bimonthly bulletin, no. 1984-5, September-October 1985
[ESA-TT-899] N86-10363
Strategies for analyzing mixed pixels in remotely sensed imagery N86-10623
RADAR TARGETS
Scattering by complicated structures: Calculation of the radar properties of metallic targets by means of physical optics
[DFVLR-FB-85-22] N86-10961
RADAR TRACKING
On the use of X-band CW nanosecond airborne radar for terrain profiling
[AD-A156886] N86-10406
RADAR TRANSMISSION
Propagation and radiation characteristics of a multimode corrugated waveguide feedhorn N86-10388
RADIAL FLOW
Three-dimensional inviscid analysis of radial turbine flow and a limited comparison with experimental data
[NASA-TM-87091] N86-10017
SUTRA (Saturated-unsaturated transport). A finite-element simulation model for saturated-unsaturated, Fluid-Density-Dependent ground-water flow with energy transport or chemically-reactive single-species solute transport
[AD-A156779] N86-10630
RADIANT FLUX DENSITY
Solar modulation of galactic cosmic rays: Techniques and applications N86-11143
RADIANT HEATING
Levitating furnance for containerless processing in space N86-10169
RADIATION DISTRIBUTION
Radiation field results from the SPEED triaxiode, a large area, high dose rate, short pulse 1MV bremsstrahlung source
[DE85-009436] N86-11005
RADIATION DOSAGE
Effect of single actions of weak electromagnetic fields of ultralow frequency on indices of endocrine system
N86-10744
Approaches to quantitative expression of dose response
[DE85-013498] N86-10772
Development and application of the electrochemical etching technique
[DE85-010302] N86-10957
Treatment planning with ion beams
[DE85-012661] N86-10990
RADIATION EFFECTS
Swelling and tensile properties of EBR-2-irradiated tantalum alloys for space reactor applications
[DE85-012687] N86-10329
Criteria for the design or selection of a bioelectromagnetics experiment
[AD-A156575] N86-10420
RADIATION HAZARDS
Approaches to quantitative expression of dose response
[DE85-013498] N86-10772
Hot cell facility design for large fusion devices
[DE85-012893] N86-11037
RADIATION MEASUREMENT
Secondary standards laboratories for ionizing radiation calibrations: The national laboratory interests
[DE85-007046] N86-10938
On-line gamma-ray data acquisition at the Power Burst facility
[DE85-011957] N86-10954
Energy efficiency of the CTX magnetized coaxial plasma source
[DE85-012735] N86-11003
RADIATION MEASURING INSTRUMENTS
On-line gamma-ray data acquisition at the Power Burst facility
[DE85-011957] N86-10954
RADIATION PRESSURE
A modeling analysis program for the JPL table mountain Io sodium cloud
[NASA-CR-176241] N86-11139
RADIATION PYROMETERS
Measurement of workpiece temperature during welding for welding robot control N86-10534
RADIATION SOURCES
Sound radiation from repetitive transient vibrations using multi-channel digital signal processing with application to impact machinery N86-10910
RADIATIVE HEAT TRANSFER
Radiative heat transfer in nonisothermal combustion products N86-10458
RADICALS
Cometary atmospheres: Modeling the spatial distribution of observed neutral radicals
[NASA-CR-176242] N86-11133
RADIO ANTENNAS
Seismic analysis of the large 70-meter antenna, part 1: Earthquake response spectra versus full transient analysis N86-10386
Load-deflection tests and computer analyses of a high-precision adhesive-bonded antenna reflector panel
N86-10389
Planning for VLA/DSN arrayed support to the Voyager at Neptune N86-10395
A VLA experiment: Planning for Voyager at Neptune
N86-10396
RADIO ASTRONOMY
Radio studies of a complete sample of quasars
N86-11093
Radio astronomy experience in image reconstruction. A history lesson for optical astronomers N86-11117
VLBI at optical and radio wavelengths: Congruences and contrasts N86-11126
RADIO CONTROL
Construction and use of a radio controlled model helicopter for research
[AD-A156547] N86-10035
RADIO EMISSION
Radio studies of a complete sample of quasars
N86-11093
RADIO EQUIPMENT
Methods for developing jam-resistant security communications networks at fixed-site facilities
[DE85-012032] N86-10408
RADIO FREQUENCIES
RFQ-funneling
[DE85-012483] N86-10194

Apparatus for locating passive intermodulation interference sources
[AD-D011796] N86-10435
High-power rf controls for the NBS-Los Alamos racetrack microtron
[DE85-012658] N86-10993
Superconductors for pulsed RF accelerators
[DE85-013378] N86-11051

RADIO FREQUENCY DISCHARGE
High-resolution phosphor screen beam profile monitor
[DE85-013074] N86-11012

RADIO FREQUENCY INTERFERENCE
SETI radio spectrum surveillance system N86-10400

RADIO SOURCES (ASTRONOMY)
Improved mapping of radio sources from VLBI data by least-square fit N86-10402
A superconducting tunnel junction receiver for millimeter-wave astronomy N86-11041

RADIO SPECTRA
SETI radio spectrum surveillance system N86-10400

RADIO TELESCOPES
Planning for VLA/DSN arrayed support to the Voyager at Neptune N86-10395
A VLA experiment: Planning for Voyager at Neptune N86-10396

RADIO TRANSMISSION
Digital radio link: Method and a measuring system for studying the radio channel during frequency selective fading
[FOA-C-30386-E2] N86-10411

RADIO TRANSMITTERS
An experimental TE sub 12 - TE sub 11 circular waveguide mode converter N86-10387

RADIOACTIVE DECAY
Relativistic wavefunction at the origin and the pion decay constant
[DE85-012392] N86-11062

RADIOACTIVE ISOTOPES
General-purpose heat source development: Safety Verification Test Program. Bullet/fragment test series
[DE85-014262] N86-10660
Impact of long-lived radionuclides on waste classification for fusion
[DE85-013205] N86-10959

RADIOACTIVE MATERIALS
Hot cell facility design for large fusion devices
[DE85-012893] N86-11037

RADIOACTIVE WASTES
Recirculation within a glass mixture subjected to external and resistive heating
[DE85-010068] N86-10348
Impact of long-lived radionuclides on waste classification for fusion
[DE85-013205] N86-10959
Hot cell facility design for large fusion devices
[DE85-012893] N86-11037

RADIOACTIVITY
Automated analysis of digital images generated by two-dimensional gel electrophoresis
[DE85-011906] N86-10526

RADIOMETERS
Mobile VLBI and GPS measurement of vertical crustal motion N86-10401

RADOMES
Attachment method-ceramic radome to metal body
[AD-D011778] N86-10032
Radome analysis and design capabilities of the RF and Microwave Technology Branch
[AD-A156662] N86-10404

RAIL TRANSPORTATION
Study of statis and dynamic stress effects in nonlinear solids
[NASA-CR-176236] N86-10578

RAILGUN ACCELERATORS
Counterpulse railgun energy recovery circuit
[DE85-011603] N86-10196
Overpulse railgun energy recovery circuit
[DE85-011607] N86-10197
EMACK railgun firing test report number 9
[AD-A156661] N86-10354

RAILS
Study of statis and dynamic stress effects in nonlinear solids
[NASA-CR-176236] N86-10578

RAMAN SPECTRA
Spontaneous Raman spectroscopy of shocked H2O
[DE85-014557] N86-10470
Real-time holography by stimulated Raman and Brillouin scattering N86-10479

RAMAN SPECTROSCOPY
Design and calibration of a flat-flame burner using line reversal techniques
[AD-A156724] N86-10294
Laser Raman spectroscopy study of the zinc and bromide ion complex equilibrium in zinc/bromine battery electrolytes
[DE85-011620] N86-10301

RAMJET ENGINES
Theoretical specific impulse for two-phase flow in nozzle of rocket-ramjet engine: A simple estimation method N86-10005

RANDOM NOISE
A study of Morrison's iterative noise removal method
[NASA-CR-176222] N86-10823

RANDOM SAMPLING
Adaptive distribution-free test for the K random sampling problem, part 1
[COMP-CENT-NOTE-14-PT-1] N86-10888
Adaptive distribution free test for the K random sampling problem, part 2
[COMP-CENT-NOTE-15-PT-2] N86-10889

RANGE (EXTREMES)
An active tracking band-pass filter
[AD-A156559] N86-10419

RANGE FINDERS
Satellite use for men — West German space program N86-10183
A nanosecond or thirty centimeters: Why atomic clocks have to be synchronized. MITREX opens new dimensions for measuring accuracy N86-10185

RANGEFINDING
Phase coded pulse expander-compressor
[AD-D011817] N86-10376

RANK TESTS
Adaptive distribution-free test for the K random sampling problem, part 1
[COMP-CENT-NOTE-14-PT-1] N86-10888
Adaptive distribution free test for the K random sampling problem, part 2
[COMP-CENT-NOTE-15-PT-2] N86-10889
Nonparametric comparison of several mean values with mild adaptation to some sample characteristics
[COMP-CENT-NOTE-20] N86-10891

RANKINE CYCLE
Fuel Cell Technology Assessment Program, work element no. 6
[DE85-008228] N86-10444

RANKING
Rank revealing QR-Factorizations
[AD-A156756] N86-10887

RARE GASES
Determination of optical properties by third-harmonic generation in noble gases in unfocused laser beams N86-10535
Experimental X-ray scattering cross sections for H2 and rare atomic gases
[DE85-011572] N86-10936

RATES (PER TIME)
Study of one- and two-dimensional filtering and deconvolution algorithms for a streaming array computer
[NASA-CR-176221] N86-10822

RATS
Evaluation of the 90-day inhalation toxicity of petroleum and oil shale JP-5 jet fuel
[AD-A156815] N86-10675

RAY TRACING
Theoretical analysis of Wolter/LSM X-ray telescope systems
[NASA-CR-176244] N86-11095

RAYLEIGH NUMBER
Rayleigh-Benard instability in systems presenting a minimum in surface tension N86-10245

REACTION KINETICS
Fundamental studies of droplet combustion at reduced gravity N86-10165
A procedure identifying a polyacetylene initiator of olefin metathesis. The reactivities of metal-carbenes toward alkenes and alkynes
[AD-A156997] N86-10283
Catalytic activity of shock modified ZnO for CO oxidation and methanol synthesis
[DE85-014704] N86-10300
Self-heating to ignition measurements and computation of critical size for solar energy collector materials
[DE85-011449] N86-10302
Chemical kinetics and cellular structure of detonations in hydrogen sulphide and air
[DE85-009406] N86-10304
Kinetics of biological ferrous iron oxidation
[DE85-014616] N86-10736
Physical acoustics: Investigation of chemical kinetic and thermodynamic properties of fluids N86-10911

REACTIVITY
The role of entrained surface oxides in RS-PM aluminum alloys on resultant structures and properties N86-10085
Study of the reactive-element effect in oxidation of Fe-Cr alloys using transverse section analytical electron microscopy N86-10087

REACTOR DESIGN
Alternative fusion concepts and the prospects for improved reactors
[DE85-009622] N86-11031

REACTOR MATERIALS
ORR core re-configuration measurements to increase the fast neutron flux in the Magnetic Fusion Energy (MFE) experiments
[DE85-013520] N86-10958

REACTOR PHYSICS
Report on a visit to CERN in February 1985. Notes on bunch monitors, high-frequency systems, linacs, kickers, magnets, vacuum and bunch extraction
[LINO-119] N86-10967

REACTOR SAFETY
Activities report in safety N86-10365

REACTORS
Dust deposition in regions of separated flow
[JUEL-1985] N86-10475

READOUT
Soudan 2 data acquisition and trigger electronics
[DE85-013864] N86-10443

REAL GASES
On the method of characteristics and its application to the calculations of annular nozzle flowfields N86-10454

REAL TIME OPERATION
Velocities of gas and plasmas from real time holographic interograms
[DE85-014618] N86-10530
Computer control of an electric hydraulic robot leg with proximity ranging system N86-10549
Efficient systolic arrays for the solution of toeplitz systems: An illustration of a methodology for the construction of systolic architectures in VLSI (Very Large Systems Integration)
[AD-A156767] N86-10795
Classification of real-time program testing tasks and methods N86-10815

REAL VARIABLES
Coordinate axes, location of origin, and redundancy for the one and two-dimensional discrete Fourier transform
[NASA-CR-176225] N86-10826

RECEIVERS
Instantaneous frequency measurement receiver with digital processing
[AD-D011759] N86-10425
Fiber optic gradient hydrophone construction and calibration for sea trial
[AD-A156469] N86-10914

RECIRCULATIVE FLUID FLOW
Confined swirling jet predictions using a multiple-scale turbulence model
[NASA-CR-178484] N86-10462

RECOMMENDATIONS
Research needs for corrosion control and prevention in energy conservation systems
[DE85-014852] N86-10326

RECORDING
Fall velocity indicator/viewer
[AD-D011769] N86-10482

RECOVERABILITY
Improved arresting and recovery system for test missiles
[AD-D011743] N86-10198

RECTANGULAR WINGS
Experimental and theoretical investigations of the flow around airfoil systems with ground effect
[DFVLR-FB-85-17] N86-10026

RECURSIVE FUNCTIONS
Acceleration-invariant approximation method for recursive digital filters
[AD-A156655] N86-10865

RED SEA
Report of the Workshop on Geologic Applications of Remote Sensing to the Study of Sedimentary Basins
[E86-10002] N86-10599
Analysis of remote sensing data N86-10605

RED SHIFT
Radio studies of a complete sample of quasars N86-11093

REDOX CELLS
High-temperature controlled redox crystallization studies N86-10178

REDUCED GRAVITY
Microgravity Science and Applications Program tasks
[NASA-TM-87568] N86-10053
Solutal convection and its effects on crystal growth and segregation in binary and pseudo-binary system with large liquidus-solidus separation N86-10056
Crystal growth research in space N86-10057
Growth of organic crystals by Ostwald ripening N86-10058
The influence of low frequency mechanical vibrations on the growth of single crystals N86-10059
The control of float zone interfaces by the use of selected boundary conditions N86-10060

Crystal growth of device quality GaAs in space N86-10061
Crystal melts under reduced gravity N86-10062
Microgravity silicon zoning investigation N86-10063
Solution growth of crystals in zero-gravity N86-10064
Growth of solid solution crystals N86-10065
HgI sub 2 crystal growth for nuclear detectors N86-10066
Fluid dynamics and thermodynamics of vapor phase crystal growth N86-10068
Vapor growth of alloy-type semiconductor crystals N86-10069
Modeling directional solidification N86-10071
Heat flow and segregation in directional solidification N86-10072
Effect of undercooling in a low-gravity containerless environment on the structure and properties of alloys N86-10073
Control of cast iron microstructure N86-10084
Solidification fundamentals N86-10090
Diffusion in immiscible melts N86-10096
Directional solidification of monotectic and hypermonotectic aluminum-indium alloys under micron-g N86-10097
Environmental degradation of materials: Surface chemistry related to stress corrosion cracking N86-10099
Graphite formation in cast iron N86-10100
Theoretical studies of the surface tension of liquid metal system N86-10101
Cloud microphysics by thermal wave methods N86-10103
Extension of Ostwald ripening theory N86-10104
Dynamic thermophysical measurements in space [NASA ORDER H-27954-B] N86-10106
Transport processes in solution crystal growth N86-10107
Free surface phenomena under low- and zero-gravity conditions N86-10108
Thermocapillary flows and their stability: Effects of surface layers and contamination N86-10109
Mass transport phenomena between bubbles and dissolved gases in liquids under reduced gravity conditions N86-10110
Suppression of Marangoni convection in float zones N86-10111
Studies of model immiscible systems N86-10112
Light scattering tests of fundamental theories of transport properties in the critical region N86-10113
Transient heat transfer in zero gravity environment [NASA ORDER H-27954B] N86-10114
Surface tensions and their variations with temperature and impurities [NASA ORDER H-27954B] N86-10115
Direct observation of critical point wetting in microgravity N86-10116
Surface tension induced instabilities in reduced gravity: The Benard problem N86-10117
Critical transport phenomena in fluid helium under low gravity N86-10119
Surface-tension driven convection N86-10124
Thermocapillary motion research N86-10125
Thermocapillary and diffusocapillary migration of a fluid drop N86-10128
Transport processes research N86-10129
Experimental and theoretical analysis of chemical vapor deposition with prediction of gravity effects N86-10132
Hormone purification by isoelectric focusing N86-10135
Cell partition in two polymer aqueous phases N86-10136
A study of blood flow and of aggregation of blood cells under conditions of zero gravity: Its relevance to the occlusive diseases and cancer N86-10137
New instrumentation for phase partitioning N86-10138
Cell separations in microgravity and development of a space bioreactor N86-10141
Cell maintenance systems N86-10142
Kidney cell electrophoresis N86-10145
Production of large-particle-size monodisperse latexes in microgravity N86-10146
Containerless processing of glass forming melts in space N86-10148
Sol-gel glasses N86-10153
Physical phenomena in containerless glass processing N86-10155
Fusion target technology N86-10156
Solid surface combustion at reduced gravity N86-10159
Buoyancy effects upon vapor flame and explosion processes N86-10161
A fundamental study of smoldering with emphasis on experimental design for zero-g N86-10162
Ignition and flame spread above liquid fuel pools N86-10163
Flammability limits of gases under low gravity conditions N86-10164
Fundamental studies of droplet combustion at reduced gravity N86-10165
Development of materials processing systems for use in space on low-g simulation devices N86-10166
Multimode acoustic research N86-10167
Levitating furnance for containerless processing in space N86-10169
Microgravity Materials Science Laboratory N86-10173
High-temperature controlled redox crystallization studies N86-10178
Fifth European symposium on Material Sciences under Microgravity. Results of Spacelab 1 [ESA-SP-222] N86-10200
The fluid physics module: A technical description — Spacelab N86-10201
Capillary forces in a low gravity environment — Spacelab N86-10202
Oscillations of semi-free liquids in microgravity: Spacelab 1 experiment ES 326 N86-10204
Axisymmetric free surface behavior of moving liquid in a cylinder in microgravity — Spacelab N86-10206
Kinetics of spreading of liquids in microgravity: Experiment 1 ES 327 — Spacelab N86-10207
Influences affecting separation in monotectic alloys under microgravity N86-10209
Particle coarsening in immiscible zinc-lead alloys under microgravity — Spacelab N86-10210
Melting and solidification of metal matrix composites under microgravity — Spacelab N86-10211
Unidirectional solidification of cast iron: Experiment ES-325 — Spacelab N86-10212
Vacuum brazing under microgravity — Spacelab N86-10214
Melting and solidification in O-g of sintered alloys: Experiments ES 311 A and B bubble reinforced materials — Spacelab N86-10215
Directional solidification of an aluminum-zinc vapor emulsion in microgravity — Spacelab N86-10218
Protein single crystal growth under microgravity — Spacelab N86-10228
Mathematical simulation of disturbing forces and material science processes under low gravity N86-10236
Numerical simulation of convections in the microgravity environment N86-10239
Verification of turbulence developing from the oscillatory Marangoni convection in a liquid column — rocket flight N86-10241
Measurements of the critical Marangoni number of the laminar-oscillatory transition of thermocapillary convection in floating zones N86-10242
Experimental study on Marangoni convection N86-10243
Stability of long liquid columns N86-10244
Separation of aqueous two-phase polymer systems in microgravity N86-10246
Rationale for two phase polymer system microgravity separation experiments N86-10247
Application of the theory of Ostwald ripening to microgravity phase separation experiments N86-10248
Nucleate pool boiling in subcooled liquid under microgravity: Results of TEXUS experimental investigations N86-10250
Surface forces in contacting solids — microgravity rocket experiment N86-10252
Shrinking of a gas bubble in a glass melt under microgravity conditions — STS-11 N86-10254
Physical and chemical properties of a nickel catalyst processed under microgravity — STS-7 N86-10255
Cellular morphologies in lead-thallium alloys — gravitational effects N86-10262
Motion analysis report [NASA-CR-171897] N86-10896
Zero-gravity movement studies [NASA-CR-171899] N86-10897
Space sciences: Perspectives of commercial utilization for the German industry N86-11068

REDUNDANCY
Coordinate axes, location of origin, and redundancy for the one and two-dimensional discrete Fourier transform [NASA-CR-176225] N86-10526

REENTRY VEHICLES
Three articles on new calculation methods in aeronautics (selected articles) [AD-A145745] N86-10007

REFINING
Glass research N86-10157

REFLECTANCE
Vision test chart and method using Gaussians [AD-D011756] N86-10778
Preliminary investigation of changes in X-ray multilayer optics subjected to high radiation flux [DE85-014074] N86-10944

REFLECTION
Total internal reflection modulator/deflector [AD-D011757] N86-10424
Laser target speckle eliminator [AD-D011775] N86-10536

REFLECTORS
A numerical method for approximating antenna surfaces defined by discrete surface points [NASA-TM-87125] N86-10381
Theoretical analysis of Wolter/LSM X-ray telescope systems [NASA-CR-176244] N86-11095

REFRACTION
Crustal structure of the southern Rio Grande rift determined from seismic refraction, surface wave dispersion, and gravity data N86-10700

REFRACTORIES
Swelling and tensile properties of EBR-2-irradiated tantalum alloys for space reactor applications [DE85-012667] N86-10329

REFRACTORY MATERIALS
Development of a sheath for sensor protection in molten steel applications [AD-A156784] N86-10315

REFRIGERANTS
Freezer model using a population balance approach for steady-state, direct-contact, secondary refrigerant, freeze desalination N86-10361
Heat transfer in condensing and evaporating two-component, two-phase flow inside a horizontal tube N86-11058

REFRIGERATING MACHINERY
Engine-driven and absorption heat pump programs [DE85-013930] N86-10472

REGRESSION ANALYSIS
Regression analysis: Assumptions, alternatives, applications N86-10895

REGULATIONS
Tendencies toward liberalization in European air traffic control [DFVLR-FB-85-23] N86-10030
Biotechnology regulation [GPO-43-778] N86-10733

RELATIVISTIC EFFECTS
Relativistic wavefunction at the origin and the pion decay constant [DE85-012392] N86-11062
A method for numerical relativity: Simulation of axisymmetric gravitational collapse and gravitational radiation generation N86-11127

RELATIVISTIC ELECTRON BEAMS
Laser generation and transport of a relativistic electron beam [DE85-011709] N86-10192
Directionality of bremsstrahlung from relativistic electrons in solar flares [NASA-TM-87509] N86-11141

RELATIVITY
Initial data for N black holes N86-11128

RELAXATION (MECHANICS)
Anelastic relaxation in irradiated Cu-Be [DE85-013693] N86-11056

RELAXATION METHOD (MATHEMATICS)
A modified Successive Over-Relaxation (SOR) method for the Poisson equation in unsteady free-surface flow calculations [TW-264] N86-10881

RELIABILITY
Microcircuit device reliability field experience database. Volume 1. Field data. Volume 2. Failure Event/Analysis data [AD-A156836] N86-10433
Load space formulation of reliability for nonlinear random structural systems N86-10570
Elektronika MS 1603 high-speed peripheral processor N86-10611

REMOTE CONSOLES
SARSAT LUC (Local user terminal) to CMCC (Canadian Mission Control Centre) alert data interface: A critical review [AD-A156881] N86-10276

REMOTE CONTROL
Construction and use of a radio controlled model helicopter for research [AD-A156547] N86-10035

REMOTE HANDLING
Beginnings of remote handling at the RAL Spallation Neutron Source [DE85-012881] N86-11001

REMOTE REGIONS
The dirigible: A catalyst for resource exploitation in remote areas? [AD-A156518] N86-10034
Geological mapping of remote mountainous regions using metric camera imagery — Spacelab N86-10503

Photovoltaic systems in remote locations: An experience summary
[NASA-TM-87106] N86-10643

REMOTE SENSING

Discussion on the progress and future of satellite communication (Japan)
[NASA-TM-77672] N86-10378

Remote sensing
[NOTA-1535] N86-10638

Remote sensing study project East Gelderland (Netherlands). Part 2: Remote sensing flights in 1982 and 1983; organization aspects N86-10639

Life sciences research on the space station: An introduction
[NASA-TM-86836] N86-10734

REMOTE SENSORS

Multiple site laser excited pollution monitoring system
[AD-D011769] N86-10674

REPORTS

X-ray satellite
[NASA-TM-77923] N86-10273

Photovoltaics: Report, 1984
[DE85-014713] N86-10658

REQUIREMENTS

Specification for the performance, design, development and test requirements for a severe environment cartridge recorder. Issue 4
[AD-A156637] N86-10523

Test, measurement, and diagnostic equipment (system peculiar)
[AD-A156669] N86-10563

RESCUE OPERATIONS

The quest for a helicopter suitable for combat rescue, 1967 - 1983
[AD-A156842] N86-10040

SARSAT LUC (Local user terminal) to CMCC (Canadian Mission Control Centre) alert data interface: A critical review
[AD-A156881] N86-10276

RESEARCH

Psychological Sciences Division 1984 programs
[AD-A156831] N86-10779

Study of one- and two-dimensional filtering and deconvolution algorithms for a streaming array computer
[NASA-CR-176226] N86-10627

RESEARCH AIRCRAFT

User manual for the Falcon system — Falcon research aircraft
[DFVLR-MITT-85-08] N86-10721

RESEARCH AND DEVELOPMENT

Research needs for corrosion control and prevention in energy conservation systems
[DE85-014852] N86-10326

Soviet free-electron laser research
[AD-A156898] N86-10542

Phosphoric and electric utility fuel technology development
[DE85-014741] N86-10651

Alternative fusion concepts and the prospects for improved reactors
[DE85-009622] N86-11031

Space research expenses of the Federal Ministry of Research and Technology (BMFT) in the period 1983-1985 N86-11070

Academic Research Equipment in selected science-engineering fields, 1982-83. An analysis of findings from the Baseline National Survey of academic research instruments and instrumentation needs N86-11088

Aerospace research at NLR N86-11089

RESEARCH FACILITIES

Collective use computer system for the Academy of Sciences KaSSR N86-10817

Academic Research Equipment in selected science-engineering fields, 1982-83. An analysis of findings from the Baseline National Survey of academic research instruments and instrumentation needs N86-11088

RESEARCH MANAGEMENT

LSRO/ONR ad hoc review process
[AD-A156590] N86-10735

Mission orientation in science N86-11066

Space utilization N86-11067

Space research expenses of the Federal Ministry of Research and Technology (BMFT) in the period 1983-1985 N86-11070

Report of the ad hoc committee to review the program of the SDI Directorate on Innovative Science and Technology (IST)
[AD-A156668] N86-11071

Activities report of the Space Flight Laboratory N86-11090

Activities Report of the Space Flight Laboratory N86-11091

RESERVES

Maximum water reserves in the snow cover in the European territory of the USSR according to data for 1892-1960
[NASA-TM-77901] N86-10611

RESERVOIRS

Geologic evaluation and reservoir properties of the PR Spring tar sand deposit, Uintah and Grand Counties, Utah
[DE85-013248] N86-10634

RESIDENTIAL ENERGY

Comparative analysis of single and continuously variable-capacity heat pump concepts
[DE85-004089] N86-10653

Analyses of advanced residential absorption heat pump cycles
[DE85-005244] N86-10664

Contribution of wind energy to the energy balance of a combined solar and wind energy system. Part 1: System description, data acquisition and system performance
[BMFT-FB-T-85-051-VOL-1] N86-10670

Contribution of wind energy to the energy balance of a combined solar and wind energy system. Part 2: Computer-assisted investigations
[BMFT-FB-T-85-052-VOL-2] N86-10671

RESIDUAL STRENGTH

Fatigue of graphite/epoxy buffer strip panels with center cracks
[NASA-TM-87595] N86-10581

RESIDUES

A fundamental study of the sticking of insect residues to aircraft wings
[NASA-CR-176231] N86-10033

RESIN BONDING

The preparation and testing of titanium and zirconium coupling agents
[SJ70] N86-10576

RESINS

Continuous fiberization of silicon-carbide-nitride precursor resin N86-10168

Carbon fiber reinforced polymide filament wound tube manufacturing
[BR64172] N86-10339

RESISTANCE

Resistance curves for crack growth under plane-stress conditions in an elastic perfectly-plastic material
[AD-A156778] N86-10593

RESISTOJET ENGINES

Compatibility of grain-stabilized platinum with candidate propellants for resistojets
[NASA-TM-87118] N86-10279

RESONANCE

Supersonic metal cluster beams
[DE85-014321] N86-10966

Analytic evaluation of LAMPF 2 Booster Cavity design
[DE85-012680] N86-11002

RESONANCE TESTING

Test and evaluate passive orbital disconnect struts (PODS 3)
[NASA-CR-177368] N86-10274

RESONANT FREQUENCIES

Electromagnetic resonances of cylinders and aircraft model with resistive wires
[NASA-CR-176250] N86-10042

RESPIRATION

Evaluation of the 90-day inhalation toxicity of petroleum and oil shale JP-5 jet fuel
[AD-A156815] N86-10675

RESPIRATORS

Conditioning potentialities of respiratory apparatus N86-10753

RESPIRATORY RATE

Dynamics of general resistance of rats during readaptation period after training in altered gas environment N86-10767

RESPIRATORY SYSTEM

Classification of changes in electrocardiogram during muscular exertion of healthy individuals N86-10755

Reaction of rabbit respiration system to hypoxic stimulus in nitrogen-oxygen medium at elevated pressure N86-10760

RESPONSE TIME (COMPUTERS)

Study of one- and two-dimensional filtering and deconvolution algorithms for a streaming array computer
[NASA-CR-176221] N86-10822

RESPONSES

Determining a physically appropriate neutron spectrum from multisphere data
[DE85-013045] N86-10299

A transformation method for the evaluation of the response moments of elastic structures with random properties
[AD-A156882] N86-10557

A study of Morrison's iterative noise removal method
[NASA-CR-176222] N86-10823

Always-convergent iterative noise removal and deconvolution for image data
[NASA-CR-176223] N86-10824

RETARDING

Suppression of Marangoni convection in float zones N86-10111

RETROFITTING

Retrofit of SAC EC-135C and RC-135 aircraft with CFM-56 engines
[AD-A156688] N86-10038

REYNOLDS STRESS

Large eddy interactions in a turbulent channel flow
[NASA-TM-86757] N86-10464

RHEOELECTRICAL SIMULATION

Determination of thermophysical characteristics of solid materials by electrical modelling of the solutions to the inverse problems in nonsteady heat conduction
[NASA-TM-77907] N86-10293

RHEOLOGY

A study of blood flow and of aggregation of blood cells under conditions of zero gravity: Its relevance to the occlusive diseases and cancer N86-10137

Geothermal influences on the long-term thickness of the mechanical lithosphere during flexure N86-10697

RHONE DELTA (FRANCE)

Interpretation of metric camera concerning hydrologic structures of the Rhone Delta --- Spacelab N86-10504

Topographic and thematic mapping: Analysis of metric camera black and white photographs of the Rhone Delta N86-10514

RIO GRANDE (NORTH AMERICA)

Crustal structure of the southern Rio Grande rift determined from seismic refraction, surface wave dispersion, and gravity data N86-10700

RISK

Development of the Multi-Attribute Hazard Assessment System (MAHAS) and its application to energy-related waste streams
[DE85-010278] N86-10676

Initial design of a relational database system for NPS computer asset identification and valuation for risk assessment
[AD-A156847] N86-10796

Framework for generating expert systems to perform computer security risk analysis
[DE85-014134] N86-10841

Risk propensity, action readiness and the roles of societal and individual decision makers
[IZF-1984-27] N86-11077

RIVER BASINS

Tertiary and quaternary research with remote sensing methods N86-10603

Paleogene vertebrate paleontology, geology and remote sensing in the Wind River Basin N86-10609

RIVERS

Report of the Workshop on Geologic Applications of Remote Sensing to the Study of Sedimentary Basins
[E86-10002] N86-10599

RIVETED JOINTS

Correlation between vibrations and buckling of cylindrical shells stiffened by spot-welded and riveted stringers
[TAE-537] N86-10584

ROBOTICS

Dynamic analysis of robotic manipulations with flexible links N86-10545

Computer control of an electric hydraulic robot leg with proximity ranging system N86-10549

ROBOTS

Measurement of workpiece temperature during welding for welding robot control N86-10534

USSR report: Cybernetics, computers and automation technology
[JPRS-UCC-85-006] N86-10809

ROBUSTNESS (MATHEMATICS)

Robust failure detection filters
[NASA-CR-176232] N86-10271

Robustness of multiple comparisons against variance heterogeneity
[COMP-CENT-NOTE-17] N86-10890

ROCKET ENGINE CASES

Ultrasonic evaluation of mechanical properties of thick, multilayered, filament wound composites
[MASA-TM-87088] N86-10561

ROCKET ENGINES

Analytical investigation of solid rocket nozzle failure
[NASA-TM-86513] N86-10278

ROCKET EXHAUST

Vibro-acoustic forecast for space shuttle launches at Vandenberg AFB: The payload changeout room and the administration building
[AD-A156944] N86-10269

ROCKET FLIGHT

Skin casting of alloys and composites: Results of Spacelab (SL)-1 and TEXUS experiments N86-10213

The TEXUS flight results on convective flows and heat transfer in simulated floating zones N86-10235

Verification of turbulence developing from the oscillatory Marangoni convection in a liquid column — rocket flight
N86-10241

A preliminary report on floating zone experiments with germanium crystals in a sounding rocket N86-10256

ROCKET LAUNCHING
Vibro-acoustic forecast for space shuttle launches at Vandenberg AFB: The payload changeout room and the administration building
[AD-A156944] N86-10269

ROCKET NOZZLES
High temperature mechanical testing of a cylindrical weave carbon-carbon composite
[AD-A156639] N86-10591

ROCKET PROPELLED SLEDS
Dynamic analysis of a sled traveling along a rough rail
[AD-A156589] N86-10191

ROCKS
Analysis of remote sensing data N86-10605

Remote stratigraphic and structural analysis: Multisensor results in the Wind River/Bighorn Basin area, Wyoming N86-10606

Geothermal influences on the long-term thickness of the mechanical lithosphere during flexure N86-10697

Fundamental study of the closure property of joints
N86-10698

ROCKY MOUNTAINS (NORTH AMERICA)
Report of the Workshop on Geologic Applications of Remote Sensing to the Study of Sedimentary Basins
[E86-10002] N86-10599

Foreland basin structures and remote sensing
N86-10608

ROLL
The influence of tactual seat-motion cues on training and performance in a roll-axis compensatory tracking task setting N86-10784

ROOM TEMPERATURE
Liquid to gas leak ratios with liquid nitrogen and liquid helium
[DE85-012950] N86-11030

ROOT-MEAN-SQUARE ERRORS
A root-mean-square pressure fluctuations model for internal flow applications
[NASA-CR-3928] N86-10460

ROTARY WINGS
Theoretical study of the unsteady linear problem for a rectangular wing with a pitching movement
[ONERA-RT-17/1841-RY-010-R] N86-10022

ROTATION
Theoretical modeling of the vapor cavitation in dynamically loaded journal bearings
[NASA-TM-87076] N86-10463

A superconducting tunnel junction receiver for millimeter-wave astronomy N86-11041

ROTOR BLADES (TURBOMACHINERY)
Forced response analysis of an aerodynamically detuned supersonic turbomachine rotor
[NASA-TM-87093] N86-10019

ROTORS
Three-dimensional inviscid analysis of radial turbine flow and a limited comparison with experimental data
[NASA-TM-87091] N86-10017

ROUGHNESS
A quantitative method for analyzing the roughness of the seafloor N86-10726

RUBBER
The rubber tube test section of the DFVLR in Goettingen, West Germany — wind tunnel walls
[DFVLR-FB-85-18] N86-10051

Whole plant utilization of sunflowers as a renewable source of strategic materials (rubber)
[AD-A155833] N86-10342

Membrane research in energy and solvent recovery from industrial effluent streams
[DE85-014583] N86-10682

RUSTING
Rusty bolt intermodulation interference reducer
[AD-D011748] N86-10313

Passivation of steel with aqueous amine solutions
[AD-D011749] N86-10314

RUTHENIUM
Application of the ruthenium and technetium thermodynamic data bases used in the EQ3/6 geochemical codes
[DE85-013766] N86-10632

S

S CURVES
Stellar s-process diagnostics
[DE85-012926] N86-11134

SACCADIC EYE MOVEMENTS
Eye-movement activity as index of functional state of brain N86-10756

SAFETY DEVICES
Evaluation of the International Atomic Energy Agency (IAEA) Safeguards Analytical Laboratory quality assurance program
[DE85-012078] N86-10953

SAFETY MANAGEMENT
Activities report in safety N86-10365

Evaluation of the International Atomic Energy Agency (IAEA) Safeguards Analytical Laboratory quality assurance program
[DE85-012078] N86-10953

SANDSTONES
Tertiary and quaternary research with remote sensing methods N86-10603

SARSAT
SARSAT LUC (Local user terminal) to CMCC (Canadian Mission Control Centre) alert data interface: A critical review
[AD-A156881] N86-10276

SATELLITE ANTENNAS
A dual frequency microstrip antenna for Ka band
[NASA-TM-87124] N86-10380

SATELLITE ATTITUDE CONTROL
Nonlinear methods for spacecraft attitude maneuvers
[AD-A156956] N86-10275

SATELLITE IMAGERY
Satellite use for men — West German space program
N86-10180

Satellite data even for a poultry farm. A development for Tanzania. Image evaluation following new ways
N86-10182

With Argus eyes from space. Satellite Diagnosis for Upper Volta. Seven maps without mystery N86-10183

LANDSAT TM image data quality analysis for energy-related applications
[E85-10109] N86-10597

Applications for three-dimensional computer graphic cloud representations produced from satellite imagery
[AD-A156903] N86-10798

SATELLITE NETWORKS
JPL emergency support of TDRSS and compatible satellites N86-10394

SATELLITE OBSERVATION
The air of life of the blue planet. Atmosphere research from space using data and facts against climate speculations N86-10184

Calibration of the multispectral scanner (MSS) satellite data to evaluate change in the reflection of coniferous stocks
[DFVLR-FB-84-44] N86-10636

SATELLITE TRANSMISSION
Digital transmission experiments with the Orbital Test Satellite
[EUT-84-E-144] N86-10270

SATELLITE-BORNE PHOTOGRAPHY
With Argus eyes from space. Satellite Diagnosis for Upper Volta. Seven maps without mystery N86-10183

SATELLITES
Lumped geopotential harmonics of order 14, from the orbit of 1967-11G
[AD-A156627] N86-10190

SCALARS
Gravitational collapse of a scalar field N86-11129

SCALE EFFECT
Freezer model using a population balance approach for steady-state, direct-contact, secondary refrigerant, freeze desalination N86-10361

SCALE MODELS
The Rhine-Meuse estuary hydraulic scale model. Experiences with computer configuration and software
[PUBL-335] N86-10637

SCALING LAWS
Ignition and flame spread above liquid fuel pools
N86-10163

Design, fabricate and test a 1.06(MU) repetitively pulsed laser
[DE85-014439] N86-10543

Critical dynamics in superfluid helium N86-11046

SCATTERING
Ultrasonic evaluation of mechanical properties of thick, multilayered, filament wound composites
[NASA-TM-87088] N86-10561

SCATTERING CROSS SECTIONS
Dielectric properties of silicon surfaces and silver thin films
[JUEL-1988] N86-10450

Charge exchange in slow collisions of atoms and molecules N86-10922

Experimental X-ray scattering cross sections for H2 and rare atomic gases
[DE85-011572] N86-10936

SCATTEROMETERS
CV-990 L-band SAR: A calibration experiment
N86-10617

SCHLIEREN PHOTOGRAPHY
Investigation of density gradient fluctuations in a turbulent free jet by means of the laser schlieren crossed-beam method
[DFVLR-FB-85-19] N86-10027

Advanced optical measurement techniques
N86-10174

SCHOTTKY DIODES
Interdigital Schottky barrier capacitor apparatus
[AD-D011799] N86-10436

Realization of a multifunction Input/Output (I/O) controller by means of a gate array
[EUT-85-E-147] N86-10804

SCIENCE
Collective use computer system for the Academy of Sciences KaSSR N86-10817

SCIENTIFIC SATELLITES
X-ray satellite
[NASA-TM-77923] N86-10273

SCREWS
Termination load carrying device
[AD-D011800] N86-10556

SEA LEVEL
Mild hypoxia and visual performance with night vision goggles
[AD-A156969] N86-10787

SEATS
The influence of tactual seat-motion cues on training and performance in a roll-axis compensatory tracking task setting N86-10784

A graphic anthropometric aid for seating and workplace design
[AD-A156988] N86-10788

SECURITY
Methods for developing jam-resistant security communications networks at fixed-site facilities
[DE85-012032] N86-10408

SEDIMENT TRANSPORT
Dust deposition in regions of separated flow
[JUEL-1985] N86-10475

SEDIMENTARY ROCKS
Structural mapping of folded sedimentary environments from satellite images: An example from Central Asia
N86-10607

Cretaceous and cenozoic stratigraphy of the upper and middle coastal plain, Harnett County area, North Carolina N86-10690

Stratigraphy, petrology, depositional and post-depositional histories and their effects upon reservoir properties of the Parkman Formation of the Mesa Verde group, Powder River Basin, Wyoming N86-10691

SEDIMENTS
Report of the Workshop on Geologic Applications of Remote Sensing to the Study of Sedimentary Basins
[E86-10002] N86-10599

Some opinions on remote sensing and geologic studies N86-10600

Position paper: Workshop on Geologic Applications of Remote Sensing to the Study of Sedimentary Basins
N86-10601

Chronologic analysis of terrestrial sediments and basin evolution N86-10602

Tertiary and quaternary research with remote sensing methods N86-10603

Analysis of remote sensing data N86-10605

Remote stratigraphic and structural analysis: Multisensor results in the Wind River/Bighorn Basin area, Wyoming N86-10606

Structural mapping of folded sedimentary environments from satellite images: An example from Central Asia
N86-10607

Foreland basin structures and remote sensing
N86-10608

Neogene compressional deformation and possible thrust faulting in southwest Dominican Republic N86-10618

Lithologic mapping in a sedimentary environment using multipolarization SAR images N86-10624

Sediment characterization. Task 2: Instream contaminant study. Volume 2: Appendices
[DE85-013503] N86-10680

Application of the dutch method for estimating storm-induced dune erosion
[AD-A156717] N86-10728

SEISMIC ENERGY
Structural discontinuity within the southern California continental margin: Seismic and gravity models of the western Transverse Ranges N86-10699

Crustal structure of the southern Rio Grande rift determined from seismic refraction, surface wave dispersion, and gravity data N86-10700

SEISMIC WAVES
Cryogenic equivalence principle experiment
N86-10171

Design, fabrication and testing of an experimental apparatus for determining particle behavior under very low intergranular stresses N86-10175

Formation of waves by ground motion
[PM/84/09] N86-10706

Understanding and improving acoustic to seismic coupling as it pertains to Sandia's helicopter detector
[DE85-009440] N86-10920

SEISMOLOGY

Seismic analysis of the large 70-meter antenna, part 1: Earthquake response spectra versus full transient analysis N86-10386

Remote stratigraphic and structural analysis: Multisensor results in the Wind River/Bighorn Basin area, Wyoming N86-10606

Time-term analysis of upper crustal structure in the Columbia Basin, Washington
[DE85-012390] N86-10633

In-situ geophysical investigations into the nature of the oceanic crust N86-10725

SELECTIVE FADING

Digital radio link: Method and a measuring system for studying the radio channel during frequency selective fading
[FOA-C-30386-E2] N86-10411

SELF ADAPTIVE CONTROL SYSTEMS

Identification of a plant's weighting sequence — self-tuning control
[OUEL-1534/84] N86-10854

SELF ALIGNMENT

Increase of the packaging density of Very Large Scale Integration (VLSI) circuits using automatic alignment
[BMFT-FB-T-85-020] N86-10451

SELF DIFFUSION (SOLID STATE)

Self diffusion of Sn112 and Sn124 in liquid tin N86-10231

SEMANTICS

Compexity of higher-order programs
[DE85-012776] N86-10834

SEMICONDUCTOR DEVICES

Magnetic properties of doped semiconductors
[DE85-012090] N86-11053

SEMICONDUCTOR JUNCTIONS

Rusty bolt intermodulation interference reducer
[AD-D011748] N86-10313

P-N junction controlled field emitter array cathode
[AD-D011815] N86-10416

Sensor system
[AD-D011767] N86-10480

Some aspects of long-range, high-risk photovoltaic research at SERI
[DE85-012144] N86-10662

Electron tunneling in metal/tunnel-oxide/degenerate silicon junctions N86-11043

SEMICONDUCTORS (MATERIALS)

Processing of complex compound semiconductors in space N86-10054

Crystal growth of device quality GaAs in space N86-10061

Growth of solid solution crystals N86-10065

Vapor growth of alloy-type semiconductor crystals N86-10069

Energy stability of thermocapillary convection in models of the float zone process N86-10123

Directional solidification of InSb-NiSb eutectic — Spacelab N86-10221

GaS-semiconductor crystals under microgravity: Experiment ES 323 — Spacelab N86-10224

Preliminary reports, memoranda and technical notes of the Materials Research Council Summer Conference, La Jolla, California
[AD-A156776] N86-10291

Electrically conducting polymers N86-10333

Polymer engineering: Polymeric and molecular electronic, dielectric and optical properties for device applications
[AD-A156671] N86-10344

Interdigital Schottky barrier capacitor apparatus
[AD-D011799] N86-10436

Non-empirical interatomic potentials for transition metals
[DE85-013448] N86-10440

Parallel pulse processing for mercuric iodide gamma-ray detectors
[DE85-013391] N86-10528

Free carrier absorption from electrons in confined systems N86-11042

Electron tunneling in metal/tunnel-oxide/degenerate silicon junctions N86-11043

SENSITIVITY

High sensitivity millimeter-wave measurement apparatus
[AD-D011786] N86-10373

Elastic wave gyrometer. Experiments with a parametric wave device
[REPT-26/5005/HF/AR] N86-10533

Design sensitivity analysis and optimization of built-up structures N86-10565

Measurement of visual contrast sensitivity
[AD-D011776] N86-10973

SEPARATED FLOW

Experiments and computations on unsteady separating flow in an expanding flume
[REPT-2-84] N86-10477

SEPARATION

Weld metal hot-cracking of hastelloy alloys C-22 and C-276: A study by analytical electron microscopy
[DE85-000437] N86-10324

SEPARATORS

Impurity extraction by droplets N86-10122

Electrophoresis technology N86-10144

Phosphoric and electric utility fuel cell technology development
[DE85-014552] N86-10652

Membrane research in energy and solvent recovery from industrial effluent streams
[DE85-014583] N86-10682

SEQUENCING

Periodic binary sequences with very good autocorrelation properties N86-10397

A binary sequence of period 60 with better autocorrelation properties than the Barker sequence of period 13 N86-10398

Effect of sequence of loading on interaction curves for buckling of stiffened shells
[TAE-536] N86-10583

SEQUENTIAL COMPUTERS

Study of one- and two-dimensional filtering and deconvolution algorithms for a streaming array computer
[NASA-CR-176221] N86-10822

SEQUENTIAL CONTROL

Dynamic analysis of robotic manipulations with flexible links N86-10545

SEROTONIN

Effect of cold on brain serotonin system and plasma corticosteroid level in different strains of mice N86-10766

SERVICE LIFE

Captive volume device as a safe life monitor
[AD-D011802] N86-10525

SET THEORY

Principal bundles on the affine line N86-10856

Two algorithms for weighted matroid intersection
[AD-A156525] N86-10861

SETTLING

High-temperature controlled redox crystallization studies N86-10178

SHAPE CONTROL

Skin casting of alloys and composites: Results of Spacelab (SL)-1 and TEXUS experiments N86-10213

Design sensitivity analysis and optimization of built-up structures N86-10565

SHAPED CHARGES

Explosive initiation by very small conical shaped charge jets
[DE85-009443] N86-10357

SHAPES

Vision test chart and method using Gaussians
[AD-D011756] N86-10778

Conducting wall and pressure profile effect on MHD stabilization of axisymmetric mirror
[DE85-013647] N86-11020

SHEAR FLOW

Finite element solution of the Navier-Stokes equations for 3-D turbulent free shear flows N86-10457

SHEAR LAYERS

Three articles on new calculation methods in aeronautics (selected articles)
[AD-A145745] N86-10007

Effect of a shear layer on the stability of an axisymmetrical external compression air intake N86-10010

SHEAR PROPERTIES

Fabrication and metallurgical properties of modified 9Cr-1 Mo steel
[DE85-012885] N86-10328

SHEAR STRENGTH

Ultrasonic evaluation of mechanical properties of thick, multilayered, filament wound composites
[MASA-TM-87088] N86-10561

SHEAR STRESS

Inelastic analysis of frame structures including member and joint shears N86-10573

SHEATHS

Development of a sheath for sensor protection in molten steel applications
[AD-A156764] N86-10315

SHELLS (STRUCTURAL FORMS)

Attachment method-ceramic radome to metal body
[AD-D011778] N86-10032

Joint research effort on vibrations of twisted plates, phase 1: Final results
[NASA-RP-1150] N86-10579

SHOCK LOADS

Shock loading and release behavior of x-cut quartz
[DE85-013954] N86-11054

SHOCK WAVE INTERACTION

A numerical solution of the shock-turbulent interaction over a compression corner for supersonic flow N86-10003

Heating and generation of suprathermal particles at collisionless shocks
[DE85-014114] N86-11034

SHOCK WAVE PROPAGATION

Heating and generation of suprathermal particles at collisionless shocks
[DE85-014114] N86-11034

Shock loading and release behavior of x-cut quartz
[DE85-013954] N86-11054

SHOCK WAVES

Second order approximation method for transonic flows over swept wings N86-10002

Catalytic activity of shock modified ZnO for CO oxidation and methanol synthesis
[DE85-014704] N86-10300

On the method of characteristics and its application to the calculations of annular nozzle flowfields N86-10454

Angle of incidence effects for underwater shock using generic computational models, rev. 1
[DE85-012921] N86-10467

Spontaneous Raman spectroscopy of shocked H2O
[DE85-014557] N86-10470

Improved particle-velocity transducer for equation-of-state experiments
[DE85-013204] N86-10532

High-pressure release-wave measurements and phase transformation in CaCO3
[DE85-012592] N86-11055

SHORT TAKEOFF AIRCRAFT

Evaluation of an aerodynamic-load prediction method on a STOL fighter configuration
[NASA-TM-86782] N86-10015

SHORT WAVE RADIO TRANSMISSION

Acoustic gravity wave chemistry model for the RAYTRACE code
[AD-A156850] N86-10405

SHRINKAGE

Shrinking of a gas bubble in a glass melt under microgravity conditions — STS-11 N86-10254

SHUTTLE IMAGING RADAR

High-resolution image data from the Space Shuttle N86-10494

Vegetation canopy discrimination and biomass assessment using multipolarized airborne SAR N86-10628

SIDELOBE REDUCTION

A binary sequence of period 60 with better autocorrelation properties than the Barker sequence of period 13 N86-10398

SIDELOBES

Periodic binary sequences with very good autocorrelation properties N86-10397

A binary sequence of period 60 with better autocorrelation properties than the Barker sequence of period 13 N86-10398

SIERRA NEVADA MOUNTAINS (CA)

Altitudinal distribution of granitic landforms in the south central Sierra Nevada, California N86-10695

SIGNAL ANALYSIS

The role of freestream turbulence scale in subsonic flow separation
[NASA-CR-176237] N86-10014

Signal analysis of gas tungsten arc welds N86-10078

Signal analysis receiver with acousto-optic delay lines
[AD-D011761] N86-10427

SIGNAL DETECTION

Apparatus for locating passive intermodulation interference sources
[AD-D011798] N86-10435

Proposed aural nondetectability limits for Army materiel
[AD-A156704] N86-10917

Optical detection of photoacoustic pulses in thin silicon wafers
[AD-A156705] N86-10977

SIGNAL DETECTORS

Constant rise AGC (Automatic Gain Control) device
[AD-D011744] N86-10421

Fiber optic gradient hydrophone construction and calibration for sea trial
[AD-A156469] N86-10914

SIGNAL ENCODING

Computational techniques for the analysis and design of digital communication systems
[AD-A156945] N86-10407

SIGNAL FADING

Digital radio link: Method and a measuring system for studying the radio channel during frequency selective fading
[FOA-C-30386-E2] N86-10411

SIGNAL MEASUREMENT

Optical detection of photoacoustic pulses in thin silicon wafers
[AD-A156705] N86-10977

SIGNAL PROCESSING

The interpolation of signals sampled at less than the Nyquist rate N86-10388

Amplitude and phase modulation in fin-lines electrical tuning
[AD-D011813] N86-10415

Pulse compression system
[AD-D011833] N86-10417

A compact bulk acousto-optic time integrating correlator
[AD-A156606] N86-10428

Multiple site laser excited pollution monitoring system
[AD-D011769] N86-10674

Parallel local interface bus
[AD-D011742] N86-10792

Efficient systolic arrays for the solution of toeplitz systems: An illustration of a methodology for the construction of systolic architectures in VLSI (Very Large Systems Integration)
[AD-A156767] N86-10795

An improved FFT (Fast fourier transform) for a four parallel pipe SIMD arithmetic processor
[AD-A156625] N86-10863

Sound radiation from repetitive transient vibrations using multi-channel digital signal processing with application to impact machinery N86-10910

Method for determining the position, angle and other injection parameters of a short pulsed beam in the Brookhaven AGS
[DE85-012523] N86-10931

Kalman filter preprocessor
[AD-D011774] N86-10972

SIGNAL TO NOISE RATIOS

Sample data phase locked loop for adaptive Doppler tracker
[AD-D011788] N86-10374

A sequential decoding performance analysis for International Comet Explorer N86-10390

High-rate convolutional code construction with the minimum required SNR criterion N86-10392

Pulse compression system
[AD-D011833] N86-10417

Variability analysis of visually induced responses in the midst of noise
[B8564052] N86-10774

A study of derivative filters using the discrete Fourier transform
[NASA-CR-176224] N86-10825

Naive approximate realization of noisy data
[ER-83/10] N86-10880

SIGNAL TRANSMISSION

Mobile VLBI and GPS measurement of vertical crustal motion N86-10401

SILANES

Modelling of laser-enhanced chemical vapor deposition N86-10105

Photovoltaic devices using a Si:H from higher order silanes
[DE85-008804] N86-10668

SILICA GLASS

Interdiffusion in the glass melt system (Na2O+Rb2O).3SiO2 — Spacelab N86-10216

SILICATES

High-temperature controlled redox crystallization studies N86-10178

SILICON

Microgravity silicon zoning investigation N86-10063

Modelling of laser-enhanced chemical vapor deposition N86-10105

Surface tension induced instabilities in reduced gravity: The Benard problem N86-10117

Bulk formation of metallic glasses and amorphous silicon from the melt N86-10154

Crystallization of a silicon sphere — Spacelab N86-10226

Crystal growth of silicon in Spacelab 1: Experiment ES-321 N86-10227

Development of metallization process
[NASA-CR-176209] N86-10312

Defect identification in high-energy semiconductors
[DE85-014533] N86-10442

Dielectric properties of silicon surfaces and silver thin films
[JUEL-1968] N86-10450

Making the right choice — silicon photodiodes N86-10669

Optical detection of photoacoustic pulses in thin silicon wafers
[AD-A156705] N86-10977

Magnetic properties of doped semiconductors
[DE85-012090] N86-11053

SILICON CARBIDES

Continuous fiberization of silicon-carbide-nitride precursor resin N86-10166

High temperature properties of SiC materials
[BMFT-FB-T-85-047] N86-10353

Characterization of mechanical damage mechanisms in ceramic composite materials
[AD-A156574] N86-10590

SILICON DIOXIDE

Investigation of metallic impurities introduced into SiO2 and silicon by various candidate VLSI metallization systems: Chemical reactions, diffusion, and electrical properties
[AD-A156609] N86-10429

SILICON FILMS

Improved blue response and efficiency of A-Si:H solar cells deposited from disilane using a dual-chamber plasma system
[DE85-013289] N86-10649

SILICON JUNCTIONS

Investigation of metallic impurities introduced into SiO2 and silicon by various candidate VLSI metallization systems: Chemical reactions, diffusion, and electrical properties
[AD-A156609] N86-10429

SILICON NITRIDES

Mixed-mode fracture of ceramics
[DE85-014067] N86-10349

High temperature properties and characterization of S3-N4 materials
[BMFT-FB-T-85-046] N86-10352

SILICON OXIDES

Colloidal oxide properties and kinetic studies N86-10147

SILVER

Dielectric properties of silicon surfaces and silver thin films
[JUEL-1968] N86-10450

SILVER ALLOYS

Reduction of noble metal stock and noble metal loss during wire production with the Conform extrusion process
[BMFT-FB-T-85-049] N86-10560

SIMULATION

Cryogenic equivalence principle experiment N86-10171

Time-implicity simulation of particle-fluid systems
[DE85-012944] N86-10471

High flux calorimetry
[AD-A156852] N86-10524

Simulation of the atmospheric boundary layer in the large wind tunnel of the TNO Institute for Building materials and Constructions (IBBC). Part 1: Theory
[BI-76-39/06.7.23100-PT-1] N86-10703

Simulation of the atmospheric boundary layer in the large wind tunnel of the TNO Institute for Building Materials and Construction (IBBC). Part 2: Experiments
[BI-76-39/06.7.23100-PT-2] N86-10704

Optical testing of large telescopes using multiple subapertures N86-10971

A method for numerical relativity: Simulation of axisymmetric gravitational collapse and gravitational radiation generation N86-11127

SIMULATORS

Simulated direct-strike lightning testing at Sandia National Laboratories
[DE85-012033] N86-10049

SINGLE CRYSTALS

Processing of complex compound semiconductors in space N86-10054

Growth of solid solution crystals N86-10065

Fluid dynamics and thermodynamics of vapor phase crystal growth N86-10066

Environmental degradation of materials: Surface chemistry related to stress corrosion cracking N86-10099

Growth of larger single crystals N86-10186

Lead telluride crystals grown in microgravity: Experiment ES 318 — Spacelab N86-10220

GaS-semiconductor crystals under microgravity: Experiment ES 323 — Spacelab N86-10224

Solution growth of cadmium telluride: Experiment ES 322 — Spacelab N86-10225

Protein single crystal growth under microgravity — Spacelab N86-10228

Growth and characterization of brushite and lead monetite, simulation and results — Spacelab N86-10230

Creep-fatigue behavior of NiCoCrAlY coated PWA 1480 superalloy single crystals
[NASA-TM-87110] N86-10311

Low temperature plastic deformation mechanisms of alpha-titanium single crystals
[ESA-TT-871] N86-10332

Extended precision in video bandwidth analog to digital converter using optical techniques
[AD-D011745] N86-10422

Adsorption of oxygen on single crystal tin at liquid helium temperatures N86-11044

High-pressure release-wave measurements and phase transformation in CaCO3
[DE85-012592] N86-11055

SINGULARITY (MATHEMATICS)

Theoretical specific impulse for two-phase flow in nozzle of rocket-ramjet engine: A simple estimation method N86-10005

Analysis of hyperlift systems. Study of a singularities method
[SNIAS-443.529/84] N86-10024

Estimates for maximal functions along hypersurfaces
[CTH-MATH-1984-29] N86-10874

SINTERED ALUMINUM POWDER

Melting and solidification in O-g of sintered alloys: Experiments ES 311 A and B bubble reinforced materials — Spacelab N86-10215

SINTERING

Melting and solidification in O-g of sintered alloys: Experiments ES 311 A and B bubble reinforced materials — Spacelab N86-10215

SIPHONS

Laminar film condensation in vertical closed two-phase thermosiphons
[IKE-5-220] N86-10476

SITE SELECTION

LANDSAT TM image data quality analysis for energy-related applications
[E85-10109] N86-10597

Overview of wind turbine siting research: Prospecting to micrositing
[DE85-013496] N86-10666

SITES

Methods for developing jam-resistant security communications networks at fixed-site facilities
[DE85-012032] N86-10408

SIZE (DIMENSIONS)

Self-heating to ignition measurements and computation of critical size for solar energy collector materials
[DE85-011449] N86-10302

Photographic catalog of selected planetary size comparisons
[NASA-TM-86207] N86-11138

SKIN TEMPERATURE (BIOLOGY)

Heat transfer mechanism in human extremities N86-10759

SKY BRIGHTNESS

Mobile VLBI and GPS measurement of vertical crustal motion N86-10401

Optical/IR telescope arrays: A study of their potential for satisfying observational requirements in astronomy for a large aperture system in the 1990s and beyond
[REPT-15] N86-11094

SLEEP

Intradiurnial organization of wakefulness-sleep sequence and energy metabolism in rats exposed to low ambient temperature N86-10764

SLEEP DEPRIVATION

The effects of age, sleep deprivation, and altitude on complex performance
[AD-A156987] N86-10771

SLOPES

Marginal terrain straddle-lift container handler
[AD-D011752] N86-10555

SLOTS

Effects of slots/holes in disks on frequencies of TM01 and EH11 waves in the disk-loaded waveguide
[DE85-013376] N86-11009

SLOTTED WIND TUNNELS

Investigations to improve the slotted-wall test section of the F+W transonic wind tunnel
[F+W-FO-1752] N86-10050

SMELTING

Multimode acoustic research N86-10167

SMOKE

Methods for developing jam-resistant security communications networks at fixed-site facilities
[DE85-012032] N86-10408

SNOW COVER

Evaluation of metric camera photos — Spacelab: alpine snow cover N86-10515

Maximum water reserves in the snow cover in the European territory of the USSR according to data for 1892-1960
[NASA-TM-77901] N86-10611

Representation of the distribution of the snow cover on the surface of the Earth's dry land
[NASA-TM-77909] N86-10612

Observations of the snow cover in the southern part of the Buryat Autonomous Soviet Socialist Republic
[NASA-TM-77910] N86-10613
Laws of distribution of the snow cover on the greater Caucasus (Soviet Union)
[NASA-TM-77911] N86-10614

SODIUM
Design and calibration of a flat-flame burner using line reversal techniques
[AD-A156724] N86-10294
A modeling analysis program for the JPL table mountain lo sodium cloud
[NASA-CR-176241] N86-11139

SODIUM SULFATES
Environmental degradation of materials: Surface chemistry related to stress corrosion cracking
N86-10099

SOFTWARE TOOLS
Ada (trademark) Programming Support Environment (APSE) Evaluation and Validation (E and V) workshop report held at Airlie, Virginia on 2-6 April 1984
[AD-A156667] N86-10829

SOIL EROSION
Erosion control and watershed management by Spacelab photography N86-10493
Application of the dutch method for estimating storm-induced dune erosion
[AD-A156717] N86-10728

SOIL MAPPING
Examples of regional environmental assessment using acid deposition data
[DE85-012903] N86-10677

SOIL MOISTURE
The effect of vegetation type, microrelief, and incidence angle on radar backscatter N86-10619
The boundary condition in a numerical model of atmospheric flows over fixed interfaces
[GKSS-85-E-10] N86-10722

SOIL SCIENCE
Development and evaluation of multispecies test protocols for assessing chemical toxicity
[DE85-013526] N86-10679

SOILS
Design, fabrication and testing of an experimental apparatus for determining particle behavior under very low intergranular stresses N86-10175
Marginal terrain straddle-lift container handler
[AD-D011752] N86-10555
Vegetation and soils field research data base: Experiment summaries
[E85-10110] N86-10610

SOLAR ARRAYS
Photovoltaics: Report, 1984
[DE85-014713] N86-10658
Photovoltaic concentrator array evaluation
[DE85-013789] N86-10665

SOLAR CELLS
Development of metallization process
[NASA-CR-176209] N86-10312
Improved blue response and efficiency of A-Si:H solar cells deposited from disilane using a dual-chamber plasma system
[DE85-013289] N86-10649
Theory of advanced, high-efficience concentrator cells
[DE85-008821] N86-10655
Photovoltaics: Report, 1984
[DE85-014713] N86-10658
Some aspects of long-range, high-risk photovoltaic research at SERI
[DE85-012144] N86-10662
Photovoltaic devices using a Si:H from higher order silanes
[DE85-008804] N86-10668
Cooperative emission by two different atoms into surface plasmons
[AD-A157033] N86-10925

SOLAR COLLECTORS
Self-heating to ignition measurements and computation of critical size for solar energy collector materials
[DE85-011449] N86-10302
Solar thermal technical information guide
[DE85-002941] N86-10657
Photovoltaics: Report, 1984
[DE85-014713] N86-10658

SOLAR COOLING
Passive and hybrid solar technologies program summary
[DE85-013100] N86-10648

SOLAR ELECTRIC PROPULSION
Solar propulsion for the TRIO interferometer
N86-11109

SOLAR ENERGY
Passive solar design handbook
[DE85-014263] N86-10656
Solar thermal technical information guide
[DE85-002941] N86-10657
Contribution of wind energy to the energy balance of a combined solar and wind energy system. Part 1: System description, data acquisition and system performance
[BMFT-FB-T-85-051-VOL-1] N86-10670

SOLAR ENERGY CONVERSION
Passive and hybrid solar technologies program summary
[DE85-013100] N86-10648
Solar thermal technical information guide
[DE85-002941] N86-10657

SOLAR FLARES
Directionality of bremsstrahlung from relativistic electrons in solar flares
[NASA-TM-87509] N86-11141
Solar flares and magnetospheric particles: Investigations based upon the ONR-602 experiment
[AD-A156583] N86-11142

SOLAR FLUX
Integrating sphere measurements of directional-hemispherical transmittance of window systems
[DE85-013926] N86-10978

SOLAR GENERATORS
Research on solar pumped liquid lasers
[NASA-CR-176235] N86-10539
Passive and hybrid solar technologies program summary
[DE85-013100] N86-10648

SOLAR HEATING
Passive and hybrid solar technologies program summary
[DE85-013100] N86-10648
Passive solar design handbook
[DE85-014263] N86-10656
Contribution of wind energy to the energy balance of a combined solar and wind energy system. Part 1: System description, data acquisition and system performance
[BMFT-FB-T-85-051-VOL-1] N86-10670

SOLAR HOUSES
Passive and hybrid solar technologies program summary
[DE85-013100] N86-10648

SOLAR RADIATION
Energy balance in a deep Colorado valley: ASCOT 84
[DE85-012441] N86-10631
Identification of chemical and physical phenomena affecting the durability of silvered polymer (PMMA) mirrors
[DE85-012131] N86-10645
A numerical model for the estimation of solar radiation on rugged terrain N86-10694
A modeling analysis program for the JPL table mountain lo sodium cloud
[NASA-CR-176241] N86-11139

SOLAR REFLECTORS
Identification of chemical and physical phenomena affecting the durability of silvered polymer (PMMA) mirrors
[DE85-012131] N86-10645

SOLAR SAILS
TRIO: A kilometric array stabilized by solar sails — Spaceborne astronomy N86-11102
Solar propulsion for the TRIO interferometer
N86-11109

SOLAR SYSTEM
Stellar s-process diagnostics
[DE85-012926] N86-11134
Photographic catalog of selected planetary size comparisons
[NASA-TM-86207] N86-11138

SOLDERS
Reduction of noble metal stock and noble metal loss during wire production with the Conform extrusion process
[BMFT-FB-T-85-049] N86-10560

SOLID PHASES
Thermal expansion of glasses in the solid and liquid phases
[DE85-013953] N86-10351

SOLID PROPELLANTS
Analytical investigation of solid rocket nozzle failure
[NASA-TM-86513] N86-10278

SOLID ROCKET BINDERS
Binder-filler interaction in energetic polymers
[AD-A156752] N86-10345

SOLID STATE DEVICES
Fluid dynamics and thermodynamics of vapor phase crystal growth N86-10068
Preliminary reports, memoranda and technical notes of the Materials Research Council Summer Conference, La Jolla, California
[AD-A156776] N86-10291
Semiconductor superlattic photodetectors
[NASA-CR-176249] N86-10484

SOLID STATE LASERS
Design, fabricate and test a 1.06(MU) repetitively pulsed laser
[DE85-014439] N86-10543

SOLID SURFACES
Solid surface combustion at reduced gravity
N86-10159

SOLID-SOLID INTERFACES
Surface forces in contacting solids — microgravity rocket experiment N86-10252

SOLIDIFICATION
Microgravity Science and Applications Program tasks
[NASA-TM-87568] N86-10053
Fluid flow in crystal growth: Analysis of the verticle Bridgman and floating zone process N86-10055
Solutal convection and its effects on crystal growth and segregation in binary and pseudo-binary system with large liquidus-solidus separation N86-10056
The influence of containerless undercooling and rapid solid-state quenching on the superconductive and magnetic properties of some clustering alloy systems
N86-10076
Convection during unidirectional solidification
N86-10077
Mephisto: Interfacial destabilization in metal alloys
N86-10079
Undercooling, remelting, and coarsening N86-10080
Dendritic growth in undercooled melts N86-10082
Influence of melt convection on solid-liquid interface under terrestrial and reduced gravity environments
N86-10083
Control of cast iron microstructure N86-10084
The development and prevention of channel segregation during alloy solidification N86-10086
Orbital processing of aligned magnetic composites
N86-10089
Solidification fundamentals N86-10090
Containerless processing of undercooled melts
N86-10093
Thermal and solutal convection damping using an applied magnetic field N86-10094
Directional solidification of monotectic and hypermonotectic aluminum-indium alloys under micron-g
N86-10097
Graphite formation in cast iron N86-10100
Studies of model immiscible systems N86-10112
Rapid solidification of magnetic oxides N86-10152
Oxidation behavior of glassy alloys N86-10158
Modification of the electromagnetic levitator (EML) hardware N86-10172
Microgravity Materials Science Laboratory
N86-10173
Melting and solidification of metal matrix composites under microgravity — Spacelab N86-10211
Melting and solidification in O-g of sintered alloys: Experiments ES 311 A and B bubble reinforced materials — Spacelab N86-10215
Directional solidification of InSb-NiSb eutectic — Spacelab N86-10221
Experimental facility for materials research in space (CSK-1) N86-10263
Measurement of the density of base fluids at pressures 0.422 to 2.20 GPa
[NASA-TM-87114] N86-10551

SOLIDS
Directional solidification of monotectic and hypermonotectic aluminum-indium alloys under micron-g
N86-10097
Dynamic thermophysical measurements in space
[NASA ORDER H-27954-B] N86-10106
Determination of thermophysical characteristics of solid materials by electrical modelling of the solutions to the inverse problems in nonsteady heat conduction
[NASA-TM-77907] N86-10293

SOLITARY WAVES
Topics in nonlinear wave theory with applications
N86-10367

SOLUBILITY
Liquid phase miscibility gap materials N86-10081
Influences affecting separation in monotectic alloys under microgravity N86-10209
Particle coarsening in immiscible zinc-lead alloys under microgravity — Spacelab N86-10210
Stability of metallic dispersions — microgravity
N86-10258
Space shuttle experiments on Al-In liquid phase miscibility gap (LPMG) alloys N86-10264

SOLUTES
Electrohydrodynamics N86-10130

SOLVATION
Rapid analysis using capillary supercritical fluid chromatography
[DE85-012460] N86-10297

SOLVENT EXTRACTION
Extraction of lanthanide ions by 2-methyl-8-quinolinol
[DE85-014277] N86-10303

SOLVENTS
Recovery of alcohol from a fermentation source by separation rather than distillation [AD-D011782] N86-10262
Rusty bolt intermodulation interference reducer [AD-D011748] N86-10313
Thermodynamics of polymer-supercritical solvent mixtures [AD-A157038] N86-11061
SONDES
Satellite use for men — West German space program N86-10180
SONIC ANEMOMETERS
Field comparison of in situ meteorological sensors [PB85-196988] N86-10723
SOOT
Microphysical/mesoscale aspects of nuclear winter and new directions in assessments [DE85-013479] N86-10718
SORET COEFFICIENT
Thermomigration of cobalt in liquid tin: Experiment 1 ES 320 — Spacelab N86-10222
Space experiment on thermal diffusion. Preparation and theoretical analysis N86-10253
SOUND TRANSMISSION
Proposed aural nondetectability limits for Army materiel [AD-A156704] N86-10917
SOUND WAVES
Multimode acoustic research N86-10167
Advanced containerless processing technology N86-10176
Elastic properties and thermal stability characterization of metallic glasses by guided wave techniques N86-10337
Tunable acousto-optic filter with improved spectral resolution and increased aperture [AD-D011758] N86-10915
SOUTHERN HEMISPHERE
Representation of the distribution of the snow cover on the surface of the Earth's dry land [NASA-TM-77909] N86-10612
SPACE CAPSULES
Guidance and control of a cable based payload pickup system N86-10045
SPACE COMMERCIALIZATION
Space utilization N86-11067
Space sciences: Perspectives of commercial utilization for the German industry N86-11068
SPACE INDUSTRIALIZATION
Space sciences: Perspectives of commercial utilization for the German industry N86-11068
SPACE MAINTENANCE
Cell maintenance systems N86-10142
SPACE MANUFACTURING
Thermocapillary and diffusocapillary migration of a fluid drop N86-10128
Development of materials processing systems for use in space on low-g simulation devices N86-10166
SPACE OBSERVATIONS (FROM EARTH)
Results and limitations of ground-based optical arrays — stellar interferometry N86-11097
SPACE POWER REACTORS
Swelling and tensile properties of EBR-2-irradiated tantalum alloys for space reactor applications [DE85-012887] N86-10329
SPACE PROBES
A sequential decoding performance analysis for International Comet Explorer N86-10390
SPACE PROCESSING
Microgravity Science and Applications Program tasks [NASA-TM-87568] N86-10053
Processing of complex compound semiconductors in space N86-10054
Fluid flow in crystal growth: Analysis of the verticle Bridgman and floating zone process N86-10055
Solutal convection and its effects on crystal growth and segregation in binary and pseudo-binary system with large liquidus-solidus separation N86-10056
Crystal growth research in space N86-10057
Crystal melts under reduced gravity N86-10062
Solution growth of crystals in zero-gravity N86-10064
Float zone experiments in space N86-10067
Modeling directional solidification N86-10071
Heat flow and segregation in directional solidification N86-10072
Measurement of high temperature thermophysical properties N86-10074
Effect of undercooling and modified microstructure on the physical properties of material synthesized in the drop tube and drop tower N86-10075
Production of large-particle-size monodisperse latexes in microgravity N86-10146
Containerless processing of glass forming melts in space N86-10148
Gel precursors as glass and ceramic starting materials for space processing applications research N86-10150
Glass formation in reluctant glass formers N86-10151
Sol-gel glasses N86-10153
Physical phenomena in containerless glass processing N86-10155
Glass research N86-10157
Electric field containerless processing technology N86-10170
Fifth European symposium on Material Sciences under Microgravity. Results of Spacelab 1 [ESA-SP-222] N86-10200
Unidirectional solidification of cast iron: Experiment ES-325 — Spacelab N86-10212
Skin casting of alloys and composites: Results of Spacelab (SL)-1 and TEXUS experiments N86-10213
Crystal growth of GaAs in space N86-10234
Mathematical simulation of disturbing forces and material science processes under low gravity N86-10236
Physical and chemical properties of a nickel catalyst processed under microgravity — STS-7 N86-10255
Stability of metallic dispersions — microgravity N86-10258
First Spacelab Payload (FSLP) experiments on composite materials N86-10265
First Spacelab Payload (FSLP) experiments in metallurgy N86-10266
SPACE PROGRAMS
Space research expenses of the Federal Ministry of Research and Technology (BMFT) in the period 1983-1985 N86-11070
SPACE SHUTTLE MISSION 41-G
High-resolution image data from the Space Shuttle N86-10494
SPACE SHUTTLE ORBITERS
Physical and chemical properties of a nickel catalyst processed under microgravity — STS-7 N86-10255
Transport processes in directional solidification during space shuttle flight N86-10257
Stability of metallic dispersions — microgravity N86-10258
SPACE SHUTTLE PAYLOADS
Modification of the electromagnetic levitator (EML) hardware N86-10172
SPACE SHUTTLES
Vibro-acoustic forecast for space shuttle launches at Vandenberg AFB: The payload changeout room and the administration building [AD-A156944] N86-10269
SPACE STATIONS
Compatibility of grain-stabilized platinum with candidate propellants for resistojets [NASA-TM-87118] N86-10279
Life sciences research on the space station: An introduction [NASA-TM-86836] N86-10734
SPACE SURVEILLANCE (GROUND BASED)
SETI radio spectrum surveillance system N86-10400
SPACEBORNE ASTRONOMY
Colloquium on Kilometric Optical Arrays in Space [ESA-SP-226] N86-11096
Extragalactic observations with optical space arrays N86-11098
Astronomical criteria for interferometric arrays — Spacecraft design N86-11099
High angular resolution in the infrared: Prospects for space observations N86-11100
Strategy for the development of space arrays N86-11101
TRIO: A kilometric array stabilized by solar sails — Spaceborne astronomy N86-11102
SAMSI: An orbiting spatial interferometer for micro-arc second astronomical observations — Spacecraft Array for Michelson Spatial interferometry (SAMSI) N86-11103
COSMIC: A high resolution, large collecting area telescope — Coherent Optical System of Modular Imaging Collectors (COSMIC) N86-11104
A fiber-linked version of project TRIO — telescope array N86-11105
OASIS: Optical Aperture Synthesis in Space N86-11106
Future space telescope design concepts N86-11107
TRIO optics — spaceborne optical interferometer (TRIO) N86-11108
Mission analysis aspects — spaceborne interferometry N86-11114
Problems in image reconstruction with optical arrays — spaceborne astronomy N86-11115
Space antenna for gravitational wave astronomy N86-11123
The DUO: Far infrared heterodyne concept for space interferometry N86-11125
SPACEBORNE EXPERIMENTS
Orbital processing of aligned magnetic composites N86-10069
Purification and cultivation of human pituitary growth hormones secreting cells N86-10140
Cell separations in microgravity and development of a space bioreactor N86-10141
Electrophoresis technology N86-10144
Space experiment on thermal diffusion. Preparation and theoretical analysis N86-10253
Shrinking of a gas bubble in a glass melt under microgravity conditions — STS-11 N86-10254
Experimental facility for materials research in space (CSK-1) N86-10263
Space shuttle experiments on Al-In liquid phase miscibility gap (LPMG) alloys N86-10264
SPACEBORNE PHOTOGRAPHY
Metric Camera Workshop — Spacelab [ESA-SP-209] N86-10485
Digital elevation model from Spacelab metric camera photographs N86-10486
Orthophotomapping from metric camera imagery — Spacelab N86-10487
Restitution of Spacelab photography by analog stereoplotter N86-10489
Evaluation of the accuracy of the metric camera images for the production of line maps and orthophotos N86-10490
Photomapping in different climatic zones — Spacelab metric camera N86-10491
A geological structural analysis of the southeastern Zagros (iran) ranges based on metric camera photos N86-10492
Erosion control and watershed management by Spacelab photography N86-10493
Identification of planimetric features from the metric camera — Spacelab N86-10497
Analysis of metric camera images from the USA and their suitability for topographic and thematic mapping — Spacelab N86-10498
Long range translocations ashore to offshore using Spacelab-1 metric camera imagery in the perspective of integrated geophysical surveys N86-10499
Role of the Economic Commission for Africa as a principal investigator in the metric camera experiment and reports of the result of the assessment for topographic and revision of maps in populated and developed areas of the world N86-10501
The role of very small scale metric images in modern geology — Spacelab metric camera N86-10502
Geological mapping of remote mountainous regions using metric camera imagery — Spacelab N86-10503
Interpretation of metric camera concerning hydrologic structures of the Rhone Delta — Spacelab N86-10504
OEEPE participation in testing metric camera photography — European Organization for Experimental Photogrammetric Investigations (OEEPE) N86-10507
Topographic interpretation of metric camera images: An example in Somalia — Spacelab N86-10508
Thematic investigations in France based on metric camera imagery — Spacelab N86-10509
Photographic catalog of selected planetary size comparisons [NASA-TM-86207] N86-11138
SPACEBORNE TELESCOPES
Extragalactic observations with optical space arrays N86-11098
Astronomical criteria for interferometric arrays — Spacecraft design N86-11099
Strategy for the development of space arrays N86-11101
TRIO: A kilometric array stabilized by solar sails — Spaceborne astronomy N86-11102
SAMSI: An orbiting spatial interferometer for micro-arc second astronomical observations — Spacecraft Array for Michelson Spatial Interferometry (SAMSI) N86-11103
COSMIC: A high resolution, large collecting area telescope — Coherent Optical System of Modular Imaging Collectors (COSMIC) N86-11104
A fiber-linked version of project TRIO — telescope array N86-11105
Future space telescope design concepts N86-11107
TRIO optics — spaceborne optical interferometer (TRIO) N86-11108
Solar propulsion for the TRIO interferometer N86-11109
Preliminary studies of a spinning tether-connected TRIO concept — spaceborne interferometer (TRIO) N86-11110
TRIO interferometer positioning — spaceborne interferometers (TRIO) N86-11111
TRIANGLE: A different design for a three satellite interferometer in space N86-11113
Problems in image reconstruction with optical arrays — spaceborne astronomy N86-11115

COSMIC image reconstruction --- Coherent Optical System of Modular Imaging Collectors (COSMIC) N86-11118
The OASIS correlator --- Optical Aperture Synthesis in Space (OASIS) N86-11119
Imaging speckle interferometer in space: Digital simulations of image reconstruction and photon noise N86-11120
The intensified multi CCD camera --- spaceborne interferometers N86-11122

SPACECRAFT ANTENNAS
A numerical method for approximating antenna surfaces defined by discrete surface points
[NASA-TM-87125] N86-10381

SPACECRAFT COMMUNICATION
SARSAT LUC (Local user terminal) to CMCC (Canadian Mission Control Centre) alert data interface: A critical review
[AD-A156681] N86-10276
Discussion on the progress and future of satellite communication (Japan)
[NASA-TM-77672] N86-10378

SPACECRAFT COMPONENTS
X-ray satellite
[NASA-TM-77923] N86-10273

SPACECRAFT CONFIGURATIONS
Preliminary studies of a spinning tether-connected TRIO concept --- spaceborne interferometer (TRIO) N86-11110

SPACECRAFT CONTROL
Evaluation of a pulse control law for flexible spacecraft
[NASA-CR-176233] N86-10272

SPACECRAFT DESIGN
Manned flight simulation: Challenge and response
[NASA-TM-86827] N86-10048
Astronomical criteria for interferometric arrays --- Spacecraft design N86-11099
SAMSI: An orbiting spatial interferometer for micro-arc second astronomical observations --- Spacecraft Array for Michelson Spatial Interferometry (SAMSI) N86-11103
Preliminary studies of a spinning tether-connected TRIO concept --- spaceborne interferometer (TRIO) N86-11110
TRIANGLE: A different design for a three satellite interferometer in space N86-11113

SPACECRAFT MANEUVERS
Nonlinear methods for spacecraft attitude maneuvers
[AD-A156956] N86-10275

SPACECRAFT POWER SUPPLIES
General-purpose heat source development: Safety Verification Test Program. Bullet/fragment test series
[DE85-014262] N86-10660

SPACECRAFT STABILITY
TRIO: A kilometric array stabilized by solar sails --- Spaceborne astronomy N86-11102

SPACELAB
The first German Spacelab mission D1 reports --- Spacelab payloads
[PR-1] N86-10187

SPACELAB PAYLOADS
Growth of larger single crystals N86-10186
The first German Spacelab mission D1 reports --- Spacelab payloads
[PR-1] N86-10187
The first German Spacelab mission D1 reports --- Spacelab payloads
[PR-2] N86-10188
The first German Spacelab mission D1 reports --- Spacelab payloads
[PR-3] N86-10189
Fifth European symposium on Material Sciences under Microgravity. Results of Spacelab 1
[ESA-SP-222] N86-10200
The fluid physics module: A technical description --- Spacelab N86-10201
Capillary forces in a low gravity environment --- Spacelab N86-10202
Some results of the Marangoni free convection experiment --- Spacelab N86-10203
Oscillations of semi-free liquids in microgravity: Spacelab 1 experiment ES 326 N86-10204
Liquid column stability: Experiment 1 ES-331 --- Spacelab N86-10205
Axisymmetric free surface behavior of moving liquid in a cylinder in microgravity --- Spacelab N86-10206
Kinetics of spreading of liquids in microgravity: Experiment 1 ES 327 --- Spacelab N86-10207
The isothermal heating facility --- Spacelab N86-10208
Influences affecting separation in monotectic alloys under microgravity N86-10209
Melting and solidification of metal matrix composites under microgravity --- Spacelab N86-10211
Unidirectional solidification of cast iron: Experiment ES-325 --- Spacelab N86-10212
Skin casting of alloys and composites: Results of Spacelab (SL)-1 and TEXUS experiments N86-10213
Vacuum brazing under microgravity --- Spacelab N86-10214
Melting and solidification in O-g of sintered alloys: Experiments ES 311 A and B bubble reinforced materials --- Spacelab N86-10215
Interdiffusion in the glass melt system (Na2O+Rb2O).3SiO2 --- Spacelab N86-10216
Gradient heating facility behavior --- Spacelab N86-10217
Directional solidification of an aluminum-zinc vapor emulsion in microgravity --- Spacelab N86-10218
Directional solidification of eutectic alloys --- Spacelab N86-10219
Lead telluride crystals grown in microgravity: Experiment ES 318 --- Spacelab N86-10220
Directional solidification of InSb-NiSb eutectic --- Spacelab N86-10221
Thermomigration of cobalt in liquid tin: Experiment 1 ES 320 --- Spacelab N86-10222
The mirror heating facility: Performance and experiences --- Spacelab N86-10223
GaS-semiconductor crystals under microgravity: Experiment ES 323 --- Spacelab N86-10224
Solution growth of cadmium telluride: Experiment ES 322 --- Spacelab N86-10225
Crystallization of a silicon sphere --- Spacelab N86-10226
Crystal growth of silicon in Spacelab 1: Experiment ES-321 N86-10227
Protein single crystal growth under microgravity --- Spacelab N86-10228
Crystal growth from solution --- Spacelab N86-10229
Growth and characterization of brushite and lead monetite, simulation and results --- Spacelab N86-10230
Self diffusion of Sn112 and Sn124 in liquid tin N86-10231
Adhesion of metals: Experiment 1 ES-340 --- Spacelab N86-10232
Holographic interferometry near gas/liquid critical points: Ground-based study of a D1 experiment --- Spacelab N86-10249
Isochoric specific heat of sulfur hexafluoride at the critical point. A Spacelab experiment for the German D1-mission in 1985 N86-10251
First Spacelab Payload (FSLP) experiments on composite materials N86-10265
First Spacelab Payload (FSLP) experiments in metallurgy N86-10266
Crystal growth from solutions and nucleation from the vapor phase --- Spacelab N86-10267
Liquids and interfaces --- Spacelab N86-10268
Metric Camera Workshop --- Spacelab
[ESA-SP-209] N86-10485
Digital elevation model from Spaculab metric camera photographs N86-10486
Orthophotomapping from metric camera imagery --- Spacelab N86-10487
Evaluation of the accuracy of the metric camera images for the production of line maps and orthophotos N86-10490
Photomapping in different climatic zones --- Spacelab metric camera N86-10491
A geological structural analysis of the southeastern Zagros (Iran) ranges based on metric camera photos N86-10492
Erosion control and watershed management by Spacelab photography N86-10493
Evaluation of metric camera images at the University of London --- Spacelab N86-10495
Partial in-flight calibration of the metric camera --- Spacelab N86-10496
Identification of planimetric features from the metric camera --- Spacelab N86-10497
Analysis of metric camera images from the USA and their suitability for topographic and thematic mapping --- Spacelab N86-10498
Long range translocations ashore to offshore using Spacelab-1 metric camera imagery in the perspective of integrated geophysical surveys N86-10499
Line mapping and resolution tests with metric camera data --- Spacelab N86-10500
Role of the Economic Commission for Africa as a principal investigator in the metric camera experiment and reports of the result of the assessment for topographic and revision of maps in populated and developed areas of the world N86-10501
The role of very small scale metric images in modern geology --- Spacelab metric camera N86-10502
Geological mapping of remote mountainous regions using metric camera imagery --- Spacelab N86-10503
Interpretation of metric camera concerning hydrologic structures of the Rhone Delta --- Spacelab N86-10504
Test on mapping application of metric camera imagery --- Spacelab N86-10505
Status of preparation activities for metric camera reflight on EOM-1/2 N86-10506
OEEPE participation in testing metric camera photography --- European Organization for Experimental Photogrammetric Investigations (OEEPE) N86-10507
Topographic interpretation of metric camera images: An example in Somalia --- Spacelab N86-10508
Thematic investigations in France based on metric camera imagery --- Spacelab N86-10509
Thematic mapping of metric camera color infrared and black and white photographs for land use classification N86-10510
Digital image processing of metric camera imagery --- Spacelab N86-10511
Land evaluation successes with the metric camera --- Spacelab N86-10512
Requirements and possibilities of Spacelab metric camera photos usage for inventories of large areas of extensively managed forests N86-10513
Topographic and thematic mapping: Analysis of metric camera black and white photographs of the Rhone Delta N86-10514
Evaluation of metric camera photos --- Spacelab; alpine snow cover N86-10515
Creation of Ground Control Points (GCP) library using ESA Spacelab metric camera imagery --- ground control point (gcp) N86-10516
Updating of topographic maps by means of metric camera photos example: Hallertau (Bavaria) N86-10517
Interpretation of Spacelab-1 photographs for the generation of 1:200000 topographic map N86-10518
Metric camera image of Munich as additional means for urban cartography --- Spacelab N86-10519
An example of single model orientation of metric camera stereophotographs --- Spacelab N86-10520
Tectonic analysis of typical fold structures in the Zagros Mountains (Iran) by the application of quantitative photogrammetric methods on metric camera data --- Spacelab N86-10521
Test results using metric camera photography for 1:250,000 mapping --- Spacelab N86-10522

SPALLATION
Beginnings of remote handling at the RAL Spallation Neutron Source
[DE85-012681] N86-11001

SPARK GAPS
Compact, low jitter, triggered spark gap
[DE85-012812] N86-10195
Delay times and jitter in triggered vacuum spark gaps using metal vapor and surface flashover types of triggers
[DE85-013966] N86-10441

SPATIAL DISTRIBUTION
Cometary atmospheres: Modeling the spatial distribution of observed neutral radicals
[NASA-CR-176242] N86-11133

SPATIAL RESOLUTION
Time resolved flow velocity and concentration measurements using a travelling thermal lens
[AD-A156706] N86-10541

SPECIFIC HEAT
Isochoric specific heat of sulfur hexafluoride at the critical point. A Spacelab experiment for the German D1-mission in 1985 N86-10251

SPECIFICATIONS
Specification for the performance, design, development and test requirements for a severe environment cartridge recorder. Issue 4
[AD-A156637] N86-10523
Partial evolution and omega completeness of algebraic specifications
[CWI-CS-R8501] N86-10884
Application of structural-mechanics methods to the design of large tandem-mirror fusion devices (MFTF-B)
[DE85-008960] N86-11017
RHIC lattice
[DE85-013289] N86-11026

SPECKLE PATTERNS
Laser target speckle eliminator
[AD-D011775] N86-10536
Imaging speckle interferometer in space: Digital simulations of image reconstruction and photon noise N86-11120

SPECTRAL METHODS
Spectral methods in adapted curved grids N86-10878

SPECTRAL REFLECTANCE
Vegetation and soils field research data base: Experiment summaries
[E85-10110] N86-10610

Integrating sphere measurements of directional-hemispherical transmittance of window systems
[DE85-013926] N86-10978

SPECTRAL RESOLUTION
Parallel pulse processing for mercuric iodide gamma-ray detectors
[DE85-013391] N86-10526

SPECTROMETERS
Lithologic mapping in a sedimentary environment using multipolarization SAR images N86-10624
NBSGSC: A FORTRAN program for quantitative X-ray fluorescence analysis
[PB85-206068] N86-10647

SPECTROSCOPY
Light scattering tests of fundamental theories of transport properties in the critical region N86-10113

SPECTRUM ANALYSIS
A superconducting tunnel junction receiver for millimeter-wave astronomy N86-11041
Theoretical analysis of Wolter/LSM X-ray telescope systems
[NASA-CR-176244] N86-11095

SPHERES
Analysis of combined natural and forced convection around cylinders and spheres N86-10456

SPHERICAL SHELLS
Fusion target technology N86-10156
Strength of shells under local transverse loads N86-10568

SPHEROIDS
Mechanics of coated fiber composites N86-10285

SPHEROMAKS
Theoretical aspects of magnetic helicity
[DE85-011846] N86-10984
Increased particle confinement with the use of external dc bias field in the CTX spheromak
[DE85-012744] N86-10988
Local drift parameter, j/n sub e and resistivity anomaly measurements in CTX spheromaks
[DE85-012740] N86-10998
Energy efficiency of the CTX magnetized coaxial plasma source
[DE85-012735] N86-11003
Generalized helicity and its time derivative
[DE85-012770] N86-11027
Recent helicity source and power supply improvements in CTX
[DE85-012741] N86-11028
Equilibrium of the kink source experiment
[DE85-012764] N86-11029

SPIN EXCHANGE
Polarization transfer in inelastic scattering and pionic models of the EMC effect
[DE85-010736] N86-10955

SPIN STABILIZATION
Preliminary studies of a spinning tether-connected TRIO concept — spaceborne interferometer (TRIO) N86-11110

SPIN TESTS
Axisymmetric free surface behavior of moving liquid in a cylinder in microgravity — Spacelab N86-10206

SPIN-SPIN COUPLING
Two-loop large Higgs mass corrections to vector boson self-couplings
[NIKHEF-H/84-15] N86-11038

SPINOR GROUPS
On class groups of lattices
[CTH-MATH-1985-08] N86-10903

SPONTANEOUS COMBUSTION
Self-heating to ignition measurements and computation of critical size for solar energy collector materials
[DE85-011449] N86-10302

SPONTANEOUS EMISSION
Spontaneous Raman spectroscopy of shocked H2O
[DE85-014557] N86-10470

SPOT WELDS
Correlation between vibrations and buckling of cylindrical shells stiffened by spot-welded and riveted stringers
[TAE-537] N86-10584

SPRAY NOZZLES
Modeling of engine sprays
[DE85-010020] N86-10559

SPRAYERS
Microcomputer aided calculations of parameters for spray dryer operation
[DE85-013466] N86-10681

SPRING (SEASON)
A composite climatological study of the frequency and distribution of severe weather associated with spring season Colorado cyclogenesis
[AD-A156981] N86-10715

SPUTTERING
Rapid evaluation of ion thruster lifetime using optical emission spectroscopy
[NASA-TM-87103] N86-10280

Identification of chemical and physical phenomena affecting the durability of silvered polymer (PMMA) mirrors
[DE85-012131] N86-10645

STABILITY
Topics in nonlinear wave theory with applications N86-10367
Beam stability in a 6 GeV synchrotron light source
[DE85-013850] N86-10979

STAINLESS STEELS
Adhesion of metals: Experiment 1 ES-340 — Spacelab N86-10232
Fracture toughness and stress relief response of irradiated type 347/348 stainless steel N86-10320
Fracture toughness of hydrogen-embrittled precipitation-hardened stainless steels
[AD-A156664] N86-10592

STANDARDIZATION
Standardization of tasks: Approach planning — human performance assessment
[IZF-1984-19] N86-10782

STANDARDS
Secondary standards laboratories for ionizing radiation calibrations: The national laboratory interests
[DE85-007046] N86-10938

STANDING WAVES
Multimode acoustic research N86-10167

STAR CLUSTERS
The dynamics and stellar content of globular star clusters N86-11131

STARS
Radio studies of a complete sample of quasars N86-11093
Stellar s-process diagnostics
[DE85-012926] N86-11134

STARTING
Gel precursors as glass and ceramic starting materials for space processing applications research N86-10150

STATISTICAL ANALYSIS
Dynamic analysis of a sled traveling along a rough rail
[AD-A156589] N86-10191
A quantitative method for analyzing the roughness of the seafloor N86-10726

STATISTICAL DISTRIBUTIONS
A modified repair strategy for two-component systems with revealed and unrevealed faults
[AD-A156715] N86-10885
Adaptive distribution-free test for the K random sampling problem, part 1
[COMP-CENT-NOTE-14-PT-1] N86-10888
Adaptive distribution free test for the K random sampling problem, part 2
[COMP-CENT-NOTE-15-PT-2] N86-10889

STATISTICAL MECHANICS
Theoretical studies of the surface tension of liquid metal system N86-10101
New approach to multiphase equilibria: Application to high-pressure physics problems
[DE85-013820] N86-10907

STATISTICAL TESTS
Robustness of multiple comparisons against variance heterogeneity
[COMP-CENT-NOTE-17] N86-10890

STEADY STATE
Mephisto: Interfacial destabilization in metal alloys N86-10079
Dendritic solidification in a binary alloy melt: Steady-state versus morphological stability theories N86-10261
Rapid evaluation of ion thruster lifetime using optical emission spectroscopy
[NASA-TM-87103] N86-10280
Steady state frictional behavior of thin film coatings N86-10335

STEAM
KRAK: A computer program for two-phase, two-component porous flow and fracture propagation, revision
[DE85-014264] N86-10489

STEELS
Application of the unloading compliance methods in fracture toughness measurements of a quenched and tempered steel
[BLL-BISI-TRANS-21628-(9022.09)] N86-10308
Passivation of steel with aqueous amine solutions
[AD-D011749] N86-10314
Development of a sheath for sensor protection in molten steel applications
[AD-A156764] N86-10315
Chemical/hydrogen energy systems
[DE85-012742] N86-10667

STEERING
Path error-neglection in straight lane driving
[IZF-1984-32] N86-10783

STELLAR ENVELOPES
The two micron spectrum of R Scuti N86-11092

STELLAR EVOLUTION
Project VESTA, exploratory mission to the asteroids: Scientific objectives and technical specifications
[NASA-TM-77669] N86-10179

STELLAR ROTATION
The dynamics and stellar content of globular star clusters N86-11131

STEPPES
Observations of the snow cover in the southern part of the Buryat Autonomous Soviet Socialist Republic
[NASA-TM-77910] N86-10613

STEREOPHOTOGRAPHY
Stereoscopic video imagery generation
[AD-D011785] N86-10481
Stereo-orthophotos in various map projections N86-10488
Restitution of Spacelab photography by analog stereoplotter N86-10489
Land evaluation successes with the metric camera — Spacelab N86-10512
An example of single model orientation of metric camera stereophotographs — Spacelab N86-10520

STEREOSCOPIC VISION
Test of a multilevel computational theory of stereoscopic visual image processing
[AD-A157011] N86-10870

STIFFNESS
Finite element analysis of statics and dynamic structural engineering problems using semi-explicit methods N86-10571

STIRLING CYCLE
Simplified analysis of Stirling engines and heat pumps
[DE85-005366] N86-10647
Stirling-engine-driven heat pump program overview
[DE85-004796] N86-10661

STOCHASTIC PROCESSES
A quantitative method for analyzing the roughness of the seafloor N86-10726
On maximal and distributional coupling
[CTH-MATH-1984-30] N86-10875

STOICHIOMETRY
Crystal growth of GaAs in space N86-10234

STORAGE RINGS (PARTICLE ACCELERATORS)
Method for compensating bellows pressure loads while accommodating thermal deformations
[DE85-013306] N86-10933
The 20 keV undulators for a 6-GeV storage ring
[DE85-013867] N86-10941
Beam profile monitor for the NSLS VUV ring employing linear photodiode arrays
[DE85-012184] N86-10947
Surface conditioning of synchrotron radiation source to improve beam lifetime
[DE84-012185] N86-10948
Parasitic mode losses versus signal sensitivity in beam position monitors
[DE85-014367] N86-10964
Superconvergent tracking and invariant surfaces in phase space
[DE85-013051] N86-10985
Ferrite kicker magnet for the IAMPF switchyard upgrade
[DE85-012657] N86-10996
Field-independent normalization of SSC Collider Ring costs
[DE85-012425] N86-10997
Thermal and structural analysis of ring components by the finite element method
[DE85-013305] N86-11021
Unicell structure for superconducting storage rings
[DE85-013303] N86-11022
Tracking studies on the effects of magnet multipoles on the aperture of the RHIC heavy ion collider
[DE85-013282] N86-11023

STORMS
A composite climatological study of the frequency and distribution of severe weather associated with spring season Colorado cyclogenesis
[AD-A156981] N86-10715
Application of the dutch method for estimating storm-induced dune erosion
[AD-A156717] N86-10728

STRAIN HARDENING
Portevin-Le Chatelier effect. 1: Model for the type-E serrations
[DE85-006879] N86-10322

STRANGENESS
Hyperon polarization: An unresolved problem
[DE85-012298] N86-10946

STRATA
Dynamic lithostratigraphy and paleoecology of upper Mississippi (Chesterian) strata of the northcentral Appalachian Basin N86-10869

STRATEGIC MATERIALS
Whole plant utilization of sunflowers as a renewable source of strategic materials (rubber) [AD-A155833] N86-10342
STRATEGY
DFVLR, strategic study of astronautics 1984, user requirements N86-11069
Report of the ad hoc committee to review the program of the SDI Directorate on Innovative Science and Technology (IST) [AD-A156666] N86-11071
STRATIGRAPHY
Report of the Workshop on Geologic Applications of Remote Sensing to the Study of Sedimentary Basins [E86-10002] N86-10599
Chronologic analysis of terrestrial sediments and basin evolution N86-10602
Multisensor data integration techniques N86-10604
Paleogene vertebrate paleontology, geology and remote sensing in the Wind River Basin N86-10609
Cretaceous and cenozoic stratigraphy of the upper and middle coastal plain, Harnett County area, North Carolina N86-10690
Stratigraphy, petrology, depositional and post-depositional histories and their effects upon reservoir properties of the Parkman Formation of the Mesa Verde group, Powder River Basin, Wyoming N86-10691
Paleontology and stratigraphy of Lower Cambrian and upper Proterozoic sediments, Caborca region, northwestern Sonora, Mexico N86-10692
Dynamic lithostratigraphy and paleecology of upper Mississippi (Chesterian) strata of the northcentral Appalachian Basin N86-10693
In-situ geophysical investigations into the nature of the oceanic crust N86-10725
STRATOSPHERE
Chemical kinetics and photochemical data for use in stratospheric modeling [NASA-CR-1[illegible]198] N86-10707
STRATUS CLOUDS
Comparative flight measurement of icing parameters for the propeller aircraft Do-28D2 of the test station 61 of the DFVLR and for the DFVLR aircraft Falcon 20e in stratus clouds [DFVLR-FB-85-16] N86-10720
STREAM FUNCTIONS (FLUIDS)
Analysis of combined natural and forced convection around cylinders and spheres N86-10456
STREAMS
Development of the Multi-Attribute Hazard Assessment System (MAHAS) and its application to energy-related waste streams [DE85-010278] N86-10676
STRESS (PHYSIOLOGY)
Classification of changes in electrocardiogram during muscular exertion of healthy individuals N86-10755
Mechanism of adaptogenic action of prickly eleuterococcus on man during heat stress N86-10757
Report on the research activities on whole-body vibrations. Human strain due to mechanical vibrations [ISBN-3-88383-107-7] N86-10773
STRESS (PSYCHOLOGY)
Effect of emotional stress on hemostasis system of healthy persons N86-10745
Eye-movement activity as index of functional state of brain N86-10758
STRESS ANALYSIS
Finite element analysis of metals at elevated temperature using unified constitutive theories N86-10569
STRESS CONCENTRATION
Mechanics of coated fiber composites N86-10295
Analytical and experimental study of cracks emanating from an elliptical hole in unidirectional composite material N86-10567
Strength of shells under local transverse loads N86-10568
STRESS CORROSION
Fatigue, static tensile strength and stress corrosion of aircraft materials and structures [VTH-LR-360-PT-1] N86-10045
Design, fabrication and testing of an experimental apparatus for determining particle behavior under very low intergranular stresses N86-10175
STRESS CORROSION CRACKING
Environmental degradation of materials: Surface chemistry related to stress corrosion cracking N86-10099
STRESS INTENSITY FACTORS
Analytical and experimental study of cracks emanating from an elliptical hole in unidirectional composite material N86-10567
Numerical simulation of crack arrest experiments on Araldite B using the finite difference method [REPT-W-8/82] N86-10586
STRESS MEASUREMENT
Study of static and dynamic stress effects in nonlinear solids [NASA-CR-176236] N86-10578
STRESS RELAXATION
Constitutive modeling for isotropic materials (HOST) [NASA-CR-174980] N86-10589
STRESS WAVES
Ultrasonic evaluation of mechanical properties of thick, multilayered, filament wound composites [NASA-TM-87066] N86-10561
STRESS-STRAIN-TIME RELATIONS
High temperature properties and characterization of Si3-N4 materials [BMFT-FB-T-85-046] N86-10352
High temperature properties of SiC materials [BMFT-FB-T-85-047] N86-10353
STRESSES
Resistance curves for crack growth under plane-stress conditions in an elastic perfectly-plastic material [AD-A156778] N86-10593
Fundamental study of the closure property of joints N86-10698
Shock loading and release behavior of x-cut quartz [DE85-013954] N86-11054
STRINGERS
The effect of debond growth on crack propagation in composite plates reinforced with adhesively bonded composite stringers N86-10287
Effect of sequence of loading on interaction curves for buckling of stiffened shells [TAE-536] N86-10583
Correlation between vibrations and buckling of cylindrical shells stiffened by spot-welded and riveted stringers [TAE-537] N86-10584
STRUCTURAL ANALYSIS
Load-deflection tests and computer analyses of a high-precision adhesive-bonded antenna reflector panel N86-10389
Marginal terrain straddle-lift container handler [AD-D011752] N86-10555
A transformation method for the evaluation of the response moments of elastic structures with random properties [AD-A156882] N86-10557
Load space formulation of reliability for nonlinear random structural systems N86-10570
Three-dimensional vibration analysis of a uniform beam with offset inertial masses at the ends [NASA-TM-86393] N86-10580
Constitutive modeling for isotropic materials (HOST) [NASA-CR-174980] N86-10589
Thermal and structural analysis of ring components by the finite element method [DE85-013305] N86-11021
STRUCTURAL BASINS
Report of the Workshop on Geologic Applications of Remote Sensing to the Study of Sedimentary Basins [E86-10002] N86-10599
Some opinions on remote sensing and geologic studies N86-10600
Position paper: Workshop on Geologic Applications of Remote Sensing to the Study of Sedimentary Basins N86-10601
Chronologic analysis of terrestrial sediments and basin evolution N86-10602
Analysis of remote sensing data N86-10605
Remote stratigraphic and structural analysis: Multisensor results in the Wind River/Bighorn Basin area, Wyoming N86-10606
Foreland basin structures and remote sensing N86-10608
Lithologic mapping in a sedimentary environment using multipolarization SAR images N86-10624
Time-term analysis of upper crustal structure in the Columbia Basin, Washington [DE85-012390] N86-10633
Dynamic lithostratigraphy and paleecology of upper Mississippi (Chesterian) strata of the northcentral Appalachian Basin N86-10693
STRUCTURAL DESIGN
Design sensitivity analysis and optimization of built-up structures N86-10565
Application of structural-mechanics methods to the design of large tandem-mirror fusion devices (MFTF-B) [DE85-008960] N86-11017
STRUCTURAL DESIGN CRITERIA
Optimum design of an aircraft wing structure with multiple constraints by the direct-vision criteria method N86-10004
Optimal design of portal frames against buckling N86-10572
Application of structural-mechanics methods to the design of large tandem-mirror fusion devices (MFTF-B) [DE85-008960] N86-11017
Astronomical criteria for interferometric arrays --- Spacecraft design N86-11099
STRUCTURAL ENGINEERING
Finite element analysis of statics and dynamic structural engineering problems using semi-explicit methods N86-10571
STRUCTURAL FAILURE
Progressive damage, fracture predictions and post mortem correlations for fiber composites [NASA-TM-87101] N86-10290
STRUCTURAL PROPERTIES (GEOLOGY)
A geological structural analysis of the southeastern Zagros (Iran) ranges based on metric camera photos N86-10492
Geologic evaluation and reservoir properties of the PR Spring tar sand deposit, Uintah and Grand Counties, Utah [DE85-013248] N86-10634
Structural discontinuity within the southern California continental margin: Seismic and gravity models of the western Transverse Ranges N86-10699
STRUCTURAL STABILITY
Application of structural-mechanics methods to the design of large tandem-mirror fusion devices (MFTF-B) [DE85-008960] N86-11017
STRUCTURAL VIBRATION
Evaluation of a pulse control law for flexible spacecraft [NASA-CR-176233] N86-10272
STRUTS
Test and evaluate passive orbital disconnect struts (PODS 3) [NASA-CR-177368] N86-10274
STUDS (STRUCTURAL MEMBERS)
Improved stud configurations for attaching laminated wood wind turbine blades [NASA-TM-87109] N86-10582
SUBMARINES
Angle of incidence effects for underwater shock using generic computational models [DE85-012936] N86-10466
Angle of incidence effects for underwater shock using generic computational models, rev. 1 [DE85-012921] N86-10467
SUBROUTINES
The development of a neutron evaporation theory code for the thermal fission of Uranium-235 [AD-A156593] N86-10951
SUBSONIC FLOW
The role of freestream turbulence scale in subsonic flow separation [NASA-CR-176237] N86-10014
Oscillations of subsonic flow in an abruptly expanding circular duct [MPIS-16/1984] N86-10028
SUBSONIC SPEED
Summary of work on jet noise prediction [ESDU-BR-62636] N86-10909
SUBSTITUTES
Coincidence densities and spectra of a class of substitution minimal sets N86-10857
SUBSTRATES
Modelling of laser-enhanced chemical vapor deposition N86-10105
Thermodynamic constraints on ion beam mixing of metals on insulators [DE85-013628] N86-10448
The influence of the substrate on the practical machining applications of cutting edges coated with different materials [BLL-RISLEY-TR-5039-(9091.9F)] N86-10546
The interaction of small metal particles with refractory oxide supports [NASA-CR-176228] N86-11047
SUCTION
Investigations on a supercritical airfoil with boundary layer suction through a perforated strip in the shock region [DFVLR-FB-85-15] N86-10025
SULFUR
Method for determining elemental sulfur in jet fuel --- differential pulse polarography [FOA-C-40211-B4] N86-10380
SULFUR DIOXIDES
Emissions of NOx, SOx and VOC from Antropogenic sources [PB85-193530] N86-10688
Seasonal variations in atmospheric chemistry in the Adirondacks [DE85-014227] N86-10719
SULFUR FLUORIDES
Isochoric specific heat of sulfur hexafluoride at the critical point. A Spacelab experiment for the German D1-mission in 1985 N86-10251

High voltage instrument transformers for outdoor service with an insulation of low pressure SF6 gas and plastic foils
[BMFT-FB-T-85-034] N86-10449

SUNFLOWERS
Whole plant utilization of sunflowers as a renewable source of strategic materials (rubber)
[AD-A155833] N86-10342

SUPERCONDUCTING MAGNETS
Cryogenic equivalence principle experiment
N86-10171
Cryogenic structural materials for superconducting magnets
[DE85-008026] N86-10908
Field-independent normalization of SSC Collider Ring costs
[DE85-012425] N86-10997
US superconducting magnet data base assessment for INTOR
[DE85-013648] N86-11000
Unicell structure for superconducting storage rings
[DE85-013303] N86-11022

SUPERCONDUCTORS
A superconducting tunnel junction receiver for millimeter-wave astronomy N86-11041
Superconductors for pulsed RF accelerators
[DE85-013378] N86-11051

SUPERCOOLING
Glass formation in reluctant glass formers
N86-10151
Bulk formation of metallic glasses and amorphous silicon from the melt N86-10154

SUPERCRITICAL FLUIDS
Rapid analysis using capillary supercritical fluid chromatography
[DE85-012460] N86-10297

SUPERCRITICAL WINGS
Investigations on a supercritical airfoil with boundary layer suction through a perforated strip in the shock region
[DFVLR-FB-85-15] N86-10025

SUPERFLUIDITY
An investigation of vortex dynamics in 2-dimensional superfluid films of helium-4 N86-11040
Critical dynamics in superfluid helium N86-11046

SUPERHIGH FREQUENCIES
On the use of X-band CW nanosecond airborne radar for terrain profiling
[AD-A156888] N86-10406
Digital radio link: Method and a measuring system for studying the radio channel during frequency selective fading
[FOA-C-30386-E2] N86-10411

SUPERLATTICES
Semiconductor superlattic photodetectors
[NASA-CR-176249] N86-10484

SUPERNOVA REMNANTS
Physical conditions in giant extragalactic H2 regions
N86-11130

SUPERSONIC FLOW
A numerical solution of the shock-turbulent interaction over a compression corner for supersonic flow
N86-10003
A new method for calculating unsteady supersonic aerodynamic forces and its application N86-10009
Forced response analysis of an aerodynamically detuned supersonic turbomachine rotor
[NASA-TM-87093] N86-10019

SUPERSONIC FLUTTER
A new method for calculating unsteady supersonic aerodynamic forces and its application N86-10009

SUPERSONIC INLETS
Effect of a shear layer on the stability of an axisymmetrical external compression air intake
N86-10010

SUPERSONIC SPEEDS
Supersonic metal cluster beams
[DE85-014321] N86-10966

SUPPLEMENTS
Advanced vehicle systems assessment. Volume 5: Appendices
[NASA-CR-176208] N86-11086

SUPPORTS
A new 70-meter antenna quadripod with reduced RF blockage N86-10385
Cryogenic structural materials for superconducting magnets
[DE85-008026] N86-10908

SURFACE COOLING
Undercooling investigations on the easy glass former Pd-Cu-Si N86-10259

SURFACE DEFECTS
Liquid crystal non-destructive inspection of metals
[AD-D011772] N86-10316

SURFACE ENERGY
Surface forces in contacting solids — microgravity rocket experiment N86-10252

SURFACE FINISHING
Mechanism of the formation of boronised layers on high carbon steel
[BLL-BISI-TRANS-23036-(9022.06)] N86-10306
Boronising of iron and steel by ionic bombardment by diborane
[BLL-BISI-TRANS-23034-(9022.06)] N86-10307
Pre-bond treatment for titanium alloys
[BAE-AL/MAT/3864] N86-10309
Fuel and lubricant behavior in boundary layers analyzed by infrared emission Fourier transform spectrometry
N86-10336

SURFACE LAYERS
Thermocapillary flows and their stability: Effects of surface layers and contamination N86-10109
Mechanism of the formation of boronised layers on high carbon steel
[BLL-BISI-TRANS-23036-(9022.06)] N86-10306

SURFACE PROPERTIES
Mixed-mode fracture of ceramics
[DE85-014087] N86-10349
Fundamental study of the closure property of joints
N85-10698

SURFACE REACTIONS
Environmental degradation of materials: Surface chemistry related to stress corrosion cracking
N86-10099
Compatibility of grain-stabilized platinum with candidate propellants for resistojets
[NASA-TM-87118] N86-10279

SURFACE ROUGHNESS
Age-dating volcanic and alluvial surfaces with multipolarization data N86-10620

SURFACE ROUGHNESS EFFECTS
Laser target speckle eliminator
[AD-D011775] N86-10536

SURFACE TEMPERATURE
LANDSAT TM image data quality analysis for energy-related applications
[E85-10109] N86-10597

SWEEP FREQUENCY
A comparison of swept frequency and FFT methods used to calibrate array test modules
[AD-A156629] N86-10430

SWELLING
Swelling and tensile properties of EBR-2-irradiated tantalum alloys for space reactor applications
[DE85-012887] N86-10329

SWEPT WINGS
Second order approximation method for transonic flows over swept wings N86-10002

SWIRLING
Confined swirling jet predictions using a multiple-scale turbulence model
[NASA-CR-178484] N86-10462

SWITCHING CIRCUITS
Counterpulse railgun energy recovery circuit
[DE85-011603] N86-10196
Contact effects in light activated GaAs switches
[AD-A156957] N86-10434
A course on field programmable logic
[EUT-85-E-148] N86-10805
State assignment in sequential circuits
[EUT-85-E-146] N86-10846

SWITCHING THEORY
Theoretical modeling of the vapor cavitation in dynamically loaded journal bearings
[NASA-TM-87076] N86-10463

SYMMETRY
Determination of symmetry and phase in human visual response functions: Theory and experiments
N86-10769
Charge exchange in slow collisions of atoms and molecules N86-10922
Conducting wall and pressure profile effect on MHD stabilization of axisymmetric mirror
[DE85-013647] N86-11020

SYNCHRONISM
Reaching approximate agreement in the presence of faults
[AD-A156541] N86-10698
Engineering high reliability, low-jitter Marx generators
[DE85-012811] N86-11013

SYNCHRONIZERS
Programmable delay unit incorporating a semi-custom integrated circuit
[DE85-013379] N86-11033

SYNCHROTRON RADIATION
Method for determining the position, angle and other injection parameters of a short pulsed beam in the Brookhaven AGS
[DE85-012523] N86-10931
Beam profile monitor for the NSLS VUV ring employing linear photodiode arrays
[DE85-012184] N86-10947
Surface conditioning of synchrotron radiation source to improve beam lifetime
[DE84-012185] N86-10948
Beam stability in a 6 GeV synchrotron light source
[DE85-013850] N86-10979
Noninterceptive techniques for the measurement of longitudinal parameters for intense H(-) beams
[DE85-012682] N86-10992

SYNCHROTRONS
Use of the MURA transformation to generate the fields and calculate the motion of protons in the designed Argonne Mini-ASPUN FFAG spiral sector accelerator
[DE85-011477] N86-10934
Report on a visit to CERN in February 1985. Notes on bunch monitors, high-frequency systems, linacs, kickers, magnets, vacuum and bunch extraction
[LINO-119] N86-10967
Performance of the H(-) ion source for the intense pulsed neutron source
[DE85-012368] N86-10991

SYNOPTIC METEOROLOGY
A composite climatological study of the frequency and distribution of severe weather associated with spring season Colorado cyclogenesis
[AD-A156981] N86-10715

SYNTHESIS (CHEMISTRY)
Catalytic activity of shock modified ZnO for CO oxidation and methanol synthesis
[DE85-014704] N86-10300
Synthesis of arylene siloxanylene polymers and copolymers
[AD-D011780] N86-10338

SYNTHETIC APERTURE RADAR
SAR image quality: A review
[DFVLR-MITT-85-07] N86-10413
Multisensor data integration techniques N86-10604
NASA/JPL Aircraft SAR Workshop Proceedings
[NASA-CR-176204] N86-10615
Radar system description N86-10616
CV-990 L-band SAR: A calibration experiment
N86-10617
Neogene compressional deformation and possible thrust faulting in southwest Dominican Republic N86-10618
The effect of vegetation type, microrelief, and incidence angle on radar backscatter N86-10619
Age-dating volcanic and alluvial surfaces with multipolarization data N86-10620
Topographic mapping from interferometric synthetic aperture radar observations N86-10622
Strategies for analyzing mixed pixels in remotely sensed imagery N86-10623
Lithologic mapping in a sedimentary environment using multipolarization SAR images N86-10624
Mapping diverse forest cover with multipolarization airborne radar N86-10625
Potential applications of multipolarization SAR for pine plantation biomass estimation N86-10626
On the use of L-band multipolarization airborne SAR for surveys of crops, vineyards, and orchards in a California irrigated agricultural region N86-10627
Vegetation canopy discrimination and biomass assessment using multipolarized airborne SAR
N86-10628

SYNTHETIC APERTURES
Optical/IR telescope arrays: A study of their potential for satisfying observational requirements in astronomy for a large aperture system in the 1990s and beyond
[REPT-15] N86-11094
OASIS: Optical Aperture Synthesis in Space
N86-11106
COSMIC image reconstruction — Coherent Optical System of Modular Imaging Collectors (COSMIC)
N86-11118
The OASIS correlator — Optical Aperture Synthesis in Space (OASIS) N86-11119
Aperture synthesis with or without phase information for kilometric arrays interpolation algorithms for stabilized image reconstruction N86-11124
VLBI at optical and radio wavelengths: Congruences and contrasts N86-11126

SYNTHETIC ARRAYS
Optical/IR telescope arrays: A study of their potential for satisfying observational requirements in astronomy for a large aperture system in the 1990s and beyond
[REPT-15] N86-11094
Colloquium on Kilometric Optical Arrays in Space
[ESA-SP-226] N86-11096
Extragalactic observations with optical space arrays
N86-11098
Astronomical criteria for interferometric arrays — Spacecraft design N86-11099
Strategy for the development of space arrays
N86-11101

TRIO: A kilometric array stabilized by solar sails — Spaceborne astronomy N86-11102

SAMSI: An orbiting spatial interferometer for micro-arc second astronomical observations — Spacecraft Array for Michelson Spatial Interferometry (SAMSI) N86-11103

COSMIC: A high resolution, large collecting area telescope — Coherent Optical System of Modular Imaging Collectors (COSMIC) N86-11104

A fiber-linked version of project TRIO — telescope array N86-11105

OASIS: Optical Aperture Synthesis in Space N86-11106

Problems in image reconstruction with optical arrays — spaceborne astronomy N86-11115

The OASIS correlator — Optical Aperture Synthesis in Space (OASIS) N86-11119

Aperture synthesis with or without phase information for kilometric arrays interpolation algorithms for stabilized image reconstruction N86-11124

SYSTEM EFFECTIVENESS

An annotated bibliography of abstracts on the use of simulators in technical training [AD-A156792] N86-11065

Advanced vehicle systems assessment. Volume 2: Subsystems assessment [NASA-CR-176205] N86-11083

SYSTEM IDENTIFICATION

The identification package SATER [ER-83/08] N86-10844

Naive approximate realization of noisy data [ER-83/10] N86-10880

SYSTEMS ANALYSIS

Annotated bibliography of publications dealing with occupational health and medical information systems, cost analysis procedures, evaluation methodology and related legal issues [AD-A156650] N86-11078

A systems development life cycle study of the information center [AD-A156977] N86-11079

SYSTEMS ENGINEERING

New directions in chemical analysis [DE85-012930] N86-10296

Initial design of a relational database system for NPS computer asset identification and valuation for risk assessment [AD-A156847] N86-10796

System integration report [NASA-CR-171900] N86-10821

Ada (trademark) Programming Support Environment (APSE) Evaluation and Validation (E and V) workshop report held at Airlie, Virginia on 2-6 April 1984 [AD-A156867] N86-10829

Fault-free behavior of reliable multiprocessor systems: FTMP experiments in AIRLAB [NASA-CR-177967] N86-10848

A systems development life cycle study of the information center [AD-A156977] N86-11079

Future space telescope design concepts N86-11107

SYSTEMS INTEGRATION

Efficient systolic arrays for the solution of toeplitz systems: An illustration of a methodology for the construction of systolic architectures in VLSI (Very Large Systems Integration) [AD-A156767] N86-10795

System integration report [NASA-CR-171900] N86-10821

SYSTEMS MANAGEMENT

Development of IS2100: An information systems laboratory [AD-A156848] N86-10797

SYSTEMS STABILITY

Stability of long liquid columns N86-10244

T

TABLES (DATA)

Monthly and Seasonal Weather Outlook for mid-April to mid-May 1985, Volume 39, Number 8 [PB85-195345] N86-10724

TANTALUM ALLOYS

Swelling and tensile properties of EBR-2-irradiated tantalum alloys for space reactor applications [DE85-012887] N86-10329

TANZANIA

Satellite data even for a poultry farm. A development for Tanzania. Image evaluation following new ways N86-10182

TAPE RECORDERS

Specification for the performance, design, development and test requirements for a severe environment cartridge recorder. Issue 4 [AD-A156837] N86-10523

TARGET ACQUISITION

Guidance and control of a cable based payload pickup system N86-10048

TARS

A fundamental study of smoldering with emphasis on experimental design for zero-g N86-10162

TASKS

Standardization of tasks: Approach planning — human performance assessment [IZF-1984-19] N86-10782

TATB

Composite explosives for metal acceleration: The effect of detonation temperature [DE85-013982] N86-10359

TAYLOR INSTABILITY

Equilibrium of the kink source experiment [DE85-012764] N86-11029

TDR SATELLITES

JPL emergency support of TDRSS and compatible satellites N86-10394

TECHNETIUM

Application of the ruthenium and technetium thermodynamic data bases used in the EQ3/6 geochemical codes [DE85-013766] N86-10632

TECHNICAL WRITING

Writer/editor and the computer [DE85-011843] N86-11080

TECHNOLOGICAL FORECASTING

Evaluation and prediction of long-term environmental effects on non metallic materials [NASA-CR-178495] N86-10340

Report of the ad hoc committee to review the program of the SDI Directorate on Innovative Science and Technology (IST) [AD-A156668] N86-11071

TECHNOLOGY ASSESSMENT

New directions in chemical analysis [DE85-012930] N86-10296

Fuel Cell Technology Assessment Program, work element no. 6 [DE85-008228] N86-10444

Photomapping in different climatic zones — Spacelab metric camera N86-10491

Analysis of metric camera images from the USA and their suitability for topographic and thematic mapping — Spacelab N86-10498

Role of the Economic Commission for Africa as a principal investigator in the metric camera experiment and reports of the result of the assessment for topographic and revision of maps in populated and developed areas of the world N86-10501

The role of very small scale metric images in modern geology — Spacelab metric camera N86-10502

OEEPE participation in testing metric camera photography — European Organization for Experimental Photogrammetric Investigations (OEEPE) N86-10507

Requirements and possibilities of Spacelab metric camera photos usage for inventories of large areas of extensively managed forests N86-10513

Updating of topographic maps by means of metric camera photos example: Hallertau (Bavaria) N86-10517

Improved particle-velocity transducer for equation-of-state experiments [DE85-013204] N86-10532

Stock-taking of data base management systems choice considerations for the Eindhoven Technical University Computing Center (THE-RC) [COMP-CENT-NOTE-18] N86-10851

US superconducting magnet data base assessment for INTOR [DE85-013648] N86-11000

Advanced vehicle systems assessment. Volume 3: Systems assessment [NASA-CR-176206] N86-11084

Advanced vehicle systems assessment. Volume 4: Supporting analyses [NASA-CR-176207] N86-11085

Results and limitations of ground-based optical arrays — stellar interferometry N86-11097

TECHNOLOGY TRANSFER

Editors rattle space N86-10586

Solar thermal technical information guide [DE85-002941] N86-10657

Publication of the Executive Office of the President, January 20, 1981 - December 31, 1984 [PB85-187110] N86-11082

TECHNOLOGY UTILIZATION

The dirigible: A catalyst for resource exploitation in remote areas? [AD-A156518] N86-10034

Wind energy in agriculture, a promise [SS-45] N86-10672

Wind energy, a feasibility investigation for wind mills in agriculture [SS-45A] N86-10673

Advanced vehicle systems assessment. Volume 5: Appendices [NASA-CR-176208] N86-11086

TECTONICS

A geological structural analysis of the southeastern Zagros (Iran) ranges based on metric camera photos N86-10492

Tectonic analysis of typical fold structures in the Zagros Mountains (Iran) by the application of quantitative photogrammetric methods on metric camera data — Spacelab N86-10521

Chronologic analysis of terrestrial sediments and basin evolution N86-10602

Remote stratigraphic and structural analysis: Multisensor results in the Wind River/Bighorn Basin area, Wyoming N86-10606

TELECOMMUNICATION

Construction and use of a radio controlled model helicopter for research [AD-A156547] N86-10035

The Telecommunications and Data Acquisition Report [NASA-CR-176203] N86-10382

DFVLR, strategic study of astronautics 1984, user requirements N86-11069

TELEMETRY

A sequential decoding performance analysis for International Comet Explorer N86-10390

TELEOPERATORS

Supervisory control of the right arm of the beam assembly teleoperator [AD-A156856] N86-10632

TELEPHONES

Methods for developing jam-resistant security communications networks at fixed-site facilities [DE85-012032] N86-10408

TELEPHONY

Digital transmission experiments with the Orbital Test Satellite [EUT-84-E-144] N86-10270

TELESCOPES

Optical testing of large telescopes using multiple subapertures N86-10971

TELEVISION CAMERAS

The intensified multi CCD camera — spaceborne interferometers N86-11122

TEMPERATURE

Mathematical models of continuous flow electrophoresis N86-10143

TEMPERATURE CONTROL

Renovated cooling at PIMU [LINO-122] N86-10452

TEMPERATURE DEPENDENCE

Surface tensions and their variations with temperature and impurities [NASA ORDER H-27954B] N86-10115

Miscibility gap systems [NASA ORDER H-27954B] N86-10131

Chemical kinetics and cellular structure of detonations in hydrogen sulphide and air [DE85-009408] N86-10304

Portevin-Le Chatelier effect. 1: Model for the type-E serrations [DE85-006879] N86-10322

Recirculation within a glass mixture subjected to external and resistive heating [DE85-010068] N86-10348

Laminar film condensation in vertical closed two-phase thermosiphons [IKE-5-220] N86-10476

Conditioning potentialities of respiratory apparatus N86-10753

Experimental investigations of thermal radiation from potassium atoms and design applications [DE85-004086] N86-11036

Critical dynamics in superfluid helium N86-11046

Anelastic relaxation in irradiated Cu-Be [DE85-013893] N86-11056

TEMPERATURE DISTRIBUTION

Design and calibration of a flat-flame burner using line reversal techniques [AD-A156724] N86-10294

TEMPERATURE EFFECTS

Composite explosives for metal acceleration: The effect of detonation temperature [DE85-013982] N86-10359

Mean turbulence structure in strongly heating air flows N86-10455

Short term heat effect on adreno- and cholino-sensitivity of rat's small intestine N86-10754

Efficiency of muscular work in white rats during adaptation to cold N86-10763

Beam line windows at LAMPF [DE85-012723] N86-10985

TEMPERATURE GRADIENTS
Graphite formation in cast iron N86-10100
Thermocapillary motion research N86-10125
Miscibility gap systems [NASA ORDER H-27954B] N86-10131
Advanced containerless processing technology N86-10176
Gradient heating facility behavior — Spacelab N86-10217
Thermomigration of cobalt in liquid tin: Experiment 1 ES 320 — Spacelab N86-10222
The influence of thermocapillarity on the migration of droplets in a liquid possessing a uniform temperature gradient N86-10237
Analysis of large, non-isothermal elastic-visco-plastic deformations [NASA-CR-176220] N86-10588
Smoke inputs to climate models: Optical properties and height distribution for nuclear winter studies [DE85-011363] N86-10717
A processor for the study of ocean fine-scale patches [AD-A157019] N86-10730

TEMPERATURE MEASUREMENT
Containerless high temperature property measurements by atomic fluorescence N86-10092
Measurement of workpiece temperature during welding for welding robot control N86-10534

TEMPERATURE MEASURING INSTRUMENTS
Development of a sheath for sensor protection in molten steel applications [AD-A156764] N86-10315

TEMPERATURE PROFILES
Float zone experiments in space N86-10067
Flammability limits of gases under low gravity conditions N86-10164

TEMPERING
Application of the unloading compliance methods in fracture toughness measurements of a quenched and tempered steel [BLL-BISI-TRANS-21628-(9022.06)] N86-10308

TENNESSEE
Ground-coupled heat pump research at the University of Tennessee Washington, D.C., 10 Dec. 1984 [DE85-005357] N86-10650

TENSILE PROPERTIES
Swelling and tensile properties of EBR-2-irradiated tantalum alloys for space reactor applications [DE85-012887] N86-10329

TENSILE STRENGTH
Fatigue, static tensile strength and stress corrosion of aircraft materials and structures [VTH-LR-360-PT-1] N86-10045
Age-life prediction of nylon 66 parachute materials. Part 2: Changes in the chemical and physical properties of materials on aging [AD-A156909] N86-10347

TENSILE TESTS
Constitutive modeling for isotropic materials (HOST) [NASA-CR-174980] N86-10589

TENSOR ANALYSIS
Gravitational collapse of a scalar field N86-11129

TERRAIN
On the use of X-band CW nanosecond airborne radar for terrain profiling [AD-A156886] N86-10406
Marginal terrain straddle-lift container handler [AD-D011752] N86-10555
A numerical model for the estimation of solar radiation on rugged terrain N86-10694
A boundary layer flow model for areas of complex terrain N86-10701

TERRAIN ANALYSIS
Multisensor data integration techniques N86-10604

TEST CHAMBERS
Fundamental studies of droplet combustion at reduced gravity N86-10165

TEST EQUIPMENT
Academic Research Equipment in selected science-engineering fields, 1982-83. An analysis of findings from the Baseline National Survey of academic research instruments and instrumentation needs N86-11088

TEST FACILITIES
Test, measurement, and diagnostic equipment (system peculiar) [AD-A156669] N86-10563
Evaluation of the International Atomic Energy Agency (IAEA) Safeguards Analytical Laboratory quality assurance program [DE85-012078] N86-10953

TEST FIRING
EMACK railgun firing test report number 9 [AD-A156861] N86-10354

TETHERED SATELLITES
Preliminary studies of a spinning tether-connected TRIO concept — spaceborne interferometer (TRIO) N86-11110

TEXTBOOKS
Catalog of Resources for Education in Ada (trademark) and Software Engineering (CREASE). Version 3.0 [AD-A156687] N86-10790

THALLIUM ALLOYS
Cellular morphologies in lead-thallium alloys — gravitational effects N86-10262

THEMATIC MAPPING
Photomapping in different climatic zones — Spacelab metric camera N86-10491
Analysis of metric camera images from the USA and their suitability for topographic and thematic mapping — Spacelab N86-10496
Thematic investigations in France based on metric camera imagery — Spacelab N86-10509
Thematic mapping of metric camera color infrared and black and white photographs for land use classification N86-10510
Topographic and thematic mapping: Analysis of metric camera black and white photographs of the Rhone Delta N86-10514
Multisensor data integration techniques N86-10604
The effects of merging TM and A/C radar on wetland classification N86-10621
Lithologic mapping in a sedimentary environment using multipolarization SAR images N86-10624

THEOREM PROVING
Principal bundles on the affine line N86-10856
Coincidence densities and spectra of a class of substitution minimal sets N86-10857

THERMAL ANALYSIS
Thermal and structural analysis of ring components by the finite element method [DE85-013305] N86-11021

THERMAL BATTERIES
Characterization of cathodic corrosion products in the Ca/CaCrO4 thermal battery [DE85-013442] N86-10644

THERMAL CONDUCTIVITY
Recirculation within a glass mixture subjected to external and resistive heating [DE85-010068] N86-10348

THERMAL CONTROL COATINGS
Steady state frictional behavior of thin film coatings N86-10335

THERMAL DEGRADATION
Age-life prediction of nylon 66 parachute materials. Part 2: Changes in the chemical and physical properties of materials on aging [AD-A156909] N86-10347

THERMAL DIFFUSION
Space experiment on thermal diffusion. Preparation and theoretical analysis N86-10253
HALFBREED: An extended capability version of the YAQUI code [DE85-014237] N86-10843

THERMAL DIFFUSIVITY
Recirculation within a glass mixture subjected to external and resistive heating [DE85-010068] N86-10348

THERMAL EMISSION
Investigation of the uncertainties of the NBS (National Bureau of Standards) thermal voltage and current converters [PB85-200178] N86-10453

THERMAL ENERGY
Time resolved flow velocity and concentration measurements using a travelling thermal lens [AD-A156706] N86-10541
Solar thermal technical information guide [DE85-002941] N86-10657

THERMAL EXPANSION
Thermal expansion of glasses in the solid and liquid phases [DE85-013953] N86-10351
Method for compensating bellows pressure loads while accommodating thermal deformations [DE85-013306] N86-10933

THERMAL INSULATION
Effect of increased body clothing insulation on hand temperature in a cold environment [AD-A156597] N86-10786

THERMAL MAPPING
LANDSAT TM image data quality analysis for energy-related applications [E85-10109] N86-10597

THERMAL NEUTRONS
Anelastic relaxation in irradiated Cu-Be [DE85-013693] N86-11056

THERMAL PROTECTION
Analytical investigation of solid rocket nozzle failure [NASA-TM-88513] N86-10278

THERMAL RADIATION
Experimental investigations of thermal radiation from potassium atoms and design applications [DE85-004086] N86-11036

THERMAL STABILITY
Elastic properties and thermal stability characterization of metalic glasses by guided wave techniques N86-10337

THERMAL STRESSES
Fracture toughness and stress relief response of irradiated type 347/348 stainless steel N86-10320

THERMOCHEMICAL PROPERTIES
Guidelines for a thermochemical kinetics computer program [DE85-014266] N86-10839

THERMOCHEMISTRY
Process models for 3D composites [AD-A156889] N86-10292

THERMOCLINES
A processor for the study of ocean fine-scale patches [AD-A157019] N86-10730

THERMODYNAMIC CYCLES
Engine-driven and absorption heat pump programs [DE85-013930] N86-10472
Analyses of advanced residential absorption heat pump cycles [DE85-005244] N86-10664

THERMODYNAMIC PROPERTIES
Application of the ruthenium and technetium thermodynamic data bases used in the EQ3/6 geochemical codes [DE85-013766] N86-10632
The effects of orography on land-atmosphere turbulent exchange processes N86-10702

THERMODYNAMICS
Thermocapillary flows and their stability: Effects of surface layers and contamination N86-10109
Thermodynamic constraints on ion beam mixing of metals on insulators [DE85-013629] N86-10448
Simplified analysis of Stirling engines and heat pumps [DE85-005366] N86-10647
Thermodynamics of polymer-supercritical solvent mixtures [AD-A157038] N86-11061

THERMOELECTRIC GENERATORS
General-purpose heat source development. Safety Verification Test Program. Bullet/fragment test series [DE85-014262] N86-10660

THERMOELECTRIC MATERIALS
Magnetic properties of doped semiconductors [DE85-012090] N86-11053

THERMOMECHANICAL TREATMENT
The influence of containerless undercooling and rapid solid-state quenching on the superconductive and magnetic properties of some clustering alloy systems N86-10076

THERMOMIGRATION
Thermomigration of cobalt in liquid tin: Experiment 1 ES 320 — Spacelab N86-10222

THERMONUCLEAR REACTIONS
ORR core re-configuration measurements to increase the fast neutron flux in the Magnetic Fusion Energy (MFE) experiments [DE85-013520] N86-10958

THERMOPHYSICAL PROPERTIES
Measurement of high temperature thermophysical properties N86-10074
Measurement of the properties of tungsten at high temperatures N86-10091
Dynamic thermophysical measurements in space [NASA ORDER H-27954-B] N86-10106
Determination of thermophysical characteristics of solid materials by electrical modelling of the solutions to the inverse problems in nonsteady heat conduction [NASA-TM-77907] N86-10293
Age-life prediction of nylon 66 parachute materials. Part 2: Changes in the chemical and physical properties of materials on aging [AD-A156909] N86-10347
A study of the applicability of nucleation theory to quasi-thermodynamic transitions of second and higher Ehrenfest-order [NASA-CR-176238] N86-11059

THERMOREGULATION
Mechanism of adaptogenic action of prickly eleutherococcus on man during heat stress N86-10757
Vestibular resistance and blood circulation changes in orthostatic position during hyperthermia N86-10758
Heat transfer mechanism in human extremities N86-10759

THERMOVISCOELASTICITY
Oscillations of a viscoelastic liquid drop in zero-gravity N86-10240

THESES

Study of one- and two-dimensional filtering and deconvolution algorithms for a streaming array computer [NASA-CR-176226] N86-10827

THICK PLATES

The effect of debond growth on crack propagation in composite plates reinforced with adhesively bonded composite stringers N86-10287

THICKNESS

Explosive initiation by very small conical shaped charge jets [DE85-009443] N86-10357

Geothermal influences on the long-term thickness of the mechanical lithosphere during flexure N86-10697

Ion beam sputter deposited zinc telluride films [NASA-TM-87119] N86-11048

THICKNESS RATIO

Joint research effort on vibrations of twisted plates, phase 1: Final results [NASA-RP-1150] N86-10579

THIN FILMS

Modelling of laser-enhanced chemical vapor deposition N86-10105

Capillary forces in a low gravity environment --- Spacelab N86-10202

Steady state frictional behavior of thin film coatings N86-10335

Fuel and lubricant behavior in boundary layers analyzed by infrared emission Fourier transform spectrometry N86-10336

Dielectric properties of silicon surfaces and silver thin films [JUEL-1968] N86-10450

Experimental studies of transition radiation and optical bremsstrahlung [DE85-0135637] N86-10949

An investigation of vortex dynamics in 2-dimensional superfluid films of helium-4 N86-11040

Ion beam sputter deposited zinc telluride films [NASA-TM-87119] N86-11048

THIN WALLED SHELLS

Stiffened and prestressed composite overwrapped pressure vessels N86-10547

Strength of shells under local transverse loads N86-10568

THIN WALLS

An analytical and numerical study of the buckling behavior of fiber-reinforced beams N86-10566

THOMSON SCATTERING

Design, fabricate and test a 1.06(MU) repetitively pulsed laser [DE85-014439] N86-10543

THREE DIMENSIONAL COMPOSITES

Mechanics of coated fiber composites N86-10285

THREE DIMENSIONAL FLOW

Three-dimensional inviscid analysis of radial turbine flow and a limited comparison with experimental data [NASA-TM-87091] N86-10017

Mathematical models of continuous flow electrophoresis N86-10143

Finite element solution of the Navier-Stokes equations for 3-D turbulent free shear flows N86-10457

THREE DIMENSIONAL MOTION

Motion analysis report [NASA-CR-171897] N86-10896

THRESHOLDS (PERCEPTION)

Dynamics of changes of statistical indicators of heart rhythm of persons with different degree of motion sickness N86-10743

Determination of symmetry and phase in human visual response functions: Theory and experiments N86-10769

THROMBOCYTES

Effect of emotional stress on hemostasis system of healthy persons N86-10745

THRUST BEARINGS

Termination load carrying device [AD-D011800] N86-10558

THRUST CHAMBERS

Rapid evaluation of ion thruster lifetime using optical emission spectroscopy [NASA-TM-87103] N86-10280

TILT ROTOR AIRCRAFT

A comparative analysis of a CV helicopter and a JVX (Joint Services Advanced Vertical Lift) tilt-rotor aircraft in an aircraft carrier based ASW (Anti-Submarine Warfare) [AD-A156871] N86-10041

TIMBER INVENTORY

Requirements and possibilities of Spacelab metric camera photos usage for inventories of large areas of extensively managed forests N86-10513

TIME CONSTANT

Timing system control software in the SLC [DE85-013380] N86-11024

TIME DEPENDENCE

Portevin-Le Chatelier effect. 1: Model for the type-E serrations [DE85-006879] N86-10322

Time-implicity simulation of particle-fluid systems [DE85-012944] N86-10471

New probabilistic modeling and simulation methods for complex time-dependent systems [DE85-009575] N86-10835

A mesh moving technique for time dependent partial differential equations in two space dimensions [AD-A156663] N86-10866

TIME LAG

Control concepts for in-flight simulation including actuator nonlinearities and time delays [DFVLR-FB-85-24] N86-10047

Signal analysis receiver with acousto-optic delay lines [AD-D011761] N86-10427

TIME MEASUREMENT

Time resolved flow velocity and concentration measurements using a travelling thermal lens [AD-A156706] N86-10541

TIME OF FLIGHT SPECTROMETERS

Direct mass measurements in the light neutron-rich region using a combined energy and time-of-flight technique [DE85-012758] N86-10963

TIME SIGNALS

DSN frequency and timing system, Mark 4-85 N86-10393

TIMING DEVICES

DSN frequency and timing system, Mark 4-85 N86-10393

TIN

Self diffusion of Sn112 and Sn124 in liquid tin N86-10231

Development of metallization process [NASA-CR-176209] N86-10312

Adsorption of oxygen on single crystal tin at liquid helium temperatures N86-11044

TIN ALLOYS

Thermomigration of cobalt in liquid tin: Experiment 1 ES 320 --- Spacelab N86-10222

TIN ISOTOPES

Self diffusion of Sn112 and Sn124 in liquid tin N86-10231

TIN OXIDES

Float zone experiments in space N86-10067

TITANIUM

Low temperature plastic deformation mechanisms of alpha-titanium single crystals [ESA-TT-871] N86-10332

TITANIUM ALLOYS

Pre-bond treatment for titanium alloys [BAE-AL/MAT/3864] N86-10309

TITANIUM COMPOUNDS

Development of metallization process [NASA-CR-176209] N86-10312

TOKAMAK DEVICES

GA Theory News, January-March 1985 [DE85-012572] N86-11007

Activities report in plasma physics N86-11039

TOPOGRAPHY

How Antarctica was unveiled. Masterpieces of Frankfurt topographic surveyors. A part of the German Antarctica research program N86-10181

On the use of X-band CW nanosecond airborne radar for terrain profiling [AD-A156886] N86-10406

Analysis of metric camera images from the USA and their suitability for topographic and thematic mapping --- Spacelab N86-10498

Line mapping and resolution tests with metric camera data --- Spacelab N86-10500

Topographic and thematic mapping: Analysis of metric camera black and white photographs of the Rhone Delta N86-10514

Updating of topographic maps by means of metric camera photos example: Hallertau (Bavaria) N86-10517

Interpretation of Spacelab-1 photographs for the generation of 1:200000 topographic map N86-10518

Multisensor data integration techniques N86-10604

Representation of the distribution of the snow cover on the surface of the Earth's dry land [NASA-TM-77909] N86-10612

Topographic mapping from interferometric synthetic aperture radar observations N86-10622

Analysis of edge detection algorithms on DIAL (Digital Image Analysis Laboratory) [AD-A156735] N86-10630

Fundamental study of the closure property of joints N86-10698

A boundary layer flow model for areas of complex terrain N86-10701

Applications for three-dimensional computer graphic cloud representations produced from satellite imagery [AD-A156903] N86-10798

contemporary Aeolian processes on Mars: Local dust storms N86-11136

TOPOLOGY

Topological properties of hypercubes [AD-A156777] N86-10850

TOROIDAL PLASMAS

Box method for finding intersections of a trajectory with axisymmetric flux surfaces [DE85-013525] N86-10840

Compact torus compression of microwaves [DE85-012919] N86-11016

Recent helicity source and power supply improvements in CTX [DE85-012741] N86-11026

TOUGHNESS

Application of the unloading compliance methods in fracture toughness measurements of a quenched and tempered steel [BLL-BISI-TRANS-21628-(9022.06)] N86-10308

TOWED BODIES

A processor for the study of ocean fine-scale patches [AD-A157019] N86-10730

TOWERS

List of publications on the 200 m meteorological mast at Cabauw, the Netherlands [KNMI-FM-85-6] N86-10711

TOXICITY

Evaluation of the 90-day inhalation toxicity of petroleum and oil shale JP-5 jet fuel [AD-A156815] N86-10675

Development and evaluation of multispecies test protocols for assessing chemical toxicity [DE85-013526] N86-10679

TRACKING (POSITION)

Digital processing of images in tracking a moving object N86-10618

TRACKING FILTERS

An active tracking band-pass filter [AD-A156559] N86-10419

TRACKING PROBLEM

Superconvergent tracking and invariant surfaces in phase space [DE85-013051] N86-10995

TRAINING AIRCRAFT

Proposed modifications for the RAAF Airtrainer CT-4A cockpit [AD-A156808] N86-10039

TRAINING DEVICES

The influence of tactual seat-motion cues on training and performance in a roll-axis compensatory tracking task setting N86-10784

An annotated bibliography of abstracts on the use of simulators in technical training [AD-A156792] N86-11065

TRAINING SIMULATORS

The first German Spacelab mission D1 reports --- Spacelab payloads [PR-3] N86-10189

The influence of tactual seat-motion cues on training and performance in a roll-axis compensatory tracking task setting N86-10784

An annotated bibliography of abstracts on the use of simulators in technical training [AD-A156792] N86-11065

TRAJECTORIES

Lumped geopotential harmonics of order 14, from the orbit of 1967-11G [AD-A156627] N86-10190

TRAJECTORY ANALYSIS

Box method for finding intersections of a trajectory with axisymmetric flux surfaces [DE85-013525] N86-10840

TRANSDUCERS

Levitating furnance for containerless processing in space N86-10169

Elastic properties and thermal stability characterization of metallic glasses by guided wave techniques N86-10337

Improved particle-velocity transducer for equation-of-state experiments [DE85-013204] N86-10532

TRANSFER FUNCTIONS

Advanced containerless processing technology N86-10176

Digital control of the hydraulic actuators of an adaptive suspension vehicle N86-10548

Acceleration-invariant approximation method for recursive digital filters [AD-A156655] N86-10865

TRANSFORMATIONS (MATHEMATICS)
A transformation method for the evaluation of the response moments of elastic structures with random properties [AD-A156882] N86-10557
Well-posed questions and exploration of the space of parameters in linear and non linear inversion [PN-84/13] N86-10858
Bounding solutions of geometrically nonlinear viscoelastic problems [NASA-CR-176219] N86-10880
Measurement and resulting first and second order approximations for a 9 deg bending magnet in LAMPF's 750-keV transport [DE85-012691] N86-10930
TRANSIENT RESPONSE
Mephisto: Interfacial destabilization in metal alloys N86-10079
A fundamental study of smoldering with emphasis on experimental design for zero-g N86-10162
TRANSITION METALS
Non-empirical interatomic potentials for transition metals [DE85-013448] N86-10440
TRANSITION TEMPERATURE
Experimental and theoretical studies of wetting and multilayer adsorption [NASA ORDER H-27954B] N86-10121
Calculation of the glass transition temperatures of linear polymers. Part 1: Rules for hierarchical ordering of the data set [AD-A156584] N86-10343
A study of the applicability of nucleation theory to quasi-thermodynamic transitions of second and higher Ehrenfest-order [NASA-CR-176236] N86-11059
TRANSLATIONAL MOTION
Multimode acoustic research N86-10167
TRANSMISSION
The generation and transmission of vibration in plain cylindrical bearings. Part 2. Experiment [AD-A156577] N86-10553
TRANSMISSION LINES
Method for tuning a phased array antenna [AD-D011768] N86-10372
TRANSMISSION LOSS
Long term statistical measurements of environmental acoustics parameters in the arctic. AEAS report number 2. Low frequency transmission loss measurements in the central arctic ocean [AD-A156576] N86-10727
TRANSMISSIVITY
Particle cloud combustion experiment N86-10160
Radome analysis and design capabilities of the RF and Microwave Technology Branch [AD-A156662] N86-10404
TRANSMITTERS
High sensitivity millimeter-wave measurement apparatus [AD-D011786] N86-10373
TRANSONIC FLOW
Acta Aeronautica et Astronautica Sinica (selected articles) [AD-A147304] N86-10001
Second order approximation method for transonic flows over swept wings N86-10002
On the design of airfoils in transonic flow using the Euler equations N86-10013
TRANSONIC WIND TUNNELS
Investigations to improve the slotted-wall test section of the F+W transonic wind tunnel [F+W-FO-1752] N86-10050
The rubber tube test section of the DFVLR in Goettingen, West Germany — wind tunnel walls [DFVLR-FB-85-18] N86-10051
TRANSPORT AIRCRAFT
The dirigible: A catalyst for resource exploitation in remote areas? [AD-A156518] N86-10034
Retrofit of SAC EC-135C and RC-135 aircraft with CFM-56 engines [AD-A156688] N86-10036
TRANSPORT PROPERTIES
Light scattering tests of fundamental theories of transport properties in the critical region N86-10113
Critical transport phenomena in fluid helium under low gravity N86-10119
Transport processes research N86-10129
Advanced containerless processing technology N86-10176
Laser generation and transport of a relativistic electron beam [DE85-011709] N86-10192
Polyacetylene polymerization, structure, and electrical transport properties N8[illegible]0334
The measurement and application of transport properties of ion swarms in gases N86-10370
Radionuclide complexation in xylem exudates of plants [DE85-013446] N86-10684
Technical considerations in regional aerosol modeling [PB85-193027] N86-10710
Indices of blood oxygen transporting properties and erythropoiesis in rats after prolonged stay in nitrogen-oxygen mixture at elevated pressure N86-10761
Beam line windows at LAMPF [DE85-012723] N86-10985
Applications of the second-order achromat concept to the design of particle accelerators [DE85-013072] N86-10994
TRANSPORT THEORY
Transport processes in solution crystal growth N86-10107
Lambda point equipment N86-10118
Critical transport phenomena in fluid helium under low gravity N86-10119
Transport processes research N86-10129
TRANSPORTATION NETWORKS
Research needs for corrosion control and prevention in energy conservation systems [DE85-014852] N86-10326
TRANSVERSE ACCELERATION
Strength of shells under local transverse loads N86-10568
TRAVELING WAVE TUBES
The Netherlands Institute for Nuclear and High Energy Physics (NIKHEF) traveling wave monitor user guide [LINO-121] N86-10969
TREES (PLANTS)
Vegetation and soils field research data base: Experiment summaries [E85-10110] N86-10610
TRIBOLOGY
Steady state frictional behavior of thin film coatings N86-10335
Tribological properties of structural ceramics [NASA-TM-87105] N86-10341
TRIGGER CIRCUITS
Compact, low jitter, triggered spark gap [DE85-012812] N86-10195
Delay times and jitter in triggered vacuum spark gaps using metal vapor and surface flashover types of triggers [DE85-013966] N86-10441
Soudan 2 data acquisition and trigger electronics [DE85-013864] N86-10443
Timing system control software in the SLC [DE85-013380] N86-11024
TROPOSPHERE
The Liu, Katsaros, and Businger (1979) bulk atmospheric flux computational iteration program in FORTRAN and BASIC [AD-A156736] N86-10714
TRYPTOPHAN
Effect of cold on brain serotonin system and plasma corticosteroid level in different strains of mice N86-10766
TSUNAMI WAVES
Formation of waves by ground motion [PM/84/09] N86-10706
TUNGSTEN
Measurement of the properties of tungsten at high temperatures N86-10091
TUNING
Effects of slots/holes in disks on frequencies of TM01 and EH11 waves in the disk-loaded waveguide [DE85-013376] N86-11009
TURBINE BLADES
Three-dimensional inviscid analysis of radial turbine flow and a limited comparison with experimental data [NASA-TM-87091] N86-10017
Film cooling on a convex wall: Heat transfer and hydrodynamic measurements for full and partial coverage [NASA-CR-174864] N86-10461
Joint research effort on vibrations of twisted plates, phase 1: Final results [NASA-RP-1150] N86-10579
Improved stud configurations for attaching laminated wood wind turbine blades [NASA-TM-87109] N86-10582
TURBINE ENGINES
Film cooling on a convex wall: Heat transfer and hydrodynamic measurements for full and partial coverage [NASA-CR-174864] N86-10461
TURBULENCE
Acta Aeronautica et Astronautica Sinica (selected articles) [AD-A147304] N86-10001
A numerical solution of the shock-turbulent interaction over a compression corner for supersonic flow N86-10003
The role of freestream turbulence scale in subsonic flow separation [NASA-CR-176237] N86-10014
Role of convection in grain refining N86-10133
Effects of chemistry and swirl on the production of turbulence in a flame [PB85-219632] N86-10305
Mean turbulence structure in strongly heating air flows N86-10455
A root-mean-square pressure fluctuations model for internal flow applications [NASA-CR-3928] N86-10460
Film cooling on a convex wall: Heat transfer and hydrodynamic measurements for full and partial coverage [NASA-CR-174864] N86-10461
The effects of orography on land-atmosphere turbulent exchange processes N86-10702
GA Theory News, January-March 1985 [DE85-012572] N86-11007
TURBULENCE EFFECTS
Buoyancy effects upon vapor flame and explosion processes N86-10161
Large eddy interactions in a turbulent channel flow [NASA-TM-86757] N86-10464
TURBULENT BOUNDARY LAYER
Evaluation of surface exchange coefficients from mildex ocean/atmosphere mixed layer data [AD-A156765] N86-10729
TURBULENT FLOW
Verification of turbulence developing from the oscillatory Marangoni convection in a liquid column — rocket flight N86-10241
Finite element solution of the Navier-Stokes equations for 3-D turbulent free shear flows N86-10457
A root-mean-square pressure fluctuations model for internal flow applications [NASA-CR-3928] N86-10460
Large eddy interactions in a turbulent channel flow [NASA-TM-86757] N86-10464
TURBULENT JETS
Investigation of density gradient fluctuations in a turbulent free jet by means of the laser schlieren crossed-beam method [DFVLR-FB-85-19] N86-10027
Confined swirling jet predictions using a multiple-scale turbulence model [NASA-CR-178484] N86-10462
TURBULENT WAKES
Effects of chemistry and swirl on the production of turbulence in a flame [PB85-219632] N86-10305
TWISTING
Joint research effort on vibrations of twisted plates, phase 1: Final results [NASA-RP-1150] N86-10579
TWO DIMENSIONAL BODIES
Automated analysis of digital images generated by two-dimensional gel electrophoresis [DE85-011906] N86-10526
An analytical and numerical study of the buckling behavior of fiber-reinforced beams N86-10566
TWO DIMENSIONAL FLOW
Numerical solution of hypersonic flow near leading edge of a flat plate N86-10008
Aerodynamics of hyperlift systems [SNIAS-443.501/85] N86-10023
Spectral methods in adapted curved grids N86-10878
TWO PHASE FLOW
Theoretical specific impulse for two-phase flow in nozzle of rocket-ramjet engine: A simple estimation method N86-10005
Analysis of annular two-phase flow with liquid entrainment N86-10459
KRAK: A computer program for two-phase, two-component porous flow and fracture propagation, revision [DE85-014264] N86-10469
Heat transfer in condensing and evaporating two-component, two-phase flow inside a horizontal tube N86-11058

U

U.S.S.R.
Soviet free-electron laser research [AD-A156896] N86-10542
Report of the Workshop on Geologic Applications of Remote Sensing to the Study of Sedimentary Basins [E86-10002] N86-10599

Structural mapping of folded sedimentary environments from satellite images: An example from Central Asia N86-10607

Maximum water reserves in the snow cover in the European territory of the USSR according to data for 1892-1960 [NASA-TM-77901] N86-10611

Observations of the snow cover in the southern part of the Buryat Autonomous Soviet Socialist Republic [NASA-TM-77910] N86-10613

ULTRAHIGH VACUUM

Report on a visit to CERN in February 1985. Notes on bunch monitors, high-frequency systems, linacs, kickers, magnets, vacuum and bunch extraction [LINO-119] N86-10967

The MEA vacuum system [LINO-120] N86-10968

ULTRALOW TEMPERATURES

Magnetic properties of doped semiconductors [DE85-012090] N86-11053

ULTRAPURE METALS

Defect identification in high-energy semiconductors [DE85-014533] N86-10442

ULTRASONIC FLAW DETECTION

Ultrasonic inspection of weldments in large size spiral box for hydroelectric plant [AS-701/85] N86-10562

ULTRASONIC SPECTROSCOPY

Characterization of vapor and aerosol flows by photothermal methods [AD-A156601] N86-10465

ULTRASONIC TESTS

Ultrasonic evaluation of mechanical properties of thick, multilayered, filament wound composites [MASA-TM-87088] N86-10561

ULTRASONIC WAVE TRANSDUCERS

Ultrasonic evaluation of mechanical properties of thick, multilayered, filament wound composites [MASA-TM-87088] N86-10561

ULTRASONICS

Exploratory development for a high reliability flaw characterization module [AD-A156632] N86-10916

ULTRAVIOLET RADIATION

Identification of chemical and physical phenomena affecting the durability of silvered polymer (PMMA) mirrors [DE85-012131] N86-10645

Somatic cell and molecular genetics approach to DNA repair and mutagenesis [DE85-014181] N86-10737

ULTRAVIOLET SPECTROSCOPY

Ultraviolet spectroscopy of the Earth's dayglow and magnetosphere cleft N86-10696

UNDERGROUND ACOUSTICS

Geothermal lost circulation zone mapping tool [DE85-008696] N86-10531

UNDERWATER ACOUSTICS

Long term statistical measurements of environmental acoustics parameters in the arctic. AEAS report number 2. Low frequency transmission loss measurements in the central arctic ocean [AD-A156576] N86-10727

UNDERWATER EXPLOSIONS

Angle of incidence effects for underwater shock using generic computational models [DE85-012936] N86-10466

UNIQUENESS

Multivariable partial realization and the aspect of uniqueness [ER-83/09] N86-10879

UNITED STATES

An anthology: Rationale for a US ballistic missile defense (1969 - 1984) [AD-A156781] N86-10199

UNIVERSITIES

NASA/American Society for Engineering Education (ASEE) Summer Faculty Fellowship Program, 1985 [NASA-CR-177972] N86-11064

Academic Research Equipment in selected science-engineering fields, 1982-83. An analysis of findings from the Baseline National Survey of academic research instruments and instrumentation needs N86-11068

UNSTEADY FLOW

A new method for calculating unsteady supersonic aerodynamic forces and its application N86-10009

A study of the aerodynamic performance of Weis-Fogh wings N86-10012

Theoretical study of the unsteady linear problem for a rectangular wing with a pitching movement [ONERA-RT-17/1841-RY-010-R] N86-10022

Numerical simulation of unsteady thermal Marangoni flows N86-10236

Experiments and computations on unsteady separating flow in an expanding flume [REPT-2-84] N86-10477

A modified Successive Over-Relaxation (SOR) method for the Poisson equation in unsteady free-surface flow calculations [TW-264] N86-10881

UPGRADING

Computer control of rf at SLAC [DE85-013065] N86-11015

URANIUM

Aluminum ion plating for corrosion protection of uranium, revision 1 [DE85-012419] N86-10330

URANIUM 235

The development of a neutron evaporation theory code for the thermal fission of Uranium-235 [AD-A156593] N86-10951

UREAS

Growth of organic crystals by Ostwald ripening N86-10058

USER MANUALS (COMPUTER PROGRAMS)

User's guide for Langley Research Center Orbital Lifetime program [NASA-TM-87587] N86-10828

USER REQUIREMENTS

Computer-based training for the US Coast Guard standard terminal microcomputer: A basis for implementation utilizing the elaboration theory of instructional design [AD-A156548] N86-10791

DFVLR, strategic study of astronautics 1984, user requirements N86-11069

UTILITIES

Photovoltaic systems in remote locations: An experience summary [NASA-TM-87106] N86-10643

Phosphoric and electric utility fuel technology development [DE85-014741] N86-10651

UTILIZATION

Operations research applications [ARW-03-THE-BDK/ORS/83-08] N86-10901

V

VACUUM CHAMBERS

Adhesion of metals: Experiment 1 ES-340 — Spacelab N86-10232

VACUUM FURNACES

The isothermal heating facility — Spacelab N86-10208

Vacuum brazing under microgravity — Spacelab N86-10214

Gradient heating facility behavior — Spacelab N86-10217

VACUUM MELTING

Melting and solidification of metal matrix composites under microgravity — Spacelab N86-10211

Shrinking of a gas bubble in a glass melt under microgravity conditions — STS-11 N86-10254

VACUUM SYSTEMS

Delay times and jitter in triggered vacuum spark gaps using metal vapor and surface flashover types of triggers [DE85-013966] N86-10441

Method for compensating bellows pressure loads while accommodating thermal deformations [DE85-013306] N86-10933

The MEA vacuum system [LINO-120] N86-10968

VALVES

Digital control of the hydraulic actuators of an adaptive suspension vehicle N86-10548

VANADIUM

Fabrication and metallurgical properties of modified 9Cr-1 Mo steel [DE85-012885] N86-10328

VAPOR DEPOSITION

Modelling of laser-enhanced chemical vapor deposition N86-10105

Morphological stability and fluid dynamics of vapor crystal growth N86-10126

Experimental and theoretical analysis of chemical vapor deposition with prediction of gravity effects N86-10132

Preliminary reports, memoranda and technical notes of the Materials Research Council Summer Conference, La Jolla, California [AD-A156776] N86-10291

The influence of the substrate on the practical machining applications of cutting edges coated with different materials [BLL-RISLEY-TR-5039-(9091.9F)] N86-10646

Improved blue response and efficiency of A-Si:H solar cells deposited from disilane using a dual-chamber plasma system [DE85-013289] N86-10649

Photovoltaic devices using a Si:H from higher order silanes [DE85-008604] N86-10666

VAPOR PHASE EPITAXY

HgI sub 2 crystal growth for nuclear detectors N86-10066

Fluid dynamics and thermodynamics of vapor phase crystal growth N86-10068

Vapor growth of alloy-type semiconductor crystals N86-10069

Experimental and theoretical analysis of chemical vapor deposition with prediction of gravity effects N86-10132

Directional solidification of an aluminum-zinc vapor emulsion in microgravity — Spacelab N86-10216

VAPOR PHASES

Modelling of laser-enhanced chemical vapor deposition N86-10105

Fundamental studies of droplet combustion at reduced gravity N86-10165

Crystal growth from solutions and nucleation from the vapor phase — Spacelab N86-10267

VAPORS

Test and evaluate passive orbital disconnect struts (PODS 3) [NASA-CR-177368] N86-10274

Characterization of vapor and aerosol flows by photothermal methods [AD-A156601] N86-10465

Scoping studies of vapor behavior during a severe accident in a metal-fueling reactor [DE85-011474] N86-10952

VARIABILITY

A quantitative method for analyzing the roughness of the seafloor N86-10726

Variability analysis of visually induced responses in the midst of noise [B8564052] N86-10774

VARIABLE STARS

The two micron spectrum of R Scuti N86-11092

VARIATIONAL PRINCIPLES

Variational estimates for the mass gap of SU(2) Euclidean lattice gauge theory [NIKHEF-H/84-13] N86-10883

VECTOR ANALYSIS

Study of one- and two-dimensional filtering and deconvolution algorithms for a streaming array computer [NASA-CR-176221] N86-10822

A mesh moving technique for time dependent partial differential equations in two space dimensions [AD-A156663] N86-10866

VECTOR MESONS

Two-loop large Higgs mass corrections to vector boson self-couplings [NIKHEF-H/84-15] N86-11038

VEGETATION

Vegetation and soils field research data base: Experiment summaries [E85-10110] N86-10610

The effect of vegetation type, microrelief, and incidence angle on radar backscatter N86-10619

The effects of merging TM and A/C radar on wetland classification N86-10621

Modelling of vegetation volumes N86-10629

VEHICLES

Marginal terrain straddle-lift container handler [AD-D011752] N86-10555

VELOCITY

Chemical kinetics and cellular structure of detonations in hydrogen sulphide and air [DE85-009408] N86-10304

Velocities of gas and plasmas from real time holographic interograms [DE85-014616] N86-10530

Ultrasonic evaluation of mechanical properties of thick, multilayered, filament wound composites [MASA-TM-87088] N86-10561

VELOCITY DISTRIBUTION

Large eddy interactions in a turbulent channel flow [NASA-TM-86757] N86-10464

Strength of shells under local transverse loads N86-10568

VELOCITY MEASUREMENT

Fall velocity indicator/viewer [AD-D011789] N86-10482

Time resolved flow velocity and concentration measurements using a travelling thermal lens [AD-A156706] N86-10541

Structural discontinuity within the southern California continental margin: Seismic and gravity models of the western Transverse Ranges N86-10699

VERTEBRATES
Paleogene vertebrate paleontology, geology and remote sensing in the Wind River Basin N86-10609

VERTICAL DISTRIBUTION
Field comparison of in situ meteorological sensors
[PB85-196988] N86-10723

VERTICAL MOTION
System modeling and identification of equivalent systems with and without compensating time delay for control-augmented aircraft
[ESA-TT-852] N86-10043

VERY LARGE SCALE INTEGRATION
The VLSI design of error trellis syndrome decoding for convolutional codes N86-10391
Investigation of metallic impurities introduced into SiO2 and silicon by various candidate VLSI metallization systems: Chemical reactions, diffusion, and electrical properties
[AD-A156609] N86-10429
Implementation issues for algorithmic VLSI (Very Large Scale Integration) processor arrays
[AD-A156699] N86-10432
Microcircuit device reliability field experience database. Volume 1. Field data. Volume 2. Failure Event/Analysis data
[AD-A156836] N86-10433
Increase of the packaging density of Very Large Scale Integration (VLSI) circuits using automatic alignment
[BMFT-FB-T-85-020] N86-10451
Efficient systolic arrays for the solution of toeplitz systems: An illustration of a methodology for the construction of systolic architectures in VLSI (Very Large Systems Integration)
[AD-A156767] N86-10795
Design of a multifunction Input-Output (I/O) controller
[EUT-84-E-143] N86-10802

VERY LONG BASE INTERFEROMETRY
A VLBI survey at 2.29 GHz N86-10383
Comparison of the calibration of ionospheric delay in VLBI data by the methods of dual frequency and Faraday rotation N86-10384
Mobile VLBI and GPS measurement of vertical crustal motion N86-10401
Improved mapping of radio sources from VLBI data by least-square fit N86-10402
Optical/IR telescope arrays: A study of their potential for satisfying observational requirements in astronomy for a large aperture system in the 1990s and beyond
[REPT-15] N86-11094
Colloquium on Kilometric Optical Arrays in Space
[ESA-SP-226] N86-11096
Radio astronomy experience in image reconstruction. A history lesson for optical astronomers N86-11117
VLBI at optical and radio wavelengths: Congruences and contrasts N86-11126

VESTIBULAR TESTS
Vestibular resistance and blood circulation changes in orthostatic position during hyperthermia N86-10758

VIBRATION
The influence of low frequency mechanical vibrations on the growth of single crystals N86-10059
Compact, low jitter, triggered spark gap
[DE85-012812] N86-10195
Vibro-acoustic forecast for space shuttle launches at Vandenberg AFB: The payload changeout room and the administration building
[AD-A156944] N86-10269
Specification for the performance, design, development and test requirements for a severe environment cartridge recorder. Issue 4
[AD-A156637] N86-10523
Passive damping concepts for slender columns in space structures
[NASA-CR-176234] N86-10577
Three-dimensional vibration analysis of a uniform beam with offset inertial masses at the ends
[NASA-TM-86393] N86-10580
The Shock and Vibration Digest, volume 17, no. 3
[AD-A154144] N86-10585
Sound radiation from repetitive transient vibrations using multi-channel digital signal processing with application to impact machinery N86-10910

VIBRATION DAMPING
Evaluation of a pulse control law for flexible spacecraft
[NASA-CR-176233] N86-10272

VIBRATION EFFECTS
Oscillations of semi-free liquids in microgravity: Spacelab 1 experiment ES 326 N86-10204
Numerical simulation of convections in the microgravity environment N86-10239
Report on the research activities on whole-body vibrations. Human strain due to mechanical vibrations
[ISBN-3-88383-107-7] N86-10773

VIBRATION ISOLATORS
Cryogenic equivalence principle experiment N86-10171

VIBRATION MEASUREMENT
Test and evaluate passive orbital disconnect struts (PODS 3)
[NASA-CR-177368] N86-10274
Joint research effort on vibrations of twisted plates, phase 1: Final results
[NASA-RP-1150] N86-10579
Correlation between vibrations and buckling of cylindrical shells stiffened by spot-welded and riveted stringers
[TAE-537] N86-10584

VIBRATION SIMULATORS
The generation and transmission of vibration in plain cylindrical bearings. Part 2. Experiment
[AD-A156577] N86-10553

VIBRATIONAL SPECTRA
The generation and transmission of vibration in plain cylindrical bearings. Part 2. Experiment
[AD-A156577] N86-10553

VIDEO DATA
Extended precision in video bandwidth analog to digital converter using optical techniques
[AD-D011745] N86-10422
Stereoscopic video imagery generation
[AD-D011785] N86-10481
Fall velocity indicator/viewer
[AD-D011789] N86-10482
Catalog of Resources for Education in Ada (trademark) and Software Engineering (CREASE). Version 3.0
[AD-A156687] N86-10790

VIEWING
Fall velocity indicator/viewer
[AD-D011789] N86-10482

VINYL POLYMERS
Electrically conducting polymers N86-10333

VISCOELASTICITY
Bounding solutions of geometrically nonlinear viscoelastic problems
[NASA-CR-176219] N86-10860

VISCOPLASTICITY
Advanced development of BEM for two and three dimensional nonlinear analysis N86-10855

VISCOSITY
Precise viscosity measurements very close to critical points
[NASA ORDER C-86129D] N86-10120
A study of blood flow and of aggregation of blood cells under conditions of zero gravity: Its relevance to the occlusive diseases and cancer N86-10137
Work-hardening and effective viscosity in solid beryllium
[DE85-013978] N86-10323
Recirculation within a glass mixture subjected to external and resistive heating
[DE85-010068] N86-10348
On the method of characteristics and its application to the calculations of annular nozzle flowfields N86-10454
Physical acoustics: Investigation of chemical kinetic and thermodynamic properties of fluids N86-10911
Acoustic cavitation and bubble dynamics
[AD-A156888] N86-10918

VISCOUS DAMPING
Inelastic analysis of frame structures including member and joint shears N86-10573

VISCOUS FLOW
A study of the aerodynamic performance of Weis-Fogh wings N86-10012
Numerical procedure for three-dimensional hypersonic viscous flow over aerobrake configuration
[NASA-TM-58269] N86-10018
Precise viscosity measurements very close to critical points
[NASA ORDER C-86129D] N86-10120
On the method of characteristics and its application to the calculations of annular nozzle flowfields N86-10454

VISION
Vision test chart and method using Gaussians
[AD-D011756] N86-10778

VISUAL ACUITY
Mild hypoxia and visual performance with night vision goggles
[AD-A156969] N86-10787

VISUAL DISCRIMINATION
Speed of work and error rate: Analyses of individual differences in a choice reaction series with a cognitive component
[DFVLR-FB-85-21] N86-10781

VISUAL PERCEPTION
Determination of symmetry and phase in human visual response functions: Theory and experiments N86-10769
The synthesis and analysis of color images
[NASA-TM-86844] N86-10777
Mild hypoxia and visual performance with night vision goggles
[AD-A156969] N86-10787
Test of a multilevel computational theory of stereoscopic visual image processing
[AD-A157011] N86-10870
Measurement of visual contrast sensitivity
[AD-D011776] N86-10973

VISUAL STIMULI
Variability analysis of visually induced responses in the midst of noise
[B8564052] N86-10774

VITAMINS
Effect of various doses of some vitamins on non-specific mechanisms of adaptation of man N86-10750

VLASOV EQUATIONS
Local conservation laws for the Maxwell-Vlasov and collisionless kinetic guiding center theories
[DE85-013122] N86-11063

VOIDS
Binder-filler interaction in energetic polymers
[AD-A156752] N86-10345

VOLATILITY
Volatile organic compounds in indoor air: A survey of various structures
[PB85-196356] N86-10687
Emissions of NOx, SOx and VOC from Antropogenic sources
[PB85-193530] N86-10688
Evaluation of Passive Sampling Devices (PSDs)
[PB85-196418] N86-10689

VOLTAGE CONVERTERS (AC TO AC)
Investigation of the uncertainties of the NBS (National Bureau of Standards) thermal voltage and current converters
[PB85-200178] N86-10453

VOLTAGE CONVERTERS (DC TO DC)
Investigation of the uncertainties of the NBS (National Bureau of Standards) thermal voltage and current converters
[PB85-200178] N86-10453

VOLUME
Captive volume device as a safe life monitor
[AD-D011802] N86-10525

VOLUMETRIC ANALYSIS
Measurement of the density of base fluids at pressures 0.422 to 2.20 GPa
[NASA-TM-87114] N86-10551

VORTICES
Large eddy interactions in a turbulent channel flow
[NASA-TM-86757] N86-10464

VORTICITY
Analysis of combined natural and forced convection around cylinders and spheres N86-10456

VOYAGER PROJECT
Planning for VLA/DSN arrayed support to the Voyager at Neptune N86-10395
A VLA experiment: Planning for Voyager at Neptune N86-10396

W

WAFERS
Contact effects in light activated GaAs switches
[AD-A156957] N86-10434
Optical detection of photoacoustic pulses in thin silicon wafers
[AD-A156705] N86-10977
Transient velocity assessment in gallium arsenide, and of other GaAs characteristics related to device functions
[AD-A156983] N86-11050

WAKEFULNESS
Intradiurnial organization of wakefulness-sleep sequence and energy metabolism in rats exposed to low ambient temperature N86-10764

WALKING MACHINES
Digital control of the hydraulic actuators of an adaptive suspension vehicle N86-10548

WALL FLOW
Mean turbulence structure in strongly heating air flows N86-10455

WALL PRESSURE
Conducting wall and pressure profile effect on MHD stabilization of axisymmetric mirror
[DE85-013647] N86-11020

WARFARE
The quest for a helicopter suitable for combat rescue, 1967 - 1983
[AD-A156842] N86-10040

WASTE DISPOSAL
Hot cell facility design for large fusion devices
[DE85-012893] N86-11037

WASTE WATER
Development of the Multi-Attribute Hazard Assessment System (MAHAS) and its application to energy-related waste streams
[DE85-010278] N86-10676
Membrane research in energy and solvent recovery from industrial effluent streams
[DE85-014583] N86-10682
WATER
Passivation of steel with aqueous amine solutions
[AD-D011749] N86-10314
KRAK: A computer program for two-phase, two-component porous flow and fracture propagation, revision
[DE85-014264] N86-10469
Spontaneous Raman spectroscopy of shocked H2O
[DE85-014557] N86-10470
Application of the dutch method for estimating storm-induced dune erosion
[AD-A156717] N86-10728
WATER FLOW
Modeling groundwater flow into lakes N86-10598
The Rhine-Meuse estuary hydraulic scale model. Experiences with computer configuration and software
[PUBL-335] N86-10637
SUTRA (Saturated-unsaturated transport). A finite-element simulation model for saturated-unsaturated, Fluid-Density-Dependent ground-water flow with energy transport or chemically-reactive single-species solute transport
[AD-A156779] N86-10830
WATER POLLUTION
Sediment characterization. Task 2: Instream contaminant study. Volume 2: Appendices
[DE85-013503] N86-10680
Sediment characterization. Task 2: Instream contaminant study, volume 1
[DE85-013502] N86-10683
WATER RESOURCES
Maximum water reserves in the snow cover in the European territory of the USSR according to data for 1892-1960
[NASA-TM-77901] N86-10611
WATER RUNOFF
Maximum water reserves in the snow cover in the European territory of the USSR according to data for 1892-1960
[NASA-TM-77901] N86-10611
WATER TABLES
Evaluating the ground-water resources of the high plains of Texas, Volume 4
[PB85-191625] N86-10641
WATER TEMPERATURE
LANDSAT TM image data quality analysis for energy-related applications
[E85-10109] N86-10597
WATER VAPOR
Mobile VLBI and GPS measurement of vertical crustal motion N86-10401
Chemical/hydrogen energy systems
[DE85-012742] N86-10667
WATER WAVES
Formation of waves by ground motion
[PM/84/09] N86-10706
WATERSHEDS
Erosion control and watershed management by Spacelab photography N86-10493
WAVE ATTENUATION
Numerical methods for analyzing electromagnetic scattering
[NASA-CR-176141] N86-10377
WAVE DISPERSION
Phase-coded pulse expander-compressor
[AD-D011812] N86-10375
WAVE EQUATIONS
Recent advances in the analysis of exhaust mufflers N86-10587
WAVE FRONTS
A mesh moving technique for time dependent partial differential equations in two space dimensions
[AD-A156663] N86-10866
WAVE FUNCTIONS
Experimental X-ray scattering cross sections for H2 and rare atomic gases
[DE85-011572] N86-10936
Relativistic wavefunction at the origin and the pion decay constant
[DE85-012392] N86-11062
WAVE INTERACTION
Large eddy interactions in a turbulent channel flow
[NASA-TM-86757] N86-10464
WAVE PROPAGATION
Nonlinear propagation of elastoplastic waves in Ke penetrators (excerpts)
[DE85-011450] N86-10318
An experimental TE sub 12 - TE sub 11 circular waveguide mode converter N86-10387
Propagation and radiation characteristics of a multimode corrugated waveguide feedhorn N86-10388
A simplified method of estimation of the specular components of radar cross section for some re-entrant conductors
[AD-A156573] N86-10403
Formation of waves by ground motion
[PM/84/09] N86-10706
WAVE REFLECTION
Radome analysis and design capabilities of the RF and Microwave Technology Branch
[AD-A156662] N86-10404
WAVE SCATTERING
Renormalization of an inverse scattering theory for inhomogeneous dielectrics
[AD-A156836] N86-11049
WAVEFORMS
Signal analysis of gas tungsten arc welds N86-10078
Periodic binary sequences with very good autocorrelation properties N86-10397
WAVEGUIDE FILTERS
Direct-coupled cavity filters with irises of arbitrary thickness
[DFVLR-FB-85-14] N86-10412
WAVEGUIDES
Numerical methods for analyzing electromagnetic scattering
[NASA-CR-176141] N86-10377
An experimental TE sub 12 - TE sub 11 circular waveguide mode converter N86-10387
Propagation and radiation characteristics of a multimode corrugated waveguide feedhorn N86-10388
High-power rf controls for the NBS-Los Alamos racetrack microtron
[DE85-012658] N86-10993
Electron wind in strong wave guide fields
[DE85-013062] N86-11004
WEAR
Tribological properties of structural ceramics
[NASA-TM-87105] N86-10341
WEAR INHIBITORS
Steady state frictional behavior of thin film coatings N86-10335
WEATHER
ELCAP instrumentation
[DE85-013042] N86-10527
WEATHER FORECASTING
Monthly and Seasonal Weather Outlook for mid-April to mid-May 1985, Volume 39, Number 8
[PB85-195345] N86-10724
WEATHERING
Altitudinal distribution of granitic landforms in the south central Sierra Nevada, California N86-10695
WEDGE FLOW
A numerical solution of the shock-turbulent interaction over a compression corner for supersonic flow N86-10003
WEIGHT (MASS)
Operating characteristics of the multiple critical Venturi System and secondary calibration nozzles used for weight-flow measurements in the Langley 16-foot transonic tunnel
[NASA-TM-86405] N86-10016
WEIGHTING FUNCTIONS
Identification of a plant's weighting sequence --- self-tuning control
[OUEL-1534/84] N86-10854
Two algorithms for weighted matroid intersection
[AD-A156525] N86-10861
WEIGHTLESSNESS
Microgravity Science and Applications Program tasks
[NASA-TM-87568] N86-10053
Solutal convection and its effects on crystal growth and segregation in binary and pseudo-binary system with large liquidus-solidus separation N86-10056
Effect of undercooling and modified microstructure on the physical properties of material synthesized in the drop tube and drop tower N86-10075
The influence of containerless undercooling and rapid solid-state quenching on the superconductive and magnetic properties of some clustering alloy systems N86-10076
Influence of melt convection on solid-liquid interface under terrestrial and reduced gravity environments N86-10083
Orbital processing of aligned magnetic composites N86-10089
Metallic foams N86-10095
Growth of larger single crystals N86-10186
Oscillations of a viscoelastic liquid drop in zero-gravity N86-10240
WEIGHTLESSNESS SIMULATION
The first German Spacelab mission D1 reports --- Spacelab payloads
[PR-2] N86-10188
The first German Spacelab mission D1 reports --- Spacelab payloads
[PR-3] N85-10189
Mathematical simulation of disturbing forces and material science processes under low gravity N86-10236
Nucleate pool boiling in subcooled liquid under microgravity: Results of TEXUS experimental investigations N86-10250
A preliminary report on floating zone experiments with germanium crystals in a sounding rocket N86-10256
WELDED JOINTS
Ultrasonic inspection of weldments in large size spiral box for hydroelectric plant
[AS-701/85] N86-10562
WELDING
Weld metal hot-cracking of hastelloy alloys C-22 and C-276: A study by analytical electron microscopy
[DE85-009437] N86-10324
WELDING MACHINES
Measurement of workpiece temperature during welding for welding robot control N86-10534
WELLS
Geothermal lost circulation zone mapping tool
[DE85-008696] N86-10531
Evaluating the ground-water resources of the high plains of Texas, Volume 4
[PB85-191625] N86-10641
WEST GERMANY
The air traffic demand in passenger travel of the Federal Republic of Germany 1990 - 2000. Update of the DFVLR air traffic forecast
[DFVLR-MITT-85-06] N86-10031
Satellite use for men --- West German space program N86-10180
Airborne measurements of the border-crossing air pollution in the area between Weiden and Hof/Bavaria
[DFVLR-FB-85-25] N86-10685
Space research expenses of the Federal Ministry of Research and Technology (BMFT) in the period 1983-1985 N86-11070
WETLANDS
The effects of merging TM and A/C radar on wetland classification N86-10621
Approaches to cumulative impact assessment
[DE85-013891] N86-10635
WETTING
Direct observation of critical point wetting in microgravity N86-10116
WIGGLER MAGNETS
Thermal and structural analysis of ring components by the finite element method
[DE85-013305] N86-11021
WIND (METEOROLOGY)
Surface winds at NWC (Naval Weapons Center): 1964 - 1982
[AD-A156660] N86-10712
Estimating wind speed as a function of height above ground: An analysis of data obtained at the Southwest Residential Experiment Station, Las Cruces, New Mexico
[DE85-013262] N86-10716
Field comparison of in situ meteorological sensors
[PB85-196988] N86-10723
Evaluation of surface exchange coefficients from mildex ocean/atmosphere mixed layer data
[AD-A156765] N86-10729
WIND DIRECTION
Overview of wind turbine siting research: Prospecting to micrositing
[DE85-013496] N86-10666
Surface winds at NWC (Naval Weapons Center): 1964 - 1982
[AD-A156660] N86-10712
Field comparison of in situ meteorological sensors
[PB85-196988] N86-10723
WIND EFFECTS
contemporary Aeolian processes on Mars: Local dust storms N86-11136
WIND MEASUREMENT
Overview of wind turbine siting research: Prospecting to micrositing
[DE85-013496] N86-10666
Contribution of wind energy to the energy balance of a combined solar and wind energy system. Part 1: System description, data acquisition and system performance
[BMFT-FB-T-85-051-VOL-1] N86-10670
WIND SHEAR
Rotary-wing operations in a microburst environment
[AD-A156695] N86-10713
WIND TUNNEL APPARATUS
Activities report of the German-Dutch wind tunnel N86-10029

The rubber tube test section of the DFVLR in Goettingen, West Germany — wind tunnel walls
[DFVLR-FB-85-18] N86-10051
Activities report of the German-Dutch wind tunnel
N86-10052

WIND TUNNEL MODELS
Simulation of the atmospheric boundary layer in the large wind tunnel of the TNO Institute for Building materials and Constructions (IBBC). Part 1: Theory
[BI-76-39/08.7.23100-PT-1] N86-10703

WIND TUNNEL TESTS
Second order approximation method for transonic flows over swept wings N86-10002
Evaluation of an aerodynamic-load prediction method on a STOL fighter configuration
[NASA-TM-86782] N86-10015
Operating characteristics of the multiple critical Venturi System and secondary calibration nozzles used for weight-flow measurements in the Langley 16-foot transonic tunnel
[NASA-TM-86405] N86-10016
Activities report of the German-Dutch wind tunnel
N86-10029
Investigations to improve the slotted-wall test section of the F+W transonic wind tunnel
[F+W-FO-1752] N86-10050
Activities report of the German-Dutch wind tunnel
N86-10052
Simulation of the atmospheric boundary layer in the large wind tunnel of the TNO Institute for Building Materials and Construction (IBBC). Part 2: Experiments
[BI-76-39/08.7.23100-PT-2] N86-10704

WIND TUNNEL WALLS
Investigations to improve the slotted-wall test section of the F+W transonic wind tunnel
[F+W-FO-1752] N86-10050
The rubber tube test section of the DFVLR in Goettingen, West Germany — wind tunnel walls
[DFVLR-FB-85-18] N86-10051

WIND TURBINES
Improved stud configurations for attaching laminated wood wind turbine blades
[NASA-TM-87109] N86-10582

WIND VANES
Field comparison of in situ meteorological sensors
[PB85-196988] N86-10723

WIND VELOCITY
Surface winds at NWC (Naval Weapons Center): 1964 - 1982
[AD-A156660] N86-10712
Estimating wind speed as a function of height above ground: An analysis of data obtained at the Southwest Residential Experiment Station, Las Cruces, New Mexico
[DE85-013262] N86-10716
Field comparison of in situ meteorological sensors
[PB85-196988] N86-10723

WIND VELOCITY MEASUREMENT
Overview of wind turbine siting research: Prospecting to micrositing
[DE85-013496] N86-10666
The boundary condition in a numerical model of atmospheric flows over fixed interfaces
[GKSS-85-E-10] N86-10722

WINDMILLS (WINDPOWERED MACHINES)
Wind energy in agriculture, a promise
[SS-45] N86-10672
Wind energy, a feasibility investigation for wind mills in agriculture
[SS-45A] N86-10673

WINDOWS (APERTURES)
Integrating sphere measurements of directional-hemispherical transmittance of window systems
[DE85-013826] N86-10678
Beam line windows at LAMPF
[DE85-012723] N86-10965

WINDPOWER UTILIZATION
Overview of wind turbine siting research: Prospecting to micrositing
[DE85-013496] N86-10666
Contribution of wind energy to the energy balance of a combined solar and wind energy system. Part 1: System description, data acquisition and system performance
[BMFT-FB-T-85-051-VOL-1] N86-10670
Contribution of wind energy to the energy balance of a combined solar and wind energy system. Part 2: Computer-assisted investigations
[BMFT-FB-T-85-052-VOL-2] N86-10671
Wind energy in agriculture, a promise
[SS-45] N86-10672

WINDPOWERED GENERATORS
Wind energy, a feasibility investigation for wind mills in agriculture
[SS-45A] N86-10673

WING PANELS
Optimum design of an aircraft wing structure with multiple constraints by the direct-vision criteria method
N86-10004

WING PROFILES
A study of the aerodynamic performance of Weis-Fogh wings N86-10012
Aerodynamics of hyperlift systems
[SNIAS-443.501/85] N86-10023

WINTER
Smoke inputs to climate models: Optical properties and height distribution for nuclear winter studies
[DE85-011363] N86-10717
Microphysical/mesoscale aspects of nuclear winter and new directions in assessments
[DE85-013479] N86-10718

WIRE
Reduction of noble metal stock and noble metal loss during wire production with the Conform extrusion process
[BMFT-FB-T-85-049] N86-10560

WOOD
Self-heating to ignition measurements and computation of critical size for solar energy collector materials
[DE85-011449] N86-10302
Improved stud configurations for attaching laminated wood wind turbine blades
[NASA-TM-87109] N86-10582

WORK CAPACITY
Adaptation of man to extreme conditions of Antarctica
N86-10751

WORKING FLUIDS
Simplified analysis of Stirling engines and heat pumps
[DE85-005366] N86-10647
Analyses of advanced residential absorption heat pump cycles
[DE85-005244] N86-10664

WORKLOADS (PSYCHOPHYSIOLOGY)
Capacity for work and hemodynamics in males residing at middle and high latitudes N86-10747
Effect of inclusion of supplementary ascorbic acid in daily diet on degree of vitamin saturation of body and thermoresistance of erythrocytes while working in arid zone N86-10749
Effect of various doses of some vitamins on non-specific mechanisms of adaptation of man N86-10750
The effects of age, sleep deprivation, and altitude on complex performance
[AD-A156967] N86-10771
Report on the research activities on whole-body vibrations. Human strain due to mechanical vibrations
[ISBN-3-88383-107-7] N86-10773

WYOMING
Report of the Workshop on Geologic Applications of Remote Sensing to the Study of Sedimentary Basins
[E86-10002] N86-10599
Paleogene vertebrate paleontology, geology and remote sensing in the Wind River Basin N86-10609

X

X RAY ABSORPTION
NBSGSC: A FORTRAN program for quantitative X-ray fluorescence analysis
[PB85-206068] N86-10847

X RAY ANALYSIS
La Recherche Aerospatiale, bimonthly bulletin, no. 1984-5, September-October 1985
[ESA-TT-899] N86-10363

X RAY ASTRONOMY
X-ray satellite
[NASA-TM-77923] N86-10273
Theoretical analysis of Wolter/LSM X-ray telescope systems
[NASA-CR-176244] N86-11095

X RAY DENSITY MEASUREMENT
Extra-galactic X-ray sources and the diffuse X-ray background N86-11144

X RAY DIFFRACTION
A simple method of obtaining concentration depth-profiles from X-ray diffraction
[NASA-CR-176262] N86-10310

X RAY FLUORESCENCE
NBSGSC: A FORTRAN program for quantitative X-ray fluorescence analysis
[PB85-206068] N86-10847

X RAY IRRADIATION
Preliminary investigation of changes in X-ray multilayer optics subjected to high radiation flux
[DE85-014074] N86-10844

X RAY SCATTERING
Experimental X-ray scattering cross sections for H2 and rare atomic gases
[DE85-011572] N86-10936

X RAY SOURCES
Device for cryogenically fabricating source material for plasma X-ray lasers
[AD-D011814] N86-10537

X RAY SPECTRA
NBSGSC: A FORTRAN program for quantitative X-ray fluorescence analysis
[PB85-206068] N86-10847

X RAY TELESCOPES
Theoretical analysis of Wolter/LSM X-ray telescope systems
[NASA-CR-176244] N86-11095

X RAYS
Dynamics of imploding neon gas puff plasmas. 1
[AD-A156916] N86-10983
Photoactivation of PBFA-2
[DE85-013439] N86-11019

XENON
Light scattering tests of fundamental theories of transport properties in the critical region N86-10113
Thermodynamic constraints on ion beam mixing of metals on insulators
[DE85-013628] N86-10448
Determination of optical properties by third-harmonic generation in noble gases in unfocused laser beams
N86-10535

Y

YAG LASERS
Contact effects in light activated GaAs switches
[AD-A156957] N86-10434

YEAST
Romanian plant produces protein concentrate from paraffin-nourished yeasts N86-10741

YTTERBIUM
Extraction of lanthanide ions by 2-methyl-8-quinolinol
[DE85-014277] N86-10303

YTTRIUM
Study of the reactive-element effect in oxidation of Fe-Cr alloys using transverse section analytical electron microscopy N86-10087
Characterization of mechanical damage mechanisms in ceramic composite materials
[AD-A156574] N86-10590

Z

ZETA PINCH
Equilibrium of the kink source experiment
[DE85-012764] N86-11029

ZINC
Diffusion in immiscible melts N86-10096
Environmental degradation of materials: Surface chemistry related to stress corrosion cracking
N86-10099
Laser Raman spectroscopy study of the zinc and bromide ion complex equilibrium in zinc/bromine battery electrolytes
[DE85-011820] N86-10301
W-shaped diffused stripe GaAs/AlGaAs laser
[AD-D011816] N86-10538

ZINC ALLOYS
Particle coarsening in immiscible zinc-lead alloys under microgravity — Spacelab N86-10210

ZINC COMPOUNDS
Directional solidification of an aluminum-zinc vapor emulsion in microgravity — Spacelab N86-10218
Laser Raman spectroscopy study of the zinc and bromide ion complex equilibrium in zinc/bromine battery electrolytes
[DE85-011820] N86-10301

ZINC OXIDES
Catalytic activity of shock modified ZnO for CO oxidation and methanol synthesis
[DE85-014704] N86-10300

ZINC TELLURIDES
Ion beam sputter deposited zinc telluride films
[NASA-TM-87119] N86-11048

ZIRCONIUM TITANATES
The preparation and testing of titanium and zirconium coupling agents
[SJ70] N86-10576

ZONE MELTING
Float zone experiments in space N86-10067

PERSONAL AUTHOR INDEX

SCIENTIFIC AND TECHNICAL AEROSPACE REPORTS VOLUME 24 NUMBER 1

Typical Personal Author Index Listing

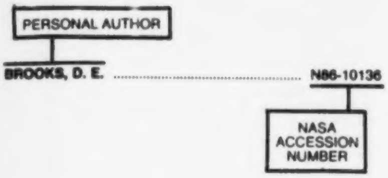

Listings in this index are arranged alphabetically by personal author. The NASA accession number denotes the number by which the citation is identified.

A

ABOLFADL, M. A. N86-10459
ABRAMOVICH, H. N86-10583
N86-10584
ACHENBACH, J. D. N86-10346
N86-10593
ACKERMANN, F. N86-10486
ACOSTA, R. N86-10381
ADAMS, J. N86-10623
ADAMSKA, H. N86-11042
ADHIKARY, K. R. N86-10505
AERTS, N. N86-11074
AGARKOV, F. T. N86-10753
AGRAWALA, M. N86-10697
AHLBORN, H. N86-10209
AHMAD, I. N86-10961
AHRENS, L. N86-10931
AKSENOV, V. V. N86-10746
ALBERTZ, J. N86-10508
ALBRECHT, J. N86-10308
ALDRICH, B. R. N86-10165
ALESSI, J. G. N86-10935
ALFORQUE, R. N86-11021
ALI, A. W. N86-10924
ALLAN, J. A. N86-10495
ALLARD, R. N86-11072
ALLEN, G. N86-10940
ALLISON, L. J. N86-10677
ALPATOV, B. A. N86-10818
ALSEM, W. H. M. N86-10212
ALTENKIRCH, R. A. N86-10159
ANDERSON, B. J. N86-10103
ANDERSON, C. M. N86-10829
ANDERSON, E. C. N86-10694
ANDERSON, K. W. N86-10039
N86-10788
ANDRESEN, U. N86-10183
ANDREWS, G. W. N86-10410
ANITLLON, A. N86-11018
AOKI, H. N86-11052
APPLETON, B. R N86-10448
ARAKAWA, E. T. N86-10949
ARAM, S. N86-11116
ARKHANGELSKIY, D. Y. N86-10739
ARNBAK, J. C. N86-10270
ARNEY, D. C. N86-10666
ARP, V. D. N86-10114
ARVIDSON, R. E. N86-10605
ASSARD, G. L. N86-10483
ATCHLEY, A. A. N86-10918
ATHALE, R. N86-10975
ATHERTON, P. D. N86-11106
N86-11119
ATTENBERGER, S. E. N86-10640
ATZMON, M. N86-10327
AUBRON, R. N86-10217
AUDU, M. L. N86-10853
AUTHIER, A. N86-10230
AUTHIER, B. N86-11102
N86-11108
N86-11111
AXLER, K. M. N86-10660
AYRES, A. N86-11065
AZOUI, N. N86-10961

B

BABUSKA, I. N86-10862
N86-10864
N86-10869
BACHMANN, K. N86-10031
N86-10054
BACKES, U. N86-10450
BADDOUR, M. F. N86-10380
BADLER, N. I. N86-10770
N86-10785
N86-10820
N86-10821
N86-10896
N86-10897
BAEHR, H. P. N86-10489
BAGLIN, J. E. F. N86-10448
BAILEY, G. B. N86-10600
BAIRD, J. N86-10104
BAIRD, J. K. N86-10248
BAKER, M. S. N86-10656
BAKER, R. W. N86-10682
BALACHANDRAN, V. N86-10573
BALANDRIN, M. F. N86-10342
BALKO, B. N86-11071
BALUDA, M. V. N86-10745
BAMBADE, P. N86-10965
BAMBERGER, S. B. N86-10246
N86-10247
BANE, K. L. N86-10964
BANGERT, L. S. N86-10016
BARBIER, F. N86-10215
BARISAS, S. G. N86-10676
BARKER, D. S. N86-10852
BARKER, R. E., JR. N86-11059
N86-11060
BARLOW, G. H. N86-10134
BARMATZ, M. N86-10167
BARNARD, J. C. N86-10597
BARNES, C. W. N86-10988
N86-10998
N86-11003
N86-11028
BARNES, H. M. N86-10710
BARNETT, C. F. N86-10926
BARNETT, R. J. N86-10014
BARR, B. N86-10821
BARRETT, R. J. N86-11037
BARRETT, T. W. N86-10344
BARTA, C. N86-10263
BARTHOLOMEW, R. J. N86-10835
BATTEN, A. L. N86-10275
BATZER, T. H. N86-11030
BAUDOIN, A. N86-10497
BAUER, H. F. N86-10240
BAUER, M. E. N86-10610
BAUGH, R. N. N86-10650
BAUMAN, T. J. N86-10531
BAYUZICK, R. J. N86-10073
BAZARNYY, Y. M. N86-10813
BEALE, J. N86-10821
BEHRINGER, R. P. N86-10119
BENCUYA, I. N86-11043
BENDER, P. L. N86-11123
BENNETT, I. F. N86-10195
BENNETT, R. H. N86-10557
BENOIT, J. N86-10217
BENZ, K. W. N86-10224
BERG, B. N86-10120
BERGGRUND, U. N86-10364
BERGSTROEM, S. I. N86-10551
BERLAD, A. L. N86-10160
BERMAN, M. N86-10474
BERNHARD, R. J. N86-10912
BERRIER, B. L. N86-10016
BERT, J. N86-10253
BERTHEL, R. O. N86-10482
BERTOLA, E. N86-11098
BEYERLE, A. N86-10526
BHASAVANICH, D. N86-10441
BIDDLE, R. S. N86-10993
BIEHL, L. L. N86-10610
BIER, M. N86-10135
BIERIG N86-10436
BIGELOW, C. A. N86-10287
N86-10581
BIGLIERI, E. N86-10407
BIJLEVELD, J. N86-10964
BILLIA, B. N86-10262
BILSKIE, J. R. N86-10950
BIRKEMEIER, W. A. N86-10728
BIRNBAUM N86-10424
BISCH, C. N86-10204
BLAAUW, G. J. N86-10776
BLAKE, P. L. N86-10601
N86-10604
BLAKE, R. L. N86-10944
BLAKEMORE, J. S. N86-11050
BLANC, T. V. N86-10714
BLAYLOCK, B. G. N86-10679
BLAZIT, A. N86-11122
BLODGETT, J. A. N86-10975
BLOOMFIELD, D. N86-10444
BOATNER, L. A. N86-10448
BOBB, L. C. N86-10976
BOBKOVA, N. N. N86-10740
BODDAERT, M. N86-10217
BODECHTEL, J. N86-10521
BODINE, F. R. N86-10481
BODNER, S. R. N86-10589
BOER, L. C. N86-10782
BOHMAN, L. N86-10960
BOICOURT, G. P. N86-10837
N86-10992
BOIT, J. L. N86-11109
BOLLEN, R. N86-10844
BONDARENKO, T. I. N86-10762
BONNELL, D. W. N86-10074
BONNET, C. N86-10023
BORGARDT N86-10525
BORQUE, R. F. N86-10468
BORTNOVSKIY, V. N. N86-10750
BOTTA, E. F. F. N86-10881
BOTTEGA, W. J. N86-10284
BOUCHIER, F. A. N86-11011
BOUDREAULT, R. N86-10239
BOUSSOUF, M. D. N86-10547
BOUTEMY, O. N86-10217
BOUTENKO, O. N86-10306
BOUWMANS, J. M. M. N86-10638
BOWDLE, D. A. N86-10103
BOWLES, K. J. N86-10288
BOYER, W. B. N86-11011
BRACCO, F. V. N86-10559
BRACEY, J. T. N86-10953
BRACKENBUSH, I. W. N86-10299
BRADBURY, K. A. N86-10365
BRAEDT, M. N86-10216
BRAETSCH, V. N86-10216
BRAND, U. N86-10449
BREAULT, R. D. N86-10651
N86-10652
BREITHAUPT, D. N86-10323
BREWE, D. E. N86-10463
BREZINSKI, D. K. N86-10693
BREZOVEC, C. N86-10661
BRIGGS, T. A. N86-10651
N86-10652
BROCKWELL, J. L. N86-10110
BROOKS, D E. N86-10136
N86-10246
N86-10247
BROOMAN, E. W. N86-10326
BROWMAN, A. A. N86-10986
BROWN, D. N86-10950
BROWN, D. W. N86-10395
BROWN, J. M. N86-10630
BROWN, K. L. N86-10994
BROWN, R. A. N86-10055
N86-10056
N86-10105
BROWN, R. D. N86-10985

BROWN, S. R. N86-10698
BROWN, W. E. N86-10616
BRUCKENTHAL, E. N86-10601
BRUNING, T. H. N86-10851
BRUST, F. W., JR. N86-10574
BRYANT, G. G. N86-10315
BRYANT, J. N86-10554
BRZEZINSKI, J. N86-10877
N86-10903
BUCH, Y. I. N86-10765
BUCHENAUER, C. J. N86-10998
BUCHROITHNER, M. F. N86-10503
BUCK, B. M. N86-10727
BUCKLEY, D. H. N86-10341
N86-10552
BULAKH, M. A. N86-10817
BUNCE, G. M. N86-10989
BUNNER, A. N. N86-11107
BURBANK, D. N86-10602
BURGDORF, K. N86-11088
BURKE, B. F. N86-11126
BURTON, L. C. N86-10431
BUSSELL, G. T. N86-11037
BUTLER, G. W. N86-10963
BUTTRAM, M. T. N86-10441
BUXBAUM, O. N86-10044
BYRD, L. W. N86-10361

C

CABE, S. N86-10690
CADA, G. F. N86-10678
CAHN, J. W. N86-10121
CAI, J. N86-10011
CALDECOTT, S. J. N86-10523
CALL, W. R. N86-11030
CALOGERO, F. N86-10859
CALVERT, P. D. N86-10576
CAMBIAGHI, D. N86-10252
CAMBON, G. N86-10217
CAMEL, D. N86-10262
CAMPBELL, G. W. N86-10938
CAMPBELL, K. W. N86-11059
CAMPISI, I. E. N86-11051
CAPBERN, P. N86-10023
CAPITAINE, G. N86-10050
CARBONELL, J. G. N86-10899
CARLBERG, T. N86-10256
CARLETON, N. P. N86-11104
CARLSON, R. L. N86-10588
CARLSSON, H. N86-10874
CARNEY, K. S. N86-10579
CASADESUS, P. N86-10307
CASSENTI, B. N. N86-10589
CASTETS, B. N86-10217
CASTOR, V. L. N86-10829
CATALDO, D. A. N86-10684
CATHEY, W. N. N86-10644
CATTROLL, S. W. N86-10786
CAVALLO, J. M. N86-11044
CEZAIRLIYAN, A. N86-10106
CHABILDAS, L. C. N86-11054
CHAI, A. T. N86-10107
N86-10117
N86-10125
CHAN, K. S. N86-10589
CHAN, T. F. N86-10887
CHANG, I. C. N86-10915
CHANG, J. N86-10439
N86-10540
N86-10940
CHANG, J. P. N86-10569
CHANG, L. W. N86-10545
CHAO, S. N86-11095
CHEN, C. P. N86-10462
CHEN, D. T. N86-10406
CHEN, F. C. N86-10661
CHEN, H. H. N86-10012
CHEN, I. W. N86-10147
CHEN, M. H. N86-10956
CHEN, N. C. J. N86-10647
CHEN, X. N86-10358
CHEN, Y. S. N86-10460
CHENG, K. T. N86-10956
CHIAN, C. T. N86-10386
N86-10389
CHING, L. N86-10400
CHIU, S. Y. N86-10676
CHO, Y. N86-10941
CHOINSKI, T. C. N86-10863
CHOO, Y. K. N86-10017
CHOU, T. S. N86-10948
CHOW, L. S. H. N86-11036
CHOWDHURY, P. N86-10961
CHRISTIANSEN, W. H. N86-10540
CHU, C. W. N86-10075
CHUANG, S. L. N86-10377
N86-10484
CHUN, C. H. N86-10241
CHUZEVILLE, G. N86-10253
CIESLAK, M. J. N86-10324
CIVINSKAS, K. C. N86-10017
CLARK, G. J. N86-10448
CLARK, R. W. N86-10983
CLARKE, D. W. N86-10854
CLAUS, J. N86-11026
CLAUSSEN, M. N86-10722
CLUNE, E. N86-10848
COHRT, H. N86-10353
COLE, R. N86-10155
COLEMAN, J. J. N86-10484
COLEMAN, R. B. N86-10910
COLES, D. N86-10108
COLIN, L. N86-11137
COLLINGS, E. W. N86-10076
COLLINS, W. E. N86-10771
COMBI, M. R. N86-11133
CONCUS, P. N86-10108
CONEIM, C. N86-10022
CONEL, J. E. N86-10603
N86-10604
N86-10606
CONGDON, J. V. N86-10651
N86-10652
CONNES, P. N86-11105
CONTI, R. N86-10438
COOPER, J. C. N86-10313
COPPLESTONE, R. W. N86-10919
CORDERMAN, R. R. N86-10649
CORIELL, S. R. N86-10077
CORNUEJOLS, G. N86-10861
CORTEZ, J. H. N86-10992
COSTES, N. N86-10175
COTTINGAME, W. B. N86-10992
COURANT, E. D. N86-11026
COUTANT, R. W. N86-10689
COX, J. D. N86-10539
CRABTREE, G. W. N86-11052
CRAWFORD, E. A. N86-10543
CREEDON, R. I. N86-10468
CRELLIN, E. B. N86-11110
CREMERS, P. N86-10894
CRIST, C. E. N86-10192
CROSBIE, E. A. N86-10934
CROUCH, R. K. N86-10057
CROW, B. N86-10400
CROWE, R. A. N86-10399
CROWLEY, F. A. N86-10269
CRUM, L. A. N86-10918
CUCCHISSI, J. J. N86-10385
CUNNINGHAM, J. C. N86-10437
CURRERI, P. A. N86-10246
CZANDERNA, A. W. N86-10645

D

DABKOWSKI, F. N86-10234
DAHLBERG, B. E. J. N86-10873
N86-10876
DALDER, E. N. C. N86-10908
DALGITY, G. G. N86-10522
DAMEN, A. N86-10879
N86-10880
DANBY, G. N86-11022
DAPKUS, D. N86-10538
DASS, N. D. H. N86-10882
N86-10883
DAUGHTRY, C. S. T. N86-10610
DAVIDSON, J. M. N86-10401
DAVIS, A. H. N86-10469
DAVIS, J. N86-10983
DAVIS, S. H. N86-10109
DAWSON, J. N86-10443
DAY, D. D. N86-10148
DEASON, V. A. N86-10530
DEB, S. K. N86-10662
DECARLO, J. L. N86-10094
DEGASPERIS, A. N86-10859
DEGOER, J. N86-10219
DEGRAAUW, T. N86-11102
DEGROEN, P. N86-10452
DEGUIRE, M. R. N86-10152
DELAHAYE, J. P. N86-11014
DELAHOY, A. E. N86-10668
DELITZSCH, V. N86-10237
DELL, G. F. N86-11023
DELOSME, J. M. N86-10795
DEMORE, W. B. N86-10707
DEMOULIN, P. D. N86-10655
DENARD, J. C. N86-10964
DENAVIT, J. N86-10471
DEPURY, P. N86-10493
DEREFELDT, G. N86-10364
DERITO, R. F. N86-10697
DERMER, C. D. N86-11141
DEROQUEFORT, T. A. N86-10878
DERRICK, M. N86-10942
DERUYTTERE, A. N86-10211
DEUPREE, R. G. N86-10469
DEVITO, B. N86-11022
DEWITT, A. N86-10991
DEWITT, K. J. N86-10110
DIAN, R. N86-10225
DIEM, W. N86-10560
DIETZ, K. R. N86-10498
DIJK, J. N86-10270
DIJKSTRA, J. B. N86-10888
N86-10889
N86-10890
N86-10891
DINTENFASS, L. N86-10137
DIVSALAR, D. N86-10390
DIXON, R. H. N86-10537
DIXON, T. H. N86-10618
DOBSON, M. C. N86-10628
DOGAN, A. U. N86-10691
DOLEV, D. N86-10898
DOLGANYUK, I. N. N86-10815
DONG, H. N86-10358
DONINA, Z. A. N86-10760
DONOVAN, N. N86-10615
DOORNBOS, R. N86-10888
N86-10889
DOREMUS, R. H. N86-10149
DOWNMAN, I. J. N86-10495
N86-10507
DOWNS, R. L. N86-10150
DOWO, J. F. N86-10598
DOYLE, F. J. N86-10494
DRESSLER, R. F. N86-10111
DRIEDONKS, A. G. M. N86-10711
DRIGERT, M. W. N86-10961
DRISCOLL, J. F. N86-10305
DROTNING, W. D. N86-10351
DRUMM, D. M. N86-10788
DRUMMOND, C. J. N86-10681
DUBOIS, M. V. N86-10719
DUFF, I. S. N86-10871
DUGAN, J. P. N86-10730
DUNN, S. A. N86-10168
N86-10169
DUPUIS, H. N86-10773
DUPUY, J. N86-10253
DURKIN, P. S. N86-10434
DUSTERBERRY, J. C. N86-10048
DUVAL, W. M. B. N86-11058
DWORAK, J. A. N86-10548
DYBDAL, R. B. N86-10373
DYBOY, V. A. N86-10811
N86-10812

E

EAGAR, T. W. N86-10078
EASTES, R. W. N86-10696
ECKELMANN, H. N86-10237
EDELMAN, R. B. N86-10161
EDEN, J. G. N86-10426
EGBERT, W. N86-10058
EGERT, C. M. N86-10330
EGGLESTON, J. M. N86-10543
EGGLESTONE, C. T. N86-10347
EISS, N. S., JR. N86-10033
EKHELIKAR, R. K. N86-10577
EKLUND, R. C. N86-10554
EL-AASSER, M. S. N86-10146
EL-KADDAH, N. N86-10133
ELACHI, C. N86-10629
ELIASON, J. R. N86-10597
ELLEMAN, D. D. N86-10170
ELLENBROEK, M. H. M. N86-10881
ELLIOTT, G. N86-10920
ELTON, R. C. N86-10537
ELWELL, D. N86-10059
EMBLING, L. V. N86-10553
EMLING, H. N86-10961
ENG, C. N86-10386
ENGEL, H. N86-10487
ENGHETA, N. N86-10629
ENGSTROEM, O. N86-10980
ENYA, S. N86-10243
ERAMUS, D. A. N86-10701
ERDOES, P. N86-10182
ESHLEMAN, R. E. N86-10586
ETCHEVERRY, R. D. N86-10373

ETHRIDGE, E. C. N86-10087
N86-10151
EVANS, C. R., II N86-11127
EVANS, D. C. N86-11005
EVANS, D. L. N86-10604
N86-10615
N86-10624
EVANS, R. A. N86-10793
EVANS, W. P. N86-10799
EVERITT, C. W. F. N86-10171
EVERT, R. W. N86-10712
EYER, A. N86-10227
EZELL, T. F. N86-11011

F

FACEMIRE, B. R. N86-10112
FACQ, P. N86-11105
FADOUL, J. R. N86-10582
FAIRBANK, W. M. N86-10118
FALA, G. N86-10820
FALICOV, L. M. N86-10321
FALIN, B. W. N86-10393
FALLER, J. E. N86-11123
FANALE, F. P. N86-11137
FANELLI, N. A. N86-10394
FANNING, U. N86-10112
FARCY, A. N86-10678
FARLOW, G. C. N86-10448
FARR, T. G. N86-10620
FAUCHERRE, M. N86-11116
FAULKNER, J. N86-10383
FAVIER, J. J. N86-10079
N86-10219
N86-10262
N86-10266
FAY, J. F. N86-10013
FEHLERT, G. P. N86-10636
FEHLING, H. N86-10451
FEIGELSON, R. S. N86-10059
FELDMAN, G. J. N86-11035
FERGER, R. N86-10670
FERGUSON, G. L. N86-10191
FERKO, P. N86-10554
FERNANDEZ-PELLO, A. C. N86-10162
FERNANDEZ, J. C. N86-10988
N86-11003
FERRELL, W. R. N86-10535
FEZER, F. E. N86-10491
FIGUROVA, M. Y. N86-10766
FILTER, W. F. N86-10940
FINE, J. N86-10115
FINGER, M. N86-10359
FINGLETON, D. J. N86-10676
FINKELSTEIN, P. L. N86-10723
FINN, R. N86-10108
FINSTERWALDER, R. N86-10518
FISCHER, M. N86-10294
FISCHER, S. K. N86-10653
FISCHMEISTER, H. N86-10210
FISHER, A. L. N86-10432
FISHER, C. E. N86-10014
FISHWICK, P. N86-10897
FLAHERTY, J. E. N86-10866
FLEETER, S. N86-10019
FLEMING, E. A. N86-10522
FLEMINGS, M. C. N86-10080
N86-10133
FOGG, D. A. B. N86-10428
FOGLER, R. J. N86-10920
FOKIN, A. A. N86-10811
N86-10812
FOLLSTAEDT, D. M. N86-10331
FOOTE, H. P. N86-10597
FORD, J. L. N86-10537
FORD, J. P. N86-10625
FOREST, J. C. E. P. E. N86-10970
FORSTREUTER, W. N86-10513
FOSS, M. H. N86-10990
FOSTER, L. M. N86-10060
FOX, C. G. N86-10726
FOXWELL N86-10020
FRANCO, N. N86-10084
FRANK, G. H. N86-10414
FRANK, L. N86-11137
FRANKE, P. R. N86-10663
FRANKLIN, T. L. N86-10195
FRANTZ, C. N86-10307
FRANZKE, K. N86-10595
FRASER, J. S. N86-10929
FRAZIER, D. O. N86-10112
FREISER, H. N86-10303
FREKERS, D. N86-10961
FRIANT, C. L. N86-10337
FRIEDRICHS, C. C. N86-11002
FRIELER, K. N86-10214
FRIPP, A. L. N86-10057
FRISCHAT, G. H. N86-10216
N86-10254
FRITSCHEN, L. J. N86-10631
FRITZE, G. N86-10488
FROEHLY, C. N86-11105
FROHBERG, G. N86-10231
FROST, C. A. N86-10192
FROST, R. T. N86-10172
FROYEN, L. N86-10211
FU, D. N86-10008
FUERST, M. N86-10492
FUNG, A. N86-10438
FURSHCHIK, A. B. N86-10813
FURUHAMA, K. N86-10461

G

GAILLARD, A. W. K. N86-10782
GALAYDA, J. N86-10947
GALIBERT, G. N86-10499
GALIBOIS, A. N86-10306
GALSTER, G. N86-10229
GAMMON, R. W. N86-10113
GANGEL, D. J. N86-10408
GANGEL, J. N86-10820
GANGOPADHYAY, P. K. N86-10922
GANGULI, B. N86-11132
GARCIA, A., III N86-10312
GARDNER, C. N86-10931
GARDNER, E. C. N86-10401
GARINTHER, G. R. N86-10917
GARLAND, T. R. N86-10684
GARTEN, C. T., JR. N86-10679
GASKELL, P. S. N86-10366
GATHERS, G. R. N86-10317
GATOS, H. C. N86-10061
N86-10234
GAWORSKI, C. L. N86-10675
GAY, J. N86-11125
GAYDA, J. N86-10311
GAYNOR, J. E. N86-10723
GEAR, C. W. N86-10871
GELBWACHS, J. A. N86-10674
GELLES, S. H. N86-10081
N86-10264
GELTIG, R. L. N86-10651
GELTING, R. L. N86-10652
GEORGE, G. A. N86-10347
GEORGE, T. F. N86-10925
GEORGE, T. G. N86-10660
GERRISH, V. N86-10528
GEZARI, D. Y. N86-11103
GHERSINI, G. N86-10232
GIARRATANO, P. G. N86-10114
GICQUEL, J. P. N86-10217
GIERLOFF-EMDEN, H. G. N86-10510
GILBERT, E. S. N86-10772
GILBODY, H. B. N86-10926
GILES, C. L. N86-10975
GILES, M. K. N86-10972
GILLESSEN, F. N86-10259
N86-10260
GILLIAM, D. R. N86-10033
GILLMAN, G. B. N86-10430
GILSON, A. P. N86-10974
GINSBERG, J. H. N86-10466
N86-10467
GLICKSMAN, M. E. N86-10082
N86-10083
N86-10088
GLOVER, D. W. N86-10633
GLOVER, F. N86-10861
GODFREY, B. B. N86-10192
GODTHELP, H. N86-10775
GODTHELP, J. N86-10783
GOETERS, K. M. N86-10780
N86-10781
GOGLIA, G. N86-11064
GOKHALE, R. B. N86-10014
GOLDBERG, B. A. N86-11139
GOLDEN, D. M. N86-10707
GOLDSTEIN, R. M. N86-10622
GOLDSTONE, J. A. N86-10932
GOLIA, C. N86-10238
GOLLER, G. J. N86-10651
N86-10652
GOLOMBEK, M. P. N86-10618
GONFALONE, A. N86-10201
GONNDI, P. N86-10215
GOPALAN, A. K. S. N86-10516
GOREAU, P. N86-10618
GORMAN, J. G. N86-10441
GORNEY, D. J. N86-10708
GRADY, D. E. N86-11055
GRAFOVA, V. A. N86-10749
GRAHAM, J. N86-10084
GRAHAM, R. A. N86-10300
GRAHAM, W. B. N86-10470
GRANATO, A. V. N86-11056
GRANT, N. J. N86-10085
GRATHWOHL, G. N86-10352
GRATHWOLH, G. N86-10353
GRAVES, M. E. N86-10723
GRAY, E. R. N86-10929
GRAY, H. F. N86-10416
GRAY, R. P., JR. N86-10372
GREENAWAY, A. H. N86-11094
N86-11106
N86-11119
GREENE, R. F. N86-10416
GREENSPAN, H. P. N86-10062
GREGORY, D. C. N86-10926
GRIEMERT, R. N86-10475
GRIFFIN, F. P. N86-10647
GRIFFIN, P. M. N86-10926
GRIFFITH, W. A. N86-10650
GRIMES, P. G. N86-10301
GRINDELAND, R. N86-10140
GRISAFFE, S. J. N86-10173
GRISHAM, D. L. N86-10965
GRISNIK, S. P. N86-10279
GROSSBECK, M. I. N86-10329
GROSSO, J. S. N86-10944
GRUBER, G. J. N86-10916
GUI, W. N86-10862
N86-10864
N86-10869
GUIDOTT, R. A. N86-10644
GUINESS, E. A. N86-10605
GULAID, A. A. N86-10506
GULINO, D. A. N86-11048
GURTOVAYA, Y. Y. N86-10614
GUYENNE, T. D. N86-10200
N86-10485
GYORKE, D. F. N86-10681

H

HABEGGER, L. J. N86-10676
HAEFNER, H. N86-10515
HAGAFORS, R. N86-11072
HAGG, E. N86-11062
HAGGAG, F. M. N86-10320
HAHN, H. N86-11026
HAJDASINSKI, A. N86-10879
N86-10880
HALL, I. J. N86-10716
HALL, J. L. N86-11123
HALLER, E. E. N86-10442
HALM, K. N86-10504
HAMDAN, M. A. N86-10458
HAMMER, J. H. N86-10984
HAMMINGER, R. N86-10353
HAMPSON, R. F. N86-10707
HAMROCK, B. J. N86-10551
HAN, C. C. N86-10283
HARDEKOPF, R. A N86-10950
N86-10996
HARDY, K. N86-11083
N86-11084
N86-11085
N86-11086
HARDY, S. C. N86-10115
HARRIS, J. M. N86-10138
N86-10139
N86-10246
N86-10247
HARSHA, P. T. N86-10161
HARTNETT, E. B. N86-10269
HARTWELL, J. K. N86-10954
HARVEY, B. N86-11007
HASELMAN, I. C., JR. N86-10717
HASS, K. C. N86-11045
HAUCK, C. A. N86-10962
HAUN, C. C. N86-10675
HAUPT, R. J. N86-10030
HAUSMAN, H. J. N86-11088
HAVENER, C. C. N86-10926
HAYES, D. C. N86-10554
HAYES, K. F. N86-10592
HAYNES, J. M. N86-10207
HAYS, R. T. N86-11065
HEADLEY, T. J. N86-10324
HEARST, P. J. N86-10314
HEATH, J. E. N86-10480
HEBSUR, M. G. N86-10311
HEDDERGOTT, A. N86-10051
HEDEMANN, M. A. N86-11005

HEERING, J. N86-10884
HEGLAND, J. R. N86-10831
HEINE, E. N86-10968
HEINEMANN, K. N86-11047
HEINICKE, M. N86-11065
HEJHAL, D. A. N86-10902
HELD, D. N. N86-10615
N86-10616
N86-10617
N86-10628
HELLAWELL, A. N86-10086
HEMSKY, J. W. N86-10932
HENDRIX, G. J. N86-10816
HENDY, K. C. N86-10039
N86-10788
HENINS, I. N86-10988
N86-10996
N86-11026
HENNINGER, W. C. N86-10274
HENRY, D. N86-10253
HENSCHEL, F. N86-10047
HEPPELMAN, S. N86-10443
HERCEG, R. N86-10659
HERLACH, D. M. N86-10259
N86-10260
HERMACH, F. L. N86-10453
HESS, K. N86-10494
HESSELINK, L. N86-10108
HESTER, J. N86-10278
HEUSTESS, J. E. N86-10408
HEWETT, D. W. N86-11016
HIGGINS, E. F. N86-10996
HIGGINS, W. W. N86-10992
HILDEBRAND, S. G. N86-10678
HILS, D. N86-11123
HINCHLIFFE, I. N86-11008
HINDS, F. T. N86-10556
HINES, R. E. N86-10842
HINTZE, C. J. N86-10035
HIRSCHFELD, T. B. N86-10296
HIRST, J. N86-11001
HOBBS, R. W. N86-10958
HOCKADAY, M. P. N86-10944
HODGE, D. C. N86-10917
HOEFER, H. R. N86-10027
HOFMANN, K. H. N86-11120
HOIDA, H. W. N86-10988
N86-10998
HOLIAN, B. L. N86-10927
HOLLAND, L. R. N86-10065
HOLLEMAN, F. B. N86-10370
HOLMES, N. C. N86-10470
HOLTKAMP, D. N86-10943
HOLZMANN, R. N86-10961
HOMOLYA, J. B. N86-10686
HOMSEY, G. M. N86-10109
HONG, C. S. N86-10538
HONG, S. K. N86-10464
HONIG, E. M. N86-10196
N86-10197
HONODEL, C. N86-10323
HOPPE, D. N86-10387
N86-10388
HOULBERG, W. A. N86-10840
HOUTEKAMER, G. E. N86-10806
N86-10807
N86-10808
HOWARD, A. M. N86-10926
HOWARD, C. J. N86-10707
HOWARD, W. M. N86-11134
HOYNIAK, D. N86-10019
HSU, I. S. N86-10391
HUGENTOBLER, F. N86-10515
HULL, K. N86-10528
HULLIGER, F. N86-11052
HUMPHRIES, C. M. N86-11094
HUMPHRIES, W. N86-10554
HUNT, J. J. N86-10200
N86-10485
HUNTEN, D. M. N86-11137
HURD, J. W. N86-10930
HURWITCH, J. W. N86-10326
HUTH, H. N86-10044
HUTTON, A. M. N86-10964
HYMER, W. C. N86-10140
HYNES, T. V. N86-10315

I

IAIRD, R. N86-10443
ICE, G. E. N86-10936
IGREVSKIY, A. V. N86-10743
ILLEGRAMS, P. F. A. N86-10534
ILYALETDINOV, A. N86-10742
IOUP, G. E. N86-10822
N86-10823
N86-10824
N86-10825
N86-10826
N86-10827
IOUP, J. W. N86-10828
IPSEN, I. C. F. N86-10796
IRIE, K. N86-10378
ISHERWOOD, D. N86-10632
ISHIHARA, A. N86-10982
ITALIANO, V. M. N86-10928
IWASHITA, Y. N86-10967

J

JABLONSKI, D. G. N86-10423
JACKSON, J. N86-11022
JACKSON, T. J. N86-10619
JACOBSON, B. G. N86-10551
JAHNKE, T. O. N86-10040
JAMGOTCHIAN, H. N86-10262
JANKOWSKI, D. F. N86-10123
JANNEY, J. I. N86-10839
JANSA, J. N86-10486
JANSSENS, R. V. F. N86-10961
JARBOE, T. R. N86-10988
N86-10998
N86-10999
N86-11000
N86-11027
N86-11028
JAUNCEY, D. L. N86-10383
JAVELLE, J. N86-10023
JAWAD, M. N86-10328
JENKINS, C. J. N86-10553
JENSEN, J. M. N86-10391
JESSER, W. A. N86-10193
JHA, S. N. N86-10516
JOBE, R. K. N86-10836
JOERGEN, P. N86-10874
JOHENNING, B. N86-11140
JOHN, C. N86-10228
JOHNSON, C. N86-10872
JOHNSON, J. D. N86-10927
JOHNSON, N. L. N86-10885
N86-10886
JOHNSON, S. E. N86-10791
JOHNSON, T. V. N86-11137
JOHNSON, W. L. N86-10327
JOHNSON, W. S. N86-10650
JOHNSTON, J. P. N86-10461
JOHNSTON, M. H. N86-10174
JONES, E. E. N86-10195
JONES, M. W. N86-10339
JONES, S. H. N86-10482
JORDAN, A. K. N86-11049
JORDAN, H. L. N86-11098
JORDAN, J. N86-10819
JOSS, W. N86-11052
JOST, G. S. N86-10036
JUN, Y. W. N86-10046
JUNGBLUTH, R. N86-10186
JUNGBLUTTH, R. N86-10181

K

KABIR, K. L. N86-10368
KAIMAL, J. C. N86-10723
KALB, J. T. N86-10917
KALDIS, E. N86-10267
KALONJI, G. N86-10152
KAMAT, D. S. N86-10516
KAMMERER, P. N86-10517
KAMOTANI, Y. N86-10124
KAMPAS, F. J. N86-10649
KARAWAS, G. K. N86-10369
KARPENKO, V. N. N86-11017
KARPOVSKIY, Y. Y. N86-10815
KASHTANOV, V. V. N86-10811
KASSEL, S. N86-10542
KATZ, J. N86-10015
KATZ, S. A. N86-10274
KATZ, T. J. N86-10283
KAUKLER, W. F. N86-10112
N86-10116
KAUTZ, H. E. N86-10561
KAYS, W. M. N86-10461
KAYSER, R. F. N86-10121
KEECH, M. A. N86-10512
KELLER, B. R. N86-10686
KELLER, R. N86-11006
KELLY, T. J. N86-10719
KELSO, A. R. N86-10712
KENNEDY, A. N86-10309
KENNEDY, R. E. N86-10198
KEOHANE, G. N86-11022
KEREN, G. B. N86-11077
KERN, E. L. N86-10063
KESNER, J. N86-11020
KESSEL, J. N86-10978
KEYANG, S. N86-10002
KHALIL, S. A. M. N86-10567
KHOMSKAYA, Y. D. N86-10756
KHOO, T. L. N86-10961
KHOVANSKAYA, T. P. N86-10745
KIBBLEWHITE, E. N86-11098
N86-11102
KIEDRON, K. N86-10386
KIEKEL, P. D. N86-10192
KIELB, R. E. N86-10579
KILLIAN, E. W. N86-10954
KIM, M. N86-11040
KIM, S. H. N86-10941
KINCAID, J. M. N86-10122
KING-HELE, D. G. N86-10190
KING, J. D. N86-10943
KING, R. J. N86-10409
KING, W. E. N86-10067
KINNEY, D. C. N86-10642
KIRKPATRICK, M. I. N86-10926
KLEIJNEN, J. P. C. N86-10893
N86-10894
N86-10895
KLEIN, H. N86-10249
N86-10257
KLEIN, M. M. N86-10944
KLEMENT, D. N86-10961
KLEMME, K. E. N86-10546
KLEMT, W. B. N86-10641
KLEY, M. N86-10521
KLINE, K. B. N86-10900
KNEISSEL, A. N86-10210
KNOTT, M. N86-10979
KNOWLES, T. N86-10641
KNOX, J. B. N86-10718
KNOX, S. O. N86-11003
N86-11028
KOECHLIN, L. N86-11112
KOEK, F. B. N86-10732
KOELBL, O. N86-10463
KOELKER, H. N86-10226
KOELLE, H. H. N86-11140
KOHLER, R. N86-10309
KOMAROV, V. D. N86-10811
KOMPENHANS, J. N86-10027
KONECNY, G. N86-10487
KONINGS, C. A. G. N86-11081
KONSTANTINOV, M. A. N86-10752
KOOPS, J. N86-10672
N86-10673
KOREIN, J. D. N86-10785
N86-10821
KOREVAAR, C. G. N86-10732
KORNFELD, M. N86-10146
KOROTKOV, Y. A. N86-10743
KORTH, M. S. N86-11046
KORYAKINA, L. A. N86-10796
KOSCHMIEDER, E. N86-10117
KOSHCHIY, G. N. N86-10762
KOSHELEV, V. N. N86-10759
KORTSOV, E. G. N86-10810
KOTZ, S. N86-10885
N86-10886
KOZDOBA, L. A. N86-10293
KPONCU, A. N86-10835
KRAATZ, K. H. N86-10231
KRAKOWSKI, R. A. N86-11031
KRAMER, J. F., JR. N86-10829
KRATIN, Y. G. N86-10765
KRAUS, K. N86-10486
KREMER, R. E. N86-11050
KRICHEVSKAYA, A. A. N86-10762
KRIENEN, F. N86-11004
KRISHTALKA, L. N86-10809
KRIVOSHEI, F. A. N86-10293
KROES, E. B. N86-10967
KROES, R. L. N86-10064
KROGER, P. M. N86-10401
KROGMANN, P. N86-10025
KUCERA, G. H. N86-10659
KULIKOV, A. V. N86-10796
KULKARNI, A. D. N86-11128
KUMAKAWA, A. N86-10114
KUNKLE, T. D. N86-10469
KUPERMAN, G. G. N86-10481
KUPFER, G. N86-10496
KURYLO, M. J. N86-10707
KURZWEG, U. H. N86-10539
KUSCHER, G. F. N86-10318
KUWAHARA, K. N86-10243
KYR, P. N86-10221

L

LABBE, P. N86-10419
N86-10865
LABEYRIE, A. N86-11097
N86-11101
N86-11102
N86-11106
N86-11115
LACASSE, M. G. N86-11118
LACH, J. N86-10846
LADOUCEUR, H. D. N86-11049
LAGOWSKI, J. N86-10234
LAL, R. B. N86-10064
LALANANDHAM, R. N86-10676
LAMBERT, J. E. N86-10865
LAMBERT, R. F. N86-10909
LANE, B. N86-11020
LANG, H. R. N86-10569
N86-10604
N86-10606
LANGBEIN, D. N86-10268
LANGDON, A. B. N86-11016
LANGE, H. G. N86-10555
LANGE, R. N86-10251
LANGER, J. S. N86-10086
LANGNER, A. N86-10506
LANHAM, W. N86-10140
LANKFORD, J. N86-10590
LANNES, A. N86-11124
LARGER, N. N86-10023
N86-10024
LARRABEE, J. A. N86-10301
LARSON, D. J. N86-10089
LATORRE, V. R. N86-10409
LAXMANAN, V. N86-10090
LAYANI, P. N86-10253
LAYLAND, J. W. N86-10385
N86-10386
LAYMAKAN, V. N86-10281
LAZAREV, V. O. N86-10811
LEAHY, H. F. N86-10675
LEAVITT, L. D. N86-10016
LEBEDEV, A. P. N86-10236
LEBER, L. L. N86-10787
LEBURTON, J. P. N86-10464
LECHLEITNER, M. L. N86-11079
LECORDIX, P. Y. N86-10509
LECURU, D. N86-10564
N86-10594
LEE, C. S. N86-10377
LEE, D. M. N86-10950
LEE, H. G. N86-10565
LEE, K. Y. N86-10356
LEE, M. J. N86-11025
LEE, P. N86-10770
LEE, P. J. N86-10382
LEE, R. Q. N86-10380
N86-10381
LEE, S. W. N86-10377
LEE, S. Y. N86-11010
N86-11026
LEE, W. A. N86-10343
LEE, Y. K. N86-10300
LEE, Y. Y. N86-11022
LEFAUCHEUX, F. N86-10230
LEHOCZKY, S. L. N86-10065
LEIFESTE, G. T. N86-10192
LEISSA, A. W. N86-10579
LEISTE, H. N86-10227
LEITH, W. N86-10607
LENA, P. N86-11100
LEVY, R. N86-10389
LEWIS, B. L. N86-10375
N86-10376
N86-10417
LI, C. J. N86-10234
LI, C. P. N86-10018
LI, X. Z. N86-11020
LI, Z. L. N86-10569
LICHTENSTEIN, S. N86-11077
LIEFELD, R. J. N86-10944
LILLYBECK, N. N86-10084
LIM, J. J. N86-10841
LIN, T. S. N86-10570
LINANG, L. N86-10004
LINDHOLM, U. S. N86-10589
LINDQUIST, T. E. N86-10629
LINSTADT, E. N86-10801
N86-11033
LIPA, J. A. N86-10118
LISKA, D. J. N86-11001
LISOWSKI, P. W. N86-10843
LITTKE, W. N86-10229
LIU, K. C. N86-10825
LIU, W. T. N86-10714
LIU, Y. Z. N86-10538
LIVINGSTONE, S. D. N86-10786
LO, Y. T. N86-10377
LOAR, J. M. N86-10678
LOCKHART, T. J. N86-10723
LOCKWOOD, G. J. N86-10439
N86-10940
N86-11013
LOEHBERG, K. N86-10209
LOFTSSON, J. N86-10397
N86-10398
LOFTUS, J. J. N86-10302
LOGAN, T. L. N86-10604
LOHMANN, P. N86-10511
LOKSHIN, A. N86-10400
LONGDON, N. N86-11096
LOUSTEAU, D. C. N86-10960
LUIJCKX, G. N86-10967
LUNDSTROM, M. S. N86-10655
LUNSFORD, J. S. N86-10996
LUOMA, W. L. N86-10651
N86-10652
LUPTON, R. H. N86-11131
LUYENDIJK, T. N86-10212
LYNCH, N. A. N86-10698
LYNN, K. G. N86-10937

M

MAAS, R. N86-10967
MAAT, L. N86-11081
MACBAIN, J. C. N86-10579
MACDONALD, G. E. N86-10914
MACE, E. E. N86-10713
MACEWEN, J. D. N86-10675
MACHENS, U. N86-10670
MACK, S. N86-10591
MACPHERSON, P. B. N86-10550
MAEKAWA, T. N86-10243
MAHAR, D. J. N86-10433
MAISH, A. B. N86-10665
MAITHREYAN, T. N86-11129
MALMEJAC, Y. N86-10079
N86-10222
MALONE, S. D. N86-10633
MALOTA, F. N86-10544
MANABAYEV, G. T. N86-10817
MANGANIELLO, A. J. N86-10832
MANINGER, R. C. N86-10959
MANN, R. C. N86-10526
MANNARA, G. N86-10235
MANOOCHEHRI, K. N86-10821
MANSFIELD, B. K. N86-10526
MANTENIEKS, M. A. N86-10280
MANTOVANI, J. C. N86-10435
MANUKHIN, B. N. N86-10754
MARCHATERRE, J. F. N86-10952
MARGITAN, J. J. N86-10707
MARGRAVE, J. L. N86-10091
MARGULIES, T. S. N86-10911
MARINA, M. N86-10400
MARKARYAN, S. S. N86-10743
MARKLIN, G. N86-11029
MARKLIN, G. J. N86-10988
N86-10998
N86-11027
MARKO, A. R. N86-10973
MARKWORTH, A. J. N86-10081
N86-10264
MARMORINO, G. O. N86-10730
MARTIN, E. A. N86-10784
MARTINEAU, J. R. N86-10342
MARTINEZ, T. N86-10205
MARTINSON, R. H. N86-10345
MASHBURN, J. B. N86-11019
MATHEWS, G. J. N86-11134
MATTHEWS, A. J. N86-10482
MATTSON, C. B. N86-11011
MATTSSON, S. N86-10411
MATUSKA, W., JR. N86-10944
MATUSOV, A. L. N86-10751
MATVEYEV, L. N. N86-10747
MAVROGENES, G. S. N86-10967
MAXAM, G. L. N86-10049
MAY, E. N86-10443
MAYA, I. N86-10466
MAZIAR, C. M. N86-10655
MCCLENNY, W. A. N86-10687
MCCLOSKE, M. W. N86-10651
MCCLOSKEY, M. W. N86-10652
MCCOY, K. E. N86-10275
MCDANIEL, E. W. N86-10926
MCDERMOTT, D. N86-10833
MCDONALD, M. M. N86-10325
MCDONNELL, M. N86-10524
MCFADDEN, D. M. N86-10684
MCFADDEN, G. B. N86-10077
MCGRAW, B. A. N86-10650
MCGUFFIE, B. A. N86-10604
MCGUIRE, R. R. N86-10359
MCHARGUE, C. J. N86-10448
MCHUGH, M. A. N86-11061
MCILWAIN, M. E. N86-10530
MCKENNA, K. F. N86-11003
MCLAREN, S. E. N86-10719
MCMENAMIN, M. A. S. N86-10692
MCMICAN, W. J. N86-10649
MCPHERSON, W. R. N86-10276
MEADE, A. C. N86-10798
MEIER, G. E. A. N86-10028
MELITA, O. N86-11086
MENEGUETTE, A. N86-10495
MENG, F. N86-10358
MENICUCCI, D. F. N86-10716
MENITSKIY, D. N. N86-10752
MENZEL, M. T. N86-10837
MERRITT, F. L. N86-10277
MERTENS, H. W. N86-10771
MESEGUER, J. N86-10244
MESZAROS, S. P. N86-11138
MEYER, C. N86-10821
MEYER, F. W. N86-10926
MEYER, H. N86-10119
MEYER, P. N86-10553
MEZIDOVA, K. A. N86-10754
MICALE, F. J. N86-10146
MIENTEK, A. P. N86-10651
N86-10652
MIKATA, Y. N86-10285
MILLER, A. P. N86-10106
MILLER, J. O. N86-10669
MILLER, W. A. N86-10473
MILLER, W. H. N86-10355
MILLER, W. J. N86-10150
MILUTINOVIC, J. N86-10921
MINER, R. V. N86-10311
MINH, N. Q. N86-10659
MITCHELL, A. C. N86-10317
MIYASHITA, K. N86-10520
MIYOSHI, K. N86-10341
MIZUSAWA, H. N86-10376
MOBLEY, J. D. N86-10688
MOEN, I. O. N86-10304
MOFFAT, R. J. N86-10461
MOHAMED-ALY, H. N. N86-10566
MOHSENI, S. N86-10362
MOLDOVER, M. R. N86-10113
N86-10120
N86-10121
MOLINA, M. J. N86-10707
MOMMADOV, I. M. N86-10749
MONDAL, N. N86-10443
MONTANARI, R. N86-10215
MONTGOMERY, D. B. N86-11000
MONTGOMERY, S. T. N86-10350
MONTH, M. N86-11018
MONTI, R. N86-10203
N86-10235
MOON, S. H. N86-10456
MOORCROFT, A. L. N86-10483
MOORE, C. E. N86-10923
MORABITO, D. D. N86-10383
MORESCHI, J. N86-10659
MORGAN, T. J. N86-10926
MORGAND, P. N86-10218
MORI, T. T. N86-10373
MORIN, A. N86-10419
N86-10865
MORIOKA, M. N86-10243
MORIONDO, A. N86-10490
MORISON, J. D. N86-10793
MOROSIN, B. N86-10300
MORRIS, J. W., JR. N86-10906
MORRISON, D. N86-10140
MORRISON, D. R. N86-10141
N86-10142
MORRISON, G. N86-10122
MORRISON, P. J. N86-11063
MORSE, M. S. N86-10106
MOSES, J. D. N86-10943
MOSS, J. M. N86-10955
MOZURKEWICH, D. N86-11092
MRAZEK, F. C. N86-10659
MSEZANE, A. Z. N86-10939
MUELLER, G. N86-10221
MUELLER, T. A. N86-10916
MUENZER, U. N86-10521
MUKHERJEE, S. P. N86-10153
MULLIGAN, P. J. N86-10621
MUNJAL, M. L. N86-10587

MURALIDHARAN, S. N56-10857
MURPHY, J. C. N86-10034

N

NAEHLE, R. N86-10257
NAGEL, G. N86-10224
NAGLE-ESHLEMAN, J. N86-10585
NAKA, S. N86-10332
NAKANISHI, S. N86-10281
NAMKUNG, M. N86-10578
NAPIER, P. J. N86-10396
NAPOLITANO, L. G. N86-10203
N86-10235
N86-10238
NAUMANN, R. N86-10058
N86-10104
NAWROCKY, R. J. N86-10947
NEEF, J. D. N86-10198
NEFEDEVA, Y. A. N86-10613
NEIDLINGER, H. H. N86-10645
NEITZEL, G. P. N86-10123
NELLIS, W. J. N86-10470
NEPOMUCENO, L. X. N86-10562
NEWCOM, C. C. N86-11011
NEWMARK, R. L. N86-10725
NEYER, B. T. N86-10439
N86-10940
NG, D. S. N86-11017
NICHOLLS, L. A. N86-10403
NICKEL, H. N86-10595
NICOLSON, G. D. N86-10383
NIELSEN, K. F. N86-10229
NIESWAAG, H. N86-10212
NIEUWENHUIS, G. J. A. N86-10638
N86-10639
NIKITIN, S. A. N86-10236
NISHIMURA, N. N86-10346
NITSCHE, K. N86-10251
NITSCHE, R. N86-10223
N86-10225
N86-10227
NOACK, R. W. N86-10021
NOLAN, R. W. N86-10786
NOOMEN, J. N86-10967
NOORDAM, J. E. N86-11106
N86-11119
NORDINE, P. C. N86-10092
NORDSTROM, P. N86-10641
NOREM, J. N86-10979
NOVIKOV, I. V. N86-10745
NOVIKOV, V. S. N86-10750
NOVOZHILOV, G. N. N86-10757
NOWICKI, C. M. N86-10792
NUNZ, G. J. N86-10663

O

OBRIEN, J. J. N86-10651
N86-10652
OCHIAI, J. N86-10243
OGATA, M. N86-10378
OLD, T. E. N86-10405
OLEM, H. N86-10736
OLIVER, K. N86-10687
OLOFSSON, B. N86-10360
OLSON, N. N86-10524
OLSON, R. J. N86-10677
OLUJOHUNGBE, O. N86-10501
ONEILL, P. E. N86-10619
ONURAL, L. N86-10478
ORGILL, M. M. N86-10631
ORMSBY, J. P. N86-10621
ORR, L. H. N86-10828
OSHIMA, T. N86-10520
OSTRACH, S. N86-10124
OTOOLE, J. A. N86-10960
OTTO, H. N86-10258
OVERFELT, P. L. N86-10404
OWE, M. N86-10619
OWEN, R. B. N86-10174

P

PADDAY, J. E. N86-10202
PAFFRATH, D. N86-10685
PAGANO, N. J. N86-10292
PAGNI, P. J. N86-10162
PAK, I. T. N86-10817
PALATUCCI, G. J. N86-10792
PALETS, B. L. N86-10739
PALMER, M. A. N86-10944
PAN, S. K. N86-11041
PANAYAPPAN, R. N86-10313
PAPAS, C. H. N86-10629
PAPAZIAN, H. N86-10340
PAPPAS, J. A. N86-10354
PAPTHEODOROU, T. N86-10071
PARIS, J. F. N86-10627
PARK, C. N86-11047
PARK, J. E. N86-10843
PARKAS, Z. D. N86-11051
PARKIN, D. M. N86-10932
PARMLEY, R. T. N86-10274
PARSONS, M. L. N86-10280
PARZEN, G. N86-11023
N86-11026
PASTUKHOV, Y. F. N86-10764
PATRIARCA, P. N86-10328
PATRICK, H. V. L. N86-10913
PATUELLI, C. N86-10215
PAUT, A. J. N86-10023
PAWLOWICZ, L. M. N86-10234
PAYLOR, E. D. N86-10604
N86-10606
N86-10608
PECH, G. J. N86-10316
PELLA, P. A. N86-10847
PELLEGRIN, J. I. N86-10964
PELLETIER, D. H. N86-10457
PENG, C. N86-10010
PENKALLA, H. J. N86-10595
PENNER, J. E. N86-10717
PENNLINE, H. W. N86-10681
PENTECOST, E. N86-10053
PEPPER, D. W. N86-10348
PEREPEZKO, J. H. N86-10093
PERKO, J. S. N86-11143
PERRY, J. S. N86-10032
PERTSOV, O. L. N86-10759
PETERFREUND, A. R. N86-11136
PETERS, J. H. N86-10715
PETERSEN, R. H. N86-10676
PETERSON, T. T. N86-10125
PETRIE, G. M. N86-10597
PETROVA, L. A. N86-10612
PETROVIC, J. J. N86-10349
PFIRSCH, D. N86-11063
PHILLIPS, B. A. N86-10664
PHILLIPS, R. N86-11022
PHILLIS, N. J. N86-10523
PHINNEY, N. N86-10836
N86-11024
PICKARD, W. F. N86-10420
PIERCE, R. D. N86-10659
PIETRI, C. E. N86-10953
PIKE, T. K. N86-10413
PILLAI, C. N86-10963
PINCOSY, P. A. N86-10962
PINTER, S. S. N86-10896
PIPEROPOULOU, H. N86-10444
PIRICH, R. G. N86-10094
PLANK, V. G. N86-10482
PLATE, S. N86-11022
PLATTEN, J. K. N86-10245
PLATTS, D. A. N86-10999
N86-11003
PLEIL, J. D. N86-10687
PODSIADLY, C. N86-10058
POEPPEL, R. B. N86-10659
POLETTI, G. N86-10252
POLEZHAEV, V. I. N86-10236
POND, R. B. N86-10095
N86-10096
POPECHITELEV, Y. P. N86-10765
POPOV, A. A. N86-10739
POPOVA, N. K. N86-10766
PORZ, F. N86-10352
POSEY, L. D. N86-11005
POSNER, E. C. N86-10382
POSOSHENKO, L. Z. N86-10613
POTARD, C. N86-10097
N86-10218
POTASH, R. I. N86-11093
POTTER, J. L. N86-10014
POTTER, J. M. N86-10987
POUKEY, J. W. N86-10192
PRAIZEY, J. P. N86-10222
PREGENZER, A. L. N86-11005
PRESTON, R. A. N86-10383
PRICE, G. R. N86-10917
PRIVON, G. T. N86-10472
PURASINGHE, R. N86-10571
PYLE, R. V. N86-10962

Q

QIPENG, C. N86-10003

R

RAALAND, D. M. N86-10298
RABBIA, Y. N86-11125
RABOUT, P. N86-11108
RADFORD, D. C. N86-10961
RAGHUNATHAN, M. S. N86-10656
RAJESWARAN, G. N86-10649
RAMANTHAN, A. N86-10856
RAMATY, R. N86-11141
RANDALL, S. A. N86-10651
N86-10652
RANNENBERG, S. N86-10027
RAO, B. C. S. N86-10552
RATAJCZAK, A. F. N86-10643
RAUBENHEIMER, T. N86-10995
RAUCHAS, A. N86-10979
RAVEENDRA, S. T. N86-10855
RAVISHANKARA, A. R. N86-10707
RAYGORODSKAYA, T. G. N86-10759
RAZZAQ, Z. N86-10577
REBER, G. N86-10195
REDDISH, V. C. N86-11094
REDEEN, W. C. N86-10006
REE, F. H. N86-10907
REED, I. S. N86-10391
REGEL, L. L. N86-10263
REHN, L. E. N86-11056
REIMANN, R. C. N86-10654
REINHARDT, F. W. N86-10644
REISCHEL, M. N86-10103
REMICK, R. J. N86-10447
REMSBERG, I. P. N86-10963
RENHORN, I. N86-10980
REPETA, L. N86-11022
REX, J. D. N86-10906
REY, C. A. N86-10177
REYNOLDS, J. R. N86-10373
REYNOLDS, L. D. N86-10530
REZAIE-KEYVAN, N. N86-10572
REZTSOV, V. P. N86-10813
RHIM, W. K. N86-10170
RICE, C. K. N86-10653
RICHARDS, J. J. N86-10849
RIEPL, H. N86-10255
RIFF, R. N86-10588
RIKHTER, G. D. N86-10612
RIVKIN, I. N86-11014
RIVKIN, L. N86-10964
ROBERSON, P. I. N86-10938
ROBERT, M. C. N86-10230
ROBERTS, G. O. N86-10705
ROBERTSON, D. K. N86-10580
ROCK, B. A. N86-10280
RODEMICH, E. R. N86-10402
RODENZ, G. W. N86-10837
N86-10929
RODOT, H. N86-10204
N86-10220
RODRIGUES, G. C. N86-10319
ROEDER, A. W. N86-10374
ROEDIG, M. N86-10595
ROFFEY, R. N86-10360
ROGERS, J. W., JR. N86-10644
ROGERS, R. B. N86-10972
ROHAY, A. C. N86-10633
ROKNI, S. H. N86-10963
ROMIG, A. D., JR. N86-10324
N86-10331
ROOIJAKKERS, R. V. H. N86-10889
ROSENBERG, H. N86-10338
ROSENBERGER, F. N86-10126
ROSENBLUM, L. J. N86-10730
ROSENER, T. J. N86-10951
ROSENKILDE, C. E. N86-10466
N86-10467
ROSENKRANZ, V. N86-10254
ROSNER, H. S. N86-10729
ROSS, M. C. N86-11025
ROSS, P. N., JR. N86-10446
ROSSI, M. J. N86-10433
ROSSITTO, F. N86-10232
ROTH, E. A. N86-11114
ROUSSEAU, R. M. N86-10847
ROUTHORT, J. N86-10659
ROUX, B. N86-10253
ROVINS, J. N86-10821
ROY, S. N86-10479
ROYLANCE, D. N86-10127
ROZENDAAL, L. T. N86-10804
RUGGLES, L. E. N86-10439
RUSSEL, W. B. N86-10129
RUSSO, G. N86-10203
RUSZKAY, J. N86-10438
RUTH, R. D. N86-10935

S

SAAD, Y. N86-10794
N86-10850
N86-10867
N86-10868
SABATIER, P. C. N86-10706
N86-10858

SABER, A. J. N86-10304
SADOWAY, D. R. N86-10096
SALBERGER, P. N86-10904
SALE, M. J. N86-10678
SANDER, O. R. N86-10992
SANDERS, M. E. N86-10957
SANDOVAL, D. P. N86-10992
SANG, Y. N86-10529
SANI, R. L. N86-10128
SANMARTIN, A. M. N86-10271
SARACHIK, M. P. N86-11053
SARGENT, F. E. N86-10728
SAVILLE, D. A. N86-10129
N86-10130
N86-10143

SAYLES, D. C. N86-10282
SAZONOV, V. S. N86-10764
SCALA, C. M. N86-10037
SCHAEFER, R. J. N86-10077
SCHARMANN, A. N86-10242
SCHEID, J. A. N86-10384
SCHEMPP, A. N86-10194
SCHEN, M. A. N86-10334
SCHENCK, L. R. N86-10604
N86-10624

SCHERPELZ, R. I. N86-10299
SCHICKEL, K. P. N86-10720
SCHIJVE, J. N86-10045
SCHISSEL, P. N86-10645
SCHLERETH, J. N86-10443
SCHMID, L. A. N86-10106
N86-10131

SCHMIDT, J. W. N86-10121
SCHMUGGE, T. J. N86-10619
SCHNEIDER, L. X. N86-11013
SCHNEIDER, R. T. N86-10539
SCHNEPPLE, W. F. N86-10066
SCHOENHOLZ, R. N86-10225
SCHOLTEN, W. N86-10637
SCHRIBER, S. O. N86-10987
SCHROEDER, M. N86-10500
SCHUBERT, F. N86-10595
SCHUERING, A. N86-10500
SCHUHR, W. N86-10500
SCHULTZ, J. H. N86-11000
SCHULTZ, K. R. N86-10468
SCHULTZ, M. H. N86-10794
N86-10850

SCHUMMERS, J. H. N86-10906
SCHUSTER, G. J. N86-10527
SCHWAB, D. N86-10184
SCHWABE, D. N86-10242
SCHWARTZ, R. J. N86-10655
SCHWARZ, H. D. N86-11015
SCHWARZ, J. A. N86-10099
SCHWARZ, R. B. N86-10322
SCHWEBEKE, H. N86-10968
SCOTT, D. H. N86-10445
SCULLY, C. N. N86-10536
SEEBAUGH, W. R. N86-10014
SEEMAN, J. T. N86-11025
SEGALL, Z. N86-10848
SEIGNEUR, C. N86-10710
SELEROWICZ, W. C. N86-10028
SELKIRK, J. K. N86-10526
SELKOWITZ, S. N86-10978
SELPH, M. M. N86-10944
SELYAYEV, A. A. N86-10818
SEMENOVA, O. S. N86-10812
SERVRANCKX, R. V. N86-10994
SEVESTRE, C. N86-10363
SEZAKI, K. N86-10243
SGAVETTI, M. N86-10502
SHALKHAUSER, K. A. N86-10379
SHARITZ, R. R. N86-10625
SHARMA, S. N86-11021
SHARR, Y. N86-10816
SHAW, M. S. N86-10927
SHEALY, D. L. N86-11095
SHEFFIELD, R. L. N86-10929
SHEHATA, A. M. T. M. N86-10455
SHEPHERD, J. E. N86-10304
SHEPPARD, J. C. N86-11025
SHIELDS, G. N86-10820
SHIGUAN, B. N86-10005
SHIH, W. H. N86-10101
SHIMAZAKI, Y. N86-10335
SHIOHARA, Y. N86-10080
N86-10133

SHISONG, M. N86-10886
SHOPE, S. L. N86-10192
SHRADER, C. R. N86-11144
SHU, D. M. N86-10947
SHULTIS, J. N86-10834
SHUMILOVA, T. Y. N86-10761
SIDOROV, Y. A. N86-10748
N86-10751

SIEGFRIED, E. N86-10214
SIEWIOREK, D. N86-10848
SIGMON, T. W. N86-10429
SIKKA, V. K. N86-10328
SILCHENKO, K. K. N86-10757
SIMITSES, G. J. N86-10588
N86-10660

SIMMONS, J. E. N86-10943
SIMMONS, T. N. N86-11019
SIMPSON, H. M. N86-10932
SIMPSON, J. R. N86-10631
SIMS, T. M. N86-10958
SINEGUB, Y. S. N86-10611
SINES, G. N86-10591
SINGER, J. N86-10584
SINGER, M. J. N86-11065
SINGER, R. B. N86-10601
N86-10604

SINKS, D. J. N86-10634
SINNO, Y. A. N86-10700
SINNOTT, M. J. N86-10291
SIOCHI, E. J. N86-10033
SIRIGNANO, W. A. N86-10163
SKAALEN, C. I. N86-10555
SKARITKA, J. N86-11022
SKILLMAN, E. D. N86-11130
SKUDRIDAKIS, J. N86-10043
SLACK, R. A. N86-10421
SLINKER, S. N86-10924
SLINN, S. Y. N86-10276
SLUIJK, I. N86-10969
SLUYTERS, T. N86-10935
SMALLEY, R. E. N86-10966
SMEULDERS, T. N86-10888
SMITH, B. R. N86-11080
SMITH, J. L. N86-10659
SMITH, L. N86-11022
SMITH, M. N86-10623
SMITH, R. D. N86-10297
SMITH, S. T. N86-10841
SMYTH, W. H. N86-11139
SNEAD, C. L., JR. N86-10937
SNELL, M. K. N86-10408
SNELLING, D. R. N86-10294
SNYDER, R. S. N86-10143
N86-10144

SOBOLEVSKIY, V. I. N86-10758
SOKOLOV, Y. I. N86-10745
SOLOMEY, N. N86-10443
SOLOVYEV, A. N. N86-10765
SOMARATNA, N. N86-10286
SOMORJAI, G. A. N86-11057
SONI, S. R. N86-10292
SONTAG, H. N86-10465
N86-10541
N86-10977

SOROKO, S. I. N86-10751
SPAEPEN, F. N86-10154
N86-10233

SPATARO, S. J. N86-10532
SPEAR, K. E. N86-10132
SPENCE, P. W. N86-11005
SPENCER, B. W. N86-10952
SPENDEL, T. N86-10476
SPRADLEY, I. N86-10274
SPRENGER, H. N86-10213
SPRINGSTON, P. S. N86-10555
SRINIVASAN, M. A. N86-10568
SRIVASTAVA, P. K. N86-10516
STACHNIK, R. V. N86-11103
N86-11116

STAPASHKIN, A. I. N86-10818
STAPAY, J. R. N86-10659
STARK, E. N86-10486
STARK, E. W. N86-10898
STEFANESCU, D. M. N86-10084
N86-10100

STEINBACH, D. N86-10026
STEINBERG, D. N86-10323
STEINER, W. R. N86-10800
STELLING, G. S. N86-10477
STEVENS, M. P. J. N86-10802
N86-10804

STICKLER, R. N86-10214
STIENING, R. F. N86-11025
STINESPRING, C. D. N86-10132
STINNETT, R. M. N86-10958
STIPP, V. N86-10991
STOECKL, H. N86-10506
STOLZ, W. N86-10514
STONE, G. A. N86-10342
STOOKE, W. N., JR. N86-10038
STORK, D. G. N86-10769
STRATHMANN, F. W. N86-10519
STRAUB, J. N86-10250
N86-10251

STREHLOW, R. A. N86-10164
STROO, R. N86-10968
STROUD, D. G. N86-10101
STUBSTAD, J. M. N86-10660
STUCKY, R. K. N86-10609
STUHLINGER, T. W. N86-10971
STURE, S. N86-10175
SUBRAMANIAN, R. S. N86-10155
SUENAGA, M. N86-10937
SUGIURA, T. N86-10520
SULAKVELIDZE, G. K. N86-10614
SULMISTRAS, A. N86-10304
SULTAN, M. N86-10605
SULTANGAZIN, U. M. N86-10817
SULTANOV, F. F. N86-10754
SUTER, G. W., JR. N86-10679
SUURA, H. N86-11062
SVENSSON, S. N86-10980
SWAB, J. J. N86-10315
SWAIN, G. R. N86-10986
SWANSON, R. M. N86-10429
SWENSON, D. A. N86-10987
SWENSON, H. W. N86-10480
SWENSON, I. W. N86-10963
SYNDER, S. N86-10246
SZEKELY, J. N86-10133
SZOFRAN, F. R. N86-10065
SZU, H. H. N86-10975
SZUMOWSKI, A. P. N86-10028

T

TAFT, N. N86-10897
TAGUCHI, S. N86-10303
TAKAHASHI, K. N86-11134
TAKENS, F. N86-10892
N86-10905
TAM, A. C. N86-10465
N86-10541
N86-10977

TANAKA, S. N86-10520
TANASAWA, I. N86-10243
TANNER, R. L. N86-10719
TAO, G. Y. N86-10847
TASK, H. L. N86-10778
TATE, R. E. N86-10660
TAVERNA, A. R. N86-10289
TAYLOR, C. H. N86-10277
TAYLOR, H. F. N86-10422
TAZETDINOV, I. G. N86-10746
TERVO, J. N. N86-10558
THEON, J. S. N86-10702
THOEMING, G. H. N86-10838
THOM, C. N86-11121
THOMPSON, A. R. N86-10396
THOMPSON, D. S. N86-10445
THOMPSON, F. W. N86-10796
THOMPSON, K. N86-10836
N86-11024

THOMPSON, L. H. N86-10737
THOMPSON, W. S. N86-10289
THOMSEN, M. F. N86-11034
THORISSON, H. N86-10875
THRON, J. N86-10443
TIAN, Y. N86-10358
TIKHONOV, M. A. N86-10739
TILANUS, C. B. N86-10901
N86-11076

TIMMERMANS, X. I. M. N86-10845
TIRCUIT, E. C. N86-10199
TKACHENKO, Y. Y. N86-10763
TODD, P. N86-10140
N86-10145

TOGLIATTI, G. N86-10490
TOLCOTT, M. A. N86-10779
TOMICH, S. D. N86-10527
TOOHIG, T. E. N86-10997
TOOTHMAN, D. A. N86-10688
TOTTEREAU, O. N86-10220
TRACY, E. R. N86-10367
TRAUB, W. A. N86-11104
N86-11118

TRAVIS, B. J. N86-10469
TRINH, E. H. N86-10102
TRINKA, J. N86-10263

TRISKA, A. N86-10263
TROSHIKHIN, G. V. N86-10761
TROST, T. F. N86-10042
TRUONG, T. K. N86-10391
TSAI, C. K. N86-10549
TSAI, T. T. N86-10338
TSAY, V. A. N86-10617
TSUI, J. B. Y. N86-10425
N86-10427
TUCKER, W. K. N86-10195
TUPIKOVA, G. A. N86-10749
TURNER, R. S. N86-10677
TYLASKA, T. T. N86-10863
TYLER, S. N86-10397
N86-10398

U

UDANI, P. M. N86-10516
ULABY, F. T. N86-10628
ULIANA, E. A. N86-10406
UNNAM, J. N86-10310
UNRUH, K. M. N86-10327
UTTAL, W. R. N86-10870
UWIRA, K. N86-10720

V

VAKILI, F. N86-11113
VANALSTINE, J. N86-10247
VANALSTINE, J. M. N86-10246
VANBELLE, F. N86-10894
VANDENBERG, L. N86-10066
VANDENBOOM, A. J. W. N86-10644
VANDENDAELE, W. N86-11066
VANDENEIJNDEN, P. M. C. M. N86-10804
N86-10805
VANDENHOF, P. N86-10679
N86-10680
VANDENHONDEL, M. N86-11061
VANDERBIJ, J. D. N86-11073
N86-11074
N86-11075
VANDERBIJ, J. J. N86-11038
VANDERHOFF, J. W. N86-10145
VANDERLINDE, F. J. G. N86-10769
VANDERSCHAAF, T. W. N86-11077
VANDYCK, O. B. V. N86-10850
VANIER, P. E. N86-10649
VANLOON, M. F. N86-10774
VANLOON, M. P. M. N86-10602
VANMIDDENDORP, H. N86-10789
VANMOERKERKEN, R. A. N86-10732
VANWEERT, M. J. M. N86-10603
VANZYL, J. J. N86-10629
VASHCHILLO, Y. G. N86-10752
VASQUEZ, M. C. N86-10637
VAZIRI, K. N86-10963
VELLA, M. C. N86-10962
VENDETTI, A. N86-10562
VENTURINI, E. L. N86-10644
VERHOEVEN, J. D. N86-10067
VERLIJSDONK, A. P. N86-10270
VERMEULEN, P. N86-10703
N86-10704
VERNOT, E. H. N86-10675
VEYSSIERE, A. N86-10418
VIEIRA, D. J. N86-10963
VIGIL, M. G. N86-10357
VILLERS, D. N86-10245
VINCENT, M. A. N86-11123
VITTORIA, C. N86-10415
VIVIANI, A. N86-10236
VOGEL, P. N86-10336
VOLZHSKAYA, A. M. N86-10761
VONGIERKE, H. E. N86-10973
VOSHALL, R. E. N86-10441
VOSS, C. I. N86-10630
VOYZELLE, B. N86-10306
VREEBURG, J. P. B. N86-10206
VYSTAVKIN, A. N. N86-10613

W

WAEGEL, K. H. N86-10412
WAGENFAR, W. A. N86-11077
WALKER, K. P. N86-10589
WALKER, R. P. N86-10906
WALLACE, J. F. N86-10090
WALRAFEN, G. E. N86-10470
WALSHAW, D. J. N86-11094
WALTER, H. U. N86-10265
WALTON, D. R. M. N86-10576
WALZ, D. R. N86-11012
WANDELL, B. A. N86-10777
WANDERS, K. N86-10249
N86-10257
WANG, B. H. N86-10454
WANG, C. S. N86-11036
WANG, J. M. N86-11010
WANG, L. X. N86-10477
WANG, P. N86-10964
WANG, Q. N86-10356
WANG, T. G. N86-10156
N86-10176
WANG, X. N86-10009
WARD, R. A. N86-11134
WARNER, P. J. N86-11117
WARNOCK, R. L. N86-10895
WARREN, J. L. N86-10637
WATKINS, J. N86-10398
WATKINS, R. W. N86-10423
WATSON, R. T. N86-10707
WEAVER, J. N. N86-10864
WEBER, P. J. N86-10030
WEBER, R. M. N86-10589
WEDEMEYER, E. N86-10051
WEFEL, J. P. N86-11142
WEIGELT, G. N86-11102
N86-11120
WEIHL, W. E. N86-10898
WEINBERG, M. C. N86-10157
WEINSTEIN, N. H. N86-10539
WEINZIERL, A. N86-10250
WEISSER, M. N86-10412
WELLER, T. N86-10583
N86-10584
WENDELL, L. L. N86-10866
WENSIERSKI, P. W. N86-10671
WERNER, C. N86-10617
WESSELS, J. N86-11073
N86-11074
N86-11075
WEST, C. D. N86-10647
WEVER, H. N86-10231
WHALEN, M. V. N86-10279
WHITE, C. W. N86-10446
WHITEHORN, M. A. N86-10624
WHITEMAN, C. D. N86-10631
WHITSEL, R. N86-10792
WHITT, W. D. N86-10166
WHYMARK, R. R. N86-10177
WICHLACZ, P. L. N86-10736
WICKLAND, D. E. N86-10625
WIEDEMANN, K. E. N86-10310
WIEDEMEIER, H. N86-10068
N86-10069
WIEDERSICH, H. N86-11056
WIESNER, K. P. N86-10491
WIFFEN, F. W. N86-10329
WIGHTMAN, J. P. N86-10033
WIJNGAARD, J. N86-11073
N86-11075
WILCOX, W. R. N86-10070
N86-10071
WILDE, R. L. N86-10041
WILDUNG, R. R. N86-10684
WILKEN, D. N86-10031
WILLIAMS, F. A. N86-10165
WILLIAMS, F. L. N86-10300
WILLIAMS, J. G. N86-10383
WILLIAMS, R. J. N86-10178
WILLIAMS, W. N86-10354
WILLMORE, R. R. N86-10371
WILLNECKER, R. N86-10259
N86-10260
WINDSOR, M. F. N86-10695
WINELAND, D. J. N86-10295
WITHEROW, W. K. N86-10112
N86-10174
WITMER, G. W. N86-10636
WITT, A. F. N86-10056
N86-10072
WITTEN, C. S. D. N86-10797
WITTMANN, K. N86-10208
WOLZ, H. D. N86-10186
WONG, S. N86-10770
WOOD, G. W. N86-10042
WOODLE, M. H. N86-10933
WOODLEY, M. D. N86-11025
WOODS, S. N86-10524
WORDEN, P. W. N86-10171
WORDSWORTH, R. N86-10550
WOUTES, J. M. N86-10663
WRIGHT, B. L. N86-10989
WRIGHT, B. W. N86-10297
WRIGHT, K. A. R. N86-10623
WU, S. T. N86-10626
WUEST, W. N86-10237
WUETHRICH, C. N86-10308
WUKELIC, G. E. N86-10697

Y

YAKIMENKO, M. A. N86-10763
YAO, C. G. N86-11009
YASHINA, A. V. N86-10614
YEATES, C. M. N86-11137
YEFIMOVA, I. V. N86-10756
YEGOROV, V. M. N86-10610
YEH, J. T. N86-10661
YENCHO, S. N86-11012
YOSHIMURA, M. N86-10520
YOUNG, I. M. N86-10980
YU, L. H. N86-10647
YU, S. N86-10010
YUREK, G. N86-10158

Z

ZAGORSKAYA, Y. A. N86-10744
ZAPOLOTSKIY, D. Y. N86-10614
ZAVYALOV, A. I. N86-10755
ZEBKER, H. A. N86-10622
ZELL, M. N86-10250
ZERLETT, G. N86-10773
ZHANG, K. N86-10010
ZIELINSKI, A. E. N86-10354
ZIMMERLE, D. N86-10912
ZSIDISIN, G. N86-10354
ZVERKOVA, Y. Y. N86-10767

CORPORATE SOURCE INDEX

SCIENTIFIC AND TECHNICAL AEROSPACE REPORTS VOLUME 24 NUMBER 1

Typical Corporate Source Index Listing

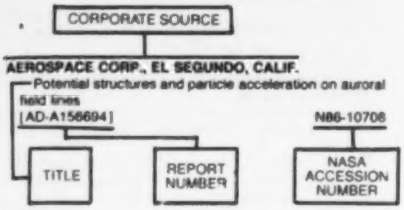
CORPORATE SOURCE
AEROSPACE CORP., EL SEGUNDO, CALIF.
Potential structures and particle acceleration on auroral field lines
[AD-A156694]
N86-10706
TITLE
REPORT NUMBER
NASA ACCESSION NUMBER

Listings in this index are arranged alphabetically by corporate source. The title of the document provides the user with a brief description of the subject matter. The report number helps to indicate the type of document cited (e.g., NASA report, translation, NASA contractor report). The NASA accession number denotes the number by which the citation is identified. The titles are arranged under each corporate source in ascending accession number order.

A

ACADEMY OF SCIENCES (USSR), MOSCOW.

Mathematical simulation of disturbing forces and material science processes under low gravity N86-10236

ADMIRALTY MARINE TECHNOLOGY ESTABLISHMENT, TEDDINGTON (ENGLAND).

The generation and transmission of vibration in plain cylindrical bearings. Part 2. Experiment [AD-A156577] N86-10553

ADVANCED ENGINEERING LAB., ADELAIDE (AUSTRALIA).

Specification for the performance, design, development and test requirements for a severe environment cartridge recorder. Issue 4 [AD-A156637] N86-10523

AERODYNE RESEARCH, INC., BILLERICA, MASS.

Experimental and theoretical analysis of chemical vapor deposition with prediction of gravity effects N86-10132

AERONAUTICAL RESEARCH LABS., MELBOURNE (AUSTRALIA).

A review of Australian investigations on aeronautical fatigue during the period April 1983 to March 1985 [AD-A156602] N86-10036

Report on an overseas visit [AD-A156603] N86-10037

Proposed modifications for the RAAF Airtrainer CT-4A cockpit [AD-A156806] N86-10039

A graphic anthropomatric aid for seating and workplace design [AD-A156988] N86-10788

AEROSPACE CORP., EL SEGUNDO, CALIF.

Potential structures and particle acceleration on auroral field lines [AD-A156694] N86-10706

AIR COMMAND AND STAFF COLL., MAXWELL AFB, ALA.

The dirigible: A catalyst for resource exploitation in remote areas? [AD-A156518] N86-10034

Retrofit of SAC EC-135C and RC-135 aircraft with CFM-56 engines [AD-A156688] N86-10038

The quest for a helicopter suitable for combat rescue, 1967 - 1983 [AD-A156842] N86-10040

An anthology: Rationale for a US ballistic missile defense (1969 - 1984) [AD-A156781] N86-10199

Rotary-wing operations in a microburst environment [AD-A156695] N86-10713

Let's get serious about software [AD-A156819] N86-10831

AIR FORCE INST. OF TECH., WRIGHT-PATTERSON AFB, OHIO.

Nonlinear methods for spacecraft attitude maneuvers [AD-A156956] N86-10275

Contact effects in light activated GaAs switches [AD-A156957] N86-10434

A transformation method for the evaluation of the response moments of elastic structures with random properties [AD-A156882] N86-10557

A composite climatological study of the frequency and distribution of severe weather associated with spring season Colorado cyclogenesis [AD-A156981] N86-10715

Mild hypoxia and visual performance with night vision goggles [AD-A156969] N86-10787

Applications for three-dimensional computer graphic cloud representations produced from satellite imagery [AD-A156903] N86-10798

Generation of flight paths using hierarchical planning [AD-A156905] N86-10900

AIR FORCE SYSTEMS COMMAND, WRIGHT-PATTERSON AFB, OHIO.

Acta Aeronautica et Astronautica Sinica (selected articles) [AD-A147304] N86-10001

Second order approximation method for transonic flows over swept wings N86-10002

A numerical solution of the shock-turbulent interaction over a compression corner for supersonic flow N86-10003

Optimum design of an aircraft wing structure with multiple constraints by the direct-vision criteria method N86-10004

Theoretical specific impulse for two-phase flow in nozzle of rocket-ramjet engine: A simple estimation method N86-10005

Three articles on new calculation methods in aeronautics (selected articles) [AD-A145745] N86-10007

Numerical solution of hypersonic flow near leading edge of a flat plate N86-10008

A new method for calculating unsteady supersonic aerodynamic forces and its application N86-10009

Effect of a shear layer on the stability of an axisymmetrical external compression air intake N86-10010

Comment on Determination of Aerodynamic Coefficients for a Reentry Body by Means of the Kalman Filter Method N86-10011

AKRON UNIV., OHIO.

Finite element analysis of metals at elevated temperature using unified constitutive theories N86-10569

ALABAMA A & M UNIV., NORMAL.

Solution growth of crystals in zero-gravity N86-10064

ALABAMA UNIV., BIRMINGHAM.

Theoretical analysis of Wolter/LSM X-ray telescope systems [NASA-CR-176244] N86-11095

ALABAMA UNIV., HUNTSVILLE.

Graphite formation in cast iron N86-10100

Direct observation of critical point wetting in microgravity N86-10116

New instrumentation for phase partitioning N86-10138

Cell partition in two polymer aqueous phases N86-10139

Application of the theory of Ostwald ripening to microgravity phase seperation experiments N86-10248

ALLIED BENDIX AEROSPACE, KANSAS CITY, MO.

Miniature radar packaging [DE85-014596] N86-10410

Software for an automated gaging system [DE85-013322] N86-10842

AMES LAB., IOWA.

Float zone experiments in space N86-10067

AMSTERDAM UNIV. (NETHERLANDS).

Variability analysis of visually induced responses in the midst of noise [B8564052] N86-10774

Mission orientation in science N86-11066

ANALYTICAL SERVICES AND MATERIALS, INC., TABB, VA.

A simple method of obtaining concentration depth-profiles from X-ray diffraction [NASA-CR-176262] N86-10310

ARGONNE NATIONAL LAB., ILL.

Portevin-Le Chatelier effect. 1: Model for the type-E serrations [DE85-006879] N86-10322

Souden 2 data acquisition and trigger electronics [DE85-013864] N86-10443

Approaches to cumulative impact assessment [DE85-013891] N86-10635

Advanced fuel cell development [DE85-014550] N86-10659

Chemical/hydrogen energy systems [DE85-012742] N86-10667

Development of the Multi-Attribute Hazard Assessment System (MAHAS) and its application to energy-related waste streams [DE85-010278] N86-10676

Computing the structural index [DE85-014370] N86-10871

Use of the MURA transformation to generate the fields and calculate the motion of protons in the designed Argonne Mini-ASPUN FFAG spiral sector accelerator [DE85-011477] N86-10934

The 20 keV undulators for a 6-GeV storage ring [DE85-013867] N86-10941

New particle searches [DE85-014073] N86-10942

Scoping studies of vapor behavior during a severe accident in a metal-fueling reactor [DE85-011474] N86-10952

Information on continuum states from feeding times and total (GAMMA) spectra measured with BGO suppressed detectors [DE85-013868] N86-10961

Beam stability in a 6 GeV synchrotron light source [DE85-013850] N86-10979

Performance of the H(-) ion source for the intense pulsed neutron source [DE85-012368] N86-10991

Experimental investigations of thermal radiation from potassium atoms and design applications [DE85-004086] N86-11036

Fermi surface study of CeSb in the ferromagnetic and antiferromagnetic phases [DE85-012122] N86-11052

Anelastic relaxation in irradiated Cu-Be [DE85-013893] N86-11056

ARIZONA STATE UNIV., TEMPE.

Energy stability of thermocapillary convection in models of the float zone process N86-10123

contemporary Aeolian processes on Mars: Local dust storms N86-11136

ARIZONA UNIV., TUCSON.

Hormone purification by isoelectric focusing N86-10135

Extraction of lanthanide ions by 2-methyl-8-quinolinol [DE85-ι .4277] N86-10303

Mean turbulence structure in strongly heating air flows N86-10455

Optical testing of large telescopes using multiple subapertures N86-10971

ARMAMENT DEVELOPMENT AND TEST CENTER, EGLIN AFB, FLA.

Dynamic analysis of a sled traveling along a rough rail [AD-A156589] N86-10191

ARMY ARMAMENT RESEARCH AND DEVELOPMENT COMMAND, DOVER, N. J.

EMACK railgun firing test report number 9 [AD-A156661] N86-10354

ARMY ENGINEER TOPOGRAPHIC LABS., FORT BELVOIR, VA.

Analysis of edge detection algorithms on DIAL (Digital Image Analysis Laboratory) [AD-A156735] N86-10630

ARMY MATERIALS AND MECHANICS RESEARCH CENTER, WATERTOWN, MASS.
Development of a sheath for sensor protection in molten steel applications
[AD-A156764] N86-10315

ARMY MILITARY PERSONNEL CENTER, ALEXANDRIA, VA.
Supervisory control of the right arm of the beam assembly teleoperator
[AD-A156856] N86-10832
The development of a neutron evaporation theory code for the thermal fission of Uranium-235
[AD-A156593] N86-10951

ARMY TEST AND EVALUATION COMMAND, ABERDEEN PROVING GROUND, MD.
Test, measurement, and diagnostic equipment (system peculiar)
[AD-A156669] N86-10563

ATLANTA UNIV., GA.
Theoretical investigation of electron-positive ion-atom interactions
[DE85-013019] N86-10939

ATMOSPHERIC AND ENVIRONMENTAL RESEARCH, INC., CAMBRIDGE, MASS.
Cometary atmospheres: Modeling the spatial distribution of observed neutral radicals
[NASA-CR-176242] N86-11133

B

BATTELLE COLUMBUS LABS., OHIO.
Research needs for corrosion control and prevention in energy conservation systems
[DE85-014852] N86-10326
Evaluation of Passive Sampling Devices (PSDs)
[PB85-196418] N86-10689

BATTELLE INST., FRANKFURT AM MAIN (WEST GERMANY).
Liquids and interfaces N86-10268

BATTELLE MEMORIAL INST., COLUMBUS, OHIO.
The influence of containerless undercooling and rapid solid-state quenching on the superconductive and magnetic properties of some clustering alloy systems
N86-10076

BJORKSTEN RESEARCH LABS., INC., MADISON, WIS.
Continuous fiberization of silicon-carbide-nitride precursor resin N86-10168
Levitating furnance for containerless processing in space N86-10169
Electric field containerless processing technology
N86-10170

BOLOGNA UNIV. (ITALY).
Melting and solidification in O-g of sintered alloys: Experiments ES 311 A and B bubble reinforced materials N86-10215

BONN UNIV. (WEST GERMANY).
Partial in-flight calibration of the metric camera
N86-10496

BONNEVILLE POWER ADMINISTRATION, PORTLAND, OREG.
Passive solar design handbook
[DE85-014263] N86-10656

BOSTON UNIV., MASS.
Gravitational collapse of a scalar field N86-11129

BRANDEIS UNIV., WALTHAM, MASS.
Radio studies of a complete sample of quasars
N86-11093

BRISTOL UNIV. (ENGLAND).
Kinetics of spreading of liquids in microgravity: Experiment 1 ES 327 N86-10207

BRITISH AEROSPACE AIRCRAFT GROUP, BRISTOL (ENGLAND).
Pre-bond treatment for titanium alloys
[BAE-AL/MAT/3864] N86-10309

BRITISH BROADCASTING CORP., KINGSWOOD (ENGLAND).
An evaluation of the use of microphone arrays for studio recording
[BBC-RD-1985/8] N86-10366

BROOKHAVEN NATIONAL LAB., UPTON, N. Y.
Streaming potentials in conductive and nonconductive tubing
[DE85-012964] N86-10438
Improved blue response and efficiency of A-Si:H solar cells deposited from disilane using a dual-chamber plasma system
[DE85-013289] N86-10649
Seasonal variations in atmospheric chemistry in the Adirondacks
[DE85-014227] N86-10719
Method for determining the position, angle and other injection parameters of a short pulsed beam in the Brookhaven AGS
[DE85-012523] N86-10931
Method for compensating bellows pressure loads while accommodating thermal deformations
[DE85-013306] N86-10933
AGS polarized H(-) source
[DE85-013296] N86-10935
Methane-bubble formation in hydrogen-charged Fe-30 ppM C
[DE85-012526] N86-10937
Beam profile monitor for the NSLS VUV ring employing linear photodiode arrays
[DE85-012184] N86-10947
Surface conditioning of synchrotron radiation source to improve beam lifetime
[DE84-012185] N86-10948
Seperated K(-) beams (10 GeV and above)
[DE85-012527] N86-10989
Microwave instability across the transition energy
[DE85-013304] N86-11010
Theory of non-planar orbits
[DE85-013284] N86-11018
Thermal and structural analysis of ring components by the finite element method
[DE85-013305] N86-11021
Unicell structure for superconducting storage rings
[DE85-013303] N86-11022
Tracking studies on the effects of magnet multipoles on the aperture of the RHIC heavy ion collider
[DE85-013282] N86-11023
RHIC lattice
[DE85-013289] N86-11026

BUNDESMINISTERIUM FUER FORSCHUNG UND TECHNOLOGIE, BONN (WEST GERMANY).
Satellite use for men N86-10180
How Antarctica was unveiled. Masterpieces of Frankfurt topographic surveyors. A part of the German Antarctica research program N86-10181
Satellite data even for a poultry farm. A development for Tanzania. Image evaluation following new ways
N86-10182
With Argus eyes from space. Satellite Diagnosis for Upper Volta. Seven maps without mystery N86-10183
The air of life of the blue planet. Atmosphere research from space using data and facts against climate speculations N86-10184
A nanosecond or thirty centimeters: Why atomic clocks have to be synchronized. MITREX opens new dimensions for measuring accuracy N86-10185
Growth of larger single crystals N86-10186
Space utilization N86-11067
Space sciences: Perspectives of commercial utilization for the German industry N86-11068
DFVLR, strategic study of astronautics 1984, user requirements N86-11069
Space research expenses of the Federal Ministry of Research and Technology (BMFT) in the period 1983-1985 N86-11070

BURNS AND ROE, INC., ORADELL, N. J.
Hot cell facility design for large fusion devices
[DE85-012893] N86-11037

C

CALIFORNIA INST. OF TECH., PASADENA.
Formation and characterization of amorphous erbium-based alloys prepared by near-isothermal cold-rolling of elemental composites
[DE85-014853] N86-10327
VLBI at optical and radio wavelengths: Congruences and contrasts N86-11126

CALIFORNIA UNIV., BERKELEY.
Free surface phenomena under low- and zero-gravity conditions N86-10108
A fundamental study of smoldering with emphasis on experimental design for zero-g N86-10162

CALIFORNIA UNIV., BERKELEY. LAWRENCE BERKELEY LAB.
Electronic and magnetic properties of noble-metal and transition-metal alloys, interfaces and overlayers
[DE85-014532] N86-10321
Defect identification in high-energy semiconductors
[DE85-014533] N86-10442
Effect of H2S and COS in the fuel gas on the performance of ambient pressure phosphoric acid fuel cells
[DE85-013913] N86-10446
Report on the engineering test of the LBL 30 second neutral beam source for the MFTF-B project
[DE85-013317] N86-10962
Integrating sphere measurements of directional-hemispherical transmittance of window systems
[DE85-013926] N86-10978
Superconvergent tracking and invariant surfaces in phase space
[DE85-013051] N86-10995
Proceedings of a Workshop on Electroweak Symmetry Breaking
[DE85-004444] N86-11008
Surface science and catalysis
[DE85-013922] N86-11057

CALIFORNIA UNIV., IRVINE, DAYTON, OHIO.
Evaluation of the 90-day inhalation toxicity of petroleum and oil shale JP-5 jet fuel
[AD-A156815] N86-10675

CALIFORNIA UNIV., LIVERMORE. LAWRENCE LIVERMORE LAB.
New directions in chemical analysis
[DE85-012930] N86-10296
Hugoniot measurements in aluminum to 420 GPa using the LLNL two-stage light-gas gun
[DE85-013821] N86-10317
Nonlinear propagation of elastoplastic waves in Ke penetrators (excerpts)
[DE85-011450] N86-10318
Work-hardening and effective viscosity in solid beryllium
[DE85-013978] N86-10323
Composite explosives for metal acceleration: The effect of detonation temperature
[DE85-013982] N86-10359
Microwave evaluation of materials
[DE85-013183] N86-10409
Angle of incidence effects for underwater shock using generic computational models
[DE85-012936] N86-10466
Angle of incidence effects for underwater shock using generic computational models, rev. 1
[DE85-012921] N86-10467
Spontaneous Raman spectroscopy of shocked H2O
[DE85-014557] N86-10470
Time-implicity simulation of particle-fluid systems
[DE85-012944] N86-10471
Improved particle-velocity transducer for equation-of-state experiments
[DE85-013204] N86-10532
Application of the ruthenium and technetium thermodynamic data bases used in the EQ3/6 geochemical codes
[DE85-013766] N86-10632
Smoke inputs to climate models: Optical properties and height distribution for nuclear winter studies
[DE85-011363] N86-10717
Microphysical/mesoscale aspects of nuclear winter and new directions in assessments
[DE85-013479] N86-10718
Somatic cell and molecular genetics approach to DNA repair and mutagenesis
[DE85-014181] N86-10737
New approach to multiphase equilibria: Application to high-pressure physics problems
[DE85-013820] N86-10907
Cryogenic structural materials for superconducting magnets
[DE85-008026] N86-10908
Mean life of the 2p(4)((1)S)3s (2)S state in fluorine
[DE85-012929] N86-10956
Impact of long-lived radionuclides on waste classification for fusion
[DE85-013205] N86-10959
Theoretical aspects of magnetic helicity
[DE85-011846] N86-10984
Compact torus compression of microwaves
[DE85-012919] N86-11016
Application of structural-mechanics methods to the design of large tandem-mirror fusion devices (MFTF-B)
[DE85-008960] N86-11017
Liquid to gas leak ratios with liquid nitrogen and liquid helium
[DE85-012950] N86-11030
Writer/editor and the computer
[DE85-011843] N86-11060
Stellar s-process diagnostics
[DE85-012926] N86-11134

CALIFORNIA UNIV., LOS ANGELES.
High temperature mechanical testing of a cylindrical weave carbon-carbon composite
[AD-A156639] N86-10591

CALIFORNIA UNIV., SAN DIEGO, LA JOLLA.
Particle cloud combustion experiment N86-10160

CALIFORNIA UNIV., SANTA BARBARA.
Theoretical problems in materials science
N86-10085
Paleontology and stratigraphy of Lower Cambrian and upper Proterozoic sediments, Caborca region, northwestern Sonora, Mexico N86-10692
Structural discontinuity within the southern California continental margin: Seismic and gravity models of the western Transverse Ranges N86-10699

CAMBRIDGE UNIV. (ENGLAND).
Astronomical criteria for interferometric arrays
N86-11099

CANADIAN ASTRONAUTICS LTD., OTTAWA (ONTARIO).
Numerical simulation of convections in the microgravity environment N86-10239

CARNEGIE-MELLON INST. OF RESEARCH, PITTSBURGH, PA.
Implementation issues for algorithmic VLSI (Very Large Scale Integration) processor arrays
[AD-A156699] N86-10432

CARNEGIE-MELLON UNIV., PITTSBURGH, PA.
Ignition and flame spread above liquid fuel pools N86-10163
Fault-free behavior of reliable multiprocessor systems: FTMP experiments in AIRLAB
[NASA-CR-177967] N86-10848
Two algorithms for weighted matroid intersection
[AD-A156525] N86-10861
Derivational analogy: A theory of reconstructive problem solving and expertise acquisition
[AD-A156817] N86-10899

CARNEGIE MUSEUM OF NATURAL HISTORY, PITTSBURGH, PA.
Paleogene vertebrate paleontology, geology and remote sensing in the Wind River Basin N86-10609

CARRIER CORP., SYRACUSE, N.Y.
Advanced absorption heat pump cycles
[DE85-003914] N86-10654

CASE WESTERN RESERVE UNIV., CLEVELAND, OHIO.
Solidification fundamentals N86-10090
Surface-tension driven convection N86-10124
Fundamental studies of low velocity impact resistance of graphite fiber reinforced polymer matrix composites N86-10288
Theoretical and numerical investigation of dipole radiation over a flat earth N86-10369
Finite element analysis of statics and dynamic structural engineering problems using semi-explicit methods N86-10571
Optimal control modeling of lower extremity musculoskeletal motion N86-10853

CENTER FOR MATHEMATICS AND COMPUTER SCIENCE, AMSTERDAM (NETHERLANDS).
Partial evolution and omega completeness of algebraic specifications
[CWI-CS-R8501] N86-10884

CENTRE D'ETUDES AERODYNAMIQUES ET THERMIQUES, POITIERS (FRANCE).
Spectral methods in adapted curved grids N86-10878

CENTRE D'ETUDES ET DE RECHERCHES GEODYNAMIQUES ET ASTRONOMIQUES, ST. VALLIER DE THIEY (FRANCE).
Results and limitations of ground-based optical arrays N86-11097
Strategy for the development of space arrays N86-11101
TRIO: A kilometric array stabilized by solar sails N86-11102
Fringe drift compensation in computer memory N86-11112
TRIANGLE: A different design for a three satellite interferometer in space N86-11113
Problems in image reconstruction with optical arrays N86-11115
On line astronomical image processing using microcomputers N86-11121
The intensified multi CCD camera N86-11122
The DUO: Far infrared heterodyne concept for space interferometry N86-11125

CENTRE NATIONAL D'ETUDES SPATIALES, TOULOUSE (FRANCE).
Gradient heating facility behavior N86-10217

CENTRE NATIONAL DE LA RECHERCHE SCIENTIFIQUE, MARSEILLES (FRANCE).
TRIO optics N86-1110
Soler propulsion for the TRIO interferometer N86-11109
TRIO interferometer positioning N86-11111

CENTRE NATIONAL DE LA RECHERCHE SCIENTIFIQUE, MEUDON-BELLEVUE (FRANCE).
Oscillations of semi-free liquids in microgravity: Spacelab 1 experiment ES 326 N86-10204
Lead telluride crystals grown in microgravity: Experiment ES 318 N86-10220

CENTRE NATIONAL DE LA RECHERCHE SCIENTIFIQUE, TOULOUSE (FRANCE).
Aperture synthesis with or without phase information for kilometric arrays interpolation algorithms for stabilized image reconstruction N86-11124

CENTRE NATIONAL DE LA RECHERCHE SCIENTIFIQUE, VERRIERES-LE BUISSON (FRANCE).
A fiber-linked version of project TRIO N86-11105

CENTRONIC LTD., CROYDON (ENGLAND).
Making the right choice N86-10669

CESKOSLOVENSKA AKADEMIE VED, PRAGUE.
Experimental facility for materials research in space (CSK-1) N86-10263

CHALMERS UNIV. OF TECHNOLOGY, GOTEBORG (SWEDEN).
Error estimates and automatic time step control for numerical methods for stiff ordinary differential equations
[CTH-MATH-1984-27] N86-10872
On the absolute continuity of elliptic measures
[CTH-MATH-1984-28] N86-10873
Estimates for maximal functions along hypersurfaces
[CTH-MATH-1984-29] N86-10874
On maximal and distributional coupling
[CTH-MATH-1984-30] N86-10875
Poisson semigroups and singular integrals
[CTH-MATH-1985-05] N86-10876
Brauer-Severi schemes of orders
[CTH-MATH-1985-06] N86-10877
Some remarks about cusp forms: Holomorphic and non-holomorphic
[CTH-MATH-1984-26] N86-10902
On class groups of lattices
[CTH-MATH-1985-08] N86-10903
Galois descent and class groups of orders
[CTH-MATH-1985-09] N86-10904

CHRONAR CORP., PRINCETON, N.J.
Photovoltaic devices using a Si:H from higher order silanes
[DE85-008804] N86-10668

CITY UNIV. OF NEW YORK, N.Y.
Magnetic properties of doped semiconductors
[DE85-012090] N86-11053

CLARKSON COLL. OF TECHNOLOGY, POTSDAM, N.Y.
Study of eutectic formation N86-10070
Modeling directional solidification N86-10071
Physical phenomena in containerless glass processing N86-10155

CLEMSON UNIV., S.C.
An analytical and numerical study of the buckling behavior of fiber-reinforced beams N86-10566

COASTAL ENGINEERING RESEARCH CENTER, VICKSBURG, MISS.
Application of the dutch method for estimating storm-induced dune erosion
[AD-A156717] N86-10728

COLLEGE OF WILLIAM AND MARY, WILLIAMSBURG, VA.
Study of statis and dynamic stress effects in nonlinear solids
[NASA-CR-176236] N86-10578

COLORADO UNIV., BOULDER.
Thermocapillary and diffusocapillary migration of a fluid drop N86-10128
Compexity of higher-order programs
[DE85-012776] N86-10834

COLUMBIA UNIV., NEW YORK.
A procedure identifying a polyacetylene initiator of olefin metathesis. The reactivities of metal-carbenes toward alkenes and alkynes
[AD-A156997] N86-10283
Fundamental study of the closure property of joints N86-10698
In-situ geophysical investigations into the nature of the oceanic crust N86-10725
A quantitative method for analyzing the roughness of the seafloor N86-10726
A superconducting tunnel junction receiver for millimeter-wave astronomy N86-11041

COMMISSARIAT A L'ENERGIE ATOMIQUE, GRENOBLE (FRANCE).
Mephisto: Interfacial destabilization in metal alloys N86-10079
Directional solidification of monotectic and hypermonotectic aluminum-indium alloys under micron-g N86-10097
Directional solidification of an aluminum-zinc vapor emulsion in microgravity N86-10218
Directional solidification of eutectic alloys N86-10219
Thermomigration of cobalt in liquid tin: Experiment 1 ES 320 N86-10222
Cellular morphologies in lead-thallium alloys N86-10262
First Spacelab Payload (FSLP) experiments in metallurgy N86-10266

COMMITTEE ON ENERGY AND COMMERCE (U. S. HOUSE).
Biotechnology regulation
[GPO-43-778] N86-10733

CONCORDIA UNIV., MONTREAL (QUEBEC).
Chemical kinetics and cellular structure of detonations in hydrogen sulphide and air
[DE85-009408] N86-10304

CONSERVATION AND RENEWABLE ENERGY INQUIRY AND REFERRAL SERVICE, SILVER SPRING, MD.
Geothermal Energy Technology Program summary
[DE85-013101] N86-10646
Passive and hybrid solar technologies program summary
[DE85-013100] N86-10648
Ocean energy technology program summary
[DE85-013102] N86-10731

D

DARTMOUTH COLL., HANOVER, N.H.
Analysis of annular two-phase flow with liquid entrainment N86-10459

DAYTON UNIV., OHIO.
Process models for 3D composites
[AD-A156869] N86-10292

DEERE AND CO., MOLINE, ILL.
Control of cast iron microstructure N86-10084

DEFENCE RESEARCH ESTABLISHMENT, OTTAWA (ONTARIO).
SARSAT LUC (Local user terminal) to CMCC (Canadian Mission Control Centre) alert data interface: A critical review
[AD-A156681] N86-10276
Design and calibration of a flat-flame burner using line reversal techniques
[AD-A156724] N86-10294
Effect of increased body clothing insulation on hand temperature in a cold environment
[AD-A156597] N86-10786

DEFENCE RESEARCH ESTABLISHMENT VALCARTIER (QUEBEC).
An active tracking band-pass filter
[AD-A156559] N86-10419
Acceleration-invariant approximation method for recursive digital filters
[AD-A156655] N86-10865

DELAWARE UNIV., NEWARK.
Mechanics of coated fiber composites N86-10285
The interpolation of signals sampled at less than the Nyquist rate N86-10368

DELFT HYDRAULICS LAB. (NETHERLANDS).
The Rhine-Meuse estuary hydraulic scale model. Experiences with computer configuration and software
[PUBL-335] N86-10637

DEPARTMENT OF ENERGY, ARGONNE, ILL.
Evaluation of the International Atomic Energy Agency (IAEA) Safeguards Analytical Laboratory quality assurance program
[DE85-012078] N86-10953

DEPARTMENT OF ENERGY, OAK RIDGE, TENN.
Computer codes: A bibliography, supplement 1
[DE85-008721] N86-10638

DEPARTMENT OF ENERGY, PITTSBURGH, PA.
Microcomputer aided calculations of parameters for spray dryer operation
[DE85-013468] N86-10681

DEPARTMENT OF ENERGY, WASHINGTON, D. C.
Counterpulse railgun energy recovery circuit
[DE85-011603] N86-10196
Overpulse railgun energy recovery circuit
[DE85-011607] N86-10197
Aluminum battery alloys
[DE85-011599] N86-10445

DEPARTMENT OF THE AIR FORCE, WASHINGTON, D.C.
Submerged ram air inlets for ECM (electronic countermeasures) pods
[AD-D011801] N86-10020
Attachment method-ceramic radome to metal body
[AD-D011778] N86-10032
Small cartridge heater
[AD-D011784] N86-10277
Erosion-resistant nosetip construction
[AD-D011787] N86-10289
Liquid crystal non-destructive inspection of metals
[AD-D011772] N86-10316
Synthesis of arylene siloxanylene polymers and copolymers
[AD-D011780] N86-10338
Gas generator fuel flow throttle control system
[AD-D011797] N86-10355
Angle set-on apparatus
[AD-D011766] N86-10371
Method for tuning a phased array antenna
[AD-D011768] N86-10372
High sensitivity millimeter-wave measurement apparatus
[AD-D011786] N86-10373
Sample data phase locked loop for adaptive Doppler tracker
[AD-D011788] N86-10374
Protection circuitry for high voltage drivers
[AD-D011781] N86-10414
Total internal reflection modulator/deflector
[AD-D011757] N86-10424

Instantaneous frequency measurement receiver with digital processing
[AD-D011759] N86-10425

Photoionization technique for growth of metallic films
[AD-D011760] N86-10426

Signal analysis receiver with acousto-optic delay lines
[AD-D011761] N86-10427

Apparatus for locating passive intermodulation interference sources
[AD-D011798] N86-10435

Interdigital Schottky barrier capacitor apparatus
[AD-D011799] N86-10436

Multi-row connector with ground plane board
[AD-D011803] N86-10437

Sensor system
[AD-D011767] N86-10460

Stereoscopic video imagery generation
[AD-D011785] N86-10481

Fall velocity indicator/viewer
[AD-D011789] N86-10482

Captive volume device as a safe life monitor
[AD-D011802] N86-10525

Laser target speckle eliminator
[AD-D011775] N86-10536

Over-center toggle latch
[AD-D011753] N86-10556

Termination load carrying device
[AD-D011800] N86-10558

Nickel-cadmium battery conditioner and tester apparatus
[AD-D011770] N86-10642

Multiple site laser excited pollution monitoring system
[AD-D011769] N86-10674

Vision test chart and method using Gaussians
[AD-D011756] N86-10778

Harmonic distortion reduction technique for data acquisition
[AD-D011771] N86-10799

Arithmetic pipeline for image processing
[AD-D011773] N86-10800

Infrared system with computerized image display
[AD-D011777] N86-10906

Tunable acousto-optic filter with improved spectral resolution and increased aperture
[AD-D011758] N86-10915

Kalman filter preprocessor
[AD-D011774] N86-10972

Measurement of visual contrast sensitivity
[AD-D011776] N86-10973

Optical disc transport system
[AD-D011779] N86-10974

DEPARTMENT OF THE ARMY, WASHINGTON, D. C.

Recovery of alcohol from a fermentation source by separation rather than distillation
[AD-D011782] N86-10282

DEPARTMENT OF THE NAVY, WASHINGTON, D. C.

Improved arresting and recovery system for test missiles
[AD-D011743] N86-10198

Rusty bolt intermodulation interference reducer
[AD-D011748] N86-10313

Passivation of steel with aqueous amine solutions
[AD-D011749] N86-10314

Phase-coded pulse expander-compressor
[AD-D011812] N86-10375

Phase coded pulse expander-compressor
[AD-D011817] N86-10376

Amplitude and phase modulation in fin-lines electrical tuning
[AD-D011813] N86-10415

P-N junction controlled field emitter array cathode
[AD-D011815] N86-10416

Pulse compression system
[AD-D011833] N86-10417

Constant rise AGC (Automatic Gain Control) device
[AD-D011744] N86-10421

Extended precision in video bandwidth analog to digital converter using optical techniques
[AD-D011745] N86-10422

High output programmable signal current source for low output impedance applications
[AD-D011751] N86-10423

Precise bearing support ditherer with piezoelectric drive means
[AD-D011819] N86-10483

Device for cryogenically fabricating source material for plasma X-ray lasers
[AD-D011814] N86-10537

W-shaped diffused stripe GaAs/AlGaAs laser
[AD-D011818] N86-10538

AIRBOC (air rapid bloom offboard chaff) chaff deployment system
[AD-D011746] N86-10554

Marginal terrain straddle-lift container handler
[AD-D011752] N86-10555

Parallel local interface bus
[AD-D011742] N86-10792

Spatial frequency multiplexed coherent optical processor for calculating generalized moments
[AD-D011816] N86-10975

Fiber optic system for measuring electric fields
[AD-D011830] N86-10976

DEUTSCHE FORSCHUNGS- UND VERSUCHSANSTALT FUER LUFT- UND RAUMFAHRT, BRUNSWICK (WEST GERMANY).

Control concepts for in-flight simulation including actuator nonlinearities and time delays
[DFVLR-FB-85-24] N86-10047

DEUTSCHE FORSCHUNGS- UND VERSUCHSANSTALT FUER LUFT- UND RAUMFAHRT, COLOGNE (WEST GERMANY).

Tendencies toward liberalization in European air traffic control
[DFVLR-FB-85-23] N86-10030

The air traffic demand in passenger travel of the Federal Republic of Germany 1990 - 2000. Update of the DFVLR air traffic forecast
[DFVLR-MITT-85-05] N86-10031

The first German Spacelab mission D1 reports
[PR-1] N86-10187

The first German Spacelab mission D1 reports
[PR-2] N86-10188

The first German Spacelab mission D1 reports
[PR-3] N86-10189

The isothermal heating facility N86-10206

Holographic interferometry near gas/liquid critical points. Ground-based study of a D1 experiment N86-10249

Transport processes in directional solidification during space shuttle flight N86-10257

Stability of metallic dispersions N86-10258

Undercooling investigations on the easy glass former Pd-Cu-Si N86-10259

Containerless undercooling of Ni N86-10260

Status of preparation activities for metric camera reflight on EOM-1/2 N86-10506

DEUTSCHE FORSCHUNGS- UND VERSUCHSANSTALT FUER LUFT- UND RAUMFAHRT, GOETTINGEN (WEST GERMANY).

Investigations on a supercritical airfoil with boundary layer suction through a perforated strip in the shock region
[DFVLR-FB-85-15] N86-10025

Experimental and theoretical investigations of the flow around airfoil systems with ground effect
[DFVLR-FB-85-17] N86-10026

Investigation of density gradient fluctuations in a turbulent free jet by means of the laser schlieren crossed-beam method
[DFVLR-FB-85-19] N86-10027

The rubber tube test section of the DFVLR in Goettingen, West Germany
[DFVLR-FB-85-18] N86-10051

DEUTSCHE FORSCHUNGS- UND VERSUCHSANSTALT FUER LUFT- UND RAUMFAHRT, HAMBURG (WEST GERMANY).

Extended analysis of the structure of error scores in psychological aptitude tests
[DFVLR-FB-85-20] N86-10780

Speed of work and error rate: Analyses of individual differences in a choice reaction series with a cognitive component
[DFVLR-FB-85-21] N86-10781

DEUTSCHE FORSCHUNGS- UND VERSUCHSANSTALT FUER LUFT- UND RAUMFAHRT, OBERPFAFFENHOFEN (WEST GERMANY).

Direct-coupled cavity filters with irises of arbitrary thickness
[DFVLR-FB-85-14] N86-10412

SAR image quality: A review
[DFVLR-MITT-85-07] N86-10413

Line mapping and resolution tests with metric camera data N86-10500

Experimental investigations of pulse-pulse interference in heterodyne detection
[DFVLR-FB-85-26] N86-10544

Calibration of the multispectral scanner (MSS) satellite data to evaluate change in the reflection of coniferous stocks
[DFVLR-FB-84-44] N86-10636

Airborne measurements of the border-crossing air pollution in the area between Weiden and Hof/Bavaria
[DFVLR-FB-85-25] N86-10685

Comparative flight measurement of icing parameters for the propeller aircraft Do-28D2 of the test station 61 of the DFVLR and for the DFVLR aircraft Falon 20e in stratus clouds
[DFVLR-FB-85-16] N86-10720

User manual for the Falcon system
[DFVLR-MITT-85-08] N86-10721

Scattering by complicated structures: Calculation of the radar properties of metallic targets by means of physical optics
[DFVLR-FB-85-22] N86-10981

DEUTSCHE GOLD- UND SILBER-SCHEIDEANSTALT, FRANKFURT AM MAIN (WEST GERMANY).

Reduction of noble metal stock and noble metal loss during wire production with the Conform extrusion process
[BMFT-FB-T-85-049] N86-10560

DU PONT DE NEMOURS (E. I.) AND CO., AIKEN, S.C.

Multipurpose pan development
[DE85-012326] N86-10319

Recirculation within a glass mixture subjected to external and resistive heating
[DE85-010088] N86-10348

DUKE UNIV., DURHAM, N. C.

Critical transport phenomena in fluid helium under low gravity N86-10119

E

ECOLE POLYTECHNIQUE FEDERALE DE LAUSANNE (SWITZERLAND).

Erosion control and watershed management by Spacelab photography N86-10493

EDGERTON, GERMESHAUSEN AND GRIER, INC., GOLETA, CALIF.

HgI sub 2 crystal growth for nuclear detectors N86-10066

Parallel pulse processing for mercuric iodide gamma-ray detectors
[DE85-013391] N86-10528

EDGERTON, GERMESHAUSEN AND GRIER, INC., IDAHO FALLS, IDAHO.

Fracture toughness and stress relief response of irradiated type 347/348 stainless steel N86-10320

Velocities of gas and plasmas from real time holographic interograms
[DE85-014618] N86-10530

Kinetics of biological ferrous iron oxidation
[DE85-014616] N86-10736

EIDGENOESSISCHE TECHNISCHE HOCHSCHULE, ZURICH (SWITZERLAND).

Crystal growth from solutions and nucleation from the vapor phase N86-10267

EIDGENOESSISCHES FLUGZEUGWERK, EMMEN (SWITZERLAND).

Investigations to improve the slotted-wall test section of the F+W transonic wind tunnel
[F+W-FO-1752] N86-10050

ELECTRONICS RESEARCH LAB., ADELAIDE (AUSTRALIA).

A compact bulk acousto-optic time integrating correlator
[AD-A158606] N86-10428

ELORET CORP., SUNNYVALE, CALIF.

The interaction of small metal particles with refractory oxide supports
[NASA-CR-176228] N86-11047

ENGINEERING-SCIENCE, INC., FAIRFAX, VA.

Emissions of NOx, SOx and VOC from Antropogenic sources
[PB85-193530] N86-10686

ENVIRONMENTAL PROTECTION AGENCY, RESEARCH TRIANGLE PARK, N.C.

Volatile organic compounds in indoor air: A survey of various structures
[PB85-198356] N86-10687

ERLANGEN-NUREMBERG UNIV. (WEST GERMANY).

Directional solidification of InSb-NiSb eutectic N86-10221

Imaging speckle interferometer in space: Digital simulations of image reconstruction and photon noise N86-11120

ESDU INTERNATIONAL LTD., LONDON (ENGLAND).

Summary of work on jet noise prediction
[ESDU-BR-62636] N86-10909

EUROPEAN ORGANIZATION FOR NUCLEAR RESEARCH, GENEVA (SWITZERLAND).

Applications of the second-order achromat concept to the design of particle accelerators
[DE85-013072] N86-10994

EUROPEAN SOUTHERN OBSERVATORY, MUNICH (WEST GERMANY).

Activities report of the European Southern Observatory N86-11135

EUROPEAN SPACE AGENCY, PARIS (FRANCE).

System modeling and identification of equivalent systems with and without compensating time delay for control-augmented aircraft
[ESA-TT-852] N86-10043

Fifth European symposium on Material Sciences under Microgravity. Results of Spacelab 1
[ESA-SP-222] N86-10200

First Spacelab Payload (FSLP) experiments on composite materials N86-10265

Low temperature plastic deformation mechanisms of alpha-titanium single crystals
[ESA-TT-871] N86-10332

Metric Camera Workshop
[ESA-SP-209] N86-10485

Colloquium on Kilometric Optical Arrays in Space
[ESA-SP-226] N86-11096

EUROPEAN SPACE AGENCY. EUROPEAN SPACE OPERATIONS CENTER, DARMSTADT (WEST GERMANY).

Mission analysis aspects N86-11114

EUROPEAN SPACE AGENCY. EUROPEAN SPACE RESEARCH AND TECHNOLOGY CENTER, ESTEC, NOORDWIJK (NETHERLANDS).

The fluid physics module: A technical description N86-10201

Preliminary studies of a spinning tether-connected TRIO concept N86-11110

EXECUTIVE OFFICE OF THE PRESIDENT, WASHINGTON, D. C.

Publication of the Executive Office of the President, January 20, 1981 - December 31, 1984
[PB85-187110] N86-11082

EXXON RESEARCH AND ENGINEERING CO., ANNANDALE, N.J.

Laser Raman spectroscopy study of the zinc and bromide ion complex equilibrium in zinc/bromine battery electrolytes
[DE85-011820] N86-10301

F

FACHHOCHSCHULE, GIESSEN (WEST GERMANY).

Contribution of wind energy to the energy balance of a combined solar and wind energy system. Part 1: System description, data acquisition and system performance
[BMFT-FB-T-85-051-VOL-1] N86-10670

FEDERAL AVIATION ADMINISTRATION, WASHINGTON, D.C.

The effects of age, sleep deprivation, and altitude on complex performance
[AD-A156987] N86-10771

FEDERATION OF AMERICAN SOCIETIES FOR EXPERIMENTAL BIOLOGY, BETHESDA, MD.

LSRO/ONR ad hoc review process
[AD-A156590] N86-10735

FERMI NATIONAL ACCELERATOR LAB., BATAVIA, ILL.

Hyperon polarization: An unresolved problem
[DE85-012298] N86-10946

Field-independent normalization of SSC Collider Ring costs
[DE85-012425] N86-10997

FLORIDA UNIV., GAINESVILLE.

Research on solar pumped liquid lasers
[NASA-CR-176235] N86-10539

Analytical and experimental study of cracks emanating from an elliptical hole in unidirectional composite material N86-10567

Inelastic analysis of frame structures including member and joint shears N86-10573

FOM-INST. VOOR PLASMAFYSICA, RIJNHUIZEN, JUTPHAAS (NETHERLANDS).

Activities report in plasma physics N86-11039

FRAUNHOFER-INST. FUER BETRIEBSFESTIGKEIT, DARMSTADT (WEST GERMANY).

Review of investigations on aeronautical fatigue in the Federal Republic of Germany
[LBF-S-173] N86-10044

FRAUNHOFER INST. FUER WERKSTOFFMECHANIK, FREIBURG (WEST GERMANY).

Numerical simulation of crack arrest experiments on Araldite B using the finite difference method
[REPT-W-9/82] N86-10596

FREIBURG UNIV. (WEST GERMANY).

The mirror heating facility: Performance and experiences N86-10223

Solution growth of cadmium telluride: Experiment ES 322 N86-10225

Crystal growth of silicon in Spacelab 1: Experiment ES-321 N86-10227

Protein single crystal growth under microgravity N86-10226

Requirements and possibilities of Spacelab metric camera photos usage for inventories of large areas of extensively managed forests N86-10513

G

GA TECHNOLOGIES, INC., SAN DIEGO, CALIF.

High efficiency heat transport and power conversion system for cascade
[DE85-012959] N86-10468

GA Theory News, January-March 1985
[DE85-012572] N86-11007

GARRETT MFG. LTD., REXDALE (ONTARIO).

Advanced Gas Turbine (AGT) powertrain system development for automotive applications report
[NASA-CR-174886] N86-11087

GELLES (S. H.) ASSOCIATES, COLUMBUS, OHIO.

Liquid phase miscibility gap materials N86-10061

Space shuttle experiments on Al-In liquid phase miscibility gap (LPMG) alloys N86-10264

GENERAL ELECTRIC CO., PHILADELPHIA, PA.

Modification of the electromagnetic levitator (EML) hardware N86-10172

GEOLOGICAL SURVEY, RESTON, VA.

High-resolution image data from the Space Shuttle N86-10494

SUTRA (Saturated-unsaturated transport). A finite-element simulation model for saturated-unsaturated, Fluid-Density-Dependent ground-water flow with energy transport or chemically-reactive single-species solute transport
[AD-A156779] N86-10830

GEOLOGICAL SURVEY, SIOUX FALLS, S. DAK.

Some opinions on remote sensing and geologic studies N86-10600

GEOLOGICAL SURVEY OF CANADA, OTTAWA (ONTARIO).

NBSGSC: A FORTRAN program for quantitative X-ray fluorescence analysis
[PB85-206068] N86-10847

GEORGE MASON UNIV., FAIRFAX, VA.

An annotated bibliography of abstracts on the use of simulators in technical training
[AD-A156792] N86-11065

GEORGE WASHINGTON UNIV., WASHINGTON, D.C.

Suppression of Marangoni convection in float zones N86-10111

GEORGIA INST. OF TECH., ATLANTA.

A study of the aerodynamic performance of Weis-Fogh wings N86-10012

The effect of debond growth on crack propagation in composite plates reinforced with adhesively bonded composite stringers N86-10287

Steady state frictional behavior of thin film coatings N86-10335

The measurement and application of transport properties of ion swarms in gases N86-10370

Angle of incidence effects for underwater shock using generic computational models
[DE85-012936] N86-10466

Angle of incidence effects for underwater shock using generic computational models, rev. 1
[DE85-012921] N86-10467

The use of new path independent integrals in elastic-plastic and creep fracture N86-10574

Analysis of large, non-isothermal elastic-visco-plastic deformations
[NASA-CR-176220] N86-10586

Bounding solutions of geometrically nonlinear viscoelastic problems
[NASA-CR-176219] N86-10860

Development and application of the electrochemical etching technique
[DE85-010302] N86-10957

GERMAN-DUTCH WIND TUNNEL, NORTH EAST POLDER (NETHERLANDS).

Activities report of the German-Dutch wind tunnel N86-10029

Activities report of the German-Dutch wind tunnel N86-10052

GESAMTHOCHSCHULE, ESSEN (WEST GERMANY).

Verification of turbulence developing from the oscillatory Marangoni convection in a liquid column N86-10241

GESELLSCHAFT FUER SCHWERIONENFORSCHUNG M.B.H., DARMSTADT (WEST GERMANY).

Information on continuum states from feeding times and total (GAMMA) spectra measured with BGO suppressed detectors
[DE85-013888] N86-10961

GIESSEN UNIV. (WEST GERMANY).

Measurements of the critical Marangoni number of the laminar-oscillatory transition of thermocapillary convection in floating zones N86-10242

GKSS-FORSCHUNGSZENTRUM GEESTHACHT (WEST GERMANY).

The boundary condition in a numerical model of atmospheric flows over fixed interfaces
[GKSS-85-E-10] N86-10722

GOETTINGEN UNIV. (WEST GERMANY).

The influence of thermocapillarity on the migration of droplets in a liquid possessing a uniform temperature gradient N86-10237

GRONINGEN RIJKSUNIVERSITEIT (NETHERLANDS).

Wind energy in agriculture, a promise
[SS-45] N86-10672

Wind energy, a feasibility investigation for wind mills in agriculture
[SS-45A] N86-10673

A modified Successive Over-Relaxation (SOR) method for the Poisson equation in unsteady free-surface flow calculations
[TW-264] N86-10891

On the numerical determination of the dimension of an attractor
[ZW-8415] N86-10892

A note on the differenciability of center manifolds
[ZW-8414] N86-10905

The OASIS correlator N86-11119

GRUMMAN AEROSPACE CORP., BETHPAGE, N.Y.

Orbital processing of aligned magnetic composites N86-10089

Thermal and solutal convection damping using an applied magnetic field N86-10094

H

HAMBURG UNIV. (WEST GERMANY).

Influences affecting separation in monotectic alloys under microgravity N86-10209

HARVARD-SMITHSONIAN CENTER FOR ASTROPHYSICS, CAMBRIDGE, MASS.

COSMIC: A high resolution, large collecting area telescope N86-11104

Numerical experiments in image reconstruction N86-11116

COSMIC image reconstruction N86-11118

HARVARD UNIV., CAMBRIDGE, MASS.

Bulk formation of metallic glasses and amorphous silicon from the melt N86-10154

Crystal nucleation and glass formation in metallic alloy melts N86-10233

Topics in the electronic theory of disordered semiconductors N86-11045

HASKONING, CONSULTING ENGINEERS, NIJMEGEN (NETHERLANDS).

Utilization of satellite remote sensing for the monitoring of oil pollution and marine ecosystems in Indonesia. A Tropical Earth Resources Satellite program (TERS) case study implemented for the NLR, Delft N86-10640

HAUPTVERBAND DER GEWERBLICHEN BERUFSGENOSSENSCHAFTEN, E. V., BONN (WEST GERMANY).

Report on the research activities on whole-body vibrations. Human strain due to mechanical vibrations
[ISBN-3-88383-107-7] N86-10773

HAWAII UNIV., HONOLULU.

Position paper: Workshop on Geologic Applications of Remote Sensing to the Study of Sedimentary Basins N86-10601

A boundary layer flow model for areas of complex terrain N86-10701

HEIDELBERG UNIV. (WEST GERMANY).

Photomapping in different climatic zones N86-10491

HELLER (JEAN), LOS ALAMOS, N. MEX.

Properties of plastic-bonded nitroguanidine
[DE85-015316] N86-10356

Type of new Chinese-produced high-speed camera and its utilization in detonation physics experiments
[DE85-015191] N86-10529

HOCHSCHULE DER BUNDESWEHR, MUNICH (WEST GERMANY).

Oscillations of a viscoelastic liquid drop in zero-gravity N86-10240

HOSEI UNIV., TOKYO (JAPAN).

An example of single model orientation of metric camera stereophotographs N86-10520

HOUSTON UNIV., TEX.

Effect of undercooling and modified microstructure on the physical properties of material synthesized in the drop tube and drop tower N86-10075

HUMAN ENGINEERING LABS., ABERDEEN PROVING GROUND, MD.

Proposed aural nondetectability limits for Army materiel
[AD-A156704] N86-10917

I

IBM RESEARCH LAB., SAN JOSE, CALIF.

Characterization of vapor and aerosol flows by photothermal methods
[AD-A156601] N86-10465

Time resolved flow velocity and concentration measurements using a travelling thermal lens
[AD-A156706] N86-10541

Optical detection of photoacoustic pulses in thin silicon wafers
[AD-A156705] N86-10977

IBM RESEARCH LAB., YORKTOWN HEIGHTS, N. Y.
Thermodynamic constraints on ion beam mixing of metals on insulators [DE85-013628] N86-10448
IDAHO NATIONAL ENGINEERING LAB., IDAHO FALLS.
On-line gamma-ray data acquisition at the Power Burst facility [DE85-011957] N86-10954
IIT RESEARCH INST., ROME, N.Y.
Catalog of Resources for Education in Ada (trademark) and Software Engineering (CREASE). Version 3.0 [AD-A156687] N86-10790
ILLINOIS INST. OF TECH., CHICAGO.
Free carrier absorption from electrons in confined systems N86-11042
ILLINOIS UNIV., CHICAGO.
Three-dimensional stress singularities in anisotropic materials and composites N86-10286
Optimal design of portal frames against buckling N86-10572
ILLINOIS UNIV., URBANA.
Flammability limits of gases under low gravity conditions N86-10164
Numerical methods for analyzing electromagnetic scattering [NASA-CR-176141] N86-10377
Anelastic relaxation in irradiated Cu-Be [DE85-013893] N86-11056
ILLINOIS UNIV., URBANA-CHAMPAIGN.
Semiconductor superlattic photodetectors [NASA-CR-176249] N86-10484
IMPERIAL METAL INDUSTRIES LTD., KIDDERMINSTER (ENGLAND).
Carbon fiber reinforced polymide filament wound tube manufacturing [BR64172] N86-10339
INDIAN INST. OF SCIENCE, BANGALORE.
Recent advances in the analysis of exhaust mufflers N86-10587
INDIAN SPACE RESEARCH ORGANIZATION, AHMEDABAD.
Creation of Ground Control Points (GCP) library using ESA Spacelab metric camera imagery N86-10516
INFORMATICS, INC., PALO ALTO, CALIF.
LANES 1 Users' Guide [NASA-CR-177334] N86-10819
INFORMATION SPECTRUM, INC., ARLINGTON, VA.
F-16X MSIP (Multi-national Staged Improvement Program) case example: Operating and support cost estimation using VAMOSC (Visibility And Management Of Operating and Support Costs) [AD-A156893] N86-10006
INSTITUT GEOGRAPHIQUE NATIONAL, PARIS (FRANCE).
Identification of planimetric features from the metric camera N86-10497
Thematic investigations in France based on metric camera imagery N86-10509
INSTITUTE FOR DEFENSE ANALYSES, ALEXANDRIA, VA.
Ada (trademark) Programming Support Environment (APSE) Evaluation and Validation (E and V) workshop report held at Airlie, Virginia on 2-6 April 1984 [AD-A156667] N86-10829
Report of the ad hoc committee to review the program of the SDI Directorate on Innovative Science and Technology (IST) [AD-A156668] N86-11071
INSTITUTE FOR PERCEPTION RVO-TNO, SOESTERBERG (NETHERLANDS).
Studies on human vehicle control [B8563352] N86-10775
Car driving as a supervisory control task [B8563351] N86-10776
Standardization of tasks: Approach planning [IZF-1984-19] N86-10782
Path error-neglection in straight lane driving [IZF-1984-32] N86-10783
The wearing comfort of the PVC: Combat back pack [IZF-1984-34] N86-10789
Risk propensity, action readiness and the roles of societal and individual decision makers [IZF-1984-27] N86-11077
INSTITUTE OF GAS TECHNOLOGY, CHICAGO, ILL.
Effects of H2S on molten carbonate fuel cells [DE85-014052] N86-10447
INSTITUUT TNO VOOR BOUWMATERIALEN EN BOUWCONSTRUCTIES, DELFT (NETHERLANDS).
Simulation of the atmospheric boundary layer in the large wind tunnel of the TNO Institute for Building materials and Constructions (IBBC). Part 1: Theory [BI-76-39/08.7.23100-PT-1] N86-10703
Simulation of the atmospheric boundary layer in the large wind tunnel of the TNO Institute for Building Materials and Construction (IBBC). Part 2: Experiments [BI-76-39/08.7.23100-PT-2] N86-10704
INSTITUUT VOOR CULTURRTECHNIEK EN WATERHUISHOUDING, WAGENINGEN (NETHERLANDS).
Remote sensing [NOTA-1536] N86-10638
Remote sensing study project East Gelderland (Netherlands). Part 2: Remote sensing flights in 1982 and 1983; organization aspects N86-10639
INTERSONICS, INC., NORTHBROOK, ILL.
Acoustic levitation: containerless processing N86-10177
IOWA UNIV., IOWA CITY.
Design sensitivity analysis and optimization of built-up structures N86-10565
Stratigraphy, petrology, depositional and post-depositional histories and their effects upon reservoir properties of the Parkman Formation of the Mesa Verde group, Powder River Basin, Wyoming N86-10691
ISHIKAWAJIMA-HARIMA HEAVY INDUSTRIES CO. LTD., YOKOHAMA (JAPAN).
Experimental study on Marangoni convection N86-10243

J

JET PROPULSION LAB., CALIFORNIA INST. OF TECH., PASADENA.
Containerless studies of nucleation and undercooling N86-10152
Sol-gel glasses N86-10153
Fusion target technology N86-10156
Glass research N86-10157
Multimode acoustic research N86-10167
Advanced containerless processing technology N86-10175
The Telecommunications and Data Acquisition Report [NASA-CR-176203] N86-10382
A VLBI survey at 2.29 GHz N86-10383
Comparison of the calibration of ionospheric delay in VLBI data by the methods of dual frequency and Faraday rotation N86-10384
A new 70-meter antenna quadripod with reduced RF blockage N86-10385
Seismic analysis of the large 70-meter antenna, part 1: Earthquake response spectra versus full transient analysis N86-10386
An experimental TE sub 12 - TE sub 11 circular waveguide mode converter N86-10387
Propagation and radiation characteristics of a multimode corrugated waveguide feedhorn N86-10388
Load-deflection tests and computer analyses of a high-precision adhesive-bonded antenna reflector panel N86-10389
A sequential decoding performance analysis for International Comet Explorer N86-10390
The VLSI design of error-trellis syndrome decoding for convolutional codes N86-10391
High-rate convolutional code construction with the minimum required SNR criterion N86-10392
DSN frequency and timing system, Mark 4-85 N86-10393
JPL emergency support of TDRSS and compatible satellites N86-10394
Planning for VLA/DSN arrayed support to the Voyager at Neptune N86-10395
A VLA experiment: Planning for Voyager at Neptune N86-10396
Periodic binary sequences with very good autocorrelation properties N86-10397
A binary sequence of period 60 with better autocorrelation properties than the Barker sequence of period 13 N86-10398
The GCF Mark 4 implementation and beyond N86-10399
SETI radio spectrum surveillance system N86-10400
Mobile VLBI and GPS measurement of vertical crustal motion N86-10401
Improved mapping of radio sources from VLBI data by least-square fit N86-10402
Report of the Workshop on Geologic Applications of Remote Sensing to the Study of Sedimentary Basins [E86-10002] N86-10599
Tertiary and quaternary research with remote sensing methods N86-10603
Multisensor data integration techniques N86-10604
Remote stratigraphic and structural analysis: Multisensor results in the Wind River/Bighorn Basin area, Wyoming N86-10606
Foreland basin structures and remote sensing N86-10608
NASA/JPL Aircraft SAR Workshop Proceedings [NASA-CR-176204] N86-10615
Radar system description N86-10616
CV-990 L-band SAR: A calibration experiment N86-10617
Neogene compressional deformation and possible thrust faulting in southwest Dominican Republic N86-10618
Age-dating volcanic and alluvial surfaces with multipolarization data N86-10620
Topographic mapping from interferometric synthetic aperture radar observations N86-10622
Lithologic mapping in a sedimentary environment using multipolarization SAR images N86-10624
Mapping diverse forest cover with multipolarization airborne radar N86-10625
On the use of L-band multipolarization airborne SAR for surveys of crops, vineyards, and orchards in a California irrigated agricultural region N86-10627
Vegetation canopy discrimination and biomass assessment using multipolarized airborne SAR N86-10628
Modelling of vegetation volumes N86-10629
Chemical kinetics and photochemical data for use in stratospheric modeling [NASA-CR-176198] N86-10707
Advanced vehicle systems assessment. Volume 2: Subsystems assessment [NASA-CR-176205] N86-11083
Advanced vehicle systems assessment. Volume 3: Systems assessment [NASA-CR-176206] N86-11084
Advanced vehicle systems assessment. Volume 4: Supporting analyses [NASA-CR-176207] N86-11085
Advanced vehicle systems assessment. Volume 5: Appendices [NASA-CR-176208] N86-11086
Galileo: Exploration of Jupiter's system [NASA-SP-479] N86-11137
A modeling analysis program for the JPL table mountain Io sodium cloud [NASA-CR-176241] N86-11139
JOHNS HOPKINS UNIV., BALTIMORE, MD.
Metallic foams N86-10095
Diffusion in immiscible melts N86-10096
Elastic properties and thermal stability characterization of metallic glasses by guided wave techniques N86-10337
Stiffened and prestressed composite overwrapped pressure vessels N86-10547
Load space formulation of reliability for nonlinear random structural systems N86-10570
Ultraviolet spectroscopy of the Earth's dayglow and magnetosphere cleft N86-10696
Physical acoustics: Investigation of chemical kinetic and thermodynamic properties of fluids N86-10911
Thermodynamics of polymer-supercritical solvent mixtures [AD-A157038] N86-11061
JOINT INST. FOR LAB. ASTROPHYSICS, BOULDER, COLO.
Space antenna for gravitational wave astronomy N86-11123
JOINT PUBLICATIONS RESEARCH SERVICE, ARLINGTON, VA.
USSR report: Life sciences. Biomedical and behavioral sciences [JPRS-UBB-85-023] N86-10738
Hemodynamics during gravitational overloads (mathematical modeling) N86-10739
Study of hypokinesia and acceleration effects on human chromosomes N86-10740
Romanian plant produces protein concentrate from paraffin-nourished yeasts N86-10741
Biotechnology: Science and practice N86-10742
Dynamics of changes of statistical indicators of heart rhythm of persons with different degree of motion sickness N86-10743
Effect of single actions of weak electromagnetic fields of ultralow frequency on indices of endocrine system N86-10744
Effect of emotional stress on hemostasis system of healthy persons N86-10745
Assessment of state of chronotropic and inotropic heart function at different degrees of physical fitness N86-10746
Capacity for work and hemodynamics in males residing at middle and high latitudes N86-10747
Individual typological features of autonomic reactions during autogenic training in polar expedition members in period of wintering in Antarctica N86-10748
Effect of inclusion of supplementary ascorbic acid in daily diet on degree of vitamin saturation of body and thermoresistance of erythrocytes while working in arid zone N86-10749
Effect of various doses of some vitamins on non-specific mechanisms of adaptation of man N86-10750
Adaptation of man to extreme conditions of Antarctica N86-10751
Individual typological self-regulation of cardio-vascular system N86-10752

Conditioning potentialities of respiratory apparatus N86-10753
Short term heat effect on adreno- and cholino-sensitivity of rat's small intestine N86-10754
Classification of changes in electrocardiogram during muscular exertion of healthy individuals N86-10755
Eye-movement activity as index of functional state of brain N86-10756
Mechanism of adaptogenic action of prickly eleuterococcus on man during heat stress N86-10757
Vestibular resistance and blood circulation changes in orthostatic position during hyperthermia N86-10758
Heat transfer mechanism in human extremities N86-10759
Reaction of rabbit respiration system to hypoxic stimulus in nitrogen-oxygen medium at elevated pressure N86-10760
Indices of blood oxygen transporting properties and erythropoiesis in rats after prolonged stay in nitrogen-oxygen mixture at elevated pressure N86-10761
Homocarnosin in rat brain during adaptation to cold N86-10762
Efficiency of muscular work in white rats during adaptation to cold N86-10763
Intradiurnial organization of wakefulness-sleep sequence and energy metabolism in rats exposed to low ambient temperature N86-10764
TV monitoring control system in electrophysiological studies N86-10765
Effect of cold on brain serotonin system and plasma corticosteroid level in different strains of mice N86-10766
Dynamics of general resistance of rats during readaptation period after training in altered gas environment N86-10767
USSR report: Cybernetics, computers and automation technology
[JPRS-UCC-85-006] N86-10809
Prospects for creation of optical digital high-performance computers N86-10810
Elektronika MS 1603 high-speed peripheral processor N86-10811
Diagnostics of peripheral processors and controllers N86-10812
An approach to implementing CAMAC microprocessor modules N86-10813
Compact, high-speed algorithm for laying out printed circuit board runs N86-10814
Classification of real-time program testing tasks and methods N86-10815
DBS/R database control system N86-10816
Collective use computer system for the Academy of Sciences KaSSR N86-10817
Digital processing of images in tracking a moving object N86-10818

K

KANNER (LEO) ASSOCIATES, REDWOOD CITY, CALIF.
RFQ-funneling
[DE85-012483] N86-10194
Ion sources for high-frequency accelerators
[DE85-012992] N86-11006
KARLSRUHE UNIV. (WEST GERMANY).
High temperature properties and characterization of S3-N4 materials
[BMFT-FB-T-85-046] N86-10352
High temperature properties of SiC materials
[BMFT-FB-T-85-047] N86-10353
Restitution of Spacelab photography by analog stereoplotter N86-10489
KATHOLIEKE UNIVERSITEIT TE LEUVEN (BELGIUM).
Melting and solidification of metal matrix composites under microgravity N86-10211
KENTUCKY UNIV., LEXINGTON.
Solid surface combustion at reduced gravity N86-10159
KERNFORSCHUNGSANLAGE, JUELICH (WEST GERMANY).
Dielectric properties of silicon surfaces and silver thin films
[JUEL-1988] N86-10450
Dust deposition in regions of separated flow
[JUEL-1985] N86-10475
Experiments with tubular probes made of INCOLOY 800 H under uniaxial and multiaxial strain
[JUEL-1979] N86-10595
Contribution of wind energy to the energy balance of a combined solar and wind energy system. Part 2: Computer-assisted investigations
[BMFT-FB-T-85-052-VOL-2] N86-10671
KIRUNA GEOPHYSICAL INST. (SWEDEN).
Activities report in geophysics
[KGI-188] N86-10709
KMS FUSION, INC., ANN ARBOR, MICH.
Gel precursors as glass and ceramic starting materials for space processing applications research N86-10150
KODAK LTD., LONDON (ENGLAND).
Capillary forces in a low gravity environment N86-10202

L

LABORATORIO DE ACUSTICA E SONICA, SAO PAULO (BRAZIL).
Ultrasonic inspection of weldments in large size spiral box for hydroelectric plant
[AS-701/85] N86-10562
LAMONT-DOHERTY GEOLOGICAL OBSERVATORY, PALISADES, N. Y.
Structural mapping of folded sedimentary environments from satellite images: An example from Central Asia N86-10607
LAPPEENRANNAN TEKNILLINEN, KORKEAKOULU (FINALAND).
Information on continuum states from feeding times and total (GAMMA) spectra measured with BGO suppressed detectors
[DE85-013868] N86-10961
LOCKHEED MISSILES AND SPACE CO., PALO ALTO, CALIF.
Test and evaluate passive orbital disconnect struts (PODS 3)
[NASA-CR-177368] N86-10274
Binder-filler interaction in energetic polymers
[AD-A156752] N86-10345
LOS ALAMOS NATIONAL LAB., N. MEX.
Mixed-mode fracture of ceramics
[DE85-014087] N86-10349
Revision of and documentation for the standard version of the Poisson-Group codes
[DE85-012659] N86-10837
Theory of dense molecular fluid equations of state with application to detonation products
[DE84-016822] N86-10927
High-brightness photoemitter injector for electron accelerators
[DE85-012673] N86-10929
Measurement and resulting first and second order approximations for a 9 deg bending magnet in LAMPF's 750-keV transport
[DE85-012691] N86-10930
Wide dynamic range beam profile monitor
[DE85-012709] N86-10950
Ferrite kicker magnet for the IAMPF switchyard upgrade
[DE85-012657] N86-10996
Local drift parameter, j/n sub e and resistivity anomaly measurements in CTX spheromaks
[DE85-012740] N86-10998
Introduction to the m = 1 helicity source
[DE85-012771] N86-10999
Beginnings of remote handling at the RAL Spallation Neutron Source
[DE85-012681] N86-11001
Analytic evaluation of LAMPF 2 Booster Cavity design
[DE85-012680] N86-11002
LOS ALAMOS SCIENTIFIC LAB., N. MEX.
RFQ-funneling
[DE85-012483] N86-10194
Development of new ammonium nitrate composite explosives
[DE85-014252] N86-10356
KRAK: A computer program for two-phase, two-component porous flow and fracture propagation, revision
[DE85-014264] N86-10469
General-purpose heat source development: Safety Verification Test Program. Bullet/fragment test series
[DE85-014262] N86-10660
Recent development in the Hot Dry Rock Geothermal Energy Program
[DE85-009562] N86-10663
New probabilistic modeling and simulation methods for complex time-dependent systems
[DE85-009575] N86-10835
Guidelines for a thermochemical kinetics computer program
[DE85-014266] N86-10839
Framework for generating expert systems to perform computer security risk analysis
[DE85-014134] N86-10841
Initial increase, peaking effect, in the internal friction of copper following pulsed neutron and electron irradiation
[DE85-012767] N86-10932
Angular distribution of neutral hydrogen following collisional electron detachment from H(-)
[DE85-014258] N86-10943
Preliminary investigation of changes in X-ray multilayer optics subjected to high radiation flux
[DE85-014074] N86-10944
Polarization transfer in inelastic scattering and pionic models of the EMC effect
[DE85-010738] N86-10955
Direct mass measurements in the light neutron-rich region using a combined energy and time-of-flight technique
[DE85-012758] N86-10963
Beam line windows at LAMPF
[DE85-012723] N86-10985
Proposed bunching scheme for a polarized H(-) injector
[DE85-012648] N86-10986
Beam-cavity interaction measurements in a DAW structure
[DE85-012660] N86-10987
Increased particle confinement with the use of external dc bias field in the CTX spheromak
[DE85-012744] N86-10988
Treatment planning with ion beams
[DE85-012661] N86-10990
Noninterceptive techniques for the measurement of longitudinal parameters for intense H(-) beams
[DE85-012662] N86-10992
High-power rf controls for the NBS-Los Alamos racetrack microtron
[DE85-012658] N86-10993
Energy efficiency of the CTX magnetized coaxial plasma source
[DE85-012735] N86-11003
Generalized helicity and its time derivative
[DE85-012770] N86-11027
Recent helicity source and power supply improvements in CTX
[DE85-012741] N86-11028
Equilibrium of the kink source experiment
[DE85-012764] N86-11029
Alternative fusion concepts and the prospects for improved reactors
[DE85-009622] N86-11031
Heating and generation of suprathermal particles at collisionless shocks
[DE85-014114] N86-11034
LOUISIANA STATE UNIV., BATON ROUGE.
Solar flares and magnetospheric particles: Investigations based upon the ONR-602 experiment
[AD-A156583] N86-11142
LYON-1 UNIV. (FRANCE).
Space experiment on thermal diffusion. Preparation and theoretical analysis N86-10253

M

MAINZ UNIV. (WEST GERMANY).
A geological structural analysis of the southeastern Zagros (Iran) ranges based on metric camera photos N86-10492
MAPPING AND CHARTING ESTABLISHMENT, OTTAWA (ONTARIO).
Test results using metric camera photography for 1:250,000 mapping N86-10522
MARTIN MARIETTA AEROSPACE, DENVER, COLO.
Evaluation and prediction of long-term environmental effects on non metallic materials
[NASA-CR-178495] N86-10340
MARTIN MARIETTA ENERGY SYSTEMS, INC., PADUCAH, KY.
Evaluation of the International Atomic Energy Agency (IAEA) Safeguards Analytical Laboratory quality assurance program
[DE85-012078] N86-10953
MARYLAND UNIV., COLLEGE PARK.
Light scattering tests of fundamental theories of transport properties in the critical region N86-10113
Topics in nonlinear wave theory with applications N86-10367
Analysis of combined natural and forced convection around cylinders and spheres N86-10456
Determination of symmetry and phase in human visual response functions: Theory and experiments N86-10769
The h, p and h-p versions of the finite element method in dimension. Part 1: The error analysis of the p-version
[AD-A156600] N86-10862
The h, p and h-p versions of the finite element method in 1 dimension. Part 3. The adaptive h-p version
[AD-A156626] N86-10864
The h, p and h-p versions of the finite element method in 1 dimension. Part 2. The error analysis of the H and h-p versions
[AD-A156835] N86-10869

A modified repair strategy for two-component systems with revealed and unrevealed faults [AD-A156715] N86-10885

Estimation by moments in a model of faulty inspection [AD-A156754] N86-10886

Matter-antimatter transition operators: A manual for modeling N86-10921

Lie algebraic methods for charged particle beams and light optics N86-10970

Adsorption of oxygen on single crystal tin at liquid helium temperatures N86-11044

Critical dynamics in superfluid helium N86-11046

MASCHINENFABRIK AUGSBURG-NUERNBERG A.G., MUNICH (WEST GERMANY).

Skin casting of alloys and composites: Results of Spacelab (SL)-1 and TEXUS experiments N86-10213

MASSACHUSETTS INST. OF TECH., CAMBRIDGE.

Fluid flow in crystal growth: Analysis of the verticle Bridgman and floating zone process N86-10055

Solutal convection and its effects on crystal growth and segregation in binary and pseudo-binary system with large liquidus-solidus separation N86-10056

Crystal growth of device quality GaAs in space N86-10061

Crystal melts under reduced gravity N86-10062

Heat flow and segregation in directional solidification N86-10072

Signal analysis of gas tungsten arc welds N86-10078

Undercooling, remelting, and coarsening N86-10080

The role of entrained surface oxides in RS-PM aluminum alloys on resultant structures and properties N86-10085

Metals electroprocessing in molten salts N86-10098

Modelling of laser-enhanced chemical vapor deposition N86-10105

Automatic processing of reactive polymers N86-10127

Role of convection in grain refining N86-10133

Colloidal oxide properties and kinetic studies N86-10147

Rapid solidification of magnetic oxides N86-10152

Oxidation behavior of glassy alloys N86-10158

Crystal growth of GaAs in space N86-10234

Robust failure detection filters [NASA-CR-176232] N86-10271

Reaching approximate agreement in the presence of faults [AD-A156541] N86-10898

US superconducting magnet data base assessment for INTOR [DE85-013648] N86-11000

Conducting wall and pressure profile effect on MHD stabilization of axisymmetric mirror [DE85-013647] N86-11020

MASSACHUSETTS UNIV., AMHERST.

Electrically conducting polymers N86-10333

Polyacetylene polymerization, structure, and electrical transport properties N86-10334

Relativistic wavefunction at the origin and the pion decay constant [DE85-012392] N86-11062

MATERIALS RESEARCH LABS., ASCOT VALE (AUSTRALIA).

Age-life prediction of nylon 66 parachute materials. Part 2: Changes in the chemical and physical properties of materials on aging [AD-A156909] N86-10347

MAX-PLANCK-INST. FUER METALLFORSCHUNG, STUTTGART (WEST GERMANY).

Particle coarsening in immiscible zinc-lead alloys under microgravity N86-10210

MAX-PLANCK-INSTITUT FUER STROEMUNGSFORSCHUNG, GOETTINGEN (WEST GERMANY).

Oscillations of subsonic flow in an abruptly expanding circular duct [MPIS-16/1984] N86-10028

MCELROY (RALPH) CO., AUSTIN, TEX.

Nonlinear propagation of elastoplastic waves in Ke penetrators (excerpts) [DE85-011450] N86-10318

MEMBRANE TECHNOLOGY AND RESEARCH, INC., MENLO PARK, CALIF.

Membrane research in energy and solvent recovery from industrial effluent streams [DE85-014583] N86-10682

MESSWANDLER-BAU G.M.B.H., BAMBERG (WEST GERMANY).

High voltage instrument transformers for outdoor service with an insulation of low pressure SF6 gas and plastic foils [BMFT-FB-T-85-034] N86-10449

METALS SOCIETY, LONDON (ENGLAND).

Mechanism of the formation of boronised layers on high carbon steel [BLL-BISI-TRANS-23036-(9022.06)] N86-10306

Boronising of iron and steel by ionic bombardment by diborane [BLL-BISI-TRANS-23034-(9022.06)] N86-10307

Application of the unloading compliance methods in fracture toughness measurements of a quenched and tempered steel [BLL-BISI-TRANS-21628-(9022.06)] N86-10308

MICHAEL REESE RESEARCH FOUNDATION, CHICAGO, ILL.

Biochemical assays of cultured cells N86-10134

MICHIGAN TECHNOLOGICAL UNIV., HOUGHTON.

The development and prevention of channel segregation during alloy solidification N86-10086

MICHIGAN UNIV., ANN ARBOR.

Preliminary reports, memoranda and technical notes of the Materials Research Council Summer Conference, La Jolla, California [AD-A156776] N86-10291

Effects of chemistry and swirl on the production of turbulence in a flame [PB85-219632] N86-10305

Test of a multilevel computational theory of stereoscopic visual image processing [AD-A157011] N86-10870

MIDWEST RESEARCH INST., GOLDEN, COLO.

Identification of chemical and physical phenomena affecting the durability of silvered polymer (PMMA) mirrors [DE85-012131] N86-10645

Solar thermal technical information guide [DE85-002941] N86-10657

Photovoltaics: Report, 1984 [DE85-014713] N86-10658

Some aspects of long-range, high-risk photovoltaic research at SERI [DE85-012144] N86-10662

MIDWEST RESEARCH INST., KANSAS CITY, MO.

Containerless high temperature property measurements by atomic fluorescence N86-10092

MILAN UNIV. (ITALY).

Surface forces in contacting solids N86-10252

MISSION RESEARCH CORP., ALBUQUERQUE, N. MEX.

Laser generation and transport of a relativistic electron beam [DE85-011709] N86-10192

MISSION RESEARCH CORP., SANTA BARBARA CALIF.

Acoustic gravity wave chemistry model for the RAYTRACE code [AD-A156850] N86-10405

MISSISSIPPI STATE UNIV., STATE COLLEGE.

Guidance and control of a cable based payload pickup system N86-10046

MISSISSIPPI UNIV., UNIVERSITY.

Acoustic cavitation and bubble dynamics [AD-A156888] N86-10918

MISSOURI UNIV., ROLLA.

Containerless processing of glass forming melts in space N86-10148

MONS UNIV. (BELGIUM).

Rayleigh-Benard instability in systems presenting a minimum in surface tension N86-10245

MULLARD RADIO ASTRONOMY OBSERVATORY, CAMBRIDGE (ENGLAND).

Radio astronomy experience in image reconstruction. A history lesson for optical astronomers N86-11117

N

NANJING UNIV. (CHINA).

Effects of slots/holes in disks on frequencies of TM01 and EH11 waves in the disk-loaded waveguide [DE85-013376] N86-11009

NAPLES UNIV. (ITALY).

Some results of the Marangoni free convection experiment N86-10203

The TEXUS flight results on convective flows and heat transfer in simulated floating zones N86-10235

Numerical simulation of unsteady thermal Marangoni flows N86-10238

NATIONAAL INST. VOOR KERNFYSICA EN HOGE ENERGIEFYSICA, AMSTERDAM (NETHERLANDS).

Activities report in safety N86-10365

Renovated cooling at PIMU [LINO-122] N86-10452

On the analytical evaluation of the partition function for unit hypercubes in four dimensions [NIKHEF-H/84-12] N86-10882

Variational estimates for the mass gap of SU(2) Euclidean lattice gauge theory [NIKHEF-H/84-13] N86-10883

Report on a visit to CERN in February 1985. Notes on bunch monitors, high-frequency systems, linacs, kickers, magnets, vacuum and bunch extraction [LINO-119] N86-10967

The MEA vacuum system [LINO-120] N86-10968

The Netherlands Institute for Nuclear and High Energy Physics (NIKHEF) traveling wave monitor user guide [LINO-121] N86-10969

Two-loop large Higgs mass corrections to vector boson self-couplings [NIKHEF-H/84-15] N86-11038

NATIONAL ACADEMY OF SCIENCES - NATIONAL RESEARCH COUNCIL, WASHINGTON, D. C.

Confined swirling jet predictions using a multiple-scale turbulence model [NASA-CR-178484] N86-10462

NATIONAL AERONAUTICS AND SPACE ADMINISTRATION, WASHINGTON, D. C.

Microgravity Science and Applications Program tasks [NASA-TM-87568] N86-10053

Project VESTA, exploratory mission to the asteroids: Scientific objectives and technical specifications [NASA-TM-77669] N86-10179

X-ray satellite [NASA-TM-77923] N86-10273

Determination of thermophysical characteristics of solid materials by electrical modelling of the solutions to the inverse problems in nonsteady heat conduction [NASA-TM-77907] N86-10293

Discussion on the progress and future of satellite communication (Japan) [NASA-TM-77672] N86-10378

Design and construction of a Faraday cup for measurement of small electronic currents [NASA-TM-77915] N86-10418

Maximum water reserves in the snow cover in the European territory of the USSR according to data for 1892-1960 [NASA-TM-77901] N86-10611

Representation of the distribution of the snow cover on the surface of the Earth's dry land [NASA-TM-77909] N86-10612

Observations of the snow cover in the southern part of the Buryat Autonomous Soviet Socialist Republic [NASA-TM-77910] N86-10613

Laws of distribution of the snow cover on the greater Caucasus (Soviet Union) [NASA-TM-77911] N86-10614

Aerospace medicine and biology: A continuing bibliography with indexes (supplement 275) [NASA-SP-7011(275)] N86-10768

NATIONAL AERONAUTICS AND SPACE ADMINISTRATION. AMES RESEARCH CENTER, MOFFETT FIELD, CALIF.

Evaluation of an aerodynamic-load prediction method on a STOL fighter configuration [NASA-TM-86782] N86-10015

Manned flight simulation: Challenge and response [NASA-TM-86827] N86-10048

Large eddy interactions in a turbulent channel flow [NASA-TM-86757] N86-10464

Life sciences research on the space station: An introduction [NASA-TM-86836] N86-10734

The synthesis and analysis of color images [NASA-TM-86844] N86-10777

NATIONAL AERONAUTICS AND SPACE ADMINISTRATION. GODDARD SPACE FLIGHT CENTER, GREENBELT, MD.

The effect of vegetation type, microrelief, and incidence angle on radar backscatter N86-10619

The effects of merging TM and A/C radar on wetland classification N86-10621

SAMSI: An orbiting spatial interferometer for micro-arc second astronomical observations N86-11103

Photographic catalog of selected planetary size comparisons [NASA-TM-86207] N86-11138

Directionality of bremsstrahlung from relativistic electrons in solar flares [NASA-TM-87509] N86-11141

NATIONAL AERONAUTICS AND SPACE ADMINISTRATION. JOHNSON (LYNDON B.) SPACE CENTER,

Numerical procedure for three-dimensional hypersonic viscous flow over aerobrake configuration [NASA-TM-58269] N86-10018

Purification and cultivation of human pituitary growth hormones secreting cells N86-10140

Cell separations in microgravity and development of a space bioreactor N86-10141

Cell maintenance systems N86-10142

High-temperature controlled redox crystallization studies N86-10178

NATIONAL AERONAUTICS AND SPACE ADMINISTRATION. LANGLEY RESEARCH CENTER, HAMPTON, VA.

Operating characteristics of the multiple critical Venturi System and secondary calibration nozzles used for weight-flow measurements in the Langley 16-foot transonic tunnel
[NASA-TM-86405] N86-10016

Crystal growth research in space N86-10057

Three-dimensional vibration analysis of a uniform beam with offset inertial masses at the ends
[NASA-TM-86393] N86-10580

Fatigue of graphite/epoxy buffer strip panels with center cracks
[NASA-TM-87595] N86-10581

User's guide for Langley Research Center Orbital Lifetime program
[NASA-TM-87587] N86-10828

Investigation of composite materials property requirements for sonic fatigue research
[NASA-TM-87601] N86-10913

NATIONAL AERONAUTICS AND SPACE ADMINISTRATION. LEWIS RESEARCH CENTER, CLEVELAND, OHIO.

Three-dimensional inviscid analysis of radial turbine flow and a limited comparison with experimental data
[NASA-TM-87091] N86-10017

Forced response analysis of an aerodynamically detuned supersonic turbomachine rotor
[NASA-TM-87093] N86-10019

Transport processes in solution crystal growth
N86-10107

Surface tension induced instabilities in reduced gravity: The Benerd problem N86-10117

Thermocapillary motion research N86-10125

Microgravity Materials Science Laboratory
N86-10173

Dendritic solidification in a binary alloy melt: Steady-state versus morphological stability theories
N86-10261

Compatibility of grain-stabilized platinum with candidate propellants for resistojets
[NASA-TM-87118] N86-10279

Rapid evaluation of ion thruster lifetime using optical emission spectroscopy
[NASA-TM-87103] N86-10280

Experimental performance of a 1-kilowatt arcjet thruster
[NASA-TM-87131] N86-10281

Progressive damage, fracture predictions and post mortem correlations for fiber composites
[NASA-TM-87101] N86-10290

Creep-fatigue behavior of NiCoCrAlY coated PWA 1480 superalloy single crystals
[NASA-TM-87110] N86-10311

Tribological properties of structural ceramics
[NASA-TM-87105] N86-10341

Test results for 20-GHz GaAs FET spacecraft power amplifier
[NASA-TM-87072] N86-10379

A dual frequency microstrip antenna for Ka band
[NASA-TM-87124] N86-10380

A numerical method for approximating antenna surfaces defined by discrete surface points
[NASA-TM-87125] N86-10381

Theoretical modeling of the vapor cavitation in dynamically loaded journal bearings
[NASA-TM-87076] N86-10463

Measurement of the density of base fluids at pressures 0.422 to 2.20 GPa
[NASA-TM-87114] N86-10551

The mechanism of erosion of metallic materials under cavitation attack
[NASA-TM-87133] N86-10552

Ultrasonic evaluation of mechanical properties of thick, multilayered, filament wound composites
[MASA-TM-87088] N86-10561

Joint research effort on vibrations of twisted plates, phase 1: Final results
[NASA-RP-1150] N86-10579

Improved stud configurations for attaching laminated wood wind turbine blades
[NASA-TM-87109] N86-10582

Photovoltaic systems in remote locations: An experience summary
[NASA-TM-87106] N86-10643

Ion beam sputter deposited zinc telluride films
[NASA-TM-87119] N86-11048

NATIONAL AERONAUTICS AND SPACE ADMINISTRATION. MARSHALL SPACE FLIGHT CENTER, HUNTSVILLE, ALA.

Growth of organic crystals by Ostwald ripening
N86-10058

Growth of solid solution crystals N86-10065

Study of the reactive-element effect in oxidation of Fe-Cr alloys using transverse section analytical electron microscopy N86-10087

Cloud microphysics by thermal wave methods
N86-10103

Extension of Ostwald ripening theory N86-10104

Studies of model immiscible systems N86-10112

Mathematical models of continuous flow electrophoresis N86-10143

Electrophoresis technology N86-10144

Production of large-particle-size monodisperse latexes in microgravity N86-10146

Glass formation in reluctant glass formers
N86-10151

Development of materials processing systems for use in space on low-g simulation devices N86-10166

Advanced optical measurement techniques
N86-10174

Design, fabrication and testing of an experimental apparatus for determining particle behavior under very low intergranular stresses N86-10175

Separation of aqueous two-phase polymer systems in microgravity N86-10246

Rationale for two phase polymer system microgravity separation experiments N86-10247

Analytical investigation of solid rocket nozzle failure
[NASA-TM-86513] N86-10278

NATIONAL AERONAUTICS AND SPACE ADMINISTRATION. NATIONAL SPACE TECHNOLOGY LABS., BAY SAINT LOUIS, MISS.

Potential applications of multipolarization SAR for pine plantation biomass estimation N86-10626

NATIONAL AEROSPACE LAB., AMSTERDAM (NETHERLANDS).

Axisymmetric free surface behavior of moving liquid in a cylinder in microgravity N86-10206

Aerospace research at NLR N86-11089

Activities report of the Space Flight Laboratory
N86-11090

Activities Report of the Space Flight Laboratory
N86-11091

NATIONAL BUREAU OF STANDARDS, BOULDER, COLO.

Transient heat transfer in zero gravity environment
[NASA ORDER H-27954B] N86-10114

Cooled ion frequency standard
[AD-A156813] N86-10295

Space antenna for gravitational wave astronomy
N86-11123

NATIONAL BUREAU OF STANDARDS, GAITHERSBURG, MD.

Investigation of the uncertainties of the NBS (National Bureau of Standards) thermal voltage and current converters
[PB85-200178] N86-10453

NBSGSC: A FORTRAN program for quantitative X-ray fluorescence analysis
[PB85-206068] N86-10847

Selected tables of atomic spectra. Atomic energy levels and multiplet table O3
[NBS/NSRDS-3/11] N86-10923

NATIONAL BUREAU OF STANDARDS, WASHINGTON, D.C.

Measurement of high temperature thermophysical properties N86-10074

Convection during unidirectional solidification
N86-10077

Dynamic thermophysical measurements in space
[NASA ORDER H-27954-B] N86-10106

Surface tensions and their variations with temperature and impurities
[NASA ORDER H-27954B] N86-10115

Precise viscosity measurements very close to critical points
[NASA ORDER C-86129D] N86-10120

Experimental and theoretical studies of wetting and multilayer adsorption
[NASA ORDER H-27954B] N86-10121

Impurity extraction by droplets N86-10122

Miscibility gap systems
[NASA ORDER H-27954B] N86-10131

Self-heating to ignition measurements and computation of critical size for solar energy collector materials
[DE85-011449] N86-10302

NATIONAL OCEANIC AND ATMOSPHERIC ADMINISTRATION, BOULDER, COLO.

Field comparison of in situ meteorological sensors
[PB85-196988] N86-10723

NATIONAL WEATHER SERVICE, WASHINGTON, D.C.

Monthly and Seasonal Weather Outlook for mid-April to mid-May 1985, Volume 39, Number 8
[PB85-195345] N86-10724

NAVAL AIR SYSTEMS COMMAND, WASHINGTON, D. C.

Polymer engineering: Polymeric and molecular electronic, dielectric and optical properties for device applications
[AD-A156671] N86-10344

NAVAL MEDICAL RESEARCH AND DEVELOPMENT COMMAND, BETHESDA, MD.

Evaluation of the 90-day inhalation toxicity of petroleum and oil shale JP-5 jet fuel
[AD-A156815] N86-10675

NAVAL POSTGRADUATE SCHOOL, MONTEREY, CALIF.

Construction and use of a radio controlled model helicopter for research
[AD-A156547] N86-10036

A comparative analysis of a CV helicopter and a JVX (Joint Services Advanced Vertical Lift) tilt-rotor aircraft in an aircraft carrier based ASW (Anti-Submarine Warfare)
[AD-A156871] N86-10041

Evaluation of surface exchange coefficients from mildex ocean/atmosphere mixed layer data
[AD-A156765] N86-10729

Computer-based training for the US Coast Guard standard terminal microcomputer: A basis for implementation utilizing the elaboration theory of instructional design
[AD-A156548] N86-10791

Initial design of a relational database system for NPS computer asset identification and valuation for risk assessment
[AD-A156847] N86-10796

Development of IS2100: An information systems laboratory
[AD-A156848] N86-10797

Shipboard non-tactical computer systems of the US Navy
[AD-A156769] N86-10849

Fiber optic gradient hydrophone construction and calibration for sea trial
[AD-A156469] N86-10914

A systems development life cycle study of the information center
[AD-A156977] N86-11079

NAVAL RESEARCH LAB., WASHINGTON, D. C.

On the use of X-band CW nanosecond airborne radar for terrain profiling
[AD-A156886] N86-10406

The Liu, Katsaros, and Businger (1979) bulk atmospheric flux computational iteration program in FORTRAN and BASIC
[AD-A156736] N86-10714

A processor for the study of ocean fine-scale patches
[AD-A157019] N86-10730

Selected tables of atomic spectra. Atomic energy levels and multiplet table O3
[NBS/NSRDS-3/11] N86-10923

Electron momentum transfer collision frequency in N(2), O(2) and air
[AD-A157030] N86-10924

Dynamics of imploding neon gas puff plasmas. 1
[AD-A156916] N86-10983

Renormalization of an inverse scattering theory for inhomogeneous dielectrics
[AD-A156636] N86-11049

NAVAL UNDERWATER SYSTEMS CENTER, NEW LONDON, CONN.

An improved FFT (Fast fourier transform) for a four parallel pipe SIMD arithmetic processor
[AD-A156625] N86-10863

NAVAL WEAPONS CENTER, CHINA LAKE, CALIF.

Radome analysis and design capabilities of the RF and Microwave Technology Branch
[AD-A156662] N86-10404

Fracture toughness of hydrogen-embrittled precipitation-hardened stainless steels
[AD-A156664] N86-10592

Surface winds at NWC (Naval Weapons Center): 1964 - 1982
[AD-A156660] N86-10712

NEVADA UNIV., RENO.

Characterization of cathodic corrosion products in the Ca/CaCrO4 thermal battery
[DE85-013442] N86-10644

NEW HAMPSHIRE UNIV., DURHAM.

Solar modulation of galactic cosmic rays: Techniques and applications N86-11143

NEW MEXICO STATE UNIV., LAS CRUCES.

Preliminary investigation of changes in X-ray multilayer optics subjected to high radiation flux
[DE85-014074] N86-10944

NEW MEXICO UNIV., ALBUQUERQUE.

Catalytic activity of shock modified ZnO for CO oxidation and methanol synthesis
[DE85-014704] N86-10300

NEW ORLEANS UNIV., LA.
Study of one- and two-dimensional filtering and deconvolution algorithms for a streaming array computer
[NASA-CR-176221] N86-10822
A study of Morrison's iterative noise removal method
[NASA-CR-176222] N86-10823
Always-convergent iterative noise removal and deconvolution for image data
[NASA-CR-176223] N86-10824
A study of derivative filters using the discrete Fourier transform
[NASA-CR-176224] N86-10825
Coordinate axes, location of origin, and redundancy for the one and two-dimensional discrete Fourier transform
[NASA-CR-176225] N86-10826
Study of one- and two-dimensional filtering and deconvolution algorithms for a streaming array computer
[NASA-CR-176226] N86-10827

NOOTER CORP., ST. LOUIS, MO.
Fabrication and metallurgical properties of modified 9Cr-1 Mo steel
[DE85-012885] N86-10328

NORTH CAROLINA STATE UNIV., RALEIGH.
Processing of complex compound semiconductors in space N86-10054
Freezer model using a population balance approach for steady-state, direct-contact, secondary refrigerant, freeze desalination N86-10361
Sound radiation from repetitive transient vibrations using multi-channel digital signal processing with application to impact machinery N86-10910

NORTH CAROLINA UNIV., CHAPEL HILL.
Cretaceous and cenozoic stratigraphy of the upper and middle coastal plain, Harnett County area, North Carolina N86-10690

NORTH CAROLINA UNIV., CHARLOTTE.
Initial increase, peaking effect, in the internal friction of copper following pulsed neutron and electron irradiation
[DE85-012767] N86-10932

NORTHROP SERVICES, INC., RESEARCH TRIANGLE PARK, N. C.
Volatile organic compounds in indoor air: A survey of various structures
[PB85-198356] N86-10687

NORTHWESTERN UNIV., EVANSTON, ILL.
Thermocapillary flows and their stability: Effects of surface layers and contamination N86-10109
Finite deformation crack-line fields in a thin elasto-plastic sheet
[AD-A156757] N86-10346
Resistance curves for crack growth under plane-stress conditions in an elastic perfectly-plastic material
[AD-A156778] N86-10593

NOTRE DAME UNIV., IND.
Information on continuum states from feeding times and total (GAMMA) spectra measured with BGO suppressed detectors
[DE85-013668] N86-10961

O

OAK RIDGE GASEOUS DIFFUSION PLANT, TENN.
HALFBREED: An extended capability version of the YAQUI code
[DE85-014237] N86-10643

OAK RIDGE NATIONAL LAB., TENN.
Fabrication and metallurgical properties of modified 9Cr-1 Mo steel
[DE85-012885] N86-10328
Swelling and tensile properties of EBR-2-irradiated tantalum alloys for space reactor applications
[DE85-012887] N86-10329
Engine-driven and absorption heat pump programs
[DE85-013930] N86-10472
Laboratory experiments of heat pump dynamic losses
[DE85-013931] N86-10473
Automated analysis of digital images generated by two-dimensional gel electrophoresis
[DE85-011906] N86-10526
Simplified analysis of Stirling engines and heat pumps
[DE85-005366] N86-10647
Comparative analysis of single and continuously variable-capacity heat pump concepts
[DE85-004089] N86-10653
Stirling-engine-driven heat pump program overview
[DE85-004796] N86-10661
Examples of regional environmental assessment using acid deposition data
[DE85-012903] N86-10677
National perspective on environmental constraints to hydroelectric development
[DE85-013111] N86-10678
Development and evaluation of multispecies test protocols for assessing chemical toxicity
[DE85-013526] N86-10679
Box method for finding intersections of a trajectory with axisymmetric flux surfaces
[DE85-013525] N86-10840
The 1984 bibliography of atomic and molecular processes
[DE85-010583] N86-10926
Experimental X-ray scattering cross sections for H2 and rare atomic gases
[DE85-011572] N86-10936
Experimental studies of transition radiation and optical bremsstrahlung
[DE85-0135637] N86-10949
ORR core re-configuration measurements to increase the fast neutron flux in the Magnetic Fusion Energy (MFE) experiments
[DE85-013520] N86-10958
Evolution of the fusion power demonstration tandem mirror reactor configuration
[DE85-012889] N86-10960
Hot cell facility design for large fusion devices
[DE85-012893] N86-11037

OAK RIDGE Y-12 PLANT, TENN.
Aluminum ion plating for corrosion protection of uranium, revision 1
[DE85-012419] N86-10330

OFFICE NATIONAL D'ETUDES ET DE RECHERCHES AEROSPATIALES, PARIS (FRANCE).
Theoretical study of the unsteady linear problem for a rectangular wing with a pitching movement
[ONERA-RT-17/1841-RY-010-R] N86-10022
La Recherche Aerospatiale, bimonthly bulletin, no. 1984-5, September-October 1985
[ESA-TT-899] N86-10363

OFFICE OF NAVAL RESEARCH, ARLINGTON, VA.
Psychological Sciences Division 1984 programs
[AD-A156631] N86-10779

OHIO STATE UNIV., COLUMBUS.
Theoretical studies of the surface tension of liquid metal system N86-10101
Digital control of the hydraulic actuators of an adaptive suspension vehicle N86-10548
Computer control of an electric hydraulic robot leg with proximity ranging system N86-10549
A numerical model for the estimation of solar radiation on rugged terrain N86-10694
The influence of tactual seat-motion cues on training and performance in a roll-axis compensatory tracking task setting N86-10784

OLD DOMINION UNIV., NORFOLK, VA.
Passive damping concepts for slender columns in space structures
[NASA-CR-176234] N86-10577
NASA/American Society for Engineering Education (ASEE) Summer Faculty Fellowship Program, 1985
[NASA-CR-177972] N86-11064

OREGON GRADUATE CENTER FOR STUDY AND RESEARCH, BEAVERTON.
Transient velocity assessment in gallium arsenide, and of other GaAs characteristics related to device functions
[AD-A156983] N86-11050

OREGON HEALTH SCIENCES UNIV., PORTLAND.
Cell partition in two polymer aqueous phases N86-10136

OREGON STATE UNIV., CORVALLIS.
Direct mass measurements in the light neutron-rich region using a combined energy and time-of-flight technique
[DE85-012758] N86-10963

OXFORD UNIV. (ENGLAND).
Identification of a plant's weighting sequence
[OUEL-1534/84] N86-10654

P

PACIFIC NORTHWEST LAB., RICHLAND, WASH.
Rapid analysis using capillary supercritical fluid chromatography
[DE85-012460] N86-10297
Determining a physically appropriate neutron spectrum from multisphere data
[DE85-013045] N86-10299
ELCAP instrumentation
[DE85-013042] N86-10527
LANDSAT TM image data quality analysis for energy-related applications
[E85-10109] N86-10597
Energy balance in a deep Colorado valley: ASCOT 84
[DE85-012441] N86-10631
Overview of wind turbine siting research: Prospecting to micrositing
[DE85-013496] N86-10666
Radionuclide complexation in xylem exudates of plants
[DE85-013446] N86-10684
Approaches to quantitative expression of dose response
[DE85-013496] N86-10772
Secondary standards laboratories for ionizing radiation calibrations: The national laboratory interests
[DE85-007046] N86-10838

PADUA UNIV. (ITALY).
Extragalactic observations with optical space arrays N86-11096

PARIS VI UNIV. (FRANCE).
Growth and characterization of brushite and lead monetite, simulation and results N86-10230

PARIS VII UNIV. (FRANCE).
High angular resolution in the infrared: Prospects for space observations N86-11100

PARMA UNIV. (ITALY).
The role of very small scale metric images in modern geology N86-10502

PENNSYLVANIA STATE UNIV., UNIVERSITY PARK.
Kidney cell electrophoresis N86-10145

PENNSYLVANIA UNIV., PHILADELPHIA.
Strength modeling report
[NASA-CR-171896] N86-10770
TEMPUS: Simulating personnel and tasks in a 3-D environment
[NASA-CR-171901] N86-10785
User interface enhancement report
[NASA-CR-171898] N86-10820
System integration report
[NASA-CR-171900] N86-10821
Motion analysis report
[NASA-CR-171897] N86-10896
Zero-gravity movement studies
[NASA-CR-171899] N86-10897

PERKIN-ELMER CORP., DANBURY, CONN.
Future space telescope design concepts N86-11107

PHILLIPS ENGINEERING CO., ST. JOSEPH, MICH.
Analyses of advanced residential absorption heat pump cycles
[DE85-005244] N86-10664

PHYSICAL SCIENCES, INC., ANDOVER, MASS.
Fuel Cell Technology Assessment Program, work element no. 6
[DE85-008228] N86-10444

PITTSBURGH UNIV., PA.
Dynamic lithostratigraphy and paleoecology of upper Mississippi (Chesterian) strata of the northcentral Appalachian Basin N86-10690
Charge exchange in slow collisions of atoms and molecules N86-10922
Electron-ion recombination studies of planetary ionospheric and astrophysical ions N86-11132

PLANT RESOURCES INST., SALT LAKE CITY, UTAH.
Whole plant utilization of sunflowers as a renewable source of strategic materials (rubber)
[AD-A155833] N86-10342

POLAR RESEARCH LAB., INC., CARPINTERIA, CALIF.
Long term statistical measurements of environmental acoustics parameters in the arctic. AEAS report number 2. Low frequency transmission loss measurements in the central arctic ocean
[AD-A156576] N86-10727

POLITECNICO DI MILANO (ITALY).
Adhesion of metals: Experiment 1 ES-340 N86-10232
Evaluation of the accuracy of the metric camera images for the production of line maps and orthophotos N86-10490

POLITECNICO DI TORINO (ITALY).
Computational techniques for the analysis and design of digital communication systems
[AD-A156945] N86-10407

PRINCETON UNIV., N. J.
On the design of airfoils in transonic flow using the Euler equations N86-10013
Transport processes research N86-10129
Electrohydrodynamics N86-10130
Fundamental studies of droplet combustion at reduced gravity N86-10165
Modeling of engine sprays
[DE85-010020] N86-10559
The dynamics and stellar content of globular star clusters N86-11131

PULSE SCIENCES, INC., SAN LEANDRO, CALIF.
Radiation field results from the SPEED triaxiode, a large area, high dose rate, short pulse 1MV bremsstrahlung source
[DE85-009438] N86-11005

PURDUE UNIV., LAFAYETTE, IND.
On the method of characteristics and its application to the calculations of annular nozzle flowfields N86-10454
Dynamic analysis of robotic manipulations with flexible links N86-10545

Vegetation and soils field research data base: Experiment summaries
[E85-10110] N86-10810
Theory of advanced, high-efficience concentrator cells
[DE85-008621] N86-10855
A study of methods to predict and measure the transmission of sound through the walls of light aircraft. Integration of certain singular boundary element integrals for applications in linear acoustics
[NASA-CR-176229] N86-10812
Information on continuum states from feeding times and total (GAMMA) spectra measured with BGO suppressed detectors
[DE85-013868] N86-10861

R

R-K RESEARCH AND SYSTEM DESIGN, MALIBU, CALIF.
Annotated bibliography of publications dealing with occupational health and medical information systems, cost analysis procedures, evaluation methodology and related legal issues
[AD-A156650] N86-11078
RADIAN CORP., MORRISVILLE, N.C.
Proceedings: First Annual Acid Deposition Emissions Inventory Symposium
[PB85-200004] N86-10886
RAND CORP., SANTA MONICA, CALIF.
Soviet free-electron laser research
[AD-A156898] N86-10542
RELIABILITY ANALYSIS CENTER, GRIFFISS AFB, N. Y.
Microcircuit device reliability field experience database. Volume 1. Field data. Volume 2. Failure Event/Analysis data
[AD-A156836] N86-10433
RENNES UNIV. (FRANCE).
Long range translocations ashore to offshore using Spacelab-1 metric camera imagery in the purspective of integrated geophysical surveys N86-10490
RENSSELAER POLYTECHNIC INST., TROY, N. Y.
Fluid dynamics and thermodynamics of vapor phase crystal growth N86-10068
Vapor growth of alloy-type semiconductor crystals N86-10069
Dendritic growth in undercooled melts N86-10082
Influence of melt convection on solid-liquid interface under terrestrial and reduced gravity environments N86-10083
Crystallization, optical and chemical properties of fluoride glasses N86-10149
Fuel and lubricant behavior in boundary layers analyzed by infrared emission Fourier transform spectrometry N86-10336
Modeling and control of nonlinear systems N86-10362
A mesh moving technique for time dependent partial differential equations in two space dimensions
[AD-A156663] N86-10666
Heat transfer in condensing and evaporating two-component, two-phase flow inside a horizontal tube N86-11058
RESEARCH INST. OF NATIONAL DEFENCE, LINKOEPING (SWEDEN).
Digital radio link: Method and a measuring system for studying the radio channel during frequency selective fading
[FOA-C-30386-E2] N86-10411
Information technique 1985: Optical technology and electro-optics, a defense technical component review
[FOA-A-30037-E] N86-10980
RESEARCH INST. OF NATIONAL DEFENCE, STOCKHOLM (SWEDEN).
Report on a visit to England
[FOA-C5-85-0006-H2] N86-10364
Management of organizational operations in dynamic environments. Towards a frame of reference.
[FOA-C5-85-0003-H2] N86-11072
RESEARCH INST. OF NATIONAL DEFENCE, UMEA (SWEDEN).
Method for determining elemental sulfur in jet fuel
[FOA-C-40211-B4] N86-10360
RICE UNIV., HOUSTON, TEX.
Measurement of the properties of tungsten at high temperatures N86-10091
Supersonic metal cluster beams
[DE85-014321] N86-10966
ROBERTS ASSOCIATES, INC., VIENNA, VA.
Computation of flow regimes in parameter space for the AGCE
[NASA-CR-176480] N86-10705
ROCHESTER UNIV., N. Y.
Cooperative emission by two different atoms into surface plasmons
[AD-A157033] N86-10925
ROCKWELL INTERNATIONAL CORP., GOLDEN, COLO.
Metallurgy and metallography of braze joints
[DE85-014563] N86-10325
Secondary standards laboratories for ionizing radiation calibrations: The national laboratory interests
[DE85-007046] N86-10938
ROCKWELL INTERNATIONAL CORP., RICHLAND, WASH.
Time-term analysis of upper crustal structure in the Columbia Basin, Washington
[DE85-012390] N86-10633
ROYAL AIRCRAFT ESTABLISHMENT, FARNBOROUGH (ENGLAND).
Lumped geopotential harmonics of order 14, from the orbit of 1967-11G
[AD-A156627] N86-10190
Calculation of the glass transition temperatures of linear polymers. Part 1: Rules for hierarchical ordering of the data set
[AD-A156584] N86-10343
Measurements of the acoustic interference between adjacent microphones
[AD-A156662] N86-10919
ROYAL GREENWICH OBSERVATORY, HERSTMONCEUX (ENGLAND).
OASIS: Optical Aperture Synthesis in Space N86-11106
ROYAL INST. OF TECH., STOCKHOLM (SWEDEN).
A preliminary report on floating zone experiments with germanium crystals in a sounding rocket N86-10256
ROYAL NETHERLANDS METEOROLOGICAL INST., DE BILT.
List of publications on the 200 m meteorological mast at Cabauw, the Netherlands
[KNMI-FM-85-6] N86-10711
Monthly Bulletin North Sea: Volume 2, January 1985
[KNMI-167-VOL-2] N86-10732
ROYAL OBSERVATORY, EDINBURGH (SCOTLAND).
Optical/IR telescope arrays: A study of their potential for satisfying observational requirements in astronomy for a large aperture system in the 1990s and beyond
[REPT-15] N86-11094
ROYAL SIGNALS AND RADAR ESTABLISHMENT, MALVERN (ENGLAND).
Special purpose hardware architectures for language recognition
[AD-A156634] N86-10793
RUTGERS - THE STATE UNIV., NEW BRUNSWICK, N. J.
An investigation of vortex dynamics in 2-dimensional superfluid films of helium-4 N86-11040
Extra-galactic X-ray sources and the diffuse X-ray background N86-11144

S

SANDIA LABS., ALBUQUERQUE, N. MEX.
Inviscid flow field analysis of maneuvering hypersonic vehicles using the SCM formulation and parabolic grid generation
[DE85-013950] N86-10021
Simulated direct-strike lightning testing at Sandia National Laboratories
[DE85-012033] N86-10049
Laser generation and transport of a relativistic electron beam
[DE85-011709] N86-10192
Compact, low jitter, triggered spark gap
[DE85-012812] N86-10195
Theoretical comparison of classical (K-matrix) and inverse (P-matrix) least-squares methods for quantitative infrared spectroscopy
[DE85-012827] N86-10298
Chemical kinetics and cellular structure of detonations in hydrogen sulphide and air
[DE85-009409] N86-10304
Weld metal hot-cracking of hastelloy alloys C-22 and C-276: A study by analytical electron microscopy
[DE85-009437] N86-10324
Metastable phase formation in Ni-implanted Al: An analytical electron microscope investigation
[DE85-009105] N86-10331
Analysis of transitions between ferroelectric and antiferroelectric states under conditioning of uniaxial strain
[DE85-014466] N86-10350
Thermal expansion of glasses in the solid and liquid phases
[DE85-013953] N86-10351
Explosive initiation by very small conical shaped charge jets
[DE85-009443] N86-10357
Methods for developing jam-resistant security communications networks at fixed-site facilities
[DE85-012032] N86-10408
Calibrated Faraday current and magnetic field sensor
[DE85-013436] N86-10439
Effects of scale and geometry on hydrogen-air detonations
[DE85-006762] N86-10474
Geothermal lost circulation zone mapping tool
[DE85-008696] N86-10531
Characterization of cathodic corrosion products in the Ca/CaCrO4 thermal battery
[DE85-013442] N86-10644
Photovoltaic concentrator array evaluation
[DE85-013789] N86-10665
Estimating wind speed as a function of height above ground: An analysis of data obtained at the Southwest Residential Experiment Station, Las Cruces, New Mexico
[DE85-013262] N86-10716
Understanding and improving acoustic to seismic coupling as it pertains to Sandia's helicopter detector
[DE85-009440] N86-10920
Providing automated control for PBFA-2
[DE85-012867] N86-10928
Photonic diagnostics and pulsed power research
[DE85-013752] N86-10940
Preliminary investigation of changes in X-ray multilayer optics subjected to high radiation flux
[DE85-014074] N86-10944
Radiation field results from the SPEED triaxiode, a large area, high dose rate, short pulse 1MV bremsstrahlung source
[DE85-009438] N86-11005
Advances in data acquisition system technology for PBFA 2
[DE85-012860] N86-11011
Engineering high reliability, low-jitter Marx generators
[DE85-012811] N86-11013
Photoactivation of PBFA-2
[DE85-013439] N86-11019
Shock loading and release behavior of x-cut quartz
[DE85-013954] N86-11054
High-pressure release-wave measurements and phase transformation in CaCO3
[DE85-012592] N86-11055
SASKATCHEWAN UNIV., SASKATOON.
Applications of the second-order achromat concept to the design of particle accelerators
[DE85-013072] N86-10994
SCIENCE APPLICATIONS, INC., CHATSWORTH, CALIF.
Buoyancy effects upon vapor flame and explosion processes N86-10161
SCIENCE APPLICATIONS, INC., HUNTSVILLE, ALA.
The control of float zone interfaces by the use of selected boundary conditions N86-10060
SCIENCE APPLICATIONS INTERNATIONAL CORP., MCLEAN, VA.
High flux calorimetry
[AD-A156852] N86-10524
SHOCK AND VIBRATION INFORMATION CENTER (DEFENSE), WASHINGTON, D. C.
The Shock and Vibration Digest, volume 17, no. 3
[AD-A154144] N86-10585
Editors rattle space N86-10586
SILSOE COLL., BEDFORD (ENGLAND).
Land evaluation successes with the metric camera N86-10512
SOCIETE CROUZET, VALENCE (FRANCE).
Elastic wave gyrometer. Experiments with a parametric wave device
[REPT-26/5005/HF/AR] N86-10533
SOCIETE NATIONALE INDUSTRIELLE AEROSPATIALE, SURESNES (FRANCE).
Nondestructive control of thick structures made without disassembling
[PV-43-954/F/3] N86-10564
Nondestructive corrosion test of aluminum alloy structures
[PV-43-954/F/2] N86-10594
SOCIETE NATIONALE INDUSTRIELLE AEROSPATIALE, TOULOUSE (FRANCE).
Aerodynamics of hyperlift systems
[SNIAS-443.501/85] N86-10023
Analysis of hyperlift systems. Study of a singularities method
[SNIAS-443.529/84] N86-10024
SOUTHWEST RESEARCH INST., SAN ANTONIO, TEX.
Constitutive modeling for isotropic materials (HOST)
[NASA-CR-174980] N86-10589
Characterization of mechanical damage mechanisms in ceramic composite materials
[AD-A156574] N86-10590
Exploratory development for a high reliability flaw characterization module
[AD-A156632] N86-10916
SPECTRA TECHNOLOGY, INC., BELLEVUE, WASH.
Design, fabricate and test a 1.06(MU) repetitively pulsed laser
[DE85-014439] N86-10543

SPECTROLAB, INC., SYLMAR, CALIF.

Development of metallization process
[NASA-CR-176209] N86-10312

STANFORD LINEAR ACCELERATOR CENTER, CALIF.

Dissecting the cow
[DE85-013369] N86-10801

Klystron control software in the SIC
[DE85-013068] N86-10836

Parasitic mode losses versus signal sensitivity in beam position monitors
[DE85-014367] N86-10964

Beam-beam deflections to measure size spot and offset at SLC IP
[DE85-014285] N86-10965

Applications of the second-order achromat concept to the design of particle accelerators
[DE85-013072] N86-10994

Superconvergent tracking and invariant surfaces in phase space
[DE85-013051] N86-10995

Electron wind in strong wave guide fields
[DE85-013062] N86-11004

Effects of slots/holes in disks on frequencies of TM01 and EH11 waves in the disk-loaded waveguide
[DE85-013376] N86-11009

High-resolution phosphor screen beam profile monitor
[DE85-013074] N86-11012

SLC positron damping ring optics design
[DE85-013054] N86-11014

Timing system control software in the SLC
[DE85-013380] N86-11024

Beam steering in the SLC linac
[DE85-013370] N86-11025

Programmable delay unit incorporating a semi-custom integrated circuit
[DE85-013379] N86-11033

Search for heavy neutrines produced in e(+)e(-) annihilation
[DE85-013372] N86-11035

Superconductors for pulsed RF accelerators
[DE85-013378] N86-11051

STANFORD UNIV., CALIF.

The influence of low frequency mechanical vibrations on the growth of single crystals N86-10059

Lambda point equipment N86-10118

Cryogenic equivalence principle experiment N86-10171

Investigation of metallic impurities introduced into SiO2 and silicon by various candidate VLSI metallization systems: Chemical reactions, diffusion, and electrical properties
[AD-A156609] N86-10429

Film cooling on a convex wall: Heat transfer and hydrodynamic measurements for full and partial coverage
[NASA-CR-174964] N86-10461

Computer control of rf at SLAC
[DE85-013065] N86-11015

STATE UNIV. COLL. OF NEW YORK, BUFFALO.

Geothermal influences on the long-term thickness of the mechanical lithosphere during flexure N86-10697

STATE UNIV. OF NEW YORK, ALBANY.

Seasonal variations in atmospheric chemistry in the Adirondacks
[DE85-014227] N86-10719

STATE UNIV. OF NEW YORK, BUFFALO.

Digital decoding of in-line holograms N86-10478

Advanced development of BEM for two and three dimensional nonlinear analysis N86-10855

Cooperative emission by two different atoms into surface plasmons
[AD-A157033] N86-10925

STATE UNIV. OF NEW YORK AT BUFFALO, AMHERST.

Two-dimensional electrons
[AD-A156894] N86-10982

STONE AND WEBSTER ENGINEERING CORP., BOSTON, MASS.

Hot cell facility design for large fusion devices
[DE85-012893] N86-11037

STUTTGART UNIV. (WEST GERMANY).

GaS-semiconductor crystals under microgravity: Experiment ES 323 N86-10224

Laminar film condensation in vertical closed two-phase thermosiphons
[IKE-5-220] N86-10476

Digital elevation model from Spacelab metric camera photographs N86-10486

SUSSEX UNIV., BRIGHTON (ENGLAND).

The preparation and testing of titanium and zirconium coupling agents
[SJ70] N86-10576

SYDNEY UNIV. (AUSTRALIA).

A study of blood flow and of aggregation of blood cells under conditions of zero gravity: Its relevance to the occlusive diseases and cancer N86-10137

SYRACUSE UNIV., N. Y.

Environmental degradation of materials: Surface chemistry related to stress corrosion cracking N86-10099

SYSTEMS APPLICATIONS, INC., SAN RAFAEL, CALIF.

Technical considerations in regional aerosol modeling
[PB85-193027] N86-10710

T

TATA INST. OF FUNDAMENTAL RESEARCH, BOMBAY (INDIA).

Principal bundles on the affine line N86-10856

Coincidence densities and spectra of a class of substitution minimal sets N86-10857

TECHNICAL UNIV. OF DENMARK, LYNGBY.

Crystal growth from solution N86-10229

TECHNION - ISRAEL INST. OF TECH., HAIFA.

Effect of sequence of loading on interaction curves for buckling of stiffened shells
[TAE-536] N86-10583

Correlation between vibrations and buckling of cylindrical shells stiffened by spot-welded and riveted stringers
[TAE-537] N86-10584

TECHNISCHE HOCHSCHULE, GRAZ (AUSTRIA).

Geological mapping of remote mountainous regions using metric camera imagery N86-10503

TECHNISCHE HOGESCHOOL, DELFT (NETHERLANDS).

Fatigue, static tensile strength and stress corrosion of aircraft materials and structures
[VTH-LR-360-PT-1] N86-10045

Unidirectional solidification of cast iron: Experiment ES-325 N86-10212

Experiments and computations on unsteady separating flow in an expanding flume
[REPT-2-84] N86-10477

The local disk controller
[REPT-1-68430-44(1985)01] N86-10806

Performance analysis of the IBM Direct Access Storage Device (DASD) subsystem, and some suggestions for improved systems
[REPT-1-68430-44(1985)02] N86-10807

An intelligent local disk control system
[REPT-051560-28(1984)08] N86-10808

Acquaintance with on line literature research. An introduction for education at the Chemical Technology Section N86-11061

TECHNISCHE HOGESCHOOL, EINDHOVEN (NETHERLANDS).

Digital transmission experiments with the Orbital Test Satellite
[EUT-84-E-144] N86-10270

Measurement of workpiece temperature during welding for welding robot control N86-10534

Design of a multifunction Input-Output (I/O) controller
[EUT-84-E-143] N86-10802

Minimization of programmable logic arrays
[EUT-84-E-145] N86-10803

Realization of a multifunction Input/Output (I/O) controller by means of a gate array
[EUT-85-E-147] N86-10804

A course on field programmable logic
[EUT-85-E-148] N86-10805

The identification package SATER
[ER-83/08] N86-10844

COMPACT: Compaction of hierarchial chip layouts based on a constraint graph method with double-sided constraints N86-10845

State assignment in sequential circuits
[EUT-85-E-146] N86-10846

Stock-taking of data base management systems choice considerations for the Eindhoven Technical University Computing Center (THE-RC)
[COMP-CENT-NOTE-18] N86-10851

Multivariable partial realization and the aspect of uniqueness
[ER-83/09] N86-10879

Naive approximate realization of noisy data
[ER-83/10] N86-10880

Adaptive distribution-free test for the K random sampling problem, part 1
[COMP-CENT-NOTE-14-PT-1] N86-10888

Adaptive distribution free test for the K random sampling problem, part 2
[COMP-CENT-NOTE-15-PT-2] N86-10889

Robustness of multiple comparisons against variance heterogeneity
[COMP-CENT-NOTE-17] N86-10890

Nonparametric comparison of several mean values with mild adaptation to some sample characteristics
[COMP-CENT-NOTE-20] N86-10891

Operations research applications
[ARW-03-THE-BDK/ORS/83-08] N86-10901

On the structure of manpower planning, a contribution of simulation experiments with decomposition methods
[MANPOWER-PLANNING-28] N86-11073

Aspects of manpower planning at a Dutch university, an example of aggregation and decomposition methods in manpower planning
[MANPOWER-PLANNING-29] N86-11074

On the structure of manpower planning, a contribution of simulation experiments with aggregation methods
[MANPOWER-PLANNING-30] N86-11075

Failures and successes of quantitative methods in management
[ARW-03-THE-BDK/ORS/83-06] N86-11076

TECHNISCHE UNIV., BERLIN (WEST GERMANY).

Self diffusion of Sn112 and Sn124 in liquid tin N86-10231

Topographic interpretation of metric camera images: An example in Somalia N86-10506

A logistics scenario for an early lunar base
[ILR-MITT-143] N86-11140

TECHNISCHE UNIV., CLAUSTHAL-ZELLERFELD (WEST GERMANY).

Interdiffusion in the glass melt system (Na2O+Rb2O).3SiO2 N86-10216

Shrinking of a gas bubble in a glass melt under microgravity conditions N86-10254

TECHNISCHE UNIV., HANOVER (WEST GERMANY).

Orthophotomapping from metric camera imagery N86-10487

Digital image processing of metric camera imagery N86-10511

TECHNISCHE UNIV., MUNICH (WEST GERMANY).

Nucleate pool boiling in subcooled liquid under microgravity: Results of TEXUS experimental investigations N86-10250

Isochoric specific heat of sulfur hexafluoride at the critical point. A Spacelab experiment for the German D1-mission in 1985 N86-10251

Physical and chemical properties of a nickel catalyst processed under microgravity N86-10255

Analysis of metric camera images from the USA and their suitability for topographic and thematic mapping N86-10498

Interpretation of metric camera concerning hydrologic structures of the Rhone Delta N86-10504

Thematic mapping of metric camera color infrared and black and white photographs for land use classification N86-10510

Topographic and thematic mapping: Analysis of metric camera black and white photographs of the Rhone Delta N86-10514

Updating of topographic maps by means of metric camera photos example: Hallertau (Bavaria) N86-10517

Interpretation of Spacelab-1 photographs for the generation of 1:200000 topographic map N86-10518

Metric camera image of Munich as additional means for urban cartography N86-10519

Tectonic analysis of typical fold structures in the Zagros Mountains (Iran) by the application of quantitative photogrammetric methods on metric camera data N86-10521

TECHNISCHE UNIV., VIENNA (AUSTRIA).

Vacuum brazing under microgravity N86-10214

Stereo-orthophotos in various map projections N86-10488

TENNESSEE UNIV., KNOXVILLE.

Thermodynamic constraints on ion beam mixing of metals on insulators
[DE85-013626] N86-10448

Determination of optical properties by third-harmonic generation in noble gases in unfocused laser beams N86-10535

Ground-coupled heat pump research at the University of Tennessee Washington, D.C., 10 Dec. 1984
[DE85-005357] N86-10650

The effects of orography on land-atmosphere turbulent exchange processes N86-10702

TENNESSEE VALLEY AUTHORITY, CHATTANOOGA.

Kinetics of biological ferrous iron oxidation
[DE85-014616] N86-10736

TENNESSEE VALLEY AUTHORITY, KNOXVILLE.

Sediment characterization. Task 2: Instream contaminant study. Volume 2: Appendices
[DE85-013503] N86-10680

Sediment characterization. Task 2: Instream contaminant study, volume 1
[DE85-013502] N86-10683

TESTWELL LTD., DAVENTRY (ENGLAND).

Fracture toughness testing of centrifugally cast nickel aluminium bronze
[REPT-MAT/720] N86-10575

TEXAS CHRISTIAN UNIV., FORT WORTH.

Real-time holography by stimulated Raman and Brillouin scattering N86-10479

TEXAS DEPT. OF WATER RESOURCES, AUSTIN.

Evaluating the ground-water resources of the high plains of Texas, Volume 4 [PB85-191625] N86-10641

TEXAS TECHNOLOGICAL UNIV., LUBBOCK.

Electromagnetic resonances of cylinders and aircraft model with resistive wires [NASA-CR-176250] N86-10042

TEXAS UNIV., AUSTIN.

Nature of photoemission into dielectric fluids [DE85-013017] N86-10945

Local conservation laws for the Maxwell-Vlasov and collisionless kinetic guiding center theories [DE85-013122] N86-11063

A method for numerical relativity: Simulation of axisymmetric gravitational collapse and gravitational radiation generation N86-11127

Initial data for N black holes N86-11128

TEXAS UNIV., EL PASO.

Crustal structure of the southern Rio Grande rift determined from seismic refraction, surface wave dispersion, and gravity data N86-10700

TILBURG UNIV. (NETHERLANDS).

Superefficient estimation of power functions in simulation experiments [B8562445] N86-10893

The power of weighted and ordinary least squares with estimated unequal variances in experimental design [B8562446] N86-10894

Regression analysis: Assumptions, alternatives, applications N86-10895

TOLEDO UNIV., OHIO.

Mass transport phenomena between bubbles and dissolved gases in liquids under reduced gravity conditions N86-10110

TOPOGRAPHICAL SURVEY BRANCH, KATHMANDU (NEPAL).

Test on mapping application of metric camera imagery N86-10505

TRW SPACE TECHNOLOGY LABS., REDONDO BEACH, CALIF.

Symmetric Tandem Mirror Program [DE85-012352] N86-11032

U

UNITED KINGDOM ATOMIC ENERGY AUTHORITY, RISLEY (ENGLAND).

The influence of the substrate on the practical machining applications of cutting edges coated with different materials [BLL-RISLEY-TR-5039-(9091.9F)] N86-10546

UNITED NATIONS ECONOMIC COMMISSION FOR AFRICA, ADDIS ABABA (ETHIOPIA).

Role of the Economic Commission for Africa as a principal investigator in the metric camera experiment and reports of the result of the assessment for topographic and revision of maps in populated and developed areas of the world N86-10501

UNITED TECHNOLOGIES CORP., SOUTH WINDSOR, CONN.

Phosphoric and electric utility fuel technology development [DE85-014741] N86-10651

Phosphoric and electric utility fuel cell technology development [DE85-014552] N86-10652

UNIVERSIDAD POLITECNICA DE MADRID (SPAIN).

Liquid column stability: Experiment 1 ES-331 N86-10205

Stability of long liquid columns N86-10244

UNIVERSITE DES SCIENCES ET TECHNIQUES DU LANGUEDOC, MONTPELLIER (FRANCE).

Formation of waves by ground motion [PM/84/09] N86-10706

Well-posed questions and exploration of the space of parameters in linear and non linear inversion [PN-84/13] N86-10858

A modified modified Korteweg-deVries equation [PN-84/27] N86-10859

UNIVERSITIES SPACE RESEARCH ASSOCIATION, COLUMBIA, MD.

A root-mean-square pressure fluctuations model for internal flow applications [NASA-CR-3928] N86-10460

UNIVERSITY COLL., LONDON (ENGLAND).

Evaluation of metric camera images at the University of London N86-10495

OEEPE participation in testing metric camera photography N86-10507

UNIVERSITY OF SOUTHERN CALIFORNIA, LOS ANGELES.

Evaluation of a pulse control law for flexible spacecraft [NASA-CR-176233] N86-10272

Chronologic analysis of terrestrial sediments and basin evolution N86-10602

UTAH UNIV., SALT LAKE CITY.

Morphological stability and fluid dynamics of vapor crystal growth N86-10126

V

VALVO ROEHREN- UND HALBLEITERWERKE DER PHILIPS G.M.B.H., HAMBURG (WEST GERMANY).

Increase of the packaging density of Very Large Scale Integration (VLSI) circuits using automatic alignment [BMFT-FB-T-85-020] N86-10451

VANDERBILT UNIV., NASHVILLE, TENN.

The role of freestream turbulence scale in subsonic flow separation [NASA-CR-176237] N86-10014

Effect of undercooling in a low-gravity containerless environment on the structure and properties of alloys N86-10073

VIRGINIA POLYTECHNIC INST., BLACKSBURG.

Intrinsic mechanisms of multilayer ceramic capacitor failure [AD-A156638] N86-10431

VIRGINIA POLYTECHNIC INST. AND STATE UNIV., BLACKSBURG.

A fundamental study of the sticking of insect residues to aircraft wings [NASA-CR-176231] N86-10033

Finite element solution of the Navier-Stokes equations for 3-D turbulent free shear flows N86-10457

VIRGINIA UNIV., CHARLOTTESVILLE.

Simulating the CTR environment in the HVBM [DE85-011745] N86-10193

A study of the applicability of nucleation theory to quasi-thermodynamic transitions of second and higher Ehrenfest-order [NASA-CR-176238] N86-11059

A study of the applicability of nucleation theory to quasi-thermodynamic transformations of second and higher Ehrenfest-order [NASA-CR-176230] N86-11060

W

WACKER-CHEMIE G.M.B.H. BURGHAUSEN (WEST GERMANY).

Crystallization of a silicon sphere N86-10226

WASHINGTON UNIV., SEATTLE.

Radiative heat transfer in nonisothermal combustion products N86-10458

Scaling studies of solar pumped lasers [NASA-CR-176240] N86-10540

Strategies for analyzing mixed pixels in remotely sensed imagery N86-10623

Energy balance in a deep Colorado valley: ASCOT 84 [DE85-012441] N86-10631

Physical conditions in giant extragalactic H2 regions N86-11130

WASHINGTON UNIV., ST. LOUIS, MO.

Criteria for the design or selection of a bioelectromagnetics experiment [AD-A156575] N86-10420

Non-empirical interatomic potentials for transition metals [DE85-013448] N86-10440

Analysis of remote sensing data N86-10605

WEAPONS SYSTEMS RESEARCH LAB., ADELAIDE (AUSTRALIA).

A simplified method of estimation of the specular components of radar cross section for some re-entrant conductors [AD-A156573] N86-10403

A comparison of swept frequency and FFT methods used to calibrate array test modules [AD-A156629] N86-10430

WESTAT RESEARCH, INC., ROCKVILLE, MD.

Academic Research Equipment in selected science-engineering fields, 1982-83. An analysis of findings from the Baseline National Survey of academic research instruments and instrumentation needs N86-11088

WESTECH SYSTEMS, INC., PHOENIX, ARIZ.

Microgravity silicon zoning investigation N86-10063

WESTERN RESEARCH INST., LARAMIE, WYO.

Geologic evaluation and reservoir properties of the PR Spring tar sand deposit, Uintah and Grand Counties, Utah [DE85-013248] N86-10634

WESTINGHOUSE RESEARCH AND DEVELOPMENT CENTER, PITTSBURGH, PA.

Delay times and jitter in triggered vacuum spark gaps using metal vapor and surface flashover types of triggers [DE85-013986] N86-10441

WESTLAND HELICOPTERS LTD., YEOVIL (ENGLAND).

Trials on the asperity counting monitoring system [RES-PAPER-670] N86-10550

WESTON OBSERVATORY, MASS.

Vibro-acoustic forecast for space shuttle launches at Vandenberg AFB: The payload changeout room and the administration building [AD-A156944] N86-10269

WISCONSIN UNIV., MADISON.

Containerless processing of undercooled melts N86-10093

WISCONSIN UNIV., MILWAUKEE.

Altitudinal distribution of granitic landforms in the south central Sierra Nevada, California N86-10695

WRIGHT STATE UNIV., DAYTON, OHIO.

Initial increase, peaking effect, in the internal friction of copper following pulsed neutron and electron irradiation [DE85-012767] N86-10932

WYOMING UNIV., LARAMIE.

Spillover minimization in self-adjoint distributed-parameter systems with direct output feedback N86-10852

The two micron spectrum of R Scuti N86-11092

Y

YALE UNIV., NEW HAVEN, CONN.

The mechanics of delamination in composite materials N86-10284

Strength of shells under local transverse loads N86-10568

Modeling groundwater flow into lakes N86-10598

Alternating direction methods on multiprocessors: An extended abstract [AD-A156722] N86-10794

Efficient systolic arrays for the solution of toeplitz systems: An illustration of a methodology for the construction of systolic architectures in VLSI (Very Large Systems Integration) [AD-A156767] N86-10795

The DUCK manual [AD-A156936] N86-10833

Topological properties of hypercubes [AD-A156777] N86-10850

Rank revealing QR-Factorizations [AD-A156756] N86-10887

Electron tunneling in metal/tunnel-oxide/degenerate silicon junctions N86-11043

YALE UNIV. OBSERVATORY, NEW HAVEN, CONN.

Partial eigensolutions of large nonsymmetric matrices [AD-A156711] N86-10867

On the lanczos method for solving symmetric linear systems with several right-hand-sides [AD-A156816] N86-10868

Z

ZURICH UNIV. (SWITZERLAND).

Evaluation of metric camera photos N86-10515

CONTRACT NUMBER INDEX

SCIENTIFIC AND TECHNICAL AEROSPACE REPORTS VOLUME 24 NUMBER 1

Typical Contract Number Index Listing

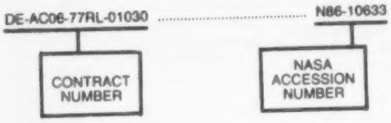

Listings in this index are arranged alphanumerically by contract number. Under each contract number the NASA accession numbers denoting documents that have been produced as a result of research done under that contract are arranged in ascending order. The NASA accession number denotes the number by which the citation is identified.

AF PROJ. TKSI N86-10191
AF PROJ. 2103 N86-10830
AF-AFOSR-0192-80 N86-10666
AF-AFOSR-0193-81 N86-10668
AF-AFOSR-0290-82 N86-11060
AMTE-NSM42D/1611 N86-10575
ARPA ORDER 4395 N86-10924
ARPA ORDER 5020 N86-11050
A12/1347 N86-10550
A79/KL/097 N86-10789
A83/K/045 N86-10782
BMFT-01-QV-148-ZA-SN-SLN-7786 N86-10242
CNR-PSN-83-070 N86-10203
N86-10238
DA PROJ. RR0-3302 N86-11049
DA PROJ. W05-270 N86-10406
DA PROJ. 1L1-61102-BH-57 N86-10407
DA PROJ. 4A7-62707-A-855 N86-10630
DA PROJ. 376-3 N86-10042
DAAG29-82-K-0197 N86-10866
DAAG29-83-C-0016 N86-10342
DAAG29-83-K-0177 N86-10887
DAJA37-80-C-0011 N86-10407
DARPA ORDER A04541 N86-10429
DARPA ORDER 4000 N86-10291
DE-AC01-83CE-30780 N86-10646
N86-10648
N86-10731
DE-AC02-76CH-00016 N86-10438
N86-10649
N86-10667
N86-10719
N86-10931
N86-10933
N86-10935
N86-10937
N86-10947
N86-10948
N86-10969
N86-11010
N86-11018
N86-11021
N86-11022
N86-11023
N86-11026
DE-AC02-76CH-03000 N86-10946
N86-10997
DE-AC02-76ER-04073 N86-10303
DE-AC02-78ET-51013 N86-11000
N86-11020
DE-AC02-81ER-10996 N86-10668
N86-10887
DE-AC02-83CH-10093 N86-10645
N86-10655
N86-10657
N86-10658
N86-10668
DE-AC02-83CH-100983 N86-10662
DE-AC02-83ER-40105 N86-11062
DE-AC03-76SF-00098 N86-10321
N86-10442
N86-10446
N86-10962
N86-10978
N86-10995
N86-11008
N86-11057
DE-AC03-76SF-00515 N86-10801
N86-10836
N86-10964
N86-10965
N86-10994
N86-10995
N86-11004
N86-11009
N86-11012
N86-11014
N86-11015
N86-11024
N86-11025
N86-11033
N86-11035
N86-11051
DE-AC03-79ET-51017 N86-11032
DE-AC03-81ER-40050 N86-11014
DE-AC04-76DP-00613 N86-10410
N86-10842
DE-AC04-76DP-00789 N86-10021
N86-10049
N86-10192
N86-10195
N86-10298
N86-10300
N86-10301
N86-10304
N86-10324
N86-10331
N86-10350
N86-10351
N86-10357
N86-10408
N86-10439
N86-10441
N86-10474
N86-10531
N86-10644
N86-10716
N86-10920
N86-10928
N86-10940
N86-11005
N86-11011
N86-11013
N86-11019
N86-11054
N86-11055
DE-AC04-76DP-03533 N86-10325
DE-AC04-81AL-16338 N86-10559
DE-AC05-84CR-21400 N86-10328
N86-10958
DE-AC05-84CT-21400 N86-10843
DE-AC05-84OR-21400 N86-10329
N86-10448
N86-10472
N86-10473
N86-10526
N86-10647
N86-10650
N86-10653
N86-10654
N86-10661
N86-10664
N86-10677
N86-10678
N86-10679
N86-10840
N86-10926
N86-10936
N86-10949
N86-10960
N86-11037
DE-AC05-84OS-21400 N86-10330
DE-AC05-84OU-21400 N86-10953
DE-AC06-76RL-01830 N86-10297
N86-10299
N86-10326
N86-10527
N86-10631
N86-10666
N86-10684
N86-10772
N86-10938
DE-AC06-77RL-01030 N86-10633
DE-AC06-83FR-53157 N86-10543
DE-AC07-76ID-01570 N86-10320
N86-10530
N86-10736
N86-10954
DE-AC07-83ID-12379 N86-10682
DE-AC08-83NV-10282 N86-10528
DE-AC09-76SF-00001 N86-10348
DE-AC09-76SR-00001 N86-10319
DE-AC21-81FE-15078 N86-10444
DE-AC21-83FE-60338 N86-10651
N86-10652
DE-AC21-83MC-20212 N86-10447
DE-AC79-83BP-13795 N86-10527
DE-AI01-76ET-20320 N86-10582
DE-AI01-78CS-54209 N86-11083
N86-11084
N86-11085
N86-11086
DE-AI01-79ET-20485 N86-10643
DE-AI05-84CR-21444 N86-10680
DE-AS05-76ET-52023 N86-10193
DE-AS05-76FV-04814 N86-10957
DE-AS05-78ER-06035 N86-10966
DE-AT01-77DP-70032 N86-10302
DE-AT03-81ER-10870 N86-10327
DE-AT03-84ER-53158 N86-11007
DE-FC21-83FE-60177 N86-10634
DE-FG02-84ER-13283 N86-10834
DE-FG02-84ER-45130 N86-10440
DE-FG02-34ER-45153 N86-11053
DE-FG05-80ET-53088 N86-11063
DE-FG05-84ER-45064 N86-10945
DE-FG05-84FR-13266 N86-10939
DFVLR-01-QV-698 N86-10224
DNA001-80-C-0022 N86-10405
DNA001-82-C-0185 N86-10524
DRET-81-668 N86-10878
DRET-83-34-051-00-470-75-01 N86-10023
DRET-83-34-135 N86-10022
DRET-83-056 N86-10533
EPA-68-02-3487 N86-10689
EPA-68-02-3994 N86-10686
EPA-68-02-3996 N86-10688
EPA-68-02-4076 N86-10710
F04701-83-C-0064 N86-10708
F19628-84-C-0011 N86-10269
F30602-84-C-0162 N86-10433
F33600-82-C-0543 N86-10006
F33615-80-C-0512 N86-10675
F33615-81-C-5056 N86-10292
F33615-81-C-5066 N86-10916
F33615-81-K-1539 N86-10432
JPL PROJ. 5030-573 N86-11083
N86-11084
N86-11085
N86-11086
JPL-955057 N86-10118
JPL-955870 N86-10149
JPL-956205 N86-10312
LFP-955147 N86-10050
MDA903-82-K-0412 N86-10429
MDA903-83-C-0306 N86-10790
MDA903-83-M-2646 N86-11065
MDA903-84-C-0031 N86-10829
N86-11071
MDA903-84-K-0232 N86-10291
MDA903-84-K-0374 N86-11050
MDA903-85-C-0030 N86-10542
MIN-DEF-A93B/1034 N86-10309
MIN-DEF-ERC/9/4/2120/034 N86-10576
MIN-DEF-K80B/33 N86-10339
MIPR-N-83-18 N86-10830
NAG-483 N86-10101

NAGW-466 N86-10099
NAGW-469 N86-10100
NAG1-26 N86-10042
NAG1-56 N86-10912
NAG1-126 N86-10271
NAG1-135 N86-10539
NAG1-176 N86-10540
NAG1-190 N86-10848
NAG1-300 N86-10033
NAG1-336 N86-10577
NAG1-354 N86-10054
NAG1-419 N86-11059
N86-11060
NAG1-471 N86-10272
NAG1-483 N86-10014
NAG1-500 N86-10484
NAG2-62 N86-10118
NAG3-3 N86-10461
NAG3-34 N86-10110
NAG3-147 N86-10108
NAG3-259 N86-10130
NAG3-303 N86-10117
NAG3-333 N86-10083
NAG3-380 N86-10165
NAG3-381 N86-10160
NAG3-404 N86-10163
NAG3-417 N86-10090
NAG3-436 N86-10093
NAG3-443 N86-10162
NAG3-447 N86-10129
NAG3-470 N86-10113
NAG3-475 N86-10377
NAG3-493 N86-10128
NAG3-534 N86-10588
N86-10860
NAG3-560 N86-10086
NAG3-568 N86-10123
NAG3-570 N86-10124
NAG4-379 N86-10119
NASA ORDER H-27954-B N86-10074
N86-10077
NASA ORDER H-34328-B N86-10067
NASA ORDER H-73830-B N86-10066
NASA ORDER H-78181-B N86-10705
NASA ORDER H-78183-B N86-11095
NASA ORDER R05-030-001 N86-11047
NASA ORDER S-12402-C N86-10597
NASW-3458 N86-10462
NASW-3755 N86-11103
NASW-3949 N86-11139
NASW-3950 N86-11133
NASW-4004 N86-10418
NASW-4005 N86-10293
N86-10611
N86-10612
N86-10613
N86-10614
NASW-4006 N86-10179
N86-10273
N86-10378
NAS2-11555 N86-10819
NAS2-11946 N86-10274
NAS3-22822 N86-10161
NAS3-23770 N86-10164
NAS3-23925 N86-10589
NAS3-23934 N86-10132
NAS7-100 N86-10150
N86-10312
NAS7-918 N86-10102
N86-10167
N86-10382
N86-10599
N86-10615
N86-10707
N86-11083
N86-11084
N86-11085
N86-11086
NAS8-32614 N86-10143
NAS8-32936 N86-10069
NAS8-32945 N86-10064
NAS8-32950 N86-10135
NAS8-32951 N86-10146
NAS8-32952 N86-10081
N86-10264
NAS8-33021 N86-10095
NAS8-33199 N86-10091
NAS8-33513 N86-10169
NAS8-33562 N86-10068
NAS8-33742 N86-10177
NAS8-33861 N86-10109
NAS8-34321 N86-10172
NAS8-34648 N86-10168
NAS8-34676 N86-10073
NAS8-34758 N86-10148
NAS8-34872 N86-10059
NAS8-34887 N86-10070
NAS8-34891 N86-10071
NAS8-34920 N86-10063
NAS8-35108 N86-10060
NAS8-35145 N86-10076
NAS8-35161 N86-10075
NAS8-35333 N86-10136
N86-10246
NAS8-35334 N86-10138
N86-10246
NAS8-35362 N86-10139
N86-10246
NAS8-35412 N86-10062
NAS8-35416 N86-10154
NAS8-35483 N86-10089
NAS8-35620 N86-10096
NAS8-35668 N86-10175
NAS8-35918 N86-10460
NAS8-36516 N86-10233
NAS9-15566 N86-10140
NAS9-15584 N86-10145
NAS9-16389 N86-10134
NAS9-16528 N86-10610
NAS9-16634 N86-10770
N86-10785
N86-10820
N86-10821
N86-10896
N86-10897
NCC1-75 N86-10578
NCC2-248 N86-11047
NGT-47-003-029 N86-11064
NSF DCR-84-07077 N86-10833
NSF DMS-83-15216 N86-10862
N86-10864
N86-10869
NSF ECS-82-05425 N86-10861
NSF PHY-77-27084 N86-10088
NSF PHY-84-01063 N86-11008
NSF SRS-80-17873 N86-11088
NSG-1468 N86-10827
NSG-1534 N86-10126
NSG-1648 N86-10822
N86-10823
N86-10824
N86-10825
N86-10826
NSG-7176 N86-11103
N86-11104
N86-11118
NSG-7331 N86-10061
NSG-7645 N86-10055
N86-10056
N86-10072
N86-10078
N86-10080
N86-10085
N86-10098
N86-10105
N86-10127
N86-10133
N86-10147
N86-10152
N86-10158
N00014-76-C-0063 N86-10346
N86-10593
N00014-76-C-0370 N86-10432
N00014-77-C-0505 N86-10591
N00014-79-C-0661 N86-10899
N00014-79-C-0683 N86-10283
N00014-80-C-0236 N86-10432
N00014-80-C-0472 N86-10925
N00014-82-C-5076 N86-10899
N00014-82-K-0184 N86-10794
N86-10795
N86-10850
N86-10867
N86-10868
N86-10887
N00014-82-K-0329 N86-10861
N00014-83-C-0170 N86-10465
N86-10541
N86-10977
N00014-83-C-0196 N86-10735
N00014-83-C-0271 N86-10345
N00014-83-K-0125 N86-10898
N00014-83-K-0168 N86-10431
N00014-83-K-0281 N86-10833
N00014-83-K-0365 N86-11142
N00014-83-K-0613 N86-11061
N00014-84-C-0123 N86-10590
N00014-84-C-0193 N86-10918
N00014-84-C-0394 N86-10727
N00014-84-C-0601 N86-11078
N00014-84-K-0092 N86-10795
N00014-84-K-0301 N86-10885
N86-10886
N00014-84-K-0387 N86-10982
N00014-84-K-0457 N86-10420
N00014-85-F-0004 N86-10295
N00014-85-K-0131 N86-10870
N00014-85-K-0169 N86-10862
N86-10864
N86-10869
RR0-1103 N86-10295
RR0-3302 N86-10714
RR0-4209 N86-10870
STPA-82-96-006 N86-10564
STPA-82-96006 N86-10594
S14-40 N86-10863
T99-QMXL N86-10983
USPN-HL-23374 N86-10247
W-31-109-ENG-38 N86-10322
N86-10443
N86-10635
N86-10659
N86-10676
N86-10871
N86-10934
N86-10941
N86-10942
N86-10952
N86-10961
N86-10979
N86-10991
N86-11036
N86-11052
N86-11056
W-7405-ENG-26 N86-10985
W-7405-ENG-36 N86-10194
N86-10349
N86-10356
N86-10358
N86-10469
N86-10529
N86-10660
N86-10663
N86-10835
N86-10837
N86-10839
N86-10841
N86-10927
N86-10929
N86-10930
N86-10932
N86-10943
N86-10944
N86-10950
N86-10963
N86-10986
N86-10987
N86-10988
N86-10990
N86-10992
N86-10993
N86-10996
N86-10998
N86-10999
N86-11001
N86-11002
N86-11003
N86-11006
N86-11027
N86-11028
N86-11029
N86-11031
N86-11034
W-7405-ENG-48 N86-10296
N86-10317
N86-10318
N86-10323
N86-10359
N86-10409
N86-10445
N86-10466
N86-10467
N86-10468
N86-10470
N86-10471
N86-10532
N86-10632
N86-10717
N86-10718
N86-10737
N86-10907
N86-10908
N86-10956
N86-10959
N86-10984
N86-11016
N86-11017
N86-11030

N86-11090
N86-11134
W-7503-ENG-36 .... N86-10955
147-51-02-40-00 .... N86-10707
199-80-42 .... N86-10734
446-01-01-01-00 .... N86-10615
503-56-11 .... N86-11047
504-64-23 .... N86-10828
505-31-01 .... N86-10464
505-31-04 .... N86-10017
N86-10461
505-33-1A N86-10290
N86-10311
505-33-53-03 .... N86-10913
505-33-78 .... N86-10579
505-34-13-32 .... N86-10848
505-35-31 .... N86-10048
505-40-90-01 .... N86-10016
505-43-01 .... N86-10015
506-53-1A N86-10561
506-53-1B N86-10552
506-53-23-05 .... N86-10581
506-54-21 .... N86-10274
506-55-22 .... N86-10279
N86-10281
506-55-72 .... N86-11048
506-57-13-01 .... N86-10580
506-57-21 .... N86-10777
506-57-27-36 .... N86-10770
N86-10785
N86-10820
N86-10821
N86-10896
N86-10897
506-58-22 .... N86-10380
N86-10381
533-04-1A N86-10589
776-33-41 .... N86-10582
776-52-41 .... N86-10643
778-36-05-01 .... N86-11083
N86-11084
N86-11085
N86-11086
953-36-00-00-72 .... N86-10018
999-43-02 .... N86-10819

REPORT/ACCESSION NUMBER INDEX

SCIENTIFIC AND TECHNICAL AEROSPACE REPORTS VOLUME 24 NUMBER 1

Typical Report Number Index Listing

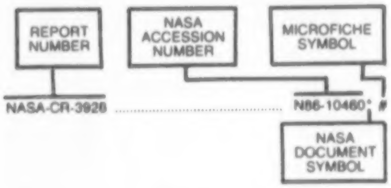

Listings in this index are arranged alphanumerically by report number. The NASA accession number denotes the number by which the citation is identified. An asterisk (*) indicates that the item is a NASA report. A pound sign (#) indicates that the item is available on microfiche.

ACSC-85-1130 .... N86-10831 #
ACSC-85-1330 .... N86-10040 #
ACSC-85-1670 .... N86-10713 #
ACSC-85-1950 .... N86-10034 #
ACSC-85-2630 .... N86-10038 #
ACSC-85-2715 .... N86-10199 #

AD-A145745 .... N86-10007 #
AD-A147304 .... N86-10001 #
AD-A154144 .... N86-10585 #
AD-A155833 .... N86-10342 #
AD-A156469 .... N86-10914 #
AD-A156518 .... N86-10034 #
AD-A156525 .... N86-10861 #
AD-A156541 .... N86-10898 #
AD-A156547 .... N86-10035 #
AD-A156548 .... N86-10791 #
AD-A156559 .... N86-10419 #
AD-A156573 .... N86-10403 #
AD-A156574 .... N86-10590 #
AD-A156575 .... N86-10420 #
AD-A156576 .... N86-10727 #
AD-A156577 .... N86-10553 #
AD-A156583 .... N86-11142 #
AD-A156584 .... N86-10343 #
AD-A156589 .... N86-10191 #
AD-A156590 .... N86-10735 #
AD-A156593 .... N86-10951 #
AD-A156597 .... N86-10786 #
AD-A156600 .... N86-10862 #
AD-A156601 .... N86-10465 #
AD-A156602 .... N86-10036 #
AD-A156603 .... N86-10037 #
AD-A156608 .... N86-10428 #
AD-A156609 .... N86-10429 #
AD-A156625 .... N86-10863 #
AD-A156626 .... N86-10864 #
AD-A156627 .... N86-10190 #
AD-A156629 .... N86-10430 #
AD-A156631 .... N86-10779 #
AD-A156632 .... N86-10916 #
AD-A156634 .... N86-10793 #
AD-A156636 .... N86-11049 #
AD-A156637 .... N86-10523 #
AD-A156638 .... N86-10431 #
AD-A156639 .... N86-10591 #
AD-A156650 .... N86-11078 #
AD-A156655 .... N86-10865 #
AD-A156660 .... N86-10712 #
AD-A156661 .... N86-10354 #
AD-A156662 .... N86-10404 #
AD-A156663 .... N86-10866 #
AD-A156664 .... N86-10592 #
AD-A156667 .... N86-10829 #
AD-A156668 .... N86-11071 #
AD-A156669 .... N86-10563 #
AD-A156671 .... N86-10344 #
AD-A156687 .... N86-10790 #
AD-A156688 .... N86-10038 #
AD-A156694 .... N86-10708 #
AD-A156695 .... N86-10713 #
AD-A156699 .... N86-10432 #
AD-A156704 .... N86-10917 #
AD-A156705 .... N86-10977 #
AD-A156706 .... N86-10541 #
AD-A156711 .... N86-10867 #
AD-A156715 .... N86-10885 #
AD-A156717 .... N86-10726 #
AD-A156722 .... N86-10794 #
AD-A156724 .... N86-10294 #
AD-A156735 .... N86-10630 #
AD-A156736 .... N86-10714 #
AD-A156752 .... N86-10345 #
AD-A156754 .... N86-10886 #
AD-A156756 .... N86-10887 #
AD-A156757 .... N86-10346 #
AD-A156764 .... N86-10315 #
AD-A156765 .... N86-10729 #
AD-A156767 .... N86-10795 #
AD-A156769 .... N86-10849 #
AD-A156776 .... N86-10291 #
AD-A156777 .... N86-10850 #
AD-A156778 .... N86-10593 #
AD-A156779 .... N86-10830 #
AD-A156781 .... N86-10199 #
AD-A156792 .... N86-11065 #
AD-A156808 .... N86-10039 #
AD-A156813 .... N86-10295 #
AD-A156815 .... N86-10675 #
AD-A156816 .... N86-10868 #
AD-A156817 .... N86-10899 #
AD-A156819 .... N86-10831 #
AD-A156835 .... N86-10869 #
AD-A156836 .... N86-10433 #
AD-A156842 .... N86-10040 #
AD-A156847 .... N86-10796 #
AD-A156848 .... N86-10797 #
AD-A156850 .... N86-10405 #
AD-A156852 .... N86-10524 #
AD-A156856 .... N86-10832 #
AD-A156871 .... N86-10041 #
AD-A156881 .... N86-10276 #
AD-A156882 .... N86-10557 #
AD-A156886 .... N86-10406 #
AD-A156888 .... N86-10918 #
AD-A156889 .... N86-10292 #
AD-A156892 .... N86-10919 #
AD-A156893 .... N86-10006 #
AD-A156894 .... N86-10982 #
AD-A156898 .... N86-10542 #
AD-A156903 .... N86-10798 #
AD-A156905 .... N86-10900 #
AD-A156909 .... N86-10347 #
AD-A156916 .... N86-10983 #
AD-A156936 .... N86-10833 #
AD-A156944 .... N86-10269 #
AD-A156945 .... N86-10407 #
AD-A156956 .... N86-10275 #
AD-A156957 .... N86-10434 #
AD-A156960 .... N86-10042* #
AD-A156969 .... N86-10787 #
AD-A156977 .... N86-11079 #
AD-A156981 .... N86-10715 #
AD-A156983 .... N86-11050 #
AD-A156987 .... N86-10771 #
AD-A156988 .... N86-10788 #
AD-A156997 .... N86-10283 #
AD-A157011 .... N86-10870 #
AD-A157019 .... N86-10730 #
AD-A157030 .... N86-10924 #
AD-A157033 .... N86-10925 #
AD-A157038 .... N86-11061 #

AD-D011742 .... N86-10792 #
AD-D011743 .... N86-10198 #
AD-D011744 .... N86-10421 #
AD-D011745 .... N86-10422 #
AD-D011746 .... N86-10554 #
AD-D011748 .... N86-10313 #
AD-D011749 .... N86-10314 #
AD-D011751 .... N86-10423 #
AD-D011752 .... N86-10555 #
AD-D011753 .... N86-10556 #
AD-D011756 .... N86-10778 #
AD-D011757 .... N86-10424 #
AD-D011758 .... N86-10915 #
AD-D011759 .... N86-10425 #
AD-D011760 .... N86-10426 #
AD-D011761 .... N86-10427 #
AD-D011766 .... N86-10371
AD-D011767 .... N86-10480
AD-D011768 .... N86-10372
AD-D011769 .... N86-10674
AD-D011770 .... N86-10642
AD-D011771 .... N86-10799 #
AD-D011772 .... N86-10316 #
AD-D011773 .... N86-10800 #
AD-D011774 .... N86-10972
AD-D011775 .... N86-10536
AD-D011776 .... N86-10973
AD-D011777 .... N86-10906
AD-D011778 .... N86-10032
AD-D011779 .... N86-10974
AD-D011780 .... N86-10338
AD-D011781 .... N86-10414
AD-D011782 .... N86-10282
AD-D011784 .... N86-10277
AD-D011785 .... N86-10481
AD-D011786 .... N86-10373
AD-D011787 .... N86-10289
AD-D011788 .... N86-10374
AD-D011789 .... N86-10482
AD-D011797 .... N86-10355 #
AD-D011798 .... N86-10435 #
AD-D011799 .... N86-10436 #
AD-D011800 .... N86-10558 #
AD-D011801 .... N86-10020 #
AD-D011802 .... N86-10525 #
AD-D011803 .... N86-10437 #
AD-D011812 .... N86-10375
AD-D011813 .... N86-10415
AD-D011814 .... N86-10537
AD-D011815 .... N86-10416
AD-D011816 .... N86-10975
AD-D011817 .... N86-10376
AD-D011818 .... N86-10538
AD-D011819 .... N86-10483
AD-D011830 .... N86-10976
AD-D011833 .... N86-10417

AD-E301723 .... N86-10040 #
AD-E301723 .... N86-10405 #
AD-E301723 .... N86-10433 #
AD-E301723 .... N86-10796 #
AD-E301723 .... N86-10797 #
AD-E301723 .... N86-10869 #
AD-E301731 .... N86-10524 #
AD-E401349 .... N86-10354 #
AD-E440287 .... N86-10866 #
AD-E500720 .... N86-11071 #
AD-E500721 .... N86-10829 #
AD-E750965 .... N86-10407 #
AD-E900456 .... N86-10712 #
AD-E900472 .... N86-10592 #
AD-E900475 .... N86-10404 #
AD-E950724 .... N86-10283 #
AD-E950724 .... N86-10715 #
AD-E950724 .... N86-10771 #
AD-E950724 .... N86-10787 #
AD-E950724 .... N86-10788 #
AD-E950724 .... N86-11050 #
AD-E950724 .... N86-11079 #

AD-TR-85-39 .... N86-10191 #

AEAS-2 .... N86-10727 #

AEL-0125-SD .... N86-10523 #

AFAMRL-TR-85-035 .... N86-10675 #

AFESC/ESL-TR-85-10 .... N86-10830 #

AFGL-TR-84-0322 .... N86-10269 #

AFIT/CI/NR-85-35T .... N86-10787 #
AFIT/CI/NR-85-37T .... N86-10900 #

AFIT/CI/NR-85-40T ..... N86-10434 #
AFIT/CI/NR-85-46D ..... N86-10557 #
AFIT/CI/NR-85-50T ..... N86-10798 #
AFIT/CI/NR-85-51D ..... N86-10275 #
AFIT/CI/NR-85-52T ..... N86-10715 #

AFWAL-TR-84-4172 ..... N86-10916 #
AFWAL-TR-85-4002 ..... N86-10292 #

AFWL-TR-84-90 ..... N86-10042* #

AIAA-85-2011 ..... N86-10280* #
AIAA-85-2014 ..... N86-10279* #

AMMRC-TR-85-9 ..... N86-10315 #

AMTE(N)/R84009-PT-2 ..... N86-10553 #

ANL-HEP-CP-85-34 ..... N86-10934 #
ANL-HEP-CP-85-44 ..... N86-10942 #

ANL-85-7 ..... N86-10659 #

ANL/MCS-TM-50 ..... N86-10871 #

ARI-RP-84-21 ..... N86-11065 #

ARL/MAT-TM-388 ..... N86-10037 #

ARL/STRUC-TM-399 ..... N86-10036 #

ARL/SYS-R-29 ..... N86-10788 #

ARL/SYS-TM-75 ..... N86-10039 #

ARLCB-TR-85016 ..... N86-10886 #

ARLCD-TR-85009 ..... N86-10354 #

ARO-20679.1-MS-S ..... N86-10342 #

ARW-03-THE-BDK/ORS/83-06 ..... N86-11076 #
ARW-03-THE-BDK/ORS/83-08 ..... N86-10901 #

AS-701/85 ..... N86-10562 #

ASR-2 ..... N86-10589* #

BAE-AL/MAT/3864 ..... N86-10309

BAO-6 ..... N86-10723 #

BBC-RD-1985/8 ..... N86-10366

BDX-613-3266 ..... N86-10410 #
BDX-613-3268 ..... N86-10842 #

BI-76-39/08.7.23100-PT-1 ..... N86-10703
BI-76-39/08.7.23100-PT-2 ..... N86-10704

BLL-BISI-TRANS-21628-(9022.06) N86-10308
BLL-BISI-TRANS-23034-(9022.06) N86-10307
BLL-BISI-TRANS-23036-(9022.06) N86-10306

BLL-RISLEY-TR-5039-(9091.9F) N86-10546

BMFT-FB-T-85-020 ..... N86-10451 #
BMFT-FB-T-85-034 ..... N86-10449 #
BMFT-FB-T-85-046 ..... N86-10352 #
BMFT-FB-T-85-047 ..... N86-10353 #
BMFT-FB-T-85-049 ..... N86-10560 #
BMFT-FB-T-85-051-VOL-1 ..... N86-10670 #
BMFT-FB-T-85-052-VOL-2 ..... N86-10671 #

BN-1036 ..... N86-10862 #
BN-1037-PT-2 ..... N86-10869 #
BN-1038 ..... N86-10864 #

BNL-36414 ..... N86-10937 #
BNL-36450 ..... N86-10989 #
BNL-36486 ..... N86-10935 #
BNL-36490 ..... N86-10931 #
BNL-36495 ..... N86-11018 #
BNL-36497 ..... N86-10947 #
BNL-36546 ..... N86-10948 #
BNL-36559 ..... N86-11022 #
BNL-36564 ..... N86-11010 #
BNL-36566 ..... N86-11023 #
BNL-36572 ..... N86-10933 #
BNL-36573 ..... N86-11021 #
BNL-36577 ..... N86-10649 #
BNL-36671 ..... N86-10719 #
BNL-51865 ..... N86-10667 #
BNL-51875 ..... N86-10438 #

BR64172 ..... N86-10339

BR91279 ..... N86-10576
BR91991 ..... N86-10309
BR93962 ..... N86-10550
BR94518 ..... N86-10575

B8475856 ..... N86-10673 #
B8476135 ..... N86-10672 #
B8561677 ..... N86-10883 #
B8561680 ..... N86-11038 #
B8562445 ..... N86-10893 #
B8562446 ..... N86-10894 #
B8562871 ..... N86-10890 #
B8562872 ..... N86-10851 #
B8562873 ..... N86-10891 #
B8563351 ..... N86-10776
B8563352 ..... N86-10775
B8564052 ..... N86-10774 #

CEA-R-3276 ..... N86-10418* #

CERC-IR-85-2 ..... N86-10726 #

CMU-CS-85-115 ..... N86-10899 #

COMP-CENT-NOTE-14-PT-1 ..... N86-10888 #
COMP-CENT-NOTE-15-PT-2 ..... N86-10889 #
COMP-CENT-NOTE-17 ..... N86-10890 #
COMP-CENT-NOTE-18 ..... N86-10851 #
COMP-CENT-NOTE-20 ..... N86-10891 #

CONF-840817-3 ..... N86-10978 #
CONF-841231-5 ..... N86-10647 #
CONF-841231-7 ..... N86-10650 #
CONF-841231-10 ..... N86-10661 #
CONF-841231-17 ..... N86-10664 #
CONF-841231-20 ..... N86-10654 #
CONF-841231-21 ..... N86-10472 #
CONF-841231-22 ..... N86-10473 #
CONF-841231-23 ..... N86-10653 #
CONF-841267-1 ..... N86-10330 #
CONF-850103-10 ..... N86-10329 #
CONF-850137-4 ..... N86-10530 #
CONF-850169-13 ..... N86-10937 #
CONF-850175-1 ..... N86-10527 #
CONF-850211-10 ..... N86-10321 #
CONF-850211-12 ..... N86-10736 #
CONF-850266-6 ..... N86-10471 #
CONF-850286-1 ..... N86-11057 #
CONF-850310-104 ..... N86-11037 #
CONF-850310-109 ..... N86-10960 #
CONF-850310-110 ..... N86-10468 #
CONF-850310-112 ..... N86-11030 #
CONF-850315-2 ..... N86-10955 #
CONF-850375-1 ..... N86-10946 #
CONF-850375-4 ..... N86-11035 #
CONF-850375-5 ..... N86-11134 #
CONF-850410-47 ..... N86-10952 #
CONF-850421-01 ..... N86-10442 #
CONF-850421-10 ..... N86-10448 #
CONF-850473-3 ..... N86-10684 #
CONF-850484-1 ..... N86-10949 #
CONF-850504-30 ..... N86-10192 #
CONF-850504-48 ..... N86-10986 #
CONF-850504-53 ..... N86-10992 #
CONF-850504-54 ..... N86-10990 #
CONF-850504-56 ..... N86-10987 #
CONF-850504-60 ..... N86-10996 #
CONF-850504-61 ..... N86-10993 #
CONF-850504-62 ..... N86-10837 #
CONF-850504-67 ..... N86-11051 #
CONF-850504-69 ..... N86-10801 #
CONF-850504-70 ..... N86-11025 #
CONF-850504-72 ..... N86-11033 #
CONF-850504-75 ..... N86-10995 #
CONF-850504-77 ..... N86-10994 #
CONF-850504-79 ..... N86-10836 #
CONF-850504-83 ..... N86-11012 #
CONF-850504-87 ..... N86-11024 #
CONF-850504-96 ..... N86-10929 #
CONF-850504-99 ..... N86-11014 #
CONF-850504-108 ..... N86-11002 #
CONF-850504-109 ..... N86-11001 #
CONF-850504-110 ..... N86-11004 #
CONF-850504-113 ..... N86-10985 #
CONF-850504-117 ..... N86-10991 #
CONF-850504-118 ..... N86-10930 #
CONF-850504-134 ..... N86-10950 #
CONF-850504-135 ..... N86-10931 #
CONF-850504-142 ..... N86-10935 #
CONF-850504-144 ..... N86-10933 #
CONF-850504-145 ..... N86-11021 #
CONF-850504-146 ..... N86-11010 #
CONF-850504-147 ..... N86-11022 #
CONF-850504-150 ..... N86-11009 #
CONF-850504-157 ..... N86-11023 #
CONF-850504-160 ..... N86-11018 #
CONF-850504-170 ..... N86-10948 #
CONF-850504-172 ..... N86-10947 #
CONF-850504-175 ..... N86-10979 #
CONF-850504-177 ..... N86-10941 #
CONF-850504-190 ..... N86-10964 #
CONF-850507-40 ..... N86-10963 #
CONF-850533-5 ..... N86-10954 #
CONF-850533-9 ..... N86-10528 #
CONF-850560-5 ..... N86-10956 #
CONF-850577-1 ..... N86-10772 #
CONF-850579-3 ..... N86-10443 #
CONF-850581-3 ..... N86-10631 #
CONF-850604-6 ..... N86-10665 #
CONF-850610-30 ..... N86-10959 #
CONF-850612-2 ..... N86-10676 #
CONF-850612-4 ..... N86-10681 #
CONF-850612-5 ..... N86-10719 #
CONF-850616-1D ..... N86-10928 #
CONF-850616-18 ..... N86-10195 #
CONF-850616-30 ..... N86-11011 #
CONF-850616-35 ..... N86-11019 #
CONF-850616-38 ..... N86-10439 #
CONF-850616-44 ..... N86-10940 #
CONF-850616-46 ..... N86-10441 #
CONF-850617-1 ..... N86-10351 #
CONF-850706-1 ..... N86-10927 #
CONF-850706-9 ..... N86-10357 #
CONF-850706-21 ..... N86-10359 #
CONF-850711-7 ..... N86-11005 #
CONF-850717-1 ..... N86-10021 #
CONF-850723-2 ..... N86-10835 #
CONF-850726-1 ..... N86-10938 #
CONF-850736-2 ..... N86-11055 #
CONF-850736-4 ..... N86-10317 #
CONF-850736-6 ..... N86-11054 #
CONF-850736-14 ..... N86-10350 #
CONF-850736-19 ..... N86-10300 #
CONF-850745-8 ..... N86-10348 #
CONF-850753-2 ..... N86-10325 #
CONF-850759-1 ..... N86-10907 #
CONF-850759-2 ..... N86-10323 #
CONF-850759-3 ..... N86-10470 #
CONF-850801-7 ..... N86-10531 #
CONF-850801-24 ..... N86-10663 #
CONF-850808-3 ..... N86-11031 #
CONF-850809-19 ..... N86-10908 #
CONF-850809-29 ..... N86-11017 #
CONF-850810-3 ..... N86-11036 #
CONF-850810-6 ..... N86-10474 #
CONF-850823-3 ..... N86-10322 #
CONF-850830-2 ..... N86-10304 #
CONF-850840-2 ..... N86-10324 #
CONF-850840-3 ..... N86-10331 #
CONF-850864-1 ..... N86-11080 #
CONF-850884-1 ..... N86-10049 #
CONF-850885-1 ..... N86-10408 #
CONF-850885-2 ..... N86-10841 #
CONF-850887-4 ..... N86-10944 #
CONF-851043-1 ..... N86-10649 #
CONF-851048-2 ..... N86-10301 #
CONF-8406190 ..... N86-11008 #
CONF-8408121-4 ..... N86-11034 #
CONF-8408122-3 ..... N86-10717 #
CONF-8408122-5 ..... N86-10718 #
CONF-8410159-2 ..... N86-10466 #
CONF-8410159-2-REV-1 ..... N86-10467 #
CONF-8503137-1 ..... N86-10984 #
CONF-8504109-2 ..... N86-10662 #
CONF-8504115-4 ..... N86-11052 #
CONF-8504133-2 ..... N86-10989 #
CONF-8504136-1 ..... N86-10936 #
CONF-8504138-1 ..... N86-10296 #
CONF-8504151-1 ..... N86-10633 #
CONF-8504155-2 ..... N86-10942 #
CONF-8505100-2 ..... N86-11003 #
CONF-8505100-4 ..... N86-11028 #
CONF-8505100-5 ..... N86-10988 #
CONF-8505100-6 ..... N86-11016 #
CONF-8505100-11 ..... N86-10999 #
CONF-8505100-12 ..... N86-10998 #
CONF-8505100-14 ..... N86-11029 #
CONF-8505100-15 ..... N86-11027 #
CONF-8505103-3 ..... N86-10299 #
CONF-8505139-2 ..... N86-10319 #
CONF-8505145-1 ..... N86-10328 #
CONF-8505148-1 ..... N86-10678 #
CONF-8505149-1 ..... N86-10677 #
CONF-8505151-1 ..... N86-10297 #
CONF-8505171-1 ..... N86-10666 #
CONF-8506115-1 ..... N86-10526 #
CONF-8506118-1 ..... N86-10298 #
CONF-8506125-2 ..... N86-10932 #
CONF-8506125-3 ..... N86-11056 #
CONF-8506128-2 ..... N86-10349 #
CONF-8506131-1 ..... N86-10532 #
CONF-8506137-4 ..... N86-10737 #

CONF-8506146-1	N86-10635	#
COO-1764-408	N86-11062	#
CTH-MATH-1984-26	N86-10902	#
CTH-MATH-1984-27	N86-10872	#
CTH-MATH-1984-28	N86-10873	#
CTH-MATH-1984-29	N86-10874	#
CTH-MATH-1984-30	N86-10875	#
CTH-MATH-1985-05	N86-10876	#
CTH-MATH-1985-06	N86-10877	#
CTH-MATH-1985-08	N86-10903	#
CTH-MATH-1985-09	N86-10904	#
CWI-CS-R8501	N86-10884	#
D-82	N86-10450	#
DE84-012185	N86-10948	#
DE84-016822	N86-10927	#
DE85-002941	N86-10657	#
DE85-003914	N86-10654	#
DE85-004086	N86-11036	#
DE85-004089	N86-10653	#
DE85-004444	N86-11008	#
DE85-004796	N86-10661	#
DE85-005244	N86-10664	#
DE85-005357	N86-10650	#
DE85-005366	N86-10647	#
DE85-006762	N86-10474	#
DE85-006879	N86-10322	#
DE85-007046	N86-10938	#
DE85-008026	N86-10908	#
DE85-008228	N86-10444	#
DE85-008696	N86-10531	#
DE85-008721	N86-10838	#
DE85-008804	N86-10668	#
DE85-008821	N86-10655	#
DE85-008960	N86-11017	#
DE85-009105	N86-10331	#
DE85-009408	N86-10304	#
DE85-009437	N86-10324	#
DE85-009438	N86-11005	#
DE85-009440	N86-10920	#
DE85-009443	N86-10357	#
DE85-009562	N86-10663	#
DE85-009575	N86-10835	#
DE85-009622	N86-11031	#
DE85-010020	N86-10559	#
DE85-010068	N86-10348	#
DE85-010278	N86-10676	#
DE85-010302	N86-10957	#
DE85-010583	N86-10926	#
DE85-010738	N86-10955	#
DE85-011363	N86-10717	#
DE85-011449	N86-10302	#
DE85-011450	N86-10318	#
DE85-011474	N86-10952	#
DE85-011477	N86-10934	#
DE85-011572	N86-10936	#
DE85-011599	N86-10445	#
DE85-011603	N86-10196	#
DE85-011607	N86-10197	#
DE85-011709	N86-10192	#
DE85-011745	N86-10193	#
DE85-011820	N86-10301	#
DE85-011843	N86-11080	#
DE85-011846	N86-10984	#
DE85-011906	N86-10526	#
DE85-011957	N86-10954	#
DE85-012032	N86-10408	#
DE85-012033	N86-10049	#
DE85-012078	N86-10953	#
DE85-012090	N86-11053	#
DE85-012122	N86-11052	#
DE85-012131	N86-10645	#
DE85-012144	N86-10662	#
DE85-012184	N86-10947	#
DE85-012298	N86-10946	#
DE85-012326	N86-10319	#
DE85-012352	N86-11032	#
DE85-012368	N86-10991	#
DE85-012390	N86-10633	#
DE85-012392	N86-11062	#
DE85-012419	N86-10330	#
DE85-012425	N86-10997	#
DE85-012441	N86-10631	#
DE85-012460	N86-10297	#
DE85-012483	N86-10194	#
DE85-012523	N86-10931	#
DE85-012526	N86-10937	#
DE85-012527	N86-10989	#
DE85-012572	N86-11007	#
DE85-012592	N86-11055	#
DE85-012648	N86-10986	#
DE85-012657	N86-10996	#
DE85-012658	N86-10993	#
DE85-012659	N86-10837	#
DE85-012660	N86-10987	#
DE85-012661	N86-10990	#
DE85-012662	N86-10992	#
DE85-012673	N86-10929	#
DE85-012680	N86-11002	#
DE85-012681	N86-11001	#
DE85-012691	N86-10930	#
DE85-012709	N86-10950	#
DE85-012723	N86-10985	#
DE85-012735	N86-11003	#
DE85-012740	N86-10998	#
DE85-012741	N86-11028	#
DE85-012742	N86-10667	#
DE85-012744	N86-10988	#
DE85-012758	N86-10963	#
DE85-012764	N86-11029	#
DE85-012767	N86-10932	#
DE85-012770	N86-11027	#
DE85-012771	N86-10999	#
DE85-012776	N86-10834	#
DE85-012811	N86-11013	#
DE85-012812	N86-10195	#
DE85-012827	N86-10298	#
DE85-012860	N86-11011	#
DE85-012867	N86-10928	#
DE85-012885	N86-10328	#
DE85-012887	N86-10329	#
DE85-012889	N86-10960	#
DE85-012893	N86-11037	#
DE85-012903	N86-10677	#
DE85-012919	N86-11016	#
DE85-012921	N86-10467	#
DE85-012926	N86-11134	#
DE85-012929	N86-10956	#
DE85-012930	N86-10296	#
DE85-012936	N86-10466	#
DE85-012944	N86-10471	#
DE85-012950	N86-11030	#
DE85-012959	N86-10468	#
DE85-012984	N86-10438	#
DE85-012992	N86-11006	#
DE85-013017	N86-10945	#
DE85-013019	N86-10939	#
DE85-013042	N86-10527	#
DE85-013045	N86-10299	#
DE85-013051	N86-10995	#
DE85-013054	N86-11014	#
DE85-013062	N86-11004	#
DE85-013065	N86-11015	#
DE85-013068	N86-10836	#
DE85-013072	N86-10994	#
DE85-013074	N86-11012	#
DE85-013100	N86-10648	#
DE85-013101	N86-10646	#
DE85-013102	N86-10731	#
DE85-013111	N86-10678	#
DE85-013122	N86-11063	#
DE85-013183	N86-10409	#
DE85-013204	N86-10532	#
DE85-013205	N86-10959	#
DE85-013248	N86-10634	#
DE85-013262	N86-10716	#
DE85-013282	N86-11023	#
DE85-013284	N86-11018	#
DE85-013289	N86-10649	#
DE85-013289	N86-11026	#
DE85-013296	N86-10935	#
DE85-013303	N86-11022	#
DE85-013304	N86-11010	#
DE85-013305	N86-11021	#
DE85-013306	N86-10933	#
DE85-013317	N86-10962	#
DE85-013322	N86-10842	#
DE85-013369	N86-10801	#
DE85-013370	N86-11025	#
DE85-013372	N86-11035	#
DE85-013376	N86-11009	#
DE85-013378	N86-11051	#
DE85-013379	N86-11033	#
DE85-013380	N86-11024	#
DE85-013391	N86-10528	#
DE85-013438	N86-10439	#
DE85-013439	N86-11019	#
DE85-013442	N86-10644	#
DE85-013446	N86-10684	#
DE85-013448	N86-10440	#
DE85-013468	N86-10681	#
DE85-013479	N86-10718	#
DE85-013496	N86-10666	#
DE85-013498	N86-10772	#
DE85-013502	N86-10683	#
DE85-013503	N86-10680	#
DE85-013520	N86-10958	#
DE85-013525	N86-10840	#
DE85-013526	N86-10679	#
DE85-013585	N86-10312*	#
DE85-013628	N86-10448	#
DE85-013647	N86-11020	#
DE85-013648	N86-11000	#
DE85-013752	N86-10940	#
DE85-013766	N86-10632	#
DE85-013789	N86-10665	#
DE85-013820	N86-10907	#
DE85-013821	N86-10317	#
DE85-013850	N86-10979	#
DE85-013864	N86-10443	#
DE85-013867	N86-10941	#
DE85-013868	N86-10961	#
DE85-013891	N86-10635	#
DE85-013893	N86-11056	#
DE85-013913	N86-10446	#
DE85-013922	N86-11057	#
DE85-013926	N86-10978	#
DE85-013930	N86-10472	#
DE85-013931	N86-10473	#
DE85-013950	N86-10021	#
DE85-013953	N86-10351	#
DE85-013954	N86-11054	#
DE85-013966	N86-10441	#
DE85-013978	N86-10323	#
DE85-013982	N86-10359	#
DE85-014052	N86-10447	#
DE85-014073	N86-10942	#
DE85-014074	N86-10944	#
DE85-014087	N86-10349	#
DE85-014114	N86-11034	#
DE85-014134	N86-10841	#
DE85-014181	N86-10737	#
DE85-014227	N86-10719	#
DE85-014237	N86-10843	#
DE85-014252	N86-10356	#
DE85-014258	N86-10943	#
DE85-014262	N86-10660	#
DE85-014263	N86-10656	#
DE85-014264	N86-10469	#
DE85-014266	N86-10839	#
DE85-014277	N86-10303	#
DE85-014285	N86-10965	#
DE85-014321	N86-10966	#
DE85-014367	N86-10964	#
DE85-014370	N86-10871	#
DE85-014439	N86-10543	#
DE85-014468	N86-10350	#
DE85-014532	N86-10321	#
DE85-014533	N86-10442	#
DE85-014550	N86-10659	#
DE85-014552	N86-10652	#
DE85-014557	N86-10470	#
DE85-014563	N86-10325	#
DE85-014583	N86-10682	#
DE85-014598	N86-10410	#
DE85-014616	N86-10736	#
DE85-014618	N86-10530	#
DE85-014704	N86-10300	#
DE85-014713	N86-10658	#
DE85-014741	N86-10651	#
DE85-014852	N86-10326	#
DE85-014853	N86-10327	#
DE85-015191	N86-10529	#
DE85-015316	N86-10358	#
DE85-0135637	N86-10949	#
DFVLR-FB-83-36	N86-10043	#
DFVLR-FB-84-44	N86-10636	#
DFVLR-FB-85-14	N86-10412	#
DFVLR-FB-85-15	N86-10025	#
DFVLR-FB-85-16	N86-10720	#
DFVLR-FB-85-17	N86-10026	#
DFVLR-FB-85-18	N86-10051	#
DFVLR-FB-85-19	N86-10027	#
DFVLR-FB-85-20	N86-10780	#
DFVLR-FB-85-21	N86-10781	#
DFVLR-FB-85-22	N86-10981	#
DFVLR-FB-85-23	N86-10030	#
DFVLR-FB-85-24	N86-10047	#
DFVLR-FB-85-25	N86-10685	#
DFVLR-FB-85-26	N86-10544	#
DFVLR-MITT-85-06	N86-10031	#
DFVLR-MITT-85-07	N86-10413	#
DFVLR-MITT-85-08	N86-10721	#
DFVLR-WF2/8734	N86-10273*	#
DNA-TR-84-127	N86-10405	#
DNA-TR-84-183	N86-10524	#
DOE/AL-16338/T1	N86-10559	#
DOE/BP-2	N86-10656	#

DOE/CE-0109 N86-10648 #
DOE/CE-0111 N86-10646 #
DOE/CE-0114 N86-10731 #
DOE/CE-0126 N86-10658 #

DOE/CS-54209/22-VOL-2 N86-11083* #
DOE/CS-54209/22-VOL-3 N86-11084* #
DOE/CS-54209/22-VOL-4 N86-11085* #
DOE/CS-54209/22-VOL-5 N86-11086* #

DOE/ER-04073/18 N86-10303 #
DOE/ER-08035/7 N86-10966 #
DOE/ER-10870/156 N86-10327 #
DOE/ER-13266/T1 N86-10939 #
DOE/ER-13283/2 N86-10834 #
DOE/ER-40105/T3 N86-11062 #
DOE/ER-40561/1 N86-10945 #
DOE/ER-45130/T1 N86-10440 #
DOE/ER-45153/1 N86-11053 #
DOE/ER-53157/T1 N86-10543 #

DOE/ET-51013/135 N86-11020 #
DOE/ET-51013/139 N86-11000 #
DOE/ET-51017/T2 N86-11032 #
DOE/ET-52023/34 N86-10193 #
DOE/ET-53088/177 N86-11063 #

DOE/EV-04814/T2 N86-10957 #

DOE/FE-15078/6-1 N86-10444 #
DOE/FE-60177/1883 N86-10634 #

DOE/ID-12379/T2 N86-10682 #

DOE/JPL/956205-85/8 N86-10312* #

DOE/MC-20212/1850 N86-10447 #

DOE/NASA/0167-9 N86-11087* #
DOE/NASA/20320-66 N86-10562* #
DOE/NASA/20485-20 N86-10643* #

DOE/NBM-5013868 N86-10961 #

DOE/OR-21444/T2-VOL-1 N86-10683 #
DOE/OR-21444/T2-VOL-2 N86-10680 #

DOE/TIC-3386-SUPPL-1 N86-10838 #

DP-MS-85-29 N86-10348 #
DP-MS-85-57 N86-10319 #

DREO-TN-84-24 N86-10276 #
DREO-TN-84-26 N86-10786 #
DREO-TN-85-4 N86-10294 #

DREV-4347/85 N86-10419 #
DREV-4371/85 N86-10865 #

DRIC-BR-94287-PT-1 N86-10343 #
DRIC-BR-94556 N86-10919 #
DRIC-BR-95198 N86-10190 #
DRIC-BR-95691-PT-2 N86-10553 #
DRIC-BR-95704 N86-10793 #

DRL-175 N86-10312* #

E-2573 N86-10379* #
E-2576 N86-10579* #
E-2649 N86-10341* #
E-2650 N86-10551* #
E-2651 N86-10463* #
E-2676 N86-10561* #
E-2679 N86-10017* #
E-2684 N86-10552* #
E-2685 N86-10019* #
E-2695 N86-10290* #
E-2700 N86-10280* #
E-2703 N86-10643* #
E-2709 N86-10582* #
E-2710 N86-10311* #
E-2725 N86-10279* #
E-2726 N86-11048* #
E-2737 N86-10380* #
E-2738 N86-10381* #
E-2744 N86-10281* #

EEB-W-84-22 N86-10978 #

EGG-M-08985 N86-10954 #
EGG-M-27064 N86-10530 #
EGG-M-27484 N86-10736 #

EGG/10282-2055 N86-10526 #

ENVIRON-SCI-DIV-2354 N86-10679 #

EPA-600/D-85-083 N86-10710 #
EPA-600/D-85-100 N86-10687 #
EPA-600/D-85-106 N86-10688 #
EPA-600/4-85-034 N86-10689 #
EPA-600/9-85-015 N86-10686 #

ER-83/08 N86-10844 #
ER-83/09 N86-10879 #
ER-83/10 N86-10880 #

ERL-0323-TR N86-10428 #

ESA-SP-209 N86-10485 #
ESA-SP-222 N86-10200 #
ESA-SP-226 N86-11096 #

ESA-TT-852 N86-10043 #
ESA-TT-871 N86-10332 #
ESA-TT-899 N86-10363 #

ESDU-AN-36B N86-10909

ESDU-BR-62636 N86-10909

ETL-0371 N86-10630 #

EUT-84-E-143 N86-10802 #
EUT-84-E-144 N86-10270 #
EUT-84-E-145 N86-10803 #
EUT-85-E-146 N86-10846 #
EUT-85-E-147 N86-10804 #
EUT-85-E-148 N86-10805 #

E85-10109 N86-10597*
E85-10110 N86-10610* #
E86-10002 N86-10599* #

F+W-FO-1752 N86-10050 #

FAA-AM-85 3 N86-10771 #

FCR-6948P N86-10651 #
FCR-6956P N86-10652 #

FNAL-TM-1306 N86-10997 #

FNAL/C-85/65 N86-10946 #

FOA-A-30037-E N86-10980 #

FOA-C-30386-E2 N86-10411 #
FOA-C-40211-B4 N86-10360 #

FOA-C5-85-0003-H2 N86-11072 #
FOA-C5-85-0006-H2 N86-10364 #

FTD-ID(RS)T-0910-84 N86-10007 #
FTD-ID(RS)T-1120-84 N86-10001 #

GA-A-17995 N86-11007 #

GKSS-85-E-10 N86-10722 #

GPO-43-778 N86-10733 #

GRI-85/0064 N86-10305 #

HEL-TM-3-85 N86-10917 #

HL-85-21 N86-10912* #

IA-UR-85-1620 N86-10998 #

IDA-M-34 N86-10829 #
IDA-M-83 N86-11071 #

IDA/HQ-84-29295 N86-10829 #
IDA/HQ-85-29861 N86-11071 #

IFSR-177 N86-11063 #

IKE-5-220 N86-10476 #

ILR-MITT-143 N86-11140 #

IPR-2 N86-10014* #

ISBN-3-88383-107-7 N86-10773 #
ISBN-90-6144-143-9 N86-10802 #
ISBN-90-6144-144 7 N86-10270 #
ISBN-90-6144-145-5 N86-10803 #
ISBN-90-6144-146-3 N86-10846 #
ISBN-90-6144-147-1 N86-10804 #
ISBN-90-6144-148-X N86-10805 #

ISI-V-4859-02 N86-10006 #

ISPO-232 N86-10953 #

ISSN-0167-9708 N86-10270 #
ISSN-0167-9708 N86-10802 #
ISSN-0167-9708 N86-10803 #
ISSN-0167-9708 N86-10804 #
ISSN-0167-9708 N86-10805 #
ISSN-0167-9708 N86-10846 #
ISSN-0168-8332 N86-10732 #
ISSN-0171-1342 N86-10025 #
ISSN-0171-1342 N86-10026 #
ISSN-0171-1342 N86-10027 #
ISSN-0171-1342 N86-10030 #
ISSN-0171-1342 N86-10047 #
ISSN-0171-1342 N86-10051 #
ISSN-0171-1342 N86-10412 #
ISSN-0171-1342 N86-10544 #
ISSN-0171-1342 N86-10636 #
ISSN-0171-1342 N86-10685 #
ISSN-0171-1342 N86-10720 #
ISSN-0171-1342 N86-10780 #
ISSN-0171-1342 N86-10781 #
ISSN-0171-1342 N86-10981 #
ISSN-0173-6892 N86-10476 #
ISSN-0176-7739 N86-10031 #
ISSN-0176-7739 N86-10413 #
ISSN-0176-7739 N86-10721 #
ISSN-0281-0212 N86-10980 #
ISSN-0309-099X N86-11094 #
ISSN-0336-0885 N86-10475 #
ISSN-0340-7608 N86-10352 #
ISSN-0340-7608 N86-10353 #
ISSN-0340-7608 N86-10449 #
ISSN-0340-7608 N86-10451 #
ISSN-0340-7608 N86-10560 #
ISSN-0340-7608 N86-10670 #
ISSN-0340-7608 N86-10671 #
ISSN-0344-9629 N86-10722 #
ISSN-0347-2124 N86-10360 #
ISSN-0347-2809 N86-10872 #
ISSN-0347-2809 N86-10873 #
ISSN-0347-2809 N86-10874 #
ISSN-0347-2809 N86-10875 #
ISSN-0347-2809 N86-10876 #
ISSN-0347-2809 N86-10877 #
ISSN-0347-2809 N86-10902 #
ISSN-0347-2809 N86-10903 #
ISSN-0347-2809 N86-10904 #
ISSN-0347-3708 N86-10411 #
ISSN-0347-6405 N86-10709 #
ISSN-0347-7665 N86-10364 #
ISSN-0347-7665 N86-11072 #
ISSN-0366-0885 N86-10450 #
ISSN-0366-0885 N86-10595 #
ISSN-0379-6566 N86-10200 #
ISSN-0379-6566 N86-10485 #
ISSN-0379-6566 N86-11096 #
ISSN-0436-1199 N86-10028 #
ISSN-0721-5320 N86-10044 #

IZF-1984-19 N86-10782 #
IZF-1984-27 N86-11077 #
IZF-1984-32 N86-10783 #
IZF-1984-34 N86-10789 #

JPL-PUB-84-79-VOL-2 N86-11083* #
JPL-PUB-84-79-VOL-3 N86-11084* #
JPL-PUB-84-79-VOL-4 N86-11085* #
JPL-PUB-84-79-VOL-5 N86-11086* #
JPL-PUB-85-37 N86-10707* #
JPL-PUB-85-39 N86-10615* #
JPL-PUB-85-44 N86-10599* #

JPL-5030-573-VOL-2 N86-11083* #
JPL-5030-573-VOL-3 N86-11084* #
JPL-5030-573-VOL-4 N86-11085* #
JPL-5030-573-VOL-5 N86-11086* #

JPRS-UBB-85-023 N86-10738 #

JPRS-UCC-85-006 N86-10809 #

JUEL-1968 N86-10450 #
JUEL-1979 N86-10595 #
JUEL-1985 N86-10475 #

K/CSD/INF-85/4 N86-10843 #

KGI-188 N86-10709 #

KNMI-FM-85-6 N86-10711

KNMI-167-VOL 2 N86-10732 #

L-15960 N86-10016* #

LA-TR-85-16 .... N86-11006 #
LA-TR-85-21 .... N86-10194 #
LA-TR-85-30 .... N86-10358 #
LA-TR-85-31 .... N86-10529 #

LA-UR-84-2753 .... N86-10927 #
LA-UR-85-828 .... N86-10835 #
LA-UR-85-934 .... N86-10663 #
LA-UR-85-1035 .... N86-11031 #
LA-UR-85-1450 .... N86-10955 #
LA-UR-85-1528 .... N86-10930 #
LA-UR-85-1585 .... N86-11001 #
LA-UR-85-1586 .... N86-11002 #
LA-UR-85-1615 .... N86-10992 #
LA-UR-85-1616 .... N86-10990 #
LA-UR-85-1618 .... N86-10837 #
LA-UR-85-1619 .... N86-10993 #
LA-UR-85-1632 .... N86-10929 #
LA-UR-85-1640 .... N86-10986 #
LA-UR-85-1651 .... N86-10950 #
LA-UR-85-1737 .... N86-10985 #
LA-UR-85-1789 .... N86-10988 #
LA-UR-85-1791 .... N86-10998 #
LA-UR-85-1818 .... N86-11003 #
LA-UR-85-1820 .... N86-10999 #
LA-UR-85-1821 .... N86-11027 #
LA-UR-85-1829 .... N86-10932 #
LA-UR-85-1837 .... N86-11029 #
LA-UR-85-1923 .... N86-10963 #
LA-UR-85-1933 .... N86-10841 #
LA-UR-85-2073 .... N86-11034 #
LA-UR-85-2195 .... N86-10349 #
LA-UR-85-2265 .... N86-10944 #
LA-UR-1790 .... N86-11028 #

LA-74-85-1617 .... N86-10987 #
LA-9703-REV .... N86-10469 #
LA-10276 .... N86-10356 #
LA-10326-ML .... N86-10943 #
LA-10361-MS .... N86-10839 #
LA-10364-MS .... N86-10660 #

LARS-TR-042382 .... N86-10610* #

LBF-S-173 .... N86-10044 #

LBL-17284 .... N86-10978 #
LBL-17550 .... N86-10962 #
LBL-18001 .... N86-10446 #
LBL-18571 .... N86-11008 #
LBL-19139 .... N86-11057 #
LBL-19218 .... N86-10442 #
LBL-19695 .... N86-10321 #

LC-64-60074 .... N86-10923 #

LINO-119 .... N86-10967 #
LINO-120 .... N86-10968 #
LINO-121 .... N86-10969 #
LINO-122 .... N86-10452 #

LMSC/F035789 .... N86-10345 #

MANPOWER-PLANNING-28 .... N86-11073 #
MANPOWER-PLANNING-29 .... N86-11074 #
MANPOWER-PLANNING-30 .... N86-11075 #

MASA-TM-87088 .... N86-10561* #

MCR-85-506-ADDN .... N86-10340* #

MDR-21A-VOL-1/2 .... N86-10433 #

MIT/BNL-84-4 .... N86-10438 #

MIT/LCS/TM-276 .... N86-10898 #

MPIS-16/1984 .... N86-10028 #

MRC-R-815 .... N86-10405 #

MRL-R-950-PT-2 .... N86-10347 #

MSRR-517 .... N86-10861 #

NAS 1.12/6:479 .... N86-11137* #
NAS 1.15:58269 .... N86-10018* #
NAS 1.15:77669 .... N86-10179* #
NAS 1.15:77672 .... N86-10378* #
NAS 1.15:77901 .... N86-10611* #
NAS 1.15:77907 .... N86-10293* #
NAS 1.15:77909 .... N86-10612* #
NAS 1.15:77910 .... N86-10613* #
NAS 1.15:77911 .... N86-10614* #
NAS 1.15:77915 .... N86-10418* #
NAS 1.15:77923 .... N86-10273* #
NAS 1.15:86207 .... N86-11138* #
NAS 1.15:86393 .... N86-10580* #
NAS 1.15:86405 .... N86-10016* #
NAS 1.15:86513 .... N86-10278* #
NAS 1.15:86757 .... N86-10464* #
NAS 1.15:86782 .... N86-10015* #
NAS 1.15:86827 .... N86-10048* #
NAS 1.15:86836 .... N86-10734* #
NAS 1.15:86844 .... N86-10777* #
NAS 1.15:87072 .... N86-10379* #
NAS 1.15:87076 .... N86-10463* #
NAS 1.15:87088 .... N86-10561* #
NAS 1.15:87091 .... N86-10017* #
NAS 1.15:87093 .... N86-10019* #
NAS 1.15:87101 .... N86-10290* #
NAS 1.15:87103 .... N86-10280* #
NAS 1.15:87105 .... N86-10341* #
NAS 1.15:87106 .... N86-10643* #
NAS 1.15:87109 .... N86-10582* #
NAS 1.15:87110 .... N86-10311* #
NAS 1.15:87114 .... N86-10551* #
NAS 1.15:87118 .... N86-10279* #
NAS 1.15:87119 .... N86-11048* #
NAS 1.15:87124 .... N86-10380* #
NAS 1.15:87125 .... N86-10381* #
NAS 1.15:87131 .... N86-10281* #
NAS 1.15:87133 .... N86-10552* #
NAS 1.15:87509 .... N86-11141* #
NAS 1.15:87568 .... N86-10053* #
NAS 1.15:87587 .... N86-10828* #
NAS 1.15:87595 .... N86-10581* #
NAS 1.15:87601 .... N86-10913* #
NAS 1.21:7011(275) N86-10768*
NAS 1.26:3928 .... N86-10460* #
NAS 1.26:171894 .... N86-10610* #
NAS 1.26:171896 .... N86-10770* #
NAS 1.26:171897 .... N86-10896* #
NAS 1.26:171898 .... N86-10820* #
NAS 1.26:171899 .... N86-10897* #
NAS 1.26:171900 .... N86-10821* #
NAS 1.26:171901 .... N86-10785* #
NAS 1.26:174886 .... N86-11087* #
NAS 1.26:174964 .... N86-10461* #
NAS 1.26:174980 .... N86-10589* #
NAS 1.26:176141 .... N86-10377* #
NAS 1.26:176198 .... N86-10707* #
NAS 1.26:176203 .... N86-10382* #
NAS 1.26:176204 .... N86-10615* #
NAS 1.26:176205 .... N86-11083* #
NAS 1.26:176206 .... N86-11084* #
NAS 1.26:176207 .... N86-11085* #
NAS 1.26:176208 .... N86-11086* #
NAS 1.26:176209 .... N86-10312* #
NAS 1.26:176211 .... N86-10599* #
NAS 1.26:176219 .... N86-10860* #
NAS 1.26:176220 .... N86-10588* #
NAS 1.26:176221 .... N86-10822* #
NAS 1.26:176222 .... N86-10823* #
NAS 1.26:176223 .... N86-10824* #
NAS 1.26:176224 .... N86-10825* #
NAS 1.26:176225 .... N86-10826* #
NAS 1.26:176226 .... N86-10827* #
NAS 1.26:176228 .... N86-11047* #
NAS 1.26:176229 .... N86-10912* #
NAS 1.26:176230 .... N86-11060* #
NAS 1.26:176231 .... N86-10033* #
NAS 1.26:176232 .... N86-10271* #
NAS 1.26:176233 .... N86-10272* #
NAS 1.26:176234 .... N86-10577* #
NAS 1.26:176235 .... N86-10539* #
NAS 1.26:176236 .... N86-10578* #
NAS 1.26:176237 .... N86-10014* #
NAS 1.26:176238 .... N86-11059* #
NAS 1.26:176240 .... N86-10540* #
NAS 1.26:176241 .... N86-11139* #
NAS 1.26:176242 .... N86-11133* #
NAS 1.26:176244 .... N86-11095* #
NAS 1.26:176249 .... N86-10484* #
NAS 1.26:176250 .... N86-10042* #
NAS 1.26:176262 .... N86-10310* #
NAS 1.26:176268 .... N86-10597*
NAS 1.26:177334 .... N86-10819* #
NAS 1.26:177368 .... N86-10274* #
NAS 1.26:177967 .... N86-10848* #
NAS 1.26:177972 .... N86-11064* #
NAS 1.26:178480 .... N86-10705* #
NAS 1.26:178484 .... N86-10462* #
NAS 1.26:178495 .... N86-10340* #
NAS 1.61:1150 .... N86-10579* #

NASA ORDER C-86129D .... N86-10120* #

NASA ORDER H-27954-B .... N86-10106* #
NASA ORDER H-27954B .... N86-10114* #
NASA ORDER H-27954B .... N86-10115* #
NASA ORDER H-27954B .... N86-10121* #
NASA ORDER H-27954B .... N86-10131* #

NASA-CR-3928 .... N86-10460* #
NASA-CR-171894 .... N86-10610* #
NASA-CR-171896 .... N86-10770* #
NASA-CR-171897 .... N86-10896* #
NASA-CR-171898 .... N86-10820* #
NASA-CR-171899 .... N86-10897* #
NASA-CR-171900 .... N86-10821* #
NASA-CR-171901 .... N86-10785* #
NASA-CR-174886 .... N86-11087* #
NASA-CR-174964 .... N86-10461* #
NASA-CR-174980 .... N86-10589* #
NASA-CR-176141 .... N86-10377* #
NASA-CR-176198 .... N86-10707* #
NASA-CR-176203 .... N86-10382* #
NASA-CR-176204 .... N86-10615* #
NASA-CR-176205 .... N86-11083 #
NASA-CR-176206 .... N86-11084* #
NASA-CR-176207 .... N86-11085* #
NASA-CR-176208 .... N86-11086* #
NASA-CR-176209 .... N86-10312* #
NASA-CR-176211 .... N86-10599* #
NASA-CR-176219 .... N86-10860* #
NASA-CR-176220 .... N86-10588* #
NASA-CR-176221 .... N86-10822* #
NASA-CR-176222 .... N86-10823* #
NASA-CR-176223 .... N86-10824* #
NASA-CR-176224 .... N86-10825* #
NASA-CR-176225 .... N86-10826* #
NASA-CR-176226 .... N86-10827* #
NASA-CR-176228 .... N86-11047* #
NASA-CR-176229 .... N86-10912* #
NASA-CR-176230 .... N86-11060* #
NASA-CR-176231 .... N86-10033* #
NASA-CR-176232 .... N86-10271* #
NASA-CR-176233 .... N86-10272* #
NASA-CR-176234 .... N86-10577* #
NASA-CR-176235 .... N86-10539* #
NASA-CR-176236 .... N86-10578* #
NASA-CR-176237 .... N86-10014* #
NASA-CR-176238 .... N86-11059* #
NASA-CR-176240 .... N86-10540* #
NASA-CR-176241 .... N86-11139* #
NASA-CR-176242 .... N86-11133* #
NASA-CR-176244 .... N86-11095* #
NASA-CR-176249 .... N86-10484* #
NASA-CR-176250 .... N86-10042* #
NASA-CR-176262 .... N86-10310* #
NASA-CR-176268 .... N86-10597*
NASA-CR-177334 .... N86-10819* #
NASA-CR-177368 .... N86-10274* #
NASA-CR-177967 .... N86-10848* #
NASA-CR-177972 .... N86-11064* #
NASA-CR-178480 .... N86-10705* #
NASA-CR-178484 .... N86-10462* #
NASA-CR-178495 .... N86-10340* #

NASA-RP-1150 .... N86-10579* #

NASA-SP-479 .... N86-11137* #
NASA-SP-7011(275) N86-10768*

NASA-TM-58269 .... N86-10018* #
NASA-TM-77669 .... N86-10179* #
NASA-TM-77672 .... N86-10378* #
NASA-TM-77901 .... N86-10611* #
NASA-TM-77907 .... N86-10293* #
NASA-TM-77909 .... N86-10612* #
NASA-TM-77910 .... N86-10613* #
NASA-TM-77911 .... N86-10614* #
NASA-TM-77915 .... N86-10418* #
NASA-TM-77923 .... N86-10273* #
NASA-TM-86207 .... N86-11138* #
NASA-TM-86393 .... N86-10580* #
NASA-TM-86405 .... N86-10016* #
NASA-TM-86513 .... N86-10278* #
NASA-TM-86757 .... N86-10464* #
NASA-TM-86782 .... N86-10015* #
NASA-TM-86827 .... N86-10048* #
NASA-TM-86836 .... N86-10734* #
NASA-TM-86844 .... N86-10777* #
NASA-TM-87072 .... N86-10379* #
NASA-TM-87076 .... N86-10463* #
NASA-TM-87091 .... N86-10017* #
NASA-TM-87093 .... N86-10019* #
NASA-TM-87101 .... N86-10290* #
NASA-TM-87103 .... N86-10280* #
NASA-TM-87105 .... N86-10341* #
NASA-TM-87106 .... N86-10643* #
NASA-TM-87109 .... N86-10582* #
NASA-TM-87110 .... N86-10311* #
NASA-TM-87114 .... N86-10551* #
NASA-TM-87118 .... N86-10279* #
NASA-TM-87119 .... N86-11048* #
NASA-TM-87124 .... N86-10380* #

NASA-TM-87125 N86-10381* #
NASA-TM-87131 N86-10281* #
NASA-TM-87133 N86-10552* #
NASA-TM-87509 N86-11141* #
NASA-TM-87566 N86-10053* #
NASA-TM-87567 N86-10828* #
NASA-TM-87595 N86-10581* #
NASA-TM-87601 N86-10913* #

NBL-312 N86-10953 #

NBS/NSRDS-3/11 N86-10923 #

NBS/TN-1213 N86-10847 #

NBSIR-84-2903 N86-10453 #
NBSIR-85-3122 N86-10302 #

NIKHEF-H/84-12 N86-10882 #
NIKHEF-H/84-13 N86-10883 #
NIKHEF-H/84-15 N86-11038 #

NOTA-1535 N86-10638 #

NRL-MR-5291 N86-10714 #
NRL-MR-5573 N86-10730 #
NRL-MR-5599 N86-10406 #
NRL-MR-5613 N86-10983 #
NRL-MR-5614 N86-10924 #

NU-SML-TR-85-1 N86-10593 #
NU-SML-TR-85-2 N86-10346 #

NUSC-TR-7363 N86-10863 #

NWC-TP-6488 N86-10592 #
NWC-TP-6572 N86-10712 #
NWC-TP-6636 N86-10404 #

ONERA-NT-1983-7 N86-10332 #

ONERA-RT-17/1841-RY-010-R N86-10022 #

ORNL-6157 N86-10926 #

ORNL/TM-9225 N86-10679 #
ORNL/TM-9483 N86-10840 #
ORNL/TM-9615 N86-10958 #

OUEL-1534/84 N86-10854 #

PB85-187110 N86-11082 #
PB85-191625 N86-10641 #
PB85-193027 N86-10710 #
PB85-193530 N86-10688 #
PB85-195345 N86-10724 #
PB85-196418 N86-10689 #
PB85-196988 N86-10723 #
PB85-198356 N86-10687 #
PB85-200004 N86-10686 #
PB85-200178 N86-10453 #
PB85-206068 N86-10847 #
PB85-219632 N86-10305 #

PERLAB-6 N86-10870 #

PFC/RR-84-15 N86-11020 #
PFC/RR-84-19 N86-11000 #

PH-273 N86-10366

PM/84/09 N86-10706 #

PN-84/13 N86-10858 #
PN-84/27 N86-10859 #

PNL-SA-12423 N86-10938 #
PNL-SA-12549 N86-10684 #
PNL-SA-12696 N86-10297 #
PNL-SA-12863 N86-10527 #
PNL-SA-12888 N86-10299 #
PNL-SA-12990 N86-10631 #
PNL-SA-13032 N86-10686 #
PNL-SA-13193 N86-10772 #

PNL-5457 N86-10326 #
PNL-5572 N86-10597*

PR-1 N86-10187 #
PR-2 N86-10188 #
PR-3 N86-10189 #

PRL-TR-56 N86-10727 #

PSI-TR-451 N86-10444 #

PUBL-335 N86-10637 #

PV-43-954/F/2 N86-10594 #
PV-43-954/F/3 N86-10564 #

QPR-6 N86-10339

RAE-TM-P-1030 N86-10919 #

RAE-TR-84109-PT-1 N86-10343 #
RAE-TR-85002 N86-10190 #

RAI-84-AG-4 N86-10705* #

RAND/R-3259-ARPA N86-10542 #

REPT-MAT/720 N86-10575

REPT-W-9/82 N86-10596 #

REPT-1-68430-44(1985)01 N86-10806 #
REPT-1-68430-44(1985)02 N86-10807 #
REPT-2-84 N86-10477 #
REPT-15 N86-11094 #
REPT-26/5005/HF/AR N86-10533 #
REPT-31-3725(9) N86-11087* #
REPT-71-521-SA-1 N86-11050 #
REPT-85B0346 N86-11138* #
REPT-442-4 N86-10779 #
REPT-0226-16 N86-10912* #
REPT-85265 N86-10464* #
REPT-85358 N86-10015* #
REPT-85392 N86-10048* #
REPT-85408 N86-10734* #
REPT-85419 N86-10777* #
REPT-051560-28(1984)08 N86-10808 #

RES-PAPER-670 N86-10550

RFP-3848 N86-10325 #

RHO-BW-SA-435P N86-10633 #

RSRE-MEMO-3806 N86-10793 #

S-549 N86-10018* #

SAIC-84/1104 N86-10524 #

SAND-84-1096 N86-10644 #
SAND-84-1775C N86-10665 #
SAND-84-2342C N86-10351 #
SAND-84-2395C N86-10195 #
SAND-84-2434C N86-10928 #
SAND-84-2499C N86-11013 #
SAND-84-2500C N86-10940 #
SAND-84-2530 N86-10716 #
SAND-84-2544C N86-10439 #
SAND-84-2576C N86-11019 #
SAND-84-2670C N86-10021 #
SAND-84-18440 N86-10357 #
SAND-85-0042C N86-10192 #
SAND-85-0063C N86-10049 #
SAND-85-0098C N86-10324 #
SAND-85-0148C N86-11055 #
SAND-85-0149C N86-11054 #
SAND-85-0171C N86-10474 #
SAND-85-0200C N86-10408 #
SAND-85-0258C N86-10304 #
SAND-85-0262C N86-10331 #
SAND-85-0459C N86-11005 #
SAND-85-0554C N86-10350 #
SAND-85-0721C N86-10300 #
SAND-85-0841C N86-10920 #
SAND-85-02980 N86-10298 #
SAND-85-71960 N86-10301 #
SAND-8402519C N86-11011 #

SAPR-2 N86-11060* #
SAPR-9 N86-11087* #

SD-TR-85-12 N86-10708 #

SERI/PR-255-2493 N86-10645 #

SERI/SP-271-2511 N86-10657 #

SERI/STR-211-2637 N86-10668 #
SERI/STR-211-2687 N86-10655 #

SERI/TP-212-2749 N86-10662 #

SJ70 N86-10576

SNIAS-443.501/85 N86-10023 #
SNIAS-443.501/85 N86-10024 #

SNIAS-443.529/84 N86-10024 #

SR-2 N86-10269 #

SS-45 N86-10672 #
SS-45A N86-10673 #

SSL-17-85 N86-10271* #

SU-SLAC-CN-303 N86-10985 #

SU-SLAC-PUB-3583 N86-11025 #
SU-SLAC-PUB-3599 N86-11009 #
SU-SLAC-PUB-3600 N86-11015 #
SU-SLAC-PUB-3616 N86-11004 #
SU-SLAC-PUB-3617 N86-11051 #
SU-SLAC-PUB-3637 N86-11033 #
SU-SLAC-PUB-3638 N86-10801 #
SU-SLAC-PUB-3649 N86-11014 #
SU-SLAC-PUB-3651 N86-11024 #
SU-SLAC-PUB-3654 N86-10964 #
SU-SLAC-PUB-3660 N86-10995 #
SU-SLAC-PUB-3667 N86-10836 #
SU-SLAC-PUB-3671 N86-11012 #
SU-SLAC-PUB-3675 N86-10994 #
SU-SLAC-PUB-3684 N86-11035 #

SWRI-7573/30 N86-10589* #

TAE-536 N86-10583 #
TAE-537 N86-10584 #

TDA-PR-42-82 N86-10382* #

TDCK-79518 N86-10782 #
TDCK-79524 N86-11077 #
TDCK-79698 N86-10783 #
TDCK-79782 N86-10789 #

TDWR/R-288-VOL-4 N86-10641 #

TEST-9 N86-10354 #

THE-RC-51408-PT-1 N86-10888 #
THE-RC-52082-PT-2 N86-10889 #

TMS-PAPER-F8415 N86-10310* #

TN-84-7104-925-46 N86-10819* #

TOP-6-2-335 N86-10563 #

TPR-20 N86-10651 #
TPR-21 N86-10652 #

TR-2-85 N86-10918 #
TR-11 N86-10283 #
TR-18 N86-10541 #
TR-19 N86-10485 #
TR-20 N86-10977 #
TR-0084A(5940-05)-6 N86-10708 #

TW-264 N86-10881 #

UCID-20437 N86-10409 #

UCLA-ENG-85-20 N86-10591 #

UCRI-92523 N86-10717 #

UCRL-TRANS-12061 N86-10318 #

UCRL-15640 N86-10468 #
UCRL-53594 N86-10632 #
UCRL-91078-REV-1 N86-10467 #
UCRL-91078-2 N86-10466 #
UCRL-91359 N86-10718 #
UCRL-91482 N86-10359 #
UCRL-91642 N86-10471 #
UCRL-91885 N86-10959 #
UCRL-91892 N86-10323 #
UCRL-91953 N86-11030 #
UCRL-92121 N86-10907 #
UCRL-92161 N86-10908 #
UCRL-92204 N86-10317 #
UCRL-92246 N86-11017 #
UCRL-92525 N86-11080 #
UCRL-92538 N86-10984 #
UCRL-92648 N86-10532 #
UCRL-92690 N86-11016 #
UCRL-92713 N86-10956 #
UCRL-92724 N86-11134 #
UCRL-92731 N86-10296 #
UCRL-92834 N86-10737 #
UCRL-92885 N86-10470 #

UMD-DMSS-85/5 N86-10885 #
UMD-DMSS-85/6 N86-10886 #

UROCHESTER/DC/85/TR-68 N86-10925 #

US-PATENT-APPL-SN-143399 N86-10417
US-PATENT-APPL-SN-329558 N86-10374
US-PATENT-APPL-SN-343032 N86-10338
US-PATENT-APPL-SN-347391 N86-10674
US-PATENT-APPL-SN-347749 N86-10371
US-PATENT-APPL-SN-361016 N86-10481
US-PATENT-APPL-SN-377107 N86-10376
US-PATENT-APPL-SN-387133 N86-10975
US-PATENT-APPL-SN-388327 N86-10373
US-PATENT-APPL-SN-388574 N86-10972
US-PATENT-APPL-SN-403246 N86-10906
US-PATENT-APPL-SN-403247 N86-10973
US-PATENT-APPL-SN-415639 N86-10538
US-PATENT-APPL-SN-420209 N86-10375
US-PATENT-APPL-SN-421766 N86-10416
US-PATENT-APPL-SN-431434 N86-10642
US-PATENT-APPL-SN-431866 N86-10480
US-PATENT-APPL-SN-442496 N86-10482
US-PATENT-APPL-SN-442497 N86-10976
US-PATENT-APPL-SN-45260 N86-10536
US-PATENT-APPL-SN-455362 N86-10282
US-PATENT-APPL-SN-471550 N86-10372
US-PATENT-APPL-SN-486477 N86-10974
US-PATENT-APPL-SN-486603 N86-10032
US-PATENT-APPL-SN-500725 N86-10537
US-PATENT-APPL-SN-505569 N86-10415
US-PATENT-APPL-SN-529412 N86-10414
US-PATENT-APPL-SN-577391 N86-10277
US-PATENT-APPL-SN-591715 N86-10355 #
US-PATENT-APPL-SN-617049 N86-10483
US-PATENT-APPL-SN-637238 N86-10198 #
US-PATENT-APPL-SN-640623 N86-10556 #
US-PATENT-APPL-SN-643140 N86-10289
US-PATENT-APPL-SN-655486 N86-10445 #
US-PATENT-APPL-SN-655490 N86-10196 #
US-PATENT-APPL-SN-655593 N86-10197 #
US-PATENT-APPL-SN-677136 N86-10792 #
US-PATENT-APPL-SN-693927 N86-10778 #
US-PATENT-APPL-SN-708909 N86-10437 #
US-PATENT-APPL-SN-715992 N86-10421 #
US-PATENT-APPL-SN-717365 N86-10422 #
US-PATENT-APPL-SN-718399 N86-10554 #
US-PATENT-APPL-SN-718762 N86-10555 #
US-PATENT-APPL-SN-719792 N86-10435 #
US-PATENT-APPL-SN-722579 N86-10313 #
US-PATENT-APPL-SN-726872 N86-10424 #
US-PATENT-APPL-SN-727507 N86-10915 #
US-PATENT-APPL-SN-729849 N86-10314 #
US-PATENT-APPL-SN-731223 N86-10436 #
US-PATENT-APPL-SN-732330 N86-10423 #
US-PATENT-APPL-SN-738817 N86-10426 #
US-PATENT-APPL-SN-739413 N86-10425 #
US-PATENT-APPL-SN-741644 N86-10800 #
US-PATENT-APPL-SN-742825 N86-10427 #
US-PATENT-APPL-SN-743853 N86-10799 #
US-PATENT-APPL-SN-744593 N86-10316 #
US-PATENT-APPL-SN-746617 N86-10558 #
US-PATENT-APPL-SN-749333 N86-10020 #
US-PATENT-APPL-SN-749335 N86-10525 #

US-PATENT-CLASS-17.2-PC N86-10376
US-PATENT-CLASS-118-724 N86-10537
US-PATENT-CLASS-250-370 N86-10480
US-PATENT-CLASS-310-323 N86-10483
US-PATENT-CLASS-324-72 N86-10976
US-PATENT-CLASS-324-433 N86-10642
US-PATENT-CLASS-332-16R N86-10415
US-PATENT-CLASS-343-17.2PC N86-10375
US-PATENT-CLASS-343-17.2PC N86-10417
US-PATENT-CLASS-343-18 N86-10371
US-PATENT-CLASS-343-372 N86-10372
US-PATENT-CLASS-343-872 N86-10032
US-PATENT-CLASS-350-162.13 N86-10975
US-PATENT-CLASS-350-388 N86-10972
US-PATENT-CLASS-350-403 N86-10536
US-PATENT-CLASS-351-243 N86-10973
US-PATENT-CLASS-356-437 N86-10674
US-PATENT-CLASS-357-55 N86-10416
US-PATENT-CLASS-358-88 N86-10481
US-PATENT-CLASS-358-93 N86-10482
US-PATENT-CLASS-361-58 N86-10414
US-PATENT-CLASS-369-37 N86-10974
US-PATENT-CLASS-372-45 N86-10538
US-PATENT-CLASS-375-120 N86-10374
US-PATENT-CLASS-382-1 N86-10906
US-PATENT-CLASS-428-107 N86-10289
US-PATENT-CLASS-455-67 N86-10373
US-PATENT-CLASS-528-35 N86-10338
US-PATENT-CLASS-568-923 N86-10282

US-PATENT-4,505,544 N86-10975
US-PATENT-4,506,234 N86-10415
US-PATENT-4,508,055 N86-10537
US-PATENT-4,508,929 N86-10282
US-PATENT-4,509,051 N86-10375
US-PATENT-4,510,377 N86-10277
US-PATENT-4,510,525 N86-10481
US-PATENT-4,510,622 N86-10373
US-PATENT-4,511,219 N86-10972
US-PATENT-4,511,220 N86-10536
US-PATENT-4,511,228 N86-10973
US-PATENT-4,513,308 N86-10416
US-PATENT-4,513,429 N86-10374
US-PATENT-4,514,758 N86-10482
US-PATENT-4,515,847 N86-10289
US-PATENT-4,516,858 N86-10674
US-PATENT-4,517,464 N86-10480
US-PATENT-4,517,517 N86-10642
US-PATENT-4,517,568 N86-10371
US-PATENT-4,517,570 N86-10372
US-PATENT-4,517,618 N86-10414
US-PATENT-4,518,759 N86-10338
US-PATENT-4,519,055 N86-10974
US-PATENT-4,520,364 N86-10032
US-PATENT-4,520,504 N86-10906
US-PATENT-4,521,779 N86-10417
US-PATENT-4,521,867 N86-10538
US-PATENT-4,523,120 N86-10483
US-PATENT-4,524,322 N86-10976
US-PATENT-4,524,362 N86-10376

USAAVSCOM-TR-85-C-12 N86-10017* #
USAAVSCOM-TR-85-C-15 N86-10463* #

USGS/WRI/84-4369 N86-10830 #

UVA/5-28230 N86-11060* #
UVA/528230/MS86/101 N86-11059* #

VTH-LR-360-PT-1 N86-10045 #

WP-29-84-85 N86-10861 #

WSRL-0383-TR N86-10430 #
WSRL-0389-TM N86-10403 #

Y/DV-404-REV-1 N86-10330 #

YALEU/DCS/RR-370 N86-10795 #
YALEU/DCS/RR-381 N86-10794 #
YALEU/DCS/RR-389 N86-10850 #
YALEU/DCS/RR-396 N86-10868 #
YALEU/DCS/RR-397 N86-10867 #
YALEU/DCS/RR-398 N86-10887 #
YALEU/DCS/RR-399 N86-10833 #

ZW-8414 N86-10905 #
ZW-8415 N86-10892 #

☆ U.S. GOVERNMENT PRINTING OFFICE: 1985-491-573/20024

FEDERAL DEPOSITORY LIBRARY PROGRAM

The Federal Depository Library Program provides Government publications to designated libraries throughout the United States. The Regional Depository Libraries listed below receive and retain at least one copy of nearly every Federal Government publication, either in printed or microfilm form, for use by the general public. These libraries provide reference services and inter-library loans; however, they are *not* sales outlets. You may wish to ask your local library to contact a Regional Depository to help you locate specific publications, or you may contact the Regional Depository yourself.

ARKANSAS STATE LIBRARY
One Capitol Mall
Little Rock, AR 72201
(501) 371-2326

AUBURN UNIV. AT MONTGOMERY LIBRARY
Documents Department
Montgomery, AL 36193
(205) 279-9110, ext. 253

UNIV. OF ALABAMA LIBRARY
Documents Dept.—Box S
University, AL 35486
(205) 348-7369

DEPT. OF LIBRARY, ARCHIVES AND PUBLIC RECORDS
Third Floor—State Cap.
1700 West Washington
Phoenix, AZ 85007
(602) 255-4121

UNIVERSITY OF ARIZONA LIB.
Government Documents Dept.
Tucson, AZ 85721
(602) 626-5233

CALIFORNIA STATE LIBRARY
Govt. Publications Section
P.O. Box 2037
Sacramento, CA 95809
(916) 322-4572

UNIV. OF COLORADO LIB.
Government Pub. Division
Campus Box 184
Boulder, CO 80309
(303) 492-8834

DENVER PUBLIC LIBRARY
Govt. Pub. Department
1357 Broadway
Denver, CO 80203
(303) 571-2131

CONNECTICUT STATE LIBRARY
Government Documents Unit
231 Capitol Avenue
Hartford, CT 06106
(203) 566-4971

UNIV. OF FLORIDA LIBRARIES
Library West
Documents Department
Gainesville, FL 32611
(904) 392-0367

UNIV. OF GEORGIA LIBRARIES
Government Reference Dept.
Athens, Ga. 30602
(404) 542-8951

UNIV. OF HAWAII LIBRARY
Govt. Documents Collection
2550 The Mall
Honolulu, HI 96822
(808) 948-8230

UNIV. OF IDAHO LIBRARY
Documents Section
Moscow, ID 83843
(208) 885-6344

ILLINOIS STATE LIBRARY
Information Services Branch
Centennial Building
Springfield, IL 62706
(217) 782-5185

INDIANA STATE LIBRARY
Serials Documents Section
140 North Senate Avenue
Indianapolis, IN 46204
(317) 232-3686

UNIV. OF IOWA LIBRARIES
Govt. Documents Department
Iowa City, IA 52242
(319) 353-3318

UNIVERSITY OF KANSAS
Doc. Collect—Spencer Lib.
Lawrence, KS 66045
(913) 864-4662

UNIV. OF KENTUCKY LIBRARIES
Govt. Pub. Department
Lexington, KY 40506
(606) 257-3139

LOUISIANA STATE UNIVERSITY
Middleton Library
Govt. Docs. Dept.
Baton Rouge, LA 70803
(504) 388-2570

LOUISIANA TECHNICAL UNIV. LIBRARY
Documents Department
Ruston, LA 71272
(318) 257-4962

UNIVERSITY OF MAINE
Raymond H. Fogler Library
Tri-State Regional Documents Depository
Orono, ME 04469
(207) 581-1680

UNIVERSITY OF MARYLAND
McKeldin Lib.—Doc. Div.
College Park, MD 20742
(301) 454-3034

BOSTON PUBLIC LIBRARY
Government Docs. Dept.
Boston, MA 02117
(617) 536-5400 ext. 226

DETROIT PUBLIC LIBRARY
Sociology Department
5201 Woodward Avenue
Detroit, MI 48202
(313) 833-1409

MICHIGAN STATE LIBRARY
P.O. Box 30007
Lansing, MI 48909
(517) 373-0640

UNIVERSITY OF MINNESOTA
Government Pubs. Division
409 Wilson Library
309 19th Avenue South
Minneapolis, MN 55455
(612) 373-7813

UNIV. OF MISSISSIPPI LIB.
Documents Department
University, MS 38677
(601) 232-5857

UNIV. OF MONTANA
Mansfield Library
Documents Division
Missoula, MT 59812
(406) 243-6700

NEBRASKA LIBRARY COMM.
Federal Documents
1420 P Street
Lincoln, NE 68508
(402) 471-2045
In cooperation with University of Nebraska-Lincoln

UNIVERSITY OF NEVADA LIB.
Govt. Pub. Department
Reno, NV 89557
(702) 784-6579

NEWARK PUBLIC LIBRARY
5 Washington Street
Newark, NJ 07101
(201) 733-7812

UNIVERSITY OF NEW MEXICO
Zimmerman Library
Government Pub. Dept.
Albuquerque, NM 87131
(505) 277-5441

NEW MEXICO STATE LIBRARY
Reference Department
325 Don Gaspar Avenue
Santa Fe, NM 87501
(505) 827-2033, ext. 22

NEW YORK STATE LIBRARY
Empire State Plaza
Albany, NY 12230
(518) 474-5563

UNIVERSITY OF NORTH CAROLINA AT CHAPEL HILL
Wilson Library
BA/SS Documents Division
Chapel Hill, NC 27515
(919) 962-1321

UNIVERSITY OF NORTH DAKOTA
Chester Fritz Library
Documents Department
Grand Forks, ND 58202
(701) 777-2617, ext. 27
(In cooperation with North Dakota State Univ. Library)

STATE LIBRARY OF OHIO
Documents Department
65 South Front Street
Columbus, OH 43215
(614) 462-7051

OKLAHOMA DEPT. OF LIB.
Government Documents
200 NE 18th Street
Oklahoma City, OK 73105
(405) 521-2502

OKLAHOMA STATE UNIV. LIB.
Documents Department
Stillwater, OK 74078
(405) 624-6546

PORTLAND STATE UNIV. LIB.
Documents Department
P.O. Box 1151
Portland, OR 97207
(503) 229-3673

STATE LIBRARY OF PENN.
Government Pub. Section
P.O. Box 1601
Harrisburg, PA 17105
(717) 787-3752

TEXAS STATE LIBRARY
Public Services Department
P.O. Box 12927—Cap. Sta.
Austin, TX 78750
(512) 471-2996

TEXAS TECH UNIV. LIBRARY
Govt. Documents Department
Lubbock, TX 79409
(806) 742-2268

UTAH STATE UNIVERSITY
Merrill Library, U.M.C. 30
Logan, UT 84322
(801) 750-2682

UNIVERSITY OF VIRGINIA
Alderman Lib.—Public Doc.
Charlottesville, VA 22901
(804) 924-3133

WASHINGTON STATE LIBRARY
Documents Section
Olympia, WA 98504
(206) 753-4027

WEST VIRGINIA UNIV. LIB.
Documents Department
Morgantown, WV 26506
(304) 293-3640

MILWAUKEE PUBLIC LIBRARY
814 West Wisconsin Avenue
Milwaukee, WI 53233
(414) 278-3000

ST. HIST LIB. OF WISCONSIN
Government Pub. Section
816 State Street
Madison, WI 53706
(608) 262-4347

WYOMING STATE LIBRARY
Supreme Ct. & Library Bld.
Cheyenne, WY 82002
(307) 777-6344

National Aeronautics and
Space Administration
Code NIT-4
Washington, D.C.
20546

Official Business
Penalty for Private Use, $300

SPECIAL FOURTH-CLASS RATE
POSTAGE & FEES PAID
NASA
WASHINGTON, D.C.
PERMIT No. G 27

POSTMASTER: If Undeliverable (Section 158
Postal Manual) Do Not Return

24/2

VOLUME 24 / NUMBER 2
JANUARY 23, 1986
ACC. NOS. N86-11145 TO N86-12198

STAR

AN ABSTRACT JOURNAL

LD
C
S & T REFERENCE
NEWARK PUBLIC LIBRARY
U.S. DOCUMENTS

Scientific and Technical Aerospace Reports

PRODUCED BY THE
SCIENTIFIC AND TECHNICAL
INFORMATION
BRANCH

NASA

READEX
FICHE
best copy available

NAS 1.9/4:

NATIONAL AERONAUTICS AND SPACE ADMINISTRATION

WHAT YOU CAN DO FOR *STAR*

All users of this abstract service are urged to forward reports to be considered for announcement in *STAR*. This will aid NASA in its efforts to provide the fullest possible coverage of all scientific and technical publications that might support aeronautics and space research and development. If you have prepared relevant reports (other than those that you will transmit to NASA, DoD, or DOE through the usual contract- or grant-reporting channels), please send them for consideration to the NASA Scientific and Technical Information Facility, P.O. Box 8757, B.W.I. Airport, Maryland 21240.

Reprints of journal articles, book chapters, and conference papers are also welcome. These will be considered for announcement in *STAR's* companion journal, *International Aerospace Abstracts*.

You may specify a particular source to be included in a report announcement if you wish; otherwise the report will be placed on public sale at the National Technical Information Service. Copyrighted publications will be announced but not distributed or sold.

PURCHASE OF *STAR*

The semimonthly issues are available for sale by the Superintendent of Documents, U.S. Government Printing Office, Washington, D.C. 20402.

PUBLISHED BY:

UNITED STATES GOVERNMENT
NATIONAL AERONAUTICS AND SPACE ADMINISTRATION
SCIENTIFIC AND TECHNICAL INFORMATION BRANCH

Scientific and Technical Aerospace Reports, Volume 24, is prepared by the NASA Scientific and Technical Information Facility operated for the National Aeronautics and Space Administration by RMS Associates.

The Administrator of the National Aeronautics and Space Administration has determined that the publication of this periodical is necessary in the transaction of the public business required by law of this Agency. Use of funds for printing this periodical has been approved by the Director of the Office of Management and Budget through March 22, 1988.

US ISSN 0036-8741

INTRODUCTION

Scientific and Technical Aerospace Reports (STAR) is a major component of a comprehensive National Aeronautics and Space Administration information system covering aeronautics, space, and supporting disciplines. *STAR* is issued on the 8th and 23rd of each month and announces current publications of the following types:

- NASA, NASA contractor, and NASA grantee reports

- Reports issued by other U.S. Government agencies, domestic and foreign institutions, universities, and private firms

- Translations in report form

- NASA-owned patents and patent applications

- Dissertations and theses

Cumulative index volumes are published annually.

Journal, book, and conference literature, cover-to-cover journal translations, and certain foreign dissertations are announced in a companion journal, *International Aerospace Abstracts (IAA)*, available on subscription from the American Institute of Aeronautics and Astronautics, Technical Information Service, 555 West 57th Street, 12th Floor, New York, New York 10019.

SUBJECT SCOPE

Subject scope of *STAR*, and *IAA* includes all aspects of aeronautics and space research and development, supporting basic and applied research, and applications. Aerospace aspects of earth resources, energy development, conservation, oceanography, environmental protection, urban transportation, and other topics of high national priority are also covered.

OTHER NASA PUBLICATIONS

Other NASA publications and information services are described in the publication, *The NASA Scientific and Technical Information System ... and How to Use It*, available without charge from the NASA Scientific and Technical Information Facility, P.O. Box 8757, B.W.I. Airport, Maryland 21240.

HOW TO USE *STAR* SUBJECT CATEGORIES

STAR is categorized by 10 major subject divisions divided into 74 specific subject categories and one general category/division. The major subject divisions are listed in the Table of Contents, together with a note for each that defines its scope and provides any cross-references. For example:

AERONAUTICS

Includes aeronautics (general); aerodynamics; air transportation and safety; aircraft communications and navigation; aircraft design, testing and performance; aircraft instrumentation; aircraft propulsion and power; aircraft stability and control; and research and support facilities (air).

For related information see also *Astronautics*.

Each major division is further divided into as many as nine specific categories, which are identified by category numbers.

Abstracts in *STAR* are grouped by specific category, the categories appearing in sequential order. Category breaks in the abstract section are identified by the category number and title, and a scope note. Cross-references to other categories are provided as appropriate. For example:

02 AERODYNAMICS

Includes aerodynamics of bodies, combinations, wings, rotors, and control surfaces; and internal flow in ducts and turbomachinery.

For related information see also *34 Fluid Mechanics and Heat Transfer*.

CROSS-REFERENCES

Individual *STAR* abstracts are not ordinarily cross-referenced, except for certain conference reports or book translations that have had separate abstracts written for their component papers or chapters. Citations and abstracts of the components follow immediately after those of the parent document. When the subject content of a component differs sufficiently from the general content of the parent, a cross-reference citation also is printed at the end of the category to which it normally would have been assigned if it were independent.

DOCUMENTS ON MICROFICHE

Documents on microfiche(1) are designated by a pound sign (#) following the accession number. The pound sign is used without regard to the source or quality of the microfiche.

AVAILABILITIES

One or more sources from which a document announced in *STAR* is available to the public is given in each citation. The most commonly indicated sources and their acronyms or abbreviations are listed below. If the publication is available from a source other than those listed, the publisher and his address will be displayed on the availability line or in combination with the corporate source line.

---

(1) A microfiche is a transparent sheet of film, 105 by 148 mm in size, containing as many as 60 to 98 pages of information reduced to micro images (not to exceed 26:1 reduction).

Avail: NTIS. Sold by the National Technical Information Service. Prices for hard copy (HC) and microfiche (MF) are indicated by a price code following the letters HC or MF in the *STAR* citation. Current values for the price codes are given in the tables on page vii.

Initially distributed microfiche under the NTIS SRIM (Selected Research in Microfiche) is available at greatly reduced unit prices. For this service and for information concerning subscription to NASA printed reports, consult the NTIS Subscription Section, Springfield, Va. 22161.

NOTE ON ORDERING DOCUMENTS: When ordering NASA publications (those followed by the * symbol), use the N accession number. NASA patent applications (only the specifications are offered) should be ordered by the US-Patent-Appl-SN number. Non-NASA publications (no asterisk) should be ordered by the AD, PB, or other *report* number shown on the last line of the citation, not by the N accession number. It is also advisable to cite the title and other bibliographic identification.

Avail: SOD (or GPO). Sold by the Superintendent of Documents, U.S. Government Printing Office, in hard copy. The current price and order number are given following the availability line. (NTIS will fill microfiche requests, as indicated above, for those documents identified by a # symbol.)

Avail: NASA Public Document Rooms. Documents so indicated may be examined at or purchased from the National Aeronautics and Space Adminstration, Public Documents Room (Room 126), 600 Independence Ave., S.W., Washington, D.C. 20546, or public document rooms located at each of the NASA research centers, the NASA Space Technology Laboratories, and the NASA Pasadena Office at the Jet Propulsion Laboratory.

Avail: DOE Depository Libraries. Organizations in U.S. cities and abroad that maintain collections of Department of Energy reports, usually in microfiche form, are listed in *Energy Research Abstracts*. Services available from the DOE and its depositories are described in a booklet, *DOE Technical Information Center - Its' Functions and Services* (TID-4660), which may be obtained without charge from the DOE Technical Information Center.

Avail: Univ. Microfilms. Documents so indicated are dissertations selected from *Dissertation Abstracts* and are sold by University Microfilms as xerographic copy (HC) and microfilm. All requests should cite the author and the Order Number as they appear in the citation.

Avail: USGS. Originals of many reports from the U.S. Geological Survey, which may contain color illustrations, or otherwise may not have the quality of illustrations preserved in the microfiche or facsimile reproduction, may be examined by the public at the libraries of the USGS field offices whose addresses are listed in this Introduction. The libraries may be queried concerning the availability of specific documents and the possible utilization of local copying services, such as color reproduction.

Avail: HMSO. Publications of Her Majesty's Stationery Office are sold in the U.S. by Pendragon House, Inc. (PHI), Redwood City, California. The U.S. price (including a service and mailing charge) is given, or a conversion table may be obtained from PHI.

Avail: BLL (formerly NLL): British Library Lending Division, Boston Spa, Wetherby, Yorkshire, England. Photocopies available from this organization at the price shown. (If none is given, inquiry should be addressed to the BLL.)

Avail: Fachinformationszentrum, Karlsruhe. Sold by the Fachinformationszentrum Energie, Physik, Mathematik GMBH, Eggenstein Leopoldshafen, Federal Republic of Germany, at the price shown in deutschmarks (DM).

Avail: Issuing Activity, or Corporate Author, or no indication of availability. Inquiries as to the availability of these documents should be addressed to the organization shown in the citation as the corporate author of the document.

Avail: U.S. Patent and Trademark Office. Sold by Commissioner of Patents and Trademarks, U.S. Patent and Trademark Office, at the standard price of 50 cents each, postage free. (See discussion of patents and patent applications below.)

Avail: ESDU. Pricing information on specific data, computer programs, and details on ESDU topic categories can be obtained from ESDU International Ltd. Requesters in North America should use the Virginia address while all other requesters should use the London address, both of which are on page vi.

NASA PATENTS AND PATENT APPLICATIONS

Patents and patent applications owned by NASA are announced in *STAR* under appropriate subject categories and are referenced in the *STAR* indexes. In the Report/Accession Number Index, patents are indexed by the NASA Case Number (which appears in lieu of the report number in other indexes), the U.S. Patent Number, the U.S. Patent Application Serial Number, and the U.S. Patent Class. Patent applications for which patents have not yet been issued are indexed by the NASA Case Number and the U.S. Patent Application Serial Number.

NASA *patent application specifications* are sold in paper copy by the National Technical Information Service at price code A02 ($9.95 domestic; $19.90 foreign). Microfiche are sold at price code A01 ($5.95 domestic; $11.90 foreign). The US-Patent-Appl-SN- number should be used in ordering either paper copy or microfiche from NTIS. Printed copies of *patents* (which are not microfiched) are available for purchase at 50 cents per copy from:

Commissioner of Patents and Trademarks
U.S. Patent and Trademark Office
Washington, D.C. 20231

When ordering patents, the U.S. Patent Number should be used, and payment must be remitted in advance, preferably by money order or check payable to the Commissioner of Patents and Trademarks. Prepaid purchase coupons for ordering are also available from the Patent and Trademark Office. The patents and patent applications announced in *STAR* are owned by NASA and are available for royalty-free licensing. Requests for licensing terms and further information should be addressed to:

Assistant General Counsel for Patent Matters/Code GP-1
National Aeronautics and Space Administration
Washington, D.C. 20546

ELIGIBILITY AND REGISTRATION FOR NASA INFORMATION PRODUCTS AND SERVICES

A variety of services is available to organizations of the following types that have registered with NASA to receive specific services or products:

1. NASA offices, research centers, contractors, subcontractors, grantees, and consultants;
2. Other U.S. Government agencies and their contractors;
3. Libraries in the United States that have arrangements with NASA to maintain collections of NASA documents for public reference;
4. Other organizations in the United States having a need for NASA documents in work related to aeronautics and space research;
5. Organizations abroad that have established reciprocal document exchange arrangements with NASA.

Only the central service points or central points of document acquisition and control within qualified organizations are eligible to register for NASA products and services. Domestic organizations that may be eligible to receive various classes of NASA publications and services should address their requests for registration or for further information to:

NASA Scientific and Technical Information Facility
ATTN: Registration Activity
P.O. Box 8757
B.W.I. Airport, Maryland 21240

Organizations abroad should direct requests to the same address, but to the attention of: International Exchange Program.

AVAILABILITY OF *STAR* ABSTRACTS ON MICROFICHE

Microfiche of the abstract sections of this issue and other issues of *STAR* are available on annual subscription from NTIS, Attn: Subscriptions, 5285 Port Royal Road, Springfield, Virginia 22161. Annual subscription rates are $60.00 North America; $120.00 foreign. Abstract sections for previous years retroactive to 1964 are available at the current rates. Microfiche for individual *STAR* issue abstract sections are not available.

PUBLIC COLLECTIONS OF NASA DOCUMENTS

DOMESTIC: NASA and NASA-sponsored documents and a large number of aerospace publications are available to the public for reference purposes at the library maintained by the American Institute of Aeronautics and Astronautics, Technical Information Service, 555 West 57th Street, 12th Floor, New York, New York 10019.

EUROPEAN: An extensive collection of NASA and NASA-sponsored publications is maintained by the British Library Lending Division, Boston Spa, Wetherby, Yorkshire, England for public access. The British Library Lending Division also has available many of the non-NASA publications cited in *STAR*. European requesters may purchase facsimile copy or microfiche of NASA and NASA-sponsored documents, those identified by both the symbols # and * from ESA - Information Retrieval Service European Space Agency, 8-10 rue Mario-Nikis, 75738 Paris CEDEX 15, France.

FEDERAL DEPOSITORY LIBRARY PROGRAM

In order to provide the general public with greater access to U.S. Government publications, Congress established the Federal Depository Library Program under the Government Printing Office (GPO), with 50 regional depositories responsible for permanent retention of material, inter-library loan, and reference services. Over 1,300 other depositories also exist. A list of the regional GPO libraries appears on the inside back cover of *STAR*.

ADDRESSES OF ORGANIZATIONS

American Institute of Aeronautics and
Astronautics
Technical Information Service
555 West 57th Street, 12th Floor
New York, New York 10019

British Library Lending Division,
Boston Spa, Wetherby, Yorkshire,
England

Commissioner of Patents and
Trademarks
U.S. Patent and Trademark Office
Washington, D.C. 20231

Department of Energy
Technical Information Center
P.O. Box 62
Oak Ridge, Tennessee 37830

ESA-Information Retrieval Service
ESRIN
Via Galileo Galilei
00044 Frascati (Rome) Italy

ESDU International, Ltd.
1495 Chain Bridge Road
McLean, Virginia 22101

ESDU International, Ltd.
251-259 Regent Street
London, W1R 7AD, England

Fachinformationszentrum Energie, Physik,
Mathematik GMBH
7514 Eggenstein Leopoldshafen
Federal Republic of Germany

Her Majesty's Stationery Office
P.O. Box 569, S.E. 1
London, England

NASA Scientific and Technical Information
Facility
P.O. Box 8757
B.W.I. Airport, Maryland 21240

National Aeronautics and Space
Administration
Scientific and Technical Information
Branch (NIT-1)
Washington, D.C. 20546

National Technical Information Service
5285 Port Royal Road
Springfield, Virginia 22161

Pendragon House, Inc.
899 Broadway Avenue
Redwood City, California 94063

Superintendent of Documents
U.S. Government Printing Office
Washington, D.C. 20402

University Microfilms
A Xerox Company
300 North Zeeb Road
Ann Arbor, Michigan 48106

University Microfilms, Ltd.
Tylers Green
London, England

U.S. Geological Survey Library
National Center – MS 950
12201 Sunrise Valley Drive
Reston, Virginia 22092

U.S. Geological Survey Library
2255 North Gemini Drive
Flagstaff, Arizona 86001

U.S. Geological Survey
345 Middlefield Road
Menlo Park, California 94025

U.S. Geological Survey Library
Box 25046
Denver Federal Center, MS 914
Denver, Colorado 80225

NTIS PRICE SCHEDULES

(Effective October 1, 1985)

Schedule A
STANDARD PRICE DOCUMENTS AND MICROFICHE

PRICE CODE	PAGE RANGE	NORTH AMERICAN PRICE	FOREIGN PRICE
A01	Microfiche	$ 5.95	$11.90
A02-A03	001-050	9.95	19.90
A04-A05	051-100	11.95	23.90
A06-A09	101-200	16.95	33.90
A10-A13	201-300	22.95	45.90
A14-A17	301-400	28.95	57.90
A18-A21	401-500	34.95	69.90
A22-A25	501-600	40.95	81.90
A99	601-up	*	*
NO1		$40.00	70.00
NO2		40.00	70.00

Schedule E
EXCEPTION PRICE DOCUMENTS AND MICROFICHE

PRICE CODE	NORTH AMERICAN PRICE	FOREIGN PRICE
E01	$ 7.50	15.00
E02	10.00	20.00
E03	11.00	22.00
E04	13.50	27.00
E05	15.50	31.00
E06	18.00	36.00
E07	20.50	41.00
E08	23.00	46.00
E09	25.50	51.00
E10	28.00	56.00
E11	30.50	61.00
E12	33.00	66.00
E13	35.50	71.00
E14	38.50	77.00
E15	42.00	84.00
E16	46.00	92.00
E17	50.00	100.00
E18	54.00	108.00
E19	60.00	120.00
E20	70.00	140.00
E99	*	*

*Contact NTIS for price quote.

IMPORTANT NOTICE

NTIS Shipping and Handling Charges (effective June 1, 1985)
U.S., Canada, Mexico — ADD $3.00 per TOTAL ORDER
All Other Countries — ADD $4.00 per TOTAL ORDER

Exceptions — Does NOT apply to:
ORDERS REQUESTING NTIS RUSH HANDLING
ORDERS FOR SUBSCRIPTION OR STANDING ORDER PRODUCTS *ONLY*

NOTE: Each additional delivery address on an order
requires a separate shipping and handling charge.

VOLUME 24 NUMBER 2 / JANUARY 23, 1986

TABLE OF CONTENTS

AERONAUTICS

Includes aeronautics (general); aerodynamics; air transportation and safety; aircraft communications and navigation; aircraft design, testing and performance; aircraft instrumentation; aircraft propulsion and power; aircraft stability and control; and research and support facilities (air).

For related information see also *Astronautics*.

01 AERONAUTICS (GENERAL) 183

02 AERODYNAMICS 189

Includes aerodynamics of bodies, combinations, wings, rotors, and control surfaces; and internal flow in ducts and turbomachinery.

For related information see also *34 Fluid Mechanics and Heat Transfer*

03 AIR TRANSPORTATION AND SAFETY 190

Includes passenger and cargo air transport operations; and aircraft accidents.

For related information see also *16 Space Transportation* and *85 Urban Technology and Transportation*.

04 AIRCRAFT COMMUNICATIONS AND NAVIGATION 190

Includes digital and voice communication with aircraft; air navigation systems (satellite and ground based); and air traffic control.

For related information see also *17 Spacecraft Communications, Command and Tracking* and *32 Communications*.

05 AIRCRAFT DESIGN, TESTING AND PERFORMANCE 191

Includes aircraft simulation technology.

For related information see also *18 Spacecraft Design, Testing and Performance* and *39 Structural Mechanics*.

06 AIRCRAFT INSTRUMENTATION N.A.

Includes cockpit and cabin display devices; and flight instruments.

For related information see also *19 Spacecraft Instrumentation* and *35 Instrumentation and Photography*.

07 AIRCRAFT PROPULSION AND POWER 192

Includes prime propulsion systems and systems components, e.g., gas turbine engines and compressors; and on-board auxiliary power plants for aircraft.

For related information see also *20 Spacecraft Propulsion and Power*, *28 Propellants and Fuels*, and *44 Energy Production and Conversion*.

08 AIRCRAFT STABILITY AND CONTROL 194

Includes aircraft handling qualities; piloting; flight controls; and autopilots.

09 RESEARCH AND SUPPORT FACILITIES (AIR) 194

Includes airports, hangars and runways; aircraft repair and overhaul facilities; wind tunnels; shock tube facilities; and engine test blocks.

For related information see also *14 Ground Support Systems and Facilities (Space)*.

ASTRONAUTICS

Includes astronautics (general); astrodynamics; ground support systems and facilities (space); launch vehicles and space vehicles; space transportation; spacecraft communications, command and tracking; spacecraft design, testing and performance; spacecraft instrumentation; and spacecraft propulsion and power.

For related information see also *Aeronautics*

12 ASTRONAUTICS (GENERAL) N.A.

For extraterrestrial exploration see *91 Lunar and Planetary Exploration*.

13 ASTRODYNAMICS 195

Includes powered and free-flight trajectories; and orbit and launching dynamics.

14 GROUND SUPPORT SYSTEMS AND FACILITIES (SPACE) 196

Includes launch complexes, research and production facilities; ground support equipment, e.g., mobile transporters; and simulators.

For related information see also *09 Research and Support Facilities (Air)*.

15 LAUNCH VEHICLES AND SPACE VEHICLES 196

Includes boosters; manned orbital laboratories; reusable vehicles; and space stations.

16 SPACE TRANSPORTATION 197

Includes passenger and cargo space transportation, e.g., shuttle operations; and rescue techniques.

For related information see also *03 Air Transportation and Safety* and *85 Urban Technology and Transportation*.

17 SPACECRAFT COMMUNICATION, COMMAND AND TRACKING N.A.

Includes telemetry; space communications networks; astronavigation; and radio blackout.

For related information see also *04 Aircraft Communications and Navigation* and *32 Communications*.

18 SPACECRAFT DESIGN, TESTING AND PERFORMANCE 197

Includes spacecraft thermal and environmental control; and attitude control.

For life support systems see *54 Man/System Technology and Life Support*. For related information see also *05 Aircraft Design, Testing and Performance* and *39 Structural Mechanics*.

19 SPACECRAFT INSTRUMENTATION N.A.

For related information see also *06 Aircraft Instrumentation* and *35 Instrumentation and Photography*.

20 SPACECRAFT PROPULSION AND POWER 198

Includes main propulsion systems and components, e.g., rocket engines; and spacecraft auxiliary power sources.

For related information see also *07 Aircraft Propulsion and Power*, *28 Propellants and Fuels*, and *44 Energy Production and Conversion*.

CHEMISTRY AND MATERIALS

Includes chemistry and materials (general); composite materials; inorganic and physical chemistry; metallic materials; nonmetallic materials; and propellants and fuels.

23 CHEMISTRY AND MATERIALS (GENERAL) 199
Includes biochemistry and organic chemistry.

24 COMPOSITE MATERIALS 204
Includes laminates.

25 INORGANIC AND PHYSICAL CHEMISTRY 211
Includes chemical analysis, e.g., chromatography; combustion theory; electrochemistry; and photochemistry.
For related information see also *77 Thermodynamics and Statistical Physics.*

26 METALLIC MATERIALS 212
Includes physical, chemical, and mechanical properties of metals, e.g., corrosion; and metallurgy.

27 NONMETALLIC MATERIALS 217
Includes physical, chemical, and mechanical properties of plastics, elastomers, lubricants, polymers, textiles, adhesives, and ceramic materials.

28 PROPELLANTS AND FUELS 221
Includes rocket propellants, igniters, and oxidizers; storage and handling; and aircraft fuels.
For related information see also *07 Aircraft Propulsion and Power, 20 Spacecraft Propulsion and Power,* and *44 Energy Production and Conversion.*

ENGINEERING

Includes engineering (general), communications; electronics and electrical engineering; fluid mechanics and heat transfer; instrumentation and photography; lasers and masers; mechanical engineering; quality assurance and reliability; and structural mechanics.
For related information see also *Physics.*

31 ENGINEERING (GENERAL) 222
Includes vacuum technology; control engineering; display engineering; and cryogenics.

32 COMMUNICATIONS 227
Includes land and global communications; communications theory; and optical communications.
For related information see also *04 Aircraft Communications and Navigation* and *17 Spacecraft Communications, Command and Tracking.*

33 ELECTRONICS AND ELECTRICAL ENGINEERING 230
Includes test equipment and maintainability; components, e.g., tunnel diodes and transistors; microminiaturization; and integrated circuity.
For related information see also *60 Computer Operations and Hardware* and *76 Solid-State Physics.*

34 FLUID MECHANICS AND HEAT TRANSFER 231
Includes boundary layers; hydrodynamics; fluidics; mass transfer; and ablation cooling.
For related information see also *02 Aerodynamics* and *77 Thermodynamics and Statistical Physics.*

35 INSTRUMENTATION AND PHOTOGRAPHY 234
Includes remote sensors; measuring instruments and gages; detectors; cameras and photographic supplies; and holography.
For aerial photography see *43 Earth Resources.* For related information see also *06 Aircraft Instrumentation* and *19 Spacecraft Instrumentation.*

36 LASERS AND MASERS 240
Includes parametric amplifiers.

37 MECHANICAL ENGINEERING 243
Includes auxiliary systems (non-power); machine elements and processes; and mechanical equipment.

38 QUALITY ASSURANCE AND RELIABILITY 246
Includes product sampling procedures and techniques; and quality control.

39 STRUCTURAL MECHANICS 247
Includes structural element design and weight analysis; fatigue; and thermal stress.
For applications see *05 Aircraft Design, Testing and Performance* and *18 Spacecraft Design, Testing and Performance.*

GEOSCIENCES

Includes geosciences (general); earth resources; energy production and conversion; environment pollution; geophysics; meteorology and climatology; and oceanography.
For related information see also *Space Sciences.*

42 GEOSCIENCES (GENERAL) 256

43 EARTH RESOURCES 266
Includes remote sensing of earth resources by aircraft and spacecraft; photogrammetry; and aerial photography.
For instrumentation see *35 Instrumentation and Photography.*

44 ENERGY PRODUCTION AND CONVERSION 274
Includes specific energy conversion systems, e.g., fuel cells and batteries; global sources of energy; fossil fuels; geophysical conversion; hydroelectric power; and wind power.
For related information see also *07 Aircraft Propulsion and Power, 20 Spacecraft Propulsion and Power, 28 Propellants and Fuels,* and *85 Urban Technology and Transportation.*

45 ENVIRONMENT POLLUTION 278
Includes air, noise, thermal and water pollution; environment monitoring; and contamination control.

46 GEOPHYSICS 280

Includes aeronomy; upper and lower atmosphere studies; ionospheric and magnetospheric physics; and geomagnetism.

For space radiation see *93 Space Radiation*.

47 METEOROLOGY AND CLIMATOLOGY 288

Includes weather forecasting and modification.

48 OCEANOGRAPHY 301

Includes biological, dynamic and physical oceanography; and marine resources.

LIFE SCIENCES

Includes sciences (general); aerospace medicine; behavioral sciences; man/system technology and life support; and planetary biology.

51 LIFE SCIENCES (GENERAL) 302

Includes genetics.

52 AEROSPACE MEDICINE 304

Includes physiological factors; biological effects of radiation; and weightlessness.

53 BEHAVIORAL SCIENCES 306

Includes psychological factors; individual and group behavior; crew training and evaluation; and psychiatric research.

54 MAN/SYSTEM TECHNOLOGY AND LIFE SUPPORT 307

Includes human engineering; biotechnology; and space suits and protective clothing.

55 PLANETARY BIOLOGY N.A.

Includes exobiology; and extraterrestrial life.

MATHEMATICAL AND COMPUTER SCIENCES

Includes mathematical and computer sciences (general); computer operations and hardware; computer programming and software; computer systems; cybernetics; numerical analysis; statistics and probability; systems analysis; and theoretical mathematics.

59 MATHEMATICAL AND COMPUTER SCIENCES (GENERAL) 307

60 COMPUTER OPERATIONS AND HARDWARE 307

Includes computer graphics and data processing.

For components see *33 Electronics and Electrical Engineering*.

61 COMPUTER PROGRAMMING AND SOFTWARE 314

Includes computer programs, routines, and algorithms.

62 COMPUTER SYSTEMS 316

Includes computer networks.

63 CYBERNETICS N.A.

Includes feedback and control theory.

For related information see also *54 Man/System Technology and Life Support*.

64 NUMERICAL ANALYSIS 317

Includes iteration, difference equations, and numerical approximation.

65 STATISTICS AND PROBABILITY N.A.

Includes data sampling and smoothing; Monte Carlo method; and stochastic processes.

66 SYSTEMS ANALYSIS N.A.

Includes mathematical modeling; network analysis; and operations research.

67 THEORETICAL MATHEMATICS N.A.

Includes topology and number theory.

PHYSICS

Includes physics (general); acoustics; atomic and molecular physics; nuclear and high-energy physics; optics; plasma physics; solid-state physics; and thermodynamics and statistical physics.

For related information see also *Engineering*.

70 PHYSICS (GENERAL) 319

For geophysics see *46 Geophysics*. For astrophysics see *90 Astrophysics*. For solar physics see *92 Solar Physics*.

71 ACOUSTICS 332

Includes sound generation, transmission, and attenuation.

For noise pollution see *45 Environment Pollution*.

72 ATOMIC AND MOLECULAR PHYSICS 335

Includes atomic structure and molecular spectra.

73 NUCLEAR AND HIGH-ENERGY PHYSICS 338

Includes elementary and nuclear particles; and reactor theory.

For space radiation see *93 Space Radiation*.

74 OPTICS 342

Includes light phenomena.

75 PLASMA PHYSICS 343

Includes magnetohydrodynamics and plasma fusion.

For ionospheric plasmas see *46 Geophysics*. For space plasmas see *90 Astrophysics*.

76 SOLID-STATE PHYSICS 352

Includes superconductivity.

For related information see also *33 Electronics and Electrical Engineering* and *36 Lasers and Masers*.

77 THERMODYNAMICS AND STATISTICAL PHYSICS 357

Includes quantum mechanics; and Bose and Fermi statistics.

For related information see also *25 Inorganic and Physical Chemistry* and *34 Fluid Mechanics and Heat Transfer*.

SOCIAL SCIENCES

Includes social sciences (general); administration and management; documentation and information science; economics and cost analysis; law and political science; and urban technology and transportation.

80 SOCIAL SCIENCES (GENERAL) 357

Includes educational matters.

81 ADMINISTRATION AND MANAGEMENT 357

Includes management planning and research.

82 DOCUMENTATION AND INFORMATION SCIENCE 357

Includes information storage and retrieval technology; micrography; and library science.

For computer documentation see *61 Computer Programming and Software.*

83 ECONOMICS AND COST ANALYSIS 358

Includes cost effectiveness studies.

84 LAW AND POLITICAL SCIENCE 358

Includes space law; international law; international cooperation; and patent policy.

85 URBAN TECHNOLOGY AND TRANSPORTATION 358

Includes applications of space technology to urban problems; technology transfer; technology assessment; and surface and mass transportation.

For related information see *03 Air Transportation and Safety, 16 Space Transportation,* and *44 Energy Production and Conversion.*

SPACE SCIENCES

Includes space sciences (general); astronomy; astrophysics; lunar and planetary exploration; solar physics; and space radiation.

For related information see also *Geosciences.*

88 SPACE SCIENCES (GENERAL) N.A.

89 ASTRONOMY 359

Includes radio and gamma-ray astronomy; celestial mechanics; and astrometry.

90 ASTROPHYSICS N.A.

Includes cosmology; and interstellar and interplanetary gases and dust.

91 LUNAR AND PLANETARY EXPLORATION 363

Includes planetology; and manned and unmanned flights.

For spacecraft design see *18 Spacecraft Design, Testing and Performance.* For space stations see *15 Launch Vehicles and Space Vehicles.*

92 SOLAR PHYSICS 363

Includes solar activity, solar flares, solar radiation and sunspots.

93 SPACE RADIATION 364

Includes cosmic radiation; and inner and outer earth's radiation belts.

For biological effects of radiation see *52 Aerospace Medicine.* For theory see *73 Nuclear and High-Energy Physics.*

GENERAL

99 GENERAL N.A.

Note: N.A. means that no abstracts were assigned to this category for this issue.

SUBJECT INDEX I-1
PERSONAL AUTHOR INDEX I-65
CORPORATE SOURCE INDEX I-73
CONTRACT NUMBER INDEX I-87
REPORT/ACCESSION NUMBER INDEX I-89

TYPICAL CITATION AND ABSTRACT

NASA SPONSORED DOCUMENT

NASA ACCESSION NUMBER

TITLE

AUTHOR

CONTRACT OR GRANT

REPORT NUMBER

N86-10462*# National Academy of Sciences - National Research Council, Washington, D. C. Systems Dynamics Lab.
CONFINED SWIRLING JET PREDICTIONS USING A MULTIPLE-SCALE TURBULENCE MODEL
C. P. Chen Aug. 1985 22 p refs
(Contract NASw-3458)
(NASA-CR-178484; NAS 1.26:178484) Avail: NTIS
HC A02/MF A01 CSCL 20D

A recently developed multiple scale turbulence model is used for the numerical prediction of isothermal, confined turbulent swirling flows. Because of the streamline curvature and nonequilibrium spectral energy transfer nature of the swirling flow, the utilized multiple scale turbulence model includes a different set of response equations for each of the large scale energetic eddies and the small scale transfer eddies. Predictions are made of a confined coaxial swirling jet in a sudden expansion and comparisons are made with experimental data and with the conventional single scale two equation model. The multiple scale model shows significant improvement of predictions of swirling flows over the single scale k epsilon model. The sensitivity study of the effect of prescribed inlet turbulence levels on the flow fields is also included. Author

AVAILABLE ON MICROFICHE

CORPORATE SOURCE

PUBLICATION DATE

AVAILABILITY SOURCE

COSATI CODE

VOLUME 24 NUMBER 2 / JANUARY 23, 1986

Scientific and Technical Aerospace Reports

A Semimonthly Publication of the National Aeronautics and Space Administration

01 AERONAUTICS (GENERAL)

N86-11145* National Aeronautics and Space Administration, Washington, D. C.
AERONAUTICAL ENGINEERING: A CONTINUING BIBLIOGRAPHY WITH INDEXES
Sep. 1985 138 p
(NASA-SP-7037(191); NAS 1.21:7037(191)) Avail: NTIS HC A07 CSCL 01A

This bibliography lists 499 reports, articles and other documents introduced into the NASA scientific and technical information system in August 1985. Author

N86-11146*# National Aeronautics and Space Administration. Lewis Research Center, Cleveland, Ohio.
DEVELOPMENT OF AN EXPLICIT MULTIGRID ALGORITHM FOR QUASI-THREE-DIMENSIONAL VISCOUS FLOWS IN TURBO-MACHINERY
Rodrick V. Chima [1985] 21 p refs Prepared for presentation at the 24th Aerospace Sci. Meeting, Reno, Nevada, 6-9 Jan. 1986; sponsored by AIAA
(NASA-TM-87128; E-2681; NAS 1.15:87128) Avail: NTIS HC A02/MF A01 CSCL 01B

A rapid quasi three-dimensional analysis was developed for blade-to-blade flows in turbomachinery. The analysis solves the unsteady Euler or thin layer Navier-Stokes equations in a body-fitted coordinate system. It accounts for the effects of rotation, radius change, and stream-surface thickness. The Baldwin-Lomax eddy-viscosity model is used for turbulent flows. The equations which are solved by a two-stage Runge-Kutta scheme made efficient by use of vectorization, a variable time-step, and a flux-based multigrid scheme, are described. A stability analysis is presented for the two-stage scheme. Results for a flat-plate model problem show the applicability of the method to axial, radial, and rotating geometries. Results for a centrifugal impeller and a radial diffuser show that the quasi three-dimensional viscous analysis can be a practical design tool. E.A.K.

N86-11147# Advisory Group for Aerospace Research and Development, Neuilly-Sur-Seine (France).
AERODYNAMICS AND ACOUSTICS OF PROPELLERS
Loughton, England Feb. 1985 458 p refs In ENGLISH and FRENCH Symp. held in Toronto, 1-4 Oct. 1984
(AGARD-CP-366; ISBN-92-835-0374-0) Avail: NTIS HC A20/MF A01

A state of the art review of the aerodynamic design and testing of modern propellers, acoustic and vibration environmental problems and their solutions, and considerations in the integration of the propeller(s) and airframe is presented. Propellers have recently become a focus of attention after having been neglected for many years. The efficient use of propellers as a propulsion medium up to Mach 0.6 was realized at the expense of high noise and vibration. Since the mid-1970s there have been many developments, including the propfan, with an aerodynamic efficiency of 80% at Mach 0.8 now seriously challenges the fanjet. The advent of the supercritical airfoil is another significant development beginning to influence propeller design. For individual titles, see N86-11148 through N86-11176.

N86-11148# Lockheed-Georgia Co., Marietta. Advanced Concepts Dept.
A REVIEW OF ADVANCED TURBOPROP TRANSPORT ACTIVITIES c07
Roy H. Lange *In* AGARD Aerodyn. and Acoustics of Propellers Feb. 1985 16 p refs (For primary document see N86-11147 02-01)
Avail: NTIS HC A20/MF A01

The application of advanced technologies shows the potential for significant improvement in the fuel efficiency and operating costs of future transport aircraft envisioned for operation in the 1990s time period. One advanced turboprop concept originated by Hamilton Standard and NASA is known as the propfan. The concept features a highly loaded, multibladed, variable pitch propeller geared to a high pressure ratio gas turbine engine. The blades have high sweepback and advanced airfoil sections to achieve 80 percent propulsive efficiency at M = 0.80 cruise speed. Aircraft system studies have shown improvements in fuel efficiency of 15 to 20 percent for propfan advanced transport aircraft as compared to equivalent turbofan transports. Beginning with the Lockheed C-130 and Electrica turboprop aircraft, an overview of the evolution of propfan aircraft design concepts and system studies is presented. These system studies include possible civil and military transport applications and data on the performance, community and far field noise characteristics and operating costs of propfan aircraft design concepts. NASA Aircraft Energy Efficiency (ACEE) program propfan projects with industry are reviewed with respect to system studies of propfan aircraft and recommended flight development programs. Author

N86-11149# Office National d'Etudes et de Recherches Aerospatiales, Paris (France).
AERODYNAMIC METHOD USED IN FRANCE FOR ADVANCED FAST PROPELLER STUDY c07
J. M. Bousquet *In* AGARD Aerodyn. and Acoustics of Propellers Feb. 1985 15 p refs In FRENCH; ENGLISH summary Original language document previously announced in IAA as A85-15840 (For primary document see N86-11147 02-01)
Avail: NTIS HC A20/MF A01

Computational techniques and programs currently in use in the design analysis of aircraft propellers are surveyed and illustrated with diagrams and graphs of typical results. Methods examined include lifting line, incompressible lifting surface, three dimensional compressible, and three dimensional Euler; both classical and advanced propeller designs are considered. The Euler analysis of the experimental propeller HT1 being developed for ONERA is explored in detail, evaluating the effects of tip speed ratio, Mach number, number of blades, hub diameter, and a tapered diameter hub shroud. T.K.

N86-11150# Centre National de la Recherche Scientifique, Orsay (France).

DESIGN CONCEPT AND PERFORMANCE PREDICTION TECHNIQUE FOR POTENTIAL FLOWS AROUND ADVANCED PROPELLERS c07

Thoai-Sum Luu and Ranjit Collercandy *In* AGARD Aerodyn. and Acoustics of Propellers Feb. 1985 12 p refs (For primary document see N86-11147 02-01)

Avail: NTIS HC A20/MF A01

The design concept and performance prediction technique for potential flows around advanced propellers is presented. The design of propellers is based on the panel method, applied to the lifting surface theory in which the flow is supposed to be incompressible. A transonic performance prediction technique is developed where the resulting potential equation is solved by a finite difference approximate factorization method in a body fitted grid system. Both two and three dimensional results are presented. Author

N86-11151# Aircraft Research Association Ltd., Bedford (England).

A REVIEW OF ARA RESEARCH INTO PROPELLER AERODYNAMIC PREDICTION METHODS c07

A. J. Bocci and J. I. Morrison *In* AGARD Aerodyn. and Acoustics of Propellers Feb. 1985 19 p refs (For primary document see N86-11147 02-01)

Avail: NTIS HC A20/MF A01

An improved wake method involving a numerical solution to Goldstein's wake flow model was developed and the effects of removing Goldstein's limiting assumptions are illustrated. The representation of ARA-D airfoil data for use with the wake methods is considered, covering the wide range of geometry and flow conditions likely to be encountered on operating blades. The importance of finite blade effects is discussed and a tip relief correction is shown to improve predictions of experimental blade pressures and loadings. A method was developed to calculate the flow induced by a prescribed wake vortex sheet and some of the issues arising in calculating the flow development from the propeller disc downstream are illustrated. A three dimensional method involving solution of the compressible potential flow equation was developed, capable of predicting the blade flow in some detail for general multiblade configurations. Comparisons with experiment are shown for two blade cases. Author

N86-11152# Office National d'Etudes et de Recherches Aerospatiales, Paris (France).

MODERN PROPELLER PROFILES c07

A. M. Rodde, J. J. Cuny (Societe Ratier Figeac, France), and J. J. Thibert *In* AGARD Aerodyn. and Acoustics of Propellers Feb. 1985 12 p refs In FRENCH Original language document previously announced in IAA as A85-15841 (For primary document see N86-11147 02-01)

Avail: NTIS HC A20/MF A01

The design of a family of advanced profile composite aircraft propellers is presented, and the results of wind tunnel tests performed at the ONERA Modane S3 and CEATY S10 facilities are reported. The design specifications are outlined; the definition of profiles with relative thicknesses 4, 7, 12, and 20 percent is explained; and the test results are presented in graphs and diagrams. Significant performance improvements (relative to a NACA 16707 reference profile) are observed, including 43 and 8 percent better lift/drag ratios for cruising and ascent, respectively, 15 percent better Cz max, and equivalent critical Mach number at lower drag. The first planned application is to the Transall C160 two engine turboprop transport aircraft. T.K.

N86-11153# National Aerospace Lab., Amsterdam (Netherlands).

AERODYNAMICS OF WIDE-CHORD PROPELLERS IN NON-AXISYMMETRIC FLOW c07

J. B. H. M. Schulten *In* AGARD Aerodyn. and Acoustics of Propellers Feb. 1985 10 p refs (For primary document see N86-11147 02-01)

Avail: NTIS HC A20/MF A01

A lifting surface analysis is presented for propellers in nonaxisymmetric flow. In the analysis the Euler equations linearized about a uniform subsonic main flow are solved after separation of variables in cylindrical coordinates. This solution is obtained via an integral equation for the force distribution over the upper and lower surfaces of the blades which replaces the action of the propeller on the surrounding fluid. The boundary condition of vanishing normal velocity is applied at the actual blade surfaces, thus leading to a nonhelicoidal, unsteady lifting surface theory for propellers. Since the integral equation is solved most efficiently per circumferential Fourier component of the inflow distortion field, symmetric inflow is included naturally as the zeroth term of the Fourier series. General blade shapes can be handled as the blades may be swept both axially and azimuthally. There is no inherent limitation to the propeller tip Mach number. Apart from the calculation of the unsteady blade loading, expressions for the velocity and pressure fields are derived, in which the propeller slipstream appears explicitly as part of the complete velocity field in a form perfectly suited for wing interference calculations. Author

N86-11154# Cranfield Inst. of Tech., Bedford (England). Coll. of Aeronautics.

ON THE AERODYNAMICS OF INSTALLED PROPELLERS c07

Martin E. Eshelby *In* AGARD Aerodyn. and Acoustics of Propellers Feb. 1985 15 p refs (For primary document see N86-11147 02-01)

Avail: NTIS HC A20/MF A01

When the propeller is installed on the aircraft there will be mutual influence between the airframe and the propeller and its slipstream, two sources of that interference are examined. First, as the aircraft angle of attack changes with forward speed the angle of attack of the propeller also changes giving rise to forces and moments other than thrust and torque. Second, the high energy slipstream may pass over the tailplane and so affect the tail lift force, and in consequence a pitching moment due to power may be produced. These two effects are considered separately and means are suggested to estimate their magnitude and their effect on the handling qualities of the aircraft. Author

N86-11155# Deutsche Forschungs- und Versuchsanstalt fuer Luft- und Raumfahrt, Brunswick (West Germany). Inst. fuer Entwurfsaerodynamik.

A UNIFIED APPROACH FOR THE AERODYNAMICS AND ACOUSTICS OF PROPELLERS IN FORWARD MOTION c07

A. Das *In* AGARD Aerodyn. and Acoustics of Propellers Feb. 1985 28 p refs (For primary document see N86-11147 02-01)

Avail: NTIS HC A20/MF A01

The aerodynamics and the acoustics of moving bodies or surfaces follow the same basic laws of disturbance propagation and hence can be treated in a unified way. Further advancements of the propeller theories have two objectives: attaining better propulsive efficiency and producing less noise at high forward speeds. A unified aerodynamic and acoustic theory of propeller in forward motion is formulated and analyzed in detail describing the aspect of disturbance propagation from singularities in arbitrary motion, derivation of the spatial and temporal dilatations concerned with the propagation process, generalized exposition of the solution method for aerodynamics and acoustics and an extended sweep technique to determine the inducing effect of moving surfaces. In view of the flow field of a propeller being not completely irrotational the use of pressure potential proves to be more suitable in the numerical methods. The results of the analysis are illustrated by diagrams. Author

N86-11156*# National Aeronautics and Space Administration. Langley Research Center, Hampton, Va.

THEORETICAL ANALYSIS OF LINEARIZED ACOUSTICS AND AERODYNAMICS OF ADVANCED SUPERSONIC PROPELLERS c07

F. Farassat *In* AGARD Aerodyn. and Acoustics of Propellers Feb. 1985 15 p refs (For primary document see N86-11147 02-01)

Avail: NTIS HC A20/MF A01 CSCL 01A

The derivation of a formula for prediction of the noise of supersonic propellers using time domain analysis is presented. This formula is a solution of the Ffowcs Williams-Hawkings equation and does not have the Doppler singularity of some other formulations. The result presented involves some surface integrals over the blade and line integrals over the leading and trailing edges. The blade geometry, motion and surface pressure are needed for noise calculation. To obtain the blade surface pressure, the observer is moved onto the blade surface and a linear singular integral equation is derived which can be solved numerically. Two examples of acoustic calculations using a computer program are currently under development. Author

N86-11157# Lockheed-California Co., Burbank.
A GENERAL THEORY OF ARBITRARY MOTION AERODYNAMICS USING AN AEROACOUSTIC APPROACH c07
Lyle N. Long and George A. Watts *In* AGARD Aerodyn. and Acoustics of Propellers Feb. 1985 12 p refs (For primary document see N86-11147 02-01)
Avail: NTIS HC A20/MF A01

The theoretical aspects of a new unsteady aerodynamics method that uses time domain aeroacoustic integral equations is described. Recent advances in theoretical aeroacoustics permit the development of general unsteady aerodynamics methods. The effects of thickness, compressibility, and arbitrary motions may be calculated for subsonic and supersonic flows. Most linearized unsteady aerodynamics methods today are limited to zero thickness effects and sinusoidal motion. The equations presented will make it possible to develop computer codes for complex three dimensional bodies, including not only complete aircraft configurations, but rotating propellers and helicopter blades as well. Panel methods for steady aerodynamics are widely used in the aircraft industry for such configurations, the present method should permit equally general configurations to be solved in unsteady motion, using a time stepping procedure. Author

N86-11158*# National Aeronautics and Space Administration. Lewis Research Center, Cleveland, Ohio.
SUMMARY OF RECENT NASA PROPELLER RESEARCH c07
Daniel C. Mikkelson, Glenn A. Mitchell, and Lawrence J. Bober *In* AGARD Aerodyn. and Acoustics of Propellers Feb. 1985 24 p refs Previously announced as N84-32344 (For primary document see N86-11147 02-01)
Avail: NTIS HC A20/MF A01 CSCL 01A

Advanced high speed propellers offer large performance improvements for aircraft that cruise in the Mach 0.7 to 0.8 speed regime. At these speeds, studies indicate that there is a 15 to near 40 percent block fuel savings and associated operating cost benefits for advanced turboprops compared to equivalent technology turbofan powered aircraft. Recent wind tunnel results for five eight to ten blade advanced models are compared with analytical predictions. Test results show that blade sweep was important in achieving net efficiencies near 80 percent at Mach 0.8 and reducing nearfield cruise noise about 6 dB. Lifting line and lifting surface aerodynamic analysis codes are under development and some results are compared with propeller force and probe data. Also, analytical predictions are compared with some initial laser velocimeter measurements of the flow field velocities of an eight bladed 45 swept propeller. Experimental aeroelastic results indicate that cascade effects and blade sweep strongly affect propeller aeroelastic characteristics. Comparisons of propeller nearfield noise data with linear acoustic theory indicate that the theory adequately predicts nearfield noise for subsonic tip speeds, but overpredicts the noise for supersonic tip speeds. B.W.

N86-11159# Societe Nationale Industrielle Aerospatiale, Marignane (France).
DYNAMIC BEHAVIOR OF A PROPFAN c07
J. M. Besson and D. Petot (ONERA, Paris) *In* AGARD Aerodyn. and Acoustics of Propellers Feb. 1985 15 p refs In FRENCH Original language document previously announced in IAA as A85-15842 (For primary document see N86-11147 02-01)
Avail: NTIS HC A20/MF A01

The dynamic behavior of a 1 m diameter 12 blade propfan model is investigated analytically and experimentally. Both the propfan and its individual blades are analyzed using two versions of a simplified beam model and the finite element codes ASTRONEFF and SAMCEF, considering blades of Dural alloy, CFRF, and foam filled CFRP. The modeling techniques are illustrated, and results are presented in graphs and tables. The single blade findings are compared with the results of wind tunnel tests performed at the ONERA Mondane S1 facility, and the errors of the models are found to be of the order 10 percent. The ASTRONEFF procedure is shown to be best adapted to the foam filled ribbed CFRP blade to be used in the actual propfan model. Preliminary computations of the aerodynamics and static deformation of the propfan are also presented. T.K.

N86-11160# De Havilland Aircraft Co. of Canada Ltd., Downsview (Ontario).
PERFORMANCE EVALUATION OF FULL SCALE PROPELLERS BY WIND TUNNEL TEST c07
D. J. Barber *In* AGARD Aerodyn. and Acoustics of Propellers Feb. 1985 12 p refs (For primary document see N86-11147 02-01)
Avail: NTIS HC A20/MF A01

A large propeller test facility was developed for the nine meter wind tunnel. The facility is described along with the propeller test rig features and associated drive system. Propeller performance measurement philosophy, test procedures and calibrations are discussed. In cooperation with Dowty Rotol Ltd. and Hartzell Inc., two currently available propeller designs were tested. The two 8.5 foot diameter propeller suitable for a DHC Twin Otter size of aircraft provided an evaluation of alternative airfoil applications: the ARA-D series and NACA 16 series. Results have demonstrated propeller efficiencies close to manufacturers estimates for clean well finished blades. Forward and reverse thrust testing results are discussed with respect to aircraft application. Prediction methods tend to over estimate efficiencies due to hardware features encompassing blade finish, blade root/spinner juncture, spinner openings, erosion protection and deicer equipment. Typical results illustrating the influence on propeller performance of such features is given. Author

N86-11161# Institut de Mecanique des Fluides de Marseille (France).
STUDY OF THE 3D WAKE OF AN AERIAL PROPELLER [ETUDE DU SILLAGE 3D D'UNE HELICE AERIENNE] c07
D. Favier and C. Maresca *In* AGARD Aerodyn. and Acoustics of Propellers Feb. 1985 22 p refs In FRENCH (For primary document see N86-11147 02-01)
Avail: NTIS HC A20/MF A01

An analysis of the near and far wake of a four blade aerial propeller, operated under various working parameters and following various adjustments, was carried out with hot wire anemometry. Empirical laws were synthesized which provide the axial translation velocity of the tip vortices, the rate of wake radial contraction, in such a way that the stability limit of the vortex system is established as a function of azimuth rotation and as an extended range of the working parameters active in the range from null to maximum thrust. For a given functional regime, the determination of the three dimensional induced velocity field is effective in different sections downstream of the wake and conducted in a detailed characterization of the geometry and associated vortex intensity, in the azimuth function and the axial distance to the downstream of the plane of rotation. E.A.K.

N86-11162# Dornier-Werke G.m.b.H., Friedrichshafen (West Germany).
INVESTIGATIONS OF MODERN GENERAL AVIATION PROPELLERS c07
H. Zimmer, R. Hoffmann (Hoffmann-Propellers, Rosenheim, West Germany), and K. H. Horstmann (DFVLR, Brunswick) *In* AGARD Aerodyn. and Acoustics of Propellers Feb. 1985 14 p refs (For primary document see N86-11147 02-01)
Avail: NTIS HC A20/MF A01

After a period of stagnation in the years following WW2 an accelerated movement towards propeller propulsion has taken place in recent years. Because of its inherent propulsive advantages the propeller propulsion has a considerable development potential. Initial analyses of the state of the art of propeller technology in the General Aviation field by means of flight and wind tunnel tests as well as by aerodynamic and acoustic calculations have shown possibilities for improvement, mainly in the lower and medium speed range. Improved propellers were designed and analyzed theoretically and experimentally. Newly designed super-critical airfoils with high lift to drag ratios at high lift were used. To find the optimum blade shapes associated with minimum supervelocities, also several tip shapes were analyzed. After wind tunnel tests the best of the propeller designs was selected for full scale flight test. A set of experimental propellers for the Do 228 Experimental aircraft was developed, constructed and tested. Improvements were achieved in the whole flight regime. The experience of this propeller development program was used to design a high performance high speed General Aviation propeller for M = 0.6 flight. Author

N86-11163# Dowty Rotol Ltd., Gloucester (England).
AERODYNAMIC AND STRUCTURAL ASPECTS OF PROPELLER AND DRIVE FOR A 1/5 SCALE WIND TUNNEL PROGRAMME c07
R. M. Bass, B. Munniksma (National Aerospace Lab., Amsterdam), and J. vanHengst (Royal Netherlands Aircraft Factories Fokker, Schiphol-Oost) *In* AGARD Aerodyn. and Acoustics of Propellers Feb. 1985 18 p refs (For primary document see N86-11147 02-01)
Avail: NTIS HC A20/MF A01

The paper describes the development of a model propeller and its calibration in association with an axisymmetric nacelle in the National Aerospace Laboratory low speed tunnel in Amsterdam before testing on a complete 1/5 scale model of the Fokker in the DNW (German-Dutch wind tunnel). The calibration so obtained, allowed the required operating propeller conditions to be set up on the complete F50 model. The influence of Reynolds number on correction for scale effects, between experimental model results and full scale prediction. A previously unsuspected and unavoidable vibration originating in the reduction gear train of the drive unit gave rise to high propeller blade stresses, ultimately leading to a blade failure. In order to continue running with minimum delay, new propeller blades with high internal damping were manufactured from composite materials, and the program was successfully concluded. Author

N86-11164# De Havilland Aircraft Co. of Canada Ltd., Downsview (Ontario).
SOME CONSIDERATIONS IN PROPELLER AND AIRFRAME INTEGRATION c07
B. Eggleston *In* AGARD Aerodyn. and Acoustics of Propellers Feb. 1985 11 p refs (For primary document see N86-11147 02-01)
Avail: NTIS HC A20/MF A01

The paper review elected items of R and D limited in support of propeller driven transport aircraft. The topics include the design of new propeller airfoils, two dimensional tests of selected airfoils, and estimates are presented of the resulting benefits in propeller performance. The application of numerical optimization to the aerodynamic design of propeller is also reviewed. Some results from wind tunnel tests of airframe/propeller installations are presented showing the benefits of alternative nacelle shape and the merits of high versus low wing locations on a transport aircraft. Author

N86-11165# Avions Marcel Dassault, Saint-Cloud (France). Div. des Etudes Avancees.
PROBLEMS OF THE INTEGRATION OF PROPELLERS IN AIRFRAMES, ESPECIALLY FOR HIGH PERFORMANCE TWIN-ENGINE AIRCRAFT [LES PROBLEMES D'INTEGRATION DE HELICES A LA CELLULE D'UN AVION ET, PLUS PARTICULIEREMENT, D'UN BIMOTEUR DE FORTE PUISSANCE] c07
Rene Taisserie *In* AGARD Aerodyn. and Acoustics of Propellers Feb. 1985 10 p In FRENCH (For primary document see N86-11147 02-01)
Avail: NTIS HC A20/MF A01

This report presents studies conducted on the integration of aircraft propellers with the airframe for general aircraft, as well as for high performance twin engine propeller aircraft. The effect of engine dimensions on the aerodynamic characteristics of the aircraft in all flight situations, including low speed flight, is presented. It is shown that detailed model tests will have to be conducted before accurate results can be obtained. The objective of these studies is to examine possible configurations for future maritime reconnaissance twin engine propeller aircraft. T.M.

N86-11166# Lockheed-Georgia Co., Marietta.
WIND TUNNEL INVESTIGATION OF THE INTERACTION OF PROPELLER SLIPSTREAM WITH NACELLE/WING/FLAP COMBINATIONS c07
A. S. Aljabri and A. C. Hughes *In* AGARD Aerodyn. and Acoustics of Propellers Feb. 1985 10 p refs (For primary document see N86-11147 02-01)
Avail: NTIS HC A20/MF A01

Until recently it was sufficient to define the propeller slipstream by the average velocity induced across the propeller disk. With the advent of the highly loaded program and the accompanying concern for the effect of the slipstream and its interaction with aircraft components be known. This paper describes a series of wind tunnel tests performed to improve the understanding of this complex aerodynamic interaction. The tests were conducted using a conventional propeller operating at low subsonic speeds. Complementary theoretical and experimental studies were used to investigate the interaction effects. Results from wind tunnel tests on propeller/nacelle/wing, and propeller/nacelle/wing/flap combinations are presented here. Force, pressure, and wake survey data from the test allow the slipstream characteristics, including its distortion by the wing and flap, to be obtained. The important parameters which govern the slipstream shape and induced velocities are identified and techniques are developed for estimating slipstream drag and the torque absorbed by a wing immersed in the slipstream. An improved understanding of the effects of wind tunnel walls on propeller powered testing is also presented. Author

N86-11167*# National Aeronautics and Space Administration. Langley Research Center, Hampton, Va.
AN ASYMPTOTIC THEORY FOR THE INTERFERENCE OF LARGE ASPECT RATIO SWEPT WINGS AND MULTIPLE PROPELLER SLIPSTREAMS c07
R. K. Prabhu (Old Dominion Univ.), C. H. Liu, and S. N. Tiwari (Old Dominion Univ.) *In* AGARD Aerodyn. and Acoustics of Propellers Feb. 1985 17 p refs (For primary document see N86-11147 02-01)
Avail: NTIS HC A20/MF A01 CSCL 01A

This paper presents an asymptotic method for the analysis of the interference of multiple tractor propeller slipstream with large aspect ratio swept wings. It is assumed that the height of the slipstream is of the order of the wing chord and its spanwise extent is of the order of the wing span. Three different flow regions are identified by employing different stretching transformations. Asymptotic expansions are made in each of the three regions, using the chord to span ratio as the small expansion parameter. The details of the nonuniform flow in the slipstream enter into the wing sectional analysis. In the outer limit, the wing shrinks to a swept lifting line, and the slipstream reduces to a thin sheet of jet carrying the momentum gain from the propeller. The curvature of this jet sheet results in a pressure difference which is represented by a vortex sheet. The governing equations are solved by discretization. Several examples are considered for which experimental data are available. Comparison of the present results with the experimental data as well as other numerical solutions showed generally good agreement. Author

N86-11168# Carleton Univ., Ottawa (Ontario). Dept. of Mechanical and Aeronautical Engineering.

DEVELOPMENT OF MODERN TURBOPROP ENGINES c07
H. I. H. Saravanamuttoo *In* AGARD Aerodyn. and Acoustics of Propellers Feb. 1985 9 p refs (For primary document see N86-11147 02-01)
Avail: NTIS HC A20/MF A01

Proposals for propfan commercial aircraft operating at high cruise speeds pose requirements for advanced turboprops of high power. The history of turboprops for long range operation is briefly reviewed and the requirements for future engines are discussed. Considerable gains in the thermodynamic cycle can be realized, and the development of high performance gas generators should be a straightforward process. Transmission designs for high power engines may be extremely difficult and may result in novel engine configurations. It appears likely that a more modest goal of M = 0.7 cruise for shorter haul aircraft could be attained with much less risk while still achieving major gains. Author

N86-11169# Deutsche Forschungs- und Versuchsanstalt fuer Luft- und Raumfahrt, Goettingen (West Germany). Inst. for Experimental Fluid Mechanics.
AEROACOUSTIC WIND TUNNEL MEASUREMENTS ON PROPELLER NOISE c71
F.-R. Grosche and H. Stiewitt *In* AGARD Aerodyn. and Acoustics of Propellers Feb. 1985 9 p refs (For primary document see N86-11147 02-01)
Avail: NTIS HC A20/MF A01

Model tests were conducted in a low speed wind tunnel to determine the sound radiation of 5 propellers with different blade designs including variations of thickness ratios, blade profiles, blade planforms and blade tip configurations. The diameter of the propellers was 0.9 m, the propeller speed was kept constant. The tip Mach number was M sub I = 0.66 and the helical tip Mach number varied between 0.66 and 0.69. The main objectives were to investigate the effects of blade geometry on near field and far field noise and to locate the dominant sound sources in the propeller plane, radiating to the observer, by means of a highly directional microphone system. The results include: (1) comparisons of noise spectra of different propeller configurations; (2) near field sound pressures as function of axial distance from the propeller plane; and (3) directivity of sound radiation from the moving blades. Author

N86-11170# Royal Aircraft Establishment, Farnborough (England). Aerodynamics Dept.
SOME AEROACOUSTIC WIND TUNNEL MEASUREMENTS, THEORETICAL PREDICTIONS, AND FLIGHT-TEST CORRELATIONS ON SUBSONIC AIRCRAFT PROPELLERS c07
W. J. G. Trebble, J. Williams (Southampton Univ., England), and R. P. Donnelly (Dowty Rotol Ltd, Gloucester, England) *In* AGARD Aerodyn. and Acoustics of Propellers Feb. 1985 21 p refs (For primary document see N86-11147 02-01)
Avail: NTIS HC A20/MF A01

Aeroacoustic experiments using the full scale propeller nacelle rig in the 24 ft anechoic tunnel were first made in 1979/80 on three alternative propellers also tested in flight on the Short's 330 aircraft. The Hartzell five bladed propeller of the production aircraft has conventional NACA 64 series sections and standard tips, the Hartzell Q-tip version of this has its tips bent as lower surface end plates in the direction of rotation, and the Dowty four bladed propeller has modern ARA-D sections and standard tips (D sub p = 2.8 m). Later complementary tunnel/flight experiments also included the Dowty four bladed R.212 propeller with classical NACA 16 series sections as fitted to the B.Ae. HS 748 aircraft (D sub p = 3.7 m). Author

N86-11171# Pratt and Whitney Aircraft of Canada Ltd., Longueuil (Quebec).
AN INVESTIGATION OF IN-FLIGHT NEAR-FIELD PROPELLER NOISE GENERATION AND TRANSMISSION c71
H. Bonneau, D. F. Wilford, and L. K. Wood *In* AGARD Aerodyn. and Acoustics of Propellers Feb. 1985 12 p refs (For primary document see N86-11147 02-01)
Avail: NTIS HC A20/MF A01

In flight near field propeller noise measurements, made on a General Aviation turboprop aircraft, are reported for a range of propeller operating conditions, and are shown to be well defined and reproducible. Measurements have been made at 8 exterior microphones, 2 located on a wing mounted boom, and 6 embedded in, and flush with the aircraft fuselage. Interior noise levels are also presented. Measured propeller harmonic levels are compared to first principle calculations of near field noise, using a modified version of the Farassat computer program, in which the blade surface pressure is described using the known aerodynamic properties of the blade (NACA 16) airfoil sections. The first few; i.e., the dominant harmonic levels of propeller noise are shown to be well predicted, while higher harmonic levels are underpredicted. The transmission loss between exterior and interior noise levels is shown to be relatively constant for varying propeller operating conditions and at two different locations along the length of the fuselage. Interior noise levels are also shown for the aircraft in gliding flight at various forward velocities, with both engines at idle and propellers feathered. A method of interpolating these measurements is discussed, which allows the interior noise due only to the forward velocity of the aircraft, to be determined. The transmission loss for this component is also discussed. Finally, interior noise levels are presented for a series of ground static tests with engine mounts of various different stiffnessses. B.W.

N86-11172# Deutsche Forschungs- und Versuchsanstalt fuer Luft- und Raumfahrt, Brunswick (West Germany). Inst. fuer Entwurfsaerodynamik.
FULL-SCALE FLIGHT AND MODEL-SCALE WIND TUNNEL TESTS ON THE NEARFIELD NOISE CHARACTERISTICS OF AIRCRAFT PROPELLERS c71
H. Heller, M. Kallergis, and B. Gehlhar *In* AGARD Aerodyn. and Acoustics of Propellers Feb. 1985 17 p refs (For primary document see N86-11147 02-01)
Avail: NTIS HC A20/MF A01

Flight noise tests employing a single engine Cessna T 207 aircraft with an array of wing mounted microphones were conducted to investigate nearfield acoustic characteristics of a 3 blade variable pitch propeller under different operational conditions, varying helical blade tip Mach number, propeller advance ratio, and blade loading. A special technique to minimize the engine exhaust influence on the propeller signature had been developed for this purpose. Supplementary, yet much more extensive tenth scale tests were performed in the DFVLR One Meter Acoustic Tunnel again in the acoustic nearfield of propellers with 2 to 6 blades over a substantial range or operational, partially interdependent, parameters, such as helical blade tip Mach number, blade pitch angle setting, blade incidence angle, rotational plane attitude, and ambient temperature. These data could also be compared to some third scale results for geometrically identical propellers. Especially the model tests allowed an exact quantification of the effect of the various parameters on the ensuing harmonic and subharmonic propeller noise spectra. Author

N86-11173# Aeritalia S.p.A., Pomigliano D'Arco (Italy).
CABIN NOISE REDUCTION FOR A NEW DEVELOPMENT TURBOPROP COMMUTER AIRCRAFT c71
A. Carbone, A. Paonessa, L. Lecce (Ist. Progetto Velivoli, Naples), and F. Marulo (Ist. Progetto Velivoli, Naples) *In* AGARD Aerodyn. and Acoustics of Propellers Feb. 1985 14 p refs (For primary document see N86-11147 02-01)
Avail: NTIS HC A20/MF A01

The program followed to attain an interior noise level similar to turbofan aircraft in a new design turboprop commuter is described. The need for an early consideration, in the definition phase of the aircraft, of the acoustic requirement for configuration development is stressed, along with some peculiar characteristics of this program. After a brief presentation of features of the aircraft related to interior noise control, the analytical and experimental models developed in the course of program are discussed. Some of the results of the studies are presented, clarifying the impact that they have had on the configuration of the aircraft. The output of three structural analysis theoretical procedures is compared to experiments. Two of these procedures, the panel stringer periodic model, and a simplified FEM analysis, are found adequate to represent experimental findings. The cylindrical shell - frame model is found not representative of test results. Sidewall treatment performance is discussed, with reference to theoretical and experimental results. The noise reductions measured in a furnished fuselage are compared to data obtained without interior treatment. Future developments and recommendations for additional work are discussed. Author

N86-11174# Lockheed-California Co., Burbank.
PROPELLER AIRCRAFT CABIN VIBRATION AND NOISE-EXCITATION, SOURCES, AND PATHS c71
R. E. Donham, F. J. Balena, E. Z. Bochary, and O. K. Liehr *In* AGARD Aerodyn. and Acoustics of Propellers Feb. 1985 14 p refs (For primary document see N86-11147 02-01)
Avail: NTIS HC A20/MF A01

The potential sources and paths by which the propeller produces structural responses resulting in vibration and noise in the cabin of a transport aircraft are discussed. New low cost, convenient experimental and analytical techniques are described for evaluating the excitations; propeller airborne pressures on the fuselage shells, slip stream induced forces on the wing and tail, and oscillatory forces on the propeller. The techniques described make use of ground determined structural signatures to relate forces with vibrations or noise, and of propeller signatures from flight which define the vibroacoustic contributions of individual propellers. Author

N86-11175# Hamilton Standard, Windsor Locks, Conn.
THE STATE OF THE ART IN PROPFAN TURBOPROP NOISE c71
Frederick B. Metzger *In* AGARD Aerodyn. and Acoustics of Propellers Feb. 1985 20 p refs (For primary document see N86-11147 02-01)
Avail: NTIS HC A20/MF A01

The evolution of propeller noise research is summarized from 1919 to the present. The early experimental and analytical work to understand and predict propeller noise is discussed. Emphasis is placed on understanding source noise. However, the major advances in cabin comfort assessment and design of airplane fuselage and cabin trim to improve passenger comfort are briefly described. Emphasis is on the recent noise research work on the propfan, a many bladed relatively small diameter unshrouded motor with swept blades that will allow future transports to cruise efficiently at speeds equal to modern turbofan transports. The most recent propfan concept, a counter rotation version with even greater efficiency potential than the propfan with a single blade row is also discussed. Author

N86-11176# Lockheed-Georgia Co., Marietta.
APPLICATION OF ACTIVE NOISE CONTROL TO MODEL PROPELLER NOISE c71
M. Salikuddin, H. K. Tanna, R. H. Burrin, and W. E. Carter *In* AGARD Aerodyn. and Acoustics of Propellers Feb. 1985 15 p refs (For primary document see N86-11147 02-01)
Avail: NTIS HC A20/MF A01

The applicability of active noise control to reduce cabin noise of turboprop aircraft is demonstrated by conducting several laboratory experiments. The principle of active noise control is to reduce the noise radiated from a primary source by superimposing a signal from a secondary source, which is made identical in amplitude but opposite in phase to the primary sound signal. A computer controlled algorithm was developed to implement this concept in a free field environment, in which, the noise from the primary source (eventually the propeller) and the noise measured at several locations on a representative surface (eventually the fuselage) were used to create the input for the secondary source. Experiments using a number of sinusoidal signals were conducted. An average noise reduction of 8 to 14 dB was achieved on the surface in the frequency range of 200 to 1000 Hz. Next the concept was applied to the propeller problem where the sound signal contains many discrete tones at harmonics of the blade passage frequency. For this purpose, a prerecorded time history of a 1/10th scale model propeller was used to drive the primary source. An average noise reduction of about 15 dB was observed at the first two blade passage frequencies, and 12 dB and 5 dB reductions were observed at the 3rd and 4th blade passage frequencies, respectively. Finally, the active noise control concept was applied to a 1/10th scale propeller, installed in an anechoic chamber with flight simulation facility. A substantial amount of noise reduction was achieved on the model fuselage surface. Author

N86-11177# Joint Publications Research Service, Arlington, Va.
USSR REPORT: TRANSPORTATION
7 Oct. 1985 106 p Transl. into ENGLISH from various Russian articles
(JPRS-UTR-85-011) Avail: NTIS HC A06

Progress in U.S.S.R. transportation is reported. Topics discussed include: civil aviation; motor vehicles and highways; rail systems; maritime and river fleets; and ports and transshipment centers. For individual titles, see N86-11178 through N86-11181.

N86-11178# Joint Publications Research Service, Arlington, Va.
DEPUTY MINISTER ON SECTOR'S TECHNICAL PROGRESS
I. Ye. Mashkivskiy *In its* USSR Rept.: Transportation (JPRS-UTR-85-011) 7 Oct. 1985 p 1-6 Transl. into ENGLISH from Grazhdanskaya Aviats. (Moscow), no. 4, Apr. 1985 p 2-3 (For primary document see N86-11177 02-01)
Avail: NTIS HC A06

Measures to accelerate the U.S.S.R.'s scientific and technical progress in the area of civil aviation are discussed. The development of more economical and efficient modifications of airplanes, helicopters, and engines to replace outdated models is described. The increased use of automated diagnostic equipment for aircraft maintenace is highlighted. B.W.

N86-11179# Joint Publications Research Service, Arlington, Va.
CHIEF OF AEROFLOT'S INTERNATIONAL ACTIVITIES c03
V. Samorukov *In its* USSR Rept.: Transportation (JPRS-UTR-85-011) 7 Oct. 1985 p 7-11 Transl. into ENGLISH from Grazhdanskaya Aviats. (Moscow), no. 6, Jun. 1985 p 6-7 (For primary document see N86-11177 02-01)
Avail: NTIS HC A06

Aeroflot's role in expanding the U.S.S.R.'s international civil aviation service in socialist countries is summarized. Intergovernmental agreements concerning new aviation routes and joint operation of individual international airroutes are discussed. B.W.

N86-11180# Joint Publications Research Service, Arlington, Va.
RECENT ACHIEVEMENTS, PROBLEMS IN CROPDUSTING WORK c05
A. Savchenko *In its* USSR Rept.: Transportation (JPRS-UTR-85-011) 7 Oct. 1985 p 12-16 Transl. into ENGLISH from Grazhdanskaya Aviats. (Moscow), no. 4, Apr. 85 p 26-27 (For primary document see N86-11177 02-01)
Avail: NTIS HC A06

The long-term program for land reclamation that was discussed and approved at the October (1984) Plenum of the CPSU Central Committee represents a major new stage in the campaign for further increases in the fertility of crop lands and for fulfillment of the food program. Many sectors of the national economy, including civil aviation, are directly involved in the realization of these goals. With the aim of carrying out the decisions of the Central Committee Plenum, measures have been worked out to expand Aeroflot's contribution to increasing the efficiency of improved lands in order to bring about a steady rise in the U.S.S.R's food stores. Aviation science is supposed to play an important role in this important statewide task. Increasing the efficiency and improving the quality of the use of aviation in agriculture are tasks that are being resolved through the creation and improvement of aircraft and agricultural equipment, the introduction of progressive methods, and efficient utilization of aircraft. An overview is presented of survey techniques used in cropdusting. B.W.

N86-11181# Joint Publications Research Service, Arlington, Va.
WORLD'S LARGEST AIRPLANE NOW BEING TESTED c05
N. Dombkovskiy *In its* USSR Rept.: Transportation (JPRS-UTR-85-011) 7 Oct. 1985 p 17-20 Transl. into ENGLISH from TRUD (Moscow), 23 May 1985 p 3 (For primary document see N86-11177 02-01)
Avail: NTIS HC A06

Unique design features of the newly developed AN-124 aircraft are described. Factors such as weight, cargo capacity, and wing configuration are discussed. Problems encountered in the construction of the AN-124 are also discussed. B.W.

02 AERODYNAMICS

Includes aerodynamics of bodies, combinations, wings, rotors, and control surfaces; and internal flow in ducts and turbomachinery.

For related information see also *34 Fluid Mechanics and Heat Transfer.*

N86-11182 Maryland Univ., College Park.
A PARAMETRIC ANALYSIS OF FLOW STRUCTURE AND PERFORMANCE IN A VORTEX CONTROLLED RADIAL DIFFUSER Ph.D. Thesis
John E. Allen 1984 155 p
Avail: Univ. Microfilms Order No. DA8512169

The air flow characteristics in a vortex controlled radial diffuser have been investigated using non-orthogonal, two-component LDV measurements in the entrance region of the diffuser. The velocity components and turbulence parameters in a plane of the axisymmetric flow field were mapped for four geometric configurations, with and without suction. These detailed measurements, supported by overall performance parameters, yielded considerable insight into the interaction between the forced recirculation region and the core flow. Particularly emphasized were the influence of suction, vortex corner size and vortex corner configuration on the diffuser geometries analyzed. The non-intrusive technique employed permitted measurements to be obtained in a particularly difficult environment requiring a series of tradeoffs to maintain a flowfield which was representative of that encountered in the practical application of such a device. Dissert. Abstr.

N86-11183 Kansas Univ., Lawrence.
INLET FLOW DYNAMIC DISTORTION PREDICTION WITHOUT rms MEASUREMENTS Ph.D. Thesis
Yen-Sen Chen 1984 118 p
Avail: Univ. Microfilms Order No. DA8513816

A two-equation turbulence model, k-epsilon model, is used in the prediction of inlet flow dynamic distortion of jet aircraft based on steady state total pressure measurements only. This Turbulence model is solved at the compressor face station by using a finite difference scheme. Total pressure rms level of the inlet flow is predicted by the turbulence model. The Melick statistical method is then employed to estimate the peak dynamic distortion based on the analytically predicted total pressure rms level. A statistical method is developed for the estimation of boundary conditions for the turbulent equations. In order to solve the set of nonlinear, coupled turbulent equations, an implicit formulation is utilized such that a set of discretized finite difference equations can be arranged into tridiagonal matrix equations for efficient numerical iterations. Results of the prediction compare well with experimental measurements of subsonic, transonic and supersonic inlets under various flight conditions. The present method can be used in the preliminary inlet design phases to reduce the design costs. Dissert. Abstr.

N86-11184 Arizona Univ., Tucson.
REFINED NUMERICAL SOLUTIONS OF THE TRANSONIC FLOW PAST A WEDGE Ph.D. Thesis
Shen-Min Liang 1985 76 p
Avail: Univ. Microfilms Order No. DA8511705

An adaptive refinement procedure combining the ideas of solving a modified difference equation and of adaptive mesh refinement is introduced. The numerical solution on a fixed grid is improved by inclusion of approximated truncation error computed from local subgrid refinement. Following this procedure, a reliable scheme has been developed for refined computations of the flow past a wedge at transonic speeds. Effects of the truncation error on the pressure, wave drag, sonic line, and shock position are investigated. By comparing the pressure drag on the wedge and the wave drag due to the shocks, the existence of a supersonic-to-supersonic shock originating from the wedge shoulder is confirmed. Dissert. Abstr.

N86-11185 Maryland Univ., College Park.
STABILITY AND INTERACTION OF COHERENT STRUCTURE IN SUPERSONIC REACTIVE WAKES Ph.D. Thesis
Suresh Menon 1984 185 p
Avail: Univ. Microfilms Order No. DA8508501

A theoretical formulation and analysis is presented for a study of the stability and interaction of coherent structure in reacting free shear layer. The physical problem under investigation is a premixed hydrogen-oxygen reacting shear layer in the wake of a thin flat plate. The coherent structure is modeled as a periodic disturbance and its stability is determined by the application of linearized hydrodynamic stability theory which results in a generalized eigenvalue problem for reactive flows. Detailed stability analysis of the reactive wake for neutral, symmetrical and antisymmetrical disturbance is presented. Reactive stability criteria is shown to be quite different from classical non-reactive stability. The interaction between the mean flow, coherent structure and fine-scale turbulence is theoretically formulated using von Karman integral technique. Both time-averaging and conditional phase averaging are necessary to separate the three types of motion. The resulting integro-differential equation can then be solved subject to initial conditions with appropriate shape functions. Dissert. Abstr.

N86-11186*# National Aeronautics and Space Administration. Langley Research Center, Hampton, Va.
EFFECT OF AILERON DEFLECTIONS ON THE AERODYNAMIC CHARACTERISTICS OF A SEMISPAN MODEL OF A SUBSONIC ENERGY-EFFICIENT TRANSPORT
Peter F. Jacobs Oct. 1985 344 p refs
(NASA-TP-2478; L-15934; NAS 1.60:2478) Avail: NTIS HC A15/MF A01 CSCL 01A

An investigation was conducted in the Langley 8 Foot Transonic Pressure Tunnel to determine the effect of aileron deflections on the aerodynamic characteristics of a subsonic energy efficient transport (EET) model. The semispan model had an aspect ratio 10 supercritical wing and was configured with a conventionally located set of ailerons (i.e., a high speed aileron located inboard and a low speed aileron located outboard). Data for the model were taken over a Mach number range from 0.30 to 0.90 and an angle of attack range from approximately -2 deg to 10 deg. The Reynolds number was 2.5 million per foot for Mach number = 0.30 and 4 million per foot for the other Mach numbers. Model force and moment data, aileron effectiveness parameters, aileron hinge moment data, otherwise pressure distributions, and spanwise load data are presented. Author

N86-11187# Cranfield Inst. of Tech., Bedford (England). Coll. of Aeronautics.
GROUND EFFECT ON A ROTOR WAKE Ph.D. Thesis - March 1985
I. Kusmarwanto Jun. 1985 116 p refs
(Coll-Aeronautics-8510) Avail: NTIS HC A06/MF A01

The effect of the ground on a rotor wake in forward flight was investigated experimentally in the working section of an 8 ft x 4 ft straight through wind tunnel. A three bladed fully articulated rotor with a solidity ratio of 0.07 and diameter of 1.06 m, powered by a hydraulic motor, was tested at a height of 0.47 rotor diameter above a solid ground board which has a elliptical leading edge. Tests were run at various low advance ratios (less than 0.1) with two collective pitch settings. A hot wire anemometer probe was used to measure the average value of the three components of velocity. The rotor wake and the ground vortices were visualized by smoke. Both experimental results and theoretical estimates show that the ground induced interference is an upwash and a decrease in forward velocity. Author

N86-11188*# National Aeronautics and Space Administration. Ames Research Center, Moffett Field, Calif.
SHOCK FITTING APPLIED TO THE PREDICTION OF HIGH-SPEED ROTOR NOISE
John W. Rutherford Oct. 1985 19 p refs
(NASA-TM-86781; Rept-85384; NAS 1.15:86781; USAAVSCOM-TR-85-A-8) Avail: NTIS HC A02/MF A01 CSCL 01A

A shock fitting method applied to the transonic small disturbance (TSD) potential equation is described. This method is then applied to a simple, two dimensional (2-D) rotating disturbance which is analogous to a shock radiating from the tip of a rotor blade in high speed hover. A comparison is made between the results of this method and the more standard shock capturing method. This comparison makes it clear that the effect of the results on the acoustic signature of the 2-D model is significant, and similar results can be expected when the method is extended to the three dimensional (3-D) case. Author

N86-11189*# National Aeronautics and Space Administration. Langley Research Center, Hampton, Va.
USER'S MANUAL FOR A 0.3-m TCT WALL INTERFERENCE ASSESSMENT/CORRECTION PROCEDURE: 8- BY 24-INCH AIRFOIL TEST SECTION
Clyde R. Gumbert Sep. 1985 49 p refs
(NASA-TM-87582; NAS 1.15:87582) Avail: NTIS HC A03/MF A01 CSCL 01A

A transonic Wall-Interference Assessment/Correction (WIAC) procedure has been developed and verified for the 8- by 24-inch airfoil test section of the Langley 0.3-m Transonic Cryogenic Tunnel. This report is a user's manual for the correction procedure. It includes a listing of the computer procedure file as well as input for and results from a step-by-step sample case. Author

N86-11926# Joint Publications Research Service, Arlington, Va.
TRANSITION EFFECTS OF BOUNDARY LAYER ON STATIC AND DYNAMIC STABILITY OF SLENDER CONE Abstract Only
Hongtian Lou *In its* China Rept.: Sci. and Technol. (JPRS-CST-85-014 2 May 1985 p 78 Transl. into ENGLISH from Yuhang Xuebao (Beijing), no. 1, 31 Jan. 1985 p 88-98 Original language document announced in IAA as A85-42783 (For primary document see N86-11918 02-70)
Avail: NTIS HC A06/MF A01

03 AIR TRANSPORTATION AND SAFETY

Includes passenger and cargo air transport operations; and aircraft accidents.

For related information see also *16 Space Transportation* and *85 Urban Technology and Transportation.*

N86-11190# Air Command and Staff Coll., Maxwell AFB, Ala.
COMING SOON TO A THEATER NEAR YOU: THE MICROWAVE LANDING SYSTEM
K. S. C. Hamilton Apr. 1985 23 p
(AD-A156468; ACSC-85-1025) Avail: NTIS HC A02/MF A01 CSCL 01/2

This informational handbook has been prepared in response to a requirement levied by the SAC Instrument Flight Course (SIFC), Castle AFB, California. The Microwave Landing System (MLS) is projected for worldwide installation and use by both civilian and military facilities. This handbook has been developed for use in conjunction with an individualized lesson plan, prepared by the SIFC faculty. The history, development, advantages, and future projections for this excellent system are explained. The handbook is not a text for engineers, but for the pilot who is interested in safety of flight, noise abatement, and increased system confidence. The author's intent in authoring this project was to provide a brief introduction to the reasons behind the transition from Instrument Landing System (ILS) to the Microwave Landing System (MLS), and the international scope of this endeavor. Through the comparison of the operational and maintenance advantages of these two systems the author hopes to capture the interest of pilots by making them aware of the tremendous technological gains embodied in the Microwave Landing System. GRA

N86-11191# Federal Aviation Administration, Atlantic City, N.J. Technical Center.
USER'S MANUAL FOR AC-20-53A PROTECTION OF AIRPLANE FUEL SYSTEMS AGAINST FUEL VAPOR IGNITION DUE TO LIGHTNING
N. Rasch Oct. 1984 72 p
(AD-A157619; DOT/FAA/CT-83/3) Avail: NTIS HC A04/MF A01 CSCL 01/2

This manual provides users of AC 20-53A, protection of aircraft fuel systems against fuel vapor ignition due to lightning, with information on the subject of fuel system lightning protection and methods of compliance of aircraft design with the Federal Aviation Regulations 23.954 and 25.954. The manual is the result of a 3-year effort requested by the FAA Technical Center of the SAE-AE4L committee which is comprised of experts in the field of lightning research and protection of aircraft and systems from the adverse effects associated with atmospheric electricity. GRA

N86-11179# Joint Publications Research Service, Arlington, Va.
CHIEF OF AEROFLOT'S INTERNATIONAL ACTIVITIES
V. Samorukov *In its* USSR Rept.: Transportation (JPRS-UTR-85-011) 7 Oct. 1985 p 7-11 Transl. into ENGLISH from Grazhdanskaya Aviats. (Moscow), no. 6, Jun. 1985 p 6-7 (For primary document see N86-11177 02-01)
Avail: NTIS HC A06

04 AIRCRAFT COMMUNICATIONS AND NAVIGATION

Includes digital and voice communication with aircraft; air navigation systems (satellite and ground based); and air traffic control.

For related information see also *17 Spacecraft Communications, Command, and Tracking* and *32 Communications.*

N86-11192# IIT Research Inst., Annapolis, Md.
TRAFFIC ALERT AND COLLISION AVOIDANCE SYSTEM SIGNAL ENVIRONMENT MODEL (TCAS SEM) PROGRAMMER'S REFERENCE MANUAL Final Report, Aug. 1984 - Feb. 1985
C. Gilchrist, E. Woods, and T. Keech Jul. 1985 169 p refs
Prepared for Dept. of Defense, Annapolis
(Contract F19628-80-C-0042)
(FAA-PM-85-22; ECAC-CR-85-031) Avail: NTIS HC A08/MF A01

A traffic alert and collision avoidance system signal environment model (TCAS SEM) was developed to predict the time-average TCAS I and minimum TCAS II signal rates in a user-selected air traffic deployment. The TCAS SEM is described which includes: the modeled systems, the data-storage and retrieval subsystems for engineering data, and the software structures of all component subsystems. E.A.K.

05 AIRCRAFT DESIGN, TESTING AND PERFORMANCE

Includes aircraft simulation technology.

For related information see also *18 Spacecraft Design, Testing and Performance* and *39 Structural Mechanics.*

N86-11193*# National Aeronautics and Space Administration. Langley Research Center, Hampton, Va.

A PERSPECTIVE ON THE STATUS OF MEASUREMENT OF ATMOSPHERIC TURBULENCE IN THE US

H. N. Murrow Sep. 1985 38 p refs Presented at the Subcomm. Meeting of 61st AGARD Struct. and Mater. Panel Meeting, Oberammergau, West Germany, 10-13 Sep. 1985
(NASA-TM-87610; NAS 1.15:87610) Avail: NTIS HC A03/MF A01 CSCL 04B

A perspective on status of measurement of atmospheric turbulence is presented. Details are given for turbulence characteristics measured in four distinct meteorological conditions. The emphasis is on identifying appropriate values of L, the integral scale value in the von Karman expression. On-going activity to measure spanwise gradients of turbulence at low altitudes is described. A resume of the NASA VGH program is given, as well as on-going utilization of flight recorder data on wide-body transports to reconstruct special turbulence encounters. Reference is made to some other activities regarding sensing, measurement, modeling, and alleviation. Author

N86-11194*# National Aeronautics and Space Administration. Ames Research Center, Moffett Field, Calif.

EXPERT SYSTEMS DEVELOPMENT AND APPLICATION

Eugene L. Duke and Victoria A. Regenie Oct. 1985 8 p Presented at the IEEE Symp. on Expert Systems in Govt., McLean, Va., 23-25 Oct. 1985
(NASA-TM-86746; H-1310; NAS 1.15:86746) Avail: NTIS HC A02/MF A01 CSCL 01C

Current research in the application of expert systems to problems in the flight research environment is discussed. In what is anticipated to be a broad research area, a real time expert system flight status monitor has been identified as the initial project. This real time expert system flight status monitor is described in terms of concept, application, development, and schedule. Author

N86-11195*# National Aeronautics and Space Administration. Ames Research Center, Moffett Field, Calif.

DESCRIPTION OF AN EXPERIMENTAL EXPERT SYSTEM FLIGHT STATUS MONITOR

Eugene L. Duke and Victoria A. Regenie Oct. 1985 11 p refs Presented at the 5th AIAA Computers in Aerospace Conf., Long Beach, Calif., 21-23 Oct. 1985
(NASA-TM-86791; H-1317; NAS 1.15:86791; AIAA-85-6042-CP) Avail: NTIS HC A02/MF A01 CSCL 01C

This paper describes an experimental version of an expert system flight status monitor being developed at the Dryden Flight Research Facility of the NASA Ames Research Center. This experimental expert system flight status monitor (ESSFSM) is supported by a specialized knowledge acquisition tool that provides the user with a powerful and easy-to-use documentation and rule construction tool. The EESFSM is designed to be a testbed for concepts in rules, inference mechanisms, and knowledge structures to be used in a real-time expert system flight status monitor that will monitor the health and status of the flight control system of state-of-the-art, high-performance, research aircraft. Author

N86-11196*# National Aeronautics and Space Administration. Ames Research Center, Moffett Field, Calif.

COMPARISON OF CALCULATED AND MEASURED VELOCITIES NEAR THE TIP OF A MODEL ROTOR BLADE AT TRANSONIC SPEEDS

Michael E. Tauber, F. Kevin Owen (Complere, Inc.), Ronald G. Langhi (Informatics General Corp., Palo Alto, Calif.), and Grant E. Palmer Aug. 1985 81 p refs
(NASA-TM-86697; Rept-85158; NAS 1.15:86697) Avail: NTIS HC A05/MF A01 CSCL 01C

The ability of the ROT22 code to predict accurately the transonic flow field in the crucial region around and beyond the tip of a high speed rotor blade was assessed. The computations were compared with extensive laser velocimetry measurements made at zero advance ratio and tip Mach numbers of 0.85, 0.88, 0.90, and 0.95. The comparison between theory and experiment was made using 300 scans for the three orthogonal velocity components covering a volume having a height of over one blade chord, a width of nearly two chords, and a length ranging from about 1 to 1.6 chords, depending on the tip speeds. The good agreement between the calculated and measured velocities established the ability of the code to predict the off blade flow field at high tip speeds. This supplements previous comparisons where surface pressures were shown to be well predicted on two different tips at advance ratios to 0.45, especially at the critical 90 deg azimuth blade position. These results demonstrate that the ROT22 code can be used with confidence to predict the important tip region flow field including the occurrence, strength, and location of shock waves causing high drag and noise. Author

N86-11197# Air Command and Staff Coll., Maxwell AFB, Ala.

EVALUATION OF FAULT REPORTING/FAULT ISOLATION FOR F-15 AIRCRAFT

C. A. Mussari Apr. 1985 26 p
(AD-A156516; ACSC-85-1955) Avail: NTIS HC A03/MF A01 CSCL 01/3

The author set out to see if the accuracy of the FR/FI manuals is a factor in their non-use. Accuracy of the manuals was determined by analyzing actual reported inflight discrepancies. Fault code accuracy was obtained by comparing each discrepancy as written on the TAC Form 122 (Debriefing Record) with the discrepancy depicted in the FR manual. Accuracy of repair actions was obtained by tracking the repair action recommended by the fault isolation manual and comparing it with that shown on the TAC Form 122. Analysis revealed the F-15 fault reporting manual can accurately represent a random inflight malfunction 83.8% of the time, and these malfunctions can be accurately isolated in the fault isolation manual 77.7% of the time. These accuracy levels are acceptable and not a major factor in the non-use of the manuals. Observation of the debriefing and maintenance process, and interviews with aircrews and maintenance technicians, revealed a general lack of understanding and confidence in the FR/FI system. This lack of understanding and confidence, exhibited by both aircrews and maintenance personnel is the primary reason for the system's non-use. Recommended actions to show the effectiveness of using the system as designed are provided. GRA

N86-11198# Naval Air Development Center, Warminster, Pa. Aircraft and Crew Systems Technology Directorate.

A COMPARISON OF THE NAVTOLAND (NAVY VERTICAL TAKEOFF AND LANDING) SH-2F HELICOPTER MODEL WITH THE REQUIREMENTS OF MIL-H-8501A AND WITH FLIGHT DATA Final Report

R. L. Nave 31 Jan. 1984 78 p
(F41-400)
(AD-A157297; NADC-84166-60) Avail: NTIS HC A05/MF A01 CSCL 01/4

This report compares the dynamic response characteristics of an SH-2F simulator model with available flight test data and with the requirements of MIL-H-8501A, Helicopter Flying and Ground Handling Qualities; General Requirements for. The Navy Vertical Takeoff and Landing (NAVTOLAND) simulator model was developed to facilitate the design of an automatic approach and landing guidance control systems for helicopters and V/STOL aircraft. The simulation was validated by comparing the model response with all available flight test data. In addition, the model was used to examine some of the requirements of MIL-H-8501A. Considerable insight was gained in the application of the specification and in understanding techniques needed to determine compliance with the requirements. The original model was developed and installed on the NASA Ames Vertical Motion Simulator. Numerous modifications were made to the software based on test pilot evaluations. A version of this simulation model including all empirical adjustments was installed on the NAVAIRDEVCEN computer system. Further evaluation of the model was carried out using this batch version of the helicopter model. This study found that it is difficult if not impossible to satisfactorily tune a helicopter simulation based on pilot opinions without a complete flight test data base. The requirements of MIL-H-8501A need to be defined in more detail and in some cases be revised. An altitude excursion limit should be added to the current quick stop maneuver. Analysis indicates that the current 2-second pilot response delay following engine failure may be excessive. GRA

N86-11199# McDonnell Automation Co., St. Louis, Mo.
FLIGHT WORTHINESS OF FIRE RESISTANT HYDRAULIC SYSTEMS: VOLUME 1 Final Report, Jan. 1981 - Dec. 1984
J. R. Jeffery, R. B. Merrell, N. J. Pierce, M. J. Stevens, and R. E. Young Dec. 1984 307 p
(Contract F33615-80-C-2074)
(AD-A157618; AFWAL-TR-84-2085-Vol-1) Avail: NTIS HC A14/MF A01 CSCL 13/7

This volume reports a study to select a flight worthy hydraulic system in which to test the chlorotrifluoroethylene (CTFE) hydraulic fluid. Aircraft selection, hardware and concept definition, system and weight analysis, and reliability, maintainability and life cycles costs (LCC) studies are reported in volume 1. The F-15 and KC-10A were selected for comparison between the present fluid and system configuraation and CTFE fluid at 8,000 psi plus various energy conservation and water hammer control concepts. The results show the weight penalty of the nonflammable fluid (CTFE) can be overcome by use of 8,000 psi operating pressures. Performance, water hammer transients, fluid pumpability, sealing, null leakage control, and demonstration system effects were investigated during Phases 2 and 3 of this contract. GRA

N86-11200# National Center for Atmospheric Research, Boulder, Colo.
CALIBRATION OF THE NCAR (NATIONAL CENTER FOR ATMOSPHERIC RESEARCH) SABRELINER RESEARCH STATIC PRESSURE SOURCE WITH A TRAILING CONE ASSEMBLY
E. N. Brown Mar. 1985 21 p refs Sponsored in part by NSF
(PB85-191005; NCAR/TN-253/EDD) Avail: NTIS HC A02/MF A01 CSCL 01B

Trailing cone results verify that pressure corrections for the NCAR Sabreliner derived from tower flyby data can be extrapolated to higher Mach numbers and higher altitudes with valid results. Residual static pressure errors are small, on the order of 0.1 to 0.3 mb, corresponding to altutide errors of 20 to 30 ft for altitudes of 15,000 to 39,000 ft and Mach numbers of 0.59 to 0.76. Author (GRA)

N86-11180# Joint Publications Research Service, Arlington, Va.
RECENT ACHIEVEMENTS, PROBLEMS IN CROPDUSTING WORK
A. Savchenko *In its* USSR Rept.: Transportation (JPRS-UTR-85-011) 7 Oct. 1985 p 12-16 Transl. into ENGLISH from Grazhdanskaya Aviats. (Moscow), no. 4, Apr. 85 p 26-27 (For primary document see N86-11177 02-01)
Avail: NTIS HC A06

N86-11181# Joint Publications Research Service, Arlington, Va.
WORLD'S LARGEST AIRPLANE NOW BEING TESTED
N. Dombkovskiy *In its* USSR Rept.: Transportation (JPRS-UTR-85-011) 7 Oct. 1985 p 17-20 Transl. into ENGLISH from TRUD (Moscow), 23 May 1985 p 3 (For primary document see N86-11177 02-01)
Avail: NTIS HC A06

06 AIRCRAFT INSTRUMENTATION

Includes cockpit and cabin display devices; and flight instruments.

For related information see also *19 Spacecraft Instrumentation* and *35 Instrumentation and Photography.*

No abstracts in this category.

07 AIRCRAFT PROPULSION AND POWER

Includes prime propulsion systems and systems components, e.g., gas turbine engines and compressors; and on-board auxiliary power plants for aircraft.

For related information see also *20 Spacecraft Propulsion and Power, 28 Propellants and Fuels,* and *44 Energy Production and Conversion.*

N86-11201# Naval Postgraduate School, Monterey, Calif.
A NOVEL OSCILLATING JET: ITS EFFECT ON EJECTOR THRUST AUGMENTATION Technical Report, Aug. 1984 - Jan. 1985
M. A. BadriNarayanan, M. F. Platzer, and E. Rickenbaker May 1985 39 p
(AD-A157480; NPS67-85-005) Avail: NTIS HC A03/MF A01 CSCL 21/5

A plane subsonic turbulent jet was excited by a special oscillating nozzle. Its overall performance compares favorably with that of the vane excited jet investigated earlier. The nozzle when installed in an ejector system yielded a thrust augmentation ratio of 1.6 at an excitation frequency of 20 Hz. The dynamics of the oscillating flow was examined in the light of the Korst theory. GRA

N86-11202# Garrett Turbine Engine Co., Phoenix, Ariz.
LOW-COST, NET-SHAPE CERAMIC RADIAL TURBINE PROGRAM Final Technical Report, 1 Feb. 1981 - 31 Dec. 1984
D. W. Richerson and J. R. Smyth May 1985 163 p
(Contract DAAG46-81-C-0006)
(AD-A157532; Rept-21-5541; AMMRC-Tr-85-2) Avail: NTIS HC A08/MF A01 CSCL 11/2

This program's technical objective was to establish an injection-molded sintered silicon nitride manufacturing process to produce net-shape ceramic radial turbine rotors with high-temperature properties suitable for operation at tip speeds of 2000 feet per second and turbine inlet temperatures of 2500 F. The program consisted of: (1) screening 14 different sintered Si3N4 compositions; (2) process optimization and rotor fabrication; and (3) rotor stress analysis and rotor spin testing. A composition of 92% Si3N4 - 6% Y2O3 - 2% Al2O3 was developed with room temperature strength in excess of the 90 ksi program goal. A second composition was developed with room temperature and 2250 F strength in excess of the 90 ksi and 80 ksi program goals respectively. The TO2 turbocharger rotors were fabricated from the improved materials and exhibited burst speeds during spin testing up to 212,000 rpm. The burst speeds were lower than were predicted analytically based on the test bar strength data. Surface defects such as knit lines and cracks were consistently present in the rotors and possibly contributed to the low burst speed. GRA

N86-11148# Lockheed-Georgia Co., Marietta. Advanced Concepts Dept.
A REVIEW OF ADVANCED TURBOPROP TRANSPORT ACTIVITIES
Roy H. Lange *In* AGARD Aerodyn. and Acoustics of Propellers Feb. 1985 16 p refs (For primary document see N86-11147 02-01)
Avail: NTIS HC A20/MF A01

N86-11149# Office National d'Etudes et de Recherches Aerospatiales, Paris (France).
AERODYNAMIC METHOD USED IN FRANCE FOR ADVANCED FAST PROPELLER STUDY
J. M. Bousquet *In* AGARD Aerodyn. and Acoustics of Propellers Feb. 1985 15 p refs In FRENCH; ENGLISH summary Original language document previously announced in IAA as A85-15840 (For primary document see N86-11147 02-01)
Avail: NTIS HC A20/MF A01

N86-11150# Centre National de la Recherche Scientifique, Orsay (France).
DESIGN CONCEPT AND PERFORMANCE PREDICTION TECHNIQUE FOR POTENTIAL FLOWS AROUND ADVANCED PROPELLERS
Thoai-Sum Luu and Ranjit Collercandy *In* AGARD Aerodyn. and Acoustics of Propellers Feb. 1985 12 p refs (For primary document see N86-11147 02-01)
Avail: NTIS HC A20/MF A01

N86-11151# Aircraft Research Association Ltd., Bedford (England).
A REVIEW OF ARA RESEARCH INTO PROPELLER AERODYNAMIC PREDICTION METHODS
A. J. Bocci and J. I. Morrison *In* AGARD Aerodyn. and Acoustics of Propellers Feb. 1985 19 p refs (For primary document see N86-11147 02-01)
Avail: NTIS HC A20/MF A01

N86-11152# Office National d'Etudes et de Recherches Aerospatiales, Paris (France).
MODERN PROPELLER PROFILES
A. M. Rodde, J. J. Cuny (Societe Ratier Figeac, France), and J. J. Thibert *In* AGARD Aerodyn. and Acoustics of Propellers Feb. 1985 12 p refs In FRENCH Original language document previously announced in IAA as A85-15841 (For primary document see N86-11147 02-01)
Avail: NTIS HC A20/MF A01

N86-11153# National Aerospace Lab., Amsterdam (Netherlands).
AERODYNAMICS OF WIDE-CHORD PROPELLERS IN NON-AXISYMMETRIC FLOW
J. B. H. M. Schulten *In* AGARD Aerodyn. and Acoustics of Propellers Feb. 1985 10 p refs (For primary document see N86-11147 02-01)
Avail: NTIS HC A20/MF A01

N86-11154# Cranfield Inst. of Tech., Bedford (England). Coll. of Aeronautics.
ON THE AERODYNAMICS OF INSTALLED PROPELLERS
Martin E. Eshelby *In* AGARD Aerodyn. and Acoustics of Propellers Feb. 1985 15 p refs (For primary document see N86-11147 02-01)
Avail: NTIS HC A20/MF A01

N86-11155# Deutsche Forschungs- und Versuchsanstalt fuer Luft- und Raumfahrt, Brunswick (West Germany). Inst. fuer Entwurfsaerodynamik.
A UNIFIED APPROACH FOR THE AERODYNAMICS AND ACOUSTICS OF PROPELLERS IN FORWARD MOTION
A. Das *In* AGARD Aerodyn. and Acoustics of Propellers Feb. 1985 28 p refs (For primary document see N86-11147 02-01)
Avail: NTIS HC A20/MF A01

N86-11156*# National Aeronautics and Space Administration. Langley Research Center, Hampton, Va.
THEORETICAL ANALYSIS OF LINEARIZED ACOUSTICS AND AERODYNAMICS OF ADVANCED SUPERSONIC PROPELLERS
F. Farassat *In* AGARD Aerodyn. and Acoustics of Propellers Feb. 1985 15 p refs (For primary document see N86-11147 02-01)
Avail: NTIS HC A20/MF A01 CSCL 01A

N86-11157# Lockheed-California Co., Burbank.
A GENERAL THEORY OF ARBITRARY MOTION AERODYNAMICS USING AN AEROACOUSTIC APPROACH
Lyle N. Long and George A. Watts *In* AGARD Aerodyn. and Acoustics of Propellers Feb. 1985 12 p refs (For primary document see N86-11147 02-01)
Avail: NTIS HC A20/MF A01

N86-11158*# National Aeronautics and Space Administration. Lewis Research Center, Cleveland, Ohio.
SUMMARY OF RECENT NASA PROPELLER RESEARCH
Daniel C. Mikkelson, Glenn A. Mitchell, and Lawrence J. Bober *In* AGARD Aerodyn. and Acoustics of Propellers Feb. 1985 24 p refs Previously announced as N84-32344 (For primary document see N86-11147 02-01)
Avail: NTIS HC A20/MF A01 CSCL 01A

N86-11159# Societe Nationale Industrielle Aerospatiale, Marignane (France).
DYNAMIC BEHAVIOR OF A PROPFAN
J. M. Besson and D. Petot (ONERA, Paris) *In* AGARD Aerodyn. and Acoustics of Propellers Feb. 1985 15 p refs In FRENCH Original language document previously announced in IAA as A85-15842 (For primary document see N86-11147 02-01)
Avail: NTIS HC A20/MF A01

N86-11160# De Havilland Aircraft Co. of Canada Ltd., Downsview (Ontario).
PERFORMANCE EVALUATION OF FULL SCALE PROPELLERS BY WIND TUNNEL TEST
D. J. Barber *In* AGARD Aerodyn. and Acoustics of Propellers Feb. 1985 12 p refs (For primary document see N86-11147 02-01)
Avail: NTIS HC A20/MF A01

N86-11161# Institut de Mecanique des Fluides de Marseille (France).
STUDY OF THE 3D WAKE OF AN AERIAL PROPELLER [ETUDE DU SILLAGE 3D D'UNE HELICE AERIENNE]
D. Favier and C. Maresca *In* AGARD Aerodyn. and Acoustics of Propellers Feb. 1985 22 p refs In FRENCH (For primary document see N86-11147 02-01)
Avail: NTIS HC A20/MF A01

N86-11162# Dornier-Werke G.m.b.H., Friedrichshafen (West Germany).
INVESTIGATIONS OF MODERN GENERAL AVIATION PROPELLERS
H. Zimmer, R. Hoffmann (Hoffmann-Propellers, Rosenheim, West Germany), and K. H. Horstmann (DFVLR, Brunswick) *In* AGARD Aerodyn. and Acoustics of Propellers Feb. 1985 14 p refs (For primary document see N86-11147 02-01)
Avail: NTIS HC A20/MF A01

N86-11163# Dowty Rotol Ltd., Gloucester (England).
AERODYNAMIC AND STRUCTURAL ASPECTS OF PROPELLER AND DRIVE FOR A 1/5 SCALE WIND TUNNEL PROGRAMME
R. M. Bass, B. Munniksma (National Aerospace Lab., Amsterdam), and J. vanHengst (Royal Netherlands Aircraft Factories Fokker, Schiphol-Oost) *In* AGARD Aerodyn. and Acoustics of Propellers Feb. 1985 18 p refs (For primary document see N86-11147 02-01)
Avail: NTIS HC A20/MF A01

N86-11164# De Havilland Aircraft Co. of Canada Ltd., Downsview (Ontario).
SOME CONSIDERATIONS IN PROPELLER AND AIRFRAME INTEGRATION
B. Eggleston *In* AGARD Aerodyn. and Acoustics of Propellers Feb. 1985 11 p refs (For primary document see N86-11147 02-01)
Avail: NTIS HC A20/MF A01

N86-11165# Avions Marcel Dassault, Saint-Cloud (France). Div. des Etudes Avancees.
PROBLEMS OF THE INTEGRATION OF PROPELLERS IN AIRFRAMES, ESPECIALLY FOR HIGH PERFORMANCE TWIN-ENGINE AIRCRAFT [LES PROBLEMES D'INTEGRATION DE HELICES A LA CELLULE D'UN AVION ET, PLUS PARTICULIEREMENT, D'UN BIMOTEUR DE FORTE PUISSANCE]
Rene Taisserie *In* AGARD Aerodyn. and Acoustics of Propellers Feb. 1985 10 p In FRENCH (For primary document see N86-11147 02-01)
Avail: NTIS HC A20/MF A01

N86-11166# Lockheed-Georgia Co., Marietta.
WIND TUNNEL INVESTIGATION OF THE INTERACTION OF PROPELLER SLIPSTREAM WITH NACELLE/WING/FLAP COMBINATIONS
A. S. Aljabri and A. C. Hughes *In* AGARD Aerodyn. and Acoustics of Propellers Feb. 1985 10 p refs (For primary document see N86-11147 02-01)
Avail: NTIS HC A20/MF A01

N86-11167*# National Aeronautics and Space Administration. Langley Research Center, Hampton, Va.
AN ASYMPTOTIC THEORY FOR THE INTERFERENCE OF LARGE ASPECT RATIO SWEPT WINGS AND MULTIPLE PROPELLER SLIPSTREAMS
R. K. Prabhu (Old Dominion Univ.), C. H. Liu, and S. N. Tiwari (Old Dominion Univ.) *In* AGARD Aerodyn. and Acoustics of Propellers Feb. 1985 17 p refs (For primary document see N86-11147 02-01)
Avail: NTIS HC A20/MF A01 CSCL 01A

N86-11168# Carleton Univ., Ottawa (Ontario). Dept. of Mechanical and Aeronautical Engineering.
DEVELOPMENT OF MODERN TURBOPROP ENGINES
H. I. H. Saravanamuttoo *In* AGARD Aerodyn. and Acoustics of Propellers Feb. 1985 9 p refs (For primary document see N86-11147 02-01)
Avail: NTIS HC A20/MF A01

N86-11170# Royal Aircraft Establishment, Farnborough (England). Aerodynamics Dept.
SOME AEROACOUSTIC WIND TUNNEL MEASUREMENTS, THEORETICAL PREDICTIONS, AND FLIGHT-TEST CORRELATIONS ON SUBSONIC AIRCRAFT PROPELLERS
W. J. G. Trebble, J. Williams (Southampton Univ., England), and R. P. Donnelly (Dowty Rotol Ltd, Gloucester, England) *In* AGARD Aerodyn. and Acoustics of Propellers Feb. 1985 21 p refs (For primary document see N86-11147 02-01)
Avail: NTIS HC A20/MF A01

N86-11512*# National Aeronautics and Space Administration. Lewis Research Center, Cleveland, Ohio.
COMBUSTION HOT SECTION TECHNOLOGY
David B. Ercegovic *In its* Turbine Eng. Hot Sect. Technol. (HOST) Oct. 1983 p 129-133 refs (For primary document see N86-11495 02-39)
Avail: NTIS HC A11/MF A01 CSCL 21E

N86-11513*# National Aeronautics and Space Administration. Lewis Research Center, Cleveland, Ohio.
HOST STRUCTURAL ANALYSIS PROGRAM OVERVIEW
R. H. Johns *In its* Turbine Eng. Hot Sect. Technol. (HOST) Oct. 1983 p 153-158 (For primary document see N86-11495 02-39)
Avail: NTIS HC A11/MF A01 CSCL 21E

N86-11515*# General Electric Co., Cincinnati, Ohio.
COMPONENT-SPECIFIC MODELING
M. L. Roberts *In* NASA. Lewis Research Center Turbine Eng. Hot Sect. Technol. (HOST) Oct. 1983 p 165-173 (For primary document see N86-11495 02-39)
(Contract NAS3-23687)
Avail: NTIS HC A11/MF A01 CSCL 21E

08 AIRCRAFT STABILITY AND CONTROL

Includes aircraft handling qualities; piloting; flight controls; and autopilots.

N86-11203*# National Aeronautics and Space Administration. Langley Research Center, Hampton, Va.
PRELIMINARY DESIGN STUDY OF A LATERAL-DIRECTIONAL CONTROL SYSTEM USING THRUST VECTORING
Frederick J. Lallman Nov. 1985 51 p refs
(NASA-TM-86425; L-15990; NAS 1.15:86425) Avail: NTIS HC A04/MF A01 CSCL 01C

A preliminary design of a lateral-directional control system for a fighter airplane capable of controlled operation at extreme angles of attack is developed. The subject airplane is representative of a modern twin-engine high-performance jet fighter, is equipped with ailerons, rudder, and independent horizontal-tail surfaces. Idealized bidirectional thrust-vectoring engine nozzles are appended to the mathematic model of the airplane to provide additional control moments. Optimal schedules for lateral and directional pseudo control variables are calculated. Use of pseudo controls results in coordinated operation of the aerodynamic and thrust-vectoring controls with minimum coupling between the lateral and directional airplane dynamics. Linear quadratic regulator designs are used to specify a preliminary flight control system to improve the stability and response characteristics of the airplane. Simulated responses to step pilot control inputs are stable and well behaved. For lateral stick deflections, peak stability axis roll rates are between 1.25 and 1.60 rad/sec over an angle-of-attack range of 10 deg to 70 deg. For rudder pedal deflections, the roll rates accompanying the sideslip responses can be arrested by small lateral stick motions. E.A.K.

N86-11204*# Calspan Advanced Technology Center, Buffalo, N.Y.
MISSION-ORIENTED REQUIREMENTS FOR UPDATING MIL-H-8501: CALSPAN PROPOSED STRUCTURE AND RATIONALE Final Report
Charles R. Chalk and Robert C. Radford Sep. 1985 294 p refs
(Contract NAS2-11303; DA Proj. 1L1-62209-AH-76-A)
(NASA-CR-177371; USAAVSCOM-TR-85-A-7; NAS 1.26:177371; Calspan-Rept-7097-F-1) Avail: NTIS HC A13/MF A01 CSCL 01C

This report documents the effort by Arvin/Calspan Corporation to formulate a revision of MIL-H-8501A in terms of Mission-Oriented Flying Qualities Requirements for Military Rotorcraft. Emphasis is placed on development of a specification structure which will permit addressing Operational Missions and Flight Phases, Flight Regions, Classification of Required Operational Capability, Categorization of Flight Phases, and Levels of Flying Qualities. A number of definitions is established to permit addressing the rotorcraft state, flight envelopes, environments, and the conditions under which degraded flying qualities are permitted. Tentative requirements are drafted for Required Operational Capability Class 1. Also included is a Background Information and Users Guide for the draft specification structure proposed for the MIL-H-8501A revision. The report also contains a discussion of critical data gaps and attempts to prioritize these data gaps and to suggest experiments that should be performed to generate data needed to support formulation of quantitative design criteria for the additional Operational Capability Classes 2, 3, and 4. Author

09 RESEARCH AND SUPPORT FACILITIES (AIR)

Includes airports, hangars and runways; aircraft repair and overhaul facilities; wind tunnels; shock tube facilities; and engine test blocks.

For related information see also *14 Ground Support Systems and Facilities (Space).*

N86-11205 Communications Research Centre, Ottawa (Ontario). Space Technology and Applications Branch.

CRC CONTROL SYSTEMS LABORATORY GYRO TEST FACILITY
W. S. McMath and S. K. Yeung Apr. 1985 21 p
(CRC-1385) Avail: Issuing Activity

The gyro test facility was developed to provide a high precision testing capability, with the versatility to simulate, monitor and analyze the performance of a wide variety of sensors. The technical features of the facility as it was developed in parallel with a Single-Degree-of-Freedom (SDOF) gyro test program are summarized. Some of the data from that test program is included as a working example of facility capability. However, the details of the complete gyro evaluation will be covered in a separate report. Author

N86-11206*# National Aeronautics and Space Administration. Ames Research Center, Moffett Field, Calif.
WATER TUNNEL FLOW VISUALIZATION USING A LASER
Christine Beckner and Robert E. Curry Oct. 1985 16 p refs
Presented at the 3rd AIAA Appl. Aerodyn. Conf., Colorado Springs, 14-16 Oct. 1985
(NASA-TM-86743; H-1307; NAS 1.15:86743) Avail: NTIS HC A02/MF A01 CSCL 14B

Laser systems for flow visualization in water tunnels (similar to the vapor screen technique used in wind tunnels) can provide two-dimensional cross-sectional views of complex flow fields. This parametric study documents the practical application of the laser-enhanced visualization (LEV) technique to water tunnel testing. Aspects of the study include laser power levels, flow seeding (using flourescent dyes and embedded particulates), model preparation, and photographic techniques. The results of this study are discussed to provide potential users with basic information to aid in the design and setup of an LEV system. Author

N86-11207*# Boeing Aerospace Co., Seattle, Wash.
LASER ANGLE SENSOR
C. R. Pond and P. D. Texeira Sep. 1985 184 p refs
(Contract NAS1-16546)
(NASA-CR-172369; NAS 1.26:172369) Avail: NTIS HC A09/MF A01 CSCL 20E

A laser angle measurement system was designed and fabricated for NASA Langley Research Center. The instrument is a fringe counting interferometer that monitors the pitch attitude of a model in a wind tunnel. A laser source and detector are mounted above the model. Interference fringes are generated by a small passive element on the model. The fringe count is accumulated and displayed by a processor in the wind tunnel control room. This report includes optical and electrical schematics, system maintenance and operation procedures. Author

N86-11208*# National Aeronautics and Space Administration. Ames Research Center, Moffett Field, Calif.
VISUAL AND MOTION CUEING IN HELICOPTER SIMULATION
Richard S. Bray Sep. 1985 19 p refs
(NASA-TM-86818; Rept-85371; NAS 1.15:86818) Avail: NTIS HC A02/MF A01 CSCL 14B

Early experience in fixed-cockpit simulators, with limited field of view, demonstrated the basic difficulties of simulating helicopter flight at the level of subjective fidelity required for confident evaluation of vehicle characteristics. More recent programs, utilizing large-amplitude cockpit motion and a multiwindow visual-simulation system have received a much higher degree of pilot acceptance. However, none of these simulations has presented critical visual-flight tasks that have been accepted by the pilots as the full equivalent of flight. In this paper, the visual cues presented in the simulator are compared with those of flight in an attempt to identify deficiencies that contribute significantly to these assessments. For the low-amplitude maneuvering tasks normally associated with the hover mode, the unique motion capabilities of the Vertical Motion Simulator (VMS) at Ames Research Center permit nearly a full representation of vehicle motion. Especially appreciated in these tasks are the vertical-acceleration responses to collective control. For larger-amplitude maneuvering, motion fidelity must suffer diminution through direct attenuation through high-pass filtering washout of the computer cockpit accelerations or both. Experiments were conducted in an attempt to determine the effects of these distortions on pilot performance of height-control tasks. Author

N86-11209*# National Aeronautics and Space Administration. Ames Research Center, Moffett Field, Calif.
AIRFLOW CALIBRATION OF A BELLMOUTH INLET FOR MEASUREMENT OF COMPRESSOR AIRFLOW IN TURBINE-POWERED PROPULSION SIMULATORS
Stephen C. Smith Nov. 1985 17 p refs
(NASA-TM-84399; Rept-85337; NAS 1.15:84399) Avail: NTIS HC A02/MF A01 CSCL 14B

The development of turbine-powered propulsion simulators for high-speed wind tunnel models requires a bellmouth inlet which can accurately measure compressor-inlet airflow. A bellmouth inlet was instrumented with total pressure probes, static pressure probes, and thermocouples for airflow measurement. The bellmouth flowmeter against a critical venturi flowmeter was calibrated. The calibration was done at four inlet pressures ranging from 58 to 114 kPa. The bellmouth discharge coefficient varied as a function of bellmouth-throat Mach number. Over the range of Reynolds number and Mach number tested the Reynolds number was not a significant influence on the discharge coefficient. The overall accuracy of the bellmouth inlet as a flowmeter was estimated to be + or - 0.5% of the flowmeter reading. E.A.K.

N86-11210# Engineering and Economics Research, Inc., Vienna, Va.
ENHANCED AIRPORT SURFACE DETECTION EQUIPMENT APPLICATIONS
H. R. Schramm 17 Apr. 1985 72 p
(AD-A157641) Avail: NTIS HC A04/MF A01 CSCL 17/7

The National Airspace Review (NAR) Enhancement Program is a cooperative government/industry effort to review airspace allocations and the procedural and regulatory aspects of scheduled improvements envisioned under the National Airspace System (NAS) Plan as well as other plans. Its purpose is to identify long-term operational considerations of enhanced systems as they evolve. Improved capabilities resulting from equipment already developed or in the process of development will be examined, with attention being focused on operational considerations rather than specific generation of system requirements. Task Group 4-6.1 of the NAR Enhancement Program convened in Washington, D.C., from January 8 to 10, 1985, and January 29, 1985. This task group was responsible for reviewing and analyzing operational considerations based on the development of enhanced airport surface detection equipment. The recommendations contained herein will be submitted to the Administrator, Federal Aviation Administration, through the NAR Enhancement Executive Steering Committee (EXCOM), for consideration and disposition. GRA

12 ASTRONAUTICS (GENERAL)

For extraterrestrial exploration see *91 Lunar and Planetary Exploration.*

No abstracts in this category.

13 ASTRODYNAMICS

Includes powered and free-flight trajectories; and orbit and launching dynamics.

N86-11211 Texas Univ., Austin.
COMPUTATIONAL ERRORS AND THEIR CONTROL IN THE

DETERMINATION OF SATELLITE ORBITS Ph.D. Thesis
John Bernard Lindberg 1984 284 p
Avail: Univ. Microfilms Order No. DA8513257

Numerical integration errors are caused by a polynomial approximation of a nonlinear function and by the use of finite computer word length. Numerical integration errors may be expected to grow in a nearly quadratic or exponential manner for the satellite problem, and they become severe for long orbital trajectories. To reduce the problem of numerical integration error in the orbit determination process, certain techniques may be employed. One option to reduce integration error is the use of an increased computer word size in the computations; another is to employ techniques which do not require a change in the computer word size. The techniques under investigation were the use of the Encke method that reformulates the differential equations to reduce roundoff error, the use of empirical model parameters to compensate for some of the numberical integration error, and the modification of the integration process to reduce the errors caused by discontinuities in the force model with emphasis on the force due to solar radiation pressure. It is indicated that the effect of numerical integration error on the batch estimation process can be reduced significantly, and provide for convergence in fewer iterations with a smaller contribution to the overall error. Numerical integration error may be reduced with only a fraction of the cost compared to increasing the computer word size. Dissert. Abstr.

N86-11212*# Ohio State Univ., Columbus. ElectroScience Lab.
CALCULATION OF ALLOWABLE ORBITAL SPACINGS FOR THE FIXED-SATELLITE SERVICE
Yoshikazu Yamamura and Curt A. Levis Jul. 1985 78 p refs
(Grant NAG3-159)
(NASA-CR-176273; NAS 1.26:176273; TR-716548-1) Avail: NTIS HC A05/MF A01 CSCL 22A

Minimum satellite separations are calculated which satisfy a given carrier-to-interference protection ratio for the Fixed-Satellite Service (FSS) on a single-entry basis, assuming circular antenna beams. The results are presented in the form of universal contour curves, in which antenna-centered angles are the coordinates, and also in terms of the more conventional longitude and latitude separations. It is shown that orbit capacity increases with decreasing service-area size and that, for practical service areas, capacity is increased if the longitude of a satellite does not differ too greatly from that of the service area it serves. Author

14 GROUND SUPPORT SYSTEMS AND FACILITIES (SPACE)

Includes launch complexes, research and production facilities; ground support equipment, e.g., mobile transporters; and simulators.

For related information see also *09 Research Support Facilities (Air).*

N86-11213# Naval Postgraduate School, Monterey, Calif.
A FLASH X-RAY FACILITY FOR THE NAVAL POSTGRADUATE SCHOOL
X. K. Maruyama and E. C. Zurey, Jr. Jun. 1985 18 p
(AD-A157278; NPS61-85-004) Avail: NTIS HC A02/MF A01 CSCL 20/7

A Pulsar Model 112A flash X-ray machine has been acquired by the Naval Postgraduate School. This brief report describes the technical aspects of the accelerator and provides documentation so that interested and affected parties may be informed on safety precautions, potential uses and practical considerations for the effective utilization of a major resource for education and research. GRA

N86-11214# Los Alamos Scientific Lab., N. Mex.
RAILGUN POWER SUPPLY SYSTEM UTILIZING TRACTION MOTORS AND VACUUM INTERRUPTERS
W. M. Parsons, J. V. Parker, and P. Thullen 1985 4 p Presented at the 5th IEEE Pulsed Power Conf., Washington, D.C., 10 Jun. 1985
(Contract W-7405-eng-36)
(DE85-014123; LA-UR-85-2022; CONF-850616-60) Avail: NTIS HC A02/MF A01

A railgun power supply has been designed that utilizes traction motors, vacuum interrupters and pulse transformers. An assembly of 28 traction motors, which store approximately 75 MJ, energize the primary windings of three pulse transformers at a peak current of 50 kA. At peak current an array of vacuum interrupters disconnects the transformer primary windings and forces the current to flow in the secondary windings. The secondary windings are connected directly to the railgun and require no opening switches. By staging the vacuum interrupter openings, a 1 MA to 1.3 MA ramped current waveform can be delivered to the railgun. DOE

15 LAUNCH VEHICLES AND SPACE VEHICLES

Includes boosters; manned orbital laboratories; reusable vehicles; and space stations.

N86-11215*# National Aeronautics and Space Administration. Marshall Space Flight Center, Huntsville, Ala.
PROBLEMS EXPERIENCED AND ENVISIONED FOR DYNAMICAL PHYSICAL SYSTEMS
Robert S. Ryan Aug. 1985 148 p refs
(NASA-TP-2508; M-494; NAS 1.60:2508) Avail: NTIS HC A07/MF A01 CSCL 22B

The use of high performance systems, which is the trend of future space systems, naturally leads to lower margins and a higher sensitivity to parameter variations and, therefore, more problems of dynamical physical systems. To circumvent dynamic problems of these systems, appropriate design, verification analysis, and tests must be planned and conducted. The basic design goal is to define the problem before it occurs. The primary approach for meeting this goal is a good understanding and reviewing of the problems experienced in the past in terms of the system under design. This paper reviews many of the dynamic problems experienced in space systems design and operation, categorizes them as to causes, and envisions future program implications, developing recommendations for analysis and test approaches. Author

N86-11216*# National Aeronautics and Space Administration. Marshall Space Flight Center, Huntsville, Ala.
HEAVY LIFT LAUNCH VEHICLES FOR 1995 AND BEYOND
Ronald Toelle, comp. Sep. 1985 149 p refs
(NASA-TM-86520; NAS 1.15:86520) Avail: NTIS HC A07/MF A01 CSCL 22B

A Heavy Lift Launch Vehicle (HLLV) designed to deliver 300,000 lb to a 540 n mi circular polar orbit may be required to meet national needs for 1995 and beyond. The vehicle described herein can accommodate payload envelopes up to 50 ft diameter by 200 ft in length. Design requirements include reusability for the more expensive components such as avionics and propulsion systems, rapid launch turnaround time, minimum hardware inventory, stage and component flexibility and commonality, and low operational costs. All ascent propulsion systems utilize liquid propellants, and overall launch vehicle stack height is minimized while maintaining a reasonable vehicle diameter. The ascent propulsion systems are based on the development of a new liquid oxygen/hydrocarbon booster engine and liquid oxygen/liquid hydrogen upper stage engine derived from today's SSME technology. Wherever possible, propulsion and avionics systems are contained in reusable propulsion/avionics modules that are recovered after each launch. Author

N86-11217# General Accounting Office, Washington, D. C. National Security and International Affairs Div.
STATUS OF THE INTERCONTINENTAL BALLISTIC MISSILE

MODERNIZATION PROGRAM
8 Jul. 1985 35 p
(AD-A157375; GAO/NSIAD-85-78) Avail: NTIS HC A03/MF A01 CSCL 16/4

The Department of Defense is taking three major actions to modernize the intercontinental ballistic missile component of the U.S. strategic forces. Specifically, DOD is: (1) developing a small ICBM and its hard mobile launcher, (2) researching other basing technology, and (3) deploying Peacekeeper (MX) missiles in Minuteman silos. Potential major issues of the small ICBM can now be identified. For instance, for a 500 missile force on hard mobile launchers: (1) life cycle cost would be about $44 billion in 1982 dollars, (2) personnel requirements would be about 20, 000 people, and (3) up to 28,000 square miles of land would be required for wartime operations. The Peacekeeper program is in production while development testing continues. Results to date have been positive. Current congressional action to limit the number of missiles deployed will affect program cost and schedule. GRA

16 SPACE TRANSPORTATION

Includes passenger and cargo space transportation, e.g., shuttle operations; and rescue techniques.

For related information see also *03 Air Transportation and Safety* and *85 Urban Technology and Transportation.*

N86-11218*# National Aeronautics and Space Administration. Lewis Research Center, Cleveland, Ohio.
NASA LEWIS RESEARCH CENTER LOW-GRAVITY FLUID MANAGEMENT TECHNOLOGY PROGRAM
John C. Aydelott, Michael J. Carney, and John I. Hochstein (Washington Univ., St. Louis) Nov. 1985 56 p refs Presented at the JANNAF Safety and Environ. Protection Subcomm. Meeting, Monterey, Calif., 4-7 Nov. 1985 and at the AIAA/GNOS 3rd Ann. Aerospace Technol. Symp., New Orleans, 7-8 Nov. 1985
(NASA-TM-87145; E-2774; NAS 1.15:87145; AIAA/GNOS-85-002) Avail: NTIS HC A04/MF A01 CSCL 22B

A history of the Lewis Research Center in space fluid management technology program is presented. Current programs which include numerical modeling of fluid systems, heat exchanger/radiator concept studies, and the design of the Cryogenic Fluid Management Facility are discussed. Recent analytical and experimental activities performed to support the Shuttle/Centaur development activity are highlighted. Author

17 SPACECRAFT COMMUNICATIONS, COMMAND AND TRACKING

Includes telemetry; space communications networks; astronavigation; and radio blackout.

For related information see also *04 Aircraft Communications and Navigation* and *32 Communications.*

No abstracts in this category.

18 SPACECRAFT DESIGN, TESTING AND PERFORMANCE

Includes spacecraft thermal and environmental control; and attitude control.

For life support systems see *54 Man/System Technology and Life Support.* For related information see also *05 Aircraft Design, Testing and Performance* and *39 Structural Mechanics.*

N86-11219 California Univ., Los Angeles.
A DIRECT MODEL REFERENCE ADAPTIVE APPROACH TO THE CONTROL OF SPACE STATIONS Ph.D. Thesis
Che-Hang Charles Ih 1985 306 p
Avail: Univ. Microfilms Order No. DA8513126

Of all large space structural systems, space stations present a unique challenge and requirement to advanced control technology. During shuttle docking the system mass may suddenly increase by more than 100% and during station assembly the mass may vary even more drastically. Large space structural systems require highly sophisticated control systems that can grow as the stations evolve and cope with the uncertainities and time-varying elements to maintain the stability and pointing of the space stations. This dissertation first deals with the aspects of space station operational properties including configurations, dynamic models, shuttle docking contact dynamics, solar panel interaction and load reduction to yield a set of system models and conditions. A model reference adaptive control algorithm along with the inner-loop plant augmentation design for controlling the space stations under severe operational conditions of shuttle docking, excessive model parameter errors, and model truncation are then investigated. DOE

N86-11220*# Columbia Univ., New York. Dept. of Civil Engineering and Engineering Mechanics.
VIBRATIONS AND STRUCTUREBORNE NOISE IN SPACE STATION Progress Report, 1 Jan. - 30 Jun. 1985
Rimas Vaicaitis 30 Jun. 1985 26 p refs
(Grant NAG1-541)
(NASA-CR-176291; NAS 1.26:176291) Avail: NTIS HC A03/MF A01 CSCL 22B

The related literature was reviewed and a preliminary analytical model was developed for simplified acoustic and structural geometries for pressurized and unpressurized space station modules. In addition to the analytical work, an experimental program on structureborne noise generation and transmission was started. A brief review of those accomplishments is given. Author

N86-11221*# National Aeronautics and Space Administration. Ames Research Center, Moffett Field, Calif.
DESIGN AND PERFORMANCE ANALYSIS OF AN AERO-MANEUVERING ORBITAL-TRANSFER VEHICLE CONCEPT
Gene P. Menees Oct. 1985 16 p refs
(NASA-TM-86848; Rept-85398; NAS 1.15:86848) Avail: NTIS HC A02/MF A01 CSCL 22B

Systems requirements for design-optimized, lateral-turn performance were determined for reusable, space-based applications and low-Earth orbits involving large multiple plane-inclination changes. The aerothermodynamic analysis is the most advanced available for rarefield-hypersonic flow over lifting surfaces at incidence. The effects of leading-edge bluntness, low-density viscous phenomena, and finite-rate flow-field chemistry and surface catalysis are accounted for. The predicted aerothermal heating characteristics are correlated with thermal-control and flight-performance capabilities. The mission payload capacity for delivery, retrieval, and combined operations was determined for round-trip sorties extending to polar orbits. Recommendations are given for future design refinements. The results help to identify technology issues required to develop prototype operational vehicles. Author

N86-11222*# National Aeronautics and Space Administration. Goddard Space Flight Center, Greenbelt, Md.
SPACEWARN BULLETIN
31 Aug. 1985 7 p
(NASA-TM-87512; NAS 1.15:87512; SPX-382) Avail: NTIS HC A02/MF A01 CSCL 22A

SPACEWARN Bulletin SPX-382, Aug. 31, 1985, lists international satellite and space probe launch events which occurred from July 31 until the end of August 1985. The Bulletin serves as an international communication mechanism for the rapid distribution of information on satellites and space probes, and is guided by COSPAR (Committee on Space Research) directives. F.M.R.

N86-11223# Los Alamos Scientific Lab., N. Mex.
ACTIVATED RECOMBINATIVE DESORPTION: A POTENTIAL COMPONENT IN MECHANISMS OF SPACECRAFT GLOW
J. B. Cross 1985 10 p Presented at the 2nd Workshop on Spacecraft Glow, Huntsville, Ala., 17 Jun. 1985
(Contract W-7405-eng-36)
(DE85-014092; LA-UR-85-2182; CONF-8506145-1) Avail: NTIS HC A02/MF A01

The concept of activated recombination of atomic species on surfaces is capable of explaining the production of vibrationally and translationally excited desorbed molecular species. Equilibrium statistical mechanics predicts that the molecular quantum state distributions of desorbing molecules is a function of only the surface temperature when the adsorption probability is unity and independent of initial collision conditions. In most cases though the adsorption probability is dependent upon initial conditions such as collision energy or internal quantum state distribution of impinging molecules. From detailed balance, such dynamical behavior is reflected in the internal quantum state distribution of the desorbing molecule. A number of surface-atom recombination systems demonstrate this nonthermal behavior: H2-Cu,N2-Fe,CO2-Pt, etc. It is proposed that this concept, activated recombinative desorption, may offer a common thread in proposed mechanisms of spacecraft glow. Ground-based experiments are proposed which will complement flight investigations probing the mechanism of the flow phenomenon. DOE

N86-11920# Joint Publications Research Service, Arlington, Va.
DESIGN OF MANEUVERABLE TRAJECTORIES OF RE-ENTRY VEHICLE Abstract Only
Xanuyan Zhao *In its* China Rept.: Sci. and Technol. (JPRS-CST-85-014) 2 May 1985 p 72 Transl. into ENGLISH from Yuhang Xuebao (Beijing), no. 1, 31 Jan. 1985 p 1-10 Original language document announced in IAA as A85-42776 (For primary document see N86-11918 02-70)
Avail: NTIS HC A06/MF A01

19 SPACECRAFT INSTRUMENTATION

For related information see also *06 Aircraft Instrumentation* and *35 Instrumentation and Photography.*

No abstracts in this category.

20 SPACECRAFT PROPULSION AND POWER

Includes main propulsion systems and components, e.g., rocket engines; and spacecraft auxiliary power sources.

For related information see also *07 Aircraft Propulsion, 28 Propellants and Fuels,* and *44 Energy Production and Conversion.*

N86-11224*# National Aeronautics and Space Administration. Lewis Research Center, Cleveland, Ohio.
AN EXPERIMENTAL STUDY OF ENERGY LOSS MECHANISMS AND EFFICIENCY CONSIDERATION IN THE LOW POWER dc ARCJET
Francis M. Curran 1985 24 p refs Presented at the 18th Intern. Elec. Propulsion Conf., Alexandria, Va., 30 Sep. - 2 Oct. 1985; sponsored by AIAA, JSASS, and DGLR
(NASA-TM-87123; E-2733; NAS 1.15:87123; AIAA-85-2017) Avail: NTIS HC A02/MF A01 CSCL 21C

The potential utility of the low power dc arcjet in auxiliary propulsion was investigated. It was indicated that improvements in the areas of stability, energy efficiency, reliability, and electrode erosion are necessary to obtain a useful device. A water-cooled arcjet simulator was tested to investigate both the energy loss mechanisms at the electrodes and the stability of different conventional arcjet configurations in the presence of a vortex flow field. It is shown that in certain configurations only 25 to 30% of the input energy is lost to the electrodes. It is also shown that vortex stabilization is not difficult to obtain in many cases at the flow rates used and that a careful starting procedure is effective in minimizing electrode damage. E.A.K.

N86-11225# RAND Corp., Santa Monica, Calif.
SOME EXAMPLES OF PROPULSION APPLICATIONS USING ANTIMATTER
B. W. Augenstein Jul. 1985 9 p refs Presented at the Antimatter Propulsion Workshop, Pasadena, Calif., 20-21 Jun. 1985
Avail: NTIS HC A02/MF A01

Macroapplications of antimatter and annihilation energies to various uses beyond very high energy physics, which presupposes the solution of basic production and storage problems is discussed. Propulsion applications identifiable missions which cannot be achieved conventionally are discussed. The use of annihilation energies provides ways to access effective exhaust velocities from 10 Km/sec to a major fraction of light velocity. The promise of antimatter is illustrated by considering a mix ratio r = amount of normal matter/amount of antimatter and calculating the effective attained temperature of the mixture as approx. 2 GeV/r. Ensuring that this mixing produces high temperatures and that the energy does not largely escape from the mix is the art of utilizing annihilation energies. The immediate product of nucleon-antinucleon annihilations is almost wholly pions. The subsequent reaction trains and the ultimate forms of the end products, their spectral attributes, the decay or capture mechanisms, are documented. E.A.K.

N86-11226# Naval Postgraduate School, Monterey, Calif.
PARTICLE SIZING IN A SOLID ROCKET MOTOR USING THE MANAGEMENT OF SCATTERED LIGHT M.S. Thesis
K. Abubakar Mar. 1985 63 p
(AD-A156480) Avail: NTIS HC A04/MF A01 CSCL 17/8

A previous study discussed the formulation of the theory for the scattering properties in the general case of particles of arbitrary size and refractive index occurring in a polydispersion of finite optical depth. Roberts and Webb concluded that the volume-surface mean diameter (Sauter) D sub 32 of the polydispersion may be determined from the intensity of diffraction scattered light from spherical particles. An experimental investigation was conducted to determine the feasibility of measuring the change in particle size across the exhaust nozzle of a small solid propellant rocket motor. Light scattering measurements were made at small forward angles at the entrance and exit of the exhaust nozzle. The experimental technique was found to be practical, especially if used in conjunction with measurements of transmitted light of multiple wave lengths. However, the determination of D sub 32 is difficult in the motor environment and is biased toward the larger particles in the size distribution. Particle size measurements were in reasonable agreement with sizes determined from collected exhaust products. GRA

N86-11921# Joint Publications Research Service, Arlington, Va.
ONE-DIMENSIONAL TWO-PHASE FLOW IN COMBUSTION CHAMBER OF SOLID PROPELLANT ROCKET MOTORS Abstract Only
Xianqi Chang *In its* China Rept.: Sci. and Technol. (JPRS-CST-85-014) 2 May 1985 p 73 Transl. into ENGLISH from Yuhang Xuebao (Beijing), no. 1, 31 Jan. 1985 p 11-23 Original language document announced in IAA as A85-42777 (For primary document see N86-11918 02-70)
Avail: NTIS HC A06/MF A01

N86-11925# Joint Publications Research Service, Arlington, Va.
THE ANALYSIS AND CALCULATION FOR THE DYNAMIC CHARACTERISTICS OF THE OMNI-AXIAL MOVABLE FLEXIBLE JOINT NOZZLE Abstract Only
Shixue Yang *In its* China Rept.: Sci. and Technol.

(JPRS-CST-85-014) 2 May 1985 p 77 Transl. into ENGLISH from Yuhang Xuebao (Beijing), no. 1, 31 Jan. 1985 p 59-77 Original language document announced in IAA as A85-42781 (For primary document see N86-11918 02-70)
Avail: NTIS HC A06/MF A01

23 CHEMISTRY AND MATERIALS (GENERAL)

Includes biochemistry and organic chemistry.

N86-11227*# National Aeronautics and Space Administration. Langley Research Center, Hampton, Va.
WELDING, BONDING AND FASTENING, 1984
John D. Buckley, ed. and Bland A. Stein, ed. Washington Sep. 1985 484 p refs Conf. held in Hampton, Va., 23-25 Oct. 1984; sponsored by NASA, American Society for Metals, George Washington Univ., American Welding Society, and Society of Mfg. Engineers
(NASA-CP-2387; L-16023; NAS 1.55:2387) Avail: NTIS HC A21/MF A01 CSCL 13H

A compilation of papers presented in a joint NASA, American Society for Metals, The George Washington University, American Welding Soceity, and Society of Manufacturing Engineers conference on Welding, Bonding, and Fastening at Langley Research Center, Hampton, VA, on October 23 to 25, 1984 is given. Papers were presented on technology developed in current research programs relevant to welding, bonding, and fastening of structural materials required in fabricating structures and mechanical systems used in the aerospace, hydrospace, and automotive industries. Topics covered in the conference included equipment, hardware and materials used when welding, brazing, and soldering, mechanical fastening, explosive welding, use of unique selected joining techniques, adhesives bonding, and nondestructive evaluation. A concept of the factory of the future was presented, followed by advanced welding techniques, automated equipment for welding, welding in a cryogenic atmosphere, blind fastening, stress corrosion resistant fasteners, fastening equipment, explosive welding of different configurations and materials, solid-state bonding, electron beam welding, new adhesives, effects of cryogenics on adhesives, and new techniques and equipment for adhesive bonding. For individual titles, see N86-11228 through N86-11255.

N86-11228*# LTV Aerospace and Defense Co., Dallas, Tex. Vought Aero Products Div.
THE FACTORY OF THE FUTURE c37
J. E. Byman *In* NASA. Langley Research Center Welding, Bonding and Fastening, 1984 Sep. 1985 p 1-9 (For primary document see N86-11227 02-23)
Avail: NTIS HC A21/MF A01 CSCL 13H

A brief history of aircraft production techniques is given. A flexible machining cell is then described. It is a computer controlled system capable of performing 4-axis machining part cleaning, dimensional inspection and materials handling functions in an unmanned environment. The cell was designed to: allow processing of similar and dissimilar parts in random order without disrupting production; allow serial (one-shipset-at-a-time) manufacturing; reduce work-in-process inventory; maximize machine utilization through remote set-up; maximize throughput and minimize labor.
R.J.F.

N86-11229*# Arc Machines, Inc., Pacoima, Calif.
AUTOMATIC ORBITAL GTAW WELDING: HIGHEST QUALITY WELDS FOR TOMORROW'S HIGH-PERFORMANCE SYSTEMS c37
Barbara K. Henon *In* NASA. Langley Research Center Welding, Bonding and Fastening, 1984 Sep. 1985 p 11-19 (For primary document see N86-11227 02-32)
Avail: NTIS HC A21/MF A01 CSCL 13H

Automatic orbital gas tungsten arc welding (GTAW) or TIG welding is certain to play an increasingly prominent role in tomorrow's technology. The welds are of the highest quality and the repeatability of automatic weldings is vastly superior to that of manual welding. Since less heat is applied to the weld during automatic welding than manual welding, there is less change in the metallurgical properties of the parent material. The possibility of accurate control and the cleanliness of the automatic GTAW welding process make it highly suitable to the welding of the more exotic and expensive materials which are now widely used in the aerospace and hydrospace industries. Titanium, stainless steel, Inconel, and Incoloy, as well as, aluminum can all be welded to the highest quality specifications automatically. Automatic orbital GTAW equipment is available for the fusion butt welding of tube-to-tube, as well as, tube to autobuttweld fittings. The same equipment can also be used for the fusion butt welding of up to 6 inch pipe with a wall thickness of up to 0.154 inches. Author

N86-11230*# National Aeronautics and Space Administration. Langley Research Center, Hampton, Va.
INVESTIGATION OF LOW-TEMPERATURE SOLDERS FOR CRYOGENIC WIND TUNNEL MODELS Interim Report c26
George C. Firth and Vernon E. Watkins, Jr. *In its* Welding, Bonding and Fastening, 1984 Sep. 1985 p 21-34 refs (For primary document see N86-11227 02-23)
Avail: NTIS HC A21/MF A01 CSCL 11F

The advent of high Reynolds number cryogenic wind tunnels has forced alteration of manufacturing and assembly techniques and eliminated usage of many materials associated with conventional wind tunnel models. One of the techniques affected is soldering. Solder alloys commonly used for wind tunnel models are susceptible to low-temperature embrittlement and phase transformation. The low-temperature performance of several solder alloys is being examined during research and development activities being conducted in support of design and fabrication of cryogenic wind tunnel models. Among the properties examined during these tests are shear strength, surface quality, joint stability, and durability when subjected to dynamic loading. Results of these tests and experiences with recent models are summarized. Author

N86-11231*# National Aeronautics and Space Administration. Langley Research Center, Hampton, Va.
NTF: SOLDERING TECHNOLOGY DEVELOPMENT FOR CRYOGENICS c26
E. Thomas Hall, Jr. *In its* Welding, Bonding and Fastening, 1984 Sep. 1985 p 35-54 refs (For primary document see N86-11227 02-23)
Avail: NTIS HC A21/MF A01 CSCL 11F

The advent of the National Transonic Facility (NTF) brought about a new application for an old joining method, soldering. Soldering for use at cryogenic temperatures requires that solders remain ductile and free from tin-pest (grey tin), have toughness to withstand aerodynamic loads associated with flight research, and maintain their surface finishes. Solders are used to attach 347 Stainless-Steel tubing in surface grooves of models. The solder must fill up the gap and metallurgically bound to the tubing and model. Cryogenic temperatures require that only specific materials for models can be used, including: Vasco Max 200 CVM, lescalloy A-286 Vac Arc, pH 13-8 Mo. Solders identified for testing at this time are: 50% Sn - 49.5% Pb - 0.5% Sb, 95% Sn - 5% Sb, 50% In 50% Pb, and 37.5% Sn - 37.5% Pb - 25% In. With these materials and solders, it is necessary to determine their solderability. After solderability is determined, tube/groove specimens are fabricated and stressed under cryogenic temperatures. Compatible solders are then used for acutual models. Author

N86-11232*# SPS Technologies, Jenkintown, Pa.
MECHANICAL FASTENERS FOR ADVANCED COMPOSITE MATERIALS c37
Richard C. Landt *In* NASA. Langley Research Center Welding, Bonding and Fastening, 1984 Sep. 1985 p 55-65 ref (For primary document see N86-11227 02-23)
Avail: NTIS HC A21/MF A01 CSCL 13E

Advanced composite materials, which are increasingly being used to build aircraft, have different properties than the metals

they replace. Fasteners intended for composite-material joints must be designed and selected to allow for these differences. For example, blind fasteners (one-sided access) used to assemble composite-to-composite joints have been redesigned to expand to larger diameters to resist pull-through and cocking failures. The fastener designs needed for composite materials are reviewed. Topics discussed are: galvanic corrosion, pull-through resistance, fastener rotation, installation damage, fastener galling and conductivity. A blind fastener recently developed by SPS Technologies is described to show how these requirements are incorporated.
Author

N86-11233*# National Aeronautics and Space Administration. Langley Research Center, Hampton, Va.
THE ALTERNATING SURFACE SEGMENTED LAP JOINT: A DESIGN FOR THIN HIGHLY LOADED JOINTS c37
Vernon E. Watkins, Jr. and George C. Firth *In its* Welding, Bonding and Fastening, 1984 Sep. 1985 p 67-76 ref (For primary document see N86-11227 02-23)
Avail: NTIS HC A21/MF A01 CSCL 13E

The combination of thin airfoil sections and high aerodynamic loads on many wind tunnel models presents a major problem for attachment of flap elements. Conventional methods of attaching fixed control elements such as lap and tongue-in-groove joints are not rigid enough to provide surface continuity required in high Reynolds number research. For the extreme cases, the solution has been to fabricate separate wings for each flap setting with the flap element being and integral part of the wing. Here an attractive solution to this problem, the alternating surface segmented lap joint, is discussed. This joint provides increased rigidity and lower stress levels than conventional joints. Additionally, attachment fastener loading is low and the joint can be designed to accommodate high shear levels due to bending without the use of dowel pins.
Author

N86-11234*# Martin Marietta Aerospace, New Orleans, La.
AUTOMATIC FASTENING LARGE STRUCTURES: A NEW APPROACH c37
Donald F. Lumley *In* NASA. Langley Research Center Welding, Bonding and Fastening, 1984 Sep. 1985 p 77-88 (For primary document see N86-11227 02-23)
Avail: NTIS HC A21/MF A01 CSCL 13E

The external tank (ET) intertank structure for the space shuttle, a 27.5 ft diameter 22.5 ft long externally stiffened mechanically fastened skin-stringer-frame structure, was a labor intensive manual structure built on a modified Saturn tooling position. A new approach was developed based on half-section subassemblies. The heart of this manufacturing approach will be 33 ft high vertical automatic riveting system with a 28 ft rotary positioner coming on-line in mid 1985. The Automatic Riveting System incorporates many of the latest automatic riveting technologies. Key features include: vertical columns with two sets of independently operating CNC drill-riveting heads; capability of drill, insert and upset any one piece fastener up to 3/8 inch diameter including slugs without displacing the workpiece offset bucking ram with programmable rotation and deep retraction; vision system for automatic parts program re-synchronization and part edge margin control; and an automatic rivet selection/handling system.
Author

N86-11235*# SPS Technologies, Jenkintown, Pa.
STRESS CORROSION RESISTANT FASTENERS c37
Thomas A. Roach *In* NASA. Langley Research Center Welding, Bonding and Fastening, 1984 Sep. 1985 p 89-104 (For primary document see N86-11227 02-23)
Avail: NTIS HC A21/MF A01 CSCL 13E

A family of high performance aerospace fasteners made from corrosion resistant alloys for use in applications where corrosion and stress-corrosion cracking are of major concern are discussed. The materials discussed are mainly A-286, Inconel 718, MP35N and MP159. Most of the fasteners utilize cold worked and aged materials to achieve the desired properties. The fasteners are unique in that they provide a combination of high strength and immunity to stress corrosion cracking not previously attainable. A discussion of fastener stress corrosion failures is presented including a review of the history and a description of the mechanism. Case histories are presented to illustrate the problems which can arise when material selection is made without proper regard for the environmental conditions. Mechanical properties and chemical compositions are included for the fasteners discussed. Several aspects of the application of high performance corrosion resistant fasteners are discussed including galvanic compatibility and torque-tension relationships.
Author

N86-11236*# National Aeronautics and Space Administration. Langley Research Center, Hampton, Va.
DERIVATION AND TEST OF ELEVATED TEMPERATURE THERMAL-STRESS-FREE FASTENER CONCEPT c37
James Wayne Sawyer, Max L. Blosser, and Robert R. McWithey *In its* Welding, Bonding and Fastening, 1984 Sep. 1985 p 105-122 refs (For primary document see N86-11227 02-23)
Avail: NTIS HC A21/MF A01 CSCL 13E

Future aerospace vehicles must withstand high temperatures and be able to function over a wide temperature range. New composite materials are being developed for use in designing high-temperature lightweight structures. Due to the difference between coefficients of thermal expansion for the new composite materials and conventional high-temperature metallic fasteners, innovative joining techniques are needed to produce tight joints at all temperatures without excessive thermal stresses. A thermal-stress-free fastening technique is presented that can be used to provide structurally tight joints at all temperatures even when the fastener and joined materials have different coefficients of thermal expansion. The derivation of thermal-stress-free fasteners and joint shapes is presented for a wide variety of fastener materials and materials being joined together. Approximations to the thermal-stress-free shapes that result in joints with low-thermal-stresses and that simplify the fastener/joint shape are discussed. The low-thermal-stress fastener concept is verified by thermal and shear tests in joints using oxide-dispersion-strengthened alloy fasteners in carbon-carbon material. The test results show no evidence of thermal stress damage for temperatures up to 2000 F and the resulting joints carried shear loads at room temperature typical of those for conventional joints.
Author

N86-11237*# Battelle Columbus Labs., Ohio.
EXPLOSIVE WELDING IN THE 1990'S c37
Narain S. Lalwaney and Vonne D. Linse *In* NASA. Langley Research Center Welding, Bonding and Fastening, 1984 Sep. 1985 p 123-140 refs (For primary document see N86-11227 02-23)
Avail: NTIS HC A21/MF A01 CSCL 13H

Explosive bonding is a unique joining process with the serious potential to produce composite materials capable of fulfilling many of the high performance materials capable of fulfilling many of the high performance materials needs of the 1990's. The process has the technological versatility to provide a true high quality metallurgical compatible and incompatible systems. Metals routinely explosively bonded include a wide variety of combinations of reactive and refractory metals, low and high density metals and their alloys, corrosion resistant and high strength alloys, and common steels. The major advantage of the process is its ability to custom design and engineer composites with physical and/or mechanical properties that meet a specific or unusual performance requirement. Explosive bonding offers the designer unique opportunities in materials selection with unique combinations of properties and high integrity bonds that cannot be achieved by any other metal joining process. The process and some applications are discussed.
Author

N86-11238*# Explosive Fabricators, Inc., Louisville, Colo.
EXPLOSIVE WELDING OF TUBULAR CONFIGURATED JOINTS FOR CRITICAL APPLICATIONS c37
Roy Hardwick *In* NASA. Langley Research Center Welding, Bonding and Fastening, 1984 Sep. 1985 p 141-155 (For primary document see N86-11227 02-23)

Avail: NTIS HC A21/MF A01 CSCL 13H

Explosive welding can provide the answer to problems of permanently joining metals typically used in the aerospace industry. The explosive bonding process is a solid state bonding process enabling material incompatibility problems associated with fusion welding to be overcome. In addition, heat affected zones are eliminated thus, enhancing joint strength, properties and performance. The process requires the parts being joined to be impelled, by means of explosives, to collide with each other. Certain critical collision parameters must be met and controlled and these parameters are defined. Various component geometries which satisfy the collision parameters are described. Examples of transition joints used in the aerospace industry are described and illustrated. Author

N86-11239*# National Aeronautics and Space Administration. Langley Research Center, Hampton, Va.

EXPLOSIVE TUBE-TO-FITTING JOINING OF SMALL-DIAMETER TUBES c37

Laurence J. Bement *In its* Welding, Bonding and Fastening, 1984 Sep. 1985 p 157-175 (For primary document see N86-11227 02-23)

Avail: NTIS HC A21/MF A01 CSCL 13H

An effort is currently under way by NASA Marshall Space Flight Center to upgrade the space shuttle main engine through the use of improved materials and processes. Under consideration is the use of the Langley Research Center explosive seam welding process. The objective is to demonstrate the feasibility of joining space shuttle main engine tube to fitting components in an oxygen heat exchanger, using the NASA LaRC explosive seam welding process. It was concluded that LaRC explosive joining is viable for this application; that there is no incompatability of materials; that ultrasonic inspection is the best nondestructive testing method; and that the .500 DIA joint experiences interface problems. R.J.F.

N86-11240*# Foster Wheeler Corp., Livingston, N.J.

THE USE OF EXPLOSIVE FORMING FOR FASTENING AND JOINING STRUCTURAL AND PRESSURE COMPONENTS c37

J. Wayne Schroeder *In* NASA. Langley Research Center Welding, Bonding and Fastening, 1984 Sep. 1985 p 177-184 (For primary document see N86-11227 02-23)

Avail: NTIS HC A21/MF A01 CSCL 13H

Explosive expansion of tubes into tubesheets has been used for over 20 years in the fabrication and repair of shell and tube heat exchangers. The use of explosives to perform these expansions has offered several distinct advantages over other methods. First, the process is fast and economical and can be performed with minimal training of personnel. Secondly, explosive forming does not cause the deleterious metallurgical effects which often result from other forming operations. In addition, the process can be performed remotely without the need for sophisticated handling equipment. The expansion of tubes into tubesheets is only one of many possible fastening and joining applications for which explosive forming can be used to achieve highly successful results. The explosive forming process and where it has been used are described. In addition, some possible adaptations to other joining applications are identified and discussed. Author

N86-11241*# Helwan Univ., Cairo (Egypt).

EXPLOSIVE WELDING OF ALUMINUM, TITANIUM AND ZIRCONIUM TO COPPER SHEET METAL c37

Abdel-Aziz Hegazy and Jim D. Mote (Denver Univ.) *In* NASA. Langley Research Center Welding, Bonding and Fastening, 1984 Sep. 1985 p 185-196 refs (For primary document see N86-11227 02-23)

Avail: NTIS HC A21/MF A01 CSCL 13H

The main material properties affecting the explosive weldability of a certain metal combination are the yield strength, the ductility, the density and the sonic velocity of the two metals. Successful welding of the metal combination depends mainly on the correct choice of the explosive welding parameters; i.e., the stand off distance, the weight of the explosive charge relative to the weight of the flyer plate and the detonation velocity of the explosive. Based on the measured and the handbook values of the properties of interest, the explosive welding parameters were calculated and the arrangements for the explosive welding of the Al alloy 6061-T6, titanium and zirconium to OFHC copper were determined. The relatively small sheet metal thickness (1/8') and the fact that the thickness of the explosive layer must exceed a certain minimum value were considered during the determination of the explosive welding conditions. The results of the metallographic investigations and the measurements of the shear strength at the interface demonstrate the usefulness of these calculations to minimize the number of experimental trials. Author

N86-11242*# National Aeronautics and Space Administration. Langley Research Center, Hampton, Va.

NONDESTRUCTIVE ULTRASONIC MEASUREMENT OF BOLT PRELOAD USING THE PULSED-PHASE LOCKED-LOOP INTERFEROMETER c39

S. G. Allison and J. S. Heyman *In its* Welding, Bonding and Fastening, 1984 Sep. 1985 p 197-209 refs (For primary document see N86-11227 02-23)

Avail: NTIS HC A21/MF A01 CSCL 20K

Achieving accurate preload in threaded fasteners is an important and often critical problem which is encountered in nearly all sectors of government and industry. Conventional tensioning methods which rely on torque carry with them the disadvantage of requiring constant friction in the fastener in order to accurately correlate torque to preload. Since most of the applied torque typically overcomes friction rather than tensioning the fastener, small variations in friction can cause large variations in preload. An instrument called a pulsed phase locked loop interferometer, which was recently developed at NASA Langley, has found widespread use for measurement of stress as well as material properties. When used to measure bolt preload, this system detects changes in the fastener length and sound velocity which are independent of friction. The system is therefore capable of accurately establishing the correct change in bolt tension. This high resolution instrument has been used for precision measurement of preload in critical fasteners for numerous applications such as the space shuttle landing gear and helicopter main rotors. Author

N86-11243*# National Aeronautics and Space Administration. Langley Research Center, Hampton, Va.

LANGLEY RESEARCH CENTER STANDARD FOR THE EVALUATION OF SOCKET WELDS c38

Robert F. Berry, Jr. *In its* Welding, Bonding and Fastening, 1984 Sep. 1985 p 211-229 (For primary document see N86-11227 02-23)

Avail: NTIS HC A21/MF A01 CSCL 14D

A specification utilized for the nondestructive evaluation of socket type pipe joints at Langley Research Center (LaRC) is discussed. The scope of hardware shall include, but is not limited to, all common pipe fittings: tees, elbows, couplings, caps, and so forth, socket type flanges, unions, and valves. In addition, the exterior weld of slip on flanges shall be inspected using this specification. At the discretion of the design engineer, standard practice engineer, Fracture Mechanics Engineering Section, Pressure Systems Committee, or other authority, four nondestructive evaluation techniques may be utilized exclusively, or in combination, to inspect socket type welds. These techniques are visual, radiographic, magnetic particle, and dye penetrant. Under special circumstances, other techniques (such as eddy current or ultrasonics) may be required and their application shall be guided by the appropriate sections of the American Society of Mechanical Engineers (ASME) Boiler and Pressure Vessel Code (B&PVC). Author

N86-11244*# Northrop Corp., Hawthorne, Calif. Aircraft Div.

SOLID-STATE BONDING OF SUPERPLASTIC ALUMINUM ALLOY 7475 SHEET c37

Thomas D. S. Byun and Ramsevak B. Vastava *In* NASA. Langley Research Center Welding, Bonding and Fastening, 1984 Sep. 1985 p 231-251 (For primary document see N86-11227 02-23)

Avail: NTIS HC A21/MF A01 CSCL 13H

Experimental works were carried out to study the feasibility of solid state bonding of superplastic aluminum 7475 sheet. Amount of deformation, bonding time, surface cleaning method and intermediate layer were the process parameters investigated. Other parameters, held constant by the superplastic forming condition which is required to obtain a concurrent solid state bonding, are bonding temperature, bonding pressure and atmosphere. Bond integrity was evaluated through metallographic examination, X-ray line scan analysis, SEM fractographic analysis and lap shear tests. The early results of the development program indicated that sound solid state bonding was accomplished for this high strength 7475 alloy with significant amounts of deformation. A thin intermediate layer of the soft 5052 aluminum alloy aided in achieving a solid state bonding by reducing the required amount of plastic deformation at the interface. Bond strength was substantially increased by a post bond heat treatment. Author

N86-11245*# National Aeronautics and Space Administration. Langley Research Center, Hampton, Va.

EVALUATION OF SUPERPLASTIC FORMING AND WELD-BRAZING FOR FABRICATION OF TITANIUM COMPRESSION PANELS c37

Dick M. Royster, Thomas T. Bales, and Randall C. Davis *In its* Welding, Bonding and Fastening, 1984 Sep. 1985 p 253-270 refs (For primary document see N86-11227 02-23)

Avail: NTIS HC A21/MF A01 CSCL 13H

The two titanium processing procedures, superplastic forming and weld brazing, are successfully combined to fabricate titanium skin stiffened structural panels. Stiffeners with complex shapes are superplastically formed using simple tooling. These stiffeners are formed to the desired configuration and required no additional sizing or shaping following removal from the mold. The weld brazing process by which the stiffeners are attached to the skins utilize spot welds to maintain alignment and no additional tooling is required for brazing. The superplastic formed/weld brazed panels having complex shaped stiffeners develop up to 60 percent higher buckling strengths than panels with conventional shaped stiffeners. The superplastic forming/weld brazing process is successfully scaled up to fabricate full size panels having multiple stiffeners. The superplastic forming/weld brazing process is also successfully refined to show its potential for fabricating multiple stiffener compression panels employing unique stiffener configurations for improved structural efficiency. Author

N86-11246*# Massachusetts Inst. of Tech., Cambridge.

FEASIBILITY OF REMOTELY MANIPULATED WELDING IN SPACE: A STEP IN THE DEVELOPMENT OF NOVEL JOINING TECHNOLOGIES c37

Koichi Masubuchi, John E. Agapakis, Andrew DeBiccari, and Christopher vonAlt *In* NASA. Langley Research Center Welding, Bonding and Fastening, 1984 Sep. 1985 p 271-296 refs (For primary document see N86-11227 02-23)

Avail: NTIS HC A21/MF A01 CSCL 13M

A six month research program entitled Feasibility of Remotely Manipulated Welding in Space - A Step in the Development of Novel Joining Technologies is performed at the Massachusetts Institute of Technology for the Office of Space Science and Applications, NASA, under Contract No. NASW-3740. The work is performed as a part of the Innovative Utilization of the Space Station Program. The final report from M.I.T. was issued in September 1983. This paper presents a summary of the work performed under this contract. The objective of this research program is to initiate research for the development of packaged, remotely controlled welding systems for space construction and repair. The research effort includes the following tasks: (1) identification of probable joining tasks in space; (2) identification of required levels of automation in space welding tasks; (3) development of novel space welding concepts; (4) development of recommended future studies; and (5) preparation of the final report. Author

N86-11247*# Douglas Aircraft Co., Inc., Long Beach, Calif.

ADVANCES IN JOINING TECHNIQUES USED IN DEVELOPMENT OF SPF/DB TITANIUM SANDWICH REINFORCED WITH METAL MATRICES c37

J. E. Fischler *In* NASA. Langley Research Center Welding, Bonding and Fastening, 1984 Sep. 1985 p 297-322 (For primary document see N86-11227 02-23)

Avail: NTIS HC A21/MF A01 CSCL 13M

Three and four-sheet expanded titanium sandwich sheets have been developed at Douglas Aircraft Company, a division of McDonnell Douglas Corporation, under contract to NASA Langley Research Center. In these contracts, spot welding and roll seam welding are used to join the core sheets. These core sheets are expanded to the face sheets and diffusion bonded to form various type cells. The advantages of various cell shapes and the design parameters for optimizing the wing and fuselage concepts are discussed versus the complexity of the spot weld pattern. In addition, metal matrix composites of fibers in an aluminum matrix encapsulated in a titanium sheath are aluminum brazed successfully to the titanium sandwich face sheets. The strength and crack growth rate of the superplastic-formed/diffusion bonded (SPF/DB) titanium sandwich with and without the metal matrix composites are described. Author

N86-11248*# Texas Instruments, Inc., Attleboro, Mass.

COMPARISON OF BOND IN ROLL-BONDED AND ADHESIVELY BONDED ALUMINUMS c38

R. J. Schwensfeir, Jr., G. Trenkler, R. G. Delagi, and J. A. Forster *In* NASA. Langley Research Center Welding, Bonding and Fastening, 1984 Sep. 1985 p 323-338 refs (For primary document see N86-11227 02-23)

Avail: NTIS HC A21/MF A01 CSCL 14D

Lap-shear and peel test measurements of bond strength have been carried out as part of an investigation of roll bonding of 2024 and 7075 aluminum alloys. Shear strengths of the bonded material in the F temper are in the range of 14 to 16 ksi. Corresponding peel strengths are 120 to 130 lb/inch. These values, which are three to five times those reported in the literature for adhesively bonded 2024 and 7075, are a result of the true metallurgical bond achieved. The effects of heat-treating the bonded material are described and the improvements in bond strength discussed relative to the shear strength of the parent material. The significance of the findings for aerospace applications is discussed. Author

N86-11249*# Lockheed-Georgia Co., Marietta.

ADHESIVES FOR AEROSPACE c27

L. E. Meade *In* NASA. Langley Research Center Welding, Bonding and Fastening, 1984 Sep. 1985 p 339-349 refs (For primary document see N86-11227 02-23)

Avail: NTIS HC A21/MF A01 CSCL 11A

The industry is hereby challenged to integrate adhesive technology with the total structure requirements in light of today's drive into automation/mechanization. The state of the art of adhesive technology is fairly well meeting the needs of the structural designers, the processing engineer, and the inspector, each on an individual basis. The total integration of these needs into the factory of the future is the next collective hurdle to be achieved. Improved processing parameters to fit the needs of automation/mechanization will necessitate some changes in the adhesive forms, formulations, and chemistries. Adhesives have, for the most part, kept up with the needs of the aerospace industry, normally leading the rest of the industry in developments. The wants of the aerospace industry still present a challenge to encompass all elements, achieving a totally integrated joined and sealed structural system. Better toughness with hot-wet strength improvements is desired. Lower cure temperatures, longer out times, and improved corrosion inhibition are desired. Author

N86-11250*# Boeing Aerospace Co., Seattle, Wash.

HIGH-TEMPERATURE ADHESIVE DEVELOPMENT AND EVALUATION c27

Carl L. Hendricks and Jeremy N. Hale *In* NASA. Langley Research

Center Welding, Bonding and Fastening, 1984 Sep. 1985 p 351-370 refs (For primary document see N86-11227 02-23)
Avail: NTIS HC A21/MF A01 CSCL 11A

High-temperature adhesive systems are evaluated for short and long-term stability at temperatures ranging from 232C to 427C. The resins selected for characterization include: NASA Langley developed polyphenylquinoxaline (PPQ), and commercially available polyimides (PI). The primary method of bond testing is single lap shear. The PPQ candidates are evaluated on 6Al-4V titanium adherends with chromic acid anodize and phosphate fluoride etch surface preparations. The remaining adhesives are evaluated on 15-5 PH stainless steel with a sulfuric acid anodize surface preparation. Preliminary data indicate that the PPQ adhesives tested have stability to 3000 hours at 450F with chromic acid anodize surface preparation. Additional studies are continuing to attempt to improve the PPQ's high-performance by formulating adhesive films with a boron filler and utilizing the phosphate fluoride surface preparation on titanium. Evaluation of the polyimide candidates on stainless-steel adherends indicates that the FM-35 (American Cyanamid), PMR-15 (U.S. Polymeric/Ferro), TRW partially fluorinated polyimide and NR 150B2S6X (DuPont) adhesives show sufficient promise to justify additional testing. Author

N86-11251*# Martin Marietta Corp., Baltimore, Md.
USE OF HYDRATION INHIBITORS TO IMPROVE BOND DURABILITY OF ALUMINUM ADHESIVE JOINTS c27
G. D. Davis, J. S. Ahearn, L. J. Matienzo, and J. D. Venables *In* NASA. Langley Research Center Welding, Bonding and Fastening, 1984 Sep. 1985 p 371-396 refs Previously announced in IAA as A85-29979 (For primary document see N86-11227 02-23)
(Contract N00014-80-C-0718)
Avail: NTIS HC A21/MF A01 CSCL 11A

An investigation is conducted of the mechanisms by which nitrilotris methylene phosphonic acid (NTMP) and related compounds are adsorbed onto oxidized aluminum surfaces to inhibit hydration and increase the durability of adhesive bonds formed with inhibitor-treated panels. P - O - Al bonds are identified as the basis of adsorption, and it is found that water initially adsorbed onto the etched aluminum surfaces is displaced by the NTMP. The hydration of the NTMP-treated surfaces occurs in three stages, namely the reversible physisorption of water, the slow dissolution of NTMP followed by rapid hydration of the freshly exposed Al2O3 to AlOOH and further hydration of the surface to Al(OH)3. Five properties of an ideal inhibitor are identified. Author

N86-11252*# United Technologies Research Center, East Hartford, Conn.
FACTORS AFFECTING THE PROCESSING OF EPOXY FILM ADHESIVES c27
R. A. Pike *In* NASA. Langley Research Center Welding, Bonding and Fastening, 1984 Sep. 1985 p 397-418 refs (For primary document see N86-11227 02-23)
Avail: NTIS HC A21/MF A01 CSCL 11A

The increasing awareness that adhesive performance is controlled not only by the condition of the adherend surface but also the condition or state of the adhesive and the process parameters used during fabrication is expected to result in improved reliability, as well as bond performance. The critical process variables which have been found to control adhesive bond formation and ultimate bond strength in 250F and 350F curing epoxy adhesives are described in terms of fabrication parameters and adhesive characteristics. These include the heat-up rate and cure temperature during processing and the adhesive moisture content and age condition (degree of advancement). The diagnostic methods used to delineate the effects of these process variables on adhesive performance are illustrated. These are dielectric, thermomechanical (TMA) and dynamic mechanical (DMA) analyses. Correlation of test results with measured mechanical tensile lap shear strengths of bonded joints is presented and the results briefly discussed in terms of the additives and hardeners used in the adhesive systems. Author

N86-11253*# National Aeronautics and Space Administration. Langley Research Center, Hampton, Va.
RAPID ADHESIVE BONDING AND FIELD REPAIR OF AEROSPACE MATERIALS c31
Bland A. Stein *In its* Welding, Bonding and Fastening, 1984 Sep. 1985 p 419-438 ref (For primary document see N86-11227 02-23)
Avail: NTIS HC A21/MF A01 CSCL 13H

Adhesive bonding in the aerospace industry typically utilizes autoclaves or presses which have considerable thermal mass. As a consequence, the rates of heatup and cooldown of the bonded parts are limited and the total time and cost of the bonding process are often relatively high. Many of the adhesives themselves do not inherently require long processing times. Bonding could be performed rapidly if the heat was concentrated in the bond lines or at least in the adherends. Rapid Adhesive Bonding concepts are developed to utilize induction heating techniques to provide heat directly to the bond line and/or adherends without heating the entire structure, supports, and fixtures of a bonding assembly. Bonding times for specimens can be cut by a factor of 10 to 100 compared to standard press or autoclave bonding. The development of Rapid Adhesive Bonding for lap shear specimens (per ASTM D1002 and D3163), for aerospace panel or component bonding, and for field repair needs of metallic and advanced fiber reinforced polymeric-matrix composite structures is reviewed. Equipment and procedures are described for bonding and repairing thin sheets, simple geometries, and honeycomb core panels. Author

N86-11254*# Naval Surface Weapons Center, White Oak, Md.
REDUCTION OF MOISTURE EFFECTS DURING THE CURE OF EPOXY ADHESIVES USED IN COMPOSITE REPAIR c27
Joseph M. Augl and George T. Sivy *In* NASA. Langley Research Center Welding, Bonding and Fastening, 1984 Sep. 1985 p 439-463 ref (For primary document see N86-11227 02-23)
Avail: NTIS HC A21/MF A01 CSCL 11A

The requirements for repair work on Naval aircraft composite wing skins that can be performed under depot conditions (or still worse, under field conditions) are quite restrictive. Equipment that can be used is rather limited as are the available repair space and time. The procedures must be simple enough so that they can be performed satisfactorily by personnel without special knowledge in composite materials technology. Repairs of small holes should not require more than perhaps a short predrying cycle (with heat guns) and a subsequent patch bonding using a heating blanket, held in place by applying a vacuum. However, it has been observed during simulated experimental repair work that the glue lines frequently show a high content of pores and bubbles which are attributed to evaporation of moisture during the curing cycle. (Of course, other volatile materials such as residual solvent would act similarly). The purpose of this paper is to give some detailed analysis of the problem of moisture transport as a function of repair conditions, and to discuss some preliminary work to reduce the effect of moisture by removing moisture chemically with carbodiimides before it reaches a critical level for bubble formations. Author

N86-11255*# National Aeronautics and Space Administration. Langley Research Center, Hampton, Va.
INITIAL INVESTIGATION OF CRYOGENIC WIND TUNNEL MODEL FILLER MATERIALS c24
George C. Firth *In its* Welding, Bonding and Fastening, 1984 Sep. 1985 p 465-481 refs (For primary document see N86-11227 02-23)
Avail: NTIS HC A21/MF A01 CSCL 11D

Filler materials are used for surface flaws, instrumentation grooves, and fastener holes in wind tunnel models. More stringent surface quality requirements and the more demanding test environment encountered by cryogenic wind tunnels eliminate filler materials such as polyester resins, plaster, and waxes used on conventional wind tunnel models. To provide a material data base for cryogenic models, various filler materials are investigated. Surface quality requirements and test temperature extremes require matching of coefficients of thermal expansion or interfacing materials. Microstrain versus temperature curves are generated for several candidate filler materials for comparison with cryogenically acceptable materials. Matches have been achieved for aluminum alloys and austenitic steels. Simulated model surfaces are filled with candidate filler materials to determine finishing characteristics, adhesion and stability when subjected to cryogenic cycling. Filler material systems are identified which meet requirements for usage with aluminum model components. Author

N86-11256# Oak Ridge National Lab., Tenn.
DETERMINATION OF THE STEADY-STATE BEHAVIOR OF IMMOBILIZED (BETA)-GALACTOSIDASE UTILIZING AN INTEGRAL REACTOR SCHEME
T. C. Scott, C. G. Hill, Jr., and C. H. Amundson 1985 32 p refs
Presented at the Symp. on Biotechnol. for Fuels and Chem., Gatlinburg, Tenn., 13 May 1985 Prepared in cooperation with Wisconsin Univ., Madison
(Contract DE-AC05-84OR-21400)
(DE85-012900; CONF-850513-1) Avail: NTIS HC A03/MF A01

Analysis of the steady-state behavior of immobilized (BETA)-galactosidase by integral reactor techniques has yielded a model which allows one to predict reactor performance under normal operating conditions. Values of the mechanistic rate constants for enzymatic hydrolysis of lactose were determined as a function of temperature by fitting the reactor model to experimental lactose conversion profiles. Use of this model along with the activity decay characteristics of the immobilized enzyme which have been presented in a previous publication could prove to be a useful tool in determining appropriate operating strategies for industrial applications of the immobilized enzyme catalyst. DOE

N86-11257# Cornell Univ., Ithaca, N.Y. Dept. of Plant Pathology.
IMPORTANCE OF PHYTOALEXIN TOLERANCE AND DETOXIFICATION FOR PATHOGENICITY Progress Report, Jun. 1983 - Jun. 1985
H. VanEtten and D. Matthews 1985 8 p refs
(Contract DE-AC02-83ER-13073)
(DE85-014759; DOE/ER-13073/T2) Avail: NTIS HC A02/MF A01

This study focuses on the biochemistry of phytoalexin detoxifying enzymes. Progress is reported on purification, substrate specificity, and the mechanism of several enzymes involved. Some aspects of the regulation of pisatin demethylase are studied since parallel genetic studies suggest its regulation is an important factor in the pathogenicity of Nectria haematococca. It is established that the detoxification of pisatin requires two components: NADPH-cytochrome c reductase and cytochrome P-450. The ability to separate and reconstitute these two components has allowed us to demonstrate that the reductase from a non-demethylating isolate of N. haematococca will support demethylating activity when combined with the cytochrome P-450 from a demethylating isolate. The finding that the critical genetic factor here is the cytochrome P-450 fraction reinforces the hypothesis that the multiple pda genes of this fungus encode different cytochrome P-450 isozymes. The evidence for monooxygenase catalyzed metabolism of maackiain suggests the existence of additional members of a phytoalexin detoxifying cytochrome P-450 family. DOE

N86-11272*# Boeing Aerospace Co., Seattle, Wash.
CHARACTERIZATION METHODOLOGY FOR PMR-15
A. B. Hunter *In* NASA. Lewis Research Center High Temp. Polymer Matrix Composites Sep. 1985 p 151-156 (For primary document see N86-11260 02-24)
(Contract NAS3-22523)
Avail: NTIS HC A18/MF A01 CSCL 07A

24 COMPOSITE MATERIALS

Includes laminates.

N86-11258 Michigan Univ., Ann Arbor.
A SIGNORINI MODEL OF BOLT FASTENED LAMINATED COMPOSITES Ph.D. Thesis
Ernest Ekeneme Nweke 1985 165 p
Avail: Univ. Microfilms Order No. DA8512479

A contact problem formulation of a failure strength predicting model of bolt fastened fiber reinforced laminated composites is presented. This model can handle any number of holes, it allows for gaps and friction on the pin-laminate interface. The contact stresses are also generated by this model. The model can also determine the slip/stick region as well as the slip that occurs of each node. It also gives a more realistic treatment of multiple hole cases without making apriori assumptions about the stress distribution on each pin. The procedure is as follows: first the stress distribution in the laminate is determined using an incremental signorini problem formulation; secondly a failure criterion (due to Yamada-Sun) is applied on a characteristics curve (due to Chang). A finite element computer code (COMRAD) was developed to implement the procedure and calculate the failure load and mode for the laminate. The results from this model were compared to experimental and theoretical results, and was found to do better in load prediction. Dissert. Abstr.

N86-11259 Illinois Univ., Urbana-Champaign.
TENSILE FATIGUE DAMAGE AND DEGRADATION OF RANDOM SHORT-FIBER SWC COMPOSITE
Edwin Siu-Man Chim 1985 169 p
Avail: Univ. Microfilms Order No. DA8511596

In the study of homogeneous damage, experiments were conducted to examine fundamental mechanisms and characteristics of fatigue damage and its evolution. The statistical nature of microcracks was evaluated by the introduction of damage distribution functions. Results showed that the cumulative distribution and density of microcrack length followed the form of a three-parameter Weibull function. In the nonhomogeneous damage study, residual tensile strength and fracture toughness were determined experimentally. Both of these quantities were found to decrease gradually with fatigue cycles. The results also revealed that the notch still dominated the fracture behavior in the damaged composite and that fracture mechanics concepts and analysis were applicable. A distributed damage model and a ligament model to study the mechanics of fatigue crack growth were examined. The distributed damage model which contains several salient features unique to the SMC-R50 composite is too complicated for analysis while the ligament model leads to results which fit the experimental data well, but the mechanics associated with the model is questionable. Dissert. Abstr.

N86-11260*# National Aeronautics and Space Administration. Lewis Research Center, Cleveland, Ohio.
HIGH TEMPERATURE POLYMER MATRIX COMPOSITES
Washington Sep. 1985 409 p refs Conf. held in Cleveland, Ohio, 16-18 Mar. 1983
(NASA-CP-2385; E-2425; NAS 1.55:2385) Avail: NTIS HC A18/MF A01 CSCL 11D

These are the proceedings of the High Temperature Polymer Matrix Composites Conference held at the NASA Lewis Research Center on March 16 to 18, 1983. The purpose of the conference is to provide scientists and engineers working in the field of high temperature polymer matrix composites an opportunity to review, exchange, and assess the latest developments in this rapidly expanding area of materials technology. Technical papers are presented in the following areas: (1) matrix development; (2) adhesive development; (3) characterization; (4) environmental effects; and (5) applications. For individual titles, see N86-11261 through N86-11291.

N86-11261*# Air Force Wright Aeronautical Labs., Wright-Patterson AFB, Ohio. Materials Lab.
ACETYLENE TERMINATED MATRIX RESINS
I. J. Goldfarb, Y. C. Lee, F. E. Arnold, and T. E. Helminiak *In* NASA. Lewis Research Center High Temp. Polymer Matrix

Composites Sep. 1985 p 1-9 refs (For primary document see N86-11260 02-24)
Avail: NTIS HC A18/MF A01 CSCL 11D

The synthesis of resins with terminal acetylene groups has provided a promising technology to yield high performance structural materials. Because these resins cure through an addition reaction, no volatile by-products are produced during the processing. The cured products have high thermal stability and good properties retention after exposure to humidity. Resins with a wide variety of different chemical structures between the terminal acetylene groups are synthesized and their mechanical properties studied. The ability of the acetylene cured polymers to give good mechanical properties is demonstrated by the resins with quinoxaline structures. Processibility of these resins can be manipulated by varying the chain length between the acetylene groups or by blending in different amounts of reactive deluents. Processing conditions similar to the state-of-the-art epoxy can be attained by using backbone structures like ether-sulfone or bis-phenol-A. The wide range of mechanical properties and processing conditions attainable by this class of resins should allow them to be used in a wide variety of applications. Author

N86-11262*# Hughes Aircraft Co., Culver City, Calif. Technology Support Div.

AN IMPROVED PROCESSIBLE ACETYLENE-TERMINATED POLYIMIDE FOR COMPOSITES

Abraham L. Landis and Arthur B. Naselow *In* NASA. Lewis Research Center High Temp. Polymer Matrix Composites Sep. 1985 p 11-22 refs (For primary document see N86-11260 02-24)
Avail: NTIS HC A18/MF A01 CSCL 11D

The newest member of a family of thermosetting acetylene-substituted polyimide oligomers is HR600P. This oligomer is the isoimide version of the oligomer known as HR600P and Thermid 600. Although both types of material yield the same heat resistant end products after cure, HR600P has much superior processing characteristics. This attributed to its lower melting temperature (160 + or - 10 C, 320 + or - 20 F) in contrast to 202 C (396 F) for Thermid MC-600, its longer gel time at its processing temperature (16 to 30 minutes bvs 3 minutes), and its excellent solubility in low boiling solvents such as tetrahydrofuran, glymes, or 4:1 methyl ethyl ketone/toluene mixtures. These advantages provide more acceptable coating and impregnation procedures, allow for more complete removal at lower temperatures, provide a longer pot life or working time, and allow composite structure fabrication in conventional autoclaves used for epoxy composite curing. The excellent processing characteristics of HR600P allow its use in large area laminated structures, structural composites, and molding compositions. Author

N86-11263*# National Aeronautics and Space Administration. Lewis Research Center, Cleveland, Ohio.

PMR POLYIMIDES FROM SOLUTIONS CONTAINING MIXED ENDCAPS c27

Peter Delvigs *In its* High Temp. Polymer Matrix Composites Sep. 1985 p 23-34 refs (For primary document see N86-11260 02-24)
Avail: NTIS HC A18/MF A01 CSCL 11B

Previous studies have shown that partial substitution of p-aminostyrene (PAS) for the monomethylester of endo-5-norbornene-2, 3-dicarboxylic acid (NE) lowered the cure temperature of PMR polyimides from 316 to 260 C, but the modified PMR polyimides required higher compression-molding pressures than state-of-the-art PMR-15. In this study PMR polyimides are prepared employing three encaps: NE, PAS, and endo-N-phenyl-5-norbornene-2,3-dicarboximide (PN). The effect of PN addition on the processing characteristics and glass transition temperatures of graphite fiber-reinforced PMR composites is studied. The room temperature and short-time 316 C mechanical properties of the composites are determined. The weight loss and mechanical property retention characteristics of the composites after exposure in air at 316 C are also determined. Author

N86-11264*# National Aeronautics and Space Administration. Langley Research Center, Hampton, Va.

MATRIX RESIN DEVELOPMENT AT NASA LANGLEY RESEARCH CENTER

Terry L. St.Clair *In* NASA. Lewis Research Center High Temp. Polymer Matrix Composites Sep. 1985 p 35-53 refs (For primary document see N86-11260 02-24)
Avail: NTIS HC A18/MF A01 CSCL 11D

The polymer program at NASA Langley Research Center involves exploratory studies in polymer science. These include the synthesis of novel polymers and their characterization. Polymer synthesis programs involve the development of novel thermoplastics, pseudothermoplastics, and thermosets. Recent investigations have led to the development of more easily processable polyimides, solvent-resistant polysulfones and polyphenylquinoxalines, and tougher high and intermediate-temperature polymers. Characterization efforts have included high-pressure liquid chromatography methodology, the development of toughness tests for fiber-reinforced composites, a study of electrical properties of metal-ion-filled polyimides, and a study of the mutagenicity of aromatic diamines. Also the mechanism of cure/degradation of experimental polymers has been studied by rheology, mechanical behavior, separation techniques and spectroscopy. Some of these programs have involved the degradation crosslinking of alkyl-containing polyimides, the separation and identification of crosslinked phenylquinoxalines, the rheological behavior of hot-melt polyimides, and the elucidation of the cure of norbornene endcapped imides. Author

N86-11265*# National Aeronautics and Space Administration. Ames Research Center, Moffett Field, Calif.

BISMALEIMIDES AND RELATED MALEIMIDO POLYMERS AS MATRIX RESINS c27

John A. Parker, Demitrius A. Kourtides, and George M. Fohlen *In* NASA. Lewis Research Center High Temp. Polymer Matrix Composites Sep. 1985 p 55-77 refs (For primary document see N86-11260 02-24)
Avail: NTIS HC A18/MF A01 CSCL 11B

Significant processing and property improvements can be achieved by copolymerization of state-of-the-art bisimides with various vinyl stilbazole derivatives to give both fire resistance and high-temperature properties from hot-melt compositions. Significant improvement in mechanical properties is achieved through these modifications, which may make these new matrix resins ideal candidates for fireworthy secondary graphite composite structures. Phosphorous modifications of maleimido polymers through phosphonate structure and tricyclophosphazene derivatives provide families of new matrix resins for short-time applications in severe thermo-oxidative environments. With further research these may provide matrix resins for long-term thermo-oxidative stability of advanced composites at temperatures up to 400 to 500 C. Author

N86-11266*# Case Western Reserve Univ., Cleveland, Ohio. Dept. of Chemistry.

THE SYNTHESIS, CHARACTERIZATION AND THERMAL CHEMISTRY OF MODIFIED NORBORNENYL PMR ENDCAPS c27

Chaim N. Sukenik, William M. Ritchey, Vinay Malhotra, and Uday Varde *In* NASA. Lewis Research Center High Temp. Polymer Matrix Composites Sep. 1985 p 79-90 refs (For primary document see N86-11260 02-24)
(Grant NAG3-163)
Avail: NTIS HC A18/MF A01 CSCL 11B

As part of a program to further the understanding of the polymerization of Nadic-Endcapped PMR systems, a series of model Norbornenyl-Imides has been synthesized and their thermal behavior explored. Their syntheses and characterizations as well as their rearrangement and polymerization chemistry are described. Monomer isomerization at temperatures as low as 125 C and oligomer formation at somewhat higher temperatures are observed. Approximate relative rates for competing isomerization pathways are established and some information is obtained about the details of oligomer formation. The relationship of this data to current PMR systems is briefly discussed. Author

N86-11267*# National Aeronautics and Space Administration. Lewis Research Center, Cleveland, Ohio.
ALL-AROMATIC BIPHENYLENE END-CAPPED POLYQUINOLINE AND POLYIMIDE MATRIX RESINS c27
John P. Droske (Colorado State Univ.), John K. Stille (Colorado State Univ.), and William B. Alston *In its* High Temp. Polymer Matrix Composites Sep. 1985 p 91-95 refs (For primary document see N86-11260 02-24)
Avail: NTIS HC A18/MF A01 CSCL 11B

Biphenylene end-capped polyquinoline and polyimide resins afford low void content graphite-reinforced composites with good initial properties. However, with both resins, rapid degradation occurs during oxidative isothermal aging at elevated temperatures. The degradation is not observed during isothermal aging under a nitrogen atmosphere which suggests that the biphenylene end-cap (or the resulting crosslink/chain extension structures) is not particularly thermooxidatively stable. The nature of the thermooxidative instability is currently under investigation. Author

N86-11268*# Boeing Aerospace Co., Seattle, Wash.
EVALUATION OF A HIGH TEMPERATURE ADHESIVE FOR FABRICATING GRAPHITE/PMR-15 POLYIMIDE STRUCTURES c27
S. G. Hill and J. B. Cushman *In* NASA. Lewis Research Center High Temp. Polymer Matrix Composites Sep. 1985 p 97-108 refs (For primary document see N86-11260 02-24)
Avail: NTIS HC A18/MF A01 CSCL 11A

Tests are conducted to measure shear strength, shear modulus and flatwise tensile strength of the A7F (amide-imide modified LARC-13) adhesive system. An investigation is also conducted to determine the effect of geometric material parameters, and elevated temperature on the static strength of standard joints. Single-lap and double-lap composite joints, and single, double and step lap composite to metal joints are characterized. A series of advanced joints consisting of preformed adherends, adherends with scalloped edges and joints with hybrid interface plies are tested and compared to baseline single and double-lap designs. Author

N86-11269*# Dexter Corp., Pittsburg, Calif. Hyson Div.
NEW PROCESSABLE MODIFIED POLYIMIDE RESINS FOR ADHESIVE AND MATRIX APPLICATIONS c27
David Landman *In* NASA. Lewis Research Center High Temp. Polymer Matrix Composites Sep. 1985 p 109-123 refs (For primary document see N86-11260 02-24)
Avail: NTIS HC A18/MF A01 CSCL 11B

A broad product line of bismaleimide modified epoxy adhesives which are cured by conventional addition curing methods is described. These products fill a market need for 232 C (450 F) service adhesives which are cured in a manner similar to conventional 177 C (350 F) epoxy adhesives. The products described include film adhesives, pastes, and a primer. Subsequent development work has resulted in a new bismaleimide modified epoxy resin which uses a unique addition curing mechanism. This has resulted in products with improved thermomechanical properties compared to conventional bismaleimide epoxy resins. A film adhesive, paste, and matrix resin for composites using this new technology are described. In all cases, the products developed are heat cured by using typical epoxy cure cycles i.e., 1 hour at 177 C (350 F) followed by 2 hours postcure at 246 C (475 F). Author

N86-11270*# American Cyanamid Co., Stamford, Conn. Chemical Research Div.
RECENT DEVELOPMENTS IN POLYIMIDE AND BISMALEIMIDE ADHESIVES c27
Robert E. Politi *In* NASA. Lewis Research Center High Temp. Polymer Matrix Composites Sep. 1985 p 125-136 (For primary document see N86-11260 02-24)
Avail: NTIS HC A18/MF A01 CSCL 11B

Research on high temperature resin systems has intensified. In the Aerospace Industry, the motivation for this increased activity has been to replace heat resistant alloys of aluminum, stainless steel and titanium by lighter weight glass and carbon fiber reinforced composites. Applications for these structures include: (1) engine nacelles involving long time exposure (thousands of hours) to temperatures in the 150 to 300 C range, (2) supersonic military aircraft involving moderately long exposure (hundreds of hours) to temperatures of 150 to 200 C, and (3) missile applications involving only brief exposure (seconds or minutes) to temperatures up to 500 C and above. Because of fatigue considerations, whenever possible, it is preferable to bond rather than mechanically fasten composite structures. For this reason, the increased usage of high temperature resin matrix systems for composites has necessitated the devlopment of compatible and equally heat stable adhesive systems. The performance of high temperature epoxy, epoxy phenolic and condensation polyimide adhesives is reviewed. This is followed by a discussion of three recently developed types of adhesives: (1) condensation reaction polyimides having improved processing characteristics; (2) addition reaction polyimides; and (3) bismaleimides. Author

N86-11271*# National Aeronautics and Space Administration. Lewis Research Center, Cleveland, Ohio.
CHEMICAL CONTROL OF RATE AND ONSET TEMPERATURE OF NADIMIDE POLYMERIZATION c27
Richard W. Lauver *In its* High Temp. Polymer Matrix Composites Sep. 1985 p 137-149 refs (For primary document see N86-11260 02-24)
Avail: NTIS HC A18/MF A01 CSCL 11B

The chemistry of norbornenyl capped imide compounds (nadimides) is briefly reviewed with emphasis on the contribution of Diels-Alder reversion in controlling the rate and onset of the thermal polymerization reaction. Control of onset temperature of the cure exotherm by adjusting the concentration of maleimide is demonstrated using selected model compounds. The effects of nitrophenyl compounds as free radical retarders on nadimide reactivity are discussed. A simple copolymerization model is proposed for the overall nadimide cure reaction. An approximate numerical analysis is carried out to demonstrate the ability of the model to simulate the trends observed for both maleimide and nitrophenyl additions. Author

N86-11272*# Boeing Aerospace Co., Seattle, Wash.
CHARACTERIZATION METHODOLOGY FOR PMR-15 c23
A. B. Hunter *In* NASA. Lewis Research Center High Temp. Polymer Matrix Composites Sep. 1985 p 151-156 (For primary document see N86-11260 02-24)
(Contract NAS3-22523)
Avail: NTIS HC A18/MF A01 CSCL 07A

Characterization of model compounds, monomers, resin solutions and cure cycles of PMR-15 polyimide are performed. Successful separation of various reaction products is also accomplished by liquid chromatography. The PMR-15 cure analysis is performed by fourier transform spectroscopy and gas chromatograph - mass spectrometry. Characterization receiving inspection tests for Quality Control are recommended. Author

N86-11273*# Lockheed Missiles and Space Co., Sunnyvale, Calif.
CHARACTERIZATION OF POLYIMIDE MATRIX RESINS AND PREPREGS
M. G. Maximovich and R. M. Galeos *In* NASA. Lewis Research Center High Temp. Polymer Matrix Composites Sep. 1985 p 157-170 refs (For primary document see N86-11260 02-24)
Avail: NTIS HC A18/MF A01 CSCL 11D

Graphite/polyimide composite materials are attractive candidates for a wide range of aerospace applications. They have many of the virtues of graphite/epoxies, i.e., high specific strengths and stiffness, and also outstanding thermal/oxidative stability. Yet they are not widely used in the aerospace industry due to problems of procesability. By their nature, modern addition polyimide (PI) resins and prepregs are more complex than epoxies; the key to processing lies in characterizing and understanding the materials. Chemical and rheological characterizations are carried out on several addition polyimide resins and graphite reinforced prepregs, including those based on PMR-15, LARC 160 (AP 22), LARC 160 (Curithane 103) and V378A. The use of a high range torque transducer with a

Rheometrics mechanical spectrometer allows rheological data to be generated on prepreg materials as well as neat resins. The use of prepreg samples instead of neat resins eliminates the need for preimidization of the samples and the data correlates well with processing behavior found in the shop. Rheological characterization of the resins and prepregs finds significant differences not readily detected by conventional chemical characterization techniques. Author

N86-11274*# Rockwell International Science Center, Thousand Oaks, Calif.

QUALITY ASSURANCE PROCEDURES FOR V378A MATRIX RESIN

Charles L. Hamermesh and Paul J. Dynes *In* NASA. Lewis Research Center High Temp. Polymer Matrix Composites Sep. 1985 p 171-185 refs Sponsored by AFWAL (For primary document see N86-11260 02-24)

Avail: NTIS HC A18/MF A01 CSCL 11D

A characterization methodology has been developed on which to base quality assurance procedures for U.S. Polymeric V378A bismaleimide matrix resin. Chemical composition is established by partition reverse phase and size exclusion liquid chromatography. Cure rheology behavior is quantitatively characterized by dynamic viscoelastic analysis using the parallel plate technique. The overall cure process is characterized by differential scanning calorimetry. The sensitivity of the procedures is evaluated by studying the effects of ambient out time on the chemical and behaviorial properties of the resin. Author

N86-11275*# National Aeronautics and Space Administration. Lewis Research Center, Cleveland, Ohio.

REPLACEMENT OF MDA WITH MORE OXIDATIVELY STABLE DIAMINES IN PMR-POLYIMIDES c27

William B. Alston *In its* High Temp. Polymer Matrix Composites Sep. 1985 p 187-205 refs (For primary document see N86-11260 02-24)

Avail: NTIS HC A18/MF A01 CSCL 11B

Studies are performed to investigate the effect of substituting 4,4'-oxydianiline and 1,1-bis(4-aminophenyl)-1-phenyl-2,2,2-trifluoroethane for the 4,4'-methylenedianiline in PMR polyimide matrix resin. Graphite fiber reinforced composites are fabricated from unsized Celion 6000 and PMR-polyimide matrix resins having formulated molecular weights in the range of 1500 to 2400. The composite processing characteristics are investigated and the initial room temperature and 316 C (600 F) composite mechanical properties are determined. Comparative 316 C composite weight losses and 316 C mechanical properties retention after prolonged 316 C air exposure are also determined. Author

N86-11276*# National Aeronautics and Space Administration. Lewis Research Center, Cleveland, Ohio.

PROPERTIES OF AUTOCLAVED Gr/PI COMPOSITES MADE FROM IMPROVED TACK PMR-15 PREPREG

Raymond D. Vannucci *In its* High Temp. Polymer Matrix Composites Sep. 1985 p 207-215 refs (For primary document see N86-11260 02-24)

Avail: NTIS HC A18/MF A01 CSCL 11D

Autoclave processing studies were conducted, using improved tack PMR-15 prepreg, to determine the effect of tack enhancing PMR resin modifications on composite processability and mechanical properties. Improved tack graphite fiber reinforced PMR-15 prepregs were prepared and exposed to ambient conditions for various times and then autoclave molded into composites. Composite specimens were prepared and tested for flexural and interlaminar shear strengths at room temperature and 316 C. The retention of flexural and interlaminar shear strength as a function of exposure in air at 316 C was also determined. The results show that the modified PMR resin solutions provide prepreg with improved tack and drape retention characteristics without adversely affecting processability or mechanical properties of autoclave molded graphite fiber reinforced PMR-15 composites. Author

N86-11277*# United Technologies Research Center, East Hartford, Conn.

THERMO-OXIDATIVE STABILITY OF GRAPHITE FIBER/PMR-15 POLYIMIDE COMPOSITES AT 350 DEG C

Daniel A. Scola *In* NASA. Lewis Research Center High Temp. Polymer Matrix Composites Sep. 1985 p 217-242 refs (For primary document see N86-11260 02-24)

Avail: NTIS HC A18/MF A01 CSCL 11D

A series of graphite fiber/PMR-15 polyimide composites were subjected to isothermal aging at 350 C in flowing air (100 cc/min and 1000 cc/min) over a 520 hr time period. The graphite fibers were analyzed by ISS/SIMS techniques before composite fabrication. Fibers exposed at the surface of the composite due to the isothermal aging process were also analyzed by the ISS/SIMS method. Component and composite weight less studies were also conducted for similarly exposed materials. Optical micrograph investigations of composites to follow the progress of the thermo-oxidative process were also conducted. Flexural and interlaminar shear strengths of the imaged and aged composites were measured. The relationship of component and composite properties as they relate to the thermo-oxidative behavior of the materials was discussed. Author

N86-11278*# National Aeronautics and Space Administration. Lewis Research Center, Cleveland, Ohio.

RHEOLOGICAL, PROCESSING, AND 371 DEG C MECHANICAL PROPERTIES OF CELION 6000/N-PHENYLNADIMIDE MODIFIED PMR COMPOSITES

Ruth H. Pater *In its* High Temp. Polymer Matrix Composites Sep. 1985 p 243-256 refs (For primary document see N86-11260 02-24)

Avail: NTIS HC A18/MF A01 CSCL 11D

The rheology, processing, and chemistry of newly developed N-phenylnadimide modified PMR (PMR-PN) polyimide resins are reviewed. The 371 C performance of their composites reinforced with Celion 6000 graphite fibers is also reviewed, along with the state of the art Celion 6000/PMR-15 composite. The effects of the 371 C exposure in air for up to 300 hr on the composite glass transition temperature, weight loss characteristics, and dimensional stability are presented. The changes in the composite 371 C interlaminar shear and flexural properties are also presented. In addition, composite interfacial degradation at a function of exposure time at 371 C was followed by scanning electron microscopy. The results suggest that the composite materials can be used at 371 C for at least 100 hr. Author

N86-11279*# Raytheon Co., Bedford, Mass. Missile Systems Div.

HIGH TEMPERATURE, SHORT TERM TENSILE STRENGTH OF C6000/PMR-15 COMPOSITES

P. R. DiGiovanni and D. Paterson *In* NASA. Lewis Research Center High Temp. Polymer Matrix Composites Sep. 1985 p 257-269 refs (For primary document see N86-11260 02-24)

Avail: NTIS HC A18/MF A01 CSCL 11D

Tensile tests were conducted on 0 unidirectionally reinforced Celion 6000 graphite fibers in PMR-15 polyimide matrix. Tensile strengths for coupons subjected to short and long term uniform temperatures were obtained. Thick coupons, heated on one side to produce significant transient through thickness temperature gradients, were tested and compared to the strength of specimens with uniform temperature distributions. All coupons were radiantly heated and reached maximum test temperatures within 15 sec. Tensile loads were applied to the coupons after 15 sec of elevated temperature exposure. Loading rates were selected so that specimen failures occurred within a maximum of 45 sec after reaching the test temperature. Results indicate that significant tensile strength remains beyond the material post cure temperature. Author

N86-11280*# TRW, Inc., Redondo Beach, Calif. Energy Development Group.

POLYIMIDE MATRIX RESINS FOR UP TO 700 DEG F SERVICE

R. J. Jones, G. E. Chang, S. H. Powell, and H. E. Green *In*

NASA. Lewis Research Center High Temp. Polymer Matrix Composites Sep. 1985 p 271-285 refs (For primary document see N86-11260 02-24)
Avail: NTIS HC A18/MF A01 CSCL 11D

TRW is in the process of data accumulation that strongly indicates that incorporation of the perfluorsisopropylidene linkage in molecular structures other than those employed in DU Pont's NR-150B polyimides likewise yield polymers demonstrating extremely high thermo-oxidative stability. Polyimide synthetic and characterization studies conducted to date on new polymers incorporating the perfluoroisopropylidene linkage are presented and discussed. G.L.C.

N86-11281*# National Aeronautics and Space Administration. Lewis Research Center, Cleveland, Ohio.
SURFACE PROTECTION OF GRAPHITE FABRIC/PMR-15 COMPOSITES SUBJECTED TO THERMAL OXIDATION
M. P. Hanson and T. T. Serafini *In its* High Temp. Polymer Matrix Composites Sep. 1985 p 287-297 refs (For primary document see N86-11260 02-24)
Avail: NTIS HC A18/MF A01 CSCL 11D

Graphite fabric/PMR-15 laminates develop matrix cracks during long-term exposure in air at temperatures in the range of 500 to 600 F. This study was performed to demonstrate the effectiveness of incorporating graphite mat surface plies as a means of reducing the developing of matrix cracks. Celion 3000 graphite fabric/PMR-15 laminates were fabricated with graphite or graphite mat/325-mesh boron powder surface plies. Laminates without mat surface plies were also fabricated for control purposes. Composite flexural strength, flexural modulus, and interlaminar shear strength were determined at 288 C before and after long-term exposure (up to 1500 hr) in air at 316 C. The results of this study showed that the incorporation of graphite mat surface plies reduces matrix cracking and improves the elevated temperature mechanical property retention characteristics of the composites. Author

N86-11282*# Naval Surface Weapons Center, White Oak, Md.
MICROSCOPIC EVALUATION OF A POLYIMIDE (PMR-15)-GRAPHITE COMPOSITE
Jeffry J. Fedderly and Joseph M. Augl *In* NASA. Lewis Research Center High Temp. Polymer Matrix Composites Sep. 1985 p 299-314 (For primary document see N86-11260 02-24)
Avail: NTIS HC A18/MF A01 CSCL 11D

An effort to evaluate the high temperature performance of a polyimide (PMR-15)-graphite composite which consists of several plies of woven strands of carbon fibers was undertaken. The longterm effect of high temperature on the dry material was studied by exposing polished test specimens of 473 F in a oven for nearly 400 hours. Periodically the specimens were removed and observed microscopically. Gradually surface cracks began to appear and the number of cracks increased over time. At the conclusion of the exposure the specimens were graudually ground down and observed in order to determine the depth of the cracks into the interior of the material. This procedure was repeated at an exposure temperature of 550 F. G.L.C.

N86-11283*# General Dynamics/Convair, San Diego, Calif.
EFFECTS OF REAL-TIME THERMAL AGING ON GRAPHITE/POLYIMIDE COMPOSITES
J. F. Haskins and J. R. Kerr *In* NASA. Lewis Research Center High Temp. Polymer Matrix Composites Sep. 1985 p 315-327 refs (For primary document see N86-11260 02-24)
(Contract NAS1-12308)
Avail: NTIS HC A18/MF A01 CSCL 11D

As part of a program to evaluate high-temperature advanced composites for use on supersonic cruise transport aircraft, two graphite/polyimide composites have been aged at elevated temperatures for times up to 5.7 years. Work on the first, HT-S/710 graphite/polyimide, was started in 1974. Evaluation of the second polyimide, Celion 6000/LARC-160, began in 1980. Baseline properties are presented, including unnotched and notched tensile data as a function of temperature, compression, flexure, shear, and constant-amplitude fatigue data at $R = 0.1$ and $R = -1$. Tensile specimens were aged in ovens where pressure and aging temperatures were controlled for various times up to and including 50,000 hours. Changes in tensile strength were determined and plotted as a function of aging time. The HT-S/710 composite aged at 450 F and 550 F if compared to the Celion 6000/LARC-160 composite aged at 350 F and 450 F. After tensile testing, many of the thermal aging specimens were examined using a scanning electron microscope. Results of these studies are presented, and changes in properties and degradation mechanisms during high-temperature aging are discussed and illustrated using metallographic techniques. Author

N86-11284*# Boeing Commercial Airplane Co., Seattle, Wash.
ENVIRONMENTAL STABILITY GRAPHITE/PMR-15 COMPOSITES
Clyde H. Sheppard and Doug McLaren *In* NASA. Lewis Research Center High Temp. Polymer Matrix Composites Sep. 1985 p 329-334 refs (For primary document see N86-11260 02-24)
Avail: NTIS HC A18/MF A01 CSCL 11D

During the past few years the Boeing Company was screening graphite composites for use in hot areas of engine nacelle structure. Structural and thermal analyses have shown that there is the potential for a 25 to 30 percent weight savings by using a graphite polyimide (Gr/PI) composite material in this type of structure. Work conducted on the NASA CASTS program (Composites for Advanced Space Transportation Systems) amply demonstrated the capability of Graphite/PMR-15 for short term service (125 hours) at temperatures up to 589 K (600 F). In addition, the CASTS program demonstrated that large structures could be fabricated using Gr/PMR-15. In commercial applications, however, the requirement exists for long term service capability (tens of thousands of hours) at temperatures ranging upwards from 449 K (350 F). The results of Graphite/PMR-15 materials characterization efforts conducted at Boeing are presented with emphasis on materials properties after isothermal aging at temperatures of 449 K (350 F) and above. Author

N86-11285*# Boeing Commercial Airplane Co., Seattle, Wash.
DEVELOPMENT OF DESIGN DATA FOR PROPULSION PMR-15 COMPOSITES
J. Postlewaite and Doug McLaren *In* NASA. Lewis Research Center High Temp. Polymer Matrix Composites Sep. 1985 p 335-338 (For primary document see N86-11260 02-24)
Avail: NTIS HC A18/MF A01 CSCL 11D

The continuing develoment of PMR-15 composite materials and their associated design properties is pacing the implementation of this technology on commercial aircraft. The guidelines that the FAA has issued regarding the certification of advanced composite structures are very significant with respect to future PMR-15 research and development activities. The FAA has issued an advisory circular dated 1-5-83 concerning guidelines for composite aircraft structures. Of particular significance to PMR-15 technology development is the reliance on combined environmental exposure and component testing, coupled with the stipulation that reliance on previous experience be limited to where common structures and materials have been used for a similar function. Critical environmental exposures for commercial propulsion structures include 50,000 cycle service life, exposure to skydrol, moisture and other fluids, and nacelle fire conditions. G.L.C.

N86-11286*# Grumman Aerospace Corp., Bethpage, N.Y.
POLYIMIDE COMPOSITES: APPLICATION HISTORIES
Leonard M. Poveromo *In* NASA. Lewis Research Center High Temp. Polymer Matrix Composites Sep. 1985 p 339-358 refs (For primary document see N86-11260 02-24)
Avail: NTIS HC A18/MF A01 CSCL 11D

Advanced composite hardware exposed to thermal environments above 127 C (260 F) must be fabricated from materials having resin matrices whose thermal/moisture resistance is superior to that of conventional epoxy-matrix systems. A family of polyimide resins has evolved in the last 10 years that exhibits the thermal-oxidative stability required for high-temperature technology applications. The weight and structural benefits for organic-matrix composites can now be extended by designers and materials engineers to include structures exposed to 316 F (600 F). Polyimide composite materials are now commercially available that can replace metallic or epoxy composite structures in a wide range of aerospace applications. Author

N86-11287*# HITCO, Gardena, Calif. Materials Div.
V-378A: A MODIFIED BISMALEIMIDE FOR ADVANCED COMPOSITES
S. W. Street *In* NASA. Lewis Research Center High Temp. Polymer Matrix Composites Sep. 1985 p 359-378 (For primary document see N86-11260 02-24)
Avail: NTIS HC A18/MF A01 CSCL 11D

Addition polyimides cure with no evolution of gaseous by-products at relatively low temperatures and may be cured at low pressures to yield composites with excellent hot-wet strength retention. These properaties have made them excellent candidates as matrix resins for advanced composites. However, commercially available bismaleimides are solids and difficult to handle in preimpregnated form. V-378A is an addition polyimide composed of a mixture of bismaleimides and other reactive ingredients formulated to provide good prepreg properties and handling, facile cure and excellent composite mechanical properties. Several curing mechanisms are utilized to provide the characteristics exhibited by V-378A. Part of the mechanism is free radial and takes place at ambient temperature and above. Other mechanisms are principally Diels-Alder in nature. V-378A prepregs are tacky at ambient temperature, but do not have long tacky outlife similar to some epoxies. V-378A yields composites which exhibit hot-wet strength retention which is superior to that provided by epoxy resin systems. G.L.C.

N86-11288*# Tribon Bearing Co., Cleveland, Ohio.
TRANSFER MOLDING OF PMR-15 POLYIMIDE RESIN c27
J. P. Reardon, D. W. Moyer, and B. E. Nowak *In* NASA. Lewis Research Center High Temp. Polymer Matrix Composites Sep. 1985 p 379-392 refs (For primary document see N86-11260 02-24)
Avail: NTIS HC A18/MF A01 CSCL 11B

Transfer molding is an economically viable method of producing small shapes of PMR-15 polyimide. It is shown that with regard to flexural, compressive, and tribological properties transfer-molded PMR-15 polyimide is essentially equivalent to PMR-15 polyimide produced by the more common method of compression molding. Minor variations in anisotropy are predictable effects of molding design and secondary finishing operations. Author

N86-11289*# Boeing Commercial Airplane Co., Seattle, Wash.
APPLICATION OF Gr/PMR-15 TO COMMERCIAL AIRCRAFT
J. Postlewaite, K. Porter, and Doug McLaren *In* NASA. Lewis Research Center High Temp. Polymer Matrix Composites Sep. 1985 p 393-400 (For primary document see N86-11260 02-24)
Avail: NTIS HC A18/MF A01 CSCL 11D

Following from early experience with polyimides on the SST program and Shuttle aft flap studies the Boeing Company is now working on collaborative programs with its principal nacelle suppliers to pursue the development of Gr/PMR-15 nacelle components. Two programs are currently in effect. The first program is directed specifically towards the flight test and service evaluation at the earliest possible date of a 747 nacelle core cowl structure. The second program seeks to firmly establish the producibility and cost of a 757 thrust reverser C duct in a production environment. The near term objectives of these programs include: (1) the comparison of estimated cost and weight of Gr/PMR-15 versus metal structure, (2) the engine test of representative composite structure, (3) the preliminary design and analysis of the C duct structure, and (4) the preparation of cost data and time schedules for the development and producibility program. In addition to powerplant structure, the propulsion ducting system has shown to be a strong candidate for Gr/PMR-15 application. Currently, the Boeing 747 Organization is evaluating the use of PMR-15 matrix composites to replace nearly 800 lbs of titanium ducting per airplane. Author

N86-11290*# General Electric Co., Cincinnati, Ohio. Aircraft Engine Business Group.
FABRICATION PROCESS OF A HIGH TEMPERATURE POLYMER MATRIX ENGINE DUCT
R. D. Pratt and A. J. Wilson *In* NASA. Lewis Research Center High Temp. Polymer Matrix Composites Sep. 1985 p 401-407 (For primary document see N86-11260 02-24)
Avail: NTIS HC A18/MF A01 CSCL 11D

The process that was used in the molding of an advanced composite outer by-pass duct planned for the F404 engine is discussed. This duct was developed as a potential replacement for the existing titanium duct in order to reduce both the weight and cost of the duct. The composite duct is now going into the manufacturing technology portion of the program. The duct is fabricated using graphite cloth impregnated with the PMR-15 matrix system. G.L.C.

N86-11291*# Pratt and Whitney Aircraft Group, West Palm Beach, Fla. Government Products Div.
CURRENT AND FUTURE ENGINE APPLICATIONS OF Gr/PI COMPOSITES
P. J. Cavano and T. E. Schmid *In* NASA. Lewis Research Center High Temp. Polymer Matrix Composites Sep. 1985 p 409-416 (For primary document see N86-11260 02-24)
Avail: NTIS HC A18/MF A01 CSCL 11D

The application of organic matrix composites to gas turbine engine components has been the subject of numerous government and company funded programs since the 1960's. The possibility of significant weight reductions, performance improvements and lower component costs have made the organic matrix composites extremely attractive to aircraft engine designers. Very little of this potential was incorporated into production engines over the years even though a significant number of components were designed, fabricated and tested. Some of the reasons behind the slow rate of incorporation include the following: (1) criticality; (2) engine operating temperature; (3) small component size; (4) small production volume; (5) high production cost; and (6) interfacing with metal parts. G.L.C.

N86-11292*# National Aeronautics and Space Administration. Langley Research Center, Hampton, Va.
A PROGRAM TO DETERMINE THE EFFECT OF LOW-VELOCITY IMPACTS ON THE STRENGTH OF THE FILAMENT-WOUND ROCKET MOTOR CASE FOR THE SPACE SHUTTLE
C. C. Poe, Jr., W. Illg, and D. P. Garber (PRC Kentron, Inc., Hampton, Va.) Sep. 1985 82 p refs
(NASA-TM-87588; NAS 1.15:87588) Avail: NTIS HC a05/MF A01 CSCL 11D

Graphite/epoxy filament-wound cases (FWC) are being developed for the solid rocket motors of the space shuttle. The FWC cases will be used on certain missions that require a structural mass less than that of the existing steel cases. The 12-foot-diameter FWC cases are wound with AS4W graphite fiber impregnated with an epoxy resin and are about 1.4 inches or more thick. Graphite-epoxy composite laminates, unlike metals, can be damaged relatively easily by low-velocity impacts of objects like dropped tools. The impact tests are conducted on a representative filament-wound laminate. The specimens are supported to simulate a fueled (stiff) and an empty (flexible) case. Impactors of various kinetic energy, mass, and shape are used. The conditions that give minimum visual evidence of damage are emphasized. The capability to characterize impact damage with various nondestructive evaluation (NDE) methods is also evaluated. After impact, the specimens are loaded uniaxially in tension to determine residual strengths. The residual strengths of impacted specimens are compared with fracture mechanics predictions based on a semi-elliptic surface cut of the same size as the impact damage. Author

N86-11293*# Rensselaer Polytechnic Inst., Troy, N. Y.
COMPOSITE STRUCTURAL MATERIALS Semiannual Progress Report, 30 Sep. 1984 - 30 Apr. 1985
Robert G. Loewy and Stephen E. Wiberley Aug. 1985 78 p refs Sponsored in cooperation with AFOSR

(Grant NGL-33-018-003)
(NASA-CR-176279; NAS 1.26:176279; SAPR-48) Avail: NTIS HC A05/MF A01 CSCL 11D

Various topics relating to composite structural materials for use in aircraft structures are discussed. The mechanical properties of high performance carbon fibers, carbon fiber-epoxy interface bonds, composite fractures, residual stress in high modulus and high strength carbon fibers, fatigue in composite materials, and the mechanical properties of polymeric matrix composite laminates are among the topics discussed. For individual titles, see N86-11294 through N86-11297.

N86-11294*# Rensselaer Polytechnic Inst., Troy, N. Y.
CONSTITUENT MATERIALS
In its Composite Struct. Mater. Aug. 1985 p 9-12 (For primary document see N86-11293 02-24)
Avail: NTIS HC A05/MF A01 CSCL 11D

This project is concerned with the study of polymer liquid crystals and oriented semicrystalline high-temperature thermoplastics in high modulus carbon fiber reinforced composites. Emphasis is being placed on the determination of the effects of polymer orientation at the fiber surfaces on composite fracture and mechanical properties. Author

N86-11295*# Rensselaer Polytechnic Inst., Troy, N. Y.
COMPOSITE MATERIALS
In its Composite Struct. Mater. Aug. 1985 p 13-25 (For primary document see N86-11293 02-24)
Avail: NTIS HC A05/MF A01 CSCL 11D

The deformation and failure behavior of graphite/epoxy tubes under biaxial (axial tension and torsion) loading is being investigated. The aim of this research is to increase basic understanding of and provide design information for the biaxial response of graphite/epoxy composites. Author

N86-11296*# Rensselaer Polytechnic Inst., Troy, N. Y.
GENERIC STRUCTURAL ELEMENTS
In its Composite Struct. Mater. Aug. 1985 p 27-37 (For primary document see N86-11293 02-24)
Avail: NTIS HC A05/MF A01 CSCL 11D

This research concentrated on improving beam theories as applicable to composite structures. Confirmation is sought for analytical predictions using a new beam theory based on the assumption that cross-sections of the beam are infinitely rigid in their own plane, but free to warp out-of-plane, of these analytical predictions were sought during the current reporting. Author

N86-11297*# Rensselaer Polytechnic Inst., Troy, N. Y.
PROCESSING SCIENCE AND TECHNOLOGY
In its Composite Struct. Mater. Aug. 1985 p 39-62 refs (For primary document see N86-11293 02-24)
Avail: NTIS HC A05/MF A01 CSCL 11D

The heat capacity at constant pressure,Cp, of poly-p-xylylene (PPX) was measured from 220 to 625 degrees K using differential scanning calorimetry. The heat capacities at constant volume, Cv, of both PPX and its isomer polystyrene (PS were interpreted using literature data on full normal mode calculations for PS and estimates from low molecular weight analogues for PPX for the 39 group vibrations. Nine skeletal vibrations were used with theta sub 1 and theta sub 3 temperatures of 534.5 degrees K and 43.1 degrees K for PS. It was also possible to calculate a heat capacity contribution of a phenylene group within a polymer chain. Single 48-vibration theta sub 1 temperatures of 3230 degrees K for PS and 2960 degrees K for PPX are sufficient to describe Cv above 220 degrees K. Below 140 deg K, PS heat capacity shows deviations from the Tarasov treatment. Author

N86-11298*# Missouri Univ., Rolla. Dept. of Engineering Mechanics.
INTERACTION OF MIXED MODE LOADING ON CYCLIC DEBONDING IN ADHESIVELY BONDED COMPOSITE JOINTS
S. Mall, M. A. Rezaizadeh, and G. Ramamurthy Oct. 1985 9 p refs
(Grant NAG1-425)
(NASA-CR-177990; NAS 1.26:177990) Avail: NTIS HC A02/MF A01 CSCL 11D

A combined experimental and analytical investigation of an adhesively-bonded composite joint was conducted to characterize the fracture mode dependence of cyclic debonding. The system studied consisted of graphite/epoxy adherends bonded with EC 3445 adhesive. Several types of specimens are tested which provide the cyclic debond growth rate measurements under various load conditions: mode 1, mixed mode 1 to 2, and mostly mode 2. This study shows that the total strain-energy-release rate is the governing factor for cyclic debonding. Author

N86-11299*# National Aeronautics and Space Administration. Langley Research Center, Hampton, Va.
MANUAL FOR LDEF TENSILE TESTS
William G. Witte, Jr. Oct. 1985 40 p refs
(NASA-TM-87624; NAS 1.15:87624) Avail: NTIS HC A03/MF A01 CSCL 11D

One of the experiments aboard the NASA Long Duration Exposure Facility (LDEF) consists of a tray of approximately one hundred tensile specimens of several candidate space structure composite materials. During the LDEF flight the materials will be subjected to the space environment and to possible contamination during launch and recovery. Tensile tests of representative samples were made before the LDEF flight to obtain baseline data. Similar tests will be made on control specimens stored on earth for the length of the LDEF flight and on recovered flight specimens. This manual codifies the details of testing, data acquisition, and handling used in obtaining the baseline data so that the same procedures and equipment will be used on the subsequent tests. Author

N86-11300# Martin Marietta Aerospace, Denver, Colo.
METALLURGICAL CHARACTERIZATION OF THE INTERFACES AND THE DAMPING MECHANISMS IN METAL MATRIX COMPOSITES Progress Report, 4 Feb. 1984 - 12 Jun. 1985
M. S. Misra 12 Jun. 1985 11 p
(Contract N00014-84-C-0413)
(AD-A156507; MCR-85-605-Issue-1; PR-1) Avail: NTIS HC A02/MF A01 CSCL 11/4

Metal matrix composites are candidate structural materials for space applications. Large structures in space encounter natural and hostile disturbances, which introduce vibrations of a broad spectrum of frequencies. These vibrations must be damped fast enough for effective maneuverability and dynamic dimensional precision. In the vibrational control designs of such structures, damping capacity of the structural material is a significant parameter. If metal matrix composites are to be used for space structures; their intrinsic damping behavior needs to be clearly understood and improved if necessary, through metallurgical modifications. In this report, a graphite-aluminum composite has been selected to study the microstructural features and mechanisms responsible for dissipating vibrational energy. The objectives of this program were to develop a reliable test technique to accurately measure the damping capacity of metal matrix composites; perform metallurgical characterization of the interface structures; investigate the damping mechanism in metal matrix composites; and recommend microstructural modifications to enhance damping in metal matrix composites. GRA

N86-11301# Oak Ridge National Lab., Tenn.
IMPROVEMENTS IN THE FABRICATION OF CERAMIC-FIBER-CERAMIC-MATRIX COMPOSITES BY CHEMICAL VAPOR INFILTRATION
A. J. Caputo, R. A. Lowden, and D. P. Stinton Jun. 1985 41 p
(Contract DE-AC05-84OR-21400)
(DE85-015971; ORNL/TM-9651) Avail: NTIS HC A03/MF A01

Development of a new, faster process for the fabrication of ceramic fiber reinforced ceramic matrix composites by chemical vapor infiltration has continued. Composites of SiC fibers infiltrated with a matrix of either SiC or Si3N4 were produced. Process and equipment improvements led to the fabrication of preforms with a higher fiber content, and infiltration improvements reduced infiltration times and increased infiltrated densities. These improvements have produced composites with high flexural strengths (up to 475 MPa) and high strain values (up to 1%). The high strength and high strain values along with the gradual loss of strength (in contrast to the sudden loss typical of ceramics) is discussed. DOE

N86-11255*# National Aeronautics and Space Administration. Langley Research Center, Hampton, Va.
INITIAL INVESTIGATION OF CRYOGENIC WIND TUNNEL MODEL FILLER MATERIALS
George C. Firth *In its* Welding, Bonding and Fastening, 1984 Sep. 1985 p 465-481 refs (For primary document see N86-11227 02-23)
Avail: NTIS HC A21/MF A01 CSCL 11D

N86-11529# Virginia Polytechnic Inst. and State Univ., Blacksburg. Dept. of Engineering Science and Mechanics.
A REVIEW OF THE LITERATURE ON FINITE-ELEMENT MODELING OF LAMINATED COMPOSITE PLATES
J. N. Reddy *In* Shock and Vibration Information Center The Shock and Vibration Digest, Vol. 17, No. 4 Apr. 1985 p 3-8 refs (For primary document see N86-11527 02-39)
Avail: SVIC, Code 5804, Naval Research Lab., Washington, D.C., 20375 CSCL 11/4

25 INORGANIC AND PHYSICAL CHEMISTRY

Includes chemical analysis, e.g., chromatography; combustion theory; electrochemistry; and photochemistry.

For related information see also *77 Thermodynamics and Statistical Physics.*

N86-11302# Air Force Academy, Colo.
IDENTIFICATION OF METAL ION CHLORO COMPLEXES IN AN AMBIENT TEMPERATURE MOLTEN SALT Interim Report, 6 Feb. 1984 - 6 Feb. 1985
G. F. Reynolds, T. B. Scheffler, and J. S. Wilkes 25 May 1985 29 p
(AD-A157295; FJSRL-TR-85-0002) Avail: NTIS HC A03/MF A01 CSCL 07/4

The chloro complexation of LiCl, AgCl, CdCl2, and ZnCl2 in a chloride ion rich ambient temperature chloroaluminate ionic liquid had been studied by nuclear magnetic resonance spectroscopy. Chloride ion reacts with added metal chloride salts according to the reversible reaction xCl(-) + MCl subscript m yields MCl subscript M + x superscript x-, where x is a small, positive integer. The proton chemical shift of the organic component of the molten salt is very sensitive to the free chloride concentration of the melt. Therefore, observing the change in the chemicals shifts of the organic cation with increasing amounts of added metal chloride salt allows the determination of the value of x. Results indicate the formation of LiCl2(-), AgCl2-, CdCl42(-), and ZnCl4(2-) at 30 C. In addition, and extended model for ion interactions in these melts is described. GRA

N86-11303# Naval Research Lab., Washington, D. C.
A MECHANISM FOR IGNITION OF HIGH-TEMPERATURE GASEOUS NITROMETHANE: THE KEY ROLE OF THE NITRO GROUP IN CHEMICAL EXPLOSIVES
R. Guirguis, D. Hsu, D. Bogan, and E. Oran 8 Jul. 1985 29 p (RR0-1306)
(AD-A157355; NRL-MR-5558) Avail: NTIS HC A03/MF A01 CSCL 07/3

A detailed chemical mechanism describing ignition of high-temperature pure gaseous nitromethane was compiled and tested using shock in the range of 1000 to 1600 K and 1 to 10 atm. Measurements were made of the time evolution of the pressure at the end wall, as well as of the simultaneous pressure and NO absorption at a short, fixed distance from the end wall. Mass and infrared spectoscopy were used to identify the final products. In the reaction mechanism proposed, initiation starts with the C-N bond breaking which yields CH3 and NO2. Methoxy and CH2NO2 propagation, initiation starts with the C-N bond breaking which yields CH and NO2. Methoxy and CH2NO2 radicals then propagate the reaction through two major parallel pathways, both producing CH2O. Formaldehyde is then reduced to HCO and careies the reaction towards completion. The radical reactions do not release enough energy to compensate for the energy consumed in breaking the C-N bond. Although most of the radicals reach their maximum concentration early in the reaction process, ignition does not occur until virtually all of the nitromethane is consumed. The calculations show that the nitro group is the key to explosion: NO2 produces OH through its reaction wilth H radicals. Hydroxyl reactions, which are fast and exothermic, lead an accelerated consumption to the explosive with heat release. Comparison with the experiments shows that the mechanism predicts correct induction times for the pressure and temperature range of the experiments. GRA

N86-11304# Eltron Research, Inc., Aurora, Ill.
INVESTIGATION OF PHOTOELECTRODE REDOX POLYMER JUNCTIONS Technical Report, 16 Nov. - 15 Jan. 1984
R. L. Cook and A. F. Sammells 15 Jan. 1985 14 p
(Contract N00014-84-C-0723)
(AD-A157556; Rept-0001AB) Avail: NTIS HC A02/MF A01 CSCL 07/4

The n-CdS flatband potential in the solid-state cell n-CdS/Nafion 117 + redox species/Au was shifted progressively in a cathode directed upon the introduction of FeCp2, FeCp2 + Ru(bpy)3(2+) into the SPE. This cathodic shift was consistent with that for the oxidation potentials seen for Ru(bpy)3(2+) (E1/2 = 1.25V vs SCE) and FeCp2 (0.285V vs SCE) in acetonitrile. Such perturbations of semiconductor properties can be expected to form the basis of a detector technology when the semiconductor/SPE junction is exposed to selected chemical species. GRA

N86-11305# California Univ., Livermore. Lawrence Livermore Lab.
FLUIDS AT HIGH DYNAMIC PRESSURES AND TEMPERATURES
W. J. Nellis, D. C. Hamilton, R. J. Trainor, H. B. Radousky, A. C. Mitchell, and N. C. Holmes Jun. 1985 10 p refs Presented at the 10th High Pressure Conf. on Res. in High Pressure Sci. and Technol., Amsterdam, 8 Jul. 1985
(Contract W-7405-eng-48)
(DE85-014812; UCRL-92924; CONF-850759-6) Avail: NTIS HC A02/MF A01

Electrical conductivity data for shocked liquid nitrogen, Hugoniot data for liquid air, shock temperatures for liquid ammonia, and double shock equation of state data for Al are discussed. The equation of state for ammonia is important for models of the outer planets Uranus and Neptune. DOE

N86-11959# Joint Publications Research Service, Arlington, Va.
SURFACE COMBUSTION OF LIQUID FUEL IN STREAM OF GASEOUS OXIDIZER Abstract Only.
N. I. Zverev and V. N. Smirnov *In its* USSR Rept.: Phys. and Math. (JPRS-UPM-85-005) 20 Aug. 1985 p 22 refs Transl. into ENGLISH from Fiz. Goreniya i Vzryva (Novosibirsk, USSR), v. 20, no. 6, Nov. - Dec. 1984 p 33-38 Original language doc. was announced as A85-25571 (For primary document see N86-11945 02-70)
Avail: NTIS HC A08/MF A01

N86-11960# Joint Publications Research Service, Arlington, Va.
EXPLOSION WAVES GENERATED BY DEFLAGRATION COMBUSTION Abstract Only
V. A. Gorev and S. A. Bystrov *In its* USSR Rept.: Phys. and Math. (JPRS-UPM-85-005) 20 Aug. 1985 P. 22 refs Transl. into ENGLISH from Fiz. Goreniya i Vzryva (Novosibirsk, USSR), v. 20, no. 6, Nov. - Dec. 1984 p 26-33 (For primary document see N86-11945 02-70)
Avail: NTIS HC A08/MF A01

N86-11963# Joint Publications Research Service, Arlington, Va.
CALCULATION OF FORMATION TIME OF MINIMAL NUCLEUS OF FLAME DURING IGNITION OF EXPLOSIVE MIXTURES BY ELECTRICAL DISCHARGES Abstract Only.
N. I. Lobyzov and N. M. Karmazinov *In its* USSR Rept.: Phys. and Math. (JPRS-UPM-85-005) 20 Aug. 1985 p 33 refs Transl. into ENGLISH from Fiz. Goreniya i Vzryva (Novosibirsk, USSR), v. 20, no. 6, Nov. - Dec. 1984 p 55-58 (For primary document see N86-11945 02-70)
Avail: NTIS HC A08/MF A01

N86-11964# Joint Publications Research Service, Arlington, Va.
FLAME PROPAGATION IN PULSED ACCELERATION FIELD Abstract Only.
V. P. Samsonov *In its* USSR Rept.: Phys. and Math. (JPRS-UPM-85-005) 20 Aug. 1985 p 33 refs Transl. into ENGLISH from Fiz. Goreniya i Vzryva (Novosibirsk, USSR), v. 20, no. 6, Nov. - Dec. 1984 p 58-61 (For primary document see N86-11945 02-70)
Avail: NTIS HC A08/MF A01

N86-11965# Joint Publications Research Service, Arlington, Va.
OCCURRENCE OF PRESSURE WAVE DURING SPONTANEOUS IGNITION OF GAS AHEAD OF FLAME FRONT IN CLOSED VESSEL Abstract Only.
V. I. Vodyanik and S. V. Tarakanov *In its* USSR Rept.: Phys. and Math. (JPRS-UPM-85-005) 20 Aug. 1985 p 36 refs Transl. into ENGLISH from Fiz. Goreniya i Vzryva (Novosibirsk, USSR), v. 21, no. 1, Jan. - Feb. 1985 p 49-53 (For primary document see N86-11945 02-70)
Avail: NTIS HC A08/MF A01

26 METALLIC MATERIALS

Includes physical, chemical, and mechanical properties of metals, e.g., corrosion; and metallurgy.

N86-11306 California Univ., Los Angeles.
ACOUSTIC EMISSION DURING DEFORMATION AND FRACTURE OF A533B PRESSURE VESSEL STEEL Ph.D. Thesis
Jong Bee Teoh 1984 209 p
Avail: Univ. Microfilms Order No. DA8505678

The acoustic emission (AE) characteristics of ASTM A533B steel during tensile and fracture testing are highly anisotropic, originating from the decohesion of flattened MnS inclusions. This source of AE and effects of various heat treatment practices on the MnS/matrix interfaces is explored. The AE characteristics associated with different fracture mechanisms are identified, and the effects of test temperature and notch geometry examined. During fracture testing, slow bend tests were performed on Charpy V-notch samples at temperatures from -75 to 150 C. Tests were also interrupted so as to isolate the fracture processes. Tear and shear fracture and dimple formation by microvoid coalescence generated low amplitude AE events. Quasi-cleavage and cleavage fracture processes emitted events with a broad range of amplitude. Decohesion of MnS showed the charactristic Weibull distribution. When decohesion occurs, AE events from this process would mask those from other processes except cleavage or quasi-cleavage. Dissert. Abstr.

N86-11307 Virginia Polytechnic Inst. and State Univ., Blacksburg.
ENVIRONMENTAL EFFECTS IN THE FATIGUE BEHAVIOR OF COPPER NICKEL ALLOYS Ph.D. Thesis
Tirumali Srinivas Sudarshan 1984 271 p
Avail: Univ. Microfilms Order No. DA8511954

Mode 1 and Mode 3 fatigue tests were performed on copper nickel alloys in helium, hydrogen, oxygen, air and salt water environments. The two alloys used this investigation were 90/10 and 70/30 copper/nickel. Both alloys contained iron which was added to improve the erosion corrosion resistance. The extent of cracking varied with the test environment. Tests showed that oxygen and humid air promoted cracking while salt water retarded cracking when helium was used as the baseline environment. Hydrogen promoted cracking when compared to helium but retarded cracking if comparisons were made with oxygen or humid air. Observations suggest that the presence of iron accelerates fatigue in copper nickel alloys exposed to aggressive environments. Thus, any application involving fatigue loading with simultaneous exposure to aggressive environments should attempt to ensure that the iron content of the copper nickel alloys is minimized. Dissert. Abstr.

N86-11308 California Univ., Berkeley.
THE HOLLOW SPHERE MODEL FOR POROUS METALS AND METAL POWDERS Ph.D. Thesis
Kitae Kim 1984 109 p
Avail: Univ. Microfilms Order No. DA8512880

The effect of strain hardening on compaction behavior of metal powders and porous metals is investigated by including strain hardening in the hollow sphere model of Torre and of Carroll and Holt. For various forms of the strain hardening law, theoretical compaction equations are obtained in terms of elementary functions. For a particular value of the characteristic strain in the saturation hardening law of Voce and Palm, the well known empirical equation of Shapiro and Kolthoff and of Konopicky is obtained. Some other hardening laws are also introduced, e.g., one for which the ultimate strength is unbounded. Because of the possibility oof nonsaturation hardening for some materials, the models presented have capabilities for fitting strain hardening data and the corresponding compaction data at a high density level. With regard to the micromechanical modeling of porous materials in tensile stress fields, spherical inflation problems are treated. The theory of unloading for compaction of an elastic perfectly plastic hollow sphere is introduced. Dissert. Abstr.

N86-11309 Stanford Univ., Calif.
CREEP AND FRACTURE OF A YTTRIA DISPERSED NICKEL-CHROMIUM ALLOY Ph.D. Thesis
John Joseph Stephens, Jr. 1985 248 p
Avail: Univ. Microfilms Order No. DA8511358

The high temperature longitudinal creep and fracture properties of a mechanically alooyed, nickel based yttria dispersion strengthened alloy, Inconel MA 754, have been examined. Two major creep deformation regimes are observed in the temperature range 1000 to 1200 C (0.76 to 0.88 T sub m). At high stresses a high stress exponent regime is encountered, with transgranular fracture and relatively high creep ductility. The strong [100] < 001 > texture of MA 754 and the high stress exponents (n approx. - 40), suggest that deformation at high stresses in MA 754 is essentially single crystal behavior. A second regime of creep deformation is observed, at low stresses. Here, a relatively low stress exponent is measured, and intergranular fracture is observed along with a decline in creep ductility. Creep resistance at low stresses is determined by the grain morphology. Electron Microprobe Analysis and Transmission Electron Microscopy indicate that cavity growth leading to intergranular fracture occurs by means of a diffusive growth mechanism. Dissert. Abstr.

N86-11310 Metals Society, London (England).
CORROSION TESTING BY RADIOGRAPHIC METHODS
G. DelojoMorcillo and J. delosRiosRubalcaba Oct. 1984 13 p refs Transl. into ENGLISH from Rev. de Soldadura (Spain), no. 2, Apr. - Jun. 1982 p 39-43
(BLL-BISI-Trans-23201-(9022.06)) Avail: British Library Lending Div., Boston Spa, Engl.: £10.00; overseas $22.50

Radiography, which was developed in its quantitative aspects recently, is discussed. It supplies qualitative information which is not always accurate. The need for quality, and other testing methods, which are capable of an accurate detection, location, and measuring contributes to the development of radiographic techniques which give quantitative evaluations of the discontinuities discovered by the method. To obtain accurate quantitative results it is essential to have means to position sources and films with great accuracy, to employ carefully standardized laboratory techniques, to apply a working style quite different from the usual one, and to have sensitive densitometric equipment. Author

N86-11311 Metals Society, London (England).
THE YIELD POINT OF COPPER-ZINC ALLOYS IN THE ALPHA SOLID SOLUTION RANGE
J. Gryziecki Oct. 1984 13 p refs Transl. into ENGLISH from Rudy Metale Niezelazne (Katowice), no. 10, 1983 p 373-376
(BLL-BISI-Trans-23046-(9022.06)) Avail: British Library Lending Div., Boston Spa, Engl.: £14.25; overseas $33.75

The effect of mechanical factors and external conditions on the lower yield point value and on the length of Luder bands is shown. The effect of grain size on the yield point value of copper zinc alloys deformed in the temperature range of 77 to 723 K which is based on the Hall-Petch relationship are discussed. E.A.K.

N86-11312*# Kentron International, Inc., Hampton, Va. Aerospace Technologies Div.
MECHANICAL PROPERTIES OF INCONEL 718 AND NICKEL 201 ALLOYS AFTER THERMAL HISTORIES SIMULATING BRAZING AND HIGH TEMPERATURE SERVICE
William F. James Sep. 1985 28 p refs
(Contract NAS1-18000)
(NASA-CR-177940; NAS 1.26:177940) Avail: NTIS HC A03/MF A01 CSCL 11F

An experimental investigation was made to evaluate two nickel base alloys (Nickel-201 and Inconel-718) in three heat treated conditions. These conditions were: (1) annealed; (2) after thermal exposure simulating a braze cycle; and (3) after a thermal exposure simulating a braze cycle plus one operational lifetime of high temperature service. For the Nickel-201, two different braze cycle temperatures were evaluated. A braze cycle utilizing a lower braze temperature resulted in less grain growth for Nickel-201 than the standard braze cycle used for joining Nickel-201 to Inconel-718. It was determined, however, that Nickel-201, was marginal for temperatures investigated due to large grain growth. After the thermal exposures described above, the mechanical properties of Nickel-201 were degraded, whereas similar exposure on Inconel-718 actually strengthened the material compared with the annealed condition. The investigation included tensile tests at both room temperature and elevated temperatures, stress-rupture tests, and metallographic examination. Author

N86-11313# Korrosionsinstitutet, Stockholm (Sweden).
CATHODIC PROTECTION OF ALUMINIUM STRUCTURES Abstract Only
Bertil Sandberg and Avtandil Bairamov 1985 4 p
(KiS-1985:4E) Avail: NTIS HC A02/MF A01

A study of the literature and a laboratory investigation of cathodic protection of aluminum structures is discussed. In the laboratory investigation the effect of the protection was studied in fresh water. In cathodic protection of aluminum complete cathodic protection is not striven for. The object is, instead, to counteract localized attack, chiefly pitting, and thus to prolong the life of the structure. Cathodic protection can in practice be achieved by three different principles: with impressed current, with sacrificial anodes, or by cladding such as Alclad. The results both of the study of the literature and of the laboratory investigation indicate that the lower limit is in practice below the -1130 mV rel. There is much to suggest that the interval in neutral electrolytes extends down to -1380 mV. Author

N86-11314# Korrosionsinstitutet, Stockholm (Sweden).
SHORT-TERM METHODS FOR ATMOSPHERIC CORROSION TESTING: SURVEY OF THE LITERATURE Abstract Only
Eva Johansson [1984] 2 p
(KiS-1985:5E) Avail: NTIS HC A02/MF A01

Different procedures for producing wetting and a sulfur dioxide bearing test atmosphere are dealt with. The study allows the following conclusions: (1) there are many standardized methods for atmospheric corrosion testing in which corrosion is accelerated by condensation, spraying of chloride solutions or addition of atmospheric pollutants; (2) the number of standardized methods that include cleaning of the specimen surface is limited; (3) several studies with salt spray tests have shown poor conformity with field exposures; and (4) short term tests with lower SO2 content and tests including cleaning of the specimen surface have yielded more promising results, compared with field exposures, than tests in which the SO2 content was higher and no cleaning took place. Author

N86-11315# Department of the Navy, Washington, D. C.
CHEMICAL BONDING AGENT FOR SUPPRESSION OF RUSTY BOLT INTERMODULATION INTERFERENCE Patent Application
J. C. Cooper, inventor (to Navy) Filed 23 Apr. 1985 20 p
(AD-D011747; US-Patent-Appl-SN-726563) Avail: NTIS HC A02/MF A01 CSCL 20/3

Intermodulation interference (IMI) occurs when high frequency (HF) transmitters and receivers are placed in close proximity, particularly on ships and aircraft, due to non-linear conduction through metal-oxide-metal (MOM) junctions in the supporting structure. Welding or clamping straps cannot be used where there is a multiplicity of MOM junctions, such as in chains or twisted cable, or where dissimilar metals are involved. Additionally, the use of non-conductive materials or conductive straps is very expensive. To overcome these limitations while effectively reducing IMI, an inexpensive method that maintains the structural integrity of supporting hardware while providing a highly conductive current path is required. The chemical composition of the present invention used to overcome IMI contains compounds similar to rust removal compositions which have incorporated the general principles of chelating the ferric ion, incorporating the ion into a polymer material, and removing the rust with one polymer material. GRA

N86-11316# California Univ., San Diego, La Jolla. Dept. of Electrical Engineering and Computer Sciences.
SURFACE AND INTERFACIAL PROPERTIES OF Ga0.47In0.53As ALLOYS Final Report, 1 Apr. 1984 - 31 Mar. 1985
H. H. Weider 15 Jul. 1985 15 p
(Contract N00019-84-C-0169)
(AD-A157343) Avail: NTIS HC A02/MF A01 CSCL 11/6

A modified Varian GenII, molecular beam epitaxial deposition system was installed and preliminary performance tests have indicated its suitability for growing binary and ternary 3 to 5 alloy semiconducting layers. Gallium arsenide layers grown with this MBE system have electrical properties which compare well with those of the best layers grown elsewhere. One 50 layer GaAs/Ga sub x Al sub 1-x (160 A per layer thick) superlattice was used to test the usefulness of the MBE system for the synthesis of conventional heterojunctions and superlattices. Preliminary results have been obtained with Ga sub 0.47 In sub 0.53 As epitaxial layers whose lattice constant matches exactly that of their InP substrates. Work is underway on the synthesis of the ternary alloy layers and heterojunctions whose lattice constants match that of InP. Author (GRA)

N86-11317# Michigan Technological Univ., Houghton. Dept. of Metallurgical Engineering.
DEFORMATION AND FRACTURE OF P/M TITANIUM ALLOYS Final Report, 1 Jul. 1975 - 30 Sep. 1984
D. A. Koss May 1985 33 p
(Contract N00014-76-C-0037)
(AD-A157416; TR-28) Avail: NTIS HC A03/MF A01 CSCL 11/6

Progress is reviewed for a research program whose primary purpose has been to provide a broad-based understanding of the deformation and fracture of high performance alloys in general and titanium alloys in particular. The research has ranged from strengthening mechanisms in titanium alloys to fundamental studies of crack propagation, localized necking, hydrogen embrittlement, and ductile fracture utilizing engineering alloy behavior. Progress for the period 1 July 1975 to 1 October 1984 is reviewed for the following portions of this research program: (1) the influence of silicon on the age hardening of beta-phase Ti alloys, (2) the flow and fracture behavior of multi-phase alloys with lamellar microstructures, (3) fracture along planar slip bands, (4) the multiaxial deformation and fracture of plastically anisotropic alloys in the form of sheet, (5) the influence of stress state on the hydrogen embrittlement of hydride-forming alloys in general and Ti in particular, and (6) the deformation and fracture of alloys containing pores and voids. GRA

N86-11318# Dayton Univ., Ohio. Research Inst.
EFFECTS OF MANUFACTURING PROCESSES ON STRUCTURAL ALLOWABLES Final Technical Report, Feb. 1983 - Nov. 1984
P. E. Doepker May 1985 180 p
(Contract F33615-82-C-5102)
(AD-A157596; UDR-TR-84-133; AFWAL-TR-85-4049) Avail: NTIS HC A09/MF A01 CSCL 11/6

This report documents the results from tests to determine mechanical property data for materials having various manufacturing processes. The materials tested were: 15-5 PH (H1025) Stainless Steel Alloy Hot Rolled Plate, 7175-T736 Aluminum Alloy Hand Forging and 7050-T736511 Aluminum Alloy Extrusion. Tensile, compression, shear and bearing properties were obtained for all three materials. Fatigue (notched and unnotched) properties were determined for the Stainless Steel Plate and the 7175-T736 Aluminum Hand Forging. GRA

N86-11319# Argonne National Lab., Ill.
DENSE RANDOM PACKED MODEL FOR AMORPHOUS NI35-Zr65: INFLUENCE OF THE HEAT OF MIXING
C. K. Saw and R. B. Schwarz May 1985 7 p Presented at the Intern. Conf. on the theory of the Struct. of Non-Crystalline Solids, Bloomfield Hills, Mich., 3 Jun. 1985
(Contract W-31-109-eng-38)
(DE85-014967; CONF-8506144-3) Avail: NTIS HC A02/MF A01

The structure of amorphous Ni35Zr65 alloy was simulated by a Dense Random Packed (DRP) model. The model was relaxed by minimizing its elastic energy through the use of a modified Keating potential that included only central forces with interatomic bonds of equal strength. The Bathia-Thornton number concentration (NC) distributions and the Warren chemical short range order parameter, (ALPHA) sub w, were deduced from the model and compared with measurements in rapidly quenched Ni35Zr65. The DRP model simulates a truly random alloy for which (ALPHA) sub w = 0. Since (ALPHA) sub w = 0.04 for the actual alloy, the fraction of Ni-Zr nearest neighbors in the alloy exceeds that in the model. The effects of decreasing the strength of any one of the interatomic bonds (Ni-Ni, Ni-Zr, or Zr-Zr) were investigated. It was found that the bond relaxations cause a sharpening of some of the peaks in NC distributions but have no effect on the value of (ALPHA) sub w. The effect of permuting Ni and Zr atoms, so as to increase the number of Ni-Zr nearest neighbors at the expense of Ni-Ni and Zr-Zr pairs, was also investigated. DOE

N86-11320# Los Alamos National Lab., N. Mex.
LOS ALAMOS UPGRADE IN METALLOGRAPHIC CAPABILITIES
J. M. Ledbetter, K. E. Dowler, and J. H. Cook 1985 5 p Presented at the Am. Nucl. Soc. Winter Meeting, San Francisco, 10 Nov. 1985
(Contract W-7405-eng-36)
(DE85-014089; LA-UR-85-2193; CONF-851115-4) Avail: NTIS HC A02/MF A01

The Los Alamos Wing 9 Hot Cell Facility is in the process of upgrading their metallographic sample preparation and examination capability. The present capability to grind, polish and etch samples from reactor fuels and materials has been in operation for 18 years. Macro photography and alpha and beta gamma autoradiography are an important part of this capability. Some of the fast breeder reactor experiments have contained sodium as a coolant. Therefore, the capability to distill sodium from some samples scheduled for microstructural examinations is a requirement. Since the reactor fuel samples are highly radioactive and contain plutonium, either as fabricated or as a result of breeding during reactor service, these samples must be handled in shielded hot cells containing alpha boxes to isolate the plutonium and hazardous fission products from personnel and the environment. Ideas that were developed during the design of new alpha boxes and new equipment for microstructural sample preparation have provided the concepts for the capability to perform the work faster and maintain the equipment in a safer manner. DOE

N86-11321# Sandia Labs., Albuquerque, N. Mex.
STRESS AND STRAIN-RATE DEPENDENCE OF SPALL STRENGTH IN TWO ALUMINUM ALLOYS
D. R. Ek and J. R. Asay 1985 6 p Presented at the Am. Phys. Soc. Topical Conf. on Shock Waves in Condensed Matter, Spokane, 22 Jul. 1985
(Contract DE-AC04-76DP-00789)
(DE85-015154; SAND-85-0156C; CONF-850736-41) Avail: NTIS HC A02/MF A01

The spallation behavior of 6061-T6 and AMg-6 aluminum alloys is studied as a function of loading stress and initial pulse duration for stress amplitudes ranging from 5 to 20 GPa and for pulse durations spanning range of 0.06 to 0.9 microns. These experiments show that the spallation strength varies from about 0.7 to 1.4 GPa for strain rates varying from 0.15 to 1 microns/sec and for impact stresses from 5 to 20 GPa. Author

N86-11322# California Univ., Berkeley. Lawrence Berkeley Lab.
ELECTRONIC AND MAGNETIC STRUCTURE OF CHROMIUM SURFACES AND CHROMIUM MONOLAYERS ON IRON
R. H. Victora and L. M. Falicov May 1985 13 p Presented at the Intern. Conf. on Magnetism, San Francisco, 26 Aug. 1985
(Contract DE-AC03-76SF-00098)
(DE85-014542; LBL-19722; CONF-850890-2) Avail: NTIS HC A02/MF A01

Chromium surfaces and Cr monolayers atop Fe have greatly enhanced magnetizations relative to bulk. The Cr (100) surface is ferromagnetic with a spin polarization of 3.00; the (110) surface is antiferromagnetic. A Cr monolayer is ferromagnetic atop either the (100) or (110) Fe surfaces; the former has a large polarization of 3.63. DOE

N86-11323# Los Alamos National Lab., N. Mex.
MAGNETIC PROPERTIES AND ELECTRONIC STRUCTURE OF THE ACTINIDE SYSTEMS UAl2, NpAl2 AND PuAl2
R. C. Albers, A. M. Boring, and D. D. Koelling 1985 11 p Presented at the Intern. Conf. on Magnetism, San Francisco, 26 Aug. 1985 Prepared in cooperation with ANL, Ill.
(Contract W-7405-eng-36)
(DE85-014102; LA-UR-85-2140; CONF-850890-4) Avail: NTIS HC A02/MF A01

The electronic ground states of UAl2, NpAl2 and PuAl2 were determined by band theory techniques. These calculations indicate that both actinide d-f hybridization and spin-orbit coupling are important in these systems. Using a new scheme for obtaining the paramagnon parameters for UAl2 it is shown that calculated and experimentally derived 5f band width are consistent. The fact that orbital angular momentum may not be quenched in these systems is suggested as a possible mechanism for damping spin-fluctuations in NpAl2 and PuAl2. DOE

N86-11324# North Carolina State Univ., Raleigh.
SHOCK-WAVE SYNTHESIS OF TITANIUM ALUMINIDES
Y. Horie, D. E. P. Hoy, I. Simonsen, R. A. Graham, and B. Morosin 1985 7 p Presented at the Am. Phys. Soc. Topical Conf. on Shock Waves in Condensed Matter, Spokane, 22 Jul. 1985 Prepared in cooperation with Sandia National Labs., Albuquerque, N. Mex.
(Contract DE-AC04-76DP-00789)
(DE85-015140; SAND-85-0484C; CONF-850736-33) Avail: NTIS HC A02/MF A01

The initiation of strong chemical reactions in a mixture of Ti and Al powders subject to high pressure shock wave loading was observed when the bulk peak temperature of the region calculated from numerical simulation was above 450 C. A high temperature with a high pressure does not promote reactions with significant yield. A reaction product has hardness twice the values for Ti rich equilibrium compounds in the Ti-Al system. There is lack of agreement between X-ray analysis and EPMA regarding the composition of the products. The X-ray diffraction showed the pattern for TiAl3 or its two ordered superstructures while EPMA favored Ti rich compounds - Ti2Al and TiAl. DOE

N86-11325# Sandia Labs., Albuquerque, N. Mex.

CHEMICAL SYNTHESIS UNDER SHOCK COMPRESSION

R. A. Graha, B. Morosin, Y. Horie, E. L. Venturini, M. Boslough, M. J. Carr, and D. L. Williamson 1985 19 p refs Presented at the Am. Phys. Soc. Topical Conf. on Shock Waves incondensed Matter, Spokane, 22 Jul. 1985 Prepared in cooperation with North Carolina State Univ., Raleigh and Colorado School of Mines, Golden
(Contract DE-AC04-76DP-00789)
(DE85-015166; SAND-85-0366C; CONF-850736-39) Avail: NTIS HC A02/MF A01

Many reports of chemical synthesis under high pressure shock loading have been published over the past thirty years, but little progress has been made in developing an understanding of the mechanisms responsible for the observed effects. This paper discusses the current status of studies in shock-induced solid state chemistry. It is observed that it is relatively easy to initiate and control chemical reactions in shock-loaded powder materials. In solids it is well known that chemical changes are controlled by defects at all levels from atomic and microstructural to continuum. A major program to study shock-induced modification of inorganic powders provides explicit evidence for unusually large plastic deformation and resulting defect structures. Shock-modified powders also show major enhancements in solid state reactivity in post-shock experiments. Currently, two systems are found to provide a basis for studying controlled chemical synthesis. Intermetallic alloys have been found to be produced in a controlled manner from mechanical mixtures of aluminum with either nickel or titanium. Optical measurements show that a strong chemical reaction is induced on a 100 nanosecond time scale in such aluminum-nickel mixtures under shock compression. DOE

N86-11326# California Univ., Livermore. Lawrence Livermore Lab.

PROCESSING AND MICROSTRUCTURAL CHARACTERIZATION OF B4C-Al CERMETS

D. C. Halverson, A. J. Pyzik, and I. A. Aksay Feb. 1985 21 p refs Presented at the 9th Ann. Conf. on Composites and Advan. Ceram. Mater. and Workshop on Testing Methods for Ceram. Matrix Composites, Cocoa Beach, Fla, 20 Jan. 1985 Prepared in cooperation with Washington Univ., Seattle
(Contract W-7405-eng-48)
(DE85-013195; UCRL-91305; CONF-850122-10) Avail: NTIS HC A02/MF A01

Reaction thermodynamics and wetting studies were employed to evaluate boron carbide-aluminum cermets. Wetting phenomenon and interfacial reactions are characterized using macroscale and microscale techniques. Macroscale evaluation involves aluminum sessile drop studies on boron carbide substrates. Microscale evaluation involves the fabrication of actual cermet microstructures their characterization through SEM, X-ray diffraction, metallography, and electron microprobe. Contact-angle measurements and interfacial-reaction products are reported. DOE

N86-11327# Rockwell International Corp., Golden, Colo.

METALLOGRAPHY OF SOLID STATE BONDS

W. L. Johns and J. H. Doyle 1985 35 p Presented at the Intern. Met. Soc. Conf., Denver, 21 Jul. 1985
(Contract DE-AC04-76DP-3533)
(DE85-014564; RFP-3847; CONF-850753) Avail: NTIS HC A03/MF A01

Two methods of bonding dissimilar metals are described: silver-assisted solid state bonding and friction welding. Both methods can produce bonds that are very strong at room temperature with ultimate strengths greater than the lower strength metal. Two distinct types of defects have been observed in friction welds between 1100 aluminum and 316 stainless steel: voids or tearing at the bond interface and formation of brittle intermetallic. Silver-assisted solid state bonds are made that have very high ultimate strengths. In the case of 1100 aluminum bonded to 316 stainless steel, as-machined surfaces are adequate. There is a definite relationship between silver microstructure and substrate temperature. The microstructures produced have significant differences in hardness and ductility. A change in microstructure does not appear to have any effect on the resulting bond strength. Low bonding pressure and/or temperature can result in low strength failures. High bonding temperatures can result in the growth of brittle intermetallics. DOE

N86-11328# New Mexico Inst. of Mining and Technology, Socorro.

SYNTHESIS OF NICKEL-ALUMINUM ALLOYS BY SHOCK COMPRESSION OF COMPOSITE PARTICLES

H. R. Pak, Y. Horie, and R. A. Graham 1985 7 p Presented at the Am. Phys. Soc. Topical Conf. on Shock Waves in Condensed Matter, Spokane, 22 Jul. 1985 Prepared in cooperation with North Carolina State Univ., and Sandia Labs.
(Contract DE-AC04-76DP-00789)
(DE85-015165; SAND-85-03330; CONF-850736-40) Avail: NTIS HC A02/MF A01

Electron microscope observations of compound formation in Ni/Al composite powders by shock loading is reported. Reactions with substantial yield are seen in outer areas of a recovered specimen, while unreacted or locally reacted regions are seen in the center and middle areas of the specimen. Ni3Al is formed in a gamma solid solution of Ni. The microstructure is very complex. DOE

N86-11329# Mound Lab., Miamisburg, Ohio.

INJECTION MOLDING-SEALING OF GLASS TO LOW MELTING METALS Final Report

D. P. Kramer, R. T. Massey, and D. D. Halcomb 15 Jul. 1985 12 p
(Contract DE-AC04-76DP-00053)
(DE85-015613; MLM-3268) Avail: NTIS HC A02/MF A01

The fabrication of complex glass or glass ceramic to metal seals which use low melting metals such as aluminum. During injection molding sealing, molten glass, which may have a higher melting temperature than that of the metal parts, is injected under pressure into the metal parts while they are held in a mold. The process, which for the first time allows the formation of seals with metals that have a lower melting temperature than the glass, allows the fabrication of seals of simplex geometry. DOE

N86-11330# Brandeis Univ., Waltham, Mass.

A 2D ACAR MOMENTUM DENSITY STUDY OF THE NATURE OF THE POSITRON SURFACE STATE ON Al(100)

S. Berko, K. F. Canter, K. G. Lynn, A. P. Mills, L. O. Roellig, and R. N. West 1985 4 p refs Presented at the 7th Intern. Conf. on Positron Annihilation, New Delhi, 6 Jan. 1985 Prepared in cooperation with BNL, Upton, N.Y., Bell Telephone Labs., Murray Hill, N.J., City Coll. of the State of New York, N.Y. and East Anglia Univ., Norwich, Engl.
(Contract DE-AC02-76CH-00016)
(DE85-014830; BNL-36701; CONF-850169-17) Avail: NTIS HC A02/MF A01

The two dimensional angular correlation of the 2(GAMMA) annihilation radiation (2D ACAR) has been measured from an Al(100) surface bombarded by 200 eV positrons. After removing the contribution of fast parapositronium annihilation, the spectrum from positrons annihilating at the surface exhibits a nearly isotropic conical shape with a (7.1 + or - 0.5) mrad FWHM. DOE

N86-11331# Oak Ridge National Lab., Tenn.

ITINERANT ELECTRON FERROMAGNETISM IN Fe-ALLOYED, NI3AI BASED MATERIALS

J. R. Thompson, H. R. Kerchner, and S. T. Sekula 1985 11 p Presented at the Intern. Conf. on Magnetism, San Francisco,

26 Sep. 1985
(Contract DE-AC05-84OR-21400)
(DE85-013989; CONF-8509102-1) Avail: NTIS HC A02/MF A01

Bulk magnetic properties of Ni3Al based alloys containing up to 10 at.% Fe have been investigated. The experimental results are compared with those for off stoichiometry Ni3Al and interpreted using Stoner and SCB spin fluctuation theory. DOE

N86-11332# Oak Ridge National Lab., Tenn.
TENSILE PROPERTIES OF 2-1/4Cr-1Mo STEEL IRRADIATED TO 23 dpa AT 390 TO 550(0)C
R. L. Klueh and J. M. Vitek 1985 29 p
(Contract DE-AC05-84OR-21400)
(DE85-015551; DOE/OR-21400/T99) Avail: NTIS HC A03/MF A01

The effect of neutron irradiation on the tensile properties of normalized and tempered 2-1/4Cr-1Mo steel was determined for specimens irradiated to 23 dpa in the Experimental Breeder Reactor II (EBR-II) at 390, 450, 500, and 550 C. Two types of unirradiated control specimens were tested: as heat treated specimens and as heat treated specimens thermally aged for 10,000 h at the irradiation temperatures. Aging caused a loss of strength at all four temperatures. Irradiation at 390 C increased the strength and decreased the ductility compared to the control specimens. At 500 and 550 C, softening occurred relative to the thermally aged specimens, with the amount of softening greatest at 550 C. At 450 C, the strength of the irradiated specimens was similar to a specimen aged 10,000 h at 450 C. The changes in tensile properties result from the displacement damage caused by the irradiation induced changes in carbide precipitates that occur during elevated temperature exposure. DOE

N86-11333# Sandia Labs., Albuquerque, N. Mex.
INFLUENCE OF EFFECTIVE RATE SENSITIVITY ON ADIABATIC SHEAR INSTABILITY
T. J. Burns 1985 8 p refs Presented at the Intern. Conf. on Met. Appl. of Shock Wave and High-Strain Rate Phenomena, Portland, Oreg., 28 Jul. 1985
(Contract DE-AC04-76DP-00789)
(DE85-013967; SAND-85-0280C; CONF-850889-1) Avail: NTIS HC A02/MF A01

An analysis is presented of the stability of dynamic simple shear in a ductile metal whose yield behavior is described by a mechanical flow rule, i.e., a material whose flow stress depends only on the instantaneous values of strain, strain rate, and temperature. It is shown that near the yield point, a region which usually has been ignored in shear stability studies, the steepness of the slope of the stress versus strain curve of the material can be large enough for inertial effects to dominate over viscous effects for short time, so that the process effectively has a rate sensitivity at early time which is much smaller than the coefficient of rate sensitivity typically measured during an experiment. This combination of inertial effects and smaller viscous effects can be sufficient to cause only the longer-wavelength components of a perturbation on simple shear to retain much energy after a small amount of plastic flow, and thus it provides an explanation for the apparent growth of only longer-wavelength modes once the material begins to soften due to adiabatic heating and becomes unstable. The conclusions of this work should also apply to other materials testing experiments, such as the loading of bars in tension. DOE

N86-11334# Arizona Univ., Tucson.
SHORT RANGE BONDING INTERACTION AT METAL-METAL INTERFACES
W. R. Bennett, J. A. Leavitt, and C. M. Falco 1984 2 p Presented at the Course on Dyn. Phenomena at Surfaces, Interfaces and Superlattices, Erice, Italy, 1 Jul. 1984
(Contract DE-AC02-83ER-45025)
(DE85-014442; DOE/ER-45025/5; CONF-8407117-3) Avail: NTIS HC A02/MF A01

Freshly deposited Mo surfaces were exposed to a beam of sputtered Ta atoms for varying, controlled lengths of time. The resultant number of deposited Ta atoms/cm(2) was subsequently measured using Rutherford Backscattering. DOE

N86-11335# Brookhaven National Lab., Upton, N. Y.
INTERGRANULAR ATTACK AND STRESS CORROSION CRACKING OF ALLOY 600 IN HIGH-TEMPERATURE CAUSTIC SOLUTIONS CONTAINING CONTAMINANTS
R. Bandy, R. Roberge, and D. vanRoyen Jun. 1985 73 p
(Contract DE-AC02-76CH-00016)
(DE85-014106; EPRI-NP-4051) Avail: NTIS HC A04/MF A01; available from Research Reports Center, Box 50490, Palo Alto, Calif. 94303

Concentrated caustic is a primary cause of stress corrosion cracking and intergranular attack of Alloy 600 tubing in PWRS. However, temperature, electrochemical potential, stress, and metallurgical state all play a role. This study provides the quantitative evidence needed to develop models of crack growth and to devise effective countermeasures. DOE

N86-11336# Sandia Labs., Albuquerque, N. Mex.
CALCULATION OF THERMAL TRAPPING IN SHEAR BANDS
J. W. Swegle and D. E. Grady 1985 48 p Presented at the Intern. Conf. on Met. Appl. of Shock Wave and High-Strain Rate Phenomena, Portland, Oreg., 28 Jul. 1985
(Contract DE-AC04-76DP-00789)
(DE85-014404; SAND-85-0269C; CONF-850889-2) Avail: NTIS HC A03/MF A01

The microstructure associated with heterogeneous shear deformation observed in shock-loaded materials implies the possibility of transient local temperatures which far exceed those expected under homogeneous deformation. The possible consequences of high local temperatures and resulting thermal softening are explored by using thermodynamic considerations to derive equations for the evolution of shear band temperatures. Inclusion of the equations in a finite-difference wavecode along with a previously developed model which accurately describes shockwave risetime behavior, allows calculation of temperature states in the shock front. At low stresses, risetimes are long compared to thermal diffusion times and shear bands that stay in thermal equilibrium with surrounding material, but at high stresses where risetimes are very short, shear band temperatures greatly exceed bulk temperatures before thermal equilibrium occurs. Decreasing yield strength with increasing shear band temperature followed by yield strength recovery as the shear bands cool produces an elastic precursor on reshock which cannot be obtained with standard elastic-plastic models. DOE

N86-11337# Sandia Labs., Albuquerque, N. Mex.
RELATIONSHIP BETWEEN INTERATOMIC BONDING AND ELECTRON TRANSPORT IN PLASMA DEPOSITED AMORPHOUS METAL ALLOYS
G. E. Pike, A. K. Hays, G. C. Nelson, and I. J. Fritz 1985 6 p refs Presented at the 2d Spring Meeting of the Mater. Res. Soc., San Francisco, 15 Apr. 1985
(Contract DE-AC04-76DP-00789)
(DE85-014710; SAND-85-0913C; CONF-850421-12) Avail: NTIS HC A02/MF A01

Amorphous metal alloy films have been produced using a new technique. Nominally NiP alloys are made by dissociating mixtures of nickel carbonyl and phosphine using a radio-frequency discharge in either an argon or a hydrogen carrier gas. This process incorporates significant amounts of carbon and oxygen impurities into the film. A previously unreported relationship between the interatomic bonding involving these impurities and the electronic transport properties of the films is discussed in this paper. The bonding studies were carried out principally using Auger lineshape analysis. Transport properties measured included 4-terminal resistivities, Hall mobilities and carrier concentrations, and Seeback coefficients. Covalent bonding of Ni with C or P with O is strongly correlated with high resistivity, mainly through a decrease in carrier density. DOE

N86-11338# Edgerton, Germeshausen and Grier, Inc., Idaho Falls, Idaho.
MECHANICAL PROPERTIES OF RAPIDLY SOLIDIFIED TYPE 304 STAINLESS STEEL
G. E. Korth and J. E. Flinn 1985 33 p Presented at the 114th AIME Ann. Meeting, New York, 24 Feb. 1985; sponsored in part by Society of Mining Engineers
(Contract DE-AC07-76ID-01570)
(DE85-014577; EGG-M-02285; CONF-850211-11) Avail: NTIS HC A03/MF A01

Rapidly solidified Type 304 stainless steel (SS) powder produced by the centrifugal atomization process was consolidated by hot extrusion techniques. Tensile, creep-rupture, and fatigue tests were performed on the extruded material and the mechanical properties data are compared with those of conventionally prepared wrought material. The properties of the rapidly solidified material are superior or equivalent to conventional Type 304 SS except in the case of tensile elongation which was somewhat lower. Attempts to explain the differences in terms of microstructural observations were only partially successful. DOE

N86-11230*# National Aeronautics and Space Administration. Langley Research Center, Hampton, Va.
INVESTIGATION OF LOW-TEMPERATURE SOLDERS FOR CRYOGENIC WIND TUNNEL MODELS Interim Report
George C. Firth and Vernon E. Watkins, Jr. *In its* Welding, Bonding and Fastening, 1984 Sep. 1985 p 21-34 refs (For primary document see N86-11227 02-23)
Avail: NTIS HC A21/MF A01 CSCL 11F

N86-11231*# National Aeronautics and Space Administration. Langley Research Center, Hampton, Va.
NTF: SOLDERING TECHNOLOGY DEVELOPMENT FOR CRYOGENICS
E. Thomas Hall, Jr. *In its* Welding, Bonding and Fastening, 1984 Sep. 1985 p 35-54 refs (For primary document see N86-11227 02-23)
Avail: NTIS HC A21/MF A01 CSCL 11F

N86-11873# Sandia Labs., Albuquerque, N. Mex. Analytical Solid Mechanics Div.
APPLICATION OF A MIXTURE THEORY TO THE BINARY ALLOY SOLIDIFICATION PROBLEM Abstract Only
Vincent C. Prantil *In* LANL 6th Bien. CUBE (Computer Use by Engineers) Symp. Aug. 1984 p 27 (For primary document see N86-11858 02-60)
Avail: NTIS HC A06/MF A01

27 NONMETALLIC MATERIALS

Includes physical, chemical, and mechanical properties of plastics, elastomers, lubricants, polymers, textiles, adhesives, and ceramic materials.

N86-11339*# College of William and Mary, Williamsburg, Va. Dept. of Chemistry.
CHARACTERIZATION OF THE RELATIONSHIP OF THE CURE CYCLE CHEMISTRY TO CURE CYCLE PROCESSING PROPERTIES Report, period ending 31 Jul. 1985
David E. Kranbuehl 23 Aug. 1985 33 p refs
(Grant NAG1-237)
(NASA-CR-176256; NAS 1.26:176256) Avail: NTIS HC A03/MF A01 CSCL 11B

Dynamic dielectric analysis (DDA) is used to study curing polymer systems and thermoplastics. Measurements are made over a frequency range of six decades. This wide range of frequencies increases the amount of information which can be obtained. The data is analyzed in terms of the frequency dependence of the complex permittivity epsilon sup *, specific conductivity sigma (ohm/cm) and the relaxation time tau, parameters which are characteristic of the cure state of the material and independent of the size of the sample. Author

N86-11340*# National Aeronautics and Space Administration. Ames Research Center, Moffett Field, Calif.
STRENGTH AND FLEXIBILITY PROPERTIES OF ADVANCED CERAMIC FABRICS
Paul M. Sawko and Huy Kim Tran (San Jose State Univ.) Sep. 1985 24 p refs
(NASA-TM-86824; Rept-85279; NAS 1.15:86824) Avail: NTIS HC A02/MF A01 CSCL 11B

The mechanical properties of four advanced ceramic fabrics are measured at a temperature range of 23 C to 1200 C. The fabrics evaluated are silica, high-and low-boria content aluminoborosilicate, and silicon carbide. Properties studied include fabric break strengths from room temperature to 1200 C, and bending durability after temperature conditioning at 1200 C and 1400 C. The interaction of the fabric and ceramic insulation is also studied for shrinkage, appearance, bend resistance, and fabric-to-insulation bonding. Based on these tests, the low-boria content aluminoborosilicate fabric retains more strength and fabric durability than the other fabrics studied at high temperature. Author

N86-11341# Naval Air Development Center, Warminster, Pa. Aircraft and Crew Systems Technology Directorate.
CORROSION-PREVENTIVE PRIMERS FOR MILITARY EQUIPMENT Final Report
S. J. Spadafora, C. R. Hegedus, and D. F. Pulley 1 Apr. 1985 30 p
(NR Proj. F61-542)
(AD-A156927; NADC-85029-60) Avail: NTIS HC A03/MF A01 CSCL 11/3

The operational readiness and life-time of military equipment can be significantly reduced by corrosion. One way of protecting equipment against this process is through the use of corrosion-preventive primers. These primers are composed of a variety of resins, pigments and solvents to produce materials with different properties to cover a broad range of operational environments. Eleven primers conforming to military and federal specifications were tested on steel and aluminum specimens. Properties such as corrosion protection, adhesion, flexibility and chemical resistance were determined for each primer. The results of this evaluation indicate a wide variety of performance properties for the eleven primers. This information is presented to enable the reader to choose a material with the most appropriate properties for a specific use. Author (GRA)

N86-11342# Naval Academy, Annapolis, Md. Dept. of Physics.
ELECTRICAL RELAXATION IN POLY(ETHYLENE OXIDE) Interim Technical Report
J. J. Fontanella and M. C. Wintergill Jun. 1985 27 p
(Contract N00014-85-F-0001)
(AD-A157301; TR-16) Avail: NTIS HC A03/MF A01 CSCL 07/4

Audio frequency complex admittance (DR) has been used to investigate electrical relaxation in poly(ethylene oxide) (PEO). The complex admittance measurements were performed at seventeen frequencies from 10 to 100,000 Hz in appropriately equal logarithmic intervals using a fully automated dielectric spectrometer and measurements were performed in vacuum over the temperature range 5.5 to 350K. Two relaxations are observed at low temperatures which is consistent with the literature. In order to gain new information concerning the gamma relaxation, measurements were made at -94, -91, and -88 C at pressures up to 0.2 GPa. The shift in the peak frequency with pressure and hence, the activation volume are found to be extremely small. This result combined with other work implies that the relaxation is associated with the motion of very small segments of the polymer chain. GRA

N86-11343# Dayton Univ., Ohio.
STUDIES ON CHALCOGENIDE FILMS Final Report, 1 Feb. 1984 - 31 Jan. 1985
B. Kumar and K. White May 1985 33 p
(Contract F33615-82-C-5001)
(AD-A157340; UDR-TR-85-32; AFWAL-TR-85-4046) Avail: NTIS HC A03/MF A01 CSCL 11/2

Three research tasks related to chalcogenide films have been studied. The first task deals with the thermal sensitivity of reflection peaks of narrow band reflection filters. It has been shown that a significant shift in the reflection peak can be expected in the reflection filters due to a change in temperature. The shift could be minimized by modifying film compositions. The dn/dT (Temperature coefficient of refractive index) has been identified as an important factor of the thermal sensitivity parameters. It has been suggested that in addition to bulk composition, impurities play and important role in determining the dn/dT. The second task reports the experimental data and discussion related to the effects of aging on the refractive index of As2S3 films. It has been shown that the refractive index increases by approximately 4% due to an aging below the glass transition temperature. The third task evaluates a relationship between the deposition rate and stoichiometry of As2S3 films. It has been observed that as the deposition rate increases, the films become sulfur deficient. GRA

N86-11344# Ohio State Univ., Columbus.
STUDIES ON THE SYNTHESES OF BORON HYDRIDE SYSTEMS Final Report, 1 Apr. 1982 - 31 Mar. 1985
S. G. Shore 25 May 1985 20 p
(Contract DAAG29-82-K-0112)
(AD-A157368; ARO-19129.5-CH) Avail: NTIS HC A02/MF A01 CSCL 07/2

Over the past three years, the principal objective of this program has been to fully develop and to extend earlier work on the conversion of pentaborane(9), B5H9, to potentially useful higher boron hydride systems. The existence of a large quantity of B5H9 in U.S. government storage provided the impetus for this work. On the whole, this objective has been achieved. Achieved were significant improvements over an earlier synthesis of decarborane (14), B10H14, both from the stand point of yield and safety. Furthermore, it has been demonstrated that B5H9 can be converted to a number of higher boron hydride species through one-pot procedures which give yields of products, in general, equivalent to or better than obtained by other methods. Thus, B5H9 in storage is a potential feedstock for these materials. In addition to these above efforts, during the grant period studies of the general chemistry of boron hydride were undertaken and report some interesting new developments are reported. GRA

N86-11345# Cincinnati Univ., Ohio. Dept. of Materials Science and Metallurgical Engineering.
COMPATIBILIZING EFFECT OF RANDOM OR BLOCK COPOLYMER ADDED TO BINARY MIXTURE OF HOMOPOLYMERS
D. Rigby, J. L. Lin, and R. J. Roe 1 Aug. 1985 29 p
(Contract N00014-85-K-0245)
(AD-A157384; TR-1) Avail: NTIS HC A03/MF A01 CSCL 11/9

When copolymer A-B is added to the mixture of homopolymer A and homopolymer B, the compatibility between the two homopolymers is enhanced under certain conditions. Analysis, based on the Flory-Huggins free energy of mixing, gives the specific conditions under which the critical, spinodal or binodal temperature of the ternary mixture is expected to be lowered linearly with the amount of the added copolymer. Experimental measurements were performed on the changes in the cloud point of the mixtures of polystyrene and polybutadiene to which varying amounts of styrene/butadiene random or diblock copolymer were added. The results agree with the theoretical expectation. From quantitative analysis of the cloud point depression, the temperature coefficient of the interaction energy density between styrene and butadiene polymers is determined. The temperature coefficient is found to give an excellent agreement with the value previously determined by a curve fitting procedure applied to the cloud point curves of binary mixtures. GRA

N86-11346# Cornell Univ., Ithaca, N.Y. Dept. of Materials Science and Engineering.
PROPERTIES OF CRAZES AND DEFORMATION ZONES IN GLASSY POLYMERS Final Report, 1976 - 1985
E. J. Kramer May 1985 17 p
(Contracts DAAG29-82-K-0092; DAAG29-79-C-0015; Grant DAAG29-76-G-0103)
(AD-A157428; ARO-12636.10-MS; ARO-18701.2-MS; ARO-16123.21-MS) Avail: NTIS HC A02/MF A01 CSCL 11/9

New experimental methods, holographic interferometry and quantitative transmission electron microscopy, have been developed to investigate the microstructure, mechanical properties and failure of crazes and deformation zones DZ's in glassy polymers. Plasticizaton by the environment is found to be the major factor in environmental crazing and cracking. Air crazing, and the transition to more ductile DZ behavior, is controlled largely by the entanglement density of the polymer glass. Low entanglement density polymer craze readily and the craze fibrils break down rapidly to form cracks. High entanglement density polymers preferentially form non-fibrillated DZ's; crazes when formed are more resistant to craze breakdown in these polymers. A comprehensive model of these entanglement effects has been developed which explain the natural extension ratios of crazes and DZ's, the craze to DZ transition and the craze fibril stability. GRA

N86-11347# Naval Research Lab., Washington, D. C.
DEVELOPMENT OF CASTOR-OIL-RESISTANT POLYURETHANE SONAR ENCAPSULANTS Final Report, Sep. 1981 - Aug. 1982
W. T. Maurice and C. M. Thompson 30 Jun. 1985 45 p
(AD-A157576; NRL-MR-5578) Avail: NTIS HC A03/MF A01 CSCL 11/9

Polyurethanes have been widely used as underwater acoustic encapsulants for over twenty years. This research was designed to produce a polyurethane encapsulant that is nonhazardous and non-proprietary for use in castor-oil-filled systems. Seven commercial diamines were evaluated as replacements for methylene bis(2-chloroaniline)(MBOCA) in the cure system. The polyurethane produced were screened according to their handling properties, strength, modulus retention on water and castor oil exposure, electrical properties, and sound speed. The final candidates are commercial Toluene Diisocyanate/ Polyoxytetramethylene glycol prepolymers cured with diamine/diol/catalyst system. The resulting polyurethanes exhibit better combined castor oil and water resistance than any commerically available material. GRA

N86-11348# Sandia Labs., Albuquerque, N. Mex.
PHOTOSENSITIVITY AND IMAGING CHARACTERISTICS OF ION-IMPLANTED PLZT CERAMICS
C. E. Land 1985 21 p Presented at the 6thIntern. Meeting on Ferroelec., Kobe, Japan, 12 Aug. 1985
(Contract DE-AC04-76DP-00789)
(DE85-015489; SAND-85-0435C; CONF-850860-2) Avail: NTIS HC A02/MF A01

It was reported in previous papers that both the near-UV and the visible photosensitivities of ferroelectric-phase PLZT (lead lanthanum zirconate titanate) ceramics are increased by as much as four orders of magnitude by ion implantation or a combination of thermal diffusion of Al and ion implantation. New results are presented here on high-energy (1 MeV) implants of Al and Ni and complaints of Al + Ne and Ni + Ne, and these results are compared with earlier 500 keV implants of Al and Cr and compliants of Al + Ne and Cr + Ne as surface modification techniques for increasing the visible photosensitivity of PLZT. The important role of grain size in determining optimum contrast and resolution of stored optical information is described in terms of new experimental results. DOE

N86-11349# Midwest Research Inst., Golden, Colo. Solar Energy Research Inst.
SOLID-MELT INTERFACE STUDIES OF HIGH-SPEED SILICON SHEET GROWTH
T. F. Ciszek Feb. 1985 67 p
(Contract DE-AC02-83CH-10098)
(DE85-008783; SERI/PR-212-2634) Avail: NTIS HC A04/MF A01

Radial growth-rate anisotropies and limiting growth forms of point-nucleated, dislocation-free silicon sheets spreading horizontally on the free surface of a silicon melt have been measured for (100), (110), (111), and (112) sheet planes. Analysis of the sheet edges leads to predicted geometries for the tip shape of unidirectional, dislocation-free, horizontally growing sheets propagating in arious directions within the above-mentioned planes. Feasibility is demonstrated for a crucible-free horizontal (CFH) ribbon growth method. High-purity, cold-crucible melt confinement is used to grow silicon sheets by edge-supported pulling (ESP). Quartz capillary filaments are used. Solar cell data on these sheets are presented. Also cell, lifetime, mobility, spreading resistance, X-ray topography, and neutron activation analysis data are obtained for dislocation-free cylindrical ingots of [111] and [100] orientation. X-ray topography analysis of dendritic web silicon sheets is conducted and the resultant topographs are presented in this report. A possible correlation between slip dislocations and web cell efficiency is seen. Float zoning studies are initiated for high-purity, dislocation-free silicon to be applied to high-efficiency silicon solar cells. DOE

N86-11350# California Univ., Livermore. Lawrence Livermore Lab.

PULSE DURATION DEPENDENCE OF 1064-nm LASER DAMAGE THRESHOLDS OF POROUS SILICA ANTIREFLECTION COATINGS ON FUSED SILICA SUBSTRATES

D. Milam, I. M. Thomas, C. Weinzapfel, and J. G. Wilder 30 May 1985 15 p refs Presented at the Boulder Damage Symp., Boulder, Colo., 15 Oct. 1985
(Contract W-7405-eng-48)
(DE85-013207; UCRL-91429; CONF-8410276-1) Avail: NTIS HC A02/MF A01

Researchers used 1064-nm pulses with durations of 1, 5, 9 ns to measure laser-damage thresholds of 10 porous silica antireflection coatings deposited from both methanol and ethanol solutions containing silica particles with diameters of 10 to 20 nm. The median thresholds measured at the three pulse durations, 10.8 J/cm(2), 26.5 J/cm(2), and 38 J/cm(2), scaled as pulse duration to the 0.56 power. DOE

N86-11351# Argonne National Lab., Ill.

CORRELATIONS OF CHEMICAL, MICROSTRUCTURAL AND MECHANICAL PROPERTIES OF POLYETHYLENE PIPING MATERIALS

L. A. Raphaelian and D. G. Ettinger 1985 8 p Presented at the 5th Ann. Plastic Piping Mater. Workshop, Rosemont, Ill., 19 Jun. 1985
(Contract W-31-109-eng-38)
(DE85-013077; CONF-8506122-1) Avail: NTIS HC A02/MF A01

A variety of analyses, including carbon-13 nuclear magnetic resonance ((13)C NMR), X-ray diffraction (XRD), and gas chromatography/mass spectrometry (GC/MS), were performed on several commercial polyethylene (PE) pipes. In many cases, not only the sample as a whole but also the inner surface, bulk, and outer surface were examined. Also, certain samples were examined before and after annealing. Correlations of the data from the analyses with data from Constant Tensile Load Tests (CTLT) of the commercial pipe samples were developed. DOE

N86-11352# Mound Lab., Miamisburg, Ohio.

PHYSICAL PROPERTY CHANGES OF A LITHIA-ALUMINA-SILICA BASED GLASS AS A FUNCTION OF COMPOSITION

D. P. Kramer, G. L. Harville, D. A. Buckner, J. P. McCarthy, A. B. Nease, and D. B. Sullenger 22 Jul. 1985 41 p
(Contract DE-AC04-76DP-00053)
(DE85-015610; MLM-3272) Avail: NTIS HC A03/MF A01

The effect of compositional changes on various physical properties (coefficient of thermal expansion, crystalline phases, and refractive index) both before and after devitrification (when appropriate) on a lithia alumina silica based glass is determined. The results obtained by adding or subtracting various amounts of the compositional oxides (lithium carbonate, potassium carbonate, ammonium phosphate, alumina, boric acid, or silica) one at a time shows that compositional changes have a pronounced influence on the resultant physical properties of these glasses. DOE

N86-11353# California Univ., Livermore. Lawrence Livermore Lab.

CRYSTAL CLASS AND THE ELECTROOPTIC EFFECT

D. Eimerl May 1985 22 p
(Contract W-7405-eng-48)
(DE85-015240; UCRL-53636) Avail: NTIS HC A02/MF A01

The propagation of light in linear electrooptic media is reviewed with emphasis on understanding the full effect of crystal symmetry. The changes in the refractive indexes and the rotation of the optic axes are calculated in detail for each of the 18 biaxial and uniaxial crystal classes. The direction of the applied field and the ray propagation are unrestricted. Under these circumstances, there is no apparent reason to prefer crystals from any particular class. However, in applications requiring large aperture electrooptic devices, there is an advantage to applying the field parallel to the ray direction. Then the most attractive crystal classes are m, mm2, 4, 4mm, 4, 42n, 23, 43n, 6, and 6mm. These crystal classes allow propagation along an optic axis, generate birefringence with the applied field parallel to the optic axis and ray direction, and are incapable of rotating the index ellipsoid. Materials from these classes will provide robust electrooptic switches at large aperture. DOE

N86-11354# Sandia Labs., Albuquerque, N. Mex.

TRANSPORTATION SYSTEM IMPACT LIMITER DESIGN USING RIGID POLYURETHANE FOAM

G. W. Wellman Jun. 1985 48 p refs
(Contract DE-AC03-76DP-00789)
(DE85-015088; SAND-84-2271; TTC-0532) Avail: NTIS HC A03/MF A01

Techniques used to apply the finite element method to the analysis of rigid polyurethane foam that is confined by a thin, ductile metallic skin were investigated. The initial investigation covered the analysis of a simple geometry and loading condition of constrained and unconstrained foam using the constitutive relationships implied in the Elastic-Plastic and Crushable Foam material models in HONDO 2 and DYNA2D/3D. The final investigation consisted of the analysis of a series of tests of scale model impact limiters and comparison of the experimental and analytical results. DOE

N86-11355# Sandia Labs., Albuquerque, N. Mex.

POLYURETHANE FOAM COMPONENT LIFETIMES

K. B. Wischmann 1985 6 p Presented at the 190th Am. Chem. Soc. Natl. Meeting, Chicago, 8 Sep. 1985
(Contract DE-AC04-76DP-00789)
(DE85-008206; SAND-84-2239C; CONF-850942-1) Avail: NTIS HC A02/MF A01

Access deterrent foams are generated by mixing two separately stored and pressurized components upon demand. Investigations have been conducted concerning the aging of both components of three separate polyurethane foam formulations. The polyol component of the first formulation, a propylene oxide adduct of phosphoric acid, hydrolyzes rapidly to give phosphoric acid. Since phosphoric acid can corrode the container as well as adversely affect the final foam properties, a second formulation not containing acid adduct is investigated. This second polyol is isothermally aged at room temperature, 60 C and 71 C and reactions follow by acid number determination. A reaction between the polyol and the blowing agent, Freon 11, is found to give high acid content. Attempts to add inhibitors to lengthen this initiation period fails. Finally, a third formulation is designed which places the Freon 11 in the isocyanate component thereby precluding the incompatibility of the blowing agent with the polyol. subsequent aging studies indicate a long term (6 to 8 years) storage foam system could be achieved. DOE

N86-11356# Aerospace Corp., El Segundo, Calif. Lab. Operations.

IMPURITY MONITORING BY LASER-INDUCED FLUORESCENCE TECHNIQUES

J. A. Gelbwachs 26 Dec. 1984 29 p
(Contract DE-AT03-76ER-71013)

(DE85-014142; ATR-84(7783)-4) Avail: NTIS HC A03/MF A01

Laser-induced fluorescence spectroscopy can provide a highly sensitive and selective means of detecting atomic and ionic impurities. Because the photodetector can be physically isolated from the laser-excited region, these techniques can be applied to monitoring in hostile environments. The basic concepts behind fluorescence detection are reviewed. Saturated optical excitation is shown to maximize impurity atom emission yield while mitigating effects of laser intensity fluctuations upon absolute density calibration. Monitoring in high- and low-pressure monitoring environments is compared. Methods to improve detection sensitivity by luminescence background suppression are presented. DOE

N86-11357# Midwest Research Inst., Golden, Colo. Solar Energy Research Inst.
POLYMER GLAZINGS FOR SILVER MIRRORS
H. H. Neidlinger and P. Schissel Jul. 1985 11 p refs Presented at the SPIE Intern. Tech. Symp. on Opt. and Electro-Opt. Engrs., San Diego, Calif., 18 Aug. 1985
(Contract DE-AC02-83CH-10093)
(DE85-012140; SERI/TP-255-2724; CONF-850887-3) Avail: NTIS HC A02/MF A01

This paper reports on an evaluation and modification of polymeric glazings to protect silver mirrors. The mirrors were made using Corning 7809 glass as a substrate onto which a thin silver film is deposited. The modified polymeric films are then cast from solution onto the silver. The mirrors were characterized by measuring the hemispherical reflectance and the specular reflectance at 660 nm and selected acceptance angles (7.5 mrad or 3.5 mrad). The mirrors were exposed to environmental degradation using accelerated weathering devices and outdoor exposure. Empirical evidence has demonstrated that polymethylmethacrylate is a stable polymer in a terrestrial environment, but the polymer does not provide adequate protection for the silver reflector. The crucial role in degradation played by ultraviolet (UV) light is shown by several experimental results. It has been demonstrated that UV stabilizers added to the polymer improve the weatherability of mirrors. DOE

N86-11249*# Lockheed-Georgia Co., Marietta.
ADHESIVES FOR AEROSPACE
L. E. Meade *In* NASA. Langley Research Center Welding, Bonding and Fastening, 1984 Sep. 1985 p 339-349 refs (For primary document see N86-11227 02-23)
Avail: NTIS HC A21/MF A01 CSCL 11A

N86-11250*# Boeing Aerospace Co., Seattle, Wash.
HIGH-TEMPERATURE ADHESIVE DEVELOPMENT AND EVALUATION
Carl L. Hendricks and Jeremy N. Hale *In* NASA. Langley Research Center Welding, Bonding and Fastening, 1984 Sep. 1985 p 351-370 refs (For primary document see N86-11227 02-23)
Avail: NTIS HC A21/MF A01 CSCL 11A

N86-11251*# Martin Marietta Corp., Baltimore, Md.
USE OF HYDRATION INHIBITORS TO IMPROVE BOND DURABILITY OF ALUMINUM ADHESIVE JOINTS
G. D. Davis, J. S. Ahearn, L. J. Matienzo, and J. D. Venables *In* NASA. Langley Research Center Welding, Bonding and Fastening, 1984 Sep. 1985 p 371-396 refs Previously announced in IAA as A85-29979 (For primary document see N86-11227 02-23)
(Contract N00014-80-C-0718)
Avail: NTIS HC A21/MF A01 CSCL 11A

N86-11252*# United Technologies Research Center, East Hartford, Conn.
FACTORS AFFECTING THE PROCESSING OF EPOXY FILM ADHESIVES
R. A. Pike *In* NASA. Langley Research Center Welding, Bonding and Fastening, 1984 Sep. 1985 p 397-418 refs (For primary document see N86-11227 02-23)
Avail: NTIS HC A21/MF A01 CSCL 11A

N86-11254*# Naval Surface Weapons Center, White Oak, Md.
REDUCTION OF MOISTURE EFFECTS DURING THE CURE OF EPOXY ADHESIVES USED IN COMPOSITE REPAIR
Joseph M. Augl and George T. Sivy *In* NASA. Langley Research Center Welding, Bonding and Fastening, 1984 Sep. 1985 p 439-463 ref (For primary document see N86-11227 02-23)
Avail: NTIS HC A21/MF A01 CSCL 11A

N86-11263*# National Aeronautics and Space Administration. Lewis Research Center, Cleveland, Ohio.
PMR POLYIMIDES FROM SOLUTIONS CONTAINING MIXED ENDCAPS
Peter Delvigs *In its* High Temp. Polymer Matrix Composites Sep. 1985 p 23-34 refs (For primary document see N86-11260 02-24)
Avail: NTIS HC A18/MF A01 CSCL 11B

N86-11265*# National Aeronautics and Space Administration. Ames Research Center, Moffett Field, Calif.
BISMALEIMIDES AND RELATED MALEIMIDO POLYMERS AS MATRIX RESINS
John A. Parker, Demitrius A. Kourtides, and George M. Fohlen *In* NASA. Lewis Research Center High Temp. Polymer Matrix Composites Sep. 1985 p 55-77 refs (For primary document see N86-11260 02-24)
Avail: NTIS HC A18/MF A01 CSCL 11B

N86-11266*# Case Western Reserve Univ., Cleveland, Ohio. Dept. of Chemistry.
THE SYNTHESIS, CHARACTERIZATION AND THERMAL CHEMISTRY OF MODIFIED NORBORNENYL PMR ENDCAPS
Chaim N. Sukenik, William M. Ritchey, Vinay Malhotra, and Uday Varde *In* NASA. Lewis Research Center High Temp. Polymer Matrix Composites Sep. 1985 p 79-90 refs (For primary document see N86-11260 02-24)
(Grant NAG3-163)
Avail: NTIS HC A18/MF A01 CSCL 11B

N86-11267*# National Aeronautics and Space Administration. Lewis Research Center, Cleveland, Ohio.
ALL-AROMATIC BIPHENYLENE END-CAPPED POLYQUINOLINE AND POLYIMIDE MATRIX RESINS
John P. Droske (Colorado State Univ.), John K. Stille (Colorado State Univ.), and William B. Alston *In its* High Temp. Polymer Matrix Composites Sep. 1985 p 91-95 refs (For primary document see N86-11260 02-24)
Avail: NTIS HC A18/MF A01 CSCL 11B

N86-11268*# Boeing Aerospace Co., Seattle, Wash.
EVALUATION OF A HIGH TEMPERATURE ADHESIVE FOR FABRICATING GRAPHITE/PMR-15 POLYIMIDE STRUCTURES
S. G. Hill and J. B. Cushman *In* NASA. Lewis Research Center High Temp. Polymer Matrix Composites Sep. 1985 p 97-108 refs (For primary document see N86-11260 02-24)
Avail: NTIS HC A18/MF A01 CSCL 11A

N86-11269*# Dexter Corp., Pittsburg, Calif. Hyson Div.
NEW PROCESSABLE MODIFIED POLYIMIDE RESINS FOR ADHESIVE AND MATRIX APPLICATIONS
David Landman *In* NASA. Lewis Research Center High Temp. Polymer Matrix Composites Sep. 1985 p 109-123 refs (For primary document see N86-11260 02-24)
Avail: NTIS HC A18/MF A01 CSCL 11B

N86-11270*# American Cyanamid Co., Stamford, Conn. Chemical Research Div.
RECENT DEVELOPMENTS IN POLYIMIDE AND BISMALEIMIDE ADHESIVES
Robert E. Politi *In* NASA. Lewis Research Center High Temp. Polymer Matrix Composites Sep. 1985 p 125-136 (For primary document see N86-11260 02-24)
Avail: NTIS HC A18/MF A01 CSCL 11B

N86-11271*# National Aeronautics and Space Administration. Lewis Research Center, Cleveland, Ohio.

CHEMICAL CONTROL OF RATE AND ONSET TEMPERATURE OF NADIMIDE POLYMERIZATION
Richard W. Lauver *In its* High Temp. Polymer Matrix Composites Sep. 1985 p 137-149 refs (For primary document see N86-11260 02-24)
Avail: NTIS HC A18/MF A01 CSCL 11B

N86-11275*# National Aeronautics and Space Administration. Lewis Research Center, Cleveland, Ohio.
REPLACEMENT OF MDA WITH MORE OXIDATIVELY STABLE DIAMINES IN PMR-POLYIMIDES
William B. Alston *In its* High Temp. Polymer Matrix Composites Sep. 1985 p 187-205 refs (For primary document see N86-11260 02-24)
Avail: NTIS HC A18/MF A01 CSCL 11B

N86-11288*# Tribon Bearing Co., Cleveland, Ohio.
TRANSFER MOLDING OF PMR-15 POLYIMIDE RESIN
J. P. Reardon, D. W. Moyer, and B. E. Nowak *In* NASA. Lewis Research Center High Temp. Polymer Matrix Composites Sep. 1985 p 379-392 refs (For primary document see N86-11260 02-24)
Avail: NTIS HC A18/MF A01 CSCL 11B

N86-11532# Yarmouk Univ., Irbid (Jordan). Dept. of Mechanical Engineering.
STIFFNESS AND DAMPING COEFFICIENTS OF RUBBER
M. Issa Abdulhadi *In* The Shock and Vibration Information Center Shock and Vibration Digest, Vol. 17, No. 5 May 1985 p 3-9 refs (For primary document see N86-11531 02-39)
Avail: SVIC, Code 5804, Naval Research Lab., Washington, D.C. 20375 CSCL 11/10

28 PROPELLANTS AND FUELS

Includes rocket propellants, igniters, and oxidizers; storage and handling; and aircraft fuels.

For related information see also *07 Aircraft Propulsion and Power, 20 Spacecraft Propulsion and Power,* and *44 Energy Production and Conversion.*

N86-11358# Naval Postgraduate School, Monterey, Calif.
AN INVESTIGATION OF THE EFFECTS OF FUEL COMPOSITION ON COMBUSTION CHARACTERISTICS IN A T-63 COMBUSTOR Progress Report, Oct. 1983 - Mar. 1985
R. W. Dubeau, P. J. Hickey, A. C. Krug, A. L. Lohman, and J. P. Weller Mar. 1985 89 p
(AD-A157325; NPS67-85-004) Avail: NTIS HC A05/MF A01 CSCL 21/4

A T63 combustor was instrumented to allow measurement of center line distributions of temperature and soot size and concentration using water-cooled probes. Three-wavelength light transmission measurements were also made at two locations to determine that mean soot size and NOx concentrations were measured in the exhaust duct. Five fuels of varying composition were used in the combustor and initial tests were conducted using two smoke-suppressant fuel additives. The data indicated that the aft region of the combustor contained a large, low temperature recirculation zone, surrounded by an annular region of higher temperature and lower soot concentration. Light transmissionn measurements appeared to yield reasonable particle size data when compared to collected samples. However, the extent of agglomeration in the collection probes was unknown. Smoke-suppressant fuel additives were found to have reduced effectiveness in the present test series, apparently due to unheated inlet air which was employed. NOx levels increased significantly with increasing combustor exhaust temperature (or fuel-air ratio). Soot concentration increased and transmittance decreased with increasing fuel-air ratio. The mean soot particle size was found to be between 0.21 and 0.26 micronns, independent of fuel composition and fuel-air ratio. GRA

N86-11359# Sandia Labs., Albuquerque, N. Mex.
SHOCK-INDUCED TEMPERATURE DISTRIBUTIONS IN POWDER COMPACT RECOVERY FIXTURES
R. A. Graham and D. M. Webb 1985 7 p refs Presented at the Am. Phys. Soc. Topical Conf. on Shock Waves in Condensed Matter, Spokane, 22 Jul. 1985
(Contract DE-AC04-76DP-00789)
(DE85-015139; SAND-85-0334C; CONF-850736-28) Avail: NTIS HC A02/MF A01

Sandia Bear and Bertha powder compact recovery fixture systems for explosive loading have been widely used to preserve powder compact samples for post-shock analysis. Shock conditions within the compacts are determined from an extensive program of numerical simulation which reveals that, even though the initial loading is planar, the sample conditions are controlled by a radial-mode compression. The wave-trapping phenomenon which occurs in the powder samples leads to relatively uniform shock-induced temperatures except for a very hot area in the outer edge region of some fixtures. DOE

N86-11360# New Mexico Inst. of Mining and Technology, Socorro.
SHOCK CONSOLIDATION OF IN-100 NICKEL-BASE SUPER-ALLOY POWDER
S. I. Wang, M. A. Meyers, and R. A. Graham 1985 5 p refs Presented at the Am. Phys. Soc. Topical Conf. on Shock Waves in Condensed Matter, Spokane, 22 Jul. 1985 Prepared in cooperation with Sandia National Labs., Albuquerque, N. Mex.
(Contract DE-AC04-76DP-00789)
(DE85-015159; SAND-85-1597C; CONF-850736-36) Avail: NTIS HC A02/MF A01

Shock consolidation of IN-100 powders was studied in Sandia Bear and Bertha fixtures over a pressure from 7.5 to 27 GPa. In addition, the influence of pulse duration from 4.5 to 19 (MU)s was investigated at 16 GPa. From the metallographic observations it was established that: (1) the mean pressure for bonding, with approx. 5% interparticle melting, is about 20 GPa; (2) the pulse duration seems to play a role in the consolidation; and (3) the stock temperature is an important parameter. It significantly enhances interparticle melting. DOE

N86-11361# Los Alamos National Lab., N. Mex.
DETONATION REACTION ZONE STUDIES ON TATB EXPLOSIVES
W. L. Seitz, H. L. Stacy, and J. Wackerle 1985 11 p refs Presented at the 8th Intern. Symp. on Detonation, Albuquerque, N. Mex., 15 Jul. 1985
(Contract W-7405-eng-36)
(DE85-015710; LA-UR-85-2460; CONF-850706-28) Avail: NTIS HC A02/MF A01

Interface velocity histories between heterogeneous detonating explosives and transparent windows, separated by a thin (13 (micron)m) aluminum shim, have been obtained with an image-intensified rotating-mirror streak camera and a Fabry-Perot velocity interferometer system. Seven TATB-based explosives were studied with PMMA windows for typically three charge lengths. Two of the explosives were also studied with LiF windows. In each case a non-steady detonation was observed, with each increasing charge length showing a corresponding increase in the interface velocity histories. Time resolution and velocity error are estimated to be about 6 ns and 2%, respectively. Numerical simulations for one of the explosives, for which a shock-strength modified Arrhenius rate law (DAGMAR) and an assumed equation of state (HOM) had been previously calibrated with shock initiation gauge data, gave good agreement with the experimental velocity histories. DOE

N86-11966# Joint Publications Research Service, Arlington, Va.
STEADY-STATE DETONATION OF CHARGES OF FINITE LENGTH Abstract Only
V. K. Ashayev, G. S. Doronin, and V. S. Zhuchenko *In its* USSR Rept.: Phys. and Math. (JPRS-UPM-85-005) 20 Aug. 1985 p 37 refs Transl. into ENGLISH from Fiz. Goreniya i Vzryva (Novosibirsk, USSR), v. 21, no. 1, Jan. - Feb. 1985 p 127-130 (For primary

document see N86-11945 02-70)
Avail: NTIS HC A08/MF A01

N86-11924# Joint Publications Research Service, Arlington, Va.
PRESSURE-COUPLED RESPONSE FUNCTION OF SOLID PROPELLANTS INCLUDING THOSE WITH NEGATIVE PRESSURE-EXPONENTS Abstract Only
Wengan Xu *In its* China Rept.: Sci. and Technol. (JPRS-CST-85-014) 2 May 1985 p 76 Transl. into ENGLISH from Yuhang Xuebao (Beijing), no. 1, 31 Jan. 1985 p 47-58 Original language document announced in IAA as A85-42780 (For primary document see N86-11918 02-70)
Avail: NTIS HC A06/MF A01

31 ENGINEERING (GENERAL)

Includes vacuum technology; control engineering; display engineering; and cryogenics.

N86-11362# New Mexico Univ., Albuquerque. Engineering Research Inst.
VALIDATION OF PROCEDURES FOR PAVEMENT DESIGN ON EXPANSIVE SOILS Final Report, May 1984 - Aug. 1985
R. Gordon McKeen Washington FAA Jul. 1985 99 p refs
(Contract F29601-84-C-0080)
(FAA-PM-85-15; NMERI-WA5-4(5.02)) Avail: NTIS HC A05/MF A01

This report documents site investigations and design recommendations for airport pavements on expansive soils at three sites. The methods used were developed previously in an FAA-sponsored research project. The design procedure involves soil characterization, determination of surface characteristics and evaluation of soil-pavement interaction. Investigations at three airports are reported; they are Murdo, South Dakota, Mesquite, Texas, and Love Field, Dallas, Texas. Soils data are used along with climatic information to obtain estimates of the equivalent thickness of pavement required for each site. The work at Love Field was somewhat different than the other sites since NMERI was not directly conducting the investigation. Results are reported in the form of pavement thickness required to adequately perform, in terms of surface roughness, on the soil surface characteristics predicted for each site. Recommendations are included for consideration in rehabilitation of each site since all were experiencing surface roughness at the time of the investigations. These results confirm that methods developed for evaluating airport pavements on expansive soils provide useful information for pavement design. B.W.

N86-11363# National Bureau of Standards, Gaithersburg, Md.
APPLIED MODEL VALIDATION Progress Report
Alan D. Davies Jul. 1985 31 p refs
(NBSIR-85-3154-1) Avail: NTIS HC A03/MF A01

The NBS Center for Fire Research (CFR) conducts scientific research bearing on the fire safety of buildings, vehicles, tunnels and other inhabited structures. Data from controlled fire experiments are collected, analyzed and reduced to the analytical formulas that appear to underly the observed phenomena. These results and more general physical principles are then combined into models to predict the development of environments that may be hostile to humans. This is a progress report of an applied model validation case study. The subject model is Transport of Fire, Smoke and Gases (FAST). Products from a fire in a burn room exit through a connected corridor to outdoors. Cooler counterflow air in a lower layer feeds the fire. The model predicts corridor layer temperatures and thicknesses vs. time, given enclosure, fire and ambient specifications. Data have been collected from 38 tests using several fire sizes, but have not been reduced. Corresponding model results, and model and test documentation are yet to come. Considerable modeling and calculation is needed to convert instrument readings to test results comparable with model outputs so that residual differences may be determined. B.W.

N86-11364# National Bureau of Standards, Gaithersburg, Md.
FIRE GROWTH IN COMBAT SHIPS
J. Quintiere, H. Baum, and R. Lawson Jun. 1985 99 p refs
(NBSIR-85/3159) Avail: NTIS HC A05/MF A01

A discussion of fire phenomenology pertaining to ships is presented. It draws a background from ship fires, combat ship construction characteristics and scientific knowledge developed for building fires. The immediate goal of this research is to assess the prospect of developing a deterministic (physics) model for ship fire growth as initiated by explosive weapon effects. A specific analysis of vented explosion flows is given as well as a procedure for computing fire growth phenomena from formulae. Author

N86-11365# National Bureau of Standards, Gaithersburg, Md.
METHODS TO CALCULATE THE RESPONSE TIME OF HEAT AND SMOKE DETECTORS INSTALLED BELOW LARGE UNOBSTRUCTED CEILINGS
David D. Evans and David W. Stroup Feb. 1985 49 p refs
(NBSIR-85/3167) Avail: NTIS HC A03/MF A01

Recently developed methods to calculate the time required for ceiling mounted heat and smoke detectors to respond to growing fires are reviewed. A computer program, that calculates activation times for both fixed temperatures and rate of rise heat detectors in response to fires that increase in heat release rate proportionally with the square of time from ignition is given. A separate method and corresponding program are provided to calculate response time for fires having arbitrary heat release rate histories. This method is based on quasi-steady ceiling layer gas flow assumptions. Assuming a constant proportionality between smoke and hat release from burning materials, a method is described to calculate smoke detector response time modeling the smoke detector as a low temperature heat detector in either of the two response time models. Author

N86-11366# National Bureau of Standards, Gaithersburg, Md.
RESPONSE BEHAVIOR OF HOT-WIRES AND FILMS TO FLOWS OF DIFFERENT GASES
William M. Pitts and Bernard J. McCaffrey Jul. 1985 123 p refs
(Grant AFOSR ISSA-00005)
(NBSIR-85/3203) Avail: NTIS HC A06/MF A01

Measurements of the voltage output for hot wire and film anemometers placed in flows of nine different gases have been made as a function of flow velocity. It has been possible to correlate the measurements quite accurately by treating the data in terms of suitably defined Reynolds and Nusselt numbers. In order to obtain these correlations it has been necessary to consider and correct for the effects of probe end conduction losses, temperature dependencies of gas molecular properties, flow slip at the probe surfaces, and gas accommodation. With the exception of the results for helium (for which accommodation effects are strong), the most important correction is shown to be that for the different temperature dependencies of the gas molecular properties. This finding is contrasted with previous studies which have assumed that the largest effect among different gases was due to variations in the Prandtl number. The importance of the nature of the flow over the cylindrical devices to the heat transfer behavior is described. A previously unreported hysteresis in the heat transfer behavior for RE 44 has been characterized and attributed to the presence or absence of eddy shedding from the heated cylinder. Author

N86-11367*# National Bureau of Standards, Gaithersburg, Md.
PROCEEDINGS OF THE THIRD CRYOCOOLER CONFERENCE Final Report
Ray Radebaugh, Beverly Louie, and Sandy McCarthy May 1985 284 p refs Conf. held in Boulder, Colo., 17-18 Sep. 1984 Sponsored by NASA. Goddard Space Flight Center
(NASA-CR-176298; NAS 1.26:176298; PB85-233369; NBS-SP-698; LC-85-600544) Avail: NTIS MF A01; also available SOD HC $10.00 as 003-003-02662-0 CSCL 13B

Mechanical and non-mechanical types of small cryocoolers in the temperature range of 4 to 80 K are discussed. Applications of these small cryocoolers include the cooling of infrared detectors, cryopumps, small superconducting devices and magnets, and electronic devices. For individual titles, see N86-11368 through N86-11393.

N86-11368*# National Bureau of Standards, Boulder, Colo. Electromagnetic Technology Div.

DESIGN OF CRYOCOOLERS FOR MICROWATT SUPERCONDUCTING DEVICES

J. E. Zimmerman *In its* Proc. of the 3rd Cryocooler Conf. May 1985 p 2-9 refs (For primary document see N86-11367 02-31)

Avail: NTIS MF A01; SOD HC $10.00 as 003-003-02662-0 CSCL 13B

The primary applications of the cryocoolers are for cooling various Josephson devices such as SQUID magnetometers and amplifiers, voltage standards, and microwave mixers and detectors. The common feature of these devices is their extremely low inherent bias power requirement, of the order of 10/1 W per junction. This provides the possibility of designing compact, low-power cryocoolers for these applications. Several concepts were explored and a number of laboratory model cryocoolers were built. These include low-power nonmagnetic regenerative machines of the Stirling or Gifford-McMahon type, three or four-stage Joule-Thomson machines, liquid-helium dewars with integral small cryocoolers to reduce the evaporation rate, and liquid-helium dewars with integral continuously or intermittently operated small helium liquefiers to permit operation of cryogenic devices for indefinite time periods. E.A.K.

N86-11369*# Nihon Univ., Tokyo (Japan). Atomic Energy Research Inst.

RECENT CRYOCOOLER PROGRESS IN JAPAN

Yoichi Matsubara *In* NBS Proc. of the 3rd Cryocooler Conf. May 1985 p 10-19 refs (For primary document see N86-11367 02-31)

Avail: NTIS MF A01; SOD HC $10.00 as 003-003-02662-0 CSCL 13B

The progress of cryocoolers and related devices in Japan is reviewed. The Japanese National Railways has developed the light weight 4 K on-board refrigerators since 1977 as part of the MAGLEV train program. Superconducting and cryogenic fundamental technology was examined which included high performance cryocooler, magnetic refrigerator and superfluid refrigeration. Space cryogenics such as the cooling systems of IR-detectors was studied. Cryocooler for special applications such as cryopump, NMR-CT and JJ devices was investigated. Compact heat exchangers, high performance regenerators and reliable compressors are investigated as a critical component technology. E.A.K.

N86-11370*# Los Alamos National Lab., N. Mex.

MAGNETIC REFRIGERATION FOR LOW-TEMPERATURE APPLICATIONS

J. A. Barclay *In* NBS Proc. of the 3rd Cryocooler Conf. May 1985 p 20-32 refs Sponsored in part by NASA. Kennedy Space Center, DOE and DARPA (For primary document see N86-11367 02-31)

Avail: NTIS MF A01; SOD HC $10.00 as 003-003-02662-0 CSCL 13B

The application of refrigeration at low temperatures ranging from production of liquid helium for medical imaging systems to cooling of infrared sensors on surveillance satellites is discussed. Cooling below about 15 K with regenerative refrigerators is difficult because of the decreasing thermal mass of the regenerator compared to that of the working material. In order to overcome this difficulty with helium gas as the working material, a heat exchanger plus a Joule-Thomson or other exponder is used. Regenerative magnetic refrigerators with magnetic solids as the working material have the same regenerator problem as gas refrigerators. This problem provides motivation for the development of nonregenerative magnetic refrigerators that span approximately 1 K to approximately 0 K. Particular emphasis is placed on high reliability and high efficiency. Calculations indicate considerable promise in this area. The principles, the potential, the problems, and the progress towards development of successful 4 to 20 K magnetic refrigerators are discussed. E.A.K.

N86-11371*# Jet Propulsion Lab., California Inst. of Tech., Pasadena.

RECIPROCATING MAGNETIC REFRIGERATOR

Dean L. Johnson *In* NBS Proc. of the 3rd Cryocooler Conf. May 1985 p 33-41 refs (For primary document see N86-11367 02-31)

Avail: NTIS MF A01; SOD HC $10.00 as 003-003-02662-0 CSCL 13B

A 4 to 15 K magnetic refrigerator to test as an alternative to the Joule-Thomson circuit as the low temperature stage of a 4 to 300 K closed-cycle refrigerator was developed. The reciprocating magnetic refrigerator consists of two matrices of gadolinium gallium garnet spheres located in tandem on a single piston which alternately moves each matrix into a 7 telsa magnetic field. A separate helium gas circuit is used as the heat exchange mechanism for the low and the high temperature extremes of the magnetic refrigerator. Details of the design and results of the initial refrigerator component tests are presented. E.A.K.

N86-11372*# Jet Propulsion Lab., California Inst. of Tech., Pasadena.

IMPROVED HEAT SWITCH FOR GAS SORPTION COMPRESSOR

Chung K. Chan *In* NBS Proc. of the 3rd Cryocooler Conf. May 1985 p 42-52 refs (For primary document see N86-11367 02-31)

Avail: NTIS MF A01; SOD HC $10.00 as 003-003-02662-0 CSCL 13B

Thermal conductivities of the charcoal bed and the copper matrix for the gas adsorption compressor were measured by the concentric-cylinder method. The presence of the copper matrix in the charcoal bed enhanced the bed conductance by at least an order of magnitude. Thermal capacities of the adsorbent cell and the heat leaks to two compressor designs were measured by the transient method. The new gas adsorption compressor had a heat switch that could transfer eight times more heat than the previous one. The cycle time for the new prototype compressor is also improved by a factor of eight to within the minute range. E.A.K.

N86-11373*# Jet Propulsion Lab., California Inst. of Tech., Pasadena. Applied Mechanics Div.

HYDRIDE ABSORPTION REFRIGERATOR SYSTEM FOR TEN KELVIN AND BELOW

Jack A. Jones *In* NBS Proc. of the 3rd Cryocooler Conf. May 1985 p 53-64 refs (For primary document see N86-11367 02-31)

Avail: NTIS MF A01; SOD HC $10.00 as 003-003-02662-0 CSCL 13B

A very long-life, lightweight and efficient hydride absorption refrigerator system was built to operate at ten Kelvin and below. The system consists of four basic stages of refrigeration. The first stage is accomplished by an active refrigeration system. The second stage is operated by a hydride absorption system, wherein a heated hydride powder drives off high pressure hydrogen through a Joule-Thomson/heat exchanger expansion loop such that the hydrogen is partially liquefied. In the third stage, the vapor pressure over the collected liquid hydrogen is lowered by absorbing the hydrogen vapor onto a different low pressure, worn hydride. With a 1.7 torr partial pressure of hydrogen gas in the hydride, liquid hydrogen is solidified and sublimes at 10 K. Long-life adiabatic demagnetization refrigerators, helium desorption, or helium diaphragm compressors are used to cool to 4 K or below. It is shown that the hydride concepts provide an extremely efficient means of refrigeration to 10 K, and that an entire sorption refrigeration process can be accomplished solely by using low grade heat energy at about 150 C. Author

N86-11374*# General Pneumatics Corp., Scottsdale, Ariz.

CLASSIFICATION OF CRYOCOOLERS

G. Walker *In* NBS Proc. of the 3rd Cryocooler Conf. May 1985

p 65-70 refs (For primary document see N86-11367 02-31)
Avail: NTIS MF A01; SOD HC $10.00 as 003-003-02662-0 CSCL 13B

A great diversity of methods and mechanisms were devised to effect cryogenic refrigeration. The basic parameters and considerations affecting the selection of a particular system are reviewed. A classification scheme for mechanical cryocoolers is presented. An important distinguishing feature is the incorporation or not of a regenerative heat exchanger, of valves, and of the method for achieving a pressure variation. E.A.K.

N86-11375*# Zhejiang Univ. (China). Cryogenic Engineering Lab.
AN EXPERIMENTAL STUDY FOR A MINIATURE STIRLING REFRIGERATOR
Shimo Li, Guobang Chen, Zhixiu Huang, Fagao Zhang, Cuangji Cui (Beijing Univ., China), and Jiazhang Li (Beijing Univ., China) *In* NBS Proc. of the 3rd Cryocooler Conf. May 1985 p 71-79 refs (For primary document see N86-11367 02-31)
Avail: NTIS MF A01; SOD HC $10.00 as 003-003-02662-0 CSCL 13B

Experimental results of a miniature two-stage Stirling cryocooler are introduced. The influence of filling gas pressure and refrigeration temperature on the refrigerating capacity along with the relationship between parameters was measured. The valley pressure corresponding to the lowest refrigeration temperature and the cooldown time versus operating pressure are discussed. The coefficient of performance and thermodynamic efficiency of the cryocooler are calculated based on experimental data. E.A.K.

N86-11376*# Philips Labs., Briarcliff Manor, New York.
PARAMETRIC TESTING OF A LINEARLY DRIVEN STIRLING CRYOGENIC REFRIGERATOR
F. R. Stolfi and A. Daniels *In* NBS Proc. of the 3rd Cryocooler Conf. May 1985 p 80-98 refs (For primary document see N86-11367 02-31)
(Contract NAS5-25172)
Avail: NTIS MF A01; SOD HC $10.00 as 003-003-02662-0 CSCL 13B

The parametric testing of a novel Stirling cycle cryogenic refrigerator which incorporates electromagnetic bearings, clearance seals and electronically controlled linear motion was studied. The last feature, which involves the use of two linear motors, position transducers and a highly accurate electronic feedback network, produces the system capability which forms the basis for the tests. The test results provide designers with an understanding of the basic operation of the Stirling cycle and give potential users some indication of the capabilities of this refrigerator under off design conditions. E.A.K.

N86-11377*# Philips Labs., Briarcliff Manor, New York.
DESIGN OF A FLIGHT QUALIFIED LONG-LIFE CRYOCOOLER
L. Knox, P. Patt, and R. Maresca *In* NBS Proc. of the 3rd Cryocooler Conf. May 1985 p 99-118 refs (For primary document see N86-11367 02-31)
(Contract NAS5-26688)
Avail: NTIS MF A01; SOD HC $10.00 as 003-003-02662-0 CSCL 13B

A second generation Stirling cycle cryogenic refrigerator with a linear drive, magnetic bearings, and clearance seals; designed to produce 5 watts of cooling at 65 Kelvin and to meet Space Shuttle mission requirements is described. The first generation refrigerator met all performance specifications, and operated with no failure for over 12,030 hours. Meeting launch requirements necessitated improvements in the electromagnetic bearings, the radial position sensors, and in the structural design of the moving elements. Organic contamination was eliminated by the use of all metal and ceramic construction. Reductions in system input power are attained by an integral magnetic spring/motor for the displacer and by more efficient linear motors and drive electronics. E.A.K.

N86-11378*# Technische Hogeschool, Delft (Netherlands). Dept. of Applied Physics.
SIMPLE CONSTRUCTION AND PERFORMANCE OF A CONICAL PLASTIC CRYOCOOLER
N. Lambert *In* NBS Proc. of the 3rd Cryocooler Conf. May 1985 p 119-126 refs (For primary document see N86-11367 02-31)
Avail: NTIS MF A01; SOD HC $10.00 as 003-003-02662-0 CSCL 13B

Low power cryocoolers with conical displacers offer several advantages over stepped displacers. The described fabrication process allows quick and reproducible manufacturing of plastic conical displacer units. This could be of commercial interest, but it also makes systematic optimization feasible by constructing a number of different models. The process allows for a wide range of displacer profiles. Low temperature performance as dominated by regenerator losses, and several effects are discussed. A simple device is described which controls gas flow during expansion. E.A.K.

N86-11379*# Philips Labs., Briarcliff Manor, New York.
EFFECTS OF LEAKAGE THROUGH CLEARANCE SEALS ON THE PERFORMANCE OF A 10 K STIRLING-CYCLE REFRIGERATOR
C. S. Keung and E. Lindale *In* NBS Proc. of the 3rd Cryocooler Conf. May 1985 p 127-134 refs Sponsored in part by Rockwell International Corp. (For primary document see N86-11367 02-31)
Avail: NTIS MF A01; SOD HC $10.00 as 003-003-02662-0 CSCL 13B

The use of clearance seals is essential to achieve long life, wear free operation of Stirling cycle cryogenic refrigerators. The effect of leakage through clearance seals on the performance of such a refrigerator operating at temperatures ranging from 20 K down to 10 K was determined. The ability of a Stirling cycle refrigerator to achieve 10 K with clearance seals was successfully demonstrated. It is indicated that the leakage flow undergoes gap regeneration before reaching the cold expansion volume. A simple model of gap regeneration was used to estimate the regeneration loss due to the leakage flow. This regeneration process minimizes the loss in refrigerator performance caused by the clearance seal leakage. It is found that clearance seals remain effective down to a refrigeration temperature of 10 K. E.A.K.

N86-11380*# Massachusetts Inst. of Tech., Cambridge. Cryogenic Engineering Lab.
AN EXPERIMENTAL RECIPROCATING EXPANDER FOR CRYOCOOLER APPLICATION
Moses Minta and Joseph L. Smith, Jr. *In* NBS Proc. of the 3rd Cryocooler Conf. May 1985 p 135-146 refs (For primary document see N86-11367 02-31)
Avail: NTIS MF A01; SOD HC $10.00 as 003-003-02662-0 CSCL 13B

An experimental reciprocating expander was designed with features appropriate for cryocooler cycles. The expander has a displacer piston, simple valves, and a hydraulic/pneumatic stroking mechanism. The expander has a valve in head configuration with the valves extending out the bottom of the vacuum enclosure while the piston extends out the top. The expander was tested using a CTI 1400 liquefier to supply 13 atm in the temperature range 4.2 to 12 K. Expander efficiency was measured in the range 84 to 93% while operating the apparatus as a supercritical wet expander and in the range 91 to 93% aa a single phase expander. The apparatus can also be modified to operate as a compressor for saturated helium vapor. E.A.K.

N86-11381*# L'Air Liquide, Sassenage (France). Advanced Technology Div.
EXPERIMENTS WITH A FULLY INSTRUMENTED SPLIT STIRLING CRYOCOOLER
Alain Faure, Serge Reale, and Philippe Bernhein *In* NBS Proc. of the 3rd Cryocooler Conf. May 1985 p 147-155 (For primary document see N86-11367 02-31)
Avail: NTIS MF A01; SOD HC $10.00 as 003-003-02662-0 CSCL 13B

A practical model that can be used to accurately size and optimally split stirling cryocoolers is discussed. A practical model that could be used to extrapolate existing designs to meet different specifications was developed. However, to do this detailed knowledge of the dynamic operating parameters of this type of cryocooler is required. The first stage is to fully instrument a refrigerator so that various dynamic parameters can be measured. The second stage involves the application of these measurements to the design and optimization of a range of coolers. E.A.K.

N86-11382*# Xian Jiaotong Univ. (China). Dept. of Power Machinery Engineering.

LOW FREQUENCY SPLIT CYCLE CRYOCOOLER

S. X. Bian, Y. D. Zhang, W. W. Wan, L. Wang, and Q. C. Hu *In* NBS Proc. of the 3rd Cryocooler Conf. May 1985 p 156-160 refs (For primary document see N86-11367 02-31)

Avail: NTIS MF A01; SOD HC $10.00 as 003-003-02662-0 CSCL 13B

A split cycle Stirling cryocooler with two different drive motors and operating at a low drive frequency can have high thermodynamic efficiency. The temperature of the cold end of the cryocooler varies with drive frequency, voltage of the input electrical power and initial charge pressure values. The cryocooler operating at 8 Hz can provide 7 watts of refrigeration at 77 K for 230 watts of electrical input power. E.A.K.

N86-11383*# Ricor Ltd., En-Harod Ihud (Israel).

PASSIVE MOTION CONTROL OF PNEUMATICALLY DRIVEN DISPLACERS IN CRYOGENIC COOLERS

N. Pundak and S. Shtrikman (Weizmann Inst. of Science) *In* NBS Proc. of the 3rd Cryocooler Conf. May 1985 p 161-167 refs (For primary document see N86-11367 02-31)

Avail: NTIS MF A01; SOD HC $10.00 as 003-003-02662-0 CSCL 13B

The split cryogenic cooler with a remote cold finger offers many advantages for use in cooling of infrared systems. A pneumatic drive for the displacer in such coolers was adopted in many cryocooler designs. This concept can be significantly improved by causing the displacer to move sinusoidally rather than in an essentially square wave, as in most of the present models. The way this motion was achieved passively is described and its advantages outlined. Data of minicoolers using this concept are presented. E.A.K.

N86-11384*# Martini Engineering, Richland, Wash.

A NONPROPRIETARY, NONSECRET PROGRAM FOR CALCULATING STIRLING CRYOCOOLERS

William R. Martini *In* NBS Proc. of the 3rd Cryocooler Conf. May 1985 p 168-176 refs (For primary document see N86-11367 02-31)

Avail: NTIS MF A01; SOD HC $10.00 as 003-003-02662-0 CSCL 13B

A design program for an integrated Stirling cycle cryocooler was written on an IBM-PC computer. The program is easy to use and shows the trends and itemizes the losses. The calculated results were compared with some measured performance values. The program predicts somewhat optimistic performance and needs to be calibrated more with experimental measurements. Adding a multiplier to the friction factor can bring the calculated rsults in line with the limited test results so far available. The program is offered as a good framework on which to build a truly useful design program for all types of cryocoolers. E.A.K.

N86-11385*# National Bureau of Standards, Boulder, Colo. Chemical Engineering Science Div.

A SIMPLE, FIRST STEP TO THE OPTIMIZATION OF REGENERATOR GEOMETRY

Ray Radebaugh and Beverly Louie *In its* Proc. of the 3rd Cryocooler Conf. May 1985 p 177-198 refs Sponsored in part by Naval Ship Research and Development Center and ONR (For primary document see N86-11367 02-31)

Avail: NTIS MF A01; SOD HC $10.00 as 003-003-02662-0 CSCL 13B

This paper presents a simplified set of equations for calculating and optimizing regenerator geometries. A number of competing parameters must be accounted for in the design of a regenerator. To obtain high values of effectiveness, there is need for a large surface area for heat transfer and high heat capacity. The void volume should be small to maintain the pressure ratio in the entire system. Moreover, the pressure drop should be small compared to the absolute pressure. With the assumptions made here, the calculations can be done with a hand calculator. The equations show that the optimum regenerator length, hydraulic radius, and porosity are independent of mass flow rate and the gas cross sectional area is proportional to the mass flow rate. It is shown that using gas gaps between parallel plates produces a significantly better regenerator than is possible with packed spheres or screens, particularly at temperatures below approximately 50%. Author

N86-11386*# National Bureau of Standards, Boulder, Colo. Scientific Computing Div.

A COMPUTATIONAL MODEL FOR A REGENERATOR

John Gary, David E. Daney, and Ray Radebaugh *In its* Proc. of the 3rd Cryocooler Conf. May 1985 p 199-211 refs (For primary document see N86-11367 02-31)

Avail: NTIS MF A01; SOD HC $10.00 as 003-003-02662-0 CSCL 13B

This paper concerns a numerical model of a regenerator running at very low temperatures. The model consists of the usual three equations for a compressible fluid with an additional equation for a matrix temperature. The main difficulty with the model is the very low Mach number (approximately 1.E-3). The divergence of the velocity is not small, the pressure divergence is small, and the pressure fluctuation in time is not small. An asymptotic expansion based on the bounded derivative method of Kreiss is used to give a reduced model which eliminates acoustic waves. The velocity is then determined by a two-point boundary value problem which does not contain a time derivative. The solution obtained from the reduced system is compared with the numerical solution of the original system. Author

N86-11387*# Massachusetts Inst. of Tech., Cambridge. Cryogenic Engineering Lab.

CRITERIA FOR SCALING HEAT EXCHANGERS TO MINIATURE SIZE

Philipp B. RudolfvonRohr and Joseph L. Smith, Jr. *In* NBS Proc. of the 3rd Cryocooler Conf. May 1985 p 212-219 refs (For primary document see N86-11367 02-31)

Avail: NTIS MF A01; SOD HC $10.00 as 003-003-02662-0 CSCL 13B

The purpose of this work is to highlight the particular aspects of miniature heat exchangers performance and to determine an appropriate design approach. A thermodynamic analysis is performed to express the generated entropy as a function of material and geometric characteristics of the heat exchangers. This expression is then used to size miniature heat exchangers. Author

N86-11388*# Jet Propulsion Lab., California Inst. of Tech., Pasadena.

A CLOSED CYCLE CASCADE JOULE THOMSON REFRIGERATOR FOR COOLING JOSEPHSON JUNCTION MAGNETOMETERS

Emanuel Tward and Raymond Sarwinski (Hansen (R. G.) and Associates, San Diego, Calif.) *In* NBS Proc. of the 3rd Cryocooler Conf. May 1985 p 220-225 refs (For primary document see N86-11367 02-31)

Avail: NTIS MF A01; SOD HC $10.00 as 003-003-02662-0 CSCL 13B

A closed cycle cascade Joule Thomson refrigerator designed to cool Josephson Junction magnetometers to liquid helium temperature is being developed. The refrigerator incorporates 4 stages of cooling using the working fluids CF4 and He. The high pressure gases are provided by a small compressor designed for this purpose. The upper stages have been operated and performance will be described. Author

N86-11389*# Quantum Technology Corp., Surrey (British Columbia).

A SMALL HELIUM LIQUIFIER WHICH PROVIDES CONTINUOUS COOLING BASED ON CYCLED ISENTROPIC EXPANSION

Calvin Winter, Suso Gygax (Simon Fraser Univ.), Ken Myrtle, and Russel Barton *In* NBS Proc. of the 3rd Cryocooler Conf. May 1985 p 226-233 refs Sponsored by Science Council of British Columbia and National Sciences and Engineering Research Council (For primary document see N86-11367 02-31)
Avail: NTIS MF A01; SOD HC $10.00 as 003-003-02662-0 CSCL 13B

This simple cryocooler provides a small reservoir of liquid helium at a stable temperature of 4.2K. It uses a novel adaptation of the Simon expansion cryocooler to provide continuous cooling. Operation is in a four stage cycle: (1) A closed vessel of helium under high pressure is cooled to 12K using a conventional Gifford-McMahon closed-cycle cryocooler. (2) The pressure is released adiabatically providing cooling to 4.2K. (3) Liquid helium is collected in a second, well insulated, vessel. (4) The first vessel is repressurized. The cycle time is 15-30 minutes. In this manner, a pool of liquid helium is continuously maintained in the second vessel, with a temperature stability of 0.03 degrees. The continuous cooling power available is 3mW. This design provides simplicity and reliability through the absence of any orifices or moving parts at cryogenic temperatures except for the conventional Gifford-McMahon cryocooler. Author

N86-11390*# Nihon Univ., Tokyo (Japan). Atomic Energy Research Inst.

VUILLEUMIER CYCLE CRYOCOOLER OPERATING BELOW 8 K

Yoichi Matsubara and Mitsuhiro Kaneko (Suzuki Shokan Co. Ltd.) *In* NBS Proc. of the 3rd Cryocooler Conf. May 1985 p 234-239 refs Sponsored in part by Science and Technology Agency (For primary document see N86-11367 02-31)
Avail: NTIS MF A01; SOD HC $10.00 as 003-003-02662-0 CSCL 13B

This paper describes the design and development of a Vuilleumier cycle cryocooler (VM cooler) operating below 8 K, for the application of small superconducting devices. Liquid nitrogen has been used as a heat sink of the hot displacer. The annular gap between the phenolic displacer and SUS 304 stainless cylinder has been used as a gap regenerator. In order to obtain the cooling temperature below 3 K, we designed a single stage VM cooler which is precooled to 10 K by another two stage VM cooler. The effect of the mean operating pressure, cycle speed and phase difference between the hot and cold displacer of each VM cooler will be also discussed, including the experimental results. Author

N86-11391*# Air Products and Chemicals, Inc., Allentown, Pa.

FOUR K REFRIGERATORS WITH A NEW COMPACT HEAT EXCHANGER

R. C. Longsworth and W. A. Steyert *In* NBS Proc. of the 3rd Cryocooler Conf. May 1985 p 240-249 refs (For primary document see N86-11367 02-31)
Avail: NTIS MF A01; SOD HC $10.00 as 003-003-02662-0 CSCL 13B

Two refrigerators have been developed which have nominal capacities of 0.25M and 0.5W at 4.2K. These use standard two stage Displex sup R expanders and compressors combined with a new compact heat exchanger which is concentric with the expander cylinder. These refrigerators can be used to cool superconducting electronic devices by direct attachment to the 4K heat station, or they can be plugged into the neck of a liquid helium superconducting magnet cryostat where they can cool the radiation shields and reliquefy helium. Author

N86-11392*# Mechanical Technology, Inc., Latham, N. Y.

THE DESIGN OF A SMALL LINEAR-RESONANT, SPLIT STIRLING CRYOGENIC REFRIGERATOR COMPRESSOR

R. A. Ackermann *In* NBS Proc. of the 3rd Cryocooler Conf. May 1985 p 250-256 (For primary document see N86-11367 02-31)
Avail: NTIS MF A01; SOD HC $10.00 as 003-003-02662-0 CSCL 13B

The development of a small linear-resonant compressor for use in a 1/4-watt, 78K, split Stirling cryogenic refrigerator is discussed. The compressor contains the following special features: (1) a permanent-magnet linear motor; (2) resonant dynamics; (3) dynamic balancing; and (4) a close-clearance seal between the compressor piston and cylinder. This paper describes the design of the compressor, and presents component test data and system test data for the compressor driving a 1/4-watt expander. Author

N86-11393*# Ball Aerospace Systems Div., Boulder, Colo. Cryogenics, Space Systems.

JOULE-THOMSON VALVES FOR LONG TERM SERVICE IN SPACE CRYOCOOLERS

James M. Lester and Becky Benedict *In* NBS Proc. of the 3rd Cryocooler Conf. May 1985 p 257-266 ref (For primary document see N86-11367 02-31)
Avail: NTIS MF A01; SOD HC $10.00 as 003-003-02662-0 CSCL 13B

Joule-Thomson valves for small cryocoolers have throttling passages on the order of 0.1 millimeter in diameter. Consequently, they can become plugged easily and stop the operation of the cooler. Plugging can be caused by solid particles, liquids or gases. Plugging is usually caused by the freezing of contaminant gases from the process stream. In small open loop coolers and in closed loop coolers where periodic maintenance is allowed, the problem is overcome by using careful assembly techniques, pure process gases, warm filters and cold adsorbers. A more thorough approach is required for closed loop cryocoolers which must operate unattended for long periods. This paper presents the results of an effort to solve this problem. The causes of plugging are examined, and various ways to eliminate plugging are discussed. Finally, the development of a J-T defroster is explained. It is concluded that a combination of preventive measures and a defroster will reduce the chance of cooler failure by plugging to such a degree that J-T coolers can be used for long term space missions. Author

N86-11394# Joint Publications Research Service, Arlington, Va.

USSR REPORT: MACHINE TOOLS AND METALWORKING EQUIPMENT

4 Sep. 1985 73 p Transl. into ENGLISH from various Russian articles
(JPRS-UMM-85-010) Avail: NTIS HC A04

Research advances in U.S.S.R. machine tools and metal working equipment are reported. Topics covered include automated lines and aggregated machining systems; robotics; and technology planning and management automation. For individual titles, see N86-11395 through N86-11397.

N86-11395# Joint Publications Research Service, Arlington, Va.

LARGE ROBOTIZED TURNING CENTERS DESCRIBED

V. V. Kirsanov and V. I. Tsarenko *In its* USSR Rept.: Machine Tools and Metalworking Equipment (JPRS-UMM-85-010) 4 Sep. 1985 p 43-47 Transl. into ENGLISH from Stroit. i Dorozhnyye Mash. (Moscow), no. 2, Feb. 1985 p 19-20 (For primary document see N86-11394 02-31)
Avail: NTIS HC A04

The introduction of numerical control (NC) machine tools has made it possible to automate machining in series and small series production. The organization of automated production sections merged NC machine tools with automated transport systems. However, both the one and the other require the presence of an operative at the machine for low skilled operations. Industrial robots perform a number of auxiliary operations, such as equipment loading-unloading and control, changing cutting and auxiliary tools, controlling workpieces and parts, and cleaning of location surfaces. When used with a group of equipment they perform transfer operations between the machine tools. Industrial robots eliminate the need for workers to form auxiliary operations. This underscores the importance of developing robotized manufacturing centers providing for minimal human participation in production and creating conditions for two and three shift operation of equipment. Work carried out at several robotized manufacturing centers for series and small series production is described. B.W.

N86-11396# Joint Publications Research Service, Arlington, Va.
ROBOTIZED PRODUCTION SYSTEMS OBSERVED IN MODERN PLANTS
A. N. Saverina *In its* USSR Rept.: Machine Tools and Metalworking Equipment (JPRS-UMM-85-010) 4 Sep. 1985 p 46-51 Transl. into ENGLISH from Avto. Prom. (Moscow), no. 12, Dec. 1984 p 26-28 (For primary document see N86-11394 02-31)
Avail: NTIS HC A04

Robots, robotized lines and sectors are no longer innovations in shops at automotive plants. The widespread robotization of automobile assembly operations is described in general terms. Robot use for machining operation is also discussed. B.W.

N86-11397# Joint Publications Research Service, Arlington, Va.
ROBOTIZED MACHINING SYSTEMS DEVELOPED AT GOMEL INSTITUTE
N. N. Gulyayev *In its* USSR Rept.: Machine Tools and Metalworking Equipment (JPRS-UMM-85-010) 4 Sep. 1985 p 58-60 Transl. into ENGLISH from Traktory i Selkhozmashiny (Moscow), no. 4, Apr. 1985 p 54 (For primary document see N86-11394 02-31)
Avail: NTIS HC A04

The development of robotized machining systems at Gomel Institute is discussed. Applications, economic benefits, and technological sophistication are discussed in detail. Effects on productivity are also discussed. B.W.

N86-11253*# National Aeronautics and Space Administration. Langley Research Center, Hampton, Va.
RAPID ADHESIVE BONDING AND FIELD REPAIR OF AEROSPACE MATERIALS
Bland A. Stein *In its* Welding, Bonding and Fastening, 1984 Sep. 1985 p 419-438 ref (For primary document see N86-11227 02-23)
Avail: NTIS HC A21/MF A01 CSCL 13H

N86-11403# Hughes Aircraft Co., Canoga Park, Calif. Missile Systems Group.
SHEET METAL WAVEGUIDE FORMING TECHNIQUE
P. K. Park and S. E. Bradshaw *In* RADC Proc. of the 1984 Antenna Appl. Symp. Jan. 1985 p 113-122 refs (For primary document see N86-11398 02-32)
Avail: NTIS HC A13/MF A01 CSCL 13/8

32 COMMUNICATIONS

Includes land and global communications; communications theory; and optical communications.

For related information see also *04 Aircraft Communications and Navigation* and *17 Spacecraft Communications, Command and Tracking.*

N86-11398# Rome Air Development Center, Griffiss AFB, N.Y.
PROCEEDINGS OF THE 1984 ANTENNA APPLICATIONS SYMPOSIUM
Jan. 1985 277 p refs Symp. held in Urbana, Ill., 19-21 Sep. 1984; sponsored by RADC and Illinois Univ., Urbana 2 Vol.
(Contract F19628-84-M-0002; AF Proj. 4600)
(AD-A153257; RADC-TR-85-14-Vol-1) Avail: NTIS HC A13/MF A01 CSCL 09/5

Antennas and their applications were discussed. The state of the art as related to: phased array antennas, millimeter wave antennas, microstrip and conformal antennas, reflector antennas, and near field antenna measurement techniques is presented. For individual titles, see N86-11399 through N86-11410.

N86-11399# Massachusetts Univ., Amherst. Dept. of Electrical and Computer Engineering.
CONSIDERATIONS FOR MILLIMETER WAVE, MONOLITHIC PHASED ARRAYS
D. H. Schaubert, D. M. Pozar, K. S. Yngvesson, and R. W. Jackson *In* RADC Proc. of the 1984 Antenna Appl. Symp. Jan. 1985 p 9-36 refs (For primary document see N86-11398 02-32)
(Contract F19628-84-K-0022)
Avail: NTIS HC A13/MF A01 CSCL 09/3

Some candidate elements for millimeter wave, monolithic phased arrays are discussed. Printed antennas on high permittivity substrates are discussed in relation to EHF array performance. Scan impedance and blindness are evaluated by analysis and experiment. Methods for interfacing active devices such as FETs with candidate array elements are discussed. E.A.K.

N86-11400# Harris Government Aerospace Systems Div., Melbourne, Fla.
THE DESIGN OF A THERMALLY EFFICIENT 1:256 KU-BAND FEED NETWORK FOR A MMIC PHASED ARRAY
C. A. Hancik, D. E. Hackaman, and E. J. Bajgrowicz *In* RADC Proc. of the 1984 Antenna Appl. Symp. Jan. 1985 p 37-56 refs (For primary document see N86-11398 02-32)
Avail: NTIS HC A13/MF A01 CSCL 09/3

A thin, thermally transparent, 1:256 corporate feed network for use in a GaAs MMIC Ku-Band phased array antenna was designed. The network will be realized using RF transmission medium, CHANNELINE. The CHANNELINE consists of a core of TFE coated copper wire placed in a channel routed through a heat exchanging metal structure which composes the backside of the array. This unique packaging arrangement conserves both volume and weight while simultaneously allowing the rapid transfer of internally generated heat. This network is expected to realize better than 15 dB of return loss with less than 1.3 dB of return loss with less than 1.3 dB insertion loss over an 8% bandwidth. The current status of array hardware is presented. E.A.K.

N86-11401*# National Aeronautics and Space Administration. Lewis Research Center, Cleveland, Ohio.
CHARACTERIZATION OF MMIC DEVICES FOR ACTIVE ARRAY ANTENNAS
Jerry Smetana, Everett Farr (Illinois Univ., Urbana), and Raj Mittra (Illinois Univ., Urbana) *In* RADC Proc. of the 1984 Antenna Appl. Symp. Jan. 1985 p 57-82 refs Previously announced as N85-15779 (For primary document see N86-11398 02-32)
Avail: NTIS HC A13/MF A01 CSCL 09C

Certain aspects of monlithic microwave integrated circuit (MMIC) interconnectivity were investigated. Considerations that lead to preserving the inherently reproducible characteristics of the MMIC are proposed. It is shown that at radio frequencies (RF) greater than 20 GHz, the transition from the MMIC device to other transmission media must be an accurate RF match. It is proposed that the RF match is sufficiently critical to include the transition as part of the delivered MMIC package. The model to analyze several transitions is presented. This model consists of a succession of abrupt discontinuities in printed circuit transmission lines. The analysis of these discontinuities is achieved by the Spectral Galerkin technique, to establish the modes and mode that special effects should be coordinated by the active array antenna industry toward standardization of MMIC packaging and characterization. Author

N86-11402# Emerson Electric Co., Calabasas, Calif.
WAVEGUIDE SLOT ARRAY WITH CSC2 THETA (DOT) COS THETA PATTERN
John J. Erlinger and Jeffrey R. Orlow *In* RADC Proc. of the 1984 Antenna Appl. Symp. Jan. 1985 p 83-112 refs (For primary document see N86-11398 02-32)
Avail: NTIS HC A13/MF A01 CSCL 20/14

A planar array of longitudinal shunt slots in rectangular waveguides has been designed to produce a CSC sup 2 theta . COS theta patern in the E-plane and -22-dB sidelobes in the H-plane. The array operates at 15 GHz. The choice of E-plane amplitude and phase distribution, to synthesize the CSC sup 2 theta COS theta pattern shape over the sector 8 deg to 50 deg below broadside, involved a tradeof study. A technique reported perturbing the roots on a Schelfunoff unit circle to obtain the disired pattern shape was used Twelve roots were perturbed in a systematic way to obtain an optimum amplitude distribution with accompanying phase angles. A method to spread the resultant E-plane distribution and the H-plane Taylor distribution over a circular aperture is described. The mutual coupling between elements is considered for the design. The predicted results show good agreement with measurements. E.A.K.

N86-11403# Hughes Aircraft Co., Canoga Park, Calif. Missile Systems Group.
SHEET METAL WAVEGUIDE FORMING TECHNIQUE c31
P. K. Park and S. E. Bradshaw *In* RADC Proc. of the 1984 Antenna Appl. Symp. Jan. 1985 p 113-122 refs (For primary document see N86-11398 02-32)
Avail: NTIS HC A13/MF A01 CSCL 13/8

A 30 element shunt slot array was designed analytically and fabricated by a sheet metal waveguide forming technique. This technique starts with 10 mil copper sheet which is then photo-etched completely through for slots and half way through for bendlines. The photo etched copper sheet is bent into waveguide with a couple of simple mandrels. Solder paste is applied to the seams and heated. The analytic design process adjusts the slot length and offset of each slot while including the effect of external mutual coupling until the desired aperture distribution and impedance match are achieved. It is shown that the cost effective sheet metal waveguide forming technique is a viable technique. E.A.K.

N86-11404# Raytheon Co., Goleta, Calif.
CONSIDERATIONS FOR EXTENDING THE BANDWIDTH OF ARRAYS BEYOND TWO OCTAVES
George J. Monser *In* RADC Proc. of the 1984 Antenna Appl. Symp. Jan. 1985 p 123-148 (For primary document see N86-11398 02-32)
Avail: NTIS HC A13/MF A01 CSCL 20/14

Array-element characteristics for a wideband, dual-polarized, array where the extension in bandwidth is achieved by extending the lower frequency limit are summarized. Array-element behavior over the lower part of the band is described. A lower frequency limit of operation is advanced based on element mismatch loss and efficiency. It is shown that low active VSWR and good efficiency can be achieved over a two octave band. E.A.K.

N86-11405# Raytheon Co., Bedford, Mass. Missile Systems Div.
MICROSTRIP MONPULSE DIPOLE ARRAY
William Miccioli, John Toth, Norbert Sa, and Michael Lewis *In* RADC Proc. of the 1984 Antenna Appl. Symp. Jan. 1985 p 149-170 refs (For primary document see N86-11398 02-32)
Avail: NTIS HC A13/MF A01 CSCL 09/3

The development of a microstrip radiating aperture utilizing multiple microstrip dipole radiators fed by a resonant feed configuration is described. This array combines an efficient capacitively coupled radiator feeding mechanism with a planar power divider configuration to achieve an extremely thin, lightweight antenna aperture. Linear array dipole matching theory and radiator bandwidth improvement techniques are also described. A quadrant based microstrip monopulse antenna was constructed. Experimental data from this array, its subassemblies and individual components are presented and compared to analytical predictions. E.A.K.

N86-11406# Saint Francis Medical Center, Peoria, Ill. Dept. of Radiology and Medical Imaging.
THEORY AND EXPERIMENT FOR INFINITE MICROSTRIP ARRAYS
Steven M. Wright and Y. T. Lo (Illinois Univ., Urbana) *In* RADC Proc. of the 1984 Antenna Appl. Symp. Jan. 1985 p 171-196 refs (For primary document see N86-11398 02-32)
Avail: NTIS HC A13/MF A01 CSCL 20/14

Microstrip antennas are well suited for use in large scanning arrays. To obtain greater bandwidth, it is useful to use thicker substrates, which can increase the effects of mutual coupling and lead to significant mismatch or blindness for certain scan angles. Using an infinite array formulation, the impedance of a single element in an infinite array environment was solved with the method of moments. Mutual coupling is built into the solution, and the presence of surface waves is accounted for by using the periodic Green's function for the grounded dielectric substrate. Blindness in arrays of microstrip dipoles on various substrates, both with and without radomes is demonstrated. E.A.K.

N86-11407*# National Aeronautics and Space Administration. Lewis Research Center, Cleveland, Ohio.
CIRCULARLY POLARIZED MICROSTRIP ANTENNAS
Y. T. Lo (Illinois Univ., Urbana), B. Engst (Illinois Univ., Urbana), and R. Q. H. Lee *In* RADC Proc. of the 1984 Antenna Appl. Symp. Jan. 1985 p 197-218 refs (For primary document see N86-11398 02-32)
Avail: NTIS HC A13/MF A01 CSCL 20N

A simple microstrip antenna can be made to radiate EM waves of any polarization, in particular, the circular polarization (CP) without any phasing network and power divider. A simple and accurate theory for this family of antennas was developed. However, the CP bandwidth, (CPBW) the bandwidth in which the axial ratio (AR) is less than a certain specified value, is very small. Most of the experimental designs were made for a feed placed along the diagonal of the patch. It is shown that there are practically infinitely many possible designs with different feed location. The speculation that other designs might give a wider bandwidth is clarified and an effective method for broadening the bandwidth is shown. E.A.K.

N86-11408# Georgia Inst. of Tech., Atlanta. Engineering Experiment Station.
RADIATION AND SCATTERING PERFORMANCE OF MICROSTRIP ANTENNAS USING EXOTIC SUBSTRATES
J. J. H. Wang *in* RADC Proc. of the 1984 Antenna Appl. Symp. Jan. 1985 p 219-234 refs (For primary document see N86-11398 02-32)
(Contract F19628-84-K-0010)
Avail: NTIS HC A13/MF A01 CSCL 20/14

The scattering and radiation properties are considered in microstrip antenna designs for airborne applications. The use of exotic substrates, instead of simple dielectric substrates, opens up a new dimension, making it much easier to meet both the radiation and scattering requirements. Two types of substrates, the ferromagnetic annd the anisotropic dielectric, are studied for their commercial availability. It was observed that the radiation mode and the scattering mode of the microstrip antenna are often distinctly different. Permittivity and permeability tensor of the substrate are selected to decouple the radiation and scattering modes to achieve simultaneously radiation and scattering performance goals. Analysis techniques used in the design study are discussed. E.A.K.

N86-11409# Rome Air Development Center, Hanscom AFB, Mass. Electromagnetic Sciences Div.
A HIGH-EFFICIENCE, LOW-PHASE ERROR WAVEGUIDE LENS FOR A TRANSFORM FEED ANTENNA
Daniel T. McGrath *In its* Proc. of the 1984 Antenna Appl. Symp. Jan. 1985 p 235-256 refs (For primary document see N86-11398 02-32)
Avail: NTIS HC A13/MF A01 CSCL 09/3

A parallel-plate waveguide microwave lens, constructed as part of the concept development of completely overlapped subarray antennas, was tested. The lens' function is comparable to that of a Rotman lens with 16 inputs and 60 outputs. However, the input face is linear with uniformly spaced monopole elements, and the output face is circular, with monopole elements spaced uniformly in angle. Using a four-way power divider at the center four inputs connected to a line-source array, low sidelobe patterns were measured over a 22% bandwidth. Two major modifications to the antenna were required: (1) it is shown that when placed in an array, the phase center is closer to the monopole, the focal array was moved farther from the circular lens face to give good focusing at the center frequency; and (2) the mismatch and coupling properties of unequally spaced elements along the circular face varied enough to distort the amplitude taper, causing higher sidelobes, an optimum uniform spacing eliminated the problem, and is shown that it is possible, to find such a spacing that will not degrade the len's performance either as a beamformer or as a transform feed. E.A.K.

N86-11410# Teledyne Micronetics, San Diego, Calif.
COMPUTER-AIDED BIFOCAL DIELECTRIC LENS ANTENNA DESIGN FOR MH WAVE APPLICATION
Sheng Y. Peng *In* RADC Proc. of the 1984 Antenna Appl. Symp. Jan. 1985 p 257-274 refs (For primary document see N86-11398 02-32)
Avail: NTIS HC A13/MF A01 CSCL 09/3

A Bifocal Dielectric Lens Computer Model was developed for the aid in the design analysis and performance evaluation for multiplebeam application. The model calculates and plots lens contour, the aperture distributions, and the corresponding radiation patterns and gain, with the feed located at any point on the focal arc. The ray lattice numerical method proposed by Holt and Mayer is very simple. The two surfaces of lens contour are determined through the ray path length constraints and Snell's refraction law. Design equation and equations for computing the aperture phase distribution at each interbeam location are derived. Sample calculations for lens contour design, aperture phase distributions, and radiation patterns of 8-multiplebeams at 94 GHz are included. E.A.K.

N86-11411# Naval Postgraduate School, Monterey, Calif.
VOICE COMMUNICATIONS OVER PACKET RADIO NETWORKS M.S. Thesis
M. M. Seah Mar. 1985 165 p
(AD-A157478) Avail: NTIS HC A08/MF A01 CSCL 17/2

The use of packet virtual circuit technique for voice communications in military radio networks was investigated. The work was concerned with various aspects of networking which include network modeling, communications techniques, traffic analysis and network control. An attempt has been made to develop a simple yet efficient time slot assignment algorithm . This was analyzed under a variety of slot depths and networks topologies using computer simulation. The Erlang' B results were used to provide more insight into the channel characteristics of the packet radio networks. The capabilities of implementing TDMA/CDMA hybrid schemes in the system were scrutinized. A method to estimate the transmission capacity of the inter-node links was found. We demonstrate its effectiveness in controlling local congestion by computer simulation. Graphical results were presented to highlight the behavior of the proposed packet radio networks. We concluded that an appropriate link weight function would provide efficient and reliable network services. GRA

N86-11412# Mitre Corp., Bedford, Mass.
EVALUATION OF THE DIGITAL ACCESS AND CROSS-CONNECT SYSTEM FOR USE IN THE DEFENSE COMMUNICATIONS SYSTEM Final Report, Oct. 1983 - Sep. 1984
C. A. Danielson and W. J. Uhrich Apr. 1985 121 p
(Contract F19628-84-C-0001)
(AD-A157570; MTR-9238; RADC-TR-85-78) Avail: NTIS HC A06/MF A01 CSCL 17/2

The Digital Access and Cross-Connect System (DACS) is communications equipment which provides electronic patching and test access to individual 64 kb/s channels of T1 digital groups (digroups). Equipment such as the DACS is envisioned for use in the Defense Communications System (DCS) where it would interface with existing digital communications equipment such as those developed in the Digital Radio and Multiplexer Acquisition (DRAMA) program. The testing reported herein addressed issues concerning the interfaces and interoperation of the DACS with the DRAMA equipment. Section 2 describes the DACS and the test installation at Scott AFB. The communications techniques used within the equipment are described and various communications terms are defined. Section 3 goes into the test methodology and relates the test configurations to potential application of the equipment in the DCS. Results of the testing are then presented in the remaining sections. Section 4 addresses various functional characteristics of the equipment. Section 5 presents results of interface testing including a characterization of the DACS and the DRAMA digroup interfaces. Section 6 describes testing related to the important topics of synchronization and timing. In Section 7, the performance parameters monitored by the DACS and the DACS alarms are discussed. Section 8 addresses operator interface characteristics of the equipment. Summary findings and conclusions are contained in Section 9. The appendix describes the test equipment employed during the testing. GRA

N86-11413# California Univ., Livermore. Lawrence Livermore Lab.
UPGRADE OF THE EM TRANSIENT RANGE MONOCONE ANTENNA
R. J. King, K. S. Kunz, H. G. Hudson, R. E. Boberg, S. T. Pennock, and D. K. Gnade May 1985 10 p
(Contract W-7405-eng-48)
(DE85-013181; UCID-20438) Avail: NTIS HC A02/MF A01

Lawrence Livermore National Laboratory has operated an electromagnetic transient range facility (EMTRF) since 1968 using a succession of antennas. This report describes the latest upgrade involving a precision monocone antenna and the use of a shroud of EM absorbing material strategically placed around the antenna to significantly enhance the clear time. This upgrade has resulted in highly repeatable measurements of exterior and interior responses of test objects for frequencies up to approximately 3 GHz for times on the order of hundreds of nanoseconds. Highly resonant interior responses can now be resolved experimentally. The radiated signal is nearly as clean as that from a simple vertical wire radiator and the field intensity is 12 dB larger. The cone is very nearly a true conic with very small azimuthal variations. As expected, the field behaves as 1/r for periods on the order of the time required for the transient pulse to each the cone edge. This perturbation is minimized by the use of strategically placed EM absorber which also serves to increase the clear time by minimizing room reflections. With improve pulsers it may be possible to extend the range of operation of this facility to 10 to 2 GHz. DOE

N86-11414# Los Alamos Scientific Lab., N. Mex.
CALCULATION OF RF FIELDS IN AXISYMMETRIC CAVITIES
Y. Iwashita 1985 5 p Presented at the 5th Conf. on the Computation of Electromagnetic Fields, Fort Collins, Colo., 3 Jun. 1985
(Contract W-7405-eng-36)
(DE85-014135; LA-UR-85-1892; CONF-850641-4) Avail: NTIS HC A02/MF A01

A new code, PISCES, was developed for calculating a complete set of RF electromagnetic modes in an axisymmetric cavity. The finite-element method is used with up to third-order shape functions. Although two components are enough to express these modes, three components are used as unknown variables to take advantage of the symmetry of the element matrix. The unknowns are taken to be either the electric field components or the magnetic field components. The zero-divergence condition will be satisfied by the shape function within each element. DOE

N86-11922# Joint Publications Research Service, Arlington, Va.
ELECTRIC OR MAGNETIC DIPOLE IN STRATIFIED UNIAXIALLY INHOMOGENEOUS ANISOTROPIC MEDIA Abstract Only
Jiasheng Wang *In its* China Rept.: Sci. and Technol. (JPRS-CST-85-014) 2 May 1985 p 74 Transl. into ENGLISH from Yuhang Xuebao (Beijing), no. 1, 31 Jan. 1985 p 24-34 Original language document announced in IAA as A85-42778 (For primary document see N86-11918 02-70)
Avail: NTIS HC A06/MF A01

N86-11923# Joint Publications Research Service, Arlington, Va.
PROPAGATION OF ELECTROMAGNETIC WAVES IN INHOMOGENEOUS AND LOSSY REENTRY PLASMA SHEATH LAYER Abstract Only

Boyi Wang, Yanhou Xu, and Zhenyu Ji *In its* China Rept.: Sci. and Technol. (JPRS-CST-85-014) 2 May 1985 p 75 Transl. into ENGLISH from Yuhang Xuebao (Beijing), no. 1, 31 Jan. 1985 p 35-46 Original language document announced in IAA as A85-42779 (For primary document see N86-11918 02-70)
Avail: NTIS HC A06/MF A01

33 ELECTRONICS AND ELECTRICAL ENGINEERING

Includes test equipment and maintainability; components, e.g., tunnel diodes and transistors; microminiaturization; and integrated circuitry.

For related information see also *60 Computer Operations and Hardware* and *76 Solid-State Physics.*

N86-11415# Air Command and Staff Coll., Maxwell AFB, Ala.
AN INTRODUCTION TO ELECTRICAL BREAKDOWN IN DIELECTRICS
T. L. Skvarenina Apr. 1985 256 p
(AD-A156465; ACSC-85-2470) Avail: NTIS HC A12/MF A01 CSCL 20/3

This report was written to serve as a text for an introductory graduate course in high voltage engineering at the Air Force Institute of Technology. However, anyone with an undergraduate electrical engineering or physics degree should be able to understand it, if they so desire. The material presented falls into three sections. The first part discusses the basics of kinetic theory of gases, atomic structure, ionization, mobility, diffusion, and electron emission. The second portion covers gas breakdown and the characteristics of the glow, corona, and arc discharges. The final portion provides a very brief introduction to the literature. GRA

N86-11416# Southeastern Center for Electrical Engineering Education, Inc., St. Cloud, Fla.
BASIC EMC TECHNOLOGY ADVANCEMENT FOR C(3) SYSTEMS. VOLUME 3B: COMPUTER SIMULATION OF EMI EFFECTS IN A DIFFERENTIAL LINE RECEIVER Final Technical Report, Sep. 1981 - Dec. 1983
Z. Chair, T. Dave, H. Ouibrahim, and D. Weiner Apr. 1985 68 p
(Contract F30602-81-C-0062)
(AD-A156505; RADC-TR-82-286-Vol-3B) Avail: NTIS HC A04/MF A01 CSCL 17/2

This paper discusses the computer simulation of sinusoidal interference in a National DS 55115 integrated circuit differential line receiver. The receiver is designed to sense differential signals (i.e., differences in the signals at the two terminals of the input port). Typically, the receiver is used in conjunction with the National DS 55114 integrated circuit differential line driver which provides differential output signals with high current capability for driving balanced lines such as twisted pairs. Attention in this effort is focused on the receiver, as opposed to the line driver, because the receiver is significantly more susceptible. Consequently, the susceptibility of the driver-receiver pair is determined by that of the receiver for most interference situations. GRA

N86-11417# Lincoln Lab., Mass. Inst. of Tech., Lexington.
SUBMILLIMETER QUANTUM ELECTRONICS Final Report, 1 Jul. 1982 - 31 Mar. 1985
P. E. Tannenwald 25 Apr. 1985 39 p
(Contracts F19628-80-C-0002; MIPR-ARO-129-85)
(AD-A157432; ARO-19626.9-PH) Avail: NTIS HC A03/MF A01 CSCL 09/3

Tunneling phenomena have been explored in quantum wells consisting of GaAs/GaAlAs (Gallium Arsenide/Aluminum Gallium Arsenide) heterostructure layers that were grown by molecular beam epitaxy. Devices such as detectors and mixers have been fabricated from these quantum wells that showed characteristic tunneling response from DC to 2.5 THz. In addition, the negative differential resistance that was observed was used to demonstrate microwave oscillations up to 20 GHz, both at low temperatures and at room temperature. A variety of other submillimeter experiments are described in the reprints included in the appendices: heterodyning from millimeter wave to optical frequencies using GaAs MESFETs above f sub T, heterodyne radiometry measurements of the 557 GHz water vapor rotational line, development of a submillimeter radiometer using a solid-state local oscillator, and submillimeter astronomical observations carried out at telescope field sites. Also mentioned are persistent photoconductivity observed in quantum wells and a low-IF submillimeter heterodyne receiver to be used in electromagnetic scattering experiments. Author (GRA)

N86-11418# University Coll., Cork (Ireland). Dept. of Chemistry.
OXIDE CATHODE MECHANISMS: ELECTRONIC AND STRUCTURAL FEATURES OF OXIDE CATHODE SURFACES Final Report, 1 Mar. 1983 - 29 Feb. 1984
J. Cunningham and J. Nunan Jan. 1985 90 p
(Grant AF-AFOSR-0074-83)
(AD-A1[illegible]7666; AFWAL-TR-84-4158) Avail: NTIS HC A[illegible]/MF A01 CSCL 09/1

This report describes studies made upon systems selected for their ability to model various important features of oxide cathodes and the mechanisms which enable them to function as efficient thermionic emitters at moderate temperatures. An account is given of experiments which aimed to simulate conditions upon the surfaces of polycrystalline samples of alkaline earth oxides (e.g., SrO and BaO/SrO or MgO and BaO/MgO) at various stages of their preparation in similiar fashion to that used in the thermal activation of oxide cathodes. Accounts are given of experiments which examined the interaction between the gases O2, N2O, H2 or Ch4 and appropriately preactivated surface of pure and mixed alkaline earth oxide samples. Accounts are given of experiments involving the controlled deposition in UHV conditions of zero-valent Ba ad-atoms-in amounts ranging from submonolayer to multilayer coverage - upon layers of SrO or BaO previously prepared in UHV conditions by evaporation of the corresponding metal and its subsequent oxidation. UPS spectra have been undertaken in order to examine surfaces of samples prepared by evaporation of barium metal or strontium metal and to study effects upon the UPS spectra by exposures to the gases N20, O2 and CH4. GRA

N86-11419# Los Alamos National Lab., N. Mex.
MULTI-MEGAMPERE CURRENT INTERRUPTION FROM EXPLOSIVE DEFORMATION OF CONDUCTORS
J. H. Goforth, A. H. Williams, and S. P. Marsh 1985 5 p Presented at the 5th IEEE Pulsed Power Conf., Washington, D.C., 10 Jan. 1985
(Contract W-7405-eng-36)
(DE85-012756; LA-UR-85-1936; CONF-850616-15) Avail: NTIS HC A02/MF A01

Two approaches for using explosives to interrupt current flowing in solid conductors are described. One concept uses explosives to extrude the switch conductor into thin regions that fuse due to current in the switch. A preliminary scaling law is presented. The second approach employs dielectric jets to sever current carrying conductors. A feasibility experiment and an improved design are described. DOE

N86-11420# Los Alamos National Lab., N. Mex.
MULTI-MEGAMPERE OPERATION OF PLASMA COMPRESSION OPENING SWITCHES IN PLANAR GEOMETRY
J. H. Goforth, D. J. Erickson, A. H. Williams, and A. E. Greene 1985 5 p Presented at the 5th IEEE Pulsed Power Conf., Washington, D.C., 10 Jun. 1985
(Contract W-7405-eng-36)
(DE85-012755; LA-UR-85-1939; CONF-850616-14) Avail: NTIS HC A02/MF A01

Experiments are described in which a plasma compression opening switch is used in planar geometry to sharpen the output pulse of an explosive-driven magnetic flux compression generator. The description includes data from tests where peak opening switch currents range from 5.7 to 9.3 MA. The switch is used to transfer current to a static low-induction load with an efficiency of 50% or better and a risetime as low as 0.45 microns. Results related to current transfer are interpreted within a simple analytical model. DOE

N86-11421# Sandia Labs., Albuquerque, N. Mex.
EXPLOSIVE GENERATORS FOR LOW-COST PULSED POWER
E. Cnare and M. Cowan 1985 22 p Presented at the 5th IEEE Pulsed Power Conf., Washington, D.C., 10 Jun. 1985
(Contract DE-AC04-76DP-00789)
(DE85-013436; SAND-84-2638C; CONF-850616-37) Avail: NTIS HC A02/MF A01

A practical application of explosive generators (MCGs) is to provide relatively low cost pulsed power at very high energy and power to explore high risk technology. A new explosive generator design, which called the Model 632, was designed to bring the cost of prime pulsed power to .001 dollars per joule and 10 to the-7 dollars per watt. The design allows the use of inexpensive liquid explosive and attempts to minimize labor costs in construction of the armature and coil. In its first test, which was carried out with only one half of the designed initial energy, the Model 632 produced 18 MJ at 0.85 TW. The results of the first two tests of the Model 632 explosive generator and a projection of the actual cost of pulse power from this source is discussed. DOE

N86-11422# Sandia Labs., Albuquerque, N. Mex.
AUTOMATED MAGNET TESTING FACILITY
K. T. Lancaster and A. W. Sharpe 1985 11 p Presented at the 5th IEEE Pulsed Power Conf., Washington, D. C., 10 Jun. 1985
(Contract DE-AC04-76DP-00789)
(DE85-012863; SAND-84-2392C; CONF-850616-12) Avail: NTIS HC A02/MF A01

The automated Magnet Testing Facility (MTF) is a computer controlled, 60 kJ, parallel capacitor bank that was constructed to pulse test solenoidal magnets. Coil sets from different vendors are evaluated on two criteria: uniformity of field and coil reliability. The first criterion, uniformity of field, is evaluated by installing a pair of coils into stainless steel housings and pulse mapping the fields at a low energy level. Forty field-strength samples are easily collected with the one button operation of the MTF. Two thousand high field pulse tests, at a 20 kG level, is the second criterion for magnet acceptance. In a manually operated system a single operator can achieve this goal in six months. In a continuous operating mode, MTF can achieve the same goal in 42 days. DOE

N86-11423# Argonne National Lab., Ill.
EFFECTS OF ADDITIVES AND TEMPERATURE ON IRON ELECTRODE BEHAVIOR IN KOH ELECTROLYTES
D. S. Poa, J. F. Miller, and N. P. Yao Apr. 1985 29 p refs
(Contract W-31-109-eng-38)
(DE85-011901; ANL/CEPM-82-2) Avail: NTIS HC A03/MF A01

The effect of temperature, electrolyte additives, and KOH concentration on the electrochemical behavior of iron electrodes in KOH electrolytes was studied by the cyclic voltammetric method. It is indicated that the charging efficiency of the iron electrode will be decreased at lower temperatures. To achieve the same state of charge as that obtained at higher temperatures, a higher charging voltage is required at lower temperatures. The higher charging voltage will increase hydrogen evolution, which will cause the charging efficiency of the iron electrode to decrease. The addition of K2S to the KOH electrolyte can effectively suppress the H2 evolution on the iron electrode during charging. The addition of LiOH to the electrolyte will be beneficial to the stability of the iron electrode, particularly at the transitions from lower to higher oxidation states. The saturation of the KOH electrolyte with FeO causes significant changes in the mechanisms and reaction rates of the electrode reduction-oxidation processes because of the competing reactions of Fe(II) species which become more available at the iron electrode surface. The decrease in reaction rates in more concentrated electrolytes was probably caused by the increased formation of solid film products of higher oxidation states at the electrode surface. DOE

N86-11424# Sandia Labs., Albuquerque, N. Mex.
PARTIAL DISCHARGE FORMATION AND BREAKDOWN IN DEIONIZED WATER UNDER REPETITIVE STRESSING
G. J. Rohwein 1985 26 p Presented at the 5th IEEE Pulsed Power Conf., Washington, D.C., 10 Jun. 1985
(Contract DE-AC04-76DP-00789)
(DE85-013114; SAND-84-2391C; CONF-850616-20) Avail: NTIS HC A03/MF A01

Partial discharges (PD) often precede breakdown in repetitively pulsed megavolt capacitors. This mode of breakdown is believed to result from ionization buildup in the electrode gap from which streamers originate. A series of partial discharge tests using a point plane gap demonstrates that streamers periodically grow out of ionized bushes which tends to support this model. The tests also show water to have well defined corona inception and quench thresholds as well as a low first shot inception level. Data from these tests and related small area breakdown experiments are presented. The random breakdown and recovery characteristics of water are also discussed. DOE

N86-11863# California Univ., Livermore. Lawrence Livermore Lab. Nuclear Energy Systems Div.
NET-2 MODELS OF CAVITIES AND DIODES Abstract Only
George E. Vogtlin *In* LANL 6th Bien. CUBE (Computer Use by Engineers) Symp. Aug. 1984 p 11 (For primary document see N86-11858 02-60)
Avail: NTIS HC A06/MF A01

N86-12002# Joint Publications Research Service, Arlington, Va.
A GENERAL PURPOSE CAD PROGRAM FOR MICROWAVE LINEAR CIRCUITS
Yenyang Shih *In its* China Rept.: Sci. and Technol. (JPRS-CST-85-015) 16 May 1985 p 93 refs Transl. into ENGLISH from Tongxin Xuebao (Beijing), no. 2, Apr. 1984 p 60-65 (For primary document see N86-11994 02-70)
Avail: NTIS HC A07/MF A01

34 FLUID MECHANICS AND HEAT TRANSFER

Includes boundary layers; hydrodynamics; fluidics; mass transfer; and ablation cooling.

For related information see also *02 Aerodynamics* and *77 Thermodynamics and Statistical Physics.*

N86-11425*# National Aeronautics and Space Administration. Lewis Research Center, Cleveland, Ohio.
THEORETICAL AND EXPERIMENTAL COMPARISON OF VAPOR CAVITATION IN DYNAMICALLY LOADED JOURNAL BEARINGS
David E. Brewe, Bernard J. Hamrock (Ohio State Univ., Columbus), and Bo A. Jacobson (Lulea Univ.) 1985 16 p refs Proposed for presentation at the Intern. Symp. on Cavitation, Sendai, Japan, 16-19 Apr. 1986 Prepared in cooperation with Army Aviation Research and Development Command, Cleveland, Ohio
(NASA-TM-87121; E-2729; NAS 1.15:87121; USAAVSCOM-TR-85-C-19) Avail: NTIS HC A02/MF A01 CSCL 20D

Vapor cavitation for a submerged journal bearing under dynamically loaded conditions was investigated. The observation of vapor cavitation in the laboratory was done by high-speed photography. It was found that vapor cavitation occurs when the tensile stress applied to the oil exceeded the tensile strength of the oil or the binding of the oil to the surface. The theoretical solution to the Reynolds equation is determined numerically using a moving boundary algorithm. This algorithm conserves mass throughout the computational domain including the region of cavitation and its boundaries. An alternating direction implicit (MDI) method is used to effect the time march. A rotor undergoing circular whirl was studied. Predicted cavitation behavior was analyzed by three-dimensional computer graphic movies. The formation, growth, and collapse of the bubble in response to the dynamic conditions is shown. For the same conditions of dynamic loading, the cavitation bubble was studied in the laboratory using high-speed photography. E.A.K.

N86-11426*# Scientific Concepts, Inc., Potsdam, N.Y.
BRIDGMAN GROWTH OF SEMICONDUCTORS
F. M. Carlson Sep. 1985 34 p refs
(Contract NAS1-16721)
(NASA-CR-177971; NAS 1.26:177971) Avail: NTIS HC A03/MF A01 CSCL 20L

The purpose of this study was to improve the understanding of the transport phenomena which occurs in the directional solidification of alloy semiconductors. In particular, emphasis was placed on the strong role of convection in the melt. Analytical solutions were not deemed possible for such an involved problem. Accordingly, a numerical model of the process was developed which simulated the transport. This translates into solving the partial differential equations of energy, mass, species, and momentum transfer subject to various boundary and initial conditions. A finite element method with simple elements was initially chosen. This simulation tool will enable the crystal grower to systematically identify and modify the important design factors within her control to produce better crystals. Author

N86-11427# Naval Research Lab., Washington, D. C.
ON STRATIFIED VORTEX MOTIONS UNDER GRAVITY Summary Report, 1981 - 1984
Y. T. Fung 20 Jun. 1985 31 p
(RR0-2301)
(AD-A156930; NRL-MR-5564) Avail: NTIS HC A03/MF A01 CSCL 20/4

A general class of stratified vortex flows in investigated in order to understand the vortex patterns developed in stratified late wakes. The flow profiles to be considered vary in both the radial and the axial directions. Three necessary conditions (obtained by the method of generalized progressing wave expansion) and three sufficient conditions (obtained by the integral method of complex conjugation) are discussed for stability of the present flow. As a result, the three necessary and sufficient conditions require that the flow be stable in the centrifugal force field, in the gravitational force field, and in the pressure field that restrains the density variations in the two force fields. A new Brunt-Vaisala frequency and a new Richardson number are proposed as a result of the third stability condition. The newly defined Brunt-Vaisala frequency can be viewed as a measure of the interaction of the density variation in one direction with the force field in the other direction. This Richardson number is a ratio between the interactions of the density variations with the force fields and the interactions of the velocity gradients in two direction. The former interaction is a result of the third stability condition. The latter interaction determines whether the velocity gradients in the second direction strengthens or weakens the resultant shear effect. Because of the generality of the flow profiles being considered, the criteria established in this investigation are valid for a wide range of problems in oceanographic and atmospheric studies. GRA

N86-11428# Scientific Research Associates, Inc., Glastonbury, Conn.
DEVELOPMENT OF A NAVIER-STOKES ANALYSIS FOR THE FLOW IN DISK PUMPS Final Report, Sep. 1984 - Mar. 1985
Y. N. Kim, R. C. Buggeln, and H. McDonald Apr. 1985 45 p
(Contract F33615-84-C-2469)
(AD-A157454; SRA-910008F; AFWAL-TR-85-2039) Avail: NTIS HC A03/MF A01 CSCL 13/7

A technique has been developed to solve the Navier-Stokes equations for the flow in disk pumps. The technique uses a linearized block implicit-alternating direction technique to efficiently solve the unsteady governing equations to a steady state with appropriate boundary conditions and initial conditions. The resulting code was used to calculate the flow in two different geometries under the same flow conditions. Demonstration calculation indicates that the code will be a valuable tool in analytically evaluating the performance of existing and future disk pumps. GRA

N86-11429# Air Force Systems Command, Wright-Patterson AFB, Ohio. Foreign Technology Div.
THE MEASUREMENTS OF AXISYMMETRIC AIR TURBULENT JET FLOW WITH AN INDIVIDUAL REALIZATION LASER VELOCIMETER SYSTEM
X. Shen, H. Yu, D. Chen, and S. Xie 29 May 1985 23 p Transl. into ENGLISH from Qinghua Daxue Xuebao (China), v. 24, no. 3, 1984 p 26-36
(AD-A157554; FTD-ID(RS)T-0326-85) Avail: NTIS HC A02/MF A01 CSCL 14/2

This paper describes the measurements of axisymmetric air turbulent jet flow with the use of an IRLV system. The distributions of axial mean velocity, turbulent intensity and probability density functions of velocity in the initial region of jet flow were obtained. The data from LV were sampled and processed automatically by a microprocessor. The experiments show that the velocity measurements can be realized even with the air particles in their natural state. The measurements of the mean velocity were also simultaneously made with a hot wire anemometer in order to compare with those made with a LV. Their results were in good coincidence in the core flow region. The velocity bias was increased with the decrease of data rate and increase of turbulent intensity in the mixing boundary layer. GRA

N86-11430# Naval Ship Research and Development Center, Bethesda, Md.
APPLICATION OF THE VORTEX-LATTICE CONCEPT TO FLOWS WITH SMOOTH-SURFACE SEPARATION Final Report
D. F. Thrasher Jul. 1985 69 p
(AD-A157571; DTNSRDC-85/041) Avail: NTIS HC A04/MF A01 CSCL 20/4

Numerical schemes based on the vortex-lattice concept have had considerable success in treating the fully three-dimensional separated potential flow over low aspect-ratio thin wings at high incidence and the attached potential flow over bodies of more general shape. In principle, the vortex-lattice method is not limited in application as long as convection dominates vorticity diffusion. A non-linear 3-D vortex-lattice method was developed which treats the steady separated flow over prolate bodies with open separation moving through an inviscid incompressible fluid. The strength and position of the body wake were found as part of the solution. Flows with smooth-surface separation were considered as opposed to flows with sharp-edge separation treated with the vortex-lattice concept in the past. Results for flow over an inclined ogive-cylinder demonstrated the technique. For attached flow, comparisons are presented of the results from the vortex-lattice method using optimal and average control point locations with the results of the source-distribution method and with experimental data. The same panel arrangement was used calculating both methods. The results of the present method are somewhat more sensitive to panel arrangement than are those for the source-distribution method. Also, the effect of control point location varies dramatically as the incidence of the body is changed. For separated flow, results of the vortex-lattice method were compared with experimental data and with the results of a typical 2-D analogy. The present method agrees favorably with the experimental data windward of a separation line. GRA

N86-11431# Los Alamos Scientific Lab., N. Mex.
ROTATING FILM RADIATORS FOR SPACE APPLICATIONS
D. R. Koenig 1985 8 p refs Presented at the 20th Intersoc. Energy Conversion Eng. Conf., Miami Beach, Fla., 18 Aug. 1985
(Contract W-7405-eng-36)
(DE85-009633; LA-UR-85-980; CONF-850808-2) Avail: NTIS HC A02/MF A01

A new class of light-weight radiators is described. This radiator consists of a thin rotating envelope that contains the working fluid. The envelope can have many shapes including redundant, foldable configurations. The working fluid, which may be a liquid or a condensable vapor, impinges on the inside surface of the radiator and is driven as a film to the periphery by centrifugal force. Heat is radiated to space by the outer surface of the envelope. Pumps located on the periphery then return the liquid to the power converter. For a 100-MW radiator operating at 800 K, specific mass approx. 0.1 kg/kW and mass density approx. 2 kg/m(2) may be achievable. DOE

N86-11432# Argonne National Lab., Ill.
BLOCK-IMPLICIT COUPLED CALCULATION OF FLUID FLOWS
S. P. Vanka 1985 7 p Presented at the 5th Symp. on Turbulent Shear Flows, Ithaca, N.Y., 7 Aug. 1985
(Contract W-31-109-eng-38)
(DE85-004038; CONF-850820-1) Avail: NTIS HC A02/MF A01

The development of turbulence models for multidimensional flows heavily relies on the availability of accurate and efficient numerical solution algorithms for the governing partial differential equations. Several techniques have been developed in the past based on finite difference and finite element methods and have employed a variety of implicitness in the differencing and solution of the equations. A popular approach in solving the equations, at least of the finite difference variety, is a decoupled sequential solution of the individual equations. Such methods are employed by the Los Alamos group and by the Imperial College group. The decoupled methods typically solve a pressure or pressure correction equation in lieu of the continuity equation and employ a guess and correct procedure for determining the pressure field. The performance of the coupled block implicit solution technique is presented in various steady flow situations. Techniques for maintaining the requirements of computer storage small and improving the computing speed through preordering and domain splitting techniques are discussed. Attempts to extend the method to three dimensions are also discussed. DOE

N86-11433# Midwest Research Inst., Golden, Colo. Solar Energy Research Inst.
HIGH TEMPERATURE MOLTEN SALT CONTAINMENT
K. Y. Wang, R. E. West, F. Kreith, and P. P. Lynn May 1985 64 p
(Contract DE-AC02-83CH-10093)
(DE85-012152; SERI/TR-252-2490) Avail: NTIS HC A04/MF A01

The feasibility of several design options for high-temperature, sensible heat storage containment is examined. The major concerns for a successful containment design include heat loss, corrosive tolerance, structural integrity, and cost. This study is aimed at identifying the most promising high-temperature storage tank among eight designs initially proposed. The study is based on the heat transfer calculations and the structure study of the tank wall and the tank foundation and the overall cost analyses. The results indicate that the single-tank, two-media sloped wall tank has the potential of being lowest in cost. Several relevant technical uncertainties that warrant further research efforts are also identified. DOE

N86-11434# Argonne National Lab., Ill.
BLOCK-IMPLICIT MULTIGRID CALCULATION OF THREE-DIMENSIONAL RECIRCULATING FLOWS
S. P. Vanka 1985 13 p Presented at the 4th Intern. Conf. on Numer. Methods in Laminar and Turbulent Flow, Swansea, England, 8 Jul. 1985
(Contract W-31-109-eng-38)
(DE85-010250; CONF-850745-3) Avail: NTIS HC A02/MF A01

An efficient finite difference calculation procedure for three-dimensional recirculating flows is presented. The algorithm is based on a coupled solution of the three-dimensional momentum and continuity equations in primitive variables by the multigrid technique. A symmetrical coupled Gauss-Siedel technique is used for iterations and is observed to provide good rates of smoothing. Calculations were made of the fluid motion in a three-dimensional cubic cavity with a moving top wall. The efficiency of the method is demonstrated by performing calculations at different Reynolds numbers with finite difference grids as large as 66 x 66 x 66 nodes. The CPU times and storage requirements for these calculations are observed to be very modest. The algorithm has the potential to be the basis for an efficient general purpose calculation procedure for practical fluid flows. DOE

N86-11435# Los Alamos Scientific Lab., N. Mex.
INTRODUCTION TO THE SESSION ON: NUMERICAL METHODS FOR TWO-PHASE FLOW
B. Wendroff 1985 7 p Presented at the 11th Intern. Assoc. of Math. and Computers Simulation World Congr., Oslo, 5 Aug. 1985
(Contract W-7405-eng-36)
(DE85-012651; LA-UR-85-1629; CONF-850861-2) Avail: NTIS HC A02/MF A01

The six equation model without artificial correction terms is the simplest one which models the physics as correctly as we can, given that the averaging process is imprecise. Once that idea is accepted the next step is to try to evaluate the limitations of standard difference schemes applied to an ill-posed problem of this type. Analysis of simple cases shows that there are schemes which are quasi-stable (q-stable), by which I mean that errors are not amplified if the mesh size is not too small. Of course, even well-posed problems have limits on mesh size; too fine a mesh will take too much computer time or have unacceptable growth of round-off error. Here we have an additional mesh constraint, but whether or not it is more restrictive than the others is a function of the particular situation being modeled. For example, if the lowest order effects such as phase changes and friction are dominant then the q-stability condition on the mesh will still allow a mesh small enough to obtain accuracy consistent with the accuracy of the data. DOE

N86-11505*# National Aeronautics and Space Administration. Lewis Research Center, Cleveland, Ohio.
TURBINE HEAT TRANSFER
John E. Rohde *In its* Turbine Eng. Hot Sect. Technol. (HOST) Oct. 1983 p 73-77 (For primary document see N86-11495 02-39)
Avail: NTIS HC A11/MF A01 CSCL 20D

N86-11506*# Tennessee Univ. Space Inst., Tullahoma.
GAS FLOW ENVIRONMENTAL AND HEAT TRANSFER NON-ROTATING 3D PROGRAM
T. Geil and J. Steinhoff *In* NASA. Lewis Research Center Turbine Eng. Hot Sect. Technol. (HOST) Oct. 1983 p 79-86 (For primary document see N86-11495 02-39)
(Contract NAS3-23278)
Avail: NTIS HC A11/MF A01 CSCL 20D

N86-11507*# Detroit Diesel Allison, Mich.
GAS SIDE HEAT TRANSFER
Larry D. Hylton *In* NASA. Lewis Research Center Turbine Eng. Hot Sect. Technol. (HOST) Oct. 1983 p 87-99 refs (For primary document see N86-11495 02-39)
(Contracts NAS3-22761; NAS3-23695)
Avail: NTIS HC A11/MF A01 CSCL 20D

N86-11508*# United Technologies Research Center, East Hartford, Conn.
ASSESSMENT OF A 3-D BOUNDARY LAYER CODE TO PREDICT HEAT TRANSFER AND FLOW LOSSES IN A TURBINE
Veer N. Vatsa *In* NASA. Lewis Research Center Turbine Eng. Hot Sect. Technol. (HOST) Oct. 1983 p 101-106 refs (For primary document see N86-11495 02-39)
(Contract NAS3-23716)
Avail: NTIS HC A11/MF A01 CSCL 20D

N86-11509*# United Technologies Research Center, East Hartford, Conn.
GAS-SIDE HEAT TRANSFER WITH ROTATION
Robert P. Dring *In* NASA. Lewis Research Center Turbine Eng. Hot Sect. Technol. (HOST) Oct. 1983 p 107-109 refs (For primary document see N86-11495 02-39)
Avail: NTIS HC A11/MF A01 CSCL 20D

N86-11510*# Pratt and Whitney Aircraft Group, East Hartford, Conn.

COOLANT PASSAGE HEAT TRANSFER WITH ROTATION. A PROGRESS REPORT ON THE COMPUTATIONAL ASPECTS
L. D. Aceto and G. J. Sturgess *In* NASA. Lewis Research Center Turbine Eng. Hot Sect. Technol. (HOST) Oct. 1983 p 111-116 refs (For primary document see N86-11495 02-39)
Avail: NTIS HC A11/MF A01 CSCL 20D

N86-11511*# Arizona State Univ., Tempe. Dept. of Mechanical and Aerospace Engineering.
JET ARRAY IMPINGEMENT HEAT TRANSFER CHARACTERISTICS
L. W. Florschuetz and D. E. Metzger *In* NASA. Lewis Research Center Turbine Eng. Hot Sect. Technol. (HOST) Oct. 1983 p 117-128 refs (For primary document see N86-11495 02-39)
Avail: NTIS HC A11/MF A01 CSCL 20D

N86-11866# California Univ., Livermore. Lawrence Livermore Lab. Nuclear Test Engineering Div.
ICARUS: A COMPUTER CODE FOR MODELING COMPLEX ONE-DIMENSIONAL HEAT CONDUCTION ON MAINFRAMES AND MICROS Abstract Only
Steven B. Sutton *In* LANL 6th Bien. CUBE (Computer Use by Engineers) Symp. Aug. 1984 p 16 (For primary document see N86-11858 02-60)
Avail: NTIS HC A06/MF A01

N86-11867# Sandia Labs., Albuquerque, N. Mex.
THREE-DIMENSIONAL HEAT TRANSFER ANALYSIS USING THE PATRAN-G SOLIDS MODELING AND Q-TRAN THERMAL ANALYSIS COMPUTER CODES Abstract Only
James M. Nelsen, Jaime L. Moya, and H. Richard Yoshimura *In* LANL 6th Bien. CUBE (Computer Use by Engineers) Symp. Aug. 1984 p 17 (For primary document see N86-11858 02-60)
Avail: NTIS HC A06/MF A01

N86-11868# Sandia Labs., Albuquerque, N. Mex. Structural Mechanics Div.
INTERFACE ELEMENTS FOR HEAT TRANSFER ANALYSIS Abstract Only
William E. Mason *In* LANL 6th Bien. CUBE (Computer Use by Engineers) Symp. Aug. 1984 p 17 (For primary document see N86-11858 02-60)
Avail: NTIS HC A06/MF A01

N86-11879# Sandia Labs., Albuquerque, N. Mex.
A TIME-SPLITTING NUMERICAL TECHNIQUE FOR SOLVING HIGHLY COUPLED TWO-PHASE FLOW CONSERVATION EQUATION Abstract Only
R. J. Gross and M. R. Baer *In* LANL 6th Bien. CUBE (Computer Use by Engineers) Symp. Aug. 1984 p 48-49 (For primary document see N86-11858 02-60)
Avail: NTIS HC A06/MF A01

N86-11882# Sandia Labs., Albuquerque, N. Mex. Thermofluids Div.
SIMULATION OF FLAME PROPAGATION THROUGH VORTICITY REGIONS USING THE DISCRETE VORTEX METHOD Abstract Only
Pamela K. Barr *In* LANL 6th Bien. CUBE (Computer Use by Engineers) Symp. Aug. 1984 p 59 (For primary document see N86-11858 02-60)
Avail: NTIS HC A06/MF A01

N86-11883# Sandia Labs., Albuquerque, N. Mex.
APPLICATION OF FLUX-CORRECTED TRANSPORT (FCT) TO HEAT TRANSFER/FLUID MECHANICS PROBLEMS Abstract Only
R. J. Gross, M. R. Baer, and C. E. Hickox *In* LANL 6th Bien. CUBE (Computer Use by Engineers) Symp. Aug. 1984 p 60 (For primary document see N86-11858 02-60)
Avail: NTIS HC A06/MF A01

N86-11884# Sandia Labs., Albuquerque, N. Mex. Analytical Thermal/Fluid Mechanics Div.
HEAT TRANSFER AND PRESSURE CHANGES DUE TO A LARGE TEMPERATURE DIFFERENCE ACROSS AN ENCLOSED VERTICAL AIR LAYER Abstract Only
D. R. Chenoweth and S. Paolucci *In* LANL 6th Bien. CUBE (Computer Use by Engineers) Symp. Aug. 1984 p 61-62 (For primary document see N86-11858 02-60)
Avail: NTIS HC A06/MF A01

N86-11886# Sandia Labs., Albuquerque, N. Mex. Thermofluids Div.
A HYBRID VORTEX-IN-CELL FINITE-DIFFERENCE NUMERICAL METHOD FOR TURBULENT SHEAR LAYER COMPUTATION Abstract Only
Nagi N. Mansour *In* LANL 6th Bien. CUBE (Computer Use by Engineers) Symp. Aug. 1984 p 95-96 (For primary document see N86-11858 02-60)
Avail: NTIS HC A06/MF A01

N86-11887# California Univ., Livermore. Lawrence Livermore Lab. Nuclear Explosives Engineering Div.
COMPUTER CODES FOR FLUID-STRUCTURE INTERACTIONS Abstract Only
W. H. McMaster *In* LANL 6th Bien. CUBE (Computer Use by Engineers) Symp. Aug. 1984 p 96 (For primary document see N86-11858 02-60)
Avail: NTIS HC A06/MF A01

N86-11954# Joint Publications Research Service, Arlington, Va.
HYDRODYNAMICS OF LIQUID-VAPOR DISPERSE ANNULAR FLOWS IN CHANNELS CONTAINIG BUNDLES OF HEATED RODS UNDER NONSTEADY-STATE CONDITIONS Abstract Only
A. Ye. Kroshilin, V. Ye. Kroshilin, and B. I. Nigmatulin *In its* USSR Rept.: Phys. and Math. (JPRS-UPM-85-005) 20 Aug. 1985 p 10 refs Transl. into ENGLISH from Teplofiz. Vys. Temp. (Moscow), v. 22, no. 5, Sep. - Oct. 1984 p 933-940 (For primary document see N86-11945 02-70)
Avail: NTIS HC A08/MF A01

N86-11962# Joint Publications Research Service, Arlington, Va.
INFLUENCE OF PHYSICAL-CHEMICAL PROPERTIES OF GASES ON INTERACTION BETWEEN SHOCKWAVES AND CONVEX CYLINDRICAL SURFACES Abstract Only.
L. G. Gvozdeva, Yu. P. Lagutov, and V. P. Fokeyev *In its* USSR Rept.: Phys. and Math. (JPRS-UPM-85-005) 20 Aug. 1985 p 31 refs Transl. into ENGLISH from Inzhenerno-Fiz. Zh. (Minsk), v. 48, no 2, Feb. 1985 p 239-244 (For primary document see N86-11945 02-70)
Avail: NTIS HC A08/MF A01

35 INSTRUMENTATION AND PHOTOGRAPHY

Includes remote sensors; measuring instruments and gages; detectors; cameras and photographic supplies; and holography.

For aerial photography see *43 Earth Resources*. For related information see also *06 Aircraft Instrumentation*, and *19 Spacecraft Instrumentation*.

N86-11436*# Virginia Polytechnic Inst. and State Univ., Blacksburg. Dept. of Chemistry.
DIRECT COUPLING OF MICROBORE HPLC COLUMNS TO MS SYSTEMS Final Report, 1 Mar. 1984 - 31 Mar. 1985
Harold M. McNair 31 Mar. 1985 16 p refs
(Grant NAG1-343)
(NASA-CR-176292; NAS 1.26:176292) Avail: NTIS HC A02/MF A01 CSCL 14B

A detailed investigation using electron microscopy was conducted which examined the conditions of materials used in the construction of stable, high performance microbore liquid chromatography (LC) columns. Small details proved to be important. The effects of temperature on the elution of several homologous series used as probe compounds was examined in reverse phase systems. They showed that accessible temperature changes provide roughly half the increase in solvent strength that would be obtained going from a 100% aqueous to a 100% organic mobile phase, which is sufficient to warrant their use in many analyses requiring the use of gradients. Air circulation temperature control systems provide the easiest means of obtaining rapid, wide range changes in column temperature. However, slow heat transfer from the gas leads to thermal nonuniformity in the column and a decrease in resolution as the temperature program progresses. B.W.

N86-11437*# National Aeronautics and Space Administration. Langley Research Center, Hampton, Va.
WIND TUNNEL SEEDING SYSTEMS FOR LASER VELOCIMETERS
William W. Hunter, Jr., comp. and Cecil E. Nichols, Jr., comp. Washington Oct. 1985 264 p refs Workshop held in Hampton, Va., 19-20 Mar. 1985
(NASA-CP-2393; L-16013; NAS 1.55:2393) Avail: NTIS HC A12/MF A01 CSCL 14B

The principal motivating factor for convening the Workshop on the Development and Application of Wind Tunnel Seeding Systems for Laser Velocimeters is the necessity to achieve efficient operation and, most importantly, to insure accurate measurements with velocimeter techniques. The ultimate accuracy of particle scattering based laser velocimeter measurements of wind tunnel flow fields depends on the ability of the scattering particle to faithfully track the local flow field in which it is embedded. A complex relationship exists between the particle motion and the local flow field. This relationship is dependent on particle size, size distribution, shape, and density. To quantify the accuracy of the velocimeter measurements of the flow field, the researcher has to know the scattering particle characteristics. In order to obtain optimum velocimeter measurements, the researcher is striving to achieve control of the particle characteristics and to verify those characteristics at the measurement point. Additionally, the researcher is attempting to achieve maximum measurement efficiency through control of particle concentration and location in the flow field. For individual titles, see N86-11438 through N86-11457.

N86-11438*# Arnold Engineering Development Center, Arnold Air Force Station, Tenn.
CALCULATION OF PARTICLE DYNAMICS EFFECTS ON LASER VELOCIMETER DATA
Robert H. Nichols *In* NASA. Langley Research Center Wind Tunnel Seeding Systems for Laser Velocimeters Oct. 1985 p 1-11 refs (For primary document see N86-11437 02-35)
Avail: NTIS HC A12/MF A01 CSCL 14B

In order to analytically assess the effects of particle dynamics on laser velocimeter measurements, the particle response to the fluid in which it is entrained must be modeled. The equation of particle motion derived at Arnold Engineering and Development Center (AEDC), is used to model the motion of the particle. The equation is derived from the Navier-Stokes equation under the assumption of unsteady Stokes flow. It should be noted that the Stokes flow eliminates the need for a far field boundary condition, and hence eliminates any normal (lift) forces. To extend the equation to higher particle slip velocities, the Stokes drag is replaced with the particle drag law, modified to include heat transfer effects. The drag coefficient accounts for inertial, rarefaction, compressibility, shape, and heat transfer effects. Author

N86-11439*# Case Western Reserve Univ., Cleveland, Ohio. Center for Complex Flow Measurements.
CORRECTING FOR PARTICLE COUNTING BIAS ERROR IN TURBULENT FLOW
Robert V. Edwards and William Baratuci *In* NASA Langley Research Center Wind Tunnel Seeding Systems for Laser Velocimeters Oct. 1985 p 13-28 refs (For primary document see N86-11437 02-35)
Avail: NTIS HC A12/MF A01 CSCL 14B

An ideal seeding device is proposed generating particles that exactly follow the flow out are still a major source of error, i.e., with a particle counting bias wherein the probability of measuring velocity is a function of velocity. The error in the measured mean can be as much as 25%. Many schemes have been put forward to correct for this error, but there is not universal agreement as to the acceptability of any one method. In particular it is sometimes difficult to know if the assumptions required in the analysis are fulfilled by any particular flow measurement system. To check various correction mechanisms in an ideal way and to gain some insight into how to correct with the fewest initial assumptions, a computer simulation is constructed to simulate laser anemometer measurements in a turbulent flow. That simulator and the results of its use are discussed. Author

N86-11440*# National Aeronautics and Space Administration. Langley Research Center, Hampton, Va.
ESTIMATION OF PARTICLE SIZE BASED ON LDV MEASUREMENTS IN A DE-ACCELERATING FLOW FIELD
James F. Meyers *In its* Wind Tunnel Seeding Systems for Laser Velocimeters Oct. 1985 p 29-51 refs (For primary document see N86-11437 02-35)
Avail: NTIS HC A12/MF A01 CSCL 14B

The accuracy of velocity measurements made with a laser velocimeter is strongly dependent upon the response of the seeding particles to the dynamics of the flow field. The smaller the particle the better the response to flow fluctuations and gradients and therefore the more accurate velocity measurement. In direct conflict is the requirement of light scattering efficiency to obtain signals with the laser velocimeter which, in general, is better as the particle size is increased. In low speed flow fields these two requirements on particle size overlap and accurate measurements may be obtained. However in high speed flows, where the velocity gradients may be severe, very small particles are required to maintain sufficient dynamic response characteristics to follow the flow. Therefore if velocity measurements are to be made in these flows, the laser velocimeter must be designed with sufficient sensitivity to obtain signals from these small particles. An insitu determination of the size distribution of kaolin particles (Al2O3, .2 + or - SiO2 . 2H2O) in the 16-foot Transonic Tunnel and the sensitivity characteristics of the laser velocimeter system is described. Author

N86-11441*# Calspan Field Services, Inc., Arnold AFS, Tenn.
PARTICLE SIZE DISTRIBUTIONS OF SEVERAL COMMONLY USED SEEDING AEROSOLS
F. L. Crosswy *In* NASA. Langley Research Center Wind Tunnel Seeding Systems for Laser Velocimeters Oct. 1985 p 53-75 refs (For primary document see N86-11437 02-35)
Avail: NTIS HC A12/MF A01 CSCL 14B

During the course of experimentation, no solid particle powder could be found which produced an aerosol with a narrow particle size distribution when fluidization was the only flow process used in producing the aerosol. The complication of adding particle size fractionation processes to the aerosol generation effort appears to be avoidable. In this regard, a simple sonic orifice is found to be effective in reducing the percentage of agglomerates in the several metal oxide powders tested. Marginally beneficial results are obtained for a 0.5/99.5 percent by weight mixture of the flow agent and metal oxide powder. However, agglomeration is observed to be enhanced when the flow agent percentage is increased to 5 percent. Liquid atomization using the Collison nebulizer as well as a version of the Laskin nozzle resulted in polydispersed aerosols with particle size distributions heavily weighted by the small particle end of the size spectrum. The aerosol particle size distributions produced by the vaporization/condensation seeder are closer to the ideal monodispersed aerosol than any of the other aerosols tested. In addition, this seeding approach affords a measure of control over particle size and particle production rate. Author

N86-11442*# National Aeronautics and Space Administration. Langley Research Center, Hampton, Va.
EXPERIMENTS WITH SOLID PARTICLE SEEDING

Cecil E. Nichols, Jr. *In its* Wind Tunnel Seeding Systems for Laser Velocimeters Oct. 1985 p 77-84 (For primary document see N86-11437 02-35)
Avail: NTIS HC A12/MF A01 CSCL 14B

Kaoline, a hydrated aluminum silicate clay, is investigated as a seeding material for laser velocimetry. It is inexpensive but is polydispersed with some of the fineparticles being too large to follow wind tunnel flow and is in the form of nonspherical platelets having an aspect ratio of approximately 4/1. Gravity sedimentation experiments as a means of narrowing the fineparticle sizes distribution are being conducted. The fineparticle size distribution of Engelhard ASP 200 kaolin suspended in ethanol (0.00792 grams kaolin/ml ethanol) as received, after 24 hours gravity sedimentation and after 48 hours sedimentation, respectively is shown. A shearing atomizer is used to inject the fineparticles. Gravity sedimentation is carried out in an 800 ml pyrex beaker. Following gravity sedimentation, the top 3.5 inches are siphoned from the liquid, which has a column height of 4.5 inches. In a like manner, longer settling times will serve to further narrow the fineparticle distribution range. As successive sedimentations are effected, the number of fineparticles per unit volume of ethanol decreased markedly.
Author

N86-11443*# National Aeronautics and Space Administration. Langley Research Center, Hampton, Va.
SEEDING TECHNIQUES USED IN THE VORTEX RESEARCH FACILITY
Dale R. Satran *In its* Wind Tunnel Seeding Systems for Laser Velocimeters Oct. 1985 p 85-92 refs (For primary document see N86-11437 02-35)
Avail: NTIS HC A12/MF A01 CSCL 14B

For many years, the Vortex Research Facility used kerosene vapor as seeding particles. The kerosene vapor formed (approx. 1 micron) particles initially. After injection into the test section, the vapor would begin to condense and form larger particles. By switching to solid particles, this has been eliminated. The uniform-sized (approx. 1 micron) solid particle seeding is used both to seed the Laser Velocimeter system and for flow visualization. After injection, the solid particles reach a uniform suspension before the vehicle is launched. It is found that the kerosene vapor poses a problem because it is a heated gas which modified the test section temperature distribution. It also produces high turbulence and secondary air currents because it was continually injected from the time of vehicle launch until model passage. In cases where the effects of either turbulence or the vertical temperature distribution are of interest, this hot gas injection method is unsuitable. Both types of seeding particles provide adequate flow visualization but are sensitive to vertical temperature distributions.
Author

N86-11444*# National Aeronautics and Space Administration. Langley Research Center, Hampton, Va.
SEEDING SYSTEMS FOR USE WITH A LASER VELOCIMETER IN LARGE SCALE WIND TUNNELS
Joe W. Elliott (Army Structures Lab.) and Cecil E. Nichols, Jr. *In its* Wind Tunnel Seeding Systems for Laser Velocimeters Oct. 1985 p 93-103 refs (For primary document see N86-11437 02-35)
Avail: NTIS HC A12/MF A01 CSCL 14B

Three seeding systems have been used in the 4- by 7- Meter Tunnel at NASA Langley Research Center: Kerosene smoke, solid particle dry dispersing, and solid particle liquid dispersing. It is anticipated that the liquid dispersing system will be used in all future applications at this facility because: (1) it has a steady output; (2) it is easy to operate and reconfigure; and, (3) it delivers particles of near uniform size.
Author

N86-11445*# United Technologies Research Center, East Hartford, Conn.
OVERVIEW OF SOLID PARTICLE LV SEEDING TECHNIQUES USED AT UTRC
William P. Patrick *In* NASA. Langley Research Center Wind Tunnel Seeding Systems for Laser Velocimeters Oct. 1985 p 105-113 refs (For primary document see N86-11437 02-35)
Avail: NTIS HC A12/MF A01 CSCL 14B

Due to the failure of existing seeders to meet the stringent specifications required for benchmark experiments in high pressure, high temperature, rapidly accelerating flowfields, an effort is made to improve an existing solid particle seeder. The goal is to produce a more monodisperse seed from the 0.3 micro alumina powder with more than 99 percent of the particles in the submicron range while maintaining a high seeding rate. Coiled-wire inserts are installed within the ends of the nitrogen injection lines in the primary seeder to produce swirling conical jets to vigorously agitate the seed bed. A secondary swirler, constructed from a 25 cm length of 3.8 cm ID steel pipe having threaded end caps, is connected to the output line of the primary seeder. The seeded nitrogen from the primary seeder is injected tangentially at near sonic velocity into the secondary swirler 9.4 cm above its base. Independently controlled auxiliary nitrogen used to increase the swirl in the secondary chamber is also injected tangentially 2.5 cm below the seeded nitrogen lines. Large seed particles are collected by bleeds in the swirler cap and directed overboard. The remaining seeded nitrogen is collected on the center line of the secondary swirler and ducted to the rig.
Author

N86-11446*# Sandia Labs., Livermore, Calif.
SEEDING REQUIREMENTS FOR SCANNING LASER VELOCIMETRY
Colin E. Hackett *In* NASA. Langley Research Center Wind Tunnel Seeding Systems for Laser Velocimeters Oct. 1985 p 115-120 (For primary document see N86-11437 02-35)
(Contract DE-AC04-76DP-00789)
Avail: NTIS HC A12/MF A01 CSCL 14B

To measure the velocity distributions within time dependent turbulent flow fields, a continuously scanning laser velocimeter system is being developed at Sandia National Laboratories Livermore (SNLL). A prototype of this system has produced results which show that spatial and temporal variations in particle seed distribution seriously compromise the overall performance and operation of this device. To alleviate some of these problems, alternate flow seeding concepts are explored. The most promising appear to be those that actively induce laser sparks within the gas flow, the velocity of which may be measured by a Fourier transformed velocimetry system.
Author

N86-11447*# Calspan Field Services, Inc., Arnold AFS, Tenn.
RECENT EXPERIENCE IN SEEDING TRANSONIC/SUPERSONIC FLOWS AT AEDC
Fred L. Heltsley *In* NASA. Langley Research Center Wind Tunnel Seeding Systems for Laser Velocimeters Oct. 1985 p 121-140 refs (For primary document see N86-11437 02-35)
Avail: NTIS HC A12/MF A01 CSCL 14B

The laser velocimeter has been utilized for several years at the Arnold Engineering and Development Center (AEDC) as a flow diagnostics tool. Most applications, following the initial proof-of-concept experiments, have involved relatively complex unknown flow fields in which the more conventional, intrusive techniques had either not been attempted or had yielded unsatisfactory results. A blunt-base nozzle-afterbody base flow study is discussed as a respresentative example of such applications. A wide variety of problems have been encountered during these tests, many of which have proven to be closely related to the size and/or size distribution of the seeding material within the fluid. Resulting measurement uncertainties could often not be conclusively resolved because of the unknown nature of the flow field. The other experiments listed were conducted to provide known aerodynamic conditions for comparison with the velocimeter results.
Author

N86-11448*# Notre Dame Univ., Ind. Dept. of Aerospace and Mechanical Engineering.
LASER VELOCIMETRY MEASUREMENT IN A TRANSONIC TUNNEL
T. Terry Ng and Thomas J. Mueller *In* NASA. Langley Research Center Wind Tunnel Seeding Systems for Laser Velocimeters Oct. 1985 p 141-148 ref (For primary document see N86-11437

02-35)
Avail: NTIS HC A12/MF A01 CSCL 14B

Some preliminary velocity measurements were carried out inside the transonic tunnel using the laser velocimeter (LV) system in association with the smoke generator. Pressure measurements were also performed using a pressure tap located on the side wall of the test section slightly upstream of the windows. Though the pressure measurements and the LV measurements were not taken at exactly the same location, extrapolation of the pressure data into the location of the LV measurements indicated a very close agreement between the velocity values obtained using the two different methods. Thus it is believed that the smoke particle is following the air flow with little or no velocity slip. Velocity measurements with airfoil at various angles of attack are now being carried out in conjuction with schlieren flow visualization. In the near future pressure distribution around and on the airfoil will be obtained by putting pressure taps on the side windows and using a pressure tap model (currently under construction) of the airfoil. Author

N86-11449*# National Aeronautics and Space Administration. Langley Research Center, Hampton, Va.
PARTICLE GENERATION EXPERIENCE IN LANGLEY'S 16-FOOT TRANSONIC TUNNEL
David E. Reubush *In its* Wind Tunnel Seeding Systems for Laser Velocimeters Oct. 1985 p 149-167 refs (For primary document see N86-11437 02-35)
Avail: NTIS HC A12/MF A01 CSCL 14B

The Langley 16-Foot Transonic Tunnel is a single-return, continuous-flow, atmospheric tunnel which uses air exchange for cooling. The tunnel speed is continuously variable from Mach 0 to 1.30. The test section is a regular octagon in cross-section with slots at the corners of the octagon. The laser velocimeter optics, laser, photomultipliers, etc. are mounted in the test section plenum chamber which surrounds the test section. The test volume is approximately a 1-meter cube about the tunnel center line centered on tunnel station 40.84 meters. The seeding system particle generators are mounted on the upstream side of the fourth set of turning vanes approximately 49 meters upstream of the test volume. At this point the tunnel has a diameter of 17.68 meters which meant that installation of the generators was a difficult procedure. It might be noted that particle generation had to be continuous as when the generators were turned off the data rate rapidly deteriorated to zero. Author

N86-11450*# National Aeronautics and Space Administration. Langley Research Center, Hampton, Va.
LDA SEEDING SYSTEM FOR THE LANGLEY LOW TURBULENCE PRESSURE TUNNEL
J. Scheiman and Laguduva R. Kubendran *In its* Wind Tunnel Seeding Systems for Laser Velocimeters Oct. 1985 p 169-178 refs (For primary document see N86-11437 02-35)
Avail: NTIS HC A12/MF A01 CSCL 14B

A Laser Velocimetry (LV) seeding system was specifically developed for the Langley Low Turbulence Wind Tunnel (LTPT), and it has been successfully used for LV measurements in two major tests (Juncture Flow Experiment and Gortler Experiment). The LTPT is capable of operating at Mach numbers from 0.05 to 0.50 and unit Reynolds numbers from 100,000 to 15,000,000 per foot. The test section is 3 feet wide and 7.5 feet high. The turbulence level in the test section is relatively low because of the high contraction ratio and because of the nine turbulence reduction screens in the settling chamber. A primary requirement of the seeding system was that the seeding material not contaminate or damage in any way these screens. Both solid and liquid seeding systems were evaluated, and the results are presented. They can provide some guidelines for setting up seeding systems in other similar tunnels. Author

N86-11451*# National Aeronautics and Space Administration. Ames Research Center, Moffett Field, Calif.
SEEDING SUBSONIC, TRANSONIC AND SUPERSONIC FLOWS WITH 0.5 MICRON POLYSTYRENE SPHERES
H. Lee Seegmiller *In* NASA. Langley Research Center Wind Tunnel Seeding Systems for Laser Velocimeters Oct. 1985 p 179-187 refs (For primary document see N86-11437 02-35)
Avail: NTIS HC A12/MF A01 CSCL 14B

Polystyrene latex particles have been successfully used as laser velocimetry seed material for flows in the Ames High Reynolds Channels (HR) 1 and 2, the pilot channel, and the one-foot low speed tunnel. These facilities provide test flows with Mach numbers from 0.1 to 3.0 and test section sizes from 4 inches by 6 inches to 18 inches by 24 inches. Tunnel mass flow in the HR-2 channel can approach 1000 lb/sec. The latex particles have the following favorable characteristics: size of 0.35 to 0.55 microns diameter; spherical shape; specific gravity of 1.05; excellent flow trackability; low toxicity; and low cost. they have the disadvantage of being packaged as an aqueous suspension which must be diluted and introduced into the test flow as an atomized mist. This must occur sufficiently far upstream of the test section to minimize flow disturbances and permit the liquid mist to evaporate before reaching the model. Several techniques which have been developed to accomplish satisfactory seeding will be described. Author

N86-11452*# National Aeronautics and Space Administration. Lewis Research Center, Cleveland, Ohio.
DEVELOPMENT OF SEEDING TECHNIQUES FOR SMALL SUPERSONIC WIND TUNNEL
Warren R. Hingst and Randall M. Chriss (Toledo Univ.) *In* NASA. Langley Research Center Wind Tunnel Seeding Systems for Laser Velocimeters Oct. 1985 p 189-202 refs (For primary document see N86-11437 02-35)
Avail: NTIS HC A12/MF A01 CSCL 14B

The NASA Lewis 1x1 foot supersonic wind tunnel is used to experimentally verify computational methods. This tunnel, which is continuous running, operates from laboratory-wide high pressure air and vacuum systems. As such, the air does not recirculate but makes a single pass through the tunnel. The Mach number is varied with interchangeable nozzle blocks and has a range from Mach 1.6 to 4.0. Dry and filtered air is available up to pressures of 3 atmospheres. The air enters the tunnel system through a plenum having flow straighteners and 6 fine mesh screens. The exit of the plenum provides smooth contraction with an area ratio of approximately 20 that, along with the screens, provides a uniform flow for the nozzle. Author

N86-11453*# Naval Surface Weapons Center, White Oak, Md.
AEROSOL SEEDING SYSTEMS FOR THE NSWC WIND TUNNELS
William J. Yanta, Timothy S. Smith, and Arnold S. Collier *In* NASA. Langley Research Center Wind Tunnel Seeding Systems for Laser Velocimeters Oct. 1985 p 203-210 refs (For primary document see N86-11437 02-35)
Avail: NTIS HC A12/MF A01 CSCL 14B

Four types of laskin nozzles which are used to generate the primary aerosol mist are illustrated. This mist may be used directly as laser doppler velocimeters (LDV) particles. However, in general, a wide range of particle size exists at this stage and requires the use of some type of mono-dispersion refinement technique. These nozzles rely on the shearing action of high speed air near a column of seeding liquid. Typically, olive oil or dioctyl phthalate (DOP) is used, but within the past year solid polystyrene particles in an alcohol suspension have been used with great success. Air, at a typical pressure of five psig, is supplied to the top of the nozzle which is merely a hollow tube. This air issues radially from one or more small jets located near the collar close to the bottom of the tube. When the collar is submerged in the seeding liquid, the hollow columns located in the collar become filled with liquid. The air from the jet shears the liquid into the fine mist. Author

N86-11454*# National Aeronautics and Space Administration. Langley Research Center, Hampton, Va.
SEEDING MATERIALS: HEALTH AND SAFETY CONSIDERATIONS
Robert D. Brown *In its* Wind Tunnel Seeding Systems for Laser Velocimeters Oct. 1985 p 211-219 refs (For primary document

see N86-11437 02-35)
Avail: NTIS HC A12/MF A01 CSCL 14B

The choice of a proper seeding material for laser velocimeters must include health and safety considerations. Failure to do so can lead to catastrophic results. All materials are toxic, and laser velocimeter seeding materials are no exception. Toxicity may be considered an inherent property of a given material. The manifestation of that property or the physiological response to the material is dependent on dose and exposure conditions. An approximate physiological classification of toxicity is given in tablular form. Toxicity in some situations is not necessarily the most restrictive factor in selection of materials. It is also very important to consider how the material is used so that actual exposure to the material in a damaging form can result. For example, nickel and cadmium are both extremely toxic as systemic poisons and in the case of nickel as a carcinogen. Seeding materials are dispersed in air under conditions that favor personnel exposure. Dispersal equipment is frequently if not normally manned, and personnel are often required to make frequent adjustments to assure proper operations. Author

N86-11455*# Thermo-Systems, Inc., St. Paul, Minn.
GENERATING AEROSOLS FOR LASER VELOCIMETER SEEDING
Jugal K. Agarwal *In* NASA. Langley Research Center Wind Tunnel Seeding Systems for Laser Velocimeters Oct. 1985 p 221-235 refs (For primary document see N86-11437 02-35)
Avail: NTIS HC A12/MF A01 CSCL 14B

The laser velocimeter (LV) is a unique tool for fluid flow measurements. In such measurements, even though the fluid velocity is of primary interest, the LV signal originates from seed particles present in the fluid and the LV actually measures the velocity of these particles. Thus it is important that a sufficient number of seed particles be present in the fluid and they scatter sufficient light to produce LV signals. Also, the seed particles should follow the fluid with high fidelity. Aerodynamic diameter is the true measure of a particle's ability to follow the flow. The aerodynamic diameter of a particle is defined as the diameter of a unit density sphere with same settling velocity as the particle in question. It is affected by geometric diameter, density and shape of the particle. For LV seeding, particles with smaller aerodynamic diameter are desirable because they follow the flow more readily. On the other hand, in general, the particle's ability to scatter light increases with its geometric diameter and its refractive index. Author

N86-11456*# Science and Technology Corp., Las Cruces, N. Mex.
PARTICLE PHASE FUNCTION MEASUREMENTS BY A NEW FIBER ARRAY NEPHELOMETER: FAN 1
W. M. Farmer, Edward J. Burlbaw, and A. Deepak (Science and Technology Corp., Hampton, Va.) *In* NASA. Langley Research Center Wind Tunnel Seeding Systems for Laser Velocimeters Oct. 1985 p 237-243 (For primary document see N86-11437 02-35)
Avail: NTIS HC A12/MF A01 CSCL 14B

A fiber array polar nephelometer of advanced design, the FAN I is capable of in-situ phase function measurements of scattered light from man-made or natural atmospheric particles. The scattered light is measured at 100 different angles throughout 360 degrees, thus providing a potential measurement of the asymmetry of irregularly shaped particles. Phase functions can be measured at 10 to 100 Hz rates and the range of measurable single particle sizes is from 5 micron m to as large as 8mm. For particles smaller than 5 micro m the ensemble average can be measured. The FAN I is microprocessor controlled and the data may be stored on floppy disk or printed out in tabular and/or graphical form. The optical head may be separated from the computer system for operation in field or adverse conditions. Examples of laboratory measured scattering phase functions obtained with the FAN I for spherical particles is given to illustrate its measurement capabilities. Author

N86-11457*# Spectron Development Labs., Inc., Costa Mesa, Calif.
A TECHNIQUE TO MEASURE THE SIZE OF PARTICLES IN LASER DOPPLER VELOCIMETRY APPLICATIONS
C. F. Hess *In* NASA. Langley Research Center Wind Tunnel Seeding Systems for Laser Velocimeters Oct. 1985 p 245-264 refs (For primary document see N86-11437 02-35)
Avail: NTIS HC A12/MF A01 CSCL 14B

A method to measure the size of particles in Laser Doppler Velocimeter (LDV) applications is discussed. Since in LDV the velocity of the flow is assocated with the velocity of particles to establish how well they follow the flow, in the present method the interferometric probe volume is surrounded by a larger beam of different polarization or wavelength. The particle size is then measured from the absolute intensity scattered from the large beam by particles crossing the fringes. Experiments using polystrene particles between 1.1 and 3.3 microns and larger glass beads are reported. It is shown that the method has an excellent size resolution and its accuracy is better than 10% for the particle size studied. Author

N86-11458# Little (Arthur D.), Inc., Cambridge, Mass.
SURFACE SAMPLING TECHNIQUES USING ULTRAVIOLET ILLUMINATION Final Report
E. M. Smith, J. R. Aronson, R. M. Cornish, B. E. Goodwin, and I. Simon Nov. 1984 68 p
(Contract DAAK11-83-C-0062)
(AD-A156457; AMXTH-TE-CR-84308) Avail: NTIS HC A04/MF A01 CSCL 19/1

In laboratory and preliminary field tests, a system that uses photography in the presence of a 254 nm UV illumination source has been shown useful for detection of explosives residues on surfaces. Analytes (TNT, 2, 4-DNT, 2, 6-DNT, Tetryl, RDX and DPA) can be detected at 10 to 20 microgram/sq cm on concrete, transite or stainless steel. The method was not successful for wood or brick surfaces or for the analyte PETN. An alternative thermal image radiometric method of detection was unsuccessful. Author (GRA)

N86-11459# Air Force Inst. of Tech., Wright-Patterson AFB, Ohio.
FEEDBACK STABILIZATION OF OPTICAL INTERFEROMETER M.S. Thesis
R. H. Nakat Feb. 1985 76 p
(AD-A156912; AFIT/CI/NR-85-41T) Avail: NTIS HC A05/MF A01 CSCL 20/6

An experimental study was carried out on the performance of a feedback stabilization scheme for optical interferometers. Optical interferometers are susceptible to acoustic noise which translates into path length fluctuations in the interferometer arms. These fluctuations induce phase noise, resulting in amplitude fluctuations on the interferometer output. The experiment was performed on a Mach-Zehnder homodyne interferometer where a RMS noise reduction of 23 dB was observed. The stabilization scheme has application to other interferometer configurations. In the future, it will be applied to stabilize cavities used in the squeezed state generation of light. Author (GRA)

N86-11460# Naval Research Lab., Washington, D. C.
SCALING CALCULATIONS FOR A RELATIVISTIC GYROTRON Memorandum Report, Mar. 1984 - Mar. 1985
A. W. Fliflet 31 Jul. 1985 41 p
(RR0-1109)
(AD-A157476; NRL-MR-5598) Avail: NTIS HC A03/MF A01 CSCL 09/1

The relativistic gyrotron is under development as an ultra-high power source of millimeter wave radiation. The purpose of the present study is to estimate the optimum operating characteristics of gyrotrons based on multi-kiloampere, mega-electron volt electron beams. Gyrotrons with weakly relativistic, moderate current electron beams have demonstrated very high efficiency and average power at millimeter wavelengths and the possibility of achieving good efficiencies at very high peak powers is of interest. Compared to other high power millimeter wave generators, gyrotrons are

relatively insensitive to electron beam velocity spread and thus appear well suited to device configurations based on high current pulseline accelerators. The results of this study indicate that the relativistic gyrotron has potential for achieving high efficiency (15-30%) using relativistic electron beams with gamma approx 2-3. Optimum efficiency occurs for short interaction lengths characterized by 4-8 cyclotron periods. Such short interaction lengths lead to the possibility of very high peak power generation using multi-kiloampere beams: 100-300 MW with a 600 ke V beam and about 1 GW with a 1 Me V beam. The output power risetime has been estimated to be a few nanoseconds for a low Q oscillator at 35 GHz which implies the gyrotron interaction can be readily investigated using a 20-100 nsec pulseline accelerator.
Author (GRA)

N86-11461# Edgerton, Germeshausen and Grier, Inc., Idaho Falls, Idaho.
FABRICATION AND USE OF ZIRCALOY/TANTALUM-SHEATHED CLADDING THERMOCOUPLES
S. Curtis Wilkins and L. K. Sepold Jan. 1985 43 p refs
(EGG-TFBP-6739; TI85-009174A) Avail: NTIS HC A03/MF A01

The thermocouples described are zircaloy/tantalum-sheathed and molybdenum/rhenium alloy-sheathed instruments intended for fuel rod cladding and fuel centerline temperature measurements, respectively. Both types incorporate beryllium oxide insulation and tungsten/rhenium alloy thermoelements. These thermocouples, operated at temperatures of 2000 C and above, are developed for use in the internationally sponsored Severe Fuel Damage test series in the Power Burst Facility at the Idaho National Engineering Laboratory. The fabrication steps for both thermocouple types are described in detail. A laser-welding attachment technique for the cladding-type thermocouple is presented, and experience with alternate materials for cladding and fuel thermocouples is discussed. DOE

N86-11462# Mound Lab., Miamisburg, Ohio.
INFRARED THERMOGRAPHY: AN ANALYTICAL TOOL FOR HIGH TEMPERATURE AND FAST RESPONSE
J. H. Mohler, M. D. Kelly, and L. D. Abney 1985 4 p Presented at the AIAA Thermophys. Conf., Williamsburg, Va., 18 Jun. 1985
(Contract DE-AC04-76DP-00053)
(DE85-013826; MLM-3271(OP); CONF-850607-3) Avail: NTIS HC A02/MF A01

The speed and noncontact properties of optical temperature measurements techniques make them particularly useful for studying dynamic, high temperature process. Several examples of the use of video thermography in chemical heat source development are shown. DOE

N86-11463# Sandia Labs., Albuquerque, N. Mex.
GEOTHERMAL INSTRUMENTATION DEVELOPMENT ACTIVITIES AT SANDIA
C. C. Carson Mar. 1985 5 p refs Presented at Intern. Symp. on Geothermal Energy, Kailua Kona, Hawaii, 26 Aug. 1985
(Contract DE-AC04-76DP-00789)
(DE85-008693; SAND-85-0647C; CONF-850801-8) Avail: NTIS HC A02/MF A01

A major element of the geothermal technology development program is directed toward development of instrumentation. This effort has two aspects: the development of high temperature components and prototype tools, and the investigation of new concepts and capabilities. Data acquisition to make geothermal drilling and resource development more efficient is emphasized. Several projects of varying nature and scope make up the instrumentation development element, and the program's emphasis on development of an advanced geothermal drilling system and the need for improved information growth is expanded. DOE

N86-11497*# National Aeronautics and Space Administration. Lewis Research Center, Cleveland, Ohio.
HOST INSTRUMENTATION R AND D PROGRAM OVERVIEW
D. R. Englund *In its* Turbine Eng. Hot Sect. Technol. (HOST) Oct. 1983 p 7-9 (For primary document see N86-11495 02-39)
Avail: NTIS HC A11/MF A01 CSCL 14B

N86-11498*# United Technologies Research Center, East Hartford, Conn.
HOT SECTION VIEWING SYSTEM
William W. Morey *In* NASA. Lewis Research Center Turbine Eng. Hot Sect. Technol. (HOST) Oct. 1983 p 11-16 (For primary document see N86-11495 02-39)
Avail: NTIS HC A11/MF A01 CSCL 14B

N86-11499*# Pratt and Whitney Aircraft, East Hartford, Conn. Engineering Div.
DYNAMIC GAS TEMPERATURE MEASUREMENT SYSTEM
Denny L. Elmore, Woodrow W. Robinson, and William B. Watkins *In* NASA. Lewis Research Center Turbine Eng. Hot Sect. Technol. (HOST) Oct. 1983 p 17-35 ref (For primary document see N86-11495 02-39)
(Contract NAS3-23154)
Avail: NTIS HC A11/MF A01 CSCL 14B

N86-11500*# United Technologies Research Center, East Hartford, Conn.
HIGH TEMPERATURE STATIC STRAIN SENSOR DEVELOPMENT PROGRAM
Charles Hulse, Richard Bailey, and Howard Grant (Pratt and Whitney Aircraft Group, East Hartford, Conn.) *In* NASA. Lewis Research Center Turbine Eng. Hot Sect. Technol. (HOST) Oct. 1983 p 37-40 (For primary document see N86-11495 02-39)
(Contract NAS3-23722)
Avail: NTIS HC A11/MF A01 CSCL 14B

N86-11502*# Pratt and Whitney Aircraft Group, East Hartford, Conn. Engineering Div.
DEVELOPMENT OF HEAT FLUX SENSORS FOR TURBINE AIRFOILS AND COMBUSTOR LINERS
William H. Atkinson *In* NASA. Lewis Research Center Turbine Eng. Hot Sect. Technol. (HOST) Oct. 1983 p 45-55 ref (For primary document see N86-11495 02-39)
Avail: NTIS HC A11/MF A01 CSCL 14B

N86-11504*# Case Western Reserve Univ., Cleveland, Ohio. Dept. of Chemical Engineering.
TIME-OF-FLIGHT ANEMOMETER FOR HOT SECTION APPLICATIONS
Robert V. Edwards *In* NASA. Lewis Research Center Turbine Eng. Hot Sect. Technol. (HOST) Oct. 1983 p 69-71 (For primary document see N86-11495 02-39)
Avail: NTIS HC A11/MF A01 CSCL 14B

N86-11880# California Univ., Livermore. Lawrence Livermore Lab. Field Test Systems Div.
PHOTOELECTRON TRAJECTORY ANALYSES OF STREAK TUBES Abstract Only
Ching C. Lai *In* LANL 6th Bien. CUBE (Computer Use by Engineers) Symp. Aug. 1984 p 53 (For primary document see N86-11858 02-60)
Avail: NTIS HC A06/MF A01

N86-11563# Technische Hochschule, Darmstadt (West Germany). Inst. fuer Physikalische Geodaesie.
MODIFICATION OF A HUGHES TILTMETER TO A BOREHOLE TILTMETER
C. Gerstenecker *In* Academy of Sciences of the GDR Proc. of the 5th Intern. Symp. Geodesy and Phys. of the Earth 1985 p 142-149 refs (For primary document see N86-11549 02-42)
Avail: NTIS HC A09/MF A01

N86-11577# Hungarian Academy of Sciences, Sopron. Geodetical and Geophysical Research Inst.
CAPACITIVE PENDULUM WITH INTELLIGENT DATA COLLECTION
Gy. Mentes *In* Academy of Sciences of the GDR Proc. of the 5th Intern. Symp. Geodesy and Phys. of the Earth, Pt. 2 1985

p 63-69 refs (For primary document see N86-11568 02-42)
Avail: NTIS HC A09/MF A01

N86-11583# Academy of Sciences, Potsdam (East Germany). Zentralinst. fuer Physik der Erde.
ON THE COMPARISON OF THE RESULTS OF TWO DIFFERENT E-W-STRAINMETERS
D. Simon, R. M. Karmaleeva (Academy of Sciences (USSR), Moscow), and L. A. Latynina (Academy of Sciences (USSR), Moscow) *In its* Proc. of the 5th Intern. Symp. Geodesy and Phys. of the Earth, Pt. 2 1985 p 115-125 refs (For primary document see N86-11568 02-42)
Avail: NTIS HC A09/MF A01

N86-11614# Hungarian Academy of Sciences, Sopron. Geodetic and Geophysical Research Inst.
A NEW APPARATUS FOR TESTING BUBBLE VIALS, ELECTRONIC LEVELS AND AUTOMATIC LEVELS
J. Somogyi, K. Krausz, and Gy. Mentes *In* Academy of Sciences of the GDR Proc. of the 5th Intern. Symp. Geodesy and Phys. of the Earth, Pt. 3 1985 p 140-147 refs (For primary document see N86-11591 02-42)
Avail: NTIS HC A08/MF A01

N86-11981# Joint Publications Research Service, Arlington, Va.
EXPERIMENTAL INVESTIGATION OF RECORDING OF DYNAMIC HOLOGRAMS WITHIN ABSORPTION CONTOUR OF RESONANT ATOMIC MEDIUM Abstract Only.
A. Ye. Korolev and D. I. Staselko *In its* USSR Rept.: Phys. and Math. (JPRS-UPM-85-005) 20 Aug. 1985 p 86 refs Transl. into ENGLISH from Opt. i Spektrosk. (Leningrad), v. 58, no. 1, Jan. 1985 p 147-152 (For primary document see N86-11945 02-70)
Avail: NTIS HC A08/MF A01

N86-11982# Joint Publications Research Service, Arlington, Va.
DIFFRACTION EFFICIENCY OF THREE-DIMENSIONAL PHASE HOLOGRAM OF DIFFUSE OBJECT Abstract Only
Yu. L. Korzinin and V. L. Sukhanov *In its* USSR Rept.: Phys. and Math. (JPRS-UPM-85-005) 20 Aug. 1985 p 87 refs Transl. into ENGLISH from Opt. i. Spektrosk. (Leningrad), v. 58, no. 1, Jan. 1985 p 142-146 (For primary document see N86-11945 02-70)
Avail: NTIS HC A08/MF A01

N86-11983# Joint Publications Research Service, Arlington, Va.
POSSIBILITY OF OPTIMAL CHOICE OF EXPOSURE TIME FOR HOLOGRAPHIC RECORDING OF OBJECTS THROUGH UNSTEADY SCATTERING MEDIA Abstract Only.
O. V. Angelskiy, V. V. Yatsenko, and D. I. Derkach *In its* USSR Rept.: Phys. and Math. (JPRS-UPM-85-005) 20 Aug. 1985 p 89 refs Transl. into ENGLISH from Zh. Prikl. Spektrosk. (Minsk, USSR), v. 42, no. 1, Jan. 1985 p 118-122 Original language doc. was announced as A85-28983 (For primary document see N86-11945 02-70)
Avail: NTIS HC A08/MF A01

36 LASERS AND MASERS

Includes parametric amplifiers.

N86-11464 Illinois Univ., Urbana-Champaign.
OPERATING RANGE OF ALUMINUM GALLIUM ARSENIDE QUANTUM-WELL HETEROSTRUCTURE LASERS: TUNABILITY, POWER OUTPUT AND HIGH ENERGY EMISSION Ph.D. Thesis
John Edward Epler 1985 99 p
Avail: Univ. Microfilms Order No. DA8511604

A quantum-well heterostructure (QWH) is the most capable form of semiconductor laser. The quantum-size effect (QSE), inherent in a QWH laser, improves the device performance compared to conventional double heterostructure lasers. One advantage provided by the QSE is the increased possibility for carrier bandfilling of the active region. Experimental results are presented in which the continuous (CW) emission wavelength of an A1(x)Ga(1-x)AsGaAs QWH laser diode is tuned over a 100-meV spectral range (with the aid of an external grating cavity). The single 90-A quantum well is an ideal active region to provide broadband (7800-8300) optical gain. To extend the power output, a QWH laser with a multiple-stripe active region is also operated in the external grating cavity. The short wavelength, high performance diodes with a single 400-AA1(x)Ga(1-x)As (x approx. 0.22) quantum-well active region region exhibit less tunability but a much greater power output than single stripe lasers fabricated on the same crystal. The trade-off between power output and tunability is discussed. Dissert. Abstr.

N86-11465*# Purdue Univ., Lafayette, Ind. School of Mechanical Engineering.
[CHARACTERISTICS OF AN AXISYMMETRIC SUDDEN EXPANSION FLOW] Progress Report, 1 Jul. 1984 - 1 Jul. 1985
W. H. Stevenson and H. D. Thompson 1 Jul. 1985 17 p refs
(Grant NAG3-502)
(NASA-CR-176278; NAS 1.26:176278) Avail: NTIS HC A02/MF A01 CSCL 20E

A two-color, two component Laser Doppler Velocimeter (LDV) system operating in forward scatter has been developed in order to make simultaneous measurements of the axial and radial velocity components in an axisymmetric sudden expansion flow with and without combustion. The LDV system includes Bragg cell modulators in the four beam paths to allow a net frequency shift of 5MHz in both the green and blue beams. This permits an unambiguous measurement of negative velocities and also eliminates incomplete signal bias. The green beam probe volume has a waist diameter of 0.200 mm and is approximately 2mm long. The blue beam has a probe volume waist of 0.250 mm and is approximately 1 mm long. The scattered light from the probe volume is separated so that approximately 80% of each color passes to its respective photomultiplier tube by using a dichroic filter. Narrow bandpass filters are used to further filter unwanted signals before they are detected. A schematic diagram of the LDV system is shown. Author

N86-11466# Westinghouse Research and Development Center, Pittsburgh, Pa.
MERCURY BROMIDE RECONSTITUTION IN THE HgBr LASER SYSTEM Final Report, 15 May 1983 - 15 Jun. 1984
C. S. Liu 11 Sep. 1984 22 p
(Contract N00014-83-C-0375)
(AD-A156502) Avail: NTIS HC A02/MF A01 CSCL 20/5

The major effort was to perform experimental life studies of an UV pre-ionized mercury bromide laser and reconstitute the reaction products such as Hg and Hg2Br2. During past years, we had conducted extensive experimental lifetime studies of a small scale HgBr laser. From these experiments, we selected suitable materials for laser construction, developed procedures to fabricate and fill the laser tube, and finally, we lifetested the laser for over 5 million shots. Those results indicate that pinhole-free gold plated nickel is chemically inert to the HgBr2 discharge and can be used for constructing long-lived high prf HgBr lasers. However, for a large system its is difficult to plate the base metal with pinhole free gold. It is this motivation for developing a HgBr2 recovery system. In this report, we describe the construction of a long-lived, high prf HgBr laser with a built-in HgBr2 reconstitution system and present experimental test data which confirm our theoretical predictions. Finally we recommend the future design of a practical 10 to the 10th power shots HgBr laser. GRA

N86-11467# Georgia Tech Research Inst., Atlanta.
PHOTON INDUCED ELECTRON ATTACHMENT Final Report, May 1982 - Nov. 1984
F. L. Eisele Wright-Patterson AFB, Ohio AFWAL Dec. 1984 64 p
(Contract F33615-82-C-2202)
(AD-A156506, AFWAL-TR-85-2015) Avail: NTIS

HC A04/MF A01 CSCL 07/5

Measurements were performed to determine the feasibility of infrared excitation of the molecules Nitrogen Fluoride, Carbon Fluoride, Carbon Dioxide, Hydrogen Chloride, and Hydrogen Cyanide to an excited state with an enhanced electron attachment rate. The former three molecules were optical pumped by a CO2 laser but no enhanced attachment was observed at any of the laser lines available. The HCl v = zero to two transition was directly pumped by optically mixing of 1.06 micron radiation from a Neodymium : YAG laser with the output of a Yttrium Aluminum Garnet pumped dye laser at .660 microns. Little or no enhanced attachment was observed suggesting a dissociative electron attachment cross section of less than 10 to the -15th power sq. cm. for HCl(v=2). A similar technique was used to excite HCN(v=2) but no enhanced electron attachment was observed. GRA

N86-11468# Oak Ridge National Lab., Tenn.
MELTING OF CRYSTALLINE AND AMORPHOUS SILICON BY RUBY, XeCl AND KrF LASER IRRADIATION
M. J. Aziz, C. W. White, J. Narayan, and B. Stritzker Jun. 1985 7 p Presented at the Mater. Res. Soc. Europe Conf., Strasbourg, 13 May 1985
(Contract DE-AC05-84OR-21400)
(DE85-015040; CONF-8505184-1) Avail: NTIS HC A02/MF A01

Depths of melting in crystalline Si were measured by TEM observations of the removal of dislocation loops created by low dose ion implanting. Depths of melting of amorphous Si layers were monitored by observing the boundaries between a large polycrystalline region, assumed to form by normal melting from and resolidification back to the free surface, and a fine polycrystalline region, assumed to form by the explosive propagation inward of a thin buried liquid layer. The comparison or predictions of heat flow calculations to the measured depth of melting in both crystalline and amorphous silicon are reported. Excellent agreement is found with the Ruby and the XeCl results. Reasonable agreement with the KrF results is obtained only if the silicon liquid phase reflectivity at 249 nm is significantly less than that obtained by extrapolation of the optical parameters from longer wavelengths. DOE

N86-11469# Stanford Univ., Calif. Dept. of Applied Physics.
IMPROVED SOLID STATE LASER SOURCES, VOLUME 3 Final Report
R. L. Dyer and R. C. Eckardt Apr. 1985 17 p
(Contract W-7405-eng-48)
(DE85-012956; UCRL-15561-Vol-3) Avail: NTIS HC A02/MF A01

Investigations have been performed in several areas of solid state laser development. Research in slab-lasers has resulted in a theory of thermal effects and optical propagation which has allowed scaling to larger slabs and extention of the slab concept to crystalline laser hosts. Study of nonlinear optical materials has been extended to include AgGaSe2 and Nd:MgO:LiNbO3. AgGaSe2 is useful for nonlinear frequency conversion in the infrared out to 17 microns. Nd:MgO:LiNbO3 allows a single crystal to be used simultaneously as both active laser material and nonlinear optical or modulator material. A single crystal fiber growth station is developed which has potential application in material surveys by the rapid growth of small samples of crystalline laser materials for spectroscopic evaluation. These research activities combined with other current research programs form a coordinated effort which has resulted in several significant advances in laser development and nonlinear optics. DOE

N86-11470# Sandia Labs., Albuquerque, N. Mex.
VELOCITY MEASUREMENTS OF LASER DRIVEN FLYERS BACKED BY HIGH IMPEDANCE WINDOWS
S. A. Sheffield, J. W. Rogers, Jr., and J. N. Castaneda 1985 13 p Presented at the Am. Phys. Soc. Topical Conf. on Shock Waves in Condensed Matter, Spokane, 22 Jul. 1985
(Contract DE-AC04-76DP-00789)
(DE85-015142; SAND-85-12350; CONF-850736-30) Avail: NTIS HC A02/MF A01

The response of free-standing foils to laser intensity levels of 1,000 to 1,000000 Gw/sq cm was characterized. The response of free-standing and backed foils at much lower intensities, i.e., in the region of 1 to 20 GW/sq cm, was characterized and these flyers are used to initiate insensitive secondary high explosives. The output of a 3.5-J Nd:glass laser with a 16 ns pulse was used to drive 1.5-mm-diameter aluminum flyers. The velocities of both free-standing flyers and flyers backed on the driven side by windows of water, fused silica, or sapphire were measured using optically recording velocity interferometer system (ORVIS). Intensities were on the order of 10 GW/sq cm and velocities as high as 5 km/s were measured for 13-micron/thick, Al flyers. Velocity and acceleration varied only slightly with the shock impedance of the window. Preliminary measurements indicate that pentaerythritol tetranitrate (PETN) at a density of 1.4 grams/cu cm, and HNS-FP (hexanitrostilbene-fine particle) at a density of 1.6 grams/cu cm, can be promptly detonated by 66-micron m-thick, Al flyers impacting at a velocity of near 2.5 km/s. DOE

N86-11471# California Univ., Livermore. Lawrence Livermore Lab.
SPECTRALLY-BROAD PICOSECOND LIGHT SOURCE
M. D. Rotter 18 Jul. 1985 5 p refs Presented at the SPIE Intern. Tech. Symp. on Optical and Elec.-Optical Eng., San Diego, Calif., 18 Aug. 1985
(Contract W-7405-eng-48)
(DE85-015177; UCRL-92170; CONF-850887-10) Avail: NTIS HC A02/MF A01

A fast (35 ps or less), spectrally broad (at least 600 nm) light source for use in characterizing and calibrating photonics equipment is described. The spectral output of the source is described, and examples of its use are given. DOE

N86-11503*# National Aeronautics and Space Administration. Lewis Research Center, Cleveland, Ohio.
LASER ANEMOMETRY FOR HOT SECTION APPLICATIONS
Richard G. Seasholtz, Lawrence G. Oberle, and Donald H. Weikle *In its* Turbine Eng. Hot Sect. Technol (HOST) Oct. 1983 p 57-67 refs (For primary document see N86-11495 02-39)
Avail: NTIS HC A11/MF A01 CSCL 20E

N86-11861# Los Alamos National Lab., N. Mex. Engineering Analysis Section.
DESIGN OPTIMIZATION OF THE POWER GENERATION SYSTEM FOR A SPACE-BASED FREE-ELECTRON LASER Abstract Only
Norman M. Schnurr *In its* 6th Bien. CUBE (Computer Use by Engineers) Symp. Aug. 1984 p 10 (For primary document see N86-11858 02-60)
Avail: NTIS HC A06/MF A01

N86-11877# California Univ., Livermore. Lawrence Livermore Lab. Nuclear Test Engineering Div.
THERMO-MECHANICAL ANALYSES OF LASER-HEATED SURFACES Abstract Only
Gary L. Johnson *In* LANL 6th Bien. CUBE (Computer Use by Engineers) Symp. Aug. 1984 p 44 (For primary document see N86-11858 02-60)
Avail: NTIS HC A06/MF A01

N86-11955# Joint Publications Research Service, Arlington, Va.
TOWARD A THEORY OF ATOMIC GAS BREAKDOWN BY LASER RADIATION NEAR A METAL SURFACE Abstract Only
V. S. Vorobev and A. L. Khomkin *In its* USSR Rept.: Phys. and Math. (JPRS-UPM-85-005) 20 Aug. 1985 p 13 refs Transl. into ENGLISH from Fiz. Plazmy (Moscow), v. 10, no. 5, Sep. - Oct. 1984 p 1025-1032 (For primary document see N86-11945 02-70)
Avail: NTIS HC A08/MF A01

N86-11957# Joint Publications Research Service, Arlington, Va.
LASER EVAPORATION OF METAL IN GASEOUS ATMOSPHERE Abstract Only
V. I. Igoshin and V. I. Kurochkin *In its* USSR Rept.: Phys. and

Math. (JPRS-UPM-85-005) 20 Aug. 1985 p 15 refs Transl. into ENGLISH from Kvantovaya Elektron. (Moscow), v. 11, no. 8, Aug. 1984 p 1555-1561 Previously announced in IAA as A85-19247 (For primary document see N86-11945 02-70)
Avail: NTIS HC A08/MF A01

N86-11961# Joint Publications Research Service, Arlington, Va.
EXCITATION OF DISCHARGE IN AIR BY LASER RADIATION Abstract Only
V. I. Bukatyy, A. A. Kobolov, and A. A. Telnikhin *In its* USSR Rept.: Phys. and Math. (JPRS-UPM-85-005) 20 Aug. 1985 p 27 refs Transl. into ENGLISH from Zh. Tekhn. Fiz. (Leningrad), v. 55, no. 2, Feb. 1985 p 312-318 (For primary document see N86-11945 02-70)
Avail: NTIS HC A08/MF A01

N86-11967# Joint Publications Research Service, Arlington, Va.
LASING ON VAPORS OF CHAIN COMPOUNDS Abstract Only
V. V. Gruzinskiy, K. M. Degtyarenko, T. N. Kopylova, and V. T. Pavlova *In its* USSR Rept.: Phys. and Math. (JPRS-UPM-85-005) 20 Aug. 1985 p 44 p 44 refs Transl. into ENGLISH from Izv. Vyssh. Ucheb. Zaved.: Fiz. (Tomsk, USSR), v. 28, no. 1, Jan. 1985 p 101-103 (For primary document see N86-11945 02-70)
Avail: NTIS HC A08/MF A01

N86-11968# Joint Publications Research Service, Arlington, Va.
ENERGY CHARACTERISTICS OF LASER WITH SATURABLE ANISOTROPIC ABSORBING MEDIUM IN CAVITY Abstract Only
A. P. Voytovich and V. V. Mashko *In its* USSR Rept.: Phys. and Math. (JPRS-UPM-85-005) 20 Aug. 1985 p 44-45 refs Transl. into ENGLISH from Zh. Prikl. Spektros. (Minsk, USSR), v. 41, no. 6, Dec. 1984 p 899-904 (For primary document see N86-11945 02-70)
Avail: NTIS HC A08/MF A01

N86-11969# Joint Publications Research Service, Arlington, Va.
INVESTIGATION OF EFFICIENCY OF GENERATION OF DIFFERENCE-FREQUENCY LASER RADIATION IN WAVEGUIDE Abstract Only
A. O. Makaryan, K. M. Movsisyan, and P. S. Pogosyan *In its* USSR Rept.: Phys. and Math. (JPRS-UPM-85-005) 20 Aug. 1985 p 45 Transl. into ENGLISH from Zh. Prikl. Spektros. (Minsk, USSR), v. 41, no. 6, Dec. 1984 p 908-911 (For primary document see N86-11945 02-70)
Avail: NTIS HC A08/MF A01

N86-11970# Joint Publications Research Service, Arlington, Va.
SPECTRUM STRUCTURE OF XeCl ELECTRIC DISCHARGE LASER Abstract Only
V. S. Burakov, A. F. Bokhonov, and V. A. Titarchuk *In its* USSR Rept.: Phys. and Math. (JPRS-UPM-85-005) 20 Aug. 1985 p 46 Transl. into ENGLISH from Zh. Prikl. Spektros. (Minsk, USSR), v. 41, no. 6, Dec. 1984 p 1029-1032 (For primary document see N86-11945 02-70)
Avail. NTIS HC A08/MF A01

N86-11971# Joint Publications Research Service, Arlington, Va.
DISTRIBUTED-FEEDBACK LASERS WITH ACTIVE FRAMING MEDIUM Abstract Only
Yu. N. Ryzhov, I. V. Cheremiskin, and T. K. Chekhlova *In its* USSR Rept.: Phys. and Math. (JPRS-UPM-85-005) 20 Aug. 1985 p 47 refs Transl. into ENGLISH from Zh. Prikl. Spektros. (Minsk, USSR), v. 42, no. 1, Jan. 1985 p 48-51 (For primary document see N86-11945 02-70)
Avail: NTIS HC A08/MF A01

N86-11972# Joint Publications Research Service, Arlington, Va.
INVESTIGATION OF POLARIZATION CHARACTERISTICS OF RADIATION FROM LASER WITH DYE-ACTIVATED POLYMER ELEMENTS Abstract Only
V. S. Burakova, N. N. Vasilev, A. Ya. Gorelenko, V. Ye. Sivenkova, and A. P. Shkadarevich *In its* USSR Rept.: Phys. and Math. (JPRS-UPM-85-005) 20 Aug. 1985 p 48 refs Transl. into ENGLISH from Zh. Prikl. Spektros. (Minsk, USSR), v. 42, no. 1, Jan. 1985 p 35-40 (For primary document see N86-11945 02-70)
Avail: NTIS HC A08/MF A01

N86-11973# Joint Publications Research Service, Arlington, Va.
HIGH-EFFICIENCY Al SUB 2 O SUB 3:Ti SUP 3+ TUNABLE LASER Abstract Only
G. S. Kruglik, G. A. Skripko, A. P. Shkadarevich, N. V. Kondratyuk, E. A. Zhdanov, and A. M. Zabaznov *In its* USSR Rept.: Phys. and Math. (JPRS-UPM-85-005) 20 Aug. 1985 p 48-49 refs Transl. into ENGLISH from Zh. Prikl. Spektros. (Minsk, USSR), v. 42, no. 1, Jan. 1985 p 126-128 Original language doc. was announced at A85-28984 (For primary document see N86-11945 02-70)
Avail: NTIS HC A08/MF A01

N86-11974# Joint Publications Research Service, Arlington, Va.
ULTRAVIOLET LASING IN HELIUM-NITROGREN MIXTURES Abstract Only
E. I. Asinovskiy, L. M. Vasilyak, V. V. Markovets, and Yu. M. Tokunov *In its* USSR Rept.: Phys. and Math. (JPRS-UPM-85-005) 20 Aug. 1985 p 49 refs Transl. into ENGLISH from Zh. Prikl. Spektros. (Minsk, USSR), v. 42, no. 1, Jan. 1985 p 131-134 (For primary document see N86-11945 02-70)
Avail: NTIS HC A08/MF A01

N86-11975# Joint Publications Research Service, Arlington, Va.
ELECTROIONIZATION IR Xe-ATOM LASER Abstract Only
N. G. Basov, V. A. Danilychev, A. Yu. Dudin, D. A. Zayarnyy, N. N. Ustinovskiy, I. V. Kholin, and A. Yu. Chugunov *In its* USSR Rept.: Phys. and Math. (JPRS-UPM-85-005) 20 Aug. 1985 p 49-50 refs Transl. into ENGLISH from Kvantovaya Elektronika (Moscow), v. 11, no. 9, Sep. 1984 p 1722-1736 Original language doc. was announced as A85-21003 (For primary document see N86-11945 02-70)
Avail: NTIS HC A08/MF A01

N86-11976# Joint Publications Research Service, Arlington, Va.
OPTIMIZATION OF PARAMETERS OF CHEMICAL CO LASER BY INCREASING LENGTH OF ACTIVE MEDIUM Abstract Only
V. A. Dudkin and V. B. Rukhin *In its* USSR Rept.: Phys. and Math. (JPRS-UPM-85-005) 20 Aug. 1985 p 51 refs Transl. into ENGLISH from Kvantovaya Elektronika (Moscow), v. 11, no. 9, Sep. 1984 p 1883-1884 Original language doc. was announced at A85-21013 (For primary document see N86-11945 02-70)
Avail: NTIS HC A08/MF A01

N86-11977# Joint Publications Research Service, Arlington, Va.
EFFICIENCY OF OPTICALLY-PUMPED XeF-LASER Abstract Only
V. S. Zuyev, L. D. Mikheyev, and D. B. Stavrovskiy *In its* USSR Rept.: Phys. and Math. (JPRS-UPM-85-005) 20 Aug. 1985 p 55 refs Transl. into ENGLISH from Kvantovaya Elektronika (Moscow), v. 11, no. 9, Sep. 1984 p 1750-1756 (For primary document see N86-11945 02-70)
Avail: NTIS HC A08/MF A01

N86-11978# Joint Publications Research Service, Arlington, Va.
ENERGY CHARACTERISTICS OF WAVEGUIDE CO SUB 2-LASER Abstract Only
Yu. B. Konev, N. I. Lipatov, P. P. Pashinin, and A. M. Prokhorov *In its* USSR Rept.: Phys. and Math. (JPRS-UPM-85-005) 20 Aug. 1985 p 59-60 refs Transl. into ENGLISH from Kvantovaya Elektron. (Moscow), v. 11, no. 8, Aug. 84 p 1641-1645 (For primary document see N86-11945 02-70)
Avail: NTIS HC A08/MF A01

N86-11979# Joint Publications Research Service, Arlington, Va.
CHROMIUM- AND NEODYMIUM-ACTIVATED GADOLINIUM-SCANDIUM-GALLIUM GARNET CRYSTAL: A NEW LASER ACTIVE MEDIUM
Ye. V. Zarikov, V. V. Yaptev, V. G. Ostroumov, Yu. S. Privos, V. A. Smirnov, and I. A. Shcherbakov *In its* USSR Rept.: Phys. and

Math. (JPRS-UPM-85-005) 20 Aug. 1985 p 61 refs Transl. into ENGLISH from Kvantovaya Elektronika (Moscow), v. 11, no. 8, Aug. 1984 p. 1565-1574 (For primary document see N86-11945 02-70)
Avail: NTIS HC A08/MF A01

N86-11980# Joint Publications Research Service, Arlington, Va.
TWO-FREQUENCY PASSIVE MODE LOCKING IN IODINE PHOTODISSOCIATION LASER Abstract Only
V. M. Kiselev, A. S Grenishin, T. N. Kotlikova, and L. I. Rodina *In its* USSR Rept.: Phys. and Math. (JPRS-UPM-85-005) 20 Aug. 1985 p 61-62 p 61-62 refs Transl. into ENGLISH from Kvantovaya Elektron. (Moscow), v. 11, no. 8, Aug. 1984 p 1542-1554 Previously announced in IAA as A85-19246 (For primary document see N86-11945 02-70)
Avail: NTIS HC A08/MF A01

N86-11928# Joint Publications Research Service, Arlington, Va.
FREQUENCY-SELECTION AND MODE-LOCKING AND Nd:YAG LASER Abstract Only
Guichen Tan and Peixia Qiu *In its* China Rept.: Sci. and Technol. (JPRS-CST-85-014) 2 May 1985 p 80 Transl. into ENGLISH from Zhongguo Jiguang (Shanghai), v. 12, no. 1, 20 Jan. 1985 p 11-14 (For primary document see N86-11918 02-70)
Avail: NTIS HC A06/MF A01

N86-11929# Joint Publications Research Service, Arlington, Va.
A LARGE AREA X-RAY SOURCE AND ITS PREIONIZATION CHARACTERISTICS FOR XeCl EXCIMER LASER Abstract Only
Qihong Lou, Runwen Wang, and Xusan Cheng *In its* China Rept.: Sci. and Technol. (JPRS-CST-85-014) 2 May 1985 p 81 Transl. into ENGLISH from Zhongguo Jiguang (Shanghai), v. 12, no. 1, 20 Jan. 1985 p 19-21 (For primary document see N86-11918 02-70)
Avail: NTIS HC A06/MF A01

N86-11930# Joint Publications Research Service, Arlington, Va.
RING CAVITY CO2 LASER FOR BRANCH-SELECTION AND NARROW RESONANCE PRODUCED BY SF6 IN CAVITY Abstract Only
Yongkai Huang and Jianmin Rong *In its* China Rept.: Sci. and Technol. (JPRS-CST-85-014) 2 May 1985 p 82 Transl. into ENGLISH from Zhongguo Jiguang (Shanghai), v. 12, no. 1, 20 Jan. 1985 p 25-28 (For primary document see N86-11918 02-70)
Avail: NTIS HC A06/MF A01

N86-11933# Joint Publications Research Service, Arlington, Va.
STATIONARY PULSE SOLUTIONS FOR A FREE ELECTRON LASER Abstract Only
Honglie Fang, Shufen Fu, and G. T. Moore *In its* China Rept.: Sci. and Technol. (JPRS-CST-85-014) 2 May 1985 p 88 Transl. into ENGLISH from Wuli Xuebao (Beijing), v. 33, no. 7, Jul. 1984 p 935-942 (For primary document see N86-11918 02-70)
Avail: NTIS HC A06/MF A01

N86-12003# Joint Publications Research Service, Arlington, Va.
DOUBLE-WAVELENGTH PULSED TUNABLE DYE LASER Abstract Only
Zaixuan Zhang, Jingyun Wang, Yiqian Yuan et al *In its* China Rept.: Sci. and Technol. (JPRS-CST-85-015) 16 May 1985 p 97 Transl. into ENGLISH from Zhongguo Jiguang (Shanghai), v. 11, no. 6, 20 Jun. 1984 p 323-326 (For primary document see N86-11994 02-70)
Avail: NTIS HC A07/MF A01

N86-12006# Joint Publications Research Service, Arlington, Va.
ON CONVECTIVE EFFECTS IN GAS LASERS Abstract Only
Zhi Gao *In its* China Rept.: Sci. and Technol. (JPRS-CST-85-015) 16 May 1985 p 116 Transl. into ENGLISH from Wuli Xuebao (Beijing), v. 33, no. 9, Sep. 1984 p 1294-1300 (For primary document see N86-11994 02-70)
Avail: NTIS HC A07/MF A01

37 MECHANICAL ENGINEERING

Includes auxiliary systems (non-power); machine elements and processes; and mechanical equipment.

N86-11472 Texas Univ., Austin.
NUMERICAL SOLUTION FOR CONTACT PRESSURE AND WEAR DISTRIBUTIONS OF UNLUBRICATED, MISALIGNED, CLOSELY CONFORMING, MULTIPLY CONNECTED SURFACES Ph.D. Thesis
Hsien Heng Chen 1984 239 p
Avail: Univ. Microfilms Order No. DA8513195

A general numerical method is presented for studying unlubricated arbitrary profile, elastic body contact problems with combined normal and shear loadings. A pressure wear theory is introduced to solve for instantaneous pressure distributions and the corresponding worn surface profiles as sliding contact continues. The modified Boussinesq point force displacement influence function and modified profile function are employed in conjunction with an integral equation discretization method and an automatic mesh generation technique to redefine the new pressure area boundary. A wide range of contact problems involving multiply connected regions can be solved. The general numerical method has been implemented in several computer programs and has been applied to the problems of misaligned and perfectly-aligned contact. The results have been verified by comparison with the experimental data presented in the literature for the self-lubricated journal bearing under various conditions of load and misalignment. Dissert. Abstr.

N86-11473*# National Aeronautics and Space Administration. Marshall Space Flight Center, Huntsville, Ala.
A COMPARISON OF THE PHYSICS OF GAS TUNGSTEN ARC WELDING (GTAW), ELECTRON BEAM WELDING (EBW), AND LASER BEAM WELDING (LBW)
A. C. Nunes, Jr. Aug. 1985 22 p refs
(NASA-TM-86503; NAS 1.15:86503) Avail: NTIS HC A02/MF A01 CSCL 13H

The physics governing the applicability and limitations of gas tungsten arc (GTA), electron beam (EB), and laser beam (LB) welding are compared. An appendix on the selection of laser welding systems is included. Author

N86-11474*# Pratt and Whitney Aircraft, East Hartford, Conn. Engineering Div.
LATERAL DAMPERS FOR THRUST BEARINGS Final Report
D. H. Hibner and D. R. Szafir Aug. 1985 79 p refs
(Contract NAS3-23932)
(NASA-CR-174924; NAS 1.26:174924; PWA-5966-17) Avail: NTIS HC A05/MF A01 CSCL 13I

The development of lateral damping schemes for thrust bearings was examined, ranking their applicability to various engine classes, selecting the best concept for each engine class and performing an in-depth evaluation. Five major engine classes were considered: large transport, military, small general aviation, turboshaft, and non-manrated. Damper concepts developed for evaluation were: curved beam, constrained and unconstrained elastomer, hybrid boost bearing, hydraulic thrust piston, conical squeeze film, and rolling element thrust face. Author

N86-11475*# National Aeronautics and Space Administration. Lewis Research Center, Cleveland, Ohio.
PROTECTIVE COATINGS OF METAL SURFACES BY COLD PLASMA TREATMENT
R. Manory and A. Grill (Ben Gurion Univ. of the Negev, Beer Sheva) Oct. 1985 15 p refs
(NASA-TM-87152; E-2747-1; NAS 1.15:87152) Avail: NTIS HC A02/MF A01 CSCL 11F

The cold plasma techniques for deposition of various types of protective coatings are reviewed. The main advantage of these techniques for deposition of ceramic films is the lower process temperature, which enables heat treating of the metal prior to deposition. In the field of surface hardening of steel, significant reduction of treatment time and energy consumption were obtained.

A simple model for the plasma - surface reactions in a cold plasma system is presented, and the plasma deposition techniques are discussed in view of this model. Author

N86-11476# California Univ., Livermore. Lawrence Livermore Lab.

SURFACE PROPERTIES OF SHOCKED LEAD

R. Couch, L. Shaw, R. Barlett, L. Steinmetz, w. Behrendt, and C. Firpo Mar. 1985 11 p Presented at the Intern. Conf. on Mech. and Phys. Behaviour of Mater. Under Dyn. Loading, Paris, 2 Sep. 1985
(Contract W-7405-eng-48)
(DE85-009582; UCRL-90817; CONF-850946-2) Avail: NTIS HC A02/MF A01

Hydrodynamic experiments often require optical observation of shocked surfaces. However, phenomena that alter surface appearance can obscure the interpretation of data. Studies of material ejection were extended to include more complicated shock structures. In addition, both thin foils and an imposed atmosphere were used as ways of sampling the surface in search for nonhomogeneous behavior. Quantitative measures of mass ejection were obtained using X-ray transmission analysis, and high speed photography, provided qualitative data. Results indicate that the amount of mass ejected is a function of shock structure. Many heterogeneous effects are observed that are presumed to be related to surface preparation, partial melting, and spall. DOE

N86-11477# Oak Ridge National Lab., Tenn.

REFRACTORY ALLOY PERFORMANCE: PRODUCT FORM PROCUREMENT AND COMPONENT FABRICATION

W. O. Harms 1985 17 p Presented at the SP-100 Systems Selection Comm. Rev. on Fuels and Mater. Conf., Los Alamos, N. Mex., 20 Jun. 1985
(Contract DE-AC05-84OR-21400)
(DE85-014658; CONF-8506153-2) Avail: NTIS HC A02/MF A01

The availability and fabricability of welded components of candidate refractory alloys is presented. Listed is the commercial facilities, procedures, properties of weldments and postweld heat treatments. E.R.

N86-11478# Honeywell, Inc., Roseville, Minn.

HERMETIC BELLOWS SEAL FOR BRAUN LINEAR ENGINE: DESIGN, TEST AND DEMONSTRATION Final Report

Jun. 1985 26 p Prepared in cooperation with Tectonics Research Inc., Roseville, Minn.
(Contract DE-AC05-87OR-21400)
(DE85-013545; ORNL/Sub-80-61613/1) Avail: NTIS HC A03/MF A01

Seal requirements were defined, seal performance to develop a design data base were analyzed and the design criteria to evolve a seal solution suitable for application to a light commercial sized heat pump was applied. Maximum life goal is 15 years with operation of at least 4000 hours per year. The seal will be exposed to an oil/refringement mixture on one side and atmosphere contaminated with combustion products on the other side. The evolved seal design consists of two or more bellows elements placed in series and joined to the underface of the piston at one end and to the crankcase at the other. The intermediary ends of the bellows are joined together so that all the joints are made leak tight. The compressor piston rod is enclosed within the bellows. Bellows elements are driven at their point of junction by a mechanism synchronized to the piston motion but so constrained as to limit the stress in each element, thereby insuring an effective, long life hermetic seal. E.A.K.

N86-11479# Sandia Labs., Albuquerque, N. Mex.

DISH ELECTRIC SYSTEMS HEAT ENGINE ASSESSMENT

L. L. Lukens Jun. 1985 44 p
(Contract DE-AC04-76DP-00789)
(DE85-013942; SAND-85-0522) Avail: NTIS HC A03/MF A01

Cost and performance estimates of several heat engine technologies were studied and their performance was evaluated with a dish electric system model. The analysis yielded the relative potential of the different heat engine technologies to meet the National Solar Thermal Technology program goal for levelized electricity cost. The heat engines evaluated were the Brayton engine, the Rankine engine the liquid metal thermoelectric converter, the Stirling engine, and two binary engines. It is indicated that the liquid metal thermoelectric converter, the Stirling engines, and the binary engines have the highest potential for cost effective dish electric systems. DOE

N86-11480# National Coal Board, Grimethorpe (England).

EVALUATION OF CANDIDATE MATERIALS IN A STATIC TURBINE CASCADE

Jun. 1985 266 p
(Contract DE-AI01-76ET-10393)
(DE85-008592; DOE/ET-10393/1859) Avail: NTIS HC A12/MF A01

A range of materials in a static cascade was evaluated. Some of these materials are considered for the manufacturing of blades for a gas turbine powered by a pressurized fluidized bed combustor. The cascade consisted of five stages of specimens. The first three stages consisted of nine impulse aerofoils, which turned the flow but did not accelerate it. The fourth stage was made up of nine reaction blades which both turned the flow and accelerated it to near sonic velocity, whereupon the flow entered the fifth stage which consisted of three erosion targets. Details of the exposure conditions and the results of the examinations of the specimens are presented. No evidence was found of erosion of the blades by particles of entrained dust; however, there was evidence of Type II, low temperature, hot corrosion on many of the specimens. DOE

N86-11481# Edgerton, Germeshausen and Grier, Inc., Idaho Falls, Idaho.

ECONOMIC EVALUATION OF CONCURRENT WELDING AND NONDESTRUCTIVE EXAMINATION

A. D. Watkins, J. A. Johnson, and H. B. Smartt 1985 20 p Presented at the 66th Am. Welding Soc. Ann. Meeting, Las Vegas, Nev., 28 Apr. 1985
(Contract DE-AC07-76ID-01570)
(DE85-014623; EGG-M-17884; CONF-8504102-3) Avail: NTIS HC A02/MF A01

The cost savings of implementing the concurrent welding and nondestructive examination technique, for a proposed welding operation, to be $73.26 per meter of weld are estimated. A hypothetical weld operation was developed using standard data from nonrepetitive work measuring programs. Proposed changes to this weld operation to implement the concurrent welding and nondestructive examination are analyzed by comparing between the proposed and hypothetical weld operation. Standard methods are used to calculate the cost savings between the sequential differences of the two weld operations. DOE

N86-11482# Argonne National Lab., Ill.

NUMERICAL SIMULATION OF AN EQUIPMENT HATCH FOR A STEEL CONTAINMENT VESSEL TO LOADING BEYOND THE DESIGN BASIS

R. F. Kulak, B. J. Hsieh, J. E. Ash, J. M. Kennedy, and G. A. McLennan 1985 13 p refs Presented at the 8th Intern. Conf. on Struct. Mech. in Reactor Technol., Brussels, 19 Aug. 1985
(Contract W-31-109-eng-38)
(DE85-010485; CONF-850809-56) Avail: NTIS HC A02/MF A01

The sealing deformations of a large equipment hatch with a pressure seated gasket due to overpressurization were analyzed. An axisymmetric finite element analysis of the penetration sleeve revealed that its surface can undergo large rotations. Values for sealing surface rotation of 7 deg were computed. The order of magnitude of leakage due to the sealing surface rotation is estimated. DOE

N86-11483# Edgerton, Germeshausen and Grier, Inc., Idaho Falls, Idaho.

ADVANCED MECHANICAL HEAT PUMP TECHNOLOGIES FOR INDUSTRIAL APPLICATIONS

J. I. Mills, D. S. Plaster, and R. N. Chappell 1985 9 p refs Presented at the 7th Ann. Ind. Energy Technol. Conf., Houston, Tex., 13 May 1985 Prepared in cooperation with DOE, Idaho Falls, Idaho
(Contract DE-AC07-76ID-01570)
(DE85-014613; EGG-M-28384; CONF-850515-2) Avail: NTIS HC A02/MF A01

Advanced chemical and mechanical heat pump technologies were developed for industrial application. Five advanced mechanical heat pump technologies are at various stages of stepped development strategy including: (1) a waste heat powered steam compression system; (2) a high temperature reverse Rankine cycle heat pump with methanol working fluid; (3) a Brayton cycle solvent recovery system; (4) magnetic cycle heat pumps; and (5) Stirling cycle heat pumps. These five advanced mechanical heat pump systems and how the development strategy allows efficient progression from concept to technology transfer to the private sector is discussed. Results are beneficial in determining how various steps of the product development plan should proceed. The results of ongoing work will determine applications suitable for industrial heat pumps and will further guide the development of advanced technologies. DOE

N86-11484# Brookhaven National Lab., Upton, N. Y.
OPTIMIZED GROUND-COUPLED HEAT PUMP SYSTEM DESIGN FOR NORTHERN CLIMATE
M. A. Catan and V. D. Baxter (ORNL) 1985 29 p refs Presented at Am. Soc. of Heating, Refrigerating and Air-Conditioning Engr. Semiann. Meeting, Honolulu, Hawaii, 23 Jun. 1985
(Contracts DE-AC02-76CH-00016; DE-AC05-84OR-21400)
(DE85-014065; CONF-850606-9) Avail: NTIS HC A03/MF A01

This paper addresses the question of the performance of a Ground Coupled Heat Pump (GCHP) system with a water - source heat pump package designed expressly for such systems operating in a northern climate. The project objective is to minimize the life-cycle cost of a GCHP system by optimizing the design of both the heat pump package and the ground coil in concert. In order to achieve this objective, a number of modelling tools are developed or modified to analyze the heat pump's performance and cost and the ground coil's performance. The life-cycle cost of a GCHP system (water-source heat pump with a horizontal ground coil) for an 1800 ft(2) (167 m(2)) house in Pittsburgh, PA, is minimized over a 7 year economic life. Simple payback for the optimized GCHP system, relative to conventional air-source heat pumps, is under 3 years. The water-source heat pump package resulting from this optimization is calculated to cost 21% more than its conventional counterpart with a heating coefficient of performance (COP) about 20% higher, and a cooling COP about 23% higher. In the GCHP system modeled, its annual energy savings are predicted to be about 11% comparred to a system designed around the conventional heat pump while having about the same installation cost. The major conclusion of this study is - GCHP system performance improvement can be attained by improving the water-source heat pump package at less cost than by buying more ground coil. DOE

N86-11485# Sandia Labs., Albuquerque, N. Mex.
NUMERICAL SIMULATION OF A SAMPLE RECOVERY FIXTURE FOR HIGH VELOCITY IMPACT
F. R. Norwood, R. A. Graham, and A. Sawaoka Jun. 1985 5 p refs Presented at the Am. Phys. Soc. Topical Conf. on Shock Waves in Condensed Matter, Spokane, Wash., 22 Jul. 1985 Prepared in cooperation with Tokyo Inst. of Technology, Japan
(Contract DE-AC04-76DP-00789)
(DE85-013965; SAND-85-1511C; CONF-850736-8) Avail: NTIS HC A02/MF A01

Numerical simulations of shock compression conditions in the sample recovery fixture for high velocity impact were carried out with two dimensional (CSQ) and three dimensional (HULL) computer codes. For the impact of stainless steel on the stainless steel capsule at a velocity of 2.5 km/sec, it is found that two dimensional effects within the low density powder samples dominate the loading process and that interactions between the four samples are nagligible. Because of the much higher pressure encountered, the two dimensional effects are qualitatively different than those found for the Sandia Bear explosive fixtures. It is shown that, in both the axisymmetric and the three dimensional geometry, the radial effects are the dominant feature. These two dimensional radial effects dominate the shock pressures and temperatures such that one dimensional analysis is incorrect and would lead to substantial errors. DOE

N86-11228*# LTV Aerospace and Defense Co., Dallas, Tex. Vought Aero Products Div.
THE FACTORY OF THE FUTURE
J. E. Byman *In* NASA. Langley Research Center Welding, Bonding and Fastening, 1984 Sep. 1985 p 1-9 (For primary document see N86-11227 02-23)
Avail: NTIS HC A21/MF A01 CSCL 13H

N86-11229*# Arc Machines, Inc., Pacoima, Calif.
AUTOMATIC ORBITAL GTAW WELDING: HIGHEST QUALITY WELDS FOR TOMORROW'S HIGH-PERFORMANCE SYSTEMS
Barbara K. Henon *In* NASA. Langley Research Center Welding, Bonding and Fastening, 1984 Sep. 1985 p 11-19 (For primary document see N86-11227 02-32)
Avail: NTIS HC A21/MF A01 CSCL 13H

N86-11232*# SPS Technologies, Jenkintown, Pa.
MECHANICAL FASTENERS FOR ADVANCED COMPOSITE MATERIALS
Richard C. Landt *In* NASA. Langley Research Center Welding, Bonding and Fastening, 1984 Sep. 1985 p 55-65 ref (For primary document see N86-11227 02-23)
Avail: NTIS HC A21/MF A01 CSCL 13E

N86-11233*# National Aeronautics and Space Administration. Langley Research Center, Hampton, Va.
THE ALTERNATING SURFACE SEGMENTED LAP JOINT: A DESIGN FOR THIN HIGHLY LOADED JOINTS
Vernon E. Watkins, Jr. and George C. Firth *In its* Welding, Bonding and Fastening, 1984 Sep. 1985 p 67-76 ref (For primary document see N86-11227 02-23)
Avail: NTIS HC A21/MF A01 CSCL 13E

N86-11234*# Martin Marietta Aerospace, New Orleans, La.
AUTOMATIC FASTENING LARGE STRUCTURES: A NEW APPROACH
Donald F. Lumley *In* NASA. Langley Research Center Welding, Bonding and Fastening, 1984 Sep. 1985 p 77-88 (For primary document see N86-11227 02-23)
Avail: NTIS HC A21/MF A01 CSCL 13E

N86-11235*# SPS Technologies, Jenkintown, Pa.
STRESS CORROSION RESISTANT FASTENERS
Thomas A. Roach *In* NASA. Langley Research Center Welding, Bonding and Fastening, 1984 Sep. 1985 p 89-104 (For primary document see N86-11227 02-23)
Avail: NTIS HC A21/MF A01 CSCL 13E

N86-11236*# National Aeronautics and Space Administration. Langley Research Center, Hampton, Va.
DERIVATION AND TEST OF ELEVATED TEMPERATURE THERMAL-STRESS-FREE FASTENER CONCEPT
James Wayne Sawyer, Max L. Blosser, and Robert R. McWithey *In its* Welding, Bonding and Fastening, 1984 Sep. 1985 p 105-122 refs (For primary document see N86-11227 02-23)
Avail: NTIS HC A21/MF A01 CSCL 13E

N86-11237*# Battelle Columbus Labs., Ohio.
EXPLOSIVE WELDING IN THE 1990'S
Narain S. Lalwaney and Vonne D. Linse *In* NASA. Langley Research Center Welding, Bonding and Fastening, 1984 Sep. 1985 p 123-140 refs (For primary document see N86-11227 02-23)
Avail: NTIS HC A21/MF A01 CSCL 13H

N86-11238*# Explosive Fabricators, Inc., Louisville, Colo.
EXPLOSIVE WELDING OF TUBULAR CONFIGURATED JOINTS FOR CRITICAL APPLICATIONS
Roy Hardwick *In* NASA. Langley Research Center Welding, Bonding and Fastening, 1984 Sep. 1985 p 141-155 (For primary document see N86-11227 02-23)
Avail: NTIS HC A21/MF A01 CSCL 13H

N86-11239*# National Aeronautics and Space Administration. Langley Research Center, Hampton, Va.
EXPLOSIVE TUBE-TO-FITTING JOINING OF SMALL-DIAMETER TUBES
Laurence J. Bement *In its* Welding, Bonding and Fastening, 1984 Sep. 1985 p 157-175 (For primary document see N86-11227 02-23)
Avail: NTIS HC A21/MF A01 CSCL 13H

N86-11240*# Foster Wheeler Corp., Livingston, N.J.
THE USE OF EXPLOSIVE FORMING FOR FASTENING AND JOINING STRUCTURAL AND PRESSURE COMPONENTS
J. Wayne Schroeder *In* NASA. Langley Research Center Welding, Bonding and Fastening, 1984 Sep. 1985 p 177-184 (For primary document see N86-11227 02-23)
Avail: NTIS HC A21/MF A01 CSCL 13H

N86-11241*# Helwan Univ., Cairo (Egypt).
EXPLOSIVE WELDING OF ALUMINUM, TITANIUM AND ZIRCONIUM TO COPPER SHEET METAL
Abdel-Aziz Hegazy and Jim D. Mote (Denver Univ.) *In* NASA. Langley Research Center Welding, Bonding and Fastening, 1984 Sep. 1985 p 185-196 refs (For primary document see N86-11227 02-23)
Avail: NTIS HC A21/MF A01 CSCL 13H

N86-11244*# Northrop Corp., Hawthorne, Calif. Aircraft Div.
SOLID-STATE BONDING OF SUPERPLASTIC ALUMINUM ALLOY 7475 SHEET
Thomas D. S. Byun and Ramsevak B. Vastava *In* NASA. Langley Research Center Welding, Bonding and Fastening, 1984 Sep. 1985 p 231-251 (For primary document see N86-11227 02-23)
Avail: NTIS HC A21/MF A01 CSCL 13H

N86-11245*# National Aeronautics and Space Administration. Langley Research Center, Hampton, Va.
EVALUATION OF SUPERPLASTIC FORMING AND WELD-BRAZING FOR FABRICATION OF TITANIUM COMPRESSION PANELS
Dick M. Royster, Thomas T. Bales, and Randall C. Davis *In its* Welding, Bonding and Fastening, 1984 Sep. 1985 p 253-270 refs (For primary document see N86-11227 02-23)
Avail: NTIS HC A21/MF A01 CSCL 13H

N86-11246*# Massachusetts Inst. of Tech., Cambridge.
FEASIBILITY OF REMOTELY MANIPULATED WELDING IN SPACE: A STEP IN THE DEVELOPMENT OF NOVEL JOINING TECHNOLOGIES
Koichi Masubuchi, John E. Agapakis, Andrew DeBiccari, and Christopher vonAlt *In* NASA. Langley Research Center Welding, Bonding and Fastening, 1984 Sep. 1985 p 271-296 refs (For primary document sec N86-11227 02-23)
Avail: NTIS HC A21/MF A01 CSCL 13M

N86-11247*# Douglas Aircraft Co., Inc., Long Beach, Calif.
ADVANCES IN JOINING TECHNIQUES USED IN DEVELOPMENT OF SPF/DB TITANIUM SANDWICH REINFORCED WITH METAL MATRICES
J. E. Fischler *In* NASA. Langley Research Center Welding, Bonding and Fastening, 1984 Sep. 1985 p 297-322 (For primary document see N86-11227 02-23)
Avail: NTIS HC A21/MF A01 CSCL 13M

N86-11530# Technion - Israel Inst. of Tech., Haifa. Dept. of Mechanical Engineering.
MECHANICAL FACE SEAL DYNAMICS UPDATE
I. Etison *In* The Shock and Vibration Information Center The Shock and Vibration Digest, Vol. 17, No. 4 Apr. 1985 p 11-15 refs (For primary document see N86-11527 02-39)
Avail: SVIC, Code 5804, Naval Research Lab., Washington, D.C. 20375 CSCL 11/1

38 QUALITY ASSURANCE AND RELIABILITY

Includes product sampling procedures and techniques; and quality control.

N86-11486 Arizona Univ., Tucson.
RELIABILITY ANALYSIS OF SERIES STRUCTURAL SYSTEMS Ph.D. Thesis
Lidvin Kjerengtroen 1985 175 p
Avail: Univ. Microfilms Order No. DA8511703

Reliability analysis of series structural systems with emphasis on problems typical for metal fatigue is addressed. Answers are sought to the following questions: (1) Given the distribution of strength of the components and the distribution of external loads on the system, what is the probability of failure of the system? (2) Given the target safety index for the system, what would be the target safety index for the components? Exact solutions in the analysis of series structural systems only exists for some special problems. Some of these special problems are investigated. In particular some special cases of the problem of unequal element reliabilities are considered and some interesting observations are made. Numerical integration is in general required even when an exact solution exists. A correction or adjustment factor is developed for an important class of problems. This factor makes it possible to relate element and system probabilities of failure without numerical integration. Dissert. Abstr.

N86-11487# Aeronautical Research Labs., Melbourne (Australia).
NERF: A COMPUTER PROGRAM FOR THE NUMERICAL EVALUATION OF RELIABILITY FUNCTIONS USER MANUAL
A. D. Graham and G. D. Mallinson Feb. 1984 241 p refs
(ARL/STRUC-R-411; AR-003-967) Avail: NTIS HC A11/MF A01

The computer program NERF and its support programs NERPRE and NERPLT provide a versatile facility for the incorporation of statistical variations in the calculation of reliability functions for fatigue failure. The reliability models that can be evaluated by NERF, the use of the NERF suite of programs, the definition of input data, the operating instructions and various results are detailed. Examples, complete with the associated input data and specimen results are also presented. E.A.K.

N86-11488# Army Construction Engineering Research Lab., Champaign, Ill.
UNCERTAINTY ASSESSMENT IN LIFE CYCLE COST ANALYSIS Final Report
May 1985 25 p
(AD-A157414; CERL-SR-P-85/12) Avail: NTIS HC A02/MF A01 CSCL 14/1

Several of the leading probabilistic methods for measuring uncertainties in construction project life cycle costs were studied to evaluate their applicability for military construction projects. The confidence index and statistical testing approaches are discussed in detail; other methods are discussed briefly. The confidence index approach is recommended as a simple, cost-effective method suitable for use in military construction design. GRA

N86-11489# Battelle Pacific Northwest Labs., Richland, Wash.
EXPLORATORY DEVELOPMENT OF FMR (FERROMAGNETIC RESONANCE) ADVANCED SURFACE FLAW DETECTION METHODS Final Report, Aug. 1982 - Aug. 1984
J. M. Prince and B. A. Auld Wright-Patterson AFB, Ohio AFWAL Apr. 1985 78 p
(Contract F33615-82-C-5100)
(AD-A157436; AFWAL-TR-85-4010) Avail: NTIS

HC A05/MF A01 CSCL 14/2

The purpose of this program was to carry forward the development of a microwave eddy current (MEC) probe, which is based on the ferromagnetic resonance (FMR) principle, to the point where its performance in a practical flaw detection breadboard system for gas turbine engine component inspection and its compatibility with the Retirement-for-Cause (RFC) modular inspection system could be demonstrated. This program studied the physical constraints related to the inspection of complex geometries in Ti 6-2-4-6 and IN-100 materials with the MEC-FMR surface flaw detection method. Based on the resulting information, a breadboard inspection system was designed and fabricated to demonstrate the MEC-FMR test method in the inspection of a jet engine interstage seal key slot.
GRA

N86-11243*# National Aeronautics and Space Administration. Langley Research Center, Hampton, Va.
LANGLEY RESEARCH CENTER STANDARD FOR THE EVALUATION OF SOCKET WELDS
Robert F. Berry, Jr. *In its* Welding, Bonding and Fastening, 1984 Sep. 1985 p 211-229 (For primary document see N86-11227 02-23)
Avail: NTIS HC A21/MF A01 CSCL 14D

N86-11248*# Texas Instruments, Inc., Attleboro, Mass.
COMPARISON OF BOND IN ROLL-BONDED AND ADHESIVELY BONDED ALUMINUMS
R. J. Schwensfeir, Jr., G. Trenkler, R. G. Delagi, and J. A. Forster *In* NASA. Langley Research Center Welding, Bonding and Fastening, 1984 Sep. 1985 p 323-338 refs (For primary document see N86-11227 02-23)
Avail: NTIS HC A21/MF A01 CSCL 14D

39 STRUCTURAL MECHANICS

Includes structural element design and weight analysis; fatigue; and thermal stress.

For applications see *05 Aircraft Design, Testing and Performance* and *18 Spacecraft Design, Testing and Performance.*

N86-11490 California Univ., Berkeley.
ELASTIC WAVE SCATTERING OF A GAUSSIAN INCIDENT BEAM FROM AN INTERFACE CRACK IN A LAYERED HALF SPACE SUBMERGED IN WATER Ph.D. Thesis
Sheryl Marie Gracewski 1984 110 p
Avail: Univ. Microfilms Order No. DA8512837

Many industrial products contain parts with thin coatings or layers bonded to thicker substrates. For quality control of these parts, there is need for a nondestructive evaluation (NDE) method to locate and characterize interface flaws and debonding. In this thesis an analytical model for a typical NDE testing configuration is presented. Time harmonic elastic wave scattering by an interface crack in a liquid-solid layer-solid substrate structure is analyzed. The solution is presented for three incident disturbances. Harmonic normal and shear loadings onto the solid structure are first considered to gain insight into the response characteristics of the structure. The solution for an incident beam of Gaussian profile is then presented since this profile approximates the output of an ultrasonic transducer. The solution of the problem leads to a set of coupled singular integral equations for the jump in displacements across the crack.
Dissert. Abstr.

N86-11491 Wisconsin Univ., Madison.
A BODY TENSOR FORMALISM FOR ELASTIC-PLASTIC CONTINUA WITH APPLICATIONS IN UNIAXIAL EXTENSION Ph.D. Thesis
Alan David Freed 1985 173 p
Avail: Univ. Microfilms Order No. DA8507241

The body tensor formalism of Lodge (1974) is extended to include elastic-plastic materials. The fundamental body tensors are defined. The field equations that govern an elastic-plastic continuum are derived from first principles. The covariant strain-rate tensor is postulated to be the sum of two tensors; they are the elastic and plastic, covariant, strain-rate tensors. The elastic and plastic, covariant, strain tensors are obtained by integration. Their sum equals the covariant strain tensor, regardless of the magnitude of the deformation. The thermoelastic relationships for stress and entropy are derived from first principles. The elastic potential must be continuous and twice-differentiable in the thermostatic state variable for these equations to be consistent with Caratheodory's (1909) theory of thermostatics. The classical theory of elasticity is obtained as a special case. Components of the fundamental tensors are determined for the process of uniform extension.
Dissert. Abstr.

N86-11492 Tennessee Univ., Knoxville.
THE STABILITY OF TIMOSHENKO BEAMS CONVEYING A COMPRESSIBLE FLUID Ph.D. Thesis
Robert Ost Johnson 1984 175 p
Avail: Univ. Microfilms Order No. DA8506899

The purpose is to formulate and solve the stability problem associated with the equations of motion of a Timoshenko beam conveying a compressible fluid. The beam is assumed to be either cantilevered or simply supported. Shear deformation and rotary inertia are considered in the Timoshenko beam theory. The beam analysis that is carried out is quite general and allows for viscous damping external to the tube as well as both internal strain rate and hysteretic damping. Interactions between these three damping mechanisms, shear deformation, and rotary inertia also are accounted for. The compressible, isenitropic flow through the tube is governed by Euler's equations of motion. Gravitational effects are neglected in the analysis. This is equivalent to assuming that the tube is horizontal. The motion of the fluid is coupled to that of the beam by a compatibility condition at the tube wall which requires that they vibrate together.
Dissert. Abstr.

N86-11493 Polytechnic Inst. of New York, Brooklyn.
BOUNDED STATE CONTROL OF LINEAR SYSTEMS WITH APPLICATION TO THE ACTIVE STRUCTURAL CONTROL Ph.D. Thesis
Sang-Kook Lee 1985 126 p
Avail: Univ. Microfilms Order No. DA8506856

A new approach to be used in active control of structures was attempted. The motivation for this research came from consideration of controlling a civil engineering structure exposed to environmental loads, such as wind gusts, earthquakes, etc. Often, the main purpose of structural control is to keep all the controlled variables, e.g., displacements and velocities, inside an allowable region which may be determined by the needs of structural safety and human comfort. The specification of structural safety and comfort of the occupants was directly formulated with a topology in state space, but not with a certain cost function to be minimized with respect to the control law. A sufficient and necessary condition on the existence of linear state feedback control law which guarantees the specified performance, i.e., bounded region, was established. The control law obtained guarantees that the motion of a structure remain within an allowable region under an assumed class of disturbances.
Dissert. Abstr.

N86-11494 Purdue Univ., Lafayette, Ind.
EFFECT OF A VISCOELASTIC BOUNDARY INSET ON VIBRATIONAL CHARACTERISTICS OF A BEAM Ph.D. Thesis
Mehdi Ilkhani-Pour 1984 144 p
Avail: Univ. Microfilms Order No. DA8507695

The effect of a viscoelastic (elastomeric) inset on the vibrational characteristics of a cantilevered beam in flexural motion is examined. The inset is placed at the support fixture of the beam. A closed form solution is obtained for the cyclic energy dissipation due to the inset. The validity of analytical results are confirmed by a good comparison with available test data in the literature. Expressions are then developed for the effect of the inset on fundamental natural frequency and damping ratio of the beam. The former is achieved by modifying the boundary conditions of a cantilevered beam, so as to allow for support rotation and displacement due to elasticity of the inset. The results of a series of experiments, concerning the fundamental natural frequency and damping ratio of two steel beams with a soft polymeric inset, are reported. Again, good agreement is observed between theory and experiments. The existence of an optimum inset length, resulting in maximum energy dissipation, was revealed by both theory and experiments. A further increase in the inset length beyond this value causes a reduction in energy dissipation. Dissert. Abstr.

N86-11495*# National Aeronautics and Space Administration. Lewis Research Center, Cleveland, Ohio.
TURBINE ENGINE HOT SECTION TECHNOLOGY (HOST)
Oct. 1983 250 p refs Workshop held in Cleveland, Ohio, 25-26 Oct. 1983
(NASA-CP-2289; E-1816; NAS 1.55:2289) Avail: NTIS HC A11/MF A01 CSCL 21E

A two-day workshop on the research and plans for turbine engine hot section durability problems was held on October 25 and 26, 1983, at the NASA Lewis Research Center. Presentations were made during six sessions, including structural analysis, fatigue and fracture, surface protective coatings, combustion, turbine heat transfer, and instrumentation, that dealt with the thermal and fluid environment around liners, blades, and vanes, and with material coatings, constitutive behavior, stress-strain response, and life prediction methods for the three components. The principal objective of each session was to disseminate the research results to date, along with future plans, in each of the six areas. Contract and government researchers presented results of their work. For individual titles, see N86-11496 through N86-11521.

N86-11496*# National Aeronautics and Space Administration. Lewis Research Center, Cleveland, Ohio.
TURBINE ENGINE HOT SECTION TECHNOLOGY (HOST) PROJECT
Daniel E. Sokolowski and C. Robert Ensign *In its* Turbine Eng. Hot Sect. Technol. (HOST) Oct. 1983 p 1-6 (For primary document see N86-11495 02-39)
Avail: NTIS HC A11/MF A01 CSCL 21E

The Hot Section Technology (HOST) Project is a NASA-sponsored endeavor to improve the durability of advanced gas turbine engines for commercial and military aircraft. Through improvements in the analytical models and life prediction systems, designs for future hot section components , the combustor and turbine, will be more accurately analyzed and will incorporate features required for longer life in the more hostile operating environment of high performance engines. G.L.C.

N86-11497*# National Aeronautics and Space Administration. Lewis Research Center, Cleveland, Ohio.
HOST INSTRUMENTATION R AND D PROGRAM OVERVIEW c35
D. R. Englund *In its* Turbine Eng. Hot Sect. Technol. (HOST) Oct. 1983 p 7-9 (For primary document see N86-11495 02-39)
Avail: NTIS HC A11/MF A01 CSCL 14B

The HOST Instrumentation R&D program is focused on two categories of instrumentation. One category is that required to characterize the environment imposed on the hot section components of turbine engines. This category includes instruments for measuring gas flow, gas temperature, and heat flux. The second category is that for measuring the effect of the environment on the hot section components. This category includes strain measuring instruments and an optical system for viewing the interior of an operating combustor to detect cracks, buckling, carbon buildup, etc. G.L.C.

N86-11498*# United Technologies Research Center, East Hartford, Conn.
HOT SECTION VIEWING SYSTEM c35
William W. Morey *In* NASA. Lewis Research Center Turbine Eng. Hot Sect. Technol. (HOST) Oct. 1983 p 11-16 (For primary document see N86-11495 02-39)
Avail: NTIS HC A11/MF A01 CSCL 14B

The objective of the hot section viewing program is to develop a prototype optical system for viewing the interior of a gas turbine combustor during high temperature, high pressure operation in order to produce a visual record of some causes of premature hot section failures. The program began by identifying and analyzing system designs that would provide clearest images while being able to survive the hostile environment inside the combustion chamber. Different illumination methods and computer techniques for image enhancement and analysis were examined during a preliminary test phase. In the final phase of the program the prototype system was designed and fabricated and is currently being tested on a high pressure combustor rig. G.L.C.

N86-11499*# Pratt and Whitney Aircraft, East Hartford, Conn. Engineering Div.
DYNAMIC GAS TEMPERATURE MEASUREMENT SYSTEM c35
Denny L. Elmore, Woodrow W. Robinson, and William B. Watkins *In* NASA. Lewis Research Center Turbine Eng. Hot Sect. Technol. (HOST) Oct. 1983 p 17-35 ref (For primary document see N86-11495 02-39)
(Contract NAS3-23154)
Avail: NTIS HC A11/MF A01 CSCL 14B

A gas temperature measurement system with compensated frequency response of 1 KHz and capability to operate in the exhaust of a gas turbine combustor was developed. Environmental guidelines for this measurement are presented, followed by a preliminary design of the selected measurement method. Transient thermal conduction effects were identified as important; a preliminary finite-element conduction model quantified the errors expected by neglecting conduction. A compensation method was developed to account for effects of conduction and convection. This method was verified in analog electrical simulations, and used to compensate dynamic temperature data from a laboratory combustor and a gas turbine engine. Detailed data compensations are presented. Analysis of error sources in the method were done to derive confidence levels for the compensated data. G.L.C.

N86-11500*# United Technologies Research Center, East Hartford, Conn.
HIGH TEMPERATURE STATIC STRAIN SENSOR DEVELOPMENT PROGRAM c35
Charles Hulse, Richard Bailey, and Howard Grant (Pratt and Whitney Aircraft Group, East Hartford, Conn.) *In* NASA. Lewis Research Center Turbine Eng. Hot Sect. Technol. (HOST) Oct. 1983 p 37-40 (For primary document see N86-11495 02-39)
(Contract NAS3-23722)
Avail: NTIS HC A11/MF A01 CSCL 14B

Electrical resistance strain gages useful for static strain measurements on nickel or cobalt superalloy parts inside a gas turbine engine on a test stand are being developed. Measurements of this type are of great importance in meeting the goals of the HOST program because, without reliable knowledge of the stresses and strains which exist in specific components, it will be difficult to fully appreciate where improvements in design and materials can be implemented. The first part of the effort consisted of a strain gage alloy development program which will be followed by an investigation of complete strain gage systems which will use the best of the alloys developed together with other system improvements. G.L.C.

N86-11501*# United Technologies Research Center, East Hartford, Conn.
DEMONSTRATION TEST OF BURNER LINER STRAIN MEASUREMENT SYSTEMS: INTERIM RESULTS
Karl A. Stetson and Howard P. Grant (Pratt and Whitney Aircraft, East Hartford, Conn.) *In* NASA. Lewis Research Center Turbine Eng. Hot Sect. Technol. (HOST) Oct. 1983 p 41-44 (For primary document see N86-11495 02-39)
(Contract NAS3-23690)
Avail: NTIS HC A11/MF A01 CSCL 20K

Work is in progress to demonstrate two techniques for static strain measurements on a jet engine burner liner. Measurements are being made with a set of resistance strain gages made from Kanthal A-1 wire and via heterodyne speckle photogrammetry.

The background of the program is presented along with current results. Author

N86-11502*# Pratt and Whitney Aircraft Group, East Hartford, Conn. Engineering Div.
DEVELOPMENT OF HEAT FLUX SENSORS FOR TURBINE AIRFOILS AND COMBUSTOR LINERS c35
William H. Atkinson *In* NASA. Lewis Research Center Turbine Eng. Hot Sect. Technol. (HOST) Oct. 1983 p 45-55 ref (For primary document see N86-11495 02-39)
Avail: NTIS HC A11/MF A01 CSCL 14B

The design of durable turbine airfoils that use a minimum amount of cooling air requires knowledge of the heat loads on the airfoils during engine operation. Measurement of these heat loads will permit the verification or modification of the analytical models used in the design process and will improve the ability to predict and confirm the thermal performance of turbine airfoil designs. Heat flux sensors for turbine blades and vanes must be compatible with the cast nickel-base and cobalt-base materials used in their fabrication and will need to operate in a hostile environment with regard to temperature, pressure and thermal cycling. There is also a need to miniaturize the sensors to obtain measurements without perturbing the heat flows that are to be measured. G.L.C.

N86-11503*# National Aeronautics and Space Administration. Lewis Research Center, Cleveland, Ohio.
LASER ANEMOMETRY FOR HOT SECTION APPLICATIONS c36
Richard G. Seasholtz, Lawrence G. Oberle, and Donald H. Weikle *In its* Turbine Eng. Hot Sect. Technol (HOST) Oct. 1983 p 57-67 refs (For primary document see N86-11495 02-39)
Avail: NTIS HC A11/MF A01 CSCL 20E

Laser anemometers (LA's) for use in the study of the hot section components of turbomachinery are being developed. Specifically, laser anemometers are being developed for use in the 50.8-cm (20-in.) diameter warm turbine and high-pressure turbine (HPT) facilities at Lewis. A brief review of the status of the program along with some preliminary data taken in an open-jet burner are presented. G.L.C.

N86-11504*# Case Western Reserve Univ., Cleveland, Ohio. Dept. of Chemical Engineering.
TIME-OF-FLIGHT ANEMOMETER FOR HOT SECTION APPLICATIONS c35
Robert V. Edwards *In* NASA. Lewis Research Center Turbine Eng. Hot Sect. Technol. (HOST) Oct. 1983 p 69-71 (For primary document see N86-11495 02-39)
Avail: NTIS HC A11/MF A01 CSCL 14B

The design, construction and testing of laser anemometer configurations for Hot Section velocity measurements is considered. Optimizing the laser anemometer system necessarily included the data processing algorithms used. It is felt that the requirements here are too demanding for standard laser anemometer systems. G.L.C.

N86-11505*# National Aeronautics and Space Administration. Lewis Research Center, Cleveland, Ohio.
TURBINE HEAT TRANSFER c34
John E. Rohde *In its* Turbine Eng. Hot Sect. Technol. (HOST) Oct. 1983 p 73-77 (For primary document see N86-11495 02-39)
Avail: NTIS HC A11/MF A01 CSCL 20D

Improved turbine durability and performance and reduced development cost will all result from impoved methods of predicting turbine metal temperatures. Better metal temperature prediction methods require improvements in the methods of predicting the hot gas flow over the turbine airfoils and the cooling air flow inside the airfoil and in the methods of predicting the heat transfer rates on both the hot gas side and coolant side of the airfoil. The overall HOST Turbine Heat Transfer effort is directed at improving all four of these areas of concern. G.L.C.

N86-11506*# Tennessee Univ. Space Inst., Tullahoma.
GAS FLOW ENVIRONMENTAL AND HEAT TRANSFER NON-ROTATING 3D PROGRAM c34
T. Geil and J. Steinhoff *In* NASA. Lewis Research Center Turbine Eng. Hot Sect. Technol. (HOST) Oct. 1983 p 79-86 (For primary document see N86-11495 02-39)
(Contract NAS3-23278)
Avail: NTIS HC A11/MF A01 CSCL 20D

A complete set of benchmark quality data for the flow and heat transfer within a large rectangular turning duct is being compiled. These data will be used to evaluate and verify three dimensional internal viscous flow models and computational codes. The analytical objective is to select such a computational code and define the capabilities of this code to predict the experimental results. Details of the proper code operation will be defined and improvements to the code modeling capabilities will be formulated. G.L.C.

N86-11507*# Detroit Diesel Allison, Mich.
GAS SIDE HEAT TRANSFER c34
Larry D. Hylton *In* NASA. Lewis Research Center Turbine Eng. Hot Sect. Technol. (HOST) Oct. 1983 p 87-98 refs (For primary document see N86-11495 02-39)
(Contracts NAS3-22761; NAS3-23695)
Avail: NTIS HC A11/MF A01 CSCL 20D

Improvements in methods for predicting heat transfer rates on the hot gas side of turbine airfoils are necessary for improved turbine durability and performance. The development and verification of improved analytical models requires a systematic, closely coupled experimental and analytical program. G.L.C.

N86-11508*# United Technologies Research Center, East Hartford, Conn.
ASSESSMENT OF A 3-D BOUNDARY LAYER CODE TO PREDICT HEAT TRANSFER AND FLOW LOSSES IN A TURBINE c34
Veer N. Vatsa *In* NASA. Lewis Research Center Turbine Eng. Hot Sect. Technol. (HOST) Oct. 1983 p 101-106 refs (For primary document see N86-11495 02-39)
(Contract NAS3-23716)
Avail: NTIS HC A11/MF A01 CSCL 20D

The prediction of the complete flow field in a turbine passage is an extremely difficult task due to the complex three dimensional pattern which contains separation and attachment lines, a saddle point and horseshoe vortex. Whereas, in principle such a problem can be solved using full Navier-Stokes equations, in reality methods based on a Navier-Stokes solution procedure encounter difficulty in accurately predicting surface quantities (e.g., heat transfer) due to grid limitations imposed by the speed and size of the existing computers. On the other hand the overall problem is strongly three dimensional and too complex to be analyzed by the current design methods based on inviscid and/or viscous strip theories. Thus there is a strong need for enhancing the current prediction techniques through inclusion of 3-D viscous effects. A potentially simple and cost effective way to achieve this is to use a prediction method based on three dimensional boundary layer (3-DBL) theory. The major objective of this program is to assess the applicability of such a 3-DBL approach for the prediction of heat loads, boundary layer growth, pressure losses and streamline skewing in critical areas of a turbine passage. A brief discussion of the physical problem addressed here along with the overall approach is presented. Author

N86-11509*# United Technologies Research Center, East Hartford, Conn.
GAS-SIDE HEAT TRANSFER WITH ROTATION c34
Robert P. Dring *In* NASA. Lewis Research Center Turbine Eng. Hot Sect. Technol. (HOST) Oct. 1983 p 107-109 refs (For primary document see N86-11495 02-39)
Avail: NTIS HC A11/MF A01 CSCL 20D

The primary basis for heat transfer analysis of turbine blades is experimental data obtained in linear cascades. These data have been very valuable in identifying the major heat transfer and fluid flow features of a turbine airfoil. The question of major interest is how well all of these data translate to the rotating turbine blade. It is known from the work of Lokay and Trushin that average heat transfer coefficients on the rotor may be as much as 40 percent above the values measured on the same blades nonrotating. Recent work by Dunn and Holt supports the Russian conclusion. What is lacking is a set of data from a rotating system which is of sufficient detail as to make careful local comparisons between static system in which there is sufficient documentation of the flow field to support the computer analyses being developed today. A second major question is the influence, if any, of the first stator row on the heat transfer of the second stator row after the flow has passed through the rotor. An objective of the present program, is to obtain a detailed set of heat transfer coefficients along the midspan of a blade in a rotating turbine. Author

N86-11510*# Pratt and Whitney Aircraft Group, East Hartford, Conn.

COOLANT PASSAGE HEAT TRANSFER WITH ROTATION. A PROGRESS REPORT ON THE COMPUTATIONAL ASPECTS

c34

L. D. Aceto and G. J. Sturgess *In* NASA. Lewis Research Center Turbine Eng. Hot Sect. Technol. (HOST) Oct. 1983 p 111-116 refs (For primary document see N86-11495 02-39)
Avail: NTIS HC A11/MF A01 CSCL 20D

Turbine airfoils are subjected to increasingly higher heat loads which escalate the cooling requirements in order to satisfy life goals for the component materials. If turbine efficiency is to be maintained, however, cooling requirements should be as low as possible. To keep the quantity of cooling air bounded, a more efficient internal cooling scheme must be developed. One approach is to employ airfoils with multipass cooling passages that contain devices to augment internal heat transfer while limiting pressure drop. Design experience with multipass cooling passage airfoils has shown that a surplus of cooling air must be provided as a margin of safety. This increased cooling air leads to a performance penalty. Reliable methods for predicting the internal thermal [illegible] aerodynamic performance of multipass cooling passage airfoils would reduce or eliminate the need for the safety margin of surplus cooling air. The objective of the program is to develop and verify improved analytical methods that will form the basis for design technology which will result in efficient turbine components with improved durability without sacrificing performance. The objective will be met by: (1) establishing a comprehensive experimental data base that can form the basis of an empirical design system; (2) developing computational fluid dynamic techniques; and (3) analyzing the information in the data base with both phenomenological modeling and mathematical modeling to derive a suitable design and analysis procedure. Author

N86-11511*# Arizona State Univ., Tempe. Dept. of Mechanical and Aerospace Engineering.

JET ARRAY IMPINGEMENT HEAT TRANSFER CHARACTERISTICS

c34

L. W. Florschuetz and D. E. Metzger *In* NASA. Lewis Research Center Turbine Eng. Hot Sect. Technol. (HOST) Oct. 1983 p 117-128 refs (For primary document see N86-11495 02-39)
Avail: NTIS HC A11/MF A01 CSCL 20D

Two dimensional arrays of circular air jets impinging on a heat transfer surface parallel to the jet orifice plate are considered. The jet flow, after impingement, is constrained to exit in a single direction along the channel formed by the jet orifice plate and the heat transfer surface. In addition to the crossflow which originates from the jets following impingement, an initial crossflow is present which approaches the array through an upstream extension of the channel. The configurations considered are intended to model the impingement cooled midchord region of gas turbine airfoils in cases where an initial crossflow is also present. A major objective is determination of the effect of initial crossflow air temperature relative to jet array air temperature on impingement surface heat fluxes. Author

N86-11512*# National Aeronautics and Space Administration. Lewis Research Center, Cleveland, Ohio.

COMBUSTION HOT SECTION TECHNOLOGY

c07

David B. Ercegovic *In its* Turbine Eng. Hot Sect. Technol. (HOST) Oct. 1983 p 129-133 refs (For primary document see N86-11495 02-39)
Avail: NTIS HC A11/MF A01 CSCL 21E

The overall objective of the Turbine Engine Hot Section Technology Combustion Project is to develop and verify improved and more accurate analysis methods for increasing the ability to design with confidence the combustion system for advanced aircraft turbine engines. The analysis methods developed will be generically applicable to combustion systems and not restricted to one specific engine or manufacturer. This project's approach was to first assess and evaluate existing combustor aerothermal analysis models by means of a contracted effort initiated during FY 1982. This evaluation effort has assessed and quantified known models' strengths and deficiencies. During FY 1984 the Aerothermal Modeling Program, Phase 2 will be initiated, which is expected to have contracted model development efforts in the areas of improved numerical methods for turbulent viscous flows, flow interactions, and fuel spray flow foekd interactions. A Phase 3 effort is planned to address remaining model deficiencies. The primary inhouse effort in this area will be the determination of high pressure flame radiation characteristics in a full annular combustor. This experiment will be conducted in the NASA LeRC High Pressure Facility with the results compiled into a comprehensive flame radiation and liner heat flux model. Author

N86-11513*# National Aeronautics and Space Administration. Lewis Research Center, Cleveland, Ohio.

HOST STRUCTURAL ANALYSIS PROGRAM OVERVIEW

c07

R. H. Johns *In its* Turbine Eng. Hot Sect. Technol. (HOST) Oct. 1983 p 153-158 (For primary document see N86-11495 02-39)
Avail: NTIS HC A11/MF A01 CSCL 21E

Hot section components of aircraft gas turbine engines are subjected to severe thermal structural loading conditions, especially during the start up and take off portions of the engine cycle. The most severe and damaging stresses and strains are those induced by the steep thermal gradients induced during the start up transient. These transient stresses and strains are also the most difficult to predict, in part because of the temperature gradients and distributions are not well known or readily predictable, and also because the cyclic elastic viscoplastic behavior of the materials at these extremes of temperature and strain are not well known or readily predictable. A broad spectrum of structures related technology programs is underway to address these deficiencies. One element of the structures program is developing improved time varying thermal mechanical load models for the entire engine mission cycle from start up to shutdown. Another major part of the program is the development of new and improved nonlinear 3-D finite elements and associated structural analysis programs, including the development of temporal elements with time dependent properties to account for creep effects in the materials and components. Author

N86-11514*# General Electric Co., Cincinnati, Ohio. Aircraft Engine Business Group.

BURNER LINER THERMAL/STRUCTURAL LOAD MODELLING

R. J. Maffeo *In* NASA. Lewis Research Center Turbine Eng. Hot Sect. Technol. (HOST) Oct. 1983 p 159-163 (For primary document see N86-11495 02-39)
(Contract NAS3-23272)
Avail: NTIS HC A11/MF A01 CSCL 20K

The objective of this program is to develop a thermal data transfer computer program module for the burner liner thermal structural load modeling program. This will be accomplished by (1) reviewing existing methodologies for thermal data transfer and selecting three heat transfer codes for application in this program; (2) evaluating the selected codes to establish criteria for developing a computer program module to transfer thermal data from the heat transfer codes to selected stress analysis codes; (3) developing the automated thermal load transfer module; and

(4) verifying and documenting the module. In aircraft turbine engine hot section components, cyclic thermal stresses are the most important damage mechanism. Consequently, accurate and reliable prediction of thermal loads is essential to improving durability. To achieve this goal, a considerable effort over the past 20 years has been devoted to the acquisition of engine temperature test data, as well as the development of accurate, reliable, and efficient computer codes for the prediction of steady state and transient temperatures and for the calculation of elastic and inelastic cyclic stresses and strains in hot section components. There is a need for continued development of these codes, because the availability of more accurate analysis techniques for complex configurations has enabled engine designers to use more sophisticated designs to achieve higher cycle efficiency and reduce weight. Author

N86-11515*# General Electric Co., Cincinnati, Ohio.
COMPONENT-SPECIFIC MODELING c07
M. L. Roberts *In* NASA. Lewis Research Center Turbine Eng. Hot Sect. Technol. (HOST) Oct. 1983 p 165-173 (For primary document see N86-11495 02-39)
(Contract NAS3-23687)
Avail: NTIS HC A11/MF A01 CSCL 21E

The overall objective of this program is to develop and verify a series of interdisciplinary modeling and analysis techniques which have been specialized to address three specific hot section components. These techniques will incorporate data as well as theoretical methods from many diverse areas, including cycle and performance analysis, heat transfer analysis, linear and nonlinear stress analysis, and mission analysis. Building on the proven techniques already available in these fields, the new methods developed through this contract will be integrated to provide an accurate, efficient, and unified approach to analyzing combustor burner liners, hollow air cooled turbine blades, and air cooled turbine vanes. For these components, the methods developed will predict temperature, deformation, stress, and strain histories throughout a complete flight mission. Author

N86-11516*# General Electric Co., Cincinnati, Ohio. Aircraft Engine Business Group.
THE 3D INELASTIC ANALYSIS METHODS FOR HOT SECTION COMPONENTS
L. T. Dame and R. L. McKnight *In* NASA. Lewis Research Center Turbine Eng. Hot Sect. Technol. (HOST) Oct. 1983 p 175-177 refs (For primary document see N86-11495 02-39)
Avail: NTIS HC A11/MF A01 CSCL 20K

The objective of this research is to develop an analytical tool capable of economically evaluating the cyclic time dependent plasticity which occurs in hot section engine components in areas of strain concentration resulting from the combination of both mechanical and thermal stresses. The techniques developed must be capable of accommodating large excursions in temperatures with the associated variations in material properties including plasticity and creep. The overall objective of this proposed program is to develop advanced 3-D inelastic structural/stress analysis methods and solution strategies for more accurate and yet more cost effective analysis of combustors, turbine blades, and vanes. The approach will be to develop four different theories, one linear and three higher order with increasing complexities including embedded singularities. Author

N86-11517*# Pratt and Whitney Aircraft, East Hartford, Conn.
THE 3-D INELASTIC ANALYSIS METHODS FOR HOT SECTION COMPONENTS (BASE PROGRAM)
E. S. Todd *In* NASA. Lewis Research Center Turbine Eng. Hot Sect. Technol. (HOST) Oct. 1983 p 179-180 (For primary document see N86-11495 02-39)
Avail: NTIS HC A11/MF A01 CSCL 20K

The objective of this program is to produce a series of new computer codes that permit more accurate and efficient three dimensional inelastic analysis of selected hot section components - combustor liners, turbine blades and turbine vanes. The computer codes embody a progression of mathematical models and are streamlined to take advantage of geometrical features, loading conditions, and forms of material response that distinguish each group of selected components. Author

N86-11518*# National Aeronautics and Space Administration. Lewis Research Center, Cleveland, Ohio.
VALIDATION OF STRUCTURAL ANALYSIS METHODS USING BURNER LINER CYCLIC RIG TEST DATA
R. Thompson *In its* Turbine Eng. Hot Sect. Technol. (HOST) Oct. 1983 p 181-193 (For primary document see N86-11495 02-39)
Avail: NTIS HC A11/MF A01 CSCL 20K

The objectives of the hot section technology (HOST) burner liner cyclic rig test program are basically threefold: (1) to assist in developing predictive tools needed to improve design analyses and procedures for the efficient and accurate prediction of burner liner structural response; (2) to calibrate, evaluate and validate these predictive tools by comparing the predicted results with the experimental data generated in the tests; and (3) to evaluate existing as well as advanced temperature and strain measurement instrumentation, both contact and noncontact, in a simulated engine cycle environment. The data generated will include measurements of the thermal environment (metal surface temperatures) as well as structural (strain) and life (fatigue) responses of simulated burner liners and specimens under controlled boundary and operating conditions. These data will be used to calibrate, compare and validate analytical theories, methodologies and design procedures, as well as improvements in them, for predicting liner temperatures, stress-strain responses and cycles to failure. Comparison of predicted results with experimental data will be used to show where the predictive theories, etc. need improvements. In addition, as the predictive tools, as well as the tests, test methods, and data acquisition and reduction techniques, are developed and validated, a proven, integrated analysis/experiment method will be developed to determine the cyclic life of a simulated burner liner. Author

N86-11519*# National Aeronautics and Space Administration. Lewis Research Center, Cleveland, Ohio.
HOST LINER CYCLIC FACILITIES
Donald Schultz *In its* Turbine Eng. Hot Sect. Technol. (HOST) Oct. 1983 p 195-204 (For primary document see N86-11495 02-39)
Avail: NTIS HC A11/MF A01 CSCL 20K

The HOST Liner Cyclic Program is utilizing two types of test apparatus, rectangular box rigs and a full annular rig. To date two quartz lamp cyclic box rigs have been tested and a third is to begin testing in late October 1983. The box rigs are used to evaluate 5x8 inch rectangular linear samples. A 21 inch diameter outer liner simulator is also being built up for testing beginning in April 1984. All rigs are atmospheric rigs. The first box rig, a three 6-kVA lamp installation, was operated under adverse conditions to determine feasibility of using quartz lamps for cyclic testing. This work was done in December 1981 and looked promising. The second box rig, again using three 6-kVA lamps, was operated to obtain instrumentation durability information and initial data input to a Finite Element Model. This limited test program was conducted in August 1983. Five test plates were run. Instrumentation consisted of strain gages, thermocouples and thermal paint. The strain gages were found to fail at 1200 F as expected though plates were heated to 1700 F. The third box rig, containing four 6-kVA lamps, is in build up for testing to begin in late October 1983. In addition to 33 percent greater power input, this rig has provision for 400 F backside line cooling air and a viewing port suitable for IR camera viewing. The casing is also water cooled for extended durability. Author

N86-11520*# National Aeronautics and Space Administration. Lewis Research Center, Cleveland, Ohio.
LIFE PREDICTION AND CONSTITUTIVE BEHAVIOR
G. R. Halford *In its* Turbine Eng. Hot Sect. Technol. (HOST) Oct. 1983 p 205-207 (For primary document see N86-11495 02-39)
Avail: NTIS HC A11/MF A01 CSCL 20K

One of the primary drivers that prompted the initiation of the hot section technology (HOST) program was the recognized need for improved cyclic durability of costly hot section components. All too frequently, fatigue in one form or another was directly responsible for the less than desired durability, and prospects for the future weren't going to improve unless a significant effort was mounted to increase our knowledge and understanding of the elements governing cyclic crack initiation and propagation lifetime. Certainly one of the important factors is the ability to perform accurate structural stress-strain analyses on a routine basis to determine the magnitudes of the localized stresses and strains since it is these localized conditions that govern the initiation and crack growth processes. Developing the ability to more accurately predict crack initiation lifetimes and cyclic crack growth rates for the complex loading conditions found in turbine engine hot sections is of course the ultimate goal of the life prediction research efforts. It has been found convenient to divide the research efforts into those dealing with nominally isotropic and anisotropic alloys; the latter for application to directionally solidified and single crystal turbine blades. Author

N86-11521*# Pratt and Whitney Aircraft, East Hartford, Conn.
CREEP FATIGUE LIFE PREDICTION FOR ENGINE HOT SECTION MATERIALS (ISOTROPIC)
Vito Moreno *In* NASA. Lewis Research Center Turbine Eng. Hot Sect. Technol. (HOST) Oct. 1983 p 209-210 (For primary document see N86-11495 02-39)
(Contract NAS3-23288)
Avail: NTIS HC A11/MF A01 CSCL 20K

The activities performed during the first year of the NASA HOST Program, Creep Fatigue Life Prediction for Engine Hot Section Materials (Isotropic), being conducted by Pratt & Whitney Aircraft are summarized. The program is a 5 year, two part effort aimed at improving the high temperature crack initiation prediction technology for gas turbine hot section components. Significant results of the program produced thus far are discussed. Cast B1900 + Hf and wrought IN 718 were selected as the base and alternate materials, respectively. A single heat of B1900 + Hf was obtained and test specimens fabricated. The material was characterized with respect to grain size, gamma prime size, carbide distribution, and dislocation density. Monotonic tensile and creep testing has shown engineering properties within anticipated scatter for this material. Examination of the tensile tests has shown a transition from inhomogeneous planar slip within the grains at lower temperatures to more homogeneous matrix deformation. Examination of the creep tests has shown a transgranular failure mode at 1400 F and an intergranular failure mode at 1600 F and 1800 F. Author

N86-11522*# National Aeronautics and Space Administration. Langley Research Center, Hampton, Va.
A STUDY OF THE CORNERING FORCES GENERATED BY AIRCRAFT TIRES ON A TILTED, FREE-SWIVELING NOSE GEAR
Robert H. Daugherty and Sandy M. Stubbs Oct. 1985 30 p refs
(NASA-TP-2481; L-15954; NAS 1.60:2481) Avail: NTIS HC A03/MF A01 CSCL 20K

An experimental investigation was conducted to study the effect of various parameters on the cornering forces produced by a rolling aircraft tire installed on a tilted, free-swiveling nose gear. The parameters studied included tilt angle, trial, tire inflation pressure, rake angle, vertical load, and whether or not a twin tire configuration corotates. These parameters were evaluated by measuring the cornering force produced by an aircraft tire installed on the nose gear of a modified vehicle as it was towed slowly. Cornering force coefficient increased with increasing tilt angle. Increasing trial or rake angle decreased the magnitude of the cornering force coefficient. Tire inflation pressure had no effect on the cornering force coefficient. Increasing vertical load decreased the cornering force coefficient. When the tires of a twin tire system rotated independently, the cornering force coefficients were the same as those for the single-tire configuration. When the twin tire system was made to corotate, however, the cornering force coefficients increased significantly. Author

N86-11523*# National Aeronautics and Space Administration. Langley Research Center, Hampton, Va.
AEROELASTIC MODEL HELICOPTER ROTOR TESTING IN THE LANGLEY TDT
Wayne R. Mantay, William T. Yeager, Jr., M-Nabil Hamouda, Robert G. Cramer, Jr., and Chester W. Langston Jun. 1985 19 p refs
Presented at AHS Specialists' Meeting on Helicopter Test Methodology, 29 Oct. - 1 Nov. 1984, Williamsburg, Va.
(DA Proj. 1L1-62209-AH-76)
(NASA-TM-86440; NAS 1.15:86440; USAAVSCOM-TM-85-B-5)
Avail: NTIS HC A02/MF A01 CSCL 20K

Wind-tunnel testing of a properly scaled aeroelastic model helicopter rotor is considered a necessary phase in the design development of new or existing rotor systems. For this reason, extensive testing of aeroelastically scaled model rotors is done in the Transonic Dynamics Tunnel (TDT) located at the NASA Langley Research Center. A unique capability of this facility, which enables proper dynamic scaling, is the use of Freon as a test medium. A description of the TDT and a discussion of the benefits of using Freon as a test medium are presented. A description of the model test bed used, the Aeroelastic Rotor Experimental System (ARES), is also provided and examples of recent rotor tests are cited to illustrate the advantages and capabilities of aeroelastic model rotor testing in the TDT. The importance of proper dynamic scaling in identifying and solving rotorcraft aeroelastic problems, and the importance of aeroelastic testing of model rotor systems in the design of advanced rotor systems are demonstrated. Author

N86-11524*# National Aeronautics and Space Administration. Ames Research Center, Moffett Field, Calif.
STRESS ANALYSES OF B-52 PYLON HOOKS
William L. Ko and Lawrence S. Schuster Oct. 1985 33 p refs
(NASA-TM-84924; H-1221; NAS 1.15:84924) Avail: NTIS HC A03/MF A01 CSCL 20K

The NASTRAN finite element computer program was used in the two dimensional stress analysis of B-52 carrier aircraft pylon hooks: (1) old rear hook (which failed), (2) new rear hook (improved geometry), (3) new DAST rear hook (derated geometry), and (4) front hook. NASTRAN model meshes were generated by the aid of PATRAN-G computer program. Brittle limit loads for all the four hooks were established. The critical stress level calculated from NASTRAN agrees reasonably well with the values predicted from the fracture mechanics for the failed old rear hook. Author

N86-11525*# National Aeronautics and Space Administration. Ames Research Center, Moffett Field, Calif.
A COMPARISON OF MEASURED AND CALCULATED THERMAL STRESSES IN A HYBRID METAL MATRIX COMPOSITE SPAR CAP ELEMENT
Jerald M. Jenkins, Allan H. Taylor (NASA, Langley Research Center), and I. Frank Sakata (Lockheed California Co., Burbank) Sep. 1985 20 p refs
(NASA-TM-86729; H-1289; NAS 1.15:86729) Avail: NTIS HC A02/MF A01 CSCL 20K

A hybrid spar of titanium with an integrally brazed composite, consisting of an aluminum matrix reinforced with boron-carbide-coated fibers, was heated in an oven and the resulting thermal stresses were measured. Uniform heating of the spar in an oven resulted in thermal stresses arising from the effects of dissimilar materials and anisotropy of the metal matrix composite. Thermal stresses were calculated from a finite element structural model using anisotropic material properties deduced from constituent properties and rules of mixtures. Comparisons of calculated thermal stresses with measured thermal stresses on the spar are presented. It was shown that failure to account for anistropy in the metal matrix composite elements would result in large errors in correlating measured and calculated thermal stresses. It was concluded that very strong material characterization efforts are required to predict accurate thermal stresses in anisotropic composite structures. Author

N86-11526*# Connecticut Univ., Storrs. School of Engineering.
ELEVATED TEMPERATURE BIAXIAL FATIGUE Final Report
Eric H. Jordan Oct. 1985 162 p refs
(Contract NAS3-160)
(NASA-CR-175009; NAS 1.26:175009) Avail: NTIS HC A08/MF A01 CSCL 20K

A 3 year experimental program for studying elevated temperature biaxial fatigue of a nickel based alloy Hastelloy-X has been completed. A new high temperature fatigue test facility with unique capabilities has been developed. Effort was directed toward understanding multiaxial fatigue and correlating the experimental data to the existing theories of fatigue failure. The difficult task of predicting fatigue lives for nonproportional loading was used as an ultimate test for various life prediction methods being considered. The primary means of reaching improved understanding were through several critical nonproportional loading experiments. The direction of cracking observed on failed specimens was also recorded and used to guide the development of the theory. Cyclic deformation responses were permanently recorded digitally during each test. It was discovered that the cracking mode switched from primarily cracking on the maximum shear planes at room temperature to cracking on the maximum normal strain planes at 649 C. In contrast to some other metals, loading path in nonproportional loading had little effect on fatigue lives. Strain rate had a small effect on fatigue lives at 649 C. Of the various correlating parameters the modified plastic work and octahedral shear stress were the most successful. Author

N86-11527# Shock and Vibration Information Center (Defense), Washington, D. C.
THE SHOCK AND VIBRATION DIGEST, VOLUME 17, NO. 4 Monthly Report
Judith Nagle-Eshleman, ed. Apr. 1985 91 p refs
(AD-A154112) Avail: SVIC, Code 5804, Naval Research Lab., Washington, D.C. 20375 CSCL 20/11

Literature surveys of extensive shock and vibration research are presented. Finite element modeling of laminated composite plates is discussed. The use of the microcomputer as an effective tool for solving many shock and vibration problems is examined. A historical overview of mechanical face seal dynamics is presented. Book reviews presented in this digest reflect new computational testing techniques and design techniques, such as model testing and isolation system design. For individual titles, see N86-11528 through N86-11530.

N86-11528# Shock and Vibration Information Center (Defense), Washington, D. C.
MICROCOMPUTERS IN SHOCK AND VIBRATION
In its The Shock and Vibration Digest, Vol. 17, No. 4 Apr. 1985 p 1 (For primary document see N86-11527 02-39)
Avail: SVIC, Code 5804, Naval Research Lab., Washington, D.C., 20375 CSCL 20/11

The use of microcomputers for solving computational tasks in shock and vibration is examined. Some of the tasks included shock spectra computations, balancing of rotating shafts, acquisition and processing of materials properties data and spectral analysis. The increased power of the microcomputer is also significantly impacting shock and vibration analyses. Many problems that may have been previously run on mainframe computers, or minicomputers, are now small enough so they may be run on microcomputers with little, if any, loss in accuracy. Exploratory dynamic analyses of complex systems are often necessary, and this is another type of problem that might be run on a microcomputer. B.W.

N86-11529# Virginia Polytechnic Inst. and State Univ., Blacksburg. Dept. of Engineering Science and Mechanics.
A REVIEW OF THE LITERATURE ON FINITE-ELEMENT MODELING OF LAMINATED COMPOSITE PLATES c24
J. N. Reddy *In* Shock and Vibration Information Center The Shock and Vibration Digest, Vol. 17, No. 4 Apr. 1985 p 3-8 refs (For primary document see N86-11527 02-39)
Avail: SVIC, Code 5804, Naval Research Lab., Washington, D.C., 20375 CSCL 11/4

This review of the literature on the finite-element modeling of natural vibrations of plates is confined to the period from 1980 to the present. A historical background of the development of shear deformation theories is also presented. Author

N86-11530# Technion - Israel Inst. of Tech., Haifa. Dept. of Mechanical Engineering.
MECHANICAL FACE SEAL DYNAMICS UPDATE c37
I. Etison *In* The Shock and Vibration Information Center The Shock and Vibration Digest, Vol. 17, No. 4 Apr. 1985 p 11-15 refs (For primary document see N86-11527 02-39)
Avail: SVIC, Code 5804, Naval Research Lab., Washington, D.C. 20375 CSCL 11/1

This review is an update of literature published since 1981 on mechanical face seal dynamics. Experimental observations as well as theoretical analyses are summarized. Future research needs in mechanical face seal dynamics are pointed out. Author

N86-11531# Shock and Vibration Information Center (Defense), Washington, D. C.
THE SHOCK AND VIBRATION DIGEST, VOLUME 17, NO. 5 Monthly Report
Judith Nagle-Eshleman, ed. May 1985 102 p refs
(AD-A156716) Avail: SVIC, Code 5804, Naval Research Lab., Washington, D.C. 20375 CSCL 20/11

The Shock and Vibrating Digest is a monthly publication of the Shock and Vibration Information Center. Its goal is to provide efficient transfer of sound, shock, and vibration technology among researchers and practicing engineers. Subjective and objective analyses of the literature are provided along with news and editorial comment. For individual titles, see N86-11532 through N86-11533.

N86-11532# Yarmouk Univ., Irbid (Jordan). Dept. of Mechanical Engineering.
STIFFNESS AND DAMPING COEFFICIENTS OF RUBBER c27
M. Issa Abdulhadi *In* The Shock and Vibration Information Center Shock and Vibration Digest, Vol. 17, No. 5 May 1985 p 3-9 refs (For primary document see N86-11531 02-39)
Avail: SVIC, Code 5804, Naval Research Lab., Washington, D.C. 20375 CSCL 11/10

A study is carried out on a rubber pad (Neoprene GN) in the shape of a solid circular cylinder. The pad is subjected to a vibrating force. A mathematical model is used to evaluate stiffness and damping coefficients for the rubber and the damped energy. A heat conduction equation describing the temperature field in the rubber specimen is formulated; analytical results agree fairly well with temperatures measured in the rubber. Author

N86-11533# California Univ., Berkeley. Dept. of Mechanical Engineering.
CURRENT RESEARCH ON CIRCULAR SAW AND BAND SAW VIBRATION AND STABILITY
C. D. DAngelo, III, N. T. Alvarado, K. W. Wang, and C. D. Mote, Jr. *In* The Shock and Vibration Information Center The Shock and Vibration Digest, Vol. 17, No. 5 May 1985 p 11-23 refs (For primary document see N86-11531 02-39)
Avail: SVIC, Code 5804, Naval Research Lab., Washington, D.C., 20375 CSCL 20/11

Topics discussed are circular saw and band saw vibration; saw guides, which are fluid-film bearings used to control saw position and vibration; guided saw vibration; and generation of noise by vibration and aerodynamic sources in high-speed sawing. Author

N86-11534# Maryland Univ., College Park. Inst. for Physical Science andd Technology.
THIN PLATES WITH RAPIDLY VARYING THICKNESS, AND THEIR RELATION TO STRUCTURAL OPTIMIZATION Final Report
R. V. Kohn and M. Vogelius Champaign, Ill. Army Construction Engineering Research Lab. Jun. 1985 37 p Prepared in cooperation with Minnesota Univ., Minneapolis

(Contracts N00014-85-K-0169; N00014-83-K-0536; Grant NSF DMS-83-12229)
(AD-A157607; IMA-Preprint-155) Avail: NTIS HC A03/MF A01 CSCL 12/1

Mathematical models are described for plates with rapidly varying thickness; we place special emphasis on their relation to problems in optimal design. Our plate models extinguish between variations on a scale larger than the mean thickness, on a scale comparable to the mean thickness and on a scale smaller than the mean thickness. We review a number of theoretical results that compare the relative strengths of these three design options. The paper also contains exact numerical values for the rigidities of certain interesting plate profiles. These values were computed by a finite element method. GRA

N86-11535# UNC Nuclear Industries, Inc., Richland, Wash.

HARDWARE AND SOFTWARE CONSTRUCTS FOR A VIBRATION ANALYSIS NETWORK

S. A. Cook, R. D. Crowe, and H. Toffer 20 Feb. 1985 10 p Presented at the Intern. Topical Meeting on Computer Appl. for Nucl. Power Plant Operation and Control, Pasco, Wash., 8 Sep. 1985
(Contract DE-AC06-76RL-01857)
(DE85-008436; UNI-SA-144; CONF-850903-4) Avail: NTIS HC A02/MF A01

Vibration level monitoring and analysis was initiated at N Reactor, a dual purpose reactor. The machinery to be monitored was located in several buildings scattered over the plant site, necessitating an approach using satellite stations to collect, monitor and temporarily store data. The satellite stations are, in turn, linked to a centralized processing computer for further analysis. The advantages of a networked data analysis system are discussed along with the hardware and software required to implement such a system. DOE

N86-11536# Massachusetts Inst. of Tech., Cambridge. Nuclear Reactor Lab.

MINIATURIZATION OF SPECIMENS FOR MECHANICAL TESTING

O. K. Harling and G. Kohse 17 Jun. 1985 30 p Presented at the Workshop on the Relation Between Mech. Properties and Micro-Struct. Under Fusion Irradiation Conditions, Ebeltoft, Denmark, 27 Jun. 1985
(Contract DE-AC02-78ER-10107)
(DE85-014506; DOE/ER-10107/28; CONF-8506165-1) Avail: NTIS HC A03/MF A01

The development of mechanical property tests based on bending of a 3 mm diameter by 0.25 mm thick disk is described. Slow strain rate testing of such a disk is used to obtain tensile properties. Finite element computer modeling is used to extract yield stress values with accuracies of at least + or - 10% of uniaxial tensile test values for a variety of materials. Analytical estimates of ductility from disk bend test values are possible for low-ductility materials. Work directed toward finite element calculations for ductility and ultimate tensile strength is also discussed. Preliminary data indicating the feasibility of high strain rate testing for estimation of ductile-to-brittle transition temperatures, and an example of the successful application of miniature bend testing in obtaining relative fatigue information are presented. DOE

N86-11537# Argonne National Lab., Ill.

SENSTIVITY OF USING BLUNT AND SHARP CRACK MODELS IN ELASTIC-PLASTIC FRACTURE MECHANICS

Y. C. Fan, J. M. Kennedy, and A. H. Marchertas 1985 16 p refs Presented at the 8th Intern. Conf. on Struct. Mech. in Reactor Technol., Brussels, 19 Aug. 1985
(Contract W-31-109-eng-38)
(DE85-010288; CONF-850809-49) Avail: NTIS HC A02/MF A01

J integral values are calculated for both the blunt (smeared) crack and the sharp (discrete) crack models in elastic-plastic fracture mechanics problems involving metallic materials. A sensitivity study is performed to show the relative strengths and weaknesses of the two cracking models. It is concluded that the blunt crack model is less dependent on the orientation of the mesh. For the mesh which is in line with the crack direction, however, the sharp crack model is less sensitive to the mesh size. Both models yield reasonable results for a properly discretized finite element mesh. A subcycling technique is used in the explicit integration scheme so that large time steps can be used for the coarse elements away from the crack tip. The savings of computation time by this technique are reported. DOE

N86-11538# Brown Univ., Providence, R. I. Div. of Engineering.

UNIAXIAL TENSILE DEFORMATION AND FRACTURE OF DUAL-PHASE STEELS

Y. L. Su Jul. 1985 211 p
(Contract DE-AC02-80ER-10556)
(DE85-015034; DOE/ER-10556/105) Avail: NTIS HC A1/MF A01

The photolithography technique was used to produce the micrograms on the specimen surface in order to study the difference in strain between the hard martensite particles and the soft ferrite matrix, and thus to determine the difference in stress between the two phases. Based on the stress-strain curves of dual phasae steels and direct observation of deformation of martensite particles and investigation of fracture behavior, analytical models were developed to explain the work hardening behavior and to formulate the expressions for uniform and fracture strains of dual phase steels. The results show that the uniform strain of dual phase steels is primarily decided by the properties and volume fraction of the ferrite, but the mechanism and strain of fracture of dual phase steels are determined by martensite. DOE

N86-11539# Argonne National Lab., Ill.

VISCOELASTIC CREEP OF HIGH-TEMPERATURE CONCRETE

P. A. Pfeiffer, A. H. Marchertas, and Z. P. Bazant 1985 13 p Presented at the 8th Intern. Conf. on Struct. Mech. in Reactor Technol., Brussels, 19 Aug. 1985 Prepared in cooperation with Northwestern Univ., Evanston, Ill.
(Contract W-31-109-eng-38)
(DE85-010511; CONF-850509-53) Avail: NTIS HC A02/MF A01

The analytical model for analysis of high temperature creep response of concrete is presented. The creep law used is linear (viscoelastic), the temperature and moisture effects on the creep rate and also aging are included. Both constant and transient temperature as well as constant and transient moisture conditions are considered. Examples are presented to correlate experimental data with parameters of the analytical model by the use of a finite element scheme. DOE

N86-11540*# National Aeronautics and Space Administration. Langley Research Center, Hampton, Va.

COMPUTATIONAL STRUCTURAL MECHANICS: A NEW ACTIVITY AT THE NASA LANGLEY RESEARCH CENTER

Norman F. Knight, Jr. and W. Jefferson Stroud Sep. 1985 39 p refs Presented at 22nd Ann. Tech. Meeting of the Soc. of Eng. Sci., University Park, Pa., 7-9 Oct. 1985
(NASA-TM-87612; NAS 1.15:87612) Avail: NTIS HC A03/MF A01 CSCL 20K

Complex structures considered for the late 1980's and early 1990's include composite primary aircraft structure and the space station. These structures will be much more difficult to analyze than today's structures and necessitate a major upgrade in computerized structural analysis technology. A new research activity in structural analysis, the computational structural mechanics (CSM) was initiated. The objective of the CSM activity is to develop advanced structural analysis technology that will exploit modern and emerging computers such as computers with vector and/or parallel processing capabilities. The three main research activities underway in CSM include: (1) structural analysis methods development; (2) a software testbed for evaluating the methods; and (3) numerical techniques for parallel processing computers. The motivation and objectives of the CSM activity are presented and CSM activity is described. The current CSM research thrusts, and near and long term CSM research thrusts are outlined. E.A.K.

N86-11541# Argonne National Lab., Ill.
EXPERIMENTAL NEEDS OF HIGH TEMPERATURE CONCRETE
J. C. Chern and A. H. Marchertas 1985 7 p Presented at 8th Intern. Conf. on Struct. Mech. in Reactor Technol., Brussels, 19 Aug. 1985
(Contract W-31-109-eng-38)
(DE85-009700; CONF-850809-35) Avail: NTIS HC A02/MF A01

The needs of experimental data on concrete structures under high temperature, ranging up to about 370 C for operating reactor conditions and to about 500 C and beyond for hypothetical accident conditions, are described. This information is required to supplement analytical methods which are implemented into the finite element code TEMP-STRESS to treat reinforced concrete structures. Recommended research ranges from material properties of reinforced/prestressed concrete, direct testing of analytical models used in the computer codes, to investigations of certain aspects of concrete behavior, the phenomenology of which is not well understood. DOE

N86-11542# Argonne National Lab., Ill.
CONCRETE CREEP AT TRANSIENT TEMPERATURE: CONSTITUTIVE LAW AND MECHANISM
J. C. Chern, Z. P. Bazant, and A. H. Marchertas 1985 13 p refs Presented at the 8th Intern. Conf. on Struct. Mech. in Reactor Technol., Brussels, 19 Aug. 1985 Prepared in cooperation with Northwestern Univ., Evanston, Ill.
(Contract W-31-109-eng-38)
(DE85-010525; CONF-850809-57) Avail: NTIS HC A02/MF A01

A constitutive law which describes the transient thermal creep of concrete is presented. Moisture and temperature are two major parameters in this constitutive law. Load, creep, cracking, thermal (shrinkage) strains, stress induced hygrothermal strains are analyzed. The theory agrees with most types of test data which include basic creep, thermal expansion, shrinkage, swelling, creep at cyclic heating or drying, and creep at heating under compression or bending. Examples are given to demonstrate agreement between the theory and the experimental data. DOE

N86-11543# Los Alamos Scientific Lab., N. Mex.
EVALUATION OF CONCRETE CREEP AND STRESS REDISTRIBUTION IN A PROTOTYPIC PCRV FOLLOWING RUPTURE OF PRESTRESSING TENDONS
E. Fugelso and C. A. Anderson 1985 13 p refs Presented at the 8th Intern. Conf. on Struct. Mech. in Reactor Technol., Brussels, 19 Aug. 1985
(Contract W-7405-eng-36)
(DE85-007673; LA-UR-85-638; CONF-850809-18) Avail: NTIS HC A02/MF A01

Numerical evaluation of the instantaneous and creep stress changes in a prototypic concrete PCRV subsequent to degradation and rupture of selected prestressing tendons is presented. Either partial or complete degradation of one prestressing tendon will slightly reduce the mean compressive stress in the same direction in the concrete. DOE

N86-11544# Sandia Labs., Albuquerque, N. Mex.
STRAIN RATE DEPENDENCE IN STEADY, PLASTIC SHOCK WAVES
J. E. Dunn and D. E. Grady 1985 7 p Presented at the Am. Phys. Soc. Topical Conf. on Shock Waves in Condensed Matter, Spokane, 22 Jul. 1985
(Contract DE-AC04-76DP-00789)
(DE85-014703; SAND-85-0635C; CONF-850736-20) Avail: NTIS HC A02/MF A01

The shock wave profile data of Barker for Al fits the empirical equation epsilon sub m = kp sub d to the 4th power. Attempts to understand the constitutive implications of the equation for the broader class of materials are summarized. DOE

N86-11545# Los Alamos National Lab., N. Mex.
MECHANICAL THRESHOLD OF DYNAMICALLY DEFORMED COPPER AND NITRONIC 40
P. S. Follansbee, U. F. Kock, and G. Regazzoni 1985 11 p Presented at the Intern. Conf. on Mech. and Phys. Behaviour of Mater. under Dynamic Loading, Paris, 2 Sep. 1985
(Contract W-7405-eng-36)
(DE85-010779; LA-UR-85-1135; CONF-850946-3) Avail: NTIS HC A02/MF A01

Measurements of the mechanical threshold, or threshold stress, are reported on quasi-statically and dynamically deformed copper and Nitronic 40. Results for copper show that the increase of the threshold stress with strain rate is similar to that of the flow stress. In Nitronic 40 the results show that the ratio of the flow stress to the threshold stress is approximately 0.6. Both results indicate that the increased rate sensitivity found in these materials at high strain rates is not due to the predominance of a viscous drag deformation mechanism, as has been previously suggested. DOE

N86-11546# Los Alamos National Lab., N. Mex.
INERTIA, STABILITY AND DUCTIBILITY IN UNIAXIAL TENSION AT HIGH STRAIN RATE
G. Regazzoni, P. S. Follansbee, and J. N. Johnson 1985 15 p Presented at the Symp. on Plastic Instability, Paris, 1 Sep. 1985
(Contract W-7405-eng-36)
(DE85-007671; LA-UR-85-632; CONF-850945-1) Avail: NTIS HC A02/MF A01

The influence of inertia on the necking process in the dynamic tensile test was studied. The equations of motion for a bar of finite length elongation dynamically were written assuming a one-dimensional state of stress, and a model for rate independent or rate dependent flow was presented. For rate dependent flow, a description of the stress-strain rate law that takes into account the increase of strain rate sensitivity in the dynamic range was introduced. The growth of an assumed perturbation located at the middle of the specimen was simulated with a finite difference code. Predictions of the model are compared with experimental results obtained on pure copper. E.A.K.

N86-11547# Sandia Labs., Albuquerque, N. Mex.
HIGH PRESSURE STRENGTH OF SHOCKED ALUMINUM
J. R. Asay, L. C. Chhabildas, G. I. Kerley, and T. G. Trucano 1985 5 p Presented at the Am. Phys. Soc. Topical Conf. on Shock Waves in Condensed Matter, Spokane, 22 Jul. 1985
(Contract DE-AC04-76DP-00789)
(DE85-014461; SAND-85-0157C; CONF-850736-15) Avail: NTIS HC A02/MF A01

Unloading wave experiments were used to determine the material strength and release adiabats in pure and 6061-T6 aluminum alloy over the stress range of 50 to 100 GPa. The experimental adiabats are in good agreement with theoretical calculations, assuming a constant rho(GAMMA). The strength measurements show that a maximum occurs for shock states above 20 GPa and that a general softening of the strength is evident between 40 and 100 GPa. DOE

N86-11548# Argonne National Lab., Ill.
EXPERIMENTAL STUDY ON IMPACT/FRETTING WEAR IN HEAT EXCHANGER TUBES
J. H. Cha, M. W. Wambsganss, and J. A. Jendrzejczyk Apr. 1985 56 p
(Contract W-31-109-eng-38)
(DE85-014597; ANL-85-38) Avail: NTIS HC A04/MF A01

A data bank of field experiences with heat exchanger tube vibration reveals numerous cases of tube failures at, or near, the baffle. Qualitative impact/fretting wear information for heat exchanger tubes through the performance of a series of tests involving the pertinent parameters were provided. They included: (1) force level, between the tube and its support; (2) tube to support plate hole clearance; (3) tube support plate thickness; and (4) tube vibration frequency. The characteristics of impact/fretting wear relative to tube motion pattern, material combination and surrounding fluid were also investigated. The test apparatus consists of a cantilevered tube with a simulated tube support plate at the free end. Tube vibration is induced by an electromagnetic exciter to simulate the flow induced tube motion occurring in a real heat exchanger at the tube/tube support plate interface. Tests are conducted in air, water, and oil, all at room temperature. Wear rate increases significantly with the magnitude of the impact force between the tube and its support plate; the degree and trend of the wear rates are highly dependent on the mechanical and metallurgical properties of the tube/support material combination; the rate of impact/fretting wear decreases with increasing frequency. An empirical formula is proposed to correlate the experimental impact/fretting wear results. DOE

N86-11242*# National Aeronautics and Space Administration. Langley Research Center, Hampton, Va.
NONDESTRUCTIVE ULTRASONIC MEASUREMENT OF BOLT PRELOAD USING THE PULSED-PHASE LOCKED-LOOP INTERFEROMETER
S. G. Allison and J. S. Heyman *In its* Welding, Bonding and Fastening, 1984 Sep. 1985 p 197-209 refs (For primary document see N86-11227 02-23)
Avail: NTIS HC A21/MF A01 CSCL 20K

N86-11885# California Univ., Livermore. Lawrence Livermore Lab. Engineering Research Div.
FLEXIBLE VIBRATIONS OF A UNIFORM ELASTIC BEAM WITH ARBITRARY SUPPORTS AND LUMPED MASSES Abstract Only
Donald T. Gavel and Howard Woo *In* LANL 6th Bien. CUBE (Computer Use by Engineers) Symp. Aug. 1984 p 73 (For primary document see N86-11858 02-60)
Avail: NTIS HC A06/MF A01

N86-12004# Joint Publications Research Service, Arlington, Va.
INVOLUTORY TRANSFORMATIONS AND VARIATION PRINCIPLES WITH MULTIVARIABLES IN THIN PLATE BENDING PROBLEMS Abstract Only
Weichang Qian *In its* China Rept.: Sci. and Technol. (JPRS-CST-85-015) 16 May 1985 p 107 Transl. into ENGLISH from Yingyong Shuxue he Lixue (Chongquing), v. 6, no. 1, Jan. 1985 p 25-40 (For primary document see N86-11994 02-70)
Avail: NTIS HC A07/MF A01

N86-12005# Joint Publications Research Service, Arlington, Va.
NUMERICAL METHOD IN DYNAMIC RESPONSE OF NONLINEAR SYSTEMS Abstract Only
Zhaochang Zheng and Mingyi Tan *In its* China Rept.: Sci. and Technol. (JPRS-CST-85-015) 16 May 1985 p 108 Transl. into ENGLISH from Yingyong Shuxue he Lixue (Chongquing), v. 6, no. 1, Jan. 1985 p 93-101 (For primary document see N86-11994 02-70)
Avail: NTIS HC A07/MF A01

N86-12009*# Naval Ship Research and Development Center, Bethesda, Md.
ON THE COMPUTATION OF STRUCTURAL VIBRATIONS INDUCED BY A LOW-SPEED TURBULENT FLOW Abstract Only
Y. F. Hwang *In* NASA. Lewis Research Center Numerical Tech. in Acoustics Oct. 1985 p 3-5 (For primary document see N86-12007 02-71)
Avail: NTIS HC A03/MF A01 CSCL 20K

N86-12010*# Houston Univ., Tex.
IMPROVING THE ACCURACY OF THE BOUNDARY INTEGRAL METHOD BASED ON THE HELMHOLTZ INTEGRAL Abstract Only
G. H. Koopmann and K. Brod *In* NASA. Lewis Research Center Numerical Tech. in Acoustics Oct. 1985 p 7-8 (For primary document see N86-12007 02-71)
Avail: NTIS HC A03/MF A01 CSCL 20K

42 GEOSCIENCES (GENERAL)

N86-11549# Academy of Sciences, Potsdam (East Germany). Zentralinst fuer Physik der Erde.
PROCEEDINGS OF THE 5TH INTERNATIONAL SYMPOSIUM GEODESY AND PHYSICS OF THE EARTH, PART 1
1985 177 p refs Symp. held in Magdeburg, East Germany, 23-29 Sep. 1984 3 Vol.
(Rept-81-Pt-1; ISSN-0514-8790) Avail: NTIS HC A09/MF A01

Numerous topics in planetary dynamics were presented. The Earth-Moon system, geodynamics, geodesy, Earth tides, Earth rotation, inverse problems in differential equations, geodetic boundary value problems, the modification of a tiltmeter to a borehole tiltmeter, and rheological parameters of the Earth are among the topics discussed. For individual titles, see N86-11550 through N86-11567.

N86-11550# Academy of Sciences, Potsdam (East Germany). Zentralinst. fuer Physik der Erde.
FIGURE OF THE EARTH, MOON, AND PLANETS Progress Report, 1981-1984 c90
M. Bursa *In its* Proc. of the 5th Intern. Symp. Geodesy and Phys. of the Earth 1985 p 10-24 refs (For primary document see N86-11549 02-42)
Avail: NTIS HC A09/MF A01

Numerous topics related to the celestial mechanics of the Sun, Moon and Earth are briefly discussed as studies by a number of authors are briefly surveyed. Orbital, rotational, and tidal dynamics of systems of celestial bodies; representation of gravitational fields of celestial bodies; gravity field parameters of Earth, Moon and planets; the boundary value of Mododensky; and density models of the Earth are discussed. R.J.F.

N86-11551# Research Inst. of Geodesy, Prague (Czechoslovakia).
RESULTS OF KAPG CO-OPERATION IN EARTH TIDE RESEARCH c48
Zdenek Simon *In* Academy of Sciences of the GDR Proc. of the 5th Intern. Symp. Geodesy and Phys. of the Earth 1985 p 24-30 refs (For primary document see N86-11549 02-42)
Avail: NTIS HC A09/MF A01

Joint Earth tide measurements with Askania gravimeters were conducted on the stations Pulkovo, Obninsk (USSR), Potsdam (GDR), Pecny (Czechoslovakia), Tihany (Hungary) and Sofia (Bulgaria). For the tidal analysis Venedikov's method M 74 was used. In contradiction with the high inner accuracy, systematic differences were found between the results of individual series of measurements on the same station, first of all in gravimetric factors delta. These differences occur sometimes also between the results obtained with the same gravimeters. The mean square value of the systematic error of delta values from one series caused by the record calibration imperfection, is s sub delta = 0.0064. For the real random mean square error of the main waves the value sigma sub delta = 0.0043 was found. With the phase lags chi there is s sub chi = 26 omega (omega - angular speed in o over s) and = 0.36 degrees. An improvement of the real accuracy of the results of gravimetric Earth tide measurements is possible either by increasing the number of measured series on the station or, more effectively, by improvement of the measuring techniques. R.J.F.

N86-11552# Martin Luther-Universitaet, Halle-Wittenberg (East Germany). Sektion Mathematik.
ON INVERSE PROBLEMS IN DIFFERENTIAL EQUATIONS: A CRITICAL ANALYSIS c64
Gottfried Anger *In* Academy of Sciences of the GDR Proc. of the 5th Intern. Symp. Geodesy and Phys. of the Earth 1985 p 38-44 refs (For primary document see N86-11549 02-42)
Avail: NTIS HC A09/MF A01

The author has conducted fundamental research in potential theory, partial differential equations, and functional analysis for 20 years, concentrating on the systematic study of the natural coupling between physical fields and modern analysis. For the past 14 years he has applied the results obtained to the study of inverse problems. He has encountered serious difficulties in this task, since, apart from the inverse spectral problem, no effective general formulation of this class of problems was available and no useful theories have been developed for coping with them. The author discusses the problem encountered in his investigations. Author

N86-11553# Academy of Sciences, Potsdam (East Germany). Zentralinst. fuer Physik der Erde.
NEW ASPECTS OF THE GEODETIC BOUNDARY VALUE PROBLEMS c43
K. Arnold *In its* Proc. of the 5th Intern. Symp. Geodesy and Phys. of the Earth 1985 p 45-50 refs (For primary document see N86-11549 02-42)
Avail: NTIS HC A09/MF A01

At first, the solution of the boundary value problem of Molodensky is considered. The identity of Green and the smoothing superposition with the visible mountain masses lead to a closed solution which does not involve series developments and instable downward continuations. The negligible remainder term has a mathematical expression that gives an insight of clear transparency into its amount. Further, the first mixed boundary value problem of geodesy is investigated. The potential values at the oceans and the free air anomalies at the continents are the boundary values. The solution consists in a representation of the potential values at the continents in terms of the boundary values. The kernel of the concerned integral equation of the first kind is symmetric, positive definitie and closed. Thus, it allows a bijective mapping. A condition for the uniqueness is derived for an arbitrary course of the coastline. Four compatibility conditions for the boundary values are found. They must be fulfilled if the solution is in the subspace of the harmonics of 2nd and higher order only. Author

N86-11554# Hungarian Academy of Sciences, Sopron. Geodetical and Geophysical Research Inst.
HIGH FREQUENCIES IN TIDAL TILT RECORDS c48
G. Bartha *In* Academy of Sciences of the GDR Proc. of the 5th Intern. Symp. Geodesy and Phys. of the Earth 1985 p 51-59 refs (For primary document see N86-11549 02-42)
Avail: NTIS HC A09/MF A01

A new type of horizontal pendulum was developed, where the motion of the beam is detected by a capacitive sensor. A possibility of dense sampling is provided by this technique. Therefore, higher frequencies than the tidal ones could be studied. The periods of the Earth's normal modes excited by big earthquakes can be found from some minutes till near one hour. Their detection was strongly hoped with the new horizontal pendulum. The free oscillation phenomenon is discussed from this aspect. Some results, produced from data series sampled densely after earthquakes, are also shown. Author

N86-11555# Institut Geographique National, Paris (France). Groupe de Recherches de Geodesie Spatiale.
ESTABLISHMENT OF THE BIH TERRESTRIAL SYSTEM BY COMBINING THE RESULTS OF DIFFERENT EARTH ROTATION SPACE GEODESY PROGRAMS Abstract Only c43
Claude Boucher and Martine Feissel (Observatoire de Paris) *In* Academy of Sciences of the GDR Proc. of the 5th Intern. Symp. Geodesy and Phys. of the Earth 1985 p 60 (For primary document see N86-11549 02-42)
Avail: NTIS HC A09/MF A01

The application of space geodesy techniques to global geodesy problems has resulted in the precise determination of positions of several tens of sites where stations are operated for Earth rotation observing programs. These sites are organized in networks, for which consistent ensembles of Sets of Stations Coordinates (SSC) and series of the Earth's rotation parameters (ERP) are obtained by analysis centers specializing in the treatment of Doppler Lacking satellite or Lunar laser ranging, and VLBI. More than ten such ensembles are presently available. The simultaneous use of the SSC and the series of ERP, constrained by common site coordinates for colocated stations, makes it possible to realize a worldwide terrestrial frame, and a series of ERP consistent with it. Starting with 1984, the terrestrial frame of the BIH will be realized along this ideas, by the method described in [C. Boucher and M. Feissel, Realization of the BIH terrestrial system, Proc. of the Internat. Symp. Space Techniques for Geodynamics, held in Sopron (Hungary), 9 to 13 July 1984]. The continuity of the orientation of the new frame with respect to the previous realization of the BIH System will be insured within 0.005 inches. The precision of site coordinates will be in the range 10 to 100 cm, depending on the observing technique operated at the site. Author

N86-11556# Ceskoslovenska Akademie Ved, Prague. Astronomical Inst.
TIDAL FRICTION, THE EARTH'S ROTATION AND HYPOTHESIS OF AN EXPANDING EARTH c43
Milan Bursa *In* Academy of Sciences of the GDR Proc. of the 5th Intern. Symp. Geodesy and Phys. of the Earth 1985 p 61-67 refs (For primary document see N86-11549 02-42)
Avail: NTIS HC A09/MF A01

It has been demonstrated that the observed decreasing of the second zonal harmonic in the geopotential and of the angular velocity of the Earth's rotation affects its dynamics significantly. The tidal budget angular momentum equation of the Earth-Moon-System is well satisfied using recent data. There is no space for the hypothesis of an expanding Earth, as well as, for secular variations in the Newtonian gravitational constant. Author

N86-11557# Zagreb Univ. (Yugoslavia). Geodetic Faculty.
ANEW ABOUT THE CORRELATION BETWEEN MOHOROVICIC DISCONTINUITY DEPTHS, GEOID UNDULATIONS AND BOUGUER GRAVITY ANOMALIES IN THE DINARIC-PANNONIAN REGION OF YUGOSLAVIA c46
K. Colic, S. Petrovic, and T. Basic *In* Academy of Sciences of the GDR Proc. of the 5th Intern. Symp. Geodesy and Phys. of the Earth 1985 p 68-76 refs (For primary document see N86-11549 02-42)
Avail: NTIS HC A09/MF A01

The continuation and the expansion of the preliminary investigations of the linear correlation between Mohorovicic discontinuity depths M and the absolute geoid undulations N (obtained from astrogeodetic and GEM 10 data) are depicted, as well as Bouguer gravity anomalies delta g in the Dinaric-Pannonian region of Yugoslavia. At this stage, an attempt was made to modify the numerical treatment. Also, a fresh deep seismic sounding profile, situated on the border of Alps massif, was included into research. Thus, it became possible for the considered region, a region which frequently shows a high degree of seismic activities, to test the relations which had been obtained previously, as well as to achieve some new interesting results in the field of M-depths predicition. Author

N86-11558# Academy of Sciences, Potsdam (East Germany). Zentralinst. fuer Physik der Erde.
AN ATTEMPT TO DETECT GEOMETRIC TIDAL INFORMATION USING LAGEOS LASER RANGING DATA c48
R. Dietrich and G. Gendt *In its* Proc. of the 5th Intern. Symp. Geodesy and Phys. of the Earth 1985 p 77-81 refs (For primary document see N86-11549 02-42)
Avail: NTIS HC A09/MF A01

Usually, in satellite geodesy, the solid earth tide effects are computed as corrections to the station coordinates. Here the Love number h was introduced as an unknown parameter into the adjustment process. Computations with the orbital program POTSDAM-5 and the data of MERIT Short Campaign led to values of h = 0.56 plus or minus 0.06 (gravity field model GEM-L2) and h = 0.55 plus or minus 0.06 (gravity field model GRIM 3B). Author

N86-11559# Academy of Sciences, Potsdam (East Germany). Zentralinst. fuer Physik der Erde.
SOME RESULTS OF AN EIGHT YEARS GRAVIMETRIC REGISTRATION SERIES c46
H.-J. Dittfeld *In its* Proc. of the 5th Intern. Symp. Geodesy and Phys. of the Earth 1985 p 82-91 refs (For primary document

see N86-11549 02-42)
Avail: NTIS HC A09/MF A01

Digital Earth tide records have been carried out since March 1974 at the Potsdam Gravimetric Observatory using the Askania gravimeter GS15 No. 222. Analyzed are 63,341 hourly readings, measured until February 1982. The inner accuracy of the main tidal amplitude factors is + or - 0.0002 + or - 0.0009, that of the phase + or - 0.01 + or - 0.04. The mean square error of an hourly reading was m sub o = + or - 0.66 microgal. The final results for the entire series are compared with model values. Temporal variations of the tidal parameters are determined by overlapping partial analyses of more than 10,000 readings. The results are compared with those of corresponding data of the Earth tide station Pecny/CSSR. In both the series of a significant increase of the 01 amplitude is detected for the same time interval in which a decrease of the length of the day was obtained by the BIH (Bureau Internationale de e'Houre). Author

N86-11560# Deutsches Geodaetisches Forschungsinstitut, Munich (West Germany).

GEOPHYSICAL INTERPRETATION OF GLOBAL GEOID UNDULATIONS AND MEAN GRAVITY ANOMALIES c46

Hermann Drewes *In* Academy of Sciences of the GDR Proc. of the 5th Intern. Symp. Geodesy and Phys. of the Earth 1985 p 95-104 refs (For primary document see N86-11549 02-42)
Avail: NTIS HC A09/MF A01

Global representations of geoid and gravity anomalies are discussed with respect to their evidence for the mass distribution inside the Earth. Two methods can be used: The first one starts from the distribution of inhomogeneous masses as known from geophysics. The effect of these masses on the gravitational potential and gravity is computed and compared with the geodetically determined parameters. The second method applies a least squares adjustment approach to estimate the inhomogeneous mass distribution from the observed geoid and gravity representations. For the latter inversion procedure a new algorithm and application is given. Author

N86-11561# Technische Hochschule, Darmstadt (West Germany). Inst. fuer Physikalische Geodaesie.

PRECISE GEOID COMPUTATIONS AT MOUNTAINOUS COASTLINES IN VIEW OF VERTICAL DATUM DETERMINATIONS c43

H. J. Euler, E. Groten, W. Hausch, and B. Stock *In* Academy of Sciences of the GDR Proc. of the 5th Intern. Symp. Geodesy and Phys. of the Earth 1985 p 109-139 refs (For primary document see N86-11549 02-42)
Avail: NTIS HC A09/MF A01

Problems inherent in precise geoid determination are considered. Conceptional ideas about the vertical datum problem are presented. Geophysical considerations and spherical spline interpolations are carried out in a test area. Truncation error coefficients for the altitude-extended Hotline function in form of recurrence relations are derived. The ellipsoidal corrections for the geoid undulation and the deflections of the vertical as well as the atmospheric correction to geoid undulations are determined with spherical harmonic models up to degree 180. Author

N86-11562# Agricultural Univ., Wroclaw (Poland). Dept. of Geodesy and Photogrammetry.

ADJUSTMENT OF THE LATITUDE DATA BY LEAST-SQUARES COLLOCATION APPROACH c64

R. Galas *In* Academy of Sciences of the GDR Proc. of the 5th Intern. Symp. Geodesy and Phys. of the Earth 1985 p 139-141 refs (For primary document see N86-11549 02-42)
Avail: NTIS HC A09/MF A01

To solve the problem of intercomparison of the polar motion data on the base of various space and astrometric techniques, many basic problems must be discussed. Among them, the proper algorithms for smoothing of the observational data should be evaluated. At the outset the stochastic-deterministic model of the latitude variations and of the polar motion is presented. Then the empirical covariance functions are defined and positive definiteness of the respective covariance matrices is checked out. Finally, smoothing of the observational series of the latitude variations by the least-squares collocation is discussed. Author

N86-11563# Technische Hochschule, Darmstadt (West Germany). Inst. fuer Physikalische Geodaesie.

MODIFICATION OF A HUGHES TILTMETER TO A BOREHOLE TILTMETER c35

C. Gerstenecker *In* Academy of Sciences of the GDR Proc. of the 5th Intern. Symp. Geodesy and Phys. of the Earth 1985 p 142-149 refs (For primary document see N86-11549 02-42)
Avail: NTIS HC A09/MF A01

Earth tidal tilt measurements in mines are influenced by cavity effects. Therefore, the modification of tiltmeters to borehole instruments is useful, since the cavity effect may be avoided in boreholes. The principle of the design of the Hughes tiltmeter and of borehole equipment is described. The diameter of the borehole case is similar to that of the Askania vertical pendulum. Hence the Hughes tiltmeter can be installed in boreholes drilled for Askania pendulums. To achieve proper operation of the instrument, the electronics had to be reconstructed and integrated in the borehole case. Devices for remote adjustment of the tiltmeter in the borehole, self test, temperature, and air pressure sensors complete the borehole equipment. The borehole tiltmeter is connected via a 60 m long cable with the control unit, containing the necessary power supplies, analog control instruments and adjustment knobs. Author

N86-11564# Technische Hochschule, Darmstadt (West Germany). Inst. fuer Physikalische Geodaesie.

ON THE DISTRIBUTION OF THE RESIDUAL VECTORS OF EARTH'S TIDE GRAVITY OBSERVATIONS IN CENTRAL EUROPE c46

C. Gerstenecker and P. Varga (Budapest Science Univ.) *In* Academy of Sciences of the GDR Proc. of the 5th Intern. Symp. Geodesy and Phys. of the Earth 1985 p 150-165 refs (For primary document see N86-11549 02-42)
Avail: NTIS HC A09/MF A01

Residual vectors of Earth tidal gravity observations should give information about inhomogenities in the Earth's crust, if all error sources such as tidal load vectors, instrumental nonlinearities and instabilities are compensated. Results of observations at 13 different stations in Central Europe with the LaCoste-Romberg Earth tide meter ET 16 are compared with residual vectors obtained at neighbor stations with other gravimeters such as Askania GS-15 and Geodynamics. The phase angles distribution obtained points out a significant correlation between the individual stations, which is independent of the instruments used, but no correlation with the thickness of the lithosphere. The behavior of the residual vectors proposes the existence of a common noise source. The reasons are mainly seen in the load tide calculation, which may be systematically biased up to 0.3 microgal with regard to amplitude. Author

N86-11565# Academia Sinica, Beijing (China). Inst. of Geodesy and Geophysics.

ON THE LUNAR TIDAL EFFECT IN THE LATITUDE OBSERVATIONS AT TIANJIN c46

Tianqi Han, Yiming Qian, Shiguang Li, and Lanzhen Ma *In* Academy of Sciences of the GDR Proc. of the 5th Intern. Symp. Geodesy and Phys. of the Earth 1985 p 166-168 refs (For primary document see N86-11549 02-42)
Avail: NTIS HC A09/MF A01

The effects of the lunar tides on the latitude observation results of 25260 star pairs with the zenith telescope ZTL-180 at Tianjin Latitude Station during 1960-1966 are analyzed. It is found that the amplitude of the M2 tidal wave is 0".0108, and the value of $1+k=1$ is 1.34. When the effects of the ocean tides are removed, the value of $1+k-1$ is reduced to 1.315, which shows good consistency with the value 1.31 given by geophysicists to the Asian area. F.M.R.

N86-11566# Slovak Technical Univ., Bratislava (Czechoslovakia). Observatory.

SOME SHORT PERIODIC TERMS DUE TO NUTATION AND TIDES FROM LATITUDE AND TIME DETERMINATIONS AT CZECHOSLOVAK OBSERVATORIES c46

Jan Hefty *In* Academy of Sciences of the GDR Proc. of the 5th Intern. Symp. Geodesy and Phys. of the Earth 1985 p 169-172 refs (For primary document see N86-11549 02-42)

Avail: NTIS HC A09/MF A01

The latitude factor lambda = 1 + k =- 1 and gamma, the ratio of observed to theoretical nutation of a rigid Earth, is estimated. For the analysis of observations by three instruments the Photographic Zenith Telescope (PZT), circum-zenithal and visual transit instruments - two independent methods are used. Results are consistent with Wahr's model of forced nutations and the theory of body tides. F.M.R.

N86-11567# Academy of Sciences, Potsdam (East Germany). Zentralinsts fuer Physik der Erde.

RESULTS CONCERNING RHEOLOGICAL PARAMETERS OF THE EARTH c43

Joachim Hoepfner *In its* Proc. of the 5th Intern. Symp. Geodesy and Phys. of the Earth 1985 p 173-176 refs (For primary document see N86-11549 02-42)

Avail: NTIS HC A09/MF A01

Using the mean Chandler period obtained from latitude observations at the astrolab in Potsdam, the deformation factor k sub d and from this the Love number k is computed. Furthermore, the heterogeneities of k sub d and k are estimated. The contribution to the Chandler period for anelasticity in the Earth's mantle is determined by comparison with a theoretical Chandler period corrected for the influence of the polar tide. Author

N86-11568# Academy of Sciences, Potsdam (East Germany). Zentralinst. fuer Physik der Erde.

PROCEEDINGS OF THE 5TH INTERNATIONAL SYMPOSIUM GEODESY AND PHYSICS OF THE EARTH, PART 2

1985 161 p refs In ENGLISH and RUSSIAN Symp. held in Magdeburg, East Germany, 23-29 Sep. 1984 3 Vol.

(Rept-81-Pt-2; ISSN-0514-8790) Avail: NTIS HC A08/MF A01

Geodesy and earth physics were discussed. Topics presented include: solving geodetic boundary value problems for topography, irregularity in the Earth's annual rotation caused by time variation, ocean tidal loading, coupling torques between the Earth's core and mantle on Earth rotation parameters, periodical variations of polar motion, oceanic and gravity interactions, convergence problems of satellite derived spherical harmonic expansion of the geopotential at Earth's surface, geodynamic effects due to Earth's deformation, comparisons between formulas of Earth's tidal correction in astronomical time and latitude observation, inelasticity the Earth mantle. For individual titles, see N86-11569 through N86-11590.

N86-11569# Research Inst. of Geodesy, Prague (Czechoslovakia).

A NEW APPROACH TO ITERATIONS IN SOLVING GEODETIC BOUNDARY VALUE PROBLEMS FOR REAL TOPOGRAPHY c43

Petr Holota *In* Academy of Sciences of the GDR Proc. of the 5th Intern. Symp. Geodesy and Phys. of the Earth, Pt. 2 1985 p 4-15 refs (For primary document see N86-11568 02-42)

Avail: NTIS HC A09/MF A01

A geodetic boundary value problem means to find a harmonic function in the domain outside a telluroid which meets conditions given on the surface of the telluroid. Following the definition, the telluroid or the surface of the Earth in the first approximation is as irregular as the physical surface of the Earth's body. However, almost all formulas which are used for practical representation of the solution of the problem are valid for what is a zero-order approximation of the solution based on a formal approximation of the real boundary surface by a sphere. This spherical approximation is habitual in the computations when it is used even at a high smoothing of the real topography. It is suggested that there is a convergent iterative process, an analytical centinuation in the interpretation which modifies the original boundary data. The simple molodensky problem is discussed. It is concluded that there is a need for a good starting approximation, which is identical with the Stokes integral. The Stokes approximate solution of the molodensky problem is the basis in the sequence of approximations of the iterative process. Author

N86-11570# Higher Inst. of Mining and Geology, Sofia (Bulgaria).

THE IRREGULARITY IN THE EARTH'S ANNUAL ROTATION AS A CAUSE OF SYSTEMATIC TIME VARIATION c43

I. B. Ivanov *In* Academy of Sciences of the GDR Proc. of the 5th Intern. Symp. Geodesy and Phys. of the Earth, Pt. 2 1985 p 16-18 refs (For primary document see N86-11568 02-42)

Avail: NTIS HC A09/MF A01

Seasonal variations in the Earth's rotational velocity phi were established and it was pointed out that they are causes of meteorological factors. The effect of the meteorological factors, can explain only about half on the observed values of these seasonal variations the unexplained 50% of the values of these seasonal variations in the Earth's angular velocity are outlined. The transport of masses through the equatorial plane were established. The angular moment of a rotational body is presented. E.A.K.

N86-11571# Freie Univ., Berlin (West Germany). Inst. fuer Geophysikalische Wissenschaften.

OCEAN TIDAL LOADING ALONG THE BLUE ROAD GEOTRAVERSE IN FENNOSCANDIA c48

Gerhard Jentzsch *In* Academy of Sciences of the GDR Proc. of the 5th Intern. Symp. Geodesy and Phys. of the Earth, Pt. 2 1985 p 18-28 refs (For primary document see N86-11568 02-42)

Avail: NTIS HC A09/MF A01

Gravity tidal measurements along the Fennoscandian Blue Road Geotraverse are presented. The residual vectors for consituents O1 and M2 are compared to ocean tidal loading, and calculated for modified Schwiderski maps. The coherence of the results for O1 shows the sufficient intercalibration of the different gravimeters. The results for M2 indicate that an improvement of the models for the spatial distribution of the marine tide of the Norwegian shelf has to be applied to fit the observed residuals near the coast. Data acquisition of the gravimeters, calibration, and data analysis are discussed. E.A.K.

N86-11572# Academy of Sciences, Potsdam (East Germany). Zentralinst. fuer Physik der Erde.

ON THE INFLUENCE OF COUPLING TORQUES BETWEEN THE EARTH'S CORE AND MANTLE ON PARAMETERS AND COMPONENTS OF THE ROTATION OF THE EARTH c46

H. Jochmann *In its* Proc. of the 5th Intern. Symp. Geodesy and Phys. of the Earth, Pt. 2 1985 p 29-31 refs (For primary document see N86-11568 02-42)

Avail: NTIS HC A09/MF A01

The physical reliability of correlations between magnetic field quantities and components and parameters of the Earth's rotation was investigated. It is found that only the correlations between variations of the magnetic field intensities and of the length of day are physically significant, while the correlations between the magnetic field and parameters of the CHANDLER-wobble are dubious. E.A.K.

N86-11573# Technische Univ., Dresden (East Germany).

TREATMENT OF THE GEODETIC BOUNDARY VALUE PROBLEM BY CONTACT-TRANSFORMATION c64

Wolfgang Keller *In* Academy of Sciences of the GDR Proc. of the 5th Intern. Symp. Geodesy and Phys. of the Earth, Pt. 2 1985 p 32-35 refs (For primary document see N86-11568 02-42)

Avail: NTIS HC A09/MF A01

Free boundary value problems for elliptical differential equations were studied use by use of the searched function V for the definition of a contact-transformation. This contact-transformation transforms the free boundary value problem for V into a boundary value problem with fixed boundary for a coordinated function psi. This approach was examined and the application of this principle in geodesy goes back to Sanso. The most simple case of a contact-transformation, is applied to Legendre's transformation. Author

N86-11574# Polish Academy of Sciences, Warsaw. Space Research Centre.
ON SHORT PERIODICAL VARIATIONS OF POLAR MOTION AND UT1-UTC c43
B. Kolaczek, A. Brzezinski, W. Kosek, J. Nastula, and B. Soloducha *In* Academy of Sciences of the GDR Proc. of the 5th Intern. Symp. Geodesy and Phys. of the Earth, Pt. 2 1985 p 35-44 refs (For primary document see N86-11568 02-42)
Avail: NTIS HC A09/MF A01

The MERIT data of pole coordinates, UT1-UTC and l.o.d. from the period between October 1983 to July 1984 were used to analysis spectra of their variations in the short periodical part from 10 to 90 days by the Maximum Entropy Spectral Analysis (MESA). A few short periodical variations detected by MESA in all series of data determined by different techiques seem to be real short periodical variations of the order of a few miliarcseconds only, are weakly determined, and they can be changeable. E.A.K.

N86-11575# Academy of Sciences, Potsdam (East Germany). Zentralinst. fuer Physik der Erde.
INFLUENCES OF SYSTEMATIC DIFFERENCES BETWEEN DIFFERENT STAR CATALOGUES ON THE RESULTS OF LATITUDE AND TIME DETERMINATIONS WITH THE PZT 2 c89
M. Mainig *In its* Proc. of the 5th Intern. Symp. Geodesy and Phys. of the Earth, Pt. 2 1985 p 45-54 refs (For primary document see N86-11568 02-42)
Avail: NTIS HC A09/MF A01

Systematic errors in the star catalogues, used for the reduction of Photographic Zenith Telescope PZT observations, effect directly the results of latitude and time determinations and the Earth rotation parameters which were derived from these results. In the geodetic-astromical observatory of the Central Institute for Physics of the Earth the catalogue PZT 80 is used. The catalogue contains star places, which were improved by own PZT results. The systematic differences between this catalogue and the catalogue of northern PZT stars NPZT 74 are approximated by analytical expressions in dependence on the right ascension. The influence of these differences on the latitude and time determinations is presented for the observation series with the PZT 2 in the years 1981 to 83. The obtained results are compared with values calculated from data of the Bureau International de l'Heure. E.A.K.

N86-11576# Belgian Royal Observatory, Uccle.
INTERACTIONS BETWEEN OCEANIC AND GRAVITY TIDES, AS ANALYSED FROM WORLD-WIDE EARTH TIDE OBSERVATIONS AND OCEAN MODELS c48
P. Melchior, B. Ducarme, M. VanRuymbeke, C. Poitevin, and M. DeBecker *In* Academy of Sciences of the GDR Proc. of the 5th Intern. Symp. Geodesy and Phys. of the Earth, Pt. 2 1985 p 55-62 refs (For primary document see N86-11568 02-42)
Avail: NTIS HC A09/MF A01

Interactions between earth tides and oceanic tides involves effects of newtonian attraction, loading and associated change of earth potential, tangential pressure and friction on the moving ocean floor. The following two facts were applied: a considerable amount of data from 223 stations including those of the Trans World Profiles were evaluated, which a Worldwide distribution including the tropical areas and the southern hemisphere; (2) in 1978 to 80, new oceanic cotidal maps of high quality became available. Eight principal tidal waves were calculated for the correlations between the observed gravity variations and those resulting from a calculation based upon the Schwiderski maps. These cotidal maps can be used as working standards for other geodetic and geophysical applications. E.A.K.

N86-11577# Hungarian Academy of Sciences, Sopron. Geodetical and Geophysical Research Inst.
CAPACITIVE PENDULUM WITH INTELLIGENT DATA COLLECTION c35
Gy. Mentes *In* Academy of Sciences of the GDR Proc. of the 5th Intern. Symp. Geodesy and Phys. of the Earth, Pt. 2 1985 p 63-69 refs (For primary document see N86-11568 02-42)
Avail: NTIS HC A09/MF A01

The improvement of horizontal pendulums in geodynamic measuring techniques. Coventional recording systems are not convenient for geodynamic phenomena, and a new capacitive horizontal pendulum with electric output and an intelligent digital data recorder was constructed. For the reproduction of the original signal this latter also uses logical decisions besides mathematical filtering of the data. Analog recording can be abandoned and it is not necessary to store all sampled data. The recorder can be programmed for various tasks. E.A.K.

N86-11578# Academia Sinica, Beijing (China). Inst. of Geodesy and Geophysics.
RESEARCH ON THE COMPUTATIONAL METHODS OF GRAVITY TOPOGRAPHIC EFFECT c46
Jiachun Meng *In* Academy of Sciences of the GDR Proc. of the 5th Intern. Symp. Geodesy and Phys. of the Earth, Pt. 2 1985 p 70-77 refs (For primary document see N86-11568 02-42)
Avail: NTIS HC A09/MF A01

Methods for computing the gravity topographic effect are presented. These methods include: topographic correction solution C are shown, MOLODENSKY's series solution G1, PELLINEN's formula G', analytic continuation g sub and BOERHAMMAR's solution. The interrelation between the formulas of topographic correction are shown the relation between the analytic continuation solution and BOERHAMMAR's solution are derived and some of their natures are deduced. In these methods, each has a common operator L. A certain connections with each other exists, but they can not be replaced mutually. The linear solution of analytic continuation solution is respectevely the approximates value of MOLODENSKY's series solution G1 and BOERHAMMAR'S solution. This suggested that these of reduction of separated rings may decrease difficulties brought about in iterative computation. E.A.K.

N86-11579# Academy of Sciences (USSR), Moscow.
THE POTENTIALOGRAPHICAL PROBLEM AND THE CONCEPTION OF GRAVITATING DISKS c46
G. A. Meshcheryakov *In* Academy of Sciences of the GDR Proc. of the 5th Intern. Symp. Geodesy and Phys. of the Earth, Pt. 2 1985 p 78-87 refs In RUSSIAN; ENGLISH summary (For primary document see N86-11568 02-42)
Avail: NTIS HC A09/MF A01

Two approaches to the Potentialographical Problem (PP) for solving the problems of convenient analytical representation of external potential planet gravitation are presented. The first one corresponds to known methods of solution of direct PP. The second is a constructive one; it presents inverse PP, which is a new kind of inverse problems of potential theory. The inverse PP in which a known potential of the planet is represented as sums of potentials of the simple and double layers, situated on the given surface in the interior of the planet is presented. The density and moments of these layers are sought. A particular case of this problem, when layers are supposed to be in the equatorial plane, brings about the conception of gravitating disks CGD. According to CGD potential of planet is represented as the sum of three potentials of the plane circular one centered disks: focal disks - FD, material, massless MMD and kipole disk - DD. Author

N86-11580# Technische Univ., Graz (Austria). Inst. of Theoretical Geodesy.
VARIATIONAL PRINCIPLES FOR EARTH ROTATION c43
Helmut Moritz *In* Academy of Sciences of the GDR Proc. of the 5th Intern. Symp. Geodesy and Phys. of the Earth, Pt. 2 1985 p 88-101 refs (For primary document see N86-11568 02-42)
Avail: NTIS HC A09/MF A01

Hamilton's principle of least action, in the form of Lagrange's equations, was applied to the rotation of a rigid earth, and to the rotation of an elastic earth with a liquid core. In the form of Hamilton's canonical equations it was applied to a rigid earth.

Modified Lagrange's equations, using nonholonomic group variables, were applied to the rotation of a rigid mantle with a homogeneous liquid core. This equation was applied to the rotation of the earth model (elastic mantle and liquid core), which results in extremely simple equations derived in a different way. Since the rotation of a rigid earth is well known, the classical approach, using holonomic variables, and, in more detail, the recent approach through equations using nonholonomic variables related to rotation groups are discussed. Author

N86-11581# Stazione Astronomica Internazionale di Latitudine, Cagliari (Italy).

SECULAR AND LONG TERM VARIATIONS IN POLAR MOTION FROM CLASSICAL AND DOPPLER OBSERVATIONS c43

A. Poma and E. Proverbio (Ist. di Astronomia e Fisica Superiore, Cagliari, Italy) *In* Academy of Sciences of the GDR Proc. of the 5th Intern. Symp. Geodesy and Phys. of the Earth, Pt. 2 1985 p 101-108 refs (For primary document see N86-11568 02-42)
Avail: NTIS HC A09/MF A01

The existence of secular and low frequency variations in the spectrum of polar motion was reported in a large number of works and discussed by several authors. However, the reality and the geophysical and/or meteorological causes of these phenomena are still a matter of discussion chiefly because the only long series of pole coordinates are essentially the ones based on the results of the five ILS stations. The comparison of classical series (ILS and BIH) of polar coordinates with those derived from Doppler observations lead to the emphasizing of some characteristic features in the secular polar motion in accordance with the crustal motion model. Author

N86-11582# Royal Inst. of Tech., Stockholm (Sweden). Dept. of Geodesy.

ON THE CONVERGENCE PROBLEM OF THE SATELLITE DERIVED SPHERICAL HARMONIC EXPANSION OF THE GEOPOTENTIAL AT THE EARTH'S SURFACE c46

Lars E. Sjoeberg *In* Academy of Sciences of the GDR Proc. of the 5th Intern. Symp. Geodesy and Phys. of the Earth, Pt. 2 1985 p 108-114 refs (For primary document see N86-11568 02-42)
Avail: NTIS HC A09/MF A01

The problem of downward continuing a satellite derived series of spherical harmonics of the Earth's gravity field to the surface is considered. An error formula is derived. Despite extensive numerical study it is concluded that the error of a high degree harmonic expansion (N > or = 300) is not yet satisfactorily known. Author

N86-11583# Academy of Sciences, Potsdam (East Germany). Zentralinst. fuer Physik der Erde.

ON THE COMPARISON OF THE RESULTS OF TWO DIFFERENT E-W-STRAINMETERS c35

D. Simon, R. M. Karmaleeva (Academy of Sciences (USSR), Moscow), and L. A. Latynina (Academy of Sciences (USSR), Moscow) *In its* Proc. of the 5th Intern. Symp. Geodesy and Phys. of the Earth, Pt. 2 1985 p 115-125 refs (For primary document see N86-11568 02-42)
Avail: NTIS HC A09/MF A01

The possible application of tidal strainmeters for measurements of recent crustal movements is discussed. The records of two E-W-strainmeter of different type were analyzed. The instruments are measuring since 1978 simultaneously at the Tiefenort station, 5 meters distant from each other. G.L.C.

N86-11584# Technische Univ., Dresden (East Germany). Sektion Geodaesie und Kartographie.

PLANETS AROUND BARNARD'S STAR? c89

Klaus-Guenter Steinert *In* Academy of Sciences of the GDR Proc. of the 5th Intern. Symp. Geodesy and Phys. of the Earth, Pt. 2 1985 p 126-128 refs *Its* Mitteilung des Lohrmann-Observatoriums No. 52 (For primary document see N86-11568 02-42)
Avail: NTIS HC A09/MF A01

From analyses of long focus observations unseen objects may be found from perturbations in the proper motions of a star. The question is discussed under what conditions it should be possible to detect planets around the nearby Barnard's star. G.L.C.

N86-11585# Ceskoslovenska Akademie Ved, Prague. Geophysical Inst.

GEODYNAMIC EFFECTS DUE TO EARTH'S DEFORMATION c43

Jiri Tresl *In* Academy of Sciences of the GDR Proc. of the 5th Intern. Symp. Geodesy and Phys. of the Earth, Pt. 2 1985 p 128-133 refs (For primary document see N86-11568 02-42)
Avail: NTIS HC A09/MF A01

Some geodynamic effects arising due to deformation of the Earth are investigated. In undeformed state the Earth is replaced by a sphere with radially depending density. Its deformed state is described by displacement vector field. Corresponding density disturbances are expressed in terms of the density and displacements. Further, displacement vector field is decomposed into irrotational and solenoidal parts. Gravitational changes on the Earth's surface are composed from: (1) the changes due to density disturbances inside the Earth; (2) the changes due to deformations of the density interfaces; and (3) the changes due to radial displacement of the observational point. Mathematical expression are derived for the deflections of the vertical, the displacements of the principal axes of inertia, the changes of Earth's rate of rotation and its center of gravity in terms of the density disturbances. G.L.C.

N86-11586# Geodetic Inst., Charlottenlund (Denmark).

ON THE LONG-WAVELENGTH CORRELATION BETWEEN GRAVITY AND TOPOGRAPHY c46

C. C. Tscherning *In* Academy of Sciences of the GDR Proc. of the 5th Intern. Symp. Geodesy and Phys. of the Earth, Pt. 2 1985 p 134-143 refs (For primary document see N86-11568 02-42)
Avail: NTIS HC A09/MF A01

Spherical harmonic expansions of the topography, the topographic isostatic reduction potential and the gravity potential of the Earth now exist complete to degree (N) and order 180. A correlation analysis of the various fields by degree was made. While the general correlation between gravity and topography for the sets is around 50% for N > 15, the correlation with GEM10C is considerably lower for N > 36. This indicates that this set is unreliable above this degree. The topographic isostatic reduction potential may be computed either rigorously by integrating the topography and is compensation or by condensing the topography and its compensating masses. In the last case the spherical harmonic coefficients of the isostatic reduction potential are related in a simple linear manner to the spherical harmonic coefficients of the expansion of the topographic heights. An optimal depth of compensation for each degree was determined by requiring the reduced field to be as smooth as possible. Despite between 35 and 15 km were found for N > 20, which are much lower than the values found earlier using another optimal depth principle. G.L.C.

N86-11587# Ceskoslovenska Akademie Ved, Prague. Astronomical Inst.

POLAR MOTION BETWEEN 1900.0 AND 1984.0 AS DETERMINED BY DIFFERENT TECHNIQUES Abstract Only c43

J. Vondrak *In* Academy of Sciences of the GDR Proc. of the 5th Intern. Symp. Geodesy and Phys. of the Earth, Pt. 2 1985 p 143 (For primary document see N86-11568 02-42)
Avail: NTIS HC A09/MF A01

Polar motion between 1900.0 and 1984.0 as determined by classical astrometry and modern techniques (after 1973.0) is studied with stress on periods equal to one year and longer. Carter's hypothesis on the frequency modulation of Chandler wobble is supported; nonlinear relationship between frequency and amplitude can explain the observed phase shifts with rms error + or - 16 deg. Westward secular drift of the mean pole (0.00329"/y in the direction 78.2 deg W) is confirmed, being present also in modern data. The most probable period of Markowitz wobble is found to be 27.5y but its real existence is highly improbable; it is

not present after 1962.0, when more reliable data are available.
G.L.C.

N86-11588# Academia Sinica, Beijing (China). Inst. of Geodesy and Geophysics.
ON THE COMPARISON AND CHOICE BETWEEN THE FORMULAS OF THE EARTH TIDAL CORRECTION IN ASTRONOMICAL TIME AND LATITUDE OBSERVATION c89
Jiongyu Xia *In* Academy of Sciences of the GDR Proc. of the 5th Intern. Symp. Geodesy and Phys. of the Earth, Pt. 2 1985 p 144-149 refs (For primary document see N86-11568 02-42)
Avail: NTIS HC A09/MF A01

Three formulas of the earth tidal correction in astronomical time and latitude observations are presented. Two of them were calculated and compared. The main conclusions are as follows: (1) the Wahr formula is more complete than the others in theory and is suitable for calculating the correction of each single wave; (2) the equilibrium tidal formula is fit for calculating the correction of all tidal waves; and (3) the calculation of 11 main tidal waves shows that the earth tidal correction in astronomical time and latitude observation is not the same as the ocean tidal one, in which the several main waves are only needed. It is necessary for the earth tidal correction to calculate as much as possible waves. Therefore the equilibrium tidal formula may more suitable in practice. Author

N86-11589# Academy of Sciences of the Ukrainian SSR, Kiev (USSR). Astronomical Observatory.
ON REDUCING THE EFFECT OF HORIZONTAL DISPLACEMENTS OF THE LITHOSPHERIC PLATES FROM THE OBSERVATIONS CARRIED OUT BY GLOBAL GEODYNAMIC NETWORK (ON EXAMPLE THE GEOSS-REA NETWORK) c46
Ya. S. Yatskiv and N. T. Mironov *In* Academy of Sciences of the GDR Proc. of the 5th Intern. Symp. Geodesy and Phys. of the Earth, Pt. 2 1985 p 150-155 refs In RUSSIAN. ENGLISH summary (For primary document see N86-11568 02-42)
Avail: NTIS HC A09/MF A01

On the base of plate tectonic model RM2 the displacements of the lithospheric plates relative to the EURA plate are calculated. This modified relative model is called RM2-REA. Relative changes of angular distances between the stations predicted by means of the RM2-REA model are compared with the observational data (BIH data and Doppler satellite data for the periods 1968-1982 and 1973-1983 respectively. It is shown that the RM2-REA model does not contradict to the observations and could be used for the reduction purpose. G.L.C.

N86-11590# Kiel Univ. (West Germany). Inst. of Geophysics.
ANELASTICITY IN THE EARTH'S MANTLE: IMPLICATIONS FOR THE FREQUENCY DEPENDENCE OF LOVE NUMBERS c46
J. Zschau *In* Academy of Sciences of the GDR Proc. of the 5th Intern. Symp. Geodesy and Phys. of the Earth, Pt. 2 1985 p 160 (For primary document see N86-11568 02-42)
Avail: NTIS HC A09/MF A01

Analytical formulas are developed which describe the anelastic and viscous behavior of solids by means of an absorption band as deduced from a Gaussian distribution of relaxation times. These formulas are applied to the Earth's mantle in order to explain post glacial rebound data as well as various observations of anelasticity over a frequency range of more than seven decades including the seismological band as well as free oscillations and the Chandler Wobble. In fitting the parameters of the absorption band to the observations, the effect of composition, structure, phase transitions, pressure and temperature on the anelastic behavior is accounted for by making use of the empirical relationship G'=CI/S sub o were G' is Gibb's free energy of a relaxation process, I the seismic parameter S sub o ambient density and c a constant which is only dependent on the relaxation mechanism itself. This relationship is shown to be well fulfilled for solid state self diffusion in various solids like metals, halides and oxides including minerals important in the mantle. Author

N86-11591# Academy of Sciences, Potsdam (East Germany). Zentralinst. fuer Physik der Erde.
PROCEEDINGS OF THE 5TH INTERNATIONAL SYMPOSIUM GEODESY AND PHYSICS OF THE EARTH, PART 3
1985 189 p refs In ENGLISH and GERMAN Symp. held in Magdeburg, East Germany, 23-29 Sep. 1984 3 Vol.
(Rept-81-Pt-3; ISSN-0514-8790) Avail: NTIS HC A08/MF A01

Studies of recent earth crust movements of local, regional and global importance is reported in this conference. Overall this science is called geodynamics. The determination of the dynamic parameters of crustal blocks in relation to subsurface is discussed. The main source of independent numeric data analyzed are repeated geodetic measurements carried out by means of either surface or space techniques. For individual titles, see N86-11592 through N86-11617.

N86-11592# Research Inst. of Geodesy, Topography and Cartography, Prague (Czechoslovakia).
CRCM AND KAPG ACTIVITY IN RECENT CRUSTAL MOVEMENT STUDIES c46
Pavel Vyskocil *In* Academy of Sciences of the GDR Proc. of the 5th Intern. Symp. Geodesy and Phys. of the Earth, Pt. 3 1985 p 4-6 refs (For primary document see N86-11591 02-42)
Avail: NTIS HC A08/MF A01

Some results of the work of both organizations in the field of recent crustal movements are discussed. The results of recent crustal movement studies are published in national or international journals and presented at special symposia on recent crustal movements. These studies are briefly discussed. E.R.

N86-11593# Mezoegazdasagi es Elelmezesuegyi Ministerium, Budapest (Hungary). Orszagos Foldugyi es Terkepeszeti Hivatal.
ON THE WORKS AND RESULTS OF INVESTIGATIONS CONCERNING THE RECENT MOVEMENTS IN THE KARPATHO-BALKAN REGION c46
I. Joo *In* Academy of Sciences of the GDR Proc. of the 5th Intern. Symp. Geodesy and Phys. of the Earth, Pt. 3 1985 p 7-15 refs In GERMAN; ENGLISH summary (For primary document see N86-11591 02-42)
Avail: NTIS HC A08/MF A01

Information is given on the purpose, conditions and method of recent investigations of vertical crustal movements as well as on the results obtained so far. The applied geodetic and oceanographic data is presented together with their reliability and the standard error of derived velocities and absolute height data in tabular form. Derived height value differences between the mean sea levels of the three seas considered (Baltic, Black and Adriatic Seas) are also shown. By now joint adjustment and compilation of national maps of movements have been completed. The derivation of movement velocity gradients and their cartographic presentation is presented. Author

N86-11594# Niedersaechsisches Landesverwaltungsamt, Hanover (West Germany). Abt. Landesvermessung.
NORTH SEA COAST LEVELLING NET: A MODEL CASE FOR THE DETERMINATION OF VERTICAL MOVEMENTS IN WESTERN EUROPE c46
Wolfgang Augath and Hans Pelzer (Hannover Univ.) *In* Academy of Sciences of the GDR Proc. of the 5th Intern. Symp. Geodesy and Phys. of the Earth, Pt. 3 1985 p 16-25 refs (For primary document see N86-11591 02-42)
Avail: NTIS HC A08/MF A01

In Northern Germany, permanent tide gauge records have been available for investigations since about 1850. As a result of such investigations it was found that in the North Sea the mean sea level (MSL) seems to increase by an amount of approximately 2 mm/year being nearly twice the amount of the eustatic change of the MSL recorded all over the world. This result suggested a coastal subsidence of about 1 mm/year. In order to study this effect in more detail a special precise leveling net (North Sea Coast Leveling Net, NKN) was established after 1910 and observed repeatedly. A tendency toward land subsidence was discovered, the amounts determined lying within their statistical confidence regions. The Hanover analysis was established for the computation of vertical crustal movements. The computation and results are detailed. Author

N86-11595# Academy of Sciences, Potsdam (East Germany). Zentralinst. fuer Physik der Erde.
SPACE-TIME VARIATING GEOLOGICAL MASSES BY SPACE-TIME VARIATING GEODETIC MEASUREMENTS c43
K. Arnold *In its* Proc. of the 5th Intern. Symp. Geodesy and Phys. of the Earth, Pt. 3 1985 p 26-31 refs (For primary document see N86-11591 02-42)
Avail: NTIS HC A08/MF A01

The gravity measurements and the repeated levelings are the space-time variating geodetic measurements which are introduced in the deductions. The plausible hypothesis is presupposed that the recent crustal movement phenomenons which are here to be investigated cover spherical caps of smaller than 1000 kilometer diameter. The other recent crustal movement phenomenons existing at some other distant places exterior of this cap are approximatively supposed to influence not the space-time geodetic measurements within the considered area. The space-time variating geological masses are represented in terms of some point masses. A relation between these geological masses and the space-time geodetic measurements is derived. Author

N86-11596# Academy of Sciences, Potsdam (East Germany). Zentralinst. fuer Physik der Erde.
GEOKINEMATIC MODELS FOR THE GRAVIMETRIC W - E PROFILE OF THE GDR c46
W. Conrad, C. Elstner, G. Schwab, W. Schwahn, and S. Thomaschewski *In its* Proc. of the 5th Intern. Symp. Geodesy and Phys. of the Earth, Pt. 3 1985 p 32-43 refs (For primary document see N86-11591 02-42)
Avail: NTIS HC A08/MF A01

The gravimetric W - E profile of the GDR crosses in its western part the Central German - Polish main fault, which forms the transition from the high lying crystalline rocks to the mesozoic-cenozoic sedimentary basin. The net slip of the step fault is about 3 km. The strongest horizontal gradient of gravity in the European region occurs here. Starting from the geological-geophysical situation simple geokinematic models are built up for the interpretation of possible temporal gravity changes, whereby also movements of the Earth's surface were included: relative movements of different blocks and mass redistributions in different geotectonic levels (Upper mantle, Earth's crust and intrasedimentary processes). The deep seated dynamics of the block structure cause in the gravity field a contribution whose extend coincides with a possible subdivision of gravity changes on the W - E profile. The intrasedimentary dynamics may be considered as a noise at the different observation points. Author

N86-11597# Hungarian Academy of Sciences, Sopron. Geodetical and Geophysical Research Inst.
MATHEMATICAL TREATMENT OF VERTICAL MOVEMENTS c46
J. Czompo *In* Academy of Sciences of the GDR Proc. of the 5th Intern. Symp. Geodesy and Phys. of the Earth, Pt. 3 1985 p 44-50 refs (For primary document see N86-11591 02-42)
Avail: NTIS HC A08/MF A01

The vertical movement is an important geodynamic phenomenon both in regional as well as in local scale. Determination of the kinematical parameters (displacement, velocity and acceleration) is the principal task in the treatment of measured data. Presently, these parameters are usually determined at measured points and some interpolation method is used between these points. The problem is tackled by an analytical method. The observed surface is approximated by a 3D harmonic series in space and in time. An application example is given using DFT to describe the surface motion over a working coal mine. Author

N86-11598# Technische Univ., Dresden (East Germany). Sektion Geodaesie und Kartographie.
GEODIMETER NET FOR THE INVESTIGATION OF HORIZONTAL CRUSTAL DEFORMATIONS [GEODIMETER-NETZ ZUR UNTERSUCHUNG HORIZONTALER KRUSTENDEFORMATIONEN] c46
Marion Dost and Guenter Lorenz *In* Academy of Sciences of the GDR Proc. of the 5th Intern. Symp. Geodesy and Phys. of the Earth, Pt. 3 1985 p 51-54 refs In GERMAN; ENGLISH summary (For primary document see N86-11591 02-42)
Avail: NTIS HC A08/MF A01

In the German Democratic Republic investigations of horizontal Earth's crustal movements referred until now to the derivation of recent horizontal deformations from multiple observed triangulation nets. They were performed for 20 percent of the territory of the GDR. To obtain more detailed information on the dynamic behavior of the Earth's crust, a special net was established for the first time. It covers by means of a chain structure the most important geological perturbations of the test field Elbe valley zone. Special stress was laid upon the reciprocal surface visibility and the identity with numerous points of older triangulations. The applied GEODIMETER 600 distance meter proved to be successful for these tasks and permits an attempt to receive a new accuracy range. The mean positional error of m sub p = + or - 10 mm obtained for the net part measured until now, makes one optimistic in expecting a considerable more accurate derivation of horizontal deformations and stress. Author

N86-11599# Uppsala Univ. (Sweden). Dept. of Geodesy.
GAUSSIAN AND MEAN CURVATURES OF POSTGLACIAL LAND UPLIFT AS EXPANDED IN SURFACE SPHERICAL HARMONICS, AND THE ORIGIN OF EARTHQUAKES IN FENNOSCANDIA c46
Martin Ekman *In* Academy of Sciences of the GDR Proc. of the 5th Intern. Symp. Geodesy and Phys. of the Earth, Pt. 3 1985 p 55-70 refs (For primary document see N86-11591 02-42)
Avail: NTIS HC A08/MF A01

Formula for Gaussian and mean curvatures of postglacial land uplift, as expanded in a series of surface spherical harmonics, are derived. These are then applied in investigating if postglacial land uplift is an origin of earthquakes. It is found that the postglacial land uplift of Fennoscandia probably is the origin of the earthquakes along the whole Swedish coast of the Gulf of Bothnia as well as possibly of those in northernmost Sweden, the earthquakes occurring mainly where the Gaussian curvature of land uplift is great enough. No such relationship exists for the earthquakes of southeastern Norway/southwestern Sweden, which then probably do not originate from the land uplift. Author

N86-11600# Academy of Sciences (USSR), Moscow. Inst. of Physics of the Earth.
NEAR-SURFACE DEFORMATIONS AND STRESSES IN THE AREA OF THE TOLBACHIK GREAT FISSURE ERUPTION OF 1975-1976 (KAMCHATKA) FROM GEODETIC DATA c46
S. V. Enman *In* Academy of Sciences of the GDR Proc. of the 5th Intern. Symp. Geodesy and Phys. of the Earth, Pt. 3 1985 p 71-75 refs (For primary document see N86-11591 02-42)
Avail: NTIS HC A08/MF A01

The analysis of displacements of the points of the triangulation network covering the area of 40x60 km around the region of eruption is presented. Angle and linear measurements were carried out before eruption, during and after eruption. The formulas of mechanics were used to determine the parameters of deformations (values and direction of the principal strain axes, maximal shears, dilatation), the basic regularities in the deformation of the region of eruption were analyzed, and the stress values were calculated with regard to different observation periods. All calculations were made under assumption that the medium is continuous and homogeneous. Author

N86-11601# Mezoegazdasagi es Elelmezesuegyi Ministerium, Budapest (Hungary). Orszagos Foldugyi es Terkepeszeti Hivatal.
METHOD OF JOINT ADJUSTMENT OF HEIGHT DIFFERENCES AND VELOCITIES c46
M. Fury, J. Gergely (Foldmeresi Intezet, Budapest), and Zs. Nemeth (Foldmeresi Intezet, Budapest) *In* Academy of Sciences of the

GDR Proc. of the 5th Intern. Symp. Geodesy and Phys. of the Earth, Pt. 3 1985 p 76-78 refs (For primary document see N86-11591 02-42)
Avail: NTIS HC A08/MF A01

The preliminary investigations of Carpatho-Balkan Region's repeated leveling network led to the conclusion that the adjustment should be carried out in a way discussed herein. According to this method the height differences of the second leveling were adjusted jointly with the velocities computed from the first and second levelings. The algorithm of the rigorous adjustment and the weighting system of correlated quantities are presented. The computer program and the network are also discussed. The computation ran in computer HWB 66/20 in FORTRAN by sparse manner. The normal matrix was factorized by means of Gauss elimination. Author

N86-11602# Mezoegazdasagi es Elelmezesuegyi Ministerium, Budapest (Hungary). Orszagos Foldugyi es Terkepeszeti Hivatal.
PRINCIPLE OF THE CONSTRUCTION OF THE LINES OF THE REPEATED LEVELLING FOR THE INVESTIGATION OF THE VERTICAL MOVEMENT IN THE CARPATHO-BALKAN REGION (CBR) c46
M. Fury, J. Gergely (Foldmeresi Intezet, Budapest), and Zs. Nemeth (Foldmeresi Intezet, Budapest) *In* Academy of Sciences of the GDR Proc. of the 5th Intern. Symp. Geodesy and Phys. of the Earth, Pt. 3 1985 p 79-83 refs In GERMAN; ENGLISH summary (For primary document see N86-11591 02-42)
Avail: NTIS HC A08/MF A01

Former levelings were carried out with different reliability and protracted for a long time. The final result is doubtlessly influenced by the calculation carried out using the sum of the height differences on the lines led between the knot-points, the mean reliability and the time of measurement of the levelings, as the experimental adjustment showed. This effect can be overcome by carrying out the adjustment of the repeated leveling network with use of leveling sections of same reliability and in a shorter time interval, which extremely increase the volume of the work. Similar results can be obtained by the joint adjustment of the velocity values deduced from both levelings and the height be summed up between the knotpoints without neglecting. It is why the height difference of the second levelling, its reliability and the time of the measurement, as wel as the sum of velocity values deduced for each section and their weight reciprocals were drawn up for each line between the knotpoints in the CBR. Author

N86-11603# Bulgarian Academy of Science, Sofia. Central Lab. for Geodesy.
SOME GEODETIC ASPECTS OF THE PROBLEM OF CHECKING THE PLATE-TECTONIC MODEL OF SEISMICITY IN SOUTH-EASTERN EUROPE c46
N. I. Georgiev, I. N. Totomanov, and C. G. Darakciev *In* Academy of Sciences of the GDR Proc. of the 5th Intern. Symp. Geodesy and Phys. of the Earth, Pt. 3 1985 p 84-89 refs (For primary document see N86-11591 02-42)
Avail: NTIS HC A08/MF A01

In the last years, due to the increased accuracy and applicability of the laser range finders of third generation and radio interferometric measuring systems of stationary and mobile types, the satellite geodesy, with its own methods and means, enters in the regional geodynamic investigations. One of the problems is the determination of the recent movements of large Earth's crustal blocks in seismoactive regions, in order to elucidate the mechanism of generation and manifestation of strong earthquakes. Here on the basis of the modern geological-geophysical conception on the mechanism of generating strong earthquakes and volcanic activity in southeastern Europe, some methodical aspects of possible geodetic investigations in the region are discussed. Author

N86-11604# Eidgenoessische Landestopographie, Bern (Switzerland).
RECENT CRUSTAL MOVEMENTS AND GEOPHYSICAL INTERPRETATION OF GEODYNAMIC PROCESSES IN THE ALPINE MOUNTAIN BELT c46
E. Gubler and H.-G. Kahle (Eidgenoessische Technische Hochschule, Zurich) *In* Academy of Sciences of the GDR Proc. of the 5th Intern. Symp. Geodesy and Phys. of the Earth, Pt. 3 1985 p 90-97 refs (For primary document see N86-11591 02-42)
Avail: NTIS HC A08/MF A01

It is a well-known fact that the surface phenomena of global plate tectonics are most convincingly seen and felt along the boundaries of the moving lithospheric plates. These boundaries are morphologically expressed as mild-ocean ridges or as subduction zones such as deep sea trenches or Himalayan/Alpine fold belts, the latter of which are the subject of this paper. On a global scale, there are kinematic models giving an idea of what kind of rates can be expected. This is due to the fact that magnetic sea floor spreading anomalies are missing in the Alpine environment. On the other hand, the structure and kinematics of the Apulian microplate are of major interest to Switzerland because its northern boundary seems to be formed by the Alpine chain. In Switzerland there are some 14 special study groups actively working in this field of geodynamics. This paper is restricted to the geodetic and gravity studies. With emphasis on the assumed northern boundary of the Apulian microplate, the kinematics of relative plate movements in the Alpine area were investigated. A simplified tectonic map of this region is shown. B.W.

N86-11605# Karlova Univ., Prague (Czechoslovakia).
DETERMINATION OF CRUSTAL MOVEMENTS IN THE HIGH TATRA MOUNTAINS c46
L. Hradilek *In* Academy of Sciences of the GDR Proc. of the 5th Intern. Symp. Geodesy and Phys. of the Earth, Pt. 3 1985 p 98-99 refs (For primary document see N86-11591 02-42)
Avail: NTIS HC A08/MF A01

A method of three-dimensional triangulation is used for determining the crustal movements in the region of the high mountain ridges where the geodetic leveling cannot be performed. The method is based on integrated observations of both horizontal and vertical angles, distances, spirit leveling lines, deflections of the vertical, and on combine processing of all observed data. Network design is discussed. B.W.

N86-11606# Geodetic Inst., Helsinki (Finland).
FINNISH MEASUREMENTS OF THE FENNOSCANDIAN LAND UPLIFT GRAVITY LINES IN FINLAND 1966-1984 c46
Aimo Kiviniemi *In* Academy of Sciences of the GDR Proc. of the 5th Intern. Symp. Geodesy and Phys. of the Earth, Pt. 3 1985 p 100-102 refs (For primary document see N86-11591 02-42)
Avail: NTIS HC A08/MF A01

According to the isostatic theory, land uplift reduces gravity. In Finland the connection between land uplift and gravity has been studied with high precision gravity measurements over the past 18 years. The results show that, although there are significant variations in gravity, the variations are not linear with the time but rather periodic ones. Author

N86-11607# Technische Univ., Dresden (East Germany).
STATIONARY HYDROSTATIC PRECISION TILTMETER SYSTEM [STATIONAERES HYDROSTATISCHES PRAEZISIONS-NEIGUNGSMESSSYSTEM] c46
G. Lorenz *In* Academy of Sciences of the GDR Proc. of the 5th Intern. Symp. Geodesy and Phys. of the Earth, Pt. 3 1985 p 102-105 refs In GERMAN; ENGLISH summary (For primary document see N86-11591 02-42)
Avail: NTIS HC A09/MF A01

About twenty years ago, a tiltmeter station was established for investigations of recent crustal movements in the most important test area of the GDR. The station is located in a sandrock tunnel system of more than 50 m, the measuring components are orientated in NNW- and ENE-direction. Standard sets of the precision instruments were used with some new constructions and auxiliary equipment. The reliability of the present measuring system is proved if the earth-tides are compared with measuring data. This system is qualified for the investigations of tectonic block tilting. Author

N86-11608# Karlsruhe Univ. (West Germany). Geodetic Inst.
HEIGHT CHANGES AND RECENT CRUSTAL MOVEMENTS IN THE RHENISH MASSIF AND IN THE UPPER RHINE GRABEN RIFT c46
H. Maelzer *In* Academy of Sciences of the GDR Proc. of the 5th Intern. Symp. Geodesy and Phys. of the Earth, Pt. 3 1985 105-112 refs (For primary document see N86-11591 02-42)
Avail: NTIS HC A08/MF A01

Height changes are computed aiming at the investigation of recent crustal movements for the Rhenish Massif and the northern Rhine Graben area. For that purpose results of first order leveling data of the Departments of Ordnance Survey are used. The Rhenish Massif is not lifting like a rigid block. At the present time uplift is restricted to limited areas. In the eastern part tendencies of alternating uplift and subsidence exist, and the western part is characterized by uplift and stability. The northern Rhine Graben area is not only an area of subsidence but also an area of uplift. A trend analysis of recent vertical crustal movements shows tilts in the directions NS and WE. Author

N86-11609# Academy of Sciences (USSR), Moscow. Inst. of Physics of the Earth.
RECENT VERTICAL CRUSTAL MOVEMENTS OF THE CARPATHIAN-BALKAN REGION AND THEIR RELATIONSHIP WITH NEOTECTONIC MOVEMENTS AND GEOPHYSICAL FIELDS c46
V. A. Magnitsky, A. F. Grachev, I. V. Kalashnikova, and V. V. Bronguleev *In* Academy of Sciences of the GDR Proc. of the 5th Intern. Symp. Geodesy and Phys. of the Earth, Pt. 3 1985 p 113-123 refs (For primary document see N86-11591 02-42)
Avail: NTIS HC A08/MF A01

On the basis of correlation analysis the high degree of inheritance of recent vertical crustal movements from neotectonic movements has been established as for the whole of the Carpathian-Balkan region. Recent vertical crustal movements, neotectonic movements and crustal thickness have a stable reverse correlation with heat flow. This suggests that thermal heating is a probable cause of neotectonic and recent tectonic activity. As a base for comparative analysis the new map of recent crustal movements was used. The map of neotectonic movements in a scale of 1 : 1 000 000, compiled by G. I. Raisner and the international heat flow map of Europe were also used. The boundaries of the studied region and the major structure units are shown. The whole territory was divided into equal quadrants 0 deg 50 x 0 deg 30 and for every quadrant the next average values were determined: recent crustal movements velocity, amplitude of neotectonic movements and crustal thickness. The 290 measurements have been used for calculation of statistics (mean values and standard deviations), correlation coefficients and factors (principal component analysis). B.W.

N86-11610# Academy of Sciences (USSR), Moscow.
ON THE RELATION BETWEEN RECENT CRUSTAL MOVEMENTS, THE SURFACE OF THE BASEMENT COMPLEX AND NEOTECTONIC DISPLACEMENTS OF THE EAST-EUROPEAN PLATFORM c46
V. A. Magnitsky, A. F. Grachev, I. V. Kalashnikova, and V. V. Bronguleev *In* Academy of Sciences of the GDR Proc. of the 5th Intern. Symp. Geodesy and Phys. of the Earth, Pt. 3 1985 p 124-130 refs (For primary document see N86-11591 02-42)
Avail: NTIS HC A08/MF A01

The problem of the origin of recent crustal movements is one of the most important problems in the field of the Earth's sciences. There exist only a few natural phenomena permitting to obtain the direct information about the processes in the interior of the Earth now in action. Recent crustal movements are one of such phenomena. In the present paper some results are reported of investigations of recent vertical movements of the Earth crust within the western part of East-European platform (to the west from longitude 42 deg E). This region represents an area with slight tectonic activity since Neogen. All the mentioned maps of geophysical and geological fields were treated by the method of trend analysis. As a result schematic maps of the regional component and their residuals were obtained from each field respectively (the radius of averaging is 1000 to 1500 km). B.W.

N86-11611# Technische Univ., Dresden (East Germany).
SIGNIFICANCE TESTS OF RECENT VERTICAL CRUSTAL MOVEMENTS BY CORRELATION FUNCTIONS Abstract Only c46
S. Meier *In* Academy of Sciences of the GDR Proc. of the 5th Intern. Symp. Geodesy and Phys. of the Earth, Pt. 3 1985 p 131 (For primary document see N86-11591 02-42)
Avail: NTIS HC A08/MF A01

Empirically estimates autocorrelation functions (ACF) of planar, homogeneous isotropic processes of the vertical rate of Earth's recent crustal movements in Central and East Europe are tested by a comparison with ACF's of band filtered leveling errors concerning their geophysical reality. The ACF of the vertical rate in the Pannonian Basin may be coordinated to a real process of movement, the others are explainable, either without restriction or by deducting a linear trend, by error correlations. The data material obviously includes no further predictable movement signals, except the above trend, the partial area Pannonian Basin, and possible local point movements. Therefore, a comprehensive revision of the appropriate maps with isolines of the vertical rate is necessary. Author

N86-11612# Geodetic Inst., Helsinki (Finland).
COMPARISONS OF DIFFERENT OBSERVATION METHODS OF A LACOSTE AND ROMBERG G GRAVIMETER c46
Leena Mikkola *In* Academy of Sciences of the GDR Proc. of the 5th Intern. Symp. Geodesy and Phys. of the Earth, Pt. 3 1985 p 132-135 refs (For primary document see N86-11591 02-42)
Avail: NTIS HC A08/MF A01

The LaCoste and Romberg gravimeters can be observed by three different methods: optically, with the gravimeters' own galvanometers and with digital voltmeters together with electronic filters. Field measurements and laboratory tests have been made by these methods with LCR G600 in the Finnish Geodetic Institute for comparing the accuracy of the method. Author

N86-11613# Bulgarian Academy of Science, Sofia. Lab. for Geotechnics.
STATISTICAL ANALYSIS AND INTERPRETATION OF EARTH CRUSTAL MOVEMENTS IN NORTHEAST BULGARIA [STATISTISCHE ANALYSE UND INTERPRETATION DER ERDKRUSTENBEWEGUNGEN IN NORDOSTBULGARIEN] c46
G. Milev and I. N. Totomanov *In* Academy of Sciences of the GDR Proc. of the 5th Intern. Symp. Geodesy and Phys. of the Earth, Pt. 3 1985 p 136-139 refs (For primary document see N86-11591 02-42)
Avail: NTIS HC A08/MF A01

A statistical analysis of the changes in height differences of representative bench marks, measured during two periods of the leveling net in northeast Bulgaria, is made. Considerable differences in exceedings are found which indicate that real changes in the heights of the leveling points exist. By means of velocity maps of the contemporary vertical movements on the same territory, with the aid of a suitable statistical test, it is found that the vertical movements on both sides of the Tvardica fault are insignificant. The methods applied and the results obtained are a contribution to the complex investigations of the contemporary dynamics of the region. Author

N86-11614# Hungarian Academy of Sciences, Sopron. Geodetic and Geophysical Research Inst.
A NEW APPARATUS FOR TESTING BUBBLE VIALS, ELECTRONIC LEVELS AND AUTOMATIC LEVELS c35
J. Somogyi, K. Krausz, and Gy. Mentes *In* Academy of Sciences of the GDR Proc. of the 5th Intern. Symp. Geodesy and Phys. of the Earth, Pt. 3 1985 p 140-147 refs (For primary document see N86-11591 02-42)
Avail: NTIS HC A08/MF A01

An important task of geodetic research is to increase the accuracy. Several significant results have been achieved in this field leading to an increase of the role of geodesy in geosciences, e.g., determination of geometric and physical parameters needed for geodynamical investigations. The accuracy of astrogeodetic measurements and high precision leveling must be also increased. A part of this task is a more correct qualification of different levels and leveling instruments. For this purpose a new level trier/tiltmeter has been constructed. The main aspects of the construction of this new apparatus are the following: (1) more accurate measurement of the tilt angle; (2) more accurate measurement of the bubble movement; (3) electronic sensing and digital display of the measured values; (4) one line connection to the computer; and (5) decrease of the effect of outer disturbances during measurements and comfortable handling. B.W.

N86-11615# Bulgarian Academy of Science, Sofia. Central Lab. for Geodesy.

RELATION BETWEEN EARTHQUAKE FOCAL INTENSITY AND RECENT VERTICAL EARTH'S CRUSTAL MOVEMENTS IN THE RILA-RHODOPE SEISMIC REGION c46

Ivan N. Totomanov *In* Academy of Sciences of the GDR Proc. of the 5th Intern. Symp. Geodesy and Phys. of the Earth, Pt. 3 1985 p 148-155 refs (For primary document see N86-11591 02-42)

Avail: NTIS HC A08/MF A01

The stable statistical relation is studied between the maximum magnitude Y of expected earthquakes with foci in the Earth's crust and the vertical velocity X of recent crustal movements, in the mountainous region of southwestern Bulgaria characterized by a particularly high seismic and tectonic activity. The two dimensional random variate (X,Y) is presented by its sample (Xk, Yk), k = 1, 2,..., 60 composed by appropriate smoothed estimates according to data of the most recent investigations. The sampling (joint and respective marginal) distributions of (X, Y) are determined and examined. Statistical hypotheses are tested and the respective recent geokinematic and tectonic predestination of the seismic activity in the Rila-Rhodope seismic region is argued in terms of the best fit, to the empirical data, regression polynomial of Y with respect to X. A comparison is made between results obtained on the region under examination and corresponding data of earlier studies. Author

N86-11616# Research Inst. of Geodesy, Topography and Cartography, Prague (Czechoslovakia).

DYNAMICS OF THE BOHEMIAN MASSIF c46

Pavel Vyskocil *In* Academy of Sciences of the GDR Proc. of the 5th Intern. Symp. Geodesy and Phys. of the Earth, Pt. 3 1985 p 156-159 refs (For primary document see N86-11591 02-42)

Avail: NTIS HC A08/MF A01

The Bohemian Massif is a solid block surrounded by the Alps and Carpathians from south and south-east respectively. The main idea of the presented paper is the controlling role of the Alps at the dynamics of the Bohemian Massif. The initial assumption is discussed with respect to the results of new repeated levelings, local horizontal measurements as well as to the disturbance lines determined from satellite images. In addition the results of local horizontal and vertical remeasurements performed at the test area of Lisov, southern Bohemia, are taken into consideration. The discussion of mentioned data leads to conclusions on the possible role of the Alpine pressure as a driving force in dynamics of the Bohemian Massif. Author

N86-11617# Academy of Sciences, Potsdam (East Germany). Zentralinst. fuer Physik der Erde.

AN OPTIMUM USE OF SEA-LEVEL RECORDINGS c46

H. Weise *In its* Proc. of the 5th Intern. Symp. Geodesy and Phys. of the Earth, Pt. 3 1985 p 160-168 refs (For primary document see N86-11591 02-42)

Avail: NTIS HC A08/MF A01

A reference niveau is necessary for proof of vertical recent crustal movements. The undisturbed surface of the sea is a suitable reference niveau. It is deduced from continuous sea level recordings at the adjacent coasts of most countries. For a significant proof it is necessary to presume: (1) modern measurement techniques, with adequate resolution in time and area; (2) homogeneous data collections for a long time range; and (3) careful analysis methods for treatment of measuring data. Propositions for working modus are offered in connection with this geoscientific assertion. Author

43 EARTH RESOURCES

Includes remote sensing of earth resources by aircraft and spacecraft; photogrammetry; and aerial photography.

For instrumentation see *35 Instrumentation and Photography.*

N86-11618*# Jet Propulsion Lab., California Inst. of Tech., Pasadena.

PROCEEDINGS OF THE AIRBORNE IMAGING SPECTROMETER DATA ANALYSIS WORKSHOP

Gregg Vane, ed. and Alexander F. H. Goetz, ed. 15 Jun. 1985 180 p refs Workshop held in Pasadena, Calif., 8-10 Apr. 1985 Original contains color imagery. Original photography may be purchased from the EROS Data Center, Sioux Falls, S.D. 57198 ERTS

(Contract NAS7-918)

(E86-10001; NASA-CR-176210; JPL-Pub-85-41; NAS 1.26:176210) Avail: NTIS HC A09/MF A01 CSCL 05B

The Airborne Imaging Spectrometer (AIS) Data Analysis Workshop was held at the Jet Propulsion Laboratory on April 3 to 10, 1985. It was attended by 92 people who heard reports on 30 investigations currently under way using AIS data that have been collected over the past two years. Written summaries of 27 of the presentations are in these Proceedings. Many of the results presented at the Workshop are preliminary because most investigators have been working with this fundamentally new type of data for only a relatively short time. Nevertheless, several conclusions can be drawn from the Workshop presentations concerning the value of imaging spectrometry to Earth remote sensing. First, work with AIS has shown that direct identification of minerals through high spectral resolution imaging is a reality for a wide range of materials and geological settings. Second, there are strong indications that high spectral resolution remote sensing will enhance the ability to map vegetation species. There are also good indications that imaging spectrometry will be useful for biochemical studies of vegetation. Finally, there are a number of new data analysis techniques under development which should lead to more efficient and complete information extraction from imaging spectrometer data. The results of the Workshop indicate that as experience is gained with this new class of data, and as new analysis methodologies are developed and applied, the value of imaging spectrometry should increase. For individual titles, see N86-11619 through N86-11644.

N86-11619*# Jet Propulsion Lab., California Inst. of Tech., Pasadena.

MINERALOGICAL MAPPING IN THE CUPRITE MINING DISTRICT, NEVADA c46

Alexander F. H. Goetz and Vinay Srivastava *In its* Proc. of the Airborne Imaging Spectrometer Data Anal. Workshop 15 Jun. 1985 p 22-31 refs Original contains color imagery. Original photography may be purchased from the EROS Data Center, Sioux Falls, S.D. 57198 ERTS (For primary document see N86-11618 02-43)

Avail: NTIS HC A09/MF A01 CSCL 08G

The airborne imaging spectrometer (AIS) has provided for the first time, the possibility to map mineralogical constituents in the Earth's surface and thus has enormously increased the value of remote-sensing data as a tool in the solution of geologic problems. The question addressed with AIS at Cuprite was how well could the mineral components at the surface of a hydrothermal alteration zone be detected, identified and mapped? The question was answered positively and is discussed. A relatively rare mineral, buddingtonie, that could not have been detected by conventional means, was discovered and mapped by the use of AIS. Author

N86-11620*# Jet Propulsion Lab., California Inst. of Tech., Pasadena.

REMOTE STRATIGRAPHIC ANALYSIS: COMBINED TM AND AIS RESULTS IN THE WIND RIVER/BIGHORN BASIN AREA, WYOMING

H. R. Lang, E. D. Paylor, and S. Adams *In its* Proc. of the Airborne Imaging Spectrometer Data Anal. Workshop 15 Jun. 1985 p 32-34 ref ERTS (For primary document see N86-11618 02-43)

Avail: NTIS HC A09/MF A01 CSCL 08B

An in-progress study demonstrates the utility of airborne imaging spectrometer (AIS) data for unraveling the stratigraphic evolution of a North American, western interior foreland basin. AIS data are used to determine the stratigraphic distribution of mineralogical facies that are diagnostic of specific depositional environments. After wavelength and amplitude calibration using natural ground targets with known spectral characteristics, AIS data identify calcite, dolomite, gypsum and montmorillonite-bearing strata in the Permian-Cretaceous sequence. Combined AIS and TM results illustrate the feasibility of spectral stratigraphy, remote analysis of stratigraphic sequences. Author

N86-11621*# Stanford Univ., Calif. Dept. of Applied Earth Sciences.

FIELD UTILIZATION AND ANALYSIS OF AIS 128-CHANNEL IMAGERY USING MICROCOMPUTERS: APPLICATION TO YERINGTON, NEVADA FIELD AREA

R. J. P. Lyon and Kai Lanz *In* JPL Proc. of the Airborne Imaging Spectrometer Data Anal. Workshop 15 Jun. 1985 p 35-40 refs Original contains imagery. Original photography may be purchased from the EROS Data Center, Sioux Falls, S.D. 57198 ERTS (For primary document see N86-11618 02-43)

Avail: NTIS HC A09/MF A01 CSCL 05B

Geologists in exploration need to be able to determine the mineral composition of a given outcrop, and then proceed to another in order to carry out the process of geologic mapping. Since April 1984 researchers have been developing a portable microcomputer-based imaging system (with a grey-scale of 16 shades of amber), which were demonstrated during the November 1984 GSA field trip in the field at Yerington, NV. A color-version of the same technology was recently demonstrated. The portable computer selected is a COLBY 10-Megabyte, hard disk-equipped repackaged-IBM/XT, which operates on either 110/220 VAC or on 12VDC from the cigarette lighter in a field vehicle. A COMPAQ PLUS or an IBM Portable will also work on modified software. The underlying concept is that the atmospheric transmission and surface albedo/slope terms are multiplicative, relating the spectral irradiance to the spectral color of the surface materials. Thus, the spectral color of a pixel remains after averaged log-albedo and log-irradiance have been estimated. All these steps can be carried out on the COLBY microcomputer, using 80 image lines of the 128-channel, 12-bit imagery. Results are shown for such an 80-line segment, showing the identification of an O-H bearing mineral group (of slightly varying specific characters) on the flight line. Author

N86-11622*# Jet Propulsion Lab., California Inst. of Tech., Pasadena.

PRELIMINARY ANALYSIS OF AIS SPECTRAL DATA ACQUIRED FROM SEMI-ARID SHRUB COMMUNITIES IN THE OWENS VALLEY, CALIFORNIA

Susan L. Ustin (California Univ., Berkeley) and Barrett N. Rock *In its* Proc. of the Airborne Imaging Spectrometer Data Anal. Workshop 15 Jun. 1985 p 41-45 refs ERTS (For primary document see N86-11618 02-43)

Avail: NTIS HC A09/MF A01 CSCL 05B

Spectral characteristics of semic-arid plant communities using 128 channel airborne imaging spectrometer (AIS) data acquired on October 30, 1984. Both field and AIS spectra of vegetation were relatively featureless and differed from substrate spectra primarily in albedo. Unvegetated sand dunes were examined to assess spectral variation resulting from topographic irregularity. Although shrub cover as low as 10% could be detected on relatively flat surfaces, such differences were obscured in more heterogeneous terrain. Sagebrush-covered fans which had been scarred by fire were studied to determine the effect of changes in plant density on reflectance. Despite noise in the atmospherically corrected spectra, these provide better resolution of differences in plant density than spectra which are solar-corrected only. A high negative correlation was found between reflectance and plant cover in areas which had uniform substrates and vegetation types. A lower correlation was found where vegetation and substrates were more diverse. Author

N86-11623*# Jet Propulsion Lab., California Inst. of Tech., Pasadena.

AIS SPECTRA FOR STRESSED AND UNSTRESSED PLANT COMMUNITIES IN THE CAROLINA SLATE BELT

Diane E. Wickland *In its* Proc. of the Airborne Imaging Spectrometer Data Anal. Workshop 15 Jun. 1985 p 46-50 refs ERTS (For primary document see N86-11618 02-43)

Avail: NTIS HC A09/MF A01 CSCL 05B

Airborne imaging spectrometer (AIS) data were collected over a number of derelict heavy metal mine sites in the Carolina slate belt of North Carolina. A 32 channel (1156 to 1456 nm) data set was acquired in October, 1983 at the time of peak fall foliage display, and a 128 channel (1220 to 2420) data set was acquired near the end of the spring leaf flush in May, 1984. Spectral curves were extracted from the AIS data for differing ground cover types (e.g., pine forests, mixed deciduous forests, mine sites, and pastures). Variation in the width of an absorption feature located at approximately 1190 nm has been related to differences in forest type. Small differences in the location and shape of features in the near infrared plateau (1156 to 1300 nm) and the region 2000 to 2420 nm have yet to be evaluated. Because these variations were subtle, and because atmospheric effects were apparent in the data, high priority must be assigned to devising a means of removing atmospheric effects from AIS spectra. Author

N86-11624*# Jet Propulsion Lab., California Inst. of Tech., Pasadena.

SPECTRAL CHARACTERIZATION OF SUSPECTED ACID DEPOSITION DAMAGE IN RED SPRUCE (PICEA RUBENS) STANDS FROM VERMONT c45

James E. Vogelmann and Barrett N. Rock *In its* Proc. of the Airborne Imaging Spectrometer Data Anal. Workshop 15 Jun. 1985 p 51-55 refs ERTS (For primary document see N86-11618 02-43)

Avail: NTIS HC A09/MF A01 CSCL 13B

In an attempt to demonstrate the utility of remote sensing systems to monitor sites of suspected acid rain deposition damage, intensive field activities, coupled with aircraft overflights, were centered on red spruce stands in Vermont during August and September of 1984. Remote sensing data were acquired using the Airborne Imaging Spectrometer, Thematic Mapper Simulator, Barnes Model 12 to 1000 Modular Multiband Radiometer and Spectron Engineering Spectrometer (the former two flown on the NASA C-130; the latter two on A Bell UH-1B Iroquois Helicopter). Field spectral data were acquired during the week of the August overflights using a high spectral resolution spectrometer and two broad-band radiometers. Preliminary analyses of these data indicate a number of spectral differences in vegetation between high and low damage sites. Some of these differences are subtle, and are observable only with high spectral resolution sensors; others are less subtle and are observable using broad-band sensors. Author

N86-11625*# Nevada Univ., Reno. School of Mines.

A FIRST LOOK AT AIRBORNE IMAGING SPECTROMETER (AIS) DATA IN AN AREA OF ALTERED VOLCANIC ROCKS AND CARBONATE FORMATIONS, HOT CREEK RANGE, SOUTH CENTRAL NEVADA

Sandra C. Feldman, James V. Taranik, and David A. Mouat (Stanford Univ.) *In* JPL Proc. of the Airborne Imaging Spectrometer

Data Anal. Workshop 15 Jun. 1985 p 56-61 refs ERTS (For primary document see N86-11618 02-43)
Avail: NTIS HC A09/MF A01 CSCL 08G

Three flight lines of Airborne Imaging Spectrometer (AIS) data were collected in 128 bands between 1.2 and 2.4 microns in the Hot Creek Range, Nevada on July 25, 1984. The flight lines are underlain by hydrothermally altered and unaltered Paleozoic carbonates and Tertiary rhyolitic to latitic volcanics in the Tybo mining district. The original project objectives were to discriminate carbonate rocks from other rock types, to distinguish limestone from dolomite, and to discriminate carbonate units from each other using AIS imagery. Because of high cloud cover over the prime carbonate flight line and because of the acquisition of another flight line in altered and unaltered volcanics, the study has been extended to the discrimination of alteration products. In an area of altered and unaltered rhyolites and latites in Red Rock Canyon, altered and unaltered rock could be discriminated from each other using spectral features in the 1.16 to 2.34 micron range. The altered spectral signatures resembled montmorillonite and kaolinite. Field samples were gathered and the presence of montmorillonite was confirmed by X-ray analysis. Author

N86-11626*# Washington Univ., Seattle. Dept. of Geological Sciences.

INTERPRETATION OF AIS IMAGES OF CUPRITE, NEVADA USING CONSTRAINTS OF SPECTRAL MIXTURES

Milton O. Smith and John B. Adams *In* JPL Proc. of the Airborne Imaging Spectrometer Data Anal. Workshop 15 Jun. 1985 p 62-67 refs ERTS (For primary document see N86-11618 02-43)
Avail: NTIS HC A09/MF A01 CSCL 05B

A technique is outlined that tests the hypothesis Airborne Imaging Spectrometer (AIS) image spectra are produced by mixtures of surface materials. This technique allows separation of AIS images into concentration images of spectral endmembers (e.g., surface materials causing spectral variation). Using a spectral reference library it was possible to uniquely identify these spectral endmembers with respect to the reference library and to calibrate the AIS images. Author

N86-11627*# Nebraska Univ., Lincoln.

EVALUATION OF AIS DATA FOR AGRONOMIC AND RANGELAND VEGETATION: PRELIMINARY RESULTS FOR AUGUST 1984 FLIGHT OVER NEBRASKA SANDHILLS AGRICULTURAL LABORATORY

Blaine L. Blad, Patrick J. Starks, Cynthia Hays, and Bronson R. Gardner (Standard Oil, Cleveland, Ohio) *In* JPL Proc. of the Airborne Imaging Spectrometer Data Anal. Workshop 15 Jun. 1985 p 68-70 ref ERTS (For primary document see N86-11618 02-43)
Avail: NTIS HC A09/MF A01 CSCL 05B

Since 1978 scientists from the Center for Agricultural Meteorology and Climatology at the University of Nebraska have been conducting research at the Sandhills Agricultural Laboratory on the effects of water stress on crop growth, development and yield using remote sensing techniques. We have been working to develop techniques, both remote and ground-based, to monitor water stress, phenological development, leaf area, phytomass production and grain yields of corn, soybeans and sorghum. Because of the sandy soils and relatively low rainfall at the site it is an excellent location to study water stress without the necessity of installing expensive rainout shelters. The primary objectives of research with the airborne imaging spectrometer (AIS) data collected during an August 1984 flight over the Sandhills Agricultural Laboratory are to evaluate the potential of using AIS to: (1) discriminate crop type; (2) to detect subtle architectural differences that exist among different cultivars or hybrids of agronomic crops; (3) to detect and quantify, if possible, the level of water stress imposed on the crops; and (4) to evaluate leaf area and biomass differences for different crops. Author

N86-11628*# Standard Oil Co., Cleveland, Ohio.

SITE DESCRIPTION FOR THE UNIVERSITY OF NEBRASKA'S SANDHILLS AGRICULTURAL LABORATORY

B. R. Gardner and Blaine L. Blad (Nebraska Univ., Lincoln) *In* JPL Proc. of the Airborne Imaging Spectrometer Data Anal. Workshop 15 Jun. 1985 p 71-73 ERTS (For primary document see N86-11618 02-43)
Avail: NTIS HC A09/MF A01 CSCL 08B

The Sandhills Agricultural Laboratory is operated by the University of Nebraska. The laboratory is located in the south-central part of the Nebraska Sandhills near Tryon, Nebraska (41 deg. 37' N; 100 deg. 50' W). The laboratory is surrounded on the west and south by native rangeland vegetation, on the south by a large field of corn irrigated by a center pivot, and on the east by wheat stubble. This site is appropriate for moisture stress studies since rainfall is almost always inadequate to meet evaporative demands of agricultural crops during most of the growing season and the sandy soils (Valentine fine sand) at the site do not store large quantities of water. Various levels of water stress are achieved through irrigation from solid set sprinklers. Author

N86-11629*# Nebraska Univ., Lincoln. Remote Sensing Center.

PRELIMINARY EVALUATION OF AIS SPECTRA ALONG A TOPOGRAPHIC/MOISTURE GRADIENT IN THE NEBRASKA SANDHILLS

Donald C. Runquist *In* JPL Proc. of the Airborne Imaging Spectrometer Data Anal. Workshop 15 Jun. 1985 p 74-78 refs ERTS (For primary document see N86-11618 02-43)
Avail: NTIS HC A09/MF A01 CSCL 08B

Six spectral plots, each summarizing single-pixel reflectance for 128 channels of Airborne Imaging Spectrometer (AIS) data, were examined. The six sample pixels were located along a topographic/moisture gradient from lake surface to dune top in the Nebraska Sandhills. AIS spectra for various moisture regimes/vegetative zones appear quite logical, with a general positive relationship between increasing elevation (i.e., decreasing access of plant roots to water) and increasing reflectance in the spectral regions diagnostic of leaf-water content (i.e., bands centered on 1.65 and 2.20 microns). Author

N86-11630*# Nebraska Univ., Lincoln. Dept. of Agronomy.

THE USE OF AIS DATA FOR IDENTIFYING AND MAPPING CALCAREOUS SOILS IN WESTERN NEBRASKA

Scott A. Samson *In* JPL Proc. of the Airborne Imaging Spectrometer Data Anal. Workshop 15 Jun. 1985 p 79-83 ERTS (For primary document see N86-11618 02-43)
Avail: NTIS HC A09/MF A01 CSCL 05B

The identification of calcareous soils, through unique spectral responses of the vegetation to the chemical nature of calcareous soils, can improve the accuracy of delineating the boundaries of soil mapping units over conventional field techniques. The objective of this experiment is to evaluate the use of the Airborne Imaging Spectrometer (AIS) in the identification and delineation of calcareous soils in the western Sandhills of Nebraska. Based upon statistical differences found in separating the spectral curves below 1.3 microns, calcareous and non-calcareous soils may be identified by differences in species of vegetation. Additional work is needed to identify biogeochemical differences between the two soils. Author

N86-11631*# Jet Propulsion Lab., California Inst. of Tech., Pasadena.

CALIBRATION OF AIS DATA USING GROUND-BASED SPECTRAL REFLECTANCE MEASUREMENTS

James E. Conel *In its* Proc. of the Airborne Imaging Spectrometer Data Anal. Workshop 15 Jun. 1985 p 84-85 ERTS (For primary document see N86-11618 02-43)
Avail: NTIS HC A09/MF A01 CSCL 05B

Present methods of correcting airborne imaging spectrometer (AIS) data for instrumental and atmospheric effects include the flat- or curved-field correction and a deviation-from-the-average adjustment performed on a line-by-line basis throughout the image. Both methods eliminate the atmospheric absorptions, but remove the possibility of studying the atmosphere for its own sake, or of using the atmospheric information present as a possible basis for theoretical modeling. The method discussed here relies on use of ground-based measurements of the surface spectral reflectance in comparison with scanner data to fix in a least-squares sense parameters in a simplified model of the atmosphere on a wavelength-by-wavelength basis. The model parameters (for optically thin conditions) are interpretable in terms of optical depth and scattering phase function, and thus, in principle, provide an approximate description of the atmosphere as a homogeneous body intervening between the sensor and the ground. Author

N86-11632*# Earth Satellite Corp., Chevy Chase, Md.
ANALYSIS OF AIS DATA OF THE RECLUSE OIL FIELD, RECLUSE, WYOMING
Jon D. Dykstra and Donald B. Segal *In* JPL Proc. of the Airborne Imaging Spectrometer Data Anal. Workshop 15 Jun. 1985 p 86-91 Original contains imagery. Original photography may be purchased from the EROS Data Center, Sioux Falls, S.D. 57198 ERTS (For primary document see N86-11618 02-43)
Avail: NTIS HC A09/MF A01 CSCL 05B

Airborne Imaging Spectrometer (AIS) data were flown over the Recluse, Wyoming oil field on September 9, 1984. Processing software was developed at Earth Satellite Corporation (EarthSat) for interactive analysis of the AIS data. EarthSat's AIS processing capabilities include destriping, solar irradiance corrections, residual calculations, geometric resampling, equal energy normalization, interactive spectral classifications and a variety of compressive algorithms to reduce the data to 8-bit format with a minimum of information loss. The in-house photolab facilities of EarthSat can routinely produce high-quality color renditions of the enhanced AIS data. A total of 80 lithologic samples were collected under the AIS flight lines. Correlation (within the atmospheric windows) between the laboratory and the AIS spectra of sample sites was generally poor. Reasonable correlation was only possible in large, freshly plowed fields. Mixed pixels and contrast between the natural and sample's surfaces were believed responsible for the poor correlation. Finally, a drift of approximately three channels was observed in the diffraction grating position within the 1.8 to 2.1 micron quadrant. Author

N86-11633*# National Aeronautics and Space Administration. Ames Research Center, Moffett Field, Calif.
HIGH RESOLUTION SPECTROMETRY OF LEAF AND CANOPY CHEMISTRY FOR BIOCHEMICAL CYCLING
Michael A. Spanner (Technicolor Government Services, Moffett Field, Calif.), David L. Peterson, William Acevedo (Technicolor Government Services, Moffett Field, Calif.), and Pamela Matson *In* JPL Proc. of the Airborne Imaging Spectrometer Data Anal. Workshop 15 Jun. 1985 p 92-99 refs ERTS (For primary document see N86-11618 02-43)
Avail: NTIS HC A09/MF A01 CSCL 05B

High-resolution laboratory spectrophotometer and Airborne Imaging Spectrometer (AIS) data were used to analyze forest leaf and canopy chemistry. Fundamental stretching frequencies of organic bonds in the visible, near infrared and short-wave infrared are indicative of concentrations and total content of nitrogen, phosphorous, starch and sugar. Laboratory spectrophotometer measurements showed very strong negative correlations with nitrogen (measured using wet chemistry) in the visible wavelengths. Strong correlations with green wet canopy weight in the atmospheric water absorption windows were observed in the AIS data. A fairly strong negative correlation between the AIS data at 1500 nm and total nitrogen and nitrogen concentration was evident. This relationship corresponds very closely to protein absorption features near 1500 nm. Author

N86-11634# Wisconsin Univ., Madison. Dept. of Forestry.
FOREST CANOPY CHEMISTRY FROM BLACKHAWK ISLAND, WISCONSIN
James H. Fownes and John D. Aber *In* JPL Proc. of the Airborne Imaging Spectrometer Data Anal. Workshop 15 Jun. 1985 p 100-104 ERTS (For primary document see N86-11618 02-43)
Avail: NTIS HC A09/MF A01 CSCL 02F

This ongoing project attempts to develop process-oriented models of forest productivity, which are driven by canopy spectral data. Concurrent with Airborne Imaging Spectrometer (AIS) flyover, a series of mixed-species hardwood forests were sampled for leaf morphological characteristics; total leaf mass, area, and vertical distribution; and overall average canopy nitrogen and lignin. Within a canopy, leaf specific weight (dry weight per unit area) varied significantly with height and between species. Species are separated ecologically by percent nitrogen and lignin. Mean total canopy percent lignin correlates well with previously published field estimates of soil nitrogen availability and total annual net primary productivity, which augurs well for the model, subject to identification of unambiguous spectral signals. Author

N86-11635*# Brown Univ., Providence, R. I. Dept. of Geological Sciences.
SPECTROSCOPY OF MOSES ROCK KIMBERLITE DIATREME
c46
Carle M. Pieters and John F. Mustard *In* JPL Proc. of the Airborne Imaging Spectrometer Data Anal. Workshop 15 Jun. 1985 p 106-110 refs ERTS (For primary document see N86-11618 02-43)
Avail: NTIS HC A09/MF A01 CSCL 08G

Three types of remote sensing data (Airborne Imaging Spectroscopy (AIS), NS001, Zeiss IR-photographs) were obtained for the Moses Rock kimberlite dike in southern Utah. The goal is to identify and characterize the mantle derived mafic component in such volcanic features. The Zeiss and NS001 images provide information on the regional setting and allow units of the dike to be distinguished from surrounding material. A potential unmapped satellite dike was identified. The AIS data provide characterizing information of the surface composition of the dike. Serpentized olivine-bearing soils are (tentatively) identified from the AIS spectra for a few areas within the dike. Author

N86-11636*# Commonwealth Scientific and Industrial Research Organization, Sydney (Australia). Div. of Mineral Physics.
ANALYSIS OF AIRCRAFT SPECTROMETER DATA WITH LOGARITHMIC RESIDUALS
A. A. Green and M. D. Craig *In* JPL Proc. of the Airborne Imaging Spectrometer Data Anal. Workshop 15 Jun. 1985 p 111-119 refs ERTS (For primary document see N86-11618 02-43)
Avail: NTIS HC A09/MF A01 CSCL 05B

Spectra from airborne systems must be analyzed in terms of their mineral-related absorption features. Methods for removing backgrounds and extracting these features one at a time from reflectance spectra are discussed. Methods for converting radiance spectra into a form similar to reflectance spectra so that the feature extraction procedures can be implemented on aircraft spectrometer data are also discussed. Author

N86-11637*# National Aeronautics and Space Administration. Goddard Space Flight Center, Greenbelt, Md.
COMPARISON OF AIS VERSUS TMS DATA COLLECTED OVER THE VIRGINIA PIEDMONT
R. Bell and C. S. Evans (Maryland Univ.) *In* JPL Proc. of the Airborne Imaging Spectrometer Data Anal. Workshop 15 Jun. 1985 p 120-122 refs ERTS (For primary document see N86-11618 02-43)
Avail: NTIS HC A09/MF A01 CSCL 05B

The Airborne Imaging Spectrometer (AIS, NS001 Thematic Mapper Simlulator (TMS), and Zeiss camera collected remotely sensed data simultaneously on October 27, 1983, at an altitude of 6860 meters (22,500 feet). AIS data were collected in 32 channels covering 1200 to 1500 nm. A simple atmospheric correction was applied to the AIS data, after which spectra for four cover types were plotted. Spectra for these ground cover classes showed a telescoping effect for the wavelength endpoints. Principal components were extracted from the shortwave region of the AIS (1200 to 1280 nm), full spectrum AIS (1200 to 1500 nm) and TMS (450 to 12,500 nm) to create three separate three-component color image composites. A comparison of the TMS band 5 (1000 to 1300 nm) to the six principal components from the shortwave AIS region (1200 to 1280 nm) showed improved visual discrimination of ground cover types. Contrast of color image composites created from principal components showed the AIS composites to exhibit a clearer demarcation between certain ground cover types but subtle differences within other regions of the imagery were not as readily seen. Author

N86-11638*# National Aeronautics and Space Administration. Goddard Space Flight Center, Greenbelt, Md.

A PRELIMINARY INVESTIGATION OF SYSTEMATIC NOISE IN DATA ACQUIRED WITH THE AIRBORNE IMAGING SPECTROMETER

Edward Masuoka *In* JPL Proc. of the Airborne Imaging Spectrometer Data Anal. Workshop 15 Jun. 1985 p 123-128 Original contains imagery. Original photography may be purchased from the EROS Data Ceter, Sioux Falls, S.D. 57198 ERTS (For primary document see N86-11618 02-43)

Avail: NTIS HC A09/MF A01 CSCL 05B

Systematic noise is present in Airborne Imaging Spectrometer (AIS) data collected on October 26, 1983 and May 5, 1984 in grating position 0 (1.2 to 1.5 microns). In the October data set the noise occurs as 135 scan lines of low DN's every 270 scan lines. The noise is particularly bad in bands nine through thirty, restricting effective analysis to at best ten of the 32 bands. In the May data the regions of severe noise have been eliminated, but systematic noise is present with three frequencies (3, 106 and 200 scan lines) in all thirty two bands. The periodic nature of the noise in both data sets suggests that it could be removed as part of routine processing. This is necessary before classification routines or statistical analyses are used with these data. Author

N86-11639*# Delaware Univ., Newark. Coll. of Marine Studies.

DISCRIMINATION OF COASTAL VEGETATION AND BIOMASS: USING AIS DATA

Michael F. Gross and V. Klemas *In* JPL Proc. of the Airborne Imaging Spectrometer Data Anal. Workshop 15 Jun. 1985 p 129-133 refs ERTS (For primary document see N86-11618 02-43)

Avail: NTIS HC A09/MF A01 CSCL 02C

The Airborne Imaging Spectrometer (AIS) was flown over a coastal wetlands region near Lewes, Delaware, adjacent to the Delaware Bay on 16 August 1984. Using the AIS data, it was possible to discriminate between four different types of wetland vegetation canopies: (1) trees; (2) broadleaf herbaceous plants (e.g., Acnida cannabina, Hisbiscus moscheutos); (3) the low marsh grass Spartina alterniflora; and (4) the high marsh grasses Distichlis spicata and Spartina patens. The single most useful region of the spectrum was that between 1.40 and 1.90 microns, where slopes of portions of the radiance curve and ratios of radiance at particular wavelengths were significantly different for the four canopy types. The ratio between the highest digital number in the 1.40 to 1.90 microns and .84 to .94 microns regions and a similar ratio between the peaks in radiance in the 1.12 to 1.40 microns and .84 to .94 microns spectral regions were also very effective at discriminating between vegetation types. Differences in radiance values at various wavelengths between samples of the same vegetation type could potentially be used to estimate biomass. Author

N86-11640*# National Aeronautics and Space Administration. Ames Research Center, Moffett Field, Calif.

AIS INVESTIGATION OF AGRICULTURAL MONOCULTURES

Byron L. Wood (Technicolor Government Services, Inc., Moffett Field, Calif.) and Robert C. Wrigley *In* JPL Proc. of the Airborne Imaging Spectrometer Data Anal. Workshop 15 Jun. 1985 p 134-140 ERTS (For primary document see N86-11618 02-43)

Avail: NTIS HC A09/MF A01 CSCL 02C

Airborne Imaging Spectrometer (AIS) data were acquired over an agricultural area in eastern San Joaquin County, California in July, 1984. Cover type information was subsequently collected for all fields along this flight line. The lack of detailed ground data on individual fields, however, limited AIS data analysis to a qualitative comparison of the spectral reflectance curves for a total of nine cover types. Based on this analysis, it appears that cover types with a positive slope in the 1550 to 1700 nm region have a higher spectral response in the 1200 to 1300 nm region compared to those cover types with a negative slope in the 1550 to 1700 nm region. Within cover type, spectral variability was also found to be greater than that between cover types. Given the lack of additional field data, the reason for these differences is a matter of speculation. Author

N86-11641*# California Univ., Santa Barbara. Remote Sensing Research Unit.

APPLICATION OF AIS TECHNOLOGY TO FOREST MAPPING

Stephen R. Yool and Jeffrey L. Star *In* JPL Proc. of the Airborne Imaging Spectrometer Data Anal. Workshop 15 Jun. 1985 p 141-145 refs ERTS (For primary document see N86-11618 02-43)

Avail: NTIS HC A09/MF A01 CSCL 02F

Concerns about environmental effects of large scale deforestation have prompted efforts to map forests over large areas using various remote sensing data and image processing techniques. Basic research on the spectral characteristics of forest vegetation are required to form a basis for development of new techniques, and for image interpretation. Examination of LANDSAT data and image processing algorithms over a portion of boreal forest have demonstrated the complexity of relations between the various expressions of forest canopies, environmental variability, and the relative capacities of different image processing algorithms to achieve high classification accuracies under these conditions. Airborne Imaging Spectrometer (AIS) data may in part provide the means to interpret the responses of standard data and techniques to the vegetation based on its relatively high spectral resolution. Author

N86-11642*# Stanford Univ., Calif. Applied Earth Sciences.

A COMPARISON OF AIS DATA WITH OTHER AIRCRAFT AND GROUND DATA FOR THE GEOBOTANICAL DISCRIMINATION OF ROCK TYPES IN SOUTHWEST OREGON

David A. Mouat *In* JPL Proc. of the Airborne Imaging Spectrometer Data Anal. Workshop 15 Jun. 1985 p 146-151 refs ERTS (For primary document see N86-11618 02-43)

Avail: NTIS HC A09/MF A01 CSCL 08G

The use of remote sensing techniques for the geobotanical discrimination of rock types is predicated upon a number of factors. These include an understanding of vegetation response to environmental (especially geochemical) conditions, the establishment of correlations between those vegetation factors and environmental factors, and the use of appropriate remote sensing techniques to discriminate the vegetation. Author

N86-11643*# Michigan Univ., Ann Arbor. School of Natural Resources.

FOREST SPECIES IDENTIFICATION WITH HIGH SPECTRAL RESOLUTION DATA

Charles E. Olson, Jr. and Zhiliang Zhu (Nanjing Inst. of Forestry, China) *In* JPL Proc. of the Airborne Imaging Spectrometer Data Anal. Workshop 15 Jun. 1985 p 152-157 refs ERTS (For primary document see N86-11618 02-43)

Avail: NTIS HC A09/MF A01 CSCL 02F

Data collected over the Sleeping Bear Sand Dunes Test Site and the Saginaw Forest Test Site (Michigan) with the JPL Airborne Imaging Spectrometer and the Collins' Airborne Spectroradiometer are being used for forest species identification. The linear discriminant function has provided higher identification accuracies than have principal components analyses. Highest identification accuracies are obtained in the 450 to 520 nm spectral region. Spectral bands near 1,300, 1,685 and 2,220 nm appear to be important, also. Author

N86-11644*# Purdue Univ., Lafayette, Ind. Lab. for Applications of Remote Sensing.

URBAN, FOREST, AND AGRICULTURAL AIS DATA: FINE SPECTRAL STRUCTURE

V. C. Vanderbilt *In* JPL Proc. of the Airborne Imaging Spectrometer Data Anal. Workshop 15 Jun. 1985 p 158-165 ERTS (For primary document see N86-11618 02-43)
Avail: NTIS HC A09/MF A01 CSCL 05B

Spectra acquired by the Airborne Imaging Spectrometer (AIS) near Lafayette, IN, Ely, MN, and over the Stanford University campus, CA were analyzed for fine spectral structure using two techniques: the ratio of radiance of a ground target to the radiance of a standard and also the correlation coefficient of radiances at adjacent wavelengths. The results show ramp like features in the ratios. These features are due to the biochemical composition of the leaf and to the optical scattering properties of its cuticle. The size and shape of the ramps vary with ground cover. Author

N86-11645*# Massachusetts Inst. of Tech., Cambridge. Research Lab. of Electronics.
REMOTE SENSING OF EARTH TERRAIN Semiannual Report, 1 Mar. - 31 Aug. 1985
J. A. Kong Aug. 1985 9 p refs
(Grant NAG5-270)
(NASA-CR-176284; NAS 1.26:176284) Avail: NTIS HC A02/MF A01 CSCL 08B

Progress on the investigation of the anisotropy of the terrain media, such as vegetation canopy and sea ice, and the study of the fluctuation-dissipation theorem in conjunction with the application of strong fluctuation theory for passive remote sensing of snowpacks is reported. The Feynman diagrammatic technique is used to derive the Dyson equation for the mean field and the Bethe-Salpeter equation for the correlation or the covariance of the field for electromagnetic wave propagation and scattering in an anisotropic random medium. With the random permittivity expressed in a general form, the bilocal and the nonlinear approximations are employed to solve the Dyson equation and the ladder approximation to the Bethe-Salpeter equation. The mean dyadic Green's function for a two layer anisotropic random medium with arbitrary three dimensional correlation function was investigated with the zeroth-order solutions to the Dyson equation under the four characteristic waves associated with the coherent vector fields propagating in an anisotropic random medium layer, which are the ordinary and extraordinary waves with upward and downward propagating vectors. Author

N86-11646*# Maryland Univ., College Park. Dept. of Geography.
ANALYSIS OF TERRESTRIAL CONDITIONS AND DYNAMICS Progress Report, 1 Sep. 1984 - 30 Jun. 1985
Samuel N. Goward Jun. 1985 103 p refs
(NCC5-26)
(NASA-CR-176308; NAS 1.26:176308) Avail: NTIS HC A06/MF A01 CSCL 05B

An ecological model is developed to estimate annual net primary productivity of vegetation in twelve major North American biomes. Three models are adapted and combined, each addressing a different factor known to govern primary productivity, i.e., photosynthesis, respiration, and moisture availability. Measures of intercepted photosynthetically active radiation (1PAR) for input to the photosynthesis model are derived from spectral vegetation index data. Normalized Difference Vegetation Index (NDVI) data are produced from NOAA-7 Advanced Very High Resolution Radiometer (AVHRR) observations for April 1982 through March 1983. NDVI values are sampled from within the biomes at locations for which climatological data are available. Monthly estimates of Net Primary Productivity (NPP) for each sample location are generated and summed over the twelve month period. These monthly estimates are averaged to produce a single annual estimated NPP value for each biomes. Comparison of estimated NPP values with figures reported in the literature produces a correlation coefficient of 85. Author

N86-11647*# National Aeronautics and Space Administration. Langley Research Center, Hampton, Va.
ACTIVE AND PASSIVE MICROWAVE MEASUREMENTS IN HURRICANE ALLEN
Victor E. Delnore (PRC Kentron, Inc.), Gilbert S. Bahn, William L. Grantham (Harris Corp., Melbourne, Fla.), Richard F. Harrington, and W. Linwood Jones Washington Nov. 1985 146 p refs
(NASA-TM-86390; L-15775; NAS 1.15:86390) Avail: NTIS HC A07/MF A01 CSCL 04B

The NASA Langley Research Center analysis of the airborne microwave remote sensing measurements of Hurricane Allen obtained on August 5 and 8, 1980 is summarized. The instruments were the C-band stepped frequency microwave radiometer and the Ku-band airborne microwave scatterometer. They were carried aboard a NOAA aircraft making storm penetrations at an altitude of 3000 m and are sensitive to rain rate, surface wind speed, and surface wind vector. The wind speed is calculated from the increase in antenna brightness temperature above the estimated calm sea value. The rain rate is obtained from the difference between antenna temperature increases measured at two frequencies, and wind vector is determined from the sea surface normalized radar cross section measured at several azimuths. Comparison wind data were provided from the inertial navigation systems aboard both the C-130 aircraft at 3000 m and a second NOAA aircraft (a P-3) operating between 500 and 1500 m. Comparison rain rate data were obtained with a rain radar aboard the P-3. Evaluation of the surface winds obtained with the two microwave instruments was limited to comparisons with each other and with the flight level winds. Two important conclusions are drawn from these comparisons: (1) the radiometer is accurate when predicting flight level wind speeds and rain; and (2) the scatterometer produces well behaved and consistent wind vectors for the rain free periods. Author

N86-11648# Army Cold Regions Research and Engineering Lab., Hanover, N. H.
THERMAL CONVECTION IN SNOW
D. J. Powers, S. C. Colbeck, and K. ONeill May 1985 69 p
(AD-A157577; CRREL-85-9) Avail: NTIS HC A04/MF A01 CSCL 08/12

Large temperature gradients applied to a snow cover drive water vapor upward and result in rapid recrystallization of snow crystals. The same temperature gradients create gradients of air density that can cause flows of air through the snow cover. This report develops formalism necessary to describe these flows in an effort to include the convection of vapor in the understanding of snow metamorphism. The theory of convection through porous media is extended to include the transport of water vapor, which is important because of its latent heat. Results are presented in terms of a Lewis number, defined as the ration of thermal to mass diffusivities. For Lewis numbers greater than 1.0, phase change intensifies convection, and for Lewis numbers less than 1.0, phase change retards convection. Two boundary conditions of special interest in the study of snow, a constant heat flux bottom and a permeable top, are investigated. Their influence on the transfer of heat is quantified, and it is found that heat transfer can be described as a linear function of the driving force for convection. The effect of a permeable top on convection at low Rayleigh numbers is derived. Experiments are performed to measure the effects of convection on heat transfer through glass beads and snow. The model results using constant flux boundary conditions are confirmed by experiments. Experiments show that convection can occur in snow, and that convection behaves in a manner consistent with our theoretical understanding of the phenomenon. Some uncertainty exists about the permeability and thermal conductivity of snow and hence it is uncertain if thermal convection would occur for a given temperature gradient, density and thickness. GRA

N86-11649# Department of Energy, Morgantown, W. Va.
ARCTIC ENERGY TECHNOLOGIES WORKSHOP: PROCEEDINGS
Apr. 1985 225 p Workshop held in Morgantown, W. Va., 14 Nov. 1984
(DE85-003360; DOE/METC-85/6014; CONF-8411108) Avail: NTIS HC A10/MF A01

Arctic oil and gas development program areas are discussed.

Technical information exchange among engineers, geologists, geophysicists, physical scientists, oceanographers, statisticians, analysts, and other participants engaged in similar research areas was provided. The first section of the proceedings is the keynote address. The second section of the proceedings includes 14 technical papers presented in two sessions at the Workshop: Sea Ice Research, and Seafloor/Soils Research. The third section of the proceedings includes the summaries of four work group discussion sessions from the second day of the meeting: (1) Arctic Offshore Structures; (2) Arctic Offshore Pipelines; (3) Subice Development Systems; and (4) Polar-Capable Ice Vessels. DOE

N86-11650# Washington State Energy Office, Olympia.
EVALUATION AND RANKING OF GEOTHERMAL RESOURCES FOR ELECTRICAL GENERATION OR ELECTRICAL OFFSET IN IDAHO, MONTANA, OREGON AND WASHINGTON Executive Summary
R. G. Bloomquist Jun. 1985 28 p refs
(Contract DE-AI79-83BP-13609)
(DE85-014661; DOE/BP-13609/3; WAOENG-85-02c) Avail: NTIS HC A03/MF A01

All geologic, environmental, legal, and institutional information in existing records and files was consolidated and evaluated, and a uniform methodology was applied to the evaluation and ranking of all known geothermal sites. The four states identified a total of 1265 potential geothermal sites. The 1265 sites were screened to eliminate those with little or no chance of providing either electrical generation and/or electrical offset. Two hundred and forty-five of the original 1265 sites were determined to warrant further study. On the basis of a developability index, 78 high temperature sites and 120 direct utilization sites were identified as having good or average potential for development and should be studied in detail. On the basis of cost, at least 29 of the high temperature sites appear to be technically capable of supporting a minimum total of at least 1000 MW of electrical generation which could be competitive with the busbar cost of conventional thermal generating technologies. DOE

N86-11651# Geological Survey, Anchorage, Alaska.
THE 1984 ANNUAL REPORT ON ALASKA'S MINERAL RESOURCES
1985 55 p
(DE85-015235; USGS-CIRC-940) Avail: NTIS HC A04/MF A01

Section 1011 of the Alaska National Interest Lands Conservation Act requires that on or before October 1, 1982, and annually thereafter, the President shall transmit to Congress all pertinent public information relating to minerals in Alaska gathered by the United States Geological Survey, the Bureau of Mines, and any other Federal agency. This is the third report to be prepared in response to that requirement. This report addresses onshore areas of Alaska only. It provides information about minerals of current interest in two broad categories: energy resources and nonfuel, critical, and strategic minerals. DOE

N86-11652# Analytic and Computational Research, Inc., Los Angeles, Calif.
PROBABILITY ENCODING OF HYDROLOGIC PARAMETERS FOR BASALT. ELICITATION OF EXPERT OPINIONS FROM A PANEL OF THREE BASALT WASTE ISOLATION PROJECT STAFF HYDROLOGISTS
A. K. Runchal, M. W. Merkhofer, E. Olmsted, and J. D. Davis Nov. 1984 73 p Prepared in cooperation with Applied Decision Analysis, Inc. and Rockwell International Corp., Richland, Wash.
(Contract DE-AC06-77RL-01030)
(DE85-014665; RHO-EW-CR-146P) Avail: NTIS HC A04/MF A01

A probability encoding method to estimate the probability distributions of selected hydrologic variables for the Cohassett basalt flow top and flow interior, and the anisotropy ratio of the interior of the Cohassett basalt flow beneath the Hanford Site was conducted. The results indicate significant differences of opinion among the experts. This was especially true of the values of the effective porosity of the Cohassett basalt flow interior for which estimates differ by more than five orders of magnitude. The experts are in greater agreement about the values of effective porosity of the Cohassett basalt flow top; their estimates for this variable are generally within one to two orders of magnitude of each other. For anisotropy ratio, the expert estimates are generally within two or three orders of magnitude of each other. Based on this study, the Rockwell hydrologists estimate the effective porosity of the Cohassett basalt flow top to be generally higher than do the independent experts. For the effective porosity of the Cohassett basalt flow top, the estimates of the Rockwell hydrologists indicate a smaller uncertainty than do the estimates of the independent experts. On the other hand, for the effective porosity and anisotropy ratio of the Cohassett basalt flow interior, the estimates of the Rockwell hydrologists indicate a larger uncertainty than do the estimates of the independence experts. DOE

N86-11653# Department of Energy, Morgantown, W. Va.
STATUS OF MODELS FOR ANALYSIS OF WESTERN GAS SANDS
A. I. Horton and A. W. Layne Apr. 1985 53 p refs
(DE85-003398; DOE/METC-85/2004) Avail: NTIS HC A04/MF A01

Existing capabilities for computer modeling of tight gas sands are summarized. The emphasis is on reservoir and stimulation model applicable to tight (low permeability), lenticular reservoirs (formations of irregularly shaped, randomly distributed sandstone bodies surrounded by relatively impermeable reservoir rock). These types of reservoirs are the focus of the Department of Energy's (DOE) Western Gas Sands (WGS) research efforts. The subject was addressed to assist DOE program managers and reservoir modelers in determining the needs for refining modeling capabilities for WGS research. Existing models are identified and their technical features and data requirements are discussed. The general benefits and problems in using models and suggested improvements for research-oriented models are covered. DOE

N86-11654# Urban Systems Research and Engineering, Inc., Cambridge, Mass.
EVALUATION OF COLOR INFRARED AERIAL SURVEYS OF WASTEWATER SOIL ABSORPTION SYSTEMS Final Report
S. O. Farrell Apr. 1985 83 p refs
(Contract EPA-68-03-3057)
(PB85-189074; EPA-600/2-85-039) Avail: NTIS HC A05/MF A01 CSCL 08B

Color infrared (CIR) aerial surveys can identify soil absorption systems in which the effluent rises rather than percolates into the ground water. This report reviews the technique's scientific basis and effectiveness, and discusses the procedures and equipment required for such surveys, and survey costs. Author (GRA)

N86-11655# Texas Dept. of Water Resources, Austin.
EVALUATING THE GROUND-WATER RESOURCES OF THE HIGH PLAINS OF TEXAS, VOLUME 3
T. Knowles, P. Norstrom, and W. B. Klemt Aug. 1985 425 p 4 Vol.
(PB85-191617; TDWR/R-2688-Vol-3) Avail: NTIS HC A18/MF A01; also available in set of 4 reports as PB85-191583 CSCL 08H

This report contains the basic data supporting counties in the middle third of the study as shown on the accompanying map which include records of approximately 12,200 wells, and county maps depicting well locations, elevation of the base of the High Plains aquifer, elevation of the water levels in 1980, and saturated thicknesses in 1980. GRA

N86-11656# Agricultural Research Service, Beltsville, Md.
HYDROLOGIC DATA FOR EXPERIMENTAL AGRICULTURAL WATERSHEDS IN THE US, 1975
J. B. Burford, J. L. Thurman, and R. T. Roberts Jan. 1985 587 p
(PB85-197317; USDA/MPUB-1446) Avail: NTIS HC A25/MF A01 CSCL 08H

Hydrologic data from 98 agricultural watersheds for calendar year 1975 are summarized. Daily and monthly total precipitation and runoff together with annual maximum peak discharge and maximum runoff for selected time intervals are included. Watershed descriptive information is presented. Maximum and minimum daily temperatures are given to many of the watersheds. GRA

N86-11657*# National Academy of Sciences - National Research Council, Washington, D. C.
GEODESY: A LOOK TO THE FUTURE
1985 193 p refs Sponsored in part by NASA, Defense Mapping Agency, NOAA and Geological Survey
(NASA-CR-176283; NAS 1.26:176283; PB85-199578) Avail: NTIS HC A09/MF A01 CSCL 08E

The report deals with the current and future uses of contemporary geodetic data and poses some questions and possibilities for the future. It is anticipated that the document will generate interest in present and future geodetic data for the solution of problems in Earth, ocean, and atmospheric sciences. GRA

N86-11658# Wisconsin Univ., Madison. Dept. of Civil and Environmental Engineering.
AERIAL PHOTOGRAPHY AND GROUND VERIFICATION AT POWER PLANT SITES: WISCONSIN POWER PLANT IMPACT STUDY
S. L. Wynn and R. W. Kiefer Apr. 1985 293 p Prepared in cooperation with Wisconsin Dept. of Natural Resources, Madison, Wisconsin Public Service Commission, Madison and Wisconsin Public Service Corp., Green Bay
(Grant EPA-R-803971)
(PB85-197358; EPA-600/3-85-034) Avail: NTIS HC A13/MF A01 CSCL 06C

Nine methods for monitoring the deterioration of a large wetland on the site of a newly constructed coal fired power plant in Columbia County, Wisconsin were demonstrated and evaluated. Four of the nine methods used data from ground sampling; two were remote sensing methods without ground verification; and three were remote sensing methods which either used ground verification or relied on the analyst's on the ground knowledge of the area. These methods were evaluated on the basis of whether they monitor change at a species or a community level, whether they monitor community change in terms of area or location or both, and whether they provide information about trends in plant communities. GRA

N86-11659# Vermont Univ., Burlington. Water Resources Research Center.
FISCAL YEAR 1983 INSTITUTE PROGRAM REPORT, VERMONT WATER RESOURCES RESEARCH CENTER Final Report
L. L. Arris and E. A. Cassell Dec. 1984 71 p
(Grant DI-14-08-0001-G-873)
(PB85 214500) Avail: NTIS HC A04/MF A01 CSCL 08H

Using the Center's Five Year Plan for Water Research as a guide, investigations studied water management problems of the highest priority in Vermont, including water quality watershed management lake processes, groundwater, acid precipitation, water resources data management, and allocation of water resources. The Water Center supported five major water research/information dissemination projects during the year. For the second year the Vermont Water Center supported research dealing with acid precipitation. GRA

N86-11660# Louisiana State Univ., Baton Rouge.
INFORMATION DISSEMINATION FOR A BETTER UNDERSTANDING OF LOUISIANA'S WATER RESOURCES
B. Worm 20 Sep. 1985 36 p Prepared in cooperation with Louisiana State Univ., Baton Rouge
(Grant DI-14-08-0001-G-845)
(PB85-219079; USGS/G-845-22) Avail: NTIS HC A03/MF A01 CSCL 08H

The project involved the assessment of Louisiana citizen's needs for water resources information, and the identification, preparation, and dissemination of the information available through the Louisiana Water Resources Research Institute to meet these needs. During the needs assessment phase, it was found that a need for information on most aspects of water resources exists in Louisiana. One topic of major concern for the State, coastal zone water problems, has been addressed by Institute supported research, and the results of the research were used to develop educational materials for the public on these problems. The project, through the evaluation of the Institute's ability to satisfy the State's needs for water information through existing Institute information, revealed gaps between needs for information and existing information. The topics not previously addressed by the Institute were recommended for incorporation into the Institute's water research priorities listing. GRA

N86-11661# Louisiana State Univ., Baton Rouge. Water Resources Research Inst.
LOUISIANA WATER RESOURCES RESEARCH INSTITUTE Program Report, FY 1983
1985 31 p
(Grant DI-14-08-0001-G-845)
(PB85-218998; USGS/G-845-01) Avail: NTIS HC A03/MF A01 CSCL 08H

Five projects were supported by the Louisiana Water Resources Research Institute during the year 1983 to 1984. One project dealt with mathematical modeling of streamflow. The other project dealt with development of techniques for sediment analysis to isolate, concentrate and detect chlorinated hydrocarbons. Another project concentrated on treatment of coal pile runoff in Louisiana and suggested ways for treating the wastewater most effectively. The last project dealt with nutrient assimilation capacity in two shallow coastal lakes. GRA

N86-11662# Cornell Univ., Ithaca, N.Y. Center for Environmental Research.
FISCAL YEAR 1983 PROGRAM REPORT OF THE WATER RESOURCES RESEARCH INSTITUTE OF NEW YORK STATE Final Report
Sep. 1984 20 p
(Grant DI-14-08-0001-G-859; Proj. G859-01)
(PB85-217024; USGS/G-859-01) Avail: NTIS HC A02/MF A01 CSCL 08H

The Institute Water Resources Research Program for FY 1983 focused on three problem areas identified as critical in the Middle Atlantic Region; groundwater protection and management; acid precipitation; and water resources planning. The groundwater protection and management research program addressed problems of quality protection and the technology transfer program focused on related problems of management and information dissemination. The acid precipitation research projects focused on the effects of the phenomenon; on tree pollen germination and tube growth and use of induced fluorescence measurements to assess aluminum organic interactions in acidified lakes. The project relating to water resources planning developed a methodology for estimating the frequency, severity and duration of water supply shortage in existing water supply systems which rely on both surface and ground water. GRA

N86-11553# Academy of Sciences, Potsdam (East Germany). Zentralinst. fuer Physik der Erde.
NEW ASPECTS OF THE GEODETIC BOUNDARY VALUE PROBLEMS
K. Arnold *In its* Proc. of the 5th Intern. Symp. Geodesy and Phys. of the Earth 1985 p 45-50 refs (For primary document see N86-11549 02-42)
Avail: NTIS HC A09/MF A01

N86-11555# Institut Geographique National, Paris (France). Groupe de Recherches de Geodesie Spatiale.
ESTABLISHMENT OF THE BIH TERRESTRIAL SYSTEM BY COMBINING THE RESULTS OF DIFFERENT EARTH ROTATION SPACE GEODESY PROGRAMS Abstract Only
Claude Boucher and Martine Feissel (Observatoire de Paris) *In* Academy of Sciences of the GDR Proc. of the 5th Intern. Symp. Geodesy and Phys. of the Earth 1985 p 60 (For primary document

see N86-11549 02-42)
Avail: NTIS HC A09/MF A01

N86-11556# Ceskoslovenska Akademie Ved, Prague. Astronomical Inst.

TIDAL FRICTION, THE EARTH'S ROTATION AND HYPOTHESIS OF AN EXPANDING EARTH

Milan Bursa *In* Academy of Sciences of the GDR Proc. of the 5th Intern. Symp. Geodesy and Phys. of the Earth 1985 p 61-67 refs (For primary document see N86-11549 02-42)
Avail: NTIS HC A09/MF A01

N86-11561# Technische Hochschule, Darmstadt (West Germany). Inst. fuer Physikalische Geodaesie.

PRECISE GEOID COMPUTATIONS AT MOUNTAINOUS COASTLINES IN VIEW OF VERTICAL DATUM DETERMINATIONS

H. J. Euler, E. Groten, W. Hausch, and B. Stock *In* Academy of Sciences of the GDR Proc. of the 5th Intern. Symp. Geodesy and Phys. of the Earth 1985 p 109-139 refs (For primary document see N86-11549 02-42)
Avail: NTIS HC A09/MF A01

N86-11567# Academy of Sciences, Potsdam (East Germany). Zentralinsts fuer Physik der Erde.

RESULTS CONCERNING RHEOLOGICAL PARAMETERS OF THE EARTH

Joachim Hoepfner *In its* Proc. of the 5th Intern. Symp. Geodesy and Phys. of the Earth 1985 p 173-176 refs (For primary document see N86-11549 02-42)
Avail: NTIS HC A09/MF A01

N86-11569# Research Inst. of Geodesy, Prague (Czechoslovakia).

A NEW APPROACH TO ITERATIONS IN SOLVING GEODETIC BOUNDARY VALUE PROBLEMS FOR REAL TOPOGRAPHY

Petr Holota *In* Academy of Sciences of the GDR Proc. of the 5th Intern. Symp. Geodesy and Phys. of the Earth, Pt. 2 1985 p 4-15 refs (For primary document see N86-11568 02-42)
Avail: NTIS HC A09/MF A01

N86-11570# Higher Inst. of Mining and Geology, Sofia (Bulgaria).

THE IRREGULARITY IN THE EARTH'S ANNUAL ROTATION AS A CAUSE OF SYSTEMATIC TIME VARIATION

I. B. Ivanov *In* Academy of Sciences of the GDR Proc. of the 5th Intern. Symp. Geodesy and Phys. of the Earth, Pt. 2 1985 p 16-18 refs (For primary document see N86-11568 02-42)
Avail: NTIS HC A09/MF A01

N86-11574# Polish Academy of Sciences, Warsaw. Space Research Centre.

ON SHORT PERIODICAL VARIATIONS OF POLAR MOTION AND UT1-UTC

B. Kolaczek, A. Brzezinski, W. Kosek, J. Nastula, and B. Soloducha *In* Academy of Sciences of the GDR Proc. of the 5th Intern. Symp. Geodesy and Phys. of the Earth, Pt. 2 1985 p 35-44 refs (For primary document see N86-11568 02-42)
Avail: NTIS HC A09/MF A01

N86-11580# Technische Univ., Graz (Austria). Inst. of Theoretical Geodesy.

VARIATIONAL PRINCIPLES FOR EARTH ROTATION

Helmut Moritz *In* Academy of Sciences of the GDR Proc. of the 5th Intern. Symp. Geodesy and Phys. of the Earth, Pt. 2 1985 p 88-101 refs (For primary document see N86-11568 02-42)
Avail: NTIS HC A09/MF A01

N86-11581# Stazione Astronomica Internazionale di Latitudine, Cagliari (Italy).

SECULAR AND LONG TERM VARIATIONS IN POLAR MOTION FROM CLASSICAL AND DOPPLER OBSERVATIONS

A. Poma and E. Proverbio (Ist. di Astronomia e Fisica Superiore, Cagliari, Italy) *In* Academy of Sciences of the GDR Proc. of the 5th Intern. Symp. Geodesy and Phys. of the Earth, Pt. 2 1985 p 101-108 refs (For primary document see N86-11568 02-42)
Avail: NTIS HC A09/MF A01

N86-11585# Ceskoslovenska Akademie Ved, Prague. Geophysical Inst.

GEODYNAMIC EFFECTS DUE TO EARTH'S DEFORMATION

Jiri Tresl *In* Academy of Sciences of the GDR Proc. of the 5th Intern. Symp. Geodesy and Phys. of the Earth, Pt. 2 1985 p 128-133 refs (For primary document see N86-11568 02-42)
Avail: NTIS HC A09/MF A01

N86-11587# Ceskoslovenska Akademie Ved, Prague. Astronomical Inst.

POLAR MOTION BETWEEN 1900.0 AND 1984.0 AS DETERMINED BY DIFFERENT TECHNIQUES Abstract Only

J. Vondrak *In* Academy of Sciences of the GDR Proc. of the 5th Intern. Symp. Geodesy and Phys. of the Earth, Pt. 2 1985 p 143 (For primary document see N86-11568 02-42)
Avail: NTIS HC A09/MF A01

N86-11595# Academy of Sciences, Potsdam (East Germany). Zentralinst. fuer Physik der Erde.

SPACE-TIME VARIATING GEOLOGICAL MASSES BY SPACE-TIME VARIATING GEODETIC MEASUREMENTS

K. Arnold *In its* Proc. of the 5th Intern. Symp. Geodesy and Phys. of the Earth, Pt. 3 1985 p 26-31 refs (For primary document see N86-11591 02-42)
Avail: NTIS HC A08/MF A01

N86-11984# Joint Publications Research Service, Arlington, Va.

GENERAL-PURPOSE EQUIPMENT FOR AIRBORNE LASER REMOTE SENSING OF OCEAN, ATMOSPHERE AND AGRICULTURAL CROPS Abstract Only.

A. F. Bunkin, D. V. Vlasov, A. S. Glaumyan, D. V. Maltsev, D. M. Mirkamilov, and V. P. Slobodyanin *In its* USSR Rept.: Phys. and Math. (JPRS-UPM-85-005) 20 Aug. 1985 p 94 refs Transl. into ENGLISH from Zh. Tekhn. Fiz. (Leningrad), v. 54, no. 11, Nov. 1984 p 2190-2195 (For primary document see N86-11945 02-70)
Avail: NTIS HC A08/MF A01

N86-11927# Joint Publications Research Service, Arlington, Va.

RESEARCH ON OPTIC SPATIAL FREQUENCY ANALYSIS OF LINEAR STRUCTURES IN REMOTE SENSING IMAGES Abstract Only

Ziqiang Zhu, Zhenpei Chen, Jitao Li, and Guangjie Tang *In its* China Rept.: Sci. and Technol. (JPRS-CST-85-014) 2 May 1985 p 79 Transl. into ENGLISH from Zhongguo Jiguang (Shanghai), v. 12, no. 1, 20 Jan. 1985 p 1-5 (For primary document see N86-11918 02-70)
Avail: NTIS HC A06/MF A01

44 ENERGY PRODUCTION AND CONVERSION

Includes specific energy conversion systems, e.g., fuel cells and batteries; global sources of energy; fossil fuels; geophysical conversion; hydroelectric power; and wind power.

For related information see also *07 Aircraft Propulsion and Power, 20 Spacecraft Propulsion and Power, 28 Propellants and Fuels,* and *85 Urban Technology and Transportation.*

N86-11663# Vitro Labs., Silver Spring, Md.

PERFORMANCE OF SOLAR COLLECTOR ARRAYS AND COLLECTOR CONTROLLERS IN THE NATIONAL SOLAR DATA NETWORK

T. L. Logee and P. W. Kendall Jul. 1984 244 p refs
(Contract DE-AC01-79CS-30027)
(DE85-001297; Solar/0015-84-32) Avail: NTIS HC A11/MF A01

The accumulated National Solar Data Network (NSDN) data has been analyzed with regard to collector and collector control performance. The collector data is presented in the ASHRAE format as efficiency vs. operating points, (Tinlet - Tambient)/insolation. Collector controls were analyzed by determining the losses caused by control problems common to the NSDN solar systems. This study of collectors and collector controls has several objectives which are: (1) to compare actual and predicted collector performance; (2) to determine which generic types of components performed well and which performed poorly; (3) to determine why predicted performance was not achieved in the field; (4) to determine the types and causes of failures; (5) to determine the reliability weaknesses; and (6) to determine whether there are any component integration problems. Author

N86-11664*# Solenergy Corp., Woburn, Mass.
INTERMEDIATE LOAD MODULES FOR TEST AND EVALUATION: FIXED PRICE RESEARCH AND DEVELOPMENT Final Report
22 Mar. 1985 16 p Prepared in cooperation with JPL, Pasadena, Calif.
(Contract NAS7-100)
(NASA-CR-176135; JPL-9950-1157; NAS 1.26:176135; DOE/JPL-956347-1; DRL-185; DRD-SE-2) Avail: NTIS HC A02/MF A01 CSCL 10B

Solenergy was contracted by JPL to furnish solar modules for evaluation of design test specification for intermediate load modules. Jet Propulsion Laboratory has performed qualification tests on Group 1 and Group 2 modules and has reported the resulting data. Modules were provided that are designed to be consistent with the Block 5 Electrical and Mechanical Design Requirements. Also these modules must meet the design requirements of Block 5 Environmental Design Requirements. It is felt that the modules performed satisfactorily although some workmanship problem were noted helping to correct production. It also appears that further work on EVA lamination by interested parties is required to address some problems associated with this method of production. Author

N86-11665# Solarex Corp., Rockville, Md.
THE INTERFACE STRUCTURE OF GRAIN BOUNDARIES IN POLYSILICON
S. M. Johnson, K. C. Yoo (Maryland Univ., College Park), R. G. Rosemeier (Maryland Univ., College Park), P. Soltani (Semix, Inc.), and H. C. Lin 1982 35 p refs Presented at Mater. Res. Soc. Ann. Meeting, Boston, 1-4 Nov., 1982
(Contract DE-FC01-80-ET-23197)
Avail: NTIS HC A03/MF A01

Normal grain growth in polysilicon material proceeds by a twinning mechanism such that the individual grain orientations are related by single or multiple twinning steps. The twinning relationship between adjacent grains can result in the alignment of their boundary interfaces along certain planar segments which have a very low electrical activity. The varying degree of electrical activity of these boundaries, and boundary positions, is attributed to the smaller dislocation portion of the larger change in orientation across the grains. Author

N86-11666*# National Aeronautics and Space Administration. Lewis Research Center, Cleveland, Ohio.
PHOTOVOLTAIC-POWERED VACCINE REFRIGERATOR: FREEZER SYSTEMS FIELD TEST RESULTS Final Report
Anthony F. Ratajczak Aug. 1985 99 p
(DE-AI01-79ET-20485; PASA-NASA/DSB-5710-2-79)
(NASA-TM-86972-Rev; E-2498; DOE/NASA/20485-18; NAS 1.15:86972-Rev) Avail: NTIS HC A05/MF A01 CSCL 10B

A project to develop and field test photovoltaic-powered refrigerator/freezers suitable for vaccine storage was undertaken. Three refrigerator/freezers were qualified; one by Solar Power Corp. and two by Solvolt. Follow-on contracts were awarded for 19 field test systems and for 10 field test systems. A total of 29 systems were installed in 24 countries between October 1981 and October 1984. The project, systems descriptions, installation experiences, performance data for the 22 systems for which field test data was reported, an operational reliability summary, and recommendations relative to system designs and future use of such systems are explained. Performance data indicate that the systems are highly reliable and are capable of maintaining proper vaccine storage temperatures in a wide range of climatological and user environments. Author

N86-11667*# Michigan State Univ., East Lansing. Div. of Engineering Research.
EFFECT OF ACCURACY OF WIND POWER PREDICTION ON POWER SYSTEM OPERATOR Final Report
Robert A. Schlueter, G. Sigari, and T. Costi Jun. 1985 188 p refs
(Grant NAG3-399)
(NASA-CR-176300; NAS 1.26:176300; MSU-ENGR-85-026) Avail: NTIS HC A09/MF A01 CSCL 10B

This research project proposed a modified unit commitment that schedules connection and disconnection of generating units in response to load. A modified generation control is also proposed that controls steam units under automatic generation control, fast responding diesels, gas turbines and hydro units under a feedforward control, and wind turbine array output under a closed loop array control. This modified generation control and unit commitment require prediction of trend wind power variation one hour ahead and the prediction of error in this trend wind power prediction one half hour ahead. An improved meter for predicting trend wind speed variation is developed. Methods for accurately simulating the wind array power from a limited number of wind speed prediction records was developed. Finally, two methods for predicting the error in the trend wind power prediction were developed. This research provides a foundation for testing and evaluating the modified unit commitment and generation control that was developed to maintain operating reliability at a greatly reduced overall production cost for utilities with wind generation capacity. Author

N86-11668*# National Aeronautics and Space Administration. Lewis Research Center, Cleveland, Ohio.
RE-1000 FREE-PISTON STIRLING ENGINE UPDATE
J. G. Schreiber 1985 20 p refs Presented at the 20th Intersoc. Energy Conversion Eng. Conf., Miami Beach, Fla., 18-23 Aug. 1985
(Contract DE-AI05-82OR-1005)
(NASA-TM-87126; E-2597; DOE/NASA/1005-6; NAS 1.15:87126) Avail: NTIS HC A02/MF A01 CSCL 10B

A free piston Stirling engine was tested. The tests performed over the past several years on the single cylinder engine were designed to investigate the dynamics of a free piston Stirling engine. The data are intended to be used primarily for computer code validation. The tests designed to investigate the sensitivity of the engine performance to variations in working space pressure, heater and cooler temperatures, regenerator porosity, power piston mass and displacer dynamics were completed. In addition, some data were recorded with alternate working fluids. A novel resonant balance system for the engine was also tested. Some preliminary test results of the tests performed are presented along with an outline of future tests to be run with the engine coupled to a hydraulic output unit. A description of the hydraulic output unit is given. Author

N86-11669*# Jet Propulsion Lab., California Inst. of Tech., Pasadena.
A SUMMARY REPORT ON THE FLAT-PLATE SOLAR ARRAY PROJECT WORKSHOP ON TRANSPARENT CONDUCTING POLYMERS
R. Kachare and J. Moacanin 1 Aug. 1985 51 p Workshop held in Santa Barbara, Calif., 11-12 Jan. 1985
(Contract NAS7-918; DE-AI01-76ET-20356)
(NASA-CR-176302; NASA-JPL-85-60; NAS 1.26:176302; DOE/JPL-1012-110) Avail: NTIS HC A04/MF A01 CSCL 10B

The proceedings and technical discussions of a workshop on Transparent Conducting Polymers (TCP) for solar cell applications are reported. This is in support of the Device Research Task of the Flat-Plate Solar Array Project. The workshop took place on January 11 and 12, 1985, in Santa Barbara, California. Participants included university and industry researchers. The discussions focused on the electronic and optical properties of TCP, and on experimental issues and problems that should be addressed for high-efficiency solar cell application. Author

N86-11670*# Michigan State Univ., East Lansing. Div. of Engineering Research.

AC MOTOR AND GENERATOR REQUIREMENTS FOR ISOLATED WECS

Gerald L. Park, Patrick J. McCleer (Michigan Univ.), Bror Hanson (SWX Corp.), Bernhard Weinberg, and Otto Krauss Oct. 1985 82 p refs
(Grant NAG3-530)
(NASA-CR-176315; DOE/NASA/0530-1; NAS 1.26:176315) Avail: NTIS HC A05/MF A01 CSCL 10A

After surveying electrically driven loads used on productive farms, the investigators chose three pumps for testing at voltages and frequencies far outside the normal operating range. These loads extract and circulate water and move heat via air, and all are critical to farm productivity. The object was to determine the envelope of supply voltage and frequency over which these loads would operate stably for time intervals under 1 hour. This information is among that needed to determine the feasibility of supplying critical loads, in case of a utility outage, from a wind driven alternator whose output voltage and frequency will vary dramatically in most continental wind regimes. Other related work is surveyed. The salient features and limitations of the test configurations used and the data reduction are described. The development of simulation models suitable for a small computer are outlined. The results are primarily displayed on the voltage frequency plane with the general conclusion that the particular pump models considered will operate over the range of 50 to 90 Hz and a voltage band which starts below rated, decreases as frequency decreases, and is limited on the high side by excessive motor heating. For example, centrifugal pump operating voltage ranges as extensive .4 to 1.4 appear possible. Particular problems with starting, stalling due to lack of motor torque, high speed cavitation, and likely overheating are addressed in a listing of required properties for wind driven alternators and their controllers needed for use in the isolated or stand alone configuration considered. Author

N86-11671*# National Aeronautics and Space Administration. Lewis Research Center, Cleveland, Ohio.

A 25.5 PERCENT AMO GALLIUM ARSENIDE GRATING SOLAR CELL

V. G. Weizer and M. P. Godlewski 1985 10 p refs Presented at the 18th Photovoltaic Specialists Conf., Las Vegas, Nev., 21-25 Oct. 1985; sponsored by IEEE
(NASA-TM-87134; E-2748; NAS 1.15:87134) Avail: NTIS HC A02/MF A01 CSCL 10A

Recent calculations have shown that significant open circuit voltage gains are possible with a dot grating junction geometry. The feasibility of applying the dot geometry to the GaAs cell was investigated. This geometry is shown to result in voltages approach 1.120 V and efficiencies well over 25 percent (AMO) if good collection efficiency can be maintained. The latter is shown to be possible if one chooses the proper base resistivity and cell thickness. The above advances in efficiency are shown to be possible in the P-base cell with only minor improvements in existing technology. Author

N86-11672# Naval Surface Weapons Center, White Oak, Md.

HIGH RATE Li/SOCl(2) CELLS. 2. EFFECT OF CATALYST ON CELL PERFORMANCE Report, Nov. 1983 - Apr. 1985

W. P. Kilroy, L. Pitts, and K. M. Abraham Apr. 1985 59 p
(AD-A157383; NSWC/TR-85-104) Avail: NTIS HC A04/MF A01 CSCL 10/3

As part of the ongoing High Energy Batteries for Weapons Programs at NSWC, various cell parameters were investigated to examine their effect on the performance, safety, and chemistry of Li/SOCl2 cells. This report summarizes the influence of cobalt dibenzo-tetraazaannulene (Co-TAA) cataylsis on the discharge and overdischarge chemistry and performance of spirally wound commercial C-size cells. Co-TAA catalyst improved the performance and safety of C-size Li/SOCl2 cells. The catalyst was most effective at high rate or low temperature operation. The presence of water increased the risk of hazards at high rates of discharge. The generation of gases such as COS, CS2, HCl, etc. was dependent on the internal temperature. GRA

N86-11673# EIC, Inc., Norwood, Mass.

BASIC STUDIES OF THE LITHIUM SECONDARY BATTERY Final Technical Report, 1 May 1984 - 30 Apr. 1985

J. S. Foos, S. M. Erker, and L. M. Rembetsy Jun. 1985 19 p
(Contract N00014-84-C-0336)
(AD-A157449; C-604; FTR-1) Avail: NTIS HC A02/MF A01 CSCL 10/3

Poly-1, 4-dimethoxybenzene has been synthesized by the anodic oxidation of 1,4-dimethoxybenzene in aprotic electrolytes. The black polymer is a doped semiconductor as formed. This material is converted to polymeric (olimeric) hydroquinone and quinone. The polymers are insoluble in all common solvents except for the polyhydroquinone in aqueous base. A coulombic titration of this quinone, using an electrode compounded with carbon and an aprotic electrolyte, gave an equivalent weight corresponding to approx. 0.5e(-) per quinone unit. Similar results were observed in the initial cycles in Li cells. However, the capacity of the electrode degraded on cycling. GRA

N86-11674# Thermo Electron Corp., Waltham, Mass.

ADVANCED THERMIONIC TECHNOLOGY PROGRAM: SUMMARY REPORT, VOLUME 3 Final Report

Oct. 1984 130 p refs Prepared in cooperation with Rasor Associates, Inc., Sunnyvale, Calif.
(Contracts DE-AC02-76ET-11292; DE-AC21-83MC-20352)
(DE85-009360; DOE/ET-11292/1893-Vol-3) Avail: NTIS HC A07/MF A01

The results of systems studies of primary interest to those involved in identifying and evaluating applications for thermionics are presented. Several of the industries which consume the largest amounts of energy have an electrical-to-thermal ratio of about ten percent. This closely matches the electrical efficiency of thermionic converters. Thermionic cogeneration has several other unique advantages relative to alternative technologies for cogeneration which should lead to a much broader application of cogeneration in industry. These advantages accrue from the much higher temperatures at which thermionic energy conversion takes place, its suitability for very small as well as large process heaters, and, of course, its production of direct heat rather than process steam. Several examples of thermionic cogeneration are presented in greater detail: copper refining by the Noranda process; thermionic topping cycles or gas turbine; and combined cycle and fossil-fuel steam power plants. DOE

N86-11675# Midwest Research Inst., Golden, Colo. Solar Energy Research Inst.

NEW-GENERATION PHOTOVOLTAIC TECHNOLOGIES

T. Surek and R. D. McConnell Jun. 1985 7 p Presented at INTERSOL '85 - Solar Energy, the Diverse Solution, Montreal, 23 Jun. 1985
(Contract DE-AC02-83CH-10093)
(DE85-012143; SERI/TP-211-2748; CONF-850604-11) Avail: NTIS HC A02/MF A01

Five generations of photovoltaic technologies are identified: single crystal silicon, polycrystalline silicon, ribbon silicon, single junction thin films, and multijunction thin films. The Solar Energy Research Institute (SERI) is the focus for the US government's research and development of the most promising, the fourth and fifth generation single-junction and multijunction thin films. Improvements in materials and solar cell fabrication techniques have resulted in remarkable progress for thin-film devices in recent years. Some recent highlights of SERI's photovoltaic research efforts are described. Author

N86-11676# Utah Geological and Mineralogical Survey, Salt Lake City.
SUMMARY OF LOW-TEMPERATURE GEOTHERMAL STUDIES CONDUCTED BY THE UTAH GEOLOGICAL AND MINERAL SURVEY FROM JULY 1, 1977 TO DECEMBER 31, 1984
R. H. Klauk Dec. 1984 20 p refs
(Contract DE-AS07-77ET-28393)
(DE85-009346; DOE/ET-28393/T9; RI-193) Avail: NTIS HC A02/MF A01

Brief summaries of the results of studies of low-temperature geothermal areas are presented. These include state-wide studies, site-specific studies, and area studies. DOE

N86-11677# GeoProducts Corp., Oakland, Calif.
HONEY LAKE GEOTHERMAL PROJECT, LASSEN COUNTY, CALIFORNIA Final Technical Report
Nov. 1984 61 p
(Contract DE-FC07-81ID-12262)
(DE85-013388; DOE/ID-12262/T1) Avail: NTIS HC A04/MF A01

The drilling, completion, and testing of deep well WEN-2 for a hybrid electric power project which will use the area's moderate temperature geothermal fluids and locally procured wood fuel is reported. The project is located within the Wendel-Amedee Known Geothermal Resource Area. DOE

N86-11678# Stanford Univ., Calif. Geothermal Program.
TRACER TEST ANALYSIS OF THE KLAMATH FALLS GEOTHERMAL RESOURCE: A COMPARISON OF MODELS
S. E. Johnson Jun. 1985 116 p refs
(Contract DE-AT03-80SF-11459)
(DE85-009924; SGP-TR-81) Avail: NTIS HC A06/MF A01

Two tracer tests on doublet systems in a fractured geothermal system were carried out to obtain data which would lead to information about the reservoir and to test the applicability of current tracer flow models. The results show rapid breakthrough times and indicate fracture flow with vigorous mixing of injector fluid before production of same are shown. It is suggested that thermal breakthrough is not directly related to tracer breakthrough in the Klamath Union doublet system. There has been no long-term enthalpy loss from exploiting the resource for 40 years. To reduce the data, models were developed to analyze the results. Along with a porous media flow model two mathematical models developed to analyze fractured geothermal systems are used to help dicipher the various tracer return curves. The flow of tracers in doublet systems was investigated. A mathematical description is used for tracer flow through fractures as a function of time and various nonlinear parameters which can be found using a curve fitting technique. DOE

N86-11679# Sandia Labs., Albuquerque, N. Mex.
VERTICAL AXIS WIND TURBINE POWER REGULATION THROUGH CENTRIFUGALLY PUMPED LIFT SPOILING
P. C. Klimas and J. F. Sladky, Jr. (Washington Univ., Seattle) 1985 5 p refs Presented at INTERSOL 1985. Solar Energy: The Diverse Solution, Montreal, 23 Jun. 1985
(Contract DE-AC04-76DP-00789)
(DE85-013787; SAND-85-1408C; CONF-850604-3) Avail: NTIS HC A02/MF A01

This paper describes an approach for lowering the rated windspeeds of Darrieus-type vertical axis wind turbines (VAWTs) whose blades are hollow aluminum extrusions. The blades, which when rotating act as centrifugal pumps, are fitted with a series of small perforations distributed along a portion of the blades' span. By valving the ends of the hollow blades, flow into the blade ends and out of the perforations may be controlled. This flow can induce premature aerodynamic stall on the blade elements, thereby reducing both the rated power of the turbine and its cost-of-energy. The concept has been proven on the Sandia National Laboratories 5-m diameter research VAWT and force balance and flow visualization wind tunnel tests have been conducted using a blade section designed for the VAWT application. DOE

N86-11680# Oak Ridge National Lab., Tenn.
STIRLING CYCLE HEAT PUMP STUDIES
N. Domingo 1984 8 p Presented at the DOE/ORNL Heat Pump Conf., Washington, D.C., 10 Dec. 1984
(Contract DE-AC05-84OR-21400)
(DE85-005365; CONF-841231-6) Avail: NTIS HC A02/MF A01

Major accomplishments for the analytical activities in Stirling cycle heat pumps include: (1) a computer simulation of a kinematic SCHP to determine the effects of source temperature, gas pressure, drive speed, dead volume, and working-space isothermalization on performance; and (2) a comparative analysis of SCHP performance and loss terms obtained with two different computer models. Simulation results indicate some performance trends and trade-off relationships which may be general enough to cover a wide range of machine configurations. It is shown that overall performance agreement between the models is farily good, but for the individual losses, agreement is very poor. DOE

N86-11681# Sandia Labs., Albuquerque, N. Mex.
DEGRADATION OF IONIC MEMBRANES IN THE ZINC/FERRICYANIDE BATTERY
R. A. Assink and O. Arnold, Jr. 1985 20 p Presented at the Spring Natl. Meeting of AIChE, Houston, Tex., 24 Mar. 1985
(Contract DE-AC04-76DP-00789)
(DE85-008469; SAND-84-1953C; CONF-850357-4) Avail: NTIS HC A02/MF A01

Homogeneous and radiatively grafted membranes were evaluated as separators for the zinc/ferricyanide storage battery. An accelerated aging test demonstrated that membrane failures could be attributed to both mechanical and chemical mechanisms. A series of radiation grafted membranes using fluorinated film substrates were prepared. One of these membranes has exhibited a 79.3% average energy efficiency for over 700 charge/discharge cycles in a test cell. DOE

N86-11682# Oak Ridge National Lab., Tenn.
THERMODYNAMICS OF CHROMIUM AND IRON IN CARBONATE SALTS AT 650(0)C
H. S. Hsu and J. H. DeVan May 1985 25 p refs
(Contract DE-AC05-84OR-21400)
(DE85-013542; ORNL-6181) Avail: NTIS HC A02/MF A01

Chemical equilibria of chromium and iron in Li2CO3-K2CO3 were investigated in conjunction with corrosion studies of current collector materials for molten-carbonate fuel cells. The SOLGASMIX-PV computer program was used to perform thermochemical calculations to establish equilibrium phase relationships under various gas atmospheres at 650(0)C. Phase stability diagrams were constructed for the systems Cr-Li-C-O, Cr-K-C-O, Cr-Li-K-C-O, Fe-Li-C-O, Fe-K-C-O, and Fe-Li-K-C-O at 650(0)C. These predicted phase relationships were checked experimentally by thermogravimetric analysis, differential thermal analysis, and X-ray diffraction. The experimental results generally confirmed that reaction paths were consistent with the calculated phase stability diagrams. DOE

N86-11683# Washington State Energy Office, Olympia.
EVALUATION AND RANKING OF GEOTHERMAL RESOURCES FOR ELECTRICAL GENERATION OR ELECTRICAL OFFSET IN IDAHO, MONTANA, OREGON AND WASHINGTON, VOLUME 2
F. G. Bloomquist Jun. 1985 528 p
(Contract DE-AI79-83BP-13609)
(DE85-014452; DOE/BP-13609/2-Vol-2; WAOENG-85-02b-Vol-2) Avail: NTIS HC A23/MF A01

Appendices are given on: (1) resource assessments of electrical generation computer results; (2) a resource assessment summary of direct use computer results; (3) an electrical generation (high temperature) resource assessment computer program listing; (4) a direct utilization (low temperature) resource assessment computer program listing; (5) an electrical generation computer program CENTPLANT and related documentation; (6) an electrical generation computer program WELLHEAD and related documentation; (7) a direct utilization computer program HEATPLAN and related documentation; (8) an electrical generation ranking computer program GEORANK and related documentation; (9) a direct utilization ranking computer program GEORANK and related documentation; and (10) a life cycle cost analysis computer program and related documentation. DOE

N86-11684# Utah Univ., Salt Lake City. Dept. of Materials Science and Engineering.
MULTISPECTROSCOPIC STUDIES OF THE ELECTRONIC STRUCTURE OF ELECTRODE MATERIALS FOR HIGH ENERGY DENSITY BATTERIES: 1-2, 1-3 INTERMETALLIC COMPOUNDS WITH B32 STRUCTURE Final Technical Report
I. M. Curelaru 2 Jul. 1985 23 p
(Contract DE-AT03-83ER-45011)
(DE85-014675; DOE/ER-45011/T1) Avail: NTIS HC A02/MF A01

The 1-2 and 1-3 intermetallic compounds with B32 (Zintl) structure which are promising candidates for electrode materials to be used in high energy density batteries or solid blankets for nuclear reactors are discussed. Optimal use of these important materials requires a satisfactory understanding of their structure and physicochemical properties. The work performed to initiate a systematic experimental study of the electronic structure and related properties of representative compounds in the 1-2 and 1-3 Zintl series is described. DOE

N86-11685# Los Alamos National Lab., N. Mex.
PASSIVE SOLAR APPLICATIONS
J. D. Balcomb 1985 8 p Presented at the Intern. Conf. on Solar and Wind Energy Appl. (ICSWEA), Beijing, China, 3 Aug. 1985
(Contract W-7405-eng-36)
(DE85-014085; LA-UR-85-2213; CONF-850888-1) Avail: NTIS HC A02/MF A01

Passive solar applications in buildings are described. The major emphasis of the research has been on devising mathematical models to characterize heat flow within buildings, on the validation of these models by comparison with test results, and on the subsequent use of the models to investigate the influence of both various design parameters and the weather on system performance. Results from both test modules and monitored buildings are discussed. Simulation analysis, the development of simplified methods, and systems analysis are outlined. Passive solar potential in China is discussed. DOE

N86-11686# Oregon State Univ., Corvallis. Wind Resources Assessment Lab.
REGIONAL WIND ENERGY ASSESSMENT PROGRAM. APPENDIX: WIND STATISTICS SUMMARIES Progress Report, Oct. 1983 - Sep. 1984
R. W. Baker, J. E. Wade, and R. J. Wittrup Feb. 1985 152 p refs
(DE85-011520; DOE/EP-388-App; BPA-84-18-App) Avail: NTIS HC A08/MF A01

The wind statistics given include summarized spectrum analyzer data, speed frequency distributions, and occurrences of winds of 50 mph or greater. Also mapped is the wind power prospecting flight path, with site locations numbered. DOE

N86-11687# Sandia Labs., Albuquerque, N. Mex.
ECONOMICS OF MAGMA POWER GENERATION
C. C. Carson and J. Haraden (Well Production Testing, Inc., Carlsbad, Calif.) 1985 5 p refs Presented at Intern. Symp. on Geothermal Energy, Kailua Kona, Hawaii, 26 Aug. 1985
(Contract DE-AC04-76DP-00789)
(DE85-008694; SAND-85-0646C; CONF-850801-6) Avail: NTIS HC A02/MF A01

An analysis of the economics of generating electricity using magma reservoirs as the energy source indicates that magma based energy could be roughly competitive with existing sources of electricity. The conclusion seems justified even though the analysis requires many assumptions that may or may not prove to be realistic as technology advances. Another important result of this analysis that is not dependent on the state of technology is the identification of the parameters that have the largest effect on the economics of magma energy. These include the initial cost and the lifetime of the wells that are drilled to reach the magma reservoir and the rate at which energy can be extracted from each well - the same parameters that control the economics of hydrothermal resources. The technological improvements that affect these parameters will be the focus of the continuing magma energy extraction program. DOE

N86-11688# Sandia Labs., Albuquerque, N. Mex.
USE OF SIO2 AND TIO2 SOL-GEL ANTIREFLECTION FILMS ON SILICON SOLAR CELLS
R. B. Pettit, C. J. Brinker, and C. S. Ashley 1985 5 p refs Presented at 13th Photovoltaic Concentrator Project Integration Meeting, Albuquerque, N. Mex., 4 Jun. 1985
(Contract DE-AC04-76DP-00789)
(DE85-011280; SAND-85-0936C; CONF-8506140-1) Avail: NTIS HC A02/MF A01

SiO2 and TiO2 sol-gel solutions were prepared for use as antireflection coatings on silicon solar cells. Multiple layers of the sol-gel were applied to silicon substrates, and the resulting reflectance curves were measured and calculated. The reflectance properties double layer coatings on silicon were calculated as a function of the thickness of the SiO2 and TiO2 layers near the optimum range. DOE

N86-11689# Sandia Labs., Albuquerque, N. Mex.
DEVELOPMENT OF MEMBRANES FOR THE ZINC/FERRICYANIDE BATTERY
R. A. Assink and C. Arnold, Jr. 1985 18 p refs Presented at 20th Intersoc. Energy Conversion Eng. Conf., Miami Beach, Fla., 18 Aug. 1985
(Contract DE-AC04-76DP-00789)
(DE85-011189; SAND-84-2358C; CONF-850808-5) Avail: NTIS HC A02/MF A01

The successful commercialization of the zinc/ferricyanide battery depends in part on the availability of an inexpensive, chemically stable membrane. The objectives of this study were to: (1) identify chemically stable commercial and/or developmental membranes, and (2) explore new approaches to the synthesis and fabrication of chemically stable membranes. The stability of membranes was evaluated by their response to a saturated solution of sodium ferricyanide in 5N sodium hydroxide for one week at 50 C. The most promising membranes were tested in cycling test cells by Lockheed Corp. The cycle tests enabled the cell's voltaic, coulombic and energy efficiency to be determined as a function of a membrane's exposure time. A radiatively grafted membrane prepared by RAI Research Corp. using fluorinated film substrates exhibited 79.3% average energy efficiency for 760 charge/discharge cycles. A membrane prepared by casting sulfonated polysulfone exhibited 75.4% average energy efficiency for 150 charge/discharge cycles. DOE

45 ENVIRONMENT POLLUTION

Includes air, noise, thermal and water pollution; environment monitoring; and contamination control.

N86-11690# Oak Ridge National Lab., Tenn.
INTEGRATED FOREST STUDY ON EFFECTS OF ATMOSPHERIC DEPOSITION. PROJECT SUMMARY
D. W. Johnson and S. E. Lindberg Jul. 1985 38 p
(Contract DE-AC05-84OR-21400)
(DE85-015972; DOE/OR-21400/T157) Avail: NTIS HC A03/MF A01

The forest effects research is divided into two major sections: atmospheric deposition and forest nutrient dynamics. Atmospheric deposition tasks will provide estimates of the rates of deposition to the canopy by precipitation, dry deposition of vapors and particles, and by cloud and fog interception, and also the wetfall return to the forest floor. The forest nutrient effects tasks will provide estimates of element fluxes in litter and soil systems, estimates of internal H(+) production, and characterization of key processes leading to S, N, and H saturation in soils. The results of these tasks will be combined in assessments of atmospheric deposition effects on forest nutrient cycles, which can in turn be applied to assessments of nutritional causes of forest dieback and long-term effects on productivity. DOE

N86-11691# California Univ., Livermore. Lawrence Livermore Lab.

UNCERTAINTIES IN THE RADIATIVE PROPERTIES OF SMOKE AND THEIR EFFECTS ON CLIMATE ASSESSMENTS

F. M. Luther Jul. 1985 13 p refs Presented at the 4th Intern. Conf. on Nucl. War, Erice, Italy, 19 Aug. 1984
(Contract W-7405-eng-48)
(DE85-015187; UCRL-92942; CONF-8408122-6) Avail: NTIS HC A02/MF A01

The sensitivity of the climatic effects of large tropospheric smoke loadings to uncertainties in the physical and radiative properties of the smoke is investigated. The extinction coefficient is shown to be very sensitive to the smoke composition and particle size distribution. The reduction in surface temperature resulting from an initial smoke mass loading of 0.5 gm(-2) varies by more than a factor of depending upon the index of refraction, particle size distribution, and vertical distribution of the smoke in the troposphere. As the smoke is modified by microphysical processes after injection into the atmosphere, the extinction coefficient for urban smoke may be reduced significantly. DOE

N86-11692# Harvard Univ., Cambridge, Mass. Biological Labs.

EFFECT OF ELEVATED ATMOSPHERIC CO2 ON PLANT COMMUNITIES. ANNUAL REPORT, 1984-1985

F. A. Bazzaz 1985 35 p
(Contract DE-FG02-84ER-60257)
(DE85-015575; DOE/ER-60257/1) Avail: NTIS HC A03/MF A01

The effects of elevated CO2 on species relationships were examined by exposing competing groups of plants to high CO2 and analyzing their ecological and physiological responses. Researchers analyzed total community productivity in these groups to learn about which combinations of species and resources show enhanced productivity with increased CO2 and which do not. DOE

N86-11693# California Univ., Livermore. Lawrence Livermore Lab.

STUDY OF HEAVY GAS EFFECTS ON THE ATMOSPHERIC DISPERSION OF DENSE GASES, REVISION 1

D. L. Ermak and S. T. Chan Apr. 1985 25 p refs Presented at 15th Intern. Tech. Survey on Air Pollution Modeling and It's Appl., St. Louis, 15 Apr. 1985
(Contract W-7405-eng-48)
(DE85-012917; UCRL-92494-Rev-1; CONF-8504135-2-Rev-1) Avail: NTIS HC A02/MF A01

In this paper, four different types of dispersion simulations are compared with the results from three heavy gas dispersion experiments. The experiments include two different release gases (LNG vapor, a cold dense gas and NO2, an isothermal dense gas) and three different wind speeds and atmospheric stabilities. The four types of dispersion simulations are a heavy gas simulation, a neutrally buoyant gas simulation, and two types of trace gas simulations. Two models (FEM3 and Steady State SLAB) are used to make the predictions. FEM3 simulates the dispersion of a heavy gas by solving the time dependent, three dimensional conservation equations and uses similarity profiles to determine the crosswind dependence. The purpose of this paper is to demonstrate how the inclusion of heavy gas phenomena and the choice in concentration averaging time affect the concentration prediction from a heavy gas release. DOE

N86-11694# PEI Associates, Inc., Cincinnati, Ohio.

LABORATORY EVALUATION OF THE PROTOCOL FOR THE VOLATILE ORGANIC SAMPLING TRAIN

T. J. Logan, R. G. Fuerst, M. R. Midgett (EPA, Research Triangle Park, N. Car.), and J. Prohaska 1985 17 p refs
(Contract EPA-68-02-3767)
(PB85-201184; EPA-600/D-85-107) Avail: NTIS HC A02/MF A01 CSCL 14B

The measurement of volatile organic emissions from a hazardous waste incinerator is one of the more difficult source testing problems. Specific compounds called Principal Organic Hazardous Constituents (POHC) are to be identified and quantified at levels of 0.5 to 100 ppb in hot, wet incinerator exhaust gas, which may also contain high particulate and acid levels. The protocol, which describes the practices used by laboratories making these measurements, allows for several alternative designs and operating procedures. This paper describes an experimental program to evaluate under controlled conditions in the laboratory as many of the acceptable practices as possible. It describes the results of sampling at various concentration levels using two tube configurations, two moisture levels and other procedural variations. These results have led to conclusions about the specific VOST procedures to be followed during the field validation studies. Author (GRA)

N86-11695# Midwest Research Inst., Kansas City, Mo.

DEVELOP, EVALUATE AND VALIDATE CONTINUOUS EMISSION MONITORS FOR DESIGNATED HAZARDOUS POLLUTANTS Final Report

G. W. Scheil May 1985 75 p
(Contract EPA-68-02-3770)
(PB85-201176; EPA-600/4-85-037) Avail: NTIS HC A03/MF A01 CSCL 14B

The objectives of the project are to assess the state of the art of continuous emission monitoring of vinyl chloride monomer (VCM) and to conduct actual experiments to evaluate two monitors in laboratory and in a six-month field testing program. A process GC with flame ionization detector and a photoionization detector were used during this study. Three one-week EPA Method 106 tests were conducted during the six-month field testing program to measure the relative accuracies of the monitors. The precisions of both types of detectors all were in the 1% range when evaluated in laboratory. The relative accuracies for both types of detectors were < 10% for VCM concentration between 2 to 10 ppm. Author (GRA)

N86-11696# Environmental Protection Agency, Research Triangle Park, N.C. Atmospheric Sciences Research Lab.

REGIONAL-SCALE (1000 KM) MODEL OF PHOTOCHEMICAL AIR POLLUTION. PART 3: TESTS OF THE NUMERICAL ALGORITHMS

R. G. Lamb and G. F. Laniak (Program Resources, Inc.) May 1985 291 p refs
(PB85-203818; EPA-600/3-85-037-Pt-3) Avail: NTIS HC A13/MF A01 CSCL 13B

The Regional Oxidant Model (ROM) developed in two earlier reports is applied to a series of hypothetical problems whose exact solutions are known. Comparisons are made between the model's predictions and the known solutions to assess the accuracies of the numerical algorithms that comprise the models's predictive equations. It is found that in the case of ozone, the solutions of the numerical algorithms on which the model is based are within 10 percent of the solutions of the corresponding differential equations that describe the chemical and physical processes that the model simulates. Extensive documentation is provided in the report of the model's performance in simulating the concentrations of 23 chemical species over a 48 hour period. Author (GRA)

N86-11697# Environmental Protection Agency, Atlanta, Ga.

SALTWATER WETLANDS FOR WASTEWATER MANAGEMENT ENVIRONMENTAL ASSESSMENT

Nov. 1984 322 p
(PB85-201267; EPA-904/10-84-128) Avail: NTIS HC A14/MF A01 CSCL 06F

Saltwater wetlands have the potential for use as municipal and seafood processing wastewater-discharge sites. However, the potential also exists for adversely impacting these important natural resources. The Saltwater Wetlands or Wastewater Management Environmental Assessment is designed to explore the feasibility of using saltwater wetlands for municipal and seafood processing wastewater management and to identify areas of concern that are important to local, state and federal agencies in making wastewater management decisions affecting saltwater wetlands in the southeastern United States. This assessment is a companion study to the previously initiated Freshwater Wetlands for Wastewater Management Environmental Impact Statement (EIS). The emphasis of this Saltwater Wetlands Environmental Assessment is to provide a description of key saltwater wetland factors, disposal practices and options, regulatory considerations for disposal implementation, and areas where additional wetland research is needed. GRA

N86-11698# Tennessee Water Resources Research Center, Knoxville.

EFFECTS OF ACID PRECIPITATION ON COMPOSITION, ELECTROKINETIC BEHAVIOR, CATION ADSORPTION AND ION EXCHANGE CAPACITY IN VARIOUS SOIL SYSTEMS

A. R. Bowers and T. Higgs Sep. 1984 94 p
(Grant DI-14-08-0001-G-870)
(PB85-217727; RR-103; UT/PUB-R01-2550-29-001-85; USGS/G-870-03) Avail: NTIS HC A05/MF A01 CSCL 08M

The effects of acidic environments on the physical/chemical behavior of natural soils from Tennessee were examined in the laboratory. Primarily, the influence of increased weathering of iron oxides on electrokinetic behavior, cation exchange capacity and adsorption of free and complexed heavy metals was studied. Natural soils, compared to samples in which iron oxides were removed showed little change in cation exchange capacity or electrokinetic behavior. Acid aging of one particular soil was also conducted. Studies showed that prolonged exposure to acidic environments may result in drastic changes in soil properties. Substantial changes in the electrokinetic behavior were found with the zero point of charge increasing from a pH of 2.0 for the unaged soil to 8.0 for the acid aged one. Also, the zinc adsorptive behavior of the soils changed significantly with acid aging. The study indicates that prolonged exposure to acidic environments may create changes in physical/chemical properties of soils rich in iron oxides. GRA

N86-11624*# Jet Propulsion Lab., California Inst. of Tech., Pasadena.

SPECTRAL CHARACTERIZATION OF SUSPECTED ACID DEPOSITION DAMAGE IN RED SPRUCE (PICEA RUBENS) STANDS FROM VERMONT

James E. Vogelmann and Barrett N. Rock *In its* Proc. of the Airborne Imaging Spectrometer Data Anal. Workshop 15 Jun. 1985 p 51-55 refs ERTS (For primary document see N86-11618 02-43)
Avail: NTIS HC A09/MF A01 CSCL 13B

46 GEOPHYSICS

Includes aeronomy; upper and lower atmosphere studies; ionospheric and magnetospheric physics; and geomagnetism.

For space radiation see *93 Space Radiation.*

N86-11699 Northwestern Univ., Evanston, Ill.

OCEANIC INTRAPLATE SEISMICITY: IMPLICATIONS FOR THE RHEOLOGY AND TECTONICS OF THE OCEAN LITHOSPHERE Ph.D. Thesis

Douglas Alvin Wiens 1985 235 p
Avail: Univ. Microfilms Order No. DA8511877

The strength of the oceanic lithosphere is constrained by the maximum depth of oceanic intraplate seismicity, which increases with lithospheric age and appears to be bounded by a 700 C isotherm. Intraplate earthquake focal mechanisms indicate that older oceanic lithosphere is in compression, models of the stresses produced by a combination of ridge push and basal drag forces require the magnitude of the drag be less than a few bars for rapidly moving plates. Focal mechanisms of intraplate earthquakes in young oceanic lithosphere indicate a diversity of faulting styles. Tensional stress in the spreading direction is concentrated in a very narrow zone at the ridge axis, suggesting the axial region has very little tensile strength. The intraplate seismicity rate is highest in young lithosphere, indicating that stress sources concentrated in young lithosphere are significant. However, most of the near-ridge seismicity occurs in five areas, suggesting local perturbations strongly affect near-ridge seismicity. It is indicated that a deconvolution method is useful for determining the depth, mechanism, source time function and rupture characteristics of an earthquake from P and SH waveforms. This technique is used to determine the source parameters of three large intraplate earthquakes. Dissert. Abstr.

N86-11700*# National Aeronautics and Space Administration. Langley Research Center, Hampton, Va.

SAGE AEROSOL MEASUREMENTS. VOLUME 1: FEBRUARY 21, 1979 TO DECEMBER 31, 1979

M. Patrick McCormick Oct. 1985 371 p refs
(NASA-RP-1144; L-15962; NAS 1.61:1144) Avail: NTIS HC A16/MF A01 CSCL 04A

The Stratospheric Aerosol and Gas Experiment (SAGE) satellite system, launched on February 18, 1979, provides profiles of aerosol extinction, ozone concentration, and nitrogen dioxide concentration between about 80 N and 80 S. Zonal averages, separated into sunrise and sunset events, and seasonal averages of the aerosol extinction at 1.00 microns and 0.45 microns ratios of the aerosol extinction to the molecular extinction at 1.00 microns, and ratios of the aerosol extinction at 0.45 microns to the aerosol extinction at 1.00 microns are given. The averages for 1979 are shown in tables and in profile and contour plots (as a function of altitude and latitude). In addition, temperature data provided by the National Oceanic and Atmospheric Administration (NOAA) for the time and location of each SAGE measurement are averaged and shown in a similar format. Typical values of the peak aerosol extinction were 0.0001 to 0.0002 km at 1.00 microns depth values for the 1.00 microns channel varied between 0.001 and 0.002 over all latitudes. Author

N86-11701*# National Aeronautics and Space Administration, Washington, D. C.

BIBLIOGRAPHY OF TERRESTRIAL IMPACT STRUCTURES

Maurice J. Grolier (Geological Survey, Flagstaff, Ariz.) Sep. 1985 532 p
(NASA Order W-13130)
(NASA-TM-87567; NAS 1.15:87567) Avail: NTIS HC A23/MF A01 CSCL 08G

This bibliography lists 105 terrestrial impact structures, of which 12 are proven structures, that is, structures associated with meteorites, and 93 are probable. Of the 93 probable structures, 18 are known to contain rocks with meteoritic components or to be enriched in meteoritic signature-elements, both of which enhance their probability of having originated by impact. Many of the structures investigated in the USSR to date are subsurface features that are completely or partly buried by sedimentary rocks. At least 16 buried impact structures have already been identified in North America and Europe. No proven nor probable submarine impact structure rising above the ocean floor is presently known; none has been found in Antarctica or Greenland. An attempt has been made to cite for each impact structure all literature published prior to mid-1983. The structures are presented in alphabetical order by continent, and their geographic distribution is indicated on a sketch map of each continent in which they occur. They are also listed tables in: (1) alphabetical order, (2) order of increasing latitude, (3) order of decreasing diameter, and (4) order of increasing geologic age. Author

N86-11702 Ceskoslovenska Akademie Ved, Prague. Scientific Information Centre.

GEOPHYSICAL WORKS, 1982, VOLUME 30

1985 277 p refs
Copyright. Avail: Issuing Activity

Volume 30 of Geophysical Works (1982) published by the Geophysical Institute of the Czechoslovak Academy of Sciences (Prague, 1985), contains 13 articles on geophysical topics. They discuss the following: earth crust-mantle boundary, Legendre polynomial applications, macroseismic effects, seismic waves from underground explosions, seismology in Civil Engineering, seismographic readings, deep geomagnetic sounding, numerical solution of ionospheric filtration of ULF waves, ion whistlers in middle latitudes, and the instability of a vortex series. For individual titles, see N86-11703 through N86-11715.

N86-11703# Ceskoslovenska Akademie Ved, Prague. Geophysical Inst.

ON THE GRAVITATIONAL EFFECT OF THE CRUST-MANTLE BOUNDARY IN CENTRAL EUROPE

Vincenc Vyskoch, Miloslav Burda, and Milada Koziskova *In its* Geophys. Works, 1982, Vol. 30 1985 p 9-31 refs (For primary document see N86-11702 02-46)

Avail: Issuing Activity

The correlation between gravity anomalies, elevations above sea level and depths of the crust-mantle boundary in Central Europe are investigated. The results of the correlation analyses are used to estimate the density jump Delta Sigma at the crust-mantle boundary in the Alps and Carpathians. In both cases Delta Sigma <0.2 g/cu cm. It is found that the density inhomogeneities in the lithosphere may compensate each other so that they are not reflected in the anomalous gravity field. This should be taken into account in dealing with the gravitational effects of deep structure and in constructing density models of the lithosphere. Author

N86-11704# Karlova Univ., Prague (Czechoslovakia). Inst. of Geophysics.

ON THE ADDITION THEOREM FOR LEGENDRE POLYNOMIALS c64

Oldrich Novotny *In* Ceskoslovenska Akademie Ved Geophys. Works, 1982, Vol. 30 1985 p 33-45 refs (For primary document see N86-11702 02-46)

Avail: Issuing Activity

The usual proofs of the addition theorem for Legendre polynomials are founded on the theory of spherical functions. Two, principally simple proofs of this theorem, founded on recurrent formulae for Legendre polynomials and associated Legendre functions, are described here. Author

N86-11705# Ceskoslovenska Akademie Ved, Prague.

ATTENUATION OF MACROSEISMIC EFFECTS OF EARTHQUAKES

Dana Prochazkova *In its* Geophys. Works, 1982, Vol. 30 1985 p 47-93 refs (For primary document see N86-11702 02-46)

Avail: Issuing Activity

One of the main tasks of seismology today is to calculate the earthquake hazard at specific localities. The calculation is also based on the detailed description of macroseismic earthquake fields, which may be manifested by their effects in a given locality. One of the parameters used to calculate the hazard is the attenuation of the macroseismic effects of earthquakes. The propagation of macroseismic effects from the earthquake focus depends on the earthquake mechanism, on the one hand, and on the physical properties of the medium through which the seismic waves propagate, on the other. Since the causes of earthquakes and, consequently, also the earthquake mechanisms and physical properties of the medium are not exactly the same in all focal regions, understandably the attenuation of the macroseismic effects of earthquakes will differ from place to place as well. The purpose of this paper is to study the dependences describing the attenuation of the macroseismic effects of earthquakes and to calculate these dependences for the focal regions of Central Europe. Author

N86-11706# Scientific Coal Research Inst., Ostrava (Czechoslovakia).

TRAVEL-TIME AND ITS RESIDUALS FOR THE BLASTS FROM ESCHENLOHE (BAVARIA)

Karel Holub *In* Ceskoslovenska Akademie Ved Geophys. Works 1982, Vol. 30 1985 p 95-117 refs (For primary document see N86-11702 02-46)

Avail: Issuing Activity

The seismic waves generated by instantaneous blasts in the stone quarry near Eschenlohe (Bavaria), for purposes of deep seismic sounding, were recorded at 9 sites in the Bohemian Massif, including seismic stations Pruhonice (PRU) and Kasperske Hory (KHC). The travel-time curves of the principal wave groups of body waves, recorded during refraction measurements within the distance range Delta = 245-410 km, are described by the following equations: t = 8.10 + Delta/8.27(Pn), t = Delta/5.85(Pg), t = 9.47 + Delta/4.47(Sn) and t = Delta/3.42(Sg). In analyzing the arrival time residuals (O-C(s)) using the experimental data from the seismic stations of PRU and KHC, and seismic wave velocities determined from the travel-time curves of near earthquakes, relatively high negative values were obtained for Pg-waves. Better agreement of the observed and calculated arrival times was achieved, on the one hand, by reinterpretation of first arrivals and on the other hand by using seismic velocities, derived from refraction measurements. Author

N86-11707# Ceskoslovenska Akademie Ved, Prague. Stavebni Geologie.

SEISMOLOGY IN CIVIL ENGINEERING

Arnost Dvorak *In its* Geophys. Works, 1982, Vol. 30 1985 p 103-117 refs (For primary document see N86-11702 02-46)

Avail: Issuing Activity

Properties of soils and rocks exposed to vibrations in the practice of civil engineering are examined. Seismic and dynamic field investigations, determination of seismic and dynamic modulus of elasticity, coefficients of damping and absorption are studied. Seismic effects of blasting and of other sources of vibrations on structures and persons, application of rock-noise and dynamic tests of piles are studied. Author

N86-11708# Ceskoslovenska Akademie Ved, Prague. Geophysical Inst.

SHORT-PERIOD SVSN-4 SEISMOGRAPH

Vladimir Tobyas *In its* Geophys. Works, 1982, Vol. 30 1985 p 119-140 refs (For primary document see N86-11702 02-46)

Avail: Issuing Activity

The procedure for calculating the parameters of a vertical short-period seismometer for an electromagnetic seismograph with galvanometric recording, and for determining the fundamental constants with a non-negligible coupling coefficient is described. A seismograph with a seismometer period of 0.96 s, a galvanometer period of 1.47 s, critical damping of both systems and a coupling coefficient of 0.17 achieves its maximum magnification of 36000 for the period motion of 0.8 s. The equivalent damping constants of 0.61 and 1.43 guarantee quick damping of the transient oscillations of the seismograph. The errors of the mean magnification under long-term operation are estimated on the basis of calculated changes of the constants caused by the changes of the parameters. The seismograph which has been operating at the seismic station of Pruhonice (PRU) for the purposes of the seismic service since 1960, permits extensive material to be collected for studying near as well as distant earthquakes. Author

N86-11709# Slovak Academy of Sciences, Hurbanova (Czechoslovakia). Geophysical Inst.

MAGNIFICATION OF LOW-SENSITIVITY CHANNELS IN SEISMOGRAPHS WITH STANDARD CHARACTERISTICS

Ivan Broucek and Vladimir Tobyas (Ceskoslovenska Akademie Ved., Prague) *In* Ceskoslovenska Akademie Ved Geophys. Works, 1982, Vol. 30 1985 p 141-153 refs (For primary document see N86-11702 02-46)

Avail: Issuing Activity

The accuracy of an approximate method of computing the magnification of the low-sensitivity channel is analyzed on an analog computer for the parameters of seismographs with standard characteristics used in the network of seismic stations of CAPG (Commission of the Academies of Sciences of the Socialist Countries for Planetary Geophysical Research). The errors of the method of computation depend on the magnitude of the coupling coefficient of the basic channel of the seismograph: for short periods of motion they approach zero and they are usually largest outside the passband in the range of long periods. The error in the magnification of the low-sensitivity channel of a short-period seismograph with an A IV amplitude characteristic and a maximum magnification of the basic channel of 100000 is 65% at the most, of an intermediate-period seismograph with a magnification of 1000 as much as 24%, and of a long-period seismograph with a maximum magnification of 900 up to 19%. Author

N86-11710# Ceskoslovenska Akademie Ved, Prague. Geophysical Inst.

STATISTICAL PROPERTIES OF GEOMAGNETIC PULSATIONS AT THE FUERSTENFELDBRUCK OBSERVATORY DETERMINED BY MEANS OF PULSATION INDICES. PART 3: CORRELATION WITH THE PARAMETERS OF THE INTERPLANETARY MAGNETIC FIELD

Jaroslav Strestik *In its* Geophys. Works, 1982, Vol. 30 1985 p 155-178 refs (For primary document see N86-11702 02-46)
Avail: Issuing Activity

Geomagnetic pulsations recorded at the observatory of Furstenfeldbruck (FRG) in the years 1963 to 1971 were processed in the form of pulsation indices. The correlation of these indices and also of the Ap-amplitudes with the Interplanetary Magnet Field (IMF) parameters is investigated: with the intensity B and its components, with the solar-wind velocity v, with the Alfven velocity V sub a with the particle concentration N, and with the components of the interplanetary electric field E sub y and E sub z. The mean values of the individual indices are determined for different polarities of the IMF components and separately for large and small values of B, v, Ap, etc. Also all the correlations are calculated separately or the above divisions. In conclusion, the mean values of some IMF quantities, corresponding to the values of the indices within certain intervals are given and used to show how the index values and Ap's can be used to estimate the magnitude of some of the IMF parameters. Author

N86-11711# Ceskoslovenska Akademie Ved, Prague. Geophysical Inst.

DETERMINATION OF THE DEPTH OF A CONDUCTIVITY ANOMALY BY SEPARATING THE GEOMAGNETIC VARIATION FIELD INTO ITS EXTERNAL AND INTERNAL PART

Jana Pecova *In its* Geophys. Works, 1982, Vol. 30 1985 p 179-197 refs (For primary document see N86-11702 02-46)
Avail: Issuing Activity

The problem in question is part of deep geomagnetic sounding carried out on a local or regional scale, whose solution requires synchronous records of the variations of the geomagnetic field components along profiles running through the area being investigated. The variation of the geomagnetic field, observed at the Earth's surface, is composed of an external and internal part. The external part represents the magnetic field of current systems in outer space, particularly in the ionosphere. Due to the incidence of corpuscular and wave radiation from the Sun, electrical current systems, which generate a variable magnetic field, are created in the outer conductive layers of the Earth. This variable primary magnetic field also induces systems of electrical currents within the conductive layers of the Earth's interior, which then generate their own secondary variable magnetic field. This secondary magnetic field provides information about the medium in which the induction has taken place and through which the electromagnetic waves propagate. It is referred to as the internal part of the variation field observed at the Earth's surface. In order to determine the properties of the medium, the internal part has to be separated from the external. Author

N86-11712# Foreign Trade Computer Centre, Prague (Czechoslovakia).

NUMERICAL SOLUTION OF IONOSPHERIC FILTRATION OF ULF WAVES. PART 1: METHOD

Vladimir Vagner *In* Ceskoslovenska Akademie Ved Geophys. Works, 1982, Vol. 30 1985 p 199-229 refs (For primary document see N86-11702 02-46)
Avail: Issuing Activity

The algorithm for solving the transmission and reflection of both homogeneous spectral natural wave modes is optimized and programmed in FORTRAN IV. The input of this program are the values of the parameters of the profiles of the ionospheric plasma, the conductivity of the Earth's crust, the dip and values of the outer magnetic induction of the Earth, as well as the values of the ranges of the variable parameters of frequencies and angles of incidence, and the data determining whether the incident mode is electron or ion. Moreover, data can be given which enable the standard spacing densities of both variable parameters to be varied and the transition layer to be discretized. The output, apart from the values of the indicators of accuracy and stability of the computations, are the matrices of the values of the amplitude and energetic real coefficients and of the supplementary energetic coefficients. Some of these characteristics describe the transition layer and document the possibilities of this program. The input parameters are chosen to simulate the situation in the mid geomagnetic latitudes. Author

N86-11713# Ceskoslovenska Akademie Ved, Prague. Geophysical Inst.

NUMERICAL SOLUTION OF IONOSPHERIC FILTRATION OF ULF WAVES. PART 2: APPLICATION

Karel Prikner and Vladimir Vagner (Foreign Trade Computer Centre) *In its* Geophys. Works, 1982, Vol. 30 1985 p 231-257 refs (For primary document see N86-11702 02-46)
Avail: Issuing Activity

The problem of ionospheric correction is still topical from the point of view of micropulsation wave diagnostics of the ionized envelope of the Earth. The micropulsation diagnostics of the magnetosphere make use of natural geomagnetic activity recorded in a network of terrestrial observatories. The material which has so far been recorded, is abundant and, to a considerable extent, also continuous in time and space. However, the available data pertaining to the wave field, recorded at the Earth's surface, do not permit a complete reconstruction of the primary signal above the ionosphere. These data provide us with a number of parameters (amplitudes, phase and polarization characteristics, energy flow, etc.) which enable us to develop methods of modeling various wave-propagation patterns. We are able to evolve a method for eliminating the effect of the ionosphere on the received signal, the method of ionospheric correction. Micropulsations, i.e., ULF signals recorded at the Earth's surface, provide information about the structure and dynamics of the plasma in the magnetosphere which is, however, distorted due to the propagation of electromagnetic (or MHD) waves through the dense layers of the ionosphere. The vertically, strongly inhomogeneous, anisotropic (magnetoactive) ionosphere, in which losses occur, may be interpreted as a stratifed inhomogeneous interference filter which deforms the original signal, generated in the magnetosphere. Author

N86-11714# Ceskoslovenska Akademie Ved, Prague. Geophysical Inst.

ION WHISTLERS IN MIDDLE LATITUDES OBSERVED BY THE INTERKOSMOS-14 SATELLITE

Jaroslava Boskova and Frantisek Jiricek *In its* Geophysical Works, 1982, Vol. 30 1985 p 259-267 refs (For primary document see N86-11702 02-46)
Avail: Issuing Activity

Ion cyclotron whistlers from higher geomagnetic latitudes, as found in the Interkosmos-14 Very Low Frequency (VLF) data set, distinctly reflect the effects of processes in the midlatitude trough of light ions. These proton whistlers indicate a marked decrease of the relative proton content in the vicinity of the satellite with increasing geomagnetic latitude. As it is further shown, proton whistlers from higher geomagnetic latitudes give additional information on some changes of the plasma parameters in the region of midlatitude plasma troughs. They are able to indicate the satellite's crossing of a point with a very steep gradient of the O(+)-H(+) transition height and to provide information on the plasma structure in the medium below the satellite along the propagation path of ion cyclotron waves. Author

N86-11715# Ceskoslovenska Akademie Ved, Prague. Inst. of the Physics of the Atmosphere.
ON THE INSTABILITY OF VORTEX SERIES c64
Jiri Horak *In its* Geophys. Works, 1982, Vol. 30 1985 p 269-285 refs (For primary document see N86-11702 02-46)
Avail: Issuing Activity

The instability of the vortex motion of an ideal liquid is examined by means of the algebraic physics method and perturbation theory. The instability criterion is based on the hydrodynamic analog of the expression for the second full differential of the kinetic energy of rotation of a rigid body, fixed at a point. Author

N86-11716# Iowa Univ., Iowa City. Dept. of Physics and Astronomy.
PLASMAS IN THE EARTH'S MAGNETOTAIL Progress Report
L. A. Frank May 1985 33 p Original contains color illustrations
(Contract N00014-76-C-0016)
(AD-A157320; U-OF-IOWA-85-12) Avail: NTIS HC A03/MF A01
CSCL 04/1

An overview of the general characteristics of plasmas within the Earths magnetotail and its environs is presented. Present knowledge of the plasmas within these regions as gained via in situ measurements provides the general theme, although observations of magnetic fields, energetic particles and plasma waves are included in the discussion. Primary plasma regimes in the magnetotail are the plasma sheet, its boundary layer, the magnetotail lobes, the boundary layer at the magnetopause and the distant magnetotail. Although the great progress in our understanding of these regions is evident in the literature of the past several years, many of their features remain as exciting enigmas to be resolved by future observational and theoretical investigation. GRA

N86-11717# Naval Research Lab., Washington, D. C.
MEASUREMENTS OF REFRACTIVE INDEX STRUCTURE FUNCTION C2N AND AEROSOL SIZE DISTRIBUTION AT CHESAPEAKE BAY Memorandum Report, Oct. 1982 - Oct. 1983
D. R. Cutten 26 Jul. 1985 36 p
(AD-A157455; NRL-MR-5593) Avail: NTIS HC A03/MF A01
CSCL 04/1

Measurements of (C sub N) square using fine wire thermal probes were obtained on a 35 m tower located between the cliff face and the shoreline at Chesapeake Bay, MD. The data collected have shown, using long averaging times, that the -4/3 height dependence of (C sub N) generally still applies in the vicinity of the cliff face with light winds coming from either over the cliff or over the water. The aerosol size distribution data revealed very little change in the distribution with height. Over the 0.15 to 0.75 micrometers radius range both bi-modal log-normal and power laws described the shape of the distribution curves. Author (GRA)

N86-11718# Army Cold Regions Research and Engineering Lab., Hanover, N. H.
PERIGLACIAL LANDFORMS AND PROCESSES IN THE SOUTHERN KENAI MOUNTAINS, ALASKA Special Report
P. K. Bailey Apr. 1985 72 p
(AD-A157459; CRREL-SR-85-3) Avail: NTIS HC A04/MF A01
CSCL 08/12

The distribution and characteristics of periglacial landforms in the southern Kenai Mountains, Alaska, were investigated during 1979 and 1980. The principal area of study was a 1300-m-high mountain mass that stood as a nunatak during the last general glaciation. Periglacial features in the area include gelifluction lobes, nivation hollows, cryoplanation terraces, tors, a string bog, and such patterned ground as sorted circles, sorted polygons, earth hummocks, sorted steps, sorted stripes, and small ice-wedge polygons. Ground temperature measurements indicate that permafrost exists in only isolated patches but may have recently been much more extensive. The sorted polygons, cryoplanation terraces, and nivation hollows are relict features that have been inactive for a considerable time. The turf-banked sorted steps and large gelifluction lobes probably were active until the recent thawing of permafrost. Cryofraction and frost sorting still are vigorous, active progresses. Finely jointed bedrock, a previous colder environment, and long exposure in the absence of glacial ice has allowed periglacial processes to be the dominant surface agents both in the principal study area and in similar areas along the western side of the Kenai Mountains. GRA

N86-11719# Army Cold Regions Research and Engineering Lab., Hanover, N. H.
WORKSHOP ON PERMAFROST GEOPHYSICS Special Report
J. Brown, M. C. Metz, and P. Hoekstra May 1985 124 p Workshop held at Golden, Colo., 23-24 Oct. 1984 Prepared in cooperation with National Academa of Sciences/National Research Council
(AD-A157485; CRREL-SR-85-5) Avail: NTIS HC A06/MF A01
CSCL 08/12

This report contains abstracts and summary papers of presentations made at a workshop in October 1984. Major topics include: deep onshore and offshore permafrost methods; shallow geophysical and borehole methods; and shallow geophysical methods and terrain analysis. GRA

N86-11720# Los Alamos National Lab., N. Mex.
SUBSURFACE GEOLOGY OF THE PAJARITO PLATEAU, ESPANCIA BASIN, NEW MEXICO
B. J. Dransfield and J. N. Gardner May 1985 23 p refs
(Contract W-7405-eng-36)
(DE85-016215; LA-10455-MS) Avail: NTIS HC A02/MF A01

Integration of data from wells, geophysical surveys, and surface exposures has enabled construction of structure contour and paleogeologic maps of the pre-Bandelier Tuff surface beneath the Pajarito Plateau. Numerous faults of the Rio Grande rift system cut the pre-Bandelier Tuff surface, and most have down-to-the-west displacements. Cumulative down-to-the-west movements across these faults from the Rio Grande on the east to the Rendija Canyon fault zone on the west exceed 600 ft (185 m). All faults in the area show evidence of recurrent activity, with increasing displacements of progressively older rock units. The southern Pajarito fault zone has over 600 ft (185 m) of pre-Bandelier Tuff down-to-the-east movement. The Pajarito fault zone and a major pre-Bandelier Tuff fault identified herein may constitute the local boundaries of the southern continuation of the intra-rift Velarde graben. The paleogeologic map shows that three major rock units (Cerros del Rio basalts, Tschicoma Formation dacites, and Puye Formation gravels) underlie the Bandelier Tuff and interfinger beneath the central Pajarito Plateau. DOE

N86-11721# Texas A&M Univ., College Station. Center for Tectonophysics.
DEFORMATION OF GRANITE AT ELEVATED TEMPERATURE AND PRESSURE Final Report, 1 Mar. 1984 - 28 Feb. 1985
N. I. Carter 15 Mar. 1985 21 p refs
(Contract DE-FG05-84ER-13216)
(DE85-014057; DOE/ER-13216/T1) Avail: NTIS HC A02/MF A01

The purpose was to determine the evolution of substructure and mechanical behavior of westerly granite, deformed under both wet and dry conditions, from the initial stages of transient creep well into the steady-state. Following calibration of the 10 kb gas apparatus at elevated temperature and pressure, the main pressure vessel burst. As a consequence, other studies were pursued. These include: (1) analysis of olivine fabrics of ophiolites; (2) upper mantle deformation in collision zones; (3) flow properties of continental lithosphere; and (4) mechanical behavior of oceanic layer 2 basalts. DOE

N86-11722# California Univ., Berkeley. Lawrence Berkeley Lab.
ELECTROMAGNETIC SOUNDINGS FOR GEOTHERMAL RESOURCES IN DIXIE VALLEY, NEVADA
M. J. Wilt and N. E. Goldstein Mar. 1985 8 p refs Presented at Intern. Symp. on Geothermal Energy, Kailua Kona, Hawaii, 26 Aug. 1985
(Contract DE-AC03-76SF-00098)

(DE85-011986; LBL-19321; CONF-850801-35) Avail: NTIS HC A02/MF A01

An electromagnetic (EM) sounding survey was performed over a region encompassing the Dixie Valley geothermal field to map the subsurface resistivity in the geothermal field and the surrounding area. The EM survey, consisting of 19 frequency domain depth soundings made with the LBL EM-60 system, was undertaken to explore a narrow region adjacent to the Stillwater Range to a depth of 2 to 3 km. Lithologic and well log resistivity information from well 66-21 show that for EM interpretation the section can be reduced to a three layer model consisting of moderately resistive alluvial sediments, low resistivity lacustrine sediments, and high resistivity Tertiary volcanics and older rocks. This three layer model was used as a starting point in interpreting EM sounding data. Variations in resistivity and thickness provided structural information and clues to the accumulation of geothermal fluids. The interpreted soundings reveal a 1 to 1.5 km deep low resistivity zone spatially associated with the geothermal field. The shallow depth suggests that the zone detected is either fluid leakage or hydrothermal alteration, rather that high temperature reservoir fluids.
DOE

N86-11723# National Oceanic and Atmospheric Administration, Silver Spring, Md. Air Resources Labs.

LIDAR OBSERVATIONS OF STRATOSPHERIC AEROSOL OVER MAUNA LOA OBSERVATORY: 1982 - 1983

J. DeLuisi, T. Defoor, K. Coulson, and F. Fernald Feb. 1985 85 p ref
(PB85-187896; NOAA-DR-ERL-ARL-5) Avail: NTIS HC A05/MF A01 CSCL 04A

One hundred and nine lidar profiles obtained during the years 1982 to 1983, are presented. Backscattering ratios are displayed in graphical form for 1-km intervals. Aerosol backscattering cross section, Rayleigh backscattering cross section, backscattering ratio and integrated optical thickness are tabulated, also for 1-km intervals. Two significant episodes of stratospheric aerosol were detected in 1982. A mystery aerosol cloud was detected on the 28th of January and the immense aerosol cloud from El Chichon was detected on the 9th of April. Some additional analysis of the lidar data is given in this report. A plot of stratospheric aerosol optical thickness above 15 km for 1974 to 1983, inclusively, is given. These tables should be useful for modeling climatic effects of El Chichon.
Author (GRA)

N86-11724# National Oceanic and Atmospheric Administration, Boulder, Colo. Space Environment Lab.

TIROS/NOAA (TELEVISION AND INFRARED OBSERVATION SATELLITE/NATIONAL OCEANIC AND ATMOSPHERIC ADMINISTRATION) SATELLITES SPACE ENVIRONMENT MONITOR ARCHIVE TAPE DOCUMENTATION

V. J. Hill, D. S. Evans, and H. H. Sauer Jan. 1985 56 p refs
(PB85-187920; NOAA-TM-34L-SEL-71) Avail: NTIS HC A03/MF A01 CSCL 04A

TIROS/NOAA satellite archive tapes containing data obtained with the Medium Energy Proton and Electron Detector (MEPED), High Energy Proton and Alpha Particle Detector (HEPAD), and Total Energy Detector (TED) are described. Descriptions of the data include orbital and housekeeping details and the information needed to decode and understand the data. Specifications of the data channels are supplied, with the timing information needed to convert the data to usable information. Description of the archive tape format gives the information needed to read the tape and unpack the data. Appendices supply the retrieval routines used by the Space Environment Services Center in Boulder.
Author (GRA)

N86-11725# University of Southern California, Los Angeles. Geophysics Lab.

EARTHQUAKE HAZARD RESEARCH IN THE LOS ANGELES BASIN AND ITS OFFSHORE AREA, OCTOBER 1, 1983 TO SEPTEMBER 30, 1984

E. Hauksson, T. Teng, T. L. Henyey, J. K. McRaney, and L. Hsu Mar. 1985 44 p refs
(Contract DI-14-08-0001-21858)
(PB85-196491; TR-85-1) Avail: NTIS HC A03/MF A01 CSCL 08K

The Geophysics Laboratory at the University of Southern California is conducting a comprehensive investigation of seismicity in the greater Los Angeles basin and its offshore area under U.S.G.S. Contract No. 14-08-0001-21858. As a part of this investigation, U.S.C. operates a seismic network in the Los Angeles basin area. During the 1984 fiscal year the authors have concentrated on seismotectonic analysis of the seismicity recorded in the Los Angeles Basin during the last 10 years. A comprehensive study of earthquakes along the Newport-Inglewood fault is in progress and the authors report the latest results. The authors are also reanalyzing the January 1, 1979 Malibu earthquake and its aftershocks.
Author (GRA)

N86-11726# University of Southern California, Los Angeles. Geophysics Lab.

DEEPWELL MONITORING ALONG THE SOUTHERN SAN ANDREAS FAULT

T. L. Henyey and S. P. Lund Mar. 1985 25 p refs
(Contract DI-14-08-0001-21879)
(PB85-196483; TR-85-3) Avail: NTIS HC A02/MF A01 CSCL 08K

Reports of strain-related changes in groundwater level flow rate, chemistry, and even turbidity accompanying large seismic events are widespread in the earthquake literature. The possibility that similar pre-seismic strains may act on groundwater basins or aquifers near the San Andreas fault cannot be ruled out, even though regional dilatancy may in fact not exist. Although flow rates in aquifers are relatively slow, the pressure response of large aquifers or even basement rocks (with interconnected fracture porosity) to changes in strain should be considerably faster. This is borne out by observation of water level changes due to solid-Earth-tides and the passage of seismic surface waves from local or even teleseismic events. In such cases, appreciable flow is not required for changes of millimeters to decameters in the apparent water tables. The authors reclaimed a set of abandoned deep wells along the San Andrea fault in the Palmdale region in order to monitor groundwater level and temperature variations that might be related to strain changes along the fault.
GRA

N86-11727# National Academy of Sciences - National Research Council, Washington, D. C.

POLAR RESEARCH BOARD ANNUAL REPORT 1984 AND FUTURE PLANS Annual Report, Jan. - Dec. 1984

1985 64 p
(PB85-204477) Avail: NTIS HC A04/MF A01 CSCL 08G

The report describes studies completed and work in progress during 1984, and projects planned for initiation in 1985. The report also describes international activities related to the Board's role as U.S. National Committee for the Scientific Committee on Antarctic Research of the International Council of Scientific Unions. Attachments provide lists of names and addresses of Board members and participants in Board special studies, as well as of reports published, in press, and in preparation.
Author (GRA)

N86-11728# Environmental Protection Agency, Research Triangle Park, N.C. Atmospheric Sciences Research Lab.

REGIONAL OXIDANT MODELING OF THE NORTHEAST US

K. L. Schere and J. H. Novak 1985 16 p refs
(PB85-201192; EPA-600/D-85-110) Avail: NTIS HC A02/MF A01 CSCL 04A

The occurrence of long range and interurban transport of ozone and/or ozone precursors across the Northeast U.S. has been documented by numerous field studies during the last ten years. The U.S. Environmental Protection Agency initiated the Northeast Corridor Regional Modeling Project (NECRMP) during the late 1970's, in part, to develop a regional model capable of simulating regional transport of ozone and its precursors on scales on the order of 1000 km. The resulting Regional Oxidant Model (ROM) is being applied to the Northeast U.S. to evaluate the effectiveness of various control strategies for reducing ozone in this region.

This paper summarizes the physical processes encompassed by the model including several that have heretofore been omitted from air quality models on smaller scales, such as cumulus cloud effects on vertical atmospheric motions and nighttime wind shear.
GRA

N86-11729# National Oceanic and Atmospheric Administration, Washington, D. C.
HIGH ALTITUDE MEASURED RADIANCE OF WHITE SANDS, NEW MEXICO IN THE 400-2000 nm BAND USING A FILTER WEDGE SPECTROMETER
G. R. Smith and R. H. Levin Apr. 1985 25 p refs
(PB85-206084; NOAA-TR-NESDIS-21) Avail: NTIS HC A02/MF A01 CSCL 04A

Activity by the National Oceanic and Atmospheric Administration (NOAA) at White Sands, New Mexico, was directed at providing visible wavelength calibration of Earth oriented satellite instruments. A Filter Wedge Spectrometer (FWS) was flown in an aircraft at an altitude of 11.28 km. The FWS viewed the Earth in a vector parallel to that of the Visible Spin Scan Radiometer (VISSR) satellite aboard a geostationary satellite, and data was taken near solar noon. Samples of FWS Sands radiance from June and September 1981 are presented. Author (GRA)

N86-11730# Environmental Protection Agency, Research Triangle Park, N.C. Atmospheric Sciences Research Lab.
PARAMETERIZATION OF THE ATMOSPHERIC BOUNDARY LAYER FOR AIR POLLUTION DISPERSION MODELS
A. A. M. Holtslag, S. E. Gryning, J. S. Irwin, and B. Sivertsen 1985 31 p refs
(PB85-193548; EPA-600/D-85-095) Avail: NTIS HC A03/MF A01 CSCL 04A

The characteristic features of the turbulent atmospheric boundary layer (ABL) are reviewed by means of scaling arguments. The goal was to characterize the meteorological conditions affecting diffusion for transport on the order of 10 km or less. The idealized ABL is divided into a number of regions, each characterized by distinct scaling parameters for the turbulence. With these scaling parameters wind and vertical dispersion are parameterized. The lateral dispersion is treated separately. Methods are suggested for estimating the surface fluxes of heat and momentum, and the mixing height. Several of the models characterize directly the crosswind integrated concentration at the surface, thus avoiding whenever justified the assumption of a Gaussian distribution of material in the vertical. Author (GRA)

N86-11557# Zagreb Univ. (Yugoslavia). Geodetic Faculty.
ANEW ABOUT THE CORRELATION BETWEEN MOHOROVICIC DISCONTINUITY DEPTHS, GEOID UNDULATIONS AND BOUGUER GRAVITY ANOMALIES IN THE DINARIC-PANNONIAN REGION OF YUGOSLAVIA
K. Colic, S. Petrovic, and T. Basic *In* Academy of Sciences of the GDR Proc. of the 5th Intern. Symp. Geodesy and Phys. of the Earth 1985 p 68-76 refs (For primary document see N86-11549 02-42)
Avail: NTIS HC A09/MF A01

N86-11559# Academy of Sciences, Potsdam (East Germany). Zentralinst. fuer Physik der Erde.
SOME RESULTS OF AN EIGHT YEARS GRAVIMETRIC REGISTRATION SERIES
H.-J. Dittfeld *In its* Proc. of the 5th Intern. Symp. Geodesy and Phys. of the Earth 1985 p 82-91 refs (For primary document see N86-11549 02-42)
Avail: NTIS HC A09/MF A01

N86-11560# Deutsches Geodaetisches Forschungsinstitut, Munich (West Germany).
GEOPHYSICAL INTERPRETATION OF GLOBAL GEOID UNDULATIONS AND MEAN GRAVITY ANOMALIES
Hermann Drewes *In* Academy of Sciences of the GDR Proc. of the 5th Intern. Symp. Geodesy and Phys. of the Earth 1985 p 95-104 refs (For primary document see N86-11549 02-42)
Avail: NTIS HC A09/MF A01

N86-11564# Technische Hochschule, Darmstadt (West Germany). Inst. fuer Physikalische Geodaesie.
ON THE DISTRIBUTION OF THE RESIDUAL VECTORS OF EARTH'S TIDE GRAVITY OBSERVATIONS IN CENTRAL EUROPE
C. Gerstenecker and P. Varga (Budapest Science Univ.) *In* Academy of Sciences of the GDR Proc. of the 5th Intern. Symp. Geodesy and Phys. of the Earth 1985 p 150-165 refs (For primary document see N86-11549 02-42)
Avail: NTIS HC A09/MF A01

N86-11565# Academia Sinica, Beijing (China). Inst. of Geodesy and Geophysics.
ON THE LUNAR TIDAL EFFECT IN THE LATITUDE OBSERVATIONS AT TIANJIN
Tianqi Han, Yiming Qian, Shiguang Li, and Lanzhen Ma *In* Academy of Sciences of the GDR Proc. of the 5th Intern. Symp. Geodesy and Phys. of the Earth 1985 p 166-168 refs (For primary document see N86-11549 02-42)
Avail: NTIS HC A09/MF A01

N86-11566# Slovak Technical Univ., Bratislava (Czechoslovakia). Observatory.
SOME SHORT PERIODIC TERMS DUE TO NUTATION AND TIDES FROM LATITUDE AND TIME DETERMINATIONS AT CZECHOSLOVAK OBSERVATORIES
Jan Hefty *In* Academy of Sciences of the GDR Proc. of the 5th Intern. Symp. Geodesy and Phys. of the Earth 1985 p 169-172 refs (For primary document see N86-11549 02-42)
Avail: NTIS HC A09/MF A01

N86-11572# Academy of Sciences, Potsdam (East Germany). Zentralinst. fuer Physik der Erde.
ON THE INFLUENCE OF COUPLING TORQUES BETWEEN THE EARTH'S CORE AND MANTLE ON PARAMETERS AND COMPONENTS OF THE ROTATION OF THE EARTH
H. Jochmann *In its* Proc. of the 5th Intern. Symp. Geodesy and Phys. of the Earth, Pt. 2 1985 p 29-31 refs (For primary document see N86-11568 02-42)
Avail: NTIS HC A09/MF A01

N86-11578# Academia Sinica, Beijing (China). Inst. of Geodesy and Geophysics.
RESEARCH ON THE COMPUTATIONAL METHODS OF GRAVITY TOPOGRAPHIC EFFECT
Jiachun Meng *In* Academy of Sciences of the GDR Proc. of the 5th Intern. Symp. Geodesy and Phys. of the Earth, Pt. 2 1985 p 70-77 refs (For primary document see N86-11568 02-42)
Avail: NTIS HC A09/MF A01

N86-11579# Academy of Sciences (USSR), Moscow.
THE POTENTIALOGRAPHICAL PROBLEM AND THE CONCEPTION OF GRAVITATING DISKS
G. A. Meshcheryakov *In* Academy of Sciences of the GDR Proc. of the 5th Intern. Symp. Geodesy and Phys. of the Earth, Pt. 2 1985 p 78-87 refs In RUSSIAN; ENGLISH summary (For primary document see N86-11568 02-42)
Avail: NTIS HC A09/MF A01

N86-11582# Royal Inst. of Tech., Stockholm (Sweden). Dept. of Geodesy.
ON THE CONVERGENCE PROBLEM OF THE SATELLITE DERIVED SPHERICAL HARMONIC EXPANSION OF THE GEOPOTENTIAL AT THE EARTH'S SURFACE
Lars E. Sjoeberg *In* Academy of Sciences of the GDR Proc. of the 5th Intern. Symp. Geodesy and Phys. of the Earth, Pt. 2 1985 p 108-114 refs (For primary document see N86-11568 02-42)
Avail: NTIS HC A09/MF A01

N86-11586# Geodetic Inst., Charlottenlund (Denmark).
ON THE LONG-WAVELENGTH CORRELATION BETWEEN GRAVITY AND TOPOGRAPHY

C. C. Tscherning *In* Academy of Sciences of the GDR Proc. of the 5th Intern. Symp. Geodesy and Phys. of the Earth, Pt. 2 1985 p 134-143 refs (For primary document see N86-11568 02-42)
Avail: NTIS HC A09/MF A01

N86-11589# Academy of Sciences of the Ukrainian SSR, Kiev (USSR). Astronomical Observatory.
ON REDUCING THE EFFECT OF HORIZONTAL DISPLACEMENTS OF THE LITHOSPHERIC PLATES FROM THE OBSERVATIONS CARRIED OUT BY GLOBAL GEODYNAMIC NETWORK (ON EXAMPLE THE GEOSS-REA NETWORK)
Ya. S. Yatskiv and N. T. Mironov *In* Academy of Sciences of the GDR Proc. of the 5th Intern. Symp. Geodesy and Phys. of the Earth, Pt. 2 1985 p 150-155 refs In RUSSIAN. ENGLISH summary (For primary document see N86-11568 02-42)
Avail: NTIS HC A09/MF A01

N86-11590# Kiel Univ. (West Germany). Inst. of Geophysics.
ANELASTICITY IN THE EARTH'S MANTLE: IMPLICATIONS FOR THE FREQUENCY DEPENDENCE OF LOVE NUMBERS
J. Zschau *In* Academy of Sciences of the GDR Proc. of the 5th Intern. Symp. Geodesy and Phys. of the Earth, Pt. 2 1985 p 160 (For primary document see N86-11568 02-42)
Avail: NTIS HC A09/MF A01

N86-11592# Research Inst. of Geodesy, Topography and Cartography, Prague (Czechoslovakia).
CRCM AND KAPG ACTIVITY IN RECENT CRUSTAL MOVEMENT STUDIES
Pavel Vyskocil *In* Academy of Sciences of the GDR Proc. of the 5th Intern. Symp. Geodesy and Phys. of the Earth, Pt. 3 1985 p 4-6 refs (For primary document see N86-11591 02-42)
Avail: NTIS HC A08/MF A01

N86-11593# Mezoegazdasagi es Elelmezesuegyi Ministerium, Budapest (Hungary). Orszagos Foldugyi es Terkepeszeti Hivatal.
ON THE WORKS AND RESULTS OF INVESTIGATIONS CONCERNING THE RECENT MOVEMENTS IN THE KARPATHO-BALKAN REGION
I. Joo *In* Academy of Sciences of the GDR Proc. of the 5th Intern. Symp. Geodesy and Phys. of the Earth, Pt. 3 1985 p 7-15 refs In GERMAN; ENGLISH summary (For primary document see N86-11591 02-42)
Avail: NTIS HC A08/MF A01

N86-11594# Niedersaechsisches Landesverwaltungsamt, Hanover (West Germany). Abt. Landesvermessung.
NORTH SEA COAST LEVELLING NET: A MODEL CASE FOR THE DETERMINATION OF VERTICAL MOVEMENTS IN WESTERN EUROPE
Wolfgang Augath and Hans Pelzer (Hannover Univ.) *In* Academy of Sciences of the GDR Proc. of the 5th Intern. Symp. Geodesy and Phys. of the Earth, Pt. 3 1985 p 16-25 refs (For primary document see N86-11591 02-42)
Avail: NTIS HC A08/MF A01

N86-11596# Academy of Sciences, Potsdam (East Germany). Zentralinst. fuer Physik der Erde.
GEOKINEMATIC MODELS FOR THE GRAVIMETRIC W - E PROFILE OF THE GDR
W. Conrad, C. Elstner, G. Schwab, W. Schwahn, and S. Thomaschewski *In its* Proc. of the 5th Intern. Symp. Geodesy and Phys. of the Earth, Pt. 3 1985 p 32-43 refs (For primary document see N86-11591 02-42)
Avail: NTIS HC A08/MF A01

N86-11597# Hungarian Academy of Sciences, Sopron. Geodetical and Geophysical Research Inst.
MATHEMATICAL TREATMENT OF VERTICAL MOVEMENTS
J. Czompo *In* Academy of Sciences of the GDR Proc. of the 5th Intern. Symp. Geodesy and Phys. of the Earth, Pt. 3 1985 p 44-50 refs (For primary document see N86-11591 02-42)
Avail: NTIS HC A08/MF A01

N86-11598# Technische Univ., Dresden (East Germany). Sektion Geodaesie und Kartographie.
GEODIMETER NET FOR THE INVESTIGATION OF HORIZONTAL CRUSTAL DEFORMATIONS [GEODIMETER-NETZ ZUR UNTERSUCHUNG HORIZONTALER KRUSTENDEFORMATIONEN]
Marion Dost and Guenter Lorenz *In* Academy of Sciences of the GDR Proc. of the 5th Intern. Symp. Geodesy and Phys. of the Earth, Pt. 3 1985 p 51-54 refs In GERMAN; ENGLISH summary (For primary document see N86-11591 02-42)
Avail: NTIS HC A08/MF A01

N86-11599# Uppsala Univ. (Sweden). Dept. of Geodesy.
GAUSSIAN AND MEAN CURVATURES OF POSTGLACIAL LAND UPLIFT AS EXPANDED IN SURFACE SPHERICAL HARMONICS, AND THE ORIGIN OF EARTHQUAKES IN FENNOSCANDIA
Martin Ekman *In* Academy of Sciences of the GDR Proc. of the 5th Intern. Symp. Geodesy and Phys. of the Earth, Pt. 3 1985 p 55-70 refs (For primary document see N86-11591 02-42)
Avail: NTIS HC A08/MF A01

N86-11600# Academy of Sciences (USSR), Moscow. Inst. of Physics of the Earth.
NEAR-SURFACE DEFORMATIONS AND STRESSES IN THE AREA OF THE TOLBACHIK GREAT FISSURE ERUPTION OF 1975-1976 (KAMCHATKA) FROM GEODETIC DATA
S. V. Enman *In* Academy of Sciences of the GDR Proc. of the 5th Intern. Symp. Geodesy and Phys. of the Earth, Pt. 3 1985 p 71-75 refs (For primary document see N86-11591 02-42)
Avail: NTIS HC A08/MF A01

N86-11601# Mezoegazdasagi es Elelmezesuegyi Ministerium, Budapest (Hungary). Orszagos Foldugyi es Terkepeszeti Hivatal.
METHOD OF JOINT ADJUSTMENT OF HEIGHT DIFFERENCES AND VELOCITIES
M. Fury, J. Gergely (Foldmeresi Intezet, Budapest), and Zs. Nemeth (Foldmeresi Intezet, Budapest) *In* Academy of Sciences of the GDR Proc. of the 5th Intern. Symp. Geodesy and Phys. of the Earth, Pt. 3 1985 p 76-78 refs (For primary document see N86-11591 02-42)
Avail: NTIS HC A08/MF A01

N86-11602# Mezoegazdasagi es Elelmezesuegyi Ministerium, Budapest (Hungary). Orszagos Foldugyi es Terkepeszeti Hivatal.
PRINCIPLE OF THE CONSTRUCTION OF THE LINES OF THE REPEATED LEVELLING FOR THE INVESTIGATION OF THE VERTICAL MOVEMENT IN THE CARPATHO-BALKAN REGION (CBR)
M. Fury, J. Gergely (Foldmeresi Intezet, Budapest), and Zs. Nemeth (Foldmeresi Intezet, Budapest) *In* Academy of Sciences of the GDR Proc. of the 5th Intern. Symp. Geodesy and Phys. of the Earth, Pt. 3 1985 p 79-83 refs In GERMAN; ENGLISH summary (For primary document see N86-11591 02-42)
Avail: NTIS HC A08/MF A01

N86-11603# Bulgarian Academy of Science, Sofia. Central Lab. for Geodesy.
SOME GEODETIC ASPECTS OF THE PROBLEM OF CHECKING THE PLATE-TECTONIC MODEL OF SEISMICITY IN SOUTH-EASTERN EUROPE
N. I. Georgiev, I. N. Totomanov, and C. G. Darakciev *In* Academy of Sciences of the GDR Proc. of the 5th Intern. Symp. Geodesy and Phys. of the Earth, Pt. 3 1985 p 84-89 refs (For primary document see N86-11591 02-42)
Avail: NTIS HC A08/MF A01

N86-11604# Eidgenoessische Landestopographie, Bern (Switzerland).
RECENT CRUSTAL MOVEMENTS AND GEOPHYSICAL INTERPRETATION OF GEODYNAMIC PROCESSES IN THE ALPINE MOUNTAIN BELT
E. Gubler and H.-G. Kahle (Eidgenoessische Technische Hochschule, Zurich) *In* Academy of Sciences of the GDR Proc. of the 5th Intern. Symp. Geodesy and Phys. of the Earth, Pt. 3 1985 p 90-97 refs (For primary document see N86-11591 02-42)
Avail: NTIS HC A08/MF A01

N86-11605# Karlova Univ., Prague (Czechoslovakia).
DETERMINATION OF CRUSTAL MOVEMENTS IN THE HIGH TATRA MOUNTAINS
L. Hradilek *In* Academy of Sciences of the GDR Proc. of the 5th Intern. Symp. Geodesy and Phys. of the Earth, Pt. 3 1985 p 98-99 refs (For primary document see N86-11591 02-42)
Avail: NTIS HC A08/MF A01

N86-11606# Geodetic Inst., Helsinki (Finland).
FINNISH MEASUREMENTS OF THE FENNOSCANDIAN LAND UPLIFT GRAVITY LINES IN FINLAND 1966-1984
Aimo Kiviniemi *In* Academy of Sciences of the GDR Proc. of the 5th Intern. Symp. Geodesy and Phys. of the Earth, Pt. 3 1985 p 100-102 refs (For primary document see N86-11591 02-42)
Avail: NTIS HC A08/MF A01

N86-11607# Technische Univ., Dresden (East Germany).
STATIONARY HYDROSTATIC PRECISION TILTMETER SYSTEM [STATIONAERES HYDROSTATISCHES PRAEZISIONS-NEIGUNGSMESSSYSTEM]
G. Lorenz *In* Academy of Sciences of the GDR Proc. of the 5th Intern. Symp. Geodesy and Phys. of the Earth, Pt. 3 1985 p 102-105 refs In GERMAN; ENGLISH summary (For primary document see N86-11591 02-42)
Avail: NTIS HC A09/MF A01

N86-11608# Karlsruhe Univ. (West Germany). Geodetic Inst.
HEIGHT CHANGES AND RECENT CRUSTAL MOVEMENTS IN THE RHENISH MASSIF AND IN THE UPPER RHINE GRABEN RIFT
H. Maelzer *In* Academy of Sciences of the GDR Proc. of the 5th Intern. Symp. Geodesy and Phys. of the Earth, Pt. 3 1985 105-112 refs (For primary document see N86-11591 02-42)
Avail: NTIS HC A08/MF A01

N86-11609# Academy of Sciences (USSR), Moscow. Inst. of Physics of the Earth.
RECENT VERTICAL CRUSTAL MOVEMENTS OF THE CARPATHIAN-BALKAN REGION AND THEIR RELATIONSHIP WITH NEOTECTONIC MOVEMENTS AND GEOPHYSICAL FIELDS
V. A. Magnitsky, A. F. Grachev, I. V. Kalashnikova, and V. V. Bronguleev *In* Academy of Sciences of the GDR Proc. of the 5th Intern. Symp. Geodesy and Phys. of the Earth, Pt. 3 1985 p 113-123 refs (For primary document see N86-11591 02-42)
Avail: NTIS HC A08/MF A01

N86-11610# Academy of Sciences (USSR), Moscow.
ON THE RELATION BETWEEN RECENT CRUSTAL MOVEMENTS, THE SURFACE OF THE BASEMENT COMPLEX AND NEOTECTONIC DISPLACEMENTS OF THE EAST-EUROPEAN PLATFORM
V. A. Magnitsky, A. F. Grachev, I. V. Kalashnikova, and V. V. Bronguleev *In* Academy of Sciences of the GDR Proc. of the 5th Intern. Symp. Geodesy and Phys. of the Earth, Pt. 3 1985 p 124-130 refs (For primary document see N86-11591 02-42)
Avail: NTIS HC A08/MF A01

N86-11611# Technische Univ., Dresden (East Germany).
SIGNIFICANCE TESTS OF RECENT VERTICAL CRUSTAL MOVEMENTS BY CORRELATION FUNCTIONS Abstract Only
S. Meier *In* Academy of Sciences of the GDR Proc. of the 5th Intern. Symp. Geodesy and Phys. of the Earth, Pt. 3 1985 p 131 (For primary document see N86-11591 02-42)
Avail: NTIS HC A08/MF A01

N86-11612# Geodetic Inst., Helsinki (Finland).
COMPARISONS OF DIFFERENT OBSERVATION METHODS OF A LACOSTE AND ROMBERG G GRAVIMETER
Leena Mikkola *In* Academy of Sciences of the GDR Proc. of the 5th Intern. Symp. Geodesy and Phys. of the Earth, Pt. 3 1985 p 132-135 refs (For primary document see N86-11591 02-42)
Avail: NTIS HC A08/MF A01

N86-11613# Bulgarian Academy of Science, Sofia. Lab. for Geotechnics.
STATISTICAL ANALYSIS AND INTERPRETATION OF EARTH CRUSTAL MOVEMENTS IN NORTHEAST BULGARIA [STATISTISCHE ANALYSE UND INTERPRETATION DER ERDKRUSTENBEWEGUNGEN IN NORDOSTBULGARIEN]
G. Milev and I. N. Totomanov *In* Academy of Sciences of the GDR Proc. of the 5th Intern. Symp. Geodesy and Phys. of the Earth, Pt. 3 1985 p 136-139 refs (For primary document see N86-11591 02-42)
Avail: NTIS HC A08/MF A01

N86-11615# Bulgarian Academy of Science, Sofia. Central Lab. for Geodesy.
RELATION BETWEEN EARTHQUAKE FOCAL INTENSITY AND RECENT VERTICAL EARTH'S CRUSTAL MOVEMENTS IN THE RILA-RHODOPE SEISMIC REGION
Ivan N. Totomanov *In* Academy of Sciences of the GDR Proc. of the 5th Intern. Symp. Geodesy and Phys. of the Earth, Pt. 3 1985 p 148-155 refs (For primary document see N86-11591 02-42)
Avail: NTIS HC A08/MF A01

N86-11616# Research Inst. of Geodesy, Topography and Cartography, Prague (Czechoslovakia).
DYNAMICS OF THE BOHEMIAN MASSIF
Pavel Vyskocil *In* Academy of Sciences of the GDR Proc. of the 5th Intern. Symp. Geodesy and Phys. of the Earth, Pt. 3 1985 p 156-159 refs (For primary document see N86-11591 02-42)
Avail: NTIS HC A08/MF A01

N86-11617# Academy of Sciences, Potsdam (East Germany). Zentralinst. fuer Physik der Erde.
AN OPTIMUM USE OF SEA-LEVEL RECORDINGS
H. Weise *In its* Proc. of the 5th Intern. Symp. Geodesy and Phys. of the Earth, Pt. 3 1985 p 160-168 refs (For primary document see N86-11591 02-42)
Avail: NTIS HC A08/MF A01

N86-11619*# Jet Propulsion Lab., California Inst. of Tech., Pasadena.
MINERALOGICAL MAPPING IN THE CUPRITE MINING DISTRICT, NEVADA
Alexander F. H. Goetz and Vinay Srivastava *In its* Proc. of the Airborne Imaging Spectrometer Data Anal. Workshop 15 Jun. 1985 p 22-31 refs Original contains color imagery. Original photography may be purchased from the EROS Data Center, Sioux Falls, S.D. 57198 ERTS (For primary document see N86-11618 02-43)
Avail: NTIS HC A09/MF A01 CSCL 08G

N86-11635*# Brown Univ., Providence, R. I. Dept. of Geological Sciences.
SPECTROSCOPY OF MOSES ROCK KIMBERLITE DIATREME
Carle M. Pieters and John F. Mustard *In* JPL Proc. of the Airborne Imaging Spectrometer Data Anal. Workshop 15 Jun. 1985 p 106-110 refs ERTS (For primary document see N86-11618 02-43)
Avail: NTIS HC A09/MF A01 CSCL 08G

N86-11872# Los Alamos National Lab., N. Mex. Advanced Engineering Technology Group.
GEOLOGICAL CALCULATIONS WITH SANGRE AND MANTLE: RECENT RESULTS Abstract Only
Lucy M. Carruthers, Peggy Goldman, and Charles A. Anderson *In its* 6th Bien. CUBE (Computer Use by Engineers) Symp. Aug. 1984 p 26 (For primary document see N86-11858 02-60)
Avail: NTIS HC A06/MF A01

47 METEOROLOGY AND CLIMATOLOGY

Includes weather forecasting and modification.

N86-11731 State Univ. of New York, Stony Brook.
CLIMATE SIMULATION AND CHANGE: A SIMPLE ENERGY BALANCE CLIMATE MODEL Ph.D. Thesis
Steven Donald Goldenberg 1984 212 p
Avail: Univ. Microfilms Order No. DA8512714

Model results are calculated for the Northern Hemisphere for nine 10 latitude zones at one month intervals. The energy balance flux equations are solved separately for open ocean, land and sea ice surface types coupled by an intra-zonal advection term. Meridional transport is via a Budyko-type parameterization, while total net outgoing IR flux is based on a linear, empirical expression. Realistic values for ocean, land, and ice albedo dependent on surface type, surface temperature, cloud fraction and solar zenith angle are used. A diffuse ocean-atmosphere subsurface heating term is used, and a simple physical model of ice freezing and melting provide the subsurface heating flux for sea ice, allowing calculation of ice thickness. With a minimum of tuning, the model accurately predicts the land and ocean seasonal temperature cycles. Model calculated temperatures show a phase lead of about 1 month relative to the observed, a situation linked to the choice of subsurface heating and intra-zonal advection parameterization. Ice thickness results are consistent with observation. Author

N86-11732 Harvard Univ., Cambridge, Mass.
THE EFFECT OF THE HADLEY CIRCULATION ON THE MERIDIONAL PROPAGATION OF STATIONARY WAVES Ph.D. Thesis
Ian Geoffrey Watterson 1985 226 p
Avail: Univ. Microfilms Order No. DA8510227

The effect on the meridional propagation of stationary planetary waves of the inclusion of the zonal mean Hadley circulation in linearized models of the atmosphere is examined. Previous models in which the Hadley circulation was ignored have not been consistent with apparent midlatitude response to tropical forcing since the easterly winds near the equator do not support meridionally propagating waves. The inclusion of a meridional wind in the basic state of a baratropic model enables wave propagation from one midlatitude through the easterlies to the other provided the wind is in that direction. Waves traveling in the other direction can be turned around by the opposing wind. These effects are shown to be consistent with the Wentzel-Kramer-Brillouin method (WKB). The zero zonal wind latitude no longer has significance. A primitive equation model is developed to test the potential significance of this tropical wave in a three dimensional atmosphere. For an idealized case ten levels in the vertical seems adequate to resolve the solution. Author

N86-11733*# National Aeronautics and Space Administration, Washington, D. C.
VARIABILITY OF SNOW COVER CHARACTERISTICS IN THE TRANSBAYKAL
R. K. Govsh Jul. 1985 12 p refs Transl. into ENGLISH from Trudy Glav. Geof. Observ., no. 130, 1962 p 78-83 Transl. by Scientific Translation Service, Inc., Santa Barbara, Calif.
(Contract NASw-4004)
(NASA-TM-77917; NAS 1.15:77917) Avail: NTIS HC A02/MF A01 CSCL 04B

The variations in snow cover characteristics in the Transbaykal were examined. Results are presented of an experimental verification of the Transbaykal theoretical developments to improve the efficiency of snow measurement photographs. E.A.K.

N86-11734*# National Aeronautics and Space Administration, Washington, D. C.
FORMATION, DISTRIBUTION AND VARIABILITY IN SNOW COVER ON THE ASIAN TERRITORY OF THE USSR
V. N. Pupkov Jul. 1985 14 p Transl. into ENGLISH from Meteorol. i Gidrolog., no. 8, 1964 p 34-40 Transl. by Scientific Translation Service, Inc., Santa Barbara, Calif.
(Contract NASw-4004)
(NASA-TM-77913; NAS 1.15:77913) Avail: NTIS HC A02/MF A01 CSCL 04B

A description is given of maps compiled for annual and average multiple-year water reserves. The annual and average multiple-year maximum snow cover height for winter, extreme values of maximum snow reserves, and the average height and snow reserves at the end of each decade are shown. These maps were made for the entire Asian territory of the USSR, excluding Central Asia, Kamchatka Peninsula, and the Sakhalin Islands. Author

N86-11735*# National Aeronautics and Space Administration. Marshall Space Flight Center, Huntsville, Ala.
METEOROLOGICAL AND ENVIRONMENTAL INPUTS TO AVIATION SYSTEMS
Dennis W. Camp, ed. and Walter Frost, ed. (Tennessee Univ. Space Inst.) Sep. 1985 144 p refs Workshop held in Tullahoma, Tenn., 26-28 Oct. 1983; sponsored by NASA, NOAA, FAA, DOD, and Office of the Federal Coordinator for Meteorology
(Contract NAS8-36177)
(NASA-CP-2388; NAS 1.55:2388) Avail: NTIS HC A07/MF A01 CSCL 04B

An overview of meteorological parameters effecting aircraft flight is presented. For individual titles, see N86-11736 through N86-11748.

N86-11736*# Federal Aviation Administration, Washington, D.C. Weather Coordination Program.
OVERVIEW OF METEOROLOGICAL INPUTS TO NASP
James C. Dziuk *In* NASA. Marshall Space Flight Center Meteorol. and Environ. Inputs to Aviation Systems Sep. 1985 p 17-21 (For primary document see N86-11735 02-47)
Avail: NTIS HC A07/MF A01 CSCL 04B

An overview of meteorological systems for forecasting flight conditions is presented. The types of equipment used to gather the information used to prepare pilot briefings and in flight advisories is described. Possible improvements to the systems are classified as short term or long term. G.L.C.

N86-11737*# Delta Air Lines, Inc., Atlanta, Ga.
AIRLINE METEOROLOGICAL REQUIREMENTS
C. L. Chandler and John Pappas (Western Airlines, Los Angeles, Calif.) *In* NASA. Marshall Space Flight Center Meteorol. and Environ. Inputs to Aviation Systems Sep. 1985 p 21-23 (For primary document see N86-11735 02-47)
Avail: NTIS HC A07/MF A01 CSCL 04B

A brief review of airline meteorological/flight planning is presented. The effects of variations in meteorological parameters upon flight and operational costs are reviewed. Flight path planning through the use of meteorological information is briefly discussed. G.L.C.

N86-11738*# Newton (Dennis W.), Reno, Nev.
GENERAL AVIATION'S METEOROLOGICAL REQUIREMENTS
Dennis Newton *In* NASA. Marshall Space Flight Center Meteorol. and Environ. Inputs to Aviation Systems Sep. 1985 p 23-26 (For primary document see N86-11735 02-47)
Avail: NTIS HC A07/MF A01 CSCL 04B

Communication of weather theory and information about weather service products to pilots in an accurate and comprehensible manner is essential to flying safety in general. Probably no one needs weather knowledge more than the people who fly through it. The specific subject of this overview is General Aviation's Meteorological Requirements. G.L.C.

N86-11739*# Business and Commercial Aviation, White Plains, N.Y.
CORPORATE/COMMUTER AIRLINES METEOROLOGICAL REQUIREMENTS
John W. Olcott *In* NASA. Marshall Space Flight Center Meteorol. and Environ. Inputs to Aviation Systems Sep. 1985 p 27-29 (For primary document see N86-11735 02-47)
Avail: NTIS HC A07/MF A01 CSCL 04B

The meteorological information requirements of corporate and commuter airlines are reviewed. The skill level and needs of this class of aviator were assessed. An overview of the methodology by which meteorological data is communicated to these users is presented. G.L.C.

N86-11740*# Federal Aviation Administration, Atlantic City, N.J.
OVERVIEW OF FAA'S AIRCRAFT ICING PROGRAM
Loni Czekalski *In* NASA. Marshall Space Flight Center Meteorol. and Environ. Inputs to Aviation Systems Sep. 1985 p 30-34 (For primary document see N86-11735 02-47)
Avail: NTIS HC A07/MF A01 CSCL 04B

An overview of the FAA's icing program is presented. The program involves certification of various types of aircraft for flight in known icing conditions, the study of icing conditions, and the preparation of certification standards. Test and technology transfer programs are also included. G.L.C.

N86-11741*# National Aeronautics and Space Administration, Washington, D. C.
OVERVIEW OF NASA'S PROGRAMS
A. Richard Tobiason *In* NASA. Marshall Space Flight Center Meteorol. and Environ. Inputs to Aviation Systems Sep. 1985 p 34-39 (For primary document see N86-11735 02-47)
Avail: NTIS HC A07/MF A01 CSCL 04B

An overview of some of NASA's aviation related programs is presented. The areas discussed include: (1) severe storms; (2) clear air turbulence; (3) icing; (4) fog; and (5) landing systems. G.L.C.

N86-11742*# Coast Guard, Elizabeth City, N.C.
ADVERSE WEATHER IMPACT ON AVIATION SAFETY, INVESTIGATION AND OVERSIGHT
Mont J. Smith *In* NASA. Marshall Space Flight Center Meteorol. and Environ. Inputs to Aviation Systems Sep. 1985 p 43-48 (For primary document see N86-11735 02-47)
Avail: NTIS HC A07/MF A01 CSCL 04B

A brief review of the weather factors that effect aviation safety with respect to U.S. Coast Guard operations is presented. Precise meteorological information is an absolute necessity to the Coast Guard which must conduct life saving and rescue operations under the worst of weather conditions. Many times the weather conditions in which they operate are the cause of or a contributing factor to the predicament from which they must execute a rescue operation. G.L.C.

N86-11743*# Naval Research Lab., Washington, D. C. Experimental Cloud Physics Section.
A NEW CHARACTERIZATION OF THE ICING ENVIRONMENT BELOW 10,000 FEET AGL FROM 7,000 MILES OF MEASUREMENTS IN SUPERCOOLED CLOUDS
Richard K. Jeck *In* NASA. Marshall Space Flight Center Meteorol. and Environ. Inputs to Aviation Systems Sep. 1985 p 51-55 refs (For primary document see N86-11735 02-47)
Avail: NTIS HC A07/MF A01 CSCL 04B

A growing requirement over the past decade for a new assessment of aircraft icing conditions in wintertime clouds at altitudes up to about 10,000 feet is discussed. The requirement was documented in past workshops and comes primarily from the helicopter community which wants ice-protected rotorcraft to meet increasing demands for all-weather operations. Currently, only a few of the larger helicopters are equipped with certification of ice-protection devices. This is because the current FAA criteria for design and certification of ice-protection equipment results in power and payload penalties that smaller rotorcraft cannot tolerate. The FAA criteria were actually designed for large, transport-category aircraft capable of flying to 20,000 feet or more. For this reason, there have been concerns that the current criteria may be too severe for low-performance aircraft, such as helicopters, which generally operate at altitudes below 10,000 feet. G.L.C.

N86-11744*# Federal Aviation Administration, Atlantic City, N.J.
A NEW CHARACTERIZATION OF SUPERCOOLED CLOUDS BELOW 10,000 FEET AGL
Charles O. Masters *In* NASA. Marshall Space Flight Center Meteorol. and Environ. Inputs to Aviation Systems Sep. 1985 p 56-59 refs (For primary document see N86-11735 02-47)
Avail: NTIS HC A07/MF A01 CSCL 04B

Icing caused by supercooled clouds below 10,000 feet were characterized with a view toward a change in FAA standards for civil aircraft ice protection standards. Current techniques in cloud physics were employed. G.L.C.

N86-11745*# Spectron Development Labs., Inc., Costa Mesa, Calif.
ADVANCE PARTICLE AND DOPPLER MEASUREMENT METHODS
Chris Busch *In* NASA. Marshall Space Flight Center Meteorol. and Environ. Inputs to Aviation Systems Sep. 1985 p 61-62 (For primary document see N86-11735 02-47)
Avail: NTIS HC A07/MF A01 CSCL 04B

Particle environments, i.e., rain, ice, and snow particles are discussed. Two types of particles addressed are: (1) the natural environment in which airplanes fly and conduct test flights; and (2) simulation environments that are encountered in ground-test facilities such as wind tunnels, ranges, etc. There are characteristics of the natural environment that one wishes to measure. The liquid water content (LWC) is the one that seems to be of most importance; size distribution may be of importance in some applications. Like snow, the shape of the particle may be an important parameter to measure. As one goes on to environment in simulated tests, additional parameters may be required such as velocity distribution, the velocity lag of the particle relative to the aerodynamic flow, and the trajectory of the particle as it goes through the aerodynamic flow and impacts on the test object. G.L.C.

N86-11746*# Flying Tigers-Retired, San Pedro, Calif.
DEVELOPMENT OF A WIND SHEAR PERFORMANCE ENVELOPE
John H. Bliss *In* NASA. Marshall Space Flight Center Meteorol. and Environ. Inputs to Aviation Systems Sep. 1985 p 62-65 (For primary document see N86-11735 02-47)
Avail: NTIS HC A07/MF A01 CSCL 04B

It is quite important that the airplane performance during a continuing headwind loss be understood. Lack of consideration of this characteristic can result in assuming almost twice the performance than that which the airplane actually has during severe wind shear at high descent rates. The example data relates to the Boeing 727-200, but the characteristics are applicable to any airplane. G.L.C.

N86-11747*# Tennessee Univ. Space Inst., Tullahoma. Atmospheric Sciences Div.
LABORATORY MODEL OF FLIGHT THROUGH WIND SHEAR
Walter Frost *In* NASA. Marshall Space Flight Center Meteorol. and Environ. Inputs to Aviation Systems Sep. 1985 p 65-67 (For primary document see N86-11735 02-47)
Avail: NTIS HC A07/MF A01 CSCL 04B

The simulation of an aircraft flying through a downdraft or microburst is presented. The simulation was performed under the conditions of constant takeoff thrust. The resulting wind shear conditions were filmed and examined for possible pilot corrective action in the future. G.L.C.

N86-11748*# Toronto Univ. (Ontario). Inst. for Aerospace Studies.
A MODEL OF A DOWNBURST, A WIND TUNNEL PROGRAM ON PLANETARY BOUNDARY LAYER, AND AIRSHIP IN TURBULENCE
Bernard Etkin *In* NASA. Marshall Space Flight Center Meteorol. and Environ. Inputs to Aviation Systems Sep. 1985 p 68-73 (For primary document see N86-11735 02-47)
Avail: NTIS HC A07/MF A01 CSCL 04B

An engineering model of microbursts was developed as an aid to possible future flight simulation in wind shear. Planetary boundary layer and high altitude turbulence were also modeled. G.L.C.

N86-11749*# Pennsylvania State Univ., University Park. Dept. of Meteorology.

THE UTILIZATION OF SATELLITE DATA AND DYNAMICS IN UNDERSTANDING AND PREDICTING GLOBAL WEATHER PHENOMENA Final Report, 15 Aug. 1980 - 31 Mar. 1985

Hamilton N. Shirer, ed. and John A. Dutton, ed. May 1985 390 p refs

(Contract NAS8-33794)

(NASA-CR-171577; NAS 1.26:171577) Avail: NTIS HC A17/MF A01 CSCL 04B

A two layer spectral quasi-geostrophic model is used to simulate the effects of topography on the equilibria, the stability, and the long term evaluation of incipient unstable waves. The flow is forced by latitudinally dependent radiational heating. The nature of the form drag instability of high index equilibria is investigated. The proximity of the equilibrium shear to a resonant value is essential for the instability, provided the equilibrium occurs at a slightly stronger shear than resonance. The properties of the steady Hadley and Rossby required for a thermally forced rotating fluid on a sphere are further explained. An objective parameterization technique is developed for general nonlinear hydrodynamical systems. The typical structure is one in which the rates of change of the dependent variables depend on homogeneous quadratic and linear forms, as well as on inhomogeneous forcing terms. Also documented is a steady, axisymmetric model of the general circulation developed as a basis for climate stability studies. The model includes the effects of heating, rotation, and internal friction, but neglects topography. Included is further research on cloud street phenomena. Orientation angles and horizontal wavelengths of boundary layer rolls and cloud streets are determined from an analysis of a truncated spectral model of three dimensional shallow moist Boussinesq convection in a shearing environment is further explained. Relatively broadly spaced roll clouds have orientations for which the Fourier component of the roll perpendicular shear is nearly zero, but the second corresponds to narrowly spaced rolls having orientations for which the Fourier coefficients of both the perpendicular and the parallel components of the shear are nearly equal. For individual titles, see N86-11750 through N86-11756.

N86-11750*# Pennsylvania State Univ., University Park.

THE EFFECT OF TOPOGRAPHY ON THE EVOLUTION OF UNSTABLE DISTURBANCES IN A BAROCLINIC ATMOSPHERE Final Report

John H. E. Clark *In its* The Util. of Satellite Data and Dyn. in Understanding and Predicting Global Weather Phenomena May 1985 p 19-68 refs (For primary document see N86-11749 02-47)

Avail: NTIS HC A17/MF A01 CSCL 04B

A two layer spectral quasi-geostrophic model is used to simulate the effects of topography on the equilibria, their stability, and the long term evolution of incipient unstable waves. The flow is forced by latitudinally dependent radiative heating. Dissipation is in the form of Rayleigh friction. An analytical solution is found for the propagating finite amplitude waves which result from baroclinic instability of the zonal winds when topography is absent. The appearance of this solution for wavelengths just longer than the Rossby radius of deformation and disappearance of ultra-long wavelengths is interpreted in terms of the Hopf bifurcation theory. Simple dynamic and thermodynamic criteria for the existence of periodic Rossby solutions are presented. A Floquet stability analysis shows that the waves are neutral. The nature of the form drag instability of high index equilibria is investigated. The proximity of the equilibrium shear to a resonant value is essential for the instability, provided the equilibrium occurs at a slightly stronger shear than resonance. F.M.R.

N86-11751*# Pennsylvania State Univ., University Park. Dept. of Meteorology.

THE HADLEY AND ROSSBY REGIMES IN A SPHERICAL ATMOSPHERE Final Report

Steven B. Feldstein and John H. E. Clark *In its* The Util. of Satellite Data and Dyn. in Understanding and Predicting Global Weather Phenomena May 1985 p 69-108 refs (For primary document see N86-11749 02-47)

Avail: NTIS HC A17/MF A01 CSCL 04B

The properties of the steady Hadley and Rossby regimes for a thermally forced rotating fluid on a sphere are studied. The two layer modified geostrophic model is employed which allows for thermal advection by the divergent wind and time dependent static stability. Heating processes are parameterized using the Newtonian approximation and Rayleigh friction is accounted for. The equations are transformed to spectral form using spherical harmonics and then truncated retaining a simple axisymmetric state and initial, one wave. A time independent Hadley circulation is obtained which is neutral to axisymmetric disturbances but unstable to wave like perturbations for intermediate values of the meridional temperature gradient, indicating the existence of both an upper and lower symmetric Hadley regime. An analytical solution for the steady Rossby circulation is determined for values of the meridional temperature gradient where the Hadley regime is unstable. Linear perturbation theory is used to show that within the steady Rossby regime two or more waves cannot exist simultaneously. F.M.R.

N86-11752*# Pennsylvania State Univ., University Park. Dept. of Meteorology.

A PARAMETERIZATION TECHNIQUE FOR NONLINEAR SPECTRAL MODELS Final Report

Ronald Gelaro and Hampton N. Shirer *In its* The Util. of Satellite Data and Dyn. in Understanding and Predicting Global Weather Phenomena May 1985 p 109-165 refs (For primary document see N86-11749 02-47)

Avail: NTIS HC A17/MF A01 CSCL 04B

An objective parameterization technique is developed for general nonlinear hydrodynamical systems. The typical structure of hydrodynamical systems, regardless of their complexity, is one in which the rates of change of the dependent variables depend on homogeneous quadratic and linear forms, as well as on inhomogeneous forcing terms. As a prototype of the generic problem containing this typical structure, the parameterization technique is applied to various three component subsets of a five component nonlinear spectral model of forced, dissipative quasi-geostrophic flow in a channel. The results obtained lead to specification of the necessary data coverage requirements for applying the technique in general. Author

N86-11753*# Pennsylvania State Univ., University Park. Dept. of Meteorology.

A NUMERICAL STUDY OF GLOBAL AXISYMMETRIC STATES AND THEIR STABILITY TO QUASI-GEOSTROPHIC DISTURBANCES Final Report

Harry W. Henderson and John A. Dutton *In its* The Util. of Satellite Data and Dyn. in Understanding and Predicting Global Weather Phenomena May 1985 p 167-222 refs (For primary document see N86-11749 02-47)

Avail: NTIS HC A17/MF A01 CSCL 04B

A steady, axisymmetric model of the general circulation is developed as a basis for climate stability studies. The model includes the effects of heating, rotation, and internal friction, but neglects topography. It is assumed that the axisymmetric flow may be modeled by making the Boussinesq and deep convection approximations. The hydrostatic assumption is not made, thus permitting the advective terms to be included in the vertical equation of motion. The initial set of five primitive equations is reduced to three equations in terms of the zonal velocity, meridional streamfunction, and the potential temperature perturbation. The application of the Boussinesq, deep convection, and quasi-geostrophic assumptions limits the ranges of the heating and rotation rates. For values not too far from typical atmospheric values, the model produces a stability boundary separating Hadley from Rossby flow. The boundary is characterized by a particular value of vertical wind shear, which suggests that baroclinic instability is the primary mechanism for the loss of stability. The initial growth rates are largest for longitudinal waves 4-7, also in agreement with studies of baroclinic instability. F.M.R.

N86-11754*# Pennsylvania State Univ., University Park. Dept. of Meteorology.
ON CLOUD STREET DEVELOPMENT IN THREE DIMENSIONAL PARALLEL AND RAYLEIGH INSTABILITIES Final Report
Hampton N. Shirer *In its* The Util. of Satellite Data and Dyn. in Understanding and Predicting Global Weather Phenomena May 1985 p 223-290 refs (For primary document see N86-11749 02-47)
Avail: NTIS HC A17/MF A01 CSCL 04B

Expected orientation angles and horizontal wavelengths of boundary layer rolls or cloud streets are determined from an analysis of a truncated spectral model of three dimensional shallow moist Boussinesq convection in a shearing environment. The nonlinear secondary circulations are organized into two dimensional forms by the height dependent wind field, and these rolls may develop from the combined effects of thermal stratification and mean wind shear. The associated thermal and parallel instability mechanisms are shown to be special cases of a single one. Only one mode is found when the stratification is unstable or neutral, but a second one is possible when the stratification is weakly stable. The first corresponds to relatively broadly spaced rolls having orientations for which the Fourier component of the roll perpendicular shear is nearly zero, but the second corresponds to relatively narrowly spaced rolls having orientations for which the Fourier coefficients of both the perpendicular and the parallel components of the shear are nearly equal. Author

N86-11755*# Pennsylvania State Univ., University Park. Dept. of Meteorology.
CLOUD STREETS DURING KONTUR: A COMPARISON OF PARALLEL/THERMAL INSTABILITY MODES WITH OBSERVATIONS Final Report
Hampton N. Shirer, Burghard Bruemmer (Max-Planck Inst. fuer Meteorologie), and Alan Grant (British Meteorological Office) *In its* The Util. of Satellite Data and Dyn. in Understanding and Predicting Global Weather Phenomena May 1985 p 291-318 refs (For primary document see N86-11749 02-47)
Avail: NTIS HC A17/MF A01 CSCL 04B

Estimates of cloud street geometry produced by a model of the parallel/thermal instability modes of shallow convection are compared with observations obtained during the 1981 KonTur experiment. Good agreement between the modeled and observed orientation angles, wavelengths and Reynolds numbers are found when the streets are assumed to derive their energy from the average shear and the lowest order sine terms of a Fourier expansion of the mean wind profile (or equivalently from the lowest order cosine terms of the mean shear profile). The modes associated with the cosine terms of the wind profile (or the sine terms of the wind shear profile) do not agree well with the observations. These results suggest that the boundary layer rolls observed during KonTur might have developed owing to a combined parallel/thermal instability originating primarily from the cosine terms of the ambient roll parallel wind shear. Author

N86-11756*# Pennsylvania State Univ., University Park. Dept. of Meteorology.
ON THE NONLINEAR CHARACTERISTICS OF THE AXISYMMETRIC FLOW REGIME: CYLINDRICAL AND SPHERICAL SYSTEMS
R. Wayne Higgins, John A. Dutton, and Hampton N. Shire *In its* The Util. of Satellite Data and Dyn. in Understanding and Predicting Global Weather Phenomena May 1985 p 319-389 refs (For primary document see N86-11749 02-47)
Avail: NTIS HC A17/MF A01 CSCL 04B

The physical relationship between steady axisymmetric flows that might be observed in the atmosphere and in laboratory vessels is investigated theoretically. This is accomplished by comparing both the nonlinear structure and the thermal forcing mechanisms in two truncated spectral models of flow in the atmosphere and the rotating laboratory cylinder, respectively. Under statically stable conditions, the response of the internally forced spherical model (which is developed here from a set of new orthonormal basis functions) exhibits steady behavior different from that in the externally forced cylindrical model. Two regions of multiple steady solutions occur in the cylindrical model, under stable conditions, that are not found in the spherical one. The possible physical relevance of these multiple solutions is investigated by determining their location in parameter space with respect to the classical Hadley-Rossby transition curve. The results suggest that the wave flow regime, in an annulus, might develop catastrophically when an upper symmetric flow ceases to exist. Author

N86-11757# Systems and Applied Sciences Corp., Vienna, Va.
SUB-CLOUD LAYER MOTIONS FROM RADAR DATA USING CORRELATION TECHNIQUES
G. R. Smythe and F. I. Harris 15 Oct. 1984 25 p
(Contract F19628-82-C-0023)
(AD-A156477; AFGL-TR-84-0272; SR-5) Avail: NTIS HC A02/MF A01 CSCL 04/2

Acquisition of a new system of Doppler weather radars (NEXRAD, Next Generation Weather Radar) will necessitate availability of appropriate automated weather analysis algorithms. In this report one such algorithm for obtaining small-scale motions from radar data by pattern recognition is evaluated. Two variations that correlate reflectivity data from scan to scan, one of which utilizes Doppler velocities, are applied to data of to intense thunderstorms. From these analyses it is found that resolution typical of most weather radars is too coarse to allow consistently reliable reconstruction of motions with temporal lags short enough to preclude discernible effects of propagation. Author (GRA)

N86-11758# Air Command and Staff Coll., Maxwell AFB, Ala.
RECOGNITION AND CONTROL OF LOW LEVEL WIND SHEAR
W. G. Rogers Apr. 1985 108 p
(AD-A156500; ACSC-85-2215) Avail: NTIS HC A06/MF A01 CSCL 04/2

This is a two hour lesson plan/handbook and slide presentation on low level wind shear. The project was developed for the SAC Instrument Flight Center to be used in their curriculum. The lesson plan is designed to enable SAC instructors to effectively teach other pilots how to understand, recognize, and cope with low level wind shear hazards. The lesson plan addresses the effects, causes, detection, and control of low level wind shear. Author (GRA)

N86-11759# Naval Postgraduate School, Monterey, Calif.
POSSIBLE CROSS EQUATORIAL INFLUENCE OF THE NORTHEAST MONSOON ON THE EQUATORIAL WESTERLIES OVER INDONESIA M.S. Thesis
K. A. Shield Mar. 1985 74 p
(AD-A156907) Avail: NTIS HC A04/MF A01 CSCL 04/2

Objectively analyzed surface, 700 and 200 mb winds of nine winters are used to study the possible cross equatorial influence of the northern winter monsoon on the zonal wind along 10 deg S in the Indonesia-Arafura Sea region and to prepare a nine-year monthly mean climatology. Key circulation features are represented by area averaged and time composited parameters in an attempt to infer correlations between their perturbation. Specifically, the acceleration of the zonal wind along 10 deg S in the Indonesia-Arafura Sea region is used to define the onset of the southern summer monsoon and illustrate the timing between circulation features of interest in both hemispheres. While no conclusive results were achieved, some basic observations can be made. Midseason active phases in the southern monsoon appear to be influenced by surges in the northeast monsoon in the Northern Hemisphere while late season events appear to be primarily a result of Southern Hemispheric, mid-latitude, baroclinic effects. In both cases, the meridional extent of the southern summer monsoon is limited. Even in the mid-season event, variability in area-averaged cross equatorial flow may not be indicative of the nature of forcing of the Northern Hemisphere's monsoonal winds on the southern summer monsoonal winds along 10 deg S. GRA

N86-11760# Air Force Inst. of Tech., Wright-Patterson AFB, Ohio.
APPLICATION OF AN OBJECTIVE ANALYSIS SCHEME TO MESOSCALE OBSERVATIONAL NETWORK DESIGN

M.S. Thesis
D. E. Harms 1985 101 p
(AD-A156911; AFIT/CI/NR-85-43T) Avail: NTIS HC A06/MF A01 CSCL 12/1

Objective analysis is a programmable method for estimating grid point values by transforming (interpolating) data from observations at irregularly spaced points into data at the points of a regular grid mesh. The gridded information can be used for diagnostic studies or in numerical weather production models. The objective of this thesis was to estimate the probable effectiveness of the proposed surface observational network (PAM (Portable Automated Mesonet) II) which will be deployed as part of the winter 1986 GALE field project. This network is to contribute to the study of mesoscale features within developing east coast cyclones and the coastal front. The process of spatial weighted-averaging interpolation of surface data was investigated by using the Barnes objective analysis scheme. Tests were conducted to determine the limitations of the Barnes analysis method and evaluate how well this technique reconstructs meteorological fields. A method was developed which enables an optimum weight parameter to be determined for a given data distribution. Barnes objective analyses were generally more accurate than kinematic fields based on detailed hand analyses. The objective analysis scheme effectively filtered random errors typical on instrumental and exposure effects from the analysis. However, interpolation near the edge of a data domain and extrapolation into data void regions led to erroneous results. GRA

N86-11761# Air Force Systems Command, Wright-Patterson AFB, Ohio. Foreign Technology Div.
METEOROLOGY OF THE PERSIAN GULF AND OF SEVERAL AIRPORTS ON THE ARABIAN COAST
G. Marcal 12 Jun. 1985 115 p Transl. into ENGLISH from Air France (France), Apr. 1980 p 1-84
(AD-A157441; FTD-ID(RS)T-0113-85) Avail: NTIS HC A06/MF A01 CSCL 04/2

Topographic location; general meteorological conditions; chief meteorological phenomena; prevailing regional winds in the gulf; Arabian Coast airports; monthly climatological statistics; hourly averages of monthly temperatures for the Persian Gulf and airports on the Arabian Coast are given. GRA

N86-11762# National Oceanic and Atmospheric Administration, Washington, D. C.
MONTHLY AND SEASONAL WEATHER OUTLOOK FOR JUNE 1985, VOLUME 39, NUMBER 11, 30 MAY 1985
Jun. 1985 10 p refs
(PB85-209526) Avail: NTIS HC A02/MF A01 CSCL 04B

Maps which give observed and probability estimates of temperature and precipitation for October and November 1984 in the United States and Canada are presented. GRA

N86-11763# National Oceanic and Atmospheric Administration, Rockville, Md.
PROCEEDINGS OF THE 9TH ANNUAL CLIMATE DIAGNOSTICS WORKSHOP
Mar. 1985 447 p refs Workshop held in Corvallis, Oreg., 22-26 Oct. 1984; sponsored by Oregon State Univ.
(PB85-183911) Avail: NTIS HC A19/MF A01 CSCL 04B

The Proceedings of the Ninth Annual Climate Diagnostic Workshop took place at Oregon State University in Corvallis, Oregon, October 22 to 26, 1984 under the auspices of the National Oceanic and Atmospheric Administration (NOAA). The session opened with a review of the world's climate fluctuations for the period September 1983 to August 1984, followed by seminars on climate diagnostics, ENSO, intraseasonal oscillations, climate variability of the west coast of the Americas, modeling, and monsoons and rainfall, prediction and specification, and special topics. For individual titles, see N86-11764 through N86-11818.

N86-11764# East Anglia Univ., Norwich (England). Climatic Research Unit.
GLOBAL SURFACE AIR TEMPERATURE VARIATIONS: 1983-1984
P. D. Jones, P. M. Kelly, and B. Santer *In* NOAA Proc. of the 9th Ann. Climate Diagnostics Workshop Mar. 1985 p 1-10 (For primary document see N86-11763 02-47)
(Contracts DE-AC02-79EV-10098; DE-AC02-81EV-10739)
Avail: NTIS HC A19/MF A01 CSCL 04B

Global surface air temperature anomaly data are discussed for the period September 1983 to August 1984 and placed in their long-term context. The values are drawn from a gridded data set updated globally using data from stations reporting on the CLIMAT network. The information is largely for the landmasses of the Northern Hemisphere and of the Southern Hemisphere north of 45 S. Data are also presented for Antarctica. Annual data for the Northern Hemisphere, the Arctic (65-85 N) and the Antarctic (65-90 S) for the period 1881 to 1983 are presented. The data are expressed as departures from the reference period 1961 to 1975. Over the Northern Hemisphere, 1983 was the fourth warmest year during the 103-year record. 1981 was the warmest year (the second and third warmest were 1938 and 1953, respectively) and 1980 to 1984 promised to be the warmest 5-year period in the record. Recent warming is close to rivalling that of the 1920s and 1930s, but is different in character. It is most noticeable in middle latitudes, whereas the earlier warming was more pronounced at high latitudes. The Antarctic warmth of the 1970s has continued into the 1980s. Author

N86-11765# National Meteorological Center, Washington, D.C. Climate Analysis Center.
MONITORING CLIMATE IN REAL TIME: AN APPLICATION OF THE CLIMATE ANOMALY MONITORING SYSTEM (CAMS)
C. F. Ropelewski *In* NOAA Proc. of the 9th Ann. Climate Diagnostics Workshop Mar. 1985 p 11-20 refs (For primary document see N86-11763 02-47)
Avail: NTIS HC A19/MF A01 CSCL 04B

The data synthesis and analysis outlined is an attempt to realistically characterize monthly and seasonal climate anomalies in real time. The system has several potential sources of uncertainty. The reliance on unvalidated data transmitted over the GTS will undoubtedly introduce some errors. The computation of the standard deviations for temperature and parameters of the Gamma distribution or precipitation based on only 30 years of data also introduces uncertainties. Finally the isopleth analyses, a modified Cressman scheme, may give rise to errors where the data density is low and or sharp gradients exist. While these limitations must be kept in mind there is little doubt that CAMS has the capacity of providing a first look at surface climate anomalies on monthly to seasonal temporal scales and quantifying these anomalies in terms of their statistical significance. Author

N86-11766# National Meteorological Center, Washington, D.C. Climate Analysis Center.
REVIEW OF THE CLIMATE OF FALL 1983 AND WINTER 1983-84
K. Bergman and R. S. Quiroz *In* NOAA Proc. of the 9th Ann. Climate Diagnostics Workshop Mar. 1985 p 21-31 refs (For primary document see N86-11763 02-47)
Avail: NTIS HC A19/MF A01 CSCL 04B

This review covers the major climatic events of the period September 1983 thru February 1984. Further details are given for September through November, 1983, and for December 1983 through February 1984. The first part of this summary covers tropical circulation and climatic statistics, with the main emphasis on the tropical Pacific area. Noted especially is the aftermath of the record El Nino event of 1982 to 1983. In the second part, the Northern Hemisphere circulation and its climatic effects are discussed and in the last part the focus is on conditions in the U.S., where the winter season is characterized by severe cold and wide swings in temperature. Author

N86-11767# Scripps Institution of Oceanography, La Jolla, Calif.
SOME EMPIRICAL EVIDENCE FOR THE INFLUENCE OF SNOW COVER ON TEMPERATURE AND PRECIPITATION
Jerome Namias *In* NOAA Proc. of the 9th Ann. Climate Diagnostics

Workshop Mar. 1985 p 32-43 (For primary document see N86-11763 02-47)
Avail: NTIS HC A19/MF A01 CSCL 04B

The thermodynamic effects of variable snow cover during a given winter can alter temperature anomalies and precipitation patterns over the contiguous United States. This background acts to modulate conditions imposed by the concomitant general circulation which deploys different air masses with variable static stability. The lower tropospheric stability is responsive to the presence or absence of snow which effects the albedo and sensible heat exchange. In turn, stability alterations affect the ease with which clouds and precipitation are formed, again feeding back to alter back radiation. The winter months of 1983 to 1984 offer some remarkable illustrations of these effects because December and January were characterized by persistent and recurrent snows over much of the eastern half of the country, while an abrupt change from a low to a high index regime at the end of January led to dramatic snow melt over this area. Author

N86-11768# National Meteorological Center, Washington, D.C. Climate Analysis Center.
BLOCKING AS AN EXPLANATION OF THE SEVERE COLD OF WINTER 1983-84
R. S. Quiroz *In* NOAA Proc. of the 9th Ann. Climate Diagnostics Workshop Mar. 1985 p 44-49 (For primary document see N86-11763 02-47)
Avail: NTIS HC A19/MF A01 CSCL 04B

The forecasting of seasonal and monthly mean temperature is often made difficult by cold-to-warm or warm-to-cold transitions within the season or month. A case in point is the winter of 1983 to 1984, which over the greater part of North America was severely cold in December (coldest December over the U.S. in at least 5 decades), very cold in January, and abnormally warm in February. The weekly resolution for surface temperature departure from normal (TDN) is given averaged over 3 U.S. latitudes, along with blocking information to be described below. The exceptional cold centered on the second half of December and middle half of January, followed by February warmth. Using flow-oriented criteria for defining blocking, a nearly four-fold increase in the number of blocking days over the east Pacific and Western North America from winter 1982 to 1983 to winter 1983 to 1984 is shown. Major winter blocking episodes (6 days or more with index of strength of associated meridional flow, N, greater than 20) were on December 15 to 30 centered near 155 deg W, January 8 to 21, nar 146 deg W; and in the Atlantic-European area on February 4 to 26, near 6 deg E. Author

N86-11769# National Meteorological Center, Washington, D.C. Climate Analysis Center.
CIRCULATION AND WEATHER FOR MAM AND JJA 1984
A. James Wagner and Chester F. Ropelewski *In* NOAA Proc. of the 9th Ann. Climate Diagnostics Workshop Mar. 1985 p 50-59 (For primary document see N86-11763 02-47)
Avail: NTIS HC A19/MF A01 CSCL 04B

Most of the equatorial Pacific indices reveal that the atmosphere was in the cool/positive phase of the El Nino Southern Oscillation (ENSO) phenomenon. The Pacific tradewind indices are all strongly positive, with magnitudes of over 2 sigma in the area west of the dateline from March through June. There is a tendency for the area of maximum anomaly to move eastward and weaken with time. The 200 mb zonal wind index east of the dateline is near or above normal, with a tendency to increase with time. The outgoing long wave radiation (OLR) index near the dateline declines slowly from strongly to moderately positive values, indicating a general supression of convective activity in that area. The Indian summer monsoon is characterized by an excess of rainfall in the northern provinces and a tendency for a deficiency in some parts of southern India. Values of the SOI itself and the sea surface temperature anomalies (SSTA) in key areas of the eastern Pacific oscillate around zero with no discernible trends. Author

N86-11770# Scripps Institution of Oceanography, La Jolla, Calif.
ON THE RELATIONSHIP BETWEEN NORTH ATLANTIC SEASONAL SST ANOMALIES WITH UNITED STATES SURFACE TEMPERATURE ANOMALIES
Daniel R. Cayan *In* NOAA Proc. of the 9th Ann. Climate Diagnostics Workshop Mar. 1985 p 60-69 (For primary document see N86-11763 02-47)
Avail: NTIS HC A19/MF A01 CSCL 04B

A North Atlantic sea surface temperature (SST) data set is used to form regional average anomalies from area exhibition relatively strong temporal persistence. The two SST areas considered are both located in the western North Atlantic Region 1 offshore of the northeastern United States, and Region 2 in the subtropic area of the Caribbean and to its east. These regions are defined in the four month lag autocorrelation field over the North Atlantic; for comparison the four month lag autocorrelation for the North Pacific is shown. (Note that in the North Pacific the amplitude and spatial extent of the maximum autocorrelation coefficients are similar to those in the North Atlantic, but clustered in around the eastern boundary rather than the weatern.) Time series of the SST in the two regions are graphed; the variance of Region 1, reflecting its midlatitude, western boundary location is quite high, while the variance of Region 2 is rather small, being a subtropical area. Both regions exhibit a fairly decided low frequency character, although Region 2 appears more homogeneous throughout the 1949 to 1981 record length. Author

N86-11771# British Meteorological Office, Bracknell (England).
WORLDWIDE MARINE TEMPERATURE VARIATIONS ON THE SEASON TO CENTURY TIME SCALE
C. K. Folland, D. E. Parker, and M. Newman *In* NOAA Proc. of the 9th Ann. Climate Diagnostics Workshop Mar. 1985 p 70-85 refs (For primary document see N86-11763 02-47)
Avail: NTIS HC A19/MF A01 CSCL 04B

Recently, an analysis of global and N. Hemisphere sea surface temperature (SST) and night marine air temperature (MATN) variations during 1856 to 1981 was published. The work is partly motivated by the desire to find out, in the context of a long-term research program on long-range forecasting for the UK, whether a deterministic explanation can be sought for any of several substantial long-lasting circulation fluctuations in the N. Atlantic region over the last century. These have sometimes led to large fluctuations in mean temperature or rainfall within the UK that have been coherent over decades. Author

N86-11772# National Climatic Center, Asheville, N. C. National Climatic Data Center.
RECENT UNUSUAL MEAN WINTER TEMPERATURE ACROSS THE CONTIGUOUS UNITED STATES
Thomas R. Karl, Robert E. Livezey (Climate Analysis Center, Camp Springs, Md.), and Edward S. Epstein (Climate Analysis Center, Camp Springs, Md.) *In* NOAA Proc. of the 9th Ann. Climate Diagnostics Workshop Mar. 1985 p 86-90 (For primary document see N86-11763 02-47)
Avail: NTIS HC A19/MF A01 CSCL 04B

A long time series (1895 to 1984) of mean areally-averaged winter temperatures in the contiguous United States depicts an unprecedented spell of abnormal winters beginning with the winter of 1975 to 1976. The data set used to obtain areally-weighted average winter temperatures consists of monthly averages of temperature for each of 344 state climatic divisions in the contiguous United States and, prior to 1931, monthly averages of statewide average of temperature derived by a simple average of the data from stations within a state. The data set is then corrected for spatial density of stations prior to 1931, systematic time of observation bias, and urban warming. Each of these corrections is empirically derived by previously published correction factors or by comparison to a fixed network in the case of station density prior to 1931. A plot of the time series with time of observation and urban warming corrections versus the series without these corrections is depicted. Author

N86-11773# Maryland Univ., College Park. Dept. of Meteorology.

TOWARDS UNDERSTANDING THE GEOGRAPHICAL DISTRIBUTION AND SEASONALITY IN PERSISTANCE OF MONTHLY MEAN SURFACE AIR TEMPERATURE OVER THE U.S.A.

H. M. VandenDool and W. H. Klein *In* NOAA Proc. of the 9th Ann. Climate Diagnostics Workshop Mar. 1985 p 91-95 refs (For primary document see N86-11763 02-47)
(Grants NSF ATM-83-14431; NA-83AA-D-00048)
Avail: NTIS HC A19/MF A01 CSCL 04B

Using the traditional linear correlation (rho) between anomalies in monthly mean air temperature (MMAT) occurring in adjacent months, we will describe the distribution of rho over the U.S.A. and its variation with season. Rho(i,s,tau,n,m) is a function of the starting month (i), the station (s), the lag (tau), and the period over which calculations were performed (starting year n, ending year m). In this report tau will be 1 month exclusively. The data set used is the 80 year (1900 to 1979) record for 61 stations over the U.S.A. Author

N86-11774# Lamont-Doherty Geological Observatory, Palisades, N. Y.

TEMPERATURE AND PRECIPITATION TRENDS IN NORTH AMERICA

G. Kukla, J. Gavin, and T. R. Karl (National Climatic Center) *In* NOAA Proc. of the 9th Ann. Climate Diagnostics Workshop Mar. 1985 p 96-100 refs (For primary document see N86-11763 02-47)
(Contract DE-AC02-83ER-60162)
Avail: NTIS HC A19/MF A01 CSCL 04B

Trends in monthly mean maximum, minimum and average temperature as well as precipitation are calculated over the 1941 to 1980 interval for 122 to 130 U.S. and Canadian stations. Correlation coefficients are used to measure the association between each element and time (in 40 equal time steps) and are tested for local significance using a Monte Carlo technique. Field significance tests are then used to determine whether the percentage of stations in the network with > or = 90% local significance level is greater than expected due to chance. Stations are selected to minimize as much as possible the potential influence of urbanization. Author

N86-11775# Oregon State Univ., Corvallis. College of Oceanography.

RECENT LONG-TERM CLIMATIC CHANGE OVER THE EASTERN TROPICAL AND SUBTROPICAL PACIFIC AND ITS RAMIFICATIONS

William H. Quinn and Victor T. Neal *In* NOAA Proc. of the 9th Ann. Climate Diagnostics Workshop Mar. 1985 p 101-109 refs Supported in part by The Tinker Foundation (For primary document see N86-11763 02-47)
(Grant NSF ATM-83-06135)
Avail: NTIS HC A19/MF A01 CSCL 04B

Information concerning the climatic change that has affected much of the tropical and subtropical Pacific over recent years is discussed and illustrated with graphs. It provides an additional approach for monitoring and assessing the ENSO events, based on changes noted at sites located in the southeast trade band. It also includes a discussion of related changes noted at tropical North Pacific sites. Author

N86-11776# Washington Univ., Seattle.

GLOBAL RELATIONSHIPS WITH THE SOUTHERN OSCILLATION

P. B. Wright, T. P. Mitchell, and J. M. Wallace *In* NOAA Proc. of the 9th Ann. Climate Diagnostics Workshop Mar. 1985 p 110-113 (For primary document see N86-11763 02-47)
Avail: NTIS HC A19/MF A01 CSCL 04B

An atlas was prepared comprising maps of correlation and regression coefficients between various surface meteorological fields over the global oceans and an index of the Southern Oscillation (SO). The fields are: sea-surface temperature (SST), sea-level pressure (SLP), sea minus air temperature (S-A), cloudiness and wind components. The data are monthly anomalies in 4 deg latitude by 10 deg longitude areas for the period 1950 to 1979, generated from the COADs set. The SO index is the SLP anomaly at Darwin averaged over the twelve months beginning in April of one year and ending in March of the next; this is reversed in sign to the traditional SO index. Global maps of correlation and regression coefficients are calculated for six seasons defined relative to the twelve months of the SO index. This choice provides a description of the time evolution of seasonal anomalies relative to fluctuations of the SO. The maps reveal many interesting features, some very familiar, others less so. Sample maps for the Indian and Pacific sectors are shown. A few of the features are monitored with emphasis on the less familiar. The anomalies mentioned tend to be associated with high Darwin pressure, and anomalies of opposite sign with low Darwin pressure. Author

N86-11777# Oregon State Univ., Corvallis. Dept. of Atmospheric Sciences.

TIME SERIES MODELING OF THE SOUTHERN OSCILLATION Abstract Only

Pao-Shin Chu and Richard W. Katz (National Center for Atmospheric Research) *In* NOAA Proc. of the 9th Ann. Climate Diagnostics Workshop Mar. 1985 p 114 (For primary document see N86-11763 02-47)
Avail: NTIS HC A19/MF A01 CSCL 04B

An index consisting of the difference of normalized sea level pressure departure between Tahiti and Darwin during 1935 to 1983 is used to monitor the Southern Oscillation (SO) fluctuation. Using a time domain approach, autoregressive moving average (ARMA) processes are applied to model the Southern Oscillation Index (SOI) on a monthly and seasonal basis. An objective model selection procedure is used to help identify the appropriate time series model. It is shown that a low order ARMA process, namely ARMA(1,1), adequately fits the monthly SOI. According to this process, the SOI for the current month can be expressed as a function of the state of the previous month SOI and a current month's random error plus a previous month's error. Strong midlatitude forcing as induced by the cold surge during winter season appears to be one of many possible mechanisms which would perturb the large scale mass circulation. For the seasonal data, an AR(3) process is found to be the most adequate time series model. For this process, the current value of the SOI can be represented in terms of its immediate three post values and a noise term. Author

N86-11778# Colorado Univ., Boulder. Cooperative Inst. for Research in Environmental Science.

SATELLITE OBSERVATIONS OF A LARGE-AMPLITUDE 40-50 DAY OSCILLATION IN UPPER TROPOSPHERIC TEMPERATURE OVER THE EQUATORIAL PACIFIC OCEAN DURING THE 1982-83 ENSO EVENT

Edward I. Tollerud *In* NOAA Proc. of the 9th Ann. Climate Diagnostics Workshop Mar. 1985 p 115-118 refs (For primary document see N86-11763 02-47)
Avail: NTIS HC A19/MF A01 CSCL 04B

An oscillation is described with a period near 50 days that was observed in the atmospheric temperature fields over the equatorial Pacific Ocean in 1982 to 1983. The results show that there is an apparent relationship between the amplitude of the oscillation and the on going ENSO event. The data used are temperature retrievals from NOAA polar orbiting satellites. The basic averaging unit applied to the retrievals was 5 days in duration and 5 deg of latitude and longitude in horizontal dimension. While providing sufficient time resolution to describe oscillations of the period of interest, this choice of averaging period and area also results in an adequate sample of retrievals in each averaging area. Fields of these averages were used to construct time series and sections like those presented here. Author

N86-11779*# National Aeronautics and Space Administration. Goddard Space Flight Center, Greenbelt, Md.

SUBSEASONAL AND INTERANNUAL VARIATIONS OF TROPICAL CONVECTION AND THE EL NINO/SOUTHERN OSCILLATION

K. M. Lau and P. H. Chan (Applied Research Corp., Landover, Md.) *In* NOAA Proc. of the 9th Ann. Climate Diagnostics Workshop Mar. 1985 p 119-122 (For primary document see N86-11763 02-47)
Avail: NTIS HC A19/MF A01 CSCL 04B

It was found that during the northern winter, fluctuation in tropical convection is dominated by eastware propagating cloud clusters from the Indian Ocean. Most of these clusters reach as far as the central Pacific. Longitude time sections of outgoing longwave radiation (OLR) anomaly along the equator show that there are about 3 to 4 such episodes each winter. Also, simultaneous OLR anomalies over the equatorial central Pacific (ECP) and the maritime continent (MC) are negatively correlated and their variations are dominated by a 40 to 60 day period, suggesting the presence of a standing wave phenomenon. Such combination of propagating and standing phenomena can be captured by the extended empirical orthogonal function (EEOF) analysis. The EEOF method combines the temporal as well as the spatial correlation information to produce eigenmodes which have space time dependence. A 5 day and a 10 day lag in addition to the simultaneous spatial correlation is used. Author

N86-11780# National Center for Atmospheric Research, Boulder, Colo.

THE ANNUAL VARIATION IN THE VERTICAL STRUCTURE OF THE 40-50-DAY TROPICAL OSCILLATION

Roland A. Madden *In* NOAA Proc. of the 9th Ann. Climate Diagnostics Workshop Mar. 1985 p 123-127 (For primary document see N86-11763 02-47)
Avail: NTIS HC A19/MF A01 CSCL 04B

Spectra based on relatively long time series (5 to 10 or more years) of station pressure and upper air data from tropical regions reveal relatively broad spectral peaks whose maxima typically fall in the 40 to 50 day period range. The lower tropospheric zonal wind is very coherent and out of phase with the upper tropospheric zonal wind. To date, these results have been based on time series which open all seasons. The aim here is to learn something of the annual variation of this vertical structure. Author

N86-11781# Wisconsin Univ., Madison. Center for Climatic Research.

LIFE CYCLE OF A 28-72 DAY ATMOSPHERIC OSCILLATION DURING NORTHERN WINTER

Klaus M. Weickmann and John E. Kutzbach *In* NOAA Proc. of the 9th Ann. Climate Diagnostics Workshop Mar. 1985 p 128-140 refs (For primary document see N86-11763 02-47)
Avail: NTIS HC A19/MF A01 CSCL 04B

The spatial and temporal characteristics of 28 to 72 day fluctuations in NMC analyzed 250mb wind and satellite derived outgoing longwave radiation (OLR) is investigated. The ensemble averaged statistics described are calculated using 9 different (1974 to 1984) Nov. to Apr. and May to Oct. periods. This data base gives approximately 36 realizations of 28 to 72 day oscillations for each season. An overview of the seasonal differences in the spatial structure and the propagation characteristics of 28 to 72 day oscillations in 250mb wind and OLR are described first. This is followed by description of the life cycle of 28 to 72 day oscillations during northern winter; the life cycle highlights a systematic relationship between the evolution of OLR and the 250mb circulation. Author

N86-11782# Scripps Institution of Oceanography, La Jolla, Calif.

THE DISTRIBUTION OF RAINFALL ALONG THE COAST OF NORTHERN PERU DURING 1982-83

J. D. Horel and A. Cornejo-Garrido *In* NOAA Proc. of the 9th Ann. Climate Diagnostics Workshop Mar. 1985 p 141-146 (For primary document see N86-11763 02-47)
Avail: NTIS HC A19/MF A01 CSCL 04B

Torrential rainfall and severe flooding along the normally arid coast of Northern Peru caused considerable hardship to its inhabitants. Although past episodes of intense convection were linked to the El Nino phenomenon, the mechanisms responsible for the changes in the regional atmospheric circulation have yet to be adequately explained. Rainfall and surface wind observations were obtained from a network of roughly 50 stations in northern Peru, in addition to gridded data sets available in the United States. Preliminary results are presented on the conditions along the west coast of South America during the 1982 to 1983 El Nino episode. Author

N86-11783# Oregon State Univ., Corvallis. College of Oceanography.

PERU COASTAL WINDS DURING 1982-1983

D. B. Enfield and P. A. Newberger *In* NOAA Proc. of the 9th Ann. Climate Diagnostics Workshop Mar. 1985 p 147-156 refs (For primary document see N86-11763 02-47)
Avail: NTIS HC A19/MF A01 CSCL 04B

Synoptic data are presented on winds from seven coastal stations from northern and central Peru, from 1 January 1981 to the last quarter of 1983. To isolate synoptic and longer time scale variability from the diurnal signal, the basic data were smoothed with a low-low pass (LLP) filter having a half amplitude at 40 hours and decimated to six hourly values. A second set of time series was formed by further smoothing the LLP data with a very low pass (VLP) filter having half-amplitude at 30 days. The LLP variability is shown as vector sticks, while both the LLP and VLP time series are shown in plots of the alongshore wind component. Author

N86-11784# Clark Univ., Worcester, Mass. Geography Dept.

CLIMATIC EVENTS OF THE WEST COAST OF SOUTHERN AFRICA

Sharon Nicholson and Dara Entekhabi *In* NOAA Proc. of the 9th Ann. Climate Diagnostics Workshop Mar. 1985 p 157-165 (For primary document see N86-11763 02-47)
Avail: NTIS HC A19/MF A01 CSCL 04B

Suggestions have been made that the warm water is here also coupled with increased coastal rainfall and possibly with the Southern Oscillation as well. That idea is tested by using time series analysis and multi-year composites to examine the relationship between rainfall, SSTs and the Southern Oscillation. The data base consists of monthly SST data for 1948 to 1972 for the Marsden squares and derived from the TDF-11 data set, monthly rainfall data for the coastal stations indicated and for 84 regions covering the entire continent. The length of the rainfall records varies considerably, but most coastal stations have data for at least the period 1948 to 1972 and the regional series generally commence around 1901 and extend to 1973. Author

N86-11785# Naval Postgraduate School, Monterey, Calif.

SEVERAL ASPECTS OF INTERANNUAL VARIABILITY IN THE CALIFORNIA CURRENT SYSTEM

C. N. K. Mooers and L. C. Breaker *In* NOAA Proc. of the 9th Ann. Climate Diagnostics Workshop Mar. 1985 p 166-172 refs (For primary document see N86-11763 02-47)
Avail: NTIS HC A19/MF A01 CSCL 04B

Sea-surface temperature (SST) time series of daily observations acquired along the Central California coast are examined for interannual variability. A 13-year record off Pt. Sur clearly reveals three warming episodes that coincide with Equatorial ENSO events. Also a warming was observed in 1979; this episode coincides with a relatively weak ENSO event observed mainly in the Western and the Northeastern Pacific. These mid-latitude responses have been referred to as California El Ninos. Trend analysis of the Pt. Sur time series revealed a significant increase in SST over the past 13 years. Both the most recent El Nino episode and a large scale warming that started in 1976, appear to have contributed to the long term increase. Author

N86-11786# Scripps Institution of Oceanography, La Jolla, Calif. Marine Life Research Group.

WARM AND COLD EPISODES IN THE CALIFORNIA CURRENT: A CASE FOR LARGE-SCALE MID-LATITUDE ATMOSPHERIC FORCING

James J. Simpson *In* NOAA Proc of the 9th Ann. Climate Diagnostics Workshop Mar. 1985 p 173-184 refs (For primary

document see N86-11763 02-47)
Avail: NTIS HC A19/MF A01 CSCL 04B

This paper examines time series of oceanographic variables which indicate the occurrence of warm (EL Nino-like) and cold (anti-El Nino-like) periods in the California Current. Large-scale distributions of atmospheric data are then used to show that the most intense mid-latitude warm periods generally are contemporaneous with periods of pronounced tropical El Nino Southern Oscillation (ENSO) activity and that the most intense mid-latitude cold periods are contemporaneous with periods of pronounced tropical El Nino Southern Oscillation ENSO activity. Strong mid-latitude warm periods, however, can occur without contemporaneous tropical ENSO activity. In all cases, however, mid-latitude warm periods are associated with an expansion and intensification of the Aleutian Low, while the corresponding cold periods are associated with an expansion and intensification of the North Pacific High. Oceanographic data support the conclusion that mid-latitude warm (cold) periods in the California Current are related to observed anomalous atmospheric circulation through enhanced onshore (offshore) large-scale wind-driven oceanic transport. B.W.

N86-11787# Colorado Univ., Boulder. Cooperative Inst. for Research in Environmental Sciences.
RELATIONSHIPS BETWEEN PACIFIC NORTHWEST COAST CLIMATE AND ENSO EVENTS
Brent Yarnal *In* NOAA Proc. of the 9th Ann. Climate Diagnostics Workshop Mar. 1985 p 185-192 (For primary document see N86-11763 02-47)
Avail: NTIS HC A19/MF A01 CSCL 04B

The extremes in climate experienced during the 1982 to 1983 El Nino Southern Oscillation (ENSO) have generated considerable interest in the effect such episodes have on regional climatic variation. Surprisingly, not much is known about the relationships between ENSO events and the climate of the Pacific Northwest. Here, associations between ENSO events and the winter climate of eight coastal climatological divisions are investigated, with special emphasis given to the Washington coast and southeastern Alaska in the later parts of the paper. B.W.

N86-11788# National Weather Service, Portland, Oreg.
EVIDENCE OF AN 18 YEAR CYCLE IN PACIFIC NORTHWEST PRECIPITATION DATA
Philip A. Peck and Vernon C. Bissell *In* NOAA Proc. of the 9th Ann. Climate Diagnostics Workshop Mar. 1985 p 193-198 (For primary document see N86-11763 02-47)
Avail: NTIS HC A19/MF A01 CSCL 04B

This is a preliminary report on the basis of evidence that a cyclical pattern of about 19 years recurrence is seen in precipitation at selected stations in Western Oregon and Western Washington. The coincidence of these climate fluctuations with total solar eclipse events having periodicities of the same interval suggests that the causation may be lunar-gravitational. Drought cycles based on tree-ring analysis by Mitchell, Stockton and Meko were then compared with pacific Northwest precipitation changes and compared with total solar eclipse periodicities. Total solar eclipse over the Northern Hemisphere were considered to provide the best lunar-rainfall relationship. Nine stations in Western Washington and Northwest Oregon were used in this study. Four of these station's records were extended by using data from adjacent stations and normalizing the data. All stations have a marked winter rainfall climate. B.W.

N86-11789# Oregon State Univ., Corvallis. Dept. of Atmospheric Sciences.
TIME-AVERAGING THE FLUX-PROFILE RELATIONSHIP
Larry Mahrt, Claude Berthou (Centre National de Recherches Meteorologiques, Toulouse, France), Pascal Marquet, and Jean-Claude Andre *In* NOAA Proc. of the 9th Ann. Climate Diagnostics Workshop Mar. 1985 p 199-200 ref (For primary document see N86-11763 02-47)
Avail: NTIS HC A19/MF A01 CSCL 04B

Surface fluxes are generally related to mean flow variables by use of the bulk aerodynamic relationship and associated surface exchange coefficient. However, use of long time steps, as well as implied averaging over grid volumes can greatly alter the formal relationship between the flux and the mean flow. Formulations are presented for determining the bulk aerodynamic relationship for the surface turbulent flux using time step averaging. B.W.

N86-11790# Oregon State Univ., Corvallis. Climatic Research Inst.
ATMOSPHERIC GENERAL CIRCULATION MODEL SIMULATIONS OF THE MODERN ANTARCTIC CLIMATE
Michael E. Schlesinger *In* NOAA Proc. of the 9th Ann. Climate Diagnostics Workshop Mar. 1985 p 201-210 refs (For primary document see N86-11763 02-47)
(Grant NSF ATM-82-05992)
Avail: NTIS HC A19/MF A01 CSCL 04B

In this paper the modern summer and winter climates in and around Antarctica simulated by six contemporary global atmospheric general circulation models (AGCMs) are compared with the corresponding observed climates. The models are listed along with their characteristics and simulations. The simulated and observed climates are presented in terms of their surface air temperatures, sea-level pressures, precipitation rates, and cyclogenesis and cyclone tracks. Results for selected model simulations are presented. A discussion of this intercomparison is given. B.W.

N86-11791# National Center for Atmospheric Research, Boulder, Colo.
ATMOSPHERIC RESPONSE TO AN EQUATORIAL PACIFIC SEA SURFACE TEMPERATURE ANOMALY: THE EFFECTS OF OROGRAPHY
M. L. Blackmon, G. T. Bates, and J. E. Geisler (Utah Univ., Salt Lake City) *In* NOAA Proc. of the 9th Ann. Climate Diagnostics Workshop Mar. 1985 p 211-217 (For primary document see N86-11763 02-47)
Avail: NTIS HC A19/MF A01 CSCL 04B

General circulation model experiments, carried out using the Community Climate Model (CCM) at the National Center for Atmospheric Research (NCAR) are described. All of these experiments are perpetual January, and they start at day 200, this being the time taken to spin up the model to some natural climatic state which is taken as the initial condition in all the experiments. A typical experiment runs for 1200 days after that. This record is divided into eight 90-day segments, each separated by a 60-day segment. Eight samples of independent 90-day realizations of winter climate averaged over the 90-day span are presented. This average is known as an ensemble average. Two basic categories of such ensemble-average winter climates are presented. One is the control ensemble; the other is the anomaly ensemble, in which the Sea Surface Temperature (SST) pattern is that used for the control experiment plus some SST anomaly in the equatorial Pacific. Two features of the anomalous response are investigated: the tropical anticyclone pair and the chain of alternating highs and lows that has come to be called the PNA pattern. B.W.

N86-11792# Canadian Climate Centre, Downsview (Ontario).
HORIZONTAL FLUXES IN REAL AND MODEL ATMOSPHERES
G. J. Boer *In* NOAA Proc. of the 9th Ann. Climate Diagnostics Workshop Mar. 1985 p 218-224 refs (For primary document see N86-11763 02-47)
Avail: NTIS HC A19/MF A01 CSCL 04B

Large-scale vertically integrated fluxes of moisture and energy, together with the associated distribution of sources and sinks, are basic climatological parameters of the atmosphere. Global distributions of these quantities have only recently become available from the PGGE 3-b data set. Quantities obtained from the FGGE 3-b data set observations are compared with those from general circulation models, such as the Canadian Climate Center GCM. B.W.

N86-11793# Royal Netherlands Meteorological Inst., De Bilt.
THE IMPACT OF HEAT SOURCES IN THE TROPICS ON THE ATMOSPHERIC CIRCULATION

R. Mureau, J. D. Opsteegh, and J. S. Winston (Maryland Univ., College Park) *In* NOAA Proc. of the 9th Ann. Climate Diagnostics Workshop Mar. 1985 p 225-230 (For primary document see N86-11763 02-47)
Avail: NTIS HC A19/MF A01 CSCL 04B

Observational and Global Circulation Model (GCM) studies have produced evidence of the importance of heat sources in the tropics for the global atmospheric circulation. Linear steady state models have been considered a useful tool to demonstrate the process of energy propagation out of the tropics, and have in a qualitative way contributed to the understanding of GCM's and also of the real atmosphere. Little is known, however, to what extent linear models can produce quantitatively realistic circulation patterns in response to observed forcing. An attempt was made to simulate with a liner 15 layer steady state model the observed anomalies for a large number of seasons. Seasonal mean outgoing longwave radiation (OLR) anomalies in the tropics were used as a proxy for the anomalous seasonal mean diabatic heating for all seasons during the years 1974 to 1983. Other forcing terms have been ignored. Simulated anomalous streamfunctions at 300 mb and 700 bm are objectively verified, by computing pattern correlation coefficients (pcc). B.W.

N86-11794# Maryland Univ., College Park. Dept. of Meteorology.

THE EFFECT OF ANOMALOUS SNOW COVER ON THE GENERAL CIRCULATION OF THE ATMOSPHERE USING A SIMPLE CLIMATE MODEL

Alan Robock and James W. Tauss *In* NOAA Proc. of the 9th Ann. Climate Diagnostics Workshop Mar. 1985 p 231-237 refs (For primary document see N86-11763 02-47)
Avail: NTIS HC A19/MF A01 CSCL 04B

The effect of anomalous snow cover has long been studied as having a pronounced influence on the temperature of the overlying atmosphere. However, little if any literature has described the incorporation of such a forcing into a climate model to investigate the anomalous atmospheric response. It is the purpose of this paper to study the effects of such anomalous forcings when imposed on a given basic state using a simple, linear, steady-state climate model. Some preliminary results are discussed. B.W.

N86-11795# Australian Numerical Meteorology Research Center, Melbourne.

INTERANNUAL CLIMATE VARIABILITY IN A LOW VERTICAL RESOLUTION SPECTRAL ATMOSPHERIC MODEL

Hal B. Gordon *In* NOAA Proc. of the 9th Ann. Climate Diagnostics Workshop Mar. 1985 p 238-245 (For primary document see N86-11763 02-47)
Avail: NTIS HC A19/MF A01 CSCL 04B

A 2-level spectral atmospheric model has been integrated for a total of 10 model years. This run is now being analyzed and some preliminary results are presented here concentrating on the interannual variability (IV) generated. B.W.

N86-11796*# National Aeronautics and Space Administration. Goddard Space Flight Center, Greenbelt, Md.

VARIABILITY SIMULATIONS WITH A STEADY, LINEARIZED PRIMITIVE EQUATIONS MODEL

James L. Kinter, III and Sumant Nigam (Massachusetts Inst. of Tech., Cambridge) *In* NOAA Proc. of the 9th Ann. Climate Diagnostics Workshop Mar. 1965 p 246-249 ref (For primary document see N86-11763 02-47)
Avail: NTIS HC A19/MF A01 CSCL 04B

Solutions of the steady, primitive equations on a sphere, linearized about a zonally symmetric basic state are computed for the purpose of simulating monthly mean variability in the troposphere. The basic states are observed, winter monthly mean, zonal means of zontal and meridional velocities, temperatures and surface pressures computed from the 15 year NMC time series. A least squares fit to a series of Legendre polynomials is used to compute the basic states between 20 H and the equator, and the hemispheres are assumed symmetric. The model is spectral in the zonal direction, and centered differences are employed in the meridional and vertical directions. Since the model is steady and linear, the solution is obtained by inversion of a block, pentediagonal matrix. The model simulates the climatology of the GFDL nine level, spectral general circulation model quite closely, particularly in middle latitudes above the boundary layer. This experiment is an extension of that simulation to examine variability of the steady, linear solution. B.W.

N86-11797# California Univ., Davis. Dept. of Land, Air and Water Resources.

UNDERSTANDING EL NINO EVENTS USING A SIMPLE DYNAMICAL ATMOSPHERE MODEL

Bryan C. Weare *In* NOAA Proc. of the 9th Ann. Climate Diagnostics Workshop Mar. 1985 p 250-256 (For primary document see N86-11763 02-47)
Avail: NTIS HC A19/MF A01 CSCL 04B

A simple model is outlined which illustrates possible feedback mechanisms linking oceanic surface conditions with tropical atmospheric heating and surface circulation. The results of the model suggest the importance of feedback mechanisms in the initiation and development of El Nino episodes. The basic model is patterned after the reduced gravity model on an equatorial Beta-plane introduced by Gill om 1980. The equations giving solutions for the perturbations of the winds pressure, vertical velocity, and potential temperature are given. Unlike most previous uses of this model, the forcing function will not be fixed but will be a function of the model circulation together with fixed oceanic conditions. R.J.F.

N86-11798# Princeton Univ., N. J. Geophysical Fluid Dynamics Lab.

ANOMALY GENERAL CIRCULATION MODELS

A. Navarra and K. Miyakoda *In* NOAA Proc. of the 9th Ann. Climate Diagnostics Workshop Mar. 1985 p 257-261 refs (For primary document see N86-11763 02-47)
Avail: NTIS HC A19/MF A01 CSCL 04B

The construction of a baroclinic anomaly model, based on an existing general circulation model (GCM) is discussed. Both a time-dependent, non-linear version, and a steady, linear version of the anomaly model were prepared, but only the application of the steady, linear model is discussed. Since the full GCM and the anomaly GCM are closely related, the anomaly model may facilitate the investigation of dynamical characteristics of the solution of full GCM, if an appropriate set of basic state and forcing is specified. The anomaly model based on a spectral general circulation model (GCM) is formulated and applied to the simulation of a January 1983 case. The steady anomaly model is solved by a matrix method using the Krylov technique to handle large linear systems. R.J.F.

N86-11799# Hawaii Univ., Honolulu. Dept. of Meteorology.

TRANSITION FROM THE SOUTHERN TO NORTHERN HEMISPHERE SUMMER MONSOON

Takio Murakami *In* NOAA Proc. of the 9th Ann. Climate Diagnostics Workshop Mar. 1985 p 262-264 (For primary document see N86-11763 02-47)
Avail: NTIS HC A19/MF A01 CSCL 04B

To facilitate the discussion, any meteorological variable is separated into two important components. The first component is symmetric about the equator and shows relatively small seasonality. The second component is asymmetric about the equator with convective zones showing a distinct seasonal pattern between the Southern and Northern Hemisphere summer. For example, OLR outgoing longwave radiation (OLR) can be partitioned into two components as follows: OLR(+) = 1/2(OLR sub N + OLR sub S), OLR(-) = 1/2(OLR sub N - OLR sub S), where OLF(+) and OLR(-) represents the symmetric and asymmetric components, respectively; OLR sub N (OLR sub S) denotes OLR in the Northern (Southern) Hemisphere. OLF(+) is small, irrespective of season, over equatorial Africa (20 to 40 E), the waritime cowntinent (100 to 160 E), and equatorial South America (110 t 70 W). These are three of the most convectively active regions near the equator.

Response to OLR(+) is generally confined to the equatorial latitudes and is often called the Walker Circulation. R.J.F.

N86-11800# National Meteorological Center, Washington, D.C. Climate Analysis Center.

LARGE-SCALE VARIABILITY IN INDIAN MONSOON RAINFALL INFERRED FROM SATELLITE DATA

Phillip A. Arkin, John E. Janowiak, and William Replane *In* NOAA Proc. of the 9th Ann. Climate Diagnostics Workshop Mar. 1985 p 265-273 (For primary document see N86-11763 02-47)

Avail: NTIS HC A19/MF A01 CSCL 04B

The object is to investigate the practicality of diagnosing rainfall variability by means of the indices constructed from the NOAA outgoing longwear radiation (OLR) data set. The principal conclusions drawn from this study are given: (1) Indices using thresholds of 240Wm(-2) appeared to define the large-scale annual cycle in monsoon area rainfall reasonably well. It seems that an index using the mean flux would provide much of the same information; (2) Onset of the monsoon, defined as three consecutive five day periods with index values above 0.4, was observed in each area/year examined here; (3) Onset progressed from south to north in a regular fashion; (4) Onset occurred latest in the Indian and Arabian Sea index areas, with differing sequences in different years. It seems possible that onset occurs first in the Arabian Sea during years in which an onset vortex occurs; (5) Important features of the interannual variability in monsoon rainfall were seen in the time series of standardized anomalies; (6) The drought of 1979 appears to have been a feature of the Indian and Arabial Sea index areas only; (7) The monsoon season of 1976 appears to have been relatively dry over the entire region; and (8) the results here are encouraging enough to warrant an effort to produce a precipitation index. R.J.F.

N86-11801# Illinois State Water Survey, Champaign. Climate and Meteorology Section.

TROPOSPHERIC STATIC STABILITY AND CENTRAL NORTH AMERICAN RAINFALL DURING 1979

Peter J. Lamb and Randy A. Peppler *In* NOAA Proc. of the 9th Ann. Climate Diagnostics Workshop Mar. 1985 p 274-283 (For primary document see N86-11763 02-47)

Avail: NTIS HC A19/MF A01 CSCL 04B

The occurrence, rate, and duration of precipitation in a continental region are likely to be functions of the existence and strength of several atmospheric processes and conditions over the region itself and, in particular, the degree to which they are simultaneously favorable. It is hypothesized that, in very general terms, such processes/conditions include the local presence and external supply of water vapor, and the troposphere's predisposition to providing the vertical motion necessary to produce the required condensation rates. One condition of potential importance in the latter regard is tropospheric static stability. This steady-state property indicates the likelihood of introduced vertical displacements or perturbations being thermodynamically damped, enhanced, or unchanged. The relation between tropospheric static stability and central North American summer (May-August) rainfall for 1979 is investigated. The first objective is to ascertain which of the many available methods of parameterizing static stability are most strongly related to the variation of the above rainfall. A rational basis is sought for the characterization of static stability. The second objective is to quantify the fraction of the 1979 rainfall variance that can be explained by static stability alone (i.e., by just one of the above processes/conditions). R.J.F.

N86-11802# Washington Univ., Seattle. Dept. of Atmospheric Sciences.

METEOROLOGICAL CONDITIONS DURING DROUGHT EPISODES IN THE UNITED STATES GREAT PLAINS

Fong-Chiau Chang and John M. Wallace *In* NOAA Proc. of the 9th Ann. Climate Diagnostics Workshop Mar. 1985 p 284-291 refs (For primary document see N86-11763 02-47)

Avail: NTIS HC A19/MF A01 CSCL 04B

Historical droughts over the central United States (1889 to 1980) and their associated large-scale circulation patterns and land-surface moisture conditions are investigated, using climatological monthly mean surface data, rawinsonde data, Palmer drought severity indices, 82 years of gridded monthly mean sea-level pressure data, and 30 years of gridded 5-day mean sea-level pressure and 500 mb height data. Surface station data include monthly mean surface pressure, maximum and minimum temperatures, temperature range, monthly total precipitation, dew point and relative humidity. Anomalies in monthly mean surface air temperature at Kansas City were used as a basis for objectively ranking the 276 months in the 92 summers, 1889 to 1980. A striking feature that emerges is the concentration of drought months in the decades of the 1910's, 1930's, and 1950's. Many of the hot months enhibit negative anomalies in relative humidity, dew point, precipitation and Palmer drought severity index. The drought months during the 1930's were characterized by extreme negative relative humidity anomalies and very low Palmer drought severity indices. These results support the view that soil moisture plays an important role in droughts. R.J.F.

N86-11803# Princeton Univ., N. J. Geophysical Fluid Dynamics Lab.

MONTHLY FORECAST EXPERIMENTS WITH SEA SURFACE TEMPERATURE ANOMALY FORCINGS AND ENVELOPE MOUNTAINS: PRELIMINARY RESULTS

J. Strutis, K. Niyakoda, Y.-H. Lu, and J. Ploshay *In* NOAA Proc. of the 9th Ann. Climate Diagnostics Workshop Mar. 1985 p 292-295 (For primary document see N86-11763 02-47)

Avail: NTIS HC A19/MF A01 CSCL 04B

A series of 30 day forecasts were made for January 1983 to assess the impact of using observed sea surface temperature and envelope mountains on medium and long range forecasting. The basic model used in these studies is the Geophysical Fluid Dynamics Laboratory global finite difference model. The model has a resolution of 1.875 deg in the north-south direction, and a variable resolution in the east-west direction, ranging from 1.875 deg in the tropics to 10 deg near the poles. The model has 9 sigma levels in the vertical. A set of four experiments has been run with this model: the control experiment using climatological sets and smooth topography; a forecast with envelope mountains which are steeper than those used in the control run; a forecast using the observed sets of January 1983; and a forecast using both observed sets and envelope mountains. Results are discussed. Author

N86-11804# Scripps Institution of Oceanography, La Jolla, Calif.

SPECTRAL STATISTICAL FORECASTS OF THE 500 MB HEIGHT FIELD

John O. Roads and Tim P. Barnett *In* NOAA Proc. of the 9th Ann. Climate Diagnostics Workshop Mar. 1985 p 296-304 (For primary document see N86-11763 02-47)

(Grants NSF ATM-82-13279; NSF ATM-82-10160; NA-81AA-D-0054)

Avail: NTIS HC A19/MF A01 CSCL 04B

A simple dynamic model used to describe global weather variations is based on damped propagating Rossby waves. For motions on the sphere, the solution is developed in terms of associated Legendre polynomials. In terms of a damped barotropic model linearized around solid body rotation for the nonzonal component, the solution can be found analytically. A data set is used consisting of twice daily spherical harmonics for the Northern Hemisphere 500 mb height field. Ten years of data are available. Coefficients for the model are determined using least squares from the first five years, which were then tested against the coefficients for the second five years. F.M.R.

N86-11805# Rutgers - The State Univ., New Brunswick, N. J. Dept. of Meteorology.

PREDICTION OF MONTHLY 700 MB HEIGHTS USING ANTECEDENT AND SIMULATED PROGNOSTIC HEIGHT PREDICTORS

Robert Harnack, Charles Kluepfel (Science Systems and Applications, Inc., Seabrook, Md.), and Robert E. Livezey (National Meteorological Center, Washington, D.C.) *In* NOAA Proc. of the

9th Ann. Climate Diagnostics Workshop Mar. 1985 p 305-316 (For primary document see N86-11763 02-47)
Avail: NTIS HC A19/MF A01 CSCL 04B

This study has two parts. The first is the study of persistence relationships by computing pattern correlations between time-averaged Northern Hemisphere 700 mb height fields ending on the 28th of the month and monthly-averaged heights for the following month. The second portion examines hindcast skill for monthly-mean 700 mb heights using antecedent heights, simulated prognostic heights, and a combination of both. Raw data consists of daily 700 mb heights in the period 1948 to 1980 for the Northern Hemisphere from 25N to 75N. Pattern correlations are computed between height fields consisting of time-averages for the last n days of an antecedent month on the one hand and the height field of the entire following (target) month on the other. Results are presented as average pattern correlations for calendar month pairs. These show a general tendency for maximum correlations at small n in the spring, and intermediate or large n in other months especially in mid-winter and mid-summer. F.M.R.

N86-11806# Maryland Univ., College Park. Dept. of Meteorology.

SPECIFICATION OF MEAN SURFACE TEMPERATURE ANOMALIES IN EUROPE AND ASIA DURING THE FALL MONTHS

William H. Klein and Runhua Yang *In* NOAA Proc. of the 9th Ann. Climate Diagnostics Workshop Mar. 1985 p 317-325 (For primary document see N86-11763 02-47)
(Grant NA-83AA-D-00048A1)
Avail: NTIS HC A19/MF A01 CSCL 04B

This paper extends research for the United States and Canada reported previously to a network of 68 surface stations in the European sector and 47 in Asia. Monthly mean air temperature anomalies near the surface (MMATA) at 134 grid points, plus the previous month's local MMATA, for the 30-year period: Jan. 1951 - Dec. 1980. Here are presented results for the 90 fall months of Sept., Oct. and Nov. F.M.R.

N86-11807# Illinois Univ., Urbana.

LAND-SURFACE FLUCTUATIONS AND ASSOCIATED CLIMATIC VARIABILITY

John E. Walsh and William H. Jasperson (Control Data Corp., Minneapolis, Minn.) *In* NOAA Proc. of the 9th Ann. Climate Diagnostics Workshop Mar. 1985 p 326-330 (For primary document see N86-11763 02-47)
Avail: NTIS HC A19/MF A01 CSCL 04B

Land surface effects are examined by constructing specification equations for the monthly surface station temperatures over the United States and Eurasia. These equations are obtained by forward stepwise screening of monthly grids of 700 mb height. Each equation is truncated according to a 1% F-test criterion. The 700 mb grids contain 91 points in the domains bounded by 20 deg N, 80 deg N, and either 50 deg W and 180 deg W (U.S.) or 0 deg E and 150 deg E (Eurasia). The 700 mb grids for 34 years (1947 to 1980, inclusive) are used in the analysis. Monthly air temperatures for the same 34 years are obtained for 61 stations in the U.S. and 231 stations in Eurasia. Missing Eurasian temperatures are obtained from the temperature anomalies at nearby stations. The snow data consists of monthly snow cover (2.5 cm and 15.0 cm) at eleven longitudes in the U.S. 120 deg W, 115 deg W, ..., 70 deg W. A monthly soil moisture index for each station is computed from monthly temperatures and precipitation amounts. F.M.R.

N86-11808# Creighton Univ., Omaha, Nebr. Dept. of Atmospheric Sciences.

CONCURRENT AND LAGGED RELATIONSHIPS BETWEEN PRECIPITATION FREQUENCY AND 700 MB HEIGHTS

Arthur V. Douglas and Phillip J. Englehart (Midwest Research Inst., Kansas City, Mo.) *In* NOAA Proc. of the 9th Ann. Climate Diagnostics Workshop Mar. 1985 p 331-340 (For primary document see N86-11763 02-47)
Avail: NTIS HC A19/MF A01 CSCL 04B

Precipitation frequency and its relationship to 700 mb heights which shows little skewedness, especially in the arid West, are discussed. A data set of recipitation frequency for 60 divisions in the United States was developed. The new data set and its properties are described. Summer precipitation in two regions, the Southwest and the Central Plains, are reported. The pattern correlation between southwestern precipitation frequency in summer and 700mb height anomalies is given. If the summer data (frequency and 700mb) are recalculated using data from the normally wet months of July and August, stronger relationships become apparent. It is indicated that the June height data have little relationship with precipitation or subsequent height fields in July and August. If precipitation totals for the southwest region are related to 700mb heights instead of frequency, the observed correlation values tend to be lower, especially in the critical region of the central Rockies. E.A.K.

N86-11809# Colorado Univ., Boulder. Cooperative Inst. for Research in Environmental Sciences.

TROPICAL CONVECTION AND NORTH AMERICAN CYCLONES DURING THE 1982-83 EL NINO

Richard A. Keen *In* NOAA Proc. of the 9th Ann. Climate Diagnostics Workshop Mar. 1985 p 341-345 refs (For primary document see N86-11763 02-47)
Avail: NTIS HC A19/MF A01 CSCL 04B

The planetary-scale wave pattern over North America responds to changes in the location and intensity of convection in the tropical Pacific. During El Nino conditions, convection shifts eastward into the central and eastern Pacific; the indicated mid-latitude response to this shift is the Pacific-North America, (PNA) pattern. One feature of the PNA pattern is an enhanced subtropical jet stream (STJ) across southern North America. During 1982 to 1983 jet stream wind velocities over the Gulf of Mexico were nearly twice their normal values. Such circulation anomalies are based on monthly or seasonal averages, and indicate the steady-state atmospheric response to persistent, large-scale tropical convection. E.A.K.

N86-11810# Massachusetts Inst. of Tech., Cambridge. Center for Meteorology and Physical Oceanography.

AN OBSERVATIONAL STUDY OF THE VERTICAL STRUCTURE OF INTERANNUAL WIND FLUCTUATIONS IN THE TROPICS

David S. Gutzler *In* NOAA Proc. of the 9th Ann. Climate Diagnostics Workshop Mar. 1985 p 346-351 refs (For primary document see N86-11763 02-47)
Avail: NTIS HC A19/MF A01 CSCL 04B

Time series of rawinsonde-derived monthly mean winds were used to document and characterize the interannual variability of the tropical wind field with emphasis on the vertical structure of the observed fluctuations. Seasonal climatology was calculated and subtracted from season's observed wind to form time series of seasonal anomalies. Empirical orthogonal functions of the vertical structure of interannual variability were derived for each station and season for zonal and meridional wind components separately, by calculating the eigenvectors of a mass-weighted covariance matrix incorporating wind anomalies at all six levels. E.A.K.

N86-11811# Washington Univ., Seattle. Dept. of Atmospheric Sciences.

LOW-FREQUENCY BAROCLINIC FEATURES OBSERVED IN THE LEE OF MAJOR MOUNTAIN RANGES

Huang-Hsiung Hsu and John M. Wallace *In* NOAA Proc. of the 9th Ann. Climate Diagnostics Workshop Mar. 1985 p 352-359 refs (For primary document see N86-11763 02-47)
Avail: NTIS HC A19/MF A01 CSCL 04B

The occurrence of the observed low-frequency variability which is inherently baroclinic in nature was addressed. The geographical dependence of the vertical structure of the geopotential height field was studied and indicated the existence of the baroclinic vertical structure on the cold or lee side of the major mountain ranges such as the Rockies and the Tibetan plateau in a wide frequency domain. The role of the highly baroclinic patterns playing in the low-frequency variability of the geopotential height field is examined. E.A.K.

N86-11812# Massachusetts Inst. of Tech., Cambridge. Dept. of Earth, Atmospheric and Planetary Science.
SLOW FLUCTUATIONS OF THE TROPICAL CIRCULATION DURING THE FGGE YEAR
Rennie Selkirk *In* NOAA Proc. of the 9th Ann. Climate Diagnostics Workshop Mar. 1985 p 360-372 (For primary document see N86-11763 02-47)
Avail: NTIS HC A19/MF A01 CSCL 04B

The fluctuations of the Walker circulation as reflected in the large scale divergent wind fields over the tropics and the subtropic during the FGGE Year are discussed. Empirical orthogonal function (EOF) analysis is used to resolve the largest spatial and largest time scale variations in the fields of velocity potential at the 850 and 200mb levels computed from the analyzed winds of the ECMWF FGGE III-b data set. The EOF results demonstrate that the 40 to 50 day time variations in both the Walker and Hadley cells are as important on the largest scale as the seasonal variability of the Hadley cell. E.A.K.

N86-11813# Maryland Univ., College Park. Dept. of Meteorology.
VERY ANOMALOUS BEHAVIOR OF OUTGOING LONGWAVE RADIATION IN THE TROPICS IN 1983-84: AFTERMATH OF ENSO?
Jay S. Winston *In* NOAA Proc. of the 9th Ann. Climate Diagnostics Workshop Mar. 1985 p 373-383 (For primary document see N86-11763 02-47)
(Grant NSF ATM-82-15090)
Avail: NTIS HC A19/MF A01 CSCL 04B

The extreme anomalies of the outgoing longwave radiation (OLR) over the tropical Pacific during the 1982 to 1983 ENSO event are discussed. As sea surface temperatures, the Southern Oscillation Index (SOI), and other features returned to more normal conditions in the second half of 1983, OLR anomalies in the tropics also became less extreme. By winter 1983 to 1984, however, strong OLR anomalies developed over the tropical Pacific and the Indian Ocean and generally persisted into spring 1984. These anomalies in tropical cloudiness and precipitation were accompanied by some pronounced anomalies of flow at 200 mb and 850 mb, but Pacific sea surface temperatures and the SOI exhibited values generally close to their normals. E.A.K.

N86-11814# World Meteorological Organization, Geneva (Switzerland). World Climate Programme Dept.
CLIMATE SYSTEM FLUCTUATIONS, MONITORING
S. Unninayar *In* NOAA Proc. of the 9th Ann. Climate Diagnostics Workshop Mar. 1985 p 384-397 refs (For primary document see N86-11763 02-47)
Avail: NTIS HC A19/MF A01 CSCL 04B

Climate fluctuations occur over a range of time scales and are associated with a magnitude of impact which are related to these time scales. The spatial extent of the phenomena seems linked with their temporal characteristics. The cause of past climate fluctuations is still a question. Theoretical and numerical modelling may be determining climate prediction. Advances in computer technology make it possible to process enormous volumes of observational data and integrate models of greater complexity. With the global deployment of satellite technology, observing systems have kept pace with the demand of models for more data, though in certain areas the availability of observations of certain variables/processes remains poor. An ideal global observing system could be implemented. The multidisciplinary nature of the atmosphere ocean cryosphere land surface climate system requires a mechanism that promotes a cross flow of information on the state of the system as a whole and on possible fluctuations that are of regional and global consequence. E.A.K.

N86-11815# National Environmental Satellite Service, Washington, D. C. Climate and Earth Sciences Lab.
THE STATUS OF THE NOAA/NESDIS RADIATION BUDGET DATA SET
Arnold Gruber *In* NOAA Proc. of the 9th Ann. Climate Diagnostics Workshop Mar. 1985 p 398-407 refs (For primary document see N86-11763 02-47)
Avail: NTIS HC A19/MF A01 CSCL 04B

Estimates of the planetary albedo and outgoing long wave radiation were obtained from polar orbiting operational spacecraft. Estimates of albedo and emitted radiation were produced from the TIROS-N series of satellites. Estimates of albedo were obtained from visible channel radiance and emitted flux were obtained from window channel measurements. Regression procedures are used to obtain the total broadband emitted flux from the window channel. The regression procedure was an empirical regression between simultaneous window data and broadband radiance observation from the Nimbus-7 ERB experiment. This is adopted as the most accurate equation for processing the data and previous calculations are adjusted to this new regression. E.A.K.

N86-11816# National Meteorological Center, Washington, D.C. Climate Analysis Center.
A SEA SURFACE TEMPERATURE ANALYSIS BASED ON IN SITU AND SATELLITE DATA
Richard W. Reynolds and William H. Gemmill *In* NOAA Proc. of the 9th Ann. Climate Diagnostics Workshop Mar. 1985 p 408-416 refs (For primary document see N86-11763 02-47)
Avail: NTIS HC A19/MF A01 CSCL 04B

The use of satellite data can significantly improve the surface temperature (SST) analysis. The monthly number of satellite SST retrievals over the globe are shown. These retrievals are obtained from the multichannel techniques using Advanced Very High Resolution Radiometer (AVHRR). The number of observations is much greater than the number of in situ observations and the satellite coverage is more uniform. The variation in the number of retrievals is due at times to satellite hardware problems but also to interpretation difficulties related to cloud cover and high level aerosols. It is reported that the aerosols introduced into the atmosphere by the El Chichon eruptions resulted in cold biases sometimes exceeding 2 C in the satellite SST retrievals relative to in situ reports. E.A.K.

N86-11817# Atmospheric and Environmental Research, Inc., Cambridge, Mass.
EFFECT OF INITIALIZATION ON DIAGNOSES OF LARGE-SCALE CIRCULATION STATISTICS FROM WMC ANALYSES
Richard D. Rosen and David A. Salstein *In* NOAA Proc. of the 9th Ann. Climate Diagnostics Workshop Mar. 1985 p 417-428 (For primary document see N86-11763 02-47)
(Contract NA-83SA-C-00738)
Avail: NTIS HC A19/MF A01 CSCL 04B

Analyses of the state of the atmosphere produced by operational weather concern are used in diagnostic studies of the large scale circulation. The degree to which these analyses may be compromised for this is analyzed to generate them. The effect of one element of the EMC global data assimilation system initialization on calculation of circulation statistics is examined. The only fields routinely archived and available to the scientific community are those that have undergone initialization. However, daily analyses made prior to the initialization step were used to examine differences between statistics generated from these preinitialized (PREI) analyses and the postinitialized (POSTI) ones. The results are generally more valid because the initialization scheme used by NMC remained unchanged during the entire period from about January 1981 through August 1984. E.A.K.

N86-11818# Texas A&M Univ., College Station. Dept. of Meteorology.
James P. McGuirk, Aylmer H. Thompson, and Neil R. Smith *In* NOAA Proc. of the 9th Ann. Climate Diagnostics Workshop Mar. 1985 p 429-436 (For primary document see N86-11763 02-47)
Avail: NTIS HC A19/MF A01 CSCL 04B

Aspects of the tropical Eastern Pacific mean meridional circulation are interpreted for the mean behavior of a synoptic event the moisture burst. Three different aspects of the interaction of moisture bursts and the Hadley cell are described: (1) the El Nino behavior; (2) mean meridional wind behavior; and (3) data quality. E.A.K.

N86-11819# National Weather Service, Silver Spring, Md.
MONTHLY AND SEASONAL WEATHER OUTLOOK FOR MAY 1985, VOLUME 39, NUMBER 9
30 Apr. 1985 10 p
(PB85-199123) Avail: NTIS HC A02/MF A01 CSCL 04B

Maps are given which contain observed and probability estimates of temperature and precipitation for October and November 1984 in the United States and Canada. GRA

N86-11820# National Oceanic and Atmospheric Administration, Washington, D. C. National Environmental Satellite, Data, and Information Service.
ATLAS OF HIGH ALTITUDE AIRCRAFT MEASURED RADIANCE OF WHITE SANDS, NEW MEXICO, IN THE 450-1050 NANOMETERS BAND
G. R. Smith, R. H. Levin, and J. S. Knoll Apr. 1985 34 p refs
(PB85-204501; NOAA-TR-NESDIS-20) Avail: NTIS HC A03/MF A01 CSCL 04B

The National Oceanic and Atmospheric Administration (NOAA) activity at White Sands, New Mexico was directed at providing visible wavelength calibration of Earth oriented satellite instruments. The best method of calibrating a satellite sensor is to make a simultaneous measurement with a calibrated instrument from a high altitude aircraft. Independent of the calibration, and as an interim product of data analysis, the aircraft instrument data is scientifically useful and is herein presented as an atlas of White Sands surface radiance. Author (GRA)

N86-11821# National Severe Storms Forecast Center, Kansas City, Mo.
MINIMUM ASSUMPTION TORNADO HAZARD PROBABILITY MODEL Final Technical Memo, 1950 - 1982
J. T. Schaefer, D. L. Kelly, and R. F. Abbey May 1985 40 p refs
(PB85-206092; NOAA-TM-NWS-NSSFC-8) Avail: NTIS HC A03/MF A01 CSCL 04B

One of the principle applications of climatological tornado data is in tornado hazard assessment. To perform such a hazard potential determination, historical tornado characteristics in either a regional or local area are compiled. A model is then used to determine a site specific point probability of a tornado greater than a specified intensity occurring. Various models require different climatological input. However, a knowledge of the mean values of tornado track length, tornado track width, tornado affected area, and tornado occurrence rate as both a function of tornado intensity and geographic area along with a violence frequency distribution enable most of the models to be applied. The NSSFC-NRC tornado data base is used to supply input for the determination of these parameters over the United States. Author (GRA)

N86-11822# North American Weather Consultants, Inc., Salt Lake City, Utah.
CONTINUING DESIGN, REVIEW, AND ANALYSIS WORK FOR THE SIERRA COOPERATIVE PILOT PROJECT Final Report
R. D. Elliot, D. A. Griffith, John A. Flueck (Flueck Associates), and Jack F. Hannaford (Sierra Hydrotech, Placerville, Calif.) Nov. 1984 228 p refs
(Contract DI-7-07-83-V0008)
(PB85-204303; NAWC/SLWM-84-2) Avail: NTIS HC A11/MF A01 CSCL 04B

North America Weather Consultants (NAWC) supplied contractual support to the Bureau of Reclamation on their Sierra Cooperative Pilot Project (SCPP). The SCPP is an on-going winter weather modification research program being conducted in the central Sierra Nevada of California. This contractual work covered a 7-year period beginning in October 1977 and ending in September 1984. NAWC's objectives in the performance of this work were threefold: (1) complete the physical and statistical design of the SCPP, (2) review the project during its lifetime to insure that operations comply with the design, and (3) perform an unbiased evaluation of the seeding results. Author (GRA)

N86-11823# National Oceanic and Atmospheric Administration, Boulder, Colo. Environmental Sciences Group.
AUTOMATED METHOD FOR THE DOCUMENTATION OF CLOUD-TOP CHARACTERISTICS OF MESOSCALE CONVECTIVE SYSTEMS
J. A. Augustine Feb. 1985 127 p
(PB85-204246; NOAA-TM-ERL-ESG-10) Avail: NTIS HC A07/MF A01 CSCL 04B

Measurements of cloud-top areas, centroid, and eccentricity for mesoscale convective systems (MCS's) were automated. The algorithm resides on the PROFS-2 VAX 11/780 computer and utilizes digital infrared imagery received at the local satellite ground station. The software is user-activated and processes one image per run. All operations are performed within the bounds of a user-defined image subsector. GRA

48 OCEANOGRAPHY

Includes biological, dynamic and physical oceanography; and marine resources.

N86-11824# Naval Postgraduate School, Monterey, Calif.
USE OF THE WAVENUMBER TECHNIQUE WITH THE LLOYDS MIRROR FOR AN ACOUSTIC DOUBLET M.S. Thesis
P. B. King Mar. 1985 113 p
(AD-A156463) Avail: NTIS HC A06/MF A01 CSCL 17/1

This thesis examines a method to determine the depth of a point source in an ocean environment. Using the Fourier Transform on the acoustic pressure field in the range domain results in the attainment of the acoustic pressure spectrum in the wave-number domain and a characteristic nodal spacing unique to the source-receiver depths. Quantitative examination of a magnitude plot of the spectrum and use of simple mathematical formulae yield the source depth. The debilitative effects of narrowband noise and surface roughness on the pressure spectrum is recognizable in noise after the pressure field in the range domain has been lost in the noise field. The effect of surface gravity waves on the pressure spectrum is similar to that on the pressure field in the range domain: the characteristic nodal spacing is suppressed as the height of the surface waves increases. Author (GRA)

N86-11825# Army Engineer Waterways Experiment Station, Vicksburg, Miss. Environmental Lab.
USER GUIDE FOR WIFM-SAL (WES IMPLICIT FLOODING MODEL-SAL): A TWO-DIMENSIONAL VERTICALLY INTEGRATED, TIME-VARYING ESTUARINE TRANSPORT MODEL Final Report, Jul. 1979 - Jun. 1983
R. A. Schmalz, Jr. Mar. 1985 113 p
(AD-A157446; WES/IR/EL-85-1) Avail: NTIS HC A06/MF A01 CSCL 08/8

WIFM-SAL is preliminary to the development of comprehensive water quality mathematical models that may be used to assist in the analysis of water quality problems in shallow estuaries and embayments which may be considered vertically well mixed. The model is two dimensional in the horizontal and generates time-varying water surface elevations, velocities, and constituent fields over a space staggered grid. Units of measure are expressed in the English system (slug-ft-second). Results computed on a global grid may be employed as boundary conditions on a more spatially limited refined grid concentrated around the area of interest. In addition, the user may select either of two distinct transport schemes. Scheme 1 is a flux-corrected transport scheme capable of resolving sharp fronts without oscillation. Scheme 2 is a full, three time level scheme directly compatible with three level hydrodynamics. The telescoping grid capability in conjunction with the user selectable constituent transport scheme is an extremely powerful concept in real world transport problem solving. GRA

N86-11826# Coast Guard Research and Development Center, Groton, Conn.

AN EVALUATION OF CASP (COMPUTER ASSISTED SEARCH PLANNING PROGRAM) DRIFT PREDICTIONS NEAR THE NEW ENGLAND SHELF/SLOPE FRONT Interim Report
D. L. Murphy and A. A. Allen Jan. 1985 49 p
(AD-A157447; CGR/DC-7/85; USCG-D-16-85; IR-19) Avail: NTIS HC A03/MF A01 CSCL 06/7

In June 1984 a series of experiments was conducted in which the drift predictions of the Coast Guard's operational search planning computer model (CASP) were evaluated. Three satellite-tracked drift buoys and a life raft were released and tracked for two 3-day periods at the New England Shelf/Slope Front. Their movement was compared with CASP drift predictions for simulated PIW's and a life raft for two sets of environmental data: historical currents and large-scale winds versus locally measured data. For the historical data, the observed drift errors were two to four times larger than drift errors calculated by CASP. The use of on-scene environmental data improved the predictions for PIW's to near the CASP-calculated drift errors, but not for the life raft. Significant differences in the surface currents occurred over 20 nautical miles and 3 to 5 days, which were not accounted for by the historical surface current files, and therefore increased the error in the drift prediction of CASP. GRA

N86-11827# Army Cold Regions Research and Engineering Lab., Hanover, N. H.
SURVEY OF ICE PROBLEM AREAS IN NAVIGABLE WATERWAYS
J. Zufelt and D. Calkins Apr. 1985 37 p
(AD-A157477; CRREL-SR-85-2) Avail: NTIS HC A03/MF A01 CSCL 13/2

This report presents the findings of a survey of ice problems encountered on the nation's major navigable waterways. A survey questionnaire was developed and, through a field review group, was distributed to lock and dam facilities on the Allegheny, Monongahela, Ohio, Kanawha, Kaskaskia, and Mississippi Rivers and the Illinois Waterway. Analysis of the completed questionnaires identified 13 ice problem categories. The report describes each category of ice problem encountered, as well as the cited methods, operational and/or structural, undertaken to reduce the impact of each ice problem. GRA

N86-11828# San Jose State Univ., Calif. Dept. of Geology.
CORAL REEF HYDROGEOLOGY
R. W. Buddemeier and J. A. Oberdorfer 21 May 1985 20 p refs Presented at the 5th Congr. Intern. Sur Les Recifs Coralliens, Rapeete, Tahiti, 27 May 1985
(Contract W-7405-eng-48)
(DE85-012923; UCRL-91772; CONF-8505162-1) Avail: NTIS HC A02/MF A01

Knowledge of internal flow velocities and pore water residence time is important in understanding pore water geochemistry, nutrient fluxes at the benthic boundary, reef diagenesis, and fresh water resources in reef islands. Hydrogeologic studies of Pacific and Indian Ocean reef and atoll islands indicate a dual aquifer systems; the major Pleistocene aquifer has hydraulic conductivities on the order of 1000 m/d, while the overlying Holocene aquifer of unconsolidated sediments is at least an order of magnitude less permeable. Studies of both submerged reefs and atoll islands give bulk pore water residence times on the order of months to a few years. Chemical analyses of pore water indicate that both carbonate solution and precipitation are taking place, which will alter porosity and permeability with time. The dual aquifer model also suggests that the Ghyben-Herzberg lens approach to reef island fresh water resources is inaccurate and can lead to a gross overestimation of the potable resource. DOE

N86-11551# Research Inst. of Geodesy, Prague (Czechoslovakia).
RESULTS OF KAPG CO-OPERATION IN EARTH TIDE RESEARCH
Zdenek Simon *In* Academy of Sciences of the GDR Proc. of the 5th Intern. Symp. Geodesy and Phys. of the Earth 1985 p 24-30 refs (For primary document see N86-11549 02-42)
Avail: NTIS HC A09/MF A01

N86-11554# Hungarian Academy of Sciences, Sopron. Geodetical and Geophysical Research Inst.
HIGH FREQUENCIES IN TIDAL TILT RECORDS
G. Bartha *In* Academy of Sciences of the GDR Proc. of the 5th Intern. Symp. Geodesy and Phys. of the Earth 1985 p 51-59 refs (For primary document see N86-11549 02-42)
Avail: NTIS HC A09/MF A01

N86-11558# Academy of Sciences, Potsdam (East Germany). Zentralinst. fuer Physik der Erde.
AN ATTEMPT TO DETECT GEOMETRIC TIDAL INFORMATION USING LAGEOS LASER RANGING DATA
R. Dietrich and G. Gendt *In its* Proc. of the 5th Intern. Symp. Geodesy and Phys. of the Earth 1985 p 77-81 refs (For primary document see N86-11549 02-42)
Avail: NTIS HC A09/MF A01

N86-11571# Freie Univ., Berlin (West Germany). Inst. fuer Geophysikalische Wissenschaften.
OCEAN TIDAL LOADING ALONG THE BLUE ROAD GEOTRAVERSE IN FENNOSCANDIA
Gerhard Jentzsch *In* Academy of Sciences of the GDR Proc. of the 5th Intern. Symp. Geodesy and Phys. of the Earth, Pt. 2 1985 p 18-28 refs (For primary document see N86-11568 02-42)
Avail: NTIS HC A09/MF A01

N86-11576# Belgian Royal Observatory, Uccle.
INTERACTIONS BETWEEN OCEANIC AND GRAVITY TIDES, AS ANALYSED FROM WORLD-WIDE EARTH TIDE OBSERVATIONS AND OCEAN MODELS
P. Melchior, B. Ducarme, M. VanRuymbeke, C. Poitevin, and M. DeBecker *In* Academy of Sciences of the GDR Proc. of the 5th Intern. Symp. Geodesy and Phys. of the Earth, Pt. 2 1985 p 55-62 refs (For primary document see N86-11568 02-42)
Avail: NTIS HC A09/MF A01

51 LIFE SCIENCES (GENERAL)

Includes genetics.

N86-11829*# Wisconsin Univ., Madison. Dept. of Horticulture.
CONTROLLED ENVIRONMENT LIFE SUPPORT SYSTEM: CALCIUM-RELATED LEAF INJURIES ON PLANTS Final Report, May 1981 - Apr. 1984
T. W. Tibbitts 1985 44 p refs
(Contract NCC2-136)
(NASA-CR-176288; NAS 1.26:176288) Avail: NTIS HC A03/MF A01 CSCL 06C

A calcium related injury in lettuce termed tipburn was the focus of this study. It affects the young developing leaves as they become enclosed during head formation. It is a good model system to study because the injury can be induced with good predictability and lettuce is one of the crops chosen by the CELSS program for concentrated study. Investigations were undertaken to study a number of different procedures, that would have the potential for encouraging movement of calcium into the young developing leaves and to study the time course and pattern of calcium accumulation in developing leaves to provide a basis for developing effective control procedures for this injury. Author

N86-11830*# Massachusetts Inst. of Tech., Cambridge. Dept. of Applied Biological Science.
UTILIZATION OF NON-CONVENTIONAL SYSTEMS FOR CONVERSION OF BIOMASS TO FOOD COMPONENTS: POTENTIAL FOR UTILIZATION OF ALGAE IN ENGINEERED FOODS Annual Report
M. Karel, A. R. Kamarei, and Z. Nakhost Mar. 1985 37 p refs
(Contract NCC2-231)
(NASA-CR-176257; NAS 1.26:176257) Avail: NTIS HC A03/MF A01 CSCL 06C

The major nutritional components of the green algae (Scenedesmus obliquus) grown in a Constant Cell density Apparatus were determined. Suitable methodology to prepare proteins from which three major undesirable components of these cells (i.e., cell walls, nucleic acids, and pigments) were either removed or substantially reduced was developed. Results showed that processing of green algae to protein isolate enhances its potential nutritional and organoleptic acceptability as a diet component in a Controlled Ecological Life Support System. Author

N86-11831*# San Francisco Univ., Calif.

STRUCTURE AND FUNCTION OF ISOZYMES: EVOLUTIONARY ASPECTS AND ROLE OF OXYGEN IN EUCARYOTIC ORGANISMS Final Report

Tanjore Satyanarayana Sep. 1985 11 p refs
(Contract NCC2-85)
(NASA-CR-176286; NAS 1.26:176286) Avail: NTIS HC A02/MF A01 CSCL 06C

Oxygen is not only one of the most abundant elements on the Earth, but it is also one of the most important elements for life. In terms of composition, the feature of the atmosphere that most distinguishes Earth from other planets is the presence of abundant amounts of oxygen. The first forms of life may have been similar to present day anaerobic bacteria such as clostridium. The relationship between prokaryotes and eukaryotes, if any, has been a topic of much speculation. With only a few exceptions eukaryotes are oxygen-utilizing organisms. This research eukaryotes or eukaryotic biochemical processes requiring oxygen, could have arisen quite early in evolution and utilized the small quantities of photocatalytically produced oxygen which are thought to have been present on the Earth prior to the evolution of massive amounts of photosynthetically-produced oxygen. B.W.

N86-11832# Army Research Inst. of Environmental Medicine, Natick, Mass.

AN ATROPINIZED HEAT-STRESSED RAT MODEL: ANTICHOLINERGIC AND ANTICHOLINESTERASE DRUG POTENCY

C. B. Matthew, R. W. Hubbard, and R. P. Francesconi Jul. 1985 18 p
(DA Proj. 3M1-62734-A-875)
(AD-A157620; USARIEM-M-34/85) Avail: NTIS HC A02/MF A01 CSCL 06/15

We have developed an animal model to evaluate the thermoregulatory effects of several anticholinergic drugs, particularly in hot environments. Our previous work on this model demonstrated that atropine, the prototype of muscarinic anticholinergic drugs, produces a dose-dependent increase in heating rate of heat-stressed rats that lasted for 3 hours after administration. By comparing the effects on heating rate of other anticholinergic drugs relative to the effects of atropine, we derived the following potency ratios: imipramine (0.004), amitriptyline (0.02), chlorpromazine (0.1), atropine (1); L-hyoscymaine (2), atropine methyl nitrate (4), and scopolamine (16). Additionally, we tested the ability of carbamates to reduce the elevated heating rate of atropinized rats as a measure of anticholinesterase efficacy, resulting in the following relative potencies: neostigmine (8), physostigmine (2) and pyridostigmine (1). Our results indicate that this is a useful model to evaluate potential drug-exacerbated increases in body temperature in hot environments. GRA

N86-11833# Oak Ridge National Lab., Tenn.

POSITIVE GENETIC HAZARD PREDICTIONS FROM SHORT-TERM TESTS HAVE PROVED FALSE FOR RESULTS IN MAMMALIAN SPERMATOGONIA WITH ALL ENVIRONMENTAL CHEMICALS SO FAR TESTED

W. L. Russell 1985 9 p refs Presented at the 4th Intern. Conf. on Environ. Mutagens, Stockholm, 24 Jun. 1985
(Contract DE-AC05-84OR-21400)
(DE85-013640; CONF-8506137-1) Avail: NTIS HC A02/MF A01

Eleven chemicals for which there has been considerable human exposure were studied by the mouse specific-locus method because of their positive mutagenic action in other test systems. All were positive in the Drosophila sex-linked recessive lethal test, and in mammalian somatic cells proved muagenic. In mouse stem-cell spermatogonia none of the chemicals, even at maximum tolerated dose, has given a specific-locus mutation frequency higher than the control, and the mutation frequency for all eleven combined (12 mutations in 298,502 offspring) was actually less than the historical control. Absence of mutation induction cannot be attributed to: (1) failure of the chemicals to reach the testis (10 of them are known to reach the testis in active form), (2) small sample size (the samples are large), and (3) insensitivity of the test (the test is not insensitive, a positive control gave a mutation frequency 132 times higher than the historical control). It is concluded that mammalian stem-cell spermatogonia have an effective repair capability. DOE

N86-11834# California Univ., Livermore. Lawrence Livermore Lab.

DETECTION OF CHROMOSOMAL ABNORMALITIES IN HUMAN SPERM

B. Brandriff, L. Gordon, A. K. Ashworth, G. Watchmaker, and A. V. Carrano 19 Jun. 1985 9 p refs Presented at the 4th Intern. Conf. on Environ. Mutgens, Stockholm, 24 Jun. 1985
(Contract W-7405-eng-48)
(DE85-014178; UCRL-92835; CONF-8506137-3) Avail: NTIS HC A02/MF A01

A new technology developed by Rudak, et al., for examining the chromosomal constitution of human sperm through fusion with eggs from the Syrian hamster was used to obtain baseline data on the types and frequencies of aberrations in sperm of normal men. The frequency of structural aberrations in 2724 sperm chromosome karyotypes from the 13 healthy non-exposed donors ranged from 2 to 15.8%, demonstrating significant interindividual variability. The most frequently occurring aberrations were chromosome breaks, followed by acentric fragments, chromatid exchanges, chromatid breaks, dicentrics and translocations, chromosome deletions and duplications, inversions, and chromatid deletions. Two donors previously reported had one cell each with multiple chromatid exchanges and breaks. In addition, the oldest donor, AA, had 5 cells out of 124 examined with multiple breaks and rearrangements too extensive to completely identify. DOE

N86-11835# Oak Ridge National Lab., Tenn.

RELATIONSHIP BETWEEN ALKYLATION SITES AND INDUCTION OF DOMINANT LETHALS AND HERITABLE TRANSLOCATIONS IN MICE

W. M. Generoso 1985 8 p refs Presented at the 4th Intern. Conf. on Environ. Mutagens, Stockholm, 24 Jun. 1985
(Contract DE-AC05-84OR-21400)
(DE85-014309; CONF-8506137-6) Avail: NTIS HC A02/MF A01

Production of dominant lethals and heritable translocations is determined by the degree of stability of alkylation products within the chromosome. If repair is not effected in the fertilized eggs and the alkylation products persist to the time of pronuclear chromosome replication or early cleavage divisions, they lead to chromatid-type aberrations and eventually to lethality. The production of heritable translocations requires a transformation of unstable alkylation products into suitable intermediate lesions. These lesions are converted into chromosome exchanges prior to the time of pronuclear chromosome replication. Dominant lethals result from both chromatid and chromosome-type aberrations while heritable translocations results primarily from the latter type. It is inherent that the production of chromosome and chromatid-type aberrations by a chemical mutagen are not necessarily mutually exclusive. E.A.K.

N86-11836# Oak Ridge National Lab., Tenn.

INFORMATION FROM SPECIFIC-LOCUS MUTANTS ON THE NATURE OF INDUCED AND SPONTANEOUS MUTATIONS IN THE MOUSE

L. B. Russell 1985 12 p refs Presented at 4th Intern. Conf. on Environ. Mutagens, Stockholm, 24 Jun. 1985
(DE85-014313; CONF-8506123-7) Avail: NTIS HC A02/MF A01

Genetic and molecular analyses of mutations are increasing the qualitative capabilities of the specific-locus test (SLT). Some mutations are found to be deletions of large numbers of genes, including some that control survival at various developmental stages, neurological functions, enzyme syntheses, etc. Smaller (including possibly single-gene) deletions are also detected. A third group of SLT mutations represents intragenic lesions. For at least three of the loci, mutations may now be qualitatively grouped on the basis of simple phenotypic findings. Type of mutagen and germ-cell stage exposed strongly influence the nature of the lesions. The qualitative information from SLT results makes possible conclusions about relative potential harmfulness of different types of exposures that may yield equal mutation rates, about difference between induced and spontaneous mutations, etc. It also identifies genetic material suitable for basic studies. DOE

N86-11837# Tulsa Univ., Okla.
TERATOGENIC EFFECTS OF MICROWAVE RADIATION Final Report, 1980 - 1985
M. E. OConnor and R. Strattan May 1985 51 p
(Contract EPA-68-02-3453)
(PB85-207462; EPA-600/1-85-007) Avail: NTIS
HC A04/MF A01 CSCL 06T

Pregnant CF-1 mice was exposed to 2450-MHz CW microwave irradiation at power densities of 0, 10, or 30 mW/sq. cm for 6 hours daily from gestational day 1 through day 18. All exposures occurred in an anechoic chamber maintained at 50% relative humidity with air temperature of 22C. A group of pregnant colon cage-control mice was maintained for each of the three exposure groups. Teratogenic examinations were performed on day 18 following Caesarean section of the maternal subject. Every third fetus was stained with alazarin red and examined for skeletal abnormalities. No significant differences between the groups observed for fetal body mass, fetal brain mass, resorption, live fetuses, gross abnormalities, or skeletal abnormalities. Author (GRA)

52 AEROSPACE MEDICINE

Includes physiological factors; biological effects of radiation; and weightlessness.

N86-11838*# Rhode Island Univ., Kingston. Dept. of Physics.
FIBER OPTIC PRESSURE SENSORS IN SKIN-FRICTION MEASUREMENTS Final Report
Robert Kidwell Sep. 1985 57 p refs
(Grant NAG1-519)
(NASA-CR-176294; NAS 1.26:176294) Avail: NTIS
HC A04/MF A01 CSCL 06B

Fiber optic lever pressure sensors intended for use in a low speed wind tunnel environment were designed, constructed and tested for the measurement of normal and shear displacements associated with the pressures acting on a flat aluminum plate. On-site tests performed along with several static and dynamic measurements made have established that, with proper modifications and improvements, the design concepts are acceptable and can be utilized for their intended use. Several elastomers were investigated for use in sensors and for their incorporation into these sensors. Design and assembly techniques for probes and complete sensors were developed. Author

N86-11839# American Inst. of Biological Sciences, Arlington, Va.
ASSESSMENTS AND VIEWPOINTS ON THE BIOLOGICAL AND HUMAN HEALTH EFFECTS OF EXTREMELY LOW FREQUENCY (ELF) ELECTROMAGNETIC FIELDS: COMPILATION OF COMMISSIONED PAPERS FOR THE ELF LITERATURE REVIEW PROJECT Final Report
May 1985 469 p
(Contract N00014-84-C-0446)
(AD-A156942) Avail: NTIS HC A20/MF A01 CSCL 06/18

The biological and human health effects of extremely low frequency (ELF) electromagnetic fields are discussed. Among the topics discussed are: The effects of ELF fields on neural development and nerve regeneration; electromagnetic fields and calcium efflux; studies of plants and animals exposed to ELF electric and magnetic fields; electromagnetic influences on birds; a review of Cell Effects Induced by Exposure of Extremely Low Frequency electromagnetic fields; the effects of ELF electric and magnetic fields on artificial cardiac pacemakers; behavioral toxicology of ELF electric and magnetic fields; electromagnetic fields and public health; influence of power frequency electric and magnetic fields on human health; ecological effects of extremely low frequency electric and magnetic fields; reproductive and developmental alterations associated with exposure of mammals to ELF (1 to 300 Hz) electromagnetic fields; behavioral effects extremely low frequency electric and magnetic fields; effects of electromagnetic fields on circadian rhythms; effects of ELF electromagnetic fields on neuroendocrine systems; immunological effects of extremely low frequency electromagnetic fields; neural effects of extremely low frequency fields as a function of induced tissue current density; magnetic and electromagnetic field effects on biological systems; and effects of extremely low frequency electric and magnetic fields on the nervous system are discussed. GRA

N86-11840# Army Research Inst. of Environmental Medicine, Natick, Mass.
PERCEPTUAL AND PHYSIOLOGICAL RESPONSES DURING EXERCISE IN COOL AND COLD WATER
M. M. Toner, L. L. Drolet, and K. B. Pandolf Jun. 1985 23 p
(DA Proj. 3E1-62777-A-879)
(AD-A157334; USARIEM-M-32/85) Avail: NTIS
HC A02/MF A01 CSCL 06/19

This investigation examined the interaction of exposure to cold water stress with both perceived exertion and thermal sensation (TS) during exercise. Eight male volunteers performed arm, leg and combined arm and leg exercise for 45 min in water at 20 and 26 C. Exercise was performed at a low and a high intensity relative to the ergometer specific peak oxygen uptake (VO2 peak). In general, percent VO2 peak did not differ ($p > 0.05$) between types of exercise in either 20 or 26 C water. During low intensity exercise when power output was matched across water temperatures (Tw), percent VO2 peak was greater ($p < 0.05$) in 20 C water (52%) compared to 26 C water (42%). Ratings of perceived exertion (RPE) did not differ ($p > 0.05$) between Tw. During high intensity exercise when percent VO2 peak was matched across Tw, RPE was lower during exercise in 20 C compared to 26 C. Multiple correlation analyses comparing both final RPE and thermal sensation with physiological and thermal measures were performed across type of exercise and Tw. RPE was moderately correlated with heart rate and ventilation, whereas very slight relationships were established with TS, skin and rectal temperatures. TS was moderately correlated with skin and rectal temperatures whereas low correlations existed between TS and both heart rate and ventilation. These data suggest that the change in oxygen uptake associated with exercise in cold water does not add to the overall perception of exertion. This perception appears to be related to cardiopulmonary variables rather than thermal measures, whereas thermal sensation is related to thermal measures and not cardiopulmonary variables. GRA

N86-11841# Army Research Inst. of Environmental Medicine, Natick, Mass.
PHYSIOLOGICAL EFFECTS OF TRAINING
W. J. Kraemer and W. L. Daniels 25 Jun. 1985 44 p
(AD-A157417; USARIEM-M-31/85) Avail: NTIS
HC A03/MF A01 CSCL 06/16

With the evolution of exercise science a vast amount of information concerning the physiological effects of training has been generated. Understanding the basic training responses and adaptations of various modes of conditioning can give the clinician insights into exercise prescription. The purpose of this manuscript is not to present an exhaustive review, but provide the reader with a basic overview of the physiological effects of training. Aerobic training results in a number of adaptations in humans. The magnitude of this response is dependent upon a number of factors. It depends upon the type, the intensity, the frequency and the duration of the training; as well as the characteristics of the person undergoing training. In this section, we will discuss the physiological changes associated with the adaptation to training and how the characteristics of the individual and the training itself affect this adaptation. GRA

N86-11842# Oregon Univ., Eugene. Dept. of Psychology.

IS THE CEREBELLUM INVOLVED IN MOTOR AND PERCEPTUAL TIMING: A CASE STUDY Final Report

S. W. Keele, D. L. Manchester, and R. D. Rafal 15 May 1985 21 p
(Contract N00014-83-K-0601)
(AD-A157452; TR-85-5-ONR) Avail: NTIS HC A02/MF A01 CSCL 06/16

A model and a technique developed by Wing and Kristofferson (1973) decomposes variance of timing into that putatively due to a central timekeeper (a clock) and that due to implementation of movement through the motor system. A patient with unilateral cerebellar damage, when attempting to tap out a regular series of intervals, showed a large increase in timing variability for the left hand compared to the right hand at target intervals of 550 msec. Application of the model suggested the increased variability was in the clock. Moreover, the patient appeared to have greater than normal difficulty in discriminating the durations of auditorially based time intervals. Earlier work (Wing, Keele, and Margolin, 1984) had suggested that basal ganglia damage in a Parkinson's patient also manifested itself as a clock disorder. The suggestion that clock variability arises from two different sources leads us to speculate that the brain's clock involves a circuit between several brain systems. These speculations are quite tentative because of interpretive problems with some of the data. GRA

N86-11843# Oregon Univ., Eugene. Dept. of Psychology.

FORCE AND TIMING COMPONENTS OF THE MOTOR PROGRAM Final Report

R. B. Ivry 15 May 1985 55 p
(Contract N00014-83-K-0601)
(AD-A157584; TR-85-3-ONR) Avail: NTIS HC A04/MF A01 CSCL 05/10

Three experiments assess the effects of variations of force and time on response latency on both simple and choice reaction time. The first two experiments demonstrate that, while latency does not vary as a function of force, increasing timing demands by requiring that a response be maintained led to increases in reaction time. These results led to the development of a model of motor programming in which force and timing are dissociated as separate components. However, the data also indicated that the force component may be further analyzed into two subcomponents: force activation and force deactivation. The model predicts that the latter subcomponent may be programmed on-line provided sufficient time elapses between the implementation of the two subcomponents. The results of Experiment 3 support this prediction and further validate the proposed model. GRA

N86-11844# Army Environmental Hygiene Agency, Aberdeen Proving Ground, Md.

HEALTH HAZARD EVALUATION OF LIQUID MONOPROPELLANTS. PHASE 4. SUBCHRONIC INHALATION OF HYDROXYLAMMONIUM NITRATE, JANUARY 1985

19 Jul. 1985 24 p
(AD-A157623; USAEHA-75-51-0132-85) Avail: NTIS HC A02/MF A01 CSCL 06/20

This study was conducted to determine the effects of repeated airborne exposures to animals of hydroxylammonium nitrate (HAN), a major component of liquid gun propellants. This evaluation will assist in advising on the potential health risks associated with handling these materials. Rats and dogs were exposed to aerosolized HAN for 90 days at concentrations of 300, 100, and 33 mg/cu m. Dose-related effects occurred in both species and were characterized in rats by weight loss and spleen and liver enlargement. In dogs, respiratory irritation and blood dyscrasia were the major toxic effects. Minimal effects were observed at the low dose, 33 mg/cu m. Personnel should be protected against all routes of HAN exposure since the systemic effects are additive. An airborne concentration of HAN at 3 mg/cu m may be considered as a basis for the development of a maximum allowable workplace atmosphere. Accidental exposures in man should be closely monitored for cyanosis, anemia and respiratory distress. Treatment for methemoglobinemia may be indicated. GRA

N86-11845# Pacific Northwest Lab., Richland, Wash.

DOSE DISTRIBUTION AND THE RELATIVE BIOLOGICAL EFFECTIVENESS OF INTERNAL ALPHA EMITTERS

D. R. Fisher, M. E. Frazier, and T. K. Andrews, Jr. Mar. 1985 15 p refs Presented at the 9th Symp. on Microdosimetry, Toulouse, 20 May 1985
(Contract DE-AC06-76RL-01330)
(DE85-013041; PNL-SA-12638; CONF-850506-9) Avail: NTIS HC A02/MF A01

The influence of dose distribution at the cellular level on the relative biological effectiveness of internally deposited alpha-particle emitters were examined. Cultured Chinese Hamster Ovary (CHO-K1) cells were irradiated in vitro by insoluble ceramic microspheres of zirconium oxide labeled with (239)Pu. The absorbed dose and dose rate were held constant at 0.7 Gy and 0.17 Gy h(-1), respectively. Relative biological effectiveness (RBE) was evaluated using three endpoints: initial cell survival, mutation frequency, and primary DNA damage. Cell death was greatest for irradiations by sources of low specific activity. Mutation frequency was greatest for cells exposed to agitated sources and least for irradiation by stationary high-specific-activity sources. The amount of DNA damage increased at the alpha radiation was more uniformly distributed amongst the cells at risk. DOE

N86-11846# Brookhaven National Lab., Upton, N. Y.

THYROID ABSORBED DOSE FOR PEOPLE AT RONGELAP, UTIRIK AND SIFO ON MARCH 1, 1954

E. T. Lessard, R. P. Miltenberger, R. A. Conrad, S. V. Musolino, J. R. Naidu, A. Moorthy, and C. J. Schopfer Mar. 1985 84 p refs
(Contract DE-AC02-76CH-00016)
(DE85-014695; BNL-51882) Avail: NTIS HC A05/MF A01

A study was undertaken to reexamine thyroid absorbed dose estimates for people accidentally exposed to fallout at Rongelap, Sifo, and Utirik Islands from the Pacific weapon test known as Operation Castle BRAVO. The study included: (1) reevaluation of radiochemical analysis, to relate results from pooled urine to intake, retention, and excretion functions; (2) analysis of neutron-irradiation studies of archival soil samples, to estimate areal activities of the iodine isotopes; (3) analysis of source term, weather data, and meteorological functions used in predicting atmospheric diffusion and fallout deposition, to estimate airborne concentrations of the iodine isotopes; and (4) reevaluation of radioactive fallout, which contaminated a Japanese fishing vessel in the vicinity of Rongelap Island on March 1, 1954, to determine fallout components. The conclusions of the acute exposure study were that the population mean thyroid absorbed doses were 21 gray (2100 rad) at Rongelap, 6.7 gray (670 rad) at Sifo, and 2.8 gray (280 rad) at Utirik. The overall thyroid cancer risk we estimated was in agreement with results published on the Japanese exposed at Nagasaki and Hiroshima. The major route for intake of fallout was by direct ingestion of food prepared and consumed outdoors. DOE

N86-11847# California Univ., Livermore. Lawrence Livermore Lab.

PROSPECTS FOR DNA METHODS TO MEASURE HUMAN HERITABLE MUTATION RATES

M. L. Mendelsohn 14 Jun. 1985 9 p Presented at the 4th Intern. Conf. on Environ. Mutagens, Stockholm, 24 Jun. 1985
(Contract W-7405-eng-48)
(DE85-014555; UCRL-92242; CONF-8506137-5) Avail: NTIS HC A02/MF A01

A workshop cosponsored by ICPEMC and the US Department of Energy was held in Alta, Utah, December 9 to 13, 1984 to examine the extent to which DNA-oriented methods might provide new approaches to the important but intractable problem of measuring mutation rates in control and exposed human populations. The workshop identified and analyzed six DNA methods for detection of human heritable mutation, including several created at the meeting, and concluded that none of the methods combine sufficient feasibility and efficiency to be recommended for general application. DOE

N86-11848# Maryland Univ., Baltimore.
ACUTE PULMONARY EFFECTS OF FORMALDEHYDE EXPOSURE IN HUMANS Progress Report, 1 Dec. 1983 - 30 Nov. 1984
Jul. 1985 6 p refs
(Contract DE-AS05-84ER-60192)
(DE85-014728; DOE/ER-60192/1) Avail: NTIS HC A02/MF A01

Nonsmoking subjects were randomly exposed at rest for 3 hours each to 0.0, 0.5, 1.0, and 2.0 ppM HCHO for establishing a dose-response curve at rest, and the effect of 2 ppM HCHO with moderate exercise with a 24-hr postexposure was evaluated. Results of exposure of the 10 subjects to the concentration are: (1) a significant or near significant decrease, compared to clean air; (2) the FVC and FEV1 time courses of response showed no clear change in function over any 3-hour exposure from 0.0 to 2.0 ppM HCHO; and (3) including the 2.0 ppM HCHO exposure only mild symptoms were experienced. DOE

N86-11849# Oak Ridge National Lab., Tenn.
IMPROVEMENT IN WEAR PERFORMANCE OF SURGICAL Ti-6Al-4V ALLOY BY ION IMPLANTATION OF NITROGEN OR CARBON
J. M. Williams, R. A. Buchanan, and E. D. Rigney, Jr. Jun. 1985 10 p refs Presented at the Am. Soc. for Met. Conf. on the Appl. of Ion Plating and Implantation to Mater., Atlanta, 3 Jun. 1985 Prepared in cooperation with Alabama Univ., Birmingham
(Contract DE-AC05-84OR-21400)
(DE85-013986; CONF-8506139-1) Avail: NTIS HC A02/MF A01

The effects of ion implantations of either nitrogen or carbon on the corrosive wear performance of surgical Ti-6Al-4V alloy were investigated. In vitro tests made use of an apparatus which could produce certain chemical and mechanical aspects of a sliding interface such as that which occurs between alloy and polyethylene components of an artificial hip (or knee) joint. Cylindrical samples of the Ti alloy were rotated between loaded, conforming pads made of ultrahigh molecular weight polyethylene (UHMWPE) while these test components were immersed either in a saline solution or a saline solution with bovine serum added. During the tests open circuit corrosion currents for the alloy were measured by the Tafel extrapolation technique. Profilometry studies were done before and after the tests. Alloy samples implanted with either nitrogen or carbon remained as new for all test conditions. Unimplanted control samples were severely scored. Corrosion currents as measured under the mechanical action were reduced by a factor of approximately one hundred by the ion implantation treatments. DOE

53 BEHAVIORAL SCIENCES

Includes psychological factors; individual and group behavior; crew training and evaluation; and psychiatric research.

N86-11850*# Old Dominion Univ., Norfolk, Va. Dept. of Psychology.
VISUAL INFORMATION TRANSFER. PART 1: ASSESSMENT OF SPECIFIC INFORMATION NEEDS. PART 2: PARAMETERS OF APPROPRIATE INSTRUMENT SCANNING BEHAVIOR Progress Report, 15 Feb. - 15 Oct. 1985
J. Raymond Comstock, Jr., Raymond H. Kirby, and Glynn D. Coates Oct. 1985 11 p refs
(Grant NAG1-451)
(NASA-CR-176277; NAS 1.26:176277) Avail: NTIS HC A02/MF A01

The present study explored eye scan behavior as a function of level of subject training. Oculometric (eye scan) measures were recorded from each of ten subjects during training trials on a CRT based flight simulation task. The task developed for the study incorporated subtasks representative of specific activities performed by pilots, but which could be performed at asymptotic levels within relatively short periods of training. Changes in eye scan behavior were examined as initially untrained subjects developed skill in the task. Eye scan predictors of performance on the task were found. Examination of eye scan in proximity to selected task events revealed differences in the distribution of looks at the instruments as a function of level of training. Author

N86-11851# Pennsylvania State Univ., University Park. Dept. of Psychology.
ADAPTIVE MOTIVATION THEORY Final Report
F. J. Landy and W. S. Becker Jun. 1985 69 p
(Contract N00014-81-K-0197)
(AD-A157440; Rept-85-1) Avail: NTIS HC A04/MF A01 CSCL 05/10

Traditional approaches to understanding motivation have not been successful. Middle range theories are necessary for progress in this area. Cognitive processes will play a major role in motivation theories of the future. Various middle range theories are likely to be more suitable for understanding some dependent variables than others. The work on adaptive motivation theory was intended to be preliminary, exploring the possible advantages of a reconceptualization of motivation theory. In this report, we see our goal as introducing some lines of speculation, sampling some recent research that gives rise to that speculation, and presenting specimens of new theory and research designs and, ultimately, persuading the reader to pick up the burden of a novel idea or approach and to carry it some distance for us. Various technical and quarterly reports have detailed the development of questionnaires and methods of measuring components of adaptive motivation theory. In this report, we identify the nature and extent of that conceptual work. In effect, we suggest that it may be valuable to explore more deeply the cognitive roots of many of the current approaches. Through such an exploration, it may be possible to develop a set of middle range theories capable, in aggregate, of explaining motivated behavior. GRA

N86-11852# Oregon Univ., Eugene. Dept. of Psychology.
COGNITIVE SCIENCE PROGRAM: DISSOCIATION OF THE CENTRAL TIMEKEEPER AND THE PERIPHERAL IMPLEMENTATION PROCESSES IN REPETITIVE MOVEMENTS Final Technical Report
R. B. Ivry and S. W. Keele 15 May 1985 23 p
(Contract N00014-83-K-0601)
(AD-A157542; TR-85-7-ONR) Avail: NTIS HC A02/MF A01 CSCL 06/5

Wing and Kristofferson (1973) have proposed a two-stage model of timing in repetitive motor behavior which assumes independence of a central timekeeper process and the peripheral implementation system. This model was tested with a patient who has incurred a peripheral motor neuropathy. The patient's inconsistent performance in a periodic tapping task with the afflicted hand was found to be attributable to increased variability in the motor implementation process only. This report, in conjunction with the previous study of Wing et al., (1984) in which a Parkinsonian patient was found to have a timekeeper deficit, provides a double dissociation of the timekeeper and implementation processes. Thus, the independence assumption of the Wing and Kristofferson model is supported. GRA

N86-11853# California Univ., Livermore. Lawrence Livermore Lab.
PSYCHOLOGICAL ASPECTS OF PERSONNEL CONTAMINATION
R. L. Wilson Apr. 1985 7 p ref Presented at the Hazardous Mater. Conf., Oakland, Calif., 23 Apr. 1985
(Contract W-7405-eng-48)
(DE85-012955; UCRL-92501; CONF-8504140-1) Avail: NTIS HC A02/MF A01

This paper discusses some of the major emotional considerations involved in the treatment of people who have been contaminated with potentially hazardous materials. Although the principal focus is the treatment of people trained to work with these materials, an attempt is also made to extend these methods to people having little or no knowledge of such matters. Accidents always result in emotional trauma. When the accident involves radioactive or other potentially toxic, carcinogenic, or mutagenic materials, there is a possibility of enhanced emotional stress due to the mystique surrounding these substances. Several psychological principles that have emerged from the treatment of radioactively contaminated workers are: (1) provide preaccident training for all radiation workers; (2) avoid secrets; (3) as rapidly as possible following a contamination accident, bring the worker into contact with others; (4) recognize the emotions of the family and the family's fears and trauma; and (5) do not desert the worker after decontamination has been completed. DOE

54 MAN/SYSTEM TECHNOLOGY AND LIFE SUPPORT

Includes human engineering; biotechnology; and space suits and protective clothing.

N86-11854*# Martin Marietta Aerospace, Denver, Colo.
TELEOPERATOR HUMAN FACTORS STUDY Progress Report, 7 Sep. - 6 Oct. 1985
K. Z. Bradford and R. T. Schappell Oct. 1985 6 p
(Contract NAS8-35184)
(NASA-CR-176310; NAS 1.26:176310; MCR-83-607) Avail: NTIS HC A02/MF A01 CSCL 05H

The progress made on the Teleoperator Human Factors Study program during the period of September 7, 1985 to October 6, 1985 is discussed. Technical and programmatic problems that were encountered are discussed along with activity planned for the following month. The main portion of the report has been separated into four sections: Work Performed, Future Work, Problems Encountered, and Cost Information. G.L.C.

N86-11855# Oak Ridge National Lab., Tenn.
MECHANICAL ACCESSORIES FOR MOBILE TELEOPERATORS
M. J. Feldman and J. N. Herndon 1985 19 p Presented at the Workshop on Requirements of Mobile Teleoperators for Radiol. Emergency Response and Recovery, Dallas, 23 Jun. 1985
(Contract DE-AC05-84OR-21400)
(DE85-014310; CONF-8506148-2) Avail: NTIS HC A02/MF A01

The choice of optimum mechanical accessories for mobile teleoperators involves matching the criteria for emergency response with the available technology. A general background is presented to teleoperations, a potpourri of the manipulator systems available, and an argument for force reflecting manipulation. The theme presented is that the accomplishment of humanlike endeavors in hostile environments will be most successful when man model capabilities are utilized. The application of recent electronic technology to manipulator development has made new tools available to be applied to emergency response activities. The development activities described are products of the Consolidated Fuel Reprocessing Program at the Oak Ridge National Laboratory. DOE

55 PLANETARY BIOLOGY

Includes exobiology; and extraterrestrial life.

No abstracts in this category.

59 MATHEMATICAL AND COMPUTER SCIENCES (GENERAL)

N86-11856*# National Aeronautics and Space Administration. Langley Research Center, Hampton, Va.
TOWARDS DEVELOPING ROBUST ALGORITHMS FOR SOLVING PARTIAL DIFFERENTIAL EQUATIONS ON MIMD MACHINES Final Report
Joel H. Saltz and Vijay K. Naik Sep. 1985 53 p refs Submitted for publication
(Contract NAS1-17070; Grants NAG1-466; NIH-HL-11307)
(NASA-CR-177979; ICASE-85-39; NAS 1.26:177979) Avail: NTIS HC A04/MF A01 CSCL 12A

Methods for efficient computation of numerical algorithms on a wide variety of MIMD machines are proposed. These techniques reorganize the data dependency patterns to improve the processor utilization. The model problem finds the time-accurate solution to a parabolic partial differential equation discretized in space and implicitly marched forward in time. The algorithms are extensions of Jacobi and SOR. The extensions consist of iterating over a window of several timesteps, allowing efficient overlap of computation with communication. The methods increase the degree to which work can be performed while data are communicated between processors. The effect of the window size and of domain partitioning on the system performance is examined both by implementing the algorithm on a simulated multiprocessor system. E.A.K.

N86-11857# Air Command and Staff Coll., Maxwell AFB, Ala.
A COMPUTER ENGINEERING CURRICULUM FOR THE AIR FORCE ACADEMY: AN IMPLEMENTATION PLAN
L. L. Burge, Jr. Apr. 1985 113 p
(AD-A156464; ACSC-85-0335) Avail: NTIS HC A06/MF A01 CSCL 05/9

The recent advances in computer technology which impact present and future Air Force systems led the Air Force Academy to include computers and information systems engineering courses in the curriculum. This analysis addresses the issue of a major in computer engineering at the Academy. The Air Force computer engineer (AFSCs 2625, 2736 and 2885) specializes in designing, developing, installing, and testing embedded computer systems in aircraft, missiles, flight simulators, and command, control, and communications systems. An embedded computer system is all computer equipment, programs, data, documentation, personnel, and supplies integral to a defense system from the design, acquisition, or operations and support point of view. This report addresses the Air Force need for computer engineers, the need for the computer engineering major at the Academy, the appropriate department to administer the major, the structure of the degree, and the implementation of the discipline at the Academy. Author (GRA)

60 COMPUTER OPERATIONS AND HARDWARE

Includes computer graphics and data processing.

For components see *33 Electronics and Electrical Engineering.*

N86-11858# Los Alamos National Lab., N. Mex.
SIXTH BIENNIAL CUBE (COMPUTER USE BY ENGINEERS) SYMPOSIUM Abstracts Only
Aug. 1984 125 p Symp. held in Los Alamos, N. Mex., 10-12 Oct. 1984
(Contract W-7405-eng-36)
(LA-10240-C) Avail: NTIS HC A06/MF A01

A symposium was conducted to exchange information on computer hardware and software developments and applications among engineers at the Los Alamos, Lawrence Livermore, and Sandia National Laboratories. The CUBE Symposium benefits the participants and their respective Laboratories by providing a forum for: (1) sharing information on recently developed and current computer codes for modeling physical processes; (2) discussing solutions to a broad range of engineering problems both in weapons and in energy programs; (3) illustrating the development and effectiveness of computer methods for design, control, and experiment interpretation; (4) describing creative approaches to the solution of engineering problems; and (5) exploring trends in hardware/software and their impact on engineering. For individual titles, see N86-11859 through N86-11887.

N86-11859# California Univ., Livermore. Lawrence Livermore Lab. Applications Systems Div.

SOFTWARE ENGINEERING TOOLS THAT WORK Abstract Only **c61**

David Balaban *In* LANL 6th Bien. CUBE (Computer Use by Engineers) Symp. Aug. 1984 p 7 (For primary document see N86-11858 02-60)

Avail: NTIS HC A06/MF A01

An overview of a very new, highly integrated, set of software engineering tools is presented. This set of tools is powerful enough to be applied to any software system including real-time systems, data base systems, and communications systems. The tools are designed for all phases of software development from preliminary analysis through detailed design. The generality and utility of this methodology result from the fact that three different software models are used and integrated. One model describes data transformation; another model describes stored data; and a third model describes dynamics. These models provide a useful basis for classifying software systems and a complete elegant methodology for developing software. G.L.C.

N86-11860# California Univ., Livermore. Lawrence Livermore Lab. Applications Systems Div.

AN APPLICATION OF REAL-TIME ANALYSIS AND DESIGN TOOLS IN SOFTWARE DEVELOPMENT Abstract Only **c61**

Don W. Freeman *In* LANL 6th Bien. CUBE (Computer Use by Engineers) Symp. Aug. 1984 p 7 (For primary document see N86-11858 02-60)

Avail: NTIS HC A06/MF A01

A software system was written to perform real-time data acquisition and analysis on a newly designed dynamic mechanical spectrometer at Sandia National Laboratory, Livermore. This research software was developed using several modern real-time analysis and design tools. These tools were not used to their maximum capability, since this would have increased the software development time significantly and unnecessarily. However, the appropriate use of these tools has made this software particularly easy to understand, construct, debug, and ungrade. The overall system architecture was first specified using data flow diagrams. These were reviewed and approved by the end user. Structure charts for the major software subsystems were then constructed. The code was easily generated from the structure charts. At the same time that this top-down analysis and design was being carried out, some software was being developed from the bottom up to deal with the instrumentation in a conceptual way. These instrumentation routines were developed to hid the nitty-gritty bit level details from the user so that he/she can interact with the instrumentation in human terms. Author

N86-11861# Los Alamos National Lab., N. Mex. Engineering Analysis Section.

DESIGN OPTIMIZATION OF THE POWER GENERATION SYSTEM FOR A SPACE-BASED FREE-ELECTRON LASER Abstract Only **c36**

Norman M. Schnurr *In its* 6th Bien. CUBE (Computer Use by Engineers) Symp. Aug. 1984 p 10 (For primary document see N86-11858 02-60)

Avail: NTIS HC A06/MF A01

A computer program, FELWT, was developed to perform a system optimization of the power generation system for a space-based free-electron laser. A detailed cooling analysis of the linear accelerator and computations of cooling requirements for the klystrons, electron dumps, and injectors are performed. A prime power-generation system consisting of a combustor, a turbine, and a generator is analyzed and hydrogen and oxygen requirements are determined. Performances of various components depend on operating temperatures so that analyses of individual components are coupled in a rather complex fashion. Several levels of iteration are used in the code to obtain a simultaneous solution of the entire system of governing equations. A parametric study is performed to determine optimum operating conditions. Author

N86-11862# Sandia Labs., Albuquerque, N. Mex. Thermophysical Properties Div.

OPTICAL MODELING OF MULTILAYER THIN/THICK FILMS Abstract Only **c76**

Richard B. Pettit *In* LANL 6th Bien. CUBE (Computer Use by Engineers) Symp. Aug. 1984 p 10-11 (For primary document see N86-11858 02-60)

Avail: NTIS HC A06/MF A01

A computer program was written to implement a calculation of the optical reflectance and transmittance characteristics of an arbitrary multilayer film k that can include both thick and thin films. For the thin films (film thickness comparable to the wavelength), complex Fresnel reflection and transmission coefficients are calculated in order to preserve phase information (interference effects) between the films. Recursion relations are then used to replace each multilayer thin film stack with effective Fresnel coefficients. For films thick compared to the wavelength, reflectance and transmittance intensity coefficients are used, together with a multiple reflection recursion relation, to calculate the overall reflectance and transmittance of the stack. This amounts to effectively averaging over phases in the thick films. Thus the optical characteristics of multiple thin films on both sides of a thick glass substrate, for example, can be accurately calculated. In the program, these properties can be calculated as a function of incident angle, polarization and wavelength. Application of this program to several practical situations will be illustrated. Author

N86-11863# California Univ., Livermore. Lawrence Livermore Lab. Nuclear Energy Systems Div.

NET-2 MODELS OF CAVITIES AND DIODES Abstract Only **c33**

George E. Vogtlin *In* LANL 6th Bien. CUBE (Computer Use by Engineers) Symp. Aug. 1984 p 11 (For primary document see N86-11858 02-60)

Avail: NTIS HC A06/MF A01

The network analysis program, Net-2, was used to model microwave cavities and wave guides. Techniques using both lumped lines and distributed transmission lines were used with good agreement compared to measured values. This technique is applicable to pill box and rectangular cavities as well as rectangular and circular wave guides. Higher order modes can be modeled in addition to the fundamental mode. Pulse driven diodes were modeled using Child-Langmuir limited current. These models use six to nine sections to represent the various radial currents and ection parameters. Complex rise-times and resonances were evaluated and measured to several giga hertz. Author

N86-11864# Sandia Labs., Albuquerque, N. Mex. Theoretical Div.

CALCULATION OF THE ELECTRON BACKSCATTERING COEFFICIENT BY MONTE CARLO SIMULATION Abstract Only **c76**

Arlyn J. Antolak and William Williamson, Jr. (Toledo Univ.) *In* LANL 6th Bien. CUBE (Computer Use by Engineers) Symp. Aug. 1984 p 11 (For primary document see N86-11858 02-60)

Avail: NTIS HC A06/MF A01

The Monte Carlo electron/photon transport code SANDYL is used to compute the total electron backscattering yield eta in the energy range 20 to 100 keV. The backscattering from bulk solids, thin self-supporting films, and from thin films on substrates is computed for various targets at normal and oblique incidence of the primary electron beam. The results of the theoretical model are compared with experimental scanning electron microscope data. Author

N86-11865# California Univ., Livermore. Lawrence Livermore Lab. Engineering Research Div.
PARTICLE PUSHING TECHNIQUES FOR USE WITH FINITE ELEMENT BASED FIELD CALCULATIONS Abstract Only c64
John C. Peterson *In* LANL 6th Bien. CUBE (Computer Use by Engineers) Symp. Aug. 1984 p 12 (For primary document see N86-11858 02-60)
Avail: NTIS HC A06/MF A01

The discrete particle-mesh method is widely used for finding self-consistent solutions to Maxwell's equations. In this approach to modeling the behavior of plasmas, one alternates between: (1) solving for the electromagnetic fields that arise from the current and charge distributions (determined by the position and velocity of all the discrete particles in the system), and (2) updating the position and velocity of all the discrete particles using the usual laws of mechanics and the forces which result from the fields calculated above. In many engineering situations, the presence of curved boundaries makes it advantageous to use finite element methods to do the field computations. The irregular aspect of the grids used with finite element methods complicates the process of locating a particle in the mesh, so that the fields acting on that particle can be determined. A method for keeping track of the particle locations was developed and implemented in the Galerkin ElectroMagnetics code, or GEM2D. The method will be described, and selected results will be presented. Author

N86-11866# California Univ., Livermore. Lawrence Livermore Lab. Nuclear Test Engineering Div.
ICARUS: A COMPUTER CODE FOR MODELING COMPLEX ONE-DIMENSIONAL HEAT CONDUCTION ON MAINFRAMES AND MICROS Abstract Only c34
Steven B. Sutton *In* LANL 6th Bien. CUBE (Computer Use by Engineers) Symp. Aug. 1984 p 16 (For primary document see N86-11858 02-60)
Avail: NTIS HC A06/MF A01

The geometry in numerous heat transfer problems can be approximated quite accurately as being one-dimensional. Under this condition, it is advantageous to use a one-dimensional computer code. The computer code ICARUS was developed to allow easy, straight forward modeling of complex one-dimensional systems. Two versions of the code exist: a large, full feature version for main-frame computers, and a smaller version written for use of micro computers. The large full feature version, written in FORTRAN, can account for material phase change (solidification or melting), multiple material regions, material gaps (across which radiation and convection can take place), temperature dependent material properties and time or temperature dependent general boundary conditions (specified temperature, applied heat flux, convection and/or thermal radiation). The phase change algorithm tracks the moving phase change front in a continuous fashion. The equations are formulated so that the solution can be fully implicit, fully explicit or Crank-Nicolsen. Output information is available in both hard-copy edits and graphics. The micro-computer version, written in IBM BASIC, can account for multiple material regions, general boundary conditions, and material gaps. In its present form, all properties and parameters must be constant in both time and temperature. The equations are formulated so that the solution can be fully implicit or fully explicit. A user friendly drive controls interactive specification of all input. Output information is presently available only in the form of printer edits. Author

N86-11867# Sandia Labs., Albuquerque, N. Mex.
THREE-DIMENSIONAL HEAT TRANSFER ANALYSIS USING THE PATRAN-G SOLIDS MODELING AND Q-TRAN THERMAL ANALYSIS COMPUTER CODES Abstract Only c34
James M. Nelsen, Jaime L. Moya, and H. Richard Yoshimura *In* LANL 6th Bien. CUBE (Computer Use by Engineers) Symp. Aug. 1984 p 17 (For primary document see N86-11858 02-60)
Avail: NTIS HC A06/MF A01

A computer program to translate PDA PATRAN-G finite element meshes to finite difference meshes for use in the Q-TRAN thermal analysis computer code was developed. PATRAN-G, a solids modeling program, was extensively used to generate finite element models for structural analyses codes. However, this code was not previously used for two- or three-dimensional heat conduction models. This translator allows pre- and post-processing for thermal analysis of arbitrary two- and three-dimensional geometries. Furthermore, Q-TRAN offers analysis capabilities not furnished by other thermal analysis codes including phase change, spectral radiation, and improved solution algorithms. Examples will be provided demonstrating the pre- and post-processing capabilities of the PATRAN-G program used in the thermal analysis of the Beneficial Uses Shipping System (BUSS) cask. Author

N86-11868# Sandia Labs., Albuquerque, N. Mex. Structural Mechanics Div.
INTERFACE ELEMENTS FOR HEAT TRANSFER ANALYSIS Abstract Only c34
William E. Mason *In* LANL 6th Bien. CUBE (Computer Use by Engineers) Symp. Aug. 1984 p 17 (For primary document see N86-11858 02-60)
Avail: NTIS HC A06/MF A01

Interface elements are desirable in finite element heat transfer analyses in situations where dissimilar meshes are to be joined or where contact resistances occur between various parts of a body. In stress codes, such elements are often termed master/slave. A general algorithm for interface elements will be described. The algorithm allows development of interface elements for both two- and three-dimensional applications. Surfaces in contact are automatically determined so that a minimum of input data is required. In addition, the algorithm allows for compatibility in thermal stress calculations with mechanical codes which have sliding interface capabilities. Implementation of the algorithm into the TACO codes will be discussed and examples will be given. Author

N86-11869# California Univ., Livermore. Lawrence Livermore Lab. Nuclear Test Engineering Div.
ANALYSIS OF ULTRASONIC WAVES IN A BOUNDED MEDIUM Abstract Only c71
Thomas A. Nelson and Gerald L. Goudreau *In* LANL 6th Bien. CUBE (Computer Use by Engineers) Symp. Aug. 1984 p 21 (For primary document see N86-11858 02-60)
Avail: NTIS HC A06/MF A01

In their effort to design an acoustic shutter for the Nova Program, the Laser Program wished to study the propagation of ultrasonic (approx. 10 MHz) waves induced in the plane of the glass by a strip piezoelectric crystal mounted on an edge of the glass. The object is to set up a clean standing wave which forms a diffraction grating in the glass window with respect to laser light entering normal to the window. Early design analysis treated the axial vibration problem with a separate optical analogy governed by a scalar wave equation. Further, assuming lateral boundaries did not interfere with the longitudinal wave, ray techniques could solve the geometric optics problem. The item of interest was finding the optimum width of the piezoelectric crystal which launches the acoustic wave. Subsequent studies showed that lateral boundary effects were important to the wave characteristics and that attempting to launch a square wave front would generate a complicated stress state. The code DYNA2D was used to study transient stress wave propagation in a solid. This required an extremely fine mesh to capture the very short wave lengths of the ultrasonic wave. More relevant was the ultra high frequency steady state and modal solution. For the solid assumption (vector valued wave equation) codes NIKE2D and GEMINI were employed. For the scalar approximation of optics, the thermal code TACO2D was successfully adapted to solve the required steady state spatial operator. Author

N86-11870# California Univ., Livermore. Lawrence Livermore Lab. Engineering Research Div.
AN EVALUATION OF THREE GRAPHICS PACKAGES: THE METHODOLOGY AND RESULTS Abstract Only c61
Brian K. Cabral *In* LANL 6th Bien. CUBE (Computer Use by

Engineers) Symp. Aug. 1984 p 24 (For primary document see N86-11858 02-60)
Avail: NTIS HC A06/MF A01

The increased use of computers in engineering environments coupled with the decreasing price of graphics equipment has resulted in the widespread use of graphics software. Much of the available graphics software is dependent on some application, machine, or graphics device. However there are a number of public domain graphics packages which attempt to be independent of these factors. A method of evaluating graphics packages as applied to three public domain graphics packages is introduced. The methodology presented is designed in a top-down fashion. It begins by exploring the high level functionality dealing with application interface issues, such as ease of use and completeness of functionality. Software design issues, documentation, and error handling are discussed in conjunction with the other high level functionalities. The methodology continues by investigating the low level functionality which includes performance measurements and the ability to add new devices to the package. The methodology was used in an evaluation of three public domain graphics packages. The evaluation took place on a VAX running VMS which supported a large number of graphics devices. By creating an environment conductive to unbiased observations, the evaluators were able to investigate all three packages concurrently. Author

N86-11871# Los Alamos National Lab., N. Mex. Analysis and Testing Group.
INTERACTIVE GRAPHICS FOR FINITE ELEMENT PRE-PROCESSING Abstract Only c61
W. Rob Oakes, Jr. *In its* 6th Bien. CUBE (Computer Use by Engineers) Symp. Aug. 1984 p 24 (For primary document see N86-11858 02-60)
Avail: NTIS HC A06/MF A01

Graphics interactivity for finite element preprocessing was increased by using newly available terminal hardware and graphics software. Interactivity between users and codes was increased by reducing input-output to graphics terminals and by increasing the information content of images. Advanced terminal design that allows higher level graphics entities is primarily responsible for more effective terminal-application communications. Hardware-zoom-and-pan, retained segments, markers, and panels are discussed, showing how each has allowed the number of images sent, the volume of data for each image, and user input volume to be reduced by increasing graphical input. The augmented CGS language used to implement the software and why this was chosen over one likely alternative will be explained. Increased information content of graphics images has improved interactivity. The uses of color, and the JONES-D hidden surface algorithm and why it is well suited by to finite element preprocessing are discussed. Author

N86-11872# Los Alamos National Lab., N. Mex. Advanced Engineering Technology Group.
GEOLOGICAL CALCULATIONS WITH SANGRE AND MANTLE: RECENT RESULTS Abstract Only c46
Lucy M. Carruthers, Peggy Goldman, and Charles A. Anderson *In its* 6th Bien. CUBE (Computer Use by Engineers) Symp. Aug. 1984 p 26 (For primary document see N86-11858 02-60)
Avail: NTIS HC A06/MF A01

Q-13 has two finite-element calculational efforts involving geological studies, both two dimensional and both with extensive graphics output. The SANGRE code was developed at Los Alamos as an extension of TSAAS. Recent code developments include introduction of pore pressure, which has made possible some calculations with geologic folds that show the behavior of fluid during the geological fold process. The code has recently been linked to the STRAP code for graphical output--results will be shown. The MANTLE code work has continued in collaboration with Gerald Schubert of UCLA. Modeling efforts include slabs extending into the fluid region, with and without initial slab motion. Coupled calculations are made of temperature and creep. Graphics are internal to the code and show velocities, pressures, temperatures, stream functions, etc. Author

N86-11873# Sandia Labs., Albuquerque, N. Mex. Analytical Solid Mechanics Div.
APPLICATION OF A MIXTURE THEORY TO THE BINARY ALLOY SOLIDIFICATION PROBLEM Abstract Only c26
Vincent C. Prantil *In* LANL 6th Bien. CUBE (Computer Use by Engineers) Symp. Aug. 1984 p 27 (For primary document see N86-11858 02-60)
Avail: NTIS HC A06/MF A01

Motivated by a principal interest in the continuous casting of alloys, an application of a mixture theory has been proposed for examining problems involving solidification of a multicomponent system. The formulation can provide a basis for studying the solidification of a binary alloy in which the two phases may be present in arbitrary amounts. The system is defined in terms of the constituent phases and alloying elements in which the volume fraction is utilized to model, in a continuous fashion, the amount of each phase present at a point. Balance laws for mass, momentum, and energy for each phase are presented which include terms for representing interactions between the mixture components. The idea of a structured continuum is adopted and the discrete nature of separable phases is discussed in light of how the system description reflects the characteristics of the solid-liquid system. The present work proposes methods for modeling rate of growth of solid as a mass exchange, using drag, buoyancy, and interfacial pressure forces in the momentum exchange, and including the latent heat and dissipation in the energy exchange for binary alloy solidification. Author

N86-11874# Sandia Labs., Albuquerque, N. Mex.
MICROCOMPUTER CONTROL AND DATA MANAGEMENT TECHNIQUES FOR TRANSIENT DIGITAL RECORDING Abstract Only c61
David A. Benson and Gary D. Miller *In* LANL 6th Bien. CUBE (Computer Use by Engineers) Symp. Aug. 1984 p 39 (For primary document see N86-11858 02-60)
Avail: NTIS HC A06/MF A01

Techniques developed for microcomputer control of waveform recorders are discussed. These techniques have been effective in collecting transient high temperature data for an application which requires frequent changes of test configuration. This system allows the user to specify the recording configuration through a data file together with suitable annotations which give a full description of the experiments performed. Communications with the digital recorders are through the IEEE-488 bus to a Z80 computer driven by compiled BASIC software. Once the test data are captured by the recorders, the system retrieves and stores the data in a form previously specified. Data files from the waveform recorders are output using a compression technique which limits the number of points to those containing significant information. These data files also contain plot legends and fields of comments specific to each test. These are placed in a compact ASC2 format and stored on floppy disk media. Ability exists to control this post processing from simple commands embedded in a data file without further operator intervention. B.W.

N86-11875# California Univ., Livermore. Lawrence Livermore Lab. Nuclear Energy Systems Div.
A DATA TRANSLATOR FOR ENGINEERING MEASUREMENTS Abstract Only c61
Mel Wieting and Robert M. Trusty *In* LANL 6th Bien. CUBE (Computer Use by Engineers) Symp. Aug. 1984 p 40 (For primary document see N86-11858 02-60)
Avail: NTIS HC A06/MF A01

The Engineering Measurements Section provides a complete measurement of service for all Lawrence Livermore National Laboratory (LLNL) programs. Because of the various types of data collected, several different acquisition systems are required, each having a different digital data format/medium. This has caused compatibility problems in analyzing and supplying the data to the end-users. The Data Translator was designed to solve these problems. The Data Translator uses either the IEEE-488 bus (GPIB) or an RS-232 serial line to receive data from the various data acquisition systems after the measurement is performed. The

488 bus provides a fast parallel transfer, but must be done locally. RS-232 transfers are much slower, but can be accomplished remotely using a modem. The Data Translator is based on an LSI-11/23 with 256k bytes of RAM and the RT-11 single job operating system. Data from the Data Translator are written to a disk file in a format compatible with SIG, an LLNL signal analysis program. Data analysis and graphics output can be accomplished using either SIG or a streamlined SIG look-alike program, on the Data Translator. B.W.

N86-11876# California Univ., Livermore. Lawrence Livermore Lab. Engineering Research Div.
SIG: A GENERAL-PURPOSE SIGNAL PROCESSING CODE Abstract Only **c61**
Darrel L. Lager and Stephen G. Azevedo *In* LANL 6th Bien. CUBE (Computer Use by Engineers) Symp. Aug. 1984 p 40-41 (For primary document see N86-11858 02-60)
Avail: NTIS HC A06/MF A01

SIG is a general-purpose signal processing, analysis, and display program for performing manipulations on time- and frequency-domain signals. It has been designed to ultimately accommodate other representations for data such as multiplexed signals and complex matrices. Many of the basic operations one would perform on digitized data are contained in the core SIG package. These range from basic arithmetic (add, subtract, multiply, divide), to resampling, filtering and graphically displaying results. More sophisticated operations include several methods of estimating transfer functions, performing spectral estimation and doing parameter estimation. Out of these core commands, more powerful signal processing algorithms may be built. SIG provides two user interfaces: a menu mode for the occasional user, and a command mode for the sophisticated daily user. In both modes, errors are detected as early as possible in the processing and are indicated by friendly, meaningful messages. Options exist for multiple commands per line, commenting lines, defining commands, executing command files with arguments and the writing of custom menus. Author

N86-11877# California Univ., Livermore. Lawrence Livermore Lab. Nuclear Test Engineering Div.
THERMO-MECHANICAL ANALYSES OF LASER-HEATED SURFACES Abstract Only **c36**
Gary L. Johnson *In* LANL 6th Bien. CUBE (Computer Use by Engineers) Symp. Aug. 1984 p 44 (For primary document see N86-11858 02-60)
Avail: NTIS HC A06/MF A01

The Lawrence Livermore National Laboratory (LLNL) needs to heat metal parts to melt temperatures using a highly focused laser. In addition to the mechanical loads applied to the part, thermally induced stresses occur near the heated area. The objective of this work was to specify the surface heat load and cooldown rate parameters which would provide the desired melt zone geometry while assuring an acceptable level and distribution of thermally-induced plastic strain and stress. To model the thermo-mechanical response of the part to various heat loads, the thermo-elastic-plastic model in the finite element structural code, NIKE2D was used based on the temperature response calculated by the thermal code, TACO2D. Author

N86-11878# Sandia Labs., Albuquerque, N. Mex. Computational Physics and Mechanics Div.
FINITE DIFFERENCE CALCULATIONS OF VOLTAGES GENERATED IN THIN DIELECTRIC LAYERS SUBJECTED TO SHOCK LOADING Abstract Only **c76**
Jeffrey W. Swegle *In* LANL 6th Bien. CUBE (Computer Use by Engineers) Symp. Aug. 1984 p 44-45 (For primary document see N86-11858 02-60)
Avail: NTIS HC A06/MF A01

Difficulties which recently developed in weapon systems tests were thought to be due to high voltages being generated in thin layers of dielectric materials in the outer shell of the device when the HE was detonated. Due to the difficulties involved in measuring these voltages, a theoretical investigation was undertaken of the mechanisms of voltage generation in these thin dielectric layers when subjected to shock loading. The situation was studied using the automatically rezoning Lagrangian finite-difference wavecode ART00 to explicitly predict the charge generated in each layer. The device was modeled including the thin layers in the outer shell, and the code was modified to predict the charge generated in each layer as well as the capacitance of each layer as the dimensions changed. The polarization of the dielectric in each layer was calculated based on the assumption that the induced polarization was a function only of the maximum pressure and did not revert during the time of interest of the calculation. The charge generated in each layer was then calculated as the layer area times the induced polarization. These calculations provided the only readily available means of assessing the cause of the problems. Author

N86-11879# Sandia Labs., Albuquerque, N. Mex.
A TIME-SPLITTING NUMERICAL TECHNIQUE FOR SOLVING HIGHLY COUPLED TWO-PHASE FLOW CONSERVATION EQUATION Abstract Only **c34**
R. J. Gross and M. R. Baer *In* LANL 6th Bien. CUBE (Computer Use by Engineers) Symp. Aug. 1984 p 48-49 (For primary document see N86-11858 02-60)
Avail: NTIS HC A06/MF A01

A time-splitting numerical technique incorporating the positive aspects of flux-corrected transport (FCT) and the method of lines (MOL) has been developed to efficiently and accurately solve systems of highly coupled hyperbolic partial differential equations. Several two-phase flow equation systems, including that of modeling deflagration-to-detonation transition (DDT) in granular explosives, are used to illustrate the method. Upwind differencing, MOL, and FCT are also used to solve the model problems so that one can compare the new technique to established methods. The results show that time-splitting offers increased accuracy for these types of problems, although in one dimension the method is computationally more costly. However, in multidimensional calculations, the time-splitting technique should offer an economy of computer cost and storage. Author

N86-11880# California Univ., Livermore. Lawrence Livermore Lab. Field Test Systems Div.
PHOTOELECTRON TRAJECTORY ANALYSES OF STREAK TUBES Abstract Only **c35**
Ching C. Lai *In* LANL 6th Bien. CUBE (Computer Use by Engineers) Symp. Aug. 1984 p 53 (For primary document see N86-11858 02-60)
Avail: NTIS HC A06/MF A01

A streak tube is a precision high voltage vacuum photonic device capable of registering the temporal variation of multiple signal channels with subnanosecond resolution. The streak tube has become the vital component of the current time-resolved prompt diagnostics instrumentation system for the Nuclear Test Program. The performance of the streak tube is predominately governed by the trajectory behavior of all the photoelectrons traveling from the photocathode through the deflection region to the phosphor anode. The trajectory analyses require a finite-element-method based on computer program to solve Poisson's equation for potential distribution and to calculate the trajectories. Two codes (GUNSLAC and EBQ) in the CDC-7600 computer were used for the designing of a prototype large-format streak tube, and the evaluation of two existing tubes, RCA-C73435 and ITT-2XIC16. Analyses were performed by varying the electrode's configuration, voltage, photoelectron's energy, emitting orientation and current. Both the computer generated trajectory plots and the numerical data summaries are presented. Author

N86-11881# California Univ., Livermore. Lawrence Livermore Lab. Nuclear Energy Systems Div.
RAMP RESPONSE ESTIMATION AND SPECTRUM EXTRAPOLATION FOR ULTRASONIC SCATTERING Abstract Only **c71**
Gregory A. Clark *In* LANL 6th Bien. CUBE (Computer Use by Engineers) Symp. Aug. 1984 p 55 (For primary document see N86-11858 02-60)

Avail: NTIS HC A06/MF A01

A combined application of digital signal processing, estimation theory, and scattering theory is used to attack the important problem of target identification. The basic problem is that of examining an object with an ultrasonic pulse and using the reflected signal to determine various properties of the object. Typically, an impulse reponse h(t) can be calculated from knowledge of the (input x(t)) signal and the reflected (output y(t)) signal. If the impulse response can be found, it can sometimes contain important information about the object. We have studied some new algorithms for impulse response estimation. It is also well-known that the ramp response contains information about the cross-sectional area of the scatterer. The ramp response can be calculated directly from the impulse response, but the estimate of cross-sectional area is degraded by the fact that the ultrasonic transducer severely bandlimits the data. Algorithms have been produced for extrapolating the ramp response spectrum to improve the cross-sectional area estimates from the ramp response technique. Experimental results demonstrating the estimation of properties of a known flaw (created by a saw cut) in a block of aluminum are presented. Author

N86-11882# Sandia Labs., Albuquerque, N. Mex. Thermofluids Div.

SIMULATION OF FLAME PROPAGATION THROUGH VORTICITY REGIONS USING THE DISCRETE VORTEX METHOD Abstract Only **c34**

Pamela K. Barr *In* LANL 6th Bien. CUBE (Computer Use by Engineers) Symp. Aug. 1984 p 59 (For primary document see N86-11858 02-60)

Avail: NTIS HC A06/MF A01

Interaction of a freely propagating premixed flame with regions of high vorticity in the flow is investigated using a computer model. These vorticity regions are formed due to the flame-generated volume expansion that pushes gas past obstacles ahead of the flame. In the computer model the discrete vortex dynamics method is used to simulate the time developent of the vorticity regions downstream of each obstacle. The flame front is modeled as a wrinkle laminar flame interface that propagates normal to itself at the laminar burning velocity, separating the two different density fluids: burned and unburned. Two different obstacle configurations are discussed. In the first case, a flame causes unburned gas to exhaust out of a planar duct, and when the flame reaches the duct exit it interacts with the vorticity which was formed at the exit. The second case involves a series of obstacles in a channel. Here, the repeated obstacles in the channel lead to acceleration of the flame, as indicated by the dramatic increase in the rate of fuel consumption. Author

N86-11883# Sandia Labs., Albuquerque, N. Mex.

APPLICATION OF FLUX-CORRECTED TRANSPORT (FCT) TO HEAT TRANSFER/FLUID MECHANICS PROBLEMS Abstract Only **c34**

R. J. Gross, M. R. Baer, and C. E. Hickox *In* LANL 6th Bien. CUBE (Computer Use by Engineers) Symp. Aug. 1984 p 60 (For primary document see N86-11858 02-60)

Avail: NTIS HC A06/MF A01

The FCT finite-difference technique was developed to minimize numerical diffusion in concert with avoiding numerical dispersion (no artificial maxima or minima). As a result, the method is well-suited for accurately solving convective-diffusive flow equations. One-dimensional and two-dimensional solvers have been developed which utilize and explicit FCT approach. The solvers are vectorized for optimum execution on the CRAY. For instance, on a 50x50 grid, the two-dimensional solver may take up to 0.06 sec, per transport equation, per timestep, on the CRAY. In addition, the solvers are essentially canned to facilitate use by others. The flexibility of the FCT technique will be illustrated by showing results obtained for a variety of fluid flow/heat and mass transfer problems. Two-dimensional results will be presented for a Riemann shock problem, the classical Kelvin-Helmholtz and Rayleigh-Taylor flow instability problems, natural convective flow in a porous medium, thermal-solutal flow in a porous medium, and solution of the acoustic-filtered conservation equations describing a fire within a room. Author

N86-11884# Sandia Labs., Albuquerque, N. Mex. Analytical Thermal/Fluid Mechanics Div.

HEAT TRANSFER AND PRESSURE CHANGES DUE TO A LARGE TEMPERATURE DIFFERENCE ACROSS AN ENCLOSED VERTICAL AIR LAYER Abstract Only **c34**

D. R. Chenoweth and S. Paolucci *In* LANL 6th Bien. CUBE (Computer Use by Engineers) Symp. Aug. 1984 p 61-62 (For primary document see N86-11858 02-60)

Avail: NTIS HC A06/MF A01

The TRACE-2D Code has been used to obtain non-Boussinesq results from transient, compressible and two-dimensional calculations using Sutherland law conductivity and viscosity property variations for air. These free convection results are limited to the laminar flow region. The aspect ratio A of the vertical air layer, with adiabatic top and bottom walls, is taken to be unity or greater, and the Rayleigh number Ra based on the layer width is as large as 10 to the 7th power when A = 1. The results are valid for large temperature differences between the hot and cold isothermal walls, epsilon = sub T(h) - sub T(c) < or = 0.6, where the limitation is due to the Sutherland law accuracy. The various flow regimes are defined in terms of epsilon, A and Ra and correlations are developed for the Nusselt number and pressure in terms of these parameters. It is shown that, with proper non-dimensionalization, much of the vast body of literature concerning Nusselt number correlations and vertical temperature stratification for the Boussinesq case (which is asymptotically approached here for epsilon < < 1) can be used where epsilon is not small. Author

N86-11885# California Univ., Livermore. Lawrence Livermore Lab. Engineering Research Div.

FLEXIBLE VIBRATIONS OF A UNIFORM ELASTIC BEAM WITH ARBITRARY SUPPORTS AND LUMPED MASSES Abstract Only **c39**

Donald T. Gavel and Howard Woo *In* LANL 6th Bien. CUBE (Computer Use by Engineers) Symp. Aug. 1984 p 73 (For primary document see N86-11858 02-60)

Avail: NTIS HC A06/MF A01

This presentation introduces a simplified and systematic method for estimating the flexible vibrations of an elastic beam of uniform thickness with arbitrary supports and lumped masses. The method used is an eigenfunction expansion approach based on the free-free beam solution. A general form of the vibration model (called FLXBEAM) has been implemented within the DELIGHT computer-aided engineering package on a VAX/11-70. Results from example runs were favorably compared against finite-element solutions. After the user specifies a beam model into the interactive DELIGHT/FLXBEAM package, the computer can calculate frequencies, pilot mode shapes, and simulate the dynamic response of the beam all within a few minutes. This interactive package provides designers with a handy tool for quickly analyzing flexible beams under dynamic loads. Author

N86-11886# Sandia Labs., Albuquerque, N. Mex. Thermofluids Div.

A HYBRID VORTEX-IN-CELL FINITE-DIFFERENCE NUMERICAL METHOD FOR TURBULENT SHEAR LAYER COMPUTATION Abstract Only **c34**

Nagi N. Mansour *In* LANL 6th Bien. CUBE (Computer Use by Engineers) Symp. Aug. 1984 p 95-96 (For primary document see N86-11858 02-60)

Avail: NTIS HC A06/MF A01

A hybrid numerical scheme is presented to compute turbulent shear flows. The scheme divides the computational domain D into two regions, D sub 1 and D sub 2 and the vorticity equation is solved by different methods in each region. In region D sub 1, a Lagrangian formulation (vortex-in-cell) is used, while in region D sub 2 an Eulerian formulation (finite-difference) is used. At the boundary between the two regions, discrete Lagangian vorticity can be convected and converted into Eulerian grid vorticity.

Conversely, Eulerian fluxes of vorticity at this boundary are discretized so that in D vorticity is conserved and vorticity transport does not realize the imposition of the artificial boundary. This particular method has been developed to compute spatially-developing turbulent shear layers in two dimensions. Turbulent shear layers have a large range of length scales from the initial thin boundary layer near the splitter plate to large coherent vortex structures which continue to grow with downstream distance. Thus, by starting with discrete Lagrangian vorticity and changing to continuous Eulerian vorticity, the advantages of both methods can be used to simulate a larger flowfield domain than achievable with either method alone. B.W.

N86-11887# California Univ., Livermore. Lawrence Livermore Lab. Nuclear Explosives Engineering Div.
COMPUTER CODES FOR FLUID-STRUCTURE INTERACTIONS Abstract Only c34
W. H. McMaster *In* LANL 6th Bien. CUBE (Computer Use by Engineers) Symp. Aug. 1984 p 96 (For primary document see N86-11858 02-60)
Avail: NTIS HC A06/MF A01

Three fluid dynamics codes, PELE-IC, PELE 3D and MAUI are available for the analysis of fluid-structure interactions where the fluid motion is drastic enough to cause difficulties in the Lagrangian formulation. The fluid-structure-interaction algorithms in these codes have been developed for the analysis of the dynamic response of coupled fluid-structure systems. The fluid motion is computed using an Eulerian differencing formulation and the structural motion is determined from a finite element code. The coupling is affected across the Lagrangian boundary defining the structure. These codes can be used over a wide range of fluid and structural motions. The incompressible fluid approach in the PELE codes is used when the effects of compressibility are minimal and the acoustic approximation suffices. The explicit algorithm of the MAUI code can handle those situations where compressible effects are important, and it can also accommodate shock waves. All three codes are in the public domain. Author

N86-11888# Stanford Univ., Calif. Computer Systems Lab.
DIRECTLY EXECUTED LANGUAGES Final Report, 19 Apr. 1982 - 30 Jun. 1985
M. J. Flynn 10 May 1985 13 p
(Contract DAAG29-82-K-0109)
(AD-A157311; ARO-18553.1-EL) Avail: NTIS HC A02/MF A01 CSCL 09/2

Computer architectures or instruction sets can be designed to be in close correspondence with high level computer languages. Techniques for designing this correspondence have been developed which produce instruction sets called Direct Correspondence Architectures, or DCAs. DCA representation minimize the number of bits needed to encode an instruction, as well as minimizing many of the dynamic parameters associated with program execution. In a Pascal-based DCA, the following reductions were achieved for a broad range of benchmarks when compared to a breadbasket of conventional architectures such as S/370, VAX, and P-code: (1) instruction bandwidth reduction: 3.46, (2) data read reduction (in bytes): 5.42, and (3) data write reduction (in bytes): 14.72. A microprocessor based implementation of a Pascal-based DCA has begun. Issues in concurrency detection for these and other architectures have been investigated. Author (GRA)

N86-11889# Michigan Univ., Ann Arbor. Coll. of Engineering.
IMPROVING THE COMPREHENSIBILITY OF A SIMULATED TECHNICAL MANUAL
D. E. Kieras 20 Jun. 1985 57 p
(Contract N00014-84-K-0729)
(AD-A157482; TR-85/ONR-20) Avail: NTIS HC A04/MF A01 CSCL 05/10

It is clear that careful rewriting can improve the comprehensibility and usability of a technical document. But exactly how the document should be modified to accomplish this improvement has been unclear. In two experiments, a simulated technical manual for a simple piece of equipment was evaluated for comprehensibility using well-defined rules, and rewritten to eliminate the specific comprehension problems detected by the rules. Unlike conventional readability formulas or writer's guidelines, these rules were based on results and theory from research on comprehension processes, and thus concern what aspects of text are actually difficult for the reader to process. Substantial improvements in performance were observed in tasks in which the subject had to learn how to operate the equipment using the manual. These results suggest that a computer-based system that could apply the comprehensibility rules would be useful in improving the quality of technical documents. Author (GRA)

N86-11890# Federal Compiler Testing Center, Falls Church, Va. Office of Software Development and Information Technology.
Ada (TRADEMARK) COMPILER VALIDATION SUMMARY REPORT: DATA GENERAL CORPORATION, ADE Ada COMPILER, VERSION 2.30.03.12, ECLIPSE DS/4000, DS/4200, MV/4000-DC, MV/8000-C, MV/8000-2, MV/10000, MV/10000 SX USING AOS/VS 5.04 AND AOS/RT32 4.001.00
May 1985 25 p
(AD-A157573) Avail: NTIS HC A02/MF A01 CSCL 09/2

The purpose of this Validation Summary Report is to present the results and conclusions of performing standardized tests on the Data General Corporation ADE Ada Compiler. On-site testing was performed between 29 April 1985 and 3 May 1985 at Data General Corporation headquarters, Westboro, Massachusetts, under the auspices of an Ada Validation Facility (AVF), the Federal Software Testing Center, according to current Ada Validation Office policies and procedures. The Data General ADE Ada Compiler is hosted on those systems listed in the table below. The hosts, as well as selected AOS/RT32 based systems served as the target systems. The suite of tests known as the Ada Compiler Validation Capability (ACVC), Version 1.5, was used. The ACVC suite of tests is used to validate conformance of the compiler ANSI/MIL-STD-1815A (Ada). This standard is described in the ANSI Ada Reference Manual, January 1983. Not all tests in the ACVC test suite are applicable to this specific implementation. Also, known test errors in Version 1.5 are present in some tests; these tests were withdrawn. The purpose of the testing is to ensure that the compiler properly implements legal language constructs and that it identifies, rejects from processing, and labels illegal constructs. GRA

N86-11891# Softech, Inc., Fairborn, Ohio.
Ada (TRADEMARK) COMPILER VALIDATION SUMMARY REPORT: VERDIX Ada COMPILER, VERDIX Ada DEVELOPMENT SYSTEM (VADS) VAda-010-1010, VERSION V05.00, FOR SUN MICROSYSTEMS MODEL 2/120 USING UNIX (TRADEMARK) 4.2 BSD, RELEASE 1.1 Final Report
Jun. 1985 48 p
(Contract F33600-84-D-0280)
(AD-A157574) Avail: NTIS HC A03/MF A01 CSCL 09/2

The purpose of this Validation Summary Report is to present the results and conclusions of performing standardized tests on the Verdix Ada compiler. On-site testing was performed 28 to 30 April 1985 at Verdix Western Operations in Aloha, Oregon, under the auspices of the Ada Validation Facility, according to the Ada Validation Office policies and procedures. The Verdix Ada compiler (Verdix Ada Development System (VADS), VAda-010-1010) is hosted on the Sun Microsystems Model 2/120 computer operating under Berkeley UNIX 4.2 BSD, Release 1.1. The suite of tests known as the Ada Compiler Validation Capability (ACVC), Version 1.5, was used. The ACVC suite of tests is used to validate conformance of the compiler to ANSI/MIL-STD-1815A (Ada). This standard is described in the ANSI Ada Reference Manual, January 1983. Not all tests in the ACVC test suite are applicable to a specific implementation. Also, known test errors in Version 1.5 are present in some tests; the tests were withdrawn. The purpose of the testing is to ensure that the compiler properly implements legal language constructs and that it identifies, rejects from processing, and labels illegal language constructs. The testing also identifies implementation-dependent behavior permitted by the standard. GRA

N86-11892# Edgerton, Germeshausen and Grier, Inc., Idaho Falls, Idaho.
DATA ANALYSIS USING A DATA BASE DRIVEN GRAPHIC ANIMATION SYSTEM
D. H. Schwieder, H. D. Stewart, and J. N. Curtis 1985 10 p refs
(Contract DE-AC07-76ID-01570)
(DE85-014635; EGG-M-14285) Avail: NTIS HC A02/MF A01

A graphics animation system was developed to assist engineers in the analysis of large amounts of time series data. Most prior attempts at computer animation of data involve the development of large and expensive problem-specific systems. A generalized interactive computer animation system designed to be used in a wide variety of data analysis applications is discussed. By using relational data storage of graphics and control information, considerable flexibility in design and development of animated displays is achieved. DOE

N86-11995# Joint Publications Research Service, Arlington, Va.
HIGH-SPEED SIGNAL PROCESSOR DEVELOPED Abstract Only
In its China Rept.: Sci. and Technol. (JPRS-CST-85-015) 16 May 1985 p 10 Transl. into ENGLISH from Jisuanji Shijie (Beijing), no. 7, 8 Apr. 1984 p 7 (For primary document see N86-11994 02-70)
Avail: NTIS HC A07/MF A01

61 COMPUTER PROGRAMMING AND SOFTWARE

Includes computer programs, routines, and algorithms.

N86-11893*# Illinois Univ., Urbana-Champaign. Software Systems Research Group.
THE EMBEDDED OPERATING SYSTEM PROJECT
Roy H. Campbell May 1985 338 p refs
(Grant NsG-1471)
(NASA-CR-176280; NAS 1.26:176280) Avail: NTIS HC A15/MF A01 CSCL 09B

The design and construction of embedded operating systems for real-time advanced aerospace applications was investigated. The applications require reliable operating system support that must accommodate computer networks. Problems that arise in the construction of such operating systems, reconfiguration, consistency and recovery in a distributed system, and the issues of real-time processing are reported. A thesis that provides theoretical foundations for the use of atomic actions to support fault tolerance and data consistency in real-time object-based system is included. The following items are addressed: (1) atomic actions and fault-tolerance issues; (2) operating system structure; (3) program development; (4) a reliable compiler for path Pascal; and (5) mediators, a mechanism for scheduling distributed system processes. E.A.K.

N86-11894*# California Univ., Santa Barbara.
ADS: A FORTRAN PROGRAM FOR AUTOMATED DESIGN SYNTHESIS: VERSION 1.10 Final Report
G. N. Vanderplaats Sep. 1985 46 p refs
(Grant NAG1-567)
(NASA-CR-177985; NAS 1.26:177985) Avail: NTIS HC A03/MF A01 CSCL 09B

A new general-purpose optimization program for engineering design is described. ADS (Automated Design Synthesis - Version 1.10) is a FORTRAN program for solution of nonlinear constrained optimization problems. The program is segmented into three levels: strategy, optimizer, and one-dimensional search. At each level, several options are available so that a total of over 100 possible combinations can be created. Examples of available strategies are sequential unconstrained minimization, the Augmented Lagrange Multiplier method, and Sequential Linear Programming. Available optimizers include variable metric methods and the Method of Feasible Directions as examples, and one-dimensional search options include polynomial interpolation and the Golden Section method as examples. Emphasis is placed on ease of use of the program. All information is transferred via a single parameter list. Default values are provided for all internal program parameters such as convergence criteria, and the user is given a simple means to over-ride these, if desired. Author

N86-11895*# Hawaii Univ., Honolulu. Dept. of Electrical Engineering.
A CASCADED CODING SCHEME FOR ERROR CONTROL
Tadao Kasami (Osaka Univ., Toyonaka, Japan) and Shu Lin 1 Oct. 1985 44 p refs
(Grant NAG5-407)
(NASA-CR-176276; NAS 1.26:176276) Avail: NTIS HC A03/MF A01 CSCL 09B

A cascaded coding scheme for error control was investigated. The scheme employs a combination of hard and soft decisions in decoding. Error performance is analyzed. If the inner and outer codes are chosen properly, extremely high reliability can be attained even for a high channel bit-error-rate. Some example schemes are studied which seem to be quite suitable for satellite down-link error control. E.A.K.

N86-11896*# Jet Propulsion Lab., California Inst. of Tech., Pasadena.
CELCAP: A COMPUTER MODEL FOR COGENERATION SYSTEM ANALYSIS
Jul. 1985 108 p refs
(Contract NAS7-918; N68305-84WR-40126)
(NASA-CR-176306; JPL-Pub-85-20; NAS 1.26:176306) Avail: NTIS HC A06/MF A01 CSCL 09B

A description of the CELCAP cogeneration analysis program is presented. A detailed description of the methodology used by the Naval Civil Engineering Laboratory in developing the CELCAP code and the procedures for analyzing cogeneration systems for a given user are given. The four engines modeled in CELCAP are: gas turbine with exhaust heat boiler, diesel engine with waste heat boiler, single automatic-extraction steam turbine, and back-pressure steam turbine. Both the design point and part-load performances are taken into account in the engine models. The load model describes how the hourly electric and steam demand of the user is represented by 24 hourly profiles. The economic model describes how the annual and life-cycle operating costs that include the costs of fuel, purchased electricity, and operation and maintenance of engines and boilers are calculated. The CELCAP code structure and principal functions of the code are described to how the various components of the code are related to each other. Three examples of the application of the CELCAP code are given to illustrate the versatility of the code. The examples shown represent cases of system selection, system modification, and system optimization. Author

N86-11897*# Illinois Univ., Urbana-Champaign. Dept. of Computer Science.
RESEARCH IN THE DESIGN OF HIGH-PERFORMANCE RECONFIGURABLE SYSTEMS Semiannual Status Report, 1 Apr. - 30 Sep. 1985
D. L. Slotnick 30 Sep. 1985 38 p
(Grant NAG5-377)
(NASA-CR-176275; NAS 1.26:176275; SASR-4) Avail: NTIS HC A03/MF A01 CSCL 09B

The initial control and programming philosophies of the RELAPSE are discussed. A block diagram showing the relationship of the Arithmetic Units (composed of Stages and Bit Processors), to the Functional Units, and other components of the RELAPSE is used to guide this discussion. The latest version of the Bit Processor design is presented. Included is a detailed discussion of the Bit Processor's new scratch pad memory component. The section also clarifies the usage of the Bit Processor's processing registers, and Input/Output functions. The final design phase of the Arithmetic Unit is underway by a study of the Proposed IEEE Floating Point Standard. The decisions on conformation to this standard will be used as inputs into the finalization of the designs of the Bit Processor, Stage, and Arithmetic Units of the RELAPSE. G.L.C.

N86-11898# Lockheed-California Co., Burbank.
KRASH85 USER'S GUIDE: INPUT/OUTPUT FORMAT Final Report, Jan. - Sep. 1984
M. A. Gamon, G. Wittlin, and W. L. LaBarge Jul. 1985 240 p refs
(Contract DTFA03-84-C-00004)
(FAA-CT-85-10; LR-30777) Avail: NTIS HC A11/MF A01

The input and output formats appropriate for the computer program KRASH 85 are presented. Features that are incorporated into KRASH85 include: (1) an improved plastic hinge moment algorithm; (2) gear-oleo metering pin coding; (3) load-interaction curves; (4) an expanded initial conditions subroutine (combined with NASTRAN); (5) a comprehensive energy balance; (6) center of gravity (c.g.) displacement, velocity, acceleration and force time histories; (7) revised vertical beam orientation coding; (8) provision to save data for post-process i.e., acceleration, mass location and forces; (9) provisions to input preprocessed data; (10) a corrected uncoupled KR curve unloading/reloading algorithm; (11) provisions to define a tire spring (remains normal to the ground plane); (12) provisions to number the masses to an arbitrary sequence; and (13) an option to compute section shear and moment distributions. Author

N86-11899# Naval Postgraduate School, Monterey, Calif.
MODIFICATION OF HUFFMAN CODING M.S. Thesis
S. Kilic Mar. 1985 92 p
(AD-A156479) Avail: NTIS HC A05/MF A01 CSCL 17/2

Huffman coding minimizes the average number of coding digits per message. Minimizing the mean time by this method raises the problem of large variance. When the variance is large there is a greater probability that an arbitrary encoded message significantly exceeds the average. The delicate point here is the danger of an urgent message taking more time than expected, in addition to larger bandwidth or buffer requirements. With this research a large reduction of variance versus a small increase in mean time is examined for the purpose of modifying Huffman coding for a particular alphabet. Author (GRA)

N86-11900# Naval Research Lab., Washington, D. C.
MICROLAN, FILE TRANSFER PROGRAM FOR MICROPROCESSORS M.S. Thesis
R. D. Jaskot and H. W. Henry Mar. 1985 156 p
(AD-A156519) Avail: NTIS HC A08/MF A01 CSCL 09/2

The age of automation has established its foothold in today's society. Computerization now affects almost everyone's job, and sharing of information is vital to successful job performance. Manual transfer of information is inefficient and prone to error, so another means is needed. One option is computer networking. Both Local Area Networks and long-haul networks presently exist, but they are either very expensive or hardware dependent. It would normally require a long lead time and high costs for the military to acquire an information transfer system. To provide a readily available, low-cost file transfer system, the authors developed an assembly language program named MICROLAN, which is written to work with three of the main microcomputer operating systems (CP.M-80, CP/M-86, and MS.DOS) and to take advantage of RS232 technology. MICROLAN was successfully tested for file transfer at up to 4800 baud, and suggestions have been included as to possible uses for MICROLAN in the military environment. Additionally, possible methods for upgrading MICROLAN are also included. Author (GRA)

N86-11901# California Univ., Berkeley. Operations Research Center.
BAYESIAN EXTENSIONS TO A BASIC MODEL OF SOFTWARE RELIABILITY
W. S. Jewell Jun. 1985 25 p
(Grant AF-AFOSR-0122-81)
(AD-A157296; ORC-85-4) Avail: NTIS HC A02/MF A01 CSCL 09/2

A Bayesian analysis of the software reliability model of Jelinski and Moranda is given, based upon Meinhold and Singpurwalla. Important extensions are provided to the stopping rule and prior distribution of the number of defects, as well as permitting uncertainity in the failure rate. It is easy to calculate the predictive distribution of unfound errors at the end of software testing, and to see the relative effects of uncertainty in the number of errors and in the detection efficiency. The behavior of the predictive mode and mean over time are examined as possible point estimators, but are clearly inferior to calculating the full predictive distribution. Author (GRA)

N86-11902# Naval Postgraduate School, Monterey, Calif.
APPROXIMATE REASONING AND THE REVEAL SOFTWARE SYSTEM. USERS GUIDE M.S. Thesis
D. W. Verhagen Mar. 1985 141 p
(AD-A157298) Avail: NTIS HC A07/MF A01 CSCL 09/2

This thesis introduces the reader to some of the principles of fuzzy set theory and approximate reasoning. Sample applications are discussed with possible military situations outlined. The REVEAL software package is reviewed and its relationship with fuzzy set theory and approximate reasoning discussed. This thesis is designed to be used as a tutorial for REVEAL. Author (GRA)

N86-11903# Yale Univ., New Haven, Conn. Dept. of Computer Science.
EASY IMPOSSIBILITY PROOFS FOR DISTRIBUTED CONCENSUS PROBLEMS
M. J. Fischer, N. A. Lynch, and M. Merritt Jul. 1985 26 p Prepared in cooperation with Massachusetts Inst. of Tech., Cambridge
(Contract N00014-82-K-0154; N00014-85-K-0168; N00014-83-K-0125; DAAG29-84-K-0058; Grant NSF DCR-84-05478)
(AD-A157411; Yaleu/DCS/TR-405) Avail: NTIS HC A03/MF A01 CSCL 09/2

Easy proofs are given, of the impossibility of solving several consensus problems (Byzantine agreement, weak agreement, Byzantine firing squad, approximate agreement and clock synchronization) in certain communication graphs. It is shown that, in the presence of m faults, no solution to these problems exists for communication graphs with fewer than 3m+1 nodes or less than 2m+1 connectivity. While some of these results had previously been proved, the new proofs are much simpler, provide considerably more insight, apply to more general needs of computation, and (particularly in the case of clock synchronization) significantly strengthen the results. GRA

N86-11904# Massachusetts Inst. of Tech., Cambridge. Lab. for Computer Science.
PROBABILISTIC ANALYSIS OF A NETWORK RESOURCE ALLOCATION ALGORITHM Interim Research Report, Apr. 1985
N. A. Lynch, N. Griffeth, M. J. Fischer, and L. J. Guibas Jun. 1985 44 p
(Contract N00014-83-K-0125)
(AD-A157553; MIT/LCS/TM-278) Avail: NTIS HC A03/MF A01 CSCL 09/2

A distributed algorithm is presented, for allocating a large number of identical resources (such as airline tickets) to requests which can arrive anywhere in a distributed network. Resources, once allocated, are never returned. The algorithm searches sequentially, exhausting certain neighborhoods of the request origin before proceeding to search at greater distances. Choice of search direction is made nondeterministically. Analysis of expected response time is simplified by assuming that the search direction is chosen probabilistically, that messages require constant time, that the network is a tree with all leaves at the same distance from the root, and that requests and resources occur only at leaves. It is shown that the response time is approximated by the number of messages of one that are sent during the execution of the algorithm, and that this number of message is a nondecreasing function of the interarrival time for requests. Therefore, the worst case occurs when requests come in so far apart that they are processed sequentially. The expected time for the sequential case of the algorithm is analyzed by standard techniques. This time is shown to be bounded by a constant, independent of the size of the network. It follows that the expected response time for the algorithm is bounded in the same way. Author (GRA)

N86-11905# Ada Joint Program Office, Arlington, Va.
MILITARY STANDARD COMMON APSE (Ada PROGRAMMING SUPPORT ENVIRONMENT) INTERFACE SET (CAIS)
Jan. 1985 334 p
(AD-A157589) Avail: NTIS HC A15/MF A01 CSCL 09/2

This document provides specifications for a set of Ada packages, with their intended semantics, which together form the set of common interfaces for Ada Programming Support Environments (APSEs). This set of interfaces is known as the Common APSE Interface Set (CAIS). This interface set is designed to promote the source-level portability of Ada programs, particularly Ada software development tools. The CAIS applies to Ada Programming Support Environments which are to become the basic software life-cycle environments for Department of Defense (DOD) mission critical computer systems (MCCS). Those Ada programs that are used in support of software development are defined as tools. This includes the spectrum of support software from project management through code development, configuration management and life-cycle support. Tools are not restricted to only those software items normally associated with program generation, such as editors, compilers, debuggers, and linker-loaders. Groups of tools that are composed of a number of independent but interrelated programs (such as a debugger which is related to a specific compiler) are classed as tool sets. The goal of the CAIS is to promote interoperability and transportability of Ada software across DoD APSEs. GRA

N86-11859# California Univ., Livermore. Lawrence Livermore Lab. Applications Systems Div.
SOFTWARE ENGINEERING TOOLS THAT WORK Abstract Only
David Balaban *In* LANL 6th Bien. CUBE (Computer Use by Engineers) Symp. Aug. 1984 p 7 (For primary document see N86-11858 02-60)
Avail: NTIS HC A06/MF A01

N86-11860# California Univ., Livermore. Lawrence Livermore Lab. Applications Systems Div.
AN APPLICATION OF REAL-TIME ANALYSIS AND DESIGN TOOLS IN SOFTWARE DEVELOPMENT Abstract Only
Don W. Freeman *In* LANL 6th Bien. CUBE (Computer Use by Engineers) Symp. Aug. 1984 p 7 (For primary document see N86-11858 02-60)
Avail: NTIS HC A06/MF A01

N86-11870# California Univ., Livermore. Lawrence Livermore Lab. Engineering Research Div.
AN EVALUATION OF THREE GRAPHICS PACKAGES: THE METHODOLOGY AND RESULTS Abstract Only
Brian K. Cabral *In* LANL 6th Bien. CUBE (Computer Use by Engineers) Symp. Aug. 1984 p 24 (For primary document see N86-11858 02-60)
Avail: NTIS HC A06/MF A01

N86-11871# Los Alamos National Lab., N. Mex. Analysis and Testing Group.
INTERACTIVE GRAPHICS FOR FINITE ELEMENT PRE-PROCESSING Abstract Only
W. Rob Oakes, Jr. *In its* 6th Bien. CUBE (Computer Use by Engineers) Symp. Aug. 1984 p 24 (For primary document see N86-11858 02-60)
Avail: NTIS HC A06/MF A01

N86-11874# Sandia Labs., Albuquerque, N. Mex.
MICROCOMPUTER CONTROL AND DATA MANAGEMENT TECHNIQUES FOR TRANSIENT DIGITAL RECORDING Abstract Only
David A. Benson and Gary D. Miller *In* LANL 6th Bien. CUBE (Computer Use by Engineers) Symp. Aug. 1984 p 39 (For primary document see N86-11858 02-60)
Avail: NTIS HC A06/MF A01

N86-11875# California Univ., Livermore. Lawrence Livermore Lab. Nuclear Energy Systems Div.
A DATA TRANSLATOR FOR ENGINEERING MEASUREMENTS Abstract Only
Mel Wieting and Robert M. Trusty *In* LANL 6th Bien. CUBE (Computer Use by Engineers) Symp. Aug. 1984 p 40 (For primary document see N86-11858 02-60)
Avail: NTIS HC A06/MF A01

N86-11876# California Univ., Livermore. Lawrence Livermore Lab. Engineering Research Div.
SIG: A GENERAL-PURPOSE SIGNAL PROCESSING CODE Abstract Only
Darrel L. Lager and Stephen G. Azevedo *In* LANL 6th Bien. CUBE (Computer Use by Engineers) Symp. Aug. 1984 p 40-41 (For primary document see N86-11858 02-60)
Avail: NTIS HC A06/MF A01

N86-11992# Joint Publications Research Service, Arlington, Va.
COMPUTER-AIDED DESIGNING, ENGINEERING, PREPARATION OF PRODUCTION
Yu. I. Topcheyev *In its* USSR Rept.: Sci. and Technol. Policy (JPRS-UST-85-014) 25 Sep. 1985 p 20-24 Transl. into ENGLISH from Vest. Vysshey Shkoly (Moscow), no. 5, May 1985 p 29-31 (For primary document see N86-11990 02-70)
Avail: NTIS HC A06

62 COMPUTER SYSTEMS

Includes computer networks.

N86-11906*# Michigan Univ., Ann Arbor. Dept. of Electrical and Computer Engineering.
INTEGRATED ANALYSIS OF ERROR DETECTION AND RECOVERY Final Report, 1 Jan. - 31 Dec. 1984
Kang G. Shin and Yann-Hang Lee Oct. 1985 115 p refs
(Grant NAG1-296)
(NASA-CR-172571; NAS 1.26:172571) Avail: NTIS HC A06/MF A01 CSCL 09B

An integrated modeling and analysis of error detection and recovery is presented. When fault latency and/or error latency exist, the system may suffer from multiple faults or error propagations which seriously deteriorate the fault-tolerant capability. Several detection models that enable analysis of the effect of detection mechanisms on the subsequent error handling operations and the overall system reliability were developed. Following detection of the faulty unit and reconfiguration of the system, the contaminated processes or tasks have to be recovered. The strategies of error recovery employed depend on the detection mechanisms and the available redundancy. Several recovery methods including the rollback recovery are considered. The recovery overhead is evaluated as an index of the capabilities of the detection and reconfiguration mechanisms. E.A.K.

63 CYBERNETICS

Includes feedback and control theory.
For related information see also *54 Man/System Technology and Life Support.*

No abstracts in this category.

64 NUMERICAL ANALYSIS

Includes iteration, difference equations, and numerical approximation.

N86-11907*# National Aeronautics and Space Administration. Ames Research Center, Moffett Field, Calif.
ON THE IMPLEMENTATION OF A CLASS OF UPWIND SCHEMES FOR SYSTEM OF HYPERBOLIC CONSERVATION LAWS
H. C. Yee Sep. 1985 17 p refs
(NASA-TM-86839; Rept-85412; NAS 1.15:86839) Avail: NTIS HC A02/MF A01 CSCL 12A

The relative computational effort among the spatially five point numerical flux functions of Harten, van Leer, and Osher and Chakravarthy is explored. These three methods typify the design principles most often used in constructing higher than first order upwind total variation diminishing (TVD) schemes. For the scalar case the difference in operation count between any two algorithms may be very small and yet the operation count for their system counterparts might be vastly different. The situation occurs even though one starts with two different yet equivalent representations for the scalar case. Author

N86-11908*# Oklahoma Univ., Norman.
ALGEBRAIC GRID GENERATION USING TENSOR PRODUCT B-SPLINES Ph.D. Thesis
Bonita V. Saunders Sep. 1985 152 p refs
(Grant NGT-47-003-802)
Avail: NTIS HC A08/MF A01 CSCL 12A

Finite difference methods are more successful if the accompanying grid has lines which are smooth and nearly orthogonal. The development of an algorithm which produces such a grid when given the boundary description. Topological considerations in structuring the grid generation mapping are discussed. The concept of the degree of a mapping and how it can be used to determine what requirements are necessary if a mapping is to produce a suitable grid is examined. The grid generation algorithm uses a mapping composed of bicubic B-splines. Boundary coefficients are chosen so that the splines produce Schoenberg's variation diminishing spline approximation to the boundary. Interior coefficients are initially chosen to give a variation diminishing approximation to the transfinite bilinear interpolant of the function mapping the boundary of the unit square onto the boundary grid. The practicality of optimizing the grid by minimizing a functional involving the Jacobian of the grid generation mapping at each interior grid point and the dot product of vectors tangent to the grid lines is investigated. Grids generated by using the algorithm are presented. E.A.K.

N86-11909*# National Aeronautics and Space Administration. Ames Research Center, Moffett Field, Calif.
ON SYMMETRIC AND UPWIND TVD SCHEMES
H. C. Yee Sep. 1985 12 p refs
(NASA-TM-86842; Rept-85417; NAS 1.15:86842) Avail: NTIS HC A02/MF A01 CSCL 12A

A class of explicit and implicit total variation diminishing (TVD) schemes for the compressible Euler and Navier-Stokes equations was developed. They do not generate spurious oscillations across shocks and contact discontinuities. In general, shocks can be captured within 1 to 2 grid points. For the inviscid case, these schemes are divided into upwind TVD schemes and symmetric (nonupwind) TVD schemes. The upwind TVD scheme is based on the second-order TVD scheme. The symmetric TVD scheme is a generalization of Roe's and Davis' TVD Lax-Wendroff scheme. The performance of these schemes on some viscous and inviscid airfoil steady-state calculations is investigated. The symmetric and upwind TVD schemes are compared. E.A.K.

N86-11910*# Ohio State Univ., Columbus. Dept. of Geodetic Science and Surveying.
LEAST SQUARES COLLOCATION APPLIED TO LOCAL GRAVIMETRIC SOLUTIONS FROM SATELLITE GRAVITY GRADIOMETRY DATA
John W. Robbins Aug. 1985 105 p refs
(Grant NGR-36-008-161)
(NASA-CR-176299; NAS 1.26:176299; OSU-368) Avail: NTIS HC A06/MF A01 CSCL 12A

An autonomous spaceborne gravity gradiometer mission is being considered as a post Geopotential Research Mission project. The introduction of satellite diometry data to geodesy is expected to improve solid earth gravity models. The possibility of utilizing gradiometer data for the determination of pertinent gravimetric quantities on a local basis is explored. The analytical technique of least squares collocation is investigated for its usefulness in local solutions of this type. It is assumed, in the error analysis, that the vertical gravity gradient component of the gradient tensor is used as the raw data signal from which the corresponding reference gradients are removed to create the centered observations required in the collocation solution. The reference gradients are computed from a high degree and order geopotential model. The solution can be made in terms of mean or point gravity anomalies, height anomalies, or other useful gravimetric quantities depending on the choice of covariance types. Selected for this study were 30 x 30 foot mean gravity and height anomalies. Existing software and new software are utilized to implement the collocation technique. It was determined that satellite gradiometry data at an altitude of 200 km can be used successfully for the determination of 30 x 30 foot mean gravity anomalies to an accuracy of 9.2 mgal from this algorithm. It is shown that the resulting accuracy estimates are sensitive to gravity model coefficient uncertainties, data reduction assumptions and satellite mission parameters. Author

N86-11911*# Hawaii Univ., Manoa. Dept. of Electrical Engineering.
A CASCADED CODING SCHEME FOR ERROR CONTROL
Shu Lin and Tadao Kasami (Osaka Univ., Toyonaka, Japan) 1 Oct. 1985 44 p refs
(Grant NAG5-407)
(NASA-CR-176287; NAS 1.26:176287) Avail: NTIS HC A03/MF A01 CSCL 12A

A cascaded coding scheme for error control was investigated. The scheme employs a combination of hard and soft decisions in decoding. Error performance is analyzed. If the inner and outer codes are chosen properly, extremely high reliability can be attained even for a high channel bit-error-rate. Some example schemes are studied. They seem to be quite suitable for satellite down-link error control. Author

N86-11912# Texas Research Inst., Inc., Austin.
FAILURE RATE MODEL FOR CATHODIC DELAMINATION OF PROTECTIVE COATINGS Memorandum Report, Jun. 1983 - Jun. 1984
J. S. Thornton, R. E. Montgomery, and J. F. Cartier 30 May 1985 22 p
(Contract N00014-83-C-2258)
(AD-A157483; NRL-MR-5584) Avail: NTIS HC A02/MF A01 CSCL 12/1

In order to improve the reliability of wet-end sonar components, the mechanisms for cathodic delamination of rubber-to-metal bonds are studied. A quantitative model for the rate of delamination is proposed. This model is based on the kinetics of the many contributing chemical processes as well as diffusion processes which lead to the failure of the protective coating. The model is solved under a set of assumptions which simplify the differential equations. However, a numerical solution to the complete set of equations would be possible. It is concluded that it will be feasible to understand and quantify the failure process in sufficient detail to formulate design specifications for protective coatings on sonar transducers which will extend the service life of equipment. It is also concluded that better testing procedures could be applied in the evaluation of future candidates for polymeric bonding systems. GRA

N86-11913# Princeton Univ., N. J. Dept. of Electrical Engineering and Computer Science.

A NUMERICAL ANALYSIS OF A QUEUE WITH NETWORK ACCESS FLOW CONTROL
D. W. Browning and J. B. Thomas 1985 9 p
(Contract DAAG29-82-K-0095; Grant NSF ECS-83-17777)
(AD-A157526; ARO-18985.19-EL) Avail: NTIS HC A02/MF A01 CSCL 12/2

A network access flow control method is considered where messages are sent to the nodes which are major users of a congested queue. The model is based on a Markovian queue embedded in the network, and analysis takes place on a sequence of fixed-length time intervals. Changes of state reflecting the control and resulting input rates occur at the ends of the intervals, and the evolution of state probabilities over the course of an internal is analyzed numerically using Euler's method with Richardson extrapolation. The results provide insight into both transient and steady-state behaviors. GRA

N86-11914# Stanford Univ., Calif. Systems Optimization Lab.
SPARSE QUASI-NEWTON METHODS AND THE CONTINUATION PROBLEM
F. F. Chadee Jun. 1985 134 p
(Contracts N00014-85-K-0343; DE-AM03-7 Grants NSF DMS-84-20623; NSF DMS-84-04121)
(AD-A157587; SU-SOL-85-8) Avail: NTIS HC A07/MF A01 CSCL 12/1

The problem of tracing a smooth path arises in many engineering problems, the solution of parametric differential equations and eigenvalue problems; it also finds application in the solution of nonlinear systems of equations by homotopy techniques. In many instances, the path is defined implicitly as the solution of a system of equations whose Jacobian matrix is large and sparse. Robust simplicial path-following techniques cannot be applied to large problems since the work involved rises rapidly with increasing dimension. This dissertation addresses the numerical problems involved in tracing the path for large sparse systems by the use of a predictor-corrector algorithm. We investigate the use of sparse quasi-Newton techniques to reduce the expense of the convector phase of the predictor-corrector algorithm inherent in Newton's method. In order to avoid the drawbacks of the sparse Broyden method - the need for a matrix factorization on each iterate and the need to store both the Jacobian matrix and its factors - we examine techniques for directly updating the LU factors of the approximation to the Jacobian matrix. Under reasonable assumptions on the systems of equations to be solved, a proof of local Q-superlinear convergence is presented for two sparse updating techniques. A predictor-corrector algorithm employing these sparse updating techniques is implemented in a Fortran code and numerical results are obtained demonstrating the advantages to be gained from the use of quasi-Newton methods for the large sparse continuation problem. GRA

N86-11915# Maryland Univ., College Park. Center for Automation Research.
COMPUTATION OF MINIMAL ISOVIST SETS
M. F. Doherty Sep. 1984 89 p
(Contract DAAK70-83-K-0018)
(AD-A157624; CAR-TR-87; CSC-TR-1430) Avail: NTIS HC A05/MF A01 CSCL 12/1

A minimal isovist set (MIS) of a simple polygonal region P is a smallest set of points in P whose union of isovists equals P (where the isovist of x is the set of all points visible from x). This thesis represents an algorithm to search for an MIS for an arbitrary P. An MIS is shown to be equivalent to a minimal covering of P with star-shaped polygons. A (non-complete) algorithm to find a minimal covering is proposed which uses the vertices of the kernels of the star-shaped polygons. The complexity of finding an MIS is reduced to a worst-case consideration of no more than n to the 4th power points in P. A comparison of the proposed algorithm with two previously published algorithms is made. Extension of this method to exterior views and interior holes is discussed, and areas for future research are mentioned. Author (ESA)

N86-11552# Martin Luther-Universitaet, Halle-Wittenberg (East Germany). Sektion Mathematik.
ON INVERSE PROBLEMS IN DIFFERENTIAL EQUATIONS: A CRITICAL ANALYSIS
Gottfried Anger *In* Academy of Sciences of the GDR Proc. of the 5th Intern. Symp. Geodesy and Phys. of the Earth 1985 p 38-44 refs (For primary document see N86-11549 02-42)
Avail: NTIS HC A09/MF A01

N86-11562# Agricultural Univ., Wroclaw (Poland). Dept. of Geodesy and Photogrammetry.
ADJUSTMENT OF THE LATITUDE DATA BY LEAST-SQUARES COLLOCATION APPROACH
R. Galas *In* Academy of Sciences of the GDR Proc. of the 5th Intern. Symp. Geodesy and Phys. of the Earth 1985 p 139-141 refs (For primary document see N86-11549 02-42)
Avail: NTIS HC A09/MF A01

N86-11573# Technische Univ., Dresden (East Germany).
TREATMENT OF THE GEODETIC BOUNDARY VALUE PROBLEM BY CONTACT-TRANSFORMATION
Wolfgang Keller *In* Academy of Sciences of the GDR Proc. of the 5th Intern. Symp. Geodesy and Phys. of the Earth, Pt. 2 1985 p 32-35 refs (For primary document see N86-11568 02-42)
Avail: NTIS HC A09/MF A01

N86-11704# Karlova Univ., Prague (Czechoslovakia). Inst. of Geophysics.
ON THE ADDITION THEOREM FOR LEGENDRE POLYNOMIALS
Oldrich Novotny *In* Ceskoslovenska Akademie Ved Geophys. Works, 1982, Vol. 30 1985 p 33-45 refs (For primary document see N86-11702 02-46)
Avail: Issuing Activity

N86-11715# Ceskoslovenska Akademie Ved, Prague. Inst. of the Physics of the Atmosphere.
ON THE INSTABILITY OF VORTEX SERIES
Jiri Horak *In its* Geophys. Works, 1982, Vol. 30 1985 p 269-285 refs (For primary document see N86-11702 02-46)
Avail: Issuing Activity

N86-11865# California Univ., Livermore. Lawrence Livermore Lab. Engineering Research Div.
PARTICLE PUSHING TECHNIQUES FOR USE WITH FINITE ELEMENT BASED FIELD CALCULATIONS Abstract Only
John C. Peterson *In* LANL 6th Bien. CUBE (Computer Use by Engineers) Symp. Aug. 1984 p 12 (For primary document see N86-11858 02-60)
Avail: NTIS HC A06/MF A01

65 STATISTICS AND PROBABILITY

Includes data sampling and smoothing; Monte Carlo method; and stochastic processes.

No abstracts in this category.

66 SYSTEMS ANALYSIS

Includes mathematical modeling; network analysis; and operations research.

No abstracts in this category.

67 THEORETICAL MATHEMATICS

Includes topology and number theory.

No abstracts in this category.

70 PHYSICS (GENERAL)

For geophysics see *46 Geophysics*. For astrophysics see *90 Astrophysics*. For solar physics see *92 Solar physics*.

N86-11916 Texas Univ., Austin.
THE VACUUM IN THE PRESENCE OF ELECTROMAGNETIC FIELDS AND ROTATING BOUNDARIES Ph.D. Thesis
Corinne Alison Manogue 1984 155 p
Avail: Univ. Microfilms Order No. DA8513258

Two investigations of the properties of the vacuum are made. The first is a reconsideration of the classic Klein paradox, particle creation due to the presence of very strong external electromagnetic potentials. Expectation values of the current, momentum, and number operators, each of which is a measure of particle creation, are calculated for both massive spin zero and massive spin one half fields. The relationship between super-radiance and pair creation is explained. The second investigation concerns the rotation of the vacuum caused by the rotation of boundaries. Just as the presence of boundaries can create a change in the vacuum expectation value of the energy density (the Casimir effect), the rotation of such boundaries can create changes in the vacuum expectation value of the momentum density. Calculations of the Casimir effect are made for a massless scalar field confined to an infinitely long square box. The change in the vacuum expectation value of the momentum density is calculated if this same box is rotating around its long central axis. In contrast, it is shown that for an infinitely long circular cylinder there is no change in the momentum density. Dissert. Abstr.

N86-11917 Clarkson Univ., Potsdam, N.Y.
MAGNETIC FILTRATION Ph.D. Thesis
Mayuree Natenapit 1985 131 p
Avail: Univ. Microfilms Order No. DA8512141

A theory for capture of magnetic particles by a bed of spheres in high gradient magnetic separation (HGMS) is presented. The studies are divided into microscopic and submicroscopic regimes according to the size of particles being filtered. In the former, two cases were considered, one where the carrier fluid can be described by ideal inviscid potential flow, and the other for carrier fluid in creeping or laminar flow. An effective medium treatment (EMI) is employed to determine the fluid velocity profile around a representative sphere in the assemblage. The same approach is used to model the magnetic field, thus taking into account the magnetic effects of neighboring spheres. Results for capture efficiency are reported for both paramagnetic and diamagnetic particles by a filter operating either in the longitudinal or transverse design mode. Dissert. Abstr.

N86-11918# Joint Publications Research Service, Arlington, Va.
CHINA REPORT: SCIENCE AND TECHNOLOGY
2 May 1985 110 p refs Transl. into ENGLISH from various Chinese articles
(JPRS-CST-85-014) Avail: NTIS HC A06/MF A01

Progress in science and technology in the People's Republic of China is reported. Topics discussed include: applied sciences, life sciences, environmental quality, astronautics, lasers, nuclear engineering, phyiscs, and semiconductors. For individual titles, see N86-11919 through N86-11943.

N86-11919# Joint Publications Research Service, Arlington, Va.
DOUBLE TEARING MODE IN PLASMA WITH MAGNETIC BRAIDING c75
Jiaqi Dong *In its* China Rept.: Sci. and Technol. (JPRS-CST-85-014) 2 May 1985 p 28-39 refs Transl. into ENGLISH from Wuli Xuebao (Beijing), v. 33, no. 10, Oct. 1984 p 1341-1349 (For primary document see N86-11918 02-70)
Avail: NTIS HC A06/MF A01

Due to the presence of low amplitude magnetic disturbances in a magnetically confined plasma, the magnetic lines are often twisted into a braid, called magnetic braiding. This type of braided magnetic field structure was investigated. It is suggested that it is possible cause for many phenomena observed in a tokamak plasma like anomalous electron heat conduction, fracture instability, and the behavior of escaped electrons. The heating made caused by anomalous electron viscosity as a possible cause of fracture instability was examined. The linear behavior of resistance double tearing made caused by electron anomalous viscosity is studied. E.A.K.

N86-11920# Joint Publications Research Service, Arlington, Va.
DESIGN OF MANEUVERABLE TRAJECTORIES OF RE-ENTRY VEHICLE Abstract Only c18
Xanuyan Zhao *In its* China Rept.: Sci. and Technol. (JPRS-CST-85-014) 2 May 1985 p 72 Transl. into ENGLISH from Yuhang Xuebao (Beijing), no. 1, 31 Jan. 1985 p 1-10 Original language document announced in IAA as A85-42776 (For primary document see N86-11918 02-70)
Avail: NTIS HC A06/MF A01

This paper mainly discussed the design of maneuverable trajectories of reentry vehicles. Two methods are discussed. The first one is to design optimal maneuverable trajectories by means of the optimal control theory. The method for calculating optimal reentry maneuverable trajectories in this paper is simple and easy, and requires less time. The second one is to attain the engineering design method of selecting reentry maneuverable trajectories from the requirement for terminal velocity to be maximal under the condition of considering the effect of attack angle on drag coefficient. The calculated results show that the deviation of trajectories designed by these two methods is not much; thus, the method of engineering design is feasible. Author (IAA)

N86-11921# Joint Publications Research Service, Arlington, Va.
ONE-DIMENSIONAL TWO-PHASE FLOW IN COMBUSTION CHAMBER OF SOLID PROPELLANT ROCKET MOTORS Abstract Only c20
Xianqi Chang *In its* China Rept.: Sci. and Technol. (JPRS-CST-85-014) 2 May 1985 p 73 Transl. into ENGLISH from Yuhang Xuebao (Beijing), no. 1, 31 Jan. 1985 p 11-23 Original language document announced in IAA as A85-42777 (For primary document see N86-11918 02-70)
Avail: NTIS HC A06/MF A01

In this paper, a numerical solution of basic equations for one dimensional two phase nonequilibrium flow in combustion chambers of solid propellant rocket motors is discussed in detail. The effect of particle size on the flow field in a chamber and pressure time curves is analyzed, and some useful conclusions are obtained in comparison with results of one dimensional two phase constant lag flow in a chamber. It is useful for predicting pressure time curves accurately and providing accurate boundary conditions for the calculation of two phase flow through a nozzle. Author (IAA)

N86-11922# Joint Publications Research Service, Arlington, Va.
ELECTRIC OR MAGNETIC DIPOLE IN STRATIFIED UNIAXIALLY INHOMOGENEOUS ANISOTROPIC MEDIA Abstract Only c32
Jiasheng Wang *In its* China Rept.: Sci. and Technol. (JPRS-CST-85-014) 2 May 1985 p 74 Transl. into ENGLISH from Yuhang Xuebao (Beijing), no. 1, 31 Jan. 1985 p 24-34 Original language document announced in IAA as A85-42778 (For primary document see N86-11918 02-70)
Avail: NTIS HC A06/MF A01

A formulation for calculating the electromagnetic field in an arbitrary layer in terms of the primary source excitation in a stratified homogeneous media is outlined. The source can be an electric or magnetic dipole which oriented in arbitrary direction This formulation is generalized for stratified uniaxially inhomogeneous and anisotropic media. This problem is facilitated by decomposing a general wave field into TE and TM modes. The procedure for calculation is discussed and some examples are presented. Author (IAA)

N86-11923# Joint Publications Research Service, Arlington, Va.
PROPAGATION OF ELECTROMAGNETIC WAVES IN INHOMOGENEOUS AND LOSSY REENTRY PLASMA SHEATH LAYER Abstract Only c32
Boyi Wang, Yanhou Xu, and Zhenyu Ji *In its* China Rept.: Sci. and Technol. (JPRS-CST-85-014) 2 May 1985 p 75 Transl. into ENGLISH from Yuhang Xuebao (Beijing), no. 1, 31 Jan. 1985 p 35-46 Original language document announced in IAA as A85-42779 (For primary document see N86-11918 02-70)
Avail: NTIS HC A06/MF A01

This paper presents a theoretical method to analyze the propagation characteristics of the electromagnetic waves through a reentry plasma sheath layer, which is based on the stratified layer model and invariant imbedding principle. The power transmission and reflection coefficients of electromagnetic waves are calculated. The theoretical results are in good agreement with the actual measurements in flight. The advantages of this method are: (1) the physical concepts are clear and direct viewing; (2) formulas are simple; and (3) its applicability is powerful. The computers program in this paper is applicable to any case of the thickness of the sheath layer, the distributions of the electronic density and electronic collision frequency, and the stratified layer media. Author (IAA)

N86-11924# Joint Publications Research Service, Arlington, Va.
PRESSURE-COUPLED RESPONSE FUNCTION OF SOLID PROPELLANTS INCLUDING THOSE WITH NEGATIVE PRESSURE-EXPONENTS Abstract Only c28
Wengan Xu *In its* China Rept.: Sci. and Technol. (JPRS-CST-85-014) 2 May 1985 p 76 Transl. into ENGLISH from Yuhang Xuebao (Beijing), no. 1, 31 Jan. 1985 p 47-58 Original language document announced in IAA as A85-42780 (For primary document see N86-11918 02-70)
Avail: NTIS HC A06/MF A01

A new pressure coupled response function of solid propellants has been theoretically derived using a combustion response model based on the steady state burning of composite solid propellants, including those with negative pressure exponents. In this model, the burning surface of a given propellant is divided into one part consisting of a region of the AF surface covered by molten binder with a corresponding binder surface and another part consisting of a region of the AP surface uncovered by molten binder with the remaining binder surface. The covered part of the surface is analyzed taking the condensed phase reaction and the gasification of covered AP into consideration. The results calculated by the derived pressure coupled response function for 504-5A propellant are in reasonable agreement with experimentally observed behavior. C.D. (IAA)

N86-11925# Joint Publications Research Service, Arlington, Va.
THE ANALYSIS AND CALCULATION FOR THE DYNAMIC CHARACTERISTICS OF THE OMNI-AXIAL MOVABLE FLEXIBLE JOINT NOZZLE Abstract Only c20
Shixue Yang *In its* China Rept.: Sci. and Technol. (JPRS-CST-85-014) 2 May 1985 p 77 Transl. into ENGLISH from Yuhang Xuebao (Beijing), no. 1, 31 Jan. 1985 p 59-77 Original language document announced in IAA as A85-42781 (For primary document see N86-11918 02-70)
Avail: NTIS HC A06/MF A01

In this paper, an analysis and calculation for the dynamic characteristics of the omni axial movable flexible joint nozzle are presented under simulated motor chamber pressure. It mainly consists of the analysis and calculation using measured data, the transient pivot point, and the vector moments. Moreover, the following parametes are calculated: the vector angle, the sweeping speed, the vector azimuth, the length of actuator, the thrust misalignment and the axial/radial displacements of the nozzle under the different pressure. The calculating method is suitable for the firing test with transducers mounted correctly, and it is suitable to measure and calculate the characteristics of the flexible joint in the neutral position. Author (IAA)

N86-11926# Joint Publications Research Service, Arlington, Va.
TRANSITION EFFECTS OF BOUNDARY LAYER ON STATIC AND DYNAMIC STABILITY OF SLENDER CONE Abstract Only c02
Hongtian Lou *In its* China Rept.: Sci. and Technol. (JPRS-CST-85-014 2 May 1985 p 78 Transl. into ENGLISH from Yuhang Xuebao (Beijing), no. 1, 31 Jan. 1985 p 88-98 Original language document announced in IAA as A85-42783 (For primary document see N86-11918 02-70)
Avail: NTIS HC A06/MF A01

This paper presents the experimental technique of transition effects of boundary layer on static and dynamic stability of a slender cone and analyzes its result. The experimental results show that the effects of Re number on static and dynamic stability of slender cone are very important. The variation of Re number induces a change in the position of the natural transition of the boundary layer in the cone face; thus, the induced moment and the induced damping moment of the transition are changed. When the transition exists on the surface of the afterbody of the cone, there is a great increase in dynamic stability and a great decrease in static stability; on the other hand, when the transition occurs forward of the center of gravity, there is some decrease in dynamic stability and some increase in static stability. Author (IAA)

N86-11927# Joint Publications Research Service, Arlington, Va.
RESEARCH ON OPTIC SPATIAL FREQUENCY ANALYSIS OF LINEAR STRUCTURES IN REMOTE SENSING IMAGES Abstract Only c43
Ziqiang Zhu, Zhenpei Chen, Jitao Li, and Guangjie Tang *In its* China Rept.: Sci. and Technol. (JPRS-CST-85-014) 2 May 1985 p 79 Transl. into ENGLISH from Zhongguo Jiguang (Shanghai), v. 12, no. 1, 20 Jan. 1985 p 1-5 (For primary document see N86-11918 02-70)
Avail: NTIS HC A06/MF A01

The fundamental principle and experimental method for spatial frequency analysis of the linear structures in remote sensing images are described. The faint geologic structures in the ERTS image of Yanting County, Sichuan Province, were analyzed by the method, and useful results are obtained. E.A.K.

N86-11928# Joint Publications Research Service, Arlington, Va.
FREQUENCY-SELECTION AND MODE-LOCKING AND Nd:YAG LASER Abstract Only c36
Guichen Tan and Peixia Qiu *In its* China Rept.: Sci. and Technol. (JPRS-CST-85-014) 2 May 1985 p 80 Transl. into ENGLISH from Zhongguo Jiguang (Shanghai), v. 12, no. 1, 20 Jan. 1985 p 11-14 (For primary document see N86-11918 02-70)
Avail: NTIS HC A06/MF A01

Mode-locking of Nd:YAG laser was achieved at four spectral lines (1.052 micron, 1.061 micron, 1.064 micron and 1.073 micron) by inserting prisms as dispersion elements in the cavity. The calculations on prisms are consistent with the experimental results. The stable output wavelength of the laser is obtained. E.A.K.

N86-11929# Joint Publications Research Service, Arlington, Va.
A LARGE AREA X-RAY SOURCE AND ITS PREIONIZATION CHARACTERISTICS FOR XeCl EXCIMER LASER Abstract Only c36
Qihong Lou, Runwen Wang, and Xusan Cheng *In its* China Rept.: Sci. and Technol. (JPRS-CST-85-014) 2 May 1985 p 81 Transl. into ENGLISH from Zhongguo Jiguang (Shanghai), v. 12, no. 1, 20 Jan. 1985 p 19-21 (For primary document see N86-11918 02-70)
Avail: NTIS HC A06/MF A01

A large area cold cathode diode X-ray source and its performances and dosage distribution along with the laser tube and the effects of X-ray intensity on the laser output energy were investigated experimentally. E.A.K.

N86-11930# Joint Publications Research Service, Arlington, Va.
RING CAVITY CO2 LASER FOR BRANCH-SELECTION AND NARROW RESONANCE PRODUCED BY SF6 IN CAVITY Abstract Only c36
Yongkai Huang and Jianmin Rong *In its* China Rept.: Sci. and Technol. (JPRS-CST-85-014) 2 May 1985 p 82 Transl. into ENGLISH from Zhongguo Jiguang (Shanghai), v. 12, no. 1, 20 Jan. 1985 p 25-28 (For primary document see N86-11918 02-70)
Avail: NTIS HC A06/MF A01

A new type of branch-selected ring CO2 laser is described. Laser output at the vibration-rotation lines was obtained at 9.5 micron and 10.6 micron. The narrow resonance behavior of SF6 in the cavity is observed. E.A.K.

N86-11931# Joint Publications Research Service, Arlington, Va.
Pb(1-x)Sn(x)Te AND Pb(1-y)Sn(y)Se LASER CRYSTALS Abstract Only c76
Xiaochun Zhu, Gendi Cao, and Weizai Zhang *In its* China Rept.: Sci. and Technol. (JPRS-CST-85-014) 2 May 1985 p 84 Transl. into ENGLISH from Zhongguo Jiguang (Shanghai), v. 12, no. 1, 20 Jan. 1985 p 48-50 (For primary document see N86-11918 02-70)
Avail: NTIS HC A06/MF A01

The Pb1- Sub xSn sub xTe and Pb1 - sub ySn sub ySe crystals with the suitable carrier concentration, low dislocation densities and a proper depth of P-N junction are reported. The crystals are directly obtained by a horizontal unseeded vapor growth technique at an appropriate controlling condition for crystal growth. They are used in fabricating the CW tunable diode lasers. E.A.K.

N86-11932# Joint Publications Research Service, Arlington, Va.
PROGRESS OF INERTIAL CONFINEMENT FUSION (ICF) RESEARCH Abstract Only c75
Ganchang Wang *In its* China Rept.: Sci. and Technol. (JPRS-CST-85-014) 2 May 1985 p 85 Transl. into ENGLISH from He Kexue Yu Gongcheng (Beijing), v. 4, no. 4, Dec. 1984 p 289-302 (For primary document see N86-11918 02-70)
Avail: NTIS HC A06/MF A01

Progress of inertial confinement fusion (ICF) research is described. Four topics in this field were selected, they are: (1) the cannonball target; (2) high power krypton fluoride (KrF) laser; (3) ion beam diodes; and (4) imploding foil/plasma. E.A.K.

N86-11933# Joint Publications Research Service, Arlington, Va.
STATIONARY PULSE SOLUTIONS FOR A FREE ELECTRON LASER Abstract Only c36
Honglie Fang, Shufen Fu, and G. T. Moore *In its* China Rept.: Sci. and Technol. (JPRS-CST-85-014) 2 May 1985 p 88 Transl. into ENGLISH from Wuli Xuebao (Beijing), v. 33, no. 7, Jul. 1984 p 935-942 (For primary document see N86-11918 02-70)
Avail: NTIS HC A06/MF A01

The stationary pulse solutions for a free electron laser are obtained by using the classical theory. Computation shows that the stationary solutions can only be found under certain conditions. The shapes of the solutions do not depend on the shapes of initial optical pulses as long as these conditions are satisfied. E.A.K.

N86-11934# Joint Publications Research Service, Arlington, Va.
THE RELATIONS BETWEEN VOLTAGE AND MAGNETIC FIELD OF SUPERCONDUCTING WEAKLINK (1) Abstract Only c76
Yuheng Zhang and Jun Wang *In its* China Rept.: Sci. and Technol. (JPRS-CST-85-014) 2 May 1985 p 89 Transl. into ENGLISH from Wuli Xuebao (Beijing), v. 33, no. 7, Jul. 1984 p 952-958 (For primary document see N86-11918 02-70)
Avail: NTIS HC A06/MF A01

The quantum diffraction of the superconducting weaklink and the quantum interference of the de-SQUID were calculated theoretically based on the constant current source RSJ model. The constant amplitude oscillation of the dc voltage component with magnetic field for double junction de-SQUID is described. E.A.K.

N86-11935# Joint Publications Research Service, Arlington, Va.
THE RELATIONS BETWEEN VOLTAGE AND MAGNETIC FIELD OF SUPERCONDUCTING WEAKLINK (2) Abstract Only c76
Yuheng Zhang and Jun Wang *In its* China Rept.: Sci. and Technol. (JPRS-CST-85-014) 2 May 1985 p 90 Transl. into ENGLISH from Wuli Xuebao (Beijing), v. 33, no. 7, Jul. 1984 p 959-966 (For primary document see N86-11918 02-70)
Avail: NTIS HC A06/MF A01

The superconducting weaklink and the influence of the feedback radiation on its I to V curve was studied based on the constant source RSJ model. The analytical solution was obtained and the relationship between the change of the I to V curve and the feedback radiation field intensity from the cavity is given for the case in which the field is very weak. The theoretical results show that the feedback radiation can change the amplitude and shape of V(H), but its period is unchanged. E.A.K.

N86-11936# Joint Publications Research Service, Arlington, Va.
DISCUSSION OF THE SUPERCONDUCTING CRITICAL TEMPERATURE IN A N-S MULTI-FILM STRUCTURE Abstract Only c76
Changde Gong, Dingyu Xing, and Mei Liu *In its* China Rept.: Sci. and Technol. (JPRS-CST-85-014) 2 May 1985 p 91 Transl. into ENGLISH from Wuli Xuebao (Beijing), v. 33, no. 7, Jul. 1984 p 967-974 (For primary document see N86-11918 02-70)
Avail: NTIS HC A06/MF A01

The McMillian tunneling model was generalized and applied to a N-S multifilm structure of which the thickness of each film is smaller than the superconducting coherent length. The order parameters and superconducting critical temperature of the structure are calculated, and the possibilities of enhancing T sub by modifying the electron-phonon coupling and contaminating with different atoms in the interface regions are discussed. E.A.K.

N86-11937# Joint Publications Research Service, Arlington, Va.
THEORY OF THE CRITICAL TEMPERATURE FOR SUPERCONDUCTORS WITH SMALL LAMBDA (1) Abstract Only c76
Hangsheng Wu and Zhengyu Weng *In its* China Rept.: Sci. and Technol. (JPRS-CST-85-014) 2 May 1985 p 92 Transl. into ENGLISH from Wuli Xuebao (Beijing), v. 33, no. 7, Jul. 1984 p 975-988 (For primary document see N86-11918 02-70)
Avail: NTIS HC A06/MF A01

A formula for the critical temperature of superconductors with small lambda is derived from the Eliashberg equation. The effective phonon spectrum is taken as the Einstein spectrum. The values of T sub c calculated from the formula are compared with the numerical solutions of the Eliashberg equation in the case of mu* = 0 and the agreement between them is fairly well within the region of lambda < lambda. E.A.K.

N86-11938# Joint Publications Research Service, Arlington, Va.
EFFECT OF HIGH ELECTRIC FIELD ON MINORITY CARRIER GENERATION IN SILICON DEPLETION LAYER Abstract Only c76
Zhijian Li, Lilin Tian, and Xinrong Ma *In its* China Rept.: Sci. and Technol. (JPRS-CST-85-014) 2 May 1985 p 94 Transl. into ENGLISH from Bandaoti Xuebao (Beijing), v. 6, no. 1, Jan. 1985 p 1-10 (For primary document see N86-11918 02-70)
Avail: NTIS HC A06/MF A01

The effect of high electric field on minority carrier generation was investigated by using MOS C(t) characteristics. A model based on Ieda's theoretical relationship between electron emissivity and field intensity is proposed for simulating the experimental results. This model is successful not only for the experiments of the present work, but also for the reasonable explanation of all experimental nonlinear Zerbst curves. It is concluded that the enhancement of minority carrier generation by electric field should exist in samples of perfect crystal structure and in samples containing high concentration of structural defects. Accompanying the kink of C(V) characteristics of deep depleted MOS structure, a jump in effective surface generation velocity is observed. This phenomenon is related to the electron injection from the valence band of the high impurity concentration region under the gate into the depletion region by tunneling. E.A.K.

N86-11939# Joint Publications Research Service, Arlington, Va.
DEEP-LEVEL DEFECTS IN ION-IMPLANTED AND CO2 LASER-ANNEALED SILICON Abstract Only c76
Ximao Bao, Xinyu Zhang, and Chengen Liu *In its* China Rept.: Sci. and Technol. (JPRS-CST-85-014) 2 May 1985 p 95 Transl. into ENGLISH from Bandaoti Xuebao (Beijing), v. 6, no. 1, Jan. 1985 p 11-18 (For primary document see N86-11918 02-70)
Avail: NTIS HC A06/MF A01

Seven deep-level traps were found in As-implanted silicon. The CW CO2 laser annealing is an effective method for removing deep-level defects induced by ion-implantation. The available laser power density range is 350 W/sq cm 600 W/sq cm, which is in keeping with that of activation of implanted impurity. A clear slip dislocation was induced by CO2 laser scanning with a power density higher than 600 W/sq cm. The deep level H(0.33 eV) of slip dislocation is measured by DLTS technique. E.A.K.

N86-11940# Joint Publications Research Service, Arlington, Va.
BINDING ENERGY OF DONORS IN GaAs-Ga(1-x) Al(x)As QUANTUM WELL STRUCTURES Abstract Only c76
Zhenping Liu and Tianke Li *In its* China Rept.: Sci. and Technol. (JPRS-CST-85-014) 2 May 1985 p 97 Transl. into ENGLISH from Bandaoti Xuebao (Beijing), v. 6, no. 1, Jan. 1985 p 32-40 (For primary document see N86-11918 02-70)
Avail: NTIS HC A06/MF A01

Binding energies of the ground state are calculated using a variational approach for shallow donors in quantum well structures consisting of a single slab of GaAs sandwiched between two semi-infinite slabs of Ga sub xAl sub As. The binding energy of donors is calculated as a function of GaAs layer thickness and of the impurity position. Two alloy compositions, $X = 0.1$ and 0.4, are studied and calculated when finite potential barriers determined by realistic conduction band are offset. The results of the present calculations are compared with previous calculations. It is found that the impurity atom is located at the center of the quantum well with composition $x = 0.4$. When the well thickness $L < 50$ A, the modification is considerable. The influence of the different effective masses of GaAs and Ga1- sub xAl sub xAs on the ground state binding energy is investigated. E.A.K.

N86-11941# Joint Publications Research Service, Arlington, Va.
AN INTERFACIAL ANALYSIS OF MoNb-GaAs SCHOTTKY BARRIER DIODES Abstract Only c76
Mingren Yu, Furong Zhu, Xun Wang, Binqi Wang, and Kai Shao *In its* China Rept.: Sci. and Technol. (JPRS-CST-85-014) 2 May 1985 p 100 Transl. into ENGLISH from Bandaoti Xuebao (Beijing), v. 6, no. 1, Jan. 1985 p 55-60 (For primary document see N86-11918 02-70)
Avail: NTIS HC A06/MF A01

The GaAs-Nb-Mo-Au Schottky barrier diodes were fabricated on epitaxial GaAs layers by electron beam evaporation of Nb and then D.C. plasma sputtering of Mo and Au. The compositional depth profiles and the interfacial characteristics of these diodes are measured by XPS associated with Ar ion etching. The results are obtained: the interdiffusion between Au and GaAs can be prevented if the thickness of the sputtered Mo layer is larger than 1000 A. The pure Nb layer no longer exists as a result of the Mo interdiffusion. This leads to a structural change of the original GaAs-Mo-Au into a GaAs-(Nb, Mo, Ga, As)-Mo-(Mo, Au multilayer. In the transition region of the interface, Mo exists in the metal form, and the Nb atoms form a low valence oxide after chemical reaction with the native oxide on the GaAs surface. The thermal stability of MoNb-GaAs Schottky barrier is better than that of the Mo-GaAs structure is because it is related to the larger heat of formation of the Nb oxides. E.A.K.

N86-11942# Joint Publications Research Service, Arlington, Va.
THERMAL POST-TREATMENT CHARACTERISTICS OF METASTABLE CARRIER CONCENTRATION IN As-IMPLANTED SILICON AFTER TRANSIENT ANNEALING Abstract Only c76
Li Xu, Peixin Qian, Dongyan Hou, Yusheng Wang, Jianhua Yan, and Shengnan Zheng *In its* China Rept.: Sci. and Technol. (JPRS-CST-85-014) 2 May 1985 p 102 Transl. into ENGLISH from Bandaoti Xuebao (Beijing), v. 6, no. 1, Jan. 1985 p 76-81 (For primary document see N86-11918 02-70)
Avail: NTIS HC A06/MF A01

Metastable carrier concentration which exceeds the value of equilibrium solid solubility of arsenic in silicon was obtained in high-dose arsenic-implanted silicon samples by transient annealing with infrared irradiation. The samples were subjected to thermal post-treatments at different temperatures ranging from 20 to 800 C, and it was observed that above 390 C the activated impurity concentrations decrease with the increase of post-treatment time. The samples were investigated by Hall effect measurement, layer-removal technique by anodic oxidation and etching, TEM, RBS and channeling effect technique. The experimental results are shown and the possible mechanism of deactivation of activated arsenic atom is discussed. E.A.K.

N86-11943# Joint Publications Research Service, Arlington, Va.
DEEP LEVELS IN SEMI-INSULATING GaAs Abstract Only c76
Binglin Zhou and Zhengxiu Chen *In its* China Rept.: Sci. and Technol. (JPRS-CST-85-014) 2 May 1985 p 103 Transl. into ENGLISH from Bandaoti Xuebao (Beijing), v. 6, no. 1, Jan. 1985 p 100-103 (For primary document see N86-11918 02-70)
Avail: NTIS HC A06/MF A01

Hall measurements were performed at a temperature range from 180 to 500 K on undoped SI-GaAs crystals. Two kinds of samples were obtained (1) the high-resistivity samples with activation energy of 0.71 to 0.64 eV determined by 0.43 eV; and (2) 0.37 eV determined by EL5 and EL6 levels. The identification of deep levels in middle-resistivity samples is different from that reported before, and the analysis is proven by the heat-treatment experiments. E.A.K.

N86-11944# Brookhaven National Lab., Upton, N. Y.
DESIGN FOR A HIGH FIELD COMBINED FUNCTION SUPERFERRIC MAGNET
R. C. Gupta and G. H. Morgan 1985 2 p refs Presented at the Particle Accelerator Conf., Vancouver, British Columbia, 13 May 1985
(Contract DE-AC02-76CH-00016)
(DE85-014827; BNL-36626; CONF-850504-215) Avail: NTIS HC A02/MF A01

A combined function superferric magnet option was investigated for the Relativistic Heavy Ion Collider (RHIC). The option requires the maximum value of the field in the magnet to be much higher than that achieved in any existing combined function accelerator magnet. A model is presented in which a good field quality can be maintained up to 2T. It is done by carefully designing the yoke structure and positioning the coils in such a way that the iron poles tend to saturate evenly across the gap. A cold iron model might be necessary for this magnet. DOE

N86-11945# Joint Publications Research Service, Arlington, Va.
USSR REPORT: PHYSICS AND MATHEMATICS Abstracts Only
20 Aug. 1985 163 p refs Transl. into ENGLISH from various Russian articles
(JPRS-UPM-85-005) Avail: NTIS HC A08/MF A01

Progress in physics and mathematics is highlighted in this U.S.S.R. report. Topics discussed include: (1) Acoustics; (2) crystals and semiconductors; (3) fluid dynamics; (4) gas dynamics; (5) high-temperature physics; (6) lasers; (7) nuclear physics; (8) optics and spectroscopy; (9) theoretical physics; (10) thermodynamics; (11) logic and game theory; (12) numerical analysis and algorithms; (13) probability and statistics; (14) control theory; (15) differential equations; and (16) group theory and combinatorics. For individual titles, see N86-11946 through N86-11989.

N86-11946# Joint Publications Research Service, Arlington, Va.
DIFFRACTION OF ULTRASONIC BEAM PASSING NORMALLY

THROUGH LAYERED MEDIA Abstract Only c71
V. S. Konenenko *In its* USSR Rept.: Phys. and Math. (JPRS-UPM-85-005) 20 Aug. 1985 p 1 refs Transl. into ENGLISH from Fiz. (Tomsk), v. 28, no. 1, Jan. 1985 p 118-119 (For primary document see N86-11945 02-70)
Avail: NTIS HC A08/MF A01

The increase in the velocity and absorption of ultrasound passing through media with different acoustic parameters normal to the interface of the media is assessed analytically. Expressions are derived for the boundary conditions for finding the velocity potentials in the media. The diffraction error occurring in measurements of ultrasound absorption in liquids which use delay lines is analyzed as an example. The analysis shows that diffraction errors can be small in spite of substantial diffraction divergence of the ultrasonic beam in delay lines. Author

N86-11947# Joint Publications Research Service, Arlington, Va.
SPEED OF SOUND IN LIQUID SODIUM NEAR GAMMA-TRANSITION POINT Abstract Only c71
D. L. Timrot, M. A. Serednitskaya, and T. D. Chkhikvadze *In its* USSR Rept.: Phys. and Math. (JPRS-UPM-85-005) 20 Aug. 1985 p 1-2 refs Transl. into ENGLISH from Dokl. Akad. Nauk SSSR (Moscow), v. 279, no. 3, Nov. 1984 p 617-621 (For primary document see N86-11945 02-70)
Avail: NTIS HC A08/MF A01

This study investigates the speed of sound, which is an accurately measurable characteristic of the behavior of liquid sulfur that changes abruptly at about 432 K, which is called a gamma-transition point. The speed of sound is measured at temperatures of 361 to 493 K, which surrounds the special point and includes a region not investigated previously. The measurements were made by fixed-distance echo pulsation. The precision of the experiment made it possible to establish a singular point in the behavior of the parameter in question as a function of temperature. This point, at which the temperature coefficient of the speed of sound changes abruptly, is approximately 432 K. Analysis of the temperature dependency of he adiabatic and isothermic compressibility also made it possible to identify a singular point in the behavior of adiabatic compressibility at the gamma-transition temperature. Author

N86-11948# Joint Publications Research Service, Arlington, Va.
RAMAN SCATTERING OF SOUND ON RANDOM OSCILLATIONS OF BUBBLES Abstract Only c71
Ye. A. Zabolotskaya *In its* USSR Rept.: Phys. and Math. (JPRS-UPM-85-005) 20 Aug. 1985 p 2 ref Transl. into ENGLISH from Kratk. Soobshch. po Fiz. (Moscow), no. 10, 1984 p 23-25 (For primary document see N86-11945 02-70)
Avail: NTIS HC A08/MF A01

This study investigates the Raman combination frequencies that occur when acoustic waves propagating in a medium containing distributed gas bubbles are scattered on the latter because of nonlinearity of the motion equation of the bubble. The spectral density of the combination-frequency scattered wave is estimated by sequential approximation. It is found that the determining role in Raman scattering of sound on bubbles is played by random forces, random noise and vibrations, the leading edge of the acoustic perturbation and non-steady-state movement when the bubbles are formed, etc. The frequency and spectral density of the oscillations of the volume of bubbles can be found from the Raman scattering spectrum. Author

N86-11949# Joint Publications Research Service, Arlington, Va.
DETERMINATION OF PARAMETERS OF ELASTIC SPHERICAL SHELL FROM SCATTERED WAVE FIELD Abstract Only c71
A. V. Sergeyev *In its* USSR Rept.: Phys. and Math. (JPRS-UPM-85-005) 20 Aug. 1985 p 2-3 refs Transl. into ENGLISH from Akust. Zh. (Moscow), v. 31, no. 1, Jan.-Feb. 1985 p 96-102 (For primary document see N86-11945 02-70)
Avail: NTIS HC A08/MF A01

This study investigates the possibility of constructing a structurally simple algorithm for determining the parameters of an elastic spherical shell in a liquid that uses the space-frequency processing of the field scattered by the shell. The characteristics of the surrounding medium are assumed to be known. A plane harmonic wave is incident on the shell; the space-frequency distribution of the field scattered by the shell is measured. The proposed algorithm is modeled on an ES1022 computer for a water-filled aluminum shell with h/R = 0.02. Investigations indicate that registering the field on a spherical surface concentric with the spherical shell is most effective in terms of measurement error. Author

N86-11950# Joint Publications Research Service, Arlington, Va.
STABILITY OF A METHOD FOR ANALYZING RADIATION PATTERN OF ACOUSTIC RADIATOR WITH NEAR-FIELD PRESSURE MEASUREMENT ERRORS Abstract Only c71
I. Ye. Tsukernikov *In its* USSR Rept.: Phys. and Math. (JPRS-UPM-85-005) 20 Aug. 1985 p 3 refs Transl. into ENGLISH from Akust. Zh. (Moscow), v. 31, no. 1, Jan.-Feb. 1985 p 111-113 (For primary document see N86-11945 02-70)
Avail: NTIS HC A08/MF A01

Two constraints are derived that facilitate the uniform convergence of the approximate solution of the integral equation for the distribution of the normal component of the oscillatory rate to its exact value. Both constraints are derived as the result of linearizing hydrodynamic equations, and therefore can be viewed as a stability criterion for the solution of the equation of the first kind in linear acoustics. It is shown by solving test problems that the algorithm presented in a previous study by the author for solving the integral equation satisfies both constraints automatically. The findings are illustrated by calculating the radiation pattern of an antenna consisting of five phased point acoustic sources spaced with a period of gamma/4 on the axis of rotation of the measurement cylinder surrounding the antenna. Author

N86-11951# Joint Publications Research Service, Arlington, Va.
REFLECTION OF SOUND FROM PLATE CONTAINING PERIODIC INHOMOGENEITIES Abstract Only c71
A. D. Lapin *In its* USSR Rept.: Phys. and Math. (JPRS-UPM-85-005) 20 Aug. 1985 p 5-6 refs Transl. into ENGLISH from Akust. Zh. (Moscow), v. 31, no. 1, Jan-Feb. 1985 p 73-76 Previously announced in IAA as A85-41647 (For primary document see N86-11945 02-70)
Avail: NTIS HC A08/MF A01

The scattering of sound by a thin plane elastic plate with small periodic inhomogeneities is investigated analytically, extending the theory developed by Lapin (1984) for a wall with elastic-reactance acoustic impedance. An equation describing the vibration of the plate is derived, and the problem of the conversion of bulk waves to surface waves is solved by combining the free and forced solutions for an infinite periodic structure. Allowance is made for the three-mode interactions, and the inclusion of higher-level interactions is shown to have no significant effect on the results. T.K. (IAA)

N86-11952# Joint Publications Research Service, Arlington, Va.
CONVERSION OF ELECTROMAGNETIC WAVE ENERGY TO ELECTRICAL CURRENT BY BULK SUPERLATTICE SEMICONDUCTORS Abstract Only c76
M. M. Kechiyev, A. A. Kostenko, V. D. Kurek, O. A. Kuznetsov, V. A. Tolomasov, O. N. Filatov, G. I. Khlopov, and V. P. Shestopalov *In its* USSR Rept.: Phys. and Math. (JPRS-UPM-85-005) 20 Aug. 1985 p 7 refs Transl. into ENGLISH from Dokl. Akad. Nauk SSSR (Moscow), v. 279, no. 3, Nov. 1984 p 606-608 (For primary document see N86-11945 02-70)
Avail: NTIS HC A08/MF A01

This study describes the experimentally observed phenomenon of conversion of millimeter-band electromagnetic wave energy to direct current by bulk superlattice semiconductors. The specimens investigated consisted of multilayer heteroepitaxial structures consisting of three hundred layers of pure germanium and a solid solution of germanium and silicon, alternating with a period of 175 A. The voltage-power sensitivity of the specimen is analyzed as a function of the electrical dc bias and the microwave power level, and the equivalent noise power is found as a function of the electrical dc bias. Analogous experiments were made for comparison using commercially produced type D404 microwave diodes, confirming a fundamental difference between the semiconductors in question and semiconductor devices with gate-type response. Author

N86-11953# Joint Publications Research Service, Arlington, Va.
CAUSE OF OCCURRENCE OF HIGH-ENERGY IONS DURING UV LASER IRRADIATION OF MOLECULAR CRYSTALS Abstract Only c76
S. Ye Yegorov and A. N. Shibanov *In its* USSR Rept.: Phys. and Math. (JPRS-UPM-85-005) 20 Aug. 1985 p 7-8 refs Transl. into ENGLISH from Zh. Teckh. Fiz. (Leningrad), v. 54, no. 11, Nov. 1984 p 2270-2274 (For primary document see N86-11945 02-70)
Avail: NTIS HC A08/MF A01

High-energy ions (up to several keV) form during pulse laser irradiation of the surface of solids at intensities of 10 to the 4th power to 10 to the 6th power UV sq cm. It is shown that high ion kinetic energy is associated with the occurrence of a potential on the surface of the specimen due to the external photoelectric effect. The investigations were performed on a transit-time mass spectrometer coupled with a storage oscilloscope with 50 MHz range. The behavior of anthracene and adenine ions is compared. It is found that ions formed near the surface of the crystal in the center of the irradiated area acquire significantly more additional energy than ions formed away from the center of the irradiated area. The conclusion reached elsewhere that ions where high kinetic energies cannot be formed in the gaseous phase is refuted. Author

N86-11954# Joint Publications Research Service, Arlington, Va.
HYDRODYNAMICS OF LIQUID-VAPOR DISPERSE ANNULAR FLOWS IN CHANNELS CONTAINIG BUNDLES OF HEATED RODS UNDER NONSTEADY-STATE CONDITIONS Abstract Only c34
A. Ye. Kroshilin, V. Ye. Kroshilin, and B. I. Nigmatulin *In its* USSR Rept.: Phys. and Math. (JPRS-UPM-85-005) 20 Aug. 1985 p 10 refs Transl. into ENGLISH from Teplofiz. Vys. Temp. (Moscow), v. 22, no. 5, Sep. - Oct. 1984 p 933-940 (For primary document see N86-11945 02-70)
Avail: NTIS HC A08/MF A01

A one-dimensional nonsteady-state hydrodynamic model is developed for liquid-vapor disperse annular flows in channels containing bundles of heated rods, (e.g., water-cooled nuclear fuel rods). The cross-section of the channel is divided into cells; continuity equations are derived for the gas-phase, liquid-film and droplet components of the mixture. A system of linear algebraic equations is derived for the unknown crossover flows and the pressure gradient along the channel. The model is used to predict the time between the drying up of the fluid layer near a heated rod and the onset of a heat release emergency, and the results agree satisfactorily with experimental findings. Author

N86-11955# Joint Publications Research Service, Arlington, Va.
TOWARD A THEORY OF ATOMIC GAS BREAKDOWN BY LASER RADIATION NEAR A METAL SURFACE Abstract Only c36
V. S. Vorobev and A. L. Khomkin *In its* USSR Rept.: Phys. and Math. (JPRS-UPM-85-005) 20 Aug. 1985 p 13 refs Transl. into ENGLISH from Fiz. Plazmy (Moscow), v. 10, no. 5, Sep. - Oct. 1984 p 1025-1032 (For primary document see N86-11945 02-70)
Avail: NTIS HC A08/MF A01

The threshold intensity of laser radiation causing the breakdown of atomic gases near a metal surface is investigated as a function of the kind of metal and gas, pressure and radius of focusing spot. The initial stage of breakdown is viewed as a clearly defined transition from the state of a gas with a very low degree of vapor ionization to a state with considerable ionization. This transition is determined by the relationship between the generation of electrons in ionization events and diffusion losses. The average electron energy and diffusion loss radius are found through two-dimensional balance equations written for a cylindrical geometry at a given surface temperature with allowance for the process of ionization and recombination, ambipolar diffusion, heat conductivity, elastic and nonelastic electron energy loss, and absorption of laser radiation energy. The laser radiation intensity is found for which ionization and recombination processes predominate over diffusion losses near the surface. The intensities thus derived are compared with experimental data for different gases and metals. Author

N86-11956# Joint Publications Research Service, Arlington, Va.
INITIAL PLASMA FORMATION DURING EXPOSURE OF ABSORBING MATERIALS TO LASER RADIATION WITH PLANE EXPANSION GEOMETRY OF THE FORMING PLASMA Abstract Only c75
L. Ya. Minko, Yu. A. Chivel, and A. N. Chumakov *In its* USSR Rept.: Phys. and Math. (JPRS-UPM-85-005) 20 Aug. 1985 p 14-15 Transl. into ENGLISH from Zh. Prikl. Spektrosk. (Minsk), v. 42, no. 1, Jan. 1985 p 55-61 (For primary document see N86-11945 02-70)
Avail: NTIS HC A08/MF A01

This study describes experimental investigations of unsteady processes of initial plasma formation, and analyzers the role of erosion and air plasma in the formation of the screening plasma plane. Complex experiments employing high speed shadow, photographic and spectrographic methods, as well as photoelectric recording of the incident and reflected laser radiation, were conducted. A Q-modulated neodymium glass laser producing from 10 to 700 MW/cm at gamma = 1.06 micrometers (tau approx. 0.0000015) sub s was the source of moderate-intensity laser radiation directed at the absorptive targets. The plasma formation times were determined to within approximately 20 ns for aluminum, zinc, bismuth and ebonite. An erosion mechanism is found to decribe initial plasma formation; the screening of the target that may develop under certain additional conditions does not occur. The initial formation of an erosion laser plasma is found to be accompanied by the occurrence of turbulence that includes the entire plasma formation in many cases, including the moving shock wave front. Author

N86-11957# Joint Publications Research Service, Arlington, Va.
LASER EVAPORATION OF METAL IN GASEOUS ATMOSPHERE Abstract Only c36
V. I. Igoshin and V. I. Kurochkin *In its* USSR Rept.: Phys. and Math. (JPRS-UPM-85-005) 20 Aug. 1985 p 15 refs Transl. into ENGLISH from Kvantovaya Elektron. (Moscow), v. 11, no. 8, Aug. 1984 p 1555-1561 Previously announced in IAA as A85-19247 (For primary document see N86-11945 02-70)
Avail: NTIS HC A08/MF A01

A gasdynamic theory is presented of the evaporation of metals by laser radiation in a wide range of external pressures for power densities of 1 to 100 MW/sq cm. The boundary between the supersonic gasdynamic and the diffusive evaporation regimes is established. The results of numerical calculations of the evaporation of aluminum and iron are presented. Author (IAA)

N86-11958# Joint Publications Research Service, Arlington, Va.
INFLUENCE OF SOLID STATE OBSTACLES ON RADIATION OF RECOMBINATION LASER PLASMA Abstract Only c75
V. A. Boyko, B. A. Bryunetkin, F. V. Bunkin, V. I. Derzhiyev, V. M. Dyakin, S. A. Mayorov, I. Yu. Skobelev, A. Ya. Fayenov, A. I. Fedosimov, and K. A. Shilov *In its* USSR Rept.: Phys. and Math. (JPRS-UPM-85-005) 20 Aug. 1985 p 16-17 refs Transl. into ENGLISH from Fiz. Plazmy (Moscow), v. 10, no. 5, Sep. - Oct. 1984 p 999-1009 (For primary document see N86-11945 02-70)
Avail: NTIS HC A08/MF A01

The influence of solid-state obstacles on the separation dynamics of laser plasma is investigated. It is found observationally, analytically and through modeling that obstacles influence the nature of plasma flow by changing such hydrodynamic parameters as the electron density and temperature. A substantial role is played by phenomena associated with shockwaves; it is suggested that an increase in recombination plasma glow behind the shockwave front is observed. Two groups of experiments are described: one with high intensity achieved by focusing thie laser pulse sharply within a spot 0.1 to 0.4 mm in diameter; and a second with comparatively low intensity, of less than 5 x 10 to the 10th power w/sq cm, obtained by focusing the pulse in a line 2 cm long and 200 m wide. It is found that obstacles increase the glow intensity of ion lines at those distances at which recombination level jumping is realized. The changes in glow intensity occurring during interaction with a cylindrical obstacle can be used to diagnose the electron density by the width of the trough in the glow ahead of the shockwave front. Author

N86-11959# Joint Publications Research Service, Arlington, Va.
SURFACE COMBUSTION OF LIQUID FUEL IN STREAM OF GASEOUS OXIDIZER Abstract Only. c25
N. I. Zverev and V. N. Smirnov *In its* USSR Rept.: Phys. and Math. (JPRS-UPM-85-005) 20 Aug. 1985 p 22 refs Transl. into ENGLISH from Fiz. Goreniya i Vzryva (Novosibirsk, USSR), v. 20, no. 6, Nov. - Dec. 1984 p 33-38 Original language doc. was announced as A85-25571 (For primary document see N86-11945 02-70)
Avail: NTIS HC A08/MF A01

The problem of the combustion of a plane surface of liquid fuel in a flow with distributed parameters is analyzed for the case where the fuel vapors over the fuel surface react in the kinetic model. The problem is solved in the content of boundary layer theory, with allowance made for the motion induced in the fuel layer and changes in the thermophysical properties of the gas associated with changes in its composition. V.L. (IAA)

N86-11960# Joint Publications Research Service, Arlington, Va.
EXPLOSION WAVES GENERATED BY DEFLAGRATION COMBUSTION Abstract Only c25
V. A. Gorev and S. A. Bystrov *In its* USSR Rept.: Phys. and Math. (JPRS-UPM-85-005) 20 Aug. 1985 P. 22 refs Transl. into ENGLISH from Fiz. Goreniya i Vzryva (Novosibirsk, USSR), v. 20, no. 6, Nov. - Dec. 1984 p 26-33 (For primary document see N86-11945 02-70)
Avail: NTIS HC A08/MF A01

This study presents an analytical solution of the problem of the flow of gas ahead of a spherical combustion front propagating at a constant velocity with the combustion products assumed stationary. The problem is also solved for a cylindrical flame bounded above and below by rigid planes. Equations are derived for the flame- and piston-associated movement of gas expanding at a constant rate. The method is advantageous in that it makes it possible to calculate the gas flow for a wide range of flame velocities, ranging from minimal, corresponding to laminar combustion, to approximately 500 m/sec. Author

N86-11961# Joint Publications Research Service, Arlington, Va.
EXCITATION OF DISCHARGE IN AIR BY LASER RADIATION Abstract Only c36
V. I. Bukatyy, A. A. Kobolov, and A. A. Telnikhin *In its* USSR Rept.: Phys. and Math. (JPRS-UPM-85-005) 20 Aug. 1985 p 27 refs Transl. into ENGLISH from Zh. Tekhn. Fiz. (Leningrad), v. 55, no. 2, Feb. 1965 p 312-318 (For primary document see N86-11945 02-70)
Avail: NTIS HC A08/MF A01

Experimental findings on the low-threshold breakdown of air by pulse infrared radiation are analyzed. The dynamics of the formation of the discharge and the properties of the low-temperature plasma that is formed are found to depend strongly upon the parameters of the perturbing radiation. The discharge produced in air by a CO2 laser is highly nonequilibrium, while that produced by a neodymium laser is quasiequilibrium. The findings indicate that discharge development in the radiation field of the neodymium laser is thermal in nature. Author

N86-11962# Joint Publications Research Service, Arlington, Va.
INFLUENCE OF PHYSICAL-CHEMICAL PROPERTIES OF GASES ON INTERACTION BETWEEN SHOCKWAVES AND CONVEX CYLINDRICAL SURFACES Abstract Only. c34
L. G. Gvozdeva. Yu. P. Lagutov, and V. P. Fokeyev *In its* USSR Rept.: Phys. and Math. (JPRS-UPM-85-005) 20 Aug. 1985 p 31 refs Transl. into ENGLISH from Inzhenerno-Fiz. Zh. (Minsk), v. 48, no 2, Feb. 1985 p 239-244 (For primary document see N86-11945 02-70)
Avail: NTIS HC A08/MF A01

The interaction of shockwaves with cylindrical surfaces is investigated in a square shock tube with Mach numbers ranging from 1.5 to 6.0 and initial pressures from 10 to 30 mm Hg. Cylindrical segments with radii 123 mm were employed. Shadowgrams and interferomgrams of the interaction regions were registered in argon, nitrogen and carbon dioxide, which were used to model different depths of physical-chemical transformations in the gas behind the shockwave. The influence of physical and chemical processes on shockwave interaction is described. The changes occurring in the flow picture are similar to those observed on plane wedges. Author

N86-11963# Joint Publications Research Service, Arlington, Va.
CALCULATION OF FORMATION TIME OF MINIMAL NUCLEUS OF FLAME DURING IGNITION OF EXPLOSIVE MIXTURES BY ELECTRICAL DISCHARGES Abstract Only. c25
N. I. Lobyzov and N. M. Karmazinov *In its* USSR Rept.: Phys. and Math. (JPRS-UPM-85-005) 20 Aug. 1985 p 33 refs Transl. into ENGLISH from Fiz. Goreniya i Vzryva (Novosibirsk, USSR), v. 20, no. 6, Nov. - Dec. 1984 p 55-58 (For primary document see N86-11945 02-70)
Avail: NTIS HC A08/MF A01

The influence of asymmetry on the formation time of the minimal flame nucleus and the sharpness of the maximum of the curve of the discharge power plotted as a function of time are analyzed from the viewpoint of thermal ignition theory. The electrical discharge is replaced by a point heat source with time-varying power; the surrounding medium during the ignition time is chemically inert. It is found that the formation time of the minimal nucleus depends little upon the rate of energy release in the discharge, and is apparently determined, like the dimension of the minimal nucleus of the flame, by the physical-chemical properties of the explosive mixture. The formation time for hydrogen-air and methane-air explosive mixtures is estimated as an example. The analytical and experimental values are found to agree well qualitatively and quantitatively. Author

N86-11964# Joint Publications Research Service, Arlington, Va.
FLAME PROPAGATION IN PULSED ACCELERATION FIELD Abstract Only. c25
V. P. Samsonov *In its* USSR Rept.: Phys. and Math. (JPRS-UPM-85-005) 20 Aug. 1985 p 33 refs Transl. into ENGLISH from Fiz. Goreniya i Vzryva (Novosibirsk, USSR), v. 20, no. 6, Nov. - Dec. 1984 p 58-61 (For primary document see N86-11945 02-70)
Avail: NTIS HC A08/MF A01

The variation in the velocity and form of a flame initially propagating under weightless conditions in a semi-open tube in a pulsed uniform acceleration field is investigated. Weightlessness is created by dropping a heavy container, within which the reaction tube is held vertically. A camera secured to the container is then used to record the flame. The stability of the flame front is studied. Differences in the change in the flame velocity during upward and downward propagation are explained primarily by different conditions for the development of the flows of cold gas and hot combustion products occurring when the reaction tube is braked, as well as convection currents in the combustion product. Author

N86-11965# Joint Publications Research Service, Arlington, Va.
OCCURRENCE OF PRESSURE WAVE DURING SPONTANEOUS IGNITION OF GAS AHEAD OF FLAME FRONT IN CLOSED VESSEL Abstract Only. c25
V. I. Vodyanik and S. V. Tarakanov *In its* USSR Rept.: Phys. and Math. (JPRS-UPM-85-005) 20 Aug. 1985 p 36 refs Transl. into ENGLISH from Fiz. Goreniya i Vzryva (Novosibirsk, USSR), v. 21, no. 1, Jan. - Feb. 1985 p 49-53 (For primary document

see N86-11945 02-70)
Avail: NTIS HC A08/MF A01

The basic stages of the propagation of a flame in a closed vessel are analyzed chronologically, starting with frontal combustion, followed by spontaneous combustion and pressure wave formation. The analytical results are tested numerically in a problem of spontaneous ignition and pressure wave formation. The conditions under which spontaneous ignition causes shockwave formation are determined. The peak pressures are found to be significantly higher than the maximum reached during frontal combustion of a gas in a vessel. Evaluation criteria are derived for the possibility of spontaneous ignition, as well as formulas for calculating the shockwave pressure. Author

N86-11966# Joint Publications Research Service, Arlington, Va.
STEADY-STATE DETONATION OF CHARGES OF FINITE LENGTH Abstract Only c28
V. K. Ashayev, G. S. Doronin, and V. S. Zhuchenko *In its* USSR Rept.: Phys. and Math. (JPRS-UPM-85-005) 20 Aug. 1985 p 37 refs Transl. into ENGLISH from Fiz. Goreniya i Vzryva (Novosibirsk, USSR), v. 21, no. 1, Jan. - Feb. 1985 p 127-130 (For primary document see N86-11945 02-70)
Avail: NTIS HC A08/MF A01

The applicability of the steady-state model to short explosive charges is demonstrated with the help of precision optical recordings. The error sources in the free surface method are analyzed, and the findings of two previous studies are interpreted within the framework of classical conceptions. The studies employ compressed trotyl and octogen in charges 10 and 50 mm long initiated by a shockwave. Steady-state detonation is found for 10 mm. Methods based on measuring the attenuation of the velocity of the shockwave front in the barrier can be used to investigate detonation processes using short charges. Author

N86-11967# Joint Publications Research Service, Arlington, Va.
LASING ON VAPORS OF CHAIN COMPOUNDS Abstract Only c36
V. V. Gruzinskiy, K. M. Degtyarenko, T. N. Kopylova, and V. T. Pavlova *In its* USSR Rept.: Phys. and Math. (JPRS-UPM-85-005) 20 Aug. 1985 p 44 p 44 refs Transl. into ENGLISH from Izv. Vyssh. Ucheb. Zaved.: Fiz. (Tomsk, USSR), v. 28, no. 1, Jan. 1985 p 101-103 (For primary document see N86-11945 02-70)
Avail: NTIS HC A08/MF A01

The lasting properties of a number of organic molecules in the gas phase and in solution are investigated. Effective lasing is achieved on the vapors of new chain-structured organic compounds; replacing a double carbon-carbon bond with a ternary bond improves the lasing characteristics of the active media in the gas phase significantly. Lasing intensity and threshold jumping power density close to the values in a Toluol solution are achieved for 1,4-diphenyl-ethynilbiphenyl. Author

N86-11968# Joint Publications Research Service, Arlington, Va.
ENERGY CHARACTERISTICS OF LASER WITH SATURABLE ANISOTROPIC ABSORBING MEDIUM IN CAVITY Abstract Only c36
A. P. Voytovich and V. V. Mashko *In its* USSR Rept.: Phys. and Math. (JPRS-UPM-85-005) 20 Aug. 1985 p 44-45 refs Transl. into ENGLISH from Zh. Prikl. Spektros. (Minsk, USSR), v. 41, no. 6, Dec. 1984 p 899-904 (For primary document see N86-11945 02-70)
Avail: NTIS HC A08/MF A01

The single-frequency steady-state lasing mode of a laser in which the cavity contains an absorbing medium in the longitudinal magnetic field and elements that create circular phase and linear amplitude anisotropy is investigated theoretically. The influence of various factors on the size of the losses introduced in the laser cavity by the absorbing medium, and the corresponding changes in the intensity of the radiation generated at the frequency of the absorption line, are investigated. The relative change in the absorption lines when a magnetic field is applied to the absorbing medium is calculated as a function of the lasing intensity in the absence of absorption in the cavity. The analytical data show good agreement with experimental values. The findings can be utilized for intracavity laser spectroscopy. Author

N86-11969# Joint Publications Research Service, Arlington, Va.
INVESTIGATION OF EFFICIENCY OF GENERATION OF DIFFERENCE-FREQUENCY LASER RADIATION IN WAVEGUIDE Abstract Only. c36
A. O. Makaryan, K. M. Movsisyan, and P. S. Pogosyan *In its* USSR Rept.: Phys. and Math. (JPRS-UPM-85-005) 20 Aug. 1985 p 45 Transl. into ENGLISH from Zh. Prikl. Spektros. (Minsk, USSR), v. 41, no. 6, Dec. 1984 p 908-911 (For primary document see N86-11945 02-70)
Avail: NTIS HC A08/MF A01

Millimeter wavelength difference-frequency lasing was obtained by mixing the frequencies produced by two temperature-detuned ruby lasers in a LiNbO3 crystal in a rectangular waveguide. The conversion efficiency is studied as a function of the angle of incidence of the exciting beams on the crystal, as well as the angle between the exciting beams and their spatial overlap, at wavelengths of 4 and 8 mm. The experimental findings are in good agreement with the analytical figures. The results can be used in developing lasers, determining the spatial parameters of lasers, etc. Author

N86-11970# Joint Publications Research Service, Arlington, Va.
SPECTRUM STRUCTURE OF XeCl ELECTRIC DISCHARGE LASER Abstract Only c36
V. S. Burakov, A. F. Bokhonov, and V. A. Titarchuk *In its* USSR Rept.: Phys. and Math. (JPRS-UPM-85-005) 20 Aug. 1985 p 46 Transl. into ENGLISH from Zh. Prikl. Spektros. (Minsk, USSR), v. 41, no. 6, Dec. 1984 p 1029-1032 (For primary document see N86-11945 02-70)
Avail: NTIS HC A08/MF A01

The influence of selective cavity elements, intra-cavity absorption, plasma reaction products in the active medium, and components of the electrode material on the spectrum structure of an XeC1 laser is investigated. The investigations employ high spectral resolution (3 x 10 to the 5th power) with widely varying pressure of the active medium, and cavity construction, incorporating a selectively absorbing cell, making it possible to identify the basic factors determining the formation of the lasing spectrum. The occurrence of an interference structure is observed experimentally, and ways of eliminating it are found. The possibility of controlling the spectrum with the help of dispersing elements and a selectively absorbing cell is demonstrated. Selective losses induced by the OH radical could not be eliminated. Author

N86-11971# Joint Publications Research Service, Arlington, Va.
DISTRIBUTED-FEEDBACK LASERS WITH ACTIVE FRAMING MEDIUM Abstract Only. c36
Yu. N. Ryzhov, I. V. Cheremiskin, and T. K. Chekhlova *In its* USSR Rept.: Phys. and Math. (JPRS-UPM-85-005) 20 Aug. 1985 p 47 refs Transl. into ENGLISH from Zh. Prikl. Spektros. (Minsk, USSR), v. 42, no. 1, Jan. 1985 p 48-51 (For primary document see N86-11945 02-70)
Avail: NTIS HC A08/MF A01

This study describes the use of transverse waveguide pumping in thin-film layers employing an active framing medium. With this approach, active particles are excited only in the thin framing layer of the waveguide, which reduces the superluminescence and lasing (non-waveguide) that occurs within the pumped layer. A laser consisting of a 0.06 micron Ta205 film applied to a glass substrate is described. The method by which the active stripline waveguides were prepared is described. The relationship between the laser gain and the waveguide parameters is investigated theoretically, and the laser parameters corresponding to the smallest threshold pumping power are found. The use of alkali-halide crystals with color centers to obtain CW lasing is discussed. The distributed feedback lasers examined require high pumping power density and give off substantial heat in the CW mode. Author

N86-11972# Joint Publications Research Service, Arlington, Va.
INVESTIGATION OF POLARIZATION CHARACTERISTICS OF RADIATION FROM LASER WITH DYE-ACTIVATED POLYMER ELEMENTS Abstract Only **c36**
V. S. Burakova, N. N. Vasilev, A. Ya. Gorelenko, V. Ye. Sivenkova, and A. P. Shkadarevich *In its* USSR Rept.: Phys. and Math. (JPRS-UPM-85-005) 20 Aug. 1985 p 48 refs Transl. into ENGLISH from Zh. Prikl. Spektros. (Minsk, USSR), v. 42, no. 1, Jan. 1985 p 35-40 (For primary document see N86-11945 02-70)
Avail: NTIS HC A08/MF A01

The polarization characteristics of a laser with active elements made of oxazine-17 activated polymethylmethacrylate are investigated and compared with the analogous parameters of a laser employing solutions of oxazine-17 in different solvents. The influence of the activator on the properties of the polymer elements activated by complex organic compounds is assessed. The lasing efficiency and degree of polarization during transverse and quasi-longitudinal excitation at the second harmonic (532 nm) of a frequency monopulse YAG laser are determined as a function of the aximuth of the polarization, the power of the exciting light, and the parameters of the cavity of the dye laser. The properties of polymer lasers are found to depend more upon the polarization of the exciting light than dye lasers, which is important when polymer is found to be the fundamental factor determining the efficiency in polarization of the laser. Author

N86-11973# Joint Publications Research Service, Arlington, Va.
HIGH-EFFICIENCY AI SUB 2 O SUB 3:TI SUP 3+ TUNABLE LASER Abstract Only **c36**
G. S. Kruglik, G. A. Skripko, A. P. Shkadarevich, N. V. Kondratyuk, E. A. Zhdanov, and A. M. Zabaznov *In its* USSR Rept.: Phys. and Math. (JPRS-UPM-85-005) 20 Aug. 1985 p 48-49 refs Transl. into ENGLISH from Zh. Prikl. Spektros. (Minsk, USSR), v. 42, no. 1, Jan. 1985 p 126-128 Original language doc. was announced at A85-28984 (For primary document see N86-11945 02-70)
Avail: NTIS HC A08/MF A01

A study is made of the lasing characteristics of an A1203:Ti(3+) laser pumped by the second harmonic of a YAG laser. A conversion efficiency of 36 percent (for a differential efficiency of 55 percent) and a tunability range of 680 to 930 nm have been demonstrated. Second harmonic generation in the LiIO3 crystal and passive Q-switching at F3(-) color centers in LiF have been achieved. Author

N86-11974# Joint Publications Research Service, Arlington, Va.
ULTRAVIOLET LASING IN HELIUM-NITROGREN MIXTURES Abstract Only **c36**
E. I. Asinovskiy, L. M. Vasilyak, V. V. Markovets, and Yu. M. Tokunov *In its* USSR Rept.: Phys. and Math. (JPRS-UPM-85-005) 20 Aug. 1985 p 49 refs Transl. into ENGLISH from Zh. Prikl. Spektros. (Minsk, USSR), v. 42, no. 1, Jan. 1985 p 131-134 (For primary document see N86-11945 02-70)
Avail: NTIS HC A08/MF A01

The influence of helium admixtures on ultraviolet lasing (337.1 nm) in a coaxial nitrogen laser is investigated experimentally. The addition of helium expands the region of pressures within which lasing exists, but the lasing intensity drops off. An experimental setup incorporating a glass discharge tube 48.5 cm long and 0.4 cm in diameter is described. Lasing in coaxial lasers is found to be determined basically by the dynamics and parameters of the breakdown waves, regardless of the composition of the gas. The addition of helium makes it possible to increase the overall working pressure of the gas in a nitrogen laser without reducing the peak power of the laser significantly. The laser pulse length is shorter in helium-nitrogen mixtures than in pure nitrogen. The length of the tube must be increased or decreased correspondingly in order to obtain the first or second laser peak for a given pressure. Author

N86-11975# Joint Publications Research Service, Arlington, Va.
ELECTROIONIZATION IR Xe-ATOM LASER Abstract Only **c36**
N. G. Basov, V. A. Danilychev, A. Yu. Dudin, D. A. Zayarnyy, N. N. Ustinovskiy, I. V. Kholin, and A. Yu. Chugunov *In its* USSR Rept.: Phys. and Math. (JPRS-UPM-85-005) 20 Aug. 1985 p 49-50 refs Transl. into ENGLISH from Kvantovaya Elektronika (Moscow), v. 11, no. 9, Sep. 1984 p 1722-1736 Original language doc. was announced as A85-21003 (For primary document see N86-11945 02-70)
Avail: NTIS HC A08/MF A01

A high-power high-pressure electroionization laser operating at the 5d-6p and 7p-7s transition of the Xe atom and having an active volume of 9 liters is investigated. Expressions are obtained which relate the electrical parameters of the electroionization discharge and the energy parameters and spectral composition of the output radiation to the type of the buffer gas, parameters of the discharge circuit, and the component ratio and pressure of the active medium. When the laser is pumped by an electron beam alone, with a current density of 6 A/sq cm and a pulse length of 0.7 microsec, the output energy is about 6 J (efficiency of about 1.5 percent); under electroionization pumping, the output energy is about 20 J. The physical efficiency of generation due to the electric field is about 5 percent. The mechanism of active medium conductivity and the level population kinetics of the lasing transitions are discussed. Author

N86-11976# Joint Publications Research Service, Arlington, Va.
OPTIMIZATION OF PARAMETERS OF CHEMICAL CO LASER BY INCREASING LENGTH OF ACTIVE MEDIUM Abstract Only **c36**
V. A. Dudkin and V. B. Rukhin *In its* USSR Rept.: Phys. and Math. (JPRS-UPM-85-005) 20 Aug. 1985 p 51 refs Transl. into ENGLISH from Kvantovaya Elektronika (Moscow), v. 11, no. 9, Sep. 1984 p 1883-1884 Original language doc. was announced at A85-21013 (For primary document see N86-11945 02-70)
Avail: NTIS HC A08/MF A01

Results of an experimental study of a chemical CO laser using a CS2-N2O-O2 flame with an active medium length of up to 3 m are reported. The importance of matching the dimensions of the active medium with the mode structure of the resonator is emphasized. A chemical efficiency of 15 percent has been achieved under 100-W continuous emission. Author

N86-11977# Joint Publications Research Service, Arlington, Va.
EFFICIENCY OF OPTICALLY-PUMPED XeF-LASER Abstract Only **c36**
V. S. Zuyev, L. D. Mikheyev, and D. B. Stavrovskiy *In its* USSR Rept.: Phys. and Math. (JPRS-UPM-85-005) 20 Aug. 1985 p 55 refs Transl. into ENGLISH from Kvantovaya Elektronika (Moscow), v. 11, no. 9, Sep. 1984 p 1750-1756 (For primary document see N86-11945 02-70)
Avail: NTIS HC A08/MF A01

A discussion is given of the findings from experiments conducted to determine the attainable inner efficiency and technical efficiency values for a photodissociation XeF-laser employing electrical-discharge vacuum UV pumping. The laser investigated employed B-X (353 nm) and C-A (485 nm) transitions in the Xe-F excimer. The possibility of attaining instantaneous efficiency of approximately 1% in discharge-pumped XeF-lasers is confirmed experimentally. The energy efficiency, defined as the ratio of the lasing energy to the energy stored in the condenser battery, can also approach 1%. It is estimated that only about 10R of the energy emitted by the source within the photodissociation band of XeF2 is utilized, considering the temporal behavior of the brightness temperature and the geometric dimensions of the pumping source. The output energy observed is the highest ever recorded for optically pumped XeF lasers. Author

N86-11978# Joint Publications Research Service, Arlington, Va.
ENERGY CHARACTERISTICS OF WAVEGUIDE CO SUB 2-LASER Abstract Only **c36**
Yu. B. Konev, N. I. Lipatov, P. P. Pashinin, and A. M. Prokhorov *In its* USSR Rept.: Phys. and Math. (JPRS-UPM-85-005) 20 Aug. 1985 p 59-60 refs Transl. into ENGLISH from Kvantovaya Elektron. (Moscow), v. 11, no. 8, Aug. 84 p 1641-1645 (For

primary document see N86-11945 02-70)
Avail: NTIS HC A08/MF A01

This study describes the numerical modeling of a waveguide CO2-laser in the linear amplification and lasing modes by the balance equation method for average numbers of individual mode quanta. The composition of the working medium is assumed to be constant, and allowance is made for quantum flow to levels above the minimum of the Triner distribution function of the assymmetrical CO2-molecule mode caused by the high degree of vibrational excitation of the medium. The approach employed takes into account the effect of surface deactivation of CO2 molecules on the inner walls of the waveguide. Calculations are made for discharge-channel diameters of 1.5 and 2.0 mm. Discharge current values are plotted as a function of the lasing output power and the electromagnetic field intensity in the cavity. It is found that surface deactivation of the excited mixture can cause substantial losses of vibrational V3-mode energy of CO2 and N2, particularly when the active medium pressures are comparatively low. Author

N86-11979# Joint Publications Research Service, Arlington, Va.
CHROMIUM- AND NEODYMIUM-ACTIVATED GADOLINIUM-SCANDIUM-GALLIUM GARNET CRYSTAL: A NEW LASER ACTIVE MEDIUM c36
Ye. V. Zarikov, V. V. Yaptev, V. G. Ostroumov, Yu. S. Privos, V. A. Smirnov, and I. A. Shcherbakov *In its* USSR Rept.: Phys. and Math. (JPRS-UPM-85-005) 20 Aug. 1985 p 61 refs Transl. into ENGLISH from Kvantovaya Elektronika (Moscow), v. 11, no. [illegible], Aug. 1984 p. 1565-1574 (For primary document see N86-11945 02-70)
Avail: NTIS HC A08/MF A01

The mechanisms underlying the population of the upper lasing level of neodymium is investigated in order to identify the optimum working conditions for the active medium in various types of lasers. A general method is proposed for calculating the population of the excited state of acceptors interacting with energy donors which allows for non-radiative losses in the acceptor subsystem for the steady-state and pulsed pumping modes for any pumping pulse form. The time evolution of the population of the upper lasing level of 4F(3/2)Nu(3+) in gadolinium-scandium-gallium garnet crystals activated with chromium and neodymium is analyzed, along with the population gain in the 4F(3/2) level of Nd(3+) due to sensitization of Nd(3+) ion luminescence by Cr(3+) ions. The proposed method for calculating the kinetics of the decay of the excied state of acceptors interacting with energy donors is used to find the optimum concentrations of Nd(3+) ions in chromium- and neodymium- activated gadolinium-scandium-gallium garnet crystals for steady-state and impulse modes. Author

N86-11980# Joint Publications Research Service, Arlington, Va.
TWO-FREQUENCY PASSIVE MODE LOCKING IN IODINE PHOTODISSOCIATION LASER Abstract Only c36
V. M. Kiselev, A. S Grenishin, T. N. Kotlikova, and L. I. Rodina *In its* USSR Rept.: Phys. and Math. (JPRS-UPM-85-005) 20 Aug. 1985 p 61-62 p 61-62 refs Transl. into ENGLISH from Kvantovaya Elektron. (Moscow), v. 11, no. 8, Aug. 1984 p 1542-1554 Previously announced in IAA as A85-19246 (For primary document see N86-11945 02-70)
Avail: NTIS HC A08/MF A01

Partially summed Maxwell-Bloch equations are used to estimate the ultimate potentialities of the passive mode-locking regime in an iodine laser under single-frequency and two-frequency lasing conditions. In the case of two-frequency passive mode locking an experimental discovery is made and an explanation is given of the appearance, in the laser emission spectrum, of the combination frequencies nu-sub 22 - Delta-nu and nu-sub 34 + Delta-nu, where Delta-nu is the spectral interval between nu-sub 22 and nu-sub 34. Author

N86-11981# Joint Publications Research Service, Arlington, Va.
EXPERIMENTAL INVESTIGATION OF RECORDING OF DYNAMIC HOLOGRAMS WITHIN ABSORPTION CONTOUR OF RESONANT ATOMIC MEDIUM Abstract Only c35
A. Ye. Korolev and D. I. Staselko *In its* USSR Rept.: Phys. and Math. (JPRS-UPM-85-005) 20 Aug. 1985 p 86 refs Transl. into ENGLISH from Opt. i Spektrosk. (Leningrad), v. 58, no. 1, Jan. 1985 p 147-152 (For primary document see N86-11945 02-70)
Avail: NTIS HC A08/MF A01

The influence of the atomic concentration, the spectral width of the recording radiation and the resonance detuning on the diffraction efficiency of dynamic holograms recorded on the resonance lines of metals were studied. The efficiency of resonant dynamic holograms is investigated as function of the exposure for different vapor concentrations and resonance off-tuning. Good agreement is noted between the experimental and theoretical results. A region is identified in which the required tuning accuracy is determined by the spectral width of the recording radiation, which makes it possible to use a significantly wider group of radiation sources to record resonant dynamic holograms. E.A.K.

N86-11982# Joint Publications Research Service, Arlington, Va.
DIFFRACTION EFFICIENCY OF THREE-DIMENSIONAL PHASE HOLOGRAM OF DIFFUSE OBJECT Abstract Only c35
Yu. L. Korzinin and V. L. Sukhanov *In its* USSR Rept.: Phys. and Math. (JPRS-UPM-85-005) 20 Aug. 1985 p 87 refs Transl. into ENGLISH from Opt. i. Spektrosk. (Leningrad), v. 58, no. 1, Jan. 1985 p 142-146 (For primary document see N86-11945 02-70)
Avail: NTIS HC A08/MF A01

The diffraction efficiency of the hologram of a diffuse object is analyzed within the framework of a space-frequency approach in which the diffraction efficiency is expressed through the spectrum of the wave recovered by the hologram. The diffraction efficiencies and the expsoures needed to achieve them are shown to be a function of the relationship between the intensities of the interfering beams, and the geometry of the hologram recording scheme. It is recommended that oblique incidence of the reference wave be employed in recording the hologram of the object. The angle of incidence of the object wave should consider that the hologram efficiency decreases as the angle becomes smaller, but that the exposure level needed to obtain maximum efficiency becomes somewhat longer. E.A.K.

N86-11983# Joint Publications Research Service, Arlington, Va.
POSSIBILITY OF OPTIMAL CHOICE OF EXPOSURE TIME FOR HOLOGRAPHIC RECORDING OF OBJECTS THROUGH UNSTEADY SCATTERING MEDIA Abstract Only c35
O. V. Angelskiy, V. V. Yatsenko, and D. I. Derkach *In its* USSR Rept.: Phys. and Math. (JPRS-UPM-85-005) 20 Aug. 1985 p 89 refs Transl. into ENGLISH from Zh. Prikl. Spektrosk. (Minsk, USSR), v. 42, no. 1, Jan. 1985 p 118-122 Original language doc. was announced as A85-28983 (For primary document see N86-11945 02-70)
Avail: NTIS HC A08/MF A01

A study of the possibility of the holographic measurement of the velocity distributions of Brownian movement in scattering media has yielded an algorithm for optimum exposure selection during holographic recording through unsteady scattering media. It is shown that by varying the hologram exposure. It is possible to obtain information on subensembles of Brownian particles of various mobilities, i.e., on the velocity distribution of the particles. The algorithm proposed here is verified experimentally. V.L. (IAA)

N86-11984# Joint Publications Research Service, Arlington, Va.
GENERAL-PURPOSE EQUIPMENT FOR AIRBORNE LASER REMOTE SENSING OF OCEAN, ATMOSPHERE AND AGRICULTURAL CROPS Abstract Only c43
A. F. Bunkin, D. V. Vlasov, A. S. Glaumyan, D. V. Maltsev, D. M. Mirkamilov, and V. P. Slobodyanin *In its* USSR Rept.: Phys. and Math. (JPRS-UPM-85-005) 20 Aug. 1985 p 94 refs Transl. into ENGLISH from Zh. Tekhn. Fiz. (Leningrad), v. 54, no. 11, Nov. 1984 p 2190-2195 (For primary document see N86-11945 02-70)
Avail: NTIS HC A08/MF A01

A general-purpose airborne laser remote sensing system is described for ocean and land research from altitudes of 800 to

1200 meters to obtain information on the thermodynamic parameters of the ocean, currents, ocean depth, and the condition and yield of agricultural crops. The system, which is carried aboard an AN-30 aircraft, employs fluorescent spectroscopy to determine small concentrations of organic impurities in sea water. The airborne system is described in detail; the results of measurements of bodies of water and land areas are discussed. The development of this system opens up fundamentally new capabilities for laser spectroscopy in environmental pollution montioring, and to map currents and turbulence in the ocean, and to diagnose crop yields. E.A.K.

N86-11985# Joint Publications Research Service, Arlington, Va.
PHOTOINDUCED RAYLEIGH SCATTERING OF LIGHT IN CRYSTALS Abstract Only c74
V. V. Obukhovskiy and A. V. Stoyanov *In its* USSR Rept.: Phys. and Math. (JPRS-UPM-85-005) 20 Aug. 1985 p 97 p 97 Transl. into ENGLISH from Opt. i Spektrosk. (Leningrad), v. 58, no. 2, Feb. 85 p 3780-385 (For primary document see N86-11945 02-70)
Avail: NTIS HC A08/MF A01

The intensity of light scattered by inhomogeneities of the dielectric constant of ferroelectric crystals was calculated. It was shown that the scattering intensity is a sum of two terms: one due to scattering by inhomogeneities present initially and the other due to scattering by inhomogeneities which are induced by the exciting radiation. It was shown that the scattering process is nonstationary. Both components of the scattering intensity increase with time, but the second component of the scattering is absent initially and approaches a finite value at infinite time. The dynamic behavior of the scattering intensity was very sensitive to the statistical properties of the exciting radiation. For incoherent light the scattering intensity relaxes to a steady-state value within a time of the order of the dark relaxation time. In coherent light, however, a holographic pattern is formed as a result of the interference of the pump wave with the induced wave. The study of the dynamic behavior of the scattering intensity provides an independent means for determining the coefficients of photoconductivity and dark conductivity and the saturation optical inhomogeneity. E.A.K.

N86-11986# Joint Publications Research Service, Arlington, Va.
MULTIPHOTON RAMAN SCATTERING OF LIGHT EXCITED IN CRYSTALS BY A COPPER-VAPOR LASER Abstract Only c74
A. M. Agaltsov, V. S. Gorelik, and M. M. Sushchinskiy *In its* USSR Rept.: Phys. and Math. (JPRS-UPM-85-005) 20 Aug. 1985 p 98 p 98 refs Transl. into ENGLISH from Opt. i Spektrosk. (Leningrad), v. 58, no. 2, Feb. 85 p 386-389 (For primary document see N86-11945 02-70)
Avail: NTIS HC A08/MF A01

Multiphoton Raman scattering was excited in lithium tantalate and potassium chloride crystals with a copper-vapor laser emitting at two wavelengths. The laser operated in a quasicontinuous mode: the pulse repetition frequency was equal to + or - 8 kHz. The pulse power and pulse duration were equal to 20 kW and 15 nsec, respectively. In lithium tantalate, the multiphoton Raman scattering was studied near the second optical harmonic under excitation with the laser radiation at lambda = 578.2 nm and in the region of the sum under excitation with laser radiation at both wavelengths. In potassium chloride, three-photon scattering was studied near the second optical harmonic. The scattered radiation was recorded in the continuous mode at 300 K with a spectral resolution of 10 to 50 cm. E.A.K.

N86-11987# Joint Publications Research Service, Arlington, Va.
PHASING OF MULTIPLE-APERTURE OPTICAL SYSTEMS Abstract Only c74
P. A. Bakut, A. D. Rayakin, K. N. Sviridov, and N. D. Ustinov *In its* USSR Rept.: Phys. and Math. (JPRS-UPM-85-005) 20 Aug. 1985 p 98 refs Transl. into ENGLISH from Opt. i Spektrosk. (Leningrad), v. 58, no. 2, Feb. 1985 p 445-448 (For primary document see N86-11945 02-70)
Avail: NTIS HC A08/MF A01

Image sharpness functions were studied for the problem of phasing multiple aperture systems. Phasing is achieved by maximizing the image-sharpness function. From an examination of the optical transfer function of the system it was determined that a image-sharpness functions are acceptable in the absence of phase distortions of the wave front while type b functions are acceptable in the presence of phase distortions. E.A.K.

N86-11988# Joint Publications Research Service, Arlington, Va.
TRANSFORMATION OF LIGHT PULSE SHAPE BY THIN PLANE-PARALLEL LAYER OF ABSORBING MATERIAL Abstract Only c74
N. I. Insarova and G. I. Olefir *In its* USSR Rept.: Phys. and Math. (JPRS-UMP-85-005) 20 Aug. 1985 p 101 refs Transl. into ENGLISH from Zh. Prikl. Spektrosk. (Minsk, USSR), v. 42, no. 2, Feb. 1985 p 255-259 (For primary document see N86-11945 02-70)
Avail: NTIS HC A08/MF A01

The properties of the reflection of radiation by a plane-parallel absorbing layer on the characteristics of a powerful light pulse reflected from or passing through the layer were investigated. Self-interaction is studied, in which the thermal nonlinearity of the index of refraction of the layer is caused by the incidence of the radiation on the layer at some angle alfa that is smaller than alfa sub 0 IC and it is found that the shape of the pulse that is reflected or passed through the layer can differ greatly from that of the incident pulse due to variation in the refractivity of the layer due to heating caused by the incident pulse. Layers that exhibit this property can be employed in quantum electronic devices as general-purpose high-sensitivity nonlinear elements. E.A.K.

N86-11989# Joint Publications Research Service, Arlington, Va.
HYDROTHERMODYNAMICS OF THE NEAR-SURFACE LAYER OF A LIQUID AND OPTICAL METHODS OF INVESTIGATING IT c77
O. D. Fedorovskyy *In its* USSR Rept.: Phys. and Math. (JPRS-UPM-85-005) 20 Aug. 1985 p 107-115 refs Transl. into ENGLISH from Visnyk Akad. Nauk Ukrayinskoyi RSR (Kiev), no. 11, Nov. 1984 p 15-21 (For primary document see N86-11945 02-70)
Avail: NTIS HC A08/MF A01

Information on the temperature distribution at the air-water interface, which is obtained by contact and remote methods is described. It is pointed out, that methods do not consider the complex thermohydrodynamic structures which form in water layers near the surface, with dimensions of the order of millimeters. Diagnosis of the dynamic processes which take place in the ocean by remote sensing of the surface is emphasized. Results of the remote measurement of the spatial scale and the values of the temperature anomalies of a homogeneous are presented. It is concluded that there is a possibility of determining the dimensions and energy of the synoptic vortex and indications of the parameters of internal waves through characteristic thermal radiations of the free surface of the ocean in the infrared region of the spectrum. E.A.K.

N86-11990# Joint Publications Research Service, Arlington, Va.
USSR REPORT: SCIENCE AND TECHNOLOGY POLICY
25 Sep. 1985 105 p Transl. into ENGLISH from various Russian articles
(JPRS-UST-85-014) Avail: NTIS HC A06

Soviet policies applied to science and technology are reported. Topics discussed include: organization, planning and coordination, automation and information policy, and training and education. For individual titles, see N86-11991 through N86-11993.

N86-11991# Joint Publications Research Service, Arlington, Va.
BOOK ON PLANNING OF SCIENTIFIC, TECHNICAL PROGRESS c81
A. N. Andrukhovich, V. Yu. Budvey, T. N. Kalinovskaya, B. P. Krasnoglazov, V. M. Likhtenshteyn, L. I. Maksimov, V. L. Mershko, Ye. V. Sapilov, P. A. Sedlov, and T. L. Sletova *In its* USSR Rept.: Sci. and Technol. Policy (JPRS-UST-85-014) 25 Sep 1985 p 11-14 Transl. into ENGLISH from Oshchestvennyye Nauki

v SSSR, Ser. 2: Ekonomika (Referativnvy Zh.) (Moscow), no. 1, Jan. - Feb. 1985 p 60-64 (For primary document see N86-11990 02-70)
Avail: NTIS HC A06

The general problems of planning scientific and technical progress were examined: the role of planning as the basic tool in the acceleration of scientific and technical development, and the structure of plans for new equipment and the basic directions of the improvement of planning are revealed. It is pointed out that the lack of precise criteria in the determination of the novelty of equipment, leads to the decrease of the rate and scale of the assimilation of advanced types of products. Author

N86-11992# Joint Publications Research Service, Arlington, Va.
COMPUTER-AIDED DESIGNING, ENGINEERING, PREPARATION OF PRODUCTION c61
Yu. I. Topcheyev *In its* USSR Rept.: Sci. and Technol. Policy (JPRS-UST-85-014) 25 Sep. 1985 p 20-24 Transl. into ENGLISH from Vest. Vysshey Shkoly (Moscow), no. 5, May 1985 p 29-31 (For primary document see N86-11990 02-70)
Avail: NTIS HC A06

The introduction of flexible manufacturing systems and robots in industry and agriculture and the complete automation of production, are impossible without the use of computer-aided design systems, engineering and the technological preparation of production (SAPR). The use of SAPR allows the combination of a single cycle and the performance of planning and design work and technological preparation. The production cycle improves the working conditions of designers and workers, frees them from routine operations and affords greater opportunities for creative activity. E.A.K.

N86-11993# Joint Publications Research Service, Arlington, Va.
PROBLEMS, TRENDS IN TECHNICAL EDUCATION OF RESEARCHERS c80
O. M. Belotserkovskiy *In its* USSR Rept.: Sci. and Technol. Policy (JPRS-UST-85-014) 25 Sep. 1985 p 52-62 Transl. into ENGLISH from Vest. Vyssey Shkoly (Moscow), no. 5, May 1985 p 25-29 (For primary document see N86-11990 02-70)
Avail: NTIS HC A06

The scientific and technical revolution has a profound influence on all levels and areas of general and specialized education, including higher education. The problems and trends in the development of modern higher technical education, which are most important in the training of research personnel in the physical-technical sciences are discussed. E.A.K.

N86-11994# Joint Publications Research Service, Arlington, Va.
CHINA REPORT: SCIENCE AND TECHNOLOGY
16 May 1985 134 p refs Transl. into ENGLISH from various Chinese articles
(JPRS-CST-85-015) Avail: NTIS HC A07/MF A01

Progress in science and technology in the People's Republic of China is reported. Topics discussed include: life sciences, environmental quality, acoustics, chemistry, communications, computer development and applications, electronics, lasers, mathematics, and mechanics. For individual titles, see N86-11995 through N86-12006.

N86-11995# Joint Publications Research Service, Arlington, Va.
HIGH-SPEED SIGNAL PROCESSOR DEVELOPED Abstract Only c60
In its China Rept.: Sci. and Technol. (JPRS-CST-85-015) 16 May 1985 p 10 Transl. into ENGLISH from Jisuanji Shijie (Beijing), no. 7, 8 Apr. 1984 p 7 (For primary document see N86-11994 02-70)
Avail: NTIS HC A07/MF A01

The Fast Fourier Transform signal processor, a special use computer used for high speed realtime signal processing was developed. The computer uses an Am2901 bit slice device, VLSI multiplier TDC 1010, and RAM2147H high speed components with FFT algorithms, automatic calibration, and microprogram control. Word length is 16-bits, the power spectrum time for 1024 real number points is 5ms, the highest sampling frequency of realtime processing is 200 KHz. With this computer as the core, the attached A/D converter and microcomputer can carry out pre and post processing. Existing functions are FFT, IFFT, automatic reciprocal power spectrum and automatic reciprocal switching. E.A.K.

N86-11996# Joint Publications Research Service, Arlington, Va.
NEW R AND D IN CHINESE LANGUAGE INFORMATION PROCESSING Abstract Only c62
In its China Rept.: Sci. and Technol. (JPRS-CST-85-015) 16 May 1985 p 11-12 Transl. into ENGLISH from Jisuanji Shijie (Beijing), no. 7, 8 Apr. 1984 p 7 (For primary document see N86-11994 02-70)
Avail: NTIS HC A07/MF A01

The Plug compatible type Chinese Character Terminal and the Plug compatible type Chinese Character Processing System was developed. The development of China's Chinese language information processing systems went through three stages: (1) simple Chinese written language processing systems with Chinese character management functions; (2) Chinese character high level language Chinese language computer systems compatible with Western languages; (3) Chinese language information processing systems with Chinese character support for high level language carried out by revising the original computer control system. The task of getting a Chinese language computer system has reached the stage where it can be used in a preliminary way. The operating systems of machines above the medium and large scale level are hard to change and the Chinese character processing function was a main computer. The search for a newer and faster way to resolve the problem of Chinese character processing which faces Chinese language information processing is discussed. E.A.K.

N86-11997# Joint Publications Research Service, Arlington, Va.
CENTER FOR HIGH TEMPERATURE PLASMA PHYSICS CERTIFIED Abstract Only c75
Hu Maolian *In its* China Rept.: Sci. and Technol. (JPRS-CST-85-015) 16 May 1985 p 13-14 Transl. into ENGLISH from Anhui Ribao (Hefei), 21 Jan. 1985 p 1 (For primary document see N86-11994 02-70)
Avail: NTIS HC A07/MF A01

The construction and functions of a research center for high temperature plasma physics and controlled thermonuclear fusion are discussed. It has four of China's largest d.c. pulse generators capable of producing 80 megawatts of power, an induction coil capable of storing 200 million joules of electric energy, and a capacitor bank that can store 8 million joules of energy. It has equipment for producing deionized water, low temperature equipment, a cooling system using refrigerated circulating water, and a heat supply system. The center is one of China's important bases for thermonuclear fusion research. E.A.K.

N86-11998# Joint Publications Research Service, Arlington, Va.
CONTROLLED THERMONUCLEAR FUSION, HIGH TEMPERATURE PLASMA PHYSICS Abstract Only c75
In its China Rept.: Sci. and Technol. (JPRS-CST-85-015) 16 May 1985 p 15 Transl. into ENGLISH from Anhui Ribao (Hefei), 21 Jan. 1985 p 1 (For primary document see N86-11994 02-70)
Avail: NTIS HC A07/MF A01

The primary source of nuclear energy comes from the fission process of heavy nuclei. To utilize the energy released by a thermonuclear fusion process, methods of controlling the fusion reaction were studied. This is controlled thermonuclear fusion technology. The fuel used in a thermonuclear fusion process are isotopes of hydrogen: deuterium and tritium. They can be extracted from the almost unlimited seawater. Nuclear fusion also produces very little radioactive waste. Thermonuclear fusion is a promising energy source with an almost unlimited supply; it is economical, safe, and relatively clean. Ways to raise plasma temperature to a very high level and to maintain it to allow fusion reactions to take place are studied. The physical laws of high temperature plasma was studied to reach this goal which resulted in the development of high temperature plasma physics. E.A.K.

N86-11999# Joint Publications Research Service, Arlington, Va.
THIRD NATIONAL ACADEMIC MACHINE RETRIEVAL CONFERENCE HELD IN ZHENJIANG Abstract Only c82
In its China Rept.: Sci. and Technol. (JPRS-CST-85-015) 16 May 1985 p 26-27 Transl. into ENGLISH from Jisuanji Shijie (Beijing), no. 1, 8 Jan. 1984 p 1 (For primary document see N86-11994 02-70)
Avail: NTIS HC A07/MF A01

The set up and build up of data base of nearly a million documents was introduced. Improvements to the Toshinari Kikuchi algorithm which is an inquiry processing algorithm widely used in selective service programs was presented. The multi-user on line book title retrieval system introduced the implementation of a small book title retrieval system which uses a minicomputer with a minimum configuration. The on line processing system for Chinese language personnel files and document materials using Chinese character terminal was introduced. A library information automated data base is proposed. The viewpoint of fuzzy set mathematics in an information retrieval system, and a mathematical model of a fuzzy set retrieval language and its implementation are presented. E.A.K.

N86-12000# Joint Publications Research Service, Arlington, Va.
MICROCOMPUTER-CONTROLLED HIGH-ALTITUDE DATA ACQUISITION SYSTEM Abstract Only c89
In its China Rept.: Sci. and Technol. (JPRS-CST-85-015) 16 May 1985 p 36 Transl. into ENGLISH from Jisuanji Shijie (Beijing), no. 7, 8 Apr. 1984 p 8 (For primary document see N86-11994 02-70)
Avail: NTIS HC A07/MF A01

A new microcomputer controlled high altitude data acquisition system was developed. The system provides a new technique for data acquisition from China's astronomical, meteorological and other high altitude experiments and opens up new territory in microcomputer applications. This microcomputer controlled high altitude data acquisition system is made up of a Z80 single board computer, 10 K memory expansion board, and keyboard and display board which can collect 16 analog signals simultaneously, and through analog/digital conversion can convert external analog signals into digital signals then encode them in a certain form through program modulation and store them on audio cassette. The data is immediately retrieved from the tape and sent to the surface microcomputer system for data processing and analysis. E.A.K.

N86-12001# Joint Publications Research Service, Arlington, Va.
COMPUTER APPLICATION IN ATOMIC ABSORPTION SPECTROMETRY c72
Hu Xinyao and Zhang Liangping *In its* China Rept.: Sci. and Technol. (JPRS-CST-85-015) 16 May 1985 p 51-57 refs Transl. into ENGLISH from Fenxi Huaxue (Changchun), no. 6, 20 Jun. 1983 p 451-454 (For primary document see N86-11994 02-70)
Avail: NTIS HC A07/MF A01

In the past the presence of sulfates interfered with the measurement of calcium and magnesium by chemical separation method or the spectrometric method of changing the spectrum condition. A mathematical model was designed by using the method of computer atomic absorption spectrometry to determine and calculate the concentrations of calcium and magnesium and the concentration of the interfering sulfate radicals. The computer processing method and the mathematical model used to measure other elements under similar conditions is discussed. E.A.K.

N86-12002# Joint Publications Research Service, Arlington, Va.
A GENERAL PURPOSE CAD PROGRAM FOR MICROWAVE LINEAR CIRCUITS c33
Yenyang Shih *In its* China Rept.: Sci. and Technol. (JPRS-CST-85-015) 16 May 1985 p 93 refs Transl. into ENGLISH from Tongxin Xuebao (Beijing), no. 2, Apr. 1984 p 60-65 (For primary document see N86-11994 02-70)
Avail: NTIS HC A07/MF A01

A general purpose computer aided design program for microwave linear circuits is presented. This program has the capability to perform frequency domain analysis, optimization, sensitivity analysis, and Monte Carlo analysis for passive or active circuits with complex topology, including lumped and/or distributed elements. Four sections are presented: (1) a mathematical description of the methodology used; (2) a flow diagram showing the logical structure of the program; (3) a summary of the types of microwave circuits that can be analyzed by the program; and; (4) numerical examples of analysis and optimization results for selected circuits of different topology. It is shown that the numerical results obtained from the program MICAD are consistent with those obtained from the program COMPACT. E.A.K.

N86-12003# Joint Publications Research Service, Arlington, Va.
DOUBLE-WAVELENGTH PULSED TUNABLE DYE LASER Abstract Only c36
Zaixuan Zhang, Jingyun Wang, Yiqian Yuan et al *In its* China Rept.: Sci. and Technol. (JPRS-CST-85-015) 16 May 1985 p 97 Transl. into ENGLISH from Zhongguo Jiguang (Shanghai), v. 11, no. 6, 20 Jun. 1984 p 323-326 (For primary document see N86-11994 02-70)
Avail: NTIS HC A07/MF A01

Simultaneous tunable two wavelength operation of the tunable dye laser pumped by SHG of a Nd:YAG pulsed repetitive Q switched laser is described. The R6G, R6G+R640 and R6G+LD473 mixtures in methanol solution were studied. The proper choice of the beam splitter and the Brewster prism pre-expander grazing incident grating cavity provided a wide tunable spectral range and low background ASE. The polarized peak output power of the laser is about 40 kW and the spectral bandwidth is 0.22 cm/1. E.A.K.

N86-12004# Joint Publications Research Service, Arlington, Va.
INVOLUTORY TRANSFORMATIONS AND VARIATION PRINCIPLES WITH MULTIVARIABLES IN THIN PLATE BENDING PROBLEMS Abstract Only c39
Weichang Qian *In its* China Rept.: Sci. and Technol. (JPRS-CST-85-015) 16 May 1985 p 107 Transl. into ENGLISH from Yingyong Shuxue he Lixue (Chongquing), v. 6, no. 1, Jan. 1985 p 25-40 (For primary document see N86-11994 02-70)
Avail: NTIS HC A07/MF A01

The generalized variational principles of plate bending problems are established from their minimum potential energy principle and minimum complementary energy principle through the elimination of their constraints by the Lagrange multipliers method. The involutory transformations are also introduced to reduce the order of differentiations for the variables in the variation. The involutory transformations become the additional constraints in the variation, and additional Lagrange multipliers may be used to remove these additional constraints. Various multivariable variational principles are obtained for the plate bending problems. It is observed that not all the constraints of variation can be removed simply by the ordinary method of linear Lagrange multipliers. In such cases, the method of high order Lagrange multipliers are used to remove those constraints left over by ordinary linear multiplier method. Functionals of more general forms are obtained for the generalized variational principles of plate bending problems. E.A.K.

N86-12005# Joint Publications Research Service, Arlington, Va.
NUMERICAL METHOD IN DYNAMIC RESPONSE OF NONLINEAR SYSTEMS Abstract Only c39
Zhaochang Zheng and Mingyi Tan *In its* China Rept.: Sci. and Technol. (JPRS-CST-85-015) 16 May 1985 p 108 Transl. into ENGLISH from Yingyong Shuxue he Lixue (Chongquing), v. 6, no. 1, Jan. 1985 p 93-101 (For primary document see N86-11994 02-70)
Avail: NTIS HC A07/MF A01

A modal synthesis technique which is applicable to vibration analysis for linear substructures with nonlinear coupling attachments is extended to nonlinear dynamic analysis. A process is suggested which modal synthesis techniques are further extended to dynamic analysis of large complex structural systems with nonlinear charracteristics of each substructure. The high efficiency of this process is shown. E.A.K.

N86-12006# Joint Publications Research Service, Arlington, Va.
ON CONVECTIVE EFFECTS IN GAS LASERS Abstract Only
c36
Zhi Gao *In its* China Rept.: Sci. and Technol. (JPRS-CST-85-015) 16 May 1985 p 116 Transl. into ENGLISH from Wuli Xuebao (Beijing), v. 33, no. 9, Sep. 1984 p 1294-1300 (For primary document see N86-11994 02-70)
Avail: NTIS HC A07/MF A01

The convection of the gain medium is a decisive factor for large increase in power output of gas lasers. It is shown that both the saturation intensity and the laser power density by which the CW laser is characterized increase nonlinearly with the flow speed and tend toward the respective limiting values. It is also shown that the increment of the saturation intensity does not go beyond 10 times, and a large increase in power density is caused by the accumulation of excited energy in the flowing gas. The quantitative results of the variation of the saturation intensity with the gas flow transient time are consistent with the experimental data of the flowing CO2 gas lasers, where the gas flow transient time denotes the time required for the flowing gas to move across the gas gain region or the probing beam section. E.A.K.

71 ACOUSTICS

Includes sound generation, transmission and attenuation.
For noise pollution see *45 Environment Pollution.*

N86-12007*# National Aeronautics and Space Administration. Lewis Research Center, Cleveland, Ohio.
NUMERICAL TECHNIQUES IN ACOUSTICS
Kenneth J. Baumeister, comp. Oct. 1985 35 p refs Meeting held in Miami Beach, Fla., 17-21 Nov. 1985; sponsored by the ASME
(NASA-CP-2404; E-2758; NAS 1.55:2404) Avail: NTIS HC A03/MF A01 CSCL 20A

This is the compilation of abstracts of the Numerical Techniques in Acoustics Forum held at the ASME's Winter Annual Meeting. This forum was for informal presentation and information exchange of ongoing acoustic work in finite elements, finite difference, boundary elements and other numerical approaches. As part of this forum, it was intended to allow the participants time to raise questions on unresolved problems and to generate discussions on possible approaches and methods of solution. For individual titles, see N86-12008 through N86-12016.

N86-12008*# Alberta Univ., Edmonton.
APPLICATION OF HIGH ORDER ACOUSTIC FINITE ELEMENTS TO TRANSMISSION LOSSES AND ENCLOSURE PROBLEMS Abstract Only
A. Craggs and G. Stevenson *In* NASA. Lewis Research Center Numerical Tech. in Acoustics Oct. 1985 p 1-2 ref (For primary document see N86-12007 02-71)
Avail: NTIS HC A03/MF A01 CSCL 20A

A family of acoustic finite elements was developed based on C continuity (acoustic pressure being the nodal variable) and the no-flow condition. The family include triangular, quadrilateral and hexahedral isoparametric elements with linear quadratic and cubic variation in modelling and distortion. Of greatest use in problems with irregular boundaries are the cubic isoparametric elements: the 32 node hexahedral element for three-dimensional systems; and the twelve node quadrilateral and ten node triangular elements for two-dimensional/axisymmetric applications. These elements were applied to problems involving cavity resonances, transmission loss in silencers and the study of end effects, using a Floating Point Systems 164 attached array processor accessed through an Amdahl 5860 mainframe. The elements are presently being used to study the end effects associated with duct terminations within finite enclosures. The transmission losses with various silencers and sidebranches in ducts is also being studied using the same elements. Author

N86-12009*# Naval Ship Research and Development Center, Bethesda, Md.
ON THE COMPUTATION OF STRUCTURAL VIBRATIONS INDUCED BY A LOW-SPEED TURBULENT FLOW Abstract Only
c39
Y. F. Hwang *In* NASA. Lewis Research Center Numerical Tech. in Acoustics Oct. 1985 p 3-5 (For primary document see N86-12007 02-71)
Avail: NTIS HC A03/MF A01 CSCL 20K

A method for numerical evaluation of the vibrations of a cylindrical shell structure induced by a low speed external turbulent flow is discussed. The direction of flow is along the axis of revolution of the shell, and the source of excitation is the pressure fluctuations in the turbulent boundary layer. For the investigation of vibration and noise problems it is usually more desirable to utilize the modal expansion approach. The axisymmetric shell structure can be modeled by the assemblage of conical-shell finite-elements. This modeling allows the eigenfunction psi sub mn (x,theta) to be represented in a rectangular product of a longitudinal modal function f sub mn (x) and a circular harmonic function cos m theta (or sin m theta). Author

N86-12010*# Houston Univ., Tex.
IMPROVING THE ACCURACY OF THE BOUNDARY INTEGRAL METHOD BASED ON THE HELMHOLTZ INTEGRAL Abstract Only
c39
G. H. Koopmann and K. Brod *In* NASA. Lewis Research Center Numerical Tech. in Acoustics Oct. 1985 p 7-8 (For primary document see N86-12007 02-71)
Avail: NTIS HC A03/MF A01 CSCL 20K

Several recent papers in the literature have been based on various forms of the Helmholtz integral to compute the radiation fields of vibrating bodies. The surface integral form is given. The symbols of P,R micron, rho,G,R,V, and S micron are acoustic pressure, source coordinate, angular frequency, fluid density, Green function, field coordinate, surface velocity and body surface respectively. A discretized form of the surface integral is also given. Solutions to the surface integral are complicated with the singularity of the Green function at R=R micron and with the uniqueness problem at interior eigen frequencies of the enclosed space. The use of the interior integral circumvents the singularity problem since the field points are chosen in the interior space of the vibrating body where a zero pressure condition exists. The interior integral form is given. The method to improve the accuracy is detailed. Examples of the method is presented for a variety of radiators. Author

N86-12011*# Texas A&M Univ., College Station. Dept. of Aerospace Engineering.
A NUMERICAL METHOD OF CALCULATING PROPELLER NOISE INCLUDING ACOUSTIC NONLINEAR EFFECTS Abstract Only
K. D. Korkan *In* NASA. Lewis Research Center Numerical Tech. in Acoustics Oct. 1985 p 9-10 refs (For primary document see N86-12007 02-71)
(Grant NAG3-354)
Avail: NTIS HC A03/MF A01 CSCL 20A

Using the transonic flow fields(s) generated by the NASPROP-E computer code for an eight blade SR3-series propeller, a theoretical method is investigated to calculate the total noise values and frequency content in the acoustic near and far field without using the Ffowcs Williams - Hawkings equation. The flow field is numerically generated using an implicit three dimensional Euler equation solver in weak conservation law form. Numerical damping is required by the differencing method for stability in three dimensions, and the influence of the damping on the calculated acoustic values is investigated. The acoustic near field is solved by integrating with respect to time the pressure oscillations induced at a stationary observer location. The acoustic far field is calculated from the near field primitive variables as generated by NASPROP-E computer code using a method involving a perturbation velocity potential as suggested by Hawkings in the calculation of the acoustic pressure time-history at a specified far field observed location. the methodologies described are valid for calculating total noise levels and are applicable to any propeller geometry for which a flow field solution is available. Author

N86-12012*# National Aeronautics and Space Administration. National Space Technology Labs., Bay Saint Louis, Miss.

A GENERAL-APPLICATIONS DIRECT GLOBAL MATRIX ALGORITHM FOR RAPID SEISMO-ACOUSTIC WAVEFIELD COMPUTATIONS

Henrik Schmidt (SACLANT ASW Research Center), Gerard J. Tango, and Michael F. Werby *In* NASA. Lewis Research Center Numerical Tech. in Acoustics Oct. 1985 p 11-15 refs (For primary document see N86-12007 02-71)

Avail: NTIS HC A03/MF A01 CSCL 20A

A new matrix method for rapid wave propagation modeling in generalized stratified media, which has recently been applied to numerical simulations in diverse areas of underwater acoustics, solid earth seismology, and nondestructive ultrasonic scattering is explained and illustrated. A portion of recent efforts jointly undertaken at NATOSACLANT and NORDA Numerical Modeling groups in developing, implementing, and testing a new fast general-applications wave propagation algorithm, SAFARI, formulated at SACLANT is summarized. The present general-applications SAFARI program uses a Direct Global Matrix Approach to multilayer Green's function calculation. A rapid and unconditionally stable solution is readily obtained via simple Gaussian ellimination on the resulting sparsely banded block system, precisely analogous to that arising in the Finite Element Method. The resulting gains in accuracy and computational speed allow consideration of much larger multilayered air/ocean/Earth/engineering material media models, for many more source-receiver configurations than previously possible. The validity and versatility of the SAFARI-DGM method is demonstrated by reviewing three practical examples of engineering interest, drawn from ocean acoustics, engineering seismology and ultrasonic scattering. Author

N86-12013*# National Aeronautics and Space Administration. National Space Technology Labs., Bay Saint Louis, Miss.

NUMERICAL TECHNIQUES FOR SCATTERING FROM SUBMERGED OBJECTS Abstract Only

Michael F. Werby, Gerald J. Tango, and G. C. Gaunaurd (Naval Surface Weapons Center, White Oak, Md.) *In* NASA. Lewis Research Center Numerical Tech. in Acoustics Oct. 1985 p 17-20 refs (For primary document see N86-12007 02-71)

Avail: NTIS HC A03/MF A01 CSCL 20A

To represent the final results in terms of matrices, one expands all appropriate physical quantities in terms of partial wave basis states. This includes expansions for the incident and scattered fields and the surface quantities. The method then utilizes the Huygen-Poincare integral representation for both the exterior and interior solutions, leading to the required matrix equations. One thus deals with matrix equations, the complexity of which depends on the nature of the problem. It is shown that in general a transition matrix T can be obtained relating the incident field A with the scattered field f having the form T = PQ(-1), where f = TA. The structure of Q can be quite complicated and can itself be composed of other matrix inversions such as arise from layered objects. Recent improvements in this method appropriate for a variety of physical problems are focused on, and on their implementation. Results are outlined from scattering simulations for very elongated submerged objects and resonance scattering from elastic solids and shells. The final improvement concerns eigenfunction expansions of surface terms, arising from solution of the interior problem, obtained via a preconditioning technique. This effectively reduces the problem to that of obtaining eigenvalues of a Hermitian operator. This formalism is reviewed for scattering from targets that are rigid, sound-soft, acoustic, elastic solids, elastic shells, and elastic layered objects. Two sets of the more interesting results are presented. The first concerns scattering from elongated objects, and the second to thin elastic spheroids. Author

N86-12014*# Purdue Univ., Lafayette, Ind.

PREDICTION OF ACOUSTICAL RESPONSE OF THREE-DIMENSIONAL CAVITIES USING AN INDIRECT BOUNDARY ELEMENT METHOD Abstract Only

Robert J. Bernhard and Carl R. Kipp (Bell Labs., Whippany, N.J.) *In* NASA. Lewis Research Center Numerical Tech. in Acoustics Oct. 1985 p 21-23 ref (For primary document see N86-12007 02-71)

Avail: NTIS HC A03/MF A01 CSCL 20A

A technique which characterizes the acoustics of generalized cavities with the minimum model possible is developed. All boundary element methods have two advantages over finite element methods: (1) the models are smaller; and (2) the assumed variable behavior, inherent in the method to allow discretization, is harmonic rather than polynomial. Further, IBEM often requires one rather than two numerical boundary integrals as required by DBEM. Thus, a quadratic, isoparametric IBEM program was developed. The source distribution in this solution is continuous and quadratically variable rather than continuous and constant. The program was also formulated to include the additional capability of interior point sources and impedance boundary conditions. To test the quadratic, isoparametric IBEM program, several simple cavity enclosure problems where studied. Results are shown. Author

N86-12015*# George Washington Univ., Hampton, Va.

VORTEX STUDIES RELATING TO BOUNDARY LAYER TURBULENCE AND NOISE Abstract Only

J. L. Adelman (George Washington Univ., Hampton, Va.) and J. C. Hardin *In* NASA. Lewis Research Center Numerical Tech. in Acoustics Oct. 1985 p 25-28 Previously announced as N85-27169 (For primary document see N86-12007 02-71)

Avail: NTIS HC A03/MF A01 CSCL 20A

The present study considers the two-dimensional case of an array of N rectilinear, like-sign vortices above an infinite flat boundary. The method of images can be employed with this configuration to reduce the problem to that of 2N vortices in free space, constrained by 2N symmetry relations. This system is Hamiltonian and therefore certain invariants of the motion are known. Further, from the Hamiltonian constant, the equations of motion are readily derived and may be integrated numerically to determine the vortex trajectories. This knowledge of the time-dependent vortex motion then allows the resulting noise radiation to be computed by standard aeroacoustic techniques. R.J.F.

N86-12016*# Iowa State Univ. of Science and Technology, Ames.

STATISTICAL SIGNAL ANALYSIS FOR SYSTEMS WITH INTERFERENCED INPUTS

Robin M. Bai and Anna L. Mielnicka-Pate *In* NASA. Lewis Research Center Numerical Tech. in Acoustics Oct. 1985 p 29-32 ref (For primary document see N86-12007 02-71)

Avail: NTIS HC A03/MF A01 CSCL 20A

A new approach is introduced, based on statistical signal analysis, which overcomes the error due to input signal interference. The model analyzed is given. The input signals u sub 1 (t) and u sub 2 (t) are assumed to be unknown. The measurable signals x sub 1 (t) and x sub 2 (t) are interferened according to the frequency response functions, H sub 12 (f) and H sub 21 (f). The goal of the analysis was to evaluate the power output due to each input, u sub 1 (t) and u sub 2 (t), for the case where both are applied to the same time. In addition, all frequency response functions are calculated. The interferenced system is described by a set of five equations with six unknown functions. An IBM XT Personal Computer, which was interfaced with the FFT, was used to solve the set of equations. The software was tested on an electrical two-input, one-output system. The results were excellent. The research presented includes the analysis of the acoustic radiation from a rectangular plate with two force inputs and the sound pressure as an output signal. Author

N86-12017# *Defence Materiel Administration, Stockholm* (Sweden). Radio Dept.

INFRASOUND: A SUMMARY OF INTERESTING ARTICLES

May 1985 271 p refs

(FMV:ELEKTRO-A12:142/83) Avail: NTIS HC A12/MF A01

A comprehensive accounting of infrasound levels under normal working conditions and in home environment, both in Sweden and in the rest of the world is discussed. Due to the fact that the results from different reports are not uniform and often incomplete, a direct comparison of results is not possible. The existence of high levels of man made low frequency noise (0 to 100 Hz), and in particular infrasonic noise, has been reported in many environments. An effort has been made over the last decade to discover whether such high levels of low frequency noise are significant. A review of the effects of low frequency noise indicates that the effects are similar to those of higher frequency noise, that noise in the 20 to 100 Hz range is much more significant than infrasound at similar sound pressure levels and that the possible danger due to infrasound has been much over rated. Author

N86-12018# Middleton (David), New York.
INTERMEDIATE AND HIGH-FREQUENCY ACOUSTIC BACKSCATTERING CROSS SECTIONS FOR WATER-ICE INTERFACES. 1: TWO-COMPONENT PROFILE MODELS Technical Report, Aug. 1983 - 30 Nov. 1984
D. Middleton 7 Mar. 1985 80 p
(Contracts N00140-83-M-PL78; N00140-84-M-MS42)
(AD-A157533; NUSC-TD-7375) Avail: NTIS HC A05/MF A01 CSCL 20/1

Two general statistical-physical models (1, 2) for underice surface elevations are constructed. These provide the basis for determining the intensities and associated frequency spectra of acoustic waves scattered from such water-ice interfaces. Both models embody two-component processes: the simpler model represents the interface as an appropriately weighted sum of two gaussian distributions of elevation, each with different nonzero means and variances. No explicit identification of keel structure is made. The second model does account for keel structure and assigns the Gaussian components of the first model respectively to two distinct physical processes: that of local iced generation and that of the intermittent, large-scale keel formation. In this report the analysis is limited to Model 1 and calculations of backscattering cross sections appropriate to intermediate and high frequencies i.e., Kirchoff-based methods. The treatment here is also restricted, for the moment, to zero gradient and single ice bottom surface interactions. In most instances, the Rayleigh numbers for both components of the underice surface are large, so that theories based solely on perturbation techniques and/or Bragg scatter are inadequate. GRA

N86-11169# Deutsche Forschungs- und Versuchsanstalt fuer Luft- und Raumfahrt, Goettingen (West Germany). Inst. for Experimental Fluid Mechanics.
AEROACOUSTIC WIND TUNNEL MEASUREMENTS ON PROPELLER NOISE
F.-R. Grosche and H. Stiewitt *In* AGARD Aerodyn. and Acoustics of Propellers Feb. 1985 9 p refs (For primary document see N86-11147 02-01)
Avail: NTIS HC A20/MF A01

N86-11171# Pratt and Whitney Aircraft of Canada Ltd., Longueuil (Quebec).
AN INVESTIGATION OF IN-FLIGHT NEAR-FIELD PROPELLER NOISE GENERATION AND TRANSMISSION
H. Bonneau, D. F. Wilford, and L. K. Wood *In* AGARD Aerodyn. and Acoustics of Propellers Feb. 1985 12 p refs (For primary document see N86-11147 02-01)
Avail: NTIS HC A20/MF A01

N86-11172# Deutsche Forschungs- und Versuchsanstalt fuer Luft- und Raumfahrt, Brunswick (West Germany). Inst. fuer Entwurfsaerodynamik.
FULL-SCALE FLIGHT AND MODEL-SCALE WIND TUNNEL TESTS ON THE NEARFIELD NOISE CHARACTERISTICS OF AIRCRAFT PROPELLERS
H. Heller, M. Kallergis, and B. Gehlhar *In* AGARD Aerodyn. and Acoustics of Propellers Feb. 1985 17 p refs (For primary document see N86-11147 02-01)
Avail: NTIS HC A20/MF A01

N86-11173# Aeritalia S.p.A., Pomigliano D'Arco (Italy).
CABIN NOISE REDUCTION FOR A NEW DEVELOPMENT TURBOPROP COMMUTER AIRCRAFT
A. Carbone, A. Paonessa, L. Lecce (Ist. Progetto Velivoli, Naples), and F. Marulo (Ist. Progetto Velivoli, Naples) *In* AGARD Aerodyn. and Acoustics of Propellers Feb. 1985 14 p refs (For primary document see N86-11147 02-01)
Avail: NTIS HC A20/MF A01

N86-11174# Lockheed-California Co., Burbank.
PROPELLER AIRCRAFT CABIN VIBRATION AND NOISE-EXCITATION, SOURCES, AND PATHS
R. E. Donham, F. J. Balena, E. Z. Bochary, and O. K. Liehr *In* AGARD Aerodyn. and Acoustics of Propellers Feb. 1985 14 p refs (For primary document see N86-11147 02-01)
Avail: NTIS HC A20/MF A01

N86-11175# Hamilton Standard, Windsor Locks, Conn.
THE STATE OF THE ART IN PROPFAN TURBOPROP NOISE
Frederick B. Metzger *In* AGARD Aerodyn. and Acoustics of Propellers Feb. 1985 20 p refs (For primary document see N86-11147 02-01)
Avail: NTIS HC A20/MF A01

N86-11176# Lockheed-Georgia Co., Marietta.
APPLICATION OF ACTIVE NOISE CONTROL TO MODEL PROPELLER NOISE
M. Salikuddin, H. K. Tanna, R. H. Burrin, and W. E. Carter *In* AGARD Aerodyn. and Acoustics of Propellers Feb. 1985 15 p refs (For primary document see N86-11147 02-01)
Avail: NTIS HC A20/MF A01

N86-11869# California Univ., Livermore. Lawrence Livermore Lab. Nuclear Test Engineering Div.
ANALYSIS OF ULTRASONIC WAVES IN A BOUNDED MEDIUM Abstract Only
Thomas A. Nelson and Gerald L. Goudreau *In* LANL 6th Bien. CUBE (Computer Use by Engineers) Symp. Aug. 1984 p 21 (For primary document see N86-11858 02-60)
Avail: NTIS HC A06/MF A01

N86-11881# California Univ., Livermore. Lawrence Livermore Lab. Nuclear Energy Systems Div.
RAMP RESPONSE ESTIMATION AND SPECTRUM EXTRAPOLATION FOR ULTRASONIC SCATTERING Abstract Only
Gregory A. Clark *In* LANL 6th Bien. CUBE (Computer Use by Engineers) Symp. Aug. 1984 p 55 (For primary document see N86-11858 02-60)
Avail: NTIS HC A06/MF A01

N86-11946# Joint Publications Research Service, Arlington, Va.
DIFFRACTION OF ULTRASONIC BEAM PASSING NORMALLY THROUGH LAYERED MEDIA Abstract Only
V. S. Konenenko *In its* USSR Rept.: Phys. and Math. (JPRS-UPM-85-005) 20 Aug. 1985 p 1 refs Transl. into ENGLISH from Fiz. (Tomsk), v. 28, no. 1, Jan. 1985 p 118-119 (For primary document see N86-11945 02-70)
Avail: NTIS HC A08/MF A01

N86-11947# Joint Publications Research Service, Arlington, Va.
SPEED OF SOUND IN LIQUID SODIUM NEAR GAMMA-TRANSITION POINT Abstract Only
D. L. Timrot, M. A. Serednitskaya, and T. D. Chkhikvadze *In its* USSR Rept.: Phys. and Math. (JPRS-UPM-85-005) 20 Aug. 1985 p 1-2 refs Transl. into ENGLISH from Dokl. Akad. Nauk SSSR (Moscow), v. 279, no. 3, Nov. 1984 p 617-621 (For primary document see N86-11945 02-70)
Avail: NTIS HC A08/MF A01

N86-11948# Joint Publications Research Service, Arlington, Va.
RAMAN SCATTERING OF SOUND ON RANDOM OSCILLATIONS OF BUBBLES Abstract Only

Ye. A. Zabolotskaya *In its* USSR Rept.: Phys. and Math. (JPRS-UPM-85-005) 20 Aug. 1985 p 2 ref Transl. into ENGLISH from Kratk. Soobshch. po Fiz. (Moscow), no. 10, 1984 p 23-25 (For primary document see N86-11945 02-70)
Avail: NTIS HC A08/MF A01

N86-11949# Joint Publications Research Service, Arlington, Va.
DETERMINATION OF PARAMETERS OF ELASTIC SPHERICAL SHELL FROM SCATTERED WAVE FIELD Abstract Only
A. V. Sergeyev *In its* USSR Rept.: Phys. and Math. (JPRS-UPM-85-005) 20 Aug. 1985 p 2-3 refs Transl. into ENGLISH from Akust. Zh. (Moscow), v. 31, no. 1, Jan.-Feb. 1985 p 96-102 (For primary document see N86-11945 02-70)
Avail: NTIS HC A08/MF A01

N86-11950# Joint Publications Research Service, Arlington, Va.
STABILITY OF A METHOD FOR ANALYZING RADIATION PATTERN OF ACOUSTIC RADIATOR WITH NEAR-FIELD PRESSURE MEASUREMENT ERRORS Abstract Only
I. Ye. Tsukernikov *In its* USSR Rept.: Phys. and Math. (JPRS-UPM-85-005) 20 Aug. 1985 p 3 refs Transl. into ENGLISH from Akust. Zh. (Moscow), v. 31, no. 1, Jan.-Feb. 1985 p 111-113 (For primary document see N86-11945 02-70)
Avail: NTIS HC A08/MF A01

N86-11951# Joint Publications Research Service, Arlington, Va.
REFLECTION OF SOUND FROM PLATE CONTAINING PERIODIC INHOMOGENEITIES Abstract Only
A. D. Lapin *In its* USSR Rept.: Phys. and Math. (JPRS-UPM-85-005) 20 Aug. 1985 p 5-6 refs Transl. into ENGLISH from Akust. Zh. (Moscow), v. 31, no. 1, Jan-Feb. 1985 p 73-76 Previously announced in IAA as A85-41647 (For primary document see N86-11945 02-70)
Avail: NTIS HC A08/MF A01

72 ATOMIC AND MOLECULAR PHYSICS

Includes atomic structure and molecular spectra.

N86-12019*# Rice Univ., Houston, Tex.
LABORATORY STUDIES OF ATOMIC COLLISION PROCESSES OF IMPORTANCE IN PLANETARY ATMOSPHERES Annual Status Report
R. F. Stebbings and Ken Smith [Aug. 1985] 25 p
(Grant NsG7-386)
(NASA-CR-176301; NAS 1.26:176301) Avail: NTIS HC A02/MF A01 CSCL 20H

A series of differential cross sections for angular scattering and charge transfer was measured. These studies employ position-sensitive detectors (PSD's) to collect collision products scattered over a wide range of angles; and the research program includes investigation of differential cross sections for total angular scattering, charge transfer, stripping, and other collisions. All of these processes can be studied with the same basic apparatus, but minor modifications in the equipment details and in the data acquisition programs and techniques are required for each individual experiment. G.L.C.

N86-12020# Pittsburgh Univ., Johnstown, Pa.
FLOW REACTOR STUDIES OVER WIDE TEMPERATURE AND PRESSURE RANGES OF ATOM AND RADICAL REACTION RATES IMPORTANT IN IGNITION AND COMBUSTION Final Report, 16 Feb. 1981 - 15 Feb. 1985
F. Kaufman May 1985 9 p
(Contract DAAG29-81-K-0050)
(AD-A156931; ARO-17967.6-CH) Avail: NTIS HC A02/MF A01 CSCL 07/4

The completed research consists of critical evaluations of atom and radical reactions in terms of rate theory, the measurement of elementary reaction rate parameters for several important reactions, and the building and use of a new flow system for the study of H + O2 + M yields HO2 + M recombination. The experimental studies include the establishment of the primary products of the O + C2H4 reaction, viz. C2H3O + H in approximately 80% yield; the measurement of five H-atom abstraction reactions of OH with C2H6 and four Cl-and F-substituted ethanes; the proof, by use of 18O, that the fast reaction O + HO2 yields OH + O2 proceeds via an intermediate HO3 asterisk adduct; and the first direct measurement, by laser-induced fluorescence, of the CH3O + NO2 reaction rate over the temperature range 250 to 473 K. The 18O + NO, O2 isotope exchange reaction rates were measured and compared with theory, and a new, higher pressure flow reactor apparatus was built and the rate constants for H + O2 + M measured at 298K for M = He, N2, CH4, and H2O. GRA

N86-12021# San Diego State Univ., Calif. Dept. of Chemistry.
THE CHEMICAL PRODUCTION OF EXCITED STATE MOLECULES Final Report, 1 Jul. 1980 - 31 Mar. 1985
W. H. Richardson 31 Mar. 1985 12 p
(Contract DAAG29-80-K-0021)
(AD-A157276; ARO-17283.8-CH) Avail: NTIS HC A02/MF A01 CSCL 07/3

Most of the research deals with the effect of electronic structural variation upon the efficiency of triplet state carbonyl production from dioxetanes. Other studies involving dioxethanes include the question of preferential n, pi* state (vs pi, pi*) carbonyl formation and attempts to trap the proposed 1,4-dioxybiradical intermediate form thermolysis of dioxetanes. Some amino peroxides were also studied as potential sources of chemilumuniscence (CL). Finally, a detailed kinetic study was made on the thermolysis of a five-membered ring peroxide in order to distinguish between concerted vs stepwise decomposition routes. This study was pertinent to the mechanism of dioxetane (a four-ring peroxide) thermolysis. GRA

N86-12022# RAND Corp., Santa Monica, Calif.
SOVIET RESEARCH ON CRYSTAL CHANNELING OF CHARGED PARTICLE BEAMS Interim Report
S. Kassel Mar. 1985 57 p
(Contract MDA903-82-C-0067)
(AD-A157353; RAND/R-3224-ARPA) Avail: NTIS HC A04/MF A01 CSCL 20/7

This report presents an overview of Soviet research in charged particle beam channeling in crystals from 1972 to the present, and the resulting electromagnetic emission, including Soviet proposals for channeling emission lasers in the X-ray region of the spectrum. It analyzes Soviet attitudes toward crystal channeling of charged particles as a subject of research, describes performers of the research, and indicates the level of effort involved. It presents a brief history of crystal channeling research, the differences between channeling and other kinds of electromagnetic radiation, the definition of the main research issues, and estimates of the potential capabilities of channeling radiation, all based on the Soviet viewpoint. It then describes Soviet proposals for laser systems utilizing the channeling radiation mechanism, and analyzes Soviet experimental work involving the observation and measurement of channeling radiation. The author concludes that the outstanding feature of Soviet research in this area is the optimistic belief of Soviet specialists in the technological potential of this research, but finds that the role of the laser proposals in Soviet planning is ambiguous. Author (GRA)

N86-12023# Polytechnic Inst. of New York, Farmingdale.
PART A. MOLECULAR DYNAMICS AND IONIC ASSOCIATIONS OF LiAsF6 IN 4-BUTYROLACTONE MIXTURES WITH 2-METHYL TETRAHYDROFURAN. PART B. MOLECULAR DYNAMICS AND IONIC ASSOCIATIONS OF LiBF4 IN 1,2-DIMETHOXYMETHANE Technical Report, 1 Jan. - 30 Jun. 1985
Y. Harada, M. Salomon, S. Petrucci, M. Delsignore, and H. Farber 30 Jun. 1985 53 p
(Contract DAAG29-85-K-0048)
(AD-A157401; TR-7-Pt-A/B; ARO-21758.1-CH-Pt-A/B) Avail: NTIS HC A04/MF A01 CSCL 07/4

Solutions of LiAsF6 at 298.2 K were studied by audiofrequency conductance in the concentrations range .0001-.01 Mol/Cu dm and by radiofrequency ultrasonic absorption in the concentration range 0.05 - 0.5 mol/cu dm. The solvents employed were mixtures of 4-butyrolactone with 2-methyl tetrahydrofuran varying in compositions from mole fractions X subscript BL = 0.10 X subscript BL = 0.75. In dilute solutions the audiofrequency conductivity data yield ion association constants which appear to represent both contact and solvent-separated ion pairs for mixtures up to X subscript BL = 0.36. At higher LiAsF6 concentrations and in solvent mixtures of composition X subscript BL = 0.75, and X subscript BL = 0.35, the ultrasonic spectrum shows a single relaxation process which again is attributed to the formation of both contact and solvent separated ion pairs. Part B: Electrical conductance data for LiBF4 in 1,2-Dimethyoxymethane (DMM)at 25 C reveal the electrolyte to be heavily associated to ion-pairs and triple ions. A theoretical expression for the triple ion association constant similar to the Bjerrum one for ion-pairs and to the Maaser-Bjerrum theory of dimers has been developed and applied to the present conductance data. Ultrasonic relaxation absorption data at much higher concentrations than the conductance data reveal association to dimers. This is also evident from the microwave dielectric data showing no electrolyte dielectric effect on the solvent and apparent lack of presence of dipoles. The ultrasonic data can be rationalized by a two-step dimerization mechanism. GRA

N86-12024# Aerospace Corp., El Segundo, Calif. Chemistry and Physics Lab.
THE USE OF WALL-COATED CELLS IN ATOMIC FREQUENCY STANDARDS
R. P. Frueholz, C. H. Volk, and J. C. Camparo 24 Jun. 1985 25 p Sponsored by Air Force
(AD-A157435; TR-0084A(5945-05)-5; SD-TR-85-18) Avail: NTIS HC A02/MF A01 CSCL 14/2

An analysis of the effect of the microwave field distribution on the application of a wall-coated, bufferless absorption cell in an atomic frequency standard has been performed. While certain advantages of using such a cell in an atomic frequency standard employing a TE sub 011 microwave cavity have been previously demonstrated, we show that a simple incorporation of this type of cell in a frequency standard using a TE sub 111 microwave cavity would not be advantageous. The role of the microwave field distribution, particularly its phase variation within the cavity, is analyzed, and suggestions concerning the use of a wall-coated cell in a TE sub 111 microwave cavity as applied to an atomic frequency standard are made. GRA

N86-12025# Naval Postgraduate School, Monterey, Calif.
EMISSION THRESHOLD FOR CERENKOV RADIATION
J. R. Neighbours, F. R. Buskirk, and X. K. Maruyama Jul. 1985 28 p
(AD-A157615; NPS61-85-005) Avail: NTIS HC A03/MF A01 CSCL 20/8

As a consequence of the phasing condition between the moving charge and radiated wave for finite beam lengths, the Cerenkov peak is broadened and the threshold energy is lowered. A criterion for the threshold energy is developed which is applicable to charged beams consisting of a single charge bunch of finite size, as well as beams consisting of periodically repeated bunches. Author (GRA)

N86-12026# California Univ., Berkeley. Lawrence Berkeley Lab.
MEDICAL HEAVY ION ACCELERATOR PROPOSALS
R. A. Gough May 1985 8 p refs Presented at the Particle Accelerator Conf., Vancouver, British Columbia, 13 May 1985
(Contract DE-AC03-76SF-00098)
(DE85-015247; LBL-18978; CONF-850504-236) Avail: NTIS HC A02/MF A01

For several decades, accelerators designed primarily for research in nuclear and high energy physics have been adapted for biomedical research including radiotherapeutic treatment of human diseases such as pituitary disorders, cancer, and more recently, arteriovascular malformations. The particles used in these treatments include pions, protons and heavier ions such as carbon, neon, silicon and argon. Maximum beam energies must be available to penetrate into an equivalent of about 30 cm of water, requiring treatment beams of 250 to 1000 MeV/nucleon. Intensities must be adequate to complete a 100 rad treatment fraction in about 1 minute. The favored technical approach in these proposals utilizes a conventional, strong-focusing synchrotron capable of fast switching between ions and energies, and servicing multiple treatment rooms. Specialized techniques for shaping the dose to conform to irregularly-shaped target volumes, while simultaneously sparing surrounding, healthy tissue and critical structures, are employed in each treatment room, together with the sophisticated dosimetry necessary for verification, monitoring, and patient safety. DOE

N86-12027# Sandia Labs., Albuquerque, N. Mex.
IFR GUIDING EXPERIMENTS
C. A. Frost, S. L. Shope, P. D. Kiekel, J. W. Poukey, C. A. Ekdahl, R. B. Miller, B. E. Godfrey, L. W. Wright, and B. B. Newberger 1985 13 p Presented at the SDIC/DARPA Ann. Propagation Rev., Monterey, Calif., 24 Jun. 1984 Prepared in cooperation with Mission Research Corp., Albuquerque, N. Mex.
(Contract DE-AC04-76DP-00789)
(DE85-014512; SAND-85-1450C; CONF-8506141-5) Avail: NTIS HC A02/MF A01

A new technique was developed for electrostatically guiding high-current electron beams in accelerators and for IFR (ion focused regime) propagation experiments. The new method allows transport of IREEs over curved paths for applications in circular accelerators such as Sandia's recirculating linac. This method uses a low-energy electron beam in place of a laser to ionize the channel and thereby allows the use of any background gas desired instead of being restricted to the use of organics with high-photoionization cross sections. A weak longitudinal magnetic field is applied to confine the low-energy beam, enabling one to precisely define the ionization channel. Using this method, a 1.2 MeV beam with currents exceeding 20 kA was guided over a 3-m straight path. In these experiments with high nu/(GAMMA) beams, the inductive erosion and the effects of ion mass on channel stability were observed. Both effects can be important for accelerator applications. DOE

N86-12028# Texas Univ., Bastrop. Center for Particle Theory.
REPRESENTATIONS OF THE GROUP OF DIFFEOMORPHISMS IN THE PHYSICS OF PARTICLES, GRAVITY AND FLUIDS
Y. Neeman Oct. 1984 14 p Prepared in cooperation with Ministry of Science and Development, Jerusalem
(Contract DE-AS05-76ER-03992)
(DE85-007031; DOE/ER-03992/569) Avail: NTIS HC A02/MF A01

The group of space-time diffeomorphisms is defined. The discovery of its double-covering group is reviewed and its representations are mentioned. Applications in several domains of physics are discussed. DOE

N86-12029# California Univ., Berkeley. Lawrence Berkeley Lab.
TWO-DIMENSIONAL LINACS
W. S. Cooper and C. A. Anderson May 1985 6 p refs Presented at the Particle Accelerator Conf., Vancouver, British Columbia, 13 May 1985
(Contract DE-AC03-76SF-00098)
(DE85-015129; LBL-18970; CONF-850504-210) Avail: NTIS HC A02/MF A01

Several schemes for RF acceleration of ribbon beams are described. (Although the ribbon edges of course, need to be focussed, these configurations are essentially 2-D). They allow simpler modeling than quadrupole systems and, if operable, provide good matching to certain types of ion sources and beam neutralizers. Four possible configurations are discussed, in chronological order of conception: (1) an RF linac with dc transverse field focussing; (2) a similar linac, also with many pairs of electrodes, but using RF focussing; (3) an RFQ-like configuration with continuous electrodes, in which energy changes slowly along the beam axis; and (4) a similar system in which the beam energy oscillates along the axis. Some of the advantages and disadvantages of these systems are considered and the last case is analyzed in some detail. DOE

N86-12030# California Univ., Berkeley. Lawrence Berkeley Lab.
SOURCES OF RADIOACTIVE IONS
J. R. Alonso May 1985 7 p Presented at the Particle Accelerator Conf., Vancouver, British Columbia, 13 May 1985
(Contract DE-AC3-76SF-00098)
(DE85-015251; LBL-18958; CONF-850504-213) Avail: NTIS HC A02/MF A01

Beams of unstable nuclei can be formed by direct injection of the radioactive atoms into an ion source, or by using momentum of the primary production beam as the basis for the secondary beam. The effectiveness of this latter mechanism in secondary beam formation, i.e., the quality of the emerging beam (emittance, intensity, energy spread), depends critically on the nuclear reaction kinematics, and on the magnitude of the incident beam energy. When this beam energy significantly exceeds the energies typical of the nuclear process, many of the qualities of the incident beam can be passed on the secondary beam. Factors affecting secondary beam quality are discussed, along with techniques for isolating and purifying a specific secondary product. The ongoing radioactive beam program at the Bevalac is used as an example, with applications, present performance and plans for improvements. DOE

N86-12031# California Univ., Livermore. Lawrence Livermore Lab.
TRANSITION RADIATION AND COHERENT ELECTRON-PHOTON SCATTERING
M. J. Moran Apr. 1985 16 p Presented at the Penetration Phenomena Workshop, Oak Ridge, Tenn., 14 Apr. 1985
(Contract W-7405-eng-48)
(DE85-014813; UCRL-92912; CONF-850484-2) Avail: NTIS HC A02/MF A01

Relativistic electron irradiation of thin solid targets is known to generate collimated beams of X-ray photons in the forward direction by a number of different processes. A variety of mechanisms are discussed that share common characteristics in the angular and spectral distributions of the generated photon beams. Some simple physical explanations are offered for the characteristics shared by these processes. Some examples are then given based on experimental results attained at the LLNL electron-positron accelerator. DOE

N86-12032# Stanford Linear Accelerator Center, Calif.
DISRUPTION ANGLES
A. Minten 25 Jun. 1985 11 p refs
(Contract DE-AC03-76SF-0051)
(DE85-015138; SU-SLAC-CN-305) Avail: NTIS HC A02/MF A01

This investigation was stimulated by the question, to what extent beam disruption of two penetrating SLC bunches will modify the initial angular distribution of the incident beam, and whether the tails of the outgoing beam will be significantly enhanced and will lead to increased losses in the vicinity of the detector. An attempt was made to answer this question in three steps. DOE

N86-12033# Los Alamos Scientific Lab., N. Mex.
STUDY OF LAMPF H (-) BEAM POSITION MOTION AND A PREDICTIVE ALGORITHM FOR NOISE REDUCTION
V. Yuan and J. D. Bowman 1985 4 p Presented at the Particle Accelerator Conf., Vancouver, British Columbia, 13 May 1985
(Contract W-7405-eng-36)
(DE85-012701; LA-UR-85-1668; CONF-850504-80) Avail: NTIS HC A02/MF A01

The position noise in the LAMPF H(-) beam has been studied through examination of the autocorrelation and spectral-density functions for position motion. The LAMPF H(-) beam is a pulsed 800-MeV beam, and the position of each beam pulse was treated as a discrete value. Also investigated was the reduction in position noise that can be attained with an algorithm that predicts beam position from the measured positions of previous beam pulses. The basis for this predictive algorithm is the calculation of the optimal linear estimator. We conclude that the majority of low-frequency noise occurs within the 10- to 16-Hz frequency range, and that, with a simple, 2-pulse predictive correction system, one could improve the noise in this frequency region by as much as a factor of 15. DOE

N86-12034# Tufts Univ., Medford, Mass. Dept. of Physics.
AMPLITUDE TESTS OF DIRECT CHANNEL RESONANCES: THE DIBARYON
G. R. Goldstein, M. J. Moravosik, and F. Arash Feb. 1985 17 p refs Prepared in cooperation with Oregon Univ., Eugene
(Contract DE-AT06-76ER-70004)
(DE85-011478; DOE/ER-70004/T4) Avail: NTIS HC A02/MF A01

A recently formulated polarization amplitude test for the existence of one-particle-exchange mechanisms is modified to deal with direct-channel resonances. The results are applied to proton-proton elastic scattering at and around 800 MeV to test the suggested existence of a dibaryon resonance. This test is sensitive to somewhat different circumstances and parameters than the methods used in the past to find dibaryon resonances. The evidence, on the basis of the SAID data set, is negative for a resonance in any singlet partial wave, but is tantalizingly subliminal for a 3F3 resonance. DOE

N86-12035# Fermi National Accelerator Lab., Batavia, Ill.
REDUCTION OF SEXTUPOLE DISTORTION BY SHUFFLING MAGNETS IN SMALL GROUPS
R. I. Gluckstern and S. Ohnuma May 1985 4 p Presented at the Particle Accelerator Conf., Vancouver, British Columbia, 13 May 1985 Prepared in cooperation with Maryland Univ., College Park
(Contract DE-AC02-76CH-03000)
(DE85-013024; FNAL-TM-1312; CONF-850504-98) Avail: NTIS HC A02/MF A01

A method is given for reducing the most troublesome sextupole harmonics in a ring by measuring the sextupole field in groups of magnets, and ordering them according to a predetermined prescription. The predicted result is a decrease in sextupole related distortions by a factor (RADICAL)(2/(J+1)/SUP 1/2) where J magnets, covering one or more betatron periods, are measured at one time. Simulations performed for typical Superconducting Super Collider (SSC) lattices confirm the expected improvements. DOE

N86-12036# California Univ., Livermore. Lawrence Livermore Lab.
TRANSITION RADIATION AS A PRACTICAL X-RAY SOURCE
M. J. Moran and P. J. Ebert May 1985 14 p refs Presented at the 6th Symp. on X-and Gamma-Ray Sources and Appl., Ann Arbor, Mich., 21 May 1985
(Contract W-7405-eng-48)
(DE85-013201; UCRL-92017; CONF-850533-8) Avail: NTIS HC A02/MF A01

Transition radiation is generated when an energetic electron crosses the boundary between two different media. Theoretical calculations predict soft X-ray spectra and angular distributions that agree with experimental results. Further, recent advances in microstructure technology create the possibility of designing transition-radiation sources for several practical applications. For example, calculations indicate that a stack of 60 1 MU m-thick beryllium foils exposed to a beam of 100 MeV electrons will produce about 120 Joules of 1 to 2 keV X-rays per Coulomb of incident charge. The highest intensity sources appear to be bright enough for application to microlithography. DOE

N86-12037# Los Alamos Scientific Lab., N. Mex.
KINETICS ANALYSIS OF DIFFUSION OF POINT DEFECTS TO DISLOCATIONS FOLLOWING PULSED NEUTRON AND ELECTRON IRRADIATIONS
D. M. Parkin, J. A. Goldstone, H. M. Simpson, and J. W. Hemsky 1985 6 p Presented at the Conf. on Internal Friction and Ultrasonic Attenuation in Solids, Urbana, Ill., 3 Jun. 1985 Prepared in

cooperation with North Carolina Univ., Charlotte and Wright State Univ.
(Contract W-7405-eng-36)
(DE85-012768; LA-UR-85-1828; CONF-8506125-1) Avail: NTIS HC A02/MF A01

The kinetics of point defect-dislocation interactions following pulsed neutron and electron irradiations have been studied in high purity copper. In all experiments, data showed a very rapid increase in the modulus defect followed by a more gradual change. The magnitude of the rapid change in the modulus defect was proportional to the fluence. The initial rapid rise was too fast to allow for kinetics analysis; however, the slower continuous process was analyzed. Results are interpreted in terms of a model wherein interstitials are rapidly depleted and responsible for the initial rapid increase; the lower process is due to vacancy diffusion and arrival at dislocations. DOE

N86-12038# Brookhaven National Lab., Upton, N. Y.
AGS POLARIZED BEAM FACILITY
I. G. Ratner 1985 3 p Presented at the 6th Intern. Symp. on Polarization Phenomena in Nucl. Phys., Osaka, 26 Aug. 1985
(Contract DE-AC02-76CH-00016)
(DE85-011834; BNL-36425; CONF-850807-1) Avail: NTIS HC A02/MF A01

Two (MU)A of polarized H(-) were accelerated through the linac to 200 MeV a polarization of 65%. One (MU)A was injected into the AGS and acceleration began. The AGS polarized beam reached 13.8 GeV/c to eclipse the previous world's high energy of 12.75 GeV/c. The polarized beam energy is raised to 16.5 GeV/c at which energy it was decided to commence high energy physics running. The accelerated beam intensity exceeds 10 to the 10th power protons per pulse with about 40% polarization. DOE

N86-12039# Sandia Labs., Albuquerque, N. Mex.
CASCADE SWITCH IMPLEMENTATION OF PBFA 1
D. D. Bloomquist, G. R. Montry, S. E. Downie, and G. R. Peterson 1985 4 p Presented at the 5th IEEE Pulsed Power Conf., Washington, D.C., 10 Jun. 1985
(Contract DE-AC04-76DP-00789)
(DE85-013955; SAND-84-2459C; CONF-850616-52) Avail: NTIS HC A02/MF A01

The triggered gas switches in Particle Beam Fusion Accelerator (PBFA) 1 were recently changed from a single gap trigatron design to a 15-stage cascade design with a relatively short triggered gap. This improved design provides a low jitter value and has an extremely low probability of prefire. The triggered section represents about one-third of the total voltage of the switch and is triggered with a pin configuration similar to the previous trigatron design. The fields in the triggered gap were adjusted to allow prompt triggering and yet avoid prefires in the trigger gap at the operating gas pressure. Operating parameters of the switch will be discussed along with an analysis of the improved machine performance with respect to jitter, prefire probability, and operating voltage. DOE

N86-12040# California Univ., Berkeley. Electronics Research Lab.
SATURATION CHARACTERISTICS OF COUNTERSTREAMING WARM ELECTRONS
A. Wendt 28 May 1985 31 p
(Contract DE-AT03-76ET-53064)
(DE85-014390; DOE/ET-53064/T4) Avail: NTIS HC A03/MF A01

An investigation was made of the electron-electron two stream instability as the beam temperatures were increased, using particle simulations. Growth rates and saturation characteristics were studied and compared to theoretical models. The final state of the system, characterized by the value of the distribution function at zero velocity, f(upsilon = 0), was found to evolve to a Maxwellian in the cold case, and to a double-peaked distribution stable by the Penrose criterion in the warm cases. DOE

N86-12041# Brandeis Univ., Waltham, Mass. Dept. of Physics.
RESEARCH IN ELEMENTARY PARTICLE PHYSICS Technical Progress Report, 1 Jun. 1984 - 31 May 1985
L. E. Kirsch, H. J. Schnitzer, J. R. Bensinger, and L. F. Abbott 1985 29 p refs
(Contract DE-AC02-76ER-03230)
(DE85-014062; DOE/ER-03230/T4) Avail: NTIS HC A03/MF A01

Research performed on both the experimental and theoretical properties of elementary particles is briefly described, including: construction of forward electromagnetic shower counters; BO test facility; gas monitor development and production; off-line simulation work for trigger studies; hyperon weak radiative decay; search for dibaryons of strangeness = -1; study of the Skyrme model; collider physics; quarkonium spectroscopy; some theoretical studies of the standard model; and studies of cosomology, the cosmological constant, and scalar fields in curved space-time. DOE

N86-12042# Sandia Labs., Albuquerque, N. Mex.
IONIZATION-RAMAN DOUBLE-RESONANCE SPECTROSCOPY
P. Esherick and A. Owyoung 1985 5 p refs Presented at the 7th Intern. Conf. on Laser Spectroscopy, Maui, Hawaii, 24 Jun. 1985
(Contract DE-AC04-76DP-00789)
(DE85-013774; SAND-85-1347C; CONF-850605-2) Avail: NTIS HC A02/MF A01

Ionization detected stimulated Raman spectroscopy (IDSRS) is a new technique for high sensitivity, high resolution Raman studies based on resonant laser ionization/detection of vibrationally excited molecules. Results are presented on the application of IDSRS to the Raman spectroscopy of benzene. The spectra concentrate on the region near 1600 cm(-1) where the overlap of transitions to the (nu16, nu2 + nu18) Fermi dyad produces a particularly complex spectrum. By taking advantage of the double resonance capabilities of IDSRS, transitions are cleanly separated to each of the two vibrational bands, and thereby greatly simplify their spectra. DOE

N86-12001# Joint Publications Research Service, Arlington, Va.
COMPUTER APPLICATION IN ATOMIC ABSORPTION SPECTROMETRY
Hu Xinyao and Zhang Liangping *In its* China Rept.: Sci. and Technol. (JPRS-CST-85-015) 16 May 1985 p 51-57 refs Transl. into ENGLISH from Fenxi Huaxue (Changchun), no. 6, 20 Jun. 1983 p 451-454 (For primary document see N86-11994 02-70) Avail: NTIS HC A07/MF A01

73 NUCLEAR AND HIGH-ENERGY PHYSICS

Includes elementary, and nuclear particles; and reactor theory.

For space radiation see *93 Space Radiation*.

N86-12043# Department of the Navy, Washington, D. C.
ION BEAM NEUTRALIZER Patent Application
J. E. Campana, inventor (to Navy) Filed 31 Oct. 1984 16 p
(AD-D011741; US-Patent-Appl-SN-666597) Avail: NTIS HC A02/MF A01 CSCL 20/3

A method and apparatus for converting an ion beam from a standard ion gun into a neutral particle beam by the processes of resonance neutralization followed by Auger deexcitation and/or Auger neutralization, established by directing the ion beam to pass in the proximity of a suitable metal surface are discussed. Author (GRA)

N86-12044# Brookhaven National Lab., Upton, N. Y.
POSSIBILITIES OF POLARIZED PROTONS IN Sp ANTI p S AND OTHER HIGH ENERGY HADRON COLLIDERS
E. D. Courant 1985 3 p Presented at the 6th Intern. Symp. on High Energy Spin Phys., Marseille, 12 Sep. 1985 Prepared in

cooperation with State Univ. of New York, Stony Brook
(Contract DE-AC02-76CH-00016)
(DE85-012517; BNL-36181; CONF-8409162-15) Avail: NTIS HC A02/MF A01

The requirements for collisions with polarized protons in hadron colliders above 200 GeV are listed and briefly discussed. Particular attention is given to the use of the Siberian snake to eliminate depolarizing resonances, which occur when the spin precession frequency equals a frequency contained in the spectrum of the field seen by the beam. The Siberien snake is a device which makes the spin precession frequency essentially constant by using spin rotators, which precess the spin by 180 deg about either the longitudinal or transverse horizontal axis. It is concluded that operation with polarized protons should be possible at all the high energy hadron colliders. DOE

N86-12045# Los Alamos Scientific Lab., N. Mex.
STATUS OF FAST NEUTRON NUCLEAR DATA FOR (239)Pu
E. D. Arthur 1985 14 p Presented at the Intern. Conf. on Nucl. Data for Basic and Appl. Sci., Santa Fe, N. Mex., 13 May 1985
(Contract W-7405-eng-36)
(DE85-012699; LA-UR-85-1674; CONF-850507-30) Avail: NTIS HC A02/MF A01

Recent energy-averaged data (fission, total cross section, scattering and anti nu sub p) describing the interaction of fast neutrons with (239)Pu are discussed, with emphasis on neutron energies higher than the inelastic scattering threshold. The linkage between such experimental data and new theoretical calculations is described in context of their influence on a new revision to the ENDF/B-V (239)Pu evaluation. Results from this new revision are compared with other current (239)Pu evaluations. Incorporation of such information pertaining to neutron emission and anti nu sub p in the new ENDF revision had a profound impact on calculations performed for fast critical assemblies. Such calculational results are presented with emphasis on systematic improvements achieved in eigenvalues and fission ratios. DOE

N86-12046# Oak Ridge National Lab., Tenn.
LIQUID METAL REACTORS PROGRAMS: SAFEGUARDS AND PROGRAM ASSURANCE Technical Progress Report, Apr. 1985
W. L. Cooper, Jr. 17 May 1985 8 p
(Contract DE-AC05-84OR-21400)
(DE85-011002; ORNL/LMP/SP-85/4) Avail: NTIS HC A02/MF A01

Significant accomplishments and progress highlights concerning the development of standards for the liquid metal reactor program are presented. DOE

N86-12047# Edgerton, Germeshausen and Grier, Inc., Idaho Falls, Idaho.
SURVEY OF ELEMENT AND ISOTOPE IMPORTANCE FOR FUSION SAFETY AND ENVIRONMENTAL ASSESSMENTS
S. J. Piet May 1985 34 p
(Contract DE-AC07-76ID-01570)
(DE85-012415; EGG-2393) Avail: NTIS HC A03/MF A01

A survey was made, using the most reliable information possible, to identify which elements and isotopes are potentially important for fusion safety and environmental assessments. It was determined that 51 elements may be exposed to fusion neutrons in either experimental devices or commercial reactors. These elements were prioritized by the relative probability of use. Also, 371 radioactive isotopes were identified that may be produced from these elements. These isotopes were prioritized by screening criteria that measured their relative importance to effluent assessments, accident assessments, and waste management assessments. Survey results presented in this report are prioritized lists of elements and isotopes of importance to neutronics researchers, effluent assessors, accident assessors, waste management assessors, maintenance assessors, and volatility and/or transport researchers. It is hoped that the results of this effort will lead to improved information in the various areas, which in turn will lead to better safety and environmental assessments. DOE

N86-12048# Los Alamos Scientific Lab., N. Mex.
APPLICATION OF DETAILED FISSION-PRODUCT DECAY GAMMA SPECTRA IN THE CALCULATION OF PHOTONEUTRON SPECTRA FROM D((GAMMA),n) REACTIONS IN PWR FUEL
W. B. Wilson, J. E. Stewart, T. R. England, and R. T. Perry 1985 5 p Presented at the Intern. Conf. on Nucl. Data for Basic and Appl. Sic., Santa Fe, N. Mex., 13 May 1985 Prepared in cooperation with Texas A&M Univ., College Station
(Contract W-7405-eng-36)
(DE85-012729; LA-UR-85-1729; CONF-850507-23) Avail: NTIS HC A02/MF A01

The magnitude, average neutron energy, and spectrum of the photoneutron source in a PWR fuel is calculated for shutdown times to 100 y using CINDER radionuclide inventory calculations, ENDF/B-V (GAMMA) line decay spectra, MCNP (GAMMA) transport calculations, and PHONEX D((GAMMA),n) reaction physics calculations. DOE

N86-12049# Stanford Linear Accelerator Center, Calif.
EXPERIMENTAL PROGRAM TO BUILD A MULTIMEGAWATT LASERTRON FOR SUPER LINEAR COLLIDERS
E. L. Garwin, W. B. Hermannsfeldt, C. Sinclair, J. N. Weaver, J. J. Welch, and P. B. Wilson Apr. 1985 4 p refs Presented at Particle Accelerator Conf., Vancouver, British Columbia, 13 May 1985
(Contract DE-AC03-76SF-00515)
(DE85-014293; SU-SLAC-Pub-3650; CONF-850504-192) Avail: NTIS HC A02/MF A01

A lasertron (a microwave triode with an RF output cavity and an RF modulated laser to illuminate a photocathode) is a possible high power RF amplifier for TeV linear colliders. As the first step toward building a 35 MW, S-band lasertron for a proof of principle demonstration, a 400 kV dc diode is being designed with a GaAs photocathode, a drift tube and a collector. After some cathode life tests are made in the diode, an RF output cavity will replace the drift tube and a mode-locked, frequency-doubled, Nd:YAG laser, modulated to produce a 1 us-long comb of 60 ps pulses at a 2856 MHz rate, will be used to illuminate the photocathode to make an RF power source out of the device. The plans for the project are discussed and numerical simulation studies results of the lasertron as well as some of the ultrahigh vacuum and mechanical design requirements for incorporating a photocathode are included. DOE

N86-12050# Stanford Linear Accelerator Center, Calif.
COLLINEAR WAKE FIELD ACCELERATION
K. L. F. Bane, P. Chen, and P. B. Wilson Apr. 1985 3 p refs Presented at Particle Accelerator Conf., Vancouver, British Columbia, 13 May 1985
(Contract DE-AC03-76SF-00515)
(DE85-014356; SU-SLAC-Pub-3662; CONF-850504-187) Avail: NTIS HC A02/MF A01

In the Voss-Weiland scheme of wake field acceleration a high current, ring shaped driving bunch is used to accelerate a low current beam following along an axis. In such a structure, the transformer ratio, i.e., the ratio of maximum voltage that can be gained by the on-axis beam and the voltage lost by the driving beam, can be large. In contrast, it was observed that for an arrangement in which driving and driven bunches follow the same path, and where the current distribution of both bunches is gaussian, the transformer ratio is not normally greater than two. Some of the possibilities and limitations of a collinear acceleration scheme are explored. In addition to its application to wake field acceleration in structures, this study is also of interest for the understanding of the plasma wake field accelerator. DOE

N86-12051# Oak Ridge National Lab., Tenn.
CALCULATIONS OF PHYSICAL AND CHEMICAL REACTIONS PRODUCED IN IRRADIATED WATER CONTAINING DNA
H. A. Wright, J. L. Magee, R. N. Hamm, A. Chatterjee, J. E. Turner, and C. E. Klots 1985 18 p refs Presented at the 9th Symp. on Microdosimetry, Toulouse, 20 May 1985 Prepared in cooperation

with California Univ., Berkeley. Lawrence Berkeley Lab.
(Contracts DE-AC05-84OR-21400; DE-AC03-76SF-00098)
(DE85-012899; CONF-850506-8) Avail: NTIS HC A02/MF A01

Initial results obtained with a Monte Carlo computer program designed to link initial physical events in irradiated liquid water with subsequent chemical and biological events are presented. A simple model for a segment of DNA was taken and calculations were performed for proton and alpha particles that traverse the medium at various distances from the DNA molecule. The number of chemical reactions were insulated. DOE

N86-12052# Oak Ridge National Lab., Tenn.
R-MATRIX ANALYSIS OF THE (239) Pu NEUTRON CROSS SECTIONS
G. Desaussure, R. B. Perez, and R. L. Macklin 1985 6 p refs Presented at the Intern. Conf. on Nucl. Data for Basic and Appl. Sci., Santa Fe, N. Mex., 13 May 1985 Prepared in cooperation with Tennessee Univ., Knoxville
(Contract DE-AC05-84OR-21400)
(DE85-013095; CONF-850507-39) Avail: NTIS HC A02/MF A01

Pu-239 neutron cross-section data in the resolved resonance region were analyzed with the R-Matrix Bayesian Program SAMMY. Below 30 eV the cross sections computed with the multilevel parameters are consistent with recent fission and transmission measurements as well as with older capture and alpha measurements. Above 30 eV no suitable transmission data were available and only fission cross-section measurements were analyzed. However, since the analysis conserves the complete covariance matrix, the analysis can be updated by the Bayes method as transmission measurements become available. To date, the analysis of the fission measurements was completed up to 300 eV. DOE

N86-12053# California Inst. of Tech., Pasadena. Lab. of Engineering Materials.
DOMINANT MOVING SPECIES IN THE FORMATION OF AMORPHOUS Nzr BY SOLID-STATE REACTION
Y. T. Cheng, W. I. Johnson, and M. A. Nicolet Jun. 1985 11 p
(Contract DE-AT03-81ER-10870)
(DE85-014855; DOE/ER-10870/155) Avail: NTIS HC A02/MF A01

The displacement of W and Hf makers were monitored by backscattering of MeV He. The growth of the amorphous NiZr phase was studied by solid-state reaction. It is found that the Ni is the dominant moving species in this reaction. DOE

N86-12054# Oak Ridge National Lab., Tenn.
CHEMICAL THERMODYNAMIC ASSESSMENT OF THE LI-U-O SYSTEM FOR POSSIBLE SPACE NUCLEAR APPLICATIONS
T. M. Besmann and R. H. Cooper, Jr. Jun. 1985 13 p
(Contract DE-AC05-84OR-21400)
(DE85-015060; ORNL/TM-9662) Avail: NTIS HC A02/MF A01

A thermochemical assessment of possible oxide fuel-lithium coolant interactions in conceptual 100-kW(e) space nuclear power reactors was performed. Results of the evaluation indicate that in the event of a cladding breach the fuel and coolant will interact with extremely negative consequences. The lithium has the potential to reduce the fuel to metallic uranium. Differences in temperature within the coolant loop can drive oxygen and uranium transport processes. DOE

N86-12055# Sandia Labs., Albuquerque, N. Mex.
MULTIDIMENSIONAL ION MICROBEAM ANALYSIS
B. L. Doyle 1985 25 p refs Presented at the 7th Intern. Conf. on Ion Beam Anal., Berlin, West Germany, 7 Jul. 1985
(Contract DE-AC04-76DP-00789)
(DE85-014699; SAND-85-0874C; CONF-850716-2) Avail: NTIS HC A02/MF A01

The nuclear microprobe is an instrument used to determine the atomic composition of the near-surface region of materials and is finding increasing use in a wide variety of scientific areas. When a scanning microprobe uses a depth-sensitive ion-beam analysis technique such as RBS, three dimensional analyses can be performed. This paper reviews current nuclear microbeam applications with emphasis on results involving such multidimensional profiling. DOE

N86-12056# Los Alamos Scientific Lab., N. Mex.
DOUBLE DIFFERENTIAL NEUTRON EMISSION CROSS SECTIONS OF (10)B AND (1)B AT 6, 10 AND 14 MeV AND OF (6)LI, (7)LI AND (12)C AT 14 MeV
M. Drosq, P. W. Lisowski, R. A. Hardegopf, D. M. Drake, and K. Treitl 1985 5 p Presented at the Intern. Conf. on Nucl. Data for Basic and Appl. Sci., Santa Fe, N. Mex. 13 May 1985 Prepared in cooperation with Wien Univ.
(Contract W-7405-eng-36)
(DE85-012749; LA-UR-85-1743; CONF-850507-28) Avail: NTIS HC A02/MF A01

Neutron emission spectra of (10)B and (11)B were measured at 6, 10, and 14.1 MeV and those of (6)li, (7)Li and carbon at 14.1 MeV using time-of-flight technique. Absolute double differential cross sections were obtained by emission cross sections. At 6 and 10 MeV excellent agreement with total cross section data is found, at 14.1 MeV the new data tend to be higher than expected. The biggest error source in the continuous spectra stems from uncertainties in the input library (FNDF/B-IV) of the Monte Carlo correction for multiple scattering. In particular, the library for (11)B appears to be very unrealistic, with a total elastic cross section at 14.1 MeV which should be higher by 50%. DOE

N86-12057# California Univ., Livermore. Lawrence Livermore Lab.
PHYSICS OVERVIEW OF AVLIS
R. W. Solarz Feb. 1985 18 p
(Contract W-7405-eng-48)
(DE85-014854; UCID-20343) Avail: NTIS HC A02/MF A01

Atomic vapor laster isotope separation (AVLIS) represents the largest-scale potential application of tunable lasers that has received serious attention. The underlying physical principles were identified and optimized, the major technology components were developed, and the integrated enrichment performance of the process was tested. The central physical processes are outlined, progress to date on the technology elements is reviewed, and scaling laws are fomulated. Two primary applications are the production of light-water reactor fuel and the conversion of fuel-grade plutonium to weapons-grade material. A variety of applications exist that all potentially use a common base of AVLIS technology. These include missions such as the enrichment of mercury isotopes to improve fluorescent lamp efficiency, the enrichment of iodine isotopes for medical isotope use, and the cleanup of strontium from defense waste for recovering strontium isotopes for radiothermal mechanical generators. The ability to radidly assess the economic and technical feasibility of each mission is derived from the general applicability of AVLIS physics and AVLIS technology. DOE

N86-12058# Sandia Labs., Albuquerque, N. Mex.
EXPERIMENTAL CHECK OF BREMSSTRAHLUNG DOSIMETRY PREDICTIONS FOR 0.75 MeV ELECTRONS
T. W. L. Sanford, J. A. Halbleib, and W. Beezhold 1985 28 p refs Presented at the 22nd Ann. Conf. on Nucl. and Space Radiation Effects, Monterey, Calif., 22 Jul. 1985
(Contract DE-AC04-76DP-00789)
(DE85-014706; SAND-85-0357C; CONF-850711-10) Avail: NTIS HC A03/MF A01

Bremsstrahlung dose in CaF2 TLDs from the radiation produced by 0.75 MeV electrons incident on Ta/C targets is measured and compared with that calculated via the CYLTRAN Monte Carlo code. The comparison was made to validate the code, which is used to predict and analyze radiation environments of flash X-ray simulators measured by TLDs. Over a wide range of Ta target thicknesses and radiation angles the code is found to agree with the 5% measurements. For Ta thickness near those that optimize the radiation output, however, the code overestimates the radiation dose at small angles. Maximum overprediction is about 14 + or - 5%. The general agreement, nonetheless, gives confidence in using the code at this energy and in the TLD calibration procedure. For the bulk of the measurements, a standard TLD employing a 2.2 mm thick Al equilibrator was used. In this paper we also show that this thickness can significantly attenuate the free-field dose and introduces significant photon buildup in the equalibrator. DOE

N86-12059# Brookhaven National Lab., Upton, N. Y.
ANTINUCLEON-NUCLEUS ELASTIC AND INELASTIC SCATTERING
C. B. Dover and D. J. Millener 1985 25 p refs Presented at the Conf. on Antinucleon and Nucleon-Nucleus Interactions, Telluride, Colo., 18 Mar. 1985
(Contract DE-AC02-76CH-00016)
(DE85-012510; BNL-36438; CONF-850315-4) Avail: NTIS HC A02/MF A01

A general overview of the utility of antinucleon (anti N)-nucleus inelastic scattering studies is presented, emphasizing both the sensitivity of the cross sections to various components of the N anti N transition amplitudes and the prospects for the exploration of some novel aspects of nuclear structure. An examination of the relation between NN and N anti N potentials, focusing on the coherences predicted for the central, spin-orbit and tensor components, and how these may be revealed by measurements of two-body spin observables was conducted. The role of the nucleus as a spin and isospin filter, and how, by a judicious choice of final state quantum numbers (natural or unnatural parity states, isospin transfer (DELTA)T = 0 or 1) and momentum transfer g, one can isolate different components of the N anti N transition amplitude was discussed. Various models for the N anti N interaction which give reasonable fits to the available two-body data are shown to lead to strikingly different predictions for certain spin-flip nuclear transitions. The antinucleon and the nucleon were considered as a probe of nuclear modes of excitation. DOE

N86-12060# Massachusetts Inst. of Tech., Cambridge.
OVERVIEW OF MIT, ADIP IRRADIATION EXPERIMENTS
G. Kohse, O. K. Harling, and N. J. Grant Jun. 1985 5 p
(Contract DE-AC02-78ER-10107)
(DE85-014469; DOE/ER-10107/27) Avail: NTIS HC A02/MF A01

Various rapidly solidified austenitic, ferritic and copper alloys have been produced at MIT for inclusion in ADIP neutron irradiation experiments. A brief summary of the alloys and their preparation and the achieved or projected irradiation parameters is provided. DOE

N86-12061# Brookhaven National Lab., Upton, N. Y.
VACANCIES IN THERMAL EQUILIBRIUM IN Nb
B. Nielsen, K. G. Lynn, J. Hurst, A. Vehanen, and P. J. Schultz Jun. 1985 4 p Presented at the 7th Intern. Conf. on Positron Annihilation, New Delhi, 6 Jan. 1985 Prepared in cooperation with Helsinki Univ. and University of Western Ontario, London
(Contract DE-AC02-76CH-00016)
(DE85-014832; BNL-36699; CONF-850169-18) Avail: NTIS HC A02/MF A01

The diffusion of positrons in Nb-110 in the temperature range from 300K to 2450K utilizing a variable energy positron beam was measured. The vacancy formation was studied, however, no significant sign of vacancy trapping was observed. This could be due to a high detrapping rate caused by a low positron binding energy or due to a high vacancy formation enthalpy H sub IV sup F. The last possibility is consistent with recent studies of the vacancy migration and with calculation of the positron binding energy. It is found that H/sub IV sup F > 3 eV. DOE

N86-12062# Argonne National Lab., Ill.
SI(LI)-NaI(TI) SANDWICH DETECTOR ARRAY FOR MEASUREMENTS OF TRACE RADIONUCLIDES IN SOIL SAMPLES
M. G. Strauss, I. S. Sherman, C. T. Roche, and R. H. Pehl (California Univ., Berkeley. Lawrence Berkeley Lab.) 1985 19 p refs Presented at 6th Symp. on X- and Gamma-Ray Sources and Appl., Ann Arbor, Mich., 21 May 1985
(Contract W-31-109-eng-38)
(DE85-013865; CONF-850533-10) Avail: NTIS HC A02/MF A01

An ultra-sensitive X-(gamma) ray detector system for assaying trace radioactivity in actinide contaminated soil and ash samples was developed. The new system consists of an array of 6 large Si(Li) X-ray detectors sensitive on both faces and mounted on edge in a paddle-shaped cryostat with a 14 cm dia Be window on each side. The paddle, with a sample of the soil placed at each window, is sandwiched between 2 large NaI(Tl) scintillators which suppress the (GAMMA) background. With X-rays being measured simultaneously from soil in 2 sample holders and background reduced by 50% using anticoincidence, the sensitivity of this detector is 4 times higher than that of conventionally mounted Si(Li) detectors. DOE

N86-12063# Colorado Univ., Boulder.
HIGH ENERGY PHYSICS Progress Report, Oct. 1984 - Jun. 1985
U. Nauenberg 2 Jul. 1985 38 p
(Contract DE-AC02-81ER-40025)
(DE85-014272; DOE/ER-40025/33) Avail: NTIS HC A03/MF A01

The tagged-photon beam effort consists of photoproduction and charm photoproduction. Progress in the broadband neutral beam program included setting up the production data analysis for hadronic charm production, and design, prototyping, procurement and fabrication of the electromagnetic calorimeter for photoproduction at the Tevatron. The electron-positron effort included data-taking and physics analysis, fabrication of a trigger/vertex drift chamber for the Mark II upgrade, and prototype studies. Studies included formal work in supergravity, supersymmetry phenomenology, lattice gauge theory approaches to hadronization, investigations of the behavior of the quark-gluon plasma in the early Universe, in heavy ion collisions, and on the lattice, and a first look at the real-time behavior of quantum systems out of thermal equilibrium. The equivalence of inertial and passive gravitational mass of high sensitivity in a cryogenic system is investigated. DOE

N86-12064# Argonne National Lab., Ill.
FEW-NUCLEON TRANSFER REACTIONS ON DEFORMED NUCLEI
A. M. vandenBerg 1985 29 p refs Presented at the Conf. on Nucl. Struct. with Heavy Ions, Padua, 27 May 1985
(Contract W-31-109-eng 38)
(DE85-013869; CONF-8505172-1) Avail: NTIS HC A03/MF A01

Development in nucleon transfer reactions on deformed nuclei were discussed. They include: alpha-transfer reactions on deformed nuclei, quasi-elastic neutron transfer reactions induced by (58)Ni beams on spherical and deformed samarium nuclei, and the population of low lying states in neutron rich nuclei using particle, GAMMA or particle, e coincidence methods. DOE

N86-12065# Argonne National Lab., Ill.
HIGH RESOLUTION SPECTROMETER IN STUDIES OF e(+)e(-) ANNIHILATION AT (RADICAL)s = 29 GeV
M. Derrick 3 May 1985 47 p refs Presented at the PEP High Luminosity Workshop, Stanford, Calif., 5-6 Apr. 1985
(Contract W-31-109-eng-38)
(DE85-013870; ANL/HEP-CP-85-45; CONF-8504155-1) Avail: NTIS HC A03/MF A01

The High Resolution Spectrometer is a general-purpose spectrometer which measures both charged particles and electromagnetic energy over 90% of the solid angle. The detection elements are in a 1.62-T magnetic field. The detector elements consist of a central drift chamber, an outer drift-chamber system, a barrel shower counter, and an end-cap shower-counter system. The goals of the program of research with the High Resolution Spectrometer include measurements of the electroweak coupling of the quarks and leptons, studies of the strong interactions of the quarks, and search for qualitatively new phenomena. DOE

N86-12066# Brookhaven National Lab., Upton, N. Y.
SPIN DEPENDENCE OF THE COHERENT SCATTERING

LENGTHS OF (27)AI AND ADMIXTURE OF s- AND d-PARTIAL WAVES
S. F. Mughab 1985 6 p Presented at the Intern. Conf. on Nucl. Data for Basic and Appl. Sci., Santa Fe, N. Mex., 13 May 1985
(Contract DE-AC02-76CH-00016)
(DE85-013299; BNL-NCS-36468; CONF-850507-36) Avail: NTIS HC A02/MF A01

A long standing discrepancy between measurements and calculations of the sign of the incoherent scattering length is attributed to two sources: (1) spin dependence of the potential scattering radius, and (2) identification of additional s-wave resonances at higher neutron energies. Detailed examination of the reaction Al-27 (n vector, (GAMMA) (28)Al induced by thermal neutrons revealed that R b +/ - R sub -/ = 0.32 +- 0.10 fm. Also shape fit analysis of the total cross section showed the presence of s-wave resonances at neutron energies 280, 386, 422, 491, 523, and 615 keV. One interesting outcome is the demonstration of the admixture of s- and d-wave partial waves in these resonances and the presence of a large d-wave neutron strength in the above energy region. DOE

N86-12067# California Univ., Berkeley. Lawrence Berkeley Lab.
MUON DECAY
H. Steiner Mar. 1985 9 p refs Presented at the 5th Moriond Workshop on Heavy Quarks, Flavor Mixing and CP Violation, La Plagne, France, 13 Jan. 1985
(Contract DE-AC03-76SF-00098)
(DE85-012590; LBL-19684; CONF-850171-2) Avail: NTIS HC A02/MF A01

Improved searches for rare processes in muon decay have substantially improved existing limits, but no evidence for any nonstandard behavior was found. The result of a recent sensitive search for right handed currents indicates that the ratio (V + A)-anokutyde/(V - A)-amplitude less than or equal to 0.029. This experiment also imposed new limits on nonstandard couplings and on the energy scales where lepton substructure and family symmetry breaking effects might manifest themselves. DOE

N86-12068# Fermi National Accelerator Lab., Batavia, Ill.
COLLIDER DETECTOR AT FERMILAB (CDF) Progress Report
D. Theriot Jun. 1985 14 p refs Presented at the Intern. Symp. on Phys. of Proton-Antiproton Collision, Tsukuba, Japan, 13-15 Mar. 1985
(Contract DE-AC02-76CH-03000)
(DE85-014423; FNAL/C-85/89; CONF-8503151-1) Avail: NTIS HC A02/MF A01

CDF, the Collider Detector at Fermilab, is a collaboration of almost 180 physicists from ten US universities, three US DOE supported national laboratories, Italy, and Japan. The primary physics goal for CDF is to study the general features of proton-antiproton collision at 2 TeV center-of-mass energy. On general grounds, it is expected that parton subenergies in the range 50 to 500 GeV will provide the most interesting physics at this energy. Work at the present CERN Collider has already demonstrated the richness of the 100 GeV scale in parton subenergies. DOE

74 OPTICS

Includes light phenomena.

N86-12069# Ceskoslovenska Akademie Ved, Ondrejov. Astronomical Inst.
PUBLICATIONS OF THE ASTRONOMICAL INSTITUTE OF THE CZECHOSLOVAK ACADEMY OF SCIENCES, NO. 61
1985 81 p refs
(Publ-61) Avail: NTIS HC A05/MF A01

An X-ray mirror system with mean resolution and a maximum effective collecting area for the spectral region of 1 to 10 nm is presented, and galvanoplastic grazing incidence mirrors for vertical experiments are discussed. For individual titles, see N86-12070 through N86-12071.

N86-12070# Ceskoslovenska Akademie Ved, Ondrejov. Astronomical Inst.
WOLTER 1 TYPE X-RAY MIRROR SYSTEM WITH MEAN RESOLUTION AND MAXIMUM EFFECTIVE COLLECTING AREA FOR THE SPECTRAL REGION OF 1-10 nm
R. Hudec, B. Valnicek, I. Solc, V. Landa, L. Svatek, R. Marecek, J. Urban, L. A. Vainshtein, M. E. Plotkin, M. M. Mitropolskii et al *In its* Publ. of the Astron. Inst. of the Czech. Acad. of Sci., No. 61 1985 p 1-41 refs (For primary document see N86-12069 02-74)
Avail: NTIS HC A05/MF A01

Parameter calculations of manufacturing procedure methods, and results are described for the Wolter 1 X-ray mirror system. The system consists of two nested pairs of mirrors: the outer pair has an input diameter of 24 cm and nickel coating, the inner pair has an input diameter of 13 cm and a gold coating. The focal distance is 41,9 cm, the length of each paraboloid and hyperboloid is 24 cm. Geometrical parameters of the mirrors are chosen to obtain a maximum effective area within the limits for overall dimensions. The mirrors are made as galavanic replicas with metallic reflecting surface and plastic base. The system is intended for use in the RT-4M X-ray telescope. E.A.K.

N86-12071# Ceskoslovenska Akademie Ved, Ondrejov. Astronomical Inst.
GALVANOPLASTIC GRAZING INCIDENCE MIRRORS FOR VERTICLE EXPERIMENTS: THE TANDEM TESTS IN SOFT X-RAYS
R. Hudec, B. Valnicek, I. Solc, M. M. Mitropolskii, I. A. Zhitnik, V. V. Krutov, and N. K. Sukhodrev *In its* Publ. of the Astron. Inst. of the Czech. Acad. of Sci., No. 61 1985 p 42-76 refs (For primary document see N86-12069 02-74)
Avail: NTIS HC A05/MF A01

The principles for calculating methodology, and laboratory tests results for grazing incidence mirrors used in solar X-ray telescopes installed in the Vertikal 8, Vertikal 9, and Vertikal 11 rockets launched as part of the Intercosmos program are described. The X-ray grazing incidence mirrors were developed by using galvanoplastic replica technology and tested according to a chart design with one of the investigated mirrors acting as a collimator. The advantages and drawbacks of this test method for X-ray mirrors are analyzed. E.A.K.

N86-12072# Clarkson Univ., Potsdam, N.Y.
ELASTIC AND INELASTIC LIGHT SCATTERING OF COLLOIDAL PARTICLES Final Report, 1982 - 1985
M. Kerker 10 Jun. 1985 6 p
(Contract DAAG29-82-K-0062)
(AD-A157335; ARO-18638.13-CH) Avail: NTIS HC A02/MF A01 CSCL 20/6

The project has been primarily concerned with both theoretical and experimental aspects of surface enhanced scattering. The theory has been extended to include concentric spherical particles, the effect of surface coverage, enhancement of coherent anti-Stokes Raman scattering and the effect of dielectric cavities. The experimental work included SERS (Surface Enhanced Raman Scattering) from citrate on silver hydrosols, surface enhanced resonance Raman scattering (SERRS) for dabsylaspartate on silver hydrosols, silver organosols and roughened silver electrodes, the effect of aggregates on SERS. In addition there have been ancillary studies dealing with absorption and luminescence by dye coated silver particles, analysis of biological cells by flow fluorimetry, and electromagnetic scattering by magnetic particles. Author (GRA)

N86-12073# Office of the Under Secretary of Defense for Research and Engineering, Washington, D. C.
ELECTRO-OPTICS MILLIMETER/MICROWAVE TECHNOLOGY IN JAPAN. REPORT OF DOD TECHNOLOGY TEAM Final Report, Jul. 1984 - May 1985
J. M. MacCallum, Jr., G. Nicholas, S. Musa, T. Hartwick, and B. Spielman May 1985 54 p
(AD-A157376) Avail: NTIS HC A04/MF A01 CSCL 20/6

This document is a report on the first DOD technology team review of Japanese programs in electro-optical (EO) millimeter and microwave technology of interest to the Department of Defense. The team visited Japan during July 1984 and April 1985 and reviewed EO/MMW activities at a number of companies and government research centers. GRA

N86-12074# Georgia Inst. of Tech., Atlanta. School of Geophysical Sciences.
ANALYSIS OF ARCTIC HAZE SCATTERING AND AEROSOL DATA OBTAINED DURING AGASP Final Report, 16 Sep. 1983 - 15 Sep. 1984
E. M. Patterson and G. W. Grams 1 May 1985 46 p
(Contract DAAG29-83-K-0163)
(AD-A157434; ARO-21001.1-GS) Avail: NTIS HC A03/MF A01
CSCL 20/6

We have analyzed polar nephelometer scattering data to infer radiative parameters for the Arctic haze aerosols. We have also used the scattering properties as measured with the nephelometer as well as other measurements of aerosol microphysical properties to improve our estimates of aerosol properties for radiative modeling. We have confirmed earlier estimates of the submicron size distribution and have demonstrated the uniformity of these distributions. We have also shown that the giant particles also have relatively uniform size distributions and have provided an estimate of the infrared effects due to these particles. We have also demonstrated an inconsistency in two of the AGASP data sets and have resolved the discrepancy in terms of the measurement limitations of the data set. GRA

N86-11985# Joint Publications Research Service, Arlington, Va.
PHOTOINDUCED RAYLEIGH SCATTERING OF LIGHT IN CRYSTALS Abstract Only.
V. V. Obukhovskiy and A. V. Stoyanov *In its* USSR Rept.: Phys. and Math. (JPRS-UPM-85-005) 20 Aug. 1985 p 97 p 97 Transl. into ENGLISH from Opt. i Spektrosk. (Leningrad), v. 58, no. 2, Feb. 85 p 3780-385 (For primary document see N86-11945 02-70)
Avail: NTIS HC A08/MF A01

N86-11986# Joint Publications Research Service, Arlington, Va.
MULTIPHOTON RAMAN SCATTERING OF LIGHT EXCITED IN CRYSTALS BY A COPPER-VAPOR LASER Abstract Only.
A. M. Agaltsov, V. S. Gorelik, and M. M. Sushchinskiy *In its* USSR Rept.: Phys. and Math. (JPRS-UPM-85-005) 20 Aug. 1985 p 98 p 98 refs Transl. into ENGLISH from Opt. i Spektrosk. (Leningrad), v. 58, no. 2, Feb. 85 p 386-389 (For primary document see N86-11945 02-70)
Avail: NTIS HC A08/MF A01

N86-11987# Joint Publications Research Service, Arlington, Va.
PHASING OF MULTIPLE-APERTURE OPTICAL SYSTEMS Abstract Only.
P. A. Bakut, A. D. Rayakin, K. N. Sviridov, and N. D. Ustinov *In its* USSR Rept.: Phys. and Math. (JPRS-UPM-85-005) 20 Aug. 1985 p 98 refs Transl. into ENGLISH from Opt. i Spektrosk. (Leningrad), v. 58, no. 2, Feb. 1985 p 445-448 (For primary document see N86-11945 02-70)
Avail: NTIS HC A08/MF A01

N86-11988# Joint Publications Research Service, Arlington, Va.
TRANSFORMATION OF LIGHT PULSE SHAPE BY THIN PLANE-PARALLEL LAYER OF ABSORBING MATERIAL Abstract Only
N. I. Insarova and G. I. Olefir *In its* USSR Rept.: Phys. and Math. (JPRS-UMP-85-005) 20 Aug. 1985 p 101 refs Transl. into ENGLISH from Zh. Prikl. Spektrosk. (Minsk, USSR), v. 42, no. 2, Feb. 1985 p 255-259 (For primary document see N86-11945 02-70)
Avail: NTIS HC A08/MF A01

75 PLASMA PHYSICS

Includes magnetohydrodynamics and plasma fusion.
For ionospheric plasmas see *46 Geophysics*. For space plasmas see *90 Astrophysics*.

N86-12075# Naval Research Lab., Washington, D. C.
A HYBRID MODE AND A CLASSIFICATION OF BEAM PLASMA INSTABILITIES
Y. Y. Lau 11 Jul. 1985 39 p
(ARPA Order 4395)
(AD-A157356; NRL-MR-5601) Avail: NTIS HC A03/MF A01
CSCL 20/9

The interactions of an electron beam with a background plasma are classified according to the beam energy and to the relative density of the beam and the plasma. Both the electron beam and plasma are assumed to be cold, unmagnetized, collisionless, and all equilibrium self-fields have been assumed negligible. Emphasis is placed on the dynamical coupling of longitudinal and transverse motions as a result of relativistic and electromagnetic effects. Over many orders of magnitudes, we find that the parameter space may be divided into just a few domains, with different instability mechanisms. The boundaries separating these domains are given, together with the instability growth rates and the characteristic wave number of the instability within each of these domains. This classification thus provides an immediate assessment of the nature specified. In addition to the classical two stream instabilities and the Weibel type instabilities, a new mode, temporarily called the hybrid mode, is discovered. The hybrid mode is dominant when the electron beam is highly relativistic. We provide several examples of current interest to demonstrate the use of this classification. The results have been tested against the dispersion relationship given by Tajima, Jones and Shoucri. Effects of a finite beam are discussed. GRA

N86-12076# Michigan Univ., Ann Arbor. Coll. of Engineering.
NEUTRAL BEAM INTERACTIONS WITH MATERIALS Annual Progress Report, 1 Jun. 1984 - 31 May 1985
R. M. Gilgenbach and J. J. Duderstadt 18 Jun. 1985 61 p
(Grant AF-AFOSR-0130-84)
(AD-A157445) Avail: NTIS HC A04/MF A01 CSCL 20/8

This annual report describes experimental and theoretical research which concerns the interaction of neutral or ion beams with surface ablation plasmas. This problem is of interest in the case of particle penetration to outgassing or ablating objects in a high vacuum environment. We have constructed a neutral beam-ablation plasma experiment which employs a Q-switched ruby laser to independently generate a dense ablation plasma. GRA

N86-12077# Naval Research Lab., Washington, D. C.
SIMPLODE: AN IMPLODING GAS PUFF PLASMA MODEL. 1: NEON
J. Davis, C. Agritellis, and D. Duston 26 Jul. 1985 46 p
(AD-A157456; NRL-MR-5615) Avail: NTIS HC A03/MF A01
CSCL 20/9

A non-LTE dynamic pinch model - SIMPLODE - has been developed and applied to describing the implosion dynamics of a K-shell radiating gas puff. Numerical simulations have been carried out with neon gas puffs and compared with recent experimental results obtained on GAMBLE II. In addition, the influence of the Plasma Erosion Opening Switch on the K-shell yield is investigated. Author (GRA)

N86-12078# Naval Research Lab., Washington, D. C.
THE IONIZATION EQUILIBRIUM OF OPTICALLY THICK ARGON z-PINCH PLASMAS FOR ELECTRON TEMPERATURES BETWEEN 25 AND 65 eV
J. P. Apruzese, P. C. Kepple, and J. Davis 2 Jul. 1985 27 p
(AD-A157484; NRL-MR-5609) Avail: NTIS HC A03/MF A01
CSCL 20/9

Calculations of the ionization balance of optically thick argon plasmas of electron temperature 25-65 eV are presented. A multistage, multilevel model of argon ions with accurate radiation transport of about 50 lines in the sodium, neon, and flourine-like stages forms the basis of the calculations. By comparison with similar optically thin calculations, the effects on ionization of radiative and collisional pumping of excited states of these stages is delineated. In particular, the broad temperature distribution of the neon-like stage is compressed by line photon pumping to a narrower regime of existence because of ionization from the excited states. The relevance to the 3p-3s lasing scheme in neon-like argon is briefly discussed. Author (GRA)

N86-12079# Naval Research Lab., Washington, D. C.
TOTAL AND PARTIAL ABSORPTION COEFFICIENTS FOR A NITROGEN PLASMA Memorandum Report, 1984 - 1985
R. D. Taylor and A. W. Ali 2 Jul. 1985 52 p
(ARPA Order 4395)
(AD-A157534; NRL-MR-5607) Avail: NTIS HC A04/MF A01 CSCL 20/9

A detailed description of the absorption cross sections in a nitrogen plasma is given. The results are presented for partial and total absorption coefficients, where the components are the bound-bound, the bound free and the free-free absorptions. Use is made of nitrogen plasma composition as a function of the electron density and temperature calculated earlier. GRA

N86-12080# Naval Research Lab., Washington, D. C.
ADVANCED CONCEPTS THEORY ANNUAL REPORT, 1984 Memorandum Report, Jan. - Dec. 1984
26 Jun. 1985 145 p
(AD-A157535; NRL-MR-5590) Avail: NTIS HC A07/MF A01 CSCL 20/9

This volume of the Annual Final Report contains the results of a number of theoretical issues related to the radiative properties and X-ray conversion efficiency of dense hot plasmas. In particular, numerical simulations and analyses are presented for the radiative properties of gas puff mixtures, the dynamics of imploding gas puff plasmas, the implosion dynamics of stagnating gas puff plasmas, the influence of radiation on the velocity scaling of gas puff implosions and radiation from an ion beam target interaction. The following topics include: radiative properties of puffed-gas mixtures; optically thin case; modeling of K-shell yields; dynamics of imploding Z-pinch; implosion of a neon puff-gas plasma onto a low-density plasma; velocity scaling of the radiatively dominated Z-pinch; and Ion-beam deposition, Heating, and radiation from an aluminum plasma. GRA

N86-12081# Massachusetts Inst. of Tech., Cambridge. Plasma Fusion Center.
MHD STABILIZATION OF HIGH (BETA) MIRROR PLASMA PARTIALLY ENCLOSED BY CONDUCTING WALL
X. Z. Li, J. Kesner, and B. Lane Apr. 1985 23 p Presented at the Sherwood Theory Conf., Madison, Wisc., 15 Apr. 1985
(Contract DE-AC02-78ET-51013)
(DE85-015579; DOE/ET-51013/148; PFC/CP-85-2; CONF-850474-1) Avail: NTIS HC A02/MF A01

An MHD formulation is used to study a wall stabilized high (BETA) mirror plasma with isotropic pressure. The stabilizing wall extends axially only a part of the distance between the mirror midplane and throat. This arrangement was modeled using a wall that approaches the plasma surface in the bad curvature region and is distant from the plasma in the good curvature region. A variational method is used to solve the equation in the distant wall region and an iterative method is used to solve the equation when the wall is close to the plasma. A jump condition is used to connect the regions of close and distant plasma-wall proximity. A simple trial function is used to perform the variational calculation (the choice of trial function is substantiated by an exact numerical solution). The results show that for a low mirror ratio case more conducting wall surface is needed for stability than in the high mirror ratio case. This agrees with the physical mechanism of the wall stabilization. DOE

N86-12082# Oak Ridge National Lab., Tenn.
EFFECTS OF TRAPPED ALPHA PARTICLES ON BALLOONING MODES IN TOKAMAKS
D. A. Spong, D. J. Sigmar, W. A. Cooper, D. E. Hastings, and K. T. Tsang Jul. 1985 34 p
(Contract DE-AC05-84OR-21400)
(DE85-015064; ORNL/TM-9598) Avail: NTIS HC A03/MF A01

The effects of a trapped, processing alpha particle population on ballooning modes are examined for a large-aspect-ratio, shifted circular flux surface tokamak equilibrium. The alphas are modeled in the deeply trapped limit and with a Maxwellian distribution in energy. The resulting kinetic ballooning equation is solved numerically, and the dependence of the eigenvalues and stability boundaries on shear, background pressure gradient, and ratio of hot to background temperatures and densities is investigated. In the low-frequency regime LC OMEGA <LC OMEGA sub dH sub dH = alpha precessional drift frequency, the alpha component has a stabilizing influence, while in the intermediate-frequency range <LC OMEGA less than or equal to <LC OMEGA sub dH the alphas destabilize ballooning modes through interaction with the trapped particle precessional drift resonance. Parameter ranges that should be typical of alpha production in near-term tokamak devices such as the Tokamak Fusion Test Reactor (TFTR) are considered. DOE

N86-12083# Massachusetts Inst. of Tech., Cambridge. Plasma Fusion Center.
IMPLICATIONS OF RF CURRENT DRIVE THEORY FOR NEXT STEP STEADY-STATE TOKAMAK DESIGN
J. H. Schultz Jun. 1985 60 p
(Contract DE-AC02-78ET-51013)
(DE85-014753; DOE/ET-51013/T3; PFC/RR-85-2) Avail: NTIS HC A04/MF A01

Two missions have been identified for a next-step tokamak experiment in the United States. The more ambitious Mission II device would be a superconducting tokamak, capable of doing long pulse ignition demonstrations, and hopefully capable of also being able to achieve steady state burn. A few interesting lines of approach were identified, using a combination of logical design criteria and parametric system scans. These include: (1) TIBER: A point design that proposes a machine with the capability of demonstrating ignition, high beta (10%) and high Q (=10), using high frequency, fast wave current drive; (2) JET Scale-up; (3) Magic 5: It is argued here that an aspect ratio of 5 is a magic number for a good steady state current drive experiment; and (4) ET-II: The concept of a highly elongated tokamak (ET) was first proposed as a low cost approach to Mission I, because of the possibility of achieving ohmic ignition with low stress copper magnets. Its best application is for commercial tokamaks, using fast wave current drive. A Mission II experiment that would be prototypical of such a reactor is suggested. DOE

N86-12084# Texas Univ., Austin. Inst. for Fusion Studies.
PLASMA KINETIC THEORY IN ACTION-ANGLE VARIABLES
S. M. Mahajan and C. Y. Chen Jun. 1985 23 p
(Contract DE-FG05-80ET-53088)
(DE85-014767; DOE/ET-53088/194; IFSR-194) Avail: NTIS HC A02/MF A01

An appropriate canonical perturbation theory to correctly deal with general electromagnetic field perturbation is developed, and is used to set up plasma kinetic theory in action-angle variables. A variety of test problems are solved to show the unifying power of the method. Basic linear, quasilinear, and nonlinear equations are derived which can serve as the starting point for a whole range of plasma problems. DOE

N86-12085# Oak Ridge National Lab., Tenn.
TOKAMAK STARTUP: PROBLEMS AND SCENARIOS RELATED TO THE TRANSIENT PHASES OF IGNITED TOKAMAK OPERATIONS
J. Sheffield 1985 37 p Presented at the Workshop on Tokamak Start-Up - Probl. and Senarios Related to the Transient Phases of Long-Burn Operations, Erice, Italy, 14 Jul. 1985
(Contract DE-AC05-84OR-21400)
(DE85-015321; CONF-850708-1) Avail: NTIS HC A03/MF A01

During recent years improvements have been made to tokamak startup procedures, which are important to the optimization of ignited tokamaks. The use of RF-assisted startup and noninductive current drive has led to substantial reduction and even complete elimination of the volt-seconds used during startup, relaxing constraints on poloidal coil, vacuum vessel, and structure design. This paper reviews these and other improvements and discusses the various bulk heating techniques that may be used to ignite a D-T plasma. DOE

N86-12086# TRW, Inc., Redondo Beach, Calif.
PHYSICS MODELING OF TANDEM MIRROR DEVICES WITH HIGH FIELD TEST CELL INSERTS
M. E. Fensternmacher and R. B. Campbell 15 Apr. 1984 64 p refs Prepared in cooperation with California Univ., Berkeley. Lawrence Livermore Lab.
(Contract W-7405-eng-48)
(DE85-011870; UCID-20405) Avail: NTIS HC A04/MF A01

Recently developed plasma physics models of tandem mirror operation with a high-field technology test cell insert in the central cell are described in detail. These models were incorporated in the TMRBAR tandem mirror reactor physics code. Results of a benchmark case for the code models against previous analysis of the MFTF - (ALPHA) (+) T configuration are given. A brief users guide to the new TMRBAR with the test cell models is also presented. Some description of the applications of the models to MFTF - (ALPHA) (+) T and FPD - II + T configurations is made. DOE

N86-12087# California Univ., Livermore. Lawrence Livermore Lab.
MIRROR FUSION TEST FACILITY (MFTF-B): STATUS
V. N. Karpenko Feb. 1985 7 p Presented at the 6th Topical Meeting on the Technol. of Fusion Energy, San Francisco, 3 Mar. 1985
(Contract W-7405-eng-48)
(DE85-012953; UCRL-92247; CONF-850310-107) Avail: NTIS HC A02/MF A01

The Mirror Fusion Test Facility (MFTF-B), now under construction at Lawrence Livermore National Laboratory, represents more than an order-of-magnitude step up from earlier magnetic mirror experiments on the way to a future mirror fusion reactor. In fact, when the device begins operating in 1988, it will be capable of achieving plasma performance approaching scientific breakeven for D-T equivalent operation. We have taken major steps to develop MFTB-B technologies for tandem mirrors. In the machine, we will use steady-state, high-field, superconducting agents on reactor-relevant scales. The 30-s beam pulses, ECRH, and ICRH will also introduce near steady-state technologies into those systems. DOE

N86-12088# Kanner (Leo) Associates, Redwood City, Calif.
DISCUSSION OF THE CURRENT LIMITS IN THE RFQ
A. Schemmp 1985 7 p Transl. into ENGLISH of "Zur Diskussion der Stromgrenzen in RFQ" rept. 85-1 Inst. fuer Angewandte Phys. der Univ. Frankfurt/Main, Jan. 1985
(Contract W-7405-eng-36)
(DE85-012909; LA-tr-85-22) Avail: NTIS HC A02/MF A01

During the introduction of the SNQ injector, various reasons were given for the structure selection without any discussion. Moreover, a current equation: I approx. V/f (e/E sub k) squared was employed without any indication of the boundary conditions, indicating that a 200 MHz-RFQ is not possible for the SNQ. On the one hand, there is a proposal for a 200 MHz high-current RFQ (CERN RFQ II); on the other hand, Junior indicates a RFQ current proportional to the vane voltage. Simple considerations demonstrate the limits of the simple assumption in equation one. When the design values in literature are compared, the linear relationship of Junior is confirmed, i.e., that the longitudinal current I1 essentially provides the limit, the radial increase does not have an effect because of the alteration in the cos(MU). DOE

N86-12089# Oak Ridge National Lab., Tenn.
VARIABLE FIELD MAGNETIC EXTRACTION CHANNEL FOR ORIC
E. D. Hudson, J. A. Martin, and R. S. Lord 1985 3 p refs Presented at the Particle Accelerator Conf., Vancouver, British Columbia, 13 May 1985
(Contract DE-AC05-84OR-21400)
(DE85-011927; CONF-850504-34) Avail: NTIS HC A02/MF A01

An improved magnetic beam extraction channel for the Oak Ridge Isochronous Cyclotron (ORIC) was designed to significantly reduce the external field disturbance and provide uniform in-channel field. This will make beam extraction near nu sub r = 1 more predictable. The new channel consists of an iron tube of constant cross section with independently adjustable windings, both inside and outside the iron. The windings have a cos theta current density distribution. The iron tube is 1 meter long with a bore of 6 cm; aperture for beam is 4 cm. The external field is negligible except for small perturbations in the field arising from the geometry modifications required at the ends so that the beam can enter and leave. The field reduction inside the channel is variable from 0.4 to 0.6 Tesla without significant change in either the internal field uniformity or the external field level. DOE

N86-12090# Sandia Labs., Albuquerque, N. Mex.
PBFA-2 VACUUM INSULATOR STACK FAILURE MECHANISMS
M. A. Sweeney 1985 14 p Presented at the 5th IEEE Pulsed Power Conf., Washington, D.C., 10 Jun. 1985
(Contract DE-AC04-76DP-00789)
(DE85-013118; SAND-84-2567C; CONF-850616-23) Avail: NTIS HC A02/MF A01

The BPFA-II accelerator includes a large-radius, vertical-axis vacuum insulator stack. The possible failure of the acrylic rings in the stack from electron- or gamma-induced charge buildup is being evaluated. The induced static charges could remain for many hours, and either type of irradiation might cause dendrites to form. Aluminum grading rings sandwiched between the acrylic affect charge accumulation; the acrylic would preferentially break down to these grading rings. The charge buildup and the bremsstrahlung dose could depend critically upon the directionality and position of the electron loss. The effects of electron loss that occurs in the vicinity of the ion diode, where the electrons have energies of about 30 MeV are considered. Monte Carlo electron-photon transport calculations indicate that the bremsstrahlung dose expected in an acrylic ring once diode experiments begin in 1986 could be as much as 5 krads per shot, with roughly half of the photon energy above 5 MeV. Moreover, the calculation indicate that the charge deposition in an individual acrylic ring might exceed 2x10 to the 11 electrons/sq cm. DOE

N86-12091# Stanford Linear Accelerator Center, Calif.
INCREASED INTENSITY PERFORMANCE OF THE BROOKHAVEN AGS
E. Raka, L. Ahrens, W. Frey, E. Gill, J. W. Glenn, R. Sanders, and W. T. Weng May 1985 4 p refs Presented at the Particle Accelerator Conf., Vancouver, British Columbia, 13 May 1985 Prepared in cooperation with BNL
(Contract DE-AC03-76SF-00515)
(DE85-013371; SU-SLAC-PUB-3689; CONF-850504-71) Avail: NTIS HC A02/MF A01

With the advent of H(-) injection into the Brookhaven AGS, circulating beams of up to 3 x 10(13) protons at 200 MeV have been obtained. RF capture of 2.2 x 10(13) and acceleration of 1.73 x 10(13) up to the transition energy (approx. = 8 GeV) and 1.64 x 10(13) to full energy (approx. = 29 GeV) has been achieved. This represents a 50% increase over the best performance obtained with H(+) injection. The increase in circulation beam current is obtained without filling the horizontal aperture. This allows the RF capture process to utilize a larger longitudinal phase space area (approx. = 1 eV sec/bunch vs less than or equal to 0.6 eV sec with H(+) operation). The resulting reduction in relative longitudinal density partially offsets the increase in space charge effects at higher currents. In order to make the capture process independent of injected beam current, a dynamic beam loading compensation loop was installed on the AGS RF system. This is the only addition to the synchrotron itself that was required to reach the new intensity records. A discussion of injection, the RF capture process, and space charge effects is presented. DOE

N86-12092# Sandia Labs., Albuquerque, N. Mex.
DESIGN AND OPTIMIZATION OF THE P3FA 2 VACUUM INTERFACE AND TRANSMISSION LINES FOR LIGHT ION FUSION
D. B. McDaniel, R. W. Stinnett, and E. W. Gray 1985 22 p Presented at the 5th IEEE Pulsed Power Conf., Washington, D.C., 10 Jun. 1985 Prepared in cooperation with Cornell Univ., Ithaca, N.Y.
(Contract DE-AC04-76DP-00789)
(DE85-012809; SAND-84-2560C; CONF-850616-5) Avail: NTIS HC A02/MF A01

The PBFA II vacuum insulator was originally designed for optimum coupling to a proton ion diode with minimum inductance. In July 1983 it was decided that lithium ions at 30 MeV would be the baseline for PBFA II. This requires the use of plasma opening switches (POS) and vacuum inductor to reach 30 MV. To achieve this, the vacuum magnetically insulated tranamission lines had to be redesigned as an inductive energy store. To gain optimum coupling to this vacuum inductors, the output impedance of the water section was increased by the use of a water-dielectric transformer. The calculations leading to the final design will be discussed. DOE

N86-12093# Los Alamos Scientific Lab., N. Mex.
LOS ALAMOS PROTON STORAGE RING FAST-EXTRACTION KICKER SYSTEM
J. F. Power, B. Blind, and A. J. Jason May 1985 4 p refs Presented at the Particle Accelerator Conf., Vancouver, British Columbia, 13 May 1985
(Contract W-7405-eng-36)
(DE85-012663; LA-UR-85-1614; CONF-850504-52) Avail: NTIS HC A02/MF A01

We describe the kicker system used by the Los Alamos Proton Storage Ring (PSR) for fast extraction of accumulated 800-MeV proton beam. The system has several severe constraints in terms of rise time, field quality, and magnet dimensions. These are, in turn, defined by characteristics of the stored beam, ring lattice, and the allowable activation of ring components. Design methods to meet the constraints are outlined here and we describe the novel modulators that produce the fast pulses required. DOE

N86-12094# California Univ., Livermore. Lawrence Livermore Lab.
ELECTRICAL SUPPLY FOR MFTF-B SUPERCONDUCTING MAGNET SYSTEM
D. W. Shimer and E. W. Owen 13 Feb. 1985 8 p Presented at the Workshop on Power Supplies for Fusion Expt., Los Alamos, N. Mex., 20 Feb. 1985
(Contract W-7405-eng-48)
(DE85-012932; UCRL-92156; CONF-850285-1) Avail: NTIS HC A02/MF A01

The MFTF-B magnet system consists of 42 superconducting magnets which must operate continuously for long periods of time. The magnet power supply system is designed to meet the operational requirements of accuracy, flexibility, and reliability. The superconducting magnets require a protection system to protect against critical magnet faults of quench, current lead overtemperature, and overcurrent. The protection system is complex because of the large number of magnets, the strong coupling between magnets, and the high reliability requirement. The power circuits and the components used in the design are described. DOE

N86-12095# Brookhaven National Lab., Upton, N. Y.
WINDOW FRAME OR SUPERFERRIC MAGNET DESIGN FOR LOW B(<3T) HEAVY ION STORAGE RING STUDY
G. Danby, B. DeVito, J. Jackson, G. Keohane, Y. Lee, R. Phillips, S. Plate, L. Repata, J. Skaritka, and L. Smith 1985 3 p refs Presented at the Particle Accelerator Conf., Vancouver, British Columbia, 13 May 1985
(Contract DE-AC02-76CH-00016)
(DE85-013288; BNL-36557; CONF-850504-154) Avail: NTIS HC A02/M A01

Double magnets share common laminations without magnetic coupling. Single layer coils of rectangular conductor are dry wound on extruded bore tubes. Magnet construction requires no molding or prestress. Absence of superconducting (SC) magnetization fields in the aperture results in very large dynamic range. The coil is wound continuously across the modplane to give unusually large dynamic aperture. Above approx. 2.2 T saturation is corrected by simple sextupole windings with no inductive coupling to the dipole. Ultrastable design requires no internal quench protection. A quadrupole pair of novel design gives excellent field quality to B . 2 T without corrections, with no SC magnetization. Experience shows magnets are accurate enough for the assembly to take place at its final location. No training is required. Test procedures (measurements with search coils or with the beam) and cooldown properties are discussed. DOE

N86-12096# Los Alamos Scientific Lab., N. Mex.
LOS ALAMOS SPHEROMAK PROGRAM
T. R. Jarboe 1985 7 p Presented at the 7th US Symp. on Compact Toroid Res., Santa Fe, N. Mex., 21 May 1985
(Contract W-7405-eng-36)
(DE85-012769; LA-UR-85-1822; CONF-8505100-10) Avail: NTIS HC A02/MF A01

The Los Alamos Spheromak has two experimental facilities. The confinement properties of sustained and decaying spheromaks are being studied in CTX. Electrodes for the production of clean sustained spheromaks are being developed on the Electrode Studies Facility. DOE

N86-12097# Stanford Linear Accelerator Center, Calif.
STATUS OF SLC
S. D. Ecklund May 1985 4 p Presented at the Particle Accelerator Conf., Vancouver, British Columbia, 13 May 1985
(Contract DE-AC03-76SF-00515)
(DE85-013071; SU-SLAC-PUB-3679; CONF-850504-138) Avail: NTIS HC A02/MF A01

The current construction status of the Stanford Linear Collider (SLC) is described along with a brief overview of the project. Tests of completed parts of the machine are summarized. DOE

N86-12098# Fermi National Accelerator Lab., Batavia, Ill.
SSC TEST LATTICES
E. D. Courant, D. R. Douglas, A. A. Garren, and D. E. Johnson 20 Apr. 1985 20 p refs
(Contract DE-AC02-76CH-03000)
(DE85-014240; FNAL-TM-1315) Avail: NTIS HC A02/MF A01

A set of eight test lattices for the Superconducting Super Collider (SSC) were devised for such purposes as the investigation of the dependence of chromatic properties and dynamic aperture on the type, field, physical aperture and errors of the magnets, on the sextupole correction scheme, on the tunes and on the cell phase advances. They are distinguished from realistic lattices in that certain features of the latter are missing - most notably the crossing magnets that bring the two counter-rotating proton beams into collision at the interaction points, nd the utility insertions, which are the sites for the injection, beam abort, and radiofrequency systems. Furthermore the placement of magnets in the cells is simplified. DOE

N86-12099# Oak Ridge National Lab., Tenn.
SPHERICAL TORUS: AN APPROACH TO COMPACT FUSION AT LOW FIELD. INITIAL IGNITION ASSESSMENTS
Y. K. M. Peng, D. J. Strickler, S. K. Borowski, W. R. Hamilton, R. L. Reid, J. R. Haines, V. D. Lee, G. E. Gorker, S. S. Kalsi, and B. W. Riemer 1985 7 p Presented at the 6th Topical Meeting on the Technol. of Fusion Energy, San Francisco, 3 Mar. 1985 Prepared in cooperation with McDonnel Douglas Astronautics Co., Huntington Beach, Calif., Florida Univ., Gainesville and Tennessee

Univ., Knoxville
(Contract DE-AC05-84OR-21400)
(DE85-012890; CONF-850310-108) Avail: NTIS HC A02/MF A01

Initial assessments of ignition devices based on the spherical torus concept suggest that an ignition spherical torus (IST) can be highly cost-effective and exceptionally small in unit size. Assuming advanced methods of current drive and confinement and beta scalings with plasma current, a D-T IST with a toroidal field of 2 to 3 T is estimated to have a major radius ranging from 1 m to 1.6 m, and a fusion power less than 60 MW. For the nominal IST (at 2 T and 1.6 m), the direst cost of the nuclear island is estimated to be about $120 M with a total direct cost about $340 M in mid-1984 dollars based on the Fusion Engineering Design Center (FEDC) cost algorithm. For ISTs with higher field and smaller size (e.g., at 3 T and 1 m), further reductions of the cost of the nuclear island are estimated. In case of confinement scaling with the plasma size only, strong plasma paramagnetism (self-generated magnetic field) in the spherical torus may still serve to compensate for the projected confinement shortfall. DOE

N86-12100# Stanford Linear Accelerator Center, Calif.
VERY HIGH ENERGY COLLIDERS
B. Richter May 1985 6 p Presented at the Particle Accelerator Conf., Vancouver, British Columbia, 13 May 1985
(Contract DE-AC03-76SF-00515)
(DE85-013075; SU-SLAC-PUB-3669; CONF-850504-136) Avail: NTIS HC A02/MF A01

The required emittance in very high energy machines are small. It will be a real challenge to produce these small emittances and to maintain them during acceleration. The small emittances probably make acceleration by laser techniques easier, if such techniques will be practical at all. The beam spot sizes are very small indeed. It will be a challenge to design beam transport systems with the necessary freedom from aberration required for these small spot sizes. It would of course help if the beta functions at the collision points could be reduced. Beam power will be large - to paraphrase the old saying, power is money - and efficient acceleration systems will be required. DOE

N86-12101# National Bureau of Standards, Washington, D.C. Fracture and Deformation Div.
MATERIALS STUDIES FOR MAGNETIC FUSION ENERGY APPLICATIONS AT LOW TEMPERATURES. 7: TECHNICAL REPORTS
R. P. Reed, ed. May 1985 332 p
(DE85-014518; NBSIR-85-3025-7) Avail: NTIS HC A15/MF A01

Results of a research program to produce material property data that will facilitate design and development of cryogenic structures for the superconducting magnets of magnetic fusion energy power plants and prototypes are presented. Research results for 1984 are summarized. The technical papers are presented under four headings reflecting the main program areas: Welding, Nonmetallics, Structural Alloys, and Technology Transfer. Objectives, approaches, and achievements are summarized in an introduction to each program area. DOE

N86-12102# City Univ. of New York, Staten Island.
NON-GEOMETRICAL OPTICS INVESTIGATION OF MODE CONVERSION IN WEAKLY RELATIVISTIC INHOMOGENOUS PLASMAS
K. Imre Jun. 1985 9 p
(Contract DE-AC02-83ER-53162)
(DE85-013480; DOE/ER-53162/6) Avail: NTIS HC A02/MF A01

Electron cyclotron resonance heating of plasmas by waves incident to the fundamental and second harmonic layer was investigated. When the wave propagation is nearly perpendicular to the equilibrium field in a weakly inhomogeneous plasma the standard geometrical optics breaks down and the relativistic corrections become significant at the resonance layer. Unlike the previous studies of this problem, the governing equations are derived from the linearized relativistic Vlasov equation coupled with Maxwell's equations, rather than using the uniform field dispersion relation to construct equations by replacing the refractive index by some spatial differential operations. A boundary layer analysis is employed at the resonance region and the inner and outer solutions are matched in the usual manner. The full wave solution of the problem, and also the set of physical parameters and their ranges in which the analysis is valid were obtained. DOE

N86-12103# Sandia Labs., Albuquerque, N. Mex.
PHOTON DIAGNOSTICS LEADING TO AN IMPROVED MARX
G. J. Lockwood, L. E. Ruggles, B. T. Neyer, and L. X. Schneider 1985 8 p Presented at 5th IEEE Pulsed Power Conf., Washington, D.C., 10 Jun. 1985
(Contract DE-AC04-76DP-00789)
(DE85-013434; SAND-84-2418C) Avail: NTIS HC A02/MF A01

Utilizing the High Speed Multi-Channel Data Recorder (HSMCDR) developed at Sandia National Laboratories, the erection pattern of a 3.2 MV particle beam fusion accelerator (PBFA) I Marx were measured. This has allowed the study variations of the erection pattern caused by changing resistors within the Marx. The effect of each resistor change was determined by monitoring the optical signal associated with switch closure using fiber optic links and the HSMCDR. Using this photonic technique, modifications that have reduced the Marx jitter by a factor of two were carried out. DOE

N86-12104# California Univ., Berkeley. Lawrence Berkeley Lab.
BEAM POSITION MONITOR FOR STORAGE RINGS
M. Nakamura and J. A. Hinkson May 1985 5 p refs Presented at Particle Accelerator Conf., Vancouver, British Columbia, 13 May 1985
(Contract DE-AC03-76SF-00098)
(DE85-013295; LBL-19554; CONF-850504-179) Avail: NTIS HC A02/MF A01

Beam position monitors (BPM) for synchrotron light storage rings usually consist of beam pickup electrodes, coaxial relays and a narrowband receiver. While accurate, these systems are slow and of limited use in the commissioning of an accelerator. A beam position monitor is described which is intended to be a principal diagnostic during debug and routine running of a storage ring. It is capable of measuring the position of a single bunch on the first or nth orbit to an accuracy of a few percent. Stored beam position is more accurately measured with averaging techniques. Beam position changes can be studied in a bandwidth from DC to a few MHz. The beam monitor electronics consist of a separate amplification, detection, and sampling channel for each beam pickup electrode. Fast switches in each channel permit selection of the nth turn for measurement (single bunch mode). A calibration pulse is injected into each channel after beam measurement to permit gain offsets to be measured and removed from the final data. While initially more costly than the usual beam position monitor system, this system will pay for itself in reduced storage ring debug and trouble shooting time. DOE

N86-12105# Fermi National Accelerator Lab., Batavia, Ill.
USING THE TEVATRON BEAM POSITION MONITOR SYSTEM TO INVESTIGATE TRANSVERSE PHASE SPACE
F. Willeke May 1985 19 p
(Contract DE-AC02-76CH-03000)
(DE85-014261; FNAL-TM-1309) Avail: NTIS HC A02/MF A01

Transverse phase space trajectories can be measured by the TEVATRON beam position monitor in the standard turn by turn operation mode if a coherent betatron oscillation is excited by a dipole kick. The measurement of phase space coordinates is influenced by incoherent and coherent synchrotron oscillations and incoherent betatron oscillations. To investigate phase space trajectories, all these effects must be understood quantitatively and if possible the measured data must be corrected. The measuring and correction procedures are investigated and the first measurements are discussed. DOE

N86-12106# Los Alamos Scientific Lab., N. Mex.
SUPERCONDUCTING MAGNETIC ENERGY STORAGE (SMES) PROGRAM Progress Report, 1 Jan. - 31 Dec. 1984

J. D. Rogers, comp. May 1985 21 p
(Contract W-7405-eng-36)
(DE85-014250; LA-10399-PR) Avail: NTIS HC A02/MF A01

The 30 MJ, 10 MW superconducting magnetic energy storage (SMES) system was devised to interact in the Western US Power System as an alternate means to damp unstable oscillations at 0.35 Hz on the Pacific HVAC Interites. The operating limits of the 30 MJ SMES unit were established, and different means of controlling real and reactive power were tested. The unit can follow a sinusoidal power demand signal with an amplitude of up to 8.6 MW with the converter working in a 12 pulse mode. When the converter operates in the constant VAR mode, a time varying real power demand signal of up to 5 MW can be met. It was shown that the Pacific ac Interite has current and reactive power variations of the same frequency as the modulating frequency of the SMES device. The reliability of the SMES subsystems with a narrow band noise input was assessed. Parameters of the ac power system were determined. Converter short circuit tests, load tests under various control conditions, dc breaker tests for coil current interruption, and converter failure mode tests were conducted. The experimental operation of the SMES system is concluded. DOE

N86-12107# Science Research Corp., Somerville, Mass.
ELECTRON BEAM POTENTIAL DIAGNOSTIC FOR TANDEM MIRRORS, PHASE 1 Final Technical Report
Apr. 1985 71 p
(Contract DE-AC02-84ER-80187)
(DE85-013515; DOE/ER-80187/1) Avail: NTIS HC A04/MF A01

The results of the Phase 1 research effort indicate that an electron beam potential diagnostic, suitable for use on the TMX-U or TARA tandem mirror experiments, would be capable of the following performance parameters: (1) accuracy of central cell potential measurement: < 200 to 500 eV, (2) time resolution 1 to 5 msec, (3) probing electron beam energy: 5 keV, (4) radial spatial resolution: 1 cm, and (5) axial spatial resolution: 1 to 5 meters. The potential measurement accuracy, time resolution and spatial resolution are interrelated, and depend on the background plasma density. These calculated performance parameters assume an X-ray flux produced by bremsstrahlung alone. Other X-ray production processes (e.g., recombination) which contribute to the X-ray production from the probing e-beam, will improve the performance of the EBPD. DOE

N86-12108# California Univ., Livermore. Lawrence Livermore Lab.
MULTIVARIABLE CURRENT CONTROL FOR ELECTRICALLY AND MAGNETICALLY COUPLED SUPERCONDUCTING MAGNETS, REVISION 1
E. W. Owen and D. W. Shimer 8 Feb. 1985 7 p Presented at the 6th Topical Meeting. on the Technol. of Fusion Energy, San Francisco, 3 Mar. 1985
(Contract W-7405-eng-48)
(DE85-012943; UCRL-92092-Rev-1; CONF-850310-113-Rev-1) Avail: NTIS HC A02/MF A01

Superconducting magnet systems under construction and projected for the future contain magnets that are magnetically coupled and electrically connected with shared power supplies. A change in one power supply voltage affects all of the magnet currents. A current controller for these system must be designed as a multivariable system. A method, based on decoupling control is described for the rational design of these systems. Dynamic decoupling is achieved by cross-feedback of the measured currents. A network of gains at the input decouples the system statically and eliminates the steady-state error. Errors are then due to component variations. The method was applied to the magnet system of the mirror fusion test facility B (MFTF-B) at the Lawrence Livermore National Laboratory. DOE

N86-12109# Sandia Labs., Albuquerque, N. Mex.
XUV PREIONIZATION EFFECTS IN HIGH POWER MAGNETICALLY INSULATED DIODES
J. Maenchen, J. R. Woodworth, B. W. Foltz, E. J. T. Burns, D. B. Seidel, L. R. Dorrell, P. R. Johnson, P. Reyes, G. Torres, and G. Williams 1985 5 p Presented at the 5th IEEE Pulsed Power Conf., Washington, D.C., 10 Jun. 1985
(Contract DE-AC04-76DP-00789)
(DE85-013142; SAND-84-2447C; CONF-850616-33) Avail: NTIS HC A02/MF A01

Electrode surface desorption and photoionization by an intense XUV pulse was shown to dramatically improve a vacuum diode impedance history. The 6-Terawatt Applied-B ion diode experiment on PBFA I is limited by a delay in both diode and ion current initiation. The insulation magnetic field impedes electron crossings which aid the ion source initiation. The diode is initially a severe overmatch to the accelerator 40-nsec, 2.2-MV, 0.5-ohm pulse. The diode current increases during the pulse, leading to a rapidly falling impedance history. The application of an intense XUV flux from an array of sixteen 60-kA spark sources is found to cause immediate diode current flow, resulting in both a greatly improved impedance history and the prompt initiation of an intense higher power ion beam. DOE

N86-12110# GA Technologies, Inc., San Diego, Calif.
ENERGY CONFINEMENT EXPERIMENTS ON DOUBLET 3 WITH HIGH POWER NEUTRAL BEAM HEATING
J. C. DeBoo and R. J. Groebner May 1985 5 p Presented at the 12th European Conf. on Controlled Fusion and Plasma Phys., Budapest, 2 Sep. 1985
(Contract DE-AC03-84ER-51044)
(DE85-014324; GA-A-18033; CONF-850927-4) Avail: NTIS HC A02/MF A01

Energy confinement experiments with up to 8 MW of both hydrogen and deuterium neutral beam power were performed in deuterium plasmas with limiter and expand boundary divertor configurations. The results of NBI-dominated experiments indicated that total stored energy W sub t and energy confinement time tau sub e had little or no variation with electron density anti n sub e and toroidal field B sub T and scaled linearly with plasma current I sub p. Previous studies in limiter discharges indicated a weak dependence on plasma elongation kappa. The confinement time dependence on elongation was not determined for divertor discharges, but assuming a dependence similar to that for limiter discharges both limiter and divertor data were consistent with W sub t and tau sub e proportional to I sub p (RADICAL)kappa. The variation of plasma stored energy with neutral beam power was consistent with a linear relationship. The linear equation describing this relationship had a non-zero intercept which illustrated the fact that energy confinement time deteriorated with neutral beam power. The energy confinement time appears to be approaching an asymptotic value at high power, consistent with a linear functional form for stored energy. However, a power law functional form for stored energy and energy confinement time can not be ruled out. DOE

N86-12111# Texas Univ., Austin. Inst. for Fusion Studies.
ENERGY CONFINEMENT IN A HIGH-CURRENT REVERSED FIELD PINCH
Z. G. An, G. S. Lee, and P. H. Diamond Jul. 1985 11 p Presented at the 7th US Symp. on Compact Toroid Res., Santa Fe, N. Mex., 21 May 1085
(Contract DE-FG05-80ET-53088)
(DE85-015009; DOE/ET-53088/196; IFSR-196; CONF-8505100-17) Avail: NTIS HC A02/MF A01

The ion temperature gradient driven (eta sub i) mode is proposed as a candidate for the cause of anomalous transport in high current reversed field pinches. A four-field fluid model is derived to describe the coupled nonlinear evolution of resistive interchange and eta sub i modes. A renormalized theory is discussed, and the saturation level of the fluctuations is analytically estimated. Transport scalings are obtained, and their implications discussed. In particular, these results indicate that pullet injection is a potentially viable mechanism for improving energy confinement in a high temperature reverse field pinch (RFP). DOE

N86-12112# California Univ., Berkeley. Electronics Research Lab.

SIMULATION OF QUIET START MAGNETIZED PLASMAS, INCLUDING MAXWELLIAN AND VELOCITY-SPACE RING DISTRIBUTIONS

K. P. Kenyon 27 Jul. 1985 32 p
(Contract DE-AT03-76ET-53064)
(DE85-014394; DOE/ET-53064/T5) Avail: NTIS HC A03/MF A01

Longitudinal electrostatic waves are simulated in a magnetized plasma, propagating perpendicular to B0. Groups of particles are arranged in one or more rings and spokes in velocity space. Using various loading schemes to represent different particle velocity-space distributions in the simulations of (upsilon sub perpendicular), these particles are then distributed uniformly in position space along the length of the system. In particular, the evolution of magnetized cold and warm rings is followed (physically unstable), and of a magnetized Maxwellian (unstable due to the particle loading) through to saturation. Rules are deduced for useful loading methods. DOE

N86-12113# California Univ., Berkeley. Electronics Research Lab.

PARTICLE SIMULATION OF THE LOW-(ALPHA) PIERCE DIODE

T. L. Crystal and S. Kuhn 20 Sep. 1984 42 p
(Contract DE-AT03-76ET-53064)
(DE85-014435; DOE/ET-53064/T3) Avail: NTIS HC A03/MF A01

The evolution of small initial perturbations of the uniform equilibrium of the classical Pierce diode is studied using particle simulations. These simulations were performed with the new bounded plasma code PDW1 and cover the parameter range 0 < (ALPHA) < 3 (PI), where (ALPHA) = (LC OMEGA)/sub p.L/v0. In the linear regime, three stages (initial-transit, adjustment, and dominant-eigenmode) are distinguished; oscillation frequencies, growth/damping rates, and potential profiles of the dominant eigenmode as well as oscillation frequencies of the next-to-dominant eigenmode are recovered and shown to agree quantitatively with recent analytical results. In the linearly unstable cases, the system evolves nonlinearly to a final state which may be either a new, nonuniform dc equilibrium, or a state of large-amplitude oscillations. In particular, for (ALPHA) = 1.5(PI) the character of the final state is found to depend on the details of the initial conditions. DOE

N86-12114# California Univ., Livermore. Lawrence Livermore Lab.

NEW CONCEPTS FOR DRIFT PUMPING A THERMAL BARRIER WITH RF

J. D. Barter, D. Baldwin, Y. Chen, and P. Poulsen 9 May 1985 8 p Presented at the 6th Topical Conf. on Radio Frequency Plasma Heating, Pine Mountain, Ga., 13 May 1985 Prepared in cooperation with TRW Systems, Redondo Beach, Calif.
(Contract W-7405-eng-48)
(DE85-013591; UCRL-92643; CONF-8505130-6) Avail: NTIS HC A02/MF A01

Pump neutral beams, which are directed into the loss cone of the TMX-U plugs, are normally used to pump ions from the thermal barriers. These neutral beams introduce cold gas that reduces pumping efficiency, require a straight line entrance and exit from the plug. Alternate methods are investigated to provide barrier pumping. To maintain the thermal barrier, either of two classes of particles can be pumped. First, the collisionally trapped ions can be pumped directly. The most promising selection criterion is the azimuthal drift frequency. Second, the excess sloshing-ion density can be removed, allowing the use of increased sloshing-beam density to pump the trapped ions. The selection mechanism is the Doppler-shifted ion-cyclotron resonance of the high-energy sloshing-ions. DOE

N86-12115# Sandia Labs., Albuquerque, N. Mex.

RIMFIRE: A SIX MEGAVOLT LASER-TRIGGERED GAS-FILLED SWITCH FOR PBFA 2

D. R. Humphreys, K. J. Penn, J. S. Cap, R. G. Adams, J. F. Seamen, and B. N. Turman 1985 5 p Presented at the 5th IEEE Pulsed Power Conf., Washington, D.C., 10 Jun. 1985
(Contract DE-AC04-76DP-00789)
(DE85-013959; SAND-84-2505C; CONF-850616-62) Avail: NTIS HC A02/MF A01

A new multiple stage laser-triggered SF6 spark gap was developed, which performed well in tests at nearly 6 megavolts and half a megampere. It has survived many hundreds of shots between 5 and 5.7 MV. A 25 millijoule ultraviolet laser pulse arriving in its trigger gap reliably closes the whole switch in 20 nanoseconds with 0.4 ns 1-sigma jitter. The closing time has a low dependence on the applied voltage, about 0.9 ns/% of self-break voltage. For a 10 mJ laser pulse, the jitter is 1.5 ns and the slope is 1.0 ns/%. No prefires occurred; the estimated prefire rate at 90% of self-breaking voltage is less than 0.1%. The switch inductance is 400 nanohenries, of which about 100 nh comes from the spark channels. The switch is 68 cm long and 61 cm in diameter. DOE

N86-12116# Sandia Labs., Albuquerque, N. Mex.

PBFA 2: A 100 TW PULSED POWER DRIVER FOR THE INERTIAL CONFINEMENT FUSION PROGRAM

B. N. Turman, T. H. Martin, E. L. Neau, D. R. Humphreys, D. D. Bloomquist, D. L. Cook, S. A. Goldstein, L. X. Schneider, D. H. McDaniel, and J. M. Wilson 1985 8 p Presented at the 5th IEEE Pulsed Power Conf., Washington, D.C., 10 Jun. 1985
(Contract DE-AC04-76DP-00789)
(DE85-013956; SAND-84-2524C; CONF-850616-61) Avail: NTIS HC A02/MF A01

The 100 TW Particle Beam Fusion Accelerator (PBFA II) is well into the procurement and assembly phases, with the first shot scheduled for January 1986. Installation of several major sub-assemblies is underway. The PBFA II output will drive a fast opening switch in the vacuum insulator stack, providing a 30 MV, 15 ns output pulse, which accelerates lithium ions. The ions will focus onto a pellet containing deuterium-tritium, producing fusion energy. Several research areas will be reviewed: low jitter, highly reliable 370 kJ Marx generators; highly synchronized gas switching at 5 MV; efficient water switch operation of 5 MV lines; series-parallel arrangements for increasing voltage or current; and plasma erosion opening switches. DOE

N86-12117# Brookhaven National Lab., Upton, N. Y.

PHYSICS OPPORTUNITIES WITH RELATIVISTIC HEAVY ION ACCELERATORS

N. P. Samios 1985 4 p Presented at the Particle Accelerator Conf., Vancouver, British Columbia, 13 May 1985
(Contract DE-AC02-76CH-00016)
(DE85-014190; BNL-36735; CONF-850504-194) Avail: NTIS HC A02/MF A01

The physics motivation for a relativistic heavy ion collider with energies of 100 GeV/amu x 100 GeV/amu for nuclei of A-200 are: (1) this will allow the production in the laboratory of a new state of matter - the quark gluon plasma, (2) the study of such interactions will provide an experimental test of statistical quantum chromodynamics (QCD), i.e., a look at the properties of the QCD vacuum at large distances, (3) such reactions will simulate the conditions of the early universe, and (4) such a collider will allow us to delve into the unknown. If history is any guide then it is clear that any time one can increase an important physics parameter by a factor of 10 (and in this case a factor of 100 over what is presently being done) then do it. At present the Bevalac at Berkeley is the premier facility for the study of heavy ions with a center of mass capability of 1 GeV/amu x 1 GeV/amu. In the near term this capability will be increased at the AGS at BNL (6 GeV/amu x 6 GeV/amu) and at the CERN SPS (10 GeV/amu x 10 GeV/amu). DOE

N86-12118# Stanford Linear Accelerator Center, Calif.

HIGHER LUMINOSITIES VIA ALTERNATIVE INCIDENT CHANNELS

J. E. Spencer Apr. 1985 13 p refs Presented at the PEP High

Luminosity Workshop, Stanford, Calif., 5 Apr. 1985
(Contract DE-AC03-76SF-00515)
(DE85-014355; SU-SLAC-PUB-3645; CONF-8504155-3) Avail: NTIS HC A02/MF A01

We show that PEP provides some unique opportunities for one and two photon physics with real photons as well as for QCD studies with internal targets. Photon beams would avoid the major limitation on the luminosity of present machines and could provide PEP an ideal b-physics factory producing the full range of J/sub c//sup PC/ and J/sub b//sup PC/ states that may not be observable otherwise as well as allow a whole new class of missing-mass experiments. These latter particles are the pseudo-Goldstone bosons and their supersymmetric counterparts. These and related possibilities like a single-pass, free electron laser facility or even synchrotron radiation beam lines all favor a mini-maxi configuration for the low-beta insertions in PEP. This allows more diverse experiments without excluding any ongoing experimental programs. Such possibilities have interesting implications for a number of proposed facilities including the SSC. Some systematic machine physics studies over a range of energies are suggested. DOE

N86-12119# Sandia Labs., Albuquerque, N. Mex.
COMPARISON OF ENERGY TRANSPORT MEASUREMENTS AND COMPUTER SIMULATIONS IN A SINGLE MODULE PROTOTYPE FOR PBFA 2
E. L. Neau, J. F. Seamen, D. D. Bloomquist, S. R. Babcock, L. X. Schneider, and B. R. Sujka 1985 5 p Presented at the 5th IEEE Pulsed Power Conf., Washington, D.C., 10 Jun. 1985
(Contract DE-AC04-76DP-00789)
(DE85-013960; SAND-84-2584C; CONF-850616-63) Avail: NTIS HC A02/MF A01

The 36-module Particle Beam Fusion Accelerator (PBFA II) is designed to provide a 30 MV pulse, with greater than 150 TW, to a centrally located lithium ion diode. Each module is driven by a 6 MV, 400 kJ Marx generator and uses three water-insulated and switched pulse compression stages followed by a voltage inversion-adder unit. All impedance matching transmissioin-line transformer couples the output pulse from the inversion-adder unit to the central vacuum insulator, plasma erosion switches, and ion diode. The prototype of a single PBFA-II module, called Demon, is being used to test component design, including a mock-up of a section of the vacuum insulator, and to determine overall module operating characteristics. The results of measurements of energy transport efficiencies through the successive pulse compression stages are presented. Results of energy transport measurements on an 18 module, one-fifth scale model, are also compared to the single-line data. A comparison of measured parameters with computer circuit code simulations of the hardware design is also included. Comparisons are used to suggest areas of possible improvements. The measured module output characteristics agree with the code simulations and meet the design requirements for the PBFA-II accelerator. DOE

N86-12120# California Univ., Livermore. Lawrence Livermore Lab.
INTERACTION OF THE ATA BEAM WITH THE TM030 MODE OF THE ACCELERATING CELLS
V. K. Neil 14 Feb. 1985 11 p
(Contract W-7405-eng-48)
(DE85-014850; UCID-20456) Avail: NTIS HC A02/MF A01

The interaction of the electron beam in the Advanced Test Accelerator with azimuthally symmetric mode of the accelerating cells is investigated theoretically. The interaction possibly could cause modulation of the beam current at the resonant frequency of the mode. Values of the shunt impedance and Q value of the mode were obtained from previous measurement and analysis. Lagrangian hydrodynamics is employed and a WKB solution to the equation of motion is obtained. Results indicate that the interaction will not be a problem in the accelerator. DOE

N86-12121# Sandia Labs., Albuquerque, N. Mex
MABE MULTIBEAM ACCELERATOR
D. E. Hasti, J. J. Ramirez, P. D. Coleman, C. W. Huddle, A. W. Sharpe, and L. I. Torrison 1985 15 p refs Presented at the 5th IEEE Pulsed Power Conf., Washington, D.C., 10 Jun. 1985
(Contract DE-AC04-76DP-00789)
(DE85-012035; SAND-84-2393C; CONF-850616-59) Avail: NTIS HC A02/MF A01

The Megamp accelerator and beam experiment (MABE) was the technology development testbed for the multiple beam, linear induction accelerator approach for Hermes III, a new 20 MeV, 0.8 MA, 40 ns accelerator under development for gamma ray simulation. Experimental studies of a high current, single beam accelerator, and a nine beam injector were completed, and experiments on a nine beam linear induction accelerator are in progress. A two beam linear induction accelerator is designed and will be built as a gamma ray simulator to be used in parallel with Hermes III. The MABE pulsed power system and accelerator for the multiple beam experiments is described. Results from these experiments and the two beam design are discussed. DOE

N86-12122# Los Alamos Scientific Lab., N. Mex.
REVIEW OF KAON FACTORY PROPOSALS
H. A. Thiessen 1985 7 p refs Presented at the Particle Accelerator Conf., Vancouver, British Columbia, 13 May 1985
(Contract W-7405-eng-36)
(DE85-014110; LA-UR-85-2081; CONF-850504-204) Avail: NTIS HC A02/MF A01

Nuclear physics issues and particle physics issues for a kaon factory are discussed. Kaon factory accelerator proposals are considered. Secondary beam considerations are covered and hardware development for a kaon factory is discussed. The prospects for construction are presented. DOE

N86-12123# Sandia Labs., Albuquerque, N. Mex.
LOW INDUCTANCE DIODE DESIGN OF THE PROTO 2 ACCELERATOR FOR IMPLODING PLASMA LOADS
W. W. Hsing, R. Coats, D. H. McDaniel, and R. B. Spielman 1985 5 p Presented at the 5th IEEE Pulsed Power Conf., Washington, D.C., 10 Jun. 1985
(Contract DE-AC04-76DP-00789)
(DE85-013783; SAND-84-2568C; CONF-850616-53) Avail: NTIS HC A02/MF A01

A new water transmission line convolute, single piece insulator, and double accelerator. The water transmission lines have a 5 cm gap to eliminate any water arcing. A two-dimensional magnetic field code was used to calculate the convolute inductance. An acrylic insulator was used as well as a single piece, laminated polycarbonate insulator. They have been successfully tested at over 90% of the Shipman criteria for classical insulator breakdown, although the laminations in the polycarbonate insulator failed after a few shots. The anode and cathode each have two pieces and are held together mechanically. The vacuum MITL tapers to a 3 mm minimum gap. The total inductance is 8.4 nH for gas puff loads and 7.8 nH for imploding foil loads. Out of a forward-going energy of 290 kJ, 175 kJ has been delivered past the insulator, and 100 kJ has been successfully delivered to the load. DOE

N86-12124# Stanford Linear Accelerator Center, Calif.
COUPLED VIRBRATIONAL MODES OF THE SLC ARC MAGNET AND SUPPORT SYSTEM
W. T. Weng and A. W. Chao Mar. 1985 4 p refs Presented at the Particle Accelerator Conf., Vancouver, British Columbia, 13 May 1985
(Contract DE-AC03-76SF-00515)
(DE85-014288; SU-SLAC-Pub-3607; CONF-850504-198) Avail: NTIS HC A02/MF A01

The magnet support system for the SIC Arcs will be a long series of pedestals with each pedestal supporting the ends of two adjacent magnets. It was pointed out by several authors that random magnet vibrations in the Arc with amplitudes larger than 0.1 (MU)m rms are potentially harmful for the SIC operation. In order to assess the vibrational behavior of the Arc magnet system, the following must be understood: (1) the sources and characteristics of the ground disturbances, (2) the coupled vibrational modes of the composite pedestal-magnet system, and (3) the response of the system to ground disturbance. DOE

N86-12125# Stanford Linear Accelerator Center, Calif.
MEASUREMENTS OF ULTIMATE ACCELERATING GRADIENTS IN THE SLAC DISK-LOADED STRUCTURE
J. W. Wang and G. A. Loew Mar. 1985 4 p refs Presented at the Particle Accelerator Conf., Vancouver, British Columbia, 13 May 1985
(Contract DE-AC03-76SF-00515)
(DE85-014287; SU-SLAC-PUB-3597; CONF-850504-201) Avail: NTIS HC A02/MF A01

A status report on an on-going program at SLAC to study accelerator structures under high-gradient electric field conditions is presented. The study is a part of a much broader program dealing with future linear colliders. The accelerating gradient that might be achievable in such machines is a crucial parameter because once the beam energy is selected, the gradient determines the length of the linac and directly or indirectly affects the choice of many other parameters. To reach 1000 MV/m in a conventional 3 m constant-gradient section without SLED, one would need a klystron with a peak power output of 900 MW. Since such a tube is not available, it was decided to use a short standing-wave section in which the resonant fields can build up. The design criteria for this section, the fabrication, matching and tuning, the experimental set-up and the results are described. Author

N86-12126# Los Alamos Scientific Lab., N. Mex.
ACCELERATION SIMULATION IN THE LAMPF 2 BOOSTER
E. P. Colton 1985 4 p refs Presented at the Particle Accelerator Conf., Vancouver, British Columbia, 13 May 1985
(Contract W-7405-eng-36)
(DE85-012695; LA-UR-85-1518; CONF-850504-209) Avail: NTIS HC A02/MF A01

The evolution of the longitudinal phase space was studied during acceleration from 0.797-7.3 GeV in the LAMPF II booster. This machine is planned to multiparticle simulation program was used to model the acceleration with space charge included. The bunch population of 2.5 x 10 ti tge 11th protons was represented by 1000 macroparticles. During acceleration the rms longitudinal emittance grows by 3% and two particles are lost out of the separatrix. DOE

N86-12127# Rochester Univ., N. Y. Lab. for Laser Energetics.
OMEGA: A 24 BEAM UV IRRADIATION FACILITY
M. C. Richardson, W. Beich, J. Delettrez, M. Dunn, L. Folnsbee, R. J. Hutchinson, S. A. Jacobs, R. Keck, T. Kessler, W. Lampeter et al 1985 27 p refs Presented at Conf. on Lasers and Electro-optics, Baltimore, 21 May 1985
(Contract DE-FC08-85DP-40200)
(DE85-014416; DOE/EP-40200/8; CONF-850558-5) Avail: NTIS HC A03/MF A01

The recent completion of the UV upconversion (351 nm) of all 24 beams of the OMEGA laser which provides a unique short wavelength symmetrical irradiation facility for direct drive laser fusion experiments is discussed. Details of the characterization of illumination uniformity and initial implosion experiments are described. DOE

N86-12128# Pulse Sciences, Inc., Oakland, Calif.
MODELLING OF THE PROTO-2 CROSSOVER NETWORK
G. A. Proulx, H. Lackner, P. Spence, and T. P. Wright (Sandia Labs., Albuquerque, N. Mex.) 1985 5 p refs Presented at 5th IEEE Pulsed Power Conf., Washington, D.C., 10 Jun. 1985
(Contract DE-AC04-76DP-00789)
(DE85-014639; SAND-84-2588C; CONF-850616-69) Avail: NTIS HC A02/MF A01

In order to drive a double ring, symmetrically fed bremsstrahlung diode, the PROTO II accelerator was redesigned. The radially converging triplate water line was reconfigured to drive radial converging triplate lines in parallel. The four output lines were connected to the two input lines via an electrically enclosed tubular crossover network. Low-voltage Time Domain Reflectrometry (TDR) experiments were conducted on a full scale water immersed model of one section of the crossover network as an aid in this design. A lumped element analysis of the power flow through the network was inadequate in explaining the observed wave transmission and reflection characteristics. A more detailed analysis was performed with a circuit code in which we considered both localized lump-element and transmission line features of the crossover network. Experimental results of the model tests are given and compared with the circuit simulations. DOE

N86-12129# Texas Univ., Austin. Inst. for Fusion Studies.
VARIATIONAL QUADRATIC FORM FOR LOW FREQUENCY ELECTROMAGNETIC PERTURBATIONS. 1: FORMALISM
H. I. Berk and B. G. lane (MIT, Cambridge) Jun. 1985 30 p refs 2 Vol.
(Contract DE-FG05-80ET-53088)
(DE85-014896; IFSR-175-1; DOE/ET-53088/175-1) Avail: NTIS HC A03/MF A01

A variational formalism is obtained in the limit of large perpendicular wavenumber which simultaneously includes electrostatic and electromagnetic perturbations, finite Larmor radius corrections, equilibrium plasma rotation and arbitrary particle bounce effects. A tractable final expression is obtained and kinetic integrals are evaluated in special limits. The more accurate non-eikonal expression is obtained from the asymptotic matching of the eikonal form to more restrictive non-eikonal quadratic forms derived elsewhere. DOE

N86-12130# California Univ., Los Angeles. Center for Plasma Physics and Fusion Engineering.
FINESSE: STUDY OF THE ISSUES, EXPERIMENTS AND FACILITIES FOR FUSION NUCLEAR TECHNOLOGY RESEARCH AND DEVELOPMENT, VOLUME 4 Interim Report
M. Abdou Oct. 1984 658 p refs
(Contract DE-AS03-84ER-52105)
(DE85-010947; UCLA-ENG-84-30-Vol-4; PGG-821-Vol-4) Avail: NTIS HC A99/MF A01

This volume contains the following chapters (1) neutronics tests, (2) fluence considerations, (3) instrumentation and test matrix, (4) non-neutron test stands, (5) accelerator-based point neutron sources, (6) utilization of fission reactors, (7) tandem mirror test facilities, (8) tokamak fusion test facilities, (9) reliability development testing impacts on fusion reactor availability, and (10) fusion development scenarios. In addition, the following appendices are included: (1) evaluation of experience from fast breeder reactors, (2) observations of experts from the fission field, (3) evaluation of experience from the aerospace industry, (4) characterization of fusion nuclear systems operating environment, (5) modelling of MFTF-(alpha)+T high gamma mode performance, and (6) small-scale, multiple effects testing at US/DOE breeder reactor in-pile facilities. DOE

N86-12131# Rochester Univ., N. Y.
WHAT EXTENT WILL SMALL-SCALE LASER-BEAM FLUCTUATIONS SEED THE RAYLEIGH-TAYLOR INSTABILITY IN DIRECT-DRIVE TARGETS
S. Skupsky, R. I. McCrory, and C. P. Verdon 1984 9 p refs Presented at Meeting of the Plasma Phys. Div. of the Am. Phys. Soc., Boston, 27 Oct. 1984
(Contract DE-AC08-80DP-40124)
(DE85-014408; DOE/DP-40124/59; CONF-841010-16) Avail: NTIS HC A02/MF A01

The nonuniformity in laser energy deposition on a spherical target is calculated for multiple overlapping beams having small-scale fluctuations. Such nonuniformities can imprint themselves on the target surface and seed the Rayleigh-Taylor instability early in the pulse before an adequate, smoothing plasma-atmosphere has been established. The resulting growth of target deformation during the implosion is estimated. DOE

N86-12132# Los Alamos Scientific Lab., N. Mex.
RECENT FRC TRANSLATION EXPERIMENTS ON FRX-C/T
D. J. Rej, W. T. Armstrong, R. E. Chrien, W. N. Hugrass, P. L.

Klingner, K. F. McKenna, E. G. Sherwood, R. E. Siemon, and M. Tuszewski 1985 6 p Presented at the 7th US Symp. on Compact Toroid Res., Santa Fe, N. Mex., 21 May 1985
(Contract DE-AC04-76DP-00789)
(DE85-012745; LA-UR-85-1788; CONF-8505100-13) Avail: NTIS HC A02/MF A01

Accomplishments in the FRC translation studies on the FRX-C/T device are presented: (1) FRCs were launched into, and trapped in, a dc magnetic guide field region without the use of any pulsed gate coils; (2) detailed studies of translation dynamics were performed which are consistent with energy conservation, adiabatic compression theory, and 2-MHD simulations; (3) the confinement properties of translated FRC was evaluated; (4) translation through either puff or static deuterium gas fill was demonstrated; (5) higher density FRCs were translated over 10-m lengths; (6) the $n = 2$ rotational instability is stabilized by FRC translation into a weak helical quadrupole field. DOE

N86-11919# Joint Publications Research Service, Arlington, Va.
DOUBLE TEARING MODE IN PLASMA WITH MAGNETIC BRAIDING
Jiaqi Dong *In its* China Rept.: Sci. and Technol. (JPRS-CST-85-014) 2 May 1985 p 28-39 refs Transl. into ENGLISH from Wuli Xuebao (Beijing), v. 33, no. 10, Oct. 1984 p 1341-1349 (For primary document see N86-11918 02-70)
Avail: NTIS HC A06/MF A01

N86-11932# Joint Publications Research Service, Arlington, Va.
PROGRESS OF INERTIAL CONFINEMENT FUSION (ICF) RESEARCH Abstract Only
Ganchang Wang *In its* China Rept.: Sci. and Technol. (JPRS-CST-85-014) 2 May 1985 p 85 Transl. into ENGLISH from He Kexue Yu Gongcheng (Beijing), v. 4, no. 4, Dec. 1984 p 289-302 (For primary document see N86-11918 02-70)
Avail: NTIS HC A06/MF A01

N86-11956# Joint Publications Research Service, Arlington, Va.
INITIAL PLASMA FORMATION DURING EXPOSURE OF ABSORBING MATERIALS TO LASER RADIATION WITH PLANE EXPANSION GEOMETRY OF THE FORMING PLASMA Abstract Only
L. Ya. Minko, Yu. A. Chivel, and A. N. Chumakov *In its* USSR Rept.: Phys. and Math. (JPRS-UPM-85-005) 20 Aug. 1985 p 14-15 Transl. into ENGLISH from Zh. Prikl. Spektrosk. (Minsk), v. 42, no. 1, Jan. 1985 p 55-61 (For primary document see N86-11945 02-70)
Avail: NTIS HC A08/MF A01

N86-11958# Joint Publications Research Service, Arlington, Va.
INFLUENCE OF SOLID STATE OBSTACLES ON RADIATION OF RECOMBINATION LASER PLASMA Abstract Only
V. A. Boyko, B. A. Bryunetkin, F. V. Bunkin, V. I. Derzhiyev, V. M. Dyakin, S. A. Mayorov, I. Yu. Skobelev, A. Ya. Fayenov, A. I. Fedosimov, and K. A. Shilov *In its* USSR Rept.: Phys. and Math. (JPRS-UPM-85-005) 20 Aug. 1985 p 16-17 refs Transl. into ENGLISH from Fiz. Plazmy (Moscow), v. 10, no. 5, Sep. - Oct. 1984 p 999-1009 (For primary document see N86-11945 02-70)
Avail: NTIS HC A08/MF A01

N86-11997# Joint Publications Research Service, Arlington, Va.
CENTER FOR HIGH TEMPERATURE PLASMA PHYSICS CERTIFIED Abstract Only
Hu Maolian *In its* China Rept.: Sci. and Technol. (JPRS-CST-85-015) 16 May 1985 p 13-14 Transl. into ENGLISH from Anhui Ribao (Hefei), 21 Jan. 1985 p 1 (For primary document see N86-11994 02-70)
Avail: NTIS HC A07/MF A01

N86-11998# Joint Publications Research Service, Arlington, Va.
CONTROLLED THERMONUCLEAR FUSION, HIGH TEMPERATURE PLASMA PHYSICS Abstract Only
In its China Rept.: Sci. and Technol. (JPRS-CST-85-015) 16 May 1985 p 15 Transl. into ENGLISH from Anhui Ribao (Hefei), 21 Jan. 1985 p 1 (For primary document see N86-11994 02-70)
Avail: NTIS HC A07/MF A01

76 SOLID-STATE PHYSICS

includes superconductivity.

For related information, see also *33 Electronics and Electrical Engineering* and *36 Lasers and Masers.*

N86-12133 California Inst. of Tech., Pasadena.
INVESTIGATIONS OF DEEP LEVEL DEFECTS IN SEMICONDUCTOR MATERIAL SYSTEMS Ph.D. Thesis
Arati Prabhakar 1985 132 p
Avail: Univ. Microfilms Order No. DA8508467

Deep level defects in semiconductor material systems were investigated. Background information on semiconductor impurities and deep level transient spectroscopy (DLTS) are reviewed. The experiments performed on transition metal silicide-silicon Schottky barrier structures to probe for the existence of deep levels are discussed. Platinum, palladium, and nickel silicides on n-type silicon which were annealed at temperatures from 300 to 800 C were investigated. Nickel silicide structures could only withstand temperatures up to 500 C. Cobalt, chromium, and erbium silicides were also studied using DLTS. These measurements constitute the first series of deep level contamination of the silicon underlying a transition metal silicide thin film. The DLTS studies of four different compositions of the alloy In sub 1 x Ga sub x As sub y P sub 1-y. The samples, with bandgaps of 0.75, 0.83, 0.95, and 1.1 eV, covered the range of compositions that are lattice-matched to InP and are used for long-wavelength optoelectric devices. Author

N86-12134*# National Aeronautics and Space Administration. Lewis Research Center, Cleveland, Ohio.
ELLIPSOMETRIC AND OPTICAL STUDY OF SOME UNCOMMON INSULATOR FILMS ON 3-5 SEMICONDUCTORS
S. A. Alterovitz, J. D. Warner, D. C. Liu, and J. J. Pouch [1985] 18 p refs Presented at the 168th Meeting of the Electrochem. Soc., Las Vegas, Nev., 13-18 Oct. 1985
(NASA-TM-87135; E-2750; NAS 1.15:87135) Avail: NTIS HC A02/MF A01 CSCL 20L

Optical properties of three types of insulating films that show promise in potential applications in the 3-4 semiconductor technology were evaluated, namely a-C:H, BN and CaF2. The plasma deposited a-C:H shows an amorphous behavior with optical energy gaps of approximately 2 to 2.4 eV. These a-C:H films have higher density and/or hardness, higher refractive index and lower optical energy gaps with increasing energy of the particles in the plasma, while the density of states remains unchanged. These results are in agreement, and give a fine-tuned positive confirmation to an existing conjecture on the nature of a-C:H films (1). Ion beam deposited BN films show amorphous behavior with energy gap of 5 eV. These films are nonstoichiometric (B/N approximately 2) and have refractive index, density and/or hardness which are dependent on the deposition conditions. The epitaxially grown CaF2 on GaAs films have optical parameters equal to bulk, but evidence of damage was found in the GaAs at the interface. Author

N86-12135*# National Aeronautics and Space Administration. Lewis Research Center, Cleveland, Ohio.
CARBON FILMS GROWN FROM PLASMA ON III-V SEMICONDUCTORS
J. J. Pouch, J. D. Warner, and D. C. Liu 1985 12 p refs Presented at the 168th Meeting of the Electrochem. Soc., Las Vegas, Nev., 11-17 Oct. 1985
(NASA-TM-87140; E-2766; NAS 1.15:87140) Avail: NTIS HC A02/MF A01 CSCL 09C

Dielectric carbon films were grown on n- and p-type GaAs and InP substrates using plasmas generated at 30 KHz from gaseous hydrocarbons. The effect of gas source, flow rate, and power on film growth were investigated. Methane and n-butane gases were utilized. The flow rate and power ranged from 30 to 50 sccm and 25 to 300 W, respectively. AES measurements show only carbon to be present in the films. The relative Ar ion sputtering rate (3 KeV) of carbon depends on the ratio power/pressure. In addition, the degree of asymmetry associated with the carbon-semiconductor interface is approximately power-independent. SIMS spectra indicate different H-C bonding configurations to be present in the films. Band gaps as high as 3.05 eV are obtained from optical absorption studies. Author

N86-12136# California Univ., Los Angeles. Dept. of Chemistry and Biochemistry.
FRACTAL-LIKE, BUT NON-FRACTAL, BEHAVIOR OF ONE STEP DIPOLAR ENERGY TRANSFER ON REGULAR LATTICES WITH EXCLUDED VOLUME Interim Technical Report
C. L. Yang, P. Evesque, and M. A. El-Sayed 24 Jul. 1985 19 p
(Contract N00014-83-K-0341)
(AD-A157382; TR-45) Avail: NTIS HC A02/MF A01 CSCL 11/2

A simulation calculation is carried out for the time dependence of the donor intensity as one-step acceptor trapping process on a simple cubic lattice of interconnected rods of dimensions comparable to those found for the pores of Vycor (Corning Glass 7930). The donor and acceptor are allowed to occupy random sites on the surface of the pore. The results are fitted using the equations of Blumen and Klafter for energy transfer on a fractal structure. An apparent fractal dimension, (d'), is determined which is shown to result from an excluded volume effect and is not due to a real fractal structure. (D') is found to depend slightly on time, the acceptor concentration, and the length and/or width of the pores. Author (GRA)

N86-12137# Arizona Univ., Tucson. Optical Sciences Center.
THIN FILM RESEARCH. VOLUME 1 Final Report, 8 Jan. 1981 - 31 Jul. 1984
H. A. MacLeod 30 May 1985 492 p
(Contract N60530-81-C-0158; ARPA Order 3343)
(AD-A157608) Avail: NTIS HC A21/MF A01 CSCL 07/4

Optical thin films are critical components in a broad range of technologies, ranging from energy conversion to information storage. In response to the demand for increasingly specialized and durable coatings, enquiry into the basic nature of these coatings has intensified. Such efforts are necessary because assumptions that thin films were similar to nominally identical bulk materials have proven unreliable. For example, while most bulk materials show a high degree of isotropy, thin films display pronounced anisotropy. Another distinction between bulk and thin film materials is the lower density of the latter, with the resulting porosity. Both anisotropy and porosity often contribute to the unpredictable performance and durability of optical coatings. This report covers three years of fruitful research aimed at better understanding and modifying film microstructure in the direction of greater isotropy and density through novel deposition techniques. We have supported this effort with an array of analysis techniques and with a major effort in film growth simulation and in the theoretical description of anisotropic films. GRA

N86-12138# Arizona Univ., Tucson. Optical Sciences Center.
THIN FILM RESEARCH. VOLUME 2 Final Report, 8 Jan. 1981 - 31 Jul. 1984
H. A. MacLeod 30 May 1985 391 p
(Contract N60530-81-C-0158; ARPA Order 3343)
(AD-A157609) Avail: NTIS HC A17/MF A01 CSCL 07/4

Optical thin films are important components in a range of technologies, ranging from energy conversion to information storage. In response to the demand for increasingly specialized and durable coatings, study of the basic nature of these coatings has intensified. This type of effort is necessary because assumptions that thin films were similar to nominally identical bulk materials have proven unreliable. While most bulk materials show a high degree of isotropy, thin films display pronounced anisotropy. Another distinction between bulk and thin film materials is the lower density of the latter, with the resulting porosity. Both anisotropy and porosity often contribute to the unpredictable performance and durability of optical coatings. Three years of sucessful research aimed at better understanding and modifying film microstructure in the direction of greater isotropy and density through novel deposition techniques are covered in this report. We have supported this effort with a wide range of analysis techniques and with a major effort in film growth simulation and in the theoretical description of anisotropic films. GRA

N86-12139# Midwest Research Inst., Golden, Colo.
INVESTIGATION OF DEFECTS IN GaAsP SUPERLATTICE STRUCTURES
M. M. Al-Jassim and K. M. Jones Jun. 1985 7 p Presented at the 4th Oxford Conf. on Microscopy of Semiconducting Mater., Oxford, 25 Mar. 1985
(Contract DE-AC02-83CH-10098)
(DE85-012134; SERI/TP-212-2753; CONF-8503131-3) Avail: NTIS HC A02/MF A01

GaAsP superlattices were incorporated in GaAs/GaAsP cascade solar cell structures in an attempt to reduce the dislocation density in the high band gap cell. The structures were grown on GaAs substrates by MOCVD. Defects and irregularities in these structures were investigated by TEM, EBIC, X-ray microanalysis and chemical etching. DOE

N86-12140# Sandia Labs., Albuquerque, N. Mex.
ANALYTICAL ELECTRON MICROSCOPY STUDY OF SHOCK SYNTHESIZED ZINC FERRITE
M. J. Carr and R. A. Graham 1985 6 p Presented at the Am. Phys. Soc. Topical Conf. on Shock Waves in Condensed Matter, Spokane, 22 Jul. 1985
(Contract DE-AC04-76DP-00789)
(DE85-015144; SAND-85-1514C; CONF-850736-32) Avail: NTIS HC A02/MF A01

Mixtures of zinc oxide and hematite were shock loaded to various conditions, some of which resulted in the formation of zinc ferrite. Selected samples of reacted and unreacted mixtures were examined for the presence of zinc ferrite. Shock synthesized ferrite, having the spinel crystal structure, was found to occur as recrystallized regions within a heavily deformed matrix of well mixed reactants. The synthesized ferrite was not stoichiometric, but rather was found to be Zn/sub 1-x/Fe/sub 2+x/O4, where x = 0.09 + or - 0.02. DOE

N86-12141# Arizona Univ., Tucson.
METALLIC MULTILAYERS AND SUPERLATTICES
C. M. Falco 1985 11 p Presented at the 5th European Soc. General Conf. of Condensed Matter Div., West Berlin, 18 Mar. 1985
(Contract DE-AC02-83ER-45025)
(DE85-014444; DOE/ER-45025/7; CONF-8503152-1) Avail: NTIS HC A02/MF A01

An introduction to metal-metal multilayers and superlattices is presented, along with a brief review of some of the materials which have been made in our lab. and phenomena which have been observed so far. Results of a number of X-ray structural characterization techniques applied to these materials are described. These include Bragg THETA-2THETA X-ray diffraction, transmission and reflection Laue diffraction, and wide-film Debye-Scherrer diffraction. Emphasis is placed on recent results obtained in our laboratory with multilayers and superlattices produced by sputtering techniques. DOE

N86-12142# Southwest Research Inst., San Antonio, Tex.
SANDIA SHOCK COMPRESSION DATABASE
C. E. Anderson, J. S. Wilbeck, J. C. Hokanson, J. R. Asay, D. E. Grady, R. A. Graham, and M. E. Kipp 1985 11 p Presented at the Am. Phys. Soc. Top. Conf. on Shock Waves in Condensed Matter, Spokane, 22 Jul. 1985 Prepared in cooperation with Sandia National Lab., Albuquerque, N. Mex.
(Contract DE-AC04-76DP-00789)
(DE85-015141; SAND-85-0308C; CONF-850736-29) Avail: NTIS HC A02/MF A01

An authoritative, updatable, and searchable bibliographic database whose topical area is shock compression is currently under development. The database is derived from published scientific articles and reports with current emphasis in the subareas of strength, phase transitions, spall, and stress-volume relations. The content of the cited work is described by keywords which are selected and reviewed by scientific advisors. Keywords are organized to provide major and minor descriptors which summarize the technical content in considerable detail. Details of theoretical and experimental approaches are described and major emphasis is identified. In addition to bibliographic information, abstracts are also included, and a field is provided for figure captions and able headings. DOE

N86-12143# Los Alamos Scientific Lab., N. Mex.
STATICS AND ADIABATIC DYNAMICS OF NONLINEAR EXCITATIONS IN DEFECTED POLYACETYLENE
S. R. Phillpot, D. Baeriswyl, A. R. Bishop, and P. S. Lomdahl 1985 12 p Presented at the Synthetic Met. 3 Workshop, Los Alamos, N. Mex., 9 Apr. 1985
(Contract W-7405-eng-36)
(DE85-014118; LA-UR-85-2055; CONF-8504157-2) Avail: NTIS HC A02/MF A01

Within the Su, Schrieffer and Heeger model the effects of model impurities on the electronic structure and lattice distortion of trans-polyacetylene were calculated both analytically and numerically. The electron-phonon coupling may result in a fundamental alteration of the impurity level location. In simulated photoexcitation experiments on the defected system it was found that, in addition to the kinks and breathers produced in undefected system, trapped kinks, excitons and polarons may also be produced. The polarons produced in this novel way may be unusually stable and play an important role in hopping conduction mechanisms. DOE

N86-12144# Brookhaven National Lab., Upton, N. Y.
NEUTRON SCATTERING STUDIES OF THE HEAVY FERMION SUPERCONDUCTORS
A. I. Goldman 1985 14 p Presented at the Mater. and Mech. of Superconductivity Conf., Ames, Iowa, 20 May 1985
(Contract DE-AC02-76CH-00016)
(DE85-014629; BNL-36647; CONF-8505138-13) Avail: NTIS HC A02/MF A01

Recent neutron scattering measurements of the heavy Fermion superconductors are described. Those materials offer an exciting opportunity for neutron scattering since the f-electrons, which couple directly to magnetic scattering measurements, seem to be the same electrons which form the superconducting state below T sub c. In addition, studies of the magnetic fluctuations in these, and other heavy Fermion systems, by inelastic magnetic neutron scattering can provide information about the nature of the low temperature Fermi liquid character of these novel compounds. DOE

N86-12145# California Univ., Berkeley. Lawrence Berkeley Lab.
MODEL OF AMORPHOUS SILICON LAYER REGROWTH
P. Ling and J. Washburn Apr. 1985 10 p refs Presented at the 2nd Spring Meeting of the Mater. Res. Soc., San Francisco, 15 Apr. 1985
(Contract DE-AC03-76SF-00098)
(DE85-012608; LBL-19452; CONF-850421-9) Avail: NTIS HC A02/MF A01

A new model which combines heterogeneous nucleation and growth process to explain the mechanism of the crystal regrowth of amorphous silicon, in contact with a Si single crystal substrate, is presented. This model explains the effects of substrate orientation and impurity concentration on the kinetics of crystal regrowth. A comparison of experimental results with the predictions of the model is also included. DOE

N86-12146# Oak Ridge National Lab., Tenn.
FORMATION, ION MODIFICATION AND ANNEALING OF VN
J. R. Thompson, J. T. Ellis, D. K. Christen, J. D. Lewis, and S. T. Sekula Apr. 1985 18 p refs Presented at the Mater. and Mech. of Syperconductivity Conf., Ames, Iowa, 29 May 1985 Prepared in cooperation with Tennessee Univ., Knoxville
(Contract DE-AC05-84OR-21400)
(DE85-012896; CONF-8505138-3) Avail: NTIS HC A02/MF A01

Thin films of vanadium nitride, formed by diffusion of N2 gas into previously characterized vanadium films, have been modified using ion beam techniques. Irradiation by N-ions produced decreases in the superconductive transition temperature T/sub c/ and electrical resistance ratio RRR, which saturated at 3.6 K and 1.0, respectively. It was found that films with higher T/sub c/ values were less susceptible to ion-damage. An isochronal annealing study revealed several annealing stages and nearly complete recovery of T/sub C/. Laser annealing of this brittle material was rather ineffective, however. The results of this work are related to the possible formation of high T/sub c/, B1 phase Mon. DOE

N86-12147# Brookhaven National Lab., Upton, N. Y.
ICOSAHEDRAL INCOMMENSURATE CRYSTALS
P. Bak 1985 11 p Presented at the NATO Advan. Study Inst. Advan. Study Inst. on Scaling Phenomena in Disordered Systems, Geilo, Norway, 4 Aug. 1985
(Contract DE-AC02-76CH-00016)
(DE85-012512; BNL-36437; CONF-850882-1) Avail: NTIS HC A02/MF A01

The icosahedral structures can be described by 6d space group symmetries and their stability can be understood from a simple Landau theory. The task of the crystallographer is to determine the basis associated with the 6d Bravais lattice. The elastic properties and the elementary excitations can be discussed in terms of these symmetries. The ideal icosahedral structures have complete long range order, with sharp Bragg peaks; it is certainly incorrect to consider them to be intermediate between crystals and glasses; they are crystals. It is not difficult to show that the structures are stable with respect to thermal fluctuations, which simply give rise to a reduction of the Bragg peak intensity. The melting transition is first order since the free energy includes third order terms. In a sense the icosahedral structures are incommensurate structures with only one length scale 2(PI)/tau sub i. The incommensurability comes about because of the relative rotations of the 6 fundamental vectors tau sub i: it is not possible to write any of the 6 vectors as sums of rational multiples of the remaining 5 vectors. DOE

N86-12148# Los Alamos Scientific Lab., N. Mex.
EOS FOR POLYCRYSTALLINE QUARTZ
J. D. Johnson and S. P. Lyon May 1985 7 p refs
(Contract W-7405-eng-36)
(DE85-014241; LA-10391-MS) Avail: NTIS HC A02/MF A01

A new equation of state for polycrystalline quartz, material number 7383, was placed on the SESAME Library. DOE

N86-12149# Los Alamos National Lab., N. Mex.
NUCLEAR INTERLEVEL TRANSFER DRIVEN BY ELECTRONIC TRANSITIONS
J. C. Solem and G. Rinker 1985 20 p refs Presented at the IDA Workshop on Gamma-Ray Lasers, Alexandria, Va., 21 May 1985
(Contract W-7405-eng-36)
(DE85-014103; LA-UR-85-2119; CONF-8505174-1) Avail: NTIS HC A02/MF A01

It is show how a gamma-ray laser might be made by optically exciting a transfer of population from a long-lived isomer to an energetically adjacent short-lived state of the same nucleus. The advantages of using are compared. Preliminary numerical investigations of the mechanism show it to be somewhat favorable. DOE

N86-12150# Argonne National Lab., Ill.
MAGNETIC MEASUREMENTS OF MONOLAYER-THICKNESS FILMS OF Cr SANDWICHED BY Au
M. B. Brodsky, L. R. Sill, and C. H. Sowers Jun. 1985 13 p Presented at the Intern. Conf. on Magnetism, San Francisco,

26 Aug. 1985
(Contract W-31-109-eng-38)
(DE85-015005; CONF-850890-9) Avail: NTIS HC A02/MF A01

Calculations show ferromagnetic moments (3.1(MU) sub B) in Au-Cr-Au sandwiches, for monolayers of Cr. The measured moment (0.41(MU) sub B at 2(0)K) is larger in Cr monolayers than for thicker Cr samples. Results are discussed in terms of other studies of this system including those which showed superconductivity. DOE

N86-12151# McElroy (Ralph) Co., Austin, Tex.
INVESTIGATION ON GROWTH AND LASER PROPERTIES OF GGG:(Nd,Cr) SINGLE CRYSTAL
L. Zhang, C. Lin, H. Liu, L. Liu, H. Zhu, and X. Lin Jun. 1985 16 p refs Transl. into ENGLISH of unknown Chinese article
(Contract W-7405-eng-48)
(DE85-014282; UCRL-Trans-12067) Avail: NTIS HC A02/MF A01

Investigation of the growth and laser properties of gadolinium gallium garnet crystal doped with Nd and Cr is reported. As the segregation coefficient of Nd in GGG is less than 1 and that of Cr is greater than 1, a modified Czochralski method for growth is adopted in order to keep the dopants from being uniform in the growth crystal. DOE

N86-12152# American Inst. of Mining, Metallurgical, and Petroleum Engineers, Inc., Washington, D. C.
INTERNATIONAL PROJECT IN HISTORY OF SOLID STATE PHYSICS Final Report
S. R. Weart Sep. 1984 5 p refs
(Contract DE-FG02-81ER-10864)
(DE85-014843; DOE/ER-10864/1) Avail: NTIS HC A02/MF A01

The International Project in History of Solid State Physics got underway in 1981, planning a large collaborative program to preserve and make known the history of this field. The Project's scholars and sponsors were spurred by the realization that although solid state physics is one of the most important influences on late twentieth century civilization, its history was all but unknown to historians, to the public at large, and even to most physicists. The chief aim of the Project was to create a new and enduring area of historical activity, and this aim was accomplished. As we hoped, most of the scholars who have been drawn to this field plan to continue to study and publish in the history of solid state physics, building upon the research and resources assembled under the Project. DOE

N86-12153# Argonne National Lab., Ill.
MICROSCOPIC INVESTIGATION OF NbN SPUTTERED FILMS
K. E. Gray, R. T. Kampwirth, D. W. Capone, II, and R. Vaglio 29 May 1985 12 p refs Presented at Mater. and Mech. of Superconductivity Conf., Ames, Iowa, 29 May 1985
(Contract W-31-109-eng-38)
(DE85-015000; CONF-8505138-11) Avail: NTIS HC A02/MF A01

Many favorable properties of niobium nitride (NbN) sputtered films for high field magnets are significantly less favorable in bulk NbN (and other high-field superconductors) so that differences in the microstructure of sputtered NbN films are likely responsible for the improvements. Very thin transverse sections of sputtered films were studied by TEM. Such studies reveal columnar grains. Tunneling measurements that directly investigate T sub c and the energy gap of individual grains are discussed. By placing electrodes above and below the film, preliminary measurements of the intrinsic resistivity of the individual columnar grains indicate values significantly less than the transport value. Measurements of the critical current density, J sub c, in NbN suggest that shearing of the flux line lattice does not limit J sub c, as in A-15 superconductors, no doubt due to the high density of pinning centers in NbN. DOE

N86-12154# Syracuse Univ., N. Y. Dept. of Physics.
NUCLEAR SPIN-POLARIZED HD, D2, HT AND DT SOLIDS, LIQUIDS AND HIGH DENSITY GASES Quarterly Status Report, 1 Mar. - 31 May 1985
27 Jun. 1985 5 p
(Contract DE-FG02-84ER-53179)
(DE85-014136; DOE/ER-53179/T4; QSR-5) Avail: NTIS HC A02/MF A01

Success is reported in attaining extremely pure o-D2 in the 0.997 to 0.999 range by symmetry species conversion at a temperature of 4K on a partially activated charcoal catalyst. Spin-lattice relaxation times were improved to over 1 minute. Long storage times and the possibility of liquefaction without depolarizing the o-D2 are expected. Super pure o-D2 may also be used to probe magnetic impurities on surfaces. In addition, 50 kV white spectrum X-ray irradiated solid D2 experiments have yielded information on defect generation rates and defect lifetimes, as well as their effect on para-ortho D2 conversion. Experiments were also begun in epitaxial deposition of D2 on HD, and HD on mostly p-H2. Tests of a dilution refrigerator were completed. DOE

N86-12155# Los Alamos National Lab., N. Mex.
SURFACE IMPEDANCE OF SEVERAL MAGNETIC SUPERCONDUCTORS
M. K. Hou, C. Y. Huang, M. B. Maple (California Univ., San Diego, La Jolla), M. S. Torikachvili (California Univ., San Diego, La Jolla), and H. C. Hamaker (California Univ., San Diego, La Jolla) 1985 13 p refs Presented at the Intern. Conf. on Magnetism, San Francisco, 26-30 Aug. 1985
(Contract W-7405-eng-36)
(DE85-014101; LA-UR-85-2142; CONF-850890-5) Avail: NTIS HC A02/MF A01

Spin fluctuation effect plays an important role in determining the surface impedance, Z/sub s/, in magnetic superconductors. The suppression of spin fluctuations in Er/sub 0.5/Ho/sub 0.5/Rh4B4 gives rise to an abrupt change of Z/sub s/ at the critical temperature T/sub c2/. However, gradual changes of Z/sub s/ for SmRh4B4 and ErRh4B4 were observed in superconducting state. DOE

N86-12156# California Univ., Livermore. Lawrence Livermore Lab.
NEW HARMONIC MATERIALS: INDEX ENGINEERING: THIN-THICK QUADRATURE FREQUENCY CONVERSION
D. Eimerl 7 Feb. 1985 4 p
(Contract W-7405-eng-48)
(DE85-012976; UCRL-92086) Avail: NTIS HC A02/MF A01

The quadrature conversion scheme is a method of generating the second harmonic. The scheme has several advantages over single-crystal or other two crystal schemes. The most important is that it is capable of high conversion efficiency over a large dynamic range of drive intensity and detuning angle. A pair of KDP crystals cut for type-II phase matching are considered. In the quadrature scheme, the optic axes of the crystals are arranged so that the plans containing the direction of the laser beam and their optic axes (the kz planes) are mutually perpendicular. This arrangemnt has two important properties in type-II phase matching, the incident wave is polarized at 45 deg to the kz plane of the crystal. This is in the quadrature scheme, if the incident wave is correctly polarized for efficient conversion in the first crystal, it is also correctly polarized for efficient conversion in the second crystal. Both crystals can convert efficiently. DOE

N86-11862# Sandia Labs., Albuquerque, N. Mex. Thermophysical Properties Div.
OPTICAL MODELING OF MULTILAYER THIN/THICK FILMS Abstract Only
Richard B. Pettit *In* LANL 6th Bien. CUBE (Computer Use by Engineers) Symp. Aug. 1984 p 10-11 (For primary document see N86-11858 02-60)
Avail: NTIS HC A06/MF A01

N86-11864# Sandia Labs., Albuquerque, N. Mex. Theoretical Div.
CALCULATION OF THE ELECTRON BACKSCATTERING COEFFICIENT BY MONTE CARLO SIMULATION Abstract Only
Arlyn J. Antolak and William Williamson, Jr. (Toledo Univ.) *In*

LANL 6th Bien. CUBE (Computer Use by Engineers) Symp. Aug. 1984 p 11 (For primary document see N86-11858 02-60)
Avail: NTIS HC A06/MF A01

N86-11878# Sandia Labs., Albuquerque, N. Mex. Computational Physics and Mechanics Div.
FINITE DIFFERENCE CALCULATIONS OF VOLTAGES GENERATED IN THIN DIELECTRIC LAYERS SUBJECTED TO SHOCK LOADING Abstract Only
Jeffrey W. Swegle *In* LANL 6th Bien. CUBE (Computer Use by Engineers) Symp. Aug. 1984 p 44-45 (For primary document see N86-11858 02-60)
Avail: NTIS HC A06/MF A01

N86-11931# Joint Publications Research Service, Arlington, Va.
Pb(1-x)Sn(x)Te AND Pb(1-y)Sn(y)Se LASER CRYSTALS Abstract Only
Xiaochun Zhu, Gendi Cao, and Weizai Zhang *In its* China Rept.: Sci. and Technol. (JPRS-CST-85-014) 2 May 1985 p 84 Transl. into ENGLISH from Zhongguo Jiguang (Shanghai), v. 12, no. 1, 20 Jan. 1985 p 48-50 (For primary document see N86-11918 02-70)
Avail: NTIS HC A06/MF A01

N86-11934# Joint Publications Research Service, Arlington, Va.
THE RELATIONS BETWEEN VOLTAGE AND MAGNETIC FIELD OF SUPERCONDUCTING WEAKLINK (1) Abstract Only
Yuheng Zhang and Jun Wang *In its* China Rept.: Sci. and Technol. (JPRS-CST-85-014) 2 May 1985 p 89 Transl. into ENGLISH from Wuli Xuebao (Beijing), v. 33, no. 7, Jul. 1984 p 952-958 (For primary document see N86-11918 02-70)
Avail: NTIS HC A06/MF A01

N86-11935# Joint Publications Research Service, Arlington, Va.
THE RELATIONS BETWEEN VOLTAGE AND MAGNETIC FIELD OF SUPERCONDUCTING WEAKLINK (2) Abstract Only
Yuheng Zhang and Jun Wang *In its* China Rept.: Sci. and Technol. (JPRS-CST-85-014) 2 May 1985 p 90 Transl. into ENGLISH from Wuli Xuebao (Beijing), v. 33, no. 7, Jul. 1984 p 959-966 (For primary document see N86-11918 02-70)
Avail: NTIS HC A06/MF A01

N86-11936# Joint Publications Research Service, Arlington, Va.
DISCUSSION OF THE SUPERCONDUCTING CRITICAL TEMPERATURE IN A N-S MULTI-FILM STRUCTURE Abstract Only
Changde Gong, Dingyu Xing, and Mei Liu *In its* China Rept.: Sci. and Technol. (JPRS-CST-85-014) 2 May 1985 p 91 Transl. into ENGLISH from Wuli Xuebao (Beijing), v. 33, no. 7, Jul. 1984 p 967-974 (For primary document see N86-11918 02-70)
Avail: NTIS HC A06/MF A01

N86-11937# Joint Publications Research Service, Arlington, Va.
THEORY OF THE CRITICAL TEMPERATURE FOR SUPERCONDUCTORS WITH SMALL LAMBDA (1) Abstract Only
Hangsheng Wu and Zhengyu Weng *In its* China Rept.: Sci. and Technol. (JPRS-CST-85-014) 2 May 1985 p 92 Transl. into ENGLISH from Wuli Xuebao (Beijing), v. 33, no. 7, Jul. 1984 p 975-988 (For primary document see N86-11918 02-70)
Avail: NTIS HC A06/MF A01

N86-11938# Joint Publications Research Service, Arlington, Va.
EFFECT OF HIGH ELECTRIC FIELD ON MINORITY CARRIER GENERATION IN SILICON DEPLETION LAYER Abstract Only
Zhijian Li, Lilin Tian, and Xinrong Ma *In its* China Rept.: Sci. and Technol. (JPRS-CST-85-014) 2 May 1985 p 94 Transl. into ENGLISH from Bandaoti Xuebao (Beijing), v. 6, no. 1, Jan. 1985 p 1-10 (For primary document see N86-11918 02-70)
Avail: NTIS HC A06/MF A01

N86-11939# Joint Publications Research Service, Arlington, Va.
DEEP-LEVEL DEFECTS IN ION-IMPLANTED AND CO2 LASER-ANNEALED SILICON Abstract Only
Ximao Bao, Xinyu Zhang, and Chengen Liu *In its* China Rept.: Sci. and Technol. (JPRS-CST-85-014) 2 May 1985 p 95 Transl. into ENGLISH from Bandaoti Xuebao (Beijing), v. 6, no. 1, Jan. 1985 p 11-18 (For primary document see N86-11918 02-70)
Avail: NTIS HC A06/MF A01

N86-11940# Joint Publications Research Service, Arlington, Va.
BINDING ENERGY OF DONORS IN GaAs-Ga(1-x) Al(x)As QUANTUM WELL STRUCTURES Abstract Only
Zhenping Liu and Tianke Li *In its* China Rept.: Sci. and Technol. (JPRS-CST-85-014) 2 May 1985 p 97 Transl. into ENGLISH from Bandaoti Xuebao (Beijing), v. 6, no. 1, Jan. 1985 p 32-40 (For primary document see N86-11918 02-70)
Avail: NTIS HC A06/MF A01

N86-11941# Joint Publications Research Service, Arlington, Va.
AN INTERFACIAL ANALYSIS OF MoNb-GaAs SCHOTTKY BARRIER DIODES Abstract Only
Mingren Yu, Furong Zhu, Xun Wang, Binqi Wang, and Kai Shao *In its* China Rept.: Sci. and Technol. (JPRS-CST-85-014) 2 May 1985 p 100 Transl. into ENGLISH from Bandaoti Xuebao (Beijing), v. 6, no. 1, Jan. 1985 p 55-60 (For primary document see N86-11918 02-70)
Avail: NTIS HC A06/MF A01

N86-11942# Joint Publications Research Service, Arlington, Va.
THERMAL POST-TREATMENT CHARACTERISTICS OF METASTABLE CARRIER CONCENTRATION IN As-IMPLANTED SILICON AFTER TRANSIENT ANNEALING Abstract Only
Li Xu, Peixin Qian, Dongyan Hou, Yusheng Wang, Jianhua Yan, and Shengnan Zheng *In its* China Rept.: Sci. and Technol. (JPRS-CST-85-014) 2 May 1985 p 102 Transl. into ENGLISH from Bandaoti Xuebao (Beijing), v. 6, no. 1, Jan. 1985 p 76-81 (For primary document see N86-11918 02-70)
Avail: NTIS HC A06/MF A01

N86-11943# Joint Publications Research Service, Arlington, Va.
DEEP LEVELS IN SEMI-INSULATING GaAs Abstract Only
Binglin Zhou and Zhengxiu Chen *In its* China Rept.: Sci. and Technol. (JPRS-CST-85-014) 2 May 1985 p 103 Transl. into ENGLISH from Bandaoti Xuebao (Beijing), v. 6, no. 1, Jan. 1985 p 100-103 (For primary document see N86-11918 02-70)
Avail: NTIS HC A06/MF A01

N86-11952# Joint Publications Research Service, Arlington, Va.
CONVERSION OF ELECTROMAGNETIC WAVE ENERGY TO ELECTRICAL CURRENT BY BULK SUPERLATTICE SEMICONDUCTORS Abstract Only
M. M. Kechiyev, A. A. Kostenko, V. D. Kurek, O. A. Kuznetsov, V. A. Tolomasov, O. N. Filatov, G. I. Khlopov, and V. P. Shestopalov *In its* USSR Rept.: Phys. and Math. (JPRS-UPM-85-005) 20 Aug. 1985 p 7 refs Transl. into ENGLISH from Dokl. Akad. Nauk SSSR (Moscow), v. 279, no. 3, Nov. 1984 p 606-608 (For primary document see N86-11945 02-70)
Avail: NTIS HC A08/MF A01

N86-11953# Joint Publications Research Service, Arlington, Va.
CAUSE OF OCCURRENCE OF HIGH-ENERGY IONS DURING UV LASER IRRADIATION OF MOLECULAR CRYSTALS Abstract Only
S. Ye Yegorov and A. N. Shibanov *In its* USSR Rept.: Phys. and Math. (JPRS-UPM-85-005) 20 Aug. 1985 p 7-8 refs Transl. into ENGLISH from Zh. Tekh. Fiz. (Leningrad), v. 54, no. 11, Nov. 1984 p 2270-2274 (For primary document see N86-11945 02-70)
Avail: NTIS HC A08/MF A01

77 THERMODYNAMICS AND STATISTICAL PHYSICS

Includes quantum mechanics; and Bose and Fermi statistics.

For related information see also *25 Inorganic and Physical Chemistry* and *34 Fluid Mechanics and Heat Transfer.*

N86-12157# California Univ., Berkeley. Lawrence Berkeley Lab.
EPR: WHAT HAS IT TAUGHT US
H. P. Stapp May 1985 9 p refs Presented at the Symp. on the Found. of Modern Phys., Joensuu, Finland, 16 Jun. 1985
(Contract DE-AC03-76SF-00098)
(DE85-014525; LBL-19642; CONF-850683-2) Avail: NTIS HC A02/MF A01

Eistein, Podoisky, and Rosen (EPR) paper is discussed. The EPR paper was counterproductive for the following reasons: (1) the work was quickly rebutted by Bohr and this rebuttal was accepted my most workers in the field; (2) scientists who adopted the position advocated by Bohr produced, useful theory, whereas those following the course suggested by EPR produced nothing of any certified practical value; (3) it was shown by Bell that the conclusion reached by EPR is incompatible with their assumptions. The behavior of quantum mechanical systems that are very small, yet large enough to influence their environment in ways that appreciably modify their own behavior, vis-a-vis the behavior they would have if isolated was investigated. Because these systems are neither small enough to be treated as isolated between preparation and detection, nor large enough to be treated classically, they do not conform to the format demanded by the Copenhagen interpretation. The behavior of these systems depends on ontological considerations that were irrelevant in the situations covered by the Copenhagen interpretation, and that were systematically ignored in that interpretation. The task of enlarging the scope of quantum theory to cover these new situations, and comparing the empirical consequences of various ontological assumptions is discussed. DOE

N86-11989# Joint Publications Research Service, Arlington, Va.
HYDROTHERMODYNAMICS OF THE NEAR-SURFACE LAYER OF A LIQUID AND OPTICAL METHODS OF INVESTIGATING IT
O. D. Fedorovskyy *In its* USSR Rept.: Phys. and Math. (JPRS-UPM-85-005) 20 Aug. 1985 p 107-115 refs Transl. into ENGLISH from Visnyk Akad. Nauk Ukrayinskoyi RSR (Kiev), no. 11, Nov. 1984 p 15-21 (For primary document see N86-11945 02-70)
Avail: NTIS HC A08/MF A01

80 SOCIAL SCIENCES (GENERAL)

Includes educational matters.

N86-12158*# National Academy of Sciences - National Research Council, Washington, D. C.
NASA-UNIVERSITIES RELATIONSHIPS IN AERO/SPACE ENGINEERING: A REVIEW OF NASA'S PROGRAM
1985 33 p refs
(NASA-CR-176307; NAS 1.26:176307) Avail: NTIS HC A03/MF A01 CSCL 05I

NASA is concerned about the health of aerospace engineering departments at U.S. universities. The number of advanced degrees in aerospace engineering has declined. There is concern that universities' facilities, research equipment, and instrumentation may be aging or outmoded and therefore affect the quality of research and education. NASA requested that the National Research Council's Aeronautics and Space Engineering Board (ASEB) review NASA's support of universities and make recommendations to improve the program's effectiveness. G.L.C.

N86-11993# Joint Publications Research Service, Arlington, Va.
PROBLEMS, TRENDS IN TECHNICAL EDUCATION OF RESEARCHERS
O. M. Belotserkovskiy *In its* USSR Rept.: Sci. and Technol. Policy (JPRS-UST-85-014) 25 Sep. 1985 p 52-62 Transl. into ENGLISH from Vest. Vyssey Shkoly (Moscow), no. 5, May 1985 p 25-29 (For primary document see N86-11990 02-70)
Avail: NTIS HC A06

81 ADMINISTRATION AND MANAGEMENT

Includes management planning and research.

N86-12159# Oak Ridge National Lab., Tenn.
DISTINCT CHARACTERISTICS OF SCIENCE
L. G. Christophorou 22 Jan. 1985 17 p
(Contract DE-AC0-584OR-21400)
(DE85-006533; DOE/OR-21400/T144) Avail: NTIS HC A01/MF A01

The following principles of science are identified: relatedness, embeddedness, coordinating principle, correspondence, scientific parsimony, complementarity, and continuity. The scientific method and the people who work in science are discussed. DOE

N86-11991# Joint Publications Research Service, Arlington, Va.
BOOK ON PLANNING OF SCIENTIFIC, TECHNICAL PROGRESS
A. N. Andrukhovich, V. Yu. Budvey, T. N. Kalinovskaya, B. P. Krasnoglazov, V. M. Likhtenshteyn, L. I. Maksimov, V. L. Mershko, Ye. V. Sapilov, P. A. Sedlov, and T. L. Sletova *In its* USSR Rept.: Sci. and Technol. Policy (JPRS-UST-85-014) 25 Sep. 1985 p 11-14 Transl. into ENGLISH from Oshchestvennyye Nauki v SSSR, Ser. 2: Ekonomika (Referativnyy Zh.) (Moscow), no. 1, Jan. - Feb. 1985 p 60-64 (For primary document see N86-11990 02-70)
Avail: NTIS HC A06

82 DOCUMENTATION AND INFORMATION SCIENCE

Includes information storage and retrieval technology; micrography; and library science.

For computer documentation see *61 Computer Programming and Software.*

N86-12160# Air Command and Staff Coll., Maxwell AFB, Ala.
A COMPUTER-BASED EDUCATIONAL APPROACH TO THE AIR COMMAND AND STAFF COLLEGE ASSOCIATE PROGRAM
J. A. Gaudet Apr. 1985 81 p
(AD-A156460; ACSC-85-0925) Avail: NTIS HC A05/MF A01 CSCL 09/2

The ACSC Associate Program will incorporate Computer-Based Education (CBE) by the Fall of 1987. The college obtained the McGraw-Hill Interactive Authoring System as an authoring tool that has the potential to aid the faculty with CBE. The study explains the reasons for using CBE and examines the McGraw-Hill computer program for its utility to ACSC. The advantages and limitations of this authoring system are discussed. A methodology is presented which will be helpful in designing CBE. The study concludes that the McGraw-Hill Interactive Authoring System will be useful in initiating CBE. However, supplementing computer programs will be necessary to perform computer management functions. GRA

N86-12161# California Univ., Livermore. Lawrence Livermore Lab.
ANNOTATED BIBLIOGRAPHY OF HUMAN FACTORS APPLICATIONS LITERATURE

D. B. McCafferty 30 Sep. 1985 315 p Prepared in cooperation with Essex Corp., Alexandria, Va.
(Contract W-7405-eng-48)
(DE85-012957; UCRL-15674) Avail: NTIS HC A14/MF A01

The material is a revision and expansion of the bibliographic material developed in FY 1982 as part of a previous human factors technology project. The previous bibliography was published September 30, 1982, as Attachment 1 to the FY 1982 Project Status Report. DOE

N86-11996# Joint Publications Research Service, Arlington, Va.
NEW R AND D IN CHINESE LANGUAGE INFORMATION PROCESSING Abstract Only
In its China Rept.: Sci. and Technol. (JPRS-CST-85-015) 16 May 1985 p 11-12 Transl. into ENGLISH from Jisuanji Shijie (Beijing), no. 7, 8 Apr. 1984 p 7 (For primary document see N86-11994 02-70)
Avail: NTIS HC A07/MF A01

N86-11999# Joint Publications Research Service, Arlington, Va.
THIRD NATIONAL ACADEMIC MACHINE RETRIEVAL CONFERENCE HELD IN ZHENJIANG Abstract Only
In its China Rept.: Sci. and Technol. (JPRS-CST-85-015) 16 May 1985 p 26-27 Transl. into ENGLISH from Jisuanji Shijie (Beijing), no. 1, 8 Jan. 1984 p 1 (For primary document see N86-11994 02-70)
Avail: NTIS HC A07/MF A01

83 ECONOMICS AND COST ANALYSIS

Includes cost effectiveness studies.

N86-12162# Air Command and Staff Coll., Maxwell AFB, Ala.
COMMERCIALIZATION OF SPACE: NATIONAL POLICY AND DEFENSE NEEDS Student Report
J. J. Taylor Apr. 1985 57 p
(AD-A156517; ACSC-85-2675) Avail: NTIS HC A04/MF A01 CSCL 22/1

This report evaluates potential impacts of commercialization of space on U.S. space policy and space defense needs for the future. Historical trends of U.S. space commercialization and U.S. space policy form a foundation for projecting space commercialization out to the year 2025. The report contains tables and figures of space vehicle launch statistics, satellite launches, satellite lifetimes, capital investment in satellites, revenues from space industry, and other quantitative data. The study concludes that future U.S. space defense must include security needs of U.S. space-based commercial assets. Author (GRA)

84 LAW AND POLITICAL SCIENCE

Includes space law; international law; international cooperation; and patent policy.

N86-12163# State Dept., Washington, D. C. Bureau of Public Affairs.
US SPACE PROGRAMS: COOPERATION AND COMPETITION FROM EUROPE
Harry R. Marshall, Jr. and Cynthia Saboe, ed. May 1985 6 p
(BPA-CP-695) Avail: NTIS HC A02/MF A01

International activities demonstrate the many applications of space science and technology for peaceful purposes and provide opportunities for contribution by scientists of other countries to the tasks of increasing human understanding and use of space. Cooperative activities range from flight of foreign spacecraft to groundbased study and analysis of data. Activities include contributions of experiments or payloads to be flown in space, joint projects to develop flight hardware, use of data provided by satellites, and joint publication of scientific results. These cooperative programs are generally carried out under government-to-government science and technology agreements coordinated by the State Department. In addition, NASA provides, on a reimbursable basis, commercial services such as deployment of telecommunication satellites.
G.L.C.

85 URBAN TECHNOLOGY AND TRANSPORTATION

Includes applications of space technology to urban problems; technology transfer; technology assessment; and surface and mass transportation.

For related information see *03 Air Transportation and Safety, 16 Space Transportation,* and *44 Energy Production and Conversion.*

N86-12164# Massachusetts Inst. of Tech., Cambridge.
[RESEARCH OBJECTIVES AND SUMMARY OF RESEARCH PERFORMED BY THE MASSACHUSETTS INSTITUTE OF TECHNOLOGY RESEARCH LABORATORY OF ELECTRONICS]
J. Allen and R. Birgeneau Jan. 1985 270 p refs
(PR-127) Avail: NTIS HC A12/MF A01

A series of Progress Reports issued by the Research Laboratory of Electronics contains the customary annual statement of research objectives and summary of research for each group. The report covers the period January 1, 1984-December 31, 1984, and the source of support is indicated for each project. The topics include: (1) submicron structures technology and research; (2) kinetic phenomena in thin film electronic materials; (3) focused ion beam fabrication; (4) chemical reaction dynamics at surfaces; (5) optics and quantum electrons; (6) infrared nonlinear optics; (7) phase transitions in chemisorbed systems; (8) X-ray diffuse scattering; (9) semiconductor surface studies; (10) electronic properties of amorphous silicon dioxide; (11) optical spectroscopy of disordered materials; (12) quantum transport in low dimensional disordered systems; (13) photon correlation spectroscopy; (14) custom integrated circuits; (15) speech communication; (16) linguistics; (17) communications biophysics; (18) physiology; (19) molecule microscopy; (20) quantum optics and photonics; (21) atomic resonance and scattering; (22) plasma dynamics; (23) radio astronomy; (24) digital signal processing; (25) cognitive information processing; (26) electromagnetic wave theory and remote sensing; (27) microwave and quantum magnetics; and (28) optical propagation and communication. E.A.K.

N86-12165# Pacific Northwest Lab., Richland, Wash.
ASSESSMENT OF TECHNICAL STRENGTHS AND INFORMATION FLOW OF ENERGY CONSERVATION RESEARCH IN JAPAN. VOLUME 2: BACKGROUND DOCUMENT
G. J. Hane, P. M. Lewis, R. A. Hutchinson, B. Rubinger, and A. Willis Jun. 1985 203 p
(Contract DE-AC06-76RL-01830)
(DE85-013759; PNL-5244-Vol-2) Avail: NTIS HC A10/MF A01

Purpose of this study is to explore the status of R and D in Japan and the ability of US researchers to keep abreast of Japanese technical advances. US researchers familiar with R and D activities in Japan were interviewed in ten fields that are relevant to the more efficient use of energy: amorphous metals, biotechnology, ceramics, combustion, electrochemical energy storage, heat engines, heat transfer, high temperature sensors, thermal and chemical energy storage, and tribology. The researchers were questioned about their perceptions of the strengths of R and D in Japan, comparative aspects of US work, and the quality of available information sources describing R and D in Japan. Of the ten related fields, the researchers expressed a strong perception that significant R and D is under way in amorphous metals, biotechnology, and ceramics, and that the US competitive position in these technologies will be significantly challenged. Researchers also identified alternative emphases in Japanese R and D programs in these areas that provide Japan with stronger technical capabilities. DOE

N86-12166# Tuskegee Inst., Ala.

PROJECT TO STUDY THE USE OF MICROCOMPUTER TECHNOLOGY IN PLANNING AND OPERATION OF SMALL CITY TRANSPORTATION SYSTEMS Final Report

T. S. Sara Sep. 1984 37 p
(Grant DOT-UMTA-AL-06-0011)
(PB85-204873; UMTA-AL-06-0011-85-1) Avail: NTIS HC A03/MF A01 CSCL 13B

The purpose of this research was to study the use of microcomputer technology in the planning and operation of small city transportation systems. Existing and potential planning and administrative applications of microcomputers were identified. Hardware and software capabilities of some of the popular microcomputers in the market were studied in order to determine their uses in small city transportation systems. The following most common activities performed in small city transportation systems were identified: Planning; Scheduling; Transportation; Maintenance; Purchasing and Maintaining Inventory; Accounting and Finance; and Personnel and Labor Relations. Flow charts were used to determine if there existed software and computer hardware to enable small cities to computerize their transportation systems. GRA

88 SPACE SCIENCES (GENERAL)

No abstracts in this category.

89 ASTRONOMY

Includes radio and gamma-ray astronomy; celestial mechanics; and astrometry.

N86-12167*# National Aeronautics and Space Administration. Ames Research Center, Moffett Field, Calif.

FAR-INFRARED OBSERVATIONS OF SAGITTARIUS B2: RECONSIDERATION OF SOURCE STRUCTURE

Harley A. Thronson, Jr. (Wyoming Univ.) and D. A. Harper (Yerkes Observatory) Oct. 1985 25 p refs Submitted for publication
(NASA-TM-88185; Rept-86009; NAS 1.15:88185; Preprint-Ser-039) Avail: NTIS HC A02/MF A01 CSCL 03A

New moderate-angular-resolution far-infrared observations of the Sagittarius B2 star-forming region are presented, discussed, and compared with recent radio molecular and continuum observations of this source. In contrast to previous analyses, its far-infrared spectrum is interpreted as the result of a massive frigid cloud overlying a more-or-less normal infrared source, a natural explanation for the object's previously-noted peculiarities. The characteristics derived for the obscuring cloud are similar to those found for the W51 MAIN object. Both sources have high sub-millimeter surface brightness, a high ratio of sub-millimeter to far-infrared flux, and numerous regions of molecular maser emission. Author

N86-12168*# National Aeronautics and Space Administration, Washington, D. C.

THE 1982-1984 ECLIPSE OF EPSILON AURIGAE

Robert E. Stencel, ed. Sep. 1985 115 p refs Working meeting held in Tucson, Ariz., 16-17 Jan. 1985
(NASA-CP-2384; NAS 1.55:2384; LC-85-13854) Avail: NTIS HC A06/MF A01 CSCL 03A

A workshop proceedings concerned with the new data collected during the 1982-1984 eclipse period of the 27-year system Epsilon Aurigae is presented. This binary star has been a classic problem in astrophysics because the opaque eclipsing object is nonstellar, and probably disk shaped. Invited papers concerning the history of the system, optical, infrared and ultraviolet photometry, optical polarimetry and ultraviolet spectroscopy are included. An invited paper concerning comprehensive theoretical interpretation in the context of stellar evolution also is included. The information collected herein is unparalleled in scope and will remain a standard reference until the next eclipse cycle in the year 2009 A.D., in all probability. For individual titles, see N86-12169 through N86-12184.

N86-12169*# Hopkins Phoenix Observatory, Ariz.

OPTICAL PHOTOMETRY OF THE 1982-1984 ECLIPSE OF EPSILON AURIGAE

Jeffrey L. Hopkins *In* NASA, Washington The 1982-1984 Eclipse of Epsilon Aurigae Sep. 1985 p 7-22 refs (For primary document see N86-12168 02-89)
Avail: NTIS HC A06/MF A01 CSCL 03A

From slightly before the 1982-1984 eclipse of Epsilon Aurigae to the present observers from around the world have been making photoelectric photometry observations of this star system. Over 2000 UBV observations have been reported as well as observations in the R, I, J, H, K, L, M, N, and Q bandpasses plus the y, b, v, and u bandpasses. Twenty nine observers from 9 countries submitted photometry data to the campaign. The data have shown many interesting features of the star system including a Cepheid-like pulsation, flare activity, mid-eclipse brightening, post egress brightening, plus other strange activity. Author

N86-12170*# Hawaii Univ., Honolulu.

INFRARED PHOTOMETRY OF THE 1982-4 ECLIPSE OF EPSILON AURIGAE

D. E. Backman *In* NASA, Washington The 1982-1984 Eclipse of Epsilon Aurigae Sep. 1985 p 23-32 refs Sponsored in part by NSF (For primary document see N86-12168 02-89)
Avail: NTIS HC A06/MF A01 CSCL 03A

The infrared photometry of epsilon Aur performed prior to and during the ingress phase of the recent eclipse allowed the first solid determination of the temperature of the secondary object. The eclipse depth was significantly less at lambda > 5 micrometers than in the near-infrared. This is explained by a model of the secondary as an opaque and very cool object with a temperature of approx. 500 K. During eclipse, the secondary blocks approximately 45% of the near infrared radiation from the primary star. At the same time, the radiation from the secondary remains completely unobscured, resulting in a shallower light curve at longer wavelengths. This phenomenon is well known in the study of eclipsing binary stars; if the two stars have different colors, then the net color of the system changes during eclipse. In the case of epsilon Aur, the eclipsing object has a color deep in the infrared, so the effect is only noticeable there. Author

N86-12171*# Oregon Univ., Eugene. Dept. of Physics.

THE OPTICAL POLARIZATION OF EPSILON AURIGAE THROUGH THE 1982-84 ECLIPSE

J. C. Kemp, G. D. Henson, D. J. Kraus, and I. S. Beardsley *In* NASA, Washington The 1982-1984 Eclipse of Epsilon Aurigae Sep. 1985 p 33-36 (For primary document see N86-12168 02-89)
Avail: NTIS HC A06/MF A01 CSCL 03A

About 350 nights observations on the 61-cm telescope at Pine Mt. Observatory were made of the variable polarization of Eps. Aurigae during 1982-85, in the U, B, and V color bands. The V data are the most complete and are shown. In terms of the overall features the curves in all three colors are quite similar. The typical errors per nightly point in the V curves are about 0.015% for either of the two normalized, equatorial Stokes parameters Q and U. Note that there is a large background or constant component of some 2.5%, position angle around 135 deg. This is presumably largely interstellar, and the intrinsic polarization probably does not much exceed the amplitude of the variable component, approx. 0.5%. A few field-star polarizations were measured but a very clear pattern was not obtained in this part of the sky. Author

N86-12172*# Computer Sciences Corp., El Segundo, Calif.

IUE OBSERVATIONS OF THE 1982-84 ECLIPSE OF EPSILON AURIGAE

Thomas B. Ake *In* NASA, Washington The 1982-1984 Eclipse

of Epsilon Aurigae Sep. 1985 p 37-42 refs (For primary document see N86-12168 02-89)
Avail: NTIS HC A06/MF A01 CSCL 03A

The major characteristics in the ultraviolet of the 1982-84 eclipse of Eps Aur as observed with IUE by various workers are summarized. This star can be observed over the entire IUE wavelength range, from 1200 to 3200 A, in low dispersion, allowing eclipse light curves to be obtained in broadband regions, but due to its steep spectral gradient and the sensitivities of IUE cameras, high resolution exposures adequately cover only the regions from 1700-1900 and 2400-3200 A. In many ways, the UV data confirms or expands upon interpretations of the system made from observations in other wavelength regions, but in other respects the system remains as enigmatic as before. Author

N86-12173*# Trieste Univ. (Italy). Inst of Astronomy.
THE ECLIPSE OF EPSILON AURIGAE VISIBLE SPECTROSCOPY AND ULTRAVIOLET ACTIVITY
S. Ferluga and M. Hack *In* NASA, Washington The 1982-1984 Eclipse of Epsilon Aurigae Sep. 1985 p 43-48 refs (For primary document see N86-12168 02-89)
Avail: NTIS HC A06/MF A01 CSCL 03A

The preliminary results of the study of several high resolution spectrograms (lambda 3500 - lambda 7000 A), obtained at the Haute Provence Observatory (OHP) in France, at different epochs before, during and after the eclipse are reported. Some of these spectrograms are compared with corresponding IUE high resolution observations, in order to study the effects of the intrinsic UV activity, towards the longer wavelengths. Author

N86-12174*# Joint Inst. for Lab. Astrophysics, Boulder, Colo.
EPSILON AURIGAE IN AN EVOLUTIONARY CONTEXT
Ronald F. Webbink *In* NASA, Washington The 1982-1984 Eclipse of Epsilon Aurigae Sep. 1985 p 49-60 refs (For primary document see N86-12168 02-89)
Avail: NTIS HC A06/MF A01 CSCL 03A

Basic observational data of Epsilon Aurigae are summarized and used as the basis of a discussion of possible evolutionary states of the system. Constraints posed by the presence of a cold disk surrounding the secondary star are also outlined. Possible evolutionary models of the F0 Ia supergiant range from pre-main sequence contraction through shell hydrogen burning, core helium burning, to shell helium burning, depending on the absolute luminosity of the system, for models in which no mass transfer has taken place. Models invoking binary interaction include core and shell helium burning stars, and pre-white dwarfs, again depending on the absolute luminosity of the system. A massive shell helium burning star or a pre-white dwarf mass transfer remnant would appear the most likely of these models at present. Observational tests of these models are briefly outlined. Author

N86-12175*# Vanderbilt Univ., Nashville, Tenn.
PHOTOMETRIC SUPPORT FOR FUTURE ASTONOMICAL RESEARCH
Douglas S. Hall and Russell M. Genet (Fairborn Observatory) *In* NASA, Washington The 1982-1984 Eclipse of Epsilon Aurigae Sep. 1985 p 61-64 refs (For primary document see N86-12168 02-89)
Avail: NTIS HC A06/MF A01 CSCL 03A

The I.A.P.P.P. is described and how that organization can provide photometric support for future astronomical research projects such as the 1982-1984 eclipse of epsilon Aurigae discussed at this workshop. I.A.P.P.P., International Amateur-Professional Photoelectric Photometry, is an organization founded in Fairborn, Ohio by the authors in 1980. Its purpose is to encourage contact between amateur and professional astronomers interested in photoelectric photometry, for their mutual benefit and for the benefit of astronomical research. Aspects dealt with include instrumentation, electronics, computer hardware and software, observing techniques, data reduction, and observing programs. Starting with the June 1980 issue, I.A.P.P.P. has published the quarterly I.A.P.P.P. Communications. The Communications contain articles dealing with all the above aspects of photoelectric photometry, although it does not publish observational results as such. Photoelectric photometry obtained by amateurs is published in the same journals which publish photometry obtained by professionals. Author

N86-12176*# Arizona State Univ., Tempe.
UBV PHOTOMETRY OF THE 1982-4 ECLIPSE OF EPSILON AURIGAE: A DISCUSSION OF THE OBSERVED LIGHT CURVES
Paul C. Schmidtke *In* NASA, Washington The 1982-1984 Eclipse of Epsilon Aurigae Sep. 1985 p 67-74 refs (For primary document see N86-12168 02-89)
Avail: NTIS HC A06/MF A01 CSCL 03A

At least 29 observers in nine countries have contributed photometric measurements of Epsilon Aurigae during the recent observational campaign. The present discussion is limited to data submitted by J. L. Hopkins of the Hopkins Phoenix Observatory and S. I. Ingvarsson of the Tjornisland Astronomical Observatory. Both sources are on the UBV system, with no significant systematic differences. Combined, these two sources cover the entire eclipse, from pre-ingress up to the present (April 1985). It should be noted that this eclipse is the first to have complete photometric coverage in all three broadband filters U, B, and V. Author

N86-12177*# Villanova Univ., Pa.
INTERMEDIATE AND NARROW BAND PHOTOMETRY OF EPSILON AURIGAE Abstract Only
Robert A. Donovan, Edward F. Guinan, and George P. McCook *In* NASA, Washington The 1982-1984 Eclipse of Epsilon Aurigae Sep. 1985 p 77-78 (For primary document see N86-12168 02-89)
Avail: NTIS HC A06/MF A01 CSCL 03A

Intermediate band blue (4530A), far red (7790A) and H-alpha intermediate and narrow band photoelectric observations of the peculiar, 27 year eclipsing binary, Epsilon Aurigae were made from December 1981 through the present (December 1984). BD +42 1170 served as the primary comparison star because of its angular proximity to the variable star. The analysis of this data along with other available photometry was undertaken to study the characteristics of the low amplitude, semi-regular light variations that appear inside and outside of eclipse. It appears that these short term light variations arise from nonradial pulsations of the luminous F supergiant in the system. Furthermore, the semi-regular light variations found for Epsilon Aurigae are similar to those found for other luminous A-F supergiants. Also, the preliminary results from the analyses of the light variations produced by the eclipse of the F-supergiant by the mysterious cooler component is discussed. Author

N86-12178*# Lowell Observatory, Flagstaff, Ariz.
SPECTROPHOTOMETRY OF EPSILON AUR, 3295-8880 A Abstract Only
G. W. Lockwood, D. T. Thompson, B. L. Lutz, and J. Sowell (Michigan Univ.) *In* NASA, Washington The 1982-1984 Eclipse of Epsilon Aurigae Sep. 1985 p 79 (For primary document see N86-12168 02-89)
Avail: NTIS HC A06/MF A01 CSCL 03A

Spectrophotometric scans were obtained at 8 A resolution from 3295 to 8880 A on twenty nights before, during, and after the recent eclipse of epsilon Aurigae, beginning with a pre-eclipse observation on 5 March 1982 U.T. The observations were reduced to absolute flux using the standard stars 109 Vir or xi(2) Ceti. The data confirm that the eclipse is essentially gray over the entire visible spectrum, as others have noted from broadband photometry. High resolution echellograms (450 to 6700 A) made through mid-eclipse and the scans show changes in the equivalent widths of H alpha, Na D, and O I as large as a factor of two. Author

N86-12179*# Kitt Peak National Observatory, Tucson, Ariz.
MICRON CO IN THE ECLIPSE SPECTRUM OF EPSILON AUR
Kenneth H. Hinkle and Theodore Simon (Hawaii Univ.) *In* NASA, Washington The 1982-1984 Eclipse of Epsilon Aurigae Sep. 1985 p 80 Sponsored in part by NSF (For primary document see N86-12168 02-89)

Avail: NTIS HC A06/MF A01 CSCL 03A

Two micrometer spectrum of epsilon Aur was observed at high resolution (lambda/delta lambda approx. 40000) with the KPNO 4m telescope and FTS approximately every 100 days during the recent eclipse. CO delta v=2 lines appeared in the spectrum only after mid-totality. No CO features were present JD 2445478 but weak absorption lines were present on 2445592. The CO strengthened in the spectrum and remained present until at least 2445812. CO was again absent after forth contact when the spectrum was observed on 2445912. The CO appears to originate in a cool (approx. 1000 K), turbulent region. Excitation temperatures, velocities, and column densities is presented. Author

N86-12180*# National Aeronautics and Space Administration, Washington, D. C.
SCATTERED LIGHT IN THE IUE SPECTRA OF EPSILON AURIGAE
Bruce Aitner (Applied Research Corp.), Robert D. Chapman (NASA. Goddard Space Flight Center), Yoji Kondo (NASA. Goddard Space Flight Center), and Robert E. Stencel *In its* The 1982-1984 Eclipse of Epsilon Aurigae Sep. 1985 p 81-90 refs (For primary document see N86-12168 02-89)
Avail: NTIS HC A06/MF A01 CSCL 03A

As a result of this work it was found that light scattered from the longer wavelengths constitutes a small but non-negligible, wavelength and time dependent fraction of the measured flux in the far UV. The reality of the UV excess has not been unambigiously ruled out. However, it is noted that there are still uncertainties in the assumed scattering profile. New measurements of the scattering properties of the cross disperser grating are planned in order to verify the results of Mount and Fastie and extend the wavelength coverage into the far wings of the profile. The results of these measurements will no doubt reduce some of these uncertainties. For the present, it is felt that the BCH approach is a significant improvement over the methods heretofore available for the treatment of scattered light in IUE spectra. Author

N86-12181*# Arizona Univ., Tucson.
MODELLING EPSILON AURIGAE WITHOUT SOLID PARTICLES
A. Y. S. Cheng and N. J. Woolf *In* NASA, Washington The 1982-1984 Eclipse of Epsilon Aurigae Sep. 1985 p 91 (For primary document see N86-12168 02-89)
Avail: NTIS HC A06/MF A01 CSCL 03A

Three components can be expected to contribute to the emission of epsilon Aurigae. There is a primary F star. There is an opaque disk which occults it, and there is a gas stream which is observed to produce absorption lines. Evidence that the disk is not responsible for the gas stream lines comes both from the radial velocities, which are too small, and from the IR energy distribution out of eclipse, which shows free-free emission that would produce inadequate optical depth in electron scattering. The color temperature of the IR excess can give misleading indications of low temperature material. Free-free emission at 10,000 K between 10 and 20 microns has a color temperature of 350 K. Attempts to mold the system are discussed. Author

N86-12182*# Hopkins Phoenix Observatory, Ariz.
ASTRONOMICAL RESEARCH AT THE HOPKINS PHOENIX OBSERVATORY
Jeffrey L. Hopkins *In* NASA, Washington The 1982-1984 Eclipse of Epsilon Aurigae Sep. 1985 p 93-97 (For primary document see N86-12168 02-89)
Avail: NTIS HC A06/MF A01 CSCL 03A

After trying astrophotography and radio astronomy it was decided that the best way to do meaningful astronomical research at a small private observatory was by doing photoelectric photometry. Having the observatory located in the back yard of a private residence affors the luxury of observing any time the sky conditions permit. Also modest equipment is all that is needed to do accurate UBV photometry of stars 8th magnitude and brighter. Since beginning in 1980 the Hopkins Phoenix Observatory has published papers on several RS CVn star systems, 31 Cygni, 22 Vul, 18 Tau Per, and has followed the 1982-1984 eclipse of Epsilon Aurigae from its start to the present with over 1000 UBV measurements. In addition the Hopkins Phoenix Observatory has developed several pieces of photometry equipment including the HPO PEPH-101 photometer head and photon counting electronics. Author

N86-12183*# Washington Univ., Seattle.
HIGH DISPERSION OBSERVATIONS OF EPSILON AUR FROM SEPT. 1982 TO MARCH 1983 Abstract Only
George Wallterstein *In* NASA, Washington The 1982-1984 Eclipse of Epsilon Aurigae Sep. 1985 p 99-102 (For primary document see N86-12168 02-89)
Avail: NTIS HC A06/MF A01 CSCL 03A

Between September 1982 and March 1983 I obtained high dispersion spectra of epsilon Aur in selected regions using the Palomar 200-inch coude spectrograph and the Dominion Astrophysical Observatory 48-coude spectrograph. All spectra were taken with the 90-mm ITT image tube and IIa-D emulsion. Radial velocities are listed for the sodium D lines, KI lines, H alpha, and a few other features. While most of the sodium and potassium features are surely circumstellar there is certainly an interstellar component present. In the direction of epsilon Aur interstellar gas is seen mostly with radial velocities between +5 and +10 km s(-1). The sodium D lines and potassium lines show incipient resolution which may involve the interstellar components. The equivalent widths of the sodium and potassium lines are given. For potassium, blending with atmospheric O2 makes the line at lambda 7664 unmeasurable on the dates of these observations. The increase in equivalent widths already noted by Pathasarathy and Lambert is evident. Blending and partial resolution of the circumstellar and interstellar features may account for much of the velocity structure which is only partially discernable at the available resolution. Author

N86-12184*# Yonsei Univ., Seoul (South Korea).
PHOTOELECTRIC OBSERVATIONS OF THE LONG-PERIOD ECLIPSING BINARIES AT YONSEI UNIVERSITY OBSERVATORY Abstract Only
Il-Seong Nha, Yong-Sam Lee, Yong-Wood Chun, Ho-Il Kim, and Young-Soo Kim *In* NASA, Washington The 1982-1984 Eclipse of Epsilon Aurigae Sep. 1985 p 103 refs Presented at the 3rd IAU-Asia Pacific Reg. Meeting, Kyoto, Japan, Oct. 1984 (For primary document see N86-12168 02-89)
Avail: NTIS HC A06/MF A01 CSCL 03A

A long term project (ten-years; 1982-92) for the photoelectric observation in the UBV passbands of selected eclipsing binaries with P > 10 days has initiated at Yonsei University Observatory using 40-cm and 61-cm reflectors. The instrumentation used and the observation techniques and the reduction procedures applied to this investigation are described. Author

N86-12185*# National Aeronautics and Space Administration. Ames Research Center, Moffett Field, Calif.
STAR FORMATION IN THE INNER GALAXY: A FAR-INFRARED AND RADIO STUDY OF TWO H2 REGIONS
D. F. Lester, H. L. Dinerstein, M. W. Werner, P. M. Harvey, N. J. Evans, and R. L. Brown Sep. 1985 44 p refs Sponsored in part by the Robert A. Welch Foundation Prepared in cooperation with Texas Univ. and National Radio Astronomy Observatory
(Grant NGR-05-003-511; NASA-Order-NCA2-OR781-201; Grant NSF AST-83-12332)
(NASA-TM-86720; Rept-85221; NAS 1.15:86720) Avail: NTIS HC A03/MF A01 CSCL 03A

Far-infrared and radio continuum maps have been made of the central 6' of the inner-galaxy HII regions G30.8-0.0 (in the W43 complex) and G25.4-0.2, along with radio and molecular line measurements at selected positions. The purpose of this study is an effort to understand star formation in the molecular ring at 5 kpc in galactic radius. Measurements at several far infrared wavelengths allow the dust temperature structures and total far infrared fluxes to be determined. Comparison of the radio and infrared maps shows a close relationship between the ionized gas and the infrared-emitting material. There is evidence that parts of G30.8 are substantially affected by extinction, even at far-infrared wavelengths. Using radio recombination line and CO line data for G25.4-0.2, the distance ambiguity for this source is resolved. The large distance previously ascribed to the entire complex is found to apply to only one of the two main components. The confusion in distance determination is found to result from an extraordinary near-superposition of two bright HII regions. Using the revised distances of 4.3 kpc for G25.4SE and 12 kpc for G25.4NW, it is found that the latter, which is apparently the fainter of the two sources, is actually the more luminous. The ratio of total luminosity to ionizing luminosity is very similar to that of HII regions in the solar circle. Assuming a coeval population of ionizing stars, a normal initial mass function is indicated. B.W.

N86-12186*# National Aeronautics and Space Administration. Ames Research Center, Moffett Field, Calif.

SUBMILLIMETER OBSERVATIONS OF OH AND CH IN M42

Paul J. Viscuso, Gordon J. Stacy, Charles E. Fuller, Noel T. Kurtz, and Martin Harwit Sep. 1985 28 p refs Submitted for publication Prepared in cooperation with Cornell Univ., Ithaca, N.Y.
(Grant NsG-2347)
(NASA-TM-86723; Rept-85224; NAS 1.15:86723; PP-Ser-32) Avail: NTIS HC A03/MF A01 CSCL 03A

The (sup 2) pi sub 1/2 (J = 3/2 to 1/2) transitions of OH at 163.12 and 163.40 micro m have been detected and upper limits have been obtained for the (sup 2) pi sub 3/2 (J = 3/2 to 1/2) transitions of CH at 149.09 and 149.39 micro m, in observations of the Kleinmann-Low Nebula of Orion. All four flux levels lie between 1 and 1.2 x 10 to the 17th power/sq.cm. The OH lines are bright when compared to the lower, (sup 2) pi sub 3/2 (J = 5/2 to 3/2) fluxes reported and imply that the 119 micro m emission observed is partially self-absorbed. The combined results provide strong constraints. Taken together with existing data on molecular hydrogen and CO and recent data on other OH transition, they suggest OH emission from post-shock regions at temperatures T approx 1000 k, densities approx. 7 x 10 to the 6th powr/cu cm N sub OH approx 80/cu cm optically thick for the (sup 2) pi sub 3/2 (J = 5/2 to 3/2), 119 micro m but only partially self-absorbing in the (J = 7/2 to 3/2), 84 micro m transitions over a Doppler velocity bandwidth of 30 km/sec. The OH column density is N sub OH approx 4 x 10 to the 16th powr/sq cm. in the emitting regions which occupy a fraction of approx 0.1 of a 1' x 1' field of view centered on the Becklin-Neugebauer source. The CO (J = 31 to 30), 84 micro m transition appears to lie sufficiently close to one of the 84 micro m OH line components to be partially absorbed as well, through a Bowen-type mechanism. Author

N86-12187*# University of Southern California, Los Angeles. Dept. of Astronomy.

APPLICATIONS OF THE MAGNETO-OPTICAL FILTER TO STELLAR PULSATION MEASUREMENTS

Edward J. Rhodes, Jr., Alessandro Cacciani, and Steven Tomczyk [1984] 17 p refs
(Grants NAGw-13; NAGw-472)
(NASA-CR-176282; NAS 1.26:176282) Avail: NTIS HC A02/MF A01 CSCL 03A

A proposed method of employing the Cacciani magneto-optical filter (MOF) for stellar seismology studies is described. The method relies on the fact that the separation of the filter bandpasses in the MOF can be changed by varying the level of input power to the filter cells. With the use of a simple servosystem the bandpass of a MOF can be tuned to compensate for the changes in the radial velocity of a star introduced by the orbital motion of the Earth. Such a tuned filter can then be used to record intensity fluctuations through the MOF bandpass over an extended period of time for each given star. Also, the use of a two cell version of the MOF makes it possible to alternately chop between the bandpass located in the stellar line wing and a second bandpass located in the stellar continuum. Rapid interchange between the two channels makes it possible for atmospheric-introduced noise to be removed from the time series. Author

N86-12188*# Smithsonian Astrophysical Observatory, Cambridge, Mass.

BALLOON-BORNE THREE-METER TELESCOPE FOR FAR-INFRARED AND SUBMILLIMETER ASTRONOMY Semiannual Status Report, 1 Mar. - 31 Aug. 1984

Giovanni G. Fazio Oct. 1985 18 p
(Grant NAGw-509)
(NASA-CR-176285; NAS 1.26:176285; SASR-2) Avail: NTIS HC A02/MF A01 CSCL 03A

This is the second Semiannual Report submitted under Grant NAGW-509 for the development of a Balloon-Borne Three-Meter Telescope for Far-Infrared and Submillimeter Astronomy. It covers the period 1 March 1984 through 31 August 1984. This grant covers work at the Smithsonian Astrophysical Observatory (SAO), University of Arizona (UA) and the University of Chicago (UC). SAO is responsible for program management, the gondola structure including the attitude control and aspect systems, mechanical systems, and telemetry and command systems; the UA is responsible for optics design and fabrication; the UC is responsible for determining provisions for focal-plane instrumentation. SAO and the UA share responsibility for the ground support data and control computer. Author

N86-12189# Aerospace Corp., Los Angeles, Calif. Space Sciences Lab.

THE MASS OF HOT, SHOCKED CO IN ORION: FIRST OBSERVATIONS OF THE J = 17 YIELDS J = 16 TRANSITION AT 153 MICRONS

G. Stacy, N. T. Kurtz, S. Smyers, M. Harwit, and R. W. Russell 24 Jun. 1985 20 p Prepared in cooperation with Cornell Univ., Ithaca, N.Y. and Harvard-Smithsonian Center for Astrophysics, Cambridge, Mass.
(Contract F04701-83-C-0084)
(AD-A157323; TR-0084A(5940-01)-3; SD-TR-85-28) Avail: NTIS HC A02/MF A01 CSCL 03/1

We have observed the Kleinmann-Low Nebula in Orion and detected the J = 17 to J = 16 transition of carbon monoxide at a flux level of 7 x 10 to the -17th power W/sq cm. Our best estimate for the total mass of hot, T approx. 750 K, CO in the nebula is 8 x 10 to the 30th power g. From this value we assess the total hydrogen mass at this temperature to be approx. 1.5 solar mass. A puzzling apparent deficit of oxygen in the nebula is discussed. GRA

N86-12190# Smithsonian Astrophysical Observatory, Cambridge, Mass.

A LASER SIDEROSTAT Final Report, 24 Apr. 1984 - 23 Apr. 1985

M. Shao 25 Jun. 1985 4 p
(Contract N00014-84-C-2137)
(AD-A157444) Avail: NTIS HC A02/MF A01 CSCL 03/1

The Mark III Astrometric Interferometer is an instrument designed to improve on our ability to measure angular positions of stars by more than an order of magnitude. The instrument makes extensive use of active optics, digital signal processing and control, and laser metrology. This report describes the efforts of the first year of a four-year program to build the Mark III interferometer, as well as obstacles to technical progress due to Navy administrative procedures. GRA

N86-11575# Academy of Sciences, Potsdam (East Germany). Zentralinst. fuer Physik der Erde.

INFLUENCES OF SYSTEMATIC DIFFERENCES BETWEEN DIFFERENT STAR CATALOGUES ON THE RESULTS OF LATITUDE AND TIME DETERMINATIONS WITH THE PZT 2

M. Mainig *In its* Proc. of the 5th Intern. Symp. Geodesy and Phys. of the Earth, Pt. 2 1985 p 45-54 refs (For primary document see N86-11568 02-42)
Avail: NTIS HC A09/MF A01

N86-11584# Technische Univ., Dresden (East Germany). Sektion Geodaesie und Kartographie.

PLANETS AROUND BARNARD'S STAR?

Klaus-Guenter Steinert *In* Academy of Sciences of the GDR Proc. of the 5th Intern. Symp. Geodesy and Phys. of the Earth, Pt. 2 1985 p 126-128 refs *Its* Mitteilung des Lohrmann-Observatoriums No. 52 (For primary document see N86-11568 02-42)
Avail: NTIS HC A09/MF A01

N86-11588# Academia Sinica, Beijing (China). Inst. of Geodesy and Geophysics.
ON THE COMPARISON AND CHOICE BETWEEN THE FORMULAS OF THE EARTH TIDAL CORRECTION IN ASTRONOMICAL TIME AND LATITUDE OBSERVATION
Jiongyu Xia *In* Academy of Sciences of the GDR Proc. of the 5th Intern. Symp. Geodesy and Phys. of the Earth, Pt. 2 1985 p 144-149 refs (For primary document see N86-11568 02-42)
Avail: NTIS HC A09/MF A01

N86-12000# Joint Publications Research Service, Arlington, Va.
MICROCOMPUTER-CONTROLLED HIGH-ALTITUDE DATA AQUISITION SYSTEM Abstract Only
In its China Rept.: Sci. and Technol. (JPRS-CST-85-015) 16 May 1985 p 36 Transl. into ENGLISH from Jisuanji Shijie (Beijing), no. 7, 8 Apr. 1984 p 8 (For primary document see N86-11994 02-70)
Avail: NTIS HC A07/MF A01

90 ASTROPHYSICS

Includes cosmology; and interstellar and interplanetary gases and dust.

N86-11550# Academy of Sciences, Potsdam (East Germany). Zentralinst. fuer Physik der Erde.
FIGURE OF THE EARTH, MOON, AND PLANETS Progress Report, 1981-1984
M. Bursa *In its* Proc. of the 5th Intern. Symp. Geodesy and Phys. of the Earth 1985 p 10-24 refs (For primary document see N86-11549 02-42)
Avail: NTIS HC A09/MF A01

91 LUNAR AND PLANETARY EXPLORATION

Includes planetology; and manned and unmanned flights. For spacecraft design see *18 Spacecraft Design Testing, and Performance*. For space stations see *15 Launch Vehicles and Space Vehicles.*

N86-12191*# Lunar and Planetary Inst., Houston, Tex. Lunar and Planetary Sample Team.
HORIZONS AND OPPORTUNITIES IN LUNAR SAMPLE SCIENCE
1985 37 p
(Contract NASw-3389)
(NASA-CR-176290; NAS 1.26:176290; LPI-TR-85-04) Avail: NTIS HC A03/MF A01 CSCL 03B

The Moon is the cornerstone of planetary science. Lunar sample studies were fundamental in developing an understanding of the early evolution and continued development of planetary bodies, and have led to major revisions in understanding of processes for the accumulation of planetesimals and the formation of planets. Studies of lunar samples have increased an understanding of impact cratering, meteoroid and micrometeoroid fluxes, the interaction of planetary surfaces with radiations and particles, and even the history of the Sun. The lunar sample research program was especially productive, but by no means have all the important answers been determined; continued study of lunar samples will further illuminate the shadows of our knowledge about the solar system. Further, the treasures returned through the Apollo program provide information that is required for a return to the Moon, beginning with new exploration (Lunar Geoscience Observer (LGO)), followed by intensive study (new sample return missions), and eventually culminating in a lunar base and lunar resource utilization. G.L.C.

N86-12192*# Lunar and Planetary Inst., Houston, Tex.
WORKSHOP ON DUST ON MARS
Steven Lee, ed. et al 1985 30 p refs Workshop held at Tempe, Ariz., 4-5 Feb. 1985
(Contract NASw-3389)
(NASA-CR-176293; NAS 1.26:176293; LPI-TR-85-02) Avail: NTIS HC A03/MF A01 CSCL 03B

A workshop was organized to stimulate and coordinate research on the properties of Martian dust, its distribution on the planet, and the processes affecting its yearly deposition, erosion, and transport. A great deal of research was carried out to understand local, regional, and global aspects of the Martian dust transport cycle, with the goal being definition of the currently active processes and their relation to those operating over the long term. To date, however, most individual research projects have centered around interpretation of single data sets (visual images, IRTM, radar, etc.), and these many efforts were not coordinated. Many of the details of short and long term dust-related processes, as inferred from the various single data sets, are still not agreed upon. It was the intent of this workshop to encourage the informal exchange of ideas among several researchers currently investigating various aspects of the problem and to investigate cooperative efforts to synthesize the individual approaches into a unified understanding of the present seasonal and yearly Martian sediment transport cycles. G.L.C.

N86-12193# Los Alamos Scientific Lab., N. Mex.
MARS BASE BUILDUP SCENARIOS
J. D. Blacic 1985 13 p Presented at the Manned Mars Mission Workshop, Huntsville, Ala., 10 Jun. 1985
(Contract W-7405-eng-36)
(DE85-014132; LA-UR-85-1989; CONF-8506149-2) Avail: NTIS HC A02/MF A01

Two surface base build up scenarios are presented in order to help visualize the mission and to serve as a basis for trade studies. In the first scenario, direct manned landings on the Martian surface occur early in the missions and scientific investigation is the main driver and rationale. In the second scenario, early development of an infrastructure to exploit the volatile resources of the Martian moons for economic purposes is emphasized. Scientific exploration of the surface is delayed at first, but once begun develops rapidly aided by the presence of a permanently manned orbital station. DOE

92 SOLAR PHYSICS

Includes solar activity, solar flares, solar radiation and sunspots.

N86-12194*# National Aeronautics and Space Administration, Washington, D. C.
INTERNATIONAL SOLAR-TERRESTRIAL PHYSICS PROGRAM: A PLAN FOR THE CORE SPACEFLIGHT MISSIONS
1985 24 p refs Prepared in cooperation with European Space Agency, Paris, France, and Tokyo Univ., Japan Original contains color illustrations
(NASA-TM-87511; NAS 1.15:87511) Avail: NTIS HC A02/MF A01 CSCL 03B

This brochure has been prepared by NASA on behalf of the European Space Agency (ESA), the Institute of Space and Astronautical Science (Japan) (ISAS), and the U.S. National Aeronautics and Space Administration (NASA) to describe the scope of the science problems to be investigated and the mission plan for the core International Solar-Terrestrial Physics (ISTP) Program. This information is intended to stimulate discussions and plans for the comprehensive worldwide ISTP Program. The plan for the study of the solar - terrestrial system is included. The Sun, geospace, and Sun-Earth interaction is discussed as is solar dynamics and the origins of solar winds. Author

N86-12195*# Jet Propulsion Lab., California Inst. of Tech., Pasadena.
THE 1984 SOLAR OSCILLATION PROGRAM OF THE MOUNT WILSON 60-FOOT TOWER
Edward J. Rhodes, Jr., Alessandro Cacciani (Rome Univ.), Steven Tomczyk (California Univ., Los Angeles), and Roger K. Ulrich [1985] 25 p refs Sponsored in part by CNR and Minestero della Pubblica Istruzione
(Grants NAGw-13; NAGw-472)
(NASA-CR-176248; NAS 1.26:176248) Avail: NTIS HC A02/MF A01 CSCL 03B

The instrumentation, data, and preliminary results from the summer, 1984, solar oscillation observing program which was carried out using the 60-foot tower telescope of the Mt. Wilson Observatory are described. This program was carried out with a dedicated solar oscillation observing system and obtained full-disk Dopplergrams every 40 seconds for up to 11 hours per day. Between June and September, 1984, observations were obtained with a Na magneto-optical filter on 90 different days. The data analysis has progressed to the point that spherical harmonic filter functions were employed to generate a few one-dimensional power spectra from a single day's observations. Author

93 SPACE RADIATION

Includes cosmic radiation; and inner and outer Earth's radiation belts.

For biological effects of radiation see *52 Aerospace Medicine*. For theory see *73 Nuclear and High-Energy Physics.*

N86-12196*# Pennsylvania State Univ., University Park.
X-RAY INVERSE COMPTON EMISSION FROM THE RADIO HALO OF M87 Final Report, 1 Nov. 1983 - 30 Oct. 1984
Eric D. Feigelson [Oct. 1984] 4 p refs
(Grant NAG8-457)
(NASA-CR-176305; NAS 1.26:176305) Avail: NTIS HC A02/MF A01 CSCL 03B

A significant fraction of known galaxies contain an active galactic nucleus (AGN) at their cores, the site of violent activity and non-stellar radiation seen across the entire electromagnetic spectrum. This activity is thought to be due to the accretion of gas onto a massive black hole. A fraction of AGNs also eject collimated beams of energetic material, usually seen by virtue of its synchrotron emission in the radio band. Efforts to study these jets from AGNs in the X-ray band with the Einstein Observatory has led to several detections, most notably the jets in the nearby radio galaxies Centaurus A and Virgo A = M87. In their study of M87, Schreier, Gorenstein and Feigelson (1982) noted that, in addition to the synchrotron jet 10'-20' from the nucleus, X-rays appear to be generated in the diffuse radio halo 2'-5' from the nucleus. This finding may be particularly important as it may constitute the first known case of X-ray inverse Compton emission from AGN ejecta, allowing for the first time direct determination of the magnetic field strengths. G.L.C.

N86-12197*# Pennsylvania State Univ., University Park. Dept. of Astronomy.
X-RAY INVERSE COMPTON EMISSION FROM THE RADIO HALO OF M87 M.S. Thesis
Perry Alan David Wood May 1985 51 p refs
(Grant NAG8-457)
(NASA-CR-176304; NAS 1.26:176304) Avail: NTIS HC A04/MF A01 CSCL 03B

M87 has been observed in the 0.2-4 KeV X-ray band using the High Resolution Imager on the Einstein Observatory, and at 1.452 GHz using the Very Large Array. The radio map showed that the halo contained prominent asymmetries to the east and southwest. The X-ray map indicated similar asymmetries, but they were imbedded in the diffuse hot gas that surrounds the core out to a radius of several arcminutes. The hot X-ray emitting gas was assumed to be spherically symmetric and could, therefore, be subtracted from the image. The resultant image was asymmetric with major lobes to the east and southwest that coincide approximately with the asymmetries in the radio halo. The data indicates that inverse Compton emission is a plausible model for the X-rays coming from the asymmetric component. Author

N86-12198# Los Alamos Scientific Lab., N. Mex.
COSMOGENIC-NUCLIDE PRODUCTION BY PRIMARY COSMIC-RAY PROTONS
R. C. Reedy 1985 5 p refs Presented at 19th Intern. Cosmic Ray Conf., La Jolla, Calif., 11 Aug. 1985
(Contract W-7405-eng-36)
(DE85-012760; LA-UR-85-1921; CONF-850883-1) Avail: NTIS HC A02/MF A01

The production rates of cosmogenic nuclides were calculated for the primary protons in the galactic and solar cosmic rays. AT 1 AU, the long-term average fluxes of solar protons usually produce many more atoms of a cosmogenic nuclide than the primary protons in the GCR, the exceptions being nuclides made only by high-energy reactions (like Fe-10). Because the particle fluxes inside meteorites and other large objects in space include many secondary neutrons, the production rates and ratios inside large objects are often very different from those by just the primary GCR protons. Thus it is possible to determine, by examining its cosmogenic nuclides, if a small object, such as found among deep-sea spherules, was small in space or broken from a meteorite. Because heliospherical modulation and other interactions change the GCR particle spectrum, the production of cosmogenic nuclides by the GCR particles outside the heliosphere will be different from that by modulated GCR primaries. Production rates and ratios for cosmogenic nuclides would be able to identify small particles, possibly interstellar in origin, that were exposed to an unmodulated spectrum of GCR particles and to characterized the spectrum of particles to which they were exposed. DOE

99 GENERAL

No abstracts in this category.

SUBJECT INDEX

SCIENTIFIC AND TECHNICAL AEROSPACE REPORTS VOLUME 24 NUMBER 2

Typical Subject Index Listing

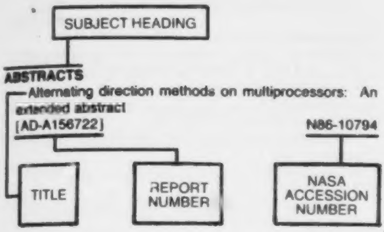

The subject heading is the key to the subject content of the document. Titles, report numbers, and accession numbers of pertinent documents are provided under each subject heading. When the title is insufficiently descriptive of the document content, a title extension has been added, separated from the title by three hyphens. The report number helps to indicate the type of document cited (e.g., NASA report, NASA translation, NASA contractor report). The NASA accession number is the number by which the document abstracts are arranged in this journal and by which the document is sold or requested. The titles, with title extensions if present, are arranged under each subject heading in ascending accession number order. The subject headings have been selected from the latest revision of the *NASA Thesaurus* (NASA SP-7051).

A

ABLATION
Neutral beam interactions with materials [AD-A157445] N86-12076
ABLATIVE MATERIALS
Neutral beam interactions with materials [AD-A157445] N86-12076
ABNORMALITIES
Detection of chromosomal abnormalities in human sperm [DE85-014178] N86-11834
Teratogenic effects of microwave radiation [PB85-207462] N86-11837
ABSORBERS (MATERIALS)
Energy characteristics of laser with saturable anisotropic absorbing medium in cavity N86-11968
Spectrum structure of XeCl electric discharge laser N86-11970
Transformation of light pulse shape by thin plane-parallel layer of absorbing material N86-11988
ABSORPTANCE
Seismology in civil engineering N86-11707
ABSORPTION
Hydride absorption refrigerator system for ten Kelvin and below N86-11373
ABSORPTION CROSS SECTIONS
Few-nucleon transfer reactions on deformed nuclei [DE85-013869] N86-12064
Total and partial absorption coefficients for a nitrogen plasma [AD-A157534] N86-12079
ABSORPTION SPECTRA
Anelasticity in the Earth's mantle: Implications for the frequency dependence of Love numbers N86-11590
Analysis of aircraft spectrometer data with logarithmic residuals N86-11636
Spectrum structure of XeCl electric discharge laser N86-11970
Computer application in atomic absorption spectrometry N86-12001
ABSORPTION SPECTROSCOPY
Micron CO in the eclipse spectrum of Epsilon Aur N86-12179
ABSORPTIVITY
Diffraction of ultrasonic beam passing normally through layered media N86-11946
ABUNDANCE
The mass of hot, shocked CO in Orion: First observations of the J = 17 yields J = 16 transition at 153 microns [AD-A157323] N86-12189
AC GENERATORS
AC motor and generator requirements for isolated WECS [NASA-CR-176315] N86-11670
ACCELERATION (PHYSICS)
Flame propagation in pulsed acceleration field N86-11964
ACCEPTOR MATERIALS
Chromium- and neodymium-activated gadolinium-scandium-gallium garnet crystal: A new laser active medium N86-11979
ACCESS CONTROL
Evaluation of the digital access and cross-connect system for use in the defense communications system [AD-A157570] N86-11412
A numerical analysis of a queue with network access flow control [AD-A157526] N86-11913
ACCURACY
Effect of accuracy of wind power prediction on power system operator [NASA-CR-176300] N86-11667
ACEE PROGRAM
A review of advanced turboprop transport activities N86-11148
ACETYLENE
Acetylene terminated matrix resins N86-11261
An improved processible acetylene-terminated polyimide for composites N86-11262
ACID RAIN
Spectral characterization of suspected acid deposition damage in red spruce (Picea rubens) stands from Vermont N86-11624
Fiscal year 1983 program report of the Water Resources Research Institute of New York State [PB85-217024] N86-11662
Effects of acid precipitation on composition, electrokinetic behavior, cation adsorption and ion exchange capacity in various soil systems [PB85-217727] N86-11698
ACOUSTIC ATTENUATION
Application of high order acoustic finite elements to transmission losses and enclosure problems N86-12008
ACOUSTIC EMISSION
Acoustic emission during deformation and fracture of A533B pressure vessel steel N86-11306
ACOUSTIC EXCITATION
Current research on circular saw and band saw vibration and stability N86-11533
ACOUSTIC PROPAGATION
Application of high order acoustic finite elements to transmission losses and enclosure problems N86-12008
ACOUSTIC SCATTERING
Reflection of sound from plate containing periodic inhomogeneities N86-11951
Numerical techniques for scattering from submerged objects N86-12013
Intermediate and high-frequency acoustic backscattering cross sections for water-ice interfaces. 1: Two-component profile models [AD-A157533] N86-12018
ACOUSTIC VELOCITY
Development of castor-oil-resistant polyurethane sonar encapsulants [AD-A157576] N86-11347
Overview of solid particle LV seeding techniques used at UTRC N86-11445
Speed of sound in liquid sodium near gamma-transition point N86-11947
ACOUSTICS
USSR report: Physics and mathematics [JPRS-UPM-85-005] N86-11945
China report: Science and technology [JPRS-CST-85-015] N86-11994
Numerical Techniques in Acoustics [NASA-CP-2404] N86-12007
Prediction of acoustical response of three-dimensional cavities using an indirect boundary element method N86-12014
ACRYLIC RESINS
PBFA-2 vacuum insulator stack failure mechanisms [DE85-013118] N86-12090
ACTINIDE SERIES
Magnetic properties and electronic structure of the actinide systems UAl2, NpAl2 and PuAl2 [DE85-014102] N86-11323
ACTIVATION
Force and timing components of the motor program [AD-A157584] N86-11843
Chromium- and neodymium-activated gadolinium-scandium-gallium garnet crystal: A new laser active medium N86-11979
ACTIVE CONTROL
Application of active noise control to model propeller noise N86-11176
Bounded state control of linear systems with application to the active structural control N86-11493
ADAPTATION
Physiological effects of training [AD-A157417] N86-11841
ADDITION THEOREM
On the addition theorem for Legendre polynomials N86-11704
ADDITIVES
Effects of additives and temperature on iron electrode behavior in KOH electrolytes [DE85-011901] N86-11423
ADDUCTS
Relationship between alkylation sites and induction of dominant lethals and heritable translocations in mice [DE85-014309] N86-11835
ADENINES
Cause of occurrence of high-energy ions during UV laser irradiation of molecular crystals N86-11953
ADHESION
Initial investigation of cryogenic wind tunnel model filler materials N86-11255
ADHESIVE BONDING
Comparison of bond in roll-bonded and adhesively bonded aluminums N86-11248
Use of hydration inhibitors to improve bond durability of aluminum adhesive joints N86-11251
Factors affecting the processing of epoxy film adhesives N86-11252
Rapid adhesive bonding and field repair of aerospace materials N86-11253
Reduction of moisture effects during the cure of epoxy adhesives used in composite repair N86-11254
ADHESIVES
Adhesives for aerospace N86-11249
High-temperature adhesive development and evaluation N86-11250
Use of hydration inhibitors to improve bond durability of aluminum adhesive joints N86-11251
High Temperature Polymer Matrix Composites [NASA-CP-2385] N86-11260
Evaluation of a high temperature adhesive for fabricating graphite/PMR-15 polyimide structures N86-11268
New processable modified polyimide resins for adhesive and matrix applications N86-11269
Recent developments in polyimide and bismaleimide adhesives N86-11270
Interaction of mixed mode loading on cyclic debonding in adhesively bonded composite joints [NASA-CR-177990] N86-11298
ADIABATIC DEMAGNETIZATION COOLING
Hydride absorption refrigerator system for ten Kelvin and below N86-11373

ADIABATIC FLOW
Influence of effective rate sensitivity on adiabatic shear instability
[DE85-013967] N86-11333

ADJUSTING
Modification of a Hughes tiltmeter to a borehole tiltmeter N86-11563
On the comparison and choice between the formulas of the Earth tidal correction in astronomical time and latitude observation N86-11588

ADSORPTION
Improved heat switch for gas sorption compressor N86-11372
Hydride absorption refrigerator system for ten Kelvin and below N86-11373

ADVECTION
Climate simulation and change: A simple energy balance climate model N86-11731
The Hadley and Rossby regimes in a spherical atmosphere N86-11751
A numerical study of global axisymmetric states and their stability to quasi-geostrophic disturbances N86-11753

AERIAL PHOTOGRAPHY
Evaluation of color infrared aerial surveys of wastewater soil absorption systems
[PB85-189074] N86-11654
Aerial photography and ground verification at power plant sites: Wisconsin power plant impact study
[PB85-197358] N86-11658

AERIAL RECONNAISSANCE
Evaluation of color infrared aerial surveys of wastewater soil absorption systems
[PB85-189074] N86-11654

AEROACOUSTICS
Aerodynamics and Acoustics of Propellers
[AGARD-CP-366] N86-11147
Theoretical analysis of linearized acoustics and aerodynamics of advanced supersonic propellers N86-11156
A general theory of arbitrary motion aerodynamics using an aeroacoustic approach N86-11157
Aeroacoustic wind tunnel measurements on propeller noise N86-11169
Some aeroacoustic wind tunnel measurements, theoretical predictions, and flight-test correlations on subsonic aircraft propellers N86-11170
Full-scale flight and model-scale wind tunnel tests on the nearfield noise characteristics of aircraft propellers N86-11172
Cabin noise reduction for a new development turboprop commuter aircraft N86-11173
Propeller aircraft cabin vibration and noise-excitation, sources, and paths N86-11174

AERODYNAMIC CHARACTERISTICS
Aerodynamics and Acoustics of Propellers
[AGARD-CP-366] N86-11147
Modern propeller profiles N86-11152
Effect of aileron deflections on the aerodynamic characteristics of a semispan model of a subsonic energy-efficient transport
[NASA-TP-2478] N86-11186

AERODYNAMIC CONFIGURATIONS
Some considerations in propeller and airframe integration N86-11164
Preliminary design study of a lateral-directional control system using thrust vectoring
[NASA-TM-86425] N86-11203

AERODYNAMIC INTERFERENCE
On the aerodynamics of installed propellers N86-11154
User's manual for a 0.3-m TCT wall interference assessment/correction procedure: 8- by 24-inch airfoil test section
[NASA-TM-87582] N86-11189

AERODYNAMIC LOADS
On the aerodynamics of installed propellers N86-11154
Seeding techniques used in the Vortex Research Facility N86-11443

AERODYNAMIC NOISE
Current research on circular saw and band saw vibration and stability N86-11533

AERODYNAMIC STABILITY
Transition effects of boundary layer on static and dynamic stability of slender cone N86-11926

AERODYNAMICS
Aeronautical Engineering: A continuing bibliography with indexes
[NASA-SP-7037(191)] N86-11145
Advance particle and Doppler measurement methods N86-11745

AEROELASTICITY
Summary of recent NASA propeller research N86-11158
Aeroelastic model helicopter rotor testing in the Langley TDT
[NASA-TM-86440] N86-11523

AERONAUTICAL ENGINEERING
Aeronautical Engineering: A continuing bibliography with indexes
[NASA-SP-7037(191)] N86-11145

AEROSOLS
Particle size distributions of several commonly used seeding aerosols N86-11441
Seeding systems for use with a laser velocimeter in large scale wind tunnels N86-11444
Seeding requirements for scanning laser velocimetry N86-11446
Aerosol seeding systems for the NSWC wind tunnels N86-11453
Generating aerosols for laser velocimeter seeding N86-11455
SAGE aerosol measurements. Volume 1: February 21, 1979 to December 31, 1979
[NASA-RP-1144] N86-11700
Measurements of refractive index structure function C2N and aerosol size distribution at Chesapeake Bay
[AD-A157455] N86-11717
Lidar observations of stratospheric aerosol over Mauna Loa Observatory: 1982 - 1983
[PB85-187896] N86-11723
Health hazard evaluation of liquid monopropellants. Phase 4. Subchronic inhalation of hydroxylammonium nitrate, January 1985
[AD-A157623] N86-11844
Analysis of arctic haze scattering and aerosol data obtained during AGASP
[AD-A157434] N86-12074

AEROSPACE ENGINEERING
The embedded operating system project
[NASA-CR-176280] N86-11893
NASA-universities relationships in aero/space engineering: A review of NASA's program
[NASA-CR-176307] N86-12158

AEROSPACE ENVIRONMENTS
Feasibility of remotely manipulated welding in space: A step in the development of novel joining technologies N86-11246
Manual for LDEF tensile tests
[NASA-TM-87624] N86-11299
TIROS/NOAA (Television and Infrared Observation Satellite/National Oceanic and Atmospheric Administration) satellites space environment monitor archive tape documentation
[PB85-187920] N86-11724

AEROSPACE INDUSTRY
Evaluation of superplastic forming and weld-brazing for fabrication of titanium compression panels N86-11245
Comparison of bond in roll-bonded and adhesively bonded aluminums N86-11248
Adhesives for aerospace N86-11249
High-temperature adhesive development and evaluation N86-11250
Rapid adhesive bonding and field repair of aerospace materials N86-11253

AEROSPACE SYSTEMS
Commercialization of space: National policy and defense needs
[AD-A156517] N86-12162

AEROTHERMODYNAMICS
Design and performance analysis of an aero-maneuvering orbital-transfer vehicle concept
[NASA-TM-86848] N86-11221
Combustion hot section technology N86-11512

AFRICA
Climatic events of the west coast of southern Africa N86-11764

AFTERBODIES
Recent experience in seeding transonic/supersonic flows at AEDC N86-11447

AGGLOMERATION
Particle size distributions of several commonly used seeding aerosols N86-11441

AGING (MATERIALS)
Factors affecting the processing of epoxy film adhesives N86-11252
Thermo-oxidative stability of graphite fiber/PMR-15 polyimide composites at 350 deg C N86-11277
Effects of real-time thermal aging on graphite/polyimide composites N86-11283
Studies on chalcogenide films
[AD-A157340] N86-11343
Polyurethane foam component lifetimes
[DE85-008206] N86-11355
Viscoelastic creep of high-temperature concrete
[DE85-010511] N86-11539
Degradation of ionic membranes in the zinc/ferricyanide battery
[DE85-008469] N86-11681

AGRICULTURE
Recent achievements, problems in cropdusting work N86-11180
Site description for the University of Nebraska's Sandhills Agricultural Laboratory N86-11626
AIS investigation of agricultural monocultures N86-11640
Urban, forest, and agricultural AIS data: Fine spectral structure N86-11644
Hydrologic data for experimental agricultural watersheds in the US, 1975
[PB85-197317] N86-11656
General-purpose equipment for airborne laser remote sensing of ocean, atmosphere and agricultural crops N86-11984

AILERONS
Effect of aileron deflections on the aerodynamic characteristics of a semispan model of a subsonic energy-efficient transport
[NASA-TP-2478] N86-11186

AIR CONDITIONING EQUIPMENT
Optimized ground-coupled heat pump system design for northern climate
[DE85-014065] N86-11484

AIR COOLING
Coolant passage heat transfer with rotation. A progress report on the computational aspects N86-11510

AIR DUCTS
Fabrication process of a high temperature polymer matrix engine duct N86-11280
Gas flow environmental and heat transfer nonrotating 3D program N86-11506

AIR FLOW
Airflow calibration of a bellmouth inlet for measurement of compressor airflow in turbine-powered propulsion simulators
[NASA-TM-84399] N86-11209

AIR JETS
The measurements of axisymmetric air turbulent jet flow with an individual realization laser velocimeter system
[AD-A157554] N86-11429
Jet array impingement heat transfer characteristics N86-11511

AIR POLLUTION
Short-term methods for atmospheric corrosion testing: Survey of the literature
[KIS-1985:5E] N86-11314
Develop, evaluate and validate continuous emission monitors for designated hazardous pollutants
[PB85-201176] N86-11695
Regional-scale (1000 KM) model of photochemical air pollution. Part 3: Tests of the numerical algorithms
[PB85-203818] N86-11696
Regional oxidant modeling of the northeast US
[PB85-201192] N86-11728
Parameterization of the atmospheric boundary layer for air pollution dispersion models
[PB85-193548] N86-11730

AIR QUALITY
Uncertainties in the radiative properties of smoke and their effects on climate assessments
[DE85-015187] N86-11691
Regional oxidant modeling of the northeast US
[PB85-201192] N86-11728

AIR SEA ICE INTERACTIONS
Global surface air temperature variations: 1983-1984 N86-11764

AIR TRAFFIC CONTROL
Traffic Alert and Collision Avoidance System Signal Environment Model (TCAS SEM) programmer's reference manual
[FAA-PM-85-22] N86-11192

AIR TRAFFIC CONTROLLERS (PERSONNEL)
Enhanced airport surface detection equipment applications
[AD-A157641] N86-11210

AIR TRANSPORTATION
Chief of Aeroflot's international activities N86-11179

AIR WATER INTERACTIONS
Proceedings of the 9th Annual Climate Diagnostics Workshop
[PB85-183911] N86-11763
Tropical convection and North American cyclones during the 1982-83 El Nino N86-11809
Observing the Eastern Pacific Hadley Circulation N86-11818

AIRBORNE EQUIPMENT
Evaluation of AIS data for agronomic and rangeland vegetation: Preliminary results for August 1984 flight over Nebraska Sandhills Agricultural Laboratory N86-11627
Geodesy: A look to the future
[NASA-CR-176283] N86-11657

AIRCRAFT ACCIDENTS
Overview of FAA's aircraft icing program N86-11740

AIRCRAFT COMPARTMENTS

Cabin noise reduction for a new development turboprop commuter aircraft N86-11173

Propeller aircraft cabin vibration and noise-excitation, sources, and paths N86-11174

The state of the art in propfan turboprop noise N86-11175

Application of active noise control to model propeller noise N86-11176

AIRCRAFT CONFIGURATIONS

World's largest airplane now being tested N86-11181

AIRCRAFT CONSTRUCTION MATERIALS

High Temperature Polymer Matrix Composites [NASA-CP-2385] N86-11260

Effects of real-time thermal aging on graphite/polyimide composites N86-11283

Environmental stability graphite/PMR-15 composites N86-11284

Development of design data for propulsion PMR-15 composites N86-11285

Polyimide composites: Application histories N86-11286

Application of Gr/PMR-15 to commercial aircraft N86-11289

Composite structural materials [NASA-CR-176279] N86-11293

AIRCRAFT CONTROL

On the aerodynamics of installed propellers N86-11154

Preliminary design study of a lateral-directional control system using thrust vectoring [NASA-TM-86425] N86-11203

AIRCRAFT DESIGN

Aerodynamics and Acoustics of Propellers [AGARD-CP-366] N86-11147

Design concept and performance prediction technique for potential flows around advanced propellers N86-11150

World's largest airplane now being tested N86-11181

AIRCRAFT DETECTION

Enhanced airport surface detection equipment applications [AD-A157641] N86-11210

AIRCRAFT ENGINES

Current and future engine applications of Gr/PI composites N86-11291

Combustion hot section technology N86-11512

HOST structural analysis program overview N86-11513

AIRCRAFT EQUIPMENT

Deputy minister on sector's technical progress N86-11178

World's largest airplane now being tested N86-11181

Chemical bonding agent for suppression of rusty bolt intermodulation interference [AD-D011747] N86-11315

AIRCRAFT FUELS

Summary of recent NASA propeller research N86-11158

User's manual for AC-20-53A protection of airplane fuel systems against fuel vapor ignition due to lightning [AD-A157619] N86-11191

AIRCRAFT HAZARDS

Development of a wind shear performance envelope N86-11746

AIRCRAFT INDUSTRY

USSR report: Transportation [JPRS-UTR-85-011] N86-11177

Deputy minister on sector's technical progress N86-11178

Chief of Aeroflot's international activities N86-11179

The factory of the future N86-11228

AIRCRAFT MAINTENANCE

Evaluation of fault reporting/fault isolation for F-15 aircraft [AD-A156516] N86-11197

AIRCRAFT MANEUVERS

Application of the vortex-lattice concept to flows with smooth-surface separation [AD-A157571] N86-11430

AIRCRAFT NOISE

Aerodynamics and Acoustics of Propellers [AGARD-CP-366] N86-11147

AIRCRAFT PERFORMANCE

Laboratory model of flight through wind shear N86-11747

AIRCRAFT RELIABILITY

Flight worthiness of fire resistant hydraulic systems: Volume 1 [AD-A157618] N86-11199

AIRCRAFT SAFETY

User's manual for AC-20-53A protection of airplane fuel systems against fuel vapor ignition due to lightning [AD-A157619] N86-11191

Meteorological and Environmental Inputs to Aviation Systems [NASA-CP-2388] N86-11735

Overview of FAA's aircraft icing program N86-11740

Advance particle and Doppler measurement methods N86-11745

AIRCRAFT SPECIFICATIONS

Development of design data for propulsion PMR-15 composites N86-11285

AIRCRAFT TIRES

A study of the cornering forces generated by aircraft tires on a tilted, free-swiveling nose gear [NASA-TP-2481] N86-11522

AIRFOIL PROFILES

Aerodynamic method used in France for advanced fast propeller study N86-11149

Modern propeller profiles N86-11152

AIRFOILS

Some considerations in propeller and airframe integration N86-11164

User's manual for a 0.3-m TCT wall interference assessment/correction procedure: 8- by 24-inch airfoil test section [NASA-TM-87582] N86-11189

Laser velocimetry measurement in a transonic tunnel N86-11448

Gas side heat transfer N86-11507

Coolant passage heat transfer with rotation. A progress report on the computational aspects N86-11510

AIRFRAMES

On the aerodynamics of installed propellers N86-11154

Full-scale flight and model-scale wind tunnel tests on the nearfield noise characteristics of aircraft propellers N86-11172

AIRPORTS

Enhanced airport surface detection equipment applications [AD-A157641] N86-11210

Validation of procedures for pavement design on expansive soils [FAA-PM-85-15] N86-11362

Meteorology of the Persian Gulf and of several airports on the Arabian Coast [AD-A157441] N86-11761

AIRSPACE

Enhanced airport surface detection equipment applications [AD-A157641] N86-11210

ALASKA

The 1984 annual report on Alaska's mineral resources [DE85-015236] N86-11651

Periglacial landforms and processes in the southern Kenai Mountains, Alaska [AD-A157459] N86-11718

ALGORITHMS

Block-implicit coupled calculation of fluid flows [DE85-004038] N86-11432

Block-implicit multigrid calculation of three-dimensional recirculating flows [DE85-010250] N86-11434

Time-of-flight anemometer for hot section applications N86-11504

Adjustment of the latitude data by least-squares collocation approach N86-11562

Regional-scale (1000 KM) model of photochemical air pollution. Part 3: Tests of the numerical algorithms [PB85-203818] N86-11696

Numerical solution of ionospheric filtration of ULF waves. Part 1: Method N86-11712

Sub-cloud layer motions from radar data using correlation techniques [AD-A156477] N86-11757

Towards developing robust algorithms for solving partial differential equations on MIMD machines [NASA-CR-177[illegible]79] N86-11856

Sixth Biennial CUBE (Computer Use By Engineers) Symposium [LA-10240-C] N86-11858

Interface elements for heat transfer analyses N86-11868

SIG: A general-purpose signal processing code N86-11876

Ramp response estimation and spectrum extrapolation for ultrasonic scattering N86-11881

Computer codes for fluid-structure interactions N86-11887

Probabilistic analysis of a network resource allocation algorithm [AD-A157553] N86-11904

Sparse quasi-Newton methods and the continuation problem [AD-A157587] N86-11914

Computation of minimal isovist sets [AD-A157624] N86-11915

Determination of parameters of elastic spherical shell from scattered wave field N86-11949

Third National Academic Machine Retrieval Conference held in Zhenjiang N86-11999

A general-applications direct global matrix algorithm for rapid seismo-acoustic wavefield computations N86-12012

ALIGNMENT

CRC control systems laboratory gyro test facility [CRC-1385] N86-11205

Coupled virbrational modes of the SLC arc magnet and support system [DE85-014288] N86-12124

ALKALI HALIDES

Distributed-feedback lasers with active framing medium N86-11971

ALKALINE EARTH OXIDES

Oxide cathode mechanisms: Electronic and structural features of oxide cathode surfaces [AD-A157666] N86-11418

ALKALOIDS

Importance of phytoalexin tolerance and detoxification for pathogenicity [DE85-014759] N86-11257

ALLOYS

Intergranular attack and stress corrosion cracking of alloy 600 in high-temperature caustic solutions containing contaminants [DE85-014106] N86-11335

Life prediction and constitutive behavior N86-11520

Binding energy of donors in GaAs-Ga(1-x) Al(x)As quantum well structures N86-11940

ALPHA PARTICLES

Effects of trapped alpha particles on ballooning modes in tokamaks [DE85-015064] N86-12082

ALPS MOUNTAINS (EUROPE)

Recent crustal movements and geophysical interpretation of geodynamic processes in the Alpine mountain belt N86-11604

Dynamics of the Bohemian Massif N86-11616

ALTITUDE

Concurrent and lagged relationships between precipitation frequency and 700 mb heights N86-11808

ALUMINUM

Advances in joining techniques used in development of SPF/DB titanium sandwich reinforced with metal matrices N86-11247

Adhesives for aerospace N86-11249

Use of hydration inhibitors to improve bond durability of aluminum adhesive joints N86-11251

Generic structural elements N86-11296

Metallurgical characterization of the interfaces and the damping mechanisms in metal matrix composites [AD-A156507] N86-11300

Cathodic protection of aluminium structures [KIS-1985:4E] N86-11313

Processing and microstructural characterization of B4C-Al cermets [DE85-013195] N86-11326

Metallography of solid state bonds [DE85-014564] N86-11327

Injection molding-sealing of glass to low melting metals [DE85-015613] N86-11329

A 2D ACAR momentum density study of the nature of the positron surface state on Al(100) [DE85-014830] N86-11330

Calculation of thermal trapping in shear bands [DE85-014404] N86-11336

Operating range of aluminum gallium arsenide quantum-well heterostructure lasers: tunability, power output and high energy emission N86-11464

Velocity measurements of laser driven flyers backed by high impedance windows [DE85-015142] N86-11470

Strain rate dependence in steady, plastic shock waves [DE85-014703] N86-11544

High pressure strength of shocked aluminum [DE85-014461] N86-11547

Vertical axis wind turbine power regulation through centrifugally pumped lift spoiling [DE85-013787] N86-11679

Spin dependence of the coherent scattering lengths of (27)Al and admixture of s- and d-partial waves [DE85-013299] N86-12066

ALUMINUM ALLOYS

Comparison of bond in roll-bonded and adhesively bonded aluminums N86-11248

Effects of manufacturing processes on structural allowables [AD-A157596] N86-11318

Stress and strain-rate dependence of spall strength in two aluminum alloys [DE85-015154] N86-11321

Shock-wave synthesis of titanium aluminides [DE85-015140] N86-11324
Synthesis of nickel-aluminum alloys by shock compression of composite particles [DE85-015165] N86-11328

ALUMINUM GALLIUM ARSENIDES
Submillimeter quantum electronics [AD-A157432] N86-11417
Binding energy of donors in GaAs-Ga(1-x) Al(x)As quantum well structures N86-11940

ALUMINUM OXIDES
Use of hydration inhibitors to improve bond durability of aluminum adhesive joints N86-11251
Physical property changes of a lithia-alumina-silica based glass as a function of composition [DE85-015610] N86-11352
Overview of solid particle LV seeding techniques used at UTRC N86-11445

ALUMINUM SILICATES
Estimation of particle size based on LDV measurements in a de-accelerating flow field N86-11440
Experiments with solid particle seeding N86-11442

AMBIENT TEMPERATURE
Identification of metal ion chloro complexes in an ambient temperature molten salt [AD-A157295] N86-11302
Worldwide marine temperature variations on the season to century time scale N86-11771

AMMONIUM NITRATES
Health hazard evaluation of liquid monopropellants. Phase 4. Subchronic inhalation of hydroxylammonium nitrate, January 1985 [AD-A157623] N86-11844

AMORPHOUS MATERIALS
Dense random packed model for amorphous Ni35Zr65: Influence of the heat of mixing [DE85-014967] N86-11319
Relationship between interatomic bonding and electron transport in plasma deposited amorphous metal alloys [DE85-014710] N86-11337
Ellipsometric and optical study of some uncommon insulator films on 3-5 semiconductors [NASA-TM-87135] N86-12134
Model of amorphous silicon layer regrowth [DE85-012608] N86-12145

AMPLITUDES
Magnification of low-sensitivity channels in seismographs with standard characteristics N86-11709

ANAEROBES
Structure and function of isozymes: Evolutionary aspects and role of oxygen in eucaryotic organisms [NASA-CR-176286] N86-11831

ANELASTICITY
Results concerning rheological parameters of the Earth N86-11567
Anelasticity in the Earth's mantle: Implications for the frequency dependence of Love numbers N86-11590

ANGLE OF ATTACK
Preliminary design study of a lateral-directional control system using thrust vectoring [NASA-TM-86425] N86-11203

ANGLES (GEOMETRY)
Laser angle sensor [NASA-CR-172369] N86-11207
A laser siderostat [AD-A157444] N86-12190

ANGULAR DISTRIBUTION
A 2D ACAR momentum density study of the nature of the positron surface state on Al(100) [DE85-014830] N86-11330
Transition radiation and coherent electron-photon scattering [DE85-014813] N86-12031
Disruption angles [DE85-015138] N86-12032
Transition radiation as a practical X-ray source [DE85-013201] N86-12036
Few-nucleon transfer reactions on deformed nuclei [DE85-013869] N86-12064

ANGULAR MOMENTUM
Tidal friction, the Earth's rotation and hypothesis of an expanding Earth N86-11556

ANISOTROPIC MEDIA
Electric or magnetic dipole in stratified uniaxially inhomogeneous anisotropic media N86-11922
Energy characteristics of laser with saturable anisotropic absorbing medium in cavity N86-11968

ANISOTROPIC PLATES
Reflection of sound from plate containing periodic inhomogeneities N86-11951

ANISOTROPY
Generic structural elements N86-11296
Remote sensing of earth terrain [NASA-CR-176284] N86-11645
Thin film research. Volume 1 [AD-A157608] N86-12137
Thin film research. Volume 2 [AD-A157609] N86-12138

ANNEALING
Mechanical properties of Inconel 718 and Nickel 201 alloys after thermal histories simulating brazing and high temperature service [NASA-CR-177940] N86-11312
Thermal post-treatment characteristics of metastable carrier concentration in As-implanted silicon after transient annealing N86-11942

ANNIHILATION REACTIONS
Some examples of propulsion applications using antimatter N86-11225
A 2D ACAR momentum density study of the nature of the positron surface state on Al(100) [DE85-014830] N86-11330
Higher luminosities via alternative incident channels [DE85-014355] N86-12118

ANNUAL VARIATIONS
The irregularity in the Earth's annual rotation as a cause of systematic time variation N86-11570
Monthly and seasonal weather outlook for June 1985, volume 39, number 11, 30 May 1985 [PB85-209526] N86-11762
Proceedings of the 9th Annual Climate Diagnostics Workshop [PB85-183911] N86-11763
Global surface air temperature variations: 1983-1984 N86-11764
Monitoring climate in real time: An application of the Climate Anomaly Monitoring System (CAMS) N86-11765
Blocking as an explanation of the severe cold of winter 1983-84 N86-11768
Subseasonal and interannual variations of tropical convection and the El Nino/Southern Oscillation N86-11779
The annual variation in the vertical structure of the 40-50-day tropical oscillation N86-11780
Life cycle of a 28-72 day atmospheric oscillation during northern winter N86-11781
Peru coastal winds during 1982-1983 N86-11783
Several aspects of interannual variability in the California current system N86-11785
Time-averaging the flux-profile relationship N86-11789
Tropical convection and North American cyclones during the 1982-83 El Nino N86-11809
An observational study of the vertical structure of interannual wind fluctuations in the tropics N86-11810
Climate system fluctuations, monitoring N86-11814
Effect of initialization on diagnoses of large-scale circulation statistics from WMC analyses N86-11817

ANOMALIES
Geophysical interpretation of global geoid undulations and mean gravity anomalies N86-11560
Monitoring climate in real time: An application of the Climate Anomaly Monitoring System (CAMS) N86-11765
Review of the climate of fall 1983 and winter 1983-84 N86-11766
Some empirical evidence for the influence of snow cover on temperature and precipitation N86-11767
Blocking as an explanation of the severe cold of winter 1983-84 N86-11768
Circulation and weather for MAM and JJA 1984 N86-11769
On the relationship between North Atlantic seasonal SST anomalies with United States surface temperature anomalies N86-11770
Recent unusual mean winter temperature across the contiguous United States N86-11772
Towards understanding the geographical distribution and seasonality in persistance of monthly mean surface air temperature over the U.S.A. N86-11773
Atmospheric response to an equatorial Pacific sea surface temperature anomaly: The effects of orography N86-11791
The impact of heat sources in the tropics on the atmospheric circulation N86-11793
Anomaly general circulation models N86-11798
Monthly forecast experiments with sea surface temperature anomaly forcings and envelope mountains: Preliminary results N86-11803
Specification of mean surface temperature anomalies in Europe and Asia during the fall months N86-11806
Very anomalous behavior of outgoing longwave radiation in the tropics in 1983-84: Aftermath of ENSO? N86-11813

ANTARCTIC REGIONS
Global surface air temperature variations: 1983-1984 N86-11764
Atmospheric general circulation model simulations of the modern Antarctic climate N86-11790

ANTENNA ARRAYS
Proceedings of the 1984 Antenna Applications Symposium [AD-A153257] N86-11398
Considerations for millimeter wave, monolithic phased arrays N86-11399
The design of a thermally efficient 1:256 KU-band feed network for a MMIC phased array N86-11400
Characterization of MMIC devices for active array antennas N86-11401
Waveguide slot array with CSC2 theta (dot) COS theta pattern N86-11402
Considerations for extending the bandwidth of arrays beyond two octaves N86-11404
Microstrip monpulse dipole array N86-11405
Theory and experiment for infinite microstrip arrays N86-11406
Circularly polarized microstrip antennas N86-11407
Radiation and scattering performance of microstrip antennas using exotic substrates N86-11408

ANTENNA COMPONENTS
Characterization of MMIC devices for active array antennas N86-11401

ANTENNA RADIATION PATTERNS
Waveguide slot array with CSC2 theta (dot) COS theta pattern N86-11402
Sheet metal waveguide forming technique N86-11403
Considerations for extending the bandwidth of arrays beyond two octaves N86-11404
Electric or magnetic dipole in stratified uniaxially inhomogeneous anisotropic media N86-11922
Stability of a method for analyzing radiation pattern of acoustic radiator with near-field pressure measurement errors N86-11950

ANTENNAS
Upgrade of the EM transient range monocone antenna [DE85-013181] N86-11413

ANTHRACENE
Cause of occurrence of high-energy ions during UV laser irradiation of molecular crystals N86-11953

ANTIFERROMAGNETISM
Electronic and magnetic structure of chromium surfaces and chromium monolayers on iron [DE85-014542] N86-11322

ANTIMATTER
Some examples of propulsion applications using antimatter N86-11225

ANTINUCLEONS
Some examples of propulsion applications using antimatter N86-11225
Antinucleon-nucleus elastic and inelastic scattering [DE85-012510] N86-12059

ANTIREFLECTION COATINGS
Pulse duration dependence of 1064-nm laser damage thresholds of porous silica antireflection coatings on fused silica substrates [DE85-013207] N86-11350
Use of SiO2 and TiO2 sol-gel antireflection films on silicon solar cells [DE85-011280] N86-11688

ANTISUBMARINE WARFARE
Use of the wavenumber technique with the Lloyds mirror for an acoustic doublet [AD-A156463] N86-11824

APERTURES
Characterization of MMIC devices for active array antennas N86-11401
Computer-aided bifocal dielectric lens antenna design for MH wave application N86-11410
Phasing of multiple-aperture optical systems N86-11987
SSC test lattices [DE85-014240] N86-12098

AQUICULTURE
Saltwater wetlands for wastewater management environmental assessment [PB85-201267] N86-11697

AQUIFERS
Evaluating the ground-water resources of the high plains of Texas, volume 3 [PB85-191617] N86-11655
Deepwell monitoring along the southern San Andreas Fault [PB85-196483] N86-11726
Coral reef hydrogeology [DE85-012923] N86-11828

ARC JET ENGINES
An experimental study of energy loss mechanisms and efficiency consideration in the low power dc arcjet [NASA-TM-87123] N86-11224

ARC WELDING
Feasibility of remotely manipulated welding in space: A step in the development of novel joining technologies N86-11246

ARCHITECTURE (COMPUTERS)
Directly executed languages [AD-A157311] N86-11888
ARCTIC REGIONS
Arctic Energy Technologies Workshop: Proceedings [DE85-003360] N86-11649
Global surface air temperature variations: 1983-1984 N86-11764
Analysis of arctic haze scattering and aerosol data obtained during AGASP [AD-A157434] N86-12074
ARGON PLASMA
The ionization equilibrium of optically thick argon z-pinch plasmas for electron temperatures between 25 and 65 eV [AD-A157484] N86-12078
ARID LANDS
Preliminary analysis of AIS spectral data acquired from semi-arid shrub communities in the Owens Valley, California N86-11622
Concurrent and lagged relationships between precipitation frequency and 700 mb heights N86-11808
ARITHMETIC AND LOGIC UNITS
Research in the design of high-performance reconfigurable systems [NASA-CR-176275] N86-11897
ARMED FORCES (UNITED STATES)
A computer engineering curriculum for the Air Force Academy: An implementation plan [AD-A156464] N86-11857
A computer-based educational approach to the Air Command and Staff College associate program [AD-A156460] N86-12160
ARRAYS
Thin film research. Volume 2 [AD-A157609] N86-12138
ARSENIC
Deep-level defects in ion-implanted and CO2 laser-annealed silicon N86-11939
ARSENIC COMPOUNDS
Studies on chalcogenide films [AD-A157340] N86-11343
Part A. Molecular dynamics and ionic associations of LiAsF6 in 4-butyrolactone mixtures with 2-methyl tetrahydrofuran. Part B. Molecular dynamics and ionic associations of LiBF4 in 1,2-dimethoxymethane [AD-A157401] N86-12023
ARSENIC ISOTOPES
Thermal post-treatment characteristics of metastable carrier concentration in As-implanted silicon after transient annealing N86-11942
ASCENT PROPULSION SYSTEMS
Heavy lift launch vehicles for 1995 and beyond [NASA-TM-86520] N86-11216
ASIA
Specification of mean surface temperature anomalies in Europe and Asia during the fall months N86-11806
Land-surface fluctuations and associated climatic variability N86-11807
ASPECT RATIO
An asymptotic theory for the interference of large aspect ratio swept wings and multiple propeller slipstreams N86-11167
Application of the vortex-lattice concept to flows with smooth-surface separation [AD-A157571] N86-11430
ASSEMBLIES
Robotized machining systems developed at Gomel Institute N86-11397
ASSESSMENTS
Uncertainties in the radiative properties of smoke and their effects on climate assessments [DE85-015187] N86-11691
ASTROLABES
Results concerning rheological parameters of the Earth N86-11567
ASTROMETRY
Adjustment of the latitude data by least-squares collocation approach N86-11562
A laser siderostat [AD-A157444] N86-12190
ASTRONAUTICS
China report: Science and technology [JPRS-CST-85-014] N86-11918
ASTRONOMICAL MAPS
Influences of systematic differences between different star catalogues on the results of latitude and time determinations with the PZT 2 N86-11575
ASTRONOMICAL MODELS
Modelling Epsilon Aurigae without solid particles N86-12181
ASTRONOMICAL PHOTOGRAPHY
Planets around Barnard's Star? N86-11584
ASTRONOMICAL PHOTOMETRY
The 1982-1984 Eclipse of Epsilon Aurigae [NASA-CP-2384] N86-12168
ASTRONOMICAL SPECTROSCOPY
The 1982-1984 Eclipse of Epsilon Aurigae [NASA-CP-2384] N86-12168
The eclipse of Epsilon Aurigae visible spectroscopy and ultraviolet activity N86-12173
ASTRONOMY
On the comparison and choice between the formulas of the Earth tidal correction in astronomical time and latitude observation N86-11588
Photometric support for future astonomical research N86-12175
A laser siderostat [AD-A157444] N86-12190
ASTROPHYSICS
Figure of the Earth, moon, and planets N86-11550
Photometric support for future astonomical research N86-12175
ASYMMETRY
Calculation of formation time of minimal nucleus of flame during ignition of explosive mixtures by electrical discharges N86-11963
Energy characteristics of waveguide CO sub 2-laser N86-11978
ASYMPTOTIC METHODS
An asymptotic theory for the interference of large aspect ratio swept wings and multiple propeller slipstreams N86-11167
ATLANTIC OCEAN
On the relationship between North Atlantic seasonal SST anomalies with United States surface temperature anomalies N86-11770
Worldwide marine temperature variations on the season to century time scale N86-11771
ATMOSPHERIC ATTENUATION
High resolution spectrometry of leaf and canopy chemistry for biochemical cycling N86-11633
ATMOSPHERIC CHEMISTRY
Study of heavy gas effects on the atmospheric dispersion of dense gases, revision 1 [DE85-012917] N86-11693
ATMOSPHERIC CIRCULATION
The Hadley and Rossby regimes in a spherical atmosphere N86-11751
A numerical study of global axisymmetric states and their stability to quasi-geostrophic disturbances N86-11753
Sub-cloud layer motions from radar data using correlation techniques [AD-A156477] N86-11757
Possible cross equatorial influence of the northeast monsoon on the equatorial westerlies over Indonesia [AD-A156907] N86-11759
Life cycle of a 28-72 day atmospheric oscillation during northern winter N86-11781
The distribution of rainfall along the coast of northern Peru during 1982-83 N86-11782
Warm and cold episodes in the California current: A case for large-scale mid-latitude atmospheric forcing N86-11786
Atmospheric general circulation model simulations of the modern Antarctic climate N86-11790
Atmospheric response to an equatorial Pacific sea surface temperature anomaly: The effects of orography N86-11791
Horizontal fluxes in real and model atmospheres N86-11792
The impact of heat sources in the tropics on the atmospheric circulation N86-11793
The effect of anomalous snow cover on the general circulation of the atmosphere using a simple climate model N86-11794
Variability simulations with a steady, linearized primitive equations model N86-11796
Understanding El Nino events using a simple dynamical atmosphere model N86-11797
Anomaly general circulation models N86-11798
Transition from the Southern to Northern Hemisphere summer monsoon N86-11799
Large-scale variability in Indian monsoon rainfall inferred from satellite data N86-11800
Tropospheric static stability and central North American rainfall during 1979 N86-11801
Meteorological conditions during drought episodes in the United States Great Plains N86-11802
An observational study of the vertical structure of interannual wind fluctuations in the tropics N86-11810
Slow fluctuations of the tropical circulation during the FGGE year N86-11812
Effect of initialization on diagnoses of large-scale circulation statistics from WMC analyses N86-11817
Observing the Eastern Pacific Hadley Circulation N86-11818
ATMOSPHERIC COMPOSITION
Effect of elevated atmospheric CO2 on plant communities. Annual report, 1984-1985 [DE85-015575] N86-11692
SAGE aerosol measurements. Volume 1: February 21, 1979 to December 31, 1979 [NASA-RP-1144] N86-11700
ATMOSPHERIC CORRECTION
Precise geoid computations at mountainous coastlines in view of vertical datum determinations N86-11561
ATMOSPHERIC EFFECTS
Short-term methods for atmospheric corrosion testing: Survey of the literature [KIS-1985:5E] N86-11314
ATMOSPHERIC ELECTRICITY
User's manual for AC-20-53A protection of airplane fuel systems against fuel vapor ignition due to lightning [AD-A157619] N86-11191
ATMOSPHERIC HEAT BUDGET
Global surface air temperature variations: 1983-1984 N86-11764
ATMOSPHERIC HEATING
Understanding El Nino events using a simple dynamical atmosphere model N86-11797
ATMOSPHERIC MODELS
Regional oxidant modeling of the northeast US [PB85-201192] N86-11728
Parameterization of the atmospheric boundary layer for air pollution dispersion models [PB85-193548] N86-11730
Climate simulation and change: A simple energy balance climate model N86-11731
The effect of the Hadley circulation on the meridional propagation of stationary waves N86-11732
The utilization of satellite data and dynamics in understanding and predicting global weather phenomena [NASA-CR-171577] N86-11749
Atmospheric general circulation model simulations of the modern Antarctic climate N86-11790
Horizontal fluxes in real and model atmospheres N86-11792
The impact of heat sources in the tropics on the atmospheric circulation N86-11793
The effect of anomalous snow cover on the general circulation of the atmosphere using a simple climate model N86-11794
Interannual climate variability in a low vertical resolution spectral atmospheric model N86-11795
Understanding El Nino events using a simple dynamical atmosphere model N86-11797
Anomaly general circulation models N86-11798
Transition from the Southern to Northern Hemisphere summer monsoon N86-11799
ATMOSPHERIC MOISTURE
Meteorological conditions during drought episodes in the United States Great Plains N86-11802
ATMOSPHERIC PHYSICS
The utilization of satellite data and dynamics in understanding and predicting global weather phenomena [NASA-CR-171577] N86-11749
ATMOSPHERIC PRESSURE
Recent long-term climatic change over the eastern tropical and subtropical Pacific and its ramifications N86-11775
Global relationships with the Southern Oscillation N86-11776
Time series modeling of the Southern Oscillation N86-11777
Life cycle of a 28-72 day atmospheric oscillation during northern winter N86-11781
ATMOSPHERIC SOUNDING
Electromagnetic soundings for geothermal resources in Dixie Valley, Nevada [DE85-011986] N86-11722
ATMOSPHERIC TEMPERATURE
Monthly and seasonal weather outlook for June 1985, volume 39, number 11, 30 May 1985 [PB85-209526] N86-11762
Monitoring climate in real time: An application of the Climate Anomaly Monitoring System (CAMS) N86-11765
Some empirical evidence for the influence of snow cover on temperature and precipitation N86-11767
Blocking as an explanation of the severe cold of winter 1983-84 N86-11768
Towards understanding the geographical distribution and seasonality in persistance of monthly mean surface air temperature over the U.S.A. N86-11773
Global relationships with the Southern Oscillation N86-11776
Satellite observations of a large-amplitude 40-50 day oscillation in upper tropospheric temperature over the equatorial Pacific Ocean during the 1982-83 ENSO event N86-11778
Specification of mean surface temperature anomalies in Europe and Asia during the fall months N86-11806
ATMOSPHERIC TURBULENCE
A perspective on the status of measurement of atmospheric turbulence in the US [NASA-TM-87610] N86-11193

ATMOSPHERICS
Applications of the magneto-optical filter to stellar pulsation measurements
[NASA-CR-176282] N86-12187
ATOMIC CLOCKS
The use of wall-coated cells in atomic frequency standards
[AD-A157435] N86-12024
ATOMIC COLLISIONS
Computer application in atomic absorption spectrometry N86-12001
Laboratory studies of atomic collision processes of importance in planetary atmospheres
[NASA-CR-176301] N86-12019
ATOMIC RECOMBINATION
Activated recombinative desorption: A potential component in mechanisms of spacecraft glow
[DE85-014092] N86-11223
Toward a theory of atomic gas breakdown by laser radiation near a metal surface N86-11955
ATOMIC SPECTRA
Experimental investigation of recording of dynamic holograms within absorption contour of resonant atomic medium N86-11981
The use of wall-coated cells in atomic frequency standards
[AD-A157435] N86-12024
ATOMIC STRUCTURE
Electronic and magnetic structure of chromium surfaces and chromium monolayers on iron
[DE85-014542] N86-11322
Magnetic properties and electronic structure of the actinide systems UAl2, NpAl2 and PuAl2
[DE85-014102] N86-11323
An introduction to electrical breakdown in dielectrics
[AD-A156465] N86-11415
Multispectroscopic studies of the electronic structure of electrode materials for high energy density batteries: 1-2, 1-3 intermetallic compounds with B32 structure
[DE85-014675] N86-11684
ATOMIZERS
Aerosol seeding systems for the NSWC wind tunnels
N86-11453
ATROPINE
An atropinized heat-stressed rat model: Anticholinergic and anticholinesterase drug potency
[AD-A157620] N86-11632
ATTITUDE (INCLINATION)
A study of the cornering forces generated by aircraft tires on a tilted, free-swiveling nose gear
[NASA-TP-2481] N86-11522
ATTITUDE CONTROL
CRC control systems laboratory gyro test facility
[CRC-1385] N86-11205
Balloon-borne three-meter telescope for far-infrared and submillimeter astronomy
[NASA-CR-176285] N86-12188
AUDIO FREQUENCIES
Electrical relaxation in poly(ethylene oxide)
[AD-A157301] N86-11342
Infrasound: A summary of interesting articles
[FMV:ELEKTRO-A12:142/83] N86-12017
Part A. Molecular dynamics and ionic associations of LiAsF6 in 4-butyrolactone mixtures with 2-methyl tetrahydrofuran. Part B. Molecular dynamics and ionic associations of LiBF4 in 1,2-dimethoxymethane
[AD-A157401] N86-12023
AUGER EFFECT
Ion beam neutralizer
[AD-D011741] N86-12043
AURIGA CONSTELLATION
The 1982-1984 Eclipse of Epsilon Aurigae
[NASA-CP-2384] N86-12168
Optical photometry of the 1982-1984 eclipse of Epsilon Aurigae N86-12169
Infrared photometry of the 1982-4 eclipse of Epsilon Aurigae N86-12170
The optical polarization of Epsilon Aurigae through the 1982-84 eclipse N86-12171
IUE observations of the 1982-84 eclipse of Epsilon Aurigae N86-12172
The eclipse of Epsilon Aurigae visible spectroscopy and ultraviolet activity N86-12173
Epsilon Aurigae in an evolutionary context
N86-12174
UBV photometry of the 1982-4 eclipse of Epsilon Aurigae: A discussion of the observed light curves
N86-12176
Intermediate and narrow band photometry of Epsilon Aurigae N86-12177
Spectrophotometry of Epsilon Aur, 3295-8880 A
N86-12178
Micron CO in the eclipse spectrum of Epsilon Aur
N86-12179
Scattered light in the IUE spectra of Epsilon Aurigae
N86-12180
Modelling Epsilon Aurigae without solid particles
N86-12181
High dispersion observations of Epsilon Aur from Sept. 1982 to March 1983 N86-12183
AURORAS
Plasmas in the Earth's magnetotail
[AD-A157320] N86-11716
AUSTENITIC STAINLESS STEELS
Mechanical threshold of dynamically deformed copper and nitronic 40
[DE85-010779] N86-11545
Overview of MIT, ADIP irradiation experiments
[DE85-014469] N86-12060
AUTOCLAVING
Properties of autoclaved Gr/PI composites made from improved tack PMR-15 prepreg N86-11276
AUTOCORRELATION
Significance tests of recent vertical crustal movements by correlation functions N86-11611
On the relationship between North Atlantic seasonal SST anomalies with United States surface temperature anomalies N86-11770
AUTOMATIC CONTROL
Automatic orbital GTAW welding: Highest quality welds for tomorrow's high-performance systems N86-11229
Adhesives for aerospace N86-11249
Automated magnet testing facility
[DE85-012863] N86-11422
USSR report: Science and technology policy
[JPRS-UST-85-014] N86-11990
Computer-aided designing, engineering, preparation of production N86-11992
AUTOMATION
USSR report: Machine tools and metalworking equipment
[JPRS-UMM-85-010] N86-11394
Large robotized turning centers described
N86-11395
Robotized production systems observed in modern plants N86-11396
AUTORADIOGRAPHY
Los Alamos upgrade in metallographic capabilities
[DE85-014089] N86-11320
AVIONICS
Expert systems development and application
[NASA-TM-86746] N86-11194
Description of an experimental expert system flight status monitor
[NASA-TM-86791] N86-11195
Heavy lift launch vehicles for 1995 and beyond
[NASA-TM-86520] N86-11216
AXIAL FLOW
Characteristics of an axisymmetric sudden expansion flow
[NASA-CR-176278] N86-11465
AXIAL STRAIN
Uniaxial tensile deformation and fracture of dual-phase steels
[DE85-015034] N86-11538
Inertia, stability and ductibility in uniaxial tension at high strain rate
[DE85-007671] N86-11546
AXISYMMETRIC FLOW
Aerodynamics of wide-chord propellers in non-axisymmetric flow N86-11153
Characteristics of an axisymmetric sudden expansion flow
[NASA-CR-176278] N86-11465
A numerical study of global axisymmetric states and their stability to quasi-geostrophic disturbances N86-11753
On the nonlinear characteristics of the axisymmetric flow regime: Cylindrical and spherical systems N86-11756
AZIMUTH
CRC control systems laboratory gyro test facility
[CRC-1385] N86-11205

B

B-52 AIRCRAFT
Stress analyses of B-52 pylon hooks
[NASA-TM-84924] N86-11524
BACKGROUND RADIATION
Si(Li)-NaI(Tl) sandwich detector array for measurements of trace radionuclides in soil samples
[DE85-013865] N86-12062
BACKSCATTERING
Seeding techniques used in the Vortex Research Facility N86-11443
Seeding systems for use with a laser velocimeter in large scale wind tunnels N86-11444
Lidar observations of stratospheric aerosol over Mauna Loa Observatory: 1982 - 1983
[PB85-187896] N86-11723
Calculation of the electron backscattering coefficient by Monte Carlo simulation N86-11864
Intermediate and high-frequency acoustic backscattering cross sections for water-ice interfaces. 1: Two-component profile models
[AD-A157533] N86-12018
Dominant moving species in the formation of amorphous NZr by solid-state reaction
[DE85-014855] N86-12053
BALLOON-BORNE INSTRUMENTS
Balloon-borne three-meter telescope for far-infrared and submillimeter astronomy
[NASA-CR-176285] N86-12188
BANDPASS FILTERS
Characteristics of an axisymmetric sudden expansion flow
[NASA-CR-176278] N86-11465
Applications of the magneto-optical filter to stellar pulsation measurements
[NASA-CR-176282] N86-12187
BANDWIDTH
Considerations for extending the bandwidth of arrays beyond two octaves N86-11404
Theory and experiment for infinite microstrip arrays
N86-11406
Circularly polarized microstrip antennas N86-11407
Directly executed languages
[AD-A157311] N86-11888
BAROCLINIC INSTABILITY
The effect of topography on the evolution of unstable disturbances in a baroclinic atmosphere N86-11750
A numerical study of global axisymmetric states and their stability to quasi-geostrophic disturbances N86-11753
BAROCLINIC WAVES
The effect of topography on the evolution of unstable disturbances in a baroclinic atmosphere N86-11750
Low-frequency baroclinic features observed in the lee of major mountain ranges N86-11811
BAROTROPIC FLOW
The effect of the Hadley circulation on the meridional propagation of stationary waves N86-11732
Low-frequency baroclinic features observed in the lee of major mountain ranges N86-11811
BAROTROPISM
Spectral statistical forecasts of the 500 mb height field
N86-11804
Specification of mean surface temperature anomalies in Europe and Asia during the fall months N86-11806
BARYON RESONANCE
Amplitude tests of direct channel resonances: The dibaryon
[DE85-011478] N86-12034
BASALT
Probability encoding of hydrologic parameters for basalt. Elicitation of expert opinions from a panel of three basalt waste isolation project staff hydrologists
[DE85-014665] N86-11652
Deformation of granite at elevated temperature and pressure
[DE85-014057] N86-11721
BAYES THEOREM
Bayesian extensions to a basic model of software reliability
[AD-A157296] N86-11901
BEAM CURRENTS
Collinear wake field acceleration
[DE85-014356] N86-12050
Discussion of the current limits in the RFQ
[DE85-012909] N86-12088
Increased intensity performance of the Brookhaven AGS
[DE85-013371] N86-12091
Interaction of the ATA beam with the TM030 mode of the accelerating cells
[DE85-014850] N86-12120
MABE multibeam accelerator
[DE85-012035] N86-12121
BEAM INJECTION
Sources of radioactive ions
[DE85-015251] N86-12030
Discussion of the current limits in the RFQ
[DE85-012909] N86-12088
Increased intensity performance of the Brookhaven AGS
[DE85-013371] N86-12091
New concepts for drift pumping a thermal barrier with RF
[DE85-013591] N86-12114
BEAM INTERACTIONS
Disruption angles
[DE85-015138] N86-12032
Collider Detector at Fermilab (CDF)
[DE85-014423] N86-12068
Neutral beam interactions with materials
[AD-A157445] N86-12076
Using the TEVATRON beam position monitor system to investigate transverse phase space
[DE85-014261] N86-12105

Higher luminosities via alternative incident channels
[DE85-014355] N86-12118
Interaction of the ATA beam with the TM030 mode of the accelerating cells
[DE85-014650] N86-12120

BEAM NEUTRALIZATION
Two-dimensional linacs
[DE85-015129] N86-12029

BEAM SPLITTERS
Double-wavelength pulsed tunable dye laser
N86-12003

BEAM WAVEGUIDES
Galvanoplastic grazing incidence mirrors for verticle experiments: The tandem tests in soft X-rays
N86-12071

BEAMS (RADIATION)
Characteristics of an axisymmetric sudden expansion flow
[NASA-CR-176278] N86-11465
Investigation of efficiency of generation of difference-frequency laser radiation in waveguide
N86-11969
AGS polarized beam facility
[DE85-011834] N86-12038
Collinear wake field acceleration
[DE85-014356] N86-12050
Very high energy colliders
[DE85-013075] N86-12100
Beam position monitor for storage rings
[DE85-013295] N86-12104
Using the TEVATRON beam position monitor system to investigate transverse phase space
[DE85-014261] N86-12105

BEAMS (SUPPORTS)
Flexible vibrations of a uniform elastic beam with arbitrary supports and lumped masses N86-11885

BEARINGS
Current research on circular saw and band saw vibration and stability N86-11533

BEDS (PROCESS ENGINEERING)
Improved heat switch for gas sorption compressor
N86-11372

BELLOWS
Hermetic bellows seal for Braun linear engine: Design, test and demonstration
[DE85-013545] N86-11478

BENDING
Involutory transformations and variation principles with multivariables in thin plate bending problems
N86-12004

BENZENE
Basic studies of the lithium secondary battery
[AD-A157449] N86-11673
Ionization-Raman double-resonance spectroscopy
[DE85-013774] N86-12042

BERYLLIUM OXIDES
Fabrication and use of zircaloy/tantalum-sheathed cladding thermocouples
[EGG-TFBP-6739] N86-11461

BIAS
Correcting for particle counting bias error in turbulent flow N86-11439

BIBLIOGRAPHIES
Aeronautical Engineering: A continuing bibliography with indexes
[NASA-SP-7037(191)] N86-11145
Bibliography of terrestrial impact structures
[NASA-TM-87567] N86-11701
Annotated bibliography of human factors applications literature
[DE85-012957] N86-12161

BINARY ALLOYS
The yield point of copper-zinc alloys in the alpha solid solution range
[BLL-BISI-TRANS-23046-(9022.06)] N86-11311
Surface and interfacial properties of Ga0.47In0.53As alloys
[AD-A157343] N86-11316

BINARY CODES
A cascaded coding scheme for error control
[NASA-CR-176276] N86-11895

BINARY MIXTURES
Shock-wave synthesis of titanium aluminides
[DE85-015140] N86-11324
Compatibilizing effect of random or block copolymer added to binary mixture of homopolymers
[AD-A157384] N86-11345
Application of a mixture theory to the binary alloy solidification problem N86-11873

BINDING
Binding energy of donors in GaAs-Ga(1-x) Al(x)As quantum well structures N86-11940

BIOCHEMISTRY
Structure and function of isozymes: Evolutionary aspects and role of oxygen in eucaryotic organisms
[NASA-CR-176286] N86-11831
Relationship between alkylation sites and induction of dominant lethals and heritable translocations in mice
[DE85-014309] N86-11835

BIOLOGICAL EFFECTS
Assessments and viewpoints on the biological and human health effects of Extremely Low Frequency (ELF) electromagnetic fields: Compilation of commissioned papers for the ELF literature review project
[AD-A156942] N86-11839
Acute pulmonary effects of formaldehyde exposure in humans
[DE85-014728] N86-11848

BIOLOGICAL EVOLUTION
Relationship between alkylation sites and induction of dominant lethals and heritable translocations in mice
[DE85-014309] N86-11835

BIOMASS
Discrimination of coastal vegetation and biomass: Using AIS data N86-11639
Utilization of non-conventional systems for conversion of biomass to food components: Potential for utilization of algae in engineered foods
[NASA-CR-176257] N86-11830

BIOMEDICAL DATA
Polar Research Board annual report 1984 and future plans
[PB85-204477] N86-11727

BIOMETEOROLOGY
Analysis of terrestrial conditions and dynamics
[NASA-CR-176308] N86-11646

BIOREACTORS
Determination of the steady-state behavior of immobilized (BETA)-galactosidase utilizing an integral reactor scheme
[DE85-012900] N86-11256

BIT ERROR RATE
A cascaded coding scheme for error control
[NASA-CR-176276] N86-11895
A cascaded coding scheme for error control
[NASA-CR-176287] N86-11911

BLACK HOLES (ASTRONOMY)
X-ray inverse Compton emission from the radio halo of M87
[NASA-CR-176305] N86-12196

BLADE SLAP NOISE
A numerical method of calculating propeller noise including acoustic nonlinear effects N86-12011

BLADES
A numerical method of calculating propeller noise including acoustic nonlinear effects N86-12011

BLOCKING
Blocking as an explanation of the severe cold of winter 1983-84 N86-11768

BLUE GREEN ALGAE
Utilization of non-conventional systems for conversion of biomass to food components: Potential for utilization of algae in engineered foods
[NASA-CR-176257] N86-11830

BODY TEMPERATURE
An atropinized heat-stressed rat model: Anticholinergic and anticholinesterase drug potency
[AD-A157620] N86-11832

BOILERS
CELCAP: A computer model for cogeneration system analysis
[NASA-CR-176306] N86-11896

BOLTS
Nondestructive ultrasonic measurement of bolt preload using the pulsed-phase locked-loop interferometer
N86-11242
A Signorini model of bolt fastened laminated composites N86-11258

BONDING
Adhesives for aerospace N86-11249
Use of hydration inhibitors to improve bond durability of aluminum adhesive joints N86-11251
Factors affecting the processing of epoxy film adhesives N86-11252
Recent developments in polyimide and bismaleimide adhesives N86-11270
Interaction of mixed mode loading on cyclic debonding in adhesively bonded composite joints
[NASA-CR-177990] N86-11298
Chemical bonding agent for suppression of rusty bolt intermodulation interference
[AD-D011747] N86-11315
Metallography of solid state bonds
[DE85-014564] N86-11327
Short range bonding interaction at metal-metal interfaces
[DE85-014442] N86-11334

BOOSTER ROCKET ENGINES
Heavy lift launch vehicles for 1995 and beyond
[NASA-TM-86520] N86-11216

BORANES
Studies on the syntheses of boron hydride systems
[AD-A157368] N86-11344

BOREHOLES
Modification of a Hughes tiltmeter to a borehole tiltmeter N86-11563
Workshop on Permafrost Geophysics
[AD-A157485] N86-11719

BORIDES
Surface impedance of several magnetic superconductors
[DE85-014101] N86-12155

BORON CARBIDES
Processing and microstructural characterization of B4C-Al cermets
[DE85-013195] N86-11326

BORON HYDRIDES
Studies on the syntheses of boron hydride systems
[AD-A157368] N86-11344

BOUNDARY ELEMENT METHOD
Prediction of acoustical response of three-dimensional cavities using an indirect boundary element method
N86-12014

BOUNDARY INTEGRAL METHOD
Numerical Techniques in Acoustics
[NASA-CP-2404] N86-12007
Improving the accuracy of the boundary integral method based on the Helmholtz integral N86-12010
Prediction of acoustical response of three-dimensional cavities using an indirect boundary element method
N86-12014

BOUNDARY LAYER COMBUSTION
Surface combustion of liquid fuel in stream of gaseous oxidizer N86-11959

BOUNDARY LAYER FLOW
On cloud street development in three dimensional parallel and Rayleigh instabilities N86-11754
Cloud streets during KonTur: A comparison of parallel/thermal instability modes with observations
N86-11755
Vortex studies relating to boundary layer turbulence and noise N86-12015

BOUNDARY LAYER PLASMAS
Plasmas in the Earth's magnetotail
[AD-A157320] N86-11716

BOUNDARY LAYER SEPARATION
Application of the vortex-lattice concept to flows with smooth-surface separation
[AD-A157571] N86-11430

BOUNDARY LAYER TRANSITION
Transition effects of boundary layer on static and dynamic stability of slender cone N86-11926

BOUNDARY LAYERS
Heat transfer and pressure changes due to a large temperature difference across an enclosed vertical air layer N86-11884

BOUNDARY VALUE PROBLEMS
New aspects of the geodetic boundary value problems
N86-11553
Proceedings of the 5th International Symposium Geodesy and Physics of the Earth, part 2
[REPT-81-PT-2] N86-11568
A new approach to iterations in solving geodetic boundary value problems for real topography
N86-11569
Treatment of the geodetic boundary value problem by contact-transformation N86-11573

BOUSSINESQ APPROXIMATION
A numerical study of global axisymmetric states and their stability to quasi-geostrophic disturbances N86-11753
On cloud street development in three dimensional parallel and Rayleigh instabilities N86-11754

BOX BEAMS
Generic structural elements N86-11296

BRAGG ANGLE
Characteristics of an axisymmetric sudden expansion flow
[NASA-CR-176278] N86-11465

BRAIN
Is the cerebellum involved in motor and perceptual timing: A case study
[AD-A157452] N86-11842

BRASSES
Experimental study on impact/fretting wear in heat exchanger tubes
[DE85-014597] N86-11548

BRAYTON CYCLE
Dish electric systems heat engine assessment
[DE85-013942] N86-11479
Advanced mechanical heat pump technologies for industrial applications
[DE85-014613] N86-11483

BRAZING
Evaluation of superplastic forming and weld-brazing for fabrication of titanium compression panels N86-11245

Feasibility of remotely manipulated welding in space: A step in the development of novel joining technologies
N86-11246
Mechanical properties of Inconel 718 and Nickel 201 alloys after thermal histories simulating brazing and high temperature service
[NASA-CR-177940] N86-11312

BREMSSTRAHLUNG
Multispectroscopic studies of the electronic structure of electrode materials for high energy density batteries: 1-2, 1-3 intermetallic compounds with B32 structure
[DE85-014675] N86-11684
Experimental check of bremsstrahlung dosimetry predictions for 0.75 MeV electrons
[DE85-014706] N86-12058
PBFA-2 vacuum insulator stack failure mechanisms
[DE85-013118] N86-12090

BREWSTER ANGLE
Double-wavelength pulsed tunable dye laser
N86-12003

BRIDGMAN METHOD
Bridgman growth of semiconductors
[NASA-CR-177971] N86-11426

BRIGHTNESS TEMPERATURE
Efficiency of optically-pumped XeF-laser N86-11977

BROMIDES
Mercury bromide reconstitution in the HgBr laser system
[AD-A156502] N86-11466

BROWNIAN MOVEMENTS
Possibility of optimal choice of exposure time for holographic recording of objects through unsteady scattering media N86-11983

BUBBLES
Raman scattering of sound on random oscillations of bubbles N86-11948

BUILDINGS
Applied model validation
[NBSIR-85-3154-1] N86-11363

BULGARIA
Statistical analysis and interpretation of Earth crustal movements in northeast Bulgaria N86-11613

BUMPY TORUSES
Spherical torus: An approach to compact fusion at low field. Initial ignition assessments
[DE85-012890] N86-12099

BUNCHING
Disruption angles
[DE85-015139] N86-12032

BURNERS
Burner liner thermal/structural load modelling
N86-11514
Component-specific modeling N86-11515
Validation of structural analysis methods using burner liner cyclic rig test data N86-11518

BURNING RATE
Pressure-coupled response function of solid propellants including those with negative pressure-exponents
N86-11924

BYPASSES
Waveguide slot array with CSC2 theta (dot) COS theta pattern N86-11402
Sheet metal waveguide forming technique
N86-11403

C

CABLES (ROPES)
Evaluation of concrete creep and stress redistribution in a prototypic PCRV following rupture of prestressing tendons
[DE85-007673] N86-11543

CADMIUM SULFIDES
Investigation of photoelectrode redox polymer junctions
[AD-A157556] N86-11304

CALCIUM
Controlled environment life support system: Calcium-related leaf injuries on plants
[NASA-CR-176288] N86-11829

CALCULUS OF VARIATIONS
On symmetric and upwind TVD schemes
[NASA-TM-86842] N86-11909
Involutory transformations and variation principles with multivariables in thin plate bending problems
N86-12004

CALIBRATING
Calibration of AIS data using ground-based spectral reflectance measurements N86-11631
High altitude measured radiance of White Sands, New Mexico in the 400-2000 nm band using a filter wedge spectrometer
[PB85-206084] N86-11729
Atlas of high altitude aircraft measured radiance of White Sands, New Mexico, in the 450-1050 nanometers band
[PB85-204501] N86-11820

CALIFORNIA
Honey Lake Geothermal Project, Lassen County, California
[DE85-013388] N86-11677
Deepwell monitoring along the southern San Andreas Fault
[PB85-196483] N86-11726
Several aspects of interannual variability in the California current system N86-11785
Warm and cold episodes in the California current: A case for large-scale mid-latitude atmospheric forcing
N86-11786

CAMERAS
Comparison of AIS versus TMS data collected over the Virginia piedmont N86-11637
Teleoperator human factors study
[NASA-CR-176310] N86-11854

CANALS
Survey of ice problem areas in navigable waterways
[AD-A157477] N86-11827

CANCER
Thyroid absorbed dose for people at Rongelap, Utirik and Sifo on March 1, 1954
[DE85-014695] N86-11846

CANOPIES (VEGETATION)
High resolution spectrometry of leaf and canopy chemistry for biochemical cycling N86-11633
Forest canopy chemistry from Blackhawk Island, Wisconsin N86-11634
Discrimination of coastal vegetation and biomass: Using AIS data N86-11639
AIS investigation of agricultural monocultures
N86-11640
Application of AIS technology to forest mapping
N86-11641

CANTILEVER BEAMS
Effect of a viscoelastic boundary inset on vibrational characteristics of a beam N86-11494

CAPACITORS
Partial discharge formation and breakdown in deionized water under repetitive stressing
[DE85-013114] N86-11424
Efficiency of optically-pumped XeF-laser N86-11977

CAPTURE EFFECT
Increased intensity performance of the Brookhaven AGS
[DE85-013371] N86-12091

CARBON
Improvement in wear performance of surgical Ti-6Al-4V alloy by ion implantation of nitrogen or carbon
[DE85-013986] N86-11849
Carbon films grown from plasma on III-V semiconductors
[NASA-TM-87140] N86-12135

CARBON DIOXIDE
Effect of elevated atmospheric CO2 on plant communities. Annual report, 1984-1985
[DE85-015575] N86-11692

CARBON DIOXIDE LASERS
Ring cavity CO2 laser for branch-selection and narrow resonance produced by SF6 in cavity N86-11930
Deep-level defects in ion-implanted and CO2 laser-annealed silicon N86-11939
Energy characteristics of waveguide CO sub 2-laser
N86-11978
On convective effects in gas lasers N86-12006

CARBON FIBER REINFORCED PLASTICS
PMR polyimides from solutions containing mixed endcaps N86-11263
Bismaleimides and related maleimido polymers as matrix resins N86-11265
All-aromatic biphenylene end-capped polyquinoline and polyimide matrix resins N86-11267
Recent developments in polyimide and bismaleimide adhesives N86-11270
Replacement of MDA with more oxidatively stable diamines in PMR-polyimides N86-11275
Composite structural materials
[NASA-CR-176279] N86-11293
Constituent materials N86-11294

CARBON FIBERS
Microscopic evaluation of a polyimide (PMR-15)-graphite composite N86-11282

CARBON MONOXIDE
Micron CO in the eclipse spectrum of Epsilon Aur
N86-12179
The mass of hot, shocked CO in Orion: First observations of the J = 17 yields J = 16 transition at 153 microns
[AD-A157323] N86-12189

CARBON MONOXIDE LASERS
Optimization of parameters of chemical CO laser by increasing length of active medium N86-11976

CARBON STEELS
Experimental study on impact/fretting wear in heat exchanger tubes
[DE85-014597] N86-11548

CARBON 13
Correlations of chemical, microstructural and mechanical properties of polyethylene piping materials
[DE85-013077] N86-11351

CARBON 14
Importance of phytoalexin tolerance and detoxification for pathogenicity
[DE85-014759] N86-11257

CARBON-CARBON COMPOSITES
Derivation and test of elevated temperature thermal-stress-free fastener concept N86-11236

CARBONATES
A first look at Airborne Imaging Spectrometer (AIS) data in an area of altered volcanic rocks and carbonate formations, Hot Creek Range, south central Nevada
N86-11625
Thermodynamics of chromium and iron in carbonate salts at 650(0)C
[DE85-013542] N86-11682

CARBONYL COMPOUNDS
The chemical production of excited state molecules
[AD-A157276] N86-12021

CARBORANE
Studies on the syntheses of boron hydride systems
[AD-A157368] N86-11344

CARBURIZING
Protective coatings of metal surfaces by cold plasma treatment
[NASA-TM-87152] N86-11475

CARGO AIRCRAFT
World's largest airplane now being tested N86-11181

CARNOT CYCLE
Magnetic refrigeration for low-temperature applications
N86-11370

CARRIER TO NOISE RATIOS
Calculation of allowable orbital spacings for the fixed-satellite service
[NASA-CR-176273] N86-11212

CASCADE CONTROL
A cascaded coding scheme for error control
[NASA-CR-176276] N86-11895
A cascaded coding scheme for error control
[NASA-CR-176287] N86-11911

CASSEGRAIN OPTICS
Balloon-borne three-meter telescope for far-infrared and submillimeter astronomy
[NASA-CR-176285] N86-12188

CATALYSIS
Nuclear spin-polarized HD, D2, HT and DT solids, liquids and high density gases
[DE85-014136] N86-12154

CATHODES
Oxide cathode mechanisms: Electronic and structural features of oxide cathode surfaces
[AD-A157666] N86-11418

CATHODIC COATINGS
Cathodic protection of aluminium structures
[KIS-1985:4E] N86-11313
Failure rate model for cathodic delamination of protective coatings
[AD-A157483] N86-11912

CATIONS
Effects of acid precipitation on composition, electrokinetic behavior, cation adsorption and ion exchange capacity in various soil systems
[PB85-217727] N86-11698

CAVITATION FLOW
Theoretical and experimental comparison of vapor cavitation in dynamically loaded journal bearings
[NASA-TM-87121] N86-11425

CAVITIES
Net-2 models of cavities and diodes N86-11863
Prediction of acoustical response of three-dimensional cavities using an indirect boundary element method
N86-12014

CAVITY RESONATORS
Calculation of RF fields in axisymmetric cavities
[DE85-014135] N86-11414

CAVITY VAPOR GENERATORS
Theoretical and experimental comparison of vapor cavitation in dynamically loaded journal bearings
[NASA-TM-87121] N86-11425

CEILINGS (ARCHITECTURE)
Methods to calculate the response time of heat and smoke detectors installed below large unobstructed ceilings
[NBSIR-85/3167] N86-11365

CELESTIAL GEODESY
Figure of the Earth, moon, and planets N86-11550
Influences of systematic differences between different star catalogues on the results of latitude and time determinations with the PZT 2 N86-11575

CELESTIAL MECHANICS
Figure of the Earth, moon, and planets N86-11550
CELESTIAL REFERENCE SYSTEMS
Influences of systematic differences between different star catalogues on the results of latitude and time determinations with the PZT 2 N86-11575
CELESTIAL SPHERE
Influences of systematic differences between different star catalogues on the results of latitude and time determinations with the PZT 2 N86-11575
CELLS (BIOLOGY)
Dose distribution and the relative biological effectiveness of internal alpha emitters
[DE85-013041] N86-11845
CENTAUR LAUNCH VEHICLE
NASA Lewis Research Center low-gravity fluid management technology program
[NASA-TM-87145] N86-11218
CENTRAL EUROPE
On the distribution of the residual vectors of Earth's tide gravity observations in Central Europe N86-11564
On the gravitational effect of the crust-mantle boundary in central Europe N86-11703
Attenuation of macroseismic effects of earthquakes N86-11705
CENTRAL NERVOUS SYSTEM
Cognitive science program: Dissociation of the central timekeeper and the peripheral implementation processes in repetitive movements
[AD-A157542] N86-11852
CENTRIFUGAL PUMPS
AC motor and generator requirements for isolated WECS
[NASA-CR-176315] N86-11670
CENTRIFUGES
Overview of solid particle LV seeding techniques used at UTRC N86-11445
CERAMIC COATINGS
Protective coatings of metal surfaces by cold plasma treatment
[NASA-TM-87152] N86-11475
CERAMIC FIBERS
Improvements in the fabrication of ceramic-fiber-ceramic-matrix composites by chemical vapor infiltration
[DE85-015971] N86-11301
Strength and flexibility properties of advanced ceramic fabrics
[NASA-TM-86824] N86-11340
CERAMIC MATRIX COMPOSITES
Improvements in the fabrication of ceramic-fiber-ceramic-matrix composites by chemical vapor infiltration
[DE85-015971] N86-11301
CERAMICS
Low-cost, net-snape ceramic radial turbine program
[AD-A157532] N86-11202
Photosensitivity and imaging characteristics of ion-implanted PLZT ceramics
[DE85-015489] N86-11348
Assessment of technical strengths and information flow of energy conservation research in Japan. Volume 2: Background document
[DE85-013759] N86-12165
CEREBELLUM
Is the cerebellum involved in motor and perceptual timing: A case study
[AD-A157452] N86-11842
CERENKOV RADIATION
Emission threshold for cerenkov radiation
[AD-A157615] N86-12025
CERMETS
Processing and microstructural characterization of B4C-Al cermets
[DE85-013195] N86-11326
CHALCOGENIDES
Studies on chalcogenide films
[AD-A157340] N86-11343
CHARACTERIZATION
High Temperature Polymer Matrix Composites
[NASA-CP-2385] N86-11260
Matrix resin development at NASA Langley Research Center N86-11264
The synthesis, characterization and thermal chemistry of modified norbornenyl PMR endcaps N86-11266
Characterization methodology for PMR-15 N86-11272
Characterization of polyimide matrix resins and prepregs N86-11273
Quality assurance procedures for V378A matrix resin N86-11274
CHARCOAL
Improved heat switch for gas sorption compressor N86-11372
CHARGED PARTICLES
The chemical production of excited state moleculea
[AD-A157276] N86-12021
Soviet research on crystal channeling of charged particle beams
[AD-A157353] N86-12022
Muon decay
[DE85-012590] N86-12067
Particle simulation of the low-(ALPHA) Pierce diode
[DE85-014435] N86-12113
CHARM (PARTICLE PHYSICS)
High energy physics
[DE85-014272] N86-12063
CHEMICAL ANALYSIS
Matrix resin development at NASA Langley Research Center N86-11264
CHEMICAL BONDS
Lasing on vapors of chain compounds N86-11967
CHEMICAL COMPOSITION
Quality assurance procedures for V378A matrix resin N86-11274
Investigation of photoelectrode redox polymer junctions
[AD-A157556] N86-11304
Physical property changes of a lithia-alumina-silica based glass as a function of composition
[DE85-015610] N86-11352
High resolution spectrometry of leaf and canopy chemistry for biochemical cycling N86-11633
Cosmogenic-nuclide production by primary cosmic-ray protons
[DE85-012760] N86-12198
CHEMICAL EQUILIBRIUM
Thermodynamics of chromium and iron in carbonate salts at 650(0)C
[DE85-013542] N86-11682
CHEMICAL EXPLOSIONS
A mechanism for ignition of high-temperature gaseous nitromethane: The key role of the nitro group in chemical explosives
[AD-A157355] N86-11303
CHEMICAL FRACTIONATION
Computer application in atomic absorption spectrometry N86-12001
CHEMICAL LASERS
Mercury bromide reconstitution in the HgBr laser system
[AD-A156502] N86-11466
Optimization of parameters of chemical CO laser by increasing length of active medium N86-11976
CHEMICAL PROPERTIES
Chemical bonding agent for suppression of rusty bolt intermodulation interference
[AD-D011747] N86-11315
Influence of physical-chemical properties of gases on interaction between shockwaves and convex cylindrical surfaces N86-11962
CHEMICAL REACTIONS
Calculations of physical and chemical reactions produced in irradiated water containing DNA
[DE85-012899] N86-12051
CHEMICAL TESTS
Characterization of polyimide matrix resins and prepregs N86-11273
CHEMILUMINESCENCE
The chemical production of excited state moleculea
[AD-A157276] N86-12021
CHESAPEAKE BAY (US)
Measurements of refractive index structure function C2N and aerosol size distribution at Chesapeake Bay
[AD-A157455] N86-11717
CHINA
New R and D in Chinese language information processing N86-11996
CHLORIDES
Develop, evaluate and validate continuous emission monitors for designated hazardous pollutants
[PB85-201176] N86-11695
CHLORINE COMPOUNDS
Identification of metal ion chloro complexes in an ambient temperature molten salt
[AD-A157295] N86-11302
CHLORINE FLUORIDES
Flight worthiness of fire resistant hydraulic systems: Volume 1
[AD-A157618] N86-11199
CHLOROPRENE RESINS
Stiffness and damping coefficients of rubber N86-11532
CHLORPROMAZINE
An atropinized heat-stressed rat model: Anticholinergic and anticholinesterase drug potency
[AD-A157620] N86-11832
CHOLINESTERASE
An atropinized heat-stressed rat model: Anticholinergic and anticholinesterase drug potency
[AD-A157620] N86-11832
CHROMIUM
Electronic and magnetic structure of chromium surfaces and chromium monolayers on iron
[DE85-014542] N86-11322
Thermodynamics of chromium and iron in carbonate salts at 650(0)C
[DE85-013542] N86-11682
Chromium- and neodymium-activated gadolinium-scandium-gallium garnet crystal: A new laser active medium N86-11979
CHROMIUM OXIDES
Intergranular attack and stress corrosion cracking of alloy 600 in high-temperature caustic solutions containing contaminants
[DE85-014106] N86-11335
CHROMIUM STEELS
Tensile properties of 2-1/4Cr-1Mo steel irradiated to 23 dpa at 390 to 550(0)C
[DE85-015551] N86-11332
CHROMOSOMES
Relationship between alkylation sites and induction of dominant lethals and heritable translocations in mice
[DE85-014309] N86-11835
CIRCUIT RELIABILITY
Electrical supply for MFTF-B superconducting magnet system
[DE85-012932] N86-12094
CIRCUITS
Sheet metal waveguide forming technique N86-11403
CIRCULAR POLARIZATION
Circularly polarized microstrip antennas N86-11407
CIRCULATION
Worldwide marine temperature variations on the season to century time scale N86-11771
Towards understanding the geographical distribution and seasonality in persistance of monthly mean surface air temperature over the U.S.A. N86-11773
CITIES
Urban, forest, and agricultural AIS data: Fine spectral structure N86-11644
Project to study the use of microcomputer technology in planning and operation of small city transportation systems
[PB85-204873] N86-12166
CIVIL AVIATION
USSR report: Transportation
[JPRS-UTR-85-011] N86-11177
Deputy minister on sector's technical progress N86-11178
Chief of Aeroflot's international activities N86-11179
Recent achievements, problems in cropdusting work N86-11[illegible]80
CLADDING
Fabrication and use of zircaloy/tantalum-sheathed cladding thermocouples
[EGG-TFBP-6739] N86-11461
CLASSICAL MECHANICS
Stationary pulse solutions for a free electron laser N86-11933
CLAYS
Experiments with solid particle seeding N86-11442
CLEANING
The factory of the future N86-11228
CLEAR AIR TURBULENCE
Development of a wind shear performance envelope N86-11746
CLEARANCES
Effects of leakage through clearance seals on the performance of a 10 K Stirling-cycle refrigerator N86-11379
CLIMATE
Optimized ground-coupled heat pump system design for northern climate
[DE85-014065] N86-11484
Uncertainties in the radiative properties of smoke and their effects on climate assessments
[DE85-015187] N86-11691
A numerical study of global axisymmetric states and their stability to quasi-geostrophic disturbances N86-11753
Proceedings of the 9th Annual Climate Diagnostics Workshop
[PB85-183911] N86-11763
Monitoring climate in real time: An application of the Climate Anomaly Monitoring System (CAMS) N86-11765
Review of the climate of fall 1983 and winter 1983-84 N86-11766
Recent long-term climatic change over the eastern tropical and subtropical Pacific and its ramifications N86-11775

Relationships between Pacific northwest coast climate and ENSO events N86-11787
Atmospheric general circulation model simulations of the modern Antarctic climate N86-11790
Atmospheric response to an equatorial Pacific sea surface temperature anomaly: The effects of orography N86-11791
The effect of anomalous snow cover on the general circulation of the atmosphere using a simple climate model N86-11794
Interannual climate variability in a low vertical resolution spectral atmospheric model N86-11795
Climate system fluctuations, monitoring N86-11814

CLIMATOLOGY
Polar Research Board annual report 1984 and future plans
[PB85-204477] N86-11727
Climate simulation and change: A simple energy balance climate model N86-11731
Climatic events of the west coast of southern Africa N86-11784
Horizontal fluxes in real and model atmospheres N86-11792
Meteorological conditions during drought episodes in the United States Great Plains N86-11802

CLOCKS
Easy impossibility proofs for distributed concensus problems
[AD-A157411] N86-11903

CLOSED CYCLES
Reciprocating magnetic refrigerator N86-11371
A closed cycle cascade Joule Thomson refrigerator for cooling Josephson junction magnetometers N86-11388
Occurrence of pressure wave during spontaneous ignition of gas ahead of flame front in closed vessel N86-11965

CLOSED ECOLOGICAL SYSTEMS
Controlled environment life support system: Calcium-related leaf injuries on plants
[NASA-CR-176288] N86-11829

CLOSURES
Numerical simulation of an equipment hatch for a steel containment vessel to loading beyond the design basis
[DE85-010485] N86-11482

CLOUD COVER
Global relationships with the Southern Oscillation N86-11776

CLOUD PHYSICS
A new characterization of supercooled clouds below 10,000 feet AGL N86-11744
The utilization of satellite data and dynamics in understanding and predicting global weather phenomena
[NASA-CR-171577] N86-11749
On cloud street development in three dimensional parallel and Rayleigh instabilities N86-11754

CLOUDS
A new characterization of the icing environment below 10,000 feet AGL from 7,000 miles of measurements in supercooled clouds N86-11743

CLOUDS (METEOROLOGY)
Continuing design, review, and analysis work for the Sierra Cooperative Pilot Project
[PB85-204303] N86-11822

COAL
Evaluation of candidate materials in a static turbine cascade
[DE85-008592] N86-11480

COASTAL WATER
Information dissemination for a better understanding of Louisiana's water resources
[PB85-219079] N86-11660
Adverse weather impact on aviation safety, investigation and oversight N86-11742

COASTS
Precise geoid computations at mountainous coastlines in view of vertical datum determinations N86-11561
Discrimination of coastal vegetation and biomass: Using AIS data N86-11639
The distribution of rainfall along the coast of northern Peru during 1982-83 N86-11782
Peru coastal winds during 1982-1983 N86-11783
Climatic events of the west coast of southern Africa N86-11784
Several aspects of interannual variability in the California current system N86-11785

COATINGS
Wolter 1 type X-ray mirror system with mean resolution and maximum effective collecting area for the spectral region of 1-10 nm N86-12070
Thin film research. Volume 2
[AD-A157609] N86-12138

COCKPITS
Visual and motion cueing in helicopter simulation
[NASA-TM-86818] N86-11208

CODING
Probability encoding of hydrologic parameters for basalt. Elicitation of expert opinions from a panel of three basalt waste isolation project staff hydrologists
[DE85-014665] N86-11652
Modification of Huffman coding
[AD-A156479] N86-11899

COEFFICIENTS
The Shock and Vibration Digest, volume 17, no. 5
[AD-A156716] N86-11531
Stiffness and damping coefficients of rubber N86-11532
Time-averaging the flux-profile relationship N86-11789

COGENERATION
Advanced Thermionic Technology Program: Summary report, Volume 3
[DE85-009360] N86-11574

COGNITION
Adaptive motivation theory
[AD-A157440] N86-11851

COHERENT SCATTERING
Transition radiation and coherent electron-photon scattering
[DE85-014313] N86-12031

COHESION
Acoustic emission during deformation and fracture of A533B pressure vessel steel N86-11306

COLD CATHODE TUBES
A large area X-ray source and its preionization characteristics for XeCl excimer laser N86-11929

COLD FRONTS
Warm and cold episodes in the California current: A case for large-scale mid-latitude atmospheric forcing N86-11780

COLD GAS
Flame propagation in pulsed acceleration field N86-11964

COLD PLASMAS
Protective coatings of metal surfaces by cold plasma treatment
[NASA-TM-87152] N86-11475

COLD WATER
Perceptual and physiological responses during exercise in cool and cold water
[AD-A157334] N86-11840

COLD WEATHER
Optimized ground-coupled heat pump system design for northern climate
[DE85-014065] N86-11484
Blocking as an explanation of the severe cold of winter 1983-84 N86-11766
Recent unusual mean winter temperature across the contiguous United States N86-11772

COLLISION AVOIDANCE
Traffic Alert and Collision Avoidance System Signal Environment Model (TCAS SEM) programmer's reference manual
[FAA-PM-85-22] N86-11192

COLLISION PARAMETERS
SSC test lattices
[DE85-014240] N86-12098
Higher luminosities via alternative incident channels
[DE85-014355] N86-12118

COLLISIONAL PLASMAS
The ionization equilibrium of optically thick argon z-pinch plasmas for electron temperatures between 25 and 65 eV
[AD-A157484] N86-12078

COLLISIONS
Measurements of ultimate accelerating gradients in the SLAC disk-loaded structure
[DE85-014287] N86-12125

COLLOIDS
Elastic and inelastic light scattering of colloidal particles
[AD-A157335] N86-12072

COLOR
The optical polarization of Epsilon Aurigae through the 1982-84 eclipse N86-12171

COMBINED CYCLE POWER GENERATION
Evaluation of candidate materials in a static turbine cascade
[DE85-008592] N86-11480

COMBUSTIBLE FLOW
One-dimensional two-phase flow in combustion chamber of solid propellant rocket motors N86-11921
Surface combustion of liquid fuel in stream of gaseous oxidizer N86-11959
Flow reactor studies over wide temperature and pressure ranges of atom and radical reaction rates important in ignition and combustion
[AD-A156931] N86-12020

COMBUSTION
Characteristics of an axisymmetric sudden expansion flow
[NASA-CR-176278] N86-11485
Turbine Engine Hot Section Technology (HOST)
[NASA-CP-2289] N86-11496
Combustion hot section technology N86-11512
Explosion waves generated by deflagration combustion N86-11960
Calculation of formation time of minimal nucleus of flame during ignition of explosive mixtures by electrical discharges N86-11963
Assessment of technical strengths and information flow of energy conservation research in Japan. Volume 2: Background document
[DE85-013759] N86-12165

COMBUSTION CHAMBERS
An investigation of the effects of fuel composition on combustion characteristics in a T-63 combustor
[AD-A157325] N86-11359
Turbine engine Hot Section Technology (HOST) project N86-11496
Hot section viewing system N86-11498
Dynamic gas temperature measurement system N86-11499
Demonstration test of burner liner strain measurement systems: Interim results N86-11501
Combustion hot section technology N86-11512
The 3D inelastic analysis methods for hot section components N86-11516
The 3-D inelastic analysis methods for hot section components (base program) N86-11517
Validation of structural analysis methods using burner liner cyclic rig test data N86-11518
HOST liner cyclic facilities N86-11519
One-dimensional two-phase flow in combustion chamber of solid propellant rocket motors N86-11921

COMBUSTION PRODUCTS
Explosion waves generated by deflagration combustion N86-11960
Flame propagation in pulsed acceleration field N86-11964

COMBUSTION STABILITY
Pressure-coupled response function of solid propellants including those with negative pressure-exponents N86-11924

COMMERCE
Commercialization of space: National policy and defense needs
[AD-A156517] N86-12162

COMMITTEE ON SPACE RESEARCH
SPACEWARN Bulletin
[NASA-TM-87512] N86-11222

COMMUNICATION
Considerations for millimeter wave, monolithic phased arrays N86-11399
Corporate/commuter airlines meteorological requirements N86-11739

COMMUNICATION NETWORKS
Voice communications over packet radio networks
[AD-A157478] N86-11411
MICROLAN, file transfer program for microprocessors
[AD-A156519] N86-11900
A numerical analysis of a queue with network access flow control
[AD-A157526] N86-11913

COMMUNICATION THEORY
New R and D in Chinese language information processing N86-11996

COMPACTING
The hollow sphere model for porous metals and metal powders N86-11308
Synthesis of nickel-aluminum alloys by shock compression of composite particles
[DE85-015165] N86-11326

COMPARISON
Comparisons of different observation methods of a LaCoste and Romberg G gravimeter N86-11612
Performance of solar collector arrays and collector controllers in the National Solar Data Network
[DE85-001297] N86-11663

COMPATIBILITY
Compatibilizing effect of random or block copolymer added to binary mixture of homopolymers
[AD-A157384] N86-11345

COMPILERS
Ada (trademark) compiler validation summary report: Data general corporation, ADE Ada Compiler, version 2.30.03.12, Eclipse DS/4000, DS/4200, MV/4000-DC, MV/8000-C, MV/8000-2, MV/10000, MV/10000 SX using AOS/VS 5.04 and AOS/RT32 4.001.00
[AD-A157573] N86-11890

Ada (trademark) compiler validation summary report: Verdix Ada Compiler, Verdix Ada Development System (VADS) VAds-010-1010, version V05.00, for Sun Microsystems Model 2/120 using UNIX (trademark) 4.2 BSD, release 1.1
[AD-A157574] N86-11891
Military standard common APSE (Ada Programming Support Environment) interface set (CAIS)
[AD-A157589] N86-11905

COMPLEX COMPOUNDS
Identification of metal ion chloro complexes in an ambient temperature molten salt
[AD-A157295] N86-11302

COMPOSITE MATERIALS
Mechanical fasteners for advanced composite materials N86-11232
Reduction of moisture effects during the cure of epoxy adhesives used in composite repair N86-11254
High Temperature Polymer Matrix Composites
[NASA-CP-2385] N86-11260
A program to determine the effect of low-velocity impacts on the strength of the filament-wound rocket motor case for the space shuttle
[NASA-TM-87588] N86-11292
Interaction of mixed mode loading on cyclic debonding in adhesively bonded composite joints
[NASA-CR-177990] N86-11298
Manual for LDEF tensile tests
[NASA-TM-87624] N86-11299
Strength and flexibility properties of advanced ceramic fabrics
[NASA-TM-86824] N86-11340

COMPOSITE PROPELLANTS
Pressure-coupled response function of solid propellants including those with negative pressure-exponents
N86-11924

COMPOSITE STRUCTURES
Feasibility of remotely manipulated welding in space: A step in the development of novel joining technologies
N86-11246
Advances in joining techniques used in development of SPF/DB titanium sandwich reinforced with metal matrices N86-11247
High-temperature adhesive development and evaluation N86-11250
Composite structural materials
[NASA-CR-176279] N86-11293
Generic structural elements N86-11296

COMPOSITION (PROPERTY)
Physical property changes of a lithia-alumina-silica based glass as a function of composition
[DE85-015610] N86-11352
An investigation of the effects of fuel composition on combustion characteristics in a T-63 combustor
[AD-A157325] N86-11358
Anelasticity in the Earth's mantle: Implications for the frequency dependence of Love numbers N86-11590

COMPRESSIBLE FLOW
Airflow calibration of a bellmouth inlet for measurement of compressor airflow in turbine-powered propulsion simulators
[NASA-TM-84399] N86-11209
A computational model for a regenerator N86-11386

COMPRESSIBLE FLUIDS
The stability of Timoshenko beams conveying a compressible fluid N86-11492

COMPRESSION LOADS
Evaluation of superplastic forming and weld-brazing for fabrication of titanium compression panels N86-11245
Chemical synthesis under shock compression
[DE85-015166] N86-11325
Numerical simulation of a sample recovery fixture for high velocity impact
[DE85-013965] N86-11485
Sandia shock compression database
[DE85-015141] N86-12142

COMPRESSORS
Improved heat switch for gas sorption compressor
N86-11372
The design of a small linear-resonant, split Stirling cryogenic refrigerator compressor N86-11392
Hermetic bellows seal for Braun linear engine: Design, test and demonstration
[DE85-013545] N86-11478

COMPTON EFFECT
X-ray inverse Compton emission from the radio halo of M87
[NASA-CR-176305] N86-12196
X-ray inverse Compton emission from the radio halo of M87
[NASA-CR-176304] N86-12197

COMPUTATION
Calculation of thermal trapping in shear bands
[DE85-014404] N86-11336
Fire growth in combat ships
[NBSIR-85/3159] N86-11364
Block-implicit coupled calculation of fluid flows
[DE85-004038] N86-11432
Experimental needs of high temperature concrete
[DE85-009700] N86-11541
Precise geoid computations at mountainous coastlines in view of vertical datum determinations N86-11561
A hybrid vortex-in-cell finite-difference numerical method for turbulent shear layer computation N86-11886
Integrated analysis of error detection and recovery
[NASA-CR-172571] N86-11906
Computation of minimal isovist sets
[AD-A157624] N86-11915
Calculation of formation time of minimal nucleus of flame during ignition of explosive mixtures by electrical discharges N86-11963

COMPUTATIONAL FLUID DYNAMICS
Aerodynamics and Acoustics of Propellers
[AGARD-CP-366] N86-11147
Aerodynamic method used in France for advanced fast propeller study N86-11149
Design concept and performance prediction technique for potential flows around advanced propellers
N86-11150
A review of ARA research into propeller aerodynamic prediction methods N86-11151
Aerodynamics of wide-chord propellers in non-axisymmetric flow N86-11153
A unified approach for the aerodynamics and acoustics of propellers in forward motion N86-11155
Theoretical analysis of linearized acoustics and aerodynamics of advanced supersonic propellers
N86-11156
A general theory of arbitrary motion aerodynamics using an aeroacoustic approach N86-11157
Development of a Navier-Stokes analysis for the flow in disk pumps
[AD-A157454] N86-11428
Coolant passage heat transfer with rotation. A progress report on the computational aspects N86-11510
On the implementation of a class of upwind schemes for system of hyperbolic conservation laws
[NASA-TM-86839] N86-11907
Algebraic grid generation using tensor product B-splines N86-11908
On symmetric and upwind TVD schemes
[NASA-TM-86842] N86-11909
One-dimensional two-phase flow in combustion chamber of solid propellant rocket motors N86-11921

COMPUTATIONAL GRIDS
Particle pushing techniques for use with finite element based field calculations N86-11865
Three-dimensional heat transfer analysis using the PATRAN-G solids modeling and Q-TRAN thermal analysis computer codes N86-11867

COMPUTER AIDED DESIGN
A nonproprietary, nonsecret program for calculating Stirling cryocoolers N86-11384
Computer-aided bifocal dielectric lens antenna design for MH wave application N86-11410
ADS: A FORTRAN program for automated design synthesis: Version 1.10
[NASA-CR-177985] N86-11894
A general purpose CAD program for microwave linear circuits N86-12002

COMPUTER ASSISTED INSTRUCTION
A computer-based educational approach to the Air Command and Staff College associate program
[AD-A156460] N86-12160

COMPUTER GRAPHICS
Sixth Biennial CUBE (Computer Use By Engineers) Symposium
[LA-10240-C] N86-11858
An evaluation of three graphics packages: The methodology and results N86-11870
Interactive graphics for finite element preprocessing
N86-11871
Geological calculations with SANGRE and MANTLE: Recent results N86-11872
A data translator for engineering measurements
N86-11875
Data analysis using a data base driven graphic animation system
[DE85-014635] N86-11892

COMPUTER NETWORKS
Hardware and software constructs for a vibration analysis network
[DE85-008436] N86-11535
The embedded operating system project
[NASA-CR-176280] N86-11893
Probabilistic analysis of a network resource allocation algorithm
[AD-A157553] N86-11904

COMPUTER PROGRAM INTEGRITY
Computational errors and their control in the determination of satellite orbits N86-11211

COMPUTER PROGRAMMING
Expert systems development and application
[NASA-TM-86746] N86-11194
Application of an objective analysis scheme to mesoscale observational network design
[AD-A156911] N86-11760
Sixth Biennial CUBE (Computer Use By Engineers) Symposium
[LA-10240-C] N86-11858
Software engineering tools that work N86-11859
Research in the design of high-performance reconfigurable systems
[NASA-CR-176275] N86-11897

COMPUTER PROGRAMS
An investigation of in-flight near-field propeller noise generation and transmission N86-11171
Methods to calculate the response time of heat and smoke detectors installed below large unobstructed ceilings
[NBSIR-85/3167] N86-11365
A nonproprietary, nonsecret program for calculating Stirling cryocoolers N86-11384
Calculation of RF fields in axisymmetric cavities
[DE85-014135] N86-11414
Introduction to the session on: Numerical methods for two-phase flow
[DE85-012651] N86-11435
NERF: A computer program for the numerical evaluation of reliability functions user manual
[ARL/STRUC-R-411] N86-11487
Hardware and software constructs for a vibration analysis network
[DE85-008436] N86-11535
Tracer test analysis of the Klamath Falls geothermal resource: A comparison of models
[DE85-009924] N86-11678
Numerical solution of ionospheric filtration of ULF waves. Part 1: Method N86-11712
Sixth Biennial CUBE (Computer Use By Engineers) Symposium
[LA-10240-C] N86-11858
Software engineering tools that work N86-11859
An application of real-time analysis and design tools in software development N86-11860
Design optimization of the power generation system for a space-based free-electron laser N86-11861
Optical modeling of multilayer thin/thick films
N86-11862
Calculation of the electron backscattering coefficient by Monte Carlo simulation N86-11864
Particle pushing techniques for use with finite element based field calculations N86-11865
ICARUS: A computer code for modeling complex one-dimensional heat conduction on mainframes and micros N86-11866
Three-dimensional heat transfer analysis using the PATRAN-G solids modeling and Q-TRAN thermal analysis computer codes N86-11867
Analysis of ultrasonic waves in a bounded medium
N86-11869
An evaluation of three graphics packages: The methodology and results N86-11870
Interactive graphics for finite element preprocessing
N86-11871
Geological calculations with SANGRE and MANTLE: Recent results N86-11872
SIG: A general-purpose signal processing code
N86-11876
Finite difference calculations of voltages generated in thin dielectric layers subjected to shock loading
N86-11878
Photoelectron trajectory analyses of streak tubes
N86-11880
Heat transfer and pressure changes due to a large temperature difference across an enclosed vertical air layer N86-11884
Flexible vibrations of a uniform elastic beam with arbitrary supports and lumped masses N86-11885
Computer codes for fluid-structure interactions
N86-11887
ADS: A FORTRAN program for automated design synthesis: Version 1.10
[NASA-CR-177985] N86-11894
KRASH85 user's guide: Input/output format
[FAA-CT-85-10] N86-11898
MICROLAN, file transfer program for microprocessors
[AD-A156519] N86-11900
Bayesian extensions to a basic model of software reliability
[AD-A157296] N86-11901
Approximate reasoning and the REVEAL software system. Users guide
[AD-A157298] N86-11902
Integrated analysis of error detection and recovery
[NASA-CR-172571] N86-11906

A general purpose CAD program for microwave linear circuits N86-12002
A numerical method of calculating propeller noise including acoustic nonlinear effects N86-12011
Physics modeling of tandem mirror devices with high field test cell inserts [DE85-011870] N86-12086

COMPUTER SYSTEMS DESIGN
Computational structural mechanics: A new activity at the NASA Langley Research Center [NASA-TM-87612] N86-11540
Research in the design of high-performance reconfigurable systems [NASA-CR-176275] N86-11897
Third National Academic Machine Retrieval Conference held in Zhenjiang N86-11999

COMPUTER SYSTEMS PROGRAMS
Traffic Alert and Collision Avoidance System Signal Environment Model (TCAS SEM) programmer's reference manual [FAA-PM-85-22] N86-11192

COMPUTER TECHNIQUES
Computational structural mechanics: A new activity at the NASA Langley Research Center [NASA-TM-87612] N86-11540
Research on the computational methods of gravity topographic effect N86-11578
Sixth Biennial CUBE (Computer Use By Engineers) Symposium [LA-10240-C] N86-11858
Software engineering tools that work N86-11859
An application of real-time analysis and design tools in software development N86-11860
Improving the comprehensibility of a simulated technical manual [AD-A157482] N86-11889
China report: Science and technology [JPRS-CST-85-014] N86-11918
China report: Science and technology [JPRS-CST-85-015] N86-11994
Third National Academic Machine Retrieval Conference held in Zhenjiang N86-11999
Computer application in atomic absorption spectrometry N86-12001
A computer-based educational approach to the Air Command and Staff College associate program [AD-A156460] N86-12160

COMPUTERIZED SIMULATION
Basic EMC technology advancement for C(3) systems. Volume 3B: Computer simulation of EMI effects in a differential line receiver [AD-A156505] N86-11416
Block-implicit multigrid calculation of three-dimensional recirculating flows [DE85-010250] N86-11434
Numerical simulation of an equipment hatch for a steel containment vessel to loading beyond the design basis [DE85-010485] N86-11482
Numerical simulation of a sample recovery fixture for high velocity impact [DE85-013965] N86-11485
Gas flow environmental and heat transfer nonrotating 3D program N86-11506
Stirling cycle heat pump studies [DE85-005365] N86-11680
Magnification of low-sensitivity channels in seismographs with standard characteristics N86-11709
User guide for WIFM-SAL (WES Implicit Flooding Model-SAL): A two-dimensional vertically integrated, time-varying estuarine transport model [AD-A157446] N86-11825
An evaluation of CASP (computer assisted search planning program) drift predictions near the New England Shelf/Slope Front [AD-A157447] N86-11826
Sixth Biennial CUBE (Computer Use By Engineers) Symposium [LA-10240-C] N86-11858
Design optimization of the power generation system for a space-based free-electron laser N86-11861
Net-2 models of cavities and diodes N86-11863
ICARUS: A computer code for modeling complex one-dimensional heat conduction on mainframes and micros N86-11866
Interface elements for heat transfer analysis N86-11868
CELCAP: A computer model for cogeneration system analysis [NASA-CR-176306] N86-11896
Computer application in atomic absorption spectrometry N86-12001
SIMPLODE: An imploding gas puff plasma model. 1. Neon [AD-A157456] N86-12077
Simulation of quiet start magnetized plasmas, including Maxwellian and velocity-space ring distributions [DE85-014394] N86-12112
Particle simulation of the low-(ALPHA) Pierce diode [DE85-014435] N86-12113
Acceleration simulation in the LAMPF 2 booster [DE85-012695] N86-12126

COMPUTERS
The factory of the future N86-11228
Hardware and software constructs for a vibration analysis network [DE85-008436] N86-11535

CONCRETE STRUCTURES
Numerical simulation of an equipment hatch for a steel containment vessel to loading beyond the design basis [DE85-010485] N86-11482
Experimental needs of high temperature concrete [DE85-009700] N86-11541
Concrete creep at transient temperature: Constitutive law and mechanism [DE85-010525] N86-11542

CONCRETES
Viscoelastic creep of high-temperature concrete [DE85-010511] N86-11539
Experimental needs of high temperature concrete [DE85-009700] N86-11541
Concrete creep at transient temperature: Constitutive law and mechanism [DE85-010525] N86-11542
Evaluation of concrete creep and stress redistribution in a prototypic PCRV following rupture of prestressing tendons [DE85-007673] N86-11543

CONDUCTIVE HEAT TRANSFER
Three-dimensional heat transfer analysis using the PATRAN-G solids modeling and Q-TRAN thermal analysis computer codes N86-11867
Double tearing mode in plasma with magnetic braiding N86-11919

CONDUCTORS
A summary report on the Flat-Plate Solar Array Project Workshop on Transparent Conducting Polymers [NASA-CR-176302] N86-11669

CONES
Calibration of the NCAR (National Center for Atmospheric Research) Sabreliner research static pressure source with a trailing cone assembly [PB85-191005] N86-11200

CONFERENCES
Welding, Bonding and Fastening, 1984 [NASA-CP-2387] N86-11227
Proceedings of the Third Cryocooler Conference [NASA-CR-176298] N86-11367
Proceedings of the 1984 Antenna Applications Symposium [AD-A153257] N86-11398
Proceedings of the 5th International Symposium Geodesy and Physics of the Earth, part 1 [REPT-81-PT-1] N86-11549
Proceedings of the 5th International Symposium Geodesy and Physics of the Earth, part 2 [REPT-81-PT-2] N86-11568
Proceedings of the Airborne Imaging Spectrometer Data Analysis Workshop [E86-10001] N86-11618
Workshop on Permafrost Geophysics [AD-A157485] N86-11719
Third National Academic Machine Retrieval Conference held in Zhenjiang N86-11999
AGS polarized beam facility [DE85-011834] N86-12038
EPR: What has it taught us [DE85-014525] N86-12157

CONFIDENCE LIMITS
Uncertainty assessment in life cycle cost analysis [AD-A157414] N86-11486

CONFINEMENT
Energy confinement experiments on Doublet 3 with high power neutral beam heating [DE85-014324] N86-12110
Energy confinement in a high-current reversed field pinch [DE85-015009] N86-12111

CONICAL BODIES
Upgrade of the EM transient range monocone antenna [DE85-013181] N86-11413

CONICAL NOZZLES
Overview of solid particle LV seeding techniques used at UTRC N86-11445

CONICAL SHELLS
Simple construction and performance of a conical plastic cryocooler N86-11378

CONSERVATION EQUATIONS
A time-splitting numerical technique for solving highly coupled two-phase flow conservation equation N86-11879

CONSERVATION LAWS
On the implementation of a class of upwind schemes for system of hyperbolic conservation laws [NASA-TM-86839] N86-11907
On symmetric and upwind TVD schemes [NASA-TM-86842] N86-11909

CONSTANTS
Probabilistic analysis of a network resource allocation algorithm [AD-A157553] N86-11904

CONSTRUCTION
Uncertainty assessment in life cycle cost analysis [AD-A157414] N86-11486

CONSTRUCTION MATERIALS
Acetylene terminated matrix resins N86-11261

CONTACT POTENTIALS
Treatment of the geodetic boundary value problem by contact-transformation N86-11573

CONTACTORS
Multi-megampere current interruption from explosive deformation of conductors [DE85-012756] N86-11419

CONTAINMENT
High temperature molten salt containment [DE85-012152] N86-11433
Numerical simulation of an equipment hatch for a steel containment vessel to loading beyond the design basis [DE85-010485] N86-11482
Experimental needs of high temperature concrete [DE85-009700] N86-11541
Concrete creep at transient temperature: Constitutive law and mechanism [DE85-010525] N86-11542

CONTAMINANTS
Intergranular attack and stress corrosion cracking of alloy 600 in high-temperature caustic solutions containing contaminants [DE85-014106] N86-11335
Current research on circular saw and band saw vibration and stability N86-11533

CONTAMINATION
Manual for LDEF tensile tests [NASA-TM-87624] N86-11299
Psychological aspects of personnel contamination [DE85-012955] N86-11853

CONTINENTAL SHELVES
An evaluation of CASP (computer assisted search planning program) drift predictions near the New England Shelf/Slope Front [AD-A157447] N86-11826

CONTINUITY EQUATION
Hydrodynamics of liquid-vapor disperse annular flows in channels containig bundles of heated rods under nonsteady-state conditions N86-11954

CONTINUOUS WAVE LASERS
Distributed-feedback lasers with active framing medium N86-11971
Optimization of parameters of chemical CO laser by increasing length of active medium N86-11976

CONTINUUM FLOW
Applications of the magneto-optical filter to stellar pulsation measurements [NASA-CR-176282] N86-12187

CONTROL
Superconducting Magnetic Energy Storage (SMES) Program [DE85-014250] N86-12106

CONTROL EQUIPMENT
Modification of a Hughes tiltmeter to a borehole tiltmeter N86-11563
Multivariable current control for electrically and magnetically coupled superconducting magnets, revision 1 [DE85-012943] N86-12108

CONTROL STABILITY
Mission-oriented requirements for updating MIL-H-8501: Calspan proposed structure and rationale [NASA-CR-177371] N86-11204
Passive motion control of pneumatically driven displacers in cryogenic coolers N86-11383

CONTROL SYSTEMS DESIGN
Description of an experimental expert system flight status monitor [NASA-TM-86791] N86-11195
Problems experienced and envisioned for dynamical physical systems [NASA-TP-2508] N86-11215
A direct model reference adaptive approach to the control of space stations N86-11219

CONTROL THEORY
Flight worthiness of fire resistant hydraulic systems: Volume 1
[AD-A157618] N86-11199
USSR report: Physics and mathematics
[JPRS-UPM-85-005] N86-11945
CONTROLLABILITY
Preliminary design study of a lateral-directional control system using thrust vectoring
[NASA-TM-86425] N86-11203
Visual and motion cueing in helicopter simulation
[NASA-TM-86818] N86-11208
CONTROLLED FUSION
Controlled thermonuclear fusion, high temperature plasma physics N86-11998
CONTROLLERS
Research in the design of high-performance reconfigurable systems
[NASA-CR-176275] N86-11897
CONVECTION
A numerical study of global axisymmetric states and their stability to quasi-geostrophic disturbances N86-11753
Cloud streets during KonTur: A comparison of parallel/thermal instability modes with observations N86-11755
Circulation and weather for MAM and JJA 1984 N86-11769
Application of Flux-Corrected Transport (FCT) to heat transfer/fluid mechanics problems N86-11883
Heat transfer and pressure changes due to a large temperature difference across an enclosed vertical air layer N86-11884
CONVECTION CLOUDS
Subseasonal and interannual variations of tropical convection and the El Nino/Southern Oscillation N86-11779
Automated method for the documentation of cloud-top characteristics of mesoscale convective systems
[PB85-204246] N86-11823
CONVECTION CURRENTS
On cloud street development in three dimensional parallel and Rayleigh instabilities N86-11754
Tropical convection and North American cyclones during the 1982-83 El Nino N86-11809
Flame propagation in pulsed acceleration field N86-11964
CONVECTIVE FLOW
Application of the vortex-lattice concept to flows with smooth-surface separation
[AD-A157571] N86-11430
CONVECTIVE HEAT TRANSFER
Thermal convection in snow
[AD-A157577] N86-11648
On convective effects in gas lasers N86-12006
CONVERGENCE
A direct model reference adaptive approach to the control of space stations N86-11219
Proceedings of the 5th International Symposium Geodesy and Physics of the Earth, part 2
[REPT-81-PT-2] N86-11568
COOLANTS
Coolant passage heat transfer with rotation. A progress report on the computational aspects N86-11510
COOLERS
Proceedings of the Third Cryocooler Conference
[NASA-CR-176298] N86-11367
Design of cryocoolers for microwatt superconducting devices N86-11368
Recent cryocooler progress in Japan N86-11369
Classification of cryocoolers N86-11374
An experimental study for a miniature Stirling refrigerator N86-11375
Design of a flight qualified long-life cryocooler N86-11377
Simple construction and performance of a conical plastic cryocooler N86-11378
Effects of leakage through clearance seals on the performance of a 10 K Stirling-cycle refrigerator N86-11379
An experimental reciprocating expander for cryocooler application N86-11380
Experiments with a fully instrumented split Stirling cryocooler N86-11381
Low frequency split cycle cryocooler N86-11382
Passive motion control of pneumatically driven displacers in cryogenic coolers N86-11383
A nonproprietary, nonsecret program for calculating Stirling cryocoolers N86-11384
COOLING SYSTEMS
Reciprocating magnetic refrigerator N86-11371
COORDINATES
Application of an objective analysis scheme to mesoscale observational network design
[AD-A156911] N86-11760
Algebraic grid generation using tensor product B-splines N86-11908
COPOLYMERIZATION
Chemical control of rate and onset temperature of nadimide polymerization N86-11271
COPOLYMERS
Compatibilizing effect of random or block copolymer added to binary mixture of homopolymers
[AD-A157384] N86-11345
COPPER
Explosive welding of aluminum, titanium and zirconium to copper sheet metal N86-11241
Improved heat switch for gas sorption compressor N86-11372
Mechanical threshold of dynamically deformed copper and nitronic 40
[DE85-010779] N86-11545
Kinetics analysis of diffusion of point defects to dislocations following pulsed neutron and electron irradiations
[DE85-012768] N86-12037
COPPER ALLOYS
Environmental effects in the fatigue behavior of copper nickel alloys N86-11307
The yield point of copper-zinc alloys in the alpha solid solution range
[BLL-BISI-TRANS-23046-(9022.06)] N86-11311
Overview of MIT, ADIP irradiation experiments
[DE85-014469] N86-12060
CORAL REEFS
Coral reef hydrogeology
[DE85-012923] N86-11828
CORPUSCULAR RADIATION
Determination of the depth of a conductivity anomaly by separating the geomagnetic variation field into its external and internal part N86-11711
CORRECTION
Correcting for particle counting bias error in turbulent flow N86-11439
Research on the computational methods of gravity topographic effect N86-11578
On the comparison and choice between the formulas of the Earth tidal correction in astronomical time and latitude observation N86-11588
SSC test lattices
[DE85-014240] N86-12098
Non-geometrical optics investigation of mode conversion in weakly relativistic inhomogenous plasmas
[DE85-013480] N86-12102
CORRELATION
Some aeroacoustic wind tunnel measurements, theoretical predictions, and flight-test correlations on subsonic aircraft propellers N86-11170
Correlations of chemical, microstructural and mechanical properties of polyethylene piping materials
[DE85-013077] N86-11351
Anew about the correlation between Mohorovicic discontinuity depths, geoid undulations and Bouguer gravity anomalies in the Dinaric-Pannonian region of Yugoslavia N86-11557
On the long-wavelength correlation between gravity and topography N86-11586
Prediction of monthly 700 mb heights using antecedent and simulated prognostic height predictors N86-11805
CORRELATION COEFFICIENTS
Temperature and precipitation trends in North America N86-11774
CORROSION
Corrosion-preventive primers for military equipment
[AD-A156927] N86-11341
Evaluation of candidate materials in a static turbine cascade
[DE85-008592] N86-11480
CORROSION PREVENTION
Adhesives for aerospace N86-11249
Cathodic protection of aluminium structures
[KIS-1985:4E] N86-11313
Corrosion-preventive primers for military equipment
[AD-A156927] N86-11341
Failure rate model for cathodic delamination of protective coatings
[AD-A157483] N86-11912
CORROSION RESISTANCE
Stress corrosion resistant fasteners N86-11235
Environmental effects in the fatigue behavior of copper nickel alloys N86-11307
Short-term methods for atmospheric corrosion testing: Survey of the literature
[KIS-1985:5E] N86-11314
High temperature molten salt containment
[DE85-012152] N86-11433
CORROSION TESTS
Corrosion testing by radiographic methods
[BLL-BISI-TRANS-23201-(9022.06)] N86-11310
Short-term methods for atmospheric corrosion testing: Survey of the literature
[KIS-1985:5E] N86-11314
COSMIC RAYS
Cosmogenic-nuclide production by primary cosmic-ray protons
[DE85-012760] N86-12198
COSMOLOGY
Research in elementary particle physics
[DE85-014062] N86-12041
COST ANALYSIS
Uncertainty assessment in life cycle cost analysis
[AD-A157414] N86-11488
COST EFFECTIVENESS
Explosive generators for low-cost pulsed power
[DE85-013436] N86-11421
COUNTING
Correcting for particle counting bias error in turbulent flow N86-11439
COUPLING
On the influence of coupling torques between the Earth's core and mantle on parameters and components of the rotation of the Earth N86-11572
High resolution spectrometer in studies of e(+)e(-) annihilation at (radical)s = 29 GeV
[DE85-013870] N86-12065
COUPLING COEFFICIENTS
Block-implicit coupled calculation of fluid flows
[DE85-004038] N86-11432
Short-period SVSN-4 seismograph N86-11708
Magnification of low-sensitivity channels in seismographs with standard characteristics N86-11709
COVARIANCE
A body tensor formalism for elastic-plastic continua with applications in uniaxial extension N86-11491
CRACK PROPAGATION
Advances in joining techniques used in development of SPF/DB titanium sandwich reinforced with metal matrices N86-11247
High-temperature adhesive development and evaluation N86-11250
Use of hydration inhibitors to improve bond durability of aluminum adhesive joints N86-11251
Deformation and fracture of P/M titanium alloys
[AD-A157416] N86-11317
Intergranular attack and stress corrosion cracking of alloy 600 in high-temperature caustic solutions containing contaminants
[DE85-014106] N86-11335
CRACKING (FRACTURING)
Interaction of mixed mode loading on cyclic debonding in adhesively bonded composite joints
[NASA-CR-177990] N86-11298
Experimental needs of high temperature concrete
[DE85-009700] N86-11541
Concrete creep at transient temperature: Constitutive law and mechanism
[DE85-010525] N86-11542
CRACKS
Senstivity of using blunt and sharp crack models in elastic-plastic fracture mechanics
[DE85-010288] N86-11537
CRASHES
KRASH85 user's guide: Input/output format
[FAA-CT-85-10] N86-11898
CRASHWORTHINESS
KRASH85 user's guide: Input/output format
[FAA-CT-85-10] N86-11898
CREEP PROPERTIES
Creep and fracture of a yttria dispersed nickel-chromium alloy N86-11309
Creep fatigue life prediction for engine hot section materials (isotropic) N86-11521
Viscoelastic creep of high-temperature concrete
[DE85-010511] N86-11539
Evaluation of concrete creep and stress redistribution in a prototypic PCRV following rupture of prestressing tendons
[DE85-007673] N86-11543
CREEP RUPTURE STRENGTH
High pressure strength of shocked aluminum
[DE85-014461] N86-11547
CRITICAL TEMPERATURE
Discussion of the superconducting critical temperature in a N-S multi-film structure N86-11936
Theory of the critical temperature for superconductors with small lambda (1) N86-11937
CROP DUSTING
Recent achievements, problems in cropdusting work N86-11180
CROP GROWTH
Evaluation of AIS data for agronomic and range and vegetation: Preliminary results for August 1984 flight over Nebraska Sandhills Agricultural Laboratory N86-11627
Controlled environment life support system: Calcium-related leaf injuries on plants
[NASA-CR-176288] N86-11829

CROP IDENTIFICATION

Evaluation of AIS data for agronomic and rangeland vegetation: Preliminary results for August 1984 flight over Nebraska Sandhills Agricultural Laboratory N86-11627

AIS investigation of agricultural monocultures N86-11640

CROP VIGOR

Evaluation of AIS data for agronomic and rangeland vegetation: Preliminary results for August 1984 flight over Nebraska Sandhills Agricultural Laboratory N86-11627

CROPS

Recent achievements, problems in cropdusting work N86-11180

CROSS COUPLING

Discussion of the superconducting critical temperature in a N-S multi-film structure N86-11936

CROSS FLOW

Jet array impingement heat transfer characteristics N86-11511

CROSSLINKING

Bismaleimides and related maleimido polymers as matrix resins N86-11265

Replacement of MDA with more oxidatively stable diamines in PMR-polyimides N86-11275

CRUSTAL FRACTURES

Tracer test analysis of the Klamath Falls geothermal resource: A comparison of models [DE85-009924] N86-11678

CRYOGENIC COOLING

Proceedings of the Third Cryocooler Conference [NASA-CR-176298] N86-11367

Design of cryocoolers for microwatt superconducting devices N86-11368

Magnetic refrigeration for low-temperature applications N86-11370

Improved heat switch for gas sorption compressor N86-11372

Hydride absorption refrigerator system for ten Kelvin and below N86-11373

A nonproprietary, nonsecret program for calculating Stirling cryocoolers N86-11384

Criteria for scaling heat exchangers to miniature size N86-11387

A small helium liquifier which provides continuous cooling based on cycled isentropic expansion N86-11389

Vuilleumier cycle cryocooler operating below 8 K N86-11390

The design of a small linear-resonant, split Stirling cryogenic refrigerator compressor N86-11392

Joule-Thomson valves for long term service in space cryocoolers N86-11393

CRYOGENIC EQUIPMENT

Recent cryocooler progress in Japan N86-11369

Classification of cryocoolers N86-11374

An experimental study for a miniature Stirling refrigerator N86-11375

Parametric testing of a linearly driven Stirling cryogenic refrigerator N86-11376

Design of a flight qualified long-life cryocooler N86-11377

Simple construction and performance of a conical plastic cryocooler N86-11378

Effects of leakage through clearance seals on the performance of a 10 K Stirling-cycle refrigerator N86-11379

An experimental reciprocating expander for cryocooler application N86-11380

Experiments with a fully instrumented split Stirling cryocooler N86-11381

Low frequency split cycle cryocooler N86-11382

Passive motion control of pneumatically driven displacers in cryogenic coolers N86-11383

Materials studies for magnetic fusion energy applications at low temperatures. 7: Technical reports [DE85-014518] N86-12101

CRYOGENIC FLUID STORAGE

NASA Lewis Research Center low-gravity fluid management technology program [NASA-TM-87145] N86-11218

CRYOGENIC FLUIDS

NASA Lewis Research Center low-gravity fluid management technology program [NASA-TM-87145] N86-11218

CRYOGENIC MAGNETS

Materials studies for magnetic fusion energy applications at low temperatures. 7: Technical reports [DE85-014518] N86-12101

CRYOGENIC WIND TUNNELS

Investigation of low-temperature solders for cryogenic wind tunnel models N86-11230

Initial investigation of cryogenic wind tunnel model filler materials N86-11255

CRYOGENICS

NTF: Soldering technology development for cryogenics N86-11231

Design of cryocoolers for microwatt superconducting devices N86-11368

Design of a flight qualified long-life cryocooler N86-11377

CRYOPUMPING

Proceedings of the Third Cryocooler Conference [NASA-CR-176298] N86-11367

CRYSTAL DEFECTS

Statics and adiabatic dynamics of nonlinear excitations in defected polyacetylene [DE85-014118] N86-12143

CRYSTAL GROWTH

Solid-melt interface studies of high-speed silicon sheet growth [DE85-008783] N86-11349

Bridgman growth of semiconductors [NASA-CR-177971] N86-11426

Improved solid state laser sources, volume 3 [DE85-012956] N86-11469

The interface structure of grain boundaries in polysilicon N86-11665

Pb(1-x)Sn(x)Te and Pb(1-y)Sn(y)Se laser crystals N86-11931

Deep levels in semi-insulating GaAs N86-11943

Model of amorphous silicon layer regrowth [DE85-012608] N86-12145

Investigation on growth and laser properties of GGG:(Nd,Cr) single crystal [DE85-014282] N86-12151

CRYSTAL LATTICES

Surface and interfacial properties of Ga0.47In0.53As alloys [AD-A157343] N86-11316

Crystal class and the electrooptic effect [DE85-015240] N86-11353

Statics and adiabatic dynamics of nonlinear excitations in defected polyacetylene [DE85-014118] N86-12143

CRYSTAL OPTICS

High-efficiency Al sub 2 O sub 3:Ti sup 3+ tunable laser N86-11973

CRYSTAL STRUCTURE

Crystal class and the electrooptic effect [DE85-015240] N86-11353

The interface structure of grain boundaries in polysilicon N86-11665

Icosahedral incommensurate crystals [DE85-012512] N86-12147

New harmonic materials: Index engineering: Thin-thick quadrature frequency conversion [DE85-012976] N86-12156

CRYSTALLINITY

Melting of crystalline and amorphous silicon by Ruby, XeCl and KrF laser irradiation [DE85-015040] N86-11468

CRYSTALLIZATION

Physical property changes of a lithia-alumina-silica based glass as a function of composition [DE85-015610] N86-11352

CRYSTALLOGRAPHY

A summary report on the Flat-Plate Solar Array Project Workshop on Transparent Conducting Polymers [NASA-CR-176302] N86-11669

Deep levels in semi-insulating GaAs N86-11943

CRYSTALS

Crystal class and the electrooptic effect [DE85-015240] N86-11353

Distributed-feedback lasers with active framing medium N86-11971

Chromium- and neodymium-activated gadolinium-scandium-gallium garnet crystal: A new laser active medium N86-11979

Soviet research on crystal channeling of charged particle beams [AD-A157353] N86-12022

Icosahedral incommensurate crystals [DE85-012512] N86-12147

CUBIC LATTICES

Fractal-like, but non-fractal, behavior of one step dipolar energy transfer on regular lattices with excluded volume [AD-A157382] N86-12136

CURIE TEMPERATURE

Itinerant electron ferromagnetism in Fe-alloyed, Ni3Al based materials [DE85-013989] N86-11331

CURING

Adhesives for aerospace N86-11249

High-temperature adhesive development and evaluation N86-11250

Factors affecting the processing of epoxy film adhesives N86-11252

Reduction of moisture effects during the cure of epoxy adhesives used in composite repair N86-11254

PMR polyimides from solutions containing mixed endcaps N86-11263

Bismaleimides and related maleimido polymers as matrix resins N86-11265

New processable modified polyimide resins for adhesive and matrix applications N86-11269

Chemical control of rate and onset temperature of nadimide polymerization N86-11271

Characterization methodology for PMR-15 N86-11272

Quality assurance procedures for V378A matrix resin N86-11274

Replacement of MDA with more oxidatively stable diamines in PMR-polyimides N86-11275

V-378A: A modified bismaleimide for advanced composites N86-11287

Characterization of the relationship of the cure cycle chemistry to cure cycle processing properties [NASA-CR-176256] N86-11339

CURVATURE

Gaussian and mean curvatures of postglacial land uplift as expanded in surface spherical harmonics, and the origin of earthquakes in Fennoscandia N86-11599

CYANIDES

Degradation of ionic membranes in the zinc/ferricyanide battery [DE85-008469] N86-11681

CYCLES

Evidence of an 18 year cycle in Pacific northwest precipitation data N86-11788

CYCLIC LOADS

Interaction of mixed mode loading on cyclic debonding in adhesively bonded composite joints [NASA-CR-177990] N86-11298

CYCLONES

Tropical convection and North American cyclones during the 1982-83 El Nino N86-11809

CYCLOTRON RADIATION

Variable field magnetic extraction channel for ORIC [DE85-011927] N86-12089

CYCLOTRON RESONANCE

Non-geometrical optics investigation of mode conversion in weakly relativistic inhomogenous plasmas [DE85-013480] N86-12102

CYCLOTRON RESONANCE DEVICES

Scaling calculations for a relativistic gyrotron [AD-A157476] N86-11460

CYLINDRICAL BODIES

Response behavior of hot-wires and films to flows of different gases [NBSIR-85/3203] N86-11366

Application of the vortex-lattice concept to flows with smooth-surface separation [AD-A157571] N86-11430

Stiffness and damping coefficients of rubber N86-11532

On the nonlinear characteristics of the axisymmetric flow regime: Cylindrical and spherical systems N86-11756

Influence of physical-chemical properties of gases on interaction between shockwaves and convex cylindrical surfaces N86-11962

CYLINDRICAL SHELLS

On the computation of structural vibrations induced by a low-speed turbulent flow N86-12009

CYLINDRICAL WAVES

On the nonlinear characteristics of the axisymmetric flow regime: Cylindrical and spherical systems N86-11756

CYTOCHROMES

Importance of phytoalexin tolerance and detoxification for pathogenicity [DE85-014759] N86-11257

D

DAMAGE

Tensile fatigue damage and degradation of random short-fiber SWC composite N86-11259

Spectral characterization of suspected acid deposition damage in red spruce (Picea rubens) stands from Vermont N86-11624

Formation, ion modification and annealing of VN [DE85-012896] N86-12146

DAMPING

Microcomputers in shock and vibration N86-11528

The Shock and Vibration Digest, volume 17, no. 5 [AD-A156716] N86-11531

Stiffness and damping coefficients of rubber N86-11532

Current research on circular saw and band saw vibration and stability N86-11533

Seismology in civil engineering N86-11707

Short-period SVSN-4 seismograph N86-11708

Magnification of low-sensitivity channels in seismographs with standard characteristics N86-11709

Spectral statistical forecasts of the 500 mb height field N86-11804

DAMPING TESTS
Stiffness and damping coefficients of rubber
N86-11532
DAMS
Survey of ice problem areas in navigable waterways
[AD-A157477] N86-11827
DATA ACQUISITION
Applied model validation
[NBSIR-85-3154-1] N86-11363
Seeding systems for use with a laser velocimeter in large scale wind tunnels N86-11444
Hardware and software constructs for a vibration analysis network
[DE85-008436] N86-11535
TIROS/NOAA (Television and Infrared Observation Satellite/National Oceanic and Atmospheric Administration) satellites space environment monitor archive tape documentation
[PB85-187920] N86-11724
An application of real-time analysis and design tools in software development N86-11860
Microcomputer-controlled high-altitude data aquisition system N86-12000
Multidimensional ion microbeam analysis
[DE85-014699] N86-12055
DATA BASES
Application of an objective analysis scheme to mesoscale observational network design
[AD-A156911] N86-11760
Data analysis using a data base driven graphic animation system
[DE85-014635] N86-11892
Third National Academic Machine Retrieval Conference held in Zhenjiang N86-11999
Sandia shock compression database
[DE85-015141] N86-12142
DATA CORRELATION
Sub-cloud layer motions from radar data using correlation techniques
[AD-A156477] N86-11757
DATA MANAGEMENT
Seeding systems for use with a laser velocimeter in large scale wind tunnels N86-11444
Microcomputer control and data management techniques for transient digital recording N86-11874
DATA PROCESSING
Introduction to the session on: Numerical methods for two-phase flow
[DE85-012651] N86-11435
Seeding requirements for scanning laser velocimetry
N86-11446
Hardware and software constructs for a vibration analysis network
[DE85-008436] N86-11535
Computational structural mechanics: A new activity at the NASA Langley Research Center
[NASA-TM-87612] N86-11540
Analysis of AIS data of the Recluse Oil Field, Recluse, Wyoming N86-11632
TIROS/NOAA (Television and Infrared Observation Satellite/National Oceanic and Atmospheric Administration) satellites space environment monitor archive tape documentation
[PB85-187920] N86-11724
Application of an objective analysis scheme to mesoscale observational network design
[AD-A156911] N86-11760
Climate system fluctuations, monitoring N86-11814
Microcomputer control and data management techniques for transient digital recording N86-11874
A data translator for engineering measurements
N86-11875
Data analysis using a data base driven graphic animation system
[DE85-014635] N86-11892
New R and D in Chinese language information processing N86-11996
DATA PROCESSING EQUIPMENT
China report: Science and technology
[JPRS-CST-85-015] N86-11994
High-speed signal processor developed N86-11995
DATA RECORDERS
Photon diagnostics leading to an improved Marx
[DE85-013434] N86-12103
DATA RECORDING
An optimum use of sea-level recordings N86-11617
Microcomputer control and data management techniques for transient digital recording N86-11874
DATA REDUCTION
Time-of-flight anemometer for hot section applications
N86-11504
Performance of solar collector arrays and collector controllers in the National Solar Data Network
[DE85-001297] N86-11663
Evidence of an 18 year cycle in Pacific northwest precipitation data N86-11788
Concurrent and lagged relationships between precipitation frequency and 700 mb heights N86-11808
Data analysis using a data base driven graphic animation system
[DE85-014635] N86-11892
DATA RETRIEVAL
Traffic Alert and Collision Avoidance System Signal Environment Model (TCAS SEM) programmer's reference manual
[FAA-PM-85-22] N86-11192
DATA STORAGE
Traffic Alert and Collision Avoidance System Signal Environment Model (TCAS SEM) programmer's reference manual
[FAA-PM-85-22] N86-11192
Thin film research. Volume 1
[AD-A157608] N86-12137
Thin film research. Volume 2
[AD-A157609] N86-12138
DATA TRANSMISSION
A sea surface temperature analysis based on in situ and satellite data N86-11816
DATUM (ELEVATION)
Precise geoid computations at mountainous coastlines in view of vertical datum determinations N86-11561
DEACTIVATION
Force and timing components of the motor program
[AD-A157584] N86-11843
Energy characteristics of waveguide CO sub 2-laser
N86-11978
DEBYE-SCHERRER METHOD
Metallic multilayers and superlattices
[DE85-014444] N86-12141
DECAY
Muon decay
[DE85-012590] N86-12067
DECAY RATES
Chromium- and neodymium-activated gadolinium-scandium-gallium garnet crystal: A new laser active medium N86-11979
DECONTAMINATION
Psychological aspects of personnel contamination
[DE85-012955] N86-11853
DEFECTS
A comparison of the physics of Gas Tungsten Arc Welding (GTAW), Electron Beam Welding (EBW), and Laser Beam Welding (LBW)
[NASA-TM-86503] N86-11473
Economic evaluation of concurrent welding and nondestructive examination
[DE85-014623] N86-11481
Exploratory development of FMR (ferromagnetic resonance) advanced surface flaw detection methods
[AD-A157438] N86-11489
Inertia, stability and ductibility in uniaxial tension at high strain rate
[DE85-007671] N86-11546
Investigation of defects in GaAsP superlattic structures
[DE85-012134] N86-12139
DEFENSE COMMUNICATIONS SYSTEM (DCS)
Evaluation of the digital access and cross-connect system for use in the defense communications system
[AD-A157570] N86-11412
DEFENSE PROGRAM
Status of the intercontinental ballistic missile modernization program
[AD-A157375] N86-11217
DEFORMATION
Composite materials N86-11295
Acoustic emission during deformation and fracture of A533B pressure vessel steel N86-11306
Creep and fracture of a yttria dispersed nickel-chromium alloy N86-11309
Deformation and fracture of P/M titanium alloys
[AD-A157416] N86-11317
Calculation of thermal trapping in shear bands
[DE85-014404] N86-11336
Multi-megampere current interruption from explosive deformation of conductors
[DE85-012756] N86-11419
A review of the literature on finite-element modeling of laminated composite plates N86-11529
Results concerning rheological parameters of the Earth N86-11567
Geodynamic effects due to Earth's deformation
N86-11585
Near-surface deformations and stresses in the area of the Tolbachik great fissure eruption of 1975-1976 (Kamchatka) from geodetic data N86-11600
Deformation of granite at elevated temperature and pressure
[DE85-014057] N86-11721
What extent will small-scale laser-beam fluctuations seed the Rayleigh-Taylor instability in direct-drive targets
[DE85-014408] N86-12131
DEGRADATION
Mission-oriented requirements for updating MIL-H-8501: Calspan proposed structure and rationale
[NASA-CR-177371] N86-11204
Tensile fatigue damage and degradation of random short-fiber SWC composite N86-11259
All-aromatic biphenylene end-capped polyquinoline and polyimide matrix resins N86-11267
Degradation of ionic membranes in the zinc/ferricyanide battery
[DE85-008469] N86-11681
DELAMINATING
Failure rate model for cathodic delamination of protective coatings
[AD-A157483] N86-11912
DELAY LINES
Diffraction of ultrasonic beam passing normally through layered media N86-11946
DENSE PLASMAS
Neutral beam interactions with materials
[AD-A157445] N86-12076
Advanced concepts theory annual report, 1984
[AD-A157535] N86-12080
DENSITOMETERS
Corrosion testing by radiographic methods
[BLL-BISI-TRANS-23201-(9022.06)] N86-11310
DENSITY (MASS/VOLUME)
Processing and microstructural characterization of B4C-Al cermets
[DE85-013195] N86-11326
A 2D ACAR momentum density study of the nature of the positron surface state on Al(100)
[DE85-014830] N86-11330
Shock-induced temperature distributions in powder compact recovery fixtures
[DE85-015139] N86-11359
Detonation reaction zone studies on TATB explosives
[DE85-015710] N86-11361
On the gravitational effect of the crust-mantle boundary in central Europe N86-11703
DENSITY MEASUREMENT
Corrosion testing by radiographic methods
[BLL-BISI-TRANS-23201-(9022.06)] N86-11310
DEOXYRIBONUCLEIC ACID
Relationship between alkylation sites and induction of dominant lethals and heritable translocations in mice
[DE85-014309] N86-11835
Dose distribution and the relative biological effectiveness of internal alpha emitters
[DE85-013041] N86-11845
Prospects for DNA methods to measure human heritable mutation rates
[DE85-014555] N86-11847
Calculations of physical and chemical reactions produced in irradiated water containing DNA
[DE85-012899] N86-12051
DEPENDENCE
Stress and strain-rate dependence of spall strength in two aluminum alloys
[DE85-015154] N86-11321
DEPENDENT VARIABLES
A parameterization technique for nonlinear spectral models N86-11752
DEPLETION
Effect of high electric field on minority carrier generation in silicon depletion layer N86-11938
The mass of hot, shocked CO in Orion: First observations of the J = 17 yields J = 16 transition at 153 microns
[AD-A157323] N86-12189
DEPOSITION
Short range bonding interaction at metal-metal interfaces
[DE85-014442] N86-11334
Oxide cathode mechanisms: Electronic and structural features of oxide cathode surfaces
[AD-A157666] N86-11418
HOST liner cyclic facilities N86-11519
Integrated forest study on effects of atmospheric deposition. Project summary
[DE85-015972] N86-11690
DEPOSITS
Evaluation of candidate materials in a static turbine cascade
[DE85-008592] N86-11480
DEPTH MEASUREMENT
Determination of the depth of a conductivity anomaly by separating the geomagnetic variation field into its external and internal part N86-11711
Use of the wavenumber technique with the Lloyds mirror for an acoustic doublet
[AD-A156463] N86-11824
DERMATITIS
Importance of phytcalexin tolerance and detoxification for pathogenicity
[DE85-014759] N86-11257

DESIGN ANALYSIS

Mission-oriented requirements for updating MIL-H-8501: Calspan proposed structure and rationale [NASA-CR-17737] N86-11204

High Temperature Polymer Matrix Composites [NASA-CP-2385] N86-11260

Optimized ground-coupled heat pump system design for northern climate [DE85-014065] N86-11484

Materials studies for magnetic fusion energy applications at low temperatures. 7: Technical reports [DE85-014518] N86-12101

Modelling of the PROTO-2 crossover network [DE85-014639] N86-12128

DESORPTION

Activated recombinative desorption: A potential component in mechanisms of spacecraft glow [DE85-014092] N86-11223

XUV preionization effects in high power magnetically insulated diodes [DE85-013142] N86-12109

DETECTION

Investigation of photoelectrode redox polymer junctions [AD-A157556] N86-11304

Surface sampling techniques using ultraviolet illumination [AD-A156457] N86-11458

DETONATION

Detonation reaction zone studies on TATB explosives [DE85-015710] N86-11361

A time-splitting numerical technique for solving highly coupled two-phase flow conservation equation N86-11879

Steady-state detonation of charges of finite length N86-11966

DETONATION WAVES

Travel-time and its residuals for the blasts from Eschenlohe (Bavaria) N86-11706

Seismology in civil engineering N86-11707

DEUTERIUM

Tokamak startup: Problems and scenarios related to the transient phases of ingnited tokamak operations [DE85-015321] N86-12085

Nuclear spin-polarized HD, D2, HT and DT solids, liquids and high density gases [DE85-014136] N86-12154

DEUTERIUM PLASMA

Energy confinement experiments on Doublet 3 with high power neutral beam heating [DE85-014324] N86-12110

DIAMINES

Replacement of MDA with more oxidatively stable diamines in PMR-polyimides N86-11275

DICHROISM

Characteristics of an axisymmetric sudden expansion flow [NASA-CR-176278] N86-11465

DIELECTRIC PROPERTIES

Factors affecting the processing of epoxy film adhesives N86-11252

Characterization of the relationship of the cure cycle chemistry to cure cycle processing properties [NASA-CR-176256] N86-11339

Finite difference calculations of voltages generated in thin dielectric layers subjected to shock loading N86-11878

DIELECTRICS

Part A. Molecular dynamics and ionic associations of LiAsF6 in 4-butyrolactone mixtures with 2-methyl tetrahydrofuran. Part B. Molecular dynamics and ionic associations of LiBF4 in 1,2-dimethoxymethane [AD-A157401] N86-12023

DIELS-ALDER REACTIONS

Chemical control of rate and onset temperature of nadimide polymerization N86-11271

DIFFERENTIAL EQUATIONS

Computational errors and their control in the determination of satellite orbits N86-11211

Treatment of the geodetic boundary value problem by contact-transformation N86-11573

On the addition theorem for Legendre polynomials N86-11704

Sparse quasi-Newton methods and the continuation problem [AD-A157587] N86-11914

DIFFRACTION

Diffraction of ultrasonic beam passing normally through layered media N86-11946

Diffraction efficiency of three-dimensional phase hologram of diffuse object N86-11982

DIFFUSERS

A parametric analysis of flow structure and performance in a vortex controlled radial diffuser N86-11182

DIFFUSION

Application of the vortex-lattice concept to flows with smooth-surface separation [AD-A157571] N86-11430

Study of heavy gas effects on the atmospheric dispersion of dense gases, revision 1 [DE85-012917] N86-11693

Application of Flux-Corrected Transport (FCT) to heat transfer/fluid mechanics problems N86-11883

Toward a theory of atomic gas breakdown by laser radiation near a metal surface N86-11955

Diffraction efficiency of three-dimensional phase hologram of diffuse object N86-11982

Dominant moving species in the formation of amorphous NZr by solid-state reaction [DE85-014855] N86-12053

DIFFUSION WELDING

Evaluation of superplastic forming and weld-brazing for fabrication of titanium compression panels N86-11245

Feasibility of remotely manipulated welding in space: A step in the development of novel joining technologies N86-11246

Advances in joining techniques used in development of SPF/DB titanium sandwich reinforced with metal matrices N86-11247

DIGITAL DATA

Microcomputer control and data management techniques for transient digital recording N86-11874

A data translator for engineering measurements N86-11875

SIG: A general-purpose signal processing code N86-11876

DIGITAL SIMULATION

Evaluating the ground-water resources of the high plains of Texas, volume 3 [PB85-191617] N86-11655

DIGITAL SYSTEMS

Evaluation of the digital access and cross-connect system for use in the defense communications system [AD-A157570] N86-11412

DIMERS

Part A. Molecular dynamics and ionic associations of LiAsF6 in 4-butyrolactone mixtures with 2-methyl tetrahydrofuran. Part B. Molecular dynamics and ionic associations of LiBF4 in 1,2-dimethoxymethene [AD-A157401] N86-12023

DIODES

Operating range of aluminum gallium arsenide quantum-well heterostructure lasers: tunability, power output and high energy emission N86-11464

Pb(1-x)Sn(x)Te and Pb(1-y)Sn(y)Se laser crystals N86-11931

Progress of Inertial Confinement Fusion (ICF) research N86-11932

XUV preionization effects in high power magnetically insulated diodes [DE85-013142] N86-12109

Particle simulation of the low-(ALPHA) Pierce diode [DE85-014435] N86-12113

Low inductance diode design of the Proto 2 accelerator for imploding plasma loads [DE85-013783] N86-12123

DIPOLE ANTENNAS

Microstrip monpulse dipole array N86-11405

Electric or magnetic dipole in stratified uniaxially inhomogeneous anisotropic media N86-11922

DIRECTIONAL SOLIDIFICATION (CRYSTALS)

Bridgman growth of semiconductors [NASA-CR-177971] N86-11426

DISCHARGE COEFFICIENT

Calculation of formation time of minimal nucleus of flame during ignition of explosive mixtures by electrical discharges N86-11963

DISPERSION

Seeding techniques used in the Vortex Research Facility N86-11443

DISPLACEMENT

Simple construction and performance of a conical plastic cryocooler N86-11378

Experiments with a fully instrumented split Stirling cryocooler N86-11381

Passive motion control of pneumatically driven displacers in cryogenic coolers N86-11383

Numerical solution for contact pressure and wear distributions of unlubricated, misaligned, closely conforming, multiply connected surfaces N86-11472

Fiber optic pressure sensors in skin-friction measurements [NASA-CR-176294] N86-11838

DISSIPATION

The effect of topography on the evolution of unstable disturbances in a baroclinic atmosphere N86-11750

A parameterization technique for nonlinear spectral models N86-11752

DISTORTION

Inlet flow dynamic distortion prediction without rms measurements N86-11183

Reduction of sextupole distortion by shuffling magnets in small groups [DE85-013024] N86-12035

DISTRIBUTED FEEDBACK LASERS

Distributed-feedback lasers with active framing medium N86-11971

DISTRIBUTION (PROPERTY)

A large area X-ray source and its preionization characteristics for XeCl excimer laser N86-11929

DIURNAL VARIATIONS

Adjustment of the latitude data by least-squares collocation approach N86-11562

Temperature and precipitation trends in North America N86-11774

Prediction of monthly 700 mb heights using antecedent and simulated prognostic height predictors N86-11805

DIVERGENCE

The Hadley and Rossby regimes in a spherical atmosphere N86-11751

DOCUMENTATION

TIROS/NOAA (Television and Infrared Observation Satellite/National Oceanic and Atmospheric Administration) satellites space environment monitor archive tape documentation [PB85-187920] N86-11724

DONOR MATERIALS

Binding energy of donors in GaAs-Ga(1-x) Al(x)As quantum well structures N86-11940

Chromium- and neodymium-activated gadolinium-scandium-gallium garnet crystal: A new laser active medium N86-11979

DOPPLER EFFECT

Applications of the magneto-optical filter to stellar pulsation measurements [NASA-CR-176282] N86-12167

DOPPLER RADAR

Sub-cloud layer motions from radar data using correlation techniques [AD-A156477] N86-11757

DOSAGE

Thyroid absorbed dose for people at Rongelap, Utirik and Sifo on March 1, 1954 [DE85-014695] N86-11846

Acute pulmonary effects of formaldehyde exposure in humans [DE85-014728] N86-11848

Psychological aspects of personnel contamination [DE85-012955] N86-11853

DOWNLINKING

A cascaded coding scheme for error control [NASA-CR-176287] N86-11911

DRAINAGE

Hydrologic data for experimental agricultural watersheds in the US, 1975 [PB85-197317] N86-11656

DRIFT RATE

Secular and long term variations in polar motion from classical and Doppler observations N86-11581

High energy physics [DE85-014272] N86-12063

DRILLING

Geothermal instrumentation development activities at Sandia [DE85-008693] N86-11463

Honey Lake Geothermal Project, Lassen County, California [DE85-013388] N86-11677

Economics of magma power generation [DE85-008694] N86-11687

DRILLS

Geothermal instrumentation development activities at Sandia [DE85-008693] N86-11463

DROUGHT

Meteorological conditions during drought episodes in the United States Great Plains N86-11802

DRUGS

An atropinized heat-stressed rat model: Anticholinergic and anticholinesterase drug potency [AD-A157620] N86-11832

DUCTED FLOW

Gas flow environmental and heat transfer nonrotating 3D program N86-11506

DUCTILITY

Influence of effective rate sensitivity on adiabatic shear instability [DE85-013967] N86-11333

Transportation system impact limiter design using rigid polyurethane foam [DE85-015088] N86-11354

Miniaturization of specimens for mechanical testing [DE85-014506] N86-11536

DUCTS
Application of Gr/PMR-15 to commercial aircraft N86-11289
DUNES
Preliminary evaluation of AIS spectra along a topographic/moisture gradient in the Nebraska Sandhills N86-11629
DURABILITY
Use of hydration inhibitors to improve bond durability of aluminum adhesive joints N86-11251
Polyimide composites: Application histories N86-11286
Gas side heat transfer N86-11507
DUST
Workshop on Dust on Mars [NASA-CR-176293] N86-12192
DUST STORMS
Workshop on Dust on Mars [NASA-CR-176293] N86-12192
DYE LASERS
Investigation of polarization characteristics of radiation from laser with dye-activated polymer elements N86-11972
Double-wavelength pulsed tunable dye laser N86-12003
DYNAMIC CHARACTERISTICS
Dynamic behavior of a propfan N86-11159
Calculation of particle dynamics effects on laser velocimeter data N86-11438
Estimation of particle size based on LDV measurements in a de-accelerating flow field N86-11440
Mechanical face seal dynamics update N86-11530
Magnification of low-sensitivity channels in seismographs with standard characteristics N86-11709
The analysis and calculation for the dynamic characteristics of the omni-axial movable flexible joint nozzle N86-11925
DYNAMIC MODELS
A direct model reference adaptive approach to the control of space stations N86-11219
Some empirical evidence for the influence of snow cover on temperature and precipitation N86-11767
Spectral statistical forecasts of the 500 mb height field N86-11804
DYNAMIC MODULUS OF ELASTICITY
Seismology in civil engineering N86-11707
DYNAMIC PRESSURE
Fluids at high dynamic pressures and temperatures [DE85-014812] N86-11305
DYNAMIC RESPONSE
A comparison of the NAVTOLAND (Navy vertical takeoff and landing) SH-2F helicopter model with the requirements of MIL-H-8501A and with flight data [AD-A157297] N86-11198
Flexible vibrations of a uniform elastic beam with arbitrary supports and lumped masses N86-11885
Computer codes for fluid-structure interactions N86-11887
DYNAMIC STRUCTURAL ANALYSIS
Bounded state control of linear systems with application to the active structural control N86-11493
Numerical method in dynamic response of nonlinear systems N86-12005
DYNAMIC TESTS
Quality assurance procedures for V378A matrix resin N86-11274
Characterization of the relationship of the cure cycle chemistry to cure cycle processing properties [NASA-CR-176256] N86-11339

E

EARTH (PLANET)
Figure of the Earth, moon, and planets N86-11550
Structure and function of isozymes: Evolutionary aspects and role of oxygen in eucaryotic organisms [NASA-CR-176286] N86-11831
EARTH ALBEDO
The status of the NOAA/NESDIS radiation budget data set N86-11815
EARTH CORE
On the influence of coupling torques between the Earth's core and mantle on parameters and components of the rotation of the Earth N86-11572
EARTH CRUST
On the distribution of the residual vectors of Earth's tide gravity observations in Central Europe N86-11564
On the lunar tidal effect in the latitude observations at Tianjin N86-11565
On the comparison of the results of two different E-W-strainmeters N86-11583
Proceedings of the 5th International Symposium Geodesy and Physics of the Earth, part 3 [REPT-81-PT-3] N86-11591
CRCM and KAPG activity in recent crustal movement studies N86-11592
On the works and results of investigations concerning the recent movements in the Karpatho-Balkan region N86-11593
North Sea coast levelling net: A model case for the determination of vertical movements in Western Europe N86-11594
Geokinematic models for the gravimetric W - E profile of the GDR N86-11596
Mathematical treatment of vertical movements N86-11597
Geodimeter net for the investigation of horizontal crustal deformations N86-11598
Gaussian and mean curvatures of postglacial land uplift as expanded in surface spherical harmonics, and the origin of earthquakes in Fennoscandia N86-11599
Near-surface deformations and stresses in the area of the Tolbachik great fissure eruption of 1975-1976 (Kamchatka) from geodetic data N86-11600
Method of joint adjustment of height differences and velocities N86-11601
Principle of the construction of the lines of the repeated levelling for the investigation of the vertical movement in the Carpatho-Balkan Region (CBR) N86-11602
Some geodetic aspects of the problem of checking the plate-tectonic model of seismicity in southeastern Europe N86-11603
Recent crustal movements and geophysical interpretation of geodynamic processes in the Alpine mountain belt N86-11604
Determination of crustal movements in the high Tatra Mountains N86-11605
Stationary hydrostatic precision tiltmeter system N86-11607
Height changes and recent crustal movements in the Rhenish Massif and in the upper Rhine Graben rift N86-11608
Recent vertical crustal movements of the Carpathian-Balkan region and their relationship with neotectonic movements and geophysical fields N86-11609
On the relation between recent crustal movements, the surface of the basement complex and neotectonic displacements of the East-European platform N86-11610
Significance tests of recent vertical crustal movements by correlation functions N86-11611
Relation between earthquake focal intensity and recent vertical Earth's crustal movements in the Rila-Rhodope seismic region N86-11615
Dynamics of the Bohemian Massif N86-11616
An optimum use of sea-level recordings N86-11617
Oceanic intraplate seismicity: Implications for the rheology and tectonics of the ocean lithosphere N86-11699
On the gravitational effect of the crust-mantle boundary in central Europe N86-11703
Numerical solution of ionospheric filtration of ULF waves. Part 1: Method N86-11712
EARTH MANTLE
On the influence of coupling torques between the Earth's core and mantle on parameters and components of the rotation of the Earth N86-11572
On the comparison of the results of two different E-W-strainmeters N86-11583
Anelasticity in the Earth's mantle: Implications for the frequency dependence of Love numbers N86-11590
On the gravitational effect of the crust-mantle boundary in central Europe N86-11703
EARTH MOVEMENTS
Capacitive pendulum with intelligent data collection N86-11577
On reducing the effect of horizontal displacements of the lithospheric plates from the observations carried out by global geodynamic network (on example the GEOSS-REA network) N86-11589
Proceedings of the 5th International Symposium Geodesy and Physics of the Earth, part 3 [REPT-81-PT-3] N86-11591
CRCM and KAPG activity in recent crustal movement studies N86-11592
On the works and results of investigations concerning the recent movements in the Karpatho-Balkan region N86-11593
North Sea coast levelling net: A model case for the determination of vertical movements in Western Europe N86-11594
Space-time variating geological masses by space-time variating geodetic measurements N86-11595
Geokinematic models for the gravimetric W - E profile of the GDR N86-11596
Mathematical treatment of vertical movements N86-11597
Geodimeter net for the investigation of horizontal crustal deformations N86-11598
Gaussian and mean curvatures of postglacial land uplift as expanded in surface spherical harmonics, and the origin of earthquakes in Fennoscandia N86-11599
Near-surface deformations and stresses in the area of the Tolbachik great fissure eruption of 1975-1976 (Kamchatka) from geodetic data N86-11600
Method of joint adjustment of height differences and velocities N86-11601
Principle of the construction of the lines of the repeated levelling for the investigation of the vertical movement in the Carpatho-Balkan Region (CBR) N86-11602
Some geodetic aspects of the problem of checking the plate-tectonic model of seismicity in southeastern Europe N86-11603
Recent crustal movements and geophysical interpretation of geodynamic processes in the Alpine mountain belt N86-11604
Determination of crustal movements in the high Tatra Mountains N86-11605
Stationary hydrostatic precision tiltmeter system N86-11607
Height changes and recent crustal movements in the Rhenish Massif and in the upper Rhine Graben rift N86-11608
Recent vertical crustal movements of the Carpathian-Balkan region and their relationship with neotectonic movements and geophysical fields N86-11609
On the relation between recent crustal movements, the surface of the basement complex and neotectonic displacements of the East-European platform N86-11610
Significance tests of recent vertical crustal movements by correlation functions N86-11611
Relation between earthquake focal intensity and recent vertical Earth's crustal movements in the Rila-Rhodope seismic region N86-11615
An optimum use of sea-level recordings N86-11617
EARTH OBSERVATIONS (FROM SPACE)
Geodesy: A look to the future [NASA-CR-176283] N86-11657
EARTH ORBITS
Design and performance analysis of an aero-maneuvering orbital-transfer vehicle concept [NASA-TM-86848] N86-11221
EARTH PLANETARY STRUCTURE
Geophysical interpretation of global geoid undulations and mean gravity anomalies N86-11560
Some short periodic terms due to nutation and tides from latitude and time determinations at Czechoslovak observatories N86-11566
On the gravitational effect of the crust-mantle boundary in central Europe N86-11703
EARTH RADIATION BUDGET EXPERIMENT
The status of the NOAA/NESDIS radiation budget data set N86-11815
EARTH ROTATION
Proceedings of the 5th International Symposium Geodesy and Physics of the Earth, part 1 [REPT-81-PT-1] N86-11549
Figure of the Earth, moon, and planets N86-11550
Establishment of the BIH terrestrial system by combining the results of different Earth rotation space geodesy programs N86-11555
Tidal friction, the Earth's rotation and hypothesis of an expanding Earth N86-11556
On the lunar tidal effect in the latitude observations at Tianjin N86-11565
Proceedings of the 5th International Symposium Geodesy and Physics of the Earth, part 2 [REPT-81-PT-2] N86-11568
The irregularity in the Earth's annual rotation as a cause of systematic time variation N86-11570
On the influence of coupling torques between the Earth's core and mantle on parameters and components of the rotation of the Earth N86-11572
Variational principles for Earth rotation N86-11580
Geodynamic effects due to Earth's deformation N86-11585
Applications of the magneto-optical filter to stellar pulsation measurements [NASA-CR-176282] N86-12187
EARTH SURFACE
Proceedings of the 5th International Symposium Geodesy and Physics of the Earth, part 2 [REPT-81-PT-2] N86-11568
A new approach to iterations in solving geodetic boundary value problems for real topography N86-11569
Remote sensing of earth terrain [NASA-CR-176234] N86-11645
Bibliography of terrestrial impact structures [NASA-TM-87567] N86-11701

EARTH TIDES
Proceedings of the 5th International Symposium Geodesy and Physics of the Earth, part 1 [REPT-81-PT-1] N86-11549
Results of KAPG co-operation in Earth tide research N86-11551
High frequencies in tidal tilt records N86-11554
Tidal friction, the Earth's rotation and hypothesis of an expanding Earth N86-11556
An attempt to detect geometric tidal information using Lageos laser ranging data N86-11558
Some results of an eight years gravimetric registration series N86-11559
Modification of a Hughes tiltmeter to a borehole tiltmeter N86-11563
On the distribution of the residual vectors of Earth's tide gravity observations in Central Europe N86-11564
On the lunar tidal effect in the latitude observations at Tianjin N86-11565
Some short periodic terms due to nutation and tides from latitude and time determinations at Czechoslovak observatories N86-11566
Results concerning rheological parameters of the Earth N86-11567
Ocean tidal loading along the Blue Road geotraverse in Fennoscandia N86-11571
Interactions between oceanic and gravity tides, as analysed from world-wide Earth tide observations and ocean models N86-11576
North Sea coast levelling net: A model case for the determination of vertical movements in Western Europe N86-11594
Stationary hydrostatic precision tiltmeter system N86-11607

EARTH-MOON SYSTEM
Proceedings of the 5th International Symposium Geodesy and Physics of the Earth, part 1 [REPT-81-PT-1] N86-11549
Figure of the Earth, moon, and planets N86-11550
Tidal friction, the Earth's rotation and hypothesis of an expanding Earth N86-11556

EARTHQUAKE DAMAGE
Geodesy: A look to the future [NASA CR-176283] N86-11657

EARTHQUAKES
Results of KAPG co-operation in Earth tide research N86-11551
Relation between earthquake focal intensity and recent vertical Earth's crustal movements in the Rila-Rhodope seismic region N86-11615
Oceanic intraplate seismicity: Implications for the rheology and tectonics of the ocean lithosphere N86-11699
Attenuation of macroseismic effects of earthquakes N86-11705
Earthquake hazard research in the Los Angeles Basin and its offshore area, October 1, 1983 to September 30, 1984 [PB85-196491] N86-11725

ECLIPSES
Optical photometry of the 1982-1984 eclipse of Epsilon Aurigae N86-12169

ECLIPSING BINARY STARS
The 1982-1984 Eclipse of Epsilon Aurigae [NASA-CP-2384] N86-12168
Optical photometry of the 1982-1984 eclipse of Epsilon Aurigae N86-12169
Infrared photometry of the 1982-4 eclipse of Epsilon Aurigae N86-12170
The optical polarization of Epsilon Aurigae through the 1982-84 eclipse N86-12171
IUE observations of the 1982-84 eclipse of Epsilon Aurigae N86-12172
The eclipse of Epsilon Aurigae visible spectroscopy and ultraviolet activity N86-12173
Epsilon Aurigae in an evolutionary context N86-12174
UBV photometry of the 1982-4 eclipse of Epsilon Aurigae: A discussion of the observed light curves N86-12176
Intermediate and narrow band photometry of Epsilon Aurigae N86-12177
Spectrophotometry of Epsilon Aur, 3295-8880 A N86-12178
Micron CO in the eclipse spectrum of Epsilon Aur N86-12179
Scattered light in the IUE spectra of Epsilon Aurigae N86-12180
Modelling Epsilon Aurigae without solid particles N86-12181
High dispersion observations of Epsilon Aur from Sept. 1982 to March 1983 N86-12183
Photoelectric observations of the long-period eclipsing binaries at Yonsei University Observatory N86-12184

ECLIPTIC
Statistical properties of geomagnetic pulsations at the Fuerstenfeldbruck Observatory determined by means of pulsation indices. Part 3: Correlation with the parameters of the interplanetary magnetic field N86-11710

ECONOMIC ANALYSIS
Recent achievements, problems in cropdusting work N86-11180
Economic evaluation of concurrent welding and nondestructive examination [DE85-014623] N86-11481
Economics of magma power generation [DE85-008694] N86-11687

ECONOMICS
Evaluation and ranking of geothermal resources for electrical generation or electrical offset in Idaho, Montana, Oregon and Washington [DE85-014661] N86-11650

ECOSYSTEMS
Effect of elevated atmospheric CO2 on plant communities. Annual report, 1984-1985 [DE85-015575] N86-11692

EDDY CURRENTS
Exploratory development of FMR (ferromagnetic resonance) advanced surface flaw detection methods [AD-A157438] N86-11489

EDITING
A data translator for engineering measurements N86-11875
Improving the comprehensibility of a simulated technical manual [AD-A157482] N86-11889

EDUCATION
A computer engineering curriculum for the Air Force Academy: An implementation plan [AD-A156464] N86-11857
Problems, trends in technical education of researchers N86-11993

EFFECTIVENESS
Dose distribution and the relative biological effectiveness of internal alpha emitters [DE85-013041] N86-11845

EFFICIENCY
Advanced mechanical heat pump technologies for industrial applications [DE85-014613] N86-11483
Development of membranes for the zinc/ferricyanide battery [DE85-011189] N86-11689
Investigation of efficiency of generation of difference-frequency laser radiation in waveguide N86-11969
Diffraction efficiency of three-dimensional phase hologram of diffuse object N86-11982
Comparison of energy transport measurements and computer simulations in a single module prototype for PBFA 2 [DE85-013960] N86-12119

EFFLUENTS
Evaluation of color infrared aerial surveys of wastewater soil absorption systems [PB85-189074] N86-11654

EIGENVALUES
Stability and interaction of coherent structure in supersonic reactive wakes N86-11185
Sparse quasi-Newton methods and the continuation problem [AD-A157587] N86-11914
Particle simulation of the low-(ALPHA) Pierce diode [DE85-014435] N86-12113

EIGENVECTORS
Flexible vibrations of a uniform elastic beam with arbitrary supports and lumped masses N86-11885

EJECTORS
A novel oscillating jet: Its effect on ejector thrust augmentation [AD-A157480] N86-11201

EL NINO
Proceedings of the 9th Annual Climate Diagnostics Workshop [PB85-183911] N86-11763
Review of the climate of fall 1983 and winter 1983-84 N86-11766
Circulation and weather for MAM and JJA 1984 N86-11769
On the relationship between North Atlantic seasonal SST anomalies with United States surface temperature anomalies N86-11770
Recent long-term climatic change over the eastern tropical and subtropical Pacific and its ramifications N86-11775
Satellite observations of a large-amplitude 40-50 day oscillation in upper tropospheric temperature over the equatorial Pacific Ocean during the 1982-83 ENSO event N86-11778
Subseasonal and interannual variations of tropical convection and the El Nino/Southern Oscillation N86-11779
The distribution of rainfall along the coast of northern Peru during 1982-83 N86-11782
Peru coastal winds during 1982-1983 N86-11783
Climatic events of the west coast of southern Africa N86-11784
Understanding El Nino events using a simple dynamical atmosphere model N86-11797
Tropical convection and North American cyclones during the 1982-83 El Nino N86-11809

ELASTIC PLATES
Reflection of sound from plate containing periodic inhomogeneities N86-11951

ELASTIC PROPERTIES
Numerical solution for contact pressure and wear distributions of unlubricated, misaligned, closely conforming, multiply connected surfaces N86-11472
A body tensor formalism for elastic-plastic continua with applications in uniaxial extension N86-11491

ELASTIC SCATTERING
Antinucleon-nucleus elastic and inelastic scattering [DE85-012510] N86-12059
Elastic and inelastic light scattering of colloidal particles [AD-A157335] N86-12072

ELASTIC WAVES
Occurrence of pressure wave during spontaneous ignition of gas ahead of flame front in closed vessel N86-11965

ELASTOPLASTICITY
Senstivity of using blunt and sharp crack models in elastic-plastic fracture mechanics [DE85-010288] N86-11537

ELECTRIC ARCS
An introduction to electrical breakdown in dielectrics [AD-A156465] N86-11415

ELECTRIC BATTERIES
Photovoltaic-powered vaccine refrigerator: Freezer systems field test results [NASA-TM-86972-REV] N86-11666
High rate Li/SOCl(2) cells. 2. Effect of catalyst on cell performance [AD-A157383] N86-11672
Degradation of ionic membranes in the zinc/ferricyanide battery [DE85-008469] N86-11681
Multispectroscopic studies of the electronic structure of electrode materials for high energy density batteries: 1-2, 1-3 intermetallic compounds with B32 structure [DE85-014675] N86-11684
Development of membranes for the zinc/ferricyanide battery [DE85-011189] N86-11689

ELECTRIC CHARGE
PBFA-2 vacuum insulator stack failure mechanisms [DE85-013118] N86-12090

ELECTRIC CORONA
An introduction to electrical breakdown in dielectrics [AD-A156465] N86-11415

ELECTRIC CURRENT
Multi-megampere current interruption from explosive deformation of conductors [DE85-012756] N86-11419
Multi-megampere operation of plasma compression opening switches in planar geometry [DE85-012755] N86-11420
Implications of rf current drive theory for next step steady-state tokamak design [DE85-014753] N86-12083

ELECTRIC DIPOLES
Electric or magnetic dipole in stratified uniaxially inhomogeneous anisotropic media N86-11922

ELECTRIC DISCHARGES
Partial discharge formation and breakdown in deionized water under repetitive stressing [DE85-013114] N86-11424
Efficiency of optically-pumped XeF-laser N86-11977
Energy characteristics of waveguide CO sub 2-laser N86-11978

ELECTRIC FIELDS
Effect of high electric field on minority carrier generation in silicon depletion layer N86-11938
Collinear wake field acceleration [DE85-014356] N86-12050
Measurements of ultimate accelerating gradients in the SLAC disk-loaded structure [DE85-014287] N86-12125
Variational quadratic form for low frequency electromagnetic perturbations. 1: Formalism [DE85-014836] N86-12129

ELECTRIC GENERATORS
Explosive generators for low-cost pulsed power [DE85-013436] N86-11421

Evaluation and ranking of geothermal resources for electrical generation or electrical offset in Idaho, Montana, Oregon and Washington
[DE85-014661] N86-11650

Design optimization of the power generation system for a space-based free-electron laser N86-11861

CELCAP: A computer model for cogeneration system analysis
[NASA-CR-176306] N86-11896

ELECTRIC POTENTIAL

Finite difference calculations of voltages generated in thin dielectric layers subjected to shock loading
N86-11878

Photoelectron trajectory analyses of streak tubes
N86-11880

The relations between voltage and magnetic field of superconducting weaklink (1) N86-11934

The relations between voltage and magnetic field of superconducting weaklink (2) N86-11935

Electron beam potential diagnostic for tandem mirrors, phase 1
[DE85-013515] N86-12107

ELECTRIC POWER PLANTS

Aerial photography and ground verification at power plant sites: Wisconsin power plant impact study
[PB85-197358] N86-11658

Evaluation and ranking of geothermal resources for electrical generation or electrical offset in Idaho, Montana, Oregon and Washington, volume 2
[DE85-014452] N86-11683

ELECTRIC POWER SUPPLIES

Intermediate load modules for test and evaluation: Fixed price research and development
[NASA-CR-176135] N86-11664

Economics of magma power generation
[DE85-008694] N86-11687

Cascade switch implementation of PBFA 1
[DE85-013955] N86-12039

Electrical supply for MFTF-B superconducting magnet system
[DE85-012932] N86-12094

Photon diagnostics leading to an improved Marx
[DE85-013434] N86-12103

Multivariable current control for electrically and magnetically coupled superconducting magnets, revision 1
[DE85-012943] N86-12108

ELECTRIC POWER TRANSMISSION

On convective effects in gas lasers N86-12006

ELECTRIC PROPULSION

An experimental study of energy loss mechanisms and efficiency consideration in the low power dc arcjet
[NASA-TM-87123] N86-11224

ELECTRIC SWITCHES

Multi-megampere operation of plasma compression opening switches in planar geometry
[DE85-012755] N86-11420

ELECTRICAL FAULTS

Partial discharge formation and breakdown in deionized water under repetitive stressing
[DE85-013114] N86-11424

ELECTRICAL IMPEDANCE

Electrical relaxation in poly(ethylene oxide)
[AD-A157301] N86-11342

ELECTRICAL INSULATION

Low inductance diode design of the Proto 2 accelerator for imploding plasma loads
[DE85-013783] N86-12123

ELECTRICAL MEASUREMENT

AC motor and generator requirements for isolated WECS
[NASA-CR-176315] N86-11670

ELECTRICAL PROPERTIES

Relationship between interatomic bonding and electron transport in plasma deposited amorphous metal alloys
[DE85-014710] N86-11337

Electrical relaxation in poly(ethylene oxide)
[AD-A157301] N86-11342

Determination of parameters of elastic spherical shell from scattered wave field N86-11949

ELECTRICAL RESISTANCE

High temperature static strain sensor development program N86-11500

Demonstration test of burner liner strain measurement systems: Interim results N86-11501

ELECTRICAL RESISTIVITY

Fluids at high dynamic pressures and temperatures
[DE85-014812] N86-11305

Electromagnetic soundings for geothermal resources in Dixie Valley, Nevada
[DE85-011986] N86-11722

ELECTRO-OPTICS

Crystal class and the electrooptic effect
[DE85-015240] N86-11353

Electro-optics Millimeter/Microwave technology in Japan. Report of DOD technology team
[AD-A157376] N86-12073

ELECTROCHEMICAL CELLS

Effects of additives and temperature on iron electrode behavior in KOH electrolytes
[DE85-011901] N86-11423

ELECTRODES

An experimental study of energy loss mechanisms and efficiency consideration in the low power dc arcjet
[NASA-TM-87123] N86-11224

Basic studies of the lithium secondary battery
[AD-A157449] N86-11673

Los Alamos Spheromak Program
[DE85-012769] N86-12096

ELECTROLYTES

Basic studies of the lithium secondary battery
[AD-A157449] N86-11673

Part A. Moleculer dynamics and ionic associations of LiAsF6 in 4-butyrolactone mixtures with 2-methyl tetrahydrofuran. Part B. Molecular dynamics and ionic associations of LiBF4 in 1,2-dimethoxymethane
[AD-A157401] N86-12023

ELECTROMAGNETIC ABSORPTION

Transformation of light pulse shape by thin plane-parallel layer of absorbing material N86-11988

ELECTROMAGNETIC COMPATIBILITY

Basic EMC technology advancement for C(3) systems. Volume 3B: Computer simulation of EMI effects in a differential line receiver
[AD-A156505] N86-11416

ELECTROMAGNETIC FIELDS

Assessments and viewpoints on the biological and human health effects of Extremely Low Frequency (ELF) electromagnetic fields: Compilation of commissioned papers for the ELF literature review project
[AD-A156942] N86-11839

The vacuum in the presence of electromagnetic fields and rotating boundaries N86-11916

Energy characteristics of waveguide CO sub 2-laser
N86-11978

Plasma kinetic theory in action-angle variables
[DE85-014767] N86-12084

Variational quadratic form for low frequency electromagnetic perturbations. 1: Formalism
[DE85-014896] N86-12129

ELECTROMAGNETIC INTERFERENCE

Calculation of allowable orbital spacings for the fixed-satellite service
[NASA-CR-176273] N86-11212

Basic EMC technology advancement for C(3) systems. Volume 3B: Computer simulation of EMI effects in a differential line receiver
[AD-A156505] N86-11416

Ion whistlers in middle latitudes observed by the Interkosmos-14 satellite N86-11714

Statistical signal analysis for systems with interferenced inputs N86-12016

ELECTROMAGNETIC NOISE

A preliminary investigation of systematic noise in data acquired with the Airborne Imaging Spectrometer
N86-11638

ELECTROMAGNETIC PROPERTIES

Parametric testing of a linearly driven Stirling cryogenic refrigerator N86-11376

ELECTROMAGNETIC RADIATION

Upgrade of the EM transient range monocone antenna
[DE85-013181] N86-11413

Conversion of electromagnetic wave energy to electrical current by bulk superlattice semiconductors N86-11952

Research in elementary particle physics
[DE85-014062] N86-12041

Applications of the magneto-optical filter to stellar pulsation measurements
[NASA-CR-176282] N86-12187

ELECTROMAGNETIC SCATTERING

Analysis of arctic haze scattering and aerosol data obtained during AGASP
[AD-A157434] N86-12074

ELECTROMAGNETIC WAVE TRANSMISSION

Numerical solution of ionospheric filtration of ULF waves. Part 2: Application N86-11713

Propagation of electromagnetic waves in inhomogeneous and lossy reentry plasma sheath layer
N86-11923

ELECTRON ACCELERATORS

Transition radiation and coherent electron-photon scattering
[DE85-014813] N86-12031

Interaction of the ATA beam with the TM030 mode of the accelerating cells
[DE85-014850] N86-12120

ELECTRON ATTACHMENT

Photon induced electron attachment
[AD-A156506] N86-11467

ELECTRON BEAM WELDING

Feasibility of remotely manipulated welding in space: A step in the development of novel joining technologies
N86-11246

A comparison of the physics of Gas Tungsten Arc Welding (GTAW), Electron Beam Welding (EBW), and Laser Beam Welding (LBW)
[NASA-TM-86503] N86-11473

Refractory alloy performance: Product form procurement and component fabrication
[DE85-014658] N86-11477

ELECTRON BEAMS

IFR guiding experiments
[DE85-014512] N86-12027

Saturation characteristics of counterstreaming warm electrons
[DE85-014390] N86-12040

A hybrid mode and a classification of beam plasma instabilities
[AD-A157356] N86-12075

Electron beam potential diagnostic for tandem mirrors, phase 1
[DE85-013515] N86-12107

Interaction of the ATA beam with the TM030 mode of the accelerating cells
[DE85-014850] N86-12120

MABE multibeam accelerator
[DE85-012035] N86-12121

ELECTRON CYCLOTRON HEATING

Non-geometrical optics investigation of mode conversion in weakly relativistic inhomogenous plasmas
[DE85-013480] N86-12102

ELECTRON DIFFRACTION

Experimental investigation of recording of dynamic holograms within absorption contour of resonant atomic medium N86-11981

ELECTRON DISTRIBUTION

Energy confinement experiments on Doublet 3 with high power neutral beam heating
[DE85-014324] N86-12110

ELECTRON EMISSION

An introduction to electrical breakdown in dielectrics
[AD-A156465] N86-11415

Double tearing mode in plesma with magnetic braiding
N86-11919

Effect of high electric field on minority carrier generation in silicon depletion layer N86-11938

ELECTRON ENERGY

A new apparatus for testing bubble vials, electronic levels and automatic levels N86-11614

ELECTRON IRRADIATION

Kinetics analysis of diffusion of point defects to dislocations following pulsed neutron and electron irradiations
[DE85-012768] N86-12037

ELECTRON MICROSCOPY

Processing and microstructural characterization of B4C-Al cermets
[DE85-013195] N86-11326

Direct coupling of microbore HPLC columns to MS systems
[NASA-CR-176292] N86-11436

Multidimensional ion microbeam analysis
[DE85-014699] N86-12055

Analytical electron microscopy study of shock synthesized zinc ferrite
[DE85-015144] N86-12140

ELECTRON MOBILITY

An introduction to electrical breakdown in dielectrics
[AD-A156465] N86-11415

A summary report on the Flat-Plate Solar Array Project Workshop on Transparent Conducting Polymers
[NASA-CR-176302] N86-11669

Effect of high electric field on minority carrier generation in silicon depletion layer N86-11938

ELECTRON PHONON INTERACTIONS

Statics and adiabatic dynamics of nonlinear excitations in defected polyacetylene
[DE85-014118] N86-12143

ELECTRON PLASMA

Relationship between interatomic bonding and electron transport in plasma deposited amorphous metal alloys
[DE85-014710] N86-11337

ELECTRON PUMPING

Electroionization IR Xe-ATOM laser N86-11975

ELECTRON SOURCES

Status of SLC
[DE85-013071] N86-12097

ELECTRON STATES

Photon induced electron attachment
[AD-A156506] N86-11467

The chemical production of excited state molecules
[AD-A157276] N86-12021

ELECTRON TRANSFER
Nuclear interlevel transfer driven by electronic transitions
[DE85-014103] N86-12149
ELECTRON TRANSITIONS
Transition radiation as a practical X-ray source
[DE85-013201] N86-12036
ELECTRON TUBES
XUV preionization effects in high power magnetically insulated diodes
[DE85-013142] N86-12109
ELECTRON TUNNELING
Submillimeter quantum electronics
[AD-A157432] N86-11417
Discussion of the superconducting critical temperature in a N-S multi-film structure N86-11936
ELECTRONIC FILTERS
Comparisons of different observation methods of a LaCoste and Romberg G gravimeter N86-11612
ELECTRONIC MAIL
MICROLAN, file transfer program for microprocessors
[AD-A156519] N86-11900
ELECTRONS
Calculation of the electron backscattering coefficient by Monte Carlo simulation N86-11864
High energy physics
[DE85-014272] N86-12063
Higher luminosities via alternative incident channels
[DE85-014355] N86-12118
ELECTROPHOTOMETRY
The 1982-1984 Eclipse of Epsilon Aurigae
[NASA-CP-2384] N86-12168
Optical photometry of the 1982-1984 eclipse of Epsilon Aurigae N86-12169
Photometric support for future astonomical research
N86-12175
Intermediate and narrow band photometry of Epsilon Aurigae N86-12177
Astronomical research at the Hopkins Phoenix Observatory N86-12182
Photoelectric observations of the long-period eclipsing binaries at Yonsei University Observatory N86-12184
ELECTROSTATIC WAVES
Simulation of quiet start magnetized plasmas, including Maxwellian and velocity-space ring distributions
[DE85-014394] N86-12112
ELEMENTARY EXCITATIONS
Theory of the critical temperature for superconductors with small lambda (1) N86-11937
ELEMENTARY PARTICLES
Representations of the group of diffeomorphisms in the physics of particles, gravity and fluids
[DE85-007031] N86-12028
Research in elementary particle physics
[DE85-014062] N86-12041
ELEVATION
CRC control systems laboratory gyro test facility
[CRC-1385] N86-11205
ELLIPSOIDS
Precise geoid computations at mountainous coastlines in view of vertical datum determinations N86-11561
ELONGATION
Inertia, stability and ductibility in uniaxial tension at high strain rate
[DE85-007671] N86-11546
EMBEDDED COMPUTER SYSTEMS
A computer engineering curriculum for the Air Force Academy: An implementation plan
[AD-A156464] N86-11857
EMBEDDING
The embedded operating system project
[NASA-CR-176280] N86-11893
EMISSION SPECTRA
Emission threshold for cerenkov radiation
[AD-A157615] N86-12025
Double differential neutron emission cross sections of (10)B and (1)B at 6, 10 and 14 MeV and of (6)Li, (7)Li and (12)C at 14 MeV
[DE85-012749] N86-12056
EMITTANCE
Disruption angles
[DE85-015138] N86-12032
Very high energy colliders
[DE85-013075] N86-12100
Using the TEVATRON beam position monitor system to investigate transverse phase space
[DE85-014261] N86-12105
EMITTERS
Dose distribution and the relative biological effectiveness of internal alpha emitters
[DE85-013041] N86-11845
EMOTIONS
Psychological aspects of personnel contamination
[DE85-012955] N86-11853
ENCAPSULATING
Development of castor-oil-resistant polyurethane sonar encapsulants
[AD-A157576] N86-11347
ENCKE METHOD
Computational errors and their control in the determination of satellite orbits N86-11211
ENERGETIC PARTICLES
Plasmas in the Earth's magnetotail
[AD-A157320] N86-11716
ENERGY ABSORPTION
Binding energy of donors in GaAs-Ga(1-x) Al(x)As quantum well structures N86-11940
ENERGY BUDGETS
Horizontal fluxes in real and model atmospheres
N86-11792
ENERGY CONSERVATION
Assessment of technical strengths and information flow of energy conservation research in Japan. Volume 2: Background document
[DE85-013759] N86-12165
ENERGY CONVERSION
Advanced Thermionic Technology Program: Summary report, Volume 3
[DE85-009360] N86-11674
Thin film research. Volume 1
[AD-A157606] N86-12137
Thin film research. Volume 2
[AD-A157609] N86-12138
ENERGY CONVERSION EFFICIENCY
A 25.5 percent AMO gallium arsenide grating solar cell
[NASA-TM-87134] N86-11671
High-efficiency Al sub 2 O sub 3:Ti sup 3+ tunable laser N86-11973
ENERGY DISSIPATION
An experimental study of energy loss mechanisms and efficiency consideration in the low power dc arcjet
[NASA-TM-87123] N86-11224
Effect of a viscoelastic boundary inset on vibrational characteristics of a beam N86-11494
ENERGY DISTRIBUTION
Climate simulation and change: A simple energy balance climate model N86-11731
ENERGY GAPS (SOLID STATE)
Dominant moving species in the formation of amorphous NZr by solid-state reaction
[DE85-014855] N86-12053
ENERGY LEVELS
A new apparatus for testing bubble vials, electronic levels and automatic levels N86-11614
Binding energy of donors in GaAs-Ga(1-x) Al(x)As quantum well structures N86-11940
ENERGY SOURCES
The 1984 annual report on Alaska's mineral resources
[DE85-015235] N86-11651
ENERGY SPECTRA
Energy characteristics of laser with saturable anisotropic absorbing medium in cavity N86-11968
AGS polarized beam facility
[DE85-011834] N86-12038
Few-nucleon transfer reactions on deformed nuclei
[DE85-013869] N86-12064
ENERGY STORAGE
Multispectroscopic studies of the electronic structure of electrode materials for high energy density batteries: 1-2, 1-3 intermetallic compounds with B32 structure
[DE85-014575] N86-11684
Efficiency of optically-pumped XeF-laser N86-11977
Assessment of technical strengths and information flow of energy conservation research in Japan. Volume 2: Background document
[DE85-013759] N86-12165
ENERGY TECHNOLOGY
Arctic Energy Technologies Workshop: Proceedings
[DE85-003360] N86-11649
ENERGY TRANSFER
Comparison of energy transport measurements and computer simulations in a single module prototype for PBFA 2
[DE85-013960] N86-12119
What extent will small-scale laser-beam fluctuations seed the Rayleigh-Taylor instability in direct-drive targets
[DE85-014408] N86-12131
Fractal-like, but non-fractal, behavior of one step dipolar energy transfer on regular lattices with excluded volume
[AD-A157382] N86-12136
ENGINE AIRFRAME INTEGRATION
Some considerations in propeller and airframe integration N86-11164
Problems of the integration of propellers in airframes, especially for high performance twin-engine aircraft
N86-11165
ENGINE DESIGN
Development of modern turboprop engines
N86-11168
Current and future engine applications of Gr/PI composites N86-11291
ENGINE INLETS
Low-cost, net-shape ceramic radial turbine program
[AD-A157532] N86-11202
ENGINE PARTS
Turbine Engine Hot Section Technology (HOST)
[NASA-CP-2289] N86-11495
High temperature static strain sensor development program N86-11500
ENGINE TESTS
Development of modern turboprop engines
N86-11168
RE-1000 free-piston Stirling engine update
[NASA-TM-87126] N86-11658
ENGINES
Dish electric systems heat engine assessment
[DE85-013942] N86-11479
CELCAP: A computer model for cogeneration system analysis
[NASA-CR-176306] N86-11896
ENTHALPY
Tracer test analysis of the Klamath Falls geothermal resource: A comparison of models
[DE85-009924] N86-11678
ENVIRONMENT EFFECTS
High Temperature Polymer Matrix Composites
[NASA-CP-2385] N86-11260
Environmental effects in the fatigue behavior of copper nickel alloys N86-11307
Aerial photography and ground verification at power plant sites: Wisconsin power plant impact study
[PB85-197358] N86-11656
Saltwater wetlands for wastewater management environmental assessment
[PB85-201267] N86-11697
ENVIRONMENTAL MONITORING
Monitoring climate in real time: An application of the Climate Anomaly Monitoring System (CAMS)
N86-11765
ENVIRONMENTAL QUALITY
China report: Science and technology
[JPRS-CST-85-014] N86-11918
China report: Science and technology
[JPRS-CST-85-015] N86-11994
ENVIRONMENTAL TESTS
Intermediate load modules for test and evaluation: Fixed price research and development
[NASA-CR-176135] N86-11664
ENZYME ACTIVITY
Importance of phytoalexin tolerance and detoxification for pathogenicity
[DE85-014759] N86-11257
ENZYMES
Determination of the steady-state behavior of immobilized (BETA)-galactosidase utilizing an integral reactor scheme
[DE85-012900] N86-11256
EPITAXY
Surface and interfacial properties on Ga0.47In0.53As alloys
[AD-A157343] N86-11316
An interfacial analysis of MoNb-GaAs Schottky barrier diodes N86-11941
EPOXY COMPOUNDS
New processable modified polyimide resins for adhesive and matrix applications N86-11269
EPOXY MATRIX COMPOSITES
New processable modified polyimide resins for adhesive and matrix applications N86-11269
Polyimide composites: Application histories
N86-11266
EPOXY RESINS
Factors affecting the processing of epoxy film adhesives N86-11252
Reduction of moisture effects during the cure of epoxy adhesives used in composite repair N86-11254
New processable modified polyimide resins for adhesive and matrix applications N86-11269
Recent developments in polyimide and bismaleimide adhesives N86-11270
Characterization of the relationship of the cure cycle chemistry to cure cycle processing properties
[NASA-CR-176256] N86-11339
EQUATIONS
Energy characteristics of waveguide CO sub 2-laser
N86-11978
EQUATIONS OF MOTION
Calculation of particle dynamics effects on laser velocimeter data N86-11438
The stability of Timoshenko beams conveying a compressible fluid N86-11492
Inertia, stability and ductibility in uniaxial tension at high strain rate
[DE85-007671] N86-11546

EQUATIONS OF STATE
Detonation reaction zone studies on TATB explosives [DE85-015710] N86-11361
Strain rate dependence in steady, plastic shock waves [DE85-014703] N86-11544
EOS for polycrystalline quartz [DE85-014241] N86-12148
EQUATORIAL ATMOSPHERE
Circulation and weather for MAM and JJA 1984 N86-11769
EQUATORIAL REGIONS
Possible cross equatorial influence of the northeast monsoon on the equatorial westerlies over Indonesia [AD-A156907] N86-11759
EQUILIBRIUM FLOW
Development of a Navier-Stokes analysis for the flow in disk pumps [AD-A157454] N86-11428
The effect of topography on the evolution of unstable disturbances in a baroclinic atmosphere N86-11750
ERBIUM COMPOUNDS
Surface impedance of several magnetic superconductors [DE85-014101] N86-12155
EROSION
An experimental study of energy loss mechanisms and efficiency consideration in the low power dc arcjet [NASA-TM-87123] N86-11224
Environmental effects in the fatigue behavior of copper nickel alloys N86-11307
Initial plasma formation during exposure of absorbing materials to laser radiation with plane expansion geometry of the forming plasma N86-11956
Los Alamos Spheromak Program [DE85-012769] N86-12096
ERROR ANALYSIS
Correcting for particle counting bias error in turbulent flow N86-11439
Influences of systematic differences between different star catalogues on the results of latitude and time determinations with the PZT 2 N86-11575
On the works and results of investigations concerning the recent movements in the Karpatho-Balkan region N86-11593
A cascaded coding scheme for error control [NASA-CR-176276] N86-11895
Integrated analysis of error detection and recovery [NASA-CR-172571] N86-11906
A cascaded coding scheme for error control [NASA-CR-176287] N86-11911
Steady-state detonation of charges of finite length N86-11966
ERROR DETECTION CODES
A cascaded coding scheme for error control [NASA-CR-176276] N86-11895
Bayesian extensions to a basic model of software reliability [AD-A157296] N86-11901
Integrated analysis of error detection and recovery [NASA-CR-172571] N86-11906
A cascaded coding scheme for error control [NASA-CR-176287] N86-11911
ESTIMATES
Estimation of particle size based on LDV measurements in a de-accelerating flow field N86-11440
ESTUARIES
User guide for WIFM-SAL (WES Implicit Flooding Model-SAL): A two-dimensional vertically integrated, time-varying estuarine transport model [AD-A157446] N86-11825
ETHANE
Flow reactor studies over wide temperature and pressure ranges of atom and radical reaction rates important in ignition and combustion [AD-A156931] N86-12020
ETHYLENE
Flight worthiness of fire resistant hydraulic systems: Volume 1 [AD-A157618] N86-11199
ETHYLENE OXIDE
Electrical relaxation in poly(ethylene oxide) [AD-A157301] N86-11342
EULER EQUATIONS OF MOTION
Development of an explicit multigrid algorithm for quasi-three-dimensional viscous flows in turbo-machinery [NASA-TM-87128] N86-11146
Aerodynamics of wide-chord propellers in non-axisymmetric flow N86-11153
EULER-CAUCHY EQUATIONS
A numerical analysis of a queue with network access flow control [AD-A157526] N86-11913
EULER-LAGRANGE EQUATION
Variational principles for Earth rotation N86-11580
Computer codes for fluid-structure interactions N86-11887
EUROPE
Specification of mean surface temperature anomalies in Europe and Asia during the fall months N86-11806
Land-surface fluctuations and associated climatic variability N86-11807
EVALUATION
Lateral dampers for thrust bearings [NASA-CR-174924] N86-11474
An evaluation of three graphics packages: The methodology and results N86-11870
EVAPORATION
Oxide cathode mechanisms: Electronic and structural features of oxide cathode surfaces [AD-A157666] N86-11418
Laser evaporation of metal in gaseous atmosphere N86-11957
EVOLUTION (LIBERATION)
Characterization of the relationship of the cure cycle chemistry to cure cycle processing properties [NASA-CR-176256] N86-11339
EXCITATION
Excitation of discharge in air by laser radiation N86-11961
Investigation of efficiency of generation of difference-frequency laser radiation in waveguide N86-11969
Distributed-feedback lasers with active framing medium N86-11971
Energy characteristics of waveguide CO sub 2-laser N86-11978
Chromium- and neodymium-activated gadolinium-scandium-gallium garnet crystal: A new laser active medium N86-11979
Multiphoton Raman scattering of light excited in crystals by a copper-vapor laser N86-11986
The chemical production of excited state moleculea [AD-A157276] N86-12021
EXERCISE PHYSIOLOGY
Perceptual and physiological responses during exercise in cool and cold water [AD-A157334] N86-11840
Physiological effects of training [AD-A157417] N86-11841
EXHAUST EMISSION
HOST liner cyclic facilities N86-11519
EXHAUST GASES
Laboratory evaluation of the protocol for the volatile organic sampling train [PB85-201184] N86-11694
EXHAUST NOZZLES
A novel oscillating jet: Its effect on ejector thrust augmentation [AD-A157480] N86-11201
Particle sizing in a solid rocket motor using the management of scattered light [AD-A156480] N86-11226
EXOTHERMIC REACTIONS
Chemical control of rate and onset temperature of nadimide polymerization N86-11271
EXPERIMENTATION
Ultraviolet lasing in helium-nitrogren mixtures N86-11974
EXPERT SYSTEMS
Expert systems development and application [NASA-TM-86746] N86-11194
Description of an experimental expert system flight status monitor [NASA-TM-86791] N86-11195
EXPLORATION
Mars base buildup scenarios [DE85-014132] N86-12193
EXPLOSION SUPPRESSION
Fire growth in combat ships [NBSIR-85/3159] N86-11364
EXPLOSIVE FORMING
Shock-wave synthesis of titanium aluminides [DE85-015140] N86-11324
Synthesis of nickel-aluminum alloys by shock compression of composite particles [DE85-015165] N86-11328
Shock consolidation of IN-100 nickel-base superalloy powder [DE85-015159] N86-11360
Analytical electron microscopy study of shock synthesized zinc ferrite [DE85-015144] N86-12140
EXPLOSIVE WELDING
Explosive welding in the 1990's N86-11237
Explosive welding of tubular configurated joints for critical applications N86-11238
Explosive tube-to-fitting joining of small-diameter tubes N86-11239
The use of explosive forming for fastening and joining structural and pressure components N86-11240
Explosive welding of aluminum, titanium and zirconium to copper sheet metal N86-11241
EXPLOSIVES
Detonation reaction zone studies on TATB explosives [DE85-015710] N86-11361
Multi-megampere current interruption from explosive deformation of conductors [DE85-012756] N86-11419
Explosive generators for low-cost pulsed power [DE85-013436] N86-11421
Surface sampling techniques using ultraviolet illumination [AD-A156457] N86-11458
Steady-state detonation of charges of finite length N86-11966
EXPOSURE
Acute pulmonary effects of formaldehyde exposure in humans [DE85-014728] N86-11848
Initial plasma formation during exposure of absorbing materials to laser radiation with plane expansion geometry of the forming plasma N86-11956
EXTERNAL TANKS
Automatic fastening large structures: A new approach N86-11234
EXTREMELY LOW FREQUENCIES
Infrasound: A summary of interesting articles [FMV:ELEKTRO-A12:142/83] N86-12017
EXTREMELY LOW RADIO FREQUENCIES
Numerical solution of ionospheric filtration of ULF waves. Part 1: Method N86-11712
Numerical solution of ionospheric filtration of ULF waves. Part 2: Application N86-11713
EXTRUDING
Effects of manufacturing processes on structural allowables [AD-A157596] N86-11318
EYE MOVEMENTS
Visual information transfer. Part 1: Assessment of specific information needs. Part 2: Parameters of appropriate instrument scanning behavior [NASA-CR-176277] N86-11850

F

F-15 AIRCRAFT
Evaluation of fault reporting/fault isolation for F-15 aircraft [AD-A156516] N86-11197
FABRICATION
Evaluation of superplastic forming and weld-brazing for fabrication of titanium compression panels N86-11245
Factors affecting the processing of epoxy film adhesives N86-11252
Evaluation of a high temperature adhesive for fabricating graphite/PMR-15 polyimide structures N86-11268
Improvements in the fabrication of ceramic-fiber-ceramic-matrix composites by chemical vapor infiltration [DE85-015971] N86-11301
Processing and microstructural characterization of B4C-Al cermets [DE85-013195] N86-11326
Fabrication and use of zircaloy/tantalum-sheathed cladding thermocouples [EGG-TFBP-6739] N86-11461
Refractory alloy performance: Product form procurement and component fabrication [DE85-014658] N86-11477
Balloon-borne three-meter telescope for far-infrared and submillimeter astronomy [NASA-CR-176285] N86-12188
FABRICS
Strength and flexibility properties of advanced ceramic fabrics [NASA-TM-86824] N86-11340
FAILURE
Metallography of solid state bonds [DE85-014564] N86-11327
NERF: A computer program for the numerical evaluation of reliability functions user manual [ARL/STRUC-R-411] N86-11487
Failure rate model for cathodic delamination of protective coatings [AD-A157483] N86-11912
PBFA-2 vacuum insulator stack failure mechanisms [DE85-013118] N86-12090
FAILURE ANALYSIS
Use of hydration inhibitors to improve bond durability of aluminum adhesive joints N86-11251
Factors affecting the processing of epoxy film adhesives N86-11252
A Signorini model of bolt fastened laminated composites N86-11258
Turbine Engine Hot Section Technology (HOST) [NASA-CP-2289] N86-11495
Hot section viewing system N86-11498

FALLOUT
Thyroid absorbed dose for people at Rongelap, Utirik and Sifo on March 1, 1954
[DE85-014695] N86-11846
FAR INFRARED RADIATION
Far-infrared observations of Sagittarius B2: Reconsideration of source structure
[NASA-TM-88185] NC6-12167
Star formation in the inner galaxy: A far-infrared and radio study of two H2 regions
[NASA-TM-86720] N86-12185
Balloon-borne three-meter telescope for far-infrared and submillimeter astronomy
[NASA-CR-176285] N86-12188
The mass of hot, shocked CO in Orion: First observations of the J = 17 yields J = 16 transition at 153 microns
[AD-A157323] N86-12189
FAST NEUTRONS
Status of fast neutron nuclear data for (239)Pu
[DE85-012699] N86-12045
FASTENERS
Welding, Bonding and Fastening, 1984
[NASA-CP-2387] N86-11227
Mechanical fasteners for advanced composite materials N86-11232
Automatic fastening large structures: A new approach N86-11234
Stress corrosion resistant fasteners N86-11235
Derivation and test of elevated temperature thermal-stress-free fastener concept N86-11236
FATIGUE (MATERIALS)
Tensile fatigue damage and degradation of random short-fiber SWC composite N86-11259
Composite materials N86-11295
NERF: A computer program for the numerical evaluation of reliability functions user manual
[ARL/STRUC-R-411] N86-11487
Exploratory development of FMR (ferromagnetic resonance) advanced surface flaw detection methods
[AD-A157438] N86-11489
Turbine Engine Hot Section Technology (HOST)
[NASA-CP-2289] N86-11495
FATIGUE LIFE
Validation of structural analysis methods using burner liner cyclic rig test data N86-11518
Life prediction and constitutive behavior N86-11520
Creep fatigue life prediction for engine hot section materials (isotropic) N86-11521
FATIGUE TESTS
Environmental effects in the fatigue behavior of copper nickel alloys N86-11307
FAULT TOLERANCE
The embedded operating system project
[NASA-CR-176280] N86-11893
Easy impossibility proofs for distributed concensus problems
[AD-A157411] N86-11903
Integrated analysis of error detection and recovery
[NASA-CR-172571] N86-11906
FEASIBILITY ANALYSIS
Mars base buildup scenarios
[DE85-014132] N86-12193
FEED SYSTEMS
The design of a thermally efficient 1:256 KU-band feed network for a MMIC phased array N86-11400
A high-efficience, low-phase error waveguide lens for a transform feed antenna N86-11409
FEEDBACK
Feedback stabilization of optical interferometer
[AD-A156912] N86-11459
FEEDBACK CONTROL
Simple construction and performance of a conical plastic cryocooler N86-11378
A cascaded coding scheme for error control
[NASA-CR-176276] N86-11895
FEEDBACK FREQUENCY MODULATION
The relations between voltage and magnetic field of superconducting weaklink (2) N86-11935
FERMIONS
Neutron scattering studies of the heavy Fermion superconductors
[DE85-014829] N86-12144
FERRIC IONS
Degradation of ionic membranes in the zinc/ferricyanide battery
[DE85-008469] N86-11681
FERRIMAGNETS
Design for a high field combined function superferric magnet
[DE85-014827] N86-11944
Window frame or superferric magnet design for low B(3T) heavy ion storage ring study
[DE85-013268] N86-12095
FERRITES
Chemical synthesis under shock compression
[DE85-015166] N86-11325
Analytical electron microscopy study of shock synthesized zinc ferrite
[DE85-015144] N86-12140
FERRITIC STAINLESS STEELS
Overview of MIT, ADIP irradiation experiments
[DE85-014469] N86-12060
FERROELECTRICITY
Photoinduced Rayleigh scattering of light in crystals N86-11985
FERROMAGNETIC RESONANCE
Exploratory development of FMR (ferromagnetic resonance) advanced surface flaw detection methods
[AD-A157438] N86-11489
FERROMAGNETISM
Electronic and magnetic structure of chromium surfaces and chromium monolayers on iron
[DE85-014542] N86-11322
Itinerant electron ferromagnetism in Fe-alloyed, Ni3Al based materials
[DE85-013989] N86-11331
Magnetic measurements of monolayer-thickness films of Cr sandwiched by Au
[DE85-015005] N86-12150
FERROUS METALS
Degradation of ionic membranes in the zinc/ferricyanide battery
[DE85-008469] N86-11681
FERTILIZATION
Relationship between alkylation sites and induction of dominant lethals and heritable translocations in mice
[DE85-014309] N86-11835
FETUSES
Teratogenic effects of microwave radiation
[PB85-207462] N86-11837
FEYNMAN DIAGRAMS
High energy physics
[DE85-014272] N86-12063
FIBER COMPOSITES
Advances in joining techniques used in development of SPF/DB titanium sandwich reinforced with metal matrices N86-11247
PMR polyimides from solutions containing mixed endcaps N86-11263
High temperature, short term tensile strength of C6000/PMR-15 composites N86-11279
FIBER OPTICS
Spectrally-broad picosecond light source
[DE85-015177] N86-11471
Fiber optic pressure sensors in skin-friction measurements
[NASA-CR-176294] N86-11838
FIBER REINFORCED COMPOSITES
Rapid adhesive bonding and field repair of aerospace materials N86-11253
Tensile fatigue damage and degradation of random short-fiber SWC composite N86-11259
Matrix resin development at NASA Langley Research Center N86-11264
Properties of autoclaved Gr/PI composites made from improved tack PMR-15 prepreg N86-11276
Thermo-oxidative stability of graphite fiber/PMR-15 polyimide composites at 350 deg C N86-11277
Surface protection of graphite fabric/PMR-15 composites subjected to thermal oxidation N86-11281
Effects of real-time thermal aging on graphite/polyimide composites N86-11283
Development of design data for propulsion PMR-15 composites N86-11285
V-378A: A modified bismaleimide for advanced composites N86-11287
Application of Gr/PMR-15 to commercial aircraft N86-11289
Fabrication process of a high temperature polymer matrix engine duct N86-11290
Current and future engine applications of Gr/PI composites N86-11291
FIBER STRENGTH
Strength and flexibility properties of advanced ceramic fabrics
[NASA-TM-86824] N86-11340
FICKS EQUATION
Reduction of moisture effects during the cure of epoxy adhesives used in composite repair N86-1125[illegible]
FIELD INTENSITY METERS
Effect of high electric field on minority carrier generation in silicon depletion layer N86-11938
FILLERS
Initial investigation of cryogenic wind tunnel model filler materials N86-11255
FILM THICKNESS
Discussion of the superconducting critical temperature in a N-S multi-film structure N86-11936
FILTRATION
Adjustment of the latitude data by least-squares collocation approach N86-11562
Magnetic filtration N86-11917
FINES
Experiments with solid particle seeding N86-11442
FINITE DIFFERENCE THEORY
Block-implicit multigrid calculation of three-dimensional recirculating flows
[DE85-010250] N86-11434
Three-dimensional heat transfer analysis using the PATRAN-G solids modeling and Q-TRAN thermal analysis computer codes N86-11867
Finite difference calculations of voltages generated in thin dielectric layers subjected to shock loading N86-11878
Application of Flux-Corrected Transport (FCT) to heat transfer/fluid mechanics problems N86-11883
A hybrid vortex-in-cell finite-difference numerical method for turbulent shear layer computation N86-11886
On the implementation of a class of upwind schemes for system of hyperbolic conservation laws
[NASA-TM-86839] N86-11907
Algebraic grid generation using tensor product B-splines N86-11908
On symmetric and upwind TVD schemes
[NASA-TM-86842] N86-11909
FINITE ELEMENT METHOD
Transportation system impact limiter design using rigid polyurethane foam
[DE85-015088] N86-11354
Calculation of RF fields in axisymmetric cavities
[DE85-014135] N86-11414
Burner liner thermal/structural load modelling N86-11514
A comparison of measured and calculated thermal stresses in a hybrid metal matrix composite spar cap element
[NASA-TM-86729] N86-11525
A review of the literature on finite-element modeling of laminated composite plates N86-11529
Thin plates with rapidly varying thickness, and their relation to structural optimization
[AD-A157607] N86-11534
Miniaturization of specimens for mechanical testing
[DE85-014506] N86-11536
Three-dimensional heat transfer analysis using the PATRAN-G solids modeling and Q-TRAN thermal analysis computer codes N86-11867
Interface elements for heat transfer analysis N86-11868
Interactive graphics for finite element preprocessing N86-11871
Geological calculations with SANGRE and MANTLE: Recent results N86-11872
Thermo-mechanical analyses of laser-heated surfaces N86-11877
Photoelectron trajectory analyses of streak tubes N86-11880
Numerical Techniques in Acoustics
[NASA-CP-2404] N86-12007
Application of high order acoustic finite elements to transmission losses and enclosure problems N86-12008
On the computation of structural vibrations induced by a low-speed turbulent flow N86-12009
FINLAND
Finnish measurements of the Fennoscandian land uplift gravity lines in Finland 1966-1984 N86-11606
FIRE CONTROL
Methods to calculate the response time of heat and smoke detectors installed below large unobstructed ceilings
[NBSIR-85/3167] N86-11365
FIRE DAMAGE
Fire growth in combat ships
[NBSIR-85/3159] N86-11364
FIRES
Flight worthiness of fire resistant hydraulic systems: Volume 1
[AD-A157618] N86-11199
Applied model validation
[NBSIR-85-3154-1] N86-11363
Fire growth in combat ships
[NBSIR-85/3159] N86-11364
Methods to calculate the response time of heat and smoke detectors installed below large unobstructed ceilings
[NBSIR-85/3167] N86-11365
FISSION
Status of fast neutron nuclear data for (239)Pu
[DE85-012699] N86-12045
R-matrix analysis of the (239) Pu neutron cross sections
[DE85-013095] N86-12052

FISSURES (GEOLOGY)
Near-surface deformations and stresses in the area of the Tolbachik great fissure eruption of 1975-1976 (Kamchatka) from geodetic data N86-11600

FITTINGS
Langley Research Center standard for the evaluation of socket welds N86-11243

FLAME IONIZATION
Optimization of parameters of chemical CO laser by increasing length of active medium N86-11976

FLAME PROPAGATION
Explosion waves generated by deflagration combustion N86-11960
Flame propagation in pulsed acceleration field N86-11964
Occurrence of pressure wave during spontaneous ignition of gas ahead of flame front in closed vessel N86-11965

FLAMES
Simulation of flame propagation through vorticity regions using the discrete vortex method N86-11882
Calculation of formation time of minimal nucleus of flame during ignition of explosive mixtures by electrical discharges N86-11963

FLAMMABLE GASES
Calculation of formation time of minimal nucleus of flame during ignition of explosive mixtures by electrical discharges N86-11963
Occurrence of pressure wave during spontaneous ignition of gas ahead of flame front in closed vessel N86-11965

FLAT PLATES
Solid-melt interface studies of high-speed silicon sheet growth [DE85-008783] N86-11349
A summary report on the Flat-Plate Solar Array Project Workshop on Transparent Conducting Polymers [NASA-CR-176302] N86-11669

FLEXIBILITY
Strength and flexibility properties of advanced ceramic fabrics [NASA-TM-86824] N86-11340
Flexible vibrations of a uniform elastic beam with arbitrary supports and lumped masses N86-11885

FLEXIBLE BODIES
The analysis and calculation for the dynamic characteristics of the omni-axial movable flexible joint nozzle N86-11925

FLEXING
Effect of a viscoelastic boundary inset on vibrational characteristics of a beam N86-11494

FLIGHT ALTITUDE
A new characterization of the icing environment below 10,000 feet AGL from 7,000 miles of measurements in supercooled clouds N86-11743

FLIGHT CHARACTERISTICS
Mission-oriented requirements for updating MIL-H-8501: Calspan proposed structure and rationale [NASA-CR-177371] N86-11204
Meteorological and Environmental Inputs to Aviation Systems [NASA-CP-2388] N86-11735
A model of a downburst, a wind tunnel program on planetary boundary layer, and airship in turbulence N86-11748

FLIGHT CONDITIONS
Mission-oriented requirements for updating MIL-H-8501: Calspan proposed structure and rationale [NASA-CR-177371] N86-11204
Overview of meteorological inputs to NASP N86-11736
Airline meteorological requirements N86-11737
General aviation's meteorological requirements N86-11738
Corporate/commuter airlines meteorological requirements N86-11739
Overview of NASA's programs N86-11741
Adverse weather impact on aviation safety, investigation and oversight N86-11742
Advance particle and Doppler measurement methods N86-11745

FLIGHT CONTROL
Expert systems development and application [NASA-TM-86746] N86-11194
Description of an experimental expert system flight status monitor [NASA-TM-86791] N86-11195

FLIGHT HAZARDS
Meteorological and Environmental Inputs to Aviation Systems [NASA-CP-2388] N86-11735
Overview of FAA's aircraft icing program N86-11740
Overview of NASA's programs N86-11741
Adverse weather impact on aviation safety, investigation and oversight N86-11742
A new characterization of supercooled clouds below 10,000 feet AGL N86-11744
Development of a wind shear performance envelope N86-11746

FLIGHT SIMULATION
A comparison of the NAVTOLAND (Navy vertical takeoff and landing) SH-2F helicopter model with the requirements of MIL-H-8501A and with flight data [AD-A157297] N86-11198
Visual and motion cueing in helicopter simulation [NASA-TM-86818] N86-11208
Visual information transfer. Part 1: Assessment of specific information needs. Part 2: Parameters of appropriate instrument scanning behavior [NASA-CR-176277] N86-11850

FLIGHT TESTS
Expert systems development and application [NASA-TM-86746] N86-11194
Description of an experimental expert system flight status monitor [NASA-TM-86791] N86-11195

FLIGHT TRAINING
Visual information transfer. Part 1: Assessment of specific information needs. Part 2: Parameters of appropriate instrument scanning behavior [NASA-CR-176277] N86-11850
A computer-based educational approach to the Air Command and Staff College associate program [AD-A156460] N86-12160

FLOODS
The distribution of rainfall along the coast of northern Peru during 1982-83 N86-11782
User guide for WIFM-SAL (WES Implicit Flooding Model-SAL): A two-dimensional vertically integrated, time-varying estuarine transport model [AD-A157446] N86-11825

FLOW CHARACTERISTICS
Design concept and performance prediction technique for potential flows around advanced propellers N86-11150

FLOW DISTRIBUTION
A review of ARA research into propeller aerodynamic prediction methods N86-11151
A unified approach for the aerodynamics and acoustics of propellers in forward motion N86-11155
A general theory of arbitrary motion aerodynamics using an aeroacoustic approach N86-11157
Summary of recent NASA propeller research N86-11158
Study of the 3D wake of an aerial propeller N86-11161
A parametric analysis of flow structure and performance in a vortex controlled radial diffuser N86-11182
Ground effect on a rotor wake [COLL-AERONAUTICS-8510] N86-11187
An experimental study of energy loss mechanisms and efficiency consideration in the low power dc arcjet [NASA-TM-87123] N86-11224
Simple construction and performance of a conical plastic cryocooler N86-11378
On stratified vortex motions under gravity [AD-A156930] N86-11427
Wind Tunnel Seeding Systems for Laser Velocimeters [NASA-CP-2393] N86-11437
Calculation of particle dynamics effects on laser velocimeter data N86-11438
Correcting for particle counting bias error in turbulent flow N86-11439
Estimation of particle size based on LDV measurements in a de-accelerating flow field N86-11440
Experiments with solid particle seeding N86-11442
Seeding techniques used in the Vortex Research Facility N86-11443
Assessment of a 3-D boundary layer code to predict heat transfer and flow losses in a turbine N86-11508
Gas-side heat transfer with rotation N86-11509

FLOW MEASUREMENT
Airflow calibration of a bellmouth inlet for measurement of compressor airflow in turbine-powered propulsion simulators [NASA-TM-84399] N86-11209
Evaluation of superplastic forming and weld-brazing for fabrication of titanium compression panels N86-11245
Correcting for particle counting bias error in turbulent flow N86-11439
Generating aerosols for laser velocimeter seeding N86-11455
Laser anemometry for hot section applications N86-11503
Time-of-flight anemometer for hot section applications N86-11504

FLOW THEORY
Block-implicit coupled calculation of fluid flows [DE85-004038] N86-11432

FLOW VELOCITY
Response behavior of hot-wires and films to flows of different gases [NBSIR-85/3203] N86-11366
A technique to measure the size of particles in laser Doppler velocimetry applications N86-11457
Characteristics of an axisymmetric sudden expansion flow [NASA-CR-176278] N86-11465
Laser anemometry for hot section applications N86-11503
Time-of-flight anemometer for hot section applications N86-11504

FLOW VISUALIZATION
Water tunnel flow visualization using a laser [NASA-TM-86743] N86-11206
Seeding techniques used in the Vortex Research Facility N86-11443
Laser velocimetry measurement in a transonic tunnel N86-11448
Development of seeding techniques for small supersonic wind tunnel N86-11452

FLUCTUATION THEORY
Remote sensing of earth terrain [NASA-CR-176284] N86-11645

FLUID DYNAMICS
USSR report: Physics and mathematics [JPRS-UPM-85-005] N86-11945

FLUID FILMS
The Shock and Vibration Digest, volume 17, no. 4 [AD-A154112] N86-11527
Mechanical face seal dynamics update N86-11530

FLUID FLOW
Block-implicit coupled calculation of fluid flows [DE85-004038] N86-11432
Particle size distributions of several commonly used seeding aerosols N86-11441
Tracer test analysis of the Klamath Falls geothermal resource: A comparison of models [DE85-009924] N86-11678

FLUID MECHANICS
A novel oscillating jet: Its effect on ejector thrust augmentation [AD-A157480] N86-11201
Application of Flux-Corrected Transport (FCT) to heat transfer/fluid mechanics problems N86-11883

FLUID SWITCHING ELEMENTS
Experiments with a fully instrumented split Stirling cryocooler N86-11381

FLUIDIZED BED PROCESSORS
Overview of solid particle LV seeding techniques used at UTRC N86-11445
Evaluation of candidate materials in a static turbine cascade [DE85-008592] N86-11480

FLUORESCENCE
Impurity monitoring by laser-induced fluorescence techniques [DE85-014142] N86-11356

FLUX (RATE)
Parameterization of the atmospheric boundary layer for air pollution dispersion models [PB85-193548] N86-11730
Horizontal fluxes in real and model atmospheres N86-11792
Nuclear interlevel transfer driven by electronic transitions [DE85-014103] N86-12149

FLUX DENSITY
Multispectroscopic studies of the electronic structure of electrode materials for high energy density batteries: 1-2, 1-3 intermetallic compounds with B32 structure [DE85-014675] N86-11684
Climate simulation and change: A simple energy balance climate model N86-11731
The vacuum in the presence of electromagnetic fields and rotating boundaries N86-11916
The mass of hot, shocked CO in Orion: First observations of the J = 17 yields J = 16 transition at 153 microns [AD-A157323] N86-12189

FLYWHEELS
Railgun power supply system utilizing traction motors and vacuum interrupters [DE85-014123] N86-11214

FOCI
Relation between earthquake focal intensity and recent vertical Earth's crustal movements in the Rila-Rhodope seismic region N86-11615
Attenuation of macroseismic effects of earthquakes N86-11705

FOCUSING
Balloon-borne three-meter telescope for far-infrared and submillimeter astronomy [NASA-CR-176285] N86-12188

FOILS (MATERIALS)
Velocity measurements of laser driven flyers backed by high impedence windows
[DE85-015142] N86-11470
Surface properties of shocked lead
[DE85-009582] N86-11476

FOOD PROCESSING
Utilization of non-conventional systems for conversion of biomass to food components: Potential for utilization of algae in engineered foods
[NASA-CR-176257] N86-11630

FORCE DISTRIBUTION
A study of the cornering forces generated by aircraft tires on a tilted, free-swiveling nose gear
[NASA-TP-2481] N86-11522

FORCED CONVECTION
The effect of the Hadley circulation on the meridional propagation of stationary waves N86-11732

FORECASTING
Mars base buildup scenarios
[DE85-014132] N86-12193

FORESTS
High resolution spectrometry of leaf and canopy chemistry for biochemical cycling N86-11633
Forest canopy chemistry from Blackhawk Island, Wisconsin N86-11634
Application of AIS technology to forest mapping N86-11641
Forest species identification with high spectral resolution data N86-11643
Urban, forest, and agricultural AIS data: Fine spectral structure N86-11644
Integrated forast study on effects of atmospheric deposition. Project summary
[DE85-015972] N86-11690

FORGING
Effects of manufacturing processes on structural allowables
[AD-A157596] N86-11318

FORMALDEHYDE
Acute pulmonary effects of formaldehyde exposure in humans
[DE85-014728] N86-11848

FORMALISM
A body tensor formalism for elastic-plastic continua with applications in uniaxial extension N86-11491

FORMING TECHNIQUES
Sheet metal waveguide forming technique N86-11403

FORTRAN
Numerical solution of ionospheric filtration of ULF waves. Part 1: Method N86-11712

FORWARD SCATTERING
Seeding techniques used in the Vortex Research Facility N86-11443
Characteristics of an axisymmetric sudden expansion flow
[NASA-CR-176278] N86-11465

FOURIER TRANSFORMATION
Characterization methodology for PMR-15 N86-11272
Seeding requirements for scanning laser velocimetry N86-11446
Use of the wavenumber technique with the Lloyds mirror for an acoustic doublet
[AD-A156463] N86-11824

FRACTIONATION
Importance of phytoalexin tolerance and detoxification for pathogenicity
[DE85-014759] N86-11257
Particle size distributions of several commonly used seeding aerosols N86-11441

FRACTURE MECHANICS
Tensile fatigue damage and degradation of random short-fiber SWC composite N86-11259
A program to determine the effect of low-velocity impacts on the strength of the filament-wound rocket motor case for the space shuttle
[NASA-TM-87588] N86-11292
Creep and fracture of a yttria dispersed nickel-chromium alloy N86-11309
Deformation and fracture of P/M titanium alloys
[AD-A157416] N86-11317
Stress analyses of B-52 pylon hooks
[NASA-TM-84924] N86-11524
Senstivity of using blunt and sharp crack models in elastic-plastic fracture mechanics
[DE85-010288] N86-11537

FRACTURE STRENGTH
Bismaleimides and related maleimido polymers as matrix resins N86-11265

FRACTURES (MATERIALS)
Acoustic emission during deformation and fracture of A533B pressure vessel steel N86-11306
Uniaxial tensile deformation and fracture of dual-phase steels
[DE85-015034] N86-11536

FRACTURING
Deformation and fracture of P/M titanium alloys
[AD-A157416] N86-11317

FREE CONVECTION
Thermal convection in snow
[AD-A157577] N86-11648

FREE ELECTRON LASERS
Design optimization of the power generation system for a space-based free-electron laser N86-11861
Stationary pulse solutions for a free electron laser N86-11933

FREE RADICALS
Chemical control of rate and onset temperature of nadimide polymerization N86-11271

FREON
Polyurethane foam component lifetimes
[DE85-008206] N86-11355

FREQUENCY ANALYZERS
Research on optic spatial frequency analysis of linear structures in remote sensing images N86-11927

FREQUENCY CONTROL
Frequency-selection and mode-locking and Nd:YAG laser N86-11928

FREQUENCY CONVERTERS
New harmonic materials: Index engineering: Thin-thick quadrature frequency conversion
[DE85-012976] N86-12156

FREQUENCY DISTRIBUTION
Worldwide marine temperature variations on the season to century time scale N86-11771
Determination of parameters of elastic spherical shell from scattered wave field N86-11949

FREQUENCY MEASUREMENT
Concurrent and lagged relationships between precipitation frequency and 700 mb heights N86-11808

FREQUENCY MODULATION
Polar motion between 1900.0 and 1984.0 as determined by different techniques N86-11567

FREQUENCY RANGES
Considerations for extending the bandwidth of arrays beyond two octaves N86-11404

FREQUENCY REUSE
Calculation of allowable orbital spacings for the fixed-satellite service
[NASA-CR-176273] N86-11212

FREQUENCY SCANNING
Theory and experiment for infinite microstrip arrays N86-11406
New harmonic materials: Index engineering: Thin-thick quadrature frequency conversion
[DE85-012976] N86-12156

FREQUENCY SHIFT
Characteristics of an axisymmetric sudden expansion flow
[NASA-CR-176278] N86-11465

FREQUENCY STABILITY
Diffraction efficiency of three-dimensional phase hologram of diffuse object N86-11982

FREQUENCY STANDARDS
The use of wall-coated cells in atomic frequency standards
[AD-A157435] N86-12024

FRESH WATER
Coral reef hydrogeology
[DE85-012923] N86-11826

FUEL CELLS
Thermodynamics of chromium and iron in carbonate salts at 650(0)C
[DE85-013542] N86-11682

FUEL COMBUSTION
An investigation of the effects of fuel composition on combustion characteristics in a T-63 combustor
[AD-A157325] N86-11358
Surface combustion of liquid fuel in stream of gaseous oxidizer N86-11959

FUEL SYSTEMS
User's manual for AC-20-53A protection of airplane fuel systems against fuel vapor ignition due to lightning
[AD-A157619] N86-11191

FULL SCALE TESTS
Performance evaluation of full scale propellers by wind tunnel test N86-11160

FUNCTIONS (MATHEMATICS)
NERF: A computer program for the numerical evaluation of reliability functions user manual
[ARL/STRUC-R-411] N86-11487
High-speed signal processor developed N86-11995

FUNGI
Importance of phytoalexin tolerance and detoxification for pathogenicity
[DE85-014759] N86-11257

FUSELAGES
The state of the art in propfan turboprop noise N86-11175

FUSION (MELTING)
XUV preionization effects in high power magnetically insulated diodes
[DE85-013142] N86-12109
Rimfire: A six megavolt laser-triggered gas-filled switch for PBFA 2
[DE85-013959] N86-12115

FUSION REACTORS
Center for High Temperature Plasma Physics certified N86-11997
Mirror Fusion Test Facility (MFTF-B): Status
[DE85-012953] N86-12087
PBFA 2: A 100 TW pulsed power driver for the inertial confinement fusion program
[DE85-013956] N86-12116

G

GADOLINIUM
Chromium- and neodymium-activated gadolinium-scandium-gallium garnet crystal: A new laser active medium N86-11979

GADOLINIUM ALLOYS
Investigation on growth and laser properties of GGG:(Nd,Cr) single crystal
[DE85-014282] N86-12151

GALACTIC RADIATION
Cosmogenic-nuclide production by primary cosmic-ray protons
[DE85-012760] N86-12198

GALLIUM
Chromium- and neodymium-activated gadolinium-scandium-gallium garnet crystal: A new laser active medium N86-11979

GALLIUM ALLOYS
Investigation on growth and laser properties of GGG:(Nd,Cr) single crystal
[DE85-014282] N86-12151

GALLIUM ARSENIDES
Surface and interfacial properties of Ga0.47In0.53As alloys
[AD-A157343] N86-11316
Operating range of aluminum gallium arsenide quantum-well heterostructure lasers: tunability, power output and high energy emission N86-11464
A 25.5 percent AMO gallium arsenide grating solar cell
[NASA-TM-87134] N86-11671
Binding energy of donors in GaAs-Ga(1-x) Al(x)As quantum well structures N86-11940
An interfacial analysis of MoNb-GaAs Schottky barrier diodes N86-11941
Deep levels in semi-insulating GaAs N86-11943
Investigations of deep level defects in semiconductor material systems N86-12133
Carbon films grown from plasma on III-V semiconductors
[NASA-TM-87140] N86-12135
Investigation of defects in GaAsP superlattic structures
[DE85-012134] N86-12139

GALLIUM PHOSPHIDES
Investigations of deep level defects in semiconductor material systems N86-12133
Investigation of defects in GaAsP superlattic structures
[DE85-012134] N86-12139

GALLIUM SELENIDES
Improved solid state laser sources, volume 3
[DE85-012956] N86-11469

GALVANOMAGNETIC EFFECTS
Publications of the Astronomical Institute of the Czechoslovak Academy of Sciences, no. 61
[PUBL-61] N86-12069

GALVANOMETERS
Short-period SVSN-4 seismograph N86-11708
Magnification of low-sensitivity channels in seismographs with standard characteristics N86-11709

GAME THEORY
USSR report: Physics and mathematics
[JPRS-UPM-85-005] N86-11945

GAMMA FUNCTION
Monitoring climate in real time: An application of the Climate Anomaly Monitoring System (CAMS) N86-11765

GAMMA RAY BEAMS
MABE multibeam accelerator
[DE85-012035] N86-12121

GAMMA RAY LASERS
Nuclear interlevel transfer driven by electronic transitions
[DE85-014103] N86-12149

GAMMA RAYS
Si(Li)-NaI(Tl) sandwich detector array for measurements of trace radionuclides in soil samples [DE85-013865] N86-12062
GANGLIA
Is the cerebellum involved in motor and perceptual timing: A case study [AD-A157452] N86-11842
GARNETS
Investigation on growth and laser properties of GGG:(Nd,Cr) single crystal [DE85-014282] N86-12151
GAS CHROMATOGRAPHY
Characterization methodology for PMR-15 N86-11272
GAS DISCHARGE TUBES
Ultraviolet lasing in helium-nitrogren mixtures N86-11974
GAS DISCHARGES
A large area X-ray source and its preionization characteristics for XeCl excimer laser N86-11929
GAS FLOW
Response behavior of hot-wires and films to flows of different gases [NBSIR-85/3203] N86-11366
Seeding requirements for scanning laser velocimetry N86-11446
Surface combustion of liquid fuel in stream of gaseous oxidizer N86-11959
Explosion waves generated by deflagration combustion N86-11960
GAS GENERATORS
Development of modern turboprop engines N86-11168
GAS INJECTION
Overview of solid particle LV seeding techniques used at UTRC N86-11445
GAS IONIZATION
Electroionization IR Xe-ATOM laser N86-11975
GAS LASERS
On convective effects in gas lasers N86-12006
GAS PRESSURE
Laser evaporation of metal in gaseous atmosphere N86-11957
GAS TEMPERATURE
Dynamic gas temperature measurement system N86-11499
GAS TUNGSTEN ARC WELDING
Automatic orbital GTAW welding: Highest quality welds for tomorrow's high-performance systems N86-11229
A comparison of the physics of Gas Tungsten Arc Welding (GTAW), Electron Beam Welding (EBW), and Laser Beam Welding (LBW) [NASA-TM-86503] N86-11473
Refractory alloy performance: Product form procurement and component fabrication [DE85-014658] N86-11477
GAS TURBINE ENGINES
Turbine Engine Hot Section Technology (HOST) [NASA-CP-2289] N86-11495
Hot section viewing system N86-11498
Dynamic gas temperature measurement system N86-11499
High temperature static strain sensor development program N86-11500
Demonstration test of burner liner strain measurement systems: Interim results N86-11501
Development of heat flux sensors for turbine airfoils and combustor liners N86-11502
Turbine heat transfer N86-11505
Gas side heat transfer N86-11507
Jet array impingement heat transfer characteristics N86-11511
Combustion hot section technology N86-11512
HOST structural analysis program overview N86-11513
Burner liner thermal/structural load modelling N86-11514
Component-specific modeling N86-11515
The 3D inelastic analysis methods for hot section components N86-11516
The 3-D inelastic analysis methods for hot section components (base program) N86-11517
HOST liner cyclic facilities N86-11519
Life prediction and constitutive behavior N86-11520
Creep fatigue life prediction for engine hot section materials (isotropic) N86-11521
GAS TURBINES
Advanced Thermionic Technology Program: Summary report, Volume 3 [DE85-009360] N86-11674
GAS WELDING
Feasibility of remotely manipulated welding in space: A step in the development of novel joining technologies N86-11246
GAS-GAS INTERACTIONS
Stability and interaction of coherent structure in supersonic reactive wakes N86-11185
GAS-METAL INTERACTIONS
Stability and interaction of coherent structure in supersonic reactive wakes N86-11185
Laser evaporation of metal in gaseous atmosphere N86-11957
GASES
Impurity monitoring by laser-induced fluorescence techniques [DE85-014142] N86-11356
An introduction to electrical breakdown in dielectrics [AD-A156465] N86-11415
Status of models for analysis of Western Gas Sands [DE85-003398] N86-11653
Study of heavy gas effects on the atmospheric dispersion of dense gases, revision 1 [DE85-012917] N86-11693
Recent FRC translation experiments on FRX-C/T [DE85-012745] N86-12132
Nuclear spin-polarized HD, D2, HT and DT solids, liquids and high density gases [DE85-014136] N86-12154
GAUSS EQUATION
On the addition theorem for Legendre polynomials N86-11704
GEARS
A study of the cornering forces generated by aircraft tires on a tilted, free-swiveling nose gear [NASA-TP-2481] N86-11522
GENERAL AVIATION AIRCRAFT
Investigations of modern general aviation propellers N86-11162
General aviation's meteorological requirements N86-11738
Corporate/commuter airlines meteorological requirements N86-11739
GENETICS
Importance of phytoalexin tolerance and detoxification for pathogenicity [DE85-014759] N86-11257
Positive genetic hazard predictions from short-term tests have proved false for results in mammalian spermatogonia with all environmental chemicals so far tested [DE85-013640] N86-11833
GEOBOTANY
A comparison of AIS data with other aircraft and ground data for the geobotanical discrimination of rock types in southwest Oregon N86-11642
GEODESY
Proceedings of the 5th International Symposium Geodesy and Physics of the Earth, part 1 [REPT-81-PT-1] N86-11549
New aspects of the geodetic boundary value problems N86-11553
Establishment of the BIH terrestrial system by combining the results of different Earth rotation space geodesy programs N86-11555
Anew about the correlation between Mohorovicic discontinuity depths, geoid undulations and Bouguer gravity anomalies in the Dinaric-Pannonian region of Yugoslavia N86-11557
An attempt to detect geometric tidal information using Lageos laser ranging data N86-11558
Proceedings of the 5th International Symposium Geodesy and Physics of the Earth, part 2 [REPT-81-PT-2] N86-11568
Treatment of the geodetic boundary value problem by contact-transformation N86-11573
Proceedings of the 5th International Symposium Geodesy and Physics of the Earth, part 3 [REPT-81-PT-3] N86-11591
A new apparatus for testing bubble vials, electronic levels and automatic levels N86-11614
Geodesy: A look to the future [NASA-CR-176283] N86-11657
Least squares collocation applied to local gravimetric solutions from satellite gravity gradiometry data [NASA-CR-176299] N86-11910
GEODETIC ACCURACY
Some geodetic aspects of the problem of checking the plate-tectonic model of seismicity in southeastern Europe N86-11603
Geodesy: A look to the future [NASA-CR-176283] N86-11657
GEODETIC COORDINATES
Establishment of the BIH terrestrial system by combining the results of different Earth rotation space geodesy programs N86-11555
GEODETIC SATELLITES
Geodesy: A look to the future [NASA-CR-176283] N86-11657
GEODETIC SURVEYS
A new approach to iterations in solving geodetic boundary value problems for real topography N86-11569
Interactions between oceanic and gravity tides, as analysed from world-wide Earth tide observations and ocean models N86-11576
Capacitive pendulum with intelligent data collection N86-11577
Research on the computational methods of gravity topographic effect N86-11578
Space-time variating geological masses by space-time variating geodetic measurements N86-11595
Least squares collocation applied to local gravimetric solutions from satellite gravity gradiometry data [NASA-CR-176299] N86-11910
GEODYNAMICS
Proceedings of the 5th International Symposium Geodesy and Physics of the Earth, part 1 [REPT-81-PT-1] N86-11549
Results of KAPG co-operation in Earth tide research N86-11551
Tidal friction, the Earth's rotation and hypothesis of an expanding Earth N86-11556
Capacitive pendulum with intelligent data collection N86-11577
On the comparison of the results of two different E-W-strainmeters N86-11583
Geodynamic effects due to Earth's deformation N86-11585
Proceedings of the 5th International Symposium Geodesy and Physics of the Earth, part 3 [REPT-81-PT-3] N86-11591
Recent crustal movements and geophysical interpretation of geodynamic processes in the Alpine mountain belt N86-11604
Determination of crustal movements in the high Tatra Mountains N86-11605
A new apparatus for testing bubble vials, electronic levels and automatic levels N86-11614
Dynamics of the Bohemian Massif N86-11616
GEOIDS
Anew about the correlation between Mohorovicic discontinuity depths, geoid undulations and Bouguer gravity anomalies in the Dinaric-Pannonian region of Yugoslavia N86-11557
Geophysical interpretation of global geoid undulations and mean gravity anomalies N86-11560
Precise geoid computations at mountainous coastlines in view of vertical datum determinations N86-11561
GEOLOGICAL FAULTS
Geokinematic models for the gravimetric W - E profile of the GDR N86-11596
Finnish measurements of the Fennoscandian land uplift gravity lines in Finland 1966-1984 N86-11606
Height changes and recent crustal movements in the Rhenish Massif and in the upper Rhine Graben rift N86-11608
Dynamics of the Bohemian Massif N86-11616
Honey Lake Geothermal Project, Lassen County, California [DE85-013388] N86-11677
Attenuation of macroseismic effects of earthquakes N86-11705
Earthquake hazard research in the Los Angeles Basin and its offshore area, October 1, 1983 to September 30, 1984 [PB85-196491] N86-11725
GEOLOGICAL SURVEYS
Summary of low-temperature geothermal studies conducted by the Utah Geological and Mineral Survey from July 1, 1977 to December 31, 1984 [DE85-009346] N86-11676
Geological calculations with SANGRE and MANTLE: Recent results N86-11872
GEOLOGY
Subsurface geology of the Pajarito Plateau, Espancia Basin, New Mexico [DE85-016215] N86-11720
Geological calculations with SANGRE and MANTLE: Recent results N86-11872
GEOMAGNETIC LATITUDE
Ion whistlers in middle latitudes observed by the Interkosmos-14 satellite N86-11714
GEOMAGNETIC MICROPULSATIONS
Numerical solution of ionospheric filtration of ULF waves. Part 2: Application N86-11713
GEOMAGNETIC PULSATIONS
Statistical properties of geomagnetic pulsations at the Fuerstenfeldbruck Observatory determined by means of pulsation indices. Part 3: Correlation with the parameters of the interplanetary magnetic field N86-11710
GEOMAGNETISM
On the influence of coupling torques between the Earth's core and mantle on parameters and components of the rotation of the Earth N86-11572

Geophysical Works, 1982, volume 30 N86-11702
On the addition theorem for Legendre polynomials N86-11704
Determination of the depth of a conductivity anomaly by separating the geomagnetic variation field into its external and internal part N86-11711

GEOMETRY
Evaluation of a high temperature adhesive for fabricating graphite/PMR-15 polyimide structures N86-11268
A simple, first step to the optimization of regenerator geometry N86-11385

GEOMORPHOLOGY
Periglacial landforms and processes in the southern Kenai Mountains, Alaska [AD-A157459] N86-11718
Horizons and opportunities in lunar sample science [NASA-CR-176290] N86-12191

GEOPHYSICS
Proceedings of the 5th International Symposium Geodesy and Physics of the Earth, part 1 [REPT-81-PT-1] N86-11549
Results of KAPG co-operation in Earth tide research N86-11551
Establishment of the BIH terrestrial system by combining the results of different Earth rotation space geodesy programs N86-11555
Tidal friction, the Earth's rotation and hypothesis of an expanding Earth N86-11556
Proceedings of the 5th International Symposium Geodesy and Physics of the Earth, part 2 [REPT-81-PT-2] N86-11568
A new approach to iterations in solving geodetic boundary value problems for real topography N86-11569
On the influence of coupling torques between the Earth's core and mantle on parameters and components of the rotation of the Earth N86-11572
Proceedings of the 5th International Symposium Geodesy and Physics of the Earth, part 3 [REPT-81-PT-3] N86-11591
Recent vertical crustal movements of the Carpathian-Balkan region and their relationship with neotectonic movements and geophysical fields N86-11609
Significance tests of recent vertical crustal movements by correlation functions N86-11611
Comparisons of different observation methods of a LaCoste and Romberg G gravimeter N86-11612
Statistical analysis and interpretation of Earth crustal movements in northeast Bulgaria N86-11613
Geophysical Works, 1982, volume 30 N86-11702
Workshop on Permafrost Geophysics [AD-A157485] N86-11719
Earthquake hazard research in the Los Angeles Basin and its offshore area, October 1, 1983 to September 30, 1984 [PB85-196491] N86-11725

GEOPOTENTIAL
Proceedings of the 5th International Symposium Geodesy and Physics of the Earth, part 2 [REPT-81-PT-2] N86-11568
Capacitive pendulum with intelligent data collection N86-11577

GEOPOTENTIAL HEIGHT
Low-frequency baroclinic features observed in the lee of major mountain ranges N86-11811

GEOSTROPHIC WIND
The effect of topography on the evolution of unstable disturbances in a baroclinic atmosphere N86-11750
The Hadley and Rossby regimes in a spherical atmosphere N86-11751
A parameterization technique for nonlinear spectral models N[illegible]752
A numerical study of global axisymmetric [illegible] and their stability to quasi-geostrophic disturbances N86-11753

GEOSYNCHRONOUS ORBITS
Calculation of allowable orbital spacings for the fixed-satellite service [NASA-CR-176273] N86-11212

GEOTHERMAL ENERGY CONVERSION
Evaluation and ranking of geothermal resources for electrical generation or electrical offset in Idaho, Montana, Oregon and Washington [DE85-014661] N86-11650

GEOTHERMAL ENERGY EXTRACTION
Economics of magma power generation [DE85-008694] N86-11687

GEOTHERMAL RESOURCES
Geothermal instrumentation development activities at Sandia [DE85-008693] N86-11463
Evaluation and ranking of geothermal resources for electrical generation or electrical offset in Idaho, Montana, Oregon and Washington [DE85-014661] N86-11650
Summary of low-temperature geothermal studies conducted by the Utah Geological and Mineral Survey from July 1, 1977 to December 31, 1984 [DE85-009346] N86-11676
Honey Lake Geothermal Project, Lassen County, California [DE85-013388] N86-11677
Tracer test analysis of the Klamath Falls geothermal resource: A comparison of models [DE85-009924] N86-11678
Evaluation and ranking of geothermal resources for electrical generation or electrical offset in Idaho, Montana, Oregon and Washington, volume 2 [DE85-014452] N86-11683
Electromagnetic soundings for geothermal resources in Dixie Valley, Nevada [DE85-011986] N86-11722

GEOTHERMAL TECHNOLOGY
Geothermal instrumentation development activities at Sandia [DE85-008693] N86-11463

GEYSERS
Honey Lake Geothermal Project, Lassen County, California [DE85-013388] N86-11677

GLACIERS
Gaussian and mean curvatures of postglacial land uplift as expanded in surface spherical harmonics, and the origin of earthquakes in Fennoscandia N86-11599
Periglacial landforms and processes in the southern Kenai Mountains, Alaska [AD-A157459] N86-11718

GLACIOLOGY
Periglacial landforms and processes in the southern Kenai Mountains, Alaska [AD-A157459] N86-11718
Polar Research Board annual report 1984 and future plans [PB85-204477] N86-11727

GLASS
Processing science and technology N86-11297
Injection molding-sealing of glass to low melting metals [DE85-015613] N86-11329
Studies on chalcogenide films [AD-A157340] N86-11343
Properties of crazes and deformation zones in glassy polymers [AD-A157428] N86-11346
Physical property changes of a lithia-alumina-silica based glass as a function of composition [DE85-015610] N86-11352
Initial plasma formation during exposure of absorbing materials to laser radiation with plane expansion geometry of the forming plasma N86-11956
Ultraviolet lasing in helium-nitrogren mixtures N86-11974
Fractal-like, but non-fractal, behavior of one step dipolar energy transfer on regular lattices with excluded volume [AD-A157382] N86-12136

GLASS FIBER REINFORCED PLASTICS
Recent developments in polyimide and bismaleimide adhesives N86-11270

GOLD
Mercury bromide reconstitution in the HgBr laser system [AD-A156502] N86-11466

GOVERNMENTS
Chief of Aeroflot's international activities N86-11179

GRAIN BOUNDARIES
The interface structure of grain boundaries in polysilicon N86-11665

GRANITE
Deformation of granite at elevated temperature and pressure [DE85-014057] N86-11721

GRAPHITE
Metallurgical characterization of the interfaces and the damping mechanisms in metal matrix composites [AD-A156507] N86-11300

GRAPHITE-EPOXY COMPOSITES
Rapid adhesive bonding and field repair of aerospace materials N86-11253
Characterization of polyimide matrix resins and prepregs N86-11273
A program to determine the effect of low-velocity impacts on the strength of the filament-wound rocket motor case for the space shuttle [NASA-TM-87586] N86-11292
Composite structural materials [NASA-CR-176279] N86-11293
Composite materials N86-11295
Generic structural elements N86-11296
Interaction of mixed mode loading on cyclic debonding in adhesively bonded composite joints [NASA-CR-177990] N86-11298

GRAPHITE-POLYIMIDE COMPOSITES
PMR polyimides from solutions containing mixed endcaps N86-11263
Properties of autoclaved Gr/PI composites made from improved tack PMR-15 prepreg N86-11276
Thermo-oxidative stability of graphite fiber/PMR-15 polyimide composites at 350 deg C N86-11277
Rheological, processing, and 371 deg C mechanical properties of Celion 6000/N-phenylnadimide modified PMR composites N86-11278
High temperature, short term tensile strength of C6000/PMR-15 composites N86-11279
Microscopic evaluation of a polyimide (PMR-15)-graphite composite N86-11282
Effects of real-time thermal aging on graphite/polyimide composites N86-11283
Environmental stability graphite/PMR-15 composites N86-11284
Development of design data for propulsion PMR-15 composites N86-11285
Polyimide composites: Application histories N86-11286
V-378A: A modified bismaleimide for advanced composites N86-11287
Transfer molding of PMR-15 polyimide resin N86-11288
Application of Gr/PMR-15 to commercial aircraft N86-11289
Fabrication process of a high temperature polymer matrix engine duct N86-11290
Current and future engine applications of Gr/PI composites N86-11291

GRAVIMETERS
Results of KAPG co-operation in Earth tide research N86-11551
Comparisons of different observation methods of a LaCoste and Romberg G gravimeter N86-11612

GRAVIMETRY
Results of KAPG co-operation in Earth tide research N86-11551
Some results of an eight years gravimetric registration series N86-11559
Ocean tidal loading along the Blue Road geotraverse in Fennoscandia N86-11571
Space-time variating geological masses by space-time variating geodetic measurements N86-11595
Geokinematic models for the gravimetric W - E profile of the GDR N86-11596
Comparisons of different observation methods of a LaCoste and Romberg G gravimeter N86-11612

GRAVITATION
On stratified vortex motions under gravity [AD-A156930] N86-11427
An attempt to detect geometric tidal information using Lageos laser ranging data N86-11558
Geophysical interpretation of global geoid undulations and mean gravity anomalies N86-11560
Geophysical Works, 1982, volume 30 N86-11702
Least squares collocation applied to local gravimetric solutions from satellite gravity gradiometry data [NASA-CR-176299] N86-11910
Representations of the group of diffeomorphisms in the physics of particles, gravity and fluids [DE85-007031] N86-12028
High energy physics [DE85-014272] N86-12063

GRAVITATIONAL CONSTANT
Tidal friction, the Earth's rotation and hypothesis of an expanding Earth N86-11556

GRAVITATIONAL EFFECTS
An attempt to detect geometric tidal information using Lageos laser ranging data N86-11558
Interactions between oceanic and gravity tides, as analysed from world-wide Earth tide observations and ocean models N86-11576
Research on the computational methods of gravity topographic effect N86-11578
On the convergence problem of the satellite derived spherical harmonic expansion of the geopotential at the Earth's surface N86-11582
On the gravitational effect of the crust-mantle boundary in central Europe N86-11703

GRAVITATIONAL FIELDS
Figure of the Earth, moon, and planets N86-11550
Some results of an eight years gravimetric registration series N86-11559
Geophysical interpretation of global geoid undulations and mean gravity anomalies N86-11560
Precise geoid computations at mountainous coastlines in view of vertical datum determinations N86-11561
Ocean tidal loading along the Blue Road geotraverse in Fennoscandia N86-11571
The potentialographical problem and the conception of gravitating disks N86-11579

On the convergence problem of the satellite derived spherical harmonic expansion of the geopotential at the Earth's surface N86-11582
Geodynamic effects due to Earth's deformation N86-11585
On the long-wavelength correlation between gravity and topography N86-11586
Geodesy: A look to the future [NASA-CR-176283] N86-11657

GRAVITATIONAL LENSES
The potentialographical problem and the conception of gravitating disks N86-11579

GRAVITATIONAL WAVES
Some results of an eight years gravimetric registration series N86-11559

GRAVITY ANOMALIES
Anew about the correlation between Mohorovicic discontinuity depths, geoid undulations and Bouguer gravity anomalies in the Dinaric-Pannonian region of Yugoslavia N86-11557
Finnish measurements of the Fennoscandian land uplift gravity lines in Finland 1966-1984 N86-11606
On the gravitational effect of the crust-mantle boundary in central Europe N86-11703

GRAVITY GRADIOMETERS
Least squares collocation applied to local gravimetric solutions from satellite gravity gradiometry data [NASA-CR-176299] N86-11910

GRAVITY WAVES
Precise geoid computations at mountainous coastlines in view of vertical datum determinations N86-11561
Interactions between oceanic and gravity tides, as analysed from world-wide Earth tide observations and ocean models N86-11576

GRAZING INCIDENCE
Double-wavelength pulsed tunable dye laser N86-12003
Galvanoplastic grazing incidence mirrors for verticle experiments: The tandem tests in soft X-rays N86-12071

GREAT PLAINS CORRIDOR (NORTH AMERICA)
Meteorological conditions during drought episodes in the United States Great Plains N86-11802

GRIST (TELESCOPE)
Publications of the Astronomical Institute of the Czechoslovak Academy of Sciences, no. 61 [PUBL-61] N86-12069
Galvanoplastic grazing incidence mirrors for verticle experiments: The tandem tests in soft X-rays N86-12071

GROOVES
Initial investigation of cryogenic wind tunnel model filler materials N86-11255

GROUND EFFECT (AERODYNAMICS)
Ground effect on a rotor wake [COLL-AERONAUTICS-8510] N86-11187

GROUND HANDLING
A comparison of the NAVTOLAND (Navy vertical takeoff and landing) SH-2F helicopter model with the requirements of MIL-H-8501A and with flight data [AD-A157297] N86-11198

GROUND STATE
Magnetic properties and electronic structure of the actinide systems UAl2, NpAl2 and PuAl2 [DE85-014102] N86-11323
Binding energy of donors in GaAs-Ga(1-x) Al(x)As quantum well structures N86-11940

GROUND STATIONS
Calculation of allowable orbital spacings for the fixed-satellite service [NASA-CR-176273] N86-11212
Establishment of the BIH terrestrial system by combining the results of different Earth rotation space geodesy programs N86-11555
An attempt to detect geometric tidal information using Lageos laser ranging data N86-11558
Specification of mean surface temperature anomalies in Europe and Asia during the fall months N86-11806

GROUND SUPPORT EQUIPMENT
Balloon-borne three-meter telescope for far-infrared and submillimeter astronomy [NASA-CR-176285] N86-12188

GROUND TRUTH
Aerial photography and ground verification at power plant sites: Wisconsin power plant impact study [PB85-197358] N86-11658

GROUND WATER
Evaluating the ground-water resources of the high plains of Texas, volume 3 [PB85-191617] N86-11655
Fiscal year 1983 institute program report, Vermont Water Resources Research Center [PB85-214500] N86-11659
Fiscal year 1983 program report of the Water Resources Research Institute of New York State [PB85-217024] N86-11662
Deepwell monitoring along the southern San Andreas Fault [PB85-196483] N86-11726
Coral reef hydrogeology [DE85-012923] N86-11828

GROUP THEORY
Representations of the group of diffeomorphisms in the physics of particles, gravity and fluids [DE85-007031] N86-12028

GROWTH
Forest canopy chemistry from Blackhawk Island, Wisconsin N86-11634
Saturation characteristics of counterstreaming warm electrons [DE85-014390] N86-12040
Particle simulation of the low-(ALPHA) Pierce diode [DE85-014435] N86-12113

GUIDANCE (MOTION)
A comparison of the NAVTOLAND (Navy vertical takeoff and landing) SH-2F helicopter model with the requirements of MIL-H-8501A and with flight data [AD-A157297] N86-11198

GUN PROPELLANTS
Health hazard evaluation of liquid monopropellants. Phase 4. Subchronic inhalation of hydroxylammonium nitrate, January 1985 [AD-A157623] N86-11844

GUSTS
A perspective on the status of measurement of atmospheric turbulence in the US [NASA-TM-87610] N86-11193

GYROSCOPES
CRC control systems laboratory gyro test facility [CRC-1385] N86-11205

H

HADRONS
Possibilities of polarized protons in Sp anti p S and other high energy hadron colliders [DE85-012517] N86-12044

HALL EFFECT
The yield point of copper-zinc alloys in the alpha solid solution range [BLL-BISI-TRANS-23046-(9022.06)] N86-11311
Thermal post-treatment characteristics of metastable carrier concentration in As-implanted silicon after transient annealing N86-11942
Deep levels in semi-insulating GaAs N86-11943

HAMILTONIAN FUNCTIONS
Variational principles for Earth rotation N86-11580

HANDBOOKS
Coming soon to a theater near you: The microwave landing system [AD-A156468] N86-11190
Recognition and control of low level wind shear [AD-A156500] N86-11758

HARMONIC ANALYSIS
Mathematical treatment of vertical movements N86-11597

HARMONICS
Reduction of sextupole distortion by shuffling magnets in small groups [DE85-013024] N86-12035
New harmonic materials: Index engineering: Thin-thick quadrature frequency conversion [DE85-012976] N86-12156

HASTELLOY (TRADEMARK)
Elevated temperature biaxial fatigue [NASA-CR-175009] N86-11526

HAZARDS
Develop, evaluate and validate continuous emission monitors for designated hazardous pollutants [PB85-201176] N86-11695
Minimum assumption tornado hazard probability model [PB85-206092] N86-11821

HAZE
Analysis of arctic haze scattering and aerosol data obtained during AGASP [AD-A157434] N86-12074

HEALTH
Seeding materials: Health and safety considerations N86-11454
Assessments and viewpoints on the biological and human health effects of Extremely Low Frequency (ELF) electromagnetic fields: Compilation of commissioned papers for the ELF literature review project [AD-A156942] N86-11839

HEAT EXCHANGERS
NASA Lewis Research Center low-gravity fluid management technology program [NASA-TM-87145] N86-11218
Recent cryocooler progress in Japan N86-11369
Reciprocating magnetic refrigerator N86-11371
Classification of cryocoolers N86-11374
A simple, first step to the optimization of regenerator geometry N86-11385
Criteria for scaling heat exchangers to miniature size N86-11387
Vuilleumier cycle cryocooler operating below 8 K N86-11390
Four K refrigerators with a new compact heat exchanger N86-11391
Experimental study on impact/fretting wear in heat exchanger tubes [DE85-014597] N86-11548

HEAT FLUX
Development of heat flux sensors for turbine airfoils and combustor liners N86-11502
Thermal convection in snow [AD-A157577] N86-11648
Time-averaging the flux-profile relationship N86-11789

HEAT GENERATION
Dense random packed model for amorphous Ni35Zr65: Influence of the heat of mixing [DE85-014967] N86-11319

HEAT MEASUREMENT
Processing science and technology N86-11297

HEAT OF FORMATION
Calculation of formation time of minimal nucleus of flame during ignition of explosive mixtures by electrical discharges N86-11963

HEAT PUMPS
Hermetic bellows seal for Braun linear engine: Design, test and demonstration [DE85-013545] N86-11478
Advanced mechanical heat pump technologies for industrial applications [DE85-014613] N86-11483
Optimized ground-coupled heat pump system design for northern climate [DE85-014065] N86-11484
Stirling cycle heat pump studies [DE85-005365] N86-11680

HEAT RADIATORS
Rotating film radiators for space applications [DE85-009633] N86-11431

HEAT RESISTANT ALLOYS
Shock consolidation of IN-100 nickel-base superalloy powder [DE85-015159] N86-11360

HEAT SOURCES
Calculation of formation time of minimal nucleus of flame during ignition of explosive mixtures by electrical discharges N86-11963

HEAT STROKE
An atropinized heat-stressed rat model: Anticholinergic and anticholinesterase drug potency [AD-A157620] N86-11832

HEAT TRANSFER
Response behavior of hot-wires and films to flows of different gases [NBSIR-85/3203] N86-11366
Effects of leakage through clearance seals on the performance of a 10 K Stirling-cycle refrigerator N86-11379
A computational model for a regenerator N86-11386
The design of a thermally efficient 1:256 KU-band feed network for a MMIC phased array N86-11400
Rotating film radiators for space applications [DE85-009633] N86-11431
Direct coupling of microbore HPLC columns to MS systems [NASA-CR-176292] N86-11436
Calculation of particle dynamics effects on laser velocimeter data N86-11438
Assessment of a 3-D boundary layer code to predict heat transfer and flow losses in a turbine N86-11508
Gas-side heat transfer with rotation N86-11509
Coolant passage heat transfer with rotation. A progress report on the computational aspects N86-11510
Jet array impingement heat transfer characteristics N86-11511
HOST structural analysis program overview N86-11513
Burner liner thermal/structural load modelling N86-11514
Component-specific modeling N86-11515
ICARUS: A computer code for modeling complex one-dimensional heat conduction on mainframes and micros N86-11866
Interface elements for heat transfer analysis N86-11868
Application of Flux-Corrected Transport (FCT) to heat transfer/fluid mechanics problems N86-11883
Heat transfer and pressure changes due to a large temperature difference across an enclosed vertical air layer N86-11884

HEAT TRANSMISSION
Melting of crystalline and amorphous silicon by Ruby, XeCl and KrF laser irradiation [DE85-015040] N86-11468
Turbine Engine Hot Section Technology (HOST) [NASA-CP-2289] N86-11495
Gas flow environmental and heat transfer nonrotating 3D program N86-11506
Gas side heat transfer N86-11507
Passive solar applications [DE85-014085] N86-11685
Hydrothermodynamics of the near-surface layer of a liquid and optical methods of investigating it N86-11989

HEAT TREATMENT
Comparison of bond in roll-bonded and adhesively bonded aluminums N86-11248
Composite structural materials [NASA-CR-176279] N86-11293
Acoustic emission during deformation and fracture of A533B pressure vessel steel N86-11306
Thermal post-treatment characteristics of metastable carrier concentration in As-implanted silicon after transient annealing N86-11942

HEATING
New concepts for drift pumping a thermal barrier with RF [DE85-013591] N86-12114

HEAVY IONS
Ion whistlers in middle latitudes observed by the Interkosmos-14 satellite N86-11714
Medical heavy ion accelerator proposals [DE85-015247] N86-12026
Window frame or superferric magnet design for low B(3T) heavy ion storage ring study [DE85-013288] N86-12095
Physics opportunities with relativistic heavy ion accelerators [DE85-014190] N86-12117

HEIGHT
Method of joint adjustment of height differences and velocities N86-11601
Principle of the construction of the lines of the repeated levelling for the investigation of the vertical movement in the Carpatho-Balkan Region (CBR) N86-11602
Height changes and recent crustal movements in the Rhenish Massif and in the upper Rhine Graben rift N86-11608
Statistical analysis and interpretation of Earth crustal movements in northeast Bulgaria N86-11613
Prediction of monthly 700 mb heights using antecedent and simulated prognostic height predictors N86-11805

HELICOPTER WAKES
Ground effect on a rotor wake [COLL-AERONAUTICS-8510] N86-11187

HELICOPTERS
Recent achievements, problems in cropdusting work N86-11180
Comparison of calculated and measured velocities near the tip of a model rotor blade at transonic speeds [NASA-TM-86697] N86-11196
Visual and motion cueing in helicopter simulation [NASA-TM-86818] N86-11208
Aeroelastic model helicopter rotor testing in the Langley TDT [NASA-TM-86440] N86-11523
A new characterization of the icing environment below 10,000 feet AGL from 7,000 miles of measurements in supercooled clouds N86-11743

HELIOSEISMOLOGY
International solar-terrestrial physics program: A plan for the core spaceflight missions [NASA-TM-87511] N86-12194

HELIUM
Proceedings of the Third Cryocooler Conference [NASA-CR-176298] N86-11367
Recent cryocooler progress in Japan N86-11369
Reciprocating magnetic refrigerator N86-11371
Ultraviolet lasing in helium-nitrogren mixtures N86-11974

HELMHOLTZ VORTICITY EQUATION
Improving the accuracy of the boundary integral method based on the Helmholtz integral N86-12010

HEREDITY
Prospects for DNA methods to measure human heritable mutation rates [DE85-014555] N86-11847

HERMETIC SEALS
Hermetic bellows seal for Braun linear engine: Design, test and demonstration [DE85-013545] N86-11478

HETEROGENEITY
Results concerning rheological parameters of the Earth N86-11567

HETEROJUNCTIONS
Surface and interfacial properties of Ga0.47In0.53As alloys [AD-A157343] N86-11316

HIGH ALTITUDE
Calibration of the NCAR (National Center for Atmospheric Research) Sabreliner research static pressure source with a trailing cone assembly [PB85-191005] N86-11200
High altitude measured radiance of White Sands, New Mexico in the 400-2000 nm band using a filter wedge spectrometer [PB85-206084] N86-11729
Atlas of high altitude aircraft measured radiance of White Sands, New Mexico, in the 450-1050 nanometers band [PB85-204501] N86-11820

HIGH ALTITUDE TESTS
Microcomputer-controlled high-altitude data aquisition system N86-12000

HIGH DISPERSION SPECTROGRAPHS
High dispersion observations of Epsilon Aur from Sept. 1982 to March 1983 N86-12183

HIGH ENERGY INTERACTIONS
Possibilities of polarized protons in Sp anti p S and other high energy hadron colliders [DE85-012517] N86-12044
Very high energy colliders [DE85-013075] N86-12100
Review of kaon factory proposals [DE85-014110] N86-12122

HIGH FIELD MAGNETS
Design for a high field combined function superferric magnet [DE85-014827] N86-11944

HIGH FREQUENCIES
High frequencies in tidal tilt records N86-11554
Intermediate and high-frequency acoustic backscattering cross sections for water-ice interfaces. 1: Two-component profile models [AD-A157533] N86-12018
New concepts for drift pumping a thermal barrier with RF [DE85-013591] N86-12114

HIGH LEVEL LANGUAGES
Directly executed languages [AD-A157311] N86-11888
New R and D in Chinese language information processing N86-11996

HIGH POWER LASERS
Electroionization IR Xe-ATOM laser N86-11975

HIGH PRESSURE
Fluids at high dynamic pressures and temperatures [DE85-014812] N86-11305
Electrical relaxation in poly(ethylene oxide) [AD-A157301] N86-11342
Shock consolidation of IN-100 nickel-base superalloy powder [DE85-015159] N86-11360
Overview of solid particle LV seeding techniques used at UTRC N86-11445
Hot section viewing system N86-11498
High pressure strength of shocked aluminum [DE85-014461] N86-11547
Deformation of granite at elevated temperature and pressure [DE85-014057] N86-11721
Occurrence of pressure wave during spontaneous ignition of gas ahead of flame front in closed vessel N86-11965

HIGH REYNOLDS NUMBER
Initial investigation of cryogenic wind tunnel model filler materials N86-11255

HIGH SPEED
Solid-melt interface studies of high-speed silicon sheet growth [DE85-008783] N86-11349
Current research on circular saw and band saw vibration and stability N86-11533

HIGH SPEED PHOTOGRAPHY
Theoretical and experimental comparison of vapor cavitation in dynamically loaded journal bearings [NASA-TM-87121] N86-11425

HIGH TEMPERATURE
High-temperature adhesive development and evaluation N86-11250
Matrix resin development at NASA Langley Research Center N86-11264
Bismaleimides and related maleimido polymers as matrix resins N86-11265
All-aromatic biphenylene end-capped polyquinoline and polyimide matrix resins N86-11267
Evaluation of a high temperature adhesive for fabricating graphite/PMR-15 polyimide structures N86-11268
Recent developments in polyimide and bismaleimide adhesives N86-11270
Rheological, processing, and 371 deg C mechanical properties of Celion 6000/N-phenylnadimide modified PMR composites N86-11278
Polyimide matrix resins for up to 700 deg F service N86-11280
Microscopic evaluation of a polyimide (PMR-15)-graphite composite N86-11282
Creep and fracture of a yttria dispersed nickel-chromium alloy N86-11309
Intergranular attack and stress corrosion cracking of alloy 600 in high-temperature caustic solutions containing contaminants [DE85-014106] N86-11335
Strength and flexibility properties of advanced ceramic fabrics [NASA-TM-86824] N86-11340
Rotating film radiators for space applications [DE85-009633] N86-11431
High temperature molten salt containment [DE85-012152] N86-11433
Overview of solid particle LV seeding techniques used at UTRC N86-11445
Infrared thermography: An analytical tool for high temperature and fast response [DE85-013826] N86-11462
Turbine Engine Hot Section Technology (HOST) [NASA-CP-2289] N86-11495
Turbine engine Hot Section Technology (HOST) project N86-11496
Hot section viewing system N86-11498
Dynamic gas temperature measurement system N86-11499
Turbine heat transfer N86-11505
Deformation of granite at elevated temperature and pressure [DE85-014057] N86-11721
Vacancies in thermal equilibrium in Nb [DE85-014832] N86-12061

HIGH TEMPERATURE ENVIRONMENTS
An atropinized heat-stressed rat model: Anticholinergic and anticholinesterase drug potency [AD-A157620] N86-11832

HIGH TEMPERATURE GASES
Seeding techniques used in the Vortex Research Facility N86-11443

HIGH TEMPERATURE PLASMAS
Center for High Temperature Plasma Physics certified N86-11997
Controlled thermonuclear fusion, high temperature plasma physics N86-11998
Advanced concepts theory annual report, 1984 [AD-A157535] N86-12080

HIGH TEMPERATURE TESTS
Derivation and test of elevated temperature thermal-stress-free fastener concept N86-11236
Surface protection of graphite fabric/PMR-15 composites subjected to thermal oxidation N86-11281
Effects of real-time thermal aging on graphite/polyimide composites N86-11283
Environmental stability graphite/PMR-15 composites N86-11284
Fabrication process of a high temperature polymer matrix engine duct N86-11290
Mechanical properties of Inconel 718 and Nickel 201 alloys after thermal histories simulating brazing and high temperature service [NASA-CR-177940] N86-11312

HIGH VOLTAGES
Multi-megampere operation of plasma compression opening switches in planar geometry [DE85-012755] N86-11420

HIGHWAYS
USSR report: Transportation [JPRS-UTR-85-011] N86-11177

HISTORIES
International project in history of solid state physics [DE85-014843] N86-12152
EPR: What has it taught us [DE85-014525] N86-12157

HOLE DISTRIBUTION (MECHANICS)
A Signorini model of bolt fastened laminated composites N86-11258

HOLMIUM
Surface impedance of several magnetic superconductors [DE85-014101] N86-12155

HOLOGRAMMETRY
Diffraction efficiency of three-dimensional phase hologram of diffuse object N86-11982

HOLOGRAPHIC INTERFEROMETRY
Photoinduced Rayleigh scattering of light in crystals N86-11985

HOLOGRAPHY
Experimental investigation of recording of dynamic holograms within absorption contour of resonant atomic medium N86-11981

Possibility of optimal choice of exposure time for holographic recording of objects through unsteady scattering media N86-11983

HOMOGENEITY
A parameterization technique for nonlinear spectral models N86-11752

HONEYCOMB CORES
Advances in joining techniques used in development of SPF/DB titanium sandwich reinforced with metal matrices N86-11247

HONEYCOMB STRUCTURES
Adhesives for aerospace N86-11249

HOOKS
Stress analyses of B-52 pylon hooks [NASA-TM-84924] N86-11524

HORIZONTAL ORIENTATION
Capacitive pendulum with intelligent data collection N86-11577
Geodimeter net for the investigation of horizontal crustal deformations N86-11598

HOT ELECTRONS
Saturation characteristics of counterstreaming warm electrons [DE85-014390] N86-12040

HOT WORKING
Mechanical properties of rapidly solidified Type 304 stainless steel [DE85-014577] N86-11338

HOT-WIRE ANEMOMETERS
Response behavior of hot-wires and films to flows of different gases [NBSIR-85/3203] N86-11366

HUGONIOT EQUATION OF STATE
Fluids at high dynamic pressures and temperatures [DE85-014812] N86-11305

HUMAN BEHAVIOR
Adaptive motivation theory [AD-A157440] N86-11851
Distinct characteristics of science [DE85-006533] N86-12159

HUMAN BEINGS
Detection of chromosomal abnormalities in human sperm [DE85-014178] N86-11834
Thyroid absorbed dose for people at Rongelap, Utirik and Sifo on March 1, 1954 [DE85-014695] N86-11846
Prospects for DNA methods to measure human heritable mutation rates [DE85-014555] N86-11847

HUMAN FACTORS ENGINEERING
Teleoperator human factors study [NASA-CR-176310] N86-11854
Distinct characteristics of science [DE85-006533] N86-12159
Annotated bibliography of human factors applications literature [DE85-012957] N86-12161

HUMAN PERFORMANCE
Cognitive science program: Dissociation of the central timekeeper and the peripheral implementation processes in repetitive movements [AD-A157542] N86-11852

HURRICANES
Active and passive microwave measurements in Hurricane Allen [NASA-TM-86390] N86-11647

HYBRID STRUCTURES
Dish electric systems heat engine assessment [DE85-013942] N86-11479

HYDRATES
Experiments with solid particle seeding N86-11442

HYDRATION
Use of hydration inhibitors to improve bond durability of aluminum adhesive joints N86-11251

HYDRAULIC EQUIPMENT
Flight worthiness of fire resistant hydraulic systems: Volume 1 [AD-A157618] N86-11199

HYDRAULIC FLUIDS
Flight worthiness of fire resistant hydraulic systems: Volume 1 [AD-A157618] N86-11199

HYDROCARBONS
Submillimeter observations of OH and CH in M42 [NASA-TM-86723] N86-12186

HYDRODYNAMICS
Theoretical and experimental comparison of vapor cavitation in dynamically loaded journal bearings [NASA-TM-87121] N86-11425
User guide for WIFM-SAL (WES Implicit Flooding Model-SAL): A two-dimensional vertically integrated, time-varying estuarine transport model [AD-A157446] N86-11825
Hydrodynamics of liquid-vapor disperse annular flows in channels containig bundles of heated rods under nonsteady-state conditions N86-11954
Influence of solid state obstacles on radiation of recombination laser plasma N86-11958
Representations of the group of diffeomorphisms in the physics of particles, gravity and fluids [DE85-007031] N86-12028

HYDROGEN
Stability and interaction of coherent structure in supersonic reactive wakes N86-11185
The mass of hot, shocked CO in Orion: First observations of the J = 17 yields J = 16 transition at 153 microns [AD-A157323] N86-12189

HYDROGEN ATOMS
Flow reactor studies over wide temperature and pressure ranges of atom and radical reaction rates important in ignition and combustion [AD-A156931] N86-12020

HYDROGEN IONS
Study of LAMPF H (-) beam position motion and a predictive algorithm for noise reduction [DE85-012701] N86-12033
AGS polarized beam facility [DE85-011834] N86-12038

HYDROGEOLOGY
Deepwell monitoring along the southern San Andreas Fault [PB85-196483] N86-11726
Coral reef hydrogeology [DE85-012923] N86-11828

HYDROLOGY
Probability encoding of hydrologic parameters for basalt. Elicitation of expert opinions from a panel of three basalt waste isolation project staff hydrologists [DE85-014665] N86-11652
Hydrologic data for experimental agricultural watersheds in the US, 1975 [PB85-197317] N86-11656
Louisiana Water Resources Research Institute [PB85-218998] N86-11661
Formation, distribution and variability in snow cover on the Asian territory of the USSR [NASA-TM-77913] N86-11734
Interannual climate variability in a low vertical resolution spectral atmospheric model N86-11795

HYDROLYSIS
Determination of the steady-state behavior of immobilized (BETA)-galactosidase utilizing an integral reactor scheme [DE85-012900] N86-11256

HYDROMECHANICS
Hydrothermodynamics of the near-surface layer of a liquid and optical methods of investigating it N86-11989

HYDROTHERMAL SYSTEMS
Hydrothermodynamics of the near-surface layer of a liquid and optical methods of investigating it N86-11989

HYDROXYL RADICALS
Health hazard evaluation of liquid monopropellants. Phase 4. Subchronic inhalation of hydroxylammonium nitrate, January 1985 [AD-A157623] N86-11844
Submillimeter observations of OH and CH in M42 [NASA-TM-86723] N86-12186

HYPERBOLIC FUNCTIONS
On symmetric and upwind TVD schemes [NASA-TM-86842] N86-11909

HYPERSONIC FLOW
Overview of solid particle LV seeding techniques used at UTRC N86-11445

I

ICE
Interannual climate variability in a low vertical resolution spectral atmospheric model N86-11795
Survey of ice problem areas in navigable waterways [AD-A157477] N86-11827
Intermediate and high-frequency acoustic backscattering cross sections for water-ice interfaces. 1: Two-component profile models [AD-A157533] N86-12018

ICE FORMATION
Overview of FAA's aircraft icing program N86-11740
A new characterization of the icing environment below 10,000 feet AGL from 7,000 miles of measurements in supercooled clouds N86-11743
A new characterization of supercooled clouds below 10,000 feet AGL N86-11744
Advance particle and Doppler measurement methods N86-11745

ICE MAPPING
Climate simulation and change: A simple energy balance climate model N86-11731

ICOSAHEDRONS
Icosahedral incommensurate crystals [DE85-012512] N86-12147

IDEAL FLUIDS
On the instability of vortex series N86-11715

IDEAL GAS
Reduction of moisture effects during the cure of epoxy adhesives used in composite repair N86-11254

IGNITION
User's manual for AC-20-53A protection of airplane fuel systems against fuel vapor ignition due to lightning [AD-A157619] N86-11191
A mechanism for ignition of high-temperature gaseous nitromethane: The key role of the nitro group in chemical explosives [AD-A157355] N86-11303
Calculation of formation time of minimal nucleus of flame during ignition of explosive mixtures by electrical discharges N86-11963
Occurrence of pressure wave during spontaneous ignition of gas ahead of flame front in closed vessel N86-11965
Flow reactor studies over wide temperature and pressure ranges of atom and radical reaction rates important in ignition and combustion [AD-A156931] N86-12020
Tokamak startup: Problems and scenarios related to the transient phases of ingnited tokamak operations [DE85-015321] N86-12085
Spherical torus: An approach to compact fusion at low field. Initial ignition assessments [DE85-012890] N86-12099

IMAGE ANALYSIS
Proceedings of the Airborne Imaging Spectrometer Data Analysis Workshop [E86-10001] N86-11618
Interpretation of AIS images of Cuprite, Nevada using constraints of spectral mixtures N86-11626
Preliminary evaluation of AIS spectra along a topographic/moisture gradient in the Nebraska Sandhills N86-11629
The use of AIS data for identifying and mapping calcareous soils in western Nebraska N86-11630
Calibration of AIS data using ground-based spectral reflectance measurements N86-11631
Analysis of AIS data of the Recluse Oil Field, Recluse, Wyoming N86-11632
A preliminary investigation of systematic noise in data acquired with the Airborne Imaging Spectrometer N86-11638
Discrimination of coastal vegetation and biomass: Using AIS data N86-11639
Application of AIS technology to forest mapping N86-11641

IMAGE PROCESSING
Field utilization and analysis of AIS 128-channel imagery using microcomputers: Application to Yerington, Nevada field area N86-11621
AIS spectra for stressed and unstressed plant communities in the Carolina slate belt N86-11623
Application of AIS technology to forest mapping N86-11641
Automated method for the documentation of cloud-top characteristics of mesoscale convective systems [PB85-204246] N86-11823
Research on optic spatial frequency analysis of linear structures in remote sensing images N86-11927

IMAGING SPECTROMETERS
Proceedings of the Airborne Imaging Spectrometer Data Analysis Workshop [E86-10001] N86-11618
Mineralogical mapping in the Cuprite Mining District, Nevada N86-11619
Remote stratigraphic analysis: Combined TM and AIS results in the Wind River/Bighorn Basin area, Wyoming N86-11620
Field utilization and analysis of AIS 128-channel imagery using microcomputers: Application to Yerington, Nevada field area N86-11621
Preliminary analysis of AIS spectral data acquired from semi-arid shrub communities in the Owens Valley, California N86-11622
AIS spectra for stressed and unstressed plant communities in the Carolina slate belt N86-11623
Spectral characterization of suspected acid deposition damage in red spruce (Picea rubens) stands from Vermont N86-11624
A first look at Airborne Imaging Spectrometer (AIS) data in an area of altered volcanic rocks and carbonate formations, Hot Creek Range, south central Nevada N86-11625
Interpretation of AIS images of Cuprite, Nevada using constraints of spectral mixtures N86-11626

Preliminary evaluation of AIS spectra along a topographic/moisture gradient in the Nebraska Sandhills N86-11629
The use of AIS data for identifying and mapping calcareous soils in western Nebraska N86-11630
Calibration of AIS data using ground-based spectral reflectance measurements N86-11631
Analysis of AIS data of the Recluse Oil Field, Recluse, Wyoming N86-11632
High resolution spectrometry of leaf and canopy chemistry for biochemical cycling N86-11633
Spectroscopy of Moses Rock kimberlite diatreme N86-11635
Analysis of aircraft spectrometer data with logarithmic residuals N86-11636
Comparison of AIS versus TMS data collected over the Virginia piedmont N86-11637
A preliminary investigation of systematic noise in data acquired with the Airborne Imaging Spectrometer N86-11638
Discrimination of coastal vegetation and biomass: Using AIS data N86-11639
AIS investigation of agricultural monocultures N86-11640
Application of AIS technology to forest mapping N86-11641
A comparison of AIS data with other aircraft and ground data for the geobotanical discrimination of rock types in southwest Oregon N86-11642
Forest species identification with high spectral resolution data N86-11643
Urban, forest, and agricultural AIS data: Fine spectral structure N86-11644

IMAGING TECHNIQUES
Photosensitivity and imaging characteristics of ion-implanted PLZT ceramics [DE85-015459] N86-11348
Hot section viewing system N86-11498
Experimental investigation of recording of dynamic holograms within absorption contour of resonant atomic medium N86-11981
Phasing of multiple-aperture optical systems N86-11987

IMIDES
Chemical control of rate and onset temperature of nadimide polymerization N86-11271

IMPACT DAMAGE
Bibliography of terrestrial impact structures [NASA-TM-87567] N86-11701

IMPACT LOADS
Surface properties of shocked lead [DE85-009582] N86-11476
Strain rate dependence in steady, plastic shock waves [DE85-014703] N86-11544

IMPACT TESTS
Experimental study on impact/fretting wear in heat exchanger tubes [DE85-014597] N86-11548

IMPEDANCE
Velocity measurements of laser driven flyers backed by high impedance windows [DE85-015142] N86-11470
Surface impedance of several magnetic superconductors [DE85-014101] N86-12155

IMPLOSIONS
Progress of Inertial Confinement Fusion (ICF) research N86-11932
SIMPLODE: An imploding gas puff plasma model. 1. Neon [AD-A157456] N86-12077
Advanced concepts theory annual report, 1984 [AD-A157535] N86-12080
OMEGA: A 24 beam UV irradiation facility [DE85-014416] N86-12127
What extent will small-scale laser-beam fluctuations seed the Rayleigh-Taylor instability in direct-drive targets [DE85-014408] N86-12131

IMPROVEMENT
Use of hydration inhibitors to improve bond durability of aluminum adhesive joints N86-11251
Reduction of moisture effects during the cure of epoxy adhesives used in composite repair N86-11254
Upgrade of the EM transient range monocone antenna [DE85-013181] N86-11413

IMPURITIES
Impurity monitoring by laser-induced fluorescence techniques [DE85-014142] N86-11356
Statics and adiabatic dynamics of nonlinear excitations in defected polyacetylene [DE85-014118] N86-12143

INCINERATORS
Laboratory evaluation of the protocol for the volatile organic sampling train [PB85-201184] N86-11694

INCOMPRESSIBLE FLOW
Application of the vortex-lattice concept to flows with smooth-surface separation [AD-A157571] N86-11430
Calculation of particle dynamics effects on laser velocimeter data N86-11438
Computer codes for fluid-structure interactions N86-11867

INCONEL (TRADEMARK)
Mechanical properties of Inconel 718 and Nickel 201 alloys after thermal histories simulating brazing and high temperature service [NASA-CR-177940] N86-11312
Intergranular attack and stress corrosion cracking of alloy 600 in high-temperature caustic solutions containing contaminants [DE85-014106] N86-11335

INDEXES (DOCUMENTATION)
Statistical properties of geomagnetic pulsations at the Fuerstenfeldbruck Observatory determined by means of pulsation indices. Part 3: Correlation with the parameters of the interplanetary magnetic field N86-11710

INDIA
Large-scale variability in Indian monsoon rainfall inferred from satellite data N86-11800

INDIUM ALLOYS
Surface and interfacial properties of Ga0.47In0.53As alloys [AD-A157343] N86-11316

INDONESIA
Possible cross equatorial influence of the northeast monsoon on the equatorial westerlies over Indonesia [AD-A156907] N86-11759

INDUCTANCE
Low inductance diode design of the Proto 2 accelerator for imploding plasma loads [DE85-013783] N86-12123

INDUCTION HEATING
Rapid adhesive bonding and field repair of aerospace materials N86-11253

INDUSTRIAL PLANTS
The factory of the future N86-11228
Robotized machining systems developed at Gomel Institute N86-11397
Advanced mechanical heat pump technologies for industrial applications [DE85-014613] N86-11483

INELASTIC SCATTERING
Antinucleon-nucleus elastic and inelastic scattering [DE85-012510] N86-12059
Elastic and inelastic light scattering of colloidal particles [AD-A157335] N86-12072
Neutron scattering studies of the heavy Fermion superconductors [DE85-014829] N86-12144

INERTIA
Inertia, stability and ductibility in uniaxial tension at high strain rate [DE85-007671] N86-11546

INERTIAL CONFINEMENT FUSION
Progress of Inertial Confinement Fusion (ICF) research N86-11932

INFILTRATION
Improvements in the fabrication of ceramic-fiber-ceramic-matrix composites by chemical vapor infiltration [DE85-015971] N86-11301

INFORMATION DISSEMINATION
Information dissemination for a better understanding of Louisiana's water resources [PB85-219079] N86-11660
Assessment of technical strengths and information flow of energy conservation research in Japan. Volume 2: Background document [DE85-013759] N86-12165

INFORMATION FLOW
New R and D in Chinese language information processing N86-11996

INFORMATION MANAGEMENT
USSR report: Science and technology policy [JPRS-UST-85-014] N86-11990
Computer-aided designing, engineering, preparation of production N86-11992

INFORMATION RETRIEVAL
Microcomputer-controlled high-altitude data aquisition system N86-12000

INFORMATION SYSTEMS
Third National Academic Machine Retrieval Conference held in Zhenjiang N86-11999
Sandia shock compression database [DE85-015141] N86-12142

INFORMATION THEORY
Third National Academic Machine Retrieval Conference held in Zhenjiang N86-11999

INFORMATION TRANSFER
MICROLAN, file transfer program for microprocessors [AD-A156519] N86-11900

INFRARED ASTRONOMY
Balloon-borne three-meter telescope for far-infrared and submillimeter astronomy [NASA-CR-176285] N86-12188

INFRARED DETECTORS
Magnetic refrigeration for low-temperature applications N86-11370
An experimental study for a miniature Stirling refrigerator N86-11375
Passive motion control of pneumatically driven displacers in cryogenic coolers N86-11383

INFRARED IMAGERY
Automated method for the documentation of cloud-top characteristics of mesoscale convective systems [PB85-204246] N86-11823

INFRARED LASERS
High-efficiency Al sub 2 O sub 3:Ti sup 3+ tunable laser N86-11973
Electroionization IR Xe-ATOM laser N86-11975

INFRARED PHOTOGRAPHY
Spectroscopy of Moses Rock kimberlite diatreme N86-11635

INFRARED PHOTOMETRY
Infrared photometry of the 1982-4 eclipse of Epsilon Aurigae N86-12170

INFRARED RADIATION
Infrared thermography: An analytical tool for high temperature and fast response [DE85-013826] N86-11462
Climate simulation and change: A simple energy balance climate model N86-11731
Thermal post-treatment characteristics of metastable carrier concentration in As-implanted silicon after transient annealing N86-11942
Excitation of discharge in air by laser radiation N86-11961

INFRARED SPECTRA
Far-infrared observations of Sagittarius B2: Reconsideration of source structure [NASA-TM-86185] N86-12167
Star formation in the inner galaxy: A far-infrared and radio study of two H2 regions [NASA-TM-86720] N86-12185

INFRARED SPECTROMETERS
Characterization methodology for PMR-15 N86-11272

INFRASONIC FREQUENCIES
Infrasound: A summary of interesting articles [FMV:ELEKTRO-A12:142/83] N86-12017

INHOMOGENEITY
Photoinduced Rayleigh scattering of light in crystals N86-11985

INJECTION MOLDING
PMR polyimides from solutions containing mixed endcaps N86-11263
Injection molding-sealing of glass to low melting metals [DE85-015613] N86-11329

INJURIES
Controlled environment life support system: Calcium-related leaf injuries on plants [NASA-CR-176288] N86-11529

INLAND WATERS
Survey of ice problem areas in navigable waterways [AD-A157477] N86-11627

INLET FLOW
Inlet flow dynamic distortion prediction without rms measurements N86-11183
Airflow calibration of a bellmouth inlet for measurement of compressor airflow in turbine-powered propulsion simulators [NASA-TM-84399] N86-11209

INLET TEMPERATURE
Low-cost, net-shape ceramic radial turbine program [AD-A157532] N86-11202

INOCULATION
Recent experience in seeding transonic/supersonic flows at AEDC N86-11447
Seeding subsonic, transonic and supersonic flows with 0.5 micron polystyrene spheres N86-11451
Aerosol seeding systems for the NSWC wind tunnels N86-11453
Seeding materials: Health and safety considerations N86-11454
Generating aerosols for laser velocimeter seeding N86-11455

INPUT
KRASH85 user's guide: Input/output format [FAA-CT-85-10] N86-11898

INSOLATION

Probability encoding of hydrologic parameters for basalt. Elicitation of expert opinions from a panel of three basalt waste isolation project staff hydrologists
[DE85-014665] N86-11652

INSPECTION

Langley Research Center standard for the evaluation of socket welds N86-11243

Adhesives for aerospace N86-11249

Exploratory development of FMR (ferromagnetic resonance) advanced surface flaw detection methods
[AD-A157436] N86-11469

INSTRUMENT COMPENSATION

On the distribution of the residual vectors of Earth's tide gravity observations in Central Europe N86-11564

INSTRUMENT PACKAGES

HOST instrumentation R and D program overview
N86-11497

INSULATION

Strength and flexibility properties of advanced ceramic fabrics
[NASA-TM-86824] N86-11340

INSULATORS

PBFA-2 vacuum insulator stack failure mechanisms
[DE85-013118] N86-12090

Ellipsometric and optical study of some uncommon insulator films on 3-5 semiconductors
[NASA-TM-87135] N86-12134

INTEGRAL EQUATIONS

Elastic wave scattering of a Gaussian incident beam from an interface crack in a layered half space submerged in water N86-11490

Stability of a method for analyzing radiation pattern of acoustic radiator with near-field pressure measurement errors N86-11950

Prediction of acoustical response of three-dimensional cavities using an indirect boundary element method
N86-12014

INTEGRATED CIRCUITS

Considerations for millimeter wave, monolithic phased arrays N86-11399

Characterization of MMIC devices for active array antennas N86-11401

Waveguide slot array with CSC2 theta (dot) COS theta pattern N86-11402

Basic EMC technology advancement for C(3) systems. Volume 3B: Computer simulation of EMI effects in a differential line receiver
[AD-A156505] N86-11416

INTERCONTINENTAL BALLISTIC MISSILES

Status of the intercontinental ballistic missile modernization program
[AD-A157375] N86-11217

INTERCOSMOS SATELLITES

Ion whistlers in middle latitudes observed by the Interkosmos-14 satellite N86-11714

INTERFACES

Comparison of bond in roll-bonded and adhesively bonded aluminums N86-11248

Initial investigation of cryogenic wind tunnel model filler materials N86-11255

Metallurgical characterization of the interfaces and the damping mechanisms in metal matrix composites
[AD-A156507] N86-11300

Short range bonding interaction at metal-metal interfaces
[DE85-014442] N86-11334

On the gravitational effect of the crust-mantle boundary in central Europe N86-11703

INTERFACIAL ENERGY

An interfacial analysis of MoNb-GaAs Schottky barrier diodes N86-11941

INTERFEROMETERS

Nondestructive ultrasonic measurement of bolt preload using the pulsed-phase locked-loop interferometer
N86-11242

Feedback stabilization of optical interferometer
[AD-A156912] N86-11459

The mass of hot, shocked CO in Orion: First observations of the J = 17 yields J = 16 transition at 153 microns
[AD-A157323] N86-12189

A laser siderostat
[AD-A157444] N86-12190

INTERGRANULAR CORROSION

Intergranular attack and stress corrosion cracking of alloy 600 in high-temperature caustic solutions containing contaminants
[DE85-014106] N86-11335

INTERMETALLICS

Shock-wave synthesis of titanium aluminides
[DE85-015140] N86-11324

Multispectroscopic studies of the electronic structure of electrode materials for high energy density batteries: 1-2, 1-3 intermetallic compounds with B32 structure
[DE85-014675] N86-11684

INTERMODULATION

Chemical bonding agent for suppression of rusty bolt intermodulation interference
[AD-D011747] N86-11315

INTERNAL COMBUSTION ENGINES

Lateral dampers for thrust bearings
[NASA-CR-174924] N86-11474

INTERNATIONAL COOPERATION

Chief of Aeroflot's international activities N86-11179

SPACEWARN Bulletin
[NASA-TM-87512] N86-11222

US space programs: Cooperation and competition from Europe
[BPA-CP-695] N86-12163

INTERPLANETARY MAGNETIC FIELDS

Statistical properties of geomagnetic pulsations at the Fuerstenfeldbruck Observatory determined by means of pulsation indices. Part 3: Correlation with the parameters of the interplanetary magnetic field N86-11710

Determination of the depth of a conductivity anomaly by separating the geomagnetic variation field into its external and internal part N86-11711

INTERPOLATION

Application of an objective analysis scheme to mesoscale observational network design
[AD-A156911] N86-11760

INTERPROCESSOR COMMUNICATION

MICROLAN, file transfer program for microprocessors
[AD-A156519] N86-11900

INTERRUPTION

Multi-megampere current interruption from explosive deformation of conductors
[DE85-012756] N86-11419

INTERSTELLAR MATTER

Submillimeter observations of OH and CH in M42
[NASA-TM-86723] N86-12186

The mass of hot, shocked CO in Orion: First observations of the J = 17 yields J = 16 transition at 153 microns
[AD-A157323] N86-12189

INTERSTELLAR SPACE

The mass of hot, shocked CO in Orion: First observations of the J = 17 yields J = 16 transition at 153 microns
[AD-A157323] N86-12189

INVENTORY CONTROLS

The factory of the future N86-11228

INVESTIGATION

Initial investigation of cryogenic wind tunnel model filler materials N86-11255

Seismology in civil engineering N86-11707

Investigation of efficiency of generation of difference-frequency laser radiation in waveguide
N86-11969

Investigation of polarization characteristics of radiation from laser with dye-activated polymer elements
N86-11972

INVISCID FLOW

Development of an explicit multigrid algorithm for quasi-three-dimensional viscous flows in turbo-machinery
[NASA-TM-87128] N86-11146

IODINE LASERS

Two-frequency passive mode locking in iodine photodissociation laser N86-11980

ION ACCELERATORS

Medical heavy ion accelerator proposals
[DE85-015247] N86-12026

Physics opportunities with relativistic heavy ion accelerators
[DE85-014190] N86-12117

ION BEAMS

Progress of Inertial Confinement Fusion (ICF) research
N86-11932

Sources of radioactive ions
[DE85-015251] N86-12030

Study of LAMPF H (-) beam position motion and a predictive algorithm for noise reduction
[DE85-012701] N86-12033

Ion beam neutralizer
[AD-D011741] N86-12043

Neutral beam interactions with materials
[AD-A157445] N86-12076

Advanced concepts theory annual report, 1984
[AD-A157535] N86-12080

Design and optimization of the PBFA 2 vacuum interface and transmission lines for light ion fusion
[DE85-012809] N86-12092

Formation, ion modification and annealing of VN
[DE85-012898] N86-12146

ION CYCLOTRON RADIATION

Ion whistlers in middle latitudes observed by the Interkosmos-14 satellite N86-11714

ION DENSITY (CONCENTRATION)

New concepts for drift pumping a thermal barrier with RF
[DE85-013591] N86-12114

ION EMISSION

Chromium- and neodymium-activated gedolinium-scandium-gallium garnet crystal: A new laser active medium N86-11979

ION IMPLANTATION

Photosensitivity and imaging characteristics of ion-implanted PLZT ceramics
[DE85-015489] N86-11348

Improvement in wear performance of surgical Ti-6Al-4V alloy by ion implantation of nitrogen or carbon
[DE85-013986] N86-11849

Deep-level defects in ion-implanted and CO2 laser-annealed silicon N86-11939

ION SCATTERING

Dominant moving species in the formation of amorphous NZr by solid-state reaction
[DE85-014855] N86-12053

ION SOURCES

Two-dimensional linacs
[DE85-015129] N86-12029

ION TEMPERATURE

Identification of metal ion chloro complexes in an ambient temperature molten salt
[AD-A157295] N86-11302

Energy confinement in a high-current reversed field pinch
[DE85-015009] N86-12111

New concepts for drift pumping a thermal barrier with RF
[DE85-013591] N86-12114

IONIC COLLISIONS

Design for a high field combined function superferric magnet
[DE85-014827] N86-11944

Laboratory studies of atomic collision processes of importance in planetary atmospheres
[NASA-CR-176301] N86-12019

IONIZATION

An introduction to electrical breakdown in dielectrics
[AD-A156465] N86-11415

Toward a theory of atomic gas breakdown by laser radiation near a metal surface N86-11955

Ionization-Raman double-resonance spectroscopy
[DE85-013774] N86-12042

IONOSPHERIC DISTURBANCES

Determination of the depth of a conductivity anomaly by separating the geomagnetic variation field into its external and internal part N86-11711

Numerical solution of ionospheric filtration of ULF waves. Part 1: Method N86-11712

Numerical solution of ionospheric filtration of ULF waves. Part 2: Application N86-11713

IONOSPHERIC NOISE

Ion whistlers in middle latitudes observed by the Interkosmos-14 satellite N86-11714

IONS

Multidimensional ion microbeam analysis
[DE85-014699] N86-12055

PBFA 2: A 100 TW pulsed power driver for the inertial confinement fusion program
[DE85-013956] N86-12116

IRON

Electronic and magnetic structure of chromium surfaces and chromium monolayers on iron
[DE85-014542] N86-11322

Thermodynamics of chromium and iron in carbonate salts at 650(0)C
[DE85-013542] N86-11682

IRON ALLOYS

Itinerant electron ferromagnetism in Fe-alloyed, Ni3Al based materials
[DE85-013989] N86-11331

IRON CYANIDES

Development of membranes for the zinc/ferricyanide battery
[DE85-011189] N86-11689

IRON OXIDES

Chemical synthesis under shock compression
[DE85-015166] N86-11325

Intergranular attack and stress corrosion cracking of alloy 600 in high-temperature caustic solutions containing contaminants
[DE85-014106] N86-11335

Effects of additives and temperature on iron electrode behavior in KOH electrolytes
[DE85-011901] N86-11423

Effects of acid precipitation on composition, electrokinetic behavior, cation adsorption and ion exchange capacity in various soil systems
[PB85-217727] N86-11698

IRRADIANCE

Intermediate load modules for test and evaluation. Fixed price research and development
[NASA-CR-176135] N86-11664

IRRADIATION
Melting of crystalline and amorphous silicon by Ruby, XeCl and KrF laser irradiation
[DE85-015040] N86-11468
Thermal post-treatment characteristics of metastable carrier concentration in As-implanted silicon after transient annealing N86-11942
Cause of occurrence of high-energy ions during UV laser irradiation of molecular crystals N86-11953
Transition radiation and coherent electron-photon scattering
[DE85-014813] N86-12031
Calculations of physical and chemical reactions produced in irradiated water containing DNA
[DE85-012899] N86-12051
Overview of MIT, ADIP irradiation experiments
[DE85-014469] N86-12060
Formation, ion modification and annealing of VN
[DE85-012896] N86-12146
ISLANDS
Coral reef hydrogeology
[DE85-012923] N86-11828
ISOMERIZATION
The synthesis, characterization and thermal chemistry of modified norbornenyl PMR endcaps N86-11266
ISOPARAMETRIC FINITE ELEMENTS
Application of high order acoustic finite elements to transmission losses and enclosure problems N86-12008
Prediction of acoustical response of three-dimensional cavities using an indirect boundary element method N86-12014
ISOSTASY
Finnish measurements of the Fennoscandian land uplift gravity lines in Finland 1966-1984 N86-11606
Stationary hydrostatic precision tiltmeter system N86-11607
ISOTOPE SEPARATION
Physics overview of AVLIS
[DE85-014854] N86-12057
ISOTOPIC LABELING
Importance of phytoalexin tolerance and detoxification for pathogenicity
[DE85-014759] N86-11257
IUE
IUE observations of the 1982-84 eclipse of Epsilon Aurigae N86-12172
Scattered light in the IUE spectra of Epsilon Aurigae N86-12180

J

JACOBI INTEGRAL
On the addition theorem for Legendre polynomials N86-11704
JACOBI MATRIX METHOD
Towards developing robust algorithms for solving partial differential equations on MIMD machines
[NASA-CR-177979] N86-11856
Algebraic grid generation using tensor product B-splines N86-11908
JAPAN
Recent cryocooler progress in Japan N86-11369
Electro-optics Millimeter/Microwave technology in Japan. Report of DOD technology team
[AD-A157376] N86-12073
Assessment of technical strengths and information flow of energy conservation research in Japan. Volume 2: Background document
[DE85-013759] N86-12165
JET AIRCRAFT
Inlet flow dynamic distortion prediction without rms measurements N86-11183
JET IMPINGEMENT
Jet array impingement heat transfer characteristics N86-11511
JET PROPULSION
A novel oscillating jet: Its effect on ejector thrust augmentation
[AD-A157480] N86-11201
JET STREAMS (METEOROLOGY)
Recent long-term climatic change over the eastern tropical and subtropical Pacific and its ramifications N86-11775
Tropical convection and North American cyclones during the 1982-83 El Nino N86-11809
JET THRUST
A novel oscillating jet: Its effect on ejector thrust augmentation
[AD-A157480] N86-11201
JET VANES
Development of heat flux sensors for turbine airfoils and combustor liners N86-11502
JOINTS (JUNCTIONS)
Mechanical fasteners for advanced composite materials N86-11232
Derivation and test of elevated temperature thermal-stress-free fastener concept N86-11236
Explosive welding of tubular configurated joints for critical applications N86-11238
Adhesives for aerospace N86-11249
Use of hydration inhibitors to improve bond durability of aluminum adhesive joints N86-11251
Factors affecting the processing of epoxy film adhesives N86-11252
Evaluation of a high temperature adhesive for fabricating graphite/PMR-15 polyimide structures N86-11268
Interaction of mixed mode loading on cyclic debonding in adhesively bonded composite joints
[NASA-CR-177990] N86-11298
JOSEPHSON JUNCTIONS
Design of cryocoolers for microwatt superconducting devices N86-11368
A closed cycle cascade Joule Thomson refrigerator for cooling Josephson junction magnetometers N86-11388
JOULE-THOMSON EFFECT
Joule-Thomson valves for long term service in space cryocoolers N86-11393
JOURNAL BEARINGS
Theoretical and experimental comparison of vapor cavitation in dynamically loaded journal bearings
[NASA-TM-87121] N86-11425

K

KAOLINITE
Estimation of particle size based on LDV measurements in a de-accelerating flow field N86-11440
Experiments with solid particle seeding N86-11442
KAON PRODUCTION
Review of kaon factory proposals
[DE85-014110] N86-12122
KAONS
Review of kaon factory proposals
[DE85-014110] N86-12122
KEROSENE
Seeding techniques used in the Vortex Research Facility N86-11443
Seeding systems for use with a laser velocimeter in large scale wind tunnels N86-11444
KINEMATICS
Geokinematic models for the gravimetric W - E profile of the GDR N86-11596
Recent crustal movements and geophysical interpretation of geodynamic processes in the Alpine mountain belt N86-11604
Relation between earthquake focal intensity and recent vertical Earth's crustal movements in the Rila-Rhodope seismic region N86-11615
KINETIC ENERGY
On the instability of vortex series N86-11715
KINETIC THEORY
An introduction to electrical breakdown in dielectrics
[AD-A156465] N86-11415
Plasma kinetic theory in action-angle variables
[DE85-014767] N86-12084
KINETICS
Interactions between oceanic and gravity tides, as analysed from world-wide Earth tide observations and ocean models N86-11576
Effects of acid precipitation on composition, electrokinetic behavior, cation adsorption and ion exchange capacity in various soil systems
[PB85-217727] N86-11698
KLYSTRONS
Status of SLC
[DE85-013071] N86-12097
KRYPTON FLUORIDE LASERS
Progress of Inertial Confinement Fusion (ICF) research N86-11932

L

LABORATORIES
Site description for the University of Nebraska's Sandhills Agricultural Laboratory N86-11628
Laboratory evaluation of the protocol for the volatile organic sampling train
[PB85-201134] N86-11694
LACTOSE
Determination of the steady-state behavior of immobilized (BETA)-galactosidase utilizing an integral reactor scheme
[DE85-012900] N86-11256
LAGEOS (SATELLITE)
An attempt to detect geometric tidal information using Lageos laser ranging data N86-11558
LAGRANGE MULTIPLIERS
ADS: A FORTRAN program for automated design synthesis: Version 1.10
[NASA-CR-177985] N86-11894
Involutory transformations and variation principles with multivariables in thin plate bending problems N86-12004
LAMINAR FLOW
Stability and interaction of coherent structure in supersonic reactive wakes N86-11185
Criteria for scaling heat exchangers to miniature size N86-11387
Simulation of flame propagation through vorticity regions using the discrete vortex method N86-11882
LAMINATES
A Signorini model of bolt fastened laminated composites N86-11258
Surface protection of graphite fabric/PMR-15 composites subjected to thermal oxidation N86-11281
LANDFORMS
Spectroscopy of Moses Rock kimberlite diatreme N86-11635
LANGUAGE PROGRAMMING
New R and D in Chinese language information processing N86-11996
LAP JOINTS
The alternating surface segmented lap joint: A design for thin highly loaded joints N86-11233
Comparison of bond in roll-bonded and adhesively bonded aluminums N86-11248
High-temperature adhesive development and evaluation N86-11250
Interaction of mixed mode loading on cyclic debonding in adhesively bonded composite joints
[NASA-CR-177990] N86-11298
LAPLACE EQUATION
On the addition theorem for Legendre polynomials N86-11704
LARGE SPACE STRUCTURES
Problems experienced and envisioned for dynamical physical systems
[NASA-TP-2508] N86-11215
A direct model reference adaptive approach to the control of space stations N86-11219
Manual for LDEF tensile tests
[NASA-TM-87624] N86-11299
LARMOR RADIUS
Variational quadratic form for low frequency electromagnetic perturbations. 1: Formalism
[DE85-014896] N86-12129
LASER ANEMOMETERS
Comparison of calculated and measured velocities near the tip of a model rotor blade at transonic speeds
[NASA-TM-86697] N86-11196
Correcting for particle counting bias error in turbulent flow N86-11439
Recent experience in seeding transonic/supersonic flows at AEDC N86-11447
Laser velocimetry measurement in a transonic tunnel N86-11448
LDA seeding system for the Langley Low Turbulence Pressure Tunnel N86-11450
Development of seeding techniques for small supersonic wind tunnel N86-11452
Seeding materials: Health and safety considerations N86-11454
Generating aerosols for laser velocimeter seeding N86-11455
Laser anemometry for hot section applications N86-11503
Time-of-flight anemometer for hot section applications N86-11504
LASER ANNEALING
Deep-level defects in ion-implanted and CO2 laser-annealed silicon N86-11939
LASER APPLICATIONS
Water tunnel flow visualization using a laser
[NASA-TM-86743] N86-11206
Laser angle sensor
[NASA-CR-172369] N86-11207
Operating range of aluminum gallium arsenide quantum-well heterostructure lasers: tunability, power output and high energy emission N86-11464
General-purpose equipment for airborne laser remote sensing of ocean, atmosphere and agricultural crops N86-11984
OMEGA: A 24 beam UV irradiation facility
[DE85-014416] N86-12127
LASER CAVITIES
Ring cavity CO2 laser for branch-selection and narrow resonance produced by SF6 in cavity N86-11930
Energy characteristics of laser with saturable anisotropic absorbing medium in cavity N86-11968
Spectrum structure of XeCl electric discharge laser N86-11970

Investigation of polarization characteristics of radiation from laser with dye-activated polymer elements N86-11972

LASER DAMAGE
Pulse duration dependence of 1064-nm laser damage thresholds of porous silica antireflection coatings on fused silica substrates [DE85-013207] N86-11350

LASER DOPPLER VELOCIMETERS
Wind Tunnel Seeding Systems for Laser Velocimeters [NASA-CP-2393] N86-11437
Calculation of particle dynamics effects on laser velocimeter data N86-11438
Experiments with solid particle seeding N86-11442
Seeding techniques used in the Vortex Research Facility N86-11443
Seeding systems for use with a laser velocimeter in large scale wind tunnels N86-11444
Seeding requirements for scanning laser velocimetry N86-11446
A technique to measure the size of particles in laser Doppler velocimetry applications N86-11457
Characteristics of an axisymmetric sudden expansion flow [NASA-CR-176278] N86-11465

LASER FUSION
OMEGA: A 24 beam UV irradiation facility [DE85-014416] N86-12127

LASER HEATING
Melting of crystalline and amorphous silicon by Ruby, XeCl and KrF laser irradiation [DE85-015040] N86-11468
Thermo-mechanical analyses of laser-heated surfaces N86-11877
Laser evaporation of metal in gaseous atmosphere N86-11957

LASER MATERIALS
Chromium- and neodymium-activated gadolinium-scandium-gallium garnet crystal: A new laser active medium N86-11979
Physics overview of AVLIS [DE85-014854] N86-12057

LASER MODE LOCKING
Two-frequency passive mode locking in iodine photodissociation laser N86-11980

LASER OUTPUTS
Seeding requirements for scanning laser velocimetry N86-11446
Operating range of aluminum gallium arsenide quantum-well heterostructure lasers: tunability, power output and high energy emission N86-11464
Melting of crystalline and amorphous silicon by Ruby, XeCl and KrF laser irradiation [DE85-015040] N86-11468
Velocity measurements of laser driven flyers backed by high impedance windows [DE85-015142] N86-11470
Frequency-selection and mode-locking and Nd:YAG laser N86-11928
Toward a theory of atomic gas breakdown by laser radiation near a metal surface N86-11955
Initial plasma formation during exposure of absorbing materials to laser radiation with plane expansion geometry of the forming plasma N86-11956
Excitation of discharge in air by laser radiation N86-11961
Lasing on vapors of chain compounds N86-11967
Energy characteristics of laser with saturable anisotropic absorbing medium in cavity N86-11968
Investigation of efficiency of generation of difference-frequency laser radiation in waveguide N86-11969
Investigation of polarization characteristics of radiation from laser with dye-activated polymer elements N86-11972
Optimization of parameters of chemical CO laser by increasing length of active medium N86-11976
Two-frequency passive mode locking in iodine photodissociation laser N86-11980
Multiphoton Raman scattering of light excited in crystals by a copper-vapor laser N86-11986
On convective effects in gas lasers N86-12006
Experimental program to build a multimegawatt lasertron for super linear colliders [DE85-014293] N86-12049
Rimfire: A six megavolt laser-triggered gas-filled switch for PBFA 2 [DE85-013959] N86-12115

LASER PLASMA INTERACTIONS
Laser evaporation of metal in gaseous atmosphere N86-11957

LASER PLASMAS
Initial plasma formation during exposure of absorbing materials to laser radiation with plane expansion geometry of the forming plasma N86-11956
Influence of solid state obstacles on radiation of recombination laser plasma N86-11958
Excitation of discharge in air by laser radiation N86-11961

LASER PUMPING
Photon induced electron attachment [AD-A156506] N86-11467
Distributed-feedback lasers with active framing medium N86-11971
High-efficiency Al sub 2 O sub 3:Ti sup 3+ tunable laser N86-11973
Chromium- and neodymium-activated gadolinium-scandium-gallium garnet crystal: A new laser active medium N86-11979

LASER RANGE FINDERS
An attempt to detect geometric tidal information using Lageos laser ranging data N86-11558

LASER SPECTROSCOPY
Impurity monitoring by laser-induced fluorescence techniques [DE85-014142] N86-11356
Ionization-Raman double-resonance spectroscopy [DE85-013774] N86-12042

LASER TARGETS
OMEGA: A 24 beam UV irradiation facility [DE85-014416] N86-12127
What extent will small-scale laser-beam fluctuations seed the Rayleigh-Taylor instability in direct-drive targets [DE85-014408] N86-12131

LASER WELDING
Feasibility of remotely manipulated welding in space: A step in the development of novel joining technologies N86-11246
Fabrication and use of zircaloy/tantalum-sheathed cladding thermocouples [EGG-TFBP-6739] N86-11461
A comparison of the physics of Gas Tungsten Arc Welding (GTAW), Electron Beam Welding (EBW), and Laser Beam Welding (LBW) [NASA-TM-86503] N86-11473

LASER WINDOWS
Velocity measurements of laser driven flyers backed by high impedance windows [DE85-015142] N86-11470

LASERS
Laser angle sensor [NASA-CR-172369] N86-11207
The measurements of axisymmetric air turbulent jet flow with an individual realization laser velocimeter system [AD-A157554] N86-11429
China report: Science and technology [JPRS-CST-85-014] N86-11918
USSR report: Physics and mathematics [JPRS-UPM-85-005] N86-11945
Soviet research on crystal channeling of charged particle beams [AD-A157353] N86-12022

LASING
Investigation of efficiency of generation of difference-frequency laser radiation in waveguide N86-11969
Distributed-feedback lasers with active framing medium N86-11971

LATITUDE MEASUREMENT
Adjustment of the latitude data by least-squares collocation approach N86-11562
On the lunar tidal effect in the latitude observations at Tianjin N86-11565
Some short periodic terms due to nutation and tides from latitude and time determinations at Czechoslovak observatories N86-11566
Results concerning rheological parameters of the Earth N86-11567

LAUNCH VEHICLES
Heavy lift launch vehicles for 1995 and beyond [NASA-TM-86520] N86-11216

LAUNCHING
Manual for LDEF tensile tests [NASA-TM-87624] N86-11299

LEAD (METAL)
Surface properties of shocked lead [DE85-009582] N86-11476

LEAD TELLURIDES
$Pb(1-x)Sn(x)Te$ and $Pb(1-y)Sn(y)Se$ laser crystals N86-11931

LEAKAGE
Effects of leakage through clearance seals on the performance of a 10 K Stirling-cycle refrigerator N86-11379

LEAST SQUARES METHOD
Adjustment of the latitude data by least-squares collocation approach N86-11562

LEAVES
Preliminary evaluation of AIS spectra along a topographic/moisture gradient in the Nebraska Sandhills N86-11629
High resolution spectrometry of leaf and canopy chemistry for biochemical cycling N86-11633
Controlled environment life support system: Calcium-related leaf injuries on plants [NASA-CR-176288] N86-11829

LEGENDRE FUNCTIONS
On the addition theorem for Legendre polynomials N86-11704
Spectral statistical forecasts of the 500 mb height field N86-11804

LENS ANTENNAS
A high-efficience, low-phase error waveguide lens for a transform feed antenna N86-11409
Computer-aided bifocal dielectric lens antenna design for MH wave application N86-11410

LENS DESIGN
A high-efficience, low-phase error waveguide lens for a transform feed antenna N86-11409
Computer-aided bifocal dielectric lens antenna design for MH wave application N86-11410
Multidimensional ion microbeam analysis [DE85-014699] N86-12055

LEPTONS
Muon decay [DE85-012590] N86-12067

LEVELING
Modification of a Hughes tiltmeter to a borehole tiltmeter N86-11563
Significance tests of recent vertical crustal movements by correlation functions N86-11611
Statistical analysis and interpretation of Earth crustal movements in northeast Bulgaria N86-11613
A new apparatus for testing bubble vials, electronic levels and automatic levels N86-11614
Dynamics of the Bohemian Massif N86-11616

LIFE (DURABILITY)
Flight worthiness of fire resistant hydraulic systems: Volume 1 [AD-A157618] N86-11199
Manual for LDEF tensile tests [NASA-TM-87624] N86-11299
Polyurethane foam component lifetimes [DE85-008206] N86-11355

LIFE CYCLE COSTS
Flight worthiness of fire resistant hydraulic systems: Volume 1 [AD-A157618] N86-11199
Status of the intercontinental ballistic missile modernization program [AD-A157375] N86-11217
Uncertainty assessment in life cycle cost analysis [AD-A157414] N86-11488

LIFE RAFTS
An evaluation of CASP (computer assisted search planning program) drift predictions near the New England Shelf/Slope Front [AD-A157447] N86-11826

LIFE SCIENCES
China report: Science and technology [JPRS-CST-85-015] N86-11994

LIFT DRAG RATIO
Investigations of modern general aviation propellers N86-11162

LIFTING BODIES
Aerodynamics of wide-chord propellers in non-axisymmetric flow N86-11153

LIGHT (VISIBLE RADIATION)
A flash X-ray facility for the Naval Postgraduate School [AD-A157278] N86-11213
Crystal class and the electrooptic effect [DE85-015240] N86-11353

LIGHT CURVE
The optical polarization of Epsilon Aurigae through the 1982-84 eclipse N86-12171
IUE observations of the 1982-84 eclipse of Epsilon Aurigae N86-12172
UBV photometry of the 1982-4 eclipse of Epsilon Aurigae: A discussion of the observed light curves N86-12 76

LIGHT EMITTING DIODES
A large area X-ray source and its preionization characteristics for XeCl excimer laser N86-11929

LIGHT IONS
Ion whistlers in middle latitudes observed by the interkosmos-14 satellite N86-11714

LIGHT SCATTERING
Particle sizing in a solid rocket motor using the management of scattered light [AD-A156480] N86-11226
Estimation of particle size based on LDV measurements in a de-accelerating flow field N86-11440
Particle phase function measurements by a new Fiber Array Nephelometer: FAN 1 N86-11456
Photoinduced Rayleigh scattering of light in crystals N86-11985

Elastic and inelastic light scattering of colloidal particles
[AD-A157335] N86-12072
Scattered light in the IUE spectra of Epsilon Aurigae N86-12180

LIGHT SOURCES
Spectrally-broad picosecond light source
[DE85-015177] N86-11471

LIGHT TRANSMISSION
An investigation of the effects of fuel composition on combustion characteristics in a T-63 combustor
[AD-A157325] N86-11356

LIGHTNING
User's manual for AC-20-53A protection of airplane fuel systems against fuel vapor ignition due to lightning
[AD-A157619] N86-11191

LINE SPECTRA
Research on optic spatial frequency analysis of linear structures in remote sensing images N86-11927
Frequency-selection and mode-locking and Nd:YAG laser N86-11928
Theory of the critical temperature for superconductors with small lambda (1) N86-11937
Diffraction efficiency of three-dimensional phase hologram of diffuse object N86-11962
Multiphoton Raman scattering of light excited in crystals by a copper-vapor laser N86-11986
Transformation of light pulse shape by thin plane-parallel layer of absorbing material N86-11988
The use of wall-coated cells in atomic frequency standards
[AD-A157435] N86-12024

LINEAR ACCELERATORS
Automated magnet testing facility
[DE85-012863] N86-11422
IFR guiding experiments
[DE85-014512] N86-12027
Disruption angles
[DE85-015138] N86-12032
Experimental program to build a multimegawatt lasertron for super linear colliders
[DE85-014293] N86-12049
Collinear wake field acceleration
[DE85-014356] N86-12050
Discussion of the current limits in the RFQ
[DE85-012909] N86-12088
Status of SLC
[DE85-013071] N86-12097
MABE multibeam accelerator
[DE85-012035] N86-12121
Low inductance diode design of the Proto 2 accelerator for imploding plasma loads
[DE85-013783] N86-12123
Measurements of ultimate accelerating gradients in the SLAC disk-loaded structure
[DE85-014287] N86-12125
Modelling of the PROTO-2 crossover network
[DE85-014639] N86-12128

LINEAR ARRAYS
Computer-aided bifocal dielectric lens antenna design for MH wave application N86-11410

LINEAR CIRCUITS
A general purpose CAD program for microwave linear circuits N86-12002

LINEAR EQUATIONS
Research on the computational methods of gravity topographic effect N86-11578
A parameterization technique for nonlinear spectral models N86-11752
Involutory transformations and variation principles with multivariables in thin plate bending problems N86-12004
Numerical method in dynamic response of nonlinear systems N86-12005

LINEAR SYSTEMS
Bounded state control of linear systems with application to the active structural control N86-11493

LINEAR VIBRATION
Design of a flight qualified long-life cryocooler N86-11377

LINEARITY
Parametric testing of a linearly driven Stirling cryogenic refrigerator N86-11376
The design of a small linear-resonant, split Stirling cryogenic refrigerator compressor N86-11392

LINEARIZATION
Stability and interaction of coherent structure in supersonic reactive wakes N86-11185
The effect of the Hadley circulation on the meridional propagation of stationary waves N86-11732

LINGUISTICS
Approximate reasoning and the REVEAL software system. Users guide
[AD-A157298] N86-11902

LININGS
Burner liner thermal/structural load modelling N86-11514
Component-specific modeling N86-11515
The 3-D inelastic analysis methods for hot section components (base program) N86-11517
Validation of structural analysis methods using burner liner cyclic rig test data N86-11518

LIQUEFACTION
Nuclear spin-polarized HD, D2, HT and DT solids, liquids and high density gases
[DE85-014136] N86-12154

LIQUEFIED NATURAL GAS
Study of heavy gas effects on the atmospheric dispersion of dense gases, revision 1
[DE85-012917] N86-11693

LIQUID ATOMIZATION
Particle size distributions of several commonly used seeding aerosols N86-11441
Seeding systems for use with a laser velocimeter in large scale wind tunnels N86-11444

LIQUID CHROMATOGRAPHY
Characterization methodology for PMR-15 N86-11272
Quality assurance procedures for V378A matrix resin N86-11274
Direct coupling of microbore HPLC columns to MS systems
[NASA-CR-176292] N86-11436

LIQUID COOLING
Optimized ground-coupled heat pump system design for northern climate
[DE85-014065] N86-11484

LIQUID CRYSTALS
Constituent materials N86-11294
Fiber optic pressure sensors in skin-friction measurements
[NASA-CR-176294] N86-11838

LIQUID FUELS
Surface combustion of liquid fuel in stream of gaseous oxidizer N86-11959

LIQUID HELIUM
Design of cryocoolers for microwatt superconducting devices N86-11368
Magnetic refrigeration for low-temperature applications N86-11370
An experimental reciprocating expander for cryocooler application N86-11380
A closed cycle cascade Joule Thomson refrigerator for cooling Josephson junction magnetometers N86-11388
A small helium liquifier which provides continuous cooling based on cycled isentropic expansion N86-11389
Four K refrigerators with a new compact heat exchanger N86-11391

LIQUID METAL FAST BREEDER REACTORS
Liquid metal reactors programs: Safeguards and program assurance
[DE85-011002] N86-12046

LIQUID METALS
Rotating film radiators for space applications
[DE85-009633] N86-11431
Dish electric systems heat engine assessment
[DE85-013942] N86-11479

LIQUID SODIUM
Speed of sound in liquid sodium near gamma-transition point N86-11947

LIQUID-SOLID INTERFACES
Solid-melt interface studies of high-speed silicon sheet growth
[DE85-008783] N86-11349

LIQUID-VAPOR INTERFACES
Hydrodynamics of liquid-vapor disperse annular flows in channels containig bundles of heated rods under nonsteady-state conditions N86-11954
Hydrothermodynamics of the near-surface layer of a liquid and optical methods of investigating it N86-11989

LITHIUM
Basic studies of the lithium secondary battery
[AD-A157449] N86-11673
Chemical thermodynamic assessment of the Li-U-O system for possible space nuclear applications
[DE85-015060] N86-12054
PBFA 2: A 100 TW pulsed power driver for the inertial confinement fusion program
[DE85-013956] N86-12116

LITHIUM CHLORIDES
High rate Li/SOCl(2) cells. 2. Effect of catalyst on cell performance
[AD-A157383] N86-11672

LITHIUM COMPOUNDS
Improved solid state laser sources, volume 3
[DE85-012956] N86-11469
Part A. Molecular dynamics and ionic associations of LiAsF6 in 4-butyrolactone mixtures with 2-methyl tetrahydrofuran. Part B. Molecular dynamics and ionic associations of LiBF4 in 1,2-dimethoxymethane
[AD-A157401] N86-12023

LITHIUM OXIDES
Physical property changes of a lithia-alumina-silica based glass as a function of composition
[DE85-015610] N86-11352
Investigation of efficiency of generation of difference-frequency laser radiation in waveguide N86-11969

LITHOSPHERE
On the distribution of the residual vectors of Earth's tide gravity observations in Central Europe N86-11564
Ocean tidal loading along the Blue Road geotraverse in Fennoscandia N86-11571
On reducing the effect of horizontal displacements of the lithospheric plates from the observations carried out by global geodynamic network (on example the GEOSS-REA network) N86-11589

LOADING MOMENTS
Interaction of mixed mode loading on cyclic debonding in adhesively bonded composite joints
[NASA-CR-177990] N86-11298

LOADS (FORCES)
Theoretical and experimental comparison of vapor cavitation in dynamically loaded journal bearings
[NASA-TM-87121] N86-11425
Elastic wave scattering of a Gaussian incident beam from an interface crack in a layered half space submerged in water N86-11490
The Shock and Vibration Digest, volume 17, no. 4
[AD-A154112] N86-11527
On the distribution of the residual vectors of Earth's tide gravity observations in Central Europe N86-11564
Ocean tidal loading along the Blue Road geotraverse in Fennoscandia N86-11571
Thermo-mechanical analyses of laser-heated surfaces N86-11877

LOGARITHMS
Analysis of aircraft spectrometer data with logarithmic residuals N86-11636

LONG DURATION SPACE FLIGHT
Manual for LDEF tensile tests
[NASA-TM-87624] N86-11299

LONG RANGE WEATHER FORECASTING
Monthly forecast experiments with sea surface temperature anomaly forcings and envelope mountains: Preliminary results N86-11803

LONG TERM EFFECTS
Worldwide marine temperature variations on the season to century time scale N86-11771
Recent unusual mean winter temperature across the contiguous United States N86-11772
Towards understanding the geographical distribution and seasonality in persistance of monthly mean surface air temperature over the U.S.A. N86-11773
Recent long-term climatic change over the eastern tropical and subtropical Pacific and its ramifications N86-11775

LONG WAVE RADIATION
The impact of heat sources in the tropics on the atmospheric circulation N86-11793
Very anomalous behavior of outgoing longwave radiation in the tropics in 1983-84: Aftermath of ENSO? N86-11813
The status of the NOAA/NESDIS radiation budget data set N86-11815

LONGERONS
A comparison of measured and calculated thermal stresses in a hybrid metal matrix composite spar cap element
[NASA-TM-86729] N86-11525

LONGITUDINAL CONTROL
Laser angle sensor
[NASA-CR-172369] N86-11207

LORENTZ FORCE
Muon decay
[DE85-012590] N86-12067

LOSSY MEDIA
Propagation of electromagnetic waves in inhomogeneous and lossy reentry plasma sheath layer N86-11923

LOUISIANA
Information dissemination for a better understanding of Louisiana's water resources
[PB85-219079] N86-11660
Louisiana Water Resources Research Institute
[PB85-218998] N86-11661

LOVE WAVES
Results concerning rheological parameters of the Earth N86-11567

LOW FREQUENCIES
Low frequency split cycle cryocooler N86-11382

Low-frequency baroclinic features observed in the lee of major mountain ranges N86-11811
Variational quadratic form for low frequency electromagnetic perturbations. 1: Formalism [DE85-014896] N86-12129

LOW TEMPERATURE
Magnetic refrigeration for low-temperature applications N86-11370
Reciprocating magnetic refrigerator N86-11371
Simple construction and performance of a conical plastic cryocooler N86-11376
Effects of leakage through clearance seals on the performance of a 10 K Stirling-cycle refrigerator N86-11379

LUBRICATION
Numerical solution for contact pressure and wear distributions of unlubricated, misaligned, closely conforming, multiply connected surfaces N86-11472
Current research on circular saw and band saw vibration and stability N86-11533

LUMINESCENCE
Activated recombinative desorption: A potential component in mechanisms of spacecraft glow [DE85-014092] N86-11223
Distributed-feedback lasers with active framing medium N86-11971
Chromium- and neodymium-activated gadolinium-scandium-gallium garnet crystal: A new laser active medium N86-11979

LUMINOSITY
Very high energy colliders [DE85-013075] N86-12100

LUMINOUS INTENSITY
A large area X-ray source and its preionization characteristics for XeCl excimer laser N86-11929

LUNAR COMPOSITION
Horizons and opportunities in lunar sample science [NASA-CR-176290] N86-12191

LUNAR GEOLOGY
Horizons and opportunities in lunar sample science [NASA-CR-176290] N86-12191

LUNAR GRAVITATIONAL EFFECTS
On the lunar tidal effect in the latitude observations at Tianjin N86-11565

LUNAR TIDES
On the lunar tidal effect in the latitude observations at Tianjin N86-11565

M

MACH NUMBER
Evaluation of a high temperature adhesive for fabricating graphite/PMR-15 polyimide structures N86-11268

MACHINE TOOLS
USSR report: Machine tools and metalworking equipment [JPRS-UMM-85-010] N86-11394
Large robotized turning centers described N86-11395
Geothermal instrumentation development activities at Sandia [DE85-008693] N86-11463

MACHINE-INDEPENDENT PROGRAMS
Third National Academic Machine Retrieval Conference held in Zhenjiang N86-11999

MACHINING
The factory of the future N86-11228
USSR report: Machine tools and metalworking equipment [JPRS-UMM-85-010] N86-11394
Robotized production systems observed in modern plants N86-11396
Robotized machining systems developed at Gomel Institute N86-11397

MAGMA
Economics of magma power generation [DE85-008694] N86-11687

MAGNESIUM ALLOYS
Stress and strain-rate dependence of spall strength in two aluminum alloys [DE85-015154] N86-11321

MAGNESIUM OXIDES
Improved solid state laser sources, volume 3 [DE85-012956] N86-11469

MAGNET COILS
Design for a high field combined function superferric magnet [DE85-014827] N86-11944
Superconducting Magnetic Energy Storage (SMES) Program [DE85-014250] N86-12106

MAGNETIC COMPRESSION
Double tearing mode in plasma with magnetic braiding N86-11919

MAGNETIC COOLING
Magnetic refrigeration for low-temperature applications N86-11370
Reciprocating magnetic refrigerator N86-11371

MAGNETIC DIFFUSION
Numerical solution of ionospheric filtration of ULF waves. Part 1: Method N86-11712

MAGNETIC DIPOLES
Electric or magnetic dipole in stratified uniaxially inhomogeneous anisotropic media N86-11922

MAGNETIC ENERGY STORAGE
Superconducting Magnetic Energy Storage (SMES) Program [DE85-014250] N86-12106

MAGNETIC FIELD CONFIGURATIONS
Variable field magnetic extraction channel for ORIC [DE85-011927] N86-12089
Recent FRC translation experiments on FRX-C/T [DE85-012745] N86-12132

MAGNETIC FIELDS
Reciprocating magnetic refrigerator N86-11371
Automated magnet testing facility [DE85-012863] N86-11422
Numerical solution of ionospheric filtration of ULF waves. Part 2: Application N86-11713
Magnetic filtration N86-11917
The relations between voltage and magnetic field of superconducting weaklink (1) N86-11934
The relations between voltage and magnetic field of superconducting weaklink (2) N86-11935
Energy characteristics of laser with saturable anisotropic absorbing medium in cavity N86-11968
IFR guiding experiments [DE85-014512] N86-12027
Reduction of sextupole distortion by shuffling magnets in small groups [DE85-013024] N86-12035
Window frame or superferric magnet design for low B(3T) heavy ion storage ring study [DE85-013288] N86-12095

MAGNETIC FLUX
Effects of trapped alpha particles on ballooning modes in tokamaks [DE85-015064] N86-12082

MAGNETIC MIRRORS
Physics modeling of tandem mirror devices with high field test cell inserts [DE85-011870] N86-12086
Mirror Fusion Test Facility (MFTF-B): Status [DE85-012953] N86-12087

MAGNETIC MOMENTS
Magnetic measurements of monolayer-thickness films of Cr sandwiched by Au [DE85-015005] N86-12150

MAGNETIC POLES
On short periodical variations of polar motion and UT1-UTC N86-11574

MAGNETIC PROPERTIES
Electronic and magnetic structure of chromium surfaces and chromium monolayers on iron [DE85-014542] N86-11322
Magnetic properties and electronic structure of the actinide systems UAl2, NpAl2 and PuAl2 [DE85-014102] N86-11323
XUV preionization effects in high power magnetically insulated diodes [DE85-013142] N86-12109

MAGNETIC SPECTROSCOPY
High resolution spectrometer in studies of e(+)e(-) annihilation at (radical)s = 29 GeV [DE85-013870] N86-12065

MAGNETIZATION
Itinerant electron ferromagnetism in Fe-alloyed, Ni3Al based materials [DE85-013989] N86-11331
Magnetic measurements of monolayer-thickness films of Cr sandwiched by Au [DE85-015005] N86-12150

MAGNETO-OPTICS
Applications of the magneto-optical filter to stellar pulsation measurements [NASA-CR-176282] N86-12187

MAGNETOHYDRODYNAMIC FLOW
International solar-terrestrial physics program: A plan for the core spaceflight missions [NASA-TM-87511] N86-12194

MAGNETOHYDRODYNAMIC STABILITY
A hybrid mode and a classification of beam plasma instabilities [AD-A157356] N86-12075
MDH stabilization of high (BETA) mirror plasma partially enclosed by conducting wall [DE85-015579] N86-12081

MAGNETOHYDRODYNAMIC WAVES
Statistical properties of geomagnetic pulsations at the Fuerstenfeldbruck Observatory determined by means of pulsation indices. Part 3: Correlation with the parameters of the interplanetary magnetic field N86-11710

MAGNETOMETERS
A closed cycle cascade Joule Thomson refrigerator for cooling Josephson junction magnetometers N86-11388

MAGNETOSPHERE
Plasmas in the Earth's magnetotail [AD-A157320] N86-11716

MAGNETS
Automated magnet testing facility [DE85-012863] N86-11422
Reduction of sextupole distortion by shuffling magnets in small groups [DE85-013024] N86-12035
Coupled virbrational modes of the SLC arc magnet and support system [DE85-014288] N86-12124

MAGNIFICATION
Magnification of low-sensitivity channels in seismographs with standard characteristics N86-11709

MAINTENANCE
Feasibility of remotely manipulated welding in space: A step in the development of novel joining technologies N86-11246
Rapid adhesive bonding and field repair of aerospace materials N86-11253
Reduction of moisture effects during the cure of epoxy adhesives used in composite repair N86-11254
Hardware and software constructs for a vibration analysis network [DE85-008436] N86-11535

MALFUNCTIONS
Evaluation of fault reporting/fault isolation for F-15 aircraft [AD-A156516] N86-11197

MANAGEMENT METHODS
Computer-aided designing, engineering, preparation of production N86-11992

MANAGEMENT SYSTEMS
USSR report: Science and technology policy [JPRS-UST-85-014] N86-11990
Book on planning of scientific, technical progress N86-11991

MANEUVERABLE REENTRY BODIES
Design of maneuverable trajectories of re-entry vehicle N86-11920

MANIPULATORS
Robotized production systems observed in modern plants N86-11396
Robotized machining systems developed at Gomel Institute N86-11397
Mechanical accessories for mobile teleoperators [DE85-014310] N86-11855

MANUALS
Evaluation of fault reporting/fault isolation for F-15 aircraft [AD-A156516] N86-11197
Improving the comprehensibility of a simulated technical manual [AD-A157482] N86-11889

MANUFACTURING
The factory of the future N86-11228
Effects of manufacturing processes on structural allowables [AD-A157596] N86-11318
Computer-aided designing, engineering, preparation of production N86-11992
Wolter 1 type X-ray mirror system with mean resolution and maximum effective collecting area for the spectral region of 1-10 nm N86-12070

MAPPING
Influences of systematic differences between different star catalogues on the results of latitude and time determinations with the PZT 2 N86-11575
Mineralogical mapping in the Cuprite Mining District, Nevada N86-11619
The use of AIS data for identifying and mapping calcareous soils in western Nebraska N86-11630
Application of AIS technology to forest mapping N86-11641
Subsurface geology of the Pajarito Plateau, Espancia Basin, New Mexico [DE85-016215] N86-11720
Algebraic grid generation using tensor product B-splines N86-11908

MAPS
Interactions between oceanic and gravity tides, as analysed from world-wide Earth tide observations and ocean models N86-11576
Formation, distribution and variability in snow cover on the Asian territory of the USSR [NASA-TM-77913] N86-11734

MARINE ENVIRONMENTS
Measurements of refractive index structure function C2N and aerosol size distribution at Chesapeake Bay
[AD-A157455] N86-11717
Worldwide marine temperature variations on the season to century time scale N86-11771
Use of the wavenumber technique with the Lloyds mirror for an acoustic doublet
[AD-A156463] N86-11824
MARKOV PROCESSES
A numerical analysis of a queue with network access flow control
[AD-A157526] N86-11913
MARS ATMOSPHERE
Workshop on Dust on Mars
[NASA-CR-176293] N86-12192
MARS ENVIRONMENT
Workshop on Dust on Mars
[NASA-CR-176293] N86-12192
MARS SURFACE
Mars base buildup scenarios
[DE85-014132] N86-12193
MASS
The mass of hot, shocked CO in Orion: First observations of the J = 17 yields J = 16 transition at 153 microns
[AD-A157323] N86-12189
MASS DISTRIBUTION
Geophysical interpretation of global geoid undulations and mean gravity anomalies N86-11560
MASS SPECTROSCOPY
Characterization methodology for PMR-15
N86-11272
Direct coupling of microbore HPLC columns to MS systems
[NASA-CR-176292] N86-11436
MATERIALS HANDLING
Manual for LDEF tensile tests
[NASA-TM-87624] N86-11299
New harmonic materials: Index engineering: Thin-thick quadrature frequency conversion
[DE85-012976] N86-12156
MATERIALS RECOVERY
Manual for LDEF tensile tests
[NASA-TM-87624] N86-11299
MATHEMATICAL MODELS
Refined numerical solutions of the transonic flow past a wedge N86-11184
Reduction of moisture effects during the cure of epoxy adhesives used in composite repair N86-11254
The hollow sphere model for porous metals and metal powders N86-11308
A computational model for a regenerator N86-11386
Optimized ground-coupled heat pump system design for northern climate
[DE85-014065] N86-11484
Component-specific modeling N86-11515
The Shock and Vibration Digest, volume 17, no. 5
[AD-A156716] N86-11531
Stiffness and damping coefficients of rubber
N86-11532
Thin plates with rapidly varying thickness, and their relation to structural optimization
[AD-A157607] N86-11534
Senstivity of using blunt and sharp crack models in elastic-plastic fracture mechanics
[DE85-010288] N86-11537
North Sea coast levelling net: A model case for the determination of vertical movements in Western Europe
N86-11594
Geokinematic models for the gravimetric W - E profile of the GDR N86-11596
Mathematical treatment of vertical movements
N86-11597
Some geodetic aspects of the problem of checking the plate-tectonic model of seismicity in southeastern Europe N86-11603
An optimum use of sea-level recordings N86-11617
Time series modeling of the Southern Oscillation
N86-11777
Sixth Biennial CUBE (Computer Use By Engineers) Symposium
[LA-10240-C] N86-11858
Magnetic filtration N86-11917
Energy characteristics of waveguide CO sub 2-laser
N86-11978
A general-applications direct global matrix algorithm for rapid seismo-acoustic wavefield computations
N86-12012
Physics modeling of tandem mirror devices with high field test cell inserts
[DE85-011870] N86-12086
Acceleration simulation in the LAMPF 2 booster
[DE85-012695] N86-12126
MATHEMATICS
USSR report: Physics and mathematics
[JPRS-UPM-85-005] N86-11945
MATRICES (MATHEMATICS)
A general-applications direct global matrix algorithm for rapid seismo-acoustic wavefield computations
N86-12012
Numerical techniques for scattering from submerged objects N86-12013
MATRIX MATERIALS
High Temperature Polymer Matrix Composites
[NASA-CP-2385] N86-11260
Acetylene terminated matrix resins N86-11261
Surface protection of graphite fabric/PMR-15 composites subjected to thermal oxidation N86-11281
Improved heat switch for gas sorption compressor
N86-11372
MATRIX METHODS
A comparison of measured and calculated thermal stresses in a hybrid metal matrix composite spar cap element
[NASA-TM-86729] N86-11525
MATTER (PHYSICS)
Some examples of propulsion applications using antimatter N86-11225
MAXIMUM LIKELIHOOD ESTIMATES
Monitoring climate in real time: An application of the Climate Anomaly Monitoring System (CAMS)
N86-11765
MAXWELL EQUATION
Particle pushing techniques for use with finite element based field calculations N86-11865
MEAN
Time-averaging the flux-profile relationship
N86-11789
Variability simulations with a steady, linearized primitive equations model N86-11796
MEASURING INSTRUMENTS
Electron beam potential diagnostic for tandem mirrors, phase 1
[DE85-013515] N86-12107
MECHANICAL DRIVES
Design of a flight qualified long-life cryocooler
N86-11377
Low frequency split cycle cryocooler N86-11382
Passive motion control of pneumatically driven displacers in cryogenic coolers N86-11383
MECHANICAL ENGINEERING
Seismology in civil engineering N86-11707
MECHANICAL PROPERTIES
Current and future engine applications of Gr/PI composites N86-11291
Effects of manufacturing processes on structural allowables
[AD-A157596] N86-11318
Mechanical properties of rapidly solidified Type 304 stainless steel
[DE85-014577] N86-11338
Correlations of chemical, microstructural and mechanical properties of polyethylene piping materials
[DE85-013077] N86-11351
Physical property changes of a lithia-alumina-silica based glass as a function of composition
[DE85-015610] N86-11352
The Shock and Vibration Digest, volume 17, no. 4
[AD-A154112] N86-11527
Thin plates with rapidly varying thickness, and their relation to structural optimization
[AD-A157607] N86-11534
Influence of physical-chemical properties of gases on interaction between shockwaves and convex cylindrical surfaces N86-11962
MECHANICAL SHOCK
The Shock and Vibration Digest, volume 17, no. 5
[AD-A156716] N86-11531
MEDIA
Diffraction of ultrasonic beam passing normally through layered media N86-11946
MEDICAL SCIENCE
Medical heavy ion accelerator proposals
[DE85-015247] N86-12026
MELTING
Melting of crystalline and amorphous silicon by Ruby, XeCl and KrF laser irradiation
[DE85-015040] N86-11468
Icosahedral incommensurate crystals
[DE85-012512] N86-12147
MELTS (CRYSTAL GROWTH)
Solid-melt interface studies of high-speed silicon sheet growth
[DE85-008783] N86-11349
MEMBRANES
Degradation of ionic membranes in the zinc/ferricyanide battery
[DE85-008469] N86-11681
Development of membranes for the zinc/ferricyanide battery
[DE85-011189] N86-11689
MENTAL PERFORMANCE
Approximate reasoning and the REVEAL software system. Users guide
[AD-A157298] N86-11902
MERCURY (METAL)
Mercury bromide reconstitution in the HgBr laser system
[AD-A156502] N86-11466
MERIDIONAL FLOW
Climate simulation and change: A simple energy balance climate model N86-11731
The effect of the Hadley circulation on the meridional propagation of stationary waves N86-11732
Slow fluctuations of the tropical circulation during the FGGE year N86-11812
Observing the Eastern Pacific Hadley Circulation
N86-11818
MESH
Introduction to the session on: Numerical methods for two-phase flow
[DE85-012651] N86-11435
Application of an objective analysis scheme to mesoscale observational network design
[AD-A156911] N86-11760
MESOSCALE PHENOMENA
Application of an objective analysis scheme to mesoscale observational network design
[AD-A156911] N86-11760
On the relationship between North Atlantic seasonal SST anomalies with United States surface temperature anomalies N86-11770
Automated method for the documentation of cloud-top characteristics of mesoscale convective systems
[PB85-204246] N86-11823
MESSAGE PROCESSING
Modification of Huffman coding
[AD-A156479] N86-11899
Probabilistic analysis of a network resource allocation algorithm
[AD-A157553] N86-11904
METAL BONDING
Solid-state bonding of superplastic aluminum alloy 7475 sheet N86-11244
Use of hydration inhibitors to improve bond durability of aluminum adhesive joints N86-11251
Failure rate model for cathodic delamination of protective coatings
[AD-A157483] N86-11912
METAL FATIGUE
Reliability analysis of series structural systems
N86-11486
Elevated temperature biaxial fatigue
[NASA-CR-175009] N86-11526
METAL IONS
Identification of metal ion chloro complexes in an ambient temperature molten salt
[AD-A157295] N86-11302
METAL MATRIX COMPOSITES
Advances in joining techniques used in development of SPF/DB titanium sandwich reinforced with metal matrices N86-11247
Metallurgical characterization of the interfaces and the damping mechanisms in metal matrix composites
[AD-A156507] N86-11300
METAL POWDER
The hollow sphere model for porous metals and metal powders N86-11308
Particle size distributions of several commonly used seeding aerosols N86-11441
METAL SHEETS
Explosive welding of aluminum, titanium and zirconium to copper sheet metal N86-11241
Solid-state bonding of superplastic aluminum alloy 7475 sheet N86-11244
Sheet metal waveguide forming technique
N86-11403
METAL SURFACES
Oxide cathode mechanisms: Electronic and structural features of oxide cathode surfaces
[AD-A157666] N86-11418
Protective coatings of metal surfaces by cold plasma treatment
[NASA-TM-87152] N86-11475
Validation of structural analysis methods using burner liner cyclic rig test data N86-11518
Toward a theory of atomic gas breakdown by laser radiation near a metal surface N86-11955
METAL VAPOR LASERS
Physics overview of AVLIS
[DE85-014854] N86-12057
METAL VAPORS
Laser evaporation of metal in gaseous atmosphere
N86-11957

METAL WORKING
USSR report: Machine tools and metalworking equipment
[JPRS-UMM-85-010] N86-11394
METAL-METAL BONDING
Welding, Bonding and Fastening, 1984
[NASA-CP-2387] N86-11227
Adhesives for aerospace N86-11249
High-temperature adhesive development and evaluation N86-11250
Evaluation of a high temperature adhesive for fabricating graphite/PMR-15 polyimide structures N86-11268
A comparison of the physics of Gas Tungsten Arc Welding (GTAW), Electron Beam Welding (EBW), and Laser Beam Welding (LBW)
[NASA-TM-86503] N86-11473
METALLIC GLASSES
Dense random packed model for amorphous Ni35Zr65: Influance of the heat of mixing
[DE85-014967] N86-11319
Relationship between interatomic bonding and electron transport in plasma deposited amorphous metal alloys
[DE85-014710] N86-11337
Dominant moving species in the formation of amorphous NZr by solid-state reaction
[DE85-014855] N86-12053
METALLOGRAPHY
Los Alamos upgrade in metallographic capabilities
[DE85-014089] N86-11320
Processing and microstructural characterization of B4C-Al cermets
[DE85-013195] N86-11326
Metallography of solid state bonds
[DE85-014564] N86-11327
METALS
The yield point of copper-zinc alloys in the alpha solid solution range
[BLL-BISI-TRANS-23046-(9022.06)] N86-11311
Metallography of solid state bonds
[DE85-014564] N86-11327
Injection molding-sealing of glass to low melting metals
[DE85-015613] N86-11329
Influence of effective rate sensitivity on adiabatic shear instability
[DE85-013967] N86-11333
Senstivity of using blunt and sharp crack models in elastic-plastic fracture mechanics
[DE85-010288] N86-11537
Experimental investigation of recording of dynamic holograms within absorption contour of resonant atomic medium N86-11981
METASTABLE STATE
Thermal post-treatment characteristics of metastable carrier concentration in As-implanted silicon after transient annealing N86-11942
METEORITE CRATERS
Bibliography of terrestrial impact structures
[NASA-TM-87567] N86-11701
METEORITIC COMPOSITION
Bibliography of terrestrial impact structures
[NASA-TM-87567] N86-11701
METEOROLOGICAL CHARTS
Monthly and seasonal weather outlook for June 1985, volume 39, number 11, 30 May 1985
[PB85-209526] N86-11762
METEOROLOGICAL INSTRUMENTS
Variability of snow cover characteristics in the Transbaykal
[NASA-TM-77917] N86-11733
METEOROLOGICAL PARAMETERS
A perspective on the status of measurement of atmospheric turbulence in the US
[NASA-TM-87610] N86-11193
Meteorological and Environmental Inputs to Aviation Systems
[NASA-CP-2388] N86-11735
The utilization of satellite data and dynamics in understanding and predicting global weather phenomena
[NASA-CR-171577] N86-11749
Meteorology of the Persian Gulf and of several airports on the Arabian Coast
[AD-A157441] N86-11761
Circulation and weather for MAM and JJA 1984 N86-11769
Global relationships with the Southern Oscillation N86-11776
Meteorological conditions during drought episodes in the United States Great Plains N86-11802
METEOROLOGICAL RADAR
Overview of meteorological inputs to NASP N86-11736
Sub-cloud layer motions from radar data using correlation techniques
[AD-A156477] N86-11757
METEOROLOGICAL SERVICES
Meteorological and Environmental Inputs to Aviation Systems
[NASA-CP-2388] N86-11735
Overview of meteorological inputs to NASP N86-11736
Airline meteorological requirements N86-11737
METEOROLOGY
The irregularity in the Earth's annual rotation as a cause of systematic time variation N86-11570
Proceedings of the 9th Annual Climate Diagnostics Workshop
[PB85-183911] N86-11763
METHOD OF MOMENTS
Theory and experiment for infinite microstrip arrays N86-11406
MICE
Teratogenic effects of microwave radiation
[PB85-207462] N86-11837
MICROBEAMS
Multidimensional ion microbeam analysis
[DE85-014699] N86-12055
MICROCOMPUTERS
Microcomputers in shock and vibration N86-11528
Field utilization and analysis of AIS 128-channel imagery using microcomputers: Application to Yerington, Nevada field area N86-11621
Microcomputer control and data management techniques for transient digital recording N86-11874
Microcomputer-controlled high-altitude data aquisition system N86-12000
Project to study the use of microcomputer technology in planning and operation of small city transportation systems
[PB85-204873] N86-12166
MICROHARDNESS
Shock-wave synthesis of titanium aluminides
[DE85-015140] N86-11324
Processing and microstructural characterization of B4C-Al cermets
[DE85-013195] N86-11326
MICROORGANISMS
Direct coupling of microbore HPLC columns to MS systems
[NASA-CR-176292] N86-11436
Structure and function of isozymes: Evolutionary aspects and role of oxygen in eucaryotic organisms
[NASA-CR-176286] N86-11831
MICROPROCESSORS
MICROLAN, file transfer program for microprocessors
[AD-A156519] N86-11900
MICROSTRIP TRANSMISSION LINES
Proceedings of the 1984 Antenna Applications Symposium
[AD-A153257] N86-11398
Microstrip monpulse dipole array N86-11405
Theory and experiment for infinite microstrip arrays N86-11406
Circularly polarized microstrip antennas N86-11407
Radiation and scattering performance of microstrip antennas using exotic substrates N86-11408
MICROSTRUCTURE
Metallurgical characterization of the interfaces and the damping mechanisms in metal matrix composites
[AD-A156507] N86-11300
Dense random packed model for amorphous Ni35Zr65: Influence of the heat of mixing
[DE85-014967] N86-11319
Los Alamos upgrade in metallographic capabilities
[DE85-014089] N86-11320
Processing and microstructural characterization of B4C-Al cermets
[DE85-013195] N86-11326
Calculation of thermal trapping in shear bands
[DE85-014404] N86-11336
Properties of crazes and deformation zones in glassy polymers
[AD-A157428] N86-11346
Correlations of chemical, microstructural and mechanical properties of polyethylene piping materials
[DE85-013077] N86-11351
Transition radiation as a practical X-ray source
[DE85-013201] N86-12036
Thin film research. Volume 1
[AD-A157608] N86-12137
MICROWAVE AMPLIFIERS
Experimental program to build a multimegawatt lasertron for super linear colliders
[DE85-014293] N86-12049
MICROWAVE ANTENNAS
Characterization of MMIC devices for active array antennas N86-11401
MICROWAVE CIRCUITS
Characterization of MMIC devices for active array antennas N86-11401
A general purpose CAD program for microwave linear circuits N86-12002
MICROWAVE EQUIPMENT
Electro-optics Millimeter/Microwave technology in Japan. Report of DOD technology team
[AD-A157376] N86-12073
MICROWAVE FREQUENCIES
A high-efficience, low-phase error waveguide lens for a transform feed antenna N86-11409
MICROWAVE LANDING SYSTEMS
Coming soon to a theater near you: The microwave landing system
[AD-A156468] N86-11190
MICROWAVE RADIOMETERS
Active and passive microwave measurements in Hurricane Allen
[NASA-TM-86390] N86-11647
MICROWAVE SCATTERING
Active and passive microwave measurements in Hurricane Allen
[NASA-TM-86390] N86-11647
MICROWAVES
Teratogenic effects of microwave radiation
[PB85-207462] N86-11837
Net-2 models of cavities and diodes N86-11863
The use of wall-coated cells in atomic frequency standards
[AD-A157435] N86-12024
MILITARY HELICOPTERS
Mission-oriented requirements for updating MIL-H-8501: Calspan proposed structure and rationale
[NASA-CR-177371] N86-11204
MILLIMETER WAVES
Proceedings of the 1984 Antenna Applications Symposium
[AD-A153257] N86-11398
Considerations for millimeter wave, monolithic phased arrays N86-11399
Circularly polarized microstrip antennas N86-11407
Computer-aided bifocal dielectric lens antenna design for MH wave application N86-11410
Scaling calculations for a relativistic gyrotron
[AD-A157476] N86-11460
Conversion of electromagnetic wave energy to electrical current by bulk superlattice semiconductors N86-11952
Investigation of efficiency of generation of difference-frequency laser radiation in waveguide N86-11969
Electro-optics Millimeter/Microwave technology in Japan. Report of DOD technology team
[AD-A157376] N86-12073
MINERAL DEPOSITS
The 1984 annual report on Alaska's mineral resources
[DE85-015235] N86-11651
MINERAL EXPLORATION
Mineralogical mapping in the Cuprite Mining District, Nevada N86-11619
Remote stratigraphic analysis: Combined TM and AIS results in the Wind River/Bighorn Basin area, Wyoming N86-11620
Field utilization and analysis of AIS 128-channel imagery using microcomputers: Application to Yerington, Nevada field area N86-11621
Preliminary analysis of AIS spectral data acquired from semi-arid shrub communities in the Owens Valley, California N86-11622
AIS spectra for stressed and unstressed plant communities in the Carolina slate belt N86-11623
A first look at Airborne Imaging Spectrometer (AIS) data in an area of altered volcanic rocks and carbonate formations, Hot Creek Range, south central Nevada N86-11625
Interpretation of AIS images of Cuprite, Nevada using constraints of spectral mixtures N86-11626
MINERALS
Analysis of aircraft spectrometer data with logarithmic residuals N86-11636
The 1984 annual report on Alaska's mineral resources
[DE85-015235] N86-11651
Polar Research Board annual report 1984 and future plans
[PB85-204477] N86-11727
MINES (EXCAVATIONS)
AIS spectra for stressed and unstressed plant communities in the Carolina slate belt N86-11623
MINIATURE ELECTRONIC EQUIPMENT
An experimental study for a miniature Stirling refrigerator N86-11375
MINIATURIZATION
Miniaturization of specimens for mechanical testing
[DE85-014506] N86-11536
MINORITY CARRIERS
Effect of high electric field on minority carrier generation in silicon depletion layer N86-11938

MIRROR FUSION
MDH stabilization of high (BETA) mirror plasma partially enclosed by conducting wall
[DE85-015579] N86-12081
Physics modeling of tandem mirror devices with high field test cell inserts
[DE85-011870] N86-12066
Mirror Fusion Test Facility (MFTF-B): Status
[DE85-012953] N86-12087
Electrical supply for MFTF-B superconducting magnet system
[DE85-012932] N86-12094
Materials studies for magnetic fusion energy applications at low temperatures. 7: Technical reports
[DE85-014518] N86-12101
Multivariable current control for electrically and magnetically coupled superconducting magnets, revision 1
[DE85-012943] N86-12108

MIRRORS
Polymer glazings for silver mirrors
[DE85-012140] N86-11357
Use of the wavenumber technique with the Lloyds mirror for an acoustic doublet
[AD-A156463] N86-11824

MISSILE LAUNCHERS
Status of the intercontinental ballistic missile modernization program
[AD-A157375] N86-11217

MISSILE SILOS
Status of the intercontinental ballistic missile modernization program
[AD-A157375] N86-11217

MISSILES
Evaluation of a high temperature adhesive for fabricating graphite/PMR-15 polyimide structures N86-11268
Recent developments in polyimide and bismaleimide adhesives N86-11270

MISSION PLANNING
International solar-terrestrial physics program: A plan for the core spaceflight missions
[NASA-TM-87511] N86-12194

MIST
Aerosol seeding systems for the NSWC wind tunnels
N86-11453

MIXING
Dense random packed model for amorphous Ni35Zr65: Influence of the heat of mixing
[DE85-014967] N86-11319

MIXING CIRCUITS
New harmonic materials: Index engineering: Thin-thick quadrature frequency conversion
[DE85-012976] N86-12156

MIXTURES
Interpretation of AIS images of Cuprite, Nevada using constraints of spectral mixtures N86-11626

MOBILITY
Mechanical accessories for mobile teleoperators
[DE85-014310] N86-11855

MODAL RESPONSE
Numerical method in dynamic response of nonlinear systems N86-12005

MODELS
Initial investigation of cryogenic wind tunnel model filler materials N86-11255
Chemical control of rate and onset temperature of nadimide polymerization N86-11271
Seeding techniques used in the Vortex Research Facility N86-11443
Laser anemometry for hot section applications
N86-11503
On reducing the effect of horizontal displacements of the lithospheric plates from the observations carried out by global geodynamic network (on example the GEOSS-REA network) N86-11589
Analysis of terrestrial conditions and dynamics
[NASA-CR-176308] N86-11646
Numerical solution of ionospheric filtration of ULF waves. Part 2: Application N86-11713
Laboratory model of flight through wind shear
N86-11747
A model of a downburst, a wind tunnel program on planetary boundary layer, and airship in turbulence
N86-11748
The effect of topography on the evolution of unstable disturbances in a baroclinic atmosphere N86-11750
The Hadley and Rossby regimes in a spherical atmosphere N86-11751
A parameterization technique for nonlinear spectral models N86-11752
A numerical study of global axisymmetric states and their stability to quasi-geostrophic disturbances N86-11753
Cloud streets during KonTur: A comparison of parallel/thermal instability modes with observations
N86-11755
Proceedings of the 9th Annual Climate Diagnostics Workshop
[PB85-183911] N86-11763
ICARUS: A computer code for modeling complex one-dimensional heat conduction on mainframes and micros N86-11866
CELCAP: A computer model for cogeneration system analysis
[NASA-CR-176306] N86-11896
Steady-state detonation of charges of finite length
N86-11966
Research in elementary particle physics
[DE85-014062] N86-12041
MDH stabilization of high (BETA) mirror plasma partially enclosed by conducting wall
[DE85-015579] N86-12081

MODULATORS
Characteristics of an axisymmetric sudden expansion flow
[NASA-CR-176278] N86-11465

MOISTURE
Viscoelastic creep of high-temperature concrete
[DE85-010511] N86-11539
Concrete creep at transient temperature: Constitutive law and mechanism
[DE85-010525] N86-11542
Analysis of terrestrial conditions and dynamics
[NASA-CR-176308] N86-11646
Horizontal fluxes in real and model atmospheres
N86-11792

MOISTURE RESISTANCE
Reduction of moisture effects during the cure of epoxy adhesives used in composite repair N86-11254
Acetylene terminated matrix resins N86-11261

MOLDING MATERIALS
Transfer molding of PMR-15 polyimide resin
N86-11266
Fabrication process of a high temperature polymer matrix engine duct N86-11290

MOLECULAR ABSORPTION
Part A. Molecular dynamics and ionic associations of LiAsF6 in 4-butyrolactone mixtures with 2-methyl tetrahydrofuran. Part B. Molecular dynamics and ionic associations of LiBF4 in 1,2-dimethoxymethane
[AD-A157401] N86-12023

MOLECULAR BEAM EPITAXY
Submillimeter quantum electronics
[AD-A157432] N86-11417

MOLECULAR BIOLOGY
Information from specific-locus mutants on the nature of induced and spontaneous mutations in the mouse
[DE85-014313] N86-11836

MOLECULAR CHAINS
Lasing on vapors of chain compounds N86-11967

MOLECULAR CLOUDS
Submillimeter observations of OH and CH in M42
[NASA-TM-86723] N86-12186

MOLECULAR EXCITATION
Photon induced electron attachment
[AD-A156506] N86-11467

MOLECULAR RELAXATION
Part A. Molecular dynamics and ionic associations of LiAsF6 in 4-butyrolactone mixtures with 2-methyl tetrahydrofuran. Part B. Molecular dynamics and ionic associations of LiBF4 in 1,2-dimethoxymethane
[AD-A157401] N86-12023

MOLECULAR SPECTROSCOPY
Seeding requirements for scanning laser velocimetry
N86-11446

MOLECULAR STRUCTURE
The chemical production of excited state molecules
[AD-A157276] N86-12021

MOLTEN SALTS
Identification of metal ion chloro complexes in an ambient temperature molten salt
[AD-A157295] N86-11302
High temperature molten salt containment
[DE85-012152] N86-11433
Thermodynamics of chromium and iron in carbonate salts at 650(0)C
[DE85-013542] N86-11682

MOLYBDENUM
Short range bonding interaction at metal-metal interfaces
[DE85-014442] N86-11334
Fabrication and use of zircaloy/tantalum-sheathed cladding thermocouples
[EGG-TFBP-6739] N86-11461
Metallic multilayers and superlattices
[DE85-014444] N86-12141

MOLYBDENUM ALLOYS
Tensile properties of 2-1/4Cr-1Mo steel irradiated to 23 dpa at 390 to 550(0)C
[DE85-015551] N86-11332

MOLYBDENUM COMPOUNDS
An interfacial analysis of MoNb-GaAs Schottky barrier diodes N86-11941

MOMENTUM
A 2D ACAR momentum density study of the nature of the positron surface state on Al(100)
[DE85-014830] N86-11330

MOMENTUM THEORY
Tidal friction, the Earth's rotation and hypothesis of an expanding Earth N86-11556

MONATOMIC GASES
Toward a theory of atomic gas breakdown by laser radiation near a metal surface N86-11965

MONITORS
Expert systems development and application
[NASA-TM-86746] N86-11194
Beam position monitor for storage rings
[DE85-013295] N86-12104

MONOMERS
PMR polyimides from solutions containing mixed endcaps N86-11263
The synthesis, characterization and thermal chemistry of modified norbornenyl PMR endcaps N86-11266
Characterization methodology for PMR-15
N86-11272
Replacement of MDA with more oxidatively stable diamines in PMR-polyimides N86-11275
Develop, evaluate and validate continuous emission monitors for designated hazardous pollutants
[PB85-201176] N86-11695

MONOPROPELLANTS
Health hazard evaluation of liquid monopropellants. Phase 4. Subchronic inhalation of hydroxylammonium nitrate, January 1985
[AD-A157623] N86-11844

MONOPULSE ANTENNAS
Microstrip monpulse dipole array N86-11405

MONSOONS
Possible cross equatorial influence of the northeast monsoon on the equatorial westerlies over Indonesia
[AD-A156907] N86-11759
Proceedings of the 9th Annual Climate Diagnostics Workshop
[PB85-183911] N86-11763
Transition from the Southern to Northern Hemisphere summer monsoon N86-11799
Large-scale variability in Indian monsoon rainfall inferred from satellite data N86-11800

MONTE CARLO METHOD
Recent unusual mean winter temperature across the contiguous United States N86-11772
Temperature and precipitation trends in North America
N86-11774
Calculation of the electron backscattering coefficient by Monte Carlo simulation N86-11864
A general purpose CAD program for microwave linear circuits N86-12002
Calculations of physical and chemical reactions produced in irradiated water containing DNA
[DE85-012899] N86-12051

MOON
Figure of the Earth, moon, and planets N86-11550

MOTION
Data analysis using a data base driven graphic animation system
[DE85-014635] N86-11892

MOTIVATION
Adaptive motivation theory
[AD-A157440] N86-11851

MOTOR VEHICLES
USSR report: Transportation
[JPRS-UTR-85-011] N86-11177

MOTORS
Railgun power supply system utilizing traction motors and vacuum interrupters
[DE85-014123] N86-11214

MOUNTAINS
Precise geoid computations at mountainous coastlines in view of vertical datum determinations N86-11561
Determination of crustal movements in the high Tatra Mountains N86-11605
Periglacial landforms and processes in the southern Kenai Mountains, Alaska
[AD-A157459] N86-11718
Low-frequency baroclinic features observed in the lee of major mountain ranges N86-11811

MULTIPHOTON ABSORPTION
Multiphoton Raman scattering of light excited in crystals by a copper-vapor laser N86-11986

MULTIPLE BEAM INTERVAL SCANNERS
Computer-aided bifocal dielectric lens antenna design for MH wave application N86-11410

MULTIPLEXING
SIG: A general-purpose signal processing code
N86-11876

MUONS
Muon decay
[DE85-012590] N86-12067

MUTAGENS
Matrix resin development at NASA Langley Research Center N86-11264
Positive genetic hazard predictions from short-term tests have proved false for results in mammalian spermatogonia with all environmental chemicals so far tested
[DE85-013640] N86-11833
Prospects for DNA methods to measure human heritable mutation rates
[DE85-014555] N86-11847

MUTATIONS
Relationship between alkylation sites and induction of dominant lethals and heritable translocations in mice
[DE85-014309] N86-11835
Information from specific-locus mutants on the nature of induced and spontaneous mutations in the mouse
[DE85-014313] N86-11836
Dose distribution and the relative biological effectiveness of internal alpha emitters
[DE85-013041] N86-11845
Prospects for DNA methods to measure human heritable mutation rates
[DE85-014555] N86-11847

N

N-TYPE SEMICONDUCTORS
Carbon films grown from plasma on III-V semiconductors
[NASA-TM-87140] N86-12135

NACELLES
Wind tunnel investigation of the interaction of propeller slipstream with nacelle/wing/flap combinations N86-11166
Recent developments in polyimide and bismaleimide adhesives N86-11270
Environmental stability graphite/PMR-15 composites N86-11284
Application of Gr/PMR-15 to commercial aircraft N86-11289

NASA PROGRAMS
Overview of NASA's programs N86-11741
NASA-universities relationships in aero/space engineering: A review of NASA's program
[NASA-CR-176307] N86-12158
US space programs: Cooperation and competition from Europe
[BPA-CP-695] N86-12163

NATURAL LANGUAGE (COMPUTERS)
New R and D in Chinese language information processing N86-11996

NAVIER-STOKES EQUATION
Development of an explicit multigrid algorithm for quasi-three-dimensional viscous flows in turbo-machinery
[NASA-TM-87128] N86-11146
Development of a Navier-Stokes analysis for the flow in disk pumps
[AD-A157454] N86-11428
Calculation of particle dynamics effects on laser velocimeter data N86-11438

NAVIGATION
Survey of ice problem areas in navigable waterways
[AD-A157477] N86-11827

NEAR FIELDS
An investigation of in-flight near-field propeller noise generation and transmission N86-11171
Full-scale flight and model-scale wind tunnel tests on the nearfield noise characteristics of aircraft propellers N86-11172
Proceedings of the 1984 Antenna Applications Symposium
[AD-A153257] N86-11398
Stability of a method for analyzing radiation pattern of acoustic radiator with near-field pressure measurement errors N86-11950

NEBRASKA
Site description for the University of Nebraska's Sandhills Agricultural Laboratory N86-11628

NEBULAE
Far-infrared observations of Sagittarius B2: Reconsideration of source structure
[NASA-TM-88185] N86-12167

NEODYMIUM
Chromium- and neodymium-activated gadolinium-scandium-gallium garnet crystal: A new laser active medium N86-11979

NEODYMIUM ALLOYS
Improved solid state laser sources, volume 3
[DE85-012956] N86-11469

NEODYMIUM LASERS
Frequency-selection and mode-locking and Nd:YAG laser N86-11928

NEON
SIMPLODE: An imploding gas puff plasma model. 1. Neon
[AD-A157456] N86-12077

NEPHELOMETERS
Particle phase function measurements by a new Fiber Array Nephelometer: FAN 1 N86-11456
Analysis of arctic haze scattering and aerosol data obtained during AGASP
[AD-A157434] N86-12074

NERVOUS SYSTEM
Cognitive science program: Dissociation of the central timekeeper and the peripheral implementation processes in repetitive movements
[AD-A157542] N86-11852

NETWORK ANALYSIS
Geodimeter net for the investigation of horizontal crustal deformations N86-11598
Principle of the construction of the lines of the repeated levelling for the investigation of the vertical movement in the Carpatho-Balkan Region (CBR) N86-11602
Application of an objective analysis scheme to mesoscale observational network design
[AD-A156911] N86-11760
Net-2 models of cavities and diodes N86-11863

NETWORK CONTROL
Voice communications over packet radio networks
[AD-A157478] N86-11411

NEUTRAL ATOMS
New concepts for drift pumping a thermal barrier with RF
[DE85-013591] N86-12114

NEUTRAL BEAMS
Neutral beam interactions with materials
[AD-A157445] N86-12076
Energy confinement experiments on Doublet 3 with high power neutral beam heating
[DE85-014324] N86-12110

NEUTRALIZERS
Ion beam neutralizer
[AD-D011741] N86-12043

NEUTRON CROSS SECTIONS
R-matrix analysis of the (239) Pu neutron cross sections
[DE85-013095] N86-12052
Double differential neutron emission cross sections of (10)B and (1)B at 6, 10 and 14 MeV and of (6)Li, (7)Li and (12)C at 14 MeV
[DE85-012749] N86-12056

NEUTRON EMISSION
Status of fast neutron nuclear data for (239)Pu
[DE85-012699] N86-12045
Double differential neutron emission cross sections of (10)B and (1)B at 6, 10 and 14 MeV and of (6)Li, (7)Li and (12)C at 14 MeV
[DE85-012749] N86-12056

NEUTRON IRRADIATION
Tensile properties of 2-1/4Cr 1Mo steel irradiated to 23 dpa at 390 to 550(0)C
[DE85-015551] N86-11332

NEUTRON SCATTERING
Neutron scattering studies of the heavy Fermion superconductors
[DE85-014829] N86-12144

NEUTRON SPECTRA
Application of detailed fission-product decay gamma spectra in the calculation of photoneutron spectra from D((GAMMA),n) reactions in PWR fuel
[DE85-012729] N86-12048
Double differential neutron emission cross sections of (10)B and (1)B at 6, 10 and 14 MeV and of (6)Li, (7)Li and (12)C at 14 MeV
[DE85-012749] N86-12056

NEUTRON STARS
High energy physics
[DE85-014272] N86-12063

NEUTRONS
Kinetics analysis of diffusion of point defects to dislocations following pulsed neutron and electron irradiations
[DE85-012768] N86-12037

NEVADA
Electromagnetic soundings for geothermal resources in Dixie Valley, Nevada
[DE85-011986] N86-11722

NEW MEXICO
Subsurface geology of the Pajarito Plateau, Espancia Basin, New Mexico
[DE85-016215] N86-11720
High altitude measured radiance of White Sands, New Mexico in the 400-2000 nm band using a filter wedge spectrometer
[PB85-206084] N86-11729
Atlas of high altitude aircraft measured radiance of White Sands, New Mexico, in the 450-1050 nanometers band
[PB85-204501] N86-11820

NEW YORK
Fiscal year 1983 program report of the Water Resources Research Institute of New York State
[PB85-217024] N86-11662

NEWTON THEORY
The Hadley and Rossby regimes in a spherical atmosphere N86-11751

NEWTON-RAPHSON METHOD
Sparse quasi-Newton methods and the continuation problem
[AD-A157587] N86-11914

NICKEL
Chemical synthesis under shock compression
[DE85-015166] N86-11325

NICKEL ALLOYS
Environmental effects in the fatigue behavior of copper nickel alloys N86-11307
Creep and fracture of a yttna dispersed nickel-chromium alloy N86-11309
Dense random packed model for amorphous Ni35Zr65: Influence of the heat of mixing
[DE85-014967] N86-11319
Synthesis of nickel-aluminum alloys by shock compression of composite particles
[DE85-015165] N86-11328
Itinerant electron ferromagnetism in Fe-alloyed, Ni3Al based materials
[DE85-013989] N86-11331
Shock consolidation of IN-100 nickel-base superalloy powder
[DE85-015159] N86-11360
Dominant moving species in the formation of amorphous NZr by solid-state reaction
[DE85-014855] N86-12053

NIOBIUM
Investigation of efficiency of generation of difference-frequency laser radiation in waveguide N86-11969

NIOBIUM COMPOUNDS
Microscopic investigation of NbN sputtered films
[DE85-015000] N86-12153

NIOBIUM ISOTOPES
Vacancies in thermal equilibrium in Nb
[DE85-014832] N86-12061

NIOBIUM OXIDES
Improved solid state laser sources, volume 3
[DE85-012956] N86-11469
An interfacial analysis of MoNb-GaAs Schottky barrier diodes N86-11941

NITRIDES
Microscopic investigation of NbN sputtered films
[DE85-015000] N86-12153

NITRIDING
Protective coatings of metal surfaces by cold plasma treatment
[NASA-TM-87152] N86-11475

NITROGEN
All-aromatic biphenylene end-capped polyquinoline and polyimide matrix resins N86-11267
Overview of solid particle LV seeding techniques used at UTRC N86-11445
Improvement in wear performance of surgical Ti-6Al-4V alloy by ion implantation of nitrogen or carbon
[DE85-013986] N86-11849
Ultraviolet lasing in helium-nitrogren mixtures N86-11974
Energy characteristics of waveguide CO sub 2-laser N86-11978

NITROGEN DIOXIDE
SAGE aerosol measurements. Volume 1: February 21, 1979 to December 31, 1979
[NASA-RP-1144] N86-11700

NITROGEN IONS
Formation, ion modification and annealing of VN
[DE85-012896] N86-12146

NITROGEN LASERS
Ultraviolet lasing in helium-nitrogren mixtures N86-11974

NITROMETHANE
A mechanism for ignition of high-temperature gaseous nitromethane: The key role of the nitro group in chemical explosives
[AD-A157355] N86-11303

NOAA SATELLITES
TIROS/NOAA (Television and Infrared Observation Satellite/National Oceanic and Atmospheric Administration) satellites space environment monitor archive tape documentation
[PB85-187920] N86-11724

NOAA 7 SATELLITE
Analysis of terrestrial conditions and dynamics
[NASA-CR-176308] N86-11646

NOCTURNAL VARIATIONS
Worldwide marine temperature variations on the season to century time scale N86-11771

NOISE (SOUND)
Vibrations and structureborne noise in space station [NASA-CR-176291] N86-11220
Numerical Techniques in Acoustics [NASA-CP-2404] N86-12007
Vortex studies relating to boundary layer turbulence and noise N86-12015
Infrasound: A summary of interesting articles [FMV:ELEKTRO-A12:142/83] N86-12017
NOISE GENERATORS
Vibrations and structureborne noise in space station [NASA-CR-176291] N86-11220
Current research on circular saw and band saw vibration and stability N86-11533
NOISE PREDICTION
Theoretical analysis of linearized acoustics and aerodynamics of advanced supersonic propellers N86-11156
Numerical Techniques in Acoustics [NASA-CP-2404] N86-12007
Prediction of acoustical response of three-dimensional cavities using an indirect boundary element method N86-12014
NOISE PREDICTION (AIRCRAFT)
Aeroacoustic wind tunnel measurements on propeller noise N86-11169
Full-scale flight and model-scale wind tunnel tests on the nearfield noise characteristics of aircraft propellers N86-11172
The state of the art in propfan turboprop noise N86-11175
Application of active noise control to model propeller noise N86-11176
Shock fitting applied to the prediction of high-speed rotor noise [NASA-TM-86781] N86-11188
A numerical method of calculating propeller noise including acoustic nonlinear effects N86-12011
NOISE PROPAGATION
A unified approach for the aerodynamics and acoustics of propellers in forward motion N86-11155
Shock fitting applied to the prediction of high-speed rotor noise [NASA-TM-86781] N86-11188
On the distribution of the residual vectors of Earth's tide gravity observations in Central Europe N86-11564
NOISE REDUCTION
Adjustment of the latitude data by least-squares collocation approach N86-11562
Study of LAMPF H (-) beam position motion and a predictive algorithm for noise reduction [DE85-012701] N86-12033
NOISE SPECTRA
Some aeroacoustic wind tunnel measurements, theoretical predictions, and flight-test correlations on subsonic aircraft propellers N86-11170
Current research on circular saw and band saw vibration and stability N86-11533
Statistical signal analysis for systems with interferenced inputs N86-12016
NONDESTRUCTIVE TESTS
Characterization of the relationship of the cure cycle chemistry to cure cycle processing properties [NASA-CR-176256] N86-11339
Economic evaluation of concurrent welding and nondestructive examination [DE85-014623] N86-11481
Exploratory development of FMR (ferromagnetic resonance) advanced surface flaw detection methods [AD-A157438] N86-11489
Elastic wave scattering of a Gaussian incident beam from an interface crack in a layered half space submerged in water N86-11490
NONFLAMMABLE MATERIALS
Flight worthiness of fire resistant hydraulic systems: Volume 1 [AD-A157618] N86-11199
NONLINEAR OPTICS
Improved solid state laser sources, volume 3 [DE85-012956] N86-11469
NONLINEAR SYSTEMS
Sparse quasi-Newton methods and the continuation problem [AD-A157587] N86-11914
NONLINEARITY
Improved solid state laser sources, volume 3 [DE85-012956] N86-11469
A parameterization technique for nonlinear spectral models N86-11752
On cloud street development in three dimensional parallel and Rayleigh instabilities N86-11754
On the nonlinear characteristics of the axisymmetric flow regime: Cylindrical and spherical systems N86-11756
Numerical method in dynamic response of nonlinear systems N86-12005
NORMAL DENSITY FUNCTIONS
Monitoring climate in real time: An application of the Climate Anomaly Monitoring System (CAMS) N86-11765
NORTH AMERICA
Analysis of terrestrial conditions and dynamics [NASA-CR-176308] N86-11646
Temperature and precipitation trends in North America N86-11774
Tropospheric static stability and central North American rainfall during 1979 N86-11801
NORTHERN HEMISPHERE
Climate simulation and change: A simple energy balance climate model N86-11731
Review of the climate of fall 1983 and winter 1983-84 N86-11766
Transition from the Southern to Northern Hemisphere summer monsoon N86-11799
Prediction of monthly 700 mb heights using antecedent and simulated prognostic height predictors N86-11805
NOSE WHEELS
A study of the cornering forces generated by aircraft tires on a tilted, free-swiveling nose gear [NASA-TP-2481] N86-11522
NOZZLE DESIGN
The analysis and calculation for the dynamic characteristics of the omni-axial movable flexible joint nozzle N86-11925
NUCLEAR EXPLOSIONS
Thyroid absorbed dose for people at Rongelap, Utirik and Sifo on March 1, 1954 [DE85-014695] N86-11846
NUCLEAR FUEL ELEMENTS
Fabrication and use of zircaloy/tantalum-sheathed cladding thermocouples [EGG-TFBP-6739] N86-11461
Hydrodynamics of liquid-vapor disperse annular flows in channels containig bundles of heated rods under nonsteady-state conditions N86-11954
Application of detailed fission-product decay gamma spectra in the calculation of photoneutron spectra from D((GAMMA),n) reactions in PWR fuel [DE85-012729] N86-12046
NUCLEAR FUELS
Los Alamos upgrade in metallographic capabilities [DE85-014089] N86-11320
Survey of element and isotope importance for fusion safety and environmental assessments [DE85-012415] N86-12047
NUCLEAR FUSION
Survey of element and isotope importance for fusion safety and environmental assessments [DE85-012415] N86-12047
FINESSE: Study of the issues, experiments and facilities for fusion nuclear technology research and development, volume 4 [DE85-010947] N86-12130
NUCLEAR PARTICLES
Review of kaon factory proposals [DE85-014110] N86-12122
NUCLEAR PHYSICS
China report: Science and technology [JPRS-CST-85-014] N86-11918
NUCLEAR POWER PLANTS
Annotated bibliography of human factors applications literature [DE85-012957] N86-12161
NUCLEAR REACTIONS
Sources of radioactive ions [DE85-015251] N86-12030
NUCLEAR REACTOR CONTROL
Progress of Inertial Confinement Fusion (ICF) research N86-11932
NUCLEATION
Continuing design, review, and analysis work for the Sierra Cooperative Pilot Project [PB85-204303] N86-11822
Model of amorphous silicon layer regrowth [DE85-012608] N86-12145
NUCLEI (NUCLEAR PHYSICS)
Few-nucleon transfer reactions on deformed nuclei [DE85-013869] N86-12064
NUCLEON-NUCLEON INTERACTIONS
Some examples of propulsion applications using antimatter N86-11225
Antinucleon-nucleus elastic and inelastic scattering [DE85-012510] N86-12059
NUCLIDES
Cosmogenic-nuclide production by primary cosmic-ray protons [DE85-012760] N86-12198
NUMERICAL ANALYSIS
Shock-induced temperature distributions in powder compact recovery fixtures [DE85-015139] N86-11359
Application of the vortex-lattice concept to flows with smooth-surface separation [AD-A157571] N86-11430
Introduction to the session on: Numerical methods for two-phase flow [DE85-012651] N86-11435
NERF: A computer program for the numerical evaluation of reliability functions user manual [ARL/STRUC-R-411] N86-11487
Numerical solution of ionospheric filtration of ULF waves. Part 1: Method N86-11712
Numerical solution of ionospheric filtration of ULF waves. Part 2: Application N86-11713
A numerical analysis of a queue with network access flow control [AD-A157526] N86-11913
Sparse quasi-Newton methods and the continuation problem [AD-A157587] N86-11914
NUMERICAL CONTROL
Traffic Alert and Collision Avoidance System Signal Environment Model (TCAS SEM) programmer's reference manual [FAA-PM-85-22] N86-11192
Large robotized turning centers described N86-11395
Computational structural mechanics: A new activity at the NASA Langley Research Center [NASA-TM-87612] N86-11540
Microcomputer-controlled high-altitude data aquisition system N86-12000
NUMERICAL INTEGRATION
Computational errors and their control in the determination of satellite orbits N86-11211
NUMERICAL WEATHER FORECASTING
Climate system fluctuations, monitoring N86-11814
NUTATION
Some short periodic terms due to nutation and tides from latitude and time determinations at Czechoslovak observatories N86-11566

O

OAK RIDGE ISOCHRONOUS CYCLOTRON
Variable field magnetic extraction channel for ORIC [DE85-011927] N86-12089
OCEAN BOTTOM
Geodesy: A look to the future [NASA-CR-176283] N86-11657
Oceanic intraplate seismicity: Implications for the rheology and tectonics of the ocean lithosphere N86-11699
OCEAN CURRENTS
Recent long-term climatic change over the eastern tropical and subtropical Pacific and its ramifications N86-11775
Climatic events of the west coast of southern Africa N86-11784
Several aspects of interannual variability in the California current system N86-11785
Warm and cold episodes in the California current: A case for large-scale mid-latitude atmospheric forcing N86-11786
An evaluation of CASP (computer assisted search planning program) drift predictions near the New England Shelf/Slope Front [AD-A157447] N86-11826
OCEAN DYNAMICS
On the lunar tidal effect in the latitude observations at Tianjin N86-11565
OCEAN MODELS
Interactions between oceanic and gravity tides, as analysed from world-wide Earth tide observations and ocean models N86-11576
Oceanic intraplate seismicity: Implications for the rheology and tectonics of the ocean lithosphere N86-11699
OCEAN SURFACE
Climate simulation and change: A simple energy balance climate model N86-11731
Understanding El Nino events using a simple dynamical atmosphere model N86-11797
Monthly forecast experiments with sea surface temperature anomaly forcings and envelope mountains: Preliminary results N86-11803
Very anomalous behavior of outgoing longwave radiation in the tropics in 1983-84: Aftermath of ENSO? N86-11813
A sea surface temperature analysis based on in situ and satellite data N86-11816
Hydrothermodynamics of the near-surface layer of a liquid and optical methods of investigating it N86-11989

OCEAN TEMPERATURE
Climate simulation and change: A simple energy balance climate model N86-11731
Global relationships with the Southern Oscillation N86-11776
Time series modeling of the Southern Oscillation N86-11777
Several aspects of interannual variability in the California current system N86-11785
Monthly forecast experiments with sea surface temperature anomaly forcings and envelope mountains: Preliminary results N86-11803
Very anomalous behavior of outgoing longwave radiation in the tropics in 1983-84: Aftermath of ENSO? N86-11813

OCEANOGRAPHIC PARAMETERS
General-purpose equipment for airborne laser remote sensing of ocean, atmosphere and agricultural crops N86-11984

OCEANS
Interannual climate variability in a low vertical resolution spectral atmospheric model N86-11795

OCTAVES
Considerations for extending the bandwidth of arrays beyond two octaves N86-11404

OFFSHORE ENERGY SOURCES
Arctic Energy Technologies Workshop: Proceedings [DE85-003360] N86-11649

OIL EXPLORATION
Arctic Energy Technologies Workshop: Proceedings [DE85-003360] N86-11649

OIL FIELDS
Analysis of AIS data of the Recluse Oil Field, Recluse, Wyoming N86-11632

OILS
Development of castor-oil-resistant polyurethane sonar encapsulants [AD-A157576] N86-11347

OLIVINE
Deformation of granite at elevated temperature and pressure [DE85-014057] N86-11721

ON-LINE PROGRAMMING
Force and timing components of the motor program [AD-A157584] N86-11843

ONE DIMENSIONAL FLOW
One-dimensional two-phase flow in combustion chamber of solid propellant rocket motors N86-11921

OPEN CIRCUIT VOLTAGE
A 25.5 percent AMO gallium arsenide grating solar cell [NASA-TM-87134] N86-11671

OPERATING SYSTEMS (COMPUTERS)
The embedded operating system project [NASA-CR-176280] N86-11893

OPERATING TEMPERATURE
Turbine Engine Hot Section Technology (HOST) [NASA-CP-2289] N86-11495
Turbine engine Hot Section Technology (HOST) project N86-11496
Turbine heat transfer N86-11505
Gas side heat transfer N86-11507

OPERATIONS RESEARCH
Book on planning of scientific, technical progress N86-11991

OPERATORS (PERSONNEL)
Evaluation of the digital access and cross-connect system for use in the defense communications system [AD-A157570] N86-11412

OPTICAL EQUIPMENT
Seeding systems for use with a laser velocimeter in large scale wind tunnels N86-11444

OPTICAL MEASUREMENT
Steady-state detonation of charges of finite length N86-11966
Photoinduced Rayleigh scattering of light in crystals N86-11985

OPTICAL MEASURING INSTRUMENTS
A laser siderostat [AD-A157444] N86-12190

OPTICAL POLARIZATION
The optical polarization of Epsilon Aurigae through the 1982-84 eclipse N86-12171

OPTICAL PROPERTIES
A summary report on the Flat-Plate Solar Array Project Workshop on Transparent Conducting Polymers [NASA-CR-176302] N86-11669
Stationary pulse solutions for a free electron laser N86-11933
Wolter 1 type X-ray mirror system with mean resolution and maximum effective collecting area for the spectral region of 1-10 nm N86-12070
Ellipsometric and optical study of some uncommon insulator films on 3-5 semiconductors [NASA-TM-87135] N86-12134

OPTICAL PUMPING
Efficiency of optically-pumped XeF-laser N86-11977

OPTICAL RADAR
Lidar observations of stratospheric aerosol over Mauna Loa Observatory: 1982 - 1983 [PB85-187896] N86-11723

OPTICAL REFLECTION
Transformation of light pulse shape by thin plane-parallel layer of absorbing material N86-11988

OPTICAL THICKNESS
Lidar observations of stratospheric aerosol over Mauna Loa Observatory: 1982 - 1983 [PB85-187896] N86-11723

OPTICS
Phasing of multiple-aperture optical systems N86-11987
Balloon-borne three-meter telescope for far-infrared and submillimeter astronomy [NASA-CR-176285] N86-12188

OPTIMAL CONTROL
Design of maneuverable trajectories of re-entry vehicle N86-11920

OPTIMIZATION
A simple, first step to the optimization of regenerator geometry N86-11385
Optimized ground-coupled heat pump system design for northern climate [DE85-014065] N86-11484
Thin plates with rapidly varying thickness, and their relation to structural optimization [AD-A157607] N86-11534
Design optimization of the power generation system for a space-based free-electron laser N86-11861
ADS: A FORTRAN program for automated design synthesis: Version 1.10 [NASA-CR-177985] N86-11894
Algebraic grid generation using tensor product B-splines N86-11908

ORBIT CALCULATION
Computational errors and their control in the determination of satellite orbits N86-11211

ORBIT DECAY
SPACEWARN Bulletin [NASA-TM-87512] N86-11222

ORBIT TRANSFER VEHICLES
Design and performance analysis of an aero-maneuvering orbital-transfer vehicle concept [NASA-TM-86848] N86-11221

ORBITAL MANEUVERS
Design and performance analysis of an aero-maneuvering orbital-transfer vehicle concept [NASA-TM-86848] N86-11221

ORGANIC CHEMISTRY
Laboratory evaluation of the protocol for the volatile organic sampling train [PB85-201184] N86-11694

ORGANIC COMPOUNDS
Develop, evaluate and validate continuous emission monitors for designated hazardous pollutants [PB85-201176] N86-11695
Lasing on vapors of chain compounds N86-11967

ORIFICES
Particle size distributions of several commonly used seeding aerosols N86-11441

ORION NEBULA
Submillimeter observations of OH and CH in M42 [NASA-TM-86723] N86-12186
The mass of hot, shocked CO in Orion: First observations of the J = 17 yields J = 16 transition at 153 microns [AD-A157323] N86-12189

OROGRAPHY
Atmospheric response to an equatorial Pacific sea surface temperature anomaly: The effects of orography N86-11791

ORTHOGONAL FUNCTIONS
On the addition theorem for Legendre polynomials N86-11704
Slow fluctuations of the tropical circulation during the FGGE year N86-11812

OSCILLATIONS
A novel oscillating jet: Its effect on ejector thrust augmentation [AD-A157480] N86-11201
Calculation of RF fields in axisymmetric cavities [DE85-014135] N86-11414
High frequencies in tidal tilt records N86-11554
Raman scattering of sound on random oscillations of bubbles N86-11948

OUTGASSING
Neutral beam interactions with materials [AD-A157445] N86-12076

OUTPUT
KRASH85 user's guide: Input/output format [FAA-CT-85-10] N86-11898

OXIDATION
Thermo-oxidative stability of graphite fiber/PMR-15 polyimide composites at 350 deg C N86-11277

OXIDATION RESISTANCE
High-temperature adhesive development and evaluation N86-11250
Bismaleimides and related maleimido polymers as matrix resins N86-11265
All-aromatic biphenylene end-capped polyquinoline and polyimide matrix resins N86-11267
Characterization of polyimide matrix resins and prepregs N86-11273
Replacement of MDA with more oxidatively stable diamines in PMR-polyimides N86-11275

OXIDES
Oxide cathode mechanisms: Electronic and structural features of oxide cathode surfaces [AD-A157666] N86-11418

OXIDIZERS
Surface combustion of liquid fuel in stream of gaseous oxidizer N86-11959

OXYGEN
Stability and interaction of coherent structure in supersonic reactive wakes N86-11185
Structure and function of isozymes: Evolutionary aspects and role of oxygen in eucaryotic organisms [NASA-CR-176286] N86-11831
The mass of hot, shocked CO in Orion: First observations of the J = 17 yields J = 16 transition at 153 microns [AD-A157323] N86-12189

OXYGEN CONSUMPTION
Perceptual and physiological responses during exercise in cool and cold water [AD-A157334] N86-11840

OZONE
Integrated forest study on effects of atmospheric deposition. Project summary [DE85-015972] N86-11690
SAGE aerosol measurements. Volume 1: February 21, 1979 to December 31, 1979 [NASA-RP-1144] N86-11700
Regional oxidant modeling of the northeast US [PB85-201192] N86-11728

P

P-N JUNCTIONS
Pb(1-x)Sn(x)Te and Pb(1-y)Sn(y)Se laser crystals N86-11931

P-TYPE SEMICONDUCTORS
Carbon films grown from plasma on III-V semiconductors [NASA-TM-87140] N86-12135

PACIFIC NORTHWEST (US)
Evaluation and ranking of geothermal resources for electrical generation or electrical offset in Idaho, Montana, Oregon and Washington [DE85-014661] N86-11650
Relationships between Pacific northwest coast climate and ENSO events N86-11787
Evidence of an 18 year cycle in Pacific northwest precipitation data N86-11788

PACIFIC OCEAN
Proceedings of the 9th Annual Climate Diagnostics Workshop [PB85-183911] N86-11763
Review of the climate of fall 1983 and winter 1983-84 N86-11766
Circulation and weather for MAM and JJA 1984 N86-11769
Satellite observations of a large-amplitude 40-50 day oscillation in upper tropospheric temperature over the equatorial Pacific Ocean during the 1982-83 ENSO event N86-11778
Very anomalous behavior of outgoing longwave radiation in the tropics in 1983-84: Aftermath of ENSO? N86-11813
Observing the Eastern Pacific Hadley Circulation N86-11818

PACKAGING
Transportation system impact limiter design using rigid polyurethane foam [DE85-015088] N86-11354

PACKETS (COMMUNICATION)
Voice communications over packet radio networks [AD-A157478] N86-11411

PANEL METHOD (FLUID DYNAMICS)
Design concept and performance prediction technique for potential flows around advanced propellers N86-11150

PANELS
Feasibility of remotely manipulated welding in space: A step in the development of novel joining technologies N86-11246

Rapid adhesive bonding and field repair of aerospace materials N86-11253

PARABOLIC ANTENNAS
Calculation of allowable orbital spacings for the fixed-satellite service
[NASA-CR-176273] N86-11212

PARABOLIC REFLECTORS
Dish electric systems heat engine assessment
[DE85-013942] N86-11479

PARALLEL FLOW
On cloud street development in three dimensional parallel and Rayleigh instabilities N86-11754
Cloud streets during KonTur: A comparison of parallel/thermal instability modes with observations
N86-11755

PARALLEL PROCESSING (COMPUTERS)
Towards developing robust algorithms for solving partial differential equations on MIMD machines
[NASA-CR-177979] N86-11856

PARAMETERIZATION
Results concerning rheological parameters of the Earth N86-11567
A parameterization technique for nonlinear spectral models N86-11752

PARTIAL DIFFERENTIAL EQUATIONS
On inverse problems in differential equations: A critical analysis N86-11552
Towards developing robust algorithms for solving partial differential equations on MIMD machines
[NASA-CR-177979] N86-11856
A time-splitting numerical technique for solving highly coupled two-phase flow conservation equation
N86-11879

PARTICLE ACCELERATION
Velocity measurements of laser driven flyers backed by high impedance windows
[DE85-015142] N86-11470

PARTICLE ACCELERATOR TARGETS
Experimental check of bremsstrahlung dosimetry predictions for 0.75 MeV electrons
[DE85-014706] N86-12058

PARTICLE ACCELERATORS
A flash X-ray facility for the Naval Postgraduate School
[AD-A157278] N86-11213
Two-dimensional linacs
[DE85-015129] N86-12029
AGS polarized beam facility
[DE85-011834] N86-12038
Cascade switch implementation of PBFA 1
[DE85-013955] N86-12039
PBFA-2 vacuum insulator stack failure mechanisms
[DE85-013118] N86-12090
Design and optimization of the PBFA 2 vacuum interface and transmission lines for light ion fusion
[DE85-012809] N86-12092
Very high energy colliders
[DE85-013075] N86-12100
Photon diagnostics leading to an improved Marx
[DE85-013434] N86-12103
XUV preionization effects in high power magnetically insulated diodes
[DE85-013142] N86-12109
Rimfire: A six megavolt laser-triggered gas-filled switch for PBFA 2
[DE85-013959] N86-12115
PBFA 2: A 100 TW pulsed power driver for the inertial confinement fusion program
[DE85-013956] N86-12116
Comparison of energy transport measurements and computer simulations in a single module prototype for PBFA 2
[DE85-013960] N86-12119
Review of kaon factory proposals
[DE85-014110] N86-12122
Coupled virbrational modes of the SLC arc magnet and support system
[DE85-0142[illegible]8] N86-12124
Acceleration simulation in the LAMPF 2 booster
[DE85-012695] N86-12126

PARTICLE BEAMS
Soviet research on crystal channeling of charged particle beams
[AD-A157353] N86-12022
Cascade switch implementation of PBFA 1
[DE85-013955] N86-12039
XUV preionization effects in high power magnetically insulated diodes
[DE85-013142] N86-12109
Rimfire: A six megavolt laser-triggered gas-filled switch for PBFA 2
[DE85-013959] N86-12115
Comparison of energy transport measurements and computer simulations in a single module prototype for PBFA 2
[DE85-013960] N86-12119

PARTICLE COLLISIONS
Status of SLC
[DE85-013071] N86-12097

PARTICLE DENSITY (CONCENTRATION)
Wind Tunnel Seeding Systems for Laser Velocimeters
[NASA-CP-2393] N86-11437
Statistical properties of geomagnetic pulsations at the Fuerstenfeldbruck Observatory determined by means of pulsation indices. Part 3: Correlation with the parameters of the interplanetary magnetic field N86-11710

PARTICLE EMISSION
Distributed-feedback lasers with active framing medium N86-11971

PARTICLE INTENSITY
The measurements of axisymmetric air turbulent jet flow with an individual realization laser velocimeter system
[AD-A157554] N86-11429

PARTICLE INTERACTIONS
Identification of metal ion chloro complexes in an ambient temperature molten salt
[AD-A157295] N86-11302
Vacancies in thermal equilibrium in Nb
[DE85-014832] N86-12061
Collider Detector at Fermilab (CDF)
[DE85-014423] N86-12068

PARTICLE MOTION
Hermetic bellows seal for Braun linear engine: Design, test and demonstration
[DE85-013545] N86-11478
Possibility of optimal choice of exposure time for holographic recording of objects through unsteady scattering media N86-11983

PARTICLE PRODUCTION
Correcting for particle counting bias error in turbulent flow N86-11439
The vacuum in the presence of electromagnetic fields and rotating boundaries N86-11916

PARTICLE SIZE DISTRIBUTION
Particle sizing in a solid rocket motor using the management of scattered light
[AD-A156480] N86-11226
An investigation of the effects of fuel composition on combustion characteristics in a T-63 combustor
[AD-A157325] N86-11358
Wind Tunnel Seeding Systems for Laser Velocimeters
[NASA-CP-2393] N86-11437
Calculation of particle dynamics effects on laser velocimeter data N86-11438
Estimation of particle size based on LDV measurements in a de-accelerating flow field N86-11440
Particle size distributions of several commonly used seeding aerosols N86-11441
Experiments with solid particle seeding N86-11442
Uncertainties in the radiative properties of smoke and their effects on climate assessments
[DE85-015187] N86-11691
Analysis of arctic haze scattering and aerosol data obtained during AGASP
[AD-A157434] N86-12074

PARTICLE TRACKS
Calculations of physical and chemical reactions produced in irradiated water containing DNA
[DE85-012899] N86-12051

PARTICLE TRAJECTORIES
Using the TEVATRON beam position monitor system to investigate transverse phase space
[DE85-014261] N86-12105

PARTICLES
Particle phase function measurements by a new Fiber Array Nephelometer: FAN 1 N86-11456
Magnetic filtration N86-11917
Elastic and inelastic light scattering of colloidal particles
[AD-A157335] N86-12072

PASTES
New processable modified polyimide resins for adhesive and matrix applications N86-11269

PATHOGENESIS
Importance of phytoalexin tolerance and detoxification for pathogenicity
[DE85-014759] N86-11257

PATTERN RECOGNITION
Sub-cloud layer motions from radar data using correlation techniques
[AD-A156477] N86-11757

PAVEMENTS
Validation of procedures for pavement design on expansive soils
[FAA-PM-85-15] N86-11362

PEELING
Comparison of bond in roll-bonded and adhesively bonded aluminums N86-11248
High-temperature adhesive development and evaluation N86-11250

PENDULUMS
High frequencies in tidal tilt records N86-11554
Modification of a Hughes tiltmeter to a borehole tiltmeter N86-11563
Capacitive pendulum with intelligent data collection
N86-11577

PENTABORANES
Studies on the syntheses of boron hydride systems
[AD-A157368] N86-11344

PERFORMANCE PREDICTION
Design concept and performance prediction technique for potential flows around advanced propellers
N86-11150
A review of ARA research into propeller aerodynamic prediction methods N86-11151
Visual information transfer. Part 1: Assessment of specific information needs. Part 2: Parameters of appropriate instrument scanning behavior
[NASA-CR-176277] N86-11850
CELCAP: A computer model for cogeneration system analysis
[NASA-CR-176306] N86-11896
Modelling of the PROTO-2 crossover network
[DE85-014639] N86-12128

PERFORMANCE TESTS
Performance evaluation of full scale propellers by wind tunnel test N86-11160
A comparison of the NAVTOLAND (Navy vertical takeoff and landing) SH-2F helicopter model with the requirements of MIL-H-8501A and with flight data
[AD-A157297] N86-11198
Modification of a Hughes tiltmeter to a borehole tiltmeter N86-11563
RE-1000 free-piston Stirling engine update
[NASA-TM-87126] N86-11668
An evaluation of three graphics packages: The methodology and results N86-11870

PERIODIC FUNCTIONS
Some short periodic terms due to nutation and tides from latitude and time determinations at Czechoslovak observatories N86-11566

PERIODIC VARIATIONS
Proceedings of the 5th International Symposium Geodesy and Physics of the Earth, part 2
[REPT-81-PT-2] N86-11568
On short periodical variations of polar motion and UT1-UTC N36-11574
Secular and long term variations in polar motion from classical and Doppler observations N86-11581
Polar motion between 1900.0 and 1984.0 as determined by different techniques N86-11587
Variability of snow cover characteristics in the Transbaykal
[NASA-TM-77917] N86-11733
Circulation and weather for MAM and JJA 1984
N86-11769
Recent unusual mean winter temperature across the contiguous United States N86-11772
Towards understanding the geographical distribution and seasonality in persistance of monthly mean surface air temperature over the U.S.A. N86-11773
Land-surface fluctuations and associated climatic variability N86-11807
Concurrent and lagged relationships between precipitation frequency and 700 mb heights N86-11808
Applications of the magneto-optical filter to stellar pulsation measurements
[NASA-CR-176282] N86-12187

PERMAFROST
Workshop on Permafrost Geophysics
[AD-A157485] N86-11719

PERMEABILITY
Experimental needs of high temperature concrete
[DE85-009700] N86-11541

PERMITTIVITY
Photoinduced Rayleigh scattering of light in crystals
N86-11985

PERSIAN GULF
Meteorology of the Persian Gulf and of several airports on the Arabian Coast
[AD-A157441] N86-11761

PERSONNEL
Distinct characteristics of science
[DE85-006533] N86-12159

PERSONNEL MANAGEMENT
Computer-aided designing, engineering, preparation of production N86-11992
Annotated bibliography of human factors applications literature
[DE85-012957] N86-12161

PERTURBATION
Investigation of photoelectrode redox polymer junctions
[AD-A157556] N86-11304
Planets around Barnard's Star? N86-11584
Particle simulation of the low-(ALPHA) Pierce diode
[DE85-014435] N86-12113

Variational quadratic form for low frequency electromagnetic perturbations. 1: Formalism
[DE85-014696] N86-12129

PERTURBATION THEORY
On the instability of vortex series N86-11715
Plasma kinetic theory in action-angle variables
[DE85-014767] N86-12084

PERU
The distribution of rainfall along the coast of northern Peru during 1982-83 N86-11782
Peru coastal winds during 1982-1983 N86-11783

PHASE DEVIATION
Phasing of multiple-aperture optical systems N86-11987

PHASE DIAGRAMS
Processing and microstructural characterization of B4C-Al cermets
[DE85-013195] N86-11326
Physical property changes of a lithia-alumina-silica based glass as a function of composition
[DE85-015610] N86-11352

PHASE SHIFT
On the distribution of the residual vectors of Earth's tide gravity observations in Central Europe N86-11564
Diffraction efficiency of three-dimensional phase hologram of diffuse object N86-11982

PHASE TRANSFORMATIONS
An interfacial analysis of MoNb-GaAs Schottky barrier diodes N86-11941
Sandia shock compression database
[DE85-015141] N86-12142

PHASED ARRAYS
Proceedings of the 1984 Antenna Applications Symposium
[AD-A153257] N86-11398
Considerations for millimeter wave, monolithic phased arrays N86-11399
The design of a thermally efficient 1:256 KU-band feed network for a MMIC phased array N86-11400

PHENOLIC EPOXY RESINS
Recent developments in polyimide and bismaleimide adhesives N86-11270

PHENYLS
Chemical control of rate and onset temperature of nadimide polymerization N86-11271
Rheological, processing, and 371 deg C mechanical properties of Celion 6000/N-phenylnadimide modified PMR composites N86-11278

PHONONS
Discussion of the superconducting critical temperature in a N-S multi-film structure N86-11936
Theory of the critical temperature for superconductors with small lambda (1) N86-11937

PHOSPHORIC ACID
Polyurethane foam component lifetimes
[DE85-008206] N86-11355

PHOTOCATHODES
Experimental program to build a multimegawatt lasertron for super linear colliders
[DE85-014293] N86-12049

PHOTOCHEMICAL OXIDANTS
Regional-scale (1000 KM) model of photochemical air pollution. Part 3: Tests of the numerical algorithms
[PB85-203818] N86-11696

PHOTOCHEMICAL REACTIONS
Regional-scale (1000 KM) model of photochemical air pollution. Part 3: Tests of the numerical algorithms
[PB85-203818] N86-11696

PHOTODISSOCIATION
Efficiency of optically-pumped XeF-laser N86-11977
Two-frequency passive mode locking in iodine photodissociation laser N86-11980

PHOTOELECTRIC EMISSION
Experimental program to build a multimegawatt lasertron for super linear colliders
[DE85-014293] N86-12049

PHOTOELECTRONS
Photoelectron trajectory analyses of streak tubes N86-11880

PHOTOGRAPHIC MEASUREMENT
Variability of snow cover characteristics in the Transbaykal
[NASA-TM-77917] N86-11733

PHOTOIONIZATION
XUV preionization effects in high power magnetically insulated diodes
[DE85-013142] N86-12109

PHOTOLITHOGRAPHY
Uniaxial tensile deformation and fracture of dual-phase steels
[DE85-015034] N86-11538

PHOTOMULTIPLIER TUBES
Characteristics of an axisymmetric sudden expansion flow
[NASA-CR-176278] N86-11465
Spectrally-broad picosecond light source
[DE85-015177] N86-11471

PHOTON BEAMS
Higher luminosities via alternative incident channels
[DE85-014355] N86-12118

PHOTONEUTRONS
Application of detailed fission-product decay gamma spectra in the calculation of photoneutron spectra from D((GAMMA),n) reactions in PWR fuel
[DE85-012729] N86-12048

PHOTONICS
Spectrally-broad picosecond light source
[DE85-015177] N86-11471

PHOTONS
Photon induced electron attachment
[AD-A156506] N86-11467
Calculation of the electron backscattering coefficient by Monte Carlo simulation N86-11864

PHOTOOXIDATION
Investigation of photoelectrode redox polymer junctions
[AD-A157556] N86-11304

PHOTOPRODUCTION
High energy physics
[DE85-014272] N86-12063

PHOTOSENSITIVITY
Photosensitivity and imaging characteristics of ion-implanted PLZT ceramics
[DE85-015489] N86-11348

PHOTOSYNTHESIS
Analysis of terrestrial conditions and dynamics
[NASA-CR-176308] N86-11646
Controlled environment life support system: Calcium-related leaf injuries on plants
[NASA-CR-176288] N86-11829
Structure and function of isozymes: Evolutionary aspects and role of oxygen in eucaryotic organisms
[NASA-CR-176286] N86-11831

PHOTOVOLTAIC CELLS
Photovoltaic-powered vaccine refrigerator: Freezer systems field test results
[NASA-TM-86972-REV] N86-11666
New-generation photovoltaic technologies
[DE85-012143] N86-11675

PHYSICAL FITNESS
Physiological effects of training
[AD-A157417] N86-11841

PHYSIOLOGICAL EFFECTS
Physiological effects of training
[AD-A157417] N86-11841

PHYSIOLOGICAL RESPONSES
Assessments and viewpoints on the biological and human health effects of Extremely Low Frequency (ELF) electromagnetic fields: Compilation of commissioned papers for the ELF literature review project
[AD-A156942] N86-11839
Perceptual and physiological responses during exercise in cool and cold water
[AD-A157334] N86-11840
Is the cerebellum involved in motor and perceptual timing: A case study
[AD-A157452] N86-11842
Force and timing components of the motor program
[AD-A157584] N86-11843

PILOT TRAINING
Recognition and control of low level wind shear
[AD-A156500] N86-11758

PIONS
Some examples of propulsion applications using antimatter N86-11225

PIPES (TUBES)
NTF: Soldering technology development for cryogenics N86-11231
Explosive welding of tubular configurated joints for critical applications N86-11238
Explosive tube-to-fitting joining of small-diameter tubes N86-11239
The use of explosive forming for fastening and joining structural and pressure components N86-11240
Langley Research Center standard for the evaluation of socket welds N86-11243
Composite materials N86-11295
The stability of Timoshenko beams conveying a compressible fluid N86-11492
HOST liner cyclic facilities N86-11519

PISTON ENGINES
RE-1000 free-piston Stirling engine update
[NASA-TM-87126] N86-11668

PLANETARY ATMOSPHERES
Laboratory studies of atomic collision processes of importance in planetary atmospheres
[NASA-CR-176301] N86-12019

PLANETARY COMPOSITION
Geophysical interpretation of global geoid undulations and mean gravity anomalies N86-11560

PLANETARY EVOLUTION
Remote stratigraphic analysis: Combined TM and AIS results in the Wind River/Bighorn Basin area, Wyoming N86-11620

PLANETARY GRAVITATION
The potentialographical problem and the conception of gravitating disks N86-11579
On the convergence problem of the satellite derived spherical harmonic expansion of the geopotential at the Earth's surface N86-11582
Geodynamic effects due to Earth's deformation N86-11585
On the long-wavelength correlation between gravity and topography N86-11586

PLANETARY MANTLES
On the comparison of the results of two different E-W-strainmeters N86-11583

PLANETARY ORBITS
Figure of the Earth, moon, and planets N86-11550

PLANETARY WAVES
The effect of the Hadley circulation on the meridional propagation of stationary waves N86-11732
Review of the climate of fall 1983 and winter 1983-84 N86-11766
Blocking as an explanation of the severe cold of winter 1983-84 N86-11768
Circulation and weather for MAM and JJA 1984 N86-11769
Spectral statistical forecasts of the 500 mb height field N86-11804

PLANETS
Planets around Barnard's Star? N86-11584

PLANNING
Project to study the use of microcomputer technology in planning and operation of small city transportation systems
[PB85-204873] N86-12166

PLANTS (BOTANY)
Preliminary analysis of AIS spectral data acquired from semi-arid shrub communities in the Owens Valley, California N86-11622
AIS spectra for stressed and unstressed plant communities in the Carolina slate belt N86-11623
Effect of elevated atmospheric CO2 on plant communities. Annual report, 1984-1985
[DE85-015575] N86-11692

PLASMA COMPRESSION
Multi-megampere operation of plasma compression opening switches in planar geometry
[DE85-012755] N86-11420

PLASMA CONTROL
Double tearing mode in plasma with magnetic braiding N86-11919
MDH stabilization of high (BETA) mirror plasma partially enclosed by conducting wall
[DE85-015579] N86-12081
Mirror Fusion Test Facility (MFTF-B): Status
[DE85-012953] N86-12087
Energy confinement experiments on Doublet 3 with high power neutral beam heating
[DE85-014324] N86-12110
Energy confinement in a high-current reversed field pinch
[DE85-015009] N86-12111
Recent FRC translation experiments on FRX-C/T
[DE85-012745] N86-12132

PLASMA CURRENTS
Spectrum structure of XeCl electric discharge laser N86-11970
Tokamak startup: Problems and scenarios related to the transient phases of ingnited tokamak operations
[DE85-015321] N86-12085
Spherical torus: An approach to compact fusion at low field. Initial ignition assessments
[DE85-012890] N86-12099

PLASMA DENSITY
Electron beam potential diagnostic for tandem mirrors, phase 1
[DE85-013515] N86-12107

PLASMA DYNAMICS
A hybrid mode and a classification of beam plasma instabilities
[AD-A157356] N86-12075
Advanced concepts theory annual report, 1984
[AD-A157535] N86-12080

PLASMA EQUILIBRIUM
The ionization equilibrium of optically thick argon z-pinch plasmas for electron temperatures between 25 and 65 eV
[AD-A157484] N86-12078

PLASMA HEATING
Spherical torus: An approach to compact fusion at low field. Initial ignition assessments
[DE85-012890] N86-12099

PLASMA INTERACTIONS
Spectrum structure of XeCl electric discharge laser N86-11970
Neutral beam interactions with materials
[AD-A157445] N86-12076
PLASMA OSCILLATIONS
Simulation of quiet start magnetized plasmas, including Maxwellian and velocity-space ring distributions
[DE85-014394] N86-12112
PLASMA PHYSICS
Particle pushing techniques for use with finite element based field calculations N86-11865
China report: Science and technology
[JPRS-CST-85-014] N86-11918
Double tearing mode in plasma with magnetic braiding N86-11919
Center for High Temperature Plasma Physics certified N86-11997
Controlled thermonuclear fusion, high temperature plasma physics N86-11998
Saturation characteristics of counterstreaming warm electrons
[DE85-014390] N86-12040
Plasma kinetic theory in action-angle variables
[DE85-014767] N86-12084
Physics modeling of tandem mirror devices with high field test cell inserts
[DE85-011870] N86-12086
Variational quadratic form for low frequency electromagnetic perturbations. 1: Formalism
[DE85-014896] N86-12129
International solar-terrestrial physics program: A plan for the core spaceflight missions
[NASA-TM-87511] N86-12194
PLASMA PUMPING
The ionization equilibrium of optically thick argon z-pinch plasmas for electron temperatures between 25 and 65 eV
[AD-A157484] N86-12078
PLASMA RADIATION
Neutral beam interactions with materials
[AD-A157445] N86-12076
PLASMA SHEATHS
Propagation of electromagnetic waves in inhomogeneous and lossy reentry plasma sheath layer N86-11923
PLASMA WAVES
Plasmas in the Earth's magnetotail
[AD-A157320] N86-11716
PLASMA-ELECTROMAGNETIC INTERACTION
Propagation of electromagnetic waves in inhomogeneous and lossy reentry plasma sheath layer N86-11923
PLASMAS (PHYSICS)
Impurity monitoring by laser-induced fluorescence techniques
[DE85-014142] N86-11356
SIMPLODE: An imploding gas puff plasma model. 1. Neon
[AD-A157456] N86-12077
PLASMASPHERE
Ion whistlers in middle latitudes observed by the Interkosmos-14 satellite N86-11714
PLASTIC DEFORMATION
The yield point of copper-zinc alloys in the alpha solid solution range
[BLL-BISI-TRANS-23046-(9022.06)] N86-11311
PLASTIC PROPERTIES
The 3D inelastic analysis methods for hot section components N86-11516
PLATEAUS
Subsurface geology of the Pajarito Plateau, Espancia Basin, New Mexico
[DE85-016215] N86-11720
PLATELETS
Experiments with solid particle seeding N86-11442
PLATES (STRUCTURAL MEMBERS)
A review of the literature on finite-element modeling of laminated composite plates N86-11529
Involutory transformations and variation principles with multivariables in thin plate bending problems N86-12004
PLATES (TECTONICS)
On reducing the effect of horizontal displacements of the lithospheric plates from the observations carried out by global geodynamic network (on example the GEOSS-REA network) N86-11589
Proceedings of the 5th International Symposium Geodesy and Physics of the Earth, part 3
[REPT-81-PT-3] N86-11591
CRCM and KAPG activity in recent crustal movement studies N86-11592
Some geodetic aspects of the problem of checking the plate-tectonic model of seismicity in southeastern Europe N86-11603
Recent vertical crustal movements of the Carpathian-Balkan region and their relationship with neotectonic movements and geophysical fields N86-11609
On the relation between recent crustal movements, the surface of the basement complex and neotectonic displacements of the East-European platform N86-11610
Dynamics of the Bohemian Massif N86-11616
Oceanic intraplate seismicity: Implications for the rheology and tectonics of the ocean lithosphere N86-11699
PLATING
Mercury bromide reconstitution in the HgBr laser system
[AD-A156502] N86-11466
PLUGGING
Joule-Thomson valves for long term service in space cryocoolers N86-11393
PLUTONIUM
Status of fast neutron nuclear data for (239)Pu
[DE85-012699] N86-12045
R-matrix analysis of the (239) Pu neutron cross sections
[DE85-013095] N86-12052
PNEUMATIC CIRCUITS
Experiments with a fully instrumented split Stirling cryocooler N86-11381
Passive motion control of pneumatically driven displacers in cryogenic coolers N86-11383
POINT DEFECTS
Kinetics analysis of diffusion of point defects to dislocations following pulsed neutron and electron irradiations
[DE85-012768] N86-12037
POINT SOURCES
Calculation of formation time of minimal nucleus of flame during ignition of explosive mixtures by electrical discharges N86-11963
POINTS (MATHEMATICS)
Computation of minimal isovist sets
[AD-A157624] N86-11915
POLAR ORBITS
Heavy lift launch vehicles for 1995 and beyond
[NASA-TM-86520] N86-11216
POLAR REGIONS
Results concerning rheological parameters of the Earth N86-11567
Polar Research Board annual report 1984 and future plans
[PB85-204477] N86-11727
POLAR WANDERING (GEOLOGY)
Adjustment of the latitude data by least-squares collocation approach N86-11562
On short periodical variations of polar motion and UT1-UTC N86-11574
Secular and long term variations in polar motion from classical and Doppler observations N86-11581
Polar motion between 1900.0 and 1984.0 as determined by different techniques N86-11587
POLARITY
Intermediate load modules for test and evaluation: Fixed price research and development
[NASA-CR-176135] N86-11664
POLARIZATION CHARACTERISTICS
Investigation of polarization characteristics of radiation from laser with dye-activated polymer elements N86-11972
POLARONS
Statics and adiabatic dynamics of nonlinear excitations in defected polyacetylene
[DE85-014118] N86-12143
POLICIES
USSR report: Science and technology policy
[JPRS-UST-85-014] N86-11990
Commercialization of space: National policy and defense needs
[AD-A156517] N86-12162
US space programs: Cooperation and competition from Europe
[BPA-CP-895] N86-12163
POLLUTION TRANSPORT
Parameterization of the atmospheric boundary layer for air pollution dispersion models
[PB85-193548] N86-11730
POLOIDAL FLUX
Tokamak startup: Problems and scenarios related to the transient phases of ingnited tokamak operations
[DE85-015321] N86-12085
POLYACETYLENE
Statics and adiabatic dynamics of nonlinear excitations in defected polyacetylene
[DE85-014118] N86-12143
POLYBUTADIENE
Compatibilizing effect of random or block copolymer added to binary mixture of homopolymers
[AD-A157384] N86-11345
POLYCRYSTALS
Oxide cathode mechanisms: Electronic and structural features of oxide cathode surfaces
[AD-A157666] N86-11416
New-generation photovoltaic technologies
[DE85-012143] N86-11675
EOS for polycrystalline quartz
[DE85-014241] N86-12148
POLYETHYLENES
Electrical relaxation in poly(ethylene oxide)
[AD-A157301] N86-11342
Correlations of chemical, microstructural and mechanical properties of polyethylene piping materials
[DE85-013077] N86-11351
POLYGONS
Computation of minimal isovist sets
[AD-A157624] N86-11915
POLYIMIDE RESINS
An improved processible acetylene-terminated polyimide for composites N86-11262
PMR polyimides from solutions containing mixed endcaps N86-11263
Matrix resin development at NASA Langley Research Center N86-11264
All-aromatic biphenylene end-capped polyquinoline and polyimide matrix resins N86-11267
New processable modified polyimide resins for adhesive and matrix applications N86-11269
Recent developments in polyimide and bismaleimide adhesives N86-11270
Characterization methodology for PMR-15 N86-11272
Characterization of polyimide matrix resins and prepregs N86-11273
Replacement of MDA with more oxidatively stable diamines in PMR-polyimides N86-11275
Polyimide matrix resins for up to 700 deg F service N86-11280
Polyimide composites: Application histories N86-11286
V-378A: A modified bismaleimide for advanced composites N86-11287
Transfer molding of PMR-15 polyimide resin N86-11288
POLYIMIDES
High-temperature adhesive development and evaluation N86-11250
Polyimide matrix resins for up to 700 deg F service N86-11280
V-378A: A modified bismaleimide for advanced composites N86-11287
Characterization of the relationship of the cure cycle chemistry to cure cycle processing properties
[NASA-CR-176256] N86-11339
POLYMER CHEMISTRY
Composite structural materials
[NASA-CR-176279] N86-11293
Constituent materials N86-11294
Characterization of the relationship of the cure cycle chemistry to cure cycle processing properties
[NASA-CR-176256] N86-11339
Investigation of polarization characteristics of radiation from laser with dye-activated polymer elements N86-11972
POLYMER MATRIX COMPOSITES
Rapid adhesive bonding and field repair of aerospace materials N86-11253
The synthesis, characterization and thermal chemistry of modified norbornenyl PMR endcaps N86-11266
Quality assurance procedures for V378A matrix resin N86-11274
Properties of autoclaved Gr/PI composites made from improved tack PMR-15 prepreg N86-11276
Rheological, processing, and 371 deg C mechanical properties of Celion 6000/N-phenylnadimide modified PMR composites N86-11278
Properties of crazes and deformation zones in glassy polymers
[AD-A157428] N86-11346
POLYMERIC FILMS
Factors affecting the processing of epoxy film adhesives N86-11252
POLYMERIZATION
PMR polyimides from solutions containing mixed endcaps N86-11263
Matrix resin development at NASA Langley Research Center N86-11264
Bismaleimides and related maleimido polymers as matrix resins N86-11265
The synthesis, characterization and thermal chemistry of modified norbornenyl PMR endcaps N86-11266

Chemical control of rate and onset temperature of nadimide polymerization N86-11271

Characterization methodology for PMR-15 N86-11272

A summary report on the Flat-Plate Solar Array Project Workshop on Transparent Conducting Polymers [NASA-CR-176302] N86-11669

POLYMERS

Investigation of photoelectrode redox polymer junctions [AD-A157556] N86-11304

Development of castor-oil-resistant polyurethane sonar encapsulants [AD-A157576] N86-11347

Polymer glazings for silver mirrors [DE85-012140] N86-11357

POLYMETHYL METHACRYLATE

Investigation of polarization characteristics of radiation from laser with dye-activated polymer elements N86-11972

POLYNOMIALS

On the addition theorem for Legendre polynomials N86-11704

POLYPHENYLS

Characterization of the relationship of the cure cycle chemistry to cure cycle processing properties [NASA-CR-176256] N86-11339

POLYQUINOXALINES

High-temperature adhesive development and evaluation N86-11250

POLYSTYRENE

Composite structural materials [NASA-CR-176279] N86-11293

Processing science and technology N86-11297

Compatibilizing effect of random or block copolymer added to binary mixture of homopolymers [AD-A157384] N86-11345

Seeding subsonic, transonic and supersonic flows with 0.5 micron polystyrene spheres N86-11451

POLYURETHANE FOAM

Transportation system impact limiter design using rigid polyurethane foam [DE85-015088] N86-11354

Polyurethane foam component lifetimes [DE85-008206] N86-11365

POROSITY

Reduction of moisture effects during the cure of epoxy adhesives used in composite repair N86-11254

Thin film research. Volume 1 [AD-A157608] N86-12137

Thin film research. Volume 2 [AD-A157609] N86-12138

POROUS MATERIALS

The hollow sphere model for porous metals and metal powders N86-11308

Thermal convection in snow [AD-A157577] N86-11648

POSITION (LOCATION)

Study of LAMPF H (-) beam position motion and a predictive algorithm for noise reduction [DE85-012701] N86-12033

POSITION INDICATORS

Beam position monitor for storage rings [DE85-013295] N86-12104

POSITIONING

Geodesy: A look to the future [NASA-CR-176283] N86-11657

POSITRON ANNIHILATION

A 2D ACAR momentum density study of the nature of the positron surface state on Al(100) [DE85-014830] N86-11330

POSITRONS

Vacancies in thermal equilibrium in Nb [DE85-014832] N86-12061

High energy physics [DE85-014272] N86-12063

Higher luminosities via alternative incident channels [DE85-014355] N86-12118

POTENTIAL FLOW

Application of the vortex-lattice concept to flows with smooth-surface separation [AD-A157571] N86-11430

POTENTIAL GRADIENTS

Measurements of ultimate accelerating gradients in the SLAC disk-loaded structure [DE85-014287] N86-12125

POTENTIAL THEORY

Investigation of photoelectrode redox polymer junctions [AD-A157556] N86-11304

On inverse problems in differential equations: A critical analysis N86-11552

POWDER (PARTICLES)

Synthesis of nickel-aluminum alloys by shock compression of composite particles [DE85-015165] N86-11328

Shock-induced temperature distributions in powder compact recovery fixtures [DE85-015139] N86-11359

Shock consolidation of IN-100 nickel-base superalloy powder [DE85-015159] N86-11360

POWER CONDITIONING

Intermediate load modules for test and evaluation: Fixed price research and development [NASA-CR-176135] N86-11664

POWER EFFICIENCY

An experimental study of energy loss mechanisms and efficiency consideration in the low power dc arcjet [NASA-TM-87123] N86-11224

POWER REACTORS

Experimental needs of high temperature concrete [DE85-009700] N86-11541

Concrete creep at transient temperature: Constitutive law and mechanism [DE85-010525] N86-11542

POWER SERIES

A parameterization technique for nonlinear spectral models N86-11752

POWER SPECTRA

The 1984 solar oscillation program of the Mount Wilson 60-foot tower [NASA-CR-176248] N86-12195

POWER SUPPLIES

Railgun power supply system utilizing traction motors and vacuum interrupters [DE85-014123] N86-11214

POWER SUPPLY CIRCUITS

Modification of a Hughes tiltmeter to a borehole tiltmeter N86-11563

POWER TRANSMISSION (LASERS)

On convective effects in gas lasers N86-12006

PRE-MAIN SEQUENCE STARS

Epsilon Aurigae in an evolutionary context N86-12174

PRECIPITATION (METEOROLOGY)

Hydrologic data for experimental agricultural watersheds in the US, 1975 [PB85-197317] N86-11656

Monthly and seasonal weather outlook for June 1985, volume 39, number 11, 30 May 1985 [PB85-209526] N86-11762

Proceedings of the 9th Annual Climate Diagnostics Workshop [PB85-183911] N86-11763

Monitoring climate in real time: An application of the Climate Anomaly Monitoring System (CAMS) N86-11765

Some empirical evidence for the influence of snow cover on temperature and precipitation N86-11767

Worldwide marine temperature variations on the season to century time scale N86-11771

Temperature and precipitation trends in North America N86-11774

Relationships between Pacific northwest coast climate and ENSO events N86-11787

Evidence of an 18 year cycle in Pacific northwest precipitation data N86-11788

Land-surface fluctuations and associated climatic variability N86-11807

Concurrent and lagged relationships between precipitation frequency and 700 mb heights N86-11808

Monthly and Seasonal Weather Outlook for May 1985, Volume 39, Number 9 [PB85-199123] N86-11819

PREDICTION ANALYSIS TECHNIQUES

Inlet flow dynamic distortion prediction without rms measurements N86-11183

Validation of procedures for pavement design on expensive soils [FAA-PM-85-15] N86-11362

Effect of accuracy of wind power prediction on power system operator [NASA-CR-176300] N86-11667

An evaluation of CASP (computer assisted search planning program) drift predictions near the New England Shelf/Slope Front [AD-A157447] N86-11826

Bayesian extensions to a basic model of software reliability [AD-A157296] N86-11901

PREDICTIONS

Gas side heat transfer N86-11507

Life prediction and constitutive behavior N86-11520

Creep fatigue life prediction for engine hot section materials (isotropic) N86-11521

Geodesy: A look to the future [NASA-CR-176283] N86-11657

Regional-scale (1000 KM) model of photochemical air pollution. Part 3: Tests of the numerical algorithms [PB85-203818] N86-11696

The utilization of satellite data and dynamics in understanding and predicting global weather phenomena [NASA-CR-171577] N86-11749

Proceedings of the 9th Annual Climate Diagnostics Workshop [PB85-183911] N86-11763

Reduction of sextupole distortion by shuffling magnets in small groups [DE85-013024] N86-12035

Mars base buildup scenarios [DE85-014132] N86-12193

PREGNANCY

Teratogenic effects of microwave radiation [PB85-207462] N86-11837

PREPREGS

Characterization of polyimide matrix resins and prepregs N86-11273

Replacement of MDA with more oxidatively stable diamines in PMR-polyimides N86-11275

PRESSURE

Variability simulations with a steady, linearized primitive equations model N86-11796

PRESSURE DEPENDENCE

Pressure-coupled response function of solid propellants including those with negative pressure-exponents N86-11924

PRESSURE GAGES

Modification of a Hughes tiltmeter to a borehole tiltmeter N86-11563

PRESSURE MEASUREMENT

Calibration of the NCAR (National Center for Atmospheric Research) Sabreliner research static pressure source with a trailing cone assembly [PB85-191005] N86-11200

Stability of a method for analyzing radiation pattern of acoustic radiator with near-field pressure measurement errors N86-11950

PRESSURE OSCILLATIONS

Recent long-term climatic change over the eastern tropical and subtropical Pacific and its ramifications N86-11775

Global relationships with the Southern Oscillation N86-11776

Time series modeling of the Southern Oscillation N86-11777

Satellite observations of a large-amplitude 40-50 day oscillation in upper tropospheric temperature over the equatorial Pacific Ocean during the 1982-83 ENSO event N86-11778

Subseasonal and interannual variations of tropical convection and the El Nino/Southern Oscillation N86-11779

The annual variation in the vertical structure of the 40-50-day tropical oscillation N86-11780

Life cycle of a 28-72 day atmospheric oscillation during northern winter N86-11781

Climatic events of the west coast of southern Africa N86-11784

On the computation of structural vibrations induced by a low-speed turbulent flow N86-12009

A numerical method of calculating propeller noise including acoustic nonlinear effects N86-12011

PRESSURE PULSES

Stationary pulse solutions for a free electron laser N86-11933

PRESSURE SENSORS

Fiber optic pressure sensors in skin-friction measurements [NASA-CR-176294] N86-11838

PRESSURE VESSELS

Acoustic emission during deformation and fracture of A533B pressure vessel steel N86-11306

Deformation of granite at elevated temperature and pressure [DE85-014057] N86-11721

PRESSURE WELDING

Solid-state bonding of superplastic aluminum alloy 7475 sheet N86-11244

PRESTRESSING

Evaluation of concrete creep and stress redistribution in a prototypic PCRV following rupture of prestressing tendons [DE85-007673] N86-11543

PRIMERS (COATINGS)

Corrosion-preventive primers for military equipment [AD-A156927] N86-11341

PRIMITIVE EQUATIONS

The effect of the Hadley circulation on the meridional propagation of stationary waves N86-11732

Variability simulations with a steady, linearized primitive equations model N86-11796

PRINTED CIRCUITS

Microstrip monpulse dipole array N86-11405

PRISMS

Frequency-selection and mode-locking and Nd:YAG laser N86-11928

PROBABILITY THEORY
Probability encoding of hydrologic parameters for basalt. Elicitation of expert opinions from a panel of three basalt waste isolation project staff hydrologists
[DE85-014665] N86-11652
Application of an objective analysis scheme to mesoscale observational network design
[AD-A156911] N86-11760
Minimum assumption tornado hazard probability model
[PB85-206092] N86-11821
Probabilistic analysis of a network resource allocation algorithm
[AD-A157553] N86-11904
PROCESS CONTROL (INDUSTRY)
Adhesives for aerospace N86-11249
PROCESS HEAT
Advanced Thermionic Technology Program: Summary report, Volume 3
[DE85-009360] N86-11674
PRODUCTION COSTS
Status of the intercontinental ballistic missile modernization program
[AD-A157375] N86-11217
PRODUCTION ENGINEERING
Adhesives for aerospace N86-11249
Robotized production systems observed in modern plants N86-11396
PRODUCTIVITY
Forest canopy chemistry from Blackhawk Island, Wisconsin N86-11634
PROGNOSIS
Prediction of monthly 700 mb heights using antecedent and simulated prognostic height predictors N86-11805
PROGRAM VERIFICATION (COMPUTERS)
Ada (trademark) compiler validation summary report: Data general corporation, ADE Ada Compiler, version 2.30.03.12, Eclipse DS/4000, DS/4200, MV/4000-DC, MV/8000-C, MV/8000-2, MV/10000, MV/10000 SX using AOS/VS 5.04 and AOS/RT32 4.001.00
[AD-A157573] N86-11890
Ada (trademark) compiler validation summary report: Verdix Ada Compiler, Verdix Ada Development System (VADS) VAda-010-1010, version V05.00, for Sun Microsystems Model 2/120 using UNIX (trademark) 4.2 BSD, release 1.1
[AD-A157574] N86-11891
Military standard common APSE (Ada Programming Support Environment) interface set (CAIS)
[AD-A157589] N86-11905
PROGRESS
Research objectives and summary of research performed by the Massachusetts Institute of Technology Research Laboratory of Electronics
[PR-127] N86-12164
PROJECT MANAGEMENT
Balloon-borne three-meter telescope for far-infrared and submillimeter astronomy
[NASA-CR-176285] N86-12188
PROPELLER BLADES
Design concept and performance prediction technique for potential flows around advanced propellers N86-11150
A review of ARA research into propeller aerodynamic prediction methods N86-11151
Aerodynamics of wide-chord propellers in non-axisymmetric flow N86-11153
Dynamic behavior of a propfan N86-11159
Investigations of modern general aviation propellers N86-11162
Aeroacoustic wind tunnel measurements on propeller noise N86-11169
Some aeroacoustic wind tunnel measurements, theoretical predictions, and flight-test correlations on subsonic aircraft propellers N86-11170
An investigation of in-flight near-field propeller noise generation and transmission N86-11171
PROPELLER DRIVE
Aerodynamic and structural aspects of propeller and drive for a 1/5 scale wind tunnel programme N86-11163
Some considerations in propeller and airframe integration N86-11164
PROPELLER EFFICIENCY
Aerodynamics of wide-chord propellers in non-axisymmetric flow N86-11153
On the aerodynamics of installed propellers N86-11154
A unified approach for the aerodynamics and acoustics of propellers in forward motion N86-11155
Theoretical analysis of linearized acoustics and aerodynamics of advanced supersonic propellers N86-11156
Performance evaluation of full scale propellers by wind tunnel test N86-11160
Aerodynamic and structural aspects of propeller and drive for a 1/5 scale wind tunnel programme N86-11163
Some considerations in propeller and airframe integration N86-11164
Wind tunnel investigation of the interaction of propeller slipstream with nacelle/wing/flap combinations N86-11166
Development of modern turboprop engines N86-11168
PROPELLER SLIPSTREAMS
On the aerodynamics of installed propellers N86-11154
A unified approach for the aerodynamics and acoustics of propellers in forward motion N86-11155
PROPELLERS
Aerodynamics and Acoustics of Propellers
[AGARD-CP-366] N86-11147
Aerodynamic method used in France for advanced fast propeller study N86-11149
A review of ARA research into propeller aerodynamic prediction methods N86-11151
Modern propeller profiles N86-11152
Summary of recent NASA propeller research N86-11158
Performance evaluation of full scale propellers by wind tunnel test N86-11160
Study of the 3D wake of an aerial propeller N86-11161
Investigations of modern general aviation propellers N86-11162
Aerodynamic and structural aspects of propeller and drive for a 1/5 scale wind tunnel programme N86-11163
Problems of the integration of propellers in airframes, especially for high performance twin-engine aircraft N86-11165
Wind tunnel investigation of the interaction of propeller slipstream with nacelle/wing/flap combinations N86-11166
An asymptotic theory for the interference of large aspect ratio swept wings and multiple propeller slipstreams N86-11167
Aeroacoustic wind tunnel measurements on propeller noise N86-11169
Some aeroacoustic wind tunnel measurements, theoretical predictions, and flight-test correlations on subsonic aircraft propellers N86-11170
An investigation of in-flight near-field propeller noise generation and transmission N86-11171
Full-scale flight and model-scale wind tunnel tests on the nearfield noise characteristics of aircraft propellers N86-11172
Application of active noise control to model propeller noise N86-11176
A numerical method of calculating propeller noise including acoustic nonlinear effects N86-12011
PROTECTION
User's manual for AC-20-53A protection of airplane fuel systems against fuel vapor ignition due to lightning
[AD-A157619] N86-11191
PROTECTIVE COATINGS
Cathodic protection of aluminium structures
[KIS-1985:4E] N86-11313
Turbine Engine Hot Section Technology (HOST)
[NASA-CP-2289] N86-11495
Failure rate model for cathodic delamination of protective coatings
[AD-A157483] N86-11912
PROTEINS
Utilization of non-conventional systems for conversion of biomass to food components: Potential for utilization of algae in engineered foods
[NASA-CR-176257] N86-11830
PROTON BEAMS
Possibilities of polarized protons in Sp anti p S and other high energy hadron colliders
[DE85-012517] N86-12044
Los Alamos proton storage ring fast-extraction kicker system
[DE85-012663] N86-12093
SSC test lattices
[DE85-014240] N86-12098
PROTON SCATTERING
Amplitude tests of direct channel resonances: The dibaryon
[DE85-011478] N86-12034
PROTON-PROTON REACTIONS
Amplitude tests of direct channel resonances: The dibaryon
[DE85-011478] N86-12034
PROTONS
Calculations of physical and chemical reactions produced in irradiated water containing DNA
[DE85-012899] N86-12051
Acceleration simulation in the LAMPF 2 booster
[DE85-012695] N86-12126
PROVING
Applied model validation
[NBSIR-85-3154-1] N86-11363
PSYCHOLOGY
Adaptive motivation theory
[AD-A157440] N86-11851
PSYCHOMOTOR PERFORMANCE
Force and timing components of the motor program
[AD-A157584] N86-11843
Cognitive science program: Dissociation of the central timekeeper and the peripheral implementation processes in repetitive movements
[AD-A157542] N86-11852
PUBLIC HEALTH
Assessments and viewpoints on the biological and human health effects of Extremely Low Frequency (ELF) electromagnetic fields: Compilation of commissioned papers for the ELF literature review project
[AD-A156942] N86-11839
PULMONARY CIRCULATION
Perceptual and physiological responses during exercise in cool and cold water
[AD-A157334] N86-11840
PULMONARY FUNCTIONS
Acute pulmonary effects of formaldehyde exposure in humans
[DE85-014728] N86-11848
PULSE COMMUNICATION
Evaluation of the digital access and cross-connect system for use in the defense communications system
[AD-A157570] N86-11412
PULSE COMPRESSION
Comparison of energy transport measurements and computer simulations in a single module prototype for PBFA 2
[DE85-013960] N86-12119
PULSE DURATION
Pulse duration dependence of 1064-nm laser damage thresholds of porous silica antireflection coatings on fused silica substrates
[DE85-013207] N86-11350
Ultraviolet lasing in helium-nitrogren mixtures N86-11974
PULSE GENERATORS
Multi-megampere operation of plasma compression opening switches in planar geometry
[DE85-012755] N86-11420
MABE multibeam accelerator
[DE85-012035] N86-12121
Modelling of the PROTO-2 crossover network
[DE85-014639] N86-12128
PULSE MODULATION
Los Alamos proton storage ring fast-extraction kicker system
[DE85-012663] N86-12093
PULSED LASERS
Stationary pulse solutions for a free electron laser N86-11933
Cause of occurrence of high-energy ions during UV laser irradiation of molecular crystals N86-11953
Two-frequency passive mode locking in iodine photodissociation laser N86-11980
Multiphoton Raman scattering of light excited in crystals by a copper-vapor laser N86-11986
Double-wavelength pulsed tunable dye laser N86-12003
PULSED RADIATION
Transformation of light pulse shape by thin plane-parallel layer of absorbing material N86-11988
Study of LAMPF H (-) beam position motion and a predictive algorithm for noise reduction
[DE85-012701] N86-12033
Los Alamos proton storage ring fast-extraction kicker system
[DE85-012663] N86-12093
PULSES
Explosive generators for low-cost pulsed power
[DE85-013436] N86-11421
PURIFICATION
Nuclear spin-polarized HD, D2, HT and DT solids, liquids and high density gases
[DE85-014136] N86-12154
PYLONS
Stress analyses of B-52 pylon hooks
[NASA-TM-84924] N86-11524

Q

Q SWITCHED LASERS
Neutral beam interactions with materials
[AD-A157445] N86-12076

QUADRATIC EQUATIONS
A parameterization technique for nonlinear spectral models N86-11752

QUADRATURES
New harmonic materials: Index engineering: Thin-thick quadrature frequency conversion
[DE85-012976] N86-12156

QUALITY CONTROL
Langley Research Center standard for the evaluation of socket welds N86-11243
High Temperature Polymer Matrix Composites
[NASA-CP-2385] N86-11260
Quality assurance procedures for V378A matrix resin N86-11274
Bayesian extensions to a basic model of software reliability
[AD-A157296] N86-11901

QUANTUM CHROMODYNAMICS
Physics opportunities with relativistic heavy ion accelerators
[DE85-014190] N86-12117

QUANTUM COUNTERS
The relations between voltage and magnetic field of superconducting weaklink (1) N86-11934
The relations between voltage and magnetic field of superconducting weaklink (2) N86-11935

QUANTUM ELECTRONICS
Submillimeter quantum electronics
[AD-A157432] N86-11417

QUANTUM MECHANICS
EPR: What has it taught us
[DE85-014525] N86-12157

QUANTUM THEORY
EPR: What has it taught us
[DE85-014525] N86-12157

QUANTUM WELLS
Binding energy of donors in GaAs-Ga(1-x) Al(x)As quantum well structures N86-11940

QUARTZ
EOS for polycrystalline quartz
[DE85-014241] N86-12148

QUEUEING THEORY
A numerical analysis of a queue with network access flow control
[AD-A157526] N86-11913

QUINOLINE
All-aromatic biphenylene end-capped polyquinoline and polyimide matrix resins N86-11267

QUINOXALINES
Acetylene terminated matrix resins N86-11261

R

RADIAL FLOW
A parametric analysis of flow structure and performance in a vortex controlled radial diffuser N86-11182
Characteristics of an axisymmetric sudden expansion flow
[NASA-CR-176278] N86-11465

RADIAL VELOCITY
Applications of the magneto-optical filter to stellar pulsation measurements
[NASA-CR-176282] N86-12187

RADIANCE
Analysis of aircraft spectrometer data with logarithmic residuals N86-11636
High altitude measured radiance of White Sands, New Mexico in the 400-2000 nm band using a filter wedge spectrometer
[PB85-206084] N86-11729
Atlas of high altitude aircraft measured radiance of White Sands, New Mexico, in the 450-1050 nanometers band
[PB85-204501] N86-11820

RADIATION
Miniaturization of specimens for mechanical testing
[DE85-014506] N86-11536
Psychological aspects of personnel contamination
[DE85-012955] N86-11853
The relations between voltage and magnetic field of superconducting weaklink (2) N86-11935

RADIATION ABSORPTION
Elastic and inelastic light scattering of colloidal particles
[AD-A157335] N86-12072

RADIATION COUNTERS
Develop, evaluate and validate continuous emission monitors for designated hazardous pollutants
[PB85-201176] N86-11695
TIROS/NOAA (Television and Infrared Observation Satellite/National Oceanic and Atmospheric Administration) satellites space environment monitor archive tape documentation
[PB85-187920] N86-11724

RADIATION DETECTORS
Si(Li)-NaI(Tl) sandwich detector array for measurements of trace radionuclides in soil samples
[DE85-013865] N86-12062
Collider Detector at Fermilab (CDF)
[DE85-014423] N86-12068

RADIATION DISTRIBUTION
Radiation and scattering performance of microstrip antennas using exotic substrates N86-11408
Improving the accuracy of the boundary integral method based on the Helmholtz integral N86-12010

RADIATION DOSAGE
Dose distribution and the relative biological effectiveness of internal alpha emitters
[DE85-013041] N86-11845
Experimental check of bremsstrahlung dosimetry predictions for 0.75 MeV electrons
[DE85-014706] N86-12058

RADIATION EFFECTS
Tensile properties of 2-1/4Cr-1Mo steel irradiated to 23 dpa at 390 to 550(0)C
[DE85-015551] N86-11332
Assessments and viewpoints on the biological and human health effects of Extremely Low Frequency (ELF) electromagnetic fields: Compilation of commissioned papers for the ELF literature review project
[AD-A156942] N86-11839
Dose distribution and the relative biological effectiveness of internal alpha emitters
[DE85-013041] N86-11845
Psychological aspects of personnel contamination
[DE85-012955] N86-11853
Experimental check of bremsstrahlung dosimetry predictions for 0.75 MeV electrons
[DE85-014706] N86-12058
PBFA-2 vacuum insulator stack failure mechanisms
[DE85-013118] N86-12090

RADIATION HAZARDS
Thyroid absorbed dose for people at Rongelap, Utirik and Sifo on March 1, 1954
[DE85-014695] N86-11846

RADIATION PROTECTION
Los Alamos upgrade in metallographic capabilities
[DE85-014089] N86-11320
Experimental needs of high temperature concrete
[DE85-009700] N86-11541

RADIATION SPECTRA
Uncertainties in the radiative properties of smoke and their effects on climate assessments
[DE85-015187] N86-11691

RADIATIVE TRANSFER
The effect of topography on the evolution of unstable disturbances in a baroclinic atmosphere N86-11750
Total and partial absorption coefficients for a nitrogen plasma
[AD-A157534] N86-12079

RADIO FREQUENCIES
Part A. Molecular dynamics and ionic associations of LiAsF6 in 4-butyrolactone mixtures with 2-methyl tetrahydrofuran. Part B. Molecular dynamics and ionic associations of LiBF4 in 1,2-dimethoxymethane
[AD-A157401] N86-12023
Implications of rf current drive theory for next step steady-state tokamak design
[DE85-014753] N86-12083

RADIO FREQUENCY DISCHARGE
Two-dimensional linacs
[DE85-015129] N86-12029

RADIO FREQUENCY HEATING
Implications of rf current drive theory for next step steady-state tokamak design
[DE85-014753] N86-12083

RADIO FREQUENCY INTERFERENCE
Chemical bonding agent for suppression of rusty bolt intermodulation interference
[AD-D011747] N86-11315

RADIO GALAXIES
Star formation in the inner galaxy: A far-infrared and radio study of two H2 regions
[NASA-TM-86720] N86-12185
X-ray inverse Compton emission from the radio halo of M87
[NASA-CR-176304] N86-12197

RADIO TRANSMISSION
Voice communications over packet radio networks
[AD-A157478] N86-11411

RADIOACTIVE ISOTOPES
Survey of element and isotope importance for fusion safety and environmental assessments
[DE85-012415] N86-12047

RADIOGRAPHY
Corrosion testing by radiographic methods
[BLL-BISI-TRANS-23201-(9022.06)] N86-11310

RADIOMETERS
Spectral characterization of suspected acid deposition damage in red spruce (Picea rubens) stands from Vermont N86-11624
Forest species identification with high spectral resolution data N86-11643
Analysis of terrestrial conditions and dynamics
[NASA-CR-176308] N86-11646

RAILGUN ACCELERATORS
Railgun power supply system utilizing traction motors and vacuum interrupters
[DE85-014123] N86-11214

RAIN
The distribution of rainfall along the coast of northern Peru during 1982-83 N86-11782
Climatic events of the west coast of southern Africa N86-11784
Large-scale variability in Indian monsoon rainfall inferred from satellite data N86-11800
Tropospheric static stability and central North American rainfall during 1979 N86-11801

RAMAN SPECTRA
Spectrally-broad picosecond light source
[DE85-015177] N86-11471
Raman scattering of sound on random oscillations of bubbles N86-11948
Multiphoton Raman scattering of light excited in crystals by a copper-vapor laser N86-11986
Elastic and inelastic light scattering of colloidal particles
[AD-A157335] N86-12072

RAMAN SPECTROSCOPY
Ionization-Raman double-resonance spectroscopy
[DE85-013774] N86-12042

RAMP FUNCTIONS
Ramp response estimation and spectrum extrapolation for ultrasonic scattering N86-11881

RANDOM NOISE
Elastic wave scattering of a Gaussian incident beam from an interface crack in a layered half space submerged in water N86-11490

RANGELANDS
Evaluation of AIS data for agronomic and rangeland vegetation: Preliminary results for August 1984 flight over Nebraska Sandhills Agricultural Laboratory N86-11627

RANKINE CYCLE
Dish electric systems heat engine assessment
[DE85-013942] N86-11479
Advanced mechanical heat pump technologies for industrial applications
[DE85-014613] N86-11483

RATIONS
A cascaded coding scheme for error control
[NASA-CR-176276] N86-11695

RATS
An atropinized heat-stressed rat model: Anticholinergic and anticholinesterase drug potency
[AD-A157620] N86-11832

RAYLEIGH EQUATIONS
On cloud street development in three dimensional parallel and Rayleigh instabilities N86-11754

RAYLEIGH SCATTERING
Photoinduced Rayleigh scattering of light in crystals N86-11985
Multiphoton Raman scattering of light excited in crystals by a copper-vapor laser N86-11986

RAYLEIGH WAVES
Thermal convection in snow
[AD-A157577] N86-11648
The effect of topography on the evolution of unstable disturbances in a baroclinic atmosphere N86-11750
The Hadley and Rossby regimes in a spherical atmosphere N86-11751

REACTION KINETICS
Determination of the steady-state behavior of immobilized (BETA)-galactosidase utilizing an integral reactor scheme
[DE85-012900] N86-11256
Importance of phytoalexin tolerance and detoxification for pathogenicity
[DE85-014759] N86-11257
A mechanism for ignition of high-temperature gaseous nitromethane: The key role of the nitro group in chemical explosives
[AD-A157355] N86-11303
Flame propagation in pulsed acceleration field N86-11964
Flow reactor studies over wide temperature and pressure ranges of atom and radical reaction rates important in ignition and combustion
[AD-A156931] N86-12020
Kinetics analysis of diffusion of point defects to dislocations following pulsed neutron and electron irradiations
[DE85-012768] N86-12037

REACTION TIME

Force and timing components of the motor program [AD-A157584] N86-11843

Probabilistic analysis of a network resource allocation algorithm [AD-A157553] N86-11904

REACTIVITY

Stability and interaction of coherent structure in supersonic reactive wakes N86-11185

REACTOR DESIGN

Liquid metal reactors programs: Safeguards and program assurance [DE85-011002] N86-12046

REACTOR MATERIALS

Los Alamos upgrade in metallographic capabilities [DE85-014089] N86-11320

Miniaturization of specimens for mechanical testing [DE85-014506] N86-11536

Liquid metal reactors programs: Safeguards and program assurance [DE85-011002] N86-12046

Survey of element and isotope importance for fusion safety and environmental assessments [DE85-012415] N86-12047

REACTOR PHYSICS

Physics modeling of tandem mirror devices with high field test cell inserts [DE85-011870] N86-12086

REACTOR SAFETY

Numerical simulation of an equipment hatch for a steel containment vessel to loading beyond the design basis [DE85-010485] N86-11482

REACTOR STARTUP TESTS

Tokamak startup: Problems and scenarios related to the transient phases of ingnited tokamak operations [DE85-015321] N86-12085

REACTOR TECHNOLOGY

Senstivity of using blunt and sharp crack models in elastic-plastic fracture mechanics [DE85-010288] N86-11537

Viscoelastic creep of high-temperature concrete [DE85-010511] N86-11539

Evaluation of concrete creep and stress redistribution in a prototypic PCRV following rupture of prestressing tendons [DE85-007673] N86-11543

China report: Science and technology [JPRS-CST-85-014] N86-11918

READING

Improving the comprehensibility of a simulated technical manual [AD-A157482] N86-11889

REAL TIME OPERATION

The irregularity in the Earth's annual rotation as a cause of systematic time variation N86-11570

Monitoring climate in real time: An application of the Climate Anomaly Monitoring System (CAMS) N86-11765

An application of real-time analysis and design tools in software development N86-11860

The embedded operating system project [NASA-CR-176280] N86-11893

High-speed signal processor developed N86-11995

RECEIVERS

Basic EMC technology advancement for C(3) systems. Volume 3B: Computer simulation of EMI effects in a differential line receiver [AD-A156505] N86-11416

RECIPROCATION

An experimental reciprocating expander for cryocooler application N86-11380

RECIRCULATIVE FLUID FLOW

A parametric analysis of flow structure and performance in a vortex controlled radial diffuser N86-11182

RECONNAISSANCE AIRCRAFT

Problems of the integration of propellers in airframes, especially for high performance twin-engine aircraft N86-11165

RECORDING INSTRUMENTS

Variability of snow cover characteristics in the Transbaykal [NASA-TM-77917] N86-11733

REDUCED GRAVITY

NASA Lewis Research Center low-gravity fluid management technology program [NASA-TM-87145] N86-11218

Bridgman growth of semiconductors [NASA-CR-177971] N86-11426

REENTRY COMMUNICATION

Propagation of electromagnetic waves in inhomogeneous and lossy reentry plasma sheath layer N86-11923

REENTRY PHYSICS

Propagation of electromagnetic waves in inhomogeneous and lossy reentry plasma sheath layer N86-11923

REENTRY TRAJECTORIES

Design of maneuverable trajectories of re-entry vehicle N86-11920

REFLECTANCE

Optical modeling of multilayer thin/thick films N86-11862

REFLECTORS

Proceedings of the 1984 Antenna Applications Symposium [AD-A153257] N86-11398

REFRACTIVITY

Particle sizing in a solid rocket motor using the management of scattered light [AD-A156460] N86-11226

Studies on chalcogenide films [AD-A157340] N86-11343

Measurements of refractive index structure function C2N and aerosol size distribution at Chesapeake Bay [AD-A157455] N86-11717

REFRACTORY METAL ALLOYS

Refractory alloy performance: Product form procurement and component fabrication [DE85-014658] N86-11477

REFRIGERATING

Proceedings of the Third Cryocooler Conference [NASA-CR-176298] N86-11367

Recent cryocooler progress in Japan N86-11369

Reciprocating magnetic refrigerator N86-11371

Improved heat switch for gas sorption compressor N86-11372

Hydride absorption refrigerator system for ten Kelvin and below N86-11373

Classification of cryocoolers N86-11374

An experimental study for a miniature Stirling refrigerator N86-11375

Parametric testing of a linearly driven Stirling cryogenic refrigerator N86-11376

Simple construction and performance of a conical plastic cryocooler N86-11378

Experiments with a fully instrumented split Stirling cryocooler N86-11381

REFRIGERATORS

A closed cycle cascade Joule Thomson refrigerator for cooling Josephson junction magnetometers N86-11388

A small helium liquifier which provides continuous cooling based on cycled isentropic expansion N86-11389

Vuilleumier cycle cryocooler operating below 8 K N86-11390

Four K refrigerators with a new compact heat exchanger N86-11391

The design of a small linear-resonant, split Stirling cryogenic refrigerator compressor N86-11392

Photovoltaic-powered vaccine refrigerator: Freezer systems field test results [NASA-TM-86972-REV] N86-11666

REGENERATIVE COOLING

Classification of cryocoolers N86-11374

Experiments with a fully instrumented split Stirling cryocooler N86-11381

A simple, first step to the optimization of regenerator geometry N86-11385

REGENERATORS

Recent cryocooler progress in Japan N86-11369

Effects of leakage through clearance seals on the performance of a 10 K Stirling-cycle refrigerator N86-11379

A simple, first step to the optimization of regenerator geometry N86-11385

A computational model for a regenerator N86-11386

Vuilleumier cycle cryocooler operating below 8 K N86-11390

Four K refrigerators with a new compact heat exchanger N86-11391

The design of a small linear-resonant, split Stirling cryogenic refrigerator compressor N86-11392

REGRESSION COEFFICIENTS

The status of the NOAA/NESDIS radiation budget data set N86-11615

REINFORCEMENT (STRUCTURES)

Evaluation of superplastic forming and weld-brazing for fabrication of titanium compression panels N86-11245

REINFORCING FIBERS

Rheological, processing, and 371 deg C mechanical properties of Celion 6000/N-phenylnadimide modified PMR composites N86-11278

RELATIVISTIC EFFECTS

Non-geometrical optics investigation of mode conversion in weakly relativistic inhomogenous plasmas [DE85-013480] N86-12102

RELATIVISTIC ELECTRON BEAMS

Scaling calculations for a relativistic gyrotron [AD-A157476] N86-11460

Design for a high field combined function superferric magnet [DE85-014827] N86-11944

Emission threshold for cerenkov radiation [AD-A157615] N86-12025

Transition radiation and coherent electron-photon scattering [DE85-014813] N86-12031

RELAXATION TIME

Anelasticity in the Earth's mantle: Implications for the frequency dependence of Love numbers N86-11590

RELIABILITY

Automated magnet testing facility [DE85-012863] N86-11422

NERF: A computer program for the numerical evaluation of reliability functions user manual [ARL/STRUC-R-411] N86-11487

Monitoring climate in real time: An application of the Climate Anomaly Monitoring System (CAMS) N86-11765

Towards understanding the geographical distribution and seasonality in persistance of monthly mean surface air temperature over the U.S.A. N86-11773

Bayesian extensions to a basic model of software reliability [AD-A157296] N86-11901

A cascaded coding scheme for error control [NASA-CR-176287] N86-11911

Photon diagnostics leading to an improved Marx [DE85-013434] N86-12103

RELIABILITY ANALYSIS

Reliability analysis of series structural systems N86-11486

REMOTE CONTROL

Feasibility of remotely manipulated welding in space: A step in the development of novel joining technologies N86-11246

Modification of a Hughes tiltmeter to a borehole tiltmeter N86-11563

Mechanical accessories for mobile teleoperators [DE85-014310] N86-11855

REMOTE HANDLING

Los Alamos upgrade in metallographic capabilities [DE85-014089] N86-11320

REMOTE SENSING

Proceedings of the Airborne Imaging Spectrometer Data Analysis Workshop [E86-10001] N86-11618

Remote sensing of earth terrain [NASA-CR-176284] N86-11645

Active and passive microwave measurements in Hurricane Allen [NASA-TM-86390] N86-11647

On the addition theorem for Legendre polynomials N86-11704

Research on optic spatial frequency analysis of linear structures in remote sensing images N86-11927

General-purpose equipment for airborne laser remote sensing of ocean, atmosphere and agricultural crops N86-11984

REMOTE SENSORS

Modification of a Hughes tiltmeter to a borehole tiltmeter N86-11563

REPLACING

Replacement of MDA with more oxidatively stable diamines in PMR-polyimides N86-11275

REPORTS

Status of SLC [DE85-013071] N86-12097

Research objectives and summary of research performed by the Massachusetts Institute of Technology Research Laboratory of Electronics [PR-127] N86-12164

REQUIREMENTS

A new characterization of supercooled clouds below 10,000 feet AGL N86-11744

RESCUE OPERATIONS

Adverse weather impact on aviation safety, investigation and oversight N86-11742

An evaluation of CASP (computer assisted search planning program) drift predictions near the New England Shelf/Slope Front [AD-A157447] N86-11626

RESEARCH

Research objectives and summary of research performed by the Massachusetts Institute of Technology Research Laboratory of Electronics [PR-127] N86-12164

RESEARCH AND DEVELOPMENT

HOST instrumentation R and D program overview N86-11497

Time-of-flight anemometer for hot section applications N86-11504

Polar Research Board annual report 1984 and future plans [PB85-204477] N86-11727

USSR report: Science and technology policy [JPRS-UST-85-014] N86-11990

FINESSE: Study of the issues, experiments and facilities for fusion nuclear technology research and development, volume 4
[DE85-010947] N86-12130
NASA-universities relationships in aero/space engineering: A review of NASA's program
[NASA-CR-176307] N86-12158

RESEARCH FACILITIES
NASA Lewis Research Center low-gravity fluid management technology program
[NASA-TM-87145] N86-11218
Center for High Temperature Plasma Physics certified N86-11997

RESEARCH MANAGEMENT
Book on planning of scientific, technical progress N86-11991
Problems, trends in technical education of researchers N86-11993
NASA-universities relationships in aero/space engineering: A review of NASA's program
[NASA-CR-176307] N86-12158

RESEARCH VEHICLES
Seeding techniques used in the Vortex Research Facility N86-11443

RESIN BONDING
Evaluation of a high temperature adhesive for fabricating graphite/PMR-15 polyimide structures N86-11268

RESIN MATRIX COMPOSITES
Adhesives for aerospace N86-11249
Acetylene terminated matrix resins N86-11261
An improved processible acetylene-terminated polyimide for composites N86-11262
Bismaleimides and related maleimido polymers as matrix resins N86-11265
All-aromatic biphenylene end-capped polyquinoline and polyimide matrix resins N86-11267
New processable modified polyimide resins for adhesive and matrix applications N86-11269
Quality assurance procedures for V378A matrix resin N86-11274
Replacement of MDA with more oxidatively stable diamines in PMR-polyimides N86-11275
Polyimide matrix resins for up to 700 deg F service N86-11280
Polyimide composites: Application histories N86-11286

RESONANCE
Numerical techniques for scattering from submerged objects N86-12013
Possibilities of polarized protons in Sp anti p S and other high energy hadron colliders
[DE85-012517] N86-12044
R-matrix analysis of the (239) Pu neutron cross sections
[DE85-013095] N86-12052
Spin dependence of the coherent scattering lengths of (27)Al and admixture of s- and d-partial waves
[DE85-013299] N86-12066
Coupled virbrational modes of the SLC arc magnet and support system
[DE85-014288] N86-12124

RESONANCE LINES
Experimental investigation of recording of dynamic holograms within absorption contour of resonant atomic medium N86-11981

RESOURCE ALLOCATION
Probabilistic analysis of a network resource allocation algorithm
[AD-A157553] N86-11904

RESOURCES MANAGEMENT
The 1984 annual report on Alaska's mineral resources
[DE85-015235] N86-11651

RESPIRATION
Analysis of terrestrial conditions and dynamics
[NASA-CR-176308] N86-11646
Acute pulmonary effects of formaldehyde exposure in humans
[DE85-014728] N86-11848

RESPIRATORY DISEASES
Health hazard evaluation of liquid monopropellants. Phase 4. Subchronic inhalation of hydroxylammonium nitrate, January 1985
[AD-A157623] N86-11844

RESPONSES
Thin film research. Volume 2
[AD-A157609] N86-12138

RETARDANTS
Chemical control of rate and onset temperature of nadimide polymerization N86-11271

REVERSE FIELD PINCH
Energy confinement in a high-current reversed field pinch
[DE85-015009] N86-12111
Recent FRC translation experiments on FRX-C/T
[DE85-012745] N86-12132

REYNOLDS NUMBER
Cloud streets during KonTur: A comparison of parallel/thermal instability modes with observations N86-11755
Transition effects of boundary layer on static and dynamic stability of slender cone N86-11926

RHENIUM
Fabrication and use of zircaloy/tantalum-sheathed cladding thermocouples
[EGG-TFBP-6739] N86-11461

RHEOLOGY
Characterization of polyimide matrix resins and prepregs N86-11273
Quality assurance procedures for V378A matrix resin N86-11274
Results concerning rheological parameters of the Earth N86-11567
Oceanic intraplate seismicity: Implications for the rheology and tectonics of the ocean lithosphere N86-11699

RHODIUM COMPOUNDS
Surface impedance of several magnetic superconductors
[DE85-014101] N86-12155

RIGIDITY
Some short periodic terms due to nutation and tides from latitude and time determinations at Czechoslovak observatories N86-11566

RING LASERS
Ring cavity CO2 laser for branch-selection and narrow resonance produced by SF6 in cavity N86-11930

RISK
High temperature molten salt containment
[DE85-012152] N86-11433

RIVERS
Survey of ice problem areas in navigable waterways
[AD-A157477] N86-11827

RIVETING
Automatic fastening large structures: A new approach N86-11234

ROBOTICS
USSR report: Machine tools and metalworking equipment
[JPRS-UMM-85-010] N86-11394
Large robotized turning centers described N86-11395
Robotized production systems observed in modern plants N86-11396
Robotized machining systems developed at Gomel Institute N86-11397

ROBOTS
Large robotized turning centers described N86-11395
Robotized production systems observed in modern plants N86-11396
Robotized machining systems developed at Gomel Institute N86-11397

ROBUSTNESS (MATHEMATICS)
Towards developing robust algorithms for solving partial differential equations on MIMD machines
[NASA-CR-177979] N86-11856

ROCK MECHANICS
Seismology in civil engineering N86-11707

ROCKET ENGINE CASES
A program to determine the effect of low-velocity impacts on the strength of the filament-wound rocket motor case for the space shuttle
[NASA-TM-87588] N86-11292

ROCKET EXHAUST
Particle sizing in a solid rocket motor using the management of scattered light
[AD-A156480] N86-11226

ROCKET NOZZLES
The analysis and calculation for the dynamic characteristics of the omni-axial movable flexible joint nozzle N86-11925

ROCKS
A first look at Airborne Imaging Spectrometer (AIS) data in an area of altered volcanic rocks and carbonate formations, Hot Creek Range, south central Nevada N86-11625
Spectroscopy of Moses Rock kimberlite diatreme N86-11635
A comparison of AIS data with other aircraft and ground data for the geobotanical discrimination of rock types in southwest Oregon N86-11642
Horizons and opportunities in lunar sample science
[NASA-CR-176290] N86-12191

ROLL FORMING
Comparison of bond in roll-bonded and adhesively bonded aluminums N86-11248

ROOM TEMPERATURE
PMR polyimides from solutions containing mixed endcaps N86-11263
Replacement of MDA with more oxidatively stable diamines in PMR-polyimides N86-11275

ROSSBY REGIMES
The effect of topography on the evolution of unstable disturbances in a baroclinic atmosphere N86-11750
The Hadley and Rossby regimes in a spherical atmosphere N86-11751
Spectral statistical forecasts of the 500 mb height field N86-11804

ROTARY WING AIRCRAFT
Mission-oriented requirements for updating MIL-H-8501: Calspan proposed structure and rationale
[NASA-CR-177371] N86-11204

ROTARY WINGS
Comparison of calculated and measured velocities near the tip of a model rotor blade at transonic speeds
[NASA-TM-86697] N86-11196
Aeroelastic model helicopter rotor testing in the Langley TDT
[NASA-TM-86440] N86-11523

ROTATING FLUIDS
The Hadley and Rossby regimes in a spherical atmosphere N86-11751

ROTATING MIRRORS
Publications of the Astronomical Institute of the Czechoslovak Academy of Sciences, no. 61
[PUBL-61] N86-12069
Wolter 1 type X-ray mirror system with mean resolution and maximum effective collecting area for the spectral region of 1-10 nm N86-12070
Galvanoplastic grazing incidence mirrors for verticle experiments: The tandem tests in soft X-rays N86-12071

ROTATION
Rotating film radiators for space applications
[DE85-009633] N86-11431
Gas-side heat transfer with rotation N86-11509
Coolant passage heat transfer with rotation. A progress report on the computational aspects N86-11510

ROTOR AERODYNAMICS
Aeroelastic model helicopter rotor testing in the Langley TDT
[NASA-TM-86440] N86-11523

ROTOR BLADES (TURBOMACHINERY)
Shock fitting applied to the prediction of high-speed rotor noise
[NASA-TM-86781] N86-11188
Low-cost, net-shape ceramic radial turbine program
[AD-A157532] N86-11202

ROTOR SPEED
Shock fitting applied to the prediction of high-speed rotor noise
[NASA-TM-86781] N86-11188

ROTORS
Ground effect on a rotor wake
[COLL-AERONAUTICS-8510] N86-11187

RUBBER
The Shock and Vibration Digest, volume 17, no. 5
[AD-A156716] N86-11531
Stiffness and damping coefficients of rubber N86-11532
Failure rate model for cathodic delamination of protective coatings
[AD-A157483] N86-11912

RUBY LASERS
Investigation of efficiency of generation of difference-frequency laser radiation in waveguide N86-11969
Neutral beam interactions with materials
[AD-A157445] N86-12076

RUPTURING
Evaluation of concrete creep and stress redistribution in a prototypic PCRV following rupture of prestressing tendons
[DE85-007673] N86-11543

S

S WAVES
Spin dependence of the coherent scattering lengths of (27)Al and admixture of s- and d-partial waves
[DE85-013299] N86-12066

SAFETY
A flash X-ray facility for the Naval Postgraduate School
[AD-A157278] N86-11213
Seeding materials: Health and safety considerations N86-11454

SAGE SATELLITE
SAGE aerosol measurements. Volume 1: February 21, 1979 to December 31, 1979
[NASA-RP-1144] N86-11700

SAGITTARIUS CONSTELLATION
Far-infrared observations of Sagittarius B2: Reconsideration of source structure
[NASA-TM-88185] N86-12167

SAMARIUM COMPOUNDS
Surface impedance of several magnetic superconductors
[DE85-014101] N86-12155

SAMPLING
Oxide cathode mechanisms: Electronic and structural features of oxide cathode surfaces
[AD-A157666] N86-11418

SAN ANDREAS FAULT
Deepwell monitoring along the southern San Andreas Fault
[PB85-196483] N86-11726

SANDS
Evaluation of AIS data for agronomic and rangeland vegetation: Preliminary results for August 1984 flight over Nebraska Sandhills Agricultural Laboratory N86-11627
Site description for the University of Nebraska's Sandhills Agricultural Laboratory N86-11628
Preliminary evaluation of AIS spectra along a topographic/moisture gradient in the Nebraska Sandhills N86-11629

SANDSTONES
Status of models for analysis of Western Gas Sands
[DE85-003398] N86-11653

SANDWICH STRUCTURES
Advances in joining techniques used in development of SPF/DB titanium sandwich reinforced with metal matrices N86-11247

SATELLITE INSTRUMENTS
Geodesy: A look to the future
[NASA-CR-176283] N86-11657

SATELLITE OBSERVATION
On the addition theorem for Legendre polynomials N86-11704
Satellite observations of a large-amplitude 40-50 day oscillation in upper tropospheric temperature over the equatorial Pacific Ocean during the 1982-83 ENSO event N86-11778
Large-scale variability in Indian monsoon rainfall inferred from satellite data N86-11800

SATELLITE TRACKING
An evaluation of CASP (computer assisted search planning program) drift predictions near the New England Shelf/Slope Front
[AD-A157447] N86-11826

SATELLITE TRANSMISSION
The utilization of satellite data and dynamics in understanding and predicting global weather phenomena
[NASA-CR-171577] N86-11749
A sea surface temperature analysis based on in situ and satellite data N86-11816

SATELLITE-BORNE INSTRUMENTS
Atlas of high altitude aircraft measured radiance of White Sands, New Mexico, in the 450-1050 nanometers band
[PB85-204501] N86-11820

SATELLITES
A sea surface temperature analysis based on in situ and satellite data N86-11816

SATURATION (CHEMISTRY)
Saturation characteristics of counterstreaming warm electrons
[DE85-014390] N86-12040

SAUDI ARABIA
Meteorology of the Persian Gulf and of several airports on the Arabian Coast
[AD-A157441] N86-11761

SAWS
The Shock and Vibration Digest, volume 17, no. 5
[AD-A156716] N86-11531
Current research on circular saw and band saw vibration and stability N86-11533

SCALE MODELS
Criteria for scaling heat exchangers to miniature size N86-11387

SCALING
Spherical torus: An approach to compact fusion at low field. Initial ignition assessments
[DE85-012890] N86-12099

SCALING LAWS
Scaling calculations for a relativistic gyrotron
[AD-A157476] N86-11460

SCANDIUM
Chromium- and neodymium-activated gadolinium-scandium-gallium garnet crystal: A new laser active medium N86-11979

SCANNING
Visual information transfer. Part 1: Assessment of specific information needs. Part 2: Parameters of appropriate instrument scanning behavior
[NASA-CR-176277] N86-11850

SCATTERING
Wind Tunnel Seeding Systems for Laser Velocimeters
[NASA-CP-2393] N86-11437
Numerical techniques for scattering from submerged objects N86-12013
Laboratory studies of atomic collision processes of importance in planetary atmospheres
[NASA-CR-176301] N86-12019

SCATTERING CROSS SECTIONS
Seeding requirements for scanning laser velocimetry N86-11446
Characteristics of an axisymmetric sudden expansion flow
[NASA-CR-176278] N86-11465
Intermediate and high-frequency acoustic backscattering cross sections for water-ice interfaces. 1: Two-component profile models
[AD-A157533] N86-12018
Laboratory studies of atomic collision processes of importance in planetary atmospheres
[NASA-CR-176301] N86-12019
Status of fast neutron nuclear data for (239)Pu
[DE85-012699] N86-12045

SCATTEROMETERS
Active and passive microwave measurements in Hurricane Allen
[NASA-TM-86390] N86-11647

SCHMIDT METHOD
On the addition theorem for Legendre polynomials N86-11704

SCHOTTKY DIODES
An interfacial analysis of MoNb-GaAs Schottky barrier diodes N86-11941

SCIENTISTS
Distinct characteristics of science
[DE85-006533] N86-12159

SEA LEVEL
North Sea coast levelling net: A model case for the determination of vertical movements in Western Europe N86-11594
Principle of the construction of the lines of the repeated levelling for the investigation of the vertical movement in the Carpatho-Balkan Region (CBR) N86-11602
An optimum use of sea-level recordings N86-11617

SEA SURFACE TEMPERATURE
Circulation and weather for MAM and JJA 1984 N86-11769
On the relationship between North Atlantic seasonal SST anomalies with United States surface temperature anomalies N86-11770
Worldwide marine temperature variations on the season to century time scale N86-11771
Atmospheric response to an equatorial Pacific sea surface temperature anomaly: The effects of orography N86-11791

SEA WATER
Saltwater wetlands for wastewater management environmental assessment
[PB85-201267] N86-11697

SEALS (STOPPERS)
Injection molding-sealing of glass to low melting metals
[DE85-015613] N86-11329
Design of a flight qualified long-life cryocooler N86-11377
Effects of leakage through clearance seals on the performance of a 10 K Stirling-cycle refrigerator N86-11379
Mechanical face seal dynamics update N86-11530

SEAMS (JOINTS)
Evaluation of a high temperature adhesive for fabricating graphite/PMR-15 polyimide structures N86-11268

SEARCHING
Probabilistic analysis of a network resource allocation algorithm
[AD-A157553] N86-11904

SECONDARY EMISSION
Sources of radioactive ions
[DE85-015251] N86-12030

SECONDARY FLOW
On the instability of vortex series N86-11715

SEDIMENTARY ROCKS
Bibliography of terrestrial impact structures
[NASA-TM-87567] N86-11701

SEDIMENTS
Experiments with solid particle seeding N86-11442
Louisiana Water Resources Research Institute
[PB85-218998] N86-11661

SEISMIC WAVES
Oceanic intraplate seismicity: Implications for the rheology and tectonics of the ocean lithosphere N86-11699
Attenuation of macroseismic effects of earthquakes N86-11705
Travel-time and its residuals for the blasts from Eschenlohe (Bavaria) N86-11706
Short-period SVSN-4 seismograph N86-11708

SEISMOGRAMS
Short-period SVSN-4 seismograph N86-11708

SEISMOGRAPHS
Short-period SVSN-4 seismograph N86-11708
Magnification of low-sensitivity channels in seismographs with standard characteristics N86-11709

SEISMOLOGY
Anew about the correlation between Mohorovicic discontinuity depths, geoid undulations and Bouguer gravity anomalies in the Dinaric-Pannonian region of Yugoslavia N86-11557
Proceedings of the 5th International Symposium Geodesy and Physics of the Earth, part 3
[REPT-81-PT-3] N86-11591
Near-surface deformations and stresses in the area of the Tolbachik great fissure eruption of 1975-1976 (Kamchatka) from geodetic data N86-11600
Some geodetic aspects of the problem of checking the plate-tectonic model of seismicity in southeastern Europe N86-11603
Geophysical Works, 1982, volume 30 N86-11702
Seismology in civil engineering N86-11707
Deepwell monitoring along the southern San Andreas Fault
[PB85-196483] N86-11726
A general-applications direct global matrix algorithm for rapid seismo-acoustic wavefield computations N86-12012

SEMICONDUCTING FILMS
Carbon films grown from plasma on III-V semiconductors
[NASA-TM-87140] N86-12135

SEMICONDUCTOR DEVICES
Investigation of photoelectrode redox polymer junctions
[AD-A157556] N86-11304
Conversion of electromagnetic wave energy to electrical current by bulk superlattice semiconductors N86-11952

SEMICONDUCTOR JUNCTIONS
Investigation of photoelectrode redox polymer junctions
[AD-A157556] N86-11304

SEMICONDUCTOR LASERS
Operating range of aluminum gallium arsenide quantum-well heterostructure lasers: tunability, power output and high energy emission N86-11464

SEMICONDUCTORS (MATERIALS)
Surface and interfacial properties of Ga0.47In0.53As alloys
[AD-A157343] N86-11316
Bridgman growth of semiconductors
[NASA-CR-177971] N86-11426
China report: Science and technology
[JPRS-CST-85-014] N86-11918
USSR report: Physics and mathematics
[JPRS-UPM-85-005] N86-11945
Investigations of deep level defects in semiconductor material systems N86-12133
Ellipsometric and optical study of some uncommon insulator films on 3-5 semiconductors
[NASA-TM-87135] N86-12134

SENSITIVITY
Influence of effective rate sensitivity on adiabatic shear instability
[DE85-013967] N86-11333
Impurity monitoring by laser-induced fluorescence techniques
[DE85-014142] N86-11356
Senstivity of using blunt and sharp crack models in elastic-plastic fracture mechanics
[DE85-010288] N86-11537
Adjustment of the latitude data by least-squares collocation approach N86-11562
RE-1000 free-piston Stirling engine update
[NASA-TM-87126] N86-11668
Si(Li)-NaI(Tl) sandwich detector array for measurements of trace radionuclides in soil samples
[DE85-013865] N86-12062

SENSORS
Laser angle sensor
[NASA-CR-172369] N86-11207
Atlas of high altitude aircraft measured radiance of White Sands, New Mexico, in the 450-1050 nanometers band
[PB85-204501] N86-11820

SENSORY PERCEPTION
Perceptual and physiological responses during exercise in cool and cold water
[AD-A157334] N86-11840

SEPARATORS
Degradation of ionic membranes in the zinc/ferricyanide battery
[DE85-008469] N86-11681

SEQUENCING
Probabilistic analysis of a network resource allocation algorithm
[AD-A157553] N86-11904

SERIES EXPANSION
Gaussian and mean curvatures of postglacial land uplift as expanded in surface spherical harmonics, and the origin of earthquakes in Fennoscandia N86-11599

SERVOCONTROL

Applications of the magneto-optical filter to stellar pulsation measurements [NASA-CR-176282] N86-12187

SERVOMECHANISMS

Mechanical accessories for mobile teleoperators [DE85-014310] N86-11855

SET THEORY

Proceedings of the 9th Annual Climate Diagnostics Workshop [PB85-183911] N86-11763

Global surface air temperature variations: 1983-1984 N86-11764

Recent unusual mean winter temperature across the contiguous United States N86-11772

Approximate reasoning and the REVEAL software system. Users guide [AD-A157298] N86-11902

SHATTER CONES

Bibliography of terrestrial impact structures [NASA-TM-87567] N86-11701

SHEAR FLOW

A hybrid vortex-in-cell finite-difference numerical method for turbulent shear layer computation N86-11886

SHEAR LAYERS

Stability and interaction of coherent structure in supersonic reactive wakes N86-11185

SHEAR PROPERTIES

Evaluation of a high temperature adhesive for fabricating graphite/PMR-15 polyimide structures N86-11268

Influence of effective rate sensitivity on adiabatic shear instability [DE85-013967] N86-11333

SHEAR STRENGTH

Comparison of bond in roll-bonded and adhesively bonded aluminums N86-11248

High-temperature adhesive development and evaluation N86-11250

Factors affecting the processing of epoxy film adhesives N86-11252

Rapid adhesive bonding and field repair of aerospace materials N86-11253

Reduction of moisture effects during the cure of epoxy adhesives used in composite repair N86-11254

Initial investigation of cryogenic wind tunnel model filler materials N86-11255

Evaluation of a high temperature adhesive for fabricating graphite/PMR-15 polyimide structures N86-11268

Recent developments in polyimide and bismaleimide adhesives N86-11270

Replacement of MDA with more oxidatively stable diamines in PMR-polyimides N86-11275

SHEAR STRESS

Interaction of mixed mode loading on cyclic debonding in adhesively bonded composite joints [NASA-CR-177990] N86-11298

Effects of manufacturing processes on structural allowables [AD-A157596] N86-11318

SHEATHS

Advances in joining techniques used in development of SPF/DB titanium sandwich reinforced with metal matrices N86-11247

Fabrication and use of zircaloy/tantalum-sheathed cladding thermocouples [EGG-TFBP-6739] N86-11461

SHIPS

USSR report: Transportation [JPRS-UTR-85-011] N86-11177

Chemical bonding agent for suppression of rusty bolt intermodulation interference [AD-D011747] N86-11315

Fire growth in combat ships [NBSIR-85/3159] N86-11364

SHOCK FRONTS

Influence of solid state obstacles on radiation of recombination laser plasma N86-11958

SHOCK LOADS

Fluids at high dynamic pressures and temperatures [DE85-014812] N86-11305

Synthesis of nickel-aluminum alloys by shock compression of composite particles [DE85-015165] N86-11328

Surface properties of shocked lead [DE85-009582] N86-11476

Numerical simulation of a sample recovery fixture for high velocity impact [DE85-013965] N86-11485

Strain rate dependence in steady, plastic shock waves [DE85-014703] N86-11544

Analytical electron microscopy study of shock synthesized zinc ferrite [DE85-015144] N86-12140

SHOCK TUBES

Influence of physical-chemical properties of gases on interaction between shockwaves and convex cylindrical surfaces N86-11962

Flame propagation in pulsed acceleration field N86-11964

SHOCK WAVE PROPAGATION

Occurrence of pressure wave during spontaneous ignition of gas ahead of flame front in closed vessel N86-11965

Steady-state detonation of charges of finite length N86-11966

SHOCK WAVES

Shock fitting applied to the prediction of high-speed rotor noise [NASA-TM-86781] N86-11188

Fluids at high dynamic pressures and temperatures [DE85-014812] N86-11305

Chemical synthesis under shock compression [DE85-015166] N86-11325

Calculation of thermal trapping in shear bands [DE85-014404] N86-11336

Shock-induced temperature distributions in powder compact recovery fixtures [DE85-015139] N86-11359

Shock consolidation of IN-100 nickel-base superalloy powder [DE85-015159] N86-11360

The Shock and Vibration Digest, volume 17, no. 4 [AD-A154112] N86-11527

Microcomputers in shock and vibration N86-11528

A review of the literature on finite-element modeling of laminated composite plates N86-11529

Mechanical face seal dynamics update N86-11530

High pressure strength of shocked aluminum [DE85-014461] N86-11547

Capacitive pendulum with intelligent data collection N86-11577

Initial plasma formation during exposure of absorbing materials to laser radiation with plane expansion geometry of the forming plasma N86-11956

Influence of solid state obstacles on radiation of recombination laser plasma N86-11958

Influence of physical-chemical properties of gases on interaction between shockwaves and convex cylindrical surfaces N86-11962

Sandia shock compression database [DE85-015141] N86-12142

SHRINKAGE

Strength and flexibility properties of advanced ceramic fabrics [NASA-TM-86824] N86-11340

SIDEREAL TIME

On the comparison and choice between the formulas of the Earth tidal correction in astronomical time and latitude observation N86-11588

SIGNAL ANALYSIS

Statistical signal analysis for systems with interferenced inputs N86-12016

SIGNAL PROCESSING

Capacitive pendulum with intelligent data collection N86-11577

SIG: A general-purpose signal processing code N86-11876

Ramp response estimation and spectrum extrapolation for ultrasonic scattering N86-11881

High-speed signal processor developed N86-11995

Superconducting Magnetic Energy Storage (SMES) Program [DE85-014250] N86-12106

SIGNAL TO NOISE RATIOS

Fiber optic pressure sensors in skin-friction measurements [NASA-CR-176294] N86-11838

SILICON

Solid-melt interface studies of high-speed silicon sheet growth [DE85-008783] N86-11349

Direct coupling of microbore HPLC columns to MS systems [NASA-CR-176292] N86-11436

Melting of crystalline and amorphous silicon by Ruby, XeCl and KrF laser irradiation [DE85-015040] N86-11468

The interface structure of grain boundaries in polysilicon N86-11665

Use of SiO2 and TiO2 sol-gel antireflection films on silicon solar cells [DE85-011280] N86-11688

Deep-level defects in ion-implanted and CO2 laser-annealed silicon N86-11939

Model of amorphous silicon layer regrowth [DE85-012608] N86-12145

SILICON CARBIDES

Strength and flexibility properties of advanced ceramic fabrics [NASA-TM-86824] N86-11340

SILICON DIOXIDE

Strength and flexibility properties of advanced ceramic fabrics [NASA-TM-86824] N86-11340

Pulse duration dependence of 1064-nm laser damage thresholds of porous silica antireflection coatings on fused silica substrates [DE85-013207] N86-11350

Physical property changes of a lithia-alumina-silica based glass as a function of composition [DE85-015610] N86-11352

SILICON FILMS

Effect of high electric field on minority carrier generation in silicon depletion layer N86-11938

Thermal post-treatment characteristics of metastable carrier concentration in As-implanted silicon after transient annealing N86-11942

SILICON NITRIDES

Low-cost, net-shape ceramic radial turbine program [AD-A157532] N86-11202

SILVER

Metallography of solid state bonds [DE85-014564] N86-11327

Polymer glazings for silver mirrors [DE85-012140] N86-11357

SILVER COMPOUNDS

Improved solid state laser sources, volume 3 [DE85-012956] N86-11469

SIMULATION

Initial investigation of cryogenic wind tunnel model filler materials N86-11255

Chemical control of rate and onset temperature of nadimide polymerization N86-11271

Oxide cathode mechanisms: Electronic and structural features of oxide cathode surfaces [AD-A157666] N86-11418

Climate simulation and change: A simple energy balance climate model N86-11731

Laboratory model of flight through wind shear N86-11747

The effect of topography on the evolution of unstable disturbances in a baroclinic atmosphere N86-11750

Prediction of monthly 700 mb heights using antecedent and simulated prognostic height predictors N86-11805

Simulation of flame propagation through vorticity regions using the discrete vortex method N86-11882

Two-dimensional linacs [DE85-015129] N86-12029

Experimental program to build a multimegawatt lasertron for super linear colliders [DE85-014293] N86-12049

SSC test lattices [DE85-014240] N86-12098

SIMULATORS

HOST liner cyclic facilities N86-11519

SINGLE CRYSTALS

USSR report: Physics and mathematics [JPRS-UPM-85-005] N86-11945

SIZE DETERMINATION

A technique to measure the size of particles in laser Doppler velocimetry applications N86-11457

SIZE DISTRIBUTION

Measurements of refractive index structure function C2N and aerosol size distribution at Chesapeake Bay [AD-A157455] N86-11717

SKIN (ANATOMY)

Importance of phytoalexin tolerance and detoxification for pathogenicity [DE85-014759] N86-11257

SKIN (STRUCTURAL MEMBER)

Evaluation of superplastic forming and weld-brazing for fabrication of titanium compression panels N86-11245

SKIN FRICTION

Fiber optic pressure sensors in skin-friction measurements [NASA-CR-176294] N86-11838

SLENDER CONES

Transition effects of boundary layer on static and dynamic stability of slender cone N86-11926

SLIP FLOW

Calculation of particle dynamics effects on laser velocimeter data N86-11438

SLIPSTREAMS

A review of ARA research into propeller aerodynamic prediction methods N86-11151

Wind tunnel investigation of the interaction of propeller slipstream with nacelle/wing/flap combinations N86-11166

An asymptotic theory for the interference of large aspect ratio swept wings and multiple propeller slipstreams N86-11167

SLOPES

A study of the cornering forces generated by aircraft tires on a tilted, free-swiveling nose gear
[NASA-TP-2481] N86-11522

SMOKE

Applied model validation
[NBSIR-85-3154-1] N86-11363

Seeding systems for use with a laser velocimeter in large scale wind tunnels N86-11[illegible]44

Uncertainties in the radiative properties of smoke and their effects on climate assessments
[DE85-015187] N86-11691

SMOKE DETECTORS

Methods to calculate the response time of heat and smoke detectors installed below large unobstructed ceilings
[NBSIR-85/3167] N86-11365

SMOOTHING

Initial investigation of cryogenic wind tunnel model filler materials N86-11255

Adjustment of the latitude data by least-squares collocation approach N86-11562

SNOW

Thermal convection in snow
[AD-A157577] N86-11648

SNOW COVER

Variability of snow cover characteristics in the Transbaykal
[NASA-TM-77917] N86-11733

Review of the climate of fall 1983 and winter 1983-84 N86-11766

Some empirical evidence for the influence of snow cover on temperature and precipitation N86-11767

The effect of anomalous snow cover on the general circulation of the atmosphere using a simple climate model N86-11794

Interannual climate variability in a low vertical resolution spectral atmospheric model N86-11795

Land-surface fluctuations and associated climatic variability N86-11807

SODIUM CARBONATES

Intergranular attack and stress corrosion cracking of alloy 600 in high-temperature caustic solutions containing contaminants
[DE85-014106] N86-11335

SODIUM HYDROXIDES

Intergranular attack and stress corrosion cracking of alloy 600 in high-temperature caustic solutions containing contaminants
[DE85-014106] N86-11335

SODIUM SULFATES

Intergranular attack and stress corrosion cracking of alloy 600 in high-temperature caustic solutions containing contaminants
[DE85-014106] N86-11335

SOIL MECHANICS

Seismology in civil engineering N86-11707

SOIL MOISTURE

Preliminary evaluation of AIS spectra along a topographic/moisture gradient in the Nebraska Sandhills N86-11629

Land-surface fluctuations and associated climatic variability N86-11807

SOILS

Validation of procedures for pavement design on expansive soils
[FAA-PM-85-15] N86-11362

The use of AIS data for identifying and mapping calcareous soils in western Nebraska N86-11630

Evaluation of color infrared aerial surveys of wastewater soil absorption systems
[PB85-189074] N86-11654

Integrated forest study on effects of atmospheric deposition. Project summary
[DE85-015972] N86-11690

Effects of acid precipitation on composition, electrokinetic behavior, cation adsorption and ion exchange capacity in various soil systems
[PB85-217727] N86-11698

Si(Li)-NaI(Tl) sandwich detector array for measurements of trace radionuclides in soil samples
[DE85-013865] N86-12062

SOLAR ARRAYS

Performance of solar collector arrays and collector controllers in the National Solar Data Network
[DE85-001297] N86-11663

A summary report on the Flat-Plate Solar Array Project Workshop on Transparent Conducting Polymers
[NASA-CR-176302] N86-11669

SOLAR CELLS

Solid-melt interface studies of high-speed silicon sheet growth
[DE85-008783] N86-11349

Intermediate load modules for test and evaluation: Fixed price research and development
[NASA-CR-176135] N86-11664

A summary report on the Flat-Plate Solar Array Project Workshop on Transparent Conducting Polymers
[NASA-CR-176302] N86-11669

A 25.5 percent AMO gallium arsenide grating solar cell
[NASA-TM-87134] N86-11671

New-generation photovoltaic technologies
[DE85-012143] N86-11675

Use of SiO2 and TiO2 sol-gel antireflection films on silicon solar cells
[DE85-011280] N86-11688

Investigation of defects in GaAsP superlattic structures
[DE85-012134] N86-12139

SOLAR COLLECTORS

Performance of solar collector arrays and collector controllers in the National Solar Data Network
[DE85-001297] N86-11663

SOLAR ECLIPSES

Evidence of an 18 year cycle in Pacific northwest precipitation data N86-11788

SOLAR ENERGY

Dish electric systems heat engine assessment
[DE85-013942] N86-11479

Performance of solar collector arrays and collector controllers in the National Solar Data Network
[DE85-001297] N86-11663

Passive solar applications
[DE85-014085] N86-11685

SOLAR ENERGY ABSORBERS

Passive solar applications
[DE85-014085] N86-11685

SOLAR GENERATORS

A summary report on the Flat-Plate Solar Array Project Workshop on Transparent Conducting Polymers
[NASA-CR-176302] N86-11669

SOLAR HEATING

Passive solar applications
[DE85-014085] N86-11685

SOLAR OSCILLATIONS

The 1984 solar oscillation program of the Mount Wilson 60-foot tower
[NASA-CR-176248] N86-12195

SOLAR PROTONS

Cosmogenic-nuclide production by primary cosmic-ray protons
[DE85-012760] N86-12198

SOLAR RADIATION

Determination of the depth of a conductivity anomaly by separating the geomagnetic variation field into its external and internal part N86-11711

SOLAR REFLECTORS

Polymer glazings for silver mirrors
[DE85-012140] N86-11357

SOLAR TERRESTRIAL INTERACTIONS

International solar-terrestrial physics program: A plan for the core spaceflight missions
[NASA-TM-87511] N86-12194

SOLAR WIND

International solar-terrestrial physics program: A plan for the core spaceflight missions
[NASA-TM-87511] N86-12194

SOLAR WIND VELOCITY

Statistical properties of geomagnetic pulsations at the Fuersterfeldbruck Observatory determined by means of pulsation indices. Part 3: Correlation with the parameters of the interplanetary magnetic field N86-11710

SOLDERING

Welding, Bonding and Fastening, 1984
[NASA-CP-2387] N86-11227

Investigation of low-temperature solders for cryogenic wind tunnel models N86-11230

NTF: Soldering technology development for cryogenics N86-11231

SOLDERS

Investigation of low-temperature solders for cryogenic wind tunnel models N86-11230

SOLENOIDS

Automated magnet testing facility
[DE85-012863] N86-11422

SOLID ELECTROLYTES

Electrical relaxation in poly(ethylene oxide)
[AD-A157301] N86-11342

SOLID PHASES

Comparison of bond in roll-bonded and adhesively bonded aluminums N86-11248

SOLID PROPELLANT COMBUSTION

Pressure-coupled response function of solid propellants including those with negative pressure-exponents N86-11924

SOLID PROPELLANT ROCKET ENGINES

Particle sizing in a solid rocket motor using the management of scattered light
[AD-A156480] N86-11226

One-dimensional two-phase flow in combustion chamber of solid propellant rocket motors N86-11921

SOLID STATE

Metallography of solid state bonds
[DE85-014564] N86-11327

Influence of solid state obstacles on radiation of recombination laser plasma N86-11958

Dominant moving species in the formation of amorphous NZr by solid-state reaction
[DE85-014855] N86-12053

International project in history of solid state physics
[DE85-014843] N86-12152

SOLID STATE LASERS

Improved solid state laser sources, volume 3
[DE85-012956] N86-11469

Investigation on growth and laser properties of GGG:(Nd,Cr) single crystal
[DE85-014282] N86-12151

SOLIDIFICATION

Mechanical properties of rapidly solidified Type 304 stainless steel
[DE85-014577] N86-11338

Application of a mixture theory to the binary alloy solidification problem N86-11873

Overview of MIT, ADIP irradiation experiments
[DE85-014469] N86-12060

SOLUTIONS

Intergranular attack and stress corrosion cracking of alloy 600 in high-temperature caustic solutions containing contaminants
[DE85-014106] N86-11335

Part A. Molecular dynamics and ionic associations of LiAsF6 in 4-butyrolactone mixtures with 2-methyl tetrahydrofuran. Part B. Molecular dynamics and ionic associations of LiBF4 in 1,2-dimethoxymethane
[AD-A157401] N86-12023

SOLVENTS

Characterization of the relationship of the cure cycle chemistry to cure cycle processing properties
[NASA-CR-176256] N86-11339

SONAR

Development of castor-oil-resistant polyurethane sonar encapsulants
[AD-A157576] N86-11347

SONIC NOZZLES

Particle size distributions of several commonly used seeding aerosols N86-11441

SOOT

An investigation of the effects of fuel composition on combustion characteristics in a T-63 combustor
[AD-A157325] N86-11358

SOUND PRESSURE

Numerical Techniques in Acoustics
[NASA-CP-2404] N86-12007

Application of high order acoustic finite elements to transmission losses and enclosure problems N86-12008

Improving the accuracy of the boundary integral method based on the Helmholtz integral N86-12010

Statistical signal analysis for systems with interferenced inputs N86-12016

Infrasound: A summary of interesting articles
[FMV:ELEKTRO-A12:142/83] N86-12017

SOUND TRANSDUCERS

Development of castor-oil-resistant polyurethane sonar encapsulants
[AD-A157576] N86-11347

SOUND TRANSMISSION

Vibrations and structureborne noise in space station
[NASA-CR-176291] N86-11220

SOUND WAVES

Use of the wavenumber technique with the Lloyds mirror for an acoustic doublet
[AD-A156463] N86-11824

Raman scattering of sound on random oscillations of bubbles N86-11946

Reflection of sound from plate containing periodic inhomogeneities N86-11951

Statistical signal analysis for systems with interferenced inputs N86-12016

SOUNDING

Determination of the depth of a conductivity anomaly by separating the geomagnetic variation field into its external and internal part N86-11711

SOUTHERN HEMISPHERE

Time series modeling of the Southern Oscillation N86-11777

Subseasonal and interannual variations of tropical convection and the El Nino/Southern Oscillation N86-11779

Transition from the Southern to Northern Hemisphere summer monsoon N86-11799

SPACE CHARGE

IFR guiding experiments
[DE85-014512] N86-12027

Discussion of the current limits in the RFQ
[DE85-012909] N86-12088

SPACE ERECTABLE STRUCTURES
Feasibility of remotely manipulated welding in space: A step in the development of novel joining technologies N86-11246

SPACE HEATING (BUILDINGS)
Passive solar applications [DE85-014085] N86-11685

SPACE POWER UNIT REACTORS
Chemical thermodynamic assessment of the Li-U-O system for possible space nuclear applications [DE85-015060] N86-12054

SPACE PROBES
SPACEWARN Bulletin [NASA-TM-87512] N86-11222

SPACE PROGRAMS
US space programs: Cooperation and competition from Europe [BPA-CP-695] N86-12163

SPACE SHUTTLE MAIN ENGINE
Explosive tube-to-fitting joining of small-diameter tubes N86-11239

SPACE SHUTTLE MISSIONS
Design of a flight qualified long-life cryocooler N86-11377

SPACE SHUTTLES
NASA Lewis Research Center low-gravity fluid management technology program [NASA-TM-87145] N86-11218
Automatic fastening large structures: A new approach N86-11234
Evaluation of a high temperature adhesive for fabricating graphite/PMR-15 polyimide structures N86-11268
A program to determine the effect of low-velocity impacts on the strength of the filament-wound rocket motor case for the space shuttle [NASA-TM-87588] N86-11292

SPACE STATIONS
A direct model reference adaptive approach to the control of space stations N86-11219
Vibrations and structureborne noise in space station [NASA-CR-176291] N86-11220
Computational structural mechanics: A new activity at the NASA Langley Research Center [NASA-TM-87612] N86-11540

SPACE-TIME FUNCTIONS
Space-time variating geological masses by space-time variating geodetic measurements N86-11595
Mathematical treatment of vertical movements N86-11597
Principle of the construction of the lines of the repeated levelling for the investigation of the vertical movement in the Carpatho-Balkan Region (CBR) N86-11602
Representations of the group of diffeomorphisms in the physics of particles, gravity and fluids [DE85-007031] N86-12028

SPACEBORNE ASTRONOMY
IUE observations of the 1982-84 eclipse of Epsilon Aurigae N86-12172

SPACEBORNE PHOTOGRAPHY
Teleoperator human factors study [NASA-CR-176310] N86-11854

SPACECRAFT
Activated recombinative desorption: A potential component in mechanisms of spacecraft glow [DE85-014092] N86-11223

SPACECRAFT CONSTRUCTION MATERIALS
Metallurgical characterization of the interfaces and the damping mechanisms in metal matrix composites [AD-A156507] N86-11300

SPACECRAFT CONTROL
CRC control systems laboratory gyro test facility [CRC-1385] N86-11205

SPACECRAFT DEFENSE
Commercialization of space: National policy and defense needs [AD-A156517] N86-12162

SPACECRAFT DESIGN
Problems experienced and envisioned for dynamical physical systems [NASA-TP-2508] N86-11215
Design and performance analysis of an aero-maneuvering orbital-transfer vehicle concept [NASA-TM-86848] N86-11221
Metallurgical characterization of the interfaces and the damping mechanisms in metal matrix composites [AD-A156507] N86-11300

SPACECRAFT LAUNCHING
SPACEWARN Bulletin [NASA-TM-87512] N86-11222

SPACECRAFT POWER SUPPLIES
Chemical thermodynamic assessment of the Li-U-O system for possible space nuclear applications [DE85-015060] N86-12054

SPALLING
Stress and strain-rate dependence of spall strength in two aluminum alloys [DE85-015154] N86-11321

SPARK GAPS
Rimfire: A six megavolt laser-triggered gas-filled switch for PBFA 2 [DE85-013959] N86-12115

SPATIAL DISTRIBUTION
Research on optic spatial frequency analysis of linear structures in remote sensing images N86-11927

SPATIAL RESOLUTION
Analysis of terrestrial conditions and dynamics [NASA-CR-176308] N86-11646

SPECIFICATIONS
Variable field magnetic extraction channel for ORIC [DE85-011927] N86-12089

SPECTRAL BANDS
UBV photometry of the 1982-4 eclipse of Epsilon Aurigae: A discussion of the observed light curves N86-12176
Intermediate and narrow band photometry of Epsilon Aurigae N86-12177
Astronomical research at the Hopkins Phoenix Observatory N86-12182
Photoelectric observations of the long-period eclipsing binaries at Yonsei University Observatory N86-12184

SPECTRAL EMISSION
Numerical solution of ionospheric filtration of ULF waves. Part 1: Method N86-11712
Modelling Epsilon Aurigae without solid particles N86-12181

SPECTRAL ENERGY DISTRIBUTION
Spin dependence of the coherent scattering lengths of (27)Al and admixture of s- and d-partial waves [DE85-013299] N86-12066
IUE observations of the 1982-84 eclipse of Epsilon Aurigae N86-12172

SPECTRAL METHODS
A parameterization technique for nonlinear spectral models N86-11752

SPECTRAL RECONNAISSANCE
Field utilization and analysis of AIS 128-channel imagery using microcomputers: Application to Yerington, Nevada field area N86-11621

SPECTRAL REFLECTANCE
Preliminary evaluation of AIS spectra along a topographic/moisture gradient in the Nebraska Sandhills N86-11629
Calibration of AIS data using ground-based spectral reflectance measurements N86-11631
Forest canopy chemistry from Blackhawk Island, Wisconsin N86-11634
Analysis of aircraft spectrometer data with logarithmic residuals N86-11636
AIS investigation of agricultural monocultures N86-11640
Use of SiO2 and TiO2 sol-gel antireflection films on silicon solar cells [DE85-011280] N86-11688

SPECTRAL RESOLUTION
Forest species identification with high spectral resolution data N86-11643
Interannual climate variability in a low vertical resolution spectral atmospheric model N86-11795
Publications of the Astronomical Institute of the Czechoslovak Academy of Sciences, no 61 [PUBL-61] N86-12069
Wolter 1 type X-ray mirror system with mean resolution and maximum effective collecting area for the spectral region of 1-10 nm N86-12070

SPECTRAL THEORY
On cloud street development in three dimensional parallel and Rayleigh instabilities N86-11754

SPECTROMETERS
High altitude measured radiance of White Sands, New Mexico in the 400-2000 nm band using a filter wedge spectrometer [PB85-206084] N86-11729
High resolution spectrometer in studies of e(+)e(-) annihilation at (radical)s = 29 GeV [DE85-013870] N86-12065

SPECTROPHOTOGRAPHY
Field utilization and analysis of AIS 128-channel imagery using microcomputers: Application to Yerington, Nevada field area N86-11621

SPECTROPHOTOMETERS
High resolution spectrometry of leaf and canopy chemistry for biochemical cycling N86-11633

SPECTROPHOTOMETRY
Spectrophotometry of Epsilon Aur, 3295-8880 A N86-12178

SPECTROSCOPIC ANALYSIS
Impurity monitoring by laser-induced fluorescence techniques [DE85-014142] N86-11356
Investigations of deep level defects in semiconductor material systems N86-12133
High dispersion observations of Epsilon Aur from Sept. 1982 to March 1983 N86-12183

SPECTROSCOPY
Characterization methodology for PMR-15 N86-11272

SPECTRUM ANALYSIS
Preliminary analysis of AIS spectral data acquired from semi-arid shrub communities in the Owens Valley, California N86-11622
AIS spectra for stressed and unstressed plant communities in the Carolina slate belt N86-11623
Spectral characterization of suspected acid deposition damage in red spruce (Picea rubens) stands from Vermont N86-11624
A first look at Airborne Imaging Spectrometer (AIS) data in an area of altered volcanic rocks and carbonate formations, Hot Creek Range, south central Nevada N86-11625
Interpretation of AIS images of Cuprite, Nevada using constraints of spectral mixtures N86-11626
Preliminary evaluation of AIS spectra along a topographic/moisture gradient in the Nebraska Sandhills N86-11629
The use of AIS data for identifying and mapping calcareous soils in western Nebraska N86-11630
Analysis of aircraft spectrometer data with logarithmic residuals N86-11636
Urban, forest, and agricultural AIS data: Fine spectral structure N86-11644
Spectral statistical forecasts of the 500 mb height field N86-11804
Spectrum structure of XeCl electric discharge laser N86-11970
Scattered light in the IUE spectra of Epsilon Aurigae N86-12180
The 1984 solar oscillation program of the Mount Wilson 60-foot tower [NASA-CR-176248] N86-12195

SPENT FUELS
Application of detailed fission-product decay gamma spectra in the calculation of photoneutron spectra from D((GAMMA),n) reactions in PWR fuel [DE85-012729] N86-12048

SPERMATOZOA
Detection of chromosomal abnormalities in human sperm [DE85-014178] N86-11834

SPHERES
Seeding subsonic, transonic and supersonic flows with 0.5 micron polystyrene spheres N86-11451

SPHERICAL COORDINATES
Precise geoid computations at mountainous coastlines in view of vertical datum determinations N86-11561

SPHERICAL HARMONICS
Precise geoid computations at mountainous coastlines in view of vertical datum determinations N86-11561
Gaussian and mean curvatures of postglacial land uplift as expanded in surface spherical harmonics, and the origin of earthquakes in Fennoscandia N86-11599
On the addition theorem for Legendre polynomials N86-11704
The Hadley and Rossby regimes in a spherical atmosphere N86-11751
Spectral statistical forecasts of the 500 mb height field N86-11804

SPHERICAL SHELLS
The hollow sphere model for porous metals and metal powders N86-11308
Determination of parameters of elastic spherical shell from scattered wave field N86-11949

SPHERICAL WAVES
On the nonlinear characteristics of the axisymmetric flow regime: Cylindrical and spherical systems N86-11756

SPHEROMAKS
Los Alamos Spheromak Program [DE85-012769] N86-12096

SPIN-LATTICE RELAXATION
Nuclear spin-polarized HD, D2, HT and DT solids, liquids and high density gases [DE85-014136] N86-12154

SPIN-ORBIT INTERACTIONS
Magnetic properties and electronic structure of the actinide systems UAl2, NpAl2 and PuAl2 [DE85-014102] N86-11323

SPONTANEOUS COMBUSTION
Occurrence of pressure wave during spontaneous ignition of gas ahead of flame front in closed vessel N86-11965

SPOT WELDS
Advances in joining techniques used in development of SPF/DB titanium sandwich reinforced with metal matrices N86-11247

SPUTTERING

Metallic multilayers and superlattices [DE85-014444] N86-12141

Microscopic investigation of NbN sputtered films [DE85-015000] N86-12153

SQUID (DETECTORS)

The relations between voltage and magnetic field of superconducting weaklink (1) N86-11934

STABILITY

Stability and interaction of coherent structure in supersonic reactive wakes N86-11185

Initial investigation of cryogenic wind tunnel model filler materials N86-11255

Influence of effective rate sensitivity on adiabatic shear instability [DE85-013967] N86-11333

Introduction to the session on: Numerical methods for two-phase flow [DE85-012651] N86-11435

Current research on circular saw and band saw vibration and stability N86-11533

On the distribution of the residual vectors of Earth's tide gravity observations in Central Europe N86-11564

Development of membranes for the zinc/ferricyanide battery [DE85-011189] N86-11689

On the instability of vortex series N86-11715

A numerical study of global axisymmetric states and their stability to quasi-geostrophic disturbances N86-11753

Flame propagation in pulsed acceleration field N86-11964

Saturation characteristics of counterstreaming warm electrons [DE85-014390] N86-12040

Particle simulation of the low-(ALPHA) Pierce diode [DE85-014435] N86-12113

STABILIZATION

Feedback stabilization of optical interferometer [AD-A156912] N86-11459

Stability of a method for analyzing radiation pattern of acoustic radiator with near-field pressure measurement errors N86-11950

STABLE OSCILLATIONS

Passive motion control of pneumatically driven displacers in cryogenic coolers N86-11383

STAINLESS STEELS

NTF: Soldering technology development for cryogenics N86-11231

Generic structural elements N86-11296

Effects of manufacturing processes on structural allowables [AD-A157596] N86-11318

Metallography of solid state bonds [DE85-014564] N86-11327

Mechanical properties of rapidly solidified Type 304 stainless steel [DE85-014577] N86-11338

Numerical simulation of a sample recovery fixture for high velocity impact [DE85-013965] N86-11485

STANDARDS

Liquid metal reactors programs: Safeguards and program assurance [DE85-011002] N86-12046

STANDING WAVES

Subseasonal and interannual variations of tropical convection and the El Nino/Southern Oscillation N86-11779

Analysis of ultrasonic waves in a bounded medium N86-11869

STAR DISTRIBUTION

On the lunar tidal effect in the latitude observations at Tianjin N86-11565

Influences of systematic differences between different star catalogues on the results of latitude and time determinations with the PZT 2 N86-11575

STARS

Planets around Barnard's Star? N86-11584

A laser siderostat [AD-A157444] N86-12190

STATIC PRESSURE

Calibration of the NCAR (National Center for Atmospheric Research) Sabreliner research static pressure source with a trailing cone assembly [PB85-191005] N86-11200

STATIC STABILITY

Evaluation of a high temperature adhesive for fabricating graphite/PMR-15 polyimide structures N86-11268

The Hadley and Rossby regimes in a spherical atmosphere N86-11751

On the nonlinear characteristics of the axisymmetric flow regime: Cylindrical and spherical systems N86-11756

Some empirical evidence for the influence of snow cover on temperature and precipitation N86-11767

Transition effects of boundary layer on static and dynamic stability of slender cone N86-11926

STATISTICAL ANALYSIS

Uncertainty assessment in life cycle cost analysis [AD-A157414] N86-11488

Statistical analysis and interpretation of Earth crustal movements in northeast Bulgaria N86-11613

Relation between earthquake focal intensity and recent vertical Earth's crustal movements in the Rila-Rhodope seismic region N86-11615

Regional Wind Energy Assessment Program. Appendix: Wind statistics summaries [DE85-011520] N86-11686

Statistical properties of geomagnetic pulsations at the Fuerstenfeldbruck Observatory determined by means of pulsation indices. Part 3: Correlation with the parameters of the interplanetary magnetic field N86-11710

Minimum assumption tornado hazard probability model [PB85-206092] N86-11821

Continuing design, review, and analysis work for the Sierra Cooperative Pilot Project [PB85-204303] N86-11822

USSR report: Physics and mathematics [JPRS-UPM-85-005] N86-11945

Statistical signal analysis for systems with interferenced inputs N86-12016

STATISTICAL MECHANICS

Activated recombinative desorption: A potential component in mechanisms of spacecraft glow [DE85-014092] N86-11223

Physics opportunities with relativistic heavy ion accelerators [DE85-014190] N86-12117

STATISTICAL WEATHER FORECASTING

Spectral statistical forecasts of the 500 mb height field N86-11804

Prediction of monthly 700 mb heights using antecedent and simulated prognostic height predictors N86-11805

Effect of initialization on diagnoses of large-scale circulation statistics from WMC analyses N86-11817

STEADY STATE

A parameterization technique for nonlinear spectral models N86-11752

The effect of anomalous snow cover on the general circulation of the atmosphere using a simple climate model N86-11794

Steady-state detonation of charges of finite length N86-11966

Energy characteristics of laser with saturable anisotropic absorbing medium in cavity N86-11968

Chromium- and neodymium-activated gadolinium-scandium-gallium garnet crystal: A new laser active medium N86-11979

Implications of rf current drive theory for next step steady-state tokamak design [DE85-014753] N86-12083

STEAM TURBINES

Advanced mechanical heat pump technologies for industrial applications [DE85-014613] N86-11483

STEELS

Acoustic emission during deformation and fracture of A533B pressure vessel steel N86-11306

Uniaxial tensile deformation and fracture of dual-phase steels [DE85-015034] N86-11538

STELLAR EVOLUTION

Epsilon Aurigae in an evolutionary context N86-12174

STELLAR FLARES

Optical photometry of the 1982-1984 eclipse of Epsilon Aurigae N86-12169

STELLAR LUMINOSITY

Optical photometry of the 1982-1984 eclipse of Epsilon Aurigae N86-12169

Star formation in the inner galaxy: A far-infrared and radio study of two H2 regions [NASA-TM-86720] N86-12185

STELLAR MAGNETIC FIELDS

X-ray inverse Compton emission from the radio halo of M87 [NASA-CR-176305] N86-12196

X-ray inverse Compton emission from the radio halo of M87 [NASA-CR-176304] N86-12197

STELLAR OSCILLATIONS

Applications of the magneto-optical filter to stellar pulsation measurements [NASA-CR-176282] N86-12187

STELLAR TEMPERATURE

Infrared photometry of the 1982-4 eclipse of Epsilon Aurigae N86-12170

Epsilon Aurigae in an evolutionary context N86-12174

STIFFENING

Evaluation of superplastic forming and weld-brazing for fabrication of titanium compression panels N86-11245

STIFFNESS

The Shock and Vibration Digest, volume 17, no. 5 [AD-A156716] N86-11531

Stiffness and damping coefficients of rubber N86-11532

STIRLING CYCLE

An experimental study for a miniature Stirling refrigerator N86-11375

Parametric testing of a linearly driven Stirling cryogenic refrigerator N86-11376

Design of a flight qualified long-life cryocooler N86-11377

Simple construction and performance of a conical plastic cryocooler N86-11378

Effects of leakage through clearance seals on the performance of a 10 K Stirling-cycle refrigerator N86-11379

Experiments with a fully instrumented split Stirling cryocooler N86-11381

Low frequency split cycle cryocooler N86-11382

A nonproprietary, nonsecret program for calculating Stirling cryocoolers N86-11384

Dish electric systems heat engine assessment [DE85-013942] N86-11479

Advanced mechanical heat pump technologies for industrial applications [DE85-014613] N86-11483

RE-1000 free-piston Stirling engine update [NASA-TM-87126] N86-11668

Stirling cycle heat pump studies [DE85-005365] N86-11680

STOICHIOMETRY

Studies on chalcogenide films [AD-A157340] N86-11343

STOKES FLOW

Calculation of particle dynamics effects on laser velocimeter data N86-11438

STORAGE BATTERIES

Basic studies of the lithium secondary battery [AD-A157449] N86-11673

STORAGE RINGS (PARTICLE ACCELERATORS)

Design for a high field combined function superferric magnet [DE85-014827] N86-11944

Reduction of sextupole distortion by shuffling magnets in small groups [DE85-013024] N86-12035

Los Alamos proton storage ring fast-extraction kicker system [DE85-012663] N86-12093

Window frame or superferric magnet design for low B(3T) heavy ion storage ring study [DE85-013288] N86-12095

Beam position monitor for storage rings [DE85-013295] N86-12104

STORAGE STABILITY

Photovoltaic-powered vaccine refrigerator. Freezer systems field test results [NASA-TM-86972-REV] N86-11666

STRAIN GAGES

High temperature static strain sensor development program N86-11500

Demonstration test of burner liner strain measurement systems: Interim results N86-11501

STRAIN HARDENING

The hollow sphere model for porous metals and metal powders N86-11308

Uniaxial tensile deformation and fracture of dual-phase steels [DE85-015034] N86-11538

STRAIN RATE

Stress and strain-rate dependence of spall strength in two aluminum alloys [DE85-015154] N86-11321

Influence of effective rate sensitivity on adiabatic shear instability [DE85-013967] N86-11333

A body tensor formalism for elastic-plastic continua with applications in uniaxial extension N86-11491

Strain rate dependence in steady, plastic shock waves [DE85-014703] N86-11544

Mechanical threshold of dynamically deformed copper and nitronic 40 [DE85-010779] N86-11545

STRATIFICATION

On stratified vortex motions under gravity [AD-A156930] N86-11427

On cloud street development in three dimensional parallel and Rayleigh instabilities N86-11754

STRATIGRAPHY

Remote stratigraphic analysis: Combined TM and AIS results in the Wind River/Bighorn Basin area, Wyoming N86-11620

STRATOSPHERE
Lidar observations of stratospheric aerosol over Mauna Loa Observatory: 1982 - 1983 [PB85-187896] N86-11723
STREAK CAMERAS
Photoelectron trajectory analyses of streak tubes N86-11880
STREAM FUNCTIONS (FLUIDS)
A numerical study of global axisymmetric states and their stability to quasi-geostrophic disturbances N86-11753
STREAMS
Louisiana Water Resources Research Institute [PB85-218998] N86-11661
STRESS (PHYSIOLOGY)
An atropinized heat-stressed rat model: Anticholinergic and anticholinesterase drug potency [AD-A157620] N86-11832
STRESS ANALYSIS
Numerical simulation of an equipment hatch for a steel containment vessel to loading beyond the design basis [DE85-010485] N86-11482
Burner liner thermal/structural load modelling N86-11514
Component-specific modeling N86-11515
Stress analyses of B-52 pylon hooks [NASA-TM-84924] N86-11524
STRESS CONCENTRATION
The 3D inelastic analysis methods for hot section components N86-11516
Stress analyses of B-52 pylon hooks [NASA-TM-84924] N86-11524
Evaluation of concrete creep and stress redistribution in a prototypic PCRV following rupture of prestressing tendons [DE85-007673] N86-11543
STRESS CORROSION
Stress corrosion resistant fasteners N86-11235
STRESS CORROSION CRACKING
Intergranular attack and stress corrosion cracking of alloy 600 in high-temperature caustic solutions containing contaminants [DE85-014106] N86-11335
STRESS MEASUREMENT
High temperature static strain sensor development program N86-11500
Demonstration test of burner liner strain measurement systems: Interim results N86-11501
STRESS RATIO
Stress and strain-rate dependence of spall strength in two aluminum alloys [DE85-015154] N86-11321
STRESS-STRAIN RELATIONSHIPS
Life prediction and constitutive behavior N86-11520
STRESSES
Hermetic bellows seal for Braun linear engine: Design, test and demonstration [DE85-013545] N86-11478
Miniaturization of specimens for mechanical testing [DE85-014506] N86-11536
Mechanical threshold of dynamically deformed copper and nitronic 40 [DE85-010779] N86-11545
Perceptual and physiological responses during exercise in cool and cold water [AD-A157334] N86-11840
STRONG INTERACTIONS (FIELD THEORY)
High resolution spectrometer in studies of e(+)e(-) annihilation at (radical)s = 29 GeV [DE85-013870] N86-12065
STRONGLY COUPLED PLASMAS
A hybrid mode and a classification of beam plasma instabilities [AD-A157356] N86-12075
STRUCTURAL ANALYSIS
Aerodynamic and structural aspects of propeller and drive for a 1/5 scale wind tunnel programme N86-11163
Cabin noise reduction for a new development turboprop commuter aircraft N86-11173
Propeller aircraft cabin vibration and noise-excitation, sources, and paths N86-11174
Reliability analysis of series structural systems N86-11486
The stability of Timoshenko beams conveying a compressible fluid N86-11492
Turbine Engine Hot Section Technology (HOST) [NASA-CP-2289] N86-11495
HOST structural analysis program overview N86-11513
Burner liner thermal/structural load modelling N86-11514
Component-specific modeling N86-11515
Validation of structural analysis methods using burner liner cyclic rig test data N86-11518
Computational structural mechanics: A new activity at the NASA Langley Research Center [NASA-TM-87612] N86-11540
STRUCTURAL BASINS
Subsurface geology of the Pajarito Plateau, Espancia Basin, New Mexico [DE85-016215] N86-11720
Earthquake hazard research in the Los Angeles Basin and its offshore area, October 1, 1983 to September 30, 1984 [PB85-196491] N86-11725
STRUCTURAL DESIGN
Adhesives for aerospace N86-11249
ADS: A FORTRAN program for automated design synthesis: Version 1.10 [NASA-CR-177985] N86-11894
STRUCTURAL ENGINEERING
Bounded state control of linear systems with application to the active structural control N86-11493
STRUCTURAL FAILURE
Reliability analysis of series structural systems N86-11486
STRUCTURAL MEMBERS
Feasibility of remotely manipulated welding in space: A step in the development of novel joining technologies N86-11246
Advances in joining techniques used in development of SPF/DB titanium sandwich reinforced with metal matrices N86-11247
High-temperature adhesive development and evaluation N86-11250
Evaluation of a high temperature adhesive for fabricating graphite/PMR-15 polyimide structures N86-11268
Manual for LDEF tensile tests [NASA-TM-87624] N86-11299
STRUCTURAL PROPERTIES (GEOLOGY)
Geophysical Works, 1982, volume 30 N86-11702
Research on optic spatial frequency analysis of linear structures in remote sensing images N86-11927
STRUCTURAL RELIABILITY
Reliability analysis of series structural systems N86-11486
STRUCTURAL STABILITY
The stability of Timoshenko beams conveying a compressible fluid N86-11492
STRUCTURAL VIBRATION
Vibrations and structureborne noise in space station [NASA-CR-176291] N86-11220
Metallurgical characterization of the interfaces and the damping mechanisms in metal matrix composites [AD-A156507] N86-11300
On the computation of structural vibrations induced by a low-speed turbulent flow N86-12009
SUBLIMATION
Hydride absorption refrigerator system for ten Kelvin and below N86-11373
SUBMERGED BODIES
Numerical techniques for scattering from submerged objects N86-12013
SUBMILLIMETER WAVES
Submillimeter quantum electronics [AD-A157432] N86-11417
Submillimeter observations of OH and CH in M42 [NASA-TM-86723] N86-12186
Balloon-borne three-meter telescope for far-infrared and submillimeter astronomy [NASA-CR-176285] N86-12188
SUBROUTINES
User guide for WIFM-SAL (WES Implicit Flooding Model-SAL): A two-dimensional vertically integrated, time-varying estuarine transport model [AD-A157446] N86-11825
SUBSONIC AIRCRAFT
Some aeroacoustic wind tunnel measurements, theoretical predictions, and flight-test correlations on subsonic aircraft propellers N86-11170
SUBSONIC FLOW
A general theory of arbitrary motion aerodynamics using an aeroacoustic approach N86-11157
SUBSONIC SPEED
Wind tunnel investigation of the interaction of propeller slipstream with nacelle/wing/flap combinations N86-11166
SUBSTRATES
Electronic and magnetic structure of chromium surfaces and chromium monolayers on iron [DE85-014542] N86-11322
Processing and microstructural characterization of B4C-Al cermets [DE85-013195] N86-11326
SUBSTRUCTURES
Numerical method in dynamic response of nonlinear systems N86-12005
SULFUR COMPOUNDS
Integrated forest study on effects of atmospheric deposition. Project summary [DE85-015972] N86-11690
SULFUR DIOXIDES
Short-term methods for atmospheric corrosion testing: Survey of the literature [KIS-1985:5E] N86-11314
SULFUR FLUORIDES
Ring cavity CO2 laser for branch-selection and narrow resonance produced by SF6 in cavity N86-11930
SUMMER
Atmospheric general circulation model simulations of the modern Antarctic climate N86-11790
Transition from the Southern to Northern Hemisphere summer monsoon N86-11799
Tropospheric static stability and central North American rainfall during 1979 N86-11801
Concurrent and lagged relationships between precipitation frequency and 700 mb heights N86-11808
SUN
Figure of the Earth, moon, and planets N86-11550
The 1984 solar oscillation program of the Mount Wilson 60-foot tower [NASA-CR-176248] N86-12195
SUPERCONDUCTING MAGNETS
Four K refrigerators with a new compact heat exchanger N86-11391
Electrical supply for MFTF-B superconducting magnet system [DE85-012932] N86-12094
Window frame or superferric magnet design for low B(3T) heavy ion storage ring study [DE85-013288] N86-12095
SSC test lattices [DE85-014240] N86-12098
Materials studies for magnetic fusion energy applications at low temperatures. 7: Technical reports [DE85-014518] N86-12101
Superconducting Magnetic Energy Storage (SMES) Program [DE85-014250] N86-12106
Multivariable current control for electrically and magnetically coupled superconducting magnets, revision 1 [DE85-012943] N86-12108
Surface impedance of several magnetic superconductors [DE85-014101] N86-12155
SUPERCONDUCTIVITY
The relations between voltage and magnetic field of superconducting weaklink (1) N86-11934
The relations between voltage and magnetic field of superconducting weaklink (2) N86-11935
Discussion of the superconducting critical temperature in a N-S multi-film structure N86-11936
Magnetic measurements of monolayer-thickness films of Cr sandwiched by Au [DE85-015005] N86-12150
SUPERCONDUCTORS
Proceedings of the Third Cryocooler Conference [NASA-CR-176298] N86-11367
Design of cryocoolers for microwatt superconducting devices N86-11368
Theory of the critical temperature for superconductors with small lambda (1) N86-11937
Neutron scattering studies of the heavy Fermion superconductors [DE85-014829] N86-12144
Microscopic investigation of NbN sputtered films [DE85-015000] N86-12153
SUPERCRITICAL WINGS
Effect of aileron deflections on the aerodynamic characteristics of a semispan model of a subsonic energy-efficient transport [NASA-TP-2478] N86-11186
SUPERHIGH FREQUENCIES
The design of a thermally efficient 1:256 KU-band feed network for a MMIC phased array N86-11400
SUPERLATTICES
Investigation of defects in GaAsP superlattic structures [DE85-012134] N86-12139
Metallic multilayers and superlattices [DE85-014444] N86-12141
SUPERPLASTICITY
Solid-state bonding of superplastic aluminum alloy 7475 sheet N86-11244
Evaluation of superplastic forming and weld-brazing for fabrication of titanium compression panels N86-11245
Advances in joining techniques used in development of SPF/DB titanium sandwich reinforced with metal matrices N86-11247
SUPERSONIC AIRCRAFT
Recent developments in polyimide and bismaleimide adhesives N86-11270

SUPERSONIC FLOW
Theoretical analysis of linearized acoustics and aerodynamics of advanced supersonic propellers N86-11156
A general theory of arbitrary motion aerodynamics using an aeroacoustic approach N86-11157
Recent experience in seeding transonic/supersonic flows at AEDC N86-11447
Seeding subsonic, transonic and supersonic flows with 0.5 micron polystyrene spheres N86-11451
SUPERSONIC WAKES
Stability and interaction of coherent structure in supersonic reactive wakes N86-11185
SUPERSONIC WIND TUNNELS
Development of seeding techniques for small supersonic wind tunnel N86-11452
SURFACE CRACKS
Properties of crazes and deformation zones in glassy polymers [AD-A157428] N86-11346
SURFACE DEFECTS
Initial investigation of cryogenic wind tunnel model filler materials N86-11255
SURFACE FINISHING
Use of hydration inhibitors to improve bond durability of aluminum adhesive joints N86-11251
Initial investigation of cryogenic wind tunnel model filler materials N86-11255
SURFACE LAYERS
Electronic and magnetic structure of chromium surfaces and chromium monolayers on iron [DE85-014542] N86-11322
SURFACE PROPERTIES
Microscopic evaluation of a polyimide (PMR-15)-graphite composite N86-11282
Surface sampling techniques using ultraviolet illumination [AD-A156457] N86-11458
Numerical solution for contact pressure and wear distributions of unlubricated, misaligned, closely conforming, multiply connected surfaces N86-11472
Surface properties of shocked lead [DE85-009582] N86-11476
SURFACE ROUGHNESS
Validation of procedures for pavement design on expansive soils [FAA-PM-85-15] N86-11362
SURFACE TEMPERATURE
Global surface air temperature variations: 1983-1984 N86-11764
Blocking as an explanation of the severe cold of winter 1983-84 N86-11768
On the relationship between North Atlantic seasonal SST anomalies with United States surface temperature anomalies N86-11770
Towards understanding the geographical distribution and seasonality in persistance of monthly mean surface air temperature over the U.S.A. N86-11773
Global relationships with the Southern Oscillation N86-11776
Several aspects of interannual variability in the California current system N86-11785
Monthly forecast experiments with sea surface temperature anomaly forcings and envelope mountains: Preliminary results N86-11803
Specification of mean surface temperature anomalies in Europe and Asia during the fall months N86-11806
Land-surface fluctuations and associated climatic variability N86-11807
SURVEYS
CRCM and KAPG activity in recent crustal movement studies N86-11592
SWEPT WINGS
An asymptotic theory for the interference of large aspect ratio swept wings and multiple propeller slipstreams N86-11167
SWIRLING
Overview of solid particle LV seeding techniques used at UTRC N86-11445
SYNCHRONISM
Easy impossibility proofs for distributed concensus problems [AD-A157411] N86-11903
SYNCHRONOUS SATELLITES
Calculation of allowable orbital spacings for the fixed-satellite service [NASA-CR-176273] N86-11212
SYNCHROTRON RADIATION
Medical heavy ion accelerator proposals [DE85-015247] N86-12026
Increased intensity performance of the Brookhaven AGS [DE85-013371] N86-12091
Beam position monitor for storage rings [DE85-013295] N86-12104
X-ray inverse Compton emission from the radio halo of M87 [NASA-CR-176305] N86-12196
SYNCHROTRONS
Using the TEVATRON beam position monitor system to investigate transverse phase space [DE85-014261] N86-12105
SYNTHESIS (CHEMISTRY)
The synthesis, characterization and thermal chemistry of modified norbornenyl PMR endcaps N86-11266
Shock-wave synthesis of titanium aluminides [DE85-015140] N86-11324
Chemical synthesis under shock compression [DE85-015166] N86-11325
Synthesis of nickel-aluminum alloys by shock compression of composite particles [DE85-015165] N86-11328
Studies on the syntheses of boron hydride systems [AD-A157368] N86-11344
Analytical electron microscopy study of shock synthesized zinc ferrite [DE85-015144] N86-12140
SYNTHETIC FOOD
Utilization of non-conventional systems for conversion of biomass to food components: Potential for utilization of algae in engineered foods [NASA-CR-176257] N86-11830
SYSTEMS ANALYSIS
Photovoltaic-powered vaccine refrigerator: Freezer systems field test results [NASA-TM-86972-REV] N86-11666
Advanced Thermionic Technology Program: Summary report, Volume 3 [DE85-009360] N86-11674
SYSTEMS ENGINEERING
Problems experienced and envisioned for dynamical physical systems [NASA-TP-2508] N86-11215
The factory of the future N86-11228
Optimized ground-coupled heat pump system design for northern climate [DE85-014065] N86-11484
The Shock and Vibration Digest, volume 17, no. 4 [AD-A154112] N86-11527
Microcomputers in shock and vibration N86-11528
Computer-aided designing, engineering, preparation of production N86-11992

T

TABLES (DATA)
Regional Wind Energy Assessment Program. Appendix: Wind statistics summaries [DE85-011520] N86-11686
Global surface air temperature variations: 1983-1984 N86-11764
Recent unusual mean winter temperature across the contiguous United States N86-11772
Spectral statistical forecasts of the 500 mb height field N86-11804
Specification of mean surface temperature anomalies in Europe and Asia during the fall months N86-11806
TANKS (CONTAINERS)
High temperature molten salt containment [DE85-012152] N86-11433
TANTALUM
Short range bonding interaction at metal-metal interfaces [DE85-014442] N86-11334
Experimental check of bremsstrahlung dosimetry predictions for 0.75 MeV electrons [DE85-014706] N86-12058
TANTALUM OXIDES
Distributed-feedback lasers with active framing medium N86-11971
TARGET RECOGNITION
Ramp response estimation and spectrum extrapolation for ultrasonic scattering N86-11881
TEARING
Strength and flexibility properties of advanced ceramic fabrics [NASA-TM-86824] N86-11340
TECHNICAL WRITING
Improving the comprehensibility of a simulated technical manual [AD-A157482] N86-11889
TECHNOLOGY ASSESSMENT
Deputy minister on sector's technical progress N86-11178
USSR report: Machine tools and metalworking equipment [JPRS-UMM-85-010] N86-11394
Proceedings of the 1984 Antenna Applications Symposium [AD-A153257] N86-11398
FINESSE: Study of the issues, experiments and facilities for fusion nuclear technology research and development, volume 4 [DE85-010947] N86-12130
Distinct characteristics of science [DE85-006533] N86-12159
Research objectives and summary of research performed by the Massachusetts Institute of Technology Research Laboratory of Electronics [PR-127] N86-12164
Project to study the use of microcomputer technology in planning and operation of small city transportation systems [PB85-204873] N86-12166
TECHNOLOGY TRANSFER
The Shock and Vibration Digest, volume 17, no. 5 [AD-A156716] N86-11531
China report: Science and technology [JPRS-CST-85-014] N86-11918
USSR report: Science and technology policy [JPRS-UST-85-014] N86-11990
Book on planning of scientific, technical progress N86-11991
Problems, trends in technical education of researchers N86-11993
China report: Science and technology [JPRS-CST-85-015] N86-11994
TECHNOLOGY UTILIZATION
Research objectives and summary of research performed by the Massachusetts Institute of Technology Research Laboratory of Electronics [PR-127] N86-12164
TECTONICS
Results of KAPG co-operation in Earth tide research N86-11551
On reducing the effect of horizontal displacements of the lithospheric plates from the observations carried out by global geodynamic network (on example the GEOSS-REA network) N86-11589
Geckinematic models for the gravimetric W - E profile of the GDR N86-11596
TELECOMMUNICATION
Evaluation of the digital access and cross-connect system for use in the defense communications system [AD-A157570] N86-11412
Easy impossibility proofs for distributed concensus problems [AD-A157411] N86-11903
TELEMETRY
Balloon-borne three-meter telescope for far-infrared and submillimeter astronomy [NASA-CR-176285] N86-12188
TELEOPERATORS
Feasibility of remotely manipulated welding in space: A step in the development of novel joining technologies N86-11246
Teleoperator human factors study [NASA-CR-176310] N86-11854
Mechanical accessories for mobile teleoperators [DE85-014310] N86-11855
TELESCOPES
On the lunar tidal effect in the latitude observations at Tianjin N86-11565
TEMPERATE REGIONS
Warm and cold episodes in the California current: A case for large-scale mid-latitude atmospheric forcing N86-11786
TEMPERATURE
Fluids at high dynamic pressures and temperatures [DE85-014812] N86-11305
Temperature and precipitation trends in North America N86-11774
Monthly and Seasonal Weather Outlook for May 1985, Volume 39, Number 9 [PB85-199123] N86-11819
Investigation of efficiency of generation of difference-frequency laser radiation in waveguide N86-11969
TEMPERATURE CONTROL
Chemical control of rate and onset temperature of nadimide polymerization N86-11271
TEMPERATURE DEPENDENCE
Effects of additives and temperature on iron electrode behavior in KOH electrolytes [DE85-011901] N86-11423
Speed of sound in liquid sodium near gamma-transition point N86-11947
TEMPERATURE DISTRIBUTION
High temperature, short term tensile strength of C6000/PMR-15 composites N86-11279
Shock-induced temperature distributions in powder compact recovery fixtures [DE85-015139] N86-11359
Stiffness and damping coefficients of rubber N86-11532

Worldwide marine temperature variations on the season to century time scale N86-11771

TEMPERATURE EFFECTS

Characterization methodology for PMR-15 N86-11272

Effects of additives and temperature on iron electrode behavior in KOH electrolytes [DE85-011901] N86-11423

Numerical simulation of an equipment hatch for a steel containment vessel to loading beyond the design basis [DE85-010485] N86-11482

Viscoelastic creep of high-temperature concrete [DE85-010511] N86-11539

Concrete creep at transient temperature: Constitutive law and mechanism [DE85-010525] N86-11542

Deep levels in semi-insulating GaAs N86-11943

TEMPERATURE GRADIENTS

Thermal convection in snow [AD-A157577] N86-11648

Temperature and precipitation trends in North America N86-11774

Heat transfer and pressure changes due to a large temperature difference across an enclosed vertical air layer N86-11884

Energy confinement in a high-current reversed field pinch [DE85-015009] N86-12111

TEMPERATURE MEASUREMENT

An investigation of the effects of fuel composition on combustion characteristics in a T-63 combustor [AD-A157325] N86-11358

Fabrication and use of zircaloy/tantalum-sheathed cladding thermocouples [EGG-TFBP-6739] N86-11461

Dynamic gas temperature measurement system N86-11499

Modification of a Hughes tiltmeter to a borehole tiltmeter N86-11563

Variability simulations with a steady, linearized primitive equations model N86-11796

A sea surface temperature analysis based on in situ and satellite data N86-11816

TEMPERATURE MEASURING INSTRUMENTS

HOST instrumentation R and D program overview N86-11497

TEMPERATURE SENSORS

Development of heat flux sensors for turbine airfoils and combustor liners N86-11502

TEMPORAL DISTRIBUTION

Photoelectron trajectory analyses of streak tubes N86-11880

Efficiency of optically-pumped XeF-laser N86-11977

TENNESSEE

Effects of acid precipitation on composition, electrokinetic behavior, cation adsorption and ion exchange capacity in various soil systems [PB85-217727] N86-11698

TENSILE DEFORMATION

Uniaxial tensile deformation and fracture of dual-phase steels [DE85-015034] N86-11538

Mechanical threshold of dynamically deformed copper and nitronic 40 [DE85-010779] N86-11545

TENSILE PROPERTIES

Tensile properties of 2-1/4Cr-1Mo steel irradiated to 23 dpa at 390 to 550(0)C [DE85-015551] N86-11332

TENSILE STRENGTH

Evaluation of superplastic forming and weld-brazing for fabrication of titanium compression panels N86-11245

Factors affecting the processing of epoxy film adhesives N86-11252

Tensile fatigue damage and degradation of random short-fiber SWC composite N86-11259

Evaluation of a high temperature adhesive for fabricating graphite/PMR-15 polyimide structures N86-11268

High temperature, short term tensile strength of C6000/PMR-15 composites N86-11279

Effects of manufacturing processes on structural allowables [AD-A157596] N86-11318

Mechanical properties of rapidly solidified Type 304 stainless steel [DE85-014577] N86-11338

Miniaturization of specimens for mechanical testing [DE85-014506] N86-11536

TENSILE STRESS

A Signorini model of bolt fastened laminated composites N86-11258

Theoretical and experimental comparison of vapor cavitation in dynamically loaded journal bearings [NASA-TM-87121] N86-11425

TENSILE TESTS

High temperature, short term tensile strength of C6000/PMR-15 composites N86-11279

Manual for LDEF tensile tests [NASA-TM-87624] N86-11299

TENSOR ANALYSIS

A body tensor formalism for elastic-plastic continua with applications in uniaxial extension N86-11491

TERNARY ALLOYS

Surface and interfacial properties of Ga0.47In0.53As alloys [AD-A157343] N86-11316

TERRAIN

Remote sensing of earth terrain [NASA-CR-176284] N86-11645

Workshop on Permafrost Geophysics [AD-A157485] N86-11719

TEST EQUIPMENT

Evaluation of the digital access and cross-connect system for use in the defense communications system [AD-A157570] N86-11412

TEST FACILITIES

CRC control systems laboratory gyro test facility [CRC-1385] N86-11205

Evaluation of the digital access and cross-connect system for use in the defense communications system [AD-A157570] N86-11412

HOST liner cyclic facilities N86-11519

Electrical supply for MFTF-B superconducting magnet system [DE85-012932] N86-12094

FINESSE: Study of the issues, experiments and facilities for fusion nuclear technology research and development, volume 4 [DE85-010947] N86-12130

TEXAS

Evaluating the ground-water resources of the high plains of Texas, volume 3 [PB85-191617] N86-11655

TEXTBOOKS

The Shock and Vibration Digest, volume 17, no. 4 [AD-A154112] N86-11527

THEMATIC MAPPING

Remote stratigraphic analysis: Combined TM and AIS results in the Wind River/Bighorn Basin area, Wyoming N86-11620

Field utilization and analysis of AIS 128-channel imagery using microcomputers: Application to Yerington, Nevada field area N86-11621

Spectral characterization of suspected acid deposition damage in red spruce (Picea rubens) stands from Vermont N86-11624

Comparison of AIS versus TMS data collected over the Virginia piedmont N86-11637

THEORETICAL PHYSICS

USSR report: Physics and mathematics [JPRS-UPM-85-005] N86-11945

EPR: What has it taught us [DE85-014525] N86-12157

THERMAL ANALYSIS

The synthesis, characterization and thermal chemistry of modified norbornenyl PMR endcaps N86-11266

Processing science and technology N86-11297

High temperature molten salt containment [DE85-012152] N86-11433

THERMAL CONDUCTIVITY

Improved heat switch for gas sorption compressor N86-11372

Thermal convection in snow [AD-A157577] N86-11648

THERMAL EXPANSION

Initial investigation of cryogenic wind tunnel model filler materials N86-11255

An experimental reciprocating expander for cryocooler application N86-11380

THERMAL FATIGUE

Elevated temperature biaxial fatigue [NASA-CR-175009] N86-11526

THERMAL INSTABILITY

Cloud streets during KonTur: A comparison of parallel/thermal instability modes with observations N86-11755

THERMAL INSULATION

High temperature molten salt containment [DE85-012152] N86-11433

THERMAL NEUTRONS

Spin dependence of the coherent scattering lengths of (27)Al and admixture of s- and d-partial waves [DE85-013299] N86-12066

THERMAL RESISTANCE

An improved processible acetylene-terminated polyimide for composites N86-11262

THERMAL STABILITY

High-temperature adhesive development and evaluation N86-11250

Acetylene terminated matrix resins N86-11261

All-aromatic biphenylene end-capped polyquinoline and polyimide matrix resins N86-11267

Recent developments in polyimide and bismaleimide adhesives N86-11270

Characterization of polyimide matrix resins and prepregs N86-11273

Replacement of MDA with more oxidatively stable diamines in PMR-polyimides N86-11275

THERMAL STRESSES

Derivation and test of elevated temperature thermal-stress-free fastener concept N86-11236

Initial investigation of cryogenic wind tunnel model filler materials N86-11255

HOST structural analysis program overview N86-11513

Burner liner thermal/structural load modelling N86-11514

The 3D inelastic analysis methods for hot section components N86-11516

The 3-D inelastic analysis methods for hot section components (base program) N86-11517

Validation of structural analysis methods using burner liner cyclic rig test data N86-11518

A comparison of measured and calculated thermal stresses in a hybrid metal matrix composite spar cap element [NASA-TM-86729] N86-11525

Current research on circular saw and band saw vibration and stability N86-11533

Thermo-mechanical analyses of laser-heated surfaces N86-11877

THERMIONIC CONVERTERS

Advanced Thermionic Technology Program: Summary report, Volume 3 [DE85-009360] N86-11674

THERMIONIC EMISSION

Oxide cathode mechanisms: Electronic and structural features of oxide cathode surfaces [AD-A157666] N86-11418

THERMOCHEMISTRY

Chemical thermodynamic assessment of the Li-U-O system for possible space nuclear applications [DE85-015060] N86-12054

THERMOCOUPLES

Fabrication and use of zircaloy/tantalum-sheathed cladding thermocouples [EGG-TFBP-6739] N86-11461

THERMODYNAMIC CYCLES

Design of cryocoolers for microwatt superconducting devices N86-11368

THERMODYNAMIC EFFICIENCY

Low frequency split cycle cryocooler N86-11382

THERMODYNAMIC EQUILIBRIUM

Vacancies in thermal equilibrium in Nb [DE85-014832] N86-12061

THERMODYNAMIC PROPERTIES

Low-cost, net-shape ceramic radial turbine program [AD-A157532] N86-11202

Factors affecting the processing of epoxy film adhesives N86-11252

Mechanical properties of Inconel 718 and Nickel 201 alloys after thermal histories simulating brazing and high temperature service [NASA-CR-177940] N86-11312

Thermodynamics of chromium and iron in carbonate salts at 650(0)C [DE85-013542] N86-11682

USSR report: Physics and mathematics [JPRS-UPM-85-005] N86-11945

General-purpose equipment for airborne laser remote sensing of ocean, atmosphere and agricultural crops N86-11984

THERMODYNAMICS

Infrared thermography: An analytical tool for high temperature and fast response [DE85-013826] N86-11462

Component-specific modeling N86-11515

Hydrothermodynamics of the near-surface layer of a liquid and optical methods of investigating it N86-11989

THERMOGRAPHY

Infrared thermography: An analytical tool for high temperature and fast response [DE85-013826] N86-11462

THERMONUCLEAR POWER GENERATION

Center for High Temperature Plasma Physics certified N86-11997

THERMONUCLEAR REACTIONS

Controlled thermonuclear fusion, high temperature plasma physics N86-11998

THERMOPHYSICAL PROPERTIES

An experimental reciprocating expander for cryocooler application N86-11380

THERMOPLASTIC RESINS

Matrix resin development at NASA Langley Research Center N86-11264

Characterization of the relationship of the cure cycle chemistry to cure cycle processing properties
[NASA-CR-176256] N86-11339

THERMOPLASTICITY
Constituent materials N86-11294

THERMOREGULATION
An atropinized heat-stressed rat model: Anticholinergic and anticholinesterase drug potency
[AD-A157620] N86-11832

THERMOSETTING RESINS
An improved processible acetylene-terminated polyimide for composites N86-11262
Matrix resin development at NASA Langley Research Center N86-11264

THICK FILMS
Optical modeling of multilayer thin/thick films N86-11862

THICK PLATES
Thin plates with rapidly varying thickness, and their relation to structural optimization
[AD-A157607] N86-11534

THICKNESS
Corrosion testing by radiographic methods
[BLL-BISI-TRANS-23201-(9022.06)] N86-11310
Recent vertical crustal movements of the Carpathian-Balkan region and their relationship with neotectonic movements and geophysical fields N86-11609

THIN FILMS
Rotating film radiators for space applications
[DE85-009633] N86-11431
Optical modeling of multilayer thin/thick films N86-11862
Distributed-feedback lasers with active framing medium N86-11971
Ellipsometric and optical study of some uncommon insulator films on 3-5 semiconductors
[NASA-TM-87135] N86-12134
Thin film research. Volume 1
[AD-A157608] N86-12137
Thin film research. Volume 2
[AD-A157609] N86-12138
Formation, ion modification and annealing of VN
[DE85-012896] N86-12146
Microscopic investigation of NbN sputtered films
[DE85-015000] N86-12153

THIN PLATES
Stability and interaction of coherent structure in supersonic reactive wakes N86-11185
Feasibility of remotely manipulated welding in space: A step in the development of novel joining technologies N86-11246
Advances in joining techniques used in development of SPF/DB titanium sandwich reinforced with metal matrices N86-11247
Rapid adhesive bonding and field repair of aerospace materials N86-11253
Thin plates with rapidly varying thickness, and their relation to structural optimization
[AD-A157607] N86-11534
Reflection of sound from plate containing periodic inhomogeneities N86-11951
Transformation of light pulse shape by thin plane-parallel layer of absorbing material N86-11988

THIN WINGS
Application of the vortex-lattice concept to flows with smooth-surface separation
[AD-A157571] N86-11430

THOMSON SCATTERING
Los Alamos Spheromak Program
[DE85-012769] N86-12096

THREE BODY PROBLEM
Figure of the Earth, moon, and planets N86-11550

THREE DIMENSIONAL BOUNDARY LAYER
Assessment of a 3-D boundary layer code to predict heat transfer and flow losses in a turbine N86-11508

THREE DIMENSIONAL FLOW
Aerodynamic method used in France for advanced fast propeller study N86-11149
Application of the vortex-lattice concept to flows with smooth-surface separation
[AD-A157571] N86-11430
Block-implicit coupled calculation of fluid flows
[DE85-004038] N86-11432
Block-implicit multigrid calculation of three-dimensional recirculating flows
[DE85-010250] N86-11434
Gas flow environmental and heat transfer nonrotating 3D program N86-11506
On cloud street development in three dimensional parallel and Rayleigh instabilities N86-11754

THRESHOLD CURRENTS
Lasing on vapors of chain compounds N86-11967

THRUST AUGMENTATION
A novel oscillating jet: Its effect on ejector thrust augmentation
[AD-A157480] N86-11201

THRUST BEARINGS
Lateral dampers for thrust bearings
[NASA-CR-174924] N86-11474

THRUST CHAMBER PRESSURE
The analysis and calculation for the dynamic characteristics of the omni-axial movable flexible joint nozzle N86-11925

THRUST REVERSAL
Application of Gr/PMR-15 to commercial aircraft N86-11269

THRUST VECTOR CONTROL
Preliminary design study of a lateral-directional control system using thrust vectoring
[NASA-TM-86425] N86-11203
The analysis and calculation for the dynamic characteristics of the omni-axial movable flexible joint nozzle N86-11925

THYROID GLAND
Thyroid absorbed dose for people at Rongelap, Utirik and Sifo on March 1, 1954
[DE85-014695] N86-11846

TIDAL WAVES
Interactions between oceanic and gravity tides, as analysed from world-wide Earth tide observations and ocean models N86-11576

TIDEPOWER
Interactions between oceanic and gravity tides, as analysed from world-wide Earth tide observations and ocean models N86-11576

TIDES
Proceedings of the 5th International Symposium Geodesy and Physics of the Earth, part 2
[REPT-81-PT-2] N86-11568
Ocean tidal loading along the Blue Road geotraverse in Fennoscandia N86-11571
On the comparison and choice between the formulas of the Earth tidal correction in astronomical time and latitude observation N86-11588

TILTMETERS
Modification of a Hughes tiltmeter to a borehole tiltmeter N86-11563
Stationary hydrostatic precision tiltmeter system N86-11607
A new apparatus for testing bubble vials, electronic levels and automatic levels N86-11614

TIME
Influences of systematic differences between different star catalogues on the results of latitude and time determinations with the PZT 2 N86-11575
Time-averaging the flux-profile relationship N86-11789

TIME DEPENDENCE
Stability and interaction of coherent structure in supersonic reactive wakes N86-11185
Seeding requirements for scanning laser velocimetry N86-11446
Adjustment of the latitude data by least-squares collocation approach N86-11562
Travel-time and its residuals for the blasts from Eschenlohe (Bavaria) N86-11706
The Hadley and Rossby regimes in a spherical atmosphere N86-11751
On the relationship between North Atlantic seasonal SST anomalies with United States surface temperature anomalies N86-11770
Prediction of monthly 700 mb heights using antecedent and simulated prognostic height predictors N86-11805
Calculation of formation time of minimal nucleus of flame during ignition of explosive mixtures by electrical discharges N86-11963
Fractal-like, but non-fractal, behavior of one step dipolar energy transfer on regular lattices with excluded volume
[AD-A157382] N86-12136

TIME FUNCTIONS
The irregularity in the Earth's annual rotation as a cause of systematic time variation N86-11570

TIME MEASUREMENT
Some short periodic terms due to nutation and tides from latitude and time determinations at Czechoslovak observatories N86-11566
Results concerning rheological parameters of the Earth N86-11567
Influences of systematic differences between different star catalogues on the results of latitude and time determinations with the PZT 2 N86-11575
Is the cerebellum involved in motor and perceptual timing: A case study
[AD-A157452] N86-11842

TIME SERIES ANALYSIS
Time series modeling of the Southern Oscillation N86-11777

An observational study of the vertical structure of interannual wind fluctuations in the tropics N86-11810
Climate system fluctuations, monitoring N86-11814

TIMOSHENKO BEAMS
The stability of Timoshenko beams conveying a compressible fluid N86-11492

TIN TELLURIDES
Pb(1-x)Sn(x)Te and Pb(1-y)Sn(y)Se laser crystals N86-11931

TIP SPEED
Comparison of calculated and measured velocities near the tip of a model rotor blade at transonic speeds
[NASA-TM-86697] N86-11196

TIROS SATELLITES
TIROS/NOAA (Television and Infrared Observation Satellite/National Oceanic and Atmospheric Administration) satellites space environment monitor archive tape documentation
[PB85-167920] N86-11724

TITANIUM
Rapid adhesive bonding and field repair of aerospace materials N86-11253
A comparison of measured and calculated thermal stresses in a hybrid metal matrix composite spar cap element
[NASA-TM-86729] N86-11525

TITANIUM ALLOYS
Evaluation of superplastic forming and weld-brazing for fabrication of titanium compression panels N86-11245
Advances in joining techniques used in development of SPF/DB titanium sandwich reinforced with metal matrices N86-11247
Deformation and fracture of P/M titanium alloys
[AD-A157416] N86-11317
Shock-wave synthesis of titanium aluminides
[DE85-015140] N86-11324
Improvement in wear performance of surgical Ti-6Al-4V alloy by ion implantation of nitrogen or carbon
[DE85-013986] N86-11849

TITANIUM OXIDES
Seeding requirements for scanning laser velocimetry N86-11446

TOBACCO
Acute pulmonary effects of formaldehyde exposure in humans
[DE85-014728] N86-11848

TOKAMAK DEVICES
Double tearing mode in plasma with magnetic braiding N86-11919
Center for High Temperature Plasma Physics certified N86-11997
Effects of trapped alpha particles on ballooning modes in tokamaks
[DE85-015064] N86-12082
Implications of rf current drive theory for next step steady-state tokamak design
[DE85-014753] N86-12083
Tokamak startup: Problems and scenarios related to the transient phases of ingnited tokamak operations
[DE85-015321] N86-12085
Spherical torus: An approach to compact fusion at low field. Initial ignition assessments
[DE85-012890] N86-12099

TOLERANCES (PHYSIOLOGY)
Assessments and viewpoints on the biological and human health effects of Extremely Low Frequency (ELF) electromagnetic fields: Compilation of commissioned papers for the ELF literature review project
[AD-A156942] N86-11839
Health hazard evaluation of liquid monopropellants. Phase 4. Subchronic inhalation of hydroxylammonium nitrate, January 1985
[AD-A157623] N86-11844

TOPOGRAPHY
A new approach to iterations in solving geodetic boundary value problems for real topography N86-11569
Research on the computational methods of gravity topographic effect N86-11578
On the long-wavelength correlation between gravity and topography N86-11586
Finnish measurements of the Fennoscandian land uplift gravity lines in Finland 1966-1984 N86-11606
The effect of topography on the evolution of unstable disturbances in a baroclinic atmosphere N86-11750
A numerical study of global axisymmetric states and their stability to quasi-geostrophic disturbances N86-11753

TOPOLOGY
A parameterization technique for nonlinear spectral models N86-11752

TORNADOES
Minimum assumption tornado hazard probability model
[PB85-206082] N86-11821

TORQUE
On the influence of coupling torques between the Earth's core and mantle on parameters and components of the rotation of the Earth N86-11572
TORUSES
Recent FRC translation experiments on FRX-C/T [DE85-012745] N86-12132
TOWING
Seeding techniques used in the Vortex Research Facility N86-11443
TOXICITY
Applied model validation [NBSIR-85-3154-1] N86-11363
TOXICOLOGY
Assessments and viewpoints on the biological and human health effects of Extremely Low Frequency (ELF) electromagnetic fields: Compilation of commissioned papers for the ELF literature review project [AD-A158942] N86-11839
TOXINS AND ANTITOXINS
Importance of phytoalexin tolerance and detoxification for pathogenicity [DE85-014759] N86-11257
TRACE ELEMENTS
Tracer test analysis of the Klamath Falls geothermal resource: A comparison of models [DE85-009924] N86-11678
TRACTION
Railgun power supply system utilizing traction motors and vacuum interrupters [DE85-014123] N86-11214
TRAINING ANALYSIS
A flash X-ray facility for the Naval Postgraduate School [AD-A157278] N86-11213
TRAJECTORY OPTIMIZATION
Design of maneuverable trajectories of re-entry vehicle N86-11920
TRANSFER FUNCTIONS
SIG: A general-purpose signal processing code N86-11876
TRANSFER OF TRAINING
Problems, trends in technical education of researchers N86-11993
TRANSFORMATIONS (MATHEMATICS)
Treatment of the geodetic boundary value problem by contact-transformation N86-11573
TRANSIENT RESPONSE
Upgrade of the EM transient range monocone antenna [DE85-013181] N86-11413
Investigations of deep level defects in semiconductor material systems N86-12133
TRANSITION FLOW
Nuclear interlevel transfer driven by electronic transitions [DE85-014103] N86-12149
TRANSITION METALS
Investigations of deep level defects in semiconductor material systems N86-12133
TRANSITION TEMPERATURE
Speed of sound in liquid sodium near gamma-transition point N86-11947
TRANSLATING
Three-dimensional heat transfer analysis using the PATRAN-G solids modeling and Q-TRAN thermal analysis computer codes N86-11867
TRANSLATIONAL MOTION
Recent FRC translation experiments on FRX-C/T [DE85-012745] N86-12132
TRANSLATORS
A data translator for engineering measurements N86-11875
TRANSMISSION LINES
Design and optimization of the PBFA 2 vacuum interface and transmission lines for light ion fusion [DE85-012609] N86-12092
Low inductance diode design of the Proto 2 accelerator for imploding plasma loads [DE85-013783] N86-12123
TRANSMISSION LOSS
Application of high order acoustic finite elements to transmission losses and enclosure problems N86-12008
TRANSMITTANCE
Optical modeling of multilayer thin/thick films N86-11862
TRANSONIC FLOW
Aerodynamic method used in France for advanced fast propeller study N86-11149
Refined numerical solutions of the transonic flow past a wedge N86-11184
Shock fitting applied to the prediction of high-speed rotor noise [NASA-TM-86781] N86-11188
Estimation of particle size based on LDV measurements in a de-accelerating flow field N86-11440
Recent experience in seeding transonic/supersonic flows at AEDC N86-11447
Laser velocimetry measurement in a transonic tunnel N86-11448
Seeding subsonic, transonic and supersonic flows with 0.5 micron polystyrene spheres N86-11451
TRANSONIC WIND TUNNELS
NTF: Soldering technology development for cryogenics N86-11231
Laser velocimetry measurement in a transonic tunnel N86-11448
Particle generation experience in Langley's 16-foot transonic tunnel N86-11449
TRANSPARENCE
A summary report on the Flat-Plate Solar Array Project Workshop on Transparent Conducting Polymers [NASA-CR-176302] N86-11669
TRANSPORT AIRCRAFT
A review of advanced turboprop transport activities N86-11148
Problems of the integration of propellers in airframes, especially for high performance twin-engine aircraft N86-11165
Effect of aileron deflections on the aerodynamic characteristics of a semispan model of a subsonic energy-efficient transport [NASA-TP-2478] N86-11186
TRANSPORT PROPERTIES
Reduction of moisture effects during the cure of epoxy adhesives used in composite repair N86-11254
Energy confinement in a high-current reversed field pinch [DE85-015009] N86-12111
Comparison of energy transport measurements and computer simulations in a single module prototype for PBFA 2 [DE85-013860] N86-12119
TRANSPORTATION
USSR report: Transportation [JPRS-UTR-85-011] N86-11177
Transportation system impact limiter design using rigid polyurethane foam [DE85-015088] N86-11354
Project to study the use of microcomputer technology in planning and operation of small city transportation systems [PB85-204873] N86-12166
TRANSVERSE WAVES
Distributed-feedback lasers with active framing medium N86-11971
Using the TEVATRON beam position monitor system to investigate transverse phase space [DE85-014261] N86-12105
TRAPPED PARTICLES
Effects of trapped alpha particles on ballooning modes in tokamaks [DE85-015064] N86-12082
TRAPPING
Vacancies in thermal equilibrium in Nb [DE85-014832] N86-12061
TREES (PLANTS)
Spectral characterization of suspected acid deposition damage in red spruce (Picea rubens) stands from Vermont N86-11624
TRENDS
Temperature and precipitation trends in North America N86-11774
TRIANGULATION
Determination of crustal movements in the high Tatra Mountains N86-11605
TRIBOLOGY
Transfer molding of PMR-15 polyimide resin N86-11288
TRIGATRONS
Cascade switch implementation of PBFA 1 [DE85-013955] N86-12039
TRIGGER CIRCUITS
Cascade switch implementation of PBFA 1 [DE85-013955] N86-12039
TRITIUM
Tokamak startup: Problems and scenarios related to the transient phases of ingnited tokamak operations [DE85-015321] N86-12085
TROPICAL METEOROLOGY
Proceedings of the 9th Annual Climate Diagnostics Workshop [PB85-183911] N86-11763
Understanding El Nino events using a simple dynamical atmosphere model N86-11797
Tropical convection and North American cyclones during the 1982-83 El Nino N86-11809
TROPICAL REGIONS
The effect of the Hadley circulation on the meridional propagation of stationary waves N86-11732
Review of the climate of fall 1983 and winter 1983-84 N86-11766
Circulation and weather for MAM and JJA 1984 N86-11769
The impact of heat sources in the tropics on the atmospheric circulation N86-11793
An observational study of the vertical structure of interannual wind fluctuations in the tropics N86-11810
Slow fluctuations of the tropical circulation during the FGGE year N86-11812
Very anomalous behavior of outgoing longwave radiation in the tropics in 1983-84: Aftermath of ENSO? N86-11813
Observing the Eastern Pacific Hadley Circulation N86-11818
TROPOSPHERE
Uncertainties in the radiative properties of smoke and their effects on climate assessments [DE85-015187] N86-11691
Review of the climate of fall 1983 and winter 1983-84 N86-11766
Circulation and weather for MAM and JJA 1984 N86-11769
Satellite observations of a large-amplitude 40-50 day oscillation in upper tropospheric temperature over the equatorial Pacific Ocean during the 1982-83 ENSO event N86-11778
The annual variation in the vertical structure of the 40-50-day tropical oscillation N86-11780
Tropospheric static stability and central North American rainfall during 1979 N86-11801
Specification of mean surface temperature anomalies in Europe and Asia during the fall months N86-11806
TRUNCATION ERRORS
Refined numerical solutions of the transonic flow past a wedge N86-11184
Computational errors and their control in the determination of satellite orbits N86-11211
Precise geoid computations at mountainous coastlines in view of vertical datum determinations N86-11561
TUNABLE LASERS
Pb(1-x)Sn(x)Te and Pb(1-y)Sn(y)Se laser crystals N86-11931
High-efficiency Al sub 2 O sub 3:Ti sup 3+ tunable laser N86-11973
Double-wavelength pulsed tunable dye laser N86-12003
Physics overview of AVLIS [DE85-014854] N86-12057
TUNGSTEN ALLOYS
Fabrication and use of zircaloy/tantalum-sheathed cladding thermocouples [EGG-TFBP-6739] N86-11461
TUNING
Investigation of efficiency of generation of difference-frequency laser radiation in waveguide N86-11969
TUNNEL DIODES
Discussion of the superconducting critical temperature in a N-S multi-film structure N86-11936
TURBINE BLADES
Evaluation of candidate materials in a static turbine cascade [DE85-008592] N86-11480
Development of heat flux sensors for turbine airfoils and combustor liners N86-11502
Assessment of a 3-D boundary layer code to predict heat transfer and flow losses in a turbine N86-11508
Gas-side heat transfer with rotation N86-11509
Coolant passage heat transfer with rotation. A progress report on the computational aspects N86-11510
The 3D inelastic analysis methods for hot section components N86-11516
The 3-D inelastic analysis methods for hot section components (base program) N86-11517
Life prediction and constitutive behavior N86-11520
Vertical axis wind turbine power regulation through centrifugally pumped lift spoiling [DE85-013787] N86-11679
TURBINE ENGINES
Turbine engine Hot Section Technology (HOST) project N86-11496
HOST instrumentation R and D program overview N86-11497
Assessment of a 3-D boundary layer code to predict heat transfer and flow losses in a turbine N86-11508
TURBOCOMPRESSORS
Airflow calibration of a bellmouth inlet for measurement of compressor airflow in turbine-powered propulsion simulators [NASA-TM-84399] N86-11209
TURBOMACHINERY
Development of an explicit multigrid algorithm for quasi-three-dimensional viscous flows in turbo-machinery [NASA-TM-87128] N86-11146

Laser anemometry for hot section applications
N86-11503

TURBOPROP AIRCRAFT

A review of advanced turboprop transport activities
N86-11148

Summary of recent NASA propeller research
N86-11158

Development of modern turboprop engines
N86-11168

An investigation of in-flight near-field propeller noise generation and transmission N86-11171

Cabin noise reduction for a new development turboprop commuter aircraft N86-11173

Propeller aircraft cabin vibration and noise-excitation, sources, and paths N86-11174

Application of active noise control to model propeller noise N86-11176

TURBOPROP ENGINES

A review of advanced turboprop transport activities
N86-11148

TURBULENCE

Block-implicit coupled calculation of fluid flows
[DE85-004038] N86-11432

LDA seeding system for the Langley Low Turbulence Pressure Tunnel N86-11450

Measurements of refractive index structure function C2N and aerosol size distribution at Chesapeake Bay
[AD-A157455] N86-11717

A model of a downburst, a wind tunnel program on planetary boundary layer, and airship in turbulence
N86-11748

TURBULENCE EFFECTS

On the computation of structural vibrations induced by a low-speed turbulent flow N86-12009

TURBULENT BOUNDARY LAYER

The measurements of axisymmetric air turbulent jet flow with an individual realization laser velocimeter system
[AD-A157554] N86-11429

Parameterization of the atmospheric boundary layer for air pollution dispersion models
[PB85-193546] N86-11730

On the computation of structural vibrations induced by a low-speed turbulent flow N86-12009

Vortex studies relating to boundary layer turbulence and noise N86-12015

TURBULENT FLOW

The measurements of axisymmetric air turbulent jet flow with an individual realization laser velocimeter system
[AD-A157554] N86-11429

Seeding requirements for scanning laser velocimetry
N86-11446

Time-averaging the flux-profile relationship
N86-11789

A hybrid vortex-in-cell finite-difference numerical method for turbulent shear layer computation N86-11886

On the computation of structural vibrations induced by a low-speed turbulent flow N86-12009

TWO DIMENSIONAL FLOW

Water tunnel flow visualization using a laser
[NASA-TM-86743] N86-11206

On cloud street development in three dimensional parallel and Rayleigh instabilities N86-11754

TWO PHASE FLOW

Introduction to the session on: Numerical methods for two-phase flow
[DE85-012651] N86-11435

A time-splitting numerical technique for solving highly coupled two-phase flow conservation equation
N86-11879

One-dimensional two-phase flow in combustion chamber of solid propellant rocket motors N86-11921

TWO-WAVELENGTH LASERS

Two-frequency passive mode locking in iodine photodissociation laser N86-11980

Double-wavelength pulsed tunable dye laser
N86-12003

U

U.S.S.R.

Formation, distribution and variability in snow cover on the Asian territory of the USSR
[NASA-TM-77913] N86-11734

USSR report: Physics and mathematics
[JPRS-UPM-85-005] N86-11945

ULTRAHIGH VACUUM

Oxide cathode mechanisms: Electronic and structural features of oxide cathode surfaces
[AD-A157666] N86-11418

ULTRASONIC RADIATION

Analysis of ultrasonic waves in a bounded medium
N86-11869

Ramp response estimation and spectrum extrapolation for ultrasonic scattering N86-11881

Diffraction of ultrasonic beam passing normally through layered media N86-11946

ULTRASONIC TESTS

Nondestructive ultrasonic measurement of bolt preload using the pulsed-phase locked-loop interferometer
N86-11242

ULTRASONIC WAVE TRANSDUCERS

Ramp response estimation and spectrum extrapolation for ultrasonic scattering N86-11881

ULTRASONICS

USSR report: Physics and mathematics
[JPRS-UPM-85-005] N86-11945

A general-applications direct global matrix algorithm for rapid seismo-acoustic wavefield computations
N86-12012

Part A. Molecular dynamics and ionic associations of LiAsF6 in 4-butyrolactone mixtures with 2-methyl tetrahydrofuran. Part B. Molecular dynamics and ionic associations of LiBF4 in 1,2-dimethoxymethane
[AD-A157401] N86-12023

ULTRAVIOLET ASTRONOMY

The eclipse of Epsilon Aurigae visible spectroscopy and ultraviolet activity N86-12173

ULTRAVIOLET LASERS

Mercury bromide reconstitution in the HgBr laser system
[AD-A156502] N86-11466

Ultraviolet lasing in helium-nitrogren mixtures
N86-11974

ULTRAVIOLET PHOTOGRAPHY

Surface sampling techniques using ultraviolet illumination
[AD-A156457] N86-11458

ULTRAVIOLET PHOTOMETRY

UBV photometry of the 1982-4 eclipse of Epsilon Aurigae: A discussion of the observed light curves
N86-12176

Astronomical research at the Hopkins Phoenix Observatory N86-12182

ULTRAVIOLET RADIATION

Polymer glazings for silver mirrors
[DE85-012140] N86-11357

Cause of occurrence of high-energy ions during UV laser irradiation of molecular crystals N86-11953

OMEGA: A 24 beam UV irradiation facility
[DE85-014416] N86-12127

ULTRAVIOLET SPECTRA

Scattered light in the IUE spectra of Epsilon Aurigae
N86-12180

ULTRAVIOLET SPECTROSCOPY

Photoelectric observations of the long-period eclipsing binaries at Yonsei University Observatory N86-12184

UNDERGROUND STRUCTURES

Bibliography of terrestrial impact structures
[NASA-TM-87567] N86-11701

UNDERWATER ACOUSTICS

Development of castor-oil-resistant polyurethane sonar encapsulants
[AD-A157576] N86-11347

Use of the wavenumber technique with the Lloyds mirror for an acoustic doublet
[AD-A156463] N86-11824

A general-applications direct global matrix algorithm for rapid seismo-acoustic wavefield computations
N86-12012

Numerical techniques for scattering from submerged objects N86-12013

Intermediate and high-frequency acoustic backscattering cross sections for water-ice interfaces. 1: Two-component profile models
[AD-A157533] N86-12018

UNDERWATER STRUCTURES

Bibliography of terrestrial impact structures
[NASA-TM-87567] N86-11701

UNITED KINGDOM

Worldwide marine temperature variations on the season to century time scale N86-11771

UNITED STATES

Regional oxidant modeling of the northeast US
[PB85-201192] N86-11728

Review of the climate of fall 1983 and winter 1983-84
N86-11766

On the relationship between North Atlantic seasonal SST anomalies with United States surface temperature anomalies N86-11770

Towards understanding the geographical distribution and seasonality in persistance of monthly mean surface air temperature over the U.S.A. N86-11773

Land-surface fluctuations and associated climatic variability N86-11807

UNIVERSITIES

A computer engineering curriculum for the Air Force Academy: An implementation plan
[AD-A156464] N86-11857

NASA-universities relationships in aero/space engineering: A review of NASA's program
[NASA-CR-176307] N86-12158

UNSTEADY FLOW

A general theory of arbitrary motion aerodynamics using an aeroacoustic approach N86-11157

A novel oscillating jet: Its effect on ejector thrust augmentation
[AD-A157480] N86-11201

Calculation of particle dynamics effects on laser velocimeter data N86-11438

Flame propagation in pulsed acceleration field
N86-11964

UPPER ATMOSPHERE

Some empirical evidence for the influence of snow cover on temperature and precipitation N86-11767

URANIUM

Chemical thermodynamic assessment of the Li-U-O system for possible space nuclear applications
[DE85-015060] N86-12054

USER MANUALS (COMPUTER PROGRAMS)

User's manual for a 0.3-m TCT wall interference assessment/correction procedure: 8- by 24-inch airfoil test section
[NASA-TM-87582] N86-11189

User's manual for AC-20-53A protection of airplane fuel systems against fuel vapor ignition due to lightning
[AD-A157619] N86-11191

Applied model validation
[NBSIR-85-3154-1] N86-11363

NERF: A computer program for the numerical evaluation of reliability functions user manual
[ARL/STRUC-R-411] N86-11487

KRASH85 user's guide: Input/output format
[FAA-CT-85-10] N86-11898

Approximate reasoning and the REVEAL software system. Users guide
[AD-A157298] N86-11902

UTILIZATION

Applications of the magneto-optical filter to stellar pulsation measurements
[NASA-CR-176282] N86-12187

V

V/STOL AIRCRAFT

A comparison of the NAVTOLAND (Navy vertical takeoff and landing) SH-2F helicopter model with the requirements of MIL-H-8501A and with flight data
[AD-A157297] N86-11198

VACANCIES (CRYSTAL DEFECTS)

Vacancies in thermal equilibrium in Nb
[DE85-014832] N86-12061

VACCINES

Photovoltaic-powered vaccine refrigerator: Freezer systems field test results
[NASA-TM-86972-REV] N86-11666

VACUUM

Railgun power supply system utilizing traction motors and vacuum interrupters
[DE85-014123] N86-11214

The vacuum in the presence of electromagnetic fields and rotating boundaries N86-11916

VALLEYS

Electromagnetic soundings for geothermal resources in Dixie Valley, Nevada
[DE85-011986] N86-11722

VALVES

Joule-Thomson valves for long term service in space cryocoolers N86-11393

VANADIUM

Formation, ion modification and annealing of VN
[DE85-012896] N86-12146

VAPOR DEPOSITION

Improvements in the fabrication of ceramic-fiber-ceramic-matrix composites by chemical vapor infiltration
[DE85-015971] N86-11301

VAPOR PHASE EPITAXY

Pb(1-x)Sn(x)Te and Pb(1-y)Sn(y)Se laser crystals
N86-11931

VAPOR PHASES

Hydrodynamics of liquid-vapor disperse annular flows in channels containig bundles of heated rods under nonsteady-state conditions N86-11954

Lasing on vapors of chain compounds N86-11967

VAPOR PRESSURE

Reduction of moisture effects during the cure of epoxy adhesives used in composite repair N86-11254

VAPORS

Seeding techniques used in the Vortex Research Facility N86-11443

VARIABILITY

Interannual climate variability in a low vertical resolution spectral atmospheric model N86-11795

Variability simulations with a steady, linearized primitive equations model N86-11796

VARIATIONAL PRINCIPLES
Variational principles for Earth rotation N86-11580
On the implementation of a class of upwind schemes for system of hyperbolic conservation laws [NASA-TM-86839] N86-11907

VARIATIONS
Worldwide marine temperature variations on the season to century time scale N86-11771
An observational study of the vertical structure of interannual wind fluctuations in the tropics N86-11810
Slow fluctuations of the tropical circulation during the FGGE year N86-11812
Flame propagation in pulsed acceleration field N86-11964

VECTOR ANALYSIS
On the distribution of the residual vectors of Earth's tide gravity observations in Central Europe N86-11564

VEGETATION
Evaluation of AIS data for agronomic and rangeland vegetation: Preliminary results for August 1984 flight over Nebraska Sandhills Agricultural Laboratory N86-11627
Preliminary evaluation of AIS spectra along a topographic/moisture gradient in the Nebraska Sandhills N86-11629
The use of AIS data for identifying and mapping calcareous soils in western Nebraska N86-11630
Comparison of AIS versus TMS data collected over the Virginia piedmont N86-11637
Analysis of terrestrial conditions and dynamics [NASA-CR-176308] N86-11646

VELOCITY
The irregularity in the Earth's annual rotation as a cause of systematic time variation N86-11570
Method of joint adjustment of height differences and velocities N86-11601
Travel-time and its residuals for the blasts from Eschenlohe (Bavaria) N86-11706

VELOCITY DISTRIBUTION
Seeding requirements for scanning laser velocimetry N86-11446
Possibility of optimal choice of exposure time for holographic recording of objects through unsteady scattering media N86-11983

VELOCITY MEASUREMENT
Ground effect on a rotor wake [COLL-AERONAUTICS-8510] N86-11187
Comparison of calculated and measured velocities near the tip of a model rotor blade at transonic speeds [NASA-TM-86697] N86-11196
Detonation reaction zone studies on TATB explosives [DE85-015710] N86-11361
The measurements of axisymmetric air turbulent jet flow with an individual realization laser velocimeter system [AD-A157554] N86-11429
Correcting for particle counting bias error in turbulent flow N86-11439
Estimation of particle size based on LDV measurements in a de-accelerating flow field N86-11440
Velocity measurements of laser driven flyers backed by high impedance windows [DE85-015142] N86-11470
Flame propagation in pulsed acceleration field N86-11964

VERMONT
Fiscal year 1983 institute program report, Vermont Water Resources Research Center [PB85-214500] N86-11659

VERTICAL AIR CURRENTS
An observational study of the vertical structure of interannual wind fluctuations in the tropics N86-11810

VERTICAL DISTRIBUTION
Precise geoid computations at mountainous coastlines in view of vertical datum determinations N86-11561
The annual variation in the vertical structure of the 40-50-day tropical oscillation N86-11780

VERTICAL MOTION
Stationary hydrostatic precision tiltmeter system N86-11607
Height changes and recent crustal movements in the Rhenish Massif and in the upper Rhine Graben rift N86-11608
On the relation between recent crustal movements, the surface of the basement complex and neotectonic displacements of the East-European platform N86-11610

VERTICAL ORIENTATION
On the works and results of investigations concerning the recent movements in the Karpatho-Balkan region N86-11593
North Sea coast levelling net: A model case for the determination of vertical movements in Western Europe N86-11594
Mathematical treatment of vertical movements N86-11597

Method of joint adjustment of height differences and velocities N86-11601

VIBRATION
Aerodynamic and structural aspects of propeller and drive for a 1/5 scale wind tunnel programme N86-11163
Propeller aircraft cabin vibration and noise-excitation, sources, and paths N86-11174
The Shock and Vibration Digest, volume 17, no. 4 [AD-A154112] N86-11527
Microcomputers in shock and vibration N86-11528
A review of the literature on finite-element modeling of laminated composite plates N86-11529
Mechanical face seal dynamics update N86-11530
The Shock and Vibration Digest, volume 17, no. 5 [AD-A156716] N86-11531
Current research on circular saw and band saw vibration and stability N86-11533
Hardware and software constructs for a vibration analysis network [DE85-008436] N86-11535
Seismology in civil engineering N86-11707
Flexible vibrations of a uniform elastic beam with arbitrary supports and lumped masses N86-11865
Numerical Techniques in Acoustics [NASA-CP-2404] N86-12007
Improving the accuracy of the boundary integral method based on the Helmholtz integral N86-12010

VIBRATION DAMPING
Metallurgical characterization of the interfaces and the damping mechanisms in metal matrix composites [AD-A156507] N86-11300
Lateral dampers for thrust bearings [NASA-CR-174924] N86-11474
Stiffness and damping coefficients of rubber N86-11532

VIBRATION MEASUREMENT
Numerical method in dynamic response of nonlinear systems N86-12005

VIBRATIONAL SPECTRA
Effect of a viscoelastic boundary inset on vibrational characteristics of a beam N86-11494
Energy characteristics of waveguide CO sub 2-laser N86-11978

VIDEO DATA
Infrared thermography: An analytical tool for high temperature and fast response [DE85-013826] N86-11462

VINYL COPOLYMERS
Develop, evaluate and validate continuous emission monitors for designated hazardous pollutants [PB85-201176] N86-11695

VISCOELASTIC DAMPING
Effect of a viscoelastic boundary inset on vibrational characteristics of a beam N86-11494

VISCOELASTICITY
Quality assurance procedures for V378A matrix resin N86-11274
Viscoelastic creep of high-temperature concrete [DE85-010511] N86-11539

VISCOSITY
Influence of effective rate sensitivity on adiabatic shear instability [DE85-013967] N86-11333
Characterization of the relationship of the cure cycle chemistry to cure cycle processing properties [NASA-CR-176256] N86-11339
Anelasticity in the Earth's mantle: Implications for the frequency dependence of Love numbers N86-11590

VISCOUS DRAG
Mechanical threshold of dynamically deformed copper and nitronic 40 [DE85-010779] N86-11545

VISCOUS FLOW
Development of an explicit multigrid algorithm for quasi-three-dimensional viscous flows in turbo-machinery [NASA-TM-87128] N86-11146

VISIBILITY
Computation of minimal isovist sets [AD-A157624] N86-11915

VISUAL FLIGHT RULES
Visual and motion cueing in helicopter simulation [NASA-TM-86818] N86-11208

VISUAL OBSERVATION
The eclipse of Epsilon Aurigae visible spectroscopy and ultraviolet activity N86-12173

VISUAL SIGNALS
Visual and motion cueing in helicopter simulation [NASA-TM-86818] N86-11208

VISUAL TASKS
Visual information transfer. Part 1: Assessment of specific information needs. Part 2: Parameters of appropriate instrument scanning behavior [NASA-CR-176277] N86-11850

VOICE COMMUNICATION
Voice communications over packet radio networks [AD-A157478] N86-11411

VOID RATIO
Reduction of moisture effects during the cure of epoxy adhesives used in composite repair N86-11254
All-aromatic ophenylene end-capped polyquinoline and polyimide matrix resins N86-11267

VOLATILITY
Laboratory evaluation of the protocol for the volatile organic sampling train [PB85-201184] N86-11694

VOLCANOES
A first look at Airborne Imaging Spectrometer (AIS) data in an area of altered volcanic rocks and carbonate formations, Hot Creek Range, south central Nevada N86-11625

VON KARMAN EQUATION
Stability and interaction of coherent structure in supersonic reactive wakes N86-11185

VORTICES
Study of the 3D wake of an aerial propeller N86-11161
A parametric analysis of flow structure and performance in a vortex controlled radial diffuser N86-11182
An experimental study of energy loss mechanisms and efficiency consideration in the low power dc arcjet [NASA-TM-87123] N86-11224
On stratified vortex motions under gravity [AD-A156930] N86-11427
Application of the vortex-lattice concept to flows with smooth-surface separation [AD-A157571] N86-11430
Seeding techniques used in the Vortex Research Facility N86-11443
On the instability of vortex series N86-11715
Simulation of flame propagation through vorticity regions using the discrete vortex method N86-11882
Vortex studies relating to boundary layer turbulence and noise N86-12015

VORTICITY
Simulation of flame propagation through vorticity regions using the discrete vortex method N86-11882
A hybrid vortex-in-cell finite-difference numerical method for turbulent shear layer computation N86-11886

W

WAKES
Study of the 3D wake of an aerial propeller N86-1116
On stratified vortex motions under gravity [AD-A156930] N86-11427
Seeding techniques used in the Vortex Research Facility N86-11443
Collinear wake field acceleration [DE85-014356] N86-12050

WARM FRONTS
Warm and cold episodes in the California current: A case for large-scale mid-latitude atmospheric forcing N86-11786

WASTE TREATMENT
Saltwater wetlands for wastewater management environmental assessment [PB85-201267] N86-11697

WASTE UTILIZATION
Advanced mechanical heat pump technologies for industrial applications [DE85-014613] N86-11483

WASTE WATER
Evaluation of color infrared aerial surveys of wastewater soil absorption systems [PB85-189074] N86-11654
Saltwater wetlands for wastewater management environmental assessment [PB85-201267] N86-11697

WASTES
Probability encoding of hydrologic parameters for basalt. Elicitation of expert opinions from a panel of three basalt waste isolation project staff hydrologists [DE85-014665] N86-11652

WATER
Partial discharge formation and breakdown in deionized water under repetitive stressing [DE85-013114] N86-11424
Elastic wave scattering of a Gaussian incident beam from an interface crack in a layered half space submerged in water N86-11490
Evaluation of AIS data for agronomic and rangeland vegetation: Preliminary results for August 1984 flight over Nebraska Sandhills Agricultural Laboratory N86-11627
Calculations of physical and chemical reactions produced in irradiated water containing DNA [DE85-012899] N86-12051

Low inductance diode design of the Proto 2 accelerator for imploding plasma loads
[DE85-013783] N86-12123

WATER CIRCULATION
Very anomalous behavior of outgoing longwave radiation in the tropics in 1983-84: Aftermath of ENSO? N86-11813

WATER FLOW
Louisiana Water Resources Research Institute
[PB85-218998] N86-11661
Deepwell monitoring along the southern San Andreas Fault
[PB85-196483] N86-11726

WATER MANAGEMENT
Fiscal year 1983 institute program report, Vermont Water Resources Research Center
[PB85-214500] N86-11659

WATER POLLUTION
Fiscal year 1983 institute program report, Vermont Water Resources Research Center
[PB85-214500] N86-11659

WATER QUALITY
Fiscal year 1983 institute program report, Vermont Water Resources Research Center
[PB85-214500] N86-11659
User guide for WIFM-SAL (WES Implicit Flooding Model-SAL): A two-dimensional vertically integrated, time-varying estuarine transport model
[AD-A157446] N86-11825

WATER RESOURCES
Fiscal year 1983 institute program report, Vermont Water Resources Research Center
[PB85-214500] N86-11659
Information dissemination for a better understanding of Louisiana's water resources
[PB85-219079] N86-11660
Louisiana Water Resources Research Institute
[PB85-218998] N86-11661
Fiscal year 1983 program report of the Water Resources Research Institute of New York State
[PB85-217024] N86-11662
Formation, distribution and variability in snow cover on the Asian territory of the USSR
[NASA-TM-77913] N86-11734

WATER TABLES
Evaluating the ground-water resources of the high plains of Texas, volume 3
[PB85-191617] N86-11655

WATER TREATMENT
Louisiana Water Resources Research Institute
[PB85-218998] N86-11661

WATER TUNNEL TESTS
Water tunnel flow visualization using a laser
[NASA-TM-86743] N86-11206

WATERSHEDS
Hydrologic data for experimental agricultural watersheds in the US, 1975
[PB85-197317] N86-11656

WAVE ATTENUATION
Attenuation of macroseismic effects of earthquakes N86-11705

WAVE EQUATIONS
Analysis of ultrasonic waves in a bounded medium N86-11869

WAVE FRONT RECONSTRUCTION
Phasing of multiple-aperture optical systems N86-11987

WAVE FRONTS
Travel-time and its residuals for the blasts from Eschenlohe (Bavaria) N86-11706

WAVE PROPAGATION
Remote sensing of earth terrain
[NASA-CR-176284] N86-11645
Attenuation of macroseismic effects of earthquakes N86-11705
Travel-time and its residuals for the blasts from Eschenlohe (Bavaria) N86-11706
Determination of the depth of a conductivity anomaly by separating the geomagnetic variation field into its external and internal part N86-11711
The effect of the Hadley circulation on the meridional propagation of stationary waves N86-11732
Analysis of ultrasonic waves in a bounded medium N86-11869
Raman scattering of sound on random oscillations of bubbles N86-11948
A general-applications direct global matrix algorithm for rapid seismo-acoustic wavefield computations N86-12012
Non-geometrical optics investigation of mode conversion in weakly relativistic inhomogenous plasmas
[DE85-013480] N86-12102
Simulation of quiet start magnetized plasmas, including Maxwellian and velocity-space ring distributions
[DE85-014394] N86-12112

WAVE REFLECTION
Reflection of sound from plate containing periodic inhomogeneities N86-11951

WAVE SCATTERING
Radiation and scattering performance of microstrip antennas using exotic substrates N86-11408
Elastic wave scattering of a Gaussian incident beam from an interface crack in a layered half space submerged in water N86-11490
Remote sensing of earth terrain
[NASA-CR-176284] N86-11645
Determination of parameters of elastic spherical shell from scattered wave field N86-11949

WAVEGUIDE ANTENNAS
A high-efficience, low-phase error waveguide lens for a transform feed antenna N86-11409

WAVEGUIDES
Waveguide slot array with CSC2 theta (dot) COS theta pattern N86-11402
Sheet metal waveguide forming technique N86-11403
Net-2 models of cavities and diodes N86-11863
Investigation of efficiency of generation of difference-frequency laser radiation in waveguide N86-11969
Distributed-feedback lasers with active framing medium N86-11971
Energy characteristics of waveguide CO sub 2-laser N86-11978

WAVELENGTHS
High altitude measured radiance of White Sands, New Mexico in the 400-2000 nm band using a filter wedge spectrometer
[PB85-206084] N86-11729
Atlas of high altitude aircraft measured radiance of White Sands, New Mexico, in the 450-1050 nanometers band
[PB85-204501] N86-11820
Frequency-selection and mode-locking and Nd:YAG laser N86-11926

WEAK INTERACTIONS (FIELD THEORY)
The relations between voltage and magnetic field of superconducting weaklink (2) N86-11935
High resolution spectrometer in studies of e(+)e(-) annihilation at (radical)s = 29 GeV
[DE85-013870] N86-12065

WEAPON SYSTEMS
Finite difference calculations of voltages generated in thin dielectric layers subjected to shock loading N86-11878

WEAR
Numerical solution for contact pressure and wear distributions of unlubricated, misaligned, closely conforming, multiply connected surfaces N86-11472
Experimental study on impact/fretting wear in heat exchanger tubes
[DE85-014597] N86-11548
Improvement in wear performance of surgical Ti-6Al-4V alloy by ion implantation of nitrogen or carbon
[DE85-013986] N86-11649

WEATHER
Overview of meteorological inputs to NASP N86-11736
Airline meteorological requirements N86-11737
General aviation's meteorological requirements N86-11738
Corporate/commuter airlines meteorological requirements N86-11739
Adverse weather impact on aviation safety, investigation and oversight N86-11742
Sub-cloud layer motions from radar data using correlation techniques
[AD-A156477] N86-11757
Application of an objective analysis scheme to mesoscale observational network design
[AD-A156911] N86-11760

WEATHER FORECASTING
Meteorological and Environmental Inputs to Aviation Systems
[NASA-CP-2388] N86-11735
Overview of meteorological inputs to NASP N86-11736
Airline meteorological requirements N86-11737
General aviation's meteorological requirements N86-11738
Corporate/commuter airlines meteorological requirements N86-11739
Overview of NASA's programs N86-11741
The utilization of satellite data and dynamics in understanding and predicting global weather phenomena
[NASA-CR-171577] N86-11749
Monthly and seasonal weather outlook for June 1985, volume 39, number 11, 30 May 1985
[PB85-209526] N86-11762
Worldwide marine temperature variations on the season to century time scale N86-11771
Large-scale variability in Indian monsoon rainfall inferred from satellite data N86-11800
Monthly and Seasonal Weather Outlook for May 1985, Volume 39, Number 9
[PB85-199123] N86-11819

WEATHER MODIFICATION
Continuing design, review, and analysis work for the Sierra Cooperative Pilot Project
[PB85-204303] N86-11822

WEATHER STATIONS
Specification of mean surface temperature anomalies in Europe and Asia during the fall months N86-11806
Land-surface fluctuations and associated climatic variability N86-11807
Effect of initialization on diagnoses of large-scale circulation statistics from WMC analyses N86-11817

WEBS (SUPPORTS)
Evaluation of superplastic forming and weld-brazing for fabrication of titanium compression panels N86-11245

WEDGE FLOW
Refined numerical solutions of the transonic flow past a wedge N86-11184

WEIGHTLESSNESS
Flame propagation in pulsed acceleration field N86-11964

WELDED JOINTS
Explosive welding in the 1990's N86-11237
Langley Research Center standard for the evaluation of socket welds N86-11243
Feasibility of remotely manipulated welding in space: A step in the development of novel joining technologies N86-11246
Metallography of solid state bonds
[DE85-014564] N86-11327
A comparison of the physics of Gas Tungsten Arc Welding (GTAW), Electron Beam Welding (EBW), and Laser Beam Welding (LBW)
[NASA-TM-86503] N86-11473
Economic evaluation of concurrent welding and nondestructive examination
[DE85-014623] N86-11481

WELDED STRUCTURES
The use of explosive forming for fastening and joining structural and pressure components N86-11240

WELDING
Welding, Bonding and Fastening, 1984
[NASA-CP-2387] N86-11227
Langley Research Center standard for the evaluation of socket welds N86-11243

WELLS
Geothermal instrumentation development activities at Sandia
[DE85-008693] N86-11463
Honey Lake Geothermal Project, Lassen County, California
[DE85-013388] N86-11677
Deepwell monitoring along the southern San Andreas Fault
[PB85-196483] N86-11726

WENTZEL-KRAMER-BRILLOUIN METHOD
The effect of the Hadley circulation on the meridional propagation of stationary waves N86-11732

WETLANDS
Discrimination of coastal vegetation and biomass: Using AIS data N86-11639
Aerial photography and ground verification at power plant sites: Wisconsin power plant impact study
[PB85-197358] N86-11658
Saltwater wetlands for wastewater management environmental assessment
[PB85-201267] N86-11697

WETTING
Short-term methods for atmospheric corrosion testing: Survey of the literature
[KIS-1985:5E] N86-11314

WHISTLERS
Ion whistlers in middle latitudes observed by the Interkosmos-14 satellite N86-11714

WIND (METEOROLOGY)
Regional Wind Energy Assessment Program. Appendix: Wind statistics summaries
[DE85-011520] N86-11686
Measurements of refractive index structure function C2N and aerosol size distribution at Chesapeake Bay
[AD-A157455] N86-11717
Sub-cloud layer motions from radar data using correlation techniques
[AD-A156477] N86-11757
Possible cross equatorial influence of the northeast monsoon on the equatorial westerlies over Indonesia
[AD-A156907] N86-11759
The annual variation in the vertical structure of the 40-50-day tropical oscillation N86-11780
The distribution of rainfall along the coast of northern Peru during 1982-83 N86-11782
Peru coastal winds during 1982-1983 N86-11783

Slow fluctuations of the tropical circulation during the FGGE year N86-11812

WIND DIRECTION
Peru coastal winds during 1982-1983 N86-11783
Observing the Eastern Pacific Hadley Circulation N86-11818

WIND PROFILES
Cloud streets during KonTur: A comparison of parallel/thermal instability modes with observations N86-11755

WIND SHEAR
Development of a wind shear performance envelope N86-11746
Laboratory model of flight through wind shear N86-11747
A model of a downburst, a wind tunnel program on planetary boundary layer, and airship in turbulence N86-11748
On cloud street development in three dimensional parallel and Rayleigh instabilities N86-11754
Cloud streets during KonTur: A comparison of parallel/thermal instability modes with observations N86-11755
Recognition and control of low level wind shear [AD-A156500] N86-11758

WIND TUNNEL APPARATUS
Laser angle sensor [NASA-CR-172369] N86-11207
Particle generation experience in Langley's 16-foot transonic tunnel N86-11449
Aerosol seeding systems for the NSWC wind tunnels N86-11453
Generating aerosols for laser velocimeter seeding N86-11455
Particle phase function measurements by a new Fiber Array Nephelometer: FAN 1 N86-11456

WIND TUNNEL DRIVES
Performance evaluation of full scale propellers by wind tunnel test N86-11160

WIND TUNNEL MODELS
Effect of aileron deflections on the aerodynamic characteristics of a semispan model of a subsonic energy-efficient transport [NASA-TP-2478] N86-11186
Investigation of low-temperature solders for cryogenic wind tunnel models N86-11230
NTF: Soldering technology development for cryogenics N86-11231
The alternating surface segmented lap joint: A design for thin highly loaded joints N86-11233
Aeroelastic model helicopter rotor testing in the Langley TDT [NASA-TM-86440] N86-11523

WIND TUNNEL TESTS
Performance evaluation of full scale propellers by wind tunnel test N86-11160
Study of the 3D wake of an aerial propeller N86-11161
Aerodynamic and structural aspects of propeller and drive for a 1/5 scale wind tunnel programme N86-11163
Wind tunnel investigation of the interaction of propeller slipstream with nacelle/wing/flap combinations N86-11166
Aeroacoustic wind tunnel measurements on propeller noise N86-11169
Some aeroacoustic wind tunnel measurements, theoretical predictions, and flight-test correlations on subsonic aircraft propellers N86-11170
Full-scale flight and model-scale wind tunnel tests on the nearfield noise characteristics of aircraft propellers N86-11172
Ground effect on a rotor wake [COLL-AERONAUTICS-8510] N86-11187
User's manual for a 0.3-m TCT wall interference assessment/correction procedure: 8- by 24-inch airfoil test section [NASA-TM-87582] N86-11189
Recent experience in seeding transonic/supersonic flows at AEDC N86-11447
LDA seeding system for the Langley Low Turbulence Pressure Tunnel N86-11450
Aerosol seeding systems for the NSWC wind tunnels N86-11453
Generating aerosols for laser velocimeter seeding N86-11455
Particle phase function measurements by a new Fiber Array Nephelometer: FAN 1 N86-11456

WIND TUNNEL WALLS
User's manual for a 0.3-m TCT wall interference assessment/correction procedure: 8- by 24-inch airfoil test section [NASA-TM-87582] N86-11189

WIND TUNNELS
Airflow calibration of a bellmouth inlet for measurement of compressor airflow in turbine-powered propulsion simulators [NASA-TM-84399] N86-11209
Wind Tunnel Seeding Systems for Laser Velocimeters [NASA-CP-2393] N86-11437
Experiments with solid particle seeding N86-11442
Seeding systems for use with a laser velocimeter in large scale wind tunnels N86-11444

WIND TURBINES
Effect of accuracy of wind power prediction on power system operator [NASA-CR-176300] N86-11667
Vertical axis wind turbine power regulation through centrifugally pumped lift spoiling [DE85-013787] N86-11679

WIND VELOCITY
Vertical axis wind turbine power regulation through centrifugally pumped lift spoiling [DE85-013787] N86-11679
Circulation and weather for MAM and JJA 1984 N86-11769
Peru coastal winds during 1982-1983 N86-11783
Variability simulations with a steady, linearized primitive equations model N86-11796
Slow fluctuations of the tropical circulation during the FGGE year N86-11812

WIND VELOCITY MEASUREMENT
A perspective on the status of measurement of atmospheric turbulence in the US [NASA-TM-87610] N86-11193

WINDOWS (INTERVALS)
The status of the NOAA/NESDIS radiation budget data set N86-11815

WINDPOWER UTILIZATION
Effect of accuracy of wind power prediction on power system operator [NASA-CR-176300] N86-11667
AC motor and generator requirements for isolated WECS [NASA-CR-176315] N86-11670
Regional Wind Energy Assessment Program. Appendix: Wind statistics summaries [DE85-011520] N86-11686

WING FLAPS
The alternating surface segmented lap joint: A design for thin highly loaded joints N86-11233

WING PANELS
Advances in joining techniques used in development of SPF/DB titanium sandwich reinforced with metal matrices N86-11247

WINGS
The alternating surface segmented lap joint: A design for thin highly loaded joints N86-11233
A comparison of measured and calculated thermal stresses in a hybrid metal matrix composite spar cap element [NASA-TM-86729] N86-11525

WINTER
Recent unusual mean winter temperature across the contiguous United States N86-11772
Life cycle of a 28-72 day atmospheric oscillation during northern winter N86-11781
Relationships between Pacific northwest coast climate and ENSO events N86-11787
Atmospheric general circulation model simulations of the modern Antarctic climate N86-11790
Variability simulations with a steady, linearized primitive equations model N86-11796

WORK
Adaptive motivation theory [AD-A157440] N86-11851

WORKING FLUIDS
Rotating film radiators for space applications [DE85-009633] N86-11431
Stirling cycle heat pump studies [DE85-005365] N86-11680

X

X RAY ANALYSIS
Corrosion testing by radiographic methods [BLL-BISI-TRANS-23201-(9022.06)] N86-11310

X RAY SCATTERING
X-ray inverse Compton emission from the radio halo of M87 [NASA-CR-176305] N86-12196
X-ray inverse Compton emission from the radio halo of M87 [NASA-CR-176304] N86-12197

X RAY SOURCES
A large area X-ray source and its preionization characteristics for XeCl excimer laser N86-11929

X RAY SPECTRA
Transition radiation as a practical X-ray source [DE85-013201] N86-12036

X RAY TELESCOPES
Publications of the Astronomical Institute of the Czechoslovak Academy of Sciences, no. 61 [PUBL-61] N86-12069
Wolter 1 type X-ray mirror system with mean resolution and maximum effective collecting area for the spectral region of 1-10 nm N86-12070
Galvanoplastic grazing incidence mirrors for verticle experiments: The tandem tests in soft X-rays N86-12071

X RAYS
A flash X-ray facility for the Naval Postgraduate School [AD-A157278] N86-11213
Si(Li)-NaI(Tl) sandwich detector array for measurements of trace radionuclides in soil samples [DE85-013865] N86-12062
Publications of the Astronomical Institute of the Czechoslovak Academy of Sciences, no. 61 [PUBL-61] N86-12069

XENON
Electroionization IR Xe-ATOM laser N86-11975

XENON CHLORIDE LASERS
A large area X-ray source and its preionization characteristics for XeCl excimer laser N86-11929
Spectrum structure of XeCl electric discharge laser N86-11970

XENON FLUORIDE LASERS
Efficiency of optically-pumped XeF-laser N86-11977

XYLENE
Processing science and technology N86-11297

Y

YAG LASERS
Frequency-selection and mode-locking and Nd:YAG laser N86-11928

YIELD POINT
The yield point of copper-zinc alloys in the alpha solid solution range [BLL-BISI-TRANS-23046-(9022.06)] N86-11311

YIELD STRENGTH
Effects of manufacturing processes on structural allowables [AD-A157596] N86-11318

YTTRIUM
Creep and fracture of a yttria dispersed nickel-chromium alloy N86-11309

YUGOSLAVIA
Anew about the correlation between Mohorovicic discontinuity depths, geoid undulations and Bouguer gravity anomalies in the Dinaric-Pannonian region of Yugoslavia N86-11557

Z

ZENITH
On the lunar tidal effect in the latitude observations at Tianjin N86-11565

ZINC ALLOYS
The yield point of copper-zinc alloys in the alpha solid solution range [BLL-BISI-TRANS-23046-(9022.06)] N86-11311

ZINC COMPOUNDS
Chemical synthesis under shock compression [DE85-015166] N86-11325
Analytical electron microscopy study of shock synthesized zinc ferrite [DE85-015144] N86-12140

ZIRCALOYS (TRADEMARK)
Fabrication and use of zircaloy/tantalum-sheathed cladding thermocouples [EGG-TFBP-6739] N86-11461

ZIRCONIUM ALLOYS
Dominant moving species in the formation of amorphous NZr by solid-state reaction [DE85-014855] N86-12053

ZONAL HARMONICS
Tidal friction, the Earth's rotation and hypothesis of an expanding Earth N86-11556

ZOOM LENSES
Seeding requirements for scanning laser velocimetry N86-11446

PERSONAL AUTHOR INDEX

SCIENTIFIC AND TECHNICAL AEROSPACE REPORTS VOLUME 24 NUMBER 2

Typical Personal Author Index Listing

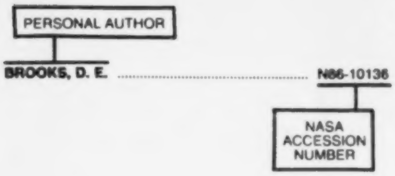

Listings in this index are arranged alphabetically by personal author. The NASA accession number denotes the number by which the citation is identified.

A

ABBEY, R. F. N86-11821
ABBOTT, L. F. N86-12041
ABDOU, M. N86-12130
ABDULHADI, M. I. N86-11532
ABER, J. D. N86-11634
ABNEY, L. D. N86-11462
ABRAHAM, K. M. N86-11672
ABUBAKAR, K. N86-11226
ACETO, L. D. N86-11510
ACEVEDO, W. N86-11633
ACKERMANN, R. A. N86-11392
ADAMS, J. B. N86-11626
ADAMS, R. G. N86-12115
ADAMS, S. N86-11620
ADELMAN, J. L. N86-12015
AGALTSOV, A. M. N86-11986
AGAPAKIS, J. E. N86-11246
AGARWAL, J. K. N86-11455
AGRITELLIS, C. N86-12077
AHEARN, J. S. N86-11251
AHRENS, L. N86-12091
AITNER, B. N86-12180
AKE, T. B. N86-12172
AKSAY, I. A. N86-11326
AL-JASSIM, M. M. N86-12139
ALBERS, R. C. N86-11323
ALI, A. W. N86-12079
ALJABRI, A. S. N86-11168
ALLEN, A. A. N86-11826
ALLEN, J. N86-12164
ALLEN, J. E. N86-11182
ALLISON, S. G. N86-11242
ALONSO, J. R. N86-12030
ALSTON, W. B. N86-11267
N86-11275
ALTEROVITZ, S. A. N86-12134
ALVARADO, N. T. N86-11533
AMUNDSON, C. H. N86-11256
AN, Z. G. N86-12111
ANDERSON, C. A. N86-11543
N86-11872
N86-12029
ANDERSON, C. E. N86-12142
ANDRE, J. C. N86-11789
ANDREWS, T. K., JR. N86-11845
ANDRUKHOVICH, A. N. N86-11991
ANGELSKIY, O. V. N86-11983
ANGER, G. N86-11552
ANTOLAK, A. J. N86-11864
APRUZESE, J. P. N86-12078
ARASH, F. N86-12034
ARKIN, P. A. N86-11800
ARMSTRONG, W. T. N86-12132
ARNOLD, C., JR. N86-11689
ARNOLD, F. E. N86-11261
ARNOLD, K. N86-11553
N86-11595
ARNOLD, O., JR. N86-11681
ARONSON, J. R. N86-11458
ARRIS, L. L. N86-11659
ARTHUR, E. D. N86-12045
ASAY, J. R. N86-11321
N86-11547
N86-12142
ASH, J. E. N86-11482
ASHAYEV, V. K. N86-11966
ASHLEY, C. S. N86-11688
ASHWORTH, A. K. N86-11834
ASINOVSKIY, E. I. N86-11974
ASSINK, R. A. N86-11681
N86-11689
ATKINSON, W. H. N86-11502
AUGATH, W. N86-11594
AUGENSTEIN, B. W. N86-11225
AUGL, J. M. N86-11254
N86-11282
AUGUSTINE, J. A. N86-11823
AULD, B. A. N86-11489
AYDELOTT, J. C. N86-11219
AZEVEDO, S. G. N86-11876
AZIZ, M. J. N86-11468

B

BABCOCK, S. R. N86-12119
BACKMAN, D. E. N86-12170
BADRINARAYANAN, M. A. N86-11201
BAER, M. R. N86-11879
N86-11883
BAERISWYL, D. N86-12143
BAHN, G. S. N86-11647
BAI, R. M. N86-12016
BAILEY, P. K. N86-11718
BAILEY, R. N86-11500
BAIRAMOV, A. N86-11313
BAJGROWICZ, E. J. N86-11400
BAK, P. N86-12147
BAKER, R. W. N86-11686
BAKUT, P. A. N86-11987
BALABAN, D. N86-11859
BALCOMB, J. D. N86-11685
BALDWIN, D. N86-12114
BALENA, F. J. N86-11174
BALES, T. T. N86-11245
BANDY, R. N86-11335
BANE, K. I. F. N86-12050
BAO, X. N86-11939
BARATUCI, W. N86-11439
BARBER, D. J. N86-11160
BARCLAY, J. A. N86-11370
BARLETT, R. N86-11476
BARNETT, T. P. N86-11804
BARR, P. K. N86-11862
BARTER, J. D. N86-12114
BARTHA, G. N86-11554
BARTON, R. N86-11389
BASIC, T. N86-11557
BASOV, N. G. N86-11975
BASS, R. M. N86-11163
BATES, G. T. N86-11791
BAUM, H. N86-11364
BAUMEISTER, K. J. N86-12007
BAXTER, V. D. N86-11484
BAZANT, Z. P. N86-11539
N86-11542
BAZZAZ, F. A. N86-11692
BEARDSLEY, I. S. N86-12171
BECKER, W. S. N86-11851
BECKNER, C. N86-11206
BEEZHOLD, W. N86-12058
BEHRENDT, W. N86-11476
BEICH, W. N86-12127
BELL, R. N86-11637
BELOTSERKOVSKIY, O. M. N86-11993
BEMENT, L. J. N86-11239
BENEDICT, B. N86-11393
BENNETT, W. R. N86-11334
BENSINGER, J. R. N86-12041
BENSON, D. A. N86-11874
BERGMAN, K. N86-11766
BERK, H. I. N86-12129
BERKO, S. N86-11330
BERNHARD, R. J. N86-12014
BERNHEIN, P. N86-11381
BERRY, R. F., JR. N86-11243
BERTHOU, C. N86-11789
BESMANN, T. M. N86-12054
BESSON, J. M. N86-11159
BIAN, S. X. N86-11382
BIRGENEAU, R. N86-12164
BISHOP, A. R. N86-12143
BISSELL, V. C. N86-11788
BLACIC, J. D. N86-12193
BLACKMON, M. L. N86-11791
BLAD, B. L. N86-11627
N86-11628
BLIND, B. N86-12093
BLISS, J. H. N86-11746
BLOOMQUIST, D. D. N86-12039
N86-12116
N86-12119
BLOOMQUIST, F. G. N86-11683
BLOOMQUIST, R. G. N86-11650
BLOSSER, M. L. N86-11236
BOBER, L. J. N86-11158
BOBERG, R. E. N86-11413
BOCCI, A. J. N86-11151
BOCHARY, E. Z. N86-11174
BOER, G. J. N86-11792
BOGAN, D. N86-11303
BOKHONOV, A. F. N86-11970
BONNEAU, H. N86-11171
BORING, A. M. N86-11323
BOROWSKI, S. K. N86-12099
BOSKOVA, J. N86-11714
BOSLOUGH, M. N86-11325
BOUCHER, C. N86-11555
BOUSQUET, J. M. N86-11149
BOWERS, A. R. N86-11698
BOWMAN, J. D. N86-12033
BOYKO, V. A. N86-11958
BRADFORD, K. Z. N86-11854
BRADSHAW, S. E. N86-11403
BRANDRIFF, B. N86-11834
BRAY, R. S. N86-11208
BREAKER, L. C. N86-11785
BREWE, D. E. N86-11425
BRINKER, C. J. N86-11688
BROD, K. N86-12010
BRODSKY, M. B. N86-12150
BRONGULEEV, V. V. N86-11609
N86-11610
BROUCEK, I. N86-11709
BROWN, E. N. N86-11200
BROWN, J. N86-11719
BROWN, R. D. N86-11454
BROWN, R. L. N86-12185
BROWNING, D. W. N86-11913
BRUEMMER, B. N86-11755
BRYUNETKIN, B. A. N86-11958
BRZEZINSKI, A. N86-11574
BUCHANAN, R. A. N86-11849
BUCKLEY, J. D. N86-11227
BUCKNER, D. A. N86-11352
BUDDEMEIER, R. W. N86-11828
BUDVEY, V. Y. N86-11991
BUGGELN, R. C. N86-11428
BUKATYY, V. I. N86-11961
BUNKIN, A. F. N86-11984
BUNKIN, F. V. N86-11958
BURAKOV, V. S. N86-11970
BURAKOVA, V. S. N86-11972
BURDA, M. N86-11703
BURFORD, J. B. N86-11656
BURGE, L. L., JR. N86-11857
BURLBAW, E. J. N86-11456
BURNS, E. J. T. N86-12109
BURNS, T. J. N86-11333
BURRIN, R. H. N86-11176
BURSA, M. N86-11550
N86-11556
BUSCH, C. N86-11745
BUSKIRK, F. R. N86-12025
BYMAN, J. E. N86-11228
BYSTROV, S. A. N86-11360

BYUN, T. D. S. N86-11244

C

CABRAL, B. K. N86-11870
CACCIANI, A. N86-12187, N86-12195
CALKINS, D. N86-11827
CAMP, D. W. N86-11735
CAMPANA, J. E. N86-12043
CAMPARO, J. C. N86-12024
CAMPBELL, R. B. N86-12086
CAMPBELL, R. H. N86-11893
CANTER, K. F. N86-11330
CAO, G. N86-11931
CAP, J. S. N86-12115
CAPONE, D. W., II N86-12153
CAPUTO, A. J. N86-11301
CARBONE, A. N86-11173
CARLSON, F. M. N86-11426
CARNEY, M. J. N86-11218
CARR, M. J. N86-11325, N86-12140
CARRANO, A. V. N86-11834
CARRUTHERS, L. M. N86-11872
CARSON, C. C. N86-11463, N86-11687
CARTER, N. I. N86-11721
CARTER, W. E. N86-11176
CARTIER, J. F. N86-11912
CASSELL, E. A. N86-11659
CASTANEDA, J. N. N86-11470
CATAN, M. A. N86-11484
CAVANO, P. J. N86-11291
CAYAN, D. R. N86-11770
CHA, J. H. N86-11548
CHADEE, F. F. N86-11914
CHAIR, Z. N86-11416
CHALK, C. R. N86-11204
CHAN, C. K. N86-11372
CHAN, P. H. N86-11779
CHAN, S. T. N86-11693
CHANDLER, C. L. N86-11737
CHANG, F. C. N86-11802
CHANG, G. E. N86-11280
CHANG, X. N86-11321
CHAO, A. W. N86-12124
CHAPMAN, R. D. N86-12180
CHAPPELL, R. N. N86-11483
CHATTERJEE, A. N86-12051
CHEKHLOVA, T. K. N86-11971
CHEN, C. Y. N86-12084
CHEN, D. N86-11429
CHEN, G. N86-11375
CHEN, H. H. N86-11472
CHEN, P. N86-12050
CHEN, Y. N86-12114
CHEN, Y. S. N86-11183
CHEN, Z. N86-11927, N86-11943
CHENG, A. Y. S. N86-12181
CHENG, X. N86-11929
CHENG, Y. T. N86-12053
CHENOWETH, D. R. N86-11884
CHEREMISKIN, I. V. N86-11971
CHERN, J. C. N86-11541, N86-11542
CHHABILDAS, L. C. N86-11547
CHIM, E. S. M. N86-11259
CHIMA, R. V. N86-11146
CHIVEL, Y. A. N86-11956
CHKHIKVADZE, T. D. N86-11947
CHRIEN, R. E. N86-12132
CHRISS, R. M. N86-11452
CHRISTEN, D. K. N86-12146
CHRISTOPHOROU, L. G. N86-12159
CHU, P. S. N86-11777
CHUGUNOV, A. Y. N86-11975
CHUMAKOV, A. N. N86-11956
CHUN, Y. W. N86-12184
CISZEK, T. F. N86-11349
CLARK, G. A. N86-11881
CLARK, J. H. E. N86-11750, N86-11751
CNARE, E. N86-11421
COATES, G. D. N86-11850
COATS, R. N86-12123
COLBECK, S. C. N86-11648
COLEMAN, P. D. N86-12121
COLIC, K. N86-11557
COLLERCANDY, R. N86-11150
COLLIER, A. S. N86-11453
COLTON, E. P. N86-12126
COMSTOCK, J. R., JR. N86-11850
CONEL, J. E. N86-11631
CONRAD, R. A. N86-11846
CONRAD, W. N86-11596
COOK, D. L. N86-12116
COOK, J. H. N86-11320
COOK, R. L. N86-11304
COOK, S. A. N86-11535
COOPER, J. C. N86-11315
COOPER, R. H., JR. N86-12054
COOPER, W. A. N86-12082
COOPER, W. L., JR. N86-12046
COOPER, W. S. N86-12029
CORNEJO-GARRIDO, A. N86-11782
CORNISH, R. M. N86-11458
COSTI, T. N86-11667
COUCH, R. N86-11476
COULSON, K. N86-11723
COURANT, E. D. N86-12044, N86-12098
COWAN, M. N86-11421
CRAGGS, A. N86-12008
CRAIG, M. D. N86-11636
CRAMER, R. G., JR. N86-11523
CROSS, J. B. N86-11223
CROSSWY, F. L. N86-11441
CROWE, R. D. N86-11535
CRYSTAL, T. L. N86-12113
CUI, C. N86-11375
CUNNINGHAM, J. N86-11418
CUNY, J. J. N86-11152
CURELARU, I. M. N86-11684
CURRAN, F. M. N86-11224
CURRY, R. E. N86-11206
CURTIS, J. N. N86-11692
CUSHMAN, J. B. N86-11268
CUTTEN, D. R. N86-11717
CZEKALSKI, L. N86-11740
CZOMPO, J. N86-11597

D

DAME, L. T. N86-11516
DANBY, G. N86-12095
DANEY, D. E. N86-11386
DANGELO, C. D., III N86-11533
DANIELS, A. N86-11376
DANIELS, W. L. N86-11841
DANIELSON, C. A. N86-11412
DANILYCHEV, V. A. N86-11975
DARAKCIEV, C. G. N86-11603
DAS, A. N86-11155
DAUGHERTY, R. H. N86-11522
DAVE, T. N86-11416
DAVIES, A. D. N86-11363
DAVIS, G. D. N86-11251
DAVIS, J. N86-12077, N86-12078
DAVIS, J. D. N86-11652
DAVIS, R. C. N86-11245
DEBECKER, M. N86-11576
DEBICCARI, A. N86-11246
DEBOO, J. C. N86-12110
DEEPAK, A. N86-11456
DEFOOR, T. N86-11723
DEGTYARENKO, K. M. N86-11967
DELAGI, R. G. N86-11248
DELETTREZ, J. N86-12127
DELNORE, V. E. N86-11647
DELOJOMORCILLO, G. N86-11310
DELOSRIOSRUBALCABA, J. N86-11310
DELSIGNORE, M. N86-12023
DELUISI, J. N86-11723
DELVIGS, P. N86-11263
DERKACH, D. I. N86-11983
DERRICK, M. N86-12065
DERZHIYEV, V. I. N86-11958
DESAUSSURE, G. N86-12052
DEVAN, J. H. N86-11682
DEVITO, B. N86-12095
DIAMOND, P. H. N86-12111
DIETRICH, R. N86-11558
DIGIOVANNI, P. R. N86-11279
DINERSTEIN, H. L. N86-12185
DITTFELD, H. J. N86-11559
DOEPKER, P. E. N86-11318
DOHERTY, M. F. N86-11915
DOMBKOVSKIY, N. N86-11181
DOMINGO, N. N86-11680
DONG, J. N86-11919
DONHAM, R. E. N86-11174
DONNELLY, R. P. N86-11170
DONOVAN, R. A. N86-12177
DORONIN, G. S. N86-11966
DORRELL, L. R. N86-12109
DOST, M. N86-11598
DOUGLAS, A. V. N86-11808
DOUGLAS, D. R. N86-12098
DOVER, C. B. N86-12059
DOWLER, K. E. N86-11320
DOWNIE, S. E. N86-12039
DOYLE, B. L. N86-12055
DOYLE, J. H. N86-11327
DRAKE, D. M. N86-12056
DRANSFIELD, B. J. N86-11720
DREWES, H. N86-11560
DRING, R. P. N86-11509
DROLET, L. L. N86-11840
DROSKE, J. P. N86-11267
DROSQ, M. N86-12056
DUBEAU, R. W. N86-11358
DUCARME, B. N86-11576
DUDERSTADT, J. J. N86-12076
DUDIN, A. Y. N86-11975
DUDKIN, V. A. N86-11976
DUKE, E. L. N86-11194, N86-11195
DUNN, J. E. N86-11544
DUNN, M. N86-12127
DUSTON, D. N86-12077
DUTTON, J. A. N86-11749, N86-11753, N86-11756
DVORAK, A. N86-11707
DYAKIN, V. M. N86-11958
DYER, R. I. N86-11469
DYKSTRA, J. D. N86-11632
DYNES, P. J. N86-11274
DZIUK, J. C. N86-11736

E

EBERT, P. J. N86-12036
ECKARDT, R. C. N86-11469
ECKLUND, S. D. N86-12097
EDWARDS, R. V. N86-11439, N86-11504
EGGLESTON, B. N86-11164
EIMERL, D. N86-11353, N86-12156
EISELE, F. L. N86-11467
EK, D. R. N86-11321
EKDAHL, C. A. N86-12027
EKMAN, M. N86-11599
EL-SAYED, M. A. N86-12136
ELLIOT, R. D. N86-11822
ELLIOTT, J. W. N86-11444
ELLIS, J. T. N86-12146
ELMORE, D. L. N86-11499
ELSTNER, C. N86-11596
ENFIELD, D. B. N86-11783
ENGLAND, T. R. N86-12048
ENGLEHART, P. J. N86-11808
ENGLUND, D. R. N86-11497
ENGST, B. N86-11407
ENMAN, S. V. N86-11600
ENSIGN, C. R. N86-11496
ENTEKHABI, D. N86-11784
EPLER, J. E. N86-11464
EPSTEIN, E. S. N86-11772
ERCEGOVIC, D. B. N86-11512
ERICKSON, D. J. N86-11420
ERKER, S. M. N86-11673
ERLINGER, J. J. N86-11402
ERMAK, D. L. N86-11693
ESHELBY, M. E. N86-11154
ESHERICK, P. N86-12042
ETISON, I. N86-11530
ETKIN, B. N86-11748
ETTINGER, D. G. N86-11351
EULER, H. J. N86-11561
EVANS, C. S. N86-11637
EVANS, D. D. N86-11365
EVANS, D. S. N86-11724
EVANS, N. J. N86-12185
EVESQUE, P. N86-12136

F

FALCO, C. M. N86-11334, N86-12141
FALICOV, L. M. N86-11322
FANG, H. N86-11933
FARASSAT, F. N86-11156
FARBER, H. N86-12023
FARMER, W. M. N86-11456
FARR, E. N86-11401
FARRELL, S. O. N86-11654
FAURE, A. N86-11381
FAVIER, D. N86-11161
FAYENOV, A. Y. N86-11958

FAZIO, G. G. N86-12188
FEDDERLY, J. J. N86-11282
FEDOROVSKYY, O. D. N86-11989
FEDOSIMOV, A. I. N86-11958
FEIGELSON, E. D. N86-12196
FEISSEL, M. N86-11555
FELDMAN, M. J. N86-11855
FELDMAN, S. C. N86-11625
FELDSTEIN, S. B. N86-11751
FENSTERNMACHER, M. E. N86-12086
FERLUGA, S. N86-12173
FERNALD, F. N86-11723
FILATOV, O. N. N86-11952
FIRPO, C. N86-11476
FIRTH, G. C. N86-11230
N86-11233
N86-11255
FISCHER, M. J. N86-11903
N86-11904
FISCHLER, J. E. N86-11247
FISHER, D. R. N86-11845
FLIFLET, A. W. N86-11460
FLINN, J. E. N86-11338
FLORSCHUETZ, L. W. N86-11511
FLUECK, J. A. N86-11822
FLYNN, M. J. N86-11888
FOHLEN, G. M. N86-11265
FOKEYEV, V. P. N86-11962
FOLLAND, C. K. N86-11771
FOLLANSBEE, P. S. N86-11545
N86-11546
FOLNSBEE, L. N86-12127
FOLTZ, B. W. N86-12109
FONTANELLA, J. J. N86-11342
FOOS, J. S. N86-11673
FORSTER, J. A. N86-11248
FOWNES, J. H. N86-11634
FRANCESCONI, R. P. N86-11832
FRANK, L. A. N86-11716
FRAZIER, M. E. N86-11845
FREED, A. D. N86-11491
FREEMAN, D. W. N86-11860
FREY, W. N86-12091
FRITZ, I. J. N86-11337
FROST, C. A. N86-12027
FROST, W. N86-11735
N86-11747
FRUEHOLZ, R. P N86-12024
FU, S. N86-11933
FUERST, R. G. N86-11694
FUGELSO, E. N86-11543
FULLER, C. E. N86-12186
FUNG, Y. T. N86-11427
FURY, M. N86-11601
N86-11602

G

GALAS, R. N86-11562
GALEOS, R. M. N86-11273
GAMON, M. A. N86-11898
GAO, Z. N86-12006
GARBER, D. P. N86-11292
GARDNER, B. R. N86-11627
N86-11628
GARDNER, J. N. N86-11720
GARREN, A. A. N86-12098
GARWIN, E. L. N86-12049
GARY, J. N86-11386
GAUDET, J. A. N86-12160
GAUNAURD, G. C. N86-12013
GAVEL, D. T. N86-11885
GAVIN, J. N86-11774
GEHLHAR, B. N86-11172
GEIL, T. N86-11506
GEISLER, J. E. N86-11791
GELARO, R. N86-11752
GELBWACHS, J. A. N86-11356
GEMMILL, W. H. N86-11816
GENDT, G. N86-11558
GENEROSO, W. M. N86-11835
GENET, R. M. N86-12175
GEORGIEV, N. I. N86-11603
GERGELY, J. N86-11601
N86-11602
GERSTENECKER, C. N86-11563
N86-11564
GILCHRIST, C. N86-11192
GILGENBACH, R. M. N86-12076
GILL, E. N86-12091
GLAUMYAN, A. S. N86-11984
GLENN, J. W. N86-12091
GLUCKSTERN, R. I. N86-12035
GNADE, D. K. N86-11413
GODFREY, B. E. N86-12027
GODLEWSKI, M. P. N86-11671
GOETZ, A. F. H. N86-11618
N86-11619
GOFORTH, J. H. N86-11419
N86-11420
GOLDENBERG, S. D. N86-11731
GOLDFARB, I. J. N86-11261
GOLDMAN, A. I. N86-12144
GOLDMAN, P. N86-11872
GOLDSTEIN, G. R. N86-12034
GOLDSTEIN, N. E. N86-11722
GOLDSTEIN, S. A. N86-12116
GOLDSTONE, J. A. N86-12037
GONG, C. N86-11936
GOODWIN, B. E. N86-11458
GORDON, H. B. N86-11795
GORDON, L. N86-11834
GORELENKO, A. Y. N86-11972
GORELIK, V. S. N86-11986
GOREV, V. A. N86-11960
GORKER, G. E. N86-12099
GOUDREAU, G. L. N86-11869
GOUGH, R. A. N86-12026
GOVSH, R. K. N86-11733
GOWARD, S. N. N86-11646
GRACEWSKI, S. M. N86-11490
GRACHEV, A. F. N86-11609
N86-11610
GRADY, D. E. N86-11336
N86-11544
N86-12142
GRAHA, R. A. N86-11325
GRAHAM, A. D. N86-11487
GRAHAM, R. A. N86-11324
N86-11328
N86-11359
N86-11360
N86-11485
N86-12140
N86-12142
GRAMS, G. W. N86-12074
GRANT, A. N86-11755
GRANT, H. N86-11500
GRANT, H. P. N86-11501
GRANT, N. J. N86-12060
GRANTHAM, W. L. N86-11647
GRAY, E. W. N86-12092
GRAY, K. E. N86-12153
GREEN, A. A. N86-11636
GREEN, H. E. N86-11280
GREENE, A. E. N86-11420
GRENISHIN, A. S. N86-11980
GRIFFETH, N. N86-11904
GRIFFITH, D. A. N86-11822
GRILL, A. N86-11475
GROEBNER, R. J. N86-12110
GROLIER, M. J. N86-11701
GROSCHE, F. R. N86-11169
GROSS, M. F. N86-11639
GROSS, R. J. N86-11879
N86-11883
GROTEN, E. N86-11561
GRUBER, A. N86-11815
GRUZINSKIY, V. V. N86-11967
GRYNING, S. E. N86-11730
GRYZIECKI, J. N86-11311
GUBLER, E. N86-11604
GUIBAS, L. J. N86-11904
GUINAN, E. F. N86-12177
GUIRGUIS, R. N86-11303
GULYAYEV, N. N. N86-11397
GUMBERT, C. R. N86-11189
GUPTA, R. C. N86-11944
GUTZLER, D. S. N86-11810
GVOZDEVA, L. G. N86-11962
GYGAX, S. N86-11369

H

HACK, M. N86-12173
HACKAMAN, D. E. N86-11400
HACKETT, C. E. N86-11446
HAINES, J. R. N86-12099
HALBLEIB, J. A. N86-12058
HALCOMB, D. D. N86-11329
HALE, J. N. N86-11250
HALFORD, G. R. N86-11520
HALL, D. S. N86-12175
HALL, E. T., JR. N86-11231
HALVERSON, D. C. N86-11326
HAMAKER, H. C. N86-12155
HAMERMESH, C. L. N86-11274
HAMILTON, D. C. N86-11305
HAMILTON, K. S. C. N86-11190
HAMILTON, W. R. N86-12099
HAMM, R. N. N86-12051
HAMOUDA, M. N. N86-11523
HAMROCK, B. J. N86-11425
HAN, T. N86-11565
HANCIK, C. A. N86-11400
HANE, G. J. N86-12165
HANNAFORD, J. F. N86-11822
HANSON, B. N86-11670
HANSON, M. P. N86-11281
HARADA, Y. N86-12023
HARADEN, J. N86-11687
HARDEGOPF, R. A. N86-12056
HARDIN, J. C. N86-12015
HARDWICK, R. N86-11238
HARLING, O. K. N86-11536
N86-12060
HARMS, D. E. N86-11760
HARMS, W. O. N86-11477
HARNACK, R. N86-11805
HARPER, D. A. N86-12167
HARRINGTON, R. F. N86-11647
HARRIS, F. I. N86-11757
HARTWICK, T. N86-12073
HARVEY, P. M. N86-12185
HARVILLE, G. L. N86-11352
HARWIT, M. N86-12186
N86-12189
HASKINS, J. F. N86-11283
HASTI, D. E. N86-12121
HASTINGS, D. E. N86-12082
HAUKSSON, E. N86-11725
HAUSCH, W. N86-11561
HAYS, A. K. N86-11337
HAYS, C. N86-11627
HEFTY, J. N86-11566
HEGAZY, A. A. N86-11241
HEGEDUS, C. R. N86-11341
HELLER, H. N86-11172
HELMINIAK, T. E. N86-11261
HELTSLEY, F. L. N86-11447
HEMSKY, J. W. N86-12037
HENDERSON, H. W. N86-11753
HENDRICKS, C. L. N86-11250
HENON, B. K. N86-11229
HENRY, H. W. N86-11900
HENSON, G. D. N86-12171
HENYEY, T. L. N86-11725
N86-11726
HERMANNSFELDT, W. B. N86-12049
HERNDON, J. N. N86-11855
HESS, C. F. N86-11457
HEYMAN, J. S. N86-11242
HIBNER, D. H. N86-11474
HICKEY, P. J. N86-11358
HICKOX, C. E. N86-11863
HIGGINS, R. W. N86-11756
HIGGS, T. N86-11698
HILL, C. G., JR. N86-11256
HILL, S. G. N86-11268
HILL, V. J. N86-11724
HINGST, W. R. N86-11452
HINKLE, K. H. N86-12179
HINKSON, J. A. N86-12104
HOCHSTEIN, J. I. N86-11218
HOEKSTRA, P. N86-11719
HOEPFNER, J. N86-11567
HOFFMANN, R. N86-11162
HOKANSON, J. C. N86-12142
HOLMES, N. C. N86-11305
HOLOTA, P. N86-11569
HOLTSLAG, A. A. M. N86-11730
HOLUB, K. N86-11706
HOPKINS, J. L. N86-12169
N86-12182
HORAK, J. N86-11715
HOREL, J. D. N86-11782
HORIE, Y. N86-11324
N86-11325
N86-11328
HORSTMANN, K. H. N86-11162
HORTON, A. I. N86-11653
HOU, D. N86-11942
HOU, M. K. N86-12155
HOY, D. E. P. N86-11324
HRADILEK, L. N86-11605
HSIEH, B. J. N86-11482
HSING, W. W. N86-12123
HSU, D. N86-11303
HSU, H. H. N86-11811
HSU, H. S. N86-11682
HSU, L. N86-11725
HU, Q. C. N86-11382
HUANG, C. Y. N86-12155
HUANG, Y. N86-11930
HUANG, Z. N86-11375
HUBBARD, R. W. N86-11832

HUDDLE, C. W. N86-12121
HUDEC, R. N86-12070
N86-12071
HUDSON, E. D. N86-12089
HUDSON, H. G. N86-11413
HUGHES, A. C. N86-11166
HUGRASS, W. N. N86-12132
HULSE, C. N86-11500
HUMPHREYS, D. R. N86-12115
N86-12116
HUNTER, A. B. N86-11272
HUNTER, W. W., JR. N86-11437
HURST, J. N86-12061
HUTCHINSON, R. A. N86-12165
HUTCHINSON, R. J. N86-12127
HWANG, Y. F. N86-12009
HYLTON, L. D. N86-11507

I

IANE, B. G. N86-12129
IGOSHIN, V. I. N86-11957
IH, C. H. C. N86-11219
ILKHANI-POUR, M. N86-11494
ILLG, W. N86-11292
IMRE, K. N86-12102
INSAROVA, N. I. N86-11968
IRWIN, J. S. N86-11730
IVANOV, I. B. N86-11570
IVRY, R. B. N86-11843
N86-11852
IWASHITA, Y. N86-11414

J

JACKSON, J. N86-12095
JACKSON, R. W. N86-11399
JACOBS, P. F. N86-11186
JACOBS, S. A. N86-12127
JACOBSON, B. A. N86-11425
JAMES, W. F. N86-11312
JANOWIAK, J. E. N86-11800
JARBOE, T. R. N86-12096
JASKOT, R. D. N86-11900
JASON, A. J. N86-12093
JASPERSON, W. H. N86-11807
JECK, R. K. N86-11743
JEFFERY, J. R. N86-11199
JENDRZEJCZYK, J. A. N86-11548
JENKINS, J. M. N86-11525
JENTZSCH, G. N86-11571
JEWELL, W. S. N86-11901
JI, Z. N86-11923
JIRICEK, F. N86-11714
JOCHMANN, H. N86-11572
JOHANSSON, E. N86-11314
JOHNS, R. H. N86-11513
JOHNS, W. L. N86-11327
JOHNSON, D. E. N86-12098
JOHNSON, D. L. N86-11371
JOHNSON, D. W. N86-11690
JOHNSON, G. L. N86-11877
JOHNSON, J. A. N86-11481
JOHNSON, J. D. N86-12148
JOHNSON, J. N. N86-11546
JOHNSON, P. R. N86-12109
JOHNSON, R. O. N86-11492
JOHNSON, S. E. N86-11678
JOHNSON, S. M. N86-11665
JOHNSON, W. I. N86-12053
JONES, J. A. N86-11373
JONES, K. M. N86-12139
JONES, P. D. N86-11764
JONES, R. J. N86-11280
JONES, W. L. N86-11647
JOO, I. N86-11593
JORDAN, E. H. N86-11526

K

KACHARE, R. N86-11669
KAHLE, H. G. N86-11604
KALASHNIKOVA, I. V. N86-11609
N86-11610
KALINOVSKAYA, T. N. N86-11991
KALLERGIS, M. N86-11172
KALSI, S. S. .... N86-12[illegible]9
KAMAREI, A. R. .... N86-11[illegible]0
KAMPWIRTH, R. T. N86-12153
KANEKO, M. N86-11390
KAREL, M. N86-11830
KARL, T. R. N86-11772
N86-11774
KARMALEEVA, R. M. N86-11583
KARMAZINOV, N. M. N86-11963
KARPENKO, V. N. N86-12087
KASAMI, T. N86-11895
N86-11911
KASSEL, S. N86-12022
KATZ, R. W. N86-11777
KAUFMAN, F. N86-12020
KECHIYEV, M. M. N86-11952
KECK, R. N86-12127
KEECH, T. N86-11192
KEELE, S. W. N86-11842
N86-11852
KEEN, R. A. N86-11809
KELLER, W. N86-11573
KELLY, D. L. N86-11821
KELLY, M. D. N86-11462
KELLY, P. M. N86-11764
KEMP, J. C. N86-12171
KENDALL, P. W. N86-11663
KENNEDY, J. M. N86-11482
N86-11537
KENYON, K. P. N86-12112
KEOHANE, G. N86-12095
KEPPLE, P. C. N86-12078
KERCHNER, H. R. N86-11331
KERKER, M. N86-12072
KERLEY, G. I. N86-11547
KERR, J. R. N86-11283
KESNER, J. N86-12081
KESSLER, T. N86-12127
KEUNG, C. S. N86-11379
KHLOPOV, G. I. N86-11952
KHOLIN, I. V. N86-11975
KHOMKIN, A. L. N86-11955
KIDWELL, R. N86-11838
KIEFER, R. W. N86-11658
KIEKEL, P. D. N86-12027
KIERAS, D. E. N86-11889
KILIC, S. N86-11899
KILROY, W. P. N86-11672
KIM, H. I. N86-12184
KIM, K. N86-11308
KIM, Y. N. N86-11428
KIM, Y. S. N86-12184
KING, P. B. N86-11824
KING, R. J. N86-11413
KINTER, J. L., III N86-11796
KIPP, C. R. N86-12014
KIPP, M. E. N86-12142
KIRBY, R. H. N86-11850
KIRSANOV, V. V. N86-11395
KIRSCH, L. E. N86-12041
KISELEV, V. M. N86-11980
KIVINIEMI, A. N86-11606
KJERENGTROEN, L. N86-11486
KLAUK, R. H. N86-11676
KLEIN, W. H. N86-11773
N86-11806
KLEMAS, V. N86-11639
KLEMT, W. B. N86-11655
KLIMAS, P. C. N86-11679
KLINGNER, P. L. N86-12132
KLOTS, C. E. N86-12051
KLUEH, R. L. N86-11332
KLUEPFEL, C. N86-11805
KNIGHT, N. F., JR. N86-11540
KNOLL, J. S. N86-11820
KNOWLES, T. N86-11655
KNOX, L. N86-11377
KO, W. L. N86-11524
KOBOLOV, A. A. N86-11961
KOCK, U. F. N86-11545
KOELLING, D. D. N86-11323
KOENIG, D. R. N86-11431
KOHN, R. V. N86-11534
KOHSE, G. N86-11536
N86-12060
KOLACZEK, B. N86-11574
KONDO, Y. N86-12180
KONDRATYUK, N. V. N86-11973
KONENENKO, V. S. N86-11946
KONEV, Y. B. N86-11978
KONG, J. A. N86-11645
KOOPMANN, G. H. N86-12010
KOPYLOVA, T. N. N86-11967
KORKAN, K. D. N86-12011
KOROLEV, A. Y. N86-11981
KORTH, G. E. N86-11336
KORZININ, Y. L. N86-11962
KOSEK, W. N86-11574
KOSS, D. A. N86-11317
KOSTENKO, A. A. N86-11952
KOTLIKOVA, T. N. N86-11980
KOURTIDES, D. A. N86-11265
KOZISKOVA, M. N86-11703
KRAEMER, W. J. N86-11841
KRAMER, D. P. N86-11329
N86-11352
KRAMER, E. J. N86-11346
KRANBUEHL, D. E. N86-11339
KRASNOGLAZOV, B. P. N86-11991
KRAUS, D. J. N86-12171
KRAUSS, O. N86-11670
KRAUSZ, K. N86-11614
KREITH, F. N86-11433
KROSHILIN, A. Y. N86-11954
KROSHILIN, V. Y. N86-11954
KRUG, A. C. N86-11358
KRUGLIK, G. S. N86-11973
KRUTOV, V. V. N86-12071
KUBENDRAN, L. R. N86-11450
KUHN, S. N86-12113
KUKLA, G. N86-11774
KULAK, R. F. N86-11482
KUMAR, B. N86-11343
KUNZ, K. S. N86-11413
KUREK, V. D. N86-11952
KUROCHKIN, V. I. N86-11957
KURTZ, N. T. N86-12186
N86-12189
KUSMARWANTO, I. N86-11187
KUTZBACH, J. E. N86-11781
KUZNETSOV, O. A. N86-11952

L

LABARGE, W. L. N86-11896
LACKNER, H. N86-12128
LAGER, D. L. N86-11876
LAGUTOV, Y. P. N86-11962
LAI, C. C. N86-11880
LALLMAN, F. J. N86-11203
LALWANEY, N. S. N86-11237
LAMB, P. J. N86-11801
LAMB, R. G. N86-11696
LAMBERT, N. N86-11378
LAMPETER, W. N86-12127
LANCASTER, K. T. N86-11422
LAND, C. E. N86-11348
LANDA, V. N86-12070
LANDIS, A. L. N86-11262
LANDMAN, D. N86-11269
LANDT, R. C. N86-11232
LANDY, F. J. N86-11851
LANE, B. N86-12081
LANG, H. R. N86-11620
LANGE, R. H. N86-11148
LANGHI, R. G. N86-11196
LANGSTON, C. W. N86-11523
LANIAK, G. F. N86-11696
LANZ, K. N86-11621
LAPIN, A. D. N86-11951
LATYNINA, L. A. N86-11583
LAU, K. M. N86-11779
LAU, Y. Y. N86-12075
LAUVER, R. W. N86-11271
LAWSON, R. N86-11364
LAYNE, A. W. N86-11653
LEAVITT, J. A. N86-11334
LECCE, L. N86-11173
LEDBETTER, J. M. N86-11320
LEE, G. S. N86-12111
LEE, R. Q. H. N86-11407
LEE, S. N86-12192
LEE, S. K. N86-11493
LEE, V. D. N86-12099
LEE, Y. N86-12095
LEE, Y. C. N86-11261
LEE, Y. H. N86-11906
LEE, Y. S. N86-12184
LESSARD, E. T. N86-11846
LESTER, D. F. N86-12185
LESTER, J. M. N86-11393
LEVIN, R. H. N86-11729
N86-11820
LEVIS, C. A. N86-11212
LEWIS, J. D. N86-12146
LEWIS, M. N86-11405
LEWIS, P. M. N86-12165
LI, J. N86-11375
N86-11927
LI, S. N86-11375
N86-11565
LI, T. N86-11940
LI, X. Z. N86-12081
LI, Z. N86-11938
LIANG, S. M. N86-11184
LIANGPING, Z. N86-12001
LIEHR, O. K. N86-11174
LIKHTENSHTEYN, V. M. N86-11991
LIN, C. N86-12151

LIN, H. C. N86-11665
LIN, J. L. N86-11345
LIN, S. N86-11895
N86-11911
LIN, X. N86-12151
LINDALE, E. N86-11379
LINDBERG, J. B. N86-11211
LINDBERG, S. E. N86-11690
LING, P. N86-12145
LINSE, V. D. N86-11237
LIPATOV, N. I. N86-11978
LISOWSKI, P. W. N86-12056
LIU, C. N86-11939
LIU, C. H. N86-11167
LIU, C. S. N86-11466
LIU, D. C. N86-12134
N86-12135
LIU, H. N86-12151
LIU, L. N86-12151
LIU, M. N86-11936
LIU, Z. N86-11940
LIVEZEY, R. E. N86-11772
N86-11805
LO, Y. T. N86-11406
N86-11407
LOBYZOV, N. I. N86-11963
LOCKWOOD, G. J. N86-12103
LOCKWOOD, G. W. N86-12178
LOEW, G. A. N86-12125
LOEWY, R. G. N86-11293
LOGAN, T. J. N86-11694
LOGEE, T. L. N86-11663
LOHMAN, A. L. N86-11358
LOMDAHL, P. S. N86-12143
LONG, L. N. N86-11157
LONGSWORTH, R. C. N86-11391
LORD, R. S. N86-12089
LORENZ, G. N86-11598
N86-11607
LOU, H. N86-11926
LOU, Q. N86-11929
LOUIE, B. N86-11367
N86-11385
LOWDEN, R. A. N86-11301
LU, Y. H. N86-11803
LUKENS, L. L. N86-11479
LUMLEY, D. F. N86-11234
LUND, S. P. N86-11726
LUTHER, F. M. N86-11691
LUTZ, B. L. N86-12178
LUU, T. S. N86-11150
LYNCH, N. A. N86-11903
N86-11904
LYNN, K. G. N86-11330
N86-12061
LYNN, P. P. N86-11433
LYON, R. J. P. N86-11621
LYON, S. P. N86-12148

M

MA, L. N86-11565
MA, X. N86-11938
MACCALLUM, J. M., JR. N86-12073
MACKLIN, R. L. N86-12052
MACLEOD, H. A. N86-12137
N86-12138
MADDEN, R. A. N86-11780
MAELZER, H. N86-11606
MAENCHEN, J. N86-12109
MAFFEO, R. J. N86-11514
MAGEE, J. L. N86-12051
MAGNITSKY, V. A. N86-11609
N86-11610
MAHAJAN, S. M. N86-12084
MAHRT, L. N86-11789
MAINIG, M. N86-11575
MAKARYAN, A. O. N86-11969
MAKSIMOV, L. I. N86-11991
MALHOTRA, V. N86-11266
MALL, S. N86-11298
MALLINSON, G. D. N86-11487
MALTSEV, D. V. N86-11984
MANCHESTER, D. L. N86-11842
MANOGUE, C. A. N86-11916
MANORY, R. N86-11475
MANSOUR, N. N. N86-11886
MANTAY, W. R. N86-11523
MAOLIAN, H. N86-11997
MAPLE, M. B. N86-12155
MARCAL, G. N86-11761
MARCHERTAS, A. H. N86-11537
N86-11539
N86-11541
N86-11542
MARECEK, R. N86-12070
MARESCA, C. N86-11161
MARESCA, R. N86-11377
MARKOVETS, V. V. N86-11974
MARQUET, P. N86-11789
MARSH, S. P. N86-11419
MARSHALL, H. R., JR. N86-12163
MARTIN, J. A. N86-12089
MARTIN, T. H. N86-12116
MARTINI, W. R. N86-11384
MARULO, F. N86-11173
MARUYAMA, X. K. N86-11213
N86-12025
MASHKIVSKIY, I. Y. N86-11178
MASHKO, V. V. N86-11968
MASON, W. E. N86-11868
MASSEY, R. T. N86-11329
MASTERS, C. O. N86-11744
MASUBUCHI, K. N86-11246
MASUOKA, E. N86-11638
MATIENZO, L. J. N86-11251
MATSON, P. N86-11633
MATSUBARA, Y. N86-11369
N86-11390
MATTHEW, C. B. N86-11832
MATTHEWS, D. N86-11257
MAURICE, W. T. N86-11347
MAXIMOVICH, M. G. N86-11273
MAYOROV, S. A. N86-11958
MCCAFFERTY, D. B. N86-12161
MCCAFFREY, B. J. N86-11366
MCCARTHY, J. P. N86-11352
MCCARTHY, S. N86-11367
MCCLEER, P. J. N86-11670
MCCONNELL, R. D. N86-11675
MCCOOK, G. P. N86-12177
MCCORMICK, M. P. N86-11700
MCCRORY, R. I. N86-12131
MCDANIEL, D. B. N86-12092
MCDANIEL, D. H. N86-12116
N86-12123
MCDONALD, H. N86-11428
MCGRATH, D. T. N86-11409
MCGUIRK, J. P. N86-11818
MCKEEN, R. G. N86-11362
MCKENNA, K. F. N86-12132
MCKNIGHT, R. L. N86-11516
MCLAREN, D. N86-11284
N86-11285
N86-11289
MCLENNAN, G. A. N86-11482
MCMASTER, W. H. N86-11887
MCMATH, W. S. N86-11205
MCNAIR, H. M. N86-11436
MCRANEY, J. K. N86-11725
MCWITHEY, R. R. N86-11236
MEADE, L. E. N86-11249
MEIER, S. N86-11611
MELCHIOR, P. N86-11576
MENDELSOHN, M. L. N86-11847
MENEES, G. P. N86-11221
MENG, J. N86-11578
MENON, S. N86-11185
MENTES, G. N86-11577
N86-11614
MERKHOFER, M. W. N86-11652
MERRELL, R. B. N86-11199
MERRITT, M. N86-11903
MERSHKO, V. L. N86-11991
MESHCHERYAKOV, G. A. N86-11579
METZ, M. C. N86-11719
METZGER, D. E. N86-11511
METZGER, F. B. N86-11175
MEYERS, J. F. N86-11440
MEYERS, M. A. N86-11360
MICCIOLI, W. N86-11405
MIDDLETON, D. N86-12018
MIDGETT, M. R. N86-11694
MIELNICKA-PATE, A. L. N86-12016
MIKHEYEV, L. D. N86-11977
MIKKELSON, D. C. N86-11158
MIKKOLA, L. N86-11612
MILAM, D. N86-11350
MILEV, G. N86-11613
MILLENER, D. J. N86-12059
MILLER, G. D. N86-11874
MILLER, J. F. N86-11423
MILLER, R. B. N86-12027
MILLS, A. P. N86-11330
MILLS, J. I. N86-11483
MILTENBERGER, R. P. N86-11846
MINKO, L. Y. N86-11956
MINTA, M. N86-11380
MINTEN, A. N86-12032
MIRKAMILOV, D. M. N86-11984
MIRONOV, N. T. N86-11589
MISRA, M. S. N86-11300
MITCHELL, A. C. N86-11305
MITCHELL, G. A. N86-11158
MITCHELL, T. P. N86-11776
MITROPOLSKII, M. M. N86-12070
N86-12071
MITTRA, R. N86-11401
MIYAKODA, K. N86-11798
MOACANIN, J. N86-11669
MOHLER, J. H. N86-11462
MONSER, G. J. N86-11404
MONTGOMERY, R. E. N86-11912
MONTRY, G. R. N86-12039
MOOERS, C. N. K. N86-11785
MOORE, G. T. N86-11933
MOORTHY, A. N86-11846
MORAN, M. J. N86-12031
N86-12036
MORAVOSIK, M. J. N86-12034
MORENO, V. N86-11521
MOREY, W. W. N86-11498
MORGAN, G. H. N86-11944
MORITZ, H. N86-11580
MOROSIN, B. N86-11324
N86-11325
MORRISON, J. I. N86-11151
MOTE, C. D., JR. N86-11533
MOTE, J. D. N86-11241
MOUAT, D. A. N86-11625
N86-11642
MOVSISYAN, K. M. N86-11969
MOYA, J. L. N86-11867
MOYER, D. W. N86-11288
MUELLER, T. J. N86-11448
MUGHAB, S. F. N86-12066
MUNNIKSMA, B. N86-11163
MURAKAMI, T. N86-11799
MUREAU, R. N86-11793
MURPHY, D. L. N86-11826
MURROW, H. N. N86-11193
MUSA, S. N86-12073
MUSOLINE, S. V. N86-11846
MUSSARI, C. A. N86-11197
MUSTARD, J. F. N86-11635
MYRTLE, K. N86-11389

N

NAGLE-ESHLEMAN, J. N86-11527
N86-11531
NAIDU, J. R. N86-11846
NAIK, V. K. N86-11856
NAKAMURA, M. N86-12104
NAKAT, R. H. N86-11459
NAKHOST, Z. N86-11830
NAMIAS, J. N86-11767
NARAYAN, J. N86-11468
NASELOW, A. B. N86-11262
NASTULA, J. N86-11574
NATENAPIT, M. N86-11917
NAUENBERG, U. N86-12063
NAVARRA, A. N86-11798
NAVE, R. L. N86-11198
NEAL, V. T. N86-11775
NEASE, A. B. N86-11352
NEAU, E. L. N86-12116
N86-12119
NEEMAN, Y. N86-12028
NEIDLINGER, H. H. N86-11357
NEIGHBOURS, J. R. N86-12025
NEIL, V. K. N86-12120
NELLIS, W. J. N86-11305
NELSEN, J. M. N86-11867
NELSON, G. C. N86-11337
NELSON, T. A. N86-11869
NEMETH, Z. N86-11601
N86-11602
NEWBERGER, B. B. N86-12027
NEWBERGER, P. A. N86-11783
NEWMAN, M. N86-11771
NEWTON, D. N86-11738
NEYER, B. T. N86-12103
NG, T. T. N86-11448
NHA, I. S. N86-12184
NICHOLAS, G. N86-12073
NICHOLS, C. E., JR. N86-11437
N86-11442
N86-11444
NICHOLS, R. H. N86-11438
NICHOLSON, S. N86-11784
NICOLET, M. A. N86-12053
NIELSEN, B. N86-12061
NIGAM, S. N86-11796
NIGMATULIN, B. I. N86-11954
NIYAKODA, K. N86-11803

NORSTROM, P. N86-11655
NORWOOD, F. R. N86-11485
NOVAK, J. H. N86-11728
NOVOTNY, O. N86-11704
NOWAK, B. E. N86-11288
NUNAN, J. N86-11418
NUNES, A. C., JR. N86-11473
NWEKE, E. E. N86-11258

O

OAKES, W. R., JR. N86-11871
OBERDORFER, J. A. N86-11828
OBERLE, L. G. N86-11503
OBUKHOVSKIY, V. V. N86-11985
OCONNOR, M. E. N86-11837
OHNUMA, S. N86-12035
OLCOTT, J. W. N86-11739
OLEFIR, G. I. N86-11988
OLMSTED, E. N86-11652
OLSON, C. E., JR. N86-11643
ONEILL, K. N86-11648
OPSTEEGH, J. D. N86-11793
ORAN, E. N86-11303
ORLOW, J. R. N86-11402
OSTROUMOV, V. G. N86-11979
OUIBRAHIM, H. N86-11416
OWEN, E. W. N86-12094
N86-12108
OWEN, F. K. N86-11196
OWYOUNG, A. N86-12042

P

PAK, H. R. N86-11328
PALMER, G. E. N86-11196
PAN, Y. C. N86-11537
PANDOLF, K. B. N86-11840
PAOLUCCI, S. N86-11884
PAONESSA, A. N86-11173
PAPPAS, J. N86-11737
PARK, G. L. N86-11670
PARK, P. K. N86-11403
PARKER, D. E. N86-11771
PARKER, J. A. N86-11265
PARKER, J. V. N86-11214
PARKIN, D. M. N86-12037
PARSONS, W. M. N86-11214
PASHININ, P. P. N86-11978
PATER, R. H. N86-11278
PATERSON, D. N86-11279
PATRICK, W. P. N86-11445
PATT, P. N86-11377
PATTERSON, E. M. N86-12074
PAVLOVA, V. T. N86-11967
PAYLOR, E. D. N86-11620
PECK, P. A. N86-11788
PECOVA, J. N86-11711
PEHL, R. H. N86-12062
PELZER, H. N86-11594
PEI[illegible], S. Y. N86-11410
PENG, Y. K. M. N86-12099
PENN, K. J. N86-12115
PENNOCK, S. T. N86-1141[illegible]
PEPPLER, R. A. N86-11801
PEREZ, R. B. N86-12052
PERRY, R. T. N86-12048
PETERSON, D. L. N86-11633
PETERSON, G. R. N86-12039
PETERSON, J. C. N86-11865
PETOT, D. N86-11159
PETROVIC, S. N86-11557
PETRUCCI, S. N86-12023
PETTIT, R. B. N86-11688
N86-11862
PFEIFFER, P. A. N86-11539
PHILLIPS, R. N86-12095
PHILLPOT, S. R. N86-12143
PIERCE, N. J. N86-11199
PIET, S. J. N86-12047
PIETERS, C. M. N86-11635
PIKE, G. E. N86-11337
PIKE, R. A. N86-11252
PITTS, L. N86-11672
PITTS, W. M. N86-11366
PLASTER, D. S. N86-11483
PLATE, S. N86-12095
PLATZER, M. F. N86-11201
PLOSHAY, J. N86-11803
PLOTKIN, M. E. N86-12070
POA, D. S. N86-11423
POE, C. C., JR. N86-11292
POGOSYAN, P. S. N86-11969
POITEVIN, C. N86-11576
POLITI, R. E. N86-11270
POMA, A. N86-11581
POND, C. R. N86-11207
PORTER, K. N86-11289
POSTLEWAITE, J. N86-11285
N86-11289
POUCH, J. J. N86-12134
N86-12135
POUKEY, J. W. N86-12027
POULSEN, P. N86-12114
POVEROMO, L. M. N86-11286
POWELL, S. H. N86-11280
POWER, J. F. N86-12093
POWERS, D. J. N86-11648
POZAR, D. M. N86-11399
PRABHAKAR, A. N86-12133
PRABHU, R. K. N86-11167
PRANTIL, V. C. N86-11873
PRATT, R. D. N86-11290
PRIKNER, K. N86-11713
PRINCE, J. M. N86-11489
PRIVOS, Y. S. N86-11979
PROCHAZKOVA, D. N86-11705
PROHASKA, J. N86-11694
PROKHOROV, A. M. N86-11978
PROULX, G. A. N86-12128
PROVERBIO, E. N86-11581
PULLEY, D. F. N86-11341
PUNDAK, N. N86-11383
PUPKOV, V. N. N86-11734
PYZIK, A. J. N86-11326

Q

QIAN, P. N86-11942
QIAN, W. N86-12004
QIAN, Y. N86-11565
QIU, P. N86-11928
QUINN, W. H. N86-11775
QUINTIERE, J. N86-11364
QUIROZ, R. S. N86-11766
N86-11768

R

RADEBAUGH, R. N86-11367
N86-11385
N86-11386
RADFORD, R. C. N86-11204
RADOUSKY, H. B. N86-11305
RAFAL, R. D. N86-11842
RAKA, E. N86-12091
RAMAMURTHY, G. N86-11298
RAMIREZ, J. J. N86-12121
RAPHAELIAN, L. A N86-11351
RASCH, N. N86-11191
RATAJCZAK, A. F. N86-11666
RATNER, I. G. N86-12038
RAYAKIN, A. D. N86-11987
REALE, S. N86-11381
REARDON, J. P. N86-11288
REDDY, J. N. N86-11529
REED, R. P. N86-12101
REEDY, R. C. N86-12198
REGAZZONI, G. N86-11545
N86-11546
REGENIE, V. A. N86-11194
N86-11195
REID, R. L. N86-12099
REJ, D. J. N86-12132
REMBETSY, L. M N86-11673
REPATA, L. N86-12095
REPLANE, W. N86-11800
REUBUSH, D. E. N86-11449
REYES, P. N86-12109
REYNOLDS, G. F. N86-11302
REYNOLDS, R. W. N86-11816
REZAIZADEH, M. A. N86-11298
RHODES, E. J., JR. N86-12187
N86-12195
RICHARDSON, M. C. N86-12127
RICHARDSON, W. H. N86-12021
RICHERSON, D. W. N86-11202
RICHTER, B. N86-12100
RICKENBAKER, E. N86-11201
RIEMER, B. W. N86-12099
RIGBY, D. N86-11345
RIGNEY, E. D., JR. N86-11849
RINKER, G. N86-12149
RITCHEY, W. M. N86-11266
ROACH, T. A. N86-11235
ROADS, J. O. N86-11804
ROBBINS, J. W. N86-11910
ROBERGE, R. N86-11335
ROBERTS, M. L. N86-11515
ROBERTS, R. T. N86-11656
ROBINSON, W. W. N86-11499
ROBOCK, A. N86-11794
ROCHE, C. T. N86-12062
ROCK, B. N. N86-11622
N86-11624
RODDE, A. M. N86-11152
RODINA, L. I. N86-11980
ROE, R. J. N86-11345
ROELLIG, L. O. N86-11330
ROGERS, J. D. N86-12106
ROGERS, J. W., JR. N86-11470
ROGERS, W. G. N86-11758
ROHDE, J. E. N86-11505
ROHWEIN, G. J. N86-11424
RONG, J. N86-11930
ROPELEWSKI, C. F. N86-11765
N86-11769
ROSEMEIER, R. G. N86-11665
ROSEN, R. D. N86-11817
ROTTER, M. D. N86-11471
ROYSTER, D. M. N86-11245
RUBINGER, B. N86-12165
RUDOLFVONROHR, P. B. N86-11387
RUGGLES, L. E. N86-12103
RUKHIN, V. B. N86-11976
RUNCHAL, A. K. N86-11652
RUNQUIST, D. C. N86-11629
RUSSELL, L. B. N86-11836
RUSSELL, R. W. N86-12189
RUSSELL, W. L. N86-11833
RUTHERFORD, J. W. N86-11188
RYAN, R. S. N86-11215
RYZHOV, Y. N. N86-11971

S

SA, N. N86-11405
SABOE, C. N86-12163
SAKATA, I. F. N86-11525
SALIKUDDIN, M. N86-11176
SALOMON, M. N86-12023
SALSTEIN, D. A. N86-11817
SALTZ, J. H. N86-11856
SAMIOS, N. P. N86-12117
SAMMELLS, A. F. N86-11304
SAMORUKOV, V. N86-11179
SAMSON, S. A. N86-11630
SAMSONOV, V. P. N86-11964
SANDBERG, B. N86-11313
SANDERS, R. N86-12091
SANFORD, T. W. L. N86-12058
SANTER, B. N86-11764
SAPILOV, Y. V. N86-11991
SARA, T. S. N86-12166
SARAVANAMUTTOO, H. I. H. N86-11168
SARWINSKI, R. N86-11388
SATRAN, D. R N86-11443
SATYANARAYANA, T. N86-11831
SAUER, H. H. N86-11724
SAUNDERS, B. V. N86-11908
SAVCHENKO, A. N86-11180
SAVERINA, A. N. N86-11396
SAW, C. K. N86-11319
SAWAOKA, A. N86-11485
SAWKO, P. M. N86-11340
SAWYER, J. W. N86-11236
SCHAEFER, J. T. N86-11821
SCHAPPELL, R. T. N86-11854
SCHAUBERT, D. H. N86-11399
SCHEFFLER, T. B. N86-11302
SCHEIL, G. W. N86-11695
SCHEIMAN, J. N86-11450
SCHEMMP, A. N86-12088
SCHERE, K. L. N86-11728
SCHISSEL, P. N86-11357
SCHLESINGER, M. E. N86-11790
SCHLUETER, R. A. N86-11667
SCHMALZ, R. A., JR. N86-11825
SCHMID, T. E. N86-11291
SCHMIDT, H. N86-12012
SCHMIDTKE, P. C. N86-12176
SCHNEIDER, L. X. N86-12103
N86-12116
N86-12119
SCHNITZER, H. J. N86-12041
SCHNURR, N. M. N86-11861
SCHOPFER, C. J. N86-11846
SCHRAMM, H. R. N86-11210
SCHREIBER, J. G. N86-11668
SCHROEDER, J. W. N86-11240
SCHULTEN, J. B. H. M. N86-11153
SCHULTZ, D. N86-11519
SCHULTZ, J. H. N86-12083

SCHULTZ, P. J. N86-12061
SCHUSTER, L. S. N86-11524
SCHWAB, G. N86-11596
SCHWAHN, W. N86-11596
SCHWARZ, R. B. N86-11319
SCHWENSFEIR, R. J., JR. N86-11248
SCHWIEDER, D. H. N86-11892
SCOLA, D. A. N86-11277
SCOTT, T. C. N86-11256
SEAH, M. M. N86-11411
SEAMEN, J. F. N86-12115
N86-12119
SEASHOLTZ, R. G. N86-11503
SEDLOV, P. A. N86-11991
SEEGMILLER, H. L. N86-11451
SEGAL, D. B. N86-11632
SEIDEL, D. B. N86-12109
SEITZ, W. L. N86-11361
SEKULA, S. T. N86-11331
N86-12146
SELKIRK, R. N86-11812
SEPOLD, L. K. N86-11461
SERAFINI, T. T. N86-11281
SEREDNITSKAYA, M. A. N86-11947
SERGEYEV, A. V. N86-11949
SHAO, K. N86-11941
SHAO, M. N86-12190
SHARPE, A. W. N86-11422
N86-12121
SHAW, L. N86-11476
SHCHERBAKOV, I. A. N86-11979
SHEFFIELD, J. N86-12085
SHEFFIELD, S. A. N86-11470
SHEN, X. N86-11429
SHEPPARD, C. H. N86-11264
SHERMAN, I. S. N86-12062
SHERWOOD, E. G. N86-12132
SHESTOPALOV, V. P. N86-11952
SHIBANOV, A. N. N86-11953
SHIELD, K. A. N86-11759
SHIH, Y. N86-12002
SHILOV, K. A. N86-11958
SHIMER, D. W. N86-12094
N86-12108
SHIN, K. G. N86-11906
SHIRE, H. N. N86-11756
SHIRER, H. N. N86-11749
N86-11752
N86-11754
N86-11755
SHKADAREVICH, A. P. N86-11972
N86-11973
SHOPE, S. L. N86-12027
SHORE, S. G. N86-11344
SHTRIKMAN, S. N86-11383
SIEMON, R. E. N86-12132
SIGARI, G. N86-11667
SIGMAR, D. J. N86-12082
SILL, L. R. N86-12150
SIMON, D. N86-11583
SIMON, I. N86-11458
SIMON, T. N86-12179
SIMON, Z. N86-11551
SIMONSEN, I. N86-11324
SIMPSON, H. M. N86-12037
SIMPSON, J. J. N86-11796
SINCLAIR, C. N86-12049
SIVENKOVA, V. Y. N86-11972
SIVERTSEN, B. N86-11730
SIVY, G. T. N86-11254
SJOEBERG, L. E. N86-11582
SKARITKA, J. N86-12095
SKOBELEV, I. Y. N86-11958
SKRIPKO, G. A. N86-11973
SKUPSKY, S. N86-12131
SKVARENINA, T. L. N86-11415
SLADKY, J. F., JR. N86-11679
SLETOVA, T. L. N86-11991
SLOBODYANIN, V. P. N86-11984
SLOTNICK, D. L. N86-11897
SMARTT, H. B. N86-11481
SMETANA, J. N86-11401
SMIRNOV, V. A. N86-11979
SMIRNOV, V. N. N86-11959
SMITH, E. M. N86-11458
SMITH, G. R. N86-11729
N86-11820
SMITH, J. L., JR. N86-11380
N86-11387
SMITH, K. N86-12019
SMITH, L. N86-12095
SMITH, M. J. N86-11742
SMITH, M. O. N86-11626
SMITH, N. R. N86-11818
SMITH, S. C. N86-11209
SMITH, T. S. N86-11453
SMYERS, S. N86-12169
SMYTH, J. R. N86-11202
SMYTHE, G. R. N86-11757
SOKOLOWSKI, D. E. N86-11496
SOLARZ, R. W. N86-12057
SOLC, I. N86-12070
N86-12071
SOLEM, J. C. N86-12149
SOLODUCHA, B. N86-11574
SOLTANI, P. N86-11665
SOMOGYI, J. N86-11614
SOWELL, J. N86-12178
SOWERS, C. H. N86-12150
SPADAFORA, S. J. N86-11341
SPANNER, M. A. N86-11633
SPENCE, P. N86-12128
SPENCER, J. E. N86-12118
SPIELMAN, B. N86-12073
SPIELMAN, R. B. N86-12123
SPONG, D. A. N86-12082
SRIVASTAVA, V. N86-11619
ST.CLAIR, T. L. N86-11264
STACY, G. N86-12189
STACY, G. J. N86-12186
STACY, H. L. N86-11361
STAPP, H. P. N86-12157
STAR, J. L. N86-11641
STARKS, P. J. N86-11627
STASELKO, D. I. N86-11981
STAVROVSKIY, D. B. N86-11977
STEBBINGS, R. F. N86-12019
STEIN, B. A. N86-11227
N86-11253
STEINER, H. N86-12067
STEINERT, K. G. N86-11584
STEINHOFF, J. N86-11506
STEINMETZ, L. N86-11476
STENCEL, R. E. N86-12168
N86-12180
STEPHENS, J. J., JR. N86-11309
STETSON, K. A. N86-11501
STEVENS, M. J. N86-11199
STEVENSON, G. N86-12008
STEVENSON, W. H. N86-11465
STEWART, H. D. N86-11892
STEWART, J. E. N86-12048
STEYERT, W. A. N86-11391
STIEWITT, H. N86-11169
STILLE, J. K. N86-11267
STINNETT, R. W. N86-12092
STINTON, D. P. N86-11301
STOCK, B. N86-11561
STOLFI, F. R. N86-11376
STOYAHOV, A. V. N86-11985
STRATTAN, R. N86-11837
STRAUSS, M. G. N86-12062
STREET, S. W. N86-11287
STRESTIK, J. N86-11710
STRICKLER, D. J. N86-12099
STRITZKER, B. N86-11468
STROUD, W. J. N86-11540
STROUP, D. W. N86-11365
STRUTIS, J. N86-11803
STUBBS, S. M. N86-11522
STURGESS, G. J. N86-11510
SU, Y. L. N86-11538
SUDARSHAN, T. S. N86-11307
SUJKA, B. R. N86-12119
SUKENIK, C. N. N86-11266
SUKHANOV, V. L. N86-11982
SUKHODREV, N. K. N86-12071
SULLENGER, D. B. N86-11352
SUREK, T. N86-11675
SUSHCHINSKIY, M. M. N86-11986
SUTTON, S. B. N86-11866
SVATEK, L. N86-12070
SVIRIDOV, K. N. N86-11987
SWEENEY, M. A. N86-12090
SWEGLE, J. W. N86-11336
N86-11878
SZAFIR, D. R. N86-11474

T

TAISSERIE, R. N86-11165
TAN, G. N86-11928
TAN, M. N86-12005
TANG, G. N86-11927
TANGO, G. J. N86-12012
N86-12013
TANNA, H. K. N86-11176
TANNENWALD, P. E. N86-11417
TARAKANOV, S. V. N86-11965
TARANIK, J. V. N86-11625
TAUBER, M. E. N86-11196
TAUSS, J. W. N86-11794
TAYLOR, A. H. N86-11525
TAYLOR, J. J. N86-12162
TAYLOR, R. D. N86-12079
TELNIKHIN, A. A. N86-11961
TENG, T. N86-11725
TEOH, J. B. N86-11306
TEXEIRA, P. D. N86-11207
THERIOT, D. N86-12068
THIBERT, J. J. N86-11152
THIESSEN, H. A. N86-12122
THOMAS, I. M. N86-11350
THOMAS, J. B. N86-11913
THOMASCHEWSKI, S. N86-11596
THOMPSON, A. H. N86-11818
THOMPSON, C. M. N86-11347
THOMPSON, D. T. N86-12178
THOMPSON, H. D. N86-11465
THOMPSON, J. R. N86-11331
N86-12146
THOMPSON, R. N86-11518
THORNTON, J. S. N86-11912
THRASHER, D. F. N86-11430
THRONSON, H. A., JR. N86-12167
THULLEN, P. N86-11214
THURMAN, J. L. N86-11656
TIAN, L. N86-11938
TIBBITTS, T. W. N86-11829
TIMROT, D. L. N86-11947
TITARCHUK, V. A. N86-11970
TIWARI, S. N. N86-11167
TOBIASON, A. R. N86-11741
TOBYAS, V. N86-11706
N86-11709
TODD, E. S. N86-11517
TOELLE, R. N86-11216
TOFFER, H. N86-11535
TOKUNOV, Y. M. N86-11974
TOLLERUD, E. I. N86-11778
TOLOMASOV, V. A. N86-11952
TOMCZYK, S. N86-12187
N86-12195
TONER, M. M. N86-11840
TOPCHEYEV, Y. I. N86-11992
TORIKACHVILI, M. S. N86-12155
TORRES, G. N86-12109
TORRISON, L. I. N86-12121
TOTH, J. N86-11405
TOTOMANOV, I. N. N86-11603
N86-11613
N86-11615
TRAINOR, R. J. N86-11305
TRAN, H. K. N86-11340
TREBBLE, W. J. G. N86-11170
TREITL, K. N86-12056
TRENKLER, G. N86-11248
TRESL, J. N86-11585
TRUCANO, T. G. N86-11547
TRUSTY, R. M. N86-11875
TSANG, K. T. N86-12082
TSARENKO, V. I. N86-11395
TSCHERNING, C. C. N86-11586
TSUKERNIKOV, I. Y. N86-11950
TURMAN, B. N. N86-12115
N86-12116
TURNER, J. E. N86-12051
TUSZEWSKI, M. N86-12132
TWARD, E. N86-11388

U

UHRICH, W. J. N86-11412
ULRICH, R. K. N86-12195
UNNINAYAR, S. N86-11814
URBAN, J. N86-12070
USTIN, S. L. N86-11622
USTINOV, N. D. N86-11987
USTINOVSKIY, N. N. N86-11975

V

VAGLIO, R. N86-12153
VAGNER, V. N86-11712
N86-11713
VAICAITIS, R. N86-11220
VAINSHTEIN, L. A. N86-12070
VALNICEK, B. N86-12070
N86-12071
VANDENBERG, A. M. N86-12064
VANDENDOO.., H. M. N86-11773
VANDERBILT, V. C. N86-11544
VANDERPLAATS, G. N. N86-11894
VANE, G. N86-11616
VANETTEN, H. N86-11257

VANHENGST, J. N86-11163
VANKA, S. P. N86-11432
N86-11434
VANNUCCI, R. D. N86-11276
VANROYEN, D. N86-11335
VANRUYMBEKE, M. N86-11576
VARDE, U. N86-11266
VARGA, P. N86-11564
VASILEV, N. N. N86-11972
VASILYAK, L. M. N86-11974
VASTAVA, R. B. N86-11244
VATSA, V. N. N86-11508
VEHANEN, A. N86-12061
VENABLES, J. D. N86-11251
VENTURINI, E. L. N86-11325
VERDON, C. P. N86-12131
VERHAGEN, D. W. N86-11902
VICTORA, R. H. N86-11322
VISCUSO, P. J. N86-12186
VITEK, J. M. N86-11332
VLASOV, D. V. N86-11984
VODYANIK, V. I. N86-11965
VOGELIUS, M. N86-11534
VOGELMANN, J. E. N86-11624
VOGTLIN, G. E. N86-11863
VOLK, C. H. N86-12024
VONALT, C. N86-11246
VONDRAK, J. N86-11587
VOROBEV, V. S. N86-11955
VOYTOVICH, A. P. N86-11568
VYSKOCH, V. N86-11703
VYSKOCIL, P. N86-11592
N86-11616

W

WACKERLE, J. N86-11361
WADE, J. E. N86-11686
WAGNER, A. J. N86-11769
WALKER, G. N86-11374
WALLACE, J. M. N86-11776
N86-11802
N36-11811
WALLTERSTEIN, G. N86-12183
WALSH, J. E. N86-11807
WAMBSGANSS, M. W. N86-11548
WAN, W. W. N86-11382
WANG, B. N86-11923
N86-11941
WANG, G. N86-11932
WANG, J. N86-11922
N86-11934
N86-11935
N86-12003
WANG, J. J. H. N86-11408
WANG, J. W. N86-12125
WANG, K. W. N86-11533
WANG, K. Y. N86-11433
WANG, L. N86-11382
WANG, R. N86-11929
WANG, S. I. N86-11360
WANG, X. N86-11941
WANG, Y. N86-11942
WARNER, J. D. N86-12134
N86-12135
WASHBURN, J. N86-12145
WATCHMAKER, G. N86-11834
WATKINS, A. D. N86-11481
WATKINS, V. E., JR. N86-11230
N86-11233
WATKINS, W. B. N86-11499
WATTERSON, I. G. N86-11732
WATTS, G. A. N86-11157
WEARE, B. C. N86-11797
WEART, S. R. N86-12152
WEAVER, J. N. N86-12049
WEBB, D. M. N86-11359
WEBBINK, R. F. N86-12174
WEICKMANN, K. M. N86-11781
WEIDER, H. H. N86-11316
WEIKLE, D. H. N86-11503
WEINBERG, B. N86-11670
WEINER, D. N86-11416
WEINZAPFEL, C. N86-11350
WEISE, H. N86-11617
WEIZER, V. G. N86-11671
WELCH, J. J. N86-12049
WELLER, J. P. N86-11358
WELLMAN, G. W. N86-11354
WENDROFF, B. N86-11435
WENDT, A. N86-12040
WENG, W. T. N86-12091
N86-12124
WENG, Z. N86-11937
WERBY, M. F. N86-12012
N86-12013

WERNER, M. W. N86-12185
WEST, R. E. N86-11433
WEST, R. N. N86-11330
WHITE, C. W. N86-11468
WHITE, K. N86-11343
WIBERLEY, S. E. N86-11293
WICKLAND, D. E. N86-11623
WIENS, D. A. N86-[illegible]699
WIETING, M. N86-11875
WILBECK, J. S. N86-12142
WILDER, J. G. N86-11350
WILFORD, D. F. N86-11171
WILKES, J. S. N86-11302
WILKINS, S. C. N86-11461
WILLEKE, F. N86-12105
WILLIAMS, A. H. N86-11419
N86-11420
WILLIAMS, G. N86-12109
WILLIAMS, J. N86-11170
WILLIAMS, J. M. N86-11849
WILLIAMSON, D. L. N86-11325
WILLIAMSON, W., JR. N86-11864
WILLIS, A. N86-12165
WILSON, A. J. N86-11290
WILSON, J. M. N86-12116
WILSON, P. B. N86-12049
N86-12050
WILSON, R. L. N86-11853
WILSON, W. B. N86-12048
WILT, M. J. N86-11722
WINSTON, J. S. N86-11793
N86-11813
WINTER, C. N86-11389
WINTERGILL, M. C. N86-11342
WISCHMANN, K. B. N86-11355
WITTE, W. G., JR. N86-11299
WITTLIN, G. N86-11898
WITTRUP, R. J. N86-11686
WOO, H. N86-11885
WOOD, B. L. N86-11640
WOOD, L. K. N86-11171
WOOD, P. A. D. N86-12197
WOODS, E. N86-11192
WOODWORTH, J. R. N86-12109
WOOLF, N. J. N86-12181
WORM, B. N86-11660
WRIGHT, H. A. N86-12051
WRIGHT, L. W. N86-12027
WRIGHT, P. B. N86-11776
WRIGHT, S. M. N36-11406
WRIGHT, T. P. N86-12128
WRIGLEY, R. C. N86-11640
WU, H. N86-11937
WYNN, S. L. N86-11658

X

XIA, J. N86-11588
XIE, S. N86-11429
XING, D. N86-11936
XINYAO, H. N86-12001
XU, L. N86-11942
XU, W. N86-11924
XU, Y. N86-11923

Y

YAMAMURA, Y. N86-11212
YAN, J. N86-11942
YANG, C. L. N86-12136
YANG, R. N86-11806
YANG, S. N86-11925
YANTA, W. J. N86-11453
YAO, N. P. N86-11423
YAPTEV, V. V. N86-11979
YAPNAL, B. N86-11787
YATSENKO, V. V. N86-11983
YATSKIV, Y. S. N86-11589
YEAGER, W. T., JR. N86-11523
YEE, H. C. N86-11907
N86-11909
YEGOROV, S. Y. N86-11953
YEUNG, S. K. N86-11205
YNGVESSON, K. S. N86-11399
YOO, K. C. N86-11665
YOOL, S. R. N86-11641
YOSHIMURA, H. R. N86-11867
YOUNG, R. E. N86-11199
YU, H. N86-11429
YU, M. N86-11941
YUAN, V. N86-12033
YUAN, Y. N86-12003

Z

ZABAZNOV, A. M. N86-11973
ZABOLOTSKAYA, Y. A. N86-11948
ZARIKOV, Y. V. N86-11979
ZAYARNYY, D. A. N86-11975
ZHANG, F. N86-11375
ZHANG, L. N86-12151
ZHANG, W. N86-11931
ZHANG, X. N86-11939
ZHANG, Y. N86-11934
N86-11935
ZHANG, Y. D. N86-11382
ZHANG, Z. N86-12003
ZHAO, X. N86-11920
ZHDANOV, E. A. N86-11973
ZHENG, S. N86-11942
ZHENG, Z. N86-12005
ZHITNIK, I. A. N86-12071
ZHOU, B. N86-11943
ZHU, F. N86-11941
ZHU, H. N86-12151
ZHU, X. N86-11931
ZHU, Z. N86-11643
N86-11927
ZHUCHENKO, V. S. N86-11966
ZIMMER, H. N86-11162
ZIMMERMAN, J. E. N86-11368
ZSCHAU, J. N86-11590
ZUFELT, J. N86-11827
ZUREY, E. C., JR. N86-11213
ZUYEV, V. S. N86-11977
ZVEREV, N. I. N86-11959

CORPORATE SOURCE INDEX

SCIENTIFIC AND TECHNICAL AEROSPACE REPORTS VOLUME 24 NUMBER 2

Typical Corporate Source Index Listing

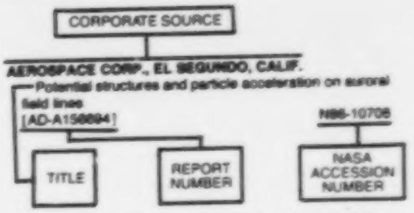
CORPORATE SOURCE
AEROSPACE CORP., EL SEGUNDO, CALIF.
Potential structures and particle acceleration on auroral field lines
[AD-A156694]
N86-10706
TITLE
REPORT NUMBER
NASA ACCESSION NUMBER

Listings in this index are arranged alphabetically by corporate source. The title of the document provides the user with a brief description of the subject matter. The report number helps to indicate the type of document cited (e.g., NASA report, translation, NASA contractor report). The NASA accession number denotes the number by which the citation is identified. The titles are arranged under each corporate source in ascending accession number order.

A

ACADEMIA SINICA, BEIJING (CHINA).

On the lunar tidal effect in the latitude observations at Tianjin N86-11565

Research on the computational methods of gravity topographic effect N86-11578

On the comparison and choice between the formulas of the Earth tidal correction in astronomical time and latitude observation N86-11588

ACADEMY OF SCIENCES, POTSDAM (EAST GERMANY).

Proceedings of the 5th International Symposium Geodesy and Physics of the Earth, part 1 [REPT-81-PT-1] N86-11549

Figure of the Earth, moon, and planets N86-11550

New aspects of the geodetic boundary value problems N86-11553

An attempt to detect geometric tidal information using Lageos laser ranging data N86-11558

Some results of an eight years gravimetric registration series N86-11559

Results concerning rheological parameters of the Earth N86-11567

Proceedings of the 5th International Symposium Geodesy and Physics of the Earth, part 2 [REPT-81-PT-2] N86-11568

On the influence of coupling torques between the Earth's core and mantle on parameters and components of the rotation of the Earth N86-11572

Influences of systematic differences between different star catalogues on the results of latitude and time determinations with the PZT 2 N86-11575

On the comparison of the results of two different E-W-strainmeters N86-11583

Proceedings of the 5th International Symposium Geodesy and Physics of the Earth, part 3 [REPT-81-PT-3] N86-11591

Space-time variating geological masses by space-time variating geodetic measurements N86-11595

Geokinematic models for the gravimetric W - E profile of the GDR N86-11596

An optimum use of sea-level recordings N86-11617

ACADEMY OF SCIENCES OF THE UKRAINIAN SSR, KIEV (USSR).

On reducing the effect of horizontal displacements of the lithospheric plates from the observations carried out by global geodynamic network (on example the GEOSS-REA network) N86-11589

ACADEMY OF SCIENCES (USSR), MOSCOW.

The potentialographical problem and the conception of gravitating disks N86-11579

Near-surface deformations and stresses in the area of the Tolbachik great fissure eruption of 1975-1976 (Kamchatka) from geodetic data N86-11600

Recent vertical crustal movements of the Carpathian-Balkan region and their relationship with neotectonic movements and geophysical fields N86-11609

On the relation between recent crustal movements, the surface of the basement complex and neotectonic displacements of the East-European platform N86-11610

ADA JOINT PROGRAM OFFICE, ARLINGTON, VA.

Military standard common APSE (Ada Programming Support Environment) interface set (CAIS) [AD-A157589] N86-11905

ADVISORY GROUP FOR AEROSPACE RESEARCH AND DEVELOPMENT, NEUILLY-SUR-SEINE (FRANCE).

Aerodynamics and Acoustics of Propellers [AGARD-CP-366] N86-11147

AERITALIA S.P.A., POMIGLIANO D'ARCO (ITALY).

Cabin noise reduction for a new development turboprop commuter aircraft N86-11173

AERONAUTICAL RESEARCH LABS., MELBOURNE (AUSTRALIA).

NERF: A computer program for the numerical evaluation of reliability functions user manual [ARL/STRUC-R-411] N86-11487

AEROSPACE CORP., EL SEGUNDO, CALIF.

Impurity monitoring by laser-induced fluorescence techniques [DE85-014142] N86-11356

The use of wall-coated cells in atomic frequency standards [AD-A157435] N86-12024

AEROSPACE CORP., LOS ANGELES, CALIF.

The mass of hot, shocked CO in Orion: First observations of the J = 17 yields J = 16 transition at 153 microns [AD-A157323] N86-12189

AGRICULTURAL RESEARCH SERVICE, BELTSVILLE, MD.

Hydrologic data for experimental agricultural watersheds in the US, 1975 [PB85-197317] N86-11656

AGRICULTURAL UNIV., WROCLAW (POLAND).

Adjustment of the latitude data by least-squares collocation approach N86-11562

AIR COMMAND AND STAFF COLL., MAXWELL AFB, ALA.

Coming soon to a theater near you: The microwave landing system [AD-A156468] N86-11190

Evaluation of fault reporting/fault isolation for F-15 aircraft [AD-A156516] N86-11197

An introduction to electrical breakdown in dielectrics [AD-A156465] N86-11415

Recognition and control of low level wind shear [AD-A156500] N86-11758

A computer engineering curriculum for the Air Force Academy: An implementation plan [AD-A156464] N86-11857

A computer-based educational approach to the Air Command and Staff College associate program [AD-A156460] N86-12160

Commercialization of space: National policy and defense needs [AD-A156517] N86-12162

AIR FORCE ACADEMY, COLO.

Identification of metal ion chloro complexes in an ambient temperature molten salt [AD-A157295] N86-11302

AIR FORCE INST. OF TECH., WRIGHT-PATTERSON AFB, OHIO.

Feedback stabilization of optical interferometer [AD-A156912] N86-11459

Application of an objective analysis scheme to mesoscale observational network design [AD-A156911] N86-11760

AIR FORCE SYSTEMS COMMAND, WRIGHT-PATTERSON AFB, OHIO

The measurements of axisymmetric air turbulent jet flow with an individual realization laser velocimeter system [AD-A157554] N86-11429

Meteorology of the Persian Gulf and of several airports on the Arabian Coast [AD-A157441] N86-11761

AIR FORCE WRIGHT AERONAUTICAL LABS., WRIGHT-PATTERSON AFB, OHIO.

Acetylene terminated matrix resins N86-11261

AIR PRODUCTS AND CHEMICALS, INC., ALLENTOWN, PA.

Four K refrigerators with a new compact heat exchanger N86-11391

AIRCRAFT RESEARCH ASSOCIATION LTD., BEDFORD (ENGLAND).

A review of ARA research into propeller aerodynamic prediction methods N86-11151

ALABAMA UNIV., BIRMINGHAM.

Improvement in wear performance of surgical Ti-6Al-4V alloy by ion implantation of nitrogen or carbon [DE85-013986] N86-11849

ALBERTA UNIV., EDMONTON.

Application of high order acoustic finite elements to transmission losses and enclosure problems N86-12006

AMERICAN CYANAMID CO., STAMFORD, CONN.

Recent developments in polyimide and bismaleimide adhesives N86-11270

AMERICAN INST. OF BIOLOGICAL SCIENCES, ARLINGTON, VA.

Assessments and viewpoints on the biological and human health effects of Extremely Low Frequency (ELF) electromagnetic fields: Compilation of commissioned papers for the ELF literature review project [AD-A156942] N86-11839

AMERICAN INST. OF MINING, METALLURGICAL, AND PETROLEUM ENGINEERS, INC., WASHINGTON, D. C.

International project in history of solid state physics [DE85-014843] N86-12152

ANALYTIC AND COMPUTATIONAL RESEARCH, INC., LOS ANGELES, CALIF.

Probability encoding of hydrologic parameters for basalt. Elicitation of expert opinions from a panel of three basalt waste isolation project staff hydrologists [DE85-014665] N86-11652

APPLIED DECISION ANALYSIS, INC., MENLO PARK, CALIF.

Probability encoding of hydrologic parameters for basalt. Elicitation of expert opinions from a panel of three basalt waste isolation project staff hydrologists [DE85-014665] N86-11652

ARC MACHINES, INC., PACOIMA, CALIF.

Automatic orbital GTAW welding: Highest quality welds for tomorrow's high-performance systems N86-11229

ARGONNE NATIONAL LAB., ILL.

Dense random packed model for amorphous Ni35Zr65: Influence of the heat of mixing [DE85-014967] N86-11319

Magnetic properties and electronic structure of the actinide systems UAl2, NpAl2 and PuAl2 [DE85-014102] N86-11323

Correlations of chemical, microstructural and mechanical properties of polyethylene piping materials [DE85-013077] N86-11351

Effects of additives and temperature on iron electrode behavior in KOH electrolytes [DE85-011901] N86-11423

Block-implicit coupled calculation of fluid flows [DE85-004038] N86-11432

Block-implicit multigrid calculation of three-dimensional recirculating flows [DE85-010250] N86-11434

Numerical simulation of an equipment hatch for a steel containment vessel to loading beyond the design basis [DE85-010485] N86-11482

Sensitivity of using blunt and sharp crack models in elastic-plastic fracture mechanics [DE85-010288] N86-11537

Viscoelastic creep of high-temperature concrete [DE85-010511] N86-11539

Experimental needs of high temperature concrete [DE85-009700] N86-11541

Concrete creep at transient temperature: Constitutive law and mechanism [DE85-010525] N86-11542

Experimental study on impact/fretting wear in heat exchanger tubes
[DE85-014597] N86-11548

Si(Li)-NaI(Tl) sandwich detector array for measurements of trace radionuclides in soil samples
[DE85-013865] N86-12062

Few-nucleon transfer reactions on deformed nuclei
[DE85-013869] N86-12064

High resolution spectrometer in studies of e(+)e(-) annihilation at (radical)s = 29 GeV
[DE85-013870] N86-12065

Magnetic measurements of monolayer-thickness films of Cr sandwiched by Au
[DE85-015005] N86-12150

Microscopic investigation of NbN sputtered films
[DE85-015000] N86-12153

ARIZONA STATE UNIV., TEMPE.

Jet array impingement heat transfer characteristics
N86-11511

UBV photometry of the 1982-4 eclipse of Epsilon Aurigae: A discussion of the observed light curves
N86-12176

ARIZONA UNIV., TUCSON.

Refined numerical solutions of the transonic flow past a wedge N86-11184

Short range bonding interaction at metal-metal interfaces
[DE85-014442] N86-11334

Reliability analysis of series structural systems
N86-11486

Thin film research. Volume 1
[AD-A157608] N86-12137

Thin film research. Volume 2
[AD-A157609] N86-12138

Metallic multilayers and superlattices
[DE85-014444] N86-12141

Modelling Epsilon Aurigae without solid particles
N86-12181

ARMY AVIATION RESEARCH AND DEVELOPMENT COMMAND, CLEVELAND, OHIO.

Theoretical and experimental comparison of vapor cavitation in dynamically loaded journal bearings
[NASA-TM-87121] N86-11425

ARMY COLD REGIONS RESEARCH AND ENGINEERING LAB., HANOVER, N. H.

Thermal convection in snow
[AD-A157577] N86-11648

Periglacial landforms and processes in the southern Kenai Mountains, Alaska
[AD-A157459] N86-11718

Workshop on Permafrost Geophysics
[AD-A157485] N86-11719

Survey of ice problem areas in navigable waterways
[AD-A157477] N86-11827

ARMY CONSTRUCTION ENGINEERING RESEARCH LAB., CHAMPAIGN, ILL.

Uncertainty assessment in life cycle cost analysis
[AD-A157414] N86-11488

ARMY ENGINEER WATERWAYS EXPERIMENT STATION, VICKSBURG, MISS.

User guide for WIFM-SAL (WES Implicit Flooding Model-SAL): A two-dimensional vertically integrated, time-varying estuarine transport model
[AD-A157446] N86-11825

ARMY ENVIRONMENTAL HYGIENE AGENCY, ABERDEEN PROVING GROUND, MD.

Health hazard evaluation of liquid monopropellants. Phase 4. Subchronic inhalation of hydroxylammonium nitrate, January 1985
[AD-A157623] N86-11844

ARMY RESEARCH INST. OF ENVIRONMENTAL MEDICINE, NATICK, MASS.

An atropinized heat-stressed rat model: Anticholinergic and anticholinesterase drug potency
[AD-A157620] N86-11832

Perceptual and physiological responses during exercise in cool and cold water
[AD-A157334] N86-11840

Physiological effects of training
[AD-A157417] N86-11841

ARNOLD ENGINEERING DEVELOPMENT CENTER, ARNOLD AIR FORCE STATION, TENN.

Calculation of particle dynamics effects on laser velocimeter data N86-11438

ATMOSPHERIC AND ENVIRONMENTAL RESEARCH, INC., CAMBRIDGE, MASS.

Effect of initialization on diagnoses of large-scale circulation statistics from WMC analyses N86-11817

AUSTRALIAN NUMERICAL METEOROLOGY RESEARCH CENTER, MELBOURNE.

Interannual climate variability in a low vertical resolution spectral atmospheric model N86-11795

AVIONS MARCEL DASSAULT, SAINT-CLOUD (FRANCE).

Problems of the integration of propellers in airframes, especially for high performance twin-engine aircraft
N86-11165

B

BALL AEROSPACE SYSTEMS DIV., BOULDER, COLO.

Joule-Thomson valves for long term service in space cryocoolers N86-11393

BATTELLE COLUMBUS LABS., OHIO.

Explosive welding in the 1990's N86-11237

BATTELLE PACIFIC NORTHWEST LABS., RICHLAND, WASH.

Exploratory development of FMR (ferromagnetic resonance) advanced surface flaw detection methods
[AD-A157438] N86-11489

BELGIAN ROYAL OBSERVATORY, UCCLE.

Interactions between oceanic and gravity tides, as analysed from world-wide Earth tide observations and ocean models N86-11576

BELL TELEPHONE LABS., INC., MURRAY HILL, N. J.

A 2D ACAR momentum density study of the nature of the positron surface state on Al(100)
[DE85-014830] N86-11330

BOEING AEROSPACE CO., SEATTLE, WASH.

Laser angle sensor
[NASA-CR-172369] N86-11207

High-temperature adhesive development and evaluation N86-11250

Evaluation of a high temperature adhesive for fabricating graphite/PMR-15 polyimide structures N86-11268

Characterization methodology for PMR-15
N86-11272

BOEING COMMERCIAL AIRPLANE CO., SEATTLE, WASH.

Environmental stability graphite/PMR-15 composites
N86-11284

Development of design data for propulsion PMR-15 composites N86-11285

Application of Gr/PMR-15 to commercial aircraft
N86-11289

BRANDEIS UNIV., WALTHAM, MASS.

A 2D ACAR momentum density study of the nature of the positron surface state on Al(100)
[DE85-014830] N86-11330

Research in elementary particle physics
[DE85-014062] N86-12041

BRITISH METEOROLOGICAL OFFICE, BRACKNELL (ENGLAND).

Worldwide marine temperature variations on the season to century time scale N86-11771

BROOKHAVEN NATIONAL LAB., UPTON, N. Y.

A 2D ACAR momentum density study of the nature of the positron surface state on Al(100)
[DE85-014830] N86-11330

Intergranular attack and stress corrosion cracking of alloy 600 in high-temperature caustic solutions containing contaminants
[DE85-014106] N86-11335

Optimized ground-coupled heat pump system design for northern climate
[DE85-014065] N86-11484

Thyroid absorbed dose for people at Rongelap, Utirik and Sifo on March 1, 1954
[DE85-014695] N86-11846

Design for a high field combined function superferric magnet
[DE85-014827] N86-11944

AGS polarized beam facility
[DE85-011834] N86-12038

Possibilities of polarized protons in Sp anti p S and other high energy hadron colliders
[DE85-012517] N86-12044

Antinucleon-nucleus elastic and inelastic scattering
[DE85-012510] N86-12059

Vacancies in thermal equilibrium in Nb
[DE85-014832] N86-12061

Spin dependence of the coherent scattering lengths of (27)Al and admixture of s- and d-partial waves
[DE85-013299] N86-12066

Increased intensity performance of the Brookhaven AGS
[DE85-013371] N86-12091

Window frame or superferric magnet design for low B(3T) heavy ion storage ring study
[DE85-013288] N86-12095

Physics opportunities with relativistic heavy ion accelerators
[DE85-014190] N86-12117

Neutron scattering studies of the heavy Fermion superconductors
[DE85-014829] N86-12144

Icosahedral incommensurate crystals
[DE85-012512] N86-12147

BROWN UNIV., PROVIDENCE, R. I.

Uniaxial tensile deformation and fracture of dual-phase steels
[DE85-015034] N86-11538

Spectroscopy of Moses Rock kimberlite diatreme
N86-11635

BULGARIAN ACADEMY OF SCIENCE, SOFIA.

Some geodetic aspects of the problem of checking the plate-tectonic model of seismicity in southeastern Europe N86-11603

Statistical analysis and interpretation of Earth crustal movements in northeast Bulgaria N86-11613

Relation between earthquake focal intensity and recent vertical Earth's crustal movements in the Rila-Rhodope seismic region N86-11615

BUSINESS AND COMMERCIAL AVIATION, WHITE PLAINS, N.Y.

Corporate/commuter airlines meteorological requirements N86-11739

C

CALIFORNIA INST. OF TECH., PASADENA.

Dominant moving species in the formation of amorphous NZr by solid-state reaction
[DE85-014855] N86-12053

Investigations of deep level defects in semiconductor material systems N86-12133

CALIFORNIA UNIV., BERKELEY.

The hollow sphere model for porous metals and metal powders N86-11308

Elastic wave scattering of a Gaussian incident beam from an interface crack in a layered half space submerged in water N86-11490

Current research on circular saw and band saw vibration and stability N86-11533

Bayesian extensions to a basic model of software reliability
[AD-A157296] N86-11901

Saturation characteristics of counterstreaming warm electrons
[DE85-014390] N86-12040

Simulation of quiet start magnetized plasmas, including Maxwellian and velocity-space ring distributions
[DE85-014394] N86-12112

Particle simulation of the low-(ALPHA) Pierce diode
[DE85-014435] N86-12113

CALIFORNIA UNIV., BERKELEY. LAWRENCE BERKELEY LAB.

Electronic and magnetic structure of chromium surfaces and chromium monolayers on iron
[DE85-014542] N86-11322

Electromagnetic soundings for geothermal resources in Dixie Valley, Nevada
[DE85-011986] N86-11722

Medical heavy ion accelerator proposals
[DE85-015247] N86-12026

Two-dimensional linacs
[DE85-015129] N86-12029

Sources of radioactive ions
[DE85-015251] N86-12030

Calculations of physical and chemical reactions produced in irradiated water containing DNA
[DE85-012699] N86-12051

Muon decay
[DE85-012590] N86-12067

Beam position monitor for storage rings
[DE85-013295] N86-12104

Model of amorphous silicon layer regrowth
[DE85-012608] N86-12145

EPR: What has it taught us
[DE85-014525] N86-12157

CALIFORNIA UNIV., DAVIS.

Understanding El Nino events using a simple dynamical atmosphere model N86-11797

CALIFORNIA UNIV., LIVERMORE. LAWRENCE LIVERMORE LAB.

Fluids at high dynamic pressures and temperatures
[DE85-014812] N86-11305

Processing and microstructural characterization of B4C-Al cermets
[DE85-013195] N86-11326

Pulse duration dependence of 1064-nm laser damage thresholds of porous silica antireflection coatings on fused silica substrates
[DE85-013207] N86-11350

Crystal class and the electrooptic effect
[DE85-015240] N86-11353

Upgrade of the EM transient range monocone antenna
[DE85-013181] N86-11413

Spectrally-broad picosecond light source
[DE85-015177] N86-11471

Surface properties of shocked lead
[DE85-009582] N86-11476
Uncertainties in the radiative properties of smoke and their effects on climate assessments
[DE85-015187] N86-11691
Study of heavy gas effects on the atmospheric dispersion of dense gases, revision 1
[DE85-012917] N86-11693
Detection of chromosomal abnormalities in human sperm
[DE85-014176] N86-11834
Prospects for DNA methods to measure human heritable mutation rates
[DE85-014555] N86-11847
Psychological aspects of personnel contamination
[DE85-012955] N86-11853
Software engineering tools that work N86-11859
An application of real-time analysis and design tools in software development N86-11860
Net-2 models of cavities and diodes N86-11863
Particle pushing techniques for use with finite element based field calculations N86-11865
ICARUS: A computer code for modeling complex one-dimensional heat conduction on mainframes and micros N86-11866
Analysis of ultrasonic waves in a bounded medium N86-11869
An evaluation of three graphics packages: The methodology and results N86-11870
A data translator for engineering measurements N86-11875
SIG: A general-purpose signal processing code N86-11876
Thermo-mechanical analyses of laser-heated surfaces N86-11877
Photoelectron trajectory analyses of streak tubes N86-11880
Ramp response estimation and spectrum extrapolation for ultrasonic scattering N86-11881
Flexible vibrations of a uniform elastic beam with arbitrary supports and lumped masses N86-11885
Computer codes for fluid-structure interactions N86-11887
Transition radiation and coherent electron-photon scattering
[DE85-014813] N86-12031
Transition radiation as a practical X-ray source
[DE85-013201] N86-12036
Physics overview of AVLIS
[DE85-014854] N86-12057
Physics modeling of tandem mirror devices with high field test cell inserts
[DE85-011870] N86-12066
Mirror Fusion Test Facility (MFTF-B): Status
[DE85-012953] N86-12087
Electrical supply for MFTF-B superconducting magnet system
[DE85-012932] N86-12094
Multivariable current control for electrically and magnetically coupled superconducting magnets, revision 1
[DE85-012943] N86-12108
New concepts for drift pumping a thermal barrier with RF
[DE85-013591] N86-12114
Interaction of the ATA beam with the TM030 mode of the accelerating cells
[DE85-014850] N86-12120
New harmonic materials: Index engineering: Thin-thick quadrature frequency conversion
[DE85-012976] N86-12156
Annotated bibliography of human factors applications literature
[DE85-012957] N86-12161

CALIFORNIA UNIV., LOS ANGELES.
A direct model reference adaptive approach to the control of space stations N86-11219
Acoustic emission during deformation and fracture of A533B pressure vessel steel N86-11306
FINESSE: Study of the issues, experiments and facilities for fusion nuclear technology research and development, volume 4
[DE85-010947] N86-12130
Fractal-like, but non-fractal, behavior of one step dipolar energy transfer on regular lattices with excluded volume
[AD-A157382] N86-12136

CALIFORNIA UNIV., SAN DIEGO, LA JOLLA.
Surface and interfacial properties of Ga0.47In0.53As alloys
[AD-A157343] N86-11316

CALIFORNIA UNIV., SANTA BARBARA.
Application of AIS technology to forest mapping N86-11641
ADS: A FORTRAN program for automated design synthesis: Version 1.10
[NASA-CR-177985] N86-11894

CALSPAN ADVANCED TECHNOLOGY CENTER, BUFFALO, N.Y.
Mission-oriented requirements for updating MIL-H-8501: Calspan proposed structure and rationale
[NASA-CR-177371] N86-11204

CALSPAN FIELD SERVICES, INC., ARNOLD AFS, TENN.
Particle size distributions of several commonly used seeding aerosols N86-11441
Recent experience in seeding transonic/supersonic flows at AEDC N86-11447

CANADIAN CLIMATE CENTRE, DOWNSVIEW (ONTARIO).
Horizontal fluxes in real and model atmospheres N86-11792

CARLETON UNIV., OTTAWA (ONTARIO).
Development of modern turboprop engines N86-11168

CASE WESTERN RESERVE UNIV., CLEVELAND, OHIO.
The synthesis, characterization and thermal chemistry of modified norbornenyl PMR endcaps N86-11266
Correcting for particle counting bias error in turbulent flow N86-11439
Time-of-flight anemometer for hot section applications N86-11504

CENTRE NATIONAL DE LA RECHERCHE SCIENTIFIQUE, ORSAY (FRANCE).
Design concept and performance prediction technique for potential flows around advanced propellers N86-11150

CESKOSLOVENSKA AKADEMIE VED, ONDREJOV.
Publications of the Astronomical Institute of the Czechoslovak Academy of Sciences, no. 61
[PUBL-61] N86-12069
Wolter 1 type X-ray mirror system with mean resolution and maximum effective collecting area for the spectral region of 1-10 nm N86-12070
Galvanoplastic grazing incidence mirrors for verticle experiments: The tandem tests in soft X-rays N86-12071

CESKOSLOVENSKA AKADEMIE VED, PRAGUE.
Tidal friction, the Earth's rotation and hypothesis of an expanding Earth N86-11556
Geodynamic effects due to Earth's deformation N86-11585
Polar motion between 1900.0 and 1984.0 as determined by different techniques N86-11587
Geophysical Works, 1982, volume 30 N86-11702
On the gravitational effect of the crust-mantle boundary in central Europe N86-11703
Attenuation of macroseismic effects of earthquakes N86-11705
Seismology in civil engineering N86-11707
Short-period SVSN-4 seismograph N86-11708
Statistical properties of geomagnetic pulsations at the Fuerstenfeldbruck Observatory determined by means of pulsation indices. Part 3: Correlation with the parameters of the interplanetary magnetic field N86-11710
Determination of the depth of a conductivity anomaly by separating the geomagnetic variation field into its external and internal part N86-11711
Numerical solution of ionospheric filtration of ULF waves. Part 2: Application N86-11713
Ion whistlers in middle latitudes observed by the Interkosmos-14 satellite N86-11714
On the instability of vortex series N86-11715

CINCINNATI UNIV., OHIO.
Compatibilizing effect of random or block copolymer added to binary mixture of homopolymers
[AD-A157384] N86-11345

CITY COLL. OF THE CITY UNIV. OF NEW YORK.
A 2D ACAR momentum density study of the nature of the positron surface state on Al(100)
[DE85-014830] N86-11330

CITY UNIV. OF NEW YORK, STATEN ISLAND.
Non-geometrical optics investigation of mode conversion in weakly relativistic inhomogenous plasmas
[DE85-013480] N86-12102

CLARK UNIV., WORCESTER, MASS.
Climatic events of the west coast of southern Africa N86-11784

CLARKSON UNIV., POTSDAM, N.Y.
Magnetic filtration N86-11917
Elastic and inelastic light scattering of colloidal particles
[AD-A157335] N86-12072

COAST GUARD, ELIZABETH CITY, N.C.
Adverse weather impact on aviation safety, investigation and oversight N86-11742

COAST GUARD RESEARCH AND DEVELOPMENT CENTER, GROTON, CONN.
An evaluation of CASP (computer assisted search planning program) drift predictions near the New England Shelf/Slope Front
[AD-A157447] N86-11826

COLLEGE OF WILLIAM AND MARY, WILLIAMSBURG, VA.
Characterization of the relationship of the cure cycle chemistry to cure cycle processing properties
[NASA-CR-176256] N86-11339

COLORADO SCHOOL OF MINES, GOLDEN.
Chemical synthesis under shock compression
[DE85-015166] N86-11325

COLORADO UNIV., BOULDER.
Satellite observations of a large-amplitude 40-50 day oscillation in upper tropospheric temperature over the equatorial Pacific Ocean during the 1982-83 ENSO event N86-11776
Relationships between Pacific northwest coast climate and ENSO events N86-11787
Tropical convection and North American cyclones during the 1982-83 El Nino N86-11809
High energy physics
[DE85-014272] N86-12063

COLUMBIA UNIV., NEW YORK.
Vibrations and structureborne noise in space station
[NASA-CR-176291] N86-11220

COMMONWEALTH SCIENTIFIC AND INDUSTRIAL RESEARCH ORGANIZATION, SYDNEY (AUSTRALIA).
Analysis of aircraft spectrometer data with logarithmic residuals N86-11636

COMMUNICATIONS RESEARCH CENTRE, OTTAWA (ONTARIO).
CRC control systems laboratory gyro test facility
[CRC-1385] N86-11205

COMPUTER SCIENCES CORP., EL SEGUNDO, CALIF.
IUE observations of the 1982-84 eclipse of Epsilon Aurigae N86-12172

CONNECTICUT UNIV., STORRS.
Elevated temperature biaxial fatigue
[NASA-CR-175009] N86-11526

CORNELL UNIV., ITHACA, N.Y.
Importance of phytoalexin tolerance and detoxification for pathogenicity
[DE85-014759] N86-11257
Properties of crazes and deformation zones in glassy polymers
[AD-A157428] N86-11346
Fiscal year 1983 program report of the Water Resources Research Institute of New York State
[PB85-217024] N86-11662
Design and optimization of the PBFA 2 vacuum interface and transmission lines for light ion fusion
[DE85-012809] N86-12092
Submillimeter observations of OH and CH in M42
[NASA-TM-86723] N86-12186
The mass of hot, shocked CO in Orion: First observations of the J = 17 yields J = 16 transition at 153 microns
[AD-A157323] N86-12189

CRANFIELD INST. OF TECH., BEDFORD (ENGLAND).
On the aerodynamics of installed propellers N86-11154
Ground effect on a rotor wake
[COLL-AERONAUTICS-8510] N86-11187

CREIGHTON UNIV., OMAHA, NEBR.
Concurrent and lagged relationships between precipitation frequency and 700 mb heights N86-11808

D

DAYTON UNIV., OHIO.
Effects of manufacturing processes on structural allowables
[AD-A157596] N86-11318
Studies on chalcogenide films
[AD-A157340] N86-11343

DE HAVILLAND AIRCRAFT CO. OF CANADA LTD., DOWNSVIEW (ONTARIO).
Performance evaluation of full scale propellers by wind tunnel test N86-11160
Some considerations in propeller and airframe integration N86-11164

DEFENCE MATERIEL ADMINISTRATION, STOCKHOLM (SWEDEN).
Infrasound: A summary of interesting articles
[FMV:ELEKTRO-A12:142/83] N86-12017

DELAWARE UNIV., NEWARK.
Discrimination of coastal vegetation and biomass: Using AIS data N86-11639

DELTA AIR LINES, INC., ATLANTA, GA.
Airline meteorological requirements N86-11737

DEPARTMENT OF ENERGY, IDAHO FALLS, IDAHO.
Advanced mechanical heat pump technologies for industrial applications
[DE85-014613] N86-11483

DEPARTMENT OF ENERGY, MORGANTOWN, W. VA.
Arctic Energy Technologies Workshop Proceedings
[DE85-003360] N86-11649

Status of models for analysis of Western Gas Sands [DE85-003398] N86-11653

DEPARTMENT OF THE NAVY, WASHINGTON, D. C.

Chemical bonding agent for suppression of rusty bolt intermodulation interference [AD-D011747] N86-11315

Ion beam neutralizer [AD-D011741] N86-12043

DETROIT DIESEL ALLISON, MICH.

Gas side heat transfer N86-11567

DEUTSCHE FORSCHUNGS- UND VERSUCHSANSTALT FUER LUFT- UND RAUMFAHRT, BRUNSWICK (WEST GERMANY).

A unified approach for the aerodynamics and acoustics of propellers in forward motion N86-11155

Full-scale flight and model-scale wind tunnel tests on the nearfield noise characteristics of aircraft propellers N86-11172

DEUTSCHE FORSCHUNGS- UND VERSUCHSANSTALT FUER LUFT- UND RAUMFAHRT, GOETTINGEN (WEST GERMANY).

Aeroacoustic wind tunnel measurements on propeller noise N86-11169

DEUTSCHES GEODAETISCHES FORSCHUNGSINSTITUT, MUNICH (WEST GERMANY).

Geophysical interpretation of global geoid undulations and mean gravity anomalies N86-11560

DEXTER CORP., PITTSBURG, CALIF.

New processable modified polyimide resins for adhesive and matrix applications N86-11269

DORNIER-WERKE G.M.B.H., FRIEDRICHSHAFEN (WEST GERMANY).

Investigations of modern general aviation propellers N86-11162

DOUGLAS AIRCRAFT CO., INC., LONG BEACH, CALIF.

Advances in joining techniques used in development of SPF/DB titanium sandwich reinforced with metal matrices N86-11247

DOWTY ROTOL LTD., GLOUCESTER (ENGLAND).

Aerodynamic and structural aspects of propeller and drive for a 1/5 scale wind tunnel programme N86-11163

E

EARTH SATELLITE CORP., CHEVY CHASE, MD.

Analysis of AIS data of the Recluse Oil Field, Recluse, Wyoming N86-11632

EAST ANGLIA UNIV., NORWICH (ENGLAND).

A 2D ACAR momentum density study of the nature of the positron surface state on Al(100) [DE85-014630] N86-11330

Global surface air temperature variations: 1983-1984 N86-11764

EDGERTON, GERMESHAUSEN AND GRIER, INC., IDAHO FALLS, IDAHO.

Mechanical properties of rapidly solidified Type 304 stainless steel [DE85-014577] N86-11338

Fabrication and use of zircaloy/tantalum-sheathed cladding thermocouples [EGG-TFBP-6739] N86-11461

Economic evaluation of concurrent welding and nondestructive examination [DE85-014623] N86-11481

Advanced mechanical heat pump technologies for industrial applications [DE85-014613] N86-11483

Data analysis using a data base driven graphic animation system [DE85-014635] N86-11892

Survey of element and isotope importance for fusion safety and environmental assessments [DE85-012415] N86-12047

EIC, INC., NORWOOD, MASS.

Basic studies of the lithium secondary battery [AD-A157449] N86-11673

EIDGENOESSISCHE LANDESTOPOGRAPHIE, BERN (SWITZERLAND).

Recent crustal movements and geophysical interpretation of geodynamic processes in the Alpine mountain belt N86-11604

ELECTROMAGNETIC COMPATIBILITY ANALYSIS CENTER, ANNAPOLIS, MD.

Traffic Alert and Collision Avoidance System Signal Environment Model (TCAS SEM) programmer's reference manual [FAA-PM-85-22] N86-11192

ELTRON RESEARCH, INC., AURORA, ILL.

Investigation of photoelectrode redox polymer junctions [AD-A157556] N86-11304

EMERSON ELECTRIC CO., CALABASAS, CALIF.

Waveguide slot array with CSC2 theta (dot) COS theta pattern N86-11402

ENGINEERING AND ECONOMICS RESEARCH, INC., VIENNA, VA.

Enhanced airport surface detection equipment applications [AD-A157641] N86-11210

ENVIRONMENTAL PROTECTION AGENCY, ATLANTA, GA.

Saltwater wetlands for wastewater management environmental assessment [PB85-201267] N86-11697

ENVIRONMENTAL PROTECTION AGENCY, RESEARCH TRIANGLE PARK, N.C.

Regional-scale (1000 KM) model of photochemical air pollution. Part 3: Tests of the numerical algorithms [PB85-203818] N86-11696

Regional oxidant modeling of the northeast US [PB85-201192] N86-11728

Parameterization of the atmospheric boundary layer for air pollution dispersion models [PB85-193548] N86-11730

ESSEX CORP., ALEXANDRIA, VA.

Annotated bibliography of human factors applications literature [DE85-012957] N86-12161

EUROPEAN SPACE AGENCY, PARIS (FRANCE).

International solar-terrestrial physics program: A plan for the core spaceflight missions [NASA-TM-87511] N86-12194

EXPLOSIVE FABRICATORS, INC., LOUISVILLE, COLO.

Explosive welding of tubular configurated joints for critical applications N86-11238

F

FEDERAL AVIATION ADMINISTRATION, ATLANTIC CITY, N.J.

User's manual for AC-20-53A protection of airplane fuel systems against fuel vapor ignition due to lightning [AD-A157619] N86-11191

Overview of FAA's aircraft icing program N86-11740

A new characterization of supercooled clouds below 10,000 feet AGL N86-11744

FEDERAL AVIATION ADMINISTRATION, WASHINGTON, D.C.

Overview of meteorological inputs to NASP N86-11736

FEDERAL COMPILER TESTING CENTER, FALLS CHURCH, VA.

Ada (trademark) compiler validation summary report: Data general corporation, ADE Ada Compiler, version 2.30.03.12, Eclipse DS/4000, DS/4200, MV/4000-DC, MV/8000-C, MV/8000-2, MV/10000, MV/10000 SX using AOS/VS 5.04 and AOS/RT32 4.001.00 [AD-A157573] N86-11890

FERMI NATIONAL ACCELERATOR LAB., BATAVIA, ILL.

Reduction of sextupole distortion by shuffling magnets in small groups [DE85-013024] N86-12035

Collider Detector at Fermilab (CDF) [DE85-014423] N86-12068

SSC test lattices [DE85-014240] N86-12098

Using the TEVATRON beam position monitor system to investigate transverse phase space [DE85-014261] N86-12105

FLORIDA UNIV., GAINESVILLE.

Spherical torus: An approach to compact fusion at low field. Initial ignition assessments [DE85-012890] N86-12099

FLYING TIGERS-RETIRED, SAN PEDRO, CALIF.

Development of a wind shear performance envelope N86-11746

FOREIGN TRADE COMPUTER CENTRE, PRAGUE (CZECHOSLOVAKIA).

Numerical solution of ionospheric filtration of ULF waves. Part 1: Method N86-11712

FOSTER WHEELER CORP., LIVINGSTON, N.J.

The use of explosive forming for fastening and joining structural and pressure components N86-11240

FREIE UNIV., BERLIN (WEST GERMANY).

Ocean tidal loading along the Blue Road geotraverse in Fennoscandia N86-11571

G

GA TECHNOLOGIES, INC., SAN DIEGO, CALIF.

Energy confinement experiments on Doublet 3 with high power neutral beam heating [DE85-014324] N86-12110

GARRETT TURBINE ENGINE CO., PHOENIX, ARIZ.

Low-cost, net-shape ceramic radial turbine program [AD-A157532] N86-11202

GENERAL ACCOUNTING OFFICE, WASHINGTON, D. C.

Status of the intercontinental ballistic missile modernization program [AD-A157375] N86-11217

GENERAL DYNAMICS/CONVAIR, SAN DIEGO, CALIF.

Effects of real-time thermal aging on graphite/polyimide composites N86-11283

GENERAL ELECTRIC CO., CINCINNATI, OHIO.

Fabrication process of a high temperature polymer matrix engine duct N86-11290

Burner liner thermal/structural load modelling N86-11514

Component-specific modeling N86-11515

The 3D inelastic analysis methods for hot section components N86-11516

GENERAL PNEUMATICS CORP., SCOTTSDALE, ARIZ.

Classification of cryocoolers N86-11374

GEODETIC INST., CHARLOTTENLUND (DENMARK).

On the long-wavelength correlation between gravity and topography N86-11586

GEODETIC INST., HELSINKI (FINLAND).

Finnish measurements of the Fennoscandian land uplift gravity lines in Finland 1966-1984 N86-11606

Comparisons of different observation methods of a LaCoste and Romberg G gravimeter N86-11612

GEOLOGICAL SURVEY, ANCHORAGE, ALASKA.

The 1984 annual report on Alaska's mineral resources [DE85-015235] N86-11651

GEOPRODUCTS CORP., OAKLAND, CALIF.

Honey Lake Geothermal Project, Lassen County, California [DE85-013388] N86-11677

GEORGE WASHINGTON UNIV., HAMPTON, VA.

Vortex studies relating to boundary layer turbulence and noise N86-12015

GEORGIA INST. OF TECH., ATLANTA.

Radiation and scattering performance of microstrip antennas using exotic substrates N86-11408

Analysis of arctic haze scattering and aerosol data obtained during AGASP [AD-A157434] N86-12074

GEORGIA TECH RESEARCH INST., ATLANTA.

Photon induced electron attachment [AD-A156506] N86-11467

GRUMMAN AEROSPACE CORP., BETHPAGE, N.Y.

Polyimide composites: Application histories N86-11286

H

HAMILTON STANDARD, WINDSOR LOCKS, CONN.

The state of the art in propfan turboprop noise N86-11175

HARRIS GOVERNMENT AEROSPACE SYSTEMS DIV., MELBOURNE, FLA.

The design of a thermally efficient 1:256 KU-band feed network for a MMIC phased array N86-11400

HARVARD-SMITHSONIAN CENTER FOR ASTROPHYSICS, CAMBRIDGE, MASS.

The mass of hot, shocked CO in Orion: First observations of the J = 17 yields J = 16 transition at 153 microns [AD-A157323] N86-12189

HARVARD UNIV., CAMBRIDGE, MASS.

Effect of elevated atmospheric CO2 on plant communities. Annual report, 1984-1985 [DE85-015575] N86-11692

The effect of the Hadley circulation on the meridional propagation of stationary waves N86-11732

HAWAII UNIV., HONOLULU.

Transition from the Southern to Northern Hemisphere summer monsoon N86-11799

A cascaded coding scheme for error control [NASA-CR-176276] N86-11895

Infrared photometry of the 1982-4 eclipse of Epsilon Aurigae N86-12170

HAWAII UNIV., MANOA.

A cascaded coding scheme for error control [NASA-CR-176287] N86-11911

HELSINKI UNIV. (FINLAND).

Vacancies in thermal equilibrium in Nb [DE85-014832] N86-12061

HELWAN UNIV., CAIRO (EGYPT).

Explosive welding of aluminum, titanium and zirconium to copper sheet metal N86-11241

HIGHER INST. OF MINING AND GEOLOGY, SOFIA (BULGARIA).

The irregularity in the Earth's annual rotation as a cause of systematic time variation N86-11570

HITCO, GARDENA, CALIF.

V-378A: A modified bismaleimide for advanced composites N86-11287

HONEYWELL, INC., ROSEVILLE, MINN.
Hermetic bellows seal for Braun linear engine: Design, test and demonstration [DE85-013545] N86-11478
HOPKINS PHOENIX OBSERVATORY, ARIZ.
Optical photometry of the 1982-1984 eclipse of Epsilon Aurigae N86-12169
Astronomical research at the Hopkins Phoenix Observatory N86-12182
HOUSTON UNIV., TEX.
Improving the accuracy of the boundary integral method based on the Helmholtz integral N86-12010
HUGHES AIRCRAFT CO., CANOGA PARK, CALIF.
Sheet metal waveguide forming technique N86-11403
HUGHES AIRCRAFT CO., CULVER CITY, CALIF.
An improved processible acetylene-terminated polyimide for composites N86-11262
HUNGARIAN ACADEMY OF SCIENCES, SOPRON.
High frequencies in tidal tilt records N86-11554
Capacitive pendulum with intelligent data collection N86-11577
Mathematical treatment of vertical movements N86-11597
A new apparatus for testing bubble vials, electronic levels and automatic levels N86-11614

I

IIT RESEARCH INST., ANNAPOLIS, MD.
Traffic Alert and Collision Avoidance System Signal Environment Model (TCAS SEM) programmer's reference manual [FAA-PM-85-22] N86-11192
ILLINOIS STATE WATER SURVEY, CHAMPAIGN.
Tropospheric static stability and central North American rainfall during 1979 N86-11801
ILLINOIS UNIV., URBANA.
Land-surface fluctuations and associated climatic variability N86-11807
ILLINOIS UNIV., URBANA-CHAMPAIGN.
Tensile fatigue damage and degradation of random short-fiber SWC composite N86-11259
Operating range of aluminum gallium arsenide quantum-well heterostructure lasers: tunability, power output and high energy emission N86-11464
The embedded operating system project [NASA-CR-176280] N86-11893
Research in the design of high-performance reconfigurable systems [NASA-CR-176275] N86-11897
INSTITUT DE MECANIQUE DES FLUIDES DE MARSEILLE (FRANCE).
Study of the 3D wake of an aerial propeller N86-11161
INSTITUT GEOGRAPHIQUE NATIONAL, PARIS (FRANCE).
Establishment of the BIH terrestrial system by combining the results of different Earth rotation space geodesy programs N86-11555
IOWA STATE UNIV. OF SCIENCE AND TECHNOLOGY, AMES.
Statistical signal analysis for systems with interferenced inputs N86-12016
IOWA UNIV., IOWA CITY.
Plasmas in the Earth's magnetotail [AD-A157320] N86-11716

J

JET PROPULSION LAB., CALIFORNIA INST. OF TECH., PASADENA.
Reciprocating magnetic refrigerator N86-11371
Improved heat switch for gas sorption compressor N86-11372
Hydride absorption refrigerator system for ten Kelvin and below N86-11373
A closed cycle cascade Joule Thomson refrigerator for cooling Josephson junction magnetometers N86-11388
Proceedings of the Airborne Imaging Spectrometer Data Analysis Workshop [E86-10001] N86-11618
Mineralogical mapping in the Cuprite Mining District, Nevada N86-11619
Remote stratigraphic analysis: Combined TM and AIS results in the Wind River/Bighorn Basin area, Wyoming N86-11620
Preliminary analysis of AIS spectral data acquired from semi-arid shrub communities in the Owens Valley, California N86-11622
AIS spectra for stressed and unstressed plant communities in the Carolina slate belt N86-11623
Spectral characterization of suspected acid deposition damage in red spruce (Picea rubens) stands from Vermont N86-11624
Calibration of AIS data using ground-based spectral reflectance measurements N86-11631
Intermediate load modules for test and evaluation: Fixed price research and development [NASA-CR-176135] N86-11664
A summary report on the Flat-Plate Solar Array Project Workshop on Transparent Conducting Polymers [NASA-CR-176302] N86-11669
CELCAP: A computer model for cogeneration system analysis [NASA-CR-176306] N86-11896
The 1984 solar oscillation program of the Mount Wilson 60-foot tower [NASA-CR-176246] N86-12195
JOINT INST. FOR LAB. ASTROPHYSICS, BOULDER, COLO.
Epsilon Aurigae in an evolutionary context N86-12174
JOINT PUBLICATIONS RESEARCH SERVICE, ARLINGTON, VA.
USSR report: Transportation [JPRS-UTR-85-011] N86-11177
Deputy minister on sector's technical progress N86-11178
Chief of Aeroflot's international activities N86-11179
Recent achievements, problems in cropdusting work N86-11180
World's largest airplane now being tested N86-11181
USSR report: Machine tools and metalworking equipment [JPRS-UMM-85-010] N86-11394
Large robotized turning centers described N86-11395
Robotized production systems observed in modern plants N86-11396
Robotized machining systems developed at Gomel Institute N86-11397
China report: Science and technology [JPRS-CST-85-014] N86-11918
Double tearing mode in plasma with magnetic braiding N86-11919
Design of maneuverable trajectories of re-entry vehicle N86-11920
One-dimensional two-phase flow in combustion chamber of solid propellant rocket motors N86-11921
Electric or magnetic dipole in stratified uniaxially inhomogeneous anisotropic media N86-11922
Propagation of electromagnetic waves in inhomogeneous and lossy reentry plasma sheath layer N86-11923
Pressure-coupled response function of solid propellants including those with negative pressure-exponents N86-11924
The analysis and calculation for the dynamic characteristics of the omni-axial movable flexible joint nozzle N86-11925
Transition effects of boundary layer on static and dynamic stability of slender cone N86-11926
Research on optic spatial frequency analysis of linear structures in remote sensing images N86-11927
Frequency-selection and mode-locking and Nd:YAG laser N86-11928
A large area X-ray source and its preionization characteristics for XeCl excimer laser N86-11929
Ring cavity CO2 laser for branch-selection and narrow resonance produced by SF6 in cavity N86-11930
Pb(1-x)Sn(x)Te and Pb(1-y)Sn(y)Se laser crystals N86-11931
Progress of Inertial Confinement Fusion (ICF) research N86-11932
Stationary pulse solutions for a free electron laser N86-11933
The relations between voltage and magnetic field of superconducting weaklink (1) N86-11934
The relations between voltage and magnetic field of superconducting weaklink (2) N86-11935
Discussion of the superconducting critical temperature in a N-S multi-film structure N86-11936
Theory of the critical temperature for superconductors with small lambda (1) N86-11937
Effect of high electric field on minority carrier generation in silicon depletion layer N86-11938
Deep-level defects in ion-implanted and CO2 laser-annealed silicon N86-11939
Binding energy of donors in GaAs-Ga(1-x) Al(x)As quantum well structures N86-11940
An interfacial analysis of MoNb-GaAs Schottky barrier diodes N86-11941
Thermal post-treatment characteristics of metastable carrier concentration in As-implanted silicon after transient annealing N86-11942
Deep levels in semi-insulating GaAs N86-11943
USSR report: Physics and mathematics [JPRS-UPM-85-005] N86-11945
Diffraction of ultrasonic beam passing normally through layered media N86-11946
Speed of sound in liquid sodium near gamma-transition point N86-11947
Raman scattering of sound on random oscillations of bubbles N86-11948
Determination of parameters of elastic spherical shell from scattered wave field N86-11949
Stability of a method for analyzing radiation pattern of acoustic radiator with near-field pressure measurement errors N86-11950
Reflection of sound from plate containing periodic inhomogeneities N86-11951
Conversion of electromagnetic wave energy to electrical current by bulk superlattice semiconductors N86-11952
Cause of occurrence of high-energy ions during UV laser irradiation of molecular crystals N86-11953
Hydrodynamics of liquid-vapor disperse annular flows in channels containig bundles of heated rods under nonsteady-state conditions N86-11954
Toward a theory of atomic gas breakdown by laser radiation near a metal surface N86-11955
Initial plasma formation during exposure of absorbing materials to laser radiation with plane expansion geometry of the forming plasma N86-11956
Laser evaporation of metal in gaseous atmosphere N86-11957
Influence of solid state obstacles on radiation of recombination laser plasma N86-11958
Surface combustion of liquid fuel in stream of gaseous oxidizer N86-11959
Explosion waves generated by deflagration combustion N86-11960
Excitation of discharge in air by laser radiation N86-11961
Influence of physical-chemical properties of gases on interaction between shockwaves and convex cylindrical surfaces N86-11962
Calculation of formation time of minimal nucleus of flame during ignition of explosive mixtures by electrical discharges N86-11963
Flame propagation in pulsed acceleration field N86-11964
Occurrence of pressure wave during spontaneous ignition of gas ahead of flame front in closed vessel N86-11965
Steady-state detonation of charges of finite length N86-11966
Lasing on vapors of chain compounds N86-11967
Energy characteristics of laser with saturable anisotropic absorbing medium in cavity N86-11968
Investigation of efficiency of generation of difference-frequency laser radiation in waveguide N86-11969
Spectrum structure of XeCl electric discharge laser N86-11970
Distributed-feedback lasers with active framing medium N86-11971
Investigation of polarization characteristics of radiation from laser with dye-activated polymer elements N86-11972
High-efficiency Al sub 2 O sub 3:Ti sup 3+ tunable laser N86-11973
Ultraviolet lasing in helium-nitrogren mixtures N86-11974
Electroionization IR Xe-ATOM laser N86-11975
Optimization of parameters of chemical CO laser by increasing length of active medium N86-11976
Efficiency of optically-pumped XeF-laser N86-11977
Energy characteristics of waveguide CO sub 2-laser N86-11978
Chromium- and neodymium-activated gadolinium-scandium-gallium garnet crystal: A new laser active medium N86-11979
Two-frequency passive mode locking in iodine photodissociation laser N86-11980
Experimental investigation of recording of dynamic holograms within absorption contour of resonant atomic medium N86-11981
Diffraction efficiency of three-dimensional phase hologram of diffuse object N86-11982
Possibility of optimal choice of exposure time for holographic recording of objects through unsteady scattering media N86-11983
General-purpose equipment for airborne laser remote sensing of ocean, atmosphere and agricultural crops N86-11984
Photoinduced Rayleigh scattering of light in crystals N86-11985
Multiphoton Raman scattering of light excited in crystals by a copper-vapor laser N86-11986
Phasing of multiple-aperture optical systems N86-11987

Transformation of light pulse shape by thin plane-parallel layer of absorbing material N86-11988
Hydrothermodynamics of the near-surface layer of a liquid and optical methods of investigating it
N86-11989
USSR report: Science and technology policy
[JPRS-UST-85-014] N86-11990
Book on planning of scientific, technical progress
N86-11991
Computer-aided designing, engineering, preparation of production N86-11992
Problems, trends in technical education of researchers
N86-11993
China report: Science and technology
[JPRS-CST-85-015] N86-11994
High-speed signal processor developed N86-11995
New R and D in Chinese language information processing N86-11996
Center for High Temperature Plasma Physics certified
N86-11997
Controlled thermonuclear fusion, high temperature plasma physics N86-11998
Third National Academic Machine Retrieval Conference held in Zhenjiang N86-11999
Microcomputer-controlled high-altitude data aquisition system N86-12000
Computer application in atomic absorption spectrometry N86-12001
A general purpose CAD program for microwave linear circuits N86-12002
Double-wavelength pulsed tunable dye laser
N86-12003
Involutory transformations and variation principles with multivariables in thin plate bending problems
N86-12004
Numerical method in dynamic response of nonlinear systems N86-12005
On convective effects in gas lasers N86-12006

K

KANNER (LEO) ASSOCIATES, REDWOOD CITY, CALIF.
Discussion of the current limits in the RFQ
[DE85-012909] N86-12088

KANSAS UNIV., LAWRENCE.
Inlet flow dynamic distortion prediction without rms measurements N86-11183

KARLOVA UNIV., PRAGUE (CZECHOSLOVAKIA).
Determination of crustal movements in the high Tatra Mountains N86-11605
On the addition theorem for Legendre polynomials
N86-11704

KARLSRUHE UNIV. (WEST GERMANY).
Height changes and recent crustal movements in the Rhenish Massif and in the upper Rhine Graben rift
N86-11608

KENTRON INTERNATIONAL, INC., HAMPTON, VA.
Mechanical properties of Inconel 718 and Nickel 201 alloys after thermal histories simulating brazing and high temperature service
[NASA-CR-177940] N86-11312

KIEL UNIV. (WEST GERMANY).
Anelasticity in the Earth's mantle: Implications for the frequency dependence of Love numbers N86-11590

KITT PEAK NATIONAL OBSERVATORY, TUCSON, ARIZ.
Micron CO in the eclipse spectrum of Epsilon Aur
N86-12179

KORROSIONSINSTITUTET, STOCKHOLM (SWEDEN).
Cathodic protection of aluminium structures
[KIS-1985:4E] N86-11313
Short-term methods for atmospharic corrosion testing: Survey of the literature
[KIS-1985:5E] N86-11314

L

L'AIR LIQUIDE, SASSENAGE (FRANCE).
Experiments with a fully instrumented split Stirling cryocooler N86-11381

LAMONT-DOHERTY GEOLOGICAL OBSERVATORY, PALISADES, N. Y.
Temperature and precipitation trends in North America
N86-11774

LINCOLN LAB., MASS. INST. OF TECH., LEXINGTON.
Submillimeter quantum electronics
[AD-A157432] N86-11417

LITTLE (ARTHUR D.), INC., CAMBRIDGE, MASS.
Surface sampling techniques using ultraviolet illumination
[AD-A156457] N86-11458

LOCKHEED-CALIFORNIA CO., BURBANK.
A general theory of arbitrary motion aerodynamics using an aeroacoustic approach N86-11157
Propeller aircraft cabin vibration and noise-excitation, sources, and paths N86-11174
KRASH85 user's guide: Input/output format
[FAA-CT-85-10] N86-11896

LOCKHEED-GEORGIA CO., MARIETTA.
A review of advanced turboprop transport activities
N86-11148
Wind tunnel investigation of the interaction of propeller slipstream with nacelle/wing/flap combinations
N86-11166
Application of active noise control to model propeller noise N86-11176
Adhesives for aerospace N86-11249

LOCKHEED MISSILES AND SPACE CO., SUNNYVALE, CALIF.
Characterization of polyimide matrix resins and prepregs N86-11273

LOS ALAMOS NATIONAL LAB., N. MEX.
Los Alamos upgrade in metallographic capabilities
[DE85-014089] N86-11320
Magnetic properties and electronic structure of the actinide systems UAl2, NpAl2 and PuAl2
[DE85-014102] N86-11323
Detonation reaction zone studies on TATB explosives
[DE85-015710] N86-11361
Magnetic refrigeration for low-temperature applications
N86-11370
Multi-megampere current interruption from explosive deformation of conductors
[DE85-012756] N86-11419
Multi-megampere operation of plasma compression opening switches in planar geometry
[DE85-012755] N86-11420
Mechanical threshold of dynamically deformed copper and nitronic 40
[DE85-010779] N86-11545
Inertia, stability and ductibility in uniaxial tension at high strain rate
[DE85-007671] N86-11546
Passive solar applications
[DE85-014085] N86-11685
Subsurface geology of the Pajarito Plateau, Espancia Basin, New Mexico
[DE85-016215] N86-11720
Sixth Biennial CUBE (Computer Use By Engineers) Symposium
[LA-10240-C] N86-11858
Design optimization of the power generation system for a space-based free-electron laser N86-11861
Interactive graphics for finite element preprocessing
N86-11871
Geological calculations with SANGRE and MANTLE: Recent results N86-11872
Sandia shock compression database
[DE85-015141] N86-12142
Nuclear interlevel transfer driven by electronic transitions
[DE85-014103] N86-12149
Surface impedance of several magnetic superconductors
[DE85-014101] N86-12155

LOS ALAMOS SCIENTIFIC LAB., N. MEX.
Railgun power supply system utilizing traction motors and vacuum interrupters
[DE85-014123] N86-11214
Activated recombinative desorption: A potential component in mechanisms of spacecraft glow
[DE85-014092] N86-11223
Calculation of RF fields in axisymmetric cavities
[DE85-014135] N86-11414
Rotating film radiators for space applications
[DE85-009633] N86-11431
Introduction to the session on: Numerical methods for two-phase flow
[DE85-012651] N86-11435
Evaluation of concrete creep and stress redistribution in a prototypic PCRV following rupture of prestressing tendons
[DE85-007673] N86-11543
Study of LAMPF H (-) beam position motion and a predictive algorithm for noise reduction
[DE85-012701] N86-12033
Kinetics analysis of diffusion of point defects to dislocations following pulsed neutron and electron irradiations
[DE85-012766] N86-12037
Status of fast neutron nuclear data for (239)Pu
[DE85-012699] N86-12045
Application of detailed fission-product decay gamma spectra in the calculation of photoneutron spectra from D((GAMMA),n) reactions in PWR fuel
[DE85-012729] N86-12048
Double differential neutron emission cross sections of (10)B and (1)B at 6, 10 and 14 MeV and of (6)Li, (7)Li and (12)C at 14 MeV
[DE85-012749] N86-12056
Los Alamos proton storage ring fast-extraction kicker system
[DE85-012663] N86-12093
Los Alamos Spheromak Program
[DE85-012769] N86-12096
Superconducting Magnetic Energy Storage (SMES) Program
[DE85-014250] N86-12106
Review of kaon factory proposals
[DE85-014110] N86-12122
Acceleration simulation in the LAMPF 2 booster
[DE85-012695] N86-12126
Recent FRC translation experiments on FRX-C/T
[DE85-012745] N86-12132
Statics and adiabatic dynamics of nonlinear excitations in defected polyacetylene
[DE85-014118] N86-12143
EOS for polycrystalline quartz
[DE85-014241] N86-12148
Mars base buildup scenarios
[DE85-014132] N86-12193
Cosmogenic-nuclide production by primary cosmic-ray protons
[DE85-012760] N86-12198

LOUISIANA STATE UNIV., BATON ROUGE.
Information dissemination for a better understanding of Louisiana's water resources
[PB85-219079] N86-11660
Louisiana Water Resources Research Institute
[PB85-218998] N86-11661

LOWELL OBSERVATORY, FLAGSTAFF, ARIZ.
Spectrophotometry of Epsilon Aur, 3295-8880 A
N86-12178

LTV AEROSPACE AND DEFENSE CO., DALLAS, TEX.
The factory of the future N86-11228

LUNAR AND PLANETARY INST., HOUSTON, TEX.
Horizons and opportunities in lunar sample science
[NASA-CR-176290] N86-12191
Workshop on Dust on Mars
[NASA-CR-176293] N86-12192

M

MARTIN LUTHER-UNIVERSITAET, HALLE-WITTENBERG (EAST GERMANY).
On inverse problems in differential equations: A critical analysis N86-11552

MARTIN MARIETTA AEROSPACE, DENVER, COLO.
Metallurgical characterization of the interfaces and the damping mechanisms in metal matrix composites
[AD-A156507] N86-11300
Teleoperator human factors study
[NASA-CR-176310] N86-11854

MARTIN MARIETTA AEROSPACE, NEW ORLEANS, LA.
Automatic fastening large structures: A new approach
N86-11234

MARTIN MARIETTA CORP., BALTIMORE, MD.
Use of hydration inhibitors to improve bond durability of aluminum adhesive joints N86-11251

MARTINI ENGINEERING, RICHLAND, WASH.
A nonproprietary, nonsecret program for calculating Stirling cryocoolers N86-11384

MARYLAND UNIV., BALTIMORE.
Acute pulmonary effects of formaldehyde exposure in humans
[DE85-014728] N86-11848

MARYLAND UNIV., COLLEGE PARK.
A parametric analysis of flow structure and performance in a vortex controlled radial diffuser N86-11182
Stability and interaction of coherent structure in supersonic reactive wakes N86-11185
Thin plates with rapidly varying thickness, and their relation to structural optimization
[AD-A157607] N86-11534
Analysis of terrestrial conditions and dynamics
[NASA-CR-176308] N86-11646
Towards understanding the geographical distribution and seasonality in persistance of monthly mean surface air temperature over the U.S.A. N86-11773
The effect of anomalous snow cover on the general circulation of the atmosphere using a simple climate model N86-11794
Specification of mean surface temperature anomalies in Europe and Asia during the fall months N86-11806
Very anomalous behavior of outgoing longwave radiation in the tropics in 1983-84: Aftermath of ENSO?
N86-11813
Computation of minimal isovist sets
[AD-A157624] N86-11915
Reduction of sextupole distortion by shuffling magnets in small groups
[DE85-013024] N86-12035

MASSACHUSETTS INST. OF TECH., CAMBRIDGE.

Feasibility of remotely manipulated welding in space: A step in the development of novel joining technologies N86-11246

An experimental reciprocating expander for cryocooler application N86-11380

Criteria for scaling heat exchangers to miniature size N86-11387

Miniaturization of specimens for mechanical testing [DE85-014506] N86-11536

Remote sensing of earth terrain [NASA-CR-176284] N86-11645

An observational study of the vertical structure of interannual wind fluctuations in the tropics N86-11810

Slow fluctuations of the tropical circulation during the FGGE year N86-11812

Utilization of non-conventional systems for conversion of biomass to food components: Potential for utilization of algae in engineered foods [NASA-CR-176257] N86-11830

Easy impossibility proofs for distributed concensus problems [AD-A157411] N86-11903

Probabilistic analysis of a network resource allocation algorithm [AD-A157553] N86-11904

Overview of MIT, ADIP irradiation experiments [DE85-014469] N86-12060

MDH stabilization of high (BETA) mirror plasma partially enclosed by conducting wall [DE85-015579] N86-12081

Implications of rf current drive theory for next step steady-state tokamak design [DE85-014753] N86-12083

Research objectives and summary of research performed by the Massachusetts Institute of Technology Research Laboratory of Electronics [PR-127] N86-12164

MASSACHUSETTS UNIV., AMHERST.

Considerations for millimeter wave, monolithic phased arrays N86-11399

MCDONNELL AUTOMATION CO., ST. LOUIS, MO.

Flight worthinnes of fire resistant hydraulic systems: Volume 1 [AD-A157618] N86-11199

MCDONNELL-DOUGLAS ASTRONAUTICS CO., HUNTINGTON BEACH, CALIF.

Spherical torus: An approach to compact fusion at low field. Initial ignition assessments [DE85-012890] N86-12099

MCELROY (RALPH) CO., AUSTIN, TEX.

Investigation on growth and laser properties of GGG:(Nd,Cr) single crystal [DE85-014282] N86-12151

MECHANICAL TECHNOLOGY, INC., LATHAM, N. Y.

The design of a small linear-resonant, split Stirling cryogenic refrigerator compressor N86-11392

METALS SOCIETY, LONDON (ENGLAND).

Corrosion testing by radiographic methods [BLL-BISI-TRANS-23201-(9022.06)] N86-11310

The yield point of copper-zinc alloys in the alpha solid solution range [BLL-BISI-TRANS-23046-(9022.06)] N86-11311

MEZOEGAZDASAGI ES ELELMEZESUEGYI MINISTERIUM, BUDAPEST (HUNGARY).

On the works and results of investigations concerning the recent movements in the Karpatho-Balkan region N86-11593

Method of joint adjustment of height differences and velocities N86-11601

Principle of the construction of the lines of the repeated levelling for the investigation of the vertical movement in the Carpatho-Balkan Region (CBR) N86-11602

MICHIGAN STATE UNIV., EAST LANSING.

Effect of accuracy of wind power prediction on power system operator [NASA-CR-176300] N86-11667

AC motor and generator requirements for isolated WECS [NASA-CR-176315] N86-11670

MICHIGAN TECHNOLOGICAL UNIV., HOUGHTON.

Deformation and fracture of P/M titanium alloys [AD-A157416] N86-11317

MICHIGAN UNIV., ANN ARBOR.

A Signorini model of bolt fastened laminated composites N86-11258

Forest species identification with high spectral resolution data N86-11643

Improving the comprehensibility of a simulated technical manual [AD-A157482] N86-11889

Integrated analysis of error detection and recovery [NASA-CR-172571] N86-11906

Neutral beam interactions with materials [AD-A157445] N86-12076

MIDDLETON (DAVID), NEW YORK.

Intermediate and high-frequency acoustic backscattering cross sections for water-ice interfaces. 1: Two-component profile models [AD-A157533] N86-12018

MIDWEST RESEARCH INST., GOLDEN, COLO.

Solid-melt interface studies of high-speed silicon sheet growth [DE85-008783] N86-11349

Polymer glazings for silver mirrors [DE85-012140] N86-11357

High temperature molten salt containment [DE85-012152] N86-11433

New-generation photovoltaic technologies [DE85-012143] N86-11675

Investigation of defects in GaAsP superlattic structures [DE85-012134] N86-12139

MIDWEST RESEARCH INST., KANSAS CITY, MO.

Develop, evaluate and validate continuous emission monitors for designated hazardous pollutants [PB85-201176] N86-11695

MINISTRY OF SCIENCE AND DEVELOPMENT, JERUSALEM (ISRAEL).

Representations of the group of diffeomorphisms in the physics of particles, gravity and fluids [DE85-007031] N86-12028

MINNESOTA UNIV., MINNEAPOLIS.

Thin plates with rapidly varying thickness, and their relation to structural optimization [AD-A157607] N86-11534

MISSION RESEARCH CORP., ALBUQUERQUE, N. MEX.

IFR guiding experiments [DE85-014512] N86-12027

MISSOURI UNIV., ROLLA.

Interaction of mixed mode loading on cyclic debonding in adhesively bonded composite joints [NASA-CR-177990] N86-11298

MITRE CORP., BEDFORD, MASS.

Evaluation of the digital access and cross-connect system for use in the defense communications system [AD-A157570] N86-11412

MOUND LAB., MIAMISBURG, OHIO.

Injection molding-sealing of glass to low melting metals [DE85-015613] N86-11329

Physical property changes of a lithia-alumina-silica based glass as a function of composition [DE85-015610] N86-11352

Infrared thermography: An analytical tool for high temperature and fast response [DE85-013826] N86-11462

N

NATIONAL ACADEMY OF SCIENCES - NATIONAL RESEARCH COUNCIL, WASHINGTON, D. C

Geodesy: A look to the future [NASA-CR-176283] N86-11657

Workshop on Permafrost Geophysics [AD-A157485] N86-11719

Polar Research Board annual report 1984 and future plans [PB85-204477] N86-11727

NASA-universities relationships in aero/space engineering: A review of NASA's program [NASA-CR-176307] N86-12158

NATIONAL AERONAUTICS AND SPACE ADMINISTRATION, WASHINGTON, D. C.

Aeronautical Engineering: A continuing bibliography with indexes [NASA-SP-7037(191)] N86-11145

Bibliography of terrestrial impact structures [NASA-TM-87567] N86-11701

Variability of snow cover characteristics in the Transbaykal [NASA-TM-77917] N86-11733

Formation, distribution and variability in snow cover on the Asian territory of the USSR [NASA-TM-77913] N86-11734

Overview of NASA's programs N86-11741

The 1982-1984 Eclipse of Epsilon Aurigae [NASA-CP-2384] N86-12166

Scattered light in the IUE spectra of Epsilon Aurigae N86-12180

International solar-terrestrial physics program: A plan for the core spaceflight missions [NASA-TM-87511] N86-12194

NATIONAL AERONAUTICS AND SPACE ADMINISTRATION. AMES RESEARCH CENTER, MOFFETT FIELD, CALIF.

Shock fitting applied to the prediction of high-speed rotor noise [NASA-TM-86761] N86-11188

Expert systems development and application [NASA-TM-86746] N86-11194

Description of an experimental expert system flight status monitor [NASA-TM-86791] N86-11195

Comparison of calculated and measured velocities near the tip of a model rotor blade at transonic speeds [NASA-TM-86697] N86-11196

Water tunnel flow visualization using a laser [NASA-TM-86743] N86-11206

Visual and motion cueing in helicopter simulation [NASA-TM-86818] N86-11208

Airflow calibration of a bellmouth inlet for measurement of compressor airflow in turbine-powered propulsion simulators [NASA-TM-84399] N86-11209

Design and performance analysis of an aero-maneuvering orbital-transfer vehicle concept [NASA-TM-86848] N86-11221

Bismaleimides and related maleimido polymers as matrix resins N86-11265

Strength and flexibility properties of advanced ceramic fabrics [NASA-TM-86824] N86-11340

Seeding subsonic, transonic and suporsonic flows with 0.5 micron polystyrene spheres N86-11451

Stress analyses of B-52 pylon hooks [NASA-TM-84924] N86-11524

A comparison of measured and calculated thermal stresses in a hybrid metal matrix composite spar cap element [NASA-TM-86729] N86-11525

High resolution spectrometry of leaf and canopy chemistry for biochemical cycling N86-11633

AIS investigation of agricultural monocultures N86-11640

On the implementation of a class of upwind schemes for system of hyperbolic conservation laws [NASA-TM-86839] N86-11907

On symmetric and upwind TVD schemes [NASA-TM-86842] N86-11909

Far-infrared observations of Sagittarius B2: Reconsideration of source structure [NASA-TM-88185] N86-12167

Star formation in the inner galaxy: A far-infrared and radio study of two H2 regions [NASA-TM-86720] N86-12185

Submillimeter observations of OH and CH in M42 [NASA-TM-86723] N86-12186

NATIONAL AERONAUTICS AND SPACE ADMINISTRATION. GODDARD SPACE FLIGHT CENTER, GREENBELT, MD.

SPACEWARN Bulletin [NASA-TM-87512] N86-11222

Comparison of AIS versus TMS data collected over the Virginia piedmont N86-11637

A preliminary investigation of systematic noise in data acquired with the Airborne Imaging Spectrometer N86-11638

Subseasonal and interannual variations of tropical convection and the El Nino/Southern Oscillation N86-11779

Variability simulations with a steady, linearized primitive equations model N86-11796

NATIONAL AERONAUTICS AND SPACE ADMINISTRATION. LANGLEY RESEARCH CENTER, HAMPTON, VA.

Theoretical analysis of linearized acoustics and aerodynamics of advanced supersonic propellers N86-11156

An asymptotic theory for the interference of large aspect ratio swept wings and multiple propeller slipstreams N86-11167

Effect of aileron deflections on the aerodynamic characteristics of a semispan model of a subsonic energy-efficient transport [NASA-TP-2478] N86-11186

User's manual for a 0.3-m TCT wall interference assessment/correction procedure: 8- by 24-inch airfoil test section [NASA-TM-87582] N86-11189

A perspective on the status of measurement of atmospheric turbulence in the US [NASA-TM-87610] N86-11193

Preliminary design study of a lateral-directional control system using thrust vectoring [NASA-TM-86425] N86-11203

Welding, Bonding and Fastening, 1984 [NASA-CP-2387] N86-11227

Investigation of low-temperature solders for cryogenic wind tunnel models N86-11230

NTF: Soldering technology development for cryogenics N86-11231

The alternating surface segmented lap joint: A design for thin highly loaded joints N86-11233

Derivation and test of elevated temperature thermal-stress-free fastener concept N86-11236

Explosive tube-to-fitting joining of small-diameter tubes N86-11239

Nondestructive ultrasonic measurement of bolt preload using the pulsed-phase locked-loop interferometer N86-11242

Langley Research Center standard for the evaluation of socket welds N86-11243

Evaluation of superplastic forming and weld-brazing for fabrication of titanium compression panels N86-11245

Rapid adhesive bonding and field repair of aerospace materials N86-11253

Initial investigation of cryogenic wind tunnel model filler materials N86-11255

Matrix resin development at NASA Langley Research Center N86-11264

A program to determine the effect of low-velocity impacts on the strength of the filament-wound rocket motor case for the space shuttle [NASA-TM-87588] N86-11292

Manual for LDEF tensile tests [NASA-TM-87624] N86-11299

Wind Tunnel Seeding Systems for Laser Velocimeters [NASA-CP-2393] N86-11437

Estimation of particle size based on LDV measurements in a de-accelerating flow field N86-11440

Experiments with solid particle seeding N86-11442

Seeding techniques used in the Vortex Research Facility N86-11443

Seeding systems for use with a laser velocimeter in large scale wind tunnels N86-11444

Particle generation experience in Langley's 16-foot transonic tunnel N86-11449

LDA seeding system for the Langley Low Turbulence Pressure Tunnel N86-11450

Seeding materials: Health and safety considerations N86-11454

A study of the cornering forces generated by aircraft tires on a tilted, free-swiveling nose gear [NASA-TP-2481] N86-11522

Aeroelastic model helicopter rotor testing in the Langley TDT [NASA-TM-86440] N86-11523

Computational structural mechanics: A new activity at the NASA Langley Research Center [NASA-TM-87612] N86-11540

Active and passive microwave measurements in Hurricane Allen [NASA-TM-86390] N86-11647

SAGE aerosol measurements. Volume 1: February 21, 1979 to December 31, 1979 [NASA-RP-1144] N86-11700

Towards developing robust algorithms for solving partial differential equations on MIMD machines [NASA-CR-177979] N86-11856

NATIONAL AERONAUTICS AND SPACE ADMINISTRATION. LEWIS RESEARCH CENTER, CLEVELAND, OHIO.

Development of an explicit multigrid algorithm for quasi-three-dimensional viscous flows in turbo-machinery [NASA-TM-87128] N86-11146

Summary of recent NASA propeller research N86-11156

NASA Lewis Research Center low-gravity fluid management technology program [NASA-TM-87145] N86-11218

An experimental study of energy loss mechanisms and efficiency consideration in the low power dc arcjet [NASA-TM-87123] N86-11224

High Temperature Polymer Matrix Composites [NASA-CP-2385] N86-11260

PMR polyimides from solutions containing mixed endcaps N86-11263

All-aromatic biphenylene end-capped polyquinoline and polyimide matrix resins N86-11267

Chemical control of rate and onset temperature of nadimide polymerization N86-11271

Replacement of MDA with more oxidatively stable diamines in PMR-polyimides N86-11275

Properties of autoclaved Gr/PI composites made from improved tack PMR-15 prepreg N86-11276

Rheological, processing, and 371 deg C mechanical properties of Celion 6000/N-phenylnadimide modified PMR composites N86-11278

Surface protection of graphite fabric/PMR-15 composites subjected to thermal oxidation N86-11281

Characterization of MMIC devices for active array antennas N86-11401

Circularly polarized microstrip antennas N86-11407

Theoretical and experimental comparison of vapor cavitation in dynamically loaded journal bearings [NASA-TM-87121] N86-11425

Development of seeding techniques for small supersonic wind tunnel N86-11452

Protective coatings of metal surfaces by cold plasma treatment [NASA-TM-87152] N86-11475

Turbine Engine Hot Section Technology (HOST) [NASA-CP-2289] N86-11495

Turbine engine Hot Section Technology (HOST) project N86-11496

HOST instrumentation R and D program overview N86-11497

Laser anemometry for hot section applications N86-11503

Turbine heat transfer N86-11505

Combustion hot section technology N86-11512

HOST structural analysis program overview N86-11513

Validation of structural analysis methods using burner liner cyclic rig test data N86-11518

HOST liner cyclic facilities N86-11519

Life prediction and constitutive behavior N86-11520

Photovoltaic-powered vaccine refrigerator: Freezer systems field test results [NASA-TM-86972-REV] N86-11666

RE-1000 free-piston Stirling engine update [NASA-TM-87126] N86-11668

A 25.5 percent AMO gallium arsenide grating solar cell [NASA-TM-87134] N86-11671

Numerical Techniques in Acoustics [NASA-CP-2404] N86-12007

Ellipsometric and optical study of some uncommon insulator films on 3-5 semiconductors [NASA-TM-87135] N86-12134

Carbon films grown from plasma on III-V semiconductors [NASA-TM-87140] N86-12135

NATIONAL AERONAUTICS AND SPACE ADMINISTRATION. MARSHALL SPACE FLIGHT CENTER, HUNTSVILLE, ALA.

Problems experienced and envisioned for dynamical physical systems [NASA-TP-2508] N86-11215

Heavy lift launch vehicles for 1995 and beyond [NASA-TM-86520] N86-11216

A comparison of the physics of Gas Tungsten Arc Welding (GTAW), Electron Beam Welding (EBW), and Laser Beam Welding (LBW) [NASA-TM-86503] N86-11473

Meteorological and Environmental Inputs to Aviation Systems [NASA-CP-2388] N86-11735

NATIONAL AERONAUTICS AND SPACE ADMINISTRATION. NATIONAL SPACE TECHNOLOGY LABS., BAY SAINT LOUIS, MISS.

A general-applications direct global matrix algorithm for rapid seismo-acoustic wavefield computations N86-12012

Numerical techniques for scattering from submerged objects N86-12013

NATIONAL AEROSPACE LAB., AMSTERDAM (NETHERLANDS).

Aerodynamics of wide-chord propellers in non-axisymmetric flow N86-11153

NATIONAL BUREAU OF STANDARDS, BOULDER, COLO.

Design of cryocoolers for microwatt superconducting devices N86-11368

A simple, first step to the optimization of regenerator geometry N86-11385

A computational model for a regenerator N86-11386

NATIONAL BUREAU OF STANDARDS, GAITHERSBURG, MD.

Applied model validation [NBSIR-85-3154-1] N86-11363

Fire growth in combat ships [NBSIR-85/3158] N86-11364

Methods to calculate the response time of heat and smoke detectors installed below large unobstructed ceilings [NBSIR-85/3167] N86-11365

Response behavior of hot-wires and films to flows of different gases [NBSIR-85/3203] N86-11366

Proceedings of the Third Cryocooler Conference [NASA-CR-176296] N86-11367

NATIONAL BUREAU OF STANDARDS, WASHINGTON, D.C.

Materials studies for magnetic fusion energy applications at low temperatures. 7: Technical reports [DE85-014518] N86-12101

NATIONAL CENTER FOR ATMOSPHERIC RESEARCH, BOULDER, COLO.

Calibration of the NCAR (National Center for Atmospheric Research) Sabreliner research static pressure source with a trailing cone assembly [PB85-191005] N86-11200

The annual variation in the vertical structure of the 40-50-day tropical oscillation N86-11780

Atmospheric response to an equatorial Pacific sea surface temperature anomaly: The effects of orography N86-11791

NATIONAL CLIMATIC CENTER, ASHEVILLE, N. C.

Recent unusual mean winter temperature across the contiguous United States N86-11772

NATIONAL COAL BOARD, GRIMETHORPE (ENGLAND).

Evaluation of candidate materials in a static turbine cascade [DE85-008592] N86-11480

NATIONAL ENVIRONMENTAL SATELLITE SERVICE, WASHINGTON, D. C.

The status of the NOAA/NESDIS radiation budget data set N86-11815

NATIONAL METEOROLOGICAL CENTER, WASHINGTON, D.C.

Monitoring climate in real time: An application of the Climate Anomaly Monitoring System (CAMS) N86-11765

Review of the climate of fall 1983 and winter 1983-84 N86-11766

Blocking as an explanation of the severe cold of winter 1983-84 N86-11768

Circulation and weather for MAM and JJA 1984 N86-11769

Large-scale variability in Indian monsoon rainfall inferred from satellite data N86-11800

A sea surface temperature analysis based on in situ and satellite data N86-11816

NATIONAL OCEANIC AND ATMOSPHERIC ADMINISTRATION, BOULDER, COLO.

TIROS/NOAA (Television and Infrared Observation Satellite/National Oceanic and Atmospheric Administration) satellites space environment monitor archive tape documentation [PB85-187920] N86-11724

Automated method for the documentation of cloud-top characteristics of mesoscale convective systems [PB85-204246] N86-11823

NATIONAL OCEANIC AND ATMOSPHERIC ADMINISTRATION, ROCKVILLE, MD.

Proceedings of the 9th Annual Climate Diagnostics Workshop [PB85-183911] N86-11763

NATIONAL OCEANIC AND ATMOSPHERIC ADMINISTRATION, SILVER SPRING, MD.

Lidar observations of stratospheric aerosol over Mauna Loa Observatory: 1982 - 1983 [PB85-187896] N86-11723

NATIONAL OCEANIC AND ATMOSPHERIC ADMINISTRATION, WASHINGTON, D. C.

High altitude measured radiance of White Sands, New Mexico in the 400-2000 nm band using a filter wedge spectrometer [PB85-206084] N86-11729

Monthly and seasonal weather outlook for June 1985, volume 39, number 11, 30 May 1985 [PB85-209526] N86-11762

Atlas of high altitude aircraft measured radiance of White Sands, New Mexico, in the 450-1050 nanometers band [PB85-204501] N86-11820

NATIONAL RADIO ASTRONOMY OBSERVATORY, CHARLOTTESVILLE, VA.

Star formation in the inner galaxy: A far-infrared and radio study of two H2 regions [NASA-TM-86720] N86-12185

NATIONAL SEVERE STORMS FORECAST CENTER, KANSAS CITY, MO.

Minimum assumption tornado hazard probability model [PB85-206092] N86-11821

NATIONAL WEATHER SERVICE, PORTLAND, OREG.

Evidence of an 18 year cycle in Pacific northwest precipitation data N86-11788

NATIONAL WEATHER SERVICE, SILVER SPRING, MD.

Monthly and Seasonal Weather Outlook for May 1985, Volume 39, Number 9 [PB85-199123] N86-11819

NAVAL ACADEMY, ANNAPOLIS, MD.

Electrical relaxation in poly(ethylene oxide) [AD-A157301] N86-11342

NAVAL AIR DEVELOPMENT CENTER, WARMINSTER, PA.

A comparison of the NAVTOLAND (Navy vertical takeoff and landing) SH-2F helicopter model with the requirements of MIL-H-8501A and with flight data [AD-A157297] N86-11198

Corrosion-preventive primers for military equipment [AD-A156927] N86-11341

NAVAL POSTGRADUATE SCHOOL, MONTEREY, CALIF.

A novel oscillating jet: its effect on ejector thrust augmentation [AD-A157480] N86-11201

A flash X-ray facility for the Naval Postgraduate School
[AD-A157278] N86-11213

Particle sizing in a solid rocket motor using the management of scattered light
[AD-A156480] N86-11226

An investigation of the effects of fuel composition on combustion characteristics in a T-63 combustor
[AD-A157325] N86-11358

Voice communications over packet radio networks
[AD-A157478] N86-11411

Possible cross equatorial influence of the northeast monsoon on the equatorial westerlies over Indonesia
[AD-A156907] N86-11759

Several aspects of interannual variability in the California current system N86-11785

Use of the wavenumber technique with the Lloyds mirror for an acoustic doublet
[AD-A156463] N86-11824

Modification of Huffman coding
[AD-A156479] N86-11899

Approximate reasoning and the REVEAL software system. Users guide
[AD-A157298] N86-11902

Emission threshold for cerenkov radiation
[AD-A157615] N86-12025

NAVAL RESEARCH LAB., WASHINGTON, D. C.

A mechanism for ignition of high-temperature gaseous nitromethane: The key role of the nitro group in chemical explosives
[AD-A157355] N86-11303

Development of castor-oil-resistant polyurethane sonar encapsulants
[AD-A157576] N86-11347

On stratified vortex motions under gravity
[AD-A156930] N86-11427

Scaling calculations for a relativistic gyrotron
[AD-A157476] N86-11460

Measurements of refractive index structure function C2N and aerosol size distribution at Chesapeake Bay
[AD-A157455] N86-11717

A new characterization of the icing environment below 10,000 feet AGL from 7,000 miles of measurements in supercooled clouds N86-11743

MICROLAN, file transfer program for microprocessors
[AD-A156519] N86-11900

A hybrid mode and a classification of beam plasma instabilities
[AD-A157356] N86-12075

SIMPLODE: An imploding gas puff plasma model. 1: Neon
[AD-A157456] N86-12077

The ionization equilibrium of optically thick argon z-pinch plasmas for electron temperatures between 25 and 65 eV
[AD-A157484] N86-12078

Total and partial absorption coefficients for a nitrogen plasma
[AD-A157534] N86-12079

Advanced concepts theory annual report, 1984
[AD-A157535] N86-12080

NAVAL SHIP RESEARCH AND DEVELOPMENT CENTER, BETHESDA, MD.

Application of the vortex-lattice concept to flows with smooth-surface separation
[AD-A157571] N86-11430

On the computation of structural vibrations induced by a low-speed turbulent flow N86-12009

NAVAL SURFACE WEAPONS CENTER, WHITE OAK, MD.

Reduction of moisture effects during the cure of epoxy adhesives used in composite repair N86-11254

Microscopic evaluation of a polyimide (PMR-15)-graphite composite N86-11282

Aerosol seeding systems for the NSWC wind tunnels N86-11453

High rate Li/SOCl(2) cells. 2: Effect of catalyst on cell performance
[AD-A157383] N86-11672

NEBRASKA UNIV., LINCOLN.

Evaluation of AIS data for agronomic and rangeland vegetation: Preliminary results for August 1984 flight over Nebraska Sandhills Agricultural Laboratory N86-11627

Preliminary evaluation of AIS spectra along a topographic/moisture gradient in the Nebraska Sandhills N86-11629

The use of AIS data for identifying and mapping calcareous soils in western Nebraska N86-11630

NEVADA UNIV., RENO.

A first look at Airborne Imaging Spectrometer (AIS) data in an area of altered volcanic rocks and carbonate formations, Hot Creek Range, south central Nevada N86-11625

NEW MEXICO INST. OF MINING AND TECHNOLOGY, SOCORRO.

Synthesis of nickel-aluminum alloys by shock compression of composite particles
[DE85-015165] N86-11328

Shock consolidation of IN-100 nickel-base superalloy powder
[DE85-015159] N86-11360

NEW MEXICO UNIV., ALBUQUERQUE.

Validation of procedures for pavement design on expansive soils
[FAA-PM-85-15] N86-11362

NEWTON (DENNIS W.), RENO, NEV.

General aviation's meteorological requirements N86-11738

NIEDERSAECHSISCHES LANDESVERWALTUNGSAMT, HANOVER (WEST GERMANY).

North Sea coast levelling net: A model case for the determination of vertical movements in Western Europe N86-11594

NIHON UNIV., TOKYO (JAPAN).

Recent cryocooler progress in Japan N86-11369

Vuilleumier cycle cryocooler operating below 8 K N86-11390

NORTH AMERICAN WEATHER CONSULTANTS, INC., SALT LAKE CITY, UTAH.

Continuing design, review, and analysis work for the Sierra Cooperative Pilot Project
[PB85-204303] N86-11822

NORTH CAROLINA STATE UNIV., RALEIGH.

Shock-wave synthesis of titanium aluminides
[DE85-015140] N86-11324

Chemical synthesis under shock compression
[DE85-015166] N86-11325

Synthesis of nickel-aluminum alloys by shock compression of composite particles
[DE85-015165] N86-11328

NORTH CAROLINA UNIV., CHARLOTTE.

Kinetics analysis of diffusion of point defects to dislocations following pulsed neutron and electron irradiations
[DE85-012768] N86-12037

NORTHROP CORP., HAWTHORNE, CALIF.

Solid-state bonding of superplastic aluminum alloy 7475 sheet N86-11244

NORTHWESTERN UNIV., EVANSTON, ILL.

Viscoelastic creep of high-temperature concrete
[DE85-010511] N86-11539

Concrete creep at transient temperature: Constitutive law and mechanism
[DE85-010525] N86-11542

Oceanic intraplate seismicity: Implications for the rheology and tectonics of the ocean lithosphere N86-11699

NOTRE DAME UNIV., IND.

Laser velocimetry measurement in a transonic tunnel N86-11448

O

OAK RIDGE NATIONAL LAB., TENN.

Determination of the steady-state behavior of immobilized (BETA)-galactosidase utilizing an integral reactor scheme
[DE85-012900] N86-11256

Improvements in the fabrication of ceramic-fiber-ceramic-matrix composites by chemical vapor infiltration
[DE85-015971] N86-11301

Itinerant electron ferromagnetism in Fe-alloyed, Ni3Al based materials
[DE85-013989] N86-11331

Tensile properties of 2-1/4Cr-1Mo steel irradiated to 23 dpa at 390 to 550(0)C
[DE85-015551] N86-11332

Melting of crystalline and amorphous silicon by Ruby, XeCl and KrF laser irradiation
[DE85-015040] N86-11466

Refractory alloy performance: Product form procurement and component fabrication
[DE85-014858] N86-11477

Stirling cycle heat pump studies
[DE85-005365] N86-11680

Thermodynamics of chromium and iron in carbonate salts at 650(0)C
[DE85-013542] N86-11682

Integrated forest study on effects of atmospheric deposition. Project summary
[DE85-015972] N86-11690

Positive genetic hazard predictions from short-term tests have proved false for results in mammalian spermatogonia with all environmental chemicals so far tested
[DE85-013640] N86-11833

Relationship between alkylation sites and induction of dominant lethals and heritable translocations in mice
[DE85-014309] N86-11835

Information from specific-locus mutants on the nature of induced and spontaneous mutations in the mouse
[DE85-014313] N86-11836

Improvement in wear performance of surgical Ti-6Al-4V alloy by ion implantation of nitrogen or carbon
[DE85-013986] N86-11849

Mechanical accessories for mobile teleoperators
[DE85-014310] N86-11855

Liquid metal reactors programs: Safeguards and program assurance
[DE85-011002] N86-12046

Calculations of physical and chemical reactions produced in irradiated water containing DNA
[DE85-012899] N86-12051

R-matrix analysis of the (239) Pu neutron cross sections
[DE85-013095] N86-12052

Chemical thermodynamic assessment of the Li-U-O system for possible space nuclear applications
[DE85-015060] N86-12054

Effects of trapped alpha particles on ballooning modes in tokamaks
[DE85-015064] N86-12082

Tokamak startup: Problems and scenarios related to the transient phases of ingnited tokamak operations
[DE85-015321] N86-12085

Variable field magnetic extraction channel for ORIC
[DE85-011927] N86-12089

Spherical torus: An approach to compact fusion at low field. Initial ignition assessements
[DE85-012890] N86-12099

Formation, ion modification and annealing of VN
[DE85-012898] N86-12146

Distinct characteristics of science
[DE85-006533] N86-12159

OFFICE NATIONAL D'ETUDES ET DE RECHERCHES AEROSPATIALES, PARIS (FRANCE).

Aerodynamic method used in France for advanced fast propeller study N86-11149

Modern propeller profiles N86-11152

OFFICE OF THE UNDER SECRETARY OF DEFENSE FOR RESEARCH AND ENGINEERING, WASHINGTON, D. C.

Electro-optics Millimeter/Microwave technology in Japan. Report of DOD technology team
[AD-A157376] N86-12073

OHIO STATE UNIV., COLUMBUS.

Calculation of allowable orbital spacings for the fixed-satellite service
[NASA-CR-176273] N86-11212

Studies on the syntheses of boron hydride systems
[AD-A157388] N86-11344

Least squares collocation applied to local gravimetric solutions from satellite gravity gradiometry data
[NASA-CR-176299] N86-11910

OKLAHOMA UNIV., NORMAN.

Algebraic grid generation using tensor product B-splines N86-11908

OLD DOMINION UNIV., NORFOLK, VA.

Visual information transfer. Part 1: Assessment of specific information needs. Part 2: Parameters of appropriate instrument scanning behavior
[NASA-CR-176277] N86-11850

OREGON STATE UNIV., CORVALLIS.

Regional Wind Energy Assessment Program. Appendix: Wind statistics summaries
[DE85-011520] N86-11686

Recent long-term climatic change over the eastern tropical and subtropical Pacific and its ramifications N86-11775

Time series modeling of the Southern Oscillation N86-11777

Peru coastal winds during 1982-1983 N86-11783

Time-averaging the flux-profile relationship N86-11789

Atmospheric general circulation model simulations of the modern Antarctic climate N86-11790

OREGON UNIV., EUGENE.

Is the cerebellum involved in motor and perceptual timing: A case study
[AD-A157452] N86-11842

Force and timing components of the motor program
[AD-A157584] N86-11843

Cognitive science program: Dissociation of the central timekeeper and the peripheral implementation processes in repetitive movements
[AD-A157542] N86-11852

Amplitude tests of direct channel resonances: The dibaryon
[DE85-011478] N86-12034

The optical polarization of Epsilon Aurigae through the 1982-84 eclipse N86-12171

P

PACIFIC NORTHWEST LAB., RICHLAND, WASH.

Dose distribution and the relative biological effectiveness of internal alpha emitters
[DE85-013041] N86-11845

Assessment of technical strengths and information flow of energy conservation research in Japan. Volume 2: Background document
[DE85-013759] N86-12165

PEI ASSOCIATES, INC., CINCINNATI, OHIO.

Laboratory evaluation of the protocol for the volatile organic sampling train
[PB85-201184] N86-11694

PENNSYLVANIA STATE UNIV., UNIVERSITY PARK.

The utilization of satellite data and dynamics in understanding and predicting global weather phenomena
[NASA-CR-171577] N86-11749

The effect of topography on the evolution of unstable disturbances in a baroclinic atmosphere N86-11750

The Hadley and Rossby regimes in a spherical atmosphere N86-11751

A parameterization technique for nonlinear spectral models N86-11752

A numerical study of global axisymmetric states and their stability to quasi-geostrophic disturbances N86-11753

On cloud street development in three dimensional parallel and Rayleigh instabilities N86-11754

Cloud streets during KonTur: A comparison of parallel/thermal instability modes with observations
N86-11755

On the nonlinear characteristics of the axisymmetric flow regime: Cylindrical and spherical systems N86-11756

Adaptive motivation theory
[AD-A157440] N86-11851

X-ray inverse Compton emission from the radio halo of M87
[NASA-CR-176305] N86-12196

X-ray inverse Compton emission from the radio halo of M87
[NASA-CR-176304] N86-12197

PHILIPS LABS., BRIARCLIFF MANOR, NEW YORK.

Parametric testing of a linearly driven Stirling cryogenic refrigerator N86-11376

Design of a flight qualified long-life cryocooler
N86-11377

Effects of leakage through clearance seals on the performance of a 10 K Stirling-cycle refrigerator
N86-11379

PITTSBURGH UNIV., JOHNSTOWN, PA.

Flow reactor studies over wide temperature and pressure ranges of atom and radical reaction rates important in ignition and combustion
[AD-A156931] N86-12020

POLISH ACADEMY OF SCIENCES, WARSAW.

On short periodical variations of polar motion and UT1-UTC N86-11574

POLYTECHNIC INST. OF NEW YORK, BROOKLYN.

Bounded state control of linear systems with application to the active structural control N86-11493

POLYTECHNIC INST. OF NEW YORK, FARMINGDALE.

Part A: Molecular dynamics and ionic associations of LiAsF6 in 4-butyrolactone mixtures with 2-methyl tetrahydrofuran. Part B: Molecular dynamics and ionic associations of LiBF4 in 1,2-dimethoxymethane
[AD-A157401] N86-12023

PRATT AND WHITNEY AIRCRAFT, EAST HARTFORD, CONN.

Lateral dampers for thrust bearings
[NASA-CR-174924] N86-11474

Dynamic gas temperature measurement system
N86-11499

The 3-D inelastic analysis methods for hot section components (base program) N86-11517

Creep fatigue life prediction for engine hot section materials (isotropic) N86-11521

PRATT AND WHITNEY AIRCRAFT GROUP, EAST HARTFORD, CONN.

Development of heat flux sensors for turbine airfoils and combustor liners N86-11502

Coolant passage heat transfer with rotation. A progress report on the computational aspects N86-11510

PRATT AND WHITNEY AIRCRAFT GROUP, WEST PALM BEACH, FLA.

Current and future engine applications of Gr/PI composites N86-11291

PRATT AND WHITNEY AIRCRAFT OF CANADA LTD., LONGUEUIL (QUEBEC).

An investigation of in-flight near-field propeller noise generation and transmission N86-11171

PRINCETON UNIV., N. J.

Anomaly general circulation models N86-11798

Monthly forecast experiments with sea surface temperature anomaly forcings and envelope mountains: Preliminary results N86-11803

A numerical analysis of a queue with network access flow control
[AD-A157526] N86-11913

PULSE SCIENCES, INC., OAKLAND, CALIF.

Modelling of the PROTO-2 crossover network
[DE85-014639] N86-12128

PURDUE UNIV., LAFAYETTE, IND.

Characteristics of an axisymmetric sudden expansion flow
[NASA-CR-176278] N86-11465

Effect of a viscoelastic boundary inset on vibrational characteristics of a beam N86-11494

Urban, forest, and agricultural AIS data: Fine spectral structure N86-11644

Prediction of acoustical response of three-dimensional cavities using an indirect boundary element method
N86-12014

Q

QUANTUM TECHNOLOGY CORP., SURREY (BRITISH COLUMBIA).

A small helium liquifier which provides continuous cooling based on cycled isentropic expansion
N86-11389

R

RAND CORP., SANTA MONICA, CALIF.

Some examples of propulsion applications using antimatter N86-11225

Soviet research on crystal channeling of charged particle beams
[AD-A157353] N86-12022

RASOR ASSOCIATES, INC., SUNNYVALE, CALIF.

Advanced Thermionic Technology Program: Summary report, Volume 3
[DE85-009360] N86-11674

RAYTHEON CO., BEDFORD, MASS.

High temperature, short term tensile strength of C6000/PMR-15 composites N86-11279

Microstrip monpulse dipole array N86-11405

RAYTHEON CO., GOLETA, CALIF.

Considerations for extending the bandwidth of arrays beyond two octaves N86-11404

RENSSELAER POLYTECHNIC INST., TROY, N. Y.

Composite structural materials
[NASA-CR-176279] N86-11293

Constituent materials N86-11294

Composite materials N86-11295

Generic structural elements N86-11296

Processing science and technology N86-11297

RESEARCH INST. OF GEODESY, PRAGUE (CZECHOSLOVAKIA).

Results of KAPG co-operation in Earth tide research
N86-11551

A new approach to iterations in solving geodetic boundary value problems for real topography
N86-11569

RESEARCH INST. OF GEODESY, TOPOGRAPHY AND CARTOGRAPHY, PRAGUE (CZECHOSLOVAKIA).

CRCM and KAPG activity in recent crustal movement studies N86-11592

Dynamics of the Bohemian Massif N86-11616

RHODE ISLAND UNIV., KINGSTON.

Fiber optic pressure sensors in skin-friction measurements
[NASA-CR-176294] N86-11838

RICE UNIV., HOUSTON, TEX.

Laboratory studies of atomic collision processes of importance in planetary atmospheres
[NASA-CR-176301] N86-12019

RICOR LTD., EN-HAROD IHUD (ISRAEL).

Passive motion control of pneumatically driven displacers in cryogenic coolers N86-11383

ROCHESTER UNIV., N. Y.

OMEGA: A 24 beam UV irradiation facility
[DE85-014416] N86-12127

What extent will small-scale laser-beam fluctuations seed the Rayleigh-Taylor instability in direct-drive targets
[DE85-014408] N86-12131

ROCKWELL INTERNATIONAL CORP., GOLDEN, COLO.

Metallography of solid state bonds
[DE85-014564] N86-11327

ROCKWELL INTERNATIONAL CORP., RICHLAND, WASH.

Probability encoding of hydrologic parameters for basalt. Elicitation of expert opinions from a panel of three basalt waste isolation project staff hydrologists
[DE85-014665] N86-11652

ROCKWELL INTERNATIONAL SCIENCE CENTER, THOUSAND OAKS, CALIF.

Quality assurance procedures for V378A matrix resin
N86-11274

ROME AIR DEVELOPMENT CENTER, GRIFFISS AFB, N.Y.

Proceedings of the 1984 Antenna Applications Symposium
[AD-A153257] N86-11398

ROME AIR DEVELOPMENT CENTER, HANSCOM AFB, MASS.

A high-efficience, low-phase error waveguide lens for a transform feed antenna N86-11409

ROYAL AIRCRAFT ESTABLISHMENT, FARNBOROUGH (ENGLAND).

Some aeroacoustic wind tunnel measurements, theoretical predictions, and flight-test correlations on subsonic aircraft propellers N86-11170

ROYAL INST. OF TECH., STOCKHOLM (SWEDEN).

On the convergence problem of the satellite derived spherical harmonic expansion of the geopotential at the Earth's surface N86-11582

ROYAL NETHERLANDS METEOROLOGICAL INST., DE BILT.

The impact of heat sources in the tropics on the atmospheric circulation N86-11793

RUTGERS - THE STATE UNIV., NEW BRUNSWICK, N. J.

Prediction of monthly 700 mb heights using antecedent and simulated prognostic height predictors N86-11805

S

SAINT FRANCIS MEDICAL CENTER, PEORIA, ILL.

Theory and experiment for infinite microstrip arrays
N86-11406

SAN DIEGO STATE UNIV., CALIF.

The chemical production of excited state molecules
[AD-A157276] N86-12021

SAN FRANCISCO UNIV., CALIF.

Structure and function of isozymes: Evolutionary aspects and role of oxygen in eucaryotic organisms
[NASA-CR-176286] N86-11831

SAN JOSE STATE UNIV., CALIF.

Coral reef hydrogeology
[DE85-012923] N86-11828

SANDIA LABS., ALBUQUERQUE, N. MEX.

Stress and strain-rate dependence of spall strength in two aluminum alloys
[DE85-015154] N86-11321

Shock-wave synthesis of titanium aluminides
[DE85-015140] N86-11324

Chemical synthesis under shock compression
[DE85-015166] N86-11325

Synthesis of nickel-aluminum alloys by shock compression of composite particles
[DE85-015165] N86-11328

Influence of effective rate sensitivity on adiabatic shear instability
[DE85-013967] N86-11333

Calculation of thermal trapping in shear bands
[DE85-014404] N86-11336

Relationship between interatomic bonding and electron transport in plasma deposited amorphous metal alloys
[DE85-014710] N86-11337

Photosensitivity and imaging characteristics of ion-implanted PLZT ceramics
[DE85-015489] N86-11348

Transportation system impact limiter design using rigid polyurethane foam
[DE85-015088] N86-11354

Polyurethane foam component lifetimes
[DE85-008208] N86-11355

Shock-induced temperature distributions in powder compact recovery fixtures
[DE85-015139] N86-11359

Shock consolidation of IN-100 nickel-base superalloy powder
[DE85-015159] N86-11360

Explosive generators for low-cost pulsed power
[DE85-013436] N86-11421

Automated magnet testing facility
[DE85-012863] N86-11422

Partial discharge formation and breakdown in deionized water under repetitive stressing
[DE85-013114] N86-11424

Geothermal instrumentation development activities at Sandia
[DE85-008693] N86-11463

Velocity measurements of laser driven flyers backed by high impedance windows
[DE85-015142] N86-11470

Dish electric systems heat engine assessment
[DE85-013942] N86-11479

Numerical simulation of a sample recovery fixture for high velocity impact
[DE85-013965] N86-11485

Strain rate dependence in steady, plastic shock waves
[DE85-014703] N86-11544

High pressure strength of shocked aluminum [DE85-014461] N86-11547
Vertical axis wind turbine power regulation through centrifugally pumped lift spoiling [DE85-013787] N86-11679
Degradation of ionic membranes in the zinc/ferricyanide battery [DE85-008469] N86-11681
Economics of magma power generation [DE85-008694] N86-11687
Use of SiO2 and TiO2 sol-gel antireflection films on silicon solar cells [DE85-011280] N86-11688
Development of membranes for the zinc/ferricyanide battery [DE85-011189] N86-11689
Optical modeling of multilayer thin/thick films N86-11862
Calculation of the electron backscattering coefficient by Monte Carlo simulation N86-11864
Three-dimensional heat transfer analysis using the PATRAN-G solids modeling and Q-TRAN thermal analysis computer codes N86-11867
Interface elements for heat transfer analysis N86-11868
Application of a mixture theory to the binary alloy solidification problem N86-11873
Microcomputer control and data management techniques for transient digital recording N86-11874
Finite difference calculations of voltages generated in thin dielectric layers subjected to shock loading N86-11878
A time-splitting numerical technique for solving highly coupled two-phase flow conservation equation N86-11879
Simulation of flame propagation through vorticity regions using the discrete vortex method N86-11882
Application of Flux-Corrected Transport (FCT) to heat transfer/fluid mechanics problems N86-11883
Heat transfer and pressure changes due to a large temperature difference across an enclosed vertical air layer N86-11884
A hybrid vortex-in-cell finite-difference numerical method for turbulent shear layer computation N86-11886
IFR guiding experiments [DE85-014512] N86-12027
Cascade switch implementation of PBFA 1 [DE85-013955] N86-12039
Ionization-Raman double-resonance spectroscopy [DE85-013774] N86-12042
Multidimensional ion microbeam analysis [DE85-014699] N86-12055
Experimental check of bremsstrahlung dosimetry predictions for 0.75 MeV electrons [DE85-014706] N86-12058
PBFA-2 vacuum insulator stack failure mechanisms [DE85-013118] N86-12090
Design and optimization of the PBFA 2 vacuum interface and transmission lines for light ion fusion [DE85-012809] N86-12092
Photon diagnostics leading to an improved Marx [DE85-013434] N86-12103
XUV preionization effects in high power magnetically insulated diodes [DE85-013142] N86-12109
Rimfire: A six megavolt laser-triggered gas-filled switch for PBFA 2 [DE85-013959] N86-12115
PBFA 2: A 100 TW pulsed power driver for the inertial confinement fusion program [DE85-013956] N86-12116
Comparison of energy transport measurements and computer simulations in a single module prototype for PBFA 2 [DE85-013960] N86-12119
MABE multibeam accelerator [DE85-012035] N86-12121
Low inductance diode design of the Proto 2 accelerator for imploding plasma loads [DE85-013783] N86-12123
Analytical electron microscopy study of shock synthesized zinc ferrite [DE85-015144] N86-12140

SANDIA LABS., LIVERMORE, CALIF.
Seeding requirements for scanning laser velocimetry N86-11446

SCIENCE AND TECHNOLOGY CORP., LAS CRUCES, N. MEX.
Particle phase function measurements by a new Fiber Array Nephelometer: FAN 1 N86-11456

SCIENCE RESEARCH CORP., SOMERVILLE, MASS.
Electron beam potential diagnostic for tandem mirrors, phase 1 [DE85-013515] N86-12107

SCIENTIFIC COAL RESEARCH INST., OSTRAVA (CZECHOSLOVAKIA).
Travel-time and its residuals for the blasts from Eschenlohe (Bavaria) N86-11706

SCIENTIFIC CONCEPTS, INC., POTSDAM, N.Y.
Bridgman growth of semiconductors [NASA-CR-177971] N86-11426

SCIENTIFIC RESEARCH ASSOCIATES, INC., GLASTONBURY, CONN.
Development of a Navier-Stokes analysis for the flow in disk pumps [AD-A157454] N86-11428

SCRIPPS INSTITUTION OF OCEANOGRAPHY, LA JOLLA, CALIF.
Some empirical evidence for the influence of snow cover on temperature and precipitation N86-11767
On the relationship between North Atlantic seasonal SST anomalies with United States surface temperature anomalies N86-11770
The distribution of rainfall along the coast of northern Peru during 1982-83 N86-11782
Warm and cold episodes in the California current: A case for large-scale mid-latitude atmospheric forcing N86-11786
Spectral statistical forecasts of the 500 mb height field N86-11804

SHOCK AND VIBRATION INFORMATION CENTER (DEFENSE), WASHINGTON, D. C.
The Shock and Vibration Digest, volume 17, no. 4 [AD-A154112] N86-11527
Microcomputers in shock and vibration N86-11528
The Shock and Vibration Digest, volume 17, no. 5 [AD-A156716] N86-11531

SLOVAK ACADEMY OF SCIENCES, HURBANOVA (CZECHOSLOVAKIA).
Magnification of low-sensitivity channels in seismographs with standard characteristics N86-11709

SLOVAK TECHNICAL UNIV., BRATISLAVA (CZECHOSLOVAKIA).
Some short periodic terms due to nutation and tides from latitude and time determinations at Czechoslovak observatories N86-11566

SMITHSONIAN ASTROPHYSICAL OBSERVATORY, CAMBRIDGE, MASS.
Balloon-borne three-meter telescope for far-infrared and submillimeter astronomy [NASA-CR-176285] N86-12188
A laser siderostat [AD-A157444] N86-12190

SOCIETE NATIONALE INDUSTRIELLE AEROSPATIALE, MARIGNANE (FRANCE).
Dynamic behavior of a propfan N86-11159

SOFTECH, INC., FAIRBORN, OHIO.
Ada (trademark) compiler validation summary report: Verdix Ada Compiler, Verdix Ada Development System (VADS) VAda-010-1010, version V05.00, for Sun Microsystems Model 2/120 using UNIX (trademark) 4.2 BSD, release 1.1 [AD-A157574] N86-11891

SOLAREX CORP., ROCKVILLE, MD.
The interface structure of grain boundaries in polysilicon N86-11665

SOLENERGY CORP., WOBURN, MASS.
Intermediate load modules for test and evaluation: Fixed price research and development [NASA-CR-176135] N86-11664

SOUTHEASTERN CENTER FOR ELECTRICAL ENGINEERING EDUCATION, INC., ST. CLOUD, FLA.
Basic EMC technology advancement for C(3) systems. Volume 3B: Computer simulation of EMI effects in a differential line receiver [AD-A156505] N86-11416

SOUTHWEST RESEARCH INST., SAN ANTONIO, TEX.
Sandia shock compression database [DE85-015141] N86-12142

SPECTRON DEVELOPMENT LABS., INC., COSTA MESA, CALIF.
A technique to measure the size of particles in laser Doppler velocimetry applications N86-11457
Advance particle and Doppler measurement methods N86-11745

SPS TECHNOLOGIES, JENKINTOWN, PA.
Mechanical fasteners for advanced composite materials N86-11232
Stress corrosion resistant fasteners N86-11235

STANDARD OIL CO., CLEVELAND, OHIO.
Site description for the University of Nebraska's Sandhills Agricultural Laboratory N86-11628

STANFORD LINEAR ACCELERATOR CENTER, CALIF.
Disruption angles [DE85-015138] N86-12032
Experimental program to build a multimegawatt lasertron for super linear colliders [DE85-014293] N86-12049
Collinear wake field acceleration [DE85-014356] N86-12050
Increased intensity performance of the Brookhaven AGS [DE85-013371] N86-12091
Status of SLC [DE85-013071] N86-12097
Very high energy colliders [DE85-013075] N86-12100
Higher luminosities via alternative incident channels [DE85-014355] N86-12118
Coupled virbrational modes of the SLC arc magnet and support system [DE85-014288] N86-12124
Measurements of ultimate accelerating gradients in the SLAC disk-loaded structure [DE85-014287] N86-12125

STANFORD UNIV., CALIF.
Creep and fracture of a yttria dispersed nickel-chromium alloy N86-11309
Improved solid state laser sources, volume 3 [DE85-012956] N86-11469
Field utilization and analysis of AIS 128-channel imagery using microcomputers: Application to Yerington, Nevada field area N86-11621
A comparison of AIS data with other aircraft and ground data for the geobotanical discrimination of rock types in southwest Oregon N86-11642
Tracer test analysis of the Klamath Falls geothermal resource: A comparison of models [DE85-009924] N86-11678
Directly executed languages [AD-A157311] N86-11888
Sparse quasi-Newton methods and the continuation problem [AD-A157587] N86-11914

STATE DEPT., WASHINGTON, D. C.
US space programs: Cooperation and competition from Europe [BPA-CP-695] N86-12163

STATE UNIV. OF NEW YORK, STONY BROOK.
Climate simulation and change: A simple energy balance climate model N86-11731
Possibilities of polarized protons in Sp anti p S and other high energy hadron colliders [DE85-012517] N86-12044

STAZIONE ASTRONOMICA INTERNAZIONALE DI LATITUDINE, CAGLIARI (ITALY).
Secular and long term variations in polar motion from classical and Doppler observations N86-11581

SYRACUSE UNIV., N. Y.
Nuclear spin-polarized HD, D2, HT and DT solids, liquids and high density gases [DE85-014136] N86-12154

SYSTEMS AND APPLIED SCIENCES CORP., VIENNA, VA.
Sub-cloud layer motions from radar data using correlation techniques [AD-A156477] N86-11757

T

TECHNION - ISRAEL INST. OF TECH., HAIFA.
Mechanical face seal dynamics update N86-11530

TECHNISCHE HOCHSCHULE, DARMSTADT (WEST GERMANY).
Precise geoid computations at mountainous coastlines in view of vertical datum determinations N86-11561
Modification of a Hughes tiltmeter to a borehole tiltmeter N86-11563
On the distribution of the residual vectors of Earth's tide gravity observations in Central Europe N86-11564

TECHNISCHE HOGESCHOOL, DELFT (NETHERLANDS).
Simple construction and performance of a conical plastic cryocooler N86-11378

TECHNISCHE UNIV., DRESDEN (EAST GERMANY).
Treatment of the geodetic boundary value problem by contact-transformation N86-11573
Planets around Barnard's Star? N86-11584
Geodimeter net for the investigation of horizontal crustal deformations N86-11598
Stationary hydrostatic precision tiltmeter system N86-11607
Significance tests of recent vertical crustal movements by correlation functions N86-11611

TECHNISCHE UNIV., GRAZ (AUSTRIA).
Variational principles for Earth rotation N86-11580

TECTONICS RESEARCH, INC., MINNEAPOLIS, MINN.
Hermetic bellows seal for Braun linear engine: Design, test and demonstration [DE85-013545] N86-11478

TELEDYNE MICRONETICS, SAN DIEGO, CALIF.
Computer-aided bifocal dielectric lens antenna design for MH wave application N86-11410

TENNESSEE UNIV., KNOXVILLE.
The stability of Timoshenko beams conveying a compressible fluid N86-11492

R-matrix analysis of the (239) Pu neutron cross sections [DE85-013095] N86-12052

Spherical torus: An approach to compact fusion at low field. Initial ignition assessments [DE85-012090] N86-12099

Formation, ion modification and annealing of VN [DE85-012806] N86-12146

TENNESSEE UNIV. SPACE INST., TULLAHOMA.

Gas flow environmental and heat transfer nonrotating 3D program N86-11506

Laboratory model of flight through wind shear N86-11747

TENNESSEE WATER RESOURCES RESEARCH CENTER, KNOXVILLE.

Effects of acid precipitation on composition, electrokinetic behavior, cation adsorption and ion exchange capacity in various soil systems [PB85-217727] N86-11698

TEXAS A&M UNIV., COLLEGE STATION.

Deformation of granite at elevated temperature and pressure [DE85-014057] N86-11721

Observing the Eastern Pacific Hadley Circulation N86-11818

A numerical method of calculating propeller noise including acoustic nonlinear effects N86-12011

Application of detailed fission-product decay gamma spectra in the calculation of photoneutron spectra from D((GAMMA),n) reactions in PWR fuel [DE85-012729] N86-12048

TEXAS DEPT. OF WATER RESOURCES, AUSTIN.

Evaluating the ground-water resources of the high plains of Texas, volume 3 [PB85-191617] N86-11655

TEXAS INSTRUMENTS, INC., ATTLEBORO, MASS.

Comparison of bond in roll-bonded and adhesively bonded aluminums N86-11248

TEXAS RESEARCH INST., INC., AUSTIN.

Failure rate model for cathodic delamination of protective coatings [AD-A157483] N86-11912

TEXAS UNIV., AUSTIN.

Computational errors and their control in the determination of satellite orbits N86-11211

Numerical solution for contact pressure and wear distributions of unlubricated, misaligned, closely conforming, multiply connected surfaces N86-11472

The vacuum in the presence of electromagnetic fields and rotating boundaries N86-11916

Plasma kinetic theory in action-angle variables [DE85-014767] N86-12084

Energy confinement in a high-current reversed field pinch [DE85-015009] N86-12111

Variational quadratic form for low frequency electromagnetic perturbations. 1: Formalism [DE85-014896] N86-12129

Star formation in the inner galaxy: A far-infrared and radio study of two H2 regions [NASA-TM-86720] N86-12185

TEXAS UNIV., BASTROP.

Representations of the group of diffeomorphisms in the physics of particles, gravity and fluids [DE85-007031] N86-12028

THERMO ELECTRON CORP., WALTHAM, MASS.

Advanced Thermionic Technology Program: Summary report, Volume 3 [DE85-009360] N86-11674

THERMO-SYSTEMS, INC., ST. PAUL, MINN.

Generating aerosols for laser velocimeter seeding N86-11455

TOKYO INST. OF TECH. (JAPAN).

Numerical simulation of a sample recovery fixture for high velocity impact [DE85-013965] N86-11485

TOKYO UNIV. (JAPAN).

International solar-terrestrial physics program: A plan for the core spaceflight missions [NASA-TM-87511] N86-12194

TORONTO UNIV. (ONTARIO).

A model of a downburst, a wind tunnel program on planetary boundary layer, and airship in turbulence N86-11748

TRIBON BEARING CO., CLEVELAND, OHIO.

Transfer molding of PMR-15 polyimide resin N86-11288

TRIESTE UNIV. (ITALY).

The eclipse of Epsilon Aurigae visible spectroscopy and ultraviolet activity N86-12173

TRW, INC., REDONDO BEACH, CALIF.

Polyimide matrix resins for up to 700 deg F service N86-11280

Physics modeling of tandem mirror devices with high field test cell inserts [DE85-011870] N86-12086

TRW SYSTEMS, REDONDO BEACH, CALIF.

New concepts for drift pumping a thermal barrier with RF [DE85-013591] N86-12114

TUFTS UNIV., MEDFORD, MASS.

Amplitude tests of direct channel resonances: The dibaryon [DE85-011476] N86-12034

TULSA UNIV., OKLA.

Teratogenic effects of microwave radiation [PB85-207462] N86-11837

TUSKEGEE INST., ALA.

Project to study the use of microcomputer technology in planning and operation of small city transportation systems [PB85-204873] N86-12166

U

UNC NUCLEAR INDUSTRIES, INC., RICHLAND, WASH.

Hardware and software constructs for a vibration analysis network [DE85-008436] N86-11535

UNITED TECHNOLOGIES RESEARCH CENTER, EAST HARTFORD, CONN.

Factors affecting the processing of epoxy film adhesives N86-11252

Thermo-oxidative stability of graphite fiber/PMR-15 polyimide composites at 350 deg C N86-11277

Overview of solid particle LV seeding techniques used at UTRC N86-11445

Hot section viewing system N86-11498

High temperature static strain sensor development program N86-11500

Demonstration test of burner liner strain measurement systems: Interim results N86-11501

Assessment of a 3-D boundary layer code to predict heat transfer and flow losses in a turbine N86-11508

Gas-side heat transfer with rotation N86-11509

UNIVERSITY COLL., CORK (IRELAND).

Oxide cathode mechanisms: Electronic and structural features of oxide cathode surfaces [AD-A157666] N86-11418

UNIVERSITY OF SOUTHERN CALIFORNIA, LOS ANGELES.

Earthquake hazard research in the Los Angeles Basin and its offshore area, October 1, 1983 to September 30, 1984 [PB85-196491] N86-11725

Deepwell monitoring along the southern San Andreas Fault [PB85-196483] N86-11726

Applications of the magneto-optical filter to stellar pulsation measurements [NASA-CR-176282] N86-12187

UNIVERSITY OF WESTERN ONTARIO, LONDON.

Vacancies in thermal equilibrium in Nb [DE85-014832] N86-12061

UPPSALA UNIV. (SWEDEN).

Gaussian and mean curvatures of postglacial land uplift as expanded in surface spherical harmonics, and the origin of earthquakes in Fennoscandia N86-11599

URBAN SYSTEMS RESEARCH AND ENGINEERING, INC., CAMBRIDGE, MASS.

Evaluation of color infrared aerial surveys of wastewater soil absorption systems [PB85-189074] N86-11654

UTAH GEOLOGICAL AND MINERALOGICAL SURVEY, SALT LAKE CITY.

Summary of low-temperature geothermal studies conducted by the Utah Geological and Mineral Survey from July 1, 1977 to December 31, 1984 [DE85-009346] N86-11676

UTAH UNIV., SALT LAKE CITY.

Multispectroscopic studies of the electronic structure of electrode materials for high energy density batteries: 1-2, 1-3 intermetallic compounds with B32 structure [DE85-014675] N86-11684

V

VANDERBILT UNIV., NASHVILLE, TENN.

Photometric support for future astonomical research N86-12175

VERMONT UNIV., BURLINGTON.

Fiscal year 1983 institute program report, Vermont Water Resources Research Center [PB85-214500] N86-11659

VILLANOVA UNIV., PA.

Intermediate and narrow band photometry of Epsilon Aurigae N86-12177

VIRGINIA POLYTECHNIC INST. AND STATE UNIV., BLACKSBURG.

Environmental effects in the fatigue behavior of copper nickel alloys N86-11307

Direct coupling of microbore HPLC columns to MS systems [NASA-CR-176292] N86-11436

A review of the literature on finite-element modeling of laminated composite plates N86-11529

VITRO LABS., SILVER SPRING, MD.

Performance of solar collector arrays and collector controllers in the National Solar Data Network [DE85-001297] N86-11663

W

WASHINGTON STATE ENERGY OFFICE, OLYMPIA.

Evaluation and ranking of geothermal resources for electrical generation or electrical offset in Idaho, Montana, Oregon and Washington [DE85-014661] N86-11650

Evaluation and ranking of geothermal resources for electrical generation or electrical offset in Idaho, Montana, Oregon and Washington, volume 2 [DE85-014452] N86-11683

WASHINGTON UNIV., SEATTLE.

Processing and microstructural characterization of B4C-Al cermets [DE85-013195] N86-11326

Interpretation of AIS images of Cuprite, Nevada using constraints of spectral mixtures N86-11626

Global relationships with the Southern Oscillation N86-11776

Meteorological conditions during drought episodes in the United States Great Plains N86-11802

Low-frequency baroclinic features observed in the lee of major mountain ranges N86-11811

High dispersion observations of Epsilon Aur from Sept. 1982 to March 1983 N86-12183

WESTINGHOUSE RESEARCH AND DEVELOPMENT CENTER, PITTSBURGH, PA.

Mercury bromide reconstitution in the HgBr laser system [AD-A156502] N86-11466

WIEN UNIV. (AUSTRIA).

Double differential neutron emission cross sections of (10)B and (1)B at 6, 10 and 14 MeV and of (6)Li, (7)Li and (12)C at 14 MeV [DE85-012749] N86-12056

WISCONSIN DEPT. OF NATURAL RESOURCES, MADISON.

Aerial photography and ground verification at power plant sites: Wisconsin power plant impact study [PB85-197358] N86-11658

WISCONSIN PUBLIC SERVICE COMMISSION, MADISON.

Aerial photography and ground verification at power plant sites: Wisconsin power plant impact study [PB85-197358] N86-11658

WISCONSIN PUBLIC SERVICE CORP., GREEN BAY.

Aerial photography and ground verification at power plant sites: Wisconsin power plant impact study [PB85-197358] N86-11658

WISCONSIN UNIV., MADISON.

Determination of the steady-state behavior of immobilized (BETA)-galactosidase utilizing an integral reactor scheme [DE85-012900] N86-11256

A body tensor formalism for elastic-plastic continua with applications in uniaxial extension N86-11491

Forest canopy chemistry from Blackhawk Island, Wisconsin N86-11634

Aerial photography and ground verification at power plant sites: Wisconsin power plant impact study [PB85-197358] N86-11658

Life cycle of a 28-72 day atmospheric oscillation during northern winter N86-11781

Controlled environment life support system: Calcium-related leaf injuries on plants [NASA-CR-176288] N86-11829

WORLD METEOROLOGICAL ORGANIZATION, GENEVA (SWITZERLAND).

Climate system fluctuations, monitoring N86-11814

WRIGHT STATE UNIV., DAYTON, OHIO.

Kinetics analysis of diffusion of point defects to dislocations following pulsed neutron and electron irradiations [DE85-012768] N86-12037

X

XIAN JIAOTONG UNIV. (CHINA).

Low frequency split cycle cryocooler N86-11382

Y

YALE UNIV., NEW HAVEN, CONN.
Easy impossibility proofs for distributed concensus problems
[AD-A157411] N86-11903

YARMOUK UNIV., IRBID (JORDAN).
Stiffness and damping coefficients of rubber N86-11532

YONSEI UNIV., SEOUL (SOUTH KOREA).
Photoelectric observations of the long-period eclipsing binaries at Yonsei University Observatory N86-12184

Z

ZAGREB UNIV. (YUGOSLAVIA).
Anew about the correlation between Mohorovicic discontinuity depths, geoid undulations and Bouguer gravity anomalies in the Dinaric-Pannonian region of Yugoslavia N86-11557

ZHEJIANG UNIV. (CHINA).
An experimental study for a miniature Stirling refrigerator N86-11375

CONTRACT NUMBER INDEX

SCIENTIFIC AND TECHNICAL AEROSPACE REPORTS VOLUME 24 NUMBER 2

Typical Contract Number Index Listing

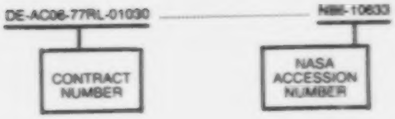

Listings in this index are arranged alphanumerically by contract number. Under each contract number the NASA accession numbers denoting documents that have been produced as a result of research done under that contract are arranged in ascending order. The NASA accession number denotes the number by which the citation is identified.

AF PROJ. 4600	N86-11398
AF-AFOSR-0074-83	N86-11418
AF-AFOSR-0122-81	N86-11901
AF-AFOSR-0130-84	N86-12076
AFOSR ISSA-00005	N86-11366
ARPA ORDER 3343	N86-12137
	N86-12138
ARPA ORDER 4395	N86-12075
	N86-12079
DA PROJ. 1L1-62209-AH-76	N86-11523
DA PROJ. 1L1-62209-AH-76-A	N86-11204
DA PROJ. 3E1-62777-A-879	N86-11840
DA PROJ. 3M1-62734-A-875	N86-11832
DAAG29-76-G-0103	N86-11346
DAAG29-79-C-0015	N86-11346
DAAG29-80-K-0021	N86-12021
DAAG29-81-K-0050	N86-12020
DAAG29-82-K-0062	N86-12072
DAAG29-82-K-0082	N86-11346
DAAG29-82-K-0085	N86-11913
DAAG29-82-K-0109	N86-11886
DAAG29-82-K-0112	N86-11344
DAAG29-83-K-0163	N86-12074
DAAG29-84-K-0058	N86-11903
DAAG29-85-K-0048	N86-12023
DAAG46-81-C-0006	N86-11202
DAAK11-83-C-0062	N86-11458
DAAK70-83-K-0018	N86-11915
DE-AC0-584OR-21400	N86-12159
DE-AC3-76SF-00098	N86-12030
DE-AC01-79CS-30027	N86-11663
DE-AC02-76CH-00016	N86-11330
	N86-11335
	N86-11484
	N86-11846
	N86-11944
	N86-12038
	N86-12044
	N86-12059
	N86-12061
	N86-12066
	N86-12095
	N86-12117
	N86-12144
	N86-12147
DE-AC02-76CH-03000	N86-12035
	N86-12066
	N86-12098
	N86-12105
DE-AC02-76ET-11292	N86-11674
DE-AC02-76FR-03230	N86-12041
DE-AC02-78ER-10107	N86-11536
	N86-12060
DE-AC02-78ET-51013	N86-12081
	N86-12083
DE-AC02-79EV-10098	N86-11764
DE-AC02-80ER-10556	N86-11538
DE-AC02-81ER-40025	N86-12063
DE-AC02-81EV-10730	N86-11764
DE-AC02-83CH-10093	N86-11357
	N86-11433
	N86-11675
DE-AC02-83CH-10098	N86-11349
	N86-12139
DE-AC02-83ER-13073	N86-11257
DE-AC02-83ER-45025	N86-11334
	N86-12141
DE-AC02-83ER-53162	N86-12102
DE-AC02-83ER-60162	N86-11774
DE-AC02-84ER-80167	N86-12107
DE-AC03-76DP-00789	N86-11354
DE-AC03-76SF-0051	N86-12032
DE-AC03-76SF-00098	N86-11322
	N86-11722
	N85-12026
	N86-12029
	N86-12051
	N86-12067
	N86-12104
	N86-12145
	N86-12157
DE-AC03-76SF-00515	N86-12049
	N86-12050
	N86-12091
	N86-12097
	N86-12100
	N86-12118
	N86-12124
	N86-12125
DE-AC03-84ER-51044	N86-12110
DE-AC04-76DP-3533	N86-11327
DE-AC04-76DP-00053	N86-11329
	N86-11352
	N86-11462
DE-AC04-76DP-00789	N86-11321
	N86-11324
	N86-11325
	N86-11328
	N86-11333
	N86-11336
	N86-11337
	N86-11348
	N86-11355
	N86-11359
	N86-11360
	N86-11421
	N86-11422
	N86-11424
	N86-11446
	N86-11463
	N86-11470
	N86-11479
	N86-11485
	N86-11544
	N86-11547
	N86-11679
	N86-11681
	N86-11687
	N86-11688
	N86-11689
	N86-12027
	N86-12039
	N86-12042
	N86-12055
	N86-12058
	N86-12090
	N86-12092
	N86-12103
	N86-12109
	N86-12115
	N86-12116
	N86-12119
	N86-12121
	N86-12123
	N86-12128
	N86-12132
	N86-12140
	N86-12142
DE-AC05-84OR-21400	N86-11256
	N86-11301
	N86-11331
	N86-11332
	N86-11468
	N86-11477
	N86-11484
	N86-11680
	N86-11682
	N86-11690
	N86-11833
	N86-11835
	N86-11849
	N86-11855
	N86-12046
	N86-12051
	N86-12052
	N86-12054
	N86-12082
	N86-12085
	N86-12089
	N86-12099
	N86-12146
DE-AC05-87OR-21400	N86-11478
DE-AC06-76RL-01380	N86-11845
DE-AC06-76RL-01830	N86-12165
DE-AC06-76RL-01857	N86-11535
DE-AC06-77RL-01030	N86-11652
DE-AC07-76ID-01570	N86-11338
	N86-11481
	N86-11483
	N86-11892
	N86-12047
DE-AC08-80DP-40124	N86-12131
DE-AC21-83MC-20352	N86-11674
DE-AI01-76ET-10393	N86-11480
DE-AI01-76ET-20356	N86-11669
DE-AI01-79ET-20485	N86-11666
DE-AI05-82OR-1005	N86-11668
DE-AI79-83BP-13609	N86-11650
	N86-11683
DE-AM03-7 NSF DMS-84-20623	N86-11914
DE-AS03-84ER-52105	N86-12130
DE-AS05-76ER-03992	N86-12028
DE-AS05-84ER-60192	N86-11848
DE-AS07-77ET-28393	N86-11676
DE-AT03-76ER-71013	N86-11356
DE-AT03-76ET-53064	N86-12040
	N86-12112
	N86-12113
DE-AT03-80SF-11459	N86-11678
DE-AT03-81ER-10870	N86-12053
DE-AT03-83ER-45011	N86-11684
DE-AT06-76ER-70004	N86-12034
DE-FC01-80-ET-23197	N86-11665
DE-FC07-81ID-12262	N86-11677
DE-FC08-85DP-40200	N86-12127
DE-FG02-81ER-10864	N86-12152
DE-FG02-84ER-53179	N86-12154
DE-FG02-84ER-60257	N86-11692
DE-FG05-80ET-53088	N86-12084
	N86-12111
	N86-12129
DE-FG05-84ER-13216	N86-11721
DI-7-07-83-V0008	N86-11822
DI-14-08-0001-G-845	N86-11660
	N86-11661
DI-14-08-0001-G-859	N86-11662
DI-14-08-0001-G-870	N86-11698
DI-14-08-0001-G-873	N86-11659
DI-14-08-0001-21858	N86-11725
DI-14-08-0001-21879	N86-11726
DOT-UMTA-AL-06-0011	N86-12166
DTFA03-84-C-00004	N86-11898
EPA-R-803971	N86-11658
EPA-68-02-3453	N86-11837
EPA-68-02-3767	N86-11694
EPA-68-02-3770	N86-11695
EPA-68-03-3057	N86-11654
F41-400	N86-11198
F04701-83-C-0084	N86-12189
F19628-80-C-0002	N86-11417
F19628-80-C-0042	N86-11192
F19628-82-C-0023	N86-11757
F19628-84-C-0001	N86-11412
F19628-84-K-0010	N86-11408
F19628-84-K-0022	N86-11399
F19628-84-M-0002	N86-11398
F29601-84-C-0080	N86-11362

F30602-81-C-0062 .... N86-11416
F33600-84-D-0280 .... N86-11891
F33615-80-C-2074 .... N86-11199
F33615-82-C-2202 .... N86-11467
F33615-82-C-5001 .... N86-11343
F33615-82-C-5100 .... N86-11489
F33615-82-C-5102 .... N86-11318
F33615-84-C-2469 .... N86-11428
MDA903-82-C-0067 .... N86-12022
MIPR-ARO-129-85 .... N86-11417
NA-81AA-D-0054 .... N86-11804
NA-83AA-D-00048 .... N86-11773
NA-83AA-D-00048A1 .... N86-11806
NA-83SA-C-00738 .... N86-11817
NAGW-13 .... N86-12187
N86-12195
NAGW-472 .... N86-12187
N86-12195
NAGW-509 .... N86-12188
NAG1-237 .... N86-11339
NAG1-296 .... N86-11906
NAG1-343 .... N86-11436
NAG1-425 .... N86-11298
NAG1-451 .... N86-11850
NAG1-463 .... N86-11856
NAG1-519 .... N86-11838
NAG1-541 .... N86-11220
NAG1-567 .... N86-11894
NAG3-159 .... N86-11212
NAG3-163 .... N86-11266
NAG3-354 .... N86-12011
NAG3-399 .... N86-11667
NAG3-502 .... N86-11465
NAG3-530 .... N86-11670
NAG5-270 .... N86-11645
NAG5-377 .... N86-11897
NAG5-407 .... N86-11895
N86-11911
NAG8-457 .... N86-12196
N86-12197
NASA ORDER W-13130 .... N86-11701
NASA-ORDER-NCA2-OR781-201 .... N86-12185
NASW-3389 .... N86-12191
N86-12192
NASW-4004 .... N86-11733
N86-11734
NAS1-12308 .... N86-11283
NAS1-16546 .... N86-11207
NAS1-16721 .... N86-11426
NAS1-17070 .... N86-11856
NAS1-18000 .... N86-11312
NAS2-11303 .... N86-11204
NAS3-180 .... N86-11526
NAS3-22523 .... N86-11272
NAS3-22761 .... N86-11507
NAS3-23154 .... N86-11499
NAS3-23272 .... N86-11514
NAS3-23278 .... N86-11506
NAS3-23288 .... N86-11521
NAS3-23687 .... N86-11515
NAS3-23690 .... N86-11501
NAS3-23695 .... N86-11507
NAS3-23716 .... N86-11508
NAS3-23722 .... N86-11500
NAS3-23932 .... N86-11474
NAS5-25172 .... N86-11376
NAS5-26688 .... N86-11377
NAS7-100 .... N86-11664
NAS7-918 .... N86-11618
N86-11669
N86-11896
NAS8-33794 .... N86-11749
NAS8-35184 .... N86-11854
NAS8-36177 .... N86-11735
NCC2-85 .... N86-11831
NCC2-136 .... N86-11829
NCC2-231 .... N86-11830
NCC5-26 .... N86-11646
NGL-33-018-003 .... N86-11293
NGR-05-003-511 .... N86-12185
NGR-36-008-161 .... N86-11910
NGT-47-003-802 .... N86-11908
NIH-HL-11307 .... N86-11856
NR PROJ. F61-542 .... N86-11341
NSF AST-83-12332 .... N86-12185
NSF ATM-82-05992 .... N86-11790
NSF ATM-82-10160 .... N86-11804
NSF ATM-82-13279 .... N86-11804
NSF ATM-82-15090 .... N86-11813
NSF ATM-83-06135 .... N86-11775
NSF ATM-83-14431 .... N86-11773
NSF DCR-84-05478 .... N86-11903
NSF DMS-83-12229 .... N86-11534
NSF DMS-84-04121 .... N86-11914
NSF ECS-83-17777 .... N86-11913
NSG-1471 .... N86-11893
NSG-2347 .... N86-12186
NSG7-386 .... N86-12019
N0014-83-K-0125 .... N86-11903
N00014-76-C-0016 .... N86-11716
N00014-76-C-0037 .... N86-11317
N00014-80-C-0718 .... N86-11251
N00014-81-K-0197 .... N86-11851
N00014-82-K-0154 .... N86-11903
N00014-83-C-0375 .... N86-11466
N00014-83-C-2258 .... N86-11912
N00014-83-K-0125 .... N86-11904
N00014-83-K-0341 .... N86-12136
N00014-83-K-0536 .... N86-11534
N00014-83-K-0601 .... N86-11842
N86-11843
N86-11852
N00014-84-C-0336 .... N86-11673
N00014-84-C-0413 .... N86-11300
N00014-84-C-0446 .... N86-11839
N00014-84-C-0723 .... N86-11304
N00014-84-C-2137 .... N86-12190
N00014-84-K-0729 .... N86-11889
N00014-85-F-0001 .... N86-11342
N00014-85-K-0168 .... N86-11903
N00014-85-K-0169 .... N86-11534
N00014-85-K-0245 .... N86-11345
N00014-85-K-0343 .... N86-11914
N00019-84-C-0169 .... N86-11316
N00140-83-M-PL78 .... N86-12018
N00140-84-M-MS42 .... N86-12018
N60530-81-C-0158 .... N86-12137
N86-12138
N68305-84WR-40126 .... N86-11896
PASA-NASA/DSB-5710-2-79 .... N86-11666
PROJ. G859-01 .... N86-11662
RR0-1109 .... N86-11460
RR0-1306 .... N86-11303
RR0-2301 .... N86-11427
W-31-109-ENG 38 .... N86-12064
W-31-109-ENG-38 .... N86-11319
N86-11351
N86-11423
N86-11432
N86-11434
N86-11482
N86-11537
N86-11539
N86-11541
N86-11542
N86-11548
N86-12062
N86-12065
N86-12150
N86-12153
W-7405-ENG-36 .... N86-11214
N86-11223
N86-11320
N86-11323
N86-11361
N86-11414
N86-11419
N86-11420
N86-11431
N86-11435
N86-11543
N86-11545
N86-11546
N86-11685
N86-11720
N86-11858
N86-12033
N86-12037
N86-12045
N86-12048
N86-12056
N86-12088
N86-12093
N86-12096
N86-12106
N86-12122
N86-12126
N86-12143
N86-12148
N86-12149
N86-12155
N86-12193
N86-12198
W-7405-ENG-48 .... N86-11305
N86-11326
N86-11350
N86-11353
N86-11413
N86-11469
N86-11471
N86-11476
N86-11691
N86-11693
N86-11828
N86-11834
N86-11847
N86-11853
N86-12031
N86-12036
N86-12057
N86-12086
N86-12087
N86-12094
N86-12108
N86-12114
N86-12120
N86-12151
N86-12156
N86-12161
352-02-03 .... N86-12167
N86-12186
505-31-01-01 .... N86-11907
N86-11909
505-31-04 .... N86-11146
505-31-21 .... N86-11206
505-31-23-07 .... N86-11186
505-31-53-09 .... N86-11207
505-31-53-12 .... N86-11189
505-31-53-13 .... N86-11437
505-31-83-01 .... N86-11856
505-31-83-02 .... N86-11908
505-33-33 .... N86-11292
505-33-33-05 .... N86-11298
505-33-53-15 .... N86-11540
505-33-53-16 .... N86-11894
505-33-62 .... N86-11425
505-34-03-02 .... N86-11203
505-34-11 .... N86-11194
N86-11195
505-34-13-32 .... N86-11906
505-35-11 .... N86-11221
505-35-31 .... N86-11208
505-40-90 .... N86-12007
505-42-11 .... N86-11196
505-42-23-03 .... N86-11227
505-42-23-05 .... N86-11523
505-43-01 .... N86-11209
505-43-31 .... N86-11524
505-43-43-06 .... N86-11312
505-45-10-01 .... N86-11193
505-45-14-01 .... N86-11522
505-63-11 .... N86-11526
506-53-18 .... N86-11475
506-53-23-08 .... N86-11299
506-53-31 .... N86-11340
506-53-51 .... N86-11525
506-55-6E N86-11668
506-55-22 .... N86-11224
506-55-42 .... N86-11671
506-58-22 .... N86-12135
506-58-23-01 .... N86-11647
506-60-42 .... N86-11218
533-04-1A N86-11495
619-12-20-21 .... N86-11700
644-11-00 .... N86-11896
694-80-70 .... N86-11426
776-52-61 .... N86-11669
776-54-01 .... N86-11666

REPORT/ACCESSION NUMBER INDEX

SCIENTIFIC AND TECHNICAL AEROSPACE REPORTS VOLUME 24 NUMBER 2

Typical Report Number Index Listing

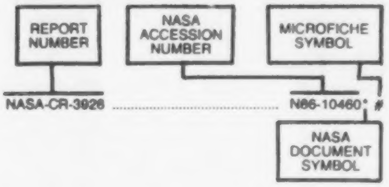

Listings in this index are arranged alphanumerically by report number. The NASA accession number denotes the number by which the citation is identified. An asterisk (*) indicates that the item is a NASA report. A pound sign (#) indicates that the item is available on microfiche.

ACSC-85-0335 N86-11857 #
ACSC-85-0925 N86-12160 #
ACSC-85-1025 N86-11190 #
ACSC-85-1955 N86-11197 #
ACSC-85-2215 N86-11758 #
ACSC-85-2470 N86-11415 #
ACSC-85-2675 N86-12162 #

AD-A153257 N86-11398 #
AD-A154112 N86-11527 #
AD-A156457 N86-11458 #
AD-A156460 N86-12160 #
AD-A156463 N86-11824 #
AD-A156464 N86-11857 #
AD-A156465 N86-11415 #
AD-A156468 N86-11190 #
AD-A156477 N86-11757 #
AD-A156479 N86-11899 #
AD-A156480 N86-11226 #
AD-A156500 N86-11758 #
AD-A156502 N86-11466 #
AD-A156505 N86-11416 #
AD-A156506 N86-11467 #
AD-A156507 N86-11300 #
AD-A156516 N86-11197 #
AD-A156517 N86-12162 #
AD-A156519 N86-11900 #
AD-A156716 N86-11531 #
AD-A156907 N86-11759 #
AD-A156911 N86-11760 #
AD-A156912 N86-11459 #
AD-A156927 N86-11341 #
AD-A156930 N86-11427 #
AD-A156931 N86-12020 #
AD-A156942 N86-11839 #
AD-A157276 N86-12021 #
AD-A157278 N86-11213 #
AD-A157295 N86-11302 #
AD-A157296 N86-11901 #
AD-A157297 N86-11198 #
AD-A157298 N86-11902 #
AD-A157301 N86-11342 #
AD-A157311 N86-11888 #
AD-A157320 N86-11716 #
AD-A157323 N86-12189 #
AD-A157325 N86-11358 #
AD-A157334 N86-11840 #
AD-A157335 N86-12072 #
AD-A157340 N86-11343 #
AD-A157343 N86-11316 #
AD-A157353 N86-12022 #
AD-A157355 N86-11303 #
AD-A157356 N86-12075 #
AD-A157368 N86-11344 #
AD-A157375 N86-11217 #
AD-A157376 N86-12073 #
AD-A157382 N86-12136 #
AD-A157383 N86-11672 #
AD-A157384 N86-11345 #
AD-A157401 N86-12023 #
AD-A157411 N86-11903 #
AD-A157414 N86-11498 #
AD-A157416 N86-11317 #
AD-A157417 N86-11841 #
AD-A157428 N86-11346 #
AD-A157432 N86-11417 #
AD-A157434 N86-12074 #
AD-A157435 N86-12024 #
AD-A157438 N86-11489 #
AD-A157440 N86-11851 #
AD-A157441 N86-11761 #
AD-A157444 N86-12190 #
AD-A157445 N86-12076 #
AD-A157446 N86-11825 #
AD-A157447 N86-11826 #
AD-A157449 N86-11673 #
AD-A157452 N86-11842 #
AD-A157454 N86-11428 #
AD-A157455 N86-11717 #
AD-A157456 N86-12077 #
AD-A157459 N86-11718 #
AD-A157476 N86-11460 #
AD-A157477 N86-11827 #
AD-A157478 N86-11411 #
AD-A157480 N86-11201 #
AD-A157482 N86-11889 #
AD-A157483 N86-11912 #
AD-A157484 N86-12078 #
AD-A157485 N86-11719 #
AD-A157526 N86-11913 #
AD-A157532 N86-11202 #
AD-A157533 N86-12018 #
AD-A157534 N86-12079 #
AD-A157535 N86-12080 #
AD-A157542 N86-11852 #
AD-A157553 N86-11904 #
AD-A157554 N86-11429 #
AD-A157556 N86-11304 #
AD-A157570 N86-11412 #
AD-A157571 N86-11430 #
AD-A157573 N86-11890 #
AD-A157574 N86-11891 #
AD-A157576 N86-11347 #
AD-A157577 N86-11648 #
AD-A157584 N86-11843 #
AD-A157587 N86-11914 #
AD-A157589 N86-11905 #
AD-A157596 N86-11318 #
AD-A157607 N86-11534 #
AD-A157608 N86-12137 #
AD-A157609 N86-12138 #
AD-A157615 N86-12025 #
AD-A157618 N86-11199 #
AD-A157619 N86-11191 #
AD-A157620 N86-11832 #
AD-A157623 N86-11844 #
AD-A157624 N86-11915 #
AD-A157641 N86-11210 #
AD-A157666 N86-11418 #

AD-D011741 N86-12043 #
AD-D011747 N86-11315 #

AFGL-TR-84-0272 N86-11757 #

AFIT/CI/NR-85-41T N86-11459 #
AFIT/CI/NR-85-43T N86-11760 #

AFWAL-TR-84-2085-VOL-1 N86-11199 #
AFWAL-TR-84-4158 N86-11418 #
AFWAL-TR-85-2015 N86-11467 #
AFWAL-TR-85-2039 N86-11428 #
AFWAL-TR-85-4010 N86-11489 #
AFWAL-TR-85-4046 N86-11343 #
AFWAL-TR-85-4049 N86-11318 #

AGARD-CP-366 N86-11147 #

AIAA-85-2017 N86-11224* #
AIAA-85-6042-CP N86-11195* #

AIAA/GNOS-85-002 N86-11218* #

AMMRC-TR-85-2 N86-11202 #

AMXTH-TE-CR-84308 N86-11458 #

ANL-85-38 N86-11548 #

ANL/CEPM-82-2 N86-11423 #

ANL/HEP-CP-85-45 N86-12065 #

AR-003-967 N86-11487 #

ARL/STRUC-R-411 N86-11487 #

ARO-12636.10-MS N86-11346 #
ARO-16123.21-MS N86-11346 #
ARO-17283.8-CH N86-12021 #
ARO-17967.6-CH N86-12020 #
ARO-18553.1-EL N86-11888 #
ARO-18638.13-CH N86-12072 #
ARO-18701.2-MS N86-11346 #
ARO-18985.19-EL N86-11913 #
ARO-19129.5-CH N86-11344 #
ARO-19626.9-PH N86-11417 #
ARO-21001.1-GS N86-12074 #
ARO-21758.1-CH-PT-A/B N86-12023 #

ATR-84(7783)-4 N86-11356 #

BLL-BISI-TRANS-23046-(9022.06) N86-11311
BLL-BISI-TRANS-23201-(9022.06) N86-11310

BNL-NCS-36468 N86-12066 #

BNL-36181 N86-12044 #
BNL-36425 N86-12038 #
BNL-36437 N86-12147 #
BNL-36438 N86-12059 #
BNL-36557 N86-12095 #
BNL-36626 N86-11944 #
BNL-36647 N86-12144 #
BNL-36699 N86-12061 #
BNL-36701 N86-11330 #
BNL-36735 N86-12117 #
BNL-51882 N86-11846 #

BPA-CP-695 N86-12163 #

BPA-84-18-APP N86-11686 #

C-804 N86-11673 #

CALSPAN-REPT-7097-F-1 N86-11204* #

CAR-TR-87 N86-11915 #

CERL-SR-P-85/12 N86-11488 #

CGR/DC-7/85 N86-11826 #

COLL-AERONAUTICS-8510 N86-11187 #

CONF-841010-16 N86-12131 #
CONF-841231-6 N86-11680 #
CONF-850122-10 N86-11326 #
CONF-850169-17 N86-11330 #
CONF-850169-18 N86-12061 #
CONF-850171-2 N86-12067 #
CONF-850211-11 N86-11338 #
CONF-850285-1 N86-12094 #
CONF-850310-107 N86-12087 #
CONF-850310-108 N86-12099 #
CONF-850310-113-REV-1 N86-12108 #
CONF-850315-4 N86-12059 #
CONF-850357-4 N86-11681 #
CONF-850421-9 N86-12145 #
CONF-850421-12 N86-11337 #
CONF-850474-1 N86-12081 #
CONF-850484-2 N86-12031 #
CONF-850504-34 N86-12089 #
CONF-850504-52 N86-12093 #
CONF-850504-71 N86-12091 #
CONF-850504-80 N86-12033 #
CONF-850504-98 N86-12035 #
CONF-850504-136 N86-12100 #

CONF-850504-138	N86-12097	#
CONF-850504-154	N86-12095	#
CONF-850504-179	N86-12104	#
CONF-850504-187	N86-12050	#
CONF-850504-192	N86-12049	#
CONF-850504-194	N86-12117	#
CONF-850504-198	N86-12124	#
CONF-850504-201	N86-12125	#
CONF-850504-204	N86-12122	#
CONF-850504-209	N86-12126	#
CONF-850504-210	N86-12029	#
CONF-850504-213	N86-12030	#
CONF-850504-215	N86-11944	#
CONF-850504-236	N86-12026	#
CONF-850506-8	N86-12051	#
CONF-850506-9	N86-11845	#
CONF-850507-23	N86-12048	#
CONF-850507-28	N86-12056	#
CONF-850507-30	N86-12045	#
CONF-850507-36	N86-12066	#
CONF-850507-39	N86-12052	#
CONF-850509-53	N86-11539	#
CONF-850513-1	N86-11256	#
CONF-850515-2	N86-11483	#
CONF-850533-8	N86-12036	#
CONF-850533-10	N86-12062	#
CONF-850558-5	N86-12127	#
CONF-850604-3	N86-11679	#
CONF-850604-11	N86-11675	#
CONF-850605-2	N86-12042	#
CONF-850606-9	N86-11484	#
CONF-850607-3	N86-11462	#
CONF-850616-5	N86-12092	#
CONF-850616-12	N86-11422	#
CONF-850616-14	N86-11420	#
CONF-850616-15	N86-11419	#
CONF-850616-20	N86-11424	#
CONF-850616-23	N86-12090	#
CONF-850616-33	N86-12109	#
CONF-850616-37	N86-11421	#
CONF-850616-52	N86-12039	#
CONF-850616-53	N86-12123	#
CONF-850616-59	N86-12121	#
CONF-850616-60	N86-11214	#
CONF-850616-61	N86-12116	#
CONF-850616-62	N86-12115	#
CONF-850616-63	N86-12119	#
CONF-850616-69	N86-12128	#
CONF-850641-4	N86-11414	#
CONF-850683-2	N86-12157	#
CONF-850706-28	N86-11361	#
CONF-850708-1	N86-12085	#
CONF-850711-10	N86-12058	#
CONF-850716-2	N86-12055	#
CONF-850736-8	N86-11485	#
CONF-850736-15	N86-11547	#
CONF-850736-20	N86-11544	#
CONF-850736-28	N86-11359	#
CONF-850736-29	N86-12142	#
CONF-850736-30	N86-11470	#
CONF-850736-32	N86-12140	#
CONF-850736-33	N86-11324	#
CONF-850736-36	N86-11360	#
CONF-850736-39	N86-11325	#
CONF-850736-40	N86-11328	#
CONF-850736-41	N86-11321	#
CONF-850745-3	N86-11434	#
CONF-850753	N86-11327	#
CONF-850759-6	N86-11305	#
CONF-850801-6	N86-11687	#
CONF-850801-8	N86-11463	#
CONF-850801-35	N86-11722	#
CONF-850807-1	N86-12038	#
CONF-850808-2	N86-11431	#
CONF-850808-5	N86-11689	#
CONF-850809-18	N86-11543	#
CONF-850809-35	N86-11541	#
CONF-850809-49	N86-11537	#
CONF-850809-56	N86-11482	#
CONF-850809-57	N86-11542	#
CONF-850820-1	N86-11432	#
CONF-850861-2	N86-11435	#
CONF-850880-2	N86-11348	#
CONF-850882-1	N86-12147	#
CONF-850883-1	N86-12198	#
CONF-850887-3	N86-11357	#
CONF-850887-10	N86-11471	#
CONF-850888-1	N86-11685	#
CONF-850889-1	N86-11333	#
CONF-850889-2	N86-11336	#
CONF-850890-2	N86-11322	#
CONF-850890-4	N86-11323	#
CONF-850890-5	N86-12155	#
CONF-850890-9	N86-12150	#
CONF-850903-4	N86-11535	#
CONF-850927-4	N86-12110	#
CONF-850942-1	N86-11355	#
CONF-850945-1	N86-11546	#
CONF-850946-2	N86-11476	#
CONF-850946-3	N86-11545	#
CONF-851115-4	N86-11320	#
CONF-8407117-3	N86-11334	#
CONF-8408122-6	N86-11691	#
CONF-8409162-15	N86-12044	#
CONF-8410276-1	N86-11350	#
CONF-8411108	N86-11649	#
CONF-8503131-3	N86-12139	#
CONF-8503151-1	N86-12068	#
CONF-8503152-1	N86-12141	#
CONF-8504102-3	N86-11481	#
CONF-8504135-2-REV-1	N86-11693	#
CONF-8504140-1	N86-11853	#
CONF-8504155-1	N86-12065	#
CONF-8504155-3	N86-12118	#
CONF-8504157-2	N86-12143	#
CONF-8505100-10	N86-12096	#
CONF-8505100-13	N86-12132	#
CONF-8505100-17	N86-12111	#
CONF-8505130-6	N86-12114	#
CONF-8505138-3	N86-12146	#
CONF-8505138-11	N86-12153	#
CONF-8505138-13	N86-12144	#
CONF-8505162-1	N86-11828	#
CONF-8505172-1	N86-12064	#
CONF-8505174-1	N86-12149	#
CONF-8505184-1	N86-11468	#
CONF-8506122-1	N86-11351	#
CONF-8506123-7	N86-11836	#
CONF-8506125-1	N86-12037	#
CONF-8506137-1	N86-11833	#
CONF-8506137-3	N86-11834	#
CONF-8506137-5	N86-11847	#
CONF-8506137-6	N86-11835	#
CONF-8506139-1	N86-11849	#
CONF-8506140-1	N86-11688	#
CONF-8506141-5	N86-12027	#
CONF-8506144-3	N86-11319	#
CONF-8506145-1	N86-11223	#
CONF-8506148-2	N86-11855	#
CONF-8506149-2	N86-12193	#
CONF-8506153-2	N86-11477	#
CONF-8506165-1	N86-11536	#
CONF-8509102-1	N86-11331	#
CRC-1385	N86-11205	
CRREL-SR-85-2	N86-11827	#
CRREL-SR-85-3	N86-11718	#
CRREL-SR-85-5	N86-11719	#
CRREL-85-9	N86-11648	#
CSC-TR-1430	N86-11915	#
DE85-001297	N86-11663	#
DE85-003360	N86-11649	#
DE85-003398	N86-11653	#
DE85-004038	N86-11432	#
DE85-005365	N86-11680	#
DE85-006533	N86-12159	#
DE85-007031	N86-12028	#
DE85-007671	N86-11546	#
DE85-007673	N86-11543	#
DE85-008206	N86-11355	#
DE85-008436	N86-11535	#
DE85-008469	N86-11681	#
DE85-008592	N86-11480	#
DE85-008693	N86-11463	#
DE85-008694	N86-11687	#
DE85-008783	N86-11349	#
DE85-009346	N86-11676	#
DE85-009360	N86-11674	#
DE85-009582	N86-11476	#
DE85-009633	N86-11431	#
DE85-009700	N86-11541	#
DE85-009924	N86-11678	#
DE85-010250	N86-11434	#
DE85-010288	N86-11537	#
DE85-010485	N86-11482	#
DE85-010511	N86-11539	#
DE85-010525	N86-11542	#
DE85-010779	N86-11545	#
DE85-010947	N86-12130	#
DE85-011002	N86-12046	#
DE85-011189	N86-11689	#
DE85-011280	N86-11688	#
DE85-011478	N86-12034	#
DE85-011520	N86-11686	#
DE85-011834	N86-12038	#
DE85-011870	N86-12086	#
DE85-011901	N86-11423	#
DE85-011927	N86-12089	#
DE85-011986	N86-11722	#
DE85-012035	N86-12121	#
DE85-012134	N86-12139	#
DE85-012140	N86-11357	#
DE85-012143	N86-11675	#
DE85-012152	N86-11433	#
DE85-012415	N86-12047	#
DE85-012510	N86-12059	#
DE85-012512	N86-12147	#
DE85-012517	N86-12044	#
DE85-012590	N86-12067	#
DE85-012608	N86-12145	#
DE85-012651	N86-11435	#
DE85-012663	N86-12093	#
DE85-012695	N86-12126	#
DE85-012699	N86-12045	#
DE85-012701	N86-12033	#
DE85-012729	N86-12048	#
DE85-012745	N86-12132	#
DE85-012749	N86-12056	#
DE85-012755	N86-11420	#
DE85-012756	N86-11419	#
DE85-012760	N86-12198	#
DE85-012768	N86-12037	#
DE85-012769	N86-12096	#
DE85-012809	N86-12092	#
DE85-012863	N86-11422	#
DE85-012890	N86-12099	#
DE85-012896	N86-12146	#
DE85-012899	N86-12051	#
DE85-012900	N86-11256	#
DE85-012909	N86-12088	#
DE85-012917	N86-11693	#
DE85-012923	N86-11828	#
DE85-012932	N86-12094	#
DE85-012943	N86-12108	#
DE85-012953	N86-12087	#
DE85-012955	N86-11853	#
DE85-012956	N86-11469	#
DE85-012957	N86-12161	#
DE85-012976	N86-12156	#
DE85-013024	N86-12035	#
DE85-013041	N86-11845	#
DE85-013071	N86-12097	#
DE85-013075	N86-12100	#
DE85-013077	N86-11351	#
DE85-013095	N86-12052	#
DE85-013114	N86-11424	#
DE85-013118	N86-12090	#
DE85-013142	N86-12109	#
DE85-013181	N86-11413	#
DE85-013195	N86-11326	#
DE85-013201	N86-12036	#
DE85-013207	N86-11350	#
DE85-013288	N86-12095	#
DE85-013295	N86-12104	#
DE85-013299	N86-12066	#
DE85-013371	N86-12091	#
DE85-013388	N86-11677	#
DE85-013434	N86-12103	#
DE85-013436	N86-11421	#
DE85-013480	N86-12102	#
DE85-013515	N86-12107	#
DE85-013542	N86-11682	#
DE85-013545	N86-11478	#
DE85-013591	N86-12114	#
DE85-013640	N86-11833	#
DE85-013759	N86-12165	#
DE85-013774	N86-12042	#
DE85-013783	N86-12123	#
DE85-013787	N86-11679	#
DE85-013826	N86-11462	#
DE85-013865	N86-12062	#
DE85-013869	N86-12064	#
DE85-013870	N86-12065	#
DE85-013942	N86-11479	#
DE85-013955	N86-12039	#
DE85-013956	N86-12116	#
DE85-013959	N86-12115	#
DE85-013960	N86-12119	#
DE85-013965	N86-11485	#
DE85-013967	N86-11333	#
DE85-013986	N86-11849	#
DE85-013989	N86-11331	#
DE85-014057	N86-11721	#
DE85-014062	N86-12041	#
DE85-014065	N86-11484	#
DE85-014085	N86-11685	#
DE85-014089	N86-11320	#
DE85-014092	N86-11223	#
DE85-014101	N86-12155	#
DE85-014102	N86-11323	#
DE85-014103	N86-12149	#
DE85-014106	N86-11335	#
DE85-014110	N86-12122	#
DE85-014118	N86-12143	#

DE85-014123 N86-11214 #
DE85-014132 N86-12193 #
DE85-014135 N86-11414 #
DE85-014136 N86-12154 #
DE85-014142 N86-11356 #
DE85-014178 N86-11834 #
DE85-014190 N86-12117 #
DE85-014240 N86-12098 #
DE85-014241 N86-12148 #
DE85-014250 N86-12106 #
DE85-014261 N86-12105 #
DE85-014272 N86-12063 #
DE85-014282 N86-12151 #
DE85-014287 N86-12125 #
DE85-014288 N86-12124 #
DE85-014293 N86-12049 #
DE85-014309 N86-11835 #
DE85-014310 N86-11855 #
DE85-014313 N86-11836 #
DE85-014324 N86-12110 #
DE85-014355 N86-12118 #
DE85-014356 N86-12050 #
DE85-014390 N86-12040 #
DE85-014394 N86-12112 #
DE85-014404 N86-11336 #
DE85-014408 N86-12131 #
DE85-014416 N86-12127 #
DE85-014423 N86-12068 #
DE85-014435 N86-12113 #
DE85-014442 N86-11334 #
DE85-014444 N86-12141 #
DE85-014452 N86-11683 #
DE85-014461 N86-11547 #
DE85-014469 N86-12060 #
DE85-014506 N86-11536 #
DE85-014512 N86-12027 #
DE85-014518 N86-12101 #
DE85-014525 N86-12157 #
DE85-014542 N86-11322 #
DE85-014555 N86-11847 #
DE85-014564 N86-11327 #
DE85-014577 N86-11338 #
DE85-014597 N86-11548 #
DE85-014613 N86-11483 #
DE85-014623 N86-11481 #
DE85-014535 N86-11892 #
DE85-014639 N86-12128 #
DE85-014658 N86-11477 #
DE85-014661 N86-11650 #
DE85-014665 N86-11652 #
DE85-014675 N86-11684 #
DE85-014695 N86-11846 #
DE85-014699 N86-12055 #
DE85-014703 N86-11544 #
DE85-014706 N86-12058 #
DE85-014710 N86-11337 #
DE85-014728 N86-11848 #
DE85-014753 N86-12083 #
DE85-014759 N86-11257 #
DE85-014767 N86-12084 #
DE85-014812 N86-11305 #
DE85-014813 N86-12031 #
DE85-014827 N86-11944 #
DE85-014829 N86-12144 #
DE85-014830 N86-11330 #
DE85-014832 N86-12061 #
DE85-014843 N86-12152 #
DE85-014850 N86-12120 #
DE85-014854 N86-12057 #
DE85-014855 N86-12053 #
DE85-014896 N86-12129 #
DE85-014967 N86-11319 #
DE85-015000 N86-12153 #
DE85-015005 N86-12150 #
DE85-015009 N86-12111 #
DE85-015034 N86-11538 #
DE85-015040 N86-11468 #
DE85-015060 N86-12054 #
DE85-015064 N86-12082 #
DE85-015088 N86-11354 #
DE85-015129 N86-12029 #
DE85-015138 N86-12032 #
DE85-015139 N86-11359 #
DE85-015140 N86-11324 #
DE85-015141 N86-12142 #
DE85-015142 N86-11470 #
DE85-015144 N86-12140 #
DE85-015154 N86-11321 #
DE85-015159 N86-11360 #
DE85-015165 N86-11328 #
DE85-015166 N86-11325 #
DE85-015177 N86-11471 #
DE85-015187 N86-11691 #
DE85-015235 N86-11651 #
DE85-015240 N86-11353 #
DE85-015247 N86-12026 #
DE85-015251 N86-12030 #
DE85-015321 N86-12085 #
DE85-015489 N86-11348 #
DE85-015551 N86-11332 #
DE85-015575 N86-11692 #
DE85-015579 N86-12081 #
DE85-015610 N86-11352 #
DE85-015613 N86-11329 #
DE85-015710 N86-11361 #
DE85-015971 N86-11301 #
DE85-015972 N86-11690 #
DE85-016215 N86-11720 #

DOE/BP-13609/2-VOL-2 N86-11683 #
DOE/BP-13609/3 N86-11650 #

DOE/DP-40124/59 N86-12131 #

DOE/EP-388-APP N86-11686 #
DOE/EP-40200/8 N86-12127 #

DOE/ER-03230/T4 N86-12041 #
DOE/ER-03992/569 N86-12028 #
DOE/ER-10107/27 N86-12060 #
DOE/ER-10107/28 N86-11536 #
DOE/ER-10556/105 N86-11538 #
DOE/ER-10864/1 N86-12152 #
DOE/ER-10870/155 N86-12053 #
DOE/ER-13073/T2 N86-11257 #
DOE/ER-13216/T1 N86-11721 #
DOE/ER-40025/33 N86-12063 #
DOE/ER-45011/T1 N86-11684 #
DOE/ER-45025/5 N86-11334 #
DOE/ER-45025/7 N86-12141 #
DOE/ER-53162/6 N86-12102 #
DOE/ER-53179/T4 N86-12154 #
DOE/ER-60192/1 N86-11848 #
DOE/ER-60257/1 N86-11692 #
DOE/ER-70004/T4 N86-12034 #
DOE/ER-80187/1 N86-12107 #

DOE/ET-10393/1859 N86-11480 #
DOE/ET-11292/1893-VOL-3 N86-11674 #
DOE/ET-28393/T9 N86-11676 #
DOE/ET-51013/T3 N86-12083 #
DOE/ET-51013/148 N86-12081 #
DOE/ET-53064/T3 N86-12113 #
DOE/ET-53064/T4 N86-12040 #
DOE/ET-53064/T5 N86-12112 #
DOE/ET-53088/175-1 N86-12129 #
DOE/ET-53088/194 N86-12084 #
DOE/ET-53088/196 N86-12111 #

DOE/ID-12262/T1 N86-11677 #

DOE/JPL-1012-110 N86-11669* #
DOE/JPL-956347-1 N86-11664* #

DOE/METC-85/2004 N86-11653 #
DOE/METC-85/6014 N86-11649 #

DOE/NASA/0530-1 N86-11670* #
DOE/NASA/1005-6 N86-11668* #
DOE/NASA/20485-18 N86-11666* #

DOE/OR-21400/T99 N86-11332 #
DOE/OR-21400/T144 N86-12159 #
DOE/OR-21400/T157 N86-11690 #

DOT/FAA/CT-83/3 N86-11191 #

DRD-SE-2 N86-11664* #

DRL-185 N86-11664* #

DTNSRDC-85/041 N86-11430 #

E-1816 N86-11495* #
E-2425 N86-11260* #
E-2498 N86-11666* #
E-2597 N86-11668* #
E-2681 N86-11146* #
E-2729 N86-11425* #
E-2733 N86-11224* #
E-2747-1 N86-11475* #
E-2748 N86-11671* #
E-2750 N86-12134* #
E-2758 N86-12007* #
E-2766 N86-12135* #
E-2774 N86-11218* #

ECAC-CR-85-031 N86-11192 #

EGG-M-02285 N86-11338 #
EGG-M-14285 N86-11892 #
EGG-M-17884 N86-11481 #
EGG-M-28384 N86-11483 #

EGG-TFBP-6739 N86-11461 #

EGG-2393 N86-12047 #

EPA-600/D-85-095 N86-11730 #
EPA-600/D-85-107 N86-11694 #
EPA-600/D-85-110 N86-11728 #
EPA-600/1-85-007 N86-11837 #
EPA-600/2-85-039 N86-11654 #
EPA-600/3-85-034 N86-11658 #
EPA-600/3-85-037-PT-3 N86-11696 #
EPA-600/4-85-037 N86-11695 #
EPA-904/10-84-128 N86-11697 #

EPRI-NP-4051 N86-11335 #

E86-10001 N86-11618* #

FAA-CT-85-10 N86-11898 #

FAA-PM-85-15 N86-11362 #
FAA-PM-85-22 N86-11192 #

FJSRL-TR-85-0002 N86-11302 #

FMV:ELEKTRO-A12:142/83 N86-12017 #

FNAL-TM-1309 N86-12105 #
FNAL-TM-1312 N86-12035 #
FNAL-TM-1315 N86-12098 #

FNAL/C-85/89 N86-12068 #

FTD-ID(RS)T-0113-85 N86-11761 #
FTD-ID(RS)T-0326-85 N86-11429 #

FTR-1 N86-11673 #

GA-A-18033 N86-12110 #

GAO/NSIAD-85-78 N86-11217 #

H-1221 N86-11524* #
H-1289 N86-11525* #
H-1307 N86-11206* #
H-1310 N86-11194* #
H-1317 N86-11195* #

ICASE-85-39 N86-11856* #

IFSR-175-1 N86-12129 #
IFSR-194 N86-12084 #
IFSR-196 N86-12111 #

IMA-PREPRINT-155 N86-11534 #

IR-19 N86-11826 #

ISBN-92-835-0374-0 N86-11147 #

ISSN-0514-8790 N86-11549 #
ISSN-0514-8790 N86-11568 #
ISSN-0514-8790 N86-11591 #

JPL-PUB-85-20 N86-11896* #
JPL-PUB-85-41 N86-11618* #

JPL-9950-1157 N86-11664* #

JPRS-CST-85-014 N86-11918 #
JPRS-CST-85-015 N86-11994 #

JPRS-UMM-85-010 N86-11394 #

JPRS-UPM-85-005 N86-11945 #

JPRS-UST-85-014 N86-11990 #

JPRS-UTR-85-011 N86-11177 #

KIS-1985:4E N86-11313 #
KIS-1985:5E N86-11314 #

L-15775 N86-11647* #
L-15934 N86-11186* #
L-15954 N86-11522* #
L-15962 N86-11700* #
L-15990 N86-11203* #
L-16013 N86-11437* #
L-16023 N86-11227* #

LA-TR-85-22 N86-12088 #

LA-UR-85-632 N86-11546 #

LA-UR-85-638 N86-11543 #
LA-UR-85-980 N86-11431 #
LA-UR-85-1135 N86-11545 #
LA-UR-85-1518 N86-12126 #
LA-UR-85-1614 N86-12093 #
LA-UR-85-1629 N86-11435 #
LA-UR-85-1666 N86-12033 #
LA-UR-85-1674 N86-12045 #
LA-UR-85-1729 N86-12048 #
LA-UR-85-1743 N86-12056 #
LA-UR-85-1798 N86-12132 #
LA-UR-85-1822 N86-12096 #
LA-UR-85-1828 N86-12037 #
LA-UR-85-1892 N86-11414 #
LA-UR-85-1921 N86-12198 #
LA-UR-85-1936 N86-11419 #
LA-UR-85-1939 N86-11420 #
LA-UR-85-1989 N86-12193 #
LA-UR-85-2022 N86-11214 #
LA-UR-85-2055 N86-12143 #
LA-UR-85-2081 N86-12122 #
LA-UR-85-2119 N86-12149 #
LA-UR-85-2140 N86-113[illegible]3 #
LA-UR-85-2142 N86-12155 #
LA-UR-85-2182 N86-11223 #
LA-UR-85-2193 N86-11320 #
LA-UR-85-2213 N86-11685 #
LA-UR-85-2460 N86-11361 #

LA-10240-C N86-11858 #
LA-10391-MS N86-12148 #
LA-10399-PR N86-12106 #
LA-10455-MS N86-11720 #

LBL-18958 N86-12030 #
LBL-18970 N86-12029 #
LBL-18978 N86-12026 #
LBL-19321 N86-11722 #
LBL-19452 N86-12145 #
LBL-19554 N86-12104 #
LBL-19642 N86-12157 #
LBL-19684 N86-12067 #
LBL-19722 N86-11322 #

LC-85-13854 N86-12168* #
LC-85-600544 N86-11367* #

LPI-TR-85-02 N86-12192* #
LPI-TR-85-04 N86-12191* #

LR-30777 N86-11898 #

M-494 N86-11215* #

MCR-83-607 N86-11854* #
MCR-85-605-ISSUE-1 N86-11300 #

MIT/LCS/TM-278 N86-11904 #

MLM-3268 N86-11329 #
MLM-3271(OP) N86-11462 #
MLM-3272 N86-11352 #

MSU-ENGR-85-026 N86-11667* #

MTR-9238 N86-11412 #

NADC-84166-60 N86-11198 #
NADC-85029-60 N86-11341 #

NAS 1.15:77913 N86-11734* #
NAS 1.15:77917 N86-11733* #
NAS 1.15:84399 N86-11209* #
NAS 1.15:84924 N86-11524* #
NAS 1.15:86390 N86-11647* #
NAS 1.15:86425 N86-11203* #
NAS 1.15:86440 N86-11523* #
NAS 1.15:86503 N86-11473* #
NAS 1.15:86520 N86-11216* #
NAS 1.15:86697 N86-11196* #
NAS 1.15:86720 N86-12185* #
NAS 1.15:86723 N86-12186* #
NAS 1.15:86729 N86-11525* #
NAS 1.15:86743 N86-11206* #
NAS 1.15:86746 N86-11194* #
NAS 1.15:86781 N86-11188* #
NAS 1.15:86791 N86-11195* #
NAS 1.15:86818 N86-11208* #
NAS 1.15:86824 N86-11340* #
NAS 1.15:86839 N86-11907* #
NAS 1.15:86842 N86-11909* #
NAS 1.15:86848 N86-11221* #
NAS 1.15:86972-REV N86-11666* #
NAS 1.15:87121 N86-11425* #
NAS 1.15:87123 N86-11224* #
NAS 1.15:87126 N86-11668* #
NAS 1.15:87128 N86-11146* #
NAS 1.15:87134 N86-11671* #
NAS 1.15:87135 N86-12134* #
NAS 1.15:87140 N86-12135* #
NAS 1.15:87145 N86-11218* #
NAS 1.15:87152 N86-11475* #
NAS 1.15:87511 N86-12194* #
NAS 1.15:87512 N86-11222* #
NAS 1.15:87567 N86-11701* #
NAS 1.15:87582 N86-11189* #
NAS 1.15:87588 N86-11292* #
NAS 1.15:87610 N86-11193* #
NAS 1.15:87612 N86-11540* #
NAS 1.15:87624 N86-11299* #
NAS 1.15:88185 N86-12167* #
NAS 1.21:7037(191) N86-11145*
NAS 1.26:171577 N86-11749* #
NAS 1.26:172369 N86-11207* #
NAS 1.26:172571 N86-11906* #
NAS 1.26:174924 N86-11474* #
NAS 1.26:175009 N86-11526* #
NAS 1.26:176135 N86-11664* #
NAS 1.26:176210 N86-11618* #
NAS 1.26:176248 N86-12195* #
NAS 1.26:176256 N86-11339* #
NAS 1.26:176257 N86-11830* #
NAS 1.26:176273 N86-11212* #
NAS 1.26:176275 N86-11897* #
NAS 1.26:176276 N86-11895* #
NAS 1.26:176277 N86-11850* #
NAS 1.26:176278 N86-11465* #
NAS 1.26:176279 N86-11293* #
NAS 1.26:176280 N86-11893* #
NAS 1.26:176282 N86-12187* #
NAS 1.26:176283 N86-11657* #
NAS 1.26:176284 N86-11645* #
NAS 1.26:176285 N86-12188* #
NAS 1.26:176286 N86-11831* #
NAS 1.26:176287 N86-11911* #
NAS 1.26:176288 N86-11829* #
NAS 1.26:176290 N86-12191* #
NAS 1.26:176291 N86-11220* #
NAS 1.26:176292 N86-11436* #
NAS 1.26:176293 N86-12192* #
NAS 1.26:176294 N86-11838* #
NAS 1.26:176298 N86-11367* #
NAS 1.26:176299 N86-11910* #
NAS 1.26:176300 N86-11667* #
NAS 1.26:176301 N86-12019* #
NAS 1.26:176302 N86-11669* #
NAS 1.26:176304 N86-12197* #
NAS 1.26:176305 N86-12196* #
NAS 1.26:176306 N86-11896* #
NAS 1.26:176307 N86-12158* #
NAS 1.26:176308 N86-11646* #
NAS 1.26:176310 N86-11854* #
NAS 1.26:176315 N86-11670* #
NAS 1.26:177371 N86-11204* #
NAS 1.26:177940 N86-11312* #
NAS 1.26:177971 N86-11426* #
NAS 1.26:177979 N86-11856* #
NAS 1.26:177985 N86-11894* #
NAS 1.26:177990 N86-11298* #
NAS 1.55:2289 N86-11495* #
NAS 1.55:2384 N86-12168* #
NAS 1.55:2385 N86-11260* #
NAS 1.55:2387 N86-11227* #
NAS 1.55:2388 N86-11735* #
NAS 1.55:2393 N86-11437* #
NAS 1.55:2404 N86-12007* #
NAS 1.60:2478 N86-11186* #
NAS 1.60:2481 N86-11522* #
NAS 1.60:2508 N86-11215* #
NAS 1.61:1144 N86-11700* #

NASA-CP-2289 N86-11495* #
NASA-CP-2384 N86-12168* #
NASA-CP-2385 N86-11260* #
NASA-CP-2387 N86-11227* #
NASA-CP-2388 N86-11735* #
NASA-CP-2393 N86-11437* #
NASA-CP-2404 N86-12007* #

NASA-CR-171577 N86-11749* #
NASA-CR-172369 N86-11207* #
NASA-CR-172571 N86-11906* #
NASA-CR-174924 N86-11474* #
NASA-CR-175009 N86-11526* #
NASA-CR-176135 N86-11664* #
NASA-CR-176210 N86-11618* #
NASA-CR-176248 N86-12195* #
NASA-CR-176256 N86-11339* #
NASA-CR-176257 N86-11830* #
NASA-CR-176273 N86-11212* #
NASA-CR-176275 N86-11897* #
NASA-CR-176276 N86-11895* #
NASA-CR-176277 N86-11850* #
NASA-CR-176278 N86-11465* #
NASA-CR-176279 N86-11293* #
NASA-CR-176280 N86-11893* #
NASA-CR-176282 N86-12187* #
NASA-CR-176283 N86-11657* #
NASA-CR-176284 N86-11645* #
NASA-CR-176285 N86-12188* #
NASA-CR-176286 N86-11831* #
NASA-CR-176287 N86-11911* #
NASA-CR-176288 N86-11829* #
NASA-CR-176290 N86-12191* #
NASA-CR-176291 N86-11220* #
NASA-CR-176292 N86-11436* #
NASA-CR-176293 N86-12192* #
NASA-CR-176294 N86-11838* #
NASA-CR-176298 N86-11367* #
NASA-CR-176299 N86-11910* #
NASA-CR-176300 N86-11667* #
NASA-CR-176301 N86-12019* #
NASA-CR-176302 N86-11669* #
NASA-CR-176304 N86-12197* #
NASA-CR-176305 N86-12196* #
NASA-CR-176306 N86-11896* #
NASA-CR-176307 N86-12158* #
NASA-CR-176308 N86-11646* #
NASA-CR-176310 N86-11854* #
NASA-CR-176315 N86-11670* #
NASA-CR-177371 N86-11204* #
NASA-CR-177940 N86-11312* #
NASA-CR-177971 N86-11426* #
NASA-CR-177979 N86-11856* #
NASA-CR-177985 N86-11894* #
NASA-CR-177990 N86-11298* #

NASA-JPL-85-60 N86-11669* #

NASA-RP-1144 N86-11700* #

NASA-SP-7037(191) N86-11145*

NASA-TM-77913 N86-11734* #
NASA-TM-77917 N86-11733* #
NASA-TM-84399 N86-11209* #
NASA-TM-84924 N86-11524* #
NASA-TM-86390 N86-11647* #
NASA-TM-86425 N86-11203* #
NASA-TM-86440 N86-11523* #
NASA-TM-86503 N86-11473* #
NASA-TM-86520 N86-11216* #
NASA-TM-86697 N86-11196* #
NASA-TM-86720 N86-12185* #
NASA-TM-86723 N86-12186* #
NASA-TM-86729 N86-11525* #
NASA-TM-86743 N86-11206* #
NASA-TM-86746 N86-11194* #
NASA-TM-86781 N86-11188* #
NASA-TM-86791 N86-11195* #
NASA-TM-86818 N86-11208* #
NASA-TM-86824 N86-11340* #
NASA-TM-86839 N86-11907* #
NASA-TM-86842 N86-11909* #
NASA-TM-86848 N86-11221* #
NASA-TM-86972-REV N86-11666* #
NASA-TM-87121 N86-11425* #
NASA-TM-87123 N86-11224* #
NASA-TM-87126 N86-11668* #
NASA-TM-87128 N86-11146* #
NASA-TM-87134 N86-11671* #
NASA-TM-87135 N86-12134* #
NASA-TM-87140 N86-12135* #
NASA-TM-87145 N86-11218* #
NASA-TM-87152 N86-11475* #
NASA-TM-87511 N86-12194* #
NASA-TM-87512 N86-11222* #
NASA-TM-87567 N86-11701* #
NASA-TM-87582 N86-11189* #
NASA-TM-87588 N86-11292* #
NASA-TM-87610 N86-11193* #
NASA-TM-87612 N86-11540* #
NASA-TM-87624 N86-11299* #
NASA-TM-88185 N86-12167* #

NASA-TP-2478 N86-11186* #
NASA-TP-2481 N86-11522* #
NASA-TP-2508 N86-11215* #

NAWC/SLWM-84-2 N86-11822 #

NBS-SP-698 N86-11367* #

NBSIR-85-3025-7 N86-12101 #
NBSIR-85-3154-1 N86-11363 #
NBSIR-85/3159 N86-11364 #
NBSIR-85/3167 N86-11365 #
NBSIR-85/3203 N86-11366 #

NCAR/TN-253/EDD	N86-11200	#
NMERI-WA5-4(5.02)	N86-11362	#
NOAA-CR-ERL-ARL-5	N86-11723	#
NOAA-TM-ERL-ESG-10	N86-11823	#
NOAA-TM-NWS-NSSFC-8	N86-11821	#
NOAA-TM-34L-SEL-71	N86-11724	#
NOAA-TR-NESDIS-20	N86-11820	#
NOAA-TR-NESDIS-21	N86-11729	#
NPS61-85-004	N86-11213	#
NPS61-85-005	N86-12025	#
NPS67-85-004	N86-11358	#
NPS67-85-005	N86-11201	#
NRL-MR-5558	N86-11303	#
NRL-MR-5564	N86-11427	#
NRL-MR-5578	N86-11347	#
NRL-MR-5584	N86-11912	#
NRL-MR-5590	N86-12080	#
NRL-MR-5593	N86-11717	#
NRL-MR-5598	N86-11460	#
NRL-MR-5601	N86-12075	#
NRL-MR-5607	N86-12079	#
NRL-MR-5609	N86-12078	#
NRL-MR-5615	N86-12077	#
NSWC/TR-85-104	N86-11672	#
NUSC-TD-7375	N86-12018	#
ORC 35-4	N86-11901	#
ORNL-6181	N86-11682	#
ORNL/LMR/SP-85/4	N86-12046	#
ORNL/SUB-80-61613/1	N86-11478	#
ORNL/TM-9598	N86-12082	#
ORNL/TM-9651	N86-11301	#
ORNL/TM-9662	N86-12054	#
OSU-368	N86-11910*	#
PB85-183911	N86-11763	#
PB85-187896	N86-11723	#
PB85-187920	N86-11724	#
PB85-189074	N86-11654	#
PB85-191005	N86-11200	#
PB85-191617	N86-11655	#
PB85-193548	N86-11730	#
PB85-196483	N86-11726	#
PB85-196491	N86-11725	#
PB85-197317	N86-11656	#
PB85-197358	N86-11658	#
PB85-199123	N86-11819	#
PB85-199578	N86-11657*	#
PB85-201176	N86-11695	#
PB85-201184	N86-11694	#
PB85-201192	N86-11728	#
PB85-201267	N86-11697	#
PB85-203818	N86-11696	#
PB85-204246	N86-11823	#
PB85-204303	N86-11822	#
PB85-204477	N86-11727	#
PB85-204501	N86-11820	#
PB85-204873	N86-12166	#
PB85-206084	N86-11729	#
PB85-206092	N86-11821	#
PB85-207462	N86-11837	#
PB85-209526	N86-11762	#
PB85-214500	N86-11659	#
PB85-217024	N86-11662	#
PB85-217727	N86-11698	#
PB85-218998	N86-11661	#
PB85-219079	N86-11660	#
PB85-233369	N86-11367*	#
PFC/CP-85-2	N86-12081	#
PFC/RR-85-2	N86-12083	#
PGG-821-VOL-4	N86-12130	#
PNL-SA-12638	N86-11845	#
PNL-5244-VOL-2	N86-12165	#
PP-SER-32	N86-12186*	#
PR-1	N86-11300	#
PR-127	N86-12164	#
PREPRINT-SER-039	N86-12167*	#
PUBL-61	N86-12069	#
PWA-5966-17	N86-11474*	#
QSR-5	N86-12154	#
RADC-TR-82-286-VOL-3B	N86-11416	#
RADC-TR-85-14-VOL-1	N86-11398	#
RADC-TR-85-76	N86-11412	#
RAND/R-3224-ARPA	N86-12022	#
REPT-21-5541	N86-11202	#
REPT-81-PT-1	N86-11549	#
REPT-81-PT-2	N86-11568	#
REPT-81-PT-3	N86-11591	#
REPT-85-1	N86-11851	#
REPT-0001AB	N86-11304	#
REPT-85158	N86-11196*	#
REPT-85221	N86-12185*	#
REPT-85224	N86-12186*	#
REPT-85279	N86-11340*	#
REPT-85337	N86-11209*	#
REPT-85371	N86-11208*	#
REPT-85384	N86-11188*	#
REPT-85398	N86-11221*	#
REPT-85412	N86-11907*	#
REPT-85417	N86-11909*	#
REPT-86009	N86-12167*	#
RFP-3847	N86-11327	#
RH0-EW-CR-146P	N86-11652	#
RI-193	N86-11676	#
RR-103	N86-11698	#
SAND-84-1953C	N86-11681	#
SAND-84-2239C	N86-11355	#
SAND-84-2271	N86-11354	#
SAND-84-2358C	N86-11689	#
SAND-84-2391C	N86-11424	#
SAND-84-2392C	N86-11422	#
SAND-84-2393C	N86-12121	#
SAND-84-2418C	N86-12103	#
SAND-84-2447C	N86-12109	#
SAND-84-2459C	N86-12039	#
SAND-84-2505C	N86-12115	#
SAND-84-2524C	N86-12116	#
SAND-84-2560C	N86-12092	#
SAND-84-2567C	N86-12090	#
SAND-84-2568C	N86-12123	#
SAND-84-2584C	N86-12119	#
SAND-84-2588C	N86-12128	#
SAND-84-2638C	N86-11421	#
SAND-85-0156C	N86-11321	#
SAND-85-0157C	N86-11547	#
SAND-85-0269C	N86-11336	#
SAND-85-0280C	N86-11333	#
SAND-85-0308C	N86-12142	#
SAND-85-0334C	N86-11359	#
SAND-85-0357C	N86-12058	#
SAND-85-0366C	N86-11325	#
SAND-85-0435C	N86-11348	#
SAND-85-0484C	N86-11324	#
SAND-85-0522	N86-11479	#
SAND-85-0635C	N86-11544	#
SAND-85-0647C	N86-11463	#
SAND-85-0648C	N86-11687	#
SAND-85-0874C	N86-12055	#
SAND-85-0913C	N86-11337	#
SAND-85-0936C	N86-11688	#
SAND-85-1347C	N86-12042	#
SAND-85-1408C	N86-11679	#
SAND-85-1450C	N86-12027	#
SAND-85-1511C	N86-11485	#
SAND-85-1514C	N86-12140	#
SAND-85-1597C	N86-11360	#
SAND-85-03330	N86-11328	#
SAND-85-12350	N86-11470	#
SAPR-48	N86-11293*	#
SASR-2	N86-12188*	#
SASR-4	N86-11897*	#
SD-TR-85-18	N86-12024	#
SD-TR-85-28	N86-12189	#
SERI/PR-212-2634	N86-11349	#
SERI/TP-211-2748	N86-11675	#
SERI/TP-212-2753	N86-12139	#
SERI/TP-255-2724	N86-11357	#
SERI/TR-252-2490	N86-11433	#
SGP-TR-81	N86-11678	#
SOLAR/0015-84-32	N86-11683	#
SPX-382	N86-11222*	#
SR-5	N86-11757	#
SRA-910008F	N86-11428	#
SU-SLAC-CN-305	N86-12032	#
SU-SLAC-PUB-3597	N86-12125	#
SU-SLAC-PUB-3607	N86-12124	#
SU-SLAC-PUB-3645	N86-12118	#
SU-SLAC-PUB-3650	N86-12049	#
SU-SLAC-PUB-3662	N86-12050	#
SU-SLAC-PUB-3669	N86-12100	#
SU-SLAC-PUB-3679	N86-12097	#
SU-SLAC-PUB-3689	N86-12091	#
SU-SOL-85-8	N86-11914	#
TDWR/R-2688-VOL-3	N86-11655	#
TI85-009174A	N86-11461	#
TR-1	N86-11345	#
TR-7-PT-A/B	N86-12023	#
TR-16	N86-11342	#
TR-28	N86-11317	#
TR-45	N86-12136	#
TR-85-1	N86-11725	#
TR-85-3	N86-11726	#
TR-85-3-ONR	N86-11843	#
TR-85-5-ONR	N86-11842	#
TR-85-7-ONR	N86-11852	#
TR-85/ONR-20	N86-11889	#
TR-0084A(5940-01)-3	N86-12189	#
TR-0084A(5945-05)-5	N86-12024	#
TR-716548-1	N86-11212*	#
TTC-0532	N86-11354	#
U-OF-IOWA-85-12	N86-11716	#
UCID-20343	N86-12057	#
UCID-20405	N86-12086	#
UCID-20438	N86-11413	#
UCID-20456	N86-12120	#
UCLA-ENG-84-30-VOL-4	N86-12130	#
UCRL-TRANS-12067	N86-12151	#
UCRL-15561-VOL-3	N86-11469	#
UCRL-15674	N86-12161	#
UCRL-53636	N86-11353	#
UCRL-90817	N86-11476	#
UCRL-91305	N86-11326	#
UCRL-91429	N86-11350	#
UCRL-91772	N86-11828	#
UCRL-92017	N86-12036	#
UCRL-92086	N86-12156	#
UCRL-92092-REV-1	N86-12108	#
UCRL-92156	N86-12094	#
UCRL-92170	N86-11471	#
UCRL-92242	N86-11847	#
UCRL-92247	N86-12087	#
UCRL-92494-REV-1	N86-11693	#
UCRL-92501	N86-11853	#
UCRL-92643	N86-12114	#
UCRL-92835	N86-11834	#
UCRL-92912	N86-12031	#
UCRL-92924	N86-11305	#
UCRL-92942	N86-11691	#
UDR-TR-84-133	N86-11318	#
UDR-TR-85-32	N86-11343	#
UMTA-AL-06-0011-85-1	N86-12166	#
UNI-SA-144	N86-11535	#
US-PATENT-APPL-SN-666597	N86-12043	#
US-PATENT-APPL-SN-726563	N86-11315	#
USAAVSCOM-TM-85-B-5	N86-11523*	#
USAAVSCOM-TR-85-A-7	N86-11204*	#

USAAVSCOM-TR-85-A-8	N86-11188* #
USAAVSCOM-TR-85-C-19	N86-11425* #
USAEHA-75-51-0132-85	N86-11844 #
USARIEM-M-31/85	N86-11841 #
USARIEM-M-32/85	N86-11840 #
USARIEM-M-34/85	N86-11832 #
USCG-D-16-85	N86-11826 #
USDA/MPUB-1446	N86-11656 #
USGS-CIRC-940	N86-11651 #
USGS/G-845-01	N86-11661 #
USGS/G-845-22	N86-11660 #
USGS/G-859-01	N86-11662 #
USGS/G-870-03	N86-11698 #
UT/PUB-R01-2550-29-001-85	N86-11698 #
WAOENG-85-02B-VOL-2	N86-11683 #
WAOENG-85-02C	N86-11650 #
WES/IR/EL-85-1	N86-11825 #
YALEU/DCS/TR-405	N86-11903 #

☆ U.S. GOVERNMENT PRINTING OFFICE: 1986-491-575/20025

FEDERAL DEPOSITORY LIBRARY PROGRAM

The Federal Depository Library Program provides Government publications to designated libraries throughout the United States. The Regional Depository Libraries listed below receive and retain at least one copy of nearly every Federal Government publication, either in printed or microfilm form, for use by the general public. These libraries provide reference services and inter-library loans; however, they are *not* sales outlets. You may wish to ask your local library to contact a Regional Depository to help you locate specific publications, or you may contact the Regional Depository yourself.

ARKANSAS STATE LIBRARY
One Capitol Mall
Little Rock, AR 72201
(501) 371-2326

AUBURN UNIV. AT MONTGOMERY LIBRARY
Documents Department
Montgomery, AL 36193
(205) 279-9110, ext. 253

UNIV. OF ALABAMA LIBRARY
Documents Dept.—Box S
University, AL 35486
(205) 348-7369

DEPT. OF LIBRARY, ARCHIVES AND PUBLIC RECORDS
Third Floor—State Cap.
1700 West Washington
Phoenix, AZ 85007
(602) 255-4121

UNIVERSITY OF ARIZONA LIB.
Government Documents Dept.
Tucson, AZ 85721
(602) 626-5233

CALIFORNIA STATE LIBRARY
Govt. Publications Section
P.O. Box 2037
Sacramento, CA 95809
(916) 322-4572

UNIV. OF COLORADO LIB.
Government Pub. Division
Campus Box 184
Boulder, CO 80309
(303) 492-8834

DENVER PUBLIC LIBRARY
Govt. Pub. Department
1357 Broadway
Denver, CO 80203
(303) 571-2131

CONNECTICUT STATE LIBRARY
Government Documents Unit
231 Capitol Avenue
Hartford, CT 06106
(203) 566-4971

UNIV. OF FLORIDA LIBRARIES
Library West
Documents Department
Gainesville, FL 32611
(904) 392-0367

UNIV. OF GEORGIA LIBRARIES
Government Reference Dept.
Athens, GA 30602
(404) 542-8951

UNIV. OF HAWAII LIBRARY
Govt. Documents Collection
2550 The Mall
Honolulu, HI 96822
(808) 948-8230

UNIV. OF IDAHO LIBRARY
Documents Section
Moscow, ID 83843
(208) 885-6344

ILLINOIS STATE LIBRARY
Information Services Branch
Centennial Building
Springfield, IL 62756
(217) 782-5185

INDIANA STATE LIBRARY
Serials Documents Section
140 North Senate Avenue
Indianapolis, IN 46204
(317) 232-3686

UNIV. OF IOWA LIBRARIES
Govt. Documents Department
Iowa City, IA 52242
(319) 353-3318

UNIVERSITY OF KANSAS
Doc. Collect.—Spencer Lib.
Lawrence, KS 66045
(913) 864-4662

UNIV. OF KENTUCKY LIBRARIES
Govt. Pub. Department
Lexington, KY 40506
(606) 257-3139

LOUISIANA STATE UNIVERSITY
Middleton Library
Govt. Docs. Dept.
Baton Rouge, LA 70803
(504) 388-2570

LOUISIANA TECHNICAL UNIV. LIBRARY
Documents Department
Ruston, LA 71272
(318) 257-4962

UNIVERSITY OF MAINE
Raymond H. Fogler Library
Tri-State Regional Documents Depository
Orono, ME 04469
(207) 581-1680

UNIVERSITY OF MARYLAND
McKeldin Lib.—Doc. Div.
College Park, MD 20742
(301) 454-3034

BOSTON PUBLIC LIBRARY
Government Docs. Dept.
Boston, MA 02117
(617) 536-5400, ext. 226

DETROIT PUBLIC LIBRARY
Sociology Department
5201 Woodward Avenue
Detroit, MI 48202
(313) 833-1409

MICHIGAN STATE LIBRARY
P.O. Box 30007
Lansing, MI 48909
(517) 373-0640

UNIVERSITY OF MINNESOTA
Government Pubs. Division
409 Wilson Library
309 19th Avenue South
Minneapolis, MN 55455
(612) 373-7813

UNIV. OF MISSISSIPPI LIB.
Documents Department
University, MS 38677
(601) 232-5857

UNIV. OF MONTANA
Mansfield Library
Documents Division
Missoula, MT 59812
(406) 243-6700

NEBRASKA LIBRARY COMM.
Federal Documents
1420 P Street
Lincoln, NE 68508
(402) 471-2045
In cooperation with University of Nebraska-Lincoln

UNIVERSITY OF NEVADA LIB.
Govt. Pub. Department
Reno, NV 89557
(702) 784-6579

NEWARK PUBLIC LIBRARY
5 Washington Street
Newark, NJ 07101
(201) 733-7812

UNIVERSITY OF NEW MEXICO
Zimmerman Library
Government Pub. Dept.
Albuquerque, NM 87131
(505) 277-5441

NEW MEXICO STATE LIBRARY
Reference Department
325 Don Gaspar Avenue
Santa Fe, NM 87503
(505) 827-3826, ext. 22

NEW YORK STATE LIBRARY
Empire State Plaza
Albany, NY 12230
(518) 474-5563

UNIVERSITY OF NORTH CAROLINA AT CHAPEL HILL
Wilson Library
BA/SS Documents Division
Chapel Hill, NC 27514
(919) 962-1151

UNIVERSITY OF NORTH DAKOTA
Chester Fritz Library
Documents Department
Grand Forks, ND 58202
(701) 777-2617, ext. 27
In cooperation with North Dakota State Univ. Library

STATE LIBRARY OF OHIO
Documents Department
65 South Front Street
Columbus, OH 43215
(614) 462-7051

OKLAHOMA DEPT. OF LIB.
Government Documents
200 NE 18th Street
Oklahoma City, OK 73105
(405) 521-2502

OKLAHOMA STATE UNIV. LIB.
Documents Department
Stillwater, OK 74078
(405) 624-6546

PORTLAND STATE UNIV. LIB.
Documents Department
P.O. Box 1151
Portland, OR 97207
(503) 229-3673

STATE LIBRARY OF PENN.
Government Pub. Section
P.O. Box 1601
Harrisburg, PA 17105
(717) 787-3752

TEXAS STATE LIBRARY
Public Services Department
P.O. Box 12927—Cap. Sta.
Austin, TX 78711
(512) 475-2996

TEXAS TECH UNIV. LIBRARY
Govt. Documents Department
Lubbock, TX 79409
(806) 742-2268

UTAH STATE UNIVERSITY
Merrill Library, U.M.C. 30
Logan, UT 84322
(801) 750-2682

UNIVERSITY OF VIRGINIA
Alderman Lib.—Public Doc.
Charlottesville, VA 22901
(804) 924-3133

WASHINGTON STATE LIBRARY
Documents Section
Olympia, WA 98504
(206) 753-4027

WEST VIRGINIA UNIV. LIB.
Documents Department
Morgantown, WV 26506
(304) 293-3640

MILWAUKEE PUBLIC LIBRARY
814 West Wisconsin Avenue
Milwaukee, WI 53233
(414) 278-3000

ST. HIST. LIB. OF WISCONSIN
Government Pub. Section
816 State Street
Madison, WI 53706
(608) 262-4347

WYOMING STATE LIBRARY
Supreme Ct. & Library Bld.
Cheyenne, WY 82002
(307) 777-6344

National Aeronautics and
Space Administration
Code NIT-4
Washington, D.C.
20546

Official Business
Penalty for Private Use, $300

SPECIAL FOURTH-CLASS RATE
POSTAGE & FEES PAID
NASA
WASHINGTON, D.C.
PERMIT No. G27

NASA

POSTMASTER: If Undeliverable (Section 158
Postal Manual) Do Not Return

24/3

VOLUME 24 / NUMBER 3
FEBRUARY 8, 1986
ACC. NOS. N86-11145 TO N86-12198

STAR

AN ABSTRACT JOURNAL

REFERENCE
NEWARK PUBLIC LIBRARY
U.S. DOCUMENTS

Scientific and Technical Aerospace Reports

PRODUCED BY THE
SCIENTIFIC AND TECHNICAL
INFORMATION
BRANCH
NASA

READEX FICHE best copy available

NAS 1.9/4:

NATIONAL AERONAUTICS AND SPACE ADMINISTRATION

WHAT YOU CAN DO FOR *STAR*

All users of this abstract service are urged to forward reports to be considered for announcement in *STAR*. This will aid NASA in its efforts to provide the fullest possible coverage of all scientific and technical publications that might support aeronautics and space research and development. If you have prepared relevant reports (other than those that you will transmit to NASA, DoD, or DOE through the usual contract- or grant-reporting channels), please send them for consideration to the NASA Scientific and Technical Information Facility, P.O. Box 8757, B.W.I. Airport, Maryland 21240.

Reprints of journal articles, book chapters, and conference papers are also welcome. These will be considered for announcement in *STAR's* companion journal, *International Aerospace Abstracts*.

You may specify a particular source to be included in a report announcement if you wish; otherwise the report will be placed on public sale at the National Technical Information Service. Copyrighted publications will be announced but not distributed or sold.

PURCHASE OF *STAR*

The semimonthly issues are available for sale by the Superintendent of Documents, U.S. Government Printing Office, Washington, D.C. 20402.

PUBLISHED BY:

UNITED STATES GOVERNMENT
NATIONAL AERONAUTICS AND SPACE ADMINISTRATION
SCIENTIFIC AND TECHNICAL INFORMATION BRANCH

Scientific and Technical Aerospace Reports, Volume 24, is prepared by the NASA Scientific and Technical Information Facility operated for the National Aeronautics and Space Administration by RMS Associates.

The Administrator of the National Aeronautics and Space Administration has determined that the publication of this periodical is necessary in the transaction of the public business required by law of this Agency. Use of funds for printing this periodical has been approved by the Director of the Office of Management and Budget through March 22, 1988.

US ISSN 0036-8741

INTRODUCTION

Scientific and Technical Aerospace Reports (STAR) is a major component of a comprehensive National Aeronautics and Space Administration information system covering aeronautics, space, and supporting disciplines. *STAR* is issued on the 8th and 23rd of each month and announces current publications of the following types:

- NASA, NASA contractor, and NASA grantee reports
- Reports issued by other U.S. Government agencies, domestic and foreign institutions, universities, and private firms
- Translations in report form
- NASA-owned patents and patent applications
- Dissertations and theses

Cumulative index volumes are published annually.

Journal, book, and conference literature, cover-to-cover journal translations, and certain foreign dissertations are announced in a companion journal, *International Aerospace Abstracts (IAA)*, available on subscription from the American Institute of Aeronautics and Astronautics, Technical Information Service, 555 West 57th Street, 12th Floor, New York, New York 10019.

SUBJECT SCOPE

Subject scope of *STAR*, and *IAA* includes all aspects of aeronautics and space research and development, supporting basic and applied research, and applications. Aerospace aspects of earth resources, energy development, conservation, oceanography, environmental protection, urban transportation, and other topics of high national priority are also covered.

OTHER NASA PUBLICATIONS

Other NASA publications and information services are described in the publication, *The NASA Scientific and Technical Information System ... and How to Use It*, available without charge from the NASA Scientific and Technical Information Facility, P.O. Box 8757, B.W.I. Airport, Maryland 21240.

HOW TO USE *STAR* SUBJECT CATEGORIES

STAR is categorized by 10 major subject divisions divided into 74 specific subject categories and one general category/division. The major subject divisions are listed in the Table of Contents, together with a note for each that defines its scope and provides any cross-references. For example:

AERONAUTICS

Includes aeronautics (general); aerodynamics; air transportation and safety; aircraft communications and navigation; aircraft design, testing and performance; aircraft instrumentation; aircraft propulsion and power; aircraft stability and control; and research and support facilities (air).

For related information see also *Astronautics*.

Each major division is further divided into as many as nine specific categories, which are identified by category numbers.

Abstracts in *STAR* are grouped by specific category, the categories appearing in sequential order. Category breaks in the abstract section are identified by the category number and title, and a scope note. Cross-references to other categories are provided as appropriate. For example:

02 AERODYNAMICS

Includes aerodynamics of bodies, combinations, wings, rotors, and control surfaces; and internal flow in ducts and turbomachinery.

For related information see also *34 Fluid Mechanics and Heat Transfer*.

CROSS-REFERENCES

Individual *STAR* abstracts are not ordinarily cross-referenced, except for certain conference reports or book translations that have had separate abstracts written for their component papers or chapters. Citations and abstracts of the components follow immediately after those of the parent document. When the subject content of a component differs sufficiently from the general content of the parent, a cross-reference citation also is printed at the end of the category to which it normally would have been assigned if it were independent.

DOCUMENTS ON MICROFICHE

Documents on microfiche(1) are designated by a pound sign (#) following the accession number. The pound sign is used without regard to the source or quality of the microfiche.

AVAILABILITIES

One or more sources from which a document announced in *STAR* is available to the public is given in each citation. The most commonly indicated sources and their acronyms or abbreviations are listed below. If the publication is available from a source other than those listed, the publisher and his address will be displayed on the availability line or in combination with the corporate source line.

---

(1) A microfiche is a transparent sheet of film, 105 by 148 mm in size, containing as many as 60 to 98 pages of information reduced to micro images (not to exceed 26:1 reduction).

Avail: NTIS. Sold by the National Technical Information Service. Prices for hard copy (HC) and microfiche (MF) are indicated by a price code following the letters HC or MF in the *STAR* citation. Current values for the price codes are given in the tables on page vii.

Initially distributed microfiche under the NTIS SRIM (Selected Research in Microfiche) is available at greatly reduced unit prices. For this service and for information concerning subscription to NASA printed reports, consult the NTIS Subscription Section, Springfield, Va. 22161.

NOTE ON ORDERING DOCUMENTS: When ordering NASA publications (those followed by the * symbol), use the N accession number. NASA patent applications (only the specifications are offered) should be ordered by the US-Patent-Appl-SN number. Non-NASA publications (no asterisk) should be ordered by the AD, PB, or other *report* number shown on the last line of the citation, not by the N accession number. It is also advisable to cite the title and other bibliographic identification.

Avail: SOD (or GPO). Sold by the Superintendent of Documents, U.S. Government Printing Office, in hard copy. The current price and order number are given following the availability line. (NTIS will fill microfiche requests, as indicated above, for those documents identified by a # symbol.)

Avail: NASA Public Document Rooms. Documents so indicated may be examined at or purchased from the National Aeronautics and Space Adminstration, Public Documents Room (Room 126), 600 Independence Ave., S.W., Washington, D.C. 20546, or public document rooms located at each of the NASA research centers, the NASA Space Technology Laboratories, and the NASA Pasadena Office at the Jet Propulsion Laboratory.

Avail: DOE Depository Libraries. Organizations in U.S. cities and abroad that maintain collections of Department of Energy reports, usually in microfiche form, are listed in *Energy Research Abstracts*. Services available from the DOE and its depositories are described in a booklet, *DOE Technical Information Center - Its' Functions and Services* (TID-4660), which may be obtained without charge from the DOE Technical Information Center.

Avail: Univ. Microfilms. Documents so indicated are dissertations selected from *Dissertation Abstracts* and are sold by University Microfilms as xerographic copy (HC) and microfilm. All requests should cite the author and the Order Number as they appear in the citation.

Avail: USGS. Originals of many reports from the U.S. Geological Survey, which may contain color illustrations, or otherwise may not have the quality of illustrations preserved in the microfiche or facsimile reproduction, may be examined by the public at the libraries of the USGS field offices whose addresses are listed in this Introduction. The libraries may be queried concerning the availability of specific documents and the possible utilization of local copying services, such as color reproduction.

Avail: HMSO. Publications of Her Majesty's Stationery Office are sold in the U.S. by Pendragon House, Inc. (PHI), Redwood City, California. The U.S. price (including a service and mailing charge) is given, or a conversion table may be obtained from PHI.

Avail: BLL (formerly NLL): British Library Lending Division, Boston Spa, Wetherby, Yorkshire, England. Photocopies available from this organization at the price shown. (If none is given, inquiry should be addressed to the BLL.)

Avail: Fachinformationszentrum, Karlsruhe. Sold by the Fachinformationszentrum Energie, Physik, Mathematik GMBH, Eggenstein Leopoldshafen, Federal Republic of Germany, at the price shown in deutschmarks (DM).

Avail: Issuing Activity, or Corporate Author, or no indication of availability. Inquiries as to the availability of these documents should be addressed to the organization shown in the citation as the corporate author of the document.

Avail: U.S. Patent and Trademark Office. Sold by Commissioner of Patents and Trademarks, U.S. Patent and Trademark Office, at the standard price of 50 cents each, postage free. (See discussion of patents and patent applications below.)

Avail: ESDU. Pricing information on specific data, computer programs, and details on ESDU topic categories can be obtained from ESDU International Ltd. Requesters in North America should use the Virginia address while all other requesters should use the London address, both of which are on page vi.

NASA PATENTS AND PATENT APPLICATIONS

Patents and patent applications owned by NASA are announced in *STAR* under appropriate subject categories and are referenced in the *STAR* indexes. In the Report/Accession Number Index, patents are indexed by the NASA Case Number (which appears in lieu of the report number in other indexes), the U.S. Patent Number, the U.S. Patent Application Serial Number, and the U.S. Patent Class. Patent applications for which patents have not yet been issued are indexed by the NASA Case Number and the U.S. Patent Application Serial Number.

NASA *patent application specifications* are sold in paper copy by the National Technical Information Service at price code A02 ($9.95 domestic; $19.90 foreign). Microfiche are sold at price code A01 ($5.95 domestic; $11.90 foreign). The US-Patent-Appl-SN- number should be used in ordering either paper copy or microfiche from NTIS. Printed copies of *patents* (which are not microfiched) are available for purchase at 50 cents per copy from:

Commissioner of Patents and Trademarks
U.S. Patent and Trademark Office
Washington, D.C. 20231

When ordering patents, the U.S. Patent Number should be used, and payment must be remitted in advance, preferably by money order or check payable to the Commissioner of Patents and Trademarks. Prepaid purchase coupons for ordering are also available from the Patent and Trademark Office. The patents and patent applications announced in *STAR* are owned by NASA and are available for royalty-free licensing. Requests for licensing terms and further information should be addressed to:

Assistant General Counsel for Patent Matters/Code GP-1
National Aeronautics and Space Administration
Washington, D.C. 20546

ELIGIBILITY AND REGISTRATION FOR NASA INFORMATION PRODUCTS AND SERVICES

A variety of services is available to organizations of the following types that have registered with NASA to receive specific services or products:

1. NASA offices, research centers, contractors, subcontractors, grantees, and consultants;
2. Other U.S. Government agencies and their contractors;
3. Libraries in the United States that have arrangements with NASA to maintain collections of NASA documents for public reference;
4. Other organizations in the United States having a need for NASA documents in work related to aeronautics and space research;
5. Organizations abroad that have established reciprocal document exchange arrangements with NASA.

Only the central service points or central points of document acquisition and control within qualified organizations are eligible to register for NASA products and services. Domestic organizations that may be eligible to receive various classes of NASA publications and services should address their requests for registration or for further information to:

NASA Scientific and Technical Information Facility
ATTN: Registration Activity
P.O. Box 8757
B.W.I. Airport, Maryland 21240

Organizations abroad should direct requests to the same address, but to the attention of: International Exchange Program.

AVAILABILITY OF *STAR* ABSTRACTS ON MICROFICHE

Microfiche of the abstract sections of this issue and other issues of *STAR* are available on annual subscription from NTIS, Attn: Subscriptions, 5285 Port Royal Road, Springfield, Virginia 22161. Annual subscription rates are $60.00 North America; $120.00 foreign. Abstract sections for previous years retroactive to 1964 are available at the current rates. Microfiche for individual *STAR* issue abstract sections are not available.

PUBLIC COLLECTIONS OF NASA DOCUMENTS

DOMESTIC: NASA and NASA-sponsored documents and a large number of aerospace publications are available to the public for reference purposes at the library maintained by the American Institute of Aeronautics and Astronautics, Technical Information Service, 555 West 57th Street, 12th Floor, New York, New York 10019.

EUROPEAN: An extensive collection of NASA and NASA-sponsored publications is maintained by the British Library Lending Division, Boston Spa, Wetherby, Yorkshire, England for public access. The British Library Lending Division also has available many of the non-NASA publications cited in *STAR*. European requesters may purchase facsimile copy or microfiche of NASA and NASA-sponsored documents, those identified by both the symbols # and * from ESA - Information Retrieval Service European Space Agency, 8-10 rue Mario-Nikis, 75738 Paris CEDEX 15, France.

FEDERAL DEPOSITORY LIBRARY PROGRAM

In order to provide the general public with greater access to U.S. Government publications, Congress established the Federal Depository Library Program under the Government Printing Office (GPO), with 50 regional depositories responsible for permanent retention of material, inter-library loan, and reference services. Over 1,300 other depositories also exist. A list of the regional GPO libraries appears on the inside back cover of *STAR*.

ADDRESSES OF ORGANIZATIONS

American Institute of Aeronautics and
Astronautics
Technical Information Service
555 West 57th Street, 12th Floor
New York, New York 10019

British Library Lending Division,
Boston Spa, Wetherby, Yorkshire,
England

Commissioner of Patents and
Trademarks
U.S. Patent and Trademark Office
Washington, D.C. 20231

Department of Energy
Technical Information Center
P.O. Box 62
Oak Ridge, Tennessee 37830

ESA-Information Retrieval Service
ESRIN
Via Galileo Galilei
00044 Frascati (Rome) Italy

ESDU International, Ltd.
1495 Chain Bridge Road
McLean, Virginia 22101

ESDU International, Ltd.
251-259 Regent Street
London, W1R 7AD, England

Fachinformationszentrum Energie, Physik,
Mathematik GMBH
7514 Eggenstein Leopoldshafen
Federal Republic of Germany

Her Majesty's Stationery Office
P.O. Box 569, S.E. 1
London, England

NASA Scientific and Technical Information
Facility
P.O. Box 8757
B.W.I. Airport, Maryland 21240

National Aeronautics and Space
Administration
Scientific and Technical Information
Branch (NIT-1)
Washington, D.C. 20546

National Technical Information Service
5285 Port Royal Road
Springfield, Virginia 22161

Pendragon House, Inc.
899 Broadway Avenue
Redwood City, California 94063

Superintendent of Documents
U.S. Government Printing Office
Washington, D.C. 20402

University Microfilms
A Xerox Company
300 North Zeeb Road
Ann Arbor, Michigan 48106

University Microfilms, Ltd.
Tylers Green
London, England

U.S. Geological Survey Library
National Center – MS 950
12201 Sunrise Valley Drive
Reston, Virginia 22092

U.S. Geological Survey Library
2255 North Gemini Drive
Flagstaff, Arizona 86001

U.S. Geological Survey
345 Middlefield Road
Menlo Park, California 94025

U.S. Geological Survey Library
Box 25046
Denver Federal Center, MS 914
Denver, Colorado 80225

NTIS PRICE SCHEDULES

(Effective October 1, 1985)

Schedule A
STANDARD PRICE DOCUMENTS AND MICROFICHE

PRICE CODE	PAGE RANGE	NORTH AMERICAN PRICE	FOREIGN PRICE
A01	Microfiche	$ 5.95	$11.90
A02-A03	001-050	9.95	19.90
A04-A05	051-100	11.95	23.90
A06-A09	101-200	16.95	33.90
A10-A13	201-300	22.95	45.90
A14-A17	301-400	28.95	57.90
A18-A21	401-500	34.95	69.90
A22-A25	501-600	40.95	81.90
A99	601-up	*	*
NO1		$40.00	70.00
NO2		40.00	70.00

Schedule E
EXCEPTION PRICE DOCUMENTS AND MICROFICHE

PRICE CODE	NORTH AMERICAN PRICE	FOREIGN PRICE
E01	$ 7.50	15.00
E02	10.00	20.00
E03	11.00	22.00
E04	13.50	27.00
E05	15.50	31.00
E06	18.00	36.00
E07	20.50	41.00
E08	23.00	46.00
E09	25.50	51.00
E10	28.00	56.00
E11	30.50	61.00
E12	33.00	66.00
E13	35.50	71.00
E14	38.50	77.00
E15	42.00	84.00
E16	46.00	92.00
E17	50.00	100.00
E18	54.00	108.00
E19	60.00	120.00
E20	70.00	140.00
E99	*	*

*Contact NTIS for price quote.

IMPORTANT NOTICE

NTIS Shipping and Handling Charges (effective June 1, 1985)

U.S., Canada, Mexico — ADD $3.00 per TOTAL ORDER

All Other Countries — ADD $4.00 per TOTAL ORDER

Exceptions — Does NOT apply to:

ORDERS REQUESTING NTIS RUSH HANDLING
ORDERS FOR SUBSCRIPTION OR STANDING ORDER PRODUCTS *ONLY*

NOTE: Each additional delivery address on an order requires a separate shipping and handling charge.

VOLUME 24 NUMBER 3 / FEBRUARY 8, 1986

TABLE OF CONTENTS

AERONAUTICS

Includes aeronautics (general); aerodynamics; air transportation and safety; aircraft communications and navigation; aircraft design, testing and performance; aircraft instrumentation; aircraft propulsion and power; aircraft stability and control; and research and support facilities (air).

For related information see also *Astronautics*.

01 AERONAUTICS (GENERAL) 365

02 AERODYNAMICS 365

Includes aerodynamics of bodies, combinations, wings, rotors, and control surfaces; and internal flow in ducts and turbomachinery.

For related information see also *34 Fluid Mechanics and Heat Transfer*

03 AIR TRANSPORTATION AND SAFETY 367

Includes passenger and cargo air transport operations; and aircraft accidents.

For related information see also *16 Space Transportation* and *85 Urban Technology and Transportation*.

04 AIRCRAFT COMMUNICATIONS AND NAVIGATION 368

Includes digital and voice communication with aircraft; air navigation systems (satellite and ground based); and air traffic control.

For related information see also *17 Spacecraft Communications, Command and Tracking* and *32 Communications*.

05 AIRCRAFT DESIGN, TESTING AND PERFORMANCE 368

Includes aircraft simulation technology.

For related information see also *18 Spacecraft Design, Testing and Performance* and *39 Structural Mechanics*.

06 AIRCRAFT INSTRUMENTATION 368

Includes cockpit and cabin display devices; and flight instruments.

For related information see also *19 Spacecraft Instrumentation* and *35 Instrumentation and Photography*.

07 AIRCRAFT PROPULSION AND POWER 369

Includes prime propulsion systems and systems components, e.g., gas turbine engines and compressors; and on-board auxiliary power plants for aircraft.

For related information see also *20 Spacecraft Propulsion and Power*, *28 Propellants and Fuels*, and *44 Energy Production and Conversion*.

08 AIRCRAFT STABILITY AND CONTROL 370

Includes aircraft handling qualities; piloting; flight controls; and autopilots.

09 RESEARCH AND SUPPORT FACILITIES (AIR) 371

Includes airports, hangars and runways; aircraft repair and overhaul facilities; wind tunnels; shock tube facilities; and engine test blocks.

For related information see also *14 Ground Support Systems and Facilities (Space)*.

ASTRONAUTICS

Includes astronautics (general); astrodynamics; ground support systems and facilities (space); launch vehicles and space vehicles; space transportation; spacecraft communications, command and tracking; spacecraft design, testing and performance; spacecraft instrumentation; and spacecraft propulsion and power.

For related information see also *Aeronautics*

12 ASTRONAUTICS (GENERAL) 372

For extraterrestrial exploration see *91 Lunar and Planetary Exploration*.

13 ASTRODYNAMICS N.A.

Includes powered and free-flight trajectories; and orbit and launching dynamics.

14 GROUND SUPPORT SYSTEMS AND FACILITIES (SPACE) 372

Includes launch complexes, research and production facilities; ground support equipment, e.g., mobile transporters; and simulators.

For related information see also *09 Research and Support Facilities (Air)*.

15 LAUNCH VEHICLES AND SPACE VEHICLES N.A.

Includes boosters; manned orbital laboratories; reusable vehicles; and space stations.

16 SPACE TRANSPORTATION N.A.

Includes passenger and cargo space transportation, e.g., shuttle operations; and rescue techniques.

For related information see also *03 Air Transportation and Safety* and *85 Urban Technology and Transportation*.

17 SPACECRAFT COMMUNICATION, COMMAND AND TRACKING N.A.

Includes telemetry; space communications networks; astronavigation; and radio blackout.

For related information see also *04 Aircraft Communications and Navigation* and *32 Communications*.

18 SPACECRAFT DESIGN, TESTING AND PERFORMANCE 373

Includes spacecraft thermal and environmental control; and attitude control.

For life support systems see *54 Man/System Technology and Life Support*. For related information see also *05 Aircraft Design, Testing and Performance* and *39 Structural Mechanics*.

19 SPACECRAFT INSTRUMENTATION N.A.

For related information see also *06 Aircraft Instrumentation* and *35 Instrumentation and Photography*.

20 SPACECRAFT PROPULSION AND POWER 374

Includes main propulsion systems and components, e.g., rocket engines; and spacecraft auxiliary power sources.

For related information see also *07 Aircraft Propulsion and Power*, *28 Propellants and Fuels*, and *44 Energy Production and Conversion*.

CHEMISTRY AND MATERIALS

Includes chemistry and materials (general); composite materials; inorganic and physical chemistry; metallic materials; nonmetallic materials; and propellants and fuels.

23 CHEMISTRY AND MATERIALS (GENERAL) 374
Includes biochemistry and organic chemistry.

24 COMPOSITE MATERIALS 375
Includes laminates.

25 INORGANIC AND PHYSICAL CHEMISTRY 377
Includes chemical analysis, e.g., chromatography; combustion theory; electrochemistry; and photochemistry.

For related information see also *77 Thermodynamics and Statistical Physics.*

26 METALLIC MATERIALS 381
Includes physical, chemical, and mechanical properties of metals, e.g., corrosion; and metallurgy.

27 NONMETALLIC MATERIALS 384
Includes physical, chemical, and mechanical properties of plastics, elastomers, lubricants, polymers, textiles, adhesives, and ceramic materials.

28 PROPELLANTS AND FUELS 387
Includes rocket propellants, igniters, and oxidizers; storage and handling; and aircraft fuels.

For related information see also *07 Aircraft Propulsion and Power, 20 Spacecraft Propulsion and Power,* and *44 Energy Production and Conversion.*

ENGINEERING

Includes engineering (general); communications; electronics and electrical engineering; fluid mechanics and heat transfer; instrumentation and photography; lasers and masers; mechanical engineering; quality assurance and reliability; and structural mechanics.

For related information see also *Physics.*

31 ENGINEERING (GENERAL) 392
Includes vacuum technology; control engineering; display engineering; and cryogenics.

32 COMMUNICATIONS 404
Includes land and global communications; communications theory; and optical communications.

For related information see also *04 Aircraft Communications and Navigation* and *17 Spacecraft Communications, Command and Tracking.*

33 ELECTRONICS AND ELECTRICAL ENGINEERING 410
Includes test equipment and maintainability; components, e.g., tunnel diodes and transistors; microminiaturization; and integrated circuity.

For related information see also *60 Computer Operations and Hardware* and *76 Solid-State Physics.*

34 FLUID MECHANICS AND HEAT TRANSFER 416
Includes boundary layers; hydrodynamics; fluidics; mass transfer; and ablation cooling.

For related information see also *02 Aerodynamics* and *77 Thermodynamics and Statistical Physics.*

35 INSTRUMENTATION AND PHOTOGRAPHY 422
Includes remote sensors; measuring instruments and gages; detectors; cameras and photographic supplies; and holography.

For aerial photography see *43 Earth Resources.* For related information see also *06 Aircraft Instrumentation* and *19 Spacecraft Instrumentation.*

36 LASERS AND MASERS 426
Includes parametric amplifiers.

37 MECHANICAL ENGINEERING 429
Includes auxiliary systems (non-power); machine elements and processes; and mechanical equipment.

38 QUALITY ASSURANCE AND RELIABILITY 431
Includes product sampling procedures and techniques; and quality control.

39 STRUCTURAL MECHANICS 431
Includes structural element design and weight analysis; fatigue; and thermal stress.

For applications see *05 Aircraft Design, Testing and Performance* and *18 Spacecraft Design, Testing and Performance.*

GEOSCIENCES

Includes geosciences (general); earth resources; energy production and conversion; environment pollution; geophysics; meteorology and climatology; and oceanography.

For related information see also *Space Sciences.*

42 GEOSCIENCES (GENERAL) 433

43 EARTH RESOURCES 453
Includes remote sensing of earth resources by aircraft and spacecraft; photogrammetry; and aerial photography.

For instrumentation see *35 Instrumentation and Photography.*

44 ENERGY PRODUCTION AND CONVERSION 455
Includes specific energy conversion systems, e.g., fuel cells and batteries; global sources of energy; fossil fuels; geophysical conversion; hydroelectric power; and wind power.

For related information see also *07 Aircraft Propulsion and Power, 20 Spacecraft Propulsion and Power, 28 Propellants and Fuels,* and *85 Urban Technology and Transportation.*

45 ENVIRONMENT POLLUTION 462
Includes air, noise, thermal and water pollution; environment monitoring; and contamination control.

46 GEOPHYSICS 465

Includes aeronomy; upper and lower atmosphere studies; ionospheric and magnetospheric physics; and geomagnetism.

For space radiation see *93 Space Radiation.*

47 METEOROLOGY AND CLIMATOLOGY 483

Includes weather forecasting and modification.

48 OCEANOGRAPHY 489

Includes biological, dynamic and physical oceanography; and marine resources.

LIFE SCIENCES

Includes sciences (general); aerospace medicine; behavioral sciences; man/system technology and life support; and planetary biology.

51 LIFE SCIENCES (GENERAL) 492

Includes genetics.

52 AEROSPACE MEDICINE 493

Includes physiological factors; biological effects of radiation; and weightlessness.

53 BEHAVIORAL SCIENCES 495

Includes psychological factors; individual and group behavior; crew training and evaluation; and psychiatric research.

54 MAN/SYSTEM TECHNOLOGY AND LIFE SUPPORT 496

Includes human engineering; biotechnology; and space suits and protective clothing.

55 PLANETARY BIOLOGY N.A.

Includes exobiology; and extraterrestrial life.

MATHEMATICAL AND COMPUTER SCIENCES

Includes mathematical and computer sciences (general); computer operations and hardware; computer programming and software; computer systems; cybernetics; numerical analysis; statistics and probability; systems analysis; and theoretical mathematics.

59 MATHEMATICAL AND COMPUTER SCIENCES (GENERAL) N.A.

60 COMPUTER OPERATIONS AND HARDWARE 497

Includes computer graphics and data processing.

For components see *33 Electronics and Electrical Engineering.*

61 COMPUTER PROGRAMMING AND SOFTWARE 499

Includes computer programs, routines, and algorithms.

62 COMPUTER SYSTEMS 504

Includes computer networks.

63 CYBERNETICS 504

Includes feedback and control theory.

For related information see also *54 Man/System Technology and Life Support.*

64 NUMERICAL ANALYSIS 505

Includes iteration, difference equations, and numerical approximation.

65 STATISTICS AND PROBABILITY 508

Includes data sampling and smoothing; Monte Carlo method; and stochastic processes.

66 SYSTEMS ANALYSIS 508

Includes mathematical modeling; network analysis; and operations research.

67 THEORETICAL MATHEMATICS N.A.

Includes topology and number theory.

PHYSICS

Includes physics (general); acoustics; atomic and molecular physics; nuclear and high-energy physics; optics; plasma physics; solid-state physics; and thermodynamics and statistical physics.

For related information see also *Engineering.*

70 PHYSICS (GENERAL) 509

For geophysics see *46 Geophysics.* For astrophysics see *90 Astrophysics.* For solar physics see *92 Solar Physics.*

71 ACOUSTICS 509

Includes sound generation, transmission, and attenuation.

For noise pollution see *45 Environment Pollution.*

72 ATOMIC AND MOLECULAR PHYSICS 511

Includes atomic structure and molecular spectra.

73 NUCLEAR AND HIGH-ENERGY PHYSICS 516

Includes elementary and nuclear particles; and reactor theory.

For space radiation see *93 Space Radiation.*

74 OPTICS 520

Includes light phenomena.

75 PLASMA PHYSICS 522

Includes magnetohydrodynamics and plasma fusion.

For ionospheric plasmas see *46 Geophysics.* For space plasmas see *90 Astrophysics.*

76 SOLID-STATE PHYSICS 529

Includes superconductivity.

For related information see also *33 Electronics and Electrical Engineering* and *36 Lasers and Masers.*

77 THERMODYNAMICS AND STATISTICAL PHYSICS 533

Includes quantum mechanics; and Bose and Fermi statistics.

For related information see also *25 Inorganic and Physical Chemistry* and *34 Fluid Mechanics and Heat Transfer.*

SOCIAL SCIENCES

Includes social sciences (general); administration and management; documentation and information science; economics and cost analysis; law and political science; and urban technology and transportation.

80 SOCIAL SCIENCES (GENERAL) 534
Includes educational matters.

81 ADMINISTRATION AND MANAGEMENT 535
Includes management planning and research.

82 DOCUMENTATION AND INFORMATION SCIENCE 535
Includes information storage and retrieval technology; micrography; and library science.
For computer documentation see *61 Computer Programming and Software.*

83 ECONOMICS AND COST ANALYSIS 536
Includes cost effectiveness studies.

84 LAW AND POLITICAL SCIENCE 536
Includes space law; international law; international cooperation; and patent policy.

85 URBAN TECHNOLOGY AND TRANSPORTATION 537
Includes applications of space technology to urban problems; technology transfer; technology assessment; and surface and mass transportation.
For related information see *03 Air Transportation and Safety, 16 Space Transportation,* and *44 Energy Production and Conversion.*

SPACE SCIENCES

Includes space sciences (general); astronomy; astrophysics; lunar and planetary exploration; solar physics; and space radiation.
For related information see also *Geosciences.*

88 SPACE SCIENCES (GENERAL) 538

89 ASTRONOMY 543
Includes radio and gamma-ray astronomy; celestial mechanics; and astrometry.

90 ASTROPHYSICS 544
Includes cosmology; and interstellar and interplanetary gases and dust.

91 LUNAR AND PLANETARY EXPLORATION 544
Includes planetology; and manned and unmanned flights.
For spacecraft design see *18 Spacecraft Design, Testing and Performance.* For space stations see *15 Launch Vehicles and Space Vehicles.*

92 SOLAR PHYSICS 545
Includes solar activity, solar flares, solar radiation and sunspots.

93 SPACE RADIATION 546
Includes cosmic radiation; and inner and outer earth's radiation belts.
For biological effects of radiation see *52 Aerospace Medicine.* For theory see *73 Nuclear and High-Energy Physics.*

GENERAL

99 GENERAL N.A.

Note: N.A. means that no abstracts were assigned to this category for this issue.

SUBJECT INDEX I-1
PERSONAL AUTHOR INDEX I-67
CORPORATE SOURCE INDEX I-77
CONTRACT NUMBER INDEX I-91
REPORT/ACCESSION NUMBER INDEX I-95

TYPICAL CITATION AND ABSTRACT

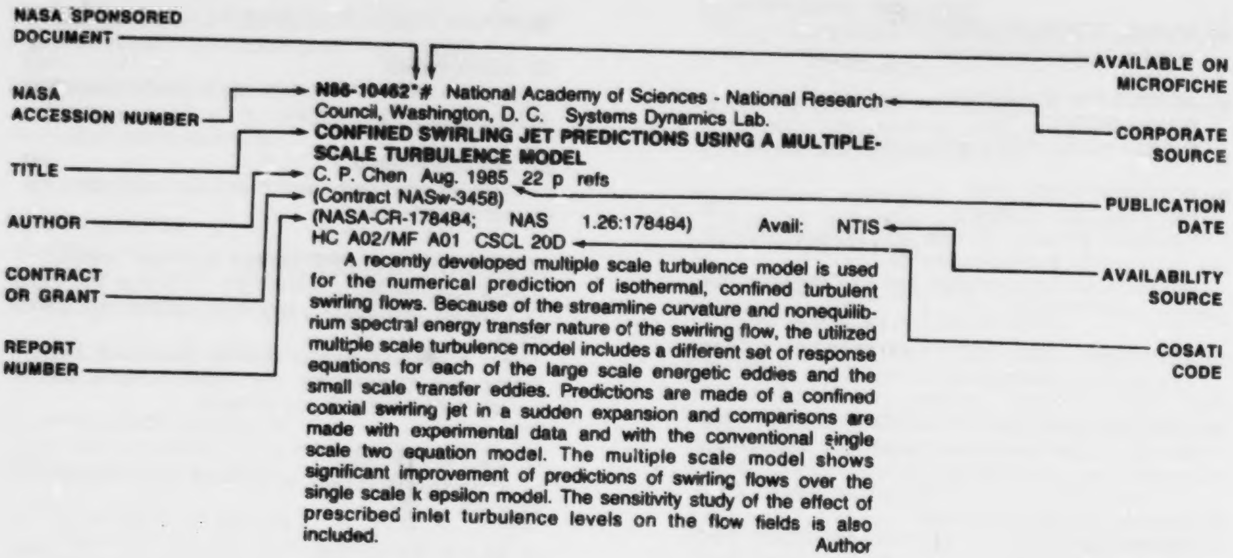
NASA SPONSORED DOCUMENT
NASA ACCESSION NUMBER
TITLE
AUTHOR
CONTRACT OR GRANT
REPORT NUMBER
AVAILABLE ON MICROFICHE
CORPORATE SOURCE
PUBLICATION DATE
AVAILABILITY SOURCE
COSATI CODE

N86-10462*# National Academy of Sciences - National Research Council, Washington, D. C. Systems Dynamics Lab.
CONFINED SWIRLING JET PREDICTIONS USING A MULTIPLE-SCALE TURBULENCE MODEL
C. P. Chen Aug. 1985 22 p refs
(Contract NASw-3458)
(NASA-CR-178484; NAS 1.26:178484) Avail: NTIS HC A02/MF A01 CSCL 20D

A recently developed multiple scale turbulence model is used for the numerical prediction of isothermal, confined turbulent swirling flows. Because of the streamline curvature and nonequilibrium spectral energy transfer nature of the swirling flow, the utilized multiple scale turbulence model includes a different set of response equations for each of the large scale energetic eddies and the small scale transfer eddies. Predictions are made of a confined coaxial swirling jet in a sudden expansion and comparisons are made with experimental data and with the conventional single scale two equation model. The multiple scale model shows significant improvement of predictions of swirling flows over the single scale k epsilon model. The sensitivity study of the effect of prescribed inlet turbulence levels on the flow fields is also included. Author

VOLUME 24 NUMBER 3 / FEBRUARY 8, 1986

Scientific and Technical Aerospace Reports

A Semimonthly Publication of the National Aeronautics and Space Administration

01 AERONAUTICS (GENERAL)

N86-12199# Aeronautical Research Labs., Melbourne (Australia).
A SURVEY OF AERONAUTICAL STRUCTURAL RESEARCH IN AUSTRALIA
F. H. Hooke Dec. 1984 45 p
(AD-A157211; ARL/STRUC-TM-394) Avail: NTIS HC A03/MF A01 CSCL 01/3

A survey of Aeronautical structural research in Australia has spanned over more than 40 years, from the establishment of the C.S.I.R. Division of Aeronautics in 1939. Industry, civil aviation and the armed services have benefited from the expertise of Structures Division in problem solving, as well as from ad-hoc research and, perhaps less immediately, from basic research. Not every avenue has been able to be explored. A major subject of research, structural fatigue, arose from an accident in 1945, and each new development in design and material has brought new problems. Standards of safety and risk have been explored. New technology of fiber composites permits better tailoring of strength and stiffness to requirements: this and the introduction to aircraft of active controls offer benefits and problems for the future. Author (GRA)

N86-12200# Air Force Academy, Colo.
AIR FORCE ACADEMY AERONAUTICS DIGEST Final Report
J. E. DeJongh, W. H. Heiser, and M. Hale Apr. 1985 269 p
(AD-A157215; USAFA-TR-85-2) Avail: NTIS HC A12/MF A01 CSCL 20/4

Some articles of the digest are entitled: The Seven-Hole Pressure Probe; Wind Tunnel Study on the Drag Effects of an Aft-Mounted Ventral Fin on a T-38 Model; An Experimental Investigation of an Airfoil Undergoing Large Amplitude Pitching Motions; Interrelated Effects of Pitch Rate and Pivot Point on Airfoil Dynamic Stall. Other topics covered are: An Examination of Curve Smoothing Using Digital Filter Theory; Flight Test Measurement of the Aerodynamic Effect of Thrust Level on Lift and Drag; and Flight Control System Design for a Computer Controlled Aircraft with Limited Sensors. GRA

02 AERODYNAMICS

Includes aerodynamics of bodies, combinations, wings, rotors, and control surfaces; and internal flow in ducts and turbomachinery.

For related information see also *34 Fluid Mechanics and Heat Transfer.*

N86-12201 Virginia Polytechnic Inst. and State Univ., Blacksburg.
EXPERIMENTAL INVESTIGATION OF 3-D TURBULENT FREE SHEAR FLOW PAST PROPELLERS AND WINDMILLS Ph.D. Thesis
Mohamed Abbas Kotb 1984 242 p
Avail: Univ. Microfilms Order No. DA8507194

An experimental investigation of the flowfield region near a 0.49 m. (1.615 ft), 3 bladed, horizontal axis rotor was conducted in the VPI 2 m x 2 m (6 ft x 6 ft) wind tunnel. Two different modes of operations were studied - propeller and windmill. For each case, tests were run with a uniform approach flow as a base line condition, and the main test series was run with a variable mesh wire grid upstream to produce an approach flow with an essentially linear velocity gradient. The results are compared to elucidate the effects of the non-uniform approach flow. Differences regarding the magnitudes and profile shapes of the mean flowfield parameters and turbulence quantities under uniform and shear flows are reported and discussed in detail. For the propeller case the measured turbulence quantities were sensitive to the upstream shear flow. This was manifested in the form of higher turbulence intensities and shear stresses. For the windmill case, the axial interference velocity was higher under the shear inflow condition while the swirl, radial flow and static pressure profiles did not show significant differences from the uniform case. Author

N86-12202*# Grumman Aerospace Corp., Bethpage, N.Y.
GRUMFOIL: A COMPUTER CODE FOR THE VISCOUS TRANSONIC FLOW OVER AIRFOILS Final Report
H. R. Mead and R. E. Melnik Washington NASA Oct. 1985 76 p refs
(Contract NAS1-12426)
(NASA-CR-3806; NAS 1.26:3806; RE-681) Avail: NTIS HC A05/MF A01 CSCL 01A

A user's manual which describes the operation of the computer program, GRUMFOIL is presented. The program computes the viscous transonic flow over two dimensional airfoils using a boundary layer type viscid-inviscid interaction approach. The inviscid solution is obtained by a multigrid method for the full potential equation. The boundary layer solution is based on integral entrainment methods. E.A.K.

N86-12203*# Southampton Univ. (England). Dept. of Aeronautics and Astronautics.
THE STATUS OF TWO-DIMENSIONAL TESTING AT HIGH TRANSONIC SPEEDS IN THE UNIVERSITY OF SOUTHAMPTON TRANSONIC SELF-STREAMLINING WIND TUNNEL Progress Report
Mark C. Lewis Washington NASA Oct. 1985 57 p refs
(Grant NsG-7172)
(NASA-CR-3919; NAS 1.26:3919) Avail: NTIS HC A04/MF A01 CSCL 01A

This report briefly outlines the progress made during the last 2 years in extending the operational range of the Transonic Self-Streamlining Wind Tunnel (at the University of Southampton) into high subsonic speeds. Analytical preparation completed in order to achieve such an extension is outlined and a summary of the preliminary model validation tests is presented. Future work necessary to allow further validation and development is discussed. Author

N86-12204*# Southampton Univ. (England). Dept. of Aeronautics and Astronautics.

DERIVATION OF JACK MOVEMENT INFLUENCE COEFFICIENTS AS A BASIS FOR SELECTING WALL CONTOURS GIVING REDUCED LEVELS OF INTERFERENCE IN FLEXIBLE WALLED TEST SECTIONS

M. J. Goodyer Oct. 1985 14 p refs Prepared for Kentron International, Inc., Hampton, Va.
(Contract NAS1-16000)
(NASA-CR-177992; NAS 1.26:177992) Avail: NTIS HC A02/MF A01 CSCL 01A

This report covers work done in a transonic wind tunnel towards providing data on the influence of the movement of wall-control jacks on the Mach number perturbations along the test section. The data is derived using an existing streamline-curvature program, and in application is reduced to matrices of influence coefficients. Author

N86-12205*# Rockwell International Corp., Columbus, Ohio. Aircraft Operations.

AERODYNAMIC CHARACTERISTICS OF A PROPULSIVE WING-CANARD CONCEPT AT STOL SPEEDS Interim Report

V. R. Stewart Nov. 1985 423 p refs
(Contract NAS1-17171)
(NASA-CR-177982; NAS 1.26:177982; NA84-0148) Avail: NTIS HC A18/MF A01 CSCL 01A

A full span model of a wing/canard concept representing a fighter configuration has been tested at STOL conditions in the NASA Langley 4 x 7 meter tunnel. The results of this test are presented, and comparisons are made to previous data of the same configuration tested as a semispan model. The potential of the propulsive wing/canard to develop very high lift coefficients was investigated with several nozzle spans (nozzle aspect ratios). Although longitudinal trim was not accomplished with the blowing distributions and configurations tested, the propulsive wing/canard appears to offer an approach to managing the large negative pitching moments associated with trailing edge flap blowing. Also presented are data showing the effects of large flap deflections and relative wing/canard positions. Presented in the appendix to the report are limited lateral-directional and ground effects data, as well as wing downwash measurements. Author

N86-12206*# National Aeronautics and Space Administration. Langley Research Center, Hampton, Va.

EFFECT OF SURFACE WAVINESS ON A SUPERCRITICAL LAMINAR-FLOW-CONTROL AIRFOIL

Dal V. Maddalon and Mark L. McMillin Oct. 1983 25 p refs
(NASA-TM-85705; NAS 1.15:85705) Avail: NTIS HC A02/MF A01 CSCL 01A

Calculations were made of the effects of surface waviness on the external pressure of a supercritical airfoil at design conditions. Wave parameters varied include amplitude, wavelength, phase, and number of cycles. Effects of single and multiple waves are calculated at various chordwise locations. General trends of surface waviness effects on pressure distribution are determined and these solutions are reported. Contour deviations are imposed on the upper surface of the airfoil. Results are presented in a manner designed to facilitate ready comparison with the ideal contour static pressure distribution. Author

N86-12207*# National Aeronautics and Space Administration. Ames Research Center, Moffett Field, Calif.

SOME RECENT ADVANCES IN COMPUTATIONAL AERODYNAMICS FOR HELICOPTER APPLICATIONS

W. J. McCroskey and J. D. Baeder (Army Aviation and Technology Activity-AVSCOM, Moffett Field, Calif.) Oct. 1985 20 p refs
(NASA-TM-86777; Rept-85345; NAS 1.15:86777; USAVSCOM-TR-85-A-06) Avail: NTIS HC A02/MF A01 CSCL 01A

The growing application of computational aerodynamics to nonlinear helicopter problems is outlined, with particular emphasis on several recent quasi-two-dimensional examples that used the thin-layer Navier-Stokes equations and an eddy-viscosity model to approximate turbulence. Rotor blade section characteristics can now be calculated accurately over a wide range of transonic flow conditions. However, a finite-difference simulation of the complete flow field about a helicopter in forward flight is not currently feasible, despite the impressive progress that is being made in both two and three dimensions. The principal limitations are today's computer speeds and memories, algorithm and solution methods, grid generation, vortex modeling, structural and aerodynamic coupling, and a shortage of engineers who are skilled in both computational fluid dynamics and helicopter aerodynamics and dynamics. Author

N86-12208*# Grumman Aerospace Corp., Bethpage, N.Y.

AN IMPROVED VISCID/INVISCID INTERACTION PROCEDURE FOR TRANSONIC FLOW OVER AIRFOILS Final Report

R. E. Melnik, R. R. Chow, H. R. Mead, and A. Jameson Washington NASA Oct. 1985 132 p refs
(Contract NAS1-12426)
(NASA-CR-3805; NAS 1.26:3805; RE-682) Avail: NTIS HC A07/MF A01 CSCL 01A

A new interacting boundary layer approach for computing the viscous transonic flow over airfoils is described. The theory includes a complete treatment of viscous interaction effects induced by the wake and accounts for normal pressure gradient effects across the boundary layer near trailing edges. The method is based on systematic expansions of the full Reynolds equation of turbulent flow in the limit of Reynolds numbers, Reynolds infinity. Procedures are developed for incorporating the local trailing edge solution into the numerical solution of the coupled full potential and integral boundary layer equations. Although the theory is strictly applicable to airfoils with cusped or nearly cusped trailing edges and to turbulent boundary layers that remain fully attached to the airfoil surface, the method was successfully applied to more general airfoils and to flows with small separation zones. Comparisons of theoretical solutions with wind tunnel data indicate the present method can accurately predict the section characteristics of airfoils including the absolute levels of drag. E.A.K.

N86-12209# Naval Ship Research and Development Center, Bethesda, Md. Ship Performance Dept.

AN EVALUATION OF FOUR METHODS OF NUMERICAL ANALYSIS FOR TWO-DIMENSIONAL AIRFOIL FLOWS. REVISION Departmental Report

R. Burke 6 Jul. 1985 29 p
(S12-66)
(AD-A157248; DTNSRDC/SPD-1139-01-Rev) Avail: NTIS HC A03/MF A01 CSCL 09/2

Four computer programs for analyzing the inviscid and boundary layer flow over two dimensional airfoils are exercised in comparisons against experimental data from two wind tunnel studies. The solution method of each computer program is discussed, followed by a description of the airfoil geometries used in the model comparisons. Measured values of pressure distribution, turbulent separation point, and boundary layer properties are compared against predicted values. GRA

N86-12210# Naval Weapons Center, China Lake, Calif.

PARACHUTE RECOVERY SYSTEMS DESIGN MANUAL, CHAPTERS 1 THROUGH 4 OFFPRINT Partial Report, Jan. 1984 - Jul. 1985

T. W. Knacke Jul. 1985 56 p
(AD-A157839; AD-E900488; NWC-TP-6575-CH-1/4) Avail: NTIS HC A04/MF A01 CSCL 01/3

This manual provides the recovery system engineer in Government and industry with tools to evaluate, select, design, test, manufacture, and operate parachute recovery systems. These systems range from simple, one-parachute assemblies to multiple-parachute systems, and may include equipment for impact attenuation, flotation, location, retrieval, and disposition. All system aspects are discussed, including the need for parachute recovery, the selection of the most suitable recovery system concept, a computerized approach to parachute performance, force and stress analysis, geometric gore design, component layout, material selection, system design, manufacturing, and in-service maintenance. GRA

N86-12211# Oregon State Univ., Corvallis. Dept. of Mechanical Engineering.
DEVELOPMENT OF AN ANALYTICAL MODEL AND CODE FOR THE FLAPPING RESPONSE OF A HAWTE ROTOR BLADE
R. W. Thresher and E. L. Hershberg Feb. 1985 233 p
(Contract DE-AC02-83CH-10093)
(DE85-008806; SERI/STR-217-2629) Avail: NTIS HC A11/MF A01

The following report is a descriptive summary of the work performed under RFP 76824 for Rockwell International's Rocky Flats, Colorado, facility as part of the Federal Wind Energy Research Program. The objectives of this project were threefold: (1) development of an analytical model of the flapping response of a wind turbine rotor; (2) development of an interactive, user-friendly computer code for performing the flapping analysis and for computing the rotor loads due to aerodynamic factors and blade flapping responses; and (3) verification of the model and the computer code with measured loads data taken from an existing machine. The model is a single-degree-of-freedom flapping response model of an individual wind turbine blade. It accounts for the blade bending deformation about the smallest blade inertia axis. The rotor is assumed to rotate at a constant speed, but the hub is allowed to move in a prescribed yawing motion. Rotors that are tilted and yawed relative to the mean wind direction can be accommodated in a straightforward manner. DOE

N86-12434# Joint Publications Research Service, Arlington, Va.
BLR STUDIES ON CONIC MODEL WITH LDA IN FL-1 WIND TUNNEL
Zhong Zhan and Yu Yong *In its* China Rept.: Sci. and Technol. (JPRS-CST-85-034) 1 Oct. 1985 p 67-70 Transl. into ENGLISH from Guoji Hangkong (Beijing), no. 6, Jun. 1985 p 9-10 (For primary document see N86-12430 03-31)
Avail: NTIS HC A08/MF A01

N86-12659# Joint Publications Research Service, Arlington, Va.
INFLUENCE OF WATER VAPOR ON DISTRIBUTION OF TURBULENT WAVE PARAMETERS Abstract Only
N. N. Pilyugin and S. G. Tikhomirov *In its* USSR Rept.: Earth Sci. (JPRS-UES-85-006) 19 Jun. 1985 p 26-27 Transl. into ENGLISH from Mekhan. Zhidkosti i Gaza (Moscow), no. 1, Jan. - Feb. 1985 p 138-142 (For primary document see N86-12630 03-42)
Avail: NTIS HC A05/MF A01

03 AIR TRANSPORTATION AND SAFETY

Includes passenger and cargo air transport operations; and aircraft accidents.

For related information see also *16 Space Transportation* and *85 Urban Technology and Transportation.*

N86-12212*# Bolt, Beranek, and Newman, Inc., Cambridge, Mass.
AN ANALYSIS OF THE APPLICATION OF AI TO THE DEVELOPMENT OF INTELLIGENT AIDS FOR FLIGHT CREW TASKS
Sheldon Baron and Carl Feehrer Washington NASA Oct. 1985 114 p refs
(Contract NAS1-17335)
(NASA-CR-3944; NAS 1.26:3944) Avail: NTIS HC A06/MF A01 CSCL 05H

This report presents the results of a study aimed at developing a basis for applying artificial intelligence to the flight deck environment of commercial transport aircraft. In particular, the study was comprised of four tasks: (1) analysis of flight crew tasks, (2) survey of the state-of-the-art of relevant artificial intelligence areas, (3) identification of human factors issues relevant to intelligent cockpit aids, and (4) identification of artificial intelligence areas requiring further research. Author

N86-12213# Naval Air Development Center, Warminster, Pa. Aircraft and Crew Systems Technology Directorate.
G PROTECTION BY AN EXTREME CROUCH POSITION Phase Report, 1 Aug. 1983 - 1 Sep. 1984
H. J. VONBeckh 4 Sep. 1984 14 p
(NR Proj. F58-523)
(AD-A157081; NADC-84162-60) Avail: NTIS HC A02/MF A01 CSCL 06/19

In World War II the pilots of diving bombers tolerated high G loads by assuming a crouch position. The Dynamic Flight Simulator (Human Centrifuge) was used to prove the advantages of the crouch position. Two subjects were located in an extreme crouch position, the upper spine being at an angle of 80 to 90 degrees from the vertical. They tolerated 6.5 and 7.5 G respectively. Both subjects have tolerated only 3.5 G in former experiments when seated upright. The use of an Anti-G suit did not improve further G tolerance. Both subjects abandoned the experiment not because of the Loss of Vision, but because of the discomfort of overfilling of the facial area with blood. It is planned to find a crouch position where the vision is still maintained and the blood filling of the facial area is mitigated. This would probably be a crouch position of 45 to 60 degrees from the vertical. Author (GRA)

N86-12214# Federal Aviation Agency, Atlantic City, N.J.
AIRCRAFT INTERIOR PANEL TEST CRITERIA DERIVED FROM FULL-SCALE FIRE TESTS Final Report
R. G. Hill, T. I. Eklund, and C. P. Sarkos Sep. 1985 65 p refs
Original contains color illustrations
(FAA/CT-85/23) Avail: NTIS HC A04/MF A01

Full scale cabin fire tests were conducted to determine potential increases in passenger survivability associated with different interior honeycomb panel constructions. The test fuselage was a C-133 with a simulated wide body door opening exposed to an 8 foot by 10 foot fuel fire. In the first series, the interior near the door was lined with the honeycomb panels to determine whether earlier studies performed with small scale enclosures were consistent with the full scale counterpart. These earlier studies resulted in the selection of the Ohio State University (OSU) Rate of Heat Release Apparatus as the most appropriate type test to evaluate aircraft panels. The first series was followed by tests that included fire blocked seats and carpeting as well as the panels to determine the type survivability increases that could be attained from low heat release materials. The scenario employed generally resulted with flashover within 2 minutes for panels considered typical in performance. A low heat release phenolic/fiberglass panel demonstrated a flashover delay until about 4 minutes into the test. An incombustible panel prevented flashover altogether. The performance of the various panels was evaluated to develop recommended flammability criteria for a modified OSU Rate of Heat Release Apparatus. Author

N86-12215# General Accounting Office, Washington, D. C. Resources Community and Economic Development Div.
FAA (FEDERAL AVIATION ADMINISTRATION) COULD IMPROVE OVERALL AVIATION SAFETY AND REDUCE COSTS ASSOCIATED WITH AIRPORT INSTRUMENT LANDING SYSTEMS
3 Apr. 1985 50 p
(PB85-195444; GAO/RCED-85-24; B-215115) Avail: NTIS HC A03/MF A01 CSCL 01E

The Federal Aviation Administration (FAA) operates and maintains over 700 instrument landing systems at airports throughout the United States. The Government Accounting Office (GAO) found that FAA could save about $31 million between now and the year 2000 if it replaced some of its older instrument landing systems with newer systems, which are less costly to operate. GAO also found that FAA could improve overall aviation safety and reduce cost by ensuring that existing systems are located where they are needed most. GRA

04 AIRCRAFT COMMUNICATIONS AND NAVIGATION

Includes digital and voice communication with aircraft; air navigation systems (satellite and ground based); and air traffic control.

For related information see also *17 Spacecraft Communications, Command, and Tracking* and *32 Communications.*

N86-12216*# Ohio State Univ., Columbus. ElectroScience Lab.
SIMULATION OF THE ENHANCED TRAFFIC ALERT AND COLLISION AVOIDANCE SYSTEM (TCAS 2) Semiannual Report
Roberto G. Rojas, Walter D. Burnside, Philip Law, and Brett Grandchamp Sep. 1985 86 p refs
(Grant NsG-1498)
(NASA-CR-176328; NAS 1.26:176328; SAR-716199-3) Avail: NTIS HC A05/MF A01 CSCL 17G

The OSU aircraft code is used to analyze and simulate the TCAS 2 circular array which is mounted on the fuselage of a Boeing 737 aircraft. It is shown that the sum and difference patterns radiated by the circular array are distorted by the various structures of the aircraft, i.e., wings, tail, etc. Furthermore, monopulse curves are calculated and plotted for several beam positions and THETA angles. As expected, the worst cases of distortion occur when the beams are pointed toward the tail of the aircraft. Author

N86-12425# Joint Publications Research Service, Arlington, Va.
NEW DUAL Z80 NAVIGAITON COMPUTER DESCRIBED
Yu Shiquan, Zhang Chunbao, and Wu Shuwei *In its* China Rept.: Sci. and Technol. (JPRS-CST-85-021) 8 Jul. 1985 p 113-122 refs Transl. into ENGLISH from Dianzi Jishu (Shanghai), v. 12, no. 1, 12 Jan. 1985 p 5-8 (For primary document see N86-12421 03-31)
Avail: NTIS HC A09/MF A01

05 AIRCRAFT DESIGN, TESTING AND PERFORMANCE

Includes aircraft simulation technology.

For related information see also *18 Spacecraft Design, Testing and Performance* and *39 Structural Mechanics.*

N86-12217 Department of the Air Force, Washington, D.C.
PNEUMATIC ACTUATOR DEVICE Patent
R. W. Gazzera, inventor (to Air Force) Issued 16 Apr. 1985 7 p Supersedes AD-D009822
(AD-D011794; US-Patent-4,510,846; US-Patent-Class-91-460)
Avail: US Patent and Trademark Office CSCL 13/11

A closed center four-way poppet actuator control device is incorporated into a pneumatic actuation system for controlling the movement of flight surfaces. The closed center four-way poppet actuator control device has a housing, a pair of two-way poppet valves in the housing, a rocker arm assembly mounted on the housing and connected to the pair of two-way poppet valves, and a diaphragm assembly also mounted in the housing and in contact with the two-way valves. A torque motor-driver assembly connected to the diaphragm assembly actuates the two-way valves as determined by control symbols. The rocker arm causes the two-way valves to function opposite each other: one allows high pressure gas to be input to a lobe motor acutator while the other allows gas to be output from the lobe motor actuator. Each two-way valve has a cylindrical poppet valve for inletting the gas to the actuator and a disk poppet valve for outputting the gas from the actuator to a vent. The actuator causes movement of the flight surfaces through a gearbox. A velocity transducer monitors this movement and transmits this movement to an electronic control unit which sends control signals to drive the torque motor-driver assembly that actuates said actuator control device. Author (GRA)

N86-12218*# Integrated Systems, Inc., Palo Alto, Calif.
REAL-TIME FLUTTER IDENTIFICATION Final Report
Richard Roy and Robert Walker Washington NASA Oct. 1985 147 p refs
(Contract NAS2-11451)
(NASA-CR-3933; NAS 1.26:3933; ISI-48) Avail: NTIS HC A07/MF A01 CSCL 01C

The techniques and a FORTRAN 77 MOdal Parameter IDentification (MOPID) computer program developed for identification of the frequencies and damping ratios of multiple flutter modes in real time are documented. Physically meaningful model parameterization was combined with state of the art recursive identification techniques and applied to the problem of real time flutter mode monitoring. The performance of the algorithm in terms of convergence speed and parameter estimation error is demonstrated for several simulated data cases, and the results of actual flight data analysis from two different vehicles are presented. It is indicated that the algorithm is capable of real time monitoring of aircraft flutter characteristics with a high degree of reliability. E.A.K.

N86-12219# Army War Coll., Carlisle Barracks, Pa.
THE C-17: WE NEED IT YESTERDAY
B. R. Hooten 25 Apr. 1985 37 p
(AD-A157147) Avail: NTIS HC A03/MF A01 CSCL 01/3

This student essay examines the historical development of the C-17, beginning in the 1970's when Tactical Airlift Command was pressing for development of the Advanced Medium Shortfield Takeoff and Landing Transport. An in-depth look is taken at the Congressionally Mandated Mobility Study and at the analyses done by the C-X Task Force that led to the final definition of the C-17. The US Air Force Airlift Master Plan is reviewed to show the importance of the C-17 to the structure of our airlift force of the future. Real world potential applications of the C-17 are projected by examination of two studies of actual airlift operations. AHUAS TARA '83, (a combined operation in Honduras) and URGENT FURY, the US rescue mission to Grenada in October 1983. This essay supports the need to buy the C-17 by showing the detailed, logistical process that led to its design, and by using two recent actual operations to show the airplane's unprecedented airlift capabilities of today and into the foreseeable future. GRA

N86-12450# Joint Publications Research Service, Arlington, Va.
WINGTIP SAILS TESTED ON Y-5 AIRCRAFT
Yang Daxi *In its* China Rept.: Sci. and Technol. (JPRS-CST-85-029) 3 Sep. 1985 p 49-53 Transl. into ENGLISH from Guoji Hangkong (Beijing), no. 5, May 1985 p 2-3 (For primary document see N86-12446 03-31)
Avail: NTIS HC A08/MF A01

06 AIRCRAFT INSTRUMENTATION

Includes cockpit and cabin display devices; and flight instruments.

For related information see also *19 Spacecraft Instrumentation* and *35 Instrumentation and Photography.*

N86-12220*# Dayton Univ., Ohio.
PERFORMANCE OF AN ALPHA-VANE AND PITOT TUBE IN SIMULATED HEAVY RAIN ENVIRONMENT Final Report
James K. Luers and Ira B. Fiscus Oct. 1985 32 p ref
(Grant NAG1-522)
(NASA-CR-176353; NAS 1.26:176353; UDR-TR-85-131) Avail: NTIS HC A03/MF A01 CSCL 01D

Experimental tests were conducted in the UDRI Environmental Wind/Rain Tunnel to establish the performance of an alpha-vane, that measures angle of attack, in a simulated heavy rain environment. The tests consisted of emersing the alpha-vane in an airstream with a concurrent water spray penetrating vertically through the airstream. The direction of the spray was varied to make an angle of 5.8 to 18 deg with the airstream direction in order to simulate the conditions that occur when an aircraft lands in a heavy rain environment. Rainrates simulated varied from 1000 to 1200 mm/hr which are the most severe ever expected to be encountered by an aircraft over even a 30 second period. Tunnel airspeeds ranged from 85 to 125 miles per hour. The results showed that even the most severe rainrates produced a misalignment in the alpha-vane of only 1 deg away from the airstream direction. Thus for normal rain conditions experienced by landing aircraft no significant deterioration in alpha-vane performance is expected. B.W.

N86-12221# Air Force Flight Test Center, Edwards AFB, Calif.
T-33 (SILVER STAR MK 3) PITOT-STATIC SYSTEM CALIBRATION Final Report, 17 Apr. - 15 May 1985
T. R. Woodford and E. P. Hansen Jun. 1985 34 p
(AD-A157854; AFFTC-TR-85-19) Avail: NTIS HC A03/MF A01 CSCL 01/4

This report presents the results of pitot-static system calibration tests performed on T-33 (Silver Star MK 3), civil registration number N83TB. The T-33 pitot-static system was calibrated in order to use the T-33 as a pacer for the T-46A pitot-static system calibration tests to be performed during the T-46A Development Test and Evaluation Program. Although the test aircraft will perform satisfactorily as a pacer, periodic checks on the pitot-static system's accuracy should be performed. GRA

N86-12222# Sanders Associates, Inc., Nashua, N. H.
ADVANCED AVIONICS COMPUTER ARCHITECTURE. VOLUME 1. EXECUTIVE SUMMARY Final Report, May 1980 - Nov. 1984
L. Greenspan and R. Singletary May 1985 19 p
(Contract F33615-79-C-1935)
(AD-A158119; AFWAL-TR-85-1041-Vol-1) Avail: NTIS HC A02/MF A01 CSCL 09/2

This exploratory development program was originally aimed at developing a computer with features to specifically support the JOVIAL (J73) programming language with considerations to Ada. Later, the program was redirected to modify the instruction set architecture (ISA) to more fully support Ada and increase performance. The new ISA supports most of the standard functions found in most ISA, but gives additional supports in: the Ada package concept, processing arrays and records, unconstrained arrays, dynamic storage allocation, detecting dangling references, detecting undefined variables, Ada-like exception handling, case instructions, for-loop instructions, Ada-like parameter passing, Ada-like tasking instructions and IEEE-standard floating point data types. GRA

N86-12223# Sanders Associates, Inc., Nashua, N. H.
ADVANCED AVIONICS COMPUTER ARCHITECTURE. VOLUME 2. INSTRUCTION SET ARCHITECTURE SPECIFICATION Final Report, May 1980 - Nov. 1984
L. Greenspan and R. Singletary May 1985 305 p 2 Vol.
(Contract F33615-79-C-1935)
(AD-A158120; AFWAL-TR-85-1041-Vol-2) Avail: NTIS HC A14/MF A01 CSCL 09/2

This exploratory development program was originally aimed at developing a computer with features to specifically support the JOVIAL (J73) programming language with considerations to Ada. Later, the program was redirected to modify the instruction set architecture (ISA) to more fully support Ada and increase performance. The new ISA supports most of the standard functions found in most ISA, but gives additional supports in: the Ada package concept, processing arrays and records, unconstrained arrays, dynamic storage allocation, detecting dangling reference, detecting undefined variables, Ada-like exception handling, case instructions, for-loop instructions, Ada-like parameter passing, Ada-like tasking instructions and IEEE-standard floating point data types. GRA

N86-12224# General Accounting Office, Washington, D. C. National Security and International Affairs Div.
NAVY SHOULD JOIN THE AIR FORCE AND ARMY PROGRAM TO DEVELOP AN ADVANCED INTEGRATED AVIONICS SYSTEM
17 Jun. 1985 17 p
(PB85-222503; GAO/NSIAD-85-94; B-215379) Avail: NTIS HC A02/MF A01 CSCL 01D

Modern technology should soon enable separate avionics systems in an aircraft to be consolidated into a single package to conserve space, save weight, and reduce costs. The report points out the potential benefits of avionics consolidation and recommends the Navy join in a demonstration program now being conducted by the Air Force and Army to exploit such benefits. GRA

07 AIRCRAFT PROPULSION AND POWER

Includes prime propulsion systems and systems components, e.g., gas turbine engines and compressors; and on-board auxiliary power plants for aircraft.

For related information see also *20 Spacecraft Propulsion and Power, 28 Propellants and Fuels,* and *44 Energy Production and Conversion.*

N86-12225 Department of the Air Force, Washington, D.C.
COMPARTMENTED, FILAMENT WOUND, ONE-PIECE AIRCRAFT FUEL TANKS Patent
E. J. Morrisey, inventor (to Air Force) Issued 16 Apr. 1985 6 p
(AD-D011793; US-Patent-4,511,105; US-Patent-Class-244-135)
Avail: US Patent and Trademark Office CSCL 01/3

An external aircraft fuel tank is provided which comprises a filament-reinforced fuel cell assembled with aerodynamic end shapes having a plurality of layers of adhesive resin-impregnated filament wrappings over the assembly. Also provided is a method for making the fuel tank. Author (GRA)

N86-12226*# Pratt and Whitney Aircraft Group, East Hartford, Conn. Engineering Div.
TURBINE BLADE AND VANE HEAT FLUX SENSOR DEVELOPMENT, PHASE 2 Final Report, Sep. 1982 - Jul. 1985
W. H. Atkinson, M. A. Cyr, and R. R. Strange Oct. 1985 85 p refs
(Contract NAS3-23629)
(NASA-CR-174995; NAS 1.26:174995; PWS-5914-39) Avail: NTIS HC A05/MF A01 CSCL 21E

The development of heat flux sensors for gas turbine blades and vanes and the demonstration of heat transfer measurement methods are reported. The performance of the heat flux sensors was evaluated in a cylinder in cross flow experiment and compared with two other heat flux measurement methods, the slug calorimeter and a dynamic method based on fluctuating gas and surface temperature. Two cylinders, each instrumented with an embedded thermocouple sensor, a Gardon gauge, and a slug calorimeter, were fabricated. Each sensor type was calibrated using a quartz lamp bank facility. The instrumented cylinders were then tested in an atmospheric pressure combustor rig at conditions up to gas stream temperatures of 1700K and velocities to Mach 0.74. The test data are compared to other measurements and analytical prediction. E.A.K.

N86-12227*# National Aeronautics and Space Administration. Lewis Research Center, Cleveland, Ohio.
FLUID MACHINES: EXPANDING THE LIMITS, PAST AND FUTURE
Melvin J. Hartmann and Donald M. Sandercock 1985 46 p refs
Presented at the Winter Ann. Meeting of the Am. Soc. of Mech. Eng., Miami Beach, Fla., 17-22 Nov. 1985
(NASA-TM-87161; E-2793; NAS 1.15:87161) Avail: NTIS HC A03/MF A01 CSCL 21E

During the 40 yr period from 1940 to 1980, the capabilities and operating limits of fluid machines were greatly extended. This was due to a research program, carried out to meet the needs of aerospace programs. Some of the events are reviewed. Overall advancements of all machinery components are discussed followed by a detailed examination of technology advancements in axial compressors and pumps. Future technology needs are suggested. E.A.K.

N86-12228# Department of the Air Force, Washington, D.C.
IMPROVED TEMPERATURE DETECTION SYSTEM FOR USE ON FILM COOLED TURBINE AIRFOILS Patent Application
R. Frederick, inventor (to Air Force) Filed 1 May 1985 13 p
(AD-D011762; US-Patent-Appl-SN-729388) Avail: NTIS
HC A02/MF A01 CSCL 21/5

This patent application discloses an improved temperature detection system for use on film cooled turbine airfoils having a showerhead assembly with a series of parallel slots defined in the leading edge of an airfoil, each slot having a multiplicity of film flow ports exiting therefrom. A plurality of sensor assemblies are affixed to the airfoil showerhead and are couplable via electrodes to electronic sensing equipment for establishing the gas flow temperature. GRA

N86-12229# Air Force Wright Aeronautical Labs., Wright-Patterson AFB, Ohio.
COMPRESSOR RESEARCH FACILITY F100 HIGH PRESSURE COMPRESSOR INLET TOTAL PRESSURE AND SWIRL PROFILE SIMULATION Final Report, Dec. 1980 - Nov. 1983
W. W. Copenhaver Oct. 1984 287 p
(AF Proj. 3066)
(AD-A157108; AFWAL-TR-84-2030) Avail: NTIS
HC A13/MF A01 CSCL 21/5

The F100 gas turbine engine currently powers the Air Force F-15 and F-16 aircraft. The compression section of this engine consists of a three-stage fan followed by a ten-stage High Pressure Compressor (HPC). A component test of the F100 HPC will be performed in the Compressor Research Facility (CRF) of the Aero Propulsion Laboratory (APL) at Wright-Patterson Air Force Base, to investigate its stall and post stall characteristics. This testing will require that the high pressure compressor entrance profiles be simulated to obtain results which correspond to actual engine operation. Since these entrance profiles had never been measured, a program was designed to experimentally measure the total and static pressure, temperature and flow angle profiles at the HPC entrance of an F100 Series 3 engine (F100 (3)), (S/NP072). The measured profile data were then used as design data for a set of inlet screens and vanes. These vanes and screens will simulate the engine fan discharge profiles for the HPC test. The manufactured screens and vanes were tested in Room 24 of Building 18 of the Air Force Wright Aeronautical Laboratories to verify their simulation capabilities. Five separate test periods were necessary to achieve the program goals. These tests are described in Sections 2 thru VI. The program discussion and conclusions are presented in Section 7 and 8. GRA

N86-12230# Battelle Columbus Labs., Ohio.
COMPOSITION AND PHOTOCHEMICAL REACTIVITY OF TURBINE ENGINE EXHAUST Final Report, Mar. 1983 - Sep. 1984
C. W. Spicer, M. W. Holdren, F. F. Lyon, and R. M. Riggin Jun. 1985 52 p
(Contract F08635-82-C-0131)
(AD-A157643; AFESC/ESL-TR-84-61) Avail: NTIS
HC A04/MF A01 CSCL 21/2

This study was carried out to augment the results of an earlier investigation of turbine engine emissions. Experiments were conducted to investigate the photochemical reactivity and biological activity of exhaust from a full-scale 60 deg. sector combustor from a TF-39 turbine engine. All experiments were carried out at idle power setting. The study utilized exhaust from two conventional petroleum fuels (JP-4 and JP-5) and a shale fuel meeting JP-4 specifications. Photochemical reactivity was studied with two large (8 cum 3)n Teflon outdoor environmental chambers. Photochemical reactivity is defined for purposes of this study as the maximum ozone concentration produced during a one day irradiation in natural sunlight. Experiments were undertaken with a TF-39 combustor operating on JP-4 and JP-5 fuels, for comparison with pervious studies of a full-scale TF-39 engine. The combustor exhaust was more effective than exhaust from the full-scale engine, regardless of which fuel was burned. The combustor exhaust was 60 percent more reactive than engine exhaust for JP-5 fuel, and between 30 and 100 percent more reactive for JP-4 fuel. The photochemical reactivity of exhaust generated from a shale oil-derived fuel meeting JP-4 specifications was studied. Exhaust from the shale fuel was no more reactive than exhaust from petroleum fuels, and under some circumstances was actually less reactive. The shale fuel exhaust also generated less secondary aerosol than exhaust from the petroleum fuels. GRA

N86-12231# Naval Weapons Center, China Lake, Calif.
ANALYSIS OF PARTICULATES IN THE EXHAUST PLUME OF A J52-P3 TURBOJET ENGINE AT MILITARY POWER Interim Report, Oct. 1983 - Sep. 1984
J. H. Johnson, E. D. Erickson, and D. J. Knight Mar. 1985 27 p
(AD-A157840; AD-E900455; NWC-TP-6618) Avail: NTIS
HC A03/MF A01 CSCL 21/5

This report presents particulate concentration, emission index, and size distribution data in the exhaust plume of a J52-P3 turbojet engine, run at military power in the open air. Recommendations are listed for future tests. GRA

N86-12232# Department of the Air Force, Washington, D.C.
LENGTH ADJUSTABLE STRUT LINK WITH LOW AERODYNAMIC DRAG Patent Application
D. Nash, inventor (to Air Force) Filed 10 Jul. 1985 25 p
(AD-D011851; US-Patent-Appl-SN-753462) Avail: NTIS
HC A02/MF A01 CSCL 13/5

This patent application discloses a low aerodynamic drag structural link suitable for use within the housing of a turbofan jet engine. The link includes length adjustment capability, pivotal end mounting provision, maintained airstream orientation capability, low mass and jam nut length and orientation locking. Several variations in link construction including a single ball and socket arrangement, varying link cross-section along its longitudinal length and the use of fairing nose and tail inserts are disclosed. GRA

08 AIRCRAFT STABILITY AND CONTROL

Includes aircraft handling qualities; piloting; flight controls; and autopilots.

N86-12233*# Purdue Univ., West Lafayette, Ind. School of Aeronautics and Astronautics.
INTERACTIVE AIRCRAFT FLIGHT CONTROL AND AEROELASTIC STABILIZATION Semiannual Report, 1 May - 31 Oct. 1985
Terrence A. Weisshaar Nov. 1985 48 p refs
(Grant NAG1-157)
(NASA-CR-176323; NAS 1.26:176323) Avail: NTIS
HC A03/MF A01 CSCL 01C

Aeroservoelastic optimization techniques were studied to determine a methodology for maximization of the stable flight envelope of an idealized, actively controlled, flexible airfoil. The equations of motion for the airfoil were developed in state-space form to include time-domain representations of aerodynamic forces and active control. The development of an optimization scheme to stabilize the aeroelastic system over a range of airspeeds, including the design airspeed is outlined. The solution approach was divided in two levels: (1) the airfoil structure, with a design variable represented by the shear center position; and (2) the control system. An objective was stated in mathematical form and a search was conducted with the restriction that each subsystem be constrained to be optimal in some sense. Analytical expressions are developed to compute the changes in the eigenvalues of the closed-loop, actively controlled system. A stability index is constructed to ensure that stability is present at the design speed and at other airspeeds away from the design speed. E.A.K.

N86-12234# Aeronautical Research Labs., Melbourne (Australia).
FLUTTER CLEARANCE TESTS ON A TRANSAVIA PL-12/T-400 SKYFARMER
A. Goldman and S. Galea Mar. 1985 66 p
(AD-A157212; ARL/STRUC-TM-400) Avail: NTIS HC A04/MF A01 CSCL 20/4

The Transavia T-400 Skyfarmer is the latest version of the twin-boom agricultural aircraft and incorporates several changes from the T-300 model previously tested. Changes which could affect the flutter characteristics are: (1) Change of engine from 6 cylinder 300 horsepower to 8 cylinder 400 horsepower; (2) Increase in length of tail booms by 750 mm; (3) Increase in stub-wing span by 900 mm; (4) Removal of the spring-tab from the elevators; and (5) Addition of a dorsal stabilizer fin along each tail boom. A ground resonance test and subsequent flight tests were conducted on a Transavia T-400 Skyfarmer. The natural modes and frequencies of vibration were measured in the ground tests, and monitored during flight tests in which attempts were made to induce flutter. The results of these tests are presented.
GRA

N86-12235# Air Force Wright Aeronautical Labs., Wright-Patterson AFB, Ohio.
POST STALL MANEUVERS AND THRUST VECTORING PERFORMANCE ANALYSIS Final Technical Report, Aug. 1983 - Jul. 1984
L. E. Miller Jul. 1984 77 p
(AF Proj. 2404)
(AD-A158100; AFWAL-TR-84-3109) Avail: NTIS HC A05/MF A01 CSCL 01/2

The purpose of this effort was to determine whether or not there are any apparent performance improvements through post stall maneuvers (PSM) or thrust vectoring. The PSM is a result of high angles of attack, greater than the stall value. Two different problems were addressed. The first examined instantaneous turning performance. The second focused on minimum time turn problems. The impact of both vectored and nonvectored thrust was considered. It was proven that minimum time turns fall in the vertical plane. For maximum instantaneous turning rate and nonvectored thrust high angle of attack results if the speed is less than the critical speed which is approximately Mach 0.2. The optimal angle of attack approaches 90 deg as the speed approaches zero. For vectored thrust, the stall angle of attack is optimum and the thrust vector angle is the complement of the angle of attack. The PSM is not optimal if thrust vectoring is available. For minimum time turning performance, maximum thrust is optimal. At the end of the trajectory, the optimal angle of attack equals that for maximum instantaneous performance. The PSM is optimal. As the thrust to weight ratio increases, the maximum angle of attack increases.
GRA

N86-12236# Air Force Inst. of Tech., Wright-Patterson AFB, Ohio.
AN APPLICATION OF ADAPTIVE LEARNING TO MALFUNCTION RECOVERY M.S. Thesis
R. E. Cruz 1985 51 p
(AD-A158129; AFIT/CI/NR-85-85T) Avail: NTIS HC A04/MF A01 CSCL 01/4

A self-organizing controller was developed for a simplified two-dimensional aircraft model. The controller learns how to pilot the aircraft through a navigational mission without exceeding pre-established position and velocity limits. The controller pilots the aircraft by activating one of eight directional actuators at all times. By continually monitoring the aircraft's position and velocity with respect to the mission, the controller progressively modifies its decision rules to improve the aircraft's performance. When the controller has learned how to pilot the aircraft, two actuators fail permanently. Despite this malfunction, the controller regains proficiency at its original task. The experimental results reported show the controller's capabilities for self-organizing control, learning, and malfunction recovery.
GRA

N86-12405# Joint Publications Research Service, Arlington, Va.
JAPANESE REPORT ON CHINA'S F-8 FIGHTER
Yu Yuebo *In its* China Rept.: Sci. and Technol. (JPRS-CST-85-035) 17 Oct. 1985 p 70-72 Transl. into ENGLISH from Hangkong Zhishi (Beijing), no. 7, Jul. 1985 p 22-23 (For primary document see N86-12399 03-31)
Avail: NTIS HC A08/MF A01

09 RESEARCH AND SUPPORT FACILITIES (AIR)

Includes airports, hangars and runways; aircraft repair and overhaul facilities; wind tunnels; shock tube facilities; and engine test blocks.

For related information see also *14 Ground Support Systems and Facilities (Space).*

N86-12237*# College of William and Mary, Williamsburg, Va. Dept. of Computer Science.
USER'S GUIDE TO STIPPAN: A PANEL METHOD PROGRAM FOR SLOTTED TUNNEL INTERFERENCE PREDICTION Report, 16 Mar. - 15 Jun. 1985
William B. Kemp, Jr. 5 Nov. 1985 33 p refs
(Contract NCC1-69)
(NASA-CR-178003; NAS 1.26:178003) Avail: NTIS HC A03/MF A01 CSCL 14B

Guidelines are presented for use of the computer program STIPPAN to simulate the subsonic flow in a slotted wind tunnel test section with a known model disturbance. Input data requirements are defined in detail and other aspects of the program usage are discussed in more general terms. The program is written for use in a CDC CYBER 200 class vector processing system.
Author

N86-12238*# Vigyan Research Associates, Inc., Hampton, Va. Dept. of Aeronautics and Astronautics.
INTRODUCTION TO CRYOGENIC WIND TUNNELS
Michael J. Goodyer (Southampton Univ.) Sep. 1985 14 p refs
(Contract NAS1-17919)
(NASA-CR-177966; NAS 1.26:177966; AGARD-722-Paper-1) Avail: NTIS HC A02/MF A01 CSCL 14B

The background to the evolution of the cryogenic wind tunnel is outlined, with particular reference to the late 60's/early 70's when efforts were begun to re-equip with larger wind tunnels. The problems of providing full scale Reynolds numbers in transonic testing were proving particularly intractible, when the notion of satisfying the needs with the cryogenic tunnel was proposed, and then adopted. The principles and advantages of the cryogenic tunnel are outlined, along with guidance on the coolant needs when this is liquid nitrogen, and with a note on energy recovery. Operational features of the tunnels are introduced with reference to a small low speed tunnel. Finally the outstanding contributions are highlighted of the 0.3-Meter Transonic Cryogenic Tunnel (TCT) at NASA Langley Research Center, and its personnel, to the furtherance of knowledge and confidence in the concept. Author

N86-12239*# National Aeronautics and Space Administration. Lewis Research Center, Cleveland, Ohio.
WIND TUNNEL TURNING VANES OF MODERN DESIGN
T. F. Gelder, R. D. Moore, J. M. Sanz, and E. R. McFarland [1985] 23 p refs Proposed for presentation at the 24th Aerospace Sci. Meeting, Reno, Nev., 6-8 Jan. 1986; sponsored by AIAA
(NASA-TM-87416; E-2775; NAS 1.15:87416; AIAA-86-0044) Avail: NTIS HC A02/MF A01 CSCL 14B

Rehabilitation of the Altitude Wind Tunnel includes the need for new corner turning vanes to match its upgraded performance. The design and experimental performance results from a 0.1-full scale model of the highest speed corner (M = 0.35) are presented and discussed along with some two dimensional inviscid analyses of two vaned corners. With a vane designed by an inverse two dimensional technique, the overall corner loss was about 12% of the inlet dynamic pressure of which about 4% was caused by vane skin friction. Comparable values with a conventionally designed circular arc vane were about 14% overall with about 7% due to skin friction. E.A.K.

N86-12240*# College of William and Mary, Williamsburg, Va.
WALL-INTERFERENCE ASSESSMENT IN THREE-DIMENSIONAL SLOTTED-WALL WIND TUNNELS Final Technical Report, 16 Jun. 1982 - 15 Oct. 1985
William B. Kemp, Jr. [Oct. 1985] 11 p refs
(NCC1-69)
(NASA-CR-176320; NAS 1.26:176320) Avail: NTIS HC A02/MF A01 CSCL 14B

The development of the slotted tunnel simulator code and lessons learned from its use are summarized. The high order panel method was selected as the basic procedure for aerodynamic computations. The panel singularities are supplemented by line sources to represent discrete wall slots. G.L.C.

N86-12241# Federal Aviation Administration, Washington, D.C. Associate Administrator for Airports.
REPORT OF ACCOMPLISHMENTS UNDER THE AIRPORT IMPROVEMENT PROGRAM Annual Report, period ending 30 Sep. 1984
V. J. Martin 30 Sep. 1984 125 p
(AD-A156834; AD-E301723; FAA-ARP-85-1; FAA-ARP-11; AR-3)
Avail: NTIS HC A06/MF A01 CSCL 01/5

Section 521 of the Airport and Airway Improvement Act of 1982 (Public Law 97-248) requires that the Secretary of Transportation submit an annual report to Congress describing the accomplishments of the airport grant program. This report covers activities for the fiscal year ending September 30, 1984. Author (GRA)

N86-12242# Florida Univ., Gainesville. Dept. of Civil Engineering.
CBR (CALIFORNIA BEARING RATIO) DESIGN OF FLEXIBLE AIRFIELD PAVEMENTS WITH CASE STUDY M.S. Thesis
T. M. Destafney 1985 94 p
(Contract N66314-72-A-3029)
(AD-A158101) Avail: NTIS HC A05/MF A01 CSCL 13/2

It is the purpose of this paper to state the fundamentals involved in the design of flexible airfield pavements utilizing the U.S. Army Corps of Engineers CBR (California Bearing Ratio) design method. This paper also discusses concepts that are considered to be prerequisites to any discussion of the subject, including basic pavement theory, aircraft loading effects, subgrade strength, and aircraft characteristics related to design. The CBR method of design is outlined, and an actual design performed in order to more clearly illustrate this method of designing flexible airfield pavements. GRA

12 ASTRONAUTICS (GENERAL)

For extraterrestrial exploration see *91 Lunar and Planetary Exploration.*

N86-12243*# ECON, Inc., Alexandria, Va.
MARKETING THE USE OF THE SPACE ENVIRONMENT FOR THE PROCESSING OF BIOLOGICAL AND PHARMACEUTICAL MATERIALS Final Report
13 Apr. 1984 162 p refs
(Contract NASw-3339)
(NASA-CR-176334; NAS 1.26:176334; ECON-81-110) Avail: NTIS HC A08/MF A01 CSCL 22A

The perceptions of U.S. biotechnology and pharmaceutical companies concerning the potential use of the space environment for the processing of biological substances was examined. Physical phenomena that may be important in space-base processing of biological materials are identified and discussed in the context of past and current experiment programs. The capabilities of NASA to support future research and development, and to engage in cooperative risk sharing programs with industry are discussed. Meetings were held with several biotechnology and pharmaceutical companies to provide data for an analysis of the attitudes and perceptions of these industries toward the use of the space environment. Recommendations are made for actions that might be taken by NASA to facilitate the marketing of the use of the space environment, and in particular the Space Shuttle, to the biotechnology and pharmaceutical industries. Author

13 ASTRODYNAMICS

Includes powered and free-flight trajectories; and orbit and launching dynamics.

N86-12396# Joint Publications Research Service, Arlington, Va.
MEAN DENSITY SCALE HEIGHTS FROM ANALYSIS OF VARIATION IN PERIGEE HEIGHT OF CHINA'S SECOND SATELLITE
Feng Zhanliang *In its* China Rept.: Sci. and Technol. (JPRS-CST-85-016) 23 May 1985 p 67-72 refs Transl. into ENGLISH from Kongjian Kexue Xuebao (Beijing), v. 4, no. 1, 1984 p 76-81 Original language document was announced in IAA as A86-45634 (For primary document see N86-12393 03-31)
Avail: NTIS HC A08/MF A01

N86-12881*# Texas Univ., Austin. Center for Space Research.
ON THE GEOGRAPHICAL CORRELATION OF ORBIT ERROR Abstract Only
B. D. Tapley and G. W. Rosborough *In* NASA, Washington Geopotential Res. Mission (GRM) Oct. 1985 p 76 (For primary document see N86-12852 03-46)
Avail: NTIS HC A07/MF A01 CSCL 22C

14 GROUND SUPPORT SYSTEMS AND FACILITIES (SPACE)

Includes launch complexes, research and production facilities; ground support equipment, e.g., mobile transporters; and simulators.

For related information see also *09 Research Support Facilities (Air).*

N86-12244# Sandia National Labs., Albuquerque, N. Mex.
RIIM ACCELERATOR BEAM EXPERIMENTS
M. G. Mazarakis, D. L. Smith, R. B. Miller, R. S. Clark, D. E. Hasti, D. L. Johnson, J. W. Poukey, K. R. Prestwich, S. I. Shope, and R. C. Richardson 1985 13 p Presented at the Particle Accelerator Conf., Vancouver, British Columbia, 13 May 1985 Prepared in cooperation with Science Applications International Corp., Albuquerque, N. Mex.
(Contract DE-AC04-76DP-00789)
(DE85-012034; SAND-85-0057C; CONF-850504-38) Avail: NTIS HC A02/MF A01

A pulsed linear accelerator assembly, RIIM 9RADLAC II Module), composed of an injector plus a number of post accelerating gaps was built and successfully operated. The injector and the post accelerating gaps were powered by water trip pulse forming and transmission lines. A high-current, high-voltage, foilless diode injector was used and an annular 40-kA relativistic electron beam was produced and further accelerated through the post accelerating gaps. The final beam energy is close to the sum of injector and gap voltages and equal to 9 MeV. DOE

N86-12245# Sandia National Labs., Albuquerque, N. Mex.
PBFA-2 INSULATOR STACK DESIGN FROM AN ENGINEERING VIEWPOINT
L. O. Seamons 1985 5 p Presented at the 5th IEEE Pulsed Power Conf., Washington, D.C., 10 Jun. 1985
(Contract DE-AC04-76DP-00789)
(DE85-013437; SAND-84-2536C; CONF-850616-36) Avail: NTIS HC A02/MF A01

The mechanical design criteria and design solution for the 3.7 meter diameter PBFA-2 vacuum insulator stack were completed. The most fundamental decision was to design a modular insulator stack interchangeable at both the module level and at the module component level. Furthermore, module physical symmetry was designed into the stack so that adjacent modules can be oriented anode-to-cathode or anode-to-anode without any module disassembly. This feature provides an easy way to reconfigure the accelerator for different voltages at the insulator stack. Dynamic response and structural stability for both static and shock loadings were identified as problem areas which required design solutions. The physical size and quality requirements of the insulator stack components were balanced against available vendor fabrication and production rate capabilities and against available Sandia assembly resources to decide the strategy to use for manufacture. DOE

15 LAUNCH VEHICLES AND SPACE VEHICLES

Includes boosters; manned orbital laboratories; reusable vehicles; and space stations.

No abstracts in this category.

16 SPACE TRANSPORTATION

Includes passenger and cargo space transportation, e.g., shuttle operations; and rescue techniques.

For related information see also *03 Air Transportation and Safety* and *85 Urban Technology and Transportation.*

No abstracts in this category.

17 SPACECRAFT COMMUNICATIONS, COMMAND AND TRACKING

Includes telemetry; space communications networks; astronavigation; and radio blackout.

For related information see also *04 Aircraft Communications and Navigation* and *32 Communications.*

No abstracts in this category.

18 SPACECRAFT DESIGN, TESTING AND PERFORMANCE

Includes spacecraft thermal and environmental control; and attitude control.

For life support systems see *54 Man/System Technology and Life Support.* For related information see also *05 Aircraft Design, Testing and Performance* and *39 Structural Mechanics.*

N86-12246*# National Aeronautics and Space Administration. Lewis Research Center, Cleveland, Ohio.
LIQUID DROPLET RADIATOR PROGRAM AT THE NASA LEWIS RESEARCH CENTER
Alden F. Presler, Carolyn E. Coles, Priscilla S. Diem-Kirsop, and K. Alan White, III [1985] 23 p refs Prepared for presentation at the 4th Thermophys. and Heat Transfer Conf., Boston, 2-4 Jun. 1986; sponsored by AIAA and ASME
(NASA-TM-87139; E-2745; NAS 1.15:87139) Avail: NTIS HC A02/MF A01 CSCL 20D

The NASA Lewis Research Center and the Air Force Rocket Propulsion Laboratory (AFRPL) are jointly engaged in a program for technical assessment of the Liquid Droplet Radiator (LDR) concept as an advanced high performance heat ejection component for future space missions. NASA Lewis has responsibility for the technology needed for the droplet generator, for working fluid qualification, and for investigating the physics of droplets in space; NASA Lewis is also conducting systems/mission analyses for potential LDR applications with candidate space power systems. For the droplet generator technology task, both micro-orifice fabrication techniques and droplet stream formation processes have been experimentally investigated. High quality micro-orifices (to 50 micron diameter) are routinely fabricated with automated equipment. Droplet formation studies have established operating boundaries for the generation of controlled and uniform droplet streams. A test rig is currently being installed for the experimental verification, under simulated space conditions, of droplet radiation heat transfer performance analyses and the determination of the effect radiative emissivity of multiple droplet streams. Initial testing has begun in the NASA Lewis Zero-Gravity Facility for investigating droplet stream behavior in microgravity conditions. This includes the effect of orifice wetting on jet dynamics and droplet formation. Results for both Brayton and Stirling power cycles have identified favorable mass and size comparisons of the LDR with conventional radiator concepts. B.W.

N86-12247# RAND Corp., Santa Monica, Calif.
COMMERCIAL AND MILITARY COMMUNICATION SATELLITE ACQUISITION PRACTICES Interim Report
G. K. Smith, J. P. Stucker, and E. J. Simmons May 1985 131 p
(Contract F49620-82-C-0018)
(AD-A157398; RAND/R-3121-AF) Avail: NTIS HC A07/MF A01 CSCL 15/5

This study tests the contention that the commercial sector consistently manages acquisition programs better than the military, by examining management practices with program outcomes associated with the acquisition of communication satellites by the Air Force and by the International Telecommunications Satellite Organization (INTELSAT). The study finds that the military and commercial programs are organized and managed in much the same way and that both produce well-functioning, useful spacecraft. Several significant differences in management practices and outcomes, however, suggest that the Air Force may be able to improve its acquisition activities. It concludes that, in carefully selected situations, there should be a place for the performance-oriented INTELSAT management practices. Author (GRA)

N86-12248# Aerospace Corp., El Segundo, Calif. Lab. Operations.
THE AEROSPACE SPACECRAFT CHARGING DOCUMENT
A. L. Vampola, P. F. Mizera, H. C. Koons, J. F. Fennell, and D. F. Hall 3 Jun. 1985 52 p
(Contract F04701-83-C-0084)
(AD-A157664; TR-0084A(5940-05)-10; SD-TR-85-26) Avail: NTIS HC A04/MF A01 CSCL 22/1

This document presents basic information on spacecraft charging in the Earth's magnetosphere, documents principal results from the engineering experiments on the USAF P78-2 satellite which was flown as part of the joint USAF-NASA spacecraft charging program (SCATHA), and makes recommendations for methods for alleviating the deleterious effects of spacecraft charging. It is intended as a primer for spacecraft designers and spacecraft program managers. GRA

N86-12249# Los Alamos National Lab., N. Mex.
GROUND-BASED INVESTIGATIONS OF ATOMIC OXYGEN INTERACTIONS WITH SPACE STATION SURFACES
J. B. Cross, D. A. Cremers, and D. F. Tucker 1985 12 p Presented at the AIAA Thermophys. Conf., Williamsburg, Va., 18 Jun. 1985
(Contract W-7405-eng-36)
(DE85-014082; LA-UR-85-2220; CONF-850607-4) Avail: NTIS HC A02/MF A01

Ground-based simulation and testing facilities were developed to investigate atomic oxygen interactions with space station surfaces which include a high kinetic energy O-atom source, a sample exposure chamber and a high sensitivity molecular beam apparatus. The sample exposure chamber is suited for surveying materials for their O-atom reactivity through weight loss measurements. The high sensitivity molecular beam apparatus will be used to determine reaction mechanisms through measurements of reaction product identity, translational and internal state of products, and angular distribution of reaction products. The O-atom source, based on the use of a laser sustained discharge, demonstrated O-atom translational temperatures of 8 to 9000 K and is presently operating with 50% oxygen in argon using 500 watts of CO2 laser power which is expected to produce velocities of 4 to 5 km/s. One hour exposures of kapton, two types of fiber glass epoxy materials, and MgF2 coated optics were accomplished and preliminary results indicate that the coated aluminum optics have very low reaction rates while kapton has the highest rate. DOE

N86-12719# Joint Publications Research Service, Arlington, Va.
LAUNCH OF KOSMOS-1653 NATURAL RESOURCES RESEARCH SATELLITE Abstract Only
In its USSR Rept.: Earth Sci. (JPRS-UES-85-008) 16 Aug. 1985 p 27 Transl. into ENGLISH from Sots. Ind. (Moscow), 24 May 1985 p 2 (For primary document see N86-12697 03-42)
Avail: NTIS HC A04/MF A01

19 SPACECRAFT INSTRUMENTATION

For related information see also *06 Aircraft Instrumentation* and *35 Instrumentation and Photography.*

No abstracts in this category.

20 SPACECRAFT PROPULSION AND POWER

Includes main propulsion systems and components, e.g., rocket engines; and spacecraft auxiliary power sources.

For related information see also *07 Aircraft Propulsion, 28 Propellants and Fuels,* and *44 Energy Production and Conversion.*

N86-12250# Air Force Rocket Propulsion Lab., Edwards AFB, Calif.
EXHAUST PLUME MEASUREMENTS OF 15-POUND BATES (BALLISTIC TEST AND EVALUATION SYSTEM) MOTORS Final Report, Jun. 1980 - Oct. 1984
J. A. Misener, P. A. Kessel, and T. W. Park Jun. 1985 116 p
(AF Proj. 5730)
(AD-A157249; AFRPL-TR-85-013) Avail: NTIS HC A06/MF A01 CSCL 21/9

This is the first AFRPL effort at taking certain rocket diagnosis experiments into the field. The major objectives were: (1) gauging use of laser transmissometer measurements as a plume visibility figure of merit; (2) measuring the ensemble particle size distribution function (PSDF) through application of Mie theory in deconvolving polarization/scattering laser signals from lightly-loaded (and therefore single-scattering) solid rocket motor plumes; (3) retrieving temperature and partial pressure profiles through multispectral infrared emission and absorption measurements; and (4) quantifying exit plan multispectral ultraviolet emission. Success was limited. Laser transmittance as a visibility figure of merit embeds many assumptions and has not been positively correlated with total plume detectability. Nonetheless, different propellants are seen to have characteristic transmittance values and a propellant visibility ranking using this criterion was undertaken using a limited experimental sample. The volume-to-surface effective mean particle diameters through applicable transmissometer/extinction measurements were made rather than PSDFs due to difficulties in size distribution inversion schemes and low experimental signal-to-noise ratios. GRA

23 CHEMISTRY AND MATERIALS (GENERAL)

Includes biochemistry and organic chemistry.

N86-12251# Brookhaven National Lab., Upton, N. Y.
ANAEROBIC MICROBIAL DISSOLUTION OF TOXIC METALS IN SUBSURFACE ENVIRONMENTS
A. J. Francis May 1985 6 p Presented at Anaerobic Biogeochem. Proc. in Subsurface Transportation - An Interactive Seminar, University Park, Pa., 14 May 1985
(DE-AC02-76CH-00016)
(DE85-013308; BNL-36571; CONF-850521-1) Avail: NTIS HC A02/MF A01

Initial laboratory and field studies indicate that under appropriate conditions, trace metal dissolution due to anaerobic microbial action in subsurface environments could be significant. Anaerobic microbial dissolution of trace metals may be from: (1) naturally occurring forms of minerals, (2) modified or altered forms due to energy related activities, or (3) trace metals co-precipitated with iron-oxides. Further research is under way to elucidate the mechanism of anaerobic microbial dissolution of toxic metals and to determine the influence of subsurface environmental variables on microbial transformations of metals and organometallics. DOE

N86-12252# Argonne National Lab., Ill.
ADSORPTION/DESORPTION PROPERTIES OF VACUUM MATERIALS FOR THE 6 GeV SYNCHROTRON
A. R. Krauss 1985 23 p Presented at the Machine Workshop on the 6 GeV Synchrotron Radiation Source, Gaithersburg, Md., 28 Mar. 1985
(Contract W-31-019-eng-38)
(DE85-010276; CONF-8503134-1) Avail: NTIS HC A02/MF A01

Considerable attention must be paid to the vacuum and adsorption/desorption properties of all materials installed inside the vacuum envelope if the design goals of the 6 GeV synchrotron are to be met. Unfortunately, the data is very sparse in several key areas. Additionally, some procedures normally associated with good vacuum practice, such as air braking, may prove to be totally unsuitable on the basis of desorption properties. A brief discussion of the adsorption, outgassing, electron-stimulated desorption (ESD), and photon-stimulated desorption (PSD) properties of vacuum materials as they relate to the design of a 6 GeV synchrotron is presented. DOE

N86-12253# Florida Univ., Gainesville.
METAL DISSOLUTION KINETICS IN ORGANIC SOLVENTS USING ROTATING RING-DISC VOLTAMMETRY Final Report
[1985] 70 p refs
(Contract DE-AS05-81ER-10951)
(DE85-013478; DOE/ER-10951/T1) Avail: NTIS HC A04/MF A01

The effect of a two phase liquid system, composed of geothermal brine and an organic heat transfer fluid, on the stability of materials used in the energy conversion system was investigated. The principle organic liquids used were isobutane and isopentane. The effects of relative fluid velocity on the corrosion behavior of representative construction materials, austenitic stainless steels, nickel, and copper alloy were determined using an autoclave incorporating a rotating ring disc electrode. DOE

24 COMPOSITE MATERIALS

Includes laminates.

N86-12254 Virginia Polytechnic Inst. and State Univ., Blacksburg.
AUTOMATED DESIGN OF COMPOSITE PLATES FOR IMPROVED DAMAGE TOLERANCE Ph.D. Thesis
Zafer Gurdal 1985 165 p
Avail: Univ. Microfilms Order No. DA8511985

An automated procedure for designing minimum-weight composite plates subject to a local damage constraint under tensile and compressive loading has been developed. A strain based criterion was used to obtain fracture toughness of cracked plates under tension. Results of an experimental investigation of the effects of simulated through-the-thickness cracks on the buckling, postbuckling, and failure characteristics of composite flat plates were presented. A model for kinking failure of fibers at the crack tip was developed for compression loadings. A finite element program based on linear elastic fracture mechanics for calculating stress intensity factor (SIF) was incorporated in the design cycle. A general purpose mathematical optimization algorithm was used for the weight minimization. Analytical sensitivity derivatives of the SIF, obtained by employing the adjoint variable technique, were used to enhance the computational efficiency of the procedure. Design results for both unstiffened and stiffened plates are presented. Dissert. Abstr.

N86-12255*# Missouri Univ., Rolla. Dept. of Engineering Mechanics.
MIXED-MODE CYCLIC DEBONDING OF ADHESIVELY BONDED COMPOSITE JOINTS M.S. Thesis
Mohammad Ali Rezaizadeh and Shankar Mall Oct. 1985 59 p refs
(Grant NAG1-425)
(NASA-CR-177991; NAS 1.26:177991) Avail: NTIS HC A04/MF A01 CSCL 11D

A combined experimental-analytical investigation to characterize the cyclic failure mechanism of a simple composite-to-composite bonded joint is conducted. The cracked lap shear (CLS) specimens of graphite/epoxy adherend bonded with EC-3445 adhesive are tested under combined mode 1 and 2 loading. In all specimens tested, fatigue failure occurs in the form of cyclic debonding. The cyclic debond growth rates are measured. The finite element analysis is employed to compute the mode 1, mode 2, and total strain energy release rates (i.e., GI, GII, and GT). A wide range of mixed-mode loading, i.e., GI/GII ranging from 0.03 to 0.38, is obtained. The total strain energy release rate, G sub T, appeared to be the driving parameter for cyclic debonding in the tested composite bonded system. Author

N86-12256*# National Aeronautics and Space Administration. Lewis Research Center, Cleveland, Ohio.
THE 371 DEG C MECHANICAL PROPERTIES OF GRAPHITE/POLYIMIDE COMPOSITES
Peter Delvigs [1985] 14 p refs Presented at the 2nd Intern. Conf. on Polyimides, Ellenville, N.Y., 30 Oct. - 1 Nov. 1985; sponsored by the Society of Plastics Engineers, Inc.
(NASA-TM-87122; E-2730; NAS 1.15:87122) Avail: NTIS HC A02/MF A01 CSCL 11D

A series of condensation polyimides based on pyromellitic dianhydride is synthesized and evaluated for potential application at 371 C. Several three-and four-ring benzenoid diamine systems containing oxygen bridging groups are investigated. Thermomechanical analysis of neat resin specimens indicate that the polyimide prepared from the dimethyl ester of pyrometallitic acid (PMDE) and 2,2-bis[4-(4'-aminophenoxy) phenyl]-1,1,1,3,3,3-hexafluoropropane (BDAF) is the only resin system which has a glass transition temperature (Tg) above 371 C. The Tg of the PMDE/BDAF polyimide is found to be 390 C after a postcure air at 371 C for 24 hr. Unidirectional composites are fabricated from the PMDE/BDAF system and unsized Celion 6000 graphite fibers. Final cure temperatures in the range of 371 to 427 C with an applied pressure of 10.34 to 13.78 MPa are investigated. The void content of the composites ranges from 4.6 to 8.6 percent. Composites cured at 399 C under a pressure of 10.34 MPa and postcured in air at 371 C for 24 hr exhibit the highest 371 C interlaminar shear strength (ILSS, 40.7 MPa) and flexural strength (758 MPa). The thermo-oxidative stability of the composites is determined by subjecting specimens to isothermal exposure at 371 C in air at atmospheric pressure, as well as a pressure of 0.52 MPa. Specimens exposed at atmospheric pressure exhibit a weight loss of 12 percent after 200 hr of exposure and 88 percent retention of its original 371 C ILSS. In contrast, the specimens exposed at 0.52 MPa pressure exhibit a comparable weight loss after only 72 hr, and a 71 percent retention of its original 371 C ILSS. Author

N86-12257*# Virginia Polytechnic Inst. and State Univ., Blacksburg. Dept. of Chemistry.
FRACTURE SURFACE ANALYSIS IN COMPOSITE AND TITANIUM BONDING
T. A. DeVilbiss and J. P. Wightman Sep. 1985 39 p refs
(Grant NAG1-343)
(NASA-CR-176309; NAS 1.26:176309) Avail: NTIS HC A03/MF A01 CSCL 11D

To understand the mechanical properties of fiber-reinforced composite materials, it is necessary to understand the mechanical properties of the matrix materials and of the reinforcing fibers. Another factor that can affect the mechanical properties of a composite material is the interaction between the fiber and the matrix. In general, composites with strong fiber matrix bonding will give higher modulus, lower toughness composites. Composites with weak bonding will have a lower modulus and more ductility. The situation becomes a bit more complex when all possibilities are examined. To be considered are the following: the properties of the surface layer on the fiber, the interactive forces between polymer and matrix, the surface roughness and porosity of the fiber, and the morphology of the matrix polymer at the fiber surface. In practice, the surface of the fibers is treated to enhance the mechanical properties of a composite. These treatments include anodization, acid etching, high temperature oxidation, and plasma oxidation, to name a few. The goal is to be able to predict the surface properties of carbon fibers treated in various ways, and then to relate surface properties to fiber matrix bonding. author

N86-12258*# Wyoming Univ., Laramie. Composite Materials Research Group.
IOSIPESCU SHEAR PROPERTIES OF GRAPHITE FABRIC/EPOXY COMPOSITE LAMINATES Final Technical Report, May 1984 - May 1985
David E. Walrath and Donald F. Adams Jun. 1985 130 p refs
(Grant NAG1-272)
(NASA-CR-176316; NAS 1.26:176316; UWME-DR-501-103-1)
Avail: NTIS HC A07/MF A01 CSCL 11D

The Iosipescu shear test method is used to measure the in-plane and interlaminar shear properties of four T300 graphite fabric/934 epoxy composite materials. Different weave geometries tested include an Oxford weave, a 5-harness satin weave, an 8-harness satin weave, and a plain weave with auxiliary warp yarns. Both orthogonal and quasi-isotropic layup laminates were tested. In-plane and interlaminar shear properties are obtained for laminates of all four fabric types. Overall, little difference in shear properties attributable to the fabric weave pattern is observed. The auxiliary warp material is significantly weaker and less stiff in interlaminar shear parallel to its fill direction. A conventional strain gage extensometer is modified to measure shear strains for use with the Iosipescu shear test. While preliminary results are encouraging, several design iterations failed to produce a reliable shear transducer prototype. Strain gages are still the most reliable shear strain transducers for use with this test method. Author

N86-12259*# National Aeronautics and Space Administration. Langley Research Center, Hampton, Va.
EFFECT OF MEASURED MATERIAL PROPERTIES ON THE FINITE ELEMENT ANALYSIS OF AN OH-58 COMPOSITE TAIL

BOOM
Lynn M. Bowman Oct. 1985 28 p refs
(DA Proj. 1L1-61102-AH-45)
(NASA-TM-86430; L-15969; NAS 1.15:86430;
AVSCOM-TR-85-B-5) Avail: NTIS HC A03/MF A01 CSCL 11D

A static and dynamic finite element analysis is conducted on a U.S. Army OH-58 composite tail boom and compared with test data. The tail boom is a filament-wound graphite/epoxy monocoque structure. The structural design of the composite tail boom skin is based on 50-percent graphite fiber volume. However, material tests on representative samples of the tail boom skin reveal that the graphite fiber-volume fraction varied from 44.6 to 49.3 percent. To determine the effect of using measured material properties, static and dynamic finite element analyses are conducted for three fiber-volume conditions of 45, 48, and 50 percent. The static and dynamic model with the 45-percent fiber-volume graphite skins gives the closest agreement with test data. Author

N86-12260# Army Materials and Mechanics Research Center, Watertown, Mass.
MATERIALS AND PROCESS CHARACTERIZATION TO DETERMINE THE EFFECT OF HIGH INTENSITY INFRARED LASER RADIATION ON A COMPOSITE MATERIAL
J. S. Perkins, P. W. Wong, D. J. Jaklitsch, L. Elandjian, and A. F. Connolly Mar. 1985 24 p
(DA Proj. 1L1-62105-AH-84)
(AD-A157094; AMMRC-TR-85-3) Avail: NTIS HC A02/MF A01
CSCL 11/4

Measurements were made of the true (black body) surface temperature of a well-characterized metal-doped carbon-carbon composite during irradiation with an intense, continuous-wave, CO2-laser beam along with spectrometric determination of the temporal variation of C2 and C3 species appearing in the laser-induced plume in a high vacuum environment. Various analytical methods used for post-burn analyses, during irradiation analyses, and material characterization are detailed. Thermodynamic aspects are considered. A synopsis of the stages in laser/beam/composite interaction derived from this study is included. GRA

N86-12261# Massachusetts Inst. of Tech., Cambridge. Materials Processing Center.
MICROSTRUCTURE/PROPERTY RELATIONSHIPS FOR CARBON FIBER REINFORCED ALUMINUM ALLOYS Final Technical Report
R. G. Dixon, J. A. Cornie, and M. C. Flemings 1984 109 p
(Contract N00017-83-K-0677)
(AD-A157858) Avail: NTIS HC A06/MF A01 CSCL 11/4

Graphite fibers with various coatings tested for strength. Longitudinal composites were produced from the coated fibers using pure aluminum as the matrix by pressure casting. The strength and microstructure of the composites was evaluated. Longitudinal and transverse composites were also produced using uncoated graphite fibers with various alloy matrices and their strength and microstructure evaluated. The coated fibers were leached from the pure aluminum matrix and examined. The uncoated graphite fibers were leached from the alloy matrices and tested for strength. The coated fibers were not found to be stronger that the uncoated fibers, nor were they effective in increasing composite strengths. Composites produced from uncoated fibers and alloy matrices were quite strong longitudinally with strengths of up to 93 percent of rule of mixtures strength. The same material, when tested in the transverse direction exhibited low strengths, with the failure being interfacial. GRA

N86-12262# Institute for Defense Analyses, Alexandria, Va.
MINUTES OF WORKSHOP ON COMPOSITE MATERIALS TEST METHODS Final Report
S. L. Channon Apr. 1985 156 p Workshop held at Alexandria, Va., 27 Feb. 1985
(Contract MDA903-84-C-0031)
(AD-A157903; AD-E500722; IDA-M-81; IDA/HQ-85-29831) Avail: NTIS HC A08/MF A01 CSCL 11/4

The advanced composite materials community has recognized the need for standardization of test methods as the most important step in improving the acceptance of composite materials, in providing a reliable data base and in qualifying new materials. A survey of advanced composites suppliers and end users showed a strong interest in developing standardized test methods, the greatest need being for shear and compression testing as well as standardized methods for test specimen preparation. A test program was formulated which is aimed at screening available methods in these areas on several types of materials, determining the repeatability of selected test methods by testing at a large number of laboratories, followed by analyses of the data. In addition, provision is made for the development of improved test methods and subsequent evaluation of these methods. The first phase of the program was estimated to cost $2.5 million and would require 2.5 years for completion. GRA

N86-12263# Lawrence Livermore National Lab., Calif.
MACROSCOPIC AND MICROSCOPIC DEFORMATION AND FAILURE PROCESSES THAT CONTROL COMPOSITE TOUGHNESS
R. J. Morgan and C. O. Pruneda 12 Feb. 1985 21 p Presented at the ASTM Symp. on Toughened Composites, Houston, Tex., 13 Mar. 1985
(Contract W-7405-eng-48)
(DE85-012938; UCRL-91366; CONF-8503142-1) Avail: NTIS HC A02/MF A01

Stress optical microscopy and fracture topography studies of a variety of fibrous composites are presented and discussed in terms of the composite macroscopic and microscopic deformation and failure processes. Composite toughening mechanisms associated with the fiber failure processes and fiber matrix interfacial strength are discussed. Molecular flow in the composite matrix, which enhances composite toughness, occurs either in the form of macroscopic homogeneous plastic flow or inhomogeneously in the form of crazing or shear banding. The physical parameters that control the toughening mechanisms in epoxy, thermoplastic and polyimide composite matrices are discussed. Effects of service environment exposure on the elimination of these toughening mechanisms which results in composite embrittlement are also considered. DOE

N86-12264# Tennessee Univ., Knoxville. Dept. of Materials Science and Engineering.
DYNAMIC SMALL ANGLE X-RAY SCATTERING STUDY OF STRESSED KEVLAR 49 EPOXY COMPOSITES
J. S. Lee, J. F. Fellers, M. Y. Tang, and J. S. Lin 1985 9 p Presented at the Soc. of Plastics Eng. Meeting, Washington, D.C., 29 Apr. 1985 Prepared in cooperation with ORNL
(Contract DE-AC05-84OR-21400)
(DE85-011408; CONF-8504143-1) Avail: NTIS HC A02/MF A01

The highly crosslinked epoxy resins gave rise to isotropic scattering patterns and applying tensile stresses resulted in very little scattering changes. The dynamic scattering studies on the epoxy resins indicate the failure process as a catastrophic dynamic process with fractures initiating from surface or internal flaws. The crack propagates across the whole sample in a very short time to complete failure. The Kevlar fibers are microporous giving rise to equatorially elongated anisotropic scattering patterns. These microvoids can be partially filled by liquid epoxy. Based on comparisons of the volume fraction of the microvoids obtained by SAXS absolute intensity measurements and by the density measurements, two sizes of microvoids are present in the Kevlar 49 fibers - one in the range of 10 to 20 nm and the other much larger. Applying tensile stresses results in an increase in the scattering intensities and in the volume fraction of smaller microvoids. The average radius of gyration of these microvoids remained constant, and hence the number of these smaller microvoids must have increased in order to account for increased scattering intensities. It is thus concluded that the failure of Kevlar 49 fibers is accompanied by the increase in number of smaller microvoids and the enlargement of the larger microvoids along the fiber axis direction. The reinforced epoxy composites of low volume fraction unidirectional Kevlar 49 fiber gave rise to anisotropic scattering patterns perpendicular to the fiber axis direction, and it is believed this scattering is due to voids within the fibers and voids entrapped along the fiber matrix interface during processing. DOE

N86-12265# Du Pont de Nemours (E. I.) and Co., Aiken, S.C.
U308 POWDER FROM URANYL-LOADED CATION EXCHANGE RESIN
W. C. Mosley 1985 29 p refs Presented at the Am. Ceram. Soc. Ann. Meeting, Cincinnati, 5 May 1985
(Contract DE-AC09076SR-00001)
(DE85-013231; DP-MS-84-126; CONF-850536-5) Avail: NTIS HC A03/MF A01

U308 powder has been produced from uranyl-loaded cation exchange resin with density, particle size distribution, and grain size suitable for powder metallurgy fabrication of reactor fuel tubes with Al-U308 cores. Macroporous sulfonate resin in granular form is used in the process. Resin conversion techniques that were evaluated include batch, rotary, and fluidized bed calcination. DOE

25 INORGANIC AND PHYSICAL CHEMISTRY

Includes chemical analysis, e.g., chromatography; combustion theory; electrochemistry; and photochemistry.

For related information see also *77 Thermodynamics and Statistical Physics.*

N86-12266 Michigan Univ., Ann Arbor.
GROUP COMBUSTION OF SPRAYS Ph.D. Thesis
Sampathkumar Palaniswamy 1985 174 p
Avail: Univ. Microfilms Order No. DA8512483

In the group combustion limit, fuel sprays evaporate and burn as a group and not as individual droplets. Only the outermost droplets in the cloud evaporate, and conditions within within the cloud remain uniform during most part of the cloud life time. The burning charcteristics of a cloud undergoing group combustion is studied using activation energy asymptotics. The relationship between the ambient temperature and the gas-phase Damkohler number is obtained for ignition and extinction of the fuel cloud. It is found that larger fuel clouds ignite at lower ambient temperature than the smaller clouds and, therefore, a single drop as well. The effect of drop-size distribution is analyzed using a phenomenological model. It is found that for a simple bimodel dropsize distribution the burning characteristics of the cloud do not change.
Dissert. Abstr.

N86-12267 Department of the Navy, Washington, D. C.
PICOSECOND BROADBAND CARS PROBE USING THE PICOSECOND CONTINUUM Patent
L. S. Goldberg, inventor (to Navy) Issued 23 Apr. 1985 8 p
Supersedes AD-D010311
(AD-D011840; US-Patent-4,512,660; US-Patent-Appl-SN-484810; US-Patent-Class-356-301) Avail: US Patent and Trademark Office CSCL 07/4

A coherent anti-Stokes Raman spectroscopy (CARS) method and apparatus for producing a broadband CARS vibrational spectrum of a sample in a single picosecond laser pulse is discussed. A laser pulse having a picosecond duration and a frequency of omega is directed into a liquid cell containing D_2O which generates a picosecond continuum pulse having a broad range of frequencies omega (WL) and a picosecond duration. A second harmonic of the laser pulse is produced to form a probe pulse having a frequency of omega (1) and a picosecond duration. The probe pulse and the continuum pulse are spatially and temporally combined and the combined pulses are directed into a sample to excite the Raman active vibrational resonances in the sample. In response the sample emits a beam of radiation which contains an anti-Stokes spectrum of energy characteristic of the sample. The anti-Stokes spectrum is separated from the beam of radiation for detection and analysis. GRA

N86-12268*# National Aeronautics and Space Administration. Lewis Research Center, Cleveland, Ohio.
EVALUATION PARAMETERS FOR THE ALKALINE FUEL CELL OXYGEN ELECTRODE
Joseph Singer and Vakula Srinivasan (Bowling Green State Univ., Ohio) Nov. 1985 13 p refs
(NASA-TM-87155; E-2669; NAS 1.15:87155) Avail: NTIS HC A02/MF A01 CSCL 07D

Studies were made of Pt- and Au-catalyzed porous electrodes, designed for the cathode of the alkaline H_2/O_2 fuel cell, employing cyclic voltammetry and the floating half-cell method. The purpose was to obtain parameters from the cyclic voltammograms which could predict performance in the fuel cell. It was found that a satisfactory relationship between these two types of measurement could not be established; however, useful observations were made of relative performance of several types of carbon used as supports for noble metal catalysts and of some Au catalysts. The best half-cell performance with H_2/O_2 in a 35 percent KOH electrolyte at 80 C was given by unsupported fine particle Au on Teflon; this electrode is used in the Orbiter fuel cell. Author

N86-12269# Air Force Systems Command, Wright-Patterson AFB, Ohio.
KINETICS OF EVAPORATION AND GROWTH OF DROPS OF AQUEOUS SOLUTIONS OF SURFACE ACTIVE SUBSTANCES AT NEGATIVE TEMPERATURES
Y. I. Sokolov 25 Jun. 1985 11 p refs Transl. into ENGLISH from Fiz. Aerodispersnkyk Sistem (USSR), no. 7, 1972 p 20-25
(AD-A156961; FTD-ID(RS)T-0938-84) Avail: NTIS HC A02/MF A01 CSCL 07/4

It is established that surface active substances (SAS), both soluble and insoluble, substantially slow the rate of evaporation of water drops. In the case of insoluble SAS the slowing of evaporation comes down to the creation of a mechanical barrier by SAS molecules, preventing the outlet of water molecules from the surface of the drop. A formula is theoretically obtained, expressing the rate of quasistationary evaporation of a drop of water covered with a layer of insoluble SAS. GRA

N86-12270# North Carolina Univ., Raleigh. Dept. of Chemistry.
CHARGE TRANSFER IN MULTIPLE SITE CHEMICAL SYSTEMS Final Report, Apr. 1982 - Apr. 1985
T. J. Meyer 30 May 1985 18 p
(Contract DAAG29-82-K-0111)
(AD-A157413; ARO-19011.1-CH) Avail: NTIS HC A02/MF A01 CSCL 07/4

This report covers work done by the author in both mixed-valence dimers and metallopolymers. Concerning the dimers, crystal structures of related monomers were obtained to judge the adequacy of classical approximations in calculating inner-sphere vibrational trapping. A series of homometallic and heterometallic dimers were prepared and a relationship between redox asymmetry and intervalence transfer absorption band energy was found. Electronic structure was observed in the intervalence transfer absorption band of an OS(II)-Os(III) mixed-valence dimer, owing to the presence of well-separated spin orbit states in Os(III). Other dimers were prepared to study the transitions between various states within the dimers. Both metal to metal and ligand to ligand electron transfer was seen in optically prepared mixed-valence dimers. Concerning the polymers, redox-site incorporation into poly-vinylpyridine, P-chlorosulfonated polystyrene and oxidatively electro-polymerized films were studied. Characterization and stability of these films as well as comparison to monomeric analogues was accomplished. Practical application of the metallopolymers include their use as a chromophore in a photoelectrochemical cell and as a catalyst for the oxidation of C1- to C12.
GRA

N86-12271# Air Force Systems Command, Wright-Patterson AFB, Ohio. Foreign Technology Div.

EXPERIMENTAL STUDY OF THE COMBUSTION OF GAS-AIR MIXTURES IN A CHANNEL AND THE DIFFUSION COMBUSTION IN A SLIPSTREAM AT HIGH VELOCITIES
V. K. Bayev, P. K. Tretyakov, and V. A. Yasakov 16 Jul. 1985 49 p Transl. into ENGLISH from mono. "Sovremennoye Sostoyaniye i Teoriya Sgoraniya Kondensirovannykh Sistem" Moscow, 1972 p 357-360, 386-391, 416-420, 421-425
(AD-A157495; FTD-ID(RS)T-1323-84) Avail: NTIS HC A03/MF A01 CSCL 21/2

This translation contains three additional papers by other authors. Their titles are: Ignition and Interruption of Combustion in the Stagnation Zone During Flow Around a Flatstep or Indentation by a Supersonic Flow of Combustible Mixture; Combustion of Rich Kerosine-Air Mixture in Tunnel Type Chamber; and Mechanism of the Process of Combustion After the Front Devices and in the Zone of the Inflow of the Jets of Secondary Air in the Chambers of Gas-Turbine Engine. GRA

N86-12272# Arnold Engineering Development Center, Arnold Air Force Station, Tenn.
METHOD TO DETECT ETHYLENE GLYCOL IN GASEOUS MIXTURES Final Report, 1 Oct. 1982 - 30 Sep. 1983
R. E. Willis Aug. 1985 53 p Prepared in cooperation with Sverdrup Technology, Inc., Arnold AFS, TN
(AD-A158109; AEDC-TR-85-39) Avail: NTIS HC A04/MF A01 CSCL 07/4

Ethylene glycol is used as a refrigerant for the intake air during simulated altitude testing. There have been some problems during these tests because of the ethylene glycol accidentally leaking into the inlet airstream. Since ethylene glycol has at times been suspected of interfering with the test article, its early detection would be greatly beneficial so that testing could be stopped before damage occurs. Because a detection scheme must indicate the presence of ethylene glycol as soon as it appears in the inlet airstream, a spectroscopic technique is preferred over other methods of gas analysis such as sampling and subsequent laboratory analysis. A study was conducted to determine if microwave spectroscopy techniques could be used to monitor the level of ethylene glycol in the inlet airstream to the Engine Test Facility (ETF) test cells during simulated altitude testing. The theory of microwave spectroscopy and the spectra of ethylene glycol are reviewed. Three separate designs of microwave spectrometers are presented which should be capable of monitoring ethylene glycol in the inlet airstreams with a sensitivity of at least 10 ppm. GRA

N86-12273# California Univ., Los Angeles. Dept. of Materials Sciences and Engineering.
PREPARATION AND PROPERTIES OF THIN FILM REVERSIBLE CATHODE MATERIALS Final Report, 1 Jun. 1982 - 31 May 1985
B. Dunn and R. F. Bunshah Jul. 1985 28 p
(Contract DAAG29-82-K-0145)
(AD-A158431; ARO-19267.3-CH) Avail: NTIS HC A03/MF A01 CSCL 09/1

The research program clearly established that a reversible cathode material with a highly anisotropic structure could be prepared as a thin film, 2 to 5 micrometers thick. The research emphasized the synthesis of TiS2 by the evaporation of titanium in a plasma-enhanced H2S gas. Nearly-stoichiometric films of TiS2 were produced. The electrical conductivity and certain electrochemical properties of the films were comparable to the bulk material. Lithium diffusion coefficients were found to be lower than the bulk material and dependent upon film composition. GRA

N86-12274# Johns Hopkins Univ., Baltimore, Md. Dept. of Chemical Engineering.
THERMODYNAMICS OF MULTI-POLAR MOLECULES: THE PERTURBED-ANISOTROPIC-CHAIN THEORY
P. Vimalchand, M. D. Donohue, and I. C. Celmins 1985 43 p refs Presented at the 189th Natl. Meeting of the Am. Chem. Soc., Miami, Fla., 28 Apr. 1985
(Contract DE-AC02-81ER-10982)
(DE85-013148; DOE/ER-10982/5; CONF-850417-22) Avail: NTIS HC A03/MF A01

The Perturbed-Hard-Chain Theory (PHCT) is modified to treat rigorously dipolar and quadrupolar fluids and their mixtures. The multi-polar interactions, expansion of Gubbins and Twu to chain molecules. Moreover, the square-well potential used to characterize the spherically symmetric interactions in the PHCT has been replaced by a soft-core (Leonard-Jones) potential. Theoretical calculations and data reduction on a number of pure fluids and mixtures indicate that the above changes result in physically more meaningful pure component parameters, and the properties of even highly non-ideal mixtures can be predicted accurately without the use of a binary interaction parameter. DOE

N86-12275# Argonne National Lab., Ill.
ELECTROCHEMICAL DEPOSITION OF GLASSY CHROMIUM ON COPPER
R. Varma, A. McKiernan, and M. J. Klugh 1985 2 p Presented at the 167th Electrochem. Soc. Meeting, Toronto, 12 May 1985
(Contract W-31-109-eng-38)
(DE85-004081; CONF-850542-1) Avail: NTIS HC A02/MF A01

Electrochemical deposition of chromium at 1.0 to 5.0 A/cu(2) from aqueous electrolytes has been investigated. Results of X-ray diffraction and scanning electron microscopy of the film deposits are presented. Also, measurements of the corrosion of such coatings in a saline environment are discussed. DOE

N86-12276# Texas Southern Univ., Houston. Dept. of Chemistry.
STUDY OF SOME TRANSITION METAL COMPLEXES AS PROCESS CATALYSTS Quarterly Report, 1 Mar. - 31 May 1985
B. L. Wilson 1985 11 p
(Contract DE-FG22-84PC-70753)
(DE85-013428; DOE/PC-70753/T3) Avail: NTIS HC A02/MF A01

The main objectives of this project are the following: (1) preparation and characterization of transition metal complexes with nitrogen, oxygen and sulfur donor ligands especially the poly(pyrazolyl)borate ligands; (2) preparation of bimetallic complexes of molybdenum and other metals such as nickel, cobalt, and iron; (3) determination of the ability of the above complexes to catalytically reduce polycyclic aromatic or heterocyclic compounds; (4) evaluation of these complexes as coal liquefaction catalysts; (5) evaluation of these complexes as desulfurization and denitrogenation catalysts; (6) training of students in transition metal complex preparation and characterization and in the evaluation of metal complexes as process catalysts. During this quarter the following complexes were prepared and characterized: Fe(H2B(P2)2)2, where P2 = C3H3N2; TiX2(H2B(P2)2)2, where x = Cl, Br, or I; Ti(H2B(P2)2)4; and Ni(H2B(P2)2)2. The following 2 complexes were tested for hyrogenation activities using 1-methylnaphthalene: Co(H2B(P2)2)2; and Zn(H2B(P2)2)2. DOE

N86-12277# Department of Energy, Washington, D. C.
THERMOPHORETIC SEPARATION OF AEROSOL PARTICLES FROM A SAMPLED GAS STREAM Patent Application
A. K. Postma, inventor (to DOE) (Hanford Engineering Development Lab.) Filed 7 Sep. 1984 10 p
(Contract DE-AC06-76FF-02170)
(DE85-011672; US-Patent-Appl-SN-648197) Avail: NTIS HC A02/MF A01

This disclosure relates to separation of aerosol particles from gas samples withdrawn from within a contained atmosphere, such as containment vessels for nuclear reactors or other process equipment where remote gaseous sampling is required. It is specifically directed to separation of dense aerosols including particles of any size and at high mass loadings and high corrosivity. The United States Government has rights in this invention pursuant to Contract DE-AC06-76FF-02170 between the US Department of Energy and Westinghouse Electric Corporation. DOE

N86-12278# Massachusetts Inst. of Tech., Cambridge.
FISCHER-TROPSCH SYNTHESIS IN SLURRY REACTOR

SYSTEMS Final Report
22 Apr. 1985 7 p
(Contract DE-FG22-81PC-40771)
(DE85-013390; DOE/PC-40771/T4) Avail: NTIS HC A02/MF A01

The purpose of this grant was to support a variety of studies of Fischer-Tropsch synthesis in a slurry reactor. Experimental reaction studies were performed in a semicontinuous mechanically stirred autoclave using iron catalysts, primarily a reduced fused magnetite catalyst promoted with potassium, as manufactured for ammonia synthesis. Our findings have been published in 14 papers with 3 more accepted and in press. These are listed together with the abstracts, which highlight our accomplishments. DOE

N86-12279# Boston Univ., Mass. Dept. of Chemistry.
FORMATION OF FUEL VIA PHOTOCHEMICAL ELECTRON TRANSFER Annual Report
G. Jones 4 Mar. 1985 5 p
(Contract DE-AC02-77ER-04380)
(DE85-011168; DOE/ER-04380/T2) Avail: NTIS HC A02/MF A01

Accomplishments for the past year are reported under the following three main headings, in addition to several other related studies: (1) heterocyclic sulfur compounds which display unusual poperties as electron relays which may be important in chemical or fuel forming reactions; (2) cationic dyes which tend to aggregate in interesting ways when bound to polyanion in water; and (3) photochemistry of viologen or pyridinium ions which are complexed or ion-paired with electron donors. A publications update is appended with references cited in this report. DOE

N86-12280# California Univ., Berkeley.
RAMAN SPECTROSCOPY OF MOLECULAR ADSORBATES Final Report
J. Hemminger 13 May 1985 16 p
(Contract DE-AT03-81ER-10820)
(DE85-012981; DOE/ER-10820/T1) Avail: NTIS HC A02/MF A01

Inelastic light scattering probes are used in conjunction with the standard electron beam probes to study the binding and structure of molecular adsorbates on well-characterized metal surfaces. The ultimate objective is to probe the details of corrosion and catalysis on metal surfaces, and the chemistry of molecular adsorbates. Inelastic light scattering spectroscopy has two outstanding advantages over various electron spectroscopic techniques: the first is that light scattering can operate in the presence of a high pressure of gases and even liquids, and the second advantage is its high resolution. Thus by inelastic light scattering spectroscopy we will be able to investigate the interaction of molecules with metal surfaces under realistic pressures for corrosion and chemistry. DOE

N86-12281# IIT Research Inst., Bartlesville, Okla. National Inst. for Petroleum and Energy Research.
LIQUID CHROMATOGRAPHY ON SILICA USING MOBILE PHASES CONTAINING TETRAALKYLAMMONIUM HYDROXIDES. 1: GENERAL SEPARATION SELECTIVITY AND BEHAVIOR OF POLAR COMPOUNDS TYPICALLY IN FUELS
J. B. Green Jun. 1985 44 p refs
(Contract DE-FC03-83FE-60149)
(DE85-014450; NIPER-75) Avail: NTIS HC A03/MF A01

The known selectivity of base-modified silicas for acidic solutes led to development of the in-situ tetraalkylammonium hydroxide (TAAH)-modified silica HPLC systems described here. These systems are generated by adding small concentrations of TAAH to normal phase eluents pumped through conventional silica columns. The in-situ approach has the following advantages: the type and concentration of TAAH can be varied to control separation behavior and selectivity; greater column-to-column consistency and separation reproducibility is achieved; commercially available columns and packings are used; and the TAAH in the mobile phase also serves as an electrolyte for electrochemical detection of solutes, if desired. Retention of 180 solutes spanning several classes of compounds is measured in four different systems; the applicability of this approach to separation of acid concentrates from fuels as well as its compatibility with electrochemical detectors is demonstrated; and in addition, general chromatographic parameters such as the effect of the mobile phase composition on retention and selectivity are discussed. DOE

N86-12282# California Univ., Berkeley. Lawrence Berkeley Lab.
NANOSECOND FLUORESCENCE SPECTROSCOPY
B. Ieskovar Mar. 1985 12 p refs Presented at IEEE Symp., San Francisco, 23 Oct. 1985
(Contract DE-AC03-76SF-00098)
(DE85-012234; LBL-19291; CONF-851097-1) Avail: NTIS HC A02/MF A01

This article is a summary of a short course lecture given in conjunction with the 1984 Nuclear Science Symposium. Measuring systems for nanosecond fluorescence spectroscopy using single photon counting techniques are presented. These involve systems based on relaxation type spark gas light pulsar and synchronously pumped mode locked dye lasers. Furthermore, typical characteristics and optimization of operating conditions of the critical components responsible for the system time resolution are discussed. A short comparison of the most important deconvolution methods for numerical analysis of experimental data is given particularly with respect to the signal to noise ratio of the fluorescence signal. DOE

N86-12283# Purdue Univ., West Lafayette, Ind. Dept. of Chemistry.
MEASUREMENT OF SPECIES CONCENTRATIONS IN FLAMES BY LASER-INDUCED FLUORESCENCE Final Report
N. M. Laurendeau and F. E. Lytle Mar. 1985 57 p refs
(Contract DE-AC02-78ER-04939)
(DE85-012092; DOE/ER-04939/T2; COO-4939) Avail: NTIS HC A04/MF A01

We are currently developing laser-induced fluorescence techniques for determining the concentrations of selected species in flames. Research proposed herein involves (1) continued application of laser-saturated fluorescence to the diatomic radicals CN, CH and NO; (2) continued development of two-photon-induced fluorescence for atomic hydrogen and atomic oxygen; and (3) continued development of single-photon fluorescence for mixtures of polycyclic aromatic hydrocarbons (PAH's). New research is proposed on: (1) application of two-photon fluorescence to diatomic species such as NO; (2) development of two-photon fluorescence for mixtures of polycyclic aromatic hydrocarbons; and (3) extension of laser-saturated fluorescence to linear and nonlinear polyatomics. DOE

N86-12284# Los Alamos Scientific Lab., N. Mex.
OXIDATION OF HETEROCYCLIC NITROGEN YIELDS TO NITROHETEROCYCLES
M. D. Coburn 1985 8 p refs Presented at the Working Group Meeting on Synthesis of High Energy Mater., Dover, N.J., 4 Jun. 1985
(Contract W-7405-eng-36)
(DE85-012757; LA-UR-85-1935; CONF-8506119-1) Avail: NTIS HC A02/MF A01

In the process of finding new routes to synthesize nitrofurazans the investigators compared the oxidation of a sulfilimide and a phosphine imine derived from 3-amino-4-(chlorophenyl)furazan. The sulfilimine, 3-(4-chlorophenyl)-4-dimethyl-sulfiliminofurazan, was prepared by treating 1 with dimethyl sulfide ditriflate. Oxidation of 1 with peroxytrifluoroacetic acid (ptfa) in dichloromethane gave a mixture that was chromatographed to give 3-(4-chlorophenyl)-4-nitro-furazan in 11% yield and azoxy (4-chlorophenylfurazan) in 32% yield. Under the same conditions, 2 gave a 96% yield of 5 with no trace of 6. Oxidation of diaminofurazan with ptfa gives 3-amino-4-nitrofurazan which was converted to the sulfilimine. Treatment of the sulfilimine with anhydrous ptfa in dichloromethane gave a solution that contained dimethyl sulfone according to (13)C-NMR analysis, but no nitrocarbon could be detected. However, the (14)N-NME spectrum contained a very sharp singlet with a width at half height of 19 Hz and a chemical shift almost identical to that of 5. Thus, it appears that we may have formed dinitrofurazan in solution, but we have not been able to isolate it in pure form as yet. DOE

N86-12285# Los Alamos Scientific Lab., N. Mex.
APPLICATION OF TIME-DEPENDENT RAMAN THEORY TO THE ANALYSIS OF INORGANIC PHOTOSYSTEMS
D. E. Morris and W. H. Woodruff 1985 5 p refs Presented at 2nd Intern. Conf. on Time-Resolved Vibrational Spectry., Bayreuth-Bischofsgrun, West Germany, 3 Jun. 1985
(Contract W-7405-eng-36)
(DE85-012752; LA-UR-85-1957; CONF-8506132-1) Avail: NTIS HC A02/MF A01

The more general formulation of Heller's theory outlined here should make it possible to characterize the excited states of real and chemically interesting systems with a high degree of reliability provided care is exercised in considering the influence of all factors in determining the scattering dynamics. The reliance of this method on ground-state Raman intensities make it particularly convenient and a valuable complement to the more direct but often experimentally prohibitive methods such as TRVS. While further testing of the predictions of this formalism is required, preliminary results as presented here are encouraging. DOE

N86-12286# Bureau of Mines, Reno, Nev.
HYDROGEN CHLORIDE SPARGING CRYSTALLIZATION OF THE CHLORIDE SALTS OF COBALT, MANGANESE, AND NICKEL
D. E. Shanks and E. G. Noble 1985 26 p refs
(PB85-197002; BM-RI-8930; LC-84-600270) Avail: NTIS HC A03/MF A01 CSCL 07D

The Bureau of Mines investigated the effects of HCl concentration and solution temperature on the solubility and crystal form of the chlorides of Co, Mn, and Ni when sparged with HCl gas at temperatures of 20 degrees, 40 degrees, and 60 degrees C. Increasing HCl concentration in solution caused the chlorides of Co, Mn, and Ni to crystallize (salt out) because of the common ion effect. The salting-out crystallization was most effective for NiCl2, which had a solubility of 0.7 pct at 20 degrees C and maximum HCl concentration. GRA

N86-12287# Little (Arthur D.), Inc., Cambridge, Mass.
DEVELOPMENT OF A ROUTINE TECHNIQUE FOR ANALYSIS OF NITRO-PAH IN DIESEL PARTICULATE EXTRACT
K. T. Menzies, C. M. Wong, L. H. Magni, and M. A. Randel Feb. 1985 79 p refs
(PB85-196657; CRC-APRAC-CAPE-30-81-03) Avail: NTIS HC A05/MF A01 CSCL 07D

Several chromatographic methods potentially suitable for routine analysis of nitro-PAH in diesel particulate extract were selected from the current literature. After limited screening, a gas chromatographic separation on a fused silica capillary column with electron capture detection (ECD) was selected for method evaluation. In order to provide accurate analysis of the nitro-PAH's, a semipreparative scale, amino bonded GPLC column was evaluated to remove other compound classes which may interfere with GC/ECD analysis. As a result of this effort, an analytical method which provides adequate precision (+ or - 20%) and accuracy (+ or - 20%) for mono-nitro PAHs in diesel exhaust particulate was validated. The accuracy of the method remains undefined due to difficulties in evaluating an independent HPLC/electrochemical detection method. Author (GRA)

N86-12288# California Inst. of Tech., Pasadena. Graduate Aeronautical Labs.
COMBUSTION IN TURBULENT JETS AND BUOYANT PLUMES Annual Report, Dec. 1983 - Dec. 1984
P. E. Dimotakis, J. E. Broadwell, and E. E. Zukoski 15 Feb. 1985 62 p refs
(PB85-220655; GRI-85/0051) Avail: NTIS HC A04/MF A01 CSCL 21B

Results are reported from an ongoing investigation of the entrainment and mixing mechanisms. In momentum dominated turbulent jets, buoyancy dominated turbulent plumes, and flows which undergo a transition between these two regimes. This investigation also addresses the effects of molecular diffusion rates (Schmidt number) and combustion heat release on these mechanisms, and incorporates these mechanisms into practical modeling and predictive techniques for combustion in these flows. These measurements in large Schmidt number momentum driven jets have revealed a similarity concentration variable for which probability density functions (PDFs) display self similarity, and show that organized large scale structures play an important role in jet entrainment and mixing. Author (GRA)

N86-12289# Princeton Univ., N. J. Dept. of Chemical Engineering.
NEW CORRESPONDING STATES THEORY USING THE SECOND VIRIAL COEFFICIENT AS THE TEMPERATURE VARIABLE Topical Report, Dec. 1982 - Dec. 1984
C. K. Hall and B. A. Hacker Dec. 1984 159 p
(PB85-219624; GRI-85/0003) Avail: NTIS HC A08/MF A01 CSCL 07A

A new corresponding states theory is presented that uses an approximation to the reduced second virial coefficient as its temperature variable. This new corresponding states variable, X(T(sub r)), is chosen to be a simple function of temperature, critical temperature and the Boyle temperature. Using data generated from an accurate equation of state, it is demonstrated graphically that pure component compressibility factors are universal functions of reduced volume and the new variable X(T(sub r)) over a wide range of densities. Homogeneous mixture compressibility factors are shown to be a function of X(T(sub r)) for the limited number of systems studied, however, the correlation cannot as yet be used for two-phase binary mixtures. The theory predicts that the saturation properties of pure fluids may be represented by a universal surface, called UNISAT, upon which the reduced vapor pressure and reduced saturated gaseous and liquid densities are universal functions of X(T(sub r)). GRA

N86-12290# SRI International Corp., Menlo Park, Calif.
REDUCTION OF CO2 TO METHANOL AND METHANE BY PHOTO AND DARK REACTIONS ON SEMICONDUCTOR ELECTRODES Annual Report, 15 Feb. 1984 - 15 Feb. 1985
K. W. Frese and D. P. Summer Mar. 1985 61 p refs
(PB85-226298; GRI-85/0085) Avail: NTIS HC A04/MF A01 CSCL 07D

This report investigates the electrochemical mechanism of reduction of CO2 or carbonate species to useful fuels using semiconductor and metal electrodes. The semiconductor electrodes may be used to convert light and CO2 into fuels such as methanol and methane. Metal electrodes could be coupled to photovoltaic arrays for solar energy storage via fuel generation. By suitable electrochemical processes this inorganic carbon may be converted to organic carbon in the form of methanol and methane, which could be used as fuel. Such electrochemical conversions can be made to occur at semiconductor electrodes. In addition, semiconductor electrodes absorb light, and this light can be converted to a voltage that causes the electrochemical transformations of interest. By combining the CO2, water, semiconductor, and sunlight, the authors can store solar energy in the fuel. GRA

N86-12291# National Bureau of Standards, Gaithersburg, Md. Center for Fire Research.
MODEL DESCRIBING THE STEADY-STATE PYROLYSIS OF BUBBLE-FORMING POLYMERS IN RESPONSE TO AN INCIDENT HEAT FLUX
I. S. Wichman May 1985 48 p refs
(PB85-225225; NBSIR-85/3130) Avail: NTIS HC A03/MF A01 CSCL 07D

A theoretical model is developed to describe the indepth effect of bubbles on the steady state transport of volatile gases (monomer) from the surface of a polymer subjected to an incident heat flux. In this model the effect of the bubbles on the surrounding (liquid) polymer is felt through the bubble number distribution function, n, which appears in the equations for conservation of mass, momentum, species and energy in the melt. The equation for the evolution of n includes the effects of bubble growth, convection and nucleation; its derivation requires preliminary study of the growth and motion of an individual bubble in a liquid with a temperature gradient. With these equations, formulas for the mass flux of volatiles from the polymer surface and the bubble void fraction are developed, for the special case of constant polymer mass fraction. Author

N86-12351# IIT Research Inst., Chicago, Ill.
HYDRAULIC FLUIDS
In its Hazards of Chem. Rockets and Propellants, Vol. 3 Sep. 1984 12 p refs (For primary document see N86-12328 03-28)
Avail: Chemical Propulsion Information Agency, Johns Hopkins Road, Laurel, Md. 20707 HC $61.56 CSCL 07/4

N86-12352# IIT Research Inst., Chicago, Ill.
MERCURY
In its Hazards of Chem. Rockets and Propellants, Vol. 3 Sep. 1984 9 p refs (For primary document see N86-12328 03-28)
Avail: Chemical Propulsion Information Agency, Johns Hopkins Road, Laurel, Md. 20707 HC $61.56 CSCL 07/4

N86-12353# IIT Research Inst., Chicago, Ill.
COMPRESSED AND LIQUID AIR
In its Hazards of Chem. Rockets and Propellants, Vol. 3 Sep. 1984 8 p refs (For primary document see N86-12328 03-28)
Avail: Chemical Propulsion Information Agency, Johns Hopkins Road, Laurel, Md. 20707 HC $61.56 CSCL 07/4

N86-12354# IIT Research Inst., Chicago, Ill.
CARBON DIOXIDE
In its Hazards of Chem. Rockets and Propellants, Vol. 3 Sep. 1984 10 p refs (For primary document see N86-12328 03-28)
Avail: Chemical Propulsion Information Agency, Johns Hopkins Road, Laurel, Md. 20707 HC $61.56 CSCL 07/4

N86-12355# IIT Research Inst., Chicago, Ill.
NITROUS OXIDE
In its Hazards of Chem. Rockets and Propellants, Vol. 3 Sep. 1984 7 p refs (For primary document see N86-12328 03-28)
Avail: Chemical Propulsion Information Agency, Johns Hopkins Road, Laurel, Md. 20707 HC $61.56 CSCL 07/4

N86-12381# Tokyo Denki Univ. (Japan). Faculty of Engineering.
THE STUDIES ON THE EFFECTS OF INTERMOLECULAR HYDROGEN BOND IN MELAMINE RESINATION PROCESS. (METHYLATED MELAMINES WERE ADOPTED AS THE MODEL COMPOUNDS OF STARTING MATERIAL)
Moritaka Tajima *In its* Res. Rept. of the Faculty of Eng., Tokyo Denki Univ., No. 32 Dec. 1984 p 131-156 refs In JAPANESE; ENGLISH summary (For primary document see N86-12372 03-31)
Avail: NTIS HC A09/MF A01

N86-12453# Joint Publications Research Service, Arlington, Va.
USAGES OF ORGANIC MEMBRANES IN ELECTROLYTIC INDUSTRY DESCRIBED
Li Jisen *In its* China Rept.: Sci. and Technol. (JPRS-CST-85-030) 4 Sep. 1985 p 25-35 refs Transl. into ENGLISH from Huaxue Tongbao (Beijing), no. 5, 18 May 1985 p 37-42 (For primary document see N86-12451 03-31)
Avail: NTIS HC A08/MF A01

26 METALLIC MATERIALS

Includes physical, chemical, and mechanical properties of metals, e.g., corrosion; and metallurgy.

N86-12292*# National Aeronautics and Space Administration. Lewis Research Center, Cleveland, Ohio.
INFLUENCE OF LOAD INTERACTIONS ON CRACK GROWTH AS RELATED TO STATE OF STRESS AND CRACK CLOSURE
Jack Telesman Sep. 1985 22 p refs
(NASA-TM-87117; E-2724; NAS 1.15:87117) Avail: NTIS HC A02/MF A01 CSCL 11F

Fatigue crack propagation (FCP) after an application of a low-high loading sequence was investigated as a function of specimen thickness and crack closure. No load interaction effects were detected for specimens in a predominant plane strain state. However, for the plane stress specimens, initially high FCP rates after transition to a higher stress intensity range were observed. The difference in observed behavior was explained by examining the effect of the resulting closure stress intensity values on the effective stress intensity range. Author

N86-12293*# National Aeronautics and Space Administration. Lewis Research Center, Cleveland, Ohio.
ELLIPSOMETRIC SURFACE ANALYSIS OF WEAR TRACKS PRODUCED BY DIFFERENT LUBRICANTS
James L. Lauer, Norbert Marxer, and William R. Jones, Jr. [Oct. 1985] 20 p refs Presented at the Tribology Conf., Atlanta, 8-10 Oct. 1985; sponsored by ASLE and ASME
(Grants NAG3-22; DAAG24-83-K-0058)
(NASA-TM-87142; E-2769; NAS 1.15:87142) Avail: NTIS HC A02/MF A01 CSCL 11H

A scanning ellipsometer with high spatial resolution was used to analyze wear tracks generated on M-50 surfaces operated in several lubricant formulations. These formulations included a pure ester base stock of trimethyol propane triheptanoate with additives of either benzotriazole (BTZ), dioctyldiphenylamine (DODPA), or tricresylphosphate (TCP). Results indicated that BTZ and TCP produced patchy oxide surface films consisting mainly of Fe304. DOPDA produced a much more uniform oxide film. These findings may explain the tendency of lubricant formulations containing TCP to scuff more readily than those containing only antioxidants. Author

N86-12294*# National Aeronautics and Space Administration. Lewis Research Center, Cleveland, Ohio.
FATIGUE CRACK PROPAGATION OF NICKEL-BASE SUPERALLOYS AT 650 DEG C
J. Gayda, T. P. Gabb, and R. V. Miner [Oct. 1985] 22 p refs Presented at the Symp. on Low-Cycle Fatigue Directions for the Future, Bolton Landing, N.Y., 30 Sep. - 4 Oct. 1985; sponsored by American Society for Testing and Materials
(NASA-TM-87150; E-2778; NAS 1.15:87150) Avail: NTIS HC A02/MF A01 CSCL 11F

The 650 C fatigue crack propagation behavior of two nickel-base superalloys, Rene 95 and Waspaloy, is studied with particular emphasis placed on understanding the roles of creep, environment, and two key grain boundary alloying additions, boron and zirconium. Comparison of air and vacuum data shows the air environment to be detrimental over a wide range of frequencies for both alloys. More in-depth analysis on Rene 95 shows at lower frequencies, such as 0.02 Hz, failure in air occurs by intergranular, environmentally-assisted creep crack growth, while at higher frequencies, up to 5.0 Hz, environmental interactions are still evident but creep effects are minimized. The effect of B and Zr in Waspaloy is found to be important where environmental and/or creep interactions are presented. In those instances, removal of B and Zr dramatically increases crack growth and it is therefore plausible that effective dilution of these elements may explain a previously observed trend in which crack growth rates increase with decreasing grain size. Author

N86-12295*# National Aeronautics and Space Administration. Lewis Research Center, Cleveland, Ohio.
AN UPDATE OF THE TOTAL-STRAIN VERSION OF SRP
James F. Saltsman and Gary R. Halford Oct. 1985 27 p refs Presented at the Symp. on Low Cycle Fatigue: Direc. for the

Future, Lake George, N.Y., 30 Sep. - 4 Oct. 1985; sponsored by American Society for Testing and Materials, American Inst. of Mining, Metallurgical and Petroleum Engineers, and American Society for Metals
(NASA-TP-2499; E-2575; NAS 1.60:2499) Avail: NTIS HC A03/MF A01 CSCL 11F

An updated procedure for characterizing an alloy and predicting cyclic life by using the total strain range version of strainrange partitioning (TS-SRP) has been developed. The principal feature of this update is a new procedure for determining the intercept of time dependent elastic strain range versus cyclic life lines. The procedure is based on an established relation between failure and the cyclic stress-strain response of an alloy. The stress-strain response is characterized by empirical equations presented in this report. These equations were determined with the aid of a cyclic constitutive model. The procedures presented herein reduce the testing required to characterize an alloy. Failure testing is done only in the high strain, low life regime; cyclic stress-strain response is determined from tests conducted in both the high and low strain regimes. These tests are carried out to stability of the stress-strain hysteresis loop but not to failure. Thus both the time and costs required to characterize an alloy are greatly reduced. This approach was evaluated and verified for two nickel base superalloys, AF2-1DA and Inconel 718. Author

N86-12296# Johns Hopkins Univ., Baltimore, Md. Center for Materials Research.
RESEARCH ON THE MICROSTRUCTURE OF RAPIDLY SOLIDIFIED ALLOYS Progress Report
D. Shechtman, L. A. Bendersk, and E. Horowitz Jun. 1985 62 p
(Contract MDA903-83-K-0400)
(AD-A157077; CMR-DARPA-10) Avail: NTIS HC A04/MF A01 CSCL 11/6

The results of research performed on rapidly solidified alloys are presented. A major breakthrough by Shechtman is reported in the first paper on Al-Mn alloys with a metallic phase (icosahedral quasicrystal) with long range of orientational order and no translational symmetry. In addition, the microstructure and phases in other rapidly solidified alloys are discussed including variations in microstructure as a function of processing conditions. GRA

N86-12297# Pennsylvania State Univ., University Park. Dept. of Materials Science and Engineering.
EFFECT OF GRAIN BOUNDARY STRUCTURE ON SENSITIZATION AND CORROSION OF STAINLESS STEEL Annual Technical Report
B. W. Bennett and H. W. Pickering Jun. 1985 21 p
(Contract N00014-81-K-0025)
(AD-A157133) Avail: NTIS HC A02/MF A01 CSCL 11/6

This paper reports on a study of intergranular corrosion, particularly the influence of the crystallography of a grain boundary (g.b.) on the sensitization and grain boundary corrosion of stainless steels. Since sensitization of stainless steels depends on g.b. energy, this study included a determination of the misorientation angle of grain boundaries in a sample. A scanning electron microscope was modified for application of the electron backscattering (EBS) technique in conjunction with normal SEM imaging of the sample surface. In austenitic stainless steel (Fe-18Cr-10Ni) samples annealed at 1200 C for 1 hour, water quenched and aged for various times at 650 C, the degree of sensitization increased with increasing aging time. This was indicated by an increasing width of the g.b. groove. A plot of groove width vs. g.b. misorientation angle obtained by the EBS technique showed a range of groove crystallography and the coincident site lattice concept provided a rationalization of this observation. Similar results were found for ferritic stainless steel (Fe-19 Cr) samples. The Cr concentration profiles as a function of time were calculated, using a finite difference method, both along the g.b. and normal to the g.b. GRA

N86-12298# Naval Air Development Center, Warminster, Pa. Aircraft and Crew Systems Technology Directorate.
PROPERTIES OF A RETROGRESSED AND RE-AGED 7075 ALUMINUM ALLOY Progress Report
E. S. Tankins, V. S. Agarwala, C. E. Neu, and J. J. Bethke 31 Dec. 1984 47 p
(NR Proj. F61-542)
(AD-A157415; NADC-84096-60) Avail: NTIS HC A03/MF A01 CSCL 11/6

Retrogression and Re-aging (RRA) is a new thermal process introduced for the purpose of enhancing corrosion resistance of 7075-T651 aluminum alloy while maintaining its T6 strength. In this study a 7075 material so treated was investigated for its mechanical and corrosion resistant properties. Results indicated that the RRA treated 7075 was significantly better than the T6 temper in resistance to stress corrosion cracking and exfoliation corrosion. The loss in strength from RRA treatment was minimal. Electron microscopy of the fractured surface showed a distinct difference in the fracture mode when compared to the T6 temper condition. Tests results indicated that the RRA heat treatment resulted in fatigue and fracture toughness properties superior to the 7075-T651. GRA

N86-12299# Department of the Navy, Washington, D. C.
SUSPENSION METHOD OF IMPREGNATING ACTIVE MATERIAL INTO COMPOSITE NICKEL PLAQUE Patent Application
W. A. Ferrando, inventor (to Navy) Filed 29 May 1985 18 p
(AD-D011826; US-Patent-Appl-SN-740115) Avail: NTIS HC A02/MF A01 CSCL 09/1

A process is described for impregnating nickel or cadmium active material into a sintered nickel coated graphite fiber composite plaque electrode in which a suspension of 1-20 micron particles of active material in ethylene glycol in a 1:1 to 1:4 weight ratio of glycol to particles is gently worked into the plaque and the ethylene glycol is then evaporated off leaving the particles of active material distributed throughout the plaque. This procedure is repeated until the desired level of loading is achieved. Author (GRA)

N86-12300# Aluminum Co. of America, Alcoa Center, Pa.
RESISTANCE TO FRACTURE, FATIGUE AND STRESS-CORROSION OF Al-Cu-Li-Zr ALLOYS Final Report, 1 Jul. 1981 - 28 Feb. 1985
A. K. Vasudevan, R. C. Malcolm, W. G. Fricke, and R. J. Rioja 19 Feb. 1985 243 p Original contains color illustrations
(Contract N00019-80-C-0569)
(AD-A158407) Avail: NTIS HC A11/MF A01 CSCL 11/6

This investigation was undertaken to characterize the role of composition/microstructure on the mechanical behavior of Al-Cu-Li-Zr alloys. This characterization is intended to serve as a baseline data for alloy development work directed at improving the mechanical properties of Al-Li alloys. The report summarizes the results on fracture, fatigue and stress corrosion behavior of Al-Cu-Li-Zr alloys. GRA

N86-12301# Oak Ridge National Lab., Tenn.
PARAMAGNETIC FORM FACTORS OF HCP TRANSITION METALS
S. H. Liu, A. J. Liu, and J. F. Cooke Jun. 1985 11 p Presented at the Intern. Conf. on Magnetics, San Francisco, 26 Aug. 1985
(Contract DE-AC05-84OR-21400)
(DE85-016301; CONF-85089-0) Avail: NTIS HC A02/MF A01

Elastic neutron scattering experiments have provided accurate information about the Fourier transform of the total induced magnetization density which consists of orbital and spin contributions. Traditionally, one analyzes the orbital part by using the atomic model. Recently we have developed a numerical technique to compute accurately the orbital moment form factor of the itinerant electrons in cubic transition metals. We have now extended the calculation to HCP metals Sc, Y, Lu, and Zr. The calculated orbital contributions deviate from atomic orbital form factors. There is reasonable overall agreement between theory and experiments. DOE

N86-12302# Oak Ridge National Lab., Tenn.
EFFECT OF PULSED IRRADIATION ON MICROSTRUCTURAL EVOLUTION

N. H. Packan 1985 21 p Presented at the Workshop on the Relation Between Mech. Properties and Micro-Struct. Under Fusion Irradiation Conditions, Ebeltoft, Denmark, 27 Jun. 1985
(Contract DE-AC05-84OR-21400)
(DE85-016317; CONF-8506165-2) Avail: NTIS HC A02/MF A01

Discontinuous irradiation, such as could ensue from the operation of a magnetic fusion reactor, may cause changes in the development of radiation damage microstructures. In this paper, the experimental observations of such pulsing effects are collected and compared. Resulting trends are related to the implications of theoretical mechanisms. Conclusions are drawn on the degree to which pulsing seems capable of affecting the major aspects of radiation damage to metals. DOE

N86-12303# Oak Ridge National Lab., Tenn. National Center for Small Angle Scattering Research.
COMBINED SMALL ANGLE X-RAY SCATTERING AND TRANSMISSION ELECTRON MICROSCOPE STUDIES OF Al-Li ALLOYS
D. Spooner, D. B. Williams (Lehigh Univ., Bethlehem, Pa.), and C. M. Sung (Lehigh Univ., Bethlehem, Pa.) 1985 15 p refs
(Contract DE-AC05-84OR-21400; Grant NSF DMR-77-24459)
(DE85-016356; CONF-850777-2) Avail: NTIS HC A02/MF A01

Combined small angle X-ray scattering (SAXS) and transmission electron microscopy (TEM) studies have been performed on two binary Al-Li alloys subjected to different pre-aging treatments. Both the SAXS and TEM data indicate that DELTA' (Al3Li) in samples of the two alloys directly quenched to the aging temperature is larger in size than in samples quenched to below room temperature prior to aging. SAXS data indicate an initial rise in scattering center size in Al-9.4 at% Li, which is not observed in the more dilute Al-6.8 at% Li, or in the TEM studies of DELTA' in both alloys. It is considered that these observations are evidence that the initial rise in the SAXS data in Al-9.4 at% Li alloys is due to a phenomenon other than DELTA' precipitation. The possibility of matrix spinodal decomposition in this alloy is one explanation. Author

N86-12304# Oak Ridge National Lab., Tenn.
REVIEW OF EFFECTS OF LONG-TERM AGING ON THE MECHANICAL PROPERTIES AND MICROSTRUCTURES OF TYPES 304 AND 316 STAINLESS STEEL
J. A. Horak, V. K. Sikka, and D. T. Raske 1985 13 p refs Presented at the Intern. Conf. on Nucl. Power Plant Aging, Availability Factor and Reliability Anal., San Diego, Calif., 7 Jul. 1985 Prepared in cooperation with Argonne National Lab., Ill.
(Contract DE-AC05-84OR-21400)
(DE85-016472; CONF-850713-7) Avail: NTIS HC A02/MF A01

Because commercial liquid metal fast breeder reactors (LMFBR) are designed to last for 40 years or more, an understanding of the mechanical behavior of the structural alloys used in them is required for times on the order of 2.5 x 10 to the 5th power h (assuming a 70% availability factor). Types 304 and 316 stainless steel are used extensively in LMFBR systems. At the beginning of life these alloys are in a metastable state and evolve to a more stable state and, therefore, more stable microstructure during plant operation. Correlations of microstructures and mechanical properties during aging under representative LMFBR temperature and loading conditions are desirable from the standpoint of assuring safe, reliable, and economic plant operation. The mechanical properties and microstructures of types 304 and 316 stainless steel wrought alloys are reviewed after long-term aging in air for times up to 9 x 10 the 4th power h (about 10-1/2 years). The principal effect of such aging is to reduce low temperature fracture toughness (as measured by Charpy impact test) and tensile ductility. Examples are cited, however, where, because stable microstructures are achieved, these as well as strength-related properties can be expected to remain adequate for anticipated service life conditions. DOE

N86-12305# Sandia National Labs., Albuquerque, N. Mex.
SPECIAL METALLOGRAPHIC PROCEDURES FOR AUSTENITIC STAINLESS STEEL WELDS
M. J. Cieslak and M. E. McAllaster 1985 34 p Presented at the Intern. Metallog. Soc. Conf., Denver, 21 Jul. 1985
(Contract DE-AC04-76DP-00789)
(DE85-010113; SAND-85-0818C; CONF-850753-1) Avail: NTIS HC A03/MF A01

The interpretation of austenitic stainless steel weld metal microstructure requires an understanding of the solidification and solid state transformation metallurgy of this class of alloys. The room temperature microstructures are complicated by the fact that ferrite is only stable at high temperatures. The alloy composition and weld cooling rates can influence both the form and amount of ferrite present in the room temperature microstructure. Optical microscopy can be a valuable tool in studying both weld metal solidification and transformation mechanisms and the related problem of solidification hot-cracking. DOE

N86-12306# Department of Energy, Washington, D. C.
METHOD AND APPARATUS FOR CONDUCTING VARIABLE THICKNESS VAPOR DEPOSITION Patent Application
G. V. Nesslage, inventor (to DOE) Filed 3 Aug. 1984 12 p Prepared in cooperation with Mound Lab., Miamisburg, Ohio
(Contract DE-AC04-76DP-00053)
(DE85-011653; US-Patent-Appl-SN-637629) Avail: NTIS HC A02/MF A01

A method of vapor depositing metal on a substrate in variable thickness comprises conducting the deposition continuously without interruption to avoid formation of grain boundaries. To achieve reduced deposition in specific regions a thin wire or ribbon blocking body is placed between source and substrate to partially block vapors from depositing in the region immediately below. DOE

N86-12307# Ames Lab., Iowa.
EFFECTS OF MICROSTRUCTURE ON THE ACOUSTOELASTIC MEASUREMENTS OF STRESS
R. B. Thompson, J. F. Smith, and S. S. Lee 1983 9 p Presented at the AIME-ASM Fall Meeting, Philadelphia, 1 Oct. 1983
(Contract W-7405-eng-82)
(DE85-015518; IS-M-538; CONF-8310394-1) Avail: NTIS HC A02/MF A01

The acoustoelastic measurement of stress is based on deformation induced shifts in the ultrasonic velocity. Although changes in stress are routinely monitored, the absolute determination of stress in a part of unknown history is rendered difficult by competing microstructurally induced velocity shifts. A number of techniques to overcome this problem are first reviewed. A more detailed discussion is then given of a potential solution under investigation by the authors. This involves measuring the difference in the velocities of two shear waves whose directions of propagation and polarization have been interchanged. According to the theory of anisotropic elastic continua, the proportionality constant relating this velocity difference to stress should be only weakly dependent on microstructure. Preliminary measurements show that this prediction is followed in mildly anisotropic (rolled 6061 Al) and plastically deformed (1100 Al loaded beyond yield) metal polycrystals. Included is a discussion of more severe microstructural conditions which must be considered to establish the ultimate limits of the technique. DOE

N86-12308# Sandia National Labs., Albuquerque, N. Mex.
OPTICAL MEASUREMENTS OF SHOCK-INDUCED CHEMICAL REACTIONS IN MIXED ALUMINUM-NICKEL POWDER
M. B. Boslough, R. A. Graham, and D. M. Webb 1985 6 p Presented at the Am. Phys. Soc. Topical Conf. on Shock Waves in Condensed Matter, Spokane, 22 Jul. 1985
(Contract DE-AC04-76DP-00789)
(DE85-014705; SAND-85-0498C; CONF-850736-21) Avail: NTIS HC A02/MF A01

Optical pyrometer and high-speed photography experiments have been carried out to determine the temperature and temporal-spatial evolution of a chemical reaction zone in shock-loaded, nickel-aluminum powder mixtures. The temperature generated is about 5000 K, and the reaction occurs on a 100 nanosecond or faster time scale. Experimental results are compared to numerical calculations, which suggest that there are threshold shock pressures and temperatures of about 15 GPa and 500 C which are required to initiate the strong exothermic reaction. Further, excessive pressure appears to inhibit reaction. This observation is in agreement with previous experiments in which nickel-aluminum alloys were recovered from shock-loaded mixtures. DOE

N86-12309# Nebraska Univ., Lincoln. Dept. of Chemistry.
STUDIES ON UNUSALLY REACTIVE METAL POWDERS: PREPARATION OF NEW ORGANOMETALLIC AND ORGANIC COMPOUNDS INCLUDING POTENTIAL NEW CATALYSTS Final Report, 1 Jul. 1980 - 31 Dec. 1984
R. D. Rieke Jun. 1985 18 p refs
(Contract DE-AC02-80ER-10603)
(DE85-014844; DOE/ER-10603/T3) Avail: NTIS HC A02/MF A01

This research project was involved with the preparation and study of highly reactive metal powders prepared by the reduction of metal salts with alkali metals. Studies concentrated on nickel, copper, cadmium, uranium, iron, and magnesium. The nickel powders have been found to react rapidly with benzylic halides, and the resulting organonickel complexes yield dibenzyl. Aryl halides react rapidly with the nickel powders to produce biaryl compounds in high yields. Benzylic halides react with the nickel powders in the presence of acylhalides to produce benzyl ketones in high yields. Reactions of ROCOCOC 1 and benzylic halides with nickel powders yield benzyl ketones. These reactions proceed with a wide variety of substituents on the phenyl ring of the benzylic halides. Highly reactive uranium has beeen prepared, and found to react with a variety of oxygen containing substrates, such as nitrobenzene to yield azo benzene. Highly reactive magnesium has opened up a totally new area of low temperature Grignard chemistry. The preparation of highly reactive copper has allowed the direct preparation of organocopper species directly from organic halides. DOE

N86-12429# Joint Publications Research Service, Arlington, Va.
TITANIUM EXTRACTANT T105-1 STUDIED
Mu Guangzhao *In its* China Rept.: Sci. and Technol. (JPRS-CST-85-021) 8 Jul. 1985 p 141-144 Transl. into ENGLISH from Huaxue Shijie (Shanghai), v. 26, no. 3, 20 Mar. 1985 p 82-83 (For primary document see N86-12421 03-31)
Avail: NTIS HC A09/MF A01

N86-12467# Joint Publications Research Service, Arlington, Va.
IRON AND STEELMAKING WITH PLASMA
Yu Dingfu *In its* China Rept.: Sci. and Technol. (JPRS-CST-85-032) 19 Sep. 1985 p 71-84 refs Transl. into ENGLISH from Gangtie (Beijing), v. 20, no. 5, May 1985 p 48-54 (For primary document see N86-12462 03-31)
Avail: NTIS HC A08/MF A01

27 NONMETALLIC MATERIALS

Includes physical, chemical, and mechanical properties of plastics, elastomers, lubricants, polymers, textiles, adhesives, and ceramic materials.

N86-12310*# National Aeronautics and Space Administration. Lewis Research Center, Cleveland, Ohio.
MOLTEN SALT CORROSION OF SIC: PITTING MECHANISM
N. S. Jacobson and J. L. Smialek [Oct. 1985] 12 p refs Presented at the 168th Meeting of the Electrochem. Soc., Las Vegas, Nev., 13-18 Oct. 1985
(NASA-TM-87143; E-2770; NAS 1.15:87143) Avail: NTIS HC A02/MF A01 CSCL 11G

Thin films of Na_2SO_4 and Na_2CO_3 at 1000 C lead to severe pitting of sintered alpha-SiC. These pits are important as they cause a strength reduction in this material. The growth of product layers is related to pit formation for the Na_2CO_3 case. The early reaction stages involve repeated oxidation and dissolution to form sodium silicate. This results in severe grain boundary attack. After this a porous silica layer forms between the sodium silicate melt and the SiC. The pores in this layer appear to act as paths for the melt to reach the SiC and create larger pits. Author

N86-12311*# National Aeronautics and Space Administration. Lewis Research Center, Cleveland, Ohio.
STRUCTURE-TO-GLASS TRANSITION TEMPERATURE RELATIONSHIPS IN HIGH TEMPERATURE STABLE CONDENSATION POLYIMIDES
William B. Alston and Roy F. Gratz (Mary Washington Coll., Fredericksburg, Va.) [1985] 19 p refs Presented at the 2nd Intern. Conf. on Polyimides, Ellenville, N.Y., 30 Oct. - 1 Nov. 1985; sponsored by the Society of Plastics Engineers, Inc.
(DA Proj. 1L1-61101-AH-45)
(NASA-TM-87113; E-2714; NAS 1.15:87113; USAAVSCOM-TR-85-C-18) Avail: NTIS HC A02/MF A01 CSCL 11B

The presence of a hexafluoroisopropylidene (6F) connecting group in aryl dianhydrides used to prepare aromatic condensation polyimides provides high glass transition temperature (T sub g) polyimides with excellent thermo-oxidative stability. The purpose of this study was to determine if a trifluorophenyl-ethylidene (3F) connecting group would have a similar effect on the T sub g of aromatic condensation polyimides. A new dianhydride containing the 3F connecting group was synthesized. This dianhydride and an aromatic diamine also containing the 3F connecting group were used together and in various combinations with known diamines or known dianhydrides, respectively, to prepare new 3F containing condensation polyimides. Known polyimides, including some with the 6F connecting linkage, were also prepared for comparison purposes. The new 3F containing polymers and the comparison polymers were prepared by condensation polymerization via the traditional amic-acid polymerization method in N,N-dimethylacetamide solvent. The solutions were characterized by determining their inherent viscosities and then were thermally converted into polyimide films under nitrogen atmosphere at 300 to 500 C, usually 350 C. The T sub g's of the films and resin discs were then determined by thermomechanical analysis and were correlated as a function of the final processing temperatures of the films and resin discs. The results showed that similarities existed in the T sub g's depending on the nature of the connecting linkage in the monomers used to prepare the condensation polyimides. B.W.

N86-12312# Solarex Corp., Rockville, Md.
SEMICRYSTALLINE CASTING PROCESS DEVELOPMENT AND VERIFICATION Final Report, 19 Jun. 1980 - 28 Feb. 1984
Feb. 1984 264 p refs
(Contract DE-FC01-80ET-23197)
(JPL-9950-1160; DOE/JPL-ET-23197) Avail: NTIS HC A12/MF A01

The development of the polycrystalline silicon ingot technology employing the ubiquitous crystallization process (UCP) is discussed. The key elements of the program are to: (1) demonstrate the technical viability of large grain polycrystalline silicon wafers and their compatibility with all industrial requirements for fabrication of efficient solar cells; (2) demonstrate the compatibility of the process economics with low-cost array production and with 1982 and 1986 price goals; (3) verify process and equipment performance at high throughput levels, demonstrating readiness for commercialization. It is shown that semicrystalline silicon production by the UCP is a viably technology. The technical feasibility of producing large quantities of high quality sheet silicon is demonstrated. E.A.K.

N86-12313*# National Aeronautics and Space Administration, Washington, D. C.
MOLECULAR CONTROL
1985 69 p Prepared in cooperation with Naval Air Systems Command, Washington, D.C.
(NASA-TM-87510; NAS 1.15:87510; AD-A156709) Avail: NTIS HC A04/MF A01 CSCL 07C

In the first two chapters, the fundamental physics both existing and required are described. Chapter 1 is the most theoretical of the chapters and introduces the theoretical platform. Chapter 2 and especially Chapter 3 moves the reader along to consider the applications of the theoretical platform to along to consider the applications of the theoretical platform to molecular dynamics and devices. Chapter 3 points out the need to extend some theoretical methods of physics itself in order to deal with the applied problems. Theoretical analyses which are necessary but require considerable time to develop and bring to engineering fruition are described in these first three chapters. Chapter 4 introduces the study of specific polymer systems, namely proteins, and Chapter 5 consides the broader area of polymer science and a specific example of energy harvesting. In Chapter 6 there is progress toward the applied with the introduction of the important field of enzyme mimics. Chapters 7 and 8 discuss basic science issues of enzymatic function. Chapters 9 and 10 define precise avenues of approach to obtaining enzyme control and also indicate the difficulties and complexities. Chapter 11 brings the reader down-to-earth to the practical and short-term requirements of bio-organic synthesis control. Chapter 12 addresses the pressing need for research and training, in general, in Polymer Science. GRA

N86-12314# Army Construction Engineering Research Lab., Champaign, Ill.
FULL-SCALE FIRE TESTS OF POLYURETHANE FOAM DOME STRUCTURES Final Report
L. A. Hrdina Jun. 1985 22 p
(DA Proj. 4A1-62731-AT-41)
(AD-A157107; CERL-TR-M-85/17) Avail: NTIS HC A02/MF A01 CSCL 11/9

This report documents research to determine the behavior and performance of uncoated rigid polyurethane foam (PUF) and of PUF coated with thermal barrier materials in full-scale fires on foam dome structures. Six PUF dome structures were tested for compliance with specified fire criteria and the results evaluated. The research showed that the coated structures complied with specific Department of Defense fire safety criteria, and furthermore that such a coating is necessary to prevent rapid spread of fire. Since the geometry of the test room apparently has no effect on a structure's ignitability or on the spread of fire, it was also concluded that reasonably fire-resistant structures may be built of PUF for housing during mobilization. Author (GRA)

N86-12315# Dayton Univ., Ohio. Dept. of Mathematics.
STATISTICAL TREATMENT OF ARAMID/EPOXY STRESS-RUPTURE DATA Final Report, 15 Feb. - 30 Apr. 1984
G. Shaughnessy Apr. 1985 17 p
(Contract F33615-82-C-5089)
(AD-A157238; AFWAL-TR-85-4001) Avail: NTIS HC A02/MF A01 CSCL 11/4

The purpose of this report is to provide statistically derived tabular design data to predict the estimated stress-rupture life of unidirectional aramid/epoxy composites subjected to sustained tensile loading. The maximum likelihood estimated life (MLEL) is tabulated for various stress levels of the fiber stress and quantile levels. The estimated lifetimes were calculated from accelerated stress-rupture tests of T.T. Chiao, who used uniaxial strand samples; therefore, the estimated lifetimes reported are considered to be conservative. GRA

N86-12316# Akron Univ., Ohio. Inst. of Polymer Science.
ROLE OF CHEMICAL BONDING IN ADHESION Final Report, Mar. 1977 - Oct. 1984
A. N. Gent and P. Dreyfuss Jun. 1985 16 p
(Contract N00014-76-C-0408)
(AD-A157251) Avail: NTIS HC A02/MF A01 CSCL 11/10

This project was concerned with the principal factors that govern the strength of elastomers when filled with rigid particles. The factors studied were: the level of adhesion between the elastomer and the rigid surface; the size and number of the rigid inclusions; and, the strength of the elastomer itself. GRA

N86-12317# Naval Academy, Annapolis, Md. Dept. of Physics.
HIGH PRESSURE AND MOLECULAR WEIGHT VARIATION OF ELECTRICAL RELAXATION IN POLY(ETHYLENE OXIDE) Interim Technical Report
J. J. Fontanella and M. C. Wintersgill Jun. 1985 32 p
(AD-A157660; TR-15) Avail: NTIS HC A03/MF A01 CSCL 07/4

Vacuum audio frequency complex admittance measurements have been performed on poly(ethylene oxide) using a fully automated dielectric spectrometer. Measurements have been made over the temperature range 5.5-320 K for molecular weights from 18,500 to 4,000,000. The gamma relaxation is essentially unchanged over the range of molecular weights studied. This represents evidence against assigning the gamma relaxation to the motion of end groups. Next, previously reported data for the gamma relaxation is reanalyzed using a reduced plot. The activation volume is found to be 3-4 cc/mol in good agreement with previous work and the small value implies that the relaxation is associated with the motion of very small segments of the polymer chain. Next, the relaxation associated with the glass transition, alpha subscript a, is only observed in temperature for some samples but is observed in both frequency and temperature for others. The strength of alpha subscript a decreases monotonically as molecular weight decreases. Finally, alpha subscript a was studied up to pressures of about 0.2 GPa for 5,000,000 molecular weight material. The results for the shift of alpha subscript a with pressure are in qualitative agreement with recent theories. GRA

N86-12318# Department of the Navy, Washington, D. C.
EPOXY PHTHALONITRILE POLYMERS Patent Application
T. M. Keller, inventor (to Navy) Filed 28 Jun. 1985 15 p
(AD-D011821; US-Patent-Appl-SN-749705) Avail: NTIS HC A02/MF A01 CSCL 11/9

A bisorthodinitrile monomer and an epoxy monomer are mixed with or without an amine curing agent and heated to a temperature sufficient to induce polymerization. The resulting epoxy-phthalonitrile copolymer has improved properties relative to the epoxy polymers including higher thermal and oxidative stability, higher glass transition temperatures, better shelf life, lower water absorptivity, and better electrical properties. The properties of the epoxy-phthalonitrile copolymer can be varied by varying the epoxy:phthalonitrile ratio. GRA

N86-12319# Pennsylvania State Univ., University Park. Dept. of Electrical Engineering.
EVALUATION OF HIGH PERMITTIVITY GLASS CERAMICS FOR MILLIMETER WAVE APPLICATIONS Final Report, 1 Dec. 1981 - 30 Nov. 1984
J. Perison, W. A. Schulze, L. E. Cross, A. Bhalla, and S. Swartz 11 May 1985 40 p
(Contract DAAG29-82-K-0015)
(AD-A158551; ARO-18209.2-PH) Avail: NTIS HC A03/MF A01 CSCL 20/3

The crystallization and dielectric properties of strontium titanate aluminosilicate glass-ceramics, containing perovskite SrTiO3 as the primary crystalline phase, have been investigated. The majority of this research was concentrated on glass-ceramics consisting of 65 wt% of SrTiO3 and 35 wt% of silica and alumina with a silica/alumina weight ratio of 2/1 (SAR-2). In glass-ceramics of this composition, the primary crystalline phase was perovskite SrTiO3; other crystalline phases included SrAl2Si2O8 (hexacelsian and anorthite) and TiO2 (anatase and rutile). The relative amounts of SrTiO3 and the other crystalline phases, and the microstructure, were a strong function of the crystallization conditions. The dielectric properties of SAR-2 glass-ceramics were extremely sensitive to the amount of SrTiO3 in the glass-ceramic, and thus to the crystallization conditions. Room temperature dielectric constants of the glass-ceramics ranged from 13 to 47. The dielectric constant increased as the crystallization temperature or time was increased, and peaks developed in the dielectric constant at low temperatures. These dielectric constant peaks were not due to dielectric mixing, and it was proposed that the peaks resulted from ferroic domains in the SrTiO3, possibly caused by an interaction of the SrTiO3 crystallites with the matrix. GRA

N86-12320# Allied Bendix Corp., Kansas City, Mo.
THERMALLY INDUCED FAILURES OF THICK-FILM GLAZE RESISTORS
M. S. Raffety and W. D. Tuchig May 1985 20 p Presented at the 35th Electron. Components Conf., Washington, D.C., 20 May 1985
(Contract DE-AC04-76DP-00613)
(DE85-012014; BDX-613-3230; CONF-850599-2) Avail: NTIS HC A02/MF A01

Thick-film glaze resistors are particularly attractive for use in environments subject to extreme changes in temperature because of their low TCR values. Recently, however, it has been shown these resistors may fail when they are subjected to extended temperature cycling. The failures are characterized by increasing resistance with cycling and may ultimately culminate in a completely open condition. Examination of the failed components using a scanning electron microscope revealed the presence of cracks in the resistive glaze. The microstructural origin and propagation of these cracks are discussed in terms of an elastic model, and solutions to the problem of thermal cycling failure are proposed. DOE

N86-12321# Oak Ridge National Lab., Tenn.
CARBOTHERMAL SYNTHESIS OF SILICON CARBIDE
M. A. Janney, G. C. Wei, C. R. Kennedy, and I. A. Harris May 1985 60 p refs
(Contract DE-AC05-84OR-21400)
(DE85-013546; ORNL-6169) Avail: NTIS HC A04/MF A01

Silicon carbide powders were synthesized from various silica and carbon sources by a carbothermal reduction process at temperatures between 1500 and 1600 C. The silica sources were fumed silica, methyltrimethoxysilane, and microcrystalline quartz. The carbon sources were petroleum pitch, phenolic resins, sucrose, and carbon black. Submicron SiC powders were synthesized. Their morphologies included equiaxed loosely-bound agglomerates, equiaxed hard-shell agglomerates, and whiskers. Morphology changes with the furnance atmosphere (argon, nitrogen, or nitrogen-4% hydrogen). The best sintering was observed in SiC derived from the fumed-silica-pitch and fumed silica-sucrose precursors. The poorest sintering was observed in SiC derived from microcrystalline quartz and carbon black. DOE

N86-12322# Lawrence Livermore National Lab., Calif.
HIGH DAMAGE THRESHOLD POROUS SILICA ANTIREFLECTIVE COATING
I. M. Thomas, J. G. Wilder, W. H. Lowdermilk, and M. C. Staggs 25 Apr. 1985 11 p refs Presented at the Damage Symp., Boulder, Colo., 15 Oct. 1984
(Contract W-7405-eng-48)
(DE85-012924; UCRL-91428; CONF-8410276-2) Avail: NTIS HC A02/MF A01

A quarterwave-thick, narrow-bandwidth, antireflective coating for fused silica optical components and KDP crystals was developed. The coating consists of porous silica prepared from a silica sol in ethanol. It is applied by dip or spin from a solution at room temperature and requires no further treatment. The damage threshold levels are about equal to the surface damage thresholds of the uncoated substrates. DOE

N86-12323# Language Services, Nashville, Tenn.
MANUFACTURING PROCESS FOR CYLINDRICAL CERAMIC TUBES WITH LOCALIZED IMPRINTS AND DEVICE FOR APPLICATION OF THIS PROCESS
[1985] 27 p Transl. into ENGLISH of French Patent no. 78-33445 (27 Nov. 1978)
(Contract DE-AC05-84OT-21400)
(DE85-012294; K-Trans-297) Avail: NTIS HC A03/MF A01

This invention involves a process for manufacturing permeable cylindrical ceramic tubes with localized relief such as annular, spiral or simple coiled or double crossed coils or even stipple imprints on their internal face. It is known that one of the techniques for the separation of the mixture of gases with close molecular masses is gaseous diffusion. According to this technique, the gas mixture is circulated under pressure inside tubes constituted by a microporous wall. These tubes, according to a known technique, are constituted by a macroporous ceramic tube, generally called a support, covered on the inside with a microporous layer deposited on this interior wall. The unit constituted by the tube itself or the support and the microporous layer makes it possible to adapt the total porosity of the covered tube or barrier in order to obtain an optimal coefficient of gas separation. This technique is used specifically for separation of two gases corresponding to various isotopes of the same simple body. DOE

N86-12324# Sandia National Labs., Albuquerque, N. Mex.
SURFACE CRYSTALLIZATION ON METALLIZED 94 PERCENT ALUMINA CERAMICS
J. R. Hellmann, W. R. Sorenson, M. J. Carr, and T. J. Headley 1985 13 p Presented at the Joint Meeting of the Electron Microscopy Soc. of Am. and the Microbeam Anal. Soc., Louisville, Ky., 5 Aug. 1985
(Contract DE-AC04-76DP-00789)
(DE85-008691; SAND-85-0500C; CONF-850840-1) Avail: NTIS HC A02/MF A01

Fabrication of 94% alumina (Wesgo AL500:94% (ALPHA) - Al2O3, balance SiO2-MgO-CaO glass) ceramic-to-metal seals involves metallization and nickel plating of the ceramic surface before brazing to the metal. To obtain a satisfactory joint, the metallized layer must be nickel plated for it to be wetted by the braze alloy. The strength and hermeticity of these seals are occasionally compromised by formation of an acicular reaction product on the metallized surface of the ceramic prior to plating. This reaction phase is electrically nonconductive and inhibits uniform nickel plating. In this study a variety of electro-optical techniques is integrated to indentify the structure and composition of this deleterious acicular phase and deduce how it forms; a means to retard its formation is suggested. DOE

N86-12325# Pacific Northwest Lab., Richland, Wash.
FIXATION OF HIGH-LEVEL WASTES IN GLASSES
J. E. Mendel May 1985 37 p Presented at the Discussion Meeting on Radioactive Waste Disposal, London, 30 May 1985
(Contract DE-AC06-76RL-01830)
(DE85-013276; PNL-SA-12921; CONF-850559-1) Avail: NTIS HC A03/MF A01

The early work that led to the selection of borosilicate glass for high-level waste disposal is described, and the important properties of borosilicate glass as they are now understood are reviewed. DOE

N86-12326# Mound Lab., Miamisburg, Ohio.
IN-SITU VACUUM-ASSISTED MOLDING OF GLASS-METAL ELECTRICAL COMPONENTS
D. P. Kramer and R. T. Massey 12 Jul. 1985 10 p
(Contract DE-AC04-76DP-00053)
(DE85-015607; MLM-3267) Avail: NTIS HC A02/MF A01

In-situ vacuum-assisted molding is an innovative processing technique, which is useful in the fabrication of complex glass or glass-ceramic-to-metal seals. During in-situ vacuum-assisted molding, molten glass is pulled with vacuum onto the metal parts, allowing the formation of the seal. The process improves glass flow, facilitates the removal of trapped gases, and makes possible the fabrication of seals of complex geometry. DOE

N86-12327# University of Southern California, Los Angeles.
DEPOSITION, MICROSTRUCTURE AND PROPERTIES OF LASER CVD SIC FILMS
S. D. Allen, S. M. Copley, R. H. Edwards, and F. Shaapur 1985 59 p
(Contract DE-FG03-84ER-45093)
(DE85-014680; DOE/ER-45093/T1) Avail: NTIS HC A04/MF A01

A nonlinear numerical integration computer code for the prediction of the laser generated surface temperature distribution in the LCVD substrate has been developed in support of the experimental measurements. Additionally, deposition initiation and rates in LCVD for various deposit/substrate/laser systems were measured and correlated with theoretically calculated laser heated surface temperature profiles. This numerical integration technique, however, needs further modifications to match our SiC/substrate/laser systems specifications. Theoretical investigation of transport effects including convective and diffusive processes influence on the LCVD film growth characteristics is currently in progress. DOE

N86-12380# Tokyo Denki Univ. (Japan). Faculty of Engineering.
STUDY ON ELECTROPAINTING USING ALKOXYMETHYLMELAMINE AS CROSSLINKING AGENT
R. Shiba, M. Takahashi, H. Yoneyama, and M. Tajima *In its* Res. Rept. of the Faculty of Eng., Tokyo Denki Univ., No. 32 Dec. 1984 p 117-130 refs In JAPANESE; ENGLISH summary (For primary document see N86-12372 03-31)
Avail: NTIS HC A09/MF A01

N86-12773*# Jet Propulsion Lab., California Inst. of Tech., Pasadena.
GLASS BREAKING STRENGTH: THE ROLE OF SURFACE FLAWS AND TREATMENTS
Donald Moore *In its* Reliability and Eng. of Thin-Film Photovoltaic Modules 1 Oct. 1985 p 235-248 (For primary document see N86-12759 03-44)
Avail: NTIS HC A13/MF A01 CSCL 11B

28 PROPELLANTS AND FUELS

Includes rocket propellants, igniters, and oxidizers; storage and handling; and aircraft fuels.

For related information see also *07 Aircraft Propulsion and Power, 20 Spacecraft Propulsion and Power,* and *44 Energy Production and Conversion.*

N86-12328# IIT Research Inst., Chicago, Ill. Chemical Propulsion Information Agency.
HAZARDS OF CHEMICAL ROCKETS AND PROPELLANTS. VOLUME 3: LIQUID PROPELLANTS Manual, 1 Jan. 1977 - 30 Jun. 1985
John A. E. Hannum, ed. 30 Jun. 1985 547 p refs 3 Vol.
(Contracts F04611-82-C-0007; N00024-83-C-5301)
(AD-A158115; CPIA-Publ-394-Vol-3) Avail: Chemical Propulsion Information Agency, Johns Hopkins Road, Laurel, Md. 20707 HC $61.56 CSCL 19/1

This manual in three volumes was prepared under the auspices of the Joint Army-Navy-NASA-Air Force (JANNAF) Interagency Propulsion Committee through the Safety and Environmental Protection Subcommittee. It is intended solely as a source of information and as a set of basic guidelines for the processing, handling, storage, and transportation of chemical rocket and gun propellants and propellant ingredients. The manual consists of three volumes, of which this is the third: Volume 1-Safety Health and the Environment; Volume 2-Solid Propellants and Ingredients; Volume 3-Liquid propellants. For individual titles, see N86-12329 through N86-12357.

N86-12329# IIT Research Inst., Chicago, Ill.
HYDROCARBON FUELS
In its Hazards of Chem. Rockets and Propellants, Vol. 3 Sep. 1984 32 p refs (For primary document see N86-12328 03-28)
Avail: Chemical Propulsion Information Agency, Johns Hopkins Road, Laurel, Md. 20707 HC $61.56 CSCL 21/9

Hydrocarbon fuels are liquid rocket propellant components. Their physical and chemical properties are listed, including specifications of commercial examples. A guideline for their safe processing, handling, storage, and transportation is given. Emergency procedures to be taken in the event of accidental spills or leaks are also given. F.M.R.

N86-12330# IIT Research Inst., Chicago, Ill.
ANHYDROUS AMMONIA
In its Hazards of Chem. Rockets and Propellants, Vol. 3 Sep. 1984 16 p refs (For primary document see N86-12328 03-28)
Avail: Chemical Propulsion Information Agency, Johns Hopkins Road, Laurel, Md. 20707 HC $61.56 CSCL 21/9

Anhydrous ammonia is a liquid rocket propellant component. Its physical and chemical properties are listed. A guideline for its safe processing, handling, storage, and transportation is given. Emergency procedures to be taken in the event of accidental spills or leaks are also given. F.M.R.

N86-12331# IIT Research Inst., Chicago, Ill.
THE HYDRAZINE FUELS
In its Hazards of Chem. Rockets and Propellants, Vol. 3 Sep. 1984 26 p refs (For primary document see N86-12328 03-28)
Avail: Chemical Propulsion Information Agency, Johns Hopkins Road, Laurel, Md. 20707 HC $61.56 CSCL 21/9

Hydrazine fuel is a liquid rocket propellant component. Its physical and chemical properties are listed. A guideline for its safe processing, handling, storage, and transportation is given. Emergency procedures to be taken in the event of accidental spills or leaks are also given. F.M.R.

N86-12332# IIT Research Inst., Chicago, Ill.
NITROMETHANE
In its Hazards of Chem. Rockets and Propellants, Vol. 3 Sep. 1984 12 p refs (For primary document see N86-12328 03-28)
Avail: Chemical Propulsion Information Agency, Johns Hopkins Road, Laurel, Md. 20707 HC $61.56 CSCL 21/9

Nitromethane is a liquid rocket propellant component. Its physical and chemical properties are listed. A guideline for its safe processing, handling, storage, and transportation is given. Emergency procedures to be taken in the event of accidental spills or leaks are also given. F.M.R.

N86-12333# IIT Research Inst., Chicago, Ill.
ETHYLENE OXIDE
In its Hazards of Chem. Rockets and Propellants, Vol. 3 Sep. 1984 15 p refs (For primary document see N86-12328 03-28)
Avail: Chemical Propulsion Information Agency, Johns Hopkins Road, Laurel, Md. 20707 HC $61.56 CSCL 21/9

Ethylene oxide is a liquid rocket propellant component. Its physical and chemical properties are listed. A guideline for its safe processing, handling, storge, and transportation is given. Emergency procedures to be taken in the event of accidental spills or leaks are also given. F.M.R.

N86-12334# IIT Research Inst., Chicago, Ill.
OTTO FUEL 2
In its Hazards of Chem. Rockets and Propellants, Vol. 3 Sep. 1984 12 p refs (For primary document see N86-12328 03-28)
Avail: Chemical Propulsion Information Agency, Johns Hopkins Road, Laurel, Md. 20707 HC $61.56 CSCL 21/9

Otto Fuel 2 is a liquid rocket propellant component. Its physical and chemical properties are listed. A guideline for its safe processing, handling, storage, and transportation is given. Emergency procedures to be taken in the event of accidental spills or leaks are also given. F.M.R.

N86-12335# IIT Research Inst., Chicago, Ill.
HYDROGEN AND DEUTERIUM
In its Hazards of Chem. Rockets and Propellants, Vol. 3 Sep. 1984 13 p refs (For primary document see N86-12328 03-28)
Avail: Chemical Propulsion Information Agency, Johns Hopkins Road, Laurel, Md. 20707 HC $61.56 CSCL 21/9

Hydrogen and deuterium are liquid rocket propellant components. Their physical and chemical properties are listed. A guideline for their safe processing, handling, storage, and transportation is given. Emergency procedures to be taken in the event of accidental spills or leaks are also given. F.M.R.

N86-12336# IIT Research Inst., Chicago, Ill.
THE BORANES
In its Hazards of Chem. Rockets and Propellants, Vol. 3 Sep. 1985 18 p refs (For primary document see N86-12328 03-28)
Avail: Chemical Propulsion Information Agency, Johns Hopkins Road, Laurel, Md. 20707 HC $61.56 CSCL 21/9

Diborane and pentaborane are liquid rocket propellant components. Their physical and chemical properties are listed. A guideline for its safe processing, handling, storage, and transportation is given. Emergency procedures to be taken in the event of accidental spills or leaks are also given. F.M.R.

N86-12337# IIT Research Inst., Chicago, Ill.
CARBON MONOXIDE
In its Hazards of Chem. Rockets and Propellants, Vol. 3 Sep. 1984 8 p refs (For primary document see N86-12328 03-28)
Avail: Chemical Propulsion Information Agency, Johns Hopkins Road, Laurel, Md. 20707 HC $61.56 CSCL 21/9

Carbon monoxide is a liquid rocket propellant component. Its physical and chemical properties are listed. A guideline for its safe processing, handling, storage, and transportation is given. Emergency procedures to be taken in the event of accidental spills or leaks are also given. F.M.R.

N86-12338# IIT Research Inst., Chicago, Ill.
OXYGEN
In its Hazards of Chem. Rockets and Propellants, Vol. 3 Sep. 1984 11 p refs (For primary document see N86-12328 03-28)
Avail: Chemical Propulsion Information Agency, Johns Hopkins Road, Laurel, Md. 20707 HC $61.56 CSCL 21/9

Liquid oxgyen is a liquid rocket propellant component. Its physical and chemical properties are listed. A guideline for its safe processing, handling, storage, and transportation is given. Emergency procedures to be taken in the event of accidental spills or leaks are also given. F.M.R.

N86-12339# IIT Research Inst., Chicago, Ill.
FLUORINE AND FLUORINE MIXTURES
In its Hazards of Chem. Rockets and Propellants, Vol. 3 Sep. 1984 18 p refs (For primary document see N86-12328 03-28)
Avail: Chemical Propulsion Information Agency, Johns Hopkins Road, Laurel, Md. 20707 HC $61.56 CSCL 21/9

Fluorine and FLOX are liquid rocket propellant components. Their physical and chemical properties are listed. A guideline for its safe processing, handling, storage, and transportation is given. Emergency procedures to be taken in the event of accidental spills or leaks are also given. F.M.R.

N86-12340# IIT Research Inst., Chicago, Ill.
THE HALOGEN FLUORIDES
In its Hazards of Chem. Rockets and Propellants, Vol. 3 Sep. 1984 16 p refs (For primary document see N86-12328 03-28)
Avail: Chemical Propulsion Information Agency, Johns Hopkins Road, Laurel, Md. 20707 HC $61.56 CSCL 21/9

Chlorine fluorides are liquid rocket propellant components. Their physical and chemical properties are listed. A guideline for their safe processing, handling, storage, and transportation is given. Emergency procedures to be taken in the event of accidental spills or leaks are also given. F.M.R.

N86-12341# IIT Research Inst., Chicago, Ill.
NITROGEN OXIDES
In its Hazards of Chem. Rockets and Propellants, Vol. 3 Sep. 1984 17 p refs (For primary document see N86-12328 03-28)
Avail: Chemical Propulsion Information Agency, Johns Hopkins Road, Laurel, Md. 20707 HC $61.56 CSCL 21/9

Nitrogen oxides are liquid rocket propellant components. Their physical and chemical properties are listed. A guideline for their safe processing, handling, storage, and transportation are given. Emergency procedures to be taken in the event of accidental spills or leaks are also given. F.M.R.

N86-12342# IIT Research Inst., Chicago, Ill.
FUMING NITRIC ACIDS
In its Hazards of Chem. Rockets and Propellants, Vol. 3 Sep. 1984 16 p refs (For primary document see N86-12328 03-28)
Avail: Chemical Propulsion Information Agency, Johns Hopkins Road, Laurel, Md. 20707 HC $61.56 CSCL 21/9

Fuming nitric acids are liquid rocket propellant components. Their physical and chemical properties are listed. A guideline for their safe processing, handling, storage, and transportation is given. Emergency procedures to be taken in the event of accidental spills or leaks are also given. F.M.R.

N86-12343# IIT Research Inst., Chicago, Ill.
IODINE
In its Hazards of Chem. Rockets and Propellants, Vol. 3 Sep. 1984 7 p refs (For primary document see N86-12328 03-28)
Avail: Chemical Propulsion Information Agency, Johns Hopkins Road, Laurel, Md. 20707 HC $61.56 CSCL 21/9

Iodine is a liquid rocket propellant component. Its physical and chemical properties are listed. A guideline for its safe processing, handling, storage, and transportation is given. Emergency procedures to be taken in the event of accidental spills or leaks are also given. F.M.R.

N86-12344# IIT Research Inst., Chicago, Ill.
CHLORINE
In its Hazards of Chem. Rockets and Propellants, Vol. 3 Sep. 1984 11 p refs (For primary document see N86-12328 03-28)
Avail: Chemical Propulsion Information Agency, Johns Hopkins Road, Laurel, Md. 20707 HC $61.56 CSCL 21/9

Chlorine is a liquid rocket propellant component. Its physical and chemical properties are listed. A guideline for its safe processing, handling, storage, and transportation is given. Emergency procedures to be taken in the event of accidental spills or leaks are also given. F.M.R.

N86-12345# IIT Research Inst., Chicago, Ill.
NITROGEN TRIFLUORIDE
In its Hazards of Chem. Rockets and Propellants, Vol. 3 Sep. 1984 17 p refs (For primary document see N86-12328 03-28)
Avail: Chemical Propulsion Information Agency, Johns Hopkins Road, Laurel, Md. 20707 HC $61.56 CSCL 21/9

Nitrogen trifluoride is a liquid rocket propellant component. Its physical and chemical properties are listed. A guideline for its safe processing, handling, storage, and transportation is given. Emergency procedures to be taken in the event of accidental spills or leaks are also given. F.M.R.

N86-12346# IIT Research Inst., Chicago, Ill.
HYDROGEN PEROXIDE
In its Hazards of Chem. Rockets and Propellants, Vol. 3 Sep. 1983 19 p refs (For primary document see N86-12328 03-28)
Avail: Chemical Propulsion Information Agency, Johns Hopkins Road, Laurel, Md. 20707 HC $61.56 CSCL 21/9

Hydrogen peroxide is a liquid rocket propellant component. Its physical and chemical properties are listed. A guideline for its safe processing, handling, storage, and transportation is given. Emergency procedures to be taken in the event of accidental spills or leaks are also given. F.M.R.

N86-12347# IIT Research Inst., Chicago, Ill.
NITROGEN
In its Hazards of Chem. Rockets and Propellants, Vol. 3 Sep. 1984 11 p refs (For primary document see N86-12328 03-28)
Avail: Chemical Propulsion Information Agency, Johns Hopkins Road, Laurel, Md. 20707 HC $61.56 CSCL 21/9

Nitrogen is a liquid rocket propellant component. Its physical and chemical properties are listed. A guideline for its safe processing, handling, storage, and transportation is given. Emergency procedures to be taken in the event of accidental spills or leaks are also given. F.M.R.

N86-12348# IIT Research Inst., Chicago, Ill.
NOBLE GASES
In its Hazards of Chem. Rockets and Propellants, Vol. 3 Sep. 1983 11 p refs (For primary document see N86-12328 03-28)

Avail: Chemical Propulsion Information Agency, Johns Hopkins Road, Laurel, Md. 20707 HC $61.56 CSCL 21/9

The rare gases are used as pressurizing agents in liquid rocket propulsion. Their physical and chemical properties are listed. A guideline for their safe processing, handling, storage, and transportation is given. Emergency procedures to be taken in the event of accidental spills or leaks are also given. F.M.R.

N86-12349# IIT Research Inst., Chicago, Ill.
THE ALCOHOLS
In its Hazards of Chem. Rockets and Propellants, Vol. 3 Sep. 1984 15 p refs (For primary document see N86-12328 03-28)
Avail: Chemical Propulsion Information Agency, Johns Hopkins Road, Laurel, Md. 20707 HC $61.56 CSCL 21/9

Alcohols are used in liquid rocket propulsion. Their physical and chemical properties are listed. A guideline for their safe processing, handling, storage, and transportation is given. Emergency procedures to be taken in the event of accidental spills or leaks are also given. F.M.R.

N86-12350# IIT Research Inst., Chicago, Ill.
HALOCARBONS
In its Hazards of Chem. Rockets and Propellants, Vol. 3 Sep. 1984 31 p refs (For primary document see N86-12328 03-28)
Avail: Chemical Propulsion Information Agency, Johns Hopkins Road, Laurel, Md. 20707 HC $61.56 CSCL 21/9

Halocarbons are used during liquid rocket propulsion. Their physical and chemical properties are listed. A guideline for their safe processing, handling, storage, and transportation is given. Emergency procedures to be taken in the event of accidental spills or leaks are also given. F.M.R.

N86-12351# IIT Research Inst., Chicago, Ill.
HYDRAULIC FLUIDS c25
In its Hazards of Chem. Rockets and Propellants, Vol. 3 Sep. 1984 12 p refs (For primary document see N86-12328 03-28)
Avail: Chemical Propulsion Information Agency, Johns Hopkins Road, Laurel, Md. 20707 HC $61.56 CSCL 07/4

Hydraulic fluids are used during liquid rocket propulsion operations. Their physical and chemical properties are listed. A guideline for their safe processing, handling, storage, and transportation is given. Emergency procedures to be taken in the event of accidental spills or leaks are also given. F.M.R.

N86-12352# IIT Research Inst., Chicago, Ill.
MERCURY c25
In its Hazards of Chem. Rockets and Propellants, Vol. 3 Sep. 1984 9 p refs (For primary document see N86-12328 03-28)
Avail: Chemical Propulsion Information Agency, Johns Hopkins Road, Laurel, Md. 20707 HC $61.56 CSCL 07/4

Mercury may be used during liquid rocket propulsion operations. Its physical and chemical properties are listed. A guideline for its safe processing, handling, storage, and transportation is given. Emergency procedures to be taken in the event of accidental spills or leaks are also given. F.M.R.

N86-12353# IIT Research Inst., Chicago, Ill.
COMPRESSED AND LIQUID AIR c25
In its Hazards of Chem. Rockets and Propellants, Vol. 3 Sep. 1984 8 p refs (For primary document see N86-12328 03-28)
Avail: Chemical Propulsion Information Agency, Johns Hopkins Road, Laurel, Md. 20707 HC $61.56 CSCL 07/4

Compressed and liquid/air may be used during liquid rocket propulsion operations. Their physical and chemical properties are listed. A guideline for their safe processing, handling, storage, and transportation is given. Emergency procedures to be taken in the event of accidental spills or leaks are also given. F.M.R.

N86-12354# IIT Research Inst., Chicago, Ill.
CARBON DIOXIDE c25
In its Hazards of Chem. Rockets and Propellants, Vol. 3 Sep. 1984 10 p refs (For primary document see N86-12328 03-28)
Avail: Chemical Propulsion Information Agency, Johns Hopkins Road, Laurel, Md. 20707 HC $61.56 CSCL 07/4

Carbon dioxide may be used during liquid rocket propulsion operations. Its physical and chemical properties are listed. A guideline for its safe processing, handling, storage, and transportation is given. Emergency procedures to be taken in the event of accidental spills or leaks are also given. F.M.R.

N86-12355# IIT Research Inst., Chicago, Ill.
NITROUS OXIDE c25
In its Hazards of Chem. Rockets and Propellants, Vol. 3 Sep. 1984 7 p refs (For primary document see N86-12328 03-28)
Avail: Chemical Propulsion Information Agency, Johns Hopkins Road, Laurel, Md. 20707 HC $61.56 CSCL 07/4

Nitrous oxide is used as a liquid rocket propellant component. Its physical and chemical properties are listed. A guideline for its safe processing, handling, storage, and transportation is given. Emergency procedures to be taken in the event of accidental spills or leaks are also given. F.M.R.

N86-12356# IIT Research Inst., Chicago, Ill.
LIQUID PROPELLANT STORAGE COMPATIBILITY
In its Hazards of Chem. Rockets and Propellants, Vol. 3 Sep. 1984 3 p refs (For primary document see N86-12328 03-28)
Avail: Chemical Propulsion Information Agency, Johns Hopkins Road, Laurel, Md. 20707 HC $61.56 CSCL 21/9

Tables are presented formalizing the safe storage of propellant materials. First of all, they are stored according to similarity and compatibility, for which they are assigned alphabetical storage compatibility group designations (A, B, C, and D). A further segregation is then made on the degree of hazard presented by certain materials, the strength of oxidation, the possibility of pressure rupture, and the danger of chemical explosion. F.M.R.

N86-12357# IIT Research Inst., Chicago, Ill.
QUANTITY-DISTANCE REQUIREMENTS
In its Hazards of Chem. Rockets and Propellants, Vol. 3 Sep. 1984 15 p refs (For primary document see N86-12328 03-28)
Avail: Chemical Propulsion Information Agency, Johns Hopkins Road, Laurel, Md. 20707 HC $61.56 CSCL 21/9

Quantity-distance standards are developed for the safe storage of liquid propellants. These are presented in table form. It is first assumed that the controlling authority has properly housed the propellant materials, assuring adequate fire protection, drainage control, insulation for cryogenic materials, cooling, etc. These standards are based on the estimated credible damage, without considering the probability of frequency of occurrence. F.M.R.

N86-12358# Army Armament Research and Development Command, Watervliet, N. Y. Large Caliber Weapon Systems Lab.
WEAR OF PROJECTILE ROTATING BANDS Final Technical Report
R. S. Montgomery Mar. 1985 27 p
(AD-A156666; AD-E440283; ARLCB-TR-85008) Avail: NTIS HC A03/MF A01 CSCL 19/1

Rotating or driving bands are relatively soft materials surrounding a projectile. They have a number of functions the chief of which is probably that they produce stabilized rotating of the projectile when they are engraved or keyed into the rifling. These bands are used on spin-stabilized projectiles as small as 20 mm caliber, but this discussion concerns especially the larger cannon, i.e., in excess of 105 mm. Excess wear of projectile rotating bands has a number of important negative consequences including inaccuracy and short rounds. There are two distinctly different mechanisms of wear. At low speeds near the beginning of motion, wear is by adhesion, abrasion, and even under some conditions, scuffing. After a few centimeters of sliding, a thin surface film of molten band material is formed and the remainder of the sliding is melt-lubricated. While metal-on-metal sliding is limited to the first few centimeters, it is very important and can result in serious wear problems down bore. The exact wear of rotating bands depends on the motion of the projectile in the bore of the cannon. Therefore, this motion can be inferred from the wear. GRA

N86-12359# Southwest Research Inst., San Antonio, Tex. Fuels and Lubricants Research Lab.

MICROEMULSION-TYPE FIRE-RESISTANT DIESEL FUEL Interim Report, 1 Jan. 1982 - 31 Dec. 1984

W. D. Weatherford, Jr., G. E. Fodor, B. R. Wright, M. D. Kanakia, and E. C. Owens 31 Dec. 1984 100 p

(Contracts DAAK20-82-C-0001; DAAK70-85-C-0001)

(AD-A157125; AFLRL-191) Avail: NTIS HC A05/MF A01 CSCL 21/4

An approach to developing a fire-resistant diesel fuel (FRF) has been identified as being potentially feasible for protecting diesel-powered armored combat vehicles. This approach involves the addition of 10 vol% water and 12 vol% emulsifier premix (equal parts surfactant and aromatic concentrate) to diesel fuel to form a stable water-in-fuel microemulsion. Water, containing less than 50 ppm of dissolved solids, is required if stable formulations are to be made with all diesel fuels which may be encountered. For the same reason, it has been found necessary to include in the formulation an additional 6 vol% of an aromatic hydrocarbon concentrate to serve as a combination microemulsion promoter and emulsifier solvent/thinner. The most significant FRF inadequacy is the filter plugging at subfreezing temperatures. This, in turn, precludes FRF use under all weather conditions. In addition to the foregoing applied research, a parallel program of basic research conducted in which the influences of changes in emulsifier chemistry on diesel microemulsion phase stability, low-temperature properties, and water purity requirements were studied, and an extensive literature survey was carried out. Overall, none of the modified systems studied produced emulsions that were unambiguously superior to those made by the standard FRF surfactant. GRA

N86-12360# SRI International Corp., Menlo Park, Calif. Chemistry Lab.

OXIDATION AND GUM FORMATION IN DIESEL FUELS Interim Report, 10 Sep. 1984 - 30 Apr. 1985

F. R. Mayo 3 May 1985 17 p

(Contract DAAG29-84-K-0161)

(AD-A157410; ARO-21165.2-EG; IR-2) Avail: NTIS HC A02/MF A01 CSCL 21/4

Rates of oxygen absorption (R sub O) and gum formation (R sub g) are now related by the R sub g/ R sub o ratio, the reciprocal of the ratio previously used. The change was made because when the oxygen content of the gum is known, the R sub g/ R sub o ratio is proportional to the fraction of oxygen absorbed that appears in the gum. Oxidations of tetralin (TET) and 2-ethyl-naphthalene (EtN) at 130 C are initially fast but the rates decrease regularly. The oxidation of n-dodecane (DOD) is clearly autocatalytic; it requires the most oxygen to produce a milligram of gum while EtN, among the pure hydrocarbons, requires the least. Rates of oxygen absorption for DOD at 100 C appear to be erratic. Part of the problem is autocatalysis; part is near exhaustion of oxygen. The best results are those for K92A and K92C. R sub o without t-Bu2O2 is autocatalytic. Trends in oxidations of Fuels 14 and 14A, which are different at 130 C, are not yet clear at 100 deg., and 60 C. The important points in the above discussion are: The oxidation of DOD is autocatalytic; oxidations of TET, EtN, and Fuel 14 are self-retarding. In our oxidations of Fuel 14 with shaking, all the deposits at 100 deg. and 130 C appear as films on glass; no deposits have yet been obtained at lower temperatures. The ratio R sub g/ R sub o, still appears to be essentially constant for any fuel at a single temperature, even with large differences in R sub o from addition of t-Bu2O2. Thus, gum can be accumulated relatively rapidly for experimental purposes. We are accumulating new data at 43 deg. and 60 deg. C. These findings should assist materially in our efforts to understand and devise a test for fuel stability. GRA

N86-12361# Naval Weapons Center, China Lake, Calif.

EFFECTS OF SURFACE INTERACTIONS AND MECHANICAL PROPERTIES OF PLASTIC BONDED EXPLOSIVES ON EXPLOSIVE SENSITIVITY. PART 2: MODEL FORMULATION Annual Report, 1 Oct. 1983 - 30 Sep. 1984

R. Y. Yee and E. C. Martin Mar. 1985 31 p

(AD-A157900; AD-E900452; NWC-TP-6619-Pt-2) Avail: NTIS HC A03/MF A01 CSCL 19/1

Eight major mixes are prepared from three baseline binders. The tensile and torsional shear mechanical properties and burning behavior of these model mixes are investigated. The binder-filler bond energy determined from the surface studies can be correlated to the energy required for the onset of dewetting. The specific impulses of the model mixes are calculated. Some of the model mixes containing energetic binder are difficult to ignite at low energy flux. This suggests that the formulations may be candidates for insensitive energetic systems. GRA

N86-12362# Georgia Inst. of Tech., Atlanta. School of Aerospace Engineering.

INVESTIGATION OF THE FLAME-ACOUSTIC WAVE INTERACTION DURING AXIAL SOLID ROCKET INSTABILITIES Interim Scientific Report

B. T. Zinn and B. R. Daniel Apr. 1985 19 p

(Grant AF-AFOSR -84-0082)

(AD-A158559; AFOSR-85-0561TR) Avail: NTIS HC A02/MF A01 CSCL 21/2

The primary objective of this study is the determination of the fundamental mechanisms responsible for the driving of axial instabilities by solid propellant flames. During the report period, the behavior of a premixed flame stabilized on the side wall of a duct in the presence of an axial acoustic field was investigated both theoretically and experimentally. The developed model solutions show that driving occurs due to the combustion process heat addition while outside the reaction zone the waves are damped by viscous processes. This damping increases as the thickness of the acoustic boundary layer increases. Experimental facilities for studying oscillating duct flow in the presence and absence of flames were developed. Cold flow studies verified the presence of an excess velocity region within the acoustic boundary layer (i.e., the Richardson Effect) and the dependence of the boundary layer thickness upon the frequency and wall injection velocity. Reactive flow studies showed that the behavior of the flame depends upon its location relative to the standing acoustic wave. When the flame was positioned next to a velocity antinode, unexpected instabilities appeared on its surface eventually resulting in severe flame distortion. Also, the measured C-C and C-H radiation signals were periodic and they oscillated with the same frequency as the acoustic wave. GRA

N86-12363# Carnegie-Mellon Univ., Pittsburgh, Pa. Dept. of Mechanical Engineering.

MULTIPLE IGNITION, COMBUSTION AND QUENCHING OF HYDROCARBON FUEL SPRAYS Annual Report, Jul. 1983 - Jul. 1984

S. Aggarwal, R. Bishop, W. A. Sirignano, and H. T. Sommer Aug. 1984 14 p

(Grant AF-AFOSR-0203-80)

(AD-A158560; AFOSR-85-0498TR) Avail: NTIS HC A02/MF A01 CSCL 21/4

A detailed parametric study of the ignition of a monodisperse fuel-air spray in contact with a hot wall was conducted. The theoretical model was one-dimensional unsteady and employed a hybrid Eulerian-Lagrangian numerical scheme. Effects of drop size, chemical kinetics, fuel-air ratios, fuel type and other parameters were examined. The results indicated the statistical character of the spray ignition, the existence of optimum droplet size and optimum fuel-air ratio for the minimum ignition delays. The study was extended to the polydisperse spray. The major conclusion was that the polydisperse results can be correlated with an equivalent monodisperse spray represented by a mean diameter based on the total spray surface area. The study of ignition for sprays flowing over a hot plate was initiated. The formulation and the numerical coding were completed. Currently the code is being employed to predict the ignition delays for the flowing sprays. Preliminary experiments were conducted to investigate the ignition of a single droplet stream along a heated surface. The results show an optimal distance from the surface for the droplet stream.

It is speculated that this distance depends on the characteristic evaporation time, diffusion time and convective time inherent to the system. Experiments separating the effects are underway to investigate this interactive process. Author (GRA)

N86-12364# Midwest Research Inst., Golden, Colo.

AQUATIC SPECIES PROGRAM REVIEW: PROCEEDINGS OF PRINCIPAL INVESTIGATORS MEETING

Jun. 1985 353 p Presented at the SERI Aquatic Species Rev. - Principle Investigators Meeting, Golden, Colo., 20 Mar. 1985
(Contract DE-AC02-83CH-10093)
(DE85-012137; SERI/CP-231-2700; CONF-8503158) Avail: NTIS HC A16/MF A01

The purpose of the Aquatic Species Program is to improve the productivity, conversion to fuels, and cost efficiency of aquatic plant culture technologies. The emphasis of the program is on developing a mass culture technology for cultivating oil-yielding microalgae in the American southwest. A technical and economic analysis indicated that such a concept would be feasible if: (1) lipid yields from microalgae are improved, (2) there is sufficient saline water for large-scale development, and (3) microalgal lipids can be economically converted to conventional fuels. It was determined that fuels from microalgal lipids presented better options than converting the microalgal biomass to either alcohols or methane. All lipids can potentially be catalytically converted to gasoline, or the fatty acids can be converted to substitute diesel fuels. The Southwest has the necessary low, flat, underutilized lands, and carbon dioxide is available from either natural deposits or flue gas from industrial plants. The amount of saline water available will probably determine how much fuel can be produced from aquatic species, and this question should be answered during 1985. The largest constraint of this technology is the economical production of an oil-rich microalgal feedstock. DOE

N86-12365# Lawrence Livermore National Lab., Calif.

ENERGETIC RESPONSE OF PROPELLANTS TO HIGH VELOCITY IMPACT, REVISION 1

L. Green, E. James, and E. Lee 11 Jun. 1985 7 p refs Presented at the 8th Intern. Symp. on Detonation, Albuquerque, N. Mex., 15 Jul. 1985
(Contract W-7405-eng-48)
(DE85-013983; UCRL-91486-Rev-1; CONF-850706-22-Rev-1) Avail: NTIS HC A02/MF A01

An impact impulse on a full density intact propellant or explosive must be of high intensity (several gigapascals) to initiate detonation. Accident situation impact impulses are typically an order of magnitude less intense. The fact that detonation can arise from such lower level impulses is almost always the result of secondary compression of damaged (i.e., lower density) material. A spectrum of possible conditions has been investigated in order to evaluate threshold impact values which will cause detonation in damaged propellants. The results of new experiments involving in situ damage and impact of two propellants are reported. DOE

N86-12366# Los Alamos Scientific Lab., N. Mex.

TATE: STRONG BASIC REACTIONS PROVIDE SOLUBLE DERIVATIONS FOR SIMPLE QUALITITATIVE HIGH EXPLOSIVE SPOT TEST

B. W. Harris May 1985 15 p refs
(Contract W-7405-eng-36)
(DE85-014259; LA-10420-MS) Avail: NTIS HC A02/MF A01

Reactions of TATB in aqueous, strongly basic solutions gave metal salts of 1,3,5-trihydroxy-2,4,6-trinitrobenzene (THTNB) also called trinitrophloroglucinol. Thus, we prepared potassium, sodium, and barium salts. The mono and diammonium salts were prepared by treating THTNB with ammonia and ammonium hydroxide, respectively. Some explosive properties of the salts were evaluated. From the physical characteristics of the salts in various solvents, a spot test was developed for known high explosives (HE) containing TATB. DOE

N86-12367# Chicago Univ., Ill.

LIMITS OF THERMOCHEMICAL AND PHOTOCHEMICAL SYNTHESES OF GASEOUS FUELS: A FINITE-TIME THERMODYNAMIC ANALYSIS Annual Report, Sep. 1983 - Feb. 1985

R. S. Berry Mar. 1985 174 p refs
Avail: NTIS HC A08/MF A01 CSCL 21D

The objectives of this project are to develop methods for the evaluation of syntheses of gaseous fuels in terms of their optimum possible performance, particularly when they are required to supply those fuels at nonzero rates. The first objective is entirely in the tradition of classical thermodynamics, the processes, given the characteristics and constraints that define them. The new element which this project introduces is the capability to set limits more realistic than those from classical thermodynamics, by the inclusion of the influence of the rate or duration of a process on its performance. A second objective is to determine how any given process should be carried out, within its constraints, in order to yield its optimum performance and to use this information whenever possible to help guide the design of that process. GRA

N86-12368# Joint Publications Research Service, Arlington, Va.

CHINA REPORT: SCIENCE AND TECHNOLOGY

25 Jul. 1985 103 p refs Transl. into ENGLISH from various Chinese articles
(JPRS-CST-85-024) Avail: NTIS HC A06/MF A01

China Report: Science and Technology (25 July 1985) contains articles from scientific literature of the Peoples' Republic on National Development, Applied Sciences, Life Sciences, Scientists and Scientific Organizations, Acoustics, Chemical Industry, Computers, Control Systems, Electronics, Lasers, Mechanics, Metallurgy, Oceanography, Physical Chemistry, Physics, and Preventive Medicine. Of particular interest in this issue are two articles on solid rocket propellants under Applied Sciences. For individual titles, see N86-12369 through N86-12370.

N86-12369# Joint Publications Research Service, Arlington, Va.

PRESSURE-COUPLED RESPONSE FUNCTION OF SOLID PROPELLANTS INCLUDING THOSE WITH NEGATIVE PRESSURE EXPONENTS

Xu Wengan *In its* China Rept.: Sci. and Technol. (JPRS-CST-85-024) 25 Jul. 1985 p 4-17 refs Transl. into ENGLISH from Yuhang Xuebao (Beijing), no. 1, Jan. 1985 p 47-58 Previously announced in IAA as A85-42780 (For primary document see N86-12368 03-28)
Avail: NTIS HC A06/MF A01

A new pressure coupled response function of solid propellants has been theoretically derived using a combustion response model based on the steady state burning of composite solid propellants, including those with negative pressure exponents. In this model, the burning surface of a given propellant is divided into one part consisting of a region of the AP surface covered by molten binder with a corresponding binder surface and another part consisting of a region of the AP surface uncovered by molten binder with the remaining binder surface. The covered part of the surface is analyzed taking the condensed phase reaction and the gasification of covered AP into consideration. The results calculated by the derived pressure coupled response function for S04-5A propellant are in reasonable agreement with experimentally observed behavior. Author

N86-12370# Joint Publications Research Service, Arlington, Va.

ONE-DIMENSIONAL TWO-PHASE FLOW IN COMBUSTION CHAMBER OF SOLID PROPELLANT ROCKET MOTORS

Chang Xianqi *In its* China Rept.: Sci. and Technol. (JPRS-CST-85-024) 25 Jul. 1985 p 18-33 Transl. into ENGLISH from Yuhang Xuebao (Beijing), no. 1, Jan. 1985 p 11-23 Previously announced in IAA as A85-42777 (For primary document see N86-12368 03-28)
Avail: NTIS HC A06/MF A01

In this paper, a numerical solution of basic equations for one dimensional two phase nonequilibrium flow in combustion chambers of solid propellant rocket motors is discussed in detail. The effect of particle size on the flow field in a chamber and pressure time curves is analyzed, and some useful conclusions are obtained in comparison with results of one dimensional two phase constant lag flow in a chamber. It is useful for predicting pressure time curves accurately and providing accurate boundary conditions for the calculation of two phase flow through a nozzle. Author

N86-12418# Joint Publications Research Service, Arlington, Va.
CHARACTERISTIC VALUE AS AN ENERGY OUTPUT INDEX FOR EXPLOSIVES
Zhang Housheng and Zhang Shanshan *In its* China Rept.: Sci. and Technol. (JPRS-CST-85-018) 12 Jun. 1985 p 89-98 refs Transl. into ENGLISH from Binggong Xuebao (Beijing), no. 1, Feb. 1984 p 36-42 (For primary document see N86-12413 03-31)
Avail: NTIS HC A09/MF A01

N86-12423# Joint Publications Research Service, Arlington, Va.
QUANTUM CHEMISTRY OF AROMATIC NITRO EXPLOSIVES
Xiao Heming, Wang Zunyao, and Yao Jianmin *In its* China Rept.: Sci. and Technol. (JPRS-CST-85-021) 8 Jul. 1985 p 85-90 refs Transl. into ENGLISH from Huaxue Xuebao (Shanghai), v. 43, no. 1, Jan. 1985 p 14-18 (For primary document see N86-12421 03-31)
Avail: NTIS HC A09/MF A01

N86-12461# Joint Publications Research Service, Arlington, Va.
APPLICATION OF HEAT-SCAN NDT TO INSPECTION OF ADHESION OF SOLID ROCKET MOTOR PROPELLANT TO ENVELOPE
Tian Enrui *In its* China Rept.: Sci. and Technol. (JPRS-CST-85-026) 15 Aug. 1985 p 77-80 Transl. into ENGLISH from Harbin Gongye Daxue (Harbin), no. 1, Mar. 1985 p 74-83 (For primary document see N86-12459 03-31)
Avail: NTIS HC A07/MF A01

31 ENGINEERING (GENERAL)

Includes vacuum technology; control engineering; display engineering; and cryogenics.

N86-12371 Ohio State Univ., Columbus.
OPTIMIZATION OF THE LOCOMOTION OF A LEGGED VEHICLE WITH RESPECT TO MANEUVERABILITY Ph.D. Thesis
Dominic Anthony Messuri 1985 299 p
Avail: Univ. Microfilms Order No. DA8510604

A legged vehicle possesses a tremendous potential for maneuverability over rough terrain, particularly in comparison to conventional wheeled or tracked vehicles. In general, a legged vehicle can offer more degrees of freedom for movement than conventional vehicles. However, the coordination of the movements of the various leg joints in such a way as to produce the desired locomotion of the vehicle is an extremely complex task. The work documented in this dissertation is aimed at improving the maneuverability of a legged vehicle and reducing the operator's burden of manipulating the body and limbs. A major contribution of this research has been the development of the Dual Tripod Leg Placement Algorithm. This represents the first hardware implementation of supervisory control for an omnidirectional walking algorithm capable of rough terrain locomotion. In this algorithm, leg motion is limited only by geometrical considerations; there are no time sequencing constraints as in the typical wave gait formulations. The result is an extremely agile walking algorithm. Dissert. Abstr.

N86-12372# Tokyo Denki Univ. (Japan). Faculty of Engineering.
RESEARCH REPORTS OF THE FACULTY OF ENGINEERING, TOKYO DENKI UNIVERSITY, NO. 32
Dec. 1984 189 p refs In JAPANESE; ENGLISH summaries (ISSN-0389-617-X) Avail: NTIS HC A09/MF A01

Various research project results in the field of physics are reported by the engineering department of the Tokyo Denki University. Topics considered include: (1) plasma diagnostics in a shock tube; (2) building response in earthquake simulated by a mathematical model; (3) computer aided stress analysis; (4) speech recognition; (5) effect of cations in nerve excitation; (6) acoustics; (7) electroplating; (8) hydrogen bonds; and (9) plastic shearing. For individual titles, see N86-12373 through N86-12382.

N86-12373# Fuji Electric Co. Ltd., Yokosuka (Japan).
DISSOCIATIVE VOLUME RECOMBINATION COEFFICIENT MEASUREMENTS IN A SUBROOM TEMPERATURE NEON PLASMA AFTERGLOW c35
K. Keskinen, Y. Ichikawa, R. M. Hobson (York Univ., Toronto), H. Fukuda (Sony Co. Ltd., Tokyo), S. Teii (Musashi Inst. of Tech., Tokyo), T. Kaneda (Tokyo Denki Univ.), and J. S. Chang (McMaster Univ.) *In* Tokyo Denki Univ. Res. Rept. of the Faculty of Eng., Tokyo Denki Univ., No. 32 Dec. 1984 p 1-11 refs Sponsored in part by the Natural Sciences and Engineering Research Council of Canada (For primary document see N86-12372 03-31)
Avail: NTIS HC A09/MF A01

A new apparatus for measuring reaction rate coefficients in gaseous plasmas at low temperature is presented. The apparatus consists of a shock tube in which the plasma is generated and the plasma diagnostics are made in the expansion region of the tube. The plasma is generated by means of a R.F. pulse. Diagnostics are primarily made by double and triple electrostatic probes. Preliminary results for the gas temperature dependence of the dissociative volume recombination coefficient of neon in a temperature range of 135K to 250K are discussed. The results indicate that the gas temperature dependence is greater than T sub g to the -1/2 in this temperature range. Author

N86-12374# Tokyo Denki Univ. (Japan). Faculty of Engineering.
EARTHQUAKE-RESPONSE SIMULATION ON HORIZONTALLY LARGE-SCALE BUILDINGS BASED ON THE METHOD OF REDUCTION CONCERNING THEIR RESTORING SPRING MATRIX. DERIVATION OF GENERAL FORM OF SPRING MATRIX AND COMPARISON OF APPLIED RESPONSE RESULTS ON AN ACTUAL BUILDING WITH MEASURED VALUES c39
Fukuzo Suto and Shyuichi Asayama *In its* Res. Rept. of the Faculty of Eng., Tokyo Denki Univ., No. 32 Dec. 1984 p 13-35 refs In JAPANESE; ENGLISH summary (For primary document see N86-12372 03-31)
Avail: NTIS HC A09/MF A01

A horizontally long building structure constituted by many frames towards spanning direction is divided into several substructural blocks of 3-D framework, their required representative forms of reduced stiffness matrices are evaluated through the method of inverting their flexibility matrices firstly calculated and the final form of stiffness matrix on the whole structure is completed through their mutual connections with horizontal slab spring systems. For the general conditions managed with the individual 3-D substructured block they have included the freedoms u, v, and theta together with rocking and swaying covering elastic and plastic regions. The treatment of comparison of the quake-responding behaviors of an actual building with the analytical ones by the above theoretical system, which if accurate physical data of materials of the real structural system are input, gives a considerably good agreement verifying the appropriateness of the method described here. G.L.C.

N86-12375# Tokyo Denki Univ. (Japan). Faculty of Engineering.
A COMPUTER ANALYSIS OF THE DISTRIBUTION OF PRINCIPAL STRESSES USING PHOTOELASTIC PATTERN c39
Shoichi Ohi, Makoto Kotani, Masataka Nisida, Seiji Nakajima, and Setsuzo Honda *In its* Res. Rept. of the Faculty of Eng., Tokyo Denki Univ., No. 32 Dec. 1984 p 37-49 refs In JAPANESE; ENGLISH summary (For primary document see N86-12372 03-31)
Avail: NTIS HC A09/MF A01

A computer system of principal stress-analysis and automatic tracing of stress trajectories employing a personal-computer is described. The boundary condition and interior distribution of principal stress-difference, both obtained from two-dimensional photoelastic pattern, are put in the computer using a digitizer and Laplace's equation with respect to sum of principal stresses is solved numerically by the iteration procedure at 20x20 points over the model area. The stress trajectories are automatically traced from the obtained sigma sub 1 and sigma sub 2 without recourse to isoclinics which tend to be blurred and troublesome to determine accurately. Author

N86-12376# Tokyo Denki Univ. (Japan). Faculty of Engineering.

EXTRACTION OF FEATURE PARAMETERS FOR SPOKEN WORD RECOGNITION c32

T. Tanaka and S. Nakamura *In its* Res. Rept. of the Faculty of Eng., Tokyo Denki Univ., No. 32 Dec. 1984 p 57-65 refs In JAPANESE; ENGLISH summary (For primary document see N86-12372 03-31)

Avail: NTIS HC A09/MF A01

Extraction of local peaks in spectra of voiced signals for a speech recognition system is discussed. Since there are differences of slopes of speech spectra between members, an adaptive correction for the slope is required. A simple method of compensating a slope using a linear phase digital filter is given and it is compared with the correcting method by a least mean square fitting. Author

N86-12377# Tokyo Denki Univ. (Japan). Faculty of Engineering.

EFFECTS OF CATION IONS IN NERVE EXCITATION c52

Kazuyuki Aihara, Makoto Kotani, and Toshio Utsunomiya *In its* Res. Rept. of the Faculty of Eng., Tokyo Denki Univ., No. 32 Dec. 1984 p 67-78 refs In JAPANESE; ENGLISH summary (For primary document see N86-12372 03-31)

Avail: NTIS HC A09/MF A01

A bifurcation process of the self-sustained oscillation state of action potentials as a dissipative structure in squid giant axons is theoretically analyzed in relation to a nonequilibrium property inherent to biological membranes. A bifurcation diagram is numerically calculated by the use of the modified Hodgkin-Huxley equations which are derived by considering both an adaptation effect of axons and an effect of divalent cations upon membrane conductance. Further, the result is confirmed by the Hopf bifurcation theory. These analyses clarify the relations between the Hopf bifurcation of the dissipative structure with the limit cycle in squid giant axons and the nonequilibrium property of the ionic concentration differences across the membrane. Author

N86-12378# Tokyo Denki Univ. (Japan). Faculty of Engineering.

A PHYSICAL METHOD FOR ESTIMATING SPEECH INTELLIGIBILITY IN A REVERBERANT SOUND FIELD c32

Yasuo Ogura *In its* Res. Rept. of the Faculty of Eng., Tokyo Denki Univ., No. 32 Dec. 1984 p 79-100 refs In JAPANESE; ENGLISH summary (For primary document see N86-12372 03-31)

Avail: NTIS HC A09/MF A01

The MTF-STI method which is a physical method for measuring the quality of speech-transmission in a tunnel was investigated and it appears that the STI, which can be deduced from the MTF, correlates highly with the sound articulation score. The character of the information loss represented by the MTF, and the calculating system of the MTF are considered. In this system the effect of the reverberation on the MTF is calculated from the impulse response in a tunnel, and the effect of the noise separate from the effect of the reverberation is considered. The MTF is converted to the STI (Speech Transmission Index), which corresponds directly to the speech intelligibility. Essentially the STI represents an extension of the Articulation Index (AI) concept, therefore we determine the values of the parameters used in the STI calculation from the parameters of the AI for Japanese. Resulting STI correlates highly with the -log(1-s), where s is a sound articulation score. The data suggest that the STI may serve as a convenient predictor of speech intelligibility in a tunnel. Author

N86-12379# Tokyo Denki Univ. (Japan). Faculty of Engineering.

DUMMY HEAD MICROPHONE AND ITS APPLICATION TO THE MEASUREMENTS OF ELECTRO-ACOUSTIC EQUIPMENTS c32

In its Res. Rept. of the Faculty of Eng., Tokyo Denki Univ., No. 32 Dec. 1984 p 101-115 refs In JAPANESE; ENGLISH summary (For primary document see N86-12372 03-31)

Avail: NTIS HC A09/MF A01

An acoustic measurement system using a dummy head microphone was developed. The system consists of a dummy head microphone and an equipment for digital signal processing, and the system can be used to measure characteristics of hearing aids and headphones. The ear simulator, newly developed for practical use, is terminated in a simple resistance element of 320 cgs acoustic ohms. The dummy head microphone with the ear simulator shows the good agreement with the acoustical characteristics of the averaged human external ear. Several measured results of hearing aids and headphones using the measurement system are shown. Author

N86-12380# Tokyo Denki Univ. (Japan). Faculty of Engineering.

STUDY ON ELECTROPAINTING USING ALKOXYMETHYLMELAMINE AS CROSSLINKING AGENT c27

R. Shiba, M. Takahashi, H. Yoneyama, and M. Tajima *In its* Res. Rept. of the Faculty of Eng., Tokyo Denki Univ., No. 32 Dec. 1984 p 117-130 refs In JAPANESE; ENGLISH summary (For primary document see N86-12372 03-31)

Avail: NTIS HC A09/MF A01

When alkoxymethylmelamine, which has unsubstituted amino hydrogens, was used as crosslinking agent with substrate resin, the stability of electropainting solution was poor. Namely polymer was formed by self-condensing polymerization of the crosslinking agent, then the resulting polymer worked as nucleus to from big colloid, and the colloid produced bad effects on the adhesiveness and the surface properties of electrodeposition film. Consequently, only hexa-alkoxymethylmelamine which do not polymerize was been able to use as crosslinking agent. Author

N86-12381# Tokyo Denki Univ. (Japan). Faculty of Engineering.

THE STUDIES ON THE EFFECTS OF INTERMOLECULAR HYDROGEN BOND IN MELAMINE RESINATION PROCESS. (METHYLATED MELAMINES WERE ADOPTED AS THE MODEL COMPOUNDS OF STARTING MATERIAL) c25

Moritaka Tajima *In its* Res. Rept. of the Faculty of Eng., Tokyo Denki Univ., No. 32 Dec. 1984 p 131-156 refs In JAPANESE; ENGLISH summary (For primary document see N86-12372 03-31)

Avail: NTIS HC A09/MF A01

The effect of intermolecular hydrogen bond formation contributing to the properties of methylolmelamines and the resin was already studied theoretically in our research group by means of CNDO method. However, it has been known that the thermohardening process of methylolmelamines is complicated. Therefore it is needed to prove the process experimentally. Concreately, active amino-hydrogen atoms of melamine was changed into methyl groups to restrict the hydrogen bond formation. Nine methylated melamines and eight methylolized methylated melamines were synthesized, and identified by NMR and IR spectroscopies. The solubility and the melting point of those compounds were measured. From these results it was clarified that the extent of hydrogen bond formation played an important role in the solubility and the melting point. G.L.C.

N86-12382# Tokyo Denki Univ. (Japan). Faculty of Engineering.

STUDY OF HIGH SPEED SHEARING OF THERMOPLASTIC POLYMER SHEETS WITH A NEW ROTARY SHEARING MACHINE c37

Isami Aoki and Teizo Maeda *In its* Res. Rept. of the Faculty of Eng., Tokyo Denki Univ., No. 32 Dec. 1984 p 157-168 refs (For primary document see N86-12372 03-31)

Avail: NTIS HC A09/MF A01

An investigation on clarifying the shearing characteristics of thermoplastic polymer sheets is presented. Shearing experiments were carried out by using a rotating shearing machine newly designed for achieving tests in a wide range of shearing speed. Shearing speed and temperature were widely varied in order to disclose those effects and to find out the optimum shearing conditions. As the result of tests on five kinds of thermoplastic sheets, it is confirmed that the smooth surface can be obtained by selecting the shearing speed and temperature. It is also known that the deformation zone decreases with increasing speed. In addition, this rotary shearing machine is made firm to be available for shearing tests in a wide range of shearing speed. Author

N86-12383# Tohoku Univ., Sendai (Japan). Research Inst. of Electrical Communication.
THE RECORD OF ELECTRICAL AND COMMUNICATION ENGINEERING CONVERSAZIONE, VOLUME 54, NO. 1
Aug. 1985 34 p refs In JAPANESE; ENGLISH summaries
(ISSN-0385-771-9) Avail: NTIS HC A03/MF A01

Progress in the fields of electrical engineering and computer science by Tohoku University are reported. Topics of interest are: (1) the development of a new high efficiency peniotron; (2) the analysis of hysteresis in a diode loaded loop antenna electromagnetic field sensor; (3) a resonant frequency method of nondestructive testing; (4) the use of high level programming language to check logic design in very large scale integrated circuits; and (5) computer programming with high level programming languages such as PROLOG. For individual titles, see N86-12384 through N86-12388.

N86-12384# Tohoku Univ., Sendai (Japan). Research Inst. of Electrical Communication.
PROPOSAL OF A HIGH EFFICIENT AND HIGH POWER PENIOTRON **c35**
Nobuyuki Sato, Mohamad Razeghi, Takehisa Suzuki, Kuniyoshi Yokoo, and Shoichi Ono *In its* The Record of Elec. and Commun. Eng. Conversazione, Vol. 54, No. 1 Aug. 1985 p 1-8 refs In JAPANESE; ENGLISH summary (For primary document see N86-12383 03-31)
Avail: NTIS HC A03/MF A01

A modified peniotron which is expected to increase both of handling power and conversion efficiency compared with the original peniotron, and the analytical results of its operational characteristics using some computer simulations are discussed. The analytical results assuming the fundamental operation of omega sub o = approx. omega sub c at 10GHz show that an extremely high transverse efficiency of nearly 100% would be attainable over a considerably wide range of out-put power. And also, this tube is capable to increase the handling power because of the use of a TE sub 11 rectangular waveguide cavity instead of the double-pair ridge waveguide cavity used for the original peniotron. Author

N86-12385# Tohoku Univ., Sendai (Japan). Research Inst. of Electrical Communication.
HYSTERESIS CHARACTERISTICS OF A DIODE LOADED E-M LOOP SENSOR **c33**
Hiroshi Echigo *In its* The Record of Elec. and Commun. Eng. Conversazione, Vol. 54, No. 1 Aug. 1985 p 9-13 refs In JAPANESE; ENGLISH summary (For primary document see N86-12383 03-31)
Avail: NTIS HC A03/MF A01

Proper sensors are required to probe the Electro-Magnetic Environment. As one of the sensors, a diode loaded loop antenna was tested. Unexpectedly, it showed hysteresis characteristics in the frequency responses. The hysteresis comes from the voltage depending capacity of the diode using the equivalent circuit. Author

N86-12386# Tohoku Univ., Sendai (Japan). Research Inst. of Electrical Communication.
ACCURACY OF A NEW ULTRASONIC APPARATUS FOR SIMPLE MEASUREMENT OF VISCOELASTICITY **c71**
Ryohji Aoyagi and Hiroshi Shimizu *In its* The Record of Elec. and Commun. Eng. Conversazione, Vol. 54, No. 1 Aug. 1985 p 14-19 refs In JAPANESE; ENGLISH summary (For primary document see N86-12383 03-31)
Avail: NTIS HC A03/MF A01

A new simple nondestructive method of measuring the complex elastic modulus by detecting the changes in the resonance frequency and the mechanical quality factor of the ultrasonic vibrator when its horn tip is pressed upon a testing material with a static force is discussed. Elastic moduli of polymers (acryl, polyacetal, polycarbonate) measured by the present method are compared with those measured by the composite resonator method. It is demonstrated that the accuracy of the measured values of the Young's modulus, E, is fairly good for the three materials in the temperature range from -10 C to 60 C and that of the elastic loss factor, tan DELTA is satisfactorily good for acryl, while not so good for polyacetal and polycarbonate. Author

N86-12387# Tohoku Univ., Sendai (Japan). Research Inst. of Electrical Communication.
THE VERIFICATION OF THE LOGIC CIRCUITS BASED ON PARTICLIZED INFORMATION BITS WITH PROLOG **c33**
Yoshiaki Takai, Fusao Nakagawa, Tadao Nakamura, and Yoshiharu Shigei *In its* The Record of Elec. and Commun. Eng. Conversazione, Vol. 54, No. 1 Aug. 1985 p 20-25 refs In JAPANESE; ENGLISH summary (For primary document see N86-12383 03-31)
Avail: NTIS HC A03/MF A01

The more logic elements are being integrated into single LSI chip, the more significant the accuracy of logic design is becoming. In order to fabricate VLSI chips costly, a reliable and effective verification system will become necessary. A formal model based on particlized information bits is presented. The logic elements of this model are represented by three kinds of functional nodes and the logic operation of those can be specified with temporal logic. Secondly, the formal verification methodology of the logic circuit constructed of the functional nodes using Prolog which is considered one of the most popular logic programming languages is discussed. Lastly, CPU time for the verification of fundamental product logic circuits, and also the possibilities of its reduction using meta-logical function are assessed. Prolog could be very convenient for the formal verification of logic circuits. Author

N86-12388# Tohoku Univ., Sendai (Japan). Research Inst. of Electrical Communication.
A METHODOLOGY FOR SYNTAX-ANALYSIS USING PROLOG **c61**
Takahika Murayama, Yoshiyuki Kawazoe, and Yoshiharu Shigei *In its* The Record of Elec. and Commun. Eng. Conversazione, Vol. 54, No. 1 Aug. 1985 p 26-30 refs In JAPANESE; ENGLISH summary (For primary document see N86-12383 03-31)
Avail: NTIS HC A03/MF A01

The information represented by the high level programming languages has been expressed for executing tasks by the computer. The series of basic construction elements called Words is admitted as pure statements that belong to a specific programming language only in the case that they follow the same rules (syntax). The metalanguage written by BNF (Backus-Naur-Form) is prepared, so as to describe the rules for construction of a sentence. BNF prescribes how the language is constructed through gathering of characters and symbols. Using prolog a methodology is presented which analyzes the rules for the construction of a metalanguage sentence written by BNF and; recognizes whether a series of symbols follow these rules or not. Author

N86-12389# Forest Products Lab., Madison, Wis.
STEAM-INJECTION PRESSING OF ISOCYANATE-BONDED ASPEN FLAKEBOARDS, LATITUDES AND LIMITATIONS
R. L. Geimer Jul. 1985 19 p
(AD-A157833; FPL-456) Avail: NTIS HC A02/MF A01 CSCL 13/8

Injection of steam into a flakeboard mat during pressing significantly reduces press times. One-half-inch-thick 0.640 specific gravity (SG) isocyanate-bonded aspen flakeboard can be cured in 60 seconds by injecting 99 Btu's of steam energy per pound (Btu/lb) of board. Press time may be reduced to 40 seconds when energy consumption is increased to 177 Btu/lb of board. Two-inch-thick 0.640 SG board can be pressed in 201 seconds with 185 Btu/lb. Blister formation in high-density thin boards and temperature variation in low-density thick boards were compensated for with press cycles individually suited for each combination of board thickness and SG. GRA

N86-12390# Rockwell International Corp., Golden, Colo.
OPTIONS FOR OPERATIONAL RISK ASSESSMENTS
S. A. Dover 1985 12 p Presented at the 7th Intern. System Safety Conf., San Jose, Calif., 25 Jul. 1985
(Contract DE-AC04-76DP-03533)
(DE85-014904; RFP-3855; CONF-850723-4) Avail: NTIS HC A02/MF A01

Risk assessment is a set of analytical tools that can be used to clarify possible outcomes of decisions where the two different courses of action are indicated or different values are in conflict. These conflicts often arise in the management of any production or support facility. This paper outlines the options for performing risk assessments of any scope and the parameters that determine their effectiveness. It highlights the relative costs of each option, useful information developed, and limitations of the information. The paper concludes with the types of decisions that are routinely made in an operating facility and could benefit from the information generated in a risk assessment. DOE

N86-12391# Sandia National Labs., Albuquerque, N. Mex.
NUMERICAL STUDIES OF THE DYNAMIC ISENTROPIC LOADING OF SOLID MOLECULAR HYDROGEN
T. G. Trucano, L. M. Barker, J. R. Asay, and G. I. Kerley 1985 6 p Presented at the Am. Phys. Soc. Topical Conf. on Shock Waves in Condensed Matter, Spokane, 22 Jul. 1985
(Contract DE-AC04-76DP-00789)
(DE85-013961; SAND-85-0411C; CONF-850736-18) Avail: NTIS HC A02/MF A01

Barker, et al., have proposed a dynamic technique for isentropically compressing solid molecular hydrogen specimens to multi-Mbar pressures. Because of the many novel features of this experimental technique, computational simulations of the experiment have been used extensively in the experimental design effort. Over the past two years, many such simulations have been performed. Our purpose in the present paper is to briefly summarize important conclusions resulting from this work. We briefly describe the equation of state of solid molecular hydrogen currently in use in our calculations. We are, of course, primarily interested in the uncertainties in the equation of state, and how these influence the calculations. We then discuss the computational approach and summarize some important conclusions of the work. Finally, we consider the relevance of these results to the proposed experiment. DOE

N86-12392# Wyle Labs., Inc., Huntsville, Ala.
SAFETY CRITERIA FOR THE OPERATION OF GASEOUS HYDROGEN PIPELINES Final Report
W. W. Youngblood 12 Nov. 1984 92 p refs
(Contract DTRS56-81-C-00043)
(PB85-206159; WR-84-24; RSPA/DMT10-85/1) Avail: NTIS HC A05/MF A01 CSCL 13B

This report discusses safety criteria for the transportation of gaseous hydrogen by pipeline. Major emphasis is placed on transmission pipelines, but distribution piping is also considered. The report concludes that under certain conditions gaseous hydrogen could pose public safety hazards that are not adequately addressed by current safety code regulations. Preliminary criteria for the design of new gaseous hydrogen transmission lines, for converting existing transmission lines to gaseous hydrogen service, for enhanced operating procedures and maintenance practices for mainline transmission systems, and for introducing hydrogen into existing or new distribution systems are recommended. GRA

N86-12393# Joint Publications Research Service, Arlington, Va.
CHINA REPORT: SCIENCE AND TECHNOLOGY
23 May 1985 152 p refs Transl. into ENGLISH from various Chinese articles
(JPRS-CST-85-016) Avail: NTIS HC A08/MF A01

China Report (23 May 1985) is a periodic collection of Chinese (People's Republic) Science and Technology articles. Subjects encompassed include national developments in the sciences and technology, applied sciences, life sciences, environmental quality, biochemistry, chemistry, computer developments and applications, oceanography, oncology, optics and radiation. Of special interest in this volume are articles on laser technology, satellite sounding, and fluid mechanics. For individual titles, see N86-12394 through N86-12398.

N86-12394# Joint Publications Research Service, Arlington, Va.
COMPACT TEA-CO2 LASER WITH LONG LIFE DEVELOPED c36
Yin Yiyan, Zhang Yixiang, Want Zongjin, Wei Xianren, and Gao Chunguang *In its* China Rept.: Sci. and Technol. (JPRS-CST-85-016) 23 May 1985 p 36-42 refs Transl. into ENGLISH from Yingyong Jiguang (Shanghai), v. 5, no. 1, Feb. 1985 p 39-42 (For primary document see N86-12393 03-31)
Avail: NTIS HC A08/MF A01

A compact TEA-CO2 laser for ranging application has been made. The laser is 100x100x300 cu mm in size, the maximum output energy per pulse is 500 mJ and the laser has been operated over 10 to the 6th power pulses at 60 mJ output energy. An experimental and theoretical study is made of the laser plasma charge. Author

N86-12395# Joint Publications Research Service, Arlington, Va.
FREQUENCY SELECTION AND MODE LOCKING OF Nd:YAG LASER c36
Tang Guichen and Qiu Peixia *In its* China Rept.: Sci. and Technol. (JPRS-CST-85-016) 23 May 1985 p 43-50 refs Transl. into ENGLISH from Zhongguo Jiguang (Shanghai), v. 12, no. 1, 20 Jan. 1985 p 11-14 (For primary document see N86-12393 03-31)
Avail: NTIS HC A08/MF A01

Using a prism as the dispersion element the mode locking of a Nd:YAG laser at four spectral lines (1.052, 1.061, 1.064, and 1.073 microns) has been achieved. The calculated output wavelength stability agreed with the experimental results. Author

N86-12396# Joint Publications Research Service, Arlington, Va.
MEAN DENSITY SCALE HEIGHTS FROM ANALYSIS OF VARIATION IN PERIGEE HEIGHT OF CHINA'S SECOND SATELLITE c13
Feng Zhanliang *In its* China Rept.: Sci. and Technol. (JPRS-CST-85-016) 23 May 1985 p 67-72 refs Transl. into ENGLISH from Kongjian Kexue Xuebao (Beijing), v. 4, no. 1, 1984 p 76-81 Original language document was announced in IAA as A86-45634 (For primary document see N86-12393 03-31)
Avail: NTIS HC A08/MF A01

A method for computing the density scale height H is discussed. Four mean values of the density scale height H are determined from the analysis of variations in the perigee height of China's second satellite. The difference between the determined values and CIRA-1972 is less than 10 percent, the mean H is 5 percent greater than that given by CIRA-1972. Author

N86-12397# Joint Publications Research Service, Arlington, Va.
NUMERICAL COMPUTATION OF FULL THREE-DIMENSIONAL FLOW IN TRANSONIC TURBINES c34
Shen Mengyu and Zhang Yaoke *In its* China Rept.: Sci. and Technol. (JPRS-CST-85-016) 23 May 1985 p 73-77 refs Transl. into ENGLISH from Shuzhi Jisuan yu Jisuanji Yingyong (Beijing), no. 2, Jun. 1984 p 125-128 (For primary document see N86-12393 03-31)
Avail: NTIS HC A08/MF A01

The scalar integral form of momentum equations in the cylindrical coordinate system is derived by a simple method. The derived equations can be applied to an arbitrary control volume. It is shown that all radial momentum equations are missing a term. The influence of the missing term on computational results is discussed using a numerical test. It is also shown that the discrete form of the radial momentum equation has a wrong sign and cannot be applied to an arbitrary control volume. Author

N86-12398# Joint Publications Research Service, Arlington, Va.
CODE OF FINITE ELEMENT ANALYSIS FOR THREE-DIMENSIONAL FLOW IN TURBOMACHINES c34
Huang Abdiang *In its* China Rept.: Sci. and Technol. (JPRS-CST-85-016) 23 May 1985 p 78-91 refs Transl. into ENGLISH from Shuzhi Jisuan yu Jisuanji Yingyong (Beijing), no. 1, Mar. 1984 p 38-47 (For primary document see N86-12393 03-31)
Avail: NTIS HC A08/MF A01

The code of finite element analysis based on the arbitrary stream surface theory of three-dimensional flow in turbomachines is presented. The structure of the code and numerical examples using this code are also provided. Author

N86-12399# Joint Publications Research Service, Arlington, Va.
CHINA REPORT: SCIENCE AND TECHNOLOGY
17 Oct. 1985 154 p refs Transl. into ENGLISH from various Chinese articles
(JPRS-CST-85-035) Avail: NTIS HC A08/MF A01

Advances in science and technology by the Peoples Republic of China are reported. Topics of discussion include; (1) national development; (2) physical sciences; (3) applied sciences; (4) astronautics; (5) chemistry; (6) computers; (7) cryogenics; (8) electronics; (9) engineering; (10) mathematics; (11) physics; (12) semiconductors; and (13) solar energy. For individual titles, see N86-12400 through N86-12407.

N86-12400# Joint Publications Research Service, Arlington, Va.
NEW CRITERION OF COMBINED-MODE BRITTLE FRACTURE DESCRIBED c39
Lin Baisong *In its* China Rept.: Sci. and Technol. (JPRS-CST-85-035) 17 Oct. 1985 p 27-33 refs Transl. into ENGLISH from Yingyong Shuxue He Lixue (Chongqing), v. 5, no. 6, Nov. 1984 p 849-853 (For primary document see N86-12399 03-31)
Avail: NTIS HC A08/MF A01

A new mixed-Mode brittle fracture criterion, the circumferential stress-strain product, is presented. It is found to be in good agreement with experimental data. Author

N86-12401# Joint Publications Research Service, Arlington, Va.
CARTOGRAPHY, NATIONAL LAND MANAGEMENT RELATED c43
Shao Wenxiang *In its* China Rept.: Sci. and Technol. (JPRS-CST-85-035) 17 Oct. 1985 p 34-35 Transl. into ENGLISH from Renmin Ribao (Beijing), 16 May 1984 p 5 (For primary document see N86-12399 03-31)
Avail: NTIS HC A08/MF A01

The practice of surveying and cartography provides one of the indispensable and fundamental preliminary task for national land management. As a matter of fact, the success of national land management is closely related to the performance of the surveying and cartography service. The development of national land management requires a thorough preliminary inventory of geographical conditions and the natural and human resources in the territory; the surveying and cartography process is one of the important means to obtain this type of information. Land management is based on the results and maps produced by the surveying and cartography service. Nearly all the land management tasks, such as land planning and management, utilization, protection and administration, require the information acquired by surveying and cartography. G.L.C.

N86-12402# Joint Publications Research Service, Arlington, Va.
BENEFITS OF SURVEYING, CARTOGRAPHY DESCRIBED c43
Yu Cang *In its* China Rept.: Sci. and Technol. (JPRS-CST-85-035) 17 Oct. 1985 p 36-39 Transl. into ENGLISH from Renmin Ribao (Beijing), 16 May 1984 p 5 (For primary document see N86-12399 03-31)
Avail: NTIS HC A08/MF A01

Surveying and cartography are two important methods for investigating nature and studying societies. They are considered to be the fundamental preparations and the preliminary procedures to a national economic development program. The basic functions of surveying and cartography include the determination of precise geographic coordinates, altitude and gravity data for all the control points and the publication of maps at various scales of China, thematic maps and map collections as well as surveying and mapping services for economic development, national defense construction, cultural education, scientific research, foreign affairs, border-area surveying, transportation, tourism and interior administration. In addition, performance of these tasks such as agricultural resource investigation and zoning, farmland water conservancy development, geological studies and mining surveys, the exploration and utilization of geothermal power, exploration of oil and coal fields, route surveying and the construction of railways and highways, hydrographic surveying and river control, earthquake prediction and advance warning, shoreline resource study and urban planning requires reliable survey data and maps provided by preliminary surveying and cartography services. G.L.C.

N86-12403# Joint Publications Research Service, Arlington, Va.
STATUS, DEVELOPMENT OF POWER ULTRASONICS IN CHINA c71
Zhang Fucheng and Cheng Cundi *In its* China Rept.: Sci. and Technol. (JPRS-CST-85-035) 17 Oct. 1985 p 40-51 refs Transl. into ENGLISH from Yingyong Shengxue (Beijing), v. 4, no. 3, Jul. 1985 p 1-6 (For primary document see N86-12399 03-31)
Avail: NTIS HC A08/MF A01

Power acoustics and the utilization of rather high ultrasonic energy for cleaning, processing, ultrasonic therapeutics, surgery and other purposes are discussed. The frequencies used generally range from 10 kHz to 60 kHz (some are 1 MHz or more) with acoustic intensities ranging from O.X watts./sq. cm. to several hundred watts/sq. cm. (the figure is even higher for some special uses). Author

N86-12404# Joint Publications Research Service, Arlington, Va.
PLASMA ARC WELDING FOR THIN TITANIUM PLATES c37
Luo Jinru and Tang Xingli *In its* China Rept.: Sci. and Technol. (JPRS-CST-85-035) 17 Oct. 1985 p 52-62 refs Transl. into ENGLISH from Shiyou Huagong Shebei (Lanzhou), v. 14, no. 4, 1985 p 11-16 (For primary document see N86-12399 03-31)
Avail: NTIS HC A08/MF A01

Techniques for flat and butt plasma arc welding are described for 3-mm-thick TAI industrial plates consisting of almost pure titanium. Welding techniques, standards, and equipment are selected experimentally, with special emphasis on the discharge of the plasma gas and the welding current, welding speed, and electric arc voltage. The parameter values recommended are compared with those for stainless steel plates, and it is concluded that the LH-300 plasma arc device can give excellent results in welding thin titanium and stainless steel plates, provided that the welding parameters and titanium and stainless steel plates, provided that the welding parameters and equipment quality are strictly controlled. Author

N86-12405# Joint Publications Research Service, Arlington, Va.
JAPANESE REPORT ON CHINA'S F-8 FIGHTER c08
Yu Yuebo *In its* China Rept.: Sci. and Technol. (JPRS-CST-85-035) 17 Oct. 1985 p 70-72 Transl. into ENGLISH from Hangkong Zhishi (Beijing), no. 7, Jul. 1985 p 22-23 (For primary document see N86-12399 03-31)
Avail: NTIS HC A08/MF A01

A new Chinese-built fighter aircraft has been unveiled. This aircraft, which is named the F-8, has a delta wing and a horizontal tail; it probably has two engines, and its maximum speed is estimated to be greater then Mach2. According to the article 1983-1984 Military Balance, approximately thirty F-8 aircraft are currently in service in the Chinese Air Force. G.L.C.

N86-12406# Joint Publications Research Service, Arlington, Va.
THE 4-BIT MICROPROCESSOR CAPABILITIES, APPLICATIONS DESCRIBED c60

Miao Xiaosheng *In its* China Rept.: Sci. and Technol. (JPRS-CST-85-035) 17 Oct. 1985 p 73-87 Transl. into ENGLISH from Dianzi Jishu Yingyong (Beijing), no. 5, 25 May 1985 p 40-45 (For primary document see N86-12399 03-31)
Avail: NTIS HC A08/MF A01

Production of China's 4-bit microprocessor circuits has currently reached the level of foreign developmental chips in the early 1980's. There are already several hundred units in China that have taken up applications with 4-bit microprocessors, and domestically produced 4-bit microprocessor circuits can already more or less fulfill domestic requirements. G.L.C.

N86-12407# Joint Publications Research Service, Arlington, Va.
MATHEMATICAL MODEL OF THE DYNAMIC RESPONSE OF THERMO-REGULATING IN 200 MeV LINEAR ACCELERATOR c73
Hu Defang and Ouyang Xiantai *In its* China Rept.: Sci. and Technol. (JPRS-CST-85-035) 17 Oct. 1985 p 90-95 refs Transl. into ENGLISH from Zhongguo Kexue Jishu Daxue Xuebao (Hefei), v. 15, no. 2, Jun. 1985 p 217-222 (For primary document see N86-12399 03-31)
Avail: NTIS HC A08/MF A01

A 200 MeV electron linear accelerator is used as the injector for the 800 MeV electron synchrotron. The traveling wave cavity of the linear accelerator is a 2p1/3 model equal-impedance, disk-loaded waveguide. The power loss inside the waveguide attenuates exponentially along the length of the accelerator (in the x direction). G.L.C.

N86-12408# Joint Publications Research Service, Arlington, Va.
CHINA REPORT: SCIENCE AND TECHNOLOGY
11 Jun. 1985 167 p refs Transl. into ENGLISH from various Chinese articles
(JPRS-CST-85-017) Avail: NTIS HC A08/MF A01

Scientific and technological research in China is reported. The journal is divided into sections on national development, applied sciences, life sciences, environmental quality, and abstracts on armaments, genetics, lasers, oceanology, pharoacology and physics. Some articles of interest might be: determination of single mode optical fiber dispersion; microcomputer controlled closed loop system for positioning radio telescope; laser anemometer using a single circuit-boards; and the step structure effect of DC Josephson current within one flux quantum period. For individual titles, see N86-12409 through N86-12412.

N86-12409# Joint Publications Research Service, Arlington, Va.
DETERMINATION OF SINGLE-MODE OPTICAL FIBER DISPERSION c74
Zhou Wenjun *In its* China Rept.: Sci. and Technol. (JPRS-CST-85-017) 11 Jun. 1985 p 42-51 refs Transl. into ENGLISH from Tongxin Xuebao (Beijing), v. 5, no. 3, Jul. 1984 p 95-101 (For primary document see N86-12408 03-31)
Avail: NTIS HC A08/MF A01

On the basis of theoretical analysis and a large number of numerical calculations, an approximate analytic formula is proposed to determine the dispersions of single mode optical fibers from the relative operating wavelength, the relative refractive index difference and the core radius of the fibers. Additionally, important parameters, such as the propagating constant and the ratio of power flow in the core of the single mode optical fibers, can also be calculated by means of the related formula given. Author

N86-12410# Joint Publications Research Service, Arlington, Va.
MICROCOMPUTER-CONTROLLED CLOSED-LOOP SYSTEM FOR POSITIONING RADIO TELESCOPE c89
Zhu Liqing, Chu Yingyi, and Zhang Zhenchao *In its* China Rept.: Sci. and Technol. (JPRS-CST-85-017) 11 Jun. 1985 p 69-77 ref Transl. into ENGLISH from Wei Jisuanji Yingyong (Beijing), no. 4, Nov. 1984 p 26-30 (For primary document see N86-12408 03-31)
Avail: NTIS HC A08/MF A01

A millimeter range radio telescope is used to track and observe stars that emit radiation at radio frequencies. The horizontal system responsible for moving the principal receiving plane is equipped with servo systems for controlling the azimuthal position and pitch of the telescope. The telescope contains six servos which employ closed loop computer controlled positioners or automatic tracking and focusing. In order to match the servo systems to the basic requirements of the closed loop computer positioning system, a microprocessor based controller was designed and tested in experiments on the control of servo systems for regulating the principal and auxiliary planes of the telescope. Methods were studied for coordinating and correcting the system. This work is briefly described. Author

N86-12411# Joint Publications Research Service, Arlington, Va.
LASER ANEMOMETER USING A SINGLE CIRCUIT BOARD c35
Gu Weiyu, Han Shouchun, Song Zhengfang, Liu Xiaochun, Ding Qiang, and Qi Fudi *In its* China Rept.: Sci. and Technol. (JPRS-CST-85-017) 11 Jun. 1985 p 78-85 Transl. into ENGLISH from Weijisuanji Yingyong (Beijing), no. 4, Nov. 1984 p 48-51 (For primary document see N86-12408 03-31)
Avail: NTIS HC A08/MF A01

Real time measurements of average wind velocities over ranges of a few hundred meters or more are important for the national economy and in scientific research; nevertheless, effective and economical measurement methods remain unavailable. We have designed a laser correlation anemometer which exploits the relationship between fluorescence induced by a laser beam traveling in air and the wind velocity in the path of the beam. The system measures the average vertical wind velocity in the path of the laser beam and employs a DBJ-80 single board computer; it makes full use of software capabilities and does not require modulus conversion systems. The device is light weight and easily transported, and tests show that accuracy of the measurements is highly satisfactory. Author

N86-12412# Joint Publications Research Service, Arlington, Va.
THE STEP STRUCTURE EFFECT OF dc JOSEPHSON CURRENT WITHIN ONE FLUX QUANTUM PERIOD phi SUB ZERO (2) c33
Zhang Yuheng, Shen Xiuling, Zheng Jiefei, and Wu Yan *In its* China Rept.: Sci. and Technol. (JPRS-CST-85-017) 11 Jun. 1985 p 104-114 refs Transl. into ENGLISH from Wuli Xuebao (Beijing), v. 33, no. 8, Aug. 1984 p 1075-1083 (For primary document see N86-12408 03-31)
Avail: NTIS HC A08/MF A01

A large Josephson junction placed in a high-Q cavity whose rth eigen-mode is excited by the Josephson frequency omega = 2 eV sub zero/h, the oscillating electromagnetic field will feedback the junction and one must recognize that the spatial parts of the eigen-mode of the feedback field are not the same on the junction. Theoretical results were obtained differently from those of a previous researcher, and experimental results showing how the step structure current vary with the magnetic field. The match condition for eigen-mode of the feedback field from the cavity and electromagnetic field radiated by Josephson junction was worked out. Finally, the physical reason for the absence of step structure with period less than phi sub zero is given. Author

N86-12413# Joint Publications Research Service, Arlington, Va.
CHINA REPORT: SCIENCE AND TECHNOLOGY
12 Jun. 1985 188 p refs Transl. into ENGLISH from various Chinese articles
(JPRS-CST-85-018) Avail: NTIS HC A09/MF A01

Progress in Chinese science and technology is reported. Topics discussed include: national developments; applied sciences; life sciences; environmental quality; applied mathematics; chemistry; computer applications; electronics, optics; physics and thermodynamics. For individual titles, see N86-12414 through N86-12420.

N86-12414# Joint Publications Research Service, Arlington, Va.
STATE-OF-THE-ART OF OPTICS IN CHINA REVIEWED c74
Wang Daheng and Wo Xinneng *In its* China Rept.: Sci. and Technol. (JPRS-CST-85-018) 12 Jun. 1985 p 50-65 refs Transl.

into ENGLISH from Guangxue Xuebao (Shanghai), v. 5, no. 1, Jan. 1985 p 1-10 (For primary document see N86-12413 03-31)
Avail: NTIS HC A09/MF A01

The state-of-the-art of optics and applied optics in China is reviewed. Developments in lasers, infrared and opto-electronic techniques, optical metrology, high-speed photography, holography and information processing, nonlinear optics, optical fiber communications and optical techniques are described. Further development of optics and applied optics in China are proposed. Author

N86-12415# Joint Publications Research Service, Arlington, Va.
SINGLE MODE PHASE LOCKING FIBEROPTIC SENSOR DEVELOPED
c74
Wang Jinghua, Xie Haiming, Cui Jianhua, and Li Dazhong *In its* China Rept.. Sci. and Technol. (JPRS-CST-85-018) 12 Jun. 1985 p 66-69 refs Transl. into ENGLISH from Yingyong Jiguang (Shanghai), v. 5, no. 1, Feb. 1985 p 43-44 (For primary document see N86-12413 03-31)
Avail: NTIS HC A09/MF A01

This paper reports a single mode phase locking strain sensor. With this sensor, earth shell deformation and solid tide could be detected. This sensor has greatly improved the measurement sensitivity. Author

N86-12416# Joint Publications Research Service, Arlington, Va.
PRACTICAL OPTICAL MULTICHANNEL ANALYZER DEVELOPED
c74
Chen Jian, Li Weiliang, Wan Wanlun, Lin Weizhu, and Li Wenchong *In its* China Rept.: Sci. and Technol. (JPRS-CST-85-018) 12 Jun. 1985 p 70-77 refs Transl. into ENGLISH from Yingyong Jiguang (Shanghai), v. 5, no. 1, Feb. 1985 p 45-48 (For primary document see N86-12413 03-31)
Avail: NTIS HC A09/MF A01

An optical multichannel analyzer of a simple construction is presented in this paper. The instrument includes a video camera, a microcomputer and some accessories. It can be used in the measurement of both transient laser optics and transient laser spectroscopy, as well as for conventional spectroscopic work. Author

N86-12417# Joint Publications Research Service, Arlington, Va.
DEVELOPMENT OF BEAM OPTICS FOR A 200 keV ION IMPLANTER
c74
Pan Xianzheng, Fan Xiangjin, Xu Zaigui, and Guo Huaigui *In its* China Rept.: Sci. and Technol. (JPRS-CST-85-018) 12 Jun. 1985 p 78-88 refs Transl. into ENGLISH from Wuhan Daxue Xuebao (Wuhan), no. 4, Dec. 1984 p 35-40 and 56 (For primary document see N86-12413 03-31)
Avail: NTIS HC A09/MF A01

The beam optics of a 200 keV ion implanter is described in this paper. At present, this ion implanter is used to generate various ion beams of energy ranging from 20 to 200 keV at mass number A < or = 50. It is also used in studying semiconductors and metals. Ion implantation has been widely used in solid state physics and materials science. It is attractive to build a low energy ion accelerator with a wide tunable energy range which is capable of implanting a large number of ions and is suited for solid material implantation. The design of the ion beam optics system has embraced the merits of similar existing machines both at home and abroad. Author

N86-12418# Joint Publications Research Service, Arlington, Va.
CHARACTERISTIC VALUE AS AN ENERGY OUTPUT INDEX FOR EXPLOSIVES
c28
Zhang Housheng and Zhang Shanshan *In its* China Rept.: Sci. and Technol. (JPRS-CST-85-018) 12 Jun. 1985 p 89-98 refs Transl. into ENGLISH from Binggong Xuebao (Beijing), no. 1, Feb. 1984 p 36-42 (For primary document see N86-12413 03-31)
Avail: NTIS HC A09/MF A01

The characteristic value of an explosive and the method of computing it are described and equations for computing the detonation velocity, detonation pressure, specific kinetic energy of detonation products, specific impulse, dent depth, ballistic mortar value, cylinder-test specific kinetic energy, penetration depth, Gurney velocity and flying plate velocity are derived. These equations have some advantages over the existing equations. It is believed that the energy output index of an explosive should have a functional relationship to the detonation parameters and measures of explosive work. The characteristic value satisfies the requirements for an energy output index and may be so used. Author

N86-12419# Joint Publications Research Service, Arlington, Va.
LONG WAVE (1.2 - 1.5 MICRONS) SEMICONDUCTOR LASERS
c36
Pan Zhonghau, Yang Guisheng, Ran Chongzhu, Zhao Songshan, and Wang Yuzhang *In its* China Rept.: Sci. and Technol. (JPRS-CST-85-018) 12 Jun. 1985 p 99-105 refs Transl. into ENGLISH from Tongxin Xuebao (Beijing), no. 1, Jan. 1984 p 68-71 (For primary document see N86-12413 03-31)
Avail: NTIS HC A09/MF A01

Long-wave semiconductors lasers are important light sources for high-capacity fiber-optic communication systems with long repeater spacings. Lasers with outputs at 1.2, 1.3 and 1.5 micrometer, power feedback and temperature feedback systems for them, and techniques for coupling their output into single-mode optical fibers are described. Author

N86-12420# Joint Publications Research Service, Arlington, Va.
COUPLING BETWEEN SPINOR FIELD, PROPAGATING TORSION
c39
Xu Jizhong *In its* China Rept.: Sci. and Technol. (JPRS-CST-85-018) 12 Jun. 1985 p 106-110 refs Transl. into ENGLISH from Wuhan Daxue Xuebao (Wuhan), no. 1, Mar. 1984 p 47-50 (For primary document see N86-12413 03-31)
Avail: NTIS HC A09/MF A01

An investigation is conducted of the coupling of the spinor field and propagating torsion. It is pointed out that there is no interaction between the spinor field and torsion in the HRRS theory, and in DG theory the action of torsion on Dirac particle is expressed as a modification of Dirac particle rest-mass and the torsion produced by the Sun makes a contribution of less than 2 x 10 to the 46th power U on the rest mass of the Dirac particle on the Earth. Einstein-Cartan gravitational theory is a natural extension of Einstein's gravitational theory. B.W.

N86-12421# Joint Publications Research Service, Arlington, Va.
CHINA REPORT: SCIENCE AND TECHNOLOGY
8 Jul. 1985 187 p refs Transl. into ENGLISH from various Chinese articles
(JPRS-CST-85-021) Avail: NTIS HC A09/MF A01

Various topics related to science and technology in China are discussed. Variational analysis of phase transition in pure lattice gauge fields, quantum chemistry of aromatic nitro explosives, pulsed radiation detection technology, and neodymium lasers are among the topics covered. For individual titles, see N86-12422 through N86-12429.

N86-12422# Joint Publications Research Service, Arlington, Va.
VARIATIONAL ANALYSIS OF PHASE TRANSITION IN PURE GAUGE FIELDS
c76
Guo Shouhong, Liu Jinming, and Chen Qizhou *In its* China Rept.: Sci. and Technol. (JPRS-CST-85-021) 8 Jul. 1985 p 76-84 refs Transl. into ENGLISH from Zhongshan Daxue Xuebao (Guangzhou), no. 4, Nov. 1984 p 48-54 (For primary document see N86-12421 03-31)
Avail: NTIS HC A09/MF A01

A modified mean field theory applying an improved variational action with mixed plaquette-like variables is used to study the phase transition of 4-dimensional pure lattice gauge systems. The theory gave the overall behavior of mean plaquette energies E sub p for U(2), U(3), SU(3) and SU(2) groups over a wide range of beta, including the phase transition or crossover region, and explained that the phase transitions in SU(2) and SU(3) pure lattice gauge systems are absent. The E sub p approx. = beta curves agree with Monte Carlo results and are better than that given by simple mean field theory. Author

N86-12423# Joint Publications Research Service, Arlington, Va.
QUANTUM CHEMISTRY OF AROMATIC NITRO EXPLOSIVES c28
Xiao Heming, Wang Zunyao, and Yao Jianmin *In its* China Rept.: Sci. and Technol. (JPRS-CST-85-021) 8 Jul. 1985 p 85-90 refs Transl. into ENGLISH from Huaxue Xuebao (Shanghai), v. 43, no. 1, Jan. 1985 p 14-18 (For primary document see N86-12421 03-31)
Avail: NTIS HC A09/MF A01

The stability of over 20 nitro derivatives of aminobenzene was studied by HMO and CNDO/2 methods. The results showed that, with increasing bond order of the C-NO2 bond, the impact sensitivity decreased. The delocalization energy criterion, using isolated double bond as reference, does not reflect the influence which positioning of functional groups has on the stability of the molecule. Its applications are limited to those conjugate systems in which the relative position of functional groups has negligible effects. As a criterion for determining the stability of this series of compound, the C-NO2 bond order is more appropriate and obvious than the often used delocalization energy. The use of the C-NO2 bond order criterion is also consistent with the mechanisms of impact initiation and thermal decomposition and also in agreement with Delpuech's deha C/iota criterion. Author

N86-12424# Joint Publications Research Service, Arlington, Va.
PULSED RADIATION DETECTION TECHNOLOGY DISCUSSED c32
Lu Min *In its* China Rept.: Sci. and Technol. (JPRS-CST-85-021) 8 Jul. 1985 p 99-112 Transl. into ENGLISH from Hedianzixue Yu Tance Jishu (Beijing), v. 4, no. 6, Nov. 1984 p 321-328 (For primary document see N86-12421 03-31)
Avail: NTIS HC A09/MF A01

Various techniques and devices used to detect pulsed radiation are briely surveyed. A typical measurement system; the selection of a measurement system; the operation of scintillation counters, photoelectric multiplier tubes, and photocells are discussed. R.J.F.

N86-12425# Joint Publications Research Service, Arlington, Va.
NEW DUAL Z80 NAVIGATION COMPUTER DESCRIBED c04
Yu Shiquan, Zhang Chunbao, and Wu Shuwei *In its* China Rept.: Sci. and Technol. (JPRS-CST-85-021) 8 Jul. 1985 p 113-122 refs Transl. into ENGLISH from Dianzi Jishu (Shanghai), v. 12, no. 1, 12 Jan. 1985 p 5-8 (For primary document see N86-12421 03-31)
Avail: NTIS HC A09/MF A01

The application of microprocessor based multiprocessing systems to ship navigation, particularily to position location, is discussed. Systems engineering, interprocessor communication, data display circuits, and the structure of computer programs are covered. R.J.F.

N86-12426# Joint Publications Research Service, Arlington, Va.
SUPERHEATED STEAM'S DENSITY COMPENSATION FOR FLOW MEASUREMENT c34
Xu Guanquan *In its* China Rept.: Sci. and Technol. (JPRS-CST-85-021) 8 Jul. 1985 p 123-128 refs Transl. into ENGLISH from Huaxue Shijie (Shanghai), v. 26, no. 2, 20 Feb. 1985 p 61-63 (For primary document see N86-12421 03-31)
Avail: NTIS HC A09/MF A01

A method for steam flow measurement using an apertured plate as a flow regulation element is described. Conditions to be satisfied when using regular meters and the selection of meters are discussed. R.J.F.

N86-12427# Joint Publications Research Service, Arlington, Va.
TITANIUM-NITROGEN ION BEAM INJECTION STUDIED c76
Jiang Xingliu, He Lianlong, Jiang Songchuan, and Chen Kefan *In its* China Rept.: Sci. and Technol. (JPRS-CST-85-021) 8 Jul. 1985 p 129-131 refs Transl. into ENGLISH from Lanzhou Daxue Xuebao (Lanzhou), v. 20, no. 4, 28 Dec. 1984 p 123-124 (For primary document see N86-12421 03-31)
Avail: NTIS HC A09/MF A01

It is well known that titanium alloys and titanium compounds have such excellent properties as heat resistance, corrosion resistance, great strength and great hardness. If a layer of titanium-nitrogen ions is injected onto the surface of steel to form TiN and Ti2N layer, it should greatly improve the properties of the material. Preliminary studies on pulse titanium-nitrogen ion beam injection onto steel surface were carried out by using multiple plate electrode capacitor for low pressure gas, which is based on the principle of progressively electric field. The distribution profile of titanium, nitrogen, oxygen and carbon within the steel was analyzed by PHI-550 electronic spectroscopy. It is seen that titanium and nitrogen have similar atom concentration distribution versus depth. The concentration distributions of titanium and nitrogen can be seen as being similar on the picture from surface line scanning. The results from corrosion resistance experiments confirm that corrosion resistance and hardness of the injected surface have been notably improved. Author

N86-12428# Joint Publications Research Service, Arlington, Va.
HIGH-POWER ND: GLASS LASER AND TARGET CHAMBER SYSTEM AND AN EXPERIMENTAL STUDY OF LASER PLASMA X-RAY c36
Wu Hongxing, Guo Dahao, Zhou Yusheng, Zhang Limin, He Weimin, and Dai Yusheng *In its* China Rept.: Sci. and Technol. (JPRS-CST-85-021 8 Jul. 1985 p 132-140 refs Transl. into ENGLISH from Zhongguo Kexue Jishu Daxue Xuebao (Hefei), v. 15, no. 1, Mar. 1985 p 30-36 (For primary document see N86-12421 03-31)
Avail: NTIS HC A09/MF A01

The structure and characteristics of a high power Nd:glass laser and target chamber system is described. The system was used in the experimental study of laser plasma X-ray (LPXO) to obtain photographs of hydrogen-like and helium-like X-ray spectra of Mg and Na. The electron temperature reached one million degrees K. The results demonstrated that the Nd:glass laser and target chamber system can be used in the study of laser plasma and other related subjects. Author

N86-12429# Joint Publications Research Service, Arlington, Va.
TITANIUM EXTRACTANT T105-1 STUDIED c26
Mu Guangzhao *In its* China Rept.: Sci. and Technol. (JPRS-CST-85-021) 8 Jul. 1985 p 141-144 Transl. into ENGLISH from Huaxue Shijie (Shanghai), v. 26, no. 3, 20 Mar. 1985 p 82-83 (For primary document see N86-12421 03-31)
Avail: NTIS HC A09/MF A01

The phase ratio (organic phase/aqueous phase) and the influence of extraction time on extraction rate in the extractions by T105-1 of titanium-sulfuric acid solutions of various concentrations were studied. Extractions were done at room temperature. R.J.F.

N86-12430# Joint Publications Research Service, Arlington, Va.
CHINA REPORT: SCIENCE AND TECHNOLOGY
1 Oct. 1985 166 p refs Transl. into ENGLISH from various Chinese articles
(JPRS-CST-85-034) Avail: NTIS HC A08/MF A01

Progress in Science and Technology in the People's Republic of China is reported. The following topics are discussed, physical sciences, applied sciences, applied mathematics, chemistry, data processing, seismology, electronics, information systems, lasers, mathematics, microbiology, nuclear power, physical chemistry, and semiconductors. For individual titles, see N86-12431 through N86-12438.

N86-12431# Joint Publications Research Service, Arlington, Va.
LASER SCATTERING IN PLASMA EXAMINED c36
Lu Quankang, Chen Hang, Yin Qi, and Wang Wenhua *In its* China Rept.: Sci. and Technol. (JPRS-CST-85-034) 1 Oct. 1985 p 49-52 refs Transl. into ENGLISH from Ziran Zazhi (Shanghai), v. 7, no. 7, Jul. 1984 p 555-557 (For primary document see N86-12430 03-31)

Avail: NTIS HC A08/MF A01

On the basis of the work of Rostoker and Rosenbluth, the laser scattering spectrum in plasma was modeled by taking the Coulombic force as well as the Lorentz force into account utilizing a heuristic particle model. The calculation was made on the total electromagnetic force interaction between charged particles in the presence of an external magnetic field. E.A.K.

N86-12432# Joint Publications Research Service, Arlington, Va.
OPTIC FIBER APPLICATIONS IN DATA COMMUNICATIONS c32
Yu Huaiquan and Lu Zinan *In its* China Rept.: Sci. and Technol. (JPRS-CST-85-034) 1 Oct. 1985 p 53-58 Transl. into ENGLISH from Dianzi Jishu (Shanghai), v. 12, no. 5, 20 May 1985 p 15-17; 19 (For primary document see N86-12430 03-31)
Avail: NTIS HC A08/MF A01

Progress in data communications systems which link together computers and terminal equipment with communications circuits to accomplish information transfer, exchange, and processing are discussed. This shared resources type of communications was developed along with the broader applications of computers, and is the third largest mode of communications continuing upon analog communications and PCM digital communications. The development in China of fiber optics for transmission in computer networks is reported. E.A.K.

N86-12433# Joint Publications Research Service, Arlington, Va.
EXPERIMENTS WITH DOMESTIC IC SUBSTRATES c33
Guan Shuzhu and Li Dunfu *In its* China Rept.: Sci. and Technol. (JPRS-CST-85-034) 1 Oct. 1985 p 59-66 refs Transl. into ENGLISH from Dianzi Jishu (Shanghai), v. 12, no. 5, 20 May 1985 p 12-14 (For primary document see N86-12430 03-31)
Avail: NTIS HC A08/MF A01

The requirement for the development of low cost, highly reliable IC circuits in millimeter wave precision tactical weapons are discussed. Different forms for such circuits are proposed: (1) microstrip circuits; (2) waveguide surface circuits, (3) dielectric waveguides; and (4) fin-line. The millimeter wave microstrip circuits require a medium with low dissipation and a low dielectric constant. The waveguide surface circuits were used in the X-band. The main problem is that there is only one conductor line. The electric waveguides were used successfully in the millimeter band. The primary problem is the incompatibility introduced by the single guidestrip with active devices, and the transient conversion from square waveguides is also too long. Fin-lines have attracted attention because of their moderate transmission loss, convenient transition, variable ciruits modes (ridge line, trough line, coplaner lines, and waveguide microstrips), multiple guide strip compatibility, and especially the convenience of installation with active devices. E.A.K.

N86-12434# Joint Publications Research Service, Arlington, Va.
BLR STUDIES ON CONIC MODEL WITH LDA IN FL-1 WIND TUNNEL c02
Zhong Zhan and Yu Yong *In its* China Rept.: Sci. and Technol. (JPRS-CST-85-034) 1 Oct. 1985 p 67-70 Transl. into ENGLISH from Guoji Hangkong (Beijing), no. 6, Jun. 1985 p 9-10 (For primary document see N86-12430 03-31)
Avail: NTIS HC A08/MF A01

Boundary layer velocity measurement over a cone using laser (LDA) was studied in the FL-1 wind tunnel of the Shengyang Aerodnamics Research Institute. Velocity distributions at two cross-sections of the boundary layer of a 20 deg conic model under different Mach numbers are measured. The measured results are in agreement with theoretical calculations. E.A.K.

N86-12435# Joint Publications Research Service, Arlington, Va.
MEASUREMENT OF 1 NANOSECOND WIDE BEAMS FOR 2.5 MeV PROTON ACCELERATOR c72
Yang Jiayou, Li Wenxue, and Li Jiarong *In its* China Rept.: Sci. and Technol. (JPRS-CST-85-034) 1 Oct. 1985 p 71-77 refs Transl. into ENGLISH from He Kexue Yu Gongcheng (Beijing), no. 1, Mar. 1984 p 67-71 (For primary document see N86-12430 03-31)
Avail: NTIS HC A08/MF A01

A measuring method for beam burst with extremely narrow width of 1 ns for a 2.5 MeV proton electrostatic accelerator is described. The measurement results are given. The system consists of a long coaxial target (wideband Faraday cup), a subnanosecond pulse amplifier (t sub x < 0.4 ns) and a sampling oscilloscope (Type AQ10). It is pointed out that secondary emissions from the target knocked by the beam have almost no effect on the waveform of the beam pulse. E.A.K.

N86-12436# Joint Publications Research Service, Arlington, Va.
MATHEMATICAL PRINCIPLE FOR GENERATING SECOND-ORDER ASPHERICAL SURFACE c64
Pan Junhua and Wang Jinaguo *In its* China Rept.: Sci. and Technol. (JPRS-CST-85-034) 1 Oct. 1985 p 78-84 ref Transl. into ENGLISH from Guangxue Xuebao (Shanghai), v. 4, no. 3, Mar. 1983 p 252-256 (For primary document see N86-12430 03-31)
Avail: NTIS HC A08/MF A01

The mathematical formulas for generating second order aspherical surfaces were derived. The aspherical surface is treated as an envelope of spheres with different radius of curvature at different zones; delta sub p and alpha sub p are taken as parameters to describe the motion of grinding tool, where delta sub p is the distance between vertex of surface and lowest point of the tool; and alpha sub p is the angle between tool axis and aspherical surface axis. For mass production, pure mechanism is better than computer control of the grinding machine, and the best mechanism is cam pair, because this mechanism can repeat the grinding process and to produces a smooth aspherical surface, to give the mathematical equations of the cam design. E.A.K.

N86-12437# Joint Publications Research Service, Arlington, Va.
SUPERCONDUCTING WIRE MANUFACTURED c33
Fu Yuexian, Sun Yue, Xu Shiming, and Peng Ying *In its* China Rept.: Sci. and Technol. (JPRS-CST-85-034) 1 Oct. 1985 p 85-86 refs Transl. into ENGLISH from Diwen Wuli (Beijing), v. 7, no. 2, Jun. 1985 p 164-165 (For primary document see N86-12430 03-31)
Avail: NTIS HC A08/MF A01

The MF Nb/Cu Extrusion Tube Method was used to manufacture 3 kg of stable practical MF Nb2Sn composite superconducting wire containing pure Cu(RRR approx. 200)/Ta. The draw state composite wire diameter was 0.56 mm, it contained 11,448 x 2.6 micron Nb core, and the twist distance was 1.5 cm. The composite wire cross-section was pure Cu/Ta/11,448 Nb core/Cu/91Sn-Cu; containing 22.8 v. % pure Cu, 13.3 v. % Ta; within the Ta layer to prevent Sn diffusion. The wire was sheathed in nonalkaline glass fiber as an insulating layer. A section of wire weighing 160 g was cut off and coiled it into a small solenoid. After reaction diffusion processing at 675 C/30 and curing by vacuum dipping in paraffin, it was measured in a Nb-Ti backfield of 7.2 T intensity, a current of 129 A was passed through the Nb3Sn solenoid and produced a strength of 2.5 T, the overall magnetic field intensity of the composite magnet reached 9.7 T. At this time, the wire full current density J sub c.w. = 5.2 x 10 to the 4th power A/sq cm; the effective current density J sub c (Nb + Sn - Cu) = 8.2 x 10 to the 4th power A/sq cm. E.A.K.

N86-12438# Joint Publications Research Service, Arlington, Va.
ULTRAHIGH VACUUM EQUIPMENT DESCRIBED c35
Li Yuzhi, Jing Shiqun, and Peng Xianhui *In its* China Rept.: Sci. and Technol. (JPRS-CST-85-034) 1 Oct. 1985 p 87-91 Transl. into ENGLISH from Diwen Wuli (Beijing), v. 7, no. 2, Jun. 1985 p 166-168 (For primary document see N86-12430 03-31)
Avail: NTIS HC A08/MF A01

Ultrahigh vacuum equipment for filming with a blockade value and a substrate at the temperature of liquid nitrogen. The equipment has the following characteristics: (1) the vacuum chamber is exposed to the atmosphere, the lockade valve can maintain a vacuum of 1 to 10 to the -9 power torr for a long period of time;

(2) it greatly reduces the working cycle compared to before the blockade valve was installed; and (3) the temperature of the sample substrate in the vacuum chamber can be adjusted continuously between 77 K and room temperature. The ultrahigh vacuum filming equipment China now produces does not have an ultrahigh vacuum valve, when inserting and removing samples, the pump casing is exposed to the atmosphere so that even after the pump has operated for a time, its limited vacuum is 10 to the -8 power torr. A bakeable metallic blockade valve is installed between the vacuum pump intake and the vacuum chamber to form a filming device. The device is simple, the vacuum is increased several levels, and it can make samples at different substrate temperatures. E.A.K.

N86-12439# Joint Publications Research Service, Arlington, Va.
CHINA REPORT: SCIENCE AND TECHNOLOGY
11 Jul. 1985 190 p refs Transl. into ENGLISH from various Chinese articles
(JPRS-CST-85-022) Avail: NTIS HC A09/MF A01

Topics discussed in this China Report included: science and Technology (11 July 1985); contains articles from the scientific literature of the People's Republic on national devlopment, applied sciences, life sciences, acoustics, environmental quality, chemical industry chemistry, computers, control systems, electronics, lasers, marine science, and medicine. Of particular interest in this issue are articles on a piezoelectric sensor, microcomputerization, and CMOS circuitry. For individual titles, see N86-12440 through N86-12443.

N86-12440# Joint Publications Research Service, Arlington, Va.
CHINA'S FIRST IMPORTED PERIPHERAL EQUIPMENT PRODUCTION LINE c35
In its China Rept.: Sci. and Technol. (JPRS-CST-85-022) 11 Jul. 1985 p 17-25 Transl. into ENGLISH from Jisuanji Shijie (Beijing), no. 11, 8 Jun. 1984 p 1 (For primary document see N86-12439 03-31)
Avail: NTIS HC A09/MF A01

The piezoelectric gyroscope is a new type of solid-state inertia sensor which utilizes crystal piezoeffect sensitive angle parameters. The piezoelectric gyroscope has eliminated the rotating part of the traditional gyroscope and thus obtained an important breakthrough in gyroscope life, the device can operate for over 10,000 hours. Author

N86-12441# Joint Publications Research Service, Arlington, Va.
METHOD OF USING CTC TO MICROCOMPUTERIZE DIGITAL INSTRUMENTS c35
Wu Naiyou *In its* China Rept.: Sci. and Technol. 11 Jul. 1985 p 26-31 Transl. into ENGLISH from Dianzi Kexue Jishu (Beijing), v. 15, no. 1, 10 Jan. 1985 p 5-6 (For primary document see N86-12439 03-31)
Avail: NTIS HC A09/MF A01

This article introduces a method of borrowing the Z80 single-board computer CTC to microcomputerize digital instruments. While preserving all the functions of the single-board computer, this method fully exploits software potential, simplifies hardware design and is characterized by high precision, high reliability, low cost, and ease of extension. Author

N86-12442# Joint Publications Research Service, Arlington, Va.
DIGITAL PHASE METER USING CMOS-LED INTRODUCED c35
Tan Benzhi *In its* China Rept.: Sci. and Technol. (JPRS-CST-85-022) 11 Jul. 1985 p 32-34 Transl. into ENGLISH from Dianzi Kexue Jishu (Beijing), v. 15, no. 1, 10 Jan. 1985 p 25 and 28 (For primary document see N86-12439 03-31)
Avail: NTIS HC A09/MF A01

The structure of the CMOS-LED digital phase meter introduced in this paper is simple, its performance is stable, it is suitable for phase testing of low frequency signals, there are no strict demands on the wave form of the tested signal, sine waves, triangular waves, and square waves can be measured, and the tested signal can be in the 0.2V - 300V range. In addition to carrying out phase testing of small signals, through attenuation switch conversion, it can be used to measure the phase difference of three-phase service power supplies, is much easier to observe than a phase sequencer, and measurement error is + or - 1%. Author

N86-12443# Joint Publications Research Service, Arlington, Va.
LATCH-UP EFFECT IN CMOS DESCRIBED c33
Zhang Lichun, Yan Timing, Ni Xuewen, Yan Guizhen, Feng Chuguang, and Zhang Ziang *In its* China Rept.: Sci. and Technol. (JPRS-CST-85-022) 11 Jul. 1985 p 35-41 refs Transl. into ENGLISH from Dianzi Kexue Jishu (Beijing), v. 15, no. 1, 10 Jan. 1985 p 2-4 (For primary document see N86-12439 03-31)
Avail: NTIS HC A09/MF A01

The latch-up effect was first discovered in a small-scale bipolar integrated circuit. As long as there are parasitic four-layer PNPN structures, under certain conditions, the latch-up effect can occur. Since bulk CMOS circuits are of four-layer structure, the latch-up effect is a failure mode which often occurs in them. With the improvement of integration and the reduction in component dimensions, the latch-up effect can become increasingly serious. Therefore, how to reduce or eliminate the latch-up effect and improve the reliability of CMOS circuits is a subject which has been getting more and more attention. The latch-up phemonenon in CMOS circuits is discussed, the conditions which produce it are analyzed, and proposals for preventative measures in design, industrial technology, and use are made. Author

N86-12444# Joint Publications Research Service, Arlington, Va.
CHINA REPORT: SCIENCE AND TECHNOLOGY
1 Aug. 1985 82 p refs Transl. into ENGLISH from various Chinese articles
(JPRS-CST-85-025) Avail: NTIS HC A05/MF A01

Advances in science and technology from the Peoples Republic of China are reported. Topics of discussion include: (1) national developments; (2) allied sciences; (3) life sciences; (4) environmental quality; (5) atomic energy; (6) chemistry; (7) energy; (8) engineering; (9) medicine; (10) microbiology; (11) nuclear engineering; (12) oceanography; and (13) physics. For individual titles, see N86-12445 through N86-12445.

N86-12445# Joint Publications Research Service, Arlington, Va.
NEW APPROACHES TO DETERMINING PHYSICAL PROPERTIES IN PISTON-CYLINDER HIGH-TEMPERATURE, HIGH-PRESSURE DEVICE
Zhang Yun, Shen Zhongyi, Yin Xiujun, Chu Shaoyan, and He Shouan *In its* China Rept.: Sci. and Technol. (JPRS-CST-85-025) 1 Aug. 1985 p 14-22 refs Transl. into ENGLISH from Wuli (Beijing), v. 13, no. 12, Dec. 1984 p 714 and 742-745 (For primary document see N86-12444 03-31)
Avail: NTIS HC A05/MF A01

High pressure has a unique effect and significant in basic and applied research in solid state physics. Measurement of physical properties under high pressure is the means of high pressure research. Its major content is how to produce various high pressure devices and measurement techniques so as to apply various measurement principles to the high pressure environment and eliminate or at least greatly dampen the interference which a high temperature and high pressure environment has on measurement so as to prevent measurement loss as well as guarantee the required precision of measurement. The merits of piston cylinder containers are: the structure is simple, the determination of pressure and temperature is accurate, and it is easy to bring measuring leads directly out of the high pressure cavity. Thus, one can efficiently and conveniently measure many kinds of behavior under high temperature and high pressure. G.L.C.

N86-12446# Joint Publications Research Service, Arlington, Va.
CHINA REPORT: SCIENCE AND TECHNOLOGY
3 Sep. 1985 171 p refs Transl. into ENGLISH from various Chinese articles
(JPRS-CST-85-029) Avail: NTIS HC A08/MF A01

Numerous topics related to science and technology in China are discussed. The progess of inertial confinement research, a programmer for a single chip microprocessor, digital voltmeter technology acquisition wing tip sails on the Y-5 aircraft are among the topics discussed. For individual titles, see N86-12447 through N86-12450.

N86-12447# Joint Publications Research Service, Arlington, Va.
PROGRESS OF INERTIAL CONFINEMENT RESEARCH DETAILED c75
Wang Ganchang *In its* China Rept.: Sci. and Technol. (JPRS-CST-85-029) 3 Sep. 1985 p 1-17 refs Transl. into ENGLISH from He Kexue Yu Gongcheng (Beijing), v. 4, no. 4, Dec. 1984 p 289-302 (For primary document see N86-12446 03-31)
Avail: NTIS HC A08/MF A01

Recent progress of inertial confinement fusion (ICF) research is discussed. The cannonball target, the high power krypton fluoride (KrF) laser, the ion beam diode, and the imploding foil plasma are discussed. The principle of the cannonball target, its advantages over ordinary ablation targets, and the problem of hole sealing are discussed. The powerful KrF excimer lasers pumped by electron beams are discussed. This type of laser is now generally regarded as one of the more promising drivers for ICF. The complex kinetics of pumping, quenching, radiation, and absorption of this very interesting laser are discussed. The present status of ion beam production, especially the diodes which produce the ion beams are covered. Three types of diodes are discussed: the pinch reflec diode (PRD), the diode with an externally applied magnetic field, and the hybrid amphion diode. Finally, the impliding foil plasma is considered. This technique produces plasmas of very high temperature and very intense soft X-rays which may either be used to produce an X-ray laser or as a new driver for ICF. R.F.J.

N86-12448# Joint Publications Research Service, Arlington, Va.
PROGRAMMER FOR SINGLE-CHIP MICROPROCESSOR c60
Li Benren, Gong Ganghua, and Meng Qi *In its* China Rept.: Sci. and Technol. (JPRS-CST-85-029) 3 Sep. 1985 p 29-40 refs Transl. into ENGLISH from Xiaoxing Weixing Jisuanji Xitong (Shenyang), no. 1, 8 Jan. 1985 p 8-15 (For primary document see N86-12446 03-31)
Avail: NTIS HC A08/MF A01

The 8748/8741/8755 single chip microprocessor programming part of the TRS-80(I)/EG3200 on-line software development system is discussed. This program can read the internal read-only memory (ROM) and program the internal EPROM of the 8748/8749, 8741/8742 and 8755 chips. It is a development tool for single chip microprocessors which is very convenient, reliable and has powerful functions. Author

N86-12449# Joint Publications Research Service, Arlington, Va.
DIGITAL VOLTMETER TECHNOLOGY ACQUISITION c35
Chen Qilin and Cui Jianping *In its* China Rept.: Sci. and Technol. (JPRS-CST-85-029) 3 Sep. 1985 p 41-44 Transl. into ENGLISH from Guoji Maoyi (Beijing), no. 3, 1985 p 33-34 (For primary document see N86-12446 03-31)
Avail: NTIS HC A08/MF A01

China began its development of digital voltmeter at a fairly early stage. In 1965, the Beijing Radio Technology Research Bureau had already built a 5 digit voltmeter whose technical performance was comparable to the international standards at that time. However, at the present time, of the more than 50 models of 5 digit voltmeters produced by State designated factories, only 2 or 3 use the international standard interface and microcomputer technology; furthermore, due to the limited capability in processing, equipment and testing, they cannot be mass produced. As a result, the gap between the Chinese standard and international standard in digital voltmeter is further widened. The Beijing Radio Technology Institute prepared a plan to import the manufacturing technology of the 8520A digital system multimeters from the U.S. FLUKE Co., by using foreign exchange funds designated for mechanical and electrical instruments under the joint technology and trade program. In September 1981, an official contract and an agreement for technology cooperation were signed. The items imported to the 8520A technology and trade program can be divided into several stages: (1) import automated test and standard systems which are built using advanced technologies of the 1980's; (2) train personnel and begin production; (3) import key production equipment to coordinate with China's existing facilities; (4) modify the production lines based on FLUKE's advanced technology and begin CKD production; and (5) use the results of imported technologies in other research projects to stimulate development in related technologies. R.J.F.

N86-12450# Joint Publications Research Service, Arlington, Va.
WINGTIP SAILS TESTED ON Y-5 AIRCRAFT c05
Yang Daxi *In its* China Rept.: Sci. and Technol. (JPRS-CST-85-029) 3 Sep. 1985 p 49-53 Transl. into ENGLISH from Guoji Hangkong (Beijing), no. 5, May 1985 p 2-3 (For primary document see N86-12446 03-31)
Avail: NTIS HC A08/MF A01

In recent years, much attention has been given to the use of wingtip ailerons or wing tip sails to reduce induced drag because for most transport airplanes, the induced drag at cruising speed is approximately 30 percent of the total drag; at lower speeds the ratio is even higher. For the Y-5 biplane, the induced drag to total drag ratio is approximately 55.6 percent, at cruising speed the ratio is approximately 33 percent, and during climb it is 58 percent. Therefore, wing tip ailerons or wing tip sails potentially can be very effective in reducing the overall drag of the aircraft. Since a large number of Y-5 airplanes are used in China for a variety of applications, a research program was initiated in August 1982 to install and test wing tip sails on the Y-5 aircraft. Results show that the use of wing tip sails improved the performance of the Y-5 aircraft. Author

N86-12451# Joint Publications Research Service, Arlington, Va.
CHINA REPORT: SCIENCE AND TECHNOLOGY
4 Sep. 1985 154 p refs Transl. into ENGLISH from various Chinese articles
(JPRS-CST-85-030) Avail: NTIS HC A08/MF A01

Research in science and technology of China is reported. Most articles are contained in the applied sciences section of the journal, with a small section devoted to life sciences. The abstracts section covers many areas including applied mathematics, chemistry, electronics, cryogenics, information science and lasers. The listing of articles include: computer aided analysis of arbitrary shaped thin wire antennas; uses of organic membranes in electrolytic industry; and a high repetition rate ultrashort pulse laser. For individual titles, see N86-12452 through N86-12458.

N86-12452# Joint Publications Research Service, Arlington, Va.
COMPUTER-AIDED ANALYSIS OF ARBITRARY-SHAPED THIN-WIRE ANTENNAS c32
Hong Wei and Zhang Wenxun *In its* China Rept.: Sci. and Technol. (JPRS-CST-85-030) 4 Sep. 1985 p 15-23 refs Transl. into ENGLISH from Nanjing Gongxueyuan Xuebao (Nanjing), no. 4, 20 Dec. 1984 p 61-67 (For primary document see N86-12451 03-31)
Avail: NTIS HC A08/MF A01

The analysis of excited and loaded arbitrary shaped thin wire antennas was carried out. The numerical results for a GAUSS-type antenna agree with the experimental results. A triangular pulse base function and Galerkin method is used, the computational formulas obtained are simple and accurate, the computer program is easy to use as a subprogram call in an optimization program. Author

N86-12453# Joint Publications Research Service, Arlington, Va.
USAGES OF ORGANIC MEMBRANES IN ELECTROLYTIC INDUSTRY DESCRIBED c25
Li Jisen *In its* China Rept.: Sci. and Technol. (JPRS-CST-85-030) 4 Sep. 1985 p 25-35 refs Transl. into ENGLISH from Huaxue Tongbao (Beijing), no. 5, 18 May 1985 p 37-42 (For primary document see N86-12451 03-31)
Avail: NTIS HC A08/MF A01

Electrosynthesis is a method of preparing chemical products through eletrode reactions. In recent years rapid advances have been made in the area of organic compound preparation. Industrial scale productions were achieved on the preparation of adiponitrile by dimerization of acrylonitrile through electro-reduction, as well as the preparation of tetraethyllead and the preparation of propylene oxide from propylene. In these electrosyntheses, the applications of organic membranes have significant impacts. Due to these applications, the variety of membranes were greatly enriched, their properties improved and many chemical reactions were realized that are impossible under ordinary conditions. These syntheses and the role played by organic membranes are described. Author

N86-12454# Joint Publications Research Service, Arlington, Va.
EFFECT OF AMPLIFIED SPONTANEOUS EMISSION ON SPACE COHERENCE OF XeCl LASER c36
Zhang Dake, Wang Xiaoyi, Ni Jinzhi, Yao Jianping, Fu Shufen, and Chen Jianwen *In its* China Rept.: Sci. and Technol. (JPRS-CST-85-030) 4 Sep. 1985 p 36-44 refs Transl. into ENGLISH from Zhongguo Jiguang (Shanghai), v. 12, no. 5, 20 May 1985 p 261-265 (For primary document see N86-12451 03-31)
Avail: NTIS HC A08/MF A01

Amplified Spontaneous Emission (ASE) is the single pass wave amplification caused by the propagation of spontaneous emission through a stimulated medium which has already reached the state of particle number reversal. Since first observed the ASE output from a pulse He-Ne laser with no cavity mirror, several researchers have conducted both theoretical and experimental studies on amplified spontaneous emissions. But so far no systematic studies have been reported on the effect of ASE on the output characteristics of excimer laser; such effect is clearly important in high gain excimer systems. This particular issue is explored. Author

N86-12455# Joint Publications Research Service, Arlington, Va.
FIRST DOMESTIC HIGH REPETITION RATE ULTRASHORT PULSE LASER c36
Guang Lin *In its* China Rept.: Sci. and Technol. (JPRS-CST-85-030) 4 Sep. 1985 p 45 Transl. into ENGLISH from Zhongguo Jiguang (Shanghai), v. 12, no. 5, 20 May 1985 p 278 (For primary document see N86-12451 03-31)
Avail: NTIS HC A08/MF A01

On 7 February 1985, certification tests were conducted on the High Repetition Rate Ultrashort Pulse Laser. Experts at the meeting pointed out that this was China's first prototype high repetition rate ultrashort pulse laser. Its performance is higher than that of similar lasers in this country and is comparable to the advanced standards of foreign products. The energy of the pulse train of this laser is greater than 8 mJ; its single pulse width is 32 ps; its pulse stability is + or - 2 percent at 10 pps and + or - 4 percent at 33 pps; and its mode locked probability is 100 percent. The repetition rates are 10 pps, 20 pps, and 33 pps. The laser not only has a smooth pulse waveform, but its operation is stable and highly reliable. The high repetition rate ultrashort pulse laser is a valuable tool in the study of ranging and spectral techniques; it can be used to improve the measurement accuracy of ranging devices on third generation artificial satellites, and to increase the time resolution of laser spectral analysis. Author

N86-12456# Joint Publications Research Service, Arlington, Va.
PRACTICAL EXCIMER LASER DEVELOPED c36
Qun Li *In its* China Rept.: Sci. and Technol. (JPRS-CST-85-030) 4 Sep. 1985 p 46 Transl. into ENGLISH from Zhongguo Jiguang (Shanghai), v. 12, no. 5, 20 May 1985 p 297 (For primary document see N86-12451 03-31)
Avail: NTIS HC A08/MF A01

After nearly 3 years of research and continuous improvement of its experimental equipment, a practical excimer laser was developed with the following properties: single pulse output energy 280 mJ, wavelength 3080 A. Its repetition rate can be adjusted between 0 to 10 Hz, its average output power is 1 w, and its single charge life exceeds 100,000 firings. The gas replacement equipment can operate at the following bands: ArF (1930 A), KrF (2490 A), N2 (3371 A), and XeF (3511 A). This equipment is also structurally very simple, and can operate reliably over a long period. Its price is only one-fourth to one-fifth of similar foreign products. This highly coherent ultraviolet source which has a constant average power is a useful tool for research in photochemistry, pump dye lasers, surface physics, and laser medicine. Author

N86-12457# Joint Publications Research Service, Arlington, Va.
A HIGH PRECISION RATE DYE LASER PUMPED BY A CuCl LASER c36
Jing Chunyang, Zhang Guiyan, Wu Zhengliang, Shu Juping, Hu Qiquan, Ying Lifeng, and Lin Fucheng *In its* China Rept.: Sci. and Technol. (JPRS-CST-85-030) 4 Sep. 1985 p 47-53 refs Transl. into ENGLISH from Zhongguo Jiguang (Shanghai), v. 12, no. 7, 20 Jul. 1985 p 394; 399-401 (For primary document see N86-12451 03-31)
Avail: NTIS HC A08/MF A01

Experimental results of several high repetition rate Rhodamine dye lasers pumped by a CuCl laser are presented. The laser radiation covers a wavelength range of 5630 A to 6320 A and has a maximum conversion efficiency of 33 percent. Author

N86-12458# Joint Publications Research Service, Arlington, Va.
HUMAN HEMODYNAMIC CHANGE UNDER HIGH ATMOSPHERIC PRESSURE c52
Zhang Hengdu and Dai Duanyang *In its* China Rept.: Sci. and Technol. (JPRS-CST-85-030) 4 Sep. 1985 p 55-56 Transl. into ENGLISH from Jiefangjun Yixue Zazhi (Beijing), no. 1, 20 Feb. 1985 p 63 (For primary document see N86-12451 03-31)
Avail: NTIS HC A08/MF A01

For the purpose of observing human hemodynamic change under high atmospheric pressure, nontraumatic means were adopted to record sphygmograms during a 26 day continuous nitrogen-oxygen saturation dive simulation trial 36.5 m. The test subjects assumed a supine position and the sphygmogram was recorded on closed vessels on the left side using a mercurial sphygmomanometer to measure blood pressure in the arteria brachialis of the left arm. The data from the initial measurements was processed through electronic computer. The voluntary test subjects were seven young males averaging 22.6 + or - 3.9 years of age. The simulated pressure measured 4.65 ATA, cabin temperature was 26.05 + or - 0.8 deg C and relative humidity measured 70.3 + or - 0.9 percent. Differential pressure measured 0.31 + or - 0.08 ATA for oxygen, 0.002 ATA for carbon dioxide and 4.34 ATA for nitrogen. The subjects lived and worked under the above conditions for 26 continuous days and nights and underwent 4 days of decompression to return to normal pressure. The results of these tests are briefly decribed. Author

N86-12459# Joint Publications Research Service, Arlington, Va.
CHINA REPORT: SCIENCE AND TECHNOLOGY
15 Aug. 1985 127 p refs Transl. into ENGLISH from various Chinese articles
(JPRS-CST-85-026) Avail: NTIS HC A07/MF A01

Advances in science and technology from the Peoples Republic of China are reported. Topics of discussion include: (1) national developments; (2) applied sciences; (3) life sciences; (4) scientists and scientific organizations; (5) acoustics; (6) applied mathematics; (7) atomic energy; (8) electricity; (9) engineering; (10) marine science; (11) nuclear physics; (12) physics; and (13) technical physics. For individual titles, see N86-12460 through N86-12461.

N86-12460# Joint Publications Research Service, Arlington, Va.
LASER INDUCED BIOLOGICAL HEATING ANALYZED c36
Liu Puhe *In its* China Rept.: Sci. and Technol. (JPRS-CST-85-026) 15 Aug. 1985 p 71-76 refs Transl. into ENGLISH from Zhongguo Jiguang (Shanghai), no. 11, 20 Nov. 1984 p 697-700 (For primary document see N86-12459 03-31)
Avail: NTIS HC A07/MF A01

A quantitative analysis of the vaporization of tumors by pulsed CO2 lasers, incision by CW CO2 lasers, tissue coagulation by argon lasers, thermal killing of cancerous cells by He-Ne lasers, and the application of heat by CO2 lasers is presented. Although the calculations are based on a simplified skin model, it may prove useful in clinical treatments. Author

N86-12461# Joint Publications Research Service, Arlington, Va.
APPLICATION OF HEAT-SCAN NDT TO INSPECTION OF ADHESION OF SOLID ROCKET MOTOR PROPELLANT TO ENVELOPE c28
Tian Enrui *In its* China Rept.: Sci. and Technol. (JPRS-CST-85-026) 15 Aug. 1985 p 77-80 Transl. into ENGLISH from Harbin Gongye Daxue (Harbin), no. 1, Mar. 1985 p 74-83 (For primary document see N86-12459 03-31)
Avail: NTIS HC A07/MF A01

Heat-scan infrared nondestruction testing technology is an effective method to inspect solid rocket motors for defects in propellant adhesion to the envelope. The basic principles of heat-scan infrared NDT are introduced. Specifically, the theoretical basis of the heat-scan method is to detect internal defects of an object by measuring the infrared radiation from its surface and calculating the surface temperature distribution so that distortions in temperature pattern can be identified. Author

N86-12462# Joint Publications Research Service, Arlington, Va.
CHINA REPORT: SCIENCE AND TECHNOLOGY
19 Sep. 1985 156 p refs Transl. into ENGLISH from various Chinese articles
(JPRS-CST-85-032) Avail: NTIS HC A08/MF A01

Advances in science and technology made by the Peoples Republic of China are reported. Topics of discussion include: (1) national developments; (2) physical sciences; (3) applied sciences; (4) life sciences; (5) aerodynamics; (6) chemistry; (7) computers; (8) engineering; (9) mathematics; (10) nuclear physics; (11) physical chemistry; and (12) physics. For individual titles, see N86-12463 through N86-12468.

N86-12463# Joint Publications Research Service, Arlington, Va.
VECTOR VALUED LONG JAMES TYPE BANACH SPACES J(eTA, l sub p)(1 < OR = p < + INFINITY) c64
Zhao Junfeng *In its* China Rept.: Sci. and Technol. (JPRS-CST-85-032) 19 Sep. 1985 p 30-39 refs Transl. into ENGLISH from Xitong yu Shuxue (Beijin), v. 5, no. 1, Jan. 1985 p 51-62 (For primary document see N86-12462 03-31)
Avail: NTIS HC A08/MF A01

The concept of the transfinite basis of a Banach space is introduced. The vector valued long James type Banach spaces is investigated. We find that J(eta, L sub p)(1 < or = p < infinity) and its dual J(eta, L sub p)' have the transfinite basis, and if a Banach space X has a transfinite basis, so does the space J(eta, X). G.L.C.

N86-12464# Joint Publications Research Service, Arlington, Va.
FINITE DIFFERENCE SCHEME FOR ONE-DIMENSIONAL MAGNETOHYDRODYNAMIC EQUATIONS c64
Liu Deming *In its* China Rept.: Sci. and Technol. (JPRS-CST-85-032) 19 Sep. 1985 p 40-54 refs Transl. into ENGLISH from Shuzhi Jisuan yu Jisuanji Yingyong (Beijing), v. 5, no. 3, Sep. 1984 p 138-150 (For primary document see N86-12462 03-31)
Avail: NTIS HC A08/MF A01

A finite difference scheme for magnetohydrodynamic equations in one dimension is presented. Numeric results have verified its effectiveness. Author

N86-12465# Joint Publications Research Service, Arlington, Va.
CHINA DEVELOPS 6J KrF LASER c36
Wang Ganchang, Zhu Xuhui, Wang Naiyan, Xie Jinggang, Li Yinghshan, Zhou Changhuai, and Wang Pu *In its* China Rept.: Sci. and Technol. (JPRS-CST-85-032) 19 Sep. 1985 p 62-66 refs Transl. into ENGLISH from He Kexuy yu Gongcheng (Beijing), v. 5, no. 1, Mar. 1985 p 1-5 (For primary document see N86-12462 03-31)
Avail: NTIS HC A08/MF A01

A KrF eximer laser pumped by a relativistic electron beam of high intensity at a gas pressure up to 3.5 atm was investigated. The experiment shows that for an Ar:Kr:F2 = 89.6:10:0.4 mixture, the maximum energy is about 7.2 J and some KrF lines were observed. Author

N86-12466# Joint Publications Research Service, Arlington, Va.
APPLICATION OF RADIOGRAPHIC IMAGE ENHANCEMENT, SEGMENTATION c74
Wang Chengye and Xia Wei *In its* China Rept.: Sci. and Technol. (JPRS-CST-85-032) 19 Sep. 1985 p 67-70 Transl. into ENGLISH from Jisuanji Yanjiu yu Fazhan (Beijing), v. 21, no. 12, Dec. 1984 p 52-53 (For primary document see N86-12462 03-31)
Avail: NTIS HC A08/MF A01

A method that enchances GAMMA ray images using a method that smooths partial images with whole information, and that uses the histogram guided convergence method to separate these images is introduced. Author

N86-12467# Joint Publications Research Service, Arlington, Va.
IRON AND STEELMAKING WITH PLASMA c26
Yu Dingfu *In its* China Rept.: Sci. and Technol. (JPRS-CST-85-032) 19 Sep. 1985 p 71-84 refs Transl. into ENGLISH from Gangtie (Beijing), v. 20, no. 5, May 1985 p 48-54 (For primary document see N86-12462 03-31)
Avail: NTIS HC A08/MF A01

Plasma iron and steelmaking uses a smelting method that converts the thermal energy in electrical power to gas, and can be called a type of electrometallurgy. For this reason, plasma iron and steelmaking first of all requires consideration of the question of electricity supply capacity and the price of electrical energy. It has attracted a great deal of attention from iron and steel workers in some regions and nations with abundant electric power resources. Research and production work in this area now is unfolding. G.L.C.

N86-12468# Joint Publications Research Service, Arlington, Va.
CAD PROGRAM FOR HIGH-POWER ELECTRON GUN WITH ANNULAR CATHODE DESCRIBED c33
Tu Yushan *In its* China Rept.: Sci. and Technol. (JPRS-CST-85-032) 19 Sep. 1985 p 113-117 refs Transl. into ENGLISH from Dianzi Xuebao (Beijing), no. 4, Nov. 1984 p 95-97 (For primary document see N86-12462 03-31)
Avail: NTIS HC A08/MF A01

The characteristics of an electron gun with an annular cathode are described. In order to compare design optimizations for different applications, a program for computer-aided design (CAD) has been compiled and typical examples given. The high-power electron gun with annular cathode can achieve higher compression with a large power density, its beam is adjustable, its static electricity focusing structure is simple, it can avoid mutual contamination of cathodes and bombarded surfaces, etc. Therefore, widespread application is possible in X-ray photoetching, electron-beam smelting and evaporation installation. Author

32 COMMUNICATIONS

Includes land and global communications; communications theory; and optical communications.

For related information see also *04 Aircraft Communications and Navigation* and *17 Spacecraft Communications, Command and Tracking.*

N86-12469 Missouri Univ., Columbia.
DESIGN OF AN ANTENNA FEED SYSTEM TO PRODUCE A UNIFORM FIELD Ph.D. Thesis
Surya Saputra 1984 209 p
Avail: Univ. Microfilms Order No. DA8512241

An analytical approach is presented to find an excitation distribution of a multiple feed horn array radiating to an offset parabolic reflector to produce a uniform field over a region on earth. The reflector antenna is installed in a communication satellite. The aperture field method is used to predict the secondary pattern generated by the reflector antenna. Two antenna synthesis problems are involved in this discussion, namely the aperture synthesis and the planar array synthesis. The aperture synthesis is formulated into an integral equation. The integral equation is solved for the array factor by applying the Zernike polynomials. Applying the Zernike polynomials, the radiation integral is converted to a Fourier-Bessel series, then the field of the secondary pattern may be expressed as a function of the observation angles. The numerical results show that the shape of the principle beam of the secondary pattern may be classified into three categories which are the convex shape, the concave shape and the shape with some ripples. Dissert. Abstr.

N86-12470 Missouri Univ., Rolla.
HYBRID RADAR WAVEFORM DESIGN UTILIZING COMPLEMENTARY PHASE CODING AND LINEAR FREQUENCY STEPPING FOR ACHIEVING IMPROVED SLANT RANGE RESOLUTION IN A SYNTHETIC APERATURE RADAR Ph.D. Thesis
Daniel Bernard Koch 1984 158 p
Avail: Univ. Microfilms Order No. DA8507615

A hybrid radar waveform design is presented for achieving improved slant range resolution in a synthetic aperture radar system., The hybrid waveform consists of K repetitions of L complementary phase coded pulses with linearly increasing carrier frequency from repetition to repetition. Processing of this frequency stepped, phase coded waveform consists of matched filtering on a pulse-by-pulse basis followed by amplitude weighting and coherent summation. Three types of complementary phase codes are analyzed with coder and decoder structures modeled by finite impulse response digital filters. Computationally efficient decoder structures are identified using the concept of a matched digital filter. The composite ambiguity function is defined and computed for several hybrid waveform examples. Author

N86-12471# Communications Research Centre, Ottawa (Ontario). Radio Progagation Lab.
THE MEASUREMENT OF TROPOSPHERIC REFRACTIVE INDEX RELEVANT TO THE STUDY OF ANOMALOUS MICROWAVE PROPAGATION: REVIEW AND RECOMMENDATIONS
B. Segal Jun. 1985 43 p refs
(CRC-1387) Avail: Issuing Activity

Radio waves propagation between a transmitter and a receiver is determined by the nature of the Earth's surface and by the tropospheric properties. Observations of the refractive index structure in the lower levels of the atmosphere where its impact on radiowave propagation is greatest are summarized. Different meteorological techniques and instrumentation for study the troposphere are reviewed and possible methods for injecting these instruments into the region of interest are discussed. The interactions between the sometimes subtle climatic and emporal changes in the troposphere and the transmission of microwave signals over terrestrial links are examined. It is concluded that a good deal of research and development remains to be done in the area of improved meteorological instrumentation. E.A.K.

N86-12472 Rensselaer Polytechnic Inst., Troy, N. Y.
BANDWIDTH EFFICIENT FREQUENCY-SHIFT KEYED COMMUNICATION SYSTEMS Ph.D. Thesis
Jone-Shyan Sher 1984 345 p
Avail: Univ. Microfilms Order No. DA8509668

The performance of Pulse Code Modulation with Frequency Modulation (PCM/FM) is evaluated. A numerical algorithm is developed to compute the power spectral density function of PCM/FM. By choosing proper baseband signaling pulse and modulation index (h), the waveform of PCM/FR can be made identical to that of MSK, SFSK, and CPFSK. Thus, the spectral property of these modulation schemes can be obtained directly from that of PCM/FM. The spectral efficiency of PCM/fm is evaluated based on the criteria of out-of-band power bandwidth and channel crosstalk bandwidth. Both spectral measures are functions of the modulation index, the baseband signaling pulse, and the shape parameter thereof. For a given bandwidth or channel separation, these two spectral measures might result in different choices of optimum baseband signaling pulses. In general, through, the rectangular pulse results in better spectral performance for very narrow bandwidths, the trapezoidal pulse outperforms for medium bandwidths, and the raised cosine pulse prevails for wider bandwidths. Author

N86-12473 Department of the Air Force, Washington, D.C.
SIMULTANEOUS DETECTION OF TIME COINCIDENT SIGNALS IN AN ADAPTIVE DOPPLER TRACKER Patent
A. W. Roeder, inventor (to Air Force) Issued 23 Apr. 1985 12 p
Supersedes AD-D011092; N85-32659
(AD-D011796; US-Patent-4,513,428; US-Patent-Class-375-120)
Avail: US Patent and Trademark Office CSCL 17/2

The performance of an adaptive digital Doppler tracker having a sample data phase locked loop is improved by a circuit that detects and demodulates interfering signals. The tracker has a coherence sensor that provides signals indicating coherence and non-coherence conditions. An amplitude sensor generates a strong signal when interfering (time coincident) signals are received. The tracker includes both a coherent data detector and SSB processor. An interference detector receives the outputs of the coherence sensor and the amplitude sensor and generates and SSB enable signal in response to the coincidence of a strong signal and a non-coherent condition signal. The SSB enables the SSB processor which detects both interfering signals. Author (GRA)

N86-12474 Department of the Navy, Washington, D. C.
LOW SIDELOBE, HIGH EFFICIENCY MIRROR ANTENNA WITH TWIST REFLECTOR Patent
D. D. Howard and D. C. Cross, inventors (to Navy) Issued 12 Mar. 1985 4 p Supersedes AD-D009714
(AD-D011835; US-Patent-4,504,835; US-Patent-Appl-SN-389139; US-Patent-Class-343-755) Avail: US Patent and Trademark Office CSCL 09/5

A mirror antenna employing a continuous mirror without a hole. A feed horn and an electromagnetic lens, located behind a rotatable twist reflector (the mirror), collimates a beam toward a polarized reflector located near the twist reflector and tilted to aim energy toward the twist reflector. Energy reflected back toward the polarized reflector from the twist reflector passes through the polarized reflector to free space. Author (GRA)

N86-12475 Department of the Navy, Washington, D. C.
P1 POLYPHASE CODE EXPANDER-COMPRESSOR Patent
F. F. Kretschmer, inventor (to Navy) Issued 23 Apr. 1985 5 p
Supersedes AD-D009615
(AD-D011838; US-Patent-4,513,289; US-Patent-Appl-SN-377106; US-Patent-Class-17.2-PC) Avail: US Patent and Trademark Office CSCL 17/9

A pulse expansion and compression system, especially useful for radar ranging, comprising a pulse coder for expanding and input pulse and a pulse compressor of the matched-filter type. The coder consists of a plurality of delay stages into which the input pulse is fed, a discrete Fourier transform (DFT) circuit to which the output signals of the delay stages are fed by way of respective phase weights and for which every other frequency port is inverted prior to entry to a time-dispersion-means (TDM) comprising an arrangement of adders interconnected by delay stages for differently delaying the output signals from the DFT. The TDM output is fed to a phase modulator and then to the transmitter. The echo signals are conjugated, time-inverted, and passed through the same DFT as the input pulse signal by way of the phase weights. The outputs of the DFT are then inverted at every other frequency port and passed through the TDM, but this tme in time-inverted order. The outputs of the TDM are fed through an envelope detector to provide a cross-correlated facsimile of the original input pulse. Author (GRA)

N86-12476 Department of the Navy, Washington, D. C.
P2 POLYPHASE CODE EXPANDER-COMPRESSOR Patent
F. F. Kretschmer, inventor (to Navy) Issued 18 Jun. 1985 5 p
Supersedes AD-D009649
(AD-D011839; US-Patent-4,524,363; US-Patent-Appl-SN-377108; US-Patent-Class-343-17.2-PC) Avail: US Patent and Trademark

Office CSCL 17/9

A pulse expansion and compression system, especially useful for radar ranging, comprising a pulse coder for expanding an input pulse and a pulse compressor of the matched-filter type. The coder consists of a plurality of delay stages into which the input pulse is fed, a discrete Fourier transform (DFT) circuit to which the output signals of the delay stages are fed by way of respective phase weights and for which every frequency port is phase-shifted prior to entry to a time-dispersion-means (TDM) comprising an arrangement of delay stages for differently delaying the output signals from the DFT. The TDM output is fed to a phase modulator and then to the transmitter. The echo signals are conjugated, time-inverted, and passed through the same DFT as the input pulse signal by way of the phase weights. The outputs of the DFT are then phase-shifted at every frequency port and passed through the TDM, but this time in time-inverted order. The outputs of the TDM are fed through an envelope detector to provide a cross-correlated facsimile of the original input pulse. Author (GRA)

N86-12477 Department of the Army, Washington, D. C.
COMMUNICATIONS NETWORK STATUS INFORMATION SYSTEM Patent
H. A. Stover, inventor (to Army) Issued 30 Jul. 1985 16 p
(AD-D011850; US-Patent-4,532,625; US-Patent-Appl-SN-542635; US-Patent-Class-370-58) Avail: US Patent and Trademark Office CSCL 17/2

This disclosure concerns a communications network information system, and provides apparatus and a method for efficiently providing survivable communications capability to every surviving node in the communications network from every other surviving node. The types of information provided can include high priority message between users of the communications system, or perhaps of even greater importance, very frequently updated status information about the communications network nodes and their interconnecting links for use in optimally utilizing the surviving resources of a heavily damaged network. With this capability every surviving node in the network will be automatically and efficiently provided with the status of every node and interconnecting link. Author (GRA)

N86-12478*# Massachusetts Univ., Amherst. Dept. of Electrical and Computer Engineering.
NEAR MILLIMETER WAVE IMAGING/MULTI-BEAM INTEGRATED ANTENNAS Technical Report, 1 Apr. - 30 Sep. 1985
K. Sigfrid Yngvesson and Daniel H. Schaubert 30 Sep. 1985 134 p refs
(Grant NAG1-279)
(NASA-CR-176332; NAS 1.26:176332) Avail: NTIS HC A07/MF A01 CSCL 20N

This report describes the most recent work on the theory of single element Linearly Tapered Slot Antennas (LTSAs) and Constant Width Slot Antennas (CWSAs). The radiation mechanism for these is presently well understood and allows quantitative calculation of beamwidths and sidelobe levels, provided that the antennas have a sufficiently wide conducting region on either side of the tapered slot. Appendices 4 to 7 represent earlier work on the grant. This work further elucidates the properties of arrays of CWSA elements, and the effects of coupling on the beam-shape. It should be noted that typical beam-efficiencies of 65% have been estimated, and that element spacings of about one Rayleigh unit are possible. Further, two-point resolution at the Rayleigh spacing has been demonstrated for a CWSA array in a 30.4 cm paraboloid at 31 GHz. These results underscore that interest in further studies of the radiation mechanism of tapered slot arrays. Appendix 7 constitutes a final, detailed report on the work leading to a 94 GHz seven element LTSA array imaging system, which has been reported previously in less detail. Experimental results are presented. For individual titles, see N86-12479 through N86-12483.

N86-12479*# Massachusetts Univ., Amherst.
ADDITIONAL RESULTS ON THE RADIATING PROPERTIES OF LTSAS AND CWSAS
In its Near Millimeter Wave Imaging/Multi-Beam Integrated Antennas 30 Sep. 1985 64 p refs (For primary document see N86-12478 03-32)
Avail: NTIS HC A07/MF A01 CSCL 20N

Results are presented on the theoretical experimental investigations of the radiating properties of Linearly Tapered Slot Antennas (LTSAs) and Constant Width Slot Antennas (CWSAs). The antenna is treated as a flared slot radiating in the presence of a conducting half plane. The aperture distribution in the flared slot is determined by approximating the tapered structure as a series of short sections of parallel slots. The slot field of a uniform slotline is determined by employing the spectral Galerkin's technique and a power conservation criterion is employed to match the fields at the step junction between two successive sections. Comparison is made between theory and experiment for several LTSAs and CWSAs etched on epsilon sub r = 2.22 and 2.55 substrates, and or flare angles 4 deg < or = gamma < or = 10 deg. It is shown that the theory adequately models the physics of the problem when the lateral dimension D of the antenna is large and when the propagation constant of a parallel slot line can be estimated very accurately. Newly observed effects of the lateral truncation on the radiation pattern of the antenna are discussed. B.W.

N86-12480*# Massachusetts Univ., Amherst. Dept. of Electrical and Computer Engineering.
CHARACTERISTIC IMPEDANCE OF A WIDE SLOT LINE ON LOW PERMITTIVITY SUBSTRATES
R. Janaswamy and D. H. Schaubert *In its* Near Millimeter Wave Imaging/Multi-Beam Integrated Antennas 30 Sep. 1985 12 p refs Submitted for publication (For primary document see N86-12478 03-32)
(Grant NAG1-279)
Avail: NTIS HC A07/MF A01 CSCL 20N

Computed results on the characteristic impedance of wide slots etched on an electrically thin substrate of low dielectric constant epsilon sub r are presented. Results are given for epsilon sub r = 2.22, 3.0, 3.8 and 9.8. Comparison is shown for the characteristic impedance between the present calculations and those available in the literature for high-epsilon sub r substrates. Author

N86-12481*# Massachusetts Univ., Amherst. Dept. of Electrical and Computer Engineering.
ANALYSIS OF THE TEM MODE LINEARLY TAPERED SLOT ANTENNA
Ramakrishna Janaswamy, Daniel H. Schaubert, and David M. Pozar *In its* Near Millimeter Wave Imaging/Multi-Beam Integrated Antennas 30 Sep. 1985 34 p refs Submitted for publication (For primary document see N86-12478 03-32)
(Grant NAG1-279)
Avail: NTIS HC A07/MF A01 CSCL 20N

The theoretical analysis of the radiation characteristics of the TEM mode Linearly Tapered Slot Antenna (LTSA) is presented. The theory presented is valid for antennas with air dielectric and forms the basis for analysis of the more popular dielectric-supported antennas. The method of analysis involves two steps. In the first step, the aperture distribution in the flared slot is determined. In the second step, the equivalent magnetic current in the slot is treated as radiating in the presence of a conducting half-plane and the far-field components are obtained. Detailed comparison with experiment is made and excellent agreement is obtained. Design curves for the variation of the 3 dB and 10 dB beamwidths as a function of the antenna length, with the flare angle as a parameter, are presented. Author

N86-12482*# Onsala Space Observatory (Sweden).
MODEL EXPERIMENTS WITH SLOT ANTENNA ARRAYS FOR IMAGING
J. F. Johansson, K. S. Yngvesson (Massachusetts Univ., Amherst), and E. L. Kollberg *In* Massachusetts Univ. Near Millimeter Wave Imaging/Multi-Beam Integrated Antenna 30 Sep. 1985 9 p refs Prepared for presentation at the 10th Intern. Conf. on Infrared and Millimeter Waves, Orlando, Fla., Dec. 1985 (For primary document see N86-12478 03-32)

Avail: NTIS HC A07/MF A01 CSCL 20N

A prototype imaging system at 31 GHz was developed, which employs a two-dimensional (5x5) array of tapered slot antennas, and integrated detector or mixer elements, in the focal plane of a prime-focus paraboloid reflector, with an f/D=1. The system can be scaled to shorter millimeter waves and submillimeter waves. The array spacing corresponds to a beam spacing of approximately one Rayleigh distance and a two-point resolution experiment showed that two point-sources at the Rayleigh distance are well resolved. Author

N86-12483*# Massachusetts Univ., Amherst. Dept. of Electrical and Computer Engineering.

A NEW INTEGRATED SLOT ELEMENT FEED ARRAY FOR MULTI-BEAM SYSTEMS

K. Sigfrid Yngvesson, J. F. Johansson, and Erik L. Kollberg *In its* Near Millimeter Wave Imaging/Multi-Beam Integrated Antennas 30 Sep. 1985 12 p refs Prepared for presentation at the SPIE Conf. on Submillimeter Spectry., Cannes, Frances, 5-6 Dec. 1985 Prepared in cooperation with Onsala Space Observatory (Sweden) (For primary document see N86-12478 03-32)

Avail: NTIS HC A07/MF A01 CSCL 20N

A feed array consisting of constant width slot antennas (CWSA's), fed from a block containing fin-line transitions, has been developed. The array has a two-dimensional configuration, with five elements each on five parallel substrates. Beam-widths are compatible with use in f/D-1.0 multi-beam systems, with optimum taper. Array element spacings are close to a factor of two smaller than for other typical arrays, and spill-over efficiency is about 65%. Author

N86-12484*# Massachusetts Univ., Amherst. Dept. of Electrical and Computer Engineering.

A 94 GHz IMAGING ARRAY USING SLOT LINE RADIATORS Ph.D. Thesis

Thomas Leo Korzeniowski Sep. 1985 142 p refs

(Grant NAG1-279)

(NASA-CR-176348; NAS 1.26:176348) Avail: NTIS HC A07/MF A01 CSCL 20N

A planar endfire slotted-line antenna structure was investigated. It was found that the H-plane beamwidths are basically dependent upon the substrate properties, whereas the E-plane beamwidths are more strongly a function of the slot's shape and size. It is shown that these antennas produce symmetrical E and H-plane beamwidths while following Zucker's standard traveling-wave antenna beamwidth curves over some range of antenna normalized length. An empircally derived design formula for effective substrate thickness is shown to predict this range for linearly tapered slotted-line antennas. The experimental imaging properties of these arrays are presented and imaging theory is discussed. It is shown that a minimum spacing of elements is necessary for exact reconstruction for a sampled image in a diffraction limited system. Because these LTSA elements employ the traveling-wave mechanism of radiation, they can be spaced two times closer than a conical feed horn of comparable beamwidth. E.A.K.

N86-12485*# National Aeronautics and Space Administration. Lewis Research Center, Cleveland, Ohio.

STRATEGY FOR REFLECTOR PATTERN CALCULATION: LET THE COMPUTER DO THE WORK

P. T. Lam (Illinois Univ., Urbana), S. W. Lee (Illinois Univ., Urbana), C. C. Hung (Lockheed Missiles and Space Co., Sunnyvale, Calif.), and R. Acousta Oct. 1985 9 p refs

(Grant NAG3-149)

(NASA-TM-87137; E-2755; NAS 1.15:87137) Avail: NTIS HC A02/MF A01 CSCL 20N

Using high frequency approximations, the secondary pattern of a reflector antenna can be calculated by numerically evaluating a radiation integral I(u,v). In recent years, tremendous effort has been expended to reducing I(u,v) to Fourier integrals. These reduction schemes are invariably reflector geometry dependent. Hence, different analyses/computer software development must be carried out for different reflector shapes/boundaries. it is pointed out, that, as the computer power improves, these reduction schemes are no longer necessary. Comparable accuracy and computation time can be achieved by evaluating I(u,v) by a brute force FFT described in this note. Furthermore, there is virtually no restriction on the reflector geometry by using the brute force FFT. Author

N86-12486 British Broadcasting Corp., Kingswood (England). Engineering Div.

ROOM MODES AND SOUND ABSORPTION: SOME PRACTICAL MEASUREMENTS COMPARED WITH THEORETICAL PREDICTIONS

E. W. Taylor and C. Eng Aug. 1985 29 p refs

(BBC-RD-1985/11) Avail: Issuing Activity

Changes in the amount of sound absorption, which occur when absorbing material is placed at different regions of a standing wave pattern in a reverberant enclosure, are discussed. Theoretical predictions of this change of absorption are compared with practical measurements. The dependence of the degree of excitation of the absorbing surface on the standing wave pattern over its area, the relative importance of the potential and kinetic energy components in the sound field, and the acceptance of energy from regions of the sound field not immediately adjacent to the absorber, are cited as causes of the observed differences between the theoretical and practical results. E.A.K.

N86-12487# Naval Postgraduate School, Monterey, Calif.

COMPARISON OF CONTINUOUS SPEECH, DISCRETE SPEECH, AND KEYBOARD INPUT TO AN INTERACTIVE WARFARE SIMULATION IN VARIOUS C3 ENVIRONMENTS M.S. Thesis

R. B. Manson and M. E. Wright Mar. 1985 122 p

(AD-A156830; AD-E301723) Avail: NTIS HC A06/MF A01 CSCL 17/2

This thesis describes an experiment conducted at the Naval Postgraduate School during the period 30 October 1984 through 30 November 1984. Specifically, the experiment compares the use of continuous speech recognition equipment, discrete speech recognition equipment, and keyboard to input commands in a command and control environment. This was accomplished by using the Naval Warfare Interactive Simulation System (NWISS) as a vehicle to pose military problems to subject in a variety of light and noise environments. Although the results are not conclusive, they do show a definite advantage in using continuous speech or keyboard entry modes over discrete speech modes. Continuous speech and keyboard methods were superior in all environmental conditions. Author (GRA)

N86-12488# Naval Postgraduate School, Monterey, Calif.

AN EVOLVING DIGITAL TELECOMMUNICATIONS INDUSTRY AND ITS IMPACT ON THE OPERATIONAL ENVIRONMENT OF THE NATIONWIDE EMERGENCY TELECOMMUNICATION SYSTEM (NETS) M.S. Thesis

R. J. Stahel Mar. 1985 101 p

(AD-A156831; AD-E301723) Avail: NTIS HC A06/MF A01 CSCL 17/2

Following a national disaster, a Nationwide Emergency Telecommunications System (NETS) would be created by combining the existing telecommunications capabilities of government, public carriers and private networks. This thesis addressed an evolving digital capabilities, reviews the digital telecommunications industry and analyzes the impact of a changing digital technology upon the desired features of a pre-emergency network. GRA

N86-12489# Bolt, Beranek, and Newman, Inc., Cambridge, Mass.

INTERNETTING AND PACKET SATELLITE PROGRAM Final Report

S. Blumenthal Jul. 1985 23 p

(Contract MDA903-80-C-0353)

(AD-A157124; BBN-5939) Avail: NTIS HC A02/MF A01 CSCL 17/2

As a means of utilizing valuable communications resources more efficiently, The Department of Defense Advanced Research Projects AGency has sponsored a program of research and development in the area of packet-switched data networks. In addition to more efficient utilization, packet switching systems with autonomous distributed control can be made robust and survivable. In support of this program, BBN has conducted research and development in the areas of Internetting and the efficient use of broadcast satellite channels by packet-switched networks. Specific work performed under this contract involved the development of Internet gateways to interconnect many different types of dissimilar packet-switched networks, Internet protocols for data communication, and a Terminal Access Controller utilizing these protocols for remote network-access to time-shared computer systems. BBN also continued the development of the Atlantic Packet Satellite Network, (SATNET) providing Internet connectivity between sites in the U.S. and Europe using a shared 64kb/s INTELSAT satellite channel, and the domestic Wideband Packet Satellite Network, providing high bandwidth communication among ten sites within the continental U.S. GRA

N86-12490# Canadian Scientific Liason Office, Washington, D.C.
ELIE: SAINT EUSTACHE FIBRE OPTIC FIELD TRIAL PROJECT EVALUATION REPORT, VOLUME 4
K. B. Harris, G. A. Tough, and M. B. Akgun Mar. 1985 429 p 2 Vol.
(AD-A157144) Avail: NTIS HC A19/MF A01 CSCL 17/2

The Elie - St. Eustache Fibre Optic Field Trial has provided voice, data and video communications through an integrated services access system to 150 residential and small business participants in a rural area. The trial has generated a wealth of information in all stages of the project such as design, implementation and operation. The uniqueness of the system makes it worthwhile to document in detail all the experience gained for use by national and international parties who have an interest in the design, manufacture and operation of similar systems in the future. GRA

N86-12491# Rio Grande Associates, Houston, Tex.
NONLINEAR ELECTROMAGNETIC SCATTERING FROM A DIODE CIRCUIT
R. R. Beland Jan. 1984 40 p
(Contract F19628-81-C-0128)
(AD-A157216; AFGL-TR-84-0151; SR-3) Avail: NTIS HC A03/MF A01 CSCL 20/14

Electromagnetic scattering from an active diode circuit is considered. The focus is on the nonlinear interaction between the incident fields and the internal circuit sources. This interaction results in a mixing of frequencies between the incident and internal sources. An equivalent circuit model of the diode circuit and dipole antenna is presented and a nonlinear differential equation derived. This equation is solved approximately by a Volterra series to third order. This solution is simulated and numerical values of total scattered power at the various frequencies are calculated. GRA

N86-12492# Naval Research Lab., Washington, D. C.
RENORMALIZATION OF AN INVERSE SCATTERING THEORY FOR INHOMOGENEOUS DIELECTRICS
H. D. Ladouceur and A. K. Jordan 19 Jul. 1985 14 p
(RR0-3302)
(AD-A157224; NRL-MR-5605) Avail: NTIS HC A02/MF A01 CSCL 20/14

Renormalized solutions are obtained for an inverse scattering problem that are equivalent to the second-order regular perturbation approximations for the exact (Gelfand-Levitan-Marchenko) theory. We have developed an inversion method for reconstructing the permittivity profiles of inhomogeneous dielectric slabs from reflection coefficient data. Solutions with increased radii of convergence are obtained. Numerical examples are demonstrated for simulated scattering data from Gaussian and parabolic profiles and homogeneous slabs. GRA

N86-12493# Southeastern Center for Electrical Engineering Education, Inc., St. Cloud, Fla.
BASIC EMC (ELECTROMAGNETIC COMPATIBILITY) TECHNOLOGY ADVANCEMENT FOR C3 (COMMAND, CONTROL, AND COMMUNICATIONS) SYSTEMS. VOLUME 6 Final Technical Report, Jun. 1982 - Dec. 1983
D. Weiner, C. R. Paul, and J. Whalen Apr. 1985 140 p
(Contract F30602-81-C-0062)
(AD-A157239; RADC-TR-82-286-Vol-6) Avail: NTIS HC A07/MF A01 CSCL 17/2

This research effort was devoted to eliminating some of the basic technological gaps in the two important areas of: (1) electromagnetic effects (EM) on microelectronic circuits and (2) EM coupling and testing. The results are presented in fourteen reports which have been organized into six volumes. The reports are briefly summarized in this volume. In addition, an experiment is described which was performed to demonstrate the feasibility of applying several of the results to a problem involving electromagnetic interference. Specifically, experimental results are provided for the randomness associated with: (1) crosstalk in cable harnesses and (2) demodulation of amplitude modulated (AM) signals in operational amplifiers. These results are combined to predict candidate probability density functions (pdf's) for the amplitude of an AM interfering signal required to turn on a light emitting diode. The candidate pdf's are shown to be statistically consistent with measured data. Author (GRA)

N86-12494# Adaptive Sensors, Inc., Santa Monica, Calif.
ANALYSIS OF CONSTANT FALSE ALARM RATE SIDELOBE CANCELLER CRITERION Final Progress Report
I. S. Reed and L. E. Brennan May 1985 24 p
(Contract N00019-84-C-0074)
(AD-A157412) Avail: NTIS HC A02/MF A01 CSCL 17/4

In this final report, the constant false alarm rate (CFAR) detection criterion for a sidelobe canceller (SLC) system, introduced in the last quarterly progress report, is found completely and analyzed. This new detection test for radar exhibits the desirable CFAR property that its probability of a false alarm (PFA) is functionally independent of the covariance of the actual noise field encountered. As a consequence, such a CFAR SLC system is ideally suited to cope with the newly evolving smart jammer threat to radar. An important objective, set in the last quarterly progress report, was to find both the false alarm and signal detection probabilities of this test. The first and most important of these two goals has been met. The probability of a false alarm (or PFA) of this CFAR SLC detection criterion is derived in closed form in this report. The success in finding the PFA is due primarily to the use of a generalization of Cochran's theorem. GRA

N86-12495# Air Force Systems Command, Wright-Patterson AFB, Ohio. Foreign Technology Div.
RADIO-ABSORBING MATERIALS
Y. A. Shneyderman 16 Jul. 1985 64 p Transl. into ENGLISH from Zarubezhneya Radioelektron. (USSR), no. 4, 1965 p 115-135
(AD-A157496; FTD-ID(RS)T-1326-84) Avail: NTIS HC A04/MF A01 CSCL 17/4

Recently abroad in connection with rapid development of radar technology methods and means of antiradar protection of flight vehicles, which facilitate breach/inrush of aircraft and rockets through lines of air defense intensively are developed/processed. On the intensification of works in this direction it is possible to judge a sharp increase in the expenditures of USAF (United States Air Force) for the development of the combat means with radar - with 35.5 million dollars in 1962 to 119 million dollars in 1963 and 155 million dollars each in 1964. Utilization of radio-absorbing materials, which ensure decrease of effective surface of scattering of aircraft and rockets, is one of effective combat means with radar. GRA

N86-12496# Rome Air Development Center, Griffiss AFB, N.Y.
SCATTERING EXPERIMENTS AT THE IPSWICH ELECTROMAGNETIC MEASUREMENTS FACILITY: BACKSCATTER FROM METAL CUBES Report, for Jan. - Dec. 1984
R. V. McGahan Feb. 1985 18 p
(AF Proj. 2305)
(AD-A157925; RADC-TR-85-24) Avail: NTIS HC A02/MF A01

CSCL 20/14

Backscatter cross section measurements at broadside incidence were made on eighteen metal cubes at X-band. The measurements are compared with theoretical predictions made using Enhanced High Frequency Diffraction and Augmented Magnetic field Integral Equation solutions. A composite solution is formed and compared with the measurements, providing a validated backscatter solution for metal cubes from arbitrarily low to arbitrarily high frequencies. GRA

N86-12497# University of Southern California, Los Angeles. Communication Sciences Inst.

ADVANCED DIGITAL COMMUNICATION RESEARCH Final Report, 1 Sep. 1982 - 31 May 1985

R. A. Scholtz and L. M. Silverman Jul. 1985 59 p
(Contract DAAG29-82-K-0142)
(AD-A158412; CSI-85-07-04; ARO-19147.37-EL) Avail: NTIS HC A04/MF A01 CSCL 17/2

The research proposed for this contract included the following topics: spread-spectrum systems (synch acquisition and performance), the design of pseudorandom sequences, digital signal design, spectral shaping via redundancy, retrodirective array processing, VLSI implementation of number-theoretic transforms, and approximation theory. GRA

N86-12498# Brookhaven National Lab., Upton, N. Y.

HIGH ORDER MODE DAMPING IN THE NSLS ACCELERATING RF CAVITIES BY THE USE OF DAMPING ANTENNAE

N. Fewell and Z. Wen 1985 4 p refs Presented at the Particle Accelerator Conf., Vancouver, British Columbia, 13 May 1985
(Contract DE-AC02-76CH-00016)
(DE85-014214; BNL-36506; CONF-850504-195) Avail: NTIS HC A02/MF A01

High order modes were successfully damped in the existing NSLS accelerating cavities by the insertion of damping antennae. The location of the antennae was aided by cavity field plots using superfish and their lengths determined experimentally. A description of their construction is presented together with the results of their insertion upon higher order cavity modes and beam stability. E.A.K.

N86-12499# Argonne National Lab., Ill.

MICROWAVE RIDGED WAVEGUIDE BEAM PICKUPS

D. Suddeth 1985 3 p Presented at the Particle Accelerator Conf., Vancouver, British Columbia, 13 May 1985
(Contract W-31-109-eng-38)
(DE85-013816; ANL-HEP-CP-85-41; CONF-850504-180) Avail: NTIS HC A02/MF A01

Sensitive broadband beam pickups are a prerequisite for improved stochastic beam cooling. The 2 to 4 GHz and the 4 to 8 GHz bands were of particular interest for stochastic cooling applications. This report summarizes the striking results of an investigation of ridged waveguide pickups at Argonne. An upper to lower frequency ratio of 2.4:1 is readily obtained with a ridged waveguide as compared to 1.5:1 with a standard waveguide. Wire measurements and tests at the Argonne beam test facility indicate an approximate 20% increase in gain per unit over a stripline with comparable longitudinal spacing. Another advantage of waveguide pickups is construction simplicity. The output is easily coupled to a transmission line. Descriptions of the design, construction, and results are reported. DOE

N86-12500# Sandia National Labs., Albuquerque, N. Mex.

RESULTS OF FIELD AND LABORATORY STUDIES OF JAM-RESISTANT AND VOICE-PRIVATE RADIOS

J. E. Heustess, M. K. Snell, and D. J. Gangel 1985 7 p Presented at the 26th Ann. Meeting of the Inst. of Nucl. Mater. Management, Albuquerque, N. Mex., 21 Jul. 1985
(Contract DE-AC04-76DP-00789)
(DE85-014841; SAND-85-1570C; CONF-850765-5) Avail: NTIS HC A02/MF A01

Radio communications systems that use voice privacy or voice scrambling exhibit varying degrees of security range reduction, message intelligibility, and susceptibilities to a jamming assault. Studies included the evaluation of Data Encryption Standard (DES) and Frequency Hopping (FH) systems. Results include voice intelligibility, jamming survivability, and range reduction percentages. DOE

N86-12501# National Telecommunications and Information Administration, Boulder, Colo. Inst. for Telecommunication Sciences.

SPECTRUM RESOURCE ASSESSMENT OF THE 1605-2000 kHz BAND

R. E. Thompson, W. B. Grant, and J. C. Carroll Apr. 1985 119 p
(PB85-225076; NTIA-85-175) Avail: NTIS HC A06/MF A01 CSCL 17B

The report is a spectrum resource assessment of the 1605 to 2000 kHz band. It includes information on rules, regulations, allocations, technical standards, frequency assignments, system characteristics, and applicable compatibility analyses pertinent to the 1605 to 2000 kHz band. Major issues are discussed concerning changes in the allocation tables due to WARC-79 decisions. Parts of the 1605 to 2000 kHz band are in transition from radiolocation service use to broadcasting service use. Major problems in this band are the sharing among travelers' information stations, radiolocation, and broadcasting and the proliferation of the cordless telephone. The report analyzes the possibility of sharing between broadcasting and travelers' information stations and radiolocation, along with addressing the problems associated with cordless telephones. GRA

N86-12502# National Telecommunications and Information Administration, Annapolis, Md.

HANDBOOK OF RADIO WAVE PROPAGATION LOSS (100-10,000 MHz)

W. E. Frazier Dec. 1984 172 p refs
(PB85-200012; NTIA-84-165) Avail: NTIS HC A08/MF A01 CSCL 20N

This handbook is intended to assist in manual analysis techniques that must be used when an automated analysis is not possible. It provides estimates of radio wave propagation loss between transmitting and receiving antennas above the assumed smooth-earth surface that were calculated using the Integrated Propagation System (IPS) computer model. For many cases involving electromagnetic compatibility analysis, the included curves of transmission loss predictions may be used for estimating transmission loss for the desired signal and the undesired signal. These loss values are given in dB as BASIC MEDIAN TRANSMISSION LOSS for antennas with effective heights up to 5000 meters, operating in the 100 to 10,000 MHz frequency range, over land or sea, at great circle earth surface distances up to 1,000 kilometers. GRA

N86-12376# Tokyo Denki Univ. (Japan). Faculty of Engineering.

EXTRACTION OF FEATURE PARAMETERS FOR SPOKEN WORD RECOGNITION

T. Tanaka and S. Nakamura *In its* Res. Rept. of the Faculty of Eng., Tokyo Denki Univ., No. 32 Dec. 1984 p 57-65 refs In JAPANESE; ENGLISH summary (For primary document see N86-12372 03-31)
Avail: NTIS HC A09/MF A01

N86-12378# Tokyo Denki Univ. (Japan). Faculty of Engineering.

A PHYSICAL METHOD FOR ESTIMATING SPEECH INTELLIGIBILITY IN A REVERBERANT SOUND FIELD

Yasuo Ogura *In its* Res. Rept. of the Faculty of Eng., Tokyo Denki Univ., No. 32 Dec. 1984 p 79-100 refs In JAPANESE; ENGLISH summary (For primary document see N86-12372 03-31)
Avail: NTIS HC A09/MF A01

N86-12379# Tokyo Denki Univ. (Japan). Faculty of Engineering.

DUMMY HEAD MICROPHONE AND ITS APPLICATION TO THE MEASUREMENTS OF ELECTRO-ACOUSTIC EQUIPMENTS
In its Res. Rept. of the Faculty of Eng., Tokyo Denki Univ., No. 32 Dec. 1984 p 101-115 refs In JAPANESE; ENGLISH summary (For primary document see N86-12372 03-31)
Avail: NTIS HC A09/MF A01

N86-12424# Joint Publications Research Service, Arlington, Va.
PULSED RADIATION DETECTION TECHNOLOGY DISCUSSED
Lu Min *In its* China Rept.: Sci. and Technol. (JPRS-CST-85-021) 8 Jul. 1985 p 99-112 Transl. into ENGLISH from Hedianzixue Yu Tance Jishu (Beijing), v. 4, no. 6, Nov. 1984 p 321-328 (For primary document see N86-12421 03-31)
Avail: NTIS HC A09/MF A01

N86-12432# Joint Publications Research Service, Arlington, Va.
OPTIC FIBER APPLICATIONS IN DATA COMMUNICATIONS
Yu Huaiquan and Lu Zinan *In its* China Rept.: Sci. and Technol. (JPRS-CST-85-034) 1 Oct. 1985 p 53-58 Transl. into ENGLISH from Dianzi Jishu (Shanghai), v. 12, no. 5, 20 May 1985 p 15-17; 19 (For primary document see N86-12430 03-31)
Avail: NTIS HC A08/MF A01

N86-12452# Joint Publications Research Service, Arlington, Va.
COMPUTER-AIDED ANALYSIS OF ARBITRARY-SHAPED THIN-WIRE ANTENNAS
Hong Wei and Zhang Wenxun *In its* China Rept.: Sci. and Technol. (JPRS-CST-85-030) 4 Sep. 1985 p 15-23 refs Transl. into ENGLISH from Nanjing Gongxueyuan Xuebao (Nanjing), no. 4, 20 Dec. 1984 p 61-67 (For primary document see N86-12451 03-31)
Avail: NTIS HC A08/MF A01

N86-12644# Joint Publications Research Service, Arlington, Va.
INFLUENCE OF SHORT GRAVITY WAVES ON THERMAL RADIO EMISSION OF WATER SURFACE Abstract Only
V. A. Ilin, A. A. Naumov, V. Yu. Rayzer, S. R. Filonovich, and V. S. Etkin *In its* USSR Rept.: Earth Sci. (JPRS-UES-85-006) 19 Jun. 1985 p 15 Transl. into ENGLISH from Izv. Akad. Nauk SSSR: Fiz. Atm. i Okeana (Moscow), v. 21, no. 1, Jan. 1985 p 83-89 (For primary document see N86-12630 03-42)
Avail: NTIS HC A05/MF A01

N86-12648# Joint Publications Research Service, Arlington, Va.
CORRELATION CHARACTERISTICS OF SIGNALS REFLECTED BY THE WAVY SURFACE OF OCEAN IN MIRROR DIRECTION Abstract Only
Yu. Yu. Zhitkovskiy, A. V. Nosov, and V. V. Savelyev *In its* USSR Rept.: Earth Sci. (JPRS-UES-85-006) 19 Jun. 1985 p 18 Transl. into ENGLISH from Akust. Zh. (Moscow), v. 30, no. 6, Nov. - Dec. 1984 p 772-776 (For primary document see N86-12630 03-42)
Avail: NTIS HC A05/MF A01

N86-12684# Joint Publications Research Service, Arlington, Va.
METHOD FOR SOLVING PROBLEMS IN ELECTRODYNAMICS OF ANISOTROPIC MEDIA WITH SLANT BEDDING Abstract Only
M. G. Savin *In its* USSR Rept.: Earth Sci. (JPRS-UES-85-006) 19 Jun. 1985 p 59-60 Transl. into ENGLISH from Izv. Akad. Nauk SSSR: Fiz. Zemli (Moscow), no. 2, Feb. 1985 p 75-82 (For primary document see N86-12630 03-42)
Avail: NTIS HC A05/MF A01

N86-12701# Joint Publications Research Service, Arlington, Va.
PHASE OPERATOR METHOD IN PROBLEM OF SCATTERING OF ELECTROMAGNETIC WAVES ON IDEALLY CONDUCTING SURFACE Abstract Only
A. G. Voronovich *In its* USSR Rept.: Earth Sci. (JPRS-UES-85-008) 16 Aug. 1985 p 7-8 Transl. into ENGLISH from Dokl. Akad. Nauk SSSR (Moscow), v. 282, no. 2, May 1985 p 286-290 (For primary document see N86-12697 03-42)
Avail: NTIS HC A04/MF A01

33 ELECTRONICS AND ELECTRICAL ENGINEERING

Includes test equipment and maintainability; components, e.g., tunnel diodes and transistors; microminiaturization; and integrated circuitry.

For related information see also *60 Computer Operations and Hardware* and *76 Solid-State Physics.*

N86-12503 Pittsburgh Univ., Pa.
ADAPTIVE KALMAN FILTERING WITH CONTROL INPUT ESTIMATION Ph.D. Thesis
Chih-Tsong Chen 1984 103 p
Avail: Univ. Microfilms Order No. DA8512551

The application of Kalman filter to a linear stochastic system requires complete information regarding the system's dynamics and observations. A major disadvantage of the Kalman filter is that it is sensitive to erroneous modeling of the system. In practice there are problems associated with unknown control inputs. In this case the solution provided by the Kalman filter is suboptimal. One way to improve the filter's performance is to estimate the unknown control inputs. The estimate is then fed back to the Kalman filter to improve its behavior. When the estimated control inputs are sent back to the Kalman filter, their estimation errors also have the tendency to increase the filter's estimation uncertainty, which, in turn, will further degrade the system's performance. By manipulating the system's observability matrix, one is able to present a new algorithm in which the degraded state estimate generated by the Kalman filter is not involved in the estimation of the unknown control inputs, so that the accumulation of the estimation errors does not have any chance to take place in our adaptive estimation system. Dissert. Abstr.

N86-12504 Michigan State Univ., East Lansing.
INTEGRAL EQUATION DESCRIPTION OF INTEGRATED DIELECTRIC WAVEGUIDES Ph.D. Thesis
Jonathan Scott Bagby 1984 205 p
Avail: Univ. Microfilms Order No. DA8507475

An equivalent polarization integral equation is advanced for use in the analysis of integrated dielectric waveguiding systems. This inhomogeneous Fredholm equation of the second kind in the unknown total waveguide core electric field provides a conceptually exact formulation of the guidance properties of a wide class of practical integrated dielectric waveguides. The integral equation is applied to a generalized axially uniform integrated dielectric waveguiding system. This axial uniformity renders the axial integral convolutional in nature, prompting the use of a spatial Fourier transform. This results in an inhomogeneous Fredholm equation for the unknown transformed total core field. Subsequent inversion of the transformed field with the aid of the residue theorem allows identification of two components of the total core field: the surface waves of the guide and the radiation spectrum. Application of moment method and Neumann series techniques to the integral equation is discussed. Author

N86-12505 Case Western Reserve Univ., Cleveland, Ohio.
DESIGN OF HIGH POWER SUPERCONDUCTING SWITCHES Ph.D. Thesis
Maher Elyon Rizkalla 1985 98 p
Avail: Univ. Microfilms Order No. DA8510104

Repetitive opening switches capable of handling 5000 Amps and holdoff voltage >10 kV operating in a very short time (approx. 1 micro sec) were designed. The maximum change of temperature during the effective time of the heat source and the cooling rate of the superconducting material were calculated. Different materials were examined in order to determine the most suitable materials to optimize acoustic matching for different interfaces. The problem of heat transfer was simulated numerically in order to establish the temperature distribution across the switch. The computer results for the different materials were used in order to determine the maximum operating conduction current that can be applied on these switches while they are operating in the free convection regime of liquid helium. Dissert. Abstr.

N86-12506 Department of the Air Force, Washington, D.C.
VARIABLE RADIUS LEAD FORMER Patent
R. L. Zahn, inventor (to Air Force) Issued 7 May 1985 5 p
Supersedes AD-D010867
(AD-D011790; US-Patent-4,515,001; US-Patent-Appl-SN-566352; US-Patent-Class-72-323) Avail: US Patent and Trademark Office CSCL 13/8

A variable radius lead former operates an axial lead electronic component wherein the bend radius may be adjusted to any desired radius within specifications. Author (GRA)

N86-12507 Department of the Navy, Washington, D. C.
DEMOUNTABLE COAXIAL ELECTRICAL CONNECTOR FOR IN-LINE AMPLIFIERS Patent
R. J. Phillips, inventor (to Navy) Issued 25 Jun. 1985 4 p
Supersedes AD-D011074
(AD-D011831; US-Patent-4,525,013; US-Patent-Appl-SN-571414; US-Patent-Class-339-7) Avail: US Patent and Trademark Office CSCL 09/1

A flexible coaxial connector assembly is used on buoyant cable antenna systems. It comprises a retainer assembly that has threads mating with a bellows assembly. Components that mate in a flexible manner are enclosed by the bellows. An electrical wire passes through these flexible mating components and terminates in a contact pin. The contact pin mates with an amplifier contact socket assembly. GRA

N86-12508*# National Aeronautics and Space Administration. Langley Research Center, Hampton, Va.
THE ROLE OF AMPLITUDE-TO-PHASE CONVERSION IN THE GENERATION OF OSCILLATOR FLICKER PHASE NOISE
Chase P. Hearn Oct. 1985 12 p refs
(NASA-TM-87590; L-16015; NAS 1.15:87590) Avail: NTIS HC A02/MF A01 CSCL 09C

The role of amplitude-to-phase conversion as a factor in feedback oscillator flicker phase noise is examined. A limiting stage consisting of parallel-connected opposite polarity diodes operating in a circuit environment contining reactance is shown to exhibit amplitude-to-phase conversion. This mechanism coupled with resistive upconversion provides an indirect route for very low frequency flicker noise to be transferred into the phase of an oscillator signal. It is concluded that this effect is more significant in the lower frequency regimes where the onlinear reactances associated with active devices are overwhelmed by linear reactive elements. Author

N86-12509*# National Aeronautics and Space Administration. Lewis Research Center, Cleveland, Ohio.
PERFORMANCE AND TEMPERATURE DEPENDENCIES OF PROTON IRRADIATED n/p GaAs AND n/p SILICON CELLS
I. Weinberg, C. K. Swartz, and R. E. Hart, Jr. 1985 10 p refs
Presented at the 18th Photovoltaic Specialists Conf., Las Vegas, Nev., 21-25 Oct. 1985; sponsored by IEEE
(NASA-TM-87136; E-2753; NAS 1.15:87136) Avail: NTIS HC A02/MF A01 CSCL 09C

The n/p homojunction GaAs cell is found to be more radiation resistant than p/nheteroface GaAs under 10 MeV proton irradiation. Both GaAs cell types outperform conventional silicon n/p cells under the same conditions. An increase temperature dependency of maximum power for the GaAs n/p cells is attributed largely to differences in Voc between the two GaAs cell types. These results and diffusion length considerations are consistent with the conclusion that p-type GaAs is more radiation resistant than n-type and therefore that the n/p configuration is possibly favored for use in the space radiation environment. However, it is concluded that additional work is required in order to choose between the two GaAs cell configurations. Author

N86-12510# North Carolina State Univ., Raleigh. Dept. of Electrical and Computer Engineering.
HIGH FREQUENCY SILICON BIPOLAR TRANSISTOR WITH SIPOS (SEMI-INSULATING POLYCRYSTALLINE SILICON) HETEROJUNCTION EMITTER AND ION IMPLANTED RAPID THERMAL ANNEALED BASE REGION Annual Report
J. J. Wortman, J. R. Hauser, M. A. Littlejohn, G. A. Rozgonyi, and V. H. Ozguz Mar. 1985 142 p
(Contract N00014-82-K-0468)
(AD-A157141) Avail: NTIS HC A07/MF A01 CSCL 09/1

The research program described in this report is directed toward the investigation of concepts for improved high-frequency, high-speed, silicon bipolar transistors. The research is focused in three major areas: (1) deposition and characterization of semi-insulating polycrystalline silicon (SIPOS) as a heterojunction emitter. (2) use of ion implantation and rapid thermal annealing (RTA) for forming the base of bipolar transistors, (3) investigation of other technologies such as oxide isolation and polycrystalline silicon contacts to reduce parasitic effects to improve limitations at high frequencies. The research ranges from fundamental studies of structural, chemical, electrical, and optical properties of SIPOS deposited over a wide range of compositions on various substrates to the fabrication of transistors with polycrystalline and SIPOS emitters. Much effort has also been directed toward the ion implanted base where numerous techniques for forming the shallow implant and maintaining the profile during further processes were investigated. GRA

N86-12511# Department of the Navy, Washington, D. C.
A TiW DIFFUSION BARRIER FOR AuZn OHMIC CONTACTS TO p-TYPE InP Patent Application
J. B. Boos, N. A. Papanicolaou, and T. H. Weng, inventors (to Navy) Filed 27 Jun. 1985 27 p
(AD-D011823; US-Patent-Appl-SN-749238) Avail: NTIS HC A03/MF A01 CSCL 09/1

This abstract discloses a low metal resistance ohmic contact alloyed to p InP material having TiW within the contact as a diffusion barrier layer between an underlay of AuZn and an overlay of Au. A process for fabricating an InP JFET containing a gate contact of respective AuZn, TiW, and Au layers and with the gate contact alloyed to p InP material of a semiconductive gate region provides an improved InP JFET having a low resistance metal alloyed ohmic contact to the gate region. Use of the TiW layer in a multilayer contact alloyed to p InP material leads to unique processing and improved InP Semiconductor devices. GRA

N86-12512# Department of the Navy, Washington, D. C.
HIGH CURRENT FIBER BRUSH COLLECTOR AND METHOD FOR MAKING SAME Patent Application
S. J. Scuro, inventor (to Navy) Filed 2 May 1985 12 p
(AD-D011827; US-Patent-Appl-SN-729761) Avail: NTIS HC A02/MF A01 CSCL 09/1

This patent application discloses an axial-type homopolar motor having high density, high current fiber brush collectors affording efficient, low contact resistance and low operating temperatures. The collectors include a ring of concentric rows of brushes in equally spaced beveled holes soldered in place using a fixture for heating the ring to just below the solder melting point and a soldering iron for the local application of additional heat at each brush. Prior to soldering, an oxide film is formed on the surfaces of the brushes and ring, and the bevels are burnished to form a wetting surface. Flux applied with the solder at each bevel removes to an effective soldering depth the oxide film on the brushes and the holes. Author (GRA)

N86-12513# Department of the Navy, Washington, D. C.
DUAL DRAIN MOSFET DETECTOR FOR CROSSTIE MEMORY SYSTEMS Patent Application
N. Bluzer, inventor (to Navy) Filed 22 Mar. 1985 14 p
(AD-D011828; US-Patent-Appl-SN-714775) Avail: NTIS HC A02/MF A01 CSCL 09/5

This patent application, which discloses a circuit for detecting binary information in crosstie memory systems includes a dual drain MOSFET device having a single channel with a common source and an integrated, thin-film strip of magnetic material suitable for the storage and propagation of Bloch line-crosstie pairs acting as both a shift register and the device's gate. Current flowing through the device, in the absence of a magnetic field, is equally distributed to each drain; however, changing magnetic fields, normal to the plane of the device and generated by Bloch line-crosstie pairs in the strip, interact with the current such that a distribution imbalance exists and one drain or the other receives a disproportionate fraction of the current depending upon the direction of the magnetic field. GRA

N86-12514# Rome Air Development Center, Griffiss AFB, N.Y.
EVALUATION OF THE USE OF p-n STRUCTURES AS PHOTODETECTORS IN SILICON INTEGRATED CIRCUITS Report, Jan. 1984 - Mar. 1985
C. A. Eldering Jun. 1985 97 p
(AF Proj. 2338)
(AD-A158104; RADC-TR-85-123) Avail: NTIS HC A05/MF A01 CSCL 09/1

The light sensitivity of p-n junctions in silicon integrated circuits has been investigated and the spectral and temporal response of several structures in an integrated circuit measured. A model for the spectral response was developed based on models previously used to study solar cell response. This model takes into account the depth and the active area of the carrier collecting junction and demonstrates the shifting of the peak spectral response towards shorter wavelengths as junction depth and active area decreases. Measurements of the spectral response of junctions in an integrated circuit were compared with the predicted responses. An investigation into the temporal response of p-n photodiodes has shown that the response time of the diode is dependent on both the geometry of the junction and the wavelength of light generating the carriers. Response times for structures in the integrated circuit were measured using a He-Ne laser operating at 0.632 micron. GRA

N86-12515# Reliability Analysis Center, Griffiss AFB, N. Y.
SEARCH AND RETRIEVAL INDEX TO EOS/ESD SYMPOSIUM PROCEEDINGS 1979 TO 1984
R. E. Rash, Jr. and R. T. Wanner 15 Apr. 1985 149 p
(Contract F30602-84-C-0162)
(AD-A158114; RAC-TRS-4) Avail: NTIS HC A07/MF A01 CSCL 09/5

This book contains indexes used in searching for information contained in papers produced in Electrical Overstress/Electrostatic Discharge (EOS/ESD) Symposium 1979 to 1984. These indexes are the Alphabetical List of Index Terms, Subject Index, Author Index, Corporate Index, Keywords in Title Index, and Chronological List of Papers Index. These indexes provide a clear, easy-to-read, and concise method of searching for and retrieving the valuable information contained in IRPS Proceedings. GRA

N86-12516# Air Force Systems Command, Wright-Patterson AFB, Ohio. Foreign Technology Div.
ELECTRICAL LOSSES AND RESISTANCE OF CRYOGENIC INDUCTORS WITH CONSIDERATION OF THE EFFECT OF MAGNETORESISTANCE
A. I. Bertinov, B. L. Aliyevskiy, A. G. Sherstyuk, V. L. Orlov, and G. P. Alabin 26 Jul. 1985 11 p Transl. into ENGLISH from Izv. Akad. Nauk SSSR Energ. i Transport (USSR), no. 6, Nov. - Dec. 1972 p 72-77
(AD-A158185; FTD-ID(RS)T-1356-84) Avail: NTIS HC A02/MF A01 CSCL 09/1

A semigraphical method of calculating the electrical losses and resistance of round induction coils made of especially high purity metals (hyperconductors) - aluminum, beryllium, copper - with cryogenic cooling was developed. The peculiarity of the calculation is that it considers the effect of magnetoresistance. It uses the experimental values of the specific electrical resistance of the metals depending on the value of the induction of the transverse magnetic field at a constant low temperature. The experimental data are approximated by polynomials. Author (GRA)

N86-12517# Department of the Army, Washington, D. C.
WIDEBAND SAW (SURFACE ACOUSTIC WAVE) CHANNELLIZER USING SLANTED ARRAY INPUT TRANSDUCER Patent Application
E. A. Mariani and W. J. Skudera, Jr., inventors (to Army) Filed 25 Jun. 1985 11 p
(AD-D011857; US-Patent-Appl-SN-749038) Avail: NTIS HC A02/MF A01 CSCL 09/1

An Acoustic signal processing apparatus for the frequency-partition processing of a wideband RF spectrum surface acoustic wave (SAW) input signal into a multiplicity of relatively narrowband individual contiguous acoustic wave output signals, utilizing a wideband, linearly-dispersive, slanted array input transducer arranged on a wave-conductive surface with multiple arrayed output transducers, each frequency-responsive to a respective band of frequencies emanated from the input transducer is described. Author (GRA)

N86-12518# North Carolina Univ., Chapel Hill.
INVESTIGATION OF PHASE TRANSITIONS Final Report, 20 Jun. 1983 - 2 Mar. 1985
W. E. Hatfield 12 Aug. 1985 10 p
(Contract DAAG29-79-D-1002)
(AD-A158434; ARO-20849.1-PH) Avail: NTIS HC A02/MF A01 CSCL 20/12

An investigation of layers of CuCl grown on the (3) face of silicon has been undertaken. Detailed studies using ESCA for analysis have led to the development of an effective etching and cleaning procedure for silicon surfaces. The CuCl layers can not be grown by vapor phase transport, nor from liquid fluxes using a dipping technique, but polycrystalline layers may be grown using an improved slider-boat technique. The CuCl/silicon specimens exhibit a dielectric anomaly. The temperature of the onset of the dielectric anomaly varies from specimen to specimen, and it also depends on the history of the specimen. Materials research designed to determine the factors which affect this phenomenon is underway. GRA

N86-12519# Los Alamos Scientific Lab., N. Mex.
FOIL FUSES AS OPENING SWITCHES FOR SLOW DISCHARGE CIRCUITS
J. V. Parker and W. M. Parsons 1985 5 p Presented at the 5th IEEE Pulsed Power Conf., Washington, D.C., 10 Jun. 1985
(Contract W-7405-eng-36)
(DE85-014124; LA-UR-85-2021; CONF-850616-64) Avail: NTIS HC A02/MF A01

Metal foil fuses embedded in various materials are widely used as opening switches in fast discharge circuits (approx. 1 (MU)s). Several technologies of current interest require opening switches in circuits which operate on a much longer time scale (approx. 100 (MU)s). We have investigated the behavior of aluminum and copper foil fuses for conduction times of 100 to 200 (MU)s. Reliable current interruption is obtained at the end of melting rather than at the end of vaporization. The ratio of initial to final resistance is > 100. In general, the performance of slow fuses can be predicted by simple scaling from fast fuse behavior. For applications where the switching function depends critically on the resistivity versus input energy characteristic, the results presented can be used in the selection of proper fuse size and geometry. DOE

N86-12520# Argonne National Lab., Ill.
LOW DISPERSION NOTCH FILTER FOR MULTI-GHz FREQUENCIES USING FIBER OPTICS DELAYS
J. D. Simpson and R. Konecny 1985 3 p Presented at the Particle Accelerator Conf., Vancouver, British Columbia, 13 May 1985
(Contract W-31-109-eng-38)
(DE85-014983; ANL/HEP-CP-85-42; CONF-850504-232) Avail: NTIS HC A02/MF A01

Although their designs appear simple and straightforward, notch filters for application in stochastic cooling systems are frequently difficult to construct with acceptable characteristics. Problems arise because the components are less than perfect, coaxial cables have loss plus dispersion and other necessary hardware has limitations. Usually it is the delay line, typically a high quality coaxial line, which is the source of most problems. We report in this paper on the development of a notch filter which uses a laser diode/fiber optic delay line instead of a coaxial cable. Measurements of its properties indicate it to be a possible alternative to other designs. Bandwidth, dispersion, notch depth, dynamic range and intermodulation are each within the bounds of typical cooling system requirements. DOE

N86-12521# California Univ., Berkeley. Lawrence Berkeley Lab.
DEACTIVATION AND POISONING OF FUEL CELL CATALYSTS
P. N. Ross, Jr. Jun. 1985 6 p Presented at the 3rd Intern. Symp. on Catalyst Deactivation and Poisoning, Berkeley, Calif., 19 Jun. 1985
(Contract DE-AC03-76SF-00098)
(DE85-015127; LBL-19755; CONF-850631-1) Avail: NTIS HC A02/MF A01

The deactivation and poisoning phenomena reviewed are: the poisoning of anode (fuel electrode) catalyst by carbon monoxide and hydrogen sulfide; the deactivation of the cathode (air electrode) catalyst by sintering; and the deactivation of the cathode by corrosion of the support. The anode catalyst is Pt supported on a conductive, high area carbon black, usually at a loading of 10 w/o. This catalyst is tolerant to some level of carbon monoxide or hydrogen sulfide or both in combination, the level depending on temperature and pressure. Much less is known about hydrogen sulfide poisoning. Typical tolerance levels are 2% CO, and 10 ppM H2S. The cathode catalyst is typically Pt supported on a raphitic carbon black, usually a furnace black heat-treated to 2700 C. The Pt loading is typically 10 w/o, and the dispersion (or percent exposed) as-prepared is typically 30%. The loss of dispersion in use depends on the operational parameters, most especially the cathode potential history, i.e., higher potentials cause more rapid decrease in dispersion. The mechanism of loss of dispersion is not well known. The graphitic carbon support corrodes at a finite rate that is also potential dependent. Support corrosion causes thickening of the electrolyte film between the gas pores and the catalyst particles, which in turn causes increased diffusional resistance and performance loss. DOE

N86-12522# Sandia National Labs., Albuquerque, N. Mex.
DESIGN INFORMATION FOR THE 4/3 SILICON-GATE CMOS TECHNOLOGY
S. J. Babicz Jun. 1985 23 p
(Contract DE-AC04-76DP-00789)
(DE85-014932; SAND-85-0052) Avail: NTIS HC A02/MF A01

Enclosed is a 3-Dimensional view of the 4/3 silicon gate layout, showing the different mask layers. The 4/3 design rules are explained in detail, both in written form and pictorially. An explanation of the VAX design rule check, plus charts showing alignment sequence, mask field tones and current biasing are included. Also included are various drawings explaining positive and negative resist, cross sectional view of a silicon gate layout and three examples of different 4/3 layouts (Flipflop, Memory, C(2)L) using the 4/3 design rules. DOE

N86-12523# Oak Ridge National Lab., Tenn.
ARC DISCHARGE CONDITIONING TEST ON THE OAK RIDGE 25 URC ACCELERATOR
N. F. Ziegler, P. H. Stelson, and C. M. Jones 1985 15 p Presented at the 4th Intern. Conf. on Electrostatic Accelerator Technol. and Assoc. Boosters, Buenos Aires, 15 Apr. 1985 Prepared in cooperation with National Electrostatics Corp., Middleton, Wisc.
(Contract DE-AC05-84OR-21400)
(DE85-016394; CONF-850470-8) Avail: NTIS HC A02/MF A01

A hydrogen arc discharge has been run in the top five units (fifteen 20 cm tube sections) of the ORNL tandem accelerator to test the effectiveness of this method of cleaning the high voltage electrodes. The discharge was maintained in both the high and low-energy tubes for a period of 6 hours. The arc current in each tube was 4.0 A and the hydrogen pressure was nominally 100 mTorr. The arc discharge does not appear to have significantly affected the operating voltage of the top five units of the accelerator. However, the voltage conditioning behavior of the tested units is markedly different. DOE

N86-12524# Sandia National Labs., Albuquerque, N. Mex.
HYBRID 0-D,1-D, AND 2-D MODEL OF HELICAL EXPLOSIVE-DRIVEN MAGNETIC FLUX COMPRESSION GENERATOR
T. J. Burgess 1985 9 p Presented at the 5th IEEE Power Conf., Washington, D.C., 10 Jun. 1985
(Contract DE-AC04-76DP-00789)
(DE85-013772; SAND-85-1293C; CONF-850616-43) Avail: NTIS HC A02/MF A01

A hybrid code model of the Sandia National Laboratories' model 632 is described is introduced. A very large explosive driven magnetic flux compression generator. This involves the use of two codes. The first is a coupled 0-D equivalent circuit model and 1-D magnetohydrodynamic computation. The second is the 2-D materials response code, CSQ. This is used to obtain an equivalent drag coefficient so that the 2-D stator coil conductor encapsulent interaction can be modeled in the 1-D code. DOE

N86-12525# Sandia National Labs., Albuquerque, N. Mex.
PREVENTATIVE MAINTENANCE FOR CONTROL SYSTEMS
G. O. Corbett May 1985 3 p Presented at the Maintenance Seminar, Albuquerque, N. Mex., 11 Jun. 1985
(Contract DE-AC04-76DP-00789)
(DE85-012029; SAND-85-1159C; CONF-8506129-1) Avail: NTIS HC A02/MF A01

Preventative maintenance of the control systems should be performed on a required interval. Most manuacturers specify 6 to 12 month intervals. However, inspections can often be accomplished when the control unit or mechanical systems are out of service for a malfunction repair. A procedural checklist for proper maintenance is given. DOE

N86-12526# California Univ., Davis. Dept. of Electrical and Computer Engineering.
EVALUATION AND IMPLEMENTATION OF TESTABILITY SCHEMES FOR GATE ARRAY INTEGRATED CIRCUIT DESIGN
Final report, 1 Feb. - 30 Sep. 1984
K. W. Current, F. Edwards, and S. Hayano 8 Mar. 1985 57 p
(Contract W-7405-eng-48)
(DE85-012874; UCRL-15676) Avail: NTIS HC A04/MF A01

The research undertaken involved efforts on two distinct testing problems associated with large-scale (LSI) and very-large-scale (VLSI) integrated circuits. One problem concerns the debugging of chip test set-ups, a chip that generates a unique identifying signal on each of its pads could be useful. Such a chip could drive each wiring connection which could then be sampled. The design, realization, and characteristics of such a tester chip are discussed. Also, several design for testability schemes for chips are summarized and their potential for use in gate array design procedures is discussed. DOE

N86-12527# Air Force Weapons Lab., Kirtland AFB, N. Mex.
PARALLEL, STAGED OPENING SWITCH POWER CONDITIONING TECHNIQUES FOR FLUX COMPRESSION GENERATOR APPLICATIONS
R. E. Reinovsky, P. S. Levi, J. C. Bueck, and J. H. Goforth 1985 31 p Presented at the 5th IEEE Pulsed Power Conf., Washington, D.C., 10 Jun. 1985 Prepared in cooperation with LANL
(Contract W-7405-eng-36)
(DE85-012761; LA-UR-85-1891; CONF-850616-8) Avail: NTIS HC A03/MF A01

The Air Force Weapons Laboratory, working jointly with Los Alamos National Laboratory, has conducted a series of experiments directed at exploring composite, or staged, switching techniques for use in opening switches in applications which require the conduction of very high currents (or current densities) with very low losses for relatively long times (several tens of microseconds), and the interruption of these currents in much shorter times (ultimately a few hundred nanoseconds). The results of those experiments are reported. DOE

N86-12528# Los Alamos National Lab., N. Mex.
CALCULATION OF SERIES CAPACITANCE FOR TRANSIENT ANALYSIS OF WINDINGS
P. Chowdhuri Jan. 1985 8 p Presented at the IEEE Power Eng. Soc. Summer Meeting, Vancouver, British Columbia, 14 Jul. 1985
Avail: NTIS HC A02/MF A01

The analysis of transient voltage oscillations inside a winding (transformer, reactor or magnet) is performed by representing the winding as a lumped ladder network. The capacitances to the return lead (or ground) C sub gi can be computed by assuming either equivalent parallel-plate or cylindrical-symmetry configuration. The equivalent series capacitances of a winding C sub si, however, are complex capacitance networks, consisting of intra- and intercoil turn-to-turn capacitances of the coil sections. Many researchers have proposed methods of computing the equivalent series capacitance of a winding. As each method is quite different from the others, the analysis of the transient behavior of a winding becomes uncertain. A method of computing the series capacitance of a winding is proposed which is mathematically rigorous but simple to execute. As a check, the equivalent series capacitance of a four-turn double-disk winding was computed by the proposed method as well as by simple circuit analysis. The computations corraborated each other. DOE

N86-12529# Los Alamos National Lab., N. Mex.
SELF-CONSISTENT KLYSTRON SIMULATIONS
E. E. Carlsten and P. J. Tallerico 1985 4 p refs Presented at the Particle Accelerator Conf., Vancouver, British Columbia, 13 May 1985
(Contract W-7405-eng-36)
(DE85-012678; LA-UR-85-1588; CONF-850504-105) Avail: NTIS HC A02/MF A01

A numerical analysis of large signal klystron behavior based on general wave particle interaction theory is presented. The computer code presented is tailored for the minimum amount of complexity needed in klystron simulation. The code includes self consistent electron motion, space charge fields, and intermediate and output fields. It also includes use of time periodicity to simplify the problem, accurate representation of the space charge fields, accurate representation of the cavity standing wave fields, and a sophisticated particle pushing routine. In the paper, examples are given that show the effects of cavity detunings, of varying the magnetic field profile, of electron beam asymmetries from the gun, and of variations in external load impedance. DOE

N86-12530# Department of Energy, Washington, D. C.
SELF-CONTAINED HOT-HOLLOW CATHODE GUN SOURCE ASSEMBLY Patent Application
J. D. Zeren, inventor (to DOE) Filed Aug. 1984 13 p
(Contract DE-AC04-76DP-03533)
(DE85-011652; US-Patent-Appl-SN-637628) Avail: NTIS HC A02/MF A01

A self contained hot hollow cathode gun source assembly for use in a vacuum chamber includes a crucible having a hot hollow cathode gun mounted underneath and providing a hole for the magnetic deflection of the ion/electron beam into a crucible on top the block. DOE

N86-12531# Sandia National Labs., Albuquerque, N. Mex.
PHOTOCONDUCTIVE SEMICONDUCTOR SWITCHING FOR PULSED POWER APPLICATIONS
F. Zutavern, M. OMalley, M. Buttram, and W. Stygar 1985 14 p Presented at the 5th IEEE Pulsed Power Conf., Washington, D.C.
(Contract DE-AC04-76DP-00789)
(DE85-013859; SAND-84-2409C; CONF-850616-31) Avail: NTIS HC A02/MF A01

Photoconductive semiconductor switches hold significant promises as high-voltage, high-current switches for pulsed power applications. Their most important contributions are picosecond rise time and jitter, and millisecond recovery times. A crucial factor in their development is their surface breakdown strength. Despite the lack of improvement shown to date, there are still many techniques to be tried and we consider the chances of significant improvement to be good. In addition to working on the surface breakdown problem, our plans include the construction of a 1 MV, 5 (UC OMEGA) PCSS. DOE

N86-12532# Los Alamos National Lab., N. Mex.
RACETRACK MICROTRON RF SYSTEM
P. J. Tallerico and D. R. Keffeler 1985 3 p refs Presented at the Particle Accelerator Conf., Vancouver, Can., 13 May 1985
(Contract W-7405-eng-36)
(DE85-012669; LA-UR-85-1608; CONF-850504-1608) Avail: NTIS HC A02/MF A01

The RF system for the National Bureau of Standards (NBS)/Los Alamos CW racetrack microtron is described. The low-power portion consists of five 75-W amplifiers that drive two input ports in each of two chopper deflection cavities and one port in the prebuncher cavity. A single 500-kW klystron drives four separate 2380-MHz cavity sections: the two main accelerator sections, a capture section, and a preaccelerator section. The phases and amplitudes in all cavities are controlled by electronic or electromechanical controls. The 1-MW klystron power supply and crowbar system were purchased as a unit; several modifications are described that improve power-supply performance. The entire RF system has been tested and shipped to the NBS, and the chopper-buncher system has been operated with beam at the NBS. DOE

N86-12533# Sandia National Labs., Albuquerque, N. Mex.
HILLOCK-FREE CONDUCTOR SYSTEM FOR USE IN MULTI-LEVEL INTERCONNECTS
B. I. Draper, T. A. Hill, and H. B. Bell 1985 13 p Presented at the VLSI Multilevel Interconnection Conf., Santa Clara, Calif., 24 Jun. 1985
(Contract DE-AC04-76DP-00789)
(DE85-012595; SAND-84-2612C; CONF-8506123-1) Avail: NTIS HC A02/MF A01

A new conducter, consisting of layers of pure aluminum and tantalum silicide, was developed for use in integrated circuit multilevel metallizations. Unlike other conductor systems commonly in use or recently proposed, this structure maintains a smooth (< 30 nm roughness), hillock-free surface and a resistivity of less than 3.5 micron (UC OMEGA)-cm even after repeated thermal cycling to 450 C. Surface roughness after thermal cycling was studied as a function of the number, thickness, and position of the tantalum silicide layers. No lateral growth of material was observed during thermal cycling of 2 mircon m wide lines. Profiling Auger spectroscopy and backscattering techniques show that layers do not interdiffuse at high temperatures. In addition, the composite conductor is easily patterned using reactive ion etching (RIE) techniques, provides for the nucleation of selectively deposited LPCVD tungsten for interlevel via fills, and forms stable, low resistance (< 3 (UC OMEGA)) interlevel contacts. DOE

N86-12534# Varian Associates, Palo Alto, Calif.
THE 140 GHz GYROTRON DEVELOPMENT PROGRAM Quarterly Report, Mar. - Jun. 1984
K. L. Felch, R. E. Bier, L. J. Craig, T. S. Fiddaman, L. J. Fox, G. Bu, H. E. Huey, H. R. Jory, P. I. Reysner, and A. Salop 1984 83 p
(Contract DE-AC05-84OR-21400)
(DE85-011923; ORNL/Sub-84-95128/2; QR-1) Avail: NTIS HC A05/MF A01

The objective of this program is to develop a gyrotron oscillator capable of producing 100 kW of CW power at 140 GHz. Most aspects of the conceptual design for the first experimental tube are reported and initial calculations for several critical elements of the second experimental tube are discussed. The specification for the superconducting gyrotron magnet is presented. The various microwave components, protective devices, and special diagnostics required to test the tubes are identified and their design summarized. DOE

N86-12535# Los Alamos National Lab., N. Mex.
DESIGN OF FOIL IMPLOSION SYSTEM FOR PIONEER 1 EXPER-

IMENTS
D. J. Erickson, R. S. Caird, C. M. Fowler, W. T. Leland, H. Oona, R. J. Trainor, J. B. VanMarter, B. L. Barthell, D. V. Duchane, and J. H. Goforth 1985 5 p Presented at the 5th IEEE Pulsed Power Conf., Washington, D.C., 10 Jun. 1985
(Contract W-7405-eng-36)
(DE85-014111; LA-UR-85-2078; CONF-850616-67) Avail: NTIS HC A02/MF A01

A foil implosion system is described that integrates an explosive flux-compression generator, a flat plate feed section with power conditioning switches, and a vacuum electrode region containing a cylindrical foil/plasma load. Power conditioning, obtained with an explosive-driven plasma compression opening switch and explosive-actuated closing switches, provides a submicrosecond multimegampere pulse for the implosion of an aluminum plasma. The flat plate section is configured for bidirectional feed to the coaxial vacuum electrodes. Important considerations in the design of the vacuum power flow region include gap failure, feed symmetry, and radial diagnostic access. The system presently accommodates a foil radius of 3 cm. Innovative foil insertion and clamping techniques are also described. DOE

N86-12536# Sandia National Labs., Albuquerque, N. Mex.
CLASSICAL PIEZOELECTRICITY: IS THE THEORY COMPLETE
P. J. Chen 1985 14 p Presented at the Workshop on Dyn. Probl. in Continuum, Minneapolis, 3 Jun. 1985
(Contract DE-AC04-76DP-00789)
(DE85-014592; SAND-85-1441C; CONF-8506159-1) Avail: NTIS HC A02/MF A01

This paper cites experimental evidences which show that the classical theory of piezoelectricity is not complete in describing the responses of ferroelectric ceramics. There are also some preliminary evidences to show that the theory as applied to piezoelectric single crystals needs more thorough investigations. DOE

N86-12537# Sandia National Labs., Albuquerque, N. Mex.
LASER-BASED FOILLESS DIODE
S. L. Shope, C. A. Frost, G. T. Leifeste, C. E. Crist, and J. W. Poukey 1985 11 p Presented at the SDIO/DARPA Ann. Propagation Rev., Monterey, Calif., 24 Jun. 1985
(Contract DE-AC04-76DP-00789)
(DE85-013958; SAND-85-1338C; CONF-8506141-3) Avail: NTIS HC A02/MF A01

A foilless diode usually requires an externally applied magnetic field to control expansion and transport of a relativistic electron beam. A new foilless diode has been developed that does not require an external magnetic field. A low pressure organic gas is introduced into the diode and the transport region. A uv laser beam is injected through the transport region and is terminated at the cathode. The laser photoionizes the low pressure gas forming an ionized channel that captures the electron beam near the cathode. The electron beam is focused and guided by electrostatic attraction to the ionized channel. A 1.5-MeV, 20-KA electron beam has been generated and transported 1 m using this technique. Author

N86-12538# Sandia National Labs., Albuquerque, N. Mex.
SEMICUSTOM INTEGRATED CIRCUIT DESIGN AT SANDIA NATIONAL LABORATORIES
C. F. Acken Jul. 1985 65 p
(Contract DE-AC04-76DR-00789)
(DE85-015661; SAND-85-8226) Avail: NTIS HC A04/MF A01

This report is intended to serve as a reference for first time or one in a while designers of semicustom integrated circuits (ICS). The contents are specific to the design style, technology, and fabrication process used by Sandia National Laboratories in the design and fabrication of 4/3 micron radiation hardened CMOS standard cell and gate array integrated circuits. The topics covered in the report include an overview of semicustom IC design at Sandia, the design methodology and specific details relating to the design of a semicustom IC. DOE

N86-12539# Lawrence Livermore National Lab., Calif.
ELECTRONICS ENGINEERING DEPARTMENT THRUST AREA REPORT FY'84
C. Minichino, ed. and P. L. Phelps, ed. 1985 252 p
(Contract W-7405-eng-48)
(DE85-014857; UCID-20110-84) Avail: NTIS HC A12/MF A01

Thrust Areas for FY'84: diagnostics and microelectronic engineering; signal and control engineering; microwave and pulsed power engineering; computer-aided engineering; engineering modeling and simulation; and systems engineering. For each Thrust Area, an overview and a description of the goals and achievements of each project is provided. DOE

N86-12540# Lawrence Livermore National Lab., Calif.
EE TECHNICAL REVIEW
Jun. 1985 40 p
(Contract W-7405-eng-48)
(DE85-015313; UCRL-50025-85-1) Avail: NTIS HC A03/F A01

Areas of research reported include: ultrafast gating of microchannel plate X-ray spectrometers, study of power MOS fast switching techniques, and lightning vulnerability of nuclear explosive test systems at the Nevada Test Site. Also included is a study of a computer model of the MFTF-B neutral beam accel dc power supply. DOE

N86-12385# Tohoku Univ., Sendai (Japan). Research Inst. of Electrical Communication.
HYSTERESIS CHARACTERISTICS OF A DIODE LOADED E-M LOOP SENSOR
Hiroshi Echigo *In its* The Record of Elec. and Commun. Eng. Conversazione, Vol. 54, No. 1 Aug. 1985 p 9-13 refs In JAPANESE; ENGLISH summary (For primary document see N86-12383 03-31)
Avail: NTIS HC A03/MF A01

N86-12387# Tohoku Univ., Sendai (Japan). Research Inst. of Electrical Communication.
THE VERIFICATION OF THE LOGIC CIRCUITS BASED ON PARTICLIZED INFORMATION BITS WITH PROLOG
Yoshiaki Takai, Fusao Nakagawa, Tadao Nakamura, and Yoshiharu Shigei *In its* The Record of Elec. and Commun. Eng. Conversazione, Vol. 54, No. 1 Aug. 1985 p 20-25 refs In JAPANESE; ENGLISH summary (For primary document see N86-12383 03-31)
Avail: NTIS HC A03/MF A01

N86-12412# Joint Publications Research Service, Arlington, Va.
THE STEP STRUCTURE EFFECT OF dc JOSEPHSON CURRENT WITHIN ONE FLUX QUANTUM PERIOD phi SUB ZERO (2)
Zhang Yuheng, Shen Xiuling, Zheng Jiefel, and Wu Yan *In its* China Rept.: Sci. and Technol. (JPRS-CST-85-017) 11 Jun. 1985 p 104-114 refs Transl. into ENGLISH from Wuli Xuebao (Beijing), v. 33, no. 8, Aug. 1984 p 1075-1083 (For primary document see N86-12408 03-31)
Avail: NTIS HC A08/MF A01

N86-12433# Joint Publications Research Service, Arlington, Va.
EXPERIMENTS WITH DOMESTIC IC SUBSTRATES
Guan Shuzhu and Li Dunfu *In its* China Rept.: Sci. and Technol. (JPRS-CST-85-034) 1 Oct. 1985 p 59-66 refs Transl. into ENGLISH from Dianzi Jishu (Shanghai), v. 12, no. 5, 20 May 1985 p 12-14 (For primary document see N86-12430 03-31)
Avail: NTIS HC A08/MF A01

N86-12437# Joint Publications Research Service, Arlington, Va.
SUPERCONDUCTING WIRE MANUFACTURED
Fu Yuexian, Sun Yue, Xu Shiming, and Peng Ying *In its* China Rept.: Sci. and Technol. (JPRS-CST-85-034) 1 Oct. 1985 p 85-86 refs Transl. into ENGLISH from Diwen Wuli (Beijing), v. 7, no. 2, Jun. 1985 p 164-165 (For primary document see N86-12430 03-31)
Avail: NTIS HC A08/MF A01

N86-12443# Joint Publications Research Service, Arlington, Va.
LATCH-UP EFFECT IN CMOS DESCRIBED

Zhang Lichun, Yan Timing, Ni Xuewen, Yan Guizhen, Feng Chuguang, and Zhang Ziang *In its* China Rept.: Sci. and Technol. (JPRS-CST-85-022) 11 Jul. 1985 p 35-41 refs Transl. into ENGLISH from Dianzi Kexue Jishu (Beijing), v. 15, no. 1, 10 Jan. 1985 p 2-4 (For primary document see N86-12439 03-31)
Avail: NTIS HC A09/MF A01

N86-12468# Joint Publications Research Service, Arlington, Va.
CAD PROGRAM FOR HIGH-POWER ELECTRON GUN WITH ANNULAR CATHODE DESCRIBED
Tu Yushan *In its* China Rept.: Sci. and Technol. (JPRS-CST-85-032) 19 Sep. 1985 p 113-117 refs Transl. into ENGLISH from Dianzi Xuebao (Beijing), no. 4, Nov. 1984 p 95-97 (For primary document see N86-12462 03-31)
Avail: NTIS HC A08/MF A01

34 FLUID MECHANICS AND HEAT TRANSFER

Includes boundary layers; hydrodynamics; fluidics; mass transfer; and ablation cooling.

For related information see also *02 Aerodynamics* and *77 Thermodynamics and Statistical Physics.*

N86-12541 California Univ., Berkeley.
NUMERICAL CALCULATION OF TURBULENT BUOYANT FLOW Ph.D. Thesis
Wai-Ming To 1984 186 p
Avail: Univ. Microfilms Order No. DA8513016

Two models were developed for predicting low Reynolds number turbulent flows in the free and mixed convection regimes. One, the KEM model, is based on the notion of eddy diffusivities for momentum and heat. The other, the ASM model, is based on algebraic relations derived for the anisotropic turbulent fluxes by suitable truncation of the parent transport equations. Both formulations apply to variable property flows with high overheat ratios. Fully elliptic forms of the differential transport equations, subject to appropriately specified boundary conditions, were solved numerically for two flow configurations. Both are two dimensional. The first corresponds to free convection along a heated vertical flat plate, the second to free and mixed convection from a heated cavity of rectangular cross-section and variable orientation. A comparison between measurements and predictions for the case of the vertical plate shows that both models yield fairly accurate results for the mean flow and heat transfer. Dissert. Abstr.

N86-12542 Cornell Univ., Ithaca, N.Y.
UNSTEADY DETONATION Ph.D. Thesis
Abraham Ayowole Oyediran 1985 182 p
Avail: University Microfilms Order No. DA8504551

This work is centered on steady and unsteady detonation waves. This work is concerned with plane one-dimensional waves with onestep irreversible reactions of the ARrhenius kind. Generic problem is considered in the transition from deflagration to detonation. IT is modelled as the overtaking of a steady deflagration wave by a steady shock wave. Such a collision produces a detonation wave (as well as a contact discontinuity, a back shock and sometimes a rarefaction wave). Here the restriction to small heat release is removed. It is shown that a detonation wave thus produced can never be steady for any amount of heat release. The analysis was done in the limit of large activation energy. The governing equation for a detonation was developed in the limit of large activation energy and (subsequently) small heat release. Steady detonation solutions were investigated and a linear stability analysis was caried out. Various numerical techniques were used to solve the Stefan problem of detonation theory.
Dissert. Abstr.

N86-12543 Michigan Univ., Ann Arbor.
SHEAR DRIVEN FILM FLOW BEHAVIOR AND CAVITATION STUDY Ph.D. Thesis
Bong-Hwa Sun 1985 331 p
Avail: Univ. Microfilms Order No. DA8512517

Two complicated important multiphase flow phenomena, shear driven thin film flow and cavitation were studied experimentally. Results were compared with available theoretical models. The main objectives were to study: (1) fluid property effects on shear driven films and interfacial wave structures, and (2) the cavitation flow fields including the effects of long-chain polymer additives (AP-30 and Hec-H) on the cavitation erosion. It is found that: (1) film temperature on the turbine blade surface is equal to the local saturated steam temperature and is independent of water flow rate and water temperature in the reservoir, (2) both high viscosity and long chain polymer additive stabilize the film flow, while low surface tension is destablizing, (3) Mikielewicz's model can be used to predict the transition between rivulet and continous film. (4) Ishii's model can be used to predict transition between continuous film and atomization film flow, (5) Von Karman's universal velocity profile can be used for modelling shear driven film flow. Dissert. Abstr.

N86-12544 Northwestern Univ., Evanston, Ill.
NUMERICAL CALCULATION OF INTERNAL FLOWS WITH CURVATURE Ph.D. Thesis
Iman Esmat Osman ElDib 1985 300 p
Avail: Univ. Microfilms Order No. DA8511815

Flow in curved pipes involves secondary flows and possibly streamwise separation. An efficient numerical scheme yielding reliable predictions for such flows is presented. This is accomplished by using a simple turbulence model that reproduces the main features of the flow in curved pipes and fits with a numerical scheme suitable for such complex flow geometries. The numerical scheme used in this study is called Bodyfit and it solves the three dimensional elliptic equations of motion using the technique of boundary fitted coordinate transformation. A two equation K-epsilon turbulence model is used. The distribution of the eddy viscosity is calculated by solving two partial differential equations for the turbulence kinetic energy and its volumetric rate of dissipation simultaneously with the set of basic equations of momentum and continuity. The finite difference equations are solved using a cell by cell successive over-relaxation method (SOR). Computations were made for both laminar and turbulent flows in straight and strongly curved pipes of circular cross section. The numerical scheme gives a table solution for mean velocity and turbulence quantities. A modified pressure equation is recommended. Dissert. Abstr.

N86-12545 State Univ. of New York, Stony Brook.
STUDY OF THE MIST COOLING AND DROPLET DYNAMICS IN TURBULENT FLOW BY USING LDA Ph.D. Thesis
SangKyu Cho 1984 225 p
Avail: Univ. Microfilms Order No. DA8513530

The schemes which allow the in-situ measurement of droplet size and two components of velocity by the Laser Doppler Anemometer system are presented. The small droplet measurement technique and the large droplet measurement technique are described. The path length correction scheme is explained and the amplitude correction scheme is proposed for small droplet size measurement scheme. A scheme of simultaneous measurement of large droplet size and the two components velocity is developed and verified by the validation experiments. The on-line data acquisition system and the signal processing instrumentation are described. A droplet deposition phenomenon from a turbulent flow on a plate is investigated. The dimensionless deposition coefficient is studied theoretically based on the droplet's frequency response characteristics to the surrounding eddy motion. An investigation was made on the droplet's behavior across the quenched grid spacer. The empirical correlations on the Sauter Mean Diameter and the Fractional Volume of the small droplets are obtained. Dissert. Abstr.

N86-12546 State Univ. of New York, Stony Brook.
THE PREDICTION OF FULLY DEVELOPED TURBULENT PRESSURE DROPS IN A TRIANGULAR DUCT FOR A POWER LAW

FLUID Ph.D. Thesis
Tiee-Dan Chang 1984 129 p
Avail: Univ. Microfilms Order No. DA8513517

A model in which the nondimensional eddy viscosity and velocity distributions in circular pipe flow are applicable to noncircular passage flows was applied to the prediction of fully developed turbulent pressure drops in triangular ducts for Newtonian and power law fluids. The numerical calculations for the predicted turbulent velocity profiles and friction factors in triangular ducts were carried out by utilizing a modified integral transformation after Krajewski and the laminar velocity solutions for power law fluids. Friction factors for Newtonian and power law fluid flows were experimentally investigated over a Reynolds number range of 500 to 40000 in isosceles triangular ducts having apex angles of 10 and 60 degrees. Comparisons were made between the theoretical and experimental results. For the 60 degree duct, the model was successful in predicting friction factor-Reynolds number relations for power law fluids in the range $0.857 < n < 1$. For the 10 degree duct, the model was unable to account for the laminarization of the flow in the apex region and the presence of secondary flows. Dissert. Abstr.

N86-12547* National Aeronautics and Space Administration. Langley Research Center, Hampton, Va.
TECHNIQUE FOR MEASURING GAS CONVERSION FACTORS Patent
Jag J. Singh and Danny R. Sprinkle, inventors (to NASA) Issued 3 Sep. 1985 6 p Filed 23 Jul. 1984 Supersedes N84-32786 (22 - 22, p 3598)
(NASA-Case-LAR-13220-1; US-Patent-4,538,446; US-Patent-Appl-SN-633179; US-Patent-Class-73-3; US-Patent-Class-73-861.07) Avail: NTIS HC A02/MF A01 CSCL 20D

A method for determining hydrocarbon conversion factors for a flowmeter. A mixture of air, O2 and C sub x H sub y is burned and the partial paressure of O2 in the resulting gas is forced to equal the partial pressure of O2 in air. The flowrate of O2 flowing into the mixture is measured by flowmeter and the flowrate of C sub x H sub y flowing into the mixture is measured by the flowmeter conversion factor is to be determined. These measured values are used to calculate the conversion factor. Dissert. Abstr.

N86-12548 Rensselaer Polytechnic Inst., Troy, N. Y.
ANALYTICAL AND EXPERIMENTAL STUDIES OF WAKES BEHIND CIRCULARLY CAPPED BUBBLES Ph.D. Thesis
Warren F. Bessler 1984 230 p
Avail: Univ. Microfilms Order No. DA8509644

The wakes behind circularly capped bubbles are examined by means of an experimental and analytical study. A single two-inch diameter bubble is injected into a six by three foot fluid column, one half inch thick, producing an essentially two-dimensional flow. Aspirin powder placed in the fluid column just prior to bubble release highlights the structure of the flow field before dissolving. High speed film and sequenced photographs are taken to document the observed results. Pressure-time measurements are made with sensitive capacitive transducers mounted in the rear column wall and are synchronized with photographs using a high speed clock. Experimental fluids, prepared by mixing water and glycerine in varying proportions, are used to study the effects of viscosity on bubble shape and wake structure. Testing is performed over a range of Reynolds numbers from 14 to 29,655 which includes the transition from circularly capped to ellipsoidal bubble shape. Experimental data is reduced and summarized in convenient dimensionless form to permit comparison with analytical predictions. Author

N86-12549 Johns Hopkins Univ., Baltimore, Md.
MEASUREMENTS ON AN AXISYMMETRIC JET IN A SLOW COFLOWING STREAM Ph.D. Thesis
Dana A. Walker 1985 136 p
Avail: Univ. Microfilms Order No. DA8510446

All previously measured round turbulent jets are either contained in a recirculation region of are immersed in a coflowing stream which is too strong to obtain normal jet development. The purpose of this research is to include a slow, coflowing stream to avoid recirculation without greatly altering the development of the jet. The flow consists of a round water jet with Reynolds number, U sub j/nu d/ = 25000, submerged in a water tunnel with external stream velocity, U sub s = U sub j 150. The width of the duct is 64 times the nozzle diameter. This combination of duct size and velocity ratio results in no recirculation while the development of the jet resembles the development of a jet with no coflow. Velocity and concentration are surveyed in the jet by optical techniques. Velocity is measured by frequency-shifted laser Doppler velocimetry; concentration is measured by laser-induced fluorescence (of fluorescein sodium). Fluorescence intensity is also used to examine the concentration of reaction-product in an acidbase reaction between the jet and surrounding fluid. Requirements and applications of the fluorescence technique are also examined. Author

N86-12550*# National Aeronautics and Space Administration. Langley Research Center, Hampton, Va. Dept. of Mathematics.
AN ASYMPTOTIC INVESTIGATION OF THE STATIONARY MODES OF INSTABILITY OF THE BOUNDARY LAYER ON A ROTATING DISC Final Report
Philip Hall (Exeter Univ.) Sep. 1985 31 p refs Submitted for publication
(Contract NAS1-17070)
(NASA-CR-177977; ICASE-85-40; NAS 1.26:177977) Avail: NTIS HC A03/MF A01 CSCL 20D

An investigation of high Reynolds number stationary instabilities in the boundary layer on a rotating disc is given. It is shown that in addition to the inviscid mode at high Reynolds numbers, there is a stationary short wavelength mode. This mode has its structure fixed by a balance between viscous and Coriolis forces and cannot be described by an inviscid theory. The asymptotic structure of the wavenumber and orientation of this mode is obtained. A similar analysis is given for the inviscid mode, the expansion procedure used is capable of taking nonparallel effects into account in a self consistent manner. The results are compared to numerical calculations and experimental observations. Author

N86-12551*# National Aeronautics and Space Administration. Marshall Space Flight Center, Huntsville, Ala.
MULTIPLE-SCALE TURBULENCE CLOSURE MODELING OF CONFINED RECIRCULATING FLOWS Interim Report
C. P. Chen Aug. 1985 23 p refs Presented at the 19th Midwestern Mech. Conf., Columbus, Ohio, Sep. 1985
(Contract NASw-3458)
(NASA-CR-178536; NAS 1.26:178536) Avail: NTIS HC A02/MF A01 CSCL 20D

A multiple-scale turbulence closure scheme is developed for the numerical predictions of confined recirculating flows. This model is based on the multiple-time-scale concepts of Hanjalic et al. (1980) and takes into account the non-equilibrium spectra energy transfer mechanism. Problems concerning new formulation of energy transfer rate equations and subsequent model coefficient redefinition and energy spectrum partition are discussed. Comparisons are made with several experiments of internal recirculating flows for the purpose of model validation. Numerical results using the present model show significant improvement of predictive capability over that obtained with the single-scale k-epsilon model and show promising potential for complex turbulent flow predictions. Author

N86-12552# Virginia Polytechnic Inst. and State Univ., Blacksburg. Dept. of Aerospace and Ocean Engineering.
NUMERICAL AND EXPERIMENT STUDIES OF 3-D AND UNSTEADY TURBULENT BODY/APPENDAGE/PROPELLER FLOWS Annual Report, No. 2, 15 May 1984 - 14 May 1985
J. A. Schetz and R. L. Simpson 15 Jun. 1985 56 p
(Contract N00014-83-K-0372)
(AD-A157078) Avail: NTIS HC A04/MF A01 CSCL 20/4

The 3-D, turbulent flowfield produced by a propeller operating in the wake of a variable mesh disk has been studied with numerical solutions of the Reynolds-averaged, Navier-Stokes equations and by detailed experiments in a wind tunnel. The mesh variations of the upstream disk were chosen to produce a simulation of the wake of a streamlined, axisymmetric body with a single, streamlined appendage. Comparisons of measurements and preliminary numerical predictions show good agreement for the velocity profiles behind the propeller. The 3-D flow in the junction between a cylindrical appendage and a hull can produce separation of the trailing portion of the appendage and produces a momentum deficient 3-D boundary layer that is more prone to detachment than the 2-D regions away from the appendage. Detailed measurements of the zero-pressure-gradient boundary layer upstream of an appendage of interest have been made. A procedure has been developed for reducing blockage effects in the test wind tunnel. GRA

N86-12553# Portland State Univ., Oreg. Dept. of Mechanical Engineering.
C0 COLLOCATION SOLUTIONS FOR WEAK-FORMULATION NAVIER-STOKES EQUATIONS Final Technical Report
H. Migliore, E. Ray, and E. McReynolds 19 Jun. 1985 18 p
Presented at IMSE (Integral Methods in Sci. and Eng.), 18-21 Mar. 1985
(Contract N00014-78-C-0631)
(AD-A157250) Avail: NTIS HC A02/MF A01 CSCL 20/4

A global collocation procedure was attempted on two-D Navier-Stokes equations, but suffered from significant ringing. Historically, multi-element collocation has been based on Hermit shape functions for Navier-Stokes. Alternative, a weak formulation Navier-Stokes solution was developed using biquadratic Lagrangian functions on element boundaries and discrete Galerkin (collocation) expressions on interiors. To account for pressure, a penalty function expression was evaluated as part of a weighted integral, using bilinear shape functions. This method was exercised on flow through a duct that included a pivoting flap that protruded into the flow where the flap motion and fluid flow interacted. GRA

N86-12554# Hebrew Univ., Jerusalem (Israel). Dept. of Atmospheric Sciences.
THE ORIENTATION DISTRIBUTION OF NONSPHERICAL AEROSOL PARTICLES WITHIN A CLOUD Interim Technical Report
I. Gallily Dec. 1984 13 p
(Contract DAJA45-83-C-0004)
(AD-A157363; ITR-2) Avail: NTIS HC A02/MF A01 CSCL 20/4

Having performed a study on the orientation density function (o.d.f.) of small spheroidal aerosol particles in a general field of an arbitrary strength, it became possible to treat the orientation problem in a turbulent medium. To this end, two interconnected physical models were applied. In the first, the Realizations Model, it was assumed that the turbulent particle field constituted an ensemble of an infinite number of realizations, j, each one of which is characterized by one set of the o.d.f., F(j) (x,t), values. The latter was taken in that model to essentially coincide with previously found solution of the Fokker-Planck equation in the field of the realization. The Micro-turbulence Model, a relation between the so-called turbulent rotational diffusion coefficient of the particles and the physical characteristics of the fluid field was supplied. This coefficient and the Brownian rotational diffusion one, compose the effective diffusion coefficient. GRA

N86-12555# Army Engineer Waterways Experiment Station, Vicksburg, Miss. Hydraulics Lab.
INVESTIGATION OF TIDALLY INDUCED TURBULENT FLOW Final Report
N. W. Scheffner Mar. 1985 123 p
(DA Proj. 4A1-61101-A-91-D)
(AD-A157841; WES/MP/HL-85-2) Avail: NTIS HC A06/MF A01 CSCL 20/4

A two-dimensional numerical model was developed for the case of tidally induced turbulent flow. An analysis of shallow-water waves is made followed by the development of a second-order closure Reynolds stress turbulence model for the specific application to shallow-water waves. Verification of the resulting numerical model is made to existing steady-state turbulent flume data. GRA

N86-12556# California Univ., Los Angeles. Dept. of Physics.
MODULATIONS OF DRIVEN NONLINEAR SURFACE WAVES ON WATER AND LIQUID HELIUM-4
R. M. Keolian Jun. 1985 256 p
(Contract N00014-85-K-0370)
(AD-A157958; TR-44) Avail: NTIS HC A12/MF A01 CSCL 20/4

When a trough of water or liquid helium-4 is oscillated vertically at frequency f, waves can form on the surface through the process of parametric resonance at half the frequency of the drive, at f/2, The principle measurement is the liquid height at the end of the trough as a function of time. Nonlinearities determine the response amplitude and give rise to hysteresis. At larger drive amplitudes, the signal at f/2 becomes modulated at frequencies much lower than that of the drive in a variety of ways. One such modulation is smooth with a frequency near one of the low modes of the trough even though it is one of the higher modes that is driven. The surface amplitude is first larger on one end of the trough then larger on the other, oscillating back and forth at the modulation frequency which is of the order of f/20. Several of these frequencies can be present at once; they may be incommensurate (irrationally related) with each other or the drive or they may phase lock. The cause of these modulations are three wave resonant triads formed by a low mode, an intermediate mode, and the driven mode of the trough. Another modulation is characterized by short, sudden drops in amplitudes. These sudden drops are localized in space and propagate back and forth in the trough at nearly the gravity wave velocity. Several drops may be present at once. A third modulation is characterized by extremely deep frequencies--as low as f/2000. it seems to be caused by two adjacent modes, nonlinearly coupled together, slowly exchanging energy back and forth. At still higher drive amplitudes the surface response is chaotic. GRA

N86-12557# Massachusetts Inst. of Tech., Cambridge.
NON-LINEAR CORRECTIONS TO THE LINEAR THEORY FOR THE PREDICTION OF THE CAVITATING FLOW AROUND HYDROFOILS Final Report
S. A. Kinnas Jun. 1985 147 p
(Contract N00014-84-K-0067)
(AD-A158105; OE-85-10) Avail: NTIS HC A07/MF A01 CSCL 02/4

The problem of a partial or supercavitating hydrofoil in linear theory is formulated in terms of integral equations of unknown vortex and cavity source distributions. The general problem is decomposed into one camber, one of thickness, and one of angle of attack. The general solution is given in terms of integrals of known functions over the cavity length for partial or over the chord length for supercavitating hydrofoils. The numerical scheme to compute the integrals is shown to be very accurate and insensitive to the variables of the problem. Cavity shapes obtained from linear and nonlinear theory are compared for certain special cases. Linear theory is shown to be accurate for supercavitating sharp-nosed hydrofoils at moderate angles of attack. The effect of the leading edge radius on the partial cavitation of a hydrofoil is introduced by incorporating Lighthill's correction in the linearized formulation of the problem. Results for certain special cases show the significant role of the leading edge radius on the cavitation of hydrofoils, something also confirmed from experiments conducted at the MIT water tunnel. GRA

N86-12558# Wisconsin Univ., Madison. Mathematics Research Center.
INTERFACIAL STABILITY IN A TWO-LAYER BENARD BAD CAPS LANGUAGE(n)PROBLEM Technical Summary Report
Y. Renardy Apr. 1985 33 p
(Contract DAAG29-80-C-0041)
(AD-A158138; MRC-TSR-2814) Avail: NTIS HC A03/MF A01 CSCL 20/4

A linear stability analysis of the benard problem for two layers

of different fluids lying on top of each other and bounded by free surfaces is considered. The fluids are assumed to be similar and perturbation methods are used to calculate the eigenvalue in closed form. The case of the Rayleigh number and wavenumber of the disturbance being close to the first criticality of the one-fluid Benard problem has been investigated in a previous paper, and was found to exhibit both overstability and convective instability. In this paper, the Rayleigh number is assumed to be less than that of the first criticality of the one-fluid problem, and in this situation, overstability does not occur. An unexpected result is that by an appropriate choice of parameters, it is possible to find linearly stable arrangements with the more dense fluid on top.
Author (GRA)

N86-12559# Department of the Air Force, Washington, D.C.
HEAT PIPE WICK Patent Application
J. E. Beam, inventor (to Air Force) Filed 3 Jul. 1985 13 p
(AD-D011852; US-Patent-Appl-SN-751399) Avail: NTIS HC A02/MF A01 CSCL 13/1

This patent application discloses a heat pipe with an improved wick design which has an unheated section of greater wick wall thickness next to the evaporator section of the heat pipe and on the opposite side of the evaporator section from the condenser section. The greater wick wall thickness acts as a reservoir of liquid heat pipe working fluid to prevent dry out of the wick during pulsed high thermal energy transfer conditions and to eliminate the need to enforce quasisteady state heat input requirements during start-up operation. GRA

N86-12560# Connecticut Univ., Storrs.
A PRELIMINARY FIELD STUDY OF TURBULENT FLOW OVER AND INSIDE A FOREST EDGE Progress Report
J. D. Lin and D. R. Miller 1 Jul. 1985 116 p
(Contract DAAG29-84-K-0017)
(AD-A158409; ARO-21156.1-GS; PR-11) Avail: NTIS HC A06/MF A01 CSCL 04/2

This study focused on field measurements to determine the spatial variability of the turbulence characteristics under various atmospheric and forest canopy conditions. A high-speed multichannel data acquisition system was configured and tested. Fixed and movable observation towers have been set up in the University experimental forest in Coventry, Conn. Two wind velocity sensors, being tested and evaluated in the laboratory for their capability to measure the three-dimensional flow with high turbulence intensity that generally characterizes the flow regime in a forest canopy; are a dual triple-split hot-film probe and a tri-diagonal hot-film probe with a wind octant electronic sensor (WOES). The response of WOES tested in the low-speed wind nozzle appears to be promising and its compatibility with the tri-diagonal hot-film probe is being evaluated. A number of field measures has been conducted over and inside the forest canopy, using a vertical array of velocity sensors which includes a propeller anemometer, and X-hot wire and hot film anemometers. GRA

N86-12561# California State Univ., Long Beach. Dept. of Mechanical Enginerring.
TURBULENCE MODELS FOR BOUNDARY LAYERS ON AXISYMMETRIC BODIES Final Technical Report, Jan. 1984 - Jul. 1985
C. Li and T. Cebeci 22 Jul. 1985 43 p
(Contract N00014-80-C-0326)
(AD-A158552; CSULB/ME-84-9) Avail: NTIS HC A03/MF A01 CSCL 20/4

This report describes two turbulence models for boundary layers on axisymmetric bodies. The turbulence models are the algebraic eddy-viscosity formulation of Cebeci and Smith and the form of the two-equation transport approach suggested by Hanjalic and Launder. In both cases, the governing equations are solved in finite-difference form using Keller's box scheme and the computer program described by Bradshaw, Cebeci, and Whitelaw. The results computed by both models are evaluated for several test cases and discussed in the report. In addition, input and output instructions of a computer program based on the K-epsilon model are given together with a sample calculation. GRA

N86-12562# Carnegie-Mellon Univ., Pittsburgh, Pa. Dept. of Mechanical Engineering.
CROSS FLOW BOILING IN TUBE BUNDLES Final Technical Report
S. C. Yao Aug. 1985 164 p
(Contract N00014-79-C-0623; RR0-2403)
(AD-A158557) Avail: NTIS HC A08/MF A01 CSCL 20/13

The objective of the research described in this thesis is to understand the boiling heat transfer characteristics in the tube bundles. The studies are performed both analytically and experimentally. Analyses are conducted for single phase flow in bundles with various geometries. The results are compared with the available experimental data. Recommendation for simple and general design correlations at special conditions are proposed. Experimental results of forced convective boiling of a horizontal tube in a channel as well as in a bundle are reported. The difference between a single tube in a channel and a tube in a bundle is attributed to the different flow field environment and thermal environment. A modified Chen's correlation can be used to predict the heat transfer performance of a single tube in a channel or in a bundle. An empirical Critical heat flux (CHF) correlation of forced convective boiling from a single tube in a channel is proposed. The agreement of this correlation with the experimental data is reasonable with the maximum deviation of 20%. GRA

N86-12563# Lawrence Livermore National Lab., Calif.
COMPUTER SIMULATION OF THE EFFECT OF FREE SURFACE REFLECTION ON SHOCK WAVE PROPAGATION IN WATER
M. Kamegai, L. S. Klein, and C. E. Rosenkilde Jul. 1985 7 p refs Presented at the Am. Phys. Soc. Topical Conf. on Shock Waves in Condensed Matter, Spokane, 22 Jul. 1985
(Contract W-7405-eng-48)
(DE85-014807; UCRL-92080; CONF-850736-23) Avail: NTIS HC A02/MF A01

A computer simulation is used to study the behavior of a fluid which has been set into motion by a point explosion below a bounding free surface. Of particular interest is the interaction between the incident shock wave and the reflected rarefaction signal which, under certain conditions, can overtake the shock front. Onset criteria for the envelope which separates the region of irregular from that of regular rarefaction, the nonspherical shape of the shock front, and the pulse profile for several depths of burst covering both strong and weak shock interactions with the surface are discussed. DOE

N86-12564# Sandia National Labs., Albuquerque, N. Mex.
FINNED TUBE CONTACT CONDUCTANCE: CHARACTERIZING THE INTEGRITY OF THE MECHANICAL BOND
T. L. Ernest, J. W. Sheffield, and H. J. Sauer, Jr. 1985 15 p Presented at the Am. Soc. of Heating, Refrig. and Air-Conditioning Eng. Semiann. Meeting, Honolulu, Hawaii, 23 Jun. 1985 Prepared in cooperation with Missouri Univ., Rolla
(Contract DE-AC04-76DP-00789)
(DE85-013747; SAND-85-1440C; CONF-850606-10) Avail: NTIS HC A02/MF A01

Thermal contact conductance of expanded tube joints is dependent upon the interfacial pressure between the mating parts. A review of the literature indicates that very little work has been done towards relating the joint stresses to the dimensional parameters for mechanically expanded plate finned-tube heat exchangers, commonly called fin coils. This paper presents an experimental testing technique to investigate the fin-to-tube mechanical bond based upon the axial pull strength of the joint. Typical coils from two manufacturers were used in this investigation. They were fabricated from 3/8 in. copper tubes and plate aluminum fins. The coils tested had fin spacings of 6, 7, 8, 12, and 20 fins per inch, fin thicknesses of 0.008 and 0.0055 in. Tube thicknesses of 0.015 and 0.016 in. and diametrical interferences of 0.001, 0.006, and 0.010 in. The maximum force attained during a tube pullout was found to be descriptive of the bond. Plots of this force versus fin number and net interference are presented that illustrate the sensitivity of this force to the fin thickness, fin number, and net interference. These plots show that the fin thickness has the predominant effect on the pullout force and, in turn, the bond between the fin collar and the tube. DOE

N86-12565# Lawrence Livermore National Lab., Calif.
MODELING SHORT PULSE DURATION SHOCK INITIATION OF SOLID EXPLOSIVES
C. M. Tarver, J. O. Hallquist, and L. M. Erickson 27 Jun. 1985 11 p refs Presented at the 8th Intern. Symp. on Detonation, Albuquerque, N. Mex., 15 Jul. 1985
(Contract W-7405-eng-48)
(DE85-014803; UCRL-91484; CONF-850706-25) Avail: NTIS HC A02/MF A01

The chemical reaction rate law in the ignition and growth model of shock initiation and detonation of solid explosives is modified so that the model can accurately simulate short pulse duration shock initiation. The reaction rate law contains three terms to model the ignition of hot spots by shock compression, the slow growth of reaction from these isolated hot spots, and the rapid completion of reaction as the hot spots coalesce. Comparisons for PBX 9404 between calculated and experimental records are presented for the electric gun mylar flyer plate system, the minimum priming charge test, embedded manganin pressure and particle velocity gauges, and VISAR particle velocity measurements for a wide variety of input pressures, rise times and pulse durations. The ignition and growth model is now a fully developed phenomenological tool that can be applied with confidence to almost any hazard, vulnerability or explosive performance problem. DOE

N86-12566# Lawrence Livermore National Lab., Calif.
DISLOCATION KINETICS BEHIND SHEAR SHOCKS
R. B. Stout and G. D. Anderson Jun. 1985 6 p refs Presented at the Am. Phys. Soc. Topical Conf. on Shock Waves in Condensed Matter, Spokane, 22 Jul. 1985
(Contract W-7405-eng-48)
(DE85-014811; UCRL-92255; CONF-850736-24) Avail: NTIS HC A02/MF A01

High velocity oblique impact experiments result in both compression and shear shock waves. Behind the shear shock wave the particle velocity is transverse to the shock front. At large transverse particle velocities, dislocation kinetics can contribute a portion of the velocity. Based on a kinematic and thermodynamic model of dislocation kinetics, an analysis is made of the transverse strain and velocity behind a shear shock. Kinematics of dislocations in transverse motion behind the shock is formulated. A solution is given for an ideal case where the dislocation density function propagates as a pulse behind the shear shock. DOE

N86-12567# Argonne National Lab., Ill.
PARTICLE-WALL INTERACTION AND WALL FRICTION IN GAS-SOLID FLOWS
E. D. Doss, M. G. Srinivasan, and A. C. Raptis 1985 13 p refs Presented at the Intern. Symp. and Workshop on Particulate and Multi-Phase Processes and the 16th Ann. Meeting of the Fine Particle Soc., Miami Beach, Fla., 22 Apr. 1985
(Contract W-31-109-eng-38)
(DE85-014984; CONF-850406-14) Avail: NTIS HC A02/MF A01

Analytical modeling based on one-dimensional two-phase flow for solid-gas suspensions in pipes is the objective of the work described here. The paper focuses on three different empirical correlations based on physical models available for expressing the effect of wall friction on the solid-gas suspension. The three correlations are described and comparisons are made for a typical case of pipe flow. Predictions of pressure drop and particle velocity based on the three models agree well with each other for certain values of empirical parameters. The actual choice of the approach will be made on the basis of experiments to be performed at the Argonne National Laboratory. DOE

N86-12568# Argonne National Lab., Ill.
HEAT EXCHANGER VIBRATION ANALYSIS (HXVA) FOR PREDICTION OF TUBE BUNDLE INSTABILITIES
T. M. Mulcahy, M. W. Wamsganss, and C. I. Yang May 1985 57 p
(Contract W-31-109-eng-38)
(DE85-017144; ANL-85-40) Avail: NTIS HC A04/MF A01

Pre and postprocessors were written for an established hydraulic program (COMMIX-IHX) which enables prediction of the internal crossflow field for each tube of Argonne's Test Heat Exchanger and identification of those tubes most likely to experience fluidelastic instability, together with the instability vibration mode. While the direct use of the HXVA method is limited to single pass, single-segmentally baffled tube bundle configurations, its algorithms and methods can be applied to any type of heat exchanger which can be analyzed by COMMIX-IHX. The processors are explained and an example problem is given along with comparisons of experimental results. DOE

N86-12569# Georgia Inst. of Tech., Atlanta.
DAA MODAL ANALYSIS FOR PARAMETRIC INVESTIGATIONS OF FLUID-STRUCTURE INTERACTION IN UNDERWATER SHOCK, REVISION 1
J. H. Ginsberg and C. E. Rosenkilde Feb. 1985 13 p Presented at the 55th Shock and Vibration Symp., Dayton, Ohio, 23 Oct. 1984 Prepared in cooperation with California Univ., Livermore, Lawrence Livermore Lab.
(Contract W-7405-eng-48)
(DE85-012935; UCRL-91079-Rev-1; CONF-8410159-1-Rev-1) Avail: NTIS HC A02/MF A01

A program was initiated with the goal to develop a simulation of the underwater shock response of submarines. This capability was to be employed for systems analysis studies of a variety of tactical parameters, especially the orientation of the shock wave relative to the structure. Generic analytical models that avoided the details of specific structures, and the number of degrees of freedom was limited by the need for computational efficiency. It is shown how these objectives were met by using the modal expansion version of the doubly asymptotic approximation (DAA). Orthogonal assumed modes for the system are identified as the modes of free vibration for the isolated substructure. Based on these concepts three variants on a basic model are described; each modification provides the capability to evaluate different aspects of the system. The basic model, consists of a rigid cylinder capped by hemispheres which is subjected to a shock wave arriving from an arbitrary leading angle. The REFLECT model extends this fundamental model to treat multiple shock waves associated with reflections from the surface and bottom. The CAPS model was extended to assess the importance of an internal dead load. The new version includes a large internal mass suspended from the cylinder by four springs that give equivalent axial, transverse and rotational suspension stiffnesses. The center of mass of this dead load is located arbitrarily along the axis of symmetry of the cylinder. DOE

N86-12570# Stanford Univ., Calif. Geothermal Program.
VELOCITY AND GRAVITY EFFECTS IN RELATIVE PERMEABILITY MEASUREMENTS
B. A. Beal and C. S. Nunes Jun. 1985 154 p refs
(Contract DE-AT03-80SF-11459)
(DE85-009925; SGP-TR-82) Avail: NTIS HC A08/MF A01

There have been several studies on the effects of gravity and flowrate on laboratory relative permeability measurements. Most of these studies have concentrated on the effect of these parameters on the flooding front. Miller's (1983) data showed that the influence of these and other variables are not understood. The study found that the calculated recovery at breakthrough was different than the observed recovery at breakthrough. The calculated recovery at breakthrough was based on theory derived from Buckley-Leverett piston-like displacement. This study attempted to determine how gravity or core positioning and flowrate of the displacing fluid might be used to achieve a stable flooding front. A relative permeameter with unsteady-state flow was used for the apparatus. The core material was an unconsolidated silica sand. It is found that gravity has no significant effect on the difference between calculated and observed recovery at breakthrough. It is also observed that an increase in flowrate could increase the flooding front instabilities. Therefore as flowrate decreased the calculated and observed breakthrough approach a single value. DOE

N86-12571# Argonne National Lab., Ill.
CONDENSATION HEAT TRANSFER IN PLATE HEAT EXCHANGERS
C. B. Panchal May 1985 9 p Presented at the Natl. Heat Transfer Conf., Denver, Aug. 1985
(Contract W-31-109-eng-38)
(DE85-012369; CONF-850810-19) Avail: NTIS HC A02/MF A01

An Alfa-Laval plate heat exchanger, previously tested as an evaporator, was retested as a condenser. Two series of tests with different chevron-angle plates were carried out using ammonia as a working fluid. The overall heat transfer coefficient and pressure drop were measured, and the effects of operating parameters were determined. The experimental data were compared with theoretical predictions. In the analysis, a gravity-controlled condensation process was modeled theoretically, and the overall performance was calculated. The analysis shows that the overall heat transfer coefficient can be predicted with an average uncertainty of about 10%. It is, however, important to consider the interfacial shear stress, because the effective friction factor is high for flow in plate heat exchangers. DOE

N86-12572# University of Northern Arizona, Flagstaff.
REFRIG-12: A GRAPHICS-AUGMENTED INTERACTIVE PROGRAM FOR DESIGNING VAPOR-COMPRESSION REFRIGERATION/HEAT PUMP CYCLES
B. W. Davis 7 Sep. 1984 103 p Prepared in cooperation with California Univ., Livermore. Lawrence Livermore Lab.
(Contract W-7405-eng-48)
(DE85-014205; UCID-30200-83-6) Avail: NTIS HC A06/MF A01

REFRIG-12 is an interactive program that serves as a tool for designing and analyzing thermodynamic vapor compression refrigeration/heatpump cycles. Graphic and alphanumeric responses to design decisions are displayed simultaneously on separate monitors. Temperature-Entropy property coordinates are used to describe the thermodynamic processes Freon-12 undergoes as it passes through the various mechanical components which ultimately produce the cycle. The processes are displayed graphically as the user makes the decisions to design a refrigeration cycle. When a design has been completed, REFRIG-12 offers the user an opportunity to make changes. The effects of design changes become graphically discernible through successive overlays on the graphics monitor. DOTPLOT can be executed to produce a hard copy of the graphics monitor display. Summaries of the cycle performance, pertinent energy transfers, and other engineering consequences of the design specifications can also be presented - at user option - on both the CRT and the printer. REFRIG-12 is organized so that a relatively small main program controls 25 subroutines. Each subroutine has stand alone characteristics and may be used with programs having other primary purposes. The subroutines can be conveniently merged (or chained) into system memory as needed. DOE

N86-12573# Science Applications, Inc., Sunnyvale, Calif.
DEVELOPMENT OF A CONTINUOUS MASS FLOW MEASURING FLOW Quarterly Report, Jan. - Mar. 1984
Jun. 1985 17 p
(Contract DE-AC22-81PC-40022)
(DE85-012492; DOE/PC-40022/T3) Avail: NTIS HC A02/MF A01

Source effectiveness and geometry studies are performed in order to prepare to measure the performance of a mass flow meter by the count rate of activated oxygen detected downstream. Several neutron sources are considered for the purpose. Shielding problems were investigated. Heat transfer calculations were performed to evaluate the duty of a refrigeration unit that will be required to maintain the neutron source at its optimum operating temperature. A densitometer source and shielding has been sized. DOE

N86-12574# Oak Ridge National Lab., Tenn.
INFLUENCE OF A SURFACTANT ADDITIVE ON ABSORPTION HEAT PUMP PERFORMANCE
J. W. Michel and H. perez-Blanco 1985 16 p refs Presented at the Am. Soc. of Heating, Refrig. and Air-Conditioning Eng. Semiann. Meeting, Honolulu, Hawaii, 23 Jun. 1985
(Contract DE-AC05-84OR-21400)
(DE85-013995; CONF-850606-11) Avail: NTIS HC A02/MF A01

Surfactant additives have been known for some time to influence the boiling characteristics of water and water-salt solutions. An enhancement of boiling transfer coefficients can be obtained by a proper choice of additives. When the capacity of an absorption heat pump is limited by its generator capacity and the generator is of the boiling-pool type, it is possible to increase the machine capacity by means of surfactant addition. In this paper, the preliminary experiments leading to the selection of a surfactant for a lithium bromide-water absorption heat pump are described. Minimum foaming was the most important consideration in this selection process. The measured machine performance shows that the generator capacity may be increased by values ranging from 5% to 10% of the original capacity. The actual value depends on the operating conditions as given by solution concentration, flow rate, and temperatures. DOE

N86-12575# Pittsburgh Univ., Pa. Dept. of Physics and Astronomy.
FLUID PHYSICS RESEARCH Progress Report, 1 Aug. 1985 - 30 Jun. 1985
J. V. Maher 25 Jun. 1985 10 p
(Contract DE-FG02-84ER-45131)
(DE85-014644; DOE/ER-45131/T1) Avail: NTIS HC A02/MF A01

Research is reported for three areas: Hele-Shaw flow; search for instability on a quenched liquid interface; and binary liquid gels. DOE

N86-12576# Argonne National Lab., Ill.
ANALYSIS OF STRATIFIED FLOW MIXING
S. L. Soo and R. W. Lyczkowski 1985 25 p refs Presented at the Natl. Heat Transfer Conf., Denver, 4 Aug. 1985
(Contract W-7405-eng-38)
(DE85-006840; CONF-850810-7) Avail: NTIS HC A02/MF A01

The Creare 1/5-scale Phase II experiments which model fluid and thermal mixing of relatively cold high pressure injection (PHI) water into a cold leg of a full-scale pressurized water reactor (PWR) having loop flow are analyzed and found that they cannot achieve complete similarity with respect to characteristic Reynolds and Froude numbers and developing hydrodynamic entry length. Several analyses show that these experiments fall into two distinct regimes of mixing: momentum controlled and gravity controlled (stratification). DOE

N86-12577# Midwest Research Inst., Golden, Colo. Solar Energy Research Inst.
ISOTHERMAL DEHUMIDIFICATION OF AIR IN A PARALLEL PASSAGE CONFIGURATION
A. A. Pesaran and F. Zangrando Jun. 1985 12 p Presented at the Natl. Heat Transfer Conf., Denver, 4 Aug. 1985
(Contract DE-AC02-83CH-10093)
(DE85-008819; SERI/TP-252-2630; CONF-850810-23) Avail: NTIS HC A02/MF A01

The performance of a single parallel passage of a dehumidifier was examined under isothermal conditions both experimentally and theoretically. The passage was coated with silica gel using a polyester tape. The transient response of the silica gel test cells to a step change in air inlet humidity was obtained experimentally and compared with the predictions of a pseudo-gas-side-controlled mass transfer model. The transient response of the test cell depended on the air flow rate, aspect ratio, and temperature.

Although the general trend of the experimental and predicted results were similar, the comparisons were not satisfactory. The observed discrepancies were attributed to the uncertainties in the pseudo-gas-side mass transfer coefficient and equilibrium isotherm. DOE

N86-12578# California Univ., Berkeley. Lawrence Berkeley Lab.
STUDY OF TWO-PHASE CONCURRENT FLOW OF STEAM AND WATER IN AN UNCONSOLIDATED POROUS MEDIUM
A. K. Verma, K. Pruess, C. F. Tsang, and P. A. Witherspoon Apr. 1985 11 p refs Presented at the Natl. Heat Transfer Conf., Denver, 4 Aug. 1985
(Contract DE-AC03-76SF-00098)
(DE85-014534; LBL-19084; CONF-850810-21) Avail: NTIS HC A02/MF A01

A combined experimental and numerical study of two-phase steam/water flow in porous media was carried out. An experiment consisting of steady state, two-phase concurrent flow of steam and water was conducted to obtain a set of relative permeability and capillary pressure curves. The experimental relative permeability and the capillary pressure curves were included in a numerical code, MULKOM, and the experiment was simulated. A good agreement between the numerical results and the experimental data was found, thus confirming the results. Upon comparing these results with gas/oil and oil/water relative permeabilities obtained by other investigators, it was found that while the wetting phase relative permeabilities in all cases are about the same, the vapor phase relative permeability is larger than the non-wetting phase relative permeabilities in gas/oil or oil/water flows. It is suggested that the phenomenon of enhanced vapor phase relative permeability is caused by channeling and/or phase transformation effects. DOE

N86-12397# Joint Publications Research Service, Arlington, Va.
NUMERICAL COMPUTATION OF FULL THREE-DIMENSIONAL FLOW IN TRANSONIC TURBINES
Shen Mengyu and Zhang Yaoke *In its* China Rept.: Sci. and Technol. (JPRS-CST-85-016) 23 May 1985 p 73-77 refs Transl. into ENGLISH from Shuzhi Jisuan yu Jisuanji Yingyong (Beijing), no. 2, Jun. 1984 p 125-128 (For primary document see N86-12393 03-31)
Avail: NTIS HC A08/MF A01

N86-12398# Joint Publications Research Service, Arlington, Va.
CODE OF FINITE ELEMENT ANALYSIS FOR THREE-DIMENSIONAL FLOW IN TURBOMACHINES
Huang Aixiang *In its* China Rept.: Sci. and Technol. (JPRS-CST-85-016) 23 May 1985 p 78-91 refs Transl. into ENGLISH from Shuzhi Jisuan yu Jisuanji Yingyong (Beijing), no. 1, Mar. 1984 p 38-47 (For primary document see N86-12393 03-31)
Avail: NTIS HC A08/MF A01

N86-12426# Joint Publications Research Service, Arlington, Va.
SUPERHEATED STEAM'S DENSITY COMPENSATION FOR FLOW MEASUREMENT
Xu Guanquan *In its* China Rept.: Sci. and Technol. (JPRS-CST-85-021) 8 Jul. 1985 p 123-128 refs Transl. into ENGLISH from Huaxue Shijie (Shanghai), v. 26, no. 2, 20 Feb. 1985 p 61-63 (For primary document see N86-12421 03-31)
Avail: NTIS HC A09/MF A01

N86-12660# Joint Publications Research Service, Arlington, Va.
DIFFRACTION OF INTERNAL WAVES DESCRIBED BY EQUATION OF SLIGHTLY STRATIFIED FLUID ON HALF-PLANE Abstract Only
A. T. Ismail-Zade *In its* USSR Rept.: Earth Sci. (JPRS-UES-85-006) 19 Jun. 1985 p 27-28 Transl. into ENGLISH from Izv. Akad. Nauk Azerb. SSR, Ser. Nauk o Zemle (USSR), no. 5, 1984 p 76-83 (For primary document see N86-12630 03-42)
Avail: NTIS HC A05/MF A01

N86-12669# Joint Publications Research Service, Arlington, Va.
THEORY OF SOLITARY ANTICYCLONES IN ROTATING FLUID Abstract Only
G. G. Sutyrin *In its* USSR Rept.: Earth Sci. (JPRS-UES-85-006) 19 Jun. 1985 p 38 Transl. into ENGLISH from Dokl. Akad. Nauk SSSR (Moscow), v. 280, no. 5, Feb. 1985 p 1101-1105 (For primary document see N86-12630 03-42)
Avail: NTIS HC A05/MF A01

N86-12671# Joint Publications Research Service, Arlington, Va.
LABORATORY STUDY OF REGULAR LOW-AMPLITUDE GRAVITY CAPILLARY WAVES IN NONSTATIONARY CURRENT Abstract Only
Ye. S. Benilov, K. V. Pokazeyev, and A. D. Rozenberg *In its* USSR Rept.: Earth Sci. (JPRS-UES-85-006) 19 Jun. 1985 p 39-40 Transl. into ENGLISH from Okeanol. (Moscow), v. 25, No. 1, Jan. - Feb. 1985 p 37-42 (For primary document see N86-12630 03-42)
Avail: NTIS HC A05/MF A01

N86-12673# Joint Publications Research Service, Arlington, Va.
STUDY OF INFLUENCE OF VERTICAL VELOCITY AND DENSITY PROFILES ON HYDRODYNAMIC STABILITY OF ZONAL FLOW Abstract Only
A. S Blatov and V. I. Ulyanova *In its* USSR Rept.: Earth Sci. (JPRS-UES-85-006) 19 Jun. 1985 p 41 Transl. into ENGLISH from Okeanol. (Moscow), v. 25, no. 1, Jan. - Feb. 1985 p 19-25 (For primary document see N86-12630 03-42)
Avail: NTIS HC A05/MF A01

35 INSTRUMENTATION AND PHOTOGRAPHY

Includes remote sensors; measuring instruments and gages; detectors; cameras and photographic supplies; and holography.

For aerial photography see *43 Earth Resources*. For related information see also *06 Aircraft Instrumentation*, and *19 Spacecraft Instrumentation*.

N86-12579*# National Aeronautics and Space Administration. Langley Research Center, Hampton, Va.
RAPID ESTIMATION OF FREQUENCY RESPONSE FUNCTIONS BY CLOSE-RANGE PHOTOGRAMMETRY
John S. Tripp Nov. 1985 30 p refs
(NASA-TP-2471; L-15955; NAS 1.60:2471) Avail: NTIS HC A03/MF A01 CSCL 14E

The accuracy of a rapid method which estimates the frequency response function from stereoscopic dynamic data is computed. It is shown that reversal of the order of the operations of coordinate transformation and Fourier transformation, which provides a significant increase in computational speed, introduces error. A portion of the error, proportional to the perturbation components normal to the camera focal planes, cannot be eliminated. The remaining error may be eliminated by proper scaling of frequency data prior to coordinate transformation. Methods are developed for least square estimation of the full 3x3 frequency response matrix for a three dimensional structure. Author

N86-12580*# Spectron Development Labs., Inc., Costa Mesa, Calif.
OPTICAL TECHNIQUE TO STUDY THE IMPACT OF HEAVY RAIN ON AIRCRAFT PERFORMANCE Final Report
Cecil F. Hess and Funming Li Oct. 1985 43 p refs
(Contract NAS1-17932)
(NASA-CR-177989; NAS 1.26:177989; SDL-85-2424-1F) Avail: NTIS HC A03/MF A01 CSCL 01C

A laser based technique was investigated and shown to have the potential to obtain measurements of the size and velocity of water droplets used in a wind tunnel to simulate rain. A theoretical model was developed which included some simple effects due to droplet nonsphericity. Parametric studies included the variation of collection distance (up to 4 m), angle of collection, effect of beam interference by the spray, and droplet shape. Accurate measurements were obtained under extremely high liquid water content and spray interference. The technique finds applications in the characterization of two phase flows where the size and velocity of particles are needed. Author

N86-12581# Department of the Navy, Washington, D. C.
TECHNIQUE FOR THE REDUCTION OF FADING IN INTERFEROMETERS Patent Application
N. J. Frigo, A. Dandridge, and A. B. Tveten, inventors (to Navy) Filed 12 Apr. 1985 12 p
(AD-D011845; US-Patent-Appl-SN-722580) Avail: NTIS HC A02/MF A01 CSCL 17/8

This patent application discloses a passive device for reducing polarization fading in interferometers without significantly degrading the signal-to-noise ratio. In one embodiment, light form an interferometer output is passed through a lens to a polarization mask. The polarization mask comprises at least three independent polarizers which pass independent states of polarizers. Each independently polarized signal is detected, demodulated and passed to a means for signal extraction. GRA

N86-12582# Automated Sciences Group, Inc., Silver Spring, Md.
OPTICAL DISK TECHNOLOGY ASSESSMENT
Jun. 1985 126 p
(Contract MDA903-84-C-0197)
(AD-A157909; ASG-TR-189-17R) Avail: NTIS HC A07/MF A01 CSCL 14/3

This report provides findings and recommendations of a technical assessment which was completed in March 1985. The primary objective was to evaluate the current state-of-the-art and feasibility of using optical disks to support future applications developed by the Office of the Secretary of Defense. The technical Assessment report contains: Section 2: Study scope, terminology, and introduction; Section 3: Management and Technical Summary; Section 4 to 6: Optical disk technology assessment details; Section 7: Conclusions and recommendations; Glossary and Bibliography. The optical disk offers the same potential as the micro-computer to impact automation of information and is an excellent random storage medium for almost any type of permanent image data. The technology is based on the use of a laser to burn (record) holes in the light sensitive surface of an optical or plastic coated disk. The disks are manufactured in different sizes with 12-in, 5.25-in, and 4.75-in, diameter disks being the most common. The 12-1n. disk has a storage capacity of two billion bytes of data when recorded on both sides. GRA

N86-12583# Royal Signals and Radar Establishment, Malvern (England).
THE THEORY AND PRACTICE OF A MULTISTATE REFLECTOMETER
J. P. Ide and L. C. Oldfield Jan. 1985 32 p
(AD-A157916; RSRE-MEMO-3824; DRIC-BR-96388) Avail: NTIS HC A03/MF A01 CSCL 14/2

This Memorandum details the way a multistate reflectometer is used to measure the reflection coefficient of waveguide devices. It contains theoretical derivations of the equations and a computer program, with explanatory notes, for solving them. The calibration procedure is also given. These techniques are suitable for all frequency bands and transmission media where suitable standards and detectors exist. Author (GRA)

N86-12584# Department of the Army, Washington, D. C.
ELECTROLYTIC PRESSURE TRANSDUCTION SYSTEM Patent Application
G. H. Bryant, inventor (to Army) Filed 3 Oct. 1984 15 p
(AD-D011847; US-Patent-Appl-SN-657438) Avail: NTIS HC A02/MF A01 CSCL 14/2

This invention is directed to a Wheatstone bridge circuit for measuring pressure in the distal esophageal sphincter (D.E.S.) as well as in other organs and bodily cavities. A flexible hollow tube having three spaced electrodes is lodged in the esophagus. The tube is partly filled with a saline solution to cover the electrodes, thereby producing two series connected, pressure sensitive resistors. The electrolytic resistors are coupled to two series connected fixed resistors to complete the bridge circuit. Electrical imbalances in the bridge circuit are measured in terms of the pressure corresponding to the pressure applied by the D.E.S. Author (GRA)

N86-12585# Department of the Air Force, Washington, D.C.
TRANSIENT TEST OF SUSPENSION ELECTRONICS FOR GYROSCOPE Patent Application
P. H. Ito, inventor (to Air Force) Filed 8 Jul. 1985 48 p
(AD-D011853; US-Patent-Appl-SN-752767) Avail: NTIS HC A03/MF A01 CSCL 17/7

The rotor suspension electronics of an electrostatic gyro suspension system is required to perform flawlessly to sustain the life of the gyro. Transient abnormalities as short as one millisecond duration will cause the spinning rotor to come in contact with the surrounding electrodes and result in destruction of the gyro. Thus, not infrequently after a catastrophic dropped rotor incident no trace of the fault is evident upon ensuing check of the system. To remedy this problem a built in test (BIT) system is used to provide fault isolation. The test circuitry is built into the navigation system electronics and integrated with the system program. The fault isolation electronics comprise sensor circuits to monitor functional subdivisions of the electronic suspension system for signal abnormality and a processing circuit which receives the sensor circuit outputs and identifies the primary source of the fault. The faults are detected and the source is flagged at the time of occurrance. The output of the fault isolation electronics is a latched coded readout which is fed to the navigation computer for memory storage and any appropriate follow-up system action, such as power shutdown. After initialization by the computer, the fault isolation function is an automatic operation by the electronic circuitry. Author (GRA)

N86-12586# Los Alamos National Lab., N. Mex.
LOS ALAMOS CONSTANT-Q SPECTROMETER
R. A. Robinson, R. Pynn, J. Eckert, and J. A. Goldstone 1985 16 p refs Presented at the 8th Meeting of Intern. Collaboration on Advan. Neutron Sources, Oxford, 7 Jul. 1985
(Contract W-7405-eng-36)
(DE85-014115; LA-UR-85-2070; CONF-850762-1) Avail: NTIS HC A02/MF A01

A constant-Q spectrometer, which has been installed on the pulsed source of the Los Alamos Neutron Scattering Center, is described. It features a number of innovations that ease sample and analyzer alignment and a novel composite crystal analyzer which exploits the mosaic properties of plastically deformed germanium in a new way. Observations of phonon dispersion in aluminum and of incoherent scattering in ZrH_2 are reported, along with background measurements. DOE

N86-12587# Lawrence Livermore National Lab., Calif.
IMPROVED APPROACH TO CHARACTERIZING AND PRESENTING STREAK CAMERA PERFORMANCE
J. D. Wiedwald and B. A. Jones 15 Jul. 1985 7 p Presented at the SPIE Intern. Tech. Symp. on Optical and Elec.-Optical Eng., San Diego, Calif., 18 Aug. 1985
(Contract W-7405-eng-48)
(DE85-015188; UCRL-92160; CONF-850887-8) Avail: NTIS HC A02/MF A01

The performance of a streak camera recording system is strongly linked to the technique used to amplify, detect and quantify the streaked image. At the Lawrence Livermore National Laboratory (LLNL) streak camera images have been recorded both on film and by fiber-optically coupling to charge-coupled devices (CCD's). During the development of a new process for recording these images (lens coupling the image onto a cooled CCD) the definitions of important performance characteristics such as resolution and dynamic range are re-examined. As a result of this development, these performance characteristics are now presented to the streak camera user in a more useful format than in the past. This paper describes how these techniques are used within the Laser Fusion Program at LLNL. The system resolution is presented as a modulation transfer function, including the seldom reported effects that flare and light scattering have at low spatial frequencies. Data are presented such that a user can adjust intensifier gain and pixel averaging to optimize the useful dynamic range in any particular application. DOE

N86-12588# Oak Ridge Y-12 Plant, Tenn.
PRECISION ION VACUUM GAGE WITH LOGARITHMIC RESPONSE
M. G. Duncan 28 Jun. 1985 81 p
(Contract DE-AC05-84OS-21400)
(DE85-015312; Y-2343) Avail: NTIS HC A05/MF A01

A new ion vacuum gage controller has been developed of use with Bayard-Alpert gage tubes. The instrument employs a logarithmic-gain electrometer to cover up to 12 decades of pressure without the gain range changing. Instrument error and repeatability is + or - 1% of the pressure reading over a 9-decade pressure range with an ideal Bayard-Alpert gage tube. The instrument also offers selectable autoranging of fixed emission-current control. Furthermore, protection circuits and a computer interface are provided. DOE

N86-12589# Los Alamos Scientific Lab., N. Mex.
NOVEL INSTRUMENT FOR HIGH-PRESSURE RESEARCH AT ULTRA-HIGH TEMPERATURES
D. Schiferl, A. I. Katz, R. L. Mills, L. C. Schmidt, C. Vanderborgh, E. F. Skelton, W. T. Elam, A. W. Webb, S. B. Qadri, and M. Schaefer 1985 8 p refs Presented at the 10th High Pressure Conf. on Res. in High Pressure Sci. and Technol., Amsterdam, 8 Jul. 1985 Prepared in cooperation with NRC, Washington, D.C., Sachs/Freeman Associates, Inc., Bowie, Md. and Carnegie Institution of Washington, D.C.
(Contract W-7405-eng-36)
(DE85-015674; LA-UR-85-2362; CONF-850759-9) Avail: NTIS HC A02/MF A01

A resistively heated diamond-anvil cell has been used to achieve pressures of 110 kbar at temperatures exceeding 1200 C for periods long enough to collect X-ray powder diffraction data with energy-dispersive techniques using white X-radiation produced at the Stanford Synchrotron Radiation Laboratory. DOE

N86-12590# Sandia National Labs., Albuquerque, N. Mex.
STUDIES OF THE BAUER PIEZOELECTRIC POLYMER GAUGE (PVF2) UNDER IMPACT LOADING
L. M. Lee, W. D. Williams, R. A. Graham, and F. Bauer 1985 11 p Presented at the Am. Phys. Soc. Topical Conf. on Shock Waves in Condensed Matter, Spokane, 22 Jul. 1985 Prepared in cooperation with Ktech Corp., Albuquerque, N. Mex. and Institut Franco-Allemand de Recherches, St. Louis, France
(Contract DE-AC04-76DP-00789)
(DE85-014707; SAND-85-0415C; CONF-850736-34) Avail: NTIS HC A02/MF A01

A cooperative program has been initiated to provide a highly reproducible PVF2 polymer film for widespread use as a gauge under shock-compression loading. The material source and electrical treatment are based on prior work but new, independent studies of gauge response are being carried out. First measurements indicate excellent agreement between the independent studies. DOE

N86-12591# Lawrence Livermore National Lab., Calif.
RESULTS OF PRIM GYROSCOPE TESTING
R. Cornell Mar. 1985 11 p Presented at the 17th Ballistics Working Group Meeting, Livermore, Calif., 17 Oct. 1984
(Contract W-7405-eng-48)
(DE85-012934; UCRL-92356; CONF-8410277-1) Avail: NTIS HC A02/MF A01

The tests were designed so that motions of the gyroscope and the partially restrained internal member (PRIM) could be measured at different conditions of spin and PRIM clearance gaps. Two types of PRIM drive were tested. A round shaft configuration was used to test theory. An octagon drive was used to simulate the XM785 design. DOE

N86-12592# Lawrence Livermore National Lab., Calif.
MEASUREMENT OF TRITIUM PERMEATION THROUGH RESISTANT MATERIALS NEAR ROOM TEMPERATURE
J. Maienschein, V. DuVal, F. McMurphy, F. Uribe, R. Musket, and D. Brown 1985 8 p refs Presented at the 2nd Natl. Topical Meeting on Tritium Technol. in Fission, Fusion and Isotopic Appl., Dayton, Ohio, 30 Apr. 1985
(Contract W-7405-eng-48)
(DE85-012942; UCRL-91469; CONF-850405-12) Avail: NTIS HC A02/MF A01

To measure tritium permeation through low permeability materials at 50 to 170 C, we use highly sensitive liquid scintillation counting to detect the permeating tritium. To validate the method, extensive experiments with copper, for which such data exists for comparison were conducted and details of the experimental technique. Further plans are outlined. DOE

N86-12593# Lawrence Livermore National Lab., Calif.
X-RAY DIFFRACTION CELL FOR DEBYE-SCHERRER AND GUINIER (HUBER) CAMERAS AT PRESSURE AND TEMPERATURE
J. F. Lakner 25 Jun. 1985 12 p refs Presented at the 10th High Pressure Conf. on Res. in High Pressure Sci. and Technol., Amsterdam, 8 Jul. 1985
(Contract W-7405-eng-48)
(DE85-014815; UCRL-91872; CONF-850759-7) Avail: NTIS HC A02/MF A01

A gas high pressure cell for X-ray diffraction studies was developed. It is capable of 2700 atm hydrogen pressure at ambient temperature, when used in a Debye-Scherrer camera, and 1020 atm to at least 300(0)C, when used in a Guinier (Huber) camera. It is suitable for weakly scattering materials. DOE

N86-12594# KMS Fusion, Inc., Ann Arbor, Mich.
RECENT DEVELOPMENTS IN MICROSHELL-TIPPED OPTICAL FIBERS AS HIGH-PRESSURE SHOCK DETECTORS
F. J. Mayer, R. L. Maynard, D. L. Musinski, N. W. Schmerberg, M. R. Wixom, and R. F. Benjamin 1985 7 p refs Presented at the Am. Phys. Soc. Topical Conf. on Shock Waves in Condensed Matter, Spokane, 22 Jul. 1985 Prepared in cooperation with Los Alamos National Lab., Albuquerque, N. Mex.
(Contract W-7405-eng-36)
(DE85-015750; LA-UR-85-2479; CONF-850736-48) Avail: NTIS HC A02/MF A01

We describe ongoing development and characterization of Microshell-tipped optical fibers used as impact sensors. We observed a risetime of 15 ns when the probe is used to measure a detonation wave in PETN. We report successful development of two nondestructive tests, radiography and fluorescence, to check the integrity of the sensor. The sensor is now commercially available. DOE

N86-12595# Sandia National Labs., Albuquerque, N. Mex.
NEW PASSIVE HELICOPTER DETECTOR
G. R. Elliott 1985 7 p Presented at the 26th Ann. Meeting of the Inst. of Nucl. Mater. Management, Albuquerque, N. Mex., 21; Jul. 1985
(Contract DE-AC04-76DP-00789)
(DE85-015160; SAND-85-1670C; CONF-850765-9) Avail: NTIS HC A02/MF A01

Sandia has developed a new helicopter detector. The device relies on the correlation between the acoustic wave from the helicopter and the resulting coupled seismic wave. A significant feature of this approach is that the detector is completely passive; there is no radio frequency radiation. Intended for deployment as a perimeter sensor around a site, the unit offers a low nuisance/false alarm rate and a high probability of detection for a wide range of helicopters. Reliable detection occurs when the target is at high altitude and also very near the earth's surface. Detection ranges start at one kilometer for the small, four-place, civilian helicopter and approach five kilometers for heavier, military types. The system has two parts: a transducer package containing a micrphone and a geophone and a digital processor. Development is underway for a model which will be AC powered and well suited to permanent facilities. A prototype unit using a lightweight, battery powered processor is being constructed for rapid-deployment applications. DOE

N86-12596# Oak Ridge National Lab., Tenn.
DROPLET FORMATION PHENOMENA IN dc ELECTRICAL FIELDS
R. A. Malinauskas and C. H. Byers Jul. 1985 80 p refs
(Contract DE-AC05-84OR-21400)
(DE85-014067; ORNL/TM-9446) Avail: NTIS HC A05/MF A01

A new method of photographing and analyzing data from pendant drops was studied. This new method included using high-speed video equipment and a digitized analyzer to evaluate data in terms of the surface tensions of drops. Experimentation on pendant drops of two different systems, water-air and water-cyclohexane, was conducted in establishing this photographic technique. The most common method of evaluating pendant drops was analyzed in helping to construct a new computer program which solves for the actual Laplacian curve and surface tension of a surface by means of a curve-fitting regression analysis. The preliminary theory and applications described in this paper led to a recommendation using the proposed analytical methods on extended experiments in this project on mass transfer of liquids and droplet formation phenomena as a function of imposed electric fields. DOE

N86-12373# Fuji Electric Co. Ltd., Yokosuka (Japan).
DISSOCIATIVE VOLUME RECOMBINATION COEFFICIENT MEASUREMENTS IN A SUBROOM TEMPERATURE NEON PLASMA AFTERGLOW
K. Keskinen, Y. Ichikawa, R. M. Hobson (York Univ., Toronto), H. Fukuda (Sony Co. Ltd., Tokyo), S. Teii (Musashi Inst. of Tech., Tokyo), T. Kaneda (Tokyo Denki Univ.), and J. S. Chang (McMaster Univ.) *In* Tokyo Denki Univ. Res. Rept. of the Faculty of Eng., Tokyo Denki Univ., No. 32 Dec. 1984 p 1-11 refs Sponsored in part by the Natural Sciences and Engineering Research Council of Canada (For primary document see N86-12372 03-31)
Avail: NTIS HC A09/MF A01

N86-12384# Tohoku Univ., Sendai (Japan). Research Inst. of Electrical Communication.
PROPOSAL OF A HIGH EFFICIENT AND HIGH POWER PENIOTRON
Nobuyuki Sato, Mohamad Razeghi, Takehisa Suzuki, Kuniyoshi Yokoo, and Shoichi Ono *In its* The Record of Elec. and Commun. Eng. Conversazione, Vol. 54, No. 1 Aug. 1985 p 1-8 refs In JAPANESE; ENGLISH summary (For primary document see N86-12383 03-31)
Avail: NTIS HC A03/MF A01

N86-12411# Joint Publications Research Service, Arlington, Va.
LASER ANEMOMETER USING A SINGLE CIRCUIT BOARD
Gu Weiyu, Han Shouchun, Song Zhengfang, Liu Xiaochun, Ding Qiang, and Qi Fudi *In its* China Rept.: Sci. and Technol. (JPRS-CST-85-017) 11 Jun. 1985 p 78-85 Transl. into ENGLISH from Weijisuanji Yingyong (Beijing), no. 4, Nov. 1984 p 48-51 (For primary document see N86-12408 03-31)
Avail: NTIS HC A08/MF A01

N86-12436# Joint Publications Research Service, Arlington, Va.
ULTRAHIGH VACUUM EQUIPMENT DESCRIBED
Li Yuzhi, Jing Shiqun, and Peng Xianhui *In its* China Rept.: Sci. and Technol. (JPRS-CST-85-034) 1 Oct. 1985 p 87-91 Transl. into ENGLISH from Diwen Wuli (Beijing), v. 7, no. 2, Jun. 1985 p 166-168 (For primary document see N86-12430 03-31)
Avail: NTIS HC A08/MF A01

N86-12440# Joint Publications Research Service, Arlington, Va.
CHINA'S FIRST IMPORTED PERIPHERAL EQUIPMENT PRODUCTION LINE
In its China Rept.: Sci. and Technol. (JPRS-CST-85-022) 11 Jul. 1985 p 17-25 Transl. into ENGLISH from Jisuanji Shijie (Beijing), no. 11, 8 Jun. 1984 p 1 (For primary document see N86-12439 03-31)
Avail: NTIS HC A09/MF A01

N86-12441# Joint Publications Research Service, Arlington, Va.
METHOD OF USING CTC TO MICROCOMPUTERIZE DIGITAL INSTRUMENTS
Wu Naiyou *In its* China Rept.: Sci. and Technol. 11 Jul. 1985 p 26-31 Transl. into ENGLISH from Dianzi Kexue Jishu (Beijing), v. 15, no. 1, 10 Jan. 1985 p 5-6 (For primary document see N86-12439 03-31)
Avail: NTIS HC A09/MF A01

N86-12442# Joint Publications Research Service, Arlington, Va.
DIGITAL PHASE METER USING CMOS-LED INTRODUCED
Tan Benzhi *In its* China Rept.: Sci. and Technol. (JPRS-CST-85-022) 11 Jul. 1985 p 32-34 Transl. into ENGLISH from Dianzi Kexue Jishu (Beijing), v. 15, no. 1, 10 Jan. 1985 p 25 and 28 (For primary document see N86-12439 03-31)
Avail: NTIS HC A09/MF A01

N86-12449# Joint Publications Research Service, Arlington, Va.
DIGITAL VOLTMETER TECHNOLOGY ACQUISITION
Chen Qilin and Cui Jianping *In its* China Rept.: Sci. and Technol. (JPRS-CST-85-029) 3 Sep. 1985 p 41-44 Transl. into ENGLISH from Guoji Maoyi (Beijing), no. 3, 1985 p 33-34 (For primary document see N86-12446 03-31)
Avail: NTIS HC A08/MF A01

N86-12688# Joint Publications Research Service, Arlington, Va.
VIDEO TERMINAL FOR ANALYZING AERIAL INFRARED PHOTOGRAPHS Abstract Only
In its USSR Rept.: Earth Sci. (JPRS-UES-85-006) 19 Jun. 1985 p 72 Transl. into ENGLISH from NTR: Probl. i Resheniya (Moscow), 5-18 Mar. 1985 p 2 (For primary document see N86-12630 03-42)
Avail: NTIS HC A05/MF A01

N86-13242*# Augsburg Univ. (West Germany). Dept. of Physics.
AE AND DE MASS SPECTROMETER OBSERVATIONS RELEVANT TO THE SHUTTLE GLOW
Mark J. Engebretson *In* NASA. Marshall Space Flight Center 2d Workshop on Spacecraft Glow Sep. 1985 p 46-54 refs (For primary document see N86-13239 03-88)
(Grant NAG5-349)
Avail: NTIS HC A13/MF A01 CSCL 03B

N86-13244*# National Research Council of Canada, Ottawa (Ontario). Inst. of Astrophysics.
ORBITER GLOW OBSERVATIONS AT HIGH SPECTRAL RESOLUTION
David J. W. Kendall, Richard L. Gattinger, Edward J. Llewellyn (Saskatchewan Univ.), Ian C. McDade (Saskatchewan Univ.), and Steven B. Mende (LMSC, Palo Alto, Calif.) *In* NASA. Marshall Space Flight Center 2d Workshop on Spacecraft Glow Sep. 1985 p 63-73 refs Sponsored in part by the Universities Space Research Association. (For primary document see N86-13239 03-88)
Avail: NTIS HC A13/MF A01 CSCL 03B

N86-13245*# National Aeronautics and Space Administration. Marshall Space Flight Center, Huntsville, Ala.
NEUTRAL MASS SPECTROMETER MEASUREMENTS IN THE SHUTTLE BAY ENVIRONMENT
E. Miller and G. Carignan (Michigan Univ.) *In its* 2d Workshop on Spacecraft Glow Sep. 1985 p 74-81 refs (For primary document see N86-13239 03-88)
Avail: NTIS HC A13/MF A01 CSCL 03B

N86-13247*# Utah State Univ., Logan. Dept. of Physics.
THE UV-VIS OPTICAL ENVIRONMENT OF THE SHUTTLE
Marsha R. Torr *In* NASA. Marshall Space Flight Center 2d Workshop on Spacecraft Glow Sep. 1985 p 98-106 refs (For primary document see N86-13239 03-88)

(Contract NAS8-33992)
Avail: NTIS HC A13/MF A01

N86-13248*# Utah State Univ., Logan. Dept. of Physics.
ENHANCED N(+) SUB 2 IN THE SHUTTLE ENVIRONMENT Abstract Only
Doug G. Torr, A. Khoyloo, and Marsha R. Torr *In* NASA. Marshall Space Flight Center 2d Workshop on Spacecraft Glow Sep. 1985 p 107 (For primary document see N86-13239 03-88)
Avail: NTIS HC A13/MF A01 CSCL 03B

N86-13249*# California Univ., Berkeley. Space Sciences Lab.
INVESTIGATION OF VEHICLE GLOW IN THE FAR ULTRAVIOLET
Supiya Chakrabarti and Timothy Sassen *In* NASA. Marshall Space Flight Center 2d Workshop on Spacecraft Glow Sep. 1985 p 108-115 refs (For primary document see N86-13239 03-88)
(Contract NAS8-32577)
Avail: NTIS HC A13/MF A01 CSCL 03B

N86-13257*# National Aeronautics and Space Administration. Marshall Space Flight Center, Huntsville, Ala.
THE PRODUCTION OF GLOW PRECURSORS BY OXIDATIVE EROSION OF SPACECRAFT SURFACES
John C. Gregory (Alabama Univ., Huntsville) and Palmer N. Peters *In its* 2d Workshop on Spacecraft Glow Sep. 1985 p 174-179 refs (For primary document see N86-13239 03-88)
(Contract NAS8-36189)
Avail: NTIS HC A13/MF A01 CSCL 03B

N86-13259*# Vanderbilt Univ., Nashville, Tenn. Dept. of Physics and Astronomy.
OPTICAL RADIATION FROM THE INTERACTION OF ENERGETIC ATOMS, IONS, ELECTRONS, AND PHOTONS WITH SURFACES
N. H. Tolk, R. G. Albridge, R. F. Haglund, Jr., and M. H. Mendenhall *In* NASA. Marshall Space Flight Center 2d Workshop on Spacecraft Glow Sep. 1985 p 191-201 refs (For primary document see N86-13239 03-88)
Avail: NTIS HC A13/MF A01 CSCL 03B

N86-13260*# Princeton Univ., N. J. Plasma Physics Lab.
A GROUND-BASED EXPERIMENTAL TEST PROGRAM TO DUPLICATE AND STUDY THE SPACECRAFT GLOW PHENOMENON
W. D. Langer, S. A. Cohen, D. M. Manos, D. H. McNeill, R. W. Motley, M. Ono, and S. Paul *In* NASA. Marshall Space Flight Center 2d Workshop on Spacecraft Glow Sep. 1985 p 202-211 refs (For primary document see N86-13239 03-88)
(Grant NAG8-521; Contract DE-AC02-76CH-03073)
Avail: NTIS HC A13/MF A01 CSCL 03B

N86-13261*# Aerospace Corp., El Segundo, Calif. Chemistry and Physics Lab.
APPLICATION OF AN ATOMIC OXYGEN BEAM FACILITY TO THE INVESTIGATION OF SHUTTLE GLOW CHEMISTRY
Graham S. Arnold and Daniel R. Peplinski *In* NASA. Marshall Space Flight Center 2d Workshop on Spacecraft Glow Sep. 1985 p 212-225 refs (For primary document see N86-13239 03-88)
Avail: NTIS HC A13/MF A01 CSCL 03B

N86-13263*# Smithsonian Astrophysical Observatory, Cambridge, Mass.
INFRARED MEASUREMENTS OF SPACECRAFT GLOW PLANNED FOR SPACELAB 2
Giovanni G. Fazio and David G. Koch *In* NASA. Marshall Space Flight Center 2d Workshop on Spacecraft Glow Sep. 1985 p 243-249 refs (For primary document see N86-13239 03-88)
(Contract NAS8-32845)
Avail: NTIS HC A13/MF A01 CSCL 03B

N86-13264*# National Aeronautics and Space Administration. Goddard Space Flight Center, Greenbelt, Md.
PLANNED INVESTIGATION OF INFRARED EMISSIONS ASSOCIATED WITH THE INDUCED SPACECRAFT GLOW: A SHUTTLE INFRARED GLOW EXPERIMENT (SIRGE)
Michael J. Mumma and Donald E. Jennings *In* NASA. Marshall Space Flight Center 2d Workshop on Spacecraft Glow Sep. 1985 p 250-259 refs (For primary document see N86-13239 03-88)
Avail: NTIS HC A13/MF A01 CSCL 03B

N86-13265*# Lockheed Missiles and Space Co., Palo Alto, Calif.
DATA REQUIREMENTS FOR VERIFICATION OF RAM GLOW CHEMISTRY
Gary R. Swenson and Steven B. Mende *In* NASA. Marshall Space Flight Center 2d Workshop on Spacecraft Glow Sep. 1985 p 260-268 (For primary document see N86-13239 03-88)
Avail: NTIS HC A13/MF A01 CSCL 03B

N86-13266*# Utah State Univ., Logan. Dept. of Physics.
A POSSIBLE GLOW EXPERIMENT FOR THE EOM 1-2 MISSION Abstract Only
Marsha R. Torr *In* NASA. Marshall Space Flight Center 2d Workshop on Spacecraft Glow Sep. 1985 p 269 (For primary document see N86-13239 03-88)
Avail: NTIS HC A13/MF A01 CSCL 03B

N86-13267*# National Aeronautics and Space Administration. Langley Research Center, Hampton, Va.
SPACE SHUTTLE MECHANISTIC STUDIES TO CHARACTERIZE ATOMIC OXYGEN INTERACTIONS WITH SURFACES
Lubert J. Leger and James T. Visentine *In* NASA. Marshall Space Flight Center 2d Workshop on Spacecraft Glow Sep. 1985 p 270-273 (For primary document see N86-13239 03-88)
Avail: NTIS HC A13/MF A01 CSCL 03B

N86-13268*# Science Applications International Corp., Bellevue, Wash.
THE SHUTTLE GLOW: A PROGRAM TO STUDY THE RAM-INDUCED PHENOMENA
Hugh R. Anderson *In* NASA. Marshall Space Flight Center 2d Workshop on Spacecraft Glow Sep. 1985 p 274-276 (For primary document see N86-13239 03-88)
Avail: NTIS HC A13/MF A01 CSCL 03B

N86-13269*# Colorado Univ., Boulder. Lab. for Atmospheric and Space Physics.
SURVEY OF ULTRAVIOLET SHUTTLE GLOW Abstract Only
Kerry A. Spear, Gregory J. Uckler, and Kent Tobiska *In* NASA. Marshall Space Flight Center 2d Workshop on Spacecraft Glow Sep. 1985 p 277 (For primary document see N86-13239 03-88)
Avail: NTIS HC A13/MF A01 CSCL 03B

36 LASERS AND MASERS

Includes parametric amplifiers.

N86-12597 Department of the Air Force, Washington, D.C.
HIGH POWER LASER DUMP Patent
M. S. Hsu and J. P. Hsu, inventors (to Air Force) Issued 16 Aug. 1985 5 p Supersedes AD-D010540
(AD-D011792; US-Patent-4,511,216; US-Patent-Class-350-311)
Avail: US Patent and Trademark Office CSCL 20/5

A high power laser dump has defined laser beam introduction angles to the internal surface of a cylinder to maximize energy dispersion and absorption and, has two zones formed of distinctive reflective and absorbing materials. Author (GRA)

N86-12598 Department of the Air Force, Washington, D.C.
CO2 LASER STABILIZATION AND SWITCHING Patent
N. E. Buholz, inventor (to Air Force) Issued 23 Apr. 1985 7 p Supersedes AD-D010358
(AD-D011795; US-Patent-4,513,422; US-Patent-Class-372-29)
Avail: US Patent and Trademark Office CSCL 20/5

A CO2 laser operating in the 10 micrometer and is stabilized by a stabilization circuit that compares the power in a selected pair of R and P lines. A switching circuit connected into the stabilization circuit causes the laser's operating point to be switched within a short interval wherein four different pairs of R/P lines can be output within about 100 ms. GRA

N86-12599 Department of the Navy, Washington, D. C.
LASER GENERATION OF ULTRASONIC WAVEFORM RECONSTRUCTIONS Patent
W. R. Scott and C. S. Ih, inventors (to Navy) Issued 18 Jun. 1985 5 p Supersedes AD-D011314
(AD-D011843; US-Patent-4,523,469; US-Patent-Appl-SN-459073; US-Patent-Class-73-603) Avail: US Patent and Trademark Office CSCL 20/5

In this patent a series of pulses are transmitted to a first laser and the same series of pulses through a time delay network to a second laser. Each laser provides pulses of light through separate diagonal mirrors and through respective transparent holograms. Each light is then brought into convergence by respective sides of a wedge shaped reflector and brought into spatially coincident focus by an imaging lens onto the surface of a sample under test. The two hologram transparencies are imaged spacially coincident but separated in time on the face of the sample. Thermal elastic waves produced by laser heating at the sample surface transform into a desired acoustic beam pattern determined by the nature of the wavefronts which the hologram transparency represents. The position of the coincident image on the sample may be moved by varying the time between the two pulses. GRA

N86-12600*# Hampton Inst., Va. Dept. of Physics and Engineering.
DIRECT SOLAR-PUMPED IODINE LASER AMPLIFIER Semiannual Progress Report, 1 Apr. - 30 Sep. 1985
Kwang S. Han 30 Sep. 1985 50 p refs
(Grant NAG1-441)
(NASA-CR-176324; NAS 1.26:176324) Avail: NTIS HC A03/MF A01 CSCL 20E

This semiannual progress report covers the period from April 1, 1985 to Sept. 30, 1985 under NASA grant NAS1-441 entitled direct solar pumped iodine laser amplifier. During this period the parametric studies of the iodine laser oscillator pumped by a Vortek simulator was carried out before the amplifier studies. The amplifier studies are postponed to the extended period following completion of the parametric studies. In addition, the kinetic modeling of a solar pumped iodine laser amplifier, and the experimental work for a solar pumped dye laser amplifier are in progress. This report contains three parts: (1) the radiation characteristics of solar simulator and the parametric characteristics of photodissociation iodine laser continuously pumped by a Vortek solar simulator; (2) kinetic modeling of a solar pumped iodine laser amplifier; and (3) the study of the dye laser amplifier pumped by a Tamarack solar simulator. Author

N86-12601# Air Force Office of Scientific Research, Bolling AFB, Washington, D.C. Foreign Technology Div.
APPLIED LASERS (SELECTED ARTICLES)
20 May 1985 74 p Transl. into ENGLISH from Ying Yong Ji Guang (China), v. 3, no. 5-6 and v. 4, no. 1, 1983 p 18-22, 25-27, 23-26, 27-30, 10, 38-42 43-48 36-37
(AD-A155948; AD-E301698; FTD-ID(RS)T-1564-84) Avail: NTIS HC A04/MF A01 CSCL 20/5

Several articles on lasers and laser applications are presented. Topics covered include: frequency stability of lasers; discharge stability; laser beam modulation; laser pumping; and wavelength demarcation. Investigations are carried out on dye lasers, helium-neon lasers, carbon dioxide lasers, and semiconductor lasers. GRA

N86-12602# Department of the Navy, Washington, D. C.
LASER VIBROMETER Patent Application
M. J. Rudd, inventor (to Navy) Filed 31 Aug. 1984 17 p
(AD-D011811; US-Patent-Appl-SN-645888) Avail: NTIS HC A02/MF A01 CSCL 14/2

This Abstract disclosures an optical interferometric apparatus for detecting and measuring discontinuities in structural materials from ultrasonic stress waves at their surfaces. The apparatus includes an acousto-optic (a/o) modulator which shifts a portion of a laser beam in frequency, producing a modulated beam of light. This modulated light beam is deflected and passes through an adjustable lens to the surface being measured. The light scattered by the surface is focused by the lens on an end mirror of the laser which produced the original beam, and is divergingly reflected therefrom. The reflected, scattered light is heterodyned with the unshifted portion of the laser beam in a photodiode to produce a phase modulated signals at the acoustic frequency of the a/o modulator. Surface displacement can be measured as a function of instantaneous phase shift, and surface velocity as a function of rate of change of phase shift. GRA

N86-12603# Department of the Army, Washington, D. C.
PULSED DIGITAL MULTIPLEXED LASER GENERATOR Patent Application
T. E. Honeycutt and T. G. Roberts, inventors (to Army) Filed 25 Jun. 1985 22 p
(AD-D011855; US-Patent-Appl-SN-758919) Avail: NTIS HC A02/MF A01 CSCL 17/2

A system of lasers which produces a single pulsed laser beam carrying many channels of digital information simultaneously is discussed. The information content of each laser output pulse is determined by the presence or absence of one or more input signal channel frequencies. The presence or absence of each frequency is provided by a plurality of low power CW lasers operating at different frequencies and which are selectively gated in a binary fashion by pulse coded digital input signals to provide digitized low power laser outputs in accordance with the digital input signals. The low level pulses of the various optical frequencies are combined and utilized to preload a relatively high power pulsed CO2 output laser. A pair of mirror assemblies are utilized to respectively combine the multifrequency channel pulses and transmit a single pulsed output laser beam generated by the pulsed output laser. The presence or absence of each frequency component in each output pulse is determined by the frequency components preloading the cavity modes of the pulsed high power output laser. Author (GRA)

N86-12604# Cornell Univ., Ithaca, N.Y. Baker Lab.
STUDIES OF ENERGY STORAGE AND TRANSFER IN GAS LASERS Final Technical Report, 1 Mar. 1982 - 28 Feb. 1985
J. Wiesenfeld 28 Apr. 1985 12 p
(Grant AF-AFOSR-0037-82)
(AD-A158553; AFOSR-85-0504TR) Avail: NTIS HC A02/MF A01 CSCL 20/5

This experimental program was designed to elucidate the behavior of electronically excited atoms and molecules in gases and examine methods by which these species might generally be detected using laser-based spectroscopic techniques. To that end, several atomic and molecular states were observed using Resonance Multiphoton Ionization. In addition, the photodissociative production of electronically excited states was investigated and the subsequent deactivation of excited atoms in collisional encounters with molecules studied. GRA

N86-12605# Lawrence Livermore National Lab., Calif.
SCIENCE, TECHNOLOGY AND THE INDUSTRIALIZATION OF LASER-DRIVEN PROCESSES
J. I. Davis and J. A. Paisner May 1985 21 p
(Contract W-7405-eng-48)
(DE85-014856; UCID-20448) Avail: NTIS HC A02/MF A01

Members of the laser program at Lawrence Livermore National Laboratory (LLNL) potential applications of lasers in industry, some of which are: isotope separation, cleanup of radioactive waste, trace impurity removal, selective chemical reactions, photochemical activation or dissociation of gases, control of combustion particulates, crystal and powder chemistry, and laser induced biochemistry are reviewed. Many of these areas are currently under active study in the community. The investigation at LLNL focused on laser isotope separation of atomic uranium because of the large demand and high product enrichment price for material used as fuel in commercial light-water nuclear power reactors. They also believed that once the technology was fully developed and deployed, it could be applied directly to separating many elements economicprogram at LLNL has an extensive uranium and plutonium program of > $100 M in Fy85 and a minor research program for other elements. This report describes the AVLIS program conducted covering the following topics: candidate elements, separative work units, sepctroscopic selectivety, major systems, facilities, integrated process model, multivariable sensitivity studies, world market, and US enrichment enterprise. DOE

N86-12606# Lawrence Livermore National Lab., Calif.
DYNAMIC ADI COMPUTATIONS OF THERMOELASTIC STRESSES IN CRYSTALLINE LASER MEDIA
R. J. Gelinas, S. K. Doss, and N. N. Carlson 1985 14 p Presented at the 4th Intern. Conf. on Numerical Methods in Laminar and Turbulent Flow, Swansea, Engl., 8 Jul. 1985 Prepared in cooperation with California Univ., Berkeley
(Contract W-7405-eng-48)
(DE85-010478; UCRL-92424; CONF-850745-2) Avail: NTIS HC A02/MF A01

This article considers thermoelastic effects which influence both the thermal engineering design and optical propagation in solid state high average power laser (HAPL) systems. The methods and computations described were developed for applications, ultimately, to crystalline slabs with arbitrary symmetry properties and with arbitrary spatial orientations between crystalline axes and slab configurations. For this, accurate numerical solutions are required simultaneously for the heat equation and Hooke's law in their most general tensor forms. Prompted by the optical problem requirements in HAPL systems, this work utilizes implementations of Eulerian discretizations and dynamic ADI methods for solving general fourth order elliptic partial differential equations (PDE's) which describe stress potentials in anisotropic media. These formulations can provide both steady state and transient PDE solutions. Computed results for trigonal Al2O3 crystal deformations in various crystal axes/slab orientations are presented. DOE

N86-12607# Oak Ridge National Lab., Tenn.
NEW BEAM NEUTRALIZATION CONCEPT: LASER PHOTODETACHMENT IN A MAGNETIC FIELD
O. H. Crawford and H. F. Krause 1985 21 p Presented at the Neutralizer Workshop, Upton, N.Y., 5 Jun. 1985
(Contract DE-AC05-84OR-21400)
(DE85-014655; CONF-8506150-1) Avail: NTIS HC A02/MF A01

The major advantage of laser photodetachment as a method for neutralizing a negative ion beam is that the emittance increase can be made as small as desired. Since the momentum of the photon is negligible, it is only the recoil from the leaving electron that causes any beam spread in photodetachment. The closer the laser is turned to the threshold frequency, the smaller the relative energy of the electron and atom, and the smaller the recoil. The problem with photodetachment is the high laser power requirement. The cross section approaches zero as the laser frequency approaches the detachment threshold. As a consequence, for a high-brightness application it is estimated that the laser power required would exceed the anticipated beam power. It is shown that the imposition of a solenoidal magnetic field in the neutralization region may make photodetachment practical, by enhancing the cross section. DOE

N86-12608# Los Alamos National Lab., N. Mex.
STRATEGIC DEFENSE INITIATIVES AT LOS ALAMOS NATIONAL LABORATORY
S. D. Rockwood 1985 3 p Presented at the Southwest Conf. on Opt., Albuquerque, N. Mex., 4 Mar. 1985
(Contract W-7405-eng-36)
(DE85-014093; LA-UR-85-2177; CONF-850345-25) Avail: NTIS HC A02/MF A01

This presentation reviews the Strategic Defense Initiative (SDI) programs, noting especially the needs for and applications of optics and optical technologies. The various activities at Los Alamos contributing to SDI programs are used. The principal, nonnuclear SDI programs are: (1) the free electron laser, and (2) neutral particle beams. Both should be considered as potential long-range-kill systems, but still in the futuristic category. DOE

N86-12394# Joint Publications Research Service, Arlington, Va.
COMPACT TEA-CO2 LASER WITH LONG LIFE DEVELOPED
Yin Yiyan, Zhang Yixiang, Want Zongjin, Wei Xianren, and Gao Chunguang *In its* China Rept.: Sci. and Technol. (JPRS-CST-85-016) 23 May 1985 p 36-42 refs Transl. into ENGLISH from Yingyong Jiguang (Shanghai), v. 5, no. 1, Feb. 1985 p 39-42 (For primary document see N86-12393 03-31)
Avail: NTIS HC A08/MF A01

N86-12395# Joint Publications Research Service, Arlington, Va.
FREQUENCY SELECTION AND MODE LOCKING OF Nd:YAG LASER
Tang Guichen and Qiu Peixia *In its* China Rept.: Sci. and Technol. (JPRS-CST-85-016) 23 May 1985 p 43-50 refs Transl. into ENGLISH from Zhongguo Jiguang (Shanghai), v. 12, no. 1, 20 Jan. 1985 p 11-14 (For primary document see N86-12393 03-31)
Avail: NTIS HC A08/MF A01

N86-12419# Joint Publications Research Service, Arlington, Va.
LONG WAVE (1.2 - 1.5 MICRONS) SEMICONDUCTOR LASERS
Pan Zhonghau, Yang Guisheng, Ran Chongzhu, Zhao Songshan, and Wang Yuzhang *In its* China Rept.: Sci. and Technol. (JPRS-CST-85-018) 12 Jun. 1985 p 99-105 refs Transl. into ENGLISH from Tongxin Xuebao (Beijing), no. 1, Jan. 1984 p 68-71 (For primary document see N86-12413 03-31)
Avail: NTIS HC A09/MF A01

N86-12428# Joint Publications Research Service, Arlington, Va.
HIGH-POWER ND: GLASS LASER AND TARGET CHAMBER SYSTEM AND AN EXPERIMENTAL STUDY OF LASER PLASMA X-RAY
Wu Hongxing, Guo Dahao, Zhou Yusheng, Zhang Limin, He Weimin, and Dai Yusheng *In its* China Rept.: Sci. and Technol. (JPRS-CST-85-021 8 Jul. 1985 p 132-140 refs Transl. into ENGLISH from Zhongguo Kexue Jishu Daxue Xuebao (Hefei), v. 15, no. 1, Mar. 1985 p 30-36 (For primary document see N86-12421 03-31)
Avail: NTIS HC A09/MF A01

N86-12431# Joint Publications Research Service, Arlington, Va.
LASER SCATTERING IN PLASMA EXAMINED
Lu Quankang, Chen Hang, Yin Qi, and Wang Wenhua *In its* China Rept.: Sci. and Technol. (JPRS-CST-85-034) 1 Oct. 1985 p 49-52 refs Transl. into ENGLISH from Ziran Zazhi (Shanghai), v. 7, no. 7, Jul. 1984 p 555-557 (For primary document see N86-12430 03-31)
Avail: NTIS HC A08/MF A01

N86-12454# Joint Publications Research Service, Arlington, Va.
EFFECT OF AMPLIFIED SPONTANEOUS EMISSION ON SPACE COHERENCE OF XeCl LASER
Zhang Dake, Wang Xiaoyi, Ni Jinzhi, Yao Jianping, Fu Shufen, and Chen Jianwen *In its* China Rept.: Sci. and Technol. (JPRS-CST-85-030) 4 Sep. 1985 p 36-44 refs Transl. into ENGLISH from Zhongguo Jiguang (Shanghai), v. 12, no. 5, 20 May 1985 p 261-265 (For primary document see N86-12451 03-31)
Avail: NTIS HC A08/MF A01

N86-12455# Joint Publications Research Service, Arlington, Va.
FIRST DOMESTIC HIGH REPETITION RATE ULTRASHORT PULSE LASER
Guang Lin *In its* China Rept.: Sci. and Technol. (JPRS-CST-85-030) 4 Sep. 1985 p 45 Transl. into ENGLISH from Zhongguo Jiguang (Shanghai), v. 12, no. 5, no. 5, 20 May 1985 p 278 (For primary document see N86-12451 03-31)
Avail: NTIS HC A08/MF A01

N86-12456# Joint Publications Research Service, Arlington, Va.
PRACTICAL EXCIMER LASER DEVELOPED
Qun Li *In its* China Rept.: Sci. and Technol. (JPRS-CST-85-030) 4 Sep. 1985 p 46 Transl. into ENGLISH from Zhongguo Jiguang (Shanghai), v. 12, no. 5, 20 May 1985 p 297 (For primary document see N86-12451 03-31)
Avail: NTIS HC A08/MF A01

N86-12457# Joint Publications Research Service, Arlington, Va.
A HIGH PRECISION RATE DYE LASER PUMPED BY A CuCl LASER
Jing Chunyang, Zhang Guiyan, Wu Zhengliang, Shu Juping, Hu Qiquan, Ying Lifeng, and Lin Fucheng *In its* China Rept.: Sci. and Technol. (JPRS-CST-85-030) 4 Sep. 1985 p 47-53 refs Transl. into ENGLISH from Zhongguo Jiguang (Shanghai), v. 12, no. 7, 20 Jul. 1985 p 394; 399-401 (For primary document see N86-12451 03-31)
Avail: NTIS HC A08/MF A01

N86-12460# Joint Publications Research Service, Arlington, Va.
LASER INDUCED BIOLOGICAL HEATING ANALYZED
Liu Puhe *In its* China Rept.: Sci. and Technol. (JPRS-CST-85-026) 15 Aug. 1985 p 71-76 refs Transl. into ENGLISH from Zhongguo Jiguang (Shanghai), no. 11, 20 Nov. 1984 p 697-700 (For primary document see N86-12459 03-31)
Avail: NTIS HC A07/MF A01

N86-12465# Joint Publications Research Service, Arlington, Va.
CHINA DEVELOPS 6J KrF LASER
Wang Ganchang, Zhu Xuhui, Wang Naiyan, Xie Jinggang, Li Yinghshan, Zhou Changhuai, and Wang Pu *In its* China Rept.: Sci. and Technol. (JPRS-CST-85-032) 19 Sep. 1985 p 62-66 refs Transl. into ENGLISH from He Kexuy yu Gongcheng (Beijing), v. 5, no. 1, Mar. 1985 p 1-5 (For primary document see N86-12462 03-31)
Avail: NTIS HC A08/MF A01

N86-12734# Joint Publications Research Service, Arlington, Va.
TRANSMISSION OF TROPOSPHERIC RADIATION OF LASERS ON MOLECULES OF DIFFERENT CARBON DIOXIDE ISOTOPES Abstract Only
V. N. Arefyev *In its* USSR Rept.: Earth Sci. (JPRS-UES-85-008) 16 Aug. 1985 p 41 Transl. into ENGLISH from Kvantovaya Elektron. (Moscow), v. 12, no. 3, Mar. 1985 p 631-634 (For primary document see N86-12697 03-42)
Avail: NTIS HC A04/MF A01

37 MECHANICAL ENGINEERING

Includes auxiliary systems (non-power); machine elements and processes; and mechanical equipment.

N86-12609*# National Aeronautics and Space Administration. Lewis Research Center, Cleveland, Ohio.
SURFACE FATIGUE LIFE AND FAILURE CHARACTERISTICS OF EX-53, CBS 1000M, AND AISI 9310 GEAR MATERIALS
Dennis P. Townsend Oct. 1985 14 p refs
(NASA-TP-2513; E-2578; NAS 1.60:2513) Avail: NTIS HC A02/MF A01 CSCL 13I

Spur gear endurance tests and rolling-element surface fatigue tests are conducted to investigate EX-53 and CBS 1000M steels for use as advanced application gear materials, to determine their endurance characteristics, and to compare the results with the standard AISI 9310 gear material. The gear pitch diameter is 8.89 cm (3.50 in). Gear test conditions are an oil inlet temperature of 320 K (116 F), an oil outlet temperature of 350 K (170 F), a maximum Hertz stress of 1.71 GPa (248 ksi), and a speed of 10,000 rpm. Bench-type rolling-element fatigue tests are conducted at ambient temperature with a bar specimen speed of 12,500 rpm and a maximum Hertz stress of 4.83 GPa (700 ksi). The EX-53 test gears have a surface fatigue life of twice that of the AISI 9310 spur gears. The CBS 1000M test gears have a surface fatigue life of more than twice that of the AISI 9310 spur gears. However, the CBS 1000M gears experience a 30-percent tooth fracture failure which limits its use as a gear material. The rolling-contact fatigue lines of RC bar specimens of EX-53 and ASISI 9310 are approximately equal. However, the CBS 1000M RC specimens have a surface fatigue life of about 50 percent that of the AISI 9310.
Author

N86-12610*# Talandic Research Corp., Pasadena, Calif.
ADVANCED TORQUE CONVERTERS FOR ROBOTICS AND SPACE APPLICATIONS Final Report
Jul. 1985 60 p refs
(NASA-CR-177987; NAS 1.26:177987) Avail: NTIS HC A04/MF A01 CSCL 13I

This report describes the results of the evaluation of a novel torque converter concept. Features of the concept include: (1) automatic and rapid adjustment of effective gear ratio in response to changes in external torque (2) maintenance of output torque at zero output velocity without loading the input power source and (3) isolation of input power source from load. Two working models of the concept were fabricated and tested, and a theoretical analysis was performed to determine the limits of performance. It was found that the devices are apparently suited to certain types of tool driver applications, such as screwdrivers, nut drivers and valve actuators. However, quantiative information was insufficient to draw final conclusion as to robotic applications.
Author

N86-12611# Massachusetts Inst. of Tech., Cambridge. Dept. of Materials Science and Engineering.
FUSION WELDING RESEARCH Annual Technical Report, 15 Feb. 1983 - 15 Feb. 1984
T. W. Eagar, G. B. Hunter, G. J. Dunn, C. D. Sorensen, and M. L. Lin 30 Apr. 1984 122 p
(Contract N00014-80-C-0384)
(AD-A158127; ATR-4) Avail: NTIS HC A06/MF A01 CSCL 13/8

Research studies on the physics of arc welding processes include: (1) vapor emission from weld pools; (2) development of a high speed infrared temperature monitor; (3) digital signal analysis of weld noise voltages; (4) convection and surface depression of the weld pool; (5) pulsed current gas metal arc welding of titanium; (6) contact tip wear in gas metal arc welding of titanium; (7) fracture toughness of HY-80 weldments; and (8) Sensitization of 304 stainless steel welds. Heavy section titanium; HY-80 weld metal; Sensors for arc welding automation.
GRA

N86-12612# Department of the Air Force, Washington, D.C.
LIGHTWEIGHT CRYOGENIC TANK WITH POSITIVE EXPULSION Patent Application
J. C. Lewis, inventor (to Air Force) Filed 12 Jul. 1984 14 p
(AD-D011856; US-Patent-Appl-SN-630148) Avail: NTIS HC A02/MF A01 CSCL 13/4

A lightweight tank structure for the storage and controlled expulsion therefrom of a cryogenic liquid is a flexible metallic bladder. An interior collapsible volume for containing the cryogenic liquid, a second high pressure container enclosing the first container, a third container enclosing the second container and including supports for maintaining the second container in a spaced relationship within the third container, a first tube operatively connected to the first container through which the cryogenic liquid may be inserted into the first container and controllably expelled therefrom, a source of pressurized gas, and a tube operatively interconnecting the second container and the gas source for controllably supplying pressurized gas to the interior of the second container whereby the contained cryogenic liquid may be controllably expelled by controlled collapsing of the bladder of the first container are described. Additional insulation in the form of a layer of foam on the exterior surface of the third container, and of a cryogenic coolant or a vacuum maintained in the space between the second and third containers may be included.
Author (GRA)

N86-12613# SKF Industries, Inc., King of Prussia, Pa.
MECHANICAL INTERACTIONS OF ROUGH SURFACES Quarterly Progress Report, 1 Apr. - 30 Jun. 1985
J. I. McCool and G. B. Hadden Jul. 1985 45 p
(Contract DE-AC02-84ER-13163)
(DE85-015011; DOE/ER-13163/7; SKF-AT85D031) Avail: NTIS HC A03/MF A01

The projects, Mechanical Interactions of Rough Surfaces addresses a number of unresolved issues which impact the design of mechanical systems in which surface microtopography per se or events which occur on the microgeometric scale play a critical role. The project is an experimental/analytical investigation to: (1) explore the behavior of lubricated concentrated contacts involving microscopically rough surfaces under conditions of combined rolling, sliding and spinning with and without the presence of contaminating particles; (2) develop processing principles and techniques for the analysis of digitized rough surface profiles to yield surface descriptors that are predictive of functional performance and which have acceptable systematic and random error. The work is conducted within two distinct tasks. In task 1, a rig designed and built by SKF is used to provide optical interferograms of the lubricated contact of rough surfaces along with measurements of the traction transmitted under conditions of combined rolling, sliding and spinning. The objective of task 2 is to develop guidelines and techniques for the processing of surface roughness data generated in a analog form by a stylus profile instrument to provide interpretable predictions of surface performance on contact. DOE

N86-12614# Aspen Systems Corp., Marlborough, Mass.
PRELIMINARY DESIGN OF LINEAR ALTERNATOR DYNAMOMETER FOR FREE PISTON STIRLING ENGINES Final Report
K. P. Lee and W. M. Toscano Jun. 1985 159 p refs
(Contract DE-AC05-84OR-21400)
(DE85-015078; ORNL/Sub-84-05907/1) Avail: NTIS HC A08/MF A01

A preliminary design of a linear alternator type dynamometer for testing free piston Stirling engines (FPSEs) is prepared. The purpose of the dynamometer is to provide the FPSEs with simulated loads such as double acting inertia compressors for heat pumps, hydraulic pumps, and linear alternators. The dynamometer has two major components: the electromechanical transducer and the control system. The dynamometer control system utilizes active force control scheme. The control system operates in two modes simultaneously: the foreground mode and the background mode. The foreground mode instantaneously regulates the current to the armature coil according to the predetermined load force profile. The background mode continually refines the load force profile and upgrades the foreground mode load force profile until convergence is reached. The digital simulation of the entire system including the control system, the dynamometer, and the RE-1000 FPSE showed that the dynamometer is capable of simulating various loads very accurately and fast. DOE

N86-12615# Oak Ridge National Lab., Tenn.
COMPARATIVE ANALYSIS OF A STIRLING HEAT PUMP WITH SECOND- AND THIRD-ORDER COMPUTER MODELS
N. Domingo Jun. 1985 37 p refs
(Contract DE-AC05-87OR-21400)
(DE85-013536; ORNL/CON-162) Avail: NTIS HC A03/MF A01

Performance and loss terms obtained with the NASA third order (nodal analysis) computer model were compared with the results obtained with the Martini ISO82 second order model for a Stirling cycle heat pump. Because no Stirling heat pump test data exist to substantiate the accuracy of these models, it was not possible to designate one model as clearly superior. Agreement between the models' overall predictions was -2 to 13% for indicated power, 18 to 29% for net heat output, and 10 to 20% for indicated heating COP. Poor agreement was found between the calculated pressure drop, mechanical friction, and conduction losses. Better identification and quantification of loss mechanisms is suggested as a more meaningful step toward the development of better design models. DOE

N86-12616# Oak Ridge Y-12 Plant, Tenn.
ELECTROCHEMICAL MACHINING OF THE OUTER PROFILE OF THE B83 LUG
J. D. Hensley 28 Jun. 1985 56 p
(Contract DE-AC05-84CS-21400)
(DE85-014934; Y-2341) Avail: NTIS HC A04/MF A01

A development program was conducted which demonstrates the capability of electrochemical machining (ECM) as a viable production method for generating the outer contour profile of the B83 Lug. It is indicated that the machining time can be reduced from hours, the time required by conventional methods of metal removal, to minutes. Ordinarily, many fixtures and setups would be required to shape the features of the outer profile, as was experienced during conventional machining of the B61 Lug. In ECM the part-feature size and location are designed into the tooling, and only one operation is required to achieve the desired contour. Due to the accuracy and complexity of the cathode design, considerable testing and evaluation would normally be required to develop the process; however, the experience obtained during development of the smaller B61 Lug ECM process made it possible to produce usable E83 Lugs on the first attempt. DOE

N86-12617# Oak Ridge Gaseous Diffusion Plant, Tenn.
CORRECTION OF COMPRESSOR CRITICAL SPEED CONDITION THROUGH FLUID-FILM BEARING OPTIMIZATION
J. W. Spencer and V. E. Obeid 1985 32 p ref Presented at the AMSE Vibration and Sound Conf., Cincinnati, 10 Sep. 1985
(Contract DE-AC05-84OT-21400)
(DE85-005507; CONF-850926-4) Avail: NTIS HC A03/MF A01

A critical speed condition for an overhung centrifugal compressor was corrected through a relatively minor bearing modification. The resonant condition was evaluated analytically through rotor dynamic analyses which included fluid film bearing characterization and rotor model generation. The importance of adequate specification, inspection, and analytical characterization, of fluid film bearings are discussed. The effects of unbalance on the stability of plain journal bearings are also commented upon. DOE

N86-12618# Foster-Miller Associates, Inc., Waltham, Mass.
DEVELOPMENT OF THE HYDROTRANSPORT BOOST PUMP Open File Report, Sep. 1981 - Dec. 1984
L. S. Rubin, R. L. Cardenas, M. Burnette, J. Roberge, and A. Harvey 31 Dec. 1984 255 p refs
(Contract DI-BM-J0-133934)
(PB85-203776; BM-OFR-49-85) Avail: NTIS HC A12/MF A01 CSCL 13K

A ventilated helical boost pump was developed that can handle varying flow rates and/or solids concentrations while operating at a single rotational speed. The boost pump developed and briefly tested was designed to accomodate flows suitable for a 3-in-diam. pipeline. The boost pump's ventilated design provides the automatic pressure regulation needed to meet the system's requirements for supporting transient pipeline flow. A maximum discharge pressure of 120 psi was achieved at an operating speed of 3,000 rpm. Coal flow rates of up to 1,000 lb/min were successfully processed with a nonshrouded single vane impeller. GRA

N86-12382# Tokyo Denki Univ. (Japan). Faculty of Engineering.
STUDY OF HIGH SPEED SHEARING OF THERMOPLASTIC POLYMER SHEETS WITH A NEW ROTARY SHEARING MACHINE
Isami Aoki and Teizo Maeda *In its* Res. Rept. of the Faculty of Eng., Tokyo Denki Univ., No. 32 Dec. 1984 p 157-168 refs
(For primary document see N86-12372 03-31)
Avail: NTIS HC A09/MF A01

N86-12404# Joint Publications Research Service, Arlington, Va.
PLASMA ARC WELDING FOR THIN TITANIUM PLATES
Luo Jinru and Tang Xingli *In its* China Rept.: Sci. and Technol. (JPRS-CST-85-035) 17 Oct. 1985 p 52-62 refs Transl. into ENGLISH from Shiyou Huagong Shebei (Lanzhou), v. 14, no. 4,

1985 p 11-16 (For primary document see N86-12399 03-31)
Avail: NTIS HC A08/MF A01

38 QUALITY ASSURANCE AND RELIABILITY

Includes product sampling procedures and techniques; and quality control.

N86-12619# Hughes Aircraft Co., Fullerton, Calif. Ground Systems Group.
STUDY AND INVESTIGATION TO UPDATE THE NONELECTRONIC RELIABILITY NOTEBOOK. REVISION A Final Technical Report, Jun. 1982 - Apr. 1984
J. E. Augus, R. G. Arno, and N. R. Mann Apr. 1985 235 p
(Contract F30602-82-C-0127)
(AD-A157242; HAC-FR-84-16-681-Rev-A; RADC-TR-85-66-Rev-A)
Avail: NTIS HC A11/MF A01 CSCL 12/1

This report describes the investigations and analyses performed in connection with revising and updating the Nonelectronic Reliability Notebook (Formerly RADC-TR-75-22). It includes detailed descriptions of the statistical analyses performed, the data base on which the Nonelectronic Reliability Notebook is based, new part classification outlines, and a section on advanced statistical techniques for analyzing life data. GRA

N86-12620# Materials Research Labs., Ascot Vale (Australia).
DEVELOPMENT AND EVALUATION OF A MICROBURST TEST APPARATUS FOR USE AS A MINIMUM DESTRUCTIVE TEST FOR PARACHUTE MATERIAL
G. T. Egglestone, N. M. Browne, and M. Taylor Apr. 1985 33 p
(AD-A158110; MRL-R-959) Avail: NTIS HC A03/MF A01 CSCL 11/5

Conventional testing of parachute canopy materials to identify the extent of polymer degradation requires large amounts of material resulting in extensive repairs if the material is found to be sound. A microburst test apparatus designed and built at the Materials Research Labs is capable of testing the canopy in-situ, with a degree of damage confined to a 3.2 mm diameter hole. This does not require repair and fits between a ripstop repeat on canopy material from modern day T-1 0 parachutes. The microburst unit gives a digital readout for maximum pressure to burst and pressure to burst/time integral. Correlations between these results and those from conventional tensile and Mullens burst tests showed the microburst test results to more closely resemble those from accepted tensile test methods. GRA

N86-12621# Brookhaven National Lab., Upton, N. Y.
ULTRASONIC ATTENUATION IN CLEAN ANISOTROPIC SUPERCONDUCTORS
S. N. Coppersmith and B. A. Klemm 29 May 1985 10 p Presented at Mater. and Mech. of Superconductivity Conf., Ames, Iowa, 29 May 1985 Prepared in cooperation with Exxon Research and Engineering Co., Annandale, N. J.
(Contract DE-AC02-76CH-00016)
(DE85-012178; DOE/BNL-036528; CONF-8505138-5) Avail: NTIS HC A02/MF A01

The ultrasonic attenuation of UPt3 in the hydrodynamic regime was found to be proportional to T sup 2 at low temperatures T. In the opposite limit, ql much larger than, it is found that the ultrasonic attenuation for an anisotropic superconductor has a temperature dependence that depends on the nodal structure of the gap and on the relative orientation of the sound wave and the nodes. Both power law and exponential temperature dependences are found to be possible for gaps with either points or lines of nodes, depending upon the sound wave orientation relative to the nodes. In some directions, finite experimental resolution must be taken into account. DOE

39 STRUCTURAL MECHANICS

Includes structural element design and weight analysis; fatigue; and thermal stress.

For applications see *05 Aircraft Design, Testing and Performance* and *18 Spacecraft Design, Testing and Performance.*

N86-12622 Texas Univ., Austin.
INFLUENCE OF BONDED REINFORCEMENT IN POST-TENSIONED PRESTRESSED CONCRETE T-BEAMS WITH UNBONDED TENDONS Ph.D. Thesis
Chaiwat Changwatchai 1984 344 p
Avail: Univ. Microfilms Order No. DA8508257

For the proper design of a prestressed member with an unbonded tendon, supplemental bonded reinforcement must be provided in the tension zone of the critical section to insure satisfactory behavior of the member. The minimum amount of bonded bar suggested in the current ACI Code is based on an empirical formula. When we apply this formula to a member with a T-shaped section, the amount of bonded reinforcing bar is often substantially higher in the negative moment region than in the positive moment region. In order to study the criteria for determining the amount of bonded bar needed, an experimental program was conducted to observe and gather information on the role of bonded reinforcement in T-shaped post-tensioned members with unbonded tendons. Four full size T-shaped specimens which represent portions of a widely used post-tensioned concrete joist system of construction were tested to failure. Author

N86-12623# Army Armament Research and Development Command, Watervliet, N. Y. Large Caliber Weapon Systems Lab.
MORE ON COMPLIANCE OF THE THREE-POINT BEND SPECIMEN Final Report
J. H. Underwood, J. A. Kapp, and F. I. Baratta May 1985 15 p
(AD-A156665; AD-E440286; ARLCB-MR-85015) Avail: NTIS HC A02/MF A01 CSCL 20/11

Comparison and analysis of load-line displacement for the three-point bend specimen was performed. Expressions were developed for displacement as a function of crack length and for crack length as a function of displacement. GRA

N86-12624# Washington Univ., Seattle. Dept. of Mechanical Engineering.
STRAIN ENERGY DENSITY CRITERIA FOR DYNAMIC FRACTURE AND DYNAMIC CRACK BRANCHING
M. Ramulu and A. S. Kobayashi Jul. 1985 24 p
(Contract N00014-85-K-0187)
(AD-A157914; UWA/DME/TR-85/51) Avail: NTIS HC A02/MF A01 CSCL 20/11

Dynamic extension of Sih's fracture criterion based on strain energy density factor, r sub c (dW/dV), is used to analyze dynamic crack propagation and branching. Influence of the nonsingular components, which are known as the higher order terms (HOT) in the crack tip stress field, on the strain energy density distribution at a critical distance surrounding the crack tip moving at constant crack velocity is examined. This r sub c (dW/dV) fracture criterion is then used to analyze available dynamic photoelastic results of crack branching and of engineering materials. Author (GRA)

N86-12625# Optimization, Inc., Blacksburg, Va.
MODELING AND CONTROL OF FLEXIBLE STRUCTURES Final Report, 31 Aug. 1984 - 4 Mar. 1985
J. A. Burns, E. M. Cliff, R. M. Goff, H. J. Kelley, and F. H. Lutze May 1985 101 p
(Contract F04611-84-C-0032)
(AD-A157959; K506-1; AFRPL-TR-85-030) Avail: NTIS HC A06/MF A01 CSCL 12/1

The principal goals of this program were a demonstration of state-space procedure for modeling and control of a flexible structure, and, more generally, increased understanding of control problems for such systems. The state-space approach is based on a model of the distributed system. The model includes the

necessary partial differential equations without modal truncation. The basic view is that it is preferable to avoid introducing approximations until they are required (e.g., for numerical calculations). The program (formal model, state-space model, optimal-control formulation, approximation procedure and numerical calculation) is carried out, in detail, for a simple structural system including a rotating hub, a flexible beam and a tip mass. A final section in this part provides some parallel results for a more complex structure comprised of a hub, two flexible support beams and a tip-body. The second part of the report is concerned with some parasitic effects on the stability of a distributed system with feedback. The approach is based on an input-output description of the system; specifically, a transfer-function approach is used. In order to keep the calculation burden reasonably small the structural model studied is a simple cable which requires only second-order spatial derivatives. The baseline system employs feedback of a force to the free-end of the cable at a magnitude proportional to the velocity at the free end. The gain parameter can be varied to produce a locus of roots; albeit one with a countable infinite number of branches.
GRA

N86-12626# Oak Ridge National Lab., Tenn.

MULTIFREQUENCY EDDY-CURRENT INSPECTION OF SEAM WELD IN STEEL SHEATH

J. H. Smith, C. V. Dodd, and I. D. Chitwood Apr. 1985 173 p
(Contract DE-AC05-84OR-21400)
(DE85-013533; ORNL/TM-9470) Avail: NTIS HC A08/MF A01

Multifrequency eddy-current techniques were used to perform a continuous on-line inspection of the seam weld in the steel jacket for a superconducting cable. The inspection was required to detect both surface and internal weld flaws in the presence of a large, highly conductive central conductor. Raw eddy-current data were recorded on magnetic tape, and test properties such as discontinuity size and weld penetration were determined by mathematically fitting these data to coefficients developed with representative standards. A sophisticated computer-controlled scanning technique was applied, and a unique scanning device was developed to provide full coverage of the weld and heat-affected zone. The techniques used to develop this multifrequency eddy-current examination are described along with the test equipment, test procedures, and computer programs.
DOE

N86-12627# Argonne National Lab., Ill.

THEORY FOR THE PORTEVIN-LECHATELIER EFFECT

R. B. Schwarz Aug. 1985 7 p Presented at the 7th Intern. Conf. on the Strength of Metals and Alloys, Montreal, 12 Aug. 1985
(Contract W-31-109-eng-38)
(DE85-004030; CONF-850823-1-Abst) Avail: NTIS HC A02/MF A01

The models advanced to explain the PL effect are concerned with the critical strain, the stress serrations occurring in a T-regime, and the negative strain-rate sensitivity. A new model is proposed which also explains the rest of the observations, including the different types of serrations, localized deformation, and grouping of type-B serrations.
DOE

N86-12628# Lawrence Livermore National Lab., Calif.

FAILURE CRITERIA USED IN A PROBABILISTIC FRACTURE MECHANICS CODE

T. Y. Lo 1985 8 p refs Presented at the 8th Intern. Conf. on Struct. Mech. in Reactor Technol., Brussels, 19 Aug. 1985
(Contract W-7405-eng-48)
(DE85-007264; UCRL-91242; CONF-850809-12) Avail: NTIS HC A02/MF A01

Two criteria are implemented in a piping reliability analysis code to assess the stability of crack growth in pipes. One is the critical net section stress criterion. It is simple and convenient but its application is limited to very ductile materials. The other is the tearing modulus stability criterion. This criterion has a solid technical base. However, calculating the J-integral, J, and the associated tearing modulus, T, usually requires a complicated finite element method (FEM). In this piping reliability code, existing J and T solutions in tabular or formula form instead of the FEM are used for computational efficiency. These two failure criteria are discussed and compared in terms of their effects on the estimation of pipe failure probability.
DOE

N86-12629# Lawrence Livermore National Lab., Calif.

MOTION OF THIN METAL WALLS AND THE EQUATION OF STATE OF DETONATION PRODUCTS

E. Lee, D. Breithaupt, C. McMillan, N. Parker, J. Kury, C. M. Tarver, W. Quirk, and J. Walton 8 Jul. 1985 11 p refs Presented at the 8th Intern. Symp. on Detonation, Albuquerque, N. Mex., 15 Jul. 1985
(DE85-014809; UCRL-91490; CONF-850705-24) Avail: NTIS HC A02/MF A01

High resolution measurements made by using cylinders and flat plates to determine detonation product behavior are reported. By using thin walled cylinders and thin plates and by utilizing both streak camera and Fabry-Perot velocimeter techniques resolution and accuracy much greater than previously are obtained. Results for an explosive formulation, LX-14, containing 95% HMX and 5% polyurethane and are presented these experimental results of hydrodynamic calculations. Thin plates and varying plate thickness are used to derive the explosive behavior independent of the metal properties. The reaction zone in the explosive is resolved in the acceleration of the thinnest plates. This reaction front behavior is considered in the equation of state description. It is shown that the cylinder test measurements sample the EOS at expansion ratios $V/VO > 1$. Thin flat plates aligned in the plane of the detonation front provide detailed information on the higher compression states. The results of earlier work with respect to the pressure derivatives are confirmed.
DOE

N86-12400# Joint Publications Research Service, Arlington, Va.

NEW CRITERION OF COMBINED-MODE BRITTLE FRACTURE DESCRIBED

Lin Baisong *In its* China Rept.: Sci. and Technol. (JPRS-CST-85-035) 17 Oct. 1985 p 27-33 refs Transl. into ENGLISH from Yingyong Shuxue He Lixue (Chongqing), v. 5, no. 6, Nov. 1984 p 849-853 (For primary document see N86-12399 03-31)
Avail: NTIS HC A08/MF A01

N86-12420# Joint Publications Research Service, Arlington, Va.

COUPLING BETWEEN SPINOR FIELD, PROPAGATING TORSION

Xu Jizhong *In its* China Rept.: Sci. and Technol. (JPRS-CST-85-018) 12 Jun. 1985 p 106-110 refs Transl. into ENGLISH from Wuhan Daxue Xuebao (Wuhan), no. 1, Mar. 1984 p 47-50 (For primary document see N86-12413 03-31)
Avail: NTIS HC A09/MF A01

N86-12374# Tokyo Denki Univ. (Japan). Faculty of Engineering.

EARTHQUAKE-RESPONSE SIMULATION ON HORIZONTALLY LARGE-SCALE BUILDINGS BASED ON THE METHOD OF REDUCTION CONCERNING THEIR RESTORING SPRING MATRIX. DERIVATION OF GENERAL FORM OF SPRING MATRIX AND COMPARISON OF APPLIED RESPONSE RESULTS ON AN ACTUAL BUILDING WITH MEASURED VALUES

Fukuzo Suto and Shyuichi Asayama *In its* Res. Rept. of the Faculty of Eng., Tokyo Denki Univ., No. 32 Dec. 1984 p 13-35 refs In JAPANESE; ENGLISH summary (For primary document see N86-12372 03-31)
Avail: NTIS HC A09/MF A01

N86-12375# Tokyo Denki Univ. (Japan). Faculty of Engineering.

A COMPUTER ANALYSIS OF THE DISTRIBUTION OF PRINCIPAL STRESSES USING PHOTOELASTIC PATTERN

Shoichi Ohi, Makoto Kotani, Masataka Nisida, Seiji Nakajima, and Setsuzo Honda *In its* Res. Rept. of the Faculty of Eng., Tokyo Denki Univ., No. 32 Dec. 1984 p 37-49 refs In JAPANESE;

ENGLISH summary (For primary document see N86-12372 03-31)
Avail: NTIS HC A09/MF A01

42 GEOSCIENCES (GENERAL)

N86-12630# Joint Publications Research Service, Arlington, Va.
USSR REPORT: EARTH SCIENCES Abstracts Only
19 Jun. 1985 91 p Transl. into ENGLISH from various Russian articles
(JPRS-UES-85-006) Avail: NTIS HC A05/MF A01

Research and progress in U.S.S.R. earth sciences are reported. Topics discussed include: meteorology, oceanography, terrestrial geophysics, atmospheric physics, and Arctic and Antarctic research. For individual titles, see N86-12631 through N86-12696.

N86-12631# Joint Publications Research Service, Arlington, Va.
METEOROLOGICAL CENTER'S FORECASTS AID VENUS PROBE TRACKING Abstract Only **c47**
M. Dmitruk *In its* USSR Rept.: Earth Sci. (JPRS-UES-85-006) 19 Jun. 1985 p 1 Transl. into ENGLISH from Sots. Ind. (Moscow), 23 Mar. 1985 p 3 (For primary document see N86-12630 03-42)
Avail: NTIS HC A05/MF A01

Severe-storm warning services provided by the hydrometeorological scientific research center are reported. Warning of hurricane-force winds, heavy precipitation, sharp temperature changes and other severe weather are furnished by this center. Weather maps are prepared by computers which perform 1.5 million operations a second. The computers make it possible to heighten the accuracy and usefulness of information on severe weather phenomena. Accurate forecasts of strong winds over a period of 8 months by the 64 meter radio telescope dish antenna save trouble-free receptions by the antenna of singlas from automatic interplanetary stations which are orbiting Venus. E.A.K.

N86-12632# Joint Publications Research Service, Arlington, Va.
DIAGNOSIS OF WEATHER STATES IN WINTER OF 1980-1981 Abstract Only **c47**
G. P. Kurbatkin *In its* USSR Rept.: Earth Sci. (JPRS-UES-85-006) 19 Jun. 1985 p 2 Transl. into ENGLISH from Izv. Akad. Nauk SSSR: Fiz. Atm. i Okeana (Moscow), v. 20, no. 11, Nov. 1984 p 1011-1016 (For primary document see N86-12630 03-42)
Avail: NTIS HC A05/MF A01

Maps of winter weather states from December 1980 through February 1981 for the Rocky Mountains and Gulf of Alaska are used to study the complex nonlinear mechanisms by which bottom boundary conditions influence changes in atmosphere circulation. The weather states for December and for January are found to differ significantly. The diagnostic estimates show that nonadiabatic processes changing global atmospheric circulation are related to unsteady fluctuations in atmospheric dynamics and are unsteady. The modeling and prediction of changes in such quasisteady weather states is complex. It is recommended that heat fluxes are studied by mathematical models and by direct measurement. E.A.K.

N86-12633# Joint Publications Research Service, Arlington, Va.
MAIN PROBLEMS IN CLIMATE MONITORING (DIAGNOSIS) Abstract Only **c47**
G. V. Gruza, K. G. Rubinshteyn, B. A. Birman, and V. N. Razuvayev *In its* USSR Rept.: Earth Sci. (JPRS-UES-85-006) 19 Jun. 1985 p 2 Transl. into ENGLISH from Izv. Akad. Nauk SSSR: Fiz. Atm. i Okeana (Moscow), v. 20, no. 11, Nov. 1984 p 1017-1026 Original language document was announced in IAA as A85-17976 (For primary document see N86-12630 03-42)
Avail: NTIS HC A05/MF A01

The problem of climate monitoring is examined in the context of the global system of environmental monitoring. In particular, attention is given to the scientific, engineering, and administrative problems involved. A possible organization for a system of climate monitoring in the USSR is proposed, and examples of the experimental monitoring of the earth atmosphere on hemispherical and regional (for the USSR) scales are presented. V.L. (IAA)

N86-12634# Joint Publications Research Service, Arlington, Va.
USE OF METHOD OF CANONICAL CORRELATIONS FOR ANALYSIS OF CLIMATIC SERIES Abstract Only **c47**
M. S. Tatarskaya and M. I. Fortus *In its* USSR Rept.: Earth Sci. (JPRS-UES-85-006) 19 Jun. 1985 p 3 Transl. into ENGLISH from Izv. Akad. Nauk SSSR: Fiz. Atm. i Okeana (Moscow), v. 20, no. 11, Nov. 1984 p 1027-1034 (For primary document see N86-12630 03-42)
Avail: NTIS HC A05/MF A01

The application of the canonical correlations method to problems of statistical climate prediction was studied. The method is applicable to the task of funding functions of future values which are predicted on the basis of past values with minimal error. The method was first applied to meteorology in 1967 to study the statistical relationship between mean monthly water temperature in the North Atlantic and the mean monthly air temperature over the European USSR in December. It is demonstrated that appliction of the method for actual climatic series allows determination of optimal predicted values. The accuracy of prediction of values in some cases such as in the prediction of mean annual temperature values in the 30-80 N latitude zone, can be significantly greater than the prediction of actual values in the series. EAK

N86-12635# Joint Publications Research Service, Arlington, Va.
EMPIRICAL ANALYSIS OF DIRECT AND INVERSE RELATIONSHIPS BETWEEN MACROSCALE CHARACTERISTICS OF ATMOSPHERIC PROCESSES IN NORTHERN HEMISPHERE AND THERMAL STATE OF NORTH ATLANTIC Abstract Only **c47**
M. I. Yudin, V. M. Mirvis, and I. Ye. Chuvashina *In its* USSR Rept.: Earth Sci. (JPRS-UES-85-006) 19 Jun. 1985 p 3-4 Transl. into ENGLISH from Izv. Akad. Nauk SSSR: Fiz. Atm. i Okeana (Moscow), v. 20, no. 11, Nov. 1984 p 1035-1041 (For primary document see N86-12630 03-42)
Avail: NTIS HC A05/MF A01

New empirical data are presented on direct and inverse relationships in the ocean-atmosphere system. The data are summarized and the hypothesis that there are a number sequences of direct and inverse relationships and self-oscillating processes is confirmed. The initial data used consisted of monthly values of changes in heat content in the upper 100-meter water layer in the North Atlantic between 1949 and 1982. The relationship of cloud cover and the thermal state of the ocean was analyzed. The statistical analysis reveals a cyclic processes in the ocean-atmosphere system, and chains of direct and inverse relationships. Cold-season North Atlantic heat content anomalies are significant for subsequent development of large-scale atmospheric processes, which in turn cause disturbances in the thermal state of the ocean. EAK

N86-12636# Joint Publications Research Service, Arlington, Va.
ATMOSPHERIC AEROSOL AND ITS EFFECTS ON CLIMATE Abstract Only **c47**
K. Ya. Kondratyev and M. A. Prokofyev *In its* USSR Rept.: Earth Sci. (JPRS-UES-85-006) 19 Jun. 1985 p 4-5 Transl. into ENGLISH from Izv. Akad. Nauk SSSR: Fiz. Atm. i Okeana (Moscow), v. 20, no. 11, Nov. 1984 p 1055-1063 (For primary document see N86-12630 03-42)
Avail: NTIS HC A05/MF A01

The influence of atmospheric aerosol on climate is discussed. The importance of the contribution of aerosol-radiation effects to the energy budget of the atmosphere was studied. It is reported that large-scale systematic dust episodes in the troposphere are related to deserts and volcanic phenomena. Formulation of models of the radiation and microphysical properties of aerosol were considered. The climatic effects of tropospheric and stratospheric are distinguished. Major trends are noted for the climatic effect of aerosols: (1) development of a realistic aerosol model for climate sensitivity studies; (2) comparison of existing radiation transfer models which take aerosol effects into account; (3) inclusion of radiation transfer parameters in the atmosphere with the aerosol in climatic models; and (4) determination of global aerosol types necessary for climatic modeling by model experiments. EAK

N86-12637# Joint Publications Research Service, Arlington, Va.
INFLUENCE OF POWER ENGINEERING ON CLIMATE Abstract Only c47
V. A. Legasov, I. I. Kuzmin, and A. N. Chernoplekov *In its* USSR Rept.: Earth Sci. (JPRS-UES-85-006) 19 Jun. 1985 p 6 Transl. into ENGLISH from Izv. Akad. Nauk SSSR: Fiz. Atm. i Okeana (Moscow), v. 20, no 11, Nov. 1984 p 1089-1103 (For primary document see N86-12630 03-42)
Avail: NTIS HC A05/MF A01

The influence of power production on changes in global climate to estimate the effect of this factor over the long term on possible limitations in the increase in power consumption and the structure and fuel power balance was studied. The scale of the effect of powerplants on climate and the possible nature of these effects was estimated and, power engineering is determined to be a significant climate-altering factor, requiring consideration of climatic effects in the determination of power development strategies. The ecological aspects of the problem of safe development of power engineering must include determination of the effectiveness of appropriations for protection of the earth from the danger from possible climatic change. Defining quantitative indices reflecting changes in climate with sufficient accuracy is a major problem. E.A.K.

N86-12638# Joint Publications Research Service, Arlington, Va.
RECENT CHANGES IN CLIMATE AND WORLD WATER BALANCE Abstract Only c47
S. G. Dobrovolskiy and R. K. Klinge *In its* USSR Rept.: Earth Sci. (JPRS-UES-85-006) 19 Jun. 1985 p 6 Transl. into ENGLISH from Izv. Akad. Nauk SSSR. Ser. Geogr. (Moscow), no. 1, Jan. - Feb. 1985 p 31-38 (For primary document see N86-12630 03-42)
Avail: NTIS HC A05/MF A01

Water exchange between the ocean and the landmasses free of continental glaciation occurs by fluxes of mositure whose deviations from the mean in individual years are not dependent on one another and which are only slightly related to changes in the global temperature regime. In the series of water balance components for the continents there are no long-term trends. The fluctuations of the mean annual mositure fluxes exchanged between the oceans and continents are determined by a combination of local evaporation factors. This is consistent with the Hasselmann stochastic theory of climate. There is only a slight correlation between iceberg runoff and macroscale changes in the temperature regime, and the correlation between iceberg runoff and precipitation series. Changes in the annual increments of water volume in the ocean also have a stochastic character. The principal contribution to variability of the annual increments of water volumes in the oceans and water reserves on the land however, iceberg runoff, primarily from Anterctica. It is suggested that the changes is in volume of continental glaciation and ocean level are less sensitive to changes in air temperature than to changes in the precipitation regime. Precipitation falling on the continental glaciers, especially in Antarctica, is the most probable mechanism of changes in ocean level in the near future. E.A.K.

N86-12639# Joint Publications Research Service, Arlington, Va.
CLIMATICALLY ACTIVE TRACE GASES IN ATMOSPHERE Abstract Only c47
I. L. Karol *In its* USSR Rept.: Earth Sci. (JPRS-UES-85-006) 19 Jun. 1985 p 5 Transl. into ENGLISH from Izv. Akad. Nauk SSSR: Fiz. Atm. i Okeana (Moscow), v. 20, no. 11, Nov. 1984 p 1064-1074 Original language document was announced in IAA as A85-17981 (For primary document see N86-12630 03-42)
Avail: NTIS HC A05/MF A01

The global atmospheric cycles of trace gases affecting solar and thermal radiation fluxes and their anthropogenic changes are briefly reviewed. The gases discussed include methane, nitrogen oxides, tropospheric ozone, and chlorofluorohydrocarbons. The contribution of these gases to the greenhouse effect and the influence of the greenhouse effect on the photochemistry of the trace gases in the atmosphere are analyzed. Model estimates of the variance of the mean annual surface air temperature in the Northern Hemisphere due to a measured increase in the content of trace gases in the atmosphere are presented. V.L. (IAA)

N86-12640# Joint Publications Research Service, Arlington, Va.
ESTIMATE OF RADIATION-CLIMATIC EFFECTS OF NATURAL AND ANTHROPOGENIC AEROSOL Abstract Only c47
N. I. Manuylova, V. K. Petukhov, T. A. Tarasova, and Ye. M. Feygelson *In its* USSR Rept.: Earth Sci. (JPRS-UES-85-006) 19 Jun. 1985 p 5 Transl. into ENGLISH from Izv. Akad. Nauk SSSR: Fiz. Atm. i Okeana (Moscow), v. 20, no. 11, Nov. 1984 p 1075-1080 (For primary document see N86-12630 03-42)
Avail: NTIS HC A05/MF A01

Investigation and parameterization of the radiation aerosol effect are presented. Radiation effects of aerosol lead to changes into the albedo and absorptive capacity of the climatic system, resulting in restructuring of its dynamic parameters. The change in mean global albedo for the system is estimated for aerosols of varying optical thickness and absorptive capacity. The absorptive capacity is the major climate-forming parameter of aerosol, along with the number and size of aerosol particles. The aerosol significantly influences the temperature status of the climatic system primarily through direct changes in system albedo, to a lesser extent by the restructuring of the system caused by the aerosol. E.A.K.

N86-12641# Joint Publications Research Service, Arlington, Va.
MODELING OF SEASONAL EVOLUTION OF CARBON CYCLE IN OCEAN-ATMOSPHERE SYSTEM Abstract Only c46
B. A. Kagan, V. A. Ryabchenko, and A. S. Safray *In its* USSR Rept.: Earth Sci. (JPRS-UES-85-006) 19 Jun. 1985 p 13 Transl. into ENGLISH from Izv. Akad. Nauk SSSR: Fiz. Atm. i Okeana (Moscow), v. 21, no. 1, Jan. 1985 p 66-75 (For primary document see N86-12630 03-42)
Avail: NTIS HC A05/MF A01

A combined model for the seasonal evolution of heat conditions and the carbon cycle in the ocean-temperature system is proposed. The atmosphere and ocean in the northern hemisphere are represented as a system of five interconnected boxes - two atmospheric and three oceanic. The two oceanic boxes are the upper quasihomogeneous layer and the deep layer of the ocean in the temperature and lower latitudes, within which the influx of heat from the atmosphere is balanced by vertical advection of cold deep waters. It is shown that the major factors determining the mean values and seasonal variability of characteristics of the carbon cycle in the ocean-atmosphere system are the existence in the ocean of cold deep water formations with sharp increases in rate of absorption of atmospheric CO2, fluctuation of sources and sinks of organic CO2 and variation of ocean water temperatures. External factors include the short-wave solar radiation flux at the upper atmosphere boundary, absorption and emission of short wave and long wave radiation, atmospheric and surface albedo, mean annual production, consumption and half-life of organic matter, ocean depth, wind speed, humidity and continental area. E.A.K.

N86-12642# Joint Publications Research Service, Arlington, Va.
STUDY OF SIGNIFICANCE OF BOTTOM RELIEF IN BAROCLINIC MODEL OF EQUATORIAL COUNTERCURRENT Abstract Only c48
T. F. Kuzmicheva, E. N. Mikhaylova, and N. B. Shapiro *In its* USSR Rept.: Earth Sci. (JPRS-UES-85-006) 19 Jun. 1985 p 14 Transl. into ENGLISH from Izv. Akad. Nauk SSSR: Fiz. Atm. i Okeana (Moscow), v. 21, no. 1, Jan. 1985 p 58-65 (For primary document see N86-12630 03-42)
Avail: NTIS HC A05/MF A01

Time variability and nonlinear interaction of barotropic and baroclinic components of current velocity was studied, taking into account bottom relief in the process of formation of an equatorial countercurrent under the influence of an easterly wind and the heat flux through the ocean surface. The wind and heat flux excite circulation in the upper layer of the ocean. Processes in the baroclinic layer, acting though vertical movements at its lower boundary, cause movement in the deeper layers. During the initial stage, deep circulation does not match the bottom relief, the velocities of barotropic currents are high, particularly in shallow areas, and may significantly influence the current in the baroclinic layer. As time passes, deep currents and currents in the baroclinic layer adapt to the bottom relief, which is accompanied by a reduction in horizontal velocity gradients over submerged elevations. E.A.K.

N86-12643# Joint Publications Research Service, Arlington, Va.
ANGULAR DISTRIBUTION OF INTENSITY OF SOUND RERADIATED BY OCEAN SURFACE AT SMALL GLANCING ANGLES Abstract Only c71
Ye. A. Kopyl *In its* USSR Rept.: Earth Sci. (JPRS-UES-85-006) 19 Jun. 1985 p 14 Transl. into ENGLISH from Izv. Akad. Nauk SSSR: Fiz. Atm. i Okeana (Moscow), v. 21, no. 1, Jan. 1985 p 98-101 (For primary document see N86-12630 03-42)
Avail: NTIS HC A05/MF A01

A quantitative interpretation of field measurements of the angular stucture of signals reradiated by the ocean surface with glancing incidence of acoustical waves is presented. Experimental and calculated values agree satisfactorily. E.A.K.

N86-12644# Joint Publications Research Service, Arlington, Va.
INFLUENCE OF SHORT GRAVITY WAVES ON THERMAL RADIO EMISSION OF WATER SURFACE Abstract Only c32
V. A. Ilin, A. A. Naumov, V. Yu. Rayzer, S. R. Filonovich, and V. S. Etkin *In its* USSR Rept.: Earth Sci. (JPRS-UES-85-006) 19 Jun. 1985 p 15 Transl. into ENGLISH from Izv. Akad. Nauk SSSR: Fiz. Atm. i Okeana (Moscow), v. 21, no. 1, Jan. 1985 p 83-89 (For primary document see N86-12630 03-42)
Avail: NTIS HC A05/MF A01

An experimental study is presented of the thermal radio emission caused by short waves, accompanied by a quantitative interpretation of the data obtained. Emphasis is on an analysis of the variation in radio brightness contrast as a function of steepness of the short gravity waves, measured by means of a high-frequency radiometer operating in the lambda = 0.8 cm range. Waves were artificially generated in a small channel, wavelength 8 to 40 cm, height 0.6 to 3 cm. Due to the high sensitivity of the radiometric apparatus used, effects were recorded which were related to the influence of the profile and steepness of the short gravity waves. The possibility of using the geometrical optics approximation for quantitative interpretation of the experimental data is demonstrated. The model is based on essentially non-Gaussian statistics of slopes corresponding to quasimonochromatic waves of finite amplitude. Author

N86-12645# Joint Publications Research Service, Arlington, Va.
UPPER MESOZOIC TURBIDITES OF SOUTHERN WEST SAKHALIN DOWNWARP Abstract Only c46
S. V. Zyabrev *In its* USSR Rept.: Earth Sci. (JPRS-UES-85-006) 19 Jun. 1985 p 15-16 Transl. into ENGLISH from Tikhookeanskaya Geol. (Novosibirsk), no. 5, Sep. - Oct. 1984 p 22-33 (For primary document see N86-12630 03-42)
Avail: NTIS HC A05/MF A01

In the west Sakhalin downwarp the Albian deposits are very thick terrigenous masses, nonuniform alternations of sandstones, siltstones and argillites with some other rocks formed by erosion of the products of underwater and continental volcanism. The textures and specifics of stratification of deposits in the southern portion of the west Sakhalin downwarp were studied in order to determine the origin of the sedimentary formations, conditions of sedimenation and their evolution. The deposits are interpreted as turbidities. Western sources of clastic material were established. The deposits were formed in deep-water alluvial fan systems at the base of a deep water slope dropping down toward the east. Ancient currents confirm the western sources of clastic material and indicate significant separation from the eastern edge of the basin. Changes in facies in the section in a lateral direction are not related to transgressions and regressions on the eastern side of the downwarp, but rather reflect the specifics of the sedimentation process. Traces of erosion and redeposition of argillite and sandstone fragments are not related to erosion of the eastern side of the downwarp but rather to the sedimentation process itself. Author

N86-12646# Joint Publications Research Service, Arlington, Va.
SPECTRUM OF TURBULENT FLUCTUATIONS IN SEA WATER DENSITY IN REGION OF LARGE WAVE NUMBERS Abstract Only c48
M. A. Bramson, A. D. Fedorovskiy, V. I. Nikishov, and G. L. Luchnik *In its* USSR Rept.: Earth Sci. (JPRS-UES-85-006) 19 Jun. 1985 p 16 Transl. into ENGLISH from Dokl. Akad. Ukr. SSR, Ser. A: Fiz-Mat. i Tekhn. Nauki (Kiev), no. 12, Dec. 1984 p 35-38 (For primary document see N86-12630 03-42)
Avail: NTIS HC A05/MF A01

The study of turbulent pulsations of velocity, temperature, salinity and density, and particularly of the behavior of spectral characteristics on the small scale, is an important subject in current studies of the ocean. The pulsation spectrum of the density of sea water in the region of large wave numbers was analyzed. Turbulent inhomogeneities of the fields of temperature and salinity on a small scale are also analyzed. The spectral characteristics of pulsations of the density field and the boundary of the viscous-convective interval are determined by two parameters which can be measured by simultaneous recording of T and S pulsations by two sensors separated by a known distance. The averaging interval for the measurements can be rather small since the spatial scale corresponding to the viscous-convective internal is small. Processing of measurements can be alternated. Author

N86-12647# Joint Publications Research Service, Arlington, Va.
INTERACTION OF SOUND WAVES WITH FINE THERMOHALINE STRUCTURES OF OCEAN Abstract Only c48
V. V. Artelnyy and M. A. Rayevskiy *In its* USSR Rept.: Earth Sci. (JPRS-UES-85-006) 19 Jun. 1985 p 17 Transl. into ENGLISH from Akust. Zh. (Moscow), v. 30, no. 6, Nov. - Dec. 1984 p 728-734 (For primary document see N86-12630 03-42)
Avail: NTIS HC A05/MF A01

The interaction of acoustical waveguides with the fine thermohaline structure of the ocean is analyzed on the assumption of multiple scattering. A study is made of a number of effects occurring in a broad class of waveguides as a result of the presence of a fine structure, including attenuation of the coherent component of the sound field, changes in its angular spectrum, transformation of normal mode energy and losses resulting from pumping of energy from nodes localized in the waveguide to modes attenuation in the surrounding ground. The results obtained are extended by means of a passage to the limit to the case of a channel with a sudden change in the speed of sound. The main results of the study are extended to the case of an underwater channel with a balanced profile. Author

N86-12648# Joint Publications Research Service, Arlington, Va.
CORRELATION CHARACTERISTICS OF SIGNALS REFLECTED BY THE WAVY SURFACE OF OCEAN IN MIRROR DIRECTION Abstract Only c32
Yu. Yu. Zhitkovskiy, A. V. Nosov, and V. V. Savelyev *In its* USSR Rept.: Earth Sci. (JPRS-UES-85-006) 19 Jun. 1985 p 18 Transl. into ENGLISH from Akust. Zh. (Moscow), v. 30, no. 6, Nov. - Dec. 1984 p 772-776 (For primary document see N86-12630 03-42)
Avail: NTIS HC A05/MF A01

An experimental study was carried out to determine the correlation characteristics of pseudonoise signals reflected from a wave-covered surface in the mirror direction. The major measured quantity was the reciprocal correlation coefficient between the transmitted signal and the reflected signal. The transmitter was lowered from a ship on a 150 m cable. The receiver and preamplifier were lowered to the same depth from a buoy which was allowed to drift from the ship to a distance of 100-500 m, the changing distance changing the angle of the beam reflected from the surface of the ocean back down to the hydrophone. The radiator transmitted a pulsed signal with a pseudonoise carrier. The results were interpreted within the framework of ordinary correlation theory by processing several recordings, calculating the sign and ordinary correlation coefficients to determine the variation in sign correlation coefficient as a function of the ordinary correlation coefficient. Graphs of the average variation are presented. It was found that the medium did not distort the signal as it propagated through the water mass (within the limits of experimental accuracy). The correlation coefficient between the transmitted and reflected signals is thus determined entirely by the characteristics of reradiation of the sound by the wavecovered surface. Author

N86-12649# Joint Publications Research Service, Arlington, Va.
NUMERICAL ESTIMATE OF EFFECTIVENESS OF APPROXIMATE EQUATIONS FOR ACOUSTIC FIELD NEAR SURFACE OF DEEP SEA
c71
M. V. Perel *In its* USSR Rept.: Earth Sci. (JPRS-UES-85-006) 19 Jun. 1985 p 18 Transl. into ENGLISH from Akust. Zh. (Moscow), v. 30, no. 6, Nov. - Dec. 1984 p 813-818 (For primary document see N86-12630 03-42)
Avail: NTIS HC A05/MF A01

The acoustic field in an oceanic waveguide is calculated. The calculations for various velocity profiles confirm the effectiveness of the approximate equations of V. S. Buslayev. Author

N86-12650# Joint Publications Research Service, Arlington, Va.
PETROCHEMICAL TYPES OF MAGMATIC ROCKS OF OCEAN FLOOR AND PATTERNS OF THEIR DISTRIBUTION Abstract Only
c46
A. V. Abramov, V. M. Ryakhovskiy, and Yu. V. Mironov *In its* USSR Rept.: Earth Sci. (JPRS-UES-85-006) 19 Jun. 1985 p 19 Transl. into ENGLISH from Byul. Mosk. Obshch. Ispytateley Prirody: Otd. Geol. (Moscow), v. 60, no. 1, Jan. - Feb. 1985 p 18-27 (For primary document see N86-12630 03-42)
Avail: NTIS HC A05/MF A01

In order to classify petrochemical data on ocean floor crustal rocks an algorithm for processing multivariate samples, a nonparametric classification method was used. The classification includes no priori assumptions concerning the structure of the sample and introduces no predefined numerical criteria. The distances between points are applicable to samples with any multivariate distrition. The initial data used were compositions of magmatic oceanic rock from a previous publication. The processing allowed the following numbers of clusters to be distinguished in the sample in each of the four steps: 239, 90, 29. 7. The seven final clusters are described. It is concluded that the absence of unidirectional petrochemical evolution of oceanic basalts upon transition from one morphological structure to another and their sharp petrochemical specialization in this case indicate the relative nondependence of the paths of development of different morphostructural zones in the ocean floor. Author

N86-12651# Joint Publications Research Service, Arlington, Va.
INTRUSIVE ROCKS OF OCEANIC LITHOSPHERE AS POSSIBLE SOURCES OF ANOMALOUS MAGNETIC FIELD OF OCEAN Abstract Only
c46
Ye. A. Nazarova *In its* USSR Rept.: Earth Sci. (JPRS-UES-85-006) 19 Jun. 1985 p 19-20 Transl. into ENGLISH from Byul. Mosk. Obshch. Ispytateley Prirody: Otd. Geol. (Moscow), v. 60, no. 1, Jan. - Feb. 1985 p 28-41 (For primary document see N86-12630 03-42)
Avail: NTIS HC A05/MF A01

Results are presented from study of rock dredged from the ocean floor, plus data published in a previous review on the magnetic characteristics of 50 oceanic intrusive rocks brought up during several cruises of the Glomar Challenger. The intrusive rocks represent a cross-section of the oceanic crust. The samples available are very few in number. Available data on ore mineralogy and magnetic characteristics are analyzed for the available specimens. Analysis of the magnetic characteristics of the rocks shows that neither fresh cumulative gabbro containing fine-grained magnetite nor amphibolitized serpentinized gabbro containing magnetite grains from pseudo-single-domain to multi-domain size can be considered regulator sources of linear magnetic anomalies. Thin dolerite sills containing fine-grained magnetite with hardened edges may be sources of local magnetic anomalies. Periodotites representing the lower portion of layer 3B and the upper mantle, upon sepentinization, as a result of the formation of secondary magnetite, take on intensive and stable chemical magnetization. Only serpentinized cumulative peridotites have the necessary magnetic characteristics to be sources of linear magnetic anomalies. Author

N86-12652# Joint Publications Research Service, Arlington, Va.
MAGMATIC PROVINCES AND TECTONICS IN PACIFIC OCEAN Abstract Only
c46
Yu. M. Pushcharovskiy *In its* USSR Rept.: Earth Sci. (JPRS-UES-85-006) 19 Jun. 1985 p 21 Transl. into ENGLISH from Izv. Akad. Nauk SSSR: Ser. Geol. (Moscow), no. 11, Nov. 1984 p 13-18 (For primary document see N86-12630 03-42)
Avail: NTIS HC A05/MF A01

A determination of correlations between the large structural formations and basalt magmatism of the Pacific Ocean floor is very important for an approach to the geological history problems of this area. There have been at least two major tectonic-magmatic stages in the central and northwestern Pacific. Each major stage reflects a unique combination of geological conditions. The possibility of distinguishing and differentiating magmatic provinces allows basaltic series differing in their petrochemical features and content of individual metals to be distinguished. Analysis of the composition of mantle tectonics has shown regional differences in the composition of the upper mantle existing before the partial melting with which the formation of specific complexes is associated. The correlation which has been observed between magmatism and major tectonic elements and regions in the Pacific indicates the complex picture of geological development of the lithosphere in this area, which cannot be reduced to simplified systems of movement of a homogeneous lithospheric monolith. Implementation of the Soviet research project Litos will provide important new data on the geology of the oceans. However, additional specialized marine expeditions in different oceans are required to supplement the available factual information. Author

N86-12653# Joint Publications Research Service, Arlington, Va.
GEOCHEMISTRY AND ENERGETICS OF CYCLING OF MATTER IN FORMATION OF CRUST IN ACTIVE STRUCTURES OF OCEAN Abstract Only
c48
V. A. Ilin and A. V. Shcherbakov *In its* USSR Rept.: Earth Sci. (JPRS-UES-85-006) 19 Jun. 1985 p 22 Transl. into ENGLISH from Dokl. Akad. Nauk SSSR (Moscow), v. 279, no. 5, Dec. 1984 p 1184-1189 (For primary document see N86-12630 03-42)
Avail: NTIS HC A05/MF A01

A geochemical model was developed to check the quantiative relationships between the sedimentary and volcanogenic matter during the course of the cycling of matter related to the formation of the crust in active ocean structures. The model shows that the subduction zone should receive iron and magnesium ions from the mantle. Remaining elements are carried into the crust, the accumulation of silica and alumina in the crust supporting constant oxidation. The problem of the high content of Ca in sedimentary rock and the shift of the Na/K ratio in the direction of K are explained. The model thus explains the observed chemical differentiation between continental and oceanic crusts, as well as the mechanism of their development and evolution. Processes of transformation of an oceanic crust to a continental crust in subduction zones are calculated to require 7.5 x 10 to the 18 calories of heat per year. the hydrothermal process on the continents and ocean floor consumes 8.0 x 10 to the 18 cal/yr, 6.4 x 10 to the 18 cal/yr being carried away by hydrotherms and 1.6 x 10 to the 18 cal/yr being absorbed by deep hydrothermal systems. This means that the major effect of hydrothermal activity is restricted to the midocean ridges, only one-fifth being associated with volcanic regions. Author

N86-12654# Joint Publications Research Service, Arlington, Va.
CONTRIBUTION OF DIFFUSION PROCESSES TO THE ELECTRIC FIELD OF THE OCEAN Abstract Only c48
P. Ya. Tishchenko *In its* USSR Rept.: Earth Sci. (JPRS-UES-85-006) 19 Jun. 1985 p 24 Transl. into ENGLISH from Dokl. Akad. Nauk SSSR (Moscow), v. 279, no. 5, Dec. 1984 p 1234-1236 (For primary document see N86-12630 03-42)
Avail: NTIS HC A05/MF A01

A study was made of that portion of the electric field in the ocean which results from diffusion of ions in sea water due to the presence of concentration gravitational and temperature fields. Methods of linear nonequilibrium thermodynamics are used in the study. An electric profile was computed to establish the magnitude and nature of the electric field in the ocean caused by the processes in question, corresponding to an arbitrary hydrophysical profile. All three contributions to the total electric field considered are of the same order of magnitude. The maximum electric field gradients are found in the upper levels of the ocean where the changes in parameters t and S are greater. Author

N86-12655# Joint Publications Research Service, Arlington, Va.
OIL AND GS DEPOSITS ON CONTINENTAL SLOPES OF THE OCEAN Abstract Only c43
A. A. Geodekyan, A. Zabanbark, and A. I. Konyukhov *In its* USSR Rept.: Earth Sci. (JPRS-UES-85-006) 19 Jun. 1985 p 24-25 Transl. into ENGLISH from Dokl. Akad. Nauk SSSR (Moscow), v. 280, no. 2, Jan. 1985 p 423-426 (For primary document see N86-12630 03-42)
Avail: NTIS HC A05/MF A01

It has been suggested that some 95% of the hydrocarbon deposits in the ocean will probably be found in shelf zones and on the continental slopes at depths of not over 3,000 m and 65% not over 300 m. Some twenty-six deposits of oil, gas and gas condensate were found to date on the continental slopes of the ocean. Almost all hydrocarbon deposits are located on the slopes of the passive continental margins of the Atlantic and Indian Oceans. The collectors for oil and gas deposits are almost exclusively sandstones. Analysis of known deposits shows that ancient delta complexes on the continental margins contain oil and gas not only because they are characterized by good collectors, but also primarily due to the optimal relationship of natural reservoirs, continental rock and cover horizons. There are two stages in the formation of regional oil- and gas-bearing terrigenous masses, genetically related to rivers: periods of rift formation and burial of continental margins, and periods of cretaceous or early Cenozoic tectonic activation within the limits of a margin already formed, during which sinking occurred in the areas where ancient transverse rifts met the ocean. Author

N86-12656# Joint Publications Research Service, Arlington, Va.
ACOUSTICAL FIELD OF DIRECTIONAL SOURCE IN OCEANIC WAVEGUIDES Abstract Only c71
G. I. Bykovtsev, G. N. Kuznetsov, and A. N. Stepanov *In its* USSR Rept.: Earth Sci. (JPRS-UES-85-006) 19 Jun. 1985 p 25 Transl. into ENGLISH from Dokl. Akad. Nauk SSSR (Moscow), v. 280, no. 1, Jan. 1985 p 57-59 (For primary document see N86-12630 03-42)
Avail: NTIS HC A05/MF A01

A model is suggested for an equivalent point source having arbitrary directionality to replace actual sound sources radiating in an ocean waveguide. The model allows calculation of the hydroacoustical fields of directional sources in a medium limited by division boundary surfaces for sufficiently low radiating frequencies. Expressions are obtained for the potential of an equivalent point source in waveguides of various types. By minimizing the maximum likelihood functional it is possible to use measured pressure values to estimate the multipole moments determining the directionality of radiation. The parameter estimation procedure using this method is better than when a Taylor expansion model is used. Author

N86-12657# Joint Publications Research Service, Arlington, Va.
PETROLOGIC ASPECT OF FORMATION OF GEOSTRUCTURES IN MARGINAL SEAS Abstract Only c46
L. L. Perchuk *In its* USSR Rept.: Earth Sci. (JPRS-UES-85-006) 19 Jun. 1985 p 25-26 Transl. into ENGLISH from Dokl. Akad. Nauk SSSR (Moscow), v. 280, no. 1, Jan. 1985 p 178-182 (For primary document see N86-12630 03-42)
Avail: NTIS HC A05/MF A01

A study was made of the petrology of formation of geological structures in the marginal seas, since data are not available relating geodynamics and magmatism of intracontinental depressions. It was demonstrated in the example of the Sea of Japan that the formation of depressions is preceded by orogeny with superimposed acid and neutral magmatism and subsequent intensive denudation of volcanic structures. A change in the direction of vertical motion corresponds to predominance of andesites and basalts in volcanism, accumulation of thick masses of tuffs in narrow geosynclinal depressions, followed by intensive underwater flows of andesite-basalts and basalts. The hypothesis suggesting formation of depressions by the mechanism of magmatic substitution must be further experimentally and theoretically developed and confirmed. Author

N86-12658# Joint Publications Research Service, Arlington, Va.
SPREADING IN DEVELOPMENT OF OCEANIC STRUCTURES Abstract Only c46
Yu. M. Pushcharovskiy and S. V. Ruzhentsev *In its* USSR Rept.: Earth Sci. (JPRS-UES-85-006) 19 Jun. 1985 p 26 Transl. into ENGLISH from Dokl. Akad. Nauk SSSR (Moscow), v. 280, no. 1, Jan. 1985 p 182-185 (For primary document see N86-12630 03-42)
Avail: NTIS HC A05/MF A01

Data on the time of formation of tholeiitic basalts of different ages in the midocean ridges are incomplete. Based on studies of the East Pacific Rise and the western limb of the Mid-Atlantic Ridge, an attempt is made to explain differences in the structure of the first and second layers of the ocean on the one hand and volcanic-sedimentary series of various stages of development of eugeosynclinal zones in the Paleozoic folded belts on the other. Among the widely varied structures of the oceanic crust, the contemporary oceans represent a type characterized by the presence of a single world system of narrow volcanically active ocean spreading centers. Reconstructed paleoocean structures arose in a more complex geodynamic situation than the oceans. They are characterized by distributed spreading, which appeared in the contemporary oceans in the early stages of their development. The essence of evolution of the Phanerozoic structures with the oceanic type crust was one of changes from smaller but more complex structures and combinations to larger and simpler structures. The mesooceans can be considered transitional structures. Author

N86-12659# Joint Publications Research Service, Arlington, Va.
INFLUENCE OF WATER VAPOR ON DISTRIBUTION OF TURBULENT WAVE PARAMETERS Abstract Only c02
N. N. Pilyugin and S. G. Tikhomirov *In its* USSR Rept.: Earth Sci. (JPRS-UES-85-006) 19 Jun. 1985 p 26-27 Transl. into ENGLISH from Mekhan. Zhidkosti i Gaza (Moscow), no. 1, Jan. - Feb. 1985 p 138-142 (For primary document see N86-12630 03-42)
Avail: NTIS HC A05/MF A01

An experimental study was made of phenomena transpiring in an air flow near models flying on an aeroballistic path at hypersonic velocities. The objective was a determination of the influence of water vapor on measurements of gas parameters such as electron concentration or radiation intensity. The results are given of computations of the distributions of nonequilibrium parameters in a wake with allowance for chemical reactions in the air and water vapor under conditions characteristic for aeroballistic experiments. Specifically, the authors give a solution of equations for an axisymmetric turbulent boundary layer describing a current of a nonequilibrium multicomponent gas in the distant wake behind such a body moving at hypersonic velocity. On this basis a model of chemical kinetics is presented which takes 22 components into account. A total of 91 reactions is possible. A list of reactions between dry air components is given, as well as reactions with the participation of components containing hydrogen. It is shown that use of the proposed chemical kinetics model and computation method make it possible to compute parameters of a distant wake more precisely than by the Schapker method. It is clearly demonstrated that in the interpretation of the results of ballistic measurements for measuring the intensity of chemiluminescent radiation and electron concentration in a distant air wake it is necessary that the influence of water vapor be taken into account. Author

N86-12660# Joint Publications Research Service, Arlington, Va.
DIFFRACTION OF INTERNAL WAVES DESCRIBED BY EQUATION OF SLIGHTLY STRATIFIED FLUID ON HALF-PLANE Abstract Only c34
A. T. Ismail-Zade *In its* USSR Rept.: Earth Sci. (JPRS-UES-85-006) 19 Jun. 1985 p 27-28 Transl. into ENGLISH from Izv. Akad. Nauk Azerb. SSR, Ser. Nauk o Zemle (USSR), no. 5, 1984 p 76-83 (For primary document see N86-12630 03-42)
Avail: NTIS HC A05/MF A01

The diffraction of plane waves in a sliightly exponentially stratified fluid on a plane barrier placed in this fluid was investigated. The problem is pertinent with respect to the study of internal waves in the ocean. The considered problem is regarded as highly unusual from the mathematical point of view because it is formulated as a boundary value problem for a hyperbolic equation with boundary conditions characteristic for elliptical equations. It was demontrated long ago that such a formulation is incorrect if only a limited region is examined but the problem is well formulated and has physical sense in the case of unlimited regions when there are appropriate conditions in the neighborhood of an infinitely distant point. The formulation and results are compared with a series of studies along these lines by S. A. Gabov, et al. It is shown that the diffraction pattern obtained with Beta squared yields O outside a restricted region differs qualitatively from the diffraction pattern examined by Gamov. Specifically, the neglecting of the term Beta squared U in the Klein-Gordon equation, employed by Gamov, gives erroneous results. Author

N86-12661# Joint Publications Research Service, Arlington, Va.
POSSIBILITY OF SOUNDING EARTH BY USING ELECTROMAGNETIC FIELD OF SEA CURRENT Abstract Only c46
V. P. Smagin, G. A. Fonarev, and V. N. Savchenko *In its* USSR Rept.: Earth Sci. (JPRS-UES-85-006) 19 Jun. 1985 p 29 Transl. into ENGLISH from Izv. Akad. Nauk SSSR: Fiz. Zemli (Moscow), no. 2, Feb. 1985 p 70-74 (For primary document see N86-12630 03-42)
Avail: NTIS HC A05/MF A01

The possibilities of determining the conductivity of bottom rocks by measuring different combinations of components of the electromagnetic field of a current on the ocean floor are analyzed. It is shown that the sea current induces an electromagnetic field in the geomagnetic field. Then a formula is derived for the magnetic component B. After determining B it is possible to find the electric field in sea water and in rocks beneath the ocean layer. The parameter epsilon is introduced which makes it possible to ascertain the vertical gradient of the magnetic field in bottom rocks; a function is derived which characterizes the magnetic field in the bottom rocks. Formulas are derived which can be used in estimating the width of a current by an electromagnetic method. It is shown, therefore, that with electromagnetic sounding in the fields of sea currents it is possible to make a simple interpretation of the experimental data within the framework of an exponential model of ocean floor conductivity. Author

N86-12662# Joint Publications Research Service, Arlington, Va.
ELECTROMAGNETIC FIELD OF THREE-DIMENSIONAL SURFACE SEA WAVES Abstract Only c48
V. V. Sochelnikov *In its* USSR Rept.: Earth Sci. (JPRS-UES-85-006) 19 Jun. 1985 p 29-30 Transl. into ENGLISH from Izv. Akad. Nauk SSSR: Fiz. Zemli (Moscow), no. 2, Feb. 1985 p 65-69 (For primary document see N86-12630 03-42)
Avail: NTIS HC A05/MF A01

Numerous attempts have been made to obtain estimates of the electromagnetic field of three-dimensional sea waves. Use has been made of hypothetical models with an eddy distribution of velocity through the entire fluid layer. Since these efforts have been largely unsuccessful, and effort was made to obtain a rigorous solution for the electromagnetic field of three-dimensional sea waves of wind origin. The same assumptions are made s for a model of a two-dimensional wave. First an expression is derived for the velocity of fluid particles, making is possible to proceed to the derivation of expressions for the induced electromagnetic field. It is shown that the induced electric field is a potential field. Formulas are then found that show that the induced electric field is not dependent on the conductivity of the ambient medium; the current does not flow into the bottom and therefore the magnetic field should not be dependent on bottom conductivity; the induced electromagnetic field is completely determined by the vertical component H sub Z (TJ-wave). All this is demonstrated and expressions are derived for the components of strength or the induced magnetic field. The induced magnetic field is dependent only on sea water conductivity. Since the EM field induced by three-dimensional sea waves is not dependent on bottom conductivity it cannot be used for its electromagnetic sounding. The induced field (as in the case of two-dimensional sea waves) is noise in electromagnetic research in the sea. Author

N86-12663# Joint Publications Research Service, Arlington, Va.
STRATIGRAPHY OF SEDIMENTS IN CENTRAL AND EASTERN MEDITERRANEAN Abstract Only c46
V. M. Sorokin, M. S. Afanasyeva, V. G. Kurenkova, and N. B. Chernyshova *In its* USSR Rept.: Earth Sci. (JPRS-UES-85-006) 19 Jun. 1985 p 30 Transl. into ENGLISH from Izv. Akad. Nauk SSSR: Ser. Geol. (Moscow), no. 2, Feb. 1985 p 59-64 (For primary document see N86-12630 03-42)
Avail: NTIS HC A05/MF A01

In many parts of the Mediterranean there have been only limited stratigraphic studies. The least attention has been given to the near-shore portions of the Adriatic, Ionian and Levantian basins where sedimentation processes are typically most diverse and complex. A total of 57 cores of sediments with a length up to 6 m were obtained during cruises of the Akademik Pokrovski in 1973, 1979 and 1980. The cores were taken along profiles intersecting the continental slope and adjacent abyssal depressions. The sediments were broken down by a number of lithological and biostratigraphic methods, including study of plankton and benthos foraminifera, pollen and spores, sapropel and ash interlayers and textural varieties. Using a combination of micropaleontological and lithological methods which mutually supplement one another it was possible with a high degree of accuracy to discriminate the following horizons in the Late Quaternary deposits of the Central and Eastern Mediterranean: Riss, Riss-Wurm and Holocene. The results confirm the principles of stratification of Mediterranean sediments proposed by Olausson, Ryan and others. As illustrated in several graphs, the correlation of sections in the studied cores made it possible to plot the nature of change in the thicknesses of sediments in horizons of the same age within margins of the basin different in their tectonic position. Author

N86-12664# Joint Publications Research Service, Arlington, Va.
STRUCTURE OF ACOUSTIC FIELD IN DEEP SEA AT SHALLOW DEPTHS AND AT GREAT RANGES Abstract Only c71
V. S. Buslayev and M. V. Perel *In its* USSR Rept.: Earth Sci. (JPRS-UES-85-006) 19 Jun. 1985 p 32-33 Transl. into ENGLISH from Vestn. Leningr. Univ.: Fiz. Khim. (Leningrad), no. 22, Nov. 1984 p 9-17 (For primary document see N86-12630 03-42)
Avail: NTIS HC A05/MF A01

A study was made of the structure of the acoustic field in a deep sea at shallow depths and with great ranges. The problem is formulated as follows. The field is examined in the half-space r = (x, y, z), z approximately > G. It is assumed that the water layer o approximately < z < h is situated over a hemogeneous underlying liquid half-space h < z (bottom). The acoustic field u = u(r) generated at the point by a harmonic source of the frequency f, situated at the point r sub O = (x sub O, y sub O, z sub O), is described by the equation delta u + p squared n squared u =

minus delta (c - r sub O), n = c sub star/c, p = 2 pif/c sub star, where c sub star is the minimum speed of sound c. It is also assumed that the speed of sound and density are dependent only on depth z; the speed of sound in the bottom is greater than the speed of sound in the water layer and bottom density is greater than water layer density. (The equation is supplemented by ordinary boundary conditions.) It is further assumed that the sea is deep and the speed of sound as a function of z has a single deeply situated minimum. An important characteristic of the medium is the function D (mu). It has a simple sense: it gives the horizontal period of the ray as a function of MU. Also examined is the structure of the acoustic field at such ranges where the convergence zone considerably overlap. Author

N86-12665# Joint Publications Research Service, Arlington, Va.
FIND OF RHEOLITES AND TRACHITES AND GEOLOGICAL SITUATION IN NORTHERN PART OF EAST INDIAN OCEAN SUBMARINE RIDGE Abstract Only **c46**
V. V. Reverdatto, V. V. Yeremeyev, A. Ya. Ilyev, A. A. Popov, P. M. Sychev, and V. N. Sharapov *In its* USSR Rept.: Earth Sci. (JPRS-UES-85-006) 19 Jun. 1985 p 34 Transl. into ENGLISH from Dokl. Akad. Nauk SSSR (Moscow), v. 280, no. 4, Feb. 1985 p 960-963 (For primary document see N86-12630 03-42)
Avail: NTIS HC A05/MF A01

Most studies of the geological structure of the Indian Ocean floor have suggested that the East Indian Ocean Ridge (90 deg. Ridge) developed as a transformed fault and that it is characterized by exclusively basic volcanism. Facts are presented which contradict this. Highly modified volcanic-sedimentary rocks were raised which can be classified as tuffites or tuff-siltstones. Clastic material is represented by fragments of relatively little-modified basalts, rhyolites, dacites and trachites, a small number of grains of quartz and plagioclase and particles of ferromanganese encrustations. The presence of rhyolites and trachites indicates that it is not basalts alone which are present in the East Indian Ocean Ridge; acidic and subalkaline effusives seem to be widespread. The association of basalts, rhyolites and trachites indicates an island arc nature of volcanism in the region. Situated to the east of the ridge is a trench with maximum depths greater than 6,000 m. In the northern part of the trench there is an increased thickness of sediments. The total crustal thickness within the ridge remains uncertain, but it is evidently not less than 23 km. The proximity of the ridge and trench and the nature of volcanism reveal a similarity to systems of island arcs and abyssal depressions in the Pacific Ocean. Author

N86-12666# Joint Publications Research Service, Arlington, Va.
EVALUATING SCREENING EFFECTS AND TUSNAMI DANGER IN BAYS Abstract Only **c46**
V. V. Ivanov, K. V. Simonov, and O. I. Garder *In its* USSR Rept.: Earth Sci. (JPRS-UES-85-006) 19 Jun. 1985 p 35 Transl. into ENGLISH from Izv. Akad. Nauk SSSR: Fiz. Atm. i Okeana (Moscow), v. 20, no. 12, Dec. 1984 p 1206-1214 (For primary document see N86-12630 03-42)
Avail: NTIS HC A05/MF A01

In selecting sites for new construction in the Kuril Islands it is important to evaluate the tsunami danger of the pertinent parts of the coastline. Recommendations for the Kuril Islands have been published, but they are only preliminary. An effort has now been made to improve them by formulatating a more adequate model of the source with defining of those peculiarities of the specific position of a bay which exert the most significant influence on formation of the maximum tsunami wave in the analyzed coastal zone. The analysis was based on observational data for the Kamchatka tsunami of 1952, which was catastrophic for the shores of Kamchatka and the Kuril Islands. The data used were for Pearl Harbor, Honolulu and Hilo. The processing method involved breakdown of the record into the signal at the source and the impulse function for penetration of the wave into a bay. it was found that the record can be represented in the form of the convolution of the source function common for all the records of one tsunami and the specific impulse function for the propagation path specific for each bay. It was found that the signal at the tsunami source is a periodic process with beats of great duration with a relatively narrow spectrum. The impulse function for the paths for closed bays contains a small number of oscillations and varies in characteristic times on the order of 1 to 1.5 hours. The characteristic time of tsunami filling of a bay is important to know for shielding the bay against a tsunami wave.

N86-12667# Joint Publications Research Service, Arlington, Va.
INFLUENCE OF SESTON PHOSPHATASE ACTIVITY ON RATE OF PHOSPHORUS MINERALIZATION AND ITS RECYCLING IN PRODUCTION-DESTRUCTION CYCLE Abstract Only **c48**
A. I. Agatova, V. V. Sapozhnikov, and V. R. Vintovkin *In its* USSR Rept.: Earth Sci. (JPRS-UES-85-006) 19 Jun. 1985 p 36-37 Transl. into ENGLISH from Okeanol. (Moscow), v. 25, no. 1, Jan. - Feb. 1985 p 66-73 (For primary document see N86-12630 03-42)
Avail: NTIS HC A05/MF A01

A study was made of the vertical distribution of organic phosphorus and phosphatase activity in the southeastern Pacific Ocean. The rate of the photosynthesis process is limited by the rate of freeing of phosphates in the regeneration process. In a normally functioning community of oligotrophic waters the most important role in the mineralization of phosphorus is played by microheterotrophs. In order to estimate the rate of phosphorus regeneration a study was made of the enzymatic activity of alkaline phosphatase and the protein content in seston, as well as a determination of organic phosphorus. A total of 290 synchronous determinations of organic phosphorus and the rate of phosphorolysis were made at 17 stations which take in the region of the open ocean along a 200-mile zone from 8 deg. S to Drake Passage. Comparison of the data indicates that the distribution of the total activity of phosphatase differs considerable both vertically and in dependence on the region. An estimate is made of the minimum times required for the recycling of phosphorus. In all the investigated regions in the layer 0 to 200 m the recycling of phosphorus occurs in the course of a 24-hour period. The contribution of mesoplankton to the recycling of phosphorus is less than in the case of microplankton, not only due to its lesser biomass, but also due to a lesser specific activity of phosphatase. Author

N86-12668# Joint Publications Research Service, Arlington, Va.
ORIGIN OF ELEMENT COMPOSITION OF OCEAN WATER Abstract Only **c48**
Yu. T. Chuburkov and I. A. Zotov *In its* USSR Rept.: Earth Sci. (JPRS-UES-85-006) 19 Jun. 1985 p 37 Transl. into ENGLISH from Dokl. Akad. Nauk SSSR (Moscow), v. 280, no. 5, Feb. 1985 p 1234-1238 (For primary document see N86-12630 03-42)
Avail: NTIS HC A05/MF A01

There is still no generally accepted theory on the origin of the salt composition of the ocean. It is most widely accepted that anions enter ocean water from the mantle, whereas cations enter with runoff from the continents. It is not possible to explain all experimental facts on that basis. The authors have derived a new expression which is useful in analyzing the element composition of ocean waters and world river runnoff, the objective of such an analysis being to clarify whether the salt composition of oceanic waters is a result of transport of elements from the continents or whether it is a product of differentiation of mantle matter. A table was prepared with data on the concentrations of elements in the ocean and in river runoff. It was found that the concentration of elements in both ocean and lake-river water is directly proportional to their volatilities. The cation composition of both types of water includes products of the outgassing of the earth's deep matter released as a result of its differentiation. The distribution of elements in the waters of the oceans and continents conforms to different patterns. At attempt can be made to explain this difference within the framework of concepts concerning the relative youthfulness of the oceans, formed primarily by the products of outgassing of the earth's deep matter in the process of its fluctuating development or expansion. In continental runoff waters, however, a significant contribution is from the products of rock destruction. Author

N86-12669# Joint Publications Research Service, Arlington, Va.
THEORY OF SOLITARY ANTICYCLONES IN ROTATING FLUID Abstract Only c34
G. G. Sutyrin *In its* USSR Rept.: Earth Sci. (JPRS-UES-85-006) 19 Jun. 1985 p 38 Transl. into ENGLISH from Dokl. Akad. Nauk SSSR (Moscow), v. 280, no. 5, Feb. 1985 p 1101-1105 (For primary document see N86-12630 03-42)
Avail: NTIS HC A05/MF A01

An experiment with a thin layer of fluid in a rotating parabolic vessel made it possible to produce long-live anticyclones called Rossby solitons. The laboratory studies were made with a considerable thickening of the fluid layer at the center of the eddy; in some cases the eddy scale was 2 to 3 times less than predicted by the theory of solitary low-amplitude waves. An effort has been made of explain this discrepancy. A study was made of a wave moving westward with the velocity u in a thin layer of rotating fluid. Equations are derived which describe solitary anticyclones moving to the west and low-amplitude waves. Analysis of the derived system shows that with a decrease in the phase velocity of a wave its amplitude decreases, the horizontal scale increases and theorbital velocity becomes close to geostrophic. It is shown that allowance for the finite amplitude of a solitary wave does not eliminate the discrepancy between theory and experiment. As a result of change in Coriolis force the eddy begins to be displaced westward. The anticyclone moves more rapidly than linear Rossby waves and can be transformed into a solitary wave. A cyclone moves more slowly than linear Rossby waves and as a result of generation of Rossby waves cannot be transformed into a stationarily moving solitary wave. The difference from an anticyclone is caused by a decrease in the level in the cyclone.
Author

N86-12670# Joint Publications Research Service, Arlington, Va.
NONLINEAR MODEL OF ADAPTATION OF FIELDS OF DENSITY AND CURRENTS IN SEA Abstract Only c48
Yu. L. Demin and D. I. Trukhchev *In its* USSR Rept.: Earth Sci. (JPRS-UES-85-006) 19 Jun. 1985 p 39 Transl. into ENGLISH from Izv Akad. Nauk SSSR: Fiz. Atm. i Okeana (Moscow), v. 20, no. 12, Dec. 1984 p 1171-1182 (For primary document see N86-12630 03-42)
Avail: NTIS HC A05/MF A01

The fields of density, wind and sea floor relief determined from observations are usually inconsistent with one another and this often results in significant errors in computation of sea currents. Accordingly, the authors have formulated a new approach in order to ensure the hydrodynamic consistency of these fields while retaining the principal advantages of diagnostic computations. In the first stage purely diagnostic computations are made. Currents are computed on the basis of a priori stipulated density, wind and bottom relief fields. A quasigeostrophic model is used as well as a nonlinear model based on primitive equations of motion. In the second state, the adaptation stage, the system of equations and boundary conditions of the nonlinear diagnostic model are supplemented by a density diffusion equation with corresponding boundary conditions and using the initial density field and solution of the diagnostic problem as the initial approximation the computed density and current fields are brought into consistency with the observed wind and bottom relief fields. Having outlined this approach, the authors discuss the results of numerical computations carried out for the western part of the Black Sea, including the shelf zone. The studied region was covered by a uniform grid with a 5-mile interval and 12 horizons (0 to 1,800 m) were considered. The initial density field data were taken from a hydrological survey made in 1976. After illustrating the approach using these data, the results are compared with other models.
Author

N86-12671# Joint Publications Research Service, Arlington, Va.
LABORATORY STUDY OF REGULAR LOW-AMPLITUDE GRAVITY CAPILLARY WAVES IN NONSTATIONARY CURRENT Abstract Only c34
Ye. S. Benilov, K. V. Pokazeyev, and A. D. Rozenberg *In its* USSR Rept.: Earth Sci. (JPRS-UES-85-006) 19 Jun. 1985 p 39-40 Transl. into ENGLISH from Okeanol. (Moscow), v. 25, No. 1, Jan. - Feb. 1985 p 37-42 (For primary document see N86-12630 03-42)
Avail: NTIS HC A05/MF A01

Laboratory experiments were carried out for study the change in wavelength, frequency and amplitude of regular low-amplitude gravity capillary waves in the range 2 to 5 Hz in a slow sinusoidal current with a velocity amplitude up to 10 to 15 cm/sec. The experiments were made in a glass flume measuring 670 x 20 x 40 cm. A nonstationary uniform current was simulated by movement of a measurement carriage (on which a wave generator and sensors were mounted) along rails. Three electrode sensors were situated at a distance of 5, 20 and 25 cm from the wave generator. The accuracy in determining frequency and amplitude was 10 and 20% respectively; the accuracy in measuring wavelength was 10%. The generation of a current, changing with tiem, resulted in a change in all the parameters of the waves. Data are given for two ranges of current velocities: 10 to 15 cm/sec and 20 to 30 cm/sec. All the observations fit well within the framework of a linear kinematic model. A control experiment with a motionless carriage and a countercurrent slowly changing with time confirmed the legitimacy of transfer of the data obtained with the carriage moving relative to calm water to the case of a uniform nonstationary current.
Author

N86-12672# Joint Publications Research Service, Arlington, Va.
EDDY FLUXES OF HEAT, VORTICITY AND MOMENTUM IN OCEAN AND ATMOSPHERE AND THEIR PARAMETERIZATION (REVIEW) Abstract Only c48
V. O. Ivchenko and A. V. Klepikov *In its* USSR Rept.: Earth Sci. (JPRS-UES-85-006) 19 Jun. 1985 p 40 Transl. into ENGLISH from Okeanol. (Moscow), v. 25, no. 1, Jan. - Feb. 1985 p 5-18 (For primary document see N86-12630 03-42)
Avail: NTIS HC A05/MF A01

A critical evaluation is given of the present status of the theory of eddy transfer of momentum, heat and vorticity in the atmosphere and ocean. Despite differences in the regimes characteristic for the ocean and atmosphere, it is possible to analyze the principal ways to solve this problem on a common basis. Systematization of studies on the parameterization of vertical fluxes in macroscale circulation models suggests that four principal directions must be pursued; (1) obtaining asymptotic solutions for model situations; (2) use of a diffusional scheme for the parameterization of vertical fluxes; (3) studies of so-called orientation effects; and (4) derivation of expressions for the zonally averaged vertical flux of momentum. (This involves hypotheses related either to the baroclinic nature of eddy formation or interaction of baroclinic waves and determination of their phase velocity). Each of these directions (and the corresponding literature) is critically examined.
Author

N86-12673# Joint Publications Research Service, Arlington, Va.
STUDY OF INFLUENCE OF VERTICAL VELOCITY AND DENSITY PROFILES ON HYDRODYNAMIC STABILITY OF ZONAL FLOW Abstract Only c34
A. S Blatov and V. I. Ulyanova *In its* USSR Rept.: Earth Sci. (JPRS-UES-85-006) 19 Jun. 1985 p 41 Transl. into ENGLISH from Okeanol. (Moscow), v. 25, no. 1, Jan. - Feb. 1985 p 19-25 (For primary document see N86-12630 03-42)
Avail: NTIS HC A05/MF A01

Within the framework of the linear theory of hydrodynamic stability and on the basis of a three-layer model of a zonal current with transverse velocity shear a study was made of the joint influence of curvature of the vertical velocity and density profiles on the parameters of unstable wave disturbances and the findings were compared with theoretical studies made earlier and data from in situ observations. The problem is formulated as follows: there is a three-layer macroscale current (with small Rossly-Kibel' numbers Ro $< <$ 1) on the Beta-plane not bounded along the longitudinal coordinate X, directed to the east, and having the width L along the transverse coordinate Y, directed to the north, with the Z axis being directed vertically upward. In this formulation a system of equations is derived which is free of shortcomings present in earlier attempts to solve this problem. This makes it possible to study the influence of the vertical curvature of the density profile, related to the simultaneous existence of a seasonal thermocline and constant pycnocline, as well as the influence of curvature of the vertical velocity profile arising in the presence of subsurface velocity maxima. The system of equations is solved numerically. B.W.

N86-12674# Joint Publications Research Service, Arlington, Va.
FEATURES OF GEOSTROPHIC CIRCULATION RELATED TO NATURE OF BOTTOM RELIEF IN NORTHWESTERN ATLANTIC Abstract Only **c48**
Z. I. Kizner *In its* USSR Rept.: Earth Sci. (JPRS-UES-85-006) 19 Jun. 1985 p 4142 Transl. into ENGLISH from Okeanol. (Moscow), v. 25, no. 1, Jan. - Feb. 1985 p 26-31 (For primary document see N86-12630 03-42)
Avail: NTIS HC A05/MF A01

A study was made of the influence exerted by bottom relief on a boundary current and the geostrophic circulation of the ocean in the neighborhood of its western shore. The investigation was made within the framework of the Ekman theory of wind currents in a barotropic ocean. The conditions characteristics for the northwestern shore was simulated; the sector from Florida to Georges Bank was considered. The modeling revealed that since to the north of Cape Hatteras the depth drops off smoothly from the abyssal plain to the outer edge of the shelf almost to zero, under some conditions the isolines of the f/H function (f is the Coriolis parameter, H is depth) near the continental slope can capture the geostrophic flow, making it virtually parallel to the edge of the shelf, this resulting in the weakening and disappearance of the western boundary current. There is little basis for expecting such a strong topographic effect as detachment under baroclinic conditions, which are clearly expressed in the subtropical latitudes, particularly near the western shore (baroclinicity to a considerable degree suppresses the bottom relief effect on current within the limits of the main thermocline). The described effect of capture of the geostrophic flow near the western shore is also possibly manifested in the South Atlantic. Author

N86-12675# Joint Publications Research Service, Arlington, Va.
CYCLONIC FRONTAL EDDY IN ANTARCTIC CIRCUMPOLAR CURRENT Abstract Only **c48**
Yu. A. Ivanov, A. Yu. Krasnopevtsev, Ye. G. Morozov, I. F. Shadrin, and A. D. Shcherbinin *In its* USSR Rept.: Earth Sci. (JPRS-UES-85-006) 19 Jun. 1985 p 42 Transl. into ENGLISH from Okeanol. (Moscow), v. 25, no. 1, Jan. - Feb. 1985 p 32-36 (For primary document see N86-12630 03-42)
Avail: NTIS HC A05/MF A01

Studies of the Antarctic Circumpolar Current were made in December 1982-February 1983 on the 30th cruise of the Dmitriy Mendeleyev in the waters between New Zealand and Antarctica. Two hydrological surveys in the broad frontal zone of the current revealed a cyclonic eddy of the frontal type. The article discusses the structure and kinematics of the eddy and analyzes the nature of its evolution. This eddy could be traced in the field of all hydrological characteristics. Against a background of water with a temperature of about 6 C surrounding the eddy, the temperature at the center drops to 1.6 C. The horizontal scale of the ring can be determined from the peripheral closed isotherm. In the first survey the axes were 90 and 60 miles; in the second 80 and 50. During the time between the surveys (15 days) the center of the eddy moved 80 miles to the northeast, giving a velocity of 5.3 miles/day. The polar front separating the antarctic and subantarctic water structures possibly forms a meander extending to 58 deg S. The young ring discussed may have been formed as a result of separation of this quasistationary meander. The geostrophic velocities in the ring were computed by the dynamic method, the maximum values being 40 cm/sec. The two time-spaced surveys made it possible to compute the Lagrangian evolution of ring characteristics, specifically the available potential energy, heat and salt content. Author

N86-12676# Joint Publications Research Service, Arlington, Va.
INFLUENCE OF SOME OCEANOGRAPHIC CHARACTERISTICS ON DECAY KINETCIS OF SURFACE-ACTIVE AGENTS IN SEA Abstract Only **c45**
N. I. Ryasintseva, V. V. Malyshkina, and L. Yu. Sekundyak *In its* USSR Rept.: Earth Sci. (JPRS-UES-85-006) 19 Jun. 1985 p 45 Transl. into ENGLISH from Okeanol. (Moscow), v. 25, no. 1, Jan. - Feb. 1985 p 88-92 (For primary document see N86-12630 03-42)
Avail: NTIS HC A05/MF A01

Those parameters which constitute conditions for the vital functioning of microorganisms, such as temperature, salinity, illumination and oxygen regime, play the decisive role in processes of destruction of surface-active agents. This article gives an experimental study of the role of these marine parameters in the process of biodegradation of surface-active agents. Two methods of model research were employed in the experimental work: static laboratory modeling in open and closed glass containers and the in situ method with polyethylene or polyvinyl chloride spheres exposed during the entire experiment in the sea and supplied with values and devices for taking samples. The object studied was the Progress washing compound, one of the most commonly used Soviet-produced surface-active agents, the active substance being sodium alkyl sulfate. In both the model and in the in situ experiments the rate of the process of decay of alky sulfates was monitored by a determination of their content in daily samples by the method of photo-colorimetry with methylene blue. A study of the kinetics of decay of alkyl sulfates in the temperature range from 0 to 36 deg revealed that at temperatures 0-2 C the biodestruction process is slowed down greatly. B.W.

N86-12677# Joint Publications Research Service, Arlington, Va.
COMPUTATIONS OF SEISMIC WAVE PROPAGATION VELOCITIES IN OCEAN BOTTOM SEDIMENTS FROM REFLECTED WAVES TRAVEL-TIME CURVES Abstract Only **c46**
V. N. Moskalenko, G. A. Semenov, and P. N. Kuzmin *In its* USSR Rept.: Earth Sci. (JPRS-UES-85-006) 19 Jun. 1985 p 46-47 Transl. into ENGLISH from Okeanol. (Moscow), v. 25, no. 1, Jan. - Feb. 1985 (For primary document see N86-12630 03-42)
Avail: NTIS HC A05/MF A01

The velocity of seismic waves in a thin layer of sediments in the ocean is usually determined using the approximate Dix formula, but the latter has a number of limitations in large part attributable to its derivation. These limitations are reviewed. In its derivation use was made only of the first two even terms in the expansion of the travel-time curve for reflected waves. S. N. Medvedev found a more precise analytical expression for velocity which is derived using the first three terms of the expansion. The Medvedev algorithm, outlined in this article, was checked in a theoretical model and using experimental data obtained on the 28th cruise of the Dmitriy Mendeleyev. The Dobrinskiy program was used in solving the direct seismic problem for horizontally bedded thick layers with a constant velocity and theoretical travel-time curves were computed from the bottom of sedimentary layers of different thicknesses; these theoretical travel-time curves were then introduced into a program for the inverse seismic problem. It is shown that the Medvedev algorithm makes it possible to compute the stratum velocities of propagation of seismic waves in thin sedimentary layers of the ocean with an accuracy to 0.05 km/sec. B.W.

N86-12678# Joint Publications Research Service, Arlington, Va.
ROLE OF AHERMATYPIC CORALS IN SEDIMENTATION AND ECOLOGY OF CORAL BANKS Abstract Only **c48**
N. B. Keller *In its* USSR Rept.: Earth Sci. (JPRS-UES-85-006) 19 Jun. 1985 p 47-48 Transl. into ENGLISH from Okeanol. (Moscow), v. 25, no. 1, Jan. - Feb. 1985 p 113-116 (For primary document see N86-12630 03-42)
Avail: NTIS HC A05/MF A01

Ahermatypic scleractiniae, not forming coral reefs, occur widely as individuals and in colonies, the skeletons in the latter being very similar to those of some hermatypic corals and being very difficult to distinguish from the latter in fossil form. Ahermatypic deep-water scleractiniae are adapted to different depths as great as 6,200 m and different temperatures down to -1.1 C. Locally in the oceans they form dense colonies in the form of banks or coral overgrowths or meadows, in the latter case playing a significant role in the formation of sediments. Coral banks and overgrowths in fossilized form constitute calcareous bodies of sedimentary origin: bioherms up to 60 m thick and up to 3 km in extent; there are biostromes in the form of relatively thin lenses with an extent from tens to several hundreds of meters. A study was made to ascertain how the geologist can distinguish bioherms and biostromes of abyssal, cold-water origin from tropical zone bioherms and reefs. B.W.

N86-12679# Joint Publications Research Service, Arlington, Va.
NEW DATA OF RELIEF OF MAZCA RIDGE Abstract Only **c48**
L. A. Zakharov *In its* USSR Rept.: Earth Sci. (JPRS-UES-85-006) 19 Jun. 1985 p 48-49 Transl. into ENGLISH from Okeanol. (Moscow), v. 25, no. 1, Jan. - Feb. 1985 p 124-129 (For primary document see N86-12630 03-42)
Avail: NTIS HC A05/MF A01

The Nazca Ridge is of particular interest because many aspects of the origin, development and structure of block-volcanic ridges as a whole do not fit in with the hypothesis of the tectonics of lithospheric plates. Four principal parameters were determined: slope, horizontal and vertical dissection, mean depth level. The Nazca Ridge, like the Walvis Ridge in the Atlantic, broken into large macroblocks: northern, central and southern. Each is distinctly different. The northern macroblock has a base at a considerable depth, minimum elevation and minimum vertical dissection. The central macroblock rises to the greatest elevations above the surrounding Peruvian and Chilean Basins, has considerable vertical dissection and a maximum slope steepness. There are mountains of typical volcanic characteristics, some with flat tops. The distinguishing characteristic of the southern macroblock is a predominance of mountains of volcanic origin, many of which are typical guyots, evidence of a relatively recent sinking of this part of the Pacific Ocean floor. B.W.

N86-12680# Joint Publications Research Service, Arlington, Va.
GRAVIMETRIC SURVEYING WITH MI-8 HELICOPTERS Abstract Only **c46**
V. Sopolev *In its* USSR Rept.: Earth Sci. (JPRS-UES-85-006) 19 Jun. 1985 p 52 Transl. into ENGLISH from Vozdushnyy Transport (Moscow), 18 Apr. 1985 p 4 (For primary document see N86-12630 03-42)
Avail: NTIS HC A05/MF A01

A new type of geophysical operation--gravimetric surveying from MI-8 helicopters with the aid of suspended gravimeters--has been mastered for the first time in the country by Far East helicopter crews. In this method, all work is performed by an operator inside a helicopter carrying a gravimeter on an outside sling. The gravimeter is equipped with a stabilizing device. Work with the suspended gravimeter requires considerable flying skill and highly precise piloting during approaches and hovering. Author

N86-12681# Joint Publications Research Service, Arlington, Va.
MAGNETIC MINERALS AND CHARACTERISTICS OF NATURAL MAGNETIC STATE OF CORE IN SAATLY SUPERDEEP HOLE IN DEPTH RANGE 3500-7500 METERS Abstract Only **c46**
V. I. Bagin and Z. A. Novruzov *In its* USSR Rept.: Earth Sci. (JPRS-UES-85-006) 19 Jun. 1985 p 57 Transl. into ENGLISH from Izv. Akad. Nauk Azerb. SSR, Ser. Nauk o Zemle (USSR), no. 5, 1984 p 61-67 (For primary document see N86-12630 03-42)
Avail: NTIS HC A05/MF A01

The SG-1 Saatly superdeep hole is one of the 15-km holes being drilled or which will be drilled for studying the deep structure of the earth's crust. This article presents data on magnetic minerals, carriers of natural remanent magnetization and determinations of the conditions under which they originated. Core rocks from depths of 3,500-7,500 m were used in the study. These are andesites, andesite-basalts, basalts, decites and others (a total of 120 samples were analyzed). Data on Curie temperatures (T sub C) and other parameters were analyzed in depth. The constancy of the composition of magnetic minerals (magnetite with T sub C = 575-585 C, magnetite with a low content of titanium with T sub C = 520-550 C and oxidized magnetite with T sub C = 600 C), found in the entire studied depth range, and its stability to temperature effects indicate not only a predominance of high-temperature oxidation, but also a constancy of conditions at the source of removal of the material. B.W.

N86-12682# Joint Publications Research Service, Arlington, Va.
NEW METHODS FOR INTERPRETING SEISMIC WAVES IN STRATIFIED MEDIA Abstract Only **c46**
B. N. Lutsenko *In its* USSR Rept.: Earth Sci. (JPRS-UES-85-006) 19 Jun. 1985 p 58 Transl. into ENGLISH from Geol. Nefti i Gaza (Moscow), no. 1, Jan. 1985 p 48-53 (For primary document see N86-12630 03-42)
Avail: NTIS HC A05/MF A01

In order to ensure the most complete exploitation of petroleum deposits it is essential to develop new methods for the study of faults and the steep slopes of salt domes. The author describes a method for achieving this goal. This involves interpretation of reflections directly from fault zones: direct waves from the boundaries of fault zones and doubly reflected waves (those forming first by reflection from a subvertical boundary and then from the subhorizontal boundaries adjacent to them). It is shown that the formation of such duplex waves does not require that the entire subvertical boundary be continuously reflecting; it is only required that its individual elements in the neighborhood of the contacts with the subhorizontal boundaries have reflecting properties. The discrimination and interpretation of such waves is possible in virtually the entire range of studied depths for seismic prospecting and petroleum exploration and also in deep seismic soundings. Each of these possibilities is illustrated in examples. B.W.

N86-12683# Joint Publications Research Service, Arlington, Va.
NEW APPROACH TO SOME PROBLEMS IN SEISMOLOGY Abstract Only **c46**
I. G. Kerimov *In its* USSR Rept.: Earth Sci. (JPRS-UES-85-006) 19 Jun. 1985 p 58-59 Transl. into ENGLISH from Izv. Akad. Nauk Azerb. SSR, Ser. Nauk o Zemle (USSR), no. 5, 1984 p 41-46 (For primary document see N86-12630 03-42)
Avail: NTIS HC A05/MF A01

Profound changes have occurred in seismology in recent years with respect to certain concepts which earlier had been unquestioned. Among these concepts are those regarding the pattern of distribution of earthquakes, the theory of propagation of weak high-frequency signals and the mechanism of induced seismicity. Each of these topics is discussed. It has been generally accepted that the curve of the dependence of the number of earthquakes on their magnitude has a shape close to a hyperbola: the stronger an earthquake, the less frequently it occurs. But 72% of all earthquakes are plotted in depth to depths of 400-450 km with an interval of 10 m earthquakes with M = 4.8-4.9 are most characteristic in all depth intervals. In such a distribution the stratification of the upper part of the Earth plays the most important role in a seismogenic sense. In seismogenic respect the Earth is homogeneous both over its surface and in depth. A study of weak seismc fields during the time directly preceding earthquakes has revealed definite amplitude and frequency changes in the process of preparation for the main earthquake tremor. B.W.

N86-12684# Joint Publications Research Service, Arlington, Va.
METHOD FOR SOLVING PROBLEMS IN ELECTRODYNAMICS OF ANISOTROPIC MEDIA WITH SLANT BEDDING Abstract Only **c32**
M. G. Savin *In its* USSR Rept.: Earth Sci. (JPRS-UES-85-006) 19 Jun. 1985 p 59-60 Transl. into ENGLISH from izv. Akad. Nauk SSSR: Fiz. Zemli (Moscow), no. 2, Feb. 1985 p 75-82 (For primary document see N86-12630 03-42)
Avail: NTIS HC A05/MF A01

This is a further development of the methodology for solution of electrodynamic problems for the case of gradient anisotropic media when the axes of the medium form quite small angles with the surface. This model approximates the geoelectric situation in the crystalline structures of the Baltic shield, where there is a contancy of the tilt of ancient rocks at angles from 45 to 60 deg to a depth of 11 km. The problem is examined in relation to work with pulsed magnetohydrodynamic generators. A geoelectric structure containing one-dimensional anisotropic layers is considered. The structure is assumed to be uniaxial, with the dielectric constant and magnetic permeability being continuous functions only of the z-coordinate. A method for solving electrodynamic problems is given for such media (the generalized functions method is employed). A fundamental solution is given for a system of Maxwell equations, represented in the for of a convergent series, whose terms are computed using recurrent formulas. Author

N86-12685# Joint Publications Research Service, Arlington, Va.
FEATURES OF FIELD OF DIRECTIONS AND VELOCITIES OF PROPAGATION OF FRACTURES AT EARTHQUAKE FOCI IN NORTHERN MUYA REGION OF BAYKAL RIFT ZONE Abstract Only c46
A. V. Solonenko and N. V. Solonenko *In its* USSR Rept.: Earth Sci. (JPRS-UES-85-006) 19 Jun. 1985 p 60 Transl. into ENGLISH from Vulkanol.' i Seysmologiya (Moscow), no. 1, Jan. - Feb. 1985 p 98-105 (For primary document see N86-12630 03-42)
Avail: NTIS HC A05/MF A01

In an earlier paper a method was formulated for determining the directions and velocities of propagation of fractures at the foci of earthquakes which is based on a joint analysis of their mechanism and the distribution of apparent periods at seismic stations in the region. The method has now been applied to the Baykal rift zone, specifically the Northern Muya region, within which there is an inversion of the field of directions of fracture propagation. The characteristics of this region are discussed in detail. In this area the velocities and directions of fracture propagation were determined at the foci of 247 earthquakes. In the analysis the data were classified into three groups: (1) hose foci at which the direction of fracture propagation has a westerly component; (2) those with an easterly component; (3) and those for which the direction of propagation could not be ascertained with certainty. The four characteristic zones were defined. These analyses revealed that the Northern Muya region is actually a place where there is a reorientation of the directions of fracture propagation. The change in direction occurs in the neighborhood of the Pereval'nyy fault. B.W.

N86-12686# Joint Publications Research Service, Arlington, Va.
HARDWARE AND SOFTWARE SUPPORT OF GEOLOGICAL-GEOPHYSICAL DATABASE Abstract Only c82
V. A. Ivanov, G. A. Ivanchenko, N. N. Karlson, and N. S. Yakovenko *In its* USSR Rept.: Earth Sci. (JPRS-UES-85-006) 19 Jun. 1985 p 68 Transl. into ENGLISH from Avtometriya (Novosibirsk), no. 6, Nov. - Dec. 1985 p 82-83 (For primary document see N86-12630 03-42)
Avail: NTIS HC A05/MF A01

The greatest difficulty in processing of geological and geophysical data on computers is that of representing the data on punch cards. The first version of a geological-geophysical database and the software which allows input and output, storage, editing and analysis of the data jointly with pictures is described. Coded graphic information is transferred from cards to magnetic tape and output is through a plotter. The objects in the database are various points on coded maps. An object has three attributes: a characteristic (reference point, isoline, profile, linearment, etc.), value of geological-geophysical quantity (e.g., temperature borehole) and coordinate of the point coded. The database is physically kept on 7.5-Mb magnetic disks using FMS-10 and FMS-D file management systems under DOS-10 on a YeS-1010 minicomputer. The first part of the geological-geophysical database allows coding, storage and editing of geological-geophysical maps, reduction of the maps to a common topographic base, as well as geometric transformation of photographic images to the same topographic base, allowing work to be started on combined analysis of data and photographs. Author

N86-12687# Joint Publications Research Service, Arlington, Va.
HIGH-ELEVATION STATION'S COSMIC-RAY RECORDING SYSTEM Abstract Only c93
In its USSR Rept.: Earth Sci. (JPRS-UES-85-006) 19 Jun. 1985 p 71 Transl. into ENGLISH from Izv. (Moscow), 5 Apr. 1985 p 3 (For primary document see N86-12630 03-42)
Avail: NTIS HC A05/MF A01

Scientists of the high elevation cosmic ray station of the Kazakh Academy of Sciences' Institute of High-Energy Physics have begun their first experiments for recording cosmic particles with a new automated system, the Adron-44. The Adron-44 is a unique complex which was developed by physicists of Kazakhstan. It is located at the Tien-Shan High-Elevation Station in the Zailiyskiy Ala-Tau Mountains, at an elevation of 3,400 meters above sea level. Experiments at the cosmic ray station will make it possible to obtain new information on processes of the interaction of cosmic-radiation particle with matter. Author

N86-12688# Joint Publications Research Service, Arlington, Va.
VIDEO TERMINAL FOR ANALYZING AERIAL INFRARED PHOTOGRAPHS Abstract Only c35
In its USSR Rept.: Earth Sci. (JPRS-UES-85-006) 19 Jun. 1985 p 72 Transl. into ENGLISH from NTR: Probl. i Resheniya (Moscow), 5-18 Mar. 1985 p 2 (For primary document see N86-12630 03-42)
Avail: NTIS HC A05/MF A01

A Self-Contained Video Information Terminal (SVIT) was developed at the USSR Academy of Sciences' Institute of Space Research in collaboration with the Kirov Polytechnical Institute. Equipment and methods which were developed at IKI for digital processing of images are finding employment in various fields of science and the economy, particularly in the solution of problems of mapping temperature patterns of the Earth's surface and atmosphere. A photograph showing a fragment of an infrared portrait of a city that was produced on the screen of the SVIT is given. Clearly distinguishable against a dark background are spots of light with different degrees of brightness: a power-and-heating plant with five cooling towers, a heat-transport line running from this plant, and a waste-water discharge channel. The SVIT is capable of subdividing an image into 256 digital gradations. Author

N86-12689# Joint Publications Research Service, Arlington, Va.
COMPARISON OF SINGLE-PARAMETER STATISTICAL MODEL WITH RESULTS OF ROUND-THE-CLOCK MEASUREMENT OF LIGHT-SCATTERING MATRICES Abstract Only c46
M. A. Sviridenkov, G. I. Gorchakov, A. A. Isakov, and V. N. Sidorov *In its* USSR Rept.: Earth Sci. (JPRS-UES-85-006) 19 Jun. 1985 p 73 Transl. into ENGLISH from Izv. Akad. Nauk SSSR: Fiz. Atm. i Okeana (Moscow), v. 21, no. 1, Jan. 1985 p 22-31 (For primary document see N86-12630 03-42)
Avail: NTIS HC A05/MF A01

A statistical model proposed previously is shown to agree with the results of round-the-clock measurements of light scattering over a range of 2 to 50 km. Exceptions include extreme situations such as dust storms. The single parameter model results from uniform matched transformations of angular variations in scattering matrix components with changes in the visibility range due to two main factors, condensation transformation of the distribution of particles by size and changes in the refractive index, including heterogeneous condention of volatile vapors, plus changes in the relative contribution of molecular scattering. The statistical model can be corrected for individual data sets by considering the mean particle concentration. At long ranges the model becomes inadequate to the observed variability in light scattering characteristics due to noncondensational processes of transformation of aerosol and the dry aerosol base, leading to significant variations in concentration. Author

N86-12690# Joint Publications Research Service, Arlington, Va.
IONIC MECHANICSM OF EXCHANGE OF ADMIXTURES BETWEEN HYDROSPHERE AND ATMOSPHERE Abstract Only c46
A. V. Savchenko and V. V. Smirnov *In its* USSR Rept.: Earth

Sci. (JPRS-UES-85-006) 19 Jun. 1985 p 74 Transl. into ENGLISH from Izv. Akad. Nauk SSSR: Fiz. Atm. i Okeana (Moscow), v. 21, no. 1, Jan. 1985 p 32-41 (For primary document see N86-12630 03-42)
Avail: NTIS HC A05/MF A01

Experiments conducted are used as the basis for a proposed quantitative model of evaporation which takes into account the microphysical and macrophysical characteristics of an ionogenic solution and the surrounding gas medium. Certain practical applications to real atmospheric processes are discussed. The experiments are based on observations of alteration of the charge exchange spectrum of an evaporated liquid-drop aerosol and changes in polar conductivities of the surrounding air. The possible contribution of the mechanism to transfer of ions in the atmosphere immediately above the ocean, in fog and clouds is studied. Author

N86-12691# Joint Publications Research Service, Arlington, Va.
IONIC MECHANICSM OF EXCHANGE OF ADMIXTURES BETWEEN HYDROSPHERE AND ATMOSPHERE Abstract Only c74
A. V. Savchenko and V. V. Smirnov *In its* USSR Rept.: Earth Sci. (JPRS-UES-85-006) 19 Jun. 1985 p 74 Transl. into ENGLISH from Izv. Akad. Nauk SSSR: Fiz. Atm. i Oikeana (Moscow), v. 21, no. 1, Jan. 1985 p 32-41 Original language document was announced in IAA as A85-26294 (For primary document see N86-12630 03-42)
Avail: NTIS HC A05/MF A01

Image quality as a function of the scattering-medium layer position relative to the shelf-luminous object under observation is experimentally studied for purposes of aerial and space photography and television. The laboratory environment consisted of a 6-m long light path with a fluoroplastic film (50 microns thick) as a scattering medium. The experimental data are shown to be in agreement with theoretical conclusions based on the linear-system theory. The large discrepancies among the previous studies on the subject are suggested to be caused by the disregard of distortion of the Fourier-transformed image function resulting from the finiteness of the receiver sighting angle in an optical system. L.T.

N86-12692# Joint Publications Research Service, Arlington, Va.
DAMPING OF HIGH-FREQUENCY WIND WAVES BY ARTIFICIAL SURFACE-ACTIVE FILMS Abstract Only c45
S. A. Yermakov, A. R. Panchenko, and T. G. Talipova *In its* USSR Rept.: Earth Sci. (JPRS-UES-85-006) 19 Jun. 1985 p 74 Transl. into ENGLISH from Izv. Akad. Nauk SSSR: Fiz. Atm. i Okeana (Moscow), v. 21, no. 1, Jan. 1985 p76-82 (For primary document see N86-12630 03-42)
Avail: NTIS HC A05/MF A01

Field experiments with artificial slicks made of surface-active agents have shown that in areas covered by such films the intensity of wind waves decreases greatly over a broad frequency range. The damping of high frequency wind waves in small artificial slicks on the order of ten meters in diameter is studied. Experiments were performed along the Black Sea coast from an oceanographic platform with winds of up to about 6 m/s. A resistance-type string wave recorder was used to measure wave heights. The high frequency (over 2 to 3 Hz) component of wind waves was sharply reduced by the artificial surface active slick. With very weak winds, the contrast in the high frequency portion of the spectrum is well described by a theoretical curve in which the major factor involved is the effect of direct dissipation of surface waves resulting from the presence of the elastic surface active film. As wind speed increases to about 6 m/s the mean contrast in the gravity capillary range of frequencies monotonically approaches 1, that is the damping effect of the film decreases. Author

N86-12693# Joint Publications Research Service, Arlington, Va.
ORGANIC COMPONENTS IN ATMOSPHERE IN REGIONS OF VOLCANIC ACTIVITY Abstract Only c45
V. A. Isidorov and I. G. Zenkevich *In its* USSR Rept.: Earth Sci. (JPRS-UES-85-006) 19 Jun. 1985 p 75 Transl. into ENGLISH from Dokl. Akad. Nauk SSSR (Moscow), v. 280, no. 1, Jan. 1985 p 223-227 (For primary document see N86-12630 03-42)
Avail: NTIS HC A05/MF A01

Model experiments and thermodynamic calculations indicate the possibility of formation of a broad range of volatile organic components in volcanic processes. In September and October 1983, the air in the region of active volcanoes on Kunashir Island was sampled, performing mass spectrometric and gas chromatographic analysis. Fifty-eight organic compounds detected in the air samples are listed. Benzene was present in the greatest quantity. The analyses agreed with model experiments involving abiogenic synthesis of organic compounds under conditions simulating volcanic activity and indicate the presence of natural sources of fluorochlorohydrocarbon which must be considered in estimating the influence of halogen-containing organic compounds on the status of the earth's ozone layer. Author

N86-12694# Joint Publications Research Service, Arlington, Va.
EVALUATING INFLUENCE OF WAVES ON DYNAMIC STRUCTURE OF ATMOSPHERIC NEAR-WATER LAYER Abstract Only c46
K. L. Yegorov *In its* USSR Rept.: Earth Sci. (JPRS-UES-85-006) 19 Jun. 1985 p 76 Transl. into ENGLISH from Izv. Akad. Nauk SSSR: Fiz. Atm. i Okeana (Moscow), v. 20, no. 12, Dec. 1984 p 1183-1188 (For primary document see N86-12630 03-42)
Avail: NTIS HC A05/MF A01

A possible clarification was sought by an analysis of the possible qualitative influence of the wave covered ocean surface on the vertical profile of the characteristics of turbulence at the interface on the basis of known hypotheses of the semiempirical theory of turbulence. Specifically, on the basis of solution of the equation for the balance of turbulent energy a study is made of the stationary turbulence regime in a flow with a velocity shear near the wave covered surface, taking into account the diffusion of the kinetic energy of turbulence from the wave layer in the case of a neutral stratification. The solution is analyzed using a generalized Karman model for the mixing path. This gives evidence of the possibility of existence of conditions characterized by a decrease in the turbulence coefficient with increasing distance from the surface. The computed wind velocity field is compared with observational data. It is shown that the peculiarities observed in structure of the atmospheric near-water layer can be qualitatively correctly taken into account by setting boundary conditions different from conditions over the land and assuming an exchange of turbulent energy between the wave layer and the air flow. Author

N86-12695# Joint Publications Research Service, Arlington, Va.
GLOBAL MODELING OF OPTICAL CHARACTERISTICS OF ATMOSPHERIC AEROSOL Abstract Only c45
K. Ya. Kondratyev, N. I. Moskalenko, S. Ya. Skvortsova, A. R. Zakirova, F. S. Yakupova, and S. V. Gusev *In its* USSR Rept.: Earth Sci. (JPRS-UES-85-006) 19 Jun. 1985 p 76-77 Transl. into ENGLISH from Dokl. Akad. Nauk SSSR (Moscow), v. 280, no. 5, Feb. 1985 p 1090-1093 (For primary document see N86-12630 03-42)
Avail: NTIS HC A05/MF A01

A system for the global modeling of the optical characteristics (OC) of atmospheric aerosol (AA) is proposed. The global structural model of AA is based on a map of the earth's natural landscapes, the temperature field of the underlying surface or the temperature of the surface air layer and the zonal and meridional components of wind velocity. At the basis of the model are the background aerosol and disturbed layers of the zone of active turbulent heat exchange (ZATHE), banded transport of the dust aerosol of the middle troposphere and volcanic stratospheric aerosol. The model is analyzed. Roughly speaking, the global monitoring of OC of AA is possible on the assumption that the optical density of AA over the land in the ZATHE zone is constant. Over the sea surface allowance must be made for the effect of wind velocity on the vertical profile of optical density in the ZATHE. Optical models of AA can be based on a data bank of OC for different AA fractions with different microstructure and chemical composition. The modeling of OC of AA revealed that the greatest optical thickness of AA is observed at the hottest time of the year and in the warmest zones when the ZATHE altitude attains 4 km and the optical thickness of AA is approx. 0.3 to 0.4. The most transparent atmosphere is in the cold season when ZATHE altitude is minimum and the optical thickness decreases to 0.01 to 0.03. Author

N86-12696# Joint Publications Research Service, Arlington, Va.
DIURNAL VARIATION OF OPTICAL AND MICROPHYSICAL CHARACTERISTICS OF NEAR-SURFACE AEROSOL Abstract Only c45
V. N. Sidorov, G. I. Gorchakov, A. S. Yemilenko, and M. A. Sviridenkov *In its* USSR Rept.: Earth Sci. (JPRS-UES-85-006) 19 Jun. 1985 p 78 Transl. into ENGLISH from Izv. Akad. Nauk SSSR: Fiz. Atm. i Okeana (Moscow), v. 20, no. 12, Dec. 1984 p 1156-1165 Original language document was announced in IAA as A85-20831 (For primary document see N86-12630 03-42)
Avail: NTIS HC A05/MF A01

Inverted optical data are used to determine the average diurnal behavior of the physical parameters of the near-ground aerosol: the in-situ light-scattering coefficient; the light-scattering coefficient for a dry aerosol; and some microstructural parameters. It is shown that the fundamental behavior of diurnal optical aerosol parameters is dominated by the condensational transformation which occurs as a result of changes in relative humidity, and by the local processes of aerosol accumulation and removal in the surface layer. The accumulation of aerosol dry matter mass during the night is associated with particle growth, while day-time accumulation is marked by an increase in submicorn aerosol concentrations. I.H.

N86-12697# Joint Publications Research Service, Arlington, Va.
USSR REPORT: EARTH SCIENCES
16 Aug. 1985 57 p Transl. into ENGLISH from various Russian articles
(JPRS-UES-85-008) Avail: NTIS HC A04/MF A01

Numerous topics in earth sciences relating to meteorology, oceanography, geophysics, atmospheric physics and polar regions are discussed. Water waves, tectonics, geodynamics, solitary waves, volcanoes, clouds, air-water interactions and remote sensing are discussed. For individual titles, see N86-12698 through N86-12737.

N86-12698# Joint Publications Research Service, Arlington, Va.
SOME RESULTS OF STUDY OF BLOCKING LAYERS ON DAYS WITH VERTICALLY DEVELOPED CLOUD COVER OF CAUCASUS-CASPIAN REGION ON BASIS OF AEROSPACE INFORMATION Abstract Only c47
A. A. Gorchiyev and T. D. Agayev *In its* USSR Rept.: Earth Sci. (JPRS-UES-85-008) 16 Aug. 1985 p 1 Transl. into ENGLISH from Izv. Akad. Nauk Azerbaydzhanskoy SSR, Ser. Nauki o Zemle (USSR), no 6, 1984 p 111-118 (For primary document see N86-12697 03-42)
Avail: NTIS HC A04/MF A01

A study of vertically developed clouds (Cu and Cb) in the presence of blocking layers was made using surface and aerological data for the period 1958 to 1980 and space photographs (1974 to 1980). The investigations covered the Causasus-Caspian region. It was found that blocking layers are present in 70% of the cases when vertically developed Cu and Cb are observed over the Apsheron Peninsula. In more than 60% of all cases the lower boundary of the blocking layers is in the layer 0.5 to 2.0 km. The lower boundary of Cu is formed in the atmospheric layer 800 to 1,500 m and Cb in the layer 400 to 1,000 m. The thickness of Cu varies from hundreds of meters to several kilometers, whereas Cb can vary from a kilometer to several kilometers, sometimes reaching the tropopause. Over the Apsheron Peninsula Cu and Cb are most frequently formed in cold and moist air masses arriving from the north. The velocities of their intrusion are 5 to 15 m/sec respectively. Near midday such types of clouds can cover from several percent of the heavens to 70 to 80%; the horizontal dimensions of individual clouds may be several hundreds of meters to 2 to G km. During summer-autumn a breeze circulation makes a definite contribution to the formation of cumulus clouds. Author

N86-12699# Joint Publications Research Service, Arlington, Va.
EXPERIMENTAL STUDY OF EQUILIBRIUM INTERVAL IN FREQUENCY SPECTRA OF WIND WAVES IN SEA OF FINITE DEPTH Abstract Only c48
I. A. Alekperov, N. I. Akhmedov, A. I. Gumbatov, A. S. Ismaylov, S. G. Magerramova, and T. M. Tatrayev *In its* USSR Rept.: Earth Sci. (JPRS-UES-85-008) 16 Aug. 1985 p 6 Transl. into ENGLISH from Izv. Akad. Nauk Azerbaydzhanskoy SSR, Ser. Nauki o Zemle (USSR), no. 6, 1984 p 119-123 (For primary document see N86-12697 03-42)
Avail: NTIS HC A04/MF A01

The frequency spectrum is one of the most important characteristics of surface wind waves, making it possible to compute the mean elements of waves such as mean height, dispersion, mean period and energy of waves. However, determination of the form of the spectrum has remained an essentially unsolved problem. Along these lines the Phillips equilibrium hypothesis on the form of frequency spectra has gained the widest acceptance (in wind wave spectra these are some frequency intervals in which the energy distribution should be dependent only on the physical parameters characterizing the formation of sharp crests and collapsing waves). Data is given on the frequency spectra of surface wind waves obtained at different wind velocities for a depth of 7 m. The measurements were made in the Caspian Sea in August 1983. An analysis revealed the legitimacy of use of the Phillips and Kitaigorodskii formulas in the range of relatively low frequencies, but there are deviations in the range of high frequencies (f approximately $>$ 0.5). Any final solution of the problem requires a thorough study of smell and currents jointly with surface wind waves. Author

N86-12700# Joint Publications Research Service, Arlington, Va.
FEATURES OF ELECTRICAL MEASUREMENTS IN SEA AS MEDIUM WITH FIELD OF EXTRANEOUS FORCES Abstract Only c48
V. I. Loptnikov *In its* USSR Rept.: Earth Sci. (JPRS-UES-85-008) 16 Aug. 1985 p 7 Transl. into ENGLISH from Geofiz. Zh. (Kiev), v. 7, no. 7, Mar. - Apr. 1985 p 59-68 (For primary document see N86-12697 03-42)
Avail: NTIS HC A04/MF A01

Electrical measurements in the sea involve both theoretical and technical difficulties because in any part of the sea there may be electrical fields generated by different sources but having a close spectral makeup. These include the telluric field associated with variations of the earth's electromagnetic field, extraneous and electrostatic fields associated with physicochemical processes and fields of biological, industrial and other origin. Electrical fields of dynamic origin determined by the Lorentz force are excited in the sea moving relative to the geomagnetic field. In addition, the measurement instruments themselves frequently have their own undermined motion in which a Lorentz force and undetermined emf can arise directly in moving parts . Different possibilities for discriminating or excluding the effects of motion under specific conditions are discussed by the vertical stratification of water masses. Various types of electrical field transducers are examined. The organization of electrical field measurements in a reference system fixed relative to the earth and the results of use of transducers of different types are also discussed. It is shown that within the framework of the electrodynamics of slowly moving media there is a possibility not only of using, but also excluding the electrical effects of movement in the magnetic field. The conclusions presented serve as a basis for different methods for measuring the electrical field in the sea when carrying out magnetotelluric soundings, invesgigating currents and the vertical physiocochemical stratification of water masses. Author

N86-12701# Joint Publications Research Service, Arlington, Va.
PHASE OPERATOR METHOD IN PROBLEM OF SCATTERING OF ELECTROMAGNETIC WAVES ON IDEALLY CONDUCTING SURFACE Abstract Only c32
A. G. Voronovich *In its* USSR Rept.: Earth Sci. (JPRS-UES-85-008) 16 Aug. 1985 p 7-8 Transl. into ENGLISH from Dokl. Akad. Nauk SSSR (Moscow), v. 282, no. 2, May 1985 p 286-290

(For primary document see N86-12697 03-42)
Avail: NTIS HC A04/MF A01

Use of an S-matrix is common in a theoretical description of the scattering of electromagnetic waves on irregular surfaces because it relates the amplitudes of the incident and scattered waves. In an earlier article by the author (DAN, Vol 272, No 6, pp 1351-1355) it was proposed that a theory of perturbations be developed not relative to the scattering matrix itself, as is usually done, but relative to its logarithm. It was shown that with such an approach even the first approximation gives results corresponding to the first two approximations in the traditional perturbation theory. The approach proposed in that article is now applied to the problem of scatteing of an electromagnetic wave on an ideally conducting surface: a monochromatic electromagnetic wave of a stipulated frequency is incident on this surface from above, this surface consisting of plane (uniform and nonuniform) waves. A scattering matrix is formed for vertically and horizontally polarized waves for such a surface, as well as a matrix which the author calls a phase operator. With this as a point of departure, a final form of the scattering matrix is proposed for the first approximation (which can be used in subsequent approximations). Not only is a solution of the formulated problem obtained, but the advantageousness of the proposed approach over traditional perturbation theory is demonstrated. Author

N86-12702# Joint Publications Research Service, Arlington, Va.
QUASIGEOSTROPHIC MODEL OF CIRCULATION IN ANTARCTIC OCEAN WITH PARAMETRIZATION OF SYNOPTIC EDDIES Abstract Only c48
V. O. Ivchenko and A. V. Klepikov *In its* USSR Rept.: Earth Sci. (JPRS-UES-85-008) 16 Aug. 1985 p 8 Transl. into ENGLISH from Dokl. Akad. Nauk SSSR (Moscow), v. 281, no. 4, Apr. 1985 p 944-948 (For primary document see N86-12697 03-42)
Avail: NTIS HC A04/MF A01

Prognostic models of large-scale oceanic circulations require correct parametrization of synoptic scale disturbances, particularly for zonal currents such as the Antarctic Circumpolar Current. Traditional semiempirical closure hypotheses generally do not reflect the interaction of large-scale fields with synoptic eddies. Previous works have demonstrated the correctness of the diffusion parametrization for the adiabatic invariant potential eddy. The major feature of this approach is averaging of tensor components k sub ij. This tensor, characterized by four components, can be represented as the sum of symmetric and anti-symmetric parts, the latter related to the so-called orientation effects, i.e., the systematic rotation of fluid elements. Only the diagonal components of the k sub ij tensor are studied. The calculations confirm that in the region of the major zontal jet, the Sverdrup balance is not satisfied. The vertical component of the tangential wind stress rotor is balanced by divergences in the upper layer of the wind flow of the potential eddy. In the lower layer an analogous eddy flow is balanced by friction with the bottom. Author

N86-12703# Joint Publications Research Service, Arlington, Va.
ESTIMATION OF INFLUENCE OF OCEAN ON DISTRIBUTION OF HEAVY METALS IN MARINE ATMOSPHERE Abstract Only c45
V. V. Anikiyev, V. I. Ilichev, A. A. Lobanov, and A. N. Medvedev *In its* USSR Rept.: Earth Sci. (JPRS-UES-85-008) 16 Aug. 1985 p 9 Transl. into ENGLISH from Dokl. Akad. Nauk SSSR (Moscow), v. 281, no. 4, Apr. 1985 p 937-940 (For primary document see N86-12697 03-42)
Avail: NTIS HC A04/MF A01

The degree of enrichment of the surface microlayer with dissolved and suspended forms of Fe, Mn, Cu and Zn was determined at nineteen stations in various areas of the Pacific Ocean. The enrichment factors for the elements were calculated as the ratio of concentrations of dissolved and suspended forms of the heavy metals in the surface microlayer 250 microns thick and at a depth of 0.5 m. Total fluxes of metals from the ocean and factors of their enrichment in the atmosphere were calculated considering the possibility that the surface of the ocean is covered with an unsaturated surfactant monolayer. The influence of the ocean is found to be insufficient to explain the distribution of metals in the maritime atmosphere. Author

N86-12704# Joint Publications Research Service, Arlington, Va.
FOLDED STRUCTURES IN CENTRAL INDIAN OCEAN TRENCH Abstract Only c46
O. V. Levchenko, L. R. Merklin, and Yu. P. Neprochnov *In its* USSR Rept.: Earth Sci. (JPRS-UES-85-008) 16 Aug. 1985 p 10 Transl. into ENGLISH from Geotektonika (Moscow), no. 1, Jan. - Feb. 1985 p 15-23 (For primary document see N86-12697 03-42)
Avail: NTIS HC A04/MF A01

Continuous seismic profiling of the central Indian Ocean trench was performed during the 58th cruise of the research vessel Vityaz in 1976, revealing large folded structures to the north of the trench and a zone of deformation of the sedimentary mass and basement at 5 to 7 S. Analysis of the continuous profiling data from this and two other cruises is used in this article to define the area of folded deformations with a northeasterly strike in the sedimentary mass. The tectonic structure of the deformed zone is discussed. The deformation area is tilted relative to the general submeridional (north-northwest) direction of existing stresses. It is postulated that there is a large shear zone with a northeasterly strike to the north of the Indian-Australian plate. Author

N86-12705# Joint Publications Research Service, Arlington, Va.
REMOTE DIAGNOSIS OF MEDIA BY COMBINATION (RAMAN) ANTI-STOKES LIGHT SCATTERING METHOD WITH INDUCED BRILLOUIN BACKSCATTERING Abstract Only c74
A. F. Bunkin, D. V. Vlasov, and A. S. Galumyan *In its* USSR Rept.: Earth Sci. (JPRS-UES-85-008) 16 Aug. 1985 p 10-11 Transl. into ENGLISH from Kvantovaya Elektron. (Moscow), v. 12, no. 3, Mar. 1985 p 619-621 (For primary document see N86-12697 03-42)
Avail: NTIS HC A04/MF A01

An examination is made of the possibilities of remote sensing of the sea surface by raman spectroscopy. A modification of the method suitable for remote measurements was proposed earlier by the authors (A. F. Bunkin, et al., KVANTOVAYA ELEKTRONIKA, 10, 669, 1983; 10, 1902, 1983). In the proposed method the pumping wave is excited in the medium due to induced backscattering, especially induced Brillouin backscattering. With this taken into account, a general case of a nondegenerate scheme for remote measurements is described. In contract to the cases examined in the articles cited above, in which the minimum angles ensuring synchronism of the interacting waves were great, here it is shown that the angles can be as small as desired and collinear interaction is also possible. Developing these ideas, it is demonstrated that remote measurements can be made of the surface of water bodies by the methods of four-photon nonlinear spectroscopy of combination (Raman) scattering when there are small and zero angles between the interacting waves. Author

N86-12706# Joint Publications Research Service, Arlington, Va.
ACOUSTIC METHODS FOR FEATURING HIGH-FREQUENCY PART OF SPECTRUM OF SEA WAVES Abstract Only c71
G. Yu. Narodnitskiy *In its* USSR Rept.: Earth Sci. (JPRS-UES-85-008) 16 Aug. 1985 p 11 Transl. into ENGLISH from Izv. Akad. Nauk SSSR: Fiz. Atm. i Okeana (Moscow), v. 21, no. 4, Apr. 1985 p 443-446 (For primary document see N86-12697 03-42)
Avail: NTIS HC A04/MF A01

Measurements of the spectrum of ripples are very difficult. Possible approaches to solution of this problem are outlined. Some integral characteristics of ripples can be measured by acoustic methods with vertical pulsed sounding of the surface provided that the linear dimensions of the irradiated sector are small in comparison with the length of large sea waves. The rms value for ripple slopes can be measured by the synchronous registry of the slopes of large waves and the intensity of backscattered ultrasonic signals. Methods for measuring the rms values of ordinates and vertical velocities of ripples are based on use of the correlation between these parameters and the corresponding frequency and time correlation intervals of fluctuations in the amplitude of backscattered ultrasonic signals. With the earlier work on this problem taken into account, revised formulas are derived for determining the rms values for the ordinates and vertical velocities of ripples. Measurements of the characteristics of ripples when a vertical sounding transmitting-receiving system was situated at a height of about 7 m above the mean level of a water body are described. The frequency of the used ultrasound was about 40 KHz (wavelength 8 mm); the diameter of the irradiated sector at the 3-db level was 0.2 m. The formulas and methods given are applicable in measurements from scientific research ships and the rms values for ordinates and slopes of ripples can be measured either at drift or while a vessel is proceeding on course. Author

N86-12707# Joint Publications Research Service, Arlington, Va.
OCEAN ALBEDO FOR ATMOSPHERIC THERMAL EMISSION Abstract Only c48
R. G. Gardashov, Zh. K. Zolotova, and K. S. Shifrin *In its* USSR Rept.: Earth Sci. (JPRS-UES-85-008) 16 Aug. 1985 p 12 Transl. into ENGLISH from Izv. Akad. Nauk SSSR: Fiz. Atm. i Okeana (Moscow), v. 21, no. 4, Apr. 1985 p 438-440 (For primary document see N86-12697 03-42)
Avail: NTIS HC A04/MF A01

In computations of components of the radiation budget of the ocean its surface albedo for atmospheric thermal emission chi is assumed equal to (1 - epsilon), where epsilon is surface emissivity, although in actuality chi approx. equals (1-epsilon). A study was made for evaluating chi under some mean standard conditions. It is assumed that the brightness of thermal emission of the sky B and surface albedo for direct radiation A subs are not dependent on azimuth (B = B((Theta, lambda) and A sub s = A sub s (theta, lambda), where theta is zenith distance, lambda, is wavelength). If B (theta, lambda) is replaced by the Planck function B sub O (T sub w, lambda) with the water surface temperature T sub w, the chi value is equal to chi prime = 1 - epsilon. The theta values were computed earlier. Atmospheric emission in the range 7 to 15 microns was determined using the formula beta (theta, lambda) = B sub O (T sub w, lambda) - f (theta, lambda). Albedo A sub s (theta, lambda was computed in the approximation of the stochastically distributed areas method with different wind velocities and with allowance for shading. Computations were made in the spectral range 2.5 to 250 microns. The results of chi computations for a cloudless atmosphere are given in a table. Computations are also given for a continuous cloud cover. The chi values for a partial cloud cover can be obtained by interpolation. A formula is derived for effective emission of the ocean, based on the difference between chi and chi prime. A correction is introduced to take into account the influence of a cold film on the sea surface. Author

N86-12708# Joint Publications Research Service, Arlington, Va.
INVESTIGATION OF ELASTIC PROPERTIES OF MARINE SURFACE-ACTIVE FILMS Abstract Only c48
B. T. Demin, S. A. Yermakov, Ye. N. Pelinovskiy, T. G. Talipova, and A. I. Sheremetyeva *In its* USSR Rept.: Earth Sci. (JPRS-UES-85-008) 16 Aug. 1985 p 12-13 Transl. into ENGLISH from Izv. Akad. Nauk SSSR: Fiz. Atm. i Okeana (Moscow), v. 21, no. 4, Apr. 1985 p 410-416 (For primary document see N86-12697 03-42)
Avail: NTIS HC A04/MF A01

The dependence of the elasticity parameter of films on wind velocity, the film relaxation effect and the dependence of the film elasticity parameter on the concentration of surface-active agents were studied. The measurements were made from an oceanographic platform in the coastal zone of the Black Sea in the autumn of 1981 and 1982. The apparatus used in measuring film parameters is described. It was found that the film elasticity parameter and the surface-active agent concentration on the average decrease with an increase in wind velocity to V approximately equals 5 to 6 m/sec. An increase in these parameters is observed when there are stronger winds. The results obtained by Huhnerfuss and Garrett on a change in the properties of films with time were confirmed. the film relaxation time increases with an increase in wind velocity. There is a good correlation between the film elasticity values and the concentration of surface-active agent. It is emphasized that these conclusions are based on the results of measurements of sea films in the coastal zone and such investigations must be made in the open ocean. Author

N86-12709# Joint Publications Research Service, Arlington, Va.
STRUCTURE OF SEDIMENTARY COVER AND BASEMENT OF SIERRA LEONE RISE DETERMINED FROM COMMON DEPTH POINT SEISMIC (EQUATORIAL ATLANTIC) Abstract Only c46
V. I. Kara, K. N. Mamoshina, and A. Ye. Shlezinger *In its* USSR Rept.: Earth Sci. (JPRS-UES-85-008) 16 Aug. 1985 p 14 Transl. into ENGLISH from Geotektonika (Moscow), no. 3, May - Jun. 1985 p 38-49 (For primary document see N86-12697 03-42)
Avail: NTIS HC A04/MF A01

A thorough study of the Sierra Leone Rise was made in 1979 by geophyiscal methods, including seismic work by the common depth point method, along runs with a total length of 2,00 km. This rise consists of two morphologically different sectors separated by a troughlike valley with an E to W orientation; the rise is separated from the continental margin of Africa by the basin of the same name. Crustal thickness within the rise is 13 km. The crustal section consists of a lower basalt layer with a thickness up to 8 km and a layer with densities 2.5 to 2.6 g. cubic centimeter with a thickness up to 5 km. In the basin the thickness of the consolidated crust does not exceed 6 km and belongs to the basalt layer. An analysis is given of bedding conditions, thicknesses and seismogeological characteristics of the sedimentary layers (deep drilling data are also used). It is concluded that the Sierra Leone Rise is a major volcanic shield with a total thickness as great as 4,000 to 5,000 m, overlying a melanocratic basement. In some sectors, outpourings continued up to the Early Quaternary, resulting in formation of underwater volcanic mountains. The region became divided into uplifted and subsided sectors by the beginning of the Late Cretaceous. Subsequent volcanic activity occurred primarily in the rise. The structural plan of the present-day bottom of the rise was doubtlessly formed by Quaternary post-sedimentation differentiated descending tectonic movements. Author

N86-12710# Joint Publications Research Service, Arlington, Va.
TECTONIC STRUCTURE OF SHIRSHOV RIDGE (BERING SEA) Abstract Only c46
Yu. P. Neprochnov, V. V. Sedov, L. R. Merklin, V. P. Zinkevich, O. V. Levchenko, B. V. Baranov, and G. B. Rudnik *In its* USSR Rept.: Earth Sci. (JPRS-UES-85-008) 16 Aug. 1985 p 15 Transl. into ENGLISH from Geotektonika (Moscow), no. 3, May - Jun. 1985 p 21-37 (For primary document see N86-12697 03-42)
Avail: NTIS HC A04/MF A01

An interpretation of the geological structure of Shirshov Ridge, until recently virtually unstudied, is regarded as highly important due to the position of this ridge at the boundary between two abyssal basins of different age. Only A full comprehension of its tectonic structure will cast light on evolution of the Bering Sea region. A geological and geophysical study of this ridge was made on the 29th cruise of the Dmitriy Mendeleyev in 1982. Dredging was carried out, accompanied by continuous seismic profiling and deep seismic sounding. The ridge extends in a submeridional direction for about 700 km and has a width up to 130 km. In the north it is an underwater extension of the Olyutorsk Peninsula, but with approach to the Aleutian arc it changes its strike to sublatitudinal and at depths of about 3,600 m almost joins the Bowers Ridge. A description of the three principal blocks of the ridge is given. Continuous seismic profiling revealed that the ridge has an asymmetric structure. Deep seismic sounding disclosed that crustal thickness beneath the ridge is as great as 18 km. Three different rock associations were defined: (1) amphibolites, dolerities, quartzy dolerites; (2) deep-water siliceous, siliceous-clayey and tuffogenic-sedimentary deposits of Triassic, late Cretaceous-Paleogene and Oligocene age; and (3) slightly lithified siliceous and terrigenous deposits of Neogene age. The totality of available data suggests that Shirshov Ridge is a zone of crowding of the oceanic crust at the boundary of two differently structured Bering Sea basins. Author

N86-12711# Joint Publications Research Service, Arlington, Va.
FINE STRUCTURE OF DENSITY RELATION IN MAIN OCEANIC THERMOCLINE Abstract Only c48
V. M. Zhurbas *In its* USSR Rept.: Earth Sci. (JPRS-UES-85-008) 16 Aug. 1985 p 17 Transl. into ENGLISH from Okeanol. (Moscow), v. 25, no. 2, Mar. - Apr. 1985 p 215-218 (For primary document see N86-12697 03-42)
Avail: NTIS HC A04/MF A01

An important problem in studying fine thermocline structure in the ocean is experimental clarification of the mechanisms of its generation. The best results have been obtained by an analysis of the ratio of the amplitudes of fine-structure temperature and salinity fluctuations. However, in cases (encountered very frequently in the main thermocline) when the thermohaline structure has a steplike character, an analysis of the ratio of the amplitudes of T and S fine-structure fluctuations is inadequate for drawing any conclusions concerning the mechanisms by which the fine structure was formed. It is suggested that in such cases additional information could be obtained by an analysis of the fine structure of the density ratio. The author discusses the degree to which different mechanisms of generation of fine thermohaline structure can exert an influence on variability of the density ratio. It is indicated that in a stepped thermocline structure formed as a result of interaction of intrusion processes and double diffusion (hypothetically, at least, occurring in the main thermocline) there will also be a fine structure of the density ratio. This will afford a possibility for distinguishing such a venture (for example) from the steps produced by local turbulent mixing. The validity of these conclusions was confirmed by probing of a stepped structure in the main thermocline in the tropical Atlantic on the third cruise of the scientific research ship Akademik Mstislav Keldysh. Author

N86-12712# Joint Publications Research Service, Arlington, Va.
VISCOUS NONLINEAR CIRCULATION IN AXISYMMETRIC BAROCLINIC EDDY Abstract Only c48
D. O. Gordeyvhev and G. G. Sutyrin *In its* USSR Rept.: Earth Sci. (JPRS-UES-85-008) 16 Aug. 1985 p 18 Transl. into ENGLISH from Okeanol. (Moscow), v. 25, no. 2, Mar. - Apr. 1985 p 186-192 (For primary document see N86-12697 03-42)
Avail: NTIS HC A04/MF A01

A study was made of vertical-radial movements arising in an axisymmetric eddy as a result of the combined influence of nonlinear effects, the most important of which are centrifugal force and the turbulent diffusion of momentum, heat and salt. Specifically, the authors examine the evolution of an axisymmetric disturbance in a rotating layer of stratified fluid in the Boussinesq and quasistatic approximations. It is assumed that the coefficients of turbulent exchange of momentum, heat and salt are equal to one another but are different for the vertical and radial directions. The role of verifical diffusion is evaluated using the value K approx. 0.0001 square meters/sec, characteristic for the main thermocline. The comparative contribution of vertical diffusion is characterized by the dimensionless coefficient K prime = Kr asterisk squared /Az asterisk squared. It is further assumed that radial movements are related to a change in aximuthal velocity. Equations are derived describing the evolution of an eddy in dimensionless variables. In this formulation of the problem a model is developed and examples are presented showing that with identical coefficients of exchange of heat, salt and momentum the joint influence of diffusional processes and nonlinearity results in a radial-vertical circulation of water, for the most part due to centrifugal force. With small values of the Kibel'-Rossby number, a subsidence of water occurs along the axes of eddies in both cyclones and anticyclones, but to a considerably lesser degree in the former than in the latter. Author

N86-12713# Joint Publications Research Service, Arlington, Va.
FACIES-GENETIC GROUPS OF COARSE CLASTIC MATERIAL ON WORLD OCEAN FLOOR Abstract Only c48
N. N. Kachanov *In its* USSR Rept.: Earth Sci. (JPRS-UES-85-008) 16 Aug. 1985 p 18-19 Transl. into ENGLISH from Dokl. Akad. Nauk Ukr. SSR, Ser. B: Geol. Khim i Biol. Nauki (Kiev), no. 4, Apr. 1985 p 27-31 (For primary document see N86-12697 03-42)
Avail: NTIS HC A04/MF A01

The author compiled the first map of the geographical distribution of hard rocks on the ocean floor. A description of the position of fragments in situ, the granulometric and morphometric parameters processed on a computer using a special program, lithological and petrochemical data and age determinations are evidence of a multistage character of the processes involved in formation of fields of large clastic material, a diversity of conditions for the mobilization and accumulation of such material in recent and ancient layers of bottom sediments. New data on the development of such deposits at great depths afford possibilities for sounder conclusions in paleogeograhy. The facies and genetic characteristics of such deposits in the Atlantic, Pacific, Indian and Arctic Oceans are described. Important conclusions are drawn concerning the agents responsible for the transport of such materials. In the Atlantic, for example, ice and icebergs played the most important roles, both in the Holocene and earlier. The greatest concentration of psephites is in the high latitudes (north of 25 N and south of 35 to 40 S), where ice and icebergs are and have been most common. However, gravitational processes have also played a role near the Mid-Atlantic Ridge, in shallow-water areas, in tectonically active regions and near strongly abraded rocky shores of continents and islands. A third source is biogenous in nature, such as in reefs and deposits of shells. Similar processes have been operative in all the oceans. The influence of hydrology, bottom geomorphology, climate and geotectonics is also examined. Areas with such deposits of rock materials and bedrock outcroppings usually are a favorite habitat of marine fauna and their study therefrom is of economic significance. Author

N86-12714# Joint Publications Research Service, Arlington, Va.
SPATIAL STRUCTURE OF HIGH-FREQUENCY SEA WIND WAVES UNDER DIFFERENT METEOROLOGICAL CONDITIONS Abstract Only c48
I. I. Strizhkin, M. P. Lapchinskaya, Yu. A. Ilin, and V. A. Malinnikov *In its* USSR Rept.: Earth Sci. (JPRS-UES-85-008) 16 Aug. 1985 p 19-20 Transl. into ENGLISH from Izv. Akad. Nauk SSSR: Fiz. Atm. i Okeana (Moscow), v. 21, no. 4, Apr. 1985 p 440-442 (For primary document see N86-12697 03-42)
Avail: NTIS HC A04/MF A01

Data are given from a study of the spatial structure of high-frequency wind waves in the range of wavelengths lambda = 1.6 to 60 cm obtained in a photographic survey of the sea surface. The photoinformation on the wavecovered water surface was obtained in stereo- and monosurveys from a platform in the Caspian Sea. The survey was made with two synchronized AFA-41/7.5 aerial cameras from a height of 12 m; survey scale was 1:60; a single photograph covered an areas of 28 square meters on the surface. About 250 photographs of waves obtained under different meteorological conditions and with waves of different classes were processed for an analysis of the spatial distribution of ripples. The total area of water surface analyzed was 150,000 to 200,000 wquare meters. The survey was made in series of 5 to 25 photographs with intervals 2.5, 5 and 10 sec. It was found that with wind velocities from 5 to 18 m/sec the entire surface of the main wave is covered by sectors of capillary and capillary-gravity waves; these sectors have distinct boundaries. Within each sector the waves have a regular structure; in the case of steady waves the capillary and capillary-gravity waves are oriented primarily perpendicularly to the wind velocity, with deviations usually not exceeding 20 deg. There are two principal types of surface spatial distribution of capillary and capillary-gravity waves. In the first on the surface of the sector there are 1-2 identical or somewhat different systems of waves, frequently oriented at an angle to one another. Author

N86-12715# Joint Publications Research Service, Arlington, Va.
NONLINEAR INTERACTION BETWEEN SOLITON AND SHORT WAVES IN IDEAL FLUID Abstract Only c46
Ye. S. Benilov *In its* USSR Rept.: Earth Sci. (JPRS-UES-85-008) 16 Aug. 1985 p 20 Transl. into ENGLISH from Izv. Akad. Nauk SSSR: Fiz. Atm. i Okeana (Moscow), v. 21, no. 4, Apr. 1985 p 417-421 (For primary document see N86-12697 03-42)
Avail: NTIS HC A04/MF A01

The problem of interaction of waves with considerably different spatial scales is examined. The objective was a determination of the steady form of a restructured soliton (when it is not destroyed by interaction with short waves) for gravity waves in a fluid. During interaction between short surface waves and internal waves resonance can develop, which results in a strong restructuring of both types of waves. The following problem is examined: there are two types of surface gravitational wave movements in an ideal fluid of the finite depth h with a free boundary -- long low-frequency waves (h/L $< <$ 1), where L is their characteristic horizontal dimensions, and quasimonochromatic short high-frequency waves (kh $> >$ 1), where k is the wave vector of the carrier harmonic. It is assumed that the LF and HF waves propagate in the same direction. The entire analysis is made in a potential, slightly nonlinear approximation. The equations derived and the solutions which are found describe the propagation of a soliton of long gravitational wave on the surface of a fluid against the background of a quashiharmonic short wave. On this basis it was possible to obtain a generalization for a broad spectrum of short waves. A solution describing a solitary internal wave accompanied by a packet of short surfce waves was obtained. Author

N86-12716# Joint Publications Research Service, Arlington, Va.
THE QUESTION OF EARTH EXPANSION AND ITS OCEANIC IMPLICATIONS c46
Vladimir Neiman *In its* USSR Rept.: Earth Sci. (JPRS-UES-85-008) 16 Aug. 1985 p 21-23 Repr. from Moscow News (Moscow), no. 13 p 10 (For primary document see N86-12697 03-42)
Avail: NTIS HC A04/MF A01

The hypothesis of Earth expansion was first advanced by Russian scientist I. Yarkovsky nearly a hundred years ago. The idea of Earth expansion was first suggested by Alfred Wegener in the 1920's. According to him, both Americas, Eurasia, Australia and Antarctica formed Panagaea, a single land mass with no oceans between the continents. But the hypothesis of the continents have drifted apart like ships over many thousands of kilometres contradicts physics. However, the continents have still moved apart. So what is the reason for this? The first geologic grounds for this were provided by Hilgenberg. He assumed that the continents do not move along the substratum but drift from one another due to the appearance of new zones between them. This process is going on deep inside the planet and this caused the fragmentation of the single continent and the formation of the seas and oceans in the gaps between the land masses. Author

N86-12717# Joint Publications Research Service, Arlington, Va.
KAMCHATKA RADIO TELEMETRIC STATION REGISTERS VOLCANO PULSE Abstract Only c46
In its USSR Rept.: Earth Sci. (JPRS-UES-85-008) 16 Aug. 1985 p 24 Repr. from TASS (Moscow), v. 5-15 20 May 1985 (For primary document see N86-12697 03-42)
Avail: NTIS HC A04/MF A01

Information which serves as the basis for forecast of volcano eruptions is supplied to scientists in the Kamchatka (the Soviet Far East). A radio telemetric station installed on the slopes of Klychevskaya Sopka volcano, one of the biggest in Euroasia, is constantly registering the pulse of the volcano and automatically supplies the information to the receiving station. This method has already helped to predict the eruption of a number of volcanoes with high accuracy. Soviet seismologists are creating a system of prompt collection of geophysical information from areas of seismic activity in thhe peninsula. A series of telemetric stations has been designed for the purpose at the Institute of Volcanology of the Far Eastern Scientific Center of the USSR Academy of Sciences. Author

N86-12718# Joint Publications Research Service, Arlington, Va.
LASERS MEASURE DRIFTING MOUNTAINS Abstract Only c46
In its USSR Rept.: Earth Sci. (JPRS-UES-85-008) 16 Aug. 1985 p 25 Transl. into ENGLISH from TASS (Moscow), no. 0447 GMT, 12 Apr. 1985 (For primary document see N86-12697 03-42)
Avail: NTIS HC A04/MF A01

Soviet Tajik scientists have established with the use of lasers that two mountain ranges in Pamir have moved closer to each other by half a meter in three decades. By taking regular measurements with a light beam of the distance between the Karategin and Petr Pervyy ranges, they noticed a previously undiscovered phenomenon. It transpires that the two giant ranges sometimes move closer, and sometimes, further apart. Scientists believe that the drifting is connected with tectonics processes deep in the Earth and is not disastrous. It is yet another natural phenomenon which was previously unknown. Author

N86-12719# Joint Publications Research Service, Arlington, Va.
LAUNCH OF KOSMOS-1653 NATURAL RESOURCES RESEARCH SATELLITE Abstract Only c18
In its USSR Rept.: Earth Sci. (JPRS-UES-85-008) 16 Aug. 1985 p 27 Transl. into ENGLISH from Sots. Ind. (Moscow), 24 May 1985 p 2 (For primary document see N86-12697 03-42)
Avail: NTIS HC A04/MF A01

An artificial Earth satellite, Kosmos-1653, was launched from the Soviet Union on May 22, 1985. Installed on board the satellite is scientific apparatus intended for the continuation of research of the Earth's natural resources in the interests of various branches of the USSR's economy and of international cooperation. The satellite was placed into an orbit with the parameters: initial period of revolution--89.6 minutes; apogee--322 kilometers; perigee-222 kilometers; orbit inclination--82.3 degrees. Incoming information is being transmitted to the State scientific Research and Production Center Priroda for processing and utilization. Author

N86-12720# Joint Publications Research Service, Arlington, Va.
MUON TOMOGRAPHY USED TO STUDY UNDERGROUND ROCK STRUCTURE Abstract Only c46
A. Alekseyev *In its* USSR Rept.: Earth Sci. (JPRS-UES-85-008) 16 Aug. 1985 p 28 Transl. into ENGLISH from NTR: Probl. i Resheniya (Moscow), 30 Apr. - 13 May 1985 p 6 (For primary document see N86-12697 03-42)
Avail: NTIS HC A04/MF A01

A method called muon tomography has been developed to study underground rock structure. The flow of cosmic rays, penetrating the Earth's atmosphere produces a downpour of various elementary particles, including muons. They are capable of penetrating for kilometers into the Earth's depths. These particles can be used as a source for x-raying underground rock and also foundations of engineering structures. Instruments used for such measurements have been given the name of muon telescopes. Usually they are installed in a tunnel beneath the object to be studied, and the object's density is measured with high accuracy according to the intensity of radiation falling on detectors. Muons help to detect hollow spaces in underground rock masses which form as a result of the washing out of soluble rock by ground water, such as in limestone. The recording principle is the same: if such hollow spaces are present in the zone of visibility of a muon telescope, the flow of recorded particles increases immediately. B.W.

N86-12721# Joint Publications Research Service, Arlington, Va.
UNDERGROUND VOLCANOES DISCOVERED WITH SATELLITE RADAR Abstract Only c46
In its USSR Rept.: Earth Sci. (JPRS-UES-85-008) 16 Aug. 1985 p 29 Transl. into ENGLISH from Sov. Belorussiya (Minsk), 23 May 1985 p 4 (For primary document see N86-12697 03-42)
Avail: NTIS HC A04/MF A01

The crates of two giant volcanoes have been discovered with the help of satellite radar. One of them is located beneath the scorching sands of the West Sahara, while the other is warming the ice of Antarctica. A radar system developed by Khar'kov scientists in collaboration with specialists of Moscow and Sevastopol made it possible to see the craters. This system is installed on board the Soviet satellites Cosmos-1500 and Cosmos-1602. Author

N86-12722# Joint Publications Research Service, Arlington, Va.
P-WAVE SPECTRA IN PROBLEM OF DETERMINING DYNAMIC

PARAMTERS OF EARTHQUAKE FOCI STANDARDIZATION OF INITIAL DATA AND PROCEDURES FOR COMPUTING AMPLITUDE SPECTRA Abstract Only c46
Zh. Ya. Aptekman, S. K. Daragan, D. V. Dolgopolov, A. I. Zakharova, V. M. Zobin, S. Ya. Kogan, O. A. Korchagina, A. G. Moskvina, L. A. Polikarpova, and L. S. Chepkunas *In its* USSR Rept.: Earth Sci. (JPRS-UES-85-008) 16 Aug. 1985 p 30 Transl. into ENGLISH from Vulkanol. i Seysmologiya (Moscow), no. 2, Mar. - Apr. 1985 p 60-70 (For primary document see N86-12697 03-42)
Avail: NTIS HC A04/MF A01

The focal parameters of earthquakes are commonly determined from the spectra of P-waves, but comparison of the results obtained by different authors for the same event on the basis of different materials often reveals serious discrepancies, as great as an order of magnitude. The authors believe that this situation is not due to any fundamental deficiency of the spectral method, but instead is attributable to the use of different hypotheses and formulas relating the spectral parameters and focal parameters of earthquake foci and the result of lack of a consistent, fully validated approach in the choice of initial material. The thrust of the article is therefore the need for standardizing requirements on the initial material, processing procedures and computation methods. The authors examine each aspect of this problem: choice of initial material; instrumentation used; seismogram quality; signal level; signal-to-noise ratio; choice of length of analyzed segment of record; zero line; beginning and end of interval on record reduced to digital form; digital interval; choice of algorithm for computing spectra; numerical range of spectrum; frequency interval; instrumental correction; averaging of spectra. Author

N86-12723# Joint Publications Research Service, Arlington, Va.
PROSPECTS FOR DEVELOPMENT OF SEISMIC PROSPECTING METHODS AND APPARATUS Abstract Only c46
Yu. V. Timoshin *In its* USSR Rept.: Earth Sci. (JPRS-UES-85-008) 16 Aug. 1985 p 31 Transl. into ENGLISH from Geofiz. Zh. (Kiev), v. 7, no. 2, Mar. - Apr. 1985 p 3-12 (For primary document see N86-12697 03-42)
Avail: NTIS HC A04/MF A01

Mobile stations (MS) for exciting oscillations and self-contained reception and registry stations (SRRS) are discussed. These ensure excitation of seismic oscillations on the land and in the water by a contectless method, that is, in the total absence of a mechanical coupling between the source and the ground. A number of stages can be defined in the development of such a seismic prospecting system. The first stage involves development of self-contained apparatus for the reception and registry of seismic oscillations mounted on a truck or other vehicle with excellent cross-country capabilities, this being the most important element in the complete mechanization of the entire observation process. The second stage involves development of sources of contactless excitation of oscillations. The third stage involves improvement of means for the reception of oscillations by use of aerial pressure detectors and antennas for the reception of the electromagnetic waves accompanying the propagation of seismic waves in geological media. The fourth stage involves the development of methods and apparatus for the remote contactless reception of seismic oscillations. B.W.

N86-12724# Joint Publications Research Service, Arlington, Va.
DETERMINATION OF DYNAMIC PARAMETERS OF REFLECTED WAVES ON SLOPES OF DEEP WATER TRENCH Abstract Only c48
V. G. Bykov, F. A. Vorobyev, V. V. Zhigulev, and S. S. Snegovskoy *In its* USSR Rept.: Earth Sci. (JPRS-UES-85-008) 16 Aug. 1985 p 32 Transl. into ENGLISH from Tikhookeanskaya Geol. (Novosibirsk), no. 1, Jan. - Feb. 1985 p 99-103 (For primary document see N86-12697 03-42)
Avail: NTIS HC A04/MF A01

An attempt is made to determine the absorption and reflection coefficients in the sedimentary mass of three different sections in the north-west Pacific in parallel with continuous seismic profiling. The area of studies is a part of the Kuril-Kamchatka deep water trench. The first section is more than 100 km from the axis of the trench in an area with a water depth of about 1200 m. The second is located at the base of the ocean slope of the island structure some 150 km from the trench axis, bottom depth about 1100 m. Section three is on the oceanic slope of the trench, some 20 km from its main portion. In all three areas there are two layers of sedimentary deposits differeing both in internal structure and in physical properties. The observed similarities in structure, lithologic composition and physical properties of the sedimentary deposits of the oceanic and deep water portions of the continental slope along the Kuril-Kamchatka trench indicate simiarity of the sedimentation process in these zones as well. Author

N86-12725# Joint Publications Research Service, Arlington, Va.
OPTIMAL DENSITY MODEL OF EARTH'S RUST AND UPPER MANTLE ALONG KAMCHATKA-PACIFIC GEOTRAVERSE Abstract Only c46
M. L. Krasnyy, V. Yu. Kosygin, and V. I. Isayev *In its* USSR Rept.: Earth Sci. (JPRS-UES-85-008) 16 Aug. 1985 p 32-33 Transl. into ENGLISH from Tikhookeanskaya Geol. (Novosibirsk), no. 1, Jan. - Feb. 1985 p 72-84 (For primary document see N86-12697 03-42)
Avail: NTIS HC A04/MF A01

An a priori density model was constructed of a geotraverse from Kamchatka to the Pacific Ocean on the basis of a seismic model and the known relationship between velocity and density, extending over 400 km on the surface and down to a depth of 250 km. Multidimensional modeling was used to solve the inverse problem producing reliable solutions for 80% of the approximating blocks greatly reducing the inaccuracies of the a priori model. It was found that at great depths the lithospheric plate apparently dissolves (is assimilated into the mantle). The lithospheric layer beneath the continental block and the boundary of the ocean section has a thickness of 50 to 60 and 80 km, the mean density of the lithosphere in the continental block being significantly less than that of the oceanic block. Density is reduced beneath the seismofocal zone in both west and east, while the seismofocal zone itself is denser than the asthenosphere and the underlying subasthenosphere layer. Author

N86-12726# Joint Publications Research Service, Arlington, Va.
VARIATION IN SEISMICITY UNDER INFLUENCE OF LUNAR-SOLAR TIDAL DEFORMATIONS Abstract Only c46
A. L. Rykunov and V. B. Smirnov *In its* USSR Rept.: Earth Sci. (JPRS-UES-85-008) 16 Aug. 1985 p 33 Transl. into ENGLISH from Izv. Akad. Nauk SSSR: Fiz. Zemli (Moscow), no. 1, Jan. 1985 p 97-103 (For primary document see N86-12697 03-42)
Avail: NTIS HC A04/MF A01

Studies of the relationship of variations of seismicity to external effects in the past have been based primarily on data from a regional network of seismic stations, resulting in the use of only large, infrequent events. This makes it impossible to use correlation and spectral analysis methods as can be done with higher frequency seismic noise, hindering comparison of the specifics of the response of the medium on various scales. These shortcomings can be avoided by analyzing the time distribution of microearthquakes, which are repeated much more frequently. Observations with highly sensitive and independent recording apparatus were performed in an area of high seismic activity in 1981 on Kamchatka. Microearthquakes were continuously recorded for 24 hours. Analysis of the distribution of these minor earthquakes indicated that there is a correlation between seismicity and tidal effects. The presence of a system of quasiperiodic variations in seismicity was noted. The distribution of microearthquakes caried over time from statistically independent tests. The existence of microearthquakes swarms related to seismicity maxima was noted. Author

N86-12727# Joint Publications Research Service, Arlington, Va.
ELECTROMAGNETIC EFFECTS IN CRUSTAL FRACTURING Abstract Only c46
M. B. Gokhberg, I. L. Gufeld, N. I. Gershenzon, and V. A. Pilipenko *In its* USSR Rept.: Earth Sci. (JPRS-UES-85-008) 16 Aug. 1985 p 34 Transl. into ENGLISH from Izv. Akad. Nauk SSSR: Fiz.

Zemli (Moscow), no. 1, Jan. 1985 p 72-87 (For primary document see N86-12697 03-42)
Avail: NTIS HC A04/MF A01

The major results from field observation of electromagnetic precursors of seismic events are presented. These phenomena, including disturbances in the atmospheric electric potential, pulsed electromagnetic radiation, electrotelluric fields and luminous effects, characteristically appear on the order of the hours to days before earthquakes, with earthquakes occurring during a decrease in the phenomena. The phenomena occur over a broad frequency range. All anomalies except for electromagnetic radiation have been observed at the epicenters of earthquakes. Foreshocks have not been recorded during these anomalies. No burst of electromagnetic, atmospheric electric or electrotelluric fields has been observed at the moment of earthquakes. Electromagnetic radiation in the radio frequency band is considered most promising for earthquake prediction purposes. The specific characteristics of electromagnetic radiation caused by seismic phenomena must be determined in order to distinguish this radiation from other electromagnetic radiation. Author

N86-12728# Joint Publications Research Service, Arlington, Va.
EXPERIENCE IN BREAKING DOWN GRAVITY FIELD INTO COMPONENTS RESULTING FROM DENSITY HETEROGENEITIES AT VARIOUS DEPTHS (USING NORTH ATLANTIC AND MEDITERRANEAN AS EXAMPLES) Abstract Only c46
M. Ye. Artemyev, T. M. Babayeva, I. Ye. Voydetskiy, and V. O. Mikhaylov *In its* USSR Rept.: Earth Sci. (JPRS-UES-85-008) 16 Aug. 1985 p 34-35 Transl. into ENGLISH from Izv. Akad. Nauk SSSR: Fiz. Zemli (Moscow), no. 1, Jan. 1985 p 44-52 (For primary document see N86-12697 03-42)
Avail: NTIS HC A04/MF A01

A spectral analysis of gravity anomalies is presented. The intitial data for the analysis were values of isostatic anomalies in the North Atlantic, Western Europe and the Mediterranean, averaged in 1 x 1 degree trapezoids based on published foreign data on the gravity field. The field was divided into components using a minimum-square Kolmogorov-Wiener filter using an algorithm which considered the spherical nature of the earth and was suitable for processing files of up to 10,000 points on a BESM-6 computer. The results indicate that the study of heterogeneities located deeper than the level of isostatic compensation requires the use of gravity anomalies after introduction of corrections for the major surface density heterogeneities and their isostatic compensation. Subasthenospheric density heterogeneities create gravitational anomalies with wavelengths of 800-1000 km. There are two classes of deep density heterogeneities which appear in the gravity field at wavelengths of between 1000 and 2000 km and greater than 2000 km. Author

N86-12729# Joint Publications Research Service, Arlington, Va.
HYPOCENTRAL AREAS OF AFTERSHOCKS AND POSSIBLE FAULT SYSTEMS AT FOCI OF TSUNAMI-GENERATING KURIL EARTHQUAKES Abstract Only c46
S. L. Solovyev and K. A. Kechekezyan *In its* USSR Rept.: Earth Sci. (JPRS-UES-85-008) 16 Aug. 1985 p 35 Transl. into ENGLISH from Izv. Akad. Nauk SSSR: Fiz. Zemli (Moscow), no. 1, Jan. 1985 p 3-15 (For primary document see N86-12697 03-42)
Avail: NTIS HC A04/MF A01

While acknowledging the limited capabilities and low reliability of the aftershock method of analyzing processes at the foci of earthquakes, particalarly in the Kuril-Kamchatka area, it was still decided to use this method as the only possible one to study the foci of five comparatively recent tsunami-generating Kuril earthquakes. The results of the analysis were compared with available information on the tectonics of the island slope of the Kuril deep water trench. Data on the foci of the tsunamis and intensity of the waves were the result of standard determination of the focal mechanism. The five earthquakes all had a magnetude greater than 7 and occurred between 1969 and 1975. The results indicate that the model of a single fault presently used to describe processes of foci of tsunami-generating and strong Kuril-Kamchatka earthquakes in general is not sufficient and is too arbitrary. More effective methods of reconstructing these processes must be developed, since they may well consist of movements along several faults simultaneously. Author

N86-12730# Joint Publications Research Service, Arlington, Va.
METHOD AND RESULTS OF ELECTROMETRIC OBSERVATIONS IN SEISMICALLY ACTIVE REGION Abstract Only c46
M. G. Ostashevskiy and A. Ya. Sidorin *In its* USSR Rept.: Earth Sci. (JPRS-UES-85-008) 16 Aug. 1985 p 36 Transl. into ENGLISH from Dokl. Akad. Nauk SSSR (Moscow), v. 282, no. 2, May 1985 p 295-299 (For primary document see N86-12697 03-42)
Avail: NTIS HC A04/MF A01

Any increases in the accuracy of measurement of rock impedance will afford new possibilities for diagnosis of its state and use of the electrometric method in research on earthquake prediction. The article describes the fundamental principles and methods for contending with noise in electrical sounding which make possible a considerable increase in the inefficiency of accumulations and gives some results of observations of variations of impedance in the Garm geophysical test range in the seismically active part of the Tajik SSR. An optimum accumulation algorithm was developed on the basis of the statistical properties of a large number of records of noise observed during electrical sounding. The great volume of research data ensured full automation of the experiment by direct input of data from a precise digital measuring instrument into a minicomputer where they were processed using different algorithms at a real time scale. Measurements are made once a day in half-hour intervals. The pulse repetition rate was 24 sec and the duration of one accumulation cycle was 132 sec. B.W.

N86-12731# Joint Publications Research Service, Arlington, Va.
SEISMIC EFFECT OF UNDERGROUND BLASTS AND PROBLEM OF ESTIMATING TOTAL EARTHQUAKE ENERGY Abstract Only c46
M. A. Sadovskiy, O. K. Kedrov, V. A. Laushkin, and I. L. Pasechnik *In its* USSR Rept.: Earth Sci. (JPRS-UES-85-008) 16 Aug. 1985 p 37 Transl. into ENGLISH from Dokl. Akad. Nauk SSSR (Moscow), v. 281, no. 4, Apr. 1985 p 825-829 (For primary document see N86-12697 03-42)
Avail: NTIS HC A04/MF A01

An estimate is presented of the upper limit of total earthquake energy based on seismic energy determined by remote seismic measurement of P waves using records of American underground nuclear blasts with known source energy. The work is a contribution to the formulation of an absolute energy scale for earthquakes based on records of P waves from 99 underground blasts in the continental USA and on Amchitka Island. Records were obtained at two experimental stations in the USSR located at distances of 30 and 90 degrees from the epicenters of the blasts. The events were recorded in a three-component short-period channel with a gain of 2 x 10 to the 5th power at 1 Hz. It is found necessary to consider signal frequency in determining the absorption coefficient. The most objective energy estimates can be obtained if integration includes only the focal P wave, suppressing P-coda oscillations by frequency and polarization filtration. Calculations should be performed in the frequency range rather than in the time range, though comparable results are produced by the two methods in the first approximation. B.W.

N86-12732# Joint Publications Research Service, Arlington, Va.
TECTONICS OF EASTERN KRONOTSKIY PENINSULA AND FORMATIONAL ASSOCIATION OF BASALTS (KAMCHATKA) Abstract Only c46
Yu. N. Raznitsin, S. A. Khubunaya, and N. V. Tsukanov *In its* USSR Rept.: Earth Sci. (JPRS-UES-85-008) 16 Aug. 1985 p 37-38 Transl. into ENGLISH from Geotektonika (Moscow), no. 1, Jan. - Feb. 1985 p 88-101 (For primary document see N86-12697 03-42)
Avail: NTIS HC A04/MF A01

Results are presented from combined tectonic and geochemical studies of Cretaceous and Paleogene effusive-pyroclastic and tuffogenous-silicaceous formations in the eastern Kronotskiy Peninsula. The region of studies is a part of the eastern Kamchatka Peninsula in the immediate vicinity of the island slope of the Kuril-Kamchatka deep water trench. The studies allow a new interpretation of the structure of this region and the relationship of ultrabasic rocks to their surroundings. The studies establish a cover-flake structure for the Late Cretaceous formations proving them to be of Senonian age. For the first time, a serpentinite melange is described in eastern Kamchatka, present at the base of overthrust planes and also making up several independent plates and small protrusions. It is concluded that there was Late Cretaceous obduction on the ocean side, the melange and ultrabasites belonging to the base of the eugeosynclinal area. The Upper Cretaceous and Paleogenic formations belong to the island arcs in their early stages of development. A new transition zone from the ocean to the continent, a sharply arched volcanic-plutonic high-alumina plagiotholeiitic province is distinguished on the basis of petrochemical and geochemical data. Author

N86-12733# Joint Publications Research Service, Arlington, Va.
GEODYNAMICS OF CRUSTAL DILATATION IN TRANSITION AREA FROM ASIAN CONTINENT TO PACIFIC OCEAN Abstract Only **c46**
V. P. Utkin *In its* USSR Rept.: Earth Sci. (JPRS-UES-85-008) 16 Aug. 1985 p 38 Transl. into NGLISH from Geotektonika (Moscow), no. 1, Jan. - Feb. 1985 p 73-87 (For primary document see N86-12697 03-42)
Avail: NTIS HC A04/MF A01

A study is presented of the kinematics of deep fractures in the Asian-Pacific transition zone in order to establish the regularities of motion of the Asian and Pacific geoblocks in time and space. Crustal dilatation is shown to result from shear activation of deep faults. The major kinematic systems of deep faults are diagrammed. A close genetic relationship is demonstrated between volcanism, intrusive magmatism and orogenesis and the shear activation of deep faults. The specifics of spatial interrelationship of the various folded dislocation elements correspond to the organization of structures with lateral displacement of the Asian continent toward the southwest and movement of the Pacific and Kula plates toward the northeast. The volcanogenic belt is controlled by straight deep faults, and only superficial analysis by other investigators has allowed many of them to consider parts of the belt to be arc shaped. Establishment of the specifics of the evolutionary development of shear dislocations is very important for a solution of the problem of space and time relationships among various forms of plicative and destructive structures in the zone. Author

N86-12734# Joint Publications Research Service, Arlington, Va.
TRANSMISSION OF TROPOSPHERIC RADIATION OF LASERS ON MOLECULES OF DIFFERENT CARBON DIOXIDE ISOTOPES Abstract Only **c36**
V. N. Arefyev *In its* USSR Rept.: Earth Sci. (JPRS-UES-85-008) 16 Aug. 1985 p 41 Transl. into ENGLISH from Kvantovaya Elektron. (Moscow), v. 12, no. 3, Mar. 1985 p 631-634 (For primary document see N86-12697 03-42)
Avail: NTIS HC A04/MF A01

CO2 lasers operating in different lines of the bands 00 sup 0 1-10 sup 0 0 and 00 sup 0 1-02 sup 0 0 of molecules of different carbon dioxide isotopes are coming into increasing use for remote measurements of the parameters of the gas composition of the atmosphere. Their generation spectrum coincides with the window of relative atmospheric transparency 8-13 micro m. However, the solution of many problems requires a reliable knowledge of the parameters of molecular absorption of the emission of CO2 lasers in the troposphere. The theoretical possibility of generation of laser radiation in 960 lines of seven CO2 isotopes has been demonstrated. In order to fill this gap partially the authors give the results of computations of the transmission of laser radiation on seven isotopes of carbon dioxide by the tropospheric layer during summer in the middle latitudes of the northern hemisphere. The most transparent microwindow has a transmission of 80-85% in the region 10 micro m, where losses for the most part are determined by the continuous absorption of water vapor. The computations make it possible to analyze the contribution of each gas to the total attenuation of the radiation of CO2 lasers by the atmosphere due to molecular absorption. B.W.

N86-12735# Joint Publications Research Service, Arlington, Va.
ATMOSPHERIC TURBULENCE INVESTIGATIONS AT TSMILYANSK SCIENTIFIC STATION, ATMOSPHERIC PHYSICS INSTITUTE, USSR ACADEMY OF SCIENCES Abstract Only **c46**
L. R. Tsvang *In its* USSR Rept.: Earth Sci. (JPRS-UES-85-008) 16 Aug. 1985 p 42-43 Transl. into ENGLISH from Izv. Akad. Nauk SSSR: Fiz. Atm. i Okeana (Moscow), v. 21, no. 4, Apr. 1985 p 339--348 (For primary document see N86-12697 03-42)
Avail: NTIS HC A04/MF A01

The Tsimlyansk Scientific Station of the Atmospheric Physics Institute was established in 1957. It is situated in a level, uncultivated steppe sector surrounded by cultivated lands. Measurements are made in a level, uniform area of virgin steppe measuring 700 x 650 m. There is an underground facility from which remote measurements can be made. There is a 40-m mast which carries 6 sets of sensors for measuring the vertical profiles of wind velocity and temperature in the range of heights from 1 to 32 m and a mobile carrier with a set of sensors (acoustic anemometer, resistance thermometer) for measuring fluctuations of the three components of wind velocity and temperature in this same range of heights. The most important work done during the last 25 years is reviewed and the most important work to be done in the future is outlined. Such work will include study of processes of interaction between the atmosphere and the underlying surface under nonstationary conditions, especially in the presence of variable cloud cover, with allowance for the influence of radiational nonuniformity of the underlying surface, for developing a model of turbulent processes transpiring under the conditions most frequently observed in nature. B.W.

N86-12736# Joint Publications Research Service, Arlington, Va.
HUMIDITY PROFILE MESUREMENTS IN ATMOSPHERIC LOWER LAYER BY SPONTANEOUS RAMAN SCATTERING METHOD Abstract Only **c47**
O. A. Bukin, S. Yu. Stolyarchuk, and V. A. Tyapkin *In its* USSR Rept.: Earth Sci. (JPRS-UES-85-008) 16 Aug. 1985 p 43-44 Transl. into ENGLISH from Zh. Prikl. Spektroskopii (Minsk), v. 42, no. 4, Apr. 1985 p 631-636 Original language document was announced in IAA as A85-38572 (For primary document see N86-12697 03-42)
Avail: NTIS HC A04/MF A01

Vertical distributions of water vapor in the lower atmospheric layer (up to 500 m) above the sea surface were obtained using a Raman lidar operating at the frequency of the second harmonic of a YAG:Nd laser. The measurements of one profile took 15 minutes; the altitude resolution was 84 m, with a humidity measurement error of less than approximately 14 percent at the end of the path. It is suggested that the use of a processing system for signals from photomultipliers, which makes it possible to count simultaneously photoelectrons from all parts of the path, will improve spatial resolution and reduce the duration of humidity measurements. Finally, a method for lidar calibration is described. L.T. (IAA)

N86-12737# Joint Publications Research Service, Arlington, Va.
SOME CHARACTERISTICS OF TRANSMISSION BY THIN CLOUDS IN VISIBLE AND INFRARED SPECTRAL REGIONS Abstract Only **c47**
Yu. S. Georgiyevskiy and A. Kh. Shukurov *In its* USSR Rept.: Earth Sci. (JPRS-UES-85-008) 16 Aug. 1985 p 44-45 Transl. into ENGLISH from Izv. Akad. Nauk SSSR: Fiz. Atm. i Okeana (Moscow), v. 21, no. 4, Apr. 1985 p 397-402 (For primary document see N86-12697 03-42)
Avail: NTIS HC A04/MF A01

The article gives the results of investigations of attenuation of radiation by thin cirrus (not less than 100 spectra) and cumulus clouds or their margins (more than 100 spectra) under spring, summer and autumn conditions in a moderately moist climatic zone in five parts of the visible and IR spectral regions. Since the principal difficulty in measuring transmission through clouds is their temporal and spatial variability, the method was proposed for measuring transmission through clouds simultaneously at several wavelengths. A solar radiation flux was directed into the laboratory room by an ATsU-24 coelostat situated in a tower at a height of 15 m. It was found that cirrus clouds are more transparent (over 80% of the cases) in the visible range, whereas cumulus clouds are more transparent in the IR range (100% of the cases). This information can be used in the reliable discrimination of ice and liquid droplet clouds on the basis of data from remote measurements. B.W.

43 EARTH RESOURCES

Includes remote sensing of earth resources by aircraft and spacecraft; photogrammetry; and aerial photography.

For instrumentation see *35 Instrumentation and Photography.*

N86-12738* National Aeronautics and Space Administration, Washington, D. C.
EARTH RESOURCES: A CONTINUING BIBLIOGRAPHY, ISSUE 46
Jul. 1985 140 p
(NASA-SP-7041(46); NAS 1.21:7041(46)) Avail: NTIS HC $12.00 CSCL 05B

This bibliography lists 467 reports, articles and other documents introdcued into the NASA scientific and technical information system between April 1 and June 30, 1985. Emphasis is placed on the use of remote sensing and geophysical instrumentation in spacecraft and aircraft to survey and inventory natural resources and urban areas. Subject matter is grouped according to agriculture and forestry, environmental cultural resources geodesy and cartography, geology and mineral resources, hydrology and water management, data processing and distribution systems, instrumentation and sensors, and economical analysis. F.M.R.

N86-12739*# Massachusetts Inst. of Tech., Cambridge. Dept. of Civil Engineering.
FEASIBILITY OF USING LANDSAT IMAGES OF VEGETATION COVER TO ESTIMATE EFFECTIVE HYDRAULIC PROPERTIES OF SOILS Semiannual Technical Report, 1 Feb. - 31 Jul. 1985
Peter S. Eagleson 31 Jul. 1985 20 p refs ERTS
(Grant NAG5-510)
(E86-10003; NASA-CR-176266; NAS 1.26:176266) Avail: NTIS HC A02/MF A01 CSCL 08H

Research activities conducted from February 1, 1985 to July 31, 1985 and preliminary conclusions regarding research objectives are summarized. The objective is to determine the feasibility of using LANDSAT data to estimate effective hydraulic properties of soils. The general approach is to apply the climatic-climax hypothesis (Ealgeson, 1982) to natural water-limited vegetation systems using canopy cover estimated from LANDSAT data. Natural water-limited systems typically consist of inhomogeneous vegetation canopies interspersed with bare soils. The ground resolution associated with one pixel from LANDSAT MSS (or TM) data is generally greater than the scale of the plant canopy or canopy clusters. Thus a method for resolving percent canopy cover at a subpixel level must be established before the Eagleson hypothesis can be tested. Two formulations are proposed which extend existing methods of analyzing mixed pixels to naturally vegetated landscapes. The first method involves use of the normalized vegetation index. The second approach is a physical model based on radiative transfer principles. Both methods are to be analyzed for their feasibility on selected sites. F.M.R.

N86-12740*# Kansas Univ. Center for Research, Inc., Lawrence. Remote Sensing Lab.
EVALUATION OF SPACE SAR AS A LAND-COVER CLASSIFICATION Final Report
B. Brisco, F. T. Ulaby, and T. H. Lee Williams [1985] 123 p refs Original contains imagery. Original photography may be purchased from the EROS Data Center, Sioux Falls, S.D. 57198 ERTS
(Contract NCC9-7)
(E86-10004; NASA-CR-176267; NAS 1.26:176267; RSL-TR-605-1) Avail: NTIS HC A06/MF A01 CSCL 02B

The multidimensional approach to the mapping of land cover, crops, and forests is reported. Dimensionality is achieved by using data from sensors such as LANDSAT to augment Seasat and Shuttle Image Radar (SIR) data, using different image features such as tone and texture, and acquiring multidate data. Seasat, Shuttle Imaging Radar (SIR-A), and LANDSAT data are used both individually and in combination to map land cover in Oklahoma. The results indicates that radar is the best single sensor (72% accuracy) and produces the best sensor combination (97.5% accuracy) for discriminating among five land cover categories. Multidate Seasat data and a single data of LANDSAT coverage are then used in a crop classification study of western Kansas. The highest accuracy for a single channel is achieved using a Seasat scene, which produces a classification accuracy of 67%. Classification accuracy increases to approximately 75% when either a multidate Seasat combination or LANDSAT data in a multisensor combination is used. The tonal and textural elements of SIR-A data are then used both alone and in combination to classify forests into five categories. Author

N86-12741*# Purdue Univ., West Lafayette, Ind. Lab. for Applications of Remote Sensing.
SOYBEAN CANOPY REFLECTANCE MODELING DATA SETS
K. J. Ranson, L. L. Biehl, and C. S. T. Daughtry Jul. 1984 55 p refs ERTS
(Contract NAS9-16528)
(E86-10005; NASA-CR-171895; NAS 1.26:171895; LARS-TR-071584) Avail: NTIS HC A04/MF A01 CSCL 05B

Numerous mathematical models of the interaction of radiation with vegetation canopies have been developed over the last two decades. However, data with which to exercise and validate these models are scarce. During three days in the summer of 1980, experiments are conducted with the objective of gaining insight about the effects of solar illumination and view angles on soybean canopy reflectance. In concert with these experiment, extensive measurements of the soybean canopies are obtained. This document is a compilation of the bidirectional reflectance factors, agronomic, characteristics, canopy geometry, and leaf, stem, and pod optical properties of the soybean canopies. These data sets should be suitable for use with most vegetation canopy reflectance models. Author

N86-12742*# Pacific Northwest Lab., Richland, Wash.
LANDSAT-4 TM IMAGE DATA QUALITY ANALYSIS FOR ENERGY-RELATED APPLICATIONS Executive Summary
G. E. Wukelic and H. P. Foote 1983 4 p refs Presented at the 3rd LANDSAT-4 Investigators' Workshop, Richland, Wash., 6-7 Dec. 1983 Sponsored by NASA ERTS
(E86-10006; NASA-CR-171074; NAS 1.26:171074; PNL-SA-11861) Avail: NTIS HC A02/MF A01 CSCL 05B

LANDSAT-4 Thematic Mapper (TM) data performance and utility characteristics from an energy research and technology perspective is evaluated. The program focuses on evaluating applicational implications of using such data, in combination with other digital data, for current and future energy research and technology activities. Prime interest is in using TM data for siting, developing and operating federal energy facilities. Secondary interests involve the use of such data for resource exploration, environmental monitoring and basic scientific initiatives such as in support of the Continental Scientific Drilling Program. Author

N86-12743*# Virginia Polytechnic Inst. and State Univ., Blacksburg.
TRANSIENT THERMAL MODELING OF THE NONSCANNING ERBE DETECTOR Final Report, 13 Nov. 1980 - 30 Sep. 1982

J. R. Mahan Nov. 1983 107 p
(Contract NAS1-16508)
(NASA-CR-172240; NAS 1.26:172240) Avail: NTIS HC A06/MF A01 CSCL 14B

A numerical model to predict the transient thermal response of the ERBE nonscanning wide field of view total radiometer channel was developed. The model, which uses Monte Carlo techniques to characterize the radiative component of heat transfer, is described and a listing of the computer program is provided. Application of the model to simulate the actual blackbody calibration procedure is discussed. The use of the model to establish a real time flight data interpretation strategy is recommended. Modification of the model to include a simulated Earth radiation source field and a filter dome is indicated. E.A.K.

N86-12744# Naval Ocean Research and Development Activity, Bay St. Louis, Miss.
DATA ANALYSIS OF AIRBORNE ELECTROMAGNETIC BATHYMETRY Final Report
R. Zollinger, A. Becker, and F. Morrison Apr. 1985 21 p
(AD-A157132; NORDA-93) Avail: NTIS HC A02/MF A01 CSCL 08/10

This report describes an experimental evaluation of the concept of airborne electromagnetic bathymetry. The airborne electromagnetic data that forms the basis of this project was acquired with the Mark VI INPUT system along a 17-mile-long flight path off Cape Breton Island in the province of Nova Scotia. The water depth beneath the flight path ranged from 0 to more than 40 m. Author (GRA)

N86-12745# Institut fuer Digitale Bildverarbeitung und Graphik, Graz (Austria).
CORRECTING A DIGITAL MAP DATA BASE WITH SCENE ANALYSIS CONCEPTS AND METHODS Interim Technical Report, 1 Jan. 1983 - 31 Dec. 1984
H. Ranzinger May 1985 94 p
(Contract DAJA45-83-C-0022)
(AD-A157913; R/D-4161-R-EN) Avail: NTIS HC A05/MF A01 CSCL 08/2

The problem of updating maps has always been of considerable interest for cartographers.. With the advent of digital cartography and the supply of aerial imagery in digital form in the near future, the question arises in which way information to update maps may automatically be derived from digital imagery by means of scene analysis. This paper proposes an approach and show how a solid set of methods, modularly designed and based on an image processing language, may serve as a toolkit for experimentation. Examples are given by applying the methods to a multitemporal sequence of digitized metric aerial photos. GRA

N86-12746# Air Force Inst. of Tech., Wright-Patterson AFB, Ohio.
STRATEGIES FOR ASSOCIATING DATA AND LOCATION IN A GEOGRAPHIC INFORMATION SYSTEM M.S. Thesis
R. G. Walton 1985 120 p
(AD-A158118; AFIT/CI/NR-85-78T) Avail: NTIS HC A06/MF A01 CSCL 08/2

Much of the existing work in the area of Geographic Information Systems (GIS) treats spatial objects, e.g., points, lines, and regions, as the primary entities of interest. In that approach, descriptive information is associated directly with each of these data items. This paper explores the feasibility of implementing an alternative design which uses Location Data Sets and Location Predicates as the basic entities managed by a Location Data Management System (LDMS). A major advantage of the proposed approach is its suitability for automatic enforcement of data consistency across multi-scale geographic entities. The central idea of the Location Data Set approach is that spatial data should be directly associated with locations rather than named regions or points. The relationships between geographic entities and data values may then be derived through the intermediate relationship of shared location. It is envisioned that each type of data which is distributive in nature would be stored in a separate set. Data values associated with conventional points, lines, and regions would then be merely restrictions on these global data sets. This is similar to the way in which the external views of a database represent a subsetting of the global data. The paper includes a survey of 15 selected GIS implementations and existing work relevant to identified implementation obstacles. Author (GRA)

N86-12747# Idaho Dept. of Water Resources, Boise.
WATER INFORMATION BULLETIN NO. 30, PART 13: GEOTHERMAL INVESTIGATIONS IN IDAHO. PRELIMINARY GEOLOGIC RECONNAISSANCE OF THE GEOTHERMAL OCCURRENCES OF THE WOOD RIVER DRAINAGE AREA
J. E. Anderson, K. Bideganeta, and J. C. Mitchell Apr. 1985 54 p refs
(Contract DE-AS07-77ET-28407)
(DE85-016972; DOE/ET-28407/T6) Avail: NTIS HC A04/MF A01

Pre-tertiary sediments of the Milligen and Wood River Formations consisting primarily of argillite, quartzite, shale and dolomite are, for the most part, exposed throughout the area and are cut locally by outliers of the Idaho Batholith. At some locations, Tertiary-age Challis Volcanics overlay these formations. Structurally the area is complex with major folding and faulting visible in many exposures. Many of the stream drainages appear to be fault controlled. Hydrologic studies indicate hot spring occurrences are related to major structural trends, as rock permeabilities are generally low. Geochemical studies using stable isotopes of hydrogen and oxygen indicate the thermal water in the Wood River region to be depleted by about 10 0/00 in D and by 1 to 2 0/00 in (18)0 relative to cold water. This suggests the water could be meteoric water that fell during the late Pleistocene. The geological data, as well as the chemical data, indicate the geothermal waters are heated at depth, and subsequently migrate along permeable structural zones. In almost all cases the chemical data suggest slightly different thermal histories and recharge areas for the water issuing from the hot springs. Sustained use of the thermal water at any of the identified springs is probably limited to flow rates approximating the existing spring discharge. DOE

N86-12748# Bohan (Walter A.) Co., Park Ridge, Ill.
HYDROLOGIC AND LAND SCIENCES APPLICATIONS OF NOAA (NATIONAL OCEANIC AND ATMOSPHERIC ADMINSTRATION) POLAR-ORBITING SATELLITE DATA Final Report
M. Matson and F. Parmenter-Holt Jan. 1985 24 p
(Contract NA83SA-C-00650)
(PB85-233385; HLSB-85) Avail: NTIS HC A02/MF A01 CSCL 14E

The satellite applications training aid focuses on the use of NOAA satellite data for hydrologic applications (snow cover mapping, flood monitoring and soil moisture analysis; Renewable Resources) monitoring vegetation progress and health, forest management, fire monitoring and detection, urban effects, dust storm monitoring, volcanic activity and geologic assessment. Annotated examples of satellite imagery detail the photointerpretation details. GRA

N86-12749# Environmental Protection Agency, Denver, Colo.
TOXIC HOT SPOT STUDY, SOUTH PLATTE RIVER ALONG THE FRONT RANGE, AUGUST AND OCTOBER, 1982
C. E. Runas, M. Martin, D. McDonough, and L. Parrish Oct. 1984 70 p
(PB85-196384; EPA/908/2-84/001) Avail: NTIS HC A04/MF A01 CSCL 08H

To implement a Consent Decree between the EPA and the National Resources Defense Council requiring that EPA identify waters which may have toxic pollution problems, a two phase study was designed to determine if any toxic hot spots exist in selected reaches of the South Platte River and selected tributary and non-tributary streams along the Front Range. Phase 1 was designed to determine if such toxic hot spots exist and Phase 2 would focus on those areas defined in Phase 1 as toxic hot spots and would include additional sampling locations. Samples of water, sediment and aquatic invertebrates were obtained for chemical and biological examination. GRA

N86-12750# Illinois Dept. of Energy and Natural Resources, Springfield.
DESIGN OF A STATEWIDE GROUNDWATER MONITORING NETWORK FOR ILLINOIS
M. OHearn and S. C. Schock Mar. 1985 84 p
(PB85-192821; IL/ENR/RE-85/02) Avail: NTIS HC A05/MF A01 CSCL 08H

The design of a groundwater monitoring network for principal aquifers in Illinois is discussed. The objective of this network is to identify and assess existing groundwater resource problems in Illinois' highest yielding aquifers and to provide base line data in uneffected areas to detect future groundwater problems. The proposed network is based upon the monitoring of 1300 public water supply wells and incorporates a three tier pioritization system to determine the degree to which major aquifers should be monitored for organic and inorganic contaminants. GRA

N86-12751# Environmental Research Lab., Duluth, Minn.
GREAT LAKES: NATURE'S OWN ENVIRONMENTAL LABORATORY
W. L. Richardson 1985 12 p
(PB85-188852; EPA/600/D-85/077) Avail: NTIS HC A02/MF A01 CSCL 08H

The Great Lakes, the world's largest ecosystem and microlab, the history of man's interaction and pollution of it, and the subsequent cleanup ordered by law in recent decades and continuing into the present time are discussed. GRA

N86-12752# Texas Dept. of Water Resources, Austin.
EVALUATING THE GROUND-WATER RESOURCES OF THE HIGH PLAINS OF TEXAS, VOLUME 2
T. Knowles, P. Nordstrom, and W. B. Klemt Aug. 1984 392 p
(PB85-191609; TDWR/R-288-Vol-1) Avail: NTIS HC A17/MF A01; also avail. in set of 4 reports as PB85-191583; MF E99 CSCL 08H

Records of approximately 12,200 wells and county maps depicting well locations in Texas are given. Also, the elevation of the base of the High Plains aquifer, elevation of water levels in 1980, and saturated thicknesses in 1980 are given. GRA

N86-12753# Geological Survey, St. Paul, Minn. Water Resources Div.
WATERS RESOURCES DATA FOR MINNESOTA. WATER YEAR 1983. VOLUME 2: UPPER MISSISSIPPI AND MISSOURI RIVER BASINS Annual Report, 1 Oct. 1982 - 30 Sep. 1983
K. T. Gunard, J. H. Hess, J. L. Zirbel, and C. E. Cornelius Feb. 1985 463 p Prepared in cooperation with Minnesota Dept. of Transportation, St. Paul and Minnesota Dept. of Natural Resources, St. Paul
(PB85-215994; USGS/WRD/HD-85/215; USGS/WRD/MN-83/2)
Avail: NTIS HC A20/MF A01 CSCL 08H

Water resources data for the 1983 water year for Minnesota consist of records of stage, discharge and water quality of streams; stage, contents, and water quality of lakes and reservoirs; and water levels and water quality in wells and springs. The volume contains discharge records for 72 gaging stations; stage and contents for 11 lakes and reservoirs; water quality for 25 stream stations, 16 partial record stations, 1 lake station, and 107 wells; and water levels for 238 observation wells. Also included are 107 high flow partial record stations. Author (GRA)

N86-12754# Geological Survey, Tallahassee, Fla. Water Resources Div.
WATER RESOURCES DATA FOR FLORIDA, WATER YEAR 1983. VOLUME 3A: SOUTHWEST FLORIDA SURFACE WATER Water-Data Annual Report, 1 Oct. 1982 - 30 Sep. 1983
R. T. Mycyk, L. D. Fayard, W. L. Fletcher, and J. K. Ogle Mar. 1985 488 p
(PB85-216000; USGS/WRD/HD-85/211; USGS/WDR/FL-84/3A)
Avail: NTIS HC A21/MF A01 CSCL 08H

Water resources data for the 1983 water year for southwest Florida include continuous or daily discharge for 74 streams, periodic discharge for 14 streams, miscellaneous discharge for 15 streams, peak discharge for 19 streams, continuous or daily stage for 18 streams; continuous elevations for 43 lakes and periodic elevations for 72 lakes. GRA

N86-12755# National Marine Fisheries Service, Galveston, Tex.
GENERALIZED GEOGRAPHIC MAPPING SYSTEM FOR COMPUTER GRAPHICS
D. B. Koi Apr. 1985 45 p
(PB85-212520; NOAA-TM-MNFS-SEFC-153) Avail: NTIS HC A03/MF A01 CSCL 08B

The Generalized Geographic Mapping System (GGMS) is a computer program that draws accurately proportioned maps virtually anywhere in the world, using a variety of land mass data bases. The GGMS is written in standard FORTRAN IV and is machine-independent except where noted. GGMS is very versatile. It not only generates maps of land masses, but it also makes maximum use of the specific available output screen regardless of the selected borders of the desired output. Two mapping projections, rectangular and Mercator, are available; as are numerous different methods of drawing the graticule (latitude and longitude line grid). The heart of the GGMS is the subroutine MAPP. MAPP is the only GGMS subprogram required to be called before user-defined application routines can be called. Essentially, MAPP computes and draws all borders, draws and labels the graticule, and draws a land mass. GRA

N86-12401# Joint Publications Research Service, Arlington, Va.
CARTOGRAPHY, NATIONAL LAND MANAGEMENT RELATED
Shao Wenxiang *In its* China Rept.: Sci. and Technol. (JPRS-CST-85-035) 17 Oct. 1985 p 34-35 Transl. into ENGLISH from Renmin Ribao (Beijing), 16 May 1984 p 5 (For primary document see N86-12399 03-31)
Avail: NTIS HC A08/MF A01

N86-12402# Joint Publications Research Service, Arlington, Va.
BENEFITS OF SURVEYING, CARTOGRAPHY DESCRIBED
Yu Cang *In its* China Rept.: Sci. and Technol. (JPRS-CST-85-035) 17 Oct. 1985 p 36-39 Transl. into ENGLISH from Renmin Ribao (Beijing), 16 May 1984 p 5 (For primary document see N86-12399 03-31)
Avail: NTIS HC A08/MF A01

N86-12655# Joint Publications Research Service, Arlington, Va.
OIL AND GS DEPOSITS ON CONTINENTAL SLOPES OF THE OCEAN Abstract Only
A. A. Geodekyan, A. Zabanbark, and A. I. Konyukhov *In its* USSR Rept.: Earth Sci. (JPRS-UES-85-006) 19 Jun. 1985 p 24-25 Transl. into ENGLISH from Dokl. Akad. Nauk SSSR (Moscow), v. 280, no. 2, Jan. 1985 p 423-426 (For primary document see N86-12630 03-42)
Avail: NTIS HC A05/MF A01

44 ENERGY PRODUCTION AND CONVERSION

Includes specific energy conversion systems, e.g., fuel cells and batteries; global sources of energy; fossil fuels; geophysical conversion; hydroelectric power; and wind power.

For related information see also *07 Aircraft Propulsion and Power, 20 Spacecraft Propulsion and Power, 28 Propellants and Fuels,* and *85 Urban Technology and Transportation.*

N86-12756# Midwest Energy Inst., Kansas City, Mo.
SOLERAS: PHOTOVOLTAIC POWER SYSTEMS PROJECT. MODULE FAILURE ANALYSIS Interim Report
F. S. Huraib, M. S. Imamura, A. A. Salim, and N. Rao Oct. 1984 100 p refs Sponsored in part by Saudi Arabian National Center for Science and Technology (SANCST)
(MRI/SOL-0101) Avail: NTIS HC A05/MF A01

The SOLERAS Photovoltaic Power System (PVPS) became operational in September 1981. The system has operated satisfactorily and has experienced very little downtime. Early in 1983 some degradation in the photovoltaic (PV) field performance was detected. A series of current voltage (I-V) tests and other analyses eventually uncovered a number of PV modules that have resulted in open circuit type failure in the four cell group, or a half module. As of August 1984, the estimated number of these defective modules in the PV field was 152. In addition, there are a total of 188 defective modules in the storage warehouse, resulting in a total of 340 modules that need repairs. At the current rate of failures (seven half modules per month), an additional 112 modules would be defective by the end of January 1986, resulting in 412 defective modules. This report presents the results of the failure analysis performed during the past several months on the open circuit modules. Background information as related to the module failures and the effects of such failures on the overall PV field power output are provided. In addition, a plan to continue the monitoring of the rate of failure and analyzing the failure mechanisms is presented. Author

N86-12757*# Engelhard Corp., Edison, N.J. Specialty Chemicals Div.

DEVELOP AND TEST FUEL CELL POWERED ON-SITE INTEGRATED TOTAL ENERGY SYSTEMS: PHASE 3, FULL-SCALE POWER PLANT DEVELOPMENT Quarterly Technical Progress Report, Aug. - Oct. 1984

A. Kaufman, S. Pudick, C. L. Wang, J. Werth, and J. A. Whelan 17 May 1985 15 p
(Contracts DEN3-241; DE-AI01-80ET-17088)
(NASA-CR-174948; DOE/NASA-0241-15; NAS 1.26:174948; QR-14) Avail: NTIS HC A02/MF A01 CSCL 10B

Two 25 cell stacks of the 13 inch x 23 inch cell size (about 4kW) remain on test after 4000 hours and 2900 hours, respectively, using simulated reformate fuel. These tests are focusing on the durability of fuel cell stack components developed through the end of 1983. Also, these stacks are serving as forerunners of a 25kW stack that will contain 175 cells of the same size and will employ the same technology base. The stack technology development program has focused on a new, low cost bipolar plate edge seal technique and evaluation of advanced cathode catalysts, an electrolyte replenishment system, and nonmetallic cooling plates in small stacks. Author

N86-12758*# Engelhard Corp., Edison, N.J. Specialty Chemicals Div.

DEVELOP AND TEST FUEL CELL POWERED ON-SITE INTEGRATED TOTAL ENERGY SYSTEMS: PHASE 3, FULL-SCALE POWER PLANT DEVELOPMENT Quarterly Technical Progress Report, Feb. - Apr. 1985

A. Kaufman, S. Pudick, C. L. Wang, J. Werth, and J. A. Whelan 22 Jul. 1985 25 p
(Contract DEN3-241; DE-AI01-80ET-17088)
(NASA-CR-174998; DOE/NASA-0241-17; NAS 1.26:174998; QR-16) Avail: NTIS HC A02/MF A01 CSCL 10B

A 25 cell stack of the 13 inch x 23 inch cell size (about 4kW) remains on test after 6000 hours, using simulated reformate fuel. A similar stack was previously shut down after 7000 hours on load. These tests were carried out for the purpose of assessing the durability of fuel cell stack components developed through the end of 1983. In light of the favorable results obtained, a 25kW stack that will contain 175 cells of the same size is being constructed using the same technology base. The components for the 25kW stack have been completed. A methanol steam reformer with a design output equivalent to 50kW has been constructed to serve as a hydrogen generator for the 25kW stack. This reformer and the balance of the fuel processing sub system are currently being tested and debugged. The stack technology development program focused on cost reduction in bipolar plates, nonmetallic cooling plates, and current collecting plates; more stable cathode catalyst support materials; more corrosion resistant metal hardware; and shutdown/start up tolerance. Author

N86-12759*# Jet Propulsion Lab., California Inst. of Tech., Pasadena.

RELIABILITY AND ENGINEERING OF THIN-FILM PHOTOVOLTAIC MODULES. RESEARCH FORUM PROCEEDINGS

R. G. Ross, Jr., ed. and E. L. Royal, ed. 1 Oct. 1985 278 p refs Forum held in Washington, D.C., 20 Mar. 1985
(Contracts NAS7-918; DE-AI01-76ET-20356; JPL Proj. 5101-284)
(NASA-CR-176217; DOE/JPL-1012-111; JPL-Pub-85-73; NAS 1.26:176217) Avail: NTIS HC A13/MF A01 CSCL 10A

A Research Forum on Reliability and Engineering of Thin Film Photovoltaic Modules, under sponsorship of the Jet Propulsion Laboratory's Flat Plate Solar Array (FSA) Project and the U.S. Department of Energy, was held in Washington, D.C., on March 20, 1985. Reliability attribute investigations of amorphous silicon cells, submodules, and modules were the subjects addressed by most of the Forum presentations. Included among the reliability research investigations reported were: Arrhenius-modeled accelerated stress tests on a Si cells, electrochemical corrosion, light induced effects and their potential effects on stability and reliability measurement methods, laser scribing considerations, and determination of degradation rates and mechanisms from both laboratory and outdoor exposure tests. For individual titles, see N86-12760 through N86-12774.

N86-12760*# Jet Propulsion Lab., California Inst. of Tech., Pasadena.

CRYSTALLINE-SILICON RELIABILITY LESSONS FOR THIN-FILM MODULES

Ronald G. Ross, Jr. *In its* Reliability and Eng. of Thin-Film Photovoltaic Modules 1 Oct. 1985 p 3-11 refs (For primary document see N86-12759 03-44)
Avail: NTIS HC A13/MF A01 CSCL 10A

The reliability of crystalline silicon modules has been brought to a high level with lifetimes approaching 20 years, and excellent industry credibility and user satisfaction. The transition from crystalline modules to thin film modules is comparable to the transition from discrete transistors to integrated circuits. New cell materials and monolithic structures will require new device processing techniques, but the package function and design will evolve to a lesser extent. Although there will be new encapsulants optimized to take advantage of the mechanical flexibility and low temperature processing features of thin films, the reliability and life degradation stresses and mechanisms will remain mostly unchanged. Key reliability technologies in common between crystalline and thin film modules include hot spot heating, galvanic and electrochemical corrosion, hail impact stresses, glass breakage, mechanical fatigue, photothermal degradation of encapsulants, operating temperature, moisture sorption, circuit design strategies, product safety issues, and the process required to achieve a reliable product from a laboratory prototype. Author

N86-12761*# Exxon Research and Engineering Co., Annandale, N.J.

LIGHT-INDUCED EFFECTS-IMPACTS TO MODULE PERFORMANCE MEASUREMENTS AND RELIABILITY TESTING: AN OVERVIEW

C. R. Wronski *In* JPL Reliability and Eng. of Thin-Film Photovoltaic Modules 1 Oct. 1985 p 13-32 refs (For primary document see N86-12759 03-44)
Avail: NTIS HC A13/MF A01 CSCL 10A

The stability of solar cells is a key factor in determining the reliability of photovoltaic modules and is of great interest in the case of solar cells having a new technology which has not yet been fully developed. In particular this question arises with hydrogenated amorphous silicon (a-Si) solar cells because a-Si exhibits reversible light induced changes in its electronic properties, commonly referred to as the Staebler-Wronski effect (SWE). Continuous progress is being made in the peak conversion efficiencies of a-Si solar cells and efficiencies in excess of 11% have been achieved. However, stability is still a problem. ARCO Solar reports results on solar cells which, after over a year's exposure to sunlight, under open circuit conditions, still have about 7% conversion efficiency. Other results show a region of fast degradation for about a month, after which the degradation diminishes rapidly. Author

N86-12762*# Solarex Corp., Newtown, Pa. Thin Film Div.

THIN-FILM MODULE CIRCUIT DESIGN: PRACTICAL AND RELIABILITY ASPECTS

R. V. DAiello and E. N. Twesme *In* JPL Reliability and Eng. of Thin-Film Photovoltaic Modules 1 Oct. 1985 p 33-46 Sponsored in part by Midwest Research Inst., Golden, Colo. (For primary document see N86-12759 03-44)
Avail: NTIS HC A13/MF A01 CSCL 10A

This paper will address several aspects of the design and construction of submodules based on thin film amorphous silicon (a-Si) p i n solar cells. Starting from presently attainable single cell characteristics, and a realistic set of specifications, practical module designs are discussed from the viewpoints of efficient designs, the fabrication requirements, and reliability concerns. The examples center mostly on series interconnected modules of the superstrate type with detailed discussions of each portion of the structure in relation to its influence on module efficiency. Emphasis is placed on engineering topics such as: area coverage, optimal geometries, and cost and reliability. Practical constraints on achieving optimal designs, along with some examples of potential pitfalls in the manufacture and subsequent performance of a-Si modules are discussed. Author

N86-12763*# Jet Propulsion Lab., California Inst. of Tech., Pasadena.

HOT-SPOT HEATING SUSCEPTIBILITY DUE TO REVERSE BIAS OPERATING CONDITIONS

C. C. Gonzalez *In its* Reliability and Eng. of Thin-Film Photovoltaic Modules 1 Oct. 1985 p 47-64 (For primary document see N86-12759 03-44)
Avail: NTIS HC A13/MF A01 CSCL 10A

Because of field experience (indicating that cell and module degradation could occur as a result of hot spot heating), a laboratory test was developed at JPL to determine hot spot susceptibility of modules. The initial hot spot testing work at JPL formed a foundation for the test development. Test parameters are selected as follows. For high shunt resistance cells, the applied back bias test current is set equal to the test cell current at maximum power. For low shunt resistance cells, the test current is set equal to the cell short circuit current. The shadow level is selected to conform to that which would lead to maximum back bias voltage under the appropriate test current level. The test voltage is determined by the bypass diode frequency. The test conditions are meant to simulate the thermal boundary conditions for 100 mW/sq cm, 40C ambient environment. The test lasts 100 hours. A key assumption made during the development of the test is that no current imbalance results from the connecting of multiparallel cell strings. Therefore, the test as originally developed was applicable for single string case only. Author

N86-12764*# Clemson Univ., S.C. Dept. of Electrical and Computer Engineering.

ACCELERATED STRESS TESTING OF THIN FILM SOLAR CELLS: DEVELOPMENT OF TEST METHODS AND PRELIMINARY RESULTS

Jay W. Lathrop *In* JPL Reliability and Eng. of Thin-Film Photovoltaic Modules 1 Oct. 1985 p 65-78 (For primary document see N86-12759 03-44)
Avail: NTIS HC A13/MF A01 CSCL 10A

If thin film cells are to be considered a viable option for terrestrial power generation their reliability attributes will need to be explored and confidence in their stability obtained through accelerated testing. Development of a thin film accelerated test program will be more difficult than was the case for crystalline cells because of the monolithic construction nature of the cells. Specially constructed test samples will need to be fabricated, requiring committment to the concept of accelerated testing by the manufacturers. A new test schedule appropriate to thin film cells will need to be developed which will be different from that used in connection with crystalline cells. Preliminary work has been started to seek thin film schedule variations to two of the simplest tests: unbiased temperature and unbiased temperature humidity. Still to be examined are tests which involve the passage of current during temperature and/or humidity stress, either by biasing in the forward (or reverse) directions or by the application of light during stress. Investigation of these current (voltage) accelerated tests will involve development of methods of reliably contacting the thin conductive films during stress. Author

N86-12765*# Jet Propulsion Lab., California Inst. of Tech., Pasadena.

ELECTRICAL SAFETY REQUIREMENTS: IMPLICATIONS FOR THE MODULE DESIGNER

R. S. Sugimura *In its* Reliability and Eng. of Thin-Film Photovoltaic Modules 1 Oct. 1985 p 79-92 refs (For primary document see N86-12759 03-44)
Avail: NTIS HC A13/MF A01 CSCL 10A

Commercial photovoltaic array installations, which include residential and intermediate applications, are subject to building and electrical codes and to product safety standards. The National Electrical Code (NEC) Article 690, titled Solar Photovoltaic Systems, contains provisions defining acceptable levels of system safety and emphasizes the system design and its installation. The Underwriters Laboratories, Inc. (UL), document titled: Proposed First Edition of the Standard for Flat Plate Photovoltaic Modules and Panels, UL-1703, identifies module and panel construction requirements that ensure product safety. Together these documents describe requirements intended to minimize hazards such as shock and fire. Although initial focus of these requirements is on single crystal silicon modules, they are generic in nature, and are equally applicable to high voltage (> 30 Vdc), multikilowatt, thin film systems. A major safety concern is insulation breakdown within the module or array wiring system, or discontinuities within the electrical conductors. These failures can result in ground faults, in circuit arcs, or exposure to hazardous electrical parts. Safeguards are discussed. Author

N86-12766*# Eastman Kodak Co., Rochester, N. Y. Research Labs.

LARGE-AREA THIN-FILM MODULES

Y.-S. Tyan and E. A. Perez-Albuerne *In* JPL Reliability and Eng. of Thin-Film Photovoltaic Modules 1 Oct. 1985 p 95-112 refs (For primary document see N86-12759 03-44)
Avail: NTIS HC A13/MF A01 CSCL 10A

The low cost potential of thin film solar cells can only be fully realized if large area modules can be made economically with good production yields. This paper deals with two of the critical challenges. A scheme is presented which allows the simple, economical realization of the long recognized, preferred module structure of monolithic integration. Another scheme reduces the impact of shorting defects and, as a result, increases the production yields. Analytical results demonstrating the utilization and advantages of such schemes are discussed. Author

N86-12767*# Chronar Corp., Princeton, N.J.

INTERCONNECT RESISTANCE OF PHOTOVOLTAIC SUBMODULES

Hermann Volltrauer, Erten Eser, and Alan E. Delahoy *In* JPL Reliability and Eng. of Thin-Film Photovoltaic Modules 1 Oct. 1985 p 113-124 (For primary document see N86-12759 03-44)
Avail: NTIS HC A13/MF A01 CSCL 10A

Small area amorphous silicon solar cells generally have higher efficiencies than large interconnected submodules. Among the reasons for the differences in performance are the lack of large area uniformity, the effect of nonzero tin oxide sheet resistance, and possibly pinholes in the various layers. Another and usually small effect that can contribute to reduced performance of interconnected cells is the resistance of the interconnection i.e., the series resistance introduced by the metal to tin oxide contact through silicon. Proper processing problems to avoid poor contacts are discussed. Author

N86-12768*# ARCO Solar, Inc., Chatsworth, Calif.
THIN FILM MODULE DEVELOPMENT
Theresa Jester *In* JPL Reliability and Eng. of Thin-Film Photovoltaic Modules 1 Oct. 1985 p 125-136 (For primary document see N86-12759 03-44)
Avail: NTIS HC A13/MF A01 CSCL 10A

The design of ARCO Solar, Inc.'s Genesis G100 photovoltaic module was driven by several criteria, including environmental stability (both electrical and mechanical), consumer aesthetics, low materials costs, and manufacturing ease. The module circuitry is designed as a 12 volt battery charger, using monolithic patterning techniques on a glass superstrate. This patterning and interconnect method proves amenable to high volume, low cost production throughput, and the use of glass serves the dual role of handling ease and availability. The mechanical design of the module centers on environmental stability. Packaging of the glass superstrate circuit must provide good resistance to thermal and humidity exposure along with hi-pot insulation and hailstone impact resistance. The options considered are given. Ethylene vinyl acetate (EVA) is chosen as the pottant material for its excellent weatherability. Author

N86-12769*# Hughes Aircraft Co., Long Beach, Calif.
AMORPHOUS SILICON PHOTOVOLTAIC MODULES AND TEST DEVICES DESIGN, FABRICATION AND TESTING
Matt VanLeeuwen *In* JPL Reliability and Eng. of Thin-Film Photovoltaic Modules 1 Oct. 1985 p 151-166 (For primary document see N86-12759 03-44)
Avail: NTIS HC A13/MF A01 CSCL 10A

In July of 1984, Hughes and JPL initiated a contract for Hughes to design, fabricate and test 10 thin film Amorphous Silicon (a-Si) photovoltaic power modules. These modules were to be 1 ft x 4 ft in size. They were to be preceded by the delivery of 10 a-Si 4 in. square test devices. This effort is very timely since thin film PV development has progressed to the point where intermediate load power applications are on the horizon. It is important to know if current a-Si submodule design and manufacturing processes yield a product that is compatible with the packaging needed to meet a 20 to 30 year life span expectancy. The term submodule is assigned to an interconnected assembly of 28 a-Si cells deposited on a 1 foot square glass superstrate. These assemblies are equipped with electrical terminations, i.e., copper tabs at the four corners of the inverted submodules. It is these submodules that are to be interconnected and packaged into power modules, as opposed to the interconnected individual crystalline cells packaged into todays PV modules. A discussion of the fabrication methods and results follows. Author

N86-12770*# ARCO Solar, Inc., Chatsworth, Calif.
THIN FILM MODULE ELECTRICAL CONFIGURATION VERSUS ELECTRICAL PERFORMANCE
Don L. Morel *In* JPL Reliability and Eng. of Thin-Film Photovoltaic Modules 1 Oct. 1985 p 167-184 refs (For primary document see N86-12759 03-44)
Avail: NTIS HC A13/MF A01 CSCL 10A

The as made and degraded states of thin film silicon (TFS) based modules have been modelled in terms of series resistance losses. The origins of these losses lie in interface and bulk regions of the devices. When modules degrade under light exposure, increases occur in both the interface and bulk components of the loss based on series resistance. Actual module performance can thus be simulated by use of only one unknown parameter, shunt losses. Use of the simulation to optimize module design indicates that the current design of 25 cells per linear foot is near optimum. Degradation performance suggests a shift to approx. 35 cells to effect maximum output for applications not constrained to 12 volts. Earlier studies of energy based performance and tandem structures should be updated to include stability factors, not only the initial loss factor tested here, but also appropriate annealing factors. Author

N86-12771*# Midwest Research Inst., Golden, Colo. Solar Energy Research Inst.
OUTDOOR PERFORMANCE TESTING OF THIN-FILM DEVICES
In JPL Reliability and Eng. of Thin-Film Photovoltaic Modules 1 Oct. 1985 p 185-196 (For primary document see N86-12759 03-44)
Avail: NTIS HC A13/MF A01 CSCL 10A

The Advanced Systems Research Group supports the photovoltaic advanced R&D (PV AR&D) project by providing outdoor (global) testing of PV cells, submodules, modules, and arrays. The group also provides in house engineering and analysis to identify and determine how technical issues such as cell/module/system adaptations, long term stability, reliability, economics, materials availability, safety, and environmental impacts affect the development and ultimate use of advanced PV thin film, innovative cell, and material technologies. A major thrust of the research effort is to develop and utilize instrumentation and procedures for monitoring and analyzing PV cells and submodules including outdoor performance and stability testing and life cycle accelerated stress testing. To accomplish the above, the solar energy research institute (SERI) outdoor PV test facility was established in 1982. The group has designed testing systems and analysis procedures for, and has tested, numerous amorphous silicon thin film submodules provided by SERI subcontractors and has performed long term outdoor stability tests on CdS/CuIr Se sub 2 and hydrogen passivated silicon solar cells. A significant contribution from this facility over the past year was the testing of large area amorphous silicon submodules. Author

N86-12772*# Jet Propulsion Lab., California Inst. of Tech., Pasadena.
MODULE VOLTAGE ISOLATION AND CORROSION RESEARCH
Gordon R. Mon *In its* Reliability and Eng. of Thin-Film Photovoltaic Modules 1 Oct. 1985 p 197-234 refs (For primary document see N86-12759 03-44)
Avail: NTIS HC A13/MF A01 CSCL 10A

A summary of recent research at JPL on two topics related to achieving long term reliability of photovoltaic modules: voltage isolation and electrochemical corrosion is presented. Special emphasis is given to similarities and differences in performance between crystalline silicon modules and amorphous silicon modules. Author

N86-12773*# Jet Propulsion Lab., California Inst. of Tech., Pasadena.
GLASS BREAKING STRENGTH: THE ROLE OF SURFACE FLAWS AND TREATMENTS c27
Donald Moore *In its* Reliability and Eng. of Thin-Film Photovoltaic Modules 1 Oct. 1985 p 235-248 (For primary document see N86-12759 03-44)
Avail: NTIS HC A13/MF A01 CSCL 11B

Although the intrinsic strength of silicon dioxide glass is of the order of 10 to the 6th power lb/sq in, the practical strength is roughly two orders of magnitude below this theoretical limit, and depends almost entirely on the surface condition of the glass, that is, the number and size of flaws and the residual surface compression (temper) in the glass. Glass parts always fail in tension when these flaws grow under sustained loading to some critical size. Research associated with glass encapsulated crystalline-Si photovoltaic (PV) modules has greatly expanded our knowledge of glass breaking strength and developed sizeable data base for commercially available glass types. A detailed design algorithm is developed for thickness sizing of rectangular glass plates subject to pressure loads. Additional studies examine the strength of glass under impact loading conditions such as that caused by hail. Although the fundamentals of glass breakage are directly applicable to thin film modules, the fracture strength of typical numerical glass must be replaced with data that reflect the high temperature tin oxide processing, laser scribing, and edge processing peculiar to thin film modules. The fundamentals of glass breakage applicable to thin film modules and preliminary fracture strength data for a variety of 1 ft square glass specimens representing preprocessed and post processed sheets from current amorphous-Si module manufacturers are presented. Author

N86-12774*# Jet Propulsion Lab., California Inst. of Tech., Pasadena.

ENCAPSULANT SELECTION AND DURABILITY TESTING EXPERIENCE

E. F. Cuddihy *In its* Reliability and Eng. of Thin-Film Photovoltaic Modules 1 Oct. 1985 p 249-274 (For primary document see N86-12759 03-44)
Avail: NTIS HC A13/MF A01 CSCL 10A

The Flat Plate Solar Array Project (FSA) has established technically challenging cost and service life goals for photovoltaic modules. These goals are a cost of $70 sq m and an expected 30 years of service life in an outdoor weathering environment. out of the cost goal, $14 sq m is allocated for encapsulation materials, which includes the cost of a structural panel. At FSA's inception in 1975, the cumulative cost of encapsulation materials in popular use, such as room temperature vulcanized (RTV) silicones, aluminum panels, etc., greatly exceeded $14/sq m. Accordingly, it became necessary to identify and/or develop new materials and new material technologies to achieve the goals. Many of these new materials are low cost polymers that satisfy module engineering and encapsulation processing requirements but unfortunately are not intrinsically weather stable. This necessitates identifying lifetime and/or weathering deficiencies inherent in these low cost materials and developing specific approaches to enhancing weather stability. Author

N86-12775# GTE Labs., Inc., Waltham, Mass. Power Sources Dept.

LITHIUM-THIONYL CHLORIDE CELL SYSTEM SAFETY HAZARD ANALYSIS Final Report, Dec. 1981 - Dec. 1984

F. W. Dampier Mar. 1985 83 p
(Contract F33615-81-C-2070)
(AD-A157089; AFWAL-TR-84-2112) Avail: NTIS HC A05/MF A01 CSCL 06/20

This system safety analysis for the lithium thionyl chloride cell is a critical review of the technical literature pertaining to cell safety and draws conclusions and makes recommendations based on this data. The thermodynamics and kinetics of the electrochemical reactions occurring during discharge are discussed with particular attention given to unstable SOCl2 reduction intermediates. Potentially hazardous reactions between the various cell components and discharge products or impurities that could occur during electrical or thermal abuse are described and the most hazardous conditions and reactions identified. Design factors influencing the safety of Li/SOCl2 cells, shipping and disposal methods and the toxicity of Li/SOCl2 battery components are additional safety issues that are also addressed. GRA

N86-12776# Naval Surface Weapons Center, Silver Spring, Md.

HIGH RATE LI/SOC1(2) CELLS. 1. EFFECT OF DESIGN VARIABLES IN UNCATALYZED CELLS Report, for Nov. 1983 - Apr. 1985

W. P. Kilroy, L. Pitts, and K. M. Abraham Apr. 1985 73 p
(AD-A157203; NSWC/TR-85-98) Avail: NTIS HC A04/MF A01 CSCL 10/3

One of the goals of the Navy's High Energy Batteries for Weapons Block Program is to achieve a better understanding of safety hazards in high energy lithium batteries. To attain this objective, a statistical survey was planned to examine how various cell parameters (cell design, cell balance, catalysis, moisture content, etc.) would affect performance and safety in Li/SOC12 cells. Five replicate tests were planned for each cell parameter during various modes of testing including overdischarge, partial discharge and storage followed by further discharge, etc. Cell performance, and individual electrode potentials, cell internal and external temperatures, and pressure were measured during discharge and forced over-discharge at different rates at ambient and subambient temperatures. The effect of partial discharge and storage on cell performance was assessed. At various stages, the cell chemistry was compared using X-ray, gas chromatography, IR and mass spectrocopy techniques. The effects of water, the presence of a catalyst and lithium vs. cathode-limited cell balance were also examined. The data have been summarized in two reports. This first report primarily addresses the effect of test conditions and cell parameters on performance and chemistry. The second report will discuss the effect of the catalyst. GRA

N86-12777# Naval Weapons Center, China Lake, Calif.

MAINTENANCE OF PHOTOVOLTAIC POWER SYSTEMS, REVISION 1

M. R. Hall Jun. 1985 71 p Previously announced as N85-27390
(AD-A157838; AD-E900491; NWC-TP-6563-REV-1) Avail: NTIS HC A04/MF A01 CSCL 10/2

This publication establishes standard practices for inspection, testing, and maintenance of photovoltaic power systems at Department of the Navy installations. The practices and procedures are recommended to ensure reliable operation of the power systems. The manual covers photovoltaic-array, battery, voltage-regulator, inverter, and wiring subsystems. In addition, this manual provides a troubleshooting guide and self-study questions and answers. GRA

N86-12778# Naval Civil Engineering Lab., Port Hueneme, Calif.

NAVY APPLICATIONS EXPERIENCE WITH SMALL WIND POWER SYSTEMS Report, Jun. 1982 - Jun. 1984

D. Pal May 1985 66 p
(AD-A158561; NCEL-TN-1724) Avail: NTIS HC A04/MF A01 CSCL 10/2

This report describes the experience gained and lesson learned from the ongoing field evaluations of seven small, 2-to 20-kW wind energy conversion systems (WECS) at Navy installations located in the Southern California desert, on San Nicolas Island, in California, and in Kaneohe Bay, Hawaii. The field tests show that the WECS's bearings and yaw slip-rings are prone to failure. The failures were attributed to the corrosive environment and poor design practices. Based upon the field tests, it is concluded that a reliable WECS must use a permanent magnet alternator without a gearbox and yaw slip-rings that are driven by a fixed pitch wind turbine rotor. The present state-of-the-art in small WECS technology, including environmental concerns, is reviewed. Also presented is how the technology is advancing to improve reliability and availability for effectively using wind power at Navy bases. The field evaluations are continuing on the small WECS in order to develop operation, maintenance, and reliability data. GRA

N86-12779# Thermo Electron Corp., Waltham, Mass.

ADVANCED THERMIONIC TECHNOLOGY PROGRAM: SUMMARY REPORT. VOLUME 1 Final Report

Oct. 1984 45 p Prepared in cooperation with Rasor Associates, Inc., Sunnyvale, Calif.
(Contracts DE-AC02-76ET-11292; DE-AC21-83MC-20352)
(DE85-009358; DOE/ET-11292/1893-Vol-1; TE-4258-5-84-Vol-1)
Avail: NTIS HC A03/MF A01

This report summarizes the progress made by the Advanced Thermionic Technology Program during the past several years. This program, sponsored by the US Department of Energy, has had as its goal adapting thermionic devices to generate electricity in a terrestrial (i.e., combustion) environment. The technology has previously been developed for astronautical applications. The report is organized in four volumes, each focused as much as possible on the needs of a particular audience. Volume 1 contains Part A, the Executive Summary. This Executive Summary describes the accomplishments of the Program in brief, but assumes the reader's familiarity with the thermionic process and the technical issues associated with the Program. For this reason, Volume 1 also contains Part B, a minimally technical overview of the Advanced Thermionic Technology Program. Volume 2 (Part C) concentrates on the progress made in developing and fabricating the current generation of hemical vapor deposited hot shell thermionic converters and is addressed to those primarily concerned with today's capabilities in terrestrial thermionic technology. Volume 3 (Part D) contains the results of systems studies of primary interest to those involved in identifying and evaluating applications for thermionics. Volume 4 (Part E) is a highly technical discussion of the attempts made by the program to push the state-of-the-art beyond the current generation of converters and is directed toward potential researchers engaged in this same task. These technical discussions are complemented with Appendices where appropriate.

DOE

N86-12780# Jet Propulsion Lab., California Inst. of Tech., Pasadena.

INVESTIGATION OF REACTIVE MAGNETRON SPUTTER DEPOSITED ZnSe FOR SOLAR CELL APPLICATION Final Report

R. J. Stirn and A. Nouhi Aug. 1985 62 p
(Contract DE-AC02-83CH-10093)
(DE85-016851; SERI/STR-211-2750) Avail: NTIS HC A04/MF A01

As a higher bandgap semiconductor with reasonable lattice constant, ZnSe is an attractive alternative to CdS for heterojunction solar cells. Previous attempts to deposit doped n-type polycrystalline ZnSe films usually produced film resistivities from 10(5) to 10(8) ohm-cm unless GaAs substrates were used. This report presents results of one year's research into depositing high-conductivity ZnSe on glass substrates by reactive magnetron sputter deposition, using pure metal sputter targets of Zn and In, Ga, and Al dopants. Using substrate temperatures as low as 150 C and sputter parameters and H2Se injection rates that maximize the Zn-to-Se ratio in the films, ZnSe bulk resistivities were reduced to as low as 40 ohm-cm. The most effective dopant to date was In, co-sputtered with Zn to In atomic concentrations of 3%. AES measurements show an average 45/52 ratio of Zn to Se; a low Zn content for such conducting films. Extended studies of dopants' effects are warranted, as are heterojunction studies using thin-film CuInSe2 and CdTe substrates.

DOE

N86-12781# Lockheed Missiles and Space Co., Palo Alto, Calif.

ZINC/FERRICYANIDE BATTERY DEVELOPMENT PHASE 4 Final Report, 9 May 1983 - 15 Feb. 1985

R. P. Hollandsworth, J. Zegarski, and J. R. Selman May 1985 264 p Prepared in cooperation with Illinois Inst. of Tech., Chicago
(Contract DE-AC04-76DP-00789)
(DE85-016026; SAND-85-7195) Avail: NTIS HC A12/MF A01

Project effort was concentrated on the technical evaluation of membrane cycle life of cost-effective membranes; and the study of the alkaline zinc/ferricyanide battery to meet goals of scale-up namely, refinement of a conceptual engineering design for a 50-kW solar photovoltaic storage system; determination of the cycle life of 60, 200, and 1000-sq cm cells operating at capacities between 70 and 200 mAh/sq cm; and, development of compatible bipolar plastic electrode technologies. Numerous cost effective membranes were cyclically evaluated to determine the effects of ferricyanide upon the long term cycle life of the membrane. The results to data indicate a vast improvement over previous tests in that the new membranes endured the ferricyanide electrolyte with minor or no changes in performance during the 100+ cycles at 70-mAh/sq cm capacity cycles which was used for preliminary performance testing. Post-mortem evaluation revealed, however, that changes to the ionic groups attached to the membrane substrate had resulted in ion exchange capacity loss and increased resistance. Present data suggests that the membrane changes occur upon initial exposure to the battery electrolyte as electrochemical testing indicates stable cyclic efficiency performance.

DOE

N86-12782# Wisconsin Univ., Milwaukee.

SYNTHESIS OF RESEARCH AND DEVELOPMENT IN MECHANICAL ENERGY STORAGE TECHNOLOGIES Progress Report, 1 Feb. - 31 Aug. 1985

G. M. Karadi May 1985 16 p
(Contract DE-AC02-79ET-26106)
(DE85-013313; DOE/ET-26106-26) Avail: NTIS HC A02/MF A01

Current research in the field of energy storage was synthesized, previous accomplishments and trends have been reassessed, and new research was initiated to improve the understanding of basic phenomena governing aquifer energy storage operations. The research effort on the Environmental and Institutional Aspects of Compressed Air Energy storage was completed and specific guidelines were proposed for planning purposes. The seasonal thermal energy storage component of the ongoing work involved the reassessment of strategies of RD and D efforts and independent research was initiated on multiple aquifer systems which has already resulted in a new approach in the analysis of dispersion in porous media. A new method is advanced for the estimation of the number of heating, freezing and degree days. In the areas of Diurnal Thermal Energy Storage, Solar Thermal Storage, District Heating and Cooling, and Storage for Solar Receivers the various options is studied by reassessing the findings of various research projects and the most promising technologies and/or combinations of technologies will be determined.

DOE

N86-12783# Oak Ridge National Lab., Tenn.

ORNL GROUND COIL ANALYTICAL AND EXPERIMENTAL STUDIES

V. C. Mei 1985 5 p refs Presented at the DOE/ORNL Heat Pump Conf., Washington, D.C., 10 Dec. 1984
(Contract DE-AC05-84OR-21400)
(DE85-005246; CONF-841231-15) Avail: NTIS HC A02/MF A01

The goal of this research program is to understand the phenomenon of soil heat transfer coupled with fluid flow, soil moisture freezing, soil moisture migration, and ground surface temperature variation. From these studies, comprehensive ground coil mathematical models are developed to better predict ground coil heat exchanger performance. The program has been loosely divided into three phases. Phase 1 was for ground coils involving heat transfer only, which was suitable for deep-well, tube-in-tube type ground heat exchanger analyses. A mathematical model based on energy balance coupled with fluid flow was solved numerically. The model was validated with laboratory experimental data obtained from a vertical, tube-in-tube heat exchanger 47 m deep are shown and shows the excellent agreement between the calculated and experimental results. The parametric study indicates that the size and material of the exchanger casing and the length of the exchanger are important factors in determining the performance of the ground heat exchanger. Table 1 shows monthly ground coil cooling and heating performance. The ground coil system performs better than an air-source heat pump system in the heating season, but the latter is better for the cooling season. Nevertheless, the ground coil system achieved a respectable annual performance factor of 2.4. Various advanced ground coil models for different types of ground coils and various factors affecting soil heat transfer are developed.

DOE

N86-12784# Argonne National Lab., Ill.

DEVELOPMENT OF A SUPPORTED LIQUID MEMBRANE AS A NICKEL-ZINC SECONDARY BATTERY SEPARATOR

D. S. Poa, J. F Miller, and N. P. Yao May 1985 36 p
(Contract W-31-109-eng-38)
(DE85-012591; ANL/OEPM-85-1) Avail: NTIS HC A03/MF A01

A liquid tertiary amine complexing agent was dissolved in an organic solvent and absorbed into and held within the pores of a microporous polymeric film by either capillary or surface force. Screening tests were performed to identify the optimum tertiary amine/organic solvent combinations, and the optimum concentration range of the amine solutions. The treatment of Celgard 2400 microporous film with certain tertiary amine/organic solvent solutions, such as triethylamine/xylene or tripropylamine/xylene, had no significant effect on either zinc penetration resistivity (ZPR) or electrolytic resistivity of the membrane. When the film was treated with tri-n-octylamine solutions of very high amine concentration, the potential difference between the zinc cathode and the Ni(OH)2 counter electrode, the electrolytic resistance of the membrane, increased sharply. Among the tertiary amine solutions tested in this study, trihexylamine/xylene, tri-n-octylamine/toluene, and tri-n-octylamine/xylene appeared to be the most promising, especially the last one. The treatment of the Celgard 2400 film with that solution increased the zinc penetration resistivity of the membrane by as much as 400%. This solution treatment also

improved the electrolytic conductivity of the Celgard 2400 film.
DOE

N86-12785# Sandia National Labs., Albuquerque, N. Mex.
CHARACTERIZATION OF SHEET CALCIUM FOR Ca/CaCr04 THERMAL BATTERIES
R. A. Guidotti, F. W. Reinhardt, and G. C. Nelson Apr. 1985 46 p
(Contract DE-AC04-76DP-00789)
(DE85-013231; SAND-83-2269) Avail: NTIS HC A03/MF A01

The physical and chemical properties of sheet calcium were examined in an attempt to explain the varied performance of different lots in five-cell Ca/CaCr04 thermal batteries. Properties evaluated included microhardness, phase and texture analysis, heat capacity, melting point, transition temperature, and heat of transition. The surface chemistry was examined by Auger electron spectroscopy, secondary ion mass spectroscopy, and low-energy ion-scattering spectroscopy. None of these properties could be correlated to battery performance. The bulk chemistry of the calcium was characterized by analysis for metallic and interstitial impurities. Only the nitrogen content exerted any measurable influence upon battery performance, with the best overall results observed for samples with > 0.40% nitrogen. DOE

N86-12786*# Springborn Labs., Inc., Enfield, Conn.
INVESTIGATION OF TEST METHODS, MATERIAL PROPERTIES AND PROCESSES FOR SOLAR CELL ENCAPSULANTS Annual Report
P. B. Willis 1985 101 p Sponsored in part by DOE Prepared for JPL
(Contracts NAS7-100; JPL-954527)
(DE85-012831; NASA-CR-176371; DOE/JPL-95452727/84; NAS 1.26:176371; AR-8) Avail: NTIS HC A06/MF A01 CSCL 10A

The historical development of ethylene vinyl acetate (EVA) is presented, including the functional requirements, polymer selection, curing, stabilization, production and module processing. The construction and use of a new method for the accelerated aging of polymers is detailed. The method more closely resembles the conditions that may be encountered in actual module field exposure and additionally may permit service life to be predicted accurately. The use of hardboard as a low cost candidate substrate material is studied. The performance of surface antisoiling treatments useful for imparting a self cleaning property to modules is updated. DOE

N86-12787# Washington State Energy Office, Olympia.
WIND GENERATION IN WASHINGTON Final Progress Report, 1 Jan. 1984 - 30 Apr. 1985
J. W. James 13 May 1985 3 p
(Contract DE-FG04-81AL-21581)
(DE85-012791; DOE/AL-21581/T1) Avail: NTIS HC A02/MF A01

A Chronology of events describing the activities completed in a wind energy project is presented. The goal of the project was to use energy from a wind turbine to preheat hot water for a Ridgefield, Washington residence. The turbine operated successfully in the spring of 1984 until the yaw mechanism and prop began to fail. An output performance sheet is included which provides estimated energy outputs and wind speeds measured from the year 1979. DOE

N86-12788# Jet Propulsion Lab., California Inst. of Tech., Pasadena.
SOLAR WALK-OFF PROTECTION
H. Awaya and R. Bedard Apr. 1985 68 p Prepared in cooperation with California Inst. of Tech., Pasadena
(Contract DE-AC04-76DP-00789)
(DE85-012112; SAND-84-7019) Avail: NTIS HC A04/MF A01

A point-focus solar concentrator is normally pointed toward the sun during operations to direct concentrated solar flux into the aperture of the receiver. If solar-tracking control is lost, severe damage may occur when the concentrated solar beam moves, or walks off the aperture across the face of the receiver. Alternative methods of solar walk-off prevention/protection for a specific assumed generic dish module and electric plant design are identified. The cost of a baseline case (no walk-off prevention/protection) is first calculated, including initial capital; recurring operating, maintenance, and capital replacement costs; and the cost of restoring the plant to operation following a solar walk-off. The alternative cases (with walk-off prevention/protection) are then evaluated by increasing the solar plant cost as a function of specific walk-off prevention/protection design alternatives and decreasing the cost of walk-off events given the specific level of prevention or protection offered by the alternative cases. The alternative plant designs are then compared with the baseline case and against each other by annualizing all costs. No single walk-off protection solution is universally applicable. Decisions concerning solar walk-off prevention/protection for specific installations must be based on engineering evaluations that consider the alternative choices given a specific plant, dish module, and site. DOE

N86-12789# Brookhaven National Lab., Upton, N. Y.
LOW-COST LIGHT-WEIGHT THIN MATERIAL SOLAR HEATING SYSTEM
W. G. Wilhelm Mar. 1985 9 p Presented at Solar Bldg.: Realities for Today - Trends for Tomorrow, Washington, D.C., 18 Mar. 1985
(Contract DE-AC02-76CH-00016)
(DE85-012531; BNL-36329; CONF-850388-11) Avail: NTIS HC A02/MF A01

Presented in this paper are innovative concepts to substantially reduce the cost of residential solar application. They were based on a research and development approach that establishes cost goals which if successfully met can insure high marketability. Included in this cost goal oriented approach is the additional need to address aesthetics and performance. With such constraints established, designs were initialized, tested, and iterated towards appropriate solutions. These solutions are based on methods for reducing the material intensity of the products, improving the simplicity for ease of production, and reducing the cost of installation. Such a development approach has yielded past proof of concept designs in the solar collector and in the other components that constitute a total solar heating system. DOE

N86-12790# Sandia National Labs., Albuquerque, N. Mex.
SOLAR THERMAL ENERGY SYSTEMS Program Summary, fiscal year 1984
May 1985 142 p Prepared in cooperation with Midwest Research Inst. Golden, Colo. and Sandia National Lab., Livermore, Calif.
(Contracts DE-AC02-83CH-10093; DE-AC04-76DP-00789; DE-AC04-76DR-00789)
(DE85-008793; SERI/SP-271-2662) Avail: NTIS HC A07/MF A01

Research and development conducted within the US Department of Energy's Solar Thermal Technology Program is described. The goal of the program is to advance the engineering and scientific understanding of solar thermal technology and to establish the technology base from which private industry can develop solar thermal power production options. Research areas emphasized include central receivers, distributed receiveres, and solar thermal materials. Brief descriptions are provided of the contractor's activities at the Sandia National Laboratories, Solar Energy Research Institute, and the San Francisco and Albuquerque DOE operations offices. A list of the FY 1984 publications is included.
DOE

N86-12791# Midwest Research Inst., Golden, Colo. Solar Energy Research Inst.
FILM STABILITY FOR DIRCT ABSORPTION RECEIVERS
K. Y. Wang, T. A. Newell (Illinois Univ., Urbana-Champaign), and R. J. Copeland Jun. 1985 6 p Presented at INTERSOL 1985, Solar Energy: The Diverse Solution, Montreal, 23 Jun. 1985
(Contract DE-AC02-83CH-10093)
(DE85-012135; SERI/TP-252-2739) Avail: NTIS HC A02/MF A01

The direct absorption receiver (DAR) concept offers the potential of high temperature operation by using concentrated solar energy. The minimum flow rate and other relevant issues required to maintain a continuous film flowing over the absorption surface are examined.
DOE

N86-12792# Institute of Gas Technology, Chicago, Ill.
ABSORPTION FLUIDS DATA SURVEY
R. A. Macriss and T. S. Zawacki 1985 13 p refs Presented at the DOE/ORNL Heat Pump Conf., Washington, D. C., 10 Dec. 1984
(Contract DE-AC05-84OR-21400)
(DE85-005279; CONF-841231-18) Avail: NTIS HC A02/MF A01

Development of improved data for the thermodynamic, transport and physical properties of absorption fluids were studied. A specific objective of this phase of the study is to compile, catalog and coarse screen the available US data of known absorption fluid systems and publish it as a first edition document to be distributed to manufacturers, researchers and others active in absorption heat pump activities. The methodology and findings of the compilation, cataloguing and coarse screening of the available US data on absorption fluid properties and presents current status and future work on this project are summarized. Both in house file and literature searches were undertaken to obtain available US publications with pertinent physical, thermodynamic and transport properties data for absorption fluids. Cross checks of literature searches were also made, using available published bibliographies and literature review articles, to eliminate secondary sources for the data and include only original sources and manuscripts. The properties of these fluids relate to the liquid and/or vapor state, as encountered in normal operation of absorption equipment employing such fluids, and to the crystallization boundary of the liquid phase, where applicable. The actual data were systematically classified according to the type of fluid and property, as well as temperature, pressure and concentration ranges over which data were available. Data were sought for 14 different properties: Vapor-Liquid Equilibria, Crystallization Temperature, Corrosion Characteristics, Heat of Mixing, Liquid-Phase-Densities, Vapor-Liquid-Phase Enthalpies, Specific Heat, Stability, Viscosity, Mass Transfer Rate, Heat Transfer Rate, Thermal Conductivity, Flammability, and Toxicity.
DOE

N86-12793# South Dakota Office of Energy Policy, Pierre.
SMALL SCALE WIND ENERGY CONVERSION PROGRAMMATIC EQUIPMENT Final Report
S. Wegman 20 May 1985 63 p
(Contract DE-FG04-82AL-20860)
(DE85-012319; DOE/AL-20860/T1) Avail: NTIS HC A04/MF A01

The purpose of this project is to provide South Dakota citizens with a case study of the institutional and technical problems encountered in the installation, maintenance and use of a small wind energy system. The project will provide information on wind turbine reliability, maintenance requirements and power production to demonstrate the feasibility of small-scale wind energy conversion projects for South Dakota. The system was installed by vocational students and instructors at Mitchell Vocational School. It has been in operation since the fall of 1983.
DOE

N86-12794# Sandia National Labs., Albuquerque, N. Mex.
PHOTOVOLTAIC CONCENTRATOR TECHNOLOGY PROJECT THIRTEENTH PROJECT INTEGRATION MEETING
May 1985 282 p Meeting held in Albuquerque, N. Mex., 4 Jun. 1984
(Contract DE-AC04-76DP-00789)
(DE85-013253; SAND-85-0791/1; CONF-8506140) Avail: NTIS HC A13/MF A01

The proceedings for a meeting on photovoltaic concentrator technology held in Albuquerque, NM on June 4 and 5, 1985 are reported. The meeting covered research on photovoltaic concentrators and their components, included: concentrator cells, cell assemblies, fresnel lenses, concentrator modules, tracking structures and control systems, and complete concentrator arrays. Abstracts of presentations and status reports for current research contracts are presented.
DOE

45 ENVIRONMENT POLLUTION

Includes air, noise, thermal and water pollution; environment monitoring; and contamination control.

N86-12795# Lawrence Livermore National Lab., Calif.
REAL-TIME COMPUTING OF THE ENVIRONMENTAL CONSEQUENCES OF AN ATMOSPHERIC ACCIDENTAL RELEASE OF RADIOACTIVE MATERIAL: USER'S POINT OF VIEW
G. Boeri, R. Caracciolo, and M. Dickerson Jul. 1985 16 p refs Presented at the Workshop on Real-Time Computing of the Environ. Consequences of an Accidental Release to the Atmosphere from a Nucl. Installation, Luxembourg, 17 Sep. 1985
(Contract W-7405-eng-48)
(DE85-016438; UCRL-93116; CONF-8509130-2) Avail: NTIS HC A02/MF A01

All calculations of the consequences of an atmospheric release must start with atmospheric dispersion calculations. Time factors make external and inhalation dose estimates of immediate concern closely followed by ground contamination of land, pastures and onch agricultural crops. In general, the difficulties in modeling the source term and atmospheric transport and diffusion account for most of the error in calculating the dose to man. Thus, sophisticated treatment of the dose part of the calcuating is not usually justified, though the relative distribution of dose in individual organs may be needed for correct decision making. This paper emphasizes the atmospheric transport and diffusion part of the dose estimate and relates how this calculation can be used to estimate dose.
DOE

N86-12796# Brookhaven National Lab., Upton, N. Y.
PERSPECTIVES TO ESTABLISH KNOWLEDGE LINKAGES BETWEEN ACIDIC DEPOSITION AND VEGETATION RESPONSES
L. S. Evans and K. F. Lewin 1985 15 p Presented at the NATO ARW Conf. on Effects of Acidic Deposition on Forests, Wetlands and Agr. Ecosystems, Toronto, 12 May 1985 Prepared in cooperation with Manhattan Coll., N.Y.
(Contract DE-AC02-76CH-00016)
(DE85-011839; BNL-36452; CONF-8505156-2) Avail: NTIS HC A02/MF A01

This paper provides perspective for present and planned reseach that seeks to establish a knowledge linkage between acidic deposition and vegetation responses. The paper can be divided into three sections: (1) experimental approaches necessary to establish knowledge linkages between acidic deposition and vegetation responses; (2) perspectives obtained from an established air pollutant (ozone) - vegetation (ponderosa pine) response linkage; and (3) current obstacles to overcome in order to establish an information linkage between acidic deposition and forest decline in the northern Appalachians.
DOE

N86-12797# Mound Lab., Miamisburg, Ohio.
OUTDOOR RADON MONITORING AT CANONSBURG, PENNSYLVANIA, 1980-1983
C. R. Rudy, P. H. Jenkins, G. R. Hagee, J. C. Miles, and W. G. Yates 31 May 1985 41 p
(Contract DE-AC04-76DP-00053)
(DE85-013320; MLM-3254) Avail: NTIS HC A03/MF A01

This report summarizes the results of radon measurements from January 1980 to July 1983 near the former Vitro Manufacturing Plant located in Canonsburg, Pennsylvania. During this period, radon monitoring was performed on a continuous basis at 40 to 50 minitoring locations surrounding the site. Weekly measurements ere made using Passive Environmental Radon Monitors (PERMs) at these locations. In addition, meteorological measurements were made at the same time using a weather station located at the site. The results indicate that increased radon concentrations occur downwind of the site. The maximum off-site concentration measured was 0.93 pCi/L (39-month average). The maximum on-site concentration measured was 3.0 pCi/L (11-month average). Background outdoor radon concentrations ranged from 0.20 to 0.26 pCi/L. Positive correlations are noted between radon concentrations and inverse wind speed and calm periods. A negative correlation is observed between precipitation frequency and radon concentration during weekly monitoring periods. DOE

N86-12798# Miami Univ., Fla. School of Marine and Atmospheric Sciences.
ATMOSPHERIC TRITIUM 1968-1984
H. G. Oestlund and A. S. Mason Apr. 1985 152 p refs
(Contract DE-AS05-76FV-03944)
(DE85-013133; DOE/EV-03944/20; Rept-14) Avail: NTIS HC A02/MF A01

Tritium in the form of water, HTO, from the atmospheric testing of nuclear devices in the 60s has disappeared from the atmosphere and entered the ocean. The additions of such tritium from Chinese and French tests in the 70s were observed but did not make a big impression on the diminishing inventory of atmospheric HTO. Tritium in elemental form, HT, went through a maximum in the mid 70s, primarily as a results of some underground testing of large nuclear devices and releases from civilian and military nuclear industry. The mid 70s maximum was 1.3 kg of tritium in this form, and in 1984 0.5 kg remain. The disappearance is slower than the decay rate of tritium, so sources must still have been present during this time. The global distribution shows smaller inventory in the Southern Hemisphere across the equator and thus southward transport of HT. The chemical lifetime of hydrogen gas in the atmosphere, assuming the elemental tritium being in the form of HT, not T2, was estimated between 6 and 10 years. It is expected that increasing activity of nuclear fuel reprocessing would in the near future again increase the global tritium gas inventory. Tritium in the form of light hydrocarbons, primarily methane, was measured, and in this form a quantity of 200 g of tritium resided in the global atmosphere 1956 to 1976. By 1982 it had decreased to 50 g. DOE

N86-12799# Pacific Northwest Lab., Richland, Wash.
STATISTICAL METHODS FOR ENVIRONMENTAL POLLUTION STUDIES
R. O. Gilbert Jun. 1985 13 p
(Contract DE-AC06-76RI-01830)
(DE85-005298; PNL-SA-12373) Avail: NTIS HC A02/MF A01

Design and analysis of environmental contaminant data is reviewed. The major tasks required to conduct a successful environmental sampling study followed by a summary of the principal field sampling designs that are commonly needed. Several criteria for choosing the most appropriate sampling designs are discussed. Some of the problems commonly encountered when statistically analyzing pollution data are considered. DOE

N86-12800# Pacific Northwest Lab., Richland, Wash.
INTERPRETATION OF INDIVIDUAL PRECIPITATION CHEMISTRY DATA SETS: GENERAL CONSIDERATIONS AND APPROACHES
E. G. Chapman Apr. 1985 13 p Presented at the EPA/USGS/EPRI Workshop on Acid Deposition Monitoring and Anal., Raleigh, N. Car., 30 Apr. 1985
(Contract DE-AC06-76RL-01830)
(DE85-012449; PNL-SA-13153; CONF-8504158-1) Avail: NTIS HC A02/MF A01

The operation of precipitation chemistry monitoring networks is an important component of research efforts to understand acid deposition processes. Operation of such networks includes locating sites, collecting precipitation, and analyzing samples, and conducting a comprehensive quality control/quality assurance program, and preparing and utilizing a high quality data set. The analysis and interpretation of individual data sets are addressed. A common thread through each of these papers is that of data flagging; the criteria for data flagging, the handling of flagged data, and the problems that unflagged data can create. This thread underscores the point that data quality affects all aspects of acid precipitation research. The purpose of this paper is threefold: (1) to identify the major components that influence interpretation of individual precipitation chemistry data sets; (2) to suggest a framework for analyzing individual data sets that provides a built in system for determining the influence of these components; and (3) to identify potential areas for standardization that will aid the data analyst. DOE

N86-12801# Tennessee Univ., Chattanooga. Div. of Air and Water Resources.
ACIDIFICATION TRENDS IN SURFACE WATERS OF THE SOUTHERN APPALACHIANS Final Report
H. Olem Mar. 1985 153 p refs
(DE85-901746; TVA/ONRED-AWR-85/13) Avail: NTIS HC A08/MF A01

Historical data was reviewed to identify any spatial or temporal trends in surface water pH and alkalinity in the Southern Blue Ridge Province of Georgia, North Carolina, Tennessee, and Virginia. DOE

N86-12802# Purdue Univ., West Lafayette, Ind.
FISCAL YEAR 1983 PROGRAM REPORT OF THE PURDUE (INDIANA) WATER RESOURCES RESEARCH CENTER Report, 1 Jun. 1983 - 31 Dec. 1984
J. H. Cushman Dec. 1984 28 p
(Contract DI-14-08-0001-G-841)
(PB85-225829; USGS/G-841-01) Avail: NTIS HC A03/MF A01 CSCL 08H

A compilation of project summaries for the Fiscal Year 1983 is given. These projects include studies of groundwater pollutant transport, overland flow, control of non-point pollution control, growth of mussels, simulation of drought management, and technology transfer. GRA

N86-12803# National Bureau of Standards, Gaithersburg, Md. Building Physics Div.
INDOOR AIR QUALITY MODELING WORKSHOP REPORT
P. E. McNail May 1985 16 p Workshop held Gaithersburg, Md., 11 Feb. 1985 Sponsored in part by Environmental Monitoring Systems Lab.
(PB85-212306; NBSIR-85/3150) Avail: NTIS HC A02/MF A01 CSCL 13B

Comprehensive modeling of emission, absorption, movement, and controls of indoor air contaminants is essential for developing national policy for assessment and controls. Several topics discussed in a workshop on indoor air quality, which was held on February 11, 1985 at the National Bureau of Standards are presented. Researchers on indoor air quality (IAQ) modeling were invited to state their current activities, identify future research needs and recommend specific parameters and contaminants to be included in the IAQ models. The input thus obtained in this workshop will be incorporated in an advanced simulation model for IAQ, to be developed by NBS under a contract with EPA. GRA

N86-12804# Environmental Protection Agency, Research Triangle Park, N.C. Environmental Monitoring Systems Lab.
ASSESSMENT OF THE LONG-TERM PRECISION OF CONTINUOUS EMISSION MONITORS
R. Rollins, T. J. Logan, and M. R. Midgett 1985 16 p refs
(PB85-201150; EPA-600/D-85-111) Avail: NTIS HC A02/MF A01 CSCL 14B

The EPA has promulgated regulations requiring certain stationary sources to show continual compliance with emission limits, by using a Continuous Emission Monitoring System (CEMS). In order to make reliable compliance determinations, the quality of the monitoring data is important. Two principal parameters in assessing and describing data quality are precision and accuracy. The paper discusses the long term precision for five CEM's installed at scrubber controlled, coal fired power plants. Precision estimates were made by utilizing available daily calibration drift data. Six to seven months of calibration drift data were analyzed for each pollutant (SO2, NOx) and diluent (O2, CO2) analyze in the CEMS.

Results show that most of the monitors exhibited significant bias and variance over the months involved. Author (GRA)

N86-12805# Environmental Protection Agency, Research Triangle Park, N.C.

SUMMARY OF PRECISION AND ACCURACY ASSESSMENTS FOR THE STATE AND LOCAL AIR MONITORING NETWORKS, 1982

E. G. Evans, R. C. Rhodes, W. J. Mitchell, and J. C. Puzak Apr. 1985 151 p

(PB85-208171; EP1/600/4-85/031) Avail: NTIS HC A08/MF A01 CSCL 13B

Precision and accuracy data obtained from State and local agencies during 1982 are summarized and evaluated. Some comparisons are made with the results previously reported for 1981 to determine the indication of any trends. Some trends indicating improvement in the precision and accuracy of monitoring data are given on a national and regional basis. The annual average results from each reporting organization are given so that comparisons may be made from 1981 to 1982 and also with other reporting organization. A comparison of the precision and accuracy from the Precision and Accuracy Reporting System and that from the independent performance audit program conducted by the Environmental Monitoring Systems Laboratory is given. GRA

N86-12806# Radian Corp., Austin, Tex.

EVALUATION OF AIR EMISSIONS FROM HAZARDOUS WASTE TREATMENT, STORAGE AND DISPOSAL FACILITIES Final Report, Jun. 1982 - Jun. 1984

W. D. Balfour, R. G. Wetherold, and D. L. Lewis May 1985 81 p refs

(Contract EPA-68-02-3171)

(PB85-203792: EPA-600/2-85/057) Avail: NTIS HC A05/MF A01 CSCL 13B

The fugitive air emissions from landfills surface impoundments, storage tanks, containers (drums), solvent recovery processes, and land treatment technologies at hazardous waste disposal facilities (HWDF's) are discussed. The main objective was to develop and demonstrate techniques for determining air emissions from the above HWDF technologies (sources). Various predictive models for estimation air emissions exist for some of the these sources. These models have been identified and evaluated for procedures for applicability to select HWDF's. Sampling approaches have been identified for the collection and qualitative and quantitative analysis of the samples. The resulting analytical data have provided general information on the level of air emissions from the sources studied. The findings from each of four HWDF's tested are given. GRA

N86-12807# National Oceanic and Atmospheric Administration, Rockville, Md. Air Resources Lab.

ANALYSIS AND ASSESSMENT OF US-WMO REGIONAL PRECIPITATION CHEMISTRY MEASUREMENTS (1972-1982), A SUBJECT OF THE NATIONAL TRENDS NETWORK

R. S. Artz and J. M. Miller Feb. 1985 274 p

(PB85-212959; NOAA-TM-ERL-ARL-135) Avail: NTIS HC A12/MF A01 CSCL 04A

Data from the entire sampling period (1972-1982) for all sites in the National Trends Network and its predecessors are presented. Annual and monthly (where appropriate) volume weighted means, medians, and standard deviations are included. Selected graphs of annual statistics are also shown. Analysis of these data indicates improvement in data quality since 1980 for all ions measured and at all sites. Post-1980 data is of high quality, well documented, and should be useful for most studies requiring a regional data base. Pre-1980 data are of lesser quality and not sufficiently accurate for seasonal evaluation or annual trend analysis. GRA

N86-12808# Cornell Univ., Ithaca, N.Y. Center for Environmental Research.

DIAGNOSING THE CAUSES OF GROUND-WATER CONTAMINATION USING A MATHEMATICAL MODEL: REPORT ON TECHNOLOGY TRANSFER WORKSHOP

S. Pacenka Sep. 1984 42 p

(PB85-217008; USGS/G-859(23)) Avail: NTIS HC A03/MF A01 CSCL 08H

Ground-water contamination casese are now being detected at a rate faster than the capability of regulatory agencies to diagnose and solve them. Automation, in the form of low-cost microcomputers and simple mathematical models of contaminant behavior, can help to gain control of the growing backlog of cases. These tools can amplify the skills of the limited number of specialists in the area now employed by the key agencies such as state-level environmental and health departments. Since the same tools can also be used in advance planning for the prevention of ground-water contamination, they could also help to foster the transition from the current, crisis-driven system to one which detects potential problems early and eventually prevents them before they start. A technology transfer workshop which employed microcomputers and associated software in training agency specialists about the movement and fate of groundwater contaminants is described. GRA

N86-12809# Analytical Sciences Corp., Research Triangle Park, N.C.

SPATIAL AND TEMPORAL PATTERNS OF ACID PRECIPITATION AND THEIR INTERPRETATION

S. K. Seilkop and P. L. Finkelstein Jun. 1985 18 p

(Contract EPA-68-02-4082)

(PB85-214377; EPA/600/D-85/113) Avail: NTIS HC A02/MF A01 CSCL 13B

Using data compiled from seven nationwide precipitation chemistry networks in the U.S. and Canada, the spatial distribution of hydrogen, sulfate, and nitrate ions in North America is discussed. Geographic patterns of concentration and deposition are characterized using isopleth maps which are presented and interpreted for the years 1980, 1981, and 1982. The maps were developed using a geostatical technique known as 'kriging'. This method allows for the estimation of confidence limits on interpolated values. Using these limits, the significance of temporal changes in spatial patterns of deposition and concentration is assessed. GRA

N86-12810# Rhode Island Univ., Kingston.

ACID PRECIPITATION: SOURCE IDENTIFICATION AND ITS EFFECTS ON WATER QUALITY

C. P. C. Poon and T. Wright Sep. 1984 92 p

(PB85-214880; USGS/G-867(04)) Avail: NTIS HC A05/MF A01 CSCL 13B

Three small watersheds in the rural area of R.I. were studied for the effects of acid precipitation on the water quality. All three rivers namely, Wood, Beaver, and Usquepaug, have Class A high water quality with very low alkalinity. Storm tracks were identified by using sequential meteorological maps including satellite photos, radar precipitation scans, and pressure maps. Precipitation samples were titrated and their acid components were quantified by the Gran Plot technique. Storms from the west and southwest direction usually carry more acids than those from west-northwest and south-southwest. All storms have similar effects on the three rivers with the chemistry change more pronounced for the Beaver river because of its smallest size. A large storm or a small storm but with high acid concentrations often reduced the alkalinity of the river water to less than 1.0 mg/l. GRA

N86-12843*# Saskatchewan Univ., Saskatoon. Inst. of Space and Atmospheric Studies.

SASKATOON M. F. RADAR SYSTEM: (52 DEG N, 107 DEG W), CANADA Abstract Only

A. H. Manson and C. E. Meek *In* International Council of Scientific Unions Middle Atmosphere Program. Handbook for MAP, Vol. 17 Aug. 1985 p 52-56 refs (For primary document see N86-12837 03-46)

Avail: NTIS HC A07/MF A01; also available from SCOSTEP Secretariat, Illinois Univ., 1406 West Green Street, Urbana, Ill. 61801 CSCL 04A

N86-12676# Joint Publications Research Service, Arlington, Va.
INFLUENCE OF SOME OCEANOGRAPHIC CHARACTERISTICS ON DECAY KINETCIS OF SURFACE-ACTIVE AGENTS IN SEA Abstract Only
N. I. Ryasintseva, V. V. Malyshkina, and L. Yu. Sekundyak *In its* USSR Rept.: Earth Sci. (JPRS-UES-85-006) 19 Jun. 1985 p 45 Transl. into ENGLISH from Okeanol. (Moscow), v. 25, no. 1, Jan. - Feb. 1985 p 88-92 (For primary document see N86-12630 03-42)
Avail: NTIS HC A05/MF A01

N86-12692# Joint Publications Research Service, Arlington, Va.
DAMPING OF HIGH-FREQUENCY WIND WAVES BY ARTIFICIAL SURFACE-ACTIVE FILMS Abstract Only
S. A. Yermakov, A. R. Panchenko, and T. G. Talipova *In its* USSR Rept.: Earth Sci. (JPRS-UES-85-006) 19 Jun. 1985 p 74 Transl. into ENGLISH from Izv. Akad. Nauk SSSR: Fiz. Atm. i Okeana (Moscow), v. 21, no. 1, Jan. 1985 p76-82 (For primary document see N86-12630 03-42)
Avail: NTIS HC A05/MF A01

N86-12693# Joint Publications Research Service, Arlington, Va.
ORGANIC COMPONENTS IN ATMOSPHERE IN REGIONS OF VOLCANIC ACTIVITY Abstract Only
V. A. Isidorov and I. G. Zenkevich *In its* USSR Rept.: Earth Sci. (JPRS-UES-85-006) 19 Jun. 1985 p 75 Transl. into ENGLISH from Dokl. Akad. Nauk SSSR (Moscow), v. 280, no. 1, Jan. 1985 p 223-227 (For primary document see N86-12630 03-42)
Avail: NTIS HC A05/MF A01

N86-12695# Joint Publications Research Service, Arlington, Va.
GLOBAL MODELING OF OPTICAL CHARACTERISTICS OF ATMOSPHERIC AEROSOL Abstract Only
K. Ya. Kondratyev, N. I. Moskalenko, S. Ya. Skvortsova, A. R. Zakirova, F. S. Yakuoova, and S. V. Gusev *In its* USSR Rept.: Earth Sci. (JPRS-UES-85-006) 19 Jun. 1985 p 76-77 Transl. into ENGLISH from Dokl. Akad. Nauk SSSR (Moscow), v. 280, no. 5, Feb. 1985 p 1090-1093 (For primary document see N86-12630 03-42)
Avail: NTIS HC A05/MF A01

N86-12696# Joint Publications Research Service, Arlington, Va.
DIURNAL VARIATION OF OPTICAL AND MICROPHYSICAL CHARACTERISTICS OF NEAR-SURFACE AEROSOL Abstract Only
V. N. Sidorov, G. I. Gorchakov, A. S. Yemilenko, and M. A. Sviridenkov *In its* USSR Rept.: Earth Sci. (JPRS-UES-85-006) 19 Jun. 1985 p 78 Transl. into ENGLISH from Izv. Akad. Nauk SSSR: Fiz. Atm. i Okeana (Moscow), v. 20, no. 12, Dec. 1984 p 1156-1165 Original language document was announced in IAA as A85-20831 (For primary document see N86-12630 03-42)
Avail: NTIS HC A05/MF A01

N86-12703# Joint Publications Research Service, Arlington, Va.
ESTIMATION OF INFLUENCE OF OCEAN ON DISTRIBUTION OF HEAVY METALS IN MARINE ATMOSPHERE Abstract Only
V. V. Anikiyev, V. I. Ilichev, A. A. Lobanov, and A. N. Medvedev *In its* USSR Rept.: Earth Sci. (JPRS-UES-85-008) 16 Aug. 1985 p 9 Transl. into ENGLISH from Dokl. Akad. Nauk SSSR (Moscow), v. 281, no. 4, Apr. 1985 p 937-940 (For primary document see N86-12697 03-42)
Avail: NTIS HC A04/MF A01

46 GEOPHYSICS

Includes aeronomy; upper and lower atmosphere studies; ionospheric and magnetospheric physics; and geomagnetism.

For space radiation see *93 Space Radiation.*

N86-12811 Illinois Univ., Urbana-Champaign.
THE DYNAMIC STABILITY OF THE STRATOSPHERE AND MESOSPHERE Ph.D. Thesis
Ke-Su Zhang 1985 201 p
Avail: Univ. Microfilms Order No. DA8511696

The normal modes of large-scale atmospheric motions have been examined in a spherical quasi-geostrophic model extending from the surface up to 80 km to investigate the stability of zonal motions in the stratosphere and mesosphere. Two sets of calculations were performed. In the first set, the basic states are representative of the Northen Hemisphere winter and summer solstice conditions. The winter basic state is able to support baroclinically unstable, quasi-stationary planetary waves, which extend into the stratosphere and the mesosphere from the troposphere at high latitudes. They are identified as Green modes. The structure of the unstable Green mode compares favorably with the observed quasi-stationary planetary waves. In the second set, a comparison is made of the stabilities of the stratospheric basic states before and after the 1976/1977 sudden warming event. Dissert. Abstr.

N86-12812 Northwestern Univ., Evanston, Ill.
SEISMOLOGICAL STUDIES OF THE TECTONICS OF DIVERGENT PLATE BOUNDARIES Ph.D. Thesis
Joseph Francis Engeln 1985 147 p
Avail: Univ. Microfilms Order No. DA8511816

Earthquakes on major Atlantic transform faults were studied. Most of the events show transform-parallel strike-slip motion on steeply dipping planes. A number of earthquakes with anomalous mechanisms occur near ridge-transform intersections where the thermal contrast is greatest and stress orientations can be oblique to both the ridge and transform. Centroid depths, determined by body wave waveform inversion, occur above the 400 C isothermal of the expected thermal structure. The maximum depth extent of faulting predicted by scaling laws corresponds to the predicted 600 C isotherm. Centroid depths for oceanic intraplate earthquakes extent to approximately the 750 C isotherm. Since transforms have higher strain rates than intraplate areas, if both have the same rheology the limiting isotherm for transforms should be higher. If a weather rheology is more appropriate, the higher strain rate and weakening effects yielding a limiting isotherm similar to that for intraplate regions. It thus appears that transforms are either weaker and/or have higher temperatures than expected. Dissert. Abstr.

N86-12813 State Univ. of New York, Stony Brook.
THEORETICAL MODELLING OF THE ELASTIC PROPERTIES OF MANTLE SILICATES Ph.D. Thesis
Andrew Yu-Chung Au 1984 146 p
Avail: Univ. Microfilms Order No. DA8513508

The elastic properties of a crystalline solid are not only the manifestation of two-body central forces, but also of noncentral and many-body forces within the crystal structure. Conventional lattice calculations, by adopting the atomistic scale as the fundamental modelling unit, are inadequate in addressing the phenomenon of cooperative interactions in atomic clusters-the non-central and many-body forces. A modified rigid-ionn model is developed based on coordination polyhedra as the fundamanetal modelling units in a crystal structure. The crystal structure is represented by its constituent coordination polyhedra that are treated as three-dimensional elastic continua. Elastic moduli, experimentally determined or otherwise assumed, are ascribed to these coordination polyhedra. Finite element analysis is applied to retrieve the interatomic force information implicit in the elastic moduli of such a polyhedron. Dissert. Abstr.

N86-12814*# International Council of Scientific Unions, Urbana, Ill.
MIDDLE ATMOSPHERE PROGRAM. HANDBOOK FOR MAP. VOLUME 16: ATMOSPHERIC STRUCTURE AND ITS VARIATION IN THE REGION 20 TO 120 km. DRAFT OF A NEW REFERENCE MIDDLE ATMOSPHERE
K. Labitzke, ed. (Freie Univ.), J. J. Barnett, ed. (Oxford Univ.), and B. Edwards, ed. Jul. 1985 323 p refs Sponsored in part by UNESCO
(NASA Order W-15897)

(NASA-CR-176321; NAS 1.26:176321; MAP-HANDBOOK-16) Avail: NTIS HC A14/MF A01; also available from SCOSTEP Secretariat, Illinois Univ., 1406 West Green Street, Urbana, Ill. 61801 CSCL 04B

A draft of a new reference atmosphere for the region between 20 and 80 km which depends largely on recent satellite experiments covering the globe from 80 deg S to 80 deg N is given. A separate international tropical reference atmosphere is given, as well as reference ozone models for the middle atmosphere. For individual titles, see N86-12815 through N86-12836.

N86-12815*# Oxford Univ. (England). Dept. of Atmospheric Physics.

TEMPERATURE DATA FROM SATELLITES

J. J. Barnett and M. Corney *In* International Council of Scientific Unions Middle Atmosphere Program. Handbook for MAP, Vol. 16 Jul. 1985 p 3-11 refs (For primary document see N86-12814 03-46)
Avail: NTIS HC A14/MF A01; also available from SCOSTEP Secretariat, Illinois Univ., 1406 West Green Street, Urbana, Ill. 61801 CSCL 04B

Several satellites and sounding systems used for measuring the temperature of the middle atmosphere are discussed. Retrieval methods, geopotential height data, the merging of data sets, and an analysis of long term temperature trends are discussed. R.J.F.

N86-12816*# National Aeronautics and Space Administration. Goddard Space Flight Center, Greenbelt, Md.

TEMPERATURE AND WIND DATA FROM METEOROLOGICAL ROCKETS

F. J. Schmidlin *In* International Council of Scientific Unions Middle Atmosphere Program. Handbook for MAP, Vol. 16 Jul. 1985 p 12-14 refs (For primary document see N86-12814 03-46)
Avail: NTIS HC A14/MF A01; also available from SCOSTEP Secretariat, Illinois Univ., 1406 West Green Street, Urbana, Ill. 61801 CSCL 04B

A brief history of the use of meteorological rockets in gathering temperature and wind data in the upper atmosphere is given. The validity of data is discussed. R.J.F.

N86-12817*# Institute of Applied Geophysics, Moscow (USSR). Central Aerological Observatory.

OBSERVED WINDS AND TEMPERATURES IN THE SOUTHERN HEMISPHERE

Yu. P. Koshelkov *In* International Council of Scientific Unions Middle Atmosphere Program. Handbook for MAP, Vol. 16 Jul. 1985 p 15-35 refs (For primary document see N86-12814 03-46)
Avail: NTIS HC A14/MF A01; also available from SCOSTEP Secretariat, Illinois Univ., 1406 West Green Street, Urbana, Ill. 61801 CSCL 04B

A brief account is given of efforts to measure the winds and temperature in the Southern Hemisphere. Results of rocketsonde soundings are analyzed. R.J.F.

N86-12818*# Saskatchewan Univ., Saskatoon. Inst. of Space and Atmospheric Studies.

MEAN WINDS OF THE MESOSPHERE (60-80 km), AS MEASURED BY MF RADARS

A. H. Manson, C. E. Meek, R. A. Vincent (Adelaide Univ.), and M. J. Smith (Inst. of Nuclear Sciences) *In* International Council of Scientific Unions Middle Atmosphere Program. Handbook for MAP, Vol. 16 Jul. 1985 p 36-46 refs (For primary document see N86-12814 03-46)
Avail: NTIS HC A14/MF A01; also available from SCOSTEP Secretariat, Illinois Univ., 1406 West Green Street, Urbana, Ill. 61801 CSCL 04B

Winds data obtained from medium frequency (MF) radars for heights of 60 to 80 km are discussed: locations are Saskatoon (52 N, 107 W), Christchurch (44 S, 173 W), Adelside (35 S, 183 E) and Townsville (20 S, 147 E). Whereas well defined summer easterly jets centered near 70 km develop in summer, no regular buildups and decays are observed in winter at midlatitudes. Part of this variability can be associated with stratospheric warmings, which develop into breakdown of the polar vortex in the Northern Hemisphere. Amplitude and phase profiles of the annual and semiannual oscillations are also presented. The radar winds from Saskatoon are compared and combined with rocket derived winds up to 60 km from Primrose Lake (54 N, 110 W) to give consistent cross sections from 20 to 110 km. The SH radar winds are compared with a model based on rocket winds which extends up to 80 km. The latter evidence considerable smoothing, as no winter variability is evident. The other consistent difference is that heights of the summer easterly maxima for the model are 5 to 10 km lower than the radar winds at all latitudes. Author

N86-12819*# Oxford Univ. (England). Dept. of Atmospheric Physics.

MIDDLE ATMOSPHERE REFERENCE MODEL DERIVED FROM SATELLITE DATA

J. J. Barnett and M. Corney *In* International Council of Scientific Unions Middle Atmosphere Program. Handbook for MAP, Vol. 16 Jul. 1985 p 47-85 refs (For primary document see N86-12814 03-46)
Avail: NTIS HC A14/MF A01; also available from SCOSTEP Secretariat, Illinois Univ., 1406 West Green Street, Urbana, Ill. 61801 CSCL 04B

Zonally averaged temperature and geostrophic zonal wind for each month and for latitudes from 80 S to 80 N with pressure scale height as a vertical coordinate are given tabular form. The pressure scale height is defined as -ln (p/P sub O) where p is pressure and P sub O is surface pressure. The height interval corresponding to one pressure scale height is proportional to absolute temperature, and is 7 km at 240 K. Values in are given at intervals of 0.5 pressure scale heights, i.e., approximately 3,5 km. The geopotential height fields for the principal seasons are given. Temperature, pressure and density with geometric height as the vertical coordinate at invervals of 5 km. The temperature values were obtained from a combination of satellite data above 30 mb with values supplied by the Berlin Free University at 30 mb and the climatology derived by OORT (1983) for 50 mb and below. The geopotential height fields were obtained from these temperature fields by integrating up and down from the 30 mb geopotential height supplied by Berlin Free University. The geostrophic winds were obtained by differentiating these geopotential height fields. Author

N86-12820*# Oxford Univ. (England). Dept. of Atmospheric Physics.

PLANETARY WAVES

J. J. Barnett and M. Corney *In* International Council of Scientific Unions Middle Atmosphere Program. Handbook for MAP, Vol. 16 Jul. 1985 p 86-137 (For primary document see N86-12814 03-46)
Avail: NTIS HC A14/MF A01; also available from SCOSTEP Secretariat, Illinois Univ., 1406 West Green Street, Urbana, Ill. 61801 CSCL 04B

The mean temperature field at various pressure levels for January and July for both hemispheres are given. In summer (July in the Northern Hemisphere, January in the Southern Hemisphere) the fields are nearly zonally symmetric, but in winter large longitudinal variations are evident. These are mainly of low wave number, i.e., they may be represented by Fourier analysis around the globe using just a few (one or two) waves. This is the basis for representing the climatology of longitudinal variation in terms of wave components, since the fields may be defined with fewer values than by using a grid in longitude that has a sufficiently small interval to adequately represent the smooth variations. The amplitude and phase of temperature and geopotential height for wave numbers one and two, with ln(pressure) as the vertical coordinate are given. The fields were calculated and plotted at pressure intervals of 0.2 in ln(pressure) and at latitude intervals of 4 deg, but were interpolated to intervals of 0.5 in ln(pressure) (approximately 3.5 km) and 10 deg latitude for tabulation. Tables and figures give wave coefficients for the monthly mean temperature fields. Thus they represent the quasi-statinary planetary waves. Author

N86-12821*# Freie Univ., Berlin (West Germany). Meteorological Inst.

PLANETARY WAVES

K. Labitzke and J. J. Barnett (Oxford Univ.) *In* International Council of Scientific Unions Middle Atmosphere Program. Handbook for MAP, Vol. 16 Jul. 1985 p 136-143 refs (For primary document see N86-12814 03-46)

Avail: NTIS HC A14/MF A01; also available from SCOSTEP Secretariat, Illinois Univ., 1406 West Green Street, Urbana, Ill. 61801 CSCL 04B

The middle atmosphere exhibits variation on a time scale of a few days. Short term variations include travelling waves which are found at all seasons (although those occurring in summer have very small amplitudes). However, stratospheric warming which are connected with a very strong intensification of the planetary waves one or two, have the largest effect. They affect the stratosphere and mesosphere over periods varying between a few days and several months. The magnitude of temperature changes which can occur are shown. At some level (e.g., 50 km) changes exceed 70 K over 15 days from 28 December to 18 January. The sudden warming is such a large phenomenon that it strongly affects individual monthly means, giving larger planetary wave amplitudes than for months without large warmings. However, sudden warmings are part of the climatology, and their mean effect needs to be included, but an average over a small number of years for a given month can possibly be inadequate to obtain a reliable mean. Consequently, the means given here must be treated with caution. During the summer season, planetary wave amplitudes are small (a few K) so the year to year variability will cause little absolute error in the amplitude. Year to year variability of the monthly mean is illustrated. Author

N86-12822*# Kyoto Univ. (Japan). Faculty of Science.

GRAVITY WAVES

I. Hirota *In* International Council of Scientific Unions Middle Atmosphere Program. Handbook for MAP, Vol. 16 Jul. 1985 p 144-148 refs (For primary document see N86-12814 03-46)

Avail: NTIS HC A14/MF A01; also available from SCOSTEP Secretariat, Illinois Univ., 1406 West Green Street, Urbana, Ill. 61801 CSCL 04B

In recent years it has been widely recognized that vertically propagating gravity waves play an important role in the dynamics of the middle atmosphere in partly determining the large scale temperature and wind structure through their energy and momentum transport. In particular, the meridional temperature distribution and the mean wind profile in the upper mesosphere are considered to be largely affected by the turbulence diffusion and friction that gravity waves induce through their breaking. For an understanding of the middle atmosphere circulation, it is therefore very important to know the global distribution and temporal variation of gravity waves in a climatological sense. The results of the statistics for gravity wave activity in the stratosphere and mesosphere are presented as a function of latitude and month, with the aid of meteorological rocket network observations. Author

N86-12823*# National Oceanic and Atmospheric Administration, Boulder, Colo. Aeronomy Lab.

GRAVITY WAVES

T. E. VanZandt *In* International Council of Scientific Unions Middle Atmosphere Program. Handbook for MAP, Vol. 16 Jul. 1985 p 149-156 refs (For primary document see N86-12814 03-46)

Avail: NTIS HC A14/MF A01; also available from SCOSTEP Secretariat, Illinois Univ., 1406 West Green Street, Urbana, Ill. 61801 CSCL 04B

Atmospheric parameters fluctuate on all scales. In the mesoscale these fluctuations are occasionally sinusoidal so that they can be interpreted as gravity waves. Usually, however, the fluctuations are noise like, so that their cause is not immediately evident. Results of mesoscale observations in the 20 to 120 m altitude range that are suitable for incorporation into a model atmosphere are very limited. In the stratosphere and lower mesosphere observations are sparse and very little data has been summarized into appropriate form. There is much more data in the upper mesosphere and lower thermosphere, but again very little of it has been summarized. The available mesoscale spectra of horizontal wind u versus vertical wave number m in the 20 to 120 km altitude range are shown together with a spectrum from the lower atmosphere for comparison. Further information about these spectra is given. In spite of the large range of altitudes and latitudes, the spectra from the lower atmosphere (NASA, 1971 and DEWAN, 1984) are remarkably similar in both shape and amplitude. The mean slopes of -2.38 for the NASA spectrum and -2.7 for the Dewan spectra are supported by the mean slope of -2.75 found by ROSENBERG et al. (1974). The mesospheric spectrum is too short to establish a shape. Its amplitude is about an order of magnitude larger than the NASA spectrum in the same wave number range. The NASA and Dewan spectra suggest that the mesoscale spectra in the lower atmosphere are insensitive to meteorological conditions. Author

N86-12824*# Boston Univ., Mass. Dept. of Electrical, Computer, and System Engineering.

ATMOSPHERIC TIDES BELOW 80 km

Jeffrey M. Forbes and Gerald V. Groves (Univ. Coll., London) *In* International Council of Scientific Unions Middle Atmosphere Program. Handbook for MAP, Vol. 16 Jul. 1985 p 157-163 refs (For primary document see N86-12814 03-46)

(Grant NSF ATM-8113078)

Avail: NTIS HC A14/MF A01; also available from SCOSTEP Secretariat, Illinois Univ., 1406 West Green Street, Urbana, Ill. 61801 CSCL 04B

Measurements of diurnal and semidiurnal tidal oscillations between about 25 and 80 km are reviewed. At latitudes greater than about 30 deg, S to N wind components are consistently in quadrature with and similar to the W to E components. The tidal structures are interpreted as a superposition of quasi-steady higher order modes excited in the troposphere by sources of limited extent (approx. 1,000 km). At latitudes less than about 30 deg, steady or quasi-steady diurnal and semidiurnal components are not necessarily the dominant components of daily variation. At high latitudes diurnal phases generally show little change with height in comparison with observations at lower latitudes in accord with the latitudinal properties of positive and negative diurnal modes. Author

N86-12825*# Control Data Corp., Minneapolis, Minn.

COMPARISON OF TIME-PERIODIC VARIATIONS IN TEMPERATURE AND WIND FROM METEOROLOGICAL ROCKETS AND SATELLITES

A. D. Belmont *In* International Council of Scientific Unions Middle Atmosphere Program. Handbook for MAP, Vol. 16 Jul. 1985 p 164-174 refs (For primary document see N86-12814 03-46)

Avail: NTIS HC A14/MF A01; also available from SCOSTEP Secretariat, Illinois Univ., 1406 West Green Street, Urbana, Ill. 61801 CSCL 04B

Although the Meteorological Rocket Network operated by or in cooperation with th United States has decreased from fourteen to nine stations in the past five years, there have been many observations accumulated in the ten years since CIRA 1972 was prepared with data up to 1969. The mean, annual and semiannual variations of temperature and wind are presented and special attention is directed to the polar semiannual wave. The results are compared with the Oxford SCR-PMR five year data set, the CDC-SCR seven year data, and CIRA 1972 with respect to both temperature and zonal winds, as far as presently available. The agreement among the data sets is very good. Author

N86-12826*# Oxford Univ. (England). Dept. of Atmospheric Physics.

ANNUAL AND SEMIANNUAL CYCLES BASED ON THE MIDDLE ATMOSPHERE REFERENCE MODEL

J. J. Barnett, M. Corney, and K. Labitzke (Freie Univ.) *In* International Council of Scientific Unions Middle Atmosphere Program. Handbook for MAP, Vol. 16 Jul. 1985 p 175-180 ref (For primary document see N86-12814 03-46)

Avail: NTIS HC A14/MF A01; also available from SCOSTEP

Secretariat, Illinois Univ., 1406 West Green Street, Urbana, Ill. 61801 CSCL 04B

The SCR/PMR monthly temperature mean values were Fourier analysed at each latitude and pressure level to obtain the annual mean and the amplitude and phase of the annual and semiannual cycles. The phase is the month of the maximum, such that 1 = January 1, 1.5 = January 16, 2 = February 1, etc. Some very marked hemispheric differences noted are: (1) at 80 N there is a maximum amplitude of the annual cycle of 26 K at 2.5 mb, the corresponding maximum at 80 S is much stronger (35 K) and at a lower altitude (11 mb); (2) the semiannual amplitudes show the well known maximum over the tropics in the upper stratosphere, but also maxima at high latitudes; and (3) the annual mean shows a minimum at 50 S, 1 mb, and a corresponding weaker minimum at 60 N. In general, the hemispheres are remarkably similar and six months out of phase above about 0.3 mb (56 km). The two hemispheres are significantly different especially in winter after allowing for a six month shift. Changes rom summer to winter are so large by comparison that the annual cycles appear to be very similar. Author

N86-12827*# Freie Univ., Berlin (West Germany). Meteorological Inst.

ON THE INTERANNUAL VARIABILITY AND ON TRENDS OF THE TEMPERATURE IN THE MIDDLE ATMOSPHERE

K. Labitzke and B. Naujokat *In* International Council of Scientific Unions Middle Atmosphere Program. Handbook for MAP, Vol. 16 Jul. 1985 p 183-196 refs (For primary document see N86-12814 03-46)

Avail: NTIS HC A14/MF A01; also available from SCOSTEP Secretariat, Illinois Univ., 1406 West Green Street, Urbana, Ill. 61801 CSCL 04B

The new Reference Atmosphere presented here is based on global satellite data and forms a very useful basis for climatological studies. When using such climatologies it is important to be aware of the well known interannual variability which n themiddle atmosphere is particularly large during the northern winters and southern springs. Variability ofthe upper and lower stratospheres is discussed in detail. Areas covered included the polar region and the middile and lower latitudes. Temperature trends, notably the alteration of the global temperature structure by a number of anthropogenically influenced tract gases or the greenhouse effect is discussed. E.R.

N86-12828*# Indian Inst. of Science, Bangalore. Dept. of Aerospace Engineering.

A PROPOSED INTERNATIONAL TROPICAL REFERENCE ATMOSPHERE UP TO 80 km

M. R. Ananthasayanam and R. Narasimha *In* International Council of Scientific Unions Middle Atmosphere Program. Handbook for MAP, Vol. 16 Jul. 1985 p 197-204 refs (For primary document see N86-12814 03-46)

Avail: NTIS HC A14/MF A01; also available from SCOSTEP Secretariat, Illinois Univ., 1406 West Green Street, Urbana, Ill. 61801 CSCL 04B

Based upon previous standard reference atmosphere, which are usually inspired by temperature regions, a proposal is made for an International Tropical Reference Atmosphere (ITRA). It is a modification of the Indian Standard Tropical Atmosphere (ISIA). The data at the available longitudinal stations in the tropics was considered in formulating the present proposal. Balloonsonde, rocketsonde, and grenade and falling sphere data was used in developing the temperature data bse fromt he stratosphere, troposphere and mesosphere. Temperature distribution and mean sea level pressures up to 80 km altitudes is discussed. E.R.

N86-12829*# National Aeronautics and Space Administration. Langley Research Center, Hampton, Va.

INTERIM REFERENCE OZONE MODELS FOR THE MIDDLE ATMOSPHERE

G. M. Keating and D. F. Young (System and Applied Science Corp., Hampton, Va.) *In* International Council of Scientific Unions Middle Atmosphere Program. Handbook for MAP, Vol. 16 Jul. 1985 p 205-229 refs (For primary document see N86-12814 03-46)

Avail: NTIS HC A14/MF A01; also available from SCOSTEP Secretariat, Illinois Univ., 1406 West Green Street, Urbana, Ill. 61801 CSCL 04A

A set of models was generated based on six satellite experiments of the monthly latitudinal variations in total column ozone and the vertical structure of ozone from 20 mb to 0.003 mb. Generally, interannual variability in monthly zonal means is only a few percent. Comparisons of measurements using various techniques to measure global ozone reveal very good agreement between the techniques. Agreement between individual satellite experiments and the reference model of monthly zonal means is generally within 10% below altitudes of 0.4 mb. This has allowed the first global model of ozone measurements to be constructed from multiple sets of satellite measurements. The ozone measurements based on the satellite data are in excellent agreement with previous midlatitude mean annual model based on rocket and balloon data. Also, models are provided of the relation between total ozone and vertical structure. Author

N86-12830*# Boston Univ., Mass. Dept. of Electrical, Computer, and Systems Engineering.

TEMPERATURE STRUCTURE OF THE 80 km TO 120 km REGION

Jeffrey M. Forbes *In* International Council of Scientific Unions Middle Atmosphere Program. Handbook for MAP, Vol. 16 Jul. 1985 p 231-238 refs (For primary document see N86-12814 03-46)

Avail: NTIS HC A14/MF A01; also available from SCOSTEP Secretariat, Illinois Univ., 1406 West Green Street, Urbana, Ill. 61801 CSCL 04B

Between 80 and 120 km the CIRA 1972 model is based heavily on NASA Meteorological Sounding Rocket Program (MSRP) data collected prior to 1967. Since about 1970 an abundance of E-region (100-130 km) temperature data from the incoherent scatter facilities at Arecibo, Millstone Hill, and St. Santin have also become available. The present study examines the temperature structure of the 80 to 120 km region given considerable additional MSRP rocket data, thus providing better seasonal, latitudinal, and longitudinal coverage in the 80 to 100 km region, and a combination of incoherent scatter and rocket data in the 100 to 120 km region which allows a much improved delineation of lower thermosphere temperature structue. Although some individual station comparisons indicate measurable asymmetries in longitude and latitude, data are still insufficient to separate these effects. Specific recommendations of the new CIRA are given. Author

N86-12831*# Saskatchewan Univ., Saskatoon. Inst. of Space and Atmospheric Studies.

MEAN WINDS OF THE UPPER MIDDLE ATMOSPHERE (60-110 km): A GLOBAL DISTRIBUTION FROM RADAR SYSTEMS (MF, METEOR, VHF)

A. H. Manson, C. E. Meek, M. Massebeuf (CNRS), J. L. Fellous (CNRS), W. G. Elford (Adelaide Univ.), R. A. Vincent (Adelaide Univ.), R. L. Craig (Adelaide Univ.), R. G. Roper (Georgia Inst. of Tech.), S. Avery (NOAA, Boulder, Colo.), B. B. Balsley (NOAA, Boulder, Colo.) et al *In* International Council of Scientific Unions Middle Atmosphere Program. Handbook for MAP, Vol. 16 Jul. 1985 p 239-268 refs (For primary document see N86-12814 03-46)

Avail: NTIS HC A14/MF A01; also available from SCOSTEP Secretariat, Illinois Univ., 1406 West Green Street, Urbana, Ill. 61801 CSCL 04B

During the last decade a large number of radars have been developed, which have produced substantial quantities of tidally corrected mean winds data in the upper middle atmosphere. The distribution of the radars is not global, but many areas are well covered. Zonal and meridional wind height-time cross sections from 60 to 80 km (MF/meteor radar) to approx. 110 km were preared for the last 5 to 6 years. They are compared with cross sections from CIRA 1972 for zonal winds, and GROVES (1969) for meridional winds. It is shown that while CIRA 1972 is still a useful model for many purposes, significant differences exist between it and the new radar data. The latter demonstrate important seasonal, latitudinal, longitudinal and hemispheric variations. The new meridional cross sections are of great value. The common features with GROVES (1969) are the equatorward cells in summer near 85 km; however, their strength (approx. 10 m/s) and size are less. Systematic and somewhat different variations emerge at (higher > 52 N) and lower (35 to 44 deg) latitudes. Author

N86-12832*# Adelaide Univ. (Australia). Dept. of Physics.
PLANETARY AND GRAVITY WAVES IN THE MESOSPHERE AND LOWER THERMOSPHERE
R. A. Vincent *In* International Council of Scientific Unions Middle Atmosphere Program. Handbook for MAP, Vol. 16 Jul. 1985 p 269-277 refs (For primary document see N86-12814 03-46)
Avail: NTIS HC A14/MF A01; also available from SCOSTEP Secretariat, Illinois Univ., 1406 West Green Street, Urbana, Ill. 61801 CSCL 04B

Rocket and ground based studies of the mesosphere and lower thermosphere show that waves play an important role in the dynamics of their region. The waves manifest themselves in wind, temperature, density, pressure, ionization and airglow fluctuations in the 80-120 km height range. Rockets have enabled the density and temperature structure to be measured with excellent height resolution, while long term studies of wind motions using MST, partial reflection and meteor radars and, more recently, lidar investigations of temperature and density, have enabled the temporal behaviour of the waves to be better understood. A composite of power spectra is shown of wind motions measured near the mesopause at widely separated locations and illustrates how wave energy is distributed as a function of frequency. The spectra show three distinct parts; (1) a long period section corresponding to periods longer than 24 h; (2) a section between 12 and 24 h priod where the spectra are dominated by narrow; peaks associated with the semidiurnal and diurnal tides and (3) a section at periods less than 12 h where the spectral density decreases montonically (except for the 8 h tidal peak). The long period section is associated with transient planetary scale waves while the short period motions are caused by gravity waves. Author

N86-12833*# Boston Univ., Mass. Dept. of Electrical, Computer, and Systems Engineering.
ATMOSPHERIC TIDES BETWEEN 80 km AND 120 km
Jeffrey M. Forbes *In* International Council of Scientific Unions Middle Atmosphere Program. Handbook for MAP, Vol. 16 Jul. 1985 p 278-289 refs (For primary document see N86-12814 03-46)
(Grant NSF ATM-81-13078)
Avail: NTIS HC A14/MF A01; also available from SCOSTEP Secretariat, Illinois Univ., 1406 West Green Street, Urbana, Ill. 61801 CSCL 04B

The structure and variability of tides in the 80 to 120 km height region are reviewed. Particulary emphasized are seasonal-latitudinal variations in the vertical structure of diurnal and semidiurnal winds between 70 to 110 km as measured by meteor and partial reflection drift radars, and tidal temperatures determined by incoherent scatter radars between 100 and 140 km. Variations in tidal structures with longitude, from day to day, and during equinoctial transition periods are also addressed. A brief summary of the current status of atmospheric tidal modelling is provided. Author

N86-12834*# Adelaide Univ. (Australia). Dept. of Physics.
TURBULENCE IN THE ALTITUDE REGION 80-120 km
W. K. Hocking *In* International Council of Scientific Unions Middle Atmosphere Program. Handbook for MAP, Vol. 16 Jul. 1985 p 290-304 refs (For primary document see N86-12814 03-46)
Avail: NTIS HC A14/MF A01; also available from SCOSTEP Secretariat, Illinois Univ., 1406 West Green Street, Urbana, Ill. 61801 CSCL 04B

Measurements of turbulent energy dissipation rates and eddy diffusion coefficients have been collated, and mean height profiles of fundamental turbulence parameters in the region 80 to 120 km are presented. Curves of Epsilon, and K vs. height are presented. A clear global and seasonal picture of turbulence variations is not yet apparent. Author

N86-12835*# Centre National de la Recherche Scientifique, Verrieres-Le Buisson (France). Service d'Aeronomie.
CONTRIBUTION TO THE CIRA MODEL FROM GROUND-BASED LIDAR
M. I. Chanin, A. Hauchecorne, and N. Smires *In* International Council of Scientific Unions Middle Atmosphere Program. Handbook for MAP, Vol. 16 Jul. 1985 p 305-314 refs (For primary document see N86-12814 03-46)
Avail: NTIS HC A14/MF A01; also available from SCOSTEP Secretariat, Illinois Univ., 1406 West Green Street, Urbana, Ill. 61801 CSCL 04B

A new technique, the Rayleigh-Lidar Sounding, has been developed recently to probe the Middle Atmosphere and has demonstrated its ability to provide density and temperature profiles in the height range 30 to 90 km. It has been limited until now to ground-based observations. The set of data, as it exists to-day, has been obtained from a unique midlatitude site. Even with this limiting factor, it is thought to be a useful complement to a global model, mainly because of its spatial and temporal resolutions, usually not available from global data. Such resolutions give an insight into the atmospheric variability as a function of height and time, for time-scale ranging from minutes to years. The process is briefly described. A description of the analysis and its results is given. Author

N86-12836*# National Oceanic and Atmospheric Administration, Boulder, Colo. Aeronomy Lab.
THE MST RADAR TECHNIQUE
Ben B. Balsley *In* International Council of Scientific Unions Middle Atmosphere Program. Handbook for MAP, Vol. 16 Jul. 1985 p 315-318 refs (For primary document see N86-12814 03-46)
Avail: NTIS HC A14/MF A01; also available from SCOSTEP Secretariat, Illinois Univ., 1406 West Green Street, Urbana, Ill. 61801 CSCL 04B

The past ten year have witnessed the development of a new radar technique to examine the structure and dynamics of the atmosphere between roughly 1 to 100 km on a continuous basis. The technique is known as the MST (for Mesosphere-Stratosphere-Troposphere) technique and is usable in all weather conditions, being unaffected by precipitation or cloud cover. MST radars make use of scattering from small scale structure in the atmospheric refractive index, with scales of the order of one-half the radar wavelength. Pertinent scale sizes for middle atmospheric studies typically range between a fraction of a meter and a few meters. The structure itself arises primarily from atmospheric turbulence. The technique is briefly described along with the meteorological parameters it measures. Author

N86-12837*# International Council of Scientific Unions, Urbana, Ill.
MIDDLE ATMOSPHERE PROGRAM. HANDBOOK FOR MAP, VOLUME 17
C. F. Sechrist, Jr., ed. Aug. 1985 150 p refs Sponsored in part by UNESCO
(NASA Order W-15897)
(NASA-CR-176345; NAS 1.26:176345; MAP-HANDBOOK-17)
Avail: NTIS HC A07/MF A01; also available from SCOSTEP Secretariat, Illinois Univ., 1406 West Green Street, Urbana, Ill. 61801 CSCL 04A

The Middle Atmosphere Program (MAP) handbook is divided into three parts. Part 1 consists of minutes of MAP steering committee meeting and MAP assembly. Part 2 consists of project and study group reports, such as: (1) Atmospheric Tides Middle Atmosphere Program (ATMAP), report of the Nov./Dec. 1981, and May 1982 observational campaigns; MAP/WINE experimenters meeting at Berlin, 1985; (3) MAP/WINE experimenters meeting at Loen, Norway, 1985; and (4) the penetration of ultraviolet solar radiation into the middle atmosphere. Part 3 consists of national reports. For individual titles, see N86-12838 through N86-12851.

N86-12838*# Max-Planck-Inst. fuer Aeronomie, Katlenburg-Lindau (West Germany).
TOWARDS A GLOBAL MAP DATA BASE
G. K. Hartmann *In* International Council of Scientific Unions Middle Atmosphere Program. Handbook for MAP, Vol. 17 Aug. 1985 p 26-35 refs Sponsored in part by the Deutsche Forschungsgemeinschaft (For primary document see N86-12837 03-46)
Avail: NTIS HC A07/MF A01; also available from SCOSTEP Secretariat, Illinois Univ., 1406 West Green Street, Urbana, Ill. 61801 CSCL 04A

Scientific and ecological needs call for the generation of a global data base of measured data from the Earth's atmosphere, similar but complementary to the data of the meteorological service. Right now there is a large gap between these needs and the available financial means. If this prevails, it might be prohibitive for the generation of such a data base. There must be a compromise between the needs and the means. Priorities must be set. Thus, discussions should be started on which data can be or should be stored. Newly generated data for storage in such a data base is recommended to be handled by the World Data Centers (WDCs). This brief report should help to stimulate discussions and ubsequent actions. Author

N86-12839*# Boston Univ., Mass.
ATMOSPHERIC TIDES MIDDLE ATMOSPHERE PROGRAM (ATMAP): REPORT OF THE NOVEMBER/DECEMBER 1981, AND MAY 1982, OBSERVATIONAL CAMPAIGNS
Jeffrey M. Forbes *In* International Council of Scientific Unions Middle Atmosphere Program. Handbook for MAP, Vol. 17 Aug. 1985 p 36-43 refs (For primary document see N86-12837 03-46) (Grant NSF ATM-83-19487)
Avail: NTIS HC A07/MF A01; also available from SCOSTEP Secretariat, Illinois Univ., 1406 West Green Street, Urbana, Ill. 61801 CSCL 04A

Atmospheric tides, oscillations in meteorological fields occurring at subharmonics of a solar or lunar day, comprise a major component of middle atmosphere global dynamics. The nature of atmospheric tides requires investigations and coordination on a global, and hence international, scale. The purpose of ATMAP is to create an interaction among observationalists, data analysts, theoreticians and modellers working towards common goals. The focus for this interaction is a series of global observational campaigns involving ground based remote sensing methods. The calendar of activities for ATMAP is presented. The results of solstice campaigns I and II are assembled, a preliminary interpretation of the results is presented. Author

N86-12840*# Colspan, Inc., Boulder, Colo. Cooperative Inst. for Research in Environment Science.
DATA DESCRIPTIONS AND VERTICAL STRUCTURE PLOTS FOR MEAN, DIURNAL, AND SEMIDURNAL COMPONENTS OF EASTWARD AND NORTHWARD (ORDERED BY LATITUDE). MEAN WINDS AND TIDES OVER POKER FLAT, ALASKA (65 DEG N, 147 DEG W), DURING NOVEMBER 1981 Abstract Only
S. K. Avery *In* International Council of Scientific Unions Middle Atmosphere Program. Handbook for MAP, Vol. 17 Aug. 1985 p 44-45 ref (For primary document see N86-12837 03-46)
Avail: NTIS HC A07/MF A01; also available from SCOSTEP Secretariat, Illinois Univ., 1406 West Green Street, Urbana, Ill. 61801 CSCL 04A

The mean zonal and meridional winds and the amplitude and phase structures for the tidal harmonics for the month of November, 1981 are given. The mean winds are weak westerlies and weak southerlies. The westerlies are approximately 10 ms (-1) lower than those during November 1980 and 1982. The diurnal amplitudes are small in both the zonal and meridional wind components. The diurnal phase structures are characteristic of a propagating wave having a ertical wavelength of approximately 50 km. The semidiurnal tidal harmonic amplitudes are slightly larger than the diurnal amplitudes. However, the phase structures are different for the zonal and meridional components. The meridional phase structure appears evanescent. The zonal phase structure has a phase reversal at 88 km with downward phase progression below that level and upward phase progression above that level. The vertical wavelength is roximately 12 km. This short vertical wavelength occurs during other months of the year but longer wavelengths are more common. Author

N86-12841*# Academy of Sciences, Berlin (East Germany). Central Inst. of Solar Terrestrial Physics.
RESULTS OF THE MAY 1982 ATMAP CAMPAIGN AT THE METEOR WIND STATION KUEHLUNGSBORN (54 DEG N, 12 DEG E), GDR Abstract Only
K. M. Greisiger *In* International Council of Scientific Unions Middle Atmosphere Program. Handbook for MAP, Vol. 17 Aug. 1985 p 46 (For primary document see N86-12837 03-46)
Avail: NTIS HC A07/MF A01; also available from SCOSTEP Secretariat, Illinois Univ., 1406 West Green Street, Urbana, Ill. 61801 CSCL 04A

A sinusoisal least squares fit over the entire data of 1 to 6 May 1982 was computed. The results are shown. Wind results refere to an average height of 95 km (no height determination). The wind results correspond, in general, to the average behavior of early May. The zonal prevailing west wind, however, is stronger than the term mean value (-5 m/s). Also, the amplitude of the semidiurnal idal wind is larger (mean value 1977 to 1983: 8 m/s). Author

N86-12842*# Geophysical Observatory, Collm (East Germany).
REMARKS ON THE ATMAP CAMPAIGNS IN NOVEMBER 1981 AND MAY 1982 AT COLLM (52 DEG N, 15 DEG E) Abstract Only
R. Schminder *In* International Council of Scientific Unions Middle Atmosphere Program. Handbook for MAP, Vol. 17 Aug. 1985 p 47-50 (For primary document see N86-12837 03-46)
Avail: NTIS HC A07/MF A01; also available from SCOSTEP Secretariat, Illinois Univ., 1406 West Green Street, Urbana, Ill. 61801 CSCL 04A

The results given are based on daily nighttime L. F. wind measurements over Central Europe on three measuring paths at 179, 227, and 272 kHz. Absolute reflection height measurements were carried out for the first time in August 1982 so that values of the months of 1982 and 1983 have been taken for the campaigns in November 1981 and May 1982. The prevailing wind and the semidiurnal tidal wind components are calculated daily. Means of the month or means of parts of a month are formed for climatological investigations. A 24 hour analysis is not possible due to the very different reflection heights during the daytime and nighttime, even with measurements being carried out the whole ay long in the winter season. The critical examination of the choice of the measuring intervals selected is dependent on the visual angle. A wind ield change is observed over Central Europe very often around the 20th of November 1981 this wind field variation being in the core period and leading over to a more stable tidal wind. Author

N86-12843*# Saskatchewan Univ., Saskatoon. Inst. of Space and Atmospheric Studies.
SASKATOON M. F. RADAR SYSTEM: (52 DEG N, 107 DEG W), CANADA Abstract Only c45
A. H. Manson and C. E. Meek *In* International Council of Scientific Unions Middle Atmosphere Program. Handbook for MAP, Vol. 17 Aug. 1985 p 52-56 refs (For primary document see N86-12837 03-46)
Avail: NTIS HC A07/MF A01; also available from SCOSTEP Secretariat, Illinois Univ., 1406 West Green Street, Urbana, Ill. 61801 CSCL 04A

The system runs continuously, producing 1-h profiles approx. 75 to 110 km, 1978 to 1983: in particular for the 30-d (Nov. 9 to Dec. 7), 10-d (Nov. 16 to 26), 4-d core periods (Nov. 19 to 23). The means (EW, NS) and fourier components (24-, 12-h) fitted for the 4-d are shown. s.d. are shown, as derived from four 24-h fits in the interval. Comparisons with the 10-, 30-d intervals confirm confidence in these data and the lack of major variability in November. The 1-h profiles are means of < 12 profiles so intrinsic errors are minimal. The 4-, 10-d fourier fits are compared and also the 30-d means from 48-h fits; in these amplitudes are N2+E2 as N/E approx. 1. Means differ slightly due to planetary wave activity; 24-h tides are variable in Novembers; and the 12-h variation is small less than 80 km. The final figure is a high resolution spectra for the November month: the 12-, 24-h dominate; the 8-h appears less than 100 km; and up to 90 km there is a 4-d Author oscillation.

N86-12844*# Saskatchewan Univ., Saskatoon. Inst. of Space and Atmospheric Studies.
MAY 1982, SASKATOON M. F. RADAR SYSTEM: (52 DEG N, 107 DEG W), CANADA Abstract Only
A. H. Manson and C. E. Meek *In* International Council of Scientific Unions Middle Atmosphere Program. Handbook for MAP, Vol. 17 Aug. 1985 p 57-59 refs (For primary document see N86-12837 03-46)
Avail: NTIS HC A07/MF A01; also available from SCOSTEP Secretariat, Illinois Univ., 1406 West Green Street, Urbana, Ill. 61801 CSCL 04A

The system runs continuously, producing 1-h profiles approx. 75 to 110 km, 1978 to 1983: in particular for the 30-d (April 20 to May 19) centered on the inner core (May 3 to 6), 10-d (May 2 to 11). Incredibly, the only days missed for April/May were May 4/5, so 4-d fits for the core could not made! However the winds and tides were stable during May, so that the 10-d fits can be taken for comparison with other locations. The means (EW/NS) and Fourier components (24-, 12-h) for the 10-d (May 2 to 11) are shown; also those for the 30 days. Standard deviations are shown to be quite small. There is also little difference between 10- and 30-d profiles. The zonal flow is quite weak, showing that the summer westward flow has not fully developed. The 24-h tide has large lambda: approx. 100 km (EW and infinity (NS). Below 90 km the tide is circular, but above almost linear with EW amplitudes larger than NS. The 12-h tide is circular and lambda is small below 95 km; and more linear and variable above. The 30-d May spectral figure shows that 12-, 24-h tides are comparable; otherwise there is a 3.85-d oscillation to approx. 90 km; there were no other Author significant peaks.

N86-12845*# New Hampshire Univ., Durham.
METEOR WIND RESULTS AT DURHAM (43 DEG N, 71 DEG W) DURING THE ATMAP NOVEMBER 1981 AND MAY 1982 CAMPAIGNS Abstract Only
Ronald R. Clark *In* International Council of Scientific Unions Middle Atmosphere Program. Handbook for MAP, Vol. 17 Aug. 1985 p 60-62 ref (For primary document see N86-12837 03-46)
Avail: NTIS HC A07/MF A01; also available from SCOSTEP Secretariat, Illinois Univ., 1406 West Green Street, Urbana, Ill. 61801 CSCL 04A

Winds modeled from data measured with the University of New Hampshire Meteor Wind Radar System at Durham, New Hampshire, over the two 4-day periods November 20 to 23, 1981 and May 8 to 11, 1982 are presented. The raw meteor wind data was fit in a least square sense to a three dimensional model containing mean, 12-, 24-, and 48-h periods. The means winds for both periods are very close to the three year average values at Durham during May and November, respectively. The semidiurnal component for the November period had a normal amplitude and phase, and an estimated veritcal wavelength of 60 km. The May period results were essentially typical except that the Northward amplitude was 3 to 4 times smaller than normal. The diurnal amplitudes measured for both periods are typical for Durham and the diurnal phase is normally not very consistent. The 48-hour component amplitude is typical for these months. The intrinsic errors fo the radar are approximately + or - 2 km in position and + or - 4 m/s in radial velocity including quantization errors. These errors are random with zero mean and should not bias the wind Author results.

N86-12846*# Illinois Univ., Urbana. Aeronomy Lab.
MEAN WINDS AND TIDES OVER URBANA, ILLINOIS DURING NOVEMBER 16-22, 1981 Abstract Only
D. Tetenbaum *In* International Council of Scientific Unions Middle Atmosphere Program. Handbook for MAP, Vol. 17 Aug. 1985 p 63-64 ref (For primary document see N86-12837 03-46)
Avail: NTIS HC A07/MF A01; also available from SCOSTEP Secretariat, Illinois Univ., 1406 West Green Street, Urbana, Ill. 61801 CSCL 04A

The Urbana Meteor Radar uses a high power pulse transmitter to achieve high echo rates, and an interferometer to spatially locate the individual echoes. The irregularly spaced observations of range, radial velocity, and direction cosines are reduced to a rectangular grid, evenly spaced in time and height, of estimates of the zonal and meridional wind. This is accomplished using the method of GROVES whereby a constant horizontal wind is fitted, using least squares, to all echoes occurring within a fixed time/height interval. This interpolation region is then stepped in time and height. the size of the interpolation region is 2 hours by 5 km, the time step is approximately 11 minutes, and the height step is 2 km. The filtering of high temporal and spatial frequencies is somewhat reduced by weighting the echoes according to their Author distance from the center of the interpolation box.

N86-12847*# Kyoto Univ. (Japan). Radio Atmospheric Science Center.
KYOTO METEOR RADAR OBSERVATION IN NOVEMBER, 1981 AND MAY, 1982 Abstract Only
Toshitaka Tsuda and Susumu kato *In* International Council of Scientific Unions Middle Atmosphere Program. Handbook for MAP, Vol. 17 Aug. 1985 p 65-69 refs (For primary document see N86-12837 03-46)
Avail: NTIS HC A07/MF A01; also available from SCOSTEP Secretariat, Illinois Univ., 1406 West Green Street, Urbana, Ill. 61801 CSCL 04A

The Kyoto meteor radar a pulsed Doppler radar and operates at 31.57 MHz ith peak power of 10 kW. An interferometer is adopted for arrival angle measurement. Height resolution is approximately 1 to 3 km depending on both azimuth and elevation angles. Data is analyzed according to an algorithm approved by GROVES. All data in height range 84 to 104 km are separated into five layers, whose altitude width is 4 km. In each layer, least square fitting is performed for ten parameters, which are amplitudes of northward/eastward mean wind and sin/cos component of diurnal/semidiurnal tide. Reliable range for each parameter is also Author calculated.

N86-12848*# EISCAT Scientific Association, Kiruna (Sweden).
MESOSPHERIC WINDS AND TIDES AT ARECIBO/PUERTO RICO (18 DEG N, 67 DEG W) NOVEMBER 20-23, 1981 Abstract Only
J. Rottger *In* International Council of Scientific Unions Middle Atmosphere Program. Handbook for MAP, Vol. 17 Aug. 1985 p 70-71 ref (For primary document see N86-12837 03-46)
Avail: NTIS HC A07/MF A01; also available from SCOSTEP Secretariat, Illinois Univ., 1406 West Green Street, Urbana, Ill. 61801 CSCL 04A

The SOUSY-VHF-Radar was operated in the period November 20 to 23, 1981 during a continuous run at the Arecibo Observatory. The data used for this analysis were recorded from 06 AST on November 20 until 06 AST on November 23. Meridional winds were measured at odd hours and zonal winds at even hours. The occurrence of mesospheric VHF radar echoes was limited as usual to the daylight hours between 06 and 18 AST. The height limits, were variable from day to day, they were roughly 62 to 90 km. The intermittency of echoes in time and height, as well as radio interference, made it fairly difficult to deduce tidal information for this time period. About 10 to 45 single velocity estimates could be used to calculate an hourly mean. The variance of the displayed resulting in data, obtained by weighted averaging over the 3 day period, is about similar to the mean. The winds were extremely low during the observation period. Velocities of the prevailing wind, observed during an earlier campaign were 5 to 10 times larger than in the period of November 20 to 23, 1981. The amplitudes of the diurnal tide are comparable. Author

N86-12849*# Kyoto Univ. (Japan). Dept. of Electrical Engineering.
MESOSPHERIC WINDS AT JICAMARACA, PERU (12 DEG S, 77 DEG SW), NOVEMBER 19-21, 1981 Abstract Only
T. Aso, Y. Maekawa, I. Hirota (Inst. Geofisico del Peru, Lima), R. F. Woodman, and S. Kato *In* International Council of Scientific Unions Middle Atmosphere Program. Handbook for MAP, Vol. 17 Aug. 1985 p 72-74 refs (For primary document see N86-12837 03-46)
Avail: NTIS HC A07/MF A01; also available from SCOSTEP Secretariat, Illinois Univ., 1406 West Green Street, Urbana, Ill. 61801 CSCL 04A

The altitude of mean zonal wind in the mesosphere during the whole daytime observations is given. Positive value refers to eastward. At around 70 km, wind corresponds to summer easterly, and changes to westerly with increasing altitude above about 77 km. These are fairly compatible with known features of zonal wind at this latitude. Contour plot shows local time variations of zonal wind with daytime mean subtracted and averaged over three days. Shaded area designated westward wind with contour level of 2 m/s. The daily variation is almost in phase with altitude in the 65 to 80 km region. Thus the semidiurnal tide with long vertical wavelength is inferred to exist. Above 80 km, phase tilt occurs which indicates the contribution of the propagating diurnal component. Here the combination of dc and 12-hr component is fitted to the data below 80 km. The altitude profiles of the amplitude and phase of this semidiurnal component are shown. Author

N86-12850*# Adelaide Univ. (Australia). Dept. of Physics.
RESULTS OF NOVEMBER 1981 AND MAY 1982 ATMAP CAMPAIGNS AT ADELAIDE (35 DEG S, 138 DEG E) Abstract Only
R. A. Vincent *In* International Council of Scientific Unions Middle Atmosphere Program. Handbook for MAP, Vol. 17 Aug. 1985 p 75-78 ref (For primary document see N86-12837 03-46)
Avail: NTIS HC A07/MF A01; also available from SCOSTEP Secretariat, Illinois Univ., 1406 West Green Street, Urbana, Ill. 61801 CSCL 04A

The mean zonal circulation for both the November and May campaigns are representative of early summer and winter conditions. The mean meridional flow in November was stable and typical of summer conditions at Adelaide. The conditions in May were, however, more variable and appeared to be changing significantly during the campaign. It is possible that there was a strong influence from a large scale wave which could account for the large meridional wind values observed. Overall, the mean tidal structures observed during the core periods were not significantly different from those observed in two-week intervals centered on the cores. In May both components show evidence for propagating components with 30 to 40 km vertical wavelengths. For the semidiurnal components, the phase structures show evidence for vertical propagation with apparent vertical wavelengths of the order of 50 km. The mean amplitudes for the semidiurnal components in May are close to the noise level. Typical errors from the harmonic analysis are + or - 1 to 2 ms(-1) in amplitude and + or - 0.5 hr in phase, but these are probably underestimates. Author

N86-12851*# Canterbury Univ., Christchurch (New Zealand). Dept. of Physics.
MIDDLE ATMOSPHERE TIDES AT CHRISTCHURCH (44 DEG S, 17 DEG E) IN NOVEMBER 1981 AND MAY 1982 Abstract Only
G. J. Fraser *In* International Council of Scientific Unions Middle Atmosphere Program. Handbook for MAP, Vol. 17 Aug. 1985 p 79-81 (For primary document see N86-12837 03-46)
Avail: NTIS HC A07/MF A01; also available from SCOSTEP Secretariat, Illinois Univ., 1406 West Green Street, Urbana, Ill. 61801 CSCL 04A

Atmospheric tides at Christchurch were measured at heights of 80 to 100 km, in 2.5 km intervals during the ATMAP campaigns of November 1981 and May 1982. Average components for the 5-day periods, November 19 to 23 and May 3 to 7, were extracted by making an equally weighted least squares fit to the hourly mean values, using the sum of mean, diurnal and semidiurnal terms. Estimates of standard deviation from the least squares fit tend to be less than the variability between successive 5-day samples, but 5 to 8 ms(-1) and 2 to 3 h are typical. At altitudes below 83 km there may be gaps of up to 6 hours during the night which may generate a systematic error in the components. Amplitude and phase characteristics are generally consistent with November 1980 and 1982 and May 1981, although the amplitude of the diurnal EW tide was low in November 1981, with consequent large phase fluctuations. Author

N86-12852*# National Aeronautics and Space Administration, Washington, D. C.
GEOPOTENTIAL RESEARCH MISSION (GRM)
Oct. 1985 141 p refs Conf. held in College Park, Md., 29-31 Oct. 1984
(NASA-CP-2390; NAS 1.55:2390) Avail: NTIS HC A07/MF A01 CSCL 08E

The Geopotential Research Mission (GRM) is a satellite system proposed to determine variations in the gravitational and magnetic fields to a resolution of about 100 kilometers. Knowledge and interpretations of the potential fields on scales of 100 kilometers and greater, to clarify the needs for better data in this range of wavelengths were reviewed. The potential contribution of these data to the determination, by satellite altimetry, of a more accurate geoidal reference was discussed. For individual titles, see N86-12853 through N86-12895.

N86-12853*# Massachusetts Inst. of Tech., Cambridge. Dept. of Earth, Atmospheric and Planetary Sciences.
IMPACT OF GRM: NEW EVIDENCE FROM THE SOVIET UNION
Marcia McNutt *In* NASA, Washington Geopotential Res. Mission (GRM) Oct. 1985 p 8-9 refs (For primary document see N86-12852 03-46)
Avail: NTIS HC A07/MF A01 CSCL 08G

Gravity information released by the Soviet Union allows the quantitative assessment of how the geopotential research mission (GRM) mission might effect the ability to use global gravity data for continental tectonic interpretation. The information is of an isostatic response spectra for eight individual tectonic units in the USSR. The regions examined include the Caroathians, Caucasus, Urals, Pamirs, Tien-Shan, Altai, Chersky Ridge, and East Siberian Platform. The 1 deg x 1 deg gravity data are used to calculate the admittances are used in two different sorts of tectonic studies of mountain belts in the USSR: (1) interpretation of isostatic responses in terms of plate models of compensation for mountainous terrain. Using geologic information concerning time of the orogeny, lithospheric plates involved, and polarity of subduction in collision zones, they convert the best-fitting flexural rigidity to an elastic plate thickness for the lithospheric plate inferred to underlie the mountains; the isostatic admittance functions is an attempt to directly model gravity and topography data for a few select regions in the Soviet Union. By knowing the value of the expected correlation between topography and gravity from the admittances, the Artemjev's map in mountainous areas can be calibrated, and the maps are converted back to Bouguer gravity. This procedure is applied to the Caucasus and southern Urals. E.A.K.

N86-12854*# Eidgenoessische Technische Hochschule, Zurich (Switzerland). Inst. fuer Geodasie und Photogrammetrie.
DYNAMICS AND STRUCTURE OF THE ALPINE FOLD BELT Abstract Only
H.-G. Kahle *In* NASA, Washington Geopotential Res. Mission (GRM) Oct. 1985 p 10 (For primary document see N86-12852 03-46)
Avail: NTIS HC A07/MF A01 CSCL 08G

The structure and present-day dynamics of the Alps interms of geodesy and gravimetry are discussed. A strong correlation of precise leveling and isostatic gravity along the central Alpine chain, especially in Canton Graubunden, East Switzerland are shown. It is assumed that the uplift is partly controlled by isostatic rebound effects. Field observations indicate that these phenomena are still active in the Alps. The study of the uplift processes by applying a number of geodetic and gravimetric measuring techniques, such as the determination of nonperiodic secular variations of gravity, of the deflections of the vertical and tilt changes monitored by hydrostatic leveling is proposed. E.A.K.

N86-12855*# Australian National Univ., Canberra. Research School for Earth Sciences.
WHY DO WE NEED DETAILED GRAVITY OVER CONTINENTS: SOME AUSTRALIAN EXAMPLES
Kurt Lambeck *In* NASA, Washington Geopotential Res. Mission (GRM) Oct. 1985 p 11 (For primary document see N86-12852 03-46)
Avail: NTIS HC A07/MF A01 CSCL 08G

Geophysical quantities available over a continent are gravity and components of the magnetic field. Direct inferences on crustal structure are difficult to make and strongly dependent on mechanical assumptions the isostatic state. The data for Australia represents one of the best continental scale gravity surveys. The gravity anomalies are generally bland over the continent which confirms that stress relaxation and erosion and rebound were instrumental in reducing nonhydrostatic stresses. In central Australia very large gravity anomalies occur and the region is out of isostatic equilibrium despite the fact that tectonic activity ceased 300 ma ago. The isostatic response functions points to a substantial horizontal compression in the crust. Similar conclusions are drawn for the large anomalies in western Australia. The tectonic implications of these anomalies are examined. In eastern Australia the gravity anomalies are explained in terms of a model of erosion of the highlands and concomitant regional isostatic rebound. E.A.K.

N86-12856*# Pennsylvania State Univ., University Park. Geophysics Program.
A MAJOR CRUSTAL FEATURE IN THE SOUTHEASTERN UNITED STATES INFERRED FROM THE MAGSAT EQUIVALENT SOURCE ANOMALY FIELD
Michal E. Ruder and Shelton S. Alexander *In* NASA, Washington Geopotential Res. Mission (GRM) Oct. 1985 p 2-15 refs (For primary document see N86-12852 03-46)
Avail: NTIS HC A07/MF A01 CSCL 08G

The MAGSAT equivalent-source anomaly field evaluated at 325 km altitude depicts a prominent anomaly centered over southeast Georgia, which is adjacent to the high-amplitude positive Kentucky anomaly. To overcome the satellite resolution constraint in studying this anomaly, conventional geophysical data were included in analysis: Bouguer gravity, seismic reflection and refraction, aeromagnetic, and in-situ stress-strain measurements. This integrated geophysical approach, infers more specifically the nature and extent of the crustal and/or lithospheric source of the Georgia MAGSAT anomaly. Physical properties and tectonic evolution of the area are all important in the interpretation. E.A.K.

N86-12857*# Toronto Univ. (Ontario). Dept. of Geology.
GEOPHYSICAL INTERPRETATION OF THE MAGNETIC ANOMALIES OF THE EARTH DERIVED FROM MAGSAT DATA
J. Arkani-Hamed and D. W. Strangway *In* NASA, Washington Geopotential Res. Mission (GRM) Oct. 1985 p 16-17 (For primary document see N86-12852 03-46)
Avail: NTIS HC A07/MF A01 CSCL 08G

The ambiguities about geophysical implications based on the correlation of scalar magnetic anomalies and geological features were investigated. A method was developed to convert scalar magnetic anomalies into a map of the lateral variations of magnetic susceptibility of the lithosphere. This map is directly correlated with the causative sources. The method is based on spherical harmonic analysis of lateral variations seen on the scalar magnetic anomaly map and those of the lithospheric magnetic susceptibility. The harmonic coefficients are related through the fundamental causality relationship governing a magnetized body and its associated scalar magnetic anomaly. The main features of the resulting magnetic susceptibility anomalies are outlined. E.A.K.

N86-12858*# Southern Methodist Univ., Dallas, Tex. Dept. of Geological Sciences.
SATELLITE MAGNETIC MODELING OF NORTH AFRICAN HOT SPOTS
Roger J. Phillips and Carolyn R. Brown *In* NASA, Washington Geopotential Res. Mission (GRM) Oct. 1985 p 18-21 refs (For primary document see N86-12852 03-46)
Avail: NTIS HC A07/MF A01 CSCL 08G

The primary objectives of the MAGSAT mission was to measure the intensity and direction of magnetization of the Earth's crust. A significant effort was directed to the large crustal anomalies first delineated by the POGO mission. The MAGSAT data are capable of spatial resolution of the crustal field to 250 km wavelength with reliability limits to less than 1 nT in the mean. The difficulties of dealing with less than the most robust of the MAGSAT anomalies is that often there is no more than the magnetic fields themselves to constrain geophysical models of the interior, and no independent means of assessing the quality of the crustal anomaly data in interpreting the subsurface are available. E.A.K.

N86-12859*# National Aeronautics and Space Administration. Goddard Space Flight Center, Greenbelt, Md.
MAGNETIC STRUCTURE OF THE CRUST
Peter Wasilewski *In* NASA, Washington Geopotential Res. Mission (GRM) Oct. 1985 p 22-25 (For primary document see N86-12852 03-46)
Avail: NTIS HC A07/MF A01 CSCL 08G

The bibuniqueness aspect of geophysical interpretation must be constrained by geological insight to limit the range of theoretically possible models. An additional step in depth understanding of the relationship between rock magnetization and geological circumstances on a grand scale is required. Views about crustal structure and the distribution of lithologies suggests a complex situation with lateral and vertical variability at all levels in the crust. Volcanic, plutonic, and metamorphic processes together with each of the observed anomalies. Important questions are addressed: (1) the location of the magnetic bottom; (2) whether the source is a discrete one or are certain parts of the crust cumulatively contributing to the overall magnetization; (3) if the anomaly to some recognizable surface expression is localized, how to arrive at a geologically realistic model incorporating magnetization contrasts which are realistic; (3) in the way the primary mineralogies are altered by metamorphism and the resulting magnetic contracts; (4) the effects of temperature and pressure on magnetization. E.A.K.

N86-12860*# Lamont-Doherty Geological Observatory, Palisades, N. Y.
GRAVITY, GEOID AND THE OCEANIC LITHOSPHERE Abstract Only
A. B. Watts *In* NASA, Washington Geopotential Res. Mission (GRM) Oct. 1985 p 28 (For primary document see N86-12852 03-46)
Avail: NTIS HC A07/MF A01 CSCL 08E

Plate tectonics and its contribution to progress in studies of the Earth's gravitational field is discussed. In acquisition, the development of forced feedback accelerometers, satellite navigation, and satellite radar altimetry significantly improved the accuracy and coverage of gravity data over the oceans. In interpretation, gravity and geoid anomalies are used to determine information on the thermal and mechanical properties of the oceanic lithosphere and the forces that drive plate motions. E.A.K.

N86-12861*# Centre National d'Etudes Spatiales, Toulouse (France).
THERMAL COOLING OF THE OCEANIC LITHOSPHERE FROM GEOID HEIGHT DATA
A. Cazenave *In* NASA, Washington Geopotential Res. Mission (GRM) Oct. 1985 p 29-30 (For primary document see N86-12852 03-46)

Avail: NTIS HC A07/MF A01 CSCL 08E

Another type of geophysical observation has proved to be very useful in the study of thermal cooling of the oceanic lithosphere. It is the geoid height derivative with respect to plate age, a quantity computed from the short wavelength geoid step across fracture zones measured by altimeter satellites. Two categories of simples models are proposed to describe cooling and contraction of the oceanic lithosphere with age. Both plate model and half space model, give almost similar results up to ages of 50 to 70 ma, but predict quite distinct behavior of seafloor depth, heat flow and other parameters in old basins. Tests of thermal models are based on heat flow and topography data. However, heat flow is not very sensitive to the form of the thermal model. Large areas of the ocean floor are particularly shallow, and as a result topography data may not be very appropriate to discriminate between plate and half space models, and no clear concensus on a preferred model yet exists. E.A.K.

N86-12862*# Lamont-Doherty Geological Observatory, Palisades, N. Y.

STUDIES OF THE MARINE CRUSTAL MAGNETIZATION AT INTERMEDIATE WAVELENGTHS Abstract Only

J. L. LaBrecque, S. C. Cande, and C. A. Raymond *In* NASA, Washington Geopotential Res. Mission (GRM) Oct. 1985 p 31 (For primary document see N86-12852 03-46)

Avail: NTIS HC A07/MF A01 CSCL 08N

The data can be filtered at intermediate wavelengths to provde a data set which complements the satellite fields of MAGSAT, TSS and GRM. The filtered marine data set provides a high resolution data set which is closer to the source bodies than satellite survey data. However, the GRM and TSS could provide the necessary resolution to match the filtered sea surface field. The added resolution determines the nature of crustal magnetizations which give rise to the intermediate wavelength field. It is found that remanent magnetization is an important component over the oceans. Crustal deformation and plate motions result in magnetization vectors which differ significantly from the present day field directions. Induced magnetization or GRM are important components over the oceanic plateaus and spreading centers. E.A.K.

N86-12863*# Johns Hopkins Univ., Baltimore, Md. Dept. of Earth and Planetary Sciences.

LITHOSPHERIC STRUCTURE IN THE PACIFIC GEOID

B. D. Marsh and J. H. Hinojosa *In* NASA, Washington Geopotential Res. Mission (GRM) Oct. 1985 p 32-35 (For primary document see N86-12852 03-46)

Avail: NTIS HC A07/MF A01 CSCL 08E

The high degree and order SEASAT geoid in the central Pacific correlates closely with the structure of the cooling lithosphere. Relative changes in plate age across major fracture zones in relatively young seafloor frame the east-west trending pattern formed by the geoid anomalies. The field removal in bathymetry corresponds to removal of some of the low degree and order geoidal components, the step like structure across fracture zones is also removed. The regional thermal subsidence was removed from the bathymetry by subtracting a mean subsidence surface from the observed bathymetry. This produces a residual bathymetry map analogous to the usual residual depth anomaly maps. The residual bathymetry obtained in this way contains shallow depths for young seafloor, and larger depths for older seafloor, thus retaining the structure of the lithosphere while removing the subsidence of the lithosphere. E.A.K.

N86-12864*# National Geodetic Survey, Rockville, Md. Charting and Geodetic Services.

THE GRAVITY FIELD OF TOPOGRAPHY BURIED BY SEDIMENTS Abstract Only

David T. Sandwell and Char-Shine Liu (California Univ., San Diego, La Jolla) *In* NASA, Washington Geopotential Res. Mission (GRM) Oct. 1985 p 36 (For primary document see N86-12852 03-46)

Avail: NTIS HC A07/MF A01 CSCL 08G

The gravity field over topography in the northern Indian Ocean that was completely buried by sediments of the Bengal Fan was investigated to understand the effect of sedimentation on the continental gravity field. An isopach map made from the seismic reflection and refraction in the Bay of Bengal shows two prominent N-S trending features in the basement topography. The northernmost portion of the Ninetyeast Ridge is totally buried by sediments north of 10 deg N. The other buried ridge trends roughly N-S for 1400 km at 85 deg E to the latitude of Sri Lanka and then curves toward the west. It has basement relief up to 6 km. Two free air gravity anomaly profiles across the region show a strong gravity low over the 85 deg E ridge, while the Ninetyeast Ridge shows a gravity high. E.A.K.

N86-12865*# National Aeronautics and Space Administration. Goddard Space Flight Center, Greenbelt, Md.

GRM CRUSTAL MAGNETIC ANOMALIES: SEPARATING THE LORD HOWE RISE AND NORFOLK RIDGE SUBMARINE STRUCTURES

Herbert Frey *In* NASA, Washington Geopotential Res. Mission (GRM) Oct. 1985 p 37-40 (For primary document see N86-12852 03-46)

Avail: NTIS HC A07/MF A01 CSCL 08G

Multiple source bodies often lie within the resolution element of the MAGSAT and POGO data. Small weak sources lying near larger stronger sources will tend to be missed, although they do contribute to the total observed anomaly. Lower elevation magnetic anomaly surveys such as GRM alleviate this problem through the combined effects of significantly greater resolution and stronger signal amplitude. This permits the detection of smaller source bodies, and analysis of their structure and nature. The improvement a GRM will provide is demonstrated in the Lord Howe Rise/Norfolk Ridge area east of Australia, between the Tasman Sea and south Fiji Basin. The submarine features origin have important plate tectonic implications. The Lord Howe Rise (LHR) is a continental fragment broken off from Australia by the opening of the Tasman Sea. It is a wide, shallow structure lying between 160 and 165 deg longitude at 23 to 37 deg S latitude. Seismic refraction data show the LHR crust extending to depths in excess of 20 km. E.A.K.

N86-12866*# Johns Hopkins Univ., Baltimore, Md. Dept. of Earth and Planetary Sciences.

SEA FLOOR SWELLS AND MANTLE PLUMES

Peter Olson *In* NASA, Washington Geopotential Res. Mission (GRM) Oct. 1985 p 41-42 refs (For primary document see N86-12852 03-46)

Avail: NTIS HC A07/MF A01 CSCL 08E

Most of the intraplate oceanic hot spots are located on the crest of broad topographic swells in the sea floor. These swells have Gaussian shaped profiles, with up to 1.6 km of relief and half widths of 200 to 300 km. Swells are accompanied by positive geoid height anomalies with amplitudes of 6 to 8 m. In the Atlantic and Pacific basins swells cover an area equal to 10% of the Earth's surface. Next to boundary layer contraction, swells are the most important cause of uplift and subsidence in oceanic lithosphere. Calculation of buoyancy supported topography and geoid height were combined with uplift data from laboratory experiments to assess whether sea floor swell can be produced by mantle plumes. The critical constraints are: (1) swell topographic profiles; (2) geoid height/topographic height ratios; and (3) uplift rates, estimated to be 0.2 km/ma. E.A.K.

N86-12867*# Cornell Univ., Ithaca, N.Y. Dept. of Geological Sciences.

PROPERTIES OF THE LITHOSPHERE AND ASTHENOSPHERE DEDUCED FROM GEOID OBSERVATIONS

Donald L. Turcotte *In* NASA, Washington Geopotential Res. Mission (GRM) Oct. 1985 p 44-45 (For primary document see N86-12852 03-46)

Avail: NTIS HC A07/MF A01 CSCL 08E

Data from the GEOS-3 and SEASAT Satellites provided a very accurate geoid map over the oceans. Broad bathymetric features in the oceans such as oceanic swells and plateaus are fully compensated. It is shown that the geoid anomalies due to the density structures of the lithosphere are proportional to the first moment of the density distribution. The deepening of the ocean basins is attributed to thermal isostasy. The thickness of the oceanic lithosphere increases with age due to the loss of heat to the sea floor. Bathymetry and the geoid provide constraints on the extent of this heat loss. Offsets in the geoid across major fracture zones can also be used to constrain this problem. Geoid bathymetry correlations show that the Hawaiian and Bermuda swells and the Cape Verde Rise are probably due to lithospheric thinning. E.A.K.

N86-12868*# National Geodetic Survey, Rockville, Md. Charting and Geodetic Services.
SUBDUCTION DYNAMICS: CONSTRAINTS FROM GRAVITY FIELD OBSERVATIONS Abstract Only
David C. McAdoo *In* NASA, Washington Geopotential Res. Mission (GRM) Oct. 1985 p 46 (For primary document see N86-12852 03-46)
Avail: NTIS HC A07/MF A01 CSCL 08E

Satellite systems do the best job of resolving the long wavelength components of the Earth's gravity field. Over the oceans, satellite-borne radar altimeters such as SEASAT provide the best resolution observations of the intermediate wavelength components. Satellite observations of gravity contributed to the understanding of the dynamics of subduction. Large, long wavelength geoidal highs generally occur over subduction zones. These highs are attributed to the superposition of two effects of subduction: (1) the positive mass anomalies of subducting slabs themselves; and (2) the surface deformations such as the trenches convectively inducted by these slabs as they sink into the mantle. Models of this subduction process suggest that the mantle behaves as a nonNewtonian fluid, its effective viscosity increases significantly with depth, and that large positive mass anomalies may occur beneath the seismically defined Benioff zones. E.A.K.

N86-12869*# Ohio State Univ., Columbus. Dept. of Geology and Mineralogy.
CONTINENTAL AND OCEANIC MAGNETIC ANOMALIES: ENHANCEMENT THROUGH GRM
Ralph R. B. vonFrese and William J. Hinze (Purdue Univ., Lafayette, Ind.) *In* NASA, Washington Geopotential Res. Mission (GRM) Oct. 1985 p 47-51 Previously announced as N85-31598 (For primary document see N86-12852 03-46)
Avail: NTIS HC A07/MF A01 CSCL 08G

In contrast to the POGO and MAGSAT satellites, the Geopotential Research Mission (GRM) satellite system will orbit at a minimum elevation to provide significantly better resolved lithospheric magnetic anomalies for more detailed and improved geologic analysis. In addition, GRM will measure corresponding gravity anomalies to enhance our understanding of the gravity field for vast regions of the Earth which are largely inaccessible to more conventional surface mapping. Crustal studies will greatly benefit from the dual data sets as modeling has shown that lithospheric sources of long wavelength magnetic anomalies frequently involve density variations which may produce detectable gravity anomalies at satellite elevations. Furthermore, GRM will provide an important replication of lithospheric magnetic anomalies as an aid to identifying and extracting these anomalies from satellite magnetic measurements. The potential benefits to the study of the origin and characterization of the continents and oceans, that may result from the increased GRM resolution are examined. M.G.

N86-12870*# Toronto Univ. (Ontario). Dept. of Geology.
THE RESOLUTION OF A MAGNETIC ANOMALY MAP EXPECTED FROM GRM DATA
D. W. Strangway, J. Arkani-Hamed, D. J. Teskey (Geological Survey of Canada, Ottawa, Ontario), and P. J. Hood (Geological Survey of Canada, Ottawa, Ontario) *In* NASA, Washington Geopotential Res. Mission (GRM) Oct. 1985 p 52-53 (For primary document see N86-12852 03-46)
Avail: NTIS HC A07/MF A01 CSCL 08G

Data from the MAGSAT mission were used to derive a global scalar magnetic anomaly map at an average altitude of about 400 km. It was possible to work with 2 data sets corresponding to dawn and dusk. The anomalies which were repeatable at dawn and at dusk was identified and the error limits of these anomalies were estimated. The repeatable anomalies were downward continued to about 10 km altitude. The anomalies over Canada were correlated quantitatively with bandpass filtered magnetic anomalies derived from aeromagnetic surveys. The close correlation indicates that the repeatable anomalies detected from orbit are due to geological causes. This correlation supports the geological significance of the global anomaly map. E.A.K.

N86-12871*# Cambridge Univ. (England). Dept. of Earth Sciences.
THE IMPORTANCE OF GRM GRAVITY OBSERVATIONS IN CONTINENTAL REGIONS Abstract Only
Dan P. McKenzie *In* NASA, Washington Geopotential Res. Mission (GRM) Oct. 1985 p 56 (For primary document see N86-12852 03-46)
Avail: NTIS HC A07/MF A01 CSCL 08E

Altimetric satellites showed the existence of gravity anomalies with wavelengths between 1500 km and 3000 km which correlated with residual depth anomalies. It was suggested that there is also an even smaller scale convective circulation with a wavelength of less than 500 km. Numerical experiments and SEASAT profiles demonstrate that similar small scale circulation must also exist near fracture zones. The mantle therefore must contain at least three scales of circulation: (1) comparable to the plate dimensions, the large scale circulation, which returns material from the Island arcs to the ridges; (2) an intermediate scale comparable to the depth of the upper mantle; and (3) a small scale comparable to the thickness of the asthenosphere. This picture was established by observations of gravity and bathymetry in oceanic regions. E.A.K.

N86-12872*# California Inst. of Tech., Pasadena. Seismological Lab.
THE SOURCE OF THE EARTH'S LONG WAVELENGTH GEOID ANOMALIES: IMPLICATIONS FOR MANTLE AND CORE DYNAMICS
Bradford H. Hager, Mark A. Richards, and Richard J. OConnell (Harvard Univ., Cambridge, Mass.) *In* NASA, Washington Geopotential Res. Mission (GRM) Oct. 1985 p 57-59 (For primary document see N86-12852 03-46)
Avail: NTIS HC A07/MF A01 CSCL 08E

The long wavelength components of the Earth's gravity field result mainly from density contrasts associated with convection in the mantle. Direct interpretation of the geoid for mantle convection is complicated by the fact that convective flow results in dynamically maintained deformation of the surface of the Earth, the core mantle boundary (CMB), and any interior chemical boundaries which might exist. These boundary deformations effect the geoid opposite in sign and are comparable in magnitude to those of the interior density contrasts driving the flow. The total difference of two relatively large quantities. E.A.K.

N86-12873*# Newcastle-upon-Tyne Univ. (England). School of Physics.
INTERPRETATION OF THE GEOID
S. K. Runcorn *In* NASA, Washington Geopotential Res. Mission (GRM) Oct. 1985 p 60-62 refs (For primary document see N86-12852 03-46)
Avail: NTIS HC A07/MF A01 CSCL 08E

The superposition of the first satellite geoid determined by Iszak upon Ootilla's geoid was based on surface gravity determinations. Good agreement was observed except over the Pacific area of the globe. The poor agreement over the Pacific was interpreted as the result of inadequate observations there. Many geoids were determined from satellite observations, including Doppler measurements. It is found that the geoid is the result of density differences in the mantle maintained since the primeval Earth by its finite strength. Various models based on this assumption are developed. E.A.K.

N86-12874*# Toronto Univ. (Ontario). Dept. of Physics.
MANTLE CONVECTION AND THE LARGE SCALE STRUCTURES OF THE EARTH'S GRAVITATIONAL FIELD Abstract Only
w. R. Peltier *In* NASA, Washington Geopotential Res. Mission (GRM) Oct. 1985 p 63 (For primary document see N86-12852 03-46)
Avail: NTIS HC A07/MF A01 CSCL 08G

The connection between the observed large scale structure of the Earths' gravitational field, as represented by the GEM10 model, and the surface kinematic manifestations of plate tectonics, as represented by the absolute plate motion model of Minster and Jordan, is explored using a somewhat novel method of analysis. Two scalar derivatives of the field of surface plate velocities, namely the horizontal divergence and the radial vorticity, are computed from the plate motion data. These two scalars are respectively determined by the poloidal and toroidal scalars in terms of which any essentially solenoidal vector field may be completely represented. They provide a compact summary of the observed plate boundary types in nature, with oceanic ridges and trenches being essentially boundaries of divergence, and transform faults being essentially boundaries of vorticity. Author

N86-12875*# Harvard Univ., Cambridge, Mass. Dept. of Geological Sciences.
CONSTRAINTS ON THE RHEOLOGICAL STRUCTURE OF THE MANTLE
Richard J. OConnell and Bradford H. Hager (California Inst. of Tech., Pasadena) *In* NASA, Washington Geopotential Res. Mission (GRM) Oct. 1985 p 64-65 (For primary document see N86-12852 03-46)
Avail: NTIS HC A07/MF A01 CSCL 08G

Rheological models of the mantle are at present limited to radial symmetry, usually with homogeneous linearly viscous or viscoelastic incompressible layers. While such models are probably overly simple, they readily allow calculation of geophysical effects, such as post glacial rebound and related changes in the Earth's shape. They are also directly applicable to problems of global mantle flow and plate motions. Author

N86-12876*# Arizona State Univ., Tempe. Dept. of Geology.
THE ROLE OF A PRESSURE-DEPENDENT RHEOLOGY IN THE DYNAMICS OF MANTLE CIRCULATION
David A. Yuen and Luce Fleitout (Paris-Sud Univ., Orsay, France) *In* NASA, Washington Geopotential Res. Mission (GRM) Oct. 1985 p 66-67 (For primary document see N86-12852 03-46)
Avail: NTIS HC A07/MF A01 CSCL 08G

A thermomechanical model for upper mantle convection was constructed such that the thickness and the structure of the lithosphere are determined self consistently by the heat transported by convection. In this study of the interaction between the lithosphere and upper mantle, strongly temperature and pressure dependent rheologies for both Newtonian and non-Newtonian creep mechanisms are employed. For a strictly temperature dependent rheology an insignificant amount of heat, less than 12.5 mW/sq m, can be transported convectively for an interior viscosity, 0(10 sup 21 Pas), compatible with post glacial rebound. On the other hand, for similar values of the interior viscosity, steady heat fluxes between 20 and 40 mW/sq m are produced by introducing pressure dependence into the rheology. For the temperature and pressure dependent flow law the horizontally averaged interior temperature displays very little variation with the amount of heat evacuated, once all of the rheological parameters are fixed. This finding may have important ramifications for parameterized convection. G.L.C.

N86-12877*# California Inst. of Tech., Pasadena. Siesmological Lab.
SMALL-SCALE CONVECTION BENEATH THE TRANSVERSE RANGES, CALIFORNIA: IMPLICATIONS FOR INTERPRETATION OF GRAVITY ANOMALIES Abstract Only
Eugene D. Humphreys and Bradford H. Hager *In* NASA, Washington Geopotential Res. Mission (GRM) Oct. 1985 p 68 ref (For primary document see N86-12852 03-46)
Avail: NTIS HC A07/MF A01 CSCL 08K

Tomograhic inversion of upper mantle P wave velocity heterogeneities beneath southern California shows two prominent features: an east-west trending curtain of high velocity material (up to 3% fast) in the upper 250 km beneath the Transverse Ranges and a region of low velocity material (up to 4% slow) in the 100 km beneath the Salton Trough. These seismic velocity anomalies were interpreted as due to small scale convection in the mantle. Using this hypothesis and assuming that temperature and density anomalies are linearly related to seismic velocity anomalies through standard coefficients of proportionality, leads to inferred variations of approx. + or - 300 C and approx. + or - 0.03 g/cc. G.L.C.

N86-12878*# Massachusetts Inst. of Tech., Cambridge. Dept. of Earth, Atmospheric and Planetary Sciences.
EVIDENCE FROM SATELLITE ALTIMETRY FOR SMALL-SCALE CONVECTION IN THE MANTLE
B. Parsons, W. F. Haxby (Lamont-Doherty Geological Observatory), D. P. McKenzie (Cambridge Univ.), A. B. Watts (Lamont-Doherty Geological Observatory), and J. K. Weissel (Lamont-Doherty Geological Observatory) *In* NASA, Washington Geopotential Res. Mission (GRM) Oct. 1985 p 69-70 refs (For primary document see N86-12852 03-46)
Avail: NTIS HC A07/MF A01 CSCL 08E

Small scale convection can be defined as that part of the mantle circulation in which upwellings and downwellings can occur beneath the lithosphere within the interiors of plates, in contrast to the large scale flow associated with plate motions where upwellings and downwellings occur at ridges and trenches. The two scales of convection will interact so that the form of the small scale convection will depend on how it arises within the large scale flow. Observations based on GEOS-3 and SEASAT altimetry suggest that small scale convection occurs in at least two different ways. G.L.C.

N86-12879*# Toronto Univ. (Ontario). Dept. of Physics.
MANTLE VISCOSITY, J2 AND THE NONTIDAL ACCELERATION OF EARTH ROTATION Abstract Only
W. R. Peltier *In* NASA, Washington Geopotential Res. Mission (GRM) Oct. 1985 p 71 (For primary document see N86-12852 03-46)
Avail: NTIS HC A07/MF A01 CSCL 08G

Recent interpretations of laser ranging for the LAGEOS satellite have rather conclusively established that the observed acceleration in the node of its orbit is just that expected to exist as a residual effect of the last deglaciation event which ended about 6000 years ago. The nontidal acceleration of rotation would be rather different than that observed if there were any significant melting of high latitude continental ice masses currently ongoing. The sensitivity of the expected nontidal acceleration to variations of several elements of the radial viscoelastic structure of the planet is explored using a new normal mode method for the computation of viscoelastic relaxation spectra. These calculations establish that the most important sensitivity is to variations in the mantle viscosity profile. Although the predicted nontidal acceleration does depend upon lithospheric thickness and on the elastic component of the radial structure, the dependence on these components of the structure is much weaker than it is upon mantle viscosity. The observed J sub 2 is therefore a particularly useful determinant of radial variations in the latter parameter. Author

N86-12880*# Geological Survey, Reston, Va.
MODELING GRAVITY AND MAGNETIC FIELDS FOR CRUSTAL AND UPPER MANTLE STRUCTURES
John M. DeNoyer *In* NASA, Washington Geopotential Res. Mission (GRM) Oct. 1985 p 72-73 (For primary document see N86-12852 03-46)
Avail: NTIS HC A07/MF A01 CSCL 08E

Research was conducted to: (1) make a direct comparison between the gravity and magnetic fields near the ellipsoid and at the height expected for the Geopotential Research Mission (GRM) for the same geologic model, (2) obtain realistic estimates of the gradients that can be expected at the orbit height of the GRM, and (3) demonstrate the value of data that the GRM could provide for investigating upper mantle and deep crustal anomalies. Author

N86-12881*# Texas Univ., Austin. Center for Space Research.
ON THE GEOGRAPHICAL CORRELATION OF ORBIT ERROR Abstract Only c13
B. D. Tapley and G. W. Rosborough *In* NASA, Washington Geopotential Res. Mission (GRM) Oct. 1985 p 76 (For primary document see N86-12852 03-46)
Avail: NTIS HC A07/MF A01 CSCL 22C

The orbit accuracies needed to support the global crustal dynamics project and recent satellite altimeter missions have placed unique demands on the data analysis and orbit analysis systems. These demands include accurate and well distributed observations, improved computational techniques and substantial enhancements in the force models which represent the satellite's motion. For example, the satellite altimeter mission (TOPEX), whose objectives will be: (1) to measure the time variable ocean surface topography, and (2) to demonstrate the ability to map the general ocean circulation, requires that the radial component of the satellite's orbit be known with an rms accuracy of 13 cm for the three year mission lifetime. The primary force model uncertainty which limits the contemporary orbit computation accuracy is the inaccuracy in the values assigned to the spherical harmonic coefficients used to model the Earth's gravity field. Author

N86-12882*# National Aeronautics and Space Administration. Goddard Space Flight Center, Greenbelt, Md.
GLOBAL MEAN SEA SURFACE COMPUTATION BASED UPON A COMBINATION OF SEASAT AND GEOS-3 SATELLITE ALTIMETER DATA Abstract Only c48
J. G. Marsh, C. J. Koblinsky, A. Brenner (Edgerton, Germeshausen and Grier, Inc., Riverdale, Md.), B. Beckley (Edgerton, Germeshausen and Grier, Inc., Riverdale, Md.), and T. Martin (Edgerton, Germeshausen and Grier, Inc., Riverdale, Md.) *In* NASA, Washington Geopotential Res. Mission (GRM) Oct. 1985 p 77 (For primary document see N86-12852 03-46)
Avail: NTIS HC A07/MF A01 CSCL 08J

A mean sea surface map was computed for the global ocean areas between 70 deg N latitude and 62 deg S latitude based upon the 70 day SEASAT and 3.5 year GEOS-3 altimeter data sets. The mean sea surface is presented in the form of a global contour map and a 0.25 deg x 0.25 deg grid. A combination of regional adjustments based upon crossover techniques and the subsequent adjustment of the regional solutions into a global reference system was employed in order to minimize the effects of radial orbit error. A global map of the crossover residuals after the crossover adjustments are made is in good agreement with earlier mesoscale variability contour maps based upon the last month of SEASAT collinear data. This high level of agreement provides good evidence that relative orbit error was removed to the decimeter level on a regional basis. This represents a significant improvement over our previous maps which contained patterns, particularly in the central Pacific, which were due to radial orbit error. Long wavelength, basin scale errors are still present with a submeter amplitude due to errors in the PGS-S4 gravity model. Such errors can only be removed through the improvement of the Earth's gravity model and associated geodetic parameters. Author

N86-12883*# Jet Propulsion Lab., California Inst. of Tech., Pasadena.
CONTRIBUTIONS OF GRM TO THE OCEAN TOPOGRAPHY EXPERIMENT (TOPEX) Abstract Only c48
Robert Stewart *In* NASA, Washington Geopotential Res. Mission (GRM) Oct. 1985 p 78 (For primary document see N86-12852 03-46)
Avail: NTIS HC A07/MF A01 CSCL 08J

The permanent shape of the sea surface, the time averaged mean sea level, is comprised of: (1) an ellipsoidal component due to the mean mass of a rotating Earth; (2) spatial undulations due to the inhomogeneous distribution of mass in the Earth; and (3) spatial undulations due to permanent ocean currents. The amplitude of the three components are in the ratio 10,000 : 100 : 1 m, the first two components comprising the marine geoid, and the third being the permanent topography of the sea surface. G.L.C.

N86-12884*# Woods Hole Oceanographic Institution, Mass.
SEPARATION OF CORE AND CRUSTAL MAGNETIC FIELD SOURCES
L. Shure, R. L. Parker, and R. A. Langel *In* NASA, Washington Geopotential Res. Mission (GRM) Oct. 1985 p 80-81 refs (For primary document see N86-12852 03-46)
Avail: NTIS HC A07/MF A01 CSCL 08G

Fluid motions in the electrically conducting core and magnetized crustal rocks are the two major sources of the magnetic field observed on or slightly above the Earth's surface. The exact separation of these two contributions is not possible without imposing a priori assumptions about the internal source distribution. Nonetheless models like these were developed for hundreds of years Gauss' method, least squares analysis with a truncated spherical harmonic expansion was the method of choice for more than 100 years although he did not address separation of core and crustal sources, but rather internal versus external ones. Using some arbitrary criterion for appropriate truncation level, we now extrapolate downward core field models through the (approximately) insulating mantle. Unfortunately our view can change dramatically depending on the degree of truncation for describing core sources. G.L.C.

N86-12885*# Cambridge Univ. (England).
THE MAGNETIC FIELD AT THE CORE-MANTLE BOUNDARY
Jeremy Bloxham and David Gubbins *In* NASA, Washington Geopotential Res. Mission (GRM) Oct. 1985 p 82-84 refs (For primary document see N86-12852 03-46)
Avail: NTIS HC A07/MF A01 CSCL 08N

Models of the geomagnetic field are, in general, produced from a least-squares fit of the coefficients in a truncated spherical harmonic expansion to the available data. Downward continuation of such models to the core-mantle boundary (CMB) is an unstable process: the results are found to be critically dependent on the choice of truncation level. Modern techniques allow this fundamental difficulty to be circumvented. The method of stochastic inversion is applied to modeling the geomagnetic field. Prior information is introduced by requiring that the spectrum of spherical harmonic coefficients to fall-off in a particular manner which is consistent with the Ohmic heating in the core having a finite lower bound. This results in models with finite errors in the radial field at the CMB. Curves of zero radial field can then be determined and integrals of the radial field over patches on the CMB bounded by these null-flux curves calculated. With the assumption of negligible magnetic diffusion in the core; frozen-flux hypothesis, these integrals are time-invariant. G.L.C.

N86-12886*# National Aeronautics and Space Administration. Goddard Space Flight Center, Greenbelt, Md.
SOME ANTICIPATED CONTRIBUTIONS TO CORE FLUID DYNAMICS FROM THE GRM
Coerte VanVorhies *In* NASA, Washington Geopotential Res. Mission (GRM) Oct. 1985 p 85-88 refs (For primary document see N86-12852 03-46)
Avail: NTIS HC A07/MF A01 CSCL 08G

It is broadly maintained that the secular variation (SV) of the large scale geomagnetic field contains information on the fluid dynamics of Earth's electrically conducting outer core. The electromagnetic theory appropriate to a simple Earth model has recently been combined with reduced geomagnetic data in order to extract some of this information and ascertain its significance. The simple Earth model consists of a rigid, electrically insulating mantle surrounding a spherical, inviscid, and perfectly conducting liquid outer core. This model was tested against seismology by using truncated spherical harmonic models of the observed geomagnetic field to locate Earth's core-mantle boundary, CMB. Further electromagnetic theory has been developed and applied to the problem of estimating the horizontal fluid motion just beneath

CMB. Of particular geophysical interest are the hypotheses that these motions: (1) include appreciable surface divergence indicative of vertical motion at depth, and (2) are steady for time intervals of a decade or more. In addition to the extended testing of the basic Earth model, the proposed GRM provides a unique opportunity to test these dynamical hypotheses. G.L.C.

N86-12887*# Brown Univ., Providence, R. I. Dept. of Geological Sciences.

RATIONALE FOR A GRAVSAT-MAGSAT MISSION: A PERSPECTIVE ON THE PROBLEM OF EXTERNAL/INTERNAL TRANSIENT FIELD EFFECTS

John F. Hermance *In* NASA, Washington Geopotential Res. Mission (GRM) Oct. 1985 p 89-91 refs (For primary document see N86-12852 03-46)

Avail: NTIS HC A07/MF A01 CSCL 08N

The Earth's magnetic field at MAGSAT altitudes not only has contributions from the Earth's core and static magnetization in the lithosphere, but also from external electric current systems in the ionosphere and magnetosphere, along with induced electric currents flowing in the conducting earth. Hermance assessed these last two contributions; the external time-varying fields and their associated internal counter-parts which are electromagnetically induced. It is readily recognized that during periods of magnetic disturbance, external currents often contribute from 10's to 100's of nanoteslas (gammas) to observations of the Earth's field. Since static anomalies from lithospheric magnetization are of this same magnitude or less, these external source fields must be taken into account when attempting to delineate gross structural features in the crust. G.L.C.

N86-12888*# Geological Survey, Denver, Colo.

RECENT MAGSAT RESULTS

Joseph C. Cain *In* NASA, Washington Geopotential Res. Mission (GRM) Oct. 1985 p 92-101 refs (For primary document see N86-12852 03-46)

Avail: NTIS HC A07/MF A01 CSCL 08N

Meyer, et al. have improved their original global crustal model and made a spherical harmonic analysis of the resulting magnetic field to n=50. The Z contours at 400 Km altitude from a field model composed of the first 15 degrees and order of their model and the terms n=16 to 29 from the MAGSAT model M051782 are presented. The main point to consider from such representations is that the lower order terms appear to contribute components comparable in magnitude to those of higher order. Thus, one should allow in making tectonic interpretations of global maps of anomalies such as those published by Langel, that there are likely continental scale (or smaller) features that have been removed along with the core field by the subtraction of the terms n=1 to 13 of the observed field. Planning for the analysis of data to be accrued by GRM should thus address this problem. G.L.C.

N86-12889*# California Univ., San Diego, La Jolla.

MODELING CURRENTS AT SATELLITE ALTITUDES Abstract Only

G. E. Backus *In* NASA, Washington Geopotential Res. Mission (GRM) Oct. 1985 p 102 (For primary document see N86-12852 03-46)

Avail: NTIS HC A07/MF A01 CSCL 20C

A mathematical formalism for modeling the poloidal magnetic field and current density at satellite altitudes is presented. G.L.C.

N86-12890*# Colorado Univ., Boulder. Dept. of Astrophysical, Planetary and Atmospheric Sciences.

EXPECTED CONTRIBUTION OF THE GEOPOTENTIAL RESEARCH MISSION (GRM) TO STUDIES OF LIQUID CORE FLUID DYNAMICS

Edward R. Benton *In* NASA, Washington Geopotential Res. Mission (GRM) Oct. 1985 p 103-104 (For primary document see N86-12852 03-46)

Avail: NTIS HC A07/M A01 CSCL 08G

Finding satisfactory models of the fluid motions at the top of the core is important for delineating what kind of dynamo is in operation, for estimating the heat flux into the base of the mantle, and for forecasting the magnetic field forward in time. Each of these aspects will be discussed. G.L.C.

N86-12891*# Miami Univ., Fla. School of Marine and Atmospheric Science.

THE SOURCE OF THE INTERMEDIATE WAVELENGTH COMPONENT OF THE EARTH'S MAGNETIC FIELD

C. G. A. Harrison *In* NASA, Washington Geopotential Res. Mission (GRM) Oct. 1985 p 105-106 (For primary document see N86-12852 03-46)

Avail: NTIS HC A07/MF A01 CSCL 08G

The intermediate wavelength component of the Earth's magnetic field has been well documented by observations made by MAGSAT. It has been shown that some significant fraction of this component is likely to be caused within the core of the Earth. Evidence for this comes from analysis of the intermediate wavelength component revealed by spherical harmonics between degrees 14 and 23, in which it is shown that it is unlikely that all of this signal is crustal. Firstly, there is no difference between average continental source strength and average oceanic source strength, which is unlikely to be the case if the anomalies reside within the crust, taking into account the very different nature and thickness of continental and oceanic crust. Secondly, there is almost no latitudinal variation in the source strength, which is puzzling if the sources are within the crust and have been formed by present or past magnetic fields with a factor of two difference in intensity between the equator and the poles. If however most of the sources for this field reside within the core, then these observations are not very surprising. G.L.C.

N86-12892*# California Univ., San Diego, La Jolla.

DOES THE GEOID DRIFT WEST? Abstract Only

G. E. Backus, R. L. Parker, and M. A. Zumberge *In* NASA, Washington Geopotential Res. Mission (GRM) Oct. 1985 p 107 (For primary document see N86-12852 03-46)

Avail: NTIS HC A07/MF A01 CSCL 08E

In 1970 Hide and Malin noted a correlation of about 0.8 between the geoid and the geomagnetic potential at the Earth's surface when the latter is rotated eastward in longitude by about 160 degrees and the spherical harmonic expansions of both functions are truncated at degree 4. From a century of magnetic observatory data, Hide and Malin inferred an average magnetic westward drift rate of about 0.27 degrees/year. They attributed the magnetic-gravitational correlation to a core event at about 1350 A.D. which impressed the mantle's gravity pattern at long wavelengths onto the core motion and the resulting magnetic field. The impressed pattern was then carried westward 160 degrees by the nsuing magnetic westward drift. An alternative possibility is some sort of steady physical coupling between the magnetic and gravitational fields (perhaps migration of Hide's bumps on the core-mantle interface). This model predicts that the geoid will drift west at the magnetic rate. On a rigid earth, the resulting changes in sea level would be easily observed, but they could be masked by adjustment of the mantle if it has a shell with viscosity considerably less than 10 to the 21 poise. However, steady westward drift of the geoid also predicts secular changes in g, the local acceleration of gravity, at land stations. These changes are now ruled out by recent independent high-accuracy absolute measurements of g made by several workers at various locations in the Northern Hemisphere. Author

N86-12893*# National Aeronautics and Space Administration. Goddard Space Flight Center, Greenbelt, Md.

GRM AS A FOLLOW-ON TO MAGSAT

R. A. Langel *In* NASA, Washington Geopotential Res. Mission (GRM) Oct. 1985 p 108-109 (For primary document see N86-12852 03-46)

Avail: NTIS HC A07/MF A01 CSCL 08G

MAGSAT was the first near-Earth spacecraft dedicated to measurement of the vector geomagnetic field. Its objectives were to use the vector measurements to measure and model both the main field and the crustal field of the Earth. The main field measurements were to be used for the 1980 world charts and to study the Earth's core. The crustal fields were to be utilized to aid in modeling large-scale variations in the geologic and geophysical characteristics of the crust. G.L.C.

N86-12894*# EROS Data Center, Sioux Falls, S. Dak.
ON THE INTERPRETATION OF SATELLITE-DERIVED GRAVITY AND MAGNETIC DATA FOR STUDIES OF CRUSTAL GEOLOGY AND METALLOGENESIS
David A. Hastings *In* NASA, Washington Geopotential Res. Mission (GRM) Oct. 1985 p 110-113 ref (For primary document see N86-12852 03-46)
Avail: NTIS HC A07/MF A01 CSCL 08G

Satellite-derived global gravity and magnetic maps have been shown to be useful in large-scale studies of the Earth's crust, despite the relative infancy of such studies. Numerous authors have made spatial associations of gravity or magnetic anomalies with geological provinces. Gravimetric interpretations are often made in terms of isostasy, regional variations of density, or of geodesy in general. Interpretations of satellite magnetic anomalies often base assumptions of overall crustal magnetism on concepts of the vertical and horizontal distribution of magnetic susceptibility, then make models of these assumed distributions. The opportunity of improving our satellite gravity and magnetic data through the proposed Geopotential Research Mission should considerably improve the scientific community's ability to analyze and interpret global magnetic and gravity data. G.L.C.

N86-12895*# EROS Data Center, Sioux Falls, S. Dak. Technicolor Government Services, Inc.
DO MAGSAT ANOMALIES CONTAIN A RECORD OF PAST AND PRESENT-DAY MANTLE CONVECTION UNDER SOUTH AMERICA? Abstract Only
David A. Hastings *In* NASA, Washington Geopotential Res. Mission (GRM) Oct. 1985 p 114 ref (For primary document see N86-12852 03-46)
Avail: NTIS HC A07/MF A01 CSCL 08G

Global anomaly maps from the National Aeronautics and Space Administration's Magnetic Field Satellite (MAGSAT) have been spatially filtered to reduce the prominence of long-wavelength east-west bands and to improve the discrimination of anomalies within structural provinces. Previous research suggested a correlation between total-field MAGSAT anomaly lows in equatorial regions with crustal bodies of relatively high average magnetic susceptibility (such as Archaean shields), and of anomaly highs with bodies of low susceptibility (such as deep parts of basins). These correlations reverse at higher latitudes. G.L.C.

N86-12896# Air Force Geophysics Lab., Hanscom AFB, Mass.
PRECIPITATING ELECTRON AND ION DETECTORS (SSJ/4) FOR THE BLOCK 5D/FLIGHTS 6-10 DMSP (DEFENSE METEOROLOGICAL SATELLITE PROGRAM) SATELLITES: CALIBRATION AND DATA PRESENTATION
D. A. Hardy, L. K. Schmitt, M. S. Gussenhoven, F. J. Marshall, and H. C. Yeh 21 Nov. 1984 59 p
(AF Proj. 7601)
(AD-A157080; AFGL-TR-84-0317; AFGL-ERP-902) Avail: NTIS HC A04/MF A01 CSCL 04/1

The satellites of the Defense Meteorological Satellite Program (DMSP) are flown operationally to provide data for the specification of terrestrial weather and the near Earth space environment. In support of space environment specification the satellites starting the F6, carry an improved set of electrostatic analyzers SSJ/4, designed to measure the flux of precipitating electrons and ions with energies between 30 eV and 30 keV. The data from these analyses are routinely processed at AFCL and are available to the scientific community. Both by itself, and in combination with other sensors on the satellite, the SSJ/4 detectors provide important data for the study of auroral processes. This report was prepared to facilitate the widespread use of the SSJ/4 data. Author (GRA)

N86-12897# Naval Research Lab., Washington, D. C.
A SIMULATION OF HIGH LATITUDE F-LAYER INSTABILITIES IN THE PRESENCE OF MAGNETOSPHERE-IONOSPHERE COUPLING
H. G. Mitchell, Jr., J. A. Fedder, M. J. Keskinen, and S. T. Zalesak 8 Jul. 1985 29 p Sponsored in part by NASA and DNA
(RR0-3302)
(NASA-CR-176296; NAS 1.26:176296; AD-A157475) Avail: NTIS HC A03/MF A01 CSCL 04A

A magnetic-field-line-integrated model of plasma interchange instabilities is developed for the high latitude ionosphere including magnetospheric coupling effects. We show that primary magnetosphere-ionosphere coupling effect is to incorporate the inertia of the magnetospheric plasma in the analysis. As a specific example, we present the first simulation of the E x B instability in the inertial regime, i.e., nu sub i < omega where nu sub i is the ion-neutral collision frequency and omega is the wave frequency. We find that the inertial E x B instability develops in a fundamentally different manner than in the collisional case ni sub i < omega. Our results show that striations produced in the inertial regime are spread and retarded by ion inertial effects, and result in more isotropic irregularities than those seen in the collisional case. GRA

N86-12898# Aerospace Corp., El Segundo, Calif. Space Sciences Lab.
AN ALTERNATIVE INTERPRETATION OF ION RING DISTRIBUTION OBSERVED BY THE S3-3 SATELLITE
D. J. Gorney 15 May 1985 18 p
(Contract F04701-83-C-0084)
(AD-A157655; TR-0084A(5940-05)-3; SD-TR-85-14) Avail: NTIS HC A02/MF A01 CSCL 04/1

Recently, theoretical interest has grown in possible plasma wave instabilities arising from free energy in auroral ion distributions, and a number of ion-mode instabilities have been identified. These instabilities typically rely on positive slopes in the ion's velocity distribution parallel (del f/del v(sub par) > 0) or perpendicular (del f/del v(sub perp) > 0) to the magnetic field. Upflowing ion beams generated by electrical potential drops along auroral field lines are obvious candidates for the parallel (beam) instability, while ion conics have been treated in the limit of the flute mode instability, assuming that a positive perpendicular gradient exists. However, ion conics are not responsible for the condition del f/del v(sub perp) > 0. Downflowing ion beam distributions can have del f/del v(sub perp) > 0 and therefore might lead to flute mode instability. Examples of both conics and downflowing beams are presented, showing that only the downflowing component leads to significant del f/del v(sub perp) > 0, while ion conics generally have del f/del v(sub perp) < 0 and are themselves stable to the flute mode. GRA

N86-12899# Aerospace Corp., Germantown, Md. Space Sciences Lab.
EFFECTS OF WHISTLER-MODE AND OTHER WAVES IN THE MAGNETOSPHERE Final Report, 1981 - 1984
M. Schultz, A. L. Vampola, and D. J. Boucher, Jr. 20 Jun. 1985 108 p
(Contract F04701-83-C-0084)
(AD-A157832; TR-0084(4613)-1; SD-TR-85-24) Avail: NTIS HC A06/MF A01 CSCL 04/1

This report covers progress on three research topics related to the dynamics of natural and artificial radiation belts, with emphasis on the consequences of interactions between geomagnetically trapped electrons and waves that propagate in the magnetospheric plasma. Part 1 includes a review of the Kennel-Petschek saturation concept and a solution of the model nonlinear differential equation that describes the evolution of charged-particle intensities above, near, and below saturation level. Part 2 provides an estimate of the limiting energy spectrum of a saturated radiation belt of specified pitch-angle anisotropy. Part 3 provides a review of eigenfunction methods in pitch-angle diffusion theory and a prescription for constructing optimal basis functions for the numerical calculation of eigenvalues and eigenfunctions of the pitch-angle diffusion operator. GRA

N86-12900# Weston Observatory, Mass.
INVESTIGATION OF MAGNETIC FIELD MEASUREMENTS Final Report, 1 Jun. 1982 - 30 Sep. 1984
J. F. Devane Mar. 1985 21 p
(Contract F19628-82-K-0040)
(AD-A157924; AFGL-TR-85-0054) Avail: NTIS HC A02/MF A01 CSCL 08/14

Weston Observatory of Boston College has cooperated with AFGL personnel in the maintenance of the Air Force Geomagnetic Magnetometer Network. The computer facilities for processing the data of the Network were upgraded. Fluxgate data for every month of the period 1978-1983 has been deposited in World Data Center A. Daily magnetograms have been produced and will be published by AFGL. Some preliminary processing data to establish substation conductivity was initiated. The Network was discontinued in December 1983. GRA

N86-12901# Alaska Univ., Fairbanks. Geophysical Inst.
CARBON DIOXIDE IN ARCTIC AND SUBARCTIC REGIONS Final Report
T. Gosnik and J. J. Melley Jun. 1985 218 p
(Contract DE-AT06-80EV-10429)
(DE85-014054; DOE/EV-10429/T2) Avail: NTIS HC A10/MF A01

Summaries and interpretations of the data collected for carbon dioxide partial pressures in the air and water are given. Sections were individually abstracted for inclusion in the data base. DOE

N86-12902# University of Southwestern Louisiana, Lafayette. Dept. of Geology.
HIGH-RESOLUTION, THREE-DIMENSIONAL, SEISMIC SURVEY OVER THE GEOPRESSURED-GEOTHERMAL RESERVOIR AT PARCPERDUE, LOUISIANA Final Report, 1 Jan. 1981 - 31 Jul. 1985
G. L. Kinsland Jul. 1985 290 p refs
(Contract DE-AC08-81NV-10185)
(DE85-016465; DOE/NV-10185/1) Avail: NTIS HC A13/MF A01

A high resolution three-dimensional seismic survey was performed over the reservoir of the geopressured-geothermal production experiment at Parcperdue, Louisiana and high quality results have been obtained. The reservoir is now mapped with more control and assurance than was possible with the previously existing data. Three differences between the map of this project and those available before are significant in the interpretation of the depletion experiment: (1) the western bounding fault is further west leading to a larger reservoir volume; (2) a down to the north (relief) fault through the reservoir has been found; and (3) there are structural highs in which small petroleum accumulations may exist within the reservoir. An original goal of testing the before and after seismic experiment idea as a production monitor has not been realized. However, the quality of the data at the stages of processing presently available is high enough that, had the well not failed, it would have been prudent to have proceeded with the project toward the second experiment. DOE

N86-12903# California Univ., Berkeley. Lawrence Berkeley Lab.
GRAVITY THEORIES IN MORE THAN FOUR DIMENSIONS
B. Zumino Mar. 1985 7 p refs Presented at the Modern Methods in Quantum Field Theory Conf., Amalfi, Italy, 7 May 1984
(Contract DE-AC03-76SF-00098)
(DE85-011164; LBL-19302; CONF-8405312-1) Avail: NTIS HC A02/MF A01

String theories suggest particular forms for gravity interactions in higher dimensions. We consider an interesting class of gravity theories in more than four dimensions, clarify their geometric meaning and discuss their special properties. DOE

N86-12904# Los Alamos National Lab., N. Mex.
MAGNETIC RECONNECTION IN THE TERRESTRIAL MAGNETOSPHERE
W. C. Feldman 1984 14 p Presented at the Am. Inst. of Phys. Conf., Taos, N. Mex., 6 Aug. 1984
(Contract W-7405-eng-36)
(DE85-014107; LA-UR-85-2092; CONF-8408121-5) Avail: NTIS HC A02/MF A01

Quantitative comparisons between measured phenomena in the terrestrial magnetosphere thought to be associated with magnetic reconnection, and related theoretical predictions based on Petschek's simple model are reviewed. Although such a comparison cannot be comprehensive because of the extended nature of the process and the relatively few in situ multipoint measurements made to date, the agreement is impressive where comparisons were possible. This result leaves little doubt that magnetic reconnection does indeed occur in the terrestrial magnetosphere. The maximum reconnection rate, expressed in terms of the inflow Mach number, M sub A, is measured to be M sub A = 0.2 + or - 0.1. DOE

N86-12905# National Geodetic Survey, Rockville, Md.
GEODETICALLY DERIVED STRAIN FROM SAN FRANCISCO BAY TO THE MENDOCINO TRIPLE JUNCTION, CALIFORNIA
M. W. Cline, R. A. Snay, and E. L. Timmerman Apr. 1985 23 p refs
(PB85-198802; NOAA-TR-NOS-109; NGS-31) Avail: NTIS HC A02/MF A01 CSCL 08G

Geodetic data comprised of triangulation, trilateration, and astronomic azimuths observed since late 1906 to 1978 are used to obtain models of horizontal crustal deformation in California. The three regional models roughly cover the California Coast Ranges from San Francisco Bay northward to the Mendocino Triple Junction and from the Great Valley westward to the Pacific Ocean. Each of the three regions is partitioned into a mosaic of districts that are allowed to individually translate, rotate, and deform homogeneously as a linear function of time. By approximating the known geologic faults with district boundaries, the relative motion between districts represents secular fault slip. To study the transient postseismic effects of the 1906 San Francisco earthquake, the data for 1931 to 1978 time interval are separately modeled, and these models are compared with those for the entire time interval. GRA

N86-12906# North Carolina State Univ., Raleigh.
EXPERIMENTAL STUDY OF FLOW AND DISPERSION IN THE WAKES OF THREE-DIMENSIONAL LOW HILLS
S. P. S. Arya and P. S. Gadiyaram 1985 49 p refs
(PB85-193266; EPA-600/D-85/094) Avail: NTIS HC A03/MF A01 CSCL 04A

The EPA Meteorological Wind Tunnel was used to simulate a rural atmospheric boundary layer. Experiments were conducted on flow and dispersion over three-dimensional, conical hills of two different slopes (26.5 degrees and 17.5 degrees) whose heights were 1/3 of the boundary layer depth. These measurements were made both in undisturbed and disturbed (in presence of hill) flow, using hot-wire anemometers and hydrocarbon analyzers. Enhanced vertical and lateral dispersion were evident in the immediate wake region of the hill. This phenomenon reflects the increased turbulence levels in the wake. The results clearly illustrate that the slope of a conical hill is a most important parameter; it determines the location of flow separation, the size of the cavity region, and the characteristics of the wake flow dispersion. GRA

N86-12641# Joint Publications Research Service, Arlington, Va.
MODELING OF SEASONAL EVOLUTION OF CARBON CYCLE IN OCEAN-ATMOSPHERE SYSTEM Abstract Only
B. A. Kagan, V. A. Ryabchenko, and A. S. Safray *In its* USSR Rept.: Earth Sci. (JPRS-UES-85-006) 19 Jun. 1985 p 13 Transl. into ENGLISH from Izv. Akad. Nauk SSSR: Fiz. Atm. i Okeana (Moscow), v. 21, no. 1, Jan. 1985 p 66-75 (For primary document see N86-12630 03-42)
Avail: NTIS HC A05/MF A01

N86-12645# Joint Publications Research Service, Arlington, Va.
UPPER MESOZOIC TURBIDITES OF SOUTHERN WEST SAKHALIN DOWNWARP Abstract Only
S. V. Zyabrev *In its* USSR Rept.: Earth Sci. (JPRS-UES-85-006)

19 Jun. 1985 p 15-16 Transl. into ENGLISH from Tikhookeanskaya Geol. (Novosibirsk), no. 5, Sep. - Oct. 1984 p 22-33 (For primary document see N86-12630 03-42)
Avail: NTIS HC A05/MF A01

N86-12650# Joint Publications Research Service, Arlington, Va.
PETROCHEMICAL TYPES OF MAGMATIC ROCKS OF OCEAN FLOOR AND PATTERNS OF THEIR DISTRIBUTION Abstract Only
A. V. Abramov, V. M. Ryakhovskiy, and Yu. V. Mironov *In its* USSR Rept.: Earth Sci. (JPRS-UES-85-006) 19 Jun. 1985 p 19 Transl. into ENGLISH from Byul. Mosk. Obshch. Ispytateley Prirody: Otd. Geol. (Moscow), v. 60, no. 1, Jan. - Feb. 1985 p 18-27 (For primary document see N86-12630 03-42)
Avail: NTIS HC A05/MF A01

N86-12651# Joint Publications Research Service, Arlington, Va.
INTRUSIVE ROCKS OF OCEANIC LITHOSPHERE AS POSSIBLE SOURCES OF ANOMALOUS MAGNETIC FIELD OF OCEAN Abstract Only
Ye. A. Nazarova *In its* USSR Rept.: Earth Sci. (JPRS-UES-85-006) 19 Jun. 1985 p 19-20 Transl. into ENGLISH from Byul. Mosk. Obshch. Ispytateley Prirody: Otd. Geol. (Moscow), v. 60, no. 1, Jan. - Feb. 1985 p 28-41 (For primary document see N86-12630 03-42)
Avail: NTIS HC A05/MF A01

N86-12652# Joint Publications Research Service, Arlington, Va.
MAGMATIC PROVINCES AND TECTONICS IN PACIFIC OCEAN Abstract Only
Yu. M. Pushcharovskiy *In its* USSR Rept.: Earth Sci. (JPRS-UES-85-006) 19 Jun. 1985 p 21 Transl. into ENGLISH from Izv. Akad. Nauk SSSR: Ser. Geol. (Moscow), no. 11, Nov. 1984 p 13-18 (For primary document see N86-12630 03-42)
Avail: NTIS HC A05/MF A01

N86-12657# Joint Publications Research Service, Arlington, Va.
PETROLOGIC ASPECT OF FORMATION OF GEOSTRUCTURES IN MARGINAL SEAS Abstract Only
L. L. Perchuk *In its* USSR Rept.: Earth Sci. (JPRS-UES-85-006) 19 Jun. 1985 p 25-26 Transl. into ENGLISH from Dokl. Akad. Nauk SSSR (Moscow), v. 280, no. 1, Jan. 1985 p 178-182 (For primary document see N86-12630 03-42)
Avail: NTIS HC A05/MF A01

N86-12658# Joint Publications Research Service, Arlington, Va.
SPREADING IN DEVELOPMENT OF OCEANIC STRUCTURES Abstract Only
Yu. M. Pushcharovskiy and S. V. Ruzhentsev *In its* USSR Rept.: Earth Sci. (JPRS-UES-85-006) 19 Jun. 1985 p 26 Transl. into ENGLISH from Dokl. Akad. Nauk SSSR (Moscow), v. 280, no. 1, Jan. 1985 p 182-185 (For primary document see N86-12630 03-42)
Avail: NTIS HC A05/MF A01

N86-12661# Joint Publications Research Service, Arlington, Va.
POSSIBILITY OF SOUNDING EARTH BY USING ELECTROMAGNETIC FIELD OF SEA CURRENT Abstract Only
V. P. Smagin, G. A. Fonarev, and V. N. Savchenko *In its* USSR Rept.: Earth Sci. (JPRS-UES-85-006) 19 Jun. 1985 p 29 Transl. into ENGLISH from Izv. Akad. Nauk SSSR: Fiz. Zemli (Moscow), no. 2, Feb. 1985 p 70-74 (For primary document see N86-12630 03-42)
Avail: NTIS HC A05/MF A01

N86-12663# Joint Publications Research Service, Arlington, Va.
STRATIGRAPHY OF SEDIMENTS IN CENTRAL AND EASTERN MEDITERRANEAN Abstract Only
V. M. Sorokin, M. S. Afanasyeva, V. G. Kurenkova, and N. B. Chernyshova *In its* USSR Rept.: Earth Sci. (JPRS-UES-85-006) 19 Jun. 1985 p 30 Transl. into ENGLISH from Izv. Akad. Nauk SSSR: Ser. Geol. (Moscow), no. 2, Feb. 1985 p 59-64 (For primary document see N86-12630 03-42)
Avail: NTIS HC A05/MF A01

N86-12665# Joint Publications Research Service, Arlington, Va.
FIND OF RHEOLITES AND TRACHITES AND GEOLOGICAL SITUATION IN NORTHERN PART OF EAST INDIAN OCEAN SUBMARINE RIDGE Abstract Only
V. V. Reverdatto, V. V. Yeremeyev, A. Ya. Ilyev, A. A. Popov, P. M. Sychev, and V. N. Sharapov *In its* USSR Rept.: Earth Sci. (JPRS-UES-85-006) 19 Jun. 1985 p 34 Transl. into ENGLISH from Dokl. Akad. Nauk SSSR (Moscow), v. 280, no. 4, Feb. 1985 p 960-963 (For primary document see N86-12630 03-42)
Avail: NTIS HC A05/MF A01

N86-12666# Joint Publications Research Service, Arlington, Va.
EVALUATING SCREENING EFFECTS AND TUSNAMI DANGER IN BAYS Abstract Only
V. V. Ivanov, K. V. Simonov, and O. I. Garder *In its* USSR Rept.: Earth Sci. (JPRS-UES-85-006) 19 Jun. 1985 p 35 Transl. into ENGLISH from Izv. Akad. Nauk SSSR: Fiz. Atm. i Okeana (Moscow), v. 20, no. 12, Dec. 1984 p 1206-1214 (For primary document see N86-12630 03-42)
Avail: NTIS HC A05/MF A01

N86-12677# Joint Publications Research Service, Arlington, Va.
COMPUTATIONS OF SEISMIC WAVE PROPAGATION VELOCITIES IN OCEAN BOTTOM SEDIMENTS FROM REFLECTED WAVES TRAVEL-TIME CURVES Abstract Only
V. N. Moskalenko, G. A. Semenov, and P. N. Kuzmin *In its* USSR Rept.: Earth Sci. (JPRS-UES-85-006) 19 Jun. 1985 p 46-47 Transl. into ENGLISH from Okeanol. (Moscow), v. 25, no. 1, Jan. - Feb. 1985 (For primary document see N86-12630 03-42)
Avail: NTIS HC A05/MF A01

N86-12680# Joint Publications Research Service, Arlington, Va.
GRAVIMETRIC SURVEYING WITH MI-8 HELICOPTERS Abstract Only
V. Sopolev *In its* USSR Rept.: Earth Sci. (JPRS-UES-85-006) 19 Jun. 1985 p 52 Transl. into ENGLISH from Vozdushnyy Transport (Moscow), 18 Apr. 1985 p 4 (For primary document see N86-12630 03-42)
Avail: NTIS HC A05/MF A01

N86-12681# Joint Publications Research Service, Arlington, Va.
MAGNETIC MINERALS AND CHARACTERISTICS OF NATURAL MAGNETIC STATE OF CORE IN SAATLY SUPERDEEP HOLE IN DEPTH RANGE 3500-7500 METERS Abstract Only
V. I. Bagin and Z. A. Novruzov *In its* USSR Rept.: Earth Sci. (JPRS-UES-85-006) 19 Jun. 1985 p 57 Transl. into ENGLISH from Izv. Akad. Nauk Azerb. SSR, Ser. Nauk o Zemle (USSR), no. 5, 1984 p 61-67 (For primary document see N86-12630 03-42)
Avail: NTIS HC A05/MF A01

N86-12682# Joint Publications Research Service, Arlington, Va.
NEW METHODS FOR INTERPRETING SEISMIC WAVES IN STRATIFIED MEDIA Abstract Only
B. N. Lutsenko *In its* USSR Rept.: Earth Sci. (JPRS-UES-85-006) 19 Jun. 1985 p 58 Transl. into ENGLISH from Geol. Nefti i Gaza (Moscow), no. 1, Jan. 1985 p 48-53 (For primary document see N86-12630 03-42)
Avail: NTIS HC A05/MF A01

N86-12683# Joint Publications Research Service, Arlington, Va.
NEW APPROACH TO SOME PROBLEMS IN SEISMOLOGY Abstract Only
I. G. Kerimov *In its* USSR Rept.: Earth Sci. (JPRS-UES-85-006) 19 Jun. 1985 p 58-59 Transl. into ENGLISH from Izv. Akad. Nauk Azerb. SSR, Ser. Nauk o Zemle (USSR), no. 5, 1984 p 41-46 (For primary document see N86-12630 03-42)
Avail: NTIS HC A05/MF A01

N86-12685# Joint Publications Research Service, Arlington, Va.
FEATURES OF FIELD OF DIRECTIONS AND VELOCITIES OF PROPAGATION OF FRACTURES AT EARTHQUAKE FOCI IN NORTHERN MUYA REGION OF BAYKAL RIFT ZONE Abstract Only

A. V. Solonenko and N. V. Solonenko *In its* USSR Rept.: Earth Sci. (JPRS-UES-85-006) 19 Jun. 1985 p 60 Transl. into ENGLISH from Vulkanol. i Seysmologiya (Moscow), no. 1, Jan. - Feb. 1985 p 98-105 (For primary document see N86-12630 03-42)
Avail: NTIS HC A05/MF A01

N86-12689# Joint Publications Research Service, Arlington, Va.
COMPARISON OF SINGLE-PARAMETER STATISTICAL MODEL WITH RESULTS OF ROUND-THE-CLOCK MEASUREMENT OF LIGHT-SCATTERING MATRICES Abstract Only
M. A. Sviridenkov, G. I. Gorchakov, A. A. Isakov, and V. N. Sidorov *In its* USSR Rept.: Earth Sci. (JPRS-UES-85-006) 19 Jun. 1985 p 73 Transl. into ENGLISH from Izv. Akad. Nauk SSSR: Fiz. Atm. i Okeana (Moscow), v. 21, no. 1, Jan. 1985 p 22-31 (For primary document see N86-12630 03-42)
Avail: NTIS HC A05/MF A01

N86-12690# Joint Publications Research Service, Arlington, Va.
IONIC MECHANICSM OF EXCHANGE OF ADMIXTURES BETWEEN HYDROSPHERE AND ATMOSPHERE Abstract Only
A. V. Savchenko and V. V. Smirnov *In its* USSR Rept.: Earth Sci. (JPRS-UES-85-006) 19 Jun. 1985 p 74 Transl. into ENGLISH from Izv. Akad. Nauk SSSR: Fiz. Atm. i Okeana (Moscow), v. 21, no. 1, Jan. 1985 p 32-41 (For primary document see N86-12630 03-42)
Avail: NTIS HC A05/MF A01

N86-12694# Joint Publications Research Service, Arlington, Va.
EVALUATING INFLUENCE OF WAVES ON DYNAMIC STRUCTURE OF ATMOSPHERIC NEAR-WATER LAYER Abstract Only
K. L. Yegorov *In its* USSR Rept.: Earth Sci. (JPRS-UES-85-006) 19 Jun. 1985 p 76 Transl. into ENGLISH from Izv. Akad. Nauk SSSR: Fiz. Atm. i Okeana (Moscow), v. 20, no. 12, Dec. 1984 p 1183-1188 (For primary document see N86-12630 03-42)
Avail: NTIS HC A05/MF A01

N86-12704# Joint Publications Research Service, Arlington, Va.
FOLDED STRUCTURES IN CENTRAL INDIAN OCEAN TRENCH Abstract Only
O. V. Levchenko, L. R. Merklin, and Yu. P. Neprochnov *In its* USSR Rept.: Earth Sci. (JPRS-UES-85-008) 16 Aug. 1985 p 10 Transl. into ENGLISH from Geotektonika (Moscow), no. 1, Jan. - Feb. 1985 p 15-23 (For primary document see N86-12697 03-42)
Avail: NTIS HC A04/MF A01

N86-12709# Joint Publications Research Service, Arlington, Va.
STRUCTURE OF SEDIMENTARY COVER AND BASEMENT OF SIERRA LEONE RISE DETERMINED FROM COMMON DEPTH POINT SEISMIC (EQUATORIAL ATLANTIC) Abstract Only
V. I. Kara, K. N. Mamoshina, and A. Ye. Shlezinger *In its* USSR Rept.: Earth Sci. (JPRS-UES-85-008) 16 Aug. 1985 p 14 Transl. into ENGLISH from Geotektonika (Moscow), no. 3, May - Jun. 1985 p 38-49 (For primary document see N86-12697 03-42)
Avail: NTIS HC A04/MF A01

N86-12710# Joint Publications Research Service, Arlington, Va.
TECTONIC STRUCTURE OF SHIRSHOV RIDGE (BERING SEA) Abstract Only
Yu. P. Neprochnov, V. V. Sedov, L. R. Merklin, V. P. Zinkevich, O. V. Levchenko, B. V. Baranov, and G. B. Rudnik *In its* USSR Rept.: Earth Sci. (JPRS-UES-85-008) 16 Aug. 1985 p 15 Transl. into ENGLISH from Geotektonika (Moscow), no. 3, May - Jun. 1985 p 21-37 (For primary document see N86-12697 03-42)
Avail: NTIS HC A04/MF A01

N86-12715# Joint Publications Research Service, Arlington, Va.
NONLINEAR INTERACTION BETWEEN SOLITON AND SHORT WAVES IN IDEAL FLUID Abstract Only
Ye. S. Benilov *In its* USSR Rept.: Earth Sci. (JPRS-UES-85-008) 16 Aug. 1985 p 20 Transl. into ENGLISH from Izv. Akad. Nauk SSSR: Fiz. Atm. i Okeana (Moscow), v. 21, no. 4, Apr. 1985 p 417-421 (For primary document see N86-12697 03-42)
Avail: NTIS HC A04/MF A01

N86-12716# Joint Publications Research Service, Arlington, Va.
THE QUESTION OF EARTH EXPANSION AND ITS OCEANIC IMPLICATIONS
Vladimir Neiman *In its* USSR Rept.: Earth Sci. (JPRS-UES-85-008) 16 Aug. 1985 p 21-23 Repr. from Moscow News (Moscow), no. 13 p 10 (For primary document see N86-12697 03-42)
Avail: NTIS HC A04/MF A01

N86-12717# Joint Publications Research Service, Arlington, Va.
KAMCHATKA RADIO TELEMETRIC STATION REGISTERS VOLCANO PULSE Abstract Only
In its USSR Rept.: Earth Sci. (JPRS-UES-85-008) 16 Aug. 1985 p 24 Repr. from TASS (Moscow), v. 5-15 20 May 1985 (For primary document see N86-12697 03-42)
Avail: NTIS HC A04/MF A01

N86-12718# Joint Publications Research Service, Arlington, Va.
LASERS MEASURE DRIFTING MOUNTAINS Abstract Only
In its USSR Rept.: Earth Sci. (JPRS-UES-85-008) 16 Aug. 1985 p 25 Transl. into ENGLISH from TASS (Moscow), no. 0447 GMT, 12 Apr. 1985 (For primary document see N86-12697 03-42)
Avail: NTIS HC A04/MF A01

N86-12720# Joint Publications Research Service, Arlington, Va.
MUON TOMOGRAPHY USED TO STUDY UNDERGROUND ROCK STRUCTURE Abstract Only
A. Alekseyev *In its* USSR Rept.: Earth Sci. (JPRS-UES-85-008) 16 Aug. 1985 p 28 Transl. into ENGLISH from NTR: Probl. i Resheniya (Moscow), 30 Apr. - 13 May 1985 p 6 (For primary document see N86-12697 03-42)
Avail: NTIS HC A04/MF A01

N86-12721# Joint Publications Research Service, Arlington, Va.
UNDERGROUND VOLCANOES DISCOVERED WITH SATELLITE RADAR Abstract Only
In its USSR Rept.: Earth Sci. (JPRS-UES-85-008) 16 Aug. 1985 p 29 Transl. into ENGLISH from Sov. Belorussiya (Minsk), 23 May 1985 p 4 (For primary document see N86-12697 03-42)
Avail: NTIS HC A04/MF A01

N86-12722# Joint Publications Research Service, Arlington, Va.
P-WAVE SPECTRA IN PROBLEM OF DETERMINING DYNAMIC PARAMTERS OF EARTHQUAKE FOCI. STANDARDIZATION OF INITIAL DATA AND PROCEDURES FOR COMPUTING AMPLITUDE SPECTRA Abstract Only
Zh. Ya. Aptekman, S. K. Daragan, D. V. Dolgopolov, A. I. Zakharova, V. M. Zobin, S. Ya. Kogan, O. A. Korchagina, A. G. Moskvina, L. A. Polikarpova, and L. S. Chepkunas *In its* USSR Rept.: Earth Sci. (JPRS-UES-85-008) 16 Aug. 1985 p 30 Transl. into ENGLISH from Vulkanol. i Seysmologiya (Moscow), no. 2, Mar. - Apr. 1985 p 60-70 (For primary document see N86-12697 03-42)
Avail: NTIS HC A04/MF A01

N86-12723# Joint Publications Research Service, Arlington, Va.
PROSPECTS FOR DEVELOPMENT OF SEISMIC PROSPECTING METHODS AND APPARATUS Abstract Only
Yu. V. Timoshin *In its* USSR Rept.: Earth Sci. (JPRS-UES-85-008) 16 Aug. 1985 p 31 Transl. into ENGLISH from Geofiz. Zh. (Kiev), v. 7, no. 2, Mar. - Apr. 1985 p 3-12 (For primary document see N86-12697 03-42)
Avail: NTIS HC A04/MF A01

N86-12725# Joint Publications Research Service, Arlington, Va.
OPTIMAL DENSITY MODEL OF EARTH'S RUST AND UPPER MANTLE ALONG KAMCHATKA-PACIFIC GEOTRAVERSE Abstract Only
M. L. Krasnyy, V. Yu. Kosygin, and V. I. Isayev *In its* USSR Rept.: Earth Sci. (JPRS-UES-85-008) 16 Aug. 1985 p 32-33 Transl. into ENGLISH from Tikhookeanskaya Geol. (Novosibirsk), no. 1, Jan. - Feb. 1985 p 72-84 (For primary document see N86-12697 03-42)
Avail: NTIS HC A04/MF A01

N86-12726# Joint Publications Research Service, Arlington, Va.
VARIATION IN SEISMICITY UNDER INFLUENCE OF LUNAR-SOLAR TIDAL DEFORMATIONS Abstract Only
A. L. Rykunov and V. B. Smirnov *In its* USSR Rept.: Earth Sci. (JPRS-UES-85-008) 16 Aug. 1985 p 33 Transl. into ENGLISH from Izv. Akad. Nauk SSSR: Fiz. Zemli (Moscow), no. 1, Jan. 1985 p 97-103 (For primary document see N86-12697 03-42)
Avail: NTIS HC A04/MF A01

N86-12727# Joint Publications Research Service, Arlington, Va.
ELECTROMAGNETIC EFFECTS IN CRUSTAL FRACTURING Abstract Only
M. B. Gokhberg, I. L. Gufeld, N. I. Gershenzon, and V. A. Pilipenko *In its* USSR Rept.: Earth Sci. (JPRS-UES-85-008) 16 Aug. 1985 p 34 Transl. into ENGLISH from Izv. Akad. Nauk SSSR: Fiz. Zemli (Moscow), no. 1, Jan. 1985 p 72-87 (For primary document see N86-12697 03-42)
Avail: NTIS HC A04/MF A01

N86-12728# Joint Publications Research Service, Arlington, Va.
EXPERIENCE IN BREAKING DOWN GRAVITY FIELD INTO COMPONENTS RESULTING FROM DENSITY HETEROGENEITIES AT VARIOUS DEPTHS (USING NORTH ATLANTIC AND MEDITERRANEAN AS EXAMPLES) Abstract Only
M. Ye. Artemyev, T. M. Babayeva, I. Ye. Voydetskiy, and V. O. Mikhaylov *In its* USSR Rept.: Earth Sci. (JPRS-UES-85-008) 16 Aug. 1985 p 34-35 Transl. into ENGLISH from Izv. Akad. Nauk SSSR: Fiz. Zemli (Moscow), no. 1, Jan. 1985 p 44-52 (For primary document see N86-12697 03-42)
Avail: NTIS HC A04/MF A01

N86-12729# Joint Publications Research Service, Arlington, Va.
HYPOCENTRAL AREAS OF AFTERSHOCKS AND POSSIBLE FAULT SYSTEMS AT FOCI OF TSUNAMI-GENERATING KURIL EARTHQUAKES Abstract Only
S. L. Solovyev and K. A. Kechekezyan *In its* USSR Rept.: Earth Sci. (JPRS-UES-85-008) 16 Aug. 1985 p 35 Transl. into ENGLISH from Izv. Akad. Nauk SSSR: Fiz. Zemli (Moscow), no. 1, Jan. 1985 p 3-15 (For primary document see N86-12697 03-42)
Avail: NTIS HC A04/MF A01

N86-12730# Joint Publications Research Service, Arlington, Va.
METHOD AND RESULTS OF ELECTROMETRIC OBSERVATIONS IN SEISMICALLY ACTIVE REGION Abstract Only
M. G. Ostashevskiy and A. Ya. Sidorin *In its* USSR Rept.: Earth Sci. (JPRS-UES-85-008) 16 Aug. 1985 p 36 Transl. into ENGLISH from Dokl. Akad. Nauk SSSR (Moscow), v. 282, no. 2, May 1985 p 295-299 (For primary document see N86-12697 03-42)
Avail: NTIS HC A04/MF A01

N86-12731# Joint Publications Research Service, Arlington, Va.
SEISMIC EFFECT OF UNDERGROUND BLASTS AND PROBLEM OF ESTIMATING TOTAL EARTHQUAKE ENERGY Abstract Only
M. A. Sadovskiy, O. K. Kedrov, V. A. Laushkin, and I. L. Pasechnik *In its* USSR Rept.: Earth Sci. (JPRS-UES-85-008) 16 Aug. 1985 p 37 Transl. into ENGLISH from Dokl. Akad. Nauk SSSR (Moscow), v. 281, no. 4, Apr. 1985 p 825-829 (For primary document see N86-12697 03-42)
Avail: NTIS HC A04/MF A01

N86-12732# Joint Publications Research Service, Arlington, Va.
TECTONICS OF EASTERN KRONOTSKIY PENINSULA AND FORMATIONAL ASSOCIATION OF BASALTS (KAMCHATKA) Abstract Only
Yu. N. Raznitsin, S. A. Khubunaya, and N. V. Tsukanov *In its* USSR Rept.: Earth Sci. (JPRS-UES-85-008) 16 Aug. 1985 p 37-38 Transl. into ENGLISH from Geotektonika (Moscow), no. 1, Jan. - Feb. 1985 p 88-101 (For primary document see N86-12697 03-42)
Avail: NTIS HC A04/MF A01

N86-12733# Joint Publications Research Service, Arlington, Va.
GEODYNAMICS OF CRUSTAL DILATATION IN TRANSITION AREA FROM ASIAN CONTINENT TO PACIFIC OCEAN Abstract Only
V. P. Utkin *In its* USSR Rept.: Earth Sci. (JPRS-UES-85-008) 16 Aug. 1985 p 38 Transl. into NGLISH from Geotektonika (Moscow), no. 1, Jan. - Feb. 1985 p 73-87 (For primary document see N86-12697 03-42)
Avail: NTIS HC A04/MF A01

N86-12735# Joint Publications Research Service, Arlington, Va.
ATMOSPHERIC TURBULENCE INVESTIGATIONS AT TSIMLYANSK SCIENTIFIC STATION, ATMOSPHERIC PHYSICS INSTITUTE, USSR ACADEMY OF SCIENCES Abstract Only
L. R. Tsvang *In its* USSR Rept.: Earth Sci. (JPRS-UES-85-008) 16 Aug. 1985 p 42-43 Transl. into ENGLISH from Izv. Akad. Nauk SSSR: Fiz. Atm. i Okeana (Moscow), v. 21, no. 4, Apr. 1985 p 339--348 (For primary document see N86-12697 03-42)
Avail: NTIS HC A04/MF A01

47 METEOROLOGY AND CLIMATOLOGY

Includes weather forecasting and modification.

N86-12907 Illinois Univ., Urbana-Champaign.
THE NUMERICAL SIMULATION OF GEOGRAPHIC STORMS Ph.D. Thesis
Michael Morgan Bradley 1985 272 p
Avail: Univ. Microfilms Order No. DA8511583

Observations of winter storms over the Glamorgan Hills of south Wales confirmed the importance of the seeder-feeder mechanism of orographic recipitation enhancement. A dynamic mountain model was used to investigate the hypothesis that mountain wave effects were responsible for increased wind speed sensitivity. The model, is formulated in terrain following coordinates. In addition to representing convective and stratiform cloud processes, the model can accurately simulate moderately nonlinear mountain waves, and is suitable for studing many aspects of orographic storms. It is shown that orographic clouds significantly alter the airflow over hills and, conversely, that mountain waves strongly influence the moist processes. Wind speed, wind shear, atmospheric stability, and relative humidity are all important factors in the complex scale interactions which occur during orographic storms. The results support the hypothesis that certain mountain wave effects greatly increase the wind speed sensitivity of the Bergeron seeder-feeder mechanism. Dissert. Abstr.

N86-12908*# Colorado State Univ., Fort Collins. Dept. of Atmospheric Science.
GLOBAL VIEW OF THE UPPER LEVEL OUTFLOW PATTERNS ASSOCIATED WITH TROPICAL CYCLONE INTENSITY CHANGES DURING FGGE Final Report
Lianshou Chen (Chinese National Meteorological Bureau) and William M. Gray Oct. 1985 133 p refs
(NASA-CR-174407; NAS 1.26:174407; ISSN-0067-0340; AS-Paper-392) Avail: NTIS HC A07/MF A01 CSCL 04B

The characteristics of the upper tropospheric outflow patterns which occur with tropical cyclone intensification and weakening over all of the global tropical cyclone basins during the year long period of the First GARP Global Experiment (FGGE) are discussed. By intensification is meant the change in the tropical cyclone's maximum wind or central pressure, not the change of the cyclone's outer 1 to 3 deg radius mean wind which we classify as cyclone strength. All the 80 tropical cyclones which existed during the FGGE year are studied. Two-hundred mb wind fields are derived from the analysis of the European Center for Medium Range Weather Forecasting (ECMWF) which makes extensive use of upper tropospheric satellite and aircraft winds. Corresponding satellite cloud pictures from the polar orbiting U.S. Defense Meteorological Satellite Program (DMSP) and other supplementary polar and geostationary satellite data are also used. Author

N86-12909# Meteorological Satellite Center, Tokyo (Japan).
METEOROLOGICAL SATELLITE CENTER TECHNICAL NOTE NO. 11, 1985
Mar. 1985 109 p refs In JAPANESE; ENGLISH summaries
(MSC-TN-11; ISSN-0388-9653) Avail: NTIS HC A06/MF A01

Research conducted at the Meteorological Satellite Center in Japan is reported. A case study is presented of the occurrence of linearly ranged Cb-clouds associated with migrating band-shaped cirriform clouds. Clear sky brightness temperature over the north Pacific Ocean is measured with the GMS spacecraft. Brightness temperature differences between GMS-1 and GMS-2 are investigated. The relaying of streteched VISSR data by GMS spacecraft is discussed. Modification of the operational program for GMS-3 is an topic of discussion. An introductory report on the ASDAR (Aircraft to Satellite Data Relay) system is presented. For individual titles, see N86-12910 through N86-12915.

N86-12910# Meteorological Satellite Center, Tokyo (Japan).
OCCURRENCE OF LINEARLY RANGED Cb-CLOUDS ASSOCIATED WITH MIGRATING BAND-SHAPED CIRRIFORM-CLOUDS: A CASE STUDY
Kazufumi Suzuki *In its* Meteorol. Satellite Center Tech. Note, No. 11, 1985 Mar. 1985 p 1-9 refs In JAPANESE; ENGLISH summary (For primary document see N86-12909 03-47)
Avail: NTIS HC A06/MF A01

In the midsummer, linearly ranged Cb-clouds along the southern coast of Japan were often observed in the southwestern leading edge of migrating band-shaped cirriform-clouds. These phenomena (rapidly moving band-shaped cirriform-clouds) are usually related to subsynoptic-scale upper troughs with a weak cold air mass. It is difficult to find out such a weak sub-synoptic-scale upper trough from the conventional data only, however, by tracing the band-shaped cirriform-clouds on the satellite pictures, the trough can be detected easily. Author

N86-12911# Meteorological Satellite Center, Tokyo (Japan).
CLEAR SKY BRIGHTNESS TEMPERATURE OVER THE WESTERN NORTH PACIFIC OCEAN FROM GMS SPACECRAFT
Hideyuki Sasaki *In its* Meteorol. Satellite Center Tech. Note, No. 11, 1985 Mar. 1985 p 11-22 refs In JAPANESE; ENGLISH summary (For primary document see N86-12909 03-47)
Avail: NTIS HC A06/MF A01

An algorithm of extracting clear sky TBB from the radiance histogram in 0.25 deg x 0.25 deg latitude/longitude box of GMS IR data has been prepared and the seasonal features of the TBB in the western north Pacific Ocean have been investigated for about a year from December 1983. The clear sky TBB fluctuates irregularly in comparison with the sea surface temperature of ocean data buoy, which are collected by GMS. The mean success rate of the extraction during the one year is found to be 5 approx. 20% in the area north of 30 deg N, 20 approx. 50% in the area between 10 deg N and 30 deg N, which may correspond to the subtropical high pressure, and 10 to 25% in the zone around 5 deg N, which is associated with the intertropical convergence zone (ITCZ). The magnitude of atmospheric correction, which is defined the difference between the TBB and the ten day mean sea surface temperature which is derived from conventional data, is 4K near Japan in winter and more than 10 K near the ITCZ in summer. Author

N86-12912# Meteorological Satellite Center, Tokyo (Japan).
SIMULTANEOUS OBSERVATION OF GMS AND GMS-2: A STUDY OF THE DIFFERENCE BETWEEN THE BRIGHTNESS TEMPERATURES BY GMS AND THOSE BY GMS-2
Masaaki Togashi, Akinori Ichiki, Taichi Takahashi, and Shuichi Katsuki *In its* Meteorol. Satellite Center Tech. Note, No. 11, 1985 Mar. 1985 p 23-32 refs In JAPANESE; ENGLISH summary (For primary document see N86-12909 03-47)
Avail: NTIS HC A06/MF A01

A simultaneous observation of GMS (160 deg E) and GMS-2 (140 deg E) was conducted on 20th October in 1982. On the basis of the data obtained from this observation at same points along 150 deg E longitude, the difference between the brightness temperatures (TBB's) obtained from two geostationary meteorological satellites was analyzed. As a result it became clear that the average difference of two TBB's derived from 0.2 deg x 0.2 deg areas along 150 deg E longitude was about 1.3 K. Author

N86-12913# Meteorological Satellite Center, Tokyo (Japan).
RELAYING OF THE STRETCHED VISSR DATA BY GMS SPACECRAFT
Takao Suzuki *In its* Meteorol. Satellite Center Tech. Note, No. 11, 1985 Mar. 1985 p 33-42 refs In JAPANESE; ENGLISH summary (For primary document see N86-12909 03-47)
Avail: NTIS HC A06/MF A01

This is the proposal of the streteched VISSR data dissemination method which will enable to relay the VISSR data simultaneously with the VISSR observation. Owing to this effective usage of GMS, hourly VISSR observation will be possible. Summary of the tests conducted at the CDAS is also mentioned in this draft. Author

N86-12914# Meteorological Satellite Center, Tokyo (Japan).
THE MODIFICATION OF THE OPERATIONAL PROGRAM FOR GMS-3
Koichi Kimura and Toshiyuki Kurino *In its* Meteorol. Satellite Center Tech. Note, No. 11, 1985 Mar. 1985 p 43-54 refs In JAPANESE; ENGLISH summary (For primary document see N86-12909 03-47)
Avail: NTIS HC A06/MF A01

GMS-3 was launched in August, 1984 to contribute to improve meteorological service, succeeding to GMS/GMS-2. This report describes the modifications of the softwares in Meteorological Satellite Center in preparation for above satellite change. Before entering the main subject, the outlines of telemetry command processing and HK processing are described. Author

N86-12915# Meteorological Satellite Center, Tokyo (Japan).
INTRODUCTION TO OPERATIONAL ASDAR SYSTEM
Michio Hitani *In its* Meteorol. Satellite Center Tech. Note, No. 11, 1985 Mar. 1985 p 55-60 refs In JAPANESE; ENGLISH summary (For primary document see N86-12909 03-47)
Avail: NTIS HC A06/MF A01

ASDAR (Aircraft to Satellite Data Relay) is the meteorological avionics systems which automatically sample, record and transmit meteorological observations. The operational ASDAR unit transmits additional information compared with the prototype unit which has continued to function still in service. The initial deliveries of the new flight units are expected dy mid-1985. The data collection system will be revised to process the new ASDAR data. Author

N86-12916*# Wisconsin Univ., Milwaukee. Dept. of Geological/Geophysical Sciences.
LARGE-SCALE CIRCULATION DEPARTURES RELATED TO WET EPISODES IN NORTHEAST BRAZIL Final Report
Dhirendra N. Sikdar and James B. Elsner Oct. 1985 70 p refs (Grant NAG5-384)
(NASA-CR-176352; NAS 1.26:176352) Avail: NTIS HC A04/MF A01 CSCL 04B

Large scale circulation features are presented as related to wet spells over northeast Brazil (Nordeste) during the rainy season (March and April) of 1979. The rainy season season is devided into dry and wet periods, the FGGE and geostationary satellite data was averaged and mean and departure fields of basic variables and cloudiness were studied. Analysis of seasonal mean circulation features show: lowest sea level easterlies beneath upper level westerlies; weak meridional winds; high relative humidity over the Amazon basin and relatively dry conditions over the South Atlantic Ocean. A fluctuation was found in the large scale circulation features on time scales of a few weeks or so over Nordeste and the South Atlantic sector. Even the subtropical High SLP's have large departures during wet episodes, implying a short period oscillation in the Southern Hemisphere Hadley circulation. Author

N86-12917*# National Aeronautics and Space Administration. Marshall Space Flight Center, Huntsville, Ala.
ATMOSPHERIC ENVIRONMENT FOR SPACE SHUTTLE

(STS-51B) LAUNCH
G. L. Jasper, D. L. Johnson, C. K. Hill, and G. W. Batts (Computer Sciences Corp., Huntsville, Ala.) Jul. 1985 45 p refs
(NASA-TM-86525; NAS 1.15:86525) Avail: NTIS HC A03/MF A01 CSCL 04B

A summary of selected atmospheric conditions observed near space shuttle STS-51B launch time on April 29, 1985, at Kennedy Space Center Florida is presented. Values of ambient pressure, temperature, moisture, ground winds, visual observations (cloud), and winds aloft are included. The sequence of prelaunch Jimsphere measured vertical wind profiles is given. The final atmospheric tape, which consists of wind and thermodynamic parameters versus altitude, for STS-51B vehicle ascent was constructed. The STS-51B ascent atmospheric data tape was constructed by Marshall Space Flight Center's Atmospheric Sciences Division to provide an internally consistent data set for use in post flight performance assessments. Author

N86-12918*# Pennsylvania State Univ., University Park. Dept. of Meteorology.
THE NATURE OF SYMMETRIC INSTABILITY AND ITS SIMILARITY TO CONVECTIVE AND INERTIAL INSTABILITY Contractor Report, 1 Jul. 1980 - 31 Mar. 1985
Quin Xu and J. H. E. Clark Washington NASA Oct. 1985 30 p refs
(Contract NAS8-33797)
(NASA-CR-3945; NAS 1.26:3945) Avail: NTIS HC A03/MF A01 CSCL 04B

It is shown that there exists a local similarity among SI (Symmetric Instability), BI (Buoyancy or Convective Instability), and II (Inertial Instability) even for fully nonlinear viscous motion. The most unstable slope angles for SI and Moist SI motions are analyzed based on parcel energetics. These considerations also suggest qualitatively that CSI (Conditional SI) circulations will be slantwise and lie between the moist most unstable slope and dry least stable slope of the basic state. Author

N86-12919*# Jet Propulsion Lab., California Inst. of Tech., Pasadena.
ADVANCED MOISTURE AND TEMPERATURE SOUNDER (AMTS) BASELINE 5 STUDY REPORT
Nathan L. Evans, Jr. and Valerie G. Wright 15 Sep. 1985 437 p
(Contract NAS7-918)
(NASA-CR-176331; JPL-Pub-85-61; NAS 1.26:176331) Avail: NTIS HC A19/MF A01 CSCL 04B

An Advanced Moisture and Temperature Sounder (AMTS) passive infrared atmospheric sounding system is described. Instrument requirements are developed. Parametric and scaling equations for a grating spectrometer instrument approach are developed which define detector noise limited performance in terms of instrument, orbit, and spatial coverage parameters. Instrument design criteria are developed and a baseline instrument design is presented. Error sources are identified and corresponding system error component values are estimated. Within narrow limits, the highest level of performance achievable with a stand alone infrared sounder using current state of the art technology is established. Additional trade offs necessary to establish a reasonably optimal system design in terms of performance, cost, and risk are identified. Author

N86-12920# Massachusetts Inst. of Tech., Lexington.
WEATHER RADAR STUDIES Quarterly Technical Summary Report, 1 Oct. - 31 Dec. 1984
J. E. Evans 31 Dec. 1984 48 p
(Contract DTFA-01-80-Y-10546)
(AD-A157093; FAA-PM-85-09) Avail: NTIS HC A03/MF A01 CSCL 04/2

THe test-bed Doppler weather radar integration testing continued in Olive Branch, Mississippi after the lightning strike damage was repaired. Preliminary tests indicate that the objective of 50-dB clutter suppression is being obtained in the field and that the system sensitivity is very close to the NEXRAD specification. Installation of an improved lightning protection system neared completion. The Lincoln mesonet continued to obtain useful data throughout October and November. A strong microburst with peak winds so 68 mph was recorded in the immediate vicinity of Memphis International Airport on 20 October. The mesonet and LLWSAS data from Memphis, and Doppler weather radar data from the National Center for Atmospheric Research JAWS program and the National Severe Storms Laboratory, are being analyzed to develop low-altitude wind shear detection algorithms. Clutter measurements were carried out at Eglin Air Force Base/Ft. Walton Beach Airport, the Memphis Airport, and the Olive Branch, Mississippi test site. Work continued on the development of weather radar products for the Central Weather Processor. This work focused on tracker refinement studies and NEXRAD-compatible processing of the existing reflectivity-only weather radars. GRA

N86-12921# Naval Postgraduate School, Monterey, Calif.
WEATHER ANALYSIS PROGRAMS USING HP-41CV Technical Report, Oct. 1983 - Sep. 1984
C. H. Wash and L. A. Spray Nov. 1984 44 p
(AD-A157389; NPS63-84-008) Avail: NTIS HC A03/MF A01 CSCL 04/2

Several synoptic problems, previously solved by graphical overlays, can be solved with a programmable calculator. The HP-41CV hand-held calculator is used to determine surface winds, the probability of average rainfall for a regional area (Monterey, California), contrail formation, and the lifting condensation level from surface data. GRA

N86-12922*# Naval Postgraduate School, Monterey, Calif.
OBSERVATIONAL-NUMERICAL STUDY OF MARITIME EXTRATROPICAL CYCLONES USING FGGE (FIRST GARP GLOBAL EXPERIMENT) DATA Final Report, Jun. 1982 - May 1985
R. L. Elsberry, C. H. Wash, C. S. Liou, and J. E. Peak May 1985 42 p
(NASA Order S-10663-C)
(NASA-CR-176297; NAS 1.26:176297; AD-A157390; NPS63-85-001) Avail: NTIS HC A03/MF A01 CSCL 04B

Analyses of First GARP Global Experiment (FGGE) data have been used to study three cases of maritime extratropical cyclone development. It has been demonstrated that these FGGE analyses are consistent with the observations through synoptic comparisons and satellite interpretations. Quasi-Lagrangian diagnostic budgets of mass, vorticity, angular momentum and heat have been computed in pressure coordinates for observed and model-generated cyclones. The roles of jet streaks and small static stability in the lower troposphere during rapid development of maritime cyclones have been documented. Vertical circulation trends in the mass budget are consistent with the sea-level pressure evolution in each case. Inward transport of vorticity due to the jet streak coincides with the rapid development phase. Vorticity budgets of these maritime cyclones appear to be consistent with earlier studies of continental cyclones. To complement the observational studies, similar diagnostic studies have been done for numerical simulations of maritime cyclogenesis under straight upper-level flow. These studies demonstrate that similar physical mechanisms are involved in the simulated storms as were found in the FGGE-based studies. Two sets of numerical model predictions from the FGGE analyses were examined for an explosively deepening cyclone over the western North Pacific Ocean. Both models predicted the most rapid deepening phase too early and resulted in too low sea-level pressures. GRA

N86-12923# Air Force Inst. of Tech., Wright-Patterson AFB, Ohio.
STATISTICAL EVALUATION OF FORECASTS OVER THE LOW-LATITUDES M.S. Thesis
C. P. Zeizer Aug. 1985 82 p
(AD-A157926) Avail: NTIS HC A05/MF A01 CSCL 04/2

A series of experiments, designed to study single level predictions with a barotropic and a primitive equation model has been carried out for 15 June to 15 September 1979 utilizing FGGE (First GARP Global Experiment) data sets. The level chosen for this study is 700 mb with two separate domains being covered. Domain 1 covered a region from 75 W and 20 S to 40 N, while

Domain 2 covered a region from 75 W to 30 W and 20 S to 45 N. This study includes a discussion of tropical storm Claudette and also an analysis of the predictions using root mean square vector wind errors and absolute correlations. The results of 93 experiments show that the simple model based on the conservation of vorticity performs worse than persistence for all time periods in Domain 1 and 2. The model based on the conservation of potential vorticity performs better than persistance for up to one day in Domain 1, and up to 4 days in Domain 2. Past experiments and performance are compared. These included the following regions: the Atlantic and West Africa during the northern summer; a region including the Indian Ocean, Indonesia and the central Pacific Ocean during the northern winter; and a similar region during the northern summer. In general, useful skill of all the regions considered is exhibited only over the following: Central America and South America during northern summer to 4 days, West Africa and eastern Atlantic during northern summer to 4 days, central Pacific Ocean during northern winter to 1 day.
GRA

N86-12924# Manchester Univ. (England). Dept. of Physics.
RADIATION FOG MODELING Interim Status Report
J. Latham Sep. 1981 8 p
(Contract DAJA37-81-C-0746)
(AD-A157971; ISR-1) Avail: NTIS HC A02/MF A01 CSCL 04/2

The radiation fog model is being developed in an attempt to predict the initiation, development and characteristics of these fogs. The model is primarily based upon three important processes which interact to determine whether a fog will form in preference to haze development and what characteristics and fluctuations are likely to occur if a fog does form. These processes are: (1) radiative exchanges; (2) droplet growth and CCN spectra; and (3) turbulence characteristics. The exact nature of these interactions is poorly understood and consequently have not yet been fully included in existing models. To date, therefore, accurate simulation of all fog characteristics on various temporal and spatial scales has not been achieved. Data from recent field studies, especially Meppen, have produced results which will enable not only the model to be fully tested, but also greatly assist in the understanding of radiation fog, which will in turn allow more accurate and detailed models to be developed.
GRA

N86-12925# Air Force Inst. of Tech., Wright-Patterson AFB, Ohio.
SQUALL AND CLOUD LINES AS STRUCTURAL COMPONENTS OF AN ARABIAN SEA CONVECTIVE CLOUD CLUSTER M.S. Thesis
C. L. Benson, Jr. 1985 101 p
(AD-A157973; AFIT/CI/NR-85-83T) Avail: NTIS HC A06/MF A01 CSCL 04/2

This research has several objectives. First, it attempts to present a description of the kinematic, thermal, and cloud structure of an eastern Arabian Sea convective cloud cluster. Secondly, this research will determine the horizontal location of updrafts, downdrafts, and gust fronts in relation to observed convection. The last objective is to determine the extent of boundary layer modification by convective. Careful study of all available data revealed several squall lines (as well as other types of convective) embedded in the larger scale cloud cluster. Numerous differences were observed between the squall lines examined in this study and squall lines observed during the Global Atmospheric Research Program's Atlantic Tropical Experiments (GATE). The main differences include: Arabian Sea squall lines were quasi-stationary. while GATE squall lines were moving; Arabian Sea squall lines existed in a more highly sheared environment than GATE squall lines were moving; Arabian Sea squall lines existed in a more highly sheared environmental than GATE convection; the low-level inflow air in Arabian Sea squall lines could be influenced by subsidence from a trailing anvil cloud, while GATE convection's low-level inflow generally was not. This thesis shows exclusively that boundary layer influences caused by convection over the Arabian Sea must be considered when attempting to describe (either qualitatively or numerically) Indian southwest monsoonal rainfall.
GRA

N86-12926# Coastal Engineering Research Center, Vicksburg, Miss.
ANNUAL DATA SUMMARY FOR 1981 CERC (COASTAL ENGINEERING RESEARCH CENTER) FIELD RESEARCH FACILITY Final Technical Report
H. C. Miller, W. E. Grogg, Jr., J. R. Rottier, M. W. Leffler, and C. R. Townsend, III Jun. 1985 262 p
(AD-A158143) Avail: NTIS HC A12/MF A01 CSCL 04/2

The annual data summary for CERC (Coastal Engineering Research Center) field research facility discusses the following topics: climatological summary: climate, waves, nearshore currents, tides and water level changes, sediment size, and bathymetry; instrumentation: wave gages, tide gages, and meteorological instruments; data collection and analysis techniques: digital wave data, tide and water level data, meteorological data, visual observations, bathymetric and pier surveys, and sediment data, photographic data; and data availability and results: meteorological data, wave data, current data, tide and water level data, water characteristics, survey data, sediment data, and photography.
Author

N86-12927# National Environmental Satellite Service, Washington, D. C. Assessment and Information Services Center.
COMPARISON OF BOUNDARY LAYER WINDS FROM NWS LFM (NATIONAL WEATHER SERVICE'S LIMITED-AREA FINE-MESH) OUTPUT AND INSTRUMENTED BUOYS
R. W. Reeves and P. J. Pytlowany May 1985 51 p
(PB85-226439; NOAA-TM-NESDIS-AISC-2) Avail: NTIS HC A04/MF A01 CSCL 08C

Measurements of the surface wind by 15 instrumented buoys are compared with boundary layer winds predicted by the National Weather Service's (NWS) Limited-area Fine-mesh Model (LFM). The buoy observations at 0600 GMT and 1800 GMT are selected and compared directly to the 6-hour LFM predictions for the nearest grid point; the predictions are made twice-daily and are valid for those times. The LFM 12-hourly distributions are skewed toward higher speeds relative to the observations, but the direction distributions show very good agreement, suggesting the usefulness of the LFM data base to construct climatologies.
GRA

N86-12928# Arizona Univ., Tucson. Dept. of Hydrology and Wate Resources.
EVALUATION OF THE NWS (NATIONAL WEATHER SERVICE) SOIL MOISUTRE ACCOUNTING MODEL FOR AUTOMATED FLASH FLOOD FORECASTING IN SMALL ARID AND SEMI-ARID WATERSHEDS Report, 1983-1984
S. Sorooshian 1985 45 p Prepared in cooperation with Arizona Water Resources Research Center
(PB85-229722; USGS/G-828-08) Avail: NTIS HC A03/MF A01

An analysis of the NWS model and the hydrological characteristics of small arid watersheds indicated that modifications to the model would be necessary for arid zone applications. One modification, based on the absence or insigificance of base-flow in the typical small, arid watershed, involves removal of the lower zone reservoirs and replacement of the complex percolation function by a proportional loss rate. In light of the extreme rainfall intensities and rapid runoff rates associated with desert floods, the infiltratoin representation was revised so that overland flow may begin before the upper zone is saturated and so that maximum infiltration capacity is a parameter. Other modifications include the use of watershed subcells and routing which simulates percolation of flows into the channel bed. The amount of data required for model calibration can be reduced by the use of the modified model in conjunction with recommended calibration procedures.
GRA

N86-12929# National Oceanic and Atmospheric Administration, Boulder, Colo. Environmental Sciences Group.
FIRST EXPERIMENT IN FORECASTING COOL-SEASON WEATHER WITH THE PROFS SYSTEM
P. Schultz, M. C. McCoy, R. E. McGowan, T. W. Schlatter, and J. S. Wakefield Apr. 1985 32 p
(PB85-230605; NOAA-TM-ERL-EST-16) Avail: NTIS

HC A03/MF A01 CSCL 04B

The Program for Regional Observing and Forecasting Services (PROFS) conducted a winter weather forecasting exercise from February through April of 1984. This was PROFS' first attempt at applying advanced data processing and display technologies to winter weather forecasting problems. Eleven events were forecast. The primary objective of the exercise was to introduce the PROFS staff and the local contingent of meteorologists to winter weather forecasting and procedures. The emphasis was on understanding some of the mesoscale aspects of winter weather and not on maximizing the accuracy of the forecasts. In addition to conventional satellite, rawinsonde, and surface data, the forecasters had access to data from the PROFS mesonet and from the Colorado wind profiling system. GRA

N86-12930# National Weather Service, Salt Lake City, Utah.

ANNUAL DATA AND VERIFICATION TABULATION EASTERN NORTH PACIFIC TROPICAL STORMS AND HURRICANES, 1984

E. B. Gunther and R. L. Cross Apr. 1985 32 p Prepared in cooperation with Eastern Pacific Hurricane Center, San Francisco, Calif.

(PB85-187888; NOAA-TM-NWS-WR-189) Avail: NTIS

HC A03/MF A01 CSCL 04B

Eastern north Pacific tropical cyclone activity is discussed. Tropical cyclone prediction models used by Eastern Pacific Hurricane Center (EPHC) forecasters are included. Verification statistics for the 1964 season are shown. Best track, operational positions, and position errors are also included. GRA

N86-12931# National Oceanic and Atmospheric Administration, Boulder, Colo. Environmental Sciences Group.

MESOSCALE CONVECTIVE SYSTEMS: A SATELLITE-DATA-BASED CLIMATOLOGY

D. L. Bartels, J. M. Skradski, and R. D. Menard Dec. 1984 65 p refs

(PB85-186862; NOAA-TM-ERL-ESG-8) Avail: NTIS

HC A04/MF A01 CSCL 04B

The occurrence of significant mesoscale Convective Systems (MCSs) over the central United States during April through July is established on the basis of satellite imagery. Track figures for previously documented 1978 to 1982 Mesoscale Convective Complexes (MCCs), as well as smaller cloud clusters and convective lines that occurred during 1979 to 1983, are presented. Other climatological attributes, including diurnal characteristics and average durations, are extracted from a tabular documentation of more than 500 mesosystems. This satellite-data-based climatology of convective weather systems may be used, in conjunction with climatologies of severe thunderstorms, as a research resource to help to improve the authors understanding of central United States convective weather. GRA

N86-12932# National Weather Service, Garden City, N.Y.

COMPARISON AMONG VARIOUS THERMODYNAMIC PARAMETERS FOR THE PREDICTION OF CONVECTIVE ACTIVITY

H. M. Stone Apr. 1985 19 p refs

(PB85-208217; NOAA-TM-NWS-ER-68) Avail: NTIS

HC A02/MF A01 CSCL 04B

The development of convection requires a sufficient moisture source, unstable air, and a triggering mechanism. The authors are concerned here only with the effect of atmospheric instability on convection. A variety of different stability indices are now in use, the most recent of these being the energy indices, EI1 and EI2. The performance of the lifted, K, Showalter, EI1 and EI2 stability indices was investigated. In addition to the investigation of the performance of the various stability indices, correlation between the heights of radar tops and occurrence of severe weather were also examined. Correlation coefficients were computed for radar top heights above ground level, above tropopause level, and above equilibrium level. GRA

N86-12933# Environmental Protection Agency, Research Triangle Park, N.C. Atmospheric Sciences Research Lab.

MODELING THE DIURNAL VARIATION OF METEORLOGICAL VARIABLES WITHIN THE BOUNDARY LAYER: PRELIMINARY COMPARISON RESULTS

J. S. Irwin May 1985 28 p refs

(PB85-196349; EPA-600/D-85/097) Avail: NTIS

HC A03/MF A01 CSCL 04B

Mean monthly patterns of the diurnal variation of the wind, temperature and turbulence over the lower 300 m are computed, using data collected on the 365 m WJBF-TV meteorological mast located 11 km southeast of Augusta, Georgia. A review is presented of the seasonal variations observed in these patterns for the five-year period from 1975 through 1979. Clearly evident were the seasonal variations in the 10-m values of wind and temperature. Little seasonal variation was evident in the diurnal profiles of turbulence. Comparison results are presented of the diurnal patterns for June 1976 simulated by a meteorological processor using as input the hourly National Weather Service reports form Augusta and twice-daily radiosonde reports from Athens, Georgia. GRA

N86-12934# National Weather Service, Garden City, N.Y.

CORRELATION AND REGRESSION EQUATION PROGRAM REGRS

H. M. Stone May 1985 34 p

(PB85-213353; NOAA-NWS-ERCP-31) Avail: NTIS

HC A03/MF A01 CSCL 04B

In focal research studies, there is frequently a need to compute correlation coefficients between some variable, which is to be predicted, and various other variables which may serve as predictors. After an appropriate data base has been collected, this program computes linear correlation coefficients between the dependent variable to be predicted and all the possible predictor variables, and also computes a multiple correlation coefficient using all the predictor variables together and partial correlations for each of the predictors. In addition, a linear regression equation is obtained relating the predictors to the dependent variable. The program also has the capability of going through a screening process, whereby one variable at a time is dropped from the regression equation, eliminating those with lowest partial correlation coefficients first, until only one predictor variable remains. Author (GRA)

N86-12935# National Weather Service, Garden City, N.Y.

SCATTER DIAGRAM AND HISTOGRAM PROGRAM - SCATR

H. M. Stone May 1985 41 p

(PB85-213346; NOAA-NWS-ERCP-32) Avail: NTIS

HC A03/MF A01 CSCL 04B

One of the laborious tasks usually required for statistical studies is the plotting of scatter diagrams and frequency histograms. These two types of displays are usually needed to visualize the relationship between two or more variables and they usually provide more useful information than a table of correlation coefficients between the variables. For example, such a diagram may reveal a good relationship between some variables over a limited range of the data, while correlation coefficients computed over the full range may indicate a poor relationship. All the conclusion of the research study considerable labor must usually be devoted to drafting finished figures of this type for publication. The preparation of these diagrams has now been automated by the program SCATR, which creates them as an AFOS graphic product. The size and dimensions of the graphic are specified by the user, so that the final product is suitable for publication. Author (GRA)

N86-12936# National Weather Service, Silver Spring, Md. Techniques Development Lab.

OBJECTIVE MAP ANALYSIS FOR THE LOCAL AFOS MOS (AUTOMATION OF FIELD OPERATIONS AND SERVICES MODEL OUTPUT STATISTICS) PROGRAM

H. R. Glahn, T. L. Chambers, W. S. Richardson, and H. P. Perrotti Mar. 1985 41 p

(PB85-212884; NOAA-TM-NWS-TDL-75) Avail: NTIS

HC A03/MF A01 CSCL 04B

A computer program was developed which can be used to analyze either spatially continuous or discontinuous hydrometeorological data. It is being used extensively in the development of a local MOS capability, and has been specifically turned for the analysis of 13 meteorological variables. The Cressman successive correction procedure, used for continuous fields, and the nearest neighbor procedure, used for discontinuous fields, and their implementation in the computer program are discussed. Control parameters and options are discussed, and several examples are presented. GRA

N86-12937# National Weather Service, Washington, D.C. Climate Analysis Center.
MONTHLY AND SEASONAL WEATHER OUTLOOK FOR MID-MAY TO MID-JUNE 1985, VOLUME 39, NUMBER 10, MAY 14, 1985
14 May 1985 10 p
(PB85-204261) Avail: NTIS HC A02/MF A01 CSCL 04B

The report describes weather observations for marine areas. Articles included are: comparison between ship and buoy climatologies; and Great Lakes navigation season, 1983; Marine observation programs; tips to the radio officer; and Marine weather review. GRA

N86-12631# Joint Publications Research Service, Arlington, Va.
METEOROLOGICAL CENTER'S FORECASTS AID VENUS PROBE TRACKING Abstract Only
M. Dmitruk *In its* USSR Rept.: Earth Sci. (JPRS-UES-85-006) 19 Jun. 1985 p 1 Transl. into ENGLISH from Sots. Ind. (Moscow), 23 Mar. 1985 p 3 (For primary document see N86-12630 03-42)
Avail: NTIS HC A05/MF A01

N86-12632# Joint Publications Research Service, Arlington, Va.
DIAGNOSIS OF WEATHER STATES IN WINTER OF 1980-1981 Abstract Only
G. P. Kurbatkin *In its* USSR Rept.: Earth Sci. (JPRS-UES-85-006) 19 Jun. 1985 p 2 Transl. into ENGLISH from Izv. Akad. Nauk SSSR: Fiz. Atm. i Okeana (Moscow), v. 20, no. 11, Nov. 1984 p 1011-1016 (For primary document see N86-12630 03-42)
Avail: NTIS HC A05/MF A01

N86-12633# Joint Publications Research Service, Arlington, Va.
MAIN PROBLEMS IN CLIMATE MONITORING (DIAGNOSIS) Abstract Only
G. V. Gruza, K. G. Rubinshteyn, B. A. Birman, and V. N. Razuvayev *In its* USSR Rept.: Earth Sci. (JPRS-UES-85-006) 19 Jun. 1985 p 2 Transl. into ENGLISH from Izv. Akad. Nauk SSSR: Fiz. Atm. i Okeana (Moscow), v. 20, no. 11, Nov. 1984 p 1017-1026 Original language document was announced in IAA as A85-17976 (For primary document see N86-12630 03-42)
Avail: NTIS HC A05/MF A01

N86-12634# Joint Publications Research Service, Arlington, Va.
USE OF METHOD OF CANONICAL CORRELATIONS FOR ANALYSIS OF CLIMATIC SERIES Abstract Only
M. S. Tatarskaya and M. I. Fortus *In its* USSR Rept.: Earth Sci. (JPRS-UES-85-006) 19 Jun. 1985 p 3 Transl. into ENGLISH from Izv. Akad. Nauk SSSR: Fiz. Atm. i Okeana (Moscow), v. 20, no. 11, Nov. 1984 p 1027-1034 (For primary document see N86-12630 03-42)
Avail: NTIS HC A05/MF A01

N86-12635# Joint Publications Research Service, Arlington, Va.
EMPIRICAL ANALYSIS OF DIRECT AND INVERSE RELATIONSHIPS BETWEEN MACROSCALE CHARACTERISTICS OF ATMOSPHERIC PROCESSES IN NORTHERN HEMISPHERE AND THERMAL STATE OF NORTH ATLANTIC Abstract Only
M. I. Yudin, V. M. Mirvis, and I. Ye. Chuvashina *In its* USSR Rept.: Earth Sci. (JPRS-UES-85-006) 19 Jun. 1985 p 3-4 Transl. into ENGLISH from Izv. Akad. Nauk SSSR: Fiz. Atm. i Okeana (Moscow), v. 20, no. 11, Nov. 1984 p 1035-1041 (For primary document see N86-12630 03-42)
Avail: NTIS HC A05/MF A01

N86-12636# Joint Publications Research Service, Arlington, Va.
ATMOSPHERIC AEROSOL AND ITS EFFECTS ON CLIMATE Abstract Only
K. Ya. Kondratyev and M. A. Prokofyev *In its* USSR Rept.: Earth Sci. (JPRS-UES-85-006) 19 Jun. 1985 p 4-5 Transl. into ENGLISH from Izv. Akad. Nauk SSSR: Fiz. Atm. i Okeana (Moscow), v. 20, no. 11, Nov. 1984 p 1055-1063 (For primary document see N86-12630 03-42)
Avail: NTIS HC A05/MF A01

N86-12637# Joint Publications Research Service, Arlington, Va.
INFLUENCE OF POWER ENGINEERING ON CLIMATE Abstract Only
V. A. Legasov, I. I. Kuzmin, and A. N. Chernoplekov *In its* USSR Rept.: Earth Sci. (JPRS-UES-85-006) 19 Jun. 1985 p 6 Transl. into ENGLISH from Izv. Akad. Nauk SSSR: Fiz. Atm. i Okeana (Moscow), v. 20, no 11, Nov. 1984 p 1089-1103 (For primary document see N86-12630 03-42)
Avail: NTIS HC A05/MF A01

N86-12638# Joint Publications Research Service, Arlington, Va.
RECENT CHANGES IN CLIMATE AND WORLD WATER BALANCE Abstract Only
S. G. Dobrovolskiy and R. K. Klinge *In its* USSR Rept.: Earth Sci. (JPRS-UES-85-006) 19 Jun. 1985 p 6 Transl. into ENGLISH from Izv. Akad. Nauk SSSR: Ser. Geogr. (Moscow), no. 1, Jan. - Feb. 1985 p 31-38 (For primary document see N86-12630 03-42)
Avail: NTIS HC A05/MF A01

N86-12639# Joint Publications Research Service, Arlington, Va.
CLIMATICALLY ACTIVE TRACE GASES IN ATMOSPHERE Abstract Only
I. L. Karol *In its* USSR Rept.: Earth Sci. (JPRS-UES-85-006) 19 Jun. 1985 p 5 Transl. into ENGLISH from Izv. Akad. Nauk SSSR: Fiz. Atm. i Okeana (Moscow), v. 20, no. 11, Nov. 1984 p 1064-1074 Original language document was announced in IAA as A85-17981 (For primary document see N86-12630 03-42)
Avail: NTIS HC A05/MF A01

N86-12640# Joint Publications Research Service, Arlington, Va.
ESTIMATE OF RADIATION-CLIMATIC EFFECTS OF NATURAL AND ANTHROPOGENIC AEROSOL Abstract Only
N. I. Manuylova, V. K. Petukhov, T. A. Tarasova, and Ye. M. Feygelson *In its* USSR Rept.: Earth Sci. (JPRS-UES-85-006) 19 Jun. 1985 p 5 Transl. into ENGLISH from Izv. Akad. Nauk SSSR: Fiz. Atm. i Okeana (Moscow), v. 20, no. 11, Nov. 1984 p 1075-1080 (For primary document see N86-12630 03-42)
Avail: NTIS HC A05/MF A01

N86-12698# Joint Publications Research Service, Arlington, Va.
SOME RESULTS OF STUDY OF BLOCKING LAYERS ON DAYS WITH VERTICALLY DEVELOPED CLOUD COVER OF CAUCASUS-CASPIAN REGION ON BASIS OF AEROSPACE INFORMATION Abstract Only
A. A. Gorchiyev and T. D. Agayev *In its* USSR Rept.: Earth Sci. (JPRS-UES-85-008) 16 Aug. 1985 p 1 Transl. into ENGLISH from Izv. Akad. Nauk Azerbaydzhanskoy SSR, Ser. Nauki o Zemle (USSR), no 6, 1984 p 111-118 (For primary document see N86-12697 03-42)
Avail: NTIS HC A04/MF A01

N86-12736# Joint Publications Research Service, Arlington, Va.
HUMIDITY PROFILE MESUREMENTS IN ATMOSPHERIC LOWER LAYER BY SPONTANEOUS RAMAN SCATTERING METHOD Abstract Only
O. A. Bukin, S. Yu. Stolyarchuk, and V. A. Tyapkin *In its* USSR Rept.: Earth Sci. (JPRS-UES-85-008) 16 Aug. 1985 p 43-44 Transl. into ENGLISH from Zh. Prikl. Spektroskopii (Minsk), v. 42, no. 4, Apr. 1985 p 631-636 Original language document was announced in IAA as A85-38572 (For primary document see N86-12697 03-42)
Avail: NTIS HC A04/MF A01

N86-12737# Joint Publications Research Service, Arlington, Va.
SOME CHARACTERISTICS OF TRANSMISSION BY THIN CLOUDS IN VISIBLE AND INFRARED SPECTRAL REGIONS Abstract Only
Yu. S. Georgiyevskiy and A. Kh. Shukurov *In its* USSR Rept.: Earth Sci. (JPRS-UES-85-008) 16 Aug. 1985 p 44-45 Transl. into ENGLISH from Izv. Akad. Nauk SSSR: Fiz. Atm. i Okeana (Moscow), v. 21, no. 4, Apr. 1985 p 397-402 (For primary document see N86-12697 03-42)
Avail: NTIS HC A04/MF A01

48 OCEANOGRAPHY

Includes biological, dynamic and physical oceanography; and marine resources.

N86-12938 Michigan Univ., Ann Arbor.
WAVE-CURRENT AND WAVE-TOPOGRAPHIC INTERACTIONS USING SEASAT SYNTHETIC APERTURE RADAR OBSERVATIONS AND ANALYTICAL OCEAN MODELS Ph.D. Thesis
Yun-Chi Tseng 1985 205 p
Avail: Univ. Microfilms Order No. DA8512527

This dissertation investigates the capability of SEASAT synthetic aperture radar (SAR) to detect wave-current and wave-topographic interactions in the Gulf Stream area by analyzing the refracted wave directions obtained from different methods. Four study methods have been employed: the optical Fourier transform (OFT), the fast Fourier transform (FFT), the kinematical, and the dynamical methods. The first two methods were applied to analyze the SAR data for estimating the dominant wave directions. The last two methods were applied to calculate the refracted wave directions for comparison with those measured by the OFT and FFT analyses. General theories of wavecurrent and wave-topographic interactions were formulated by assuming the ocean waves to be linear and steady-state. The SAR data from Rev. 0974 on September 3, 1978 over the Gulf Stream off Cape Hatteras, N.C. were utilized. Some 49 study positions located within this study area were chosen for this investigation. Results showed that the refracted wave directions obtained from the analyses of SAR data, from both the OFT and FFT methods, were in reasonable agreement with those obtained from kinematical and dynamical methods. Dissert. Abstr.

N86-12939 Harvard Univ., Cambridge, Mass.
FLOW RATES IN THE EAST PACIFIC RISE (21 DEG N) HOT SPRINGS, AND NUMERICAL INVESTIGATIONS OF TWO REGIMES OF HYDROTHERMAL CIRCULATION Ph.D. Thesis
David Rhys Converse 1985 473 p
Avail: Univ. Microfilms Order No. DA8510197

Flow rates of 0.7 to 2.4 m/s were measured in the hot springs on the East Pacific Rise (21 deg N). It is estimated that the Southwest, National Geographic, and the OBS vents collectively discharge 2 x 1 10 to the 8th power watts and 150 kg H2O/s. The rate of heat transport exceeds the steady-state rate of heat input to the ridge system. The lifetimes of hot springs can not exceed 40,000 years because of the limited heat supply. Mechanical or chemical clogging of the flow routes may shorten these lifetimes significantly. It is predicted that less than 3% of the sulfide particle debouched by the hot springs settle near the vents. Large massive sulfide deposits (ex. Mavrouni) must form under different conditions. A new model of the time-averaged transfer of heat and momentum predicts the linear variation of Nusselt number and root-mean-square velocity with Rayleigh number observed in numerical experiments of two-dimensional convection in a homogeneous porous medium with a closed top. Dissert. Abstr.

N86-12940 Northwestern Univ., Evanston, Ill.
MOTION OF THE PACIFIC PLATE RELATIVE TO THE HOTSPOTS SINCE THE JURASSIC AND MODEL OF OCEANIC PLATEAUS OF THE FARALLON PLATE Ph.D. Thesis
Laurel Jean Henderson 1985 329 p
Avail: Univ. Microfilms Order No. DA8511827

A model of the motion since the Jurassic of the Pacific plate relative to the hotspots predicts the formation of nearly all the midplate and excess on-rise volcanism of the Pacific plate. All the aseismic ridges, seamount chains, and even the hitherto unexplained oceanic plateaus of the Pacific plate were produced by hotspots that remained nearly stationary relative to each other. During late Jurassic and Cretaceous time (ca. 155 to 80 Ma) the Pacific plate oceanic plateaus were produced by still-active hotspots that were located near the risecrest surrounding the Pacific plate. This model uses several newly proposed hotspots, which have tracks that are visible on maps of residual depth and gravity anomalies, but have no known active volcanos. Edifices formed near the risecrests on the Pacific plate were likely to have had counterparts on the Farallon and Kula plates. It is proposed that an Early Cretaceous aseismic-ridge of the Farallon plate was subducted beneath the United States Cordillera during the Laramide orogeny. Dissert. Abstr.

N86-12941# SACLANT ASW Research Center, La Spezia (Italy).
SACLANTCEN'S USE OF SCUBA DIVING IN OCEANOGRAPHIC AND ACOUSTIC RESEARCH
F. deStrobel, T. Akal, and O. F. Hastrup 15 Dec. 1984 20 p
Original contains color illustrations
(AD-A156714; SACLANTCEN-SM-175) Avail: NTIS HC A02/MF A01 CSCL 05/9

Over 10 years of scientific diving for oceanographic and acoustics research is described. Examples show the need for a scientist to dive even in highly automated activities. Diving operations in oceanographic research have included: deployment of oceanographic buoys and sensors, check-and-recovery operations, installation of bottom-mounted systems, placing fluorescent dye releasers for oceanographic investigations, in situ calibration of neutrally buoyant floats, and evaluations of low-speed towed bodies. Diving operations in underwater acoustics research have included: visual and stereophotographic investigations and sampling of the sea floor and in situ measurements of the acoustic characteristics of sediments using geophones and electroacoustic transducers. These operations and techniques are described and some reference is given to organization, safety rules, and operational limits. GRA

N86-12942# SACLANT ASW Research Center, La Spezia (Italy).
TEMPORAL AND SPATIAL VARIABILITIES IN SHALLOW WATER ACOUSTICS: MEASUREMENTS AND PREDICTIONS
H. B. Ali, M. C. Ferla, and T. Akal 15 Mar. 1985 14 p
(AD-A156718; SACLANTCEN-SM-178) Avail: NTIS HC A02/MF A01 CSCL 20/1

An acoustic signal propagating in the sea is generally degraded not only by interactions with the bottom and surface boundaries, but also by volume inhomogeneities caused by non-uniformities in temperature, density, and salinity distributions. The degradations in the acoustical signal are manifested by fluctuations in its amplitude and phase and by an accompanying loss in its coherence properties. The results of experiments conducted in a shallow water area of the Mediterranean are used to establish correlations between fluctuations in acoustic transmission loss and variability in the environmental parameters. The physical processes responsible for the observed fluctuations are identified primarily with inertial effects, semidiurnal tides, and fine-structure. Using a modified version of SNAP (SACLANTCEN Normal Mode Acoustic Propagation Model) comparisons are made between measured and predicted acoustic transmission loss. GRA

N86-12943# SACLANT ASW Research Center, La Spezia (Italy).
UNDERWATER PHOTOGRAPHY FOR QUANTITATIVE DESCRIPTION OF BOTTOM ROUGHNESS
T. Akal 1 Apr. 1985 21 p
(AD-A156753; SACLANTCEN-SR-87) Avail: NTIS HC A02/MF A01 CSCL 08/10

Knowledge of the roughness of the sea floor is obviously of great importance in marine geology for understanding the processes of the ocean bottom, and in underwater acoustics for

understanding acoustics for understanding the scattering process. The ocean bottom contains a wide spectrum of roughness, ranging from a few millimeters to several kilometers, where small features are superimposed on much larger topographic features. This complex structure, formed by different physical, chemical, and biological forces can be quantitatively described in terms of their statistical properties, i.e., power spectral density and autocorrelation functions. The gross-scale roughness of the sea floor is reasonably well known due to well-developed echo-sounding techniques. However, little is known about small-scale roughness (amplitudes and wavelengths ranging from centimeters to meters) due to the difficulties of measuring them. The major technique for studying this small-scale roughness is bottom photography. By using photogrammetric techniques, a single pair of overlapping photographs taken with underwater stereo cameras can subsequently be used to provide fine-scale contour charts of the sea floor. To analyze these contoured charts quantitatively, a numerical method had been developed to calculate the two-dimensional bottom-roughness power spectral density and autocorrelation functions.
GRA

N86-12944# Helsinki Univ. Technology, Otaniemi (Finland).
INVESTIGATION OF ICE DYNAMICS IN THE MARGINAL ICE ZONE Interim Technical Report, 1 Sep. 1984 - 15 May 1985
M. Leppaeranta 15 May 1985 10 p
(Contract DAJA45-83-C-0034)
(AD-A157557) Avail: NTIS HC A02/MF A01 CSCL 08/12

Most of the work this year was involved with processing the data of MIZEX-83 and MIZEX-84 experiments in the Greenland Sea. MIZEX-83 was a pilot study program where ice kinematics data could be collected for about ten days. (see Fourth Interim Report). Ocean current measurements were made simultaneously by the Univ. of Bergen, and they had three stations in the same ice floes as we had transponders for the ice kinematics study. MIZEX-84 was the main summer experiment of the MIZEX program. Iced kinematics data was collected for forty days from R/V Polarqueen, which was the main drifting station. A manuscript was prepared on one-dimensional modeling studies of ice drift in the marginal ice drift in the marginal ice zone.
GRA

N86-12945# Massachusetts Univ., Amherst.
AUTOMATIC DETECTION OF GULF STREAM RINGS Technical Report, Mar. 1984 - Jun. 1985
M. F. Janowitz Jun. 1985 20 p
(Contract N00014-79-C-0629)
(AD-A157934; TR-J8501) Avail: NTIS HC A02/MF A01 CSCL 17/5

A prototype for a program for the automatic detection of Gulf Stream rings from satellite IR images is described and illustrated. It includes a comparative study of 40 different filters on real data. The program involves a number of components: image smoothing, image simplification, edge detection, removal of small objects, and ellipse detection.
Author (GRA)

N86-12946# Coastal Engineering Research Center, Vicksburg, Miss.
A USER'S GUIDE TO THE COASTAL ENGINEERING RESEARCH CENTER'S (CERC'S) FIELD RESEARCH FACILITY Final Report
W. A. Birkemeier, H. C. Miller, S. D. Wilhelm, A. E. DeWall, and C. S. Gorbics May 1985 139 p
(AD-A157966; CERC-IR-85-1) Avail: NTIS HC A07/MF A01 CSCL 13/2

The Coastal Engineering Research Center's (CERC's) Field Research Facility (FRF) at Duck, N.C., is a 561-m-(1,840-ft-) long pier and laboratory dedicated to basic and applied coastal research. This report, which describes the facility, the instrumentation and data being collected, and the local area, is designed to be used as an aid in planning experiments to be conducted at the facility. Use of the FRF by coastal researchers is encouraged.
Author (GRA)

N86-12947# Coastal Engineering Research Center, Vicksburg, Miss.
EXTREMAL ANALYSIS OF HINDCAST AND MEASURED WIND AND WAVE DATA AT KODIAK, ALASKA Final Technical Report
M. E. Andrew, O. P. Smith, and J. M. McKee Jun. 1985 78 p
(AD-A158136; CERC-TR-85-4) Avail: NTIS HC A05/MF A01 CSCL 08/3

This study was conducted to provide an analysis of hindcast and measured wave and wind data for Kodiak, Alaska. The purpose of the analysis was to obtain long-term extreme wave conditions for the St. Paul Harbor at Kodiak. This study was accomplished by means of extremal analyses of deepwater hindcast data from the nearest Wave Information Study (WIS) grid point outside Chiniak Bay. Long-term wind measurements were used to validate the results obtained from the analyses of the hindcast data. The local wave climate and attenuation factor for swell crossing the reef into St. Paul Harbor were derived using measured wave data from the area.
GRA

N86-12948# National Center for Atmospheric Research, Boulder, Colo.
MARINE BOUNDARY LAYER FROM AIR-SEA INTERFACE TO INVERSION
J. A. Businger Mar. 1985 94 p refs Sponsored in part by NSF
(PB85-188274; NCAR/TN-252/STR) Avail: NTIS HC A05/MF A01 CSCL 08C

An overview is given of the structure of the marine boundary layer including the molecular interaction at the interface, the transfer processes in the surface layer, and the entrainment at the top of the boundary layer both for the clear and cloud topped case. Special emphasis is given on a qualitative physical understanding of the processes in and the structure of the boundary layer. The response of the boundary layer to mesoscale variations in sea surface temperature is discussed. Some evidence is given that the effect on the fluxes is larger than what is calculated for the boundary layer assuming a quasisteady state.
GRA

N86-12642# Joint Publications Research Service, Arlington, Va.
STUDY OF SIGNIFICANCE OF BOTTOM RELIEF IN BAROCLINIC MODEL OF EQUATORIAL COUNTERCURRENT Abstract Only
T. F. Kuzmicheva, E. N. Mikhaylova, and N. B. Shapiro *In its* USSR Rept.: Earth Sci. (JPRS-UES-85-006) 19 Jun. 1985 p 14 Transl. into ENGLISH from Izv. Akad. Nauk SSSR: Fiz. Atm. i Okeana (Moscow), v. 21, no. 1, Jan. 1985 p 58-65 (For primary document see N86-12630 03-42)
Avail: NTIS HC A05/MF A01

N86-12646# Joint Publications Research Service, Arlington, Va.
SPECTRUM OF TURBULENT FLUCTUATIONS IN SEA WATER DENSITY IN REGION OF LARGE WAVE NUMBERS Abstract Only
M. A. Bramson, A. D. Fedorovskiy, V. I. Nikishov, and G. L. Luchnik *In its* USSR Rept.: Earth Sci. (JPRS-UES-85-006) 19 Jun. 1985 p 16 Transl. into ENGLISH from Dokl. Akad. Ukr. SSR, Ser. A: Fiz-Mat. i Tekhn. Nauki (Kiev), no. 12, Dec. 1984 p 35-38 (For primary document see N86-12630 03-42)
Avail: NTIS HC A05/MF A01

N86-12647# Joint Publications Research Service, Arlington, Va.
INTERACTION OF SOUND WAVES WITH FINE THERMOHALINE STRUCTURES OF OCEAN Abstract Only
V. V. Artelnyy and M. A. Rayevskiy *In its* USSR Rept.: Earth Sci. (JPRS-UES-85-006) 19 Jun. 1985 p 17 Transl. into ENGLISH from Akust. Zh. (Moscow), v. 30, no. 6, Nov. - Dec. 1984 p 728-734 (For primary document see N86-12630 03-42)
Avail: NTIS HC A05/MF A01

N86-12653# Joint Publications Research Service, Arlington, Va.
GEOCHEMISTRY AND ENERGETICS OF CYCLING OF MATTER IN FORMATION OF CRUST IN ACTIVE STRUCTURES OF OCEAN Abstract Only

V. A. Ilin and A. V. Shcherbakov *In its* USSR Rept.: Earth Sci. (JPRS-UES-85-006) 19 Jun. 1985 p 22 Transl. into ENGLISH from Dokl. Akad. Nauk SSSR (Moscow), v. 279, no. 5, Dec. 1984 p 1184-1189 (For primary document see N86-12630 03-42)
Avail: NTIS HC A05/MF A01

N86-12654# Joint Publications Research Service, Arlington, Va.
CONTRIBUTION OF DIFFUSION PROCESSES TO THE ELECTRIC FIELD OF THE OCEAN Abstract Only
P. Ya. Tishchenko *In its* USSR Rept.: Earth Sci. (JPRS-UES-85-006) 19 Jun. 1985 p 24 Transl. into ENGLISH from Dokl. Akad. Nauk SSSR (Moscow), v. 279, no. 5, Dec. 1984 p 1234-1238 (For primary document see N86-12630 03-42)
Avail: NTIS HC A05/MF A01

N86-12662# Joint Publications Research Service, Arlington, Va.
ELECTROMAGNETIC FIELD OF THREE-DIMENSIONAL SURFACE SEA WAVES Abstract Only
V. V. Sochelnikov *In its* USSR Rept.: Earth Sci. (JPRS-UES-85-006) 19 Jun. 1985 p 29-30 Transl. into ENGLISH from Izv. Akad. Nauk SSSR: Fiz. Zemli (Moscow), no. 2, Feb. 1985 p 65-69 (For primary document see N86-12630 03-42)
Avail: NTIS HC A05/MF A01

N86-12667# Joint Publications Research Service, Arlington, Va.
INFLUENCE OF SESTON PHOSPHATASE ACTIVITY ON RATE OF PHOSPHORUS MINERALIZATION AND ITS RECYCLING IN PRODUCTION-DESTRUCTION CYCLE Abstract Only
A. I. Agatova, V. V. Sapozhnikov, and V. R. Vintovkin *In its* USSR Rept.: Earth Sci. (JPRS-UES-85-006) 19 Jun. 1985 p 36-37 Transl. into ENGLISH from Okeanol. (Moscow), v. 25, no. 1, Jan. - Feb. 1985 p 66-73 (For primary document see N86-12630 03-42)
Avail: NTIS HC A05/MF A01

N86-12668# Joint Publications Research Service, Arlington, Va.
ORIGIN OF ELEMENT COMPOSITION OF OCEAN WATER Abstract Only
Yu. T. Chuburkov and I. A. Zotov *In its* USSR Rept.: Earth Sci. (JPRS-UES-85-006) 19 Jun. 1985 p 37 Transl. into ENGLISH from Dokl. Akad. Nauk SSSR (Moscow), v. 280, no. 5, Feb. 1985 p 1234-1238 (For primary document see N86-12630 03-42)
Avail: NTIS HC A05/MF A01

N86-12670# Joint Publications Research Service, Arlington, Va.
NONLINEAR MODEL OF ADAPTATION OF FIELDS OF DENSITY AND CURRENTS IN SEA Abstract Only
Yu. L. Demin and D. I. Trukhchev *In its* USSR Rept.: Earth Sci. (JPRS-UES-85-006) 19 Jun. 1985 p 39 Transl. into ENGLISH from Izv Akad. Nauk SSSR: Fiz. Atm. i Okeana (Moscow), v. 20, no. 12, Dec. 1984 p 1171-1182 (For primary document see N86-12630 03-42)
Avail: NTIS HC A05/MF A01

N86-12672# Joint Publications Research Service, Arlington, Va.
EDDY FLUXES OF HEAT, VORTICITY AND MOMENTUM IN OCEAN AND ATMOSPHERE AND THEIR PARAMETERIZATION (REVIEW) Abstract Only
V. O. Ivchenko and A. V. Klepikov *In its* USSR Rept.: Earth Sci. (JPRS-UES-85-006) 19 Jun. 1985 p 40 Transl. into ENGLISH from Okeanol. (Moscow), v. 25, no. 1, Jan. - Feb. 1985 p 5-18 (For primary document see N86-12630 03-42)
Avail: NTIS HC A05/MF A01

N86-12674# Joint Publications Research Service, Arlington, Va.
FEATURES OF GEOSTROPHIC CIRCULATION RELATED TO NATURE OF BOTTOM RELIEF IN NORTHWESTERN ATLANTIC Abstract Only
Z. I. Kizner *In its* USSR Rept.: Earth Sci. (JPRS-UES-85-006) 19 Jun. 1985 p 4142 Transl. into ENGLISH from Okeanol. (Moscow), v. 25, no. 1, Jan. - Feb. 1985 p 26-31 (For primary document see N86-12630 03-42)
Avail: NTIS HC A05/MF A01

N86-12675# Joint Publications Research Service, Arlington, Va.
CYCLONIC FRONTAL EDDY IN ANTARCTIC CIRCUMPOLAR CURRENT Abstract Only
Yu. A. Ivanov, A. Yu. Krasnopevtsev, Ye. G. Morozov, I. F. Shadrin, and A. D. Shcherbinin *In its* USSR Rept.: Earth Sci. (JPRS-UES-85-006) 19 Jun. 1985 p 42 Transl. into ENGLISH from Okeanol. (Moscow), v. 25, no. 1, Jan. - Feb. 1985 p 32-36 (For primary document see N86-12630 03-42)
Avail: NTIS HC A05/MF A01

N86-12678# Joint Publications Research Service, Arlington, Va.
ROLE OF AHERMATYPIC CORALS IN SEDIMENTATION AND ECOLOGY OF CORAL BANKS Abstract Only
N. B. Keller *In its* USSR Rept.: Earth Sci. (JPRS-UES-85-006) 19 Jun. 1985 p 47-48 Transl. into ENGLISH from Okeanol. (Moscow), v. 25, no. 1, Jan. - Feb. 1985 p 113-116 (For primary document see N86-12630 03-42)
Avail: NTIS HC A05/MF A01

N86-12679# Joint Publications Research Service, Arlington, Va.
NEW DATA OF RELIEF OF MAZCA RIDGE Abstract Only
L. A. Zakharov *In its* USSR Rept.: Earth Sci. (JPRS-UES-85-006) 19 Jun. 1985 p 48-49 Transl. into ENGLISH from Okeanol. (Moscow), v. 25, no. 1, Jan. - Feb. 1985 p 124-129 (For primary document see N86-12630 03-42)
Avail: NTIS HC A05/MF A01

N86-12699# Joint Publications Research Service, Arlington, Va.
EXPERIMENTAL STUDY OF EQUILIBRIUM INTERVAL IN FREQUENCY SPECTRA OF WIND WAVES IN SEA OF FINITE DEPTH Abstract Only
I. A. Alekperov, N. I. Akhmedov, A. I. Gumbatov, A. S. Ismaylov, S. G. Magerramova, and T. M. Tatrayev *In its* USSR Rept.: Earth Sci. (JPRS-UES-85-008) 16 Aug. 1985 p 6 Transl. into ENGLISH from Izv. Akad. Nauk Azerbaydzhanskoy SSR, Ser. Nauki o Zemle (USSR), no. 6, 1984 p 119-123 (For primary document see N86-12697 03-42)
Avail: NTIS HC A04/MF A01

N86-12700# Joint Publications Research Service, Arlington, Va.
FEATURES OF ELECTRICAL MEASUREMENTS IN SEA AS MEDIUM WITH FIELD OF EXTRANEOUS FORCES Abstract Only
V. I. Loptnikov *In its* USSR Rept.: Earth Sci. (JPRS-UES-85-008) 16 Aug. 1985 p 7 Transl. into ENGLISH from Geofiz. Zh. (Kiev), v. 7, no. 7, Mar. - Apr. 1985 p 59-68 (For primary document see N86-12697 03-42)
Avail: NTIS HC A04/MF A01

N86-12702# Joint Publications Research Service, Arlington, Va.
QUASIGEOSTROPHIC MODEL OF CIRCULATION IN ANTARCTIC OCEAN WITH PARAMETRIZATION OF SYNOPTIC EDDIES Abstract Only
V. O. Ivchenko and A. V. Klepikov *In its* USSR Rept.: Earth Sci. (JPRS-UES-85-008) 16 Aug. 1985 p 8 Transl. into ENGLISH from Dokl. Akad. Nauk SSSR (Moscow), v. 281, no. 4, Apr. 1985 p 944-948 (For primary document see N86-12697 03-42)
Avail: NTIS HC A04/MF A01

N86-12707# Joint Publications Research Service, Arlington, Va.
OCEAN ALBEDO FOR ATMOSPHERIC THERMAL EMISSION Abstract Only
R. G. Gardashov, Zh. K. Zolotova, and K. S. Shifrin *In its* USSR Rept.: Earth Sci. (JPRS-UES-85-008) 16 Aug. 1985 p 12 Transl. into ENGLISH from Izv. Akad. Nauk SSSR: Fiz. Atm. i Okeana (Moscow), v. 21, no. 4, Apr. 1985 p 438-440 (For primary document see N86-12697 03-42)
Avail: NTIS HC A04/MF A01

N86-12708# Joint Publications Research Service, Arlington, Va.
INVESTIGATION OF ELASTIC PROPERTIES OF MARINE SURFACE-ACTIVE FILMS Abstract Only

B. T. Demin, S. A. Yermakov, Ye. N. Pelinovskiy, T. G. Talipova, and A. I. Sheremetyeva *In its* USSR Rept.: Earth Sci. (JPRS-UES-85-008) 16 Aug. 1985 p 12-13 Transl. into ENGLISH from Izv. Akad. Nauk SSSR: Fiz. Atm. i Okeana (Moscow), v. 21, no. 4, Apr. 1985 p 410-416 (For primary document see N86-12697 03-42)
Avail: NTIS HC A04/MF A01

N86-12711# Joint Publications Research Service, Arlington, Va.
FINE STRUCTURE OF DENSITY RELATION IN MAIN OCEANIC THERMOCLINE Abstract Only
V. M. Zhurbas *In its* USSR Rept.: Earth Sci. (JPRS-UES-85-008) 16 Aug. 1985 p 17 Transl. into ENGLISH from Okeanol. (Moscow), v. 25, no. 2, Mar. - Apr. 1985 p 215-218 (For primary document see N86-12697 03-42)
Avail: NTIS HC A04/MF A01

N86-12712# Joint Publications Research Service, Arlington, Va.
VISCOUS NONLINEAR CIRCULATION IN AXISYMMETRIC BAROCLINIC EDDY Abstract Only
D. O. Gordeyvhev and G. G. Sutyrin *In its* USSR Rept.: Earth Sci. (JPRS-UES-85-008) 16 Aug. 1985 p 18 Transl. into ENGLISH from Okeanol. (Moscow), v. 25, no. 2, Mar. - Apr. 1985 p 186-192 (For primary document see N86-12697 03-42)
Avail: NTIS HC A04/MF A01

N86-12713# Joint Publications Research Service, Arlington, Va.
FACIES-GENETIC GROUPS OF COARSE CLASTIC MATERIAL ON WORLD OCEAN FLOOR Abstract Only
N. N. Kachanov *In its* USSR Rept.: Earth Sci. (JPRS-UES-85-008) 16 Aug. 1985 p 18-19 Transl. into ENGLISH from Dokl. Akad. Nauk Ukr. SSR, Ser. B: Geol. Khim i Biol. Nauki (Kiev), no. 4, Apr. 1985 p 27-31 (For primary document see N86-12697 03-42)
Avail: NTIS HC A04/MF A01

N86-12714# Joint Publications Research Service, Arlington, Va.
SPATIAL STRUCTURE OF HIGH-FREQUENCY SEA WIND WAVES UNDER DIFFERENT METEOROLOGICAL CONDITIONS Abstract Only
I. I. Strizhkin, M. P. Lapchinskaya, Yu. A. Ilin, and V. A. Malinnikov *In its* USSR Rept.: Earth Sci. (JPRS-UES-85-008) 16 Aug. 1985 p 19-20 Transl. into ENGLISH from Izv. Akad. Nauk SSSR: Fiz. Atm. i Okeana (Moscow), v. 21, no. 4, Apr. 1985 p 440-442 (For primary document see N86-12697 03-42)
Avail: NTIS HC A04/MF A01

N86-12724# Joint Publications Research Service, Arlington, Va.
DETERMINATION OF DYNAMIC PARAMETERS OF REFLECTED WAVES ON SLOPES OF DEEP WATER TRENCH Abstract Only
V. G. Bykov, F. A. Vorobyev, V. V. Zhigulev, and S. S. Snegovskoy *In its* USSR Rept.: Earth Sci. (JPRS-UES-85-008) 16 Aug. 1985 p 32 Transl. into ENGLISH from Tikhookeanskaya Geol. (Novosibirsk), no. 1, Jan. - Feb. 1985 p 99-103 (For primary document

N86-12882*# National Aeronautics and Space Administration. Goddard Space Flight Center, Greenbelt, Md.
GLOBAL MEAN SEA SURFACE COMPUTATION BASED UPON A COMBINATION OF SEASAT AND GEOS-3 SATELLITE ALTIMETER DATA Abstract Only
J. G. Marsh, C. J. Koblinsky, A. Brenner (Edgerton, Germeshausen and Grier, Inc., Riverdale, Md.), B. Beckley (Edgerton, Germeshausen and Grier, Inc., Riverdale, Md.), and T. Martin (Edgerton, Germeshausen and Grier, Inc., Riverdale, Md.) *In* NASA, Washington Geopotential Res. Mission (GRM) Oct. 1985 p 77 (For primary document see N86-12852 03-46)
Avail: NTIS HC A07/MF A01 CSCL 08J

N86-12883*# Jet Propulsion Lab., California Inst. of Tech., Pasadena.
CONTRIBUTIONS OF GRM TO THE OCEAN TOPOGRAPHY EXPERIMENT (TOPEX) Abstract Only
Robert Stewart *In* NASA, Washington Geopotential Res. Mission (GRM) Oct. 1985 p 78 (For primary document see N86-12852 see N86-12697 03-42)
Avail: NTIS HC A04/MF A01

03-46)
Avail: NTIS HC A07/MF A01 CSCL 08J

51 LIFE SCIENCES (GENERAL)

Includes genetics.

N86-12949*# Management and Technical Services Co., Washington, D.C.
USSR SPACE LIFE SCIENCES DIGEST, ISSUE 2
Lydia Razran Hooke, ed., Mike Radtke, ed., Victoria Garshnek, ed., Joseph E. Rowe, ed., and Ronald Teeter, ed. Washington NASA Oct. 1985 96 p
(Contract NASw-3676)
(NASA-CR-3922(02); NAS 1.26:3922(02)) Avail: NTIS HC A05/MF A01 CSCL 06C

The second issue of the bimonthly digest of USSR Space Life Sciences is presented. Abstracts are included for 39 Soviet periodical articles in 16 areas of aerospace medicine and space biology and published in Russian during the first half of 1985. Selected articles are illustrated with figures from the original. Translated introductions and tables of contents for 14 Russian books on 11 topics related to NASA's life science concerns are presented. Areas covered are: adaptation, biospheric, body fluids, botany, cardiovascular and respiratory systems, cybernetics and biomedical data processing, gastrointestinal system, group dynamics, habitability and environmental effects, health and medical treatment, hematology, immunology, life support systems, metabolism, musculoskeletal system, neurophysiology, psychology, radiobiology, and space biology. Two book reviews translated from Russian are included and lists of additional relevant titles available either in English or in Russian only are appended. E.A.K.

N86-12950# Army Engineer Waterways Experiment Station, Vicksburg, Miss. Environmental Lab.
ENVIRONMENTAL IMPACT RESEARCH PROGRAM. STATUS AND SOURCE OF HABITAT MODELS AND LITERATURE REVIEWS, DECEMBER 1984 Final Report
T. H. Roberts, L. J. ONeil, and W. E. Jabour Apr. 1985 18 p Revised
(AD-A156899; WES/MP/EL-85-1-Rev) Avail: NTIS HC A02/MF A01 CSCL 06/6

This report summarizes the status and availability of selected species habitat models and other habitat-related documents developed by the US Fish and Wildlife Service and other agencies. This listing is not comprehensive since many universities and other organizations are now involved with model development and testing. Animal groups included are birds, mammals, amphibians, reptiles, fish, molluscs, and other crustaceans. Information listed includes scientific name, special status of the species (if any), the organization responsible for the development of the model or the literature review, the stage of development of the document, and whether the document has received outside review or testing. GRA

N86-12951# Los Alamos National Lab., N. Mex.
RAMAN ACTIVITY IN SYNCHRONOUSLY DIVIDING BACTERIA
S. P. Layne 1985 12 p refs Presented at the Computer Anal. for Life Sci., Okayama, Japan, 9 Jul. 1985
(Contract W-7405-eng-36)
(DE85-015672; LA-UR-85-2368; CONF-850784-1) Avail: NTIS HC A02/MF A01

Using a spectrometer equipped with an optical-multichannel analyzer as the detector (OMA), we have observed the Stokes laser-Raman spectra of metabolically active Escherichia coli and Bacillus magaterium from 100 to 2100 cm(-1). After lengthy investigation, no Raman lines attributable to the metabolic process nor the cells themselves were found. Previous Raman spectra of active bacteria cannot be used to support nonlinear theories in biology. DOE

N86-12952# California Univ., Berkeley. Lawrence Berkeley Lab.
MONITORING OF CIRCADIAN WAVEFORMS IN RODENTS EXPOSED TO HIGH-INTENSITY STATIC MAGNETIC FIELDS
T. S. Tenforde, L. Levy, and E. Veklerov Oct. 1984 38 p refs
Presented at the 23rd Hanford Life Sci. Symp., Interaction of Biol. Systems with Static and ELF Elec. and Magnetic Fields, Richland, Wash., 2 Oct. 1984
(Contract DE-AC03-76SF-00098)
(DE85-015225; LBL-18384; CONF-841041-2) Avail: NTIS HC A03/MF A01

A system was developed for the noninvasive monitoring of circadian variables in mice exposed to a 1.50 T static magnetic field. The ambient light level, temperature and relative humidity within the exposure chamber are closely regulated, and physiological monitoring systems provide simultaneous measurements of seven circadian variables: (1) climbing activity on a triangular bar; (2) migratory activity; (3) body mass; (4) respired carbon dioxide; (5) nutrient consumption; (6) urine excretion; and (7) fecal excretion. Data from the various transducers and environmental monitoring devices within the exposure system are recorded on magnetic tapes at 5-min intervals throughout experiments of 50 to 60 days duration, and the circadian waveforms of behavior and physiological parameters are analyzed by a modification of the cosiner method using a high-speed computer. Exposure of adult female LAF-1 mice to a 1.50-T homogeneous field for 5 continuous days, or for 10 consecutive days with intermittent daily exposures on an 8-hr-on/16-hr-off cycle, is found to produce no significant alterations in the circadian waveforms of behavioral or physiological parameters. DOE

N86-12953# Oak Ridge National Lab., Tenn.
BIOMEDICAL AND ENVIRONMENTAL SCIENCES PROGRAM PUBLICATIONS 1984
H. E. Gerstner, K. M. Branam, L. W. Littleton, V. S. Norman, and E. H. Thompson Jul. 1985 86 p
(Contract DE-AC05-84OR-21400)
(DE85-015070; ORNL-6201) Avail: NTIS HC A05/MF A01

A bibliography is given containing 665 references to journal articles, books, book chapters, proceedings, reports, and abstracts. Certain types of publications are not included: theses, book reviews, internal documents, and periodic progress reports (with the exception of annual reports). Publications from divisions that report to the Associate Laboratory Director for Biomedical and Environmental Sciences (ADBES) are listed here, as well as publications from divisions that receive funding through the ADBES office. The references are sorted by type (journal articles, etc.), then by division, and, within each division, alphabetically by first author. Author and journal indexes are included in the back. DOE

52 AEROSPACE MEDICINE

Includes physiological factors; biological effects of radiation; and weightlessness.

N86-12954* National Aeronautics and Space Administration, Washington, D. C.
AEROSPACE MEDICINE AND BIOLOGY CONTINUING BIBLIOGRAPH: A CONTINUING BIBLIOGRAPHY WITH INDEXES
Oct. 1985 64 p
(NASA-SP-7011(276); NAS 1.21:7011(276)) Avail: NTIS HC A04 CSCL 06E

This bibliography lists 184 reports, articles, and other documents introduced into the NASA scientific and technical information system in September 1985. F.M.R.

N86-12955 Department of the Navy, Washington, D. C.
INFRARED OPTICAL MEASUREMENT OF BLOOD GAS CONCENTRATIONS AND FIBER OPTIC CATHETER Patent
T. J. Manuccia and J. G. Eden, inventors (to Navy) Issued 9 Apr. 1985 7 p
(AD-D011836; US-Patent-4,509,522; US-Patent-Appl-SN-331091; US-Patent-Class-128-634) Avail: US Patent and Trademark Office CSCL 06/12

This patent pertains to a simple compact optical device and method for quickly measuring the concentration of CO and CO2, bound to hemoglobin or dissolved in a person's blood using optical techniques which do not require removing a blood sample from the body. It also provides a simple fiber optic device for measuring blood-gas concentrations of critical internal points of the circulatory system such as the aorta. GRA

N86-12956*# National Aeronautics and Space Administration. Ames Research Center, Moffett Field, Calif.
PLASMA VOLUME METHODOLOGY: EVANS BLUE, HEMOGLOBIN-HEMATOCRIT, AND MASS DENSITY TRANSFORMATIONS
J. E. Greenleaf and H. Hinghofer-Szalkay Nov. 1985 25 p refs
(NASA-TM-86834; Rept-85406; NAS 1.15:86834) Avail: NTIS HC A02/MF A01 CSCL 06P

Methods for measuring absolute levels and changes in plasma volume are presented along with derivations of pertinent equations. Reduction in variability of the Evans blue dye dilution technique using chromatographic column purification suggests that the day-to-day variability in the plasma volume in humans is less than + or - 20 m1. Mass density determination using the mechanical-oscillator technique provides a method for measuring vascular fluid shifts continuously for assessing the density of the filtrate, and for quantifying movements of protein across microvascular walls. Equations for the calculation of volume and density of shifted fluid are presented. E.A.K.

N86-12957# Department of the Army, Washington, D. C.
FORWARD FIELD AUTOTRANSFUSION DEVICE Patent Application
E. I. Schweitzer and K. G. Swan, inventors (to Army) Filed 10 May 1985 12 p
(AD-D011763; US-Patent-Appl-SN-732335) Avail: NTIS HC A02/MF A01 CSCL 06/12

A typical embodiment of the invention enables blood to be drawn from the pleural cavity of an injured patient for autotransfusion purposes. A chest tube is connected to an inlet check valve within a resilient bulb suction pump. Blood, drawn into the bulb, is expelled therefrom by manipulating the bulb to cause the blood to flow out of the bulb through a filter and a discharge check valve to a blood collection bag. GRA

N86-12958# Department of the Army, Washington, D. C.
SUTURE NEEDLE HOLDER Patent Application
E. J. Schweitzer and J. R. Bresch, inventors (to Army) Filed 3 Jun. 1985 15 p
(AD-D011764; US-Patent-Appl-SN-740610) Avail: NTIS HC A02/MF A01 CSCL 06/12

A typical embodiment on the invention enables a surgeon to occupy only one hand in manipulating a suture needle. The instrument thumb handle has, on one end, a freely rotatable short roller. The ring finger handle, moveover, has a long roller that is journalled within that handle. One end of the long roller bears against the short roller to form a nip that engages the suture needle. The other end of the long roller terminates near the ring finger handle grip to enable the surgeon to rotate the long roller with another finger of the same hand and thereby draw the needle through the nip, repositioning the needle for another stitch. GRA

N86-12959# School of Aerospace Medicine, Brooks AFB, Tex.
PROCEEDINGS OF A WORKSHOP ON RADIOFREQUENCY RADIATION BIOEFFECTS HELD AT WACHTBERG-WERTHHOVEN, WEST GERMANY ON 11-13 SEPTEMBER 1984 Final Report
J. C. Mitchell Apr. 1985 241 p Presented at Workshop held at Wachtberg-Werthhoven, West Germany, 11-13 Sep. 1984
(AF Proj. 7757)
(AD-A157090; USAFSAM-TP-85-14) Avail: NTIS HC A11/MF A01 CSCL 06/18

The workshop was convened to address new developments in the setting and application of RFR (Radiofrequency Radiation) safety standards, assessment of RFR levels in the military environment, RFR instrumentation and dosimetry, the medical approach to specific problems, and important state-of-the-art research regarding the biological effects of long-term low-level RFR exposures, pulsed versus continuous wave effects, and the effects of unique pulse modulation. The collected papers represent the contributions of various experts in the field from the NATO countries, brought together under the the sponsorship of Defense Research Group, Panel 8, NATO AS/243, at the Research Establishment for Applied Science, D-5307 Wachtberg-Werthhoven, Federal Republic of Germany. GRA

N86-12960# Letterman Army Inst. of Research, San Francisco, Calif.
ENERGY EXPENDITURE AND ACTIVITY PATTERNS OF CADETS AT THE UNITED STATES MILITARY ACADEMY, WEST POINT, NEW YORK Final Report, for Period Ending Oct. 1979
M. J. Kretsch, M. O. OConnor, and H. E. Sauberlich Jun. 1985 42 p
(AD-A157857; LAIR-IR-200) Avail: NTIS HC A03/MF A01 CSCL 06/16

A study was conducted in October, 1979, at the United States Military Academy, West Point, New York, to evaluate factors contributing to weight gain in cadets over the course of their academic career. This report presents the average daily energy expenditure (EE) and activity patterns of male and female cadets. A total of 136 male and 54 female cadets from the classes of 1980, 1981, 1982, and 1983 were studied. Five consecutive days (Wednesday through Sunday) of activity data were collected from each study participant by the factorial method. The average pattern of EE usage was similar between male and female cadets: about 20% at rest; 35 to 40% in very light activities; 5 to 10% in light activities; about 25% in moderate activities; and the remaining 5 to 15% in heavy or very heavy activities. Average energy expenditure when expressed as kcal/kg body weight was not significantly different between male and female cadets of the same class for weekdays or weekend days. There was a tendency for the cadets to become more sedentary with advance in class. This was more noticeable for the females than for the males. There was a significant decrease in weekday, but not weekend day, EE for the females with advance in class. This same decrease was not significant for the male cadets, but there was a weekday trend in that direction. For the females, the lower weekday EE for the 1980 and 1981 classes may be explained by the lower amount of energy and time spent in running and sports activities. Whether the decrease in weekday EE with advance in class is due to differences in program requirements should be examined. GRA

N86-12961# Brown Univ., Providence, R. I. Center for Neural Science.
CORTICAL PLASTICITY: THEORETICAL ANALYSIS, EXPERIMENTAL RESULTS
L. N. Cooper 31 Jul. 1985 34 p
(Contract N00014-81-K-0136)
(AD-A157965; TR-27) Avail: NTIS HC A03/MF A01 CSCL 06/15

An account is given of a theory of and experimental results on development and modification of selectivity and ocular dominance in visual cortex. The single cell theory is generalized to be applicable to a neural network. Also discussed, in the context of the theoretical ideas, are experiments on the modifiability of inhibitory cells and on possible candidates for global controllers of learning. GRA

N86-12962# Department of the Army, Washington, D. C.
DERMAL SUBSTANCE COLLECTION DEVICE Patent Application
C. C. Peck, inventor (to Army) Filed 11 Feb. 1985 29 p
(AD-D011848; US-Patent-Appl-SN-660778) Avail: NTIS HC A03/MF A01 CSCL 14/2

This patent application describes a dermal substance collection device (DSCD) which provides means for the non-invasive, instantaneous and continuous monitoring of chemical substances which are present in a detectable amount in either or both interstitial fluid or sweat or which are on or in the skin. The transdermal substance collection device of this invention is comprised of three essential components: (1) a substance binding reservoir, wettable by, (2) a liquid transfer medium which allows for liquid bridge transfer of a soluble substance from the skin surface to the binding reservoir by virtue of its wettability by the liquid, and (3) an occlusive cover. GRA

N86-12963# School of Aerospace Medicine, Brooks AFB, Tex.
THE EFFECTS OF HYPOXIA INDUCED BY LOW ATMOSPHERIC PRESSURE ON SOFT CONTACT LENS WEAR Final Report, 1 Jun. 1983 - 1 Jan. 1985
W. J. Flynn, R. E. Miller, II, M. G. Block, and T. J. Tredici Jun. 1985 16 p
(AF Proj. 2729)
(AD-A158556; USAFSAM-TR-85-30) Avail: NTIS HC A02/MF A01 CSCL 06/12

Contact lens use in aviation has long been a subject of debate and controversy. One of the major concerns for contact lens wear at altitude is the potential for corneal edema and subsequent visual degradation, due to the reduced levels of oxygen available for normal corneal metabolism. Four subjects were tested, wearing both high-and low-water content soft contact lenses, for visual changes and adverse corneal physiological responses due to hypoxia induced by an atmospheric pressure level equivalent to 10,000 ft. Results of this study indicate that, although the cornea is placed under higher levels of physiological stress at an altitude of 10,000 ft, the absence of visual degradation or significant symptoms suggests that lenses can be safely worn under the conditions of this study. Author (GRA)

N86-12964# National Academy of Sciences - National Research Council, Washington, D. C.
STUDIES OF PARTICIPANTS IN NUCLEAR TESTS Final Report, 1 Sep. 1978 - 31 Oct. 1984
C. D. Robinette, S. Jablon, and T. L. Preston May 1985 102 p refs
(Contract DE85-AI08-78EV-01577)
Avail: NTIS HC A06/MF A01

Mortality, by cause of death, was studied on a cohort of 46,186 participants in one or more of five test series. The series studied were UPSHOT-KNOTHOLE (1953) and PLUMBBOB (1957) at the Nevada Test Site, and GREENHOUSE (1951), CASTLE (1954), and REDWING (1956) which were conducted at the Pacific Proving Ground at Enewetak and Bikini. The number of deaths attributed to particular causes was compared with the number expected to occur at US cause and age-specific mortality rates. A total of 5113 deaths from all causes was ascertained; this was 11.1% of the number of participants. The number was, however, only 83.5% of the number expected at US mortality rates. Mortality from leukemia among the 3554 participants at SMOKY - 10 deaths below age 85 - were 2.5 times the expected number. When the leukemia deaths are compared to other deaths in all six data sets, the differences among the series are not significant. No cancer other than leukemia was ascertained to have occurred in significant excess among SMOKY participants and the number of deaths from other cancers (67) was less than the number expected at population rates (83.8). The total body of evidence cannot convincingly affirm or deny that the higher than statistically expected incidence of leukemia among SMOKY participants (or of prostate cancer among REDWING participants) is the result of radiation exposure incident to the tests. DOE

N86-12965# Pacific Northwest Lab., Richland, Wash.
ACCIDENTAL EXPOSURE TO AMERICIUM
K. R. Heid Apr. 1985 13 p refs Presented at the Health Phys. Summer School Conf., Evanston, Ill., 3 Jun. 1985
(Contract DE-AC06-76RL-01830)
(DE85-012794; PNL-SA-13155; CONF-8506136-1) Avail: NTIS HC A02/MF A01

An accident in which a 64 year old Hanford nuclear worker was exposed to high levels of americium while working in an americium recovery facility in 1976 is described. As a result of the accident, he was heavily externally contaminated with americium, sustained with a substantial internal deposition of this isotope, and was burned with concentrated nitric acid and injured by flying debris about the face and neck. The immediate and longer term treatment given the patient, including the decontamination efforts and clinical laboratory studies, are discussed. Special in vivo equipment and techniques were used to measure the americium deposited in the patient. These and subsequent in vivo measurements were used to estimate the dose rates and the accumulated doses to body organs. Urinary and fecal excreta were collected and analyzed for americium content. The interpretation of these data was complicated by the fact that the intake resulted both from inhalation and from solubilization of the americium embedded in facial tissues as a result of the accident. A total of 1100 (MU)Ci was excreted in urine and feces during the first 2 years following the accident. The long term use of diethylenetriaminepentaacetic acid (DTPA), used principally as the zinc salt, is discussed including the method, route of administration, and effectiveness. To date, the patient has apparently experienced no complications attributable to this extensive course of therapy, even though he was given approximately 560 g of DTPA. DOE

N86-12966# Joint Publications Research Service, Arlington, Va.
CHINA REPORT: SCIENCE AND TECHNOLOGY
18 Jun. 1985 117 p refs Transl. into ENGLISH from various Chinese articles
(JPRS-CST-85-019) Avail: NTIS HC A06/MF A01

Progress in science and technology in the People's Republic of China is reported. Topics discussed include: national developments, life sciences, biochemistry, biology, cement industry, chemistry, computers, engineering, industrial hygiene, medical science, microbiology, pharmacology, radiology, semiconductor materials, and telecommunications. For individual titles, see N86-12967 through N86-12967.

N86-12967# Joint Publications Research Service, Arlington, Va.
PROTECTION OF EYES AGAINST LASER DAMAGE STUDIED
Guan Chongwen, Wang Rongzhen, and Jin Humei *In its* China Rept.: Sci. and Technol. (JPRS-CST-85-019) 18 Jun. 1985 p 41-48 refs Transl. into ENGLISH from Zhongguo Jiguang (Shanghai), no. 2, 20 Feb. 1985 p 113-117 (For primary document see N86-12966 03-52)
Avail: NTIS HC A06/MF A01

The potential hazards of lasers were analyzed in eye injuries caused by lasers. Hygienic physical experiments were performed on reflected laser light from hitting spots which caused most eye injuries. Measures for the protection of eyes against laser damage are discussed. E.A.K.

N86-12377# Tokyo Denki Univ. (Japan). Faculty of Engineering.
EFFECTS OF CATION IONS IN NERVE EXCITATION
Kazuyuki Aihara, Makoto Kotani, and Toshio Utsunomiya *In its* Res. Rept. of the Faculty of Eng., Tokyo Denki Univ., No. 32 Dec. 1984 p 67-78 refs In JAPANESE; ENGLISH summary (For primary document see N86-12372 03-31)
Avail: NTIS HC A09/MF A01

N86-12458# Joint Publications Research Service, Arlington, Va.
HUMAN HEMODYNAMIC CHANGE UNDER HIGH ATMOSPHERIC PRESSURE
Zhang Hengdu and Dai Duanyang *In its* China Rept.: Sci. and Technol. (JPRS-CST-85-030) 4 Sep. 1985 p 55-56 Transl. into ENGLISH from Jiefangjun Yixue Zazhi (Beijing), no. 1, 20 Feb. 1985 p 63 (For primary document see N86-12451 03-31)
Avail: NTIS HC A08/MF A01

53 BEHAVIORAL SCIENCES

Includes psychological factors; individual and group behavior; crew training and evaluation; and psychiatric research.

N86-12968# Air Command and Staff Coll., Maxwell AFB, Ala.
THE HELICOPTER TO FIXED WING CONVERSION PROGRAM: A CRITICAL REVIEW
L. T. Massey Apr. 1985 39 p
(AD-A156820; ACSC-85-1750) Avail: NTIS HC A03/MF A01 CSCL 05/9

USAF helicopter pilots are initially trained by the U.S. Army through their undergraduate helicopter pilot training program. Four to seven years later, some of these pilots have the opportunity to convert to fixed wing aircraft via the fixed wing conversion program currently conducted by sending selected helicopter pilots through Air Force undergraduate pilot training. This study reviews these programs and assesses the impact this training philosophy has on career opportunities for helicopter pilots, both for those who convert to fixed wing systems, as well as for those who remain in helicopters. Two alternatives are presented which would resolve the problems identified. The study concludes that the USAF could provide better career opportunities for helicopter pilots, as well as improve experience levels in the helicopter force, by enacting changes to current training programs. Author (GRA)

N86-12969# Chicago Univ., Ill. Graduate School of Business.
STIMULUS STRUCTURES AND MENTAL REPRESENTATIONS IN EXPERT COMPREHENSION OF COMPUTER PROGRAMS Technical Report, Sep. 1982 - Jan. 1985
N. Pennington Jan. 1985 110 p
(Contract N00014-82-K-0759)
(AD-A157520; TR-2-ONR) Avail: NTIS HC A06/MF A01 CSCL 05/10

The difficulty of computer programming and other design tasks is a function of the multiple abstractions that combine to form a program's meaning. Thus, comprehension of the final form of a program design, the program text, involves retrieving multiple sets of relationships between parts. The research presented here addresses which, if any, abstraction is dominant psychologically in programmers' mental representation of programs, specifically whether procedural (control flow) or functional (goal hierarchy) abstractions dominate, and the relative ease or difficulty of inferring different kinds of information from the text. Eighty professional programmers were tested on comprehension and recognition of short program texts. The results, which suggest that procedural rather than functional units form the basis of expert programmers' mental representations, support work in other areas of test comprehension showing the importance of test structure knowledge in understanding. The results also raise questions concerning claims that chunking found in comprehension and memory tasks in skilled problem solving domains is due to pattern matching to schematic content knowledge rather than to knowledge of more abstract text or design structure units. GRA

N86-12970# California Univ., San Diego, La Jolla. Inst. for Cognitive Science.
HUMAN COGNITION AND PERFORMANCE Final Report, Apr. 1979 - Mar. 1985
D. A. Norman, D. E. Rumelhart, and D. R. Gentner 1 May 1985 101 p
(Contract N00014-79-C-0323)
(AD-A157665) Avail: NTIS HC A06/MF A01 CSCL 05/10

The Cognitive Science Laboratory is a part of both the Institute for Cognitive Science and the Center for Human Information Processing at their University of California, San Diego. Work in the laboratory is aimed at developing a deeper understanding of the theory and applications of human information processing. The research aims of the laboratory are broad, but all the work follows a common theoretical view of cognition, providing a cohesion that binds the separate studies together, despite the apparent wide differences in content. All of the work can be characterized as being Studies of Human Cognition. This is the main focus of the laboratory's efforts, and over the years the work has covered in-depth problems within the areas of preception, attention, learning, memory, language, thought, and action. Special emphasis has been placed on knowledge representation, and one major contribution of the laboratory has been within the area: The representational structure known as Active Structural Networks. Work in this general area is always in process elaborated and modulated by the results and progress of work in the speciality areas. Three specialty areas can be talked about separately. GRA

N86-12971# Navy Personnel Research and Development Center, San Diego, Calif.
A NEW HAZARD FUNCTION ESTIMATOR OF PERFORMANCE TIME Technical Report, Oct. 1983 - Jul. 1984
B. Bloxom Nov. 1984 35 p
(AD-A157843; NPRDC-TR-85-10) Avail: NTIS HC A03/MF A01 CSCL 05/10

The analysis of performance time is used to study a wide variety of manpower, training, and human factors problems in the Navy. The cumulative distribution of performance time provides some indication of the rate of performance, but it can lead to false conclusions as well. One method of measuring the rate of performance with a shifting residual basis of analysis, called hazard analysis, consists of estimating a hazard function, which shows the rate of performance as a function of time. Although various procedures have been developed for estimating a hazard function, none of the procedures has been shown to produce plausibly smooth and precise estimates under a variety of conditions. This research proposed a constrained quadratic spline as an estimator or the hazard function of performance time. A maximum penalized likelihood procedure was used to fit the estimator to a sample of psychological response times. The procedure was also used in a simulation study of the precision of the estimator. GRA

N86-12972# Illinois Univ., Urbana. Computer-based Education Research Lab.
DIAGNOSING COGNITIVE ERRORS: STATISTICAL PATTERN CLASSIFICATION AND RECOGNITION APPROACH
K. K. Tatsuoka Jan. 1985 36 p
(Contract N00014-82-K-0604; RR0-4204)
(AD-A158108; IU-CERL-RR-85-1-ONR) Avail: NTIS HC A03/MF A01 CSCL 05/10

This paper introduces a probabilistic model that is capable of diagnosing and classifying cognitive errors in a general problem-solving domain. The model is different from the usual deterministic strategies common in the area of artificial intelligence because the item response theory is utilized for handling the variability of response errors. As for illustrating the model, the dataset obtained form a 38-item fraction addition test is used, and the students' responses are classified into 34 groups of misconceptions. These groups are predetermined by the result of an error analysis previously done, and validated with the error diagnostic program written by a typical formal logic approach. GRA

54 MAN/SYSTEM TECHNOLOGY AND LIFE SUPPORT

Includes human engineering; biotechnology; and space suits and protective clothing.

N86-12973# Systems Research Labs., Inc., Dayton, Ohio.
CRITERIA FOR A STATE-OF-THE-ART VISION TEST SYSTEM Final Report
K. Moffitt and L. V. Genco May 1985 109 p
(Contract F33615-82-C-0511)
(AD-A157099; AFAMRL-TR-85-004) Avail: NTIS HC A06/MF A01 CSCL 06/16

Many vision test/screening devices used in the Armed Services have not changed since the 1940's. The reduction in the size of the pool of qualified aircrew candidates has caused operational Commands to question the validity of these tests. Current objectives of vision testing have evolved from a means to eliminate pilot candidates to methods of predicting aircrew performance. The Naval Aerospace Medical Research Laboratory (NAMRL) is attempting to correlate the results of several vision tests with the visual abilities of pilot trainees as demonstrated during monitored training flights. This report describes status that could be considered as useful parameters for testing in the Armed Forces vision test battery of the future. One major conclusion is that the operational visual task(s) must be suitably described in order to select appropriate clinical and laboratory test measures. Correlations and validation studies can then be performed with cooperative efforts such as those between NAMRL and AFAMRL. GRA

N86-12974# Department of the Navy, Washington, D. C.
LOW TEMPERATURE INFLATOR APPARATUS Patent Application
J. J. Esposito, inventor (to Navy) Filed 2 May 1985 9 p
(AD-D011810; US-Patent-Appl-SN-729725) Avail: NTIS HC A02/MF A01 CSCL 06/7

This invention relates to inflator apparatus for inflating emergency flotation gear such as life rafts and life jackets; and more particularly to an inflator for flotation gear which may be stored at, and operated in, extremely low temperatures. Liquid CO2 (carbon dioxide) cartridges have been used for many years as the main source of pressurized gas for inflating various types of inflatable life saving devices such as rafts, vests, and jackets. Emergency use of these devices by downed aircrewman has occurred mostly in temperate zones. However, these situations now occur more frequently in the arctic region where temperatures below -20 F are not uncommon. At these low temperatures, liquid CO2 changes too slowly to the gaseous phase to provide immediate buoyancy. A rapid change is especially needed in a life raft to enable a downed person in frigid water to board as soon as possible. The longer he or she remains exposed to the cold water awaiting the formation of a boardable raft, the more likely hypothermia will set in. Raft inflation time in excess of five minutes has been observed when CO2 cartridges were stored in an aircraft at sub-zero temperatures and then activated in water at 32 F. Consequently, lives have been needlessly lost. In lieu of liquid CO2 cartridges, solid pyrotechnic inflators have been tried which generate gas from a compacted solid material, but the gas of combustion does not attain the pressure level needed for buoyancy of inflatable gear. GRA

N86-12975# Oak Ridge National Lab., Tenn.
POWER AND SIGNAL TRANSMISSION FOR MOBILE TELE-OPERATED SYSTEMS
A. C. Morris, Jr. and W. R. Hamel ,1985 31 p Presented at the Japan/US Spec. Meeting on Remote Systems Technol., Oak Ridge, Tenn., 26 Apr. 1985
(Contract DE-AC05-84OR-21400)
(DE85-013994; CONF-8504132-1) Avail: NTIS HC A03/MF A01

Appropriate means must be furnished for supplying power and for sending controlling commands to mobile teleoperated systems. Because a sizable number of possibilities are available for such applications, methods used in designing both the power and communications systems built into mobile vehicles that serve in radiological emergencies must be carefully selected. This paper describes a number of umbilical, onboard, and wireless systems used in transmitting power that are available for mobile teleoperator services. The pros and cons of selecting appropriate methods from a list of possible communication systems are also examined. Moreover, hybrid systems combining wireless power transmissions with command-information signals are also possible. DOE

N86-12976# Oak Ridge National Lab., Tenn.
FUTURE DIRECTIONS IN MOBILE TELEOPERATION
W. R. Hamel 1985 22 p Presented at the Workshop on Requirements of Mobile Teleoperators for Radiol. Emergency Response and Recovery, Dallas, 23 Jun. 1985
(Contract DE-AC05-84OR-21400)

(DE85-014308; CONF-8506148-3) Avail: NTIS HC A02/MF A01

Mobile teleoperator systems are the subject of an increasing amount of research and development. This work is motivated by general problems of remote operations in hazardous environments, some of which are very similar to the challenges of radiological emergency response and recovery. Current work appears to fall into two broad economic classes, one in the $100 K range and the other in the $1000 K range. Both are believed to be important for technology development and deployment. Recent developments confirm that we are at the technical doorstep of next-generation mobile systems which integrate dexterous manipulation, high mobility, and telerobotic operation. DOE

55 PLANETARY BIOLOGY

Includes exobiology; and extraterrestrial life.

No abstracts in this category.

59 MATHEMATICAL AND COMPUTER SCIENCES (GENERAL)

No abstracts in this category.

60 COMPUTER OPERATIONS AND HARDWARE

Includes computer graphics and data processing.

For components see *33 Electronics and Electrical Engineering.*

N86-12977# Illinois Univ., Urbana. Computer Systems Group.
A THEORY FOR ALGORITHM-BASED FAULT TOLERANCE IN ARRAY PROCESSOR SYSTEMS M.S. Thesis
P. Banerjee 10 Dec. 1984 166 p
(AD-A156244; CSG-39) Avail: NTIS HC A08/MF A01 CSCL 09/2

The concept of algorithm-based fault tolerance deals with system-level methods for obtaining reliable results from computations, especially when performed on array processor systems. In this scheme, algorithms have their outputs encoded in a system-level error-detecting or error-correcting code. This report deals with a theoretical study of the scheme of algorithm-based fault tolerance and addresses four issues. First, it deals with some design issues of specific fault-tolerant and fault-secure schemes. Algorithms are classified into broad classes called paradigms which are determined exclusively by the communication patterns of the processors. The second part deals with the development of a model which can be used to analyze the fault-detecting and fault-locating capabilities of such algorithms. The model uses a broad interpretation of errors, faults and checks, which are represented as a tripartite graph. In the third part, some graph-theoretic bounds are presented on various useful characteristics in algorithm-based fault tolerance. The model is used to determine bounds on the number of data elements that a processor may affect while allowing t-fault detection or t-fault location. The last part deals with a probabilistic study of the scheme. Expressions for the reliability of the results of the computation, and the time for completion of the computation using a particular algorithm, are derived in terms of various parameters. GRA

N86-12978# Johns Hopkins Univ., Baltimore, Md. Dept. of Electrical Engineering and Computer Science.
FAULT TOLERANT STATISTICAL SIGNAL PROCESSING ALGORITHMS FOR PARALLEL ARCHITECTURES Final Technical Report
G. G. L. Meyer and H. L. Weinert 26 Jun. 1985 28 p
(Contract N00014-81-K-0813)
(AD-A157393) Avail: NTIS HC A03/MF A01 CSCL 09/2

We analyze the effects of hardware faults on the performance of computer-implemented signal detectors, as measured by the probability of detection and the probability of false alarm. We then use these results to design fault-tolerant detectors using hardware redundancy. GRA

N86-12979# Massachusetts Inst. of Tech., Cambridge. Lab. for Computer Science.
GENERIC SOFTWARE FOR EMULATING MULTIPROCESSOR ARCHITECTURES M.S. Thesis
R. M. Soley May 1985 99 p
(Contract N00014-75-C-0661)
(AD-A157662; MIT/LCS/TR-339) Avail: NTIS HC A05/MF A01 CSCL 09/2

The expense of designing, prototyping, and testing a new computer architecture, (particularly non-traditional supercomputer architectures, such as the dataflow machine) is enormous. The relative inflexibility of hardware to experimental changes increases the need to fully test a new architectural idea. A software architecture for prototyping and testing single and multiprocessor computer architectures is outlined. An overall design is discussed, noting the need for such a system, how it would be used to model and test various architectures, and possible implementation paths. Various extensions and uses of such a generic prototyping system are also described, including extensions for modelling shared-resource systems, centrally synchronized systems, and distributed timing simulation systems. In addition, two uses of the system are presented, in particular the Tagged Token Dataflow Architecture, noting various methods in which such a machine may be simulated under a generic emulation package. Author (GRA)

N86-12980# Department of the Army, Washington, D. C.
CONTROL FOR DOT MATRIX PRINTERS OPERATING IN HARSH ENVIRONMENT Patent Application
S. L. Everett, Jr., inventor (to Army) Filed 6 Jun. 1985 115 p
(AD-D011846; US-Patent-Appl-SN-741940) Avail: NTIS HC A06/MF A01 CSCL 09/2

A control processing method and apparatus for DOT matrix printers which are subjected to relatively high levels of vibration and shock are discussed. Vibration and shock are detected and, in the event that a known safe vibration or shock level is exceeded, print line data being fed alternately to the print head from a pair of data print buffers coupled to the output of a logic data input buffer are inhibited while the input buffer temporarily stores the incoming data. Drive pulses applied to the stepper motor used to move the print head carriage are simultaneously stopped. When the detected level falls below a set threshold indicative of a safe operating level, normal operation is resumed with the print data again being fed from the input buffer to the print line buffers which are reactivated along with the carriage stepper motor. Additionally, any positional change of print head carriage during the existence of shock or vibration levels above the threshold value from the last valid driven position is determined and accordingly repositioned prior to continuing the printing operation upon cessation of the disturbance. Author (GRA)

N86-12981# Air Force Inst. of Tech., Wright-Patterson AFB, Ohio.
THE DESIGN AND HARDWARE EVALUATION OF AN ADVANCED 16-BIT, LOW-POWER, HIGH PERFORMANCE MICROCOMPUTER SYSTEM FOR DIGITAL SIGNAL PROCESSING M.S. Thesis
G. S. Mauersberger 1985 117 p
(AD-A158130; AFIT/CI/NR-85-72T) Avail: NTIS HC A06/MF A01 CSCL 09/2

This thesis is a hardware evaluation of Rockwell International's Advanced Architecture Microprocessor (AAMP) which is a single-chip, CMOS/SOS device. The microprocessor is evaluated by designing and testing and testing an AAMP based microcomputer system. The Electrical and Computer Engineering Department at Kansas State University has an ongoing program to evaluate microprocessors and identify those with low power consumption, easy interfacing and programming, and capability of rapid multiplications. The AAMP is a microprocessor which appears to possess these qualities. It is a high-performance, 16-bit, CMOS/SOS microprocessor and operates from a 20 MHz clock. The AAMP's instruction set is well suited for compiling from high level languages, such as Jovial and Ada, and includes, and integer, fractional, and floating-point arithmetic operations. This thesis covers the AAMP's operational characteristics, the developed microcomputer system, and the evaluation process. Special emphasis is given to the aspects of the AAMP's architecture and operational characteristics which are important in the design of a microcomputer system. GRA

N86-12982# Sandia National Labs., Albuquerque, N. Mex.
CURRENT CIM ACTIVITIES IN THE MATERIALS PROCESS ENGINEERING AND FABRICATION DIRECTORATE 7400
P. Plomp 28 Nov. 1985 4 p
(Contract DE-AC04-76DP-00789)
(DE85-015491; SAND-84-1472) Avail: NTIS HC A02/MF A01

The Sandia Process Engineering and Fabrication (P/F) Directorate, 7400, is steadily procuring and installing computer controlled manufacturing and inspection equipment. To program this equipment effectively and to take maximum advantage of the Sandia engineering design database, a network of VAX computers and a set of high performance color graphics terminals are proposed. This report briefly explains this program. DOE

N86-12983# Argonne National Lab., Ill.
MANAGING PERSONAL DESKTOP COMPUTING AT ARGONNE NATIONAL LABORATORY
D. W. Coultis and M. A. Gallo 1985 14 p Presented at the Conf. of the ACM SIGUCCS User Services Pulling It All Together, Toledo, 30 Sep. 1985
(Contract W-31-109-eng-38)
(DE85-014976; CONF-8509140-1) Avail: NTIS HC A02/MF A01

The increasing number of personal desktop computer users, coupled with rapidly changing personal desktop computer technology, has increased the demand for computing services at many computing centers. However, for many computing centers, budgets have not increased as rapidly as the demand for services. These centers can use several methods to help balance increasing demands and fixed resources. Providing personal desktop computing recommendations and encouraging users to follow them are effective means of meeting demands for computing services, even while operating within a constant or slowly growing budget. Providing personal desktop computing recommendations reduces evaluation costs, shifts the burden of evaluating personal desktop computing products, and encourages expertise. Making the acquisition of personal desktop computer hardware and software easier benefits the user, as well as the computing center. Users receive evaluated products for which they can obtain assistance from the computing center, while computing centers encourage the use of recommended products. Computing centers can also encourage and nurture personal desktop computing users groups. These users groups identify areas of need, participate in the evaluation process, and help reduce the demand for computing center resources. This paper discusses issues associated with managing personal desktop computing, proposes guidelines for instituting a management program, and discusses our experiences with managing personal desktop computing at Argonne National Laboratory. DOE

N86-12984# Argonne National Lab., Ill.
DAPHNE: THE DESIGN OF A PARALLEL MULTIPROCESSOR DATA ACQUISITION SYSTEM
R. T. Daly, T. H. Moog, and L. C. Welch 1985 6 p Presented at the 4th Topical Conf. on Computerized Data Acquisition in Particle and Nucl. Phys., Chicago, 19 May 1985
(Contract W-31-109-eng-38)
(DE85-013875; CONF-850579-12) Avail: NTIS HC A02/MF A01

The DAPHNE data acquisition system is designed to collect data at high rates from CAMAC instruments and to analyze the data on-line with multiple single board computers using the National 32016 microprocessor. It will be the standard data acquisition system used on all instruments at the Argonne Tandem-Linac Accelerator (ATLAS), a heavy ion accelerator. The system includes a programmable event handler to acquire the data from CAMAC instruments, event processors operating in parallel to analyze the data, an event distributor to supply the data to the parallel processors, and an intelligent event processor interface to control the event processors and transfer data between the host computer and the event processors. Functional characteristics of each of these system components are discussed and the design of the custom event distributor and intelligent event processor interface will be described in detail. DOE

N86-12985# Los Alamos Scientific Lab., N. Mex.
DATA ACQUISITION INTERFACES FOR THE IBM PERSONAL COMPUTER
F. McGirt and K. Moore May 1985 11 p
(Contract W-7405-eng-36)
(DE85-014256; LA-10432-MS) Avail: NTIS HC A02/MF A01

Data acquisition interfaces composed of standard bus structures such as CAMAC and IEEE-488 have been used with the IBM personal computer (PC). These interfaces have proved to be invaluable for applications that require automation of laboratory and field experiments and laboratory development station. Software libraries have been developed to provide easy access to these interfaces from high level programming languages such as C. DOE

N86-12986# Los Alamos Scientific Lab., N. Mex.
THE 32-BIT COMPUTER FOR LARGE MEMORY APPLICATIONS ON FASTBUS
J. M. Blossom, J. P. Hong, and R. G. Kellner 1985 4 p Presented at the 4th Topical Conf. on Computerized Data Acquisition in Particle and Nucl. Phys., Chicago, 19 May 1985
(Contract W-7405-eng-36)
(DE85-012726; LA-UR-85-1733; CONF-850579-4) Avail: NTIS HC A02/MF A01

A FASTBUS based 32 bit computer is being built at Los Alamos National Laboratory for use in systems requiring large fast memory in the FASTBUS environment. A separate local execution bus allows data reduction to proceed concurrently with other FASTBUS operations. The computer, which can operate in either master or slave mode, includes the National Semiconductor NS32032 chip set with demand paged memory management, floating point slave processor, interrupt control unit, timers, and time of day clock. The 16.0 megabytes of random access memory are interleaved to allow windowed direct memory access on and off the FASTBUS at 80 megabytes per second. DOE

N86-12987# Lister Hill National Center for Biomedical Communications, Bethesda, Md.
SYSTEMS FOR AUTHORING COMPUTER-BASED INSTRUCTION
C. Locatis and V. Carr Jan. 1985 68 p refs
(PB85-198950; LHNCBC-85-1) Avail: NTIS HC A03/MF A01 CSCL 09B

A three part report that provides an overview to authoring system technology is discussed. In part one, the technology is described and evaluation concepts and procedures are introduced. In part two, descriptive summaries of several systems are presented. Part three contains a keyword descriptive listing of over 80 systems. The focus is on systems that are primarily microcomputer based. GRA

N86-12988# National Bureau of Standards, Gaithersburg, Md. Center for Programming Science and Technology.

USING THE INFORMATION RESOURCE DICTIONARY SYSTEM COMMAND LANGUAGE Final Report
A. Goldfine Apr. 1985 86 p
(PB85-227783; NBSIR-85/3165) Avail: NTIS HC A05/MF A01 CSCL 09B

The document introduces and provides examples of the Command Language of the draft proposed Information Resource Dictionary System (IRDS). A dictionary maintained by the U.S. Air Force is defined in the IRDS and used as a continuing example throughout the document. The dictionary is populated, manipulated; and reported on using the precise syntax of the Command Language. An appendix to the document provides a complete listing of the creation of the example. Other appendices provide indices of all command appearances and all clause appearances.
GRA

N86-12406# Joint Publications Research Service, Arlington, Va.
THE 4-BIT MICROPROCESSOR CAPABILITIES, APPLICATIONS DESCRIBED
Miao Xiaosheng *In its* China Rept.: Sci. and Technol. (JPRS-CST-85-035) 17 Oct. 1985 p 73-87 Transl. into ENGLISH from Dianzi Jishu Yingyong (Beijing), no. 5, 25 May 1985 p 40-45 (For primary document see N86-12399 03-31)
Avail: NTIS HC A08/MF A01

N86-12448# Joint Publications Research Service, Arlington, Va.
PROGRAMMER FOR SINGLE-CHIP MICROPROCESSOR
Li Benren, Gong Ganghua, and Meng Qi *In its* China Rept.: Sci. and Technol. (JPRS-CST-85-029) 3 Sep. 1985 p 29-40 refs Transl. into ENGLISH from Xiaoxing Weixing Jisuanji Xitong (Shenyang), no. 1, 8 Jan. 1985 p 8-15 (For primary document see N86-12446 03-31)
Avail: NTIS HC A08/MF A01

61 COMPUTER PROGRAMMING AND SOFTWARE

Includes computer programs, routines, and algorithms.

N86-12989# Naval Biodynamics Lab., New Orleans, La.
GENERAL PLOT SUBROUTINE PACKAGE FOR THE HEWLETT PACKARD 5451C FOURIER ANALYZER
D. A. Francis Dec. 1984 88 p
(NR Proj. F58-524)
(AD-A157127; NBDL-84R008) Avail: NTIS HC A05/MF A01 CSCL 09/2

The Hewlett Packard (HP) 5451C Fourier Analyzer formerly supported two plot packages: One in the Fourier environment and one in the Real Time Executive (RTE) environment. Thus, programs which produced graphic output in the Fourier environment could not run in the RTE environment and conversely. Therefore, it was necessary to develop a standard package of plot subroutines that could run under any operating system. The package is comprised of several FORTRAN subroutines which interact directly with the plot devices, and also provide the capability to plot to the operator's terminal. The data plotting package has been found to be extremely useful for graphic output on the HP-5451C because it can run under any operating system. The plot package has been tested on the HP-5451C system and can be recommended to users with a similar need.
Author (GRA)

N86-12990# Mitre Corp., Bedford, Mass.
AISIM (AUTOMATED INTERACTIVE SIMULATION MODELING SYSTEM) OVERVIEW: REVISION 1 Final Report
H. P. Schultz Mar. 1985 22 p
(Contract F19628-84-C-0001)
(AD-A157392; MTR-8707-Rev-1; ESD-TR-85-149-Rev-1) Avail: NTIS HC A02/MF A01 CSCL 09/2

A new general purpose simulation modeling tool, Automated Interactive Simulation Modeling System (AISIM), has been developed by the Air Force System Command's Electronic Systems Division and funded by Air Force Program Element 64740F, Computer Resource Management Technology. AISIM is designed to provide quick answers to system performance questions during the conceptual phase of system acquisitions. It is currently operational on IBM and VAX computers. AISIM has undergone many tests and is now in the initial operating capability phase. Results indicate potential for wide application to the study of communications nets, computer system architectures, and data processing functions. This document introduces the reader to AISIM: its model building capabilities and its functional interfaces.
GRA

N86-12991# Yale Univ., New Haven, Conn. Dept. of Computer Science.
MICRO-PROUST
W. L. Johnson and E. Soloway Jun. 1985 123 p
(Contract N00014-82-K-0714)
(AD-A157505; YALEU/CSD/RR-402) Avail: NTIS HC A06/MF A01 CSCL 09/2

PROUST (Program Understander for Students) is a knowledge-based system that finds nonsyntactic bugs in Pascal programs written by novice programmers. When students compile a program successfully, PROUST is automatically invoked to analyze it. PROUST reports any bugs that are in the program to the student. PROUST is a 15,000 LISP program and runs on a VAX. Micro-PROUST is a program meant to capture the essence of PROUST. Micro-PROUST is a 1500 line LISP program and runs on an IBM PC (with 512 K). This document presents the inner workings of Micro-PROUST. Its intent is to enable those who so are inclined to see at a nuts and bolts level how a system like PROUST actually works.
GRA

N86-12992# Massachusetts Inst. of Tech., Cambridge. Statistics Center.
NUMERICAL ALGORITHMS AND MATHEMATICAL SOFTWARE FOR LINEAR CONTROL AND ESTIMATION THEORY Final Report, 14 Dec. 1981 - 13 Dec. 1984
V. Klema 30 May 1985 4 p
(Contract DAAG29-82-K-0028)
(AD-A157525; ARO-18441.2-MA) Avail: NTIS HC A02/MF A01 CSCL 09/2

Research concentrated on designing and implementing a microprocessor based concurrent computing environment consisting of a number of Intel microprocessors with IEEE floating point arithmetic implemented in hardware. The major focus of our work was the design of a concurrent tasker in software to locate code can data, monitor computation and communication and report results to the user. The construction of viable numerical algebra modules in an IEEE floating point arithmetic was and continues to be part of the research.
Author (GRA)

N86-12993# Stanford Univ., Calif. Systems Optimization Lab.
IMPACT OF LINEAR PROGRAMMING ON COMPUTER DEVELOPMENT
G. B. Dantzig Jun. 1985 24 p
(Contracts N00014-85-K-0343; DE-AM03-76SF00326; DE-AT03-76ER-72018; Grants NSF DMS-84-20623; NSF ECS-83-12142)
(AD-A157659; SU-SOL-85-7) Avail: NTIS HC A02/MF A01 CSCL 09/2

In the post-War period 1947 to 1952, the United States Air Force transferred considerable funds to the National Bureau of Standards to subsidize the early development of computers, and peripherals such as high speed tapes and printers. These funds, over a million dollars, help finance SEAC, SWAC UNIVAC and early research of IBM. This paper presents an intimate view of the network of colleagues of the author during this early period, their contributions, their sponsors, and why computers were needed for the solution of a broad range of planning problems. The story of how the simplex method was discovered is told once again.
Author (GRA)

N86-12994# Massachusetts Inst. of Tech., Cambridge. Artificial Intelligence Lab.

ACTORS: A MODEL OF CONCURRENT COMPUTATION IN DISTRIBUTED SYSTEMS Ph.D. Thesis

G. A. Agha Jun. 1985 203 p
(Contract N00014-80-C-0505)
(AD-A157917; AI-TR-844) Avail: NTIS HC A10/MF A01 CSCL 09/2

A foundational model of concurrency is developed in this thesis. It examines issues in the design of parallel systems and show why the actor model is suitable for exploiting large-scale parallelism. Concurrency in actors is constrained only by the availability of hardware resources and by the logical dependence inherent in the computation. Unlike dataflow and functional programming, however, actors are dynamically reconfigurable and can model shared resources with changing local state. Concurrency is spawned in actors using asynchronous message-passing, pipelining, and the dynamic creation of actors. The author defines an abstract actor machine and provide a minimal programming language for it. A more expressive language, which includes higher level constructs such as delayed and eager evaluation, can be defined in terms of the primitives. Examples are given to illustrate the ease with which concurrent data and control structures can be programmed. This thesis deals with some central issues in distributed computing. Specifically, problems of divergence and deadlock are addressed. GRA

N86-12995# Army Cold Regions Research and Engineering Lab., Hanover, N. H.

A USER'S GUIDE FOR THE BIBSORT PROGRAM FOR THE IBM-PC PERSONAL COMPUTER

T. Kyriakakis and I. K. Iskandar Apr. 1985 66 p
(DA Proj. 4A1-61102-AT-24)
(AD-A157936; CRREL-SR-85-4) Avail: NTIS HC A04/MF A01 CSCL 09/2

This report is intended to provide the reader with step-by-step instructions on how to use the BIBSORT computer program on the IBM Personal Computer. THe program allows storage and retrieval of bibliographic data. The program has been tested on an IBM-XT, using DOS 1.1 or 2.1. The program requires a monitor and a printer. This user's guide discusses how to prepare diskettes to enter the data, how to name categories and files, how to open categories and files, and how to enter data. The guide also shows how to sort and store data, edit, delete, or append the data, and how to obtain a hard copy of the sorted data. Each data diskette can take up to 500 entries, assuming 512 characters per entry. A section on how to change the program to fit specific needs is presented in Appendix A, and the program listing is in Appendix B. GRA

N86-12996# Air Force Inst. of Tech., Wright-Patterson AFB, Ohio.

A META SYSTEM FOR GENERATING SOFTWARE ENGINEERING ENVIRONMENTS Ph.D. Thesis

W. L. McKnight 1985 281 p
(AD-A158102; AFIT/CI/NR-85-71D) Avail: NTIS HC A13/MF A01 CSCL 09/2

TRIAD is a generic meta environment that has a knowledge base of methods from which a user can select a method to customize the TRIAD environment into a specific software environment. When a method is selected to customize the TRIAD environment, it becomes an instantiated method which provides guidelines and enforcement policies for developing and recording project information. The main contribution of this dissertation is in developing a kernel tool for TRIAD. This tool called the tuner can create method representations for the knowledge base of methods and can transform method representations already in the knowledge base of methods. The tuner is a parser generator like tool. However, instead of building representations in a batch and static mode, the tuner is able to create and transform the method representation in an incremental and dynamic way. Even when a method is instantiated and a part of the TRIAD environment, the method representation can be transformed. Methods are modeled by attributed grammar forms. A genesis grammar form was developed which can be used to generate all other grammar forms. The tuner is built upon the model of the genesis grammar form. The tuner is able to reflect experience gained with using a method back into the method by program transformation on the method representation. The power of the tuner is illustrated by three examples discussed in the dissertation. Problems discovered while implementing the three examples that are associated with designing interfaces for software environment are also discussed. GRA

N86-12997# Argonne National Lab., Ill.

AUTOMATED REASONING AND VARIOUS APPLICATIONS

L. Wos 1985 17 p Presented at the Autotestcon Conf., Long Island, N.Y., 22 Oct. 1985
(Contract W-31-109-eng-38)
(DE85-014998; CONF-8510116-1) Avail: NTIS HC A02/MF A01

Automated reasoning has reached an important goal - the design and implementation of a computer program that functions as a valuable automated reasoning assistant. Automated reasoning assistants are currently used to verify properties of other computer programs, design and validate logic circuits, solve problems in control systems and robotics, and answer open questions in mathematics. Of the various reasoning programs, the most flexible is ITP, a program written in PASCAL and offering the user many different options for attacking problems. The options include various types of reasoning, diverse strategies for restricting the reasoning and for directing it according to the user's knowledge and intuition, and auxiliary procedures that contribute to effectiveness. ITP can be used in interactive mode and in batch mode. It has been ported to various machines including the VAX, IBM 3033, PERQ, Apollo, Ridge, and Sun. The program is now being used by more than 100 institutions for research and for diverse applications. DOE

N86-12998# Los Alamos National Lab., N. Mex.

GUIDELINES FOR A THERMOCHEMICAL KINETICS COMPUTER PROGRAM

J. L. Janney and R. N. Rogers 1985 9 p Presented at the 14th North Am. Thermal Anal. Soc. Conf., San Francisco, 1 Sep. 1985
(Contract W-7405-eng-36)
(DE85-015671; LA-UR-85-2373; CONF-8509144-1) Avail: NTIS HC A02/MF A01

Guidelines are given for an interactive computer program that will analyze thermochemical decomposition rate data obtained by isothermal differential-scanning calorimetry. Data from any portion of the rate curve may be analyzed, and either normal or autocatalytic rate laws may be used. The computer calculates and displays normalized data listings, rate curves, order plots, and autocatalytic rate law plots. It calculates rate constants by linear regression treatment of data from curve segments chosen by the user. Many options are available, and many forms of the rate laws may be selected. This program was desighed primarily for research rather than routine use. DOE

N86-12999# Pacific Northwest Lab., Richland, Wash.

MANAGING DATA ANALYSIS THROUGH SAVE-STATES

P. J. Cowley and M. A. Whiting Apr. 1985 8 p Presented at the 17th Symp. on the Interface of Computer Sci. and Statist., Lexington, Ky., 17 Mar. 1985
(Contract DE-AC06-76RL-01830)
(DE85-012456; PNL-21-13023; CONF-8503116-2) Avail: NTIS HC A02/MF A01

Data analysis management is a methodology intended to increase the productivity of the data analyst. A primary entity for data analysis mangement is the save-state, collection of metadata and data that captures a state of the analysis. The analyst may create a save-state to designate a milestone of the analysis. The save-state may be used later to return to that milestone by restoring the conditions of the analysis that existed at the time the save-state was created. Scientists at Pacific Northwest Laboratory (PNL) have developed a prototype data analysis management system. In that system, a save-state includes pointers to the data sets and command procedures active at the time the save-state was created, active plot descriptions and other graphics parameters, and comments supplied by the analyst. Associated with each save-state is a record of the sequence of commands or operations used to accomplish the transition from the previous (parent) save-state. Metadata also describes the overall relationships between the save-states that have been created during the analysis. DOE

N86-13000# Oak Ridge National Lab., Tenn.
UNCERTAINTY PROPAGATION FROM RAW DATA TO FINAL RESULTS
N. M. Larson 1985 5 p Presented at the Intern. Conf. on Nucl. Data for Basic and Appl. Sci., Santa Fe, N. Mex., 13 May 1985
(Contract DE-AC05-84OR-21400)
(DE85-011937; CONF-850507-11) Avail: NTIS HC A02/MF A01

Reduction of data from raw numbers (counts per channel) to physically meaningful quantities (such as cross sections) is in itself a complicated procedure. Propagation of experimental uncertainties through that reduction process has sometimes been perceived as even more difficult, if not impossible. At the Oak Ridge Electron Linear Accelerator, a computer code ALEX has been developed to assist in the propagation process. The purpose of ALEX is to carefully and correctly propagate all experimental uncertainties through the entire reduction procedure, yielding the complete covariance matrix for the reduced data, while requiring little additional input from the experimentalist beyond that which is needed for the data reduction itself. The theoretical method used in ALEX is described, with emphasis on transmission measurements. Application to the natural iron and natural nickel measurements of D.C. Larson is shown. DOE

N86-13001# Rockwell International Corp., Richardson, Tex.
MAGNUM-2D COMPUTER CODE: USER'S GUIDE
R. L. England, N. W. Kline, K. J. Ekblad, and R. G. Baca Jan. 1985 176 p refs
(Contract DE-AC06-77RL-01030)
(DE85-013315; RHO-BW-CR-143P) Avail: NTIS HC A09/MF A01

Information relevant to the general use of the MAGNUM-2D computer code is presented. This computer code was developed for the purpose of modeling (i.e., simulating) the thermal and hydraulic conditions in the vicinity of a waste package emplaced in a deep geologic repository. The MAGNUM-2D computer computes: (1) the temperature field surrounding the waste package as a function of the heat generation rate of the nuclear waste and thermal properties of the basalt, and (2) the hydraulic head distribution and associated groundwater flow fields as a function of the temperature gradients and hydraulic properties of the basalt. MAGNUM-2D is a two dimensional numerical model for transient or steady state analysis of coupled heat transfer and groundwater flow in a fractured porous medium. The governing equations consist of a set of coupled, quasilinear partial differential equations that are solved using a Galerkin finite element technique. A Newton-Raphson algorithm is embedded in the Galerkin functional to formulate the problem in terms of the incremental changes in the dependent variables. Both triangular and quadrilateral finite elements are used to represent the continuum portions of the spatial domain. Line elements may be used to represent discrete conduits. DOE

N86-13002# George Washington Univ., Washington, D.C. Dept. of Electrical Engineering and Computer Science.
SCIENTIFIC WORKSTATION RESEARCH Annual Report, Aug. 1984 - Jul. 1985
J. D. Foley May 1985 6 p
(Contract DE-AS05-83ER-13122)
(DE85-013385; DOE/ER-13122/T1; AR-2) Avail: NTIS HC A02/MF A01

During the past year we have continued to develop key concepts needed in graphics programming languages. The overall language structure consists of geometric modeling, viewing, interaction management, and display management subsystems. Within each area, we have been developing descriptions of the semantic capabilities required. Several important themes run through these capabilities. The themes are important because they will form the basis for constructs in the programming language. One of the themes is that of dynamic links. Links maintain dependencies between data variables (which might include graphic/geometric objects). Thus, when variable A changes, so too do the other variables which have functional dependencies on A. Another theme is that of coordinate system. It seems natural that a graphics language deal with coordinate systems, and declare an object's coordinate system as one of its attributes. We then use another theme, that of a transformer, to relate one coordinate system to another. Transformers are useful in input (to relate the coordinate system of a mouse or tablet to the world coordinate system), and in viewing (to relate world coordinates to the screen). Another concept used is that of additional dimensions as a means of specifying attributes. The intensity of a point, for example, is just another (non-geometrical) coordinate of the point. By treating attributes in this way, the attribute values can be operated on by transformers; a separate language construct is not needed. DOE

N86-13003# George Washington Univ., Washington, D.C. Dept. of Electrical Engineering and Computer Science.
IMAGYS GRAPHICS PROGRAMMING LANGUAGE: DESCRIPTION AND ANALYSIS
J. B. Acquah and J. D. Foley 15 Nov. 1985 57 p
(Contract DE-AS05-83ER-13122)
(DE85-013384; DOE/ER-13122/2) Avail: NTIS HC A04/MF A01

IMAGYS (Interactive Modelling and Graphics System) is a high-level modelling and graphics programming language being developed at GWU. The language is designed to considerably reduce the difficulty of writing highly interactive engineering-oriented graphics programs, and is based on the paradigms of object-oriented systems and functional, or value-oriented systems. Although these are generally considered alternative approaches to designing languages, they are combined in IMAGYS to produce a language which we believe combines the best features of both and has few of the drawbacks of either. DOE

N86-13004# Sandia National Labs., Albuquerque, N. Mex.
GRAFAID: AN ENGINEERING TOOL
C. R. Adams 1985 29 p Presented at the 41st Meeting of the IMOG Subgroup on Environ. Testing, Miamisburg, Ohio, 18 Jun. 1985
(Contract DE-AC04-76DP-00789)
(DE85-013115; SAND-85-1325C; CONF-8506117-1) Avail: NTIS HC A03/MF A01

The GRAFAID code is an interactive X-Y data tool developed for use on the digital equipment corporation (DEC) VAX computers that use DEC's VAX/VMS operating system. The code was initially developed for the analysis and comparison of shock and vibration data for the generation of weapons component specifications, but has since evolved into a more general purpose data summary and analysis tool. The GRAFAID provides an interactive capability for simultaneously plotting and comparing multiple sets of X-Y data. The GRAFAID has various X-Y data analysis, manipulation, and creation capabilities. A direct access data base for storing sets of X-Y data and their plot definitions is created and maintained by GRAFAID. A neutral file system is provided for communicating X-Y data into, and out of, a GRAFAID data base. DOE

N86-13005# Sandia National Labs., Albuquerque, N. Mex.
SECOND REFERENCE CALCULATION FOR THE WIPP
L. J. Branstetter Mar. 1985 53 p refs
(Contract DE-AC04-76DP-00789)
(DE85-013180; SAND-83-2461) Avail: NTIS HC A04/MF A01

Results of the second reference calculation for the Waste Isolation Pilot Plant (WIPP) project using the dynamic relaxation finite element code SANCHO are presented. This reference calculation is intended to predict the response of a typical panel of excavated rooms designed for storage of nonheat producing nuclear waste. Results are presented that include relevant deformations, relative clay seam displacements, and stress and strain profiles. This calculation is a particular solution obtained by a computer code, which has proven analytic capabilities when compared with other structural finite element codes. It is hoped that the results presented here will be useful in providing scoping values for defining experiments and for developing instrumentation. It is also hoped that the calculation will be useful as part of an exercise in developing a methodology for performing important design calculations by more than one analyst using more than one computer code, and for defining internal Quality Assurance (QA) procedures for such calculations. DOE

N86-13006# Oak Ridge National Lab., Tenn.
TANDEM MIRROR REACTOR SYSTEMS CODE (TMRSC)
R. L. Reid, K. E. Rothe, and R. J. Barrett 1985 7 p Presented at the 6th Topical Meeting on the Technol. of Fusion Energy, San Francisco, 3 Mar. 1985 Prepared in cooperation with Burns and Roe, Inc., Oak Ridge, Tenn.
(Contract DE-AC05-84OR-21400)
(DE85-012891; CONF-850310-103) Avail: NTIS HC A02/MF A01

This paper describes a computer code developed to model a tandem mirror reactor. This is the first tandem mirror reactor model to couple the highly linked physics, magnetics, and neutronic analysis into a single code. Results from this code for two sensitivity studies are included in this paper. These studies are designed: (1) to determine the impact of center cell plasma radius, length, and ion temperature on reactor cost and performance at constant fusion power, and (2) to determine the impact of reactor power level on cost. DOE

N86-13007# Sandia National Labs., Albuquerque, N. Mex.
APPLICATION OF A BINARY CYCLIC ERROR-CORRECTING CODE
K. L. Hiebert-Dodd May 1985 32 p
(Contract DE-AC04-76DP-00789)
(DE85-013232; SAND-85-0129) Avail: NTIS HC A03/MF A01

The purpose of this report is to explain the choice and implementation of a particular error correcting code. Error correcting codes are a signal processing technique that is used to improve the reliability of communication on digital channels. DOE

N86-13008# Hanford Engineering Development Lab., Richland, Wash.
APPLICATION OF AUTOMATED REASONING SOFTWARE PROCEDURE GENERATION SYSTEM VERIFIER
D. E. Smith and S. E. Seeman Sep. 1984 4 p refs Presented at ANS/ENS Fast Reactor Safety Meeting, Knoxville, Tenn., 21 Apr. 1985
(Contract DE-AC06-76FF-02170)
(DE85-014000; HEDL-SA-3214-FP; CONF-850410-58) Avail: NTIS HC A02/MF A01

An on-line, automated reasoning software system for verifying the actions of other software or human control systems has been developed. It was demonstrated by verifying the actions of an automated procedure generation system. The verifier uses an interactive theorem prover as its inference engine with the rules included as logic axioms. Operation of the verifier is generally transparent except when the verifier disagrees with the actions of the monitored software. Testing with an automated procedure generation system demonstrates the successful application of automated reasoning software for verification of logical actions in a diverse, redundant manner. A higher degree of confidence may be placed in the verified actions gathered by the combined system. DOE

N86-13009# Lawrence Livermore National Lab., Calif.
DATA STRUCTURES AND VECTORIZATION IN A TWO-DIMENSIONAL FREE-LAGRANGIAN CODE
R. E. Cooper 1 Mar. 1985 13 p Presented at the Free-Langrangian Methods Conf., Hilton Head Island, S. Car., 4 Mar. 1985
(Contract W-7405-eng-48)
(DE85-012948; UCRL-92390; CONF-8503139-1) Avail: NTIS HC A02/MF A01

The data structures used to define the mesh, drive and the physics calculations of a 2-D Free Lagrangian hydro code are described. The mesh contains three and four sided zones but the data structures can be generalized to support n-sided zones. The mesh is redundantly described by three different data structures: zone oriented, node oriented, and edge oriented. Physics algorithms, graphics routines, and reconnection algorithms use the data structure that is easiest to use or that results in the best execution rate. On the Cray computer, these data structures are sufficient to vectorize most of the physics algorithms. The basic vectorization methods will be discussed. From experience, given a physics algorithm, a data structure can be constructed that will vectorize the algorithm. DOE

N86-13010# Sandia National Labs., Albuquerque, N. Mex.
CONTROL OF STEP SIZE AND ORDER IN EXTRAPOLATION CODES
L. F. Shampine Apr. 1985 33 p refs
(Contract DE-AC04-76DP-00789)
(DE85-013261; SAND-85-0725) Avail: NTIS HC A03/MF A01

Extrapolation of the semi-implicit midpoint rule is an effective way to solve stiff initial value problems for a system of ordinary differential equations. The theory of the control of step size and order is advanced by investigating questions not taken up before, providing additional justification for some algorithms, and providing support for procedures not properly justified by the information theory of Deuflhard. An experimental code SIMP implementing the algorithms proposed is shown to be as good as, and in some respects much better than, the research code METAN1 of Bader and Deuflhard. DOE

N86-13011# Sandia National Labs., Albuquerque, N. Mex.
FDSC: A MICROWAVE COUPLING CODE FOR SLOTS OF FINITE DEPTH
L. D. Bacon Apr. 1985 6 p
(Contract DE-AC04-76DP-00789)
(DE85-013443; SAND-85-0561) Avail: NTIS HC A02/MF A01

Joints of narrow cracks in systems that serve as ports of entry for electromagnetic waves are normally modeled as slots in an infinitesimally thick conducting surface. Although this model works well at lower frequencies, it is questionable in the microwave region, where conductor thickness can be a nonnegligible fraction of a wavelength. Measurements have shown that conductor depth does have a significant effect on the transmission properties of slots, changing both the amplitude and the resonant frequencies from those predicted by zero depth codes. This report discusses an implementation of a moments code that directly accounts for finite conductor thickness. The code indicates that slot depth has a significant effect on transmission properties. For example, resonances due to depth are found that greatly enhance the transmission at frequencies that are not directly related to slot length. These results are validated by slot transmission measurements. DOE

N86-13012# Sandia National Labs., Albuquerque, N. Mex.
DESIGN AND USE OF DIGITAL FILTERS WITH PERSONAL COMPUTER SPREADSHEET PROGRAMS
D. E. Ryerson Jun. 1985 53 p
(Contract DE-AC04-76DP-00789)
(DE85-013805; SAND-85-1073) Avail: NTIS HC A04/MF A01

Spreadsheet programs for personal computers were designed for financial analysis but have also become very useful in engineering design and analysis. This report discusses the use of spreadsheets in designing digital filters, filtering digital data, and plotting the results. DOE

N86-13013# New York Univ., New York. Inst. of Mathematical Sciences.
PROGRAM FOR SIMPLE ALGEBRA
D. Stevens Mar. 1985 44 p
(Contract DE-AC02-76ER-03077)
(DE85-013426; DOE/ER-03077/239) Avail: NTIS HC A03/MF A01

PFSA (Program For Simple Algebra) is designed to be helpful to people doing algebra and calculus with polynomial expressions. It is written entirely in FORTRAN and hence is portable and easily modified. It is much (approximately 90 times) faster than Macsyma. PFSA uses FORTRAN integer arithmetic to compute coefficients, and so the occurrence of an excessively large number in a numerator or denominator during a computation bombs the computation. The program was developed to enable a computation (of a canonical transformation for a Hamiltonian system) which was too big to be run in other systems available at the time. The intent in creating PFSA was to make a program which would do the Hamiltonian computation and similar computations easily and fast. The only language available (on the Cray) was FORTRAN. Example C in Section 3 is a very simple canonical transformation. In running the problem for which PFSA was written some intermediate expressions have more than 20,000 terms and some answers have more than 1000 terms. DOE

N86-13014# Sandia National Labs., Albuquerque, N. Mex.
SCREAMER: A SINGLE-LINE PULSED-POWER DESIGN TOOL
M. I. Kiefer and M. M. Widner 1985 12 p Presented at the 5th IEEE Pulsed Power Conf., Washington, D.C., 10 Jun. 1985
(Contract DE-AC04-76DP-00789)
(DE85-012837; SAND-84-2402C; CONF-850616-28) Avail: NTIS HC A02/MF A01

SCREAMER is a special purpose circuit code developed as a design tool for single module accelerations. It is fast, accurate, flexible, and user friendly. Its development was motivated by the excessive costs and long turn around times incurred when using the SCEPTRE circuit analysis code to perform simulations of circuits with large numbers of nodes and with nonlinear components. Comparable simulations between SCREAMER running on a VAX 11/780 and SCEPTRE running on a CRAY-1S show that turn around times and costs can be two orders of magnitude lower when using SCREAMER. DOE

N86-13015# Argonne National Lab., Ill.
PARALLEL IMPLEMENTATION OF MULTIFRONTAL SCHEMES
I. S. Duff Mar. 1985 19 p
(Contract W-31-109-eng-38)
(DE85-014295; ANL/MCS-TM-49) Avail: NTIS HC A02/MF A01

The direct solution of large sparse sets of linear equations in an MIMD environment is considered. Algorithm are based on a multifrontal approach and shwos how to distribute tasks among processors according to an elimination tree that can be automatically generated from any pivot strategy. Organizational aspects of the scheme for shared memory multiprocessor configurations are studied and implications for multiprocessors with local memories and a communication network are considered. DOE

N86-13016# Sandia National Labs., Albuquerque, N. Mex.
FUNDAMENTALS OF ADAPTIVE SIGNAL PROCESSING
S. D. Stearns Jun. 1985 42 p
(Contract DE-AC04-76DP-00789)
(DE85-014933; SAND-84-2646) Avail: NTIS HC A03/MF A01

This report describes some of the basic concepts of adaptive signal processing, including a summary of applications, the mean square error performance surface, adaptive search methods, the LMS algorithm, and the adaptive lattice. It is intended primarily to be a short review of the subject for engineers at Sandia National Laboratories. DOE

N86-13017# Los Alamos Scientific Lab., N. Mex.
ATTEMPT TO DEVELOP AN INTELLIGENT LENS DESIGN PROGRAM
V. K. Viswanathan, I. O. Bohachevsky, and T. P. Cotter 1985 13 p refs Presented at the Intern. Lens Design Conf., Cherry Hill, N.J., 10 Jun. 1985
(Contract W-7405-eng-36)
(DE85-014122; LA-74-85-2035; CONF-8506142-2) Avail: NTIS HC A02/MF A01

A Lens Design Program intended to operate without user intervention, and to improve its performance with repeated usage is being developed. The methodology and current status is discussed in this paper. DOE

N86-13018# Sandia National Labs., Albuquerque, N. Mex.
BUILDING VERSATILE TAPE HANDLING SOFTWARE
E. L. Witzke 1985 14 p Presented at the ISE Conf., Albuquerque, N. Mex., 7 May 1985
(Contract DE-AC04-76DP-00789)
(DE85-009333; SAND-85-7174C; CONF-8505177-2) Avail: NTIS HC A02/MF A01

This paper presents solutions to some of the problems involved in building versatile tape handling software. These problems were discovered while designing and implementing a media conversion facility for Sandia National Laboratories. Following a description of the purpose and capabilities of the Sandia Media Conversion and Labeling Center, the three major design problems and their solutions will be discussed. The first problem was the many possible combinations of tracks, densities, parities, and code sets, not all of which are valid. The second problem was translating one code set into another without developing N(2) translation routines. The third problem was handling the multitude of labeling combinations that can arise. Also described is how the technologies used on the Media Conversion and Labeling Center software apply to other applications. DOE

N86-13019# Los Alamos Scientific Lab., N. Mex.
DATA ACQUISITION COMMAND INTERFACE USING VAX/VMS DCL
R. V. Poore, D. M. Barrus, G. Cort, J. A. Goldstone, L. B. Miller, and R. O. Nelson 1985 10 p Presented at the 4th Topical Conf. on Computerized Data Acquisition in Particle and Nucl. Phys., Chicago, 19 May 1985
(Contract W-7405-eng-36)
(DE85-012747; LA-UR-85-1757; CONF-850579-8) Avail: NTIS HC A02/MF A01

The user interface to a data acquisition system is being developed at the Los Alamos Weapons Neutron Research Facility using the VAX/VMS command language interface DCL. Commands are being implemented which provide for system initialization and control functions and FASTBUS diagnostics. The data acquisition system incorporates the concept of a data acquisition state (running, halted, etc.) where a certain subset of input commands is allowed. DOE

N86-13020# Oak Ridge National Lab., Tenn.
TWOPOT: A COMPUTER MODEL OF THE TWO-POT EXTRACTIVE DISTILLATION CONCEPT FOR NITRIC ACID
R. T. Jubin, W. D. Holland, R. M. Counce, and D. R. Beckwith May 1985 71 p refs
(Contract DE-AC05-84OR-21400)
(DE85-013523; ORNL/TM-9241) Avail: NTIS HC A04/MF A01

A mathematical model, TWOPOT, of the two-pot extractive distillation concept for nitric acid concentration has been developed. Prediction from a computer simulation using this model shows excellent agreement with the experimental data. This model is recommended for use in the design of large-scale, similer-purpose equipment. DOE

N86-13021# Detroit Diesel Allison, Indianapolis, Ind. Gas Turbine Div.
USER'S MANUAL FOR USING MASON: A FREQUENCY RESPONSE PROGRAM WHICH HANDLES A SYSTEM OF TRANSFER FUNCTIONS DESCRIBED BY A SIGNAL FLOW GRAPH
L. C. Boger Jul. 1985 100 p
(PB85-227106; DDAD/EDR-11187; NTIS/SW/MT-85/001A) Avail: NTIS HC A05/MF A01 CSCL 09B

MASON is a frequency response computer program useful in the design and analysis of linear control systems. Complex signal flowgraphs involving either Laplace Transform or Z-Transform transmittances are reduced via a computational algorithm based on Mason's Gain Formula. Continuous time systems are evaluated with s=jw and discrete line systems use z=exp(sT). The transmittances may include polynomial expressions, transport tags or actual gain/phase data from experimental testing. The input structure is user oriented providing for simple transfer function representation between nodes. Frequency response, resonant peak, resonant frequency and gain and phase margin are calculated where appropriate and form the program output. GRA

N86-12388# Tohoku Univ., Sendai (Japan). Research Inst. of Electrical Communication.
A METHODOLOGY FOR SYNTAX-ANALYSIS USING PROLOG
Takahika Murayama, Yoshiyuki Kawazoe, and Yoshiharu Shigei *In its* The Record of Elec. and Commun. Eng. Conversazione, Vol. 54, No. 1 Aug. 1985 p 26-30 refs In JAPANESE; ENGLISH summary (For primary document see N86-12383 03-31)
Avail: NTIS HC A03/MF A01

62 COMPUTER SYSTEMS

Includes computer networks.

N86-13022# Naval Postgraduate School, Monterey, Calif.
DESIGN AND IMPLEMENTATION OF THE COMPUTER SYSTEMS DESIGN ENVIRONMENT NETWORK M.S. Thesis
J. L. Poole Mar. 1985 93 p
(AD-A156832; AD-E301723) Avail: NTIS HC A05/MF A01 CSCL 09/2

This thesis develops and implements a computer network for the Computer System Design Environment (CSDE). The CSDE network is based upon the use of the Zenith-100 (Z100) computer as an intelligent workstation. The Z100 provides direct communication with the VAX 11/780 mainframe and Prolog computer systems. Included on line in the Z100 workstation is a users manual which describes network operations. The users manual is designed to take the first-time CSDE user through all phases of the CSDE process in a step-by-step manner. Author (GRA)

N86-13023# Lawrence Livermore National Lab., Calif.
ROLE OF SUPERCOMPUTERS IN MAGNETIC FUSION AND ENERGY RESEARCH PROGRAMS
J. Killeen Jun. 1985 22 p
(Contract W-7405-eng-48)
(DE85-013200; UCRL-92792) Avail: NTIS HC A02/MF A01

The importance of computer modeling in magnetic fusion (MFE) and energy research (ER) programs is discussed. The need for the most advanced supercomputers is described, and the role of the National Magnetic Fusion Energy Computer Center in meeting these needs is explained. DOE

N86-13024# Lawrence Livermore National Lab., Calif.
LABNET PROJECT PLAN
G. Pavel 24 Jun. 1985 41 p
(Contract W-7405-eng-48)
(DE85-014860; UCID-20471) Avail: NTIS HC A03/MF A01

LabNet value-added service is a high-speed packet-switched network that ties computers together. From the point-of-view of a single computer, or of a local network of computers within a building or a group of buildings, the LabNet high-speed network is a long-haul network (like Tymnet or ARPANET) for getting to other buildings. This service is provided through channels of the backbone that are shared by everyone at the Laboratory. The focus of the high-speed network is the efficient transfer of data between computers as opposed to the interconnection of people's terminals to these computers. The latter function is best served by the local networks, or by a separate network. DOE

63 CYBERNETICS

Includes feedback and control theory.
For related information see also *54 Man/System Technology and Life Support.*

N86-13025# Air Force Human Resources Lab., Brooks AFB, Tex.
ARTIFICIAL INTELLIGENCE IN Ada: PATTERN-DIRECTED PROCESSING Final Report
L. H. Reeker, J. Kreuter, and K. Wauchope May 1985 45 p
(AD-A157097; AFHRL-TR-85-12) Avail: NTIS HC A03/MF A01 CSCL 09/2

If the programming language Ada is to be widely used in artificial intelligence applications, it will be necessary to demonstrate to programmers that it can provide superior facilities for use in that domain. One means of doing this is to provide facilities for pattern-directed programming within Ada. This report includes three papers, of which the first is designed to serve as an introduction to pattern-directed programming and to the significance of the two papers that follow. It includes discussions of artificial intelligence programming and the facilities provided by the Ada language, pattern-directed computation, pattern matching, and parsing. The other two papers deal with the use of Ada for pattern-directed programming. One paper deals with efficient implementation of pattern matching (within Ada), important because pattern matching tends to be inefficient, leading to problems with excessive processing time. Another paper treats extensions of pattern-direction from strings to more general data structures of the sort used in artificial intelligence. Author (GRA)

N86-13026# Perceptronics, Inc., Ann Arbor, Mich.
PILOT'S ASSOCIATE DEFINITION STUDY Final Report, Jul. 1984 - May 1985
R. G. Eisenhardt, G. H. Eisenhardt, and D. Z. Douthat May 1985 139 p
(Contract MDA903-84-C-0329; ARPA Order 5116)
(AD-A157106; FR2213U/4577) Avail: NTIS HC A07/MF A01 CSCL 15/7

Air combat operational and technological problems in the 1995 technology time frame are analyzed for application of artificial intelligence technology under the DARPA's Strategic Computing Program. Operational missions are examined to identify those functions most critical for mission success. Applicable technology is reviewed including sources other than the SCP. A case is made for application of information processing architectural concepts new to airborne weapon systems, but matured in other disciplines over several decades, to accommodate AI technology. Such architecture are developed and reviewed. Onboard information processing hierarchies are developed to support mission requirements for both air-to-air and air-to-ground missions. These are then grouped into five processors, including a pilot/vehicle interface, to transition from the output of sensor signal processing to highly symbolic information for presentation to the pilot/crew. These processors are a Situation Awareness Manager to develop and maintain a current world model external to the airplane, a System Status Manager to perform the same function for the world inside the plane, a Tactical Manager to assess tactical implications of the world and make recommendations to the pilot for action, and a Mission Manager to evaluate mission plans vis-a-vis current situation and assist the pilot in revising plans as necessary. Artificial intelligence technology, both hardware and software, is reviewed and areas and degree of application efforts, measures of effectiveness (MOE) and performance (MOP) are suggested and defined. GRA

N86-13027# Allied Bendix Corp., Kansas City, Mo.
KNOWLEDGE-BASED SYSTEMS: HOW WILL THEY AFFECT MANUFACTURING IN THE 80'S
M. S. King, S. L. Brooks, and R. M. Schaefer Apr. 1985 19 p refs Presented at the ASME Intern. Computers in Eng. Conf. and Exhibition, Boston, 4 Aug. 1985
(Contract DE-AC04-76DP-00613)
(DE85-010601; BDX-613-3185; CONF-850862-1) Avail: NTIS HC A02/MF A01

Knowledge-based or expert systems have been in various stages of development and use for a long time in the academic world. Some of these systems have come out of the lab in recent years in the fields of medicine, geology, and computer system design. The use of knowledge-based systems in conjunction with manufacturing process planning and the emerging CAD/CAM/CAE technologies promises significant increases in engineering productivity. Areas in manufacturing where knowledge-based systems could most benefit the engineer and industry are emphasized. DOE

64 NUMERICAL ANALYSIS

Includes iteration, difference equations, and numerical approximation.

N86-13028*# Drexel Univ., Philadelphia, Pa. Dept. of Mechanical Engineering and Mechanics.
RESEARCH ON OUTPUT FEEDBACK CONTROL Interim Report, Jan. - Sep. 1985
Anthony J. Calise and Friedrich S. Kramer Nov. 1985 20 p refs
(Grant NAG1-243)
(NASA-CR-174253; NAS 1.26:174253) Avail: NTIS HC A02/MF A01 CSCL 12A

In designing fixed order compensators, an output feedback formulation has been adopted by suitably augmenting the system description to include the compensator states. However, the minimization of the performance index over the range of possible compensator descriptions was impeded due to the nonuniqueness of the compensator transfer function. A controller canonical form of the compensator was chosen to reduce the number of free parameters to its minimal number in the optimization. In the MIMO case, the controller form requires a prespecified set of ascending controllability indices. This constraint on the compensator structure is rather innocuous in relation to the increase in convergence rate of the optimization. Moreover, the controller form is easily relatable to a unique controller transfer function description. This structure of the compensator does not require penalizing the compensator states for a nonzero or coupled solution, a problem that occurs when following a standard output feedback synthesis formulation. G.L.C.

N86-13029# Camerino Univ. (Italy).
A NEW METHOD FOR GLOBAL OPTIMIZATION BASED ON STOCHASTIC DIFFERENTIAL EQUATIONS Final Technical Report, Dec. 1981 - Dec. 1984
F. Aluffi-Pentini, V. Parisi, and F. Zirilli Dec. 1984 282 p In ENGLISH and ITALIAN
(Contract DAJA37-81-C-0740; DA Proj. 1T1-61102-BH-57)
(AD-A157546) Avail: NTIS HC A13/MF A01 CSCL 12/1

A new approach is presented to the problem of finding a global (i.e., absolute) minimizer of a function of several real variables, and some of its mathematical properties are investigated. The approach is based on the idea of following the solution trajectories of a stochastic differential equation inspired by statistical mechanics. This document also describes a complete algorithm (SIGMA) based on the above approach, which looks for a point of global minimum by monitoring the values of the function to be minimized along a number of simultaneously-evolving trajectories generated by a new (stochastic) scheme for the numerical integration of the stochastic differential equation. Finally described is the software package SIGMA which implements the above algorithm in a portable subset of the A.N.S. FORTRAN 4 language, a number of carefully selected test problems designed for testing the software for global optimization, and the results of testing SIGMA on the above problems, and on a problem of theoretical chemistry. The main conclusion is that the performance of SIGMA is very good, even on some very hard problems. Author (GRA)

N86-13030# Naval Surface Weapons Center, Silver Spring, Md.
RELATIONSHIPS BETWEEN PRIME-RICH EULER TYPE EQUATIONS AND A TRIANGULAR ARRAY OF THE ODD INTEGERS
R. S. Sery Feb. 1985 33 p
(AD-A157928; NSWC/TR-85-120) Avail: NTIS HC A03/MF A01 CSCL 12/1

A certain triangular array of the odd integers, which is built up along successive diagonals of a rectangular grid, is correlated with equations of the form x squared-x+c, c=2n-1, n+1,2,3... where n indicates the number of the column (and also the row number for equations x squared + x - r). Primitive cell arrays are derived from the above array. Each such array consists of a prime value p(of c) which is substituted for every integer in the triangular array who is identical to 0(mod p) with all other locations corresponding to integers not identical to (mod p) left blank. Various relationships between the triangular array, the equations x squared - x + c, c=1,3,5,... and the derived primitive cell arrays are brought out. These show how: (1) Euler type prime-rich equations can be found; (2) why and how nonrandom structures exists in the way prime numbers occur in the sequence of the positive integers 1,2,3....are presented. GRA

N86-13031# Army Armament Research and Development Command, Watervliet, N. Y. Large Caliber Weapon Systems Lab.
VARIATIONAL PRINCIPLE FOR PENETRATOR DYNAMICS USING BILINEAR FUNCTIONAL AND ADJOINT FORMULATION Final Technical Report
C. N. Shen Jun. 1985 24 p Presented at 2nd Army Conf., Appl. Math. and Computing, Troy, NY, 22-24 May 1984
(AD-A157964; AD-E440290; ARLCB-TR-85021) Avail: NTIS HC A02/MF A01 CSCL 19/4

The solution to problems in both spatial and time domains using the finite element method can be based on the variational principle employing bilinear functional and adjoint formulation. The principle is extended to matrix vector coupling systems such as in penetration dynamics. The present hyperbolic type partial differential equation of interest has two dependent and two independent variables with the coupling in the spatial domain. GRA

N86-13032# Wisconsin Univ., Madison. Mathematics Research Center.
ON HIGH-ORDER ACCURATE INTERPOLATION FOR NON-OSCILLATORY SHOCK CAPTURING SCHEMES Technical Summary Report
A. Harten Jun. 1985 43 p
(Contracts DAAG29-82-C-0090; DAAG29-80-C-0041)
(AD-A158131; MRC-TSR-2829) Avail: NTIS HC A03/MF A01 CSCL 12/1

This paper describes high-order accurate Godunov-type schemes for the computation of weak solutions of hyperbolic conservation laws that are essentially non-oscillatory. It is shown that the problem of designing such schemes reduces to a problem in approximation of functions, namely that of reconstructing a piecewise smooth function from its given oscillations. To solve this reconstruction problem we introduce a new interpolation technique that when applied to piecewise smooth data gives high-order accuracy wherever the function is smooth but avoids having a Gibbs-phenomenon at discontinuities. Author (GRA)

N86-13033# Wisconsin Univ., Madison. Mathematics Research Center.
TWO RESULTS ON DENSE IMBEDDINGS Technical Summary Report
M. Renardy Jun. 1985 8 p
(Contract DAAG29-80-C-0041; Grant NSF MCS-82-15064)
(AD-A158132; MRC-TSR-2833) Avail: NTIS HC A02/MF A01 CSCL 12/1

In a recent paper J. U. Kim studied the Cauchy problem for a Bingham fluid in R sub 2. He points out that the extension of his results to R sub 3 depends on two lemmas concerning dense imbedding of C sub 0 infinity functions in certain spaces. In this paper these lemmas are proved. Author (GRA)

N86-13034# Wisconsin Univ., Madison. Mathematics Research Center.
PENALIZED LIKELIHOOD FOR GENERAL SEMI-PARAMETRIC REGRESSION MODELS Technical Summary Report
P. J. Green May 1985 31 p
(Contract DAAG29-80-C-0041)

(AD-A158133; MRC-TSR-2819) Avail: NTIS HC A03/MF A01 CSCL 12/1

This paper examines maximum penalized likelihood estimation in the context of general regression problems, characterized as probability models with composite; likelihood functions. The emphasis is on the common situation where a parametric model is considered satisfactory but for inhomogeneity with respect to a few extra variables. A finite-dimensional formulation is adopted, using a suitable set of basis functions. Appropriate definitions of deviance, degrees of freedom, and residual are provided, and the method of cross-validation for choice of the tuning constant is discussed. Quadratic approximations are derived for all the required statistics. Author (GRA)

N86-13035# Wisconsin Univ., Madison. Mathematics Research Center.

HAMILTON-JACOBI EQUATIONS IN INFINITE DIMENSIONS. PART 2: EXISTENCE OF VISCOSITY SOLUTIONS Technical Summary Report

M. G. Crandall and P. L. Lions Jun. 1985 46 p
(Contract DAAG29-80-C-0041)
(AD-A158137; MRC-TSR-2826) Avail: NTIS HC A03/MF A01 CSCL 12/1

This paper is the second in a series by the authors concerned with the theory of viscosity solutions Hamilton-Jacobi equations in infinite dimensional spaces. The first paper introduced a notion of viscosity solution appropriate for the study of Hamilton-Jacobi equations in spaces with the so-called Radon-Nikodym property and obtained uniqueness theorems under assumptions paralleling the finite dimensional theory. The main results of the current paper concern existence of solutions of stationary and time-dependent Hamilton-Jacobi equations. In order to establish these results it is necessary to overcome the difficulties associated with the fact that bounded sets are not precompact in infinite dimensions and this is done by sharp constructive estimates coupled with the use of differential games to solve regularized problems. Interest in this subject arises on the abstract side from the desire to contribute to the theory of linear partial differential equations in infinite dimensional spaces to treat natural questions raised by the finite dimensional theory. Interest also arises from potential applications to the theory of control of partial differential equations. However, the results herein do not apply directly to problems of the form arising in the control of partial differential equations, a question which will be treated in the next paper of the series. Author (GRA)

N86-13036# Wisconsin Univ., Madison. Mathematics Research Center.

C INFINITY-REGULARITY FOR THE POROUS MEDIAN EQUATION Technical Summary Report

K. Hoellig and H. O. Kreiss Jun. 1985 14 p
(Contract DAAG29-80-C-0041; Grant NSF DMS-83-51187)
(AD-A158147; MRC-TSR-2828) Avail: NTIS HC A02/MF A01 CSCL 20/4

The equation stated in the abstract describes the expansion of a gas in a one dimensional porous medium. While existence of weak solutions can be obtained by standard energy methods, not much was known about regularity of the solution near the free boundaries. The difficulty is that the equation degenerates at the boundary and the hyperbolic term becomes dominant. The authors show in this report that despite of the degeneracy the free boundary is smooth with the possible exception of a discontinuity in the derivative at the waiting time. Their method is based on energy estimates in weighted norms using some of the ideas in another document. GRA

N86-13037# Wisconsin Univ., Madison. Mathematics Research Center.

A FLOQUET DECOMPOSITION FOR VOLTERRA EQUATIONS WITH PERIODIC KERNEL AND A TRANSFORM APPROACH TO LINEAR RECURSION EQUATIONS Technical Summary Report

D. L. Russell Jun. 1985 38 p
(Contract DAAG29-80-C-0041; Grant AF-AFOSR-0088-84)
(AD-A158148; MRC-TSR-2824) Avail: NTIS HC A03/MF A01 CSCL 12/1

This report provides the theoretical background for an earlier report (Frequency/Period Estimation and Adaptive Rejection of Sinusoidal Disturbances). It also lays the foundation for a new type of transform analysis for linear recursion equations which appears to be quite useful in analyzing their spectral properties. Author (GRA)

N86-13038# Wisconsin Univ., Madison. Mathematics Research Center.

THE UNIQUENESS OF HILL'S SPHERICAL VORTEX Technical Summary Report

C. J. Amick and L. E. Fraenkel May 1985 50 p
(Contract DAAG29-80-C-0041)
(AD-A158149; MRC-TSR-2820) Avail: NTIS HC A03/MF A01 CSCL 12/1

The only explicit exact solution of the problem of steady vortex rings is that found, for a particular case, by Hill in 1984; it solves a semilinear elliptic equation, of order two, involving a Stokes stream function psi (r,z) and a non-linearity sub H (psi) that has a simple discontinuity at psi = 0. This paper proves that: (1) any weak solution of the corresponding boundary-value problem is Hill's solution, modulo translation along the axis of symmetry (r = 0), and (2) any solution of the isoperimetric variational problem in another paper is a weak solution, indeed, any local maximizer is a weak solution. The result (2) is not immediate because f sub H is discontinuous; consequently, the functional that is maximized is not Frechet differentiable on the whole Hilbert space in question. Author (GRA)

N86-13039# Wisconsin Univ., Madison. Mathematics Research Center.

GLOBAL OPTIMIZATION USING AUTOMATIC DIFFERENTIATION AND INTERVAL ITERATION Technical Summary Report

L. B. Rall Jun. 1985 34 p
(Contract DAAG29-80-C-0041)
(AD-A158150; MRC-TSR-2832) Avail: NTIS HC A03/MF A01 CSCL 12/1

A standard problem in scientific computation is the optimization of a smooth (at least twice differentiable) function, possibly subject to smooth constraints. Here, optimization means finding the maximum or minimum value of the function in some region, or perhaps its stationary points. The algorithm presented in this paper solves this problem for regions which are rectangular in form. The method used is a version of interval iteration which finds one or all of the critical points of the function in the given region (the point or points at which its gradient vector vanishes), or just the critical points at which the function has its maximum or minimum values. The required values of the gradient vector and Hessian matrix of the function are obtained by automatic differentiation, which does not involve symbolic differentiation or numerical approximation of the derivatives of the function being investigated. Unlike algorithms which sample function values only at a discrete set of points, the ones given here use interval computation to furnish guaranteed bounds for all quantities of interest over the required subregions of the initial region. The results given by these optimization algorithms are thus self-validating. The algorithms presented here have been programmed using standard implementations of automatic differentiation and interval computation. Numerical examples are given to illustrate the effectiveness of this approach to the type of optimization problem considered. GRA

N86-13040# Army Cold Regions Research and Engineering Lab., Hanover, N. H.

STEFAN'S PROBLEM IN A FINITE DOMAIN WITH CONSTANT BOUNDARY AND INITIAL CONDITIONS ANALYSIS

S. Takagi Jun. 1985 36 p
(AD-A158558; CRREL-SR-85-8) Avail: NTIS HC A03/MF A01 CSCL 12/1

Stefan's problem in a finite domain is solved under constant boundary and initial conditions. Starting in a semi-infinite domain, the solution passes infinitely many stages of lead times in a finite domain and finally becomes stationary. The singularity at the finite terminal necessitates introduction of lead times. Including lead times, parameters defining the solution vary with time. Only the analytical result is reported in this paper. Partial contents: Mathematical preliminaries- Elemental functions, Integral formulas, Functions of a series; and Stefan's problem in a finite domain-Problem, Widder's solution of heat conduction, Temperature with embedding unknowns, Lead times, The Nth stage, and The final stage. GRA

N86-13041# Sandia National Labs., Albuquerque, N. Mex.
CONTROL OF STEP SIZE AND ORDER IN EXTRAPOLATION CODES
L. F. Shampine 1985 29 p refs Presented at the South African Symp. on Numerical Math, Durban, South Africa, 8 Jul. 1985
(Contract DE-AC04-76DP-00789)
(DE85-010122; SAND-85-0725C; CONF-850752-1) Avail: NTIS HC A03/MF A01

Extrapolation of the semi-implicit midpoint rule is an effective way to solve stiff initial value problems for a system of ordinary differential equations. The theory of the control of step size and order is advanced by investigating questions not taken up before, providing additional justification for some algorithms, and providing support for procedures not properly justified by the information theory approach of Deuflhard. An experimental code SIMP implementing the algorithms proposed is shown to be as good as, and in some respects much better than, the research code METAN1 of Ba[illegible]r and Deuflhard. DOE

N86-13042# New York Univ., New York. Mathematics and Computing Lab.
HYPERBOLIC SYSTEMS OF CONSERVATION LAWS IN SEVERAL SPACE VARIABLES
P. D. Lax May 1985 18 p
(Contract DE-AC02-76ER-03077)
(DE85-014019; DOE/ER-03077/246) Avail: NTIS HC A02/MF A01

We show how to associate to each analytic function f of one variable a complex conservation law. When written in terms of real variables, this equation turns into a symmetric hyperbolic system of two first order conservation laws in time and two space variables for two unknowns. The hope is that the theory of analytic functions can be explicited to study the properties of the solutions of these model equations. These systems are strictly hyperbolic where f' is unequal to zero, and nonlinear where f'' is unequal to zero. There is, however, in every state at least one direction of propagation which is not genuinely nonlinear. We then show that every 2 x 2 quasilinear first order hyperbolic system fails to be genuinely nonlinear in some direction of propagation. The notions of the first section are easily extended to analytic functions of several variables. DOE

N86-13043# Edgerton, Germeshausen and Grier, Inc., Idaho Falls, Idaho.
TRANSISTORIZED MULTIGRID METHODS. 1: LINEAR ELLIPTIC PROBLEMS ON TWO- AND THREE-DIMENSIONAL REGIONS
A. Shieh Mar. 1985 46 p Presented at the 2nd Copper Mountain Conf. on Multigrid Methods, Copper Mountain, Colo., 1 Apr. 1985
(Contract DE-AC07-76ID-01570)
(DE85-014632; EGG-M-07685; CONF-8504100-2) Avail: NTIS HC A03/MF A01

Suitable combination of mathematical transistors and half-weighting filters gives accurate estimate of local truncation error for moderate size problems with reasonable smooth solutions without up and down cycling. The use of symmetric mathematical transistors is particularly effective for supercomputing. DOE

N86-13044# Oak Ridge Y-12 Plant, Tenn.
PADE AND RECIPROCAL APPROXIMANTS AND LINEAR NOLOR FUNCTIONS
R. W. Johnson and P. I. Tinnel 28 Jun. 1985 21 p refs
(Contract DE-AC05-84OS-21400)
(DE85-015057; Y-2350) Avail: NTIS HC A02/MF A01

Converting a truncated infinite series to a rational fraction such as the Pade' Approximant (PA) can improve the accuracy of numerical calculations. The numerical integration of differential equations is an example. We have discovered a simpler method of reducing truncation errors and we call the new approximation the Reciprocal Approximant (RA). Although the RA is the easier to compute; nevertheless, for certain truncated infinite series the RA is more accurate than the PA. The NOLOR is the normal at any point of the curve of the natural logarithm of y'(dy/dx or rate) vs x (or time). It is like an instantaneous time constant which is not necessarily constant. The Nth order chemical reaction is an example of a linear NOLOR function; the derivative of NOLOR is a constant. Complex functions can often be adequately approximated with two or more segments of different linear NOLOR functions. For slab diffusion, the time derivative of NOLOR is approximately 2 before the process is 50% complete and approximately 0 after the process if 50% complete. The N value (for a chemical reaction) is the reciprocal of 1 minus the derivative of NOLOR with respect to x (or time). The inverse function of a linear NOLOR function is also a linear NOLOR function. The first derivatives are reciprocals. The inverse NOLOR is the negative of the product of NOLOR multiplied by the first derivative. The sum of the derivative of NOLOR with respect to x plus the derivative of the inverse NOLOR with respect to y is equal to 1. DOE

N86-13045# New York Univ., New York. Mathematics and Computing Lab.
ELEMENTARY WAVES AND RIEMANN SOLUTIONS: THEIR THEORY AND THEIR ROLE IN SCIENCE
J. Glimm May 1985 11 p
(Contract DE-AC02-76ER-03077)
(DE85-014018; DOE/ER-03077/249) Avail: NTIS HC A02/MF A01

Elementary waves and Riemann solutions are solutions of a nonlinear conservation law which are distinguished by symmetry properties. In this paper we discuss the theory of elementary waves and Riemann solutions with an emphasis on general concepts and open problems. The importance of these solutions to science will also be discussed. DOE

N86-12436# Joint Publications Research Service, Arlington, Va.
MATHEMATICAL PRINCIPLE FOR GENERATING SECOND-ORDER ASPHERICAL SURFACE
Pan Junhua and Wang Jinaguo *In its* China Rept.: Sci. and Technol. (JPRS-CST-85-034) 1 Oct. 1985 p 78-84 ref Transl. into ENGLISH from Guangxue Xuebao (Shanghai), v. 4, no. 3, Mar. 1983 p 252-256 (For primary document see N86-12430 03-31)
Avail: NTIS HC A08/MF A01

N86-12463# Joint Publications Research Service, Arlington, Va.
VECTOR VALUED LONG JAMES TYPE BANACH SPACES J(eTA, l sub p)(1 < OR = p < + INFINITY)
Zhao Junfeng *In its* China Rept.: Sci. and Technol. (JPRS-CST-85-032) 19 Sep. 1985 p 30-39 refs Transl. into ENGLISH from Xitong yu Shuxue (Beijin), v. 5, no. 1, Jan. 1985 p 51-62 (For primary document see N86-12462 03-31)
Avail: NTIS HC A08/MF A01

N86-12464# Joint Publications Research Service, Arlington, Va.
FINITE DIFFERENCE SCHEME FOR ONE-DIMENSIONAL MAGNETOHYDRODYNAMIC EQUATIONS
Liu Deming *In its* China Rept.: Sci. and Technol. (JPRS-CST-85-032) 19 Sep. 1985 p 40-54 refs Transl. into ENGLISH from Shuzhi Jisuan yu Jisuanji Yingyong (Beijing), v. 5, no. 3, Sep. 1984 p 138-150 (For primary document see N86-12462 03-31)
Avail: NTIS HC A08/MF A01

65 STATISTICS AND PROBABILITY

Includes data sampling and smoothing; Monte Carlo method; and stochastic processes.

N86-13046# Southern Methodist Univ., Dallas, Tex.
NEW REPRESENTATIONS OF THE NON-CENTRAL chi-SQUARE DENSITY AND CUMULATIVE Technical Report, 1 Jan. 1984 - Jun. 1985
Y. M. Chou, K. H. Arthur, R. B. Rosentein, and D. B. Owen 1984 11 p
(Contract N00014-84-K-0146)
(AD-A157227; Rept-5-184-85) Avail: NTIS HC A02/MF A01 CSCL 12/1

In this reprint Representations of noncentral chi-square cumulative distribution function and probability density function are reveiwed and new representations are given. One representation of the cdf in terms of an integral is easily computed on any machine which has an accurate algorithm for computing the normal cdf. GRA

N86-13047# Maryland Univ., College Park. Dept. of Management Sciences and Statistics.
A SURVEY OF SOME RECENT RESULTS IN CONTINUOUS UNIVARIATE DISTRIBUTIONS Technical Report, Sep. 1984 - Aug. 1985
S. Kotz and N. L. Johnson Jul. 1985 17 p
(Contract N00014-84-K-0301)
(AD-A157450; UMD-DMSS-85/7) Avail: NTIS HC A02/MF A01 CSCL 12/1

Pursuant to the authors on advances in discrete distributions (Johnson and Kotz (1982)) they have commenced work on advances in continuous univariate distributions from 1971 onwards. In contrast to the situation for discrete distributions, this field was markedly more fully developed by 1970, in regard to both variety of available distributions and sophistication of methods for fitting. Possibly as a consequence, there is now available a number of very useful survey articles for particular families of distributions. This document makes reference to these at appropriate points, indicating the nature of their contents. The interested reader is recommended to study these sources for more precise information. While taking advantage of the existence of these valuable summaries to reduce the volume of our own work, the authors believed they should include enough descriptive material to provide an adequate picture of the current situation. In this discussion of distributions already in use before 1971, this document focuses mostly on methods of fitting (including the closely related topic of estimation of parameters), though there will often be examples of new applications and occasionally some new properties to report. In regard to distributions which have come into use since 1971 we will, in addition, endeavor to provide some indication of the genesis of the distribution, its properties and relations to other distributions. GRA

N86-13048# Stanford Univ., Calif. Dept. of Statistics.
TRANSFORMING CENSORED SAMPLES AND TESTING FIT
F. J. OReilly and M. A. Stephens 23 Jul. 1985 29 p
(Contract N00014-76-C-0475)
(AD-A157957; TR-361) Avail: NTIS HC A03/MF A01 CSCL 12/1

One approach to testing the goodness-of-fit of a completely specified continuous distribution with a censored sample, is to transform the corresponding uniform censored sample into a complete uniform sample and then to use any of the classical uniformity tests. Two systematic procedures for transforming a censored uniform sample are proposed. A Monte Carlo power study was conducted to analyze the relative merits of these procedures when followed by the Anderson-Darling A2 test for uniformity. The suggested transformations are versatile and with A2, give good power for most alternatives. Author (GRA)

N86-13049# Georgia Inst. of Tech., Atlanta. School of Industrial and Systems Engineering.
COMPOUND POISSON APPROXIMATIONS FOR SUMS OF RANDOM VARIABLES
R. F. Serfozo May 1985 17 p
(Grant AF-AFOSR-0367-84)
(AD-A158555; AFOSR-85-0623TR) Avail: NTIS HC A02/MF A01 CSCL 12/1

This document shows that a sum of dependent random variables is approximately compound Poisson when the variables are rarely nonzero and, given they are nonzero, their conditional distributions are nearly identical. It gives several upper bounds on the total-variation distance between the distribution of such a sum and a compund Poisson distribution. Included is an example for Markovian occurrences of a rare event. The bounds are consistent with those that are known for Poisson approximations for sums of uniformly small random variables. Author (GRA)

N86-13050# Los Alamos National Lab., N. Mex.
SYSTEMS ANALYSIS APPROACH TO PROBABILISTIC MODELING OF FAULT TREES
R. J. Bartholomew and C. R. Qualls 1985 12 p Presented at the 8th Intern. Conf. On Struct. Mech. In Reactor Technol., Brussels, 19 Aug. 1985 Prepared in cooperation with New Mexico Univ., Albuquerque
(Contract W-7405-eng-36)
(DE85-007705; LA-UR-85-494; CONF-850809-15) Avail: NTIS HC A02/MF A01

A method of probabilistic modeling of fault tree logic combined with stochastic process theory (Markov modeling) has been developed. Systems are then quantitatively analyzed probabilistically in terms of their failure mechanisms including common cause/common mode effects and time dependent failure and/or repair rate effects that include synergistic and propagational mechanisms. The modeling procedure results in a state vector set of first order, linear, inhomogeneous, differential equations describing the time dependent probabilities of failure described by the fault tree. The solutions of this Failure Mode State Variable (FMSV) model are cumulative probability distribution functions of the system. A method of appropriate synthesis of subsystems to form larger systems is developed and applied to practical nuclear power safety systems. DOE

66 SYSTEMS ANALYSIS

Includes mathematical modeling; network analysis; and operations research.

N86-13051# Federal Aviation Administration, Washington, D.C. Office of Aviation Policy and Plans.
STATISTICAL SAMPLING OF AIRCRAFT OPERATIONS AT NON-TOWERED AIRPORTS
M. Ford and R. Shirack Apr. 1985 49 p
(AD-A157095; FAA-APO-85-7) Avail: NTIS HC A03/MF A01 CSCL 12/1

The purpose of this handbook is to provide a statistically sound method of estimating aircraft operations at non-towered airports from sampling counts. The handbook is written for planners, engineers, airport operators responsible for aircraft planning, and persons that collect data for FAA Airport Master Records (Form 5010.1). Many of these users will be familiar with general aviation airports, but not necessarily with statistical methods. Accurate information on aircraft activity at non-towered airports is a major need of airport owners and operators as well as planners and administrators charged with the planning and development of the airport system. Unlike towered airports, where air traffic controllers keep constant tallies of activity, most non-towered airports have no accurate record of usage. Obtaining accurate aircraft activity counts will provide a variety of benefits. Investment decisions can be made with more confidence if benefit-cost analysis is based on accurate information about use of the facility. Design criteria, which may have a significant impact on development and operating costs, can be more efficiently applied. Even when decisions

are based on forecasts rather than present circumstances, accurate base data is necessary to make accurate forecasts of activity.
GRA

N86-13052# Stanford Univ., Calif. Dept. of Computer Science.
DEALS AMONG RATIONAL AGENTS
J. S. Rosenschein and M. R. Genesereth Mar. 1985 28 p
(Contract N00039-83-C-0136)
(AD-A157960; AD-E401371; SU-STAN-CS-85-1042; HPP-84-44)
Avail: NTIS HC A03/MF A01 CSCL 12/1

A formal framework is presented that models communication and promises in multi-agent interactions. This framework generalizes previous work on cooperation without communication, and shows the ability of communication to resolve conflicts among agents having disparate goals. Using a deal-making mechanism, agents are able to coordinate and cooperate more easily than in the communication-free model. In addition, there are certain types of interactions where communication makes possible mutually beneficial activity that is otherwise impossible to coordinate.
Author (GRA)

67 THEORETICAL MATHEMATICS

Includes topology and number theory.

No abstracts in this category.

70 PHYSICS (GENERAL)

For geophysics see *46 Geophysics*. For astrophysics see *90 Astrophysics*. For solar physics see *92 Solar physics*.

N86-13053# Brookhaven National Lab., Upton, N. Y.
USE OF AN ELLIPTICAL APERTURE TO CONTROL SATURATION IN CLOSELY-COUPLED, COLD IRON, SUPERCONDUCTING DIPOLE MAGNETS
G. Morgan 1985 11 p refs Presented at the Particle Accelerator Conf., Vancouver, British Columbia, 13 May 1985
(Contract DE-AC02-76CH-00016)
(DE85-012259; BNL-36623; CONF-850504-167) Avail: NTIS HC A02/MF A01

The high fields permitted by superconducting windings result in saturation of closely-coupled iron in dipole and quadrupole beam transport magnets. Coupland suggested using a triangular cutout at the poles to reduce the change in the sextuple (b2) term due to saturation. The use of an elliptical aperture in a close-coupled dipole for the Relativistic Heavy Ion Collider (RHIC) has been studied using the BNl computer program MDP (a version of GFUN). The ellipse aspect ratio was varied while holding the horizontal (minor) radius constant. The proper aspect ratio gives no shift in b2 due to saturation, and a reduction in the b4 shift. A modification of the ellipse also reduces b4. The elliptical aperture introduces a large b2 term at low field which must be compensated for by the coil design. A practical coil design which does this for the RHIC magnet is presented.
DOE

N86-13054# California Univ., Berkeley. Lawrence Berkeley Lab.
DESIGN AND PERFORMANCE OF 40 mm, 6.5 T, COLLARED, COLD-IRON MODEL MAGNETS
C. Peters, W. Gilbert, W. Hassenzahl, K. Mirk, J. Rechen, R. Scanlan, and C. Taylor May 1985 6 p Presented at the Particle Accelerator Conf., Vancouver, British Columbia, 13 May 1985
(Contract DE-AC03-76SF-00098)
(DE85-015277; LBL-19579; CONF-850504-224) Avail: NTIS HC A02/MF A01

Model magnets have been built and tested at the Lawrence Berkeley Laboratory to verify a candidate design for the main bending magnets of the SSC. Construction of thesis series of dipole models was begun in October 1984 and will be completed in October 1985. To date, Three models with collars, C1, C2, and C3, have been completed. Models C1 and C2 have been tested.
Author

N86-13055# Brookhaven National Lab., Upton, N. Y.
REPLICA-SPACE RENORMALIZATION IN RANDOM-FIELD SYSTEMS
Y. Shapir 1985 10 p refs Presented at the Intern. Conf. on Magnetism, San Francisco, 26 Aug. 1985
(Contract DE-AC02-76CH-00016)
(DE85-014800; BNL-36708; CONF-850890-3) Avail: NTIS HC A02/MF A01

The critical behavior of random field systems is characterized by exponentially long relaxation times. They may differ by orders of magnitude and slow modes have to be considered quenched with respect to the faster ones. This requires a drastic modification of the renormalization process in which the degrees of freedom are integrated out. A new replica space renormalization procedure, to carry out the coarse graining of the time intervals, is presented. We relate by recursion relations the effective reduced dimensions of consecutive time scales. Their stable fixed points yield the apparent dimensionalities for the longest and shortest time scales, which are insensitive to the exact behavior on intermediate scales. For Ising systems we find that d = 2 is the lower critical dimension in both regimes. The thermal exponents for d = 3, in the short time observable regime, are related to those of the pure system in d = 2. This is consistent with the observations in field cooled random antiferromagnets of the correlation length exponent nu approx. = 1 (by neutron scattering) and of the symmetric logarithmic divergence in the specific heat (by linear birefrigence).
DOE

71 ACOUSTICS

Includes sound generation, transmission and attenuation. For noise pollution see *45 Environment Pollution*.

N86-13056*# National Aeronautics and Space Administration. Langley Research Center, Hampton, Va.
A METHOD FOR DETERMINING ACOUSTIC-LINER ADMITTANCE IN DUCTS WITH SHEARED FLOW IN TWO-CROSS-SECTIONAL DIRECTIONS
Willie R. Watson Oct. 1985 40 p refs
(NASA-TP-2518; L-15997; NAS 1.60:2518) Avail: NTIS HC A03/MF A01 CSCL 20A

A method is developed for determining the acoustic admittance of a test liner installed in the wall of a grazing flow impedance tube. The mean flow is permitted flow gradients in both cross-sectional directions of the tube. The unknown admittance value is obtained by solving an eigenvalue problem. This eigenvalue problem results from the application of the finite-element method to the partial differential equation and boundary conditions governing the acoustic field. The credibility of the method is established by comparing results with exact solutions obtained for a constant mean-flow profile and with previous results for cases involving shear in only one cross-sectional direction. Excellent comparisons are obtained in both cases. The analysis is used in conjunction with a limited amount of experimental data and shows that the flow must be accurately modeled in order to determine the acoustic-liner properties.
Author

N86-13057*# Purdue Univ., West Lafayette, Ind. School of Mechanical Engineering.
PREDICTION OF SOUND FIELDS IN ACOUSTICAL CAVITIES USING THE BOUNDARY ELEMENT METHOD M.S. Thesis
Carl R. Kipp and R. J. Bernhard Aug. 1985 163 p refs
(Grant NAG1-58)
(NASA-CR-176295; NAS 1.26:176295; HL-85-26) Avail: NTIS HC A08/MF A01 CSCL 20A

A method was developed to predict sound fields in acoustical cavities. The method is based on the indirect boundary element method. An isoparametric quadratic boundary element is incorporated. Pressure, velocity and/or impedance boundary conditions may be applied to a cavity by using this method. The capability to include acoustic point sources within the cavity is implemented. The method is applied to the prediction of sound fields in spherical and rectangular cavities. All three boundary condition types are verified. Cases with a point source within the cavity domain are also studied. Numerically determined cavity pressure distributions and responses are presented. The numerical results correlate well with available analytical results. E.A.K.

N86-13058# Max-Planck-Institut fuer Stroemungsforschung, Goettingen (West Germany).
TRANSONIC NOISE GENERATION BY DUCT AND PROFILE FLOW Annual Technical Report
G. E. A. Meier Oct. 1984 106 p
(Contract DAJA37-81-C-0251; DA Proj. 1T1-61102-BH-57)
(AD-A157163; ATR-3) Avail: NTIS HC A06/MF A01 CSCL 20/1

Acoustic distortions which are generated by a downstream instability of shear layers are travelling upstream in the subsonic part of the laval flow and are acting on the shock wave at the end of the supersonic part. This interaction causes strong oscillations. Different kinds of separation and secondary vortex generation have a governing influence on profile-vortex interaction flow. GRA

N86-13059# Mississippi Univ., University. Physical Acoustics Research Lab.
BIOLOGICAL EFFECTS OF ACOUSTIC CAVITATION
L. A. Crum 15 Jun. 1985 100 p
(Contract N00014-84-C-0193)
(AD-A157513; TR-3-85) Avail: NTIS HC A05/MF A01 CSCL 06/16

This report contains the lecture notes of the author for a short course entitled Biological Effects of Acoustic Cavitation presented at the University of Rochester, May 13 to 16, 1985. Lecture 2 notes pertain to: Nucleation, rectified diffusion, stable cavitation and experimental measurements. Contents of lecture 2 notes include: stabilization and nucleation of cavitation nuclei; rectified diffusion; stable cavitation; experimental measurements of cavitation produced by short acoustic pulses. GRA

N86-13060# Admiralty Marine Technology Establishment, Teddington (England).
SOUND SCATTERING BY A LAYERED SPHERE
S. J. Ansley and E. A. Skelton May 1985 27 p
(AD-A157915; AMTE(N)/TM85057; DRIC-BR-96422) Avail: NTIS HC A03/MF A01 CSCL 20/1

The sphere, which is located in an acoustic fluid, is composed of an arbitrary number of concentric layers of elastic solids and fluids. It is excited by a time-harmonic incident plane wave. The exact linear equations of elasto-dynamics, visco-dynamics and acoustics are solved to obtain, via the finite element method, a matrix equation which connects the interface displacements and external stresses in the spectral domain. The pressure scattered to the far-field is obtained from the radial spectral displacements of the outer surface. Numerical results of scattered sound spectra are presented for the case of an aluminium shell with and without a GRP (Glass Reinforced Plastics) coating. GRA

N86-13061# Pennsylvania State Univ., University Park.
DEVELOPMENT OF ACOUSTIC AGGLOMERATOR. TEST PLAN FOR HIGH TEMPERATURE HIGH PRESSURE ACOUSTIC AGGLOMERATOR
12 Aug. 1985 16 p Prepared in cooperation with Aerojet Energy Conversion Co., Sacramento, Calif.
(Contract DE-AC21-84MC-20107)
(DE85-017221; DOE/MC-20107/T3) Avail: NTIS HC A02/MF A01

The design specifications for the HTHP AA Facility are listed. The facility is an open-loop, air flow system with subsystems and components to provide the high temperature, high pressure, residence time, dust loading and acoustic irradiation to simulate the aerosol and Hot Gas Cleanup (HGCU) AA system of a Pressurized Fluid Bed Combustor (PFBC), Combined Cycle Power Plant. Data sampling, instrumentation, and automatic controls and data analysis systems are also provided. This test plan describes the testing to be done on the high temperature, high pressure acoustic agglomerator (HTHP AA) at Pen State University's High Intensity Acoustic Laboratory. DOE

N86-13062# Los Alamos Scientific Lab., N. Mex.
SOUND VELOCITIES IN LIQUID LEAD AT HIGH TEMPERATURES
R. S. Hixson, M. A. Winkler, and J. W. Shaner 1985 10 p Presented at the 9th Symp. on Thermophys. Properties, Boulder, Colo., 24 Jun. 1985
(Contract W-7405-eng-36)
(DE85-014091; LA-UR-85-2190; CONF-850617-2) Avail: NTIS HC A02/MF A01

A dynamic technique, the isobaric expansion experiment (IEX) is used to reach high temperature and pressure states in liquid lead. A unique technique is described for making sound speed measurements once a final equilibrium end state is obtained. Data over an extended density range are presented. The sound speed in liquid lead over this range appears to vary linearly with density, and has no dependence on temperature within our experimental precision. DOE

N86-13063# New Jersey State Dept. of Transportation, Trenton. Div. of Research and Demonstration.
EVALUATION OF HONEYCOMB HIGHWAY SOUND BARRIER I-280 SECTION 8B, HARRISON, NEW JERSEY Final Report, Feb. 1981 - Jul. 1983
M. Marsella Oct. 1984 51 p
(PB85-231157; Rept-85-004-7799-10; FHWA/NJ-85/004) Avail: NTIS HC A04/MF A01 CSCL 13B

The insertion loss of a traffic noise barrier erected along I-280 in Harrison, N.J. was determined. This barrier was constructed of a phenolic-impregnated paper honeycomb core faced with aluminum panels on both sides a type not previously used in New Jersey. Noise data was recorded both before and after barrier construction, from several microphones placed at two locations at a site adjacent to the highway. Also recorded were traffic counts by type of vehicle for both eastbound and westbound traffic and traffic speeds for westbound traffic only. For comparison purposes, small samples were randomly selected from the full size samples and analyzed using the same method. GRA

N86-12386# Tohoku Univ., Sendai (Japan). Research Inst. of Electrical Communication.
ACCURACY OF A NEW ULTRASONIC APPARATUS FOR SIMPLE MEASUREMENT OF VISCOELASTICITY
Ryohji Aoyagi and Hiroshi Shimizu *In its* The Record of Elec. and Commun. Eng. Conversazione, Vol. 54, No. 1 Aug. 1985 p 14-19 refs In JAPANESE; ENGLISH summary (For primary document see N86-12383 03-31)
Avail: NTIS HC A03/MF A01

N86-12403# Joint Publications Research Service, Arlington, Va.
STATUS, DEVELOPMENT OF POWER ULTRASONICS IN CHINA
Zhang Fucheng and Cheng Cundi *In its* China Rept.: Sci. and Technol. (JPRS-CST-85-035) 17 Oct. 1985 p 40-51 refs Transl. into ENGLISH from Yingyong Shengxue (Beijing), v. 4, no. 3, Jul. 1985 p 1-6 (For primary document see N86-12399 03-31)
Avail: NTIS HC A08/MF A01

N86-12643# Joint Publications Research Service, Arlington, Va.
ANGULAR DISTRIBUTION OF INTENSITY OF SOUND RERADIATED BY OCEAN SURFACE AT SMALL GLANCING ANGLES Abstract Only
Ye. A. Kopyl *In its* USSR Rept.: Earth Sci. (JPRS-UES-85-006) 19 Jun. 1985 p 14 Transl. into ENGLISH from Izv. Akad. Nauk

SSSR: Fiz. Atm. i Okeana (Moscow), v. 21, no. 1, Jan. 1985 p 96-101 (For primary document see N86-12630 03-42)
Avail: NTIS HC A05/MF A01

N86-12649# Joint Publications Research Service, Arlington, Va.
NUMERICAL ESTIMATE OF EFFECTIVENESS OF APPROXIMATE EQUATIONS FOR ACOUSTIC FIELD NEAR SURFACE OF DEEP SEA
M. V. Perel *In its* USSR Rept.: Earth Sci. (JPRS-UES-85-006) 19 Jun. 1985 p 18 Transl. into ENGLISH from Akust. Zh. (Moscow), v. 30, no. 6, Nov. - Dec. 1984 p 813-818 (For primary document see N86-12630 03-42)
Avail: NTIS HC A05/MF A01

N86-12656# Joint Publications Research Service, Arlington, Va.
ACOUSTICAL FIELD OF DIRECTIONAL SOURCE IN OCEANIC WAVEGUIDES Abstract Only
G. I. Bykovtsev, G. N. Kuznetsov, and A. N. Stepanov *In its* USSR Rept.: Earth Sci. (JPRS-UES-85-006) 19 Jun. 1985 p 25 Transl. into ENGLISH from Dokl. Akad. Nauk SSSR (Moscow), v. 280, no. 1, Jan. 1985 p 57-59 (For primary document see N86-12630 03-42)
Avail: NTIS HC A05/MF A01

N86-12664# Joint Publications Research Service, Arlington, Va.
STRUCTURE OF ACOUSTIC FIELD IN DEEP SEA AT SHALLOW DEPTHS AND AT GREAT RANGES Abstract Only
V. S. Buslayev and M. V. Perel *In its* USSR Rept.: Earth Sci. (JPRS-UES-85-006) 19 Jun. 1985 p 32-33 Transl. into ENGLISH from Vestn. Leningr. Univ.: Fiz. Khim. (Leningrad), no. 22, Nov. 1984 p 9-17 (For primary document see N86-12630 03-42)
Avail: NTIS HC A05/MF A01

N86-12706# Joint Publications Research Service, Arlington, Va.
ACOUSTIC METHODS FOR FEATURING HIGH-FREQUENCY PART OF SPECTRUM OF SEA WAVES Abstract Only
G. Yu. Narodnitskiy *In its* USSR Rept.: Earth Sci. (JPRS-UES-85-008) 16 Aug. 1985 p 11 Transl. into ENGLISH from Izv. Akad. Nauk SSSR: Fiz. Atm. i Okeana (Moscow), v. 21, no. 4, Apr. 1985 p 443-446 (For primary document see N86-12697 03-42)
Avail: NTIS HC A04/MF A01

72 ATOMIC AND MOLECULAR PHYSICS

Includes atomic structure and molecular spectra.

N86-13064*# National Aeronautics and Space Administration. Langley Research Center, Hampton, Va.
REVIEW OF SPECTROSCOPIC PARAMETERS FOR UPPER ATMOSPHERIC MEASUREMENTS
Mary Ann H. Smith, ed. Oct. 1985 28 p refs Presented at the Spectroscopic Parameters Workshop, Hampton, Va., 17-18 Oct. 1984
(NASA-CP-2396; L-16022; NAS 1.55:2396) Avail: NTIS HC A03/MF A01 CSCL 04A

The workshop included communication of spectroscopic data requirements for the planned upper atmosphere research satellite (UARS) mission, review of the status of currently available spectroscopic parameters, and recommendation of additional studies. The objectives were accomplished and resulted in a series of general and specific recommendations for laboratory spectroscopy research to meet the needs of UARS and other atmospheric remote sensing programs. E.A.K.

N86-13065# Aerospace Corp., El Segundo, Calif. Chemistry and Physics Lab.
MICROWAVE FIELD STRENGTH MEASUREMENT IN A RUBIDIUM CLOCK CAVITY VIA ADIABATIC RAPID PASSAGE
R. P. Frueholz and J. C. Camparo 24 Jun. 1985 23 p
(Contract F04701-83-C-0084)
(AD-A157070; TR-0084A(5945-05)-3; SD-TR-85-16) Avail: NTIS HC A02/MF A01 CSCL 14/2

Rubidium (Rb) atomic frequency standards have been found to display a strong frequency dependence on the microwave power density or field intensity. It is therefore desirable to have simple and easily applied techniques for measuring not only the field strength but also the field distribution within the clock's microwave cavity. A technique that makes use of adiabatic rapid passage (ARP) to measure field strengths in Rb clock cavities is described and demonstrated. Measurements using this technique are found to agree with field strengths extracted by means of standard microwave procedures. The ARP technique is particularly valuable in cavities where standard microwave measurements can not be made. GRA

N86-13066# Aerospace Corp., El Segundo, Calif. Chemistry and Physics Lab.
A DRESSED ATOM INTERPRETATION OF ADIABATIC RAPID PASSAGE
J. C. Camparo and R. P. Frueholz 24 Jun. 1985 25 p
(Contract F04701-83-C-0084)
(AD-A157071; TR-0084A(5945-05)-2; SD-TR-85-15) Avail: NTIS HC A02/MF A01 CSCL 20/10

Consider the problem of adiabatic rapid passage (ARP) in a dressed atom formalism. The conditions for ARP can be understood as conditions for minimizing the probability of dressed atomic-state transitions, and that these probabilities can be used to obtain an estimate of the degree of population reversal. Furthermore, by considering ARP in the dressed atom formalism, the similarity between ARP and the Landau-Zener nonadiabatic transition problem is made quite apparent. GRA

N86-13067# Aerospace Corp., El Segundo, Calif. Chemistry and Physics Lab.
THE INHOMOGENEOUS LIGHT SHIFT IN ALKALI ATOMS
J. C. Camparo, R. P. Frueholz, and C. H. Volk 24 Jun. 1985 43 p
(Contract F04701-83-C-0084)
(AD-A157498; TR-0084A(5945-05)-6; SD-TR-85-19) Avail: NTIS HC A03/MF A01 CSCL 07/4

The dynamic Stark shift of an inhomogeneously broadened spectral transition has been studied. Our measurements show a shift in the observed 87 Rb ground-state hyperfine transition, which has a nonlinear dependence on light intensity when the conditions for inhomogeneous broadening are met. The nonlinearity is the result of light-intensity gradients in the signal volume, which produce an inhomogeneously broadened asymmetric microwave transition. We show that our measurements are in full agreement with the second-order perturbation-theory treatment of light-induced energy-level shifts when the effects of inhomogeneities are properly taken into consideration. The effects of inhomogeneous broadening must be carefully considered when one extracts oscillator strengths from light-shift data, or performs high-precision laser spectroscopy. GRA

N86-13068# Department of the Navy, Washington, D. C.
GENERATION OF A MODULATED IREB (INTENSE RELATIVISTIC ELECTRON BEAM) WITH A FREQUENCY TUNABLE BY A MAGNETIC FIELD Patent Application
M. Friedman and V. Serlin, inventors (to Navy) Filed 8 Jul. 1985 24 p
(AD-D011820; US-Patent-Appl-SN-752867) Avail: NTIS HC A02/MF A01 CSCL 20/7

The present invention comprises a device for generating a modulated intense relativistic beam (IREB) with an electronically tunable frequency, comprising: a longitudinally running drift tube; a plurality of gaps in the drift tube including first gap and a second gap, disposed with a predetermined distance therebetween; and a plurality of cavities, with a first cavity disposed around the drift tube at the location of the first gap, and a second cavity disposed around the drift tube at the location of the second gap. These first and second cavities are provided with volumes and a geometry such as to excite a predetermined frequency band below the plasma frequency for the device. A circuit is provided for generating an IREB and injecting this IREB to propagate within the drift tube with a predetermined plasma frequency. Additionally, a main magnetic field generating means is provided for generating an IREB and injecting this IREB to a desired beam diameter. The frequency tuning is obtained by providing an auxiliary magnetic field running parallel to and within the drift tube and located only along a predetermined length between the first and second gaps, with this auxiliary magnetic field running parallel to and within the drift tube and located along a predetermined length between first and second gaps, with this auxiliary magnetic field being tunable to thereby tune the frequencies of excitations in the first and second gaps. Finally, a means is provided at one end of the drift tube for converting the kinetic energy of the IREB into electrical energy. GRA

N86-13069# Oak Ridge National Lab., Tenn.
CHARGE-STATE DISTRIBUTIONS OF 100, 175, 275 AND 352 MeV GOLD IONS EMERGING FROM THIN CARBON FOILS
J. A. Martin, R. L. Auble, K. A. Erb, C. M. Jones, and D. K. Olsen 1985 17 p refs Presented at the 4th Intern. Conf. on Electrostatic Accelerator Technol. and Assoc. Boosters, Buenos Aires, 15 Apr. 1985
(Contract DE-AC05-84OR-21400)
(DE85-014651; CONF-850470-6) Avail: NTIS HC A02/MF A01

These measurements were undertaken as a consequence of our failure early this year to accelerate Au(+46) ions in the Oak Ridge Isochronous Cyclotron using an injected beam of 352 MeV (197)Au(+17) from the 25 MV tandem accelerator. Following that unsuccessful test, we made a preliminary measurement of the charge-state distribution of 352 MeV (197) Au ions emerging from a carbon foil using the bending magnet that is a part of the cyclotron beam injection system. The measured mean charge was approx. 38.5, about 4.5 charge-states lower than predicted by the Sayer semi-empirical formula. The measurements reported here were done more precisely and systematically confirm that preliminary result. DOE

N86-13070# Stanford Linear Accelerator Center, Calif.
BEAM EMITTANCE AND BEAM DISRUPTION
R. Hollebeek and A. Minten 1 Jun. 1985 5 p ref
(Contract DE-AC03-76SF-00515)
(DE85-015136; SU-SLAC-CN-301) Avail: NTIS HC A02/MF A01

Beam disruption during the collision of intense relativistic bunches has been studied by R. Hollebeek. In the case of oppositely charged bunches, focussing effects occur causing a decrease in the effective bunch cross section, and therby an increase of luminosity by an ehancement factor H. The term disruption derives from the fact that the beam emittance changes markedly during the collision. DOE

N86-13071# Stanford Linear Accelerator Center, Calif.
DISRUPTION AND LUMINOSITY OF FLAT BEAMS
R. Hollebeek and A. Minten 10 Jun. 1985 8 p refs
(Contract DE-AC03-76SF-00515)
(DE85-015137; SU-SLAC-CN-302) Avail: NTIS HC A02/MF A01

It has been suggested that high energy linear colliders might operate with non-round beam profiles, i.e., with different signa sub x and sigma sub y, described by an aspect ratio R = sigma sub x. The advantage of flat beams is the expectation, that bremsstrahlung, i.e., beam-beam synchrotron radiation is reduced with increasing R. The reason for this reduction comes from the fact that for constant bunch area and therefore constant luminosity the mean physical distance between the particles increases with R. When the physical distances are larger, the electromagnetic fields and therefore particle acceleration and radiation decrease. This would be of particular importance for very large linear colliders (VLC), where bremsstrahlung may consume an appreciable fraction of the incident energy. The underlying assumption is that the emittance quality can be preserved in the deformed bunch. DOE

N86-13072# California Univ., Berkeley. Lawrence Berkeley Lab.
SPIN-POLARIZATION OBSERVABLES IN ELASTIC ELECTRON SCATTERING FROM SPIN-1/2 NUCLEI
H. E. Conzett May 1985 4 p refs Presented at the 6th Intern. Symp. on Polarization Phenomena in Nucl. Phys., Osaka, 26 Aug. 1985
(Contract DE-AC03-76SF-00098)
(DE85-016639; LBL-19827; CONF-850807-5) Avail: NTIS HC A02/MF A01

Using the formalism nucleon-nucleon scattering as a starting point, electron scattering from spin-1/2 nuclei is examined. It is seen that high-energy electron-nucleon scattering, for example, exhibits a remarkable simplicity when compared with that of nucleon-nucleon scattering. The 6 amplitudes and 36 nucleon-nucleon observables are reduced to 3 and 9, respectively, by the relativistic nature of the electron. The one-photon exchange mechanism finally reduces the number of amplitudes and independent observables to 2. This treatment serves to extend the spin-polarization language of hadronic scattering to that of electron scattering also. DOE

N86-13073# Brookhaven National Lab., Upton, N. Y.
COLLIDER PERFORMANCE WITH IDEAL COLLISIONS
M. Month 1 Jun. 1985 12 p
(Contract DE-AC02-76CH-00016)
(DE85-017011; BNL-51909) Avail: NTIS HC A02/MF A01

Performance is estimated for head-on bunch collisions. The luminosity is written as a distribution in time and length along the collision path, using a Gaussian distribution in all space dimensions. Computations are made for the Tevatron. Sources of luminosity reduction are listed in the case of non-ideal conditions. DOE

N86-13074# California Univ., Berkeley. Lawrence Berkeley Lab.
SUPPRESSION OF PROPAGATING TE MODES IN THE FNAL ANTIPROTON SOURCE STOCHASTIC BEAM COOLING SYSTEM
W. C. Barry May 1985 5 p Presented at the Particle Accelerator Conf., Vancouver, British Columbia, 13 May 1985
(Contract DE-AC03-76SF-00098)
(DE85-016559; LBL-18797; CONF-850504-280) Avail: NTIS HC A02/MF A01

A method of attenuating the propagation of waveguide modes in the stochastic cooling array beam pipes to be utilized in the accumulator and debuncher rings of the Fermilab antiproton source is described. The attenuation method treated involves lining the vertical walls of the beam pipes with a ferromagnetic material. The general solution for propagation in a nonhomogeneously loaded waveguide is presented along with numerical results specific to the antiproton source beam cooling system. Also described is a broadband, automated technique for the simultaneous measurement of complex (MU) and epsilon developed to aid in the characterization of different ferrite materials. Permittivity and permeability data for a typical ferrite are presented along with a discussion of the effects of these parameters on waveguide mode attenuation in the ferrite lined beam pipes. DOE

N86-13075# Stanford Linear Accelerator Center, Calif.
CONTROL PROBLEMS IN VERY LARGE ACCELERATORS
M. C. Crowley-Milling Jun. 1985 14 p Presented at the Particle Accelerator Conf., Vancouver, British Columbia, 13 May 1985
(Contract DE-AC03-76SF-00515)
(DE85-014956; SU-SLAC-Pub-3624-Rev; CONF-850504-103-Rev) Avail: NTIS HC A02/MF A01

There is no fundamental difference of kind in the control requirements between a small and a large accelerator since they are built of the same types of components, which individually have similar control inputs and outputs. The main difference is one of scale; the large machine has many more components of each type, and the distances involved are much greater. Both of these factors must be taken into account in determining the optimum way of carrying out the control functions. Small machines should use standard equipment and software for control as much as possible, as special developments for small quantities cannot normally be justified if all costs are taken into account. On the other hand, the very great number of devices needed for a large machine means that, if special developments can result in simplification, they may make possible an appreciable reduction in the control equipment costs. It is the purpose of this report to look at the special control problems of large accelerators, which the author shall arbitarily define as those with a length of circumference in excess of 10 km, and point out where special developments, or the adoption of developments from outside the accelerator control field, can be of assistance in minimizing the cost of the control system. Most of the first part of this report was presented as a paper to the 1985 Particle Accelerator Conference. It has now been extended to include a discussion on the special case of the controls for the SSC. DOE

N86-13076# California Univ., Berkeley. Lawrence Berkeley Lab.
THEORETICAL STUDIES OF MOLECULAR INTERACTIONS
W. A. Lester, Jr. May 1985 6 p refs Presented at the DOE/BES Contractors' Combustion Meeting, Lake Geneva, Wisc., 22 May 1985
(Contract DE-AC03-76SF-00098)
(DE85-012604; LBL-19583; CONF-850578-3) Avail: NTIS HC A02/MF A01

The goal of this program is to extend fundamental knowledge of combustion processes by theoretical studies of the dynamics of energy transfer, reactive, and photodissociative processes. The approach is based on the reliable description of inter and intramolecular interactions using ab initio methods and a variety of approaches to describe the dynamics of nuclear motion. A summary of recent results and future plans follows. DOE

N86-13077# Brookhaven National Lab., Upton, N. Y.
CHAOTIC DYNAMICAL APERTURE
S. Y. Lee and S. Tepikian 1985 3 p Presented at the Particle Accelerator Conf., Vancouver, British Columbia, 13 May 1985
(Contract DE-AC02-76CH-00016)
(DE85-013285; BNL-36565; CONF-850504-159) Avail: NTIS HC A02/MF A01

Nonlinear magnetic forces become more important for particles in the modern large accelerators. These nonlinear elements are introduced either intentionally to control beam dynamics or by uncontrollable random errors. Equations of motion in the nonlinear Hamiltonian are usually non-integrable. Because of the nonlinear part of the Hamiltonian, the tune diagram of accelerators is a jungle. Nonlinear magnet multipoles are important in keeping the accelerator operation point in the safe quarter of the hostile jungle of resonant tunes. Indeed, all the modern accelerator designs have taken advantages of nonlinear mechanics. On the other hand, the effect of the uncontrollable random multipoles should be evaluated carefully. A powerful method of studying the effect of these nonlinear multipoles is using a particle tracking calculations, where a group of test particles are tracing through these magnetic multipoles in the accelerator hundreds to millions of turns in order to test the dynamical aperture of the machine. These methods are extremely useful in the design of a large accelerator such as SSC, LEP, HERA and RHIC. These calculations unfortunately take a tremendous amount of computing time. In this review the method of determining chaotic orbit and applying the method to nonlinear problems in accelerator physics is discussed. We then discuss the scaling properties and effect of random sextupoles. DOE

N86-13078# Los Alamos Scientific Lab., N. Mex.
RECONSTRUCTION OF LONGITUDINAL BEAM PROFILES FROM NONDESTRUCTIVE ELECTROMAGNETIC PROBES
J. D. Gilpatrick and C. A. Watson May 1985 3 p refs Presented at the Particle Accelerator Conf., Vancouver, British Columbia, 13 May 1985
(Contract W-7405-eng-36)
(DE85-012675; LA-UR-85-1598; CONF-850504-101) Avail: NTIS HC A02/MF A01

The Fusion Materials Irradiation Test (FMIT) 2-MeV accelerator has nondestructive diagnostic probes that sense changes in the electromagnetic fields of the bunched beam. These probes accurately perform their primary functions, but do not have well-behaved, frequency-domain characteristics from which the longitudinal beam profile can be measured using convolution-integral processing techniques. Therefore, each of the probes' transfer function was determined using a tightly bunched electron beam as a source for impulse response tests. Using the Signal Processing Analyzer (SPA) code, output signals from these probes mounted on the FMIT beamline were deconvolved with sampled impulse response data to produce a longitudinal electromagnetic field distribution of a beam bunch. With SPA's signal-processing techniques, any electromagnetic probe shorter than (BETA)lambda and having significant signal-to-noise ratios can reconstruct longitudinal profiles, provided the probe's transfer function is known. DOE

N86-13079# California Univ., Berkeley. Lawrence Berkeley Lab.
STOCHASTIC BEAM COOLING AMPLIFIER SYSTEM FRONT END COMPONENTS PERFORMANCE CHARACTERISTICS
C. C. Lo May 1985 14 p Presented at Particle Accelerator Conf., Vancouver, British Columbia,
(Contract DE-AC03-76SF-00098)
(DE85-013925; LBL-18711; CONF-850504-186) Avail: NTIS HC A02/MF A01 13 May 1985

The stochastic beam cooling amplifier front end consists of 180(0) hybrids, cables, directional couplers, power dividers/combiners and low noise preamplifiers. Most front ends will be operating at near liquid nitrogen (LN) temperature. Components used in the front ends should be able to operate at this temperature satisfactorily. Since the noise performance of the front end is of utmost importance to the beam cooling process, the insertion losses of cables, 180(0) hybrids, directional couplers and power combiners have been measured at room temperature and near liquid nitrogen temperature. The purpose of this report is to describe and present some measurements and data on the components mentioned, with the exception of the 1 to 2 and 2 to 4 GHz preamplifiers, which have been described elsewhere. DOE

N86-13080# Fermi National Accelerator Lab., Batavia, Ill.
THEORIES OF STATISTICAL EQUILIBRIUM IN ELECTRON-POSITRON COLLIDING-BEAM STORAGE RINGS
J. F. Shonfeld Jan. 1985 15 p Presented at the Joint US/CERN School on Particle Accelerators Topical Course on Non-Linear Dyn., Sardinia, Italy, 31 Jan. 1985
(Contract DE-AC02-76CH-03000)
(DE85-012303; FNAL/C-85/18-T; CONF-850114-2) Avail: NTIS HC A02/MF A01

In this lecture I introduce you to some recent theoretical work that represents a significant and long overdue departure from the mainstream of ideas on the physics of colliding-beam storage rings. The goal of the work in question is to understand analytically - without recourse to computer simulation - the role that dissipation and noise play in the observed colliding-beam behavior of electron-positron storage rings. DOE

N86-13081# Los Alamos National Lab., N. Mex.
LAMPF TRANSITION-REGION MECHANICAL FABRICATION
E. D. Bush, Jr., J. D. F. Gallegos, R. Harrison, V. E. Hart, W. T. Hunter, S. E. Rislove, J. R. Sims, and W. J. VanDyke 1985 4 p Presented at the Particle Accelerator Conf., Vancouver, British Columbia, 13 May 1985
(Contract W-7405-eng-36)
(DE85-012688; LA-UR-85-1546; CONF-850504-129) Avail: NTIS HC A02/MF A01

The new Transition Region (TR-II) optimizes phase matching of H(+) and H(-) beams during simultaneous transport between the drift-tube linac and side-coupled linac at LAMPF. Improvements include, larger aperture, a straight beam track, greater beam patch length adjustments, and better utility routing. Hardware density required innovative designs for magnets, mounting, vacuum, and utilities. Dipoles are powered by one constant current and one variable current supply which cause the fields to add or buck providing + or - 20 mm path length variation for phase matching. Alignment was done using two digital theodolites coupled to a computer to give real-time three-dimensional data. Production beams up to 950 (MU)A at 100 MeV have been routinely transported since September 1983. DOE

N86-13082# Los Alamos National Lab., N. Mex.
FUNNELING: AN INITIAL BEAM DYNAMICS STUDY
F. W. Guy and T. P. Wangler 20 Apr. 1985 8 p refs Presented at the Workshop on High Brightness, High Current, High Duty Factor Ion Injectors, San Diego, Calif., 21 May 1985
(Contract W-7405-eng-36)
(DE85-012652; LA-UR-85-1625; CONF-8505164-1) Avail: NTIS HC A02/MF A01

Funneling two H(-) beams into a single beam of twice the current has been examined as a means of doubling beam current without significantly increasing transverse emittance. Using the PARMILA particle-following code, two 100-mA RFQ output beams at 2 MeV were injected into idealized transport lines for merging two beams into one. Two approaches were studied: (1) the minimum-element method, in which a minimum number of discrete elements such as quadrupole triplets, buncher cavities, and bending magnets were used to transport and deflect the beam; and (2) the quasi-adiabatic method, in which a periodic lattice similar to the RFQ provided focusing and minimized abrupt changes in the beam environment. The minimum-element method resulted in an emittance growth ratio epsilon0/epsilon/sub i/ = 2.5, whereas the quasi-adiabatic emittance growth ratio was about 1.1 (albeit with an idealized line configuration). DOE

N86-13083# Los Alamos National Lab., N. Mex.
DEVELOPMENT OF A CURRENT MONITOR SYSTEM FOR MEASURING PULSED-BEAM CURRENT OVER A WIDE DYNAMIC RANGE
F. R. Gallegos, L. J. Morrison, and A. A. Browman 1985 4 p Presented at the Particle Accelerator Conf., Vancouver, British Columbia, 13 May 1985
(Contract W-7405-eng-36)
(DE85-012692; LA-UR-85-1527; CONF-850504-119) Avail: NTIS HC A02/MF A01

This report documents the development of a current transformer system to measure pulsed ion beam currents at the LAMPF accelerator. Measured peak currents typically range from 100 nA to 30 mA with pulse widths varying from 30 (MU)s to 1 ms. Signal conditioning of the peak current output provides an average current readout with a range of 1 nA to 2 mA, noise of approximately + or - 0.5 nA, and accuracy of + or - 0.1%. The system requires no operating adjustments and has proved stable and reliable during a year of operation. DOE

N86-13084# Los Alamos National Lab., N. Mex.
ELECTRON EMISSION OF OVER 200 A/cm (2) FROM A PULSED-LASER IRRADIATED PHOTOCATHODE
J. S. Fraser, C. H. Lee, P. E. Gettinger, E. R. Pugh, R. Klinkowstein, J. H. Jacob, and R. L. Sheffield 1985 4 p refs Presented at the Particle Accelerator Conf., Vancouver, British Columbia, 13 May 1985 Prepared in cooperation with Thermo Electron Corp., Waltham, Mass., Physical Sciences, Inc, Andover, Mass., and Science Research Corp., Cambridge, Mass.
(Contract W-7405-eng-36)
(DE85-012656; LA-UR-85-1621; CONF-850504-59) Avail: NTIS HC A02/MF A01

High current density, bunched electron beams with low emittance are required for efficient operation of RF linac driven free electron lasers (FELs). Laser irradiated, photoemissive electron sources are suitable for this application. Currents of over 200 A have been generated in an ultrahigh vacuum chamber from a 1-cm(2) Cs3Sb photocathode irradiated by a frequency doubled, Q switched pulse from a Nd:glass laser. These currents are over two times larger than previously reported from any photocathode. The duration of the electron pulse was 50 ns (FWHM), corresponding to the width of the 532 nm laser pulse. DOE

N86-13085# Fermi National Accelerator Lab., Batavia, Ill.
TESTS OF ORBITAL DYNAMICS USING THE TEVATRON
D. A. Edwards, R. P. Johnson, and F. Willeke Apr. 1985 9 p refs Presented at the Orbital Dyn. and Appl. to Accelerators Workshop, Berkeley, Calif., 7 Mar. 1985 Prepared in cooperation with Deutsches Elektronen-Synchrotron, Hamburg, West Germany
(Contract DE-AC02-76CH-03000)
(DE85-012296; FNAL/C-85/59; CONF-8503105-5) Avail: NTIS HC A02/MF A01

Measurements of Tevatron beam behavior relevant to questions of orbital dynamics are described. General techniques and some preliminary results from phase space distortion experiments are presented. DOE

N86-13086# Pacific Northwest Lab., Richland, Wash.
SECONDARY ELECTRON SPECTRA: A SEMIEMPIRICAL MODEL
J. H. Miller, W. E. Wilson, and S. T. Manson May 1985 18 p refs Presented at the 8th Symp. on Microdosimetry, Toulouse, 20 May 1985 Prepared in cooperation with Georgia State Univ., Atlanta
(Contract DE-AC06-76RL-01830)
(DE85-012448; PNL-21-12756; CONF-850506-7) Avail: NTIS HC A02/MF A01

A model based on evaluation of coefficients in Bethe's asymptotic expansion of the first Born approximation has been developed to extend the data base of differential ionization cross sections needed in track structure calculations. The coefficient of the lowest-order term in this expansion is related to the photoionization cross section of the target, but optical data alone are generally not sufficient to determine differential cross sections for ionization by charged particles. We have used proton-impact, differential ionization data to evaluate the coefficient of the next higher-order term in the expansion. Since these coefficients are independent of the projectile, the experimentally derived coefficients can be used to predict differential cross sections for ionization of the target by bare ions and electrons that are sufficiently energetic to make the Bethe theory valid. This paper compares model calculations with recent experimental data on ionization of water vapor by high-energy electrons and protons. DOE

N86-13087# Los Alamos National Lab., N. Mex.
FMIT DIAGNOSTIC INSTRUMENTATION
J. D. Gilpatrick and D. D. Chamberlin 1985 4 p refs Presented at the Particle Accelerator Conf., Vancouver, British Columbia, 13 May 1985
(Contract W-7405-eng-36)
(DE85-012668; LA-UR-85-1609; CONF-850504-93) Avail: NTIS HC A02/MF A01

The Fusion Materials Irradiation Test facility (FMIT) CW prototype accelerator has noninterceptive beamline instrumentation to measure beam parameters. The transverse emittances and beam profiles are measured with an array of photodiode sensors viewing light emitted from the beam region. Tomographic reconstructions of both spatial-density distributions and of transverse-emittance distributions are performed throughout a quadrupole focusing section. Beam bunches passing through capacitive probes produce bipolar waveforms whose zero crossing corresponds to the bunch's longitudinal centroid. By measuring the time required for a bunch to travel the known distance between two probes, velocity and energy are determined. A toroidal transformer measures the average ac beam current. Beam still is measured by a set of movable jaws that intercept the beam edges. Each jaw contains a water flow channel whose flow rate and differential temperature are measured to derive a transverse power distribution. Beam centroid position is measured by a four-lobe, magnetic-loop pickup. DOE

N86-13088# Sandia National Labs., Albuquerque, N. Mex.
LARGE SCALE OPERATIONAL PULSED POWER RESEARCH FACILITIES: HOW WELL HAVE WE MADE THEM A REALITY
G. D. Peterson, S. A. Goldstein, G. T. Holman, and W. H. McAtee 1985 6 p Presented at the 5th IEEE Pulsed Power Conf., Washington, D.C., 10 Jun. 1985
(Contract DE-AC04-76DP-00789)
(DE85-013784; SAND-84-2497C; CONF-850616-47) Avail: NTIS HC A02/MF A01

Many factors contribute to the successful long term operation of large scale, multiterawatt pulsed power facilities. Some of these are: staffing considerations for optimum operational effectiveness including the impact of manpower inertia and operational mode momentum, effective management of the factors that govern experimental shot rate, and hardware preventive maintenance scheduling considerations on multimodule operational accelerators. The strategies used to keep large facilities operational at optimum performance including the merits of planning to accommodate component failure will be discussed by presenting specific solutions to problems on the Particle Beam Fusion Accelerator-I (PEFA-I) at Sandia. DOE

N86-13089# Argonne National Lab., Ill.
PARTITION OF CROSS SECTIONS IN ASYMMETRIC NUCLEUS-NUCLEUS REACTIONS AND THE ORIGIN OF FAST ALPHA PARTICLES
R. H. Siemssen 1985 22 p refs Presented at the Conf. on Nucl. Struct. with Heavy Ions, Legnaro, Italy, 27 May 1985 Prepared in cooperation with Groningen Rijksuniversiteit, Netherlands
(Contract W-31-109-eng-38)
(DE85-014989; CONF-8505172-2) Avail: NTIS HC A02/MF A01

To investigate the mechanism of asymmetric nucleus-nucleus reactions from the coulomb barrier to intermediate energies the (14) N + (159)Tb reaction was studied at five bombarding energies between 8 and 23 MeV/u via particle-particle correlations (at selected energies) and particle KX-ray coincidences to identify the specific reaction channels. With the KX-ray method partial cross sections for projectile-like fragments (PLF) as a function of the atomic number (Z/sub res/) of the residual nucleus can be determined. The charge balance yields the missing charge dZ = Z/sub proj/ + Z/sub targ/ - Z/sub PLF/ - Z/sub TIF/ that indicates whether, in addition to the PLF, other charged particles are emitted. A large fraction of the inclusive cross sections is found to originate from such channels with two or more fragments in the exit channel, and this fraction increases as the PLF is further removed in mass from the incident projectile, and with increasing bombarding energy. From the particle-particle correlation studies it is found that sequential decays of PLFs are dominant. Non-sequential processes, if present, are associated with inelastic reactions involving excitations of both projectile and target. From (GAMMA)-ray multiplicity measurements and from the broad distribution of the strength with Z/sub res/ it is concluded that these alpha particles originate from inelastic (damped) processes. DOE

N86-13090# Arizona State Univ., Tempe.
HIGH NUCLEAR TEMPERATURES BY ANTIMATTER-MATTER ANNIHILATION
W. R. Gibbs and D. Strottman 1985 12 p refs Presented at the Conf. on Antinucleon and Nucleon-Nucleus Interactions, Telluride, Colo., 18 Mar. 1985 Prepared in cooperation with LANL
(DE85-014113; LA-UR-85-2075; CONF-850315-8) Avail: NTIS HC A02/MF A01

It is suggested that the quark-gluon phase be created through the use of antiproton or antideuteron beams. The first advantage to this method, using higher energy antiprotons than 1.5 GeV/c, is that the higher momenta antiprotons penetrate more deeply so that mesons produced are more nearly contained within the nucleus. Another advantage is that the annihilation products are very forward-peaked and tend to form a beam of mesons so that the energy density does not disperse very rapidly. Calculations were performed using the intranuclear cascade to try to follow the process of annihilation in some detail. The intranuclear cascade type calculation method is compared to the hydrodynamic approach. DOE

N86-13091# Argonne National Lab., Ill.
REVIEW OF HEAVY ION COLLIDER PROPOSALS
A. G. Ruggiero 1985 6 p Presented at the Particle Accelerator Conf., Vancouver, British Columbia, 13 May 1985
(Contract W-31-109-eng-38)
(DE85-014985; ANL/EEP-CP-85-43; CONF-850504-211) Avail: NTIS HC A02/MF A01

In this paper we review proposals for heavy-ion colliders generated during the last few years for several national laboratories. The proposals span over a large range of energy and luminosity to accommodate the experimental needs of both the nuclear and the high-energy physicists. We report also briefly efforts in the same field happening in Europe. DOE

N86-13092# California Univ., Berkeley. Lawrence Berkeley Lab.
ACHIEVEMENT OF BEVALAC RAPID MODE SWITCHING
F. Lothrop, R. Stevenson, R. Miller, and J. Alonso May 1985 6 p Presented at the Particle Accelerator Conf., Vancouver, British Columbia, 13 May 1985
(Contract DE-AC03-76SF-00098)
(DE85-015130; LBL-18939; CONF-850504-220) Avail: NTIS HC A02/MF A01

Rapid changes of ion, intensity, beam line, and output energy between two modes have been achieved. The techniques for switching among the Bevalac's several injectors are described. Energy level limits at the output (for q/A = 1/2) are 470 to 2100 MeV/n (high power) or 50 to 1050 MeV/n (low power). Depending on specific field value differences, the total time required for a mode change is less than one minute. This mode of operation greatly improves program efficiency in interleaving medical and nuclear science programs at the Bevalac. DOE

N86-13093# California Univ., Berkeley. Lawrence Berkeley Lab.
OVERVIEW AND STATUS OF THE TRANSVERSE-FIELD FOCUSING (TFF) ACCELERATOR
O. A. Anderson, C. F. Chan, W. S. Cooper, J. W. Kwan, C. A. Matuk, H. M. Owren, J. A. Paterson, P. Purgalis, and L. Soroka May 1985 6 p refs Presented at the Particle Accelerator Conf., Vancouver, British Columbia, 13 May 1985
(Contract DE-AC03-76SF-00098)
(DE85-015276; LBL-19593; CONF-850504-225) Avail: NTIS HC A02/MF A01

The Transverse Field focusing (TFF) system described here is a prototype for a negative-ion based neutral beam line with possible applications in the US magnetic fusion energy program. The prototype system consists of four main modules: (1) H(-) source, (2) 80 keV pre-accelerator, (3) TFF matching/pumping (M/P) section, and (4) 180 keV TFF accelerator. The first three modules have been installed on the beam line, with the fourth to follow soon. The crucial module, invoking the most difficult (and interesting) physics and engineering issues, is the M/P section. It performs: (1) gas removal from the beam by differential pumping, (2) electron removal, (3) beam thickness reduction to match the TFF accelerator parameters, and (4) beam-edge confinement. The four beamline modules are discussed in this survey, with emphasis on design features of the M/P section. DOE

N86-13094# Oak Ridge National Lab., Tenn.
MULTIPHOTON IONIZATION OF NO-RARE GAS VAN DER WAALS SPECIES
J. C. Miller 1985 3 p Presented at the 7th Intern. Conf. on Laser Spectry., Maui, Hawaii, 24 Jun. 1985
(Contract DE-AC05-84OR-21400)
(DE85-014650; CONF-850605-1) Avail: NTIS HC A02/MF A01

To date, most spectroscopic studies of electronic states of clusters involving small molecules and rare gas (RG) atoms have employed laser-induced fluorescence techniques. Consequently, such studies (e.g., levy and co-workers) on I2-RG species have been limited to the lowest lying electronic states, which are usually velance in character. Furthermore, the identification of the cluster often must be inferred from spectral shifts, pressure dependence, etc. We have applied the technique of multiphoton ionization (MPI) to the study of electronic spectroscopy of NO-RG van der Waals species and extended the previous experiments of SATO, et al. These works show several of the advantages of the MPI technique relative to the LIF method. Specifically, mass analysis can provide identification of the new species formed as well as allowing discrimination against other species (the parent monomer or higher clusters) while recording spectra. Futhermore, the use of MPI photoelectron spectroscopy can provide data on the states of the cluster ion as well. DOE

N86-13095# California Univ., Berkeley. Lawrence Berkeley Lab.
ON-LINE VELOCITY MEASUREMENTS USING PHASE PROBES AT THE SUPERHILAC
B. Leemann, D. Brodzik, B. Feinberg, and D. Howard May 1985 6 p ref Presented at the Particle Accelerator Conf., Vancouver, British Columbia, 13 May 1985
(Contract DE-AC03-76SF-00098)
(DE85-015279; LBL-18961; CONF-850504-226) Avail: NTIS HC A02/MF A01

Phase probes have been placed in several external beam lines at the SuperHILAC to provide velocity measurements independent of the type of particle being accelerated. The system uses three probes in each line to obtain accurate velocity measurements at all beam energies. Automatic gain control and signal analysis are performed so that the energy/nucleon along with a representative probe signal are displayed on an oscilloscope every eight seconds. The system is accurate to within about +-0.25%, and has provisions for on-line calibration tests. The phase probes thus provide a velocity measurement independent of the mass defect associated with the use of crystal detectors, which can become significant for heavy elements. DOE

N86-13096# Hughes Aircraft Co., Torrance, Calif. Electron Dynamics Div.
DEVELOPMENT PROGRAM FOR A 200 kW, cw GYROTRON Final Report
W. J. DeHope, P. E. Ferguson, S. L. Hart, V. A. Matranga, J. J. Sandoval, M. J. Schmitt, J. J. Tancredi, and M. A. Wozniak Feb. 1984 122 p
(Contract DE-AC05-87OR-21400)
(DE85-014887; ORNL/SUB-79/33200/18) Avail: NTIS HC A06/MF A01

Development of a millimeter-wave device to produce 200 kW of continuous wave power at 60 GHz is described. The device, a gyrotron oscillator, is intended for electron-cyclotron heating of fusion plasmas. The design philosophy is herein discussed and experimental results, both diagnostic and long pulse, are given. DOE

N86-13097# Fermi National Accelerator Lab., Batavia, Ill.
A p ANTI p COLLIDER PHYSICS: SUMMARY TALK
J. D. Bjorken Jun. 1985 24 p refs Presented at the Intern. Symp. on Phys. of Proton-Antiproton Collision, Tsukuba, Japan, 13 May 1985
(Contract DE-AC02-76CH-03000)
(DE85-014782; FNAL/C-85/84; CONF-8503151-2) Avail: NTIS HC A02/MF A01

Progress is very briefly summarized in these areas: Drell-Yan production of W and Z; inclusive spectra of jets; angular distribution of two jet final states; Dalitz plot analysis of three jet final states; interior structure of jets; minijets; issues and relevent data in soft-collision physics; structure of the pomeron; W, Z, and electroweak theory; heavy quark, and possibly anomalous same-sign isolated dimuons. Future directions are anticipated for the Sp anti pS, Tevatron I, instrumentation and detectors, group theory, and the physics at SSC energies. DOE

N86-12435# Joint Publications Research Service, Arlington, Va.
MEASUREMENT OF 1 NANOSECOND WIDE BEAMS FOR 2.5 MeV PROTON ACCELERATOR
Yang Jiayou, Li Wenxue, and Li Jiarong *In its* China Rept.: Sci. and Technol. (JPRS-CST-85-034) 1 Oct. 1985 p 71-77 refs Transl. into ENGLISH from He Kexue Yu Gongcheng (Beijing), no. 1, Mar. 1984 p 67-71 (For primary document see N86-12430 03-31)
Avail: NTIS HC A08/MF A01

73 NUCLEAR AND HIGH-ENERGY PHYSICS

Includes elementary and nuclear particles; and reactor theory.

For space radiation see *93 Space Radiation.*

N86-13098# Nova Univ., Dania, Fla. Jolla Ca.
THEORY SUPPORT OF PULSED POWER EXPERIMENTS. VOLUME 3. E-BEAM CHAMBER DESIGN Technical Report, 15 Nov. 1978 - 30 Sep. 1982
A. Wilson, D. E. Parks, E. M. Waisman, M. C. Friedman, and P. G. Steen 1 Jul. 1984 26 p
(Contract DNA001-79-C-0027)
(AD-A158417; AD-E301765; SSS-R-84-6709-3-Vol-3; DNA-TR-84-288-V3-Vol-3) Avail: NTIS HC A03/MF A01 CSCL 20/5

The progress made in understanding the physics of X-ray simulators is presented. The work includes sections on diode power flow, plasma stability and dynamics, e-beam test chambers and the DNA BACCARAT program. GRA

N86-13099# Edgerton, Germeshausen and Grier, Inc., Idaho Falls, Idaho.
GROUND TEST FACILITY FOR NUCLEAR TESTING OF SPACE REACTOR SUBSYSTEMS
W. J. Quapp and K. D. Watts 1985 4 p Presented at the 2nd Symp. on Space Nucl. Power Systems, Albsuquerque, N. Mex., 14 Jan. 1985
(Contract DE-AC07-76ID-01570)
(DE85-014634; EGG-M-13484; CONF-850103-11) Avail: NTIS HC A02/MF A01

Two major reactor facilities at the INEL have been identified as easily adaptable for supporting the nuclear testing of the SP-100 reactor subsystem. They are the Engineering Test Reactor (ETR) and the Loss of Fluid Test Reactor (LOFT). In addition, there are machine shops, analytical laboratories, hot cells, and the supporting services (fire protection, safety, security, medical, waste management, etc.) necessary to conducting a nuclear test program. This paper presents the conceptual approach for modifying these reactor facilities for the ground engineering test facility for the SP-100 nuclear subsystem. DOE

N86-13100# Argonne National Lab., Ill.
MULTIPLICITIES IN HIGH ENERGY INTERACTIONS
M. Derrick 13 May 1985 52 p refs Presented at the Aspen Winter Phys. Conf., Aspen, Colo., 14 Jan. 1985
(Contract W-31-109-eng-38)
(DE85-013847; ANL-HEP-CP-85-17; CONF-850146-7) Avail: NTIS HC A04/MF A01

Data on multiplicities in high energy interactions are reviewed. Results from e(+)e(-) annihilation, from neutrino interactions, and from hadronic collisions, both diffractive and nondiffractive, are compared and contrasted. The energy dependence of the mean charged multiplicity, <n/sub ch>, as well as the rapidity density at Y = 0 are presented. For hadronic collisions, the data on neutral pion production shows a strong correlation with <n/sub ch>. The heavy particle fractions increase with (RADICAL) s up to the highest energies. The charged particle multiplicity distributions for each type of reaction show a scaling behavior when expressed in terms of the mean. Attempts to understand this behavior, which was first predicted by Koba, Nielsen, and Olesen, are discussed. The multiplicity correlations and the energy variation of the shape of the KNO scaling distribution provide important constraints on models. Some extrapolations to the energies of the Superconducting Super Collider are made. DOE

N86-13101# Fermi National Accelerator Lab., Batavia, Ill.
TEVATRON GLOBAL RADIUS AND Os SYSTEM
S. Bristol, C. Kerns, Q. Kerns, and H. W. Miller Jun. 1985 4 p refs Presented at the Particle Accelerator Conf., Vancouver, British Columbia, 13 May 1985

(Contract DE-AC02-76CH-03000)
(DE85-017442; FNAL-TM-1328; CONF-850504-269) Avail: NTIS HC A02/MF A01

It has been found to be practical to extract a turn-average measurement of bunch beam phase relative to cavity gap voltage. This 0s signal shows the bunch position on the RF wave throughout injection, acceleration and extraction, including coherent synchrotron oscillations when present. In turn, the time derivative of 0s is a direct measure of global radial position error. We use the 0s signal, driving a phase shifter in the RF low-level system, to damp coherent synchrotron oscillations. Design and operation is discussed including single beam bunch operation if available. DOE

N86-13102# Los Alamos National Lab., N. Mex.
CHEMISTRY OF BERKELIUM: A REVIEW
D. E. Hobart and J. R. Peterson 1985 5 p Presented at ACTINIDES '85, Aix-en-Provence, France, 1 Sep. 1985 Prepared in cooperation with Tennessee Univ., Knoxville and ORNL
(Contracts DE-AS05-76ER-04447; DE-AC05-84OR-21400; W-7405-eng-36)
(DE85-017523; LA-UR-85-3112; CONF-8509147-2) Avail: NTIS HC A02/MF A01

Element 97 was first produced in December 1949, by the bombardment of americium-241 with accelerated alpha particles. This new element was named berkelium (Bk) after Berkeley, California, the city of its discovery. In the 36 years since the discovery of Bk, a substantial amount of knowledge concerning the physicochemical properties of this relatively scarce transplutonium element was acquired. All of the Bk isotopes of mass numbers 240 and 242 through 251 are presently known, but only berkelium-249 is available in sufficient quantities for bulk chemical studies. About 0.7 gram of this isotope was isolated at the HFIR/TRU Complex in Oak Ridge, Tennessee in the last 18 years. Over the same time period, the scale of experimental work using berkelium-249 has increased from the tracer level to bulk studies at the microgram level to solution and solid state investigations with milligram quantities. Extended knowledge of the physicochemical behavior of berkelium is important in its own right, because Bk is the first member of the second half of the actinide series. In addition, such information should enable more accurate extrapolations to the predicted behavior of heavier elements for which experimental studies are severely limited by lack of material and/or by intense radioactivity. DOE

N86-13103# Stanford Linear Accelerator Center, Calif.
DATA ACQUISITION SYSTEM FOR SLD
D. J. Sherden May 1985 6 p Presented at the 4th Topical Conf. On Computerized Data Acquisition in Particle and Nucl. Phys., Chicago, 19 May 1985
(Contract DE-AC03-76SF-00515)
(DE85-014361; SU-SLAC-Pub-3695, CONF-850579-10) Avail: NTIS HC A02/MF A01

This paper describes the data acquisition system planned for the SLD detector which is being constructed for use with the SLAC Linear Collider (SLC). An exclusively FASTBUS front-end system is used together with a VAX-based host system. While the volume of data transferred does not challenge the band-width capabilities of FASTBUS, extensive use is made of the parallel processing capabilities allowed by FASTBUS to reduce the data to a size which can be handled by the host system. The low repetition rate of the SLC allows a relatively simple software-based trigger. The principal components and overall architecture of the hardware and software are described. DOE

N86-13104# Stanford Linear Accelerator Center, Calif.
HIGH AND ULTRA-HIGH GRADIENT QUADRUPOLE MAGNETS
W. O. Brunk and D. R. Walz May 1985 4 p Presented at the Particle Accelerator Conf., Vancouver, British Columbia, 13 May 1985
(Contract DE-AC03-76SF-00515)
(DE85-014360; SU-SLAC-Pub-3672; CONF-850504-185) Avail: NTIS HC A02/MF A01

Small bore conventional dc quadrupoles with apertures from 1 to 2.578 cm were designed and prototypes built and measured. New fabrication techniques including the use of wire electric discharge milling (EDM) to economically generate the pole tip contours and aperture tolerances are described. Magnetic measurement data from a prototype of a 1cm aperture quadrupole with possible use in future e(+)/e(-) super colliders are presented. At a current of 400A, the lens achieved a gradient of 2.475 T/cm, and had an efficiency of 76.6%. DOE

N86-13105# Lawrence Livermore National Lab., Calif.
MEASUREMENTS AND CALCULATIONS OF NEUTRON SCATTERING ANGULAR DISTRIBUTIONS OVER A WIDE MASS AND ENERGY RANGE
I. F. Hansen May 1985 13 p refs Presented at the Intern. Conf. on Nucl. Data for Basic and Appl. Sci., Santa Fe, N. Mex., 13 May 1985
(Contract W-7405-eng-48)
(DE85-012912; UCRL-92666; CONF-850507-19) Avail: NTIS HC A02/MF A01

Neutron elastic and inelastic differential cross sections for targets between (9)Be and (239)Pu at energies, E > 14 MeV have been measured using the Livermore and Ohio University neutron time-of-flight facilities. We review here the data and the analyses based on two local microscopic optical potentials: that of Jeukenne, Lejeune and Mahaux, and that of Brieva and Rook. The results are also compared with calculations using global potentials. Coupled channel formalism has been used in the analysis of targets with strong deformations, such as Be, C, Ta, and actinides. The value of the microscopic optical potentials as a tool to predict elastic and inelastic neutron cross sections over a wide mass and energy range is discussed. The need for neutron measurements up to higher energies and their analysis in conjunction with (p,p) and charge exchange (p,n) data is addressed. DOE

N86-13106# Los Alamos National Lab., N. Mex.
ISOVECTOR RESONANCES IN PION CHARGE EXCHANGE
J. D. Bowman 1985 5 p Presented at the Symp. on Nucl. Struct., Copenhagen, 20 May 1985
(Contract W-7405-eng-36)
(DE85-012746; LA-UR-85-1777; CONF-85051661) Avail: NTIS HC A02/MF A01

The ((PI) (+-), (PI) (0)) reactions as probes of isovector resonances are discussed. Experimental observation of the isovector monopole resonance is reported. Experimental results are presented for L = 0, 1, and 2 isovector resonances and are compared to random-phase approximation [illegible]tions. DOE

N86-13107# Los Alamos National Lab., [illegible]
SHOCKING BEHAVIOR OF FLUID FLOW [illegible]RMABLE JOINTS
H. Murphy and Z. Dash 1985 14 p Presented at the Intern. Symp. on Geothermal Energy, Kailua Kona, Hawaii, 26 Aug. 1985
(Contract W-7405-ent-36)
(DE85-010104; LA-UR-85-1007; CONF-850801-13) Avail: NTIS HC A02/MF A01

If fluid is injected into joints in rock masses, several types of joint deformations can take place. At first the pressure rise in the joint is small enough that the joint does not actually open. Nevertheless the effective closure stress, i.e., the difference between the total earth stress acting normal to the joint plane and the fluid pressure, is reduced. Consequently the tightness of joint closure is lessened, resulting in a small increase of the effective open space, or aperture, of the joint. If the fluid pressure rise is small enough, the aperture can still be treated as nearly constant, and the pressure response therefore follows the usual laws of linear diffusion. But if the pressure increase is large, aperture increases must be accounted for, and the flow will be affected by nonlinear diffusion due to pressure-dependent aperture, as well as a new storativity term due to joint compressibility. Eventually the fluid pressure may attain a value equal to, and even slightly greater than, the original total earth stress, and the opposing surfaces of the rock that meet at the joint can actually part. We refer to this behavior as joint lift off, or jacking. During lift off, the changes in joint aperture and compressibility are very large compared to changes while the joint is still in roughness-to-roughness contact and the flow equation becomes so highly nonlinear that pressure pulses are no longer transmitted in a smooth, diffusive manner, but more like a propagating shock wave. DOE

N86-13108# Sandia National Labs., Albuquerque, N. Mex.
IBEX MAGNETIC COUPLING EXPERIMENTS
C. A. Frost, P. D. Kiekel, R. B. Miller, C. A. Ekdahl, J. Wagner, and J. J. Ramirez 1985 5 p Presented at the SDIO/DARPA Ann. Propagation Rev., Monterey, Calif., 24 Jun. 1985
(Contract DE-AC04-76DP-00789)
(DE85-014331; SAND-85-1460C; CONF-8506141-4) Avail: NTIS HC A02/MF A01

The magnetic coupling of one pulse to another is a key issue for some modes of high-current beam propagation. Experiments are in progress on Sandia's IBEX accelerator to address issues relevant to magnetic coupling. The IBEX experiments differ from previous experiments in that the B/sub theta/ field acting on the second pulse is the result of residual plasma current from the first pulse rather than current applied by an external means. This new feature makes the propagation sensitive to beam and plasma current profiles that are key to the physics of the magnetic coupling problem. These experiments do not attempt to study the air chemistry issues, as this would require much higher current densities than are available from IBEX. We are using the IBEX accelerator with a mismatched magnetized diode to produce two high-current pulses separated by approx. 130 nsec. A pulse pair has been propagated over a 1.5-m path in low pressure air. Extraction of two pulses, each having different parameters, complicates the experiment but also provides new insight into the magnetic coupling problem. DOE

N86-13109# Sandia National Labs., Albuquerque, N. Mex.
RADLAC PROGRAM STATUS
C. A. Ekdahl and R. W. lemke 1985 4 p Presented at the SDIO/DARPA Ann. Propagation Rev., Monterey, Calif., 24 Jun. 1985 Prepared in cooperation with AFWL, Kirtland AFB, N. Mex.
(Contract DE-AC04-76DP-00789)
(DE85-014708; SAND-85-1453C; CONF-85061 1-7) Avail: NTIS HC A02/MF A01

Regardless of the propagation mode, the critical physics issue facing the use of intense relativistic electron beams in the lower atmosphere is the stability of the first pulse. The ATA was built at LLNL to address this question for low-current beams, and in RADIAC II at Sandia we now have the means for resolving the lead pulse stability issue for high-current beams. RADLAC II is now operational, and we can proceed with experiments that have the objective of demonstrating that the instabilities on a propagating beam with current greater than 40 KA can be suppressed to a maximum amplitude less than a beam radius. DOE

N86-13110# Los Alamos Scientific Lab., N. Mex.
EXPERIMENT TO STUDY K(+) (YIELDS) (PI)(+) + NOTHING AT LAMPF 2
D. R. Marlow May 1985 8 p refs
(Contract W-7405-eng-36)
(DE85-014267; LA-10395-MS) Avail: NTIS HC A02/MF A01

An experiment to measure K(+) (YIELDS) (PI) (+) nothing (where nothing denotes unobservable neutral particles) at LAMPF II is described. This experiment is capable of measuring one K(+) (YIELDS) (PI) (+) nu anti nu event for branching ratio of 10(-12). DOE

N86-13111# Lawrence Livermore National Lab., Calif.
HIGH INTENSITY POSITRON BEAM AND ANGULAR CORRELATION EXPERIMENTS AT LIVERMORE
R. H. Howell, I. J. Rosenberg, P. Meyer, and M. J. Fluss Mar. 1985 5 p Presented at the 7th Intern. Conf. on Positron Annihilation, New Delhi, 6 Jan. 1985 Prepared in cooperation with Argonne National Lab., N. Mex.
(Contract W-7405-eng-48)
(DE85-012961; UCRL-90936; CONF-850169-12) Avail: NTIS HC A02/MF A01

A positron beam apparatus that produces a variable energy positron beam with sufficient intensity to perform new positron experiments in an ultrahigh vacuum environment has been installed at the Lawrence Livermore 100 MeV electron linac. We have installed two large area position sensitive gamma-ray detectors to measure angular correlations in two dimensions and a separate highly collimated detector to measure positronium energy distributions by time-of-flight velocity determination. Data from measurements on single crystals of Cu will be described. DOE

N86-13112# Lawrence Livermore National Lab., Calif.
NUCLEAR PERFORMANCE OPTIMIZATION OF THE Be/Li/Th BLANKET FOR THE FUSION BREEDER
J. D. Lee and B. R. Bandini 26 Feb. 1985 7 p Presented at the 6th Topical Meeting on the Technol. of Fusion Energy, San Francisco, 3 Mar. 1985 Prepared in cooperation with Pennsylvania State Univ., University Park
(Contract W-7405-eng-48)
(DE85-012949; UCRL-92252; CONF-850310-111) Avail: NTIS HC A02/MF A01

More rigorous nuclear analysis, including treatment of resonance self shielding effects coupled with an optimization procedure, has resulted in improved performance of the Be/Li/Th blanket. Net U-233 breeding ratio has increased 36% (to 0.84) while at an average U-233/Th ratio of 0.5 a/o average energy multiplication has increased only 12% (to 2.1) compared with earlier results. DOE

N86-13113# Maryland Univ., College Park.
ACCELERATOR RESEARCH STUDIES
Nov. 1984 75 p
(Contract DE-AS05-78ER-05940)
(DE85-014878; DOE/ER-05940/T1) Avail: NTIS HC A04/MF A01

During the past contract period, major progress was made in both tasks of the accelerator research program in the Charged Particle Beam Laboratory at the University of Maryland. The major event in Task A was the completion of phase two of the transport channel. This phase consists of 12 lenses in addition to the two matching lenses. The first measurements of beam transport indicate 100% beam transmission in the range 40(0) < sigma0 < 90(0). Major highlights in Task B were new results in collective acceleration from laser-produced plasmas (considerably higher ion energies and currents than reported previously), successful studies of electron beam propagation in drift-tube and helix structures, construction of a novel, compact pulse-powered generator as well as new ion and electron spectroscopy results in the plasma focus area. DOE

N86-13114# Washington Univ., Seattle. Dept. of Physics.
CONFERENCE SUMMARY: ANTINUCLEON- AND NUCLEON-NUCLEUS INTERACTIONS
L. Wilets 1985 13 p Presented at the Conf. on Antinucleon and Nucleon-Nucleus Interactions, Telluride, Colo., 18 Mar. 1985
(Contract DE-AC06-81ER-40048)
(DE85-013905; DOE/ER-40048/10-N5) Avail: NTIS HC A02/MF A01

Topics summarized include: the hadronic substructure, the EMC effect, observations on relativity and the Dirac equation, and relativistic Lagrangian field theories for N-N interactions and nuclear matter. DOE

N86-13115# Brookhaven National Lab., Upton, N. Y.
LIGHT MASS ELEMENTS TOTAL HALF-LIVES FOR SELECTED LONG-LIVED NUCLIDES
N. E. Holden 1985 12 p refs Presented at Intern. Comm. for Radionuclide Metrology Meeting, Grenoble, France, 3 Jun. 1985
(Contract DE-AC02-76CH-00016)
(DE85-014217; BNL-NCS-36553; CONF-8506130-4) Avail: NTIS HC A02/MF A01

In the past, many compilations and evaluations of half lives have been made which have uncritically accepted authors' values and uncertainties. They have merely recommended weight averaged reported results. This evaluation attempts to reanalyze each experiment in the literature including an estimate of the standard deviation utilizing, where possible, an estimate of the systematic error. This paper constitutes a preliminary step in the process of recommending values. The long lived nuclides of light elements are of interest for their use in dating methods and for calculating cosmic ray exposure ages of meteorites. Experimental data on the half lives of selected nuclides have been evaluated and recommended values and uncertainties are presented for the following nuclides: (3)H, (10)Be, (14)C, (26)Al, (39)Ar, (40)K, (50)V, (53)Mn, (76)Ge, (87)Eb, (92)Nb, (107)Pd, (113)Cd, (115)In and (123)Te. The impact of the recommended (14)C half life of 5715 years on the carbon dating techniques, which uses the Libby value of 5568 years, will be discussed. Also the possible primordial occurrence of (92)Nb is now definitely ruled out by the recommended half life of 3.7 x 10(7). Finally, based on the recommended (26)Al half life value, the (21)Ne production rate for calculating cosmic ray exposure ages remains too high, compared to rates using the (53)Mn and (10)Be half life values. DOE

N86-13116# GA Technologies, Inc., San Diego, Calif.

TRITIUM CONTROL IN HELIUM-COOLED BLANKETS

C. P. C. Wong, I. Maya, C. Kessel (California Univ., Los Angeles), D. Roelant (Michigan Univ., Ann Arbor), and K. R. Schultz Jun. 1985 12 p Presented at 2nd Natl. Topical Meeting on Tritium Technol. in Fission, Fusion and Isotropic Appl., Dayton, Ohio, 30 Apr. 1985

(Contract DE-AC03-84-ER-53158)

(DE85-014783; GA-A-17940; CONF-850405-16) Avail: NTIS HC A02/MF A01

As a part of the Blanket Comparison and Selection study (BCSS), GA Technologies as responsible for the design of helium-cooled, solid- and liquid-metal breeder blankets. Conceptual blanket designs are developed, including the consideration of the generation, transport, and extraction of tritium. Evaluations are made of the inventory and leakage of tritium for helium-cooled Li2O and LiAlO2 and liquid lithium breeder blankets for tokamak and tandem mirror reactors. To facilitate the evaluation, a solid breeder tritium code TRIT4 is developed. The results from this study indicate that tritium inventories and leakages are acceptable for the proposed helium-cooled blankets. An assumption made in the tritium leakage calculations is that tritium is released to the helium purge and coolant streams as T2 and remains in that form. If oxidation to T2O is possible, significant reduction in the tritium leakage will be possible. It is concluded that more experimental data on breeder material properties and tritium permeation behavior are needed. However, an adequate number of techniques is available to control the breeder tritium inventory and leakage to an acceptable level in helium-cooled solid- and lithium-breeder blankets. DOE

N86-13117# Brookhaven National Lab., Upton, N. Y.

PROMPT NEUTRON FISSION SPECTRUM MEAN ENERGIES FOR THE FISSILE NUCLIDES AND (252)Cf

N. E. Holden 1985 7 p refs Presented at Intern. Comm. for Radionuclide Metrology Meeting, Grenoble, France, 3 Jun. 1985

(DE85-012181; BNL-NCS-36552) Avail: NTIS HC A02/MF A01

The international standard for a neutron spectrum is that produced from the spontaneous fission of (252) Cf, while the thermal neutron induced fission neutron spectra for the four fissile nuclides, (233)U, (239)Pu, and (241)Pu are of interest from the standpoint of nuclear reactors. The average neutron energies of these spectra are tabulated. The individual measurements are recorded with the neutron energy range measured, the method of detection as well as the average neutron energy for each author. Also tabulated are the measurements of the ratio of mean energies for pairs of fission neutron spectra. DOE

N86-13118# Edgerton, Germeshausen and Grier, Inc., Idaho Falls, Idaho.

TRITIUM SAFETY ISSUES FOR TFCX

H. J. Reilly, S. J. Piet, and B. J. Merrill 1985 15 p Presented at the 2nd Natl. Topical Meeting on Tritium Technol. in Fission, Fusion and Isotopic Appl., Dayton, Ohio, 30 Apr. 1985

(Contract DE-AC07-76ID-01570)

(DE85-014621; EGG-M-20684; CONF-850405-14) Avail: NTIS HC A02/MF A01

Estimated tritium releases from the Tokamak Fusion Core Experiment are compared to the expected limits. A reaction kinetics model is described that predicts the conversion of tritium to the oxide form in free space. An analysis of the required capacity of the Emergency Tritium Cleanup System is also presented. The conclusions of this work are expected to be applicable to other experimental fusion devices that are now being considered. DOE

N86-13119# Brookhaven National Lab., Upton, N. Y.

SEARCH FOR NARROW STRUCTURE IN PROTON-ANTIPROTON ANNIHILATION CROSS SECTIONS FROM 1900 TO 1960 MeV

D. I. Lowenstein, D. C. Pealsee, R. J. Miller, R. A. Lewis, B. Y. Oh, G. A. Smith, J. Whitmore, T. Brando, L. Daftari, and A. deGuzman 1985 8 p Presented at the Intern. Conf. on Hadron Spectry., Coll. Park, Md., 20 Apr. 1985

(Contract DE-AC02-76CH-00016)

(DE85-013302; BNL-36569; CONF-8504133-3) Avail: NTIS HC A02/MF A01

The anti pp annihilation cross section has been measured with good resolution (approx. 2 MeV rms) in the mass range 1900-1960 MeV. No narrow structures are seen, the 90% confidence level upper limit being 8-12 mb-MeV for the integrated area of a resonance in this mass range. However, we do not rule out a very narrow bump dip structure seen in an earlier experiment in the 1935-1941 MeV mass interval. The data also do not support the existence of a broad structure previously reported at 1937 MeV. DOE

N86-13120# Washington Univ., Seattle. Inst. for Nuclear Theory.

DYNAMICAL MODEL OF QUARK REARRANGEMENT IN NUCLEON-ANTINUCLEON ANNIHILATION

G. A. Crawford, J. L. Dethier, L. Wilets, and M. Alberg (Seattle Univ.) May 1985 7 p refs Presented at Conf. on Antinucleon and Nucleon-Nucleus Interactions, Telluride, Colo., 18 Mar. 1985

(Contract DE-AC06-81ER-40048)

(DE85-013904; CONF-850315-6) Avail: NTIS HC A02/MF A01

The total inclusive cross-section for nucleon-antinucleon annihilation is being calculated, following a reaction mechanism in which the quarks undergo a rearrangement to form a doorway state consisting of a meson plus a two-quark, two-antiquark exotic. The soliton bag model is used for the quark interactions. Bag-bag dynamics are solved using the generator coordinate method formalism. DOE

N86-13121# Stanford Linear Accelerator Center, Calif.

PHYSICS OF e(+) - e(-) COLLIDERS: PRESENT, FUTURE AND FAR FUTURE

M. E. Peskin Oct. 1984 25 p refs Presented at 3rd Ann. Summer School on High Energy Accelerators, Upton, N.Y., 6 Jul. 1983

(Contract DE-AC03-76SF-00515)

(DE85-009895; SU-SLAC-Pub-3495; CONF-8307126-8) Avail: NTIS HC A02/MF A01

A lecture on e(+)-e(-) colliders contains the following: Section 2 reviews the features of e(+)-e(-) collisions according to the standard gauge theory of strong, weak, and electromagnetic interactions. This discussion reviews a few of the most important features of Ee(+)-e(-) collisions at currently accessible energies and the expectations for e(+)-e(-) reactions which produce the intermediate vector bosons Z(0) and W(+-). Section 3 reviews some of the experimental work done at the current generation of e(+)-e(-) colliders; this discussion emphasizes the search for new types of elementary particles. Section 4 is a theoretical digression, introducing a number of ideas about physics at the energy scale of 1 TeV. Section 5 discusses a number of technical aspects of electron-positron colliders designed to reach the TeV energies. Finally, Section 6 discusses various possible effects which could appear in e(+)-e(-) collisions as the result of new physics appearing at 1 TeV or above. DOE

N86-13122# British Columbia Univ., Vancouver.
FASTBUS FOR THE PARTICLE ACCELERATOR LABORATORIES
W. K. Dawson, L. Costrell, H. Ikeda, P. J. Ponting, and H. V. Walz May 1985 3 p refs Presented at the Particle Accelerator Conf., Vancouver, British Columbia, 13 May 1985 Prepared in cooperation with NBS, Washington, D.C., National Lab. for High Energy Physics, Ibaraki, Japan, European Organization for Nuclear Research, Geneva, Switzerland and Stanford Linear Accelerator Center, Calif.
(DE85-014352; SU-SLAC-Pub-3697; CONF-850504-189) Avail: NTIS HC A02/MF A01

The FASTBUS modular high speed data acquisition and control system for high energy physics and other applications was described by Costrell and Dawson at the 1983 Particle Accelerator Conference. Both the specification and the implementation of this interlaboratory development have progressed considerably since that time. Because of its many attractive features, FASTBUS is currently in use in several major nuclear and high energy physics laboratories and is also finding application in other areas. DOE

N86-12407# Joint Publications Research Service, Arlington, Va.
MATHEMATICAL MODEL OF THE DYNAMIC RESPONSE OF THERMO-REGULATING IN 200 MeV LINEAR ACCELERATOR
Hu Defang and Ouyang Xiantai *In its* China Rept.: Sci. and Technol. (JPRS-CST-85-035) 17 Oct. 1985 p 90-95 refs Transl. into ENGLISH from Zhongguo Kexue Jishu Daxue Xuebao (Hefei), v. 15, no. 2, Jun. 1985 p 217-222 (For primary document see N86-12399 03-31)
Avail: NTIS HC A06/MF A01

74 OPTICS

Includes light phenomena.

N86-13123 Department of the Navy, Washington, D. C.
OPTICAL SENSING DEVICES Patent
P. Shajenko, inventor (to Navy) Issued 11 Jun. 1985 6 p Supersedes AD-D011038
(AD-D011829; US-Patent-4,522,495; US-Patent-Appl-SN-503913; US-Patent-Class-356-345) Avail: US Patent and Trademark Office CSCL 17/8

This patent describes optical sensing devices comprising dual chamber apparati which use signal and reference light beams together with interferometric methods for detection of physical quantities of interest. The signal part of the chamber experiences the effects of a particular physical quantity to be measured which produce variations in the optical length of the light beam by movement of a mirror, thereby modulating that beam in proportion thereto. Concurrently, the reference beam, of equal pathlength, is passed through an adjacent chamber, isolated from such effects. The modulated signal beam and unmodulated reference beam are then combined to form a fringe pattern, the zero and first order fringes which are superimposed on apertures of an optical fibers, which carry the resultant light beams to a photodetector for converting the resultant light beams to a photodetectors for converting the optical signals to proportional electrical signals. GRA

N86-13124 Department of the Navy, Washington, D. C.
REVERSIBLE OPTICAL WAVEGUIDE VAPOR SENSOR Patent
J. F. Giuliani and H. Wohltjen, inventors (to Navy) Issued 23 Apr. 1985 5 p Supersedes AD-D010178
(AD-D011834; US-Patent-4,513,087; US-Patent-Appl-SN-462493; US-Patent-Class-436-96) Avail: US Patent and Trademark Office CSCL 09/1

A device for detecting small amounts of a chemical such as ammonia, and other ammonia-like molecules such as hydrazine or pyridine, in air and in other gases is disclosed. A capillary tube serves as a multiple total reflective medium for an optical beam from a light-emitting diode. The outer surface of the capillary tube is coated with a dye which, when exposed to the chemical, changes color so that the multiply reflected light is modified. The resultant change in the output light intensity from the capillary tube is photodetected and recorded to sense the presence of the chemical. When the chemical is removed, the dye returns to its original color so that the device can be reused. Author (GRA)

N86-13125# Department of the Army, Washington, D. C.
PHOTOSENSITIVE CARTRIDGE FOR WEAPONS ZEROING AND MARKSMANSHIP TRAINING Patent Application
F. N. Dyer and J. R. Schjelderup, inventors (to Army) Filed 3 May 1985 17 p
(AD-D011765; US-Patent-Appl-SN-730125) Avail: NTIS HC A02/MF A01 CSCL 19/1

The invention provides a light sensitive dummy cartridge for insertion into the chamber of a magazine-type weapon. A muzzle collimator is inserted into the barrel in alignment with the cartridge photosensor and the longitudinal axis of the bore. The power supply, audible scoring apparatus, and electrical circuit for the photosensor, moreover, are mounted in a dummy magazine. This combination provides an easy-to-install apparatus for temporarily converting a conventional firearm into a photoresponsive training device. This is a patent application. GRA

N86-13126# California Inst. of Tech., Pasadena.
ADAPTIVE OPTICAL FILTERING TECHNIQUES Final Technical Report, Apr. - Sep. 1984
D. Psaltis May 1985 31 p
(Contract F30602-81-C-0169)
(AD-A157072; RADC-TR-85-80) Avail: NTIS HC A03/MF A01 CSCL 20/6

The purpose of this study was to examine the potential of using optical information processing technology for adaptive antenna beamforming and null steering. The adaptive beamforming-/null steering problem consists of estimation of the covariance matrix of the noise field and inversion of the covariance matrix to obtain the antenna element weights which optimize the antenna's directional characteristics (gain pattern). This report examines the adaptive beamforming/nulling problem in view of the capabilities of optics and identifies areas where optics can be used to benefit. Benefits and drawbacks of various optical implementations of open and closed loop adaptive algorithms are discussed as well as the issues involved with optically processing digital binary numbers. GRA

N86-13127# Rome Air Development Center, Griffiss AFB, N.Y.
ANALYTIC MODELS FOR RADIATION INDUCED LOSS IN OPTICAL FIBERS. 3. TRANSIENT RADIATION EFFECTS
J. A. Wall Wright-Patterson AFB, Ohio AFWAL Feb. 1985 13 p
(AF Proj. 2306)
(AD-A157408; RADC-TR-85-39) Avail: NTIS HC A02/MF A01 CSCL 20/6

A number of physical models used to describe the recovery of transient radiation induced loss in optical fibers were evaluated and found unacceptable for various reasons. Based on an approximation to some of these models, the analytic expression L = a/(1 + b(t to the nth power)) where L = loss, time = time after pulse, and a, b, and n are constants, was formulated and found to give very good fits to transient radiation effects data obtained at RADC. GRA

N86-13128# University Coll., Galway (Ireland).
ELECTRO-OPTICAL TRANSMISSION AND LIQUID WATER CONTENT OF FOGS AND CLOUDS Final Technical Report
S. G. Jennings May 1985 73 p
(Contract DAJA37-81-C-0003)
(AD-A157506; R/D-2827-EN) Avail: NTIS HC A04/MF A01 CSCL 20/6

Research conducted during the term of this contract consisted of measurement of transmission and backscatter of electromagnetic (em) energy through water droplet clouds with known size distribution and liquid water content at visible and infra-red (IR) wavelengths. Theoretical analyses of relations between extinction, absorption and backscatter which incorporate size distribution dependencies were also made. Author (GRA)

N86-13129# Electronics Research Lab., Adelaide (Australia).
ATMOSPHERIC IR TRANSMISSION MEASUREMENTS IN A TROPICAL MARITIME ENVIRONMENT: COMPARISON WITH THE LOWTRAN 6 MODEL
D. R. Cutten Feb. 1985 38 p
(AD-A157920; ERL-0331-TM) Avail: NTIS HC A03/MF A01 CSCL 20/6

Broadband IR transmission data measured at a coastal, tropical maritime site have been compared with LOWTRAN 6 model predictions. Transmittance data for a 7 km path plotted as a function of absolute humidity have been examined in six spectral regions from 1.5 to 12 micrometers. A significant discrepancy, which increases with water vapor content, has been found between the measured and predicted data for the 8 to 12 micrometer region. This discrepancy is believed to be due to errors in the laboratory-determined self-broadening coefficients of water continuum absorption. Reasonable agreement has been obtained in the 4.4 to 5.4 micrometer and the 3.5 to 4.0 micrometer regions, particularly for the former region when water continuum absorption is included in the LOWTRAN model. GRA

N86-13130# Decilog, Inc., Melville, N. Y.
IMPROVEMENT OF MANUFACTURING TECHNIQUES AND QUALITY OF OPTICAL SCRATCH STANDARDS FOR FIRE CONTROL SYSTEMS
J. R. Goldgraben and J. Salerno Aug. 1985 53 p
(Contract DAAK10-81-C-0308)
(AD-A157963; AD-E401373; ARPAD-CR-85001) Avail: NTIS HC A04/MF A01 CSCL 20/6

Manufacture of the Optical Surface Quality Standards (Scratch and Dig) has been a problem since their introduction. The present technique of diamond scribing the scratch standard is haphazard mainly because there are no controlling dimensions for the scratch. The problem arises because there is no correlation between the physical and the visual parameters of the scratch. An evaluation was conducted of manufacturing techniques that would reliably reproduce the standards. Additionally, work was coordinated with the National Bureau of Standards who developed a measuring technique and generated a configuration for the new standard. The manufacturing process developed under this project utilized an electron beam writing instrument to produce the scratch pattern on photomasks. The photomasks were then processed by wet chemical etching to produce the scratch standards. The pattern generated was a 10-line pattern with individual line structure on the order of 1 micron in width. The results demonstrated a correlation of the scratch pattern to its visual appearance. However, the chemical etching produced low yield due to the non-repeatibility of the process. The results, therefore, while demonstrating for the first time a relationship between the physical characteristics and the visual appearance, also indicate that further refinement of the chemical etching portion of the process is necessary before the technique can be considered cost effective. GRA

N86-13131# Arizona Univ., Tucson.
MASKING OF LIGHT SCATTERING INFORMATION ON MATRIX ELEMENTS FROM COMPLEX SCATTERING Contractor Report, Sep. 1982 - Aug. 1984
W. S. Bickel Jul. 1985 73 p
(Contract DAAK11-82-K-0006)
(AD-A158144; CRDC-CR-85035) Avail: NTIS HC A04/MF A01 CSCL 20/6

Changes in light scattering curves due to perturbation on scattering systems are considered, using both measured data and, where possible, computer generated data. It is demonstrated that polydispersivity in size or real refractive index quickly destroys phase information from systems of perfect spheres, while absorption destroys phase information mainly in the backscatter directions and decreases the ratio of backscatter to forward scatter intensity. Several measured Mueller matrices are presented for perfect, bent, rotated, tilted, and surface roughened fibers, and for a highly irregular scatter, road dust. An introductory tutorial on the Mueller matrix description of light scatterings is included. GRA

N86-13132# Tetra Corp., Albuquerque, N. Mex.
UV SUSTAINED GLOW DISCHARGE OPENING SWITCH Final Report, 1 Jul. 1982 - 31 Dec. 1984
M. VonDadelszen and W. M. Moeny Jun. 1985 115 p
(Contract DAAG29-82-C-0018)
(AD-A158411; TETRA-TR-85-015; ARO-18965.2-PH) Avail: NTIS HC A06/MF A01 CSCL 09/1

This was a combined theoretical and experimental research program to determine discharge performance characteristics and the influence of various gas mixture additives on discharge performance for UV-sustained glow discharges. This research has a significant technological application in opening switches. The approach was a coordinated theoretical and experimental research effort to gain understanding of the characteristics and physics of UV-sustained glow discharges. A major portion of the research program was an experimental investigation of discharge physics using a single-pulse, UV-sustained 1.5 liter discharge chamber. By measuring discharge characteristics as a function of the electrode separation, pressure, applied voltage, source characteristics, and gas mixture, we determined the relationship between the gas mixture and the discharge kinetics, and between the UV-sustainer characteristics and the glow discharge performance characteristics. The experimental facility included the capability of studying the influence of seedants on discharge performance and measuring glow discharge kinetic rates. GRA

N86-13133# Sandia National Labs., Albuquerque, N. Mex.
RADIATION EFFECTS ON LIGHT SOURCES AND DETECTORS
C. E. Barnes 1985 15 p Presented at the Soc. of Photo-Optical Instr. Eng. Conf., Albuquerque, N. Mex., 1 Mar. 1985
(Contract DE-AC04-76DP-00789)
(DE85-014746; SAND-85-0685C; CONF-8503156-1) Avail: NTIS HC A02/MF A01

The rapidly expanding field of optoelectronics includes a wide variety of both military and non-military applications in which the systems must meet radiation exposure requirements. Herein, we review the work on radiation effects on sources and detectors for such optoelectronic systems. For sources the principal problem is permanent damage-induced light output degradation, while for detectors it is ionizing radiation-induced photocurrents. DOE

N86-13134# Los Alamos National Lab., N. Mex.
NEARLY IDEAL LENS OPTIMIZATION PROCEDURE
B. Brixner 1985 7 p refs Presented at the Intern. Lens Design Conf., Cherry Hill, N.J., 10 Jun. 1985
(Contract W-7405-eng-36)
(DE85-014116; LA-UR-85-2062; CONF-8506142-1) Avail: NTIS HC A02/MF A01

The Brixner lens optimization procedure, in which a lens design moves steadily toward diffraction-limited performance, samples lens performance with bundles of precisely traced skew rays, analyzes performance by calculating the image spot sizes and positions, and optimizes performance in a least squares system that minimizes the lateral ray deviations from their ideal image points. Minimizing the rms image spot size minimizes the rms optical path differences (OPDs). Minimizing the rms OPDs also optimizes the diffraction modulation transfer function (DMTF). Minimizing the image spot size and position errors also minimizes and balances the Seidel and high order aberrations. DOE

N86-13135# Los Alamos Scientific Lab., N. Mex. Materials Science and Technology Div.
STUDY OF POSSIBLE SOLARIZATION - RELATED IMPURITIES IN CaF2 AND OTHER FLUORIDES
Lawrence B. Edgett and Suzanne C. Stotlar 1985 7 p Presented

at the Southwest Conf. on Optics, Albuquerque, N. Mex., 4-8 Mar. 1985 Submitted for publication
(Contract W-7405-eng-36)
(DE85-014100; LA-UR-85-2157; CONF-850345-28) Avail: NTIS HC A02/MF A01

CaF2, MgF2 and SrF2 representative samples are obtained from three commercial single crystal sources. After repolishing their surfaces, all samples are subjected to spectographic quantitative spectrophotometry. A correlation of optical properties observed and trace impurities or dopants found by chemical analysis are observed, and details presented. DOE

N86-13136# Lawrence Livermore National Lab., Calif.
ESTIMATING THE RELIABILITY OF FIBER OPTICS CABLES
L. I. George 7 May 1985 23 p
(Contract W-7405-eng-48)
(DE85-014892; UCID-20459) Avail: NTIS HC A02/MF A01

This report estimates the reliability of fiber optics cables used in underground nuclear tests. Reliability is the probability of receiving signals transmitted from tests. This report uses the numbers of cable and fiber failures to estimate cable and fiber reliabilities. It uses cable and fiber reliability estimates to estimate the reliability of a signal transmission design, the probability of receiving at least one copy of each signal from a test. It shows that reliability estimates differ due to manufacturer, user, and depth of burial. And it shows one way to quantify the uncertainty in reliability estimates. This report should be used to help design reliable signal transmission systems. The data came from 43 tests done prior to FY 85 which used fiber optics cables. The users are Lawrence Livermore National Laboratory, Los Alamos National Laboratory, and Department of Defense. The data are numbers of fiber and cable failures, manufacturers and users, and depths of burial. Samples proportions estimate the fiber and cable reliabilities. Statistics test whether reliability estimates differ significantly between manufacturers and between users. Linear regression models failure rates as functions of depths of burial and tests whether failure rates depend on depths of burial. Probability theory quantifies the uncertainty in the reliability of one test with percentiles of the reliability estimate. Designers may use these results to compare alternatives for sending signals through fiber optics cables and to increase reliability with redundancy. DOE

N86-13137# National Oceanic and Atmospheric Administration, Boulder, Colo. Wave Propagation Lab.
FOLDED-PATH OPTICAL (C SUB n, SUP 2) INSTRUMENT
G. R. Ochs, D. S. Reynolds, and R. L. Zurawski Mar. 1985 33 p
Sponsored in part by AFGL, Hanscom AFB, Mass.
(PB85-216398; NOAA-TM-ERL-WPL-123) Avail: NTIS HC A03/MF A01 CSCL 20F

An optical instrument that measures the refractive-index structure parameter (C sub n, sup 2) on a folded path to a cat's eye retroreflector is described. The measurement is heavily weighted toward the retroreflector. Using optimum path lengths of 150 to 250 meters, (C sub n, sup 2) can be measured over a range from 1 x 10 the -12th power to 1 x 10 to the -16th power (m to the -2/3 power). Author (GRA)

N86-12409# Joint Publications Research Service, Arlington, Va.
DETERMINATION OF SINGLE-MODE OPTICAL FIBER DISPERSION
Zhou Wenjun *In its* China Rept.: Sci. and Technol. (JPRS-CST-85-017) 11 Jun. 1985 p 42-51 refs Transl. into ENGLISH from Tongxin Xuebao (Beijing), v. 5, no. 3, Jul. 1984 p 95-101 (For primary document see N86-12408 03-31)
Avail: NTIS HC A08/MF A01

N86-12414# Joint Publications Research Service, Arlington, Va.
STATE-OF-THE-ART OF OPTICS IN CHINA REVIEWED
Wang Daheng and Wo Xinneng *In its* China Rept.: Sci. and Technol. (JPRS-CST-85-018) 12 Jun. 1985 p 50-65 refs Transl. into ENGLISH from Guangxue Xuebao (Shanghai), v. 5, no. 1, Jan. 1985 p 1-10 (For primary document see N86-12413 03-31)
Avail: NTIS HC A09/MF A01

N86-12415# Joint Publications Research Service, Arlington, Va.
SINGLE MODE PHASE LOCKING FIBEROPTIC SENSOR DEVELOPED
Wang Jinghua, Xie Haiming, Cui Jianhua, and Li Dazhong *In its* China Rept.: Sci. and Technol. (JPRS-CST-85-018) 12 Jun. 1985 p 66-69 refs Transl. into ENGLISH from Yingyong Jiguang (Shanghai), v. 5, no. 1, Feb. 1985 p 43-44 (For primary document see N86-12413 03-31)
Avail: NTIS HC A09/MF A01

N86-12416# Joint Publications Research Service, Arlington, Va.
PRACTICAL OPTICAL MULTICHANNEL ANALYZER DEVELOPED
Chen Jian, Li Weiliang, Wan Wanlun, Lin Weizhu, and Li Wenchong *In its* China Rept.: Sci. and Technol. (JPRS-CST-85-018) 12 Jun. 1985 p 70-77 refs Transl. into ENGLISH from Yingyong Jiguang (Shanghai), v. 5, no. 1, Feb. 1985 p 45-48 (For primary document see N86-12413 03-31)
Avail: NTIS HC A09/MF A01

N86-12417# Joint Publications Research Service, Arlington, Va.
DEVELOPMENT OF BEAM OPTICS FOR A 200 keV ION IMPLANTER
Pan Xianzheng, Fan Xiangjin, Xu Zaigui, and Guo Huaigui *In its* China Rept.: Sci. and Technol. (JPRS-CST-85-018) 12 Jun. 1985 p 78-88 refs Transl. into ENGLISH from Wuhan Daxue Xuebao (Wuhan), no. 4, Dec. 1984 p 35-40 and 56 (For primary document see N86-12413 03-31)
Avail: NTIS HC A09/MF A01

N86-12466# Joint Publications Research Service, Arlington, Va.
APPLICATION OF RADIOGRAPHIC IMAGE ENHANCEMENT, SEGMENTATION
Wang Chengye and Xia Wei *In its* China Rept.: Sci. and Technol. (JPRS-CST-85-032) 19 Sep. 1985 p 67-70 Transl. into ENGLISH from Jisuanji Yanjiu yu Fazhan (Beijing), v. 21, no. 12, Dec. 1984 p 52-53 (For primary document see N86-12462 03-31)
Avail: NTIS HC A08/MF A01

N86-12691# Joint Publications Research Service, Arlington, Va.
IONIC MECHANICSM OF EXCHANGE OF ADMIXTURES BETWEEN HYDROSPHERE AND ATMOSPHERE Abstract Only
A. V. Savchenko and V. V. Smirnov *In its* USSR Rept.: Earth Sci. (JPRS-UES-85-006) 19 Jun. 1985 p 74 Transl. into ENGLISH from Izv. Akad. Nauk SSSR: Fiz. Atm. i Okeana (Moscow), v. 21, no. 1, Jan. 1985 p 32-41 Original language document was announced in IAA as A85-26294 (For primary document see N86-12630 03-42)
Avail: NTIS HC A05/MF A01

N86-12705# Joint Publications Research Service, Arlington, Va.
REMOTE DIAGNOSIS OF MEDIA BY COMBINATION (RAMAN) ANTI-STOKES LIGHT SCATTERING METHOD WITH INDUCED BRILLOUIN BACKSCATTERING Abstract Only
A. F. Bunkin, D. V. Vlasov, and A. S. Galumyan *In its* USSR Rept.: Earth Sci. (JPRS-UES-85-008) 16 Aug. 1985 p 10-11 Transl. into ENGLISH from Kvantovaya Elektron. (Moscow), v. 12, no. 3, Mar. 1985 p 619-621 (For primary document see N86-12697 03-42)
Avail: NTIS HC A04/MF A01

75 PLASMA PHYSICS

Includes magnetohydrodynamics and plasma fusion.
For ionospheric plasmas see *46 Geophysics.* For space plasmas see *90 Astrophysics.*

N86-13138*# Alabama Univ., Huntsville. School of Science.
PLASMA AND MAGNETOSPHERIC RESEARCH Quarterly Progress Report, Jul. - Sep. 1985
Richard H. Comfort and James L. Horwitz Oct. 1985 12 p refs
(Contract NAS8-33982)

(NASA-CR-176326; NAS 1.26:176326) Avail: NTIS HC A02/MF A01 CSCL 20I

Several programs and variations have been developed to determine statistical means of different plasma parameters when binned in different variables. These parameters include temperature, densities and spacecraft potentials for any of the ion species, as well as ratios of these variables for any other ion species to the corresponding variable for H(+). The variables for binning include L, radial distance, and geomagnetic latitude; and separate statistics are automatically run for local morning and local evening data. These programs all run from output files from the plasma parameter thin sheath analysis program. A variant program also bins for magnetic activity, using either Kp or Dst, which requires an additional magnetic activity input file. These programs can be run either interactively or in batch mode, using file listings generated by a DIRECTORY command. In addition to printed output, these programs generate output files which can be used to plot the results. Programs to plot these averaged data are under development. Author

N86-13139# Air Force Geophysics Lab., Hanscom AFB, Mass.
CALCULATION OF THRESHOLD CONDITIONS FOR MATERIALS CHARGING IN MAXWELLIAN PLASMAS Interim Report
A. G. Rubin and M. Tautz 25 Jan. 1985 18 p
(AF Proj. 7661)
(AD-A157123; AFGL-TR-85-0020; AFGL-ERP-907) Avail: NTIS HC A02/MF A01 CSCL 20/9

Space Plasmas at geosynchronous orbit are usually not characterized by a single Maxwellian distribution function. Plasmas are characterized as single Maxwellians to first order and as a sum of two Maxwellians as a better approximation. A threshold electron temperature condition for charging of materials in the single Maxwellian is derived. Conditions for materials charging in the dual Maxwellian case are derived and illustrated. These are threefold: an initial negative current; a threshold electron temperature and a threshold electron current. GRA

N86-13140# Naval Research Lab., Washington, D. C.
BEHAVIOR OF IONIZED PLASMA IN THE HIGH LATITUDE TOPSIDE IONOSPHERE
S. G. Ganguli, H. G. Mitchell, Jr., and P. J. Palmadesso 27 Aug. 1985 40 p
(AD-A157930; NRL-MR-5623) Avail: NTIS HC A03/MF A01 CSCL 04/1

We have developed a numerical model to study the steady state behavior of a fully ionized plasma (H+, O+ and the electrons) encompassing the geomagnetic field lines. The theoretical formulation is based on the 16-moment system of transport equations. The electron gas collision is dominated below 2500 km. Above this altitude electron temperature anisotropy develops with temperature perpendicular to the field line being higher than that parallel to the field line. The H+ ion temperature anisotropy shows H+ temperature parallel to the field line being higher than that perpendicular to the field line. H+ ion temperature also exhibits adiabatic cooling as to the supersonic ion gas cools down as it expands in a diverging magnetic field. Our results are in good agreement with the previous theoretical studies of the polar wind and recent experimental observations. This is the first successful steady state solution to the 16-moment set of transport equations. GRA

N86-13141# Los Alamos National Lab., N. Mex.
FIELD-REVERSED CONFIGURATION FORMATION, TRANSLATION, AND CONFINEMENT STUDIES ON THE FRX-C/T EXPERIMENT
R. E. Siemon, W. T. Armstrong, R. E. Chrien, W. A. Hugrass, K. F. McKenna, D. J. Rej, and M. Tuszewski 1985 5 p Presented at the 12th European Conf. on Controlled Fusion and Plasma Phys., Budapest, 2 Sep. 1985
(Contract W-7405-eng-36)
(DE85-014095; LA-UR-85-2174; CONF-850927-2) Avail: NTIS HC A02/MF A01

The field-reversed configuration (FRC) is a high (BETA) (> 50%), prolate compact toroid plasma contained primarily by poloidal magnetic fields. FRC plasmas with parameters, anti n = 1-5 x 10 to the 15th power/cu cm., T/sub i/ = 0.1-0.8 keV, T/sub e/ = 0.1-0.2 keV, R approx. = 7 cm, B = 5-8 kG, lifetimes less than or equal to 300 (MU)s, are studied on the FRX-C/T experiment at Los Alamos. FRX-C/T consists of a 0.5-m-dia, 1.0-m-long field-reversed theta-pinch coil, and a 0.4-m-dia, 5-m-long translation region into which FRC's are launched, translated, and trapped. A 5-20 mtorr pressure D2 fill is introduced into the device by either a gas puff (localized in the theta-pinch source) or static fill system. DOE

N86-13142# Oak Ridge National Lab., Tenn.
TPSS PLASMA ENGINEERING STUDIES: PROFILE EFFECTS AND PLASMA POWER BALANCE
S. K. Borowski and D. J. Strickler 1985 12 p Presented at the TPSS Meeting, Atlanta, 15 May 1985
(Contract DE-AC05-84OR-21400)
(DE85-013638; CONF-8505175-1) Avail: NTIS HC A02/MF A01

A computationally fast profile-averaged, steady-state plasma model has been developed to allow studies of radial effects in ignited and driven tokamak systems. This code was used to search for the smallest size tokamak consistent with power balance calculation. DOE

N86-13143# Lawrence Livermore National Lab., Calif.
DIFFUSION IN BINARY PLASMA MIXTURES
D. B. Boercker, A. J. Ladd, and E. L. Pollock 16 Aug. 1985 15 p refs
(Contract W-7405-eng-48)
(DE85-017694; UCID-20507) Avail: NTIS HC A02/MF A01

Ion diffusion in binary plasma mixtures is considered. After first defining the diffusion coefficients for a binary mixture, it is shown how it is related to concentration fluctuations. The relation between diffusion and self diffusion is discussed. Specializing to a model of classical ions in a uniform, charge neutralizing, background molecular dynamics simulations and kinetic theory calculations are discussed. Results for H(+)-He(++) mixtures at a temperature of 5 eV and Si(+14)-Sr(+36) mixtures at 1 keV, all at 10 to the 22d power ions cu cm (3), are presented and discussed. DOE

N86-13144# Sandia National Labs., Albuquerque, N. Mex.
IMPLEMENTING THE AUTOMATED FEATURES OF THE PBFA-I CONTROL/MONITOR SYSTEMS
J. L. Spiller 1985 16 p Presented at the 5th IEEE Pulsed Power Conf., Washington, D.C., 10 Jun. 1985
(Contract DE-AC04-76DP-00789)
(DE85-012841; SAND-84-2537C; CONF-850616-29) Avail: NTIS HC A02/MF A01

A control system is being provided for PBFA-I, an operational accelerator, to control subsystem functions such as sequencing of oil, water, gas, and vacuum controls, to coordinate charging and firing sequences, and to control safe and idle modes of the machine. Important design concepts in automating this system are: reliability, flexibility, and operability. Reliability is a primary criterion for executing single pulsed power and physics experiments as well as for supporting extended experimental series without a failure that would cause downtime. Flexibility to respond to changes in operating parameters and experimenter needs is being implemented in two major areas: a modular I/O system to provide hardware flexibility, and structured software to ease software maintenance. Operability is increased with user friendly software, and automatic sequencing. DOE

N86-13145# Los Alamos Scientific Lab., N. Mex.
GENERALIZATION OF THE CHILD-LANGMUIR RELATION FOR ONE-DIMENSIONAL TIME-DEPENDENT DIODES
A. Kadish, W. Peter, and M. E. Jones 1985 4 p Presented at the Particle Accelerator Conf., Vancouver, British Columbia, 13 May 1985
(Contract W-7405-eng-36)
(DE85-012677; LA-74-85-1596; CONF-850504-102) Avail: NTIS HC A02/MF A01

The steady-state Child-Langmuir relation between current and applied voltage has been a basic principle upon which all modern diode physics has been based. With advances in pulsed power technology and diode design, new devices which operate in vastly different parameter regimes have recently become of interest. Many of these devices cannot be said to satisfy the strict requirements necessary for Child-Langmuir flow. For instance, in a recent pulsed electron device for use in high-current accelerators, the applied voltage is sinusoidal in time. In another case, development of sources for heavy ion fusion necessitates understanding of transient current oscillations when the voltage is applied abruptly. We derive the time-dependent relationship between the emitted current and time-dependent applied voltage in a nonrelativistic planar diode. The relationship is valid for arbitrary voltage shape V(t) applied to the diode for times less than the beam-front transit time across the gap. Using this relationship, transient and time-dependent effects in the start-up phase of any nonrelativistic diode can be analzyed. DOE

N86-13146# Stanford Linear Accelerator Center, Calif.

RF BEAM DEFLECTION MEASUREMENTS AND CORRECTIONS IN THE SLC LINAC

J. R. Seeman, M. C. Ross, J. C. Sheppard, and R. F. Stiening 13 May 1985 3 p refs Presented at the Particle Accelerator Conf., Vancouver, British Columbia, 13 May 1985
(Contract DE-AC03-76SF-00515)
(DE85-013061; SU-SLAC-Pub-3621; CONF-850504-111) Avail: NTIS HC A02/MF A01

The requirements of RF acceleration in the SLC linac to produce high energy beams are complicated by the presence of small transverse RF beam deflections which arise from several sources. These RF deflections place stringent tolerances on the phase and amplitude stability of the klystrons. They also force the use of special magnetic bumps to correct the trajectories of oppositely charged beams that will pass down the linac. If left unabated, RF deflections can limit the performance of the SLC. There are several methods to reduce the deflections. Many measurements of RF deflections have been made in the low energy part of the linac where the beams are most sensitive. DOE

N86-13147# Fermi National Accelerator Lab., Batavia, Ill.

DEPRIT'S ALGORITHM, GREEN'S FUNCTIONS AND MULTIPOLE PERTURBATION THEORY

L. Michelotti Apr. 1985 5 p refs Presented at the Orbital Dyn. and Appl. to Accelerators Workshop, Berkeley, Calif., 7 Mar. 1985
(Contract DE-AC02-76CH-03000)
(DE85-012297; FNAL/C-85/63; CONF-8503105-4) Avail: NTIS HC A02/MF A01

Within the context of accelerator multipole theory, we describe a method for solving Deprit's equations using a periodic Green's function. This procedure, implemented in a MACSYMA program, has been applied to a Hamiltonian with a normal sextupoles term, and the averaged or renormalized Hamiltonian has been calculated to fourth order in sextupole strength. Anticommutativity of the bracket algebra explains the observed slow growth in the number of induced resonances with order. DOE

N86-13148# Los Alamos Scientific Lab., N. Mex.

R-MATRIX ANALYSIS OF THE (7) LI SYSTEM WITH PERIPHERAL CHANNEL OVERLAP EXCHANGE EFFECTS

G. M. Hale 1985 5 p Presented at the Intern. Conf. on Nucl. Data for Basic and Appl. Sci., Santa Fe, N. Mex., 13 May 1985
(Contract W-7405-eng-36)
(DE85-012751; LA-UR-85-1961; CONF-850507-18) Avail: NTIS HC A02/MF A01

The parameters of an R-matrix analysis that include data for all reactions open in the (7)Li system at E sub x less than or equal to 10MeV suggest that deuteron exchange contributes to the low-energy (6)Li(n,t) reaction. A method for including this mechanism directly in the theory is discussed and preliminary results are given. DOE

N86-13149# Argonne National Lab., Ill.

COMPARISON BETWEEN THEORETICAL PREDICTIONS AND TRACKING

A. G. Ruggiero 1985 38 p refs Presented at the Orbital Dyn. and Appl. to Accelerators Workshop, Berkeley, Calif., 7 Mar. 1985
(Contract W-31-109-eng-38)
(DE85-012104; ANL-EEP-CP-85-27; CONF-8503105-3) Avail: NTIS HC A03/MF A01

The beam-beam interaction in a proton-antiproton collider has been an outstanding issue for a long time. Several theoretical predictions have been made in the past which range from the appearance of single beam-beam driven resonances to the onset of stochasticity and Arnold diffusion and the presence of chaotic trajectories. All these effects would cause a limit on the maximum strength of the beam-beam interactions, the so called beam-beam tune-shift, and speculative values have been offered ranging from as low as 0.0005 to as large as a fraction of unit. The lower limit could be caused in a more complicated situation where the external focussing forces which keep the two beams in the same storage ring are also modulated in time. These theoretical predictions have been compared with extensive computer tracking where the motion of the particles is followed turn after turn over very long periods of time. Though it is indeed possible to observe the formation of several resonances, nevertheless the onset of connected stochasticity seems to occur at too large beam-beam tune-shift to be of any practical relevance. Moreover no Arnold diffusion has been observed to have any practical significance. Chaotic trajectories have been found to embed the phase space in disconnected regions of appreciable extension. They increase in numbers considerably when time modulation of external focussing forces is added. DOE

N86-13150# KMS Fusion, Inc., Ann Arbor, Mich.

ABSOLUTELY UNSTABLE TWO-PLASMON DECAY IN TWO DIMENSIONS

L. V. Powers Feb. 1985 15 p
(Contract DE-AC08-82DP-40152)
(DE85-008157; DOE/DP-40152/T7; KMSF-U-1567) Avail: NTIS HC A02/MF A01

The purpose of the work reported herein is to examine absolute modes of the TPD instability in two dimensions in an infinite homogeneous plasma. Briggs has shown that the condition for absolute instability in this case is the existence of a solution of the coupled mode dispersion relation. Analytic solutions for eigenmodes in inhomogeneous plasma have been obtained as expansions about the solutions which satisfy the Briggs criteria in one dimension; hence finding TPD solutions which satisfy the Briggs criteria in two dimensions may give a basis for identifying two-dimensional eigenvalues in the inhomogeneous case as well. DOE

N86-13151# Stanford Linear Accelerator Center, Calif.

MINIMIZING THE ENERGY SPREAD WITHIN A SINGLE BUNCH BY SHAPING ITS CHARGE DISTRIBUTION

G. A. Loew and J. W. Wang Mar. 1985 3 p refs Presented at the Particle Accelerator Conf., Vancouver, British Columbia, 13 May 1985
(Contract DE-AC03-76SF-00515)
(DE85-013064; SU-SLAC-Pub-3598; CONF-850504-126) Avail: NTIS HC A02/MF A01

It has been known for some time that partial compensation of the longitudinal wake field effects can be obtained for any bunch by placing it ahead of the accelerating crest (in space), thereby letting the positive rising sinusoidal field offset the negative beam loading field. The work presented in this paper shows that it is possible to obtain complete compensation, i.e., to reduce the energy spread essentially to zero by properly shaping the longitudinal charge distribution of the bunch and by placing it at the correct position on the wave. DOE

N86-13152# Los Alamos National Lab., N. Mex.

FRC FORMATION STUDIES WITH Z-DISCHARGE IONIZATION ON FRX-C

W. T. Armstrong, R. E. Chrien, W. A. Hugrass, P. L. Klingner, K.

F. McKenna, R. D. Milroy, D. J. Rej, E. G. Sherwood, R. E. Siemon, and M. Tuszewski 1985 6 p Presented at the 7th US Symp. on Compact Toroid Res., Santa Fe, N. Mex., 21 May 1985 Prepared in cooperation with Spectra Technology, Inc., Bellevue, Wash.
(Contract W-7405-eng-36)
(DE85-012765; LA-UR-85-1834; CONF-8505100-9) Avail: NTIS HC A02/MF A01

Recent exploratory operation at high bias levels on FRX-C is discussed. The motivation of these in situ formation studies was to explore the use of Z-discharge ionization (Z-PI) for achieving larger trapped poloidal flux and commensurately large x/sub s/ values, where x/sub s/ is the ratio of the separatrix radius r/sub s/ to the coil radius r/sub c/. Such studies are of interest in ascertaining predicted improvements of particle confinement and degradation of stability with the associated increase of anti s, the approximate number of ion gyroradii across the minor radius of the FRC. The results of these studies may be summarized briefly as: (1) the Z-PI worked well in conjunction with conventional theta-PI to extend the level of trapped flux at high fill pressure (20 mtorr), but the Z-PI worked poorly at low fill pressure (5 mtorr), and (2) increased trapped flux at 5 mtorr quickly led to degradation of the flux lifetime and no significant increase in x/sub s/, while at 20 mtorr the initial value of x/sub s/ was increased significantly but with degraded flux lifetimes. DOE

N86-13153# Stanford Linear Accelerator Center, Calif.
SLC INJECTOR MODELING
H. Hanerfeld, W. B. Herrmannsfeldt, M. B. James, and R. H. Miller Mar. 1985 4 p Presented at the Particle Accelerator Conf., Vancouver, British Columbia, 13 May 1985
(Contract DE-AC03-76SF-00515)
(DE85-013067; SU-SLAC-Pub-3614; CONF-850504-123) Avail: NTIS HC A02/MF A01

The injector for the Stanford Linear Collider is being studied using the fully electromagnetic particle-in-cell program MASK. The program takes account of cylindrically symmetrical RF fields from the external source, as well as fields produced by the beam and dc magnetic fields. It calculates the radial and longitudinal motion of electrons and plots their positions in various planes in phase space. Bunching parameters can be optimized and insights into the bunching process and emittance growth have been gained. The results of the simulations are compared to the experimental results. DOE

N86-13154# Oak Ridge National Lab., Tenn.
SUBMILLIMETER WAVE PROPAGATION IN TOKAMAK PLASMAS
C. H. Ma, D. P. Hutchinson, P. A. Staats, K. L. VanderSluis, D. K. Mansfield, H. Park, and I. C. Johnson 1985 6 p Presented at the Intern. Symp. on Antennas and Propagation, Kyoto, 20 Aug. 1985 Prepared in cooperation with Princeton Univ., N.J.
(Contracts DE-AC02-76CH-03073; DE-AC05-84OR-21400)
(DE85-007747; CONF-850839-1) Avail: NTIS HC A02/MF A01

The propagation of submillimeter-waves (smm) in tokamak plasmas has been investigated both theoretically and experimentally to ensure successful measurements of electron density and plasma current distributions in tokamak devices. Theoretical analyses have been carried out to study the polarization of the smm waves in TFTR and ISX-B tokamaks. A multichord smm wave interferometer/polarimeter system has been employed to simultaneously measure the line electron density and poloidal field-induced Faraday rotation in the ISX-B tokamak. The experimental study of TFTR is under way. Computer codes have been developed and have been used to study the wave propagation and to reconstruct the distributions of plasma current and density from the measured data. The results are compared with other measurements. DOE

N86-13155# Brookhaven National Lab., Upton, N. Y.
FULLY STRIPPED HEAVY ION YIELD VS ENERGY FOR Xe AND Au IONS
P. Thieberger, H. E. Wegner, J. Alonzo, H. Gould, R. E. Anholt, and W. E. Meyerhof 1985 4 p refs Presented at the Particle Accelerator Conf., Vancouver, British Columbia, 13 May 1985
(DE85-013281; BNL-36555; CONF-850504-156) Avail: NTIS HC A02/MF A02

The Bevalac is now capable of accelerating U-238 ions to approximately 1 GeV/amu and measurements have shown that fully stripped U-238 ions are produced with good yield at these energies. However, knowing the stripping yields at different energies for U-238 does not allow an accurate prediction for other, lower Z projectiles. Consequently, extensive stripping yield measurements were made for Au-197 and Xe-139 ions. In addition to the stripping measurements from the direct Bevalac beam, pickup measurements were also made with specially prepared bare, one electron, and two electron ions. Since many research groups are considering heavy ion storage rings and/or synchrotrons, the pickup cross section for bare ions is important to estimate beam lifetime in terms of the average machine vacuum. Since the Mylar target provides a pickup probability similar to air, a preliminary analysis of the Xe(54+) and U(92+) data are presented along with predictions for other ions ranging down to Fe(26+). DOE

N86-13156# Brookhaven National Lab., Upton, N. Y.
TRACKING STUDIES ON THE EFFECTS OF RANDOM MULTIPOLES IN THE 6.5 T LATTICE OF THE SSC REFERENCE DESIGNS STUDY
G. F. Dell 1985 4 p Presented at the Particle Acclerator Conf., Vancouver, British Columbia, 13 May 1985
(Contract DE-AC02-76CH-00016)
(DE85-013286; BNL-36567; CONF-850504-158) Avail: NTIS HC A02/MF A01

The acceptance of lattice A (6.5 T) of the SSC Reference Designs Study is determined for ten different sets of random errors as various multipole orders are set to zero. On the basis of 400 turn studies it is concluded that all multipole orders in the dipoles are important. Further studies show that the beam crossing dipoles limit the acceptance - when their multipoles are scaled as r(-)/sup (n+1)/, corresponding to an increased coil radius, the acceptance of the lattice essentially doubles. DOE

N86-13157# Brookhaven National Lab., Upton, N. Y.
LARGE ACCEPTANCE MAGNETIC FOCUSSING HORNS FOR PRODUCTION OF A HIGH INTENSITY NARROW BAND NEUTRINO BEAM AT THE AGS
A. Carroll, I. Chimienti, W. Leonhardt, R. Monaghan, G. Ryan, J. Sandberg, W. Sims, G. Smith, P. Stillman, and H. Thorwarth 1985 4 p Prepared in cooperation with Columbia Univ., N.Y.
(Contract DE-AC02-76CH-00016)
(DE85-013300; BNL-36491; CONF-850504-148) Avail: NTIS HC A02/MF A01

A set of two large acceptance (20 to 140 mrad) horns have been designed and built to form a parallel beam of 3 GeV/c pions and kaons for the production of an intense, dichromatic neutrino beam. A set of beam plugs and collimators determined the momentum of the particles which pass through the horns. The ooling and maintenance of the horns and target was a particular concern since they were operated with an incident intensity of over 10(13) proton/sec. These systems were designed for simplicity, reliability, and easy replacement. DOE

N86-13158# New York Univ., New York. Inst. of Mathematical Sciences.
WAVE PROPAGATION IN A PLASMA BASED ON THE COLD PLASMA MODEL
H. Weitzner Aug. 1985 51 p
(Contract DE-AC02-76ER-03077)
(DE85-013649; DOE/ER-03077/225) Avail: NTIS HC A04/MF A01

The cold plasma conductivity tensor is employed to explore the problem of wave propagation in a plasma without the use of the geometrical optics approximation or a plane stratified model. After the introduction of the appropriate electromagnetic potentials, the wave propagation problem reduces to a sixth order self-adjoint set of partial differential equations derivable from a self-adjoint variation principle. The usual lower and upper hybrid resonances as well as the plasma resonances can be identified as surfaces across which the system of equations changes from elliptic to partially elliptic and partially hyperbolic. In addition, the ion and electron cyclotron resonance surfaces, near which the cold plasma approximation breaks down, are also transition surfaces. DOE

N86-13159# Stanford Linear Accelerator Center, Calif.
COMMISSIONING AND OPERATION OF THE NUCLEAR PHYSICS INJECTOR AT SLAC
R. F. Koontz, R. H. Miller, G. K. Leger, and R. Iverson Mar. 1985 4 p Presented at the Particle Accelerator Conf., Vancouver, British Columbia, 13 May 195
(Contract DE-AC03-76SF-00515)
(DE85-013374; SU-SLAC-Pub-3615; CONF-850504-68) Avail: NTIS HC A02/MF A01

The new Nuclear Physics Injector (NPI) approved for construction in October of 1983 was completed by September of 1984, and delivered short pulse beams for SPEAR ring checkout in mid-October. Long pulse beams of up to 1.6 microsecond length were also demonstrated. The paper describes the startup operation, reviews the performance characteristics, and discusses the beam transport optics used to deliver 1 to 4 GeV beams to nuclear physics experiments in End Station A. DOE

N86-13160# Lawrence Livermore National Lab., Calif.
CONVERSION OF THE BOUNCE-AVERAGED FOKKER-PLANCK CODE TO CONVERSION FORM
T. D. Rognlien 1 Jul. 1985 16 p
(Contract W-7405-eng-48)
(DE85-014861; UCID-20474) Avail: NTIS HC A02/MF A01

This report describes a major modification to the bounce-averaged Fokker-Planck code of Cutler, et al. The new version of the code is written in conservation form which results in the line density being conserved exactly except at phase space boundaries. The notation and procedure for writing the code in conservation form closely follows the work of Mirin on the square well code Hybrid II, and Kerbel and McCoy on their bounce-average code CQL. Much of the original code has been perserved, and the input is the same as before; old input files should run on the new version. The major modifications to the code have occurred in subroutines COFF, IADVANCE, and RFTERMS. A new subroutine, FLUX, has been added to compute the flux across loss boundaries. DOE

N86-13161# Rochester Univ., N. Y. Lab. for Laser Energetics.
ABSORPTION AND HOT ELECTRON GENERATION IN uv (351 nm) DRIVEN SPHERICAL IMPLODING TARGETS
R. L. Keck, M. C. Richardson, J. M. Soures, and J. Delletrez 1984 7 p Presented at the Meeting of the Plasma Phys. Div. of the Am. Phys. Soc., Boston, 27 Oct. 1984
(Contract DE-AC08-80EP-40124)
(DE85-014405; DOE/DP-40124/53; CONF-841010-21) Avail: NTIS HC A02/MF A01

The advantages of short wave-length radiation for laser fusion in terms of laser absorption and low levels of suprathermal electron preheat are well known. Recently, these have been characterized for 6 beam 351 nm irradiation on solid spherical targets. In this report, we extend these studies to imploding shell targets driven by 6 or 12 beams from the OMEGA laser system. With these targets, the critical density surface is expected to move toward the target center during the laser pulse, reducing the absorption. The measurements will be compared to the predictions of hydrodynamic code calculations. DOE

N86-13162# Rochester Univ., N. Y. Lab. for Laser Energetics.
SPATIAL STRUCTURE OF HEAT FLOW INSTABILITIES IN LASER PLASMAS
R. W. Short 1984 16 p Presented at the Meeting of the Plasma Phys. Div. of the Am. Phys. Soc., Boston, 27 Oct. 1984
(Contract DE-AC08-80DP-40124)
(DE85-014407; DOE/EP-40124/57; CONF-841010-20) Avail: NTIS HC A02/MF A01

The steep temperature gradients characteristic of laser-produced plasmas generate strong thermal fluxes which can be unstable. Previous theoretical investigations of these instabilities have found temporal growth rates for modes which are uniform in the direction of heat flow. Here the analysis is extended to modes with spatial dependence in this direction. Spatial growth rates and the conditions for which the instability is absolute are determined, and the consequences for thermal transport and smoothing are discussed. DOE

N86-13163# Lawrence Livermore National Lab., Calif.
MULTIVARIABLE CURRENT CONTROL FOR ELECTRICALLY AND MAGNETICALLY COUPLED SUPERCONDUCTING MAGNETS
E. W. Owen and D. W. Shimer 8 Feb. 1985 7 p Presented at the 6th Topical Meeting on the Technol. of Fusion Energy, San Francisco, 3 Mar. 1985
(Contract W-7405-eng-48)
(DE85-012941; UCRL-92092; CONF-850310-113) Avail: NTIS HC A02/MF A01

Superconducting magnet systems under construction and projected for the future contain magnets that are magnetically coupled and electrically connected with shared power supplies. A change in one power supply voltage affects all of the magnet currents. A current controller for these systems must be designed as a multivariable system. The paper describes a method, based on decoupling control, for the rational design of these systems. Dynamic decoupling is achieved by cross feedback of the measured currents. A network of gains at the input decouples the system statically and eliminates the steady state error. Errors are then due to component variations. The method has been applied to the magnet system of the MFTF-B, at the Lawrence Livermore National Laboratory. DOE

N86-13164# Lawrence Livermore National Lab., Calif.
HIGH EFFICIENCY ICF DRIVER EMPLOYING MAGNETICALLY CONFINED PLASMA RINGS
D. J. Meeker, J. H. Hammer, and C. W. Hartman 4 Mar. 1985 8 p Presented at the 6th Topical Meeting on the Technol. of Fusion Energy, San Francisco, 3 Mar. 1985
(Contract W-7405-eng-48)
(DE85-012939; UCRL-91693; CONF-850310-114) Avail: NTIS HC A02/MF A01

We discuss the possibility of achieving energy, power and power density necessary for ICF by magnetically accelerating plasma confined by a compact torus (CT) field configuration. The CT, which consists of a dipole (poloidal) field and imbedded toroidal field formed by force free, plasma current, is compressed and accelerated between coaxial electrodes by B/sub THETA/ fields as in a coaxial railgun. Compression and acceleration over several meters by a 9.4 MJ capacitor bank is predicted to give a 5.7 cm radius, 0.001 gm CT 5 MJ kinetic energy (10(7) m/sec). Transport and focussing several meters by a disposable lithium pipe across the containment vessel is predicted to bring 4.8 MJ into the pellet region in 0.5 cm(2) area in 0.3 ns. The high efficiency (approx. 50%) and high energy delivery of the CT accelerator could lead to low cost, few hundred MW power plants that are economically viable. DOE

N86-13165# Wisconsin Univ., Madison.
MULTIPOLE AND TOKAMAK RESEARCH AT THE UNIVERSITY OF WISCONSIN
J. C. Sprott and S. C. Prager May 1985 12 p
(Contract DE-AC02-76ET-53051)
(DE85-014862; DOE/ET-53051/83) Avail: NTIS HC A02/MF A01

Experimental axisymmetric toroidal confinement research has been pursued at the University of Wisconsin through the utilization of multipole and tokamak devices. Multipoles facilitated the controlled study of key confinement issues since in a single device one is able to vary, over a wide range, critical plasma parameters including ohmic current level, collisionality, field transform, magnetic shear and plasma beta. This feature, and the natural quiescence of multipole plasmas, has been exploited for over twenty years at Wisconsin through a sequence of different multipole devices culminating in the Levitated Toroidal Octupole. Important aspects of toroidal plasma equilibrium, stability, heating and transport have been studied which often could not be addressed in existing tokamak. Toroidal confinement research using the Tokapole II poloidal divertor tokamak began in 1977, with emphasis on issues relating to the magnetic limiter topology. DOE

N86-13166# Oak Ridge National Lab., Tenn.
SPECTRAL METHOD FOR OBTAINING THREE-DIMENSIONAL MAGNETOHYDRODYNAMIC EQUILIBRIA
S. P. Hirshman and D. K. Lee Jul. 1985 35 p
(Contract DE-AC05-84OR-21400)
(DE85-015065; ORNL/TM-9531) Avail: NTIS HC A03/MF A01

A description is given of a new code, MOMCON (spectral moments with constraints), that obtains three-dimensional ideal magnetohydrodynamic (MHD) equilibria in a fixed toroidal domain using a Fourier expansion for the inverse coordinates (R,Z) representing nested magnetic surfaccs. A set of nonlinear coupled ordinary differential equations for the spectral coefficients of (R,Z) is solved using an accelerated steepest descent method. A stream function lambda is introduced to improve the mode convergence properties of the Fourier series for R and Z. Constraint equations relating the m greater than or equal to 2 moments of R and Z are solved to define a unique poloidal angle. DOE

N86-13167# Los Alamos Scientific Lab., N. Mex.
PLANE-WAVE THEORY OF ELECTRICAL TRANSPORT IN DISORDERED SYSTEMS
G. Rinker May 1985 20 p
(Contract W-7405-eng-36)
(DE85-015353; LA-10404-MS) Avail: NTIS HC A02/MF A01

This is the third in a series of reports concerning the electrical and thermal transport properties of dense plasma. In the present work we construct a plane-wave theory that approximates, with moderate success, our previous partial-wave calculations of electrical and thermal transport coefficients. Regions of validity are indicated. Comparisons are made with experimental measurements of source libraries that contain the transport coefficients calculated by the present method for all elements from Z = 1 to Z = 96. DOE

N86-13168# Brookhaven National Lab., Upton, N. Y.
MAGNET POWER SUPPLY CONTROL OF THE NSLS VUV AND X-RAY STORAGE RINGS TRANSFER LINES
J. D. Klein, S. Ramamoorthy, O. Singh, and J. D. Smith 1985 4 p Presented at the Particle Accelerator Conf., Vancouver, British Columbia, 13 May 1985
(Contract DE-AC02-76CH-00016)
(DE85-014213; BNL-36504; CONF-850504-196) Avail: NTIS HC A02/MF A01

The transfer lines for NSLS VUV and X-ray storage rings have been split. New power supplies have been incorporated with existing cones. The existing microprocessor system has been upgraded in order to control the additional functions. This system expands the input/output port of the microprocessor to an addressable serial/parallel link to each magnet power supply. The implementation of this system will be discussed. DOE

N86-13169# Stanford Linear Accelerator Center, Calif.
REAL TIME BUNCH LENGTH MEASUREMENTS IN THE SLC LINAC
J. C. Sheppard, J. E. Clendenin, M. B. James, R. H. Miller, and M. C. Ross Feb. 1985 4 p refs Presented at the Particle Accelerator Conf., Vancouver, British Columbia, 13 May 1985
(Contract DE-AC03-76SF-00515)
(DE85-014362; SU-SLAC-Pub-3584; CONF-850504-205) Avail: NTIS HC A02/MF A01

The longitudinal charge distribution of bunches accelerated in the Stanford Linear Collider (SLC) linac will strongly affect the performance of the Collider. Bunch lengths are chosen in a balance between the deleterious effects of longitudinal and transverse wakefields. The former impacts on the beam energy spread whereas the latter is important to the transverse emittance. Two bunch length measurement ports have been installed in the SLC linac: one in the injector region and one after the emittance damping ring to linac reinjection point. These ports utilize a fused quartz Cerenkov radiator in conjunction with an electrooptic streak camera to permit real time monitoring of single s-band buckets with a resolution of several picoseconds. The design of the radiators and light collection optics is discussed with an emphasis on those issues important to high resolution. Experimental results are presented. DOE

N86-13170# Massachusetts Inst. of Tech., Cambridge. Plasma Fusion Center.
THEORY OF THE ANOMALOUS DOPPLER INSTABILITY DURING LOWER-HYBRID CURRENT DRIVE
S. C. Luckhardt 1985 13 p Presented at the 6th Topical Conf. on Radio Frequency Plasma Heating, Pine Mountain, Ga., 13 May 1985
(Contract DE-AC08-78ET-51013)
(DE85-014064; DOE/ET-51013/149; PFC/CP-85-3; CONF-8505130-8) Avail: NTIS HC A02/MF A01

An instability condition is derived for electrostatic waves obeying the dispersion relation (LC OMEGA) = (LC OMEGA)/sub pe/k/sub parallel// k using a two dimensional electron distribution function, f(v/sub parallel/, v/sub< perpendicular/), appropriate for lower-hybrid current drive. It is found that when the raised plateau in f in the velocity range v1<v/sub parallel <v2 has a sufficiently large anisotropy, T/sub p parallel/ <T/sub p perpendicular/, this mode can become unstabie. If the plateau velocities satisfy the condition v2/v1> 1 + (LC OMEGA)/sub ce// (LC MEGA) /sub cee//LC OMEGA)/sub pe/ then waves exist with phase velocities in the plateau region and these waves are most easily destabilized by the anomalous Doppler resonance, (LC OMEGA) - k/sub parallel/v/sub parallel/ = (LC OMEGA)/sub ce/. DOE

N86-13171# Texas Univ., Austin. Inst. for Fusion Studies.
SOLITARY VORTICES IN A ROTATING PLASMA
W. Horton, J. Liu, J. D. Meiss, and J. E. Sedlak May 1985 32 p
(Contract DE-FG05-80ET-53088)
(DE85-014766; DOE/ET-53088/193; IFSR-193) Avail: NTIS HC A03/MF A01

Nonlinear equations describing the flute dynamics of rotating plasma are derived and solitary vortex solutions are obtained. The solution takes the form of a shielded dipole vortex, similar to that found for nonlinear Rossby waves. The nonlinear dispersion relation, relating propagation speed to vortex radius is obtained. Vortex speeds are shown to take values complementary to the phase velocities of the linear modes of the system. The E x B circulation velocity of the plasma trapped in the vortex is comparable to the diamagnetic drift velocity in the equilibrium plasma. DOE

N86-13172# Texas Univ., Austin. Inst. for Fusion Studies.
EXPLOSIVE COALESCENCE OF MAGNETIC ISLANDS
T. Tajima and J. I. Sakai Apr. 1985 14 p
(Contract DE-FG05-80FT-53088)
(DE85-015083; DOE/ET-53088/186; IFSR-186) Avail: NTIS HC A02/MF A01

An explosive reconnection process associated with nonlinear evolution of the coalescence instability is found through studies of particle and magnetohydrodynamic simulations. The explosive coalescence is a self-similar process of magnetic collapse, in which the magnetic and electrostatic energies and temperatures explode toward the explosion time t0 as (t0-t) sup 8/3, (t0-t) (-4), and (t0-t)/sup -8/3, respectively. Ensuing amplitude oscillations in these quantities are identified by deriving an equation of motion for the scale factor in the Sagdeev potential. DOE

N86-13173# Los Alamos Scientific Lab., N. Mex.
WNR/PSR FACILITY: NEUTRON PHYSICS CAPABILITIES FROM SUB-THERMAL TO 800 MeV
P. W. Liscwski, S. A. Wender, and G. F. Auchampaugh 1985

14 p refs Presented at the Intern. Conf. on Nucl. Data for Basic and Appl. Sci., Santa Fe, N. Mex., 13 May 1985
(Contract W-7405-eng-36)
(DE85-014072; LA-UR-85-2272; CONF-850507-45) Avail: NTIS HC A02/MF A01

The Weapons Neutron Research facility (WNR) is a versatile pulsed neutron source used in a variety of research programs ranging from fundamental neutron properties with ultra cold neutrons to medium energy charge exchange reaction studies. Here we describe the WNR facility and the improvements presently in progress as the Proton Storage Ring (PSR) becomes operational. DOE

N86-13174# California Univ., Berkeley. Lawrence Berkeley Lab.
ELECTRON-SPIN-POLARIZED TARGETS FOR A COLLISIONALLY-PUMPED POLARIZED-ION SOURCE
S. N. Kaplan, C. F. Burrell, R. V. Pyle, L. Ruby, A. S. Schlacheter, and J. W. Stearns May 1985 6 p refs Presented at Particle Accelerator Conf., Vancouver, British Columbia, 13 May 1985
(Contract DE-AC03-76SF-00098)
(DE85-015276; LBL-19011; CONF-850504-227) Avail: NTIS HC A02/MF A01

Collisional pumping has been proposed as a mechanism for producing polarized ion beams more intense by orders of magnitude than those from the best existing sources. One implementation of this method employs a very thick electron-spin-polarized alkali-vapor target in a low magnetic field, and is characterized by a predicted 100% spin-transfer efficiency from the target to the beam. Target characteristics and design constraints are discussed. DOE

N86-13175# Rochester Univ., N. Y. Lab. for Laser Energetics.
ABSORPTION SPECTROSCOPY AS A DENSITY DIAGNOSTIC FOR DENSE IMPLODED SHELLS
R. Epstein, S. Skupsky, and B. Yaakobi 1985 16 p Presented at the 5th Topical Conf. on Atomic Processes in High Temp. Plasmas, Pacific Grove, Calif., 25 Feb. 1985
(Contract DE-AC08-80DP-40124)
(DE85-014413; DOE/DP-40124/72; CONF-850238-1) Avail: NTIS HC A02/MF A01

Absorption lines of tamper layer additives may serve as diagnostics of the shell areal density (rhoR) and thus of the core compression in high compression target implosion experiments. The range of implosion conditions for which this technique would be applicable is investigated. Nou-LTE simulations of absorption spectra are presented to illustrate cases of interest. DOE

N86-13176# California Univ., Berkeley. Lawrence Berkeley Lab.
COMPACT MICROWAVE ION SOURCE
K. N. Leung, S. Walther, and H. W. Owren May 1985 5 p refs Presented at Particle Accelerator Conf., Vancouver, British Columbia, 13 May 1985
(Contract DE-AC03-76SF-00098)
(DE85-014536; LBL-18985; CONF-850504-206) Avail: NTIS HC A02/MF A01

A small microwave ion source has been fabricated from a quartz tube with one end enclosed by a two grid accelerator. The source is also enclosed by a cavity operated at a frequency of 2.45 GHz. Microwave power as high as 500 W can be coupled to the source plasma. The source has been operated with and without multicusp fields for different gases. In the case of hydrogen, ion current density of 200 mA/sq.cm with atomic ion species concentration as high as 80% has been extracted from the source. DOE

N86-13177# Los Alamos Scientific Lab., N. Mex.
RECENT RESULTS OF AN INTERNAL TILT MODE CALCULATION IN FRCS
D. C. Barnes, J. L. Schwarzmeier, and H. R. Lewis 1985 6 p refs Presented at 7th US Symp. on Compact Toroidal Res., Santa Fe, N. Mex., 21 May 1985
(Contract W-7405-eng-36)
(DE85-014121; LA-UR-85-2040; CONF-8505100-16) Avail: NTIS HC A02/MF A01

Recent theoretical results on the stability of FRCs to the internal tilt mode are presented. An approximate treatment of collisions shows that collisions have a small effect on the growth rate of the mode until the plasma becomes very collisional (lambda/sub ii/ less than or equal to r/sub s/2). Finite Larmor radius theory predicts that the growth rate of the instability normalized to that of MHD depends only on the combination and s/e, where e is the plasma elongation. However, a full Vlasov stability calculation does not appear to show such a scaling. DOE

N86-13178# Sandia National Labs., Albuquerque, N. Mex.
LASER DIAGNOSTIC STUDIES OF PLASMA ETCHING AND DEPOSITION
P. J. Hargis, Jr., R. W. Light, and J. M. Gee 1985 7 p refs Presented at the Intern. Conf. on Laser Process. and Diagn. Appl. in Electron. Mater., Linz, Austria, 15 Jul. 1984
(Contract DE-AC04-76DP-00789)
(DE85-009494; SAND-85-0082C; CONF-840761-2) Avail: NTIS HC A02/MF A01

Laser excited fluorescence spectroscopy was used to determine that CF2 radicals control the silicon dioxide to silicon etch-rate ratio in fluorocarbon discharges used to etch silicon and silicon dioxide. CF2 was found to control the etch-rate ratio through polymer formation which selectively inhibits the silicon etch rate. DOE

N86-13179# Wisconsin Univ., Madison.
ALFVEN WAVE HEATING ON TOKAPOLE 2
D. Korthawi and O. Eldridge May 1985 6 p Presented at the 6th Topical Conf. on Radio Frequency Plasma Heating, Pine Mountain, Ga., 13 May 1985
(Contract DE-AC02-76ET-53051)
(DE85-014859; DOE/ET-53051/84; CONF-8505130-10) Avail: NTIS HC A02/MF A01

Alfven wave experiments are being conducted on the Tokapole 2 tokamak, backed up by theoretical work. Several antenna designs are being tested. Earlier results with antennas carrying current in a primarily toroidal direction have shown significant loading with a strong dependence on the angle of the currents w.r.t. the equilibrium field. In such cases magnetic probes detect strong signals in the scrape-off region, and there is little or no evidence of bulk heating despite P/sub RF/p/sub OHMIC approx. 30 to 50%. A new antenna design to allow launching with any polarization and upgraded diagnostics is being installed. The experimental antenna loading is compared to a slab model in the MHD limit, with given density and current profiles and zero pressure. The antenna is modeled by a single, thin folded strap in vacuum, with variable orientation. The effects of the far wall and of eigenmodes are removed by assuming that each Fourier component of the wave damps exponentially on the far side of the Alfven resonant surface. The calculated radiation resistance is in the milliohm range and varies slowly with antenna orientation. DOE

N86-13180# Rochester Univ., N. Y. Lab. for Laser Energetics.
NEW DIRECTIONS FOR SHORT-WAVELENGTH LASER FUSION AND HIGH-ENERGY-DENSITY PHYSICS
R. L. McCrory, J. M. Soures, L. M. Goldman, M. C. Richardson, W. D. Seka, A. Simon, S. Skupsky, C. P. Verdon, and B. Yaakobi Nov. 1984 46 p
(Contract DE-FC-08-85DP-40200)
(DE85-014414; DOE/DP-40200/6) Avail: NTIS HC A03/MF A01

New directions in inertial fusion research using short-wavelength, direct-drive targets have increased the prospects for demonstrating inertial fusion feasibility and have generated new interest and opportunities in high-energy-density research. DOE

N86-13181# Lawrence Livermore National Lab., Calif.
IDENTIFYING HEAVY-ION-BEAM FUSION DESIGN AND SYSTEM FEATURES WITH HIGH ECONOMIC LEVERAGE
W. R. Meier and W. J. Hogan 3 Mar. 1985 43 p
(Contract W-7405-eng-48)
(DE85-014849; UCID-20470) Avail: NTIS HC A03/MF A01

We have conducted parametric economic studies for heavy-ion-beam fusion electric power plants. We examined the effects on the cost of electricity of several design parameters: maximum achievable chamber pulse rate, driver cost, target gain, and electric conversion efficiency, and net electric power. We found with reasonable assumptions on driver cost, target gain, and electric conversion efficiency, a 2 to 3 GWe heavy-ion-beam fusion power plant, with a chamber pulse rate of 5 to 10 Hz, can be competitive with nuclear and coal power plants. DOE

N86-13182# Brookhaven National Lab., Upton, N. Y.
AGS IMPROVEMENT PROGRAM
Y. Y. Lee 1985 3 p Presented at the Particle Accelerator Conf., Vancouver, British Columbia, 13 May 1985
(Contract DE-AC02-76CH-00016)
(DE85-013293; BNL-36484; CONF-850504-162) Avail: NTIS HC A02/MF A01

The interest of both particle and nuclear physicists are converging on the alternating gradient synchrotrons (AGS). This machine is almost ideally and uniquely suited to perform a new class of frontier experimunts. Particle physicists would like to study the extremely heavy (multi-TeV) particles posited by new theories by searching for rare k-decays. Nuclear physicists want to create the extremely denser form of nuclear matter which exists within neutron stars by studying heavy ion collisions. The particle physicists require extremely intense proton beams in order to produce enough k's. The nuclear physicists require heavy ions accelerated in the top energies of the AGS. The AGS recently acquired a new capability of accelerating polarized protons to 16.5-GeV and will extend its energy to full energy of the machine. This new capability will open the way to extend the surprising lower energy result of spin-spin correlation of high momentum transfer collisions to much higher energy. DOE

N86-13183# National Bureau of Standards, Boulder, Colo. Fracture and Deformation Div.
MATERIALS STUDIES FOR MAGNETIC FUSION ENERGY APPLICATIONS AT LOW TEMPERATURES - 8
R. P. Reed May 1985 335 p Sponsored in part by DOE
(PB85-236362; NBSIR-85/3025-8) Avail: NTIS HC A15/MF A01 CSCL 18A

Results of a research program to produce material property data that will facilitate design and development of cryogenic structures for the superconducting magnets of magnetic fusion energy power plants and prototypes are presented. Research results for 1984 are summarized in an initial 'Highlights of Results' section and reported in detail in the technical papers that form the main body. The technical papers are presented under four headings reflecting the main program areas: Welding, Nonmetallics, Structural Alloys, and Technology Transfer. Objectives, approaches, and achievements are summarized in an introduction to each program area. GRA

N86-12447# Joint Publications Research Service, Arlington, Va.
PROGRESS OF INERTIAL CONFINEMENT RESEARCH DETAILED
Wang Ganchang *In its* China Rept.: Sci. and Technol. (JPRS-CST-85-029) 3 Sep. 1985 p 1-17 refs Transl. into ENGLISH from He Kexue Yu Gongcheng (Beijing), v. 4, no. 4, Dec. 1984 p 289-302 (For primary document see N86-12446 03-31)
Avail: NTIS HC A08/MF A01

76 SOLID-STATE PHYSICS

Includes superconductivity.

For related information, see also *33 Electronics and Electrical Engineering* and *36 Lasers and Masers.*

N86-13184 Department of the Air Force, Washington, D.C.
ACOUSTICALLY TUNED OPTICAL FILTER SYSTEM Patent
V. Azgapetian and A. M. Azgapetian, inventors (to Air Force) Issued 30 Apr. 1985 4 p Supersedes AD-D010417
(AD-D011791; US-Patent-4,514,056; US-Patent-Appl-SN-439493; US-Patent-Class-350-372) Avail: US Patent and Trademark Office CSCL 20/6

Two crystals, made of acousto-optical material and having their respective extraordinary axes at a predetermined angle to each other, are acoustically excited; and, in combination with a polarizer and an analyzer, the acoustically excited crystals permit the complete transmission or rejection of a preselected narrow band of polarized light in the visible/infrared wavelength of the region. Author (GRA)

N86-13185 Department of the Navy, Washington, D. C.
RECOVERY OF FRAGILE LAYERS PRODUCED ON SUBSTRATES BY CHEMICAL VAPOR DEPOSITION Patent
A. Addamiano and P. H. Klein, inventors (to Navy) Issued 23 Apr. 1985 5 p Supersedes AD-D010378
(AD-D011841; US-Patent-4,512,825; US-Patent-Appl-SN-484346; US-Patent-Class-148-175) Avail: US Patent and Trademark Office CSCL 20/12

This patent pertains to a method of recovering intact at room temperature a layer of a first material, such as silicon carbide, produced by depositing it from the gas phase at a deposition temperature above room temperature on a substrate of a second material, such as silicon, having a different coefficient of thermal expansion than that of the first material. The substrate is separated from the layer prior to cooling, and then the separated layer is cooled to room temperature free of stresses otherwise present as a result of the different thermal expansions of the substrate and layer. The present invention relates generally to coating and more particularly to coating wherein a semiconductor product is produced. GRA

N86-13186 Department of the Navy, Washington, D. C.
METHOD FOR THE DEPOSITION OF HIGH-QUALITY CRYSTAL EPITAXIAL FILMS OF IRON Patent
R. Kaplan and N. Bottka, inventors (to Navy) Issued 2 Apr. 1985 5 p Supersedes AD-D010588
(AD-D011842; US-Patent-4,508,590; US-Patent-Appl-SN-532938) Avail: US Patent and Trademark Office CSCL 20/2

This patent pertains to a method for forming a single crystal epitaxial film of a selected metal on the surface of a substrate. The method includes the steps of positioning the substrate in an ultra high vacuum environment and exposing the substrate surface to a metalorganic vapor including ions of the selected metal while maintaining an ultra high vacuum environment. GRA

N86-13187*# Auburn Univ., Ala. Engineering Experiment Station.
DEVELOPMENT OF A RADIATION-HARD CMOS PROCESS Final Technical Report
W. L. Power 4 Aug. 1983 22 p refs
(Contract NAS8-33092)
(NASA-CR-170925; NAS 1.26:170925) Avail: NTIS HC A02/MF A01 CSCL 20L

It is recommended that various techniques be investigated which appear to have the potential for improving the radiation hardness of CMOS devices for prolonged space flight mission. The three key recommended processing techniques are: (1) making the gate oxide thin. It has been shown that radiation degradation is proportional to the cube of oxide thickness so that a relatively small reduction in thickness can greatly improve radiation resistance; (2) cleanliness and contamination control; and (3) to investigate different oxide growth (low temperature dry, TCE and HCL). All three produce high quality clean oxides, which are more radiation tolerant. Technique 2 addresses the reduction of metallic contamination. Technique 3 will produce a higher quality oxide by using slow growth rate conditions, and will minimize the effects of any residual sodium contamination through the introduction of hydrogen and chlorine into the oxide during growth. Author

N86-13188*# Clarkson Univ., Potsdam, N.Y. Dept. of Mechanical and Industrial Engineering.
MODELING OF CONVECTION PHENOMENA IN BRIDGMAN-STOCKBARGER CRYSTAL GROWTH Semiannual Progress

Report, 1 Feb. - 4 Aug. 1985
Frederick M. Carlson, Arsev H. Eraslan, and Ji-Zen Sheu 5 Nov. 1985 17 p refs
(Grant NAG1-397)
(NASA-CR-176325; NAS 1.26:176325) Avail: NTIS HC A02/MF A01 CSCL 20B

Thermal convection phenomena in a vertically oriented Bridgman-Stockbarger apparatus were modeled by computer simulations for different gravity conditions, ranging from earth conditions to extremely low gravity, approximate space conditions. The modeling results were obtained by the application of a state-of-the art, transient, multi-dimensional, completely densimetrically coupled, discrete-element computational model which was specifically developed for the simulation of flow, temperature, and species concentration conditions in two-phase (solid-liquid) systems. The computational model was applied to the simulation of the flow and the thermal conditions associated with the convection phenomena in a modified Germanium-Silicon charge enclosed in a stationary fused-silica ampoule. The results clearly indicated that the gravitational field strength influences the characteristics of the coherent vortical flow patterns, interface shape and position, maximum melt velocity, and interfacial normal temperature gradient. Author

N86-13189# North Carolina State Univ., Raleigh. Dept. of Physics.
COMPOUND SEMICONDUCTOR INSULATOR INTERFACE RESEARCH Final Report, Jul. 1981 - Jan. 1985
G. Lucovsky May 1985 37 p
(Contract F33615-81-C-1428)
(AD-A157277; AFWAL-TR-85-1035) Avail: NTIS HC A03/MF A01 CSCL 09/1

Work under this contact has been performed in two departments at North Carolina State University; the Departments of Physics and Chemistry. The major thrust of the research program has been in the area of semiconductor/insulator interfaces with the emphasis on the development of materials that could be used for gate insulators in Insulated Gate Field Effect Transistor Devices (IGFET's). To achieve this goal we collaborated with the research group at the Research Triangle Institute (RTI), (with additional support under NAVELEC Contract N00039-81-C-0661), and targeted our research efforts to the development of a gate insulator for (In,Ga)As IGFET's. We have designed and built a low temperature CVD deposition system, and developed a process, using Remote Plasma Enhanced CVD (RPECVD), for depositing a multilayer dielectric consisting of Si3N4 and SiO2 layers onto (In, Ga)As. We have determined the conditions necessary to achieve stoichiometry in each of the constituents layers. We have also determined the deposition conditions which minimize the incorporation of defect and impurity atom bonding groups. We have developed a model for the deposition process which can serve as a guideline for deposition of other silicon based insulators, e.g., SiN F and SiO F alloys. GRA

N86-13190# Air Force Systems Command, Wright-Patterson AFB, Ohio. Foreign Technology Div.
JOURNAL OF THE CHINESE SILICATE SOCIETY (SELECTED ARTICLES)
11 Jun. 1985 32 p Transl. into ENGLISH from Guisuanyan Xuebao (China), v. 11, no. 3, 1983 p 333-341, 357-360
(AD-A157497; FTD-ID(RS)T-0160-85) Avail: NTIS HC A03/MF A01 CSCL 20/2

The contents of a Chinese journal are given. The two titles of articles are: (1) The EFG Growth and Application of Small Diameter Sapphire Crystals in Tubular and Rod Shapes; and Study on the Surface Microtopography of Corundums Grown by Verneuil Method; Growing of Excellent Nd:YAG Crystals by Temperature Gradient Technique. GRA

N86-13191# Department of the Navy, Washington, D. C.
LIQUID PHASE EPITAXY (LPE) OF SILICON CARBIDE Patent Application
A. Addamiano, inventor (to Navy) Filed 6 Jun. 1985 16 p
(AD-D011825; US-Patent-Appl-SN-741784) Avail: NTIS HC A02/MF A01 CSCL 20/2

A method is described for making cubic SiC devices comprising the steps of preparing a preform consisting of high purity Si on which a layer of cubic SiC has been deposited by CVD; transferring the preform to a furnace containing a molten bath of Si saturated with SiC at a temperature of between 1600 to 1800 C, the saturation being insured by the use of a high purity graphite crucible for the Si; dipping the Si-SiC preform into the molten bath and allowing deposition of more cubic SiC on the SiC layer by reducing the temperature of the already formed cubic SiC layer from the preparing step in relation to the rest of the molten bath. Additional steps include adding P-type or N-type dopants to the molten bath or into the CVD process and repeating the above-mentioned steps to create cubic SiC homojunctions; and eliminating any Si adhereing to the surface of the cubic SiC layer. Author (GRA)

N86-13192# Stanford Univ., Calif. Center for Materials Research.
IMPROVED TECHNIQUES FOR THE GROWTH OF HIGH QUALITY CADMIUM TELLURIDE CRYSTALS Final Technical Report, 1 Jan. 1982 - 31 Dec. 1984
R. S. Feigelson and R. R. Route Jun. 1985 277 p
(Contract DAAG29-83-K-0023)
(AD-A157669; SU-CMR-85-3; ARO-19489.3-EL) Avail: NTIS HC A13/MF A01 CSCL 20/2

This report summarizes two years' work as part of a multiyear program on improved techniques for the growth of high quality cadmium telluride crystals and represents one of the most comprehensive studies of melt growth and defect characterization in CdTe reported to date. Extensive melt growth studied were carried out using the vertical Bridgman method. Growth parameters were systematically varied in order to determine the influence of seed orientation, thermal environment, and growth rate on crystal quality. Growth interface shapes were revealed using autoradiographic dopant tracing methods. Melt thermal profiling was also carried out to further evaluate growth interface shapes. Controlled convex growth interface shapes were generated by using the heat exchanger method. By this means some improvement in grain structure of the typically polycrystalline boules was accomplished. Low frequency melt vibrations during growth were also observed to improve grain structure and reduce dislocation density. Extensive defect characterization was also carried out using chemical etching methods, and later, synchrotron X-ray topography. Comparative studies of a broad selection of commercial CdTe substrates was carried out, and extensive defect structure was observed in all cases. Reduced dislocation densities and defect structures were accomplished using both low amplitude melt vibrations and doping with In 1IIC13. In the second case, solution hardening was assumed to be the mechanism responsible. For the case of melt vibration, the mechanism is not yet understood. GRA

N86-13193# Illinois Univ., Urbana. Dept. of Physics.
THEORETICAL STUDIES OF DEEP IMPURITY LEVELS IN TERNARY SEMICONDUCTOR ALLOYS Final Report, 1 Jul. 1977 - 31 May 1984
J. D. Dow 5 Jul. 1985 26 p
(Contract N00014-77-C-0537)
(AD-A157929) Avail: NTIS HC A03/MF A01 CSCL 20/12

The principal investigator has completed a sizeable research program studying superlattices, impurities in semiconductors, surface and interface states, Schottky barriers, many-body effects in X-ray and Auger spectra of metals, and the physics of semiconductive alloys. Here we list a few of the recent results pertaining to: Substitutional point defects; laser degradation; Central-cell scattering effects on mobility; Pressure dependence of deep levels; Deep levels in quaternary 3 to 5 alloys; Deep levels in SixGe1-x alloys; Deep levels in CuCl; Deep levels in 2 to 6 semiconductors; Hg1-xCdxTe; 4 to 6 semiconductors; Paired substitutional defects; Technological significance of the theory of paired and clustered defects; Defects at interfaces; Defects at surfaces and Schottky barrier heights; Intrinsic surface state; Intrinsic interface states;

Core excitons; Disordered systems; Thermal conductivity of superlattices; Metastable semiconductors; Technological importance of metastable semiconductors; Disordered superlattices; Phonons in 3 to 5 alloys; Deep levels in superlattices. GRA

N86-13194# Air Force Systems Command, Wright-Patterson AFB, Ohio. Foreign Technology Div.
NEW METHOD OF DETERMINING THE CURRENT CARRIER CONCENTRATION IN A SUBSTANCE IN THE STATE OF SUPERCONDUCTIVITY
F. P. Golotyuk 2 Aug. 1985 6 p Transl. into ENGLISH from Tr. Nikolayevskogo Korablestroitelnogo Inst. imeni Admirala S.O. Makarova (USSR), no. 57, 1972 p 110-112
(AD-A158182; FTD-ID(RS)T-1355-84) Avail: NTIS HC A02/MF A01 CSCL 20/3

This report proposes a fundamentally new solution to the problem of determining the current carrier concentration in a substance. The basis of the corresponding experimental method is a theory which considers the electron drift energy when considering the oscillatory processes in certain circuits. GRA

N86-13195# Little (Arthur D.), Inc., Cambridge, Mass.
DERIVATION OF THE OPTICAL CONSTANTS OF ANISOTROPIC Final Report, Jul. 1982 - Jul. 1985
J. R. Aronson, A. G. Emslie, E. M. Smith, and P. F. Strong 31 Jul. 1985 34 p
(Contract DAAG29-82-C-0017)
(AD-A158396; ARO-18649.5-CH) Avail: NTIS HC A03/MF A01 CSCL 20/2

This report concerns the development of methods for obtaining the optical constants of anisotropic crystals of the triclinic and monoclinic systems. The principal method used, classical dispersion theory, is adapted to these crystal systems by extending the Lorentz line parameters to include the angles characterizing the individual resonances, and by replacing the dielectric constant by a dielectric tensor. The sample crystals are gypsium, orthoclase and chalcanthite. The derived optical constants are shown to be suitable for modeling the optical properties of particulate media in the infrared spectral region. For those materials where suitable size single crystals are not available, an extension of a previously used method is applied to alabaster, a polycrystalline material of the monoclinic crystal system. GRA

N86-13196# California Univ., Berkeley. Lawrence Berkeley Lab.
IMPROVED BEVATRON LOCAL INJECTOR ION SOURCE PERFORMANCE
G. Stover and E. Zagec May 1985 6 p refs Presented at the Particle Accelerator Conf., Vancouver, British Columbia, 13 May 1985
(Contract DE-AC03-76SF-00098)
(DE85-015271; LBL-18964; CONF-850504-221) Avail: NTIS HC A02/MF A01

Performance tests of the improved Bevatron Local Injector PIG Ion source using particles of Si 4(+), Ne 3(+), and He 2(+) are described. Initial measurements of the 8.4 keV/nucleon Si 4(+) beam show an intensity of 100 particle microamperes with a normalized emittance of .06 (PI) cm-mrad. A low energy beam transport line provides mass analysis, diagnostics, and matching into a 200 MHz RFQ linac. The RFQ accelerates the beam from 8.4 to 200 keV/nucleon. The injector is unusual in the sense that all ion source power supplies, the ac distribution network, vacuum control equipment, and computer control system are contained in a four bay rack mounted on insulators which is located on a floor immediately above the ion source. The rack, transmission line, and the ion source housing are raised by a dc power supply to 80 kilovolts above the ground. All power supplies, which are referenced to rack ground, are modular in construction and easily removable for maintenance. The ac power is delivered to the rack via a 21 kVThe a, 3-phase transformer. DOE

N86-13197# Sandia National Labs., Albuquerque, N. Mex.
CHANNELING ANALYSIS OF STRAIN IN SUPERLATTICES
S. T. Picraux, W. K. Chu, W. R. Allen, and J. A. Ellison 1985 25 p Presented at the 7th Intern. Conf. on Ion Beam Anal., Berlin, 7 Jul. 1985 Prepared in cooperation with North Carolina Univ., Chapel Hill and New Mexico Univ., Albuquerque
(Contract DE-AC04-76DP-00789)
(DE85-014437; SAND-85-0592C; CONF-850716-1) Avail: NTIS HC A02/MF aA01

We review recent ion channeling methods for the analysis of the strain in epitaxially grow structures known as strained-layer superlattices (SLSs). These strain measurements have primarily utilized inclined-direction axial dechanneling or angular scans. More recently, a new channeling phenomenon, which involves as resonance between the planar channeling trajectory wavelength and the superlattice period, has been discovered in superlattices. Resonant conditions leading to both catastrophic dechanneling and resonant channeling are demonstrated for inclined planar directions in SLSs. Catastrophic dechanneling is shown to be the most sensitive of the channeling techniques for strain analysis. Comparison with detailed theoretical calculations shows that a simple modified-harmonic model can be used to extract the strain with relatively good accuracy from angular measurements of the catastropic dechanneling. DOE

N86-13198# Cornell Univ., Ithaca, N.Y. Dept. of Materials Science and Engineering.
DIFFRACTION AND MICROSCOPY STUDIES OF THE STRUCTURE OF GRAIN BOUNDARIES IN Fe, Fe-BASE ALLOYS AND CERAMIC MATERIALS Final Technical Report
S. L. Sass Aug. 1985 35 p
(Contract DE-AC02-81ER-10956)
(DE85-016950; DOE/ER-10956/18) Avail: NTIS HC A03/MF A01

The long range goal of this research program has been to obtain information on the atomic structure of grain boundaries in bcc metals and ceramics, to understand how segregation influences grain boundary structure and causes boundaries to become embrittled in Fe-base alloys, to understand how segregation and the ionization state of the solute influences the boundary structure in ceramic materials, and to study faceting and the frequency of its occurrence in ceramic materials. Electron microscopy and electron diffraction techniques were used to carry out the studies on grain boundaries. The research progress made during the support period of the contract is reviewed. DOE

N86-13199# Los Alamos National Lab., N. Mex.
TEMPERATURE AND CONCENTRATION DEPENDENCE OF HYDROGEN SITE OCCUPANCY IN SEVERAL RARE-EARTH DIHYDRIDES
J. A. Goldstone, J. Eckert, P. M. Richards, and E. L. Venturini 1985 13 p Presented at the Intern. Conf. on Neutron Scattering, Santa Fe, N. Mex., 19 Aug. 1985 Prepared in cooperation with Sandia Labs., Albuquerque, N. Mex.
(Contract W-7405-eng-36)
(DE85-015739; LA-UR-85-2683; CONF-850871-1) Avail: NTIS HC A02/MF A01

Neutron inelastic scattering and diffraction techniques are used to study the hydrogen site distribution in several rare earth dihydrides as a function of temperature and concentration. For Y, La, and Ce the fraction of hydrogen on octahedral sites is approximately a constant from 15K to 200K followed by a decrease with increasing temperature. A model is presented which qualitatively explains this behavior. DOE

N86-13200# Naval Research Lab., Washington, D. C.
ENERGY DISPERSIVE SPECTROSCOPY USING SYNCHROTRON RADIATION: INTENSITY CONSIDERATIONS
E. F. Skelton, W. T. Elam, S. B. Qadri, A. W. Webb, and D. Schiferl 1985 21 p refs Presented at the 10th High Conf. On Res. in High Pressure Sci. and Technol., Amsterdam, 8 Jul. 1985 Prepared in cooperation with Los Alamos National Lab., N. Mex.
(Contract W-7405-eng-36)
(DE85-017530; LA-UR-85-3064; CONF-850759-13) Avail: NTIS HC A02/MF A01

Detailed considerations are given to the reliability of energy dependent integrated intensity data collected from the pressure cavity of a diamond-anvil pressure cell illuminated with heterochromatic radiation from a synchrotron storage ring. It is demonstrated that at least in one run, the electron beam current cannot be used to correct for energy-intensity variations of the incident beam. Rather there appears to be an additional linear relationship between the decay of the synchrotron beam and the magnitude of the background intensity. DOE

N86-13201# Oak Ridge National Lab., Tenn.
WEAR OF ION IMPLANTED TIB SUB 2 SURFACES
C. S. Yust, C. J. McHargue, C. L. White, P. Angelini, and M. B. Lewis 1985 10 p Presented at the Symp. on Tribology, Lyon, 3 Sep. 1985
(Contract DE-AC05-84OR-21400)
(DE85-017091; CONF-850952-1) Avail: NTIS HC A02/MF A01

The properties of polycrystalline titanium diboride surfaces were significantly modified by ion implantation. Nickel ion implantation at room temperature (1 x 10 to the 12th power ions/sq cm., 1 MeV) produced a damage, crystalline surface in which dislocation tangles and defects were observed to a depth of 750 nm. Surface hardness values as measured by the Knoop method were 1.7 to 2.2 times those of unimplanted material, and the indentation fracture toughness was increased 50 to 90%. Wear resistance was evaluated by pin-on-disc tests in which a diamond stylus rubs against a polished surface containing both implanted and unimplanted regions. Auger electron spectroscopy was used to identify the constituents of an adhered debris layer on the resultant wear tracks. The debris layer was found to contain some oxygen, but was composed primarily of carbon. DOE

N86-13202# Oak Ridge National Lab., Tenn.
RECENT DEVELOPMENTS IN THE STRUCTURAL CRYSTALLOGRAPHY OF BORON AND THE HIGHER BORIDES
H. L. Yakel 1985 13 p refs Presented at the Intern. Conf. on the Phys. and Chem. of Boron and Boron-Rich Borides, Albuquerque, N. Mex., 29 Jul. 1985
(Contract DE-AC05-84OR-21400)
(DE85-016930; CONF-850786-1) Avail: NTIS HC A02/MF A01

This paper reviews structural studies of boron and boron-rich borides over the last decade using as a framework the classification scheme proposed by Matkovich and Economy. Chemical bonding in boron polyhedral units and the packing of these units in normal 3D space lattices are described with emphasis on stabilization effects that may be produced by impurity elements. Potentially useful areas for structural work with several new scattering and spectroscopic techniques are suggested. The paper concludes with a discussion of possible connections between boride crystal chemistry and the developing subject of quasicrystalline structure. DOE

N86-13203# Oak Ridge National Lab., Tenn.
TEMPERATURE DEPENDENCE OF THE MAGNETIC EXCITATIONS IN Gd
J. W. Cable, R. M. Nicklow, and N. Wakabayashi Aug. 1985 13 p Presented at the Intern. Conf. on Magnetism, San Francisco, 26 Aug. 1985
(Contract DE-AC05-84OR-21400)
(DE85-016303; CONF-850890-14) Avail: NTIS HC A02/MF A01

Magnetic excitation spectra were measured for Gd in the ,001. and ,hh0. directions over the temperature range from 9 to 320 K (T sub c = 292.7, k). Spin-wave-like modes are observed at T greater than or equal to T sub c. The critical wavevector for the appearance of these modes is proportional to the inverse correlation length. DOE

N86-13204# Los Alamos Scientific Lab., N. Mex.
SUPERCONDUCTIVITY IN THE W-Tc AND W2C-Tc SYSTEMS
A. L. Giorgi 1985 11 p refs Presented at the Mater. and Mech. of Superconductivity Conf., Ames, Iowa, 29 May 1985
(Contract W-7405-eng-36)
(DE85-012711; LA-UR-85-1648; CONF-8505138-4) Avail: NTIS HC A02/MF A01

A series of compositions in the W-Tc, W2C-Re and W2C-Tc systems were prepared and examined for superconductivity. The crystal structure, lattice parameters and superconducting transition temperatures of the W2C-Tc are reported for the first time. Similar measurements were made on the W-Tc and W2C-Re systems and the results compared with previous published results for these systems. DOE

N86-13205# Kent State Univ., Ohio. Dept. of Physics.
QUANTUM SIMULATIONS OF SMALL ELECTRON-HOLE COMPLEXES
M. A. Lee, R. K. Kalia, and P. D. Vashishta Sep. 1984 13 p refs Presented at Midwest Solid State Theory Symp., in Microfiche Prod., Minneapolis, 6 Sep. 1984 Prepared in cooperation with Argonne National Lab., Ill.
(Contract W-31-109-eng-38)
(DE85-013895; CONF-8409228-2) Avail: NTIS HC A02/MF A01

The Green's Function Monte Carlo method is applied to the calculation of the binding energies of electron-hole complexes in semiconductors. The quantum simulation method allows the unambiguous determination of the ground state energy and the effects of band anisotropy on the binding energy. DOE

N86-13206# Edgerton, Germeshausen and Grier, Inc., Idaho Falls, Idaho.
MICROLUMINESCENCE SPECTRA OF TI-ACTIVATED ZrO2-Y2O3
T. E. Doyle and J. L. Alvarez 1985 12 p Presented at the Joint Meeting of the Electron Microscopy Soc. of Am. and Microbeam Anal. Soc., Louisville, Ky., 5 Aug. 1985
(Contract DE-AC07-76ID-01570)
(DE85-010131; EGG-M-09185; CONF-850840-5) Avail: NTIS HC A02/MF A01

Sharp-line luminescence of titanium impurities in the system ZrO-Y2O3 has been investigated. Cubic ZrO2 and Zr3Y4O12 exhibit broadening of the luminescence lines which can be attributed to structural disorder. The sharp-line luminescence also provides a method for determining the phonon modes in cubic ZrC2. DOE

N86-13207# Argonne National Lab., Ill.
DECONFINEMENT TRANSITION ON A BCH LATTICE
E. Kovacs May 1985 10 p Presented at the 20th Recontre de Moriond, Les Arcs, France, 10 Mar. 1985
(Contract W-31-109-eng-38)
(DE85-013887; ANL-HEP-CP-85-33; CONF-850375-10) Avail: NTIS HC A02/MF A01

The results of a Monte Carlo simulation of pure SU(2) gauge theory at finite temperature on a body-centered hypercubic (BCH) lattice are presented. The behavior of the transition temperature as a function of the critical lattice coupling g' is compared with the prediction of asymptotic scaling as given by the perturbative (BETA) function. A comparison of the results for the BCH lattice and the simple hypercubic(SH) lattice provides important tests of universality. DOE

N86-13208# Oak Ridge National Lab., Tenn.
NEW INTERPRETATION OF SPIN-WAVE BEHAVIOR IN NICKEL AND IRON
J. F. Cooke, J. A. Blackman, and T. Morgan Jul. 1985 30 p Presented at the Intern. Conf. on Magnetism, San Francisco, 26 Aug. 1985 Prepared in cooperation with Reading Univ.
(Contract DE-AC05-84OR-21400)
(DE85-015323; CONF-850890-10) Avail: NTIS HC A03/MF A01

Calculations of the dynamic susceptibility based on itinerant electron theory for energies up to 1 eV have led to a new picture of spin-wave behavior in nickel and iron, in which spin-waves exist throughout most of the Brillouin zone and to much higher energies than previously thought possible. DOE

N86-13209# Los Alamos National Lab., N. Mex.
X-RAY DIFFRACTION STUDIES OF SHOCK-MODIFIED INORGANIC MATERIALS

B. Morosin and R. A. Graham 1985 16 p Presented at the Intern. Conf. on Met. Appl. of Shock Wave and High-Strain Rate Phenomena, Portland, Oreg., 28 Jul. 1985
(Contract DE-AC04-76DP-00789)
(DE85-015150; SAND-85-0405C; CONF-850889-4) Avail: NTIS HC A02/MF A01

Detailed analysis of broadened X-ray diffraction peak profiles has yielded information on the resulting residual lattice strain and reduced coherent crystallite size on a range of materials subjected to high pressure shock loading. Strain and size values are dependent on various procedures and models used for analysis of such peak profiles; however, trends on such strain and size data as a function of shock loading pressure and shock temperature depend very strongly on the material. For example, shock modified rutile shows annealing behavior at modest shock compression (20 to 27 GPa) due to shock temperature. Alumina and aluminum nitride appear to saturate to high strain values at the same conditions. Titanium diboride appears to show a pressure threshold in excess of 10 GPa before any plastic deformation occurs. The unusually large plastic deformation achieved in brittle inorganic powders indicates the unique nature of shock deformation; such deformations are not typically achieved by using other techniques. Such defective materials exhibit increased chemical activity and present the potential for synthesis of new substances as well as an opportunity to influence materials technology. DOE

N86-13210# University of Northern Illinois, De Kalb.
MOSSBAUER EFFECT AND NEUTRON DIFFRACTION STUDY OF THE ANOMALOUS LATTICE BEHAVIOR OF U6Fe
P. P. Vaishnava, A. E. Dwight, C. W. Kimball, J. D. Jorgensen, and F. Y. Fradin Jun. 1985 13 p Presented at the Mater. and Mech. of Superconductivity Conf., Ames, Iowa, 29 May 1985 Prepared in cooperation with Argonne National Lab., Ill.
(Contract W-31-109-eng-38)
(DE85-014912; CONF-8505138-10) Avail: NTIS HC A02/MF A01

Neutron diffraction and (57)Fe Moessbauer effect measurements have been made on the exchange-enhanced superconductor U6Fe. The neutron diffraction results indicate a pronounced anisotropy in the thermal expansion of the unit cell and an anomalous temperature dependence for the c-axis component of the total Debye-Waller factor of Fe below 100K. The Moessbauer effect measurements show non-Debye behavior in the mean-squared displacement of Fe, with phonon hardening occurring below 100K. The absence of a temperature dependence to the relative intensities of the lines in the Fe quadrupole doublet indicates almost isotropic lattice vibrations. Taken together these observations imply that Fe undergoes static displacements along the c-axis that begin below 100K and increase with decreasing temperature. Both the Moessbauer shift and the quadrupole coupling indicate electronic changes in the valence of Fe in the temperature region in which the displacement takes place. DOE

N86-13211# Ames Lab., Iowa.
JOSEPHSON EFFECT IN THE UNUSUAL SUPERCONDUCTORS Lu2Fe3Si5, LiTi2O4 AND UBe13
E. L. Wolf, R. J. Noer, S. Han, K. W. Ng, T. P. Chen, D. K. Finnemore, and L. Tanner 1985 12 p Presented at the Mater. and Mech. of Superconductivity Conf., Ames, Iowa, 29 May 1985
(Contract W-7405-eng-82)
(DE85-015260; IS-M-553; CONF-8505138-14) Avail: NTIS HC A02/MF A01

A Josephson supercurrent, which can be split by microwave photons of frequency nu into Shapiro steps of spacing (DELTA) V = hnu/2e, is expected between superconductors of like pairing type, either s or p-wave. A weaker, and possibly unobservable effect, with step spacing (DELTA)V/2 was predicted by Pals and van Haeringen between electrons of unlike pairing type. Experiments using K-band microwaves and a Nb point contact have been carried out at 1.2 K on the d-band superconductors LiTi2O4 and Lu2Fe3Si5. In both cases we find unambiguous indication of s-wave pairing, as in Nb. The same experiment on the heavy-fermion superconductor UBe13 in the range UBe13 has been induced into a state of s-wave superconductivity by proximity with the s-wave superconductor Nb. DOE

N86-13212# Illinois Univ., Urbana. Dept. of Physics.
SECOND ORDER ELASTIC CONTENTS OF Pd, PdH(0.7) AND PdD(0.7) BETWEEN 1.7 AND 50 K
D. B. Pokert, R. B. Schwarz (LANL), and A. V. Granato 1985 5 p Presented at Conf. on Internal Friction and Ultrasonic Attenuation in Solids, Urbana, Ill., 3 Jun. 1985
(Contract DE-AC05-84OR-21400)
(DE85-014316; CONF-8506125-4) Avail: NTIS HC A02/MF A01

The second order elastic constants, c11, c44, and c' are measured in pure Pd, PdH(sub 0.7) and PdD(sub 0.7) as a function of temperature between 1.8 and 50K. The data are fitted with polynomials c(sub ij) (1 - a(sub ij)T(2) - b(sub ij)T(4)). For Pd, a(sub ij)approx.10 to the -6 power and b(sub ij)approx.10 to the -10 power. With the addition of H or D, c11(0) decreases by 4%, c44(0) decreases by 7%, and c'(0) increases by 8%. The most significant change occurs for the a(sub ij), which decrease by a factor of 100. Furthermore, b11 remains unchanged, while b44 and b' decrease by factors of approximately 2-4. The changes in the c(sub ij)(0) cannot be explained simply in terms of the expansion of the Pd lattice with the addition of H or D. The decreases of the a(sub ij) are attributed to a decrease in the first and second derivatives of the electronic density of states at the Fermi energy of Pd that occurs with the filling of the d-states by the electrons from H or D. DOE

N86-13213# Oak Ridge National Lab., Tenn.
ELECTRONIC STAKES IN DISORDERED SOLIDS. PART 3: APPLICATIONS TO MATERIALS SCIENCE
J. S. Faulkner 1985 28 p Presented at the Sanibel Symp., Sanibel, Fla., 18 Mar. 1985
(Contract DE-AC05-84OR-21400)
(DE85-011416; CONF-8503147-1) Avail: NTIS HC A03/MF A01

The electronic states of many alloy systems have now been calculated using a framework of theory that is based on the coherent potential approximation. Some of the results of classic experiments on alloys are explained on the basis of these calculations. DOE

N86-12422# Joint Publications Research Service, Arlington, Va.
VARIATIONAL ANALYSIS OF PHASE TRANSITION IN PURE GAUGE FIELDS
Guo Shouhong, Liu Jinming, and Chen Qizhou *In its* China Rept.: Sci. and Technol. (JPRS-CST-85-021) 8 Jul. 1985 p 76-84 refs Transl. into ENGLISH from Zhongshan Daxue Xuebao (Guangzhou), no. 4, Nov. 1984 p 48-54 (For primary document see N86-12421 03-31)
Avail: NTIS HC A09/MF A01

N86-12427# Joint Publications Research Service, Arlington, Va.
TITANIUM-NITROGEN ION BEAM INJECTION STUDIED
Jiang Xingliu, He Lianlong, Jiang Songchuan, and Chen Kefan *In its* China Rept.: Sci. and Technol. (JPRS-CST-85-021) 8 Jul. 1985 p 129-131 refs Transl. into ENGLISH from Lanzhou Daxue Xuebao (Lanzhou), v. 20, no. 4, 28 Dec. 1984 p 123-124 (For primary document see N86-12421 03-31)
Avail: NTIS HC A09/MF A01

77 THERMODYNAMICS AND STATISTICAL PHYSICS

Includes quantum mechanics; and Bose and Fermi statistics.

For related information see also *25 Inorganic and Physical Chemistry* and *34 Fluid Mechanics and Heat Transfer.*

N86-13214# California Univ., Berkeley. Lawrence Berkeley Lab.
CLASSICAL GEOMETRICAL INTERPRETATION OF GHOST FIELDS AND ANOMALIES IN YANG-MILLS THEORY AND

QUANTUM GRAVITY
J. Thierry-Mieg 14 May 1985 7 p Presented at the Symp. on Anomalies, Geometry and Topology, Argonne, Ill., 28 Mar. 1985 Prepared in cooperation with Centre National de la Recherche Scientifique, Meudon-Bellevue, France
(Contract DE-AC03-76SF-00098)
(DE85-014537; LBL-19671; CONF-8503141-3) Avail: NTIS HC A02/MF A01

The reinterpretation of the ERS equations of Quantum Field Theory as the Maurer Cartan equation of a classical principal fiber bundle leads to a simple gauge invariant classification of the anomalies in Yang Mills theory and gravity. DOE

N86-13215# Oak Ridge National Lab., Tenn.
COMPARATIVE FIRST- AND SECOND-LAW ANALYSIS OF AN ABSORPTION CYCLE
H. Perez-Blanco and L. Pan Jul. 1985 37 p refs
(Contract DE-AC05-84OR-21400)
(DE85-015066; ORNL/TM-9595) Avail: NTIS HC A03/MF A01

Generally, the basis of efficiency calculations and optimization studies of absorption cycles is the first law of thermodynamics. It is often argued that a first-law analysis does not produce all the information needed to optimize the absorption system. According to this line of thought, only an analysis based on the second law of thermodynamics gives the needed information. Assessment of the usefulness of second-law analysis as applied to absorption cycles seems adequate to determine the potential benefits of gathering the additional data for the absorbent-refrigerant combinations currently under consideration. To this end, a comparative first- and second-law analysis of a single-effect, lithium bromide-water absorption cycle is carried out here. An existing computer program and entropy values from the literature are used to analyze the cycle. The effects of temperature approaches in each heat exchanger and external heating/cooling fluid flow rates on the cycle performance are determined. A comparison of the results obtained via first- and second-law analyses reveals that the usefulness of the information depends on the boundaries of the system under consideration. Optimization of the absorption cycle itself, without considering the effect of external heating/cooling fluid flow rates at all, can be accomplished by first-law analysis. However, optimization of not only the cycle but also the external flow rates (i.e., the overall thermal system) is better accomplished by second-law analysis. Another interesting result of this study is that a critical temperature approach for cycle optimization can be found for the generator. In practical terms, this means that improving the heat exchanger in the generator will not always enhance the thermal performance of the cycle. DOE

N86-13216# Lawrence Livermore National Lab., Calif.
LARGE-BASIS SHELL-MODEL TECHNOLOGY IN NUCLEOSYNTHESIS AND COSMOLOGY
G. J. Mathews, S. D. Bloom, K. Takahashi, G. M. Fuller, and R. P. Hausman, Jr. May 1985 11 p refs Presented at the 20th Recontre de Moriond, Les Arcs, France, 10 Mar. 1985 Prepared in cooperation with Los Alamos National Lab., N. Mex.
(Contract W-7405-eng-48)
(DE85-012925; UCRL-92723; CONF-850375-3) Avail: NTIS HC A02/MF A01

We discuss various applications of the Lanczos method to describe properties of many-body microscopic systems in nucleosynthesis and cosmology. These calculations include: solar neutrino detectors; beta-decay of excited nuclear states; electron-capture rates during a core-bounce supernova; exotic quarked nuclei as a catalyst for hydrogen burning; and the quark-hadron phase transition during the early universe. DOE

N86-13217# Texas Univ., Austin. Inst. for Fusion Studies.
ALFVEN CONTINUUM WITH TOROIDICITY
S. Riyopoulos and S. M. Mahajan Jun. 1985 29 p
(Contract DE-FG05-80ET-53088)
(DE85-015821; DOE/ET-53088/185; IFSR-185) Avail: NTIS HC A03/MF A01

The symmetry property of the MHD wave propagation operator is utilized to express the toroidal eigenmodes as a superposition of the mutually orthogonal cylindrical modes. Because of the degeneracy among cylindrical modes with the same frequency but resonant surfaces of different helicity the toroidal perturbation produces a zeroth order mixing of the above modes. The toroidal eigenmodes of frequency (LC OMEGA)0(2) have multiple resonant surfaces, with each surface shifted relative to its cylindrical position and carrying a multispectral content. Thus a single helicity toroidal antenna of frequency (LC OMEGA)0 couples strongly to all different helicity resonant surfaces with matching local Alfven frequency. Zeroth order coupling between modes in the continuum and global Alfven modes also results from toroidicity and degeneracy. Our perturbation technique is the MHD counterpart of the quantum mechanical methods and is applicable through the entire range of the MHD spectrum. DOE

N86-13218# Texas Univ., Austin. Inst. for Fusion Studies.
TRANSPORT NEAR THE ONSET OF STOCHASTICITY
J. D. Meiss May 1985 28 p
(Contract DE-FG05-80ET-53088)
(DE85-014765; DOE/ET-53088/189; IFSR-189) Avail: NTIS HC A03/MF A01

For two-degree-of-freedom Hamiltonians, (e.g., a particle in a 2-D potential or the flow of magnetic field lines) an invariant torus in phase space acts as an absolute barrier for trajectories. When an invariant torus is destroyed by a perturbation, a remnant remains with gaps. This cantorus forms a formidable barrier even well into the stochastic regime. We show that correlation functions decay algebraically invalidating the common assumptions of chaos. The decay rate is given by a universal exponent, obtained from self-similar scaling. DOE

80 SOCIAL SCIENCES (GENERAL)

Includes educational matters.

N86-13219*# Akron Univ., Ohio. Dept. of Civil Engineering.
NASA LERC/AKRON UNIVERSITY GRADUATE COOPERATIVE FELLOWSHIP PROGRAM AND GRADUATE STUDENT RESEARCHERS PROGRAM Interim Report, Nov. 1981 - Oct. 1983
Demeter G. Fertis Oct. 1983 59 p refs
(Grants NAG3-50; NGT36-001-800; NGT36-001-801)
(NASA-CR-174826; NAS 1.26:174826; NAUFP-202-3) Avail: NTIS HC A04/MF A01 CSCL 05I

On June 1, 1980, the University of Akron and the NASA Lewis Research Center (LERC) established a Graduate Cooperative Fellowship Program in the specialized areas of Engine Structural Analysis and Dynamics, Computational Mechanics, Mechanics of Composite Materials, and Structural Optimization, in order to promote and develop requisite technologies in these areas of engine technology. The objectives of this program are consistent with those of the NASA Engine Structure Program in which graduate students of the University of Akron participate by conducting research at Lewis. This report is the second on this grant and summarizes the second and third year research effort, which includes the participation of five graduate students where each student selects one of the above areas as his special field of interest. Each student is required to spend 30 percent of his educational training time at the NASA Lewis Research Center and the balance at the University of Akron. His course work is judiciously selected and tailored to prepare him for research work in his field of interest. A research topic is selected for each student while in residence at the NASA Lewis Research Center, which is also approved by the faculty of the University of Akron as his thesis topic for a Master's and/or a Ph.D. degree. Author

N86-13220# Naval Postgraduate School, Monterey, Calif.
COMPUTER AIDED INSTRUCTION IN ENGINEERING M.S. Thesis
T. S. Rose Mar. 1985 53 p

(AD-A156828; AD-E301723) Avail: NTIS HC A04/MF A01 CSCL 05/9

This thesis presents evidence that computer aided instruction (CAI) is effective and can improve instructional efficiency when it is properly implemented. An overview of CAI in other colleges is presented as a source of ideas. The Department of Aeronautics of the Naval Postgraduate School is used as an example of where CAI can be applied. Procedures for the proper implementation of CAI are presented; and the summary includes specific recommendations for the Aeronautics Department. GRA

81 ADMINISTRATION AND MANAGEMENT

Includes management planning and research.

N86-13221*# ECON, Inc., Princeton, N.J.
R AND D LIMITED PARTNERSHIPS (POSSIBLE APPLICATIONS IN ADVANCED COMMUNICATIONS SATELLITE TECHNOLOGY EXPERIMENT PROGRAM)
22 Jun. 1985 75 p refs
(Contract NASw-3339)
(NASA-CR-176333; NAS 1.26:176333; ECON-80-111) Avail: NTIS HC A04/MF A01 CSCL 05A

Typical R&D limited partnership arrangements, advantages and disadvantages of R&D limited partnership (RDLPs) and antitrust and tax implications are described. A number of typical forms of RDLPs are described that may be applicable for use in stimulating R&D and experimental programs using tho advanced communications technology satellite. The ultimate goal is to increase the rate of market penetration of goods and/or services based upon advanced satellite communications technology. The conditions necessary for these RDLP forms to be advantageous are outlined. E.A.K.

N86-13222# Massachusetts Univ., Amherst. Dept. of Electrical and Computer Engineering.
DECENTRALIZED CONTROL OF SCHEDULING IN DISTRIBUTED SYSTEMS Final Report, 15 Dec. 1981 - 15 Feb. 1985
J. A. Stankovic 15 Feb. 1985 22 p
(AD-A157656) Avail: NTIS HC A02/MF A01 CSCL 09/2

A distributed processing system is defined as a collection of processor-memory pairs (hosts) that are physically and logically interconnected, with decentralized system-wide control of all resources, for the cooperative execution of application programs. Such systems may be dedicated to a single application or may implement a general purpose computing facility. By decentralized system-wide control is meant that there exists distributed resources in the system, that there is decentralized control of these resources (i.e., there is no single, central host in charge, nor is there a central state table), that there is system-wide cooperation between independent hosts which results in a single unified system. By system-wide cooperation is meant that the algorithms of the system operate for the good of the whole and not for a particular host. For systems meeting this restrictive definition of distributed processing, it is hypothesized that their reliability, extensibility, and performance will be better than a what is generally available today. In this report the term distributed processing refers to this very specific type of highly integrated distributed system. The major objective of this research project was to develop and compare decentralized scheduling algorithms for distributed processing systems. GRA

82 DOCUMENTATION AND INFORMATION SCIENCE

Includes information storage and retrieval technology; micrography; and library science.

For computer documentation see *61 Computer Programming and Software.*

N86-13223 Virginia Polytechnic Inst. and State Univ., Blacksburg.
IDENTIFYING AND EVALUATING COBOL COMPETENCIES FOR FOUR-YEAR INFORMATION SYSTEMS PROGRAMS Ph.D. Thesis
Doris Peeples Mason 1984 148 p
Avail: Univ. Microfilms Order No. DA8507199

This study determines how the COBOL competencies taught in information systems programs and those attained by information systems students compare to those needed on the job. Five research questions were posed: (1) What are introductory COBOL programming competencies required to be a COBOL programmer? (2) To what extent do information systems program faculty perceive that they have taught COBOL programming competencies? (3) What level of competence in COBOL programming do prospective employers expect information systems graduates to have on the job? (4) To what extent do information systems seniors perceive that they have developed COBOL programming competencies? (5) Which COBOL programming competencies did the faculty, prospective employers, and seniors rate similarly in regard to level of skill? The respondents in the study were information systems faculty, prospective employers of information systems graduates, and information systems seniors. Usable responses were received from 85.4% of the total population. Author

N86-13224*# National Aeronautics and Space Administration, Washington, D. C.
INDEX TO NASA NEWS RELEASES AND SPEECHES, 1984
1985 163 p
(NASA-TM-87514; NAS 1.15:87514) Avail: NTIS HC A08/MF A01 CSCL 05B

The Index to NASA News Releases and Speeches (1984) contains selected speeches and news releases issued by NASA Headquarters during the year 1984. The index was prepared by the NASA Scientific and Technical Information Facility operated for the National Aeronautical and Space Administration by PRC Government Information Systems. F.M.R.

N86-13225*# National Aeronautics and Space Administration, Washington, D. C.
MICROGRAVITY SCIENCE AND APPLICATIONS BIBLIOGRAPHY, 1985 REVISION
Elizabeth Pentecost, comp. (Universities Space Research Association, Washington, D.C.) Oct. 1985 106 p
(NASA-TM-88178; NAS 1.15:88178) Avail: NTIS HC A06/MF A01 CSCL 05B

This edition of the Microgravity Science and Applications (MSA) Bibliography is a compilation of Government reports, contractor reports, conference proceedings, and journal articles dealing with flight experiments utilizing a low-gravity environment to elucidate and control various processes or with ground-based activities that provide supporting research. It encompasses literature published but not cited in the 1984 Revision and that literature which has been published in the past year. Subdivisions of the bibliography include six major categories: Electronic Materials; Metal, Alloys, and Composites; Fluid Dynamics and Transports; Biotechnology; Glass and Ceramics; and Combustion. Also included are publications from the European, Soviet, and Japanese MSA programs. In addition, there is a list of patents and appendices providing a compilation of anonymously authored collection of reports and a cross reference index. Author

N86-13226# Air Force Inst. of Tech., Wright-Patterson AFB, Ohio. School of Engineering.

AGGREGATING INDIVIDUAL PREFERENCES IN THE ANALYTIC HIERARCHY PROCESS APPLIED TO THE 1983 BATTELLE TAV STUDY M.S. Thesis
S. E. Reed 15 Mar. 1985 293 p
(AD-A155858; AFIT/GST/OS/85M-13) Avail: NTIS HC A13/MF A01 CSCL 09/2

This thesis showed that the Analytical Hierarchy Process (AHP) group priority vector was independent of three aggregation techniques: geometric mean input, arithmetic mean vector output, and majority rule output. The AHP consistency index was correlated (Kendall's Tau) with Kendall's Coefficient of Consistence when the AHP inputs were converted to a voting matrix - 0, 1/2, 1 for each pairwise comparison. Minor respondent dissatisfaction with the AHP priority vector suggested that the scale in surveys should be presented to reflect the ratio versus interval scale. Eleven judges from the 1983 Trans-Atmospheric Vehicle (TAV) steering committee participated. They completed pairwise comparisons throughout a revised hierarchy of the 1983 Battelle TAV study. The study includes Apple PASCAL computer codes to manipulate the input files. GRA

N86-13227# Corps of Engineers, St. Paul, Minn.
INFORMATION SYSTEMS PLAN
Apr. 1985 272 p
(AD-A157911) Avail: NTIS HC A12/MF A01 CSCL 09/2

The purpose of this study is to analyze what information the St. Paul District uses, who needs to share data, what are the costs of information management, and who should be responsible for information management. This pilot project authorizes the District to demonstrate the feasibility of automated approaches through the acquisition and use of high technology equipment. GRA

N86-13228# Naval Training Analysis and Evaluation Group, Orlando, Fla.
WORD LISTS TO LIMIT VOCABULARY IN TECHNICAL INFORMATION Final Report
J. P. Kincaid, W. C. McDaniel, and M. Pierce Feb. 1985 165 p
(AD-A157931; TAEG-TR-164) Avail: NTIS HC A08/MF A01 CSCL 05/2

This report describes eight word lists for use as part of an automated publishing system for technical information. The lists were developed under sponsorship of the Naval Technical Information Presentation Program (NTIPP), which has been designated as the focal point for research and development in DOD's project to automate the production of technical information (TI). DOD policy required accurate, current, and comprehensible technical information (TI) to carry out a variety of functions supporting DOD weapons systems and equipment. One of the specific goals of NTIPP is to increase comprehensibility of TI. The eight word lists in this report were developed to help achieve this by simplifying vocabulary. The first is a revision of the common word list originally developed with CRES (Computer Readability Editing System). It represents the core vocabulary of junior Navy enlisted personnel. GRA

N86-13229# Society for Industrial and Applied Mathematics, Philadelphia, Pa.
SURVEY AND EXPOSITORY PAPERS ON TOPICS OF CURRENT INTEREST IN APPLIED MATHEMATICS Final Report, 15 Mar. 1980 - 15 Mar. 1985
A. K. Kapila 24 Jul. 1985 6 p
(Contract DAAG29-80-C-0091)
(AD-A158418; ARO-13926.1-MA) Avail: NTIS HC A02/MF A01 CSCL 12/1

This report lists the titles and abstracts of survey and expository papers published in SIAM (Society for Industrial and Applied Mathematics) Review under a contract. Author (GRA)

N86-12686# Joint Publications Research Service, Arlington, Va.
HARDWARE AND SOFTWARE SUPPORT OF GEOLOGICAL-GEOPHYSICAL DATABASE Abstract Only
V. A. Ivanov, G. A. Ivanchenko, N. N. Karlson, and N. S. Yakovenko *In its* USSR Rept.: Earth Sci. (JPRS-UES-85-006) 19 Jun. 1985 p 68 Transl. into ENGLISH from Avtometriya (Novosibirsk), no. 6, Nov. - Dec. 1985 p 82-83 (For primary document see N86-12630 03-42)
Avail: NTIS HC A05/MF A01

83 ECONOMICS AND COST ANALYSIS

Includes cost effectiveness studies.

N86-13230*# ECON, Inc., Alexandria, Va.
FEDERAL GOVERNMENT PROVISION OF THIRD-PARTY LIABILITY INSURANCE TO SPACE VEHICLE USERS Final Report
2 Jan. 1985 138 p refs
(Contract NASw-3339)
(NASA-CR-176346; NAS 1.26:176346; ECON-84-101) Avail: NTIS HC A07/MF A01 CSCL 05C

Support decisions concerning the provision by the Federal Government of third-party liability insurance for commercial space activities were studied. The practices associated with third-party liability insurance in the marine, aviation, and electric utility industries in addition to those industries associated with space missions were reviewed. Theoretical considerations of rate setting are discussed and a methodology to determine the period of time over which the insurers of each industry intend to set aside reserves to recover from a maximum liability loss should one occur is introduced. The data were analyzed to determine the setaside period in each industry, and to suggest reasonable standards from the insurer's point of view. Criteria for Federal provision of insurance are discussed, an interpretation of the Price-Anderson Act, determinants of the availability of commercial insurance, potential insurer liability, and measures of reasonableness for premium rates from the user's point of view are presented. Options available to the government regarding third part liability protection are presented. Author

84 LAW AND POLITICAL SCIENCE

Includes space law; international law; international cooperation; and patent policy.

N86-13231# Committee of Conference (U. S. Congress).
MAKING APPROPRIATIONS FOR THE DEPARTMENT OF HOUSING AND URBAN DEVELOPMENT, AND FOR SUNDRY INDEPENDENT AGENCIES, BOARDS, COMMISSIONS, CORPORATIONS, AND OFFICES FOR THE FISCAL YEAR ENDING SEPTEMBER 30, 1986, AND FOR OTHER PURPOSES
Edward P. Boland Washington GPO 1985 28 p Conf. rept. to accompany H.R. 3038 presented by the Comm. of Conf., 99th Congr., 1st Sess., 8 Nov. 1985
(H-Rept-99-363; GPO-54-494) Avail: US Capitol, House Document Room

Testimony and support of appropriations for the Department of Housing and Urban Development, and for sundry independent agencies, boards, commissions, corporations, and offices are reported. For individual titles, see N86-13232 through N86-13232.

N86-13232# Committee of Conference (U. S. Congress).
NATIONAL AERONAUTICS AND SPACE ADMINISTRATION
In its Making Appropriations for the Dept. of HUD, and for Sundry Independent Agencies, Boards, Comm., Corp., and Offices for the Fiscal Year Ending Sep. 30, 1986, and for Other Purposes 1985 p 18-20 (For primary document see N86-13231 03-84)
Avail: US Capitol, House Document Room

Appropriations for the Following agencies: Department of Health and Human Services, NASA, National Science Foundation, Department of the Treasury, Veterans Administration, and Federal Home loan Bank Board, are reported. E.A.K.

N86-13233# Committee on Appropriations (U. S. Senate).
DEPARTMENT OF HOUSING AND URBAN DEVELOPMENT, AND CERTAIN OTHER INDEPENDENT AGENCIES APPROPRIATIONS FOR FISCAL YEAR 1986, PART 1
Washington GPO 1985 877 p refs Hearings on H.R. 3629 before the Comm. on Appropriations, 99th Cong., 1st Sess., 14 Mar. 1985
(S-Hrg-99-221-Pt-1; GPO-43-660) Avail: Subcommittee of the Committee on Appropriations

James Beggs, NASA Administrator, presented his 1986 Fiscal Budget to the Senate Committee on Appropriations (99th Congress), during hearings on 14 May 1985, the Honorable Jake Garn presiding. The NASA request was $7.9 billion of which 2.9 billion is for research and development, including $354 million for aeronautical research and technology; $3.5 billion for space flight, control, and data communications; $149 million for construction of facilities; and $1.3 billion for research and program management. This was followed by a University of California (California Space Institute) report on Automation and Robotics, and Volumes 1 (executive Overview) and 2 (Technical Report) of NASA's Advanced Technology Advisory Committee (ATAC), entitled, Advancing Automation and Robotics Technology for the Space Station and the U.S. Economy. For individual titles, see N86-13234 through N86-13234.

N86-13234# Committee on Appropriations (U. S. Senate).
NATIONAL AERONAUTICS AND SPACE ADMINISTRATION
In its Dept. of HUD, and Certain Independent Agencies Appropriations for Fiscal Year 1986, Pt. 1 1985 p 1-407 refs (For primary document see N86-13233 03-84)
Avail: Subcommittee of the Committee on Appropriations

In response to Public Law 98-371, dated July 18, 1984, the NASA Advanced Technology Advisory Committee (ATAC) has studied automation and robotics for use in the Space Station and prepared this report to the House and Senate Committees on Appropriations. The report is divided into two volumes: the Executive Overview, Volume 1, presents the major findings of the study and recommends to NASA principles for advancing automation and robotics technologies for the benefit of the Space Station and of the U.S. economy in general; the Technical Report, Volume 2, provides background information on automation and robotics technologies and their potential. As a result of its study, the Advanced Technology Advisory Committee believes that a key element of technology for the Space Station is extensive use of advanced general-purpose automation and robotics. This could include many systems and devices (such as computer vision, expert systems, and dexterous manipulators) that have been made possible by recent advances in artificial intelligence, robotics, computer science, and microelectronics. Author

85 URBAN TECHNOLOGY AND TRANSPORTATION

Includes applications of space technology to urban problems; technology transfer; technology assessment; and surface and mass transportation.

For related information see *03 Air Transportation and Safety, 16 Space Transportation,* and *44 Energy Production and Conversion.*

N86-13235*# National Academy of Sciences - National Research Council, Washington, D. C. Panel on Vehicle Applications.
AERONAUTICAL TECHNOLOGY 2000: A PROJECTION OF ADVANCED VEHICLE CONCEPTS
1985 116 p
(Contract NASw-3455)
(NASA-CR-176322; NAS 1.26:176322) Avail: NTIS HC A06/MF A01; also available from Aeronautics and Space Engineering Board, National Research Council, 2101 Constitution Ave., N.W., Washington, D.C. 20418 CSCL 05A

The Aeronautics and Space Engineering Board (ASEB) of the National Research Council conducted a Workshop on Aeronautical Technology: a Projection to the Year 2000 (Aerotech 2000 Workshop). The panels were asked to project advances in aeronautical technologies that could be available by the year 2000. As the workshop was drawing to a close, it became evident that a more comprehensive investigation of advanced air vehicle concepts than was possible in the limited time available at the workshop would be valuable. Thus, a special panel on vehicle applications was organized. In the course of two meetings, the panel identified and described representative types of aircraft judged possible with the workshop's technology projections. These representative aircraft types include: military aircraft; transport aircraft; rotorcraft; extremely high altitude aircraft; and transatmospheric aircraft. Improvements in performance, efficiency, and operational characteristics possible through the application of the workshop's year 2000 technology projections were discussed. The subgroups also identified the technologies considered essential and enhancing or supporting to achieve the projected aircraft improvements. B.W.

N86-13236*# National Aeronautics and Space Administration. Lewis Research Center, Cleveland, Ohio.
OVERVIEW OF FREE-PISTON STIRLING TECHNOLOGY AT THE NASA LEWIS RESEARCH CENTER
Jack G. Slaby 1985 21 p refs Presented at the 23rd Automotive Technol. Develop. Contractors' Coordination Meeting, Dearborn, Mich., 21-24 Oct. 1985; sponsored by DOE
(Contract DE-AI05-82OR-1005)
(NASA-TM-87156; E-2783; DOE/NASA-1006/7; NAS 1.15:87156)
Avail: NTIS HC A02/MF A01 CSCL 10B

An overview of the National Aeronautics and Space Administration (NASA) Lewis Research Center (Lewis) free-piston Stirling engine activities is presented. These activities include: (1) a generic free-piston Stirling technology project being conducted to develop technologies synergistic to both space power and terrestrial heat pump applications in a cooperative, cost-shared effort with the Department of Energy (DOE/Oak Ridge National Laboratory (ONRL)), and (2) a free-piston Stirling space-power technology demonstration project as part of the SP-100 program being conducted in support of the Department of Defense (DOD), DOE, and NASA/Lewis. The generic technology effort includes extensive parametric testing of a 1 kw free-piston Stirling engine (RE-1000), development and validation of a free-piston Stirling performance computer code, and fabrication and initial testing of an hydraulic output modification for the RE-1000 engine. The space power technology effort, under SP-100, addresses the status of the 25 kWe Space Power Demonstrator Engine (SPDE) including early test results. Author

N86-13237# Office of Naval Research, London (England).
EUROPEAN SCIENCE NOTES. VOLUME 39, NUMBER 8
L. E. Shaffer Aug. 1985 52 p
(AD-A157146; ESN-39-8) Avail: NTIS HC A04/MF A01 CSCL 05/2

Volume 9, Number 8 of European Space Notes, contains articles on the following topics: the psychology of left-handedness; the International Low-Temperature Biological Microscopy and Analysis Meeting; the AGARD lecture series on the Impact of Proposed Radio Frequency Radiation Standards on Military Operations; the Brain Research Institute, University of Zurich; advances in Command, Control, and Communication systems; the Spete Institute for Strength of Materials and Welding Technology, University of Ghent, Belgium; Mathematicians Working With Industry -- the Oxford Example; Surface-Wave and Ship-Resistance Research in Israel; Electro-Optics, Quantum Electronics, and Related Topics Pursued at the Hirst Research Center; and the Laser Research Center at Hull University, UK. GRA

N86-13238# Naval Surface Weapons Center, Silver Spring, Md.
NAVAL SURFACE WEAPONS CENTER TECHNOLOGY TRANSFER BIENNIAL REPORT (FISCAL YEAR 1983/1984) Biennial Report, Fiscal Year 1983-1984
R. D. Johnson 1 Oct. 1984 51 p

(AD-A157919; NSWC/MP-85-58) Avail: NTIS HC A04/MF A01 CSCL 13/10

This report describes the Naval Surface Weapons Center Technology Transfer Program and presents narrative summaries of related projects performed during FY83/84422. Technology Application Assessments and a listing of patents/Navy cases for this time period are also presented. The objectives of Navy technology transfer are (1) to disseminate non-critical technology, originally developed in support of military applications, for potentially alternative uses in the public and private sectors; and (2) to promote joint cooperative development programs that address problems of mutual concern to the Navy and other agencies or organizations. Representative Narrative Summaries are: Manufacturing Technology, U.S. Coast Guard Diving Equipment Program, Space Shuttle Booster Water Entry, Solid Rocket Booster (SRB) Hazard Study, Hydroballistic Facility, High Altitude Parachute Deployment, College Computer Science Program, Hydrogen Gas Generator, Undersea Weapons Tank. GRA

88 SPACE SCIENCES (GENERAL)

N86-13239*# National Aeronautics and Space Administration. Marshall Space Flight Center, Huntsville, Ala.

SECOND WORKSHOP ON SPACECRAFT GLOW

J. Hunter Waite, Jr., ed. and T. W. Moorehead, ed. Sep. 1985 294 p refs Workshop held in Huntsville, Ala., 6-7 May 1985; sponsored in part by the Universities Space Research Association

(NASA-CP-2391; M-502; NAS 1.55:2391) Avail: NTIS HC A13/MF A01 CSCL 03B

Various aspects of space glow were considered. Results of a workshop held on May 6 to 7, 1985, at the Space Science Laboratory of NASA/Marshall Space Flight Center, Huntsville, Alabama are presented. The topics of discussion are divided as follows: (1) in situ observations; (2) theoretical calculations; (3) laboratory measurements; and (4) future experiments. For individual titles, see N86-13240 through N86-13269.

N86-13240*# Lockheed Missiles and Space Co., Palo Alto, Calif.

VEHICLE GLOW MEASUREMENTS ON THE SPACE SHUTTLE

Steven B. Mende and Gary R. Swenson *In* NASA. Marshall Space Flight Center 2d Workshop on Spacecraft Glow Sep. 1985 p 1-34 refs (For primary document see N86-13239 03-88)
(Contract NAS8-32579)
Avail: NTIS HC A13/MF A01 CSCL 03B

From the combined data set of glow observations on shuttle flight STS-3, STS-4, STS-5, STS-8, STS-9, 41-E, and 41-G some of the properties of the shuttle glow are discussed. Comparison of the STS-3 and STS-5 (240 and 305 km altitude, respectively) photographs shows that the intensity of the glow is about a factor of 3.5 brighter on the low-altitude (STS-3) flight. In an experiment to observe the dependence of the intensity on the ram angle, the angle of incidence between the spacecraft surface normal and the velocity vector, the Orbiter was purposely rotated about the x axis on the STS-5 mission. For a relatively large angle between the velocity vector and the surface normal there is an appreciable glow, provided the surface is not shadowed by some other spacecraft structure. As the angle becomes less the glow intensifies. Material samples were also exposed in the ram direction during nightside orbits and the glow surrounding the samples was photographed. Author

N86-13241*# National Aeronautics and Space Administration. Marshall Space Flight Center, Huntsville, Ala.

SPACE SHUTTLE RAM GLOW: IMPLICATION OF NO2 RECOMBINATION CONTINUUM

Gary R. Swenson (LMSC, Palo Alto, Calif.), Steven B. Mende (LMSC, Palo Alto, Calif.), and Stu Clifton *In its* 2d Workshop on Spacecraft Glow Sep. 1985 p 25-45 refs (For primary document see N86-13239 03-88)
Avail: NTIS HC A13/MF A01 CSCL 03B

The ram glow data gathered to data from imaging experiments on space shuttle suggest the glow is a continuum (within 34 angstrom resolution); the continuum shape is such that the peak is near 7000 angstroms decreasing to the blue and red, and the average molecular travel leading to emission after leaving the surface is 20 cm (assuming isotropic scattering from the surface). Emission continuum is rare in molecular systems but the measured spectrum does resemble the laboratory spectrum of NO2 (B) recombination continuum. The thickness of the observed emission is consistent with the NO2 hypothesis given an exit velocity of approx. 2.5 km/sec (1.3 eV) which leaves approx. 3.7 eV of ramming OI energy available for unbonding the recombined NO2 from the surface. The NO2 is formed in a 3-body recombination of OI + NO + [m] = NO2 + [m] where OI originates from the atmosphere and NO is chemically formed on the surface from atmospheric NI and OI. The spacecraft surface then acts as the [n] for the reaction: Evidence exists from orbital mass spectrometer data that the NO and NO2 chemistry described in this process does occur on surfaces of spectrometer orifices in orbit. Surface temperature effects are likely a factor in the NO sticking efficiency and, therefore, glow intensities. Author

N86-13242*# Augsburg Univ. (West Germany). Dept. of Physics.

AE AND DE MASS SPECTROMETER OBSERVATIONS RELEVANT TO THE SHUTTLE GLOW c35

Mark J. Engebretson *In* NASA. Marshall Space Flight Center 2d Workshop on Spacecraft Glow Sep. 1985 p 46-54 refs (For primary document see N86-13239 03-88)
(Grant NAG5-349)
Avail: NTIS HC A13/MF A01 CSCL 03B

Recent work suggested that NO2 may be responsible for the observed continuum glow near surfaces of the space shuttle. The observations of atomic nitrogen (N) are reported at shuttle altitudes using mass spectrometers, giving special attention to the surface reactions of N relevant to the production of NO2 on spacecraft surfaces. Data from two semi-open sources mass spectrometers, the OSS instruments on the Atmosphere Explorer-C and -D satellites, and the closed source Neutral Atmospheric Composition Spectrometer (NACS) on the Dynamic Explorer-2 satellite are presented to show the similar behavior of NO in each case and the contrasting behavior of NO2. Although signals of NO and NO2 are highly dependent on surface temperature and surface composition, it appears that direct exposure of ion source surfaces to rammed gas is a necessary condition for the production of large amounts of NO2. Evidence that elevated surface temperatures can significantly reduce the production of NO2, likely by causing more rapid desorption of NO from these surfaces, is presented. Author

N86-13243*# Harvard-Smithsonian Center for Astrophysics, Cambridge, Mass.

THE ATMOSPHERE EXPLORER AND THE SHUTTLE GLOW

A. Dalgarno, J.-H. Yee, and M. LeCompte *In* NASA. Marshall Space Flight Center 2d Workshop on Spacecraft Glow Sep. 1985 p 55-62 refs (For primary document see N86-13239 03-88)
(Grant NAGw-496; Contract F19628-88-C-0034; Grant NSF ATM-84-07314)
Avail: NTIS HC A13/MF A01 CSCL 03B

Recent analyses of the Atmosphere Explorer data are discussed in which it is demonstrated that the satellite glows have two components, one at high altitudes which is consistent with excitation in single collisions of atmospheric oxygen atoms with the vehicle surface and the other at low altitudes which is consistent with double collisions of nitrogen molecules. Contrary to an earlier suggestion, the low-altitude data are not consistent with collisions of oxygen molecules. The separation of the two components strengthens the conclusion that the high-altitude glow arises from vibrationally excited OH molecules produced by a formation mechanism that is different from that leading to the normal atmospheric OH airglow. The spectrum is consistent with association of oxygen and hydrogen atoms at sites on the surface into the vibrational levels of OH. The low-altitude glow is consistent with the green mechanism but there are difficulties with it. The shuttle glows are different and have the spectral appearance of emission from NO2. The characteristics of the shuttle glows and the satellite glows will be contrasted and a tentative resolution of the differences in the Atmosphere Explorer and shuttle glows will be offered. Author

N86-13244*# National Research Council of Canada, Ottawa (Ontario). Inst. of Astrophysics.
ORBITER GLOW OBSERVATIONS AT HIGH SPECTRAL RESOLUTION c35
David J. W. Kendall, Richard L. Gattinger, Edward J. Llewellyn (Saskatchewan Univ.), Ian C. McDade (Saskatchewan Univ.), and Steven B. Mende (LMSC, Palo Alto, Calif.) *In* NASA. Marshall Space Flight Center 2d Workshop on Spacecraft Glow Sep. 1985 p 63-73 refs Sponsored in part by the Universities Space Research Association. (For primary document see N86-13239 03-88)
Avail: NTIS HC A13/MF A01 CSCL 03B

An experiment flow on mission STS 41-G as part of the Canadian complement of experiments was designed to obtain relatively high resolution spectra of the Orbiter glow phenomenon over limited spectral regions centered on prominent upper atmospheric emissions. Observations were carried out successfully at altitudes of 360 km and 230 km although those at the lower altitude were limited by degradation of the image intensifier. Definitive glow results were obtained at the end of a thruster firing which showed the spectrum to be a continuum at a resolution of approximately 0.4 nm centered at a wavelength of 360 nm. Results at other wavelengths in the absence of any firings strongly suggest that the Orbiter glow is a continuum throughout the spectral region 550 nm to 760 nm. A discussion is presented that considers the reaction NO + O2 as being a possible candidate for the mechanism producing the shuttle glow. Author

N86-13245*# National Aeronautics and Space Administration. Marshall Space Flight Center, Huntsville, Ala.
NEUTRAL MASS SPECTROMETER MEASUREMENTS IN THE SHUTTLE BAY ENVIRONMENT c35
E. Miller and G. Carignan (Michigan Univ.) *In its* 2d Workshop on Spacecraft Glow Sep. 1985 p 74-81 refs (For primary document see N86-13239 03-88)
Avail: NTIS HC A13/MF A01 CSCL 03B

A neutral mass spectrometer, flown as part of the Induced Environment Contamination Monitor (IECM), is briefly described. Results from STS-2, -3, -4, and Spacelab 1 are qualitatively summarized. The gases observed were, for the most part, those with molecular weights below 45 amu with sources attributable to instrument background, shuttle-induced environment, and the ambient atmosphere. The most abundant gases were H2O, N2, and He. Heavier gases consisted primarily of fluorocarbons. Author

N86-13246*# Physical Sciences, Inc., Andover, Mass. Atmospheric Sciences Group.
SPECTRAL IDENTIFICATION/ELIMINATION OF MOLECULAR SPECIES IN SPACECRAFT GLOW
B. D. Green, W. J. Marinelli, and W. T. Rawlins *In* NASA. Marshall Space Flight Center 2d Workshop on Spacecraft Glow Sep. 1985 p 82-97 refs Sponsored by AFGL (For primary document see N86-13239 03-88)
Avail: NTIS HC A13/MF A01 CSCL 03B

Computer models of molecular electronic and vibrational emission intensities were developed. Known radiative emission rates (Einstein coefficients) permit the determination of relative excited state densities from spectral intensities. These codes were applied to the published spectra of glow above shuttle surface and to the Spacelab 1 results of Torr and Torr. The theoretical high-resolution spectra were convolved with the appropriate instrumental slit functions to allow accurate comparison with data. The published spacelab spectrum is complex but N2+ Meinel emission can be clearly identified in the ram spectrum. M2 First Positive emission does not correlate well with observed features, nor does the CN Red System. Spectral overlay comparisons are presented. The spectrum of glow above shuttle surfaces, in contrast to the ISO data, is not highly structured. Diatomic molecular emission was matched to the observed spectral shape. Source excitation mechanisms such as (oxygen atom)-(surface species) reaction product chemiluminescence, surface recombination, or resonance fluorescent re-emission will be discussed for each tentative assignment. These assignments are the necessary first analytical step toward mechanism identification. Different glow mechanisms will occur above surfaces under different orbital conditions. Author

N86-13247*# Utah State Univ., Logan. Dept. of Physics.
THE UV-VIS OPTICAL ENVIRONMENT OF THE SHUTTLE c35
Marsha R. Torr *In* NASA. Marshall Space Flight Center 2d Workshop on Spacecraft Glow Sep. 1985 p 98-106 refs (For primary document see N86-13239 03-88)
(Contract NAS8-33992)
Avail: NTIS HC A13/MF A01

During the Spacelab 1 shuttle mission, spectroscopic measurements were made of the atmospheric emissions over a broad wavelength range extending from the extreme ultraviolet to the near infrared. Those measurements were made under a variety of vehicle attitude and sunlight conditions. Superimposed on such spectra would be any features associated with the induced vehicle environment and its interaction with solar photons and the ambient neutral atmosphere and plasma. Various anomalies and unexpected features in the spectra from the perspective of possible shuttle-induced origins are discussed. The data indicate a dramatic cleanup of the vehicle environment over the course of the 10-day mission, a strong non-atmospheric red continuum underlying the spectra at night and at large angles to the velocity vector, and a variety of molecular band distributions which are not explained by the present understanding of the atmosphere. Author

N86-13248*# Utah State Univ., Logan. Dept. of Physics.
ENHANCED N(+) SUB 2 IN THE SHUTTLE ENVIRONMENT Abstract Only c35
Doug G. Torr, A. Khoyloo, and Marsha R. Torr *In* NASA. Marshall Space Flight Center 2d Workshop on Spacecraft Glow Sep. 1985 p 107 (For primary document see N86-13239 03-88)
Avail: NTIS HC A13/MF A01 CSCL 03B

Observations were made of the N2 first negative and Meinel emission bands with the Imaging Spectrometric Observatory (ISO) on Spacelab 1. These observations have revealed the presence of N2 emissions which exceed those expected on the basis of current ionospheric models by up to a factor of 10. If the emission is of terrestrial origin, large unidentified ionospheric sources of N2 ions must exist. On the other hand, if the source is local to the shuttle environment, a mechanism must be found which is capable of generating emissions of such unexpectedly large intensity. Charge exchange of ambient ionospheric O+ ions with shuttle environmental N2, followed by resonance scattering of sunlight, as a candidate were suggested. However, this model implies that a cloud of N2 gases must surround the vehicle in concentrations in excess of 10 to the 11 c.c. cm with a scale length of tens of meters. In addition, the N2 residence time must be of the order of 10 sec. Author

N86-13249*# California Univ., Berkeley. Space Sciences Lab.
INVESTIGATION OF VEHICLE GLOW IN THE FAR ULTRAVIOLET c35
Supiya Chakrabarti and Timothy Sassen *In* NASA. Marshall Space Flight Center 2d Workshop on Spacecraft Glow Sep. 1985 p 108-115 refs (For primary document see N86-13239 03-88)
(Contract NAS8-32577)
Avail: NTIS HC A13/MF A01 CSCL 03B

To data, all vehicle glow observations have been conducted in the visible and near infrared wavelength regions. As the Space Telescope's wavelength coverage extends to the far ultraviolet range and current plasma theory of the spacecraft glow phenomena predicts bright glow intensities, a study of the ram glow effects in the 800-1400 angstrom region was undertaken. The data were collected between March 21-28, 1979, from 600 km altitude near local midnight by the University of California, Berkeley's extreme ultraviolet spectrometer on board the polar orbiting STP78-1 satellite. Data from several nighttime orbits obtained outside the South Atlantic Anomaly region and within + or - 30 deg magnetic latitude range were separated into forward (south viewing) and backward (north viewing) bins. Each of these binds was subdivided into three directional categories: (1) up (zenith angles 30-80 deg), (2) side (zenith angles 80-100 deg), and (3) down (zenith angles 120-150 deg). The maximum ram glow effects are expected in the side viewing directions. Our data include possible effects of ram glow signatures in the 800-1400 angstrom wavelength region. Author

N86-13250*# Science Applications International Corp., McLean, Va.

SPACECRAFT-INDUCED PLASMA ENERGIZATION AND ITS ROLE IN FLOW PHENOMENA

K. Papadopoulos (Maryland Univ., College Park) and R. A. Smith *In* NASA. Marshall Space Flight Center 2d Workshop on Spacecraft Glow Sep. 1985 p 119-128 refs (For primary document see N86-13239 03-88)
(Contract F19628-85-C-0024)
Avail: NTIS HC A13/MF A01 CSCL 03B

Plasma instabilities induced by orbiting vehicles can cause many important phenomena ranging from electron and ion heating and suprathermal electron tail energization, to enhanced ionization and optical emissions. We outline the basic collective processes leading to plasma energization near plasma sheaths and in regions of neutral gas streaming through plasma, and discuss the role of the induced collective effects in producing the optical emission spectra. Author

N86-13251*# National Aeronautics and Space Administration. Langley Research Center, Hampton, Va.

SHUTTLE VERTICAL FIN FLOWFIELD BY THE DIRECT SIMULATION MONTE CARLO METHOD

J. E. Hueser (Old Dominion Univ.), F. J. Brock (Old Dominion Univ.), and L. T. Melfi *In* NASA. Marshall Space Flight Center 2d Workshop on Spacecraft Glow Sep. 1985 p 129-138 refs (For primary document see N86-13239 03-88)
Avail: NTIS HC A13/MF A01 CSCL 03B

The flow properties in a model flowfield, simulating the shuttle vertical fin, determined using the Direct Simulation Monte Carlo method. The case analyzed corresponds to an orbit height of 225 km with the freestream velocity vector orthogonal to the fin surface. Contour plots of the flowfield distributions of density, temperature, velocity and flow angle are presented. The results also include mean molecular collision frequency (which reaches 1/60 sec near the surface), collision frequency density (approaches 7 x 10 to the 18/cu m sec at the surface) and the mean free path (19 m at the surface). Author

N86-13252*# Science and Engineering Associates, Inc., Englewood, Colo.

A MECHANISM FOR THE LOCAL CONCENTRATION ENHANCEMENT OF THE SHUTTLE ATMOSPHERE

Ray Rantanen, Roy Swanson (Boeing Aerospace Co.), and Doug G. Torr (Utah State Univ., Logan) *In* NASA. Marshall Space Flight Center 2d Workshop on Spacecraft Glow Sep. 1985 p 139-148 refs (For primary document see N86-13239 03-88)
Avail: NTIS HC A13/MF A01 CSCL 03B

Preliminary calculations suggest that collisions between instreaming atmospheric constituents and secondary backscattered molecules can generate unexpectedly large enhancements in neutral gas concentrations in the vicinity of the shuttle. This effect is a result of a rapid decrease in the mean free path length of the scattered components following the initial expected concentration enhancement. A study will be outlined for the theoretical investigation of this mechanism. The shape dependence of associated glow halos on vehicle configuration will be discussed. Author

N86-13253*# Photometrics, Inc., Woburn, Mass.

SURFACE-CATALYZED RECOMBINATION INTO EXCITED ELECTRONIC, VIBRATIONAL, ROTATIONAL, AND KINETIC ENERGY STATES: A REVIEW

I. L. Kofsky and J. L. Barrett *In* NASA. Marshall Space Flight Center 2d Workshop on Spacecraft Glow Sep. 1985 p 149-154 refs (For primary document see N86-13239 03-88)
Avail: NTIS HC A13/MF A01 CSCL 03B

Laboratory experiments in which recombined CO, CO2, D2O, OH, N2, H2, and O2 molecules desorb from surfaces in excited internal and translational states are briefly reviewed. Unequilibrated distributions predominate from the principally catalytic metal substrates so far investigated. Mean kinetic energies have been observed up to approx. 3x, and in some cases less than, wall-thermal; the velocity distributions generally vary with emission angle, with non-Lambertian particle fluxes. The excitation state populations are found to depend on surface impurities, in an as yet unexplained way. Author

N86-13254*# Photometrics, Inc., Woburn, Mass.

INFRARED EMISSION FROM DESORBED NO2(*) AND NO(*)

I. L. Kofsky and J. L. Barrett *In* NASA. Marshall Space Flight Center 2d Workshop on Spacecraft Glow Sep. 1985 p 155-164 refs (For primary document see N86-13239 03-88)
Avail: NTIS HC A13/MF A01 CSCL 03B

Infrared photons from the radiative cascade accompany both the gas phase NO2 continuum chemiluminescence (which originates from its 2B2 and 2B1 states) and the NO beta bands. When these upper electronic states are excited by recombination/desorption at surfaces of low Earth orbiting spacecraft, similar IR emission spectrums will be observed. The principal NO2 features (other than the long wavelength tail of its electronic transitions) are the nu sub 3 fundamental sequence near 6.2 microns and nu sub 1 + nu sub 3 intercombination bands near 3.6 microns; NO would emit the delta v=1 and delta v=2 systems above 5.3 and 2.7 microns. Because of the long radiative lifetimes of the upper vibrational states, the infrared radiances in projections parallel to the vehicle surface (which we estimate) are substantially less than those of the visible and ultraviolet glows. Author

N86-13255*# Photometrics, Inc., Woburn, Mass.

THE NO-NO2 SYSTEM AT LABORATORY SURFACES

J. L. Barrett and I. L. Kofsky *In* NASA. Marshall Space Flight Center 2d Workshop on Spacecraft Glow Sep. 1985 p 165-168 refs (For primary document see N86-13239 03-88)
Avail: NTIS HC A13/MF A01 CSCL 03B

Experiments on formation and excitation of NO2 and NO molecules at (and near) laboratory surfaces of varying degrees of characterization are reviewed. On some transition metals NO is desorbed in the B sub 2 pi state, from which it radiates the familiar beta (B yields x) bands. In contrast while an ONO intermediate is inferred from isotope interchange measurements on platinum, neither ground state nor excited NO2 has been found to be desorbed under the relatively limited number of laboratory conditions so far investigated. Author

N86-13256*# National Aeronautics and Space Administration. Marshall Space Flight Center, Huntsville, Ala.

A MODEL FOR EXPLAINING SOME FEATURES OF SHUTTLE GLOW

Palmer N. Peters *In its* 2d Workshop on Spacecraft Glow Sep. 1985 p 169-173 refs (For primary document see N86-13239 03-88)
Avail: NTIS HC A13/MF A01 CSCL 03B

A solid state model is proposed which hopefully removes some of the objections to excited atoms being sources for light emanating from surfaces. Glow features are discussed in terms of excited oxygen atoms impinged on the surface, although other species could be treated similarly. Band formation, excited lifetime shortening and glow color are discussed in terms of this model.

The model's inability to explain glow emanating above surfaces indicates a necessity for other mechanisms to satisfy this requirements. Several ways of testing the model are described. Author

N86-13257*# National Aeronautics and Space Administration. Marshall Space Flight Center, Huntsville, Ala.
THE PRODUCTION OF GLOW PRECURSORS BY OXIDATIVE EROSION OF SPACECRAFT SURFACES c35
John C. Gregory (Alabama Univ., Huntsville) and Palmer N. Peters *In its* 2d Workshop on Spacecraft Glow Sep. 1985 p 174-179 refs (For primary document see N86-13239 03-88)
(Contract NAS8-36189)
Avail: NTIS HC A13/MF A01 CSCL 03B

Erosion rates of organic materials are measured during a recent flight of the shuttle (STS-8). Several forms of carbon and a variety of thermosetting and thermoplastic polymers are exposed to the ram beam of atomic oxygen. Arrhenius energies of about 1000 to 2000 cal/mole were measured from the rate dependencies on temperature. If some simple assumptions are made about the chemical nature of the desorbed species, the data can be used to estimate production rates at surfaces in orbit under different conditions of temperature, oxygen atom flux, and material surface conditions. Author

N86-13258*# Los Alamos National Lab., N. Mex.
ACTIVATED RECOMBINATIVE DESORPTION: A POTENTIAL COMPONENT IN MECHANISMS OF SPACECRAFT GLOW
Jon B. Cross *In* NASA. Marshall Space Flight Center 2d Workshop on Spacecraft Glow Sep. 1985 p 180-188 refs (For primary document see N86-13239 03-88)
Avail: NTIS HC A13/MF A01 CSCL 03B

The concept of activated recombination of atomic species on surfaces can explain the production of vibrationally and translationally excited desorbed molecular species. Equilibrium statistical mechanics predicts that the molecular quantum state distributions of desorbing molecules is a function of surface temperature only when the adsorption probability is unity and independent of initial collision conditions. In most cases, the adsorption probability is dependent upon initial conditions such as collision energy or internal quantum state distribution of impinging molecules. From detailed balance, such dynamical behavior is reflected in the internal quantum state distribution of the desorbing molecule. This concept, activated recombinative desorption, may offer a common thread in proposed mechanisms of spacecraft glow. Using molecular beam techniques and equipment available at Los Alamos, which includes a high translational energy 0-atom beam source, mass spectrometric detection of desorbed species, chemiluminescence/laser induced fluorescence detection of electronic and vibrationally excited reaction products, and Auger detection of surface adsorbed reaction products, a fundamental study of the gas surface chemistry underlying the glow process is proposed. Author

N86-13259*# Vanderbilt Univ., Nashville, Tenn. Dept. of Physics and Astronomy.
OPTICAL RADIATION FROM THE INTERACTION OF ENERGETIC ATOMS, IONS, ELECTRONS, AND PHOTONS WITH SURFACES c35
N. H. Tolk, R. G. Albridge, R. F. Haglund, Jr., and M. H. Mendenhall *In* NASA. Marshall Space Flight Center 2d Workshop on Spacecraft Glow Sep. 1985 p 191-201 refs (For primary document see N86-13239 03-88)
Avail: NTIS HC A13/MF A01 CSCL 03B

Heavy particle, electron, and UV photon bombardment of solid surfaces has been recently observed to result in the emission of infrared, visible, and ultraviolet radiation. This effect occurs over a wide range of incident projectile energies. Line radiation arising from transitions between discrete atomic or molecular levels may be attributed to the decay of excited particles which have been sputtered or electronically/chemically desorbed from the surface. Broadband continuum radiation, which is also observed, is believed to arise either from fluorescence of the near surface bulk or from the radiative decay of desorbed excited clusters. Spacecraft, in the ambient near Earth environment, are subject to such bombardment. The dynamics of energetic particle and photon beam interactions with surfaces which lead to surface erosion and glow phenomena will be treated. In addition, projected experimental and theoretical studies of oxygen and nitrogen beam surface interactions on materials characteristic of spacecraft surfaces will be discussed. Author

N86-13260*# Princeton Univ., N. J. Plasma Physics Lab.
A GROUND-BASED EXPERIMENTAL TEST PROGRAM TO DUPLICATE AND STUDY THE SPACECRAFT GLOW PHENOMENON c35
W. D. Langer, S. A. Cohen, D. M. Manos, D. H. McNeill, R. W. Motley, M. Ono, and S. Paul *In* NASA. Marshall Space Flight Center 2d Workshop on Spacecraft Glow Sep. 1985 p 202-211 refs (For primary document see N86-13239 03-88)
(Grant NAG8-521; Contract DE-AC02-76CH-03073)
Avail: NTIS HC A13/MF A01 CSCL 03B

The use of a plasma device, the Advanced Concepts Torus-I, for producing atoms and molecules to study spacecraft glow mechanisms is discussed. A biased metal plate, located in the plasma edge, is used to accelerate and neutralize plasma ions, thus generating a neutral beam with a flux approx. > 5 x 10 to the 14th power/sq cm/sec at the end of a drift tube. Our initial experiments are to produce a 10 eV molecular and atomic nitrogen beam directed onto material targets. Photon emission in the spectral range 2000 to 9000 A from excited species formed on the target surface will be investigated. Author

N86-13261*# Aerospace Corp., El Segundo, Calif. Chemistry and Physics Lab.
APPLICATION OF AN ATOMIC OXYGEN BEAM FACILITY TO THE INVESTIGATION OF SHUTTLE GLOW CHEMISTRY c35
Graham S. Arnold and Daniel R. Peplinski *In* NASA. Marshall Space Flight Center 2d Workshop on Spacecraft Glow Sep. 1985 p 212-225 refs (For primary document see N86-13239 03-88)
Avail: NTIS HC A13/MF A01 CSCL 03B

A facility for the investigation of the interactions of energetic atomic oxygen with solids is described. The facility is comprised of a four chambered, differentially pumped molecular beam apparatus which can be equipped with one of a variety of sources of atomic oxygen. The primary source is a dc arc heated supersonic nozzle source which produces a flux of atomic oxygen in excess of 10 to the 15th power sq cm/sec at the target, at a velocity of 3.5 km/sec. Results of applications of this facility to the study of the reactions of atomic oxygen with carbon and polyimide films are briefly reviewed and compared to data obtained on various flights of the space shuttle. A brief discussion of possible application of this facility to investigation of chemical reactions which might contribute to atmosphere induced vehicle glow is presented. Author

N86-13262*# National Aeronautics and Space Administration. Marshall Space Flight Center, Huntsville, Ala.
AN ASSESSMENT OF THE IMPACT OF SPACECRAFT GLOW ON THE HUBBLE SPACE TELESCOPE. SUMMARY OF EXISTING OBSERVATIONS AND THEORY
John T. Clarke *In its* 2d Workshop on Spacecraft Glow Sep. 1985 p 229-242 refs (For primary document see N86-13239 03-88)
Avail: NTIS HC A13/MF A01 CSCL 03B

Visible spacecraft glow was first observed on the Atmospheric Explorer spacecraft (AE-E) and studied in some detail with the Visible Airglow Experiment (VAE). The AE-E was a spin-stabilized spacecraft without thrusters at an altitude of 140 to 280 km. The VAE contained six visible wavelength photometers that measured a glow spectrum which: (1) rose steeply in the red, (2) decreased with a cos cubed PH1 dependence from pointing into the ram direction of the spacecraft orbital motion, and (3) decreased in intensity with increasing altitude with the same dependence as the measured atomic oxygen number atmospheric density (O) and not with the measured molecular nitrogen density (N sub 2). It is proposed that the glow is produced by chemical reactions on the spacecraft surface as it sweeps through the atmospheric O, with roughly 5-8 eV per O atom available for excitation from the orbital motion of the spacecraft. This glow may in principle be produced by any of a number of species, including molecular band emission from OH, NO, and NO2. An attempt is made to scale the observed glow to the Hubble space telescope. Author

N86-13263*# Smithsonian Astrophysical Observatory, Cambridge, Mass.
INFRARED MEASUREMENTS OF SPACECRAFT GLOW PLANNED FOR SPACELAB 2 c35
Giovanni G. Fazio and David G. Koch *In* NASA. Marshall Space Flight Center 2d Workshop on Spacecraft Glow Sep. 1985 p 243-249 refs (For primary document see N86-13239 03-88)
(Contract NAS8-32845)
Avail: NTIS HC A13/MF A01 CSCL 03B

A liquid helium cooled infrared telescope (IRT) was to be flown in July 1985 on Spacelab 2. The instrument is designed to measure both diffuse and discrete infrared astronomical sources, including the zodiacal light, galactic, and extragalactic components, as well as to evaluate the induced Orbiter environment. The focal plane contains ten photoconductive detectors covering six broad bands from 2 to 120 microns. Each detector has a 0.5 by 1.0 deg field of view optimized for detection of extended sources of IR radiation. Except for the 2 micron detector, the system noise is limited by the sky background noise. The measurements planned for the IRT use the 1 meter base of the Plasma Diagnostic Package (PDP), an already existing SL 2 experiment, as the glow generating surface. The measurements are repeated changing the position of the PDP, the attitude of the Orbiter, and the ram direction in an effort to remove both the thermal component of the PDP emission and the cosmic background radiation. Author

N86-13264*# National Aeronautics and Space Administration. Goddard Space Flight Center, Greenbelt, Md.
PLANNED INVESTIGATION OF INFRARED EMISSIONS ASSOCIATED WITH THE INDUCED SPACECRAFT GLOW: A SHUTTLE INFRARED GLOW EXPERIMENT (SIRGE) c35
Michael J. Mumma and Donald E. Jennings *In* NASA. Marshall Space Flight Center 2d Workshop on Spacecraft Glow Sep. 1985 p 250-259 refs (For primary document see N86-13239 03-88)
Avail: NTIS HC A13/MF A01 CSCL 03B

The characteristics of infrared molecular emissions induced by energetic collisions between ambient atmospheric species and surfaces in Earth orbit are investigated, using a low-nitrogen-cooled filter wheel photometer covering the wavelength range 0.9-.5 microns with a resolving power Lambda/Delta Lambda of approximately 100. This resolving power is sufficient for identification of the molecular or atomic fluorescent spaces causing the glow. Author

N86-13265*# Lockheed Missiles and Space Co., Palo Alto, Calif.
DATA REQUIREMENTS FOR VERIFICATION OF RAM GLOW CHEMISTRY c35
Gary R. Swenson and Steven B. Mende *In* NASA. Marshall Space Flight Center 2d Workshop on Spacecraft Glow Sep. 1985 p 260-268 (For primary document see N86-13239 03-88)
Avail: NTIS HC A13/MF A01 CSCL 03B

A set of questions is posed regarding the surface chemistry producing the ram glow on the space shuttle. The questions surround verification of the chemical cycle involved in the physical processes leading to the glow. The questions, and a matrix of measurements required for most answers, are presented. The measurements include knowledge of the flux composition to and from a ram surface as well as spectroscopic signatures from the U to visible to IR. A pallet set of experiments proposed to accomplish the measurements is discussed. An interim experiment involving an available infrared instrument to be operated from the shuttle Orbiter cabin is also be discussed. Author

N86-13266*# Utah State Univ., Logan. Dept. of Physics.
A POSSIBLE GLOW EXPERIMENT FOR THE EOM 1-2 MISSION Abstract Only c35
Marsha R. Torr *In* NASA. Marshall Space Flight Center 2d Workshop on Spacecraft Glow Sep. 1985 p 269 (For primary document see N86-13239 03-88)
Avail: NTIS HC A13/MF A01 CSCL 03B

A possible opportunity for study of surface glow exists during the Environmental Observation Mission (EOM) 1-2 mission scheduled for launch on September 3, 1986. The EOM 1-2 payload includes spectroscopic and photometric instruments which operate in wavelength regions of great interest to the glow assessment activity. However, as in the case of many remote sensing instruments, these are located in the payload bay in such a way as to avoid viewing any shuttle or payload surfaces. If these instruments are to measure the spectral characteristics of surfaces, it is necessary for such surfaces to be positioned in the field of view of these instruments for the duration of the particular measurement sequence. It is possible that the shuttle of which the EOM 1-2 payload flies will have an Remote Manipulator System (RMS) in place. An assessment has shown that it is indeed feasible to place a four-sided cuff around the end of the RMS. The four sides, each coated with a different material, can then be positioned in turn above the instruments, and in such a way that the surface is alternately pointed into the ram and into the wake. Author

N86-13267*# National Aeronautics and Space Administration. Langley Research Center, Hampton, Va.
SPACE SHUTTLE MECHANISTIC STUDIES TO CHARACTERIZE ATOMIC OXYGEN INTERACTIONS WITH SURFACES c35
Lubert J. Leger and James T. Visentine *In* NASA. Marshall Space Flight Center 2d Workshop on Spacecraft Glow Sep. 1985 p 270-273 (For primary document see N86-13239 03-88)
Avail: NTIS HC A13/MF A01 CSCL 03B

A materials interaction experiment has been approved to study atomic oxygen interaction mechanisms and develop coatings for Space Station elements requiring long-lived operation in the LEO environment. A brief summary of this experiment is presented and the required exposure conditions are reviewed. Author

N86-13268*# Science Applications International Corp., Bellevue, Wash.
THE SHUTTLE GLOW: A PROGRAM TO STUDY THE RAM-INDUCED PHENOMENA c35
Hugh R. Anderson *In* NASA. Marshall Space Flight Center 2d Workshop on Spacecraft Glow Sep. 1985 p 274-276 (For primary document see N86-13239 03-88)
Avail: NTIS HC A13/MF A01 CSCL 03B

In January 1984, a proposal was submitted to NASA Headquarters entitled The Shuttle Glow: A Program to Determine the Physics of the Ram induced Phenomena. This proposal included the following elements in a shuttlebased experiment: (1) The use of a special flat generating surface > 1 x 3 m on which the glow can be produced and observed. This surface will be maneuvered to vary the orientation of ram flow and of projected component of geomagnetic field. (2) Remotely mounted optical instruments to view the glowing layer on the plate. By scanning, the variation of radiance as a function of wavelength and standoff distance from the plate will be observed looking parallel to the plate. (3) The preferred location of the generating plate and in situ diagnostics is on the end of the Remote Manipulator System (RMS) arm. F.M.R.

N86-13269*# Colorado Univ., Boulder. Lab. for Atmospheric and Space Physics.
SURVEY OF ULTRAVIOLET SHUTTLE GLOW Abstract Only c35
Kerry A. Spear, Gregory J. Uckler, and Kent Tobiska *In* NASA. Marshall Space Flight Center 2d Workshop on Spacecraft Glow Sep. 1985 p 277 (For primary document see N86-13239 03-88)
Avail: NTIS HC A13/MF A01 CSCL 03B

The University of Colorado Get Away Special (GAS) project utilizes the efforts of its students to place experiments on the shuttle. The objective of one experiment, the shuttle glow study, is to conduct a general survey of emissions in the ultraviolet near vehicle surfaces. An approximate wavelength range of 1900 to 3000 A will be scanned to observe predominant features. Special emphasis will be placed on studying the band structure of NO near 2000 A and the Mg+ line at 2800 A. The spectrometer, of Ebert-Faste 1/8-meter design, will perform the experiment during spacecraft night. It will be oriented such that the optical axis points to the cargo bay zenith. In order to direct the field-of-view of the instrument onto the shuttle vertical stabilizer (tail), a mirror assembly is employed. The mirror system has been designed to rotate through 7.5 degrees of arc using 10 positions resulting in a spatial resolution of 30 x 3 cm, with the larger dimension corresponding to the horizontal direction. Such a configuration can be attained from the forwardmost position in the cargo bay. Each spatial position will be subjected to a full spectral scan with a resolution on the order of 10 A. Author

89 ASTRONOMY

Includes radio and gamma-ray astronomy; celestial mechanics; and astrometry.

N86-13270 California Univ., Berkeley.
NEII OBSERVATIONS OF THE GALACTIC CENTER: THE VELOCITY FIELD AND MASS DISTRIBUTION Ph.D. Thesis
Eugene Serabyn 1984 132 p
Avail: Univ. Microfilms Order No. DA8512986

The velocity field within 2% of the galactic center was investigated by observing the 12.8 micron fine-structure line emission from Sgr A West. The observations show regular variations in velocity along several of the most prominent radio continuum features, indicating the presence of at least two large-scale flows of ionized gas. The inferred mass distribution is too centrally peaked to be due to a spherical isothermal stellar cluster implying that a substantial fraction of the mass located within 1.7% of the center is contained in a centrally condensed form, possibly in a massive black hole of mass approx. 3.4 x 1000,000 M sub. The best fit orbits occur under the assumption that the point mass is near the 2 micron source IRS 16 NE. The flow at r approx. 1.7% is most probably located on the inner edge of the ring of dust and neutral gas which orbits about the center at larger radii. Consequently, the source or sources of the ionization must be centrally located. Shielding of various portions of the ring from the center ionizing flux may play a role in determining the distribution of the ionized gas in Sgr A West. It is concluded that a single object may be the primary source of energy for the central few parsecs of the galaxy. Author

N86-13271*# Smithsonian Astrophysical Observatory, Cambridge, Mass.
BALLOON-BORNE THREE-METER TELESCOPE FOR FAR-INFRARED AND SUBMILLIMETER ASTRONOMY Semiannual Status Report, 1 Mar. - 31 Aug. 1985
Giovanni G. Fazio Oct. 1985 163 p refs
(Grant NAGw-509)
(NASA-CR-176347; NAS 1.26:176347; SASR-4) Avail: NTIS HC A08/MF A01 CSCL 03A

Presented are scientific objectives, engineering analysis and design, and results of technology development for a Three-Meter Balloon-Borne Far-Infrared and Submillimeter Telescope. The scientific rationale is based on two crucial instrumental capabilities: high angular resolution which approaches eight arcseconds at one hundred micron wavelength, and high resolving power spectroscopy with good sensitivity throughout the telescope's 30-micron to 1-mm wavelength range. The high angular resolution will allow us to resolve and study in detail such objects as collapsing protostellar condensations in our own galaxy, clusters of protostars in the Magellanic clouds, giant molecular clouds in nearby galaxies, and spiral arms in distant galaxies. The large aperture of the telescope will permit sensitive spectral line measurements of molecules, atoms, and ions, which can be used to probe the physical, chemical, and dynamical conditions in a wide variety of objects. Author

N86-13272*# Citadel Coll., Charleston, S.C.
THE FIELD HORIZONTAL-BRANCH STAR HD 109995: NEW RESULTS WITH COADDED ULTRAVIOLET AND OPTICAL REGION SPECTRA
Saul J. Adelman and David S. Leckrone 1985 8 p refs
(Grant NAG5-218)
(NASA-CR-176327; NAS 1.26:176327) Avail: NTIS HC A02/MF A01 CSCL 03A

A comprehensive ultraviolet and optical region abundance analysis of the field horizontal branch Population 2 A-type star HD 109995 is described. Coaddition of IUE high dispersion images and DAO 6.5 A/mm IIaO spectrograms improved the signal-to-noise ratio of the data. We have identified ultraviolet lines whose analysis will provide more complete and accurate elemental abundances than those obtained from optical region spectra alone. A preliminary elemental abundance analysis of the optical region shows that log Z/Z (solar) approx. = -2. A first attempt to synthesize two Fe 2 ultraviolet resonance lines yields an iron abundance a few tenths of a deg higher than the average obtained from optical region Fe 2 lines. Author

N86-13273*# Missouri Univ., St. Louis. Dept. of Physics.
ULTRAVIOLET OBSERVATIONS OF LOW-EXCITATION HERBIG-HARO OBJECTS Final Technical Report, Jul. 1982 - Sep. 1985
Richard D. Schwartz 1985 4 p refs
(Grant NAG5-243)
(NASA-CR-176164; NAS 1.26:176164) Avail: NTIS HC A02/MF A01 CSCL 03A

The Herbig-Haro (HH) objects rank among the faintest objects (v approx. 17) observed with the I.U.E. Expectations that the low-excitation shock-excited HHs should be dominated by H two-photon (2q) UV emission were borne out in the first observation of HH 43 and 47 obtained in 1982. The UV continuous energy distributions in the SWP spectra of these objects were found to peak near 1500 Angstroms as predicted by the 2q hypothesis. In addition, emission lines in the Lyman band of H sub 2, excited by Lyman alpha fluorescence, were detected in HH 43. It is not clear if the molecular gas is coextensive with the atomic gas responsible for the optical emission, or if the molecular gas is immediately adjacent to the region of optical emission. The two-photon energy distribution and H sub 2 fluorescent emission were previously discussed. G.L.C.

N86-13274*# Smithsonian Astrophysical Observatory, Cambridge, Mass.
COMBINED ULTRAVIOLET STUDIES OF ASTRONOMICAL SOURCE Semiannual Progress Report, 1 Feb. - 31 Jul. 1985
A. K. Dupress, S. L. Baliunas, W. P. Blair, L. W. Hartmann, J. P. Huchra, J. C. Raymond, G. H. Smith, and D. R. Soderblom Aug. 1985 12 p refs
(Grant NAG5-87)
(NASA-CR-176165; NAS 1.26:176165; SAPR-10) Avail: NTIS HC A02/MF A01 CSCL 03A

As part of its Ultraviolet Studies of Astronomical Sources the Smithsonian Astrophysical Observatory for the period 1 Feb. 1985 to 31 July 1985 observed the following: the Cygnus Loop; oxygen-rich supernova remnants in 1E0102-72; the Large Magellanic Cloud supernova remnants; P Cygni profiles in dwarf novae; soft X-ray photoionization of interstellar gas; spectral variations in AM Her stars; the mass of Feige 24; atmospheric inhomogeneities in Lambda Andromedae and FF Aquarii; photometric and spectroscopic observation of Capella; Alpha Orionis; metal deficient giant stars; M 67 giants; high-velocity winds from giant stars; accretion disk parameters in cataclysmic variables; chromospheric emission of late-type dwarfs in visual binaries; chromospheres and transient regions of stars in the Ursa Major group; and low-metallicity blue galaxies. F.M.R.

N86-12410# Joint Publications Research Service, Arlington, Va.
MICROCOMPUTER-CONTROLLED CLOSED-LOOP SYSTEM FOR POSITIONING RADIO TELESCOPE
Zhu Liqing, Chu Yingyi, and Zhang Zhenchao *In its* China Rept.:

Sci. and Technol. (JPRS-CST-85-017) 11 Jun. 1985 p 69-77 ref Transl. into ENGLISH from Wei Jisuanji Yingyong (Beijing), no. 4, Nov. 1984 p 26-30 (For primary document see N86-12408 03-31)
Avail: NTIS HC A08/MF A01

90 ASTROPHYSICS

Includes cosmology; and interstellar and interplanetary gases and dust.

N86-13275 Texas Univ., Austin.
PHYSICO-CHEMICAL CONDITIONS IN CIRCUMSTELLAR SHELLS OF EVOLVED OXYGEN-RICH M STARS Ph.D. Thesis
David Bruce Slavsky 1985 287 p
Avail: Univ. Microfilms Order No. DA8513301

The physical and chemical conditions in circumstellar shells of evolved oxygen-rich stars were studied. Time dependent non-equilibrium chemical calculations for several gas phase species were performed to determine their radially dependent abundances. The species are formed from the eight elements H, C, N, O, S, Si, Al, and Cl. The energy equation included contributions from the cooling of the gas due to expansion, heating from gas-grain collisions, and molecular cooling from 2CO, and H_2O. The circumstellar chemistry is also affected by ultraviolet radiation. It was found that the total column density through the shell determines two important shell characteristics. Higher densities result in large non-adiabatic contributions to the energy equation, and it is shown that for the highest densities studied, the temperature profile is determined by the non-adiabatic terms. The total column density determines the optical depth through the shell in the UV, which controls the position in the shell where photo-induced chemistry can begin. Radial abundances of species such as OH, SiO, and SO, which can be formed as a result of H_2O dissociation, are diagnostic of the total column density of gas through the shell. Observations of H_2O and other molecules in shells of stars possessing chromospheres place constraints on the total density through the shell. It is shown that changing the total density by an order of magnitude leads to large changes in the total attenuation of UV radiation, which determines the level of molecular association. Author

N86-13276 California Univ., Berkeley.
WAVE PROPAGATION AND PAIR FORMATION IN PULSAR MAGNETOSPHERES Ph.D. Thesis
John Juil Barnard 1984 215 p
Avail: Univ. Microfilms Order No. DA8512748

The propagation of electromagnetic waves through a relativistically outflowing electron positron plasma is investigated. The requirements for the formation of such a plasma in pulsar magnetospheres are determined. The refraction of electromagnetic waves through pulsar magnetosphere is investigated. The dispersion relation is derived for propagation in an equal density electron positron plasma in the approximation that the magnetic field is infinite, for both cold and hot distribution functions. The energy transfer rate of Alfven waves is calculated into fast mode waves from two different mechanisms: linear gradient coupling and nonlinear wave-wave coupling. The relevancy of these mechanisms to pulsars is discussed. The minimum requirements are calculated for pair creation in a pulsar magnetic field with dipolar and quadrupolar components, for several scenarios concerning the evolutionary history of the magnetic field. Dissert. Abstr.

N86-13277 California Univ., Berkeley.
DIFFRACTION-LIMITED TEN MICRON IMAGING OF CIRCUMSTELLAR DUST WITH A DETECTOR ARRAY Ph.D. Thesis
Eric Edward Bloemhof 1984 148 p
Avail: Univ. Microfilms Order No. DA8512759

An imaging system has been constructed which achieves diffraction limited spatial resolution (about 0.6) at a wavelength of 10 micro m on large telescopes. The system uses an array of 25 photovoltaic detectors in the focal plane, arranged along two crossed arms. The very small physical size of individual detectors, and the use of drift scans made with a stationary telescope, permit reliable imaging on a spatial scale not easily probed before. Several broad band interference filters (with delta lambda/lambda approx. 0.1) permit imaging on and off the 9.7 micro m spectral feature due to silicate dust particles. The array system has been used to map the circumstellar dust envelopes of several late type stars, including alpha Scorpii, Orionis, and IRC + 10216. The first two objects, oxygen rich type M supergiants, show faint extended emission around an unresolved stellar photosphere which dominates the surface brightness. Particularly accurate east-west profiles of the brightness distributions are obtained, and in the case of alpha Orionis a distinct east-west asymmetry was observed in February 1983. Dissert. Abstr.

N86-13278# Lawrence Livermore National Lab., Calif.
NUCLEAR INFORMATION NEEDS FOR THE ASTROPHYSICAL s-PROCESS
G. J. Mathews, W. M. Howard, K. Takahashi, and R. A. Ward May 1985 6 p Presented at the Intern. Conf. on Nucl. Data for Basic and Appl. Sci., Santa Fe, N. Mex., 13 May 1985
(Contract W-7405-eng-48)
(DE85-012913; UCRL-917-5; CONF-850507-32) Avail: NTIS HC A02/MF A01

The astrophysical s process is a sequence of neutron capture and beta decay reactions on a slow time scale compared to beta decay lifetimes near the line of stability. We systematically study this detailed sequence of neutron capture, continuum and bound state beta decay, positron decay, and electron capture reactions that comprise the s process for a broad range of astrophysical environments. Our results are then compared with the solar system abundances of heavy elements to determine the range of physical conditions responsible for their nucleosynthesis. The nuclear data needs are extensive but have begun to be precise enough to allow for a consistent interpretation of the astrophysical site for the s process. DOE

91 LUNAR AND PLANETARY EXPLORATION

Includes planetology; and manned and unmanned flights. For spacecraft design see *18 Spacecraft Design Testing, and Performance*. For space stations see *15 Launch Vehicles and Space Vehicles*.

N86-13279*# California Univ., San Diego, La Jolla. Center for Astrophysics and Space Sciences.
TRAPPED PARTICLE ABSORPTION BY THE RING OF JUPITER Final Report, 1 Sep. 1984 - 31 Aug. 1985
Walker Fillius 31 Aug. 1985 48 p refs
(Grant NAGw-652)
(NASA-CR-174408; NAS 1.26:174408) Avail: NTIS HC A03/MF A01 CSCL 03B

The ring systems of Jupiter and Saturn, and their interaction with the magnetosphere were studied. Opportunities to improve the understanding of the sweeping effect of orbiting material on trapped radiation, and the use of this process to gain insight on both the trapped radiation and the target material are outlined. Within the cosmogony of Hannes Alfven, this mechanism is also the key to understanding the formation of many of the features of the Saturnian rings. A better understanding of the sweeping effect would also help to clarify this process. For individual titles, see N86-13280 through N86-13281.

N86-13280*# National Aeronautics and Space Administration. Goddard Space Flight Center, Greenbelt, Md.
A NOTE ON JUPITER'S GOSSAMER RING Final Report
D. A. Mendis, J. R. Hill, W. Fillius, and T. G. Northrop *In* California Univ., San Diego, La Jolla Trapped Particle Absorption by the Ring of Jupiter 31 Aug. 1985 9 p refs Prepared in cooperation

with California Univ., San Diego, La Jolla (For primary document see N86-13279 03-91)
(Grants NsG-7102; NAGw-399; NAGw-336)
Avail: NTIS HC A03/MF A01 CSCL 03B

The newly discovered gossamer ring of Jupiter, composed largely of micron-sized grains, exhibits a significant peak very near the synchronous radius. It is believed that this peak is associated with an unobserved source consisting of large bodies that straddle the synchronous orbit. An alternative evolutionary mechanism is offered, which is the gyrophase drift towards the synchronous orbit, of fine grains, which necessarily are electrostatically charged within the Jovian magnetosphere. E.A.K.

N86-13281*# National Aeronautics and Space Administration. Goddard Space Flight Center, Greenbelt, Md.
ELECTRONS AND COSMIC RAY PRODUCED IN SATURN'S INNER MAGNETOSPHERE
T. G. Northrop and Walker Fillius (California Univ., San Diego, La Jolla) *In* California Univ., San Diego, La Jolla Trapped Particle Absorption by the Ring of Jupiter 31 Aug. 1985 30 p refs
Previously announced as N85-26546 (For primary document see N86-13279 03-91)
(Grants NAGw-336; NAGw-652)
Avail: NTIS HC A03/MF A01 CSCL 03B

The Cerenkov detector on Pioneer 11 previously observed Crand protons above 600 MeV in Saturn's inner magnetosphere, mixed with a poorly understood background of energetic electrons. The electron count is separated from the proton counts and the first-order angular distributions are established for each species. To do this the theoretical relationships among the harmonic coefficients of the count rate is used as a function of spacecraft roll angle. The majority of the counts were electrons with energy above several MeV; i.e., with drift periods shorter than the satellite orbital resonance. The electrons have isotropic pitch angle distributions, and the protons pancake over most of the region between Nimas and the rings, although there is a small region of dumbbell proton distributions in the vicinity of Janus and Epimetheus. Author

N86-13282*# Lunar and Planetary Inst., Houston, Tex.
WORKSHOP ON WATER ON MARS
Stephen Clifford, ed. Dec. 1984 109 p refs Workshop held at Moffett Field, Calif., 30 Nov. - 1 Dec. 1984
(Contract NASw-3389)
(NASA-CR-176289; NAS 1.26:176289; LPI-TR-85-03) Avail: NTIS HC A06/MF A01 CSCL 03B

The opening session of the Workshop focused on one of the most debated areas of Mars volatiles research-the size of the planet's past and present bulk water content. Current estimates of the inventory of H2O on Mars range from an equivalent layer of liquid 10-1000 meters deep averaged over the planet's surface. The most recent of these estimates, presented at the Workshop, is based on the now popular belief that the SNC class of meteorites represent actual samples of the Martian crust. From a model of planetary accretion and degassing founded on this assumption, it was determined that the present inventory of H2O on Mars is equivalent to a global layer no more than 50 meters deep. During the discussion generated by this estimate, several investigators expressed reservations about an H2O inventory as small as a few tens of meters, for it appears to directly contradict the seemingly abundant morphologic evidence that Mars is (or has been) water rich. Others, however, argued that the interpretation of much of this morphologic evidence is at best equivocal and that the case for a wet Mars is far from established. Atmospheric water vapor measurements, compiled by Earth based telescopes and the Viking Orbiter Mars Atmospheric Water Detectors (MAWD), now span a period of over six Martian years. Analysis of this data suggests that the seasonal cycle is governed by both the sublimation and condensation of H2O at the poles and by its adsorption/desorption within the regolith. So far, efforts to simulate the seasonal vapor cycle have failed to reproduce the observed behavior. B.W.

92 SOLAR PHYSICS

Includes solar activity, solar flares, solar radiation and sunspots.

N86-13283# Iowa Univ., Iowa City. Dept. of Physics and Astronomy.
ANALYSIS AND INTERPRETATION OF THE SHOCK-LIKE ELECTROSTATIC NOISE OBSERVED DURING THE AMPTE (ACTIVE MAGNETOSPHERIC PARTICLE TRACER EXPLORERS) SOLAR WIND LITHIUM RELEASES Progress Report
D. A. Gurnett, T. Z. Ma, R. R. Anderson, O. H. Bauer, and G. Haerendel May 1985 51 p
(Contracts N00014-76-C-0016; N00014-82-K-0183)
(AD-A157512; U-OF-IOWA-85-13) Avail: NTIS HC A04/MF A01 CSCL 03/2

During the AMPTE (Active Magnetospheric Particle Tracer Explorers) solar wind lithium release on September 11, and again on September 20, 1984, an intense burst of electrostatic noise was observed near the upstream edge of the ion cloud. Comparisons with measurements by the IMP-6 and ISEE-1 spacecraft show that the spectrum and overall features of this noise are very similar to electrostatic noise observed at the Earth's bow shock. A stability analysis using realistic parameters shows that the electrostatic noise can be accounted for by an ion beam-plasma instability caused by the solar wind proton beam streaming through the nearly stationary lithium cloud. The growth rate of this instability is largest when the ion density and solar wind proton density are similar, which explains why the noise only occurs near the outer edge of the ion cloud. The similarity to the noise in the Earth's bow shock suggest that a shock may exist in the solar wind plasma flow upstream of the ion cloud. If the noise is associated with a shock, then it must be an electrostatic shock, since the ion cyclotron radii are too small for the existence of a MHD shock. Since the electrostatic instability occurs at phase velocities near the lithium thermal velocity, the electrostatic turbulence may play a role in heating the lithium ions and transferring momentum from the solar wind to the ion cloud. GRA

N86-13284# Iowa Univ., Iowa City. Dept. of Physics and Astronomy.
A STATISTICAL STUDY OF SOLAR TYPE-3 BURSTS AND AURORAL KILOMETRIC RADIATION ONSETS Progress Report
W. M. Farrell and D. A. Gurnett Mar. 1985 38 p
(Contract N00014-76-C-0016)
(AD-A158408; U-OF-IOWA-85-7) Avail: NTIS HC A03/MF A01 CSCL 04/1

Simultaneous occurrences of Type-3 solar radio bursts and auroral kilometric radiation were observed by Calvert using ISEE-1 spectrograms. He presented evidence suggesting that the incoming Type-3 burst stimulates the onset of auroral kilometric radiation. This paper presents a statistical study of the correlation between Type-3 bursts and auroral kilometric radiation. A superposed epoch analysis was performed on as many as 186 Type-3 events. The Type-3 bursts were detected by the ISEE-3 spacecraft on the sunward side of the Earth. At the same time the IMP-8 spacecraft was used to detect onsets of kilometric radiation on the nightside of the Earth. For each event, the intensities measured by ISEE-3 (Type-3 intensities) were subtracted from the intensities measured by IMP-8 (Type 3 and possible AKR intensities). The resulting intensities for each event were then added to determine if kilometric radiation was preferentially observed following a Type-3 burst. This analysis was performed at frequencies of 100 kHz, 178 kHz and 500 kHz. The results of this study show that a statistically significant correlation exists between incoming Type-3 bursts from the Sun and kilometric radiation from the Earth. GRA

93 SPACE RADIATION

Includes cosmic radiation; and inner and outer Earth's radiation belts.

For biological effects of radiation see *52 Aerospace Medicine*. For theory see *73 Nuclear and High-Energy Physics*.

N86-13285*# Carnegie Institution of Washington, D. C.
X-RAYS FROM THE RADIO HALO OF VIRGO A = M87
[1985] 43 p refs
(Grants NAG8-357; NSF AST-83-51447)
(NASA-CR-176303; NAS 1.26:176303) Avail: NTIS HC A03/MF A01 CSCL 03B

The purpose of this study is to investigate in more detail the associated X-ray and radio emission in the Virgo A halo discovered by SGF. Improved Einstein HRI data and new radio maps obtained with the Very Large Array are described and the relation between the X-ray and radio structures is carefully examined. Several possible explanations are presented for the X-ray emission. The inverse compton model is found to be viable only if the magnetic field is variable and substantially weaker than the equipartition value. The principal alternative is excess thermal X-rays due to compression of the intracluster medium by the radio lobe. In either case, the association of such prominent radio and X-ray structures is unique among known radio galaxies. B.W.

N86-12687# Joint Publications Research Service, Arlington, Va.
HIGH-ELEVATION STATION'S COSMIC-RAY RECORDING SYSTEM Abstract Only
In its USSR Rept.: Earth Sci. (JPRS-UES-85-006) 19 Jun. 1985 p 71 Transl. into ENGLISH from Izv. (Moscow), 5 Apr. 1985 p 3
(For primary document see N86-12630 03-42)
Avail: NTIS HC A05/MF A01

99 GENERAL

No abstracts in this category.

SUBJECT INDEX

SCIENTIFIC AND TECHNICAL AEROSPACE REPORTS VOLUME 24 NUMBER 3

Typical Subject Index Listing

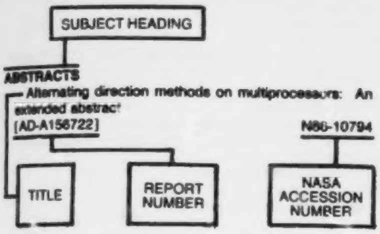

The subject heading is the key to the subject content of the document. Titles, report numbers, and accession numbers of pertinent documents are provided under each subject heading. When the title is insufficiently descriptive of the document content, a title extension has been added, separated from the title by three hyphens. The report number helps to indicate the type of document cited (e.g., NASA report, NASA translation, NASA contractor report). The NASA accession number is the number by which the document abstracts are arranged in this journal and by which the document is sold or requested. The titles, with title extensions if present, are arranged under each subject heading in ascending accession number order. The subject headings have been selected from the latest revision of the *NASA Thesaurus* (NASA SP-7051).

A

ABIOGENESIS
Organic components in atmosphere in regions of volcanic activity N86-12693

ABSORBERS (MATERIALS)
Absorption fluids data survey
[DE85-005279] N86-12792

ABSORPTION
Room modes and sound absorption: Some practical measurements compared with theoretical predictions
[BBC-RD-1985/11] N86-12486

ABSORPTION COOLING
Comparative first- and second-law analysis of an absorption cycle
[DE85-015066] N86-13215

ABSORPTION SPECTRA
Film stability for dirct absorption receivers
[DE85-012135] N86-12791
Study of possible solarization - related impurities in CaF2 and other fluorides
[DE85-014100] N86-13135
Absorption spectroscopy as a density diagnostic for dense imploded shells
[DE85-014413] N86-13175

ABSORPTION SPECTROSCOPY
Absorption spectroscopy as a density diagnostic for dense imploded shells
[DE85-014413] N86-13175

ABSORPTIVITY
Influence of a surfactant additive on absorption heat pump performance
[DE85-013995] N86-12574
Estimate of radiation-climatic effects of natural and anthropogenic aerosol N86-12640
Modeling of seasonal evolution of carbon cycle in ocean-atmosphere system N86-12641

ABSTRACTS
Survey and expository papers on topics of current interest in applied mathematics
[AD-A158418] N86-13229

ABUNDANCE
The field horizontal-branch star HD 109995: New results with coadded ultraviolet and optical region spectra
[NASA-CR-176327] N86-13272

AC GENERATORS
Preliminary design of linear alternator dynamometer for free piston Stirling engines
[DE85-015078] N86-12614

ACCELERATION (PHYSICS)
Mantle viscosity, J2 and the nontidal acceleration of Earth rotation N86-12879

ACCELERATION STRESSES (PHYSIOLOGY)
G protection by an extreme crouch position
[AD-A157081] N86-12213

ACCELERATION TOLERANCE
G protection by an extreme crouch position
[AD-A157081] N86-12213

ACCELEROMETERS
BLR studies on conic model with LDA in FL-1 wind tunnel N86-12434

ACCEPTABILITY
Development and evaluation of a microburst test apparatus for use as a minimum destructive test for parachute material
[AD-A158110] N86-12620

ACCIDENT PREVENTION
Hydrocarbon fuels N86-12329
Anhydrous ammonia N86-12330
The hydrazine fuels N86-12331
Nitromethane N86-12332
Ethylene oxide N86-12333
Otto fuel 2 N86-12334
Hydrogen and deuterium N86-12335
The boranes N86-12336
Carbon monoxide N86-12337
Oxygen N86-12338
Fluorine and fluorine mixtures N86-12339
The halogen fluorides N86-12340
Nitrogen oxides N86-12341
Fuming nitric acids N86-12342
Iodine N86-12343
Chlorine N86-12344
Nitrogen trifluoride N86-12345
Hydrogen peroxide N86-12346
Nitrogen N86-12347
Noble gases N86-12348
The alcohols N86-12349
Halocarbons N86-12350
Hydraulic fluids N86-12351
Mercury N86-12352
Compressed and liquid air N86-12353
Carbon dioxide N86-12354
Nitrous oxide N86-12355
Liquid propellant storage compatibility N86-12356
Quantity-distance requirements N86-12357

ACCUMULATORS
High current fiber brush collector and method for making same
[AD-D011627] N86-12512

ACETATES
Investigation of test methods, material properties and processes for solar cell encapsulants
[DE85-012831] N86-12786

ACETYL COMPOUNDS
Cortical plasticity: Theoretical analysis, experimental results
[AD-A157965] N86-12961

ACID RAIN
Perspectives to establish knowledge linkages between acidic deposition and vegetation responses
[DE85-011839] N86-12796
Interpretation of individual precipitation chemistry data sets: General condiserations and approaches
[DE85-012449] N86-12800
Spatial and temporal patterns of acid precipitation and their interpretation
[PB85-214377] N86-12809
Acid precipitation: Source identification and its effects on water quality
[PB85-214880] N86-12810

ACIDITY
Acidification trends in surface waters of the Southern Appalachians
[DE85-901746] N86-12801

ACOUSTIC ATTENUATION
Ultrasonic attenuation in clean anisotropic superconductors
[DE85-012178] N86-12621
Evaluation of honeycomb highway sound barrier I-280 section 8B, Harrison, New Jersey
[PB85-231157] N86-13063

ACOUSTIC DUCTS
A method for determining acoustic-liner admittance in ducts with sheared flow in two-cross-sectional directions
[NASA-TP-2518] N86-13056

ACOUSTIC IMPEDANCE
A method for determining acoustic-liner admittance in ducts with sheared flow in two-cross sectional directions
[NASA-TP-2518] N86-13056

ACOUSTIC MEASUREMENTS
Dummy head microphone and its application to the measurements of electro-acoustic equipments N86-12379
A method for determining acoustic-liner admittance in ducts with sheared flow in two-cross-sectional directions
[NASA-TP-2518] N86-13056

ACOUSTIC PROPAGATION
Temporal and spatial variabilities in shallow water acoustics: Measurements and predictions
[AD-A156718] N86-12942

ACOUSTIC PROPERTIES
Effects of microstructure on the acoustoelastic measurements of stress
[DE85-015518] N86-12307

ACOUSTIC SCATTERING
Sound scattering by a layered sphere
[AD-A157915] N86-13060

ACOUSTIC SOUNDING
Acoustic methods for featuring high-frequency part of spectrum of sea waves N86-12706
Atmospheric turbulence investigations at Tsimlyansk Scientific Station, Atmospheric Physics Institute, USSR Academy of Sciences N86-12735
Prediction of sound fields in acoustical cavities using the boundary element method
[NASA-CR-176295] N86-13057

ACOUSTIC VELOCITY
Interaction of sound waves with fine thermohaline structures of ocean N86-12647
Sound velocities in liquid lead at high temperatures
[DE85-014091] N86-13062

ACOUSTICS
Investigation of the flame-acoustic wave interaction during axial solid rocket instabilities
[AD-A158559] N86-12362
China report: Science and technology
[JPRS-CST-85-024] N86-12368
Research Reports of the Faculty of Engineering, Tokyo Denki University, no. 32
[ISSN-0389-617-X] N86-12372
China report: Science and technology
[JPRS-CST-85-022] N86-12439
China report: Science and technology
[JPRS-CST-85-026] N86-12459
Wideband SAW (Surface Acoustic Wave) channelizer using slanted array input transducer
[AD-D011857] N86-12517
Development of acoustic agglomerator. Test plan for high temperature high pressure acoustic agglomerator
[DE85-017221] N86-13061

ACOUSTO-OPTICS
Acoustically tuned optical filter system
[AD-D011791] N86-13184

ACQUISITION
AISIM (Automated Interactive-Simulation Modeling System) overview: Revision 1
[AD-A157392] N86-12990

ACRYLIC RESINS
Study on electropainting using alkoxymethylmelamine as crosslinking agent N86-12380
ACTIVITY (BIOLOGY)
Composition and photochemical reactivity of turbine engine exhaust
[AD-A157643] N86-12230
Raman activity in synchronously dividing bacteria
[DE85-015672] N86-12951
ACTUATORS
Pneumatic actuator device
[AD-D011794] N86-12217
Advanced torque converters for robotics and space applications
[NASA-CR-177987] N86-12610
ADA (PROGRAMMING LANGUAGE)
Advanced avionics computer architecture. Volume 1. Executive summary
[AD-A158119] N86-12222
Advanced avionics computer architecture. Volume 2. Instruction set architecture specification
[AD-A158120] N86-12223
ADAPTIVE CONTROL
An application of adaptive learning to malfunction recovery
[AD-A158129] N86-12236
Adaptive Kalman filtering with control input estimation
N86-12503
ADAPTIVE OPTICS
Adaptive optical filtering techniques
[AD-A157072] N86-13126
ADDITIVES
Fatigue crack propagation of nickel-base superalloys at 650 deg C
[NASA-TM-87150] N86-12294
Influence of a surfactant additive on absorption heat pump performance
[DE85-013995] N86-12574
ADHESION TESTS
Application of heat-scan NDT to inspection of adhesion of solid rocket motor propellant to envelope
N86-12461
ADHESIVE BONDING
Mixed-mode cyclic debonding of adhesively bonded composite joints
[NASA-CR-177991] N86-12255
ADHESIVES
Compartmented, filament wound, one-piece aircraft fuel tanks
[AD-D011793] N86-12225
ADIABATIC CONDITIONS
Microwave field strength measurement in a Rubidium clock cavity via adiabatic rapid passage
[AD-A157070] N86-13065
A dressed atom interpretation of adiabatic rapid passage
[AD-A157071] N86-13066
ADIABATIC EQUATIONS
Behavior of ionized plasma in the high latitude topside ionosphere
[AD-A157930] N86-13140
ADJOINTS
Variational principle for penetrator dynamics using bilinear functional and adjoint formulation
[AD-A157964] N86-13031
ADSORPTION
Adsorption/desorption properties of vacuum materials for the 6 GeV synchrotron
[DE85-010276] N86-12252
Raman spectroscopy of molecular adsorbates
[DE85-012981] N86-12280
Development of a supported liquid membrane as a nickel-zinc secondary battery separator
[DE85-012591] N86-12784
AERIAL PHOTOGRAPHY
Video terminal for analyzing aerial infrared photographs N86-12688
Correcting a digital map data base with scene analysis concepts and methods
[AD-A157913] N86-12745
AERODYNAMIC CHARACTERISTICS
Aerodynamic characteristics of a propulsive wing-canard concept at STOL speeds
[NASA-CR-177982] N86-12205
AERODYNAMIC CONFIGURATIONS
Aerodynamic characteristics of a propulsive wing-canard concept at STOL speeds
[NASA-CR-177982] N86-12205
Development of an analytical model and code for the flapping response of a Hawte rotor blade
[DE85-008806] N86-12211
AERODYNAMIC DRAG
Length adjustable strut link with low aerodynamic drag
[AD-D011851] N86-12232
AERODYNAMIC INTERFERENCE
Derivation of jack movement influence coefficients as a basis for selecting wall contours giving reduced levels of interference in flexible walled test sections
[NASA-CR-177992] N86-12204
AERODYNAMIC STABILITY
Development of an analytical model and code for the flapping response of a Hawte rotor blade
[DE85-008806] N86-12211
Interactive aircraft flight control and aeroelastic stabilization
[NASA-CR-176323] N86-12233
AERODYNAMIC STALLING
Air Force Academy Aeronautics Digest
[AD-A157215] N86-12200
Compressor research facility F100 high pressure compressor inlet total pressure and swirl profile simulation
[AD-A157108] N86-12229
Post stall maneuvers and thrust vectoring performance analysis
[AD-A158100] N86-12235
AERODYNAMICS
China report: Science and technology
[JPRS-CST-85-032] N86-12462
AEROELASTICITY
Interactive aircraft flight control and aeroelastic stabilization
[NASA-CR-176323] N86-12233
AERONAUTICAL ENGINEERING
A survey of aeronautical structural research in Australia
[AD-A157211] N86-12199
Computer aided instruction in engineering
[AD-A156828] N86-13220
Aeronautical technology 2000: A projection of advanced vehicle concepts
[NASA-CR-176322] N86-13235
AERONAUTICS
Computer aided instruction in engineering
[AD-A156828] N86-13220
AEROSOLS
Thermophoretic separation of aerosol particles from a sampled gas stream
[DE85-011672] N86-12277
The orientation distribution of nonspherical aerosol particles within a cloud
[AD-A157363] N86-12554
Atmospheric aerosol and its effects on climate
N86-12636
Estimate of radiation-climatic effects of natural and anthropogenic aerosol N86-12640
Global modeling of optical characteristics of atmospheric aerosol N86-12695
Diurnal variation of optical and microphysical characteristics of near-surface aerosol N86-12696
AEROSPACE ENGINEERING
The aerospace spacecraft charging document
[AD-A157664] N86-12248
AEROSPACE ENVIRONMENTS
China report: Science and technology
[JPRS-CST-85-035] N86-12399
Precipitating electron and ion detectors (SSJ/4) for the block 5D/Flights 6-10 DMSP (Defense Meteorological Satellite Program) satellites: Calibration and data presentation
[AD-A157080] N86-12896
USSR Space Life Sciences Digest, Issue 2
[NASA-CR-3922(02)] N86-12949
Microgravity science and applications bibliography, 1985 revision
[NASA-TM-86176] N86-13225
Neutral mass spectrometer measurements in the shuttle bay environment N86-13245
Enhanced N(+) sub 2 in the shuttle environment
N86-13248
Spacecraft-induced plasma energization and its role in flow phenomena N86-13250
A mechanism for the local concentration enhancement of the shuttle atmosphere N86-13252
AEROSPACE MEDICINE
USSR Space Life Sciences Digest, Issue 2
[NASA-CR-3922(02)] N86-12949
Aerospace Medicine and Biology Continuing Bibliograph: A continuing bibliography with indexes
[NASA-SP-7011(276)] N86-12954
AEROSPACE VEHICLES
The aerospace spacecraft charging document
[AD-A157664] N86-12248
AGGLOMERATION
Development of acoustic agglomerator. Test plan for high temperature high pressure acoustic agglomerator
[DE85-017221] N86-13061
AGING (MATERIALS)
Investigation of test methods, material properties and processes for solar cell encapsulants
[DE85-012831] N86-12786
AGING (METALLURGY)
Properties of a retrogressed and re-aged 7075 aluminum alloy
[AD-A157415] N86-12298
Combined small angle X-ray scattering and transmission electron microscope studies of Al-Li alloys
[DE85-016356] N86-12303
Review of effects of long-term aging on the mechanical properties and microstructures of types 304 and 316 stainless steel
[DE85-016472] N86-12304
AGRICULTURE
Flutter clearance tests on a Transavia PL-12/T-400 Skyfarmer
[AD-A157212] N86-12234
AIR CONDITIONING
Indoor Air Quality Modeling Workshop report
[PB85-212306] N86-12803
AIR DEFENSE
Radio-absorbing materials
[AD-A157496] N86-12495
Pilot's associate definition study
[AD-A157106] N86-13028
AIR DROP OPERATIONS
Parachute recovery systems design manual, chapters 1 through 4 offprint
[AD-A157639] N86-12210
AIR FLOW
Isothermal dehumidification of air in a parallel passage configuration
[DE85-008819] N86-12577
Experimental study of flow and dispersion in the wakes of three-dimensional low hills
[PB85-193266] N86-12906
AIR LAND INTERACTIONS
Recent changes in climate and world water balance
N86-12638
AIR MASSES
Some results of study of blocking layers on days with vertically developed cloud cover of Caucasus-Caspian region on basis of aerospace information N86-12698
AIR POLLUTION
Analysis of particulates in the exhaust plume of a J52-P3 turbojet engine at military power
[AD-A157640] N86-12231
China report: Science and technology
[JPRS-CST-85-018] N86-12413
Climatically active trace gases in atmosphere
N86-12639
Indoor Air Quality Modeling Workshop report
[PB85-212306] N86-12803
Assessment of the long-term precision of continuous emission monitors
[PB85-201150] N86-12804
Evaluation of air emissions from hazardous waste treatment, storage and disposal facilities
[PB85-203792] N86-12806
AIR QUALITY
Indoor Air Quality Modeling Workshop report
[PB85-212306] N86-12803
Assessment of the long-term precision of continuous emission monitors
[PB85-201150] N86-12804
Summary of precision and accurace assessments for the state and local air monitoring netowrks, 1982
[PB85-208171] N86-12805
AIR SAMPLING
Organic components in atmosphere in regions of volcanic activity N86-12693
AIR TRAFFIC CONTROL
Statistical sampling of aircraft operations at non-towered airports
[AD-A157095] N86-13051
AIR TRANSPORTATION
Report of accomplishments under the airport improvement program
[AD-A156834] N86-12241
AIR WATER INTERACTIONS
Empirical analysis of direct and inverse relationships between macroscale characteristics of atmospheric processes in northern hemisphere and thermal state of north Atlantic N86-12635
Modeling of seasonal evolution of carbon cycle in ocean-atmosphere system N86-12641
Ionic mechanicsm of exchange of admixtures between hydrosphere and atmosphere N86-12690
Evaluating influence of waves on dynamic structure of atmospheric near-water layer N86-12694
Quasigeostrophic model of circulation in Antarctic Ocean with parametrization of synoptic eddies N86-12702

Marine boundary layer from air-sea interface to inversion
[PB85-188274] N86-12948

AIRBORNE EQUIPMENT
Advanced Moisture and Temperature Sounder (AMTS) baseline 5 study report
[NASA-CR-176331] N86-12919

AIRCRAFT ANTENNAS
Simulation of the enhanced traffic alert and collision avoidance system (TCAS 2)
[NASA-CR-176326] N86-12216

AIRCRAFT COMPARTMENTS
Aircraft interior panel test criteria derived from full-scale fire tests
[FAA/CT-85/23] N86-12214

AIRCRAFT CONFIGURATIONS
The helicopter to fixed wing conversion program: A critical review
[AD-A156820] N86-12968

AIRCRAFT DESIGN
Flutter clearance tests on a Transavia PL-12/T-400 Skyfarmer
[AD-A157212] N86-12234
Aeronautical technology 2000: A projection of advanced vehicle concepts
[NASA-CR-176322] N86-13235

AIRCRAFT EQUIPMENT
Navy should join the Air Force and Army program to develop an advanced integrated avionics system
[PB85-222503] N86-12224
Compartmented, filament wound, one-piece aircraft fuel tanks
[AD-D011793] N86-12225

AIRCRAFT INSTRUMENTS
T-33 (Silver Star MK 3) pitot-static system calibration
[AD-A157854] N86-12221
Navy should join the Air Force and Army program to develop an advanced integrated avionics system
[PB85-222503] N86-12224

AIRCRAFT PERFORMANCE
Optical technique to study the impact of heavy rain on aircraft performance
[NASA-CR-177969] N86-12580

AIRCRAFT PILOTS
An application of adaptive learning to malfunction recovery
[AD-A158129] N86-12236

AIRCRAFT SAFETY
FAA (Federal Aviation Administration) could improve overall aviation safety and reduce costs associated with airport instrument landing systems
[PB85-195444] N86-12215

AIRCRAFT STRUCTURES
Flutter clearance tests on a Transavia PL-12/T-400 Skyfarmer
[AD-A157212] N86-12234

AIRFOILS
Air Force Academy Aeronautics Digest
[AD-A157215] N86-12200
GRUMFOIL: A computer code for the viscous transonic flow over airfoils
[NASA-CR-3806] N86-12202
The status of two-dimensional testing at high transonic speeds in the University of Southampton transonic self-streamlining wind tunnel
[NASA-CR-3919] N86-12203
Aerodynamic characteristics of a propulsive wing-canard concept at STOL speeds
[NASA-CR-177982] N86-12205
An improved viscid/inviscid interaction procedure for transonic flow over airfoils
[NASA-CR-3805] N86-12208
An evaluation of four methods of numerical analysis for two-dimensional airfoil flows. Revision
[AD-A157248] N86-12209
Improved temperature detection system for use on film cooled turbine airfoils
[AD-D011762] N86-12228

AIRFRAMES
A survey of aeronautical structural research in Australia
[AD-A157211] N86-12199

AIRGLOW
The Atmosphere Explorer and the shuttle glow
N86-13243
Orbiter glow observations at high spectral resolution
N86-13244
The UV-VIS optical environment of the shuttle
N86-13247

AIRPORT PLANNING
Statistical sampling of aircraft operations at non-towered airports
[AD-A157095] N86-13051

AIRPORTS
FAA (Federal Aviation Administration) could improve overall aviation safety and reduce costs associated with airport instrument landing systems
[PB85-195444] N86-12215
Report of accomplishments under the airport improvement program
[AD-A156834] N86-12241
CBR (California Bearing Ratio) design of flexible airfield pavements with case study
[AD-A158101] N86-12242

AIRSPEED
T-33 (Silver Star MK 3) pitot-static system calibration
[AD-A157854] N86-12221
Interactive aircraft flight control and aeroelastic stabilization
[NASA-CR-176323] N86-12233

ALBEDO
Ocean albedo for atmospheric thermal emission
N86-12707

ALCOHOLS
Liquid chromatography on silica using mobile phases containing tetraalkylammonium hydroxides. 1: General separation selectivity and behavior of polar compounds typically in fuels
[DE85-014450] N86-12281

ALGAE
Aquatic Species Program review: Proceedings of Principal Investigators Meeting
[DE85-012137] N86-12364

ALGEBRA
Program for simple algebra
[DE85-013426] N86-13013

ALGORITHMS
Derivation of jack movement influence coefficients as a basis for selecting wall contours giving reduced levels of interference in flexible walled test sections
[NASA-CR-177992] N86-12204
Optimization of the locomotion of a legged vehicle with respect to maneuverability N86-12371
Bandwidth efficient frequency-shift keyed communication systems N86-12472
DAA modal analysis for parametric investigations of fluid-structure interaction in underwater shock, revision 1
[DE85-012935] N86-12569
Kyoto meteor radar observation in November, 1981 and May, 1982 N86-12847
Clear sky brightness temperature over the western north Pacific Ocean from GMS spacecraft N86-12911
A theory for algorithm-based fault tolerance in array processor systems
[AD-A156244] N86-12977
Numerical algorithms and mathematical software for linear control and estimation theory
[AD-A157525] N86-12992
Control of step size and order in extrapolation codes
[DE85-013261] N86-13010
Penalized likelihood for general semi-parametric regression models
[AD-A158133] N86-13034
Global optimization using automatic differentiation and interval iteration
[AD-A158150] N86-13039
Control of step size and order in extrapolation codes
[DE85-010122] N86-13041
New representations of the non-central chi-square density and cumulative
[AD-A157227] N86-13046
Conversion of the bounce-averaged Fokker-Planck code to conversion form
[DE85-014861] N86-13160
Decentralized control of scheduling in distributed systems
[AD-A157656] N86-13222

ALIGNMENT
LAMPF transition-region mechanical fabrication
[DE85-012688] N86-13081

ALIPHATIC COMPOUNDS
Studies of the Bauer piezoelectric polymer gauge (PVF2) under impact loading
[DE85-014707] N86-12590

ALKALI METALS
Electron-spin-polarized targets for a collisionally-pumped polarized-ion source
[DE85-015276] N86-13174

ALKALIES
The inhomogeneous light shift in alkali atoms
[AD-A157498] N86-13067

ALKALINE BATTERIES
Evaluation parameters for the alkaline fuel cell oxygen electrode
[NASA-TM-87155] N86-12266

ALLOCATIONS
Spectrum resource assessment of the 1605-2000 kHz band
[PB85-225076] N86-12501

ALLOYS
Effect of pulsed irradiation on microstructural evolution
[DE85-016317] N86-12302

ALPHA PARTICLES
Partition of cross sections in asymmetric nucleus-nucleus reactions and the origin of fast alpha particles
[DE85-014989] N86-13089
Chemistry of berkelium: A review
[DE85-017523] N86-13102

ALPS MOUNTAINS (EUROPE)
Dynamics and structure of the Alpine Fold Belt
N86-12854

ALTIMETERS
Geopotential Research Mission (GRM)
[NASA-CP-2390] N86-12852

ALTITUDE SIMULATION
Wind tunnel turning vanes of modern design
[NASA-TM-87416] N86-12239
Method to detect ethylene glycol in gaseous mixtures
[AD-A158109] N86-12272

ALTITUDE TESTS
T-33 (Silver Star MK 3) pitot-static system calibration
[AD-A157854] N86-12221

ALUMINUM
Effects of microstructure on the acoustoelastic measurements of stress
[DE85-015518] N86-12307
Foil fuses as opening switches for slow discharge circuits
[DE85-014124] N86-12519
Hillock-free conductor system for use in multilevel interconnects
[DE85-012595] N86-12533
Design of foil implosion system for Pioneer 1 experiments
[DE85-014111] N86-12535
Encapsulant selection and durability testing experience N86-12774

ALUMINUM ALLOYS
Microstructure/Property relationships for carbon fiber reinforced aluminum alloys
[AD-A157858] N86-12261
Research on the microstructure of rapidly solidified alloys
[AD-A157077] N86-12296
Properties of a retrogressed and re-aged 7075 aluminum alloy
[AD-A157415] N86-12298
Resistance to fracture, fatigue and stress-corrosion of Al-Cu-Li-Zr alloys
[AD-A158407] N86-12300
Combined small angle X-ray scattering and transmission electron microscope studies of Al-Li alloys
[DE85-016356] N86-12303
Theory for the Portevin-LeChatelier effect
[DE85-004030] N86-12627

ALUMINUM NITRIDES
X-ray diffraction studies of shock-modified inorganic materials
[DE85-015150] N86-13209

ALUMINUM OXIDES
Surface crystallization on metallized 94 percent alumina ceramics
[DE85-008691] N86-12324
Dynamic ADI computations of thermoelastic stresses in crystalline laser media
[DE85-010478] N86-12606
Tritium control in helium-cooled blankets
[DE85-014783] N86-13116
X-ray diffraction studies of shock-modified inorganic materials
[DE85-015150] N86-13209

AMBIENT TEMPERATURE
Surface fatigue life and failure characteristics of EX-53, CBS 1000M, and AISI 9310 gear materials
[NASA-TP-2513] N86-12609

AMERICIUM
Accidental exposure to americium
[DE85-012794] N86-12965

AMERICIUM 241
Chemistry of berkelium: A review
[DE85-017523] N86-13102

AMINES
Development of a supported liquid membrane as a nickel-zinc secondary battery separator
[DE85-012591] N86-12784

AMMONIA
Anhydrous ammonia N86-12330
TATE: Strong basic reactions provide soluble derivations for simple qualititative high explosive spot test
[DE85-014259] N86-12366

AMMUNITION
Wear of projectile rotating bands
[AD-A156666] N86-12358

AMORPHOUS MATERIALS
Reliability and Engineering of Thin-Film Photovoltaic Modules. Research forum proceedings [NASA-CR-176217] N86-12759
Light-induced effects-impacts to module performance measurements and reliability testing: An overview N86-12761
Thin-film module circuit design: Practical and reliability aspects N86-12762
Accelerated stress testing of thin film solar cells: Development of test methods and preliminary results N86-12764
Interconnect resistance of photovoltaic submodules N86-12767
Amorphous silicon photovoltaic modules and test devices design, fabrication and testing N86-12769
Module voltage isolation and corrosion research N86-12772
Glass breaking strength: The role of surface flaws and treatments N86-12773

AMPLIFICATION
Improved approach to characterizing and presenting streak camera performance [DE85-015188] N86-12587
User's manual for using MASON: A frequency response program which handles a system of transfer functions described by a signal flow graph [PB85-227106] N86-13021
Adaptive optical filtering techniques [AD-A157072] N86-13126

AMPLIFIERS
Demountable coaxial electrical connector for in-line amplifiers [AD-D011831] N86-12507
Stochastic beam cooling amplifier system front end components performance characteristics [DE85-013925] N86-13079

AMPLITUDE DISTRIBUTION ANALYSIS
Hybrid radar waveform design utilizing complementary phase coding and linear frequency stepping for achieving improved slant range resolution in a synthetic aperature radar N86-12470

AMPLITUDE MODULATION
The role of amplitude-to-phase conversion in the generation of oscillator flicker phase noise [NASA-TM-87590] N86-12508

AMPLITUDES
Effect of surface waviness on a supercritical laminar-flow-control airfoil [NASA-TM-85705] N86-12206
Laboratory study of regular low-amplitude gravity capillary waves in nonstationary current N86-12671
Results of the May 1982 ATMAP campaign at the Meteor Wind Station Kuehlungsborn (54 deg N, 12 deg E), GDR N86-12841

ANAEROBES
Anaerobic microbial dissolution of toxic metals in subsurface environments [DE85-013308] N86-12251

ANALYSIS (MATHEMATICS)
China report: Science and technology [JPRS-CST-85-026] N86-12459
Analytical and experimental studies of wakes behind circularly capped bubbles N86-12548
Automated reasoning and various applications [DE85-014998] N86-12997
Stefan's problem in a finite domain with constant boundary and initial conditions analysis [AD-A158558] N86-13040
Plasma and magnetospheric research [NASA-CR-176326] N86-13138

ANALYTIC FUNCTIONS
Hyperbolic systems of conservation laws in several space variables [DE85-014019] N86-13042

ANALYTICAL CHEMISTRY
China report: Science and technology [JPRS-CST-85-018] N86-12413

ANGLE OF ATTACK
Performance of an alpha-vane and pitot tube in simulated heavy rain environment [NASA-CR-176353] N86-12220
Post stall maneuvers and thrust vectoring performance analysis [AD-A158100] N86-12235
Non-linear corrections to the linear theory for the prediction of the cavitating flow around hydrofoils [AD-A158105] N86-12557

ANGLES (GEOMETRY)
Compressor research facility F100 high pressure compressor inlet total pressure and swirl profile simulation [AD-A157108] N86-12229
Space shuttle ram glow: Implication of NO2 recombination continuum N86-13241

ANGULAR DISTRIBUTION
Angular distribution of intensity of sound reradiated by ocean surface at small glancing angles N86-12643
High nuclear temperatures by antimatter-matter annihilation [DE85-014113] N86-13090
Measurements and calculations of neutron scattering angular distributions over a wide mass and energy range [DE85-012912] N86-13105

ANGULAR RESOLUTION
Soybean canopy reflectance modeling data sets [E86-10005] N86-12741
Balloon-borne three-meter telescope for far-infrared and submillimeter astronomy [NASA-CR-176347] N86-13271

ANISOTROPIC MEDIA
Method for solving problems in electrodynamics of anisotropic media with slant bedding N86-12684
Derivation of the optical constants of anisotropic [AD-A158396] N86-13195

ANISOTROPY
Preparation and properties of thin film reversible cathode materials [AD-A158431] N86-12273
Thermodynamics of multi-polar molecules: The perturbed-anisotropic-chain theory [DE85-013148] N86-12274
Behavior of ionized plasma in the high latitude topside ionosphere [AD-A157930] N86-13140
Mossbauer effect and neutron diffraction study of the anomalous lattice behavior of U6Fe [DE85-014912] N86-13210

ANNEALING
High frequency silicon bipolar transistor with SIPOS (Semi-insulating polycrystalline silicon) heterojunction emitter and ion implanted rapid thermal annealed base region [AD-A157141] N86-12510
Thin film module electrical configuration versus electrical performance N86-12770

ANNIHILATION REACTIONS
High nuclear temperatures by antimatter-matter annihilation [DE85-014113] N86-13090
A p anti p collider physics: Summary talk [DE85-014782] N86-13097
Multiplicities in high energy interactions [DE85-013847] N86-13100
Search for narrow structure in proton-antiproton annihilation cross sections from 1900 to 1960 MeV [DE85-013302] N86-13119
Dynamical model of quark rearrangement in nucleon-antinucleon annihilation [DE85-013904] N86-13120

ANNUAL VARIATIONS
Recent changes in climate and world water balance N86-12638
Synthesis of research and development in mechanical energy storage technologies [DE85-013313] N86-12782
Planetary waves N86-12821
Gravity waves N86-12822
Annual and semiannual cycles based on the middle atmosphere reference model N86-12826
On the interannual variability and on trends of the temperature in the middle atmosphere N86-12827
A proposed international tropical reference atmosphere up to 80 km N86-12828

ANODES
Deactivation and poisoning of fuel cell catalysts [DE85-015127] N86-12521

ANOMALIES
The source of the Earth's long wavelength geoid anomalies: Implications for mantle and core dynamics N86-12872
Do MAGSAT anomalies contain a record of past and present-day mantle convection under South America? N86-12895
Theory of the anomalous Doppler instability during lower-hybrid current drive [DE85-014064] N86-13170
Classical geometrical interpretation of ghost fields and anomalies in Yang-Mills theory and quantum gravity [DE85-014537] N86-13214

ANTARCTIC REGIONS
Recent changes in climate and world water balance N86-12638
Cyclonic frontal eddy in Antarctic circumpolar current N86-12675
USSR report: Earth sciences [JPRS-UES-85-008] N86-12697
Quasigeostrophic model of circulation in Antarctic Ocean with parametrization of synoptic eddies N86-12702
Underground volcanoes discovered with satellite radar N86-12721

ANTENNA ARRAYS
Design of an antenna feed system to produce a uniform field N86-12469
Model experiments with slot antenna arrays for imaging N86-12482
A new integrated slot element feed array for multi-beam systems N86-12483
A 94 GHz imaging array using slot line radiators [NASA-CR-176348] N86-12484

ANTENNA COMPONENTS
Analysis of the tem mode linearly tapered slot antenna N86-12481

ANTENNA DESIGN
China report: Science and technology [JPRS-CST-85-030] N86-12451
Computer-aided analysis of arbitrary-shaped thin-wire antennas N86-12452
Design of an antenna feed system to produce a uniform field N86-12469
Near millimeter wave imaging/multi-beam integrated antennas [NASA-CR-176332] N86-12478
Analysis of the tem mode linearly tapered slot antenna N86-12481
Model experiments with slot antenna arrays for imaging N86-12482
A new integrated slot element feed array for multi-beam systems N86-12483

ANTENNA FEEDS
Design of an antenna feed system to produce a uniform field N86-12469
Additional results on the radiating properties of LTSAs and CWSAs N86-12479

ANTENNA RADIATION PATTERNS
Design of an antenna feed system to produce a uniform field N86-12469
Near millimeter wave imaging/multi-beam integrated antennas [NASA-CR-176332] N86-12478
Additional results on the radiating properties of LTSAs and CWSAs N86-12479
Characteristic impedance of a wide slot line on low permittivity substrates N86-12480
Analysis of the tem mode linearly tapered slot antenna N86-12481
Model experiments with slot antenna arrays for imaging N86-12482
Strategy for reflector pattern calculation: Let the computer do the work [NASA-TM-87137] N86-12485

ANTENNAS
Computer-aided analysis of arbitrary-shaped thin-wire antennas N86-12452
Demountable coaxial electrical connector for in-line amplifiers [AD-D011831] N86-12507
Adaptive optical filtering techniques [AD-A157072] N86-13126
Alfven wave heating on Tokapole 2 [DE85-014859] N86-13179

ANTICYCLONES
Theory of solitary anticyclones in rotating fluid N86-12669

ANTINUCLEONS
Dynamical model of quark rearrangement in nucleon-antinucleon annihilation [DE85-013904] N86-13120

ANTIPARTICLES
Conference summary: Antinucleon- and nucleon-nucleus interactions [DE85-013905] N86-13114

ANTIPROTONS
Suppression of propagating TE modes in the FNAL antiproton source stochastic beam cooling system [DE85-016559] N86-13074
Tests of orbital dynamics using the Tevatron [DE85-012296] N86-13085
A p anti p collider physics: Summary talk [DE85-014782] N86-13097
Search for narrow structure in proton-antiproton annihilation cross sections from 1900 to 1960 MeV [DE85-013302] N86-13119
Comparison between theoretical predictions and tracking [DE85-012104] N86-13149

ANTIRADAR COATINGS
Radio-absorbing materials [AD-A157496] N86-12495

ANTIREFLECTION COATINGS
High damage threshold porous silica antireflective coating [DE85-012924] N86-12322

APERTURES
Design of an antenna feed system to produce a uniform field N86-12469

Analysis of the tem mode linearly tapered slot antenna N86-12481
Use of an elliptical aperture to control saturation in closely-coupled, cold iron, superconducting dipole magnets [DE85-012259] N86-13053
Shocking behavior of fluid flow in deformable joints [DE85-010104] N86-13107

APPENDAGES
Numerical and experimental studies of 3-D and unsteady turbulent body/appendage/propeller flows [AD-A157078] N86-12552

APPROPRIATIONS
Making appropriations for the Department of Housing and Urban Development, and for sundry independent agencies, boards, commissions, corporations, and offices for the fiscal year ending September 30, 1986, and for other purposes [H-REPT-99-363] N86-13231
National Aeronautics and Space Administration N86-13232

APPROXIMATION
New corresponding states theory using the second virial coefficient as the temperature variable [PB85-219624] N86-12289
Finite difference scheme for one-dimensional magnetohydrodynamic equations N86-12464
Renormalization of an inverse scattering theory for inhomogeneous dielectrics [AD-A157224] N86-12492
Interfacial stability in a two-layer benard problem [AD-A158138] N86-12558
Modeling and control of flexible structures [AD-A157959] N86-12625
Compound poisson approximations for sums of random variables [AD-A158555] N86-13049
Plane-wave theory of electrical transport in disordered systems [DE85-015353] N86-13167

AQUATIC PLANTS
Aquatic Species Program review: Proceedings of Principal Investigators Meeting [DE85-012137] N86-12364

AQUEOUS SOLUTIONS
Kinetics of evaporation and growth of drops of aqueous solutions of surface active substances at negative temperatures [AD-A156961] N86-12269
TATE: Strong basic reactions provide soluble derivations for simple qualititative high explosive spot test [DE85-014259] N86-12366

AQUICULTURE
Aquatic Species Program review: Proceedings of Principal Investigators Meeting [DE85-012137] N86-12364

AQUIFERS
Design of a statewide groundwater monitoring network for Illinois [PB85-192821] N86-12750
Synthesis of research and development in mechanical energy storage technologies [DE85-013313] N86-12782

ARABIAN SEA
Squall and cloud lines as structural components of an Arabian Sea convective cloud cluster [AD-A157973] N86-12925

ARC DISCHARGES
Arc discharge conditioning test on the Oak Ridge 25 URC accelerator [DE85-016394] N86-12523

ARC WELDING
Fusion welding research [AD-A158127] N86-12611

ARCHITECTURE
CBR (California Bearing Ratio) design of flexible airfield pavements with case study [AD-A158101] N86-12242

ARCHITECTURE (COMPUTERS)
Advanced avionics computer architecture. Volume 1. Executive summary [AD-A158119] N86-12222
Advanced avionics computer architecture. Volume 2. Instruction set architecture specification [AD-A158120] N86-12223
Method of using CTC to microcomputerize digital instruments N86-12441
Fault tolerant statistical signal processing algorithms for parallel architectures [AD-A157393] N86-12978
Generic software for emulating multiprocessor architectures [AD-A157662] N86-12979
The design and hardware evaluation of an advanced 16-bit, low-power, high performance microcomputer system for digital signal processing [AD-A158130] N86-12981

ARCTIC REGIONS
USSR report: Earth sciences [JPRS-UES-85-008] N86-12697
Carbon dioxide in arctic and subarctic regions [DE85-014054] N86-12901
Low temperature inflator apparatus [AD-D011810] N86-12974

AREA
Large-area thin-film modules N86-12766
Interconnect resistance of photovoltaic submodules N86-12767

ARGON
China develops 6J KrF laser N86-12465

ARID LANDS
Evaluation of the NWS (National Weather Service) soil moisutre accounting model for automated flash flood forecasting in small arid and semi-arid watersheds [PB85-229722] N86-12928

ARMED FORCES (UNITED STATES)
The C-17: We need it yesterday [AD-A157147] N86-12219
Energy expenditure and activity patterns of cadets at the United States Military Academy, West Point, New York [AD-A157857] N86-12960
The helicopter to fixed wing conversion program: A critical review [AD-A156820] N86-12968
Using the information resource dictionary system command language [PB85-227783] N86-12988
Information systems plan [AD-A157911] N86-13227

ARRAYS
Numerical computation of full three-dimensional flow in transonic turbines N86-12397
Evaluation and implementation of testability schemes for gate array integrated circuit design [DE85-012874] N86-12526
Thin-film module circuit design: Practical and reliability aspects N86-12762
Accelerated stress testing of thin film solar cells: Development of test methods and preliminary results N86-12764
Electrical safety requirements: Implications for the module designer N86-12765
Outdoor performance testing of thin-film devices N86-12771
A theory for algorithm-based fault tolerance in array processor systems [AD-A156244] N86-12977
Parallel implementation of multifrontal schemes [DE85-014295] N86-13015
Relationships between prime-rich Euler type equations and a triangular array of the odd integers [AD-A157928] N86-13030

ARSENIC
Anaerobic microbial dissolution of toxic metals in subsurface environments [DE85-013308] N86-12251

ARTIFICIAL INTELLIGENCE
An analysis of the application of AI to the development of intelligent aids for flight crew tasks [NASA-CR-3944] N86-12212
Diagnosing cognitive errors: Statistical pattern classification and recognition approach [AD-A158108] N86-12972
Automated reasoning and various applications [DE85-014998] N86-12997
Application of automated reasoning software procedure generation system verifier [DE85-014000] N86-13008
Attempt to develop an intelligent lens design program [DE85-014122] N86-13017
Artificial intelligence in Ada: Pattern-directed processing [AD-A157097] N86-13025
Pilot's associate definition study [AD-A157106] N86-13026
Knowledge-based systems: How will they affect manufacturing in the 80's [DE85-010601] N86-13027
Department of Housing and Urban Development, and Certain Other Independent Agencies Appropriations for Fiscal Year 1986, part 1 [S-HRG-99-221-PT-1] N86-13233
National Aeronautics and Space Administration N86-13234

ARTIFICIAL SATELLITES
Launch of Kosmos-1653 natural resources research satellite N86-12719

ARTILLERY
Wear of projectile rotating bands [AD-A156666] N86-12358

ASPECT RATIO
Disruption and luminosity of flat beams [DE85-015137] N86-13071

ASPHERICITY
Mathematical principle for generating second-order aspherical surface N86-12436

ASSESSMENTS
Options for operational risk assessments [DE85-014904] N86-12390
Spectrum resource assessment of the 1605-2000 kHz band [PB85-225076] N86-12501

ASSIMILATION
Petrochemical types of magmatic rocks of ocean floor and patterns of their distribution N86-12650

ASTRODYNAMICS
China report: Science and technology [JPRS-CST-85-035] N86-12399

ASYMMETRY
Partition of cross sections in asymmetric nucleus-nucleus reactions and the origin of fast alpha particles [DE85-014989] N86-13089

ASYMPTOTIC SERIES
Secondary electron spectra: A semiempirical model [DE85-012448] N86-13086

ATLANTIC OCEAN
Features of geostrophic circulation related to nature of bottom relief in northwestern Atlantic N86-12674
Structure of sedimentary cover and basement of Sierra Leone Rise determined from common depth point seismic (equatorial Atlantic) N86-12709
Fine structure of density relation in main oceanic thermocline N86-12711

ATMOSPHERIC ATTENUATION
Ionic mechanicsm of exchange of admixtures between hydrosphere and atmosphere N86-12691

ATMOSPHERIC BOUNDARY LAYER
Diurnal variation of optical and microphysical characteristics of near-surface aerosol N86-12696
Experimental study of flow and dispersion in the wakes of three-dimensional low hills [PB85-193266] N86-12906
Modeling the diurnal variation of meteorological variables within the boundary layer: Preliminary comparison results [PB85-198349] N86-12933
Marine boundary layer from air-sea interface to inversion [PB85-188274] N86-12948

ATMOSPHERIC CHEMISTRY
Perspectives to establish knowledge linkages between acidic deposition and vegetation responses [DE85-011839] N86-12796
Interpretation of individual precipitation chemistry data sets: General condiserations and approaches [DE85-012449] N86-12800
Analysis and assessment of US-WMO regional precipitation chemistry measurements (1972-1982), a subject of the National Trends Network [PB85-212959] N86-12807

ATMOSPHERIC CIRCULATION
Diagnosis of weather states in winter of 1980-1981 N86-12632
Empirical analysis of direct and inverse relationships between macroscale characteristics of atmospheric processes in northern hemisphere and thermal state of north Atlantic N86-12635
Study of significance of bottom relief in baroclinic model of equatorial countercurrent N86-12642
Some results of study of blocking layers on days with vertically developed cloud cover of Caucasus-Caspian region on basis of aerospace information N86-12698
Real-time computing of the environmental consequences of an atmospheric accidental release of radioactive material: User's point of view [DE85-016438] N86-12795
Middle Atmosphere Program. Handbook for MAP. Volume 16: Atmospheric structure and its variation in the region 20 to 120 km. Draft of a new reference middle atmosphere [NASA-CR-176321] N86-12814
Gravity waves N86-12822
Results of November 1981 and May 1982 ATMAP campaigns at Adelaide (35 deg S, 138 deg E) N86-12850
Large-scale circulation departures related to wet episodes in northeast Brazil [NASA-CR-176352] N86-12916
The nature of symmetric instability and its similarity to convective and inertial instability [NASA-CR-3945] N86-12918

Observational-numerical study of maritime extratropical cyclones using FGGE (First GARP Global Experiment) data [NASA-CR-176297] N86-12922
Comparison among various thermodynamic parameters for the prediction of convective activity [PB85-208217] N86-12932

ATMOSPHERIC COMPOSITION
Organic components in atmosphere in regions of volcanic activity N86-12693
Spatial and temporal patterns of acid precipitation and their interpretation [PB85-214377] N86-12809
Carbon dioxide in arctic and subarctic regions [DE85-014054] N86-12901

ATMOSPHERIC DENSITY
Mean density scale heights from analysis of variation in perigee height of China's second satellite N86-12396
Contribution to the CIRA model from ground-based lidar N86-12835

ATMOSPHERIC EFFECTS
Atmospheric aerosol and its effects on climate N86-12636
Influence of power engineering on climate N86-12637
Climatically active trace gases in atmosphere N86-12639
Estimate of radiation-climatic effects of natural and anthropogenic aerosol N86-12640
Modeling of seasonal evolution of carbon cycle in ocean-atmosphere system N86-12641
Real-time computing of the environmental consequences of an atmospheric accidental release of radioactive material: User's point of view [DE85-016438] N86-12795

ATMOSPHERIC ELECTRICITY
Electromagnetic effects in crustal fracturing N86-12727

ATMOSPHERIC MODELS
Diagnosis of weather states in winter of 1980-1981 N86-12632
Atmospheric aerosol and its effects on climate N86-12636
Global modeling of optical characteristics of atmospheric aerosol N86-12695
Interim reference ozone models for the middle atmosphere N86-12829
Mean winds of the upper middle atmosphere (60-110 km): A global distribution from radar systems (MF, meteor, VHF) N86-12831

ATMOSPHERIC MOISTURE
Humidity profile mesurements in atmospheric lower layer by spontaneous Raman scattering method N86-12736

ATMOSPHERIC OPTICS
Ionic mechanicsm of exchange of admixtures between hydrosphere and atmosphere N86-12691
Global modeling of optical characteristics of atmospheric aerosol N86-12695
Diurnal variation of optical and microphysical characteristics of near-surface aerosol N86-12696

ATMOSPHERIC PHYSICS
USSR report: Earth sciences [JPRS-UES-85-006] N86-12630
High-elevation station's cosmic-ray recording system N86-12687
USSR report: Earth sciences [JPRS-UES-85-008] N86-12697
Atmospheric turbulence investigations at Tsimlyansk Scientific Station, Atmospheric Physics Institute, USSR Academy of Sciences N86-12735

ATMOSPHERIC PRESSURE
Human hemodynamic change under high atmospheric pressure N86-12458
A proposed international tropical reference atmosphere up to 80 km N86-12828

ATMOSPHERIC REFRACTION
The measurement of tropospheric refractive index relevant to the study of anomalous microwave propagation: Review and recommendations [CRC-1387] N86-12471

ATMOSPHERIC SCATTERING
Ionic mechanicsm of exchange of admixtures between hydrosphere and atmosphere N86-12691

ATMOSPHERIC SOUNDING
Temperature data from satellites N86-12815
Advanced Moisture and Temperature Sounder (AMTS) baseline 5 study report [NASA-CR-176331] N86-12919

ATMOSPHERIC STRATIFICATION
Some results of study of blocking layers on days with vertically developed cloud cover of Caucasus-Caspian region on basis of aerospace information N86-12698

ATMOSPHERIC TEMPERATURE
Temperature data from satellites N86-12815
Observed winds and temperatures in the Southern Hemisphere N86-12817
Middle atmosphere reference model derived from satellite data N86-12819
Planetary waves N86-12821
Comparison of time-periodic variations in temperature and wind from meteorological rockets and satellites N86-12825
Annual and semiannual cycles based on the middle atmosphere reference model N86-12826
On the interannual variability and on trends of the temperature in the middle atmosphere N86-12827
A proposed international tropical reference atmosphere up to 80 km N86-12828

ATMOSPHERIC TIDES
Atmospheric tides below 80 km N86-12824
Atmospheric tides between 80 km and 120 km N86-12833
Middle Atmosphere Program. Handbook for MAP, volume 17 [NASA-CR-176345] N86-12837
Atmospheric Tides Middle Atmosphere Program (ATMAP): Report of the November/December 1981, and May 1982, observational campaigns N86-12839
Data descriptions and vertical structure plots for mean, diurnal, and semidurnal components of eastward and northward (ordered by latitude). Mean winds and tides over Poker Flat, Alaska (65 deg N, 147 deg W), during November 1981 N86-12840
Remarks on the ATMAP campaigns in November 1981 and May 1982 at Collm (52 deg N, 15 deg E) N86-12842
Saskatoon M. F. radar system: (52 deg N, 107 deg W), Canada N86-12843
May 1982, Saskatoon M. F. radar system: (52 deg N, 107 deg W), Canada N86-12844
Meteor wind results at Durham (43 deg N, 71 deg W) during the ATMAP November 1981 and May 1982 campaigns N86-12845
Mean winds and tides over Urbana, Illinois during November 16-22, 1981 N86-12846
Kyoto meteor radar observation in November, 1981 and May, 1982 N86-12847
Mesospheric winds and tides at Arecibo/puerto Rico (18 deg N, 67 deg W) November 20-23, 1981 N86-12848
Mesospheric winds at Jicamaraca, Peru (12 deg S, 77 deg SW), November 19-21, 1981 N86-12849
Results of November 1981 and May 1982 ATMAP campaigns at Adelaide (35 deg S, 138 deg E) N86-12850
Middle atmosphere tides at Christchurch (44 deg S, 17 deg E) in November 1981 and May 1982 N86-12851

ATMOSPHERIC TURBULENCE
Turbulence in the altitude region 80-120 km N86-12834
Data descriptions and vertical structure plots for mean, diurnal, and semidurnal components of eastward and northward (ordered by latitude). Mean winds and tides over Poker Flat, Alaska (65 deg N, 147 deg W), during November 1981 N86-12840

ATMOSPHERICS
Diagnosis of weather states in winter of 1980-1981 N86-12632

ATOMIC BEAMS
Activated recombinative desorption: A potential component in mechanisms of spacecraft glow N86-13258
A ground-based experimental test program to duplicate and study the spacecraft glow phenomenon N86-13260
Application of an atomic oxygen beam facility to the investigation of shuttle glow chemistry N86-13261

ATOMIC CLOCKS
Microwave field strength measurement in a Rubidium clock cavity via adiabatic rapid passage [AD-A157070] N86-13065
The inhomogeneous light shift in alkali atoms [AD-A157498] N86-13067

ATOMIC COLLISIONS
Ground-based investigations of atomic oxygen interactions with space station surfaces [DE85-014082] N86-12249

ATOMIC ENERGY LEVELS
Studies of energy storage and transfer in gas lasers [AD-A158553] N86-12604

ATOMIC EXCITATIONS
A model for explaining some features of shuttle glow N86-13256
The production of glow precursors by oxidative erosion of spacecraft surfaces N86-13257
Activated recombinative desorption: A potential component in mechanisms of spacecraft glow N86-13258
Optical radiation from the interaction of energetic atoms, ions, electrons, and photons with surfaces N86-13259
Application of an atomic oxygen beam facility to the investigation of shuttle glow chemistry N86-13261

ATOMIC PHYSICS
A dressed atom interpretation of adiabatic rapid passage [AD-A157071] N86-13066

ATOMIC SPECTRA
The inhomogeneous light shift in alkali atoms [AD-A157498] N86-13067
A model for explaining some features of shuttle glow N86-13256
The field horizontal-branch star HD 109995: New results with coadded ultraviolet and optical region spectra [NASA-CR-176327] N86-13272

ATOMIC STRUCTURE
Diffraction and microscopy studies of the structure of grain boundaries in Fe, Fe-base alloys and ceramic materials [DE85-016950] N86-13198
Electronic stakes in disordered solids. Part 3: Applications to materials science [DE85-011416] N86-13213

ATOMS
The inhomogeneous light shift in alkali atoms [AD-A157498] N86-13067

ATTENUATION
Suppression of propagating TE modes in the FNAL antiproton source stochastic beam cooling system [DE85-016559] N86-13074

ATTITUDE (INCLINATION)
Recent results of an internal tilt mode calculation in FRCs [DE85-014121] N86-13177

AUDIO FREQUENCIES
High pressure and molecular weight variation of electrical relaxation in poly(ethylene oxide) [AD-A157660] N86-12317

AUGER EFFECT
Activated recombinative desorption: A potential component in mechanisms of spacecraft glow N86-13258

AUGER SPECTROSCOPY
Raman spectroscopy of molecular adsorbates [DE85-012981] N86-12280
Ellipsometric surface analysis of wear tracks produced by different lubricants [NASA-TM-87142] N86-12293
Theoretical studies of deep impurity levels in ternary semiconductor alloys [AD-A157929] N86-13193

AURORAL IRRADIATION
A statistical study of solar Type-3 bursts and auroral kilometric radiation onsets [AD-A158408] N86-13284

AURORAS
Precipitating electron and ion detectors (SSJ/4) for the block 5D/Flights 6-10 DMSP (Defense Meteorological Satellite Program) satellites: Calibration and data presentation [AD-A157080] N86-12896
An alternative interpretation of ion ring distribution observed by the S3-3 satellite [AD-A157655] N86-12898

AUSTENITIC STAINLESS STEELS
Special metallographic procedures for austenitic stainless steel welds [DE85-010113] N86-12305

AUSTRALIA
Why do we need detailed gravity over continents: Some Australian examples N86-12855

AUTOCLAVES
Metal dissolution kinetics in organic solvents using rotating ring-disc voltammetry [DE85-013478] N86-12253
Fischer-Tropsch synthesis in slurry reactor systems [DE85-013390] N86-12278

AUTOMATA THEORY
Automated reasoning and various applications [DE85-014998] N86-12997

AUTOMATIC CONTROL
Investigation of magnetic field measurements [AD-A157924] N86-12900
Automatic detection of gulf stream rings [AD-A157934] N86-12945
Attempt to develop an intelligent lens design program [DE85-014122] N86-13017
Department of Housing and Urban Development, and Certain Other Independent Agencies Appropriations for Fiscal Year 1986, part 1 [S-HRG-99-221-PT-1] N86-13233
National Aeronautics and Space Administration N86-13234

AUTOMATION
Word lists to limit vocabulary in technical information [AD-A157931] N86-13228

AVIONICS

Advanced avionics computer architecture. Volume 1. Executive summary [AD-A158119] N86-12222

Advanced avionics computer architecture. Volume 2. Instruction set architecture specification [AD-A158120] N86-12223

Navy should join the Air Force and Army program to develop an advanced integrated avionics system [PB85-222503] N86-12224

Introduction to operational ASDAR system N86-12915

AXIAL FLOW PUMPS

Fluid machines: Expanding the limits, past and future [NASA-TM-87161] N86-12227

AXISYMMETRIC BODIES

Turbulence models for boundary layers on axisymmetric bodies [AD-A158552] N86-12561

AXISYMMETRIC FLOW

Measurements on an axisymmetric jet in a slow coflowing stream N86-12549

AXONS

Effects of cation ions in nerve excitation N86-12377

B

BACKGROUND NOISE

Data requirements for verification of ram glow chemistry N86-13265

BACKSCATTERING

Scattering experiments at the Ipswich Electromagnetic Measurements Facility: Backscatter from metal cubes [AD-A157925] N86-12496

Remote diagnosis of media by combination (Raman) anti-Stokes light scattering method with induced Brillouin backscattering N86-12705

BACTERIA

Raman activity in synchronously dividing bacteria [DE85-015672] N86-12951

BAGS

Forward field autotransfusion device [AD-D011763] N86-12957

BAKING

Adsorption/desorption properties of vacuum materials for the 6 GeV synchrotron [DE85-010276] N86-12252

BALLISTICS

Influence of water vapor on distribution of turuulent wave parameters N86-12659

BALLOON-BORNE INSTRUMENTS

Balloon-borne three-meter telescope for far-infrared and submillimeter astronomy [NASA-CR-176347] N86-13271

BANACH SPACE

Vector valued long James type Banach spaces J(eta, l sub p)(1 or = p + infinity) N86-12463

Hamilton-Jacobi equations in infinite dimensions. Part 2: Existence of viscosity solutions [AD-A158137] N86-13035

BANDS

Wear of projectile rotating bands [AD-A156666] N86-12358

BANDWIDTH

Bandwidth efficient frequency-shift keyed communication systems N86-12472

A 94 GHz imaging array using slot line radiators [NASA-CR-176348] N86-12484

Microwave ridged waveguide beam pickups [DE85-013816] N86-12499

BAROCLINIC INSTABILITY

Study of significance of bottom relief in baroclinic model of equatorial countercurrent N86-12642

BAROTROPIC FLOW

Study of significance of bottom relief in baroclinic model of equatorial countercurrent N86-12642

BARREN LAND

Feasibility of using LANDSAT images of vegetation cover to estimate effective hydraulic properties of soils [E86-10003] N86-12739

BARRIER LAYERS

A TiW diffusion barrier for AuZn ohmic contacts to p-type InP [AD-D011823] N86-12511

BASALT

Petrologic aspect of formation of geostructures in marginal seas N86-12657

Spreading in development of oceanic structures N86-12658

Tectonics of eastern Kronotskiy Peninsula and formational association of basalts (Kamchatka) N86-12732

MAGNUM-2D computer code: User's guide [DE85-013315] N86-13001

BATHYMETERS

Data analysis of airborne electromagnetic bathymetry [AD-A157132] N86-12744

Lithospheric structure in the Pacific geoid N86-12863

Properties of the lithosphere and asthenosphere deduced from geoid observations N86-12867

BATTERY CHARGERS

Thin film module development N86-12766

BAYARD-ALPERT IONIZATION GAGES

Precision ion vacuum gage with logarithmic response [DE85-015312] N86-12588

BAYS (STRUCTURAL UNITS)

Survey of ultraviolet shuttle glow N86-13269

BAYS (TOPOGRAPHIC FEATURES)

Evaluating screening effects and Tusnami danger in bays N86-12666

BEAM CURRENTS

Funneling: An initial beam dynamics study [DE85-012652] N86-13082

Development of a current monitor system for measuring pulsed-beam current over a wide dynamic range [DE85-012682] N86-13083

Electron emission of over 200 A/cm (2) from a pulsed-laser irradiated photocathode [DE85-012656] N86-13084

RADLAC program status [DE85-014706] N86-13109

AGS improvement program [DE85-013293] N86-13182

BEAM INJECTION

China report: Science and technology [JPRS-CST-85-021] N86-12421

Titanium-nitrogen ion beam injection studied N86-12427

Funneling: An initial beam dynamics study [DE85-012652] N86-13082

Achievement of Bevalac rapid mode switching [DE85-015130] N86-13092

SLC injector modeling [DE85-013067] N86-13153

Commissioning and operation of the Nuclear Physics Injector at SLAC [DE85-013374] N86-13159

AGS improvement program [DE85-013293] N86-13182

Improved Bevatron local injector ion source performance [DE85-015271] N86-13196

BEAM INTERACTIONS

Beam emittance and beam disruption [DE85-015136] N86-13070

Disruption and luminosity of flat beams [DE85-015137] N86-13071

LAMPF transition-region mechanical fabrication [DE85-012686] N86-13081

Tests of orbital dynamics using the Tevatron [DE85-012296] N86-13085

Comparison between theoretical predictions and tracking [DE85-012104] N86-13149

Tracking studies on the effects of random multipoles in the 6.5 T lattice of the SSC Reference Designs Study [DE85-013286] N86-13156

The production of glow precursors by oxidative erosion of spacecraft surfaces N86-13257

BEAM NEUTRALIZATION

New beam neutralization concept: Laser photodetachment in a magnetic field [DE85-014655] N86-12607

BEAM SWITCHING

Achievement of Bevalac rapid mode switching [DE85-015130] N86-13092

BEAM WAVEGUIDES

Microwave ridged waveguide beam pickups [DE85-013816] N86-12499

BEAMS (RADIATION)

Measurement of 1 nanosecond wide beams for 2.5 MeV proton accelerator N86-12435

Microwave ridged waveguide beam pickups [DE85-013816] N86-12499

Laser-based foilless diode [DE85-013958] N86-12537

New beam neutralization concept: Laser photodetachment in a magnetic field [DE85-014655] N86-12607

Stochastic beam cooling amplifier system front end components performance characteristics [DE85-013925] N86-13079

Tevatron global radius and Os system [DE85-017442] N86-13101

Physics of e(+) - e(-) colliders: Present, future and far future [DE85-009895] N86-13121

RF beam deflection measurements and corrections in the SLC linac [DE85-013061] N86-13146

Minimizing the energy spread within a single bunch by shaping its charge distribution [DE85-013064] N86-13151

BEAMS (SUPPORTS)

Influence of bonded reinforcement in post-tensioned prestressed concrete T-beams with unbonded tendons N86-12622

BEARINGS

Correction of compressor critical speed condition through fluid-film bearing optimization [DE85-005507] N86-12617

BEDROCK

Structure of sedimentary cover and basement of Sierra Leone Rise determined from common depth point seismic (equatorial Atlantic) N86-12709

BEHAVIOR

Shear driven film flow behavior and cavitation study N86-12543

Monitoring of circadian waveforms in rodents exposed to high-intensity static magnetic fields [DE85-015225] N86-12952

New interpretation of spin-wave behavior in nickel and iron [DE85-015323] N86-13208

BENDING

Variable radius lead former [AD-D011790] N86-12506

More on compliance of the three-point bend specimen [AD-A156665] N86-12623

BENDING FATIGUE

More on compliance of the three-point bend specimen [AD-A156665] N86-12623

BENZENE

Quantum chemistry of aromatic nitro explosives N86-12423

BERING SEA

Tectonic structure of Shirshov Ridge (Bering Sea) N86-12710

BERKELIUM

Chemistry of berkelium: A review [DE85-017523] N86-13102

BERYLLIUM

Nuclear performance optimization of the Be/Li/Th blanket for the fusion breeder [DE85-012949] N86-13112

BERYLLIUM 9

Partition of cross sections in asymmetric nucleus-nucleus reactions and the origin of fast alpha particles [DE85-014989] N86-13089

BETA FACTOR

Multipole and tokamak research at the University of Wisconsin [DE85-014862] N86-13165

BETA PARTICLES

Nuclear information needs for the astrophysical s-process [DE85-012913] N86-13278

BEVATRON

Improved Bevatron local injector ion source performance [DE85-015271] N86-13196

BIBLIOGRAPHIES

Earth resources: A continuing bibliography, issue 46 [NASA-SP-7041(46)] N86-12738

Biomedical and Environmental Sciences Program publications 1984 [DE85-015070] N86-12953

Aerospace Medicine and Biology Continuing Bibliograph: A continuing bibliography with indexes [NASA-SP-7011(276)] N86-12954

A user's guide for the BIBSORT program for the IBM-PC personal computer [AD-A157936] N86-12995

Microgravity science and applications bibliography, 1985 revision [NASA-TM-88178] N86-13225

BIFURCATION (BIOLOGY)

Effects of cation ions in nerve excitation N86-12377

BINARY ALLOYS

Combined small angle X-ray scattering and transmission electron microscope studies of Al-Li alloys [DE85-016356] N86-12303

BINARY CODES

Application of a binary cyclic error-correcting code [DE85-013232] N86-13007

BINARY DATA

Dual drain MOSFET detector for crosstie memory systems [AD-D011828] N86-12513

BINARY FLUIDS

Fluid physics research [DE85-014644] N86-12575

BINARY MIXTURES
Optical measurements of shock-induced chemical reactions in mixed aluminum-nickel powder
[DE85-014705] N86-12306
Diffusion in binary plasma mixtures
[DE85-017694] N86-13143
BINARY STARS
Combined ultraviolet studies of astronomical source
[NASA-CR-176165] N86-13274
BINARY SYSTEMS (MATERIALS)
Fluid physics research
[DE85-014644] N86-12575
BIOACOUSTICS
Dummy head microphone and its application to the measurements of electro-acoustic equipments
N86-12379
BIOCHEMISTRY
China report: Science and technology
[JPRS-CST-85-016] N86-12393
BIOLOGICAL EFFECTS
Monitoring of circadian waveforms in rodents exposed to high-intensity static magnetic fields
[DE85-015225] N86-12952
Biomedical and Environmental Sciences Program publications 1984
[DE85-015070] N86-12953
Aerospace Medicine and Biology Continuing Bibliograph: A continuing bibliography with indexes
[NASA-SP-7011(276)] N86-12954
Proceedings of a workshop on Radiofrequency Radiation bioeffects held at Wachtberg-Werthhoven, West Germany on 11-13 September 1984
[AD-A157090] N86-12959
Biological effects of acoustic cavitation
[AD-A157513] N86-13059
BIOMASS
Aquatic Species Program review: Proceedings of Principal Investigators Meeting
[DE85-012137] N86-12364
BIOMEDICAL DATA
Biomedical and Environmental Sciences Program publications 1984
[DE85-015070] N86-12953
BIOSYNTHESIS
Molecular control
[NASA-TM-87510] N86-12313
BIOTECHNOLOGY
Marketing the use of the space environment for the processing of biological and pharmaceutical materials
[NASA-CR-176334] N86-12243
Laser induced biological heating analyzed
N86-12460
BIPLANES
China report: Science and technology
[JPRS-CST-85-029] N86-12446
Wingtip sails tested on Y-5 aircraft N86-12450
BIPOLAR TRANSISTORS
High frequency silicon bipolar transistor with SIPOS (Semi-insulating polycrystalline silicon) heterojunction emitter and ion implanted rapid thermal annealed base region
[AD-A157141] N86-12510
BLACK BODY RADIATION
Materials and process characterization to determine the effect of high intensity infrared laser radiation on a composite material
[AD-A157094] N86-12260
BLANKETS (FISSION REACTORS)
Tritium control in helium-cooled blankets
[DE85-014783] N86-13116
BLANKETS (FUSION REACTORS)
Nuclear performance optimization of the Be/Li/Th blanket for the fusion breeder
[DE85-012949] N86-13112
BLOCKING
Ultrahigh vacuum equipment described N86-12438
BLOOD
Infrared optical measurement of blood gas concentrations and fiber optic catheter
[AD-D011836] N86-12955
Forward field autotransfusion device
[AD-D011763] N86-12957
BLOOD PLASMA
Plasma volume methodology: Evans blue, hemoglobin-hematocrit, and mass density transformations
[NASA-TM-86834] N86-12956
BLOOD PRESSURE
Human hemodynamic change under high atmospheric pressure N86-12458
BLOOD VOLUME
Plasma volume methodology: Evans blue, hemoglobin-hematocrit, and mass density transformations
[NASA-TM-86834] N86-12956
BOARDS (PAPER)
Steam-injection pressing of isocyanate-bonded aspen flakeboards, latitudes and limitations
[AD-A157833] N86-12389
BODY FLUIDS
Dermal substance collection device
[AD-D011848] N86-12962
BOILING
Cross flow boiling in tube bundles
[AD-A158557] N86-12562
Influence of a surfactant additive on absorption heat pump performance
[DE85-013995] N86-12574
BONDING
Mixed-mode cyclic debonding of adhesively bonded composite joints
[NASA-CR-177991] N86-12255
Fracture surface analysis in composite and titanium bonding
[NASA-CR-176309] N86-12257
Effects of surface interactions and mechanical properties of plastic bonded explosives on explosive sensitivity. Part 2: Model formulation
[AD-A157900] N86-12361
Influence of bonded reinforcement in post-tensioned prestressed concrete T-beams with unbonded tendons
N86-12622
BOOSTER ROCKET ENGINES
Naval surface weapons center technology transfer biennial report (Fiscal year 1983/1984)
[AD-A157919] N86-13238
BORIDES
Recent developments in the structural crystallography of boron and the higher borides
[DE85-016930] N86-13202
BORN APPROXIMATION
Secondary electron spectra: A semiempirical model
[DE85-012448] N86-13086
BORON
Plane-wave theory of electrical transport in disordered systems
[DE85-015353] N86-13167
Recent developments in the structural crystallography of boron and the higher borides
[DE85-016930] N86-13202
BORON ISOTOPES
Partition of cross sections in asymmetric nucleus-nucleus reactions and the origin of fast alpha particles
[DE85-014989] N86-13089
BOROSILICATE GLASS
Fixation of high-level wastes in glasses
[DE85-013276] N86-12325
BOSONS
Physics of e(+) - e(-) colliders: Present, future and far future
[DE85-009895] N86-13121
BOUGUER LAW
Impact of GRM: New evidence from the Soviet Union
N86-12853
A major crustal feature in the southeastern United States inferred from the MAGSAT equivalent source anomaly field N86-12856
BOUNDARIES
Seismological studies of the tectonics of divergent plate boundaries N86-12812
C infinity-regularity for the porous median equation
[AD-A158147] N86-13036
Stefan's problem in a finite domain with constant boundary and initial conditions analysis
[AD-A158558] N86-13040
Prediction of sound fields in acoustical cavities using the boundary element method
[NASA-CR-176295] N86-13057
BOUNDARY ELEMENT METHOD
Prediction of sound fields in acoustical cavities using the boundary element method
[NASA-CR-176295] N86-13057
BOUNDARY LAYER COMBUSTION
Investigation of the flame-acoustic wave interaction during axial solid rocket instabilities
[AD-A158559] N86-12362
BOUNDARY LAYER FLOW
An evaluation of four methods of numerical analysis for two-dimensional airfoil flows. Revision
[AD-A157248] N86-12209
BLR studies on conic model with LDA in FL-1 wind tunnel N86-12434
BOUNDARY LAYER SEPARATION
An evaluation of four methods of numerical analysis for two-dimensional airfoil flows. Revision
[AD-A157248] N86-12209
Numerical and experimental studies of 3-D and unsteady turbulent body/appendage/propeller flows
[AD-A157078] N86-12552
Transonic noise generation by duct and profile flow
[AD-A157163] N86-13056
BOUNDARY LAYER STABILITY
An asymptotic investigation of the stationary modes of instability of the boundary layer on a rotating disc
[NASA-CR-177977] N86-12550
BOUNDARY LAYER TRANSITION
Numerical and experimental studies of 3-D and unsteady turbulent body/appendage/propeller flows
[AD-A157078] N86-12552
BOUNDARY LAYERS
Code of finite element analysis for three-dimensional flow in turbomachines N86-12398
Comparison of boundary layer winds from NWS LFM (National Weather Service's Limited-Area Fine-Mesh) output and instrumented buoys
[PB85-226439] N86-12927
BOUNDARY VALUE PROBLEMS
The uniqueness of Hill's spherical vortex
[AD-A158149] N86-13038
BRAIN
European Science Notes. Volume 39, number 8
[AD-A157146] N86-13237
BRANCHING (PHYSICS)
Experiment to study K(+) (YIELDS) (PI)(+) + nothing at LAMPF 2
[DE85-014267] N86-13110
BRAYTON CYCLE
Liquid droplet radiator program at the NASA Lewis Research Center
[NASA-TM-87139] N86-12246
BREEDER REACTORS
Tritium control in helium-cooled blankets
[DE85-014783] N86-13116
BRIGHTNESS TEMPERATURE
Clear sky brightness temperature over the western north Pacific Ocean from GMS spacecraft N86-12911
Simultaneous observation of GMS and GMS-2: A study of the difference between the brightness temperatures by GMS and those by GMS-2 N86-12912
BRILLOUIN EFFECT
Remote diagnosis of media by combination (Raman) anti-Stokes light scattering method with induced Brillouin backscattering N86-12705
BRILLOUIN ZONES
New interpretation of spin-wave behavior in nickel and iron
[DE85-015323] N86-13206
BRINES
Metal dissolution kinetics in organic solvents using rotating ring-disc voltammetry
[DE85-013478] N86-12253
BROADBAND
Picosecond broadband CARS probe using the picosecond continuum
[AD-D011840] N86-12267
A model for explaining some features of shuttle glow
N86-13256
BROWNIAN MOVEMENTS
The orientation distribution of nonspherical aerosol particles within a cloud
[AD-A157383] N86-12554
BRUSHES (ELECTRICAL CONTACTS)
High current fiber brush collector and method for making same
[AD-D011827] N86-12512
BUBBLES
Model describing the steady-state pyrolysis of bubble-forming polymers in response to an incident heat flux
[PB85-225225] N86-12291
Analytical and experimental studies of wakes behind circularly capped bubbles N86-12546
Module voltage isolation and corrosion research
N86-12772
BUDGETING
Making appropriations for the Department of Housing and Urban Development, and for sundry independent agencies, boards, commissions, corporations, and offices for the fiscal year ending September 30, 1986, and for other purposes
[H-REPT-99-363] N86-13231
BULK MODULUS
Thin film module electrical configuration versus electrical performance N86-12770
BUNCHING
SLC injector modeling
[DE85-013067] N86-13153
BUNDLES
Cross flow boiling in tube bundles
[AD-A158557] N86-12562
BUOYANCY
Combustion in turbulent jets and buoyant plumes
[PB85-220655] N86-12288
Numerical calculation of turbulent buoyant flow
N86-12541

Sea floor swells and mantle plumes N86-12866
The nature of symmetric instability and its similarity to convective and inertial instability
[NASA-CR-3945] N86-12918
Low temperature inflator apparatus
[AD-D011810] N86-12974

BUOYS
Comparison of boundary layer winds from NWS LFM (National Weather Service's Limited-Area Fine-Mesh) output and instrumented buoys
[PB85-226439] N86-12927

BURNING RATE
Pressure-coupled response function of solid propellants including those with negative pressure exponents
N86-12369

BYPASSES
Hot-spot heating susceptibility due to reverse bias operating conditions N86-12763
Thin film module electrical configuration versus electrical performance N86-12770

C

CADMIUM TELLURIDES
Improved techniques for the growth of high quality cadmium telluride cryatals
[AD-A157669] N86-13192

CALCIUM COMPOUNDS
Characterization of sheet calcium for Ca/CaCr04 thermal batteries
[DE85-013231] N86-12785

CALCIUM FLUORIDES
Study of possible solarization - related impurities in CaF2 and other fluorides
[DE85-014100] N86-13135

CALCIUM ISOTOPES
Isovector resonances in pion charge exchange
[DE85-012746] N86-13106

CALCULATORS
Weather analysis programs using HP-41CV
[AD-A157389] N86-12921

CALIBRATING
T-33 (Silver Star MK 3) pitot-static system calibration
[AD-A157854] N86-12221
The theory and practice of a multistate reflectometer
[AD-A157916] N86-12583
Assessment of the long-term precision of continuous emission monitors
[PB85-201150] N86-12804
Precipitating electron and ion detectors (SSJ/4) for the block 5D/Flights 6-10 DMSP (Defense Meteorological Satellite Program) satellites: Calibration and data presentation
[AD-A157080] N86-12896

CALIFORNIA
Geodetically derived strain from San Francisco Bay to the Mendocino Triple Junction, California
[PB85-198802] N86-12905

CAMERAS
X-ray diffraction cell for Debye-Scherrer and Guinier (Huber) cameras at pressure and temperature
[DE85-014815] N86-12593

CANARD CONFIGURATIONS
Aerodynamic characteristics of a propulsive wing-canard concept at STOL speeds
[NASA-CR-177982] N86-12205

CANONICAL FORMS
Use of method of canonical correlations for analysis of climatic series N86-12634

CANOPIES
Development and evaluation of a microburst test apparatus for use as a minimum destructive test for parachute material
[AD-A158110] N86-12620

CANOPIES (VEGETATION)
Feasibility of using LANDSAT images of vegetation cover to estimate effective hydraulic properties of soils
[E86-10003] N86-12739
Soybean canopy reflectance modeling data sets
[E86-10005] N86-12741

CAP CLOUDS
The numerical simulation of geographic storms
N86-12907

CAPACITANCE
Calculation of series capacitance for transient analysis of windings N86-12528
Analytical and experimental studies of wakes behind circularly capped bubbles N86-12548

CARBON CYCLE
Modeling of seasonal evolution of carbon cycle in ocean-atmosphere system N86-12641

CARBON DIOXIDE
Carbon dioxide N86-12354
Modeling of seasonal evolution of carbon cycle in ocean-atmosphere system N86-12641
Transmission of tropospheric radiation of lasers on molecules of different carbon dioxide isotopes
N86-12734
Carbon dioxide in arctic and subarctic regions
[DE85-014054] N86-12901

CARBON DIOXIDE CONCENTRATION
Infrared optical measurement of blood gas concentrations and fiber optic catheter
[AD-D011836] N86-12955

CARBON DIOXIDE LASERS
Materials and process characterization to determine the effect of high intensity infrared laser radiation on a composite material
[AD-A157094] N86-12260
Deposition, microstructure and properties of laser CVD SiC films
[DE85-014680] N86-12327
Compact TEA-CO2 laser with long life developed
N86-12394
Laser induced biological heating analyzed
N86-12460
CO2 laser stabilization and switching
[AD-D011795] N86-12598
Applied lasers (selected articles)
[AD-A155948] N86-12601

CARBON FIBERS
Ground-based investigations of atomic oxygen interactions with space station surfaces
[DE85-014062] N86-12249
Microstructure/Property relationships for carbon fiber reinforced aluminum alloys
[AD-A157858] N86-12261
Suspension method of impregnating active material into composite nickel plaque
[AD-D011826] N86-12299

CARBON MONOXIDE
Carbon monoxide N86-12337
Deactivation and poisoning of fuel cell catalysts
[DE85-015127] N86-12521
Infrared optical measurement of blood gas concentrations and fiber optic catheter
[AD-D011836] N86-12955
Physico-chemical conditions in circumstellar shells of evolved oxygen-rich M stars N86-13275

CARBON 13
Partition of cross sections in asymmetric nucleus-nucleus reactions and the origin of fast alpha particles
[DE85-014989] N86-13089

CARBON-CARBON COMPOSITES
Materials and process characterization to determine the effect of high intensity infrared laser radiation on a composite material
[AD-A157094] N86-12260

CARBONATES
Film stability for dirct absorption receivers
[DE85-012135] N86-12791

CARBOXYLIC ACIDS
Liquid chromatography on silica using mobile phases containing tetraalkylammonium hydroxides. 1: General separation selectivity and behavior of polar compounds typically in fuels
[DE85-014450] N86-12281

CARCINOGENS
Measurement of species concentrations in flames by laser-induced fluorescence
[DE85-012092] N86-12283

CARGO
Survey of ultraviolet shuttle glow N86-13269

CARTRIDGES
Low temperature inflator apparatus
[AD-D011810] N86-12974
Photosensitive cartridge for weapons zeroing and marksmanship training
[AD-D011765] N86-13125

CASCADE WIND TUNNELS
Wind tunnel turning vanes of modern design
[NASA-TM-87416] N86-12239

CASPIAN SEA
Spatial structure of high-frequency sea wind waves under different meteorological conditions N86-12714

CASSEGRAIN ANTENNAS
A 94 GHz imaging array using slot line radiators
[NASA-CR-176348] N86-12484

CATACLYSMIC VARIABLES
Combined ultraviolet studies of astronomical source
[NASA-CR-176165] N86-13274

CATALYSIS
Raman spectroscopy of molecular adsorbates
[DE85-012981] N86-12280
Surface-catalyzed recombination into excited electronic, vibrational, rotational, and kinetic energy states: A review N86-13253

CATALYSTS
Study of some transition metal complexes as process catalysts
[DE85-013426] N86-12276

CATHODES
Deactivation and poisoning of fuel cell catalysts
[DE85-015127] N86-12521
Develop and test fuel cell powered on-site integrated total energy systems: Phase 3, full-scale power plant development
[NASA-CR-174948] N86-12757
Develop and test fuel cell powered on-site integrated total energy systems: Phase 3, full-scale power plant development
[NASA-CR-174998] N86-12758

CATHODIC COATINGS
Preparation and properties of thin film reversible cathode materials
[AD-A158431] N86-12273

CATIONS
U308 powder from uranyl-loaded cation exchange resin
[DE85-013231] N86-12265
Formation of fuel via photochemical electron transfer
[DE85-011168] N86-12279
Effects of cation ions in nerve excitation N86-12377

CAUCHY PROBLEM
Two results on dense imbeddings
[AD-A158132] N86-13033

CAVITATION FLOW
Shear driven film flow behavior and cavitation study
N86-12543
Non-linear corrections to the linear theory for the prediction of the cavitating flow around hydrofoils
[AD-A158105] N86-12557
Biological effects of acoustic cavitation
[AD-A157513] N86-13059

CAVITIES
Forward field autotransfusion device
[AD-D011763] N86-12957
Prediction of sound fields in acoustical cavities using the boundary element method
[NASA-CR-176295] N86-13057
Microwave field strength measurement in a Rubidium clock cavity via adiabatic rapid passage
[AD-A157070] N86-13065

CAVITY RESONATORS
The step structure effect of dc Josephson current within one flux quantum period phi sub zero (2) N86-12412
High order mode damping in the NSLS accelerating RF cavities by the use of damping antennae
[DE85-014214] N86-12498
Compact microwave ion source
[DE85-014536] N86-13176

CELL CATHODES
Preparation and properties of thin film reversible cathode materials
[AD-A158431] N86-12273

CELL DIVISION
Raman activity in synchronously dividing bacteria
[DE85-015672] N86-12951

CEMENTS
China report: Science and technology
[JPRS-CST-85-019] N86-12966

CENSORED DATA (MATHEMATICS)
Transforming censored samples and testing fit
[AD-A157957] N86-13048

CENTRIFUGAL FORCE
Viscous nonlinear circulation in axisymmetric baroclinic eddy N86-12712

CENTRIFUGAL PUMPS
Fluid machines: Expanding the limits, past and future
[NASA-TM-87161] N86-12227
Development of the hydrotransport boost pump
[PB85-203776] N86-12618

CERAMICS
Evaluation of high permittivity glass ceramics for millimeter wave applications
[AD-A158551] N86-12319
Manufacturing process for cylindrical ceramic tubes with localized imprints and device for application of this process
[DE85-012294] N86-12323
Surface crystallization on metallized 94 percent alumina ceramics
[DE85-008691] N86-12324
Classical piezoelectricity: Is the theory complete
[DE85-014592] N86-12536
Solar thermal energy systems
[DE85-008793] N86-12790
Tritium control in helium-cooled blankets
[DE85-014783] N86-13116
Diffraction and microscopy studies of the structure of grain boundaries in Fe, Fe-base alloys and ceramic materials
[DE85-016950] N86-13196

CEREBRAL CORTEX
Cortical plasticity: Theoretical analysis, experimental results
[AD-A157965] N86-12961
CERENKOV COUNTERS
Electrons and cosmic ray produced in Saturn's inner magnetosphere N86-13281
CERIUM ISOTOPES
Isovector resonances in pion charge exchange
[DE85-012746] N86-13106
CERMETS
U308 powder from uranyl-loaded cation exchange resin
[DE85-013231] N86-12265
CHANNEL FLOW
Wall-interference assessment in three-dimensional slotted-wall wind tunnels
[NASA-CR-176320] N86-12240
Experimental study of the combustion of gas-air mixtures in a channel and the diffusion combustion in a slipstream at high velocities
[AD-A157495] N86-12271
CHANNELS (DATA TRANSMISSION)
Data acquisition interfaces for the IBM personal computer
[DE85-014256] N86-12985
The 32-bit computer for large memory applications on FASTBUS
[DE85-012726] N86-12986
CHARACTERIZATION
Improved approach to characterizing and presenting streak camera performance
[DE85-015186] N86-12587
CHARGE CARRIERS
New method of determining the current carrier concentration in a substance in the state of superconductivity
[AD-A158182] N86-13194
CHARGE DISTRIBUTION
Minimizing the energy spread within a single bunch by shaping its charge distribution
[DE85-013064] N86-13151
CHARGE EXCHANGE
Isovector resonances in pion charge exchange
[DE85-012746] N86-13106
Electron-spin-polarized targets for a collisionally-pumped polarized-ion source
[DE85-015276] N86-13174
CHARGE TRANSFER
Charge transfer in multiple site chemical systems
[AD-A157413] N86-12270
CHARGED PARTICLES
Charge transfer in multiple site chemical systems
[AD-A157413] N86-12270
The NO-NO2 system at laboratory surfaces
N86-13255
CHEMICAL ANALYSIS
Application of time-dependent Raman theory to the analysis of inorganic photosystems
[DE85-012752] N86-12285
Infrared optical measurement of blood gas concentrations and fiber optic catheter
[AD-D011836] N86-12955
CHEMICAL BONDS
Recent developments in the structural crystallography of boron and the higher borides
[DE85-016930] N86-13202
CHEMICAL COMPOSITION
Composition and photochemical reactivity of turbine engine exhaust
[AD-A157643] N86-12230
Carbothermal synthesis of silicon carbide
[DE85-013546] N86-12321
Origin of element composition of ocean water
N86-12668
Dermal substance collection device
[AD-D011848] N86-12962
CHEMICAL EFFECTS
Effects of surface interactions and mechanical properties of plastic bonded explosives on explosive sensitivity. Part 2: Model formulation
[AD-A157900] N86-12361
CHEMICAL ENGINEERING
China report: Science and technology
[JPRS-CST-85-022] N86-12439
China report: Science and technology
[JPRS-CST-85-019] N86-12966
CHEMICAL LASERS
A high precision rate dye laser pumped by a CuCl laser N86-12457
Applied lasers (selected articles)
[AD-A155948] N86-12601
CHEMICAL PROPERTIES
Adsorption/desorption properties of vacuum materials for the 6 GeV synchrotron
[DE85-010276] N86-12252
Role of chemical bonding in adhesion
[AD-A157251] N86-12316
Characterization of sheet calcium for Ca/CaCr04 thermal batteries
[DE85-013231] N86-12785
Chemistry of berkelium: A review
[DE85-017523] N86-13102
CHEMICAL REACTIONS
Optical measurements of shock-induced chemical reactions in mixed aluminum-nickel powder
[DE85-014705] N86-12306
Studies on unusually reactive metal powders: Preparation of new organometallic and organic compounds including potential new catalysts
[DE85-014644] N86-12309
TATE: Strong basic reactions provide soluble derivations for simple qualitative high explosive spot test
[DE85-014259] N86-12366
China report: Science and technology
[JPRS-CST-85-035] N86-12399
China report: Science and technology
[JPRS-CST-85-032] N86-12462
Guidelines for a thermochemical kinetics computer program
[DE85-015671] N86-12996
CHEMICAL REACTORS
Fischer-Tropsch synthesis in slurry reactor systems
[DE85-013390] N86-12278
CHEMILUMINESCENCE
Infrared emission from desorbed NO2(*) and NO(*)
N86-13254
CHEMISORPTION
Raman spectroscopy of molecular adsorbates
[DE85-012981] N86-12280
CHINA
China report: Science and technology
[JPRS-CST-85-024] N86-12368
China report: Science and technology
[JPRS-CST-85-018] N86-12413
China report: Science and technology
[JPRS-CST-85-034] N86-12430
China report: Science and technology
[JPRS-CST-85-022] N86-12439
China report: Science and technology
[JPRS-CST-85-029] N86-12446
China report: Science and technology
[JPRS-CST-85-032] N86-12462
CHINESE SPACE PROGRAM
Mean density scale heights from analysis of variation in perigee height of China's second satellite
N86-12396
CHINESE SPACECRAFT
Mean density scale heights from analysis of variation in perigee height of China's second satellite
N86-12396
CHIPS (ELECTRONICS)
China report: Science and technology
[JPRS-CST-85-029] N86-12446
Programmer for single-chip microprocessor
N86-12448
Evaluation and implementation of testability schemes for gate array integrated circuit design
[DE85-012674] N86-12526
CHLORIDES
Lithium-thionyl chloride cell system safety hazard analysis
[AD-A157089] N86-12775
CHLORINE
Chlorine N86-12344
Development of a radiation-hard CMOS process
[NASA-CR-170925] N86-13187
CHLORINE FLUORIDES
The halogen fluorides N86-12340
CHOLINE
Cortical plasticity: Theoretical analysis, experimental results
[AD-A157965] N86-12961
CHROMATES
Characterization of sheet calcium for Ca/CaCr04 thermal batteries
[DE85-013231] N86-12785
CHROMATOGRAPHY
Oxidation of heterocyclic nitrogen yields to nitroheterocycles
[DE85-012757] N86-12284
CHROMIUM
Anaerobic microbial dissolution of toxic metals in subsurface environments
[DE85-013308] N86-12251
Electrochemical deposition of glassy chromium on copper
[DE85-004061] N86-12275
CHROMOSPHERE
Combined ultraviolet studies of astronomical source
[NASA-CR-176165] N86-13274
CIRCADIAN RHYTHMS
Monitoring of circadian waveforms in rodents exposed to high-intensity static magnetic fields
[DE85-015225] N86-12962
CIRCUIT BOARDS
Laser anemometer using a single circuit board
N86-12411
CIRCUIT DIAGRAMS
Design information for the 4/3 silicon-gate CMOS technology
[DE85-014932] N86-12522
CIRCUITS
Nonlinear electromagnetic scattering from a diode circuit
[AD-A157216] N86-12491
Electrolytic pressure transduction system
[AD-D011847] N86-12584
Transient test of suspension electronics for gyroscope
[AD-D011853] N86-12585
Thin-film module circuit design: Practical and reliability aspects N86-12782
Acoustically tuned optical filter system
[AD-D011791] N86-13184
CIRCULATION
Measurements on an axisymmetric jet in a slow coflowing stream N86-12549
CIRRUS CLOUDS
Occurrence of linearly ranged Cb-clouds associated with migrating band-shaped cirriform-clouds: A case study
N86-12910
CLASSICAL MECHANICS
China report: Science and technology
[JPRS-CST-85-024] N86-12368
CLIMATE
Atmospheric aerosol and its effects on climate
N86-12636
Influence of power engineering on climate
N86-12637
CLIMATOLOGY
Main problems in climate monitoring (diagnosis)
N86-12633
Use of method of canonical correlations for analysis of climatic series N86-12634
Climatically active trace gases in atmosphere
N86-12639
Planetary waves N86-12820
Planetary waves N86-12821
Advanced Moisture and Temperature Sounder (AMTS) baseline 5 study report
[NASA-CR-176331] N86-12919
CLINICAL MEDICINE
Protection of eyes against laser damage studied
N86-12967
Criteria for a state-of-the-art vision test system
[AD-A157099] N86-12973
CLOSE PACKED LATTICES
Paramagnetic form factors of HCP transiton metals
[DE85-016301] N86-12301
CLOSURE LAW
Multiple-scale turbulence closure modeling of confined recirculating flows
[NASA-CR-178536] N86-12551
CLOUD COVER
Empirical analysis of direct and inverse relationships between macroscale characteristics of atmospheric processes in northern hemisphere and thermal state of north Atlantic N86-12635
Large-scale circulation departures related to wet episodes in northeast Brazil
[NASA-CR-176352] N86-12916
CLOUD PHOTOGRAPHY
Global view of the upper level outflow patterns associated with tropical cyclone intensity changes during FGGE
[NASA-CR-174407] N86-12908
CLOUD PHYSICS
Some characteristics of transmission by thin clouds in visible and infrared spectral regions N86-12737
Squall and cloud lines as structural components of an Arabian Sea convective cloud cluster
[AD-A157973] N86-12925
CLOUD SEEDING
The numerical simulation of geographic storms
N86-12907
CLOUDS
The orientation distribution of nonspherical aerosol particles within a cloud
[AD-A157363] N86-12554
Some characteristics of transmission by thin clouds in visible and infrared spectral regions N86-12737
Electro-optical transmission and liquid water content of fogs and clouds
[AD-A157506] N86-13128

CLOUDS (METEOROLOGY)
Some results of study of blocking layers on days with vertically developed cloud cover of Caucasus-Caspian region on basis of aerospace information N86-12898
Meteorological Satellite Center Technical Note No. 11, 1985
[MSC-TN-11] N86-12909
Squall and cloud lines as structural components of an Arabian Sea convective cloud cluster
[AD-A157973] N86-12925
CLUMPS
Squall and cloud lines as structural components of an Arabian Sea convective cloud cluster
[AD-A157973] N86-12925
CLUSTER ANALYSIS
Feasibility of using LANDSAT images of vegetation cover to estimate effective hydraulic properties of soils
[E86-10003] N86-12739
CLUTTER
Weather radar studies
[AD-A157093] N86-12920
CMOS
Digital phase meter using CMOS-LED introduced N86-12442
Latch-up effect in CMOS described N86-12443
Design information for the 4/3 silicon-gate CMOS technology
[DE85-014932] N85-12522
Semicustom integrated circuit design at Sandia National Laboratories
[DE85-015661] N86-12538
Development of a radiation-hard CMOS process
[NASA-CR-170925] N86-13167
COALESCING
Explosive coalescence of magnetic islands
[DE85-015063] N86-13172
COASTAL WATER
Annual data summary for 1981 CERC (Coastal Engineering Research Center) field research facility
[AD-A158143] N86-12926
A user's guide to the Coastal Engineering Research Center's (CERC'S) field research facility
[AD-A157966] N86-12946
COASTS
Structure of sedimentary cover and basement of Sierra Leone Rise determined from common depth point seismic (equatorial Atlantic) N86-12709
COATING
High damage threshold porous silica antireflective coating
[DE85-012924] N86-12322
COATINGS
Recovery of fragile layers produced on substrates by chemical vapor deposition
[AD-D011841] N86-13185
Space shuttle mechanistic studies to characterize atomic oxygen interactions with surfaces N86-13267
COAXIAL CABLES
Demountable coaxial electrical connector for in-line amplifiers
[AD-D011831] N86-12507
COBALT
Hydrogen chloride sparging crystallization of the chloride salts of cobalt, manganese, and nickel
[PB85-197002] N86-12286
COBOL
Identifying and evaluating COBOL competencies for four-year information systems programs N86-13223
COCKPITS
An analysis of the application of AI to the development of intelligent aids for flight crew tasks
[NASA-CR-3944] N86-12212
CODERS
P1 polyphase code expander-compressor
[AD-D011838] N86-12475
P2 polyphase code expander-compressor
[AD-D011839] N86-12476
CODING
Hybrid radar waveform design utilizing complementary phase coding and linear frequency stepping for achieving improved slant range resolution in a synthetic aperature radar N86-12470
Self-consistent klystron simulations
[DE85-012676] N86-12529
REFRIG-12: A graphics-augmented interactive program for designing vapor-compression refrigeration/heat pump cycles
[DE85-014205] N86-12572
Uncertainty propagation from raw data to final results
[DE85-011937] N86-13000
IMAGYS graphics programming language: Description and analysis
[DE85-013384] N86-13003
Control of step size and order in extrapolation codes
[DE85-013261] N86-13010
FDSC: A microwave coupling code for slots of finite depth
[DE85-013443] N86-13011
COGNITION
Human cognition and performance
[AD-A157865] N86-12970
Diagnosing cognitive errors: Statistical pattern classification and recognition approach
[AD-A158108] N86-12972
COHERENT ACOUSTIC RADIATION
Status, development of power ultrasonics in China N86-12403
COHERENT SCATTERING
Picosecond broadband CARS probe using the picosecond continuum
[AD-D011840] N86-12267
COLD PLASMAS
Wave propagation in a plasma based on the cold plasma model
[DE85-013649] N86-13158
COLD WATER
Low temperature inflator apparatus
[AD-D011810] N86-12974
COLD WEATHER
First experiment in forecasting cool-season weather with the PROFS System
[PB85-230605] N86-12929
Low temperature inflator apparatus
[AD-D011810] N86-12974
COLLECTION
Forward field autotransfusion device
[AD-D011763] N86-12957
Dermal substance collection device
[AD-D011848] N86-12962
COLLIMATORS
Los Alamos constant-Q spectrometer
[DE85-014115] N86-12586
COLLISION AVOIDANCE
Simulation of the enhanced traffic alert and collision avoidance system (TCAS 2)
[NASA-CR-176328] N86-12216
COLLISION PARAMETERS
Beam emittance and beam disruption
[DE85-015136] N86-13070
Disruption and luminosity of flat beams
[DE85-015137] N86-13071
Physics of e(+) - e(-) colliders: Present, future and far future
[DE85-009895] N86-13121
Comparison between theoretical predictions and tracking
[DE85-012104] N86-13149
A model for explaining some features of shuttle glow N86-13256
The production of glow precursors by oxidative erosion of spacecraft surfaces N86-13257
Activated recombinative desorption: A potential component in mechanisms of spacecraft glow N86-13258
Planned investigation of infrared emissions associated with the induced spacecraft glow: A shuttle infrared glow experiment (SIRGE) N86-13264
COLLISIONS
Collider performance with ideal collisions
[DE85-017011] N86-13073
Recent results of an internal tilt mode calculation in FRCs
[DE85-014121] N86-13177
COLLOCATION
C0 collocation solutions for weak-formulation Navier-Stokes equations
[AD-A157250] N86-12553
COLOR VISION
Criteria for a state-of-the-art vision test system
[AD-A157090] N86-12973
COMBAT
Pilot's associate definition study
[AD-A157106] N86-13026
COMBUSTIBLE FLOW
One-dimensional two-phase flow in combustion chamber of solid propellant rocket motors N86-12370
COMBUSTION
Experimental study of the combustion of gas-air mixtures in a channel and the diffusion combustion in a slipstream at high velocities
[AD-A157495] N86-12271
Combustion in turbulent jets and buoyant plumes
[PB85-220655] N86-12288
COMBUSTION CHAMBERS
Composition and photochemical reactivity of turbine engine exhaust
[AD-A157643] N86-12230
One-dimensional two-phase flow in combustion chamber of solid propellant rocket motors N86-12370
COMBUSTION PHYSICS
Theoretical studies of molecular interactions
[DE85-012604] N86-13076
COMBUSTION PRODUCTS
Motion of thin metal walls and the equation of state of detonation products
[DE85-014809] N86-12629
COMBUSTION STABILITY
Investigation of the flame-acoustic wave interaction during axial solid rocket instabilities
[AD-A158559] N86-12362
Pressure-coupled response function of solid propellants including those with negative pressure exponents N86-12369
COMMAND AND CONTROL
Comparison of continuous speech, discrete speech, and keyboard input to an interactive warfare simulation in various C3 environments
[AD-A156830] N86-12487
European Science Notes. Volume 39, number 8
[AD-A157146] N86-13237
COMMAND GUIDANCE
Basic EMC (Electromagnetic compatibility) technology advancement for C3 (Command, control, and communications) systems. Volume 6
[AD-A157239] N86-12493
COMMAND LANGUAGES
Using the information resource dictionary system command language
[PB85-2277[illegible]3] N86-12988
Data acquisition command interface using VAX/VMS DCL
[DE85-012747] N86-13019
COMMERCIAL SPACECRAFT
Federal government provision of third-party liability insurance to space vehicle users
[NASA-CR-176346] N86-13230
COMMUNICATION
Deals among rational agents
[AD-A157960] N86-13052
COMMUNICATION CABLES
Estimating the reliability of fiber optics cables
[DE85-014892] N86-13136
COMMUNICATION EQUIPMENT
Simultaneous detection of time coincident signals in an adaptive Doppler tracker
[AD-D011796] N86-12473
COMMUNICATION NETWORKS
Communications network status information system
[AD-D011850] N86-12477
Elie: Saint Eustache fibre Optic Field Trial project evaluation report, volume 4
[AD-A157144] N86-12490
COMMUNICATION SATELLITES
Commercial and military communication satellite acquisition practices
[AD-A157398] N86-12247
R and D limited partnerships (possible applications in advanced communications satellite technology experiment program)
[NASA-CR-176333] N86-13221
COMMUNICATIONS TECHNOLOGY SATELLITE
R and D limited partnerships (possible applications in advanced communications satellite technology experiment program)
[NASA-CR-176333] N86-13221
COMPARISON
Commercial and military communication satellite acquisition practices
[AD-A157398] N86-12247
Comparison of continuous speech, discrete speech, and keyboard input to an interactive warfare simulation in various C3 environments
[AD-A156830] N86-12487
More on compliance of the three-point bend specimen
[AD-A156665] N86-12623
COMPENSATORS
Research on output feedback control
[NASA-CR-174253] N86-13028
COMPOSITE MATERIALS
Aircraft interior panel test criteria derived from full-scale fire tests
[FAA/CT-85/23] N86-12214
Mixed-mode cyclic debonding of adhesively bonded composite joints
[NASA-CR-177991] N86-12255
Fracture surface analysis in composite and titanium bonding
[NASA-CR-176309] N86-12257
Effect of measured material properties on the finite element analysis of an OH-58 composite tail boom
[NASA-TM-86430] N86-12259
Minutes of Workshop on Composite Materials Test Methods
[AD-A157903] N86-12262

Macroscopic and microscopic deformation and failure processes that control composite toughness
[DE85-012938] N86-12263
Dynamic small angle X-ray scattering study of stressed Kevlar 49 epoxy composites
[DE85-011408] N86-12264
Statistical treatment of aramid/epoxy stress-rupture data
[AD-A157238] N86-12315
Role of chemical bonding in adhesion
[AD-A157251] N86-12316

COMPOSITE PROPELLANTS
Pressure-coupled response function of solid propellants including those with negative pressure exponents
N86-12369

COMPOSITE STRUCTURES
Automated design of composite plates for improved damage tolerance N86-12254

COMPRESSED AIR
Compressed and liquid air N86-12353
Synthesis of research and development in mechanical energy storage technologies
[DE85-013313] N86-12782

COMPRESSIBLE FLOW
Code of finite element analysis for three-dimensional flow in turbomachines N86-12398

COMPRESSION LOADS
Motion of thin metal walls and the equation of state of detonation products
[DE85-014809] N86-12629
X-ray diffraction studies of shock-modified inorganic materials
[DE85-015150] N86-13209

COMPRESSION TESTS
Compressor research facility F100 high pressure compressor inlet total pressure and swirl profile simulation
[AD-A157108] N86-12229
Minutes of Workshop on Composite Materials Test Methods
[AD-A157903] N86-12262

COMPRESSOR BLADES
Numerical computation of full three-dimensional flow in transonic turbines N86-12397

COMPRESSORS
Compressor research facility F100 high pressure compressor inlet total pressure and swirl profile simulation
[AD-A157108] N86-12229
Correction of compressor critical speed condition through fluid-film bearing optimization
[DE85-005507] N86-12617

COMPTON EFFECT
X-rays from the radio halo of Virgo A = M87
[NASA-CR-176303] N86-13285

COMPUTATION
High order mode damping in the NSLS accelerating RF cavities by the use of damping antennae
[DE85-014214] N86-12498
Calculation of series capacitance for transient analysis of windings N86-12526
P-wave spectra in problem of determining dynamic paramters of earthquake foci. Standardization of initial data and procedures for computing amplitude spectra
N86-12722
Actors: A model of concurrent computation in distributed systems
[AD-A157917] N86-12994
Global optimization using automatic differentiation and interval iteration
[AD-A156150] N86-13039

COMPUTATIONAL FLUID DYNAMICS
Some recent advances in computational aerodynamics for helicopter applications
[NASA-TM-86777] N86-12207
One-dimensional two-phase flow in combustion chamber of solid propellant rocket motors N86-12370
Numerical computation of full three-dimensional flow in transonic turbines N86-12397
Multiple-scale turbulence closure modeling of confined recirculating flows
[NASA-CR-178536] N86-12551

COMPUTATIONAL GRIDS
Transistorized multigrid methods. 1: Linear elliptic problems on two- and three-dimensional regions
[DE85-014632] N86-13043

COMPUTER AIDED DESIGN
Automated design of composite plates for improved damage tolerance N86-12254
CAD program for high-power electron gun with annular cathode described N86-12468
Electronics Engineering Department Thrust Area report FY'84
[DE85-014857] N86-12539
Current CIM activities in the materials process engineering and fabrication directorate 7400
[DE85-015491] N86-12982
SCREAMER: A single-line pulsed-power design tool
[DE85-012837] N86-13014
Attempt to develop an intelligent lens design program
[DE85-014122] N86-13017
Design and implementation of the computer systems design environment network
[AD-A156832] N86-13022
Knowledge-based systems: How will they affect manufacturing in the 80's
[DE85-010601] N86-13027

COMPUTER AIDED MANUFACTURING
Current CIM activities in the materials process engineering and fabrication directorate 7400
[DE85-015491] N86-12982
Knowledge-based systems: How will they affect manufacturing in the 80's
[DE85-010601] N86-13027

COMPUTER AIDED MAPPING
Strategies for associating data and location in a geographic information system
[AD-A156118] N86-12746

COMPUTER ASSISTED INSTRUCTION
Systems for authoring computer-based instruction
[PB85-198950] N86-12987
Computer aided instruction in engineering
[AD-A156828] N86-13220

COMPUTER DESIGN
China report: Science and technology
[JPRS-CST-85-016] N86-12393

COMPUTER GRAPHICS
REFRIG-12: A graphics-augmented interactive program for designing vapor-compression refrigeration/heat pump cycles
[DE85-014205] N86-12572
Meteorological center's forecasts aid Venus probe tracking N85-12631
Hardware and software support of geological-geophysical database N86-12686
Generalized geographic mapping system for computer graphics
[PB85-212520] N86-12755
Scatter Diagram and Histogram Program - SCATR
[PB85-213346] N86-12935
Current CIM activities in the materials process engineering and fabrication directorate 7400
[DE85-015491] N86-12982
AISIM (Automated Interactive Simulation Modeling System) overview: Revision 1
[AD-A157392] N86-12990
Scientific workstation research
[DE85-013385] N86-13002
IMAGYS graphics programming language: Description and analysis
[DE85-013384] N86-13003
GRAFAID: An engineering tool
[DE85-013115] N86-13004

COMPUTER NETWORKS
Optic fiber applications in data communications
N86-12432
Investigation of magnetic field measurements
[AD-A157924] N86-12900
Current CIM activities in the materials process engineering and fabrication directorate 7400
[DE85-015491] N86-12982
Impact of linear programming on computer development
[AD-A157659] N86-12993
Design and implementation of the computer systems design environment network
[AD-A156832] N86-13022
LabNet Project plan
[DE85-014860] N86-13024

COMPUTER PROGRAMMING
Code of finite element analysis for three-dimensional flow in turbomachines N86-12398
Handbook of radio wave propagation loss (100-10,000 MHz)
[PB85-200012] N86-12502
A user's guide for the BIBSORT program for the IBM-PC personal computer
[AD-A157936] N86-12995
Automated reasoning and various applications
[DE85-014998] N86-12997
Data acquisition command interface using VAX/VMS DCL
[DE85-012747] N86-13019
Transistorized multigrid methods. 1: Linear elliptic problems on two- and three-dimensional regions
[DE85-014632] N86-13043
National Aeronautics and Space Administration
N85-13234

COMPUTER PROGRAMS
GRUMFOIL: A computer code for the viscous transonic flow over airfoils
[NASA-CR-3806] N86-12202
An evaluation of four methods of numerical analysis for two-dimensional airfoil flows. Revision
[AD-A157248] N86-12209
Development of an analytical model and code for the flapping response of a Hawte rotor blade
[D[illegible]08806] N86-12211
Real time flutter identification
[NASA-CR-3933] N86-12218
User's guide to STIPPAN: A panel method program for slotted tunnel interference prediction
[NASA-CR-178003] N86-12237
Deposition, microstructure and properties of laser CVD SiC films
[DE85-014680] N86-12327
A computer analysis of the distribution of principal stresses using photoelastic pattern N86-12375
Laser anemometer using a single circuit board
N86-12411
Programmer for single-chip microprocessor
N86-12448
Computer-aided analysis of arbitrary-shaped thin-wire antennas N86-12452
Hybrid 0-D,1-D, and 2-D model of helical explosive-driven magnetic flux compression generator
[DE85-013772] N86-12524
Heat Exchanger Vibration Analysis (HXVA) for prediction of tube bundle instabilities
[DE85-017144] N86-12568
DAA modal analysis for parametric investigations of fluid-structure interaction in underwater shock, revision 1
[DE85-012935] N86-12569
REFRIG-12: A graphics-augmented interactive program for designing vapor-compression refrigeration/heat pump cycles
[DE85-014205] N86-12572
Hardware and software support of geological-geophysical database N86-12686
First experiment in forecasting cool-season weather with the PROFS System
[PB85-230605] N86-12929
Correlation and Regression Equation Program REGRS
[PB85-213353] N86-12934
Scatter Diagram and Histogram Program - SCATR
[PB85-213346] N86-12935
Objective map analysis for the local AFOS MOS (Automation of Field Operations and Services Model Output Statistics) Program
[PB85-212884] N86-12936
Stimulus structures and mental representations in expert comprehension of computer programs
[AD-A157520] N86-12969
Generic software for emulating multiprocessor architectures
[AD-A157662] N86-12979
Current CIM activities in the materials process engineering and fabrication directorate 7400
[DE85-015491] N86-12982
Managing personal desktop computing at Argonne National Laboratory
[DE85-014976] N86-12983
Using the information resource dictionary system command language
[PB85-227783] N86-12988
Micro-PROUST
[AD-A157505] N86-12991
Numerical algorithms and mathematical software for linear control and estimation theory
[AD-A157525] N86-12992
Automated reasoning and various applications
[DE85-014998] N86-12997
Guidelines for a thermochemical kinetics computer program
[DE85-015671] N86-12998
Uncertainty propagation from raw data to final results
[DE85-011937] N86-13000
GRAFAID: An engineering tool
[DE85-013115] N86-13004
Second reference calculation for the WIPP
[DE85-013180] N86-13005
Tandem Mirror Reactor Systems Code (TMRSC)
[DE85-012891] N86-13006
Application of a binary cyclic error-correcting code
[DE85-013232] N86-13007
Application of automated reasoning software procedure generation system verifier
[DE85-014000] N86-13008
Data structures and vectorization in a two-dimensional free-Lagrangian code
[DE85-012948] N86-13009
Control of step size and order in extrapolation codes
[DE85-013261] N86-13010

FDSC: A microwave coupling code for slots of finite depth [DE85-013443] N86-13011

Design and use of digital filters with personal computer spreadsheet programs [DE85-013605] N86-13012

Program for simple algebra [DE85-013426] N86-13013

SCREAMER: A single-line pulsed-power design tool [DE85-012837] N86-13014

Building versatile tape handling software [DE85-009333] N86-13018

Spectral method for obtaining three-dimensional magnetohydrodynamic equilibria [DE85-015065] N86-13166

Identifying and evaluating COBOL competencies for four-year information systems programs N86-13223

COMPUTER STORAGE DEVICES

Dual drain MOSFET detector for crosstie memory systems [AD-D011828] N86-12513

COMPUTER SYSTEMS DESIGN

Microcomputer-controlled closed-loop system for positioning radio telescope N86-12410

Optic fiber applications in data communications N86-12432

Impact of linear programming on computer development [AD-A157659] N86-12993

A meta system for generating software engineering environments [AD-A158102] N86-12996

GRAFAID: An engineering tool [DE85-013115] N86-13004

Building versatile tape handling software [DE85-009333] N86-13018

COMPUTER SYSTEMS PERFORMANCE

Data acquisition interfaces for the IBM personal computer [DE85-014256] N86-12985

COMPUTER TECHNIQUES

Microcomputer-controlled closed-loop system for positioning radio telescope N86-12410

Human hemodynamic change under high atmospheric pressure N86-12458

Weather analysis programs using HP-41CV [AD-A157389] N86-12921

A theory for algorithm-based fault tolerance in array processor systems [AD-A156244] N86-12977

IMAGYS graphics programming language: Description and analysis [DE85-013384] N86-13003

Pilot's associate definition study [AD-A157106] N86-13026

Data acquisition system for SLD [DE85-014361] N86-13103

Implementing the automated features of the PBFA-I control/monitor systems [DE85-012841] N86-13144

COMPUTERIZED SIMULATION

Simulation of the enhanced traffic alert and collision avoidance system (TCAS 2) [NASA-CR-176328] N86-12216

The Record of Electrical and Communication Engineering Conversazione, volume 54, no. 1 [ISSN-0385-771-9] N86-12383

Proposal of a high efficient and high power peniotron N86-12384

Handbook of radio wave propagation loss (100-10,000 MHz) [PB85-200012] N86-12502

Self-consistent klystron simulations [DE85-012678] N86-12529

EE technical review [DE85-015313] N86-12540

Computer simulation of the effect of free surface reflection on shock wave propagation in water [DE85-014807] N86-12563

DAA modal analysis for parametric investigations of fluid-structure interaction in underwater shock, revision 1 [DE85-012935] N86-12569

Analysis of stratified flow mixing [DE85-006840] N86-12576

Droplet formation phenomena in dc electrical fields [DE85-014067] N86-12596

AISIM (Automated Interactive Simulation Modeling System) overview: Revision 1 [AD-A157392] N86-12990

MAGNUM-2D computer code: User's guide [DE85-013315] N86-13001

FDSC: A microwave coupling code for slots of finite depth [DE85-013443] N86-13011

TWOPOT: A computer model of the two-pot extractive distillation concept for nitric acid [DE85-013523] N86-13020

SLC injector modeling [DE85-013067] N86-13153

Conversion of the bounce-averaged Fokker-Planck code to conversion form [DE85-014861] N86-13160

Modeling of convection phenomena in Bridgman-Stockbarger crystal growth [NASA-CR-176325] N86-13188

Overview of free-piston Stirling technology at the NASA Lewis Research Center [NASA-TM-87156] N86-13236

Spectral identification/elimination of molecular species in spacecraft glow N86-13246

COMPUTERS

China report: Science and technology [JPRS-CST-85-024] N86-12368

China report: Science and technology [JPRS-CST-85-035] N86-12399

China report: Science and technology [JPRS-CST-85-022] N86-12439

China report: Science and technology [JPRS-CST-85-032] N86-12462

Velocity and gravity effects in relative permeability measurements [DE85-009925] N86-12570

The 32-bit computer for large memory applications on FASTBUS [DE85-012726] N86-12986

Impact of linear programming on computer development [AD-A157659] N86-12993

Parallel implementation of multifrontal schemes [DE85-014295] N86-13015

CONCENTRATION (COMPOSITION)

Influence of water vapor on distribution of turbulent wave parameters N86-12659

CONCRETE STRUCTURES

Influence of bonded reinforcement in post-tensioned prestressed concrete T-beams with unbonded tendons N86-12622

CONDENSATION

Structure-to-glass transition temperature relationships in high temperature stable condensation polyimides [NASA-TM-87113] N86-12311

CONDENSERS (LIQUEFIERS)

Condensation heat transfer in plate heat exchangers [DE85-012369] N86-12571

CONDUCTORS

Hillock-free conductor system for use in multilevel interconnects [DE85-012595] N86-12533

CONFERENCES

Search and retrieval index to EOS/ESD Symposium Proceedings 1979 to 1984 [AD-A158114] N86-12515

Photovoltaic Concentrator Technology Project Thirteenth Project Integration Meeting [DE85-013253] N86-12794

Indoor Air Quality Modeling Workshop report [PB85-212306] N86-12803

Geopotential Research Mission (GRM) [NASA-CP-2390] N86-12852

Review of spectroscopic parameters for upper atmospheric measurements [NASA-CP-2396] N86-13064

Conference summary: Antinucleon- and nucleon-nucleus interactions [DE85-013905] N86-13114

Making appropriations for the Department of Housing and Urban Development, and for sundry independent agencies, boards, commissions, corporations, and offices for the fiscal year ending September 30, 1986, and for other purposes [H-REPT-99-363] N86-13231

National Aeronautics and Space Administration N86-13232

Workshop on Water on Mars [NASA-CR-176289] N86-13282

CONFORMAL MAPPING

High-resolution, three-dimensional, seismic survey over the geopressured-geothermal reservoir at Parcperdue, Louisiana [DE85-016465] N86-12902

CONGRESSIONAL REPORTS

Making appropriations for the Department of Housing and Urban Development, and for sundry independent agencies, boards, commissions, corporations, and offices for the fiscal year ending September 30 1986, and for other purposes [H-REPT-99-363] N86-13231

Department of Housing and Urban Development, and Certain Other Independent Agencies Appropriations for Fiscal Year 1986, part 1 [S-HRG-99-221-PT-1] N86-13233

CONICS

BLR studies on conic model with LDA in FL-1 wind tunnel N86-12434

CONNECTORS

Length adjustable strut link with low aerodynamic drag [AD-D011851] N86-12232

CONSERVATION LAWS

Hyperbolic systems of conservation laws in several space variables [DE85-014019] N86-13042

Elementary waves and Riemann solutions: Their theory and their role in science [DE85-014018] N86-13045

CONSISTENCY

Aggregating individual preferences in the Analytic Hierarchy Process applied to the 1983 Battelle TAV study [AD-A155858] N86-13226

CONSTANTS

Stefan's problem in a finite domain with constant boundary and initial conditions analysis [AD-A158558] N86-13040

CONSTRUCTION INDUSTRY

China report: Science and technology [JPRS-CST-85-019] N86-12966

CONTACT LENSES

The effects of hypoxia induced by low atmospheric pressure on soft contact lens wear [AD-A158556] N86-12963

CONTAMINANTS

Design of a statewide groundwater monitoring network for Illinois [PB85-192821] N86-12750

Indoor Air Quality Modeling Workshop report [PB85-212306] N86-12803

CONTAMINATION

Diagnosing the causes of ground-water contamination using a mathematical model: Report on Technology Transfer Workshop [PB85-217008] N86-12808

Accidental exposure to americium [DE85-012794] N86-12965

Development of a radiation-hard CMOS process [NASA-CR-170925] N86-13187

CONTINENTAL DRIFT

The question of Earth expansion and its oceanic implications N86-12716

CONTINENTAL SHELVES

Oil and gs deposits on continental slopes of the ocean N86-12655

Gravity, geoid and the oceanic lithosphere N86-12860

CONTINENTS

The question of Earth expansion and its oceanic implications N86-12716

Continental and oceanic magnetic anomalies: Enhancement through GRM N86-12869

CONTINUITY (MATHEMATICS)

Transforming censored samples and testing fit [AD-A157957] N86-13048

CONTINUOUS SPECTRA

A model for explaining some features of shuttle glow N86-13256

CONTINUOUS WAVE LASERS

Pulsed digital multiplexed laser generator [AD-D011855] N86-12603

CONTROL

China report: Science and technology [JPRS-CST-85-024] N86-12368

Preventative maintenance for control systems [DE85-012029] N86-12525

Power and signal transmission for mobile teleoperated systems [DE85-013994] N86-12975

Future directions in mobile teleoperation [DE85-014308] N86-12976

User's manual for using MASON: A frequency response program which handles a system of transfer functions described by a signal flow graph [PB85-227106] N86-13021

CONTROL EQUIPMENT

Derivation of jack movement influence coefficients as a basis for selecting wall contours giving reduced levels of interference in flexible walled test sections [NASA-CR-177992] N86-12204

The 4-bit microprocessor capabilities, applications described N86-12406

Precision ion vacuum gage with logarithmic response [DE85-015312] N86-12588

Control problems in very large accelerators [DE85-014956] N86-13075

Implementing the automated features of the PBFA-I control/monitor systems
[DE85-012841] N86-13144
Multivariable current control for electrically and magnetically coupled superconducting magnets
[DE85-012941] N86-13163

CONTROL SYSTEMS DESIGN
China report: Science and technology
[JPRS-CST-85-022] N86-12439

CONTROL THEORY
Modeling and control of flexible structures
[AD-A157959] N86-12625
Numerical algorithms and mathematical software for linear control and estimation theory
[AD-A157525] N86-12992
Control of step size and order in extrapolation codes
[DE85-013261] N86-13010

CONTROL UNITS (COMPUTERS)
Internetting and packet satellite program
[AD-A157124] N86-12489
Design and implementation of the computer systems design environment network
[AD-A156832] N86-13022

CONTROL VALVES
Ultrahigh vacuum equipment described N86-12438

CONTROLLED ATMOSPHERES
Microgravity science and applications bibliography, 1985 revision
[NASA-TM-88178] N86-13225

CONTROLLERS
The 4-bit microprocessor capabilities, applications described N86-12406
Research on output feedback control
[NASA-CR-174253] N36-13028
Control problems in very large accelerators
[DE85-014956] N86-13075
Tritium control in helium-cooled blankets
[DE85-014783] N86-13116

CONVECTION
The source of the Earth's long wavelength geoid anomalies: Implications for mantle and core dynamics
N86-12872
The nature of symmetric instability and its similarity to convective and inertial instability
[NASA-CR-3945] N86-12918
Squall and cloud lines as structural components of an Arabian Sea convective cloud cluster
[AD-A157973] N86-12925
Mesoscale convective systems. A satellite-data-based climatology
[PB85-186862] N86-12931
Comparison among various thermodynamic parameters for the prediction of convective activity
[PB85-208217] N86-12932
Flow rates in the East Pacific rise (21 deg N) hot springs, and numerical investigations of two regimes of hydrothermal circulation N86-12939

CONVECTIVE FLOW
Interfacial stability in a two-layer benard problem
[AD-A158138] N86-12558
Modeling of convection phenomena in Bridgman-Stockbarger crystal growth
[NASA-CR-176325] N86-13188

CONVECTIVE HEAT TRANSFER
Cross flow boiling in tube bundles
[AD-A158557] N86-12562
The role of a pressure-dependent rheology in the dynamics of mantle circulation N86-12676
Small-scale convection beneath the transverse ranges, California: Implications for interpretation of gravity anomalies N86-12877
Evidence from satellite altimetry for small-scale convection in the mantle N86-12878
Modeling of convection phenomena in Bridgman-Stockbarger crystal growth
[NASA-CR-176325] N86-13188

CONVERGENT-DIVERGENT NOZZLES
Transonic noise generation by duct and profile flow
[AD-A157163] N86-13058

CONVERSION
Technique for measuring gas conversion factors
[NASA-CASE-LAR-13220-1] N86-12547

COOLANTS
Analysis of stratified flow mixing
[DE85-006840] N86-12576
Tritium control in helium-cooled blankets
[DE85-014783] N86-13116

COOLING
Comparative analysis of a Stirling heat pump with second- and third-order computer models
[DE85-013536] N86-12615
Properties of the lithosphere and asthenosphere deduced from geoid observations N86-12867

COOLING SYSTEMS
Analysis of stratified flow mixing
[DE85-006840] N86-12576
Suppression of propagating TE modes in the FNAL antiproton source stochastic beam cooling system
[DE85-016559] N86-13074
Stochastic beam cooling amplifier system front end components performance characteristics
[DE85-013925] N86-13079

COORDINATES
Scientific workstation research
[DE85-013385] N86-13002

COPOLYMERS
Epoxy phthalonitrile polymers
[AD-D011821] N86-12318

COPPER
Studies on unusally reactive metal powders: Preparation of new organometallic and organic compounds including potential new catalysts
[DE85-014844] N86-12309
Superconducting wire manufactured N86-12437
Foil fuses as opening switches for slow discharge circuits
[DE85-014124] N86-12519
Estimation of influence of ocean on distribution of heavy metals in marine atmosphere N86-12703

COPPER ALLOYS
Resistance to fracture, fatigue and stress-corrosion of Al-Cu-Li-Zr alloys
[AD-A158407] N86-12300
Electronic stakes in disordered solids. Part 3: Applications to materials science
[DE85-011416] N86-13213

COPPER OXIDES
Anaerobic microbial dissolution of toxic metals in subsurface environments
[DE85-013308] N86-12251

CORAL REEFS
Role of ahermatypic corals in sedimentation and ecology of coral banks N86-12678

CORES
Superconducting wire manufactured N86-12437

CORRELATION
Does the geoid drift west? N86-12892
Statistical evaluation of forecasts over the low-latitudes
[AD-A157926] N86-12923
Correlation and Regression Equation Program REGRS
[PB85-213353] N86-12934

CORRELATION COEFFICIENTS
Correlation characteristics of signals reflected by the wavy surface of ocean in mirror direction N86-12648
Scatter Diagram and Histogram Program - SCATR
[PB85-213346] N86-12935

CORROSION
Raman spectroscopy of molecular adsorbates
[DE85-012981] N86-12280
Effect of grain boundary structure on sensitization and corrosion of stainless steel
[AD-A157133] N86-12297
Deactivation and poisoning of fuel cell catalysts
[DE85-015127] N86-12521
Navy applications experience with small wind power systems
[AD-A158561] N86-12778
Absorption fluids data survey
[DE85-005279] N86-12792

CORROSION RESISTANCE
Properties of a retrogressed and re-aged 7075 aluminum alloy
[AD-A157415] N86-12298

COSMIC NOISE
Infrared measurements of spacecraft glow planned for Spacelab 2 N86-13263

COSMIC RAYS
High-elevation station's cosmic-ray recording system
N86-12687

COSMOLOGY
Large-basis shell-model technology in nucleosynthesis and cosmology
[DE85-012925] N86-13216
Trapped particle absorption by the ring of Jupiter
[NASA-CR-174408] N86-13279

COST ANALYSIS
Options for operational risk assessments
[DE85-014904] N86-12390
Control problems in very large accelerators
[DE85-014956] N86-13075
Information systems plan
[AD-A157911] N86-13227

COST EFFECTIVENESS
Method of using CTC to microcomputerize digital instruments N86-12441
Accelerated stress testing of thin film solar cells: Development of test methods and preliminary results
N86-12764
Large-area thin-film modules N86-12766
Thin film module development N86-12768
Outdoor performance testing of thin-film devices
N86-12771
Encapsulant selection and durability testing experience N86-12774
Low-cost light-weight thin material solar heating system
[DE85-012531] N86-12789

COST REDUCTION
FAA (Federal Aviation Administration) could improve overall aviation safety and reduce costs associated with airport instrument landing systems
[PB85-195444] N86-12215

COSTS
Towards a global MAP data base N86-12838
Tandem Mirror Reactor Systems Code (TMRSC)
[DE85-012891] N86-13006

COULOMB COLLISIONS
Laser scattering in plasma examined N86-12431

COUNTERFLOW
Study of significance of bottom relief in baroclinic model of equatorial countercurrent N86-12642

COUPLING
Coupling between spinor field, propagating torsion
N86-12420
FDSC: A microwave coupling code for slots of finite depth
[DE85-013443] N86-13011
IBEX magnetic coupling experiments
[DE85-014331] N86-13108
Deconfinement transition on a BCH lattice
[DE85-013887] N86-13207

COUPLING CIRCUITS
Stochastic beam cooling amplifier system front end components performance characteristics
[DE85-013925] N86-13079

COVARIANCE
Uncertainty propagation from raw data to final results
[DE85-011937] N86-13000

CRACK CLOSURE
Influence of load interactions on crack growth as related to state of stress and crack closure
[NASA-TM-87117] N86-12292

CRACK INITIATION
Fatigue crack propagation of nickel-base superalloys at 650 deg C
[NASA-TM-87150] N86-12294
Influence of bonded reinforcement in post-tensioned prestressed concrete T-beams with unbonded tendons
N86-12622

CRACK PROPAGATION
Influence of load interactions on crack growth as related to state of stress and crack closure
[NASA-TM-87117] N86-12292
Fatigue crack propagation of nickel-base superalloys at 650 deg C
[NASA-TM-87150] N86-12294
Thermally induced failures of thick-film glaze resistors
[DE85-012014] N86-12320
More on compliance of the three-point bend specimen
[AD-A156665] N86-12623
Strain energy density criteria for dynamic fracture and dynamic crack branching
[AD-A157914] N86-12624
Failure criteria used in a probabilistic fracture mechanics code
[DE85-007264] N86-12628

CRACKING (FRACTURING)
Mixed-mode cyclic debonding of adhesively bonded composite joints
[NASA-CR-177991] N86-12255

CRACKS
FDSC: A microwave coupling code for slots of finite depth
[DE85-013443] N86-13011

CRATERS
Underground volcanoes discovered with satellite radar
N86-12721

CREEP ANALYSIS
Fatigue crack propagation of nickel-base superalloys at 650 deg C
[NASA-TM-87150] N86-12294

CREEP PROPERTIES
An update of the total-strain version of SRP
[NASA-TP-2499] N86-12295

CRITICAL VELOCITY
Correction of compressor critical speed condition through fluid-film bearing optimization
[DE85-005507] N86-12617

CROP IDENTIFICATION
Evaluation of space SAR as a land-cover classification
[E86-10004] N86-12740

CROSS FLOW
Turbine blade and vane heat flux sensor development, phase 2
[NASA-CR-174995] N86-12226

CROSSLINKING
Study on electropainting using alkoxymethylmelamine as crosslinking agent N86-12380
CROSSTALK
Bandwidth efficient frequency-shift keyed communication systems N86-12472
CRUCIBLES
Self-contained hot-hollow cathode gun source assembly
[DE85-011652] N86-12530
CRUDE OIL
New methods for interpreting seismic waves in stratified media N86-12682
CRUSTAL FRACTURES
A major crustal feature in the southeastern United States inferred from the MAGSAT equivalent source anomaly field N86-12856
CRYOGENIC COMPUTER STORAGE
Lightweight cryogenic tank with positive expulsion
[AD-D011856] N86-12612
CRYOGENIC COOLING
Electrical losses and resistance of cryogenic inductors with consideration of the effect of magnetoresistance
[AD-A158185] N86-12516
Temperature and concentration dependence of hydrogen site occupancy in several rare-earth dihydrides
[DE85-015739] N86-13199
CRYOGENIC WIND TUNNELS
Introduction to cryogenic wind tunnels
[NASA-CR-177966] N86-12238
CRYOGENICS
China report: Science and technology
[JPRS-CST-85-035] N86-12399
CRYOPUMPING
Application of an atomic oxygen beam facility to the investigation of shuttle glow chemistry N86-13261
CRYSTAL DEFECTS
Wear of ion implanted TiB sub 2 surfaces
[DE85-017091] N86-13201
CRYSTAL GROWTH
Journal of the Chinese Silicate Society (selected articles)
[AD-A157497] N86-13190
CRYSTAL LATTICES
Theoretical studies of deep impurity levels in ternary semiconductor alloys
[AD-A157929] N86-13193
Deconfinement transition on a BCH lattice
[DE85-013887] N86-13207
Mossbauer effect and neutron diffraction study of the anomalous lattice behavior of U6Fe
[DE85-014912] N86-13210
CRYSTAL STRUCTURE
Effect of grain boundary structure on sensitization and corrosion of stainless steel
[AD-A157133] N86-12297
Theoretical modelling of the elastic properties of mantle silicates N86-12813
Derivation of the optical constants of anisotropic
[AD-A158396] N86-13195
CRYSTAL SURFACES
Surface crystallization on metallized 94 percent alumina ceramics
[DE85-008691] N86-12324
Journal of the Chinese Silicate Society (selected articles)
[AD-A157497] N86-13190
CRYSTALLINITY
Method for solving problems in electrodynamics of anisotropic media with slant bedding N86-12684
CRYSTALLIZATION
Hydrogen chloride sparging crystallization of the chloride salts of cobalt, manganese, and nickel
[PB85-197002] N86-12286
Semicrystalline casting process development and verification
[JPL-9950-1160] N86-12312
Surface crystallization on metallized 94 percent alumina ceramics
[DE85-008691] N86-12324
CRYSTALLOGRAPHY
Effect of grain boundary structure on sensitization and corrosion of stainless steel
[AD-A157133] N86-12297
Reliability and Engineering of Thin-Film Photovoltaic Modules. Research forum proceedings
[NASA-CR-176217] N86-12759
Recent developments in the structural crystallography of boron and the higher borides
[DE85-016930] N86-13202
CRYSTALS
Crystalline-silicon reliability lessons for thin-film modules N86-12760
Acoustically tuned optical filter system
[AD-D011791] N86-13184
CULTIVATION
Aquatic Species Program review: Proceedings of Principal Investigators Meeting
[DE85-012137] N86-12364
CURING
The 371 deg C mechanical properties of graphite/polyimide composites
[NASA-TM-87122] N86-12256
Steam-injection pressing of isocyanate-bonded aspen flakeboards, latitudes and limitations
[AD-A157833] N86-12389
CURRENT DISTRIBUTION
Computer-aided analysis of arbitrary-shaped thin-wire antennas N86-12452
CURRENT REGULATORS
Development of a current monitor system for measuring pulsed-beam current over a wide dynamic range
[DE85-012692] N86-13083
CURRENTS
Achievement of Bevalac rapid mode switching
[DE85-015130] N86-13092
CURVATURE
Numerical calculation of internal flows with curvature N86-12544
CYCLIC ACCELERATORS
Chaotic dynamical aperture
[DE85-013285] N86-13077
CYCLIC LOADS
Mixed-mode cyclic debonding of adhesively bonded composite joints
[NASA-CR-177991] N86-12255
CYCLOHEXANE
Thermodynamics of multi-polar molecules: The perturbed-anisotropic-chain theory
[DE85-013148] N86-12274
Droplet formation phenomena in dc electrical fields
[DE85-014067] N86-12596
CYCLONES
Observational-numerical study of maritime extratropical cyclones using FGGE (First GARP Global Experiment) data
[NASA-CR-176297] N86-12922
Annual data and verification tabulation eastern North Pacific tropical storms and hurricanes, 1984
[PB85-187888] N86-12930
CYCLOTRON RADIATION
Charge-state distributions of 100, 175, 275 and 352 MeV gold ions emerging from thin carbon foils
[DE85-014651] N86-13069
CYCLOTRON RESONANCE DEVICES
Development program for a 200 kW, cw gyrotron
[DE85-014887] N86-13096
CYGNUS CONSTELLATION
Combined ultraviolet studies of astronomical source
[NASA-CR-176165] N86-13274
CYLINDRICAL BODIES
Numerical and experimental studies of 3-D and unsteady turbulent body/appendage/propeller flows
[AD-A157078] N86-12552

D

DAMAGE
Automated design of composite plates for improved damage tolerance N86-12254
DAMPING
High order mode damping in the NSLS accelerating RF cavities by the use of damping antennae
[DE85-014214] N86-12498
Damping of high-frequency wind waves by artifical surface-active films N86-12692
DATA ACQUISITION
Absorption fluids data survey
[DE85-005279] N86-12792
Introduction to operational ASDAR system N86-12915
DAPHNE: The design of a parallel multiprocessor data acquisition system
[DE85-013875] N86-12984
Data acquisition interfaces for the IBM personal computer
[DE85-014256] N86-12985
Data acquisition command interface using VAX/VMS DCL
[DE85-012747] N86-13019
Data acquisition system for SLD
[DE85-014361] N86-13103
FASTBUS for the particle accelerator laboratories
[DE85-014352] N86-13122
DATA BASE MANAGEMENT SYSTEMS
Strategies for associating data and location in a geographic information system
[AD-A158118] N86-12746
Information systems plan
[AD-A157911] N86-13227
DATA BASES
Minutes of Workshop on Composite Materials Test Methods
[AD-A157903] N86-12262
Study and investigation to update the nonelectronic reliability notebook. Revision A
[AD-A157242] N86-12619
Hardware and software support of geological-geophysical database N86-12686
Towards a global MAP data base N86-12838
Statistical evaluation of forecasts over the low-latitudes
[AD-A157926] N86-12923
Correlation and Regression Equation Program REGRS
[PB85-213353] N86-12934
DATA CONVERSION ROUTINES
Building versatile tape handling software
[DE85-009333] N86-13018
DATA LINKS
Optic fiber applications in data communications N86-12432
DATA MANAGEMENT
Hardware and software support of geological-geophysical database N86-12686
DATA PROCESSING
Real-time flutter identification
[NASA-CR-3933] N86-12218
China report: Science and technology
[JPRS-CST-85-034] N86-12430
Influence of short gravity waves on thermal radio emission of water surface N86-12644
Hardware and software support of geological-geophysical database N86-12686
Managing data analysis through save-states
[DE85-012456] N86-12999
GRAFAID: An engineering tool
[DE85-013115] N86-13004
Building versatile tape handling software
[DE85-009333] N86-13018
DATA PROCESSING EQUIPMENT
Information systems plan
[AD-A157911] N86-13227
DATA PROCESSING TERMINALS
General plot subroutine package for the Hewlett Packard 5451C Fourier analyzer
[AD-A157127] N86-12989
DATA REDUCTION
Analytical and experimental studies of wakes behind circularly capped bubbles N86-12548
Study and investigation to update the nonelectronic reliability notebook. Revision A
[AD-A157242] N86-12619
Feasibility of using LANDSAT images of vegetation cover to estimate effective hydraulic properties of soils
[E86-10003] N86-12739
The 32-bit computer for large memory applications on FASTBUS
[DE85-012726] N86-12986
Managing data analysis through save-states
[DE85-012456] N86-12999
Uncertainty propagation from raw data to final results
[DE85-011937] N86-13000
Light mass elements total half-lives for selected long-lived nuclides
[DE85-014217] N86-13115
DATA STORAGE
The 32-bit computer for large memory applications on FASTBUS
[DE85-012726] N86-12986
Managing data analysis through save-states
[DE85-012456] N86-12999
DATA STRUCTURES
Data structures and vectorization in a two-dimensional free-Lagrangian code
[DE85-012948] N86-13009
DATA TRANSMISSION
Optic fiber applications in data communications N86-12432
Internetting and packet satellite program
[AD-A157124] N86-12489
Power and signal transmission for mobile teleoperated systems
[DE85-013994] N86-12975
LabNet Project plan
[DE85-014860] N86-13024
DEACTIVATION
Deactivation and poisoning of fuel cell catalysts
[DE85-015127] N86-12521
DEBYE-SCHERRER METHOD
X-ray diffraction cell for Debye-Scherrer and Guinier (Huber) cameras at pressure and temperature
[DE85-014815] N86-12593
DECAY
Influence of some oceanographic characteristics on decay kinetcis of surface-active agents in sea N86-12676

Optical radiation from the interaction of energetic atoms, ions, electrons, and photons with surfaces N86-13259
DECISION MAKING
Real-time computing of the environmental consequences of an atmospheric accidental release of radioactive material: User's point of view
[DE85-016438] N86-12795
Aggregating individual preferences in the Analytic Hierarchy Process applied to the 1983 Battelle TAV study
[AD-A155858] N86-13226
DECISION THEORY
Options for operational risk assessments
[DE85-014904] N86-12390
DECONTAMINATION
Accidental exposure to americium
[DE85-012794] N86-12965
DEFENSE PROGRAM
Strategic defense initiatives at Los Alamos National Laboratory
[DE85-014093] N86-12608
Naval surface weapons center technology transfer biennial report (Fiscal year 1983/1984)
[AD-A157919] N86-13238
DEFLAGRATION
Unsteady detonation N86-12542
DEFORMATION
Macroscopic and microscopic deformation and failure processes that control composite toughness
[DE85-012938] N86-12263
Review of effects of long-term aging on the mechanical properties and microstructures of types 304 and 316 stainless steel
[DE85-016472] N86-12304
Theory for the Portevin-LeChatelier effect
[DE85-004030] N86-12627
Variation in seismicity under influence of lunar-solar tidal deformations N86-12726
Geodetically derived strain from San Francisco Bay to the Mendocino Triple Junction, California
[PB85-198802] N86-12905
Shocking behavior of fluid flow in deformable joints
[DE85-010104] N86-13107
X-ray diffraction studies of shock-modified inorganic materials
[DE85-015150] N86-13209
DEGASSING
Adsorption/desorption properties of vacuum materials for the 6 GeV synchrotron
[DE85-010276] N86-12252
DEGRADATION
Hot-spot heating susceptibility due to reverse bias operating conditions N86-12763
Thin film module development N86-12768
Thin film module electrical configuration versus electrical performance N86-12770
Development of a radiation-hard CMOS process
[NASA-CR-170925] N86-13187
Theoretical studies of deep impurity levels in ternary semiconductor alloys
[AD-A157929] N86-13193
DEGREES OF FREEDOM
Transport near the onset of stochasticity
[DE85-014765] N86-13218
DEHUMIDIFICATION
Isothermal dehumidification of air in a parallel passage configuration
[DE85-008819] N86-12577
DELAY CIRCUITS
Low dispersion notch filter for multi-GHz frequencies using fiber optics delays
[DE85-014983] N86-12520
DEMODULATION
Technique for the reduction of fading in interferometers
[AD-D011845] N86-12581
DENSE PLASMAS
Plane-wave theory of electrical transport in disordered systems
[DE85-015353] N86-13167
DENSIMETERS
Development of a continuous mass flow measuring flow
[DE85-012492] N86-12573
DENSITY (MASS/VOLUME)
Superheated steam's density compensation for flow measurement N86-12426
Spectrum of turbulent fluctuations in sea water density in region of large wave numbers N86-12646
Plasma volume methodology: Evans blue, hemoglobin-hematocrit, and mass density transformations
[NASA-TM-86834] N86-12956
Space shuttle mechanistic studies to characterize atomic oxygen interactions with surfaces N86-13267
DENSITY DISTRIBUTION
Bandwidth efficient frequency-shift keyed communication systems N86-12472
Temperature structure of the 80 km to 120 km region N86-12830
Properties of the lithosphere and asthenosphere deduced from geoid observations N86-12867
Microwave field strength measurement in a Rubidium clock cavity via adiabatic rapid passage
[AD-A157070] N86-13065
Plasma and magnetospheric research
[NASA-CR-176326] N86-13138
DENSITY MEASUREMENT
The shuttle glow: A program to study the ram-induced phenomena N86-13268
DEPOSITION
Deposition, microstructure and properties of laser CVD SiC films
[DE85-014680] N86-12327
Spatial and temporal patterns of acid precipitation and their interpretation
[PB85-214377] N86-12809
DEPOSITS
Oxidation and gum formation in diesel fuels
[AD-A157410] N86-12360
DEPTH
Experience in breaking down gravity field into components resulting from density heterogeneities at various depths (using North Atlantic and Mediterranean as examples) N86-12728
DEPTH MEASUREMENT
New data of relief of Mazca Ridge N86-12679
New approach to some problems in seismology N86-12683
DESERTS
Navy applications experience with small wind power systems
[AD-A158561] N86-12778
DESIGN
Attempt to develop an intelligent lens design program
[DE85-014122] N86-13017
DESIGN ANALYSIS
Latch-up effect in CMOS described N86-12443
REFRIG-12: A graphics-augmented interactive program for designing vapor-compression refrigeration/heat pump cycles
[DE85-014205] N86-12572
Precision ion vacuum gage with logarithmic response
[DE85-015312] N86-12588
Electrical safety requirements: Implications for the module designer N86-12765
User's manual for using MASON: A frequency response program which handles a system of transfer functions described by a signal flow graph
[PB85-227106] N86-13021
Research on output feedback control
[NASA-CR-174253] N86-13028
Nearly ideal lens optimization procedure
[DE85-014116] N86-13134
DESORPTION
Adsorption/desorption properties of vacuum materials for the 6 GeV synchrotron
[DE85-010276] N86-12252
Infrared emission from desorbed NO2(*) and NO(*) N86-13254
The NO-NO2 system at laboratory surfaces N86-13255
Activated recombinative desorption: A potential component in mechanisms of spacecraft glow N86-13256
DESTRUCTIVE TESTS
Development and evaluation of a microburst test apparatus for use as a minimum destructive test for parachute material
[AD-A158110] N86-12620
DETECTION
Pulsed radiation detection technology discussed N86-12424
Simultaneous detection of time coincident signals in an adaptive Doppler tracker
[AD-D011796] N86-12473
Dual drain MOSFET detector for crosstie memory systems
[AD-D011826] N86-12513
Recent developments in microshell-tipped optical fibers as high-pressure shock detectors
[DE85-015750] N86-12594
New passive helicopter detector
[DE85-015160] N86-12595
Reversible optical waveguide vapor sensor
[AD-D011834] N86-13124
DETONATION
Energetic response of propellants to high velocity impact, revision 1
[DE85-013983] N86-12365
Characteristic value as an energy output index for explosives N86-12418
Motion of thin metal walls and the equation of state of detonation products
[DE85-014809] N86-12629
DETONATION WAVES
Unsteady detonation N86-12542
DEUTERIDES
Second order elastic contents of Pd, PdH(0.7) and PdD(0.7) between 1.7 and 50 K
[DE85-014316] N86-13212
DEUTERIUM
Hydrogen and deuterium N86-12335
Field-reversed configuration formation, translation, and confinement studies on the FRX-C/T experiment
[DE85-014095] N86-13141
DIAMONDS
Novel instrument for high-pressure research at ultra-high temperatures
[DE85-015674] N86-12589
DIAPHRAGMS
Frequency selection and mode locking of Nd:YAG laser N86-12395
DIBORANE
The boranes N86-12336
DICTIONARIES
Using the information resource dictionary system command language
[PB85-227783] N86-12968
DIELECTRIC PROPERTIES
Renormalization of an inverse scattering theory for inhomogeneous dielectrics
[AD-A157224] N86-12492
DIELECTRICS
Evaluation of high permittivity glass ceramics for millimeter wave applications
[AD-A158551] N86-12319
Experiments with domestic IC substrates N86-12433
Integral equation description of integrated dielectric waveguides N86-12504
Derivation of the optical constants of anisotropic
[AD-A158396] N86-13195
DIESEL ENGINES
Solar walk-off protection
[DE85-012112] N86-12788
DIESEL FUELS
Microemulsion-type fire-resistant diesel fuel
[AD-A157125] N86-12359
Oxidation and gum formation in diesel fuels
[AD-A157410] N86-12360
DIFFERENCE EQUATIONS
A Floquet decomposition for Volterra equations with periodic kernel and a transform approach to linear recursion equations
[AD-A158148] N86-13037
DIFFERENTIAL CALCULUS
Program for simple algebra
[DE85-013426] N86-13013
DIFFERENTIAL EQUATIONS
Numerical calculation of turbulent buoyant flow N86-12541
A new method for global optimization based on stochastic differential equations
[AD-A157546] N86-13029
Hamilton-Jacobi equations in infinite dimensions. Part 2: Existence of viscosity solutions
[AD-A158137] N86-13035
Control of step size and order in extrapolation codes
[DE85-010122] N86-13041
Pade and reciprocal approximants and linear NOLOR functions
[DE85-015057] N86-13044
DIFFERENTIATION
Global optimization using automatic differentiation and interval iteration
[AD-A158150] N86-13039
DIFFUSION
Experimental study of the combustion of gas-air mixtures in a channel and the diffusion combustion in a slipstream at high velocities
[AD-A157495] N86-12271
A TiW diffusion barrier for AuZn ohmic contacts to p-type InP
[AD-D011823] N86-12511
Viscous nonlinear circulation in axisymmetric baroclinic eddy N86-12712
Real-time computing of the environmental consequences of an atmospheric accidental release of radioactive material: User's point of view
[DE85-016438] N86-12795
Biological effects of acoustic cavitation
[AD-A157513] N86-13059
Diffusion in binary plasma mixtures
[DE85-017694] N86-13143

DIFFUSION COEFFICIENT
The orientation distribution of nonspherical aerosol particles within a cloud
[AD-A157363] N86-12554
DIGITAL DATA
Correcting a digital map data base with scene analysis concepts and methods
[AD-A157913] N86-12745
DIGITAL FILTERS
Hybrid radar waveform design utilizing complementary phase coding and linear frequency stepping for achieving improved slant range resolution in a synthetic aperature radar N86-12470
Design and use of digital filters with personal computer spreadsheet programs
[DE85-013805] N86-13012
DIGITAL INTEGRATORS
Semicustom integrated circuit design at Sandia National Laboratories
[DE85-015661] N86-12538
DIGITAL SYSTEMS
Method of using CTC to microcomputerize digital instruments N86-12441
An evolving digital telecommunications industry and its impact on the operational environment of the Nationwide Emergency Telecommunication System (NETS)
[AD-A156831] N86-12488
Advanced digital communication research
[AD-A158412] N86-12497
LANDSAT-4 TM image data quality analysis for energy-related applications
[E86-10006] N86-12742
The design and hardware evaluation of an advanced 16-bit, low-power, high performance microcomputer system for digital signal processing
[AD-A158130] N86-12981
DIGITAL TECHNIQUES
Digital phase meter using CMOS-LED introduced N86-12442
Design and use of digital filters with personal computer spreadsheet programs
[DE85-013805] N86-13012
Fundamentals of adaptive signal processing
[DE85-014933] N86-13016
DIHYDRIDES
Temperature and concentration dependence of hydrogen site occupancy in several rare-earth dihydrides
[DE85-015739] N86-13199
DIMENSIONS
Evaluation of space SAR as a land-cover classification
[E86-10004] N86-12740
Gravity theories in more than four dimensions
[DE85-011164] N86-12903
DIMERS
Application of time-dependent Raman theory to the analysis of inorganic photosystems
[DE85-012752] N86-12285
DINITRATES
Otto fuel 2 N86-12334
DIODES
Hysteresis characteristics of a diode loaded E-M loop sensor N86-12385
Nonlinear electromagnetic scattering from a diode circuit
[AD-A157216] N86-12491
Laser-based foilless diode
[DE85-013958] N86-12537
Thin-film module circuit design: Practical and reliability aspects N86-12762
Generalization of the Child-Langmuir relation for one-dimensional time-dependent diodes
[DE85-012677] N86-13145
DIRECT CURRENT
The step structure effect of dc Josephson current within one flux quantum period phi sub zero (2) N86-12412
DISASTERS
An evolving digital telecommunications industry and its impact on the operational environment of the Nationwide Emergency Telecommunication System (NETS)
[AD-A156831] N86-12488
DISCRETE FUNCTIONS
A survey of some recent results in continuous univariate distributions
[AD-A157450] N86-13047
DISKS (SHAPES)
A user's guide for the BIBSORT program for the IBM-PC personal computer
[AD-A157936] N86-12995
DISPERSING
Determination of single-mode optical fiber dispersion N86-12409
High power laser dump
[AD-D011792] N86-12597
Experimental study of flow and dispersion in the wakes of three-dimensional low hills
[PB85-193266] N86-12906
DISPERSIONS
Frequency selection and mode locking of Nd:YAG laser N86-12395
Low dispersion notch filter for multi-GHz frequencies using fiber optics delays
[DE85-014983] N86-12520
DISPLACEMENT
Classical piezoelectricity: Is the theory complete
[DE85-014592] N86-12536
Dislocation kinetics behind shear shocks
[DE85-014811] N86-12566
More on compliance of the three-point bend specimen
[AD-A156665] N86-12623
DISPLACEMENT MEASUREMENT
Laser vibrometer
[AD-D011811] N86-12602
DISSOLVING
Molten salt corrosion of SiC: Pitting mechanism
[NASA-TM-87143] N86-12310
Estimation of influence of ocean on distribution of heavy metals in marine atmosphere N86-12703
DISTANCE MEASURING EQUIPMENT
Lasers measure drifting mountains N86-12718
DISTILLATION
TWOPOT: A computer model of the two-pot extractive distillation concept for nitric acid
[DE85-013523] N86-13020
DISTRIBUTED PROCESSING
Human cognition and performance
[AD-A157665] N86-12970
Actors: A model of concurrent computation in distributed systems
[AD-A157917] N86-12994
Decentralized control of scheduling in distributed systems
[AD-A157656] N86-13222
DISTRIBUTION (PROPERTY)
A survey of some recent results in continuous univariate distributions
[AD-A157450] N86-13047
DISTRIBUTION FUNCTIONS
New representations of the non-central chi-square density and cumulative
[AD-A157227] N86-13046
Compound poisson approximations for sums of random variables
[AD-A158555] N86-13049
DIURNAL VARIATIONS
Atmospheric tides below 80 km N86-12824
Modeling the diurnal variation of meteorlogical variables within the boundary layer: Preliminary comparison results
[PB85-198349] N86-12933
DIVING (UNDERWATER)
Saclantcen's use of scuba diving in oceanographic and acoustic research
[AD-A156714] N86-12941
DMSP SATELLITES
Precipitating electron and ion detectors (SSJ/4) for the block 5D/Flights 6-10 DMSP (Defense Meteorological Satellite Program) satellites: Calibration and data presentation
[AD-A157080] N86-12896
Global view of the upper level outflow patterns associated with tropical cyclone intensity changes during FGGE
[NASA-CR-174407] N86-12908
DOCUMENTS
Word lists to limit vocabulary in technical information
[AD-A157931] N86-13228
DOMES (STRUCTURAL FORMS)
Full-scale fire tests of polyurethane foam dome structures
[AD-A157107] N86-12314
DOPPLER EFFECT
Interpretation of the geoid N86-12873
Theory of the anomalous Doppler instability during lower-hybrid current drive
[DE85-014064] N86-13170
DRAG MEASUREMENT
Air Force Academy Aeronautics Digest
[AD-A157215] N86-12200
DRAG REDUCTION
Length adjustable strut link with low aerodynamic drag
[AD-D011851] N86-12232
China report: Science and technology
[JPRS-CST-85-029] N86-12446
Wingtip sails tested on Y-5 aircraft N86-12450
DRAINAGE
Recent changes in climate and world water balance N86-12638
Water Information Bulletin No. 30, Part 13: Geothermal investigations in Idaho. Preliminary geologic reconnaissance of the geothermal occurrences of the Wood River drainage area
[DE85-016972] N86-12747
Waters resources data for Minnesota. Water year 1983. Volume 2: Upper Mississippi and Missouri River Basins
[PB85-215994] N86-12753
DRAINAGE PATTERNS
Upper mesozoic turbidites of southern west Sakhalin downwarp N86-12645
DROP SIZE
Kinetics of evaporation and growth of drops of aqueous solutions of surface active substances at negative temperatures
[AD-A156961] N86-12269
Study of the mist cooling and droplet dynamics in turbulent flow by using LDA N86-12545
Optical technique to study the impact of heavy rain on aircraft performance
[NASA-CR-177989] N86-12580
Radiation fog modeling
[AD-A157971] N86-12924
DROPS (LIQUIDS)
Liquid droplet radiator program at the NASA Lewis Research Center
[NASA-TM-87139] N86-12246
Droplet formation phenomena in dc electrical fields
[DE85-014067] N86-12596
DUCTED FLOW
The prediction of fully developed turbulent pressure drops in a triangular duct for a power law fluid N86-12546
Measurements on an axisymmetric jet in a slow coflowing stream N86-12549
DUCTILITY
Fracture surface analysis in composite and titanium bonding
[NASA-CR-176309] N86-12257
DUCTS
Transonic noise generation by duct and profile flow
[AD-A157163] N86-13058
DWARF NOVAE
Combined ultraviolet studies of astronomical source
[NASA-CR-176165] N86-13274
DWARF STARS
Combined ultraviolet studies of astronomical source
[NASA-CR-176165] N86-13274
DYE LASERS
A high precision rate dye laser pumped by a CuCl laser N86-12457
Direct solar-pumped iodine laser amplifier
[NASA-CR-176324] N86-12600
Applied lasers (selected articles)
[AD-A155948] N86-12601
DYNAMIC CHARACTERISTICS
Variational principle for penetrator dynamics using bilinear functional and adjoint formulation
[AD-A157964] N86-13031
Tevatron global radius and Os system
[DE85-017442] N86-13101
Diffusion in binary plasma mixtures
[DE85-017694] N86-13143
DYNAMIC CONTROL
Molecular control
[NASA-TM-87510] N86-12313
DYNAMIC MODELS
Modeling of seasonal evolution of carbon cycle in ocean-atmosphere system N86-12641
DYNAMIC RESPONSE
Rapid estimation of frequency response functions by close-range photogrammetry
[NASA-TP-2471] N86-12579
Sound scattering by a layered sphere
[AD-A157915] N86-13060
DYNAMIC STABILITY
The dynamic stability of the stratosphere and mesosphere N86-12811
DYNAMIC STRUCTURAL ANALYSIS
NASA LeRC/Akron University Graduate Cooperative Fellowship Program and Graduate Student Researchers Program
[NASA-CR-174826] N86-13219
DYNAMICAL SYSTEMS
Adaptive Kalman filtering with control input estimation N86-12503
DYNAMOMETERS
Preliminary design of linear alternator dynamometer for free piston Stirling engines
[DE85-015078] N86-12614

E

E REGION
Theory support of pulsed power experiments. Volume 3. E-beam chamber design
[AD-A158417] N86-13098

EAR
Dummy head microphone and its application to the measurements of electro-acoustic equipments N86-12379
EARTH (PLANET)
USSR report: Earth sciences [JPRS-UES-85-006] N86-12630
The question of Earth expansion and its oceanic implications N86-12716
EARTH ALBEDO
Estimate of radiation-climatic effects of natural and anthropogenic aerosol N86-12640
EARTH ATMOSPHERE
Eddy fluxes of heat, vorticity and momentum in ocean and atmosphere and their parameterization (review) N86-12672
Ionic mechanicsm of exchange of admixtures between hydrosphere and atmosphere N86-12690
Ocean albedo for atmospheric thermal emission N86-12707
Atmospheric tritium 1968-1984 [DE85-013133] N86-12798
Carbon dioxide in arctic and subarctic regions [DE85-014054] N86-12901
Magnetic reconnection in the terrestrial magnetosphere [DE85-014107] N86-12904
EARTH CORE
magnetic minerals and characteristics of natural magnetic state of core in Saatly superdeep hole in depth range 3500-7500 meters N86-12681
The source of the Earth's long wavelength geoid anomalies: Implications for mantle and core dynamics N86-12872
Separation of core and crustal magnetic field sources N86-12884
The magnetic field at the core-mantle boundary N86-12885
Some anticipated contributions to core fluid dynamics from the GRM N86-12886
Expected contribution of the Geopotential Research Mission (GRM) to studies of liquid core fluid dynamics N86-12890
The source of the intermediate wavelength component of the Earth's magnetic field N86-12891
Does the geoid drift west? N86-12892
EARTH CRUST
Intrusive rocks of oceanic lithosphere as possible sources of anomalous magnetic field of ocean N86-12651
Geochemistry and energetics of cycling of matter in formation of crust in active structures of ocean N86-12653
magnetic minerals and characteristics of natural magnetic state of core in Saatly superdeep hole in depth range 3500-7500 meters N86-12681
Optimal density model of Earth's rust and upper mantle along Kamchatka-Pacific Geotraverse N86-12725
Geopotential Research Mission (GRM) [NASA-CP-2390] N86-12852
Why do we need detailed gravity over continents: Some Australian examples N86-12855
Satellite magnetic modeling of north African hot spots N86-12858
Magnetic structure of the crust N86-12859
Studies of the marine crustal magnetization at intermediate wavelengths N86-12862
GRM crustal magnetic anomalies: Separating the Lord Howe Rise and Norfolk Ridge submarine structures N86-12865
Continental and oceanic magnetic anomalies: Enhancement through GRM N86-12869
Modeling gravity and magnetic fields for crustal and upper mantle structures N86-12880
Separation of core and crustal magnetic field sources N86-12884
Recent MAGSAT results N86-12888
Do MAGSAT anomalies contain a record of past and present-day mantle convection under South America? N86-12895
Geodetically derived strain from San Francisco Bay to the Mendocino Triple Junction, California [PB85-198802] N86-12905
EARTH HYDROSPHERE
Ionic mechanicsm of exchange of admixtures between hydrosphere and atmosphere N86-12690
EARTH MANTLE
Magmatic provinces and tectonics in Pacific Ocean N86-12652
Geochemistry and energetics of cycling of matter in formation of crust in active structures of ocean N86-12653
Theoretical modelling of the elastic properties of mantle silicates N86-12813
Sea floor swells and mantle plumes N86-12866
The importance of GRM gravity observations in continental regions N86-12871
The source of the Earth's long wavelength geoid anomalies: Implications for mantle and core dynamics N86-12872
Interpretation of the geoid N86-12873
Mantle convection and the large scale structures of the Earth's gravitational field N86-12874
Small-scale convection beneath the transverse ranges, California: Implications for interpretation of gravity anomalies N86-12877
Evidence from satellite altimetry for small-scale convection in the mantle N86-12878
Mantle viscosity, J2 and the nontidal acceleration of Earth rotation N86-12879
Modeling gravity and magnetic fields for crustal and upper mantle structures N86-12880
The magnetic field at the core-mantle boundary N86-12885
Some anticipated contributions to core fluid dynamics from the GRM N86-12886
Expected contribution of the Geopotential Research Mission (GRM) to studies of liquid core fluid dynamics N86-12890
Does the geoid drift west? N86-12892
Do MAGSAT anomalies contain a record of past and present-day mantle convection under South America? N86-12895
EARTH MOVEMENTS
Lasers measure drifting mountains N86-12718
Hypocentral areas of aftershocks and possible fault systems at foci of Tsunami-generating Kuril earthquakes N86-12729
EARTH OBSERVATIONS (FROM SPACE)
Comparison of time-periodic variations in temperature and wind from meteorological rockets and satellites N86-12825
EARTH ORBITS
Vehicle glow measurements on the space shuttle N86-13240
Investigation of vehicle glow in the far ultraviolet N86-13249
EARTH PLANETARY STRUCTURE
The question of Earth expansion and its oceanic implications N86-12716
Geophysical interpretation of the magnetic anomalies of the Earth derived from MAGSAT data N86-12857
Magnetic structure of the crust N86-12859
Gravity, geoid and the oceanic lithosphere N86-12860
Thermal cooling of the oceanic lithosphere from geoid height data N86-12861
Lithospheric structure in the Pacific geoid N86-12863
GRM crustal magnetic anomalies: Separating the Lord Howe Rise and Norfolk Ridge submarine structures N86-12865
Sea floor swells and mantle plumes N86-12866
The importance of GRM gravity observations in continental regions N86-12871
EARTH RESOURCES
Launch of Kosmos-1653 natural resources research satellite N86-12719
EARTH RESOURCES PROGRAM
Earth resources: A continuing bibliography, issue 46 [NASA-SP-7041(46)] N86-12738
EARTH ROTATION
Mantle viscosity, J2 and the nontidal acceleration of Earth rotation N86-12879
Contributions of GRM to the ocean topography experiment (TOPEX) N86-12883
EARTH SURFACE
Global modeling of optical characteristics of atmospheric aerosol N86-12695
EARTHQUAKE RESISTANT STRUCTURES
Earthquake-response simulation on horizontally large-scale buildings based on the method of reduction concerning their restoring spring matrix. Derivation of general form of spring matrix and comparison of applied response results on an actual building with measured values N86-12374
EARTHQUAKES
Research Reports of the Faculty of Engineering, Tokyo Denki University, no. 32 [ISSN-0389-617-X] N86-12372
New approach to some problems in seismology N86-12683
Features of field of directions and velocities of propagation of fractures at earthquake foci in northern Muya region of Baykal Rift Zone N86-12685
P-wave spectra in problem of determining dynamic paramters of earthquake foci. Standardization of initial data and procedures for computing amplitude spectra N86-12722
Variation in seismicity under influence of lunar-solar tidal deformations N86-12726
Electromagnetic effects in crustal fracturing N86-12727
Hypocentral areas of aftershocks and possible fault systems at foci of Tsunami-generating Kuril earthquakes N86-12729
Method and results of electrometric observations in seismically active region N86-12730
Seismic effect of underground blasts and problem of estimating total earthquake energy N86-12731
Seismological studies of the tectonics of divergent plate boundaries N86-12812
ECOLOGY
Role of ahermatypic corals in sedimentation and ecology of coral banks N86-12678
Atmospheric tritium 1968-1984 [DE85-013133] N86-12798
ECONOMIC ANALYSIS
Radio-absorbing materials [AD-A157496] N86-12495
Identifying heavy-ion-beam fusion design and system features with high economic leverage [DE85-014849] N86-13181
ECONOMIC DEVELOPMENT
Benefits of surveying, cartography described N86-12402
ECONOMICS
Science, technology and the industrialization of laser-driven processes [DE85-014656] N86-12605
R and D limited partnerships (possible applications in advanced communications satellite technology experiment program) [NASA-CR-176333] N86-13221
ECOSYSTEMS
Towards a global MAP data base N86-12838
Environmental impact research program. Status and source of habitat models and literature reviews, December 1984 [AD-A156899] N86-12950
EDDY CURRENTS
Multifrequency eddy-current inspection of seam weld in steel sheath [DE85-013533] N86-12626
EDITING
Word lists to limit vocabulary in technical information [AD-A157931] N86-13228
EDITING ROUTINES (COMPUTERS)
A user's guide for the BIBSORT program for the IBM-PC personal computer [AD-A157936] N86-12995
EDUCATION
The helicopter to fixed wing conversion program: A critical review [AD-A156820] N86-12968
Systems for authoring computer-based instruction [PB85-198950] N86-12987
Identifying and evaluating COBOL competencies for four-year information systems programs N86-13223
EFFICIENCY
Thin-film module circuit design: Practical and reliability aspects N86-12762
Interconnect resistance of photovoltaic submodules N86-12767
Thin film module development N86-12768
Aeronautical technology 2000: A projection of advanced vehicle concepts [NASA-CR-176322] N86-13235
EIGENVALUES
Effects of whistler-mode and other waves in the magnetosphere [AD-A157832] N86-12899
Alfven continuum with toroidicity [DE85-015821] N86-13217
EIGENVECTORS
Effects of whistler-mode and other waves in the magnetosphere [AD-A157832] N86-12899
ELASTIC PROPERTIES
The 371 deg C mechanical properties of graphite/polyimide composites [NASA-TM-87122] N86-12256
Effects of microstructure on the acoustoelastic measurements of stress [DE85-015518] N86-12307
Investigation of elastic properties of marine surface-active films N86-12708
Theoretical modelling of the elastic properties of mantle silicates N86-12813
Sound scattering by a layered sphere [AD-A157915] N86-13060
Second order elastic contents of Pd, PdH(0.7) and PdD(0.7) between 1.7 and 50 K [DE85-014316] N86-13212

ELASTIC SCATTERING
Spin-polarization observables in elastic electron scattering from spin-1/2 nuclei
[DE85-016639] N86-13072
R-matrix analysis of the (7) Li system with peripheral channel overlap exchange effects
[DE85-012751] N86-13148
ELASTOMERS
Role of chemical bonding in adhesion
[AD-A157251] N86-12316
ELECTRIC BATTERIES
High rate Li/SOC1(2) cells. 1. Effect of design variables in uncatalyzed cells
[AD-A157203] N86-12776
Zinc/ferricyanide battery development phase 4
[DE85-016026] N86-12781
Solar walk-off protection
[DE85-012112] N86-12788
ELECTRIC COILS
Calculation of series capacitance for transient analysis of windings N86-12528
ORNL ground coil analytical and experimental studies
[DE85-005246] N86-12783
ELECTRIC CONNECTORS
Demountable coaxial electrical connector for in-line amplifiers
[AD-D011831] N86-12507
ELECTRIC CONTACTS
A TiW diffusion barrier for AuZn ohmic contacts to p-type InP
[AD-D011823] N86-12511
ELECTRIC CURRENT
Parallel, staged opening switch power conditioning techniques for flux compression generator applications
[DE85-012761] N86-12527
ELECTRIC FIELDS
Droplet formation phenomena in dc electrical fields
[DE85-014067] N86-12596
Contribution of diffusion processes to the electric field of the ocean N86-12654
Features of electrical measurements in sea as medium with field of extraneous forces N86-12700
Minimizing the energy spread within a single bunch by shaping its charge distribution
[DE85-013064] N86-13151
ELECTRIC FILTERS
Low dispersion notch filter for multi-GHz frequencies using fiber optics delays
[DE85-014983] N86-12520
ELECTRIC GENERATORS
SOLERAS: Photovoltaic power systems project. Module failure analysis
[MRI/SOL-0101] N86-12756
Crystalline-silicon reliability lessons for thin-film modules N86-12760
Accelerated stress testing of thin film solar cells: Development of test methods and preliminary results
N86-12764
Navy applications experience with small wind power systems
[AD-A158561] N86-12778
Identifying heavy-ion-beam fusion design and system features with high economic leverage
[DE85-014849] N86-13181
ELECTRIC POTENTIAL
Design of high power superconducting switches
N86-12505
Laser-based foilless diode
[DE85-013958] N86-12537
Electromagnetic effects in crustal fracturing
N86-12727
Module voltage isolation and corrosion research
N86-12772
ELECTRIC POWER PLANTS
Photovoltaic Concentrator Technology Project Thirteenth Project Integration Meeting
[DE85-013253] N86-12794
Assessment of the long-term precision of continuous emission monitors
[PB85-201150] N86-12804
ELECTRIC POWER SUPPLIES
EE technical review
[DE85-015313] N86-12540
Maintenance of photovoltaic power systems, revision 1
[AD-A157838] N86-12777
Multivariable current control for electrically and magnetically coupled superconducting magnets
[DE85-012941] N86-13163
Magnet power supply control of the NSLS VUV and X-ray storage rings transfer lines
[DE85-014213] N86-13168
ELECTRIC SWITCHES
Photoconductive semiconductor switching for pulsed power applications
[DE85-013859] N86-12531
ELECTRIC TERMINALS
Amorphous silicon photovoltaic modules and test devices design, fabrication and testing N86-12769
ELECTRIC WIRE
Superconducting wire manufactured N86-12437
ELECTRICAL ENGINEERING
PBFA-2 insulator stack design from an engineering viewpoint
[DE85-013437] N86-12245
China report: Science and technology
[JPRS-CST-85-035] N86-12399
Search and retrieval index to EOS/ESD Symposium Proceedings 1979 to 1984
[AD-A158114] N86-12515
ELECTRICAL FAULTS
Photoconductive semiconductor switching for pulsed power applications
[DE85-013859] N86-12531
SOLERAS: Photovoltaic power systems project. Module failure analysis
[MRI/SOL-0101] N86-12756
Electrical safety requirements: Implications for the module designer N86-12765
Large-area thin-film modules N86-12766
Module voltage isolation and corrosion research
N86-12772
ELECTRICAL IMPEDANCE
A method for determining acoustic-liner admittance in ducts with sheared flow in two-cross-sectional directions
[NASA-TP-2518] N86-13056
ELECTRICAL INSULATION
PBFA-2 insulator stack design from an engineering viewpoint
[DE85-013437] N86-12245
Electrical safety requirements: Implications for the module designer N86-12765
Compound semiconductor insulator interface research
[AD-A157277] N86-13189
ELECTRICAL MEASUREMENT
Features of electrical measurements in sea as medium with field of extraneous forces N86-12700
SOLERAS: Photovoltaic power systems project. Module failure analysis
[MRI/SOL-0101] N86-12756
ELECTRICAL PROPERTIES
Investigation of reactive magnetron sputter deposited ZnSe for solar cell application
[DE85-016851] N86-12780
Some anticipated contributions to core fluid dynamics from the GRM N86-12886
ELECTRICAL RESISTANCE
Electrical losses and resistance of cryogenic inductors with consideration of the effect of magnetoresistance
[AD-A158185] N86-12516
Hot-spot heating susceptibility due to reverse bias operating conditions N86-12763
Interconnect resistance of photovoltaic submodules
N86-12767
Thin film module electrical configuration versus electrical performance N86-12770
ELECTRICAL RESISTIVITY
Preparation and properties of thin film reversible cathode materials
[AD-A158431] N86-12273
Possibility of sounding Earth by using electromagnetic field of sea current N86-12661
Plane-wave theory of electrical transport in disordered systems
[DE85-015353] N86-13167
Electronic stakes in disordered solids. Part 3: Applications to materials science
[DE85-011416] N86-13213
ELECTRO-OPTICAL PHOTOGRAPHY
Improved approach to characterizing and presenting streak camera performance
[DE85-015188] N86-12587
ELECTRO-OPTICS
Electro-optical transmission and liquid water content of fogs and clouds
[AD-A157506] N86-13128
Radiation effects on light sources and detectors
[DE85-014746] N86-13133
European Science Notes. Volume 39, number 8
[AD-A157146] N86-13237
ELECTROACOUSTIC TRANSDUCERS
Saclantcen's use of scuba diving in oceanographic and acoustic research
[AD-A156714] N86-12941
ELECTROCATALYSTS
Deactivation and poisoning of fuel cell catalysts
[DE85-015127] N86-12521
Develop and test fuel cell powered on-site integrated total energy systems: Phase 3, full-scale power plant development
[NASA-CR-174948] N86-12757
Develop and test fuel cell powered on-site integrated total energy systems: Phase 3, full-scale power plant development
[NASA-CR-174996] N86-12758
ELECTROCHEMICAL CELLS
Preparation and properties of thin film reversible cathode materials
[AD-A158431] N86-12273
Lithium-thionyl chloride cell system safety hazard analysis
[AD-A157089] N86-12775
High rate Li/SOC1(2) cells. 1. Effect of design variables in uncatalyzed cells
[AD-A157203] N86-12776
ELECTROCHEMICAL CORROSION
Metal dissolution kinetics in organic solvents using rotating ring-disc voltammetry
[DE85-013478] N86-12253
Module voltage isolation and corrosion research
N86-12772
ELECTROCHEMICAL MACHINING
Electrochemical machining of the outer profile of the B83 Lug
[DE85-014934] N86-12616
ELECTROCHEMISTRY
Electrochemical deposition of glassy chromium on copper
[DE85-004081] N86-12275
Reduction of CO2 to methanol and methane by photo and dark reactions on semiconductor electrodes
[PB85-226298] N86-12290
ELECTRODEPOSITION
Electrochemical deposition of glassy chromium on copper
[DE85-004081] N86-12275
ELECTRODES
Evaluation parameters for the alkaline fuel cell oxygen electrode
[NASA-TM-87155] N86-12268
Reduction of CO2 to methanol and methane by photo and dark reactions on semiconductor electrodes
[PB85-226298] N86-12290
Arc discharge conditioning test on the Oak Ridge 25 URC accelerator
[DE85-016394] N86-12523
Electrolytic pressure transduction system
[AD-D011847] N86-12584
Zinc/ferricyanide battery development phase 4
[DE85-016026] N86-12781
ELECTRODYNAMICS
Method for solving problems in electrodynamics of anisotropic media with slant bedding N86-12684
Features of electrical measurements in sea as medium with field of extraneous forces N86-12700
ELECTROLYSIS
China report: Science and technology
[JPRS-CST-85-030] N86-12451
Usages of organic membranes in electrolytic industry described N86-12453
ELECTROLYTES
Electrochemical deposition of glassy chromium on copper
[DE85-004081] N86-12275
Develop and test fuel cell powered on-site integrated total energy systems: Phase 3, full-scale power plant development
[NASA-CR-174948] N86-12757
Zinc/ferricyanide battery development phase 4
[DE85-016026] N86-12781
ELECTROMAGNETIC ABSORPTION
Impact of GRM: New evidence from the Soviet Union
N86-12853
ELECTROMAGNETIC COMPATIBILITY
Basic EMC (Electromagnetic compatibility) technology advancement for C3 (Command, control, and communications) systems. Volume 6
[AD-A157239] N86-12493
ELECTROMAGNETIC FIELDS
Hysteresis characteristics of a diode loaded E-M loop sensor N86-12385
The step structure effect of dc Josephson current within one flux quantum period phi sub zero (2) N86-12412
Coupling between spinor field, propagating torsion
N86-12420
Possibility of sounding Earth by using electromagnetic field of sea current N86-12661
Electromagnetic field of three-dimensional surface sea waves N86-12662
Features of electrical measurements in sea as medium with field of extraneous forces N86-12700
Replica-space renormalization in random-field systems
[DE85-014800] N86-13055
Microwave field strength measurement in a Rubidium clock cavity via adiabatic rapid passage
[AD-A157070] N86-13065

Reconstruction of longitudinal beam profiles from nondestructive electromagnetic probes
[DE85-012675] N86-13078
ELECTROMAGNETIC INTERFERENCE
Basic EMC (Electromagnetic compatibility) technology advancement for C3 (Command, control, and communications) systems. Volume 6
[AD-A157239] N86-12493
ELECTROMAGNETIC MEASUREMENT
Scattering experiments at the Ipswich Electromagnetic Measurements Facility: Backscatter from metal cubes
[AD-A157925] N86-12496
ELECTROMAGNETIC NOISE
The role of amplitude-to-phase conversion in the generation of oscillator flicker phase noise
[NASA-TM-87590] N86-12508
Theories of statistical equilibrium in electron-positron colliding-beam storage rings
[DE85-012303] N86-13080
Analysis and interpretation of the shock-like electrostatic noise observed during the AMPTE (Active Magnetospheric Particle Tracer Explorers) solar wind lithium releases
[AD-A157512] N86-13283
ELECTROMAGNETIC PROPERTIES
Theory support of pulsed power experiments. Volume 3. E-beam chamber design
[AD-A158417] N86-13098
ELECTROMAGNETIC PULSES
FDSC: A microwave coupling code for slots of finite depth
[DE85-013443] N86-13011
ELECTROMAGNETIC RADIATION
Electromagnetic effects in crustal fracturing
N86-12727
Wave propagation and pair formation in pulsar magnetospheres N86-13276
ELECTROMAGNETIC SCATTERING
Nonlinear electromagnetic scattering from a diode circuit
[AD-A157216] N86-12491
Scattering experiments at the Ipswich Electromagnetic Measurements Facility: Backscatter from metal cubes
[AD-A157925] N86-12496
Phase operator method in problem of scattering of electromagnetic waves on ideally conducting surface
N86-12701
ELECTROMAGNETIC WAVE TRANSMISSION
PRospects for development of seismic prospecting methods and apparatus N86-12723
Atmospheric IR transmission measurements in a tropical maritime environment: Comparison with the LOWTRAN 6 model
[AD-A157920] N86-13129
ELECTROMAGNETISM
Strategy for reflector pattern calculation: Let the computer do the work
[NASA-TM-87137] N86-12485
Phase operator method in problem of scattering of electromagnetic waves on ideally conducting surface
N86-12701
Data analysis of airborne electromagnetic bathymetry
[AD-A157132] N86-12744
ELECTROMAGNETS
Magnet power supply control of the NSLS VUV and X-ray storage rings transfer lines
[DE85-014213] N86-13168
ELECTROMECHANICS
Method and results of electrometric observations in seismically active region N86-12730
ELECTROMETERS
Precision ion vacuum gage with logarithmic response
[DE85-015312] N86-12588
ELECTRON ACCELERATORS
Mathematical model of the dynamic response of thermo-regulating in 200 MeV linear accelerator
N86-12407
ELECTRON ATTACHMENT
New beam neutralization concept: Laser photodetachment in a magnetic field
[DE85-014655] N86-12607
ELECTRON BEAMS
RIIM accelerator beam experiments
[DE85-012034] N86-12244
China develops 6J KrF laser N86-12465
CAD program for high-power electron gun with annular cathode described N86-12468
Self-contained hot-hollow cathode gun source assembly
[DE85-011652] N86-12530
Reconstruction of longitudinal beam profiles from nondestructive electromagnetic probes
[DE85-012675] N86-13078
Electron emission of over 200 A/cm (2) from a pulsed-laser irradiated photocathode
[DE85-012656] N86-13084
Theory support of pulsed power experiments. Volume 3. E-beam chamber design
[AD-A158417] N86-13098
IBEX magnetic coupling experiments
[DE85-014331] N86-13108
RADLAC program status
[DE85-014708] N86-13109
Improvement of manufacturing techniques and quality of optical scratch standards for fire control systems
[AD-A157963] N86-13130
Generalization of the Child-Langmuir relation for one-dimensional time-dependent diodes
[DE85-012677] N86-13145
Commissioning and operation of the Nuclear Physics Injector at SLAC
[DE85-013374] N86-13159
ELECTRON BOMBARDMENT
Optical radiation from the interaction of energetic atoms, ions, electrons, and photons with surfaces N86-13259
ELECTRON BUNCHES
Racetrack microtron rf system
[DE85-012669] N86-12532
Beam emittance and beam disruption
[DE85-015136] N86-13070
Reconstruction of longitudinal beam profiles from nondestructive electromagnetic probes
[DE85-012675] N86-13078
Tevatron global radius and Os system
[DE85-017442] N86-13101
Minimizing the energy spread within a single bunch by shaping its charge distribution
[DE85-013064] N86-13151
Real time bunch length measurements in the SLC linac
[DE85-014362] N86-13169
ELECTRON COUNTERS
The shuttle glow: A program to study the ram-induced phenomena N86-13268
ELECTRON CYCLOTRON HEATING
The 140 GHz gyrotron development program
[DE85-011923] N86-12534
Development program for a 200 kW, cw gyrotron
[DE85-014887] N86-13096
ELECTRON DENSITY (CONCENTRATION)
Submillimeter wave propagation in tokamak plasmas
[DE85-007747] N86-13154
ELECTRON DENSITY PROFILES
Electrons and cosmic ray produced in Saturn's inner magnetosphere N86-13281
ELECTRON DIFFRACTION
Diffraction and microscopy studies of the structure of grain boundaries in Fe, Fe-base alloys and ceramic materials
[DE85-016950] N86-13198
ELECTRON EMISSION
Electron emission of over 200 A/cm (2) from a pulsed-laser irradiated photocathode
[DE85-012656] N86-13084
ELECTRON ENERGY
Behavior of ionized plasma in the high latitude topside ionosphere
[AD-A157930] N86-13140
Absorption and hot electron generation in uv (351 nm) driven spherical imploding targets
[DE85-014405] N86-13161
New method of determining the current carrier concentration in a substance in the state of superconductivity
[AD-A158182] N86-13194
ELECTRON GAS
Behavior of ionized plasma in the high latitude topside ionosphere
[AD-A157930] N86-13140
ELECTRON GUNS
CAD program for high-power electron gun with annular cathode described N86-12468
Self-contained hot-hollow cathode gun source assembly
[DE85-011652] N86-12530
The 140 GHz gyrotron development program
[DE85-011923] N86-12534
ELECTRON MICROSCOPES
Effect of grain boundary structure on sensitization and corrosion of stainless steel
[AD-A157133] N86-12297
ELECTRON MICROSCOPY
Combined small angle X-ray scattering and transmission electron microscope studies of Al-Li alloys
[DE85-016356] N86-12303
Thermally induced failures of thick-film glaze resistors
[DE85-012014] N86-12320
Diffraction and microscopy studies of the structure of grain boundaries in Fe, Fe-base alloys and ceramic materials
[DE85-016950] N86-13198
ELECTRON PRECIPITATION
Precipitating electron and ion detectors (SSJ/4) for the block 5D/Flights 6-10 DMSP (Defense Meteorological Satellite Program) satellites: Calibration and data presentation
[AD-A157080] N86-12896
ELECTRON SCATTERING
Spin-polarization observables in elastic electron scattering from spin-1/2 nuclei
[DE85-016639] N86-13072
Theories of statistical equilibrium in electron-positron colliding-beam storage rings
[DE85-012303] N86-13080
ELECTRON SPECTROSCOPY
Theoretical studies of deep impurity levels in ternary semiconductor alloys
[AD-A157929] N86-13193
ELECTRON STATES
Quantum simulations of small electron-hole complexes
[DE85-013895] N86-13205
ELECTRON TRANSFER
Charge transfer in multiple site chemical systems
[AD-A157413] N86-12270
ELECTRON TRANSITIONS
A dressed atom interpretation of adiabatic rapid passage
[AD-A157071] N86-13066
Isovector resonances in pion charge exchange
[DE85-012746] N86-13106
ELECTRONIC CONTROL
Electronics Engineering Department Thrust Area report FY'84
[DE85-014857] N86-12539
ELECTRONIC COUNTERMEASURES
Radio-absorbing materials
[AD-A157496] N86-12495
ELECTRONIC EQUIPMENT
Improved temperature detection system for use on film cooled turbine airfoils
[AD-D011762] N86-12228
China report: Science and technology
[JPRS-CST-85-022] N86-12439
Preventative maintenance for control systems
[DE85-012029] N86-12525
Electronics Engineering Department Thrust Area report FY'84
[DE85-014857] N86-12539
ELECTRONIC SPECTRA
Secondary electron spectra: A semiempirical model
[DE85-012448] N86-13086
ELECTRONIC TRANSDUCERS
The Record of Electrical and Communication Engineering Conversazione, volume 54, no. 1
[ISSN-0385-771-9] N86-12383
Hysteresis characteristics of a diode loaded E-M loop sensor N86-12385
ELECTRONS
Influence of water vapor on distribution of turbulent wave parameters N86-12659
Effects of whistler-mode and other waves in the magnetosphere
[AD-A157832] N86-12899
Multiplicities in high energy interactions
[DE85-013847] N86-13100
Physics of e(+) - e(-) colliders: Present, future and far future
[DE85-009895] N86-13121
ELECTROPLATING
Research Reports of the Faculty of Engineering, Tokyo Denki University, no. 32
[ISSN-0389-617-X] N86-12372
Study on electropainting using alkoxymethylmelamine as crosslinking agent N86-12380
ELECTROSTATIC CHARGE
A note on Jupiter's gossamer ring N86-13280
ELECTROSTATIC GYROSCOPES
Transient test of suspension electronics for gyroscope
[AD-D011853] N86-12585
ELECTROSTATIC PROBES
Precipitating electron and ion detectors (SSJ/4) for the block 5D/Flights 6-10 DMSP (Defense Meteorological Satellite Program) satellites: Calibration and data presentation
[AD-A157080] N86-12896
ELECTROSTATIC WAVES
Theory of the anomalous Doppler instability during lower-hybrid current drive
[DE85-014064] N86-13170
ELECTROSTATICS
Arc discharge conditioning test on the Oak Ridge 25 URC accelerator
[DE85-016394] N86-12523
Analysis and interpretation of the shock-like electrostatic noise observed during the AMPTE (Active Magnetospheric Particle Tracer Explorers) solar wind lithium releases
[AD-A157512] N86-13283

ELEMENTARY EXCITATIONS
Temperature dependence of the magnetic excitations in Gd
[DE85-016303] N86-13203

ELLIPSOIDS
Analytical and experimental studies of wakes behind circularly capped bubbles N86-12548

ELLIPSOMETERS
Ellipsometric surface analysis of wear tracks produced by different lubricants
[NASA-TM-87142] N86-12293

ELLIPTIC FUNCTIONS
Transistorized multigrid methods. 1: Linear elliptic problems on two- and three-dimensional regions
[DE85-014632] N86-13043

ELLIPTICITY
Use of an elliptical aperture to control saturation in closely-coupled, cold iron, superconducting dipole magnets
[DE85-012259] N86-13053

EMBRITTLEMENT
Macroscopic and microscopic deformation and failure processes that control composite toughness
[DE85-012936] N86-12263

EMERGENCIES
An evolving digital telecommunications industry and its impact on the operational environment of the Nationwide Emergency Telecommunication System (NETS)
[AD-A156831] N86-12466

EMISSION
Evaluation of air emissions from hazardous waste treatment, storage and disposal facilities
[PB85-203792] N86-12806

EMISSION SPECTRA
Materials and process characterization to determine the effect of high intensity infrared laser radiation on a composite material
[AD-A157094] N86-12260
Spectral identification/elimination of molecular species in spacecraft glow N86-13246
The UV-VIS optical environment of the shuttle N86-13247
A model for explaining some features of shuttle glow N86-13256
Ultraviolet observations of low-excitation Herbig-Haro objects
[NASA-CR-176164] N86-13273

EMITTANCE
Funneling: An initial beam dynamics study
[DE85-012652] N86-13082
FMIT diagnostic instrumentation
[DE85-012668] N86-13087
SLC injector modeling
[DE85-013067] N86-13153
Real time bunch length measurements in the SLC linac
[DE85-014362] N86-13169
Second Workshop on Spacecraft Glow
[NASA-CP-2391] N86-13239
The UV-VIS optical environment of the shuttle N86-13247

EMITTERS
High frequency silicon bipolar transistor with SIPOS (Semi-insulating polycrystalline silicon) heterojunction emitter and ion implanted rapid thermal annealed base region
[AD-A157141] N86-12510

ENCAPSULATED MICROCIRCUITS
Crystalline-silicon reliability lessons for thin-film modules N86-12760
Hot-spot heating susceptibility due to reverse bias operating conditions N86-12763

ENCAPSULATING
Module voltage isolation and corrosion research N86-12772
Glass breaking strength: The role of surface flaws and treatments N86-12773
Encapsulant selection and durability testing experience N86-12774
Investigation of test methods, material properties and processes for solar cell encapsulants
[DE85-012831] N86-12786

ENDOTHERMIC REACTIONS
Materials and process characterization to determine the effect of high intensity infrared laser radiation on a composite material
[AD-A157094] N86-12260

ENERGY ABSORPTION
Trapped particle absorption by the ring of Jupiter
[NASA-CR-174408] N86-13279

ENERGY ABSORPTION FILMS
Film stability for dirct absorption receivers
[DE85-012135] N86-12791

ENERGY CONSUMPTION
Energy expenditure and activity patterns of cadets at the United States Military Academy, West Point, New York
[AD-A157857] N86-12960

ENERGY CONVERSION
Small scale wind energy conversion programmatic equipment
[DE85-012319] N86-12793

ENERGY DISSIPATION
Turbulence in the altitude region 80-120 km N86-12834
Theories of statistical equilibrium in electron-positron colliding-beam storage rings
[DE85-012303] N86-13080
Energy dispersive spectroscopy using synchrotron radiation: Intensity considerations
[DE85-017530] N86-13200

ENERGY DISTRIBUTION
FMIT diagnostic instrumentation
[DE85-012668] N86-13087
Measurements and calculations of neutron scattering angular distributions over a wide mass and energy range
[DE85-012812] N86-13105
Minimizing the energy spread within a single bunch by shaping its charge distribution
[DE85-013064] N86-13151
Surface-catalyzed recombination into excited electronic, vibrational, rotational, and kinetic energy states: A review N86-13253
Physico-chemical conditions in circumstellar shells of evolved oxygen-rich M stars N86-13275

ENERGY LEVELS
Isovector resonances in pion charge exchange
[DE85-012746] N86-13106

ENERGY POLICY
LANDSAT-4 TM image data quality analysis for energy-related applications
[E86-10006] N86-12742

ENERGY SPECTRA
RIIM accelerator beam experiments
[DE85-012034] N86-12244
Multiple-scale turbulence closure modeling of confined recirculating flows
[NASA-CR-178536] N86-12551
Effects of whistler-mode and other waves in the magnetosphere
[AD-A157832] N86-12899
Partition of cross sections in asymmetric nucleus-nucleus reactions and the origin of fast alpha particles
[DE85-014989] N86-13089
Multiplicities in high energy interactions
[DE85-013847] N86-13100
Isovector resonances in pion charge exchange
[DE85-012746] N86-13106

ENERGY STORAGE
Reduction of CO2 to methanol and methane by photo and dark reactions on semiconductor electrodes
[PB85-226298] N86-12290
Studies of energy storage and transfer in gas lasers
[AD-A158553] N86-12604
Synthesis of research and development in mechanical energy storage technologies
[DE85-013313] N86-12782

ENERGY TECHNOLOGY
China report: Science and technology
[JPRS-CST-85-025] N86-12444
Role of supercomputers in magnetic fusion and energy research programs
[DE85-013200] N86-13023

ENERGY TRANSFER
Energetic response of propellants to high velocity impact, revision 1
[DE85-013983] N86-12365
Theoretical studies of molecular interactions
[DE85-012604] N86-13076

ENGINE DESIGN
NASA LeRC/Akron University Graduate Cooperative Fellowship Program and Graduate Student Researchers Program
[NASA-CR-174826] N86-13219

ENGINE INLETS
Compressor research facility F100 high pressure compressor inlet total pressure and swirl profile simulation
[AD-A157108] N86-12229

ENGINEERING DRAWINGS
Precision ion vacuum gage with logarithmic response
[DE85-015312] N86-12588

ENGINES
Overview of free-piston Stirling technology at the NASA Lewis Research Center
[NASA-TM-87156] N86-13236

ENTRAINMENT
Combustion in turbulent jets and buoyant plumes
[PB85-220655] N86-12288

ENVIRONMENT EFFECTS
Influence of power engineering on climate N86-12637
Towards a global MAP data base N86-12838

ENVIRONMENT POLLUTION
Statistical methods for environmental pollution studies
[DE85-005298] N86-12799

ENVIRONMENT SIMULATION
Comparison of continuous speech, discrete speech, and keyboard input to an interactive warfare simulation in various C3 environments
[AD-A156830] N86-12487

ENVIRONMENTAL MONITORING
Main problems in climate monitoring (diagnosis) N86-12633
Statistical methods for environmental pollution studies
[DE85-005298] N86-12799
Environmental impact research program. Status and source of habitat models and literature reviews, December 1984
[AD-A156899] N86-12950

ENVIRONMENTAL QUALITY
China report: Science and technology
[JPRS-CST-85-016] N86-12393
China report: Science and technology
[JPRS-CST-85-017] N86-12406
China report: Science and technology
[JPRS-CST-85-022] N86-12439
China report: Science and technology
[JPRS-CST-85-025] N86-12444

ENVIRONMENTAL SURVEYS
Environmental impact research program. Status and source of habitat models and literature reviews, December 1984
[AD-A156899] N86-12950

ENZYMES
Molecular control
[NASA-TM-87510] N86-12313
Influence of seston phosphatase activity on rate of phosphorus mineralization and its recycling in production-destruction cycle N86-12667

EPIDEMIOLOGY
Studies of participants in nuclear tests N86-12964

EPITAXY
Method for the deposition of high-quality crystal epitaxial films of iron
[AD-D011842] N86-13186
Channeling analysis of strain in superlattices
[DE85-014437] N86-13197

EPOXY COMPOUNDS
Ground-based investigations of atomic oxygen interactions with space station surfaces
[DE85-014082] N86-12249
Statistical treatment of aramid/epoxy stress-rupture data
[AD-A157239] N86-12315

EPOXY RESINS
Dynamic small angle X-ray scattering study of stressed Kevlar 49 epoxy composites
[DE85-011408] N86-12264
Epoxy phthalonitrile polymers
[AD-D011821] N86-12318

EQUATIONS OF MOTION
Numerical computation of full three-dimensional flow in transonic turbines N86-12397
Numerical calculation of internal flows with curvature N86-12544
Relationships between prime-rich Euler type equations and a triangular array of the odd integers
[AD-A157928] N86-13030
Chaotic dynamical aperture
[DE85-013285] N86-13077

EQUATIONS OF STATE
New corresponding states theory using the second virial coefficient as the temperature variable
[PB85-219624] N86-12289
Numerical studies of the dynamic isentropic loading of solid molecular hydrogen
[DE85-013961] N86-12391
Motion of thin metal walls and the equation of state of detonation products
[DE85-014809] N86-12629

EQUATORS
Study of significance of bottom relief in baroclinic model of equatorial countercurrent N86-12342

EQUILIBRIUM EQUATIONS
Theories of statistical equilibrium in electron-positron colliding-beam storage rings
[DE85-012303] N86-13080

EROSION
Wear of projectile rotating bands
[AD-A156666] N86-12358

The production of glow precursors by oxidative erosion of spacecraft surfaces N86-13257
ERROR ANALYSIS
On the geographical correlation of orbit error N86-12881
Fundamentals of adaptive signal processing [DE85-014933] N86-13016
ERROR CORRECTING DEVICES
Application of a binary cyclic error-correcting code [DE85-013232] N86-13007
ERROR DETECTION CODES
A theory for algorithm-based fault tolerance in array processor systems [AD-A156244] N86-12977
ERRORS
Rationale for a GRAVSAT-MAGSAT mission: A perspective on the problem of external/internal transient field effects N86-12887
ESCAPE SYSTEMS
Parachute recovery systems design manual, chapters 1 through 4 offprint [AD-A157839] N86-12210
ESOPHAGUS
Electrolytic pressure transduction system [AD-D011847] N86-12584
ESTERS
Ellipsometric surface analysis of wear tracks produced by different lubricants [NASA-TM-87142] N86-12293
ESTIMATES
Seismic effect of underground blasts and problem of estimating total earthquake energy N86-12731
Assessment of the long-term precision of continuous emission monitors [PB85-201150] N86-12804
A new hazard function estimator of performance time [AD-A157843] N86-12971
C infinity-regularity for the porous median equation [AD-A158147] N86-13036
Estimating the reliability of fiber optics cables [DE85-014892] N86-13136
Space shuttle mechanistic studies to characterize atomic oxygen interactions with surfaces N86-13267
ESTIMATING
Numerical algorithms and mathematical software for linear control and estimation theory [AD-A157525] N86-12992
ETCHING
Ground-based investigations of atomic oxygen interactions with space station surfaces [DE85-014082] N86-12249
Large-area thin-film modules N86-12766
Improvement of manufacturing techniques and quality of optical scratch standards for fire control systems [AD-A157963] N86-13130
Laser diagnostic studies of plasma etching and deposition [DE85-009494] N86-13178
ETHYL ALCOHOL
The alcohols N86-12349
ETHYLENE
Investigation of test methods, material properties and processes for solar cell encapsulants [DE85-012831] N86-12786
ETHYLENE COMPOUNDS
Method to detect ethylene glycol in gaseous mixtures [AD-A158109] N86-12272
ETHYLENE OXIDE
High pressure and molecular weight variation of electrical relaxation in poly(ethylene oxide) [AD-A157660] N86-12317
Ethylene oxide N86-12333
EULER-LAGRANGE EQUATION
Gravity theories in more than four dimensions [DE85-011164] N86-12903
EVALUATION
Optical disk technology assessment [AD-A157909] N86-12582
Light mass elements total half-lives for selected long-lived nuclides [DE85-014217] N86-13115
Identifying and evaluating COBOL competencies for four-year information systems programs N86-13223
EVAPORATION
Kinetics of evaporation and growth of drops of aqueous solutions of surface active substances at negative temperatures [AD-A156961] N86-12269
Ionic mechanicsm of exchange of admixtures between hydrosphere and atmosphere N86-12690
EVAPORATORS
Heat pipe wick [AD-D011852] N86-12559
EVENTS
DAPHNE: The design of a parallel multiprocessor data acquisition system [DE85-013875] N86-12984
EVOLUTION (DEVELOPMENT)
Role of ahermatypic corals in sedimentation and ecology of coral banks N86-12678
EXCHANGING
U308 powder from uranyl-loaded cation exchange resin [DE85-013231] N86-12265
EXCIMER LASERS
Effect of amplified spontaneous emission on space coherence of XeCl laser N86-12454
Practical excimer laser developed N86-12456
China develops 6J KrF laser N86-12465
EXERCISE PHYSIOLOGY
Energy expenditure and activity patterns of cadets at the United States Military Academy, West Point, New York [AD-A157857] N86-12960
EXHAUST EMISSION
Composition and photochemical reactivity of turbine engine exhaust [AD-A157643] N86-12230
Development of a routine technique for analysis of nitro-PAH in diesel particulate extract [PB85-196657] N86-12287
Assessment of the long-term precision of continuous emission monitors [PB85-201150] N86-12804
EXHAUST GASES
Composition and photochemical reactivity of turbine engine exhaust [AD-A157643] N86-12230
EXHAUST SYSTEMS
Exhaust plume measurements of 15-pound BATES (Ballistic Test and Evaluation System) motors [AD-A157249] N86-12250
EXOBIOLOGY
Aerospace Medicine and Biology Continuing Bibliograph: A continuing bibliography with indexes [NASA-SP-7011(276)] N86-12954
EXPANSION
The question of Earth expansion and its oceanic implications N86-12716
EXPERIMENTATION
Experimental investigation of 3-D turbulent free shear flow past propellers and windmills N86-12201
Analytical and experimental studies of wakes behind circularly capped bubbles N86-12548
A ground-based experimental test program to duplicate and study the spacecraft glow phenomenon N86-13260
EXPERT SYSTEMS
Attempt to develop an intelligent lens design program [DE85-014122] N86-13017
Knowledge-based systems: How will they affect manufacturing in the 80's [DE85-010601] N86-13027
National Aeronautics and Space Administration N86-13234
EXPLORATION
PRospects for development of seismic prospecting methods and apparatus N86-12723
EXPLOSIONS
Parallel, staged opening switch power conditioning techniques for flux compression generator applications [DE85-012761] N86-12527
Explosive coalescence of magnetic islands [DE85-015083] N86-13172
EXPLOSIVES
Effects of surface interactions and mechanical properties of plastic bonded explosives on explosive sensitivity. Part 2: Model formulation [AD-A157900] N86-12361
TATE: Strong basic reactions provide soluble derivations for simple qualititative high explosive spot test [DE85-014259] N86-12366
Characteristic value as an energy output index for explosives N86-12418
Quantum chemistry of aromatic nitro explosives N86-12423
EXPOSURE
Thin film module development N86-12768
Outdoor performance testing of thin-film devices N86-12771
Encapsulant selection and durability testing experience N86-12774
Accidental exposure to americium [DE85-012794] N86-12965
EXPULSION BLADDERS
Lightweight cryogenic tank with positive expulsion [AD-D011856] N86-12612
EXTRACTION
China report: Science and technology [JPRS-CST-85-021] N86-12421
Titanium extractant T105-1 studied N86-12429
EXTRAGALACTIC RADIO SOURCES
X-rays from the radio halo of Virgo A = M87 [NASA-CR-176303] N86-13285
EXTRAPOLATION
Control of step size and order in extrapolation codes [DE85-013261] N86-13010
Control of step size and order in extrapolation codes [DE85-010122] N86-13041
EXTRATERRESTRIAL RADIO WAVES
A statistical study of solar Type-3 bursts and auroral kilometric radiation onsets [AD-A158408] N86-13284
EXTRUDING
Superconducting wire manufactured N86-12437
EYE (ANATOMY)
Cortical plasticity: Theoretical analysis, experimental results [AD-A157965] N86-12961
Protection of eyes against laser damage studied N86-12967
EYE DOMINANCE
Cortical plasticity: Theoretical analysis, experimental results [AD-A157965] N86-12961
EYE PROTECTION
Protection of eyes against laser damage studied N86-12967

F

F REGION
A simulation of high latitude F-layer instabilities in the presence of magnetosphere-ionosphere coupling [NASA-CR-176296] N86-12897
FABRICATION
Semicustom integrated circuit design at Sandia National Laboratories [DE85-015661] N86-12538
Thin-film module circuit design: Practical and reliability aspects N86-12762
Thin film module development N86-12768
Amorphous silicon photovoltaic modules and test devices design, fabrication and testing N86-12769
Nearly ideal lens optimization procedure [DE85-014116] N86-13134
FACILITIES
Scattering experiments at the Ipswich Electromagnetic Measurements Facility: Backscatter from metal cubes [AD-A157925] N86-12496
FAILURE
Failure criteria used in a probabilistic fracture mechanics code [DE85-007264] N86-12628
Solar walk-off protection [DE85-012112] N86-12788
Estimating the reliability of fiber optics cables [DE85-014892] N86-13136
FAILURE ANALYSIS
Macroscopic and microscopic deformation and failure processes that control composite toughness [DE85-012938] N86-12263
Surface fatigue life and failure characteristics of EX-53, CBS 1000M, and AISI 9310 gear materials [NASA-TP-2513] N86-12609
SOLERAS: Photovoltaic power systems project. Module failure analysis [MRI/SOL-0101] N86-12756
Systems analysis approach to probabilistic modeling of fault trees [DE85-007705] N86-13050
FAILURE MODES
Latch-up effect in CMOS described N86-12443
Failure criteria used in a probabilistic fracture mechanics code [DE85-007264] N86-12628
SOLERAS: Photovoltaic power systems project. Module failure analysis [MRI/SOL-0101] N86-12756
FALLOUT
Atmospheric tritium 1968-1984 [DE85-013133] N86-12798
FAR INFRARED RADIATION
Compact TEA-CO2 laser with long life developed N86-12394
Balloon-borne three-meter telescope for far-infrared and submillimeter astronomy [NASA-CR-176347] N86-13271
FAR ULTRAVIOLET RADIATION
Investigation of vehicle glow in the far ultraviolet N86-13249

FATIGUE (MATERIALS)
Influence of load interactions on crack growth as related to state of stress and crack closure
[NASA-TM-87117] N86-12292
Fatigue crack propagation of nickel-base superalloys at 650 deg C
[NASA-TM-87150] N86-12294
An update of the total-strain version of SRP
[NASA-TP-2499] N86-12295
Resistance to fracture, fatigue and stress-corrosion of Al-Cu-Li-Zr alloys
[AD-A158407] N86-12300

FATIGUE LIFE
Surface fatigue life and failure characteristics of EX-53, CBS 1000M, and AISI 9310 gear materials
[NASA-TP-2513] N86-12609

FAULT TOLERANCE
A theory for algorithm-based fault tolerance in array processor systems
[AD-A156244] N86-12977
Fault tolerant statistical signal processing algorithms for parallel architectures
[AD-A157393] N86-12978

FAULT TREES
Systems analysis approach to probabilistic modeling of fault trees
[DE85-007705] N86-13050

FEASIBILITY ANALYSIS
Feasibility of using LANDSAT images of vegetation cover to estimate effective hydraulic properties of soils
[E86-10003] N86-12739

FEDERAL BUDGETS
National Aeronautics and Space Administration N86-13232
Department of Housing and Urban Development, and Certain Other Independent Agencies Appropriations for Fiscal Year 1986, part 1
[S-HRG-99-221-PT-1] N86-13233

FEEDBACK CONTROL
Microcomputer-controlled closed-loop system for positioning radio telescope N86-12410
Long wave (1.2 - 1.5 microns) semiconductor lasers N86-12419
Adaptive Kalman filtering with control input estimation N86-12503
Attempt to develop an intelligent lens design program
[DE85-014122] N86-13017
Research on output feedback control
[NASA-CR-174253] N86-13028
Multivariable current control for electrically and magnetically coupled superconducting magnets
[DE85-012941] N86-13163
National Aeronautics and Space Administration N86-13234

FERMI SURFACES
Second order elastic contents of Pd, PdH(0.7) and PdD(0.7) between 1.7 and 50 K
[DE85-014316] N86-13212

FERROELECTRICITY
Classical piezoelectricity: Is the theory complete
[DE85-014592] N86-12536

FIBER COMPOSITES
Effect of measured material properties on the finite element analysis of an OH-58 composite tail boom
[NASA-TM-86430] N86-12259
Suspension method of impregnating active material into composite nickel plaque
[AD-D011826] N86-12299
Development and evaluation of a microburst test apparatus for use as a minimum destructive test for parachute material
[AD-A158110] N86-12620

FIBER OPTICS
China report: Science and technology
[JPRS-CST-85-017] N86-12408
Determination of single-mode optical fiber dispersion N86-12409
Single mode phase locking fiberoptic sensor developed N86-12415
Long wave (1.2 - 1.5 microns) semiconductor lasers N86-12419
Optic fiber applications in data communications N86-12432
Elie: Saint Eustache fibre Optic Field Trial project evaluation report, volume 4
[AD-A157144] N86-12490
Low dispersion notch filter for multi-GHz frequencies using fiber optics delays
[DE85-014983] N86-12520
Recent developments in microshell-tipped optical fibers as high-pressure shock detectors
[DE85-015750] N86-12594
Infrared optical measurement of blood gas concentrations and fiber optic catheter
[AD-D011836] N86-12955
Optical sensing devices
[AD-D011829] N86-13123
Analytic models for radiation induced loss in optical fibers. 3. Transient radiation effects
[AD-A157408] N86-13127
Estimating the reliability of fiber optics cables
[DE85-014892] N86-13136

FIBER REINFORCED COMPOSITES
Microstructure/Property relationships for carbon fiber reinforced aluminum alloys
[AD-A157858] N86-12261

FIBER STRENGTH
Microstructure/Property relationships for carbon fiber reinforced aluminum alloys
[AD-A157858] N86-12261

FIELD STRENGTH
Rationale for a GRAVSAT-MAGSAT mission: A perspective on the problem of external/internal transient field effects N86-12887
The source of the intermediate wavelength component of the Earth's magnetic field N86-12891
GRM as a follow-on to MAGSAT N86-12893

FIELD THEORY (PHYSICS)
China report: Science and technology
[JPRS-CST-85-021] N86-12421
Variational analysis of phase transition in pure gauge fields N86-12422
Mantle convection and the large scale structures of the Earth's gravitational field N86-12874

FIGHTER AIRCRAFT
Aerodynamic characteristics of a propulsive wing-canard concept at STOL speeds
[NASA-CR-177982] N86-12205
Compressor research facility F100 high pressure compressor inlet total pressure and swirl profile simulation
[AD-A157108] N86-12229
Japanese report on China's F-8 fighter N86-12405

FILAMENT WINDING
Compartmented, filament wound, one-piece aircraft fuel tanks
[AD-D011793] N86-12225
Effect of measured material properties on the finite element analysis of an OH-58 composite tail boom
[NASA-TM-86430] N86-12259

FILM COOLING
Improved temperature detection system for use on film cooled turbine airfoils
[AD-D011762] N86-12228

FINGERS
Suture needle holder
[AD-D011764] N86-12958

FINITE DIFFERENCE THEORY
Finite difference scheme for one-dimensional magnetohydrodynamic equations N86-12464
SCREAMER: A single-line pulsed-power design tool
[DE85-012837] N86-13014

FINITE ELEMENT METHOD
Effect of measured material properties on the finite element analysis of an OH-58 composite tail boom
[NASA-TM-86430] N86-12259
Code of finite element analysis for three-dimensional flow in turbomachines N86-12398
Determination of single-mode optical fiber dispersion N86-12409
C0 collocation solutions for weak-formulation Navier-Stokes equations
[AD-A157250] N86-12553
Failure criteria used in a probabilistic fracture mechanics code
[DE85-007264] N86-12628
Second reference calculation for the WIPP
[DE85-013180] N86-13005
Variational principle for penetrator dynamics using bilinear functional and adjoint formulation
[AD-A157964] N86-13031
Sound scattering by a layered sphere
[AD-A157915] N86-13060

FINNED BODIES
Finned tube contact conductance: Characterizing the integrity of the mechanical bond
[DE85-013747] N86-12564

FIR FILTERS
Hybrid radar waveform design utilizing complementary phase coding and linear frequency stepping for achieving improved slant range resolution in a synthetic aperature radar N86-12470

FIRE CONTROL
Improvement of manufacturing techniques and quality of optical scratch standards for fire control systems
[AD-A157963] N86-13130

FIRE PREVENTION
Aircraft interior panel test criteria derived from full-scale fire tests
[FAA/CT-85/23] N86-12214

FIRES
Aircraft interior panel test criteria derived from full-scale fire tests
[FAA/CT-85/23] N86-12214
Electrical safety requirements: Implications for the module designer N86-12765

FISCHER-TROPSCH PROCESS
Fischer-Tropsch synthesis in slurry reactor systems
[DE85-013390] N86-12276

FISSION
Prompt neutron fission spectrum mean energies for the fissile nuclides and (252)Cf
[DE85-012181] N86-13117

FIXED WINGS
The helicopter to fixed wing conversion program: A critical review
[AD-A156820] N86-12968

FLAME RETARDANTS
Full-scale fire tests of polyurethane foam dome structures
[AD-A157107] N86-12314
Microemulsion-type fire-resistant diesel fuel
[AD-A157125] N86-12359

FLAMES
Measurement of species concentrations in flames by laser-induced fluorescence
[DE85-012092] N86-12283
Investigation of the flame-acoustic wave interaction during axial solid rocket instabilities
[AD-A158559] N86-12362

FLAMMABILITY
Aircraft interior panel test criteria derived from full-scale fire tests
[FAA/CT-85/23] N86-12214

FLAT PLATES
Automated design of composite plates for improved damage tolerance N86-12254
Superheated steam's density compensation for flow measurement N86-12426
Interconnect resistance of photovoltaic submodules N86-12767
Encapsulant selection and durability testing experience N86-12774
Low-cost light-weight thin material solar heating system
[DE85-012531] N86-12789

FLEXIBLE BODIES
Modeling and control of flexible structures
[AD-A157959] N86-12625

FLIGHT CONTROL
Air Force Academy Aeronautics Digest
[AD-A157215] N86-12200
Pneumatic actuator device
[AD-D011794] N86-12217
Interactive aircraft flight control and aeroelastic stabilization
[NASA-CR-176323] N86-12233

FLIGHT CREWS
An analysis of the application of AI to the development of intelligent aids for flight crew tasks
[NASA-CR-3944] N86-12212

FLIGHT OPERATIONS
Statistical sampling of aircraft operations at non-towered airports
[AD-A157095] N86-13051

FLIGHT PATHS
Data analysis of airborne electromagnetic bathymetry
[AD-A157132] N86-12744

FLIGHT SIMULATORS
G protection by an extreme crouch position
[AD-A157081] N86-12213

FLIGHT TESTS
Flutter clearance tests on a Transavia PL-12/T-400 Skyfarmer
[AD-A157212] N86-12234

FLOATING POINT ARITHMETIC
Numerical algorithms and mathematical software for linear control and estimation theory
[AD-A157525] N86-12992

FLOOD PREDICTIONS
Evaluation of the NWS (National Weather Service) soil moisutre accounting model for automated flash flood forecasting in small arid and semi-arid watersheds
[PB85-229722] N86-12928

FLOQUET THEOREM
A Floquet decomposition for Volterra equations with periodic kernel and a transform approach to linear recursion equations
[AD-A158148] N86-13037

FLOTATION
Low temperature inflator apparatus
[AD-D011810] N86-12974

FLOW CHARACTERISTICS
An improved viscid/inviscid interaction procedure for transonic flow over airfoils
[NASA-CR-3805] N86-12208

FLOW CHARTS
User's manual for using MASON: A frequency response program which handles a system of transfer functions described by a signal flow graph
[PB85-227106] N86-13021

FLOW DISTORTION
Investigation of the flame-acoustic wave interaction during axial solid rocket instabilities
[AD-A158559] N86-12362

FLOW DISTRIBUTION
Some recent advances in computational aerodynamics for helicopter applications
[NASA-TM-86777] N86-12207
Analytical and experimental studies of wakes behind circularly capped bubbles N86-12548
Numerical and experimental studies of 3-D and unsteady turbulent body/appendage/propeller flows
[AD-A157078] N86-12552
Non-linear corrections to the linear theory for the prediction of the cavitating flow around hydrofoils
[AD-A158105] N86-12557
A method for determining acoustic-liner admittance in ducts with sheared flow in two-cross-sectional directions
[NASA-TP-2518] N86-13056

FLOW EQUATIONS
Finite difference scheme for one-dimensional magnetohydrodynamic equations N86-12464

FLOW MEASUREMENT
Superheated steam's density compensation for flow measurement N86-12426

FLOW VELOCITY
BLR studies on conic model with LDA in FL-1 wind tunnel N86-12434
Measurements on an axisymmetric jet in a slow coflowing stream N86-12549
Velocity and gravity effects in relative permeability measurements
[DE85-009925] N86-12570
Condensation heat transfer in plate heat exchangers
[DE85-012369] N86-12571
Development of the hydrotransport boost pump
[PB85-203776] N86-12618
Film stability for dirct absorption receivers
[DE85-012135] N86-12791

FLOWMETERS
Superheated steam's density compensation for flow measurement N86-12426
Technique for measuring gas conversion factors
[NASA-CASE-LAR-13220-1] N86-12547
Development of a continuous mass flow measuring flow
[DE85-012492] N86-12573

FLOX
Fluorine and fluorine mixtures N86-12339

FLUID DYNAMICS
Development of the hydrotransport boost pump
[PB85-203776] N86-12618
Expected contribution of the Geopotential Research Mission (GRM) to studies of liquid core fluid dynamics N86-12890
Second Workshop on Spacecraft Glow
[NASA-CP-2391] N86-13239

FLUID FILMS
Wear of projectile rotating bands
[AD-A156666] N86-12358
Film stability for dirct absorption receivers
[DE85-012135] N86-12791

FLUID FLOW
C0 collocation solutions for weak-formulation Navier-Stokes equations
[AD-A157250] N86-12553
Analysis of stratified flow mixing
[DE85-006840] N86-12576
Study of two-phase concurrent flow of steam and water in an unconsolidated porous medium
[DE85-014534] N86-12578
Viscous nonlinear circulation in axisymmetric baroclinic eddy N86-12712
ORNL ground coil analytical and experimental studies
[DE85-005246] N86-12783
MAGNUM-2D computer code: User's guide
[DE85-013315] N86-13001
Shocking behavior of fluid flow in deformable joints
[DE85-010104] N86-13107

FLUID INJECTION
Analysis of stratified flow mixing
[DE85-006840] N86-12576

FLUID MECHANICS
Fluid machines: Expanding the limits, past and future
[NASA-TM-87161] N86-12227

FLUID POWER
The prediction of fully developed turbulent pressure drops in a triangular duct for a power law fluid N86-12546

FLUORESCENCE
Nanosecond fluorescence spectroscopy
[DE85-012234] N86-12282
Measurement of species concentrations in flames by laser-induced fluorescence
[DE85-012092] N86-12283
Measurements on an axisymmetric jet in a slow coflowing stream N86-12549
Activated recombinative desorption: A potential component in mechanisms of spacecraft glow N86-13258

FLUORINE
Fluorine and fluorine mixtures N86-12339

FLUOROCARBONS
Laser diagnostic studies of plasma etching and deposition
[DE85-009494] N86-13178

FLUOROHYDROCARBONS
Studies of the Bauer piezoelectric polymer gauge (PVF2) under impact loading
[DE85-014707] N86-12590

FLUTTER ANALYSIS
Real-time flutter identification
[NASA-CR-3933] N86-12218

FLUX DENSITY
Strain energy density criteria for dynamic fracture and dynamic crack branching
[AD-A157914] N86-12624
Data requirements for verification of ram glow chemistry N86-13265

FLUX PINNING
Field-reversed configuration formation, translation, and confinement studies on the FRX-C/T experiment
[DE85-014095] N86-13141

FOCI
Features of field of directions and velocities of propagation of fractures at earthquake foci in northern Muya region of Baykal Rift Zone N86-12685

FOCUSING
Overview and status of the Transverse-Field Focusing (TFF) accelerator
[DE85-015278] N86-13093
Nearly ideal lens optimization procedure
[DE85-014116] N86-13134
Large acceptance magnetic focussing horns for production of a high intensity narrow band neutrino beam at the AGS
[DE85-013300] N86-13157

FOG
Radiation fog modeling
[AD-A157971] N86-12924
Electro-optical transmission and liquid water content of fogs and clouds
[AD-A157506] N86-13128

FOILS (MATERIALS)
Foil fuses as opening switches for slow discharge circuits
[DE85-014124] N86-12519
Design of foil implosion system for Pioneer 1 experiments
[DE85-014111] N86-12535
Laser-based foilless diode
[DE85-013958] N86-12537

FOKKER-PLANCK EQUATION
Conversion of the bounce-averaged Fokker-Planck code to conversion form
[DE85-014861] N86-13160

FORESTS
A preliminary field study of turbulent flow over and inside a forest edge
[AD-A158409] N86-12580
Evaluation of space SAR as a land-cover classification
[E86-10004] N86-12740
Perspectives to establish knowledge linkages between acidic deposition and vegetation responses
[DE85-011839] N86-12796

FORM FACTORS
Paramagnetic form factors of HCP transiton metals
[DE85-016301] N86-12301

FORMAT
A methodology for syntax-analysis using PROLOG N86-12388

FORMATIONS
Tectonics of eastern Kronotskiy Peninsula and formational association of basalts (Kamchatka) N86-12732

FORMING TECHNIQUES
Variable radius lead former
[AD-D011790] N86-12506

FORMULATIONS
Variational principle for penetrator dynamics using bilinear functional and adjoint formulation
[AD-A157964] N86-13031

FORTRAN
Development of an analytical model and code for the flapping response of a Hawte rotor blade
[DE85-008606] N86-12211
Simulation of the enhanced traffic alert and collision avoidance system (TCAS 2)
[NASA-CR-178328] N86-12216
Program for simple algebra
[DE85-013426] N86-13013

FOURIER ANALYSIS
Annual and semiannual cycles based on the middle atmosphere reference model N86-12828
General plot subroutine package for the Hewlett Packard 5451C Fourier analyzer
[AD-A157127] N86-12969
Spectral method for obtaining three-dimensional magnetohydrodynamic equilibria
[DE85-015065] N86-13166

FOURIER TRANSFORMATION
Paramagnetic form factors of HCP transiton metals
[DE85-016301] N86-12301
P1 polyphase code expander-compressor
[AD-D011838] N86-12475
P2 polyphase code expander-compressor
[AD-D011839] N86-12476

FOURIER-BESSEL TRANSFORMATIONS
Strategy for reflector pattern calculation: Let the computer do the work
[NASA-TM-87137] N86-12485

FRACTURE MECHANICS
Fracture surface analysis in composite and titanium bonding
[NASA-CR-176309] N86-12257
New criterion of combined-mode brittle fracture described N86-12400
Fusion welding research
[AD-A158127] N86-12611
More on compliance of the three-point bend specimen
[AD-A156665] N86-12623
Features of field of directions and velocities of propagation of fractures at earthquake foci in northern Muya region of Baykal Rift Zone N86-12685
Wear of ion implanted TiB sub 2 surfaces
[DE85-017091] N86-13201

FRACTURE STRENGTH
Glass breaking strength: The role of surface flaws and treatments N86-12773

FRACTURES (MATERIALS)
Strain energy density criteria for dynamic fracture and dynamic crack branching
[AD-A157914] N86-12624

FRACTURING
Surface fatigue life and failure characteristics of EX-53, CBS 1000M, and AISI 9310 gear materials
[NASA-TP-2513] N86-12609

FREDHOLM EQUATIONS
Integral equation description of integrated dielectric waveguides N86-12504

FREE ELECTRON LASERS
Strategic defense initiatives at Los Alamos National Laboratory
[DE85-014093] N86-12608
Electron emission of over 200 A/cm (2) from a pulsed-laser irradiated photocathode
[DE85-012656] N86-13084

FREQUENCIES
Modulations of driven nonlinear surface waves on water and liquid Helium-4
[AD-A157958] N86-12556
Experimental study of equilibrium interval in frequency spectra of wind waves in sea of finite depth N86-12699

FREQUENCY ASSIGNMENT
Spectrum resource assessment of the 1605-2000 kHz band
[PB85-225076] N86-12501

FREQUENCY CONTROL
Frequency selection and mode locking of Nd:YAG laser N86-12395

FREQUENCY DISTRIBUTION
Planetary and gravity waves in the mesosphere and lower thermosphere N86-12832

FREQUENCY HOPPING
Results of field and laboratory studies of jam-resistant and voice-private radios
[DE85-014841] N86-12500

FREQUENCY MODULATION
Bandwidth efficient frequency-shift keyed communication systems N86-12472

FREQUENCY RANGES
New approach to some problems in seismology N86-12653

FREQUENCY SHIFT KEYING
Bandwidth efficient frequency-shift keyed communication systems N86-12472

FREQUENCY STABILITY
Biological effects of acoustic cavitation
[AD-A157513] N86-13059
FREQUENCY STANDARDS
Microwave field strength measurement in a Rubidium clock cavity via adiabatic rapid passage
[AD-A157070] N86-13065
FRESNEL LENSES
Photovoltaic Concentrator Technology Project Thirteenth Project Integration Meeting
[DE85-013253] N86-12794
FRICTION
Particle-wall interaction and wall friction in gas-solid flows
[DE85-014984] N86-12567
Comparative analysis of a Stirling heat pump with second- and third-order computer models
[DE85-013536] N86-12615
FRONTS (METEOROLOGY)
Squall and cloud lines as structural components of an Arabian Sea convective cloud cluster
[AD-A157973] N86-12925
FUEL CELLS
Deactivation and poisoning of fuel cell catalysts
[DE85-015127] N86-12521
FUEL COMBUSTION
Group combustion of sprays N86-12266
Multiple ignition, combustion and quenching of hydrocarbon fuel sprays
[AD-A158560] N86-12363
FUEL PRODUCTION
Aquatic Species Program review: Proceedings of Principal Investigators Meeting
[DE85-012137] N86-12364
FUEL SPRAYS
Group combustion of sprays N86-12266
Multiple ignition, combustion and quenching of hydrocarbon fuel sprays
[AD-A158560] N86-12363
FUEL TANKS
Compartmented, filament wound, one-piece aircraft fuel tanks
[AD-D011793] N86-12225
FUELS
Liquid chromatography on silica using mobile phases containing tetraalkylammonium hydroxides. 1: General separation selectivity and behavior of polar compounds typically in fuels
[DE85-014450] N86-12281
FULL SCALE TESTS
Full-scale fire tests of polyurethane foam dome structures
[AD-A157107] N85-12314
FUMES
Fuming nitric acids N86-12342
FUNCTIONS (MATHEMATICS)
Gravity theories in more than four dimensions
[DE85-011164] N86-12903
FURFURYL ALCOHOL
The alcohols N86-12349
FUSELAGES
Simulation of the enhanced traffic alert and collision avoidance system (TCAS 2)
[NASA-CR-176328] N86-12216
FUSION (MELTING)
PBFA-2 insulator stack design from an engineering viewpoint
[DE85-013437] N86-12245
FUSION REACTORS
Effect of pulsed irradiation on microstructural evolution
[DE85-016317] N86-12302
Tandem Mirror Reactor Systems Code (TMRSC)
[DE85-012891] N86-13008
Tritium safety issues for TFCX
[DE85-014621] N86-13118
Implementing the automated features of the PBFA-I control/monitor systems
[DE85-012841] N86-13144
Identifying heavy-ion-beam fusion design and system features with high economic leverage
[DE85-014849] N86-13181
FUSION WELDING
Fusion welding research
[AD-A158127] N86-12611

G

GADOLINIUM
Temperature dependence of the magnetic excitations in Gd
[DE85-016303] N86-13203
GALACTIC NUCLEI
NeII observations of the galactic center: The velocity field and mass distribution N86-13270
GALACTIC RADIATION
Infrared measurements of spacecraft glow planned for Spacelab 2 N86-13263
GALERKIN METHOD
Computer-aided analysis of arbitrary-shaped thin-wire antennas N86-12452
GALLIUM ARSENIDES
Applied lasers (selected articles)
[AD-A155948] N86-12601
Photovoltaic Concentrator Technology Project Thirteenth Project Integration Meeting
[DE85-013253] N86-12794
GAME THEORY
Deals among rational agents
[AD-A157960] N86-13052
GAMMA RAYS
Application of radiographic image enhancement, segmentation N86-12466
GAS ANALYSIS
Method to detect ethylene glycol in gaseous mixtures
[AD-A158109] N86-12272
Infrared optical measurement of blood gas concentrations and fiber optic catheter
[AD-D011836] N86-12955
GAS CHROMATOGRAPHY
Development of a routine technique for analysis of nitro-PAH in diesel particulate extract
[PB85-196657] N86-12287
GAS COMPOSITION
Climatically active trace gases in atmosphere
N86-12639
Transmission of tropospheric radiation of lasers on molecules of different carbon dioxide isotopes
N86-12734
GAS COOLING
Behavior of ionized plasma in the high latitude topside ionosphere
[AD-A157930] N86-13140
GAS DETECTORS
Reversible optical waveguide vapor sensor
[AD-D011834] N86-13124
GAS DYNAMICS
Numerical studies of the dynamic isentropic loading of solid molecular hydrogen
[DE85-013961] N86-12391
GAS EXPANSION
C infinity-regularity for the porous median equation
[AD-A158147] N86-13036
GAS FLOW
Improved temperature detection system for use on film cooled turbine airfoils
[AD-D011762] N86-12228
Technique for measuring gas conversion factors
[NASA-CASE-LAR-13220-1] N86-12547
Particle-wall interaction and wall friction in gas-solid flows
[DE85-014984] N86-12567
GAS GENERATORS
Low temperature inflator apparatus
[AD-D011810] N86-12974
GAS LASERS
Applied lasers (selected articles)
[AD-A155948] N86-12601
Studies of energy storage and transfer in gas lasers
[AD-A158553] N86-12604
GAS MIXTURES
Experimental study of the combustion of gas-air mixtures in a channel and the diffusion combustion in a slipstream at high velocities
[AD-A157495] N86-12271
GAS TEMPERATURE
Dissociative volume recombination coefficient measurements in a subroom temperature neon plasma afterglow N86-12373
Behavior of ionized plasma in the high latitude topside ionosphere
[AD-A157930] N86-13140
GAS-SOLID INTERACTIONS
Application of an atomic oxygen beam facility to the investigation of shuttle glow chemistry N86-13261
Space shuttle mechanistic studies to characterize atomic oxygen interactions with surfaces N86-13267
GAS-SOLID INTERFACES
Data requirements for verification of ram glow chemistry N86-13265
A possible glow experiment for the EOM 1-2 mission
N86-13266
GASEOUS DIFFUSION
Manufacturing process for cylindrical ceramic tubes with localized imprints and device for application of this process
[DE85-012294] N86-12323
GASEOUS FUELS
Limits of thermochemical and photochemical syntheses of gaseous fuels: A finite-time thermodynamic analysis
N86-12367
GASKETS
Novel instrument for high-pressure research at ultra-high temperatures
[DE85-015674] N86-12589
GATES (CIRCUITS)
Design information for the 4/3 silicon-gate CMOS technology
[DE85-014932] N86-12522
Evaluation and implementation of testability schemes for gate array integrated circuit design
[DE85-012874] N86-12526
GAUGE INVARIANCE
Classical geometrical interpretation of ghost fields and anomalies in Yang-Mills theory and quantum gravity
[DE85-014537] N86-13214
GAUGE THEORY
China report: Science and technology
[JPRS-CST-85-021] N86-12421
Variational analysis of phase transition in pure gauge fields N86-12422
Deconfinement transition on a BCH lattice
[DE85-013887] N86-13207
GAUSS EQUATION
Parallel implementation of multifrontal schemes
[DE85-014295] N86-13015
GEAR TEETH
Surface fatigue life and failure characteristics of EX-53, CBS 1000M, and AISI 9310 gear materials
[NASA-TP-2513] N86-12609
GEARS
Surface fatigue life and failure characteristics of EX-53, CBS 1000M, and AISI 9310 gear materials
[NASA-TP-2513] N86-12609
Advanced torque converters for robotics and space applications
[NASA-CR-177987] N86-12610
GELS
Fluid physics research
[DE85-014644] N86-12575
GEOCHEMISTRY
Geochemistry and energetics of cycling of matter in formation of crust in active structures of ocean
N86-12653
magnetic minerals and characteristics of natural magnetic state of core in Saatly superdeep hole in depth range 3500-7500 meters N86-12681
Tectonics of eastern Kronotskiy Peninsula and formational association of basalts (Kamchatka)
N86-12732
GEODESY
Geopotential Research Mission (GRM)
[NASA-CP-2390] N86-12852
Dynamics and structure of the Alpine Fold Belt
N86-12854
Interpretation of the geoid N86-12873
Geodetically derived strain from San Francisco Bay to the Mendocino Triple Junction, California
[PB85-198802] N86-12905
GEODETIC SURVEYS
Thermal cooling of the oceanic lithosphere from geoid height data N86-12861
GEODYNAMICS
The question of Earth expansion and its oceanic implications N86-12716
Geodynamics of crustal dilatation in transition area from Asian continent to Pacific Ocean N86-12733
Geopotential Research Mission (GRM)
[NASA-CP-2390] N86-12852
GEOELECTRICITY
Possibility of sounding Earth by using electromagnetic field of sea current N86-12661
Method for solving problems in electrodynamics of anisotropic media with slant bedding N86-12684
GEOGRAPHIC INFORMATION SYSTEMS
Strategies for associating data and location in a geographic information system
[AD-A158118] N86-12746
GEOGRAPHY
USSR report: Earth sciences
[JPRS-UES-85-006] N86-12630
Generalized geographic mapping system for computer graphics
[PB85-212520] N86-12755
The numerical simulation of geographic storms
N86-12907
GEOIDS
Lithospheric structure in the Pacific geoid N86-12863
The source of the Earth's long wavelength geoid anomalies: Implications for mantle and core dynamics
N86-12872
Interpretation of the geoid N86-12873
GEOLOGICAL FAULTS
New methods for interpreting seismic waves in stratified media N86-12682

Features of field of directions and velocities of propagation of fractures at earthquake foci in northern Muya region of Baykal Rift Zone N86-12685
Geodynamics of crustal dilatation in transition area from Asian continent to Pacific Ocean N86-12733
Geodetically derived strain from San Francisco Bay to the Mendocino Triple Junction, California
[PB85-196602] N86-12905

GEOLOGICAL SURVEYS
Oil and gas deposits on continental slopes of the ocean N86-12655
Petrologic aspect of formation of geostructures in marginal seas N86-12657
Water Information Bulletin No. 30, Part 13: Geothermal investigations in Idaho. Preliminary geologic reconnaissance of the geothermal occurrences of the Wood River drainage area
[DE85-016972] N86-12747

GEOLOGY
USSR report: Earth sciences
[JPRS-UES-85-006] N86-12630
Magmatic provinces and tectonics in Pacific Ocean N86-12652
Spreading in development of oceanic structures N86-12658

GEOMAGNETISM
Petrologic aspect of formation of geostructures in marginal seas N86-12657
Features of electrical measurements in sea as medium with field of extraneous forces N86-12700
A major crustal feature in the southeastern United States inferred from the MAGSAT equivalent source anomaly field N86-12856
The gravity field of topography buried by sediments N86-12864
Continental and oceanic magnetic anomalies: Enhancement through GRM N86-12869
The resolution of a magnetic anomaly map expected from GRM data N86-12870
Interpretation of the geoid N86-12873
The magnetic field at the core-mantle boundary N86-12885
Some anticipated contributions to core fluid dynamics from the GRM N86-12886
Rationale for a GRAVSAT-MAGSAT mission: A perspective on the problem of external/internal transient field effects N86-12887
Recent MAGSAT results N86-12888
Modeling currents at satellite altitudes N86-12889
The source of the intermediate wavelength component of the Earth's magnetic field N86-12891
Does the geoid drift west? N86-12892
GRM as a follow-on to MAGSAT N86-12893
On the interpretation of satellite-derived gravity and magnetic data for studies of crustal geology and metallogenesis N86-12894
Do MAGSAT anomalies contain a record of past and present-day mantle convection under South America? N86-12895
Investigation of magnetic field measurements
[AD-A157924] N86-12900
Behavior of ionized plasma in the high latitude topside ionosphere
[AD-A157930] N86-13140

GEOMETRIC RECTIFICATION (IMAGERY)
LANDSAT-4 TM image data quality analysis for energy-related applications
[E86-10006] N86-12742

GEOPHYSICS
USSR report: Earth sciences
[JPRS-UES-85-006] N86-12630
magnetic minerals and characteristics of natural magnetic state of core in Saatly superdeep hole in depth range 3500-7500 meters N86-12681
USSR report: Earth sciences
[JPRS-UES-85-008] N86-12697
Tectonic structure of Shirshov Ridge (Bering Sea) N86-12710
The question of Earth expansion and its oceanic implications N86-12716
Why do we need detailed gravity over continents: Some Australian examples N86-12855
Expected contribution of the Geopotential Research Mission (GRM) to studies of liquid core fluid dynamics N86-12890

GEOPOTENTIAL
Geopotential Research Mission (GRM)
[NASA-CP-2390] N86-12852
Impact of GRM: New evidence from the Soviet Union N86-12853
Dynamics and structure of the Alpine Fold Belt N86-12854
Geophysical interpretation of the magnetic anomalies of the Earth derived from MAGSAT data N86-12857
Satellite magnetic modeling of north African hot spots N86-12858
Thermal cooling of the oceanic lithosphere from geoid height data N86-12861
The gravity field of topography buried by sediments N86-12864
GRM crustal magnetic anomalies: Separating the Lord Howe Rise and Norfolk Ridge submarine structures N86-12865
Subduction dynamics: Constraints from gravity field observations N86-12868
Continental and oceanic magnetic anomalies: Enhancement through GRM N86-12869
The resolution of a magnetic anomaly map expected from GRM data N86-12870
The importance of GRM gravity observations in continental regions N86-12871
Expected contribution of the Geopotential Research Mission (GRM) to studies of liquid core fluid dynamics N86-12890

GEOPOTENTIAL HEIGHT
Turbulence in the altitude region 80-120 km N86-12834

GEORGIA
Modeling the diurnal variation of meteoriogical variables within the boundary layer: Preliminary comparison results
[PB85-198349] N86-12933

GEOS 3 SATELLITE
Properties of the lithosphere and asthenosphere deduced from geoid observations N86-12867

GEOSTROPHIC WIND
Features of geostrophic circulation related to nature of bottom relief in northwestern Atlantic N86-12674
Cyclonic frontal eddy in Antarctic circumpolar current N86-12675
Middle atmosphere reference model derived from satellite data N86-12819

GEOSYNCHRONOUS ORBITS
Simultaneous observation of GMS and GMS-2: A study of the difference between the brightness temperatures by GMS and those by GMS-2 N86-12912
Calculation of threshold conditions for materials charging in Maxwellian plasmas
[AD-A157123] N86-13139

GEOTHERMAL RESOURCES
Water Information Bulletin No. 30, Part 13: Geothermal investigations in Idaho. Preliminary geologic reconnaissance of the geothermal occurrences of the Wood River drainage area
[DE85-016972] N86-12747
High-resolution, three-dimensional, seismic survey over the geopressured-geothermal reservoir at Parcperdue, Louisiana
[DE85-016465] N86-12902

GERMANIUM DIODES
Performance and temperature dependencies of proton irradiated n/p GaAs and n/p silicon cells
[NASA-TM-87136] N86-12509

GIANT STARS
Combined ultraviolet studies of astronomical source
[NASA-CR-176165] N86-13274

GLASS
The 371 deg C mechanical properties of graphite/polyimide composites
[NASA-TM-87122] N86-12256
Structure-to-glass transition temperature relationships in high temperature stable condensation polyimides
[NASA-TM-87113] N86-12311
Evaluation of high permittivity glass ceramics for millimeter wave applications
[AD A158551] N86-12319
In-situ vacuum-assisted molding of glass-metal electrical components
[DE85-015607] N86-12326
Glass breaking strength: The role of surface flaws and treatments N86-12773

GLASS FIBER REINFORCED PLASTICS
Sound scattering by a layered sphere
[AD-A157915] N86-13060

GLASS LASERS
High-power ND: Glass laser and target chamber system and an experimental study of laser plasma X-ray N86-12428

GLAZES
Thermally induced failures of thick-film glaze resistors
[DE85-012014] N86-12320

GLOBAL AIR POLLUTION
Atmospheric tritium 1968-1984
[DE85-013133] N86-12798

GLOBAL ATMOSPHERIC RESEARCH PROGRAM
Global view of the upper level outflow patterns associated with tropical cyclone intensity changes during FGGE
[NASA-CR-174407] N86-12906
Observational-numerical study of maritime extratropical cyclones using FGGE (First GARP Global Experiment) data
[NASA-CR-176297] N86-12922

GLOW DISCHARGES
Arc discharge conditioning test on the Oak Ridge 25 URC accelerator
[DE85-016394] N86-12523
UV sustained glow discharge opening switch
[AD-A158411] N86-13132

GLYCOLS
Method to detect ethylene glycol in gaseous mixtures
[AD-A158109] N86-12272
Otto fuel 2 N86-12334

GOLD
Charge-state distributions of 100, 175, 275 and 352 MeV gold ions emerging from thin carbon foils
[DE85-014651] N86-13069

GOODNESS OF FIT
Transforming censored samples and testing fit
[AD-A157957] N86-13048

GOVERNMENT PROCUREMENT
The C-17: We need it yesterday
[AD-A157147] N86-12219
Commercial and military communication satellite acquisition practices
[AD-A157398] N86-12247

GOVERNMENT/INDUSTRY RELATIONS
R and D limited partnerships (possible applications in advanced communications satellite technology experiment program)
[NASA-CR-176333] N86-13221
Federal government provision of third-party liability insurance to space vehicle users
[NASA-CR-176346] N86-13230
Making appropriations for the Department of Housing and Urban Development, and for sundry independent agencies, boards, commissions, corporations, and offices for the fiscal year ending September 30, 1986, and for other purposes
[H-REPT-99-363] N86-13231
National Aeronautics and Space Administration N86-13232

GRADIENTS
High and ultra-high gradient quadrupole magnets
[DE85-014360] N86-13104

GRAIN BOUNDARIES
Fatigue crack propagation of nickel-base superalloys at 650 deg C
[NASA-TM-87150] N86-12294
Effect of grain boundary structure on sensitization and corrosion of stainless steel
[AD-A157133] N86-12297
Method and apparatus for conducting variable thickness vapor deposition
[DE85-011653] N86-12306
Molten salt corrosion of SiC: Pitting mechanism
[NASA-TM-87143] N86-12310
Diffraction and microscopy studies of the structure of grain boundaries in Fe, Fe-base alloys and ceramic materials
[DE85-016950] N86-13198

GRAIN SIZE
Fatigue crack propagation of nickel-base superalloys at 650 deg C
[NASA-TM-87150] N86-12294
Effects of microstructure on the acoustoelastic measurements of stress
[DE85-015513] N86-12307

GRANTS
Report of accomplishments under the airport improvement program
[AD-A156834] N86-12241
NASA LeRC/Akron University Graduate Cooperative Fellowship Program and Graduate Student Researchers Program
[NASA-CR-174826] N86-13219

GRAPHITE
Microstructure/Property relationships for carbon fiber reinforced aluminum alloys
[AD-A157858] N86-12261

GRAPHITE-EPOXY COMPOSITES
Mixed-mode cyclic debonding of adhesively bonded composite joints
[NASA-CR-177991] N86-12255
Iosipescu shear properties of graphite fabric/epoxy composite laminates
[NASA-CR-176316] N86-12258
Effect of measured material properties on the finite element analysis of an OH-58 composite tail boom
[NASA-TM-86430] N86-12259

GRAPHITE-POLYIMIDE COMPOSITES
The 371 deg C mechanical properties of graphite/polyimide composites
[NASA-TM-87122] N86-12256

GRAPHS (CHARTS)
Improvement of manufacturing techniques and quality of optical scratch standards for fire control systems [AD-A157963] N86-13130
GRAVIMETERS
Gravimetric surveying with MI-8 helicopters N86-12680
GRAVIMETRY
Gravimetric surveying with MI-8 helicopters N86-12680
Dynamics and structure of the Alpine Fold Belt N86-12854
GRAVITATION
Velocity and gravity effects in relative permeability measurements [DE85-009925] N86-12570
Gravity theories in more than four dimensions [DE85-011164] N86-12903
Modeling of convection phenomena in Bridgman-Stockbarger crystal growth [NASA-CR-176325] N86-13188
GRAVITATION THEORY
Classical geometrical interpretation of ghost fields and anomalies in Yang-Mills theory and quantum gravity [DE85-014537] N86-13214
GRAVITATIONAL FIELDS
Coupling between spinor field, propagating torsion N86-12420
Experience in breaking down gravity field into components resulting from density heterogeneities at various depths (using North Atlantic and Mediterranean as examples) N86-12728
Geopotential Research Mission (GRM) [NASA-CP-2390] N86-12852
Impact of GRM: New evidence from the Soviet Union N86-12853
Why do we need detailed gravity over continents: Some Australian examples N86-12855
A major crustal feature in the southeastern United States inferred from the MAGSAT equivalent source anomaly field N86-12856
Gravity, geoid and the oceanic lithosphere N86-12860
The gravity field of topography buried by sediments N86-12864
Subduction dynamics: Constraints from gravity field observations N86-12868
The source of the Earth's long wavelength geoid anomalies: Implications for mantle and core dynamics N86-12872
Interpretation of the geoid N86-12873
Mantle convection and the large scale structures of the Earth's gravitational field N86-12874
Small-scale convection beneath the transverse ranges, California: Implications for interpretation of gravity anomalies N86-12877
Modeling gravity and magnetic fields for crustal and upper mantle structures N86-12880
Contributions of GRM to the ocean topography experiment (TOPEX) N86-12883
On the interpretation of satellite-derived gravity and magnetic data for studies of crustal geology and metallogenesis N86-12894
GRAVITY ANOMALIES
Experience in breaking down gravity field into components resulting from density heterogeneities at various depths (using North Atlantic and Mediterranean as examples) N86-12728
A major crustal feature in the southeastern United States inferred from the MAGSAT equivalent source anomaly field N86-12856
The gravity field of topography buried by sediments N86-12864
The importance of GRM gravity observations in continental regions N86-12871
GRAVITY WAVES
Influence of short gravity waves on thermal radio emission of water surface N86-12644
Laboratory study of regular low-amplitude gravity capillary waves in nonstationary current N86-12671
Damping of high-frequency wind waves by artifical surface-active films N86-12692
Evaluating influence of waves on dynamic structure of atmospheric near-water layer N86-12694
Nonlinear interaction between soliton and short waves in ideal fluid N86-12715
Gravity waves N86-12822
Gravity waves N86-12823
Mean winds of the upper middle atmosphere (60-110 km): A global distribution from radar systems (MF, meteor, VHF) N86-12831
Planetary and gravity waves in the mesosphere and lower thermosphere N86-12832
Atmospheric Tides Middle Atmosphere Program (ATMAP): Report of the November/December 1981, and May 1982, observational campaigns N86-12839
GRAZING FLOW
A method for determining acoustic-liner admittance in ducts with sheared flow in two-cross-sectional directions [NASA-TP-2518] N86-13053
GREAT LAKES (NORTH AMERICA)
Great Lakes: Nature's own environmental laboratory [PB85-188852] N86-12751
GREEN'S FUNCTIONS
Deprit's algorithm, Green's functions and multipole perturbation theory [DE85-012297] N86-13147
GREENLAND
Investigation of ice dynamics in the marginal ice zone [AD-A157557] N86-12944
GROUND HANDLING
A ground-based experimental test program to duplicate and study the spacecraft glow phenomenon N86-13260
GROUND STATE
The inhomogeneous light shift in alkali atoms [AD-A157498] N86-13067
GROUND TESTS
Flutter clearance tests on a Transavia PL-12/T-400 Skyfarmer [AD-A157212] N86-12234
Ground test facility for nuclear testing of space reactor subsystems [DE85-014634] N86-13099
GROUND WATER
Muon tomography used to study underground rock structure N86-12720
Design of a statewide groundwater monitoring network for Illinois [PB85-192821] N86-12750
Evaluating the ground-water resources of the high plains of Texas, volume 2 [PB85-191609] N86-12752
Fiscal year 1983 program report of the Purdue (Indiana) Water Resources Research Center [PB85-225829] N86-12802
Diagnosing the causes of ground-water contamination using a mathematical model: Report on Technology Transfer Workshop [PB85-217008] N86-12808
MAGNUM-2D computer code: User's guide [DE85-013315] N86-13001
GROWTH
Development of a radiation-hard CMOS process [NASA-CR-170925] N86-13187
GUIDE VANES
Compressor research facility F100 high pressure compressor inlet total pressure and swirl profile simulation [AD-A157108] N86-12229
Wind tunnel turning vanes of modern design [NASA-TM-87416] N86-12239
GULF STREAM
Automatic detection of gulf stream rings [AD-A157934] N86-12945
GUMS (SUBSTANCES)
Oxidation and gum formation in diesel fuels [AD-A157410] N86-12360
GUNNERY TRAINING
Photosensitive cartridge for weapons zeroing and marksmanship training [AD-D011765] N86-13125
GUNS (ORDNANCE)
Photosensitive cartridge for weapons zeroing and marksmanship training [AD-D011765] N86-13125
GUSTS
Squall and cloud lines as structural components of an Arabian Sea convective cloud cluster [AD-A157973] N86-12925
GYROSCOPES
China's first imported peripheral equipment production line N86-12440
Results of PRIM gyroscope testing [DE85-012934] N86-12591
GYROSCOPIC STABILITY
China's first imported peripheral equipment production line N86-12440

H

HABITABILITY
Environmental impact research program. Status and source of habitat models and literature reviews, December 1984 [AD-A156899] N86-12950
HALF LIFE
Light mass elements total half-lives for selected long-lived nuclides [DE85-014217] N86-13115
HALF PLANES
Diffraction of internal waves described by equation of slightly stratified fluid on half-plane N86-12660
HALOCARBONS
Halocarbons N86-12350
HAMILTON-JACOBI EQUATION
Hamilton-Jacobi equations in infinite dimensions. Part 2: Existence of viscosity solutions [AD-A158137] N86-13035
HANDBOOKS
Statistical sampling of aircraft operations at non-towered airports [AD-A157095] N86-13051
HARBORS
Extremal analysis of hindcast and measured wind and wave data at Kodiak, Alaska [AD-A158136] N86-12947
HARDENING (MATERIALS)
The studies on the effects of intermolecular hydrogen bond in melamine resination process. (Methylated melamines were adopted as the model compounds of starting material) N86-12381
HARDNESS
Wear of ion implanted TiB sub 2 surfaces [DE85-017091] N86-13201
HARMONIC ANALYSIS
Vector valued long James type Banach spaces J(eta, I sub p)(1 or = p + infinity) N86-12463
Results of November 1981 and May 1982 ATMAP campaigns at Adelaide (35 deg S, 138 deg E) N86-12850
HARMONIC OSCILLATION
Modulations of driven nonlinear surface waves on water and liquid Helium-4 [AD-A157958] N86-12556
HARMONICS
New directions for short-wavelength laser fusion and high-energy-density physics [DE85-014414] N86-13180
HAZARDOUS MATERIAL DISPOSAL (IN SPACE)
Halocarbons N86-12350
HAZARDS
Hazards of chemical rockets and propellants. Volume 3: Liquid propellants [AD-A158115] N86-12328
Hydrocarbon fuels N86-12329
Anhydrous ammonia N86-12330
The hydrazine fuels N86-12331
Nitromethane N86-12332
Ethylene oxide N86-12333
Otto fuel 2 N86-12334
Hydrogen and deuterium N86-12335
The boranes N86-12336
Carbon monoxide N86-12337
Oxygen N86-12338
Fluorine and fluorine mixtures N86-12339
The halogen fluorides N86-12340
Nitrogen oxides N86-12341
Fuming nitric acids N86-12342
Iodine N86-12343
Chlorine N86-12344
Nitrogen trifluoride N86-12345
Hydrogen peroxide N86-12346
Nitrogen N86-12347
Noble gases N86-12348
The alcohols N86-12349
Hydraulic fluids N86-12351
Mercury N86-12352
Compressed and liquid air N86-12353
Carbon dioxide N86-12354
Nitrous oxide N86-12355
Liquid propellant storage compatibility N86-12356
Quantity-distance requirements N86-12357
Electrical safety requirements: Implications for the module designer N86-12765
High rate Li/SOC1(2) cells. 1. Effect of design variables in uncatalyzed cells [AD-A157203] N86-12776
A new hazard function estimator of performance time [AD-A157843] N86-12971
HEAT BUDGET
Ocean albedo for atmospheric thermal emission N86-12707
HEAT EXCHANGERS
Finned tube contact conductance: Characterizing the integrity of the mechanical bond [DE85-013747] N86-12564
Heat Exchanger Vibration Analysis (HXVA) for prediction of tube bundle instabilities [DE85-017144] N86-12568
Condensation heat transfer in plate heat exchangers [DE85-012369] N86-12571
Comparative first- and second-law analysis of an absorption cycle [DE85-015066] N86-13215

HEAT FLUX
Turbine blade and vane heat flux sensor development, phase 2
[NASA-CR-174995] N86-12226
Model describing the steady-state pyrolysis of bubble-forming polymers in response to an incident heat flux
[PB85-225225] N86-12291
Diagnosis of weather states in winter of 1980-1981
N86-12632
Study of significance of bottom relief in baroclinic model of equatorial countercurrent N86-12642
HEAT OF VAPORIZATION
Foil fuses as opening switches for slow discharge circuits
[DE85-014124] N86-12519
HEAT PIPES
Heat pipe wick
[AD-D011852] N86-12559
HEAT PUMPS
REFRIG-12: A graphics-augmented interactive program for designing vapor-compression refrigeration/heat pump cycles
[DE85-014205] N86-12572
Influence of a surfactant additive on absorption heat pump performance
[DE85-013995] N86-12574
Comparative analysis of a Stirling heat pump with second- and third-order computer models
[DE85-013536] N86-12615
ORNL ground coil analytical and experimental studies
[DE85-005246] N86-12783
Absorption fluids data survey
[DE85-005279] N86-12792
HEAT RADIATORS
Liquid droplet radiator program at the NASA Lewis Research Center
[NASA-TM-87139] N86-12246
HEAT RESISTANT ALLOYS
Fatigue crack propagation of nickel-base superalloys at 650 deg C
[NASA-TM-87150] N86-12294
HEAT TRANSFER
Design of high power superconducting switches
N86-12505
Heat pipe wick
[AD-D011852] N86-12559
Condensation heat transfer in plate heat exchangers
[DE85-012369] N86-12571
Development of a continuous mass flow measuring flow
[DE35-012492] N86-12573
Study of two-phase concurrent flow of steam and water in an unconsolidated porous medium
[DE85-014534] N86-12578
Comparative analysis of a Stirling heat pump with second- and third-order computer models
[DE85-013536] N86-12615
Eddy fluxes of heat, vorticity and momentum in ocean and atmosphere and their parameterization (review)
N86-12672
Viscous nonlinear circulation in axisymmetric baroclinic eddy N86-12712
Transient thermal modeling of the nonscanning ERBE detector
[NASA-CR-172240] N86-12743
ORNL ground coil analytical and experimental studies
[DE85-005246] N86-12783
Flow rates in the East Pacific rise (21 deg N) hot springs, and numerical investigations of two regimes of hydrothermal circulation N86-12939
MAGNUM-2D computer code: User's guide
[DE85-013315] N86-13001
HEAT TRANSFER COEFFICIENTS
Turbine blade and vane heat flux sensor development, phase 2
[NASA-CR-174995] N86-12226
HEAT TREATMENT
Properties of a retrogressed and re-aged 7075 aluminum alloy
[AD-A157415] N86-12298
HEAVY IONS
Review of heavy ion collider proposals
[DE85-014985] N86-13091
On-line velocity measurements using phase probes at the SuperHILAC
[DE85-015279] N86-13095
Fully stripped heavy ion yield vs energy for Xe and Au ions
[DE85-013281] N86-13155
Identifying heavy-ion-beam fusion design and system features with high economic leverage
[DE85-014849] N86-13181
AGS improvement program
[DE85-013293] N86-13182
HEIGHT
Results of the May 1982 ATMAP campaign at the Meteor Wind Station Kuehlungsborn (54 deg N, 12 deg E), GDR
N86-12841
Remarks on the ATMAP campaigns in November 1981 and May 1982 at Collm (52 deg N, 15 deg E)
N86-12842
HELICAL FLOW
Development of the hydrotransport boost pump
[PB85-203776] N86-12618
HELICAL WINDINGS
Calculation of series capacitance for transient analysis of windings N86-12528
HELICOPTERS
Some recent advances in computational aerodynamics for helicopter applications
[NASA-TM-86777] N86-12207
New passive helicopter detector
[DE85-015160] N86-12595
Gravimetric surveying with Mi-8 helicopters
N86-12680
The helicopter to fixed wing conversion program: A critical review
[AD-A156820] N86-12968
HELIOSTATS
Solar thermal energy systems
[DE85-008793] N86-12790
HELIUM
Noble gases N86-12348
Numerical studies of the dynamic isentropic loading of solid molecular hydrogen
[DE85-013961] N86-12391
Tritium control in helium-cooled blankets
[DE85-014783] N86-13116
HELIUM-NEON LASERS
Single mode phase locking fiberoptic sensor developed N86-12415
Laser induced biological heating analyzed
N86-12460
Evaluation of the use of p-n structures as photodetectors in silicon integrated circuits
[AD-A158104] N86-12514
Applied lasers (selected articles)
[AD-A155948] N86-12601
HEMATOCRIT RATIO
Plasma volume methodology: Evans blue, hemoglobin-hematocrit, and mass density transformations
[NASA-TM-86834] N86-12956
HEMATOLOGY
Plasma volume methodology: Evans blue, hemoglobin-hematocrit, and mass density transformations
[NASA-TM-86834] N86-12956
HEMODYNAMIC RESPONSES
China report: Science and technology
[JPRS-CST-85-030] N86-12451
Human hemodynamic change under high atmospheric pressure N86-12458
HEMOGLOBIN
Plasma volume methodology: Evans blue, hemoglobin-hematocrit, and mass density transformations
[NASA-TM-86834] N86-12956
HERBIG-HARO OBJECTS
Ultraviolet observations of low-excitation Herbig-Haro objects
[NASA-CR-176164] N86-13273
HERCULES NOVA
Combined ultraviolet studies of astronomical source
[NASA-CR-176165] N86-13274
HETEROCYCLIC COMPOUNDS
Formation of fuel via photochemical electron transfer
[DE85-011168] N86-12279
Oxidation of heterocyclic nitrogen yields to nitroheterocycles
[DE85-012757] N86-12284
HETEROGENEITY
Experience in breaking down gravity field into components resulting from density heterogeneities at various depths (using North Atlantic and Mediterranean as examples) N86-12728
HETEROJUNCTIONS
Performance and temperature dependencies of proton irradiated n/p GaAs and n/p silicon cells
[NASA-TM-87136] N86-12509
High frequency silicon bipolar transistor with SIPOS (Semi-insulating polycrystalline silicon) heterojunction emitter and ion implanted rapid thermal annealed base region
[AD-A157141] N86-12510
Investigation of reactive magnetron sputter deposited ZnSe for solar cell application
[DE85-016851] N86-12780
HEWLETT-PACKARD COMPUTERS
General plot subroutine package for the Hewlett Packard 5451C Fourier analyzer
[AD-A157127] N86-12989
HIERARCHIES
Stimulus structures and mental representations in expert comprehension of computer programs
[AD-A157520] N86-12969
Aggregating individual preferences in the Analytic Hierarchy Process applied to the 1983 Battelle TAV study
[AD-A155858] N86-13226
HIGH ALTITUDE
Aeronautical technology 2000: A projection of advanced vehicle concepts
[NASA-CR-176322] N86-13235
Naval surface weapons center technology transfer biennial report (Fiscal year 1983/1984)
[AD-A157919] N86-13238
HIGH CURRENT
High current fiber brush collector and method for making same
[AD-D011827] N86-12512
HIGH ENERGY INTERACTIONS
Multiplicities in high energy interactions
[DE85-013847] N86-13100
HIGH FREQUENCIES
Status, development of power ultrasonics in China
N86-12403
Scattering experiments at the Ipswich Electromagnetic Measurements Facility: Backscatter from metal cubes
[AD-A157925] N86-12496
High frequency silicon bipolar transistor with SIPOS (Semi-insulating polycrystalline silicon) heterojunction emitter and ion implanted rapid thermal annealed base region
[AD-A157141] N86-12510
Damping of high-frequency wind waves by artifical surface-active films N86-12692
Acoustic methods for featuring high-frequency part of spectrum of sea waves N86-12706
Spatial structure of high-frequency sea wind waves under different meteorological conditions N86-12714
HIGH LEVEL LANGUAGES
Advanced avionics computer architecture. Volume 1. Executive summary
[AD-A158119] N86-12222
Advanced avionics computer architecture. Volume 2. Instruction set architecture specification
[AD-A158120] N86-12223
The Record of Electrical and Communication Engineering Conversazione, volume 54, no. 1
[ISSN-0385-771-9] N86-12383
A methodology for syntax-analysis using PROLOG
N86-12388
HIGH POWER LASERS
High power laser dump
[AD-D011792] N86-12597
HIGH PRESSURE
Compressor research facility F100 high pressure compressor inlet total pressure and swirl profile simulation
[AD-A157108] N86-12229
High pressure and molecular weight variation of electrical relaxation in poly(ethylene oxide)
[AD-A157660] N86-12317
New approaches to determining physical properties in piston-cylinder high-temperature, high-pressure device
N86-12445
Analysis of stratified flow mixing
[DE85-006840] N86-12576
Novel instrument for high-pressure research at ultra-high temperatures
[DE85-015674] N86-12589
Development of acoustic agglomerator. Test plan for high temperature high pressure acoustic agglomerator
[DE85-017221] N86-13061
Sound velocities in liquid lead at high temperatures
[DE85-014091] N86-13062
HIGH RESOLUTION
Balloon-borne three-meter telescope for far-infrared and submillimeter astronomy
[NASA-CR-176347] N86-13271
HIGH SPEED
Experimental study of the combustion of gas-air mixtures in a channel and the diffusion combustion in a slipstream at high velocities
[AD-A157495] N86-12271
HIGH SPEED PHOTOGRAPHY
Analytical and experimental studies of wakes behind circularly capped bubbles N86-12548
HIGH TEMPERATURE
U308 powder from uranyl-loaded cation exchange resin
[DE85-013231] N86-12265

Review of effects of long-term aging on the mechanical properties and microstructures of types 304 and 316 stainless steel
[DE85-016472] N86-12304
Structure-to-glass transition temperature relationships in high temperature stable condensation polyimides
[NASA-TM-87113] N86-12311
New approaches to determining physical properties in piston-cylinder high-temperature, high-pressure device
N86-12445
Novel instrument for high-pressure research at ultra-high temperatures
[DE85-015674] N86-12589
Development of acoustic agglomerator. Test plan for high temperature high pressure acoustic agglomerator
[DE85-017221] N86-13061
Sound velocities in liquid lead at high temperatures
[DE85-014091] N86-13062
High nuclear temperatures by antimatter-matter annihilation
[DE85-014113] N86-13090

HIGH VOLTAGES
Parallel, staged opening switch power conditioning techniques for flux compression generator applications
[DE85-012761] N86-12527

HIGHWAYS
Evaluation of honeycomb highway sound barrier I-280 section 8B, Harrison, New Jersey
[PB85-231157] N86-13063

HISTOGRAMS
Scatter Diagram and Histogram Program - SCATR
[PB85-213346] N86-12935

HOLDERS
Suture needle holder
[AD-D011764] N86-12958

HOLES (ELECTRON DEFICIENCIES)
Quantum simulations of small electron-hole complexes
[DE85-013895] N86-13205

HOLLOW CATHODES
Self-contained hot-hollow cathode gun source assembly
[DE85-011652] N86-12530

HOLOGRAPHY
State-of-the-art of optics in China reviewed
N86-12414
Laser generation of ultrasonic waveform reconstructions
[AD-D011843] N86-12599

HOMOJUNCTIONS
Performance and temperature dependencies of proton irradiated n/p GaAs and n/p silicon cells
[NASA-TM-87136] N86-12509

HONEYCOMB STRUCTURES
Evaluation of honeycomb highway sound barrier I-280 section 8B, Harrison, New Jersey
[PB85-231157] N86-13063

HORIZONTAL ORIENTATION
Squall and cloud lines as structural components of an Arabian Sea convective cloud cluster
[AD-A157973] N86-12925

HORN ANTENNAS
Low sidelobe, high efficiency mirror antenna with twist reflector
[AD-D011835] N86-12474

HORNS
Large acceptance magnetic focussing horns for production of a high intensity narrow band neutrino beam at the AGS
[DE85-013300] N86-13157

HOT PRESSING
Carbothermal synthesis of silicon carbide
[DE85-013546] N86-12321

HOT SURFACES
Multiple ignition, combustion and quenching of hydrocarbon fuel sprays
[AD-A158560] N86-12363

HOUSINGS
Length adjustable strut link with low aerodynamic drag
[AD-D011651] N86-12232

HUBBLE SPACE TELESCOPE
An assessment of the impact of spacecraft glow on the Hubble space telescope. Summary of existing observations and theory N86-13262

HUMAN FACTORS ENGINEERING
An analysis of the application of AI to the development of intelligent aids for flight crew tasks
[NASA-CR-3944] N86-12212

HUMAN PERFORMANCE
Human cognition and performance
[AD-A157665] N86-12970
A new hazard function estimator of performance time
[AD-A157843] N86-12971

HUMIDITY MEASUREMENT
Humidity profile mesurements in atmospheric lower layer by spontaneous Raman scattering method N86-12736
Atmospheric IR transmission measurements in a tropical maritime environment: Comparison with the LOWTRAN 6 model
[AD-A157920] N86-13129

HURRICANES
Meteorological center's forecasts aid Venus probe tracking N86-12631

HYBRID CIRCUITS
Hybrid radar waveform design utilizing complementary phase coding and linear frequency stepping for achieving improved slant range resolution in a synthetic aperature radar N86-12470

HYDRAULIC EQUIPMENT
Fluid machines: Expanding the limits, past and future
[NASA-TM-87161] N86-12227

HYDRAULIC FLUIDS
Hydraulic fluids N86-12351

HYDRAULIC TEST TUNNELS
Measurements on an axisymmetric jet in a slow coflowing stream N86-12549

HYDRAZINES
The hydrazine fuels N86-12331

HYDRIDES
Temperature and concentration dependence of hydrogen site occupancy in several rare-earth dihydrides
[DE85-015739] N86-13199

HYDROBALLISTICS
Naval surface weapons center technology transfer biennial report (Fiscal year 1983/1984)
[AD-A157919] N86-13238

HYDROCARBON FUELS
Hydrocarbon fuels N86-12329
Oil and gs deposits on continental slopes of the ocean N86-12655

HYDROCARBONS
Microemulsion-type fire-resistant diesel fuel
[AD-A157125] N86-12359
Technique for measuring gas conversion factors
[NASA-CASE-LAR-13220-1] N86-12547

HYDRODYNAMICS
Study of influence of vertical velocity and density profiles on hydrodynamic stability of zonal flow N86-12673
Data structures and vectorization in a two-dimensional free-Lagrangian code
[DE85-012948] N86-13009
New directions for short-wavelength laser fusion and high-energy-density physics
[DE85-014414] N86-13180

HYDROFOILS
Non-linear corrections to the linear theory for the prediction of the cavitating flow around hydrofoils
[AD-A158105] N86-12557

HYDROGEN
Carbothermal synthesis of silicon carbide
[DE85-013546] N86-12321
Hydrogen and deuterium N86-12335
Numerical studies of the dynamic isentropic loading of solid molecular hydrogen
[DE85-013961] N86-12391
Safety criteria for the operation of gaseous hydrogen pipelines
[PB85-206159] N86-12392
Arc discharge conditioning test on the Oak Ridge 25 URC accelerator
[DE85-016394] N86-12523
Develop and test fuel cell powered on-site integrated total energy systems: Phase 3, full-scale power plant development
[NASA-CR-174998] N86-12758
Spatial and temporal patterns of acid precipitation and their interpretation
[PB85-214377] N86-12809
Development of a radiation-hard CMOS process
[NASA-CR-170925] N86-13187
Temperature and concentration dependence of hydrogen site occupancy in several rare-earth dihydrides
[DE85-015739] N86-13199
Ultraviolet observations of low-excitation Herbig-Haro objects
[NASA-CR-176164] N86-13273
Physico-chemical conditions in circumstellar shells of evolved oxygen-rich M stars N86-13275

HYDROGEN BONDS
Research Reports of the Faculty of Engineering, Tokyo Denki University, no. 32
[ISSN-0389-617-X] N86-12372
The studies on the effects of intermolecular hydrogen bond in melamine resination process. (Methylated melamines were adopted as the model compounds of starting material) N86-12381

HYDROGEN CHLORIDES
Hydrogen chloride sparging crystallization of the chloride salts of cobalt, manganese, and nickel
[PB85-197002] N86-12286

HYDROGEN IONS
Overview and status of the Transverse-Field Focusing (TFF) accelerator
[DE85-015278] N86-13093
Behavior of ionized plasma in the high latitude topside ionosphere
[AD-A157930] N86-13140

HYDROGEN OXYGEN FUEL CELLS
Evaluation parameters for the alkaline fuel cell oxygen electrode
[NASA-TM-87155] N86-12268

HYDROGEN PEROXIDE
Hydrogen peroxide N86-12346

HYDROGEN PRODUCTION
Solar thermal energy systems
[DE85-008793] N86-12790

HYDROGEN SULFIDE
Thermodynamics of multi-polar molecules: The perturbed-anisotropic-chain theory
[DE85-013148] N86-12274

HYDROGENATION
Study of some transition metal complexes as process catalysts
[DE85-013428] N86-12276

HYDROLOGY
Nonlinear model of adaptation of fields of density and currents in sea N86-12670
Cyclonic frontal eddy in Antarctic circumpolar current
N86-12675
Hydrologic and land sciences applications of NOAA (National Oceanic and Atmospheric Adminstration) polar-orbiting satellite data
[PB85-233385] N86-12748

HYDROMETEOROLOGY
Objective map analysis for the local AFOS MOS (Automation of Field Operations and Services Model Output Statistics) Program
[PB85-212884] N86-12936

HYDROTHERMAL SYSTEMS
Flow rates in the East Pacific rise (21 deg N) hot springs, and numerical investigations of two regimes of hydrothermal circulation N86-12939

HYDROXYL RADICALS
The Atmosphere Explorer and the shuttle glow
N86-13243

HYPERBOLIC FUNCTIONS
On high-order accurate interpolation for non-oscillatory shock capturing schemes
[AD-A158131] N86-13032
Hyperbolic systems of conservation laws in several space variables
[DE85-014019] N86-13042

HYPERFINE STRUCTURE
The inhomogeneous light shift in alkali atoms
[AD-A157498] N86-13067

HYSTERESIS
Hysteresis characteristics of a diode loaded E-M loop sensor N86-12385

I

ICE
Workshop on Water on Mars
[NASA-CR-176289] N86-13282

ICEBERGS
Recent changes in climate and world water balance
N86-12638
Investigation of ice dynamics in the marginal ice zone
[AD-A157557] N86-129[illegible]4

IDEAL FLUIDS
Nonlinear interaction between soliton and short waves in ideal fluid N86-12715

IDENTIFYING
Identifying and evaluating COBOL competencies for four year information systems programs N86-13223

IGNITION
Multiple ignition, combustion and quenching of hydrocarbon fuel sprays
[AD-A158560] N86-12363
Modeling short pulse duration shock initiation of solid explosives
[DE85-014803] N86-12565

ILLINOIS
Design of a statewide groundwater monitoring network for Illinois
[PB85-192821] N86-12750

IMAGE ANALYSIS
Video terminal for analyzing aerial infrared photographs N86-12688

IMAGE CONVERTERS
Application of radiographic image enhancement, segmentation N86-12486

IMAGE ENHANCEMENT
Application of radiographic image enhancement, segmentation N86-12486

IMAGE PROCESSING
LANDSAT-4 TM image data quality analysis for energy-related applications [E86-10006] N86-12742
Correcting a digital map data base with scene analysis concepts and methods [AD-A157913] N86-12745
Automatic detection of gulf stream rings [AD-A157934] N86-12945

IMAGE RESOLUTION
Ionic mechanicsm of exchange of admixtures between hydrosphere and atmosphere N86-12691
Feasibility of using LANDSAT images of vegetation cover to estimate effective hydraulic properties of soils [E86-10003] N86-12739

IMAGING TECHNIQUES
Model experiments with slot antenna arrays for imaging N86-12482
A new integrated slot element feed array for multi-beam systems N86-12483
Evaluation of space SAR as a land-cover classification [E86-10004] N86-12740
Soybean canopy reflectance modeling data sets [E86-10005] N86-12741
Diffraction-limited ten micron imaging of circumstellar dust with a detector array N86-13277

IMBEDDINGS (MATHEMATICS)
Two results on dense imbeddings [AD-A158132] N86-13033

IMPACT
Light-induced effects-impacts to module performance measurements and reliability testing: An overview N86-12761

IMPACT LOADS
Dislocation kinetics behind shear shocks [DE85-014811] N86-12566
Studies of the Bauer piezoelectric polymer gauge (PVF2) under impact loading [DE85-014707] N86-12590
Glass breaking strength: The role of surface flaws and treatments N86-12773

IMPACT TESTS
Energetic response of propellants to high velocity impact, revision 1 [DE85-013983] N86-12365

IMPEDANCE
Characteristic impedance of a wide slot line on low permittivity substrates N86-12480
Calculation of series capacitance for transient analysis of windings N86-12528
Method and results of electrometric observations in seismically active region N86-12730
Impact of GRM: New evidence from the Soviet Union N86-12853

IMPEDANCE PROBES
A method for determining acoustic-liner admittance in ducts with sheared flow in two-cross-sectional directions [NASA-TP-2518] N86-13056

IMPLOSIONS
Parallel, staged opening switch power conditioning techniques for flux compression generator applications [DE85-012761] N86-12527
Design of foil implosion system for Pioneer 1 experiments [DE85-014111] N86-12535
Absorption and hot electron generation in uv (351 nm) driven spherical imploding targets [DE85-014405] N86-13161
Absorption spectroscopy as a density diagnostic for dense imploded shells [DE85-014413] N86-13175

IMPREGNATING
Suspension method of impregnating active material into composite nickel plaque [AD-D011826] N86-12299

IMPROVEMENT
Wind tunnel turning vanes of modern design [NASA-TM-87416] N86-12239
Latch-up effect in CMOS described N86-12443
Improvement of manufacturing techniques and quality of optical scratch standards for fire control systems [AD-A157963] N86-13130

IMPURITIES
Study of possible solarization - related impurities in CaF2 and other fluorides [DE85-014100] N86-13135
Recent developments in the structural crystallography of boron and the higher borides [DE85-016930] N86-13202
Microluminescence spectra of Ti-activated ZrO2-Y2O3 [DE85-010131] N86-13206

INCIDENCE
Optical radiation from the interaction of energetic atoms, ions, electrons, and photons with surfaces N86-13259

INCIDENT RADIATION
Energy dispersive spectroscopy using synchrotron radiation: Intensity considerations [DE85-017530] N86-13200

INCOHERENT SCATTERING
Temperature structure of the 80 km to 120 km region N86-12830

INDEXES (DOCUMENTATION)
Search and retrieval index to EOS/ESD Symposium Proceedings 1979 to 1984 [AD-A158114] N86-12515
Index to NASA news releases and speeches, 1984 [NASA-TM-87514] N86-13224

INDIAN OCEAN
Find of rheolites and trachites and geological situation in northern part of East Indian Ocean Submarine Ridge N86-12665
Folded structures in central Indian Ocean trench N86-12704

INDUCTORS
Electrical losses and resistance of cryogenic inductors with consideration of the effect of magnetoresistance [AD-A158185] N86-12516

INDUSTRIAL MANAGEMENT
Commercial and military communication satellite acquisition practices [AD-A157398] N86-12247

INDUSTRIAL PLANTS
Influence of power engineering on climate N86-12637

INDUSTRIAL SAFETY
Accidental exposure to americium [DE85-012794] N86-12965

INDUSTRIES
Minutes of Workshop on Composite Materials Test Methods [AD-A157903] N86-12262
An evolving digital telecommunications industry and its impact on the operational environment of the Nationwide Emergency Telecommunication System (NETS) [AD-A156831] N86-12488

INELASTIC SCATTERING
Los Alamos constant-Q spectrometer [DE85-014115] N86-12586

INERTIAL CONFINEMENT FUSION
China report: Science and technology [JPRS-CST-85-029] N86-12446
Progress of inertial confinement research detailed N86-12447
New directions for short-wavelength laser fusion and high-energy-density physics [DE85-014414] N86-13180

INERTIAL FUSION (REACTOR)
Progress of inertial confinement research detailed N86-12447

INERTIAL GUIDANCE
China's first imported peripheral equipment production line N86-12440

INFLATABLE STRUCTURES
Low temperature inflator apparatus [AD-D011810] N86-12974

INFLATING
Low temperature inflator apparatus [AD-D011810] N86-12974

INFLUENCE COEFFICIENT
Derivation of jack movement influence coefficients as a basis for selecting wall contours giving reduced levels of interference in flexible walled test sections [NASA-CR-177992] N86-12204

INFORMATION DISSEMINATION
Strategies for associating data and location in a geographic information system [AD-A158118] N86-12746

INFORMATION RETRIEVAL
Search and retrieval index to EOS/ESD Symposium Proceedings 1979 to 1984 [AD-A158114] N86-12515
Using the information resource dictionary system command language [PB85-227783] N86-12988
A user's guide for the BIBSORT program for the IBM-PC personal computer [AD-A157936] N86-12995

INFORMATION SYSTEMS
China report: Science and technology [JPRS-CST-85-034] N86-12430
Communications network status information system [AD-D011850] N86-12477
Towards a global MAP data base N86-12838
Identifying and evaluating COBOL competencies for four-year information systems programs N86-13223

INFRARED DETECTORS
Automatic detection of gulf stream rings [AD-A157934] N86-12945

INFRARED LASERS
Compact TEA-CO2 laser with long life developed N86-12394
Infrared optical measurement of blood gas concentrations and fiber optic catheter [AD-D011836] N86-12955

INFRARED PHOTOGRAPHY
Video terminal for analyzing aerial infrared photographs N86-12686

INFRARED PHOTOMETRY
The shuttle glow: A program to study the ram-induced phenomena N86-13258

INFRARED RADIATION
Atmospheric IR transmission measurements in a tropical maritime environment: Comparison with the LOWTRAN 6 model [AD-A157920] N86-13129
The NO-NO2 system at laboratory surfaces N86-13255
Optical radiation from the interaction of energetic atoms, ions, electrons, and photons with surfaces N86-13259
Planned investigation of infrared emissions associated with the induced spacecraft glow: A shuttle infrared glow experiment (SIRGE) N86-13264

INFRARED SCANNERS
Application of heat-scan NDT to inspection of adhesion of solid rocket motor propellant to envelope N86-12461

INFRARED SIGNATURES
Exhaust plume measurements of 15-pound BATES (Ballistic Test and Evaluation System) motors [AD-A157249] N86-12250

INFRARED SPECTRA
Study of some transition metal complexes as process catalysts [DE85-013428] N86-12276
Some characteristics of transmission by thin clouds in visible and infrared spectral regions N86-12737
Infrared optical measurement of blood gas concentrations and fiber optic catheter [AD-D011836] N86-12955

INFRARED SPECTROSCOPY
Planned investigation of infrared emissions associated with the induced spacecraft glow: A shuttle infrared glow experiment (SIRGE) N86-13264
Data requirements for verification of ram glow chemistry N86-13265

INFRARED TELESCOPES
Infrared measurements of spacecraft glow planned for Spacelab 2 N86-13263
Balloon-borne three-meter telescope for far-infrared and submillimeter astronomy [NASA-CR-176347] N86-13271

INGOTS
Semicrystalline casting process development and verification [JPL-9950-1160] N86-12312

INHOMOGENEITY
Integral equation description of integrated dielectric waveguides N86-12504

INITIATORS (EXPLOSIVES)
Modeling short pulse duration shock initiation of solid explosives [DE85-014603] N86-12565

INJECTION
Steam-injection pressing of isocyanate-bonded aspen flakeboards, latitudes and limitations [AD-A157833] N86-12389

INJECTION MOLDING
In-situ vacuum-assisted molding of glass-metal electrical components [DE85-015607] N86-12326

INJURIES
Accidental exposure to americium [DE85-012794] N86-12965

INORGANIC COMPOUNDS
X-ray diffraction studies of shock-modified inorganic materials [DE85-015150] N86-13209

INSERTION LOSS
Evaluation of honeycomb highway sound barrier I-280 section 8B, Harrison, New Jersey [PB85-231157] N86-13063

INSPECTION
Current CIM activities in the materials process engineering and fabrication directorate 7400 [DE85-015491] N86-12982

INSTRUMENT LANDING SYSTEMS
FAA (Federal Aviation Administration) could improve overall aviation safety and reduce costs associated with airport instrument landing systems [PB85-195444] N86-12215

INSULATION

High frequency silicon bipolar transistor with SIPOS (Semi-insulating polycrystalline silicon) heterojunction emitter and ion implanted rapid thermal annealed base region [AD-A157141] N86-12510

INTAKE SYSTEMS

Forward field autotransfusion device [AD-D011763] N86-12957

INTEGERS

Relationships between prime-rich Euler type equations and a triangular array of the odd integers [AD-A157028] N86-13030

INTEGRAL EQUATIONS

Integral equation description of integrated dielectric waveguides N86-12504

Pade and reciprocal approximants and linear NOLOR functions [DE85-015057] N86-13044

INTEGRATED CIRCUITS

The verification of the logic circuits based on particlized information bits with PROLOG N86-12387

The 4-bit microprocessor capabilities, applications described N86-12406

Experiments with domestic IC substrates N86-12433

Latch-up effect in CMOS described N86-12443

Programmer for single-chip microprocessor N86-12448

Integral equation description of integrated dielectric waveguides N86-12504

Evaluation and implementation of testability schemes for gate array integrated circuit design [DE85-012874] N86-12526

Hillock-free conductor system for use in multilevel interconnects [DE85-012595] N86-12533

Semicustom integrated circuit design at Sandia National Laboratories [DE85-015661] N86-12536

Large-area thin-film modules N86-12766

Thin film module development N86-12768

The 32-bit computer for large memory applications on FASTBUS [DE85-012726] N86-12986

INTERATOMIC FORCES

Theoretical modelling of the elastic properties of mantle silicates N86-12813

INTERFACE STABILITY

Interfacial stability in a two-layer benard problem [AD-A158138] N86-12558

INTERFACES

Thin film module electrical configuration versus electrical performance N86-12770

Data acquisition interfaces for the IBM personal computer [DE85-014256] N86-12985

Data acquisition command interface using VAX/VMS DCL [DE85-012747] N86-13019

Compound semiconductor insulator interface research [AD-A157277] N86-13189

INTERFEROMETERS

Technique for the reduction of fading in interferometers [AD-D011845] N86-12581

Optical sensing devices [AD-D011829] N86-13123

INTERFEROMETRY

Mechanical interactions of rough surfaces [DE85-015011] N86-12613

Kyoto meteor radar observation in November, 1981 and May, 1982 N86-12847

Diffraction-limited ten micron imaging of circumstellar dust with a detector array N86-13277

INTERIOR BALLISTICS

Wear of projectile rotating bands [AD-A156666] N86-12358

INTERMEDIATE FREQUENCIES

Studies of the marine crustal magnetization at intermediate wavelengths N86-12862

INTERMETALLICS

Ultrasonic attenuation in clean anisotropic superconductors [DE85-012178] N86-12621

INTERMOLECULAR FORCES

Thermodynamics of multi-polar molecules: The perturbed-anisotropic-chain theory [DE85-013148] N86-12274

INTERNATIONAL COOPERATION

China report: Science and technology [JPRS-CST-85-018] N86-12413

Microgravity science and applications bibliography, 1985 revision [NASA-TM-86178] N86-13225

INTERPOLATION

On high-order accurate interpolation for non-oscillatory shock capturing schemes [AD-A158131] N86-13032

INVERSE SCATTERING

Renormalization of an inverse scattering theory for inhomogeneous dielectrics [AD-A157224] N86-12492

INVERTERS

Maintenance of photovoltaic power systems, revision 1 [AD-A157838] N86-12777

INVESTIGATION

Experimental investigation of 3-D turbulent free shear flow past propellers and windmills N86-12201

Results of field and laboratory studies of jam-resistant and voice-private radios [DE85-014841] N86-12500

Investigation of test methods, material properties and processes for solar cell encapsulants [DE85-012831] N86-12786

Improvement of manufacturing techniques and quality of optical scratch standards for fire control systems [AD-A157963] N86-13130

INVESTMENTS

R and D limited partnerships (possible applications in advanced communications satellite technology experiment program) [NASA-CR-176333] N86-13221

INVISCID FLOW

GRUMFOIL: A computer code for the viscous transonic flow over airfoils [NASA-CR-3806] N86-12202

An improved viscid/inviscid interaction procedure for transonic flow over airfoils [NASA-CR-3805] N86-12208

An evaluation of four methods of numerical analysis for two-dimensional airfoil flows. Revision [AD-A157248] N86-12209

Code of finite element analysis for three-dimensional flow in turbomachines N86-12398

An asymptotic investigation of the stationary modes of instability of the boundary layer on a rotating disc [NASA-CR-177977] N86-12550

IODINE

Iodine N86-12343

IODINE LASERS

Direct solar-pumped iodine laser amplifier [NASA-CR-176324] N86-12600

ION ACCELERATORS

Development of beam optics for a 200 keV ion implanter N86-12417

Review of heavy ion collider proposals [DE85-014985] N86-13091

On-line velocity measurements using phase probes at the SuperHILAC [DE85-015279] N86-13095

Fully stripped heavy ion yield vs energy for Xe and Au ions [DE85-013281] N86-13155

AGS improvement program [DE85-013293] N86-13182

ION BEAMS

Development of beam optics for a 200 keV ion implanter N86-12417

China report: Science and technology [JPRS-CST-85-021] N86-12421

Titanium-nitrogen ion beam injection studied N86-12427

An alternative interpretation of ion ring distribution observed by the S3-3 satellite [AD-A157655] N86-12898

Development of a current monitor system for measuring pulsed-beam current over a wide dynamic range [DE85-012692] N86-13083

Review of heavy ion collider proposals [DE85-014985] N86-13091

Achievement of Bevalac rapid mode switching [DE85-015130] N86-13092

Overview and status of the Transverse-Field Focusing (TFF) accelerator [DE85-015278] N86-13093

Fully stripped heavy ion yield vs energy for Xe and Au ions [DE85-013281] N86-13155

Identifying heavy-ion-beam fusion design and system features with high economic leverage [DE85-014849] N86-13181

Analysis and interpretation of the shock-like electrostatic noise observed during the AMPTE (Active Magnetospheric Particle Tracer Explorers) solar wind lithium releases [AD-A157512] N86-13283

ION DISTRIBUTION

An alternative interpretation of ion ring distribution observed by the S3-3 satellite [AD-A157655] N86-12898

Plasma and magnetospheric research [NASA-CR-176326] N86-13138

ION EXCHANGING

Usages of organic membranes in electrolytic industry described N86-12453

Ionic mechanicsm of exchange of admixtures between hydrosphere and atmosphere N86-12690

ION IMPLANTATION

Development of beam optics for a 200 keV ion implanter N86-12417

High frequency silicon bipolar transistor with SIPOS (Semi-insulating polycrystalline silicon) heterojunction emitter and ion implanted rapid thermal annealed base region [AD-A157141] N86-12510

Wear of ion implanted TiB sub 2 surfaces [DE85-017091] N86-13201

ION SOURCES

Electron-spin-polarized targets for a collisionally-pumped polarized-ion source [DE85-015276] N86-13174

Compact microwave ion source [DE85-014536] N86-13176

Improved Bevatron local injector ion source performance [DE85-015271] N86-13196

A ground-based experimental test program to duplicate and study the spacecraft glow phenomenon N86-13260

IONIC DIFFUSION

Contribution of diffusion processes to the electric field of the ocean N86-12654

IONIZATION

Studies of energy storage and transfer in gas lasers [AD-A158553] N86-12604

Multiphoton ionization of NO-rare gas van der Waals species [DE85-014650] N86-13094

FRC formation studies with Z-discharge ionization on FRX-C [DE85-012765] N86-13152

Development of a radiation-hard CMOS process [NASA-CR-170925] N86-13187

IONIZATION CROSS SECTIONS

Secondary electron spectra: A semiempirical model [DE85-012448] N86-13086

IONIZATION GAGES

Precision ion vacuum gage with logarithmic response [DE85-015312] N86-12588

IONIZED GASES

NeII observations of the galactic center: The velocity field and mass distribution N86-13270

IONOSPHERE

Rationale for a GRAVSAT-MAGSAT mission: A perspective on the problem of external/internal transient field effects N86-12887

A simulation of high latitude F-layer instabilities in the presence of magnetosphere-ionosphere coupling [NASA-CR-176296] N86-12897

Behavior of ionized plasma in the high latitude topside ionosphere [AD-A157930] N86-13140

Enhanced N(+) sub 2 in the shuttle environment N86-13248

IONS

Contribution of diffusion processes to the electric field of the ocean N86-12654

Charge-state distributions of 100, 175, 275 and 352 MeV gold ions emerging from thin carbon foils [DE85-014651] N86-13069

IRON

Fischer-Tropsch synthesis in slurry reactor systems [DE85-013390] N86-12278

Iron and steelmaking with plasma N86-12467

Estimation of influence of ocean on distribution of heavy metals in marine atmosphere N86-12703

Uncertainty propagation from raw data to final results [DE85-011937] N86-13000

Design and performance of 40 mm, 6.5 T, collared, cold-iron model magnets [DE85-015277] N86-13054

Method for the deposition of high-quality crystal epitaxial films of iron [AD-D011842] N86-13186

New interpretation of spin-wave behavior in nickel and iron [DE85-015323] N86-13208

The field horizontal-branch star HD 109995: New results with coadded ultraviolet and optical region spectra [NASA-CR-176327] N86-13272

IRON ALLOYS

Diffraction and microscopy studies of the structure of grain boundaries in Fe, Fe-base alloys and ceramic materials [DE85-016950] N86-13198

Mossbauer effect and neutron diffraction study of the anomalous lattice behavior of U6Fe
[DE85-014912] N86-13210

IRON CYANIDES
Zinc/ferricyanide battery development phase 4
[DE85-010026] N86-12781

IRRADIATION
Chemistry of berkelium: A review
[DE85-017523] N86-13102

ISOLATION
High frequency silicon bipolar transistor with SIPOS (Semi-insulating polycrystalline silicon) heterojunction emitter and ion implanted rapid thermal annealed base region
[AD-A157141] N86-12510
Module voltage isolation and corrosion research
N86-12772

ISOPROPYL ALCOHOL
The alcohols N86-12349

ISOSTASY
Why do we need detailed gravity over continents: Some Australian examples N86-12855

ISOTHERMAL PROCESSES
Isothermal dehumidification of air in a parallel passage configuration
[DE85-008819] N86-12577

ISOTHERMS
Seismological studies of the tectonics of divergent plate boundaries N86-12812

ISOTOPE SEPARATION
Science, technology and the industrialization of laser-driven processes
[DE85-014856] N86-12605

ISOTOPES
Transmission of tropospheric radiation of lasers on molecules of different carbon dioxide isotopes
N86-12734

ISOTOPIC ENRICHMENT
Tritium control in helium-cooled blankets
[DE85-014783] N86-13116

ISOTROPIC MEDIA
Iosipescu shear properties of graphite fabric/epoxy composite laminates
[NASA-CR-176316] N86-12258

ITERATIVE SOLUTION
Integral equation description of integrated dielectric waveguides N86-12504

IUE
The field horizontal-branch star HD 109995: New results with coadded ultraviolet and optical region spectra
[NASA-CR-176327] N86-13272

J

JACKETS
Low temperature inflator apparatus
[AD-D011810] N86-12974

JACKS (LIFTS)
Derivation of jack movement influence coefficients as a basis for selecting wall contours giving reduced levels of interference in flexible walled test sections
[NASA-CR-177992] N86-12204

JAMMING
Analysis of constant false alarm rate sidelobe canceller criterion
[AD-A157412] N86-12494
Results of field and laboratory studies of jam-resistant and voice-private radios
[DE85-014841] N86-12500

JET AIRCRAFT
The C-17: We need it yesterday
[AD-A157147] N86-12219
Japanese report on China's F-8 fighter N86-12405

JET ENGINE FUELS
Composition and photochemical reactivity of turbine engine exhaust
[AD-A157643] N86-12230

JET EXHAUST
Analysis of particulates in the exhaust plume of a J52-P3 turbojet engine at military power
[AD-A157840] N86-12231

JET FLOW
Measurements on an axisymmetric jet in a slow coflowing stream N86-12549

JOINING
Thin-film module circuit design: Practical and reliability aspects N86-12762
Interconnect resistance of photovoltaic submodules
N86-12767
Thin film module development N86-12768

JOINTS (JUNCTIONS)
Mixed-mode cyclic debonding of adhesively bonded composite joints
[NASA-CR-177991] N86-12255

Finned tube contact conductance: Characterizing the integrity of the mechanical bond
[DE85-013747] N86-12564
FDSC: A microwave coupling code for slots of finite depth
[DE85-013443] N86-13011

JOSEPHSON JUNCTIONS
China report: Science and technology
[JPRS-CST-85-017] N86-12408
The step structure effect of dc Josephson current within one flux quantum period phi sub zero (2) N86-12412
Josephson effect in the unusual superconductors Lu2Fe3Si5, LiTi2O4 and UBe13
[DE85-015260] N86-13211

JUPITER ATMOSPHERE
Trapped particle absorption by the ring of Jupiter
[NASA-CR-174408] N86-13279
A note on Jupiter's gossamer ring N86-13280

JUPITER RINGS
Trapped particle absorption by the ring of Jupiter
[NASA-CR-174408] N86-13279
A note on Jupiter's gossamer ring N86-13280

K

KALMAN FILTERS
Real-time flutter identification
[NASA-CR-3933] N86-12218
Adaptive Kalman filtering with control input estimation
N86-12503

KAONS
Experiment to study K(+) (YIELDS) (PI)(+) + nothing at LAMPF 2
[DE85-014267] N86-13110
Large acceptance magnetic focussing horns for production of a high intensity narrow band neutrino beam at the AGS
[DE85-013300] N86-13157

KEVLAR (TRADEMARK)
Dynamic small angle X-ray scattering study of stressed Kevlar 49 epoxy composites
[DE85-011408] N86-12264

KINEMATICS
Optimization of the locomotion of a legged vehicle with respect to maneuverability N86-12371
Cyclonic frontal eddy in Antarctic circumpolar current
N86-12675
New methods for interpreting seismic waves in stratified media N86-12682
Geodynamics of crustal dilatation in transition area from Asian continent to Pacific Ocean N86-12733
Investigation of ice dynamics in the marginal ice zone
[AD-A157557] N86-12944

KINETIC ENERGY
Characteristic value as an energy output index for explosives N86-12418
Dislocation kinetics behind shear shocks
[DE85-014811] N86-12566
Surface-catalyzed recombination into excited electronic, vibrational, rotational, and kinetic energy states: A review N86-13253

KINETIC EQUATIONS
New corresponding states theory using the second virial coefficient as the temperature variable
[PB85-219624] N86-12289

KINETIC THEORY
Diffusion in binary plasma mixtures
[DE85-017694] N86-13143

KINETICS
Metal dissolution kinetics in organic solvents using rotating ring-disc voltammetry
[DE85-013478] N86-12253
Direct solar-pumped iodine laser amplifier
[NASA-CR-176324] N86-12600
Theory for the Portevin-LeChatelier effect
[DE85-004030] N86-12627
Influence of some oceanographic characteristics on decay kinetcis of surface-active agents in sea
N86-12676

KLYSTRONS
Self-consistent klystron simulations
[DE85-012678] N86-12529
Racetrack microtron rf system
[DE85-012669] N86-12532

KRYPTON
Noble gases N86-12348

KRYPTON FLUORIDE LASERS
China develops 6J KrF laser N86-12465

KURILE ISLANDS
Evaluating screening effects and Tusnami danger in bays N86-12666

L

LABORATORIES
A user's guide to the Coastal Engineering Research Center's (CERC'S) field research facility
[AD-A157965] N86-12946
FASTBUS for the particle accelerator laboratories
[DE85-014352] N86-13122
A ground-based experimental test program to duplicate and study the spacecraft glow phenomenon
N86-13260

LAGRANGE COORDINATES
Data structures and vectorization in a two-dimensional free-Lagrangian code
[DE85-012948] N86-13009

LAKES
Water resources data for Florida, water year 1983. Volume 3A: Southwest Florida surface water
[PB85-216000] N86-12754

LAMINAR FLOW
Derivation of jack movement influence coefficients as a basis for selecting wall contours giving reduced levels of interference in flexible walled test sections
[NASA-CR-177992] N86-12204
Effect of surface waviness on a supercritical laminar-flow-control airfoil
[NASA-TM-85705] N86-12206
Code of finite element analysis for three-dimensional flow in turbomachines N86-12398

LAMINATES
Iosipescu shear properties of graphite fabric/epoxy composite laminates
[NASA-CR-176316] N86-12258

LAND MANAGEMENT
Cartography, national land management related
N86-12401
Benefits of surveying, cartography described
N86-12402
Evaluation of space SAR as a land-cover classification
[E86-10004] N86-12740

LAND USE
Evaluation of space SAR as a land-cover classification
[E86-10004] N86-12740

LANDFILLS
Evaluation of air emissions from hazardous waste treatment, storage and disposal facilities
[PB85-203792] N86-12806

LANDFORMS
Folded structures in central Indian Ocean trench
N86-12704
Structure of sedimentary cover and basement of Sierra Leone Rise determined from common depth point seismic (equatorial Atlantic) N86-12709
Tectonic structure of Shirshov Ridge (Bering Sea)
N86-12710
Experimental study of flow and dispersion in the wakes of three-dimensional low hills
[PB85-193266] N86-12906

LANDING SITES
CBR (California Bearing Ratio) design of flexible airfield pavements with case study
[AD-A158101] N86-12242

LANDSAT SATELLITES
Feasibility of using LANDSAT images of vegetation cover to estimate effective hydraulic properties of soils
[E86-10003] N86-12739

LANGUAGE PROGRAMMING
Advanced avionics computer architecture. Volume 1. Executive summary
[AD-A158119] N86-12222
A methodology for syntax-analysis using PROLOG
N86-12388

LAP JOINTS
Mixed-mode cyclic debonding of adhesively bonded composite joints
[NASA-CR-177991] N86-12255

LASER ANEMOMETERS
Laser anemometer using a single circuit board
N86-12411
Study of the mist cooling and droplet dynamics in turbulent flow by using LDA N86-12545

LASER APPLICATIONS
Measurement of species concentrations in flames by laser-induced fluorescence
[DE85-012092] N86-12283
China report: Science and technology
[JPRS-CST-85-034] N86-12430
China report: Science and technology
[JPRS-CST-85-030] N86-12451
Laser induced biological heating analyzed
N86-12460
Science, technology and the industrialization of laser-driven processes
[DE85-014856] N86-12605
Lasers measure drifting mountains N86-12718

Large-area thin-film modules N86-12766
LASER CAVITIES
Direct solar-pumped iodine laser amplifier [NASA-CR-176324] N86-12600
LASER DAMAGE
China report: Science and technology [JPRS-CST-85-019] N86-12966
Protection of eyes against laser damage studied N86-12967
LASER DOPPLER VELOCIMETERS
BLR studies on conic model with LDA in FL-1 wind tunnel N86-12434
Study of the mist cooling and droplet dynamics in turbulent flow by using LDA N86-12545
Optical technique to study the impact of heavy rain on aircraft performance [NASA-CR-177989] N86-12580
LASER FUSION
Absorption and hot electron generation in uv (351 nm) driven spherical imploding targets [DE85-014405] N86-13161
New directions for short-wavelength laser fusion and high-energy-density physics [DE85-014414] N86-13180
LASER INTERFEROMETRY
Laser vibrometer [AD-D011811] N86-12602
LASER MODES
Frequency selection and mode locking of Nd:YAG laser N86-12295
Single mode phase locking fiberoptic sensor developed N86-12415
Long wave (1.2 - 1.5 microns) semiconductor lasers N86-12419
First domestic high repetition rate ultrashort pulse laser N86-12455
LASER OUTPUTS
Materials and process characterization to determine the effect of high intensity infrared laser radiation on a composite material [AD-A157094] N86-12260
Picosecond broadband CARS probe using the picosecond continuum [AD-D011840] N86-12267
High damage threshold porous silica antireflective coating [DE85-012924] N86-12322
Practical excimer laser developed N86-12456
A high precision rate dye laser pumped by a CuCl laser N86-12457
Laser-based foilless diode [DE85-013958] N86-12537
High power laser dump [AD-D011792] N86-12597
Laser generation of ultrasonic waveform reconstructions [AD-D011843] N86-12599
Direct solar-pumped iodine laser amplifier [NASA-CR-176324] N86-12600
Applied lasers (selected articles) [AD-A155948] N86-12601
Laser vibrometer [AD-D011811] N86-12602
Pulsed digital multiplexed laser generator [AD-D011855] N86-12603
Activated recombinative desorption: A potential component in mechanisms of spacecraft glow N86-13258
LASER PLASMA INTERACTIONS
Laser scattering in plasma examined N86-12431
LASER PLASMAS
Compact TEA-CO2 laser with long life developed N86-12394
High-power ND: Glass laser and target chamber system and an experimental study of laser plasma X-ray N86-12428
Improved approach to characterizing and presenting streak camera performance [DE85-015188] N86-12587
Accelerator research studies [DE85-014878] N86-13113
Spatial structure of heat flow instabilities in laser plasmas [DE85-014407] N86-13162
Absorption spectroscopy as a density diagnostic for dense imploded shells [DE85-014413] N86-13175
LASER PUMPING
A high precision rate dye laser pumped by a CuCl laser N86-12457
LASER RANGE FINDERS
Compact TEA-CO2 laser with long life developed N86-12394
LASER SPECTROMETERS
Practical optical multichannel analyzer developed N86-12416
LASER SPECTROSCOPY
Measurement of species concentrations in flames by laser-induced fluorescence [DE85-012092] N86-12283
Practical optical multichannel analyzer developed N86-12416
LASER STABILITY
First domestic high repetition rate ultrashort pulse laser N86-12455
Applied lasers (selected articles) [AD-A155948] N86-12601
LASER TARGET INTERACTIONS
Materials and process characterization to determine the effect of high intensity infrared laser radiation on a composite material [AD-A157094] N86-12260
Absorption and hot electron generation in uv (351 nm) driven spherical imploding targets [DE85-014405] N86-13161
LASER TARGETS
High-power ND: Glass laser and target chamber system and an experimental study of laser plasma X-ray N86-12428
Improved approach to characterizing and presenting streak camera performance [DE85-015188] N86-12587
Absorption and hot electron generation in uv (351 nm) driven spherical imploding targets [DE85-014405] N86-13161
Absorption spectroscopy as a density diagnostic for dense imploded shells [DE85-014413] N86-13175
New directions for short-wavelength laser fusion and high-energy-density physics [DE85-014414] N86-13180
LASER WEAPONS
Strategic defense initiatives at Los Alamos National Laboratory [DE85-014093] N86-12608
LASERS
China report: Science and technology [JPRS-CST-85-034] N86-12430
China report: Science and technology [JPRS-CST-85-022] N86-12439
China report: Science and technology [JPRS-CST-85-030] N86-12451
Low dispersion notch filter for multi-GHz frequencies using fiber optics delays [DE85-014983] N86-12520
Laser vibrometer [AD-D011811] N86-12602
Transmission of tropospheric radiation of lasers on molecules of different carbon dioxide isotopes N86-12734
European Science Notes. Volume 39, number 8 [AD-A157146] N86-13237
LATCH-UP
Latch-up effect in CMOS described N86-12443
LATE STARS
Combined ultraviolet studies of astronomical source [NASA-CR-176165] N86-13274
LATTICE PARAMETERS
Tracking studies on the effects of random multipoles in the 6.5 T lattice of the SSC Reference Designs Study [DE85-013286] N86-13156
LEAD (METAL)
Sound velocities in liquid lead at high temperatures [DE85-014091] N86-13062
LEAD ISOTOPES
Isovector resonances in pion charge exchange [DE85-012746] N86-13106
LEARNING
Human cognition and performance [AD-A157665] N86-12970
Systems for authoring computer-based instruction [PB85-198950] N86-12987
LEARNING MACHINES
An application of adaptive learning to malfunction recovery [AD-A158129] N86-12236
LEAST SQUARES METHOD
Results of the May 1982 ATMAP campaign at the Meteor Wind Station Kuehlungsborn (54 deg N, 12 deg E), GDR N86-12841
Meteor wind results at Durham (43 deg N, 71 deg W) during the ATMAP November 1981 and May 1982 campaigns N86-12845
Mean winds and tides over Urbana, Illinois during November 16-22, 1981 N86-12846
Kyoto meteor radar observation in November, 1981 and May, 1982 N86-12847
Middle atmosphere tides at Christchurch (44 deg S, 17 deg E) in November 1981 and May 1982 N86-12851
Fundamentals of adaptive signal processing [DE85-014933] N86-13016
LEAVES
Soybean canopy reflectance modeling data sets [E86-10005] N86-12741
LECTURES
Index to NASA news releases and speeches, 1984 [NASA-TM-87514] N86-13224
LEGAL LIABILITY
Federal government provision of third-party liability insurance to space vehicle users [NASA-CR-176346] N86-13230
LENSES
Accelerator research studies [DE85-014878] N86-13113
Nearly ideal lens optimization procedure [DE85-014116] N86-13134
LEUKEMIAS
Studies of participants in nuclear tests N86-12964
LIFE (DURABILITY)
Review of effects of long-term aging on the mechanical properties and microstructures of types 304 and 316 stainless steel [DE85-016472] N86-12304
Compact TEA-CO2 laser with long life developed N86-12394
China's first imported peripheral equipment production line N86-12440
SOLERAS: Photovoltaic power systems project. Module failure analysis [MRI/SOL-0101] N86-12756
Crystalline-silicon reliability lessons for thin-film modules N86-12760
Accelerated stress testing of thin film solar cells: Development of test methods and preliminary results N86-12764
Amorphous silicon photovoltaic modules and test devices design, fabrication and testing N86-12769
Outdoor performance testing of thin-film devices N86-12771
Encapsulant selection and durability testing experience N86-12774
Light mass elements total half-lives for selected long-lived nuclides [DE85-014217] N86-13115
LIFE RAFTS
Low temperature inflator apparatus [AD-D011810] N86-12974
LIFE SCIENCES
China report: Science and technology [JPRS-CST-85-024] N86-12388
China report: Science and technology [JPRS-CST-85-016] N86-12393
China report: Science and technology [JPRS-CST-85-017] N86-12408
China report: Science and technology [JPRS-CST-85-018] N86-12413
China report: Science and technology [JPRS-CST-85-022] N86-12439
China report: Science and technology [JPRS-CST-85-025] N86-12444
China report: Science and technology [JPRS-CST-85-026] N86-12459
USSR Space Life Sciences Digest, Issue 2 [NASA-CR-3922(02)] N86-12949
China report: Science and technology [JPRS-CST-85-019] N86-12966
Protection of eyes against laser damage studied N86-12967
LIGHT (VISIBLE RADIATION)
Light-induced effects-impacts to module performance measurements and reliability testing: An overview N86-12761
Thin film module electrical configuration versus electrical performance N86-12770
Nearly ideal lens optimization procedure [DE85-014116] N86-13134
LIGHT BEAMS
Optical sensing devices [AD-D011829] N86-13123
LIGHT ELEMENTS
Light mass elements total half-lives for selected long-lived nuclides [DE85-014217] N86-13115
LIGHT EMISSION
The Atmosphere Explorer and the shuttle glow N86-13243
Orbiter glow observations at high spectral resolution N86-13244
Spacecraft-induced plasma energization and its role in flow phenomena N86-13250
LIGHT EMITTING DIODES
Digital phase meter using CMOS-LED introduced N86-12442
LIGHT SCATTERING
Comparison of single-parameter statistical model with results of round-the-clock measurement of light-scattering matrices N86-12689

Masking of light scattering information on matrix elements from complex scattering
[AD-A158144] N86-13131
A note on Jupiter's gossamer ring N86-13280

LIGHT SOURCES
Optical sensing devices
[AD-D011829] N86-13123

LIGHT TRANSMISSION
Electro-optical transmission and liquid water content of fogs and clouds
[AD-A157506] N86-13128
Study of possible solarization - related impurities in CaF2 and other fluorides
[DE85-014100] N86-13135

LIGHTNING
Weather radar studies
[AD-A157093] N86-12920

LIGHTNING SUPPRESSION
EE technical review
[DE85-015313] N86-12540

LIMITS (MATHEMATICS)
Interactive aircraft flight control and aeroelastic stabilization
[NASA-CR-176323] N86-12233

LINE SPECTRA
Frequency selection and mode locking of Nd:YAG laser N86-12395
The inhomogeneous light shift in alkali atoms
[AD-A157498] N86-13067
Balloon-borne three-meter telescope for far-infrared and submillimeter astronomy
[NASA-CR-176347] N86-13271
The field horizontal-branch star HD 109995: New results with coadded ultraviolet and optical region spectra
[NASA-CR-176327] N86-13272

LINEAR ACCELERATORS
RIIM accelerator beam experiments
[DE85-012034] N86-12244
Mathematical model of the dynamic response of thermo-regulating in 200 MeV linear accelerator
N86-12407
Beam emittance and beam disruption
[DE85-015136] N86-13070
LAMPF transition-region mechanical fabrication
[DE85-012688] N86-13081
Electron emission of over 200 A/cm (2) from a pulsed-laser irradiated photocathode
[DE85-012656] N86-13084
Data acquisition system for SLD
[DE85-014361] N86-13103
High intensity positron beam and angular correlation experiments at Livermore
[DE85-012961] N86-13111
Generalization of the Child-Langmuir relation for one-dimensional time-dependent diodes
[DE85-012677] N86-13145
Real time bunch length measurements in the SLC linac
[DE85-014362] N86-13169

LINEAR EQUATIONS
A Floquet decomposition for Volterra equations with periodic kernel and a transform approach to linear recursion equations
[AD-A159148] N86-13037

LINEAR PREDICTION
Non-linear corrections to the linear theory for the prediction of the cavitating flow around hydrofoils
[AD-A158105] N86-12557

LINEAR PROGRAMMING
Impact of linear programming on computer development
[AD-A157659] N86-12993

LINEAR SYSTEMS
Hybrid radar waveform design utilizing complementary phase coding and linear frequency stepping for achieving improved slant range resolution in a synthetic aperature radar N86-12470
User's manual for using MASON: A frequency response program which handles a system of transfer functions described by a signal flow graph
[PB85-227106] N86-13021

LINEARITY
Additional results on the radiating properties of LTSAs and CWSAs N86-12479
Preliminary design of linear alternator dynamometer for free piston Stirling engines
[DE85-015078] N86-12614
Transistorized multigrid methods. 1: Linear elliptic problems on two- and three-dimensional regions
[DE85-014632] N86-13043

LINGUISTICS
Artificial intelligence in Ada: Pattern-directed processing
[AD-A157097] N86-13025

LININGS
A method for determining acoustic-liner admittance in ducts with sheared flow in two-cross-sectional directions
[NASA-TP-2516] N86-13056

LIQUID AIR
Compressed and liquid air N86-12353

LIQUID CHROMATOGRAPHY
Liquid chromatography on silica using mobile phases containing tetraalkylammonium hydroxides. 1: General separation selectivity and behavior of polar compounds typically in fuels
[DE85-014450] N86-12281

LIQUID COOLING
Study of the mist cooling and droplet dynamics in turbulent flow by using LDA N86-12545

LIQUID HELIUM
Modulations of driven nonlinear surface waves on water and liquid Helium-4
[AD-A157958] N86-12556

LIQUID METAL COOLED REACTORS
Thermophoretic separation of aerosol particles from a sampled gas stream
[DE85-011672] N86-12277

LIQUID METAL FAST BREEDER REACTORS
Review of effects of long-term aging on the mechanical properties and microstructures of types 304 and 316 stainless steel
[DE85-016472] N86-12304

LIQUID METALS
Sound velocities in liquid lead at high temperatures
[DE85-014091] N86-13062

LIQUID NITROGEN
Ultrahigh vacuum equipment described N86-12438
Application of an atomic oxygen beam facility to the investigation of shuttle glow chemistry N86-13261

LIQUID OXYGEN
Oxygen N86-12338

LIQUID PHASE EPITAXY
Liquid Phase Epitaxy (LPE) of silicon carbide
[AD-D011825] N86-13191

LIQUID ROCKET PROPELLANTS
Hazards of chemical rockets and propellants. Volume 3: Liquid propellants
[AD-A158115] N86-12328
Hydrocarbon fuels N86-12329
Anhydrous ammonia N86-12330
The hydrazine fuels N86-12331
Nitromethane N86-12332
Ethylene oxide N86-12333
Otto fuel 2 N86-12334
Hydrogen and deuterium N86-12335
The boranes N86-12336
Carbon monoxide N86-12337
Oxygen N86-12338
Fluorine and fluorine mixtures N86-12339
The halogen fluorides N86-12340
Nitrogen oxides N86-12341
Fuming nitric acids N86-12342
Iodine N86-12343
Chlorine N86-12344
Nitrogen trifluoride N86-12345
Hydrogen peroxide N86-12346
Nitrogen N86-12347
Noble gases N86-12348
The alcohols N86-12349
Halocarbons N86-12350
Hydraulic fluids N86-12351
Mercury N86-12352
Compressed and liquid air N86-12353
Carbon dioxide N86-12354
Nitrous oxide N86-12355
Liquid propellant storage compatibility N86-12356
Quanity-distance requirements N86-12357

LIQUID-SOLID INTERFACES
Sound scattering by a layered sphere
[AD-A157915] N86-13060

LIQUIDS
Absorption fluids data survey
[DE85-005279] N86-12792

LITHIUM
Lithium-thionyl chloride cell system safety hazard analysis
[AD-A157089] N86-12775
Nuclear performance optimization of the Be/Li/Th blanket for the fusion breeder
[DE85-012949] N86-13112
Analysis and interpretation of the shock-like electrostatic noise observed during the AMPTE (Active Magnetospheric Particle Tracer Explorers) solar wind lithium releases
[AD-A157512] N86-13283

LITHIUM ALLOYS
Resistance to fracture, fatigue and stress-corrosion of Al-Cu-Li-Zr alloys
[AD-A158407] N86-12300
Combined small angle X-ray scattering and transmission electron microscope studies of Al-Li alloys
[DE85-016356] N86-12303

LITHIUM CHLORIDES
High rate Li/SOC1(2) cells. 1. Effect of design variables in uncatalyzed cells
[AD-A157203] N86-12776

LITHIUM ISOTOPES
Partition of cross sections in asymmetric nucleus-nucleus reactions and the origin of fast alpha particles
[DE85-014989] N86-13089
R-matrix analysis of the (7) Li system with peripheral channel overlap exchange effects
[DE85-012751] N86-13148

LITHIUM OXIDES
Tritium control in helium-cooled blankets
[DE85-014783] N86-13116

LITHOSPHERE
New data of relief of Mazca Ridge N86-12679
A major crustal feature in the southeastern United States inferred from the MAGSAT equivalent source anomaly field N86-12856
Geophysical interpretation of the magnetic anomalies of the Earth derived from MAGSAT data N86-12857
Gravity, geoid and the oceanic lithosphere
N86-12860
Thermal cooling of the oceanic lithosphere from geoid height data N86-12861
Lithospheric structure in the Pacific geoid N86-12863
Sea floor swells and mantle plumes N86-12866
Properties of the lithosphere and asthenosphere deduced from geoid observations N86-12867
The resolution of a magnetic anomaly map expected from GRM data N86-12870

LOADING MOMENTS
Influence of bonded reinforcement in post-tensioned prestressed concrete T-beams with unbonded tendons
N86-12622

LOADS (FORCES)
Surface fatigue life and failure characteristics of EX-53, CBS 1000M, and AISI 9310 gear materials
[NASA-TP-2513] N86-12609

LOCOMOTION
Optimization of the locomotion of a legged vehicle with respect to maneuverability N86-12371

LOGIC DESIGN
The Record of Electrical and Communication Engineering Conversazione, volume 54, no. 1
[ISSN-0385-771-9] N86-12383
The verification of the logic circuits based on particlized information bits with PROLOG N86-12387

LONG DURATION SPACE FLIGHT
Development of a radiation-hard CMOS process
[NASA-CR-170925] N86-13187
Space shuttle mechanistic studies to characterize atomic oxygen interactions with surfaces N86-13267

LONG TERM EFFECTS
Atmospheric aerosol and its effects on climate
N86-12636
Influence of power engineering on climate
N86-12637
Proceedings of a workshop on Radiofrequency Radiation bioeffects held at Wachtberg-Werthhoven, West Germany on 11-13 September 1984
[AD-A157090] N86-12959

LONGITUDINAL WAVES
The source of the Earth's long wavelength geoid anomalies: Implications for mantle and core dynamics
N86-12872

LORENTZ FORCE
Laser scattering in plasma examined N86-12431
Derivation of the optical constants of anisotropic
[AD-A158396] N86-13195

LOSSES
Electrical losses and resistance of cryogenic inductors with consideration of the effect of magnetoresistance
[AD-A158165] N86-12516
Thin film module electrical configuration versus electrical performance N86-12770
Analytic models for radiation induced loss in optical fibers. 3. Transient radiation effects
[AD-A157408] N86-13127
Federal government provision of third-party liability insurance to space vehicle users
[NASA-CR-176348] N86-13230

LOUISIANA
High-resolution, three-dimensional, seismic survey over the geopressured-geothermal reservoir at Parcperdue, Louisiana
[DE85-016465] N86-12902

LOW FREQUENCIES
Digital phase meter using CMOS-LED introduced
N86-12442

LOW TEMPERATURE

Dissociative volume recombination coefficient measurements in a subroom temperature neon plasma afterglow N86-12373

Materials studies for magnetic fusion energy applications at low temperatures - 8 [PB85-236362] N86-13183

Temperature and concentration dependence of hydrogen site occupancy in several rare-earth dihydrides [DE85-015739] N86-13199

LOWER ATMOSPHERE

Humidity profile mesurements in atmospheric lower layer by spontaneous Raman scattering method N86-12736

RADLAC program status [DE85-014708] N86-13109

LUBRICANTS

Ellipsometric surface analysis of wear tracks produced by different lubricants [NASA-TM-87142] N86-12293

LUBRICATION

Mechanical interactions of rough surfaces [DE85-015011] N86-12613

LUBRICATION SYSTEMS

Wear of projectile rotating bands [AD-A156668] N86-12358

LUGS

Electrochemical machining of the outer profile of the B83 Lug [DE85-014934] N86-12616

LUMINESCENCE

Microluminescence spectra of Ti-activated ZrO2-Y2O3 [DE85-010131] N86-13206

The NO-NO2 system at laboratory surfaces N86-13255

A model for explaining some features of shuttle glow N86-13256

The production of glow precursors by oxidative erosion of spacecraft surfaces N86-13257

Activated recombinative desorption: A potential component in mechanisms of spacecraft glow N86-13258

Optical radiation from the interaction of energetic atoms, ions, electrons, and photons with surfaces N86-13259

A ground-based experimental test program to duplicate and study the spacecraft glow phenomenon N86-13260

Application of an atomic oxygen beam facility to the investigation of shuttle glow chemistry N86-13261

An assessment of the impact of spacecraft glow on the Hubble space telescope. Summary of existing observations and theory N86-13262

Infrared measurements of spacecraft glow planned for Spacelab 2 N86-13263

Planned investigation of infrared emissions associated with the induced spacecraft glow: A shuttle infrared glow experiment (SIRGE) N86-13264

Data requirements for verification of ram glow chemistry N86-13265

A possible glow experiment for the EOM 1-2 mission N86-13266

Space shuttle mechanistic studies to characterize atomic oxygen interactions with surfaces N86-13267

The shuttle glow: A program to study the ram-induced phenomena N86-13268

Survey of ultraviolet shuttle glow N86-13269

LUMINOSITY

Ionic mechanicsm of exchange of admixtures between hydrosphere and atmosphere N86-12691

Collider performance with ideal collisions [DE85-017011] N86-13073

Second Workshop on Spacecraft Glow [NASA-CP-2391] N86-13239

Vehicle glow measurements on the space shuttle N86-13240

Space shuttle ram glow: Implication of NO2 recombination continuum N86-13241

AE and DE mass spectrometer observations relevant to the shuttle glow N86-13242

The Atmosphere Explorer and the shuttle glow N86-13243

Orbiter glow observations at high spectral resolution N86-13244

Spectral identification/elimination of molecular species in spacecraft glow N86-13246

The UV-VIS optical environment of the shuttle N86-13247

Investigation of vehicle glow in the far ultraviolet N86-13249

A mechanism for the local concentration enhancement of the shuttle atmosphere N86-13252

Infrared emission from desorbed NO2(*) and NO(*) N86-13254

LUNAR TIDES

Variation in seismicity under influence of lunar-solar tidal deformations N86-12726

LUTETIUM

Paramagnetic form factors of HCP transiton metals [DE85-016301] N86-12301

M

MAGAZINES (SUPPLY CHAMBERS)

Photosensitive cartridge for weapons zeroing and marksmanship training [AD-D011765] N86-13125

MAGELLANIC CLOUDS

Balloon-borne three-meter telescope for far-infrared and submillimeter astronomy [NASA-CR-176347] N86-13271

Combined ultraviolet studies of astronomical source [NASA-CR-176165] N86-13274

MAGNESIUM FLUORIDES

Study of possible solarization - related impurities in CaF2 and other fluorides [DE85-014100] N86-13135

MAGNETIC ANOMALIES

A major crustal feature in the southeastern United States inferred from the MAGSAT equivalent source anomaly field N86-12856

Geophysical interpretation of the magnetic anomalies of the Earth derived from MAGSAT data N86-12857

Satellite magnetic modeling of north African hot spots N86-12858

Magnetic structure of the crust N86-12859

GRM crustal magnetic anomalies: Separating the Lord Howe Rise and Norfolk Ridge submarine structures N86-12865

Continental and oceanic magnetic anomalies: Enhancement through GRM N86-12869

The resolution of a magnetic anomaly map expected from GRM data N86-12870

MAGNETIC COILS

Design and performance of 40 mm, 6.5 T, collared, cold-iron model magnets [DE85-015277] N86-13054

MAGNETIC CORES

Design and performance of 40 mm, 6.5 T, collared, cold-iron model magnets [DE85-015277] N86-13054

MAGNETIC FIELD CONFIGURATIONS

Magnetic reconnection in the terrestrial magnetosphere [DE85-014107] N86-12904

Field-reversed configuration formation, translation, and confinement studies on the FRX-C/T experiment [DE85-014095] N86-13141

Deprit's algorithm, Green's functions and multipole perturbation theory [DE85-012297] N86-13147

Multipole and tokamak research at the University of Wisconsin [DE85-014862] N86-13165

MAGNETIC FIELDS

Effect of pulsed irradiation on microstructural evolution [DE85-016317] N86-12302

Dual drain MOSFET detector for crosstie memory systems [AD-D011828] N86-12513

Self-consistent klystron simulations [DE85-012678] N86-12529

Laser-based foilless diode [DE85-013958] N86-12537

Data analysis of airborne electromagnetic bathymetry [AD-A157132] N86-12744

Geopotential Research Mission (GRM) [NASA-CP-2390] N86-12852

Why do we need detailed gravity over continents: Some Australian examples N86-12855

Magnetic structure of the crust N86-12859

Studies of the marine crustal magnetization at intermediate wavelengths N86-12862

Modeling gravity and magnetic fields for crustal and upper mantle structures N86-12880

Separation of core and crustal magnetic field sources N86-12884

An alternative interpretation of ion ring distribution observed by the S3-3 satellite [AD-A157655] N86-12898

Investigation of magnetic field measurements [AD-A157924] N86-12900

Monitoring of circadian waveforms in rodents exposed to high-intensity static magnetic fields [DE85-015225] N86-12952

Role of supercomputers in magnetic fusion and energy research programs [DE85-013200] N86-13023

Generation of a modulated IREB (Intense Relativistic Electron Beam) with a frequency tunable by a magnetic field [AD-D011820] N86-13068

Chaotic dynamical aperture [DE85-013285] N86-13077

High and ultra-high gradient quadrupole magnets [DE85-014360] N86-13104

RF beam deflection measurements and corrections in the SLC linac [DE85-013061] N86-13146

Electron-spin-polarized targets for a collisionally-pumped polarized-ion source [DE85-015276] N86-13174

MAGNETIC FLUX

Hybrid 0-D,1-D, and 2-D model of helical explosive-driven magnetic flux compression generator [DE85-013772] N86-12524

Field-reversed configuration formation, translation, and confinement studies on the FRX-C/T experiment [DE85-014095] N86-13141

MAGNETIC LENSES

High and ultra-high gradient quadrupole magnets [DE85-014360] N86-13104

MAGNETIC MATERIALS

Separation of core and crustal magnetic field sources N86-12884

MAGNETIC PROPERTIES

Intrusive rocks of oceanic lithosphere as possible sources of anomalous magnetic field of ocean N86-12651

Temperature dependence of the magnetic excitations in Gd [DE85-016303] N86-13203

MAGNETIC TAPES

Building versatile tape handling software [DE85-009333] N86-13018

MAGNETICALLY TRAPPED PARTICLES

FRC formation studies with Z-discharge ionization on FRX-C [DE85-012765] N86-13152

MAGNETITE

Fischer-Tropsch synthesis in slurry reactor systems [DE85-013390] N86-12278

MAGNETIZATION

Satellite magnetic modeling of north African hot spots N86-12858

Studies of the marine crustal magnetization at intermediate wavelengths N86-12862

MAGNETOHYDRODYNAMIC FLOW

Finite difference scheme for one-dimensional magnetohydrodynamic equations N86-12464

Shuttle vertical fin flowfield by the direct simulation Monte Carlo method N86-13251

MAGNETOHYDRODYNAMIC STABILITY

TPSS plasma engineering studies: Profile effects and plasma power balance [DE85-013638] N86-13142

Absolutely unstable two-plasmon decay in two dimensions [DE85-008157] N86-13150

Spatial structure of heat flow instabilities in laser plasmas [DE85-014407] N86-13162

Theory of the anomalous Doppler instability during lower-hybrid current drive [DE85-014064] N86-13170

Explosive coalescence of magnetic islands [DE85-015083] N86-13172

Recent results of an internal tilt mode calculation in FRCs [DE85-014121] N86-13177

Spacecraft-induced plasma energization and its role in flow phenomena N86-13250

MAGNETOHYDRODYNAMIC WAVES

Alfven wave heating on Tokapole 2 [DE85-014859] N86-13179

Alfven continuum with toroidicity [DE85-015821] N86-13217

MAGNETOHYDRODYNAMICS

Hybrid 0-D,1-D, and 2-D model of helical explosive-driven magnetic flux compression generator [DE85-013772] N86-12524

Spectral method for obtaining three-dimensional magnetohydrodynamic equilibria [DE85-015085] N86-13166

MAGNETOMETERS

Investigation of magnetic field measurements [AD-A157924] N86-12900

MAGNETORESISTIVITY

Electrical losses and resistance of cryogenic inductors with consideration of the effect of magnetoresistance [AD-A158185] N86-12516

MAGNETOSPHERE

The aerospace spacecraft charging document [AD-A157664] N86-12248

Rationale for a GRAVSAT-MAGSAT mission: A perspective on the problem of external/internal transient field effects N86-12887

A simulation of high latitude F-layer instabilities in the presence of magnetosphere-ionosphere coupling [NASA-CR-176296] N86-12897
Effects of whistler-mode and other waves in the magnetosphere [AD-A157632] N86-12899
Magnetic reconnection in the terrestrial magnetosphere [DE85-014107] N86-12904
Wave propagation and pair formation in pulsar magnetospheres N86-13276
Trapped particle absorption by the ring of Jupiter [NASA-CR-174406] N86-13279
A note on Jupiter's gossamer ring N86-13280
Electrons and cosmic ray produced in Saturn's inner magnetosphere N86-13281

MAGNETOSPHERIC INSTABILITY
Analysis and interpretation of the shock-like electrostatic noise observed during the AMPTE (Active Magnetospheric Particle Tracer Explorers) solar wind lithium releases [AD-A157512] N86-13283

MAGNETOSPHERIC ION DENSITY
Plasma and magnetospheric research [NASA-CR-176326] N86-13138
Analysis and interpretation of the shock-like electrostatic noise observed during the AMPTE (Active Magnetospheric Particle Tracer Explorers) solar wind lithium releases [AD-A157512] N86-13283

MAGNETRON SPUTTERING
Investigation of renctive magnetron sputter deposited ZnSe for solar cell application [DE85-016651] N86-12780

MAGNETS
Accelerator research studies [DE85-014878] N86-13113

MAGNONS
New interpretation of spin-wave behavior in nickel and iron [DE85-015323] N86-13208

MAGSAT SATELLITES
Geophysical interpretation of the magnetic anomalies of the Earth derived from MAGSAT data N86-12857
Satellite magnetic modeling of north African hot spots N86-12858
Studies of the marine crustal magnetization at intermediate wavelengths N86-12862

MAINTENANCE
Maintenance of photovoltaic power systems, revision 1 [AD-A157838] N86-12777

MALFUNCTIONS
An application of adaptive learning to malfunction recovery [AD-A158129] N86-12236

MAN MACHINE SYSTEMS
Human cognition and performance [AD-A157685] N86-12970
Future directions in mobile teleoperation [DE85-014308] N86-12976

MANAGEMENT INFORMATION SYSTEMS
Aggregating individual preferences in the Analytic Hierarchy Process applied to the 1983 Battelle TAV study [AD-A155858] N86-13226

MANAGEMENT PLANNING
Managing personal desktop computing at Argonne National Laboratory [DE85-014976] N86-12983

MANAGEMENT SYSTEMS
R and D limited partnerships (possible applications in advanced communications satellite technology experiment program) [NASA-CR-176333] N86-13221

MANEUVERABILITY
Optimization of the locomotion of a legged vehicle with respect to maneuverability N86-12371

MANGANESE
Hydrogen chloride sparging crystallization of the chloride salts of cobalt, manganese, and nickel [PB85-197002] N86-12286
Estimation of influence of ocean on distribution of heavy metals in marine atmosphere N86-12703

MANGANESE ALLOYS
Research on the microstructure of rapidly solidified alloys [AD-A157077] N86-12296

MANUALS
Study and investigation to update the nonelectronic reliability notebook. Revision A [AD-A157242] N86-12619

MANUFACTURING
China report: Science and technology [JPRS-CST-85-018] N86-12413
Superconducting wire manufactured N86-12437
Digital voltmeter technology acquisition N86-12449
Improvement of manufacturing techniques and quality of optical scratch standards for fire control systems [AD-A157963] N86-13130

MANY BODY PROBLEM
Large-basis shell-model technology in nucleosynthesis and cosmology [DE85-012925] N86-13216

MAPPING
Cartography, national land management related N86-12401
Benefits of surveying, cartography described N86-12402
Generalized geographic mapping system for computer graphics [PB85-212520] N86-12755
Geophysical interpretation of the magnetic anomalies of the Earth derived from MAGSAT data N86-12857
Global mean sea surface computation based upon a combination of SEASAT and GEOS-3 satellite altimeter data N86-12882
Monthly and seasonal weather outlook for mid-May to mid-June 1985, volume 39, number 10, May 14, 1985 [PB85-204261] N86-12937

MAPS
Meteorological center's forecasts aid Venus probe tracking N86-12631
Correcting a digital map data base with scene analysis concepts and methods [AD-A157913] N86-12745
Generalized geographic mapping system for computer graphics [PB85-212520] N86-12755
Properties of the lithosphere and asthenosphere deduced from geoid observations N86-12867
The resolution of a magnetic anomaly map expected from GRM data N86-12870
Global mean sea surface computation based upon a combination of SEASAT and GEOS-3 satellite altimeter data N86-12882
Recent MAGSAT results N86-12888
On the interpretation of satellite-derived gravity and magnetic data for studies of crustal geology and metallogenesis N86-12894
Do MAGSAT anomalies contain a record of past and present-day mantle convection under South America? N86-12895

MARINE ENVIRONMENTS
Optimal density model of Earth's rust and upper mantle along Kamchatka-Pacific Geotraverse N86-12725
Studies of the marine crustal magnetization at intermediate wavelengths N86-12862
Monthly and seasonal weather outlook for mid-May to mid-June 1985, volume 39, number 10, May 14, 1985 [PB85-204261] N86-12937
Saclantcen's use of scuba diving in oceanographic and acoustic research [AD-A156714] N86-12941
A user's guide to the Coastal Engineering Research Center's (CERC'S) field research facility [AD-A157966] N86-12946
Marine boundary layer from air-sea interface to inversion [PB85-188274] N86-12948
Atmospheric IR transmission measurements in a tropical maritime environment: Comparison with the LOWTRAN 6 model [AD-A157920] N86-13129

MARINE RESOURCES
Aquatic Species Program review: Proceedings of Principal Investigators Meeting [DE85-012137] N86-12364

MARINE TECHNOLOGY
China report: Science and technology [JPRS-CST-85-022] N86-12439
Naval surface weapons center technology transfer biennial report (Fiscal year 1983/1984) [AD-A157919] N86-13238

MARS (PLANET)
Workshop on Water on Mars [NASA-CR-176289] N86-13282

MARS ENVIRONMENT
Workshop on Water on Mars [NASA-CR-176289] N86-13282

MARS SURFACE
Workshop on Water on Mars [NASA-CR-176289] N86-13282

MASS
Determination of dynamic parameters of reflected waves on slopes of deep water trench N86-12724
Measurements and calculations of neutron scattering angular distributions over a wide mass and energy range [DE85-012912] N86-13105
Light mass elements total half-lives for selected long-lived nuclides [DE85-014217] N86-13115

MASS DISTRIBUTION
NeII observations of the galactic center: The velocity field and mass distribution N86-13270

MASS SPECTROMETERS
The shuttle glow: A program to study the ram-induced phenomena N86-13268

MASS SPECTROSCOPY
AE and DE mass spectrometer observations relevant to the shuttle glow N86-13242
Neutral mass spectrometer measurements in the shuttle bay environment N86-13245

MASS TRANSFER
Isothermal dehumidification of air in a parallel passage configuration [DE85-008819] N86-12577
Droplet formation phenomena in dc electrical fields [DE85-014067] N86-12596

MATERIALS HANDLING
Minutes of Workshop on Composite Materials Test Methods [AD-A157903] N86-12262
European Science Notes. Volume 39, number 8 [AD-A157146] N86-13237

MATHEMATICAL LOGIC
China report: Science and technology [JPRS-CST-85-032] N86-12462

MATHEMATICAL MODELS
Multiple ignition, combustion and quenching of hydrocarbon fuel sprays [AD-A158560] N86-12363
Effects of cation ions in nerve excitation N86-12377
New criterion of combined-mode brittle fracture described N86-12400
Mathematical model of the dynamic response of thermo-regulating in 200 MeV linear accelerator N86-12407
Variational analysis of phase transition in pure gauge fields N86-12422
Laser scattering in plasma examined N86-12431
Numerical calculation of turbulent buoyant flow N86-12541
The prediction of fully developed turbulent pressure drops in a triangular duct for a power law fluid N86-12546
Turbulence models for boundary layers on axisymmetric bodies [AD-A158552] N86-12561
Modeling short pulse duration shock initiation of solid explosives [DE85-014803] N86-12565
Modeling and control of flexible structures [AD-A157959] N86-12625
Theory for the Portevin-LeChatelier effect [DE85-004030] N86-12627
Acoustical field of directional source in oceanic waveguides N86-12656
Comparison of single-parameter statistical model with results of round-the-clock measurement of light-scattering matrices N86-12689
Ionic mechanicsm of exchange of admixtures between hydrosphere and atmosphere N86-12690
Evaluating influence of waves on dynamic structure of atmospheric near-water layer N86-12694
Soybean canopy reflectance modeling data sets [E86-10005] N86-12741
Diagnosing the causes of ground-water contamination using a mathematical model: Report on Technology Transfer Workshop [PB85-217008] N86-12808
Evaluation of the NWS (National Weather Service) soil moisutre accounting model for automated flash flood forecasting in small arid and semi-arid watersheds [PB85-229722] N86-12928
A meta system for generating software engineering environments [AD-A158102] N86-12996
MAGNUM-2D computer code: User's guide [DE85-013315] N86-13001
Tandem Mirror Reactor Systems Code (TMRSC) [DE85-012891] N86-13006
TWOPOT: A computer model of the two-pot extractive distillation concept for nitric acid [DE85-013523] N86-13020
Penalized likelihood for general semi-parametric regression models [AD-A158133] N86-13034
Systems analysis approach to probabilistic modeling of fault trees [DE85-007705] N86-13050
Deals among rational agents [AD-A157960] N86-13052
Secondary electron spectra: A semiempirical model [DE85-012448] N86-13086
Analytic models for radiation induced loss in optical fibers. 3. Transient radiation effects [AD-A157408] N86-13127

TPSS plasma engineering studies: Profile effects and plasma power balance [DE85-013638] N86-13142
Generalization of the Child-Langmuir relation for one-dimensional time-dependent diodes [DE85-012677] N86-13145
Deprit's algorithm, Green's functions and multipole perturbation theory [DE85-012297] N86-13147
Absolutely unstable two-plasmon decay in two dimensions [DE85-008157] N86-13150
Wave propagation in a plasma based on the cold plasma model [DE85-013649] N86-13158
Conversion of the bounce-averaged Fokker-Planck code to conversion form [DE85-014861] N86-13160
Solitary vortices in a rotating plasma [DE85-014766] N86-13171
Quantum simulations of small electron-hole complexes [DE85-013895] N86-13205
Comparative first- and second-law analysis of an absorption cycle [DE85-015066] N86-13215

MATHEMATICAL PROGRAMMING
Numerical algorithms and mathematical software for linear control and estimation theory [AD-A157525] N86-12992
A new method for global optimization based on stochastic differential equations [AD-A157546] N86-13029

MATHEMATICS
China report: Science and technology [JPRS-CST-85-034] N86-12430

MATRICES (MATHEMATICS)
Earthquake-response simulation on horizontally large-scale buildings based on the method of reduction concerning their restoring spring matrix. Derivation of general form of spring matrix and comparison of applied response results on an actual building with measured values N86-12374
Comparison of single-parameter statistical model with results of round-the-clock measurement of light-scattering matrices N86-12689
Uncertainty propagation from raw data to final results [DE85-011937] N86-13000
Variational principle for penetrator dynamics using bilinear functional and adjoint formulation [AD-A157964] N86-13031

MATRIX MATERIALS
Fracture surface analysis in composite and titanium bonding [NASA-CR-176309] N86-12257

MATRIX METHODS
Derivation of jack movement influence coefficients as a basis for selecting wall contours giving reduced levels of interference in flexible walled test sections [NASA-CR-177992] N86-12204

MAXIMUM LIKELIHOOD ESTIMATES
Penalized likelihood for general semi-parametric regression models [AD-A158133] N86-13034

MAXWELL EQUATION
Calculation of threshold conditions for materials charging in Maxwellian plasmas [AD-A157123] N86-13139

MECHANICAL DRIVES
Pneumatic actuator device [AD-D011794] N86-12217
Modulations of driven nonlinear surface waves on water and liquid Helium-4 [AD-A157958] N86-12556
Results of PRIM gyroscope testing [DE85-012934] N86-12591

MECHANICAL MEASUREMENT
Mathematical principle for generating second-order aspherical surface N86-12436

MECHANICAL PROPERTIES
The 371 deg C mechanical properties of graphite/polyimide composites [NASA-TM-87122] N86-12256
Fracture surface analysis in composite and titanium bonding [NASA-CR-176309] N86-12257
Effect of measured material properties on the finite element analysis of an OH-58 composite tail boom [NASA-TM-86430] N86-12259
Macroscopic and microscopic deformation and failure processes that control composite toughness [DE85-012938] N86-12263
Role of chemical bonding in adhesion [AD-A157251] N86-12316
Fixation of high-level wastes in glasses [DE85-013276] N86-12325
Effects of surface interactions and mechanical properties of plastic bonded explosives on explosive sensitivity. Part 2: Model formulation [AD-A157900] N86-12381
Investigation of test methods, material properties and processes for solar cell encapsulants [DE85-012831] N86-12786
Materials studies for magnetic fusion energy applications at low temperatures - 8 [PB85-236362] N86-13183

MEDICAL EQUIPMENT
Infrared optical measurement of blood gas concentrations and fiber optic catheter [AD-D011836] N86-12955
Suture needle holder [AD-D011764] N86-12958

MEDICAL SCIENCE
China report: Science and technology [JPRS-CST-85-022] N86-12439
China report: Science and technology [JPRS-CST-85-025] N86-12444
Laser induced biological heating analyzed N86-12460
Studies of participants in nuclear tests N86-12964
China report: Science and technology [JPRS-CST-85-019] N86-12966

MEDITERRANEAN SEA
Stratigraphy of sediments in central and eastern Mediterranean N86-12663

MELAMINE
The studies on the effects of intermolecular hydrogen bond in melamine resination process. (Methylated melamines were adopted as the model compounds of starting material) N86-12381

MELTING POINTS
Foil fuses as opening switches for slow discharge circuits [DE85-014124] N86-12519

MELTS (CRYSTAL GROWTH)
Improved techniques for the growth of high quality cadmium telluride crystals [AD-A157669] N86-13192

MEMBRANE STRUCTURES
China report: Science and technology [JPRS-CST-85-030] N86-12451
Usages of organic membranes in electrolytic industry described N86-12453

MEMBRANES
Development of a supported liquid membrane as a nickel-zinc secondary battery separator [DE85-012591] N86-12784

MEMORY
Stimulus structures and mental representations in expert comprehension of computer programs [AD-A157520] N86-12969

MENTAL PERFORMANCE
Stimulus structures and mental representations in expert comprehension of computer programs [AD-A157520] N86-12969
Human cognition and performance [AD-A157665] N86-12970

MERCURY (METAL)
Mercury N86-12352

MERIDIONAL FLOW
Mesospheric winds and tides at Arecibo/puerto Rico (18 deg N, 67 deg W) November 20-23, 1981 N86-12848
Large-scale circulation departures related to wet episodes in northeast Brazil [NASA-CR-176352] N86-12916

MESOSCALE PHENOMENA
Gravity waves N86-12823
Mesoscale convective systems: A satellite-data-based climatology [PB85-186862] N86-12931

MESOSPHERE
The dynamic stability of the stratosphere and mesosphere N86-12811
Planetary and gravity waves in the mesosphere and lower thermosphere N86-12832
The MST radar technique N86-12836
Mesospheric winds and tides at Arecibo/puerto Rico (18 deg N, 67 deg W) November 20-23, 1981 N86-12848
Mesospheric winds at Jicamaraca, Peru (12 deg S, 77 deg SW), November 19-21, 1981 N86-12849

MESSAGE PROCESSING
Communications network status information system [AD-D011850] N86-12477

METAL FILMS
Method for the deposition of high-quality crystal epitaxial films of iron [AD-D011842] N86-13186
The production of glow precursors by oxidative erosion of spacecraft surfaces N86-13257

METAL MATRIX COMPOSITES
Microstructure/Property relationships for carbon fiber reinforced aluminum alloys [AD-A157858] N86-12261

METAL OXIDE SEMICONDUCTORS
Dual drain MOSFET detector for crosstie memory systems [AD-D011828] N86-12513

METAL SURFACES
Theoretical studies of deep impurity levels in ternary semiconductor alloys [AD-A157929] N86-13193

METALLICITY
Combined ultraviolet studies of astronomical source [NASA-CR-176165] N86-13274

METALS
Anaerobic microbial dissolution of toxic metals in subsurface environments [DE85-013308] N86-12251
Method and apparatus for conducting variable thickness vapor deposition [DE85-011653] N86-12306
Surface crystallization on metallized 94 percent alumina ceramics [DE85-006691] N86-12324
In-situ vacuum-assisted molding of glass-metal electrical components [DE85-015607] N86-12326
Foil fuses as opening switches for slow discharge circuits [DE85-014124] N86-12519
Motion of thin metal walls and the equation of state of detonation products [DE85-014809] N86-12629

METASTABLE STATE
Theoretical studies of deep impurity levels in ternary semiconductor alloys [AD-A157929] N86-13193

METEOROIDS
Data descriptions and vertical structure plots for mean, diurnal, and semidurnal components of eastward and northward (ordered by latitude). Mean winds and tides over Poker Flat, Alaska (65 deg N, 147 deg W), during November 1981 N86-12840

METEOROLOGICAL CHARTS
Diagnosis of weather states in winter of 1980-1981 N86-12632

METEOROLOGICAL FLIGHT
Temperature and wind data from meteorological rockets N86-12816
Observed winds and temperatures in the Southern Hemisphere N86-12817

METEOROLOGICAL PARAMETERS
Main problems in climate monitoring (diagnosis) N86-12633
Evaluating influence of waves on dynamic structure of atmospheric near-water layer N86-12694
Spatial structure of high-frequency sea wind waves under different meteorological conditions N86-12714
Meteorological Satellite Center Technical Note No. 11, 1985 [MSC-TN-11] N86-12909
Atmospheric environment for space shuttle (STS-51B) launch [NASA-TM-86525] N86-12917
Weather analysis programs using HP-41CV [AD-A157389] N86-12921
Modeling the diurnal variation of meteorlogical variables within the boundary layer: Preliminary comparison results [PB85-198349] N86-12933

METEOROLOGICAL RADAR
Mean winds of the mesosphere (60-80 km), as measured by MF radars N86-12818
Data descriptions and vertical structure plots for mean, diurnal, and semidurnal components of eastward and northward (ordered by latitude). Mean winds and tides over Poker Flat, Alaska (65 deg N, 147 deg W), during November 1981 N86-12840
Weather radar studies [AD-A157093] N86-12920

METEOROLOGICAL SATELLITES
Temperature data from satellites N86-12815
Middle atmosphere reference model derived from satellite data N86-12819
Meteorological Satellite Center Technical Note No. 11, 1985 [MSC-TN-11] N86-12909
Clear sky brightness temperature over the western north Pacific Ocean from GMS spacecraft N86-12911
Simultaneous observation of GMS and GMS-2: A study of the difference between the brightness temperatures by GMS and those by GMS-2 N86-12912
Relaying of the stretched VISSR data by GMS spacecraft N86-12913

The modification of the operational program for GMS-3 N86-12914
Introduction to operational ASDAR system N86-12915

METEOROLOGICAL SERVICES
First experiment in forecasting cool-season weather with the PROFS System [PB85-230605] N86-12929

METEOROLOGY
USSR report: Earth sciences [JPRS-UES-85-006] N86-12630
USSR report: Earth sciences [JPRS-UES-85-008] N86-12697
Advanced Moisture and Temperature Sounder (AMTS) baseline 5 study report [NASA-CR-176331] N86-12919

METHANE
Reduction of CO2 to methanol and methane by photo and dark reactions on semiconductor electrodes [PB85-226298] N86-12290

METHYL ALCOHOLS
The alcohols N86-12349

METRIC SPACE
Vector valued long James type Banach spaces J(eta, l sub p)(1 or = p + infinity) N86-12463

MICROBIOLOGY
China report: Science and technology [JPRS-CST-85-025] N86-12444

MICROCOMPUTERS
A computer analysis of the distribution of principal stresses using photoelastic pattern N86-12375
Microcomputer-controlled closed-loop system for positioning radio telescope N86-12410
China report: Science and technology [JPRS-CST-85-018] N86-12413
Method of using CTC to microcomputerize digital instruments N86-12441
China report: Science and technology [JPRS-CST-85-019] N86-12966
The design and hardware evaluation of an advanced 16-bit, low-power, high performance microcomputer system for digital signal processing [AD-A158130] N86-12981
Systems for authoring computer-based instruction [PB85-198950] N86-12987

MICROELECTRONICS
Basic EMC (Electromagnetic compatibility) technology advancement for C3 (Command, control, and communications) systems. Volume 6 [AD-A157239] N86-12493
Electronics Engineering Department Thrust Area report FY'84 [DE85-014857] N86-12539

MICROORGANISMS
Influence of some oceanographic characteristics on decay kinetcis of surface-active agents in sea N86-12676

MICROPROCESSORS
The 4-bit microprocessor capabilities, applications described N86-12406
New dual Z80 navigaiton computer described N86-12425
China report: Science and technology [JPRS-CST-85-029] N86-12446
Programmer for single-chip microprocessor N86-12448
Magnet power supply control of the NSLS VUV and X-ray storage rings transfer lines [DE85-014213] N86-13168

MICROSCOPY
European Science Notes. Volume 39, number 8 [AD-A157146] N86-13237

MICROSTRUCTURE
Research on the microstructure of rapidly solidified alloys [AD-A157077] N86-12296
Resistance to fracture, fatigue and stress-corrosion of Al-Cu-Li-Zr alloys [AD-A158407] N86-12300
Effect of pulsed irradiation on microstructural evolution [DE85-016317] N86-12302
Review of effects of long-term aging on the mechanical properties and microstructures of types 304 and 316 stainless steel [DE85-016472] N86-12304
Special metallographic procedures for austenitic stainless steel welds [DE85-010113] N86-12305
Effects of microstructure on the acoustoelastic measurements of stress [DE85-015518] N86-12307
Thermally induced failures of thick-film glaze resistors [DE85-012014] N86-12320
Deposition, microstructure and properties of laser CVD SiC films [DE85-014680] N86-12327
Mechanical interactions of rough surfaces [DE85-015011] N86-12813

MICROTRONS
Racetrack microtron rf system [DE85-012669] N86-12532

MICROWAVE AMPLIFIERS
Development program for a 200 kW, cw gyrotron [DE85-014867] N86-13096

MICROWAVE SENSORS
Microwave ridged waveguide beam pickups [DE85-013816] N86-12499

MICROWAVE SPECTRA
Evaluation of space SAR as a land-cover classification [E86-10004] N86-12740

MICROWAVE SPECTROMETERS
Method to detect ethylene glycol in gaseous mixtures [AD-A158109] N86-12272

MICROWAVE TUBES
The Record of Electrical and Communication Engineering Conversazione, volume 54, no. 1 [ISSN-0385-771-9] N86-12383
Proposal of a high efficient and high power peniotron N86-12384

MICROWAVES
Electronics Engineering Department Thrust Area report FY'84 [DE85-014857] N86-12539
FDSC: A microwave coupling code for slots of finite depth [DE85-013443] N86-13011
Compact microwave ion source [DE85-014536] N86-13176
Josephson effect in the unusual superconductors Lu2Fe3Si5, LiTi2O4 and UBe13 [DE85-015260] N86-13211

MIDDLE ATMOSPHERE
Middle Atmosphere Program. Handbook for MAP. Volume 16: Atmospheric structure and its variation in the region 20 to 120 km. Draft of a new reference middle atmosphere [NASA-CR-176321] N86-12814
Temperature data from satellites N86-12815
Observed winds and temperatures in the Southern Hemisphere N86-12817
Mean winds of the mesosphere (60-80 km), as measured by MF radars N86-12818
Middle atmosphere reference model derived from satellite data N86-12819
Planetary waves N86-12821
Gravity waves N86-12822
Gravity waves N86-12823
Atmospheric tides below 80 km N86-12824
Annual and semiannual cycles based on the middle atmosphere reference model N86-12826
On the interannual variability and on trends of the temperature in the middle atmosphere N86-12827
Interim reference ozone models for the middle atmosphere N86-12829
Mean winds of the upper middle atmosphere (60-110 km): A global distribution from radar systems (MF, meteor, VHF) N86-12831
Contribution to the CIRA model from ground-based lidar N86-12835
Middle Atmosphere Program. Handbook for MAP, volume 17 [NASA-CR-176345] N86-12837
Towards a global MAP data base N86-12838
Atmospheric Tides Middle Atmosphere Program (ATMAP): Report of the November/December 1981, and May 1982, observational campaigns N86-12839
Remarks on the ATMAP campaigns in November 1981 and May 1982 at Collm (52 deg N, 15 deg E) N86-12842
Saskatoon M. F. radar system: (52 deg N, 107 deg W), Canada N86-12843
May 1982, Saskatoon M. F. radar system: (52 deg N, 107 deg W), Canada N86-12844
Meteor wind results at Durham (43 deg N, 71 deg W) during the ATMAP November 1981 and May 1982 campaigns N86-12845
Mean winds and tides over Urbana, Illinois during November 16-22, 1981 N86-12846
Results of November 1981 and May 1982 ATMAP campaigns at Adelaide (35 deg S, 138 deg E) N86-12850
Middle atmosphere tides at Christchurch (44 deg S, 17 deg E) in November 1981 and May 1982 N86-12851

MILITARY OPERATIONS
The C-17: We need it yesterday [AD-A157147] N86-12219
European Science Notes. Volume 39, number 8 [AD-A157146] N86-13237

MILITARY TECHNOLOGY
Japanese report on China's F-8 fighter N86-12405
Word lists to limit vocabulary in technical information [AD-A157931] N86-13226
Naval surface weapons center technology transfer biennial report (Fiscal year 1983/1984) [AD-A157919] N86-13236

MILLIMETER WAVES
Evaluation of high permittivity glass ceramics for millimeter wave applications [AD-A158551] N86-12319
Proposal of a high efficient and high power peniotron N86-12384
Experiments with domestic IC substrates N86-12433
Near millimeter wave imaging/multi-beam integrated antennas [NASA-CR-176332] N86-12478
Development program for a 200 kW, cw gyrotron [DE85-014867] N86-13096

MINERAL OILS
Velocity and gravity effects in relative permeability measurements [DE85-009925] N86-12570

MINERALS
magnetic minerals and characteristics of natural magnetic state of core in Saatly superdeep hole in depth range 3500-7500 meters N86-12681

MINICOMPUTERS
Hardware and software support of geological-geophysical database N86-12686

MINKOWSKI SPACE
Gravity theories in more than four dimensions [DE85-011164] N86-12903

MINNESOTA
Waters resources data for Minnesota. Water year 1983. Volume 2: Upper Mississippi and Missouri River Basins [PB85-215994] N86-12753

MIRROR FUSION
Tandem Mirror Reactor Systems Code (TMRSC) [DE85-012891] N86-13006

MIRRORS
Low sidelobe, high efficiency mirror antenna with twist reflector [AD-D011635] N86-12474

MIST
Study of the mist cooling and droplet dynamics in turbulent flow by using LDA N86-12545

MIXING
Analysis of stratified flow mixing [DE85-006840] N86-12576

MIXTURES
Thermodynamics of multi-polar molecules: The perturbed-anisotropic-chain theory [DE85-013148] N86-12274
Absorption fluids data survey [DE85-005279] N86-12792

MOBILITY
Power and signal transmission for mobile teleoperated systems [DE85-013994] N86-12975
Future directions in mobile teleoperation [DE85-014308] N86-12976

MODELS
Effects of surface interactions and mechanical properties of plastic bonded explosives on explosive sensitivity. Part 2: Model formulation [AD-A157900] N86-12361
Investigation of the flame-acoustic wave interaction during axial solid rocket instabilities [AD-A158559] N86-12362
Multiple-scale turbulence closure modeling of confined recirculating flows [NASA-CR-178536] N86-12551
Analysis of stratified flow mixing [DE85-006840] N86-12576
Direct solar-pumped iodine laser amplifier [NASA-CR-176324] N86-12600
Feasibility of using LANDSAT images of vegetation cover to estimate effective hydraulic properties of soils [E86-10003] N86-12739
Soybean canopy reflectance modeling data sets [E86-10005] N86-12741
Constraints on the rheological structure of the mantle N86-12875
The role of a pressure-dependent rheology in the dynamics of mantle circulation N86-12876
Small-scale convection beneath the transverse ranges, California: Implications for interpretation of gravity anomalies N86-12877
Modeling gravity and magnetic fields for crustal and upper mantle structures N86-12880
Separation of core and crustal magnetic field sources N86-12884
The magnetic field at the core-mantle boundary N86-12885
Some anticipated contributions to core fluid dynamics from the GRM N86-12886
Recent MAGSAT results N86-12888
Modeling currents at satellite altitudes N86-12889

The source of the intermediate wavelength component of the Earth's magnetic field N86-12891
GRM as a follow-on to MAGSAT N86-12893
On the interpretation of satellite-derived gravity and magnetic data for studies of crustal geology and metallogenesis N86-12894
Radiation fog modeling
[AD-A157971] N86-12924
Environmental impact research program. Status and source of habitat models and literature reviews, December 1984
[AD-A156899] N86-12950
Actors: A model of concurrent computation in distributed systems
[AD-A157917] N86-12994
Overview of free-piston Stirling technology at the NASA Lewis Research Center
[NASA-TM-87156] N86-13236
Spectral identification/elimination of molecular species in spacecraft glow N86-13246
Shuttle vertical fin flowfield by the direct simulation Monte Carlo method N86-13251
A model for explaining some features of shuttle glow N86-13256
Ultraviolet observations of low-excitation Herbig-Haro objects
[NASA-CR-176164] N86-13273

MODULATION
Modulations of driven nonlinear surface waves on water and liquid Helium-4
[AD-A157958] N86-12556

MODULES
Reliability and Engineering of Thin-Film Photovoltaic Modules. Research forum proceedings
[NASA-CR-176217] N86-12759
Crystalline-silicon reliability lessons for thin-film modules N86-12760
Light-induced effects-impacts to module performance measurements and reliability testing: An overview N86-12761
Thin-film module circuit design: Practical and reliability aspects N86-12762
Hot-spot heating susceptibility due to reverse bias operating conditions N86-12763
Accelerated stress testing of thin film solar cells: Development of test methods and preliminary results N86-12764
Electrical safety requirements: Implications for the module designer N86-12765
Large-area thin-film modules N86-12766
Interconnect resistance of photovoltaic submodules N86-12767
Thin film module development N86-12768
Amorphous silicon photovoltaic modules and test devices design, fabrication and testing N86-12769
Thin film module electrical configuration versus electrical performance N86-12770
Outdoor performance testing of thin-film devices N86-12771
Module voltage isolation and corrosion research N86-12772
Glass breaking strength: The role of surface flaws and treatments N86-12773
Encapsulant selection and durability testing experience N86-12774

MODULUS OF ELASTICITY
Fracture surface analysis in composite and titanium bonding
[NASA-CR-176309] N86-12257
Accuracy of a new ultrasonic apparatus for simple measurement of viscoelasticity N86-12386

MOISTURE CONTENT
Electro-optical transmission and liquid water content of fogs and clouds
[AD-A157506] N86-13128
Workshop on Water on Mars
[NASA-CR-176289] N86-13262

MOISTURE METERS
Advanced Moisture and Temperature Sounder (AMTS) baseline 5 study report
[NASA-CR-176331] N86-12919

MOLECULAR ABSORPTION
Raman spectroscopy of molecular adsorbates
[DE85-012981] N86-12280
Transmission of tropospheric radiation of lasers on molecules of different carbon dioxide isotopes N86-12734

MOLECULAR BEAMS
Application of an atomic oxygen beam facility to the investigation of shuttle glow chemistry N86-13261

MOLECULAR COLLISIONS
Planned investigation of infrared emissions associated with the induced spacecraft glow: A shuttle infrared glow experiment (SIRGE) N86-13264

MOLECULAR ENERGY LEVELS
Physico-chemical conditions in circumstellar shells of evolved oxygen-rich M stars N86-13275

MOLECULAR EXCITATION
Diffusion in binary plasma mixtures
[DE85-017694] N86-13143
Activated recombinative desorption: A potential component in mechanisms of spacecraft glow N86-13258
Optical radiation from the interaction of energetic atoms, ions, electrons, and photons with surfaces N86-13259

MOLECULAR INTERACTIONS
Theoretical studies of molecular interactions
[DE85-012604] N86-13076

MOLECULAR RELAXATION
High pressure and molecular weight variation of electrical relaxation in poly(ethylene oxide)
[AD-A157660] N86-12317

MOLECULAR SPECTRA
Spectral identification/elimination of molecular species in spacecraft glow N86-13246

MOLECULAR SPECTROSCOPY
Review of spectroscopic parameters for upper atmospheric measurements
[NASA-CP-2396] N86-13064

MOLECULAR STRUCTURE
Nanosecond fluorescence spectroscopy
[DE85-012234] N86-12282
Molecular control
[NASA-TM-87510] N86-12313

MOLECULAR WEIGHT
High pressure and molecular weight variation of electrical relaxation in poly(ethylene oxide)
[AD-A157660] N86-12317

MOLECULES
Thermodynamics of multi-polar molecules: The perturbed-anisotropic-chain theory
[DE85-013148] N86-12274
Molecular control
[NASA-TM-87510] N86-12313

MOLTEN SALTS
Molten salt corrosion of SiC: Pitting mechanism
[NASA-TM-87143] N86-12310
Solar thermal energy systems
[DE85-008793] N86-12790

MOM (SEMICONDUCTORS)
Interconnect resistance of photovoltaic submodules N86-12767

MOMENTS OF INERTIA
Numerical computation of full three-dimensional flow in transonic turbines N86-12397

MOMENTUM
Model describing the steady-state pyrolysis of bubble-forming polymers in response to an incident heat flux
[PB85-225225] N86-12291
Numerical and experimental studies of 3-D and unsteady turbulent body/appendage/propeller flows
[AD-A157078] N86-12552
Flow rates in the East Pacific rise (21 deg N) hot springs, and numerical investigations of two regimes of hydrothermal circulation N86-12939

MOMENTUM TRANSFER
Analysis of stratified flow mixing
[DE85-006840] N86-12576
Eddy fluxes of heat, vorticity and momentum in ocean and atmosphere and their parameterization (review) N86-12672
Viscous nonlinear circulation in axisymmetric baroclinic eddy N86-12712

MONATOMIC GASES
Space shuttle mechanistic studies to characterize atomic oxygen interactions with surfaces N86-13267

MONITORS
Microwave ridged waveguide beam pickups
[DE85-013816] N86-12499
Outdoor radon monitoring at Canonsburg, Pennsylvania, 1980-1983
[DE85-013320] N86-12797
Development of a current monitor system for measuring pulsed-beam current over a wide dynamic range
[DE85-012692] N86-13083

MONOMERS
Epoxy phthalonitrile polymers
[AD-D011821] N86-12318

MONTE CARLO METHOD
Transient thermal modeling of the nonscanning ERBE detector
[NASA-CR-172240] N86-12743
Transforming censored samples and testing fit
[AD-A157957] N86-13048
Nearly ideal lens optimization procedure
[DE85-014116] N86-13134

MORPHOLOGY
Petrochemical types of magmatic rocks of ocean floor and patterns of their distribution N86-12650

Workshop on Water on Mars
[NASA-CR-176289] N86-13262

MORTALITY
Studies of participants in nuclear tests N86-12964

MOTION
The dynamic stability of the stratosphere and mesosphere N86-12811

MOUNTAINS
Lasers measure drifting mountains N86-12718
The numerical simulation of geographic storms N86-12907

MULTICHANNEL COMMUNICATION
Practical optical multichannel analyzer developed N86-12416

MULTIPLE BEAM INTERVAL SCANNERS
Near millimeter wave imaging/multi-beam integrated antennas
[NASA-CR-176332] N86-12478

MULTIPOLES
Deprit's algorithm, Green's functions and multipole perturbation theory
[DE85-012297] N86-13147
Tracking studies on the effects of random multipoles in the 6.5 T lattice of the SSC Reference Designs Study
[DE85-013286] N86-13156
Multipole and tokamak research at the University of Wisconsin
[DE85-014862] N86-13165

MULTIPROCESSING (COMPUTERS)
New dual Z80 navigaiton computer described N86-12425
Generic software for emulating multiprocessor architectures
[AD-A157662] N86-12979
DAPHNE: The design of a parallel multiprocessor data acquisition system
[DE85-013875] N86-12984

MUONS
Muon tomography used to study underground rock structure N86-12720

N

NASA PROGRAMS
NASA LeRC/Akron University Graduate Cooperative Fellowship Program and Graduate Student Researchers Program
[NASA-CR-174826] N86-13219
Index to NASA news releases and speeches, 1984
[NASA-TM-87514] N86-13224
Department of Housing and Urban Development, and Certain Other Independent Agencies Appropriations for Fiscal Year 1986, part 1
[S-HRG-99-221-PT-1] N86-13233

NAVIER-STOKES EQUATION
Numerical and experimental studies of 3-D and unsteady turbulent body/appendage/propeller flows
[AD-A157078] N86-12552
C0 collocation solutions for weak-formulation Navier-Stokes equations
[AD-A157250] N86-12553

NAVIGATION
Monthly and seasonal weather outlook for mid-May to mid-June 1985, volume 39, number 10, May 14, 1985
[PB85-204261] N86-12937

NAVIGATION AIDS
New dual Z80 navigaiton computer described N86-12425

NEAR FIELDS
Near millimeter wave imaging/multi-beam integrated antennas
[NASA-CR-176332] N86-12478

NEARSHORE WATER
Annual data summary for 1981 CERC (Coastal Engineering Research Center) field research facility
[AD-A158143] N86-12926

NEEDLES
Suture needle holder
[AD-D011764] N86-12958

NEODYMIUM LASERS
China report: Science and technology
[JPRS-CST-85-021] N86-12421
High-power ND: Glass laser and target chamber system and an experimental study of laser plasma X-ray N86-12428

NEON
Noble gases N86-12348

NERVOUS SYSTEM
Research Reports of the Faculty of Engineering, Tokyo Denki University, no. 32
[ISSN-0389-617-X] N86-12372

NETWORK CONTROL
Survey and expository papers on topics of current interest in applied mathematics
[AD-A158418] N86-13229

NEUMANN PROBLEM
Integral equation description of integrated dielectric waveguides N86-12504
NEURAL NETS
Cortical plasticity: Theoretical analysis, experimental results
[AD-A157965] N86-12961
NEUROLOGY
Criteria for a state-of-the-art vision test system
[AD-A157099] N86-12973
NEUTRAL BEAMS
Strategic defense initiatives at Los Alamos National Laboratory
[DE85-014093] N86-12606
A ground-based experimental test program to duplicate and study the spacecraft glow phenomenon
N86-13260
Data requirements for verification of ram glow chemistry N86-13265
Space shuttle mechanistic studies to characterize atomic oxygen interactions with surfaces N86-13267
NEUTRAL PARTICLES
Experiment to study K(+) (YIELDS) (PI)(+) + nothing at LAMPF 2
[DE85-014267] N86-13110
The NO-NO2 system at laboratory surfaces
N86-13255
NEUTRINO BEAMS
Large acceptance magnetic focussing horns for production of a high intensity narrow band neutrino beam at the AGS
[DE85-013300] N86-13157
NEUTRINOS
Multiplicities in high energy interactions
[DE85-013847] N86-13100
NEUTRON DIFFRACTION
Temperature and concentration dependence of hydrogen site occupancy in several rare-earth dihydrides
[DE85-015739] N86-13199
Mossbauer effect and neutron diffraction study of the anomalous lattice behavior of U6Fe
[DE85-014912] N86-13210
NEUTRON SCATTERING
Measurements and calculations of neutron scattering angular distributions over a wide mass and energy range
[DE85-012912] N86-13105
NEUTRON SOURCES
Development of a continuous mass flow measuring flow
[DE85-012492] N86-12573
WNR/PSR facility: Neutron physics capabilities from sub-thermal to 800 MeV
[DE85-014072] N86-13173
NEUTRON SPECTRA
Prompt neutron fission spectrum mean energies for the fissile nuclides and (252)Cf
[DE85-012181] N86-13117
NEUTRON SPECTROMETERS
Los Alamos constant-Q spectrometer
[DE85-014115] N86-12586
NEUTRONS
Nuclear information needs for the astrophysical s-process
[DE85-012913] N86-13278
NEWS
Index to NASA news releases and speeches, 1984
[NASA-TM-87514] N86-13224
NICKEL
Hydrogen chloride sparging crystallization of the chloride salts of cobalt, manganese, and nickel
[PB85-197002] N86-12286
An update of the total-strain version of SRP
[NASA-TP-2499] N86-12295
Suspension method of impregnating active material into composite nickel plaque
[AD-D011626] N86-12299
Uncertainty propagation from raw data to final results
[DE85-011937] N86-13000
New interpretation of spin-wave behavior in nickel and iron
[DE85-015323] N86-13208
NICKEL ALLOYS
Metal dissolution kinetics in organic solvents using rotating ring-disc voltammetry
[DE85-013478] N86-12253
Fatigue crack propagation of nickel-base superalloys at 650 deg C
[NASA-TM-87150] N86-12294
NICKEL ISOTOPES
Isovector resonances in pion charge exchange
[DE85-012746] N86-13106
NICKEL ZINC BATTERIES
Development of a supported liquid membrane as a nickel-zinc secondary battery separator
[DE85-012591] N86-12784
NIOBIUM
Frequency selection and mode locking of Nd:YAG laser N86-12395
Superconducting wire manufactured N86-12437
NITRATES
Spatial and temporal patterns of acid precipitation and their interpretation
[PB85-214377] N86-12809
NITRIC ACID
Fuming nitric acids N86-12342
TWOPOT: A computer model of the two-pot extractive distillation concept for nitric acid
[DE85-013523] N86-13020
NITRIC OXIDE
Multiphoton ionization of NO-rare gas van der Waals species
[DE85-014650] N86-13094
NITRO COMPOUNDS
Oxidation of heterocyclic nitrogen yields to nitroheterocycles
[DE85-012757] N86-12284
Development of a routine technique for analysis of nitro-PAH in diesel particulate extract
[PB85-198657] N86-12287
Quantum chemistry of aromatic nitro explosives
N86-12423
NITROGEN
Oxidation of heterocyclic nitrogen yields to nitroheterocycles
[DE85-012757] N86-12284
Nitrogen N86-12347
Titanium-nitrogen ion beam injection studied
N86-12427
An assessment of the impact of spacecraft glow on the Hubble space telescope. Summary of existing observations and theory N86-13262
NITROGEN ATOMS
AE and DE mass spectrometer observations relevant to the shuttle glow N86-13242
NITROGEN DIOXIDE
Space shuttle ram glow: Implication of NO2 recombination continuum N86-13241
AE and DE mass spectrometer observations relevant to the shuttle glow N86-13242
The Atmosphere Explorer and the shuttle glow
N86-13243
NITROGEN FLUORIDES
Nitrogen trifluoride N86-12345
NITROGEN IONS
Enhanced N(+) sub 2 in the shuttle environment
N86-13248
NITROGEN ISOTOPES
Partition of cross sections in asymmetric nucleus-nucleus reactions and the origin of fast alpha particles
[DE85-014989] N86-13089
NITROGEN OXIDES
Nitrogen oxides N86-12341
NITROGEN PLASMA
A ground-based experimental test program to duplicate and study the spacecraft glow phenomenon
N86-13260
NITROMETHANE
Nitromethane N86-12332
NITROUS OXIDES
Nitrous oxide N86-12355
The NO-NO2 system at laboratory surfaces
N86-13255
NOISE GENERATORS
Transonic noise generation by duct and profile flow
[AD-A157163] N86-13058
NOISE INTENSITY
Angular distribution of intensity of sound reradiated by ocean surface at small glancing angles N86-12643
NOISE REDUCTION
Evaluation of honeycomb highway sound barrier I-280 section 8B, Harrison, New Jersey
[PB85-231157] N86-13063
NONADIABATIC CONDITIONS
Diagnosis of weather states in winter of 1980-1981
N86-12632
NONDESTRUCTIVE TESTS
The Record of Electrical and Communication Engineering Conversazione, volume 54, no. 1
[ISSN-0385-771-9] N86-12383
Accuracy of a new ultrasonic apparatus for simple measurement of viscoelasticity N86-12386
Application of heat-scan NDT to inspection of adhesion of solid rocket motor propellant to envelope
N86-12461
NONEQUILIBRIUM FLOW
Multiple-scale turbulence closure modeling of confined recirculating flows
[NASA-CR-178536] N86-12551
NONFLAMMABLE MATERIALS
Microemulsion-type fire-resistant diesel fuel
[AD-A157125] N86-12359
NONLINEAR EQUATIONS
Chaotic dynamical aperture
[DE85-013285] N86-13077
NONLINEAR OPTICS
State-of-the-art of optics in China reviewed
N86-12414
NONLINEAR SYSTEMS
Modulations of driven nonlinear surface waves on water and liquid Helium-4
[AD-A157958] N86-12556
Variational principle for penetrator dynamics using bilinear functional and adjoint formulation
[AD-A157964] N86-13031
Survey and expository papers on topics of current interest in applied mathematics
[AD-A158418] N86-13229
NONLINEARITY
Nonlinear electromagnetic scattering from a diode circuit
[AD-A157216] N86-12491
The role of amplitude-to-phase conversion in the generation of oscillator flicker phase noise
[NASA-TM-87590] N86-12508
Modulations of driven nonlinear surface waves on water and liquid Helium-4
[AD-A157958] N86-12556
The nature of symmetric instability and its similarity to convective and inertial instability
[NASA-CR-3945] N86-12918
NONNEWTONIAN FLOW
Subduction dynamics: Constraints from gravity field observations N86-12868
NOREPINEPHRINE
Cortical plasticity: Theoretical analysis, experimental results
[AD-A157965] N86-12961
NORMALIZING (STATISTICS)
Replica-space renormalization in random-field systems
[DE85-014800] N86-13055
NOTCHES
Low dispersion notch filter for multi-GHz frequencies using fiber optics delays
[DE85-014983] N86-12520
NOZZLE FLOW
Measurements on an axisymmetric jet in a slow coflowing stream N86-12549
NUCLEAR CAPTURE
Nuclear information needs for the astrophysical s-process
[DE85-012913] N86-13278
NUCLEAR ENERGY
China report: Science and technology
[JPRS-CST-85-026] N86-12459
NUCLEAR EXPLOSIONS
Studies of participants in nuclear tests N86-12964
NUCLEAR FUSION
Role of supercomputers in magnetic fusion and energy research programs
[DE85-013200] N86-13023
Nuclear performance optimization of the Be/Li/Th blanket for the fusion breeder
[DE85-012949] N86-13112
Materials studies for magnetic fusion energy applications at low temperatures - 8
[PB85-236362] N86-13183
Large-basis shell-model technology in nucleosynthesis and cosmology
[DE85-012925] N86-13216
NUCLEAR PARTICLES
Partition of cross sections in asymmetric nucleus-nucleus reactions and the origin of fast alpha particles
[DE85-014989] N86-13089
NUCLEAR PHYSICS
China report: Science and technology
[JPRS-CST-85-026] N86-12459
China report: Science and technology
[JPRS-CST-85-032] N86-12462
A dressed atom interpretation of adiabatic rapid passage
[AD-A157071] N86-13066
NUCLEAR POTENTIAL
Measurements and calculations of neutron scattering angular distributions over a wide mass and energy range
[DE85-012912] N86-13105
NUCLEAR POWER PLANTS
Results of field and laboratory studies of jam-resistant and voice-private radios
[DE85-014841] N86-12500
New passive helicopter detector
[DE85-015160] N86-12595

Failure criteria used in a probabilistic fracture mechanics code
[DE85-007264] N86-12628

NUCLEAR REACTORS
Role of supercomputers in magnetic fusion and energy research programs
[DE85-013200] N86-13023
Prompt neutron fission spectrum mean energies for the fissile nuclides and (252)Cf
[DE85-012181] N86-13117

NUCLEAR WEAPONS
Electrochemical machining of the outer profile of the B83 Lug
[DE85-014934] N86-12616

NUCLEON-NUCLEON SCATTERING
Conference summary: Antinucleon- and nucleon-nucleus interactions
[DE85-013905] N86-13114

NUCLEONS
Multiplicities in high energy interactions
[DE85-013847] N86-13100
Dynamical model of quark rearrangement in nucleon-antinucleon annihilation
[DE85-013904] N86-13120

NUCLIDES
Light mass elements total half-lives for selected long-lived nuclides
[DE85-014217] N86-13115

NUMERICAL ANALYSIS
Numerical calculation of turbulent buoyant flow N86-12541
Numerical and experimental studies of 3-D and unsteady turbulent body/appendage/propeller flows
[AD-A157078] N86-12552
A new method for global optimization based on stochastic differential equations
[AD-A157546] N86-13029

NUMERICAL CONTROL
The 32-bit computer for large memory applications on FASTBUS
[DE85-012726] N86-12986
Numerical algorithms and mathematical software for linear control and estimation theory
[AD-A157525] N86-12992
Magnet power supply control of the NSLS VUV and X-ray storage rings transfer lines
[DE85-014213] N86-13168

NUMERICAL INTEGRATION
Deposition, microstructure and properties of laser CVD SiC films
[DE85-014680] N86-12327

NUMERICAL WEATHER FORECASTING
Meteorological center's forecasts aid Venus probe tracking N86-12631

O

O STARS
Physico-chemical conditions in circumstellar shells of evolved oxygen-rich M stars N86-13275

OAK RIDGE ISOCHRONOUS CYCLOTRON
Charge-state distributions of 100, 175, 275 and 352 MeV gold ions emerging from thin carbon foils
[DE85-014651] N86-13069

OCEAN BOTTOM
Petrochemical types of magmatic rocks of ocean floor and patterns of their distribution N86-12650
Intrusive rocks of oceanic lithosphere as possible sources of anomalous magnetic field of ocean N86-12651
Magmatic provinces and tectonics in Pacific Ocean N86-12652
Oil and gs deposits on continental slopes of the ocean N86-12655
Possibility of sounding Earth by using electromagnetic field of sea current N86-12661
Find of rheolites and trachites and geological situation in northern part of East Indian Ocean Submarine Ridge N86-12665
Nonlinear model of adaptation of fields of density and currents in sea N86-12670
Features of geostrophic circulation related to nature of bottom relief in northwestern Atlantic N86-12674
Computations of seismic wave propagation velocities in ocean bottom sediments from reflected waves travel-time curves N86-12677
Folded structures in central Indian Ocean trench N86-12704
Structure of sedimentary cover and basement of Sierra Leone Rise determined from common depth point seismic (equatorial Atlantic) N86-12709
Tectonic structure of Shirshov Ridge (Bering Sea) N86-12710
Facies-genetic groups of coarse clastic material on world ocean floor N86-12713
Studies of the marine crustal magnetization at intermediate wavelengths N86-12862
Lithospheric structure in the Pacific geoid N86-12863
GRM crustal magnetic anomalies: Separating the Lord Howe Rise and Norfolk Ridge submarine structures N86-12865
Sea floor swells and mantle plumes N86-12866
Saclantcen's use of scuba diving in oceanographic and acoustic research
[AD-A156714] N86-12941
Underwater photography for quantitative description of bottom roughness
[AD-A156753] N86-12943

OCEAN CURRENTS
Nonlinear model of adaptation of fields of density and currents in sea N86-12670
Eddy fluxes of heat, vorticity and momentum in ocean and atmosphere and their parameterization (review) N86-12672
Study of influence of vertical velocity and density profiles on hydrodynamic stability of zonal flow N86-12673
Features of geostrophic circulation related to nature of bottom relief in northwestern Atlantic N86-12674
Cyclonic frontal eddy in Antarctic circumpolar current N86-12675
Computations of seismic wave propagation velocities in ocean bottom sediments from reflected waves travel-time curves N86-12677
Quasigeostrophic model of circulation in Antarctic Ocean with parametrization of synoptic eddies N86-12702
Contributions of GRM to the ocean topography experiment (TOPEX) N86-12883
Wave-current and wave-topographic interactions using SEASAT synthetic aperture radar observations and analytical ocean models N86-12938
Automatic detection of gulf stream rings
[AD-A157934] N86-12945

OCEAN DATA ACQUISITIONS SYSTEMS
Annual data summary for 1981 CERC (Coastal Engineering Research Center) field research facility
[AD-A158143] N86-12926

OCEAN DYNAMICS
USSR report: Earth sciences
[JPRS-UES-85-006] N86-12630
Empirical analysis of direct and inverse relationships between macroscale characteristics of atmospheric processes in northern hemisphere and thermal state of north Atlantic N86-12635
Recent changes in climate and world water balance N86-12638
Interaction of sound waves with fine thermohaline structures of ocean N86-12647
Geochemistry and energetics of cycling of matter in formation of crust in active structures of ocean N86-12653
Spreading in development of oceanic structures N86-12658
Quasigeostrophic model of circulation in Antarctic Ocean with parametrization of synoptic eddies N86-12702

OCEAN MODELS
Geochemistry and energetics of cycling of matter in formation of crust in active structures of ocean N86-12653
Nonlinear model of adaptation of fields of density and currents in sea N86-12670
Quasigeostrophic model of circulation in Antarctic Ocean with parametrization of synoptic eddies N86-12702

OCEAN SURFACE
Angular distribution of intensity of sound reradiated by ocean surface at small glancing angles N86-12643
Correlation characteristics of signals reflected by the wavy surface of ocean in mirror direction N86-12648
Electromagnetic field of three-dimensional surface sea waves N86-12662
Study of influence of vertical velocity and density profiles on hydrodynamic stability of zonal flow N86-12673
Influence of some oceanographic characteristics on decay kinetcis of surface-active agents in sea N86-12676
Evaluating influence of waves on dynamic structure of atmospheric near-water layer N86-12694
Investigation of elastic properties of marine surface-active films N86-12708
Spatial structure of high-frequency sea wind waves under different meteorological conditions N86-12714
Global mean sea surface computation based upon a combination of SEASAT and GEOS-3 satellite altimeter data N86-12882
Contributions of GRM to the ocean topography experiment (TOPEX) N86-12883
Marine boundary layer from air-sea interface to inversion
[PB85-188274] N86-12948

OCEAN TEMPERATURE
Fine structure of density relation in main oceanic thermocline N86-12711

OCEANOGRAPHIC PARAMETERS
Spreading in development of oceanic structures N86-12658
Properties of the lithosphere and asthenosphere deduced from geoid observations N86-12867
Extremal analysis of hindcast and measured wind and wave data at Kodiak, Alaska
[AD-A158136] N86-12947

OCEANOGRAPHY
China report: Science and technology
[JPRS-CST-85-024] N86-12366
China report: Science and technology
[JPRS-CST-85-016] N86-12393
China report: Science and technology
[JPRS-CST-85-025] N86-12444
China report: Science and technology
[JPRS-CST-85-026] N86-12459
USSR report: Earth sciences
[JPRS-UES-85-006] N86-12630
Influence of some oceanographic characteristics on decay kinetcis of surface-active agents in sea N86-12676
USSR report: Earth sciences
[JPRS-UES-85-008] N86-12697
Fine structure of density relation in main oceanic thermocline N86-12711
Temporal and spatial variabilities in shallow water acoustics: Measurements and predictions
[AD-A156718] N86-12942
A user's guide to the Coastal Engineering Research Center's (CERC'S) field research facility
[AD-A157966] N86-12946

OCEANS
Contribution of diffusion processes to the electric field of the ocean N86-12654
Electromagnetic field of three-dimensional surface sea waves N86-12662
Structure of acoustic field in deep sea at shallow depths and at great ranges N86-12664
Origin of element composition of ocean water N86-12668
Eddy fluxes of heat, vorticity and momentum in ocean and atmosphere and their parameterization (review) N86-12672
Experimental study of equilibrium interval in frequency spectra of wind waves in sea of finite depth N86-12699
Features of electrical measurements in sea as medium with field of extraneous forces N86-12700
Quasigeostrophic model of circulation in Antarctic Ocean with parametrization of synoptic eddies N86-12702
Remote diagnosis of media by combination (Raman) anti-Stokes light scattering method with induced Brillouin backscattering N86-12705
Acoustic methods for featuring high-frequency part of spectrum of sea waves N86-12706
Ocean albedo for atmospheric thermal emission N86-12707
The question of Earth expansion and its oceanic implications N86-12716
Gravity, geoid and the oceanic lithosphere N86-12860
Properties of the lithosphere and asthenosphere deduced from geoid observations N86-12867
Continental and oceanic magnetic anomalies: Enhancement through GRM N86-12869
Wave-current and wave-topographic interactions using SEASAT synthetic aperture radar observations and analytical ocean models N86-12938
Motion of the Pacific plate relative to the hotspots since the Jurassic and model of oceanic plateaus of the Faralion plate N86-12940

OH-58 HELICOPTER
Effect of measured material properties on the finite element analysis of an OH-58 composite tail boom
[NASA-TM-86430] N86-12259

ON-LINE SYSTEMS
DAPHNE: The design of a parallel multiprocessor data acquisition system
[DE85-013875] N86-12984

ONE DIMENSIONAL FLOW
One-dimensional two-phase flow in combustion chamber of solid propellant rocket motors N86-12370
Finite difference scheme for one-dimensional magnetohydrodynamic equations N86-12464

OPEN CIRCUIT VOLTAGE
Hot-spot heating susceptibility due to reverse bias operating conditions N86-12763

OPENINGS
UV sustained glow discharge opening switch
[AD-A158411] N86-13132

OPERATIONAL AMPLIFIERS
Basic EMC (Electromagnetic compatibility) technology advancement for C3 (Command, control, and communications) systems. Volume 6
[AD-A157239] N86-12493

OPERATIONAL HAZARDS
Future directions in mobile teleoperation
[DE85-014306] N86-12976
OPERATORS (MATHEMATICS)
On high-order accurate interpolation for non-oscillatory shock capturing schemes
[AD-A158131] N86-13032
Transistorized multigrid methods. 1: Linear elliptic problems on two- and three-dimensional regions
[DE85-014632] N86-13043
OPTICAL COMMUNICATION
Determination of single-mode optical fiber dispersion N86-12409
Optic fiber applications in data communications N86-12432
Pulsed digital multiplexed laser generator
[AD-D011855] N86-12603
OPTICAL DATA PROCESSING
Adaptive optical filtering techniques
[AD-A157072] N86-13126
OPTICAL DATA STORAGE MATERIALS
Optical disk technology assessment
[AD-A157909] N86-12582
OPTICAL EQUIPMENT
Improved approach to characterizing and presenting streak camera performance
[DE85-015186] N86-12587
Radiation effects on light sources and detectors
[DE85-014746] N86-13133
OPTICAL FILTERS
Acoustically tuned optical filter system
[AD-D011791] N86-13184
OPTICAL MEASUREMENT
Optical measurements of shock-induced chemical reactions in mixed aluminum-nickel powder
[DE85-014705] N86-12308
State-of-the-art of optics in China reviewed N86-12414
Infrared optical measurement of blood gas concentrations and fiber optic catheter
[AD-D011836] N86-12955
OPTICAL MEASURING INSTRUMENTS
The shuttle glow: A program to study the ram-induced phenomena N86-13268
OPTICAL MEMORY (DATA STORAGE)
Optical disk technology assessment
[AD-A157909] N86-12582
OPTICAL PATHS
Nearly ideal lens optimization procedure
[DE85-014116] N86-13134
OPTICAL PROPERTIES
Liquid droplet radiator program at the NASA Lewis Research Center
[NASA-TM-87139] N86-12246
China report: Science and technology
[JPRS-CST-85-016] N86-12393
Evaluation of the use of p-n structures as photodetectors in silicon integrated circuits
[AD-A158104] N86-12514
Soybean canopy reflectance modeling data sets
[E86-10005] N86-12741
Improvement of manufacturing techniques and quality of optical scratch standards for fire control systems
[AD-A157963] N86-13130
Nearly ideal lens optimization procedure
[DE85-014116] N86-13134
Study of possible solarization - related impurities in CaF2 and other fluorides
[DE85-014100] N86-13135
OPTICAL PUMPING
China develops 6J KrF laser N86-12465
OPTICAL RADAR
Humidity profile mesurements in atmospheric lower layer by spontaneous Raman scattering method N86-12736
Contribution to the CIRA model from ground-based lidar N86-12835
OPTICAL WAVEGUIDES
Reversible optical waveguide vapor sensor
[AD-D011834] N86-13124
OPTIMIZATION
Interactive aircraft flight control and aeroelastic stabilization
[NASA-CR-176323] N86-12233
Options for operational risk assessments
[DE85-014904] N86-12390
Computer-aided analysis of arbitrary-shaped thin-wire antennas N86-12452
CAD program for high-power electron gun with annular cathode described N86-12488
Research on output feedback control
[NASA-CR-174253] N86-13028
A new method for global optimization based on stochastic differential equations
[AD-A157546] N86-13029
Global optimization using automatic differentiation and interval iteration
[AD-A158150] N86-13039
Nearly ideal lens optimization procedure
[DE85-014116] N86-13134
OPTIONS
Options for operational risk assessments
[DE85-014904] N86-12390
OPTOMETRY
Criteria for a state-of-the-art vision test system
[AD-A157099] N86-12973
ORBIT CALCULATION
Calculation of threshold conditions for materials charging in Maxwellian plasmas
[AD-A157123] N86-13139
ORBITAL POSITION ESTIMATION
On the geographical correlation of orbit error N86-12881
ORBITS
Tests of orbital dynamics using the Tevatron
[DE85-012296] N86-13085
ORDER-DISORDER TRANSFORMATIONS
Theoretical studies of deep impurity levels in ternary semiconductor alloys
[AD-A157929] N86-13193
ORGANIC COMPOUNDS
Studies on unusally reactive metal powders: Preparation of new organometallic and organic compounds including potential new catalysts
[DE85-014844] N86-12309
Usages of organic membranes in electrolytic industry described N86-12453
Influence of seston phosphatase activity on rate of phosphorus mineralization and its recycling in production-destruction cycle N86-12667
ORGANIC MATERIALS
Organic components in atmosphere in regions of volcanic activity N86-12693
ORGANIC SULFUR COMPOUNDS
Formation of fuel via photochemical electron transfer
[DE85-011166] N86-12279
ORGANOMETALLIC COMPOUNDS
Anaerobic microbial dissolution of toxic metals in subsurface environments
[DE85-013308] N86-12251
Studies on unusally reactive metal powders: Preparation of new organometallic and organic compounds including potential new catalysts
[DE85-014844] N86-12309
OROGRAPHY
The numerical simulation of geographic storms N86-12907
ORTHOGONALITY
Iosipescu shear properties of graphite fabric/epoxy composite laminates
[NASA-CR-176316] N86-12258
OSCILLATION DAMPERS
High order mode damping in the NSLS accelerating RF cavities by the use of damping antennae
[DE85-014214] N86-12498
OSCILLATIONS
The role of amplitude-to-phase conversion in the generation of oscillator flicker phase noise
[NASA-TM-87590] N86-12508
PRospects for development of seismic prospecting methods and apparatus N86-12723
Tevatron global radius and Os system
[DE85-017442] N86-13101
Explosive coalescence of magnetic islands
[DE85-015083] N86-13172
New method of determining the current carrier concentration in a substance in the state of superconductivity
[AD-A158182] N86-13194
OTTO CYCLE
Otto fuel 2 N86-12334
OUTPUT
Frequency selection and mode locking of Nd:YAG laser N86-12395
OXIDATION
Oxidation of heterocyclic nitrogen yields to nitroheterocycles
[DE85-012757] N86-12284
Molten salt corrosion of SiC: Pitting mechanism
[NASA-TM-87143] N86-12310
Oxidation and gum formation in diesel fuels
[AD-A157410] N86-12360
Tritium control in helium-cooled blankets
[DE85-014783] N86-13116
OXIDATION-REDUCTION REACTIONS
Charge transfer in multiple site chemical systems
[AD-A157413] N86-12270
OXIDE FILMS
High current fiber brush collector and method for making same
[AD-D011827] N86-12512
The production of glow precursors by oxidative erosion of spacecraft surfaces N86-13257
OXIDES
High frequency silicon bipolar transistor with SIPOS (Semi-insulating polycrystalline silicon) heterojunction emitter and ion implanted rapid thermal annealed base region
[AD-A157141] N86-12510
Development of a radiation-hard CMOS process
[NASA-CR-170925] N86-13187
OXYGEN
Technique for measuring gas conversion factors
[NASA-CASE-LAR-13220-1] N86-12547
Space shuttle mechanistic studies to characterize atomic oxygen interactions with surfaces N86-13267
Physico-chemical conditions in circumstellar shells of evolved oxygen-rich M stars N86-13275
OXYGEN AFTERGLOW
A model for explaining some features of shuttle glow N86-13256
An assessment of the impact of spacecraft glow on the Hubble space telescope. Summary of existing observations and theory N86-13262
OXYGEN ATOMS
Ground-based investigations of atomic oxygen interactions with space station surfaces
[DE85-014082] N86-12249
A model for explaining some features of shuttle glow N86-13256
The production of glow precursors by oxidative erosion of spacecraft surfaces N86-13257
Application of an atomic oxygen beam facility to the investigation of shuttle glow chemistry N86-13261
An assessment of the impact of spacecraft glow on the Hubble space telescope. Summary of existing observations and theory N86-13262
OXYGEN SPECTRA
Combined ultraviolet studies of astronomical source
[NASA-CR-176165] N86-13274
OZONE
Perspectives to establish knowledge linkages between acidic deposition and vegetation responses
[DE85-011839] N86-12796
Interim reference ozone models for the middle atmosphere N86-12829
OZONOMETRY
Interim reference ozone models for the middle atmosphere N86-12829

P

P WAVES
P-wave spectra in problem of determining dynamic paramters of earthquake foci. Standardization of initial data and procedures for computing amplitude spectra N86-12722
Seismic effect of underground blasts and problem of estimating total earthquake energy N86-12731
P-I-N JUNCTIONS
Thin-film module circuit design: Practical and reliability aspects N86-12762
P-N JUNCTIONS
Performance and temperature dependencies of proton irradiated n/p GaAs and n/p silicon cells
[NASA-TM-87136] N86-12509
Evaluation of the use of p-n structures as photodetectors in silicon integrated circuits
[AD-A158104] N86-12514
P-N-P JUNCTIONS
Latch-up effect in CMOS described N86-12443
P-TYPE SEMICONDUCTORS
A TiW diffusion barrier for AuZn ohmic contacts to p-type InP
[AD-D011823] N86-12511
PACIFIC OCEAN
Magmatic provinces and tectonics in Pacific Ocean N86-12652
Influence of seston phosphatase activity on rate of phosphorus mineralization and its recycling in production-destruction cycle N86-12667
Estimation of influence of ocean on distribution of heavy metals in marine atmosphere N86-12703
Tectonic structure of Shirshov Ridge (Bering Sea) N86-12710
Optimal density model of Earth's rust and upper mantle along Kamchatka-Pacific Geotraverse N86-12725
Geodynamics of crustal dilatation in transition area from Asian continent to Pacific Ocean N86-12733
Clear sky brightness temperature over the western north Pacific Ocean from GMS spacecraft N86-12911
Observational-numerical study of maritime extratropical cyclones using FGGE (First GARP Global Experiment) data
[NASA-CR-176297] N86-12922

Annual data and verification tabulation eastern North Pacific tropical storms and hurricanes, 1984
[PB85-187888] N86-12930

PACKETS (COMMUNICATION)

Internetting and packet satellite program
[AD-A157124] N86-12489

PACKING DENSITY

Temperature and concentration dependence of hydrogen site occupancy in several rare-earth dihydrides
[DE85-015739] N86-13199

PADE APPROXIMATION

Pade and reciprocal approximants and linear NOLOR functions
[DE85-015057] N86-13044

PALLADIUM

Second order elastic contents of Pd, PdH(0.7) and PdD(0.7) between 1.7 and 50 K
[DE85-014316] N86-13212

PALLADIUM ALLOYS

Electronic stakes in disordered solids. Part 3: Applications to materials science
[DE85-011416] N86-13213

PALLADIUM COMPOUNDS

Second order elastic contents of Pd, PdH(0.7) and PdD(0.7) between 1.7 and 50 K
[DE85-014316] N86-13212

PANELS

Aircraft interior panel test criteria derived from full-scale fire tests
[FAA/CT-85/23] N86-12214

Encapsulant selection and durability testing experience N86-12774

PARABOLIC ANTENNAS

Design of an antenna feed system to produce a uniform field N86-12469

Low sidelobe, high efficiency mirror antenna with twist reflector
[AD-D011835] N86-12474

PARABOLIC REFLECTORS

Solar walk-off protection
[DE85-012112] N86-12788

PARACHUTE FABRICS

Development and evaluation of a microburst test apparatus for use as a minimum destructive test for parachute material
[AD-A158110] N86-12620

PARACHUTES

Parachute recovery systems design manual, chapters 1 through 4 offprint
[AD-A157838] N86-12210

Naval surface weapons center technology transfer biennial report (Fiscal year 1983/1984)
[AD-A157919] N86-13238

PARALLEL FLOW

Isothermal dehumidification of air in a parallel passage configuration
[DE85-008819] N86-12577

PARALLEL PROCESSING (COMPUTERS)

A theory for algorithm-based fault tolerance in array processor systems
[AD-A156244] N86-12977

DAPHNE: The design of a parallel multiprocessor data acquisition system
[DE85-013875] N86-12984

Parallel implementation of multifrontal schemes
[DE85-014295] N86-13015

PARALLEL PROGRAMMING

Parallel implementation of multifrontal schemes
[DE85-014295] N86-13015

PARAMAGNETISM

Paramagnetic form factors of HCP transiton metals
[DE85-016301] N86-12301

PARAMETER IDENTIFICATION

Real-time flutter identification
[NASA-CR-3833] N86-12218

PARAMETERIZATION

Modulations of driven nonlinear surface waves on water and liquid Helium-4
[AD-A157858] N86-12556

Eddy fluxes of heat, vorticity and momentum in ocean and atmosphere and their parameterization (review) N86-12672

Penalized likelihood for general semi-parametric regression models
[AD-A158133] N86-13034

PARTIAL DIFFERENTIAL EQUATIONS

Modeling and control of flexible structures
[AD-A157959] N86-12625

Survey and expository papers on topics of current interest in applied mathematics
[AD-A158418] N86-13229

PARTICLE ACCELERATOR TARGETS

Measurements and calculations of neutron scattering angular distributions over a wide mass and energy range
[DE85-012912] N86-13105

Isovector resonances in pion charge exchange
[DE85-012746] N86-13106

R-matrix analysis of the (7) Li system with peripheral channel overlap exchange effects
[DE85-012751] N86-13148

High efficiency ICF driver employing magnetically confined plasma rings
[DE85-012939] N86-13164

PARTICLE ACCELERATORS

PBFA-2 insulator stack design from an engineering viewpoint
[DE85-013437] N86-12245

Measurement of 1 nanosecond wide beams for 2.5 MeV proton accelerator N86-12435

Generation of a modulated IREB (Intense Relativistic Electron Beam) with a frequency tunable by a magnetic field
[AD-D011820] N86-13068

Control problems in very large accelerators
[DE85-014956] N86-13075

Tests of orbital dynamics using the Tevatron
[DE85-012296] N86-13085

FMIT diagnostic instrumentation
[DE85-012668] N86-13087

Large scale operational pulsed power research facilities: How well have we made them a reality
[DE85-013784] N86-13088

Overview and status of the Transverse-Field Focusing (TFF) accelerator
[DE85-015278] N86-13093

Tevatron global radius and Os system
[DE85-017442] N86-13101

Accelerator research studies
[DE85-014878] N86-13113

FASTBUS for the particle accelerator laboratories
[DE85-014352] N86-13122

Implementing the automated features of the PBFA-I control/monitor systems
[DE85-012841] N86-13144

Deprit's algorithm, Green's functions and multipole perturbation theory
[DE85-012297] N86-13147

PARTICLE BEAMS

PBFA-2 insulator stack design from an engineering viewpoint
[DE85-013437] N86-12245

Suppression of propagating TE modes in the FNAL antiproton source stochastic beam cooling system
[DE85-016559] N86-13074

Chaotic dynamical aperture
[DE85-013285] N86-13077

Large scale operational pulsed power research facilities: How well have we made them a reality
[DE85-013784] N86-13088

High intensity positron beam and angular correlation experiments at Livermore
[DE85-012961] N86-13111

Implementing the automated features of the PBFA-I control/monitor systems
[DE85-012841] N86-13144

PARTICLE COLLISIONS

New beam neutralization concept: Laser photodetachment in a magnetic field
[DE85-014655] N86-12607

Theories of statistical equilibrium in electron-positron colliding-beam storage rings
[DE85-012303] N86-13080

PARTICLE DIFFUSION

The orientation distribution of nonspherical aerosol particles within a cloud
[AD-A157363] N86-12554

PARTICLE INTERACTIONS

Self-consistent klystron simulations
[DE85-012678] N86-12529

Partition of cross sections in asymmetric nucleus-nucleus reactions and the origin of fast alpha particles
[DE85-014989] N86-13089

Physics of e(+) - e(-) colliders: Present, future and far future
[DE85-009695] N86-13121

Optical radiation from the interaction of energetic atoms, ions, electrons, and photons with surfaces N86-13259

PARTICLE MOTION

Multiplicities in high energy interactions
[DE85-013847] N86-13100

PARTICLE PRODUCTION

A p anti p collider physics: Summary talk
[DE85-014782] N86-13097

Multiplicities in high energy interactions
[DE85-013847] N86-13100

PARTICLE SIZE DISTRIBUTION

The orientation distribution of nonspherical aerosol particles within a cloud
[AD-A157363] N86-12554

Comparison of single-parameter statistical model with results of round-the-clock measurement of light-scattering matrices N86-12689

PARTICLE TRACKS

Tracking studies on the effects of random multipoles in the 6.5 T lattice of the SSC Reference Designs Study
[DE85-013286] N86-13156

PARTICLE TRAJECTORIES

Estimate of radiation-climatic effects of natural and anthropogenic aerosol N86-12640

PARTICULATE SAMPLING

Analysis of particulates in the exhaust plume of a J52-P3 turbojet engine at military power
[AD-A157840] N86-12231

Thermophoretic separation of aerosol particles from a sampled gas stream
[DE85-011672] N86-12277

PASCAL (PROGRAMMING LANGUAGE)

Micro-PROUST
[AD-A157505] N86-12991

PATENT APPLICATIONS

Suture needle holder
[AD-D011764] N86-12958

PATENTS

Forward field autotransfusion device
[AD-D011763] N86-12957

PATTERN RECOGNITION

Diagnosing cognitive errors: Statistical pattern classification and recognition approach
[AD-A158108] N86-12972

PATTERN REGISTRATION

Stimulus structures and mental representations in expert comprehension of computer programs
[AD-A157520] N86-12969

PAVEMENTS

CBR (California Bearing Ratio) design of flexible airfield pavements with case study
[AD-A158101] N86-12242

PAYLOADS

Federal government provision of third-party liability insurance to space vehicle users
[NASA-CR-176346] N86-13230

PENETRATION

Variational principle for penetrator dynamics using bilinear functional and adjoint formulation
[AD-A157964] N86-13031

PENINSULAS

Tectonics of eastern Kronotskiy Peninsula and formational association of basalts (Kamchatka) N86-12732

PENNSYLVANIA

Outdoor radon monitoring at Canonsburg, Pennsylvania, 1980-1983
[DE85-013320] N86-12797

PENTABORANES

The boranes N86-12336

PERFORMANCE PREDICTION

Performance and temperature dependencies of proton irradiated n/p GaAs and n/p silicon cells
[NASA-TM-87136] N86-12509

Reconstruction of longitudinal beam profiles from nondestructive electromagnetic probes
[DE85-012675] N86-13078

PERFORMANCE TESTS

Minutes of Workshop on Composite Materials Test Methods
[AD-A157903] N86-12262

Evaluation parameters for the alkaline fuel cell oxygen electrode
[NASA-TM-87155] N86-12268

The verification of the logic circuits based on particlized information bits with PROLOG N86-12387

Foil fuses as opening switches for slow discharge circuits
[DE85-014124] N86-12519

Optical disk technology assessment
[AD-A157909] N86-12582

Improved approach to characterizing and presenting streak camera performance
[DE85-015188] N86-12587

Develop and test fuel cell powered on-site integrated total energy systems: Phase 3, full-scale power plant development
[NASA-CR-174948] N86-12757

Develop and test fuel cell powered on-site integrated total energy systems: Phase 3, full-scale power plant development
[NASA-CR-174998] N86-12758

Light-induced effects-impacts to module performance measurements and reliability testing: An overview N86-12761

Amorphous silicon photovoltaic modules and test devices design, fabrication and testing N86-12769

Outdoor performance testing of thin-film devices N86-12771

Encapsulant selection and durability testing experience N86-12774
Navy applications experience with small wind power systems
[AD-A158561] N86-12776
Investigation of test methods, material properties and processes for solar cell encapsulants
[DE85-012831] N86-12786
Development of acoustic agglomerator. Test plan for high temperature high pressure acoustic agglomerator
[DE85-017221] N86-13061
Commissioning and operation of the Nuclear Physics Injector at SLAC
[DE85-013374] N86-13159
PERIGEES
Mean density scale heights from analysis of variation in perigee height of China's second satellite
N86-12396
PERIODIC VARIATIONS
Use of method of canonical correlations for analysis of climatic series N86-12634
Comparison of time-periodic variations in temperature and wind from meteorological rockets and satellites
N86-12825
Atmospheric tides between 80 km and 120 km
N86-12833
Middle atmosphere tides at Christchurch (44 deg S, 17 deg E) in November 1981 and May 1982 N86-12851
PERMEABILITY
Measurement of tritium permeation through resistant materials near room temperature
[DE85-012942] N86-12582
PERMITTIVITY
Evaluation of high permittivity glass ceramics for millimeter wave applications
[AD-A158551] N86-12319
Characteristic impedance of a wide slot line on low permittivity substrates N86-12480
PERSONAL COMPUTERS
Managing personal desktop computing at Argonne National Laboratory
[DE85-014976] N86-12983
Data acquisition interfaces for the IBM personal computer
[DE85-014256] N86-12985
A user's guide for the BIBSORT program for the IBM-PC personal computer
[AD-A157936] N86-12995
Design and use of digital filters with personal computer spreadsheet programs
[DE85-013805] N86-13012
PERSONNEL
Word lists to limit vocabulary in technical information
[AD-A157931] N86-13228
PERTURBATION
Thermodynamics of multi-polar molecules: The perturbed-anisotropic-chain theory
[DE85-013148] N86-12274
Renormalization of an inverse scattering theory for inhomogeneous dielectrics
[AD-A157224] N86-12492
Masking of light scattering information on matrix elements from complex scattering
[AD-A158144] N86-13131
Survey and expository papers on topics of current interest in applied mathematics
[AD-A158418] N86-13229
PERTURBATION THEORY
Rapid estimation of frequency response functions by close-range photogrammetry
[NASA-TP-2471] N86-12579
Phase operator method in problem of scattering of electromagnetic waves on ideally conducting surface
N86-12701
PETROLOGY
Petrologic aspect of formation of geostructures in marginal seas N86-12657
PH
Acidification trends in surface waters of the Southern Appalachians
[DE85-901746] N86-12801
PH FACTOR
Perspectives to establish knowledge linkages between acidic deposition and vegetation responses
[DE85-011839] N86-12796
PHARMACOLOGY
Marketing the use of the space environment for the processing of biological and pharmaceutical materials
[NASA-CR-176334] N86-12243
PHASE CHANGE MATERIALS
Investigation of phase transitions
[AD-A158434] N86-12518
PHASE DETECTORS
Digital phase meter using CMOS-LED introduced
N86-12442
PHASE DIAGRAMS
Surface crystallization on metallized 94 percent alumina ceramics
[DE85-008601] N86-12324
PHASE LOCKED SYSTEMS
Single mode phase locking fiberoptic sensor developed N86-12415
Simultaneous detection of time coincident signals in an adaptive Doppler tracker
[AD-D011796] N86-12473
PHASE MODULATION
The role of amplitude-to-phase conversion in the generation of oscillator flicker phase noise
[NASA-TM-87590] N86-12508
PHASE SHIFT
Tevatron global radius and Os system
[DE85-017442] N86-13101
PHASE TRANSFORMATIONS
Investigation of phase transitions
[AD-A158434] N86-12518
Study of two-phase concurrent flow of steam and water in an unconsolidated porous medium
[DE85-014534] N86-12578
TWOPOT: A computer model of the two-pot extractive distillation concept for nitric acid
[DE85-013523] N86-13020
PHOSPHORIC ACID FUEL CELLS
Develop and test fuel cell powered on-site integrated total energy systems: Phase 3, full-scale power plant development
[NASA-CR-174948] N86-12757
Develop and test fuel cell powered on-site integrated total energy systems: Phase 3, full-scale power plant development
[NASA-CR-174998] N86-12758
PHOSPHORUS
Influence of seston phosphatase activity on rate of phosphorus mineralization and its recycling in production-destruction cycle N86-12667
PHOTOCATHODES
Electron emission of over 200 A/cm (2) from a pulsed-laser irradiated photocathode
[DE85-012656] N86-13084
PHOTOCHEMICAL REACTIONS
Composition and photochemical reactivity of turbine engine exhaust
[AD-A157643] N86-12230
Materials and process characterization to determine the effect of high intensity infrared laser radiation on a composite material
[AD-A157094] N86-12280
Formation of fuel via photochemical electron transfer
[DE85-011168] N86-12279
Studies of energy storage and transfer in gas lasers
[AD-A158553] N86-12604
PHOTOCONDUCTIVE CELLS
Infrared measurements of spacecraft glow planned for Spacelab 2 N86-13263
PHOTOCONDUCTIVITY
Photoconductive semiconductor switching for pulsed power applications
[DE85-013859] N86-12531
PHOTODIODES
Evaluation of the use of p-n structures as photodetectors in silicon integrated circuits
[AD-A158104] N86-12514
Laser-based foilless diode
[DE85-013958] N86-12537
PHOTODISSOCIATION
Direct solar-pumped iodine laser amplifier
[NASA-CR-176324] N86-12600
Theoretical studies of molecular interactions
[DE85-012604] N86-13076
PHOTOELASTIC MATERIALS
Strain energy density criteria for dynamic fracture and dynamic crack branching
[AD-A157914] N86-12624
PHOTOELECTRON SPECTROSCOPY
Multiphoton ionization of NO-rare gas van der Waals species
[DE85-014650] N86-13094
PHOTOGEOLOGY
LANDSAT-4 TM image data quality analysis for energy-related applications
[E86-10006] N86-12742
PHOTOGRAMMETRY
Rapid estimation of frequency response functions by close-range photogrammetry
[NASA-TP-2471] N86-12579
Earth resources: A continuing bibliography, issue 46
[NASA-SP-7041(46)] N86-12738
PHOTOGRAPHIC EQUIPMENT
The shuttle glow: A program to study the ram-induced phenomena N86-13268
PHOTOGRAPHY
Advanced Moisture and Temperature Sounder (AMTS) baseline 5 study report
[NASA-CR-176331] N86-12910
PHOTOINTERPRETATION
Video terminal for analyzing aerial infrared photographs N86-12699
Hydrologic and land sciences applications of NOAA (National Oceanic and Atmospheric Administration) polar-orbiting satellite data
[PB85-233385] N86-12748
PHOTOIONIZATION
Combined ultraviolet studies of astronomical source
[NASA-CR-176165] N86-13274
PHOTOMASKS
Improvement of manufacturing techniques and quality of optical scratch standards for fire control systems
[AD-A157963] N86-13130
PHOTOMETERS
Recent developments in microshell-tipped optical fibers as high-pressure shock detectors
[DE85-015750] N86-12584
Optical sensing devices
[AD-D011829] N86-13123
Photosensitive cartridge for weapons zeroing and marksmanship training
[AD-D011765] N86-13125
PHOTOMETRY
A possible glow experiment for the EOM 1-2 mission
N86-13256
PHOTON BEAMS
Optical radiation from the interaction of energetic atoms, ions, electrons, and photons with surfaces N86-13259
A ground-based experimental test program to duplicate and study the spacecraft glow phenomenon
N86-13260
PHOTONS
Ultraviolet observations of low-excitation Herbig-Haro objects
[NASA-CR-176164] N86-13273
X-rays from the radio halo of Virgo A = M87
[NASA-CR-176303] N86-13285
PHOTOSENSITIVITY
Photosensitive cartridge for weapons zeroing and marksmanship training
[AD-D011765] N86-13125
PHOTOVOLTAIC CELLS
SOLERAS: Photovoltaic power systems project. Module failure analysis
[MRI/SOL-0101] N86-12756
Reliability and Engineering of Thin-Film Photovoltaic Modules. Research forum proceedings
[NASA-CR-176217] N86-12759
Crystalline-silicon reliability lessons for thin-film modules N86-12760
Light-induced effects-impacts to module performance measurements and reliability testing: An overview
N86-12761
Electrical safety requirements: Implications for the module designer N86-12765
Interconnect resistance of photovoltaic submodules
N86-12767
Thin film module development N86-12768
Amorphous silicon photovoltaic modules and test devices design, fabrication and testing N86-12769
Outdoor performance testing of thin-film devices
N86-12771
Zinc/ferricyanide battery development phase 4
[DE85-016026] N86-12781
Photovoltaic Concentrator Technology Project Thirteenth Project Integration Meeting
[DE85-013253] N86-12794
PHOTOVOLTAIC CONVERSION
SOLERAS: Photovoltaic power systems project. Module failure analysis
[MRI/SOL-0101] N86-12756
PHOTOVOLTAIC EFFECT
Maintenance of photovoltaic power systems, revision 1
[AD-A157838] N86-12777
Diffraction-limited ten micron imaging of circumstellar dust with a detector array N86-13277
PHTHALATES
Epoxy phthalonitrile polymers
[AD-D011821] N86-12318
PHYSICAL CHEMISTRY
China report: Science and technology
[JPRS-CST-85-024] N86-12368
China report: Science and technology
[JPRS-CST-85-032] N86-12462
PHYSIOLOGICAL RESPONSES
The effects of hypoxia induced by low atmospheric pressure on soft contact lens wear
[AD-A158556] N86-12965
Biological effects of acoustic cavitation
[AD-A157513] N86-13059

PIEZOELECTRIC CRYSTALS
China's first imported peripheral equipment production line N86-12440

PIEZOELECTRICITY
Classical piezoelectricity: Is the theory complete [DE85-014592] N86-12536
Studies of the Bauer piezoelectric polymer gauge (PVF2) under impact loading [DE85-014707] N86-12590

PILOT TRAINING
The helicopter to fixed wing conversion program: A critical review [AD-A156820] N86-12968

PILOTS (PERSONNEL)
Gravimetric surveying with MI-8 helicopters N86-12680

PINHOLES
Interconnect resistance of photovoltaic submodules N86-12767

PIONEER SPACE PROBES
Design of foil implosion system for Pioneer 1 experiments [DE85-014111] N86-12535

PIONEER 11 SPACE PROBE
Electrons and cosmic ray produced in Saturn's inner magnetosphere N86-13281

PIONS
Multiplicities in high energy interactions [DE85-013847] N86-13100
Isovector resonances in pion charge exchange [DE85-012746] N86-13106
Experiment to study K(+) (YIELDS) (PI)(+) + nothing at LAMPF 2 [DE85-014267] N86-13110
Large acceptance magnetic focussing horns for production of a high intensity narrow band neutrino beam at the AGS [DE85-013300] N86-13157

PIPE FLOW
Numerical calculation of internal flows with curvature N86-12544
The prediction of fully developed turbulent pressure drops in a triangular duct for a power law fluid N86-12546

PIPELINES
Safety criteria for the operation of gaseous hydrogen pipelines [PB85-206159] N86-12392
Particle-wall interaction and wall friction in gas-solid flows [DE85-014984] N86-12587

PIPES (TUBES)
Manufacturing process for cylindrical ceramic tubes with localized imprints and device for application of this process [DE85-012294] N86-12323
Cross flow boiling in tube bundles [AD-A158557] N86-12562
Finned tube contact conductance: Characterizing the integrity of the mechanical bond [DE85-013747] N86-12564

PISTON ENGINES
Preliminary design of linear alternator dynamometer for free piston Stirling engines [DE85-015078] N86-12614

PISTONS
New approaches to determining physical properties in piston-cylinder high-temperature, high-pressure device N86-12445

PITCH (INCLINATION)
Air Force Academy Auronautics Digest [AD-A157215] N86-12200

PITOT TUBES
Performance of an alpha-vane and pitot tube in simulated heavy rain environment [NASA-CR-176353] N86-12220
T-33 (Silver Star MK 3) pitot-static system calibration [AD-A157854] N86-12221

PITTING
Molten salt corrosion of SiC: Pitting mechanism [NASA-TM-87143] N86-12310

PLANE WAVES
Diffraction of internal waves described by equation of slightly stratified fluid on half-plane N86-12660
Plane-wave theory of electrical transport in disordered systems [DE85-015353] N86-13167

PLANETARY BOUNDARY LAYER
The magnetic field at the core-mantle boundary N86-12865

PLANETARY EVOLUTION
Trapped particle absorption by the ring of Jupiter [NASA-CR-174408] N86-13279
A note on Jupiter's gossamer ring N86-13280

PLANETARY WAVES
Study of significance of bottom relief in baroclinic model of equatorial countercurrent N86-12642
The dynamic stability of the stratosphere and mesosphere N86-12811
Planetary waves N86-12820
Planetary waves N86-12821
Annual and semiannual cycles based on the middle atmosphere reference model N86-12826
Planetary and gravity waves in the mesosphere and lower thermosphere N86-12832

PLASMA ACCELERATION
High efficiency ICF driver employing magnetically confined plasma rings [DE85-012939] N86-13164

PLASMA ARC WELDING
Plasma arc welding for thin titanium plates N86-12404

PLASMA CLOUDS
Analysis and interpretation of the shock-like electrostatic noise observed during the AMPTE (Active Magnetospheric Particle Tracer Explorers) solar wind lithium releases [AD-A157512] N86-13283

PLASMA CONTROL
Field-reversed configuration formation, translation, and confinement studies on the FRX-C/T experiment [DE85-014095] N86-13141
FRC formation studies with Z-discharge ionization on FRX-C [DE85-012785] N86-13152
High efficiency ICF driver employing magnetically confined plasma rings [DE85-012939] N86-13164

PLASMA CURRENTS
Submillimeter wave propagation in tokamak plasmas [DE85-007747] N86-13154

PLASMA DECAY
Absolutely unstable two-plasmon decay in two dimensions [DE85-008157] N86-13150

PLASMA DENSITY
Laser scattering in plasma examined N86-12431
Absolutely unstable two-plasmon decay in two dimensions [DE85-008157] N86-13150
The shuttle glow: A program to study the ram-induced phenomena N86-13268

PLASMA DIAGNOSTICS
Research Reports of the Faculty of Engineering, Tokyo Denki University, no. 32 [ISSN-0389-617-X] N86-12372
Dissociative volume recombination coefficient measurements in a subroom temperature neon plasma afterglow N86-12373
Laser scattering in plasma examined N86-12431
Improved approach to characterizing and presenting streak camera performance [DE85-015188] N86-12587

PLASMA DIFFUSION
Effects of whistler-mode and other waves in the magnetosphere [AD-A157832] N86-12899

PLASMA DRIFT
Solitary vortices in a rotating plasma [DE85-014766] N86-13171

PLASMA DYNAMICS
Effects of whistler-mode and other waves in the magnetosphere [AD-A157832] N86-12899

PLASMA ETCHING
Laser diagnostic studies of plasma etching and deposition [DE85-009494] N86-13178

PLASMA FLUX MEASUREMENT
Plasma and magnetospheric research [NASA-CR-176326] N86-13138

PLASMA FREQUENCIES
Generation of a modulated IREB (Intense Relativistic Electron Beam) with a frequency tunable by a magnetic field [AD-D011820] N86-13068

PLASMA HEATING
The 140 GHz gyrotron development program [DE85-011923] N86-12534
Theory of the anomalous Doppler instability during lower-hybrid current drive [DE85-014064] N86-13170
Alfven wave heating on Tokapole 2 [DE85-014859] N86-13179

PLASMA PHYSICS
Progress of inertial confinement research detailed N86-12447
Tandem Mirror Reactor Systems Code (TMRSC) [DE85-012891] N86-13006
Submillimeter wave propagation in tokamak plasmas [DE85-007747] N86-13154
Second Workshop on Spacecraft Glow [NASA-CP-2391] N86-13239

PLASMA SHEATHS
Plasma and magnetospheric research [NASA-CR-176326] N86-13138

PLASMA SPECTRA
Effects of whistler-mode and other waves in the magnetosphere [AD-A157832] N86-12899

PLASMA TEMPERATURE
Behavior of ionized plasma in the high latitude topside ionosphere [AD-A157930] N86-13140
Spatial structure of heat flow instabilities in laser plasmas [DE85-014407] N86-13162

PLASMA WAVES
An alternative interpretation of ion ring distribution observed by the S3-3 satellite [AD-A157655] N86-12898
Wave propagation in a plasma based on the cold plasma model [DE85-013649] N86-13158
Theory of the anomalous Doppler instability during lower-hybrid current drive [DE85-014064] N86-13170

PLASMA-ELECTROMAGNETIC INTERACTION
Laser scattering in plasma examined N86-12431

PLASMAS (PHYSICS)
Iron and steelmaking with plasma N86-12467
Magnetic reconnection in the terrestrial magnetosphere [DE85-014107] N86-12904
Calculation of threshold conditions for materials charging in Maxwellian plasmas [AD-A157123] N86-13139
Behavior of ionized plasma in the high latitude topside ionosphere [AD-A157930] N86-13140
TPSS plasma engineering studies: Profile effects and plasma power balance [DE85-013638] N86-13142
Diffusion in binary plasma mixtures [DE85-017694] N86-13143
Compact microwave ion source [DE85-014536] N86-13176

PLASTIC PROPELLANTS
Effects of surface interactions and mechanical properties of plastic bonded explosives on explosive sensitivity. Part 2: Model formulation [AD-A157900] N86-12361

PLASTIC PROPERTIES
Cortical plasticity: Theoretical analysis, experimental results [AD-A157965] N86-12961

PLATEAUS
Motion of the Pacific plate relative to the hotspots since the Jurassic and model of oceanic plateaus of the Farallon plate N86-12940

PLATES (STRUCTURAL MEMBERS)
Finned tube contact conductance: Characterizing the integrity of the mechanical bond [DE85-013747] N86-12564

PLATES (TECTONICS)
New data of relief of Mazca Ridge N86-12679
Hypocentral areas of aftershocks and possible fault systems at foci of Tsunami-generating Kuril earthquakes N86-12729
Tectonics of eastern Kronotskiy Peninsula and formational association of basalts (Kamchatka) N86-12732
Seismological studies of the tectonics of divergent plate boundaries N86-12812
Mantle convection and the large scale structures of the Earth's gravitational field N86-12874
Constraints on the rheological structure of the mantle N86-12875
Evidence from satellite altimetry for small-scale convection in the mantle N86-12878
Motion of the Pacific plate relative to the hotspots since the Jurassic and model of oceanic plateaus of the Farallon plate N86-12940

PLATING
Surface crystallization on metallized 94 percent alumina ceramics [DE85-008691] N86-12324

PLEURAE
Forward field autotransfusion device [AD-D011763] N86-12957

PLUMES
Analysis of particulates in the exhaust plume of a J52-P3 turbojet engine at military power [AD-A157840] N86-12231
Exhaust plume measurements of 15-pound BATES (Ballistic Test and Evaluation System) motors [AD-A157249] N86-12250

Sea floor swells and mantle plumes N86-12866

PNEUMATIC EQUIPMENT
Pneumatic actuator device [AD-D011794] N86-12217

POINT DEFECTS
Theoretical studies of deep impurity levels in ternary semiconductor alloys [AD-A157929] N86-13193

POINT SOURCES
Acoustical field of directional source in oceanic waveguides N86-12656
Prediction of sound fields in acoustical cavities using the boundary element method [NASA-CR-176295] N86-13057

POISONING (REACTION INHIBITION)
Deactivation and poisoning of fuel cell catalysts [DE85-015127] N86-12521

POISSON DENSITY FUNCTIONS
Compound poisson approximations for sums of random variables [AD-A158555] N86-13049

POLAR METEOROLOGY
Comparison of time-periodic variations in temperature and wind from meteorological rockets and satellites N86-12825

POLAR ORBITS
Hydrologic and land sciences applications of NOAA (National Oceanic and Atmospheric Adminstration) polar-orbiting satellite data [PB85-233365] N86-12748
Global view of the upper level outflow patterns associated with tropical cyclone intensity changes during FGGE [NASA-CR-174407] N86-12908

POLAR REGIONS
On the interannual variability and on trends of the temperature in the middle atmosphere N86-12827
Behavior of ionized plasma in the high latitude topside ionosphere [AD-A157930] N86-13140

POLARITY
Thermodynamics of multi-polar molecules: The perturbed-anisotropic-chain theory [DE85-013148] N86-12274

POLARIZATION (WAVES)
Measurement of 1 nanosecond wide beams for 2.5 MeV proton accelerator N86-12435
Spin-polarization observables in elastic electron scattering from spin-1/2 nuclei [DE85-016639] N86-13072

POLARIZERS
Technique for the reduction of fading in interferometers [AD-D011845] N86-12581

POLITICS
Report of accomplishments under the airport improvement program [AD-A156834] N86-12241

POLLUTION CONTROL
Fiscal year 1983 program report of the Purdue (Indiana) Water Resources Research Center [PB85-225829] N86-12802

POLLUTION MONITORING
Summary of precision and accurace assessments for the state and local air monitoring netowrks, 1982 [PB85-208171] N86-12805

POLLUTION TRANSPORT
Fiscal year 1983 program report of the Purdue (Indiana) Water Resources Research Center [PB85-225829] N86-12802

POLOIDAL FLUX
FRC formation studies with Z-discharge ionization on FRX-C [DE85-012765] N86-13152

POLYCRYSTALS
Semicrystalline casting process development and verification [JPL-9950-1160] N86-12312
High frequency silicon bipolar transistor with SIPOS (Semi-insulating polycrystalline silicon) heterojunction emitter and ion implanted rapid thermal annealed base region [AD-A157141] N86-12510
Large-area thin-film modules N86-12766
Wear of ion implanted TiB sub 2 surfaces [DE85-017091] N86-13201

POLYETHYLENES
High pressure and molecular weight variation of electrical relaxation in poly(ethylene oxide) [AD-A157660] N86-12317

POLYIMIDE RESINS
The 371 deg C mechanical properties of graphite/polyimide composites [NASA-TM-87122] N86-12256

POLYIMIDES
Structure-to-glass transition temperature relationships in high temperature stable condensation polyimides [NASA-TM-87113] N86-12311

POLYMER CHEMISTRY
Structure-to-glass transition temperature relationships in high temperature stable condensation polyimides [NASA-TM-87113] N86-12311

POLYMER MATRIX COMPOSITES
Fracture surface analysis in composite and titanium bonding [NASA-CR-176309] N86-12257

POLYMER PHYSICS
Molecular control [NASA-TM-87510] N86-12313
Accuracy of a new ultrasonic apparatus for simple measurement of viscoelasticity N86-12386

POLYMERIC FILMS
Studies of the Bauer piezoelectric polymer gauge (PVF2) under impact loading [DE85-014707] N86-12590

POLYMERIZATION
Epoxy phthalonitrile polymers [AD-D011821] N86-12318

POLYMERS
Model describing the steady-state pyrolysis of bubble-forming polymers in response to an incident heat flux [PB85-225225] N86-12291

POLYNOMIALS
Electrical losses and resistance of cryogenic inductors with consideration of the effect of magnetoresistance [AD-A158185] N86-12516

POLYPROPYLENE
Development of a supported liquid membrane as a nickel-zinc secondary battery separator [DE85-012591] N86-12784

POLYURETHANE FOAM
Full-scale fire tests of polyurethane foam dome structures [AD-A157107] N86-12314

POLYVINYL CHLORIDE
Studies of the Bauer piezoelectric polymer gauge (PVF2) under impact loading [DE85-014707] N86-12590

POROSITY
Molten salt corrosion of SiC: Pitting mechanism [NASA-TM-87143] N86-12310

POSITION (LOCATION)
Strategies for associating data and location in a geographic information system [AD-A158118] N86-12746

POSITION INDICATORS
New dual Z80 navigaiton computer described N86-12425

POSITIONING
Microcomputer-controlled closed-loop system for positioning radio telescope N86-12410
Petrochemical types of magmatic rocks of ocean floor and patterns of their distribution N86-12650

POSITRONS
Multiplicities in high energy interactions [DE85-013847] N86-13100
High intensity positron beam and angular correlation experiments at Livermore [DE85-012961] N86-13111
Physics of e(+) - e(-) colliders: Present, future and far future [DE85-009695] N86-13121

POTASSIUM
Fischer-Tropsch synthesis in slurry reactor systems [DE85-013390] N86-12278

POTENTIAL FIELDS
Modeling currents at satellite altitudes N86-12889

POTENTIAL GRADIENTS
Plasma and magnetospheric research [NASA-CR-176326] N86-13138

POWDER (PARTICLES)
U308 powder from uranyl-loaded cation exchange resin [DE85-013231] N86-12265
Optical measurements of shock-induced chemical reactions in mixed aluminum-nickel powder [DE85-014705] N86-12306

POWER CONDITIONING
Parallel, staged opening switch power conditioning techniques for flux compression generator applications [DE85-012761] N86-12527

POWER CONVERTERS
Advanced torque converters for robotics and space applications [NASA-CR-177987] N86-12610

POWER LINES
Stochastic beam cooling amplifier system front end components performance characteristics [DE85-013925] N86-13079

POWER SPECTRA
Bandwidth efficient frequency-shift keyed communication systems N86-12472

POWER SUPPLIES
Design of foil implosion system for Pioneer 1 experiments [DE85-014111] N86-12535

POWER SUPPLY CIRCUITS
Digital phase meter using CMOS-LED introduced N86-12442
Parallel, staged opening switch power conditioning techniques for flux compression generator applications [DE85-012761] N86-12527
SCREAMER: A single-line pulsed-power design tool [DE85-012837] N86-13014
Photosensitive cartridge for weapons zeroing and marksmanship training [AD-D011765] N86-13125

POWER TRANSMISSION
Power and signal transmission for mobile teleoperated systems [DE85-013994] N86-12975

PRECIPITATION (CHEMISTRY)
Interpretation of individual precipitation chemistry data sets: General condiserations and approaches [DE85-012449] N86-12800

PRECIPITATION (METEOROLOGY)
Perspectives to establish knowledge linkages between acidic deposition and vegetation responses [DE85-011639] N86-12796
Atmospheric tritium 1968-1984 [DE85-013133] N86-12798
Analysis and assessment of US-WMO regional precipitation chemistry measurements (1972-1982), a subject of the National Trends Network [PB85-212959] N86-12807
Large-scale circulation departures related to wet episodes in northeast Brazil [NASA-CR-176352] N86-12916

PRECISION
Precision ion vacuum gage with logarithmic response [DE85-015312] N86-12588

PREDICTION ANALYSIS TECHNIQUES
Development of a routine technique for analysis of nitro-PAH in diesel particulate extract [PB85-196657] N86-12287
An update of the total-strain version of SRP [NASA-TP-2499] N86-12295
Scattering experiments at the Ipswich Electromagnetic Measurements Facility: Backscatter from metal cubes [AD-A157925] N86-12496
Numerical calculation of internal flows with curvature N86-12544
Numerical and experimental studies of 3-D and unsteady turbulent body/appendage/propeller flows [AD-A157078] N86-12552
Method and results of electrometric observations in seismically active region N86-12730
Statistical evaluation of forecasts over the low-latitudes [AD-A157926] N86-12923

PREDICTIONS
Heat Exchanger Vibration Analysis (HXVA) for prediction of tube bundle instabilities [DE85-017144] N86-12568
Temporal and spatial variabilities in shallow water acoustics: Measurements and predictions [AD-A156718] N86-12942
Comparison between theoretical predictions and tracking [DE85-012104] N86-13149

PRESSING (FORMING)
Steam-injection pressing of isocyanate-bonded aspen flakeboards, latitudes and limitations [AD-A157833] N86-12389

PRESSURE DEPENDENCE
Pressure-coupled response function of solid propellants including those with negative pressure exponents N86-12369
X-ray diffraction cell for Debye-Scherrer and Guinier (Huber) cameras at pressure and temperature [DE85-014815] N86-12593
Shocking behavior of fluid flow in deformable joints [DE85-010104] N86-13107

PRESSURE DISTRIBUTION
Effect of surface waviness on a supercritical laminar-flow-control airfoil [NASA-TM-85705] N86-12206
Temperature structure of the 80 km to 120 km region N86-12830
Prediction of sound fields in acoustical cavities using the boundary element method [NASA-CR-176295] N86-13057

PRESSURE EFFECTS
The effects of hypoxia induced by low atmospheric pressure on soft contact lens wear
[AD-A158556] N86-12963
PRESSURE GRADIENTS
Numerical and experimental studies of 3-D and unsteady turbulent body/appendage/propeller flows
[AD-A157078] N86-12552
PRESSURE MEASUREMENT
Analytical and experimental studies of wakes behind circularly capped bubbles N86-12548
PRESSURE REDUCTION
The prediction of fully developed turbulent pressure drops in a triangular duct for a power law fluid
N86-12546
Particle-wall interaction and wall friction in gas-solid flows
[DE85-014984] N86-12567
PRESSURE SENSORS
Electrolytic pressure transduction system
[AD-D011847] N86-12584
PRESSURE VESSELS
New approaches to determining physical properties in piston-cylinder high-temperature, high-pressure device
N86-12445
Novel instrument for high-pressure research at ultra-high temperatures
[DE85-015674] N86-12589
Energy dispersive spectroscopy using synchrotron radiation: Intensity considerations
[DE85-017530] N86-13200
PRESSURIZED WATER REACTORS
Analysis of stratified flow mixing
[DE85-006840] N86-12576
PRESTRESSING
Influence of bonded reinforcement in post-tensioned prestressed concrete T-beams with unbonded tendons
N86-12622
PRIMITIVE EQUATIONS
Statistical evaluation of forecasts over the low-latitudes
[AD-A157926] N86-12923
PRINTERS
Impact of linear programming on computer development
[AD-A157659] N86-12993
PRINTERS (DATA PROCESSING)
Control for DOT matrix printers operating in harsh environment
[AD-D011846] N86-12980
PRINTING
Control for DOT matrix printers operating in harsh environment
[AD-D011846] N86-12980
PRISMS
Frequency selection and mode locking of Nd:YAG laser N86-12395
PROBABILITY DENSITY FUNCTIONS
Basic EMC (Electromagnetic compatibility) technology advancement for C3 (Command, control, and communications) systems. Volume 6
[AD-A157239] N86-12493
Soybean canopy reflectance modeling data sets
[E86-10005] N86-12741
New representations of the non-central chi-square density and cumulative
[AD-A157227] N86-13046
PROBABILITY DISTRIBUTION FUNCTIONS
A survey of some recent results in continuous univariate distributions
[AD-A157450] N86-13047
PROBABILITY THEORY
Weather analysis programs using HP-41CV
[AD-A157389] N86-12921
Systems analysis approach to probabilistic modeling of fault trees
[DE85-007705] N86-13050
PROBLEM SOLVING
Stefan's problem in a finite domain with constant boundary and initial conditions analysis
[AD-A153558] N86-13040
Deals among rational agents
[AD-A157960] N86-13052
PRODUCT DEVELOPMENT
Design information for the 4/3 silicon-gate CMOS technology
[DE85-014932] N86-12522
Semicustom integrated circuit design at Sandia National Laboratories
[DE85-015661] N86-12538
Development of the hydrotransport boost pump
[PB85-203776] N86-12618
Development of acoustic agglomerator. Test plan for high temperature high pressure acoustic agglomerator
[DE85-017221] N86-13061
PRODUCTION MANAGEMENT
Large-area thin-film modules N86-12766
PROGRAM VERIFICATION (COMPUTERS)
Micro-PROUST
[AD-A157505] N86-12991
Application of automated reasoning software procedure generation system verifier
[DE85-014000] N86-13006
PROGRAMMERS
Micro-PROUST
[AD-A157505] N86-12991
PROGRAMMING LANGUAGES
Advanced avionics computer architecture. Volume 2. Instruction set architecture specification
[AD-A158120] N86-12223
A meta system for generating software engineering environments
[AD-A158102] N86-12996
Scientific workstation research
[DE85-013385] N86-13002
IMAGYS graphics programming language: Description and analysis
[DE85-013384] N86-13003
Design and implementation of the computer systems design environment network
[AD-A156832] N86-13022
PROJECT MANAGEMENT
Large scale operational pulsed power research facilities: How well have we made them a reality
[DE85-013784] N86-13088
PROJECT PLANNING
LabNet Project plan
[DE85-014860] N86-13024
PROJECTILES
Wear of projectile rotating bands
[AD-A156666] N86-12358
PROPAGATION
Coupling between spinor field, propagating torsion
N86-12420
PROPAGATION MODES
Uncertainty propagation from raw data to final results
[DE85-011937] N86-13000
Suppression of propagating TE modes in the FNAL antiproton source stochastic beam cooling system
[DE85-016559] N86-13074
IBEX magnetic coupling experiments
[DE85-014331] N86-13108
PROPELLANT SENSITIVITY
Energetic response of propellants to high velocity impact, revision 1
[DE85-013983] N86-12365
PROPELLANT STORAGE
Liquid propellant storage compatibility N86-12356
Quantity-distance requirements N86-12357
PROPELLANTS
Hazards of chemical rockets and propellants. Volume 3: Liquid propellants
[AD-A158115] N86-12328
Energetic response of propellants to high velocity impact, revision 1
[DE85-013983] N86-12365
PROPELLERS
Experimental investigation of 3-D turbulent free shear flow past propellers and windmills N86-12201
Numerical and experimental studies of 3-D and unsteady turbulent body/appendage/propeller flows
[AD-A157078] N86-12552
PROPYLENE
Otto fuel 2 N86-12334
PROTECTION
Options for operational risk assessments
[DE85-014904] N86-12390
PROTEINS
Influence of seston phosphatase activity on rate of phosphorus mineralization and its recycling in production-destruction cycle N86-12667
PROTON BEAMS
Measurement of 1 nanosecond wide beams for 2.5 MeV proton accelerator N86-12435
LAMPF transition-region mechanical fabrication
[DE85-012688] N86-13081
Tests of orbital dynamics using the Tevatron
[DE85-012296] N86-13085
Comparison between theoretical predictions and tracking
[DE85-012104] N86-13149
PROTON IRRADIATION
Performance and temperature dependencies of proton irradiated n/p GaAs and n/p silicon cells
[NASA-TM-87136] N86-12509
PROTON-PROTON REACTIONS
Multiplicities in high energy interactions
[DE85-013847] N86-13100
Search for narrow structure in proton-antiproton annihilation cross sections from 1900 to 1960 MeV
[DE85-013302] N86-13119
PROTONS
A p anti p collider physics: Summary talk
[DE85-014782] N86-13097
Search for narrow structure in proton-antiproton annihilation cross sections from 1900 to 1960 MeV
[DE85-013302] N86-13119
Comparison between theoretical predictions and tracking
[DE85-012104] N86-13149
WNR/PSR facility: Neutron physics capabilities from sub-thermal to 800 MeV
[DE85-014072] N86-13173
PROTOSTARS
Balloon-borne three-meter telescope for far-infrared and submillimeter astronomy
[NASA-CR-176347] N86-13271
PROTOTYPES
FMIT diagnostic instrumentation
[DE85-012668] N86-13087
PSYCHOLOGY
European Science Notes. Volume 39, number 8
[AD-A157146] N86-13237
PUBLIC RELATIONS
Index to NASA news releases and speeches, 1984
[NASA-TM-87514] N86-13224
PULSARS
Wave propagation and pair formation in pulsar magnetospheres N86-13276
PULSE CODE MODULATION
Bandwidth efficient frequency-shift keyed communication systems N86-12472
P1 polyphase code expander-compressor
[AD-D011838] N86-12475
P2 polyphase code expander-compressor
[AD-D011839] N86-12476
PULSE COMMUNICATION
Advanced digital communication research
[AD-A158412] N86-12497
PULSE COMPRESSION
P1 polyphase code expander-compressor
[AD-D011838] N86-12475
P2 polyphase code expander-compressor
[AD-D011839] N86-12476
PULSE DURATION
Practical excimer laser developed N86-12456
Modeling short pulse duration shock initiation of solid explosives
[DE85-014803] N86-12565
Biological effects of acoustic cavitation
[AD-A157513] N86-13059
IBEX magnetic coupling experiments
[DE85-014331] N86-13108
PULSE GENERATORS
Hybrid 0-D,1-D, and 2-D model of helical explosive-driven magnetic flux compression generator
[DE85-013772] N86-12524
Parallel, staged opening switch power conditioning techniques for flux compression generator applications
[DE85-012761] N86-12527
Large scale operational pulsed power research facilities: How well have we made them a reality
[DE85-013784] N86-13088
Accelerator research studies
[DE85-014878] N86-13113
PULSE RADAR
P1 polyphase code expander-compressor
[AD-D011838] N86-12475
P2 polyphase code expander-compressor
[AD-D011839] N86-12476
PULSE REPETITION RATE
First domestic high repetition rate ultrashort pulse laser N86-12455
Practical excimer laser developed N86-12456
PULSED LASERS
Picosecond broadband CARS probe using the picosecond continuum
[AD-D011840] N86-12267
Pulsed digital multiplexed laser generator
[AD-D011855] N86-12603
PULSED RADIATION
Effect of pulsed irradiation on microstructural evolution
[DE85-016317] N86-12302
China report: Science and technology
[JPRS-CST-85-021] N86-12421
Pulsed radiation detection technology discussed
N86-12424
RADLAC program status
[DE85-014706] N86-13109

Q

QUADRUPOLES
High and ultra-high gradient quadrupole magnets
[DE85-014360] N86-13104

QUALITY CONTROL
Investigation of test methods, material properties and processes for solar cell encapsulants
[DE85-012831] N86-12786
Interpretation of individual precipitation chemistry data sets: General condiserations and approaches
[DE85-012449] N86-12800
Improvement of manufacturing techniques and quality of optical scratch standards for fire control systems
[AD-A157963] N86-13130
QUANTITATIVE ANALYSIS
Applied lasers (selected articles)
[AD-A155948] N86-12601
QUANTUM CHEMISTRY
Quantum chemistry of aromatic nitro explosives
N86-12423
QUANTUM ELECTRONICS
European Science Notes. Volume 39, number 8
[AD-A157146] N86-13237
QUANTUM MECHANICS
A dressed atom interpretation of adiabatic rapid passage
[AD-A157071] N86-13066
Quantum simulations of small electron-hole complexes
[DE85-013895] N86-13205
Large-basis shell-model technology in nucleosynthesis and cosmology
[DE85-012925] N86-13216
QUANTUM THEORY
A dressed atom interpretation of adiabatic rapid passage
[AD-A157071] N86-13066
QUARKS
Dynamical model of quark rearrangement in nucleon-antinucleon annihilation
[DE85-013904] N86-13120

R

RADAR
Analysis of constant false alarm rate sidelobe canceller criterion
[AD-A157412] N86-12494
RADAR ABSORBERS
Radio-absorbing materials
[AD-A157496] N86-12495
RADAR CROSS SECTIONS
Scattering experiments at the Ipswich Electromagnetic Measurements Facility: Backscatter from metal cubes
[AD-A157925] N86-12496
RADAR DETECTION
Analysis of constant false alarm rate sidelobe canceller criterion
[AD-A157412] N86-12494
RADAR IMAGERY
Underground volcanoes discovered with satellite radar
N86-12721
RADAR MEASUREMENT
Mean winds of the upper middle atmosphere (60-110 km): A global distribution from radar systems (MF, meteor, VHF) N86-12831
Atmospheric tides between 80 km and 120 km
N86-12833
Contribution to the CIRA model from ground-based lidar N86-12835
The MST radar technique N86-12836
Saskatoon M. F. radar system: (52 deg N, 107 deg W), Canada N86-12843
May 1982, Saskatoon M. F. radar system: (52 deg N, 107 deg W), Canada N86-12844
Meteor wind results at Durham (43 deg N, 71 deg W) during the ATMAP November 1981 and May 1982 campaigns N86-12845
Mean winds and tides over Urbana, Illinois during November 16-22, 1981 N86-12846
Kyoto meteor radar observation in November, 1981 and May, 1982 N86-12847
Mesospheric winds and tides at Arecibo/puerto Rico (18 deg N, 67 deg W) November 20-23, 1981
N86-12848
RADAR SCANNING
Evaluation of space SAR as a land-cover classification
[E86-10004] N86-12740
RADAR SCATTERING
The MST radar technique N86-12836
RADIAL DISTRIBUTION
Numerical computation of full three-dimensional flow in transonic turbines N86-12397
Plasma and magnetospheric research
[NASA-CR-176326] N86-13138
RADIAL VELOCITY
Mean winds and tides over Urbana, Illinois during November 16-22, 1981 N86-12846

RADIANCE
Clear sky brightness temperature over the western north Pacific Ocean from GMS spacecraft N86-12911
RADIANT FLUX DENSITY
Influence of water vapor on distribution of turbulent wave parameters N86-12659
A note on Jupiter's gossamer ring N86-13260
RADIATION ABSORPTION
High power laser dump
[AD-D011792] N86-12597
Atmospheric IR transmission measurements in a tropical maritime environment: Comparison with the LOWTRAN 6 model
[AD-A157920] N86-13129
RADIATION BELTS
Effects of whistler-mode and other waves in the magnetosphere
[AD-A157832] N86-12899
RADIATION DETECTORS
Data acquisition system for SLD
[DE85-014361] N86-13103
RADIATION DISTRIBUTION
A 94 GHz imaging array using slot line radiators
[NASA-CR-176346] N86-12484
RADIATION DOSAGE
Accidental exposure to americium
[DE85-012794] N86-12965
RADIATION EFFECTS
Effect of pulsed irradiation on microstructural evolution
[DE85-016317] N86-12302
Review of effects of long-term aging on the mechanical properties and microstructures of types 304 and 316 stainless steel
[DE85-016472] N86-12304
Estimate of radiation-climatic effects of natural and anthropogenic aerosol N86-12640
Proceedings of a workshop on Radiofrequency Radiation bioeffects held at Wachtberg-Werthhoven, West Germany on 11-13 September 1984
[AD-A157090] N86-12959
Studies of participants in nuclear tests N86-12964
Analytic models for radiation induced loss in optical fibers. 3. Transient radiation effects
[AD-A157408] N86-13127
Radiation effects on light sources and detectors
[DE85-014746] N86-13133
RADIATION HARDENING
High damage threshold porous silica antireflective coating
[DE85-012924] N86-12322
Development of a radiation-hard CMOS process
[NASA-CR-170925] N86-13187
RADIATION HAZARDS
China report: Science and technology
[JPRS-CST-85-019] N86-12966
RADIATION MEASUREMENT
High-elevation station's cosmic-ray recording system
N86-12687
RADIATION MEASURING INSTRUMENTS
Pulsed radiation detection technology discussed
N86-12424
RADIATION PROTECTION
Proceedings of a workshop on Radiofrequency Radiation bioeffects held at Wachtberg-Werthhoven, West Germany on 11-13 September 1984
[AD-A157090] N86-12959
RADIATION SPECTRA
Integral equation description of integrated dielectric waveguides N86-12504
RADIATION THERAPY
China report: Science and technology
[JPRS-CST-85-016] N86-12393
RADIATION TOLERANCE
Development of a radiation-hard CMOS process
[NASA-CR-170925] N86-13187
RADIATIVE HEAT TRANSFER
Atmospheric aerosol and its effects on climate
N86-12636
RADIATIVE LIFETIME
The NO-NO2 system at laboratory surfaces
N86-13255
Optical radiation from the interaction of energetic atoms, ions, electrons, and photons with surfaces N86-13259
RADIATIVE TRANSFER
Feasibility of using LANDSAT images of vegetation cover to estimate effective hydraulic properties of soils
[E86-10003] N86-12739
Radiation fog modeling
[AD-A157971] N86-12924
RADII
Variable radius lead former
[AD-D011790] N86-12506
RADIO BURSTS
Measurement of 1 nanosecond wide beams for 2.5 MeV proton accelerator N86-12435

A statistical study of solar Type-3 bursts and auroral kilometric radiation onset:
[AD-A156408] N86-13284
RADIO EMISSION
Influence of short gravity waves on thermal radio emission of water surface N86-12644
RADIO EQUIPMENT
Results of field and laboratory studies of jam-resistant and voice-private radios
[DE85-014841] N86-12500
RADIO FREQUENCIES
High order mode damping in the NSLS accelerating RF cavities by the use of damping antennae
[DE85-014214] N86-12498
Racetrack microtron rf system
[DE85-012669] N86-12532
Proceedings of a workshop on Radiofrequency Radiation bioeffects held at Wachtberg-Werthhoven, West Germany on 11-13 September 1984
[AD-A157090] N86-12959
RF beam deflection measurements and corrections in the SLC linac
[DE85-013061] N86-13146
RADIO FREQUENCY HEATING
Theory of the anomalous Doppler instability during lower-hybrid current drive
[DE85-014064] N86-13170
RADIO SPECTRA
Spectrum resource assessment of the 1605-2000 kHz band
[PB85-225076] N86-12501
RADIO TELEMETRY
Kamchatka radio telemetric station registers volcano pulse N86-12717
RADIO TELESCOPES
China report: Science and technology
[JPRS-CST-85-017] N86-12408
Microcomputer-controlled closed-loop system for positioning radio telescope N86-12410
RADIO TRANSMISSION
The measurement of tropospheric refractive index relevant to the study of anomalous microwave propagation: Review and recommendations
[CRC-1387] N86-12471
RADIO WAVE REFRACTION
The measurement of tropospheric refractive index relevant to the study of anomalous microwave propagation: Review and recommendations
[CRC-1387] N86-12471
RADIO WAVES
The measurement of tropospheric refractive index relevant to the study of anomalous microwave propagation: Review and recommendations
[CRC-1387] N86-12471
Handbook of radio wave propagation loss (100-10,000 MHz)
[PB85-200012] N86-12502
European Science Notes. Volume 39, number 8
[AD-A157146] N86-13237
RADIOACTIVE DECAY
Nuclear information needs for the astrophysical s-process
[DE85-012913] N86-13278
RADIOACTIVE ISOTOPES
Chemistry of berkelium: A review
[DE85-017523] N86-13102
RADIOACTIVE MATERIALS
Real-time computing of the environmental consequences of an atmospheric accidental release of radioactive material: User's point of view
[DE85-016438] N86-12795
RADIOACTIVE WASTES
Fixation of high-level wastes in glasses
[DE85-013276] N86-12325
MAGNUM-2D computer code: User's guide
[DE85-013315] N86-13001
Second reference calculation for the WIPP
[DE85-013180] N86-13005
RADIOACTIVITY
Outdoor radon monitoring at Canonsburg, Pennsylvania, 1980-1983
[DE85-013320] N86-12797
RADIOBIOLOGY
Biomedical and Environmental Sciences Program publications 1984
[DE85-015070] N86-12953
RADIOGRAPHY
Application of radiographic image enhancement, segmentation N86-12466
RADIOMETRIC RESOLUTION
LANDSAT-4 TM image data quality analysis for energy-related applications
[E86-10006] N86-12742
RADIOSONDES
A proposed international tropical reference atmosphere up to 80 km N86-12828

RADIOTELEPHONES
Spectrum resource assessment of the 1605-2000 kHz band [PB85-225076] N86-12501

RADON ISOTOPES
Outdoor radon monitoring at Canonsburg, Pennsylvania, 1980-1983 [DE85-013320] N86-12797

RAILGUN ACCELERATORS
High efficiency ICF driver employing magnetically confined plasma rings [DE85-012939] N86-13164

RAIN
Performance of an alpha-vane and pitot tube in simulated heavy rain environment [NASA-CR-176353] N86-12220

RAIN IMPACT DAMAGE
Optical technique to study the impact of heavy rain on aircraft performance [NASA-CR-177989] N86-12580

RAMAN SPECTRA
Raman spectroscopy of molecular adsorbates [DE85-012981] N86-12280
Application of time-dependent Raman theory to the analysis of inorganic photosystems [DE85-012752] N86-12285

RAMAN SPECTROSCOPY
Picosecond broadband CARS probe using the picosecond continuum [AD-D011840] N86-12267
Remote diagnosis of media by combination (Raman) anti-Stokes light scattering method with induced Brillouin backscattering N86-12705
Raman activity in synchronously dividing bacteria [DE85-015672] N86-12951

RAMP FUNCTIONS
Rapid estimation of frequency response functions by close-range photogrammetry [NASA-TP-2471] N86-12579

RANDOM ACCESS MEMORY
The 32-bit computer for large memory applications on FASTBUS [DE85-012726] N86-12986

RANDOM ERRORS
Tracking studies on the effects of random multipoles in the 6.5 T lattice of the SSC Reference Designs Study [DE85-013286] N86-13156

RANDOM VARIABLES
Compound poisson approximations for sums of random variables [AD-A158555] N86-13049

RANGEFINDING
P2 polyphase code expander-compressor [AD-D011839] N86-12476

RARE EARTH COMPOUNDS
Temperature and concentration dependence of hydrogen site occupancy in several rare-earth dihydrides [DE85-015739] N86-13199

RARE GAS COMPOUNDS
Multiphoton ionization of NO-rare gas van der Waals species [DE85-014650] N86-13094

RARE GASES
Noble gases N86-12348
Outdoor radon monitoring at Canonsburg, Pennsylvania, 1980-1983 [DE85-013320] N86-12797

RATES (PER TIME)
Kinetics of evaporation and growth of drops of aqueous solutions of surface active substances at negative temperatures [AD-A156961] N86-12269

RATIOS
Temperature and concentration dependence of hydrogen site occupancy in several rare-earth dihydrides [DE85-015739] N86-13199

RAYLEIGH SCATTERING
Contribution to the CIRA model from ground-based lidar N86-12835

REACTION KINETICS
Kinetics of evaporation and growth of drops of aqueous solutions of surface active substances at negative temperatures [AD-A156961] N86-12269
Dissociative volume recombination coefficient measurements in a subroom temperature neon plasma afterglow N86-12373
Guidelines for a thermochemical kinetics computer program [DE85-015671] N86-12998
Surface-catalyzed recombination into excited electronic, vibrational, rotational, and kinetic energy states: A review N86-13253
The production of glow precursors by oxidative erosion of spacecraft surfaces N86-13257

REACTOR DESIGN
Materials studies for magnetic fusion energy applications at low temperatures - 8 [PB85-236362] N86-13183

REACTOR MATERIALS
Review of effects of long-term aging on the mechanical properties and microstructures of types 304 and 316 stainless steel [DE85-016472] N86-12304
New passive helicopter detector [DE85-015160] N86-12595

REACTOR SAFETY
Tritium safety issues for TFCX [DE85-014621] N86-13118

REAL TIME OPERATION
Real-time flutter identification [NASA-CR-3933] N86-12218
Laser anemometer using a single circuit board N86-12411
Real-time computing of the environmental consequences of an atmospheric accidental release of radioactive material: User's point of view [DE85-016438] N86-12795

REAL VARIABLES
Hyperbolic systems of conservation laws in several space variables [DE85-014019] N86-13042

RECEIVERS
Film stability for dirct absorption receivers [DE85-012135] N86-12791

RECIRCULATIVE FLUID FLOW
Multiple-scale turbulence closure modeling of confined recirculating flows [NASA-CR-178536] N86-12551

RECOGNITION
Diagnosing cognitive errors: Statistical pattern classification and recognition approach [AD-A156108] N86-12972

RECOMBINATION REACTIONS
Infrared emission from desorbed NO2(*) and NO(*) N86-13254
Activated recombinative desorption: A potential component in mechanisms of spacecraft glow N86-13258

RECORDING INSTRUMENTS
High-elevation station's cosmic-ray recording system N86-12687

RECOVERABILITY
Parachute recovery systems design manual, chapters 1 through 4 offprint [AD-A157839] N86-12210

RECTANGULAR WAVEGUIDES
Integral equation description of integrated dielectric waveguides N86-12504

RECURSIVE FUNCTIONS
A Floquet decomposition for Volterra equations with periodic kernel and a transform approach to linear recursion equations [AD-A158148] N86-13037

REDUCED GRAVITY
Microgravity science and applications bibliography, 1985 revision [NASA-TM-88178] N86-13225

REDUCTION (CHEMISTRY)
Usages of organic membranes in electrolytic industry described N86-12453

REFERENCE ATMOSPHERES
Middle Atmosphere Program. Handbook for MAP. Volume 16: Atmospheric structure and its variation in the region 20 to 120 km. Draft of a new reference middle atmosphere [NASA-CR-176321] N86-12814
Middle atmosphere reference model derived from satellite data N86-12819

REFLECTANCE
The theory and practice of a multistate reflectometer [AD-A157916] N86-12583
Soybean canopy reflectance modeling data sets [E86-10005] N86-12741

REFLECTED WAVES
Folded-path optical (C sub n, sup 2) instrument [PB85-216398] N86-13137

REFLECTION
Computer simulation of the effect of free surface reflection on shock wave propagation in water [DE85-014807] N86-12563

REFLECTOMETERS
The theory and practice of a multistate reflectometer [AD-A157916] N86-12583

REFLECTORS
Strategy for reflector pattern calculation: Let the computer do the work [NASA-TM-87137] N86-12485

REFRACTIVITY
Determination of single-mode optical fiber dispersion N86-12409
Comparison of single-parameter statistical model with results of round-the-clock measurement of light-scattering matrices N86-12689
The MST radar technique N86-12836
Masking of light scattering information on matrix elements from complex scattering [AD-A158144] N86-13131
Folded-path optical (C sub n, sup 2) instrument [PB85-216398] N86-13137

REFRACTOMETERS
Folded-path optical (C sub n, sup 2) instrument [PB85-216398] N86-13137

REFRIGERANTS
Comparative first- and second-law analysis of an absorption cycle [DE85-015066] N86-13215

REFRIGERATING
Influence of a surfactant additive on absorption heat pump performance [DE85-013995] N86-12574

REFRIGERATING MACHINERY
REFRIG-12: A graphics-augmented interactive program for designing vapor-compression refrigeration/heat pump cycles [DE85-014205] N86-12572

REGRESSION ANALYSIS
Comparison of time-periodic variations in temperature and wind from meteorological rockets and satellites N86-12825
Correlation and Regression Equation Program REGRS [PB85-213353] N86-12934

REGULATIONS
Assessment of the long-term precision of continuous emission monitors [PB85-201150] N86-12804

REINFORCEMENT (STRUCTURES)
Influence of bonded reinforcement in post-tensioned prestressed concrete T-beams with unbonded tendons N86-12622

RELATIVISTIC ELECTRON BEAMS
Laser-based foilless diode [DE85-013958] N86-12537
Generation of a modulated IREB (Intense Relativistic Electron Beam) with a frequency tunable by a magnetic field [AD-D011820] N86-13068

RELAXATION TIME
Replica-space renormalization in random-field systems [DE85-014800] N86-13055

RELIABILITY
Latch-up effect in CMOS described N86-12443
Crystalline-silicon reliability lessons for thin-film modules N86-12760
Light-induced effects-impacts to module performance measurements and reliability testing: An overview N86-12761
Thin-film module circuit design: Practical and reliability aspects N86-12762
Accelerated stress testing of thin film solar cells: Development of test methods and preliminary results N86-12764
Thin film module development N86-12768
Outdoor performance testing of thin-film devices N86-12771
Navy applications experience with small wind power systems [AD-A158561] N86-12778
Estimating the reliability of fiber optics cables [DE85-014892] N86-13136

RELIABILITY ENGINEERING
Reliability and Engineering of Thin-Film Photovoltaic Modules. Research forum proceedings [NASA-CR-176217] N86-12759

RELIEF MAPS
New data of relief of Mazca Ridge N86-12679

REMOTE CONTROL
Future directions in mobile teleoperation [DE85-014308] N86-12976
The shuttle glow: A program to study the ram-induced phenomena N86-13268

REMOTE HANDLING
National Aeronautics and Space Administration N86-13234

REMOTE SENSING
Remote diagnosis of media by combination (Raman) anti-Stokes light scattering method with induced Brillouin backscattering N86-12705
Earth resources: A continuing bibliography, issue 46 [NASA-SP-7041(46)] N86-12738
Atmospheric Tides Middle Atmosphere Program (ATMAP): Report of the November/December 1981, and May 1982, observational campaigns N86-12839
Review of spectroscopic parameters for upper atmospheric measurements [NASA-CP-2396] N86-13064

REPLENISHMENT
Develop and test fuel cell powered on-site integrated total energy systems: Phase 3, full-scale power plant development
[NASA-CR-174948] N86-12757
Develop and test fuel cell powered on-site integrated total energy systems: Phase 3, full-scale power plant development
[NASA-CR-174998] N86-12758
REPORTS
China report: Science and technology
[JPRS-CST-85-024] N86-12368
China report: Science and technology
[JPRS-CST-85-016] N86-12393
China report: Science and technology
[JPRS-CST-85-022] N86-12439
RESCUE OPERATIONS
The C-17: We need it yesterday
[AD-A157147] N86-12219
RESEARCH
Naval surface weapons center technology transfer biennial report (Fiscal year 1983/1984)
[AD-A157919] N86-13238
RESEARCH AND DEVELOPMENT
Marketing the use of the space environment for the processing of biological and pharmaceutical materials
[NASA-CR-176334] N86-12243
LANDSAT-4 TM image data quality analysis for energy-related applications
[E86-10006] N86-12742
Control problems in very large accelerators
[DE85-014956] N86-13075
RESEARCH FACILITIES
Annual data summary for 1981 CERC (Coastal Engineering Research Center) field research facility
[AD-A158143] N86-12926
A user's guide to the Coastal Engineering Research Center's (CERC'S) field research facility
[AD-A157966] N86-12946
Large scale operational pulsed power research facilities: How well have we made them a reality
[DE85-013784] N86-13088
Review of heavy ion collider proposals
[DE85-014985] N86-13091
WNR/PSR facility: Neutron physics capabilities from sub-thermal to 800 MeV
[DE85-014072] N86-13173
European Science Notes. Volume 39, number 8
[AD-A157146] N86-13237
RESEARCH MANAGEMENT
Environmental impact research program. Status and source of habitat models and literature reviews, December 1984
[AD-A156899] N86-12950
R and D limited partnerships (possible applications in advanced communications satellite technology experiment program)
[NASA-CR-176333] N86-13221
RESERVOIRS
High-resolution, three-dimensional, seismic survey over the geopressured-geothermal reservoir at Parcperdue, Louisiana
[DE85-016465] N86-12902
RESIDENTIAL ENERGY
Wind generation in Washington
[DE85-012791] N86-12787
Low-cost light-weight thin material solar heating system
[DE85-012531] N86-12789
RESIDUAL STRESS
X-ray diffraction studies of shock-modified inorganic materials
[DE85-015150] N86-13209
RESIN MATRIX COMPOSITES
The 371 deg C mechanical properties of graphite/polyimide composites
[NASA-TM-87122] N86-12256
RESINS
The studies on the effects of intermolecular hydrogen bond in melamine resination process. (Methylated melamines were adopted as the model compounds of starting material) N86-12381
RESISTANCE HEATING
Novel instrument for high-pressure research at ultra-high temperatures
[DE85-015674] N86-12589
RESISTORS
Thermally induced failures of thick-film glaze resistors
[DE85-012014] N86-12320
RESONANCE
Classical piezoelectricity: Is the theory complete
[DE85-014592] N86-12536
Modulations of driven nonlinear surface waves on water and liquid Helium-4
[AD-A157958] N86-12556
Nuclear performance optimization of the Be/Li/Th blanket for the fusion breeder
[DE85-012949] N86-13112
R-matrix analysis of the (7) Li system with peripheral channel overlap exchange effects
[DE85-012751] N86-13148
RESONANCE PROBES
Picosecond broadband CARS probe using the picosecond continuum
[AD-D011840] N86-12267
RESONANT FREQUENCIES
Room modes and sound absorption: Some practical measurements compared with theoretical predictions
[BBC-RD-1985/11] N86-12486
User's manual for using MASON: A frequency response program which handles a system of transfer functions described by a signal flow graph
[PB85-227106] N86-13021
RESOURCES MANAGEMENT
Minutes of Workshop on Composite Materials Test Methods
[AD-A157903] N86-12262
AISIM (Automated Interactive Simulation Modeling System) overview: Revision 1
[AD-A157392] N86-12990
RETARDING
A method for determining acoustic-liner admittance in ducts with sheared flow in two-cross-sectional directions
[NASA-TP-2518] N86-13056
RETROFITTING
Ground test facility for nuclear testing of space reactor subsystems
[DE85-014634] N86-13099
RETROREFLECTION
Folded-path optical (C sub n, sup 2) instrument
[PB85-216398] N86-13137
REVERSE FIELD PINCH
Recent results of an internal tilt mode calculation in FRCs
[DE85-014121] N86-13177
REYNOLDS NUMBER
Introduction to cryogenic wind tunnels
[NASA-CR-177966] N86-12238
Measurements on an axisymmetric jet in a slow coflowing stream N86-12549
An asymptotic investigation of the stationary modes of instability of the boundary layer on a rotating disc
[NASA-CR-177977] N86-12550
RHENIUM ALLOYS
Superconductivity in the W-Tc and W2C-Tc systems
[DE85-012711] N86-13204
RHEOLOGY
Constraints on the rheological structure of the mantle N86-12875
The role of a pressure-dependent rheology in the dynamics of mantle circulation N86-12876
RIDGES
New data of relief of Mazca Ridge N86-12679
RIEMANN MANIFOLD
Gravity theories in more than four dimensions
[DE85-011164] N86-12903
RIEMANN WAVES
Elementary waves and Riemann solutions: Their theory and their role in science
[DE85-014018] N86-13045
RISK
Options for operational risk assessments
[DE85-014904] N86-12390
RIVERS
Toxic hot spot study, South Platte River along the Front Range, August and October, 1982
[PB85-196384] N86-12749
ROBOTICS
Department of Housing and Urban Development, and Certain Other Independent Agencies Appropriations for Fiscal Year 1986, part 1
[S-HRG-99-221-PT-1] N86-13233
National Aeronautics and Space Administration N86-13234
ROCKET EXHAUST
Exhaust plume measurements of 15-pound BATES (Ballistic Test and Evaluation System) motors
[AD-A157249] N86-12250
ROCKET SOUNDING
Temperature structure of the 80 km to 120 km region N86-12830
ROCKS
Possibility of sounding Earth by using electromagnetic field of sea current N86-12661
Find of rheolites and trachites and geological situation in northern part of East Indian Ocean Submarine Ridge N86-12665
magnetic minerals and characteristics of natural magnetic state of core in Saatly superdeep hole in depth range 3500-7500 meters N86-12681
Method for solving problems in electrodynamics of anisotropic media with slant bedding N86-12684
Facies-genetic groups of coarse clastic material on world ocean floor N86-12713
Muon tomography used to study underground rock structure N86-12720
Method and results of electrometric observations in seismically active region N86-12730
Shocking behavior of fluid flow in deformable joints
[DE85-010104] N86-13107
RODENTS
Monitoring of circadian waveforms in rodents exposed to high-intensity static magnetic fields
[DE85-015225] N86-12952
ROLLING CONTACT LOADS
Surface fatigue life and failure characteristics of EX-53, CBS 1000M, and AISI 9310 gear materials
[NASA-TP-2513] N86-12609
ROOM TEMPERATURE
Measurement of tritium permeation through resistant materials near room temperature
[DE85-012942] N86-12592
ROOMS
Room modes and sound absorption: Some practical measurements compared with theoretical predictions
[BBC-RD-1985/11] N86-12486
ROTATING BODIES
Wear of projectile rotating bands
[AD-A156666] N86-12358
ROTATING DISKS
An asymptotic investigation of the stationary modes of instability of the boundary layer on a rotating disc
[NASA-CR-177977] N86-12550
ROTATING FLUIDS
Theory of solitary anticyclones in rotating fluid N86-12669
ROTATING PLASMAS
Solitary vortices in a rotating plasma
[DE85-014766] N86-13171
ROTATING SPHERES
Mathematical principle for generating second-order aspherical surface N86-12438
ROTORS
Development of an analytical model and code for the flapping response of a Hawte rotor blade
[DE85-008806] N86-12211
RUBIDIUM
Microwave field strength measurement in a Rubidium clock cavity via adiabatic rapid passage
[AD-A157070] N86-13065
RUNWAYS
CBR (California Bearing Ratio) design of flexible airfield pavements with case study
[AD-A158101] N86-12242

S

S MATRIX THEORY
Phase operator method in problem of scattering of electromagnetic waves on ideally conducting surface N86-12701
SAFETY
Hazards of chemical rockets and propellants. Volume 3: Liquid propellants
[AD-A158115] N86-12328
Safety criteria for the operation of gaseous hydrogen pipelines
[PB85-206159] N86-12392
High rate Li/SOCl(2) cells. 1. Effect of design variables in uncatalyzed cells
[AD-A157203] N86-12776
SAFETY MANAGEMENT
Hydrocarbon fuels N86-12329
Anhydrous ammonia N86-12330
The hydrazine fuels N86-12331
Nitromethane N86-12332
Ethylene oxide N86-12333
Otto fuel 2 N86-12334
Hydrogen and deuterium N86-12335
The boranes N86-12336
Carbon monoxide N86-12337
Oxygen N86-12338
Fluorine and fluorine mixtures N86-12339
The halogen fluorides N86-12340
Nitrogen oxides N86-12341
Fuming nitric acids N86-12342
Iodine N86-12343
Chlorine N86-12344
Nitrogen trifluoride N86-12345
Hydrogen peroxide N86-12346
Nitrogen N86-12347
Noble gases N86-12348
The alcohols N86-12349
Halocarbons N86-12350
Hydraulic fluids N86-12351

Mercury N86-12352
Compressed and liquid air N86-12353
Carbon dioxide N86-12354
Nitrous oxide N86-12355
Liquid propellant storage compatibility N86-12356
Quantity-distance requirements N86-12357
Options for operational risk assessments [DE85-014904] N86-12390
Electrical safety requirements: Implications for the module designer N86-12765
Outdoor performance testing of thin-film devices N86-12771
Proceedings of a workshop on Radiofrequency Radiation bioeffects held at Wachtberg-Werthhoven, West Germany on 11-13 September 1984 [AD-A157090] N86-12959

SAILS
China report: Science and technology [JPRS-CST-85-029] N86-12446
Wingtip sails tested on Y-5 aircraft N86-12450

SALINITY
Spectrum of turbulent fluctuations in sea water density in region of large wave numbers N86-12646
Viscous nonlinear circulation in axisymmetric baroclinic eddy N86-12712

SAMPLING
Development of a routine technique for analysis of nitro-PAH in diesel particulate extract [PB85-196657] N86-12287
Interpretation of individual precipitation chemistry data sets: General condiserations and approaches [DE85-012449] N86-12800

SATELLITE IMAGERY
Feasibility of using LANDSAT images of vegetation cover to estimate effective hydraulic properties of soils [E86-10003] N86-12739

SATELLITE NETWORKS
Meteorological Satellite Center Technical Note No. 11, 1985 [MSC-TN-11] N86-12909

SATELLITE OBSERVATION
Underground volcanoes discovered with satellite radar N86-12721
Earth resources: A continuing bibliography, issue 46 [NASA-SP-7041(46)] N86-12738
Hydrologic and land sciences applications of NOAA (National Oceanic and Atmospheric Adminstration) polar-orbiting satellite data [PB85-233385] N86-12748
Interim reference ozone models for the middle atmosphere N86-12829
GRM crustal magnetic anomalies: Separating the Lord Howe Rise and Norfolk Ridge submarine structures N86-12865
Continental and oceanic magnetic anomalies: Enhancement through GRM N86-12869
The resolution of a magnetic anomaly map expected from GRM data N86-12870
The importance of GRM gravity observations in continental regions N86-12871
Interpretation of the geoid N86-12873
Mantle viscosity, J2 and the nontidal acceleration of Earth rotation N86-12879
Global mean sea surface computation based upon a combination of SEASAT and GEOS-3 satellite altimeter data N86-12882
Contributions of GRM to the ocean topography experiment (TOPEX) N86-12883
Rationale for a GRAVSAT-MAGSAT mission: A perspective on the problem of external/internal transient field effects N86-12887
Recent MAGSAT results N86-12888
Modeling currents at satellite altitudes N86-12889
GRM as a follow-on to MAGSAT N86-12893
On the interpretation of satellite-derived gravity and magnetic data for studies of crustal geology and metallogenesis N86-12894
Do MAGSAT anomalies contain a record of past and present-day mantle convection under South America? N86-12895
Meteorological Satellite Center Technical Note No. 11, 1985 [MSC-TN-11] N86-12909
Occurrence of linearly ranged Cb-clouds associated with migrating band-shaped cirriform-clouds: A case study N86-12910
Relaying of the stretched VISSR data by GMS spacecraft N86-12913
Introduction to operational ASDAR system N86-12915

SATELLITE ORBITS
On the geographical correlation of orbit error N86-12881

SATELLITE SOUNDING
Mean density scale heights from analysis of variation in perigee height of China's second satellite N86-12396

SATELLITE TRANSMISSION
Feasibility of using LANDSAT images of vegetation cover to estimate effective hydraulic properties of soils [E86-10003] N86-12739
Introduction to operational ASDAR system N86-12915

SATELLITE-BORNE PHOTOGRAPHY
Hydrologic and land sciences applications of NOAA (National Oceanic and Atmospheric Adminstration) polar-orbiting satellite data [PB85-233385] N86-12748
Global view of the upper level outflow patterns associated with tropical cyclone intensity changes during FGGE [NASA-CR-174407] N86-12908

SATELLITES
Internetting and packet satellite program [AD-A157124] N86-12489

SATURATION (CHEMISTRY)
Use of an elliptical aperture to control saturation in closely-coupled, cold iron, superconducting dipole magnets [DE85-012259] N86-13053

SATURN (PLANET)
Electrons and cosmic ray produced in Saturn's inner magnetosphere N86-13281

SATURN RINGS
Trapped particle absorption by the ring of Jupiter [NASA-CR-174408] N86-13279

SCALE EFFECT
Numerical computation of full three-dimensional flow in transonic turbines N86-12397

SCALE HEIGHT
Mean density scale heights from analysis of variation in perigee height of China's second satellite N86-12396

SCALING LAWS
Multiplicities in high energy interactions [DE85-013847] N86-13100

SCANDIUM
Paramagnetic form factors of HCP transiton metals [DE85-016301] N86-12301

SCATHA SATELLITE
The aerospace spacecraft charging document [AD-A157664] N86-12248

SCATTERING
The production of glow precursors by oxidative erosion of spacecraft surfaces N86-13257

SCATTERING CROSS SECTIONS
Partition of cross sections in asymmetric nucleus-nucleus reactions and the origin of fast alpha particles [DE85-014989] N86-13089
Multiplicities in high energy interactions [DE85-013847] N86-13100
Isovector resonances in pion charge exchange [DE85-012746] N86-13106

SCENE ANALYSIS
Correcting a digital map data base with scene analysis concepts and methods [AD-A157913] N86-12745

SCHEDULING
Decentralized control of scheduling in distributed systems [AD-A157656] N86-13222

SCHROEDINGER EQUATION
Large-basis shell-model technology in nucleosynthesis and cosmology [DE85-012925] N86-13216

SCINTILLATION COUNTERS
Measurement of tritium permeation through resistant materials near room temperature [DE85-012942] N86-12592

SCORING
Large-area thin-film modules N86-12766
Module voltage isolation and corrosion research N86-12772

SCRAMBLING (COMMUNICATION)
Results of field and laboratory studies of jam-resistant and voice-private radios [DE85-014841] N86-12500

SEA LEVEL
Recent changes in climate and world water balance N86-12638

SEA WATER
Aquatic Species Program review: Proceedings of Principal Investigators Meeting [DE85-012137] N86-12364
Spectrum of turbulent fluctuations in sea water density in region of large wave numbers N86-12646
Contribution of diffusion processes to the electric field of the ocean N86-12654
Possibility of sounding Earth by using electromagnetic field of sea current N86-12661
Structure of acoustic field in deep sea at shallow depths and at great ranges N86-12664
Origin of element composition of ocean water N86-12668
Nonlinear model of adaptation of fields of density and currents in sea N86-12670
Carbon dioxide in arctic and subarctic regions [DE85-014054] N86-12901

SEALS (STOPPERS)
Surface crystallization on metallized 94 percent alumina ceramics [DE85-008891] N86-12324
In-situ vacuum-assisted molding of glass-metal electrical components [DE85-015607] N86-12326

SEAMOUNTS
Role of ahermatypic corals in sedimentation and ecology of coral banks N86-12678

SEAS
Investigation of ice dynamics in the marginal ice zone [AD-A157557] N86-12944

SEASAT SATELLITES
Wave-current and wave-topographic interactions using SEASAT synthetic aperture radar observations and analytical ocean models N86-12938

SEASONS
Modeling of seasonal evolution of carbon cycle in ocean-atmosphere system N86-12641
Synthesis of research and development in mechanical energy storage technologies [DE85-013313] N86-12782
Monthly and seasonal weather outlook for mid-May to mid-June 1985, volume 39, number 10, May 14, 1985 [PB85-204261] N86-12937

SECONDARY FLOW
Numerical calculation of internal flows with curvature N86-12544

SECURITY
Results of field and laboratory studies of jam-resistant and voice-private radios [DE85-014841] N86-12500

SEDIMENT TRANSPORT
Upper mesozoic turbidites of southern west Sakhalin downwarp N86-12645

SEDIMENTARY ROCKS
Petrochemical types of magmatic rocks of ocean floor and patterns of their distribution N86-12650
Intrusive rocks of oceanic lithosphere as possible sources of anomalous magnetic field of ocean N86-12651
Water Information Bulletin No. 30, Part 13: Geothermal investigations in Idaho. Preliminary geologic reconnaissance of the geothermal occurrences of the Wood River drainage area [DE85-016972] N86-12747

SEDIMENTS
Spreading in development of oceanic structures N86-12658
Stratigraphy of sediments in central and eastern Mediterranean N86-12663
Find of rheolites and trachites and geological situation in northern part of East Indian Ocean Submarine Ridge N86-12665
Computations of seismic wave propagation velocities in ocean bottom sediments from reflected waves travel-time curves N86-12677
Role of ahermatypic corals in sedimentation and ecology of coral banks N86-12678
Structure of sedimentary cover and basement of Sierra Leone Rise determined from common depth point seismic (equatorial Atlantic) N86-12709
Facies-genetic groups of coarse clastic material on world ocean floor N86-12713
Determination of dynamic parameters of reflected waves on slopes of deep water trench N86-12724
The gravity field of topography buried by sediments N86-12864

SEISMIC ENERGY
Variation in seismicity under influence of lunar-solar tidal deformations N86-12726
Seismic effect of underground blasts and problem of estimating total earthquake energy N86-12731

SEISMIC WAVES
New passive helicopter detector [DE85-015180] N86-12595
Computations of seismic wave propagation velocities in ocean bottom sediments from reflected waves travel-time curves N86-12677
New methods for interpreting seismic waves in stratified media N86-12682
PRospects for development of seismic prospecting methods and apparatus N86-12723
Determination of dynamic parameters of reflected waves on slopes of deep water trench N86-12724

Optimal density model of Earth's rust and upper mantle along Kamchatka-Pacific Geotraverse N86-12725

Variation in seismicity under influence of lunar-solar tidal deformations N86-12726

Electromagnetic effects in crustal fracturing N86-12727

Method and results of electrometric observations in seismically active region N86-12730

Seismic effect of underground blasts and problem of estimating total earthquake energy N86-12731

Small-scale convection beneath the transverse ranges, California: Implications for interpretation of gravity anomalies N86-12877

SEISMOLOGY

New approach to some problems in seismology N86-12683

Structure of sedimentary cover and basement of Sierra Leone Rise determined from common depth point seismic (equatorial Atlantic) N86-12709

Tectonic structure of Shirshov Ridge (Bering Sea) N86-12710

Kamchatka radio telemetric station registers volcano pulse N86-12717

PRospects for development of seismic prospecting methods and apparatus N86-12723

Optimal density model of Earth's rust and upper mantle along Kamchatka-Pacific Geotraverse N86-12725

Electromagnetic effects in crustal fracturing N86-12727

Seismological studies of the tectonics of divergent plate boundaries N86-12812

The source of the Earth's long wavelength geoid anomalies: Implications for mantle and core dynamics N86-12872

High-resolution, three-dimensional, seismic survey over the geopressured-geothermal reservoir at Parcperdue, Louisiana [DE85-016465] N86-12902

Motion of the Pacific plate relative to the hotspots since the Jurassic and model of oceanic plateaus of the Farallon plate N86-12940

SELECTION

Encapsulant selection and durability testing experience N86-12774

SELF ORGANIZING SYSTEMS

An application of adaptive learning to malfunction recovery [AD-A158129] N86-12236

SELF SUSTAINED EMISSION

Self-consistent klystron simulations [DE85-012676] N86-12529

Self-contained hot-hollow cathode gun source assembly [DE85-011652] N86-12530

SEMANTICS

Actors: A model of concurrent computation in distributed systems [AD-A157917] N86-12994

SEMICONDUCTING FILMS

Recovery of fragile layers produced on substrates by chemical vapor deposition [AD-D011841] N86-13165

Compound semiconductor insulator interface research [AD-A157277] N86-13189

SEMICONDUCTOR DEVICES

Reduction of CO2 to methanol and methane by photo and dark reactions on semiconductor electrodes [PB85-223298] N86-12290

China report: Science and technology [JPRS-CST-85-035] N86-12399

Photoconductive semiconductor switching for pulsed power applications [DE85-013859] N86-12531

SEMICONDUCTOR JUNCTIONS

Evaluation of the use of p-n structures as photodetectors in silicon integrated circuits [AD-A158104] N86-12514

Liquid Phase Epitaxy (LPE) of silicon carbide [AD-D011825] N86-13191

SEMICONDUCTOR LASERS

Long wave (1.2 - 1.5 microns) semiconductor lasers N86-12419

SEMICONDUCTORS (MATERIALS)

Investigation of phase transitions [AD-A158434] N86-12516

Photoconductive semiconductor switching for pulsed power applications [DE85-013859] N86-12531

Compound semiconductor insulator interface research [AD-A157277] N86-13189

Theoretical studies of deep impurity levels in ternary semiconductor alloys [AD-A157929] N86-13193

Quantum simulations of small electron-hole complexes [DE85-013895] N86-13205

SENSITIVITY

Effects of surface interactions and mechanical properties of plastic bonded explosives on explosive sensitivity. Part 2: Model formulation [AD-A157900] N86-12361

Weather radar studies [AD-A157093] N86-12920

SENSITIZING

Effect of grain boundary structure on sensitization and corrosion of stainless steel [AD-A157133] N86-12297

SENSORS

Single mode phase locking fiberoptic sensor developed N86-12415

SEPARATORS

Development of a supported liquid membrane as a nickel-zinc secondary battery separator [DE85-012591] N86-12784

SERIES EXPANSION

Secondary electron spectra: A semiempirical model [DE85-012446] N86-13086

SERVICE LIFE

Statistical treatment of aramid/epoxy stress-rupture data [AD-A157238] N86-12315

SHAFTS (MACHINE ELEMENTS)

Results of PRIM gyroscope testing [DE85-012934] N86-12591

SHALLOW WATER

Investigation of tidally induced turbulent flow [AD-A157841] N86-12555

Temporal and spatial variabilities in shallow water acoustics: Measurements and predictions [AD-A156718] N86-12942

SHAPE CONTROL

Minimizing the energy spread within a single bunch by shaping its charge distribution [DE85-013064] N86-13151

SHAPES

Journal of the Chinese Silicate Society (selected articles) [AD-A157497] N86-13190

SHEAR FLOW

Experimental investigation of 3-D turbulent free shear flow past propellers and windmills N86-12201

Shear driven film flow behavior and cavitation study N86-12543

A method for determining acoustic-liner admittance in ducts with sheared flow in two-cross-sectional directions [NASA-TP-2518] N86-13056

SHEAR PROPERTIES

Iosipescu shear properties of graphite fabric/epoxy composite laminates [NASA-CR-176316] N86-12258

Minutes of Workshop on Composite Materials Test Methods [AD-A157903] N86-12262

Study of high speed shearing of thermoplastic polymer sheets with a new rotary shearing machine N86-12382

SHEAR STRENGTH

The 371 deg C mechanical properties of graphite/polyimide composites [NASA-TM-87122] N86-12256

Iosipescu shear properties of graphite fabric/epoxy composite laminates [NASA-CR-176316] N86-12258

SHEAR STRESS

Mixed-mode cyclic debonding of adhesively bonded composite joints [NASA-CR-177991] N86-12255

Effects of microstructure on the acoustoelastic measurements of stress [DE85-015518] N86-12307

Dislocation kinetics behind shear shocks [DE85-014811] N86-12586

SHEARING

Research Reports of the Faculty of Engineering, Tokyo Denki University, no. 32 [ISSN-0389-617-X] N86-12372

Study of high speed shearing of thermoplastic polymer sheets with a new rotary shearing machine N86-12382

SHEARS

Particle-wall interaction and wall friction in gas-solid flows [DE85-014984] N86-12567

SHEATHS

Multifrequency eddy-current inspection of seam weld in steel sheath [DE85-013533] N86-12626

SHELL THEORY

Large-basis shell-model technology in nucleosynthesis and cosmology [DE85-012925] N86-13216

SHELLS (STRUCTURAL FORMS)

Sound scattering by a layered sphere [AD-A157915] N86-13060

SHIELDING

Los Alamos constant-Q spectrometer [DE85-014115] N86-12586

Nuclear performance optimization of the Be/Li/Th blanket for the fusion breeder [DE85-012949] N86-13112

SHIPS

European Science Notes. Volume 39, number 8 [AD-A157146] N86-13237

SHOCK WAVE INTERACTION

Computer simulation of the effect of free surface reflection on shock wave propagation in water [DE85-014807] N86-12563

Transonic noise generation by duct and profile flow [AD-A157163] N86-13058

SHOCK WAVE PROPAGATION

Computer simulation of the effect of free surface reflection on shock wave propagation in water [DE85-014807] N86-12563

SHOCK WAVES

Energetic response of propellants to high velocity impact, revision 1 [DE85-013983] N86-12365

Numerical computation of full three-dimensional flow in transonic turbines N86-12387

Unsteady detonation N86-12542

Modeling short pulse duration shock initiation of solid explosives [DE85-014803] N86-12565

Dislocation kinetics behind shear shocks [DE85-014811] N86-12586

DAA modal analysis for parametric investigations of fluid-structure interaction in underwater shock, revision 1 [DE85-012935] N86-12569

Recent developments in microshell-tipped optical fibers as high-pressure shock detectors [DE85-015750] N86-12594

Shocking behavior of fluid flow in deformable joints [DE85-010104] N86-13107

X-ray diffraction studies of shock-modified inorganic materials [DE85-015150] N86-13209

SHORELINES

Features of geostrophic circulation related to nature of bottom relief in northwestern Atlantic N86-12674

SHORT CIRCUIT CURRENTS

Hot-spot heating susceptibility due to reverse bias operating conditions N86-12763

SHORT TAKEOFF AIRCRAFT

The C-17: We need it yesterday [AD-A157147] N86-12219

SIDELOBES

Low sidelobe, high efficiency mirror antenna with twist reflector [AD-D011835] N86-12474

SIERRA LEONE

Structure of sedimentary cover and basement of Sierra Leone Rise determined from common depth point seismic (equatorial Atlantic) N86-12709

SIGNAL DETECTION

Analysis of constant false alarm rate sidelobe canceller criterion [AD-A157412] N86-12494

Fault tolerant statistical signal processing algorithms for parallel architectures [AD-A157393] N86-12978

SIGNAL DETECTORS

P1 polyphase code expander-compressor [AD-D011838] N86-12475

P2 polyphase code expander-compressor [AD-D011839] N86-12476

SIGNAL MEASUREMENT

Exhaust plume measurements of 15-pound BATES (Ballistic Test and Evaluation System) motors [AD-A157249] N86-12250

Laser vibrometer [AD-D011811] N86-12602

SIGNAL PROCESSING

Extraction of feature parameters for spoken word recognition N86-12376

Advanced digital communication research [AD-A158412] N86-12497

Wideband SAW (Surface Acoustic Wave) channelizer using slanted array input transducer [AD-D011857] N86-12517

Fault tolerant statistical signal processing algorithms for parallel architectures [AD-A157393] N86-12978

The design and hardware evaluation of an advanced 16-bit, low-power, high performance microcomputer system for digital signal processing [AD-A158130] N86-12981

Application of a binary cyclic error-correcting code [DE85-013232] N86-13007

Fundamentals of adaptive signal processing [DE85-014933] N86-13016

Pilot's associate definition study [AD-A157106] N86-13026
Adaptive optical filtering techniques [AD-A157072] N86-13126

SIGNAL RECEPTION
Handbook of radio wave propagation loss (100-10,000 MHz) [PB85-200012] N86-12502

SIGNAL TO NOISE RATIOS
Technique for the reduction of fading in interferometers [AD-D011845] N86-12581

SIGNAL TRANSMISSION
A physical method for estimating speech intelligibility in a reverberant sound field N86-12378
Handbook of radio wave propagation loss (100-10,000 MHz) [PB85-200012] N86-12502
Power and signal transmission for mobile teleoperated systems [DE85-013994] N86-12975

SILICATES
Theoretical modelling of the elastic properties of mantle silicates N86-12813
Journal of the Chinese Silicate Society (selected articles) [AD-A157497] N86-13190

SILICIDES
Hillock-free conductor system for use in multilevel interconnects [DE85-012595] N86-12533

SILICON
Semicrystalline casting process development and verification [JPL-9950-1160] N86-12312
Crystalline-silicon reliability lessons for thin-film modules N86-12760
Light-induced effects-impacts to module performance measurements and reliability testing: An overview N86-12761
Thin-film module circuit design: Practical and reliability aspects N86-12762
Hot-spot heating susceptibility due to reverse bias operating conditions N86-12763
Accelerated stress testing of thin film solar cells: Development of test methods and preliminary results N86-12764
Electrical safety requirements: Implications for the module designer N86-12765
Interconnect resistance of photovoltaic submodules N86-12767
Amorphous silicon photovoltaic modules and test devices design, fabrication and testing N86-12769
Thin film module electrical configuration versus electrical performance N86-12770
Module voltage isolation and corrosion research N86-12772
Glass breaking strength: The role of surface flaws and treatments N86-12773
Laser diagnostic studies of plasma etching and deposition [DE85-009494] N86-13178

SILICON CARBIDES
Molten salt corrosion of SiC: Pitting mechanism [NASA-TM-87143] N86-12310
Carbothermal synthesis of silicon carbide [DE85-013546] N86-12321
Deposition, microstructure and properties of laser CVD SiC films [DE85-014680] N86-12327
Liquid Phase Epitaxy (LPE) of silicon carbide [AD-D011825] N86-13191

SILICON DIOXIDE
Liquid chromatography on silica using mobile phases containing tetraalkylammonium hydroxides. 1: General separation selectivity and behavior of polar compounds typically in fuels [DE85-014450] N86-12281
High damage threshold porous silica antireflective coating [DE85-012924] N86-12322
Glass breaking strength: The role of surface flaws and treatments N86-12773
Laser diagnostic studies of plasma etching and deposition [DE85-009494] N86-13178

SILICON FILMS
Design information for the 4/3 silicon-gate CMOS technology [DE85-014932] N86-12522

SILICON TRANSISTORS
High frequency silicon bipolar transistor with SIPOS (Semi-insulating polycrystalline silicon) heterojunction emitter and ion implanted rapid thermal annealed base region [AD-A157141] N86-12510

SILVER ALLOYS
Electronic stakes in disordered solids. Part 3: Applications to materials science [DE85-011416] N86-13213

SIMULATION
Wall-interference assessment in three-dimensional slotted-wall wind tunnels [NASA-CR-176320] N86-12240
Research Reports of the Faculty of Engineering, Tokyo Denki University, no. 32 [ISSN-0389-617-X] N86-12372
Earthquake-response simulation on horizontally large-scale buildings based on the method of reduction concerning their restoring spring matrix. Derivation of general form of spring matrix and comparison of applied response results on an actual building with measured values N86-12374
Dummy head microphone and its application to the measurements of electro-acoustic equipments N86-12379
Thin film module electrical configuration versus electrical performance N86-12770
Radiation fog modeling [AD-A157971] N86-12924
Wave propagation in a plasma based on the cold plasma model [DE85-013649] N86-13158
Explosive coalescence of magnetic islands [DE85-015083] N86-13172
Quantum simulations of small electron-hole complexes [DE85-013895] N86-13205
Shuttle vertical fin flowfield by the direct simulation Monte Carlo method N86-13251

SINE WAVES
Digital phase meter using CMOS-LED introduced N86-12442
Laboratory study of regular low-amplitude gravity capillary waves in nonstationary current N86-12671

SINGLE CRYSTALS
Classical piezoelectricity: Is the theory complete [DE85-014592] N86-12536
Thin-film module circuit design: Practical and reliability aspects N86-12762
Hot-spot heating susceptibility due to reverse bias operating conditions N86-12763
Accelerated stress testing of thin film solar cells: Development of test methods and preliminary results N86-12764
Electrical safety requirements: Implications for the module designer N86-12765
Thin film module electrical configuration versus electrical performance N86-12770
Module voltage isolation and corrosion research N86-12772
Glass breaking strength: The role of surface flaws and treatments N86-12773
Study of possible solarization - related impurities in CaF2 and other fluorides [DE85-014100] N86-13135
Method for the deposition of high-quality crystal epitaxial films of iron [AD-D011842] N86-13186

SINGLE SIDEBAND TRANSMISSION
Simultaneous detection of time coincident signals in an adaptive Doppler tracker [AD-D011796] N86-12473

SINTERING
Molten salt corrosion of SiC: Pitting mechanism [NASA-TM-87143] N86-12310

SITES
Temperature and concentration dependence of hydrogen site occupancy in several rare-earth dihydrides [DE85-015739] N86-13199

SKEWNESS
Nearly ideal lens optimization procedure [DE85-014116] N86-13134

SKIN (ANATOMY)
Dermal substance collection device [AD-D011848] N86-12962

SKY BRIGHTNESS
Clear sky brightness temperature over the western north Pacific Ocean from GMS spacecraft N86-12911

SLIPSTREAMS
Experimental study of the combustion of gas-air mixtures in a channel and the diffusion combustion in a slipstream at high velocities [AD-A157495] N86-12271

SLOPES
New data of relief of Mazca Ridge N86-12679
Determination of dynamic parameters of reflected waves on slopes of deep water trench N86-12724

SLOT ANTENNAS
Near millimeter wave imaging/multi-beam integrated antennas [NASA-CR-176332] N86-12478
Additional results on the radiating properties of LTSAs and CWSAs N86-12479
Characteristic impedance of a wide slot line on low permittivity substrates N86-12480
Analysis of the tem mode linearly tapered slot antenna N86-12481
A new integrated slot element feed array for multi-beam systems N86-12483

SLOTS
FDSC: A microwave coupling code for slots of finite depth [DE85-013443] N86-13011

SLOTTED WIND TUNNELS
User's guide to STIPPAN: A panel method program for slotted tunnel interference prediction [NASA-CR-178003] N86-12237
Wall-interference assessment in three-dimensional slotted-wall wind tunnels [NASA-CR-176320] N86-12240

SMELTING
Iron and steelmaking with plasma N86-12467

SODIUM
Development of a radiation-hard CMOS process [NASA-CR-170925] N86-13187

SODIUM CHLORIDES
Origin of element composition of ocean water N86-12868

SODIUM SILICATES
Molten salt corrosion of SiC: Pitting mechanism [NASA-TM-87143] N86-12310

SOFTWARE ENGINEERING
Programmer for single-chip microprocessor N86-12448
The modification of the operational program for GMS-3 N86-12914
A meta system for generating software engineering environments [AD-A158102] N86-12996
Plasma and magnetospheric research [NASA-CR-176326] N86-13138

SOFTWARE TOOLS
The modification of the operational program for GMS-3 N86-12914
A meta system for generating software engineering environments [AD-A158102] N86-12996

SOIL MECHANICS
Feasibility of using LANDSAT images of vegetation cover to estimate effective hydraulic properties of soils [E86-10003] N86-12739

SOIL MOISTURE
Feasibility of using LANDSAT images of vegetation cover to estimate effective hydraulic properties of soils [E86-10003] N86-12739
ORNL ground coil analytical and experimental studies [DE85-005246] N86-12783
Evaluation of the NWS (National Weather Service) soil moisutre accounting model for automated flash flood forecasting in small arid and semi-arid watersheds [PB85-229722] N86-12928

SOIL SCIENCE
ORNL ground coil analytical and experimental studies [DE85-005246] N86-12783

SOLAR ARRAYS
Encapsulant selection and durability testing experience N86-12774

SOLAR CELLS
Performance and temperature dependencies of proton irradiated n/p GaAs and n/p silicon cells [NASA-TM-87136] N86-12509
Evaluation of the use of p-n structures as photodetectors in silicon integrated circuits [AD-A158104] N86-12514
Reliability and Engineering of Thin-Film Photovoltaic Modules. Research forum proceedings [NASA-CR-176217] N86-12759
Light-induced effects-impacts to module performance measurements and reliability testing: An overview N86-12761
Thin-film module circuit design: Practical and reliability aspects N86-12762
Hot-spot heating susceptibility due to reverse bias operating conditions N86-12763
Accelerated stress testing of thin film solar cells: Development of test methods and preliminary results N86-12764
Large-area thin-film modules N86-12766
Interconnect resistance of photovoltaic submodules N86-12767
Encapsulant selection and durability testing experience N86-12774
Maintenance of photovoltaic power systems, revision 1 [AD-A157636] N86-12777

Investigation of reactive magnetron sputter deposited ZnSe for solar cell application
[DE85-016851] N86-12780
Investigation of test methods, material properties and processes for solar cell encapsulants
[DE85-012831] N86-12786
Photovoltaic Concentrator Technology Project Thirteenth Project Integration Meeting
[DE85-013253] N86-12794

SOLAR COLLECTORS
Solar walk-off protection
[DE85-012112] N86-12788
Low-cost light-weight thin material solar heating system
[DE85-012531] N86-12789
Solar thermal energy systems
[DE85-008793] N86-12790
Photovoltaic Concentrator Technology Project Thirteenth Project Integration Meeting
[DE85-013253] N86-12794

SOLAR ENERGY
Reduction of CO2 to methanol and methane by photo and dark reactions on semiconductor electrodes
[PB85-226298] N86-12290

SOLAR ENERGY CONVERSION
Solar thermal energy systems
[DE85-008793] N86-12790

SOLAR HEATING
Low-cost light-weight thin material solar heating system
[DE85-012531] N86-12789

SOLAR RADIATION
Soybean canopy reflectance modeling data sets
[E86-10005] N86-12741
Middle Atmosphere Program. Handbook for MAP, volume 17
[NASA-CR-176345] N86-12837
A statistical study of solar Type-3 bursts and auroral kilometric radiation onsets
[AD-A158408] N86-13284

SOLAR SIMULATORS
Direct solar-pumped iodine laser amplifier
[NASA-CR-176324] N86-12600

SOLAR WIND
Analysis and interpretation of the shock-like electrostatic noise observed during the AMPTE (Active Magnetospheric Particle Tracer Explorers) solar wind lithium releases
[AD-A157512] N86-13283

SOLID PROPELLANT COMBUSTION
Pressure-coupled response function of solid propellants including those with negative pressure exponents
N86-12369

SOLID PROPELLANT ROCKET ENGINES
Exhaust plume measurements of 15-pound BATES (Ballistic Test and Evaluation System) motors
[AD-A157249] N86-12250
One-dimensional two-phase flow in combustion chamber of solid propellant rocket motors N86-12370
Application of heat-scan NDT to inspection of adhesion of solid rocket motor propellant to envelope
N86-12461
Naval surface weapons center technology transfer biennial report (Fiscal year 1983/1984)
[AD-A157919] N86-13236

SOLID ROCKET BINDERS
Pressure-coupled response function of solid propellants including those with negative pressure exponents
N86-12369

SOLID ROCKET PROPELLANTS
Investigation of the flame-acoustic wave interaction during axial solid rocket instabilities
[AD-A158559] N86-12362

SOLID STATE
China's first imported peripheral equipment production line N86-12440
Reliability and Engineering of Thin-Film Photovoltaic Modules. Research forum proceedings
[NASA-CR-176217] N86-12759

SOLID STATE LASERS
Compact TEA-CO2 laser with long life developed
N86-12394
Dynamic ADI computations of thermoelastic stresses in crystalline laser media
[DE85-010478] N86-12606

SOLID STATE PHYSICS
Development of beam optics for a 200 keV ion implanter N86-12417

SOLIDIFICATION
Research on the microstructure of rapidly solidified alloys
[AD-A157077] N86-12296

SOLIDS
Numerical studies of the dynamic isentropic loading of solid molecular hydrogen
[DE85-013961] N86-12391

Particle-wall interaction and wall friction in gas-solid flows
[DE85-014964] N86-12567

SOLITARY WAVES
Theory of solitary anticyclones in rotating fluid
N86-12669
Nonlinear interaction between soliton and short waves in ideal fluid N86-12715

SOLUTIONS
Kinetics of evaporation and growth of drops of aqueous solutions of surface active substances at negative temperatures
[AD-A156961] N86-12269

SOLVENTS
Metal dissolution kinetics in organic solvents using rotating ring-disc voltammetry
[DE85-013478] N86-12253

SORPTION
Raman spectroscopy of molecular adsorbates
[DE85-012981] N86-12280

SOUND FIELDS
Room modes and sound absorption: Some practical measurements compared with theoretical predictions
[BBC-RD-1985/11] N86-12486
Numerical estimate of effectiveness of approximate equations for acoustic field near surface of deep sea
N86-12649
Structure of acoustic field in deep sea at shallow depths and at great ranges N86-12664
Prediction of sound fields in acoustical cavities using the boundary element method
[NASA-CR-176295] N86-13057
Adaptive optical filtering techniques
[AD-A157072] N86-13126

SOUND PROPAGATION
Angular distribution of intensity of sound reradiated by ocean surface at small glancing angles N86-12643

SOUND TRANSMISSION
Room modes and sound absorption: Some practical measurements compared with theoretical predictions
[BBC-RD-1985/11] N86-12486
Evaluation of honeycomb highway sound barrier I-280 section 8B, Harrison, New Jersey
[PB85-231157] N86-13063

SOUND WAVES
New passive helicopter detector
[DE85-015160] N86-12595
Angular distribution of intensity of sound reradiated by ocean surface at small glancing angles N86-12643
Transonic noise generation by duct and profile flow
[AD-A157163] N86-13056

SOUNDING
Possibility of sounding Earth by using electromagnetic field of sea current N86-12661

SOUNDING ROCKETS
Temperature and wind data from meteorological rockets N86-12816
Observed winds and temperatures in the Southern Hemisphere N86-12817

SOUTHERN HEMISPHERE
Observed winds and temperatures in the Southern Hemisphere N86-12817

SOYBEANS
Soybean canopy reflectance modeling data sets
[E86-10005] N86-12741

SPACE CHARGE
Self-consistent klystron simulations
[DE85-012678] N86-12529
Collider performance with ideal collisions
[DE85-017011] N86-13073

SPACE ENVIRONMENT SIMULATION
Space shuttle mechanistic studies to characterize atomic oxygen interactions with surfaces N86-13267

SPACE MANUFACTURING
Marketing the use of the space environment for the processing of biological and pharmaceutical materials
[NASA-CR-176334] N86-12243

SPACE PERCEPTION
Hybrid radar waveform design utilizing complementary phase coding and linear frequency stepping for achieving improved slant range resolution in a synthetic aperature radar N86-12470

SPACE PLASMAS
Second Workshop on Spacecraft Glow
[NASA-CP-2391] N86-13239
Investigation of vehicle glow in the far ultraviolet
N86-13249
Spacecraft-induced plasma energization and its role in flow phenomena N86-13250
Shuttle vertical fin flowfield by the direct simulation Monte Carlo method N86-13251
A mechanism for the local concentration enhancement of the shuttle atmosphere N86-13252

SPACE POWER REACTORS
Ground test facility for nuclear testing of space reactor subsystems
[DE85-014634] N86-13099

SPACE SHUTTLE MISSION 51-B
Atmospheric environment for space shuttle (STS-51B) launch
[NASA-TM-86525] N86-12917

SPACE SHUTTLE ORBITERS
The NO-NO2 system at laboratory surfaces
N86-13255
A model for explaining some features of shuttle glow
N86-13256
The production of glow precursors by oxidative erosion of spacecraft surfaces N86-13257
Activated recombinative desorption: A potential component in mechanisms of spacecraft glow
N86-13258
Optical radiation from the interaction of energetic atoms, ions, electrons, and photons with surfaces N86-13259
A ground-based experimental test program to duplicate and study the spacecraft glow phenomenon
N86-13260
Application of an atomic oxygen beam facility to the investigation of shuttle glow chemistry N86-13261
An assessment of the impact of spacecraft glow on the Hubble space telescope. Summary of existing observations and theory N86-13262
Infrared measurements of spacecraft glow planned for Spacelab 2 N86-13263
Planned investigation of infrared emissions associated with the induced spacecraft glow: A shuttle infrared glow experiment (SIRGE) N86-13264
Data requirements for verification of ram glow chemistry N86-13265
A possible glow experiment for the EOM 1-2 mission
N86-13266
Space shuttle mechanistic studies to characterize atomic oxygen interactions with surfaces N86-13267
The shuttle glow: A program to study the ram-induced phenomena N86-13268
Survey of ultraviolet shuttle glow N86-13269

SPACE SHUTTLES
Vehicle glow measurements on the space shuttle
N86-13240

SPACE STATIONS
Department of Housing and Urban Development, and Certain Other Independent Agencies Appropriations for Fiscal Year 1986, part 1
[S-HRG-99-221-PT-1] N86-13233

SPACEBORNE EXPERIMENTS
USSR Space Life Sciences Digest, Issue 2
[NASA-CR-3922(02)] N86-12949
Neutral mass spectrometer measurements in the shuttle bay environment N86-13245

SPACECRAFT CHARGING
The aerospace spacecraft charging document
[AD-A157664] N86-12248

SPACECRAFT ENVIRONMENTS
Neutral mass spectrometer measurements in the shuttle bay environment N86-13245
The UV-VIS optical environment of the shuttle
N86-13247

SPACECRAFT INSTRUMENTS
Advanced Moisture and Temperature Sounder (AMTS) baseline 5 study report
[NASA-CR-176331] N86-12919

SPACECRAFT LAUNCHING
Launch of Kosmos-1653 natural resources research satellite N86-12719
Atmospheric environment for space shuttle (STS-51B) launch
[NASA-TM-86525] N86-12917

SPACECRAFT ORBITS
Second Workshop on Spacecraft Glow
[NASA-CP-2391] N86-13239
Vehicle glow measurements on the space shuttle
N86-13240
Space shuttle ram glow: Implication of NO2 recombination continuum N86-13241
AE and DE mass spectrometer observations relevant to the shuttle glow N86-13242
The Atmosphere Explorer and the shuttle glow
N86-13243
Orbiter glow observations at high spectral resolution
N86-13244
Investigation of vehicle glow in the far ultraviolet
N86-13249
Spacecraft-induced plasma energization and its role in flow phenomena N86-13250
Shuttle vertical fin flowfield by the direct simulation Monte Carlo method N86-13251
A mechanism for the local concentration enhancement of the shuttle atmosphere N86-13252
Infrared emission from desorbed NO2(*) and NO(*)
N86-13254

SPACECRAFT POWER SUPPLIES
Liquid droplet radiator program at the NASA Lewis Research Center
[NASA-TM-87139] N86-12246
SPATIAL DEPENDENCIES
Spatial structure of heat flow instabilities in laser plasmas
[DE85-014407] N86-13162
SPATIAL DISTRIBUTION
Facies-genetic groups of coarse clastic material on world ocean floor N86-12713
Strategies for associating data and location in a geographic information system
[AD-A158118] N86-12746
Spatial and temporal patterns of acid precipitation and their interpretation
[PB85-214377] N86-12809
Temporal and spatial variabilities in shallow water acoustics: Measurements and predictions
[AD-A156718] N86-12942
The NO-NO2 system at laboratory surfaces
N86-13255
SPECIFIC IMPULSE
Characteristic value as an energy output index for explosives N86-12418
SPECIFICATIONS
LabNet Project plan
[DE85-014860] N86-13024
Design and performance of 40 mm, 6.5 T, collared, cold-iron model magnets
[DE85-015277] N86-13054
FASTBUS for the particle accelerator laboratories
[DE85-014352] N86-13122
SPECTRA
Experimental study of equilibrium interval in frequency spectra of wind waves in sea of finite depth N86-12699
Acoustic methods for featuring high-frequency part of spectrum of sea waves N86-12706
SPECTRAL EMISSION
Frequency selection and mode locking of Nd:YAG laser N86-12395
SPECTRAL ENERGY DISTRIBUTION
The NO-NO2 system at laboratory surfaces
N86-13255
SPECTRAL METHODS
Spectral method for obtaining three-dimensional magnetohydrodynamic equilibria
[DE85-015065] N86-13166
SPECTRAL RECONNAISSANCE
Earth resources: A continuing bibliography, issue 46
[NASA-SP-7041(46)] N86-12738
SPECTRAL REFLECTANCE
A possible glow experiment for the EOM 1-2 mission
N86-13266
SPECTRAL SIGNATURES
Soybean canopy reflectance modeling data sets
[E86-10005] N86-12741
SPECTROMETERS
Activated recombinative desorption: A potential component in mechanisms of spacecraft glow
N86-13258
Survey of ultraviolet shuttle glow N86-13269
SPECTROSCOPY
Method to detect ethylene glycol in gaseous mixtures
[AD-A158109] N86-12272
Nanosecond fluorescence spectroscopy
[DE85-012234] N86-12282
Second Workshop on Spacecraft Glow
[NASA-CP-2391] N86-13239
Enhanced N(+) sub 2 in the shuttle environment
N86-13248
A possible glow experiment for the EOM 1-2 mission
N86-13266
Balloon-borne three-meter telescope for far-infrared and submillimeter astronomy
[NASA-CR-176347] N86-13271
SPECTRUM ANALYSIS
P-wave spectra in problem of determining dynamic paramters of earthquake foci. Standardization of initial data and procedures for computing amplitude spectra
N86-12722
Experience in breaking down gravity field into components resulting from density heterogeneities at various depths (using North Atlantic and Mediterranean as examples) N86-12728
SPEECH
Research Reports of the Faculty of Engineering, Tokyo Denki University, no. 32
[ISSN-0389-617-X] N86-12372
A physical method for estimating speech intelligibility in a reverberant sound field N86-12378
SPEECH RECOGNITION
Extraction of feature parameters for spoken word recognition N86-12376
Comparison of continuous speech, discrete speech, and keyboard input to an interactive warfare simulation in various C3 environments
[AD-A156830] N86-12487
SPHERES
Sound scattering by a layered sphere
[AD-A157915] N86-13060
Masking of light scattering information on matrix elements from complex scattering
[AD-A158144] N86-13131
SPHERICAL COORDINATES
Mathematical principle for generating second-order aspherical surface N86-12436
SPHYGMOGRAPHY
Human hemodynamic change under high atmospheric pressure N86-12458
SPIN
Spin-polarization observables in elastic electron scattering from spin-1/2 nuclei
[DE85-016639] N86-13072
SPIN RESONANCE
Isovector resonances in pion charge exchange
[DE85-012746] N86-13106
SPINOR GROUPS
Coupling between spinor field, propagating torsion
N86-12420
SPIRAL GALAXIES
Balloon-borne three-meter telescope for far-infrared and submillimeter astronomy
[NASA-CR-176347] N86-13271
SPONTANEOUS EMISSION
Effect of amplified spontaneous emission on space coherence of XeCl laser N86-12454
SPREADING
Real time bunch length measurements in the SLC linac
[DE85-014362] N86-13169
SPRING (SEASON)
On the interannual variability and on trends of the temperature in the middle atmosphere N86-12827
SPRINGS (WATER)
Flow rates in the East Pacific rise (21 deg N) hot springs, and numerical investigations of two regimes of hydrothermal circulation N86-12939
SQUALLS
Squall and cloud lines as structural components of an Arabian Sea convective cloud cluster
[AD-A157973] N86-12925
SQUARE WAVES
Digital phase meter using CMOS-LED introduced
N86-12442
STABILITY
Microemulsion-type fire-resistant diesel fuel
[AD-A157125] N86-12359
Frequency selection and mode locking of Nd:YAG laser N86-12395
Heat Exchanger Vibration Analysis (HXVA) for prediction of tube bundle instabilities
[DE85-017144] N86-12568
Fluid physics research
[DE85-014644] N86-12575
Correction of compressor critical speed condition through fluid-film bearing optimization
[DE85-005507] N86-12617
Light-induced effects-impacts to module performance measurements and reliability testing: An overview
N86-12761
Accelerated stress testing of thin film solar cells: Development of test methods and preliminary results
N86-12764
Thin film module development N86-12768
Thin film module electrical configuration versus electrical performance N86-12770
Outdoor performance testing of thin-film devices
N86-12771
STABILIZATION
CO2 laser stabilization and switching
[AD-D011795] N86-12598
STABLE OSCILLATIONS
Biological effects of acoustic cavitation
[AD-A157513] N86-13059
STAINLESS STEELS
Effect of grain boundary structure on sensitization and corrosion of stainless steel
[AD-A157133] N86-12297
Review of effects of long-term aging on the mechanical properties and microstructures of types 304 and 316 stainless steel
[DE85-016472] N86-12304
STANDARD DEVIATION
Atmospheric tides between 80 km and 120 km
N86-12833
STANDARDIZATION
Navy should join the Air Force and Army program to develop an advanced integrated avionics system
[PB85-222503] N86-12224
Minutes of Workshop on Composite Materials Test Methods
[AD-A157903] N86-12262
P-wave spectra in problem of determining dynamic paramters of earthquake foci. Standardization of initial data and procedures for computing amplitude spectra
N86-12722
STANDARDS
Spectrum resource assessment of the 1605-2000 kHz band
[PB85-225076] N86-12501
Prompt neutron fission spectrum mean energies for the fissile nuclides and (252)Cf
[DE85-012181] N86-13117
Improvement of manufacturing techniques and quality of optical scratch standards for fire control systems
[AD-A157963] N86-13130
European Science Notes. Volume 39, number 8
[AD-A157146] N86-13237
STANDING WAVES
Room modes and sound absorption: Some practical measurements compared with theoretical predictions
[BBC-RD-1985/11] N86-12486
STARK EFFECT
The inhomogeneous light shift in alkali atoms
[AD-A157498] N86-13067
STATIC PRESSURE
Compressor research facility F100 high pressure compressor inlet total pressure and swirl profile simulation
[AD-A157108] N86-12229
STATIONS
Internetting and packet satellite program
[AD-A157124] N86-12469
STATISTICAL ANALYSIS
Study and investigation to update the nonelectronic reliability notebook. Revision A
[AD-A157242] N86-12619
Comparison of single-parameter statistical model with results of round-the-clock measurement of light-scattering matrices N86-12689
Statistical methods for environmental pollution studies
[DE85-005298] N86-12799
A proposed international tropical reference atmosphere up to 80 km N86-12828
Interim reference ozone models for the middle atmosphere N86-12829
Mean winds of the upper middle atmosphere (60-110 km): A global distribution from radar systems (MF, meteor, VHF) N86-12831
Statistical evaluation of forecasts over the low-latitudes
[AD-A157926] N86-12923
Scatter Diagram and Histogram Program - SCATR
[PB85-213346] N86-12935
Diagnosing cognitive errors: Statistical pattern classification and recognition approach
[AD-A158108] N86-12972
Managing data analysis through save-states
[DE85-012456] N86-12999
Transforming censored samples and testing fit
[AD-A157957] N86-13048
Statistical sampling of aircraft operations at non-towered airports
[AD-A157095] N86-13051
STATISTICAL DISTRIBUTIONS
Transforming censored samples and testing fit
[AD-A157957] N86-13048
STATISTICAL MECHANICS
A new method for global optimization based on stochastic differential equations
[AD-A157546] N86-13029
NASA LeRC/Akron University Graduate Cooperative Fellowship Program and Graduate Student Researchers Program
[NASA-CR-174826] N86-13219
STATISTICAL TESTS
New representations of the non-central chi-square density and cumulative
[AD-A157227] N86-13046
STATISTICAL WEATHER FORECASTING
Use of method of canonical correlations for analysis of climatic series N86-12634
STEADY STATE
Model describing the steady-state pyrolysis of bubble-forming polymers in response to an incident heat flux
[PB85-225225] N86-12291
STEAM
Steam-injection pressing of isocyanate-bonded aspen flakeboards, latitudes and limitations
[AD-A157833] N86-12389
Superheated steam's density compensation for flow measurement N86-12426

Study of two-phase concurrent flow of steam and water in an unconsolidated porous medium
[DE85-014534] N86-12578

STEAM FLOW
China report: Science and technology
[JPRS-CST-85-021] N86-12421
Superheated steam's density compensation for flow measurement N86-12426

STEELS
Titanium-nitrogen ion beam injection studied N86-12427
Iron and steelmaking with plasma N86-12467
Surface fatigue life and failure characteristics of EX-53, CBS 1000M, and AISI 9310 gear materials
[NASA-TP-2513] N86-12609
Multifrequency eddy-current inspection of seam weld in steel sheath
[DE85-013533] N86-12626

STELLAR CORONAS
NeII observations of the galactic center: The velocity field and mass distribution N86-13270

STELLAR ENVELOPES
Physico-chemical conditions in circumstellar shells of evolved oxygen-rich M stars N86-13275
Diffraction-limited ten micron imaging of circumstellar dust with a detector array N86-13277

STELLAR MASS ACCRETION
Balloon-borne three-meter telescope for far-infrared and submillimeter astronomy
[NASA-CR-176347] N86-13271

STELLAR WINDS
Combined ultraviolet studies of astronomical source
[NASA-CR-176165] N86-13274

STEP FUNCTIONS
Control of step size and order in extrapolation codes
[DE85-013261] N86-13010

STEP RECOVERY DIODES
The step structure effect of dc Josephson current within one flux quantum period phi sub zero (2) N86-12412

STEREOPHOTOGRAPHY
Rapid estimation of frequency response functions by close-range photogrammetry
[NASA-TP-2471] N86-12579

STIRLING CYCLE
Liquid droplet radiator program at the NASA Lewis Research Center
[NASA-TM-87139] N86-12246
Preliminary design of linear alternator dynamometer for free piston Stirling engines
[DE85-015078] N86-12614
Comparative analysis of a Stirling heat pump with second- and third-order computer models
[DE85-013536] N86-12615
Overview of free-piston Stirling technology at the NASA Lewis Research Center
[NASA-TM-87156] N86-13236

STOCHASTIC PROCESSES
Adaptive Kalman filtering with control input estimation N86-12503
DAPHNE: The design of a parallel multiprocessor data acquisition system
[DE85-013875] N86-12984
A new method for global optimization based on stochastic differential equations
[AD-A157546] N86-13029
Systems analysis approach to probabilistic modeling of fault trees
[DE85-007705] N86-13050
Nearly ideal lens optimization procedure
[DE85-014116] N86-13134
Transport near the onset of stochasticity
[DE85-014765] N86-13218

STORAGE BATTERIES
High rate Li/SOC1(2) cells. 1. Effect of design variables in uncatalyzed cells
[AD-A157203] N86-12776
Maintenance of photovoltaic power systems, revision 1
[AD-A157838] N86-12777

STORAGE RINGS (PARTICLE ACCELERATORS)
Use of an elliptical aperture to control saturation in closely-coupled, cold iron, superconducting dipole magnets
[DE85-012259] N86-13053
Collider performance with ideal collisions
[DE85-017011] N86-13073
Theories of statistical equilibrium in electron-positron colliding-beam storage rings
[DE85-012303] N86-13080
Fully stripped heavy ion yield vs energy for Xe and Au ions
[DE85-013281] N86-13155
Magnet power supply control of the NSLS VUV and X-ray storage rings transfer lines
[DE85-014213] N86-13168
WNR/PSR facility: Neutron physics capabilities from sub-thermal to 800 MeV
[DE85-014072] N86-13173

STORMS (METEOROLOGY)
Meteorological center's forecasts aid Venus probe tracking N86-12631

STRAIN ENERGY METHODS
Mixed-mode cyclic debonding of adhesively bonded composite joints
[NASA-CR-177991] N86-12255
Strain energy density criteria for dynamic fracture and dynamic crack branching
[AD-A157914] N86-12624

STRAIN GAGES
Single mode phase locking fiberoptic sensor developed N86-12415

STRAIN RATE
An update of the total-strain version of SRP
[NASA-TP-2499] N86-12295
Theory for the Portevin-LeChatelier effect
[DE85-004030] N86-12627

STRATIFICATION
Viscous nonlinear circulation in axisymmetric baroclinic eddy N86-12712

STRATIFIED FLOW
Analysis of stratified flow mixing
[DE85-006840] N86-12576
Diffraction of internal waves described by equation of slightly stratified fluid on half-plane N86-12660
New methods for interpreting seismic waves in stratified media N86-12682

STRATIGRAPHY
Stratigraphy of sediments in central and eastern Mediterranean N86-12663

STRATOSPHERE
The dynamic stability of the stratosphere and mesosphere N86-12811
The MST radar technique N86-12836

STREAK CAMERAS
Improved approach to characterizing and presenting streak camera performance
[DE85-015188] N86-12587

STREAK PHOTOGRAPHY
Optical measurements of shock-induced chemical reactions in mixed aluminum-nickel powder
[DE85-014705] N86-12308
Recent developments in microshell-tipped optical fibers as high-pressure shock detectors
[DE85-015750] N86-12594

STREAMLINING
The status of two-dimensional testing at high transonic speeds in the University of Southampton transonic self-streamlining wind tunnel
[NASA-CR-3919] N86-12203

STREAMS
Water resources data for Florida, water year 1983. Volume 3A: Southwest Florida surface water
[PB85-216000] N86-12754

STRESS ANALYSIS
Research Reports of the Faculty of Engineering, Tokyo Denki University, no. 32
[ISSN-0389-617-X] N86-12372
A computer analysis of the distribution of principal stresses using photoelastic pattern N86-12375
More on compliance of the three-point bend specimen
[AD-A156665] N86-12623
Channeling analysis of strain in superlattices
[DE85-014437] N86-13197

STRESS CONCENTRATION
Influence of load interactions on crack growth as related to state of stress and crack closure
[NASA-TM-87117] N86-12292
Statistical treatment of aramid/epoxy stress-rupture data
[AD-A157238] N86-12315
New criterion of combined-mode brittle fracture described N86-12400

STRESS MEASUREMENT
Accelerated stress testing of thin film solar cells: Development of test methods and preliminary results N86-12764
Channeling analysis of strain in superlattices
[DE85-014437] N86-13197

STRESS PROPAGATION
A computer analysis of the distribution of principal stresses using photoelastic pattern N86-12375

STRESS-STRAIN RELATIONSHIPS
New criterion of combined-mode brittle fracture described N86-12400
Theory for the Portevin-LeChatelier effect
[DE85-004030] N86-12627

STRESSES
Dynamic ADI computations of thermoelastic stresses in crystalline laser media
[DE85-010478] N86-12606

STRIATION
A simulation of high latitude F-layer instabilities in the presence of magnetosphere-ionosphere coupling
[NASA-CR-176296] N86-12897

STRONGLY COUPLED PLASMAS
A simulation of high latitude F-layer instabilities in the presence of magnetosphere-ionosphere coupling
[NASA-CR-176296] N86-12897

STRONTIUM FLUORIDES
Study of possible solarization - related impurities in CaF2 and other fluorides
[DE85-014100] N86-13135

STRUCTURAL ANALYSIS
DAA modal analysis for parametric investigations of fluid-structure interaction in underwater shock, revision 1
[DE85-012935] N86-12569
Modeling and control of flexible structures
[AD-A157959] N86-12625
NASA LeRC/Akron University Graduate Cooperative Fellowship Program and Graduate Student Researchers Program
[NASA-CR-174826] N86-13219

STRUCTURAL BASINS
Gravity, geoid and the oceanic lithosphere N86-12860
Studies of the marine crustal magnetization at intermediate wavelengths N86-12862
Properties of the lithosphere and asthenosphere deduced from geoid observations N86-12867

STRUCTURAL DESIGN CRITERIA
A survey of aeronautical structural research in Australia
[AD-A157211] N86-12199
Earthquake-response simulation on horizontally large-scale buildings based on the method of reduction concerning their restoring spring matrix. Derivation of general form of spring matrix and comparison of applied response results on an actual building with measured values N86-12374
Second reference calculation for the WIPP
[DE85-013180] N86-13005
Materials studies for magnetic fusion energy applications at low temperatures - 8
[PB85-236362] N86-13183
NASA LeRC/Akron University Graduate Cooperative Fellowship Program and Graduate Student Researchers Program
[NASA-CR-174826] N86-13219

STRUCTURAL ENGINEERING
A survey of aeronautical structural research in Australia
[AD-A157211] N86-12199
CBR (California Bearing Ratio) design of flexible airfield pavements with case study
[AD-A158101] N86-12242
A user's guide to the Coastal Engineering Research Center's (CERC'S) field research facility
[AD-A157966] N86-12946

STRUCTURAL MEMBERS
Electrochemical machining of the outer profile of the B83 Lug
[DE85-014934] N86-12616
Encapsulant selection and durability testing experience N86-12774

STRUCTURAL PROPERTIES (GEOLOGY)
Dynamics and structure of the Alpine Fold Belt N86-12854

STRUCTURAL STABILITY
Modeling and control of flexible structures
[AD-A157959] N86-12625

STUDENTS
Energy expenditure and activity patterns of cadets at the United States Military Academy, West Point, New York
[AD-A157857] N86-12960
Micro-PROUST
[AD-A157505] N86-12991

SUBARCTIC REGIONS
Carbon dioxide in arctic and subarctic regions
[DE85-014054] N86-12901

SUBDUCTION (GEOLOGY)
Subduction dynamics: Constraints from gravity field observations N86-12868

SUBMARINES
DAA modal analysis for parametric investigations of fluid-structure interaction in underwater shock, revision 1
[DE85-012935] N86-12569

SUBMILLIMETER WAVES
Submillimeter wave propagation in tokamak plasmas
[DE85-007747] N86-13154
Balloon-borne three-meter telescope for far-infrared and submillimeter astronomy
[NASA-CR-176347] N86-13271

SUBROUTINES
General plot subroutine package for the Hewlett Packard 5451C Fourier analyzer
[AD-A157127] N86-12989
SUBSONIC FLOW
User's guide to STIPPAN: A panel method program for slotted tunnel interference prediction
[NASA-CR-178003] N86-12237
Code of finite element analysis for three-dimensional flow in turbomachines N86-12396
SUBSTRATES
Method and apparatus for conducting variable thickness vapor deposition
[DE85-011653] N86-12306
Experiments with domestic IC substrates N86-12433
Characteristic impedance of a wide slot line on low permittivity substrates N86-12480
A new integrated slot element feed array for multi-beam systems N86-12483
SULFATES
Spatial and temporal patterns of acid precipitation and their interpretation
[PB85-214377] N86-12809
SUMMARIES
Annual data summary for 1981 CERC (Coastal Engineering Research Center) field research facility
[AD-A158143] N86-12926
Conference summary: Antinucleon- and nucleon-nucleus interactions
[DE85-013905] N86-13114
SUPERCOMPUTERS
Generic software for emulating multiprocessor architectures
[AD-A157662] N86-12979
Role of supercomputers in magnetic fusion and energy research programs
[DE85-013200] N86-13023
SUPERCONDUCTING MAGNETS
The 140 GHz gyrotron development program
[DE85-011923] N86-12534
Multifrequency eddy-current inspection of seam weld in steel sheath
[DE85-013533] N86-12626
Use of an elliptical aperture to control saturation in closely-coupled, cold iron, superconducting dipole magnets
[DE85-012259] N86-13053
Design and performance of 40 mm, 6.5 T, collared, cold-iron model magnets
[DE85-015277] N86-13054
Tracking studies on the effects of random multipoles in the 6.5 T lattice of the SSC Reference Designs Study
[DE85-013286] N86-13156
Multivariable current control for electrically and magnetically coupled superconducting magnets
[DE85-012941] N86-13163
Materials studies for magnetic fusion energy applications at low temperatures - 8
[PB85-236362] N86-13183
SUPERCONDUCTIVITY
Ultrasonic attenuation in clean anisotropic superconductors
[DE85-012178] N86-12621
Superconductivity in the W-Tc and W2C-Tc systems
[DE85-012711] N86-13204
Josephson effect in the unusual superconductors Lu2Fe3Si5, LiTi2O4 and UBe13
[DE85-015260] N86-13211
SUPERCONDUCTORS
Superconducting wire manufactured N86-12437
Design of high power superconducting switches
N86-12505
Josephson effect in the unusual superconductors Lu2Fe3Si5, LiTi2O4 and UBe13
[DE85-015260] N86-13211
SUPERCRITICAL AIRFOILS
Effect of surface waviness on a supercritical laminar-flow-control airfoil
[NASA-TM-85705] N86-12206
SUPERHEATING
Superheated steam's density compensation for flow measurement N86-12426
SUPERLATTICES
Channeling analysis of strain in superlattices
[DE85-014437] N86-13197
SUPERNOVA REMNANTS
Combined ultraviolet studies of astronomical source
[NASA-CR-176165] N86-13274
SUPERSONIC AIRCRAFT
Introduction to cryogenic wind tunnels
[NASA-CR-177966] N86-12238
Japanese report on China's F-8 fighter N86-12405
SUPERSONIC NOZZLES
Application of an atomic oxygen beam facility to the investigation of shuttle glow chemistry N86-13261
SUPERSONIC TURBINES
Numerical computation of full three-dimensional flow in transonic turbines N86-12397
SURFACE ACOUSTIC WAVE DEVICES
Wideband SAW (Surface Acoustic Wave) channellizer using slanted array input transducer
[AD-D011857] N86-12517
SURFACE DEFECTS
Glass breaking strength: The role of surface flaws and treatments N86-12773
SURFACE LAYERS
Fracture surface analysis in composite and titanium bonding
[NASA-CR-176309] N86-12257
Interfacial stability in a two-layer benard problem
[AD-A158138] N86-12558
Sound scattering by a layered sphere
[AD-A157915] N86-13060
SURFACE NAVIGATION
China report: Science and technology
[JPRS-CST-85-021] N86-12421
New dual Z80 navigaiton computer described
N86-12425
SURFACE PROPERTIES
Ellipsometric surface analysis of wear tracks produced by different lubricants
[NASA-TM-87142] N86-12293
Mathematical principle for generating second-order aspherical surface N86-12436
Mechanical interactions of rough surfaces
[DE85-015011] N86-12613
SURFACE REACTIONS
Kinetics of evaporation and growth of drops of aqueous solutions of surface active substances at negative temperatures
[AD-A156961] N86-12269
Effects of surface interactions and mechanical properties of plastic bonded explosives on explosive sensitivity. Part 2: Model formulation
[AD-A157900] N86-12361
Surface fatigue life and failure characteristics of EX-53, CBS 1000M, and AISI 9310 gear materials
[NASA-TP-2513] N86-12609
The NO-NO2 system at laboratory surfaces
N86-13255
SURFACE ROUGHNESS
Fracture surface analysis in composite and titanium bonding
[NASA-CR-176309] N86-12257
Underwater photography for quantitative description of bottom roughness
[AD-A156753] N86-12943
SURFACE STABILITY
Interfacial stability in a two-layer benard problem
[AD-A158138] N86-12558
SURFACE TEMPERATURE
Materials and process characterization to determine the effect of high intensity infrared laser radiation on a composite material
[AD-A157094] N86-12260
SURFACE VEHICLES
Optimization of the locomotion of a legged vehicle with respect to maneuverability N86-12371
SURFACE WATER
Acidification trends in surface waters of the Southern Appalachians
[DE85-901746] N86-12801
SURFACE WAVES
Wideband SAW (Surface Acoustic Wave) channellizer using slanted array input transducer
[AD-D011857] N86-12517
Modulations of driven nonlinear surface waves on water and liquid Helium-4
[AD-A157958] N86-12556
Experimental study of equilibrium interval in frequency spectra of wind waves in sea of finite depth N86-12699
European Science Notes. Volume 39, number 8
[AD-A157146] N86-13237
SURFACTANTS
Microemulsion-type fire-resistant diesel fuel
[AD-A157125] N86-12359
Influence of a surfactant additive on absorption heat pump performance
[DE85-013995] N86-12574
SURGEONS
Suture needle holder
[AD-D011764] N86-12958
SURVEYS
Cartography, national land management related
N86-12401
Benefits of surveying, cartography described
N86-12402
High rate *Li/SOC1(2) cells.* 1. Effect of design variables in uncatalyzed cells
[AD-A157203] N86-12776
SURVIVAL EQUIPMENT
Low temperature inflator apparatus
[AD-D011810] N86-12974
SWELLING
Sea floor swells and mantle plumes N86-12866
SWITCHES
Design of high power superconducting switches
N86-12505
Parallel, staged opening switch power conditioning techniques for flux compression generator applications
[DE85-012761] N86-12527
UV sustained glow discharge opening switch
[AD-A158411] N86-13132
SWITCHING CIRCUITS
Internetting and packet satellite program
[AD-A157124] N86-12480
Foil fuses as opening switches for slow discharge circuits
[DE85-014124] N86-12519
Hybrid 0-D,1-D, and 2-D model of helical explosive-driven magnetic flux compression generator
[DE85-013772] N86-12524
EE technical review
[DE85-015313] N86-12540
CO2 laser stabilization and switching
[AD-D011795] N86-12598
SYMMETRY
Elementary waves and Riemann solutions: Their theory and their role in science
[DE85-014018] N86-13045
Alfven continuum with toroidicity
[DE85-015821] N86-13217
SYNCHRONOUS SATELLITES
Global view of the upper level outflow patterns associated with tropical cyclone intensity changes during FGGE
[NASA-CR-174407] N86-12908
Meteorological Satellite Center Technical Note No. 11, 1985
[MSC-TN-11] N86-12909
Relaying of the stretched VISSR data by GMS spacecraft N86-12913
The modification of the operational program for GMS-3 N86-12914
SYNCHROTRON RADIATION
Adsorption/desorption properties of vacuum materials for the 6 GeV synchrotron
[DE85-010276] N86-12252
Disruption and luminosity of flat beams
[DE85-015137] N86-13071
Fully stripped heavy ion yield vs energy for Xe and Au ions
[DE85-013281] N86-13155
Energy dispersive spectroscopy using synchrotron radiation: Intensity considerations
[DE85-017530] N86-13200
X-rays from the radio halo of Virgo A = M87
[NASA-CR-176303] N86-13285
SYNCHROTRONS
Adsorption/desorption properties of vacuum materials for the 6 GeV synchrotron
[DE85-010276] N86-12252
Mathematical model of the dynamic response of thermo-regulating in 200 MeV linear accelerator
N86-12407
Tevatron global radius and Os system
[DE85-017442] N86-13101
AGS improvement program
[DE85-013293] N86-13182
SYNOPTIC METEOROLOGY
Occurrence of linearly ranged Cb-clouds associated with migrating band-shaped cirriform-clouds: A case study
N86-12910
SYNTAX
A methodology for syntax-analysis using PROLOG
N86-12388
SYNTHESIS (CHEMISTRY)
Oxidation of heterocyclic nitrogen yields to nitroheterocycles
[DE85-012757] N86-12284
Limits of thermochemical and photochemical syntheses of gaseous fuels: A finite-time thermodynamic analysis
N86-12367
Usages of organic membranes in electrolytic industry described N86-12453
SYNTHETIC APERTURE RADAR
Hybrid radar waveform design utilizing complementary phase coding and linear frequency stepping for achieving improved slant range resolution in a synthetic aperature radar N86-12470
Evaluation of space SAR as a land-cover classification
[E86-10004] N86-12740
Wave-current and wave-topographic interactions using SEASAT synthetic aperture radar observations and analytical ocean models N86-12938

SYNTHETIC ARRAYS
A 94 GHz imaging array using slot line radiators
[NASA-CR-176348] N86-12484
SYSTEM EFFECTIVENESS
Stochastic beam cooling amplifier system front end components performance characteristics
[DE85-013925] N86-13079
SYSTEMS ANALYSIS
Advanced Thermionic Technology Program: Summary Report. Volume 1
[DE85-009358] N86-12779
Systems analysis approach to probabilistic modeling of fault trees
[DE85-007705] N86-13050
SYSTEMS ENGINEERING
Parachute recovery systems design manual, chapters 1 through 4 offprint
[AD-A157639] N86-12210
Preventative maintenance for control systems
[DE85-012029] N86-12525
A meta system for generating software engineering environments
[AD-A158102] N86-12996
SYSTEMS INTEGRATION
Decentralized control of scheduling in distributed systems
[AD-A157656] N86-13222
SYSTEMS MANAGEMENT
Managing personal desktop computing at Argonne National Laboratory
[DE85-014976] N86-12983

T

TAIL ASSEMBLIES
Simulation of the enhanced traffic alert and collision avoidance system (TCAS 2)
[NASA-CR-176328] N86-12216
Effect of measured material properties on the finite element analysis of an OH-58 composite tail boom
[NASA-TM-86430] N86-12259
TANKS (COMBAT VEHICLES)
Microemulsion-type fire-resistant diesel fuel
[AD-A157125] N86-12359
TANKS (CONTAINERS)
Lightweight cryogenic tank with positive expulsion
[AD-D011856] N86-12612
TANTALUM
Superconducting wire manufactured N86-12437
TANTALUM COMPOUNDS
Hillock-free conductor system for use in multilevel interconnects
[DE85-012595] N86-12533
TAPERING
Additional results on the radiating properties of LTSAs and CWSAs N86-12479
Analysis of the tem mode linearly tapered slot antenna N86-12481
TASKS
An analysis of the application of AI to the development of intelligent aids for flight crew tasks
[NASA-CR-3944] N86-12212
TEA LASERS
Compact TEA-CO2 laser with long life developed
N86-12394
TECHNOLOGY ASSESSMENT
Status, development of power ultrasonics in China
N86-12403
China report: Science and technology
[JPRS-CST-85-018] N86-12413
State-of-the-art of optics in China reviewed
N86-12414
China report: Science and technology
[JPRS-CST-85-034] N86-12430
Optical disk technology assessment
[AD-A157909] N86-12582
Aeronautical technology 2000: A projection of advanced vehicle concepts
[NASA-CR-176322] N86-13235
TECHNOLOGY TRANSFER
Digital voltmeter technology acquisition N86-12449
China report: Science and technology
[JPRS-CST-85-032] N86-12462
Science, technology and the industrialization of laser-driven processes
[DE85-014856] N86-12605
Diagnosing the causes of ground-water contamination using a mathematical model: Report on Technology Transfer Workshop
[PB85-217008] N86-12808
Naval surface weapons center technology transfer biennial report (Fiscal year 1983/1984)
[AD-A157919] N86-13238
TECHNOLOGY UTILIZATION
LANDSAT-4 TM image data quality analysis for energy-related applications
[E86-10006] N86-12742
TECTONICS
Magnetic provinces and tectonics in Pacific Ocean
N86-12662
Folded structures in central Indian Ocean trench
N86-12704
Tectonic structure of Shirshov Ridge (Bering Sea)
N86-12710
Geopotential Research Mission (GRM)
[NASA-CP-2390] N86-12852
Impact of GRM: New evidence from the Soviet Union
N86-12853
Why do we need detailed gravity over continents: Some Australian examples N86-12855
A major crustal feature in the southeastern United States inferred from the MAGSAT equivalent source anomaly field N86-12856
Mantle convection and the large scale structures of the Earth's gravitational field N86-12874
Constraints on the rheological structure of the mantle
N86-12875
TELECOMMUNICATION
Bandwidth efficient frequency-shift keyed communication systems N86-12472
An evolving digital telecommunications industry and its impact on the operational environment of the Nationwide Emergency Telecommunication System (NETS)
[AD-A156831] N86-12488
Internetting and packet satellite program
[AD-A157124] N86-12489
Results of field and laboratory studies of jam-resistant and voice-private radios
[DE85-014841] N86-12500
Spectrum resource assessment of the 1605-2000 kHz band
[PB85-225076] N86-12501
China report: Science and technology
[JPRS-CST-85-019] N86-12965
Power and signal transmission for mobile teleoperated systems
[DE85-013994] N86-12975
Future directions in mobile teleoperation
[DE85-014308] N86-12976
Design and implementation of the computer systems design environment network
[AD-A156832] N86-13022
TELEOPERATORS
Future directions in mobile teleoperation
[DE85-014308] N86-12976
Attempt to develop an intelligent lens design program
[DE85-014122] N86-13017
TELEVISION SYSTEMS
Elie: Saint Eustache fibre Optic Field Trial project evaluation report, volume 4
[AD-A157144] N86-12490
TELLURIC CURRENTS
Features of electrical measurements in sea as medium with field of extraneous forces N86-12700
TEMPER (METALLURGY)
Glass breaking strength: The role of surface flaws and treatments N86-12773
TEMPERATURE DEPENDENCE
Kinetics of evaporation and growth of drops of aqueous solutions of surface active substances at negative temperatures
[AD-A156961] N86-12269
Thermodynamics of multi-polar molecules: The perturbed-anisotropic-chain theory
[DE85-013148] N86-12274
Oxidation and gum formation in diesel fuels
[AD-A157410] N86-12360
Dissociative volume recombination coefficient measurements in a subroom temperature neon plasma afterglow N86-12373
Study of high speed shearing of thermoplastic polymer sheets with a new rotary shearing machine N86-12382
Performance and temperature dependencies of proton irradiated n/p GaAs and n/p silicon cells
[NASA-TM-87136] N86-12509
REFRIG-12: A graphics-augmented interactive program for designing vapor-compression refrigeration/heat pump cycles
[DE85-014205] N86-12572
Measurement of tritium permeation through resistant materials near room temperature
[DE85-012942] N86-12592
X-ray diffraction cell for Debye-Scherrer and Guinier (Huber) cameras at pressure and temperature
[DE85-014815] N86-12593
Ultrasonic attenuation in clean anisotropic superconductors
[DE85-012178] N86-12621
High nuclear temperatures by antimatter-matter annihilation
[DE85-014113] N86-13090
Temperature and concentration dependence of hydrogen site occupancy in several rare-earth dihydrides
[DE85-015739] N86-13199
Temperature dependence of the magnetic excitations in Gd
[DE85-016303] N86-13213
Mossbauer effect and neutron diffraction study of the anomalous lattice behavior of U6Fe
[DE85-014912] N86-13210
Second order elastic contants of Pd, PdH(0.7) and PdD(0.7) between 1.7 and 50 K
[DE85-014316] N86-13212
TEMPERATURE DISTRIBUTION
Global modeling of optical characteristics of atmospheric aerosol N86-12685
Annual and semiannual cycles based on the middle atmosphere reference model N86-12826
On the interannual variability and on trends of the temperature in the middle atmosphere N86-12827
A proposed international tropical reference atmosphere up to 80 km N86-12828
Temperature structure of the 80 km to 120 km region
N86-12830
Atmospheric Tides Middle Atmosphere Program (ATMAP): Report of the November/December 1981, and May 1982, observational campaigns N86-12839
TEMPERATURE EFFECTS
Fixation of high-level wastes in glasses
[DE85-013276] N86-12325
Empirical analysis of direct and inverse relationships between macroscale characteristics of atmospheric processes in northern hemisphere and thermal state of north Atlantic N86-12635
Recent changes in climate and world water balance
N86-12638
Modeling of seasonal evolution of carbon cycle in ocean-atmosphere system N86-12641
The production of glow precursors by oxidative erosion of spacecraft surfaces N86-13257
TEMPERATURE GRADIENTS
New corresponding states theory using the second virial coefficient as the temperature variable
[PB85-219624] N86-12289
Spatial structure of heat flow instabilities in laser plasmas
[DE85-014407] N86-13182
TEMPERATURE MEASUREMENT
Temperature and wind data from meteorological rockets N86-12916
Advanced Moisture and Temperature Sounder (AMTS) baseline 5 study report
[NASA-CR-176331] N86-12919
TEMPERATURE PROBES
The shuttle glow: A program to study the ram-induced phenomena N86-13268
TEMPERATURE PROFILES
Contribution to the CIRA model from ground-based lidar N86-12835
Plasma and magnetospheric research
[NASA-CR-176326] N86-13138
TEMPERATURE SENSORS
Improved temperature detection system for use on film cooled turbine airfoils
[AD-D011762] N86-12229
TEMPORAL DISTRIBUTION
Temporal and spatial variabilities in shallow water acoustics: Measurements and predictions
[AD-A156718] N86-12942
TENDONS
Influence of bonded reinforcement in post-tensioned prestressed concrete T-beams with unbonded tendons
N86-12622
TENSORS
Quasigeostrophic model of circulation in Antarctic Ocean with parametrization of synoptic eddies N86-12702
TERBIUM ISOTOPES
Partition of cross sections in asymmetric nucleus-nucleus reactions and the origin of fast alpha particles
[DE85-014989] N86-13089
TERMINAL BALLISTICS
Variational principle for penetrator dynamics using bilinear functional and adjoint formulation
[AD-A157964] N86-13031
TERNARY ALLOYS
Theoretical studies of deep impurity levels in ternary semiconductor alloys
[AD-A157929] N86-13180
TERRAIN
Optimization of the locomotion of a legged vehicle with respect to maneuverability N86-12371

TERRAIN ANALYSIS
The numerical simulation of geographic storms N86-12907
TERRESTRIAL RADIATION
A statistical study of solar Type-3 bursts and auroral kilometric radiation onsets
[AD-A158408] N86-13284
TEST FACILITIES
Development of acoustic agglomerator. Test plan for high temperature high pressure acoustic agglomerator
[DE85-017221] N86-13081
Ground test facility for nuclear testing of space reactor subsystems
[DE85-014634] N86-13099
TEXAS
Evaluating the ground-water resources of the high plains of Texas, volume 2
[PB85-191609] N86-12752
THEMATIC MAPPING
LANDSAT-4 TM image data quality analysis for energy-related applications
[E86-10006] N86-12742
THEOREMS
Two results on dense imbeddings
[AD-A158132] N86-13033
THERMAL BATTERIES
Characterization of sheet calcium for Ca/CaCr04 thermal batteries
[DE85-013231] N86-12785
THERMAL CONDUCTIVITY
Finned tube contact conductance: Characterizing the integrity of the mechanical bond
[DE85-013747] N86-12564
Absorption fluids data survey
[DE85-005279] N86-12792
MAGNUM-2D computer code: User's guide
[DE85-013315] N86-13001
Plane-wave theory of electrical transport in disordered systems
[DE85-015353] N86-13167
THERMAL DIFFUSIVITY
Turbulence in the altitude region 80-120 km N86-12834
THERMAL EMISSION
Influence of short gravity waves on thermal radio emission of water surface N86-12644
Ocean albedo for atmospheric thermal emission N86-12707
THERMAL FATIGUE
Review of effects of long-term aging on the mechanical properties and microstructures of types 304 and 316 stainless steel
[DE85-016472] N86-12304
THERMAL MAPPING
Water Information Bulletin No. 30, Part 13: Geothermal investigations in Idaho. Preliminary geologic reconnaissance of the geothermal occurrences of the Wood River drainage area
[DE85-016972] N86-12747
THERMAL PLASMAS
Laser scattering in plasma examined N86-12431
THERMAL RADIATION
LANDSAT-4 TM image data quality analysis for energy-related applications
[E86-10006] N86-12742
THERMAL RESISTANCE
The 371 deg C mechanical properties of graphite/polyimide composites
[NASA-TM-87122] N86-12256
THERMAL STRESSES
Analysis of stratified flow mixing
[DE85-006840] N86-12576
THERMIONIC CONVERTERS
Advanced Thermionic Technology Program: Summary Report. Volume 1
[DE85-009358] N86-12779
THERMOCHEMISTRY
Limits of thermochemical and photochemical syntheses of gaseous fuels: A finite-time thermodynamic analysis N86-12367
Guidelines for a thermochemical kinetics computer program
[DE85-015671] N86-12898
THERMOCLINES
Fine structure of density relation in main oceanic thermocline N86-12711
THERMODYNAMIC PROPERTIES
Thermodynamics of multi-polar molecules: The perturbed-anisotropic-chain theory
[DE85-013148] N86-12274
Limits of thermochemical and photochemical syntheses of gaseous fuels: A finite-time thermodynamic analysis N86-12367
Use of method of canonical correlations for analysis of climatic series N86-12834
Transient thermal modeling of the nonscanning ERBE detector
[NASA-CR-172240] N86-12743
Atmospheric environment for space shuttle (STS-51B) launch
[NASA-TM-86525] N86-12917
THERMODYNAMICS
Comparison among various thermodynamic parameters for the prediction of convective activity
[PB85-208217] N86-12932
THERMOELASTICITY
Dynamic ADI computations of thermoelastic stresses in crystalline laser media
[DE85-010478] N86-12606
THERMOMAGNETIC COOLING
Thermal cooling of the oceanic lithosphere from geoid height data N86-12861
Lithospheric structure in the Pacific geoid N86-12863
THERMOPLASTIC FILMS
Research Reports of the Faculty of Engineering, Tokyo Denki University, no. 32
[ISSN-0389-617-X] N86-12372
Study of high speed shearing of thermoplastic polymer sheets with a new rotary shearing machine N86-12382
THERMOPLASTIC RESINS
The production of glow precursors by oxidative erosion of spacecraft surfaces N86-13257
THERMOSETTING RESINS
The production of glow precursors by oxidative erosion of spacecraft surfaces N86-13257
THERMOSPHERE
Temperature structure of the 80 km to 120 km region N86-12830
Planetary and gravity waves in the mesosphere and lower thermosphere N86-12832
THIN FILMS
Preparation and properties of thin film reversible cathode materials
[AD-A158431] N86-12273
Wear of projectile rotating bands
[AD-A156666] N86-12356
Hillock-free conductor system for use in multilevel interconnects
[DE85-012595] N86-12533
Shear driven film flow behavior and cavitation study N86-12543
Investigation of elastic properties of marine surface-active films N86-12708
Reliability and Engineering of Thin-Film Photovoltaic Modules. Research forum proceedings
[NASA-CR-176217] N86-12759
Crystalline-silicon reliability lessons for thin-film modules N86-12760
Thin-film module circuit design: Practical and reliability aspects N86-12762
Accelerated stress testing of thin film solar cells: Development of test methods and preliminary results N86-12764
Large-area thin-film modules N86-12766
Thin film module development N86-12768
Amorphous silicon photovoltaic modules and test devices design, fabrication and testing N86-12769
Thin film module electrical configuration versus electrical performance N86-12770
Outdoor performance testing of thin-film devices N86-12771
Glass breaking strength: The role of surface flaws and treatments N86-12773
Method for the deposition of high-quality crystal epitaxial films of iron
[AD-D011842] N86-13186
THIN PLATES
Plasma arc welding for thin titanium plates N86-12404
THIN WALLS
Motion of thin metal walls and the equation of state of detonation products
[DE85-014809] N86-12629
THIOLS
Lithium-thionyl chloride cell system safety hazard analysis
[AD-A157089] N86-12775
THORIUM
Nuclear performance optimization of the Be/Li/Th blanket for the fusion breeder
[DE85-012949] N86-13112
THREE DIMENSIONAL FLOW
Experimental investigation of 3-D turbulent free shear flow past propellers and windmills N86-12201
Numerical computation of full three-dimensional flow in transonic turbines N86-12397
Code of finite element analysis for three-dimensional flow in turbomachines N86-12398
A preliminary field study of turbulent flow over and inside a forest edge
[AD-A158409] N86-12560
THRESHOLD LOGIC
Evaluation and implementation of testability schemes for gate array integrated circuit design
[DE85-012874] N86-12526
THRUST
Electronics Engineering Department Thrust Area report FY'84
[DE85-014857] N86-12539
THRUST VECTOR CONTROL
Post stall maneuvers and thrust vectoring performance analysis
[AD-A158100] N86-12235
THUNDERSTORMS
Mesoscale convective systems: A satellite-data-based climatology
[PB85-186662] N86-12931
TIDES
Investigation of tidally induced turbulent flow
[AD-A157841] N86-12555
Planetary and gravity waves in the mesosphere and lower thermosphere N86-12832
TIME
A new hazard function estimator of performance time
[AD-A157843] N86-12971
TIME DEPENDENCE
Nanosecond fluorescence spectroscopy
[DE85-012234] N86-12282
Application of time-dependent Raman theory to the analysis of inorganic photosystems
[DE85-012752] N86-12285
Foil fuses as opening switches for slow discharge circuits
[DE85-014124] N86-12519
Self-consistent klystron simulations
[DE85-012678] N86-12529
Multiple-scale turbulence closure modeling of confined recirculating flows
[NASA-CR-178536] N86-12551
User's manual for using MASON: A frequency response program which handles a system of transfer functions described by a signal flow graph
[PB85-227106] N86-13021
Hamilton-Jacobi equations in infinite dimensions. Part 2: Existence of viscosity solutions
[AD-A158137] N86-13035
TIME LAG
Multiple ignition, combustion and quenching of hydrocarbon fuel sprays
[AD-A158560] N86-12363
Studies of participants in nuclear tests N86-12964
TIME MEASUREMENT
Analytical and experimental studies of wakes behind circularly capped bubbles N86-12548
TIME OF FLIGHT SPECTROMETERS
Los Alamos constant-Q spectrometer
[DE85-014115] N86-12586
TIME SERIES ANALYSIS
Fundamentals of adaptive signal processing
[DE85-014933] N86-13016
TIME SHARING
Internetting and packet satellite program
[AD-A157124] N86-12489
TIME SIGNALS
Simultaneous detection of time coincident signals in an adaptive Doppler tracker
[AD-D011796] N86-12473
TIN
Superconducting wire manufactured N86-12437
TIN ISOTOPES
Isovector resonances in pion charge exchange
[DE85-012746] N86-13106
TIN OXIDES
Interconnect resistance of photovoltaic submodules N86-12767
TITANIUM
Plasma arc welding for thin titanium plates N86-12404
Titanium-nitrogen ion beam injection studied N86-12427
Titanium extractant T105-1 studied N86-12429
Microluminescence spectra of Ti-activated ZrO2-Y2O3
[DE85-010131] N86-13206
X-ray diffraction studies of shock-modified inorganic materials
[DE85-015150] N86-13209
TITANIUM BORIDES
X-ray diffraction studies of shock-modified inorganic materials
[DE85-015150] N86-13209
TITANIUM CARBIDES
X-ray diffraction studies of shock-modified inorganic materials
[DE85-015150] N86-13209

TITANIUM COMPOUNDS
Preparation and properties of thin film reversible cathode materials
[AD-A158431] N86-12273

TITANIUM OXIDES
Surface crystallization on metallized 94 percent alumina ceramics
[DE85-008691] N86-12324

TOKAMAK DEVICES
Tritium safety issues for TFCX
[DE85-014621] N86-13118
TPSS plasma engineering studies: Profile effects and plasma power balance
[DE85-013638] N86-13142
Submillimeter wave propagation in tokamak plasmas
[DE85-007747] N86-13154
Multipole and tokamak research at the University of Wisconsin
[DE85-014862] N86-13165
Alfven wave heating on Tokapole 2
[DE85-014859] N86-13179

TOLERANCES (PHYSIOLOGY)
G protection by an extreme crouch position
[AD-A157081] N86-12213

TOMOGRAPHY
Muon tomography used to study underground rock structure N86-12720

TOPOGRAPHY
Cartography, national land management related
N86-12401
Benefits of surveying, cartography described
N86-12402
The gravity field of topography buried by sediments
N86-12864
Sea floor swells and mantle plumes N86-12866
Contributions of GRM to the ocean topography experiment (TOPEX) N86-12883
The numerical simulation of geographic storms
N86-12907
Wave-current and wave-topographic interactions using SEASAT synthetic aperture radar observations and analytical ocean models N86-12938
Journal of the Chinese Silicate Society (selected articles)
[AD-A157497] N86-13190

TOROIDAL PLASMAS
A ground-based experimental test program to duplicate and study the spacecraft glow phenomenon
N86-13260

TORQUE CONVERTERS
Advanced torque converters for robotics and space applications
[NASA-CR-177987] N86-12610

TORSION
Coupling between spinor field, propagating torsion
N86-12420

TOUGHNESS
Properties of a retrogressed and re-aged 7075 aluminum alloy
[AD-A157415] N86-12298

TOXIC HAZARDS
Toxic hot spot study, South Platte River along the Front Range, August and October, 1982
[PB85-196384] N86-12749
Evaluation of air emissions from hazardous waste treatment, storage and disposal facilities
[PB85-203792] N86-12806

TOXICITY AND SAFETY HAZARD
Lithium-thionyl chloride cell system safety hazard analysis
[AD-A157089] N86-12775

TRACE CONTAMINANTS
Climatically active trace gases in atmosphere
N86-12639

TRACKING (POSITION)
Simultaneous detection of time coincident signals in an adaptive Doppler tracker
[AD-D011796] N86-12473

TRAFFIC CONTROL
Simulation of the enhanced traffic alert and collision avoidance system (TCAS 2)
[NASA-CR-176328] N86-12216

TRAILING EDGES
An improved viscid/inviscid interaction procedure for transonic flow over airfoils
[NASA-CR-3805] N86-12208

TRAINING DEVICES
Systems for authoring computer-based instruction
[PB85-198950] N86-12987
Photosensitive cartridge for weapons zeroing and marksmanship training
[AD-D011765] N86-13125

TRAJECTORIES
Transport near the onset of stochasticity
[DE85-014765] N86-13218

TRANSDUCERS
Wideband SAW (Surface Acoustic Wave) channelizer using slanted array input transducer
[AD-D011857] N86-12517
Analytical and experimental studies of wakes behind circularly capped bubbles N86-12548

TRANSFER FUNCTIONS
User's manual for using MASON: A frequency response program which handles a system of transfer functions described by a signal flow graph
[PB85-227106] N86-13021

TRANSFER TUNNELS
A physical method for estimating speech intelligibility in a reverberant sound field N86-12378

TRANSFORMATIONS (MATHEMATICS)
Scientific workstation research
[DE85-013385] N86-13002
A Floquet decomposition for Volterra equations with periodic kernel and a transform approach to linear recursion equations
[AD-A158148] N86-13037
The uniqueness of Hill's spherical vortex
[AD-A158149] N86-13038
Transforming censored samples and testing fit
[AD-A157957] N86-13048

TRANSFORMERS
Calculation of series capacitance for transient analysis of windings N86-12528
Development of a current monitor system for measuring pulsed-beam current over a wide dynamic range
[DE85-012692] N86-13083

TRANSFUSION
Forward field autotransfusion device
[AD-D011763] N86-12957

TRANSIENT RESPONSE
Transient thermal modeling of the nonscanning ERBE detector
[NASA-CR-172240] N86-12743

TRANSISTORS
Design information for the 4/3 silicon-gate CMOS technology
[DE85-014932] N86-12522
Transistorized multigrid methods. 1: Linear elliptic problems on two- and three-dimensional regions
[DE85-014632] N86-13043

TRANSITION METALS
Study of some transition metal complexes as process catalysts
[DE85-013428] N86-12276
Paramagnetic form factors of HCP transiton metals
[DE85-016301] N86-12301

TRANSITION TEMPERATURE
The 371 deg C mechanical properties of graphite/polyimide composites
[NASA-TM-87122] N86-12256
Structure-to-glass transition temperature relationships in high temperature stable condensation polyimides
[NASA-TM-87113] N86-12311
Deconfinement transition on a BCH lattice
[DE85-013887] N86-13207

TRANSMISSION
Combined small angle X-ray scattering and transmission electron microscope studies of Al-Li alloys
[DE85-016356] N86-12303

TRANSMISSION LINES
Experiments with domestic IC substrates N86-12433

TRANSMISSION LOSS
Experiments with domestic IC substrates N86-12433
Handbook of radio wave propagation loss (100-10,000 MHz)
[PB85-200012] N86-12502

TRANSMITTANCE
Atmospheric IR transmission measurements in a tropical maritime environment: Comparison with the LOWTRAN 6 model
[AD-A157920] N86-13129

TRANSONIC FLOW
GRUMFOIL: A computer code for the viscous transonic flow over airfoils
[NASA-CR-3806] N86-12202
Some recent advances in computational aerodynamics for helicopter applications
[NASA-TM-86777] N86-12207
An improved viscid/inviscid interaction procedure for transonic flow over airfoils
[NASA-CR-3805] N86-12208
Introduction to cryogenic wind tunnels
[NASA-CR-177966] N86-12238
Numerical computation of full three-dimensional flow in transonic turbines N86-12397
Transonic noise generation by duct and profile flow
[AD-A157163] N86-13058

TRANSONIC WIND TUNNELS
The status of two-dimensional testing at high transonic speeds in the University of Southampton transonic self-streamlining wind tunnel
[NASA-CR-3919] N86-12203
Derivation of jack movement influence coefficients as a basis for selecting wall contours giving reduced levels of interference in flexible walled test sections
[NASA-CR-177992] N86-12204

TRANSPORT AIRCRAFT
An analysis of the application of AI to the development of intelligent aids for flight crew tasks
[NASA-CR-3944] N86-12212

TRANSPORT PROPERTIES
Model describing the steady-state pyrolysis of bubble-forming polymers in response to an incident heat flux
[PB85-225225] N86-12291
Laser-based foilless diode
[DE85-013958] N86-12537
Funneling: An initial beam dynamics study
[DE85-012652] N86-13082
Commissioning and operation of the Nuclear Physics Injector at SLAC
[DE85-013374] N86-13159

TRANSPORT THEORY
Numerical calculation of turbulent buoyant flow
N86-12541
Transport near the onset of stochasticity
[DE85-014765] N86-13218

TRANSPORTATION
Safety criteria for the operation of gaseous hydrogen pipelines
[PB85-206159] N86-12392

TRANSURANIUM ELEMENTS
Chemistry of berkelium: A review
[DE85-017523] N86-13102

TRAPPED PARTICLES
Trapped particle absorption by the ring of Jupiter
[NASA-CR-174408] N86-13279

TRAVELING WAVES
A 94 GHz imaging array using slot line radiators
[NASA-CR-176348] N86-12484

TRIANGLES
The prediction of fully developed turbulent pressure drops in a triangular duct for a power law fluid
N86-12546

TRIANGULATION
Relationships between prime-rich Euler type equations and a triangular array of the odd integers
[AD-A157928] N86-13030

TRIBUTARIES
Upper mesozoic turbidites of southern west Sakhalin downwarp N86-12645

TRITIUM
Measurement of tritium permeation through resistant materials near room temperature
[DE85-012942] N85-12592
Tritium control in helium-cooled blankets
[DE85-014783] N86-13116
Tritium safety issues for TFCX
[DE85-014621] N86-13118

TROPICAL REGIONS
A proposed international tropical reference atmosphere up to 80 km N86-12828

TROPICAL STORMS
Global view of the upper level outflow patterns associated with tropical cyclone intensity changes during FGGE
[NASA-CR-174407] N86-12908
Statistical evaluation of forecasts over the low-latitudes
[AD-A157926] N86-12923
Annual data and verification tabulation eastern North Pacific tropical storms and hurricanes, 1984
[PB85-187888] N86-12930

TROPOSPHERE
The MST radar technique N86-12836

TROPOSPHERIC RADIATION
The measurement of tropospheric refractive index relevant to the study of anomalous microwave propagation: Review and recommendations
[CRC-1387] N86-12471

TROUGHS
Modulations of driven nonlinear surface waves on water and liquid Helium-4
[AD-A157958] N86-12556

TRUNCATION ERRORS
Transistorized multigrid methods. 1: Linear elliptic problems on two- and three-dimensional regions
[DE85-014632] N86-13043
Pade and reciprocal approximants and linear NOLOR functions
[DE85-015057] N86-13044

TSUNAMI WAVES
Evaluating screening effects and Tusnami danger in bays N86-12666
Hypocentral areas of aftershocks and possible fault systems at foci of Tsunami-generating Kuril earthquakes N86-12729
TUBE CATHODES
CAD program for high-power electron gun with annular cathode described N86-12468
TUNGSTEN ALLOYS
Superconductivity in the W-Tc and W2C-Tc systems [DE85-012711] N86-13204
TUNGSTEN CARBIDES
Superconductivity in the W-Tc and W2C-Tc systems [DE85-012711] N86-13204
TUNING
A meta system for generating software engineering environments [AD-A158102] N86-12996
Generation of a modulated IREB (Intense Relativistic Electron Beam) with a frequency tunable by a magnetic field [AD-D011820] N86-13068
Acoustically tuned optical filter system [AD-D011791] N86-13184
TURBINE BLADES
Development of an analytical model and code for the flapping response of a Hawte rotor blade [DE85-008806] N86-12211
Turbine blade and vane heat flux sensor development, phase 2 [NASA-CR-174995] N86-12226
Shear driven film flow behavior and cavitation study N86-12543
TURBINE ENGINES
Composition and photochemical reactivity of turbine engine exhaust [AD-A157643] N86-12230
TURBINES
Improved temperature detection system for use on film cooled turbine airfoils [AD-D011762] N86-12228
TURBOCOMPRESSORS
Fluid machines: Expanding the limits, past and future [NASA-TM-87161] N86-12227
TURBOFAN ENGINES
Length adjustable strut link with low aerodynamic drag [AD-D011851] N86-12232
TURBOJET ENGINES
Analysis of particulates in the exhaust plume of a J52-P3 turbojet engine at military power [AD-A157840] N86-12231
TURBOMACHINERY
Code of finite element analysis for three-dimensional flow in turbomachines N86-12398
TURBULENCE
Multiple-scale turbulence closure modeling of confined recirculating flows [NASA-CR-178536] N86-12551
The orientation distribution of nonspherical aerosol particles within a cloud [AD-A157363] N86-12554
Viscous nonlinear circulation in axisymmetric baroclinic eddy N86-12712
Atmospheric turbulence investigations at Tsimlyansk Scientific Station, Atmospheric Physics Institute, USSR Academy of Sciences N86-12735
Weather radar studies [AD-A157093] N86-12920
TURBULENCE EFFECTS
Evaluating influence of waves on dynamic structure of atmospheric near-water layer N86-12694
TURBULENT BOUNDARY LAYER
An evaluation of four methods of numerical analysis for two-dimensional airfoil flows. Revision [AD-A157248] N86-12209
Investigation of tidally induced turbulent flow [AD-A157841] N86-12555
Turbulence models for boundary layers on axisymmetric bodies [AD-A158552] N86-12561
Influence of water vapor on distribution of turbulent wave parameters N86-12659
TURBULENT DIFFUSION
Turbulence in the altitude region 80-120 km N86-12834
TURBULENT FLOW
Experimental investigation of 3-D turbulent free shear flow past propellers and windmills N86-12201
Numerical calculation of turbulent buoyant flow N86-12541
Numerical calculation of internal flows with curvature N86-12544
Study of the mist cooling and droplet dynamics in turbulent flow by using LDA N86-12545
The prediction of fully developed turbulent pressure drops in a triangular duct for a power law fluid N86-12546
Numerical and experimental studies of 3-D and unsteady turbulent body/appendage/propeller flows [AD-A157078] N86-12552
Investigation of tidally induced turbulent flow [AD-A157841] N86-12555
A preliminary field study of turbulent flow over and inside a forest edge [AD-A158409] N86-12560
TURBULENT JETS
Combustion in turbulent jets and buoyant plumes [PB85-220655] N86-12288
Measurements on an axisymmetric jet in a slow coflowing stream N86-12549
TURBULENT WAKES
Influence of water vapor on distribution of turbulent wave parameters N86-12659
TURNING FLIGHT
Post stall maneuvers and thrust vectoring performance analysis [AD-A158100] N86-12235
TWO DIMENSIONAL FLOW
An evaluation of four methods of numerical analysis for two-dimensional airfoil flows. Revision [AD-A157248] N86-12209
Analytical and experimental studies of wakes behind circularly capped bubbles N86-12548
TWO PHASE FLOW
Metal dissolution kinetics in organic solvents using rotating ring-disc voltammetry [DE85-013478] N86-12253
One-dimensional two-phase flow in combustion chamber of solid propellant rocket motors N86-12370
Particle-wall interaction and wall friction in gas-solid flows [DE85-014984] N86-12567
Velocity and gravity effects in relative permeability measurements [DE85-009925] N86-12570
Study of two-phase concurrent flow of steam and water in an unconsolidated porous medium [DE85-014534] N86-12578
Optical technique to study the impact of heavy rain on aircraft performance [NASA-CR-177989] N86-12580
TYPHOONS
Global view of the upper level outflow patterns associated with tropical cyclone intensity changes during FGGE [NASA-CR-174407] N86-12908

U

U.S.S.R.
USSR report: Earth sciences [JPRS-UES-85-008] N86-12697
Kamchatka radio telemetric station registers volcano pulse N86-12717
Impact of GRM: New evidence from the Soviet Union N86-12853
ULTRAHIGH VACUUM
Ultrahigh vacuum equipment described N86-12438
High intensity positron beam and angular correlation experiments at Livermore [DE85-012961] N86-13111
ULTRASHORT PULSED LASERS
First domestic high repetition rate ultrashort pulse laser N86-12455
ULTRASONIC LIGHT MODULATION
Laser vibrometer [AD-D011811] N86-12602
ULTRASONIC RADIATION
Effects of microstructure on the acoustoelastic measurements of stress [DE85-015518] N86-12307
Status, development of power ultrasonics in China N86-12403
Laser generation of ultrasonic waveform reconstructions [AD-D011843] N86-12599
Ultrasonic attenuation in clean anisotropic superconductors [DE85-012178] N86-12621
ULTRASONICS
Laser generation of ultrasonic waveform reconstructions [AD-D011843] N86-12599
ULTRAVIOLET ASTRONOMY
Combined ultraviolet studies of astronomical source [NASA-CR-176165] N86-13274
ULTRAVIOLET RADIATION
Middle Atmosphere Program. Handbook for MAP, volume 17 [NASA-CR-176345] N86-12837
UV sustained glow discharge opening switch [AD-A158411] N86-13132
Optical radiation from the interaction of energetic atoms, ions, electrons, and photons with surfaces N86-13259
Survey of ultraviolet shuttle glow N86-13269
ULTRAVIOLET SPECTRA
The field horizontal-branch star HD 109995: New results with coadded ultraviolet and optical region spectra [NASA-CR-176327] N86-13272
Ultraviolet observations of low-excitation Herbig-Haro objects [NASA-CR-176164] N86-13273
UNDERGROUND EXPLOSIONS
Seismic effect of underground blasts and problem of estimating total earthquake energy N86-12731
UNDERGROUND STORAGE
MAGNUM-2D computer code: User's guide [DE85-013315] N86-13001
Second reference calculation for the WIPP [DE85-013180] N86-13005
UNDERWATER ACOUSTICS
Interaction of sound waves with fine thermohaline structures of ocean N86-12647
Correlation characteristics of signals reflected by the wavy surface of ocean in mirror direction N86-12648
Numerical estimate of effectiveness of approximate equations for acoustic field near surface of deep sea N86-12649
Acoustical field of directional source in oceanic waveguides N86-12656
Structure of acoustic field in deep sea at shallow depths and at great ranges N86-12664
Saclantcen's use of scuba diving in oceanographic and acoustic research [AD-A156714] N86-12941
Underwater photography for quantitative description of bottom roughness [AD-A156753] N86-12943
UNDERWATER PHOTOGRAPHY
Underwater photography for quantitative description of bottom roughness [AD-A156753] N86-12943
UNIFORM FLOW
Experimental investigation of 3-D turbulent free shear flow past propellers and windmills N86-12201
UNIVERSITIES
The status of two-dimensional testing at high transonic speeds in the University of Southampton transonic self-streamlining wind tunnel [NASA-CR-3919] N86-12203
Energy expenditure and activity patterns of cadets at the United States Military Academy, West Point, New York [AD-A157857] N86-12960
UNSTEADY FLOW
Unsteady detonation N86-12542
UPPER ATMOSPHERE
Temperature and wind data from meteorological rockets N86-12816
Review of spectroscopic parameters for upper atmospheric measurements [NASA-CP-2396] N86-13064
Orbiter glow observations at high spectral resolution N86-13244
UPSTREAM
Experimental investigation of 3-D turbulent free shear flow past propellers and windmills N86-12201
UPWELLING WATER
Evidence from satellite altimetry for small-scale convection in the mantle N86-12878
URANIUM OXIDES
U308 powder from uranyl-loaded cation exchange resin [DE85-013231] N86-12265
USER MANUALS (COMPUTER PROGRAMS)
GRUMFOIL: A computer code for the viscous transonic flow over airfoils [NASA-CR-3806] N86-12202
MAGNUM-2D computer code: User's guide [DE85-013315] N86-13001
User's manual for using MASON: A frequency response program which handles a system of transfer functions described by a signal flow graph [PB85-227106] N86-13021
USER REQUIREMENTS
Crystalline-silicon reliability lessons for thin-film modules N86-12760
Thin film module development N86-12768
A user's guide to the Coastal Engineering Research Center's (CERC'S) field research facility [AD-A157966] N86-12946

UTILITY AIRCRAFT
Flutter clearance tests on a Transavia PL-12/T-400 Skyfarmer
[AD-A157212] N86-12234

V

VACUUM
In-situ vacuum-assisted molding of glass-metal electrical components
[DE85-015607] N86-12326

VACUUM APPARATUS
Ultrahigh vacuum equipment described N86-12438

VACUUM CHAMBERS
High-power ND: Glass laser and target chamber system and an experimental study of laser plasma X-ray N86-12428
Self-contained hot-hollow cathode gun source assembly
[DE85-011652] N86-12530

VACUUM GAGES
Precision ion vacuum gage with logarithmic response
[DE85-015312] N86-12588

VACUUM PUMPS
Ultrahigh vacuum equipment described N86-12438

VACUUM SYSTEMS
Adsorption/desorption properties of vacuum materials for the 6 GeV synchrotron
[DE85-010276] N86-12252

VALVES
Forward field autotransfusion device
[AD-D011763] N86-12957

VAN DER WAAL FORCES
Multiphoton ionization of NO-rare gas van der Waals species
[DE85-014850] N86-13094

VANES
Turbine blade and vane heat flux sensor development, phase 2
[NASA-CR-174995] N86-12226
Wind tunnel turning vanes of modern design
[NASA-TM-87416] N86-12239

VAPOR DEPOSITION
Method and apparatus for conducting variable thickness vapor deposition
[DE85-011653] N86-12306
Recovery of fragile layers produced on substrates by chemical vapor deposition
[AD-D011841] N86-13185
Method for the deposition of high-quality crystal epitaxial films of iron
[AD-D011842] N86-13186
Compound semiconductor insulator interface research
[AD-A157277] N86-13189
Liquid Phase Epitaxy (LPE) of silicon carbide
[AD-D011825] N86-13191

VAPOR PHASE EPITAXY
Investigation of phase transitions
[AD-A158434] N86-12518

VAPOR PRESSURE
Thermodynamics of multi-polar molecules: The perturbed-anisotropic-chain theory
[DE85-013148] N86-12274

VAPORS
Reversible optical waveguide vapor sensor
[AD-D011834] N86-13124

VARIATIONAL PRINCIPLES
China report: Science and technology
[JPRS-CST-85-021] N86-12421
Variational analysis of phase transition in pure gauge fields N86-12422
Variational principle for penetrator dynamics using bilinear functional and adjoint formulation
[AD-A157964] N86-13031

VARIATIONS
Variable radius lead former
[AD-D011790] N86-12506
Spectrum of turbulent fluctuations in sea water density in region of large wave numbers N86-12646
Correlation characteristics of signals reflected by the wavy surface of ocean in mirror direction N86-12648
Middle Atmosphere Program. Handbook for MAP. Volume 16: Atmospheric structure and its variation in the region 20 to 120 km. Draft of a new reference middle atmosphere
[NASA-CR-176321] N86-12814

VAX COMPUTERS
Data acquisition command interface using VAX/VMS DCL
[DE85-012747] N86-13019

VECTOR ANALYSIS
Data structures and vectorization in a two-dimensional free-Lagrangian code
[DE85-012948] N86-13009

VECTOR DOMINANCE MODEL
Physics of e(+) - e(-) colliders: Present, future and far future
[DE85-009895] N86-13121

VEGETATION GROWTH
Feasibility of using LANDSAT images of vegetation cover to estimate effective hydraulic properties of soils
[E86-10003] N86-12739

VEGETATIVE INDEX
Evaluation of space SAR as a land-cover classification
[E86-10004] N86-12740

VELOCITY
Energetic response of propellants to high velocity impact, revision 1
[DE85-013983] N86-12365
Spectrum of turbulent fluctuations in sea water density in region of large wave numbers N86-12646
The NO-NO2 system at laboratory surfaces N86-13255

VELOCITY DISTRIBUTION
BLR studies on conic model with LDA in FL-1 wind tunnel N86-12434
Measurements on an axisymmetric jet in a slow coflowing stream N86-12549
Numerical estimate of effectiveness of approximate equations for acoustic field near surface of deep sea N86-12649
Survey of ultraviolet shuttle glow N86-13269
NeII observations of the galactic center: The velocity field and mass distribution N86-13270

VELOCITY MEASUREMENT
Velocity and gravity effects in relative permeability measurements
[DE85-009925] N86-12570
Advanced torque converters for robotics and space applications
[NASA-CR-177987] N86-12610
Study of influence of vertical velocity and density profiles on hydrodynamic stability of zonal flow N86-12673
On-line velocity measurements using phase probes at the SuperHILAC
[DE85-015279] N86-13095

VENUS PROBES
Meteorological center's forecasts aid Venus probe tracking N86-12631

VERBAL COMMUNICATION
A physical method for estimating speech intelligibility in a reverberant sound field N86-12378

VERTICAL AIR CURRENTS
Some results of study of blocking layers on days with vertically developed cloud cover of Caucasus-Caspian region on basis of aerospace information N86-12698

VERTICAL JUNCTION SOLAR CELLS
Semicrystalline casting process development and verification
[JPL-9950-1160] N86-12312

VERTICAL ORIENTATION
Interim reference ozone models for the middle atmosphere N86-12829
Atmospheric tides between 80 km and 120 km N86-12633

VERY LARGE SCALE INTEGRATION
The Record of Electrical and Communication Engineering Conversazione, volume 54, no. 1
[ISSN-0385-771-9] N86-12383
The verification of the logic circuits based on particlized information bits with PROLOG N86-12387

VIBRATION
DAA modal analysis for parametric investigations of fluid-structure interaction in underwater shock, revision 1
[DE85-012935] N86-12569
Control for DOT matrix printers operating in harsh environment
[AD-D011846] N86-12980

VIBRATION ISOLATORS
Transient test of suspension electronics for gyroscope
[AD-D011853] N86-12585

VIBRATION METERS
Laser vibrometer
[AD-D011811] N86-12602

VIBRATIONAL SPECTRA
Picosecond broadband CARS probe using the picosecond continuum
[AD-D011840] N86-12267
Application of time-dependent Raman theory to the analysis of inorganic photosystems
[DE85-012752] N86-12285

VIDEO COMMUNICATION
Elie: Saint Eustache fibre Optic Field Trial project evaluation report, volume 4
[AD-A157144] N86-12490

VIDEO DISKS
Optical disk technology assessment
[AD-A157909] N86-12582

VIDEO EQUIPMENT
Video terminal for analyzing aerial infrared photographs N86-12068

VIEW EFFECTS
Soybean canopy reflectance modeling data sets
[E86-10005] N86-12741

VINYL POLYMERS
Investigation of test methods, material properties and processes for solar cell encapsulants
[DE85-012831] N86-12786

VIRGO GALACTIC CLUSTER
X-rays from the radio halo of Virgo A = M87
[NASA-CR-176303] N86-13265

VIRIAL THEOREM
New corresponding states theory using the second virial coefficient as the temperature variable
[PB85-219624] N86-12289

VISCOELASTICITY
The Record of Electrical and Communication Engineering Conversazione, volume 54, no. 1
[ISSN-0385-771-9] N86-12383
Accuracy of a new ultrasonic apparatus for simple measurement of viscoelasticity N86-12388
Mantle viscosity, J2 and the nontidal acceleration of Earth rotation N86-12879

VISCOSITY
Particle-wall interaction and wall friction in gas-solid flows
[DE85-014984] N86-12567
Subduction dynamics: Constraints from gravity field observations N86-12868
The nature of symmetric instability and its similarity to convective and inertial instability
[NASA-CR-3945] N86-12918
Hamilton-Jacobi equations in infinite dimensions. Part 2: Existence of viscosity solutions
[AD-A158137] N86-13035

VISCOUS FLOW
GRUMFOIL: A computer code for the viscous transonic flow over airfoils
[NASA-CR-3806] N86-12202
Effect of surface waviness on a supercritical laminar-flow-control airfoil
[NASA-TM-85705] N86-12206
An improved viscid/inviscid interaction procedure for transonic flow over airfoils
[NASA-CR-3805] N86-12208
Fluid physics research
[DE85-014644] N86-12575

VISIBLE INFRARED SPIN SCAN RADIOMETER
Relaying of the stretched VISSR data by GMS spacecraft N86-12913

VISIBLE SPECTRUM
Some characteristics of transmission by thin clouds in visible and infrared spectral regions N86-12737
The field horizontal-branch star HD 109995: New results with coadded ultraviolet and optical region spectra
[NASA-CR-176327] N86-13272

VISION
The effects of hypoxia induced by low atmospheric pressure on soft contact lens wear
[AD-A158556] N86-12963

VISUAL ACUITY
Criteria for a state-of-the-art vision test system
[AD-A157099] N86-12973

VISUAL OBSERVATION
Improvement of manufacturing techniques and quality of optical scratch standards for fire control systems
[AD-A157963] N86-13130

VISUAL PERCEPTION
Criteria for a state-of-the-art vision test system
[AD-A157099] N86-12973

VITRIFICATION
Fixation of high-level wastes in glasses
[DE85-013276] N86-12325

VOICE COMMUNICATION
Results of field and laboratory studies of jam-resistant and voice-private radios
[DE85-014841] N86-12500

VOIDS
The 371 deg C mechanical properties of graphite/polyimide composites
[NASA-TM-87122] N86-12256
Module voltage isolation and corrosion research N86-12772

VOLCANOES
Find of rheolites and trachites and geological situation in northern part of East Indian Ocean Submarine Ridge N86-12665
Organic components in atmosphere in regions of volcanic activity N86-12693
Kamchatka radio telemetric station registers volcano pulse N86-12717
Underground volcanoes discovered with satellite radar N86-12721

Motion of the Pacific plate relative to the hotspots since the Jurassic and model of oceanic plateaus of the Farallon plate N86-12940
VOLCANOLOGY
Spreading in development of oceanic structures N86-12658
Kamchatka radio telemetric station registers volcano pulse N86-12717
VOLTAGE REGULATORS
Maintenance of photovoltaic power systems, revision 1
[AD-A157838] N86-12777
VOLTMETERS
Evaluation parameters for the alkaline fuel cell oxygen electrode
[NASA-TM-87155] N86-12268
China report: Science and technology
[JPRS-CST-85-029] N86-12446
Digital voltmeter technology acquisition N86-12449
VORTEX GENERATORS
Transonic noise generation by duct and profile flow
[AD-A157163] N86-13058
VORTICES
Some recent advances in computational aerodynamics for helicopter applications
[NASA-TM-86777] N86-12207
Turbulence models for boundary layers on axisymmetric bodies
[AD-A158552] N86-12561
Solitary vortices in a rotating plasma
[DE85-014766] N86-13171
VORTICITY
Eddy fluxes of heat, vorticity and momentum in ocean and atmosphere and their parameterization (review) N86-12672
VORTICITY EQUATIONS
Statistical evaluation of forecasts over the low-latitudes
[AD-A157926] N86-12923
The uniqueness of Hill's spherical vortex
[AD-A158149] N86-13038
VULNERABILITY
Communications network status information system
[AD-D011850] N86-12477
Hot-spot heating susceptibility due to reverse bias operating conditions N86-12763

W

WAFERS
Semicrystalline casting process development and verification
[JPL-9950-1160] N86-12312
WAKES
Analytical and experimental studies of wakes behind circularly capped bubbles N86-12548
Experimental study of flow and dispersion in the wakes of three-dimensional low hills
[PB85-193266] N86-12906
A possible glow experiment for the EOM 1-2 mission N86-13266
WALL FLOW
Wall-interference assessment in three-dimensional slotted-wall wind tunnels
[NASA-CR-176320] N86-12240
Particle-wall interaction and wall friction in gas-solid flows
[DE85-014984] N86-12567
WALL PRESSURE
Derivation of jack movement influence coefficients as a basis for selecting wall contours giving reduced levels of interference in flexible walled test sections
[NASA-CR-177992] N86-12204
WALL TEMPERATURE
The NO-NO2 system at laboratory surfaces N86-13255
WARFARE
Comparison of continuous speech, discrete speech, and keyboard input to an interactive warfare simulation in various C3 environments
[AD-A156830] N86-12487
WARNING SYSTEMS
Kamchatka radio telemetric station registers volcano pulse N86-12717
WASTE DISPOSAL
Evaluation of air emissions from hazardous waste treatment, storage and disposal facilities
[PB85-203792] N86-12806
Second reference calculation for the WIPP
[DE85-013180] N86-13005
WASTE TREATMENT
Evaluation of air emissions from hazardous waste treatment, storage and disposal facilities
[PB85-203792] N86-12806
WASTES
Evaluation of air emissions from hazardous waste treatment, storage and disposal facilities
[PB85-203792] N86-12806
WATER
Modulations of driven nonlinear surface waves on water and liquid Helium-4
[AD-A157958] N86-12556
Computer simulation of the effect of free surface reflection on shock wave propagation in water
[DE85-014807] N86-12563
Velocity and gravity effects in relative permeability measurements
[DE85-009925] N86-12570
Study of two-phase concurrent flow of steam and water in an unconsolidated porous medium
[DE85-014534] N86-12576
Laboratory study of regular low-amplitude gravity capillary waves in nonstationary current N86-12671
WATER BALANCE
Recent changes in climate and world water balance N86-12638
WATER CIRCULATION
Viscous nonlinear circulation in axisymmetric baroclinic eddy N86-12712
WATER FLOW
Fiscal year 1983 program report of the Purdue (indiana) Water Resources Research Center
[PB85-225829] N86-12802
WATER POLLUTION
Toxic hot spot study, South Platte River along the Front Range, August and October, 1982
[PB85-196364] N86-12749
Design of a statewide groundwater monitoring network for Illinois
[PB85-192821] N86-12750
Great Lakes: Nature's own environmental laboratory
[PB85-188852] N86-12751
Diagnosing the causes of ground-water contamination using a mathematical model: Report on Technology Transfer Workshop
[PB85-217008] N86-12808
Acid precipitation: Source identification and its effects on water quality
[PB85-214880] N86-12810
WATER QUALITY
China report: Science and technology
[JPRS-CST-85-018] N86-12413
Waters resources data for Minnesota. Water year 1983. Volume 2: Upper Mississippi and Missouri River Basins
[PB85-215994] N86-12753
Acid precipitation: Source identification and its effects on water quality
[PB85-214880] N86-12810
WATER RECLAMATION
Great Lakes: Nature's own environmental laboratory
[PB85-188852] N86-12751
WATER RESOURCES
Design of a statewide groundwater monitoring network for Illinois
[PB85-192821] N86-12750
Evaluating the ground-water resources of the high plains of Texas, volume 2
[PB85-191609] N86-12752
Waters resources data for Minnesota. Water year 1983. Volume 2: Upper Mississippi and Missouri River Basins
[PB85-215994] N86-12753
Water resources data for Florida, water year 1983. Volume 3A: Southwest Florida surface water
[PB85-216000] N86 12754
Acid precipitation: Source identification and its effects on water quality
[PB85-214880] N86-12810
WATER RUNOFF
Water Information Bulletin No. 30, Part 13: Geothermal investigations in Idaho. Preliminary geologic reconnaissance of the geothermal occurrences of the Wood River drainage area
[DE85-016972] N86-12747
WATER TEMPERATURE
Spectrum of turbulent fluctuations in sea water density in region of large wave numbers N86-12646
WATER VAPOR
Influence of water vapor on distribution of turbulent wave parameters N86-12659
Humidity profile mesurements in atmospheric lower layer by spontaneous Raman scattering method N86-12736
Atmospheric IR transmission measurements in a tropical maritime environment: Comparison with the LOWTRAN 6 model
[AD-A157920] N86-13129
WATER WAVES
Investigation of tidally induced turbulent flow
[AD-A157841] N86-12555
Electromagnetic field of three-dimensional surface sea waves N86-12662
Study of influence of vertical velocity and density profiles on hydrodynamic stability of zonal flow N86-12673
Experimental study of equilibrium interval in frequency spectra of wind waves in sea of finite depth N86-12699
Acoustic methods for featuring high-frequency part of spectrum of sea waves N86-12706
Spatial structure of high-frequency sea wind waves under different meteorological conditions N86-12714
Extremal analysis of hindcast and measured wind and wave data at Kodiak, Alaska
[AD-A158136] N86-12947
WATERSHEDS
Evaluation of the NWS (National Weather Service) soil moisutre accounting model for automated flash flood forecasting in small arid and semi-arid watersheds
[PB85-229722] N86-12928
WAVE AMPLIFICATION
Effect of amplified spontaneous emission on space coherence of XeCl laser N86-12454
WAVE DIFFRACTION
Diffraction of internal waves described by equation of slightly stratified fluid on half-plane N86-12660
WAVE GENERATION
Laser generation of ultrasonic waveform reconstructions
[AD-D011843] N86-12599
WAVE INTERACTION
Self-consistent klystron simulations
[DE85-012678] N86-12529
Damping of high-frequency wind waves by artifical surface-active films N86-12692
Nonlinear interaction between soliton and short waves in ideal fluid N86-12715
WAVE PROPAGATION
Handbook of radio wave propagation loss (100-10,000 MHz)
[PB85-200012] N86-12502
Ultrasonic attenuation in clean anisotropic superconductors
[DE85-012178] N86-12621
Computations of seismic wave propagation velocities in ocean bottom sediments from reflected waves travel-time curves N86-12677
Nonlinear interaction between soliton and short waves in ideal fluid N86-12715
Submillimeter wave propagation in tokamak plasmas
[DE85-007747] N86-13154
Wave propagation in a plasma based on the cold plasma model
[DE85-013649] N86-13158
Alfven continuum with toroidicity
[DE85-015821] N86-13217
Wave propagation and pair formation in pulsar magnetospheres N86-13276
WAVE REFLECTION
Correlation characteristics of signals reflected by the wavy surface of ocean in mirror direction N86-12648
Determination of dynamic parameters of reflected waves on slopes of deep water trench N86-12724
WAVE SCATTERING
Elementary waves and Riemann solutions: Their theory and their role in science
[DE85-014018] N86-13045
WAVEFORMS
Measurement of 1 nanosecond wide beams for 2.5 MeV proton accelerator N86-12435
Hybrid radar waveform design utilizing complementary phase coding and linear frequency stepping for achieving improved slant range resolution in a synthetic aperature radar N86-12470
Laser generation of ultrasonic waveform reconstructions
[AD-D011843] N86-12599
Monitoring of circadian waveforms in rodents exposed to high-intensity static magnetic fields
[DE85-015225] N86-12952
WAVEGUIDES
Proposal of a high efficient and high power peniotron N86-12384
Experiments with domestic IC substrates N86-12433
Integral equation description of integrated dielectric waveguides N86-12504
The theory and practice of a multistate reflectometer
[AD-A157916] N86-12583
Interaction of sound waves with fine thermohaline structures of ocean N86-12647
Numerical estimate of effectiveness of approximate equations for acoustic field near surface of deep sea N86-12649
Acoustical field of directional source in oceanic waveguides N86-12656
Suppression of propagating TE modes in the FNAL antiproton source stochastic beam cooling system
[DE85-016559] N86-13074

WAVELENGTHS
Frequency selection and mode locking of Nd:YAG laser N86-12395
Studies of the marine crustal magnetization at intermediate wavelengths N86-12862
Subduction dynamics: Constraints from gravity field observations N86-12868
WEAPON SYSTEMS
Pilot's associate definition study [AD-A157106] N86-13026
Word lists to limit vocabulary in technical information [AD-A157931] N86-13228
WEAPONS
Photosensitive cartridge for weapons zeroing and marksmanship training [AD-D011765] N86-13125
WEAPONS DEVELOPMENT
Strategic defense initiatives at Los Alamos National Laboratory [DE85-014093] N86-12608
WEAR
Ellipsometric surface analysis of wear tracks produced by different lubricants [NASA-TM-87142] N86-12293
Wear of projectile rotating bands [AD-A156666] N86-12358
The effects of hypoxia induced by low atmospheric pressure on soft contact lens wear [AD-A158556] N86-12963
WEATHER
Weather analysis programs using HP-41CV [AD-A157389] N86-12921
Comparison among various thermodynamic parameters for the prediction of convective activity [PB85-208217] N86-12932
WEATHER FORECASTING
Main problems in climate monitoring (diagnosis) N86-12633
Statistical evaluation of forecasts over the low-latitudes [AD-A157926] N86-12923
First experiment in forecasting cool-season weather with the PROFS System [PB85-230605] N86-12929
Monthly and seasonal weather outlook for mid-May to mid-June 1985, volume 39, number 10, May 14, 1985 [PB85-204261] N86-12937
WEATHERING
Thin film module development N86-12768
Outdoor performance testing of thin-film devices N86-12771
Encapsulant selection and durability testing experience N86-12774
WEIGHT (MASS)
Energy expenditure and activity patterns of cadets at the United States Military Academy, West Point, New York [AD-A157857] N86-12960
WEIGHTING FUNCTIONS
Extraction of feature parameters for spoken word recognition N86-12376
WEIGHTLESSNESS
Microgravity science and applications bibliography, 1985 revision [NASA-TM-88178] N86-13225
WELD STRENGTH
Special metallographic procedures for austenitic stainless steel welds [DE85-010113] N86-12305
WELDABILITY
Plasma arc welding for thin titanium plates N86-12404
WELDED JOINTS
Special metallographic procedures for austenitic stainless steel welds [DE85-010113] N86-12305
Fusion welding research [AD-A158127] N86-12611
Multifrequency eddy-current inspection of seam weld in steel sheath [DE85-013533] N86-12626
WELDING
European Science Notes. Volume 39, number 8 [AD-A157146] N86-13237
WHEATSTONE BRIDGES
Electrolytic pressure transduction system [AD-D011847] N86-12584
WHISTLERS
Effects of whistler-mode and other waves in the magnetosphere [AD-A157832] N86-12899
WHITE NOISE
Data requirements for verification of ram glow chemistry N86-13265
WICKS
Heat pipe wick [AD-D011852] N86-12559
WIDTH
A new integrated slot element feed array for multi-beam systems N86-12483
WILDLIFE
Environmental impact research program. Status and source of habitat models and literature reviews, December 1984 [AD-A156699] N86-12950
WIND (METEOROLOGY)
Nonlinear model of adaptation of fields of density and currents in sea N86-12670
Damping of high-frequency wind waves by artifical surface-active films N86-12692
Experimental study of equilibrium interval in frequency spectra of wind waves in sea of finite depth N86-12699
Spatial structure of high-frequency sea wind waves under different meteorological conditions N86-12714
Observed winds and temperatures in the Southern Hemisphere N86-12817
Mean winds of the mesosphere (60-80 km), as measured by MF radars N86-12818
Comparison of time-periodic variations in temperature and wind from meteorological rockets and satellites N86-12825
Middle Atmosphere Program. Handbook for MAP, volume 17 [NASA-CR-176345] N86-12837
Atmospheric Tides Middle Atmosphere Program (ATMAP): Report of the November/December 1981, and May 1982, observational campaigns N86-12839
Results of the May 1982 ATMAP campaign at the Meteor Wind Station Kuehlungsborn (54 deg N, 12 deg E), GDR N86-12841
Saskatoon M. F. radar system: (52 deg N, 107 deg W), Canada N86-12843
Meteor wind results at Durham (43 deg N, 71 deg W) during the ATMAP November 1981 and May 1982 campaigns N86-12845
Mesospheric winds and tides at Arecibo/puerto Rico (18 deg N, 67 deg W) November 20-23, 1981 N86-12848
Mesospheric winds at Jicamaraca, Peru (12 deg S, 77 deg SW), November 19-21, 1981 N86-12849
Squall and cloud lines as structural components of an Arabian Sea convective cloud cluster [AD-A157973] N86-12925
Comparison of boundary layer winds from NWS LFM (National Weather Service's Limited-Area Fine-Mesh) output and instrumented buoys [PB85-226439] N86-12927
Behavior of ionized plasma in the high latitude topside ionosphere [AD-A157930] N86-13140
WIND DIRECTION
Middle Atmosphere Program. Handbook for MAP, volume 17 [NASA-CR-176345] N86-12837
May 1982, Saskatoon M. F. radar system: (52 deg N, 107 deg W), Canada N86-12844
Mean winds and tides over Urbana, Illinois during November 16-22, 1981 N86-12846
Kyoto meteor radar observation in November, 1981 and May, 1982 N86-12847
Mesospheric winds at Jicamaraca, Peru (12 deg S, 77 deg SW), November 19-21, 1981 N86-12849
WIND EFFECTS
Investigation of elastic properties of marine surface-active films N86-12708
Spatial structure of high-frequency sea wind waves under different meteorological conditions N86-12714
WIND MEASUREMENT
Temperature and wind data from meteorological rockets N86-12816
Mean winds of the mesosphere (60-80 km), as measured by MF radars N86-12818
Remarks on the ATMAP campaigns in November 1981 and May 1982 at Collm (52 deg N, 15 deg E) N86-12842
May 1982, Saskatoon M. F. radar system: (52 deg N, 107 deg W), Canada N86-12844
Comparison of boundary layer winds from NWS LFM (National Weather Service's Limited-Area Fine-Mesh) output and instrumented buoys [PB85-226439] N86-12927
Extremal analysis of hindcast and measured wind and wave data at Kodiak, Alaska [AD-A158136] N86-12947
WIND PROFILES
Mean winds of the upper middle atmosphere (60-110 km): A global distribution from radar systems (MF, meteor, VHF) N86-12831
Atmospheric tides between 80 km and 120 km N86-12833
Middle Atmosphere Program. Handbook for MAP, volume 17 [NASA-CR-176345] N86-12837
Saskatoon M. F. radar system: (52 deg N, 107 deg W), Canada N86-12843
May 1982, Saskatoon M. F. radar system: (52 deg N, 107 deg W), Canada N86-12844
Mesospheric winds at Jicamaraca, Peru (12 deg S, 77 deg SW), November 19-21, 1981 N86-12849
Results of November 1981 and May 1982 ATMAP campaigns at Adelaide (35 deg S, 138 deg E) N86-12850
Large-scale circulation departures related to wet episodes in northeast Brazil [NASA-CR-176352] N86-12916
Atmospheric environment for space shuttle (STS-51B) launch [NASA-TM-86525] N86-12917
WIND SHEAR
Weather radar studies [AD-A157093] N86-12920
WIND TUNNEL TESTS
Air Force Academy Aeronautics Digest [AD-A157215] N86-12200
The status of two-dimensional testing at high transonic speeds in the University of Southampton transonic self-streamlining wind tunnel [NASA-CR-3919] N86-12203
Performance of an alpha-vane and pitot tube in simulated heavy rain environment [NASA-CR-176353] N86-12220
User's guide to STIPPAN: A panel method program for slotted tunnel interference prediction [NASA-CR-178003] N86-12237
BLR studies on conic model with LDA in FL-1 wind tunnel N86-12434
Experimental study of flow and dispersion in the wakes of three-dimensional low hills [PB85-193266] N86-12906
WIND TUNNEL WALLS
The status of two-dimensional testing at high transonic speeds in the University of Southampton transonic self-streamlining wind tunnel [NASA-CR-3919] N86-12203
Derivation of jack movement influence coefficients as a basis for selecting wall contours giving reduced levels of interference in flexible walled test sections [NASA-CR-177992] N86-12204
WIND TUNNELS
Experimental investigation of 3-D turbulent free shear flow past propellers and windmills N86-12201
Wind tunnel turning vanes of modern design [NASA-TM-87416] N86-12239
WIND TURBINES
Development of an analytical model and code for the flapping response of a Hawte rotor blade [DE85-008806] N86-12211
Navy applications experience with small wind power systems [AD-A158561] N86-12778
Wind generation in Washington [DE85-012791] N86-12787
Small scale wind energy conversion programmatic equipment [DE85-012319] N86-12793
WIND VANES
Performance of an alpha-vane and pitot tube in simulated heavy rain environment [NASA-CR-176353] N86-12220
WIND VARIATIONS
A preliminary field study of turbulent flow over and inside a forest edge [AD-A158409] N86-12560
Middle Atmosphere Program. Handbook for MAP, volume 17 [NASA-CR-176345] N86-12837
Data descriptions and vertical structure plots for mean, diurnal, and semidurnal components of eastward and northward (ordered by latitude). Mean winds and tides over Poker Flat, Alaska (65 deg N, 147 deg W), during November 1981 N86-12840
Results of the May 1982 ATMAP campaign at the Meteor Wind Station Kuehlungsborn (54 deg N, 12 deg E), GDR N86-12841
Remarks on the ATMAP campaigns in November 1981 and May 1982 at Collm (52 deg N, 15 deg E) N86-12842
Saskatoon M. F. radar system: (52 deg N, 107 deg W), Canada N86-12843
Meteor wind results at Durham (43 deg N, 71 deg W) during the ATMAP November 1981 and May 1982 campaigns N86-12845
Kyoto meteor radar observation in November, 1981 and May, 1982 N86-12847

WIND VELOCITY
Global modeling of optical characteristics of atmospheric aerosol N86-12695
Investigation of elastic properties of marine surface-active films N86-12708
Wind generation in Washington
[DE85-012791] N86-12787
Planetary and gravity waves in the mesosphere and lower thermosphere N86-12832
Middle Atmosphere Program. Handbook for MAP, volume 17
[NASA-CR-176345] N86-12837
Data descriptions and vertical structure plots for mean, diurnal, and semidurnal components of eastward and northward (ordered by latitude). Mean winds and tides over Poker Flat, Alaska (65 deg N, 147 deg W), during November 1981 N86-12840
Mesospheric winds and tides at Arecibo/puerto Rico (18 deg N, 67 deg W) November 20-23, 1981 N86-12848
Mesospheric winds at Jicamaraca, Peru (12 deg S, 77 deg SW), November 19-21, 1981 N86-12849
The numerical simulation of geographic storms N86-12907
Large-scale circulation departures related to wet episodes in northeast Brazil
[NASA-CR-176352] N86-12916
Weather radar studies
[AD-A157093] N86-12920

WIND VELOCITY MEASUREMENT
Laser anemometer using a single circuit board N86-12411
Atmospheric turbulence investigations at Tsimlyansk Scientific Station, Atmospheric Physics Institute, USSR Academy of Sciences N86-12735

WINDPOWER UTILIZATION
Navy applications experience with small wind power systems
[AD-A158561] N86-12778
Wind generation in Washington
[DE85-012791] N86-12787
Small scale wind energy conversion programmatic equipment
[DE85-012319] N86-12793

WINDPOWERED GENERATORS
Wind generation in Washington
[DE85-012791] N86-12787

WINDS ALOFT
Global view of the upper level outflow patterns associated with tropical cyclone intensity changes during FGGE
[NASA-CR-174407] N86-12908

WING TIPS
China report: Science and technology
[JPRS-CST-85-029] N86-12446
Wingtip sails tested on Y-5 aircraft N86-12450

WINGS
Simulation of the enhanced traffic alert and collision avoidance system (TCAS 2)
[NASA-CR-176328] N86-12216

WINTER
Diagnosis of weather states in winter of 1980-1981 N86-12632
On the interannual variability and on trends of the temperature in the middle atmosphere N86-12827

WOOD
Steam-injection pressing of isocyanate-bonded aspen flakeboards, latitudes and limitations
[AD-A157833] N86-12389

WORK CAPACITY
Stimulus structures and mental representations in expert comprehension of computer programs
[AD-A157520] N86-12969

WORKING FLUIDS
Condensation heat transfer in plate heat exchangers
[DE85-012369] N86-12571
Absorption fluids data survey
[DE85-005279] N86-12792

X

X RAY ANALYSIS
Muon tomography used to study underground rock structure N86-12720

X RAY ASTRONOMY
Combined ultraviolet studies of astronomical source
[NASA-CR-176165] N86-13274

X RAY DIFFRACTION
Novel instrument for high-pressure research at ultra-high temperatures
[DE85-015674] N86-12589
X-ray diffraction cell for Debye-Scherrer and Guinier (Huber) cameras at pressure and temperature
[DE85-014815] N86-12593
X-ray diffraction studies of shock-modified inorganic materials
[DE85-015150] N86-13209

X RAY FLUORESCENCE
Energy dispersive spectroscopy using synchrotron radiation: Intensity considerations
[DE85-017530] N86-13200

X RAY SCATTERING
Dynamic small angle X-ray scattering study of stressed Kevlar 49 epoxy composites
[DE85-011408] N86-12264
Combined small angle X-ray scattering and transmission electron microscope studies of Al-Li alloys
[DE85-016356] N86-12303

X RAY SOURCES
RIIM accelerator beam experiments
[DE85-012034] N86-12244

X RAY SPECTRA
High-power ND: Glass laser and target chamber system and an experimental study of laser plasma X-ray N86-12428

X RAY SPECTROSCOPY
EE technical review
[DE85-015313] N86-12540
Energy dispersive spectroscopy using synchrotron radiation: Intensity considerations
[DE85-017530] N86-13200

X RAYS
Theory support of pulsed power experiments. Volume 3. E-beam chamber design
[AD-A158417] N86-13098
X-rays from the radio halo of Virgo A = M87
[NASA-CR-176303] N86-13285

XENON
Noble gases N86-12348

XENON CHLORIDE LASERS
Effect of amplified spontaneous emission on space coherence of XeCl laser N86-12454

Y

YAG LASERS
Frequency selection and mode locking of Nd:YAG laser N86-12395

YIELD POINT
High damage threshold porous silica antireflective coating
[DE85-012924] N86-12322

YIELD STRENGTH
Review of effects of long-term aging on the mechanical properties and microstructures of types 304 and 316 stainless steel
[DE85-016472] N86-12304

YTTRIUM
Paramagnetic form factors of HCP transiton metals
[DE85-016301] N86-12301

Z

ZINC
Anaerobic microbial dissolution of toxic metals in subsurface environments
[DE85-013308] N86-12251
Estimation of influence of ocean on distribution of heavy metals in marine atmosphere N86-12703
Zinc/ferricyanide battery development phase 4
[DE85-016026] N86-12781

ZINC ALLOYS
Electronic stakes in disordered solids. Part 3: Applications to materials science
[DE85-011416] N86-13213

ZINC SELENIDES
Investigation of reactive magnetron sputter deposited ZnSe for solar cell application
[DE85-016851] N86-12780

ZIRCONIUM
Paramagnetic form factors of HCP transiton metals
[DE85-016301] N86-12301

ZIRCONIUM ALLOYS
Resistance to fracture, fatigue and stress-corrosion of Al-Cu-Li-Zr alloys
[AD-A158407] N86-12300

ZIRCONIUM ISOTOPES
Isovector resonances in pion charge exchange
[DE85-012746] N86-13106

ZIRCONIUM OXIDES
Microluminescence spectra of Ti-activated ZrO2-Y2O3
[DE85-010131] N86-13206

ZODIACAL LIGHT
Infrared measurements of spacecraft glow planned for Spacelab 2 N86-13263

PERSONAL AUTHOR INDEX

SCIENTIFIC AND TECHNICAL AEROSPACE REPORTS VOLUME 24 NUMBER 3

Typical Personal Author Index Listing

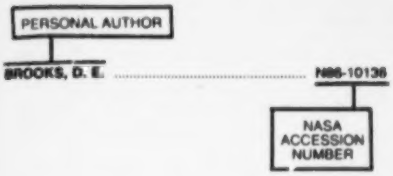

- Listings in this index are arranged alphabetically by personal author. The NASA accession number denotes the number by which the citation is identified.

A

ABRAHAM, K. M. N86-12776
ABRAMOV, A. V. N86-12650
ACKEN, C. F. N86-12538
ACOUSTA, R. N86-12485
ACQUAH, J. B. N86-13003
ADAMS, C. R. N86-13004
ADAMS, D. F. N86-12258
ADDAMIANO, A. N86-13185
N86-13191
ADELMAN, S. J. N86-13272
AFANASYEVA, M. S. N86-12663
AGARWALA, V. S. N86-12298
AGATOVA, A. I. N86-12667
AGAYEV, T. D. N86-12698
AGGARWAL, S. N86-12363
AGHA, G. A. N86-12994
AIHARA, K. N86-12377
AIXIANG, H. N86-12398
AKAL, T. N86-12941
N86-12942
N86-12943
AKGUN, M. B. N86-12490
AKHMEDOV, N. I. N86-12699
ALABIN, G. P. N86-12516
ALBERG, M. N86-13120
ALBRIDGE, R. G. N86-13259
ALEKPEROV, I. A. N86-12699
ALEKSEYEV, A. N86-12720
ALEXANDER, S. S. N86-12856
ALI, H. B. N86-12942
ALIYEVSKIY, B. L. N86-12516
ALLEN, S. D. N86-12327
ALLEN, W. R. N86-13197
ALONSO, J. N86-13092
ALONZO, J. N86-13155
ALSTON, W. B. N86-12311
ALUFFI-PENTINI, F. N86-13029
ALVAREZ, J. L. N86-13206
AMICK, C. J. N86-13038
ANANTHASAYANAM, M. R. N86-12828
ANDERSON, G. D. N86-12566
ANDERSON, H. R. N86-13268
ANDERSON, J. E. N86-12747
ANDERSON, O. A. N86-13093
ANDERSON, R. R. N86-13283
ANDREW, M. E. N86-12947
ANGELINI, P. N86-13201
ANHOLT, R. E. N86-13155
ANIKIYEV, V. V. N86-12703
ANSLEY, S. J. N86-13060
AOKI, I. N86-12382
AOYAGI, R. N86-12386
APTEKMAN, Z. Y. N86-12722
AREFYEV, V. N. N86-12734
ARKANI-HAMED, J. N86-12857
N86-12870
ARMSTRONG, W. T. N86-13141
N86-13152
ARNO, R. G. N86-12619
ARNOLD, G. S. N86-13261
ARONSON, J. R. N86-13195
ARTELNYY, V. V. N86-12647
ARTEMYEV, M. Y. N86-12728
ARTHUR, K. H. N86-13046
ARTZ, R. S. N86-12807
ARYA, S. P. S. N86-12906
ASAY, J. R. N86-12391
ASAYAMA, S. N86-12374
ASO, T. N86-12849
ATKINSON, W. H. N86-12226
AU, A. Y. C. N86-12813
AUBLE, R. L. N86-13069
AUCHAMPAUGH, G. F. N86-13173
AUGUS, J. E. N86-12619
AVERY, S. N86-12831
AVERY, S. K. N86-12840
AWAYA, H. N86-12788
AZGAPETIAN, A. M. N86-13184
AZGAPETIAN, V. N86-13184

B

BABAYEVA, T. M. N86-12728
BABICZ, S. J. N86-12522
BACA, R. G. N86-13001
BACKUS, G. E. N86-12889
N86-12892
BACON, L. D. N86-13011
BAEDER, J. D. N86-12207
BAGBY, J. S. N86-12504
BAGIN, V. I. N86-12681
BAISONG, L. N86-12400
BALFOUR, W. D. N86-12806
BALIUNAS, S. L. N86-13274
BALSLEY, B. B. N86-12831
N86-12836
BANDINI, B. R. N86-13112
BANERJEE, P. N86-12977
BARANOV, B. V. N86-12710
BARATTA, F. I. N86-12623
BARKER, L. M. N86-12391
BARNARD, J. J. N86-13276
BARNES, C. E. N86-13133
BARNES, D. C. N86-13177
BARNETT, J. J. N86-12814
N86-12815
N86-12819
N86-12820
N86-12821
N86-12826
BARON, S. N86-12212
BARRETT, J. L. N86-13253
N86-13254
N86-13255
BARRETT, R. J. N86-13006
BARRUS, D. M. N86-13019
BARRY, W. C. N86-13074
BARTELS, D. L. N86-12931
BARTHELL, B. L. N86-12535
BARTHOLOMEW, R. J. N86-13050
BATTS, G. W. N86-12917
BAUER, F. N86-12590
BAUER, O. H. N86-13283
BAYEV, V. K. N86-12271
BEAL, B. A. N86-12570
BEAM, J. E. N86-12559
BECKER, A. N86-12744
BECKLEY, B. N86-12882
BECKWITH, D. R. N86-13020
BEDARD, R. N86-12788
BELAND, R. R. N86-12491
BELL, H. B. N86-12533
BELMONT, A. D. N86-12825
BENDERSK, L. A. N86-12296
BENILOV, Y. S. N86-12671
N86-12715
BENJAMIN, R. F. N86-12594
BENNETT, B. W. N86-12297
BENREN, L. N86-12448
BENSON, C. L., JR. N86-12925
BENTON, E. R. N86-12890
BENZHI, T. N86-12442
BERNHARD, R. J. N86-13057
BERRY, R. S. N86-12367
BERTINOV, A. I. N86-12516
BESSLER, W. F. N86-12548
BETHKE, J. J. N86-12298
BHALLA, A. N86-12319
BICKEL, W. S. N86-13131
BIDEGANETA, K. N86-12747
BIEHL, L. L. N86-12741
BIER, R. E. N86-12534
BIRKEMEIER, W. A. N86-12946
BIRMAN, B. A. N86-12633
BISHOP, R. N86-12363
BJORKEN, J. D. N86-13097
BLACKMAN, J. A. N86-13208
BLAIR, W. P. N86-13274
BLATOV, A. S. N86-12673
BLOCK, M. G. N86-12963
BLOEMHOF, E. E. N86-13277
BLOOM, S. D. N86-13216
BLOSSOM, J. M. N86-12986
BLOXHAM, J. N86-12865
BLOXOM, B. N86-12971
BLUMENTHAL, S. N86-12489
BLUZER, N. N86-12513
BOERCKER, D. B. N86-13143
BOERI, G. N86-12795
BOGER, L. C. N86-13021
BOHACHEVSKY, I. O. N86-13017
BOLAND, E. P. N86-13231
BOOS, J. B. N86-12511
BOROWSKI, S. K. N86-13142
BOSLOUGH, M. B N86-12308
BOTTKA, N. N86-13186
BOUCHER, D. J., JR. N86-12899
BOWMAN, J. D. N86-13106
BOWMAN, L. M. N86-12259
BRADLEY, M. M. N86-12907
BRAMSON, M. A. N86-12646
BRANAM, K. M. N86-12953
BRANDO, T. N86-13119
BRANSTETTER, L. J. N86-13005
BREITHAUPT, D. N86-12629
BRENNAN, L. E. N86-12494
BRENNER, A. N86-12882
BRESCH, J. R. N86-12958
BRISCO, B. N86-12740
BRISTOL, S. N86-13101
BRIXNER, B. N86-13134
BROADWELL, J. E. N86-12288
BROCK, F. J. N86-13251
BRODZIK, D. N86-13095
BROOKS, S. L. N86-13027
BROWMAN, A. A. N86-13083
BROWN, C. R. N86-12858
BROWN, D. N86-12592
BROWNE, N. M. N86-12620
BRUNK, W. O. N86-13104
BRYANT, G. H. N86-12584
BU, G. N86-12534
BUECK, J. C. N86-12527
BUHOLZ, N. E. N86-12598
BUKIN, O. A. N86-12736
BUNKIN, A. F. N86-12705
BUNSHAH, R. F. N86-12273
BURGESS, T. J. N86-12524
BURKE, R. N86-12209
BURNETTE, M. N86-12618
BURNS, J. A. N86-12625
BURNSIDE, W. D. N86-12216
BURRELL, C. F. N86-13174
BUSH, E. D., JR. N86-13081
BUSINGER, J. A. N86-12948
BUSLAYEV, V. S. N86-12664
BUTTRAM, M. N86-12531
BYERS, C. H. N86-12596
BYKOV, V. G. N86-12724
BYKOVTSEV, G. I. N86-12656

C

CABLE, J. W. N86-13203

CAIN, J. C. N86-12888
CAIRD, R. S. N86-12535
CALISE, A. J. N86-13028
CAMPARO, J. C. N86-13065
N86-13066
N86-13067
CANDE, S. C. N86-12862
CANG, Y. N86-12402
CARACCIOLO, R. N86-12795
CARDENAS, R. L. N86-.2618
CARIGNAN, G. N86-13245
CARLSON, F. M. N86-13186
CARLSON, N. N. N86-12606
CARLSTEN, E. E. N86-12529
CARR, M. J. N86-12324
CARR, V. N86-12987
CARROLL, A. N86-13157
CARROLL, J. C. N86-12501
CAZENAE, A. N86-12861
CEBECI, T. N86-12561
CELMINS, I. C. N86-12274
CHAKRABARTI, S. N86-13249
CHAMBERLIN, D. D. N86-13067
CHAMBERS, T. L. N86-12936
CHAN, C. F. N86-13093
CHANG, J. S. N86-12373
CHANG, T. D. N86-12546
CHANGH'UAI, Z. N86-12465
CHANGWATCHAI, C. N86-12622
CHANIN, M. I. N86-12835
CHANNON, S. L. N86-12262
CHAPMAN, E. G. N86-12800
CHEN, C. P. N86-12551
CHEN, C. T. N86-12503
CHEN, L. N86-12908
CHEN, P. J. N86-12536
CHEN, T. P. N86-13211
CHENGYE, W. N86-12466
CHEPKUNAS, L. S. N86-12722
CHERNOPLEKOV, A. N. N86-12637
CHERNYSHOVA, N. B. N86-12663
CHIMIENTI, I. N86-13157
CHITWOOD, I. D. N86-12626
CHO, S. N86-12545
CHONGWEN, G. N86-12967
CHONGZHU, R. N86-12419
CHOU, Y. M. N86-13046
CHOW, R. R. N86-12208
CHOWDHURI, P. N86-12528
CHRIEN, R. E. N86-13141
N86-13152
CHU, W. K. N86-13197
CHUBURKOV, Y. T. N86-12668
CHUGUANG, F. N86-12443
CHUNBAO, Z. N86-12425
CHUNGUANG, G. N86-12394
CHUNYANG, J. N86-12457
CHUVASHINA, I. Y. N86-12635
CIESLAK, M. J. N86-12305
CLARK, J. H. E. N86-12918
CLARK, R. R. N86-12845
CLARK, R. S. N86-12244
CLARKE, J. T. N86-13262
CLENDENIN, J. E. N86-13169
CLIFF, E. M. N86-12625
CLIFFORD, S. N86-13282
CLIFTON, S. N86-13241
CLINE, M. W. N86-12905
COBURN, M. D. N86-12284
COHEN, S. A. N86-13260
COLES, C. E. N86-12246
COMFORT, R. H. N86-13138
CONNOLLY, A. F. N86-12260
CONVERSE, D. R. N86-12939
CONZETT, H. E. N86-13072
COOKE, J. F. N86-12301
N86-13208
COOPER, L. N. N86-12961
COOPER, R. E. N86-13009
COOPER, W. S. N86-13093
COPELAND, R. J. N86-12791
COPENHAVER, W. W. N86-12229
COPLEY, S. M. N86-12327
COPPERSMITH, S. N. N86-12621
CORBETT, G. O. N86-12525
CORNELIUS, C. E. N86-12753
CORNELL, R. N86-12591
CORNEY, M. N86-12615
N86-12619
N86-12620
N86-12626
CORNIE, J. A. N86-12261
CORT, G. N86-13019
COSTRELL, L. N86-13122
COTTER, T. P. N86-13017
COULTIS, D. W. N86-12983
COUNCE, R. M. N86-13020
COWLEY, P. J. N86-12999
CRAIG, L. J. N86-12534
CRAIG, R. L. N86-12831
CRANDALL, M. G. N86-13035
CRAWFORD, G. A. N86-13120
CRAWFORD, O. H. N86-12607
CREMERS, D. A. N86-12249
CRIST, C. E. N86-12537
CROSS, D. C. N86-12474
CROSS, J. B. N86-12249
N86-13258
CROSS, L. E. N86-12319
CROSS, R. L. N86-12930
CROWLEY-MILLING, M. C. N86-13075
CRUM, L. A. N85-13059
CRUZ, R. E. N86-12236
CUDDIHY, E. F. N86-12774
CUNDI, C. N86-12403
CURRENT, K. W. N86-12526
CUSHMAN, J. H. N86-12802
CUTTEN, D. R. N86-13129
CYR, M. A. N86-12226

D

DAFTARI, L. N86-13119
DAHAO, G. N86-12428
DAHENG, W. N86-12414
DAIELLO, R. V. N86-12762
DAKE, Z. N86-12454
DALGARNO, A. N86-13243
DALY, R. T. N86-12964
DAMPIER, F. W. N86-12775
DANDRIDGE, A. N86-12581
DANIEL, B. R. N86-12362
DANTZ'G, G. B. N86-12993
DARAGAN, S. K. N86-12722
DASH, Z. N86-13107
DAUGHTRY, C. S. T. N86-12741
DAVIS, B. W. N86-12572
DAVIS, J. I. N86-12605
DAWSON, W. K. N86-13122
DAXI, Y. N86-12450
DAZHONG, L. N86-12415
DEFANG, H. N86-12407
DEGUZMAN, A. N86-13119
DEHOPE, W. J. N86-13096
DEJONGH, J. E. N86-12200
DELAHOY, A. E. N86-12767
DELL, G. F. N86-13156
DELLETREZ, J. N86-13161
DELVIGS, P. N86-12256
DEMIN, J. T. N86-12708
DEMIN, Y. L. N86-12670
DEMING, L. N86-12464
DENOYER, J. M. N86-12880
DERRICK, M. N86-13100
DESTAFNEY, T. M. N86-12242
DESTROBEL, F. N86-12941
DETHIER, J. L. N86-13120
DEVANE, J. F. N86-12900
DEVILBISS, T. A. N86-12257
DEWALL, A. E. N86-12946
DICKERSON, M. N86-12795
DIEM-KIRSOP, P. S. N86-12246
DIMOTAKIS, P. E. N86-12288
DINGFU, Y. N86-12467
DIXON, R. G. N86-12261
DMITRUK, M. N86-12631
DOBROVOLSKIY, S. G. N86-12638
DODD, C. V. N86-12626
DOLGOPOLOV, D. V. N86-12722
DOMINGO, N. N86-12615
DONOHUE, M. D. N86-12274
DOSS, E. D. N86-12567
DOSS, S. K. N86-12606
DOUTHAT, D. Z. N86-13026
DOVER, S. A. N86-12390
DOW, J. D. N86-13193
DOYLE, T. E. N86-13206
DRAPER, B. I. N86-12533
DREYFUSS, P. N86-12316
DUANYANG, D. N86-12458
DUCHANE, D. V. N86-12535
DUFF, I. S. N86-13015
DUNCAN, M. G. N86-12588
DUNFU, L. N86-12433
DUNN, B. N86-12273
DUNN, G. J. N86-12611
DUPRESS, A. K. N86-13274
DUVAL, V. N86-12592
DWIGHT, A. E. N86-13210
DYER, F. N. N86-13125

E

EAGAR, T. W. N86-12611
EAGLESON, P. S. N86-12739
ECHIGO, H. N86-12385
ECKERT, J. N86-12586
N86-13199
EDEN, J. G. N86-12955
EDGETT, L. B. N86-13135
EDWARDS, B. N86-12814
EDWARDS, D. A. N86-13085
EDWARDS, F. N86-12526
EDWARDS, R. H. N86-12327
EGGLESTONE, G. T. N86-12620
EISENHARDT, G. H. N86-13026
EISENHARDT, R. G. N86-13026
EKBLAD, K. J. N86-13001
EKDAHL, C. A. N86-13108
N86-13109
EKLUND, T. I. N86-12214
ELAM, W. T. N86-12589
N86-13200
ELANDJIAN, L. N86-12260
ELDERING, C. A. N86-12514
ELDIB, I. E. O. N86-12544
ELDRIDGE, O. N86-13179
ELFORD, W. G. N86-12831
ELLIOTT, G. R. N86-12595
ELLISON, J. A. N86-13197
ELSBERRY, R. L. N86-12922
ELSNER, J. B. N86-12916
EMSLIE, A. G. N86-13195
ENG, C. N86-12486
ENGEBRETSON, M. J. N86-13242
ENGELN, J. F. N86-12812
ENGLAND, R. L. N86-13001
ENRUI, T. N86-12461
EPSTEIN, R. N86-13175
ERASLAN, A. H. N86-13186
ERB, K. A. N86-13069
ERICKSON, D. J. N86-12535
ERICKSON, E. D. N86-12231
ERICKSON, L. M. N86-12565
ERNEST, T. L. N86-12564
ESER, E. N86-12767
ESPOSITO, J. J. N86-12974
ETKIN, V. S. N86-12644
EVANS, E. G. N86-12805
EVANS, J. E. N86-12920
EVANS, L. S. N86-12796
EVANS, N. L., JR. N86-12919
EVERETT, S. L., JR. N86-12980

F

FARRELL, W. M. N86-13264
FAULKNER, J. S. N86-13213
FAYARD, L. D. N86-12754
FAZIO, G. G. N86-13263
N86-13271
FEDDER, J. A. N86-12897
FEDOROVSKIY, A. D. N86-12646
FEEHRER, C. N86-12212
FEIGELSON, R. S. N86-13'92
FEINBERG, B. N86-13095
FELCH, K. L. N86-12534
FELDMAN, W. C. N86-12904
FELLERS, J. F. N86-12264
FELLOUS, J. L. N86-12831
FENNELL, J. F. N86-12248
FERGUSON, P. E. N86-13096
FERLA, M. C. N86-12942
FERRANDO, W. A. N86-12299
FERTIS, D. G. N86-13219
FEWELL, N. N86-12498
FEYGELSON, Y. M. N86-12640
FIDDAMAN, T. S. N86-12534
FILLIUS, W. N86-13279
N86-13280
N86-13281
FILONOVICH, S. R. N86-12644
FINKELSTEIN, P. L. N86-12809
FINNEMORE, D. K. N86-13211
FISCUS, I. B. N86-12220
FLEITOUT, L. N86-12876
FLEMINGS, M. C. N86-12261
FLETCHER, W. L. N86-12754
FLUSS, M. J. N86-13111
FLYNN, W. J. N86-12963
FODOR, G. E. N86-12359
FOLEY, J. D. N86-13002
N86-13003
FONAREV, G. A. N86-12661
FONTANELLA, J. J. N86-12317

FOOTE, H. P. N86-12742
FORBES, J. M. N86-12824
N86-12830
N86-12833
N86-12839
FORD, M. N86-13051
FORTUS, M. I. N86-12634
FOWLER, C. M. N86-12535
FOX, L. J. N86-12534
FRADIN, F. Y. N86-13210
FRAENKEL, L. E. N86-13038
FRANCIS, A. J. N86-12251
FRANCIS, D. A. N86-12989
FRASER, G. J. N86-12851
FRASER, J. S. N86-13084
FRAZIER, W. E. N86-12502
FREDERICK, R. N86-12228
FRESE, K. W. N86-12290
FREY, H. N86-12865
FRICKE, W. G. N86-12300
FRIEDMAN, M. N86-13068
FRIEDMAN, M. C. N86-13098
FRIGO, N. J. N86-12581
FROST, C. A. N86-12537
N86-13108
FRUEHOLZ, R. P. N86-13065
N86-13066
N86-13067
FUCHENG, L. N86-12457
FUCHENG, Z. N86-12403
FUDI, Q. N86-12411
FUKUDA, H. N86-12373
FULLER, G. M. N86-13216

G

GABB, T. P. N86-12294
GADIYARAM, P. S. N86-12906
GALEA, S. N86-12234
GALLEGOS, F. R. N86-13083
GALLEGOS, J. D. F. N86-13081
GALLILY, I. N86-12554
GALLO, M. A. N86-12983
GALUMYAN, A. S. N86-12705
GANCHANG, W. N86-12447
N86-12465
GANGEL, D. J. N86-12500
GANGHUA, G. N86-12448
GANGULI, S. G. N86-13140
GARDASHOV, R. G. N86-12707
GARDER, O. I. N86-12666
GARSHNEK, V. N86-12949
GATTINGER, R. L. N86-13244
GAYDA, J. N86-12294
GAZZERA, R. W. N86-12217
GEE, J. M. N86-13178
GEIMER, R. L. N86-12389
GELDER, T. F. N86-12239
GELINAS, R. J. N86-12606
GENCO, L. V. N86-12973
GENESERETH, M. R. N86-13052
GENT, A. N. N86-12316
GENTNER, D. R. N86-12970
GEODEKYAN, A. A. N86-12655
GEORGE, L. I. N86-13136
GEORGIYEVSKIY, Y. S. N86-12737
GERSHENZON, N. I. N86-12727
GERSTNER, H. E. N86-12953
GETTINGER, P. E. N86-13084
GIBBS, W. R. N86-13090
GILBERT, R. O. N86-12799
GILBERT, W. N86-13054
GILPATRICK, J. D. N86-13078
N86-13087
GINSBERG, J. H. N86-12569
GIORGI, A. L. N86-13204
GIULIANI, J. F. N86-13124
GLAHN, H. R. N86-12936
GLIMM, J. N86-13045
GOFF, R. M. N86-12625
GOFORTH, J. H. N86-12527
N86-12535
GOKHBERG, M. B. N86-12727
GOLDBERG, L. S. N86-12267
GOLDFINE, A. N86-12988
GOLDGRABEN, J. R. N86-13130
GOLDMAN, A. N86-12234
GOLDMAN, L. M. N86-13180
GOLDSTEIN, S. A. N86-13088
GOLDSTONE, J. A. N86-12586
N86-13019
N86-13199
GOLOTYUK, F. P. N86-13194
GONZALEZ, C. C. N86-12763
GOODYER, M. J. N86-12204
N86-12238
GORBICS, C. S. N86-12946
GORCHAKOV, G. I. N86-12689
N86-12696
GORCHIYEV, A. A. N86-12698
GORDEYVHEV, D. O. N86-12712
GORNEY, D. J. N86-12898
GOSNIK, T. N86-12901
GOULD, H. N86-13155
GRAHAM, R. A. N86-12308
N86-12590
N86-13209
GRANATO, A. V. N86-13212
GRANDCHAMP, B. N86-12216
GRANT, W. B. N86-12501
GRATZ, R. F. N86-12311
GRAY, W. M. N86-12908
GREEN, B. D. N86-13246
GREEN, J. B. N86-12281
GREEN, L. N86-12365
GREEN, P. J. N86-13034
GREENLEAF, J. E. N86-12956
GREENSPAN, L. N86-12222
N86-12223
GREGORY, J. C. N86-13257
GREISIGER, K. M. N86-12841
GROGG, W. E., JR. N86-12926
GROVES, G. V. N86-12824
GRUZA, G. V. N86-12633
GUANGZHAO, M. N86-12429
GUANQUAN, X. N86-12426
GUBBINS, D. N86-12885
GUFELD, I. L. N86-12727
GUICHEN, T. N86-12395
GUIDOTTI, R. A. N86-12785
GUISHENG, Y. N86-12419
GUIYAN, Z. N86-12457
GUIZHEN, Y. N86-12443
GUMBATOV, A. I. N86-12699
GUNARD, K. T. N86-12753
GUNTHER, E. B. N86-12930
GURDAL, Z. N86-12254
GURNETT, D. A. N86-13283
N86-13284
GUSEV, S. V. N86-12695
GUSSENHOVEN, M. S. N86-12896
GUY, F. W. N86-13082

H

HACKER, B. A. N86-12289
HADDEN, G. B. N86-12613
HAERENDEL, G. N86-13283
HAGEE, G. R. N86-12797
HAGER, B. H. N86-12872
N86-12875
N86-12877
HAGLUND, R. F., JR. N86-13259
HAIMING, X. N86-12415
HALE, G. M. N86-13148
HALE, M. N86-12200
HALFORD, G. R. N86-12295
HALL, C. K. N86-12289
HALL, D. F. N86-12248
HALL, M. R. N86-12777
HALL, P. N86-12550
HALLQUIST, J. O. N86-12565
HAMEL, W. R. N86-12975
N86-12976
HAMMER, J. H. N86-13164
HAN, K. S. N86-12600
HAN, S. N86-13211
HANERFELD, H. N86-13153
HANG, C. N86-12431
HANNUM, J. A. E. N86-12328
HANSEN, E. P. N86-12221
HANSEN, I. F. N86-13105
HARDY, D. A. N86-12896
HARGIS, P. J., JR. N86-13178
HARRIS, B. W. N86-12366
HARRIS, I. A. N86-12321
HARRIS, K. B. N86-12490
HARRISON, C. G. A. N86-12891
HARRISON, R. N86-13081
HART, R. E., JR. N86-12509
HART, S. L. N86-13096
HART, V. E. N86-13081
HARTEN, A. N86-13032
HARTMAN, C. W. N86-13164
HARTMANN, G. K. N86-12838
HARTMANN, L. W. N86-13274
HARTMANN, M. J. N86-12227
HARVEY, A. N86-12618
HASSENZAHL, W. N86-13054
HASTI, D. E. N86-12244
HASTINGS, D. A. N86-12894
N86-12895
HASTRUP, O. F. N86-12941
HATFIELD, W. E. N86-12518
HAUCHECORNE, A. N86-12835
HAUSER, J. R. N86-12510
HAUSMAN, R. P., JR. N86-13216
HAXBY, W. F. N86-12878
HAYANO, S. N86-12526
HEADLEY, T. J. N86-12324
HEARN, C. P. N86-12508
HEID, K. R. N86-12965
HEISER, W. H. N86-12200
HELLMANN, J. R. N86-12324
HEMING, X. N86-12423
HEMMINGER, J. N86-12280
HENDERSON, L. J. N86-12940
HENGDU, Z. N86-12458
HENSLEY, J. D. N86-12616
HERMANCE, J. F. N86-12887
HERRAMANNSFELDT, W. B. N86-13153
HERSHBERG, E. L. N86-12211
HESS, C. F. N86-12580
HESS, J. H. N86-12753
HEUSTESS, J. E. N86-12500
HIEBERT-DODD, K. L. N86-13007
HILL, C. K. N86-12917
HILL, J. R. N86-13280
HILL, R. G. N86-12214
HILL, T. A. N86-12533
HINGHOFER-SZALKAY, H. N86-12956
HINOJOSA, J. H. N86-12863
HINZE, W. J. N86-12869
HIROTA, I. N86-12822
N86-12849
HIRSHMAN, S. P. N86-13166
HITANI, M. N86-12915
HIXSON, R. S. N86-13062
HOBART, D. E. N86-13102
HOBSON, R. M. N86-12373
HOCKING, W. K. N86-12834
HOELLIG, K. N86-13036
HOGAN, W. J. N86-13181
HOLDEN, N. E. N86-13115
N86-13117
HOLDREN, M. W. N86-12230
HOLLAND, W. D. N86-13020
HOLLANDSWORTH, R. P. N86-12781
HOLLEBEEK, R. N86-13070
N86-13071
HOLMAN, G. T. N86-13088
HONDA, S. N86-12375
HONEYCUTT, T. E. N86-12603
HONG, J. P. N86-12986
HONGXING, W. N86-12428
HOOD, P. J. N86-12870
HOOKE, F. H. N86-12199
HOOKE, L. R. N86-12949
HOOTEN, B. R. N86-12219
HORAK, J. A. N86-12304
HOROWITZ, E. N86-12296
HORTON, W. N86-13171
HORWITZ, J. L. N86-13138
HOUSHENG, Z. N86-12418
HOWARD, D. N86-13095
HOWARD, D. D. N86-12474
HOWARD, W. M. N86-13278
HOWELL, R. H. N86-13111
HRDINA, L. A. N86-12314
HSU, J. P. N86-12597
HSU, M. S. N86-12597
HUAIGUI, G. N86-12417
HUAIQUAN, Y. N86-12432
HUCHRA, J. P. N86-13274
HUESER, J. E. N86-13251
HUEY, H. E. N86-12534
HUGRASS, W. A. N86-13141
N86-13152
HUMEI, J. N86-12967
HUMPHREYS, E. D. N86-12877
HUNG, C. C. N86-12485
HUNTER, G. B. N86-12611
HUNTER, W. T. N86-13081
HURAIB, F. S. N86-12756
HUTCHINSON, D. P. N86-13154

I

ICHIKAWA, Y. N86-12373
ICHIKI, A. N86-12912
IDE, J. P. N86-12583
IEMKE, R. W. N86-13109
IESKOVAR, B. N86-12282
IH, C. S. N86-12599
IKEDA, H. N86-13122
ILICHEV, V. I. N86-12703
ILIN, V. A. N86-12644
N86-12653

ILIN, Y. A. N86-12714
ILYEV, A. Y. N86-12665
IMAMURA, M. S. N86-12756
IRWIN, J. B. N86-12933
ISAKOV, A. A. N86-12689
ISAYEV, V. I. N86-12725
ISIDOROV, V. A. N86-12693
ISKANDAR, I. K. N86-12995
ISMAIL-ZADE, A. T. N86-12660
ISMAYLOV, A. S. N86-12699
ITO, P. H. N86-12585
IVANCHENKO, G. A. N86-12686
IVANOV, V. A. N86-12686
IVANOV, V. V. N86-12666
IVANOV, Y. A. N86-12675
IVCHENKO, V. O. N86-12672
N86-12702
IVERSON, R. N86-13159

J

JABLON, S. N86-12964
JABOUR, W. E. N86-12950
JACOB, J. H. N86-13084
JACOBSON, N. S. N86-12310
JAKLITSCH, D. J. N86-12260
JAMES, E. N86-12365
JAMES, J. W. N86-12787
JAMES, M. B. N86-13153
N86-13169
JAMESON, A. N86-12208
JANASWAMY, R. N86-12480
N86-12481
JANNEY, J. L. N86-12998
JANNEY, M. A. N86-12321
JANOWITZ, M. F. N86-12945
JASPER, G. L. N86-12917
JENKINS, P. H. N86-12797
JENNINGS, D. E. N86-13264
JENNINGS, S. G. N86-13128
JESTER, T. N86-12768
JIAN, C. N86-12416
JIANHUA, C. N86-12415
JIANMIN, Y. N86-12423
JIANPING, C. N86-12449
JIANPING, Y. N86-12454
JIANWEN, C. N86-12454
JIARONG, L. N86-12435
JIAYOU, Y. N86-12435
JIEFEL, Z. N86-12412
JINAGUO, W. N86-12436
JINGGANG, X. N86-12465
JINGHUA, W. N86-12415
JINMING, L. N86-12422
JINRU, L. N86-12404
JINZHI, N. N86-12454
JISEN, L. N86-12453
JIZHONG, X. N86-12420
JOHANSSON, J. F. N86-12482
N86-12483
JOHNSON, D. L. N86-12244
N86-12917
JOHNSON, I. C. N86-13154
JOHNSON, J. H. N86-12231
JOHNSON, N. L. N86-13047
JOHNSON, R. D. N86-13238
JOHNSON, R. P. N86-13085
JOHNSON, R. W. N86-13044
JOHNSON, W. L. N86-12991
JONES, B. A. N86-12587
JONES, C. M. N86-12523
N86-13069
JONES, G. N86-12279
JONES, M. E. N86-13145
JONES, W. R., JR. N86-12293
JORDAN, A. K. N86-12492
JORGENSEN, J. D. N86-13210
JORY, H. R. N86-12534
JUBIN, R. T. N86-13020
JUNFENG, Z. N86-12463
JUNHUA, P. N86-12436
JUPING, S. N86-12457

K

KACHANOV, N. N. N86-12713
KADISH, A. N86-13145
KAGAN, B. A. N86-12641
KAHLE, H. G. N86-12854
KALIA, R. K. N86-13205
KAMEGAI, M. N86-12563
KANAKIA, M. D. N86-12359
KANEDA, T. N86-12373
KAPILA, A. K. N86-13229
KAPLAN, R. N86-13186
KAPLAN, S. N. N86-13174
KAPP, J. A. N86-12623
KARA, V. I. N86-12709
KARADI, G. M. N86-12782
KARLSON, N. N. N86-12686
KAROL, I. L. N86-12639
KATO, S. N86-12847
N86-12849
KATSUKI, S. N86-12912
KATZ, A. I. N86-12589
KAUFMAN, A. N86-12757
N86-12758
KAWAZOE, Y. N86-12388
KEATING, G. M. N86-12829
KECHEKEZYAN, K. A. N86-12729
KECK, R. L. N86-13161
KEDROV, O. K. N86-12731
KEFAN, C. N86-12427
KEFFELER, D. R. N86-12532
KELLER, N. B. N86-12678
KELLER, T. M. N86-12318
KELLEY, H. J. N86-12625
KELLNER, R. G. N86-12986
KEMP, W. B., JR. N86-12237
N86-12240
KENDALL, D. J. W. N86-13244
KENNEDY, C. R. N86-12321
KEOLIAN, R. M. N86-12556
KERIMOV, I. G. N86-12683
KERLEY, G. I. N86-12391
KERNS, C. N86-13101
KERNS, Q. N86-13101
KESKINEN, K. N86-12373
KESKINEN, M. J. N86-12897
KESSEL, C. N86-13116
KESSEL, P. A. N86-12250
KHOYLOO, A. N86-13248
KHUBUNAYA, S. A. N86-12732
KIEFER, M. I. N86-13014
KIEKEL, P. D. N86-13108
KILLEEN, J. N86-13023
KILROY, W. P. N86-12776
KIMBALL, C. W. N86-13210
KIMURA, K. N86-12914
KINCAID, J. P. N86-13228
KING, M. S. N86-13027
KINNAS, S. A. N86-12557
KINSLAND, G. L. N86-12902
KIPP, C. R. N86-13057
KIZNER, Z. I. N86-12674
KLEIN, J. D. N86-13168
KLEIN, L. S. N86-12563
KLEIN, P. H. N86-13185
KLEMA, V. N86-12992
KLEMM, B. A. N86-12621
KLEMT, W. B. N86-12752
KLEPIKOV, A. V. N86-12672
N86-12702
KLINE, N. W. N86-13001
KLINGE, R. K. N86-12638
KLINGNER, P. L. N86-13152
KLINKOWSTEIN, R. N86-13084
KLUGH, M. J. N86-12275
KNACKE, T. W. N86-12210
KNIGHT, D. J. N86-12231
KNOWLES, T. N86-12752
KOBAYASHI, A. S. N86-12624
KOBLINSKY, C. J. N86-12882
KOCH, D. B. N86-12470
KOCH, D. G. N86-13263
KOFSKY, I. L. N86-13253
N86-13254
N86-13255
KOGAN, S. Y. N86-12722
KOI, D. B. N86-12755
KOLLBERG, E. L. N86-12482
N86-12483
KONDRATYEV, K. Y. N86-12636
N86-12695
KONECNY, R. N86-12520
KONYUKHOV, A. I. N86-12655
KOONS, H. C. N86-12248
KOONTZ, R. F. N86-13159
KOPYL, Y. A. N86-12643
KORCHAGINA, O. A. N86-12722
KORTHAWI, D. N86-13179
KORZENIOWSKI, T. L. N86-12484
KOSHELKOV, Y. P. N86-12817
KOSYGIN, V. Y. N86-12725
KOTANI, M. N86-12375
N86-12377
KOTB, M. A. N86-12201
KOTZ, S. N86-13047
KOVACS, E. N86-13207
KRAMER, D. P. N86-12326
KRAMER, F. S. N86-13028
KRASNOPEVTSEV, A. Y. N86-12675
KRASNYY, M. L. N86-12725
KRAUSE, H. F. N86-12607
KRAUSS, A. R. N86-12252
KREISS, H. O. N86-13036
KRETSCH, M. J. N86-12960
KRETSCHMER, F. F. N86-12475
N86-12476
KREUTER, J. N86-13025
KURBATKIN, G. P. N86-12632
KURENKOVA, V. G. N86-12663
KURINO, T. N86-12914
KURY, J. N86-12629
KUZMICHEVA, T. F. N86-12642
KUZMIN, I. I. N86-12637
KUZMIN, P. N. N86-12677
KUZNETSOV, G. N. N86-12656
KWAN, J. W. N86-13093
KYRIAKAKIS, T. N86-12995

L

LABITZKE, K. N86-12814
N86-12821
N86-12826
N86-12827
LABRECQUE, J. L. N86-12862
LADD, A. J. N86-13143
LADOUCEUR, H. D. N86-12492
LAKNER, J. F. N86-12593
LAM, P. T. N86-12485
LAMBECK, K. N86-12855
LANGEL, R. A. N86-12884
N86-12893
LANGER, W. D. N86-13260
LAPCHINSKAYA, M. P. N86-12714
LARSON, N. M. N86-13000
LATHAM, J. N86-12924
LATHROP, J. W. N86-12764
LAUER, J. L. N86-12293
LAURENDEAU, N. M. N86-12283
LAUSHKIN, V. A. N86-12731
LAW, P. N86-12216
LAX, P. D. N86-13042
LAYNE, S. P. N86-12951
LECKRONE, D. S. N86-13272
LECOMPTE, M. N86-13243
LEE, C. H. N86-13084
LEE, D. K. N86-13166
LEE, E. N86-12365
N86-12629
LEE, J. D. N86-13112
LEE, J. S. N86-12264
LEE, K. P. N86-12614
LEE, L. M. N86-12590
LEE, M. A. N86-13205
LEE, S. S. N86-12307
LEE, S. W. N86-12485
LEE, S. Y. N86-13077
LEE, Y. Y. N86-13182
LEEMANN, B. N86-13095
LEFFLER, M. W. N86-12926
LEGASOV, V. A. N86-12637
LEGER, G. K. N86-13159
LEGER, L. J. N86-13267
LEIFESTE, G. T. N86-12537
LELAND, W. T. N86-12535
LEONHARDT, W. N86-13157
LEPPAERANTA, M. N86-12944
LESTER, W. A., JR. N86-13076
LEUNG, K. N. N86-13176
LEVCHENKO, O. V. N86-12704
N86-12710
LEVI, P. S. N86-12527
LEVY, L. N86-12952
LEWIN, K. F. N86-12796
LEWIS, D. L. N86-12806
LEWIS, H. R. N86-13177
LEWIS, J. C. N86-12612
LEWIS, M. B. N86-13201
LEWIS, M. C. N86-12203
LEWIS, R. A. N86-13119
LI, C. N86-12561
LI, F. N86-12580
LI, Q. N86-12456
LIANLONG, H. N86-12427
LICHUN, Z. N86-12443
LIFENG, Y. N86-12457
LIGHT, R. W. N86-13178
LIMIN, Z. N86-12428
LIN, G. N86-12455
LIN, J. D. N86-12560
LIN, J. S. N86-12264
LIN, M. L. N86-12611

LIONS, P. L. N86-13035
LIOU, C. S. N86-12922
LIQING, Z. N86-12410
LISOWSKI, P. W. N86-13173
LITTLEJOHN, M. A. N86-12510
LITTLETON, L. W. N86-12953
LIU, A. J. N86-12301
LIU, C. S. N86-12864
LIU, J. N86-13171
LIU, S. H. N86-12301
LLEWELLYN, E. J. N86-13244
LO, C. C. N86-13079
LO, T. Y. N86-12628
LOBANOV, A. A. N86-12703
LOCATIS, C. N86-12987
LOEW, G. A. N86-13151
LOGAN, T. J. N86-12804
LOPTNIKOV, V. I. N86-12700
LOTHROP, F. N86-13092
LOWDERMILK, W. H. N86-12322
LOWENSTEIN, D. I. N86-13119
LUCHNIK, G. L. N86-12646
LUCKHARDT, S. C. N86-13170
LUCOVSKY, G. N86-13189
LUERS, J. K. N86-12220
LUTSENKO, B. N. N86-12682
LUTZE, F. H. N86-12625
LYCZKOWSKI, R. W. N86-12576
LYON, F. F. N86-12230
LYTLE, F. E. N86-12283

M

MA, C. H. N86-13154
MA, T. Z. N86-13283
MACRISS, R. A. N86-12792
MADDALON, D. V. N86-12206
MAEDA, T. N86-12382
MAEKAWA, Y. N86-12849
MAGERRAMOVA, S. G. N86-12699
MAGNI, L. H. N86-12287
MAHAJAN, S. M. N86-13217
MAHAN, J. R. N86-12743
MAHER, J. V. N86-12575
MAIENSCHEIN, J. N86-12592
MALCOLM, R. C. N86-12300
MALINAUSKAS, R. A. N86-12596
MALINNIKOV, V. A. N86-12714
MALL, S. N86-12255
MALYSHKINA, V. V. N86-12676
MAMOSHINA, K. N. N86-12709
MANN, N. R. N86-12619
MANOS, D. M. N86-13260
MANSFIELD, D. K. N86-13154
MANSON, A. H. N86-12818
N86-12831
N86-12843
N86-12844
MANSON, R. B. N86-12487
MANSON, S. T. N86-13086
MANUCCIA, T. J. N86-12955
MANUYLOVA, N. I. N86-12640
MARIANI, E. A. N86-12517
MARINELLI, W. J. N86-13246
MARLOW, D. R. N86-13110
MARSELLA, M. N86-13063
MARSH, B. D. N86-12863
MARSH, J. G. N86-12882
MARSHALL, F. J. N86-12696
MARTIN, E. C. N86-12361
MARTIN, J. A. N86-13069
MARTIN, M. N86-12749
MARTIN, T. N86-12882
MARTIN, V. J. N86-12241
MARXER, N. N86-12293
MASON, A. S. N86-12798
MASON, D. P. N86-13223
MASSEBEUF, M. N86-12831
MASSEY, L. T. N86-12968
MASSEY, R. T. N86-12326
MATHEWS, G. J. N86-13216
N86-13278
MATRANGA, V. A. N86-13096
MATSON, M. N86-12748
MATUK, C. A. N86-13093
MAUERSBERGER, G. S. N86-12981
MAYA, I. N86-13116
MAYER, F. J. N86-12594
MAYNARD, R. L. N86-12594
MAYO, F. R. N86-12360
MAZARAKIS, M. G. N86-12244
MCADOO, D. C. N86-12868
MCALLASTER, M. E. N86-12305
MCATEE, W. H. N86-13088
MCCOOL, J. I. N86-12613
MCCOY, M. C. N86-12929
MCCRORY, R. L. N86-13100
MCCROSKEY, W. J. N86-12207
MCDADE, I. C. N86-13244
MCDANIEL, W. C. N86-13228
MCDONOUGH, D. N86-12749
MCFARLAND, E. R. N86-12239
MCGAHAN, R. V. N86-12486
MCGIRT, F. N86-12985
MCGOWAN, R. E. N86-12929
MCHARGUE, C. J. N86-13201
MCKEE, J. M. N86-12947
MCKENNA, K. F. N86-13141
N86-13152
MCKENZIE, D. P. N86-12871
N86-12878
MCKIERNAN, A. N86-12275
MCKNIGHT, W. L. N86-12996
MCMILLAN, C. N86-12629
MCMILLIN, M. L. N86-12206
MCMURPHY, F. N86-12592
MCNAIL, P. E. N86-12803
MCNEILL, D. H. N86-13260
MCNUTT, M. N86-12853
MCREYNOLDS, E. N86-12553
MEAD, H. R. N86-12202
N86-12208
MEDVEDEV, A. N. N86-12703
MEEK, C. E. N86-12818
N86-12831
N86-12843
N86-12844
MEEKER, D. J. N86-13164
MEI, V. C. N86-12783
MEIER, G. E. A. N86-13058
MEIER, W. R. N86-13181
MEISS, J. D. N86-13171
N86-13218
MELFI, L. T. N86-13251
MELLEY, J. J. N86-12901
MELNIK, R. E. N86-12202
N86-12208
MENARD, R. D. N86-12931
MENDE, S. B. N86-13240
N86-13241
N86-13244
N86-13265
MENDEL, J. E. N86-12325
MENDENHALL, M. H. N86-13259
MENDIS, D. A. N86-13280
MENGYU, S. N86-12397
MENZIES, K. T. N86-12287
MERKLIN, L. R. N86-12704
N86-12710
MERRILL, B. J. N86-13118
MESSURI, D. A. N86-12371
MEYER, G. G. L. N86-12978
MEYER, P. N86-13111
MEYER, T. J. N86-12270
MEYERHOF, W. E. N86-13155
MICHEL, J. W. N86-12574
MICHELOTTI, L. N86-13147
MIDGETT, M. R. N86-12804
MIGLIORE, H. N86-12553
MIKHAYLOV, V. O. N86-12728
MIKHAYLOVA, E. N. N86-12642
MILES, J. C. N86-12797
MILLER, D. R. N86-12560
MILLER, E. N86-13245
MILLER, H. C. N86-12926
N86-12946
MILLER, H. W. N86-13101
MILLER, J. C. N86-13094
MILLER, J. F. N86-12784
MILLER, J. H. N86-13086
MILLER, J. M. N86-12807
MILLER, L. B. N86-13019
MILLER, L. E. N86-12235
MILLER, R. N86-13092
MILLER, R. B. N86-12244
N86-13108
MILLER, R. E., II N86-12963
MILLER, R. H. N86-13153
N86-13159
N86-13169
MILLER, R. J. N86-13119
MILLS, R. L. N86-12589
MILROY, R. D. N86-13152
MIN, L. N86-12424
MINER, R. V. N86-12294
MINICHINO, C. N86-12539
MINTEN, A. N86-13070
N86-13071
MIRK, K. N86-13054
MIRONOV, Y. V. N86-12650
MIRVIS, V. M. N86-12635
MISENER, J. A. N86-12250
MITCHELL, H. G., JR. N86-12897
N86-13140
MITCHELL, J. C. N86-12747
N86-12959
MITCHELL, W. J. N86-12805
MIZERA, P. F. N86-12248
MOENY, W. M. N86-13132
MOFFITT, K. N86-12973
MON, G. R. N86-12772
MONAGHAN, R. N86-13157
MONTGOMERY, R. S. N86-12358
MONTH, M. N86-13073
MOOG, T. H. N86-12984
MOORE, D. N86-12773
MOORE, K. N86-12985
MOORE, R. D. N86-12239
MOOREHEAD, T. W. N86-13239
MOREL, D. L. N86-12770
MORGAN, G. N86-13053
MORGAN, R. J. N86-12283
MORGAN, T. N86-13208
MOROSIN, B. N86-13209
MOROZOV, Y. G. N86-12675
MORRIS, A. C., JR. N86-12975
MORRIS, D. E. N86-12285
MORRISEY, E. J. N86-12225
MORRISON, F. N86-12744
MORRISON, L. J. N86-13083
MOSKALENKO, N. I. N86-12695
MOSKALENKO, V. N. N86-12677
MOSKVINA, A. G. N86-12722
MOSLEY, W. C. N86-12265
MOTLEY, R. W. N86-13260
MULCAHY, T. M. N86-12568
MUMMA, M. J. N86-13264
MURAYAMA, T. N86-12388
MURPHY, H. N86-13107
MUSINSKI, D. L. N86-12594
MUSKET, R. N86-12592
MYCYK, R. T. N86-12754

N

NAIYAN, W. N86-12465
NAIYOU, W. N86-12441
NAKAGAWA, F. N86-12387
NAKAJIMA, S. N86-12375
NAKAMURA, S. N86-12376
NAKAMURA, T. N86-12387
NARASIMHA, R. N86-12828
NARODNITSKIY, G. Y. N86-12706
NASH, D. N86-12232
NAUJOKAT, B. N86-12827
NAUMOV, A. A. N86-12644
NAZAROVA, Y. A. N86-12651
NEIMAN, V. N86-12716
NELSON, G. C. N86-12785
NELSON, R. O. N86-13019
NEPROCHNOV, Y. P. N86-12704
N86-12710
NESSLAGE, G. V. N86-12306
NEU, C. E. N86-12298
NEWELL, T. A. N86-12791
NG, K. W. N86-13211
NICKLOW, R. M. N86-13203
NIKISHOV, V. I. N86-12646
NISIDA, M. N86-12375
NOBLE, E. G. N86-12286
NOER, R. J. N86-13211
NORDSTROM, P. N86-12752
NORMAN, D. A. N86-12970
NORMAN, V. S. N86-12953
NORTHROP, T. G. N86-13280
N86-13281
NOSOV, A. V. N86-12648
NOUHI, A. N86-12780
NOVRUZOV, Z. A. N86-12681
NUNES, C. S. N86-12570

O

OBEID, V. E. N86-12617
OCHS, G. R. N86-13137
OCONNELL, R. J. N86-12872
N86-12875
OCONNOR, M. O. N86-12960
OESTLUND, H. G. N86-12798
OGLE, J. K. N86-12754
OGURA, Y. N86-12378
OH, B. Y. N86-13119
OHEARN, M. N86-12750
OHI, S. N86-12375
OLDFIELD, L. C. N86-12583

OLEM, H. N86-12801
OLSEN, D. K. N86-13089
OLSON, P. N86-12886
OMALLEY, M. N86-12531
ONEIL, L. J. N86-12950
ONO, M. N86-13260
ONO, S. N86-12384
OOHA, H. N86-12535
OREILLY, F. J. N86-13048
ORLOV, V. L. N86-12516
OSTASHEVSKIY, M. G. N86-12730
OWEN, D. B. N86-13046
OWEN, E. W. N86-13163
OWENS, E. C. N86-12359
OWREN, H. M. N86-13083
OWREN, H. W. N86-13176
OYEDIRAN, A. A. N86-12542
OZGUZ, V. H. N86-12510

P

PACENKA, S. N86-12808
PACKAN, N. H. N86-12302
PAISNER, J. A. N86-12805
PAL, D. N86-12778
PALANISWAMY, S. N86-12266
PALMADESSO, P. J. N86-13140
PAN, L. N86-13215
PANCHAL, C. B. N86-12571
PANCHENKO, A. R. N86-12692
PAPADOPOULOS, K. N86-13250
PAPANICOLAOU, N. A. N86-12511
PARISI, V. N86-13029
PARK, H. N86-13154
PARK, T. W. N86-12250
PARKER, J. V. N86-12519
PARKER, N. N86-12629
PARKER, R. L. N86-12884
N86-12892
PARKS, D. E. N86-13098
PARMENTER-HOLT, F. N86-12746
PARRISH, L. N86-12749
PARSONS, B. N86-12878
PARSONS, W. M. N86-12519
PASECHNIK, I. L. N86-12731
PATERSON, J. A. N86-13093
PAUL, C. R. N86-12493
PAUL, S. N86-13260
PAVEL, G. N86-13024
PEAK, J. E. N86-12922
PEALSEE, D. C. N86-13119
PECK, C. C. N86-12962
PEIXIA, Q. N86-12395
PELINOVSKIY, Y. N. N86-12708
PELTIER, W. R. N86-12874
N86-12879
PENNINGTON, N. N86-12969
PENTECOST, E. N86-13225
PEPLINSKI, D. R. N86-13261
PERCHUK, L. L. N86-12657
PEREL, M. V. N86-12649
N86-12664
PEREZ-ALBUERNE, E. A. N86-12766
PEREZ-BLANCO, H. N86-12574
N86-13215
PERISON, J. N86-12319
PERKINS, J. S. N86-12260
PERROTTI, H. P. N86-12936
PESARAN, A. A. N86-12577
PESKIN, M. E. N86-13121
PETER, W. N86-13145
PETERS, C. N86-13054
PETERS, P. N. N86-13256
N86-13257
PETERSON, G. D. N86-13088
PETERSON, J. R. N86-13102
PETUKHOV, V. K. N86-12640
PHELPS, P. L. N86-12539
PHILLIPS, R. J. N86-12507
N86-12858
PICKERING, H. W. N86-12297
PICRAUX, S. T. N86-13197
PIERCE, M. N86-13228
PIET, S. J. N86-13118
PILIPENKO, V. A. N86-12727
PILYUGIN, N. N. N86-12659
PITTS, L. N86-12776
PLOMP, P. N86-12982
POA, D. S. N86-12784
POKAZEYEV, K. V. N86-12671
POKERT, D. B. N86-13212
POLIKARPOVA, L. A. N86-12722
POLLOCK, E. L. N86-13143
PONTING, P. J. N86-13122
POOLE, J. L. N86-13022
POON, C. P. C. N86-12810
POORE, R. V. N86-13019
POPOV, A. A. N86-12885
POSTMA, A. K. N86-12277
POUKEY, J. W. N86-12244
N86-12537
POWER, W. L. N86-13187
POWERS, L. V. N86-13150
POZAR, D. M. N86-12481
PRAGER, S. C. N86-13165
PRESLER, A. F. N86-12248
PRESTON, T. L. N86-12964
PRESTWICH, K. R. N86-12244
PROKOFYEV, M. A. N86-12636
PRUESS, K. N86-12578
PRUNEDA, C. O. N86-12263
PSALTIS, D. N86-13126
PU, W. N86-12465
PUDICK, S. N86-12757
N86-12758
PUGH, E. R. N86-13084
PUHE, L. N86-12480
PURGALIS, P. N86-13093
PUSHCHAROVSKIY, Y. M. N86-12652
N86-12658
PUZAK, J. C. N86-12805
PYLE, R. V. N86-13174
PYNN, R. N86-12586
PYTLOWANY, P. J. N86-12927

Q

QADRI, S. B. N86-12589
N86-13200
QI, M. N86-12448
QI, Y. N86-12431
QIANG, D. N86-12411
QILIN, C. N86-12449
QIQUAN, H. N86-12457
QIZHOU, C. N86-12422
QUALLS, C. R. N86-13050
QUANKANG, L. N86-12431
QUAPP, W. J. N86-13089
QUIRK, W. N86-12629

R

RADTKE, M. N86-12949
RAFFETY, M. S. N86-12320
RALL, L. B. N86-13039
RAMAMOORTHY, S. N86-13168
RAMIREZ, J. J. N86-13108
RAMULU, M. N86-12624
RANDEL, M. A. N86-12287
RANSON, K. J. N86-12741
RANTANEN, R. N86-13252
RANZINGER, H. N86-12745
RAO, N. N86-12756
RAPTIS, A. C. N86-12567
RASH, R. E., JR. N86-12515
RASKE, D. T. N86-12304
RAWLINS, W. T. N86-13246
RAY, E. N86-12553
RAYEVSKIY, M. A. N86-12647
RAYMOND, C. A. N86-12862
RAYMOND, J. C. N86-13274
RAYZER, V. Y. N86-12644
RAZEGHI, M. N86-12384
RAZNITSIN, V. N. N86-12732
RAZUVAYEV, V. N. N86-12633
RECHEN, J. N86-13054
REED, I. S. N86-12494
REED, R. P. N86-13183
REED, S. E. N86-13226
REEKER, L. H. N86-13025
REEVES, R. W. N86-12927
REID, R. L. N86-13006
REILLY, H. J. N86-13118
REINHARDT, F. W. N86-12785
REINOVSKY, R. E. N86-12527
REJ, D. J. N86-13141
N86-13152
RENARDY, M. N86-13033
RENARDY, Y. N86-12558
REVERDATTO, V. V. N86-12685
REYNOLDS, D. S. N86-13137
REYSNER, P. I. N86-12534
REZAIZADEH, M. A. N86-12255
RHODES, R. C. N86-12805
RICHARDS, M. A. N86-12872
RICHARDS, P. M. N86-13199
RICHARDSON, M. C. N86-13161
N86-13180
RICHARDSON, R. D. N86-12244
RICHARDSON, W. L. N86-12751
RICHARDSON, W. S. N86-12906
RIEKE, R. D. N86-12309
RIGGIN, R. M. N86-12230
RINKER, G. N86-13167
RIOJA, R. J. N86-12300
RISLOVE, S. E. N86-13081
RIYOPOULOS, S. N86-13217
RIZKALLA, M. E. N86-12506
ROBERGE, J. N86-12618
ROBERTS, T. G. N86-12603
ROBERTS, T. H. N86-12950
ROBINETTE, C. D. N86-12964
ROBINSON, R. A. N86-12586
ROCKWOOD, S. D. N86-12808
ROEDER, A. W. N86-12473
ROELANT, D. N86-13116
ROGERS, R. N. N86-12998
ROGNLIEN, T. D. N86-13160
ROJAS, R. G. N86-12216
ROLLINS, R. N86-12804
RONGZHEN, W. N86-12967
ROPER, R. G. N86-12831
ROSBOROUGH, G. W. N86-12881
ROSE, T. S. N86-13220
ROSENBERG, I. J. N86-13111
ROSENKILDE, C. E. N86-12563
N86-12569
ROSENSCHEIN, J. S. N86-13052
ROSENTEIN, R. B. N86-13046
ROSS, M. C. N86-13146
N86-13169
ROSS, P. H., JR. N86-12521
ROSS, R. G., JR. N86-12759
N86-12760
ROTHE, K. E. N86-13006
ROTTGER, J. N86-12848
ROTTIER, J. R. N86-12926
ROUTE, R. R. N86-13192
ROWE, J. E. N86-12949
ROY, R. N86-12218
ROYAL, E. L. N86-12759
ROZENBERG, A. D. N86-12671
ROZGONYI, G. A. N86-12510
RUBIN, A. G. N86-13139
RUBIN, L. S. N86-12618
RUBINSHTEYN, K. G. N86-12633
RUBY, L. N86-13174
RUDD, M. J. N86-12602
RUDER, M. E. N86-12856
RUDNIK, G. B. N86-12710
RUDY, C. R. N86-12797
RUGGIERO, A. G. N86-13091
N86-13149
RUMELHART, D. E. N86-12970
RUNAS, C. E. N86-12749
RUNCORN, S. K. N86-12873
RUSSELL, D. L. N86-13037
RUZHENTSEV, S. V. N86-12658
RYABCHENKO, V. A. N86-12641
RYAKHOVSKIY, V. M. N86-12650
RYAN, G. N86-13157
RYASINTSEVA, N. I. N86-12676
RYERSON, D. E. N86-13012
RYKUNOV, A. L. N86-12726

S

SADOVSKIY, M. A. N86-12731
SAFRAY, A. S. N86-12641
SAKAI, J. I. N86-13172
SALERNO, J. N86-13130
SALIM, A. A. N86-12756
SALOP, A. N86-12534
SALTSMAN, J. F. N86-12295
SANDBERG, J. N86-13157
SANDERCOCK, D. M. N86-12227
SANDOVAL, J. J. N86-13096
SANDWELL, D. T. N86-12864
SANZ, J. M. N86-12239
SAPOZHNIKOV, V. V. N86-12667
SAPUTRA, S. N86-12469
SARKOS, C. P. N86-12214
SASAKI, H. N86-12911
SASS, S. L. N86-13198
SASSEN, T. N86-13249
SATO, N. N86-12384
SAUBERLICH, H. E. N86-12980
SAUER, H. J., JR. N86-12564
SAVCHENKO, A. V. N86-12690
N86-12691
SAVCHENKO, V. M. N86-12661
SAVELYEV, V. V. N86-12648
SAVIN, M. G. N86-12484
SCANLAN, R. N86-13054

SCHAEFER, M. N86-12589
SCHAEFER, R. M. N86-13027
SCHAUBERT, D. H. N86-12479
N86-12480
N86-12481
SCHEFFNER, N. W. N86-12555
SCHETZ, J. A. N86-12552
SCHIFERL, D. N86-12589
N86-13200
SCHJELDERUP, J. R. N86-13125
SCHLACHETER, A. S. N86-13174
SCHLATTER, T. W. N86-12929
SCHMERBERG, N. W. N86-12594
SCHMIDLIN, F. J. N86-12816
SCHMIDT, L. C. N86-12589
SCHMINDER, R. N86-12842
SCHMITT, L. K. N86-12886
SCHMITT, M. J. N86-13096
SCHOCK, S. C. N86-12750
SCHOLTZ, R. A. N86-12497
SCHULTZ, H. P. N86-12990
SCHULTZ, K. R. N86-13116
SCHULTZ, M. N86-12889
SCHULTZ, P. N86-12929
SCHULZE, W. A. N86-12319
SCHWARTZ, R. D. N86-13273
SCHWARZ, R. B. N86-12627
N86-13212
SCHWARZMEIER, J. L. N86-13177
SCHWEITZER, E. L. N86-12957
SCHWEITZER, E. J. N86-12958
SCOTT, W. R. N86-12589
SCURO, S. J. N86-12512
SEAMONS, L. O. N86-12245
SECHRIST, C. F., JR. N86-12837
SEDLAK, J. E. N86-13171
SEDOV, V. V. N86-12710
SEEMAN, J. R. N86-13146
SEEMAN, S. E. N86-13008
SEGAL, B. N86-12471
SEILKOP, S. K. N86-12809
SEKA, W. D. N86-13180
SEKUNDYAK, L. Y. N86-12676
SELMAN, J. R. N86-12781
SEMENOV, G. A. N86-12677
SERABYN, E. N86-13270
SERFOZO, R. F. N86-13049
SERLIN, V. N86-13068
SERY, R. S. N86-13030
SHAAPUR, F. N86-12327
SHADRIN, I. F. N86-12675
SHAFFER, L. E. N86-13237
SHAJENKO, P. N86-13123
SHAMPINE, L. F. N86-13010
N86-13041
SHANER, J. W. N86-13062
SHANKS, D. E. N86-12296
SHANSHAN, Z. N86-12418
SHAOYAN, C. N86-12445
SHAPIR, Y. N86-13055
SHAPIRO, N. B. N86-12642
SHARAPOV, V. N. N86-12685
SHAUGHNESSY, G. N86-12315
SHCHERBAKOV, A. V. N86-12653
SHCHERBININ, A. D. N86-12675
SHECHTMAN, D. N86-12296
SHEFFIELD, J. W. N86-12564
SHEFFIELD, R. L. N86-13084
SHEN, C. N. N86-13031
SHEPPARD, J. C. N86-13146
N86-13169
SHER, J. S. N86-12472
SHERDEN, D. J. N86-13103
SHEREMETYEVA, A. I. N86-12708
SHERSTYUK, A. G. N86-12516
SHERWOOD, E. G. N86-13152
SHEU, J. Z. N86-13169
SHIBA, R. N86-12380
SHIEH, A. N86-13043
SHIFRIN, K. S. N86-12707
SHIGEI, Y. N86-12387
N86-12388
SHIMER, D. W. N86-13163
SHIMING, X. N86-12437
SHIMIZU, H. N86-12386
SHIQUAN, Y. N86-12425
SHIQUN, J. N86-12438
SHIRACK, R. N86-13051
SHLEZINGER, A. Y. N86-12709
SHNEYDERMAN, Y. A. N86-12495
SHONFELD, J. F. N86-13080
SHOPE, S. I. N86-12244
SHOPE, S. L. N86-12537
SHORT, R. W. N86-13162
SHOUAN, H. N86-12445
SHOUCHUN, H. N86-12411
SHOUHONG, G. N86-12422
SHUFEN, F. N86-12454
SHUKUROV, A. K. N86-12737
SHURE, L. N86-12884
SHUWEI, W. N86-12425
SHUZHU, G. N86-12433
SIDORIN, A. Y. N86-12730
SIDOROV, V. N. N86-12689
N86-12696
SIEMON, R. E. N86-13141
N86-13152
SIEMSSEN, R. H. N86-13089
SIKDAR, D. N. N86-12916
SIKKA, V. K. N86-12304
SILVERMAN, L. M. N86-12497
SIMMONS, E. J. N86-12247
SIMON, A. N86-13180
SIMONOV, K. V. N86-12686
SIMPSON, J. D. N86-12520
SIMPSON, R. L. N86-12552
SIMS, J. R. N86-13081
SIMS, W. N86-13157
SINGER, J. N86-12268
SINGH, J. J. N86-12547
SINGH, O. N86-13168
SINGLETARY, R. N86-12222
N86-12223
SIRIGNANO, W. A. N86-12363
SKELTON, E. A. N86-13060
SKELTON, E. F. N86-12589
N86-13200
SKRADSKI, J. M. N86-12931
SKUDERA, W. J., JR. N86-12517
SKUPSKY, S. N86-13175
N86-13180
SKVORTSOVA, S. Y. N86-12695
SLABY, J. G. N86-13236
SLAVSKY, D. B. N86-13275
SMAGIN, V. P. N86-12661
SMALEK, J. L. N86-12310
SMIRES, N. N86-12835
SMIRNOV, V. B. N86-12726
SMIRNOV, V. V. N86-12690
N86-12691
SMITH, D. E. N86-13008
SMITH, D. L. N86-12244
SMITH, E. M. N86-13195
SMITH, G. N86-13157
SMITH G. A. N86-13119
SMITH, G. H. N86-13274
SMITH, G. K. N86-12247
SMITH, J. D. N86-13168
SMITH, J. F. N86-12307
SMITH, J. H. N86-12626
SMITH, M. A. H. N86-13064
SMITH, M. J. N86-12818
SMITH, O. P. N86-12947
SMITH, R. A. N86-13250
SNAY, R. A. N86-12905
SNEGOVSKOY, S. S. N86-12724
SNELL, M. K. N86-12500
SOCHELNIKOV, V. V. N86-12662
SODERBLOM, D. R. N86-13274
SOKOLOV, Y. I. N86-12269
SOLEY, R. M. N86-12979
SOLONENKO, A. V. N86-12685
SOLONENKO, N. V. N86-12685
SOLOVYEV, S. L. N86-12729
SOLOWAY, E. N86-12991
SOMMER, H. T. N86-12363
SONGCHUAN, J. N86-12427
SONGSHAN, Z. N86-12419
SOO, S. L. N86-12576
SOPOLEV, V. N86-12680
SORENSEN, C. D. N86-12611
SORENSON, W. R. N86-12324
SOROKA, L. N86-13093
SOROKIN, V. M. N86-12663
SOROOSHIAN, S. N86-12926
SOURES, J. M. N86-13161
N86-13180
SPEAR, K. A. N86-13269
SPENCER, J. W. N86-12617
SPICER, C. W. N86-12230
SPILLER, J. L. N86-13144
SPOONER, D. N86-12303
SPRAY, L. A. N86-12921
SPRINKLE, D. R. N86-12547
SPROTT, J. C. N86-13165
SRINIVASAN, M. G. N86-12567
SRINIVASAN, V. N86-12268
STAATS, P. A. N86-13154
STAGGS, M. C. N86-12322
STAHEL, R. J. N86-12488
STANKOVIC, J. A. N86-13222
STEARNS, J. W. N86-13174
STEARNS, S. D. N86-13016
STEEN, P. G. N86-13098
STELSON, P. H. N86-12523
STEPANOV, A. N. N86-12656
STEPHENS, M. A. N86-13048
STEVENS, D. N86-13013
STEVENSON, R. N86-13092
STEWART, R. N86-12883
STEWART, V. R. N86-12205
STIENING, R. F. N86-13146
STILLMAN, P. N86-13157
STIRN, R. J. N86-12780
STOLYARCHUK, S. Y. N86-12736
STONE, H. M. N86-12932
N86-12934
N86-12935
STOTLAR, S. C. N86-13135
STOUT, R. B. N86-12566
STOVER, G. N86-13196
STOVER, H. A. N86-12477
STRANGE, R. R. N86-12226
STRANGWAY, D. W. N86-12857
N86-12870
STRICKLER, D. J. N86-13142
STRIZHKIN, I. I. N86-12714
STRONG, P. F. N86-13195
STROTTMAN, D. N86-13090
STUCKER, J. P. N86-12247
STYGAR, W. N86-12531
SUDDETH, D. N86-12499
SUGIMURA, R. S. N86-12765
SUMMER, D. P. N86-12290
SUN, B. H. N86-12543
SUNG, C. M. N86-12303
SUTO, F. N86-12374
SUTYRIN, G. G. N86-12669
N86-12712
SUZUKI, K. N86-12910
SUZUKI, T. N86-12384
N86-12913
SVIRIDENKOV, M. A. N86-12689
N86-12696
SWAN, K. G. N86-12957
SWANSON, R. N86-13252
SWARTZ, C. K. N86-12509
SWARTZ, S. N86-12319
SWENSON, G. R. N86-13240
N86-13241
N86-13265
SYCHEV, P. M. N86-12665

T

TAJIMA, M. N86-12380
N86-12381
TAJIMA, T. N86-13172
TAKAGI, S. N86-13040
TAKAHASHI, K. N86-13216
N86-13273
TAKAHASHI, M. N86-12380
TAKAHASHI, T. N86-12912
TAKAI, Y. N86-12387
TALIPOVA, T. G. N86-12692
N86-12708
TALLERICO, P. J. N86-12529
N86-12532
TANAKA, T. N86-12376
TANCREDI, J. J. N86-13096
TANG, M. Y. N86-12264
TANKINS, E. S. N86-12298
TANNER, L. N86-13211
TAPLEY, B. D. N86-12881
TARASOVA, T. A. N86-12640
TARVER, C. M. N86-12565
N86-12629
TATARSKAYA, M. S. N86-12634
TATRAYEV, T. M. N86-12699
TATSUOKA, K. K. N86-12972
TAUTZ, M. N86-13139
TAYLOR, C. N86-13054
TAYLOR, E. W. N86-12486
TAYLOR, M. N86-12620
TEETER, R. N86-12949
TEII, S. N86-12373
TELESMAN, J. N86-12292
TENFORDE, T. S. N86-12952
TEPIKIAN, S. N86-13077
TESKEY, D. J. N86-12870
TETENBAUM, D. N86-12846
THIEBERGER, P. N86-13155
THIERRY-MIEG, J. N86-13214
THOMAS, I. M. N86-12322
THOMPSON, E. H. N86-12953
THOMPSON, R. B. N86-12307
THOMPSON, R. E. N86-12501

THORWARTH, H. N86-13157
THRESHER, R. W. N86-12211
TIKHOMIROV, S. G. N86-12659
TIMING, Y. N86-12443
TIMMERMAN, E. L. N86-12905
TIMOSHIN, Y. V. N86-12723
TINNEL, P. I. N86-13044
TISHCHENKO, P. Y. N86-12654
TO, W. M. N86-12541
TOBISKA, K. N86-13269
TOGASHI, M. N86-12912
TOLK, N. H. N86-13259
TORR, D. G. N86-13248
N86-13252
TORR, M. R. N86-13247
N86-13248
N86-13266
TOSCANO, W. M. N86-12614
TOUGH, G. A. N86-12490
TOWNSEND, C. R., III N86-12926
TOWNSEND, D. P. N86-12609
TRAINOR, R. J. N86-12535
TREDICI, T. J. N86-12963
TRETYAKOV, P. K. N86-12271
TRIPP, J. S. N86-12579
TRUCANO, T. G. N86-12391
TRUKHCHEV, D. I. N86-12670
TSANG, C. F. N86-12578
TSENG, Y. C. N86-12938
TSUDA, T. N86-12647
TSUKANOV, N. V. N86-12732
TSVANG, L. R. N86-12735
TUCHIG, W. D. N86-12320
TUCKER, D. F. N86-12249
TURCOTTE, D. L. N86-12667
TUSZEWSKI, M. N86-13141
N86-13152
TVETEN, A. B. N86-12581
TWESME, E. N. N86-12762
TYAN, Y. S. N86-12766
TYAPKIN, V. A. N86-12736

U

UCKLER, G. J. N86-13269
ULABY, F. T. N86-12740
ULYANOVA, V. I. N86-12673
UNDERWOOD, J. H. N86-12623
URIBE, F. N86-12592
UTKIN, V. P. N86-12733
UTSUNOMIYA, T. N86-12377

V

VAISHNAVA, P. P. N86-13210
VAMPOLA, A. L. N86-12248
N86-12899
VANDERBORGH, C. N86-12589
VANDERSLUIS, K. L. N86-13154
VANDYKE, W. J. N86-13081
VANLEEUWEN, M. N86-12769
VANMARTER, J. B. N86-12535
VANVORHIES, C. N86-12886
VANZANDT, T. E. N86-12823
VARMA, R. N86-12275
VASHISHTA, P. D. N86-13205
VASUDEVAN, A. K. N86-12300
VEKLEROV, E. N86-12952
VENTURINI, E. L. N86-13199
VERDON, C. P. N86-13180
VERMA, A. K. N86-12578
VIMALCHAND, P. N86-12274
VINCENT, R. A. N86-12818
N86-12831
N86-12832
N86-12850
VINTOVKIN, V. R. N86-12667
VISENTINE, J. T. N86-13267
VISWANATHAN, V. K. N86-13017
VLASOV, D. V. N86-12705
VOLK, C. H. N86-13067
VOLLTRAUER, H. N86-12767
VONBECKH, H. J. N86-12213
VONDADELSZEN, M. N86-13132
VONFRESE, R. R. B. N86-12869
VOROBYEV, F. A. N86-12724
VORONOVICH, A. G. N86-12701
VOYDETSKIY, I. Y. N86-12728

W

WAGNER, J. N86-13106
WAISMAN, E. M. N86-13098
WAITE, J. H., JR. N86-13239
WAITON, R. G. N86-12746
WAKABAYASHI, N. N86-13203
WAKEFIELD, J. S. N86-12929
WALKER, D. A. N86-12549
WALKER, R. N86-12218
WALL, J. A. N86-13127
WALRATH, D. E. N86-12258
WALTHER, S. N86-13176
WALTON, J. N86-12629
WALZ, D. R. N86-13104
WALZ, H. V. N86-13122
WAMSGANSS, M. W. N86-12568
WANG, C. L. N86-12757
N86-12758
WANG, J. W. N86-13151
WANG, K. Y. N86-12791
WANGLER, T. P. N86-13082
WANLUN, W. N86-12416
WANNER, R. T. N86-12515
WARD, R. A. N86-13278
WASH, C. H. N86-12921
N86-12922
WASILEWSKI, P. N86-12859
WATSON, C. A. N86-13078
WATSON, W. R. N86-13056
WATTS, A. B. N86-12860
N86-12878
WATTS, K. D. N86-13099
WAUCHOPE, K. N86-13025
WEATHERFORD, W. D., JR. N86-12359
WEBB, A. W. N86-12589
N86-13200
WEBB, D. M. N86-12308
WEGMAN, S. N86-12793
WEGNER, H. E. N86-13155
WEI, G. C. N86-12321
WEI, H. N86-12452
WEI, X. N86-12466
WEILIANG, L. N86-12416
WEIMIN, H. N86-12428
WEINBERG, I. N86-12509
WEINER, D. N86-12493
WEINERT, H. L. N86-12978
WEISSEL, J. K. N86-12878
WEISSHAAR, T. A. N86-12233
WEITZNER, H. N86-13158
WEIYU, G. N86-12411
WEIZHU, L. N86-12416
WELCH, L. C. N86-12984
WEN, Z. N86-12498
WENCHONG, L. N86-12416
WENDER, S. A. N86-13173
WENG, T. H. N86-12511
WENGAN, X. N86-12369
WENHUA, W. N86-12431
WENJUN, Z. N86-12409
WENXIANG, S. N86-12401
WENXUE, L. N86-12435
WENXUN, Z. N86-12452
WERTH, J. N86-12757
N86-12758
WETHEROLD, R. G. N86-12806
WHALEN, J. N86-12493
WHELAN, J. A. N86-12757
N86-12758
WHITE, C. L. N86-13201
WHITE, K. A., III N86-12246
WHITING, M. A. N86-12999
WHITMORE, J. N86-13119
WICHMAN, I. S. N86-12291
WIDNER, M. M. N86-13014
WIEDWALD, J. D. N86-12587
WIESENFELD, J. N86-12604
WIGHTMAN, J. P. N86-12257
WILDER, J. G. N86-12322
WILETS, L. N86-13114
N86-13120
WILHELM, S. D. N86-12946
WILHELM, W. G. N86-12789
WILLEKE, F. N86-13085
WILLIAMS, D. B. N86-12303
WILLIAMS, T. H. L. N86-12740
WILLIAMS, W. D. N86-12590
WILLIS, P. B. N86-12786
WILLIS, R. E. N86-12272
WILSON, A. N86-13098
WILSON, B. L. N86-12276
WILSON, W. E. N86-13036
WINKLER, M. A. N86-13062
WINTERSGILL, M. C. N86-12317
WITHERSPOON, P. A. N86-12578
WITZKE, E. L. N86-13018
WIXOM, M. R. N86-12594
WOHLTJEN, H. N86-13124
WOLF, E. L. N86-13211
WONG, C. M. N86-12287
WONG, C. P. C. N86-13116
WONG, P. W. N86-12260
WOODFORD, T. R. N86-12221
WOODMAN, R. F. N86-12849
WOODRUFF, W. H. N86-12285
WORTMAN, J. J. N86-12510
WOS, L. N86-12997
WOZNIAK, M. A. N86-13096
WRIGHT, B. R. N86-12359
WRIGHT, M. E. N86-12487
WRIGHT, T. N86-12810
WRIGHT, V. G. N86-12919
WRONSKI, C. R. N86-12761
WUKELIC, G. E. N86-12742

X

XIANGJIN, F. N86-12417
XIANHUI, P. N86-12438
XIANQI, C. N86-12370
XIANREN, W. N86-12394
XIANTAI, O. N86-12407
XIANZHENG, P. N86-12417
XIAOCHUN, L. N86-12411
XIAOSHENG, M. N86-12406
XIAOYI, W. N86-12454
XINGLI, T. N86-12404
XINGLIU, J. N86-12427
XINNENG, W. N86-12414
XIUJUN, Y. N86-12445
XIULING, S. N86-12412
XU, Q. N86-12918
XUEWEN, N. N86-12443
XUHUI, Z. N86-12465

Y

YAAKOBI, B. N86-13175
N86-13180
YAKEL, H. L. N86-13202
YAKOVENKO, N. S. N86-12686
YAKUPOVA, F. S. N86-12695
YAN, W. N86-12412
YANG, C. I. N86-12568
YAO, N. P. N86-12784
YAO, S. C. N86-12562
YAOKE, Z. N86-12397
YASAKOV, V. A. N86-12271
YATES, W. G. N86-12797
YEE, J. H. N86-13243
YEE, R. Y. N86-12361
YEGOROV, K. L. N86-12694
YEH, H. C. N86-12896
YEMILENKO, A. S. N86-12696
YEREMEYEV, V. V. N86-12665
YERMAKOV, S. A. N86-12692
N86-12708
YING, P. N86-12437
YINGHSHAN, L. N86-12465
YINGYI, C. N86-12410
YIXIANG, Z. N86-12394
YIYAN, Y. N86-12394
YNGVESSON, K. S. N86-12478
N86-12482
N86-12483
YOKOO, K. N86-12384
YONEYAMA, H. N86-12380
YONG, Y. N86-12434
YOUNG, D. F. N86-12829
YOUNGBLOOD, W. W. N86-12392
YUDIN, M. I. N86-12635
YUE, S. N86-12437
YUEBO, Y. N86-12405
YUEN, D. A. N86-12676
YUEXIAN, F. N86-12437
YUHENG, Z. N86-12412
YUN, Z. N86-12445
YUSHAN, T. N86-12468
YUSHENG, D. N86-12428
YUSHENG, Z. N86-12428
YUST, C. S. N86-13201
YUZHANG, W. N86-12419
YUZHI, L. N86-12438

Z

ZABANBARK, A. N86-12655
ZAGEC, E. N86-13196
ZAHN, R. L. N86-12506
ZAIGUI, X. N86-12417
ZAKHAROV, L. A. N86-12679
ZAKHAROVA, A. I. N86-12722
ZAKIROVA, A. R. N86-12695
ZALESAK, S. T. N86-12897

ZANGRANDO, F. N86-12577
ZAWACKI, T. S. N86-12792
ZEGARSKI, J. N86-12781
ZELZER, C. P. N86-12923
ZENKEVICH, I. G. N86-12693
ZEREN, J. D. N86-12530
ZHAN, Z. N86-12434
ZHANG, K. S. N86-12811
ZHANLIANG, F. N86-12396
ZHENCHAO, Z. N86-12410
ZHENGFANG, S. N86-12411
ZHENGLIANG, W. N86-12457
ZHIGULEV, V. V. N86-12724
ZHITKOVSKIY, Y. Y. N86-12648
ZHONGHAU, P. N86-12419
ZHONGYI, S. N86-12445
ZHURBAS, V. M. N86-12711
ZIANG, Z. N86-12443
ZIEGLER, N. F. N86-12523
ZINAN, L. N86-12432
ZINKEVICH, V. P. N86-12710
ZINN, B. T. N86-12362
ZIRBEL, J. L. N86-12753
ZIRILLI, F. N86-13029
ZOBIN, V. M. N86-12722
ZOLLINGER, R. N86-12744
ZOLOTOVA, Z. K. N86-12707
ZONGJIN, W. N86-12394
ZOTOV, I. A. N86-12668
ZUKOSKI, E. E. N86-12288
ZUMBERGE, M. A. N86-12892
ZUMINO, B. N86-12903
ZUNYAO, W. N86-12423
ZURAWSKI, R. L. N86-13137
ZUTAVERN, F. N86-12531
ZYABREV, S. V. N86-12645

CORPORATE SOURCE INDEX

SCIENTIFIC AND TECHNICAL AEROSPACE REPORTS VOLUME 24 NUMBER 3

Typical Corporate Source Index Listing

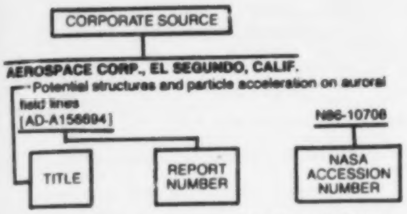
CORPORATE SOURCE
AEROSPACE CORP., EL SEGUNDO, CALIF.
Potential structures and particle acceleration on auroral field lines
[AD-A156694]
N86-10706
TITLE
REPORT NUMBER
NASA ACCESSION NUMBER

Listings in this index are arranged alphabetically by corporate source. The title of the document provides the user with a brief description of the subject matter. The report number helps to indicate the type of document cited (e.g., NASA report, translation, NASA contractor report). The NASA accession number denotes the number by which the citation is identified. The titles are arranged under each corporate source in ascending accession number order.

A

ACADEMY OF SCIENCES, BERLIN (EAST GERMANY).
Results of the May 1982 ATMAP campaign at the Meteor Wind Station Kuehlungsborn (54 deg N, 12 deg E), GDR
N86-12641

ADAPTIVE SENSORS, INC., SANTA MONICA, CALIF.
Analysis of constant false alarm rate sidelobe canceller criterion
[AD-A157412] N86-12494

ADELAIDE UNIV. (AUSTRALIA).
Planetary and gravity waves in the mesosphere and lower thermosphere N86-12832
Turbulence in the altitude region 80-120 km
N86-12834
Results of November 1981 and May 1982 ATMAP campaigns at Adelaide (35 deg S, 138 deg E)
N86-12850

ADMIRALTY MARINE TECHNOLOGY ESTABLISHMENT, TEDDINGTON (ENGLAND).
Sound scattering by a layered sphere
[AD-A157915] N86-13060

AEROJET ENERGY CONVERSION CO., SACRAMENTO, CALIF.
Development of acoustic agglomerator. Test plan for high temperature high pressure acoustic agglomerator
[DE85-017221] N86-13061

AERONAUTICAL RESEARCH LABS., MELBOURNE (AUSTRALIA).
A survey of aeronautical structural research in Australia
[AD-A157211] N86-12199
Flutter clearance tests on a Transavia PL-12/T-400 Skyfarmer
[AD-A157212] N86-12234

AEROSPACE CORP., EL SEGUNDO, CALIF.
The aerospace spacecraft charging document
[AD-A157684] N86-12248
An alternative interpretation of ion ring distribution observed by the S3-3 satellite
[AD-A157655] N86-12898
Microwave field strength measurement in a Rubidium clock cavity via adiabatic rapid passage
[AD-A157070] N86-13065
A dressed atom interpretation of adiabatic rapid passage
[AD-A157071] N86-13066
The inhomogeneous light shift in alkali atoms
[AD-A157498] N86-13067
Application of an atomic oxygen beam facility to the investigation of shuttle glow chemistry N86-13261

AEROSPACE CORP., GERMANTOWN, MD.
Effects of whistler-mode and other waves in the magnetosphere
[AD-A157832] N86-12899

AIR COMMAND AND STAFF COLL., MAXWELL AFB, ALA.
The helicopter to fixed wing conversion program: A critical review
[AD-A156820] N86-12968

AIR FORCE ACADEMY, COLO.
Air Force Academy Aeronautics Digest
[AD-A157215] N86-12200

AIR FORCE FLIGHT TEST CENTER, EDWARDS AFB, CALIF.
T-33 (Silver Star MK 3) pitot-static system calibration
[AD-A157854] N86-12221

AIR FORCE GEOPHYSICS LAB., HANSCOM AFB, MASS.
Precipitating electron and ion detectors (SSJ/4) for the block 5D/Flights 6-10 DMSP (Defense Meteorological Satellite Program) satellites: Calibration and data presentation
[AD-A157080] N86-12896
Calculation of threshold conditions for materials charging in Maxwellian plasmas
[AD-A157123] N86-13139

AIR FORCE HUMAN RESOURCES LAB., BROOKS AFB, TEX.
Artificial intelligence in Ada: Pattern-directed processing
[AD-A157097] N86-13025

AIR FORCE INST. OF TECH., WRIGHT-PATTERSON AFB, OHIO.
An application of adaptive learning to malfunction recovery
[AD-A158129] N86-12236
Strategies for associating data and location in a geographic information system
[AD-A158118] N86-12746
Statistical evaluation of forecasts over the low-latitunes
[AD-A157926] N86-12923
Squall and cloud lines as structural components of an Arabian Sea convective cloud cluster
[AD-A157973] N86-12925
The design and hardware evaluation of an advanced 16-bit, low-power, high performance microcomputer system for digital signal processing
[AD-A158130] N86-12981
A meta system for generating software engineering environments
[AD-A158102] N86-12996
Aggregating individual preferences in the Analytic Hierarchy Process applied to the 1983 Battelle TAV study
[AD-A155858] N86-13226

AIR FORCE OFFICE OF SCIENTIFIC RESEARCH, BOLLING AFB, WASHINGTON, D.C.
Applied lasers (selected articles)
[AD-A155948] N86-12601

AIR FORCE ROCKET PROPULSION LAB., EDWARDS AFB, CALIF.
Exhaust plume measurements of 15-pound BATES (Ballistic Test and Evaluation System) motors
[AD-A157249] N86-12250

AIR FORCE SYSTEMS COMMAND, WRIGHT-PATTERSON AFB, OHIO.
Kinetics of evaporation and growth of drops of aqueous solutions of surface active substances at negative temperatures
[AD-A156961] N86-12269
Experimental study of the combustion of gas-air mixtures in a channel and the diffusion combustion in a slipstream at high velocities
[AD-A157495] N86-12271
Radio-absorbing materials
[AD-A157496] N86-12495
Electrical losses and resistance of cryogenic inductors with consideration of the effect of magnetoresistance
[AD-A158165] N86-12516
Journal of the Chinese Silicate Society (selected articles)
[AD-A157497] N86-13190
New method of determining the current carrier concentration in a substance in the state of superconductivity
[AD-A158182] N86-13194

AIR FORCE WEAPONS LAB., KIRTLAND AFB, N. MEX.
Parallel, staged opening switch power conditioning techniques for flux compression generator applications
[DE85-012761] N86-12527
RADLAC program status
[DE85-014708] N86-13109

AIR FORCE WRIGHT AERONAUTICAL LABS., WRIGHT-PATTERSON AFB, OHIO.
Compressor research facility F100 high pressure compressor inlet total pressure and swirl profile simulation
[AD-A157108] N86-12229
Post stall maneuvers and thrust vectoring performance analysis
[AD-A158100] N86-12235

AKRON UNIV., OHIO.
Role of chemical bonding in adhesion
[AD-A157251] N86-12316
NASA LeRC/Akron University Graduate Cooperative Fellowship Program and Graduate Student Researchers Program
[NASA-CR-174826] N86-13219

ALABAMA UNIV., HUNTSVILLE.
Plasma and magnetospheric research
[NASA-CR-176326] N86-13138

ALASKA UNIV., FAIRBANKS.
Carbon dioxide in arctic and subarctic regions
[DE85-014054] N86-12901

ALLIED BENDIX CORP., KANSAS CITY, MO.
Thermally induced failures of thick-film glaze resistors
[DE85-012014] N86-12320
Knowledge-based systems: How will they affect manufacturing in the 80's
[DE85-010601] N86-13027

ALUMINUM CO. OF AMERICA, ALCOA CENTER, PA.
Resistance to fracture, fatigue and stress-corrosion of Al-Cu-Li-Zr alloys
[AD-A158407] N86-12300

AMES LAB., IOWA.
Effects of microstructure on the acoustoelastic measurements of stress
[DE85-015518] N86-12307
Josephson effect in the unusual superconductors Lu2Fe3Si5, LiTi2O4 and UBe13
[DE85-015260] N86-13211

ANALYTICAL SCIENCES CORP., RESEARCH TRIANGLE PARK, N.C.
Spatial and temporal patterns of acid precipitation and their interpretation
[PB85-214377] N86-12809

ARCO SOLAR, INC., CHATSWORTH, CALIF.
Thin film module development N86-12768
Thin film module electrical configuration versus electrical performance N86-12770

ARGONNE NATIONAL LAB., ILL.
Adsorption/desorption properties of vacuum materials for the 6 GeV synchrotron
[DE85-010276] N86-12252
Electrochemical deposition of glassy chromium on copper
[DE85-004081] N86-12275
Review of effects of long-term aging on the mechanical properties and microstructures of types 304 and 316 stainless steel
[DE85-016472] N86-12304
Microwave ridged waveguide beam pickups
[DE85-013816] N86-12499
Low dispersion notch filter for multi-GHz frequencies using fiber optics delays
[DE85-014983] N86-12520
Particle-wall interaction and wall friction in gas-solid flows
[DE85-014984] N86-12567
Heat Exchanger Vibration Analysis (HXVA) for prediction of tube bundle instabilities
[DE85-017144] N86-12566
Condensation heat transfer in plate heat exchangers
[DE85-012369] N86-12571

Analysis of stratified flow mixing
[DE85-006840] N86-12576

Theory for the Portevin-LeChatelier effect
[DE85-004030] N86-12627

Development of a supported liquid membrane as a nickel-zinc secondary battery separator
[DE85-012591] N86-12784

Managing personal desktop computing at Argonne National Laboratory
[DE85-014976] N86-12983

DAPHNE: The design of a parallel multiprocessor data acquisition system
[DE85-013875] N86-12984

Automated reasoning and various applications
[DE85-014998] N86-12997

Parallel implementation of multifrontal schemes
[DE85-014205] N86-13015

Partition of cross sections in asymmetric nucleus-nucleus reactions and the origin of fast alpha particles
[DE85-014989] N86-13089

Review of heavy ion collider proposals
[DE85-014985] N86-13091

Multiplicities in high energy interactions
[DE85-013847] N86-13100

High intensity positron beam and angular correlation experiments at Livermore
[DE85-012961] N86-13111

Comparison between theoretical predictions and tracking
[DE85-012104] N86-13149

Quantum simulations of small electron-hole complexes
[DE85-013895] N86-13205

Deconfinement transition on a BCH lattice
[DE85-013887] N86-13207

Mossbauer effect and neutron diffraction study of the anomalous lattice behavior of U6Fe
[DE85-014912] N86-13210

ARIZONA STATE UNIV., TEMPE.

The role of a pressure-dependent rheology in the dynamics of mantle circulation N86-12876

High nuclear temperatures by antimatter-matter annihilation
[DE85-014113] N86-13090

ARIZONA UNIV., TUCSON.

Evaluation of the NWS (National Weather Service) soil moisutre accounting model for automated flash flood forecasting in small arid and semi-arid watersheds
[PB85-229722] N86-12928

Masking of light scattering information on matrix elements from complex scattering
[AD-A158144] N86-13131

ARIZONA WATER RESOURCES RESEARCH CENTER, TUCSON.

Evaluation of the NWS (National Weather Service) soil moisutre accounting model for automated flash flood forecasting in small arid and semi-arid watersheds
[PB85-229722] N86-12928

ARMY ARMAMENT RESEARCH AND DEVELOPMENT COMMAND, WATERVLIET, N. Y.

Wear of projectile rotating bands
[AD-A156666] N86-12358

More on compliance of the three-point bend specimen
[AD-A156665] N86-12623

Variational principle for penetrator dynamics using bilinear functional and adjoint formulation
[AD-A157964] N86-13031

ARMY COLD REGIONS RESEARCH AND ENGINEERING LAB., HANOVER, N. H.

A user's guide for the BIBSORT program for the IBM-PC personal computer
[AD-A157936] N86-12995

Stefan's problem in a finite domain with constant boundary and initial conditions analysis
[AD-A158558] N86-13040

ARMY CONSTRUCTION ENGINEERING RESEARCH LAB., CHAMPAIGN, ILL.

Full-scale fire tests of polyurethane foam dome structures
[AD-A157107] N86-12314

ARMY ENGINEER WATERWAYS EXPERIMENT STATION, VICKSBURG, MISS.

Investigation of tidally induced turbulent flow
[AD-A157841] N86-12555

Environmental impact research program. Status and source of habitat models and literature reviews, December 1984
[AD-A156899] N86-12950

ARMY MATERIALS AND MECHANICS RESEARCH CENTER, WATERTOWN, MASS.

Materials and process characterization to determine the effect of high intensity infrared laser radiation on a composite material
[AD-A157094] N86-12260

ARMY WAR COLL., CARLISLE BARRACKS, PA.

The C-17: We need it yesterday
[AD-A157147] N86-12219

ARNOLD ENGINEERING DEVELOPMENT CENTER, ARNOLD AIR FORCE STATION, TENN.

Method to detect ethylene glycol in gaseous mixtures
[AD-A158109] N86-12272

ASPEN SYSTEMS CORP., MARLBOROUGH, MASS.

Preliminary design of linear alternator dynamometer for free piston Stirling engines
[DE85-015078] N86-12614

AUBURN UNIV., ALA.

Development of a radiation-hard CMOS process
[NASA-CR-170925] N86-13187

AUGSBURG UNIV. (WEST GERMANY).

AE and DE mass spectrometer observations relevant to the shuttle glow N86-13242

AUSTRALIAN NATIONAL UNIV., CANBERRA.

Why do we need detailed gravity over continents: Some Australian examples N86-12855

AUTOMATED SCIENCES GROUP, INC., SILVER SPRING, MD.

Optical disk technology assessment
[AD-A157909] N86-12562

B

BATTELLE COLUMBUS LABS., OHIO.

Composition and photochemical reactivity of turbine engine exhaust
[AD-A157643] N86-12230

BOHAN (WALTER A.) CO., PARK RIDGE, ILL.

Hydrologic and land sciences applications of NOAA (National Oceanic and Atmospheric Adminstration) polar-orbiting satellite data
[PB85-233385] N86-12748

BOLT, BERANEK, AND NEWMAN, INC., CAMBRIDGE, MASS.

An analysis of the application of AI to the development of intelligent aids for flight crew tasks
[NASA-CR-3944] N86-12212

Internetting and packet satellite program
[AD-A157124] N86-12489

BOSTON UNIV., MASS.

Formation of fuel via photochemical electron transfer
[DE85-011168] N86-12279

Atmospheric tides below 80 km N86-12824

Temperature structure of the 80 km to 120 km region N86-12830

Atmospheric tides between 80 km and 120 km N86-12833

Atmospheric Tides Middle Atmosphere Program (ATMAP): Report of the November/December 1981, and May 1982, observational campaigns N86-12839

BRITISH BROADCASTING CORP., KINGSWOOD (ENGLAND).

Room modes and sound absorption: Some practical measurements compared with theoretical predictions
[BBC-RD-1985/11] N86-12486

BRITISH COLUMBIA UNIV., VANCOUVER.

FASTBUS for the particle accelerator laboratories
[DE85-014352] N86-13122

BROOKHAVEN NATIONAL LAB., UPTON, N. Y.

Anaerobic microbial dissolution of toxic metals in subsurface environments
[DE85-013306] N86-12251

High order mode damping in the NSLS accelerating RF cavities by the use of damping antennae
[DE85-014214] N86-12498

Ultrasonic attenuation in clean anisotropic superconductors
[DE85-012178] N86-12621

Low-cost light-weight thin material solar heating system
[DE85-012531] N86-12789

Perspectives to establish knowledge linkages between acidic deposition and vegetation responses
[DE85-011839] N86-12796

Use of an elliptical aperture to control saturation in closely-coupled, cold iron, superconducting dipole magnets
[DE85-012259] N86-13053

Replica-space renormalization in random-field systems
[DE85-014800] N86-13055

Collider performance with ideal collisions
[DE85-017011] N86-13073

Chaotic dynamical aperture
[DE85-013285] N86-13077

Light mass elements total half-lives for selected long-lived nuclides
[DE85-014217] N86-13115

Prompt neutron fission spectrum mean energies for the fissile nuclides and (252)Cf
[DE85-012181] N86-13117

Search for narrow structure in proton-antiproton annihilation cross sections from 1900 to 1960 MeV
[DE85-013302] N86-13119

Fully stripped heavy ion yield vs energy for Xe and Au ions
[DE85-013281] N86-13155

Tracking studies on the effects of random multipoles in the 6.5 T lattice of the SSC Reference Designs Study
[DE85-013286] N86-13156

Large acceptance magnetic focussing horns for production of a high intensity narrow band neutrino beam at the AGS
[DE85-013300] N86-13157

Magnet power supply control of the NSLS VUV and X-ray storage rings transfer lines
[DE85-014213] N86-13168

AGS improvement program
[DE85-013293] N86-13182

BROWN UNIV., PROVIDENCE, R. I.

Rationale for a GRAVSAT-MAGSAT mission: A perspective on the problem of external/internal transient field effects N86-12887

Cortical plasticity: Theoretical analysis, experimental results
[AD-A157965] N86-12961

BUREAU OF MINES, RENO, NEV.

Hydrogen chloride sparging crystallization of the chloride salts of cobalt, manganese, and nickel
[PB85-197002] N86-12286

BURNS AND ROE, INC., OAK RIDGE, TENN.

Tandem Mirror Reactor Systems Code (TMRSC)
[DE85-012891] N86-13006

C

CALIFORNIA INST. OF TECH., PASADENA.

Combustion in turbulent jets and buoyant plumes
[PB85-220655] N86-12288

Solar walk-off protection
[DE85-012112] N86-12788

The source of the Earth's long wavelength geoid anomalies: Implications for mantle and core dynamics N86-12872

Small-scale convection beneath the transverse ranges, California: Implications for interpretation of gravity anomalies N86-12877

Adaptive optical filtering techniques
[AD-A157072] N86-13126

CALIFORNIA STATE UNIV., LONG BEACH.

Turbulence models for boundary layers on axisymmetric bodies
[AD-A158552] N86-12561

CALIFORNIA UNIV., BERKELEY.

Raman spectroscopy of molecular adsorbates
[DE85-012981] N86-12280

Numerical calculation of turbulent buoyant flow N86-12541

Dynamic ADI computations of thermoelastic stresses in crystalline laser media
[DE85-010478] N86-12606

Investigation of vehicle glow in the far ultraviolet N86-13249

NeII observations of the galactic center: The velocity field and mass distribution N86-13270

Wave propagation and pair formation in pulsar magnetospheres N86-13276

Diffraction-limited ten micron imaging of circumstellar dust with a detector array N86-13277

CALIFORNIA UNIV., BERKELEY. LAWRENCE BERKELEY LAB.

Nanosecond fluorescence spectroscopy
[DE85-012234] N86-12282

Deactivation and poisoning of fuel cell catalysts
[DE85-015127] N86-12521

Study of two-phase concurrent flow of steam and water in an unconsolidated porous medium
[DE85-014534] N86-12578

Gravity theories in more than four dimensions
[DE85-011164] N86-12903

Monitoring of circadian waveforms in rodents exposed to high-intensity static magnetic fields
[DE85-015225] N86-12952

Design and performance of 40 mm, 6.5 T, collared, cold-iron model magnets
[DE85-015277] N86-13054

Spin-polarization observables in elastic electron scattering from spin-1/2 nuclei
[DE85-016639] N86-13072

Suppression of propagating TE modes in the FNAL antiproton source stochastic beam cooling system
[DE85-016559] N86-13074

Theoretical studies of molecular interactions
[DE85-012604] N86-13076

Stochastic beam cooling amplifier system front end components performance characteristics
[DE85-013925] N86-13079

Achievement of Bevalac rapid mode switching
[DE85-015130] N86-13092

Overview and status of the Transverse-Field Focusing (TFF) accelerator
[DE85-015278] N86-13093

On-line velocity measurements using phase probes at the SuperHILAC
[DE85-015279] N86-13095

Electron-spin-polarized targets for a collisionally-pumped polarized-ion source
[DE85-015276] N86-13174

Compact microwave ion source
[DE85-014536] N86-13176

Improved Bevatron local injector ion source performance
[DE85-015271] N86-13196

Classical geometrical interpretation of ghost fields and anomalies in Yang-Mills theory and quantum gravity
[DE85-014537] N86-13214

CALIFORNIA UNIV., DAVIS.

Evaluation and implementation of testability schemes for gate array integrated circuit design
[DE85-012674] N86-12526

CALIFORNIA UNIV., LOS ANGELES.

Preparation and properties of thin film reversible cathode materials
[AD-A158431] N86-12273

Modulations of driven nonlinear surface waves on water and liquid Helium-4
[AD-A157958] N86-12556

CALIFORNIA UNIV., SAN DIEGO, LA JOLLA.

Modeling currents at satellite altitudes N86-12889

Does the geoid drift west? N86-12892

Human cognition and performance
[AD-A157665] N86-12970

Trapped particle absorption by the ring of Jupiter
[NASA-CR-174408] N86-13279

A note on Jupiter's gossamer ring N86-13280

CAMBRIDGE UNIV. (ENGLAND).

The importance of GRM gravity observations in continental regions N86-12871

The magnetic field at the core-mantle boundary
N86-12885

CAMERINO UNIV. (ITALY).

A new method for global optimization based on stochastic differential equations
[AD-A157546] N86-13029

CANADIAN SCIENTIFIC LIASON OFFICE, WASHINGTON, D.C.

Elie: Saint Eustache fibre Optic Field Trial project evaluation report, volume 4
[AD-A157144] N86-12490

CANTERBURY UNIV., CHRISTCHURCH (NEW ZEALAND).

Middle atmosphere tides at Christchurch (44 deg S, 17 deg E) in November 1981 and May 1982 N86-12851

CARNEGIE INSTITUTION OF WASHINGTON, D. C.

Novel instrument for high-pressure research at ultra-high temperatures
[DE85-015674] N86-12589

X-rays from the radio halo of Virgo A = M87
[NASA-CR-176303] N86-13285

CARNEGIE-MELLON UNIV., PITTSBURGH, PA.

Multiple ignition, combustion and quenching of hydrocarbon fuel sprays
[AD-A158560] N86-12363

Cross flow boiling in tube bundles
[AD-A158557] N86-12562

CASE WESTERN RESERVE UNIV., CLEVELAND, OHIO.

Design of high power superconducting switches
N86-12505

CENTRE NATIONAL D'ETUDES SPATIALES, TOULOUSE (FRANCE).

Thermal cooling of the oceanic lithosphere from geoid height data N86-12861

CENTRE NATIONAL DE LA RECHERCHE SCIENTIFIQUE, MEUDON-BELLEVUE (FRANCE).

Classical geometrical interpretation of ghost fields and anomalies in Yang-Mills theory and quantum gravity
[DE85-014537] N86-13214

CENTRE NATIONAL DE LA RECHERCHE SCIENTIFIQUE, VERRIERES-LE BUISSON (FRANCE).

Contribution to the CIRA model from ground-based lidar N86-12835

CHICAGO UNIV., ILL.

Limits of thermochemical and photochemical syntheses of gaseous fuels: A finite-time thermodynamic analysis
N86-12367

Stimulus structures and mental representations in expert comprehension of computer programs
[AD-A157520] N86-12969

CHRONAR CORP., PRINCETON, N.J.

Interconnect resistance of photovoltaic submodules
N86-12767

CITADEL COLL., CHARLESTON, S.C.

The field horizontal-branch star HD 109995: New results with coadded ultraviolet and optical region spectra
[NASA-CR-176327] N86-13272

CLARKSON UNIV., POTSDAM, N.Y.

Modeling of convection phenomena in Bridgman-Stockbarger crystal growth
[NASA-CR-176325] N86-13188

CLEMSON UNIV., S.C.

Accelerated stress testing of thin film solar cells: Development of test methods and preliminary results
N86-12764

COASTAL ENGINEERING RESEARCH CENTER, VICKSBURG, MISS.

Annual data summary for 1981 CERC (Coastal Engineering Research Center) field research facility
[AD-A158143] N86-12926

A user's guide to the Coastal Engineering Research Center's (CERC'S) field research facility
[AD-A157966] N86-12946

Extremal analysis of hindcast and measured wind and wave data at Kodiak, Alaska
[AD-A158136] N86-12947

COLLEGE OF WILLIAM AND MARY, WILLIAMSBURG, VA.

User's guide to STIPPAN: A panel method program for slotted tunnel interference prediction
[NASA-CR-176003] N86-12237

Wall-interference assessment in three-dimensional slotted-wall wind tunnels
[NASA-CR-176320] N86-12240

COLORADO STATE UNIV., FORT COLLINS.

Global view of the upper level outflow patterns associated with tropical cyclone intensity changes during FGGE
[NASA-CR-174407] N86-12906

COLORADO UNIV., BOULDER.

Expected contribution of the Geopotential Research Mission (GRM) to studies of liquid core fluid dynamics
N86-12890

Survey of ultraviolet shuttle glow N86-13269

COLSPAN, INC., BOULDER, COLO.

Data descriptions and vertical structure plots for mean, diurnal, and semidurnal components of eastward and northward (ordered by latitude). Mean winds and tides over Poker Flat, Alaska (65 deg N, 147 deg W), during November 1981 N86-12840

COLUMBIA UNIV., NEW YORK.

Large acceptance magnetic focussing horns for production of a high intensity narrow band neutrino beam at the AGS
[DE85-013300] N86-13157

COMMITTEE OF CONFERENCE (U. S. CONGRESS).

Making appropriations for the Department of Housing and Urban Development, and for sundry independent agencies, boards, commissions, corporations, and offices for the fiscal year ending September 30, 1986, and for other purposes
[H-REPT-99-363] N86-13231

National Aeronautics and Space Administration
N86-13232

COMMITTEE ON APPROPRIATIONS (U. S. SENATE).

Department of Housing and Urban Development, and Certain Other Independent Agencies Appropriations for Fiscal Year 1986, part 1
[S-HRG-99-221-PT-1] N86-13233

National Aeronautics and Space Administration
N86-13234

COMMUNICATIONS RESEARCH CENTRE, OTTAWA (ONTARIO).

The measurement of tropospheric refractive index relevant to the study of anomalous microwave propagation: Review and recommendations
[CRC-1387] N86-12471

CONNECTICUT UNIV., STORRS.

A preliminary field study of turbulent flow over and inside a forest edge
[AD-A158409] N86-12560

CONTROL DATA CORP., MINNEAPOLIS, MINN.

Comparison of time-periodic variations in temperature and wind from meteorological rockets and satellites
N86-12825

CORNELL UNIV., ITHACA, N.Y.

Unsteady detonation N86-12542

Studies of energy storage and transfer in gas lasers
[AD-A158553] N86-12604

Diagnosing the causes of ground-water contamination using a mathematical model: Report on Technology Transfer Workshop
[PB85-217006] N86-12808

Properties of the lithosphere and asthenosphere deduced from geoid observations N86-12867

Diffraction and microscopy studies of the structure of grain boundaries in Fe, Fe-base alloys and ceramic materials
[DE85-016950] N86-13198

CORPS OF ENGINEERS, ST. PAUL, MINN.

Information systems plan
[AD-A157911] N86-13227

D

DAYTON UNIV., OHIO.

Performance of an alpha-vane and pilot tube in simulated heavy rain environment
[NASA-CR-176353] N86-12220

Statistical treatment of aramid/epoxy stress-rupture data
[AD-A157238] N86-12315

DECILOG, INC., MELVILLE, N. Y.

Improvement of manufacturing techniques and quality of optical scratch standards for fire control systems
[AD-A157963] N86-13130

DEPARTMENT OF ENERGY, WASHINGTON, D. C.

Thermophoretic separation of aerosol particles from a sampled gas stream
[DE85-011672] N86-12277

Method and apparatus for conducting variable thickness vapor deposition
[DE85-011653] N86-12306

Self-contained hot-hollow cathode gun source assembly
[DE85-011652] N86-12530

DEPARTMENT OF THE AIR FORCE, WASHINGTON, D.C.

Pneumatic actuator device
[AD-D011794] N86-12217

Compartmented, filament wound, one-piece aircraft fuel tanks
[AD-D011793] N86-12225

Improved temperature detection system for use on film cooled turbine airfoils
[AD-D011762] N86-12228

Length adjustable strut link with low aerodynamic drag
[AD-D011851] N86-12232

Simultaneous detection of time coincident signals in an adaptive Doppler tracker
[AD-D011796] N86-12473

Variable radius lead former
[AD-D011790] N86-12506

Heat pipe wick
[AD-D011852] N86-12559

Transient test of suspension electronics for gyroscope
[AD-D011853] N86-12585

High power laser dump
[AD-D011792] N86-12597

CO2 laser stabilization and switching
[AD-D011795] N86-12598

Lightweight cryogenic tank with positive expulsion
[AD-D011856] N86-12612

Acoustically tuned optical filter system
[AD-D011791] N86-13184

DEPARTMENT OF THE ARMY, WASHINGTON, D. C.

Communications network status information system
[AD-D011850] N86-12477

Wideband SAW (Surface Acoustic Wave) channellizer using slanted array input transducer
[AD-D011857] N86-12517

Electrolytic pressure transduction system
[AD-D011847] N86-12584

Pulsed digital multiplexed laser generator
[AD-D011855] N86-12603

Forward field autotransfusion device
[AD-D011763] N86-12957

Suture needle holder
[AD-D011764] N86-12958

Dermal substance collection device
[AD-D011848] N86-12962

Control for DOT matrix printers operating in harsh environment
[AD-D011846] N86-12980

Photosensitive cartridge for weapons zeroing and marksmanship training
[AD-D011765] N86-13125

DEPARTMENT OF THE NAVY, WASHINGTON, D. C.

Picosecond broadband CARS probe using the picosecond continuum
[AD-D011840] N86-12267

Suspension method of impregnating active material into composite nickel plaque
[AD-D011826] N86-12299

Epoxy phthalonitrile polymers
[AD-D011821] N86-12318

Low sidelobe, high efficiency mirror antenna with twist reflector
[AD-D011835] N86-12474

P1 polyphase code expander-compressor [AD-D011838] N86-12475

P2 polyphase code expander-compressor [AD-D011839] N86-12476

Demountable coaxial electrical connector for in-line amplifiers [AD-D011831] N86-12507

A TiW diffusion barrier for AuZn ohmic contacts to p-type InP [AD-D011823] N86-12511

High current fiber brush collector and method for making same [AD-D011827] N86-12512

Dual drain MOSFET detector for crosstie memory systems [AD-D011828] N86-12513

Technique for the reduction of fading in interferometers [AD-D011845] N86-12581

Laser generation of ultrasonic waveform reconstructions [AD-D011843] N86-12599

Laser vibrometer [AD-D011811] N86-12602

Infrared optical measurement of blood gas concentrations and fiber optic catheter [AD-D011836] N86-12655

Low temperature inflator apparatus [AD-D011810] N86-12674

Generation of a modulated IREB (Intense Relativistic Electron Beam) with a frequency tunable by a magnetic field [AD-D011820] N86-13068

Optical sensing devices [AD-D011829] N86-13123

Reversible optical waveguide vapor sensor [AD-D011834] N86-13124

Recovery of fragile layers produced on substrates by chemical vapor deposition [AD-D011841] N86-13185

Method for the deposition of high-quality crystal epitaxial films of iron [AD-D011842] N86-13186

Liquid Phase Epitaxy (LPE) of silicon carbide [AD-D011825] N86-13191

DETROIT DIESEL ALLISON, INDIANAPOLIS, IND.

User's manual for using MASON: A frequency response program which handles a system of transfer functions described by a signal flow graph [PB85-227106] N86-13021

DEUTSCHES ELEKTRONEN-SYNCHROTRON, HAMBURG (WEST GERMANY).

Tests of orbital dynamics using the Tevatron [DE85-012296] N86-13085

DREXEL UNIV., PHILADELPHIA, PA.

Research on output feedback control [NASA-CR-174253] N86-13028

DU PONT DE NEMOURS (E. I.) AND CO., AIKEN, S.C.

U308 powder from uranyl-loaded cation exchange resin [DE85-013231] N86-12265

E

EASTERN PACIFIC HURRICANE CENTER, SAN FRANCISCO, CALIF.

Annual data and verification tabulation eastern North Pacific tropical storms and hurricanes, 1984 [PB85-187886] N86-12930

EASTMAN KODAK CO., ROCHESTER, N. Y.

Large-area thin-film modules N86-12766

ECON, INC., ALEXANDRIA, VA.

Marketing the use of the space environment for the processing of biological and pharmaceutical materials [NASA-CR-176334] N86-12243

Federal government provision of third-party liability insurance to space vehicle users [NASA-CR-176346] N86-13230

ECON, INC., PRINCETON, N.J.

R and D limited partnerships (possible applications in advanced communications satellite technology experiment program) [NASA-CR-176333] N86-13221

EDGERTON, GERMESHAUSEN AND GRIER, INC., IDAHO FALLS, IDAHO.

Transistorized multigrid methods. 1: Linear elliptic problems on two- and three-dimensional regions [DE85-014632] N86-13043

Ground test facility for nuclear testing of space reactor subsystems [DE85-014634] N86-13099

Tritium safety issues for TFCX [DE85-014621] N86-13118

Microluminescence spectra of Ti-activated ZrO2-Y2O3 [DE85-010131] N86-13206

EIDGENOESSISCHE TECHNISCHE HOCHSCHULE, ZURICH (SWITZERLAND).

Dynamics and structure of the Alpine Fold Belt N86-12854

EISCAT SCIENTIFIC ASSOCIATION, KIRUNA (SWEDEN).

Mesospheric winds and tides at Arecibo/puerto Rico (18 deg N, 67 deg W) November 20-23, 1981 N86-12848

ELECTRONICS RESEARCH LAB., ADELAIDE (AUSTRALIA).

Atmospheric IR transmission measurements in a tropical maritime environment: Comparison with the LOWTRAN 6 model [AD-A157920] N86-13129

ENGELHARD CORP., EDISON, N.J.

Develop and test fuel cell powered on-site integrated total energy systems: Phase 3, full-scale power plant development [NASA-CR-174946] N86-12757

Develop and test fuel cell powered on-site integrated total energy systems: Phase 3, full-scale power plant development [NASA-CR-174998] N86-12758

ENVIRONMENTAL PROTECTION AGENCY, DENVER, COLO.

Toxic hot spot study, South Platte River along the Front Range, August and October, 1982 [PB85-196384] N86-12749

ENVIRONMENTAL PROTECTION AGENCY, RESEARCH TRIANGLE PARK, N.C.

Assessment of the long-term precision of continuous emission monitors [PB85-201150] N86-12804

Summary of precision and accurace assessments for the state and local air monitoring netowrks, 1982 [PB85-208171] N86-12805

Modeling the diurnal variation of meteorological variables within the boundary layer: Preliminary comparison results [PB85-198349] N86-12933

ENVIRONMENTAL RESEARCH LAB., DULUTH, MINN.

Great Lakes: Nature's own environmental laboratory [PB85-188852] N86-12751

EROS DATA CENTER, SIOUX FALLS, S. DAK.

On the interpretation of satellite-derived gravity and magnetic data for studies of crustal geology and metallogenesis N86-12694

Do MAGSAT anomalies contain a record of past and present-day mantle convection under South America? N86-12695

EUROPEAN ORGANIZATION FOR NUCLEAR RESEARCH, GENEVA (SWITZERLAND).

FASTBUS for the particle accelerator laboratories [DE85-014352] N86-13122

EXXON RESEARCH AND ENGINEERING CO., ANNANDALE, N.J.

Ultrasonic attenuation in clean anisotropic superconductors [DE85-012178] N86-12621

Light-induced effects-impacts to module performance measurements and reliability testing: An overview N86-12761

F

FEDERAL AVIATION ADMINISTRATION, WASHINGTON, D.C.

Report of accomplishments under the airport improvement program [AD-A156834] N86-12241

Statistical sampling of aircraft operations at non-towered airports [AD-A157095] N86-13051

FEDERAL AVIATION AGENCY, ATLANTIC CITY, N.J.

Aircraft interior panel test criteria derived from full-scale fire tests [FAA/CT-85/23] N86-12214

FERMI NATIONAL ACCELERATOR LAB., BATAVIA, ILL.

Theories of statistical equilibrium in electron-positron colliding-beam storage rings [DE85-012303] N86-13080

Tests of orbital dynamics using the Tevatron [DE85-012296] N86-13085

A p anti p collider physics: Summary talk [DE85-014782] N86-13097

Tevatron global radius and Os system [DE85-017442] N86-13101

Deprit's algorithm, Green's functions and multipole perturbation theory [DE85-012297] N86-13147

FLORIDA UNIV., GAINESVILLE.

CBR (California Bearing Ratio) design of flexible airfield pavements with case study [AD-A158101] N86-12242

Metal dissolution kinetics in organic solvents using rotating ring-disc voltammetry [DE85-013478] N86 12253

FOREST PRODUCTS LAB., MADISON, WIS.

Steam-injection pressing of isocyanate-bonded aspen flakeboards, latitudes and limitations [AD-A157833] N86-12389

FOSTER-MILLER ASSOCIATES, INC., WALTHAM, MASS.

Development of the hydrotransport boost pump [PB85-203776] N86-12618

FREIE UNIV., BERLIN (WEST GERMANY).

Planetary waves N86-12821

On the interannual variability and on trends of the temperature in the middle atmosphere N86-12827

FUJI ELECTRIC CO. LTD., YOKOSUKA (JAPAN).

Dissociative volume recombination coefficient measurements in a subroom temperature neon plasma afterglow N86-12373

G

GA TECHNOLOGIES, INC., SAN DIEGO, CALIF.

Tritium control in helium-cooled blankets [DE85-014783] N86-13116

GENERAL ACCOUNTING OFFICE, WASHINGTON, D. C.

FAA (Federal Aviation Administration) could improve overall aviation safety and reduce costs associated with airport instrument landing systems [PB85-195444] N86-12215

Navy should join the Air Force and Army program to develop an advanced integrated avionics system [PB85-222503] N86-12224

GEOLOGICAL SURVEY, DENVER, COLO.

Recent MAGSAT results N86-12886

GEOLOGICAL SURVEY, RESTON, VA.

Modeling gravity and magnetic fields for crustal and upper mantle structures N86-12880

GEOLOGICAL SURVEY, ST. PAUL, MINN.

Waters resources data for Minnesota. Water year 1983. Volume 2: Upper Mississippi and Missouri River Basins [PB85-215994] N86-12753

GEOLOGICAL SURVEY, TALLAHASSEE, FLA.

Water resources data for Florida, water year 1983. Volume 3A: Southwest Florida surface water [PB85-216000] N86-12754

GEOPHYSICAL OBSERVATORY, COLLM (EAST GERMANY).

Remarks on the ATMAP campaigns in November 1981 and May 1982 at Collm (52 deg N, 15 deg E) N86-12842

GEORGE WASHINGTON UNIV., WASHINGTON, D.C.

Scientific workstation research [DE85-013386] N86-13002

IMAGYS graphics programming language: Description and analysis [DE85-013384] N86-13003

GEORGIA INST. OF TECH., ATLANTA.

Investigation of the flame-acoustic wave interaction during axial solid rocket instabilities [AD-A158569] N86-12362

DAA modal analyses for parametric investigations of fluid-structure interaction in underwater shock, revision 1 [DE85-012935] N86-12569

Compound poisson approximations for sums of random variables [AD-A158555] N86-13049

GEORGIA STATE UNIV., ATLANTA.

Secondary electron spectra: A semiempirical model [DE85-012448] N86-13086

GRONINGEN RIJKSUNIVERSITEIT (NETHERLANDS).

Partition of cross sections in asymmetric nucleus-nucleus reactions and the origin of fast alpha particles [DE85-014989] N86-13089

GRUMMAN AEROSPACE CORP., BETHPAGE, N.Y.

GRUMFOIL: A computer code for the viscous transonic flow over airfoils [NASA-CR-3906] N86-12202

An improved viscid/inviscid interaction procedure for transonic flow over airfoils [NASA-CR-3905] N86-12208

GTE LABS., INC., WALTHAM, MASS.

Lithium-thionyl chloride cell system safety hazard analysis [AD-A157089] N86-12775

H

HAMPTON INST., VA.

Direct solar-pumped iodine laser amplifier [NASA-CR-176324] N86-12800

HANFORD ENGINEERING DEVELOPMENT LAB., RICHLAND, WASH.
Application of automated reasoning software procedure generation system verifier
[DE85-014000] N86-13006

HARVARD-SMITHSONIAN CENTER FOR ASTROPHYSICS, CAMBRIDGE, MASS.
The Atmosphere Explorer and the shuttle glow
N86-13243

HARVARD UNIV., CAMBRIDGE, MASS.
Constraints on the rheological structure of the mantle
N86-12675
Flow rates in the East Pacific rise (21 deg N) hot springs, and numerical investigations of two regimes of hydrothermal circulation N86-12939

HEBREW UNIV., JERUSALEM (ISRAEL).
The orientation distribution of nonspherical aerosol particles within a cloud
[AD-A157363] N86-12554

HELSINKI UNIV. TECHNOLOGY, OTANIEMI (FINLAND).
Investigation of ice dynamics in the marginal ice zone
[AD-A157557] N86-12944

HUGHES AIRCRAFT CO., FULLERTON, CALIF.
Study and investigation to update the nonelectronic reliability notebook. Revision A
[AD-A157242] N86-12619

HUGHES AIRCRAFT CO., LONG BEACH, CALIF.
Amorphous silicon photovoltaic modules and test devices design, fabrication and testing N86-12769

HUGHES AIRCRAFT CO., TORRANCE, CALIF.
Development program for a 200 kW, cw gyrotron
[DE85-014887] N86-13096

I

IDAHO DEPT. OF WATER RESOURCES, BOISE.
Water Information Bulletin No. 30, Part 13: Geothermal investigations in Idaho. Preliminary geologic reconnaissance of the geothermal occurrences of the Wood River drainage area
[DE85-016972] N86-12747

IIT RESEARCH INST., BARTLESVILLE, OKLA.
Liquid chromatography on silica using mobile phases containing tetraalkylammonium hydroxides. 1: General separation selectivity and behavior of polar compounds typically in fuels
[DE85-014450] N86-12261

IIT RESEARCH INST., CHICAGO, ILL.
Hazards of chemical rockets and propellants. Volume 3: Liquid propellants
[AD-A158115] N86-12328
Hydrocarbon fuels N86-12329
Anhydrous ammonia N86-12330
The hydrazine fuels N86-12331
Nitromethane N86-12332
Ethylene oxide N86-12333
Otto fuel 2 N86-12334
Hydrogen and deuterium N86-12335
The boranes N86-12336
Carbon monoxide N86-12337
Oxygen N86-12338
Fluorine and fluorine mixtures N86-12339
The halogen fluorides N86-12340
Nitrogen oxides N86-12341
Fuming nitric acids N86-12342
Iodine N86-12343
Chlorine N86-12344
Nitrogen trifluoride N86-12345
Hydrogen peroxide N86-12346
Nitrogen N86-12347
Noble gases N86-12348
The alcohols N86-12349
Halocarbons N86-12350
Hydraulic fluids N86-12351
Mercury N86-12352
Compressed and liquid air N86-12353
Carbon dioxide N86-12354
Nitrous oxide N86-12355
Liquid propellant storage compatibility N86-12356
Quantity-distance requirements N86-12357

ILLINOIS DEPT. OF ENERGY AND NATURAL RESOURCES, SPRINGFIELD.
Design of a statewide groundwater monitoring network for Illinois
[PB85-192821] N86-12750

ILLINOIS INST. OF TECH., CHICAGO.
Zinc/ferricyanide battery development phase 4
[DE85-016026] N86-12781

ILLINOIS UNIV., URBANA.
Mean winds and tides over Urbana, Illinois during November 16-22, 1981 N86-12846
Diagnosing cognitive errors: Statistical pattern classification and recognition approach
[AD-A158106] N86-12972
A theory for algorithm-based fault tolerance in array processor systems
[AD-A158244] N86-12977
Theoretical studies of deep impurity levels in ternary semiconductor alloys
[AD-A157929] N86-13193
Second order elastic contents of Pd, PdH(0.7) and PdD(0.7) between 1.7 and 50 K
[DE85-014316] N86-13212

ILLINOIS UNIV., URBANA-CHAMPAIGN.
The dynamic stability of the stratosphere and mesosphere N86-12811
The numerical simulation of geographic storms
N86-12907

INDIAN INST. OF SCIENCE, BANGALORE.
A proposed international tropical reference atmosphere up to 80 km N86-12828

INSTITUT FRANCO-ALLEMAND DE RECHERCHES, ST. LOUIS (FRANCE).
Studies of the Bauer piezoelectric polymer gauge (PVF2) under impact loading
[DE85-014707] N86-12590

INSTITUT FUER DIGITALE BILDVERARBEITUNG UND GRAPHIK, GRAZ (AUSTRIA).
Correcting a digital map data base with scene analysis concepts and methods
[AD-A157913] N86-12745

INSTITUTE FOR DEFENSE ANALYSES, ALEXANDRIA, VA.
Minutes of Workshop on Composite Materials Test Methods
[AD-A157903] N86-12262

INSTITUTE OF APPLIED GEOPHYSICS, MOSCOW (USSR).
Observed winds and temperatures in the Southern Hemisphere N86-12817

INSTITUTE OF GAS TECHNOLOGY, CHICAGO, ILL.
Absorption fluids data survey
[DE85-005279] N86-12792

INTEGRATED SYSTEMS, INC., PALO ALTO, CALIF.
Real-time flutter identification
[NASA-CR-3933] N86-12218

INTERNATIONAL COUNCIL OF SCIENTIFIC UNIONS, URBANA, ILL.
Middle Atmosphere Program. Handbook for MAP. Volume 16: Atmospheric structure and its variation in the region 20 to 120 km. Draft of a new reference middle atmosphere
[NASA-CR-176321] N86-12814
Middle Atmosphere Program. Handbook for MAP, volume 17
[NASA-CR-176345] N86-12837

IOWA UNIV., IOWA CITY.
Analysis and interpretation of the shock-like electrostatic noise observed during the AMPTE (Active Magnetospheric Particle Tracer Explorers) solar wind lithium releases
[AD-A157512] N86-13283
A statistical study of solar Type-3 bursts and auroral kilometric radiation onsets
[AD-A158408] N86-13284

J

JET PROPULSION LAB., CALIFORNIA INST. OF TECH., PASADENA.
Reliability and Engineering of Thin-Film Photovoltaic Modules. Research forum proceedings
[NASA-CR-176217] N86-12759
Crystalline-silicon reliability lessons for thin-film modules N86-12760
Hot-spot heating susceptibility due to reverse bias operating conditions N86-12763
Electrical safety requirements: Implications for the module designer N86-12765
Module voltage isolation and corrosion research
N86-12772
Glass breaking strength: The role of surface flaws and treatments N86-12773
Encapsulant selection and durability testing experience N86-12774
Investigation of reactive magnetron sputter deposited ZnSe for solar cell application
[DE85-016851] N86-12780
Investigation of test methods, material properties and processes for solar cell encapsulants
[DE85-012831] N86-12786
Solar walk-off protection
[DE85-012112] N86-12788
Contributions of GRM to the ocean topography experiment (TOPEX) N86-12883
Advanced Moisture and Temperature Sounder (AMTS) baseline 5 study report
[NASA-CR-176331] N86-12919

JOHNS HOPKINS UNIV., BALTIMORE, MD.
Thermodynamics of multi-polar molecules: The perturbed-anisotropic-chain theory
[DE85-013148] N86-12274
Research on the microstructure of rapidly solidified alloys
[AD-A157077] N86-12296
Measurements on an axisymmetric jet in a slow coflowing stream N86-12549
Lithospheric structure in the Pacific geoid N86-12863
Sea floor swells and mantle plumes N86-12866
Fault tolerant statistical signal processing algorithms for parallel architectures
[AD-A157393] N86-12978

JOINT PUBLICATIONS RESEARCH SERVICE, ARLINGTON, VA.
China report: Science and technology
[JPRS-CST-85-024] N86-12368
Pressure-coupled response function of solid propellants including those with negative pressure exponents
N86-12369
One-dimensional two-phase flow in combustion chamber of solid propellant rocket motors N86-12370
China report: Science and technology
[JPRS-CST-85-016] N86-12393
Compact TEA-CO2 laser with long life developed
N86-12394
Frequency selection and mode locking of Nd:YAG laser N86-12395
Mean density scale heights from analysis of variation in perigee height of China's second satellite
N86-12396
Numerical computation of full three-dimensional flow in transonic turbines N86-12397
Code of finite element analysis for three-dimensional flow in turbomachines N86-12398
China report: Science and technology
[JPRS-CST-85-035] N86-12399
New criterion of combined-mode brittle fracture described N86-12400
Cartography, national land management related
N86-12401
Benefits of surveying, cartography described
N86-12402
Status, development of power ultrasonics in China
N86-12403
Plasma arc welding for thin titanium plates
N86-12404
Japanese report on China's F-8 fighter N86-12405
The 4-bit microprocessor capabilities, applications described N86-12406
Mathematical model of the dynamic response of thermo-regulating in 200 MeV linear accelerator
N86-12407
China report: Science and technology
[JPRS-CST-85-017] N86-12408
Determination of single-mode optical fiber dispersion
N86-12409
Microcomputer-controlled closed-loop system for positioning radio telescope N86-12410
Laser anemometer using a single circuit board
N86-12411
The step structure effect of dc Josephson current within one flux quantum period phi sub zero (2) N86-12412
China report: Science and technology
[JPRS-CST-85-018] N86-12413
State-of-the-art of optics in China reviewed
N86-12414
Single mode phase locking fiberoptic sensor developed N86-12415
Practical optical multichannel analyzer developed
N86-12416
Development of beam optics for a 200 keV ion implanter N86-12417
Characteristic value as an energy output index for explosives N86-12418
Long wave (1.2 - 1.5 microns) semiconductor lasers
N86-12419
Coupling between spinor field, propagating torsion
N86-12420
China report: Science and technology
[JPRS-CST-85-021] N86-12421
Variational analysis of phase transition in pure gauge fields N86-12422
Quantum chemistry of aromatic nitro explosives
N86-12423
Pulsed radiation detection technology discussed
N86-12424
New dual Z80 navigation computer described
N86-12425
Superheated steam's density compensation for flow measurement N86-12426
Titanium-nitrogen ion beam injection studied
N86-12427

JOINT PUBLICATIONS RESEARCH SERVICE, ARLINGTON, VA.

High-power ND: Glass laser and target chamber system and an experimental study of laser plasma X-ray N86-12428
Titanium extractant T105-1 studied N86-12429
China report: Science and technology [JPRS-CST-85-034] N86-12430
Laser scattering in plasma examined N86-12431
Optic fiber applications in data communications N86-12432
Experiments with domestic IC substrates N86-12433
BLR studies on conic model with LDA in FL-1 wind tunnel N86-12434
Measurement of 1 nanosecond wide beams for 2.5 MeV proton accelerator N86-12435
Mathematical principle for generating second-order aspherical surface N86-12436
Superconducting wire manufactured N86-12437
Ultrahigh vacuum equipment described N86-12438
China report: Science and technology [JPRS-CST-85-022] N86-12439
China's first imported peripheral equipment production line N86-12440
Method of using CTC to microcomputerize digital instruments N86-12441
Digital phase meter using CMOS-LED introduced N86-12442
Latch-up effect in CMOS described N86-12443
China report: Science and technology [JPRS-CST-85-025] N86-12444
New approaches to determining physical properties in piston-cylinder high-temperature, high-pressure device N86-12445
China report: Science and technology [JPRS-CST-85-029] N86-12446
Progress of inertial confinement research detailed N86-12447
Programmer for single-chip microprocessor N86-12448
Digital voltmeter technology acquisition N86-12449
Wingtip sails tested on Y-5 aircraft N86-12450
China report: Science and technology [JPRS-CST-85-030] N86-12451
Computer-aided analysis of arbitrary-shaped thin-wire antennas N86-12452
Usages of organic membranes in electrolytic industry described N86-12453
Effect of amplified spontaneous emission on space coherence of XeCl laser N86-12454
First domestic high repetition rate ultrashort pulse laser N86-12455
Practical excimer laser developed N86-12456
A high precision rate dye laser pumped by a CuCl laser N86-12457
Human hemodynamic change under high atmospheric pressure N86-12458
China report: Science and technology [JPRS-CST-85-026] N86-12459
Laser induced biological heating analyzed N86-12460
Application of heat-scan NDT to inspection of adhesion of solid rocket motor propellant to envelope N86-12461
China report: Science and technology [JPRS-CST-85-032] N86-12462
Vector valued long James type Banach spaces J(eta, l sub p)(1 or = p + infinity) N86-12463
Finite difference scheme for one-dimensional magnetohydrodynamic equations N86-12464
China develops 6J KrF laser N86-12465
Application of radiographic image enhancement, segmentation N86-12466
Iron and steelmaking with plasma N86-12467
CAD program for high-power electron gun with annular cathode described N86-12468
USSR report: Earth sciences [JPRS-UES-85-006] N86-12630
Meteorological center's forecasts aid Venus probe tracking N86-12631
Diagnosis of weather states in winter of 1980-1981 N86-12632
Main problems in climate monitoring (diagnosis) N86-12633
Use of method of canonical correlations for analysis of climatic series N86-12634
Empirical analysis of direct and inverse relationships between macroscale characteristics of atmospheric processes in northern hemisphere and thermal state of north Atlantic N86-12635
Atmospheric aerosol and its effects on climate N86-12636
Influence of power engineering on climate N86-12637
Recent changes in climate and world water balance N86-12638
Climatically active trace gases in atmosphere N86-12639
Estimate of radiation-climatic effects of natural and anthropogenic aerosol N86-12640
Modeling of seasonal evolution of carbon cycle in ocean-atmosphere system N86-12641
Study of significance of bottom relief in baroclinic model of equatorial countercurrent N86-12642
Angular distribution of intensity of sound reradiated by ocean surface at small glancing angles N86-12643
Influence of short gravity waves on thermal radio emission of water surface N86-12644
Upper mesozoic turbidites of southern west Sakhalin downwarp N86-12645
Spectrum of turbulent fluctuations in sea water density in region of large wave numbers N86-12646
Interaction of sound waves with fine thermohaline structures of ocean N86-12647
Correlation characteristics of signals reflected by the wavy surface of ocean in mirror direction N86-12648
Numerical estimate of effectiveness of approximate equations for acoustic field near surface of deep sea N86-12649
Petrochemical types of magmatic rocks of ocean floor and patterns of their distribution N86-12650
Intrusive rocks of oceanic lithosphere as possible sources of anomalous magnetic field of ocean N86-12651
Magmatic provinces and tectonics in Pacific Ocean N86-12652
Geochemistry and energetics of cycling of matter in formation of crust in active structures of ocean N86-12653
Contribution of diffusion processes to the electric field of the ocean N86-12654
Oil and gs deposits on continental slopes of the ocean N86-12655
Acoustical field of directional source in oceanic waveguides N86-12656
Petrologic aspect of formation of geostructures in marginal seas N86-12657
Spreading in development of oceanic structures N86-12658
Influence of water vapor on distribution of turbulent wave parameters N86-12659
Diffraction of internal waves described by equation of slightly stratified fluid on half-plane N86-12660
Possibility of sounding Earth by using electromagnetic field of sea current N86-12661
Electromagnetic field of three-dimensional surface sea waves N86-12662
Stratigraphy of sediments in central and eastern Mediterranean N86-12663
Structure of acoustic field in deep sea at shallow depths and at great ranges N86-12664
Find of rheolites and trachites and geological situation in northern part of East Indian Ocean Submarine Ridge N86-12665
Evaluating screening effects and Tusnami danger in bays N86-12666
Influence of seston phosphatase activity on rate of phosphorus mineralization and its recycling in production-destruction cycle N86-12667
Origin of element composition of ocean water N86-12668
Theory of solitary anticyclones in rotating fluid N86-12669
Nonlinear model of adaptation of fields of density and currents in sea N86-12670
Laboratory study of regular low-amplitude gravity capillary waves in nonstationary current N86-12671
Eddy fluxes of heat, vorticity and momentum in ocean and atmosphere and their parameterization (review) N86-12672
Study of influence of vertical velocity and density profiles on hydrodynamic stability of zonal flow N86-12673
Features of geostrophic circulation related to nature of bottom relief in northwestern Atlantic N86-12674
Cyclonic frontal eddy in Antarctic circumpolar current N86-12675
Influence of some oceanographic characteristics on decay kinetcis of surface-active agents in sea N86-12676
Computations of seismic wave propagation velocities in ocean bottom sediments from reflected waves travel-time curves N86-12677
Role of ahermatypic corals in sedimentation and ecology of coral banks N86-12678
New data of relief of Mazca Ridge N86-12679
Gravimetric surveying with MI-8 helicopters N86-12680
magnetic minerals and characteristics of natural magnetic state of core in Saatly superdeep hole in depth range 3500-7500 meters N86-12681
New methods for interpreting seismic waves in stratified media N86-12682
New approach to some problems in seismology N86-12683
Method for solving problems in electrodynamics of anisotropic media with slant bedding N86-12684
Features of field of directions and velocities of propagation of fractures at earthquake foci in northern Muya region of Baykal Rift Zone N86-12685
Hardware and softeare support of geological-geophysical database N86-12686
High-elevation station's cosmic-ray recording system N86-12687
Vidro terminal for analyzing aerial infrared photographs N86-12688
Comparison of single-parameter statistical model with results of round-the-clock measurement of light-scattering matrices N86-12689
Ionic mechanicsm of exchange of admixtures between hydrosphere and atmosphere N86-12690
Ionic mechanicsm of exchange of admixtures between hydrosphere and atmosphere N86-12691
Damping of high-frequency wind waves by artifical surface-active films N86-12692
Organic components in atmosphere in regions of volcanic activity N86-12693
Evaluating influence of waves on dynamic structure of atmospheric near-water laver N86-12694
Global modeling of optical characteristics of atmospheric aerosol N86-12695
Diurnal variation of optical and microphysical characteristics of near-surface aerosol N86-12696
USSR report: Earth sciences [JPRS-UES-85-008] N86-12697
Some results of study of blocking layers on days with vertically developed cloud cover of Caucasus-Caspian region on basis of aerospace information N86-12698
Experimental study of equilibrium interval in frequency spectra of wind waves in sea of finite depth N86-12699
Features of electrical measurements in sea as medium with field of extraneous forces N86-12700
Phase operator method in problem of scattering of electromagnetic waves on ideally conducting surface N86-12701
Quasigeostrophic model of circulation in Antarctic Ocean with parametrization of synoptic eddies N86-12702
Estimation of influence of ocean on distribution of heavy metals in marine atmosphere N86-12703
Folded structures in central Indian Ocean trench N86-12704
Remote diagnosis of media by combination (Raman) anti-Stokes light scattering method with induced Brillouin backscattering N86-12705
Acoustic methods for featuring high-frequency part of spectrum of sea waves N86-12706
Ocean albedo for atmospheric thermal emission N86-12707
Investigation of elastic properties of marine surface-active films N86-12708
Structure of sedimentary cover and basement of Sierra Leone Rise determined from common depth point seismic (equatorial Atlantic) N86-12709
Tectonic structure of Shirshov Ridge (Bering Sea) N86-12710
Fine structure of density relation in main oceanic thermocline N86-12711
Viscous nonlinear circulation in axisymmetric baroclinic eddy N86-12712
Facies-genetic groups of coarse clastic material on world ocean floor N86-12713
Spatial structure of high-frequency sea wind waves under different meteorological conditions N86-12714
Nonlinear interaction between soliton and short waves in ideal fluid N86-12715
The question of Earth expansion and its oceanic implications N86-12716
Kamchatka radio telemetric station registers volcano pulse N86-12717
Lasers measure drifting mountains N86-12718
Launch of Kosmos-1653 natural resources research satellite N86-12719
Muon tomography used to study underground rock structure N86-12720
Underground volcanoes discovered with satellite radar N86-12721
P-wave spectra in problem of determining dynamic paramters of earthquake foci. Standardization of initial data and procedures for computing amplitude spectra N86-12722
PRospects for development of seismic prospecting methods and apparatus N86-12723
Determination of dynamic parameters of reflected waves on slopes of deep water trench N86-12724
Optimal density model of Earth's rust and upper mantle along Kamchatka-Pacific Geotraverse N86-12725
Variation in seismicity under influence of lunar-solar tidal deformations N86-12726
Electromagnetic effects in crustal fracturing N86-12727

Experience in breaking down gravity field into components resulting from density heterogeneities at various depths (using North Atlantic and Mediterranean as examples) N86-12728
Hypocentral areas of aftershocks and possible fault systems at foci of Tsunami-generating Kuril earthquakes N86-12729
Method and results of electrometric observations in seismically active region N86-12730
Seismic effect of underground blasts and problem of estimating total earthquake energy N86-12731
Tectonics of eastern Kronotskiy Peninsula and formational association of basalts (Kamchatka) N86-12732
Geodynamics of crustal dilatation in transition area from Asian continent to Pacific Ocean N86-12733
Transmission of tropospheric radiation of lasers on molecules of different carbon dioxide isotopes N86-12734
Atmospheric turbulence investigations at Tsimlyansk Scientific Station, Atmospheric Physics Institute, USSR Academy of Sciences N86-12735
Humidity profile measurements in atmospheric lower layer by spontaneous Raman scattering method N86-12736
Some characteristics of transmission by thin clouds in visible and infrared spectral regions N86-12737
China report: Science and technology [JPRS-CST-85-019] N86-12966
Protection of eyes against laser damage studied N86-12967

K

KANSAS UNIV. CENTER FOR RESEARCH, INC., LAWRENCE.
Evaluation of space SAR as a land-cover classification [E86-10004] N86-12740
KENT STATE UNIV., OHIO.
Quantum simulations of small electron-hole complexes [DE85-013695] N86-13205
KENTRON INTERNATIONAL, INC., HAMPTON, VA.
Derivation of jack movement influence coefficients as a basis for selecting wall contours giving reduced levels of interference in flexible walled test sections [NASA-CR-177992] N86-12204
KMS FUSION, INC., ANN ARBOR, MICH.
Recent developments in microshell-tipped optical fibers as high-pressure shock detectors [DE85-015750] N86-12594
Absolutely unstable two-plasmon decay in two dimensions [DE85-008157] N86-13150
KTECH CORP., ALBUQUERQUE, N. MEX.
Studies of the Bauer piezoelectric polymer gauge (PVF2) under impact loading [DE85-014707] N86-12590
KYOTO UNIV. (JAPAN).
Gravity waves N86-12822
Kyoto meteor radar observation in November, 1981 and May, 1982 N86-12847
Mesospheric winds at Jicamaraca, Peru (12 deg S, 77 deg SW), November 19-21, 1981 N86-12849

L

LAMONT-DOHERTY GEOLOGICAL OBSERVATORY, PALISADES, N. Y.
Gravity, geoid and the oceanic lithosphere N86-12860
Studies of the marine crustal magnetization at intermediate wavelengths N86-12862
LANGUAGE SERVICES, NASHVILLE, TENN.
Manufacturing process for cylindrical ceramic tubes with localized imprints and device for application of this process [DE85-012294] N86-12323
LAWRENCE LIVERMORE NATIONAL LAB., CALIF.
Macroscopic and microscopic deformation and failure processes that control composite toughness [DE85-012938] N86-12263
High damage threshold porous silica antireflective coating [DE85-012924] N86-12322
Energetic response of propellants to high velocity impact, revision 1 [DE85-013983] N86-12365
Electronics Engineering Department Thrust Area report FY'84 [DE85-014857] N86-12539
EE technical review [DE85-015313] N86-12540
Computer simulation of the effect of free surface reflection on shock wave propagation in water [DE85-014807] N86-12563
Modeling short pulse duration shock initiation of solid explosives [DE85-014803] N86-12565
Dislocation kinetics behind shear shocks [DE85-014811] N86-12566
DAA modal analysis for parametric investigations of fluid-structure interaction in underwater shock, revision 1 [DE85-012935] N86-12569
REFRIG-12: A graphics-augmented interactive program for designing vapor-compression refrigeration/heat pump cycles [DE85-014205] N86-12572
Improved approach to characterizing and presenting streak camera performance [DE85-015188] N86-12587
Results of PRIM gyroscope testing [DE85-012934] N86-12591
Measurement of tritium permeation through resistant materials near room temperature [DE85-012942] N86-12592
X-ray diffraction cell for Debye-Scherrer and Guinier (Huber) cameras at pressure and temperature [DE85-014815] N86-12593
Science, technology and the industrialization of laser-driven processes [DE85-014856] N86-12605
Dynamic ADI computations of thermoelastic stresses in crystalline laser media [DE85-010478] N86-12606
Failure criteria used in a probabilistic fracture mechanics code [DE85-007264] N86-12628
Motion of thin metal walls and the equation of state of detonation products [DE85-014809] N86-12629
Real-time computing of the environmental consequences of an atmospheric accidental release of radioactive material: User's point of view [DE85-016438] N86-12795
Data structures and vectorization in a two-dimensional free-Lagrangian code [DE85-012948] N86-13009
Role of supercomputers in magnetic fusion and energy research programs [DE85-013200] N86-13023
LabNet Project plan [DE85-014860] N86-13024
Measurements and calculations of neutron scattering angular distributions over a wide mass and energy range [DE85-012912] N86-13105
High intensity positron beam and angular correlation experiments at Livermore [DE85-012961] N86-13111
Nuclear performance optimization of the Be/Li/Th blanket for the fusion breeder [DE85-012949] N86-13112
Estimating the reliability of fiber optics cables [DE85-014892] N86-13136
Diffusion in binary plasma mixtures [DE85-017694] N86-13143
Conversion of the bounce-averaged Fokker-Planck code to conversion form [DE85-014861] N86-13160
Multivariable current control for electrically and magnetically coupled superconducting magnets [DE85-012941] N86-13163
High efficiency ICF driver employing magnetically confined plasma rings [DE85-012939] N86-13164
Identifying heavy-ion-beam fusion design and system features with high economic leverage [DE85-014849] N86-13181
Large-basis shell-model technology in nucleosynthesis and cosmology [DE85-012925] N86-13216
Nuclear information needs for the astrophysical s-process [DE85-012913] N86-13278
LETTERMAN ARMY INST. OF RESEARCH, SAN FRANCISCO, CALIF.
Energy expenditure and activity patterns of cadets at the United States Military Academy, West Point, New York [AD-A157857] N86-12960
LISTER HILL NATIONAL CENTER FOR BIOMEDICAL COMMUNICATIONS, BETHESDA, MD.
Systems for authoring computer-based instruction [PB85-198950] N86-12987
LITTLE (ARTHUR D.), INC., CAMBRIDGE, MASS.
Development of a routine technique for analysis of nitro-PAH in diesel particulate extract [PB85-196657] N86-12287
Derivation of the optical constants of anisotropic [AD-A158396] N86-13195
LOCKHEED MISSILES AND SPACE CO., PALO ALTO, CALIF.
Zinc/ferricyanide battery development phase 4 [DE85-016026] N86-12781
Vehicle glow measurements on the space shuttle N86-13240
Data requirements for verification of ram glow chemistry N86-13265
LOS ALAMOS NATIONAL LAB., N. MEX.
Ground-based investigations of atomic oxygen interactions with space station surfaces [DE85-014082] N86-12249
Parallel, staged opening switch power conditioning techniques for flux compression generator applications [DE85-012761] N86-12527
Calculation of series capacitance for transient analysis of windings N86-12528
Self-consistent klystron simulations [DE85-012678] N86-12529
Racetrack microtron rf system [DE85-012669] N86-12532
Design of foil implosion system for Pioneer 1 experiments [DE85-014111] N86-12535
Los Alamos constant-Q spectrometer [DE85-014115] N86-12586
Recent developments in microshell-tipped optical fibers as high-pressure shock detectors [DE85-015750] N86-12594
Strategic defense initiatives at Los Alamos National Laboratory [DE85-014093] N86-12608
Magnetic reconnection in the terrestrial magnetosphere [DE85-014107] N86-12904
Raman activity in synchronously dividing bacteria [DE85-015672] N86-12951
Guidelines for a thermochemical kinetics computer program [DE85-015671] N86-12998
Systems analysis approach to probabilistic modeling of fault trees [DE85-007705] N86-13050
LAMPF transition-region mechanical fabrication [DE85-012688] N86-13081
Funneling: An initial beam dynamics study [DE85-012652] N86-13082
Development of a current monitor system for measuring pulsed-beam current over a wide dynamic range [DE85-012692] N86-13083
Electron emission of over 200 A/cm (2) from a pulsed-laser irradiated photocathode [DE85-012656] N86-13084
FMIT diagnostic instrumentation [DE85-012668] N86-13087
High nuclear temperatures by antimatter-matter annihilation [DE85-014113] N86-13090
Chemistry of berkelium: A review [DE85-017523] N86-13102
Isovector resonances in pion charge exchange [DE85-012746] N86-13106
Shocking behavior of fluid flow in deformable joints [DE85-010104] N86-13107
Nearly ideal lens optimization procedure [DE85-014116] N86-13134
Field-reversed configuration formation, translation, and confinement studies on the FRX-C/T experiment [DE85-014095] N86-13141
FRC formation studies with Z-discharge ionization on FRX-C [DE85-012765] N86-13152
Temperature and concentration dependence of hydrogen site occupancy in several rare-earth dihydrides [DE85-015739] N86-13199
Energy dispersive spectroscopy using synchrotron radiation: Intensity considerations [DE85-017530] N86-13200
X-ray diffraction studies of shock-modified inorganic materials [DE85-015150] N86-13209
Large-basis shell-model technology in nucleosynthesis and cosmology [DE85-012925] N86-13216
Activated recombinative desorption: A potential component in mechanisms of spacecraft glow N86-13258
LOS ALAMOS SCIENTIFIC LAB., N. MEX.
Oxidation of heterocyclic nitrogen yields to nitroheterocycles [DE85-012757] N86-12284
Application of time-dependent Raman theory to the analysis of inorganic photosystems [DE85-012752] N86-12285

TATE: Strong basic reactions provide soluble derivations for simple qualititative high explosive spot test [DE85-014259] N86-12366

Foil fuses as opening switches for slow discharge circuits [DE85-014124] N86-12519

Novel instrument for high-pressure research at ultra-high temperatures [DE85-015674] N86-12589

Data acquisition interfaces for the IBM personal computer [DE85-014256] N86-12985

The 32-bit computer for large memory applications on FASTBUS [DE85-012726] N85-12985

Attempt to develop an intelligent lens design program [DE85-014122] N86-13017

Data acquisition command interface using VAX/VMS DCL [DE85-012747] N86-13019

Sound velocities in liquid lead at high temperatures [DE85-014091] N86-13062

Reconstruction of longitudinal beam profiles from nondestructive electromagnetic probes [DE85-012675] N86-13078

Experiment to study K(+) (YIELDS) (PI)(+) + nothing at LAMPF 2 [DE85-014267] N86-13110

Study of possible solarization - related impurities in CaF2 and other fluorides [DE85-014100] N86-13135

Generalization of the Child-Langmuir relation for one-dimensional time-dependent diodes [DE85-012677] N86-13145

R-matrix analysis of the (7) Li system with peripheral channel overlap exchange effects [DE85-012751] N86-13148

Plane-wave theory of electrical transport in disordered systems [DE85-015353] N86-13167

WNR/PSR facility: Neutron physics capabilities from sub-thermal to 800 MeV [DE85-014072] N86-13173

Recent results of an internal tilt mode calculation in FRCs [DE85-014121] N86-13177

Superconductivity in the W-Tc and W2C-Tc systems [DE85-012711] N86-13204

LUNAR AND PLANETARY INST., HOUSTON, TEX.

Workshop on Water on Mars [NASA-CR-176289] N86-13282

M

MANAGEMENT AND TECHNICAL SERVICES CO., WASHINGTON, D.C.

USSR Space Life Sciences Digest, Issue 2 [NASA-CR-3922(02)] N86-12949

MANCHESTER UNIV. (ENGLAND).

Radiation fog modeling [AD-A157971] N86-12924

MANHATTAN COLL., NEW YORK.

Perspectives to establish knowledge linkages between acidic deposition and vegetation responses [DE85-011839] N86-12796

MARYLAND UNIV., COLLEGE PARK.

A survey of some recent results in continuous univariate distributions [AD-A157450] N86-13047

Accelerator research studies [DE85-014876] N86-13113

MASSACHUSETTS INST. OF TECH., CAMBRIDGE.

Microstructure/Property relationships for carbon fiber reinforced aluminum alloys [AD-A157858] N86-12261

Fischer-Tropsch synthesis in slurry reactor systems [DE85-013390] N86-12278

Non-linear corrections to the linear theory for the prediction of the cavitating flow around hydrofoils [AD-A158105] N86-12557

Fusion welding research [AD-A158127] N86-12611

Feasibility of using LANDSAT images of vegetation cover to estimate effective hydraulic properties of soils [E86-10003] N86-12739

Impact of GRM: New evidence from the Soviet Union N86-12853

Evidence from satellite altimetry for small-scale convection in the mantle N86-12878

Generic software for emulating multiprocessor architectures [AD-A157662] N86-12979

Numerical algorithms and mathematical software for linear control and estimation theory [AD-A157525] N86-12992

Actors: A model of concurrent computation in distributed systems [AD-A157917] N86-12994

Theory of the anomalous Doppler instability during lower-hybrid current drive [DE85-014064] N86-13170

MASSACHUSETTS INST. OF TECH., LEXINGTON.

Weather radar studies [AD-A157093] N86-12920

MASSACHUSETTS UNIV., AMHERST.

Near millimeter wave imaging/multi-beam integrated antennas [NASA-CR-176332] N86-12478

Additional results on the radiating properties of LTSAs and CWSAs N86-12479

Characteristic impedance of a wide slot line on low permittivity substrates N86-12480

Analysis of the tem mode linearly tapered slot antenna N86-12481

A new integrated slot element feed array for multi-beam systems N86-12483

A 94 GHz imaging array using slot line radiators [NASA-CR-176348] N86-12484

Automatic detection of gulf stream rings [AD-A157934] N86-12945

Decentralized control of scheduling in distributed systems [AD-A157656] N86-13222

MATERIALS RESEARCH LABS., ASCOT VALE (AUSTRALIA).

Development and evaluation of a microburst test apparatus for use as a minimum destructive test for parachute material [AD-A158110] N86-12620

MAX-PLANCK-INST. FUER AERONOMIE, KATLENBURG-LINDAU (WEST GERMANY).

Towards a global MAP data base N86-12838

MAX-PLANCK-INSTITUT FUER STROEMUNGSFORSCHUNG, GOETTINGEN (WEST GERMANY).

Transonic noise generation by duct and profile flow [AD-A157163] N86-13058

METEOROLOGICAL SATELLITE CENTER, TOKYO (JAPAN).

Meteorological Satellite Center Technical Note No. 11, 1985 [MSC-TN-11] N86-12909

Occurrence of linearly ranged Cb-clouds associated with migrating band-shaped cirriform-clouds: A case study N86-12910

Clear sky brightness temperature over the western north Pacific Ocean from GMS spacecraft N86-12911

Simultaneous observation of GMS and GMS-2: A study of the difference between the brightness temperatures by GMS and those by GMS-2 N86-12912

Relaying of the stretched VISSR data by GMS spacecraft N86-12913

The modification of the operational program for GMS-3 N86-12914

Introduction to operational ASDAR system N86-12915

MIAMI UNIV., FLA.

Atmospheric tritium 1968-1984 [DE85-0131[illegible]3] N86-12798

The source of the intermediate wavelength component of the Earth's magnetic field N86-12891

MICHIGAN STATE UNIV., EAST LANSING.

Integral equation description of integrated dielectric waveguides N86-12504

MICHIGAN UNIV., ANN ARBOR.

Group combustion of sprays N86-12266

Shear driven film flow behavior and cavitation study N86-12543

Wave-current and wave-topographic interactions using SEASAT synthetic aperture radar observations and analytical ocean models N86-12938

MIDWEST ENERGY INST., KANSAS CITY, MO.

SOLERAS: Photovoltaic power systems project. Module failure analysis [MRI/SOL-0101] N86-12756

MIDWEST RESEARCH INST., GOLDEN, COLO.

Aquatic Species Program review: Proceedings of Principal Investigators Meeting [DE85-012137] N86-12364

Isothermal dehumidification of air in a parallel passage configuration [DE85-008819] N86-12577

Outdoor performance testing of thin-film devices N86-12771

Solar thermal energy systems [DE85-008793] N86-12790

Film stability for dirct absorption receivers [DE85-012135] N86-12791

MINNESOTA DEPT. OF NATURAL RESOURCES, ST. PAUL.

Waters resources data for Minnesota. Water year 1983. Volume 2: Upper Mississippi and Missouri River Basins [PB85-215994] N86-12753

MINNESOTA DEPT. OF TRANSPORTATION, ST. PAUL.

Waters resources data for Minnesota. Water year 1983. Volume 2: Upper Mississippi and Missouri River Basins [PB85-215994] N86-12753

MISSISSIPPI UNIV., UNIVERSITY.

Biological effects of acoustic cavitation [AD-A157513] N86-13059

MISSOURI UNIV., COLUMBIA.

Design of an antenna feed system to produce a uniform field N86-12469

MISSOURI UNIV., POLLA.

Mixed-mode cyclic debonding of adhesively bonded composite joints [NASA-CR-177991] N86-12255

Hybrid radar waveform design utilizing complementary phase coding and linear frequency stepping for achieving improved slant range resolution in a synthetic aperature radar N86-12470

Finned tube contact conductance: Characterizing the integrity of the mechanical bond [DE85-013747] N86-12564

MISSOURI UNIV., ST. LOUIS.

Ultraviolet observations of low-excitation Herbig-Haro objects [NASA-CR-176164] N86-13273

MITRE CORP., BEDFORD, MASS.

AISIM (Automated Interactive Simulation Modeling System) overview: Revision 1 [AD-A157392] N86-12990

MOUND LAB., MIAMISBURG, OHIO.

Method and apparatus for conducting variable thickness vapor deposition [DE85-011653] N86-12306

In-situ vacuum-assisted molding of glass-metal electrical components [DE85-015607] N86-12326

Outdoor radon monitoring at Canonsburg, Pennsylvania, 1980-1983 [DE85-013320] N86-12797

N

NATIONAL ACADEMY OF SCIENCES - NATIONAL RESEARCH COUNCIL, WASHINGTON, D. C.

Studies of participants in nuclear tests N86-12964

Aeronautical technology 2000: A projection of advanced vehicle concepts [NASA-CR-176322] N86-13235

NATIONAL AERONAUTICS AND SPACE ADMINISTRATION, WASHINGTON, D. C.

Molecular control [NASA-TM-87510] N86-12313

Earth resources: A continuing bibliography, issue 46 [NASA-SP-7041(46)] N86-12738

Geopotential Research Mission (GRM) [NASA-CP-2390] N86-12852

Aerospace Medicine and Biology Continuing Bibliograph: A continuing bibliography with indexes [NASA-SP-7011(276)] N86-12954

Index to NASA news releases and speeches, 1984 [NASA-TM-87514] N86-13224

Microgravity science and applications bibliography, 1985 revision [NASA-TM-88178] N86-13225

NATIONAL AERONAUTICS AND SPACE ADMINISTRATION. AMES RESEARCH CENTER, MOFFETT FIELD, CALIF.

Some recent advances in computational aerodynamics for helicopter applications [NASA-TM-86777] N86-12207

Plasma volume methodology: Evans blue, hemoglobin-hematocrit, and mass density transformations [NASA-TM-86834] N86-12956

NATIONAL AERONAUTICS AND SPACE ADMINISTRATION. GODDARD SPACE FLIGHT CENTER, GREENBELT, MD.

Temperature and wind data from meteorological rockets N86-12616

Magnetic structure of the crust N86-12859

GRM crustal magnetic anomalies: Separating the Lord Howe Rise and Norfolk Ridge submarine structures N86-12865

Global mean sea surface computation based upon a combination of SEASAT and GEOS-3 satellite altimeter data N86-12882

Some anticipated contributions to core fluid dynamics from the GRM N86-12886

GRM as a follow-on to MAGSAT N86-12893

Planned investigation of infrared emissions associated with the induced spacecraft glow: A shuttle infrared glow experiment (SIRGE) N86-13264

A note on Jupiter's gossamer ring N86-13280

Electrons and cosmic ray produced in Saturn's inner magnetosphere N86-13281

NATIONAL AERONAUTICS AND SPACE ADMINISTRATION. LANGLEY RESEARCH CENTER, HAMPTON, VA.

Effect of surface waviness on a supercritical laminar-flow-control airfoil
[NASA-TM-85705] N86-12206

Effect of measured material properties on the finite element analysis of an OH-58 composite tail boom
[NASA-TM-86430] N86-12259

The role of amplitude-to-phase conversion in the generation of oscillator flicker phase noise
[NASA-TM-87590] N86-12508

Technique for measuring gas conversion factors
[NASA-CASE-LAR-13220-1] N86-12547

An asymptotic investigation of the stationary modes of instability of the boundary layer on a rotating disc
[NASA-CR-177977] N86-12550

Rapid estimation of frequency response functions by close-range photogrammetry
[NASA-TP-2471] N86-12579

Interim reference ozone models for the middle atmosphere N86-12829

A method for determining acoustic-liner admittance in ducts with sheared flow in two-cross sectional directions
[NASA-TP-2518] N86-13056

Review of spectroscopic parameters for upper atmospheric measurements
[NASA-CP-2396] N86-13064

Shuttle vertical fin flowfield by the direct simulation Monte Carlo method N86-13251

Space shuttle mechanistic studies to characterize atomic oxygen interactions with surfaces N86-13267

NATIONAL AERONAUTICS AND SPACE ADMINISTRATION. LEWIS RESEARCH CENTER, CLEVELAND, OHIO.

Fluid machines: Expanding the limits, past and future
[NASA-TM-87161] N86-12227

Wind tunnel turning vanes of modern design
[NASA-TM-87416] N86-12239

Liquid droplet radiator program at the NASA Lewis Research Center
[NASA-TM-87139] N86-12246

The 371 deg C mechanical properties of graphite/polyimide composites
[NASA-TM-87122] N86-12256

Evaluation parameters for the alkaline fuel cell oxygen electrode
[NASA-TM-87155] N86-12268

Influence of load interactions on crack growth as related to state of stress and crack closure
[NASA-TM-87117] N86-12292

Ellipsometric surface analysis of wear tracks produced by different lubricants
[NASA-TM-87142] N86-12293

Fatigue crack propagation of nickel-base superalloys at 650 deg C
[NASA-TM-87150] N86-12294

An update of the total-strain version of SRP
[NASA-TP-2499] N86-12295

Molten salt corrosion of SiC: Pitting mechanism
[NASA-TM-87143] N86-12310

Structure-to-glass transition temperature relationships in high temperature stable condensation polyimides
[NASA-TM-87113] N86-12311

Strategy for reflector pattern calculation: Let the computer do the work
[NASA-TM-87137] N86-12485

Performance and temperature dependencies of proton irradiated n/p GaAs and n/p silicon cells
[NASA-TM-87136] N86-12509

Surface fatigue life and failure characteristics of EX-53, CBS 1000M, and AISI 9310 gear materials
[NASA-TP-2513] N86-12609

Overview of free-piston Stirling technology at the NASA Lewis Research Center
[NASA-TM-87156] N86-13236

NATIONAL AERONAUTICS AND SPACE ADMINISTRATION. MARSHALL SPACE FLIGHT CENTER, HUNTSVILLE, ALA.

Multiple-scale turbulence closure modeling of confined recirculating flows
[NASA-CR-178536] N86-12551

Atmospheric environment for space shuttle (STS-51B) launch
[NASA-TM-86525] N86-12917

Second Workshop on Spacecraft Glow
[NASA-CP-2391] N86-13239

Space shuttle ram glow: Implication of NO2 recombination continuum N86-13241

Neutral mass spectrometer measurements in the shuttle bay environment N86-13245

A model for explaining some features of shuttle glow N86-13256

The production of glow precursors by oxidative erosion of spacecraft surfaces N86-13257

An assessment of the impact of spacecraft glow on the Hubble space telescope. Summary of existing observations and theory N86-13262

NATIONAL BUREAU OF STANDARDS, BOULDER, COLO.

Materials studies for magnetic fusion energy applications at low temperatures - 8
[PB85-236362] N86-13183

NATIONAL BUREAU OF STANDARDS, GAITHERSBURG, MD.

Model describing the steady-state pyrolysis of bubble-forming polymers in response to an incident heat flux
[PB85-225225] N86-12291

Indoor Air Quality Modeling Workshop report
[PB85-212306] N86-12803

Using the information resource dictionary system command language
[PB85-227783] N86-12988

NATIONAL BUREAU OF STANDARDS, WASHINGTON, D.C.

FASTBUS for the particle accelerator laboratories
[DE85-014352] N86-13122

NATIONAL CENTER FOR ATMOSPHERIC RESEARCH, BOULDER, COLO.

Marine boundary layer from air-sea interface to inversion
[PB85-188274] N86-12948

NATIONAL ELECTROSTATIC CORP., MIDDLETON, WIS.

Arc discharge conditioning test on the Oak Ridge 25 URC accelerator
[DE85-016394] N86-12523

NATIONAL ENVIRONMENTAL SATELLITE SERVICE, WASHINGTON, D. C.

Comparison of boundary layer winds from NWS LFM (National Weather Service's Limited-Area Fine-Mesh) output and instrumented buoys
[PB85-226439] N86-12927

NATIONAL GEODETIC SURVEY, ROCKVILLE, MD.

The gravity field of topography buried by sediments N86-12864

Subduction dynamics: Constraints from gravity field observations N86-12868

Geodetically derived strain from San Francisco Bay to the Mendocino Triple Junction, California
[PB85-198802] N86-12905

NATIONAL LAB. FOR HIGH ENERGY PHYSICS, OHO (JAPAN).

FASTBUS for the particle accelerator laboratories
[DE85-014352] N86-13122

NATIONAL MARINE FISHERIES SERVICE, GALVESTON, TEX.

Generalized geographic mapping system for computer graphics
[PB85-212520] N86-12755

NATIONAL OCEANIC AND ATMOSPHERIC ADMINISTRATION, BOULDER, COLO.

Gravity waves N86-12823

The MST radar technique N86-12836

First experiment in forecasting cool-season weather with the PROFS System
[PB85-230605] N86-12929

Mesoscale convective systems: A satellite-data-based climatology
[PB85-186862] N86-12931

Folded-path optical (C sub n, sup 2) instrument
[PB85-216398] N86-13137

NATIONAL OCEANIC AND ATMOSPHERIC ADMINISTRATION, ROCKVILLE, MD.

Analysis and assessment of US-WMO regional precipitation chemistry measurements (1972-1982), a subject of the National Trends Network
[PB85-212959] N86-12807

NATIONAL RESEARCH COUNCIL OF CANADA, OTTAWA (ONTARIO).

Orbiter glow observations at high spectral resolution N86-13244

NATIONAL TELECOMMUNICATIONS AND INFORMATION ADMINISTRATION, ANNAPOLIS, MD.

Handbook of radio wave propagation loss (100-10,000 MHz)
[PB85-200012] N86-12502

NATIONAL TELECOMMUNICATIONS AND INFORMATION ADMINISTRATION, BOULDER, COLO.

Spectrum resource assessment of the 1605-2000 kHz band
[PB85-225076] N86-12501

NATIONAL WEATHER SERVICE, GARDEN CITY, N.Y.

Comparison among various thermodynamic parameters for the prediction of convective activity
[PB85-208217] N86-12932

Correlation and Regression Equation Program REGRS
[PB85-213353] N86-12934

Scatter Diagram and Histogram Program - SCATR
[PB85-213346] N86-12935

NATIONAL WEATHER SERVICE, SALT LAKE CITY, UTAH.

Annual data and verification tabulation eastern North Pacific tropical storms and hurricanes, 1984
[PB85-187888] N86-12930

NATIONAL WEATHER SERVICE, SILVER SPRING, MD.

Objective map analysis for the local AFOS MOS (Automation of Field Operations and Services Model Output Statistics) Program
[PB85-212884] N86-12936

NATIONAL WEATHER SERVICE, WASHINGTON, D.C.

Monthly and seasonal weather outlook for mid-May to mid-June 1985, volume 39, number 10, May 14, 1985
[PB85-204261] N86-12937

NAVAL ACADEMY, ANNAPOLIS, MD.

High pressure and molecular weight variation of electrical relaxation in poly(ethylene oxide)
[AD-A157660] N86-12317

NAVAL AIR DEVELOPMENT CENTER, WARMINSTER, PA.

G protection by an extreme crouch position
[AD-A157081] N86-12213

Properties of a retrogressed and re-aged 7075 aluminum alloy
[AD-A157415] N86-12298

NAVAL AIR SYSTEMS COMMAND, WASHINGTON, D. C.

Molecular control
[NASA-TM-87510] N86-12313

NAVAL BIODYNAMICS LAB., NEW ORLEANS, LA.

General plot subroutine package for the Hewlett Packard 5451C Fourier analyzer
[AD-A157127] N86-12989

NAVAL CIVIL ENGINEERING LAB., PORT HUENEME, CALIF.

Navy applications experience with small wind power systems
[AD-A158561] N86-12778

NAVAL OCEAN RESEARCH AND DEVELOPMENT ACTIVITY, BAY ST. LOUIS, MISS.

Data analysis of airborne electromagnetic bathymetry
[AD-A157132] N86-12744

NAVAL POSTGRADUATE SCHOOL, MONTEREY, CALIF.

Comparison of continuous speech, discrete speech, and keyboard input to an interactive warfare simulation in various C3 environments
[AD-A156830] N86-12487

An evolving digital telecommunications industry and its impact on the operational environment of the Nationwide Emergency Telecommunication System (NETS)
[AD-A156831] N86-12488

Weather analysis programs using HP-41CV
[AD-A157389] N86-12921

Observational-numerical study of maritime extratropical cyclones using FGGE (First GARP Global Experiment) data
[NASA-CR-176297] N86-12922

Design and implementation of the computer systems design environment network
[AD-A156832] N86-13022

Computer aided instruction in engineering
[AD-A156828] N86-13220

NAVAL RESEARCH LAB., WASHINGTON, D. C.

Renormalization of an inverse scattering theory for inhomogeneous dielectrics
[AD-A157224] N86-12492

Novel instrument for high-pressure research at ultra-high temperatures
[DE85-015674] N86-12589

A simulation of high latitude F-layer instabilities in the presence of magnetosphere-ionosphere coupling
[NASA-CR-176296] N86-12897

Behavior of ionized plasma in the high latitude topside ionosphere
[AD-A157930] N86-13140

Energy dispersive spectroscopy using synchrotron radiation: Intensity considerations
[DE85-017530] N86-13200

NAVAL SHIP RESEARCH AND DEVELOPMENT CENTER, BETHESDA, MD.

An evaluation of four methods of numerical analysis for two-dimensional airfoil flows. Revision
[AD-A157248] N86-12209

NAVAL SURFACE WEAPONS CENTER, SILVER SPRING, MD.

High rate Li/SOC1(2) cells. 1. Effect of design variables in uncatalyzed cells
[AD-A157203] N86-12776

Relationships between prime-rich Euler type equations and a triangular array of the odd integers [AD-A157928] N86-13030

Naval surface weapons center technology transfer biennial report (Fiscal year 1983/1984) [AD-A157919] N86-13238

NAVAL TRAINING ANALYSIS AND EVALUATION GROUP, ORLANDO, FLA.

Word lists to limit vocabulary in technical information [AD-A157931] N86-13223

NAVAL WEAPONS CENTER, CHINA LAKE, CALIF.

Parachute recovery systems design manual, chapters 1 through 4 offprint [AD-A157839] N86-12210

Analysis of particulates in the exhaust plume of a J52-P3 turbojet engine at military power [AD-A157840] N86-12231

Effects of surface interactions and mechanical properties of plastic bonded explosives on explosive sensitivity. Part 2: Model formulation [AD-A157900] N86-12381

Maintenance of photovoltaic power systems, revision 1 [AD-A157838] N86-12777

NAVY PERSONNEL RESEARCH AND DEVELOPMENT CENTER, SAN DIEGO, CALIF.

A new hazard function estimator of performance time [AD-A157843] N86-12971

NEBRASKA UNIV., LINCOLN.

Studies on unusally reactive metal powders: Preparation of new organometallic and organic compounds including potential new catalysts [DE85-014844] N86-12309

NEW HAMPSHIRE UNIV., DURHAM.

Meteor wind results at Durham (43 deg N, 71 deg W) during the ATMAP November 1981 and May 1982 campaigns N86-12845

NEW JERSEY STATE DEPT. OF TRANSPORTATION, TRENTON.

Evaluation of honeycomb highway sound barrier I-280 section 8B, Harrison, New Jersey [PB85-231157] N86-13063

NEW MEXICO UNIV., ALBUQUERQUE.

Systems analysis approach to probabilistic modeling of fault trees [DE85-007705] N86-13050

Channeling analysis of strain in superlattices [DE85-014437] N86-13197

NEW YORK UNIV., NEW YORK.

Program for simple algebra [DE85-013426] N86-13013

Hyperbolic systems of conservation laws in several space variables [DE85-014019] N86-13042

Elementary waves and Riemann solutions: Their theory and their role in science [DE85-014018] N86-13045

Wave propagation in a plasma based on the cold plasma model [DE85-013849] N86-13158

NEWCASTLE-UPON-TYNE UNIV. (ENGLAND).

Interpretation of the geoid N86-12873

NORTH CAROLINA STATE UNIV., RALEIGH.

High frequency silicon bipolar transistor with SIPOS (Semi-insulating polycrystalline silicon) heterojunction emitter and ion implanted rapid thermal annealed base region [AD-A157141] N86-12510

Experimental study of flow and dispersion in the wakes of three-dimensional low hills [PB85-193266] N86-12906

Compound semiconductor insulator interface research [AD-A157277] N86-13189

NORTH CAROLINA UNIV., CHAPEL HILL.

Investigation of phase transitions [AD-A158434] N86-12518

Channeling analysis of strain in superlattices [DE85-014437] N86-13197

NORTH CAROLINA UNIV., RALEIGH.

Charge transfer in multiple site chemical systems [AD-A157413] N86-12270

NORTHWESTERN UNIV., EVANSTON, ILL.

Numerical calculation of internal flows with curvature N86-12544

Seismological studies of the tectonics of divergent plate boundaries N86-12812

Motion of the Pacific plate relative to the hotspots since the Jurassic and model of oceanic plateaus of the Farallon plate N86-12940

NOVA UNIV., DANIA, FLA.

Theory support of pulsed power experiments. Volume 3. E-beam chamber design [AD-A158417] N86-13098

O

OAK RIDGE GASEOUS DIFFUSION PLANT, TENN.

Correction of compressor critical speed condition through fluid-film bearing optimization [DE85-005507] N86-12617

OAK RIDGE NATIONAL LAB., TENN.

Dynamic small angle X-ray scattering study of stressed Kevlar 49 epoxy composites [DE85-011408] N86-12264

Paramagnetic form factors of HCP transition metals [DE85-016301] N86-12301

Effect of pulsed irradiation on microstructural evolution [DE85-016317] N86-12302

Combined small angle X-ray scattering and transmission electron microscope studies of Al-Li alloys [DE85-016356] N86-12303

Review of effects of long-term aging on the mechanical properties and microstructures of types 304 and 316 stainless steel [DE85-016472] N86-12304

Carbothermal synthesis of silicon carbide [DE85-013546] N86-12321

Arc discharge conditioning test on the Oak Ridge 25 URC accelerator [DE85-016394] N86-12523

Influence of a surfactant additive on absorption heat pump performance [DE85-013995] N86-12574

Droplet formation phenomena in dc electrical fields [DE85-014067] N86-12596

New beam neutralization concept: Laser photodetachment in a magnetic field [DE85-014655] N86-12607

Comparative analysis of a Stirling heat pump with second- and third-order computer models [DE85-013536] N86-12615

Multifrequency eddy-current inspection of seam weld in steel sheath [DE85-013533] N86-12626

ORNL ground coil analytical and experimental studies [DE85-005246] N86-12783

Biomedical and Environmental Sciences Program publications 1984 [DE85-015070] N86-12963

Power and signal transmission for mobile teleoperated systems [DE85-013994] N86-12975

Future directions in mobile teleoperation [DE85-014308] N86-12976

Uncertainty propagation from raw data to final results [DE85-011937] N86-13000

Tandem Mirror Reactor Systems Code (TMRSC) [DE85-012891] N86-13006

TWOPOT: A computer model of the two-pot extractive distillation concept for nitric acid [DE85-013523] N86-13020

Charge-state distributions of 100, 175, 275 and 352 MeV gold ions emerging from thin carbon foils [DE85-014651] N86-13069

Multiphoton ionization of NO-rare gas van der Waals species [DE85-014650] N86-13084

Chemistry of berkelium: A review [DE85-017523] N86-13102

TPSS plasma engineering studies: Profile effects and plasma power balance [DE85-013638] N86-13142

Submillimeter wave propagation in tokamak plasmas [DE85-007747] N86-13154

Spectral method for obtaining three-dimensional magnetohydrodynamic equilibria [DE85-015065] N86-13166

Wear of ion implanted TiB sub 2 surfaces [DE85-017091] N86-13201

Recent developments in the structural crystallography of boron and the higher borides [DE85-016930] N86-13202

Temperature dependence of the magnetic excitations in Gd [DE85-016303] N86-13203

New interpretation of spin-wave behavior in nickel and iron [DE85-015323] N86-13208

Electronic states in disordered solids. Part 3: Applications to materials science [DE85-011416] N86-13213

Comparative first- and second-law analysis of an absorption cycle [DE85-015066] N86-13215

OAK RIDGE Y-12 PLANT, TENN.

Precision ion vacuum gage with logarithmic response [DE85-015312] N86-12586

Electrochemical machining of the outer profile of the B83 Lug [DE85-014804] N86-12616

Pade and reciprocal approximants and linear NOLOR functions [DE85-015057] N86-13044

OFFICE OF NAVAL RESEARCH, LONDON (ENGLAND).

European Science Notes. Volume 39, number 8 [AD-A157146] N86-13237

OHIO STATE UNIV., COLUMBUS.

Simulation of the enhanced traffic alert and collision avoidance system (TCAS 2) [NASA-CR-176328] N86-12216

Optimization of the locomotion of a legged vehicle with respect to maneuverability N86-12371

Continental and oceanic magnetic anomalies: Enhancement through GRM N86-12860

ONSALA SPACE OBSERVATORY (SWEDEN).

Model experiments with slot antenna arrays for imaging N86-12482

A new integrated slot element feed array for multi-beam systems N86-12483

OPTIMIZATION, INC., BLACKSBURG, VA.

Modeling and control of flexible structures [AD-A157959] N86-12625

OREGON STATE UNIV., CORVALLIS.

Development of an analytical model and code for the flapping response of a Hawte rotor blade [DE85-008806] N86-12211

OXFORD UNIV. (ENGLAND).

Temperature data from satellites N86-12815

Middle atmosphere reference model derived from satellite data N86-12819

Planetary waves N86-12820

Annual and semiannual cycles based on the middle atmosphere reference model N86-12826

P

PACIFIC NORTHWEST LAB., RICHLAND, WASH.

Fixation of high-level wastes in glasses [DE85-013276] N86-12325

LANDSAT-4 TM image data quality analysis for energy-related applications [E86-10006] N86-12742

Statistical methods for environmental pollution studies [DE85-005298] N86-12799

Interpretation of individual precipitation chemistry data sets: General condiserations and approaches [DE85-012449] N86-12800

Accidental exposure to americium [DE85-012794] N86-12965

Managing data analysis through save-states [DE85-012456] N86-12969

Secondary electron spectra: A semiempirical model [DE85-012448] N86-13066

PENNSYLVANIA STATE UNIV., UNIVERSITY PARK.

Effect of grain boundary structure on sensitization and corrosion of stainless steel [AD-A157133] N86-12297

Evaluation of high permittivity glass ceramics for millimeter wave applications [AD-A158551] N86-12319

A major crustal feature in the southeastern United States inferred from the MAGSAT equivalent source anomaly field N86-12856

The nature of symmetric instability and its similarity to convective and inertial instability [NASA-CR-3945] N86-12918

Development of acoustic agglomerator. Test plan for high temperature high pressure acoustic agglomerator [DE85-017221] N86-13061

Nuclear performance optimization of the Be/Li/Th blanket for the fusion breeder [DE85-012949] N86-13112

PERCEPTRONICS, INC., ANN ARBOR, MICH.

Pilot's associate definition study [AD-A157106] N86-13026

PHOTOMETRICS, INC., WOBURN, MASS.

Surface-catalyzed recombination into excited electronic, vibrational, rotational, and kinetic energy states: A review N86-13253

Infrared emission from desorbed NO2(*) and NO(*) N86-13254

The NO-NO2 system at laboratory surfaces N86-13255

PHYSICAL SCIENCES, INC., ANDOVER, MASS.

Electron emission of over 200 A/cm (2) from a pulsed-laser irradiated photocathode [DE85-012656] N86-13084

Spectral identification/elimination of molecular species in spacecraft glow N86-13246

PITTSBURGH UNIV., PA.

Adaptive Kalman filtering with control input estimation N86-12503

Fluid physics research
[DE85-014644] N86-12575

PORTLAND STATE UNIV., OREG.
C0 collocation solutions for weak-formulation Navier-Stokes equations
[AD-A157250] N86-12553

PRATT AND WHITNEY AIRCRAFT GROUP, EAST HARTFORD, CONN.
Turbine blade and vane heat flux sensor development, phase 2
[NASA-CR-174995] N86-12225

PRINCETON UNIV., N. J.
New corresponding states theory using the second virial coefficient as the temperature variable
[PB85-219624] N86-12289
Submillimeter wave propagation in tokamak plasmas
[DE85-007747] N86-13154
A ground-based experimental test program to duplicate and study the spacecraft glow phenomenon
N86-13260

PURDUE UNIV., WEST LAFAYETTE, IND.
Interactive aircraft flight control and aeroelastic stabilization
[NASA-CR-176323] N86-12233
Measurement of species concentrations in flames by laser-induced fluorescence
[DE85-012082] N86-12283
Soybean canopy reflectance modeling data sets
[E86-10005] N86-12741
Fiscal year 1983 program report of the Purdue (Indiana) Water Resources Research Center
[PB85-225829] N86-12802
Prediction of sound fields in acoustical cavities using the boundary element method
[NASA-CR-176295] N86-13057

R

RADIAN CORP., AUSTIN, TEX.
Evaluation of air emissions from hazardous waste treatment, storage and disposal facilities
[PB85-203792] N86-12806

RAND CORP., SANTA MONICA, CALIF.
Commercial and military communication satellite acquisition practices
[AD-A157398] N86-12247

RASOR ASSOCIATES, INC., SUNNYVALE, CALIF.
Advanced Thermionic Technology Program: Summary Report. Volume 1
[DE85-008358] N86-12779

READING UNIV. (ENGLAND).
New interpretation of spin-wave behavior in nickel and iron
[DE85-015323] N86-13208

RELIABILITY ANALYSIS CENTER, GRIFFISS AFB, N. Y.
Search and retrieval index to EOS/ESD Symposium Proceedings 1979 to 1984
[AD-A158114] N86-12515

RENSSELAER POLYTECHNIC INST., TROY, N. Y.
Bandwidth efficient frequency-shift keyed communication systems N86-12472
Analytical and experimental studies of wakes behind circularly capped bubbles N86-12548

RHODE ISLAND UNIV., KINGSTON.
Acid precipitation: Source identification and its effects on water quality
[PB85-214880] N86-12810

RIO GRANDE ASSOCIATES, HOUSTON, TEX.
Nonlinear electromagnetic scattering from a diode circuit
[AD-A157216] N86-12481

ROCHESTER UNIV., N. Y.
Absorption and hot electron generation in uv (351 nm) driven spherical imploding targets
[DE85-014405] N86-13161
Spatial structure of heat flow instabilities in laser plasmas
[DE85-014407] N86-13162
Absorption spectroscopy as a density diagnostic for dense imploded shells
[DE85-014413] N86-13175
New directions for short-wavelength laser fusion and high-energy-density physics
[DE85-014414] N86-13160

ROCKWELL INTERNATIONAL CORP., COLUMBUS, OHIO.
Aerodynamic characteristics of a propulsive wing-canard concept at STOL speeds
[NASA-CR-177982] N86-12205

ROCKWELL INTERNATIONAL CORP., GOLDEN, COLO.
Options for operational risk assessments
[DE85-014904] N86-12380

ROCKWELL INTERNATIONAL CORP., RICHARDSON, TEX.
MAGNUM-2D computer code: User's guide
[DE85-013315] N86-13001

ROME AIR DEVELOPMENT CENTER, GRIFFISS AFB, N.Y.
Scattering experiments at the Ipswich Electromagnetic Measurements Facility: Backscatter from metal cubes
[AD-A157925] N86-12496
Evaluation of the use of p-n structures as photodetectors in silicon integrated circuits
[AD-A158104] N86-12514
Analytic models for radiation induced loss in optical fibers. 3. Transient radiation effects
[AD-A157408] N86-13127

ROYAL SIGNALS AND RADAR ESTABLISHMENT, MALVERN (ENGLAND).
The theory and practice of a multistate reflectometer
[AD-A157916] N86-12583

S

SACHS/FREEMAN ASSOCIATES, INC., BOWIE, MD.
Novel instrument for high-pressure research at ultra-high temperatures
[DE85-015674] N86-12589

SACLANT ASW RESEARCH CENTER, LA SPEZIA (ITALY).
Saclantcen's use of scuba diving in oceanographic and acoustic research
[AD-A156714] N86-12941
Temporal and spatial variabilities in shallow water acoustics: Measurements and predictions
[AD-A156718] N86-12942
Underwater photography for quantitative description of bottom roughness
[AD-A156753] N86-12943

SANDERS ASSOCIATES, INC., NASHUA, N. H.
Advanced avionics computer architecture. Volume 1. Executive summary
[AD-A158119] N86-12222
Advanced avionics computer architecture. Volume 2. Instruction set architecture specification
[AD-A158120] N86-12223

SANDIA NATIONAL LABS., ALBUQUERQUE, N. MEX.
RIIM accelerator beam experiments
[DE85-012034] N86-12244
PBFA-2 insulator stack design from an engineering viewpoint
[DE85-013437] N86-12245
Special metallographic procedures for austenitic stainless steel welds
[DE85-010113] N86-12305
Optical measurements of shock-induced chemical reactions in mixed aluminum-nickel powder
[DE85-014705] N86-12308
Surface crystallization on metallized 94 percent alumina ceramics
[DE85-008691] N86-12324
Numerical studies of the dynamic isentropic loading of solid molecular hydrogen
[DE85-013961] N86-12391
Results of field and laboratory studies of jam-resistant and voice-private radios
[DE85-014841] N86-12500
Design information for the 4/3 silicon-gate CMOS technology
[DE85-014932] N86-12522
Hybrid 0-D,1-D, and 2-D model of helical explosive-driven magnetic flux compression generator
[DE85-013772] N86-12524
Preventative maintenance for control systems
[DE85-012029] N86-12525
Photoconductive semiconductor switching for pulsed power applications
[DE85-013859] N86-12531
Hillock-free conductor system for use in multilevel interconnects
[DE85-012595] N86-12533
Classical piezoelectricity: Is the theory complete
[DE85-014592] N86-12536
Laser-based foilless diode
[DE85-013958] N86-12537
Semicustom integrated circuit design at Sandia National Laboratories
[DE85-015661] N86-12538
Finned tube contact conductance: Characterizing the integrity of the mechanical bond
[DE85-013747] N86-12564
Studies of the Bauer piezoelectric polymer gauge (PVF2) under impact loading
[DE85-014707] N86-12590
New passive helicopter detector
[DE85-015160] N86-12595
Characterization of sheet calcium for Ca/CaCrO4 thermal batteries
[DE85-013231] N86-12785
Solar thermal energy systems
[DE85-008793] N86-12790
Photovoltaic Concentrator Technology Project Thirteenth Project Integration Meeting
[DE85-013253] N86-12794
Current CIM activities in the materials process engineering and fabrication directorate 7400
[DE85-015491] N86-12982
GRAFAID: An engineering tool
[DE85-013115] N86-13004
Second reference calculation for the WIPP
[DE85-013180] N86-13005
Application of a binary cyclic error-correcting code
[DE85-013232] N86-13007
Control of step size and order in extrapolation codes
[DE85-013261] N86-13010
FDSC: A microwave coupling code for slots of finite depth
[DE85-013443] N86-13011
Design and use of digital filters with personal computer spreadsheet programs
[DE85-013805] N86-13012
SCREAMER: A single-line pulsed-power design tool
[DE85-012637] N86-13014
Fundamentals of adaptive signal processing
[DE85-014933] N86-13016
Building versatile tape handling software
[DE85-009333] N86-13018
Control of step size and order in extrapolation codes
[DE85-010122] N86-13041
Large scale operational pulsed power research facilities: How well have we made them a reality
[DE85-013784] N86-13068
IBEX magnetic coupling experiments
[DE85-014331] N86-13108
RADLAC program status
[DE85-014706] N86-13109
Radiation effects on light sources and detectors
[DE85-014746] N86-13133
Implementing the automated features of the PBFA-I control/monitor systems
[DE85-012641] N86-13144
Laser diagnostic studies of plasma etching and deposition
[DE85-009494] N86-13178
Channeling analysis of strain in superlattices
[DE85-014437] N86-13197
Temperature and concentration dependence of hydrogen site occupancy in several rare-earth dihydrides
[DE85-015739] N86-13199

SANDIA NATIONAL LABS., LIVERMORE, CALIF.
Solar thermal energy systems
[DE85-008793] N86-12790

SASKATCHEWAN UNIV., SASKATOON.
Mean winds of the mesosphere (60-80 km), as measured by MF radars N86-12818
Mean winds of the upper middle atmosphere (60-110 km): A global distribution from radar systems (MF, meteor, VHF) N86-12831
Saskatoon M. F. radar system: (52 deg N, 107 deg W), Canada N86-12843
May 1982, Saskatoon M. F. radar system: (52 deg N, 107 deg W), Canada N86-12844

SCHOOL OF AEROSPACE MEDICINE, BROOKS AFB, TEX.
Proceedings of a workshop on Radiofrequency Radiation bioeffects held at Wachtberg-Werthhoven, West Germany on 11-13 September 1984
[AD-A157090] N86-12959
The effects of hypoxia induced by low atmospheric pressure on soft contact lens wear
[AD-A158556] N86-12963

SCIENCE AND ENGINEERING ASSOCIATES, INC., ENGLEWOOD, COLO.
A mechanism for the local concentration enhancement of the shuttle atmosphere N86-13252

SCIENCE APPLICATIONS, INC., ALBUQUERQUE, N. MEX.
RIIM accelerator beam experiments
[DE85-012034] N86-12244

SCIENCE APPLICATIONS, INC., SUNNYVALE, CALIF.
Development of a continuous mass flow measuring flow
[DE85-012492] N86-12573

SCIENCE APPLICATIONS INTERNATIONAL CORP., BELLEVUE, WASH.
The shuttle glow: A program to study the ram-induced phenomena N86-13268

SCIENCE APPLICATIONS INTERNATIONAL CORP., MCLEAN, VA.
Spacecraft-induced plasma energization and its role in flow phenomena N86-13250

SCIENCE RESEARCH CORP., CAMBRIDGE, MASS.
Electron emission of over 200 A/cm (2) from a pulsed-laser irradiated photocathode
[DE85-012656] N86-13084

SKF INDUSTRIES, INC., KING OF PRUSSIA, PA.
Mechanical interactions of rough surfaces
[DE85-015011] N86-12613

SMITHSONIAN ASTROPHYSICAL OBSERVATORY, CAMBRIDGE, MASS.
Infrared measurements of spacecraft glow planned for Spacelab 2 N86-13263
Balloon-borne three-meter telescope for far-infrared and submillimeter actronomy
[NASA-CR-176347] N86-13271
Combined ultraviolet studies of astronomical source
[NASA-CR-176165] N86-13274

SOCIETY FOR INDUSTRIAL AND APPLIED MATHEMATICS, PHILADELPHIA, PA.
Survey and expository papers on topics of current interest in applied mathematics
[AD-A158418] N86-13229

SOLAREX CORP., NEWTOWN, PA.
Thin-film module circuit design: Practical and reliability aspects N86-12762

SOLAREX CORP., ROCKVILLE, MD.
Semicrystalline casting process development and verification
[JPL-9950-1160] N86-12312

SOUTH DAKOTA OFFICE OF ENERGY POLICY, PIERRE.
Small scale wind energy conversion programmatic equipment
[DE85-012319] N86-12793

SOUTHAMPTON UNIV. (ENGLAND).
The status of two-dimensional testing at high transonic speeds in the University of Southampton transonic self-streamlining wind tunnel
[NASA-CR-3919] N86-12203
Derivation of jack movement influence coefficients as a basis for selecting wall contours giving reduced levels of interference in flexible walled test sections
[NASA-CR-177992] N86-12204

SOUTHEASTERN CENTER FOR ELECTRICAL ENGINEERING EDUCATION, INC., ST. CLOUD, FLA.
Basic EMC (Electromagnetic compatibility) technology advancement for C3 (Command, control, and communications) systems. Volume 6
[AD-A157239] N86-12493

SOUTHERN METHODIST UNIV., DALLAS, TEX.
Satellite magnetic modeling of north African hot spots N86-12656
New representations of the non-central chi-square density and cumulative
[AD-A157227] N86-13046

SOUTHWEST RESEARCH INST., SAN ANTONIO, TEX.
Microemulsion-type fire-resistant diesel fuel
[AD-A157125] N86-12359

SPECTRA TECHNOLOGY, INC., BELLEVUE, WASH.
FRC formation studies with Z-discharge ionization on FRX-C
[DE85-012765] N86-13152

SPECTRON DEVELOPMENT LABS., INC., COSTA MESA, CALIF.
Optical technique to study the impact of heavy rain on aircraft performance
[NASA-CR-177989] N86-12580

SPRINGBORN LABS., INC., ENFIELD, CONN.
Investigation of test methods, material properties and processes for solar cell encapsulants
[DE85-012831] N86-12786

SRI INTERNATIONAL CORP., MENLO PARK, CALIF.
Reduction of CO2 to methanol and methane by photo and dark reactions on semiconductor electrodes
[PB85-226296] N86-12290
Oxidation and gum formation in diesel fuels
[AD-A157410] N86-12360

STANFORD LINEAR ACCELERATOR CENTER, CALIF.
Beam emittance and beam disruption
[DE85-015136] N86-13070
Disruption and luminosity of flat beams
[DE85-015137] N86-13071
Control problems in very large accelerators
[DE85-014956] N86-13075
Data acquisition system for SLD
[DE85-014361] N86-13103
High and ultra-high gradient quadrupole magnets
[DE85-014360] N86-13104
Physics of e(+) - e(-) colliders: Present, future and far future
[DE85-009895] N86-13121
FASTBUS for the particle accelerator laboratories
[DE85-014352] N86-13122
RF beam deflection measurements and corrections in the SLC linac
[DE85-013061] N86-13146
Minimizing the energy spread within a single bunch by shaping its charge distribution
[DE85-013064] N86-13151
SLC injector modeling
[DE85-013067] N86-13153
Commissioning and operation of the Nuclear Physics Injector at SLAC
[DE85-013374] N86-13159
Real time bunch length measurements in the SLC linac
[DE85-014362] N86-13169

STANFORD UNIV., CALIF.
Velocity and gravity effects in relative permeability measurements
[DE85-009925] N86-12570
Impact of linear programming on computer development
[AD-A157659] N86-12993
Transforming censored samples and testing fit
[AD-A157957] N86-13048
Deals among rational agents
[AD-A157960] N86-13052
Improved techniques for the growth of high quality cadmium telluride crystals
[AD-A157669] N86-13192

STATE UNIV. OF NEW YORK, STONY BROOK.
Study of the mist cooling and droplet dynamics in turbulent flow by using LDA N86-12545
The prediction of fully developed turbulent pressure drops in a triangular duct for a power law fluid N86-12546
Theoretical modelling of the elastic properties of mantle silicates N86-12813

SVERDRUP TECHNOLOGY, INC., ARNOLD AIR FORCE STATION, TENN.
Method to detect ethylene glycol in gaseous mixtures
[AD-A158109] N86-12272

SYSTEMS RESEARCH LABS., INC., DAYTON, OHIO.
Criteria for a state-of-the-art vision test system
[AD-A157099] N86-12973

T

TALANDIC RESEARCH CORP., PASADENA, CALIF.
Advanced torque converters for robotics and space applications
[NASA-CR-177987] N86-12610

TENNESSEE UNIV., CHATTANOOGA.
Acidification trends in surface waters of the Southern Appalachians
[DE85-901746] N86-12801

TENNESSEE UNIV., KNOXVILLE.
Dynamic small angle X-ray scattering study of stressed Kevlar 49 epoxy composites
[DE85-011408] N86-12264
Chemistry of berkelium: A review
[DE85-017523] N86-13102

TETRA CORP., ALBUQUERQUE, N. MEX.
UV sustained glow discharge opening switch
[AD-A158411] N86-13132

TEXAS DEPT. OF WATER RESOURCES, AUSTIN.
Evaluating the ground-water resources of the high plains of Texas, volume 2
[PB85-191609] N86-12752

TEXAS SOUTHERN UNIV., HOUSTON.
Study of some transition metal complexes as process catalysts
[DE85-013428] N86-12276

TEXAS UNIV., AUSTIN.
Influence of bonded reinforcement in post-tensioned prestressed concrete T-beams with unbonded tendons N86-12622
On the geographical correlation of orbit error N86-12881
Solitary vortices in a rotating plasma
[DE85-014766] N86-13171
Explosive coalescence of magnetic islands
[DE85-015083] N86-13172
Alfven continuum with toroidicity
[DE85-015821] N86-13217
Transport near the onset of stochasticity
[DE85-014765] N86-13218
Physico-chemical conditions in circumstellar shells of evolved oxygen-rich M stars N86-13275

THERMO ELECTRON CORP., WALTHAM, MASS.
Advanced Thermionic Technology Program: Summary Report. Volume 1
[DE85-009358] N86-12779
Electron emission of over 200 A/cm (2) from a pulsed-laser irradiated photocathode
[DE85-012656] N86-13084

TOHOKU UNIV., SENDAI (JAPAN).
The Record of Electrical and Communication Engineering Conversazione, volume 54, no. 1
[ISSN-0385-771-9] N86-12383
Proposal of a high efficient and high power peniotron N86-12384
Hysteresis characteristics of a diode loaded E-M loop sensor N86-12385
Accuracy of a new ultrasonic apparatus for simple measurement of viscoelasticity N86-12386
The verification of the logic circuits based on particlized information bits with PROLOG N86-12387
A methodology for syntax-analysis using PROLOG N86-12388

TOKYO DENKI UNIV. (JAPAN).
Research Reports of the Faculty of Engineering, Tokyo Denki University, no. 32
[ISSN-0389-617-X] N86-12372
Earthquake-response simulation on horizontally large-scale buildings based on the method of reduction concerning their restoring spring matrix. Derivation of general form of spring matrix and comparison of applied response results on an actual building with measured values N86-12374
A computer analysis of the distribution of principal stresses using photoelastic pattern N86-12375
Extraction of feature parameters for spoken word recognition N86-12376
Effects of cation ions in nerve excitation N86-12377
A physical method for estimating speech intelligibility in a reverberant sound field N86-12378
Dummy head microphone and its application to the measurements of electro-acoustic equipments N86-12379
Study on electropainting using alkoxymethylmelamine as crosslinking agent N86-12380
The studies on the effects of intermolecular hydrogen bond in melamine resination process. (Methylated melamines were adopted as the model compounds of starting material) N86-12381
Study of high speed shearing of thermoplastic polymer sheets with a new rotary shearing machine N86-12382

TORONTO UNIV. (ONTARIO).
Geophysical interpretation of the magnetic anomalies of the Earth derived from MAGSAT data N86-12857
The resolution of a magnetic anomaly map expected from GRM data N86-12870
Mantle convection and the large scale structures of the Earth's gravitational field N86-12874
Mantle viscosity, J2 and the nontidal acceleration of Earth rotation N86-12879

U

UNIVERSITY COLL., GALWAY (IRELAND).
Electro-optical transmission and liquid water content of fogs and clouds
[AD-A157506] N86-13128

UNIVERSITY OF NORTHERN ARIZONA, FLAGSTAFF.
REFRIG-12: A graphics-augmented interactive program for designing vapor-compression refrigeration/heat pump cycles
[DE85-014205] N86-12572

UNIVERSITY OF NORTHERN ILLINOIS, DE KALB.
Mossbauer effect and neutron diffraction study of the anomalous lattice behavior of U6Fe
[DE85-014912] N86-13210

UNIVERSITY OF SOUTHERN CALIFORNIA, LOS ANGELES.
Deposition, microstructure and properties of laser CVD SiC films
[DE85-014680] N86-12327
Advanced digital communication research
[AD-A158412] N86-12497

UNIVERSITY OF SOUTHWESTERN LOUISIANA, LAFAYETTE.
High-resolution, three-dimensional, seismic survey over the geopressured-geothermal reservoir at Parcperdue, Louisiana
[DE85-016465] N86-12902

UTAH STATE UNIV., LOGAN.
The UV-VIS optical environment of the shuttle N86-13247
Enhanced N(+) sub 2 in the shuttle environment N86-13248
A possible glow experiment for the EOM 1-2 mission N86-13266

V

VANDERBILT UNIV., NASHVILLE, TENN.
Optical radiation from the interaction of energetic atoms, ions, electrons, and photons with surfaces N86-13259

VARIAN ASSOCIATES, PALO ALTO, CALIF.
The 140 GHz gyrotron development program
[DE85-011923] N86-12534

VIGYAN RESEARCH ASSOCIATES, INC., HAMPTON, VA.
Introduction to cryogenic wind tunnels
[NASA-CR-177968] N86-12238
VIRGINIA POLYTECHNIC INST. AND STATE UNIV., BLACKSBURG.
Experimental investigation of 3-D turbulent free shear flow past propellers and windmills N86-12201
Automated design of composite plates for improved damage tolerance N86-12254
Fracture surface analysis in composite and titanium bonding
[NASA-CR-176309] N86-12257
Numerical and experimental studies of 3-D and unsteady turbulent body/appendage/propeller flows
[AD-A157078] N86-12552
Transient thermal modeling of the nonscanning ERBE detector
[NASA-CR-172240] N86-12743
Identifying and evaluating COBOL competencies for four-year information systems programs N86-13223

W

WASHINGTON STATE ENERGY OFFICE, OLYMPIA.
Wind generation in Washington
[DE85-012791] N86-12787
WASHINGTON UNIV., SEATTLE.
Strain energy density criteria for dynamic fracture and dynamic crack branching
[AD-A157914] N86-12624
Conference summary: Antinucleon- and nucleon-nucleus interactions
[DE85-013905] N86-13114
Dynamical model of quark rearrangement in nucleon-antinucleon annihilation
[DE85-013904] N86-13120
WESTON OBSERVATORY, MASS.
Investigation of magnetic field measurements
[AD-A157924] N86-12900
WISCONSIN UNIV., MADISON.
Interfacial stability in a two-layer benard problem
[AD-A158138] N86-12558
On high-order accurate interpolation for non-oscillatory shock capturing schemes
[AD-A158131] N86-13032
Two results on dense imbeddings
[AD-A158132] N86-13033
Penalized likelihood for general semi-parametric regression models
[AD-A158133] N86-13034
Hamilton-Jacobi equations in infinite dimensions. Part 2: Existence of viscosity solutions
[AD-A158137] N86-13035
C infinity-regularity for the porous median equation
[AD-A158147] N86-13036
A Floquet decomposition for Volterra equations with periodic kernel and a transform approach to linear recursion equations
[AD-A158148] N86-13037
The uniqueness of Hill's spherical vortex
[AD-A158149] N86-13038
Global optimization using automatic differentiation and interval iteration
[AD-A158150] N86-13039
Multipole and tokamak research at the University of Wisconsin
[DE85-014862] N86-13165
Alfven wave heating on Tokapole 2
[DE85-014859] N86-13179
WISCONSIN UNIV., MILWAUKEE.
Synthesis of research and development in mechanical energy storage technologies
[DE85-013313] N86-12782
Large-scale circulation departures related to wet episodes in northeast Brazil
[NASA-CR-176352] N86-12916
WOODS HOLE OCEANOGRAPHIC INSTITUTION, MASS.
Separation of core and crustal magnetic field sources N86-12884
WYLE LABS., INC., HUNTSVILLE, ALA.
Safety criteria for the operation of gaseous hydrogen pipelines
[PB85-206159] N86-12392
WYOMING UNIV., LARAMIE.
Iosipescu shear properties of graphite fabric/epoxy composite laminates
[NASA-CR-176316] N86-12258

Y

YALE UNIV., NEW HAVEN, CONN.
Micro-PROUST
[AD-A157505] N86-12991

CONTRACT NUMBER INDEX

SCIENTIFIC AND TECHNICAL AEROSPACE REPORTS VOLUME 24 NUMBER 3

Typical Contract Number Index Listing

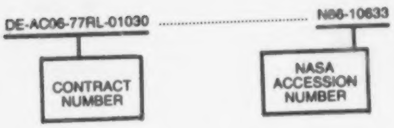

Listings in this index are arranged alphanumerically by contract number. Under each contract number the NASA accession numbers denoting documents that have been produced as a result of research done under that contract are arranged in ascending order. The NASA accession number denotes the number by which the citation is identified.

AF PROJ. 2305 .... N86-12496
AF PROJ. 2306 .... N86-13127
AF PROJ. 2338 .... N86-12514
AF PROJ. 2404 .... N86-12235
AF PROJ. 2729 .... N86-12963
AF PROJ. 3066 .... N86-12229
AF PROJ. 5730 .... N86-12250
AF PROJ. 7601 .... N86-12896
AF PROJ. 7661 .... N86-13139
AF PROJ. 7757 .... N86-12959
AF-AFOSR -84-0082 .... N86-12362
AF-AFOSR-0037-82 .... N86-12604
AF-AFOSR-0088-84 .... N86-13037
AF-AFOSR-0203-80 .... N86-12363
AF-AFOSR-0367-84 .... N86-13049
ARPA ORDER 5116 .... N86-13026
DA PROJ. 1L1-61101-AH-45 .... N86-12311
DA PROJ. 1L1-61102-AH-45 .... N86-12259
DA PROJ. 1L1-62105-AH-84 .... N86-12260
DA PROJ. 1T1-61102-BH-57 .... N86-13029
N86-13058
DA PROJ. 4A1-61101-A-91-D N86-12555
DA PROJ. 4A1-61102-AT-24 .... N86-12995
DA PROJ. 4A1-62731-AT-41 .... N86-12314
DAAG24-83-K-0058 .... N86-12293
DAAG29-79-D-1002 .... N86-12518
DAAG29-80-C-0041 .... N86-12558
N86-13032
N86-13033
N86-13034
N86-13035
N86-13036
N86-13037
N86-13038
N86-13039
DAAG29-80-C-0091 .... N86-13229
DAAG29-82-C-0017 .... N86-13195
DAAG29-82-C-0018 .... N86-13132
DAAG29-82-C-0090 .... N86-13032
DAAG29-82-K-0015 .... N86-12319
DAAG29-82-K-0028 .... N86-12992
DAAG29-82-K-0111 .... N86-12270
DAAG29-82-K-0142 .... N86-12497
DAAG29-82-K-0145 .... N86-12273
DAAG29-83-K-0023 .... N86-13192
DAAG29-84-K-0017 .... N86-12560
DAAG29-84-K-0161 .... N86-12360
DAAK10-81-C-0308 .... N86-13130
DAAK11-82-K-0008 .... N86-13131
DAAK20-82-C-0001 .... N86-12359
DAAK70-85-C-0001 .... N86-12359
DAJA37-81-C-0003 .... N86-13128
DAJA37-81-C-0251 .... N86-13058
DAJA37-81-C-0740 .... N86-13029
DAJA37-81-C-0746 .... N86-12924
DAJA45-83-C-0004 .... N86-12554
DAJA45-83-C-0022 .... N86-12745
DAJA45-83-C-0034 .... N86-12944
DE-AC02-76CH-00016 .... N86-12251
N86-12498
N86-12621
N86-12789
N86-12796
N86-13053
N86-13055
N86-13073
N86-13077
N86-13115
N86-13119
N86-13156
N86-13157
N86-13168
N86-13182
DE-AC02-76CH-03000 .... N86-13080
N86-13085
N86-13097
N86-13101
N86-13147
DE-AC02-76CH-03073 .... N86-13154
N86-13260
DE-AC02-76ER-03077 .... N86-13013
N86-13042
N86-13045
N86-13158
DE-AC02-76ET-11292 .... N86-12779
DE-AC02-76ET-53051 .... N86-13165
N86-13179
DE-AC02-77ER-04380 .... N86-12279
DE-AC02-78ER-04939 .... N86-12283
DE-AC02-79ET-26106 .... N86-12782
DE-AC02-80ER-10603 .... N86-12309
DE-AC02-81ER-10956 .... N86-13198
DE-AC02-81ER-10982 .... N86-12274
DE-AC02-83CH-10093 .... N86-12211
N86-12364
N86-12577
N86-12780
N86-12790
N86-12791
DE-AC02-84ER-13163 .... N86-12613
DE-AC03-76SF-00098 .... N86-12282
N86-12521
N86-12578
N86-12903
N86-12952
N86-13054
N86-13072
N86-13074
N86-13076
N86-13079
N86-13092
N86-13093
N86-13095
N86-13174
N86-13176
N86-13196
N86-13214
DE-AC03-76SF-00515 .... N86-13070
N86-13071
N86-13075
N86-13103
N86-13104
N86-13121
N86-13146
N86-13151
N86-13153
N86-13159
N86-13169
DE-AC03-84-ER-53158 .... N86-13116
DE-AC04-76DP-00053 .... N86-12306
N86-12326
N86-12797
DE-AC04-76DP-00613 .... N86-12320
N86-13027
DE-AC04-76DP-00789 .... N86-12244
N86-12245
N86-12305
N86-12308
N86-12324
N86-12391
N86-12500
N86-12522
N86-12524
N86-12525
N86-12531
N86-12533
N86-12536
N86-12537
N86-12564
N86-12590
N86-12595
N86-12781
N86-12785
N86-12788
N86-12790
N86-12794
N86-12982
N86-13004
N86-13005
N86-13007
N86-13010
N86-13011
N86-13012
N86-13014
N86-13016
N86-13018
N86-13041
N86-13088
N86-13108
N86-13109
N86-13133
N86-13144
N86-13178
N86-13197
N86-13209
DE-AC04-76DP-03533 .... N86-12390
N86-12530
DE-AC04-76DR-00789 .... N86-12538
N86-12790
DE-AC05-84CR-21400 .... N86-13213
DE-AC05-84CS-21400 .... N86-12616
DE-AC05-84OR-21400 .... N86-12264
N86-12301
N86-12302
N86-12303
N86-12304
N86-12321
N86-12523
N86-12534
N86-12574
N86-12596
N86-12607
N86-12614
N86-12626
N86-12783
N86-12792
N86-12953
N86-12975
N86-12976
N86-13000
N86-13006
N86-13020
N86-13069
N86-13094
N86-13102
N86-13142
N86-13154
N86-13166
N86-13201
N86-13202
N86-13203
N86-13208
N86-13212
N86-13215
DE-AC05-84OS-21400 .... N86-12588
N86-13044
DE-AC05-84OT-21400 .... N86-12323
N86-12617
DE-AC05-87OR-21400 .... N86-12615
N86-13096
DE-AC06-76FF-02170 .... N86-12277
N85-13008
DE-AC06-76RI-01830 .... N86-12799
DE-AC06-76RL-01830 .... N86-12325
N86-12800
N86-12965
N86-12999

N86-13066
DE-AC06-77RL-01030 .... N86-13001
DE-AC06-81ER-40046 .... N86-13114
N86-13120
DE-AC07-76ID-01570 .... N86-13043
N86-13099
N86-13118
N86-13206
DE-AC06-76ET-51013 .... N86-13170
DE-AC06-80DP-40124 .... N86-13162
N86-13175
DE-AC06-80EP-40124 .... N86-13161
DE-AC06-81NV-10185 .... N86-12902
DE-AC06-82DP-40152 .... N86-13150
DE-AC21-83MC-20352 .... N86-12779
DE-AC21-84MC-20107 .... N86-13061
DE-AC22-81PC-40022 .... N86-12573
DE-AC09076SR-00001 .... N86-12265
DE-AI01-76ET-20356 .... N86-12759
DE-AI01-80ET-17088 .... N86-12757
N86-12758
DE-AI05-82OR-1005 .... N86-13236
DE-AM03-76SF00326 .... N86-12993
DE-AS05-76ER-04447 .... N86-13102
DE-AS05-76FV-03944 .... N86-12798
DE-AS05-78ER-05940 .... N86-13113
DE-AS05-81ER-10951 .... N86-12253
DE-AS05-83ER-13122 .... N86-13002
N86-13003
DE-AS07-77ET-28407 .... N86-12747
DE-AT03-76ER-72018 .... N86-12993
DE-AT03-80SF-11459 .... N86-12570
DE-AT03-81ER-10820 .... N86-12280
DE-AT06-80EV-10429 .... N86-12901
DE-FC-08-85DP-40200 .... N86-13180
DE-FC01-80ET-23197 .... N86-12312
DE-FC03-83FE-60149 .... N86-12281
DE-FG02-84ER-45131 .... N86-12575
DE-FG03-84ER-45093 .... N86-12327
DE-FG04-81AL-21581 .... N86-12787
DE-FG04-82AL-20860 .... N86-12793
DE-FG05-80ET-53088 .... N86-13171
N86-13217
N86-13218
DE-FG05-80FT-53088 .... N86-13172
DE-FG22-81PC-40771 .... N86-12278
DE-FG22-84PC-70753 .... N86-12276
DEN3-241 .... N86-12757
N86-12758
DE85-AI08-78EV-01577 .... N86-12964
DI-BM-J0-133934 .... N86-12618
DI-14-08-0001-G-841 .... N86-12802
DNA001-79-C-0027 .... N86-13098
DTFA-01-80-Y-10546 .... N86-12920
DTRS56-81-C-00043 .... N86-12392
EPA-68-02-3171 .... N86-12806
EPA-68-02-4082 .... N86-12809
F04611-82-C-0007 .... N86-12328
F04611-84-C-0032 .... N86-12625
F04701-83-C-0084 .... N86-12248
N86-12898
N86-12899
N86-13065
N86-13066
N86-13067
F08635-82-C-0131 .... N86-12230
F19628-81-C-0128 .... N86-12491
F19628-82-K-0040 .... N86-12900
F19628-84-C-0001 .... N86-12990
F19628-85-C-0024 .... N86-13250
F19628-88-C-0034 .... N86-13243
F30602-81-C-0062 .... N86-12493
F30602-81-C-0169 .... N86-13126
F30602-82-C-0127 .... N86-12619
F30602-84-C-0162 .... N86-12515
F33615-79-C-1935 .... N86-12222
N86-12223
F33615-81-C-1428 .... N86-13189
F33615-81-C-2070 .... N86-12775
F33615-82-C-0511 .... N86-12973
F33615-82-C-5089 .... N86-12315
F49620-82-C-0018 .... N86-12247
JPL PROJ. 5101-264 .... N86-12759
JPL-954527 .... N86-12786
MDA903-80-C-0353 .... N86-12489
MDA903-83-K-0400 .... N86-12296
MDA903-84-C-0031 .... N86-12262
MDA903-84-C-0197 .... N86-12582
MDA903-84-C-0329 .... N86-13026
NAGW-336 .... N86-13280
N86-13281
NAGW-399 .... N86-13280
NAGW-496 .... N86-13243
NAGW-509 .... N86-13271
NAGW-652 .... N96-13279
N86-13281
NAG1-58 .... N86-13057
NAG1-157 .... N86-12233
NAG1-243 .... N86-13028
NAG1-272 .... N86-12258
NAG1-279 .... N86-12478
N86-12480
N86-12481
N86-12484
NAG1-343 .... N86-12257
NAG1-397 .... N86-13188
NAG1-425 .... N86-12255
NAG1-441 .... N86-12600
NAG1-522 .... N86-12220
NAG3-22 .... N86-12293
NAG3-50 .... N86-13219
NAG3-149 .... N86-12485
NAG5-87 .... N86-13274
NAG5-218 .... N86-13272
NAG5-243 .... N86-13273
NAG5-349 .... N86-13242
NAG5-384 .... N86-12916
NAG5-510 .... N86-12739
NAG8-357 .... N86-13285
NAG8-521 .... N86-13260
NASA ORDER S-10663-C N86-12922
NASA ORDER W-15897 .... N86-12814
N86-12837
NASW-3339 .... N86-12243
N86-13221
N86-13230
NASW-3389 .... N86-13282
NASW-3455 .... N86-13235
NASW-3458 .... N86-12551
NASW-3676 .... N86-12949
NAS1-12426 .... N86-12202
N86-12208
NAS1-16000 .... N86-12204
NAS1-16508 .... N86-12743
NAS1-17070 .... N86-12550
NAS1-17171 .... N86-12205
NAS1-17335 .... N86-12212
NAS1-17919 .... N86-12238
NAS1-17932 .... N86-12560
NAS2-11451 .... N86-12218
NAS3-23629 .... N86-12226
NAS7-100 .... N86-12786
NAS7-918 .... N86-12759
N86-12919
NAS8-32577 .... N86-13249
NAS8-32579 .... N86-13240
NAS8-32845 .... N86-13263
NAS8-33092 .... N86-13187
NAS8-33797 .... N86-12918
NAS8-33982 .... N86-13138
NAS8-33992 .... N86-13247
NAS8-36189 .... N86-13257
NAS9-16528 .... N86-12741
NA83SA-C-00650 .... N86-12748
NCC1-69 .... N86-12237
N86-12240
NCC9-7 .... N86-12740
NGT36-001-800 .... N86-13219
NGT36-001-801 .... N86-13219
NR PROJ. F58-523 .... N86-12213
NR PROJ. F58-524 .... N86-12989
NR PROJ. F61-542 .... N86-12298
NSF AST-83-51447 .... N86-13285
NSF ATM-81-13078 .... N86-12833
NSF ATM-83-19487 .... N86-12839
NSF ATM-84-07314 .... N86-13243
NSF ATM-8113078 .... N86-12824
NSF DMR-77-24459 .... N86-12303
NSF DMS-83-51187 .... N86-13036
NSF DMS-84-20623 .... N86-12993
NSF ECS-83-12142 .... N86-12993
NSF MCS-82-15064 .... N86-13033
NSG-1498 .... N86-12216
NSG-7102 .... N86-13280
NSG-7172 .... N86-12203
N00014-75-C-0661 .... N86-12979
N00014-76-C-0016 .... N86-13283
N86-13284
N00014-76-C-0408 .... N86-12316
N00014-76-C-0475 .... N86-13048
N00014-77-C-0537 .... N86-13193
N00014-78-C-0631 .... N86-12553
N00014-79-C-0323 .... N86-12970
N00014-79-C-0623 .... N86-12562
N00014-79-C-0629 .... N86-12945
N00014-80-C-0326 .... N86-12561
N00014-80-C-0384 .... N86-12611
N00014-80-C-0505 .... N86-12994
N00014-81-K-0025 .... N86-12297
N00014-81-K-0136 .... N86-12961
N00014-81-K-0813 .... N86-12978
N00014-82-K-0183 .... N86-13283
N00014-82-K-0468 .... N86-12510
N00014-82-K-0604 .... N86-12972
N00014-82-K-0714 .... N86-12991
N00014-82-K-0759 .... N86-12969
N00014-83-K-0372 .... N86-12552
N00014-84-C-0193 .... N86-13059
N00014-84-K-0067 .... N86-12557
N00014-84-K-0146 .... N86-13046
N00014-84-K-0301 .... N86-13047
N00014-85-K-0187 .... N86-12624
N00014-85-K-0343 .... N86-12993
N00014-85-K-0370 .... N86-12556
N00017-83-K-0677 .... N86-12261
N00019-80-C-0569 .... N86-12300
N00019-84-C-0074 .... N86-12494
N00024-83-C-5301 .... N86-12328
N00039-83-C-0136 .... N86-13052
N66314-72-A-3029 .... N86-12242
RR0-2403 .... N86-12562
RR0-3302 .... N86-12492
N86-12897
RR0-4204 .... N86-12972
S12-66 .... N86-12209
W-31-019-ENG-38 .... N86-12252
W-31-109-ENG-38 .... N86-12275
N86-12499
N86-12520
N86-12567
N86-12568
N86-12571
N86-12627
N86-12784
N86-12983
N86-12984
N86-12997
N86-13015
N86-13089
N86-13091
N86-13100
N86-13149
N86-13205
N86-13207
N86-13210
W-7405-ENG-36 .... N86-12249
N86-12284
N86-12285
N86-12366
N86-12519
N86-12527
N86-12529
N86-12532
N86-12535
N86-12586
N86-12589
N86-12594
N86-12608
N86-12904
N86-12951
N86-12985
N86-12986
N86-12998
N86-13017
N86-13019
N86-13050
N86-13062
N86-13078
N86-13081
N86-13082
N86-13083
N86-13084
N86-13087
N86-13102
N86-13106
N86-13110
N86-13134
N86-13135
N86-13141
N86-13145
N86-13148
N86-13152
N86-13167
N86-13173
N86-13177
N86-13199
N86-13200
N86-13204
W-7405-ENG-38 .... N86-12576
W-7405-ENG-48 .... N86-12263
N86-12322
N86-12365
N86-12526
N86-12539
N86-12540
N86-12563
N86-12565
N86-12566

N86-12569
N86-12572
N86-12587
N86-12591
N86-12592
N86-12593
N86-12605
N86-12606
N86-12628
N86-12795
N86-13009
N86-13023
N86-13024
N86-13105
N86-13111
N86-13112
N86-13136
N86-13143
N86-13160
N86-13163
N86-13164
N86-13181
N86-13216
N86-13278
W-7405-ENG-82 .... N86-12307
N86-13211
W-7405-ENT-36 .... N86-13107
144-44-02-70 .... N86-13064
146-72-02-40 .... N86-12919
199-21-12-07 .... N86-12956
324-01-00 .... N86-12580
N86-12610
505-31-13-01 .... N86-12202
N86-12208
505-31-33-13 .... N86-13056
505-31-53-09 .... N86-12579
505-31-53-10 .... N86-12203
505-31-83-01 .... N86-12550
505-33-1A N86-12294
505-33-7C N86-12292
505-33-33-05 .... N86-12255
505-33-41 .... N86-12218
505-33-62 .... N86-12256
505-35-13-04 .... N86-12212
505-42-94 .... N86-12609
505-43-03-02 .... N86-12205
505-62-3A N86-12239
505-90-01 .... N86-12227
506-41-5A N86-12246
506-41-21 .... N86-12268
506-41-42 .... N86-12509
506-55-62B N86-13236
506-58-23-01 .... N86-12508
506-60-12 .... N86-12295
506-62-52 .... N86-12485
533-05-12 .... N86-12310
534-01-13 .... N86-12206
776-52-61 .... N86-12759

REPORT/ACCESSION NUMBER INDEX

SCIENTIFIC AND TECHNICAL AEROSPACE REPORTS VOLUME 24 NUMBER 3

Typical Report Number Index Listing

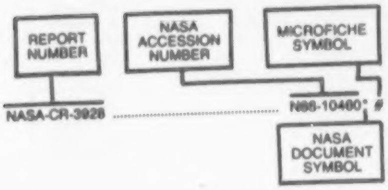

Listings in this index are arranged alphanumerically by report number. The NASA accession number denotes the number by which the citation is identified. An asterisk (*) indicates that the item is a NASA report. A pound sign (#) indicates that the item is available on microfiche.

ACSC-85-1750 .... N86-12968 #

AD-A155858 .... N86-13226 #
AD-A155948 .... N86-12601 #
AD-A156244 .... N86-12977 #
AD-A156665 .... N86-12623 #
AD-A156666 .... N86-12358 #
AD-A156709 .... N86-12313* #
AD-A156714 .... N86-12941 #
AD-A156718 .... N86-12942 #
AD-A156753 .... N86-12943 #
AD-A156820 .... N86-12968 #
AD-A156828 .... N86-13220 #
AD-A156830 .... N86-12487 #
AD-A156831 .... N86-12488 #
AD-A156832 .... N86-13022 #
AD-A156834 .... N86-12241 #
AD-A156899 .... N86-12950 #
AD-A156961 .... N86-12269 #
AD-A157070 .... N86-13065 #
AD-A157071 .... N86-13066 #
AD-A157072 .... N86-13126 #
AD-A157077 .... N86-12296 #
AD-A157078 .... N86-12552 #
AD-A157080 .... N86-12896 #
AD-A157081 .... N86-12213 #
AD-A157089 .... N86-12775 #
AD-A157090 .... N86-12959 #
AD-A157093 .... N86-12920 #
AD-A157094 .... N86-12260 #
AD-A157095 .... N86-13051 #
AD-A157097 .... N86-13025 #
AD-A157099 .... N86-12973 #
AD-A157106 .... N86-13026 #
AD-A157107 .... N86-12314 #
AD-A157108 .... N86-12229 #
AD-A157123 .... N86-13139 #
AD-A157124 .... N86-12489 #
AD-A157125 .... N86-12359 #
AD-A157127 .... N86-12989 #
AD-A157132 .... N86-12744 #
AD-A157133 .... N86-12297 #
AD-A157141 .... N86-12510 #
AD-A157144 .... N86-12490 #
AD-A157146 .... N86-13237 #
AD-A157147 .... N86-12219 #
AD-A157163 .... N86-13058 #
AD-A157203 .... N86-12776 #
AD-A157211 .... N86-12199 #
AD-A157212 .... N86-12234 #
AD-A157215 .... N86-12200 #
AD-A157216 .... N86-12491 #
AD-A157224 .... N86-12492 #
AD-A157227 .... N86-13046 #
AD-A157238 .... N86-12315 #
AD-A157239 .... N86-12493 #
AD-A157242 .... N86-12619 #
AD-A157246 .... N86-12209 #
AD-A157249 .... N86-12250 #
AD-A157250 .... N86-12553 #
AD-A157251 .... N86-12316 #
AD-A157277 .... N86-13189 #
AD-A157363 .... N86-12554 #
AD-A157389 .... N86-12921 #
AD-A157390 .... N86-12922* #
AD-A157392 .... N86-12990 #
AD-A157393 .... N86-12978 #
AD-A157398 .... N86-12247 #
AD-A157408 .... N86-13127 #
AD-A157410 .... N86-12360 #
AD-A157412 .... N86-12494 #
AD-A157413 .... N86-12270 #
AD-A157415 .... N86-12298 #
AD-A157450 .... N86-13047 #
AD-A157475 .... N86-12897 #
AD-A157495 .... N86-12271 #
AD-A157496 .... N86-12495 #
AD-A157497 .... N86-13190 #
AD-A157498 .... N86-13067 #
AD-A157505 .... N86-12991 #
AD-A157506 .... N86-13128 #
AD-A157512 .... N86-13283 #
AD-A157513 .... N86-13059 #
AD-A157520 .... N86-12969 #
AD-A157525 .... N86-12992 #
AD-A157546 .... N86-13029 #
AD-A157557 .... N86-12944 #
AD-A157643 .... N86-12230 #
AD-A157655 .... N86-12898 #
AD-A157656 .... N86-13222 #
AD-A157659 .... N86-12993 #
AD-A157660 .... N86-12317 #
AD-A157662 .... N86-12979 #
AD-A157664 .... N86-12248 #
AD-A157665 .... N86-12970 #
AD-A157669 .... N86-13192 #
AD-A157832 .... N86-12899 #
AD-A157833 .... N86-12389 #
AD-A157838 .... N86-12777 #
AD-A157839 .... N86-12210 #
AD-A157840 .... N86-12231 #
AD-A167841 .... N86-12555 #
AD-A157843 .... N86-12971 #
AD-A157854 .... N86-12221 #
AD-A157857 .... N86-12960 #
AD-A157858 .... N86-12261 #
AD-A157900 .... N86-12361 #
AD-A157903 .... N86-12262 #
AD-A157909 .... N86-12582 #
AD-A157911 .... N86-13227 #
AD-A157913 .... N86-12745 #
AD-A157914 .... N86-12624 #
AD-A157915 .... N86-13060 #
AD-A157916 .... N86-12583 #
AD-A157917 .... N86-12994 #
AD-A157919 .... N86-13238 #
AD-A157920 .... N86-13129 #
AD-A157924 .... N86-12900 #
AD-A157925 .... N86-12496 #
AD-A157926 .... N86-12923 #
AD-A157928 .... N86-13030 #
AD-A157929 .... N86-13193 #
AD-A157930 .... N86-13140 #
AD-A157931 .... N86-13228 #
AD-A157934 .... N86-12945 #
AD-A157936 .... N86-12995 #
AD-A157957 .... N86-13048 #
AD-A157958 .... N86-12556 #
AD-A157959 .... N86-12625 #
AD-A157960 .... N86-13052 #
AD-A157963 .... N86-13130 #
AD-A157964 .... N86-13031 #
AD-A157965 .... N86-12961 #
AD-A157966 .... N86-12946 #
AD-A157971 .... N86-12924 #
AD-A157973 .... N86-12925 #
AD-A158100 .... N86-12235 #
AD-A158101 .... N86-12242 #
AD-A158102 .... N86-12996 #
AD-A158104 .... N86-12514 #
AD-A158105 .... N86-12557 #
AD-A158108 .... N86-12972 #
AD-A158109 .... N86-12272 #
AD-A158110 .... N86-12620 #
AD-A158114 .... N86-12515 #
AD-A158115 .... N86-12328 #
AD-A158118 .... N86-12746 #
AD-A158119 .... N86-12222 #
AD-A158120 .... N86-12223 #
AD-A158127 .... N86-12611 #
AD-A158129 .... N86-12236 #
AD-A158130 .... N86-12981 #
AD-A158131 .... N86-13032 #
AD-A158132 .... N86-13033 #
AD-A158133 .... N86-13034 #
AD-A158136 .... N86-12947 #
AD-A158137 .... N86-13035 #
AD-A158138 .... N86-12558 #
AD-A158143 .... N86-12926 #
AD-A158144 .... N86-13131 #
AD-A158147 .... N86-13036 #
AD-A158148 .... N86-13037 #
AD-A158149 .... N86-13038 #
AD-A158150 .... N86-13039 #
AD-A158182 .... N86-13194 #
AD-A158185 .... N86-12516 #
AD-A158396 .... N86-13195 #
AD-A158407 .... N86-12300 #
AD-A158408 .... N86-13284 #
AD-A158409 .... N86-12560 #
AD-A158411 .... N86-13132 #
AD-A158412 .... N86-12497 #
AD-A158417 .... N86-13098 #
AD-A158418 .... N86-13229 #
AD-A158431 .... N86-12273 #
AD-A158434 .... N86-12518 #
AD-A158551 .... N86-12319 #
AD-A158552 .... N86-12561 #
AD-A158553 .... N86-12604 #
AD-A158555 .... N86-13049 #
AD-A158556 .... N86-12963 #
AD-A158557 .... N86-12562 #
AD-A158558 .... N86-13040 #
AD-A158559 .... N86-12362 #
AD-A158560 .... N86-12363 #
AD-A158561 .... N86-12778 #

AD-D011762 .... N86-12228 #
AD-D011763 .... N86-12957 #
AD-D011764 .... N86-12958 #
AD-D011765 .... N86-13125 #
AD-D011790 .... N86-12506
AD-D011791 .... N86-13184
AD-D011792 .... N86-12597
AD-D011793 .... N86-12225
AD-D011794 .... N86-12217
AD-D011795 .... N86-12598
AD-D011796 .... N86-12473
AD-D011810 .... N86-12974 #
AD-D011811 .... N86-12602 #
AD-D011820 .... N86-13068 #
AD-D011821 .... N86-12318 #
AD-D011823 .... N86-12511 #
AD-D011825 .... N86-13191 #
AD-D011826 .... N86-12299 #
AD-D011827 .... N86-12512 #
AD-D011828 .... N86-12513 #
AD-D011829 .... N86-13123
AD-D011831 .... N86-12507
AD-D011834 .... N86-13124
AD-D011835 .... N86-12474
AD-D011836 .... N86-12955
AD-D011838 .... N86-12475
AD-D011839 .... N86-12476
AD-D011840 .... N86-12267
AD-D011841 .... N86-13185
AD-D011842 .... N86-13186
AD-D011843 .... N86-12599
AD-D011845 .... N86-12581 #
AD-D011846 .... N86-12980 #
AD-D011847 .... N86-12584 #
AD-D011848 .... N86-12962 #
AD-D011850 .... N86-12477
AD-D011851 .... N86-12232 #
AD-D011852 .... N86-12559 #
AD-D011853 .... N86-12585 #
AD-D011855 .... N86-12603 #

AD-D011856 N86-12612 #
AD-D011857 N86-12517 #

AD-E301698 N86-12601 #
AD-E301723 N86-12241 #
AD-E301723 N86-12487 #
AD-E301723 N86-12488 #
AD-E301723 N86-13022 #
AD-EJ01723 N86-13220 #
AD-E301765 N86-13098 #
AD-E401371 N86-13052 #
AD-E401373 N86-13130 #
AD-E440283 N86-12358 #
AD-E440286 N86-12623 #
AD-E440290 N86-13031 #
AD-E500722 N86-12262 #
AD-E900452 N86-12361 #
AD-E900455 N86-12231 #
AD-E900488 N86-12210 #
AD-E900491 N86-12777 #

AEDC-TR-85-39 N86-12272 #

AFAMRL-TR-85-004 N86-12973 #

AFESC/ESL-TR-84-61 N86-12230 #

AFFTC-TR-85-19 N86-12221 #

AFGL-ERP-902 N86-12896 #
AFGL-ERP-907 N86-13139 #

AFGL-TR-84-0151 N86-12491 #
AFGL-TR-84-0317 N86-12896 #
AFGL-TR-85-0020 N86-13139 #
AFGL-TR-85-0054 N86-12900 #

AFHRL-TR-85-12 N86-13025 #

AFIT/CI/NR-85-71D N86-12996 #
AFIT/CI/NR-85-72T N86-12981 #
AFIT/CI/NR-85-78T N86-12746 #
AFIT/CI/NR-85-83T N86-12925 #
AFIT/CI/NR-85-85T N86-12236 #

AFIT/GST/OS/85M-13 N86-13226 #

AFLRL-191 N86-12359 #

AFOSR-85-0498TR N86-12363 #
AFOSR-85-0504TR N86-12604 #
AFOSP-85-0561TR N86-12362 #
AFOSR-85-0623TR N86-13049 #

AFRPL-TR-85-013 N86-12250 #
AFRPL-TR-85-030 N86-12625 #

AFWAL-TR-84-2030 N86-12229 #
AFWAL-TR-84-2112 N86-12775 #
AFWAL-TR-84-3109 N86-12235 #
AFWAL-TR-85-1035 N86-13189 #
AFWAL-TR-85-1041-VOL-1 N86-12222 #
AFWAL-TR-85-1041-VOL-2 N86-12223 #
AFWAL-TR-85-4001 N86-12315 #

AGARD-722-PAPER-1 N86-12238* #

AI-TR-844 N86-12994 #

AIAA-86-0044 N86-12239* #

AMMRC-TR-85-3 N86-12260 #

AMTE(N)/TM85057 N86-13060 #

ANL-EEP-CP-85-27 N86-13149 #

ANL-HEP-CP-85-17 N86-13100 #
ANL-HEP-CP-85-33 N86-13207 #
ANL-HEP-CP-85-41 N86-12499 #

ANL-85-40 N86-12568 #

ANL/EEP-CP-85-43 N86-13091 #

ANL/HEP-CP-85-42 N86-12520 #

ANL/MCS-TM-49 N86-13015 #

ANL/OEPM-85-1 N86-12784 #

AR-2 N86-13002 #
AR-3 N86-12241 #
AR-8 N86-12786* #

ARL/STRUC-TM-394 N86-12199 #

ARL/STRUC-TM-400 N86-12234 #

ARLCB-MR-85015 N86-12623 #

ARLCB-TR-85006 N86-12358 #
ARLCB-TR-85021 N86-13031 #

ARO-13926.1-MA N86-13229 #
ARO-18209.2-PH N86-12319 #
ARO-18441.2-MA N86-12992 #
ARO-18649.5-CH N86-13195 #
ARO-18965.2-PH N86-13132 #
ARO-19011.1-CH N86-12270 #
ARO-19147.37-EL N86-12497 #
ARO-19267.3-CH N86-12273 #
ARO-19489.3-EL N86-13192 #
ARO-20849.1-PH N86-12518 #
ARO-21156.1-GS N86-12560 #
ARO-21165.2-EG N86-12360 #

ARPAD-CR-85001 N86-13130 #

AS-PAPER-392 N86-12906* #

ASG-TR-189-17R N86-12582 #

ATR-3 N86-13058 #
ATR-4 N86-12611 #

AVSCOM-TR-85-B-5 N86-12259* #

B-215115 N86-12215 #
B-215379 N86-12224 #

BBC-RD-1985/11 N86-12486

BBN-5939 N86-12489 #

BDX-613-3185 N86-13027 #
BDX-613-3230 N86-12320 #

BM-OFR-49-85 N86-12618 #

BM-RI-8930 N86-12286 #

BNL-NCS-36552 N86-13117 #
BNL-NCS-36553 N86-13115 #

BNL-36329 N86-12789 #
BNL-36452 N86-12796 #
BNL-36484 N86-13182 #
BNL-36491 N86-13157 #
BNL-36504 N86-13168 #
BNL-36506 N86-12498 #
BNL-36555 N86-13155 #
BNL-36565 N86-13077 #
BNL-36567 N86-13156 #
BNL-36569 N86-13119 #
BNL-36571 N86-12251 #
BNL-36623 N86-13053 #
BNL-36708 N86-13055 #
BNL-51909 N86-13073 #

CERC-IR-85-1 N86-12946 #

CERC-TR-85-4 N86-12947 #

CERL-TR-M-85/17 N86-12314 #

CMR-DARPA-10 N86-12296 #

CONF-85089-0 N86-12301 #
CONF-840761-2 N86-13178 #
CONF-841010-20 N86-13162 #
CONF-841010-21 N86-13161 #
CONF-841041-2 N86-12952 #
CONF-841231-15 N86-12783 #
CONF-841231-18 N86-12792 #
CONF-850103-11 N86-13099 #
CONF-850114-2 N86-13080 #
CONF-850146-7 N86-13100 #
CONF-850169-12 N86-13111 #
CONF-850238-1 N86-13175 #
CONF-850310-103 N86-13006 #
CONF-850310-111 N86-13112 #
CONF-850310-113 N86-13163 #
CONF-850310-114 N86-13164 #
CONF-850315-6 N86-13120 #
CONF-850315-8 N86-13090 #
CONF-850345-25 N86-12608 #
CONF-850345-28 N86-13135 #
CONF-850375-3 N86-13216 #
CONF-850375-10 N86-13207 #
CONF-850388-11 N86-12789 #
CONF-850405-12 N86-12592 #
CONF-850405-14 N86-13118 #
CONF-850405-16 N86-13116 #
CONF-850406-14 N86-12567 #
CONF-850410-58 N86-13008 #
CONF-850417-22 N86-12271 #
CONF-850470-6 N86-13069 #
CONF-850470-8 N86-12523 #
CONF-850504-38 N86-12244 #
CONF-850504-59 N86-13084 #
CONF-850504-88 N86-13159 #
CONF-850504-93 N86-13087 #
CONF-850504-101 N86-13078 #
CONF-850504-102 N86-13145 #
CONF-850504-103-REV N86-13075 #
CONF-850504-105 N86-12529 #
CONF-850504-111 N86-13146 #
CONF-850504-119 N86-13083 #
CONF-850504-123 N86-13153 #
CONF-850504-126 N86-13151 #
CONF-850504-129 N86-13081 #
CONF-850504-148 N86-13157 #
CONF-850504-156 N86-13155 #
CONF-850504-158 N86-13156 #
CONF-850504-159 N86-13077 #
CONF-850504-162 N86-13182 #
CONF-850504-167 N86-13053 #
CONF-850504-180 N86-12499 #
CONF-850504-185 N86-13104 #
CONF-850504-186 N86-13079 #
CONF-850504-189 N86-13122 #
CONF-850504-195 N86-12498 #
CONF-850504-196 N86-13168 #
CONF-850504-205 N86-13169 #
CONF-850504-206 N86-13176 #
CONF-850504-211 N86-13091 #
CONF-850504-220 N86-13092 #
CONF-850504-221 N86-13196 #
CONF-850504-224 N86-13054 #
CONF-850504-225 N86-13093 #
CONF-850504-226 N86-13095 #
CONF-850504-227 N86-13174 #
CONF-850504-232 N86-12520 #
CONF-850504-269 N86-13101 #
CONF-850504-280 N86-13074 #
CONF-850504-1608 N86-12532 #
CONF-850506-7 N86-13086 #
CONF-850507-11 N86-13000 #
CONF-850507-18 N86-13148 #
CONF-850507-19 N86-13105 #
CONF-850507-32 N86-13278 #
CONF-850507-45 N86-13173 #
CONF-850521-1 N86-12251 #
CONF-850536-5 N86-12265 #
CONF-850542-1 N86-12275 #
CONF-850559-1 N86-12325 #
CONF-850578-3 N86-13076 #
CONF-850579-4 N86-12986 #
CONF-850579-8 N86-13019 #
CONF-850579-10 N86-13103 #
CONF-850579-12 N86-12984 #
CONF-850599-2 N86-12320 #
CONF-850605-1 N86-13094 #
CONF-850606-10 N86-12564 #
CONF-850606-11 N86-12574 #
CONF-850607-4 N86-12249 #
CONF-850616-8 N86-12527 #
CONF-850616-28 N86-13014 #
CONF-850616-29 N86-13144 #
CONF-850616-31 N86-12531 #
CONF-850616-36 N86-12245 #
CONF-850616-43 N86-12524 #
CONF-850616-47 N86-13088 #
CONF-850616-64 N86-12519 #
CONF-850616-67 N86-12535 #
CONF-850617-2 N86-13062 #
CONF-850631-1 N86-12521 #
CONF-850705-24 N86-12629 #
CONF-850706-22-REV-1 N86-12365 #
CONF-850706-25 N86-12565 #
CONF-850713-7 N86-12304 #
CONF-850716-1 N86-13197 #
CONF-850723-4 N86-12390 #
CONF-850736-18 N86-12391 #
CONF-850736-21 N86-12308 #
CONF-850736-23 N86-12563 #
CONF-850736-24 N86-12566 #
CONF-850736-34 N86-12590 #
CONF-850736-48 N86-12594 #
CONF-850745-2 N86-12606 #
CONF-850752-1 N86-13041 #
CONF-850753-1 N86-12305 #
CONF-850759-7 N86-12593 #
CONF-850759-9 N86-12589 #
CONF-850759-13 N86-13200 #
CONF-850762-1 N86-12586 #
CONF-850765-5 N86-12500 #
CONF-850765-9 N86-12595 #

CONF-850777-2	N86-12303 #
CONF-850784-1	N86-12951 #
CONF-850786-1	N86-13202 #
CONF-850801-13	N86-13107 #
CONF-850807-5	N86-13072 #
CONF-850809-12	N86-12628 #
CONF-850809-15	N86-13050 #
CONF-850810-7	N86-12576 #
CONF-850810-19	N86-12571 #
CONF-850810-21	N86-12578 #
CONF-850810-23	N86-12577 #
CONF-850823-1-ABST	N86-12627 #
CONF-850839-1	N86-13154 #
CONF-850840-1	N86-12324 #
CONF-850840-5	N86-13206 #
CONF-850862-1	N86-13027 #
CONF-850871-1	N86-13199 #
CONF-850887-8	N86-12587 #
CONF-850889-4	N86-13209 #
CONF-850890-3	N86-13055 #
CONF-850890-10	N86-13208 #
CONF-850890-14	N86-13203 #
CONF-850926-4	N86-12617 #
CONF-850927-2	N86-13141 #
CONF-850952-1	N86-13201 #
CONF-851097-1	N86-12282 #
CONF-8307126-8	N86-13121 #
CONF-8310394-1	N86-12307 #
CONF-8405312-1	N86-12903 #
CONF-8408121-5	N86-12904 #
CONF-8409228-2	N86-13205 #
CONF-8410159-1-REV-1	N86-12569 #
CONF-8410276-2	N86-12322 #
CONF-8410277-1	N86-12591 #
CONF-8503105-3	N86-13149 #
CONF-8503105-4	N86-13147 #
CONF-8503105-5	N86-13085 #
CONF-8503116-2	N86-12999 #
CONF-8503134-1	N86-12252 #
CONF-8503139-1	N86-13009 #
CONF-8503141-3	N86-13214 #
CONF-8503142-1	N86-12263 #
CONF-8503147-1	N86-13213 #
CONF-8503151-2	N86-13097 #
CONF-8503156-1	N86-13133 #
CONF-8503158	N86-12364 #
CONF-8504100-2	N86-13043 #
CONF-8504132-1	N86-12975 #
CONF-8504133-3	N86-13119 #
CONF-8504143-1	N86-12264 #
CONF-8504158-1	N86-12800 #
CONF-8505100-9	N86-13152 #
CONF-8505100-16	N86-13177 #
CONF-8505130-8	N86-13170 #
CONF-8505130-10	N86-13179 #
CONF-8505138-4	N86-13204 #
CONF-8505138-5	N86-12621 #
CONF-8505138-10	N86-13210 #
CONF-8505138-14	N86-13211 #
CONF-8505156-2	N86-12796 #
CONF-8505164-1	N86-13082 #
CONF-8505172-2	N86-13089 #
CONF-8505175-1	N86-13142 #
CONF-8505177-2	N86-13018 #
CONF-8506117-1	N86-13004 #
CONF-8506119-1	N86-12284 #
CONF-8506123-1	N86-12533 #
CONF-8506125-4	N86-13212 #
CONF-8506129-1	N86-12525 #
CONF-8506130-4	N86-13115 #
CONF-8506132-1	N86-12285 #
CONF-8506136-1	N86-12965 #
CONF-8506140	N86-12794 #
CONF-8506141-3	N86-12537 #
CONF-8506141-4	N86-13108 #
CONF-8506141-7	N86-13109 #
CONF-8506142-1	N86-13134 #
CONF-8506142-2	N86-13017 #
CONF-8506148-3	N86-12976 #
CONF-8506150-1	N86-12607 #
CONF-8506159-1	N86-12536 #
CONF-8506165-2	N86-12302 #
CONF-8509130-2	N86-12795 #
CONF-8509140-1	N86-12983 #
CONF-8509144-1	N86-12998 #
CONF-8509147-2	N86-13102 #
CONF-8510116-1	N86-12997 #
CONF-85051661	N86-13106 #
COO-4939	N86-12283 #
CPIA-PUBL-394-VOL-3	N86-12328 #
CRC-APRAC-CAPE-30-81-03	N86-12287 #
CRC-1387	N86-12471 #
CRDC-CR-85035	N86-13131 #
CRREL-SR-85-4	N86-12995 #
CRREL-SR-85-8	N86-13040 #
CSG-39	N86-12977 #
CSI-85-07-04	N86-12497 #
CSULB/ME-84-9	N86-12561 #
DDAD/EDR-11187	N86-13021 #
DE85-004030	N86-12627 #
DE85-004081	N86-12275 #
DE85-005246	N86-12783 #
DE85-005279	N86-12792 #
DE85-005298	N86-12799 #
DE85-005507	N86-12617 #
DE85-006840	N86-12576 #
DE85-007264	N86-12628 #
DE85-007705	N86-13050 #
DE85-007747	N86-13154 #
DE85-008157	N86-13150 #
DE85-008691	N86-12324 #
DE85-008793	N86-12790 #
DE85-008806	N86-12211 #
DE85-008819	N86-12577 #
DE85-009333	N86-13018 #
DE85-009358	N86-12779 #
DE85-009494	N86-13178 #
DE85-009895	N86-13121 #
DE85-009925	N86-12570 #
DE85-010104	N86-13107 #
DE85-010113	N86-12305 #
DE85-010122	N86-13041 #
DE85-010131	N86-13206 #
DE85-010276	N86-12252 #
DE85-010478	N86-12606 #
DE85-010601	N86-13027 #
DE85-011164	N86-12903 #
DE85-011168	N86-12279 #
DE85-011408	N86-12264 #
DE85-011416	N86-13213 #
DE85-011652	N86-12530 #
DE85-011653	N86-12306 #
DE85-011672	N86-12277 #
DE85-011839	N86-12796 #
DE85-011923	N86-12534 #
DE85-011937	N86-13000 #
DE85-012014	N86-12320 #
DE85-012029	N86-12525 #
DE85-012034	N86-12244 #
DE85-012092	N86-12283 #
DE85-012104	N86-13149 #
DE85-012112	N86-12788 #
DE85-012135	N86-12791 #
DE85-012137	N86-12364 #
DE85-012178	N86-12621 #
DE85-012181	N86-13117 #
DE85-012234	N86-12282 #
DE85-012259	N86-13053 #
DE85-012294	N86-12323 #
DE85-012296	N86-13085 #
DE85-012297	N86-13147 #
DE85-012303	N86-13080 #
DE85-012319	N86-12793 #
DE85-012369	N86-12571 #
DE85-012448	N86-13086 #
DE85-012449	N86-12800 #
DE85-012456	N86-12999 #
DE85-012492	N86-12573 #
DE85-012531	N86-12789 #
DE85-012591	N86-12784 #
DE85-012595	N86-12533 #
DE85-012604	N86-13076 #
DE85-012652	N86-13082 #
DE85-012656	N86-13084 #
DE85-012668	N86-13087 #
DE85-012669	N86-12532 #
DE85-012675	N86-13078 #
DE85-012677	N86-13145 #
DE85-012678	N86-12529 #
DE85-012688	N86-13081 #
DE85-012692	N86-13083 #
DE85-012711	N86-13204 #
DE85-012726	N86-12986 #
DE85-012746	N86-13106 #
DE85-012747	N86-13019 #
DE85-012751	N86-13148 #
DE85-012752	N86-12285 #
DE85-012757	N86-12284 #
DE85-012761	N86-12527 #
DE85-012765	N86-13152 #
DE85-012791	N86-12787 #
DE85-012794	N86-12965 #
DE85-012831	N86-12786* #
DE85-012837	N86-13014 #
DE85-012841	N86-13144 #
DE85-012874	N86-12526 #
DE85-012891	N86-13006 #
DE85-012912	N86-13105 #
DE85-012913	N86-13278 #
DE85-012924	N86-12322 #
DE85-012925	N86-13216 #
DE85-012934	N86-12591 #
DE85-012935	N86-12569 #
DE85-012938	N86-12263 #
DE85-012939	N86-13164 #
DE85-012941	N86-13163 #
DE85-012942	N86-12592 #
DE85-012948	N86-13009 #
DE85-012949	N86-13112 #
DE85-012961	N86-13111 #
DE85-012981	N86-12280 #
DE85-013061	N86-13146 #
DE85-013064	N86-13151 #
DE85-013067	N86-13153 #
DE85-013115	N86-13004 #
DE85-013133	N86-12798 #
DE85-013148	N86-12274 #
DE85-013180	N86-13005 #
DE85-013200	N86-13023 #
DE85-013231	N86-12265 #
DE85-013231	N86-12785 #
DE85-013232	N86-13007 #
DE85-013253	N86-12794 #
DE85-013261	N86-13010 #
DE85-013276	N86-12325 #
DE85-013281	N86-13155 #
DE85-013285	N86-13077 #
DE85-013286	N86-13156 #
DE85-013293	N86-13182 #
DE85-013300	N86-13157 #
DE85-013302	N86-13119 #
DE85-013308	N86-12251 #
DE85-013313	N86-12782 #
DE85-013315	N86-13001 #
DE85-013320	N86-12797 #
DE85-013374	N86-13159 #
DE85-013384	N86-13003 #
DE85-013385	N86-13002 #
DE85-013390	N86-12278 #
DE85-013426	N86-13013 #
DE85-013428	N86-12276 #
DE85-013437	N86-12245 #
DE85-013443	N86-13011 #
DE85-013478	N86-12253 #
DE85-013523	N86-13020 #
DE85-013533	N86-12626 #
DE85-013536	N86-12615 #
DE85-013546	N86-12321 #
DE85-013638	N86-13142 #
DE85-013649	N86-13158 #
DE85-013747	N86-12564 #
DE85-013772	N86-12524 #
DE85-013784	N86-13088 #
DE85-013805	N86-13012 #
DE85-013816	N86-12499 #
DE85-013847	N86-13100 #
DE85-013859	N86-12531 #
DE85-013875	N86-12984 #
DE85-013887	N86-13207 #
DE85-013895	N86-13205 #
DE85-013904	N86-13120 #
DE85-013905	N86-13114 #
DE85-013925	N86-13079 #
DE85-013958	N86-12537 #
DE85-013961	N86-12391 #
DE85-013983	N86-12365 #
DE85-013994	N86-12975 #
DE85-013995	N86-12574 #
DE85-014000	N86-13008 #
DE85-014018	N86-13045 #
DE85-014019	N86-13042 #
DE85-014054	N86-12901 #
DE85-014064	N86-13170 #
DE85-014067	N86-12596 #
DE85-014072	N86-13173 #
DE85-014082	N86-12249 #
DE85-014091	N86-13062 #
DE85-014093	N86-12608 #
DE85-014095	N86-13141 #
DE85-014100	N86-13135 #
DE85-014107	N86-12904 #
DE85-014111	N86-12535 #
DE85-014113	N86-13090 #
DE85-014115	N86-12586 #
DE85-014116	N86-13134 #
DE85-014121	N86-13177 #
DE85-014122	N86-13017 #
DE85-014124	N86-12519 #

DE85-014205 .... N86-12572 #
DE85-014213 .... N86-13168 #
DE85-014214 .... N86-12498 #
DE85-014217 .... N86-13115 #
DE85-014256 .... N86-12985 #
DE85-014259 .... N86-12366 #
DE85-014267 .... N86-13110 #
DE85-014295 .... N86-13015 #
DE85-014308 .... N86-12976 #
DE85-014316 .... N86-13212 #
DE85-014331 .... N86-13108 #
DE85-014352 .... N86-13122 #
DE85-014360 .... N86-13104 #
DE85-014361 .... N86-13103 #
DE85-014362 .... N86-13169 #
DE85-014405 .... N86-13161 #
DE85-014407 .... N86-13162 #
DE85-014413 .... N86-13175 #
DE85-014414 .... N86-13180 #
DE85-014437 .... N86-13197 #
DE85-014450 .... N86-12281 #
DE85-014534 .... N86-12578 #
DE85-014536 .... N86-13176 #
DE85-014537 .... N86-13214 #
DE85-014592 .... N86-12536 #
DE85-014621 .... N86-13118 #
DE85-014632 .... N86-13043 #
DE85-014634 .... N86-13099 #
DE85-014644 .... N86-12575 #
DE85-014650 .... N86-13094 #
DE85-014651 .... N86-13069 #
DE85-014655 .... N86-12607 #
DE85-014680 .... N86-12327 #
DE85-014705 .... N86-12308 #
DE85-014707 .... N86-12590 #
DE85-014708 .... N86-13109 #
DE85-014746 .... N86-13133 #
DE85-014765 .... N86-13218 #
DE85-014766 .... N86-13171 #
DE85-014782 .... N86-13097 #
DE85-014783 .... N86-13116 #
DE85-014800 .... N86-13055 #
DE85-014803 .... N86-12565 #
DE85-014807 .... N86-12563 #
DE85-014809 .... N86-12629 #
DE85-014811 .... N86-12566 #
DE85-014815 .... N86-12593 #
DE85-014841 .... N86-12500 #
DE85-014844 .... N86-12309 #
DE85-014849 .... N86-13181 #
DE85-014856 .... N86-12605 #
DE85-014857 .... N86-12539 #
DE85-014859 .... N86-13179 #
DE85-014860 .... N86-13024 #
DE85-014861 .... N86-13160 #
DE85-014862 .... N86-13165 #
DE85-014878 .... N86-13113 #
DE85-014887 .... N86-13096 #
DE85-014892 .... N86-13136 #
DE85-014904 .... N86-12390 #
DE85-014912 .... N86-13210 #
DE85-014932 .... N86-12522 #
DE85-014933 .... N86-13016 #
DE85-014934 .... N86-12616 #
DE85-014956 .... N86-13075 #
DE85-014976 .... N86-12983 #
DE85-014983 .... N86-12520 #
DE85-014984 .... N86-12567 #
DE85-014985 .... N86-13091 #
DE85-014989 .... N86-13089 #
DE85-014998 .... N86-12997 #
DE85-015011 .... N86-12613 #
DE85-015057 .... N86-13044 #
DE85-015065 .... N86-13166 #
DE85-015066 .... N86-13215 #
DE85-015070 .... N86-12953 #
DE85-015078 .... N86-12614 #
DE85-015083 .... N86-13172 #
DE85-015127 .... N86-12521 #
DE85-015130 .... N86-13092 #
DE85-015136 .... N86-13070 #
DE85-015137 .... N86-13071 #
DE85-015150 .... N86-13209 #
DE85-015160 .... N86-12595 #
DE85-015188 .... N86-12587 #
DE85-015225 .... N86-12952 #
DE85-015260 .... N86-13211 #
DE85-015271 .... N86-13196 #
DE85-015276 .... N86-13174 #
DE85-015277 .... N86-13054 #
DE85-015278 .... N86-13093 #
DE85-015279 .... N86-13095 #
DE85-015312 .... N86-12588 #
DE85-015313 .... N86-12540 #
DE85-015323 .... N86-13208 #
DE85-015353 .... N86-13167 #
DE85-015491 .... N86-12982 #
DE85-015518 .... N86-12307 #
DE85-015607 .... N86-12326 #
DE85-015661 .... N86-12538 #
DE85-015671 .... N86-12998 #
DE85-015672 .... N86-12951 #
DE85-015674 .... N86-12589 #
DE85-015739 .... N86-13199 #
DE85-015750 .... N86-12594 #
DE85-015821 .... N86-13217 #
DE85-016026 .... N86-12781 #
DE85-016301 .... N86-12301 #
DE85-016303 .... N86-13203 #
DE85-016317 .... N86-12302 #
DE85-016356 .... N86-12303 #
DE85-016394 .... N86-12523 #
DE85-016438 .... N86-12795 #
DE85-016465 .... N86-12902 #
DE85-016472 .... N86-12304 #
DE85-016559 .... N86-13074 #
DE85-016639 .... N86-13072 #
DE85-016851 .... N86-12780 #
DE85-016930 .... N86-13202 #
DE85-016950 .... N86-13198 #
DE85-016972 .... N86-12747 #
DE85-017011 .... N86-13073 #
DE85-017091 .... N86-13201 #
DE85-017144 .... N86-12568 #
DE85-017221 .... N86-13061 #
DE85-017442 .... N86-13101 #
DE85-017523 .... N86-13102 #
DE85-017530 .... N86-13200 #
DE85-017694 .... N86-13143 #
DE85-901746 .... N86-12801 #

DNA-TR-84-288-V3-VOL-3 .... N86-13098 #

DOE/AL-20860/T1 .... N86-12793 #
DOE/AL-21581/T1 .... N86-12787 #

DOE/BNL-036528 .... N86-12621 #

DOE/DP-40124/53 .... N86-13161 #
DOE/DP-40124/72 .... N86-13175 #
DOE/DP-40152/T7 .... N86-13150 #
DOE/DP-40200/6 .... N86-13180 #

DOE/EP-40124/57 .... N86-13162 #

DOE/ER-03077/225 .... N86-13158 #
DOE/ER-03077/239 .... N86-13013 #
DOE/ER-03077/246 .... N86-13042 #
DOE/ER-03077/249 .... N86-13045 #
DOE/ER-04380/T2 .... N86-12279 #
DOE/ER-04939/T2 .... N86-12283 #
DOE/ER-05940/T1 .... N86-13113 #
DOE/ER-10603/T3 .... N86-12309 #
DOE/ER-10820/T1 .... N86-12280 #
DOE/ER-10951/T1 .... N86-12253 #
DOE/ER-10956/18 .... N86-13198 #
DOE/ER-10982/5 .... N86-12274 #
DOE/ER-13122/T1 .... N86-13002 #
DOE/ER-13122/2 .... N86-13003 #
DOE/ER-13163/7 .... N86-12613 #
DOE/ER-40048/10-N5 .... N86-13114 #
DOE/ER-45093/T1 .... N86-12327 #
DOE/ER-45131/T1 .... N86-12575 #

DOE/ET-11292/1893-VOL-1 .... N86-12779 #
DOE/ET-26106-26 .... N86-12782 #
DOE/ET-28407/T6 .... N86-12747 #
DOE/ET-51013/149 .... N86-13170 #
DOE/ET-53051/83 .... N86-13165 #
DOE/ET-53051/84 .... N86-13179 #
DOE/ET-53088/185 .... N86-13217 #
DOE/ET-53088/186 .... N86-13172 #
DOE/ET-53088/189 .... N86-13218 #
DOE/ET-53088/193 .... N86-13171 #

DOE/EV-03944/20 .... N86-12798 #
DOE/EV-10429/T2 .... N86-12901 #

DOE/JPL-ET-23197 .... N86-12312 #

DOE/JPL-1012-111 .... N86-12759* #
DOE/JPL-95452727/84 .... N86-12786* #

DOE/MC-20107/T3 .... N86-13061 #

DOE/NASA-0241-15 .... N86-12757* #
DOE/NASA-0241-17 .... N86-12758* #
DOE/NASA-1006/7 .... N86-13236* #

DOE/NV-10185/1 .... N86-12902 #

DOE/PC-40022/T3 .... N86-12573 #
DOE/PC-40771/T4 .... N86-12278 #
DOE/PC-70753/T3 .... N86-12276 #

DP-MS-84-126 .... N86-12265 #

DRIC-BR-96368 .... N86-12583 #
DRIC-BR-96422 .... N86-13060 #

DTNSRDC/SPD-1139-01-REV .... N86-12209 #

E-2575 .... N86-12295* #
E-2578 .... N86-12609* #
E-2669 .... N86-12268* #
E-2714 .... N86-12311* #
E-2724 .... N86-12292* #
E-2730 .... N86-12256* #
E-2745 .... N86-12246* #
E-2753 .... N86-12509* #
E-2755 .... N86-12485* #
E-2769 .... N86-12293* #
E-2770 .... N86-12310* #
E-2775 .... N86-12239* #
E-2778 .... N86-12294* #
E-2783 .... N86-13236* #
E-2793 .... N86-12227* #

ECON-80-111 .... N86-13221* #
ECON-81-110 .... N86-12243* #
ECON-84-101 .... N86-13230* #

EGG-M-07685 .... N86-13043 #
EGG-M-09185 .... N86-13206 #
EGG-M-13484 .... N86-13099 #
EGG-M-20684 .... N86-13118 #

EPA-600/D-85-111 .... N86-12804 #
EPA-600/D-85/094 .... N86-12906 #
EPA-600/D-85/097 .... N86-12933 #
EPA-600/2-85/057 .... N86-12806 #

EPA/600/D-85/077 .... N86-12751 #
EPA/600/D-85/113 .... N86-12809 #
EPA/908/2-84/001 .... N86-12749 #

EP1/600/4-85/031 .... N86-12805 #

ERL-0331-TM .... N86-13129 #

ESD-TR-85-149-REV-1 .... N86-12990 #

ESN-39-8 .... N86-13237 #

E86-10003 .... N86-12739* #
E86-10004 .... N86-12740* #
E86-10005 .... N86-12741* #
E86-10006 .... N86-12742* #

FAA-APO-85-7 .... N86-13051 #

FAA-ARP-11 .... N86-12241 #
FAA-ARP-85-1 .... N86-12241 #

FAA-PM-85-09 .... N86-12920 #

FAA/CT-85/23 .... N86-12214 #

FHWA/NJ-85/004 .... N86-13063 #

FNAL-TM-1328 .... N86-13101 #

FNAL/C-85/18-T .... N86-13080 #
FNAL/C-85/59 .... N86-13085 #
FNAL/C-85/63 .... N86-13147 #
FNAL/C-85/84 .... N86-13097 #

FPL-456 .... N86-12389 #

FR2213U/4577 .... N86-13026 #

FTD-ID(RS)T-0160-85 .... N86-13190 #
FTD-ID(RS)T-0938-84 .... N86-12269 #
FTD-ID(RS)T-1323-84 .... N86-12271 #
FTD-ID(RS)T-1326-84 .... N86-12495 #
FTD-ID(RS)T-1355-84 .... N86-13194 #
FTD-ID(RS)T-1356-84 .... N86-12516 #
FTD-ID(RS)T-1564-84 .... N86-12601 #

GA-A-17940 .... N86-13116 #

GAO/NSIAD-85-94 .... N86-12224 #

GAO/RCED-85-24 .... N86-12215 #

GPO-43-660 .... N86-13233 #
GPO-54-494 .... N86-13231 #

GRI-85/0003 N86-12289 #
GRI-85/0051 N86-12288 #
GRI-85/0065 N86-12290 #

H-REPT-99-363 N86-13231 #

HAC-FR-84-16-881-REV-A N86-12619 #

HEDL-SA-3214-FP N86-13008 #

HL-85-26 N86-13057* #

HLSB-85 N86-12748 #

HPP-84-44 N86-13052 #

IA-UR-85-2220 N86-12249 #

ICASE-85-40 N86-12550* #

IDA-M-81 N86-12262 #

IDA/HQ-85-29831 N86-12262 #

IFSR-185 N86-13217 #
IFSR-186 N86-13172 #
IFSR-189 N86-13218 #
IFSR-193 N86-13171 #

IL/ENR/RE-85/02 N86-12750 #

IR-2 N86-12360 #

IS-M-538 N86-12307 #
IS-M-553 N86-13211 #

ISI-48 N86-12218* #

ISR-1 N86-12924 #

ISSN-0067-0340 N86-12908* #
ISSN-0385-771-9 N86-12383 #
ISSN-0388-9653 N86-12909 #
ISSN-0389-617-X N86-12372 #

ITR-2 N86-12554 #

IU-CERL-RR-85-1-ONR N86-12972 #

JPL-PUB-85-61 N86-12919* #
JPL-PUB-85-73 N86-12759* #

JPL-0950-1160 N86-12312 #

JPRS-CST-85-016 N86-12393 #
JPRS-CST-85-017 N86-12408 #
JPRS-CST-85-018 N86-12413 #
JPRS-CST-85-019 N86-12966 #
JPRS-CST-85-021 N86-12421 #
JPRS-CST-85-022 N86-12439 #
JPRS-CST-85-024 N86-12368 #
JPRS-CST-85-025 N86-12444 #
JPRS-CST-85-026 N86-12459 #
JPRS-CST-85-029 N86-12446 #
JPRS-CST-85-030 N86-12451 #
JPRS-CST-85-032 N86-12462 #
JPRS-CST-85-034 N86-12430 #
JPRS-CST-85-035 N86-12399 #

JPRS-UES-85-006 N86-12630 #
JPRS-UES-85-008 N86-12697 #

K-TRANS-297 N86-12323 #

KMSF-U-1567 N86-13150 #

K506-1 N86-12625 #

L-15955 N86-12579* #
L-15969 N86-12259* #
L-15997 N86-13056* #
L-16015 N86-12508* #
L-16022 N86-13064* #

LA-UR-85-494 N86-13050 #
LA-UR-85-1007 N86-13107 #
LA-UR-85-1527 N86-13083 #
LA-UR-85-1546 N86-13081 #
LA-UR-85-1588 N86-12529 #
LA-UR-85-1598 N86-13078 #
LA-UR-85-1608 N86-12532 #
LA-UR-85-1609 N86-13087 #
LA-UR-85-1621 N86-13084 #
LA-UR-85-1625 N86-13082 #
LA-UR-85-1646 N86-13204 #
LA-UR-85-1733 N86-12986 #
LA-UR-85-1757 N86-13019 #
LA-UR-85-1777 N86-13106 #
LA-UR-85-1834 N86-13152 #
LA-UR-85-1891 N86-12527 #
LA-UR-85-1935 N86-12284 #
LA-UR-85-1957 N86-12285 #
LA-UR-85-1961 N86-13148 #
LA-UR-85-2021 N86-12519 #
LA-UR-85-2040 N86-13177 #
LA-UR-85-2062 N86-13134 #
LA-UR-85-2070 N86-12588 #
LA-UR-85-2075 N86-13090 #
LA-UR-85-2078 N86-12535 #
LA-UR-85-2092 N86-12904 #
LA-UR-85-2157 N86-13135 #
LA-UR-85-2174 N86-13141 #
LA-UR-85-2177 N86-12608 #
LA-UR-85-2190 N86-13062 #
LA-UR-85-2272 N86-13173 #
LA-UR-85-2362 N86-12589 #
LA-UR-85-2368 N86-12951 #
LA-UR-85-2373 N86-12998 #
LA-UR-85-2479 N86-12594 #
LA-UR-85-2683 N86-13199 #
LA-UR-85-3064 N86-13200 #
LA-UR-85-3112 N86-13102 #

LA-74-85-1596 N86-13145 #
LA-74-85-2035 N86-13017 #
LA-10395-MS N86-13110 #
LA-10404-MS N86-13167 #
LA-10420-MS N86-12368 #
LA-10432-MS N86-12985 #

LAIR-IR-200 N86-12960 #

LARS-TR-071584 N86-12741* #

LBL-18384 N86-12952 #
LBL-18711 N86-13079 #
LBL-18797 N86-13074 #
LBL-18939 N86-13092 #
LBL-18961 N86-13095 #
LBL-18964 N86-13196 #
LBL-18965 N86-13176 #
LBL-19011 N86-13174 #
LBL-19084 N86-12578 #
LBL-19291 N86-12282 #
LBL-19302 N86-12903 #
LBL-19579 N86-13054 #
LBL-19583 N86-13076 #
LBL-19593 N86-13093 #
LBL-19671 N86-13214 #
LBL-19755 N86-12521 #
LBL-19827 N86-13072 #

LC-84-600270 N86-12286 #

LHNCBC-85-1 N86-12987 #

LPI-TR-85-03 N86-13282* #

M-502 N86-13239* #

MAP-HANDBOOK-16 N86-12814* #
MAP-HANDBOOK-17 N86-12837* #

MIT/LCS/TR-339 N86-12979 #

MLM-3254 N86-12797 #
MLM-3267 N86-12326 #

MRC-TSR-2814 N86-12558 #
MRC-TSR-2819 N86-13034 #
MRC-TSR-2820 N86-13038 #
MRC-TSR-2824 N86-13037 #
MRC-TSR-2826 N86-13035 #
MRC-TSR-2828 N86-13036 #
MRC-TSR-2829 N86-13032 #
MRC-TSR-2832 N86-13039 #
MRC-TSR-2833 N86-13033 #

MRI/SOL-0101 N86-12756 #

MRL-R-959 N86-12620 #

MSC-TN-11 N86-12909 #

MTR-8707-REV-1 N86-12990 #

NADC-84096-60 N86-12298 #
NADC-84162-60 N86-12213 #

NAS 1.15:85705 N86-12206* #
NAS 1.15:86430 N86-12259* #
NAS 1.15:86525 N86-12917* #
NAS 1.15:86777 N86-12207* #
NAS 1.15:86834 N86-12956* #
NAS 1.15:87113 N86-12311* #
NAS 1.15:87117 N86-12292* #
NAS 1.15:87122 N86-12256* #
NAS 1.15:87136 N86-12509* #
NAS 1.15:87137 N86-12485* #
NAS 1.15:87139 N86-12246* #
NAS 1.15:87142 N86-12293* #
NAS 1.15:87143 N86-12310* #
NAS 1.15:87150 N86-12294* #
NAS 1.15:87155 N86-12268* #
NAS 1.15:87156 N86-13236* #
NAS 1.15:87161 N86-12227* #
NAS 1.15:87416 N86-12239* #
NAS 1.15:87510 N86-12313* #
NAS 1.15:87514 N86-13224* #
NAS 1.15:87590 N86-12508* #
NAS 1.15:88178 N86-13225* #
NAS 1.21:7011(276) N86-12954*
NAS 1.21:7041(46) N86-12738*
NAS 1.26:3805 N86-12208* #
NAS 1.26:3806 N86-12202* #
NAS 1.26:3919 N86-12203* #
NAS 1.26:3922(02) N86-12949* #
NAS 1.26:3933 N86-12218* #
NAS 1.26:3944 N86-12212* #
NAS 1.26:3945 N86-12918* #
NAS 1.26:170925 N86-13187* #
NAS 1.26:171074 N86-12742* #
NAS 1.26:171895 N86-12741* #
NAS 1.26:172240 N86-12743* #
NAS 1.26:174253 N86-13028* #
NAS 1.26:174407 N86-12906* #
NAS 1.26:174408 N86-13279* #
NAS 1.26:174826 N86-13219* #
NAS 1.26:174948 N86-12757* #
NAS 1.26:174995 N86-12226* #
NAS 1.26:174998 N86-12758* #
NAS 1.26:176164 N86-13273* #
NAS 1.26:176165 N86-13274* #
NAS 1.26:176217 N86-12759* #
NAS 1.26:176266 N86-12739* #
NAS 1.26:176267 N86-12740* #
NAS 1.26:176289 N86-13282* #
NAS 1.26:176295 N86-13057* #
NAS 1.26:176296 N86-12697 #
NAS 1.26:176297 N86-12922* #
NAS 1.26:176303 N86-13285* #
NAS 1.26:176309 N86-12257* #
NAS 1.26:176316 N86-12258* #
NAS 1.26:176320 N86-12240* #
NAS 1.26:176321 N86-12814* #
NAS 1.26:176322 N86-13235* #
NAS 1.26:176323 N86-12233* #
NAS 1.26:176324 N86-12600* #
NAS 1.26:176325 N86-13188* #
NAS 1.26:176326 N86-13138* #
NAS 1.26:176327 N86-13272* #
NAS 1.26:176328 N86-12216* #
NAS 1.26:176331 N86-12919* #
NAS 1.26:176332 N86-12478* #
NAS 1.26:176333 N86-13221* #
NAS 1.26:176334 N86-12243* #
NAS 1.26:176345 N86-12837* #
NAS 1.26:176346 N86-13230* #
NAS 1.26:176347 N86-13271* #
NAS 1.26:176348 N86-12484* #
NAS 1.26:176352 N86-12916* #
NAS 1.26:176353 N86-12220* #
NAS 1.26:176371 N86-12786* #
NAS 1.26:177966 N86-12238* #
NAS 1.26:177977 N86-12550* #
NAS 1.26:177982 N86-12205* #
NAS 1.26:177987 N86-12610* #
NAS 1.26:177989 N86-12580* #
NAS 1.26:177991 N86-12255* #
NAS 1.26:177992 N86-12204* #
NAS 1.26:178003 N86-12237* #
NAS 1.26:178536 N86-12551* #
NAS 1.55:2390 N86-12852* #
NAS 1.55:2391 N86-13239* #
NAS 1.55:2396 N86-13064* #
NAS 1.60:2471 N86-12579* #
NAS 1.60:2499 N86-12295* #
NAS 1.60:2513 N86-12609* #
NAS 1.60:2518 N86-13056* #

NASA-CASE-LAR-13220-1 N86-12547*

NASA-CP-2390 N86-12852* #
NASA-CP-2391 N86-13239* #
NASA-CP-2396 N86-13064* #

NASA-CR-3805 N86-12208* #
NASA-CR-3806 N86-12202* #

NASA-CR-3919	N86-12203* #
NASA-CR-3922(02)	N86-12949* #
NASA-CR-3933	N86-12218* #
NASA-CR-3944	N86-12212* #
NASA-CR-3945	N86-12918* #
NASA-CR-170925	N86-13187* #
NASA-CR-171074	N86-12742* #
NASA-CR-171895	N86-12741* #
NASA-CR-172240	N86-12743* #
NASA-CR-174253	N86-13028* #
NASA-CR-174407	N86-12908* #
NASA-CR-174408	N86-13279* #
NASA-CR-174826	N86-13219* #
NASA-CR-174948	N86-12757* #
NASA-CR-174995	N86-12226* #
NASA-CR-174998	N86-12758* #
NASA-CR-176164	N86-13273* #
NASA-CR-176165	N86-13274* #
NASA-CR-176217	N86-12759* #
NASA-CR-176266	N86-12739* #
NASA-CR-176267	N86-12740* #
NASA-CR-176289	N86-13262* #
NASA-CR-176295	N86-13057* #
NASA-CR-176296	N86-12897 #
NASA-CR-176297	N86-12922* #
NASA-CR-176303	N86-13285* #
NASA-CR-176309	N86-12257* #
NASA-CR-176316	N86-12258* #
NASA-CR-176320	N86-12240* #
NASA-CR-176321	N86-12814* #
NASA-CR-176322	N86-13235* #
NASA-CR-176323	N86-12233* #
NASA-CR-176324	N86-12600* #
NASA-CR-176325	N86-13188* #
NASA-CR-176326	N86-13138* #
NASA-CR-176327	N86-13272* #
NASA-CR-176328	N86-12216* #
NASA-CR-176331	N86-12919* #
NASA-CR-176332	N86-12478* #
NASA-CR-176333	N86-13221* #
NASA-CR-176334	N86-12243* #
NASA-CR-176345	N86-12837* #
NASA-CR-176346	N86-13230* #
NASA-CR-176347	N86-13271* #
NASA-CR-176348	N86-12484* #
NASA-CR-176352	N86-12916* #
NASA-CR-176353	N86-12220* #
NASA-CR-176371	N86-12786* #
NASA-CR-177966	N86-12238* #
NASA-CR-177977	N86-12550* #
NASA-CR-177982	N86-12205* #
NASA-CR-177987	N86-12610* #
NASA-CR-177989	N86-12580* #
NASA-CR-177991	N86-12255* #
NASA-CR-177992	N86-12204* #
NASA-CR-178003	N86-12237* #
NASA-CR-178536	N86-12551* #
NASA-SP-7011(276)	N86-12954*
NASA-SP-7041(46)	N86-12738*
NASA-TM-85705	N86-12206* #
NASA-TM-86430	N86-12259* #
NASA-TM-86525	N86-12917* #
NASA-TM-86777	N86-12207* #
NASA-TM-86834	N86-12956* #
NASA-TM-87113	N86-12311* #
NASA-TM-87117	N86-12292* #
NASA-TM-87122	N86-12256* #
NASA-TM-87136	N86-12509* #
NASA-TM-87137	N86-12485* #
NASA-TM-87139	N86-12246* #
NASA-TM-87142	N86-12293* #
NASA-TM-87143	N86-12310* #
NASA-TM-87150	N86-12294* #
NASA-TM-87155	N86-12268* #
NASA-TM-87156	N86-13236* #
NASA-TM-87161	N86-12227* #
NASA-TM-87416	N86-12239* #
NASA-TM-87510	N86-12313* #
NASA-TM-87514	N86-13224* #
NASA-TM-87590	N86-12508* #
NASA-TM-88178	N86-13225* #
NASA-TP-2471	N86-12579* #
NASA-TP-2499	N86-12295* #
NASA-TP-2513	N86-12609* #
NASA-TP-2518	N86-13056* #
NAUFP-202-3	N86-13219* #
NA84-0148	N86-12205* #
NBDL-84R008	N86-12989 #
NBSIR-05/3025-8	N86-13183 #

NBSIR-85/3130	N86-12291 #
NBSIR-85/3150	N86-12803 #
NBSIR-85/3165	N86-12988 #
NCAR/TN-252/STR	N86-12948 #
NCEL-TN-1724	N86-12778 #
NGS-31	N86-12905 #
NIPER-75	N86-12281 #
NOAA-NWS-ERCP-31	N86-12934 #
NOAA-NWS-ERCP-32	N86-12935 #
NOAA-TM-ERL-ARL-135	N86-12807 #
NOAA-TM-ERL-ESG-8	N86-12931 #
NOAA-TM-ERL-EST-16	N86-12929 #
NOAA-TM-ERL-WPL-123	N86-13137 #
NOAA-TM-MNFS-SEFC-153	N86-12755 #
NOAA-TM-NESDIS-AISC-2	N86-12927 #
NOAA-TM-NWS-ER-68	N86-12932 #
NOAA-TM-NWS-TDL-75	N86-12936 #
NOAA-TM-NWS-WR-189	N86-12930 #
NOAA-TR-NOS-109	N86-12905 #
NORDA-93	N86-12744 #
NPRDC-TR-85-10	N86-12971 #
NPS63-84-008	N86-12921 #
NPS63-85-001	N86-12922* #
NRL-MR-5605	N86-12492 #
NRL-MR-5623	N86-13140 #
NSWC/MP-85-58	N86-13238 #
NSWC/TR-85-98	N86-12776 #
NSWC/TR-85-120	N86-13030 #
NTIA-84-165	N86-12502 #
NTIA-85-175	N86-12501 #
NTIS/SW/MT-85/001A	N86-13021 #
NWC-TP-6563-REV-1	N86-12777 #
NWC-TP-6575-CH-1/4	N86-12210 #
NWC-TP-6618	N86-12231 #
NWC-TP-6619-PT-2	N86-12361 #
OE-85-10	N86-12557 #
ORNL-6169	N86-12321 #
ORNL-6201	N86-12953 #
ORNL/CON-162	N86-12615 #
ORNL/SUB-79/33200/18	N86-13096 #
ORNL/SUB-84-05907/1	N86-12614 #
ORNL/SUB-84-95128/2	N86-12534 #
ORNL/TM-9241	N86-13020 #
ORNL/TM-9446	N86-12596 #
ORNL/TM-9470	N86-12626 #
ORNL/TM-9531	N86-13166 #
ORNL/TM-9595	N86-13215 #
PB85-186862	N86-12931 #
PB85-187868	N86-12930 #
PB85-188274	N86-12948 #
PB85-188852	N86-12751 #
PB85-191609	N86-12752 #
PB85-192821	N86-12750 #
PB85-193266	N86-12906 #
PB85-195444	N86-12215 #
PB85-196384	N86-12749 #
PB85-196657	N86-12287 #
PB85-197002	N86-12286 #
PB85-198349	N86-12933 #
PB85-198802	N86-12905 #
PB85-198950	N86-12987 #
PB85-200012	N86-12502 #
PB85-201150	N86-12804 #
PB85-203776	N86-12618 #
PB85-203792	N86-12806 #
PB85-204261	N86-12937 #

PB85-206159	N86-12392 #
PB85-206171	N86-12805 #
PB85-208217	N86-12932 #
PB85-212306	N86-12803 #
PB85-212520	N86-12755 #
PB85-212884	N86-12936 #
PB85-212959	N86-12807 #
PB85-213346	N86-12935 #
PB85-213353	N86-12934 #
PB85-214377	N86-12809 #
PB85-214880	N86-12810 #
PB85-215994	N86-12753 #
PB85-216000	N86-12754 #
PB85-216398	N86-13137 #
PB85-217008	N86-12808 #
PB85-219624	N86-12289 #
PB85-220655	N86-12288 #
PB85-222503	N86-12224 #
PB85-225076	N86-12501 #
PB85-225225	N86-12291 #
PB85-225829	N86-12802 #
PB85-226298	N86-12290 #
PB85-226439	N86-12927 #
PB85-227106	N86-13021 #
PB85-227783	N86-12988 #
PB85-229722	N86-12928 #
PB85-230605	N86-12929 #
PB85-231157	N86-13063 #
PB85-233385	N86-12748 #
PB85-236362	N86-13183 #
PFC/CP-85-3	N86-13170 #
PNL-SA-11861	N86-12742* #
PNL-SA-12373	N86-12799 #
PNL-SA-12921	N86-12325 #
PNL-SA-13153	N86-12800 #
PNL-SA-13155	N86-12965 #
PNL-21-12756	N86-13086 #
PNL-21-13023	N86-12999 #
PR-11	N86-12560 #
PWS-5914-39	N86-12226* #
QR-1	N86-12534 #
QR-14	N86-12757* #
QR-16	N86-12758* #
R/D-2827-EN	N86-13128 #
R/D-4161-R-EN	N86-12745 #
RAC-TRS-4	N86-12515 #
RADC-TR-82-266-VOL-6	N86-12493 #
RADC-TR-85-24	N86-12496 #
RADC-TR-85-39	N86-13127 #
RADC-TR-85-66-REV-A	N86-12619 #
RADC-TR-85-80	N86-13126 #
RADC-TR-85-123	N86-12514 #
RAND/R-3121-AF	N86-12247 #
RE-681	N86-12202* #
RE-682	N86-12208* #
REPT-5-184-85	N86-13046 #
REPT-14	N86-12798 #
REPT-85-004-7799-10	N86-13063 #
REPT-85345	N86-12207* #
REPT-85406	N86-12956* #
RFP-3855	N86-12390 #
RHO-BW-CR-143P	N86-13001 #
RSL-TR-605-1	N86-12740* #
RSPA/DMT10-85/1	N86-12392 #
RSRE-MEMO-3824	N86-12583 #
S-HRG-99-221-PT-1	N86-13233 #
SACLANTCEN-SM-175	N86-12941 #
SACLANTCEN-SM-178	N86-12942 #
SACLANTCEN-SR-87	N86-12943 #
SAND-83-2269	N86-12785 #
SAND-83-2461	N86-13005 #
SAND-84-1472	N86-12982 #
SAND-84-2402C	N86-13014 #
SAND-84-2409C	N86-12531 #
SAND-84-2497C	N86-13088 #

SAND-84-2536C N86-12245 #
SAND-84-2537C N86-13144 #
SAND-84-2612C N86-12533 #
SAND-84-2646 N86-13016 #
SAND-84-7019 N86-12788 #
SAND-85-0052 N86-12522 #
SAND-85-0057C N86-12244 #
SAND-85-0082C N86-13178 #
SAND-85-0129 N86-13007 #
SAND-85-0405C N86-13209 #
SAND-85-0411C N86-12391 #
SAND-85-0415C N86-12590 #
SAND-85-0498C N86-12308 #
SAND-85-0500C N86-12324 #
SAND-85-0561 N86-13011 #
SAND-85-0592C N86-13197 #
SAND-85-0685C N86-13133 #
SAND-85-0725 N86-13010 #
SAND-85-0725C N86-13041 #
SAND-85-0791/1 N86-12794 #
SAND-85-0818C N86-12305 #
SAND-85-1073 N86-13012 #
SAND-85-1159C N86-12525 #
SAND-85-1293C N86-12524 #
SAND-85-1325C N86-13004 #
SAND-85-1338C N86-12537 #
SAND-85-1440C N86-12564 #
SAND-85-1441C N86-12536 #
SAND-85-1453C N86-13109 #
SAND-85-1460C N86-13108 #
SAND-85-1570C N86-12500 #
SAND-85-1670C N86-12595 #
SAND-85-7174C N86-13018 #
SAND-85-7195 N86-12781 #
SAND-85-8226 N86-12538 #

SAPR-10 N86-13274* #

SAR-716199-3 N86-12216* #

SASR-4 N86-13271* #

SD-TR-85-14 N86-12898 #
SD-TR-85-15 N86-13066 #
SD-TR-85-16 N86-13065 #
SD-TR-85-19 N86-13067 #
SD-TR-85-24 N86-12899 #
SD-TR-85-26 N86-12248 #

SDL-85-2424-1F N86-12580* #

SERI/CP-231-2700 N86-12364 #

SERI/SP-271-2662 N86-12790 #

SERI/STR-211-2750 N86-12780 #
SERI/STR-217-2629 N86-12211 #

SERI/TP-252-2630 N86-12577 #
SERI/TP-252-2739 N86-12791 #

SGP-TR-82 N86-12570 #

SKF-AT85D031 N86-12613 #

SR-3 N86-12491 #

SSS-R-84-6709-3-VOL-3 N86-13098 #

SU-CMR-85-3 N86-131[illegible] #

SU-SLAC-CN-301 N86-13070 #
SU-SLAC-CN-302 N86-13071 #

SU-SLAC-PUB-3495 N86-13121 #
SU-SLAC-PUB-3584 N86-13169 #
SU-SLAC-PUB-3598 N86-13151 #
SU-SLAC-PUB-3614 N86-13153 #
SU-SLAC-PUB-3615 N86-13159 #
SU-SLAC-PUB-3621 N86-13146 #
SU-SLAC-PUB-3624-REV N86-13075 #
SU-SLAC-PUB-3672 N86-13104 #
SU-SLAC-PUB-3695 N86-13103 #
SU-SLAC-PUB-3697 N86-13122 #

SU-SOL-85-7 N86-12993 #

SU-STAN-CS-85-1042 N86-13052 #

TAEG-TR-164 N86-13226 #

TDWR/R-288-VOL-1 N86-12752 #

TE-4258-5-84-VOL-1 N86-12779 #

TETRA-TR-85-015 N86-13132 #

TR-J8501 N86-12945 #

TR-2-ONR N86-12969 #
TR-3-85 N86-13059 #
TR-15 N86-12317 #
TR-27 N86-12961 #
TR-44 N86-12556 #
TR-361 N86-13048 #
TR-0084(4613)-1 N86-12899 #
TR-0084A(5940-05)-3 N86-12898 #
TR-0084A(5940-05)-10 N86-12248 #
TR-0084A(5945-05)-2 N86-13066 #
TR-0084A(5945-05)-3 N86-13065 #
TR-0084A(5945-05)-6 N86-13067 #

TVA/ONRED-AWR-85/13 N86-12801 #

U-OF-IOWA-85-7 N86-13284 #
U-OF-IOWA-85-13 N86-13283 #

UCID-20110-84 N86-12539 #
UCID-20448 N86-12605 #
UCID-20459 N86-13136 #
UCID-20470 N86-13181 #
UCID-20471 N86-13024 #
UCID-20474 N86-13160 #
UCID-20507 N86-13143 #
UCID-30200-83-6 N86-12572 #

UCRL-917-5 N86-13278 #
UCRL-15676 N86-12526 #
UCRL-50025-85-1 N86-12540 #
UCRL-90936 N86-13111 #
UCRL-91079-REV-1 N86-12569 #
UCRL-91242 N86-12628 #
UCRL-91366 N86-12263 #
UCRL-91428 N86-12322 #
UCRL-91469 N86-12592 #
UCRL-91484 N86-12565 #
UCRL-91486-REV-1 N86-12365 #
UCRL-91490 N86-12629 #
UCRL-91693 N86-13164 #
UCRL-91872 N86-12593 #
UCRL-92080 N86-12563 #
UCRL-92092 N86-13163 #
UCRL-92160 N86-12587 #
UCRL-92252 N86-13112 #
UCRL-92255 N86-12566 #
UCRL-92356 N86-12591 #
UCRL-92390 N86-13009 #
UCRL-92424 N86-12606 #
UCRL-92666 N86-13105 #
UCRL-92723 N86-13216 #
UCRL-92792 N86-13023 #
UCRL-93116 N86-12795 #

UDR-TR-85-131 N86-12220* #

UMD-DMSS-85/7 N86-13047 #

US-PATENT-APPL-SN-331091 N86-12955
US-PATENT-APPL-SN-377105 N86-12475
US-PATENT-APPL-SN-377108 N86-12476
US-PATENT-APPL-SN-389139 N86-12474
US-PATENT-APPL-SN-439493 N86-13184
US-PATENT-APPL-SN-459073 N86-12599
US-PATENT-APPL-SN-462493 N86-13124
US-PATENT-APPL-SN-484346 N86-13185
US-PATENT-APPL-SN-484810 N86-12267
US-PATENT-APPL-SN-503913 N86-13123
US-PATENT-APPL-SN-532938 N86-13186
US-PATENT-APPL-SN-542635 N86-12477
US-PATENT-APPL-SN-566352 N86-12506
US-PATENT-APPL-SN-571414 N86-12507
US-PATENT-APPL-SN-630148 N86-12612 #
US-PATENT-APPL-SN-633179 N86-12547*
US-PATENT-APPL-SN-637628 N86-12530 #
US-PATENT-APPL-SN-637629 N86-12306 #
US-PATENT-APPL-SN-645888 N86-12602 #
US-PATENT-APPL-SN-648197 N86-12277 #
US-PATENT-APPL-SN-657438 N86-12584 #
US-PATENT-APPL-SN-660778 N86-12962 #
US-PATENT-APPL-SN-714775 N86-12513 #
US-PATENT-APPL-SN-722580 N86-12581 #
US-PATENT-APPL-SN-729388 N86-12228 #
US-PATENT-APPL-SN-729725 N86-12974 #
US-PATENT-APPL-SN-729761 N86-12512 #
US-PATENT-APPL-SN-730125 N86-13125 #
US-PATENT-APPL-SN-732335 N86-12957 #
US-PATENT-APPL-SN-740115 N86-12299 #
US-PATENT-APPL-SN-740610 N86-12958 #
US-PATENT-APPL-SN-741784 N86-13191 #
US-PATENT-APPL-SN-741940 N86-12980 #
US-PATENT-APPL-SN-749038 N86-12517 #
US-PATENT-APPL-SN-749238 N86-12511 #
US-PATENT-APPL-SN-749705 N86-12318 #
US-PATENT-APPL-SN-751399 N86-12559 #
US-PATENT-APPL-SN-752767 N86-12585 #
US-PATENT-APPL-SN-752867 N86-13068 #
US-PATENT-APPL-SN-753462 N86-12232 #
US-PATENT-APPL-SN-758919 N86-12603 #

US-PATENT-CLASS-17.2-PC N86-12475
US-PATENT-CLASS-72-323 N86-12506
US-PATENT-CLASS-73-3 N86-12547*
US-PATENT-CLASS-73-603 N86-12599
US-PATENT-CLASS-73-861.07 N86-12547*
US-PATENT-CLASS-91-460 N86-12217
US-PATENT-CLASS-128-634 N86-12955
US-PATENT-CLASS-148-175 N86-13185
US-PATENT-CLASS-244-135 N86-12225
US-PATENT-CLASS-339-7 N86-12507
US-PATENT-CLASS-343-17.2-PC N86-12476
US-PATENT-CLASS-343-755 N86-12474
US-PATENT-CLASS-350-311 N86-12597
US-PATENT-CLASS-350-372 N86-13184
US-PATENT-CLASS-356-301 N86-12267
US-PATENT-CLASS-356-345 N86-13123
US-PATENT-CLASS-370-58 N86-12477
US-PATENT-CLASS-372-29 N86-12598
US-PATENT-CLASS-375-120 N86-12473
US-PATENT-CLASS-436-96 N86-13124

US-PATENT-4,504,835 N86-12474
US-PATENT-4,508,590 N86-13186
US-PATENT-4,509,522 N86-12955
US-PATENT-4,510,846 N86-12217
US-PATENT-4,511,105 N86-12225
US-PATENT-4,511,216 N86-12597
US-PATENT-4,512,660 N86-12267
US-PATENT-4,512,825 N86-13185
US-PATENT-4,513,087 N86-13124
US-PATENT-4,513,289 N86-12475
US-PATENT-4,513,422 N86-12598
US-PATENT-4,513,428 N86-12473
US-PATENT-4,514,056 N86-13184
US-PATENT-4,515,001 N86-12506
US-PATENT-4,522,495 N86-13123
US-PATENT-4,523,469 N86-12599
US-PATENT-4,524,363 N86-12476
US-PATENT-4,525,013 N86-12507
US-PATENT-4,532,625 N86-12477
US-PATENT-4,538,446 N86-12547*

USAAVSCOM-TR-85-C-18 N86-12311* #

USAFA-TR-85-2 N86-12200 #

USAFSAM-TP-85-14 N86-12959 #

USAFSAM-TR-85-30 N86-12963 #

USAVSCOM-TR-85-A-06 N86-12207* #

USGS/G-628-08 N86-12928 #
USGS/G-841-01 N86-12802 #
USGS/G-859(23) N86-12808 #
USGS/G-867(04) N86-12810 #

USGS/WDR/FL-84/3A N86-12754 #

USGS/WRD/HD-85/211 N86-12754 #
USGS/WRD/HD-85/215 N86-12753 #

USGS/WRD/MN-83/2 N86-12753 #

UWA/DME/TR-85/51 N86-12624 #

UWME-DR-501-103-1 N86-12258* #

WES/MP/EL-85-1-REV N86-12950 #

WES/MP/HL-85-2 N86-12555 #

WR-84-24 N86-12392 #

Y-2341 N86-12616 #
Y-2343 N86-12588 #
Y-2350 N86-13044 #

YALEU/CSD/RR-402 N86-12991 #

✩U.S.GOVERNMENT PRINTING OFFICE:1986-491-573/40001

FEDERAL DEPOSITORY LIBRARY PROGRAM

The Federal Depository Library Program provides Government publications to designated libraries throughout the United States. The Regional Depository Libraries listed below receive and retain at least one copy of nearly every Federal Government publication, either in printed or microfilm form, for use by the general public. These libraries provide reference services and inter-library loans; however, they are *not* sales outlets. You may wish to ask your local library to contact a Regional Depository to help you locate specific publications, or you may contact the Regional Depository yourself.

ARKANSAS STATE LIBRARY
One Capitol Mall
Little Rock, AR 72201
(501) 371-2326

AUBURN UNIV. AT MONTGOMERY LIBRARY
Documents Department
Montgomery, AL 36193
(205) 279-9110, ext. 253

UNIV. OF ALABAMA LIBRARY
Documents Dept.—Box S
University, AL 35486
(205) 348-7369

DEPT. OF LIBRARY, ARCHIVES AND PUBLIC RECORDS
Third Floor—State Cap.
1700 West Washington
Phoenix, AZ 85007
(602) 255-4121

UNIVERSITY OF ARIZONA LIB.
Government Documents Dept.
Tucson, AZ 85721
(602) 626-5233

CALIFORNIA STATE LIBRARY
Govt. Publications Section
P.O. Box 2037
Sacramento, CA 95809
(916) 322-4572

UNIV. OF COLORADO LIB.
Government Pub. Division
Campus Box 184
Boulder, CO 80309
(303) 492-8834

DENVER PUBLIC LIBRARY
Govt. Pub. Department
1357 Broadway
Denver, CO 80203
(303) 571-2131

CONNECTICUT STATE LIBRARY
Government Documents Unit
231 Capitol Avenue
Hartford, CT 06106
(203) 566-4971

UNIV. OF FLORIDA LIBRARIES
Library West
Documents Department
Gainesville, FL 32611
(904) 392-0367

UNIV. OF GEORGIA LIBRARIES
Government Reference Dept.
Athens, Ga. 30602
(404) 542-8951

UNIV. OF HAWAII LIBRARY
Govt. Documents Collection
2550 The Mall
Honolulu, HI 96822
(808) 948-8230

UNIV. OF IDAHO LIBRARY
Documents Section
Moscow, ID 83843
(208) 885-6344

ILLINOIS STATE LIBRARY
Information Services Branch
Centennial Building
Springfield, IL 62706
(217) 782-5185

INDIANA STATE LIBRARY
Serials Documents Section
140 North Senate Avenue
Indianapolis, IN 46204
(317) 232-3686

UNIV. OF IOWA LIBRARIES
Govt. Documents Department
Iowa City, IA 52242
(319) 353-3318

UNIVERSITY OF KANSAS
Doc. Collect—Spencer Lib.
Lawrence, KS 66045
(913) 864-4662

UNIV. OF KENTUCKY LIBRARIES
Govt. Pub. Department
Lexington, KY 40506
(606) 257-3139

LOUISIANA STATE UNIVERSITY
Middleton Library
Govt. Docs. Dept.
Baton Rouge, LA 70803
(504) 388-2570

LOUISIANA TECHNICAL UNIV. LIBRARY
Documents Department
Ruston, LA 71272
(318) 257-4962

UNIVERSITY OF MAINE
Raymond H. Fogler Library
Tri-State Regional Documents Depository
Orono, ME 04469
(207) 581-1680

UNIVERSITY OF MARYLAND
McKeldin Lib.—Doc. Div.
College Park, MD 20742
(301) 454-3034

BOSTON PUBLIC LIBRARY
Government Docs. Dept.
Boston, MA 02117
(617) 536-5400 ext. 226

DETROIT PUBLIC LIBRARY
Sociology Department
5201 Woodward Avenue
Detroit, MI 48202
(313) 833-1409

MICHIGAN STATE LIBRARY
P.O. Box 30007
Lansing, MI 48909
(517) 373-0640

UNIVERSITY OF MINNESOTA
Government Pubs. Division
409 Wilson Library
309 19th Avenue South
Minneapolis, MN 55455
(612) 373-7813

UNIV. OF MISSISSIPPI LIB.
Documents Department
University, MS 38677
(601) 232-5857

UNIV. OF MONTANA
Mansfield Library
Documents Division
Missoula, MT 59812
(406) 243-6700

NEBRASKA LIBRARY COMM.
Federal Documents
1420 P Street
Lincoln, NE 68508
(402) 471-2045
In cooperation with University of Nebraska-Lincoln

UNIVERSITY OF NEVADA LIB.
Govt. Pub. Department
Reno, NV 89557
(702) 784-6579

NEWARK PUBLIC LIBRARY
5 Washington Street
Newark, NJ 07101
(201) 733-7812

UNIVERSITY OF NEW MEXICO
Zimmerman Library
Government Pub. Dept.
Albuquerque, NM 87131
(505) 277-5441

NEW MEXICO STATE LIBRARY
Reference Department
325 Don Gaspar Avenue
Santa Fe, NM 87501
(505) 827-2033, ext. 22

NEW YORK STATE LIBRARY
Empire State Plaza
Albany, NY 12230
(518) 474-5563

UNIVERSITY OF NORTH CAROLINA AT CHAPEL HILL
Wilson Library
BA SS Documents Division
Chapel Hill, NC 27515
(919) 962-1321

UNIVERSITY OF NORTH DAKOTA
Chester Fritz Library
Documents Department
Grand Forks, ND 58202
(701) 777-2617, ext. 27
(In cooperation with North Dakota State Univ. Library)

STATE LIBRARY OF OHIO
Documents Department
65 South Front Street
Columbus, OH 43215
(614) 462-7051

OKLAHOMA DEPT. OF LIB.
Government Documents
200 NE 18th Street
Oklahoma City, OK 73105
(405) 521-2502

OKLAHOMA STATE UNIV. LIB.
Documents Department
Stillwater, OK 74078
(405) 624-6546

PORTLAND STATE UNIV. LIB.
Documents Department
P.O. Box 1151
Portland, OR 97207
(503) 229-3673

STATE LIBRARY OF PENN.
Government Pub. Section
P.O. Box 1601
Harrisburg, PA 17105
(717) 787-3752

TEXAS STATE LIBRARY
Public Services Department
P.O. Box 12927—Cap. Sta.
Austin, TX 78753
(512) 471-2996

TEXAS TECH UNIV. LIBRARY
Govt. Documents Department
Lubbock, TX 79409
(806) 742-2268

UTAH STATE UNIVERSITY
Merrill Library, U.M.C. 30
Logan, UT 84322
(801) 750-2682

UNIVERSITY OF VIRGINIA
Alderman Lib.—Public Doc.
Charlottesville, VA 22901
(804) 924-3133

WASHINGTON STATE LIBRARY
Documents Section
Olympia, WA 98504
(206) 753-4027

WEST VIRGINIA UNIV. LIB.
Documents Department
Morgantown, WV 26506
(304) 293-3640

MILWAUKEE PUBLIC LIBRARY
814 West Wisconsin Avenue
Milwaukee, WI 53233
(414) 278-3000

ST. HIST. LIB. OF WISCONSIN
Government Pub. Section
816 State Street
Madison, WI 53706
(608) 262-4347

WYOMING STATE LIBRARY
Supreme Ct. & Library Bld.
Cheyenne, WY 82002
(307) 777-6344

National Aeronautics and
Space Administration
Code NIT-4
Washington, D.C.
20546

Official Business

Penalty for Private Use $300

SPECIAL FOURTH-CLASS RATE
POSTAGE & FEES PAID
NASA
WASHINGTON, D.C.
PERMIT No. G 27

NASA

POSTMASTER: If Undeliverable (Section 158
Postal Manual) Do Not Return

24/4

VOLUME 24 / NUMBER 4
FEBRUARY 23, 1986
ACC. NOS. N86-13286 TO N86-14213

STAR

AN ABSTRACT JOURNAL

S & T
LD REFERENCE
C
U.S. DOCUMENTS
NEWARK PUBLIC LIBRARY

Scientific and Technical Aerospace Reports

NEWARK PUBLIC LIBRARY
MAR 5 1986
[illegible]
DEPOSITORY [illegible]

PRODUCED BY THE
SCIENTIFIC AND TECHNICAL
INFORMATION
BRANCH

NASA

READEX FICHE best copy available

NAS 1.9/4:

NATIONAL AERONAUTICS AND SPACE ADMINISTRATION

WHAT YOU CAN DO FOR *STAR*

All users of this abstract service are urged to forward reports to be considered for announcement in *STAR*. This will aid NASA in its efforts to provide the fullest possible coverage of all scientific and technical publications that might support aeronautics and space research and development. If you have prepared relevant reports (other than those that you will transmit to NASA, DoD, or DOE through the usual contract- or grant-reporting channels), please send them for consideration to the NASA Scientific and Technical Information Facility, P.O. Box 8757, B.W.I. Airport, Maryland 21240.

Reprints of journal articles, book chapters, and conference papers are also welcome. These will be considered for announcement in *STAR's* companion journal, *International Aerospace Abstracts*.

You may specify a particular source to be included in a report announcement if you wish; otherwise the report will be placed on public sale at the National Technical Information Service. Copyrighted publications will be announced but not distributed or sold.

PURCHASE OF *STAR*

The semimonthly issues are available for sale by the Superintendent of Documents, U.S. Government Printing Office, Washington, D.C. 20402.

PUBLISHED BY:

UNITED STATES GOVERNMENT
NATIONAL AERONAUTICS AND SPACE ADMINISTRATION
SCIENTIFIC AND TECHNICAL INFORMATION BRANCH

Scientific and Technical Aerospace Reports, Volume 24, is prepared by the NASA Scientific and Technical Information Facility operated for the National Aeronautics and Space Administration by RMS Associates.

The Administrator of the National Aeronautics and Space Administration has determined that the publication of this periodical is necessary in the transaction of the public business required by law of this Agency. Use of funds for printing this periodical has been approved by the Director of the Office of Management and Budget through March 22, 1988.

US ISSN 0036-8741

INTRODUCTION

Scientific and Technical Aerospace Reports (STAR) is a major component of a comprehensive National Aeronautics and Space Administration information system covering aeronautics, space, and supporting disciplines. *STAR* is issued on the 8th and 23rd of each month and announces current publications of the following types:

- NASA, NASA contractor, and NASA grantee reports
- Reports issued by other U.S. Government agencies, domestic and foreign institutions, universities, and private firms
- Translations in report form
- NASA-owned patents and patent applications
- Dissertations and theses

Cumulative index volumes are published annually.

Journal, book, and conference literature, cover-to-cover journal translations, and certain foreign dissertations are announced in a companion journal, *International Aerospace Abstracts (IAA)*, available on subscription from the American Institute of Aeronautics and Astronautics, Technical Information Service, 555 West 57th Street, 12th Floor, New York, New York 10019.

SUBJECT SCOPE

Subject scope of *STAR*, and *IAA* includes all aspects of aeronautics and space research and development, supporting basic and applied research, and applications. Aerospace aspects of earth resources, energy development, conservation, oceanography, environmental protection, urban transportation, and other topics of high national priority are also covered.

OTHER NASA PUBLICATIONS

Other NASA publications and information services are described in the publication, *The NASA Scientific and Technical Information System ... and How to Use It*, available without charge from the NASA Scientific and Technical Information Facility, P.O. Box 8757, B.W.I. Airport, Maryland 21240.

NEWARK PUBLIC LIBRARY
MAR
[illegible]
DEPOSITORY 375

HOW TO USE *STAR* SUBJECT CATEGORIES

STAR is categorized by 10 major subject divisions divided into 74 specific subject categories and one general category/division. The major subject divisions are listed in the Table of Contents, together with a note for each that defines its scope and provides any cross-references. For example:

> **AERONAUTICS**
>
> Includes aeronautics (general); aerodynamics; air transportation and safety; aircraft communications and navigation; aircraft design, testing and performance; aircraft instrumentation; aircraft propulsion and power; aircraft stability and control; and research and support facilities (air).
>
> For related information see also *Astronautics*.

Each major division is further divided into as many as nine specific categories, which are identified by category numbers.

Abstracts in *STAR* are grouped by specific category, the categories appearing in sequential order. Category breaks in the abstract section are identified by the category number and title, and a scope note. Cross-references to other categories are provided as appropriate. For example:

> **02 AERODYNAMICS**
>
> Includes aerodynamics of bodies, combinations, wings, rotors, and control surfaces; and internal flow in ducts and turbomachinery.
>
> For related information see also *34 Fluid Mechanics and Heat Transfer.*

CROSS-REFERENCES

Individual *STAR* abstracts are not ordinarily cross-referenced, except for certain conference reports or book translations that have had separate abstracts written for their component papers or chapters. Citations and abstracts of the components follow immediately after those of the parent document. When the subject content of a component differs sufficiently from the general content of the parent, a cross-reference citation also is printed at the end of the category to which it normally would have been assigned if it were independent.

DOCUMENTS ON MICROFICHE

Documents on microfiche(1) are designated by a pound sign (#) following the accession number. The pound sign is used without regard to the source or quality of the microfiche.

AVAILABILITIES

One or more sources from which a document announced in *STAR* is available to the public is given in each citation. The most commonly indicated sources and their acronyms or abbreviations are listed below. If the publication is available from a source other than those listed, the publisher and his address will be displayed on the availability line or in combination with the corporate source line.

---

(1) A microfiche is a transparent sheet of film, 105 by 148 mm in size, containing as many as 60 to 98 pages of information reduced to micro images (not to exceed 26:1 reduction).

Avail: NTIS. Sold by the National Technical Information Service. Prices for hard copy (HC) and microfiche (MF) are indicated by a price code following the letters HC or MF in the *STAR* citation. Current values for the price codes are given in the tables on page vii.

Initially distributed microfiche under the NTIS SRIM (Selected Research in Microfiche) is available at greatly reduced unit prices. For this service and for information concerning subscription to NASA printed reports, consult the NTIS Subscription Section, Springfield, Va. 22161.

NOTE ON ORDERING DOCUMENTS: When ordering NASA publications (those followed by the * symbol), use the N accession number. NASA patent applications (only the specifications are offered) should be ordered by the US-Patent-Appl-SN number. Non-NASA publications (no asterisk) should be ordered by the AD, PB, or other *report* number shown on the last line of the citation, not by the N accession number. It is also advisable to cite the title and other bibliographic identification.

Avail: SOD (or GPO). Sold by the Superintendent of Documents, U.S. Government Printing Office, in hard copy. The current price and order number are given following the availability line. (NTIS will fill microfiche requests, as indicated above, for those documents identified by a # symbol.)

Avail: NASA Public Document Rooms. Documents so indicated may be examined at or purchased from the National Aeronautics and Space Adminstration, Public Documents Room (Room 126), 600 Independence Ave., S.W., Washington, D.C. 20546, or public document rooms located at each of the NASA research centers, the NASA Space Technology Laboratories, and the NASA Pasadena Office at the Jet Propulsion Laboratory.

Avail: DOE Depository Libraries. Organizations in U.S. cities and abroad that maintain collections of Department of Energy reports, usually in microfiche form, are listed in *Energy Research Abstracts*. Services available from the DOE and its depositories are described in a booklet, *DOE Technical Information Center - Its' Functions and Services* (TID-4660), which may be obtained without charge from the DOE Technical Information Center.

Avail: Univ. Microfilms. Documents so indicated are dissertations selected from *Dissertation Abstracts* and are sold by University Microfilms as xerographic copy (HC) and microfilm. All requests should cite the author and the Order Number as they appear in the citation.

Avail: USGS. Originals of many reports from the U.S. Geological Survey, which may contain color illustrations, or otherwise may not have the quality of illustrations preserved in the microfiche or facsimile reproduction, may be examined by the public at the libraries of the USGS field offices whose addresses are listed in this Introduction. The libraries may be queried concerning the availability of specific documents and the possible utilization of local copying services, such as color reproduction.

Avail: HMSO. Publications of Her Majesty's Stationery Office are sold in the U.S. by Pendragon House, Inc. (PHI), Redwood City, California. The U.S. price (including a service and mailing charge) is given, or a conversion table may be obtained from PHI.

Avail: BLL (formerly NLL): British Library Lending Division, Boston Spa, Wetherby, Yorkshire, England. Photocopies available from this organization at the price shown. (If none is given, inquiry should be addressed to the BLL.)

Avail: Fachinformationszentrum, Karlsruhe. Sold by the Fachinformationszentrum Energie, Physik, Mathematik GMBH, Eggenstein Leopoldshafen, Federal Republic of Germany, at the price shown in deutschmarks (DM).

Avail: Issuing Activity, or Corporate Author, or no indication of availability. Inquiries as to the availability of these documents should be addressed to the organization shown in the citation as the corporate author of the document.

Avail: U.S. Patent and Trademark Office. Sold by Commissioner of Patents and Trademarks, U.S. Patent and Trademark Office, at the standard price of 50 cents each, postage free. (See discussion of patents and patent applications below.)

Avail: ESDU. Pricing information on specific data, computer programs, and details on ESDU topic categories can be obtained from ESDU International Ltd. Requesters in North America should use the Virginia address while all other requesters should use the London address, both of which are on page vi.

NASA PATENTS AND PATENT APPLICATIONS

Patents and patent applications owned by NASA are announced in *STAR* under appropriate subject categories and are referenced in the *STAR* indexes. In the Report/Accession Number Index, patents are indexed by the NASA Case Number (which appears in lieu of the report number in other indexes), the U.S. Patent Number, the U.S. Patent Application Serial Number, and the U.S. Patent Class. Patent applications for which patents have not yet been issued are indexed by the NASA Case Number and the U.S. Patent Application Serial Number.

NASA *patent application specifications* are sold in paper copy by the National Technical Information Service at price code A02 ($9.95 domestic; $19.90 foreign). Microfiche are sold at price code A01 ($5.95 domestic; $11.90 foreign). The US-Patent-Appl-SN- number should be used in ordering either paper copy or microfiche from NTIS. Printed copies of *patents* (which are not microfiched) are available for purchase at 50 cents per copy from:

Commissioner of Patents and Trademarks
U.S. Patent and Trademark Office
Washington, D.C. 20231

When ordering patents, the U.S. Patent Number should be used, and payment must be remitted in advance, preferably by money order or check payable to the Commissioner of Patents and Trademarks. Prepaid purchase coupons for ordering are also available from the Patent and Trademark Office. The patents and patent applications announced in *STAR* are owned by NASA and are available for royalty-free licensing. Requests for licensing terms and further information should be addressed to:

Assistant General Counsel for Patent Matters/Code GP-1
National Aeronautics and Space Administration
Washington, D.C. 20546

ELIGIBILITY AND REGISTRATION FOR NASA INFORMATION PRODUCTS AND SERVICES

A variety of services is available to organizations of the following types that have registered with NASA to receive specific services or products:

1. NASA offices, research centers, contractors, subcontractors, grantees, and consultants;
2. Other U.S. Government agencies and their contractors;
3. Libraries in the United States that have arrangements with NASA to maintain collections of NASA documents for public reference;
4. Other organizations in the United States having a need for NASA documents in work related to aeronautics and space research;
5. Organizations abroad that have established reciprocal document exchange arrangements with NASA.

Only the central service points or central points of document acquisition and control within qualified organizations are eligible to register for NASA products and services. Domestic organizations that may be eligible to receive various classes of NASA publications and services should address their requests for registration or for further information to:

NASA Scientific and Technical Information Facility
ATTN: Registration Activity
P.O. Box 8757
B.W.I. Airport, Maryland 21240

Organizations abroad should direct requests to the same address, but to the attention of: International Exchange Program.

AVAILABILITY OF *STAR* ABSTRACTS ON MICROFICHE

Microfiche of the abstract sections of this issue and other issues of *STAR* are available on annual subscription from NTIS, Attn: Subscriptions, 5285 Port Royal Road, Springfield, Virginia 22161. Annual subscription rates are $70.00 North America; $140.00 foreign. Abstract sections for previous years retroactive to 1964 are available at the current rates. Microfiche for individual *STAR* issue abstract sections are not available.

PUBLIC COLLECTIONS OF NASA DOCUMENTS

DOMESTIC: NASA and NASA-sponsored documents and a large number of aerospace publications are available to the public for reference purposes at the library maintained by the American Institute of Aeronautics and Astronautics, Technical Information Service, 555 West 57th Street, 12th Floor, New York, New York 10019.

EUROPEAN: An extensive collection of NASA and NASA-sponsored publications is maintained by the British Library Lending Division, Boston Spa, Wetherby, Yorkshire, England for public access. The British Library Lending Division also has available many of the non-NASA publications cited in *STAR*. European requesters may purchase facsimile copy or microfiche of NASA and NASA-sponsored documents, those identified by both the symbols # and * from ESA - Information Retrieval Service European Space Agency, 8-10 rue Mario-Nikis, 75738 Paris CEDEX 15, France.

FEDERAL DEPOSITORY LIBRARY PROGRAM

In order to provide the general public with greater access to U.S. Government publications, Congress established the Federal Depository Library Program under the Government Printing Office (GPO), with 50 regional depositories responsible for permanent retention of material, inter-library loan, and reference services. Over 1,300 other depositories also exist. A list of the regional GPO libraries appears on the inside back cover of *STAR*.

ADDRESSES OF ORGANIZATIONS

American Institute of Aeronautics and Astronautics
Technical Information Service
555 West 57th Street, 12th Floor
New York, New York 10019

British Library Lending Division,
Boston Spa, Wetherby, Yorkshire,
England

Commissioner of Patents and Trademarks
U.S. Patent and Trademark Office
Washington, D.C. 20231

Department of Energy
Technical Information Center
P.O. Box 62
Oak Ridge, Tennessee 37830

ESA-Information Retrieval Service
ESRIN
Via Galileo Galilei
00044 Frascati (Rome) Italy

ESDU International, Ltd.
1495 Chain Bridge Road
McLean, Virginia 22101

ESDU International, Ltd.
251-259 Regent Street
London, W1R 7AD, England

Fachinformationszentrum Energie, Physik, Mathematik GMBH
7514 Eggenstein Leopoldshafen
Federal Republic of Germany

Her Majesty's Stationery Office
P.O. Box 569, S.E. 1
London, England

NASA Scientific and Technical Information Facility
P.O. Box 8757
B.W.I. Airport, Maryland 21240

National Aeronautics and Space Administration
Scientific and Technical Information Branch (NIT-1)
Washington, D.C. 20546

National Technical Information Service
5285 Port Royal Road
Springfield, Virginia 22161

Pendragon House, Inc.
899 Broadway Avenue
Redwood City, California 94063

Superintendent of Documents
U.S. Government Printing Office
Washington, D.C. 20402

University Microfilms
A Xerox Company
300 North Zeeb Road
Ann Arbor, Michigan 48106

University Microfilms, Ltd.
Tylers Green
London, England

U.S. Geological Survey Library
National Center – MS 950
12201 Sunrise Valley Drive
Reston, Virginia 22092

U.S. Geological Survey Library
2255 North Gemini Drive
Flagstaff, Arizona 86001

U.S. Geological Survey
345 Middlefield Road
Menlo Park, California 94025

U.S. Geological Survey Library
Box 25046
Denver Federal Center, MS 914
Denver, Colorado 80225

NTIS PRICE SCHEDULES

(Effective October 1, 1985)

Schedule A
STANDARD PRICE DOCUMENTS AND MICROFICHE

PRICE CODE	PAGE RANGE	NORTH AMERICAN PRICE	FOREIGN PRICE
A01	Microfiche	$ 5.95	$11.90
A02-A03	001-050	9.95	19.90
A04-A05	051-100	11.95	23.90
A06-A09	101-200	16.95	33.90
A10-A13	201-300	22.95	45.90
A14-A17	301-400	28.95	57.90
A18-A21	401-500	34.95	69.90
A22-A25	501-600	40.95	81.90
A99	601-up	*	*
NO1		$40.00	70.00
NO2		40.00	70.00

Schedule E
EXCEPTION PRICE DOCUMENTS AND MICROFICHE

PRICE CODE	NORTH AMERICAN PRICE	FOREIGN PRICE
E01	$ 7.50	15.00
E02	10.00	20.00
E03	11.00	22.00
E04	13.50	27.00
E05	15.50	31.00
E06	18.00	36.00
E07	20.50	41.00
E08	23.00	46.00
E09	25.50	51.00
E10	28.00	56.00
E11	30.50	61.00
E12	33.00	66.00
E13	35.50	71.00
E14	38.50	77.00
E15	42.00	84.00
E16	46.00	92.00
E17	50.00	100.00
E18	54.00	108.00
E19	60.00	120.00
E20	70.00	140.00
E99	*	*

*Contact NTIS for price quote.

IMPORTANT NOTICE

NTIS Shipping and Handling Charges (effective June 1, 1985)
U.S., Canada, Mexico — ADD $3.00 per TOTAL ORDER
All Other Countries — ADD $4.00 per TOTAL ORDER

Exceptions — Does NOT apply to:
ORDERS REQUESTING NTIS RUSH HANDLING
ORDERS FOR SUBSCRIPTION OR STANDING ORDER PRODUCTS *ONLY*

NOTE: Each additional delivery address on an order
requires a separate shipping and handling charge.

VOLUME 24 NUMBER 4 / FEBRUARY 23, 1986

TABLE OF CONTENTS

AERONAUTICS

Includes aeronautics (general); aerodynamics; air transportation and safety; aircraft communications and navigation; aircraft design, testing and performance; aircraft instrumentation; aircraft propulsion and power; aircraft stability and control; and research and support facilities (air).

For related information see also *Astronautics*.

01 AERONAUTICS (GENERAL) 547

02 AERODYNAMICS 547

Includes aerodynamics of bodies, combinations, wings, rotors, and control surfaces; and internal flow in ducts and turbomachinery.

For related information see also *34 Fluid Mechanics and Heat Transfer*

03 AIR TRANSPORTATION AND SAFETY 550

Includes passenger and cargo air transport operations; and aircraft accidents.

For related information see also *16 Space Transportation* and *85 Urban Technology and Transportation*.

04 AIRCRAFT COMMUNICATIONS AND NAVIGATION 551

Includes digital and voice communication with aircraft; air navigation systems (satellite and ground based); and air traffic control.

For related information see also *17 Spacecraft Communications, Command and Tracking* and *32 Communications*.

05 AIRCRAFT DESIGN, TESTING AND PERFORMANCE 552

Includes aircraft simulation technology.

For related information see also *18 Spacecraft Design, Testing and Performance* and *39 Structural Mechanics*.

06 AIRCRAFT INSTRUMENTATION N.A.

Includes cockpit and cabin display devices; and flight instruments.

For related information see also *19 Spacecraft Instrumentation* and *35 Instrumentation and Photography*.

07 AIRCRAFT PROPULSION AND POWER 554

Includes prime propulsion systems and systems components, e.g., gas turbine engines and compressors; and on-board auxiliary power plants for aircraft.

For related information see also *20 Spacecraft Propulsion and Power*, *28 Propellants and Fuels*, and *44 Energy Production and Conversion*.

08 AIRCRAFT STABILITY AND CONTROL 555

Includes aircraft handling qualities; piloting; flight controls; and autopilots.

09 RESEARCH AND SUPPORT FACILITIES (AIR) 555

Includes airports, hangars and runways; aircraft repair and overhaul facilities; wind tunnels; shock tube facilities; and engine test blocks.

For related information see also *14 Ground Support Systems and Facilities (Space)*.

ASTRONAUTICS

Includes astronautics (general); astrodynamics; ground support systems and facilities (space); launch vehicles and space vehicles; space transportation; spacecraft communications, command and tracking; spacecraft design, testing and performance; spacecraft instrumentation; and spacecraft propulsion and power.

For related information see also *Aeronautics*

12 ASTRONAUTICS (GENERAL) 556

For extraterrestrial exploration see *91 Lunar and Planetary Exploration*.

13 ASTRODYNAMICS 557

Includes powered and free-flight trajectories; and orbit and launching dynamics.

14 GROUND SUPPORT SYSTEMS AND FACILITIES (SPACE) 557

Includes launch complexes, research and production facilities; ground support equipment, e.g., mobile transporters; and simulators.

For related information see also *09 Research and Support Facilities (Air)*.

15 LAUNCH VEHICLES AND SPACE VEHICLES 557

Includes boosters; manned orbital laboratories; reusable vehicles; and space stations.

16 SPACE TRANSPORTATION 558

Includes passenger and cargo space transportation, e.g., shuttle operations; and rescue techniques.

For related information see also *03 Air Transportation and Safety* and *85 Urban Technology and Transportation*.

17 SPACECRAFT COMMUNICATION, COMMAND AND TRACKING 558

Includes telemetry; space communications networks; astronavigation; and radio blackout.

For related information see also *04 Aircraft Communications and Navigation* and *32 Communications*.

18 SPACECRAFT DESIGN, TESTING AND PERFORMANCE 559

Includes spacecraft thermal and environmental control; and attitude control.

For life support systems see *54 Man/System Technology and Life Support*. For related information see also *05 Aircraft Design, Testing and Performance* and *39 Structural Mechanics*.

19 SPACECRAFT INSTRUMENTATION 562

For related information see also *06 Aircraft Instrumentation* and *35 Instrumentation and Photography*.

20 SPACECRAFT PROPULSION AND POWER 562

Includes main propulsion systems and components, e.g., rocket engines; and spacecraft auxiliary power sources.

For related information see also *07 Aircraft Propulsion and Power*, *28 Propellants and Fuels*, and *44 Energy Production and Conversion*.

CHEMISTRY AND MATERIALS

Includes chemistry and materials (general); composite materials; inorganic and physical chemistry; metallic materials; nonmetallic materials; and propellants and fuels.

23 CHEMISTRY AND MATERIALS (GENERAL) 563

Includes biochemistry and organic chemistry.

24 COMPOSITE MATERIALS 564

Includes laminates.

25 INORGANIC AND PHYSICAL CHEMISTRY 566

Includes chemical analysis, e.g., chromatography; combustion theory; electrochemistry; and photochemistry.

For related information see also *77 Thermodynamics and Statistical Physics.*

26 METALLIC MATERIALS 569

Includes physical, chemical, and mechanical properties of metals, e.g., corrosion; and metallurgy.

27 NONMETALLIC MATERIALS 584

Includes physical, chemical, and mechanical properties of plastics, elastomers, lubricants, polymers, textiles, adhesives, and ceramic materials.

28 PROPELLANTS AND FUELS 586

Includes rocket propellants, igniters, and oxidizers; storage and handling; and aircraft fuels.

For related information see also *07 Aircraft Propulsion and Power, 20 Spacecraft Propulsion and Power,* and *44 Energy Production and Conversion.*

ENGINEERING

Includes engineering (general); communications; electronics and electrical engineering; fluid mechanics and heat transfer; instrumentation and photography; lasers and masers; mechanical engineering; quality assurance and reliability; and structural mechanics.

For related information see also *Physics.*

31 ENGINEERING (GENERAL) 600

Includes vacuum technology; control engineering; display engineering; and cryogenics.

32 COMMUNICATIONS 605

Includes land and global communications; communications theory; and optical communications.

For related information see also *04 Aircraft Communications and Navigation* and *17 Spacecraft Communications, Command and Tracking.*

33 ELECTRONICS AND ELECTRICAL ENGINEERING 608

Includes test equipment and maintainability; components, e.g., tunnel diodes and transistors; microminiaturization; and integrated circuity.

For related information see also *60 Computer Operations and Hardware* and *76 Solid-State Physics.*

34 FLUID MECHANICS AND HEAT TRANSFER 612

Includes boundary layers; hydrodynamics; fluidics; mass transfer; and ablation cooling.

For related information see also *02 Aerodynamics* and *77 Thermodynamics and Statistical Physics.*

35 INSTRUMENTATION AND PHOTOGRAPHY 619

Includes remote sensors; measuring instruments and gages; detectors; cameras and photographic supplies; and holography.

For aerial photography see *43 Earth Resources.* For related information see also *06 Aircraft Instrumentation* and *19 Spacecraft Instrumentation.*

36 LASERS AND MASERS 622

Includes parametric amplifiers.

37 MECHANICAL ENGINEERING 624

Includes auxiliary systems (non-power); machine elements and processes; and mechanical equipment.

38 QUALITY ASSURANCE AND RELIABILITY 626

Includes product sampling procedures and techniques; and quality control.

39 STRUCTURAL MECHANICS 627

Includes structural element design and weight analysis; fatigue; and thermal stress.

For applications see *05 Aircraft Design, Testing and Performance* and *18 Spacecraft Design, Testing and Performance.*

GEOSCIENCES

Includes geosciences (general); earth resources; energy production and conversion; environment pollution; geophysics; meteorology and climatology; and oceanography.

For related information see also *Space Sciences.*

42 GEOSCIENCES (GENERAL) 629

43 EARTH RESOURCES 634

Includes remote sensing of earth resources by aircraft and spacecraft; photogrammetry; and aerial photography.

For instrumentation see *35 Instrumentation and Photography.*

44 ENERGY PRODUCTION AND CONVERSION 641

Includes specific energy conversion systems, e.g., fuel cells and batteries; global sources of energy; fossil fuels; geophysical conversion; hydroelectric power; and wind power.

For related information see also *07 Aircraft Propulsion and Power, 20 Spacecraft Propulsion and Power, 28 Propellants and Fuels,* and *85 Urban Technology and Transportation.*

45 ENVIRONMENT POLLUTION 644

Includes air, noise, thermal and water pollution; environment monitoring; and contamination control.

46 GEOPHYSICS 645

Includes aeronomy; upper and lower atmosphere studies; ionospheric and magnetospheric physics; and geomagnetism.

For space radiation see *93 Space Radiation*.

47 METEOROLOGY AND CLIMATOLOGY 649

Includes weather forecasting and modification.

48 OCEANOGRAPHY 651

Includes biological, dynamic and physical oceanography; and marine resources.

LIFE SCIENCES

Includes sciences (general); aerospace medicine; behavioral sciences; man/system technology and life support; and planetary biology.

51 LIFE SCIENCES (GENERAL) 652

Includes genetics.

52 AEROSPACE MEDICINE 654

Includes physiological factors; biological effects of radiation; and weightlessness.

53 BEHAVIORAL SCIENCES 655

Includes psychological factors; individual and group behavior; crew training and evaluation; and psychiatric research.

54 MAN/SYSTEM TECHNOLOGY AND LIFE SUPPORT 656

Includes human engineering; biotechnology; and space suits and protective clothing.

55 PLANETARY BIOLOGY N.A.

Includes exobiology; and extraterrestrial life.

MATHEMATICAL AND COMPUTER SCIENCES

Includes mathematical and computer sciences (general); computer operations and hardware; computer programming and software; computer systems; cybernetics; numerical analysis; statistics and probability; systems analysis; and theoretical mathematics.

59 MATHEMATICAL AND COMPUTER SCIENCES (GENERAL) N.A.

60 COMPUTER OPERATIONS AND HARDWARE 658

Includes computer graphics and data processing.

For components see *33 Electronics and Electrical Engineering*.

61 COMPUTER PROGRAMMING AND SOFTWARE 658

Includes computer programs, routines, and algorithms.

62 COMPUTER SYSTEMS 663

Includes computer networks.

63 CYBERNETICS 664

Includes feedback and control theory.

For related information see also *54 Man/System Technology and Life Support*.

64 NUMERICAL ANALYSIS 665

Includes iteration, difference equations, and numerical approximation.

65 STATISTICS AND PROBABILITY 670

Includes data sampling and smoothing; Monte Carlo method; and stochastic processes.

66 SYSTEMS ANALYSIS 671

Includes mathematical modeling; network analysis; and operations research.

67 THEORETICAL MATHEMATICS 671

Includes topology and number theory.

PHYSICS

Includes physics (general); acoustics; atomic and molecular physics; nuclear and high-energy physics; optics; plasma physics; solid-state physics; and thermodynamics and statistical physics.

For related information see also *Engineering*.

70 PHYSICS (GENERAL) 672

For geophysics see *46 Geophysics*. For astrophysics see *90 Astrophysics*. For solar physics see *92 Solar Physics*.

71 ACOUSTICS 673

Includes sound generation, transmission, and attenuation.

For noise pollution see *45 Environment Pollution*.

72 ATOMIC AND MOLECULAR PHYSICS 674

Includes atomic structure and molecular spectra.

73 NUCLEAR AND HIGH-ENERGY PHYSICS 676

Includes elementary and nuclear particles; and reactor theory.

For space radiation see *93 Space Radiation*.

74 OPTICS 677

Includes light phenomena.

75 PLASMA PHYSICS 680

Includes magnetohydrodynamics and plasma fusion.

For ionospheric plasmas see *46 Geophysics*. For space plasmas see *90 Astrophysics*.

76 SOLID-STATE PHYSICS 685

Includes superconductivity.

For related information see also *33 Electronics and Electrical Engineering* and *36 Lasers and Masers*.

77 THERMODYNAMICS AND STATISTICAL PHYSICS N.A.

Includes quantum mechanics; and Bose and Fermi statistics.

For related information see also *25 Inorganic and Physical Chemistry* and *34 Fluid Mechanics and Heat Transfer*.

SOCIAL SCIENCES

Includes social sciences (general); administration and management; documentation and information science; economics and cost analysis; law and political science; and urban technology and transportation.

80 SOCIAL SCIENCES (GENERAL) N.A.
Includes educational matters.

81 ADMINISTRATION AND MANAGEMENT N.A.
Includes management planning and research.

82 DOCUMENTATION AND INFORMATION SCIENCE 686
Includes information storage and retrieval technology; micrography; and library science.
For computer documentation see *61 Computer Programming and Software*.

83 ECONOMICS AND COST ANALYSIS N.A.
Includes cost effectiveness studies.

84 LAW AND POLITICAL SCIENCE N.A.
Includes space law; international law; international cooperation; and patent policy.

85 URBAN TECHNOLOGY AND TRANSPORTATION 686
Includes applications of space technology to urban problems; technology transfer; technology assessment; and surface and mass transportation.
For related information see *03 Air Transportation and Safety, 16 Space Transportation*, and *44 Energy Production and Conversion*.

SPACE SCIENCES

Includes space sciences (general); astronomy; astrophysics; lunar and planetary exploration; solar physics; and space radiation.
For related information see also *Geosciences*.

88 SPACE SCIENCES (GENERAL) 691

89 ASTRONOMY 706
Includes radio and gamma-ray astronomy; celestial mechanics; and astrometry.

90 ASTROPHYSICS 707
Includes cosmology; and interstellar and interplanetary gases and dust.

91 LUNAR AND PLANETARY EXPLORATION 708
Includes planetology; and manned and unmanned flights.
For spacecraft design see *18 Spacecraft Design, Testing and Performance*. For space stations see *15 Launch Vehicles and Space Vehicles*.

92 SOLAR PHYSICS N.A.
Includes solar activity, solar flares, solar radiation and sunspots.

93 SPACE RADIATION N.A.
Includes cosmic radiation; and inner and outer earth's radiation belts.
For biological effects of radiation see *52 Aerospace Medicine*. For theory see *73 Nuclear and High-Energy Physics*.

GENERAL

99 GENERAL 710

Note: N.A. means that no abstracts were assigned to this category for this issue.

SUBJECT INDEX I-1
PERSONAL AUTHOR INDEX I-61
CORPORATE SOURCE INDEX I-69
CONTRACT NUMBER INDEX I-81
REPORT/ACCESSION NUMBER INDEX I-83

TYPICAL CITATION AND ABSTRACT

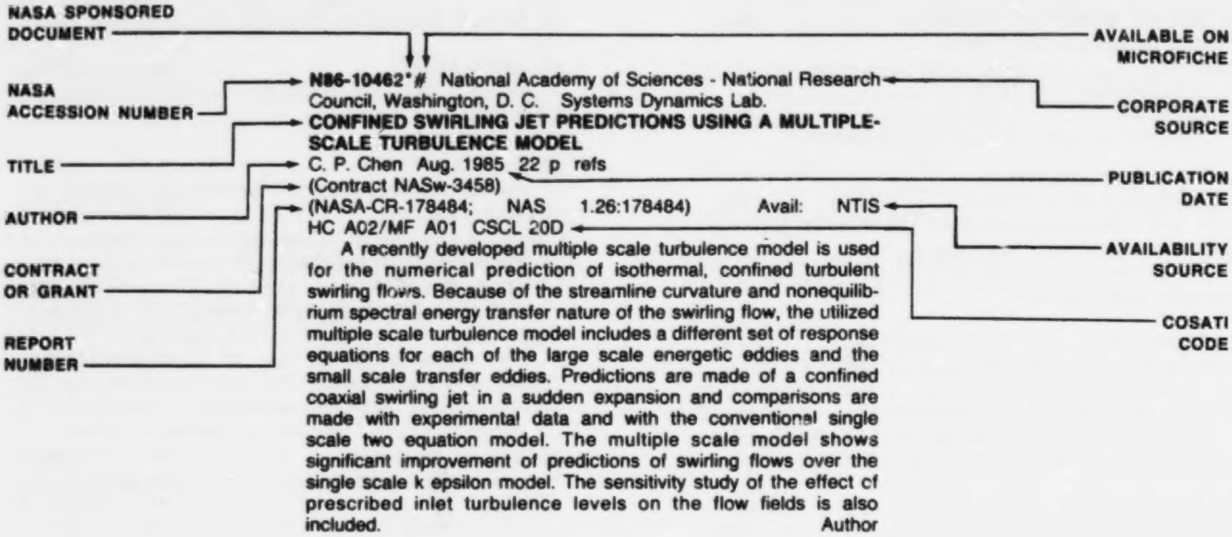
NASA SPONSORED DOCUMENT
NASA ACCESSION NUMBER
TITLE
AUTHOR
CONTRACT OR GRANT
REPORT NUMBER
AVAILABLE ON MICROFICHE
CORPORATE SOURCE
PUBLICATION DATE
AVAILABILITY SOURCE
COSATI CODE

N86-10462*# National Academy of Sciences - National Research Council, Washington, D. C. Systems Dynamics Lab.
CONFINED SWIRLING JET PREDICTIONS USING A MULTIPLE-SCALE TURBULENCE MODEL
C. P. Chen Aug. 1985 22 p refs
(Contract NASw-3458)
(NASA-CR-178484; NAS 1.26:178484) Avail: NTIS
HC A02/MF A01 CSCL 20D

A recently developed multiple scale turbulence model is used for the numerical prediction of isothermal, confined turbulent swirling flows. Because of the streamline curvature and nonequilibrium spectral energy transfer nature of the swirling flow, the utilized multiple scale turbulence model includes a different set of response equations for each of the large scale energetic eddies and the small scale transfer eddies. Predictions are made of a confined coaxial swirling jet in a sudden expansion and comparisons are made with experimental data and with the conventional single scale two equation model. The multiple scale model shows significant improvement of predictions of swirling flows over the single scale k epsilon model. The sensitivity study of the effect of prescribed inlet turbulence levels on the flow fields is also included. Author

VOLUME 24 NUMBER 4 / FEBRUARY 23, 1986

Scientific and Technical Aerospace Reports

A Semimonthly Publication of the National Aeronautics and Space Administration

01 AERONAUTICS (GENERAL)

N86-13286*# National Aeronautics and Space Administration. Ames Research Center, Moffett Field, Calif.
ASSESSMENT OF AERODYNAMIC AND DYNAMIC MODELS IN A COMPREHENSIVE ANALYSIS
Wayne Johnson Oct. 1985 39 p refs
(NASA-TM-86835; Rept-85047; NAS 1.15:86835) Avail: NTIS HC A03/MF A01 CSCL 01B

The history, status, and lessons of a comprehensive analysis for rotorcraft are reviewed. The development, features, and capabilities of the analysis are summarized, including the aerodynamic and dynamic models that were used. Examples of correlation of the computational results with experimental data are given, extensions of the analysis for research in several topics of helicopter technology are discussed, and the experiences of outside users are summarized. Finally, the required capabilities and approach for the next comprehensive analysis are described.
Author

N86-13618# Joint Publications Research Service, Arlington, Va.
ATR 42 PRODUCTION WORK IN FRENCH, ITALIAN PLANTS DETAILED
In its West Europe Rept.: Sci. and Technol. (JPRS-WST-85-031) 8 Nov. 1985 p 14-19 Repr. from Rev. Aerospatiale (France), Oct. 1985 p 16; 18; 20; 22; 27 (For primary document see N86-13616 04-31)
Avail: NTIS HC A03/MF A01

02 AERODYNAMICS

Includes aerodynamics of bodies, combinations, wings, rotors, and control surfaces; and internal flow in ducts and turbomachinery.

For related information see also *34 Fluid Mechanics and Heat Transfer.*

N86-13287*# Virginia Polytechnic Inst. and State Univ., Blacksburg. Dept. of Aerospace and Ocean Engineering.
EFFECTS OF VELOCITY PROFILE AND INCLINATION ON DUAL-JET-INDUCED PRESSURES ON A FLAT PLATE IN A CROSSWIND
A. L. Jakubowski, J. A. Schetz, C. L. Moore, and R. Joag Oct. 1985 52 p refs
(Grant NAG2-256)
(NASA-CR-177361; NAS 1.26:177361) Avail: NTIS HC A04/MF A01 CSCL 01A

An experimental study was conducted to determine surface pressure distributions on a flat plate with dual subsonic, circular jets exhausting from the surface into a crossflow. The jets were arranged in both side-by-side and tandem configurations and were injected at 90 deg and 60 deg angles to the plate, with jet-to-crossflow velocity ratio of 2.2 and 4. The major objective of the study was to determine the effect of a nonuniform (vs uniform) jet velocity profile, simulating the exhaust of a turbo-fan engine. Nonuniform jets with a high-velocity outer annulus and a low-velocity core induced stronger negative pressure fields than uniform jets with the same mass flow rate. However, nondimensional lift losses (lift loss/jet thrust lift) due to such nonuniform jets were lower than lift losses due to uniform jets. Changing the injection angle from 90 deg to 60 deg resulted in moderate (for tandem jets) to significant (for side-by-side jets) increases in the induced negative pressures, even though the surface area influenced by the jets tended to reduce as the angle decreased. Jets arranged in the side-by-side configuration led to significant jet-induced lift losses exceeding, in some cases, lift losses reported for single jets.
B.W.

N86-13288# National Aerospace Lab., Tokyo (Japan).
A METHOD FOR CALCULATING FLOW FIELDS AROUND MOVING BODIES
Sataru Ogawa and Tomiko Ishiguro May 1985 23 p refs
(NAL-TR-859T; ISSN-0389-4010) Avail: NTIS HC A02/MF A01

A new method for calculating flow fields with arbitrarily moving boundaries is proposed. Under the concept of Lie derivative, field equation moving coordinates are derived. There are several kinds of such equations; an example is one written in Viviand's conservative form. According to the formulation presented, it is natural and reasonable to consider that the computation coordinates fitted to the body move in space. This is the reverse of the usual computational procedures. The two dimensional incompressible Navier-Stokes equations in general moving coordinates are solved by a finite difference method. Using the third-order upwind scheme (Kawamura scheme), the present calculations are made for the dynamic stall process on an oscillating airfoil, and the flow generated by a moving cylinder. Consequently it is shown that the flow generated by a moving body can easily be analyzed by the present method.
Author

N86-13289*# Santa Clara Univ., Calif. Dept. of Physics.
WIND TUNNEL SIMULATIONS OF AEROLIAN PROCESSES Final Technical Report, Mar. 1980 - Nov. 1984
Ronald Greeley 31 Dec. 1984 19 p refs
(Contract NCC2-60)
(NASA-CR-176382; NAS 1.26:176382) Avail: NTIS HC A02/MF A01 CSCL 01A

The characteristics of aerolian (wind) activity as a surface modifying process on Earth, Mars, Venus, and appropriate satellites was determined. A combination of spacecraft data analysis, wind tunnel simulations, and terrestrial field analog studies were used to determine these characteristics. Wind tunnel experiments simulating Venusian surface conditions demonstrate that rolling of particles may be an important mode of transport by winds on Venus and that aerolian processes in the dense atmosphere may share attributes of both aerolian and aqueous environments on Earth.
Author

N86-13290*# Informatics General Corp., Palo Alto, Calif.
DAB USER'S GUIDE
Jeff Trosin Nov. 1985 20 p
(Contract NAS2-11555)
(NASA-CR-177393; NAS 1.26:177393; TN-85-7104-306-26) Avail: NTIS HC A02/MF A01 CSCL 01A

Use of the Display AButments (DAB) which plots PAN AIR geometries is presented. The DAB program creates hidden line displays of PAN AIR geometries and labels specified geometry components, such as abutments, networks, and network edges. It is used to alleviate the very time consuming and error prone abutment list checking phase of developing a valid PAN AIR geometry, and therefore represents a valuable tool for debugging complex PAN AIR geometry definitions. DAB is written in FORTRAN 77 and runs on a Digital Equipment Corporation VAX 11/780 under VMS. It utilizes a special color version of the SKETCH hidden line analysis routine. Author

N86-13291*# Informatics General Corp., Palo Alto, Calif.
PLTTER USER'S GUIDE
Alice Barlow, Dexter Hermstad, and Jeff Trosin Nov. 1985 64 p
(Contract NAS2-11555)
(NASA-CR-177385; NAS 1.26:177385; TN-85-7104-306-23) Avail: NTIS HC A04/MF A01 CSCL 01A

The PLTTER graphics system, which is part of CDDMS is discussed. CDDMS is a comprehensive system for data basing and subsequent plotting of data acquired during wind tunnel tests or from computational flow analyses. The PLTTER is a system which creates report-quality plots of data which is stored on a CDDMS data base. The Requests file system allows plot-controlling information to be arranged in the way which is most appropriate for any application. The PLTTER system features many capabilities which are especially useful when plotting wind tunnel data. The PLTTER offers a variety of page formats, different grid options and parametric curve fitting algorithms, and a powerful legend capability to identify relevant information about individual curves. One or more plots on a page can be suppressed if desired so that an established page format can be maintained. Final plot output may be standard Versatec plots, QMS Laser printer plots, or microfiche. E.A.K.

N86-13292*# National Aeronautics and Space Administration. Ames Research Center, Moffett Field, Calif.
ON APPLICATIONS OF CHIMERA GRID SCHEMES TO STORE SEPARATION
F. Carroll Cougherty, John A. Benek (Calspan Field Services, Arnold Air Force Station, Tenn.), and Joseph L. Steger Oct. 1985 14 p refs
(NASA-TM-88193; Rept-86045; NAS 1.15:88193) Avail: NTIS HC A02/MF A01 CSCL 01A

A finite difference scheme which uses multiple overset meshes to simulate the aerodynamics of aircraft/store interaction and store separation is described. In this chimera, or multiple mesh, scheme, a complex configuration is mapped using a major grid about the main component of the configuration, and minor overset meshes are used to map each additional component such as a store. As a first step in modeling the aerodynamics of store separation, two dimensional inviscid flow calculations were carried out in which one of the minor meshes is allowed to move with respect to the major grid. Solutions of calibrated two dimensional problems indicate that allowing one mesh to move with respect to another does not adversely affect the time accuracy of an unsteady solution. Steady, inviscid three dimensional computations demonstrate the capability to simulate complex configurations, including closely packed multiple bodies. Author

N86-13293*# Old Dominion Univ., Norfolk, Va. Dept. of Mechanical Engineering and Mechanics.
NUMERICAL SOLUTIONS OF NAVIER-STOKES EQUATIONS FOR A BUTLER WING Progress Report, 1 Jan. - 31 Aug. 1985
Jamshid S. Abolhassani and S. N. Tiwari Oct. 1985 50 p refs
(Contract NCC1-68)
(NASA-CR-174202; NAS 1.26:174202) Avail: NTIS HC A03/MF A01 CSCL 01A

The flow field is simulated on the surface of a given delta wing (Butler wing) at zero incident in a uniform stream. The simulation is done by integrating a set of flow field equations. This set of equations governs the unsteady, viscous, compressible, heat conducting flow of an ideal gas. The equations are written in curvilinear coordinates so that the wing surface is represented accurately. These equations are solved by the finite difference method, and results obtained for high-speed freestream conditions are compared with theoretical and experimental results. In this study, the Navier-Stokes equations are solved numerically. These equations are unsteady, compressible, viscous, and three-dimensional without neglecting any terms. The time dependency of the governing equations allows the solution to progress naturally for an arbitrary initial initial guess to an asymptotic steady state, if one exists. The equations are transformed from physical coordinates to the computational coordinates, allowing the solution of the governing equations in a rectangular parallel-piped domain. The equations are solved by the MacCormack time-split technique which is vectorized and programmed to run on the CDC VPS 32 computer. Author

N86-13294*# Kansas Univ. Center for Research, Inc., Lawrence. Flight Research Lab.
AN INVESTIGATION INTO THE VERTICAL AXIS CONTROL POWER REQUIREMENTS FOR LANDING VTOL TYPE AIRCRAFT ONBOARD NONAVIATION SHIPS IN VARIOUS SEA STATES
Mark E. Stevens and Jan Roskam Jul. 1985 216 p
(Contract NCC2-242)
(NASA-CR-176355; NAS 1.26:176355; KU-FRL-623-1) Avail: NTIS HC A10/MF A01 CSCL 01A

The problem of determining the vertical axis control requirements for landing a VTOL aircraft on a moving ship deck in various sea states is examined. Both a fixed-base piloted simulation and a nonpiloted simulation were used to determine the landing performance as influenced by thrust-to-weight ratio, vertical damping, and engine lags. The piloted simulation was run using a fixed-based simulator at Ames Research center. Simplified versions of an existing AV-8A Harrier model and an existing head-up display format were used. The ship model used was that of a DD963 class destroyer. Simplified linear models of the pilot, aircraft, ship motion, and ship air-wake turbulence were developed for the nonpiloted simulation. A unique aspect of the nonpiloted simulation was the development of a model of the piloting strategy used for shipboard landing. This model was refined during the piloted simulation until it provided a reasonably good representation of observed pilot behavior. B.W.

N86-13295*# National Aeronautics and Space Administration. Lewis Research Center, Cleveland, Ohio.
A FORTRAN COMPUTER CODE FOR CALCULATING FLOWS IN MULTIPLE-BLADE-ELEMENT CASCADES
Eric R. McFarland Nov. 1985 29 p refs
(NASA-TM-87104; E-2701; NAS 1.15:87104) Avail: NTIS HC A03/MF A01 CSCL 01A

A solution technique has been developed for solving the multiple-blade-element, surface-of-revolution, blade-to-blade flow problem in turbomachinery. The calculation solves approximate flow equations which include the effects of compressibility, radius change, blade-row rotation, and variable stream sheet thickness. An integral equation solution (i.e., panel method) is used to solve the equations. A description of the computer code and computer code input is given in this report. Author

N86-13296*# National Aeronautics and Space Administration. Ames Research Center, Moffett Field, Calif.
COMPUTATIONAL ASPECTS OF ZONAL ALGORITHMS FOR SOLVING THE COMPRESSIBLE NAVIER-STOKES EQUATIONS IN THREE DIMENSIONS
Terry L. Holst, Scott D. Thomas (Informatics General Corp., Palo Alto, Calif.), Unver Kaynak, Karen L. Gundy, Jolen Flores, and

Neal M. Chaderjian Oct. 1985 15 p refs
(NASA-TM-86774; Rept-85340; NAS 1.15:86774) Avail: NTIS HC A02/MF A01 CSCL 01A

Transonic flow fields about wing geometries are computed using an Euler/Navier-Stokes approach in which the flow field is divided into several zones. The flow field immediately adjacent to the wing surface is resolved with fine grid zones and solved using a Navier-Stokes algorithm. Flow field regions removed from the wing are resolved with less finely clustered grid zones and are solved with an Euler algorithm. Computational issues associated with this zonal approach, including data base management aspects, are discussed. Solutions are obtained that are in good agreement with experiment, including cases with significant wind tunnel wall effects. Additional cases with significant shock induced separation on the upper wing surface are also presented. Author

N86-13297*# National Aeronautics and Space Administration. Ames Research Center, Moffett Field, Calif.

A TOMOGRAPHIC TECHNIQUE FOR AERODYNAMICS AT TRANSONIC SPEEDS

George Lee Oct. 1985 11 p refs
(NASA-TM-86766; Rept-85318; NAS 1.15:86766) Avail: NTIS HC A02/MF A01 CSCL 01A

Computer aided tomography (CAT) provides a means of noninvasively measuring the air density distribution around an aerodynamic model. This technique is global in that a large portion of the flow field can be measured. A test of the applicability of CAT to transonic velocities was studied. A hemispherical-nose cylinder afterbody model was tested at a Mach number of 0.8 with a new laser holographic interferometer at the 2- by 2-Foot Transonic Wind Tunnel. Holograms of the flow field were taken and were reconstructed into interferograms. The fringe distribution (a measure of the local densities) was digitized for subsequent data reduction. A computer program based on the Fourier-transform technique was developed to convert the fringe distribution into three-dimensional densities around the model. Theoretical aerodynamic densities were calculated for evaluating and assessing the accuracy of the data obtained from the tomographic method. Author

N86-13298*# National Aeronautics and Space Administration. Ames Research Center, Moffett Field, Calif.

DOUBLE-BRANCHED VORTEX GENERATOR

Elizabeth R. Cantwell, Russell V. Westphal, and R. D. Mehta (Stanford Univ., Calif.) Nov. 1985 25 p refs
(NASA-TM-88201; Rept-86064; NAS 1.15:88201) Avail: NTIS HC A02/MF A01 CSCL 01A

In order to assess the suitability of using a double branched vortex generator in parametric studies involving vortex interactions, an experimental study of the main vortex and secondary flows produced by a double branched vortex generator was conducted in a 20-by-40 cm indraft wind tunnel. Measurements of the cross flow velocities were made with a five hole pressure probe from which vorticity contours and vortex parameters were derived. The results showed that the optimum configuration consisted of chord extensions with the absence of a centerbody. Author

N86-13299*# National Aeronautics and Space Administration. Ames Research Center, Moffett Field, Calif.

GROUND EFFECTS ON V/STOL AND STOL AIRCRAFT: A SURVEY

Richard E. Kuhn and James Eshleman Nov. 1985 27 p refs
(NASA-TM-86825; A-85356; NAS 1.15:86825) Avail: NTIS HC A03/MF A01 CSCL 01A

The flow fields encountered by jet- and fan-powered Vertical/Short Takeoff and Landing (V/STOL) aircraft operating in ground effect are reviewed and their general effects on the aerodynamic characteristics are discussed. The ground effects considered include: (1) the suckdown experienced by a single jet configuration in hover; (2) the fountain flow and additional suckdown experienced by multiple jet configurations in hover; (3) the ground vortex generated by jet and jet flap configurations in short takeoff and landing (STOL) operation and the associated aerodynamic and hot-gas-ingestion effects; and (4) the change in the downwash at the tail due to ground proximity. After over 30 years of research on V/STOL aircraft, the general flow phenomena are well-known and, in most areas, the effects of ground proximity can be established or can be determined experimentally. However, there are some anomalies in the current data base which are discussed. Author

N86-13300*# Texas A&M Univ., College Station. Dept. of Aerospace Engineering.

A DIRECT-INVERSE METHOD FOR TRANSONIC AND SEPARATED FLOWS ABOUT AIRFOILS Final Report

Leland A. Carlson Dec. 1985 80 p refs
(Grant NsG-1174)
(NASA-CR-176403; NAS 1.26:176403; TAMRF-3224-85-12) Avail: NTIS HC A05/MF A01 CSCL 01A

A direct-inverse technique and computer program called TAMSEP that can be sued for the analysis of the flow about airfoils at subsonic and low transonic freestream velocities is presented. The method is based upon a direct-inverse nonconservative full potential inviscid method, a Thwaites laminar boundary layer technique, and the Barnwell turbulent momentum integral scheme; and it is formulated using Cartesian coordinates. Since the method utilizes inverse boundary conditions in regions of separated flow, it is suitable for predicing the flowfield about airfoils having trailing edge separated flow under high lift conditions. Comparisons with experimental data indicate that the method should be a useful tool for applied aerodynamic analyses. Author

N86-13301# Royal Aircraft Establishment, Farnborough (England).

STUDIES OF THE FLOW FIELD NEAR A NACA 4412 AEROFOIL AT NEARLY MAXIMUM LIFT

R. C. Hastings and B. R. Williams Dec. 1984 35 p
(AD-A157750; RAE-TM-AERO-2026; DRIC-BR-96009) Avail: NTIS HC A03/MF A01 CSCL 02/4

Measurements made at a Mach number of 0.18 and a chord-based Reynolds number of 4.2 x million on a constant-chord model having a NACA 4412 aerofoil section are described and compared with the results of flow field calculations. Both the experimental arrangement and the difficulties initially experienced in achieving an adequate approximation to two-dimensional flow above the wing are briefly outlined. The measurements include static pressure distributions on the wing surface and on the wind tunnel walls above and below the mid-span section of the wing. The main emphasis in the experiment was, however, on defining the development of the upper surface boundary layer through separation (at about 20% chord ahead of the trailing-edge) and on into the wake, making extensive use of laser anemometry. The flow field calculations are the semi-inverse kind in which an inverse momentum-integral treatment of the shear flow, used to avoid difficulties at separation, is coupled to a direct solution of the inviscid flow problem. The main features of the method are outlined. GRA

N86-13302# Royal Aircraft Establishment, Bedford (England).

RECENT EXPERIENCE IN THE RAE (ROYAL AIRCRAFT ESTABLISHMENT) 5-METRE WIND TUNNEL OF A CHINA CLAY METHOD FOR INDICATING BOUNDARY LAYER TRANSITION

I. R. M. Moir Aug. 1984 11 p
(AD-A157943; RAE-TM-AERO-2007; DRIC-BR-94478) Avail: NTIS HC A02/MF A01 CSCL 14/2

The china clay method is based on the differential rate of evaporation, beneath laminar and turbulent boundary layers, of a liquid absorbed on a solid spread on the surface. The liquid is chosen to have a similar refractive index to the solid so that the mixture appears to be transparent until evaporation has taken place, when the color of the solid becomes visible. The solid layer consists of china clay powder mixture with certain chemicals to form a lacquer, which is sprayed onto the surface. When dry, this forms a semi-permanent white absorbent film. A suitable liquid sprayed on to this film is absorbed by it, causing it to become transparent. Details of a visual method for indicating boundary layer transition are given, with particular reference to tests at high Reynolds number in the RAE 5-meter pressurized low-speed wind tunnel on a slender-body model. The method is compared with other techniques on the basis of ease of use and quality of the indication. GRA

N86-13303# Institut de Mecanique des Fluides de Lille (France).
STUDY OF THE INFLUENCE OF AN OSCILLATING SPOILER ON THE SURROUNDING AERODYNAMIC FIELD [ETUDE DE L'INFLUENCE D'UNE PROTUBERANCE DE PAROI OSCILLANTE SUR LE CHAMP AERODYNAMIQUE ENVIRONNANT]
O. Rodriguez and J. M. Desse 12 Nov. 1984 69 p refs In FRENCH
(Contract DRET-83-250)
(IMFL-3119) Avail: NTIS HC A04/MF A01

Transonic wind tunnel tests were carried out on a wall protuberance vibrating with sinudoidal oscillations. The experiments studied spoiler efficiency. The unsteady phenomena following the sinusoidal excitation were studied by ultrafast visualization and by unsteady pressure measurement on the obstacle. The free stream Mach number was 0.5. Spectrum analysis proves the nonlinear nature of the flow. The dimension of the separated flow region varies with the position of the spoiler on the body. The results show that at the frequences considered the response to the oscillations can be studied in steady flow tests. Author (ESA)

N86-13304*# National Aeronautics and Space Administration. Ames Research Center, Moffett Field, Calif.
PRESSURE-DISTRIBUTION MEASUREMENTS ON A TRANSONIC LOW-ASPECT RATIO WING
Earl R. Keener Sep. 1985 77 p refs
(NASA-TM-86683; Rept-85131; NAS 1.15:86683) Avail: NTIS HC A05/MF A01 CSCL 01A

Experimental surface pressure distributions and oil flow photographs are presented for a 0.90 m semispan model of NASA/Lockheed Wing C, a generic transonic, supercritical, low aspect ratio, highly 3-dimensional configuration. This wing was tested at the design angle of attack of 5 deg over a Mach number range from 0.25 to 0.96, and a Reynolds number range from 3.4 x 1,000,000 to 10 x 1,000,000. Pressures were measured with both the tunnel floor and ceiling suction slots open for most of the tests but taped closed for some tests to simulate solid walls. A comparison is made with the measured pressures from a small model in high Reynolds number facility and with predicted pressures using two three dimesional, transonic full potential flow wing codes: design code FLO22 (nonconservative) and TWING code (conservative). At the given design condition, a small region of flow separation occurred. At a Mach number of 0.82 the flow was unseparated and the surface flow angles were less than 10 deg, indicating that the boundary layer flow was not 3-D. Evidence indicate that wings that are optimized for mild shock waves and mild pressure recovery gradients generally have small 3-D boundary layer flow at design conditions for unseparated flow. Author

03 AIR TRANSPORTATION AND SAFETY

Includes passenger and cargo air transport operations; and aircraft accidents.

For related information see also *16 Space Transportation* and *85 Urban Technology and Transportation.*

N86-13305*# National Aeronautics and Space Administration. Langley Research Center, Hampton, Va.
ADVANCED EMERGENCY OPENINGS FOR COMMERCIAL AIRCRAFT
Laurence J. Bement and Morry L. Schimmel Nov. 1985 18 p refs Presented at the 30th Corporate Aviation Safety Seminar, Dallas, Texas, 14-16 Apr. 1985
(NASA-TM-87580; L-16012; NAS 1.15:87580) Avail: NTIS HC A02/MF A01 CSCL 01C

Explosively actuated openings in composite panels are proposed to enhance passenger survivability within commercial aircraft by providing improvements in emergency openings, fuselage venting, and fuel dump. The concept is to embed a tiny, highly stable explosive cord in the periphery of a load-carrying composite panel; on initiation of the cord, the panel is fractured to create a well-defined opening. The panel would be installed in the sides of the fuselage for passenger egress, in the top of the fuselage for smoke venting, and in the bottoms of the fuel cells for fuel dump. Described are the concerns with the use of explosive systems, safety improvements, advantages, experimental results, and recommended approach to gain acceptance and develop this concept. Author

N86-13306* Ecosystems International, Inc., Crofton, Md.
NASA FLIGHT OPERATIONS REVIEW Final Report
Sep. 1985 113 p Sponsored by NASA
(NASA-CR-176393; NAS 1.26:176393) Avail: Issuing Activity CSCL 01C

Independent assessments of the provisions taken by NASA to assure the safety of their aviation operations are reported. Aviation operations conducted at the Lewis Research Center (LeRC) are reviewed. These reviews and independent assessments were undertaken as part of an on-going effort to provide NASA management with a qualitative evaluation of the overall organizational structure, administrative policy. A report which provides NASA management with a broad overview of the current status and safety of aviation operations at LeRC is presented. Recommendations for improvements are provided whenever a significant impact on the present level of safety assurance is judged to be feasible, or an existing situation has the potential for creating a hazardous condition. E.A.K.

N86-13307# Department of the Navy, Washington, D. C.
PASSIVE ARM RETENTION CURTAIN Patent Application
T. J. Zenobi, inventor (to Navy) Filed 2 Nov. 1984 12 p
(AD-D011876; US-Patent-Appl-SN-667685) Avail: NTIS HC A02/MF A01 CSCL 01/3

A pilot arm retention system for an aircraft ejection seat which includes inertia reels and a parachute is comprised of a pair of nets connected between respective sides of the seat and a pair of deployment straps which are releasably coupled to the inertia reel straps and parachute risers and routed down over the front of the seat through a pair of snubbers to fixed points on the cockpit floor. Author (GRA)

N86-13308# Institut de Mecanique des Fluides de Lille (France).
AIRCRAFT CRASHING. ANALYSIS AND IDENTIFICATION METHODS. PRESENTATION OF A SOLUTION METHOD [CRASH D'AVIONS. METHODES D'ANALYSE ET D'IDENTIFICATION. PRESENTATION D'UNE METHODOLOGIE DE RESOLUTION]
P. Geoffroy and E. Haug (ESI SA) 19 Feb. 1985 102 p refs In FRENCH
(Contract DRET-83-452)
(IMFL-4116) Avail: NTIS HC A06/MF A01

An aircraft landing crash with a vertical velocity > 5 m/sec is discussed. The tail section is assumed to make first contact. The nonlinear aspect of the problem is emphasized and a numerical solution is worked out. Superelements methods are found to be best suited to the problem. They conserve existing programs and finite element computations. An identification method is used to adjust the physical parameters in the superelements. The implementation of these techniques in the NL-CRASH program is proposed. Author (ESA)

N86-13617# Joint Publications Research Service, Arlington, Va.
CERTIFICATION GRANTED TO FRANCO-ITALIAN ATR 42
In its West Europe Rept.: Sci. and Technol. (JPRS-WST-85-031) 8 Nov. 1985 p 10-13 Repr. from Rev. Aerospatiale (France), Oct. 1985 p 10; 12 (For primary document see N86-13616 04-31)
Avail: NTIS HC A03/MF A01

04 AIRCRAFT COMMUNICATIONS AND NAVIGATION

Includes digital and voice communication with aircraft; air navigation systems (satellite and ground based); and air traffic control.

For related information see also *17 Spacecraft Communications, Command, and Tracking* and *32 Communications.*

N86-13309# Aeronautical Research Labs., Melbourne (Australia).
AN ANALYTICAL COMPARISON OF THREE VISUAL APPROACH SLOPE INDICATORS: VASIS, T-VASIS AND PAPI
Jane Millar Aug. 1984 56 p refs Original contains color illustrations
(ARL/SYS-R-33; AR-003-963; SR-33) Avail: NTIS HC A04/MF A01

The three Visual Approach Slope Indicators (VASIs), VASIS, T-VASIS and PAPI, approved by the International Civil Aviation Organization (ICAO) for use by turbojet aeroplanes are compared. The discussion is based upon published performance data including approach path measurements and pilot opinion, ergonomics and the ability to fulfill operational requirements. It is concluded from flight trial data and operational experience that T-VASIS is a more precise and sensitive aid than Red-White VASIS which has several deficiencies. The current policy of not using Red-White VASIS for routine operations in Australia is supported by the conclusions. It is predicted that PAPI also will be less satisfactory than T-VASIS. This prediction is based mainly on ergonomic principles. Performance data about PAPI is limited and consists mainly of relatively uninformative pilot acceptance surveys. Because insufficient objective parameters describing trajectories of aircraft from the intended user-population have been published, most of the claims for PAPI superiority remain unsubstantiated. Accordingly, it is recommended that PAPI be evaluated using objective measures in a controlled experimental environment with transport aircraft. Author

N86-13310*# Draper (Charles Stark) Lab., Inc., Cambridge, Mass.
THE EVALUATION OF FAILURE DETECTION AND ISOLATION ALGORITHMS FOR RESTRUCTURABLE CONTROL Interim Report, Dec. 1983 - May 1984
P. Motyka, W. Bonnice, S. Hall, and E. Wagner Aug. 1984 207 p refs
(Contract NAS1-17556)
(NASA-CR-177983; NAS 1.26:177983; CSDL-R-1799) Avail: NTIS HC A10/MF A01 CSCL 01C

Three failure detection and identification techniques were compared to determine their usefulness in detecting and isolating failures in an aircraft flight control system; excluding sensor and flight control computer failures. The algorithms considered were the detection filter, the Generalized Likelihood Ratio test and the Orthogonal Series Generalized Likelihood Ratio test. A modification to the basic detection filter is also considered which uses secondary filtering of the residuals to produce unidirectional failure signals. The algorithms were evaluated by testing their ability to detect and isolate control surface failures in a nonlinear simulation of a C-130 aircraft. It was found that failures of some aircraft controls are difficult to distinguish because they have a similar effect on the dynamics of the vehicle. Quantitative measures for evaluating the distinguishability of failures are considered. A system monitoring strategy for implementing the failure detection and identification techniques was considered. This strategy identified the mix of direct measurement of failures versus the computation of failure necessary for implementation of the technology in an aircraft system. Author

N86-13311*# National Aeronautics and Space Administration. Ames Research Center, Moffett Field, Calif.
DISCOVERY OF THE KALMAN FILTER AS A PRACTICAL TOOL FOR AEROSPACE AND INDUSTRY
Leonard A. McGee and Stanley F. Schmidt Nov. 1985 24 p refs
(NASA-TM-86847; Rept-85424; NAS 1.15:86847) Avail: NTIS HC A02/MF A01 CSCL 17G

The sequence of events which led the researchers at Ames Research Center to the early discovery of the Kalman filter shortly after its introduction into the literature is recounted. The scientific breakthroughs and reformulations that were necessary to transform Kalman's work into a useful tool for a specific aerospace application are described. The resulting extended Kalman filter, as it is now known, is often still referred to simply as the Kalman filter. As the filter's use gained in popularity in the scientific community, the problems of implementation on small spaceborne and airborne computers led to a square-root formulation of the filter to overcome numerical difficulties associated with computer word length. The work that led to this new formulation is also discussed, including the first airborne computer implementation and flight test. Since then the applications of the extended and square-root formulations of the Kalman filter have grown rapidly throughout the aerospace industry. Author

N86-13312# National Airspace System Program Office, Washington, D.C.
NATIONAL AIRSPACE SYSTEM, SYSTEM REQUIREMENTS SPECIFICATION
21 Mar. 1985 209 p
(AD-A157944; NAS-SR-1000) Avail: NTIS HC A10/MF A01 CSCL 01/5

The NAS System Requirements Specification (NASSRS) is a compilation of requirements which describe the operational capabilities for the National Airspace System (NAS) as the NAS is envisioned to exist by the year 1995. In that context, it includes those existing and transitional capabilities that will also exist in the 1995 system. It is intended primarily for use as an internal FAA management tool to support the NAS design, engineering, and acquisition activities and to manage and control change to the NAS. The document provides a ground-based systems representation of the proposed operational capabilities planned for the NAS. As programs and subsystems are developed and implemented the capabilities they provide will be compared to this document as a measure of success of NAS Plan Implementation. The contents of the document include: overview, flight planning; traffic control and airspace management; monitoring; navigation; air defense and law enforcement surveillance; aircraft detection and identification; communications; maintenance and support: system effectiveness. GRA

N86-13313# Eclectech Associates, Inc., North Stonington, Conn.
SHORT RANGE AIDS TO NAVIGATION SYSTEMS. DESIGN MANUAL FOR RESTRICTED WATERWAYS Final Draft Report
M. W. Smith, K. L. Marino, and J. Multer Jun. 1985 332 p
(Grant DOT-CG-835285-A)
(AD-A158213; EA-85-U-305; USCG-D-18-85) Avail: NTIS HC A15/MF A01 CSCL 17/7

This manual is intended to supplement the system design guidelines presented in Chapter 4 of the Aids to Navigation Manual - Administration (COMDTINST M16500.7). It provides procedures for designing or evaluating systems of aids in restricted waterways navigated by deep draft vessels. As such, it is an appropriate tool for use by the District Aids to Navigation Branch when conducting regularly scheduled waterways evaluations under the Waterways Analysis and Management System (WAMS) (COMDTINST M16500.11). Besides its structured approach to system design and evaluation, the manual provides a measure of quality for candidate aid configurations. This measure of quality is presented as an assessment of risk, providing the District or Headquarters analyst with an objective, quantifiable measure of effectiveness to support operational and budgetary decisions. GRA

N86-13314# Army Construction Engineering Research Lab., Champaign, Ill.
DESIGN CRITERIA UPGRADE FOR US ARMY TYPE 2 AIR TRAFFIC CONTROL TOWERS Final Report
T. R. Napier, W. E. Back, and M. McCulley Jun. 1985 72 p

(AD-A159115; CERL-TR-P-85/13) Avail: NTIS HC A04/MF A01 CSCL 17/7

This report documents research conducted to identify problem areas in; the design of existing Type 2 Air Traffic Control Tower (ATCT) installations and to develop standard design criteria to avoid these problems in future installations. Many design problem areas were identified in the ATCT structure's architectural design, substructure, superstructure, roof systems, exterior walls, interior construction, mechanical systems, electrical systems, and air traffic control interfaces. For each of these areas, specific solutions to the problems were recommended. However, incorporation of these solutions must consider a specific site location and environmental conditions. GRA

N86-13315# Air Force Inst. of Tech., Wright-Patterson AFB, Ohio. School of Engineering.
TIME DELAY OF ARRIVAL LOCATION ASSESSMENT USING FOUR SATELLITES M.S. Thesis
C. M. Wozniakowski Dec. 1984 97 p
(AD-A159243; AFIT/GSO/PH/84D-5) Avail: NTIS HC A05/MF A01 CSCL 17/7

The Time of Arrival (TOA)/Time Delay of Arrival (TDOA) concepts for locating a source are reviewed. The Vela satellite program and how it was used in conjunction with the TOA concept is discussed. NAVSTAR/GPS is reviewed next and how this interrelates with the other concepts discussed is mentioned. The last concept mentioned is that of nuclear detection. Again, examples on how this idea interrelates with the previous mentioned concepts shown. The problem addressed here is to develop mathematical formulas that describe the problem of having four satellites viewing an event. The first method uses a TOA technique to solve the event's location and time. The second method employs the solution from the first method to predict uncertainty in location and time. Also this uncertainty is determined through the use of implicit differentiation. These results are then compared with the projected difference from the standard solution when the associated value is varied by an equivalent amount in the first method. Results from one example are discussed. Author (GRA)

N86-14165# Joint Publications Research Service, Arlington, Va.
DETERMINING QUASI-REAL-TIME LOCATION OF SHIPS USING GEOSTATIONARY NAVIGATIONAL SATELLITES
V. E. Abdullayev, K. Kh. Ismalilov, V. N. Vintayev, and G. A. Sosunov *In its* USSR Rept.: Space (JPRS-USP-85-005) 30 Sep. 1985 p 83-89 refs Transl. into ENGLISH from Izv. Akad. Nauk Azerb. SSR: Ser. Fiz.-Tekhn. i Mat. Nauk (Baku), v. 6, no. 1, Jan. - Feb. 1985 p 96-101 (For primary document see N86-14111 04-88)
Avail: NTIS HC A08

05 AIRCRAFT DESIGN, TESTING AND PERFORMANCE

Includes aircraft simulation technology.

For related information see also *18 Spacecraft Design, Testing and Performance* and *39 Structural Mechanics.*

N86-13316*# National Aeronautics and Space Administration. Langley Research Center, Hampton, Va.
ABRASION BEHAVIOR OF ALUMINUM AND COMPOSITE SKIN COUPONS, STIFFENED SKINS AND STIFFENED PANELS REPRESENTATIVE OF TRANSPORT AIRPLANE STRUCTURES
Karen E. Jackson Nov. 1985 33 p refs
(DA Proj. 1L1-61102-AH-45)
(NASA-TP-2520; L-16018; NAS 1.60:2520; AVSCOM-TR-85-B-7)
Avail: NTIS HC A03/MF A01 CSCL 01C

A three-phase investigation was conducted to compare the friction and wear response of aluminum and graphite-epoxy composite materials when subjected to loading conditions similar to those experienced by the skin panels on the underside of a transport airplane during an emergency belly landing on a runway surface. The first phase involved a laboratory test which used a standard belt sander to provide the sliding abrasive surface. Small skin-coupon test specimens were abraded over a range of pressures and velocities to determine the effects of these variables on the coefficient of friction and wear rate. The second phase involved abrading I-beam stiffened skins on actual runway surface over the same range of pressures and velocities used in the first phase. In the third phase, large stiffened panels which most closely resembled transport fuelage skin construction were abraded on a runway surface. This report presents results from each phase of the investigation and shows comparisons between the friction and wear behavior of the aluminum and graphite-epoxy composite materials. Author

N86-13317*# Operations Research, Inc., Rockville, Md.
TRADEOFF ANALYSIS OF TECHNOLOGY NEEDS FOR PUBLIC SERVICE HELICOPTERS
James S. Bauchspies, William R. Bryant, Jr., and William E. Simpson Aug. 1985 120 p refs
(Contract NASw-3554)
(NASA-CR-3927; NAS 1.26:3927; ORI-TR-2459) Avail: NTIS HC A06/MF A01 CSCL 01C

The design requirements for a family or type of Public Service Helicopter (PSH) is examined which will satisfy the needs of municipal and state governments in the following mission areas: Emergency Medical Service--Airborne Rescue Squad; Law Enforcement; Search and Rescue; and Environmental Control (Fire Fighting, Pollution, Resource Management). The report compares both design and performance requirements as specified by the PSH user's group against current technological capabilities, RTOPS and US Army LHX design requirements. The study explores various design trade-offs and options available to the aircraft designer/manufacturer in order to meet the several criteria specified by the PSH user's group. In addition, the report includes a brief assessment of the feasibility of employing certain advanced rotorcraft designs to meet the stringent combination of operational capabilities desired by the Public Service Helicopter Users. Author

N86-13318*# National Aeronautics and Space Administration, Washington, D. C.
AIRCRAFT OF THE FUTURE
S. Yeger (OKB Tupolev, USSR) Nov. 1985 9 p Transl. into ENGLISH from Techn.-Oekonomische Inform. der Zivilen Luftfahrt (West Germany), v. 13, no. 2, 1977 p 88-90 Original language document was announced in IAA as A77-39452 Transl. by The Corporate Word, Inc., Pittsburgh, Pa.
(Contract NASw-4006)
(NASA-TM-77952; NAS 1.15:77952) Avail: NTIS HC A02/MF A01 CSCL 01C

Some basic problems connected with attempts to increase the size and capacity of transport aircraft are discussed. According to the square-cubic law, the increase in structural weight is proportional to the third power of the increase in the linear dimensions of the aircraft when geomettric similarity is maintained, while the surface area of the aircraft increases according to the second power. A consequence is that the fraction of useful weight will decrease as aircraft increase in size. However, in flying-wing designs in which the whole load on the wing is proportional to the distribution of lifting forces, the total bending moment on the wing will be sharply reduced, enabling lighter construction. Flying wings may have an ultimate capacity of 3000 passengers. DOE

N86-13319*# National Aeronautics and Space Administration. Ames Research Center, Moffett Field, Calif.
PRELIMINARY REPORT ON IN-FLIGHT MEASUREMENT OF ROTOR HUB DRAG AND LIFT USING THE RSRA
C. W. Acree, Jr. Oct. 1985 28 p refs
(NASA-TM-86764; Rept-85288; NAS 1.15:86764) Avail: NTIS HC A03/MF A01 CSCL 01C

The Rotor Systems Research Aircraft (RSRA) is a compound helicopter that was test flown as a fixed wing aircraft, with the main rotor blades removed and the rotor hub installed. An onboard rotor load measurement system measured the resulting rotor hub drag and lift. Measured hub drag and lift are plotted for comparison to that predicted by full scale and 1/6 scale model wind tunnel tests. The success of the demonstration gives confidence that planned improvements to the RSRA will allow high accuracy hub drag and lift measurements to be made in flight on a routine research basis. Author

N86-13320*# Texas Technological Univ., Lubbock. Dept. of Electrical Engineering/Computer Science.
INTERPRETATION OF F-106B IN-FLIGHT LIGHTNING SIGNATURES
T. F. Trost, M. G. Grothaus, and C. T. Wen Aug. 1985 51 p refs
(Grant NAG1-28)
(NASA-CR-176387; NAS 1.26:176387) Avail: NTIS HC A04/MF A01 CSCL 01C

Various characteristics of the electromagnetic data obtained on a NASA F-106B aircraft during direct lightning strikes are presented. Time scales of interest range from 10 ns to 400 microsecond. The following topics are discussed: (1) Lightning current, I, measured directly versus I obtained from computer integration of measured I-dot; (2) A method of compensation for the low frequency cutoff of the current transformer used to measure I; (3) Properties of fast pulses observed in the lightning time-derivative waveforms; (4) The characteristic D-dot signature of the F-106B aircraft; (5) An RC-discharge interpretation for some lightning waveforms; (6) A method for inferring the locations of lightning channel attachment points on the aircraft by using B-dot data; (7) Simple, approximate relationships between D-dot and I-dot and between B and I; and (8) Estimates of energy, charge, voltage, and resistance for a particular lightning event. Author

N86-13321*# National Aeronautics and Space Administration. Langley Research Center, Hampton, Va.
GROUND VIBRATION TEST OF THE LAMINAR FLOW CONTROL Jstar AIRPLANE
Michael W. Kehoe (NASA. Ames Research Center), F. W. Cazier, Jr. (NASA. Ames Research Center), and Joseph F. Ellison Oct. 1985 61 p
(NASA-TM-86398; L-15949; NAS 1.15:86398) Avail: NTIS HC A04/MF A01 CSCL 01C

A ground vibration test was conducted on a Lockheed JetStar airplane that had been modified for the purpose of conducting laminar flow control experiments. The test was performed prior to initial flight flutter tests. Both sine-dwell and single-point-random excitation methods were used. The data presented include frequency response functions and a comparison of mode frequencies and mode shapes from both methods. Author

N86-13322# Royal Aircraft Establishment, Farnborough (England).
STANDARDISED FATIGUE LOADING SEQUENCES FOR HELICOPTER ROTORS (HELIX AND FELIX). PART 2: FINAL DEFINITION OF HELIX AND FELIX
P. R. Edwards and J. Darts Aug. 1984 124 p
(AD-A156622; RAE-TR-84085; DRIC-BR-95846) Avail: NTIS HC A06/MF A01 CSCL 14/2

This report defines two loading standards for the fatigue evaluation of helicopter rotor materials and components. They were developed as a collaborative study between West Germany, the Netherlands and UK. Details of the contributing organizations are given in Appendix A. The new loading standards follow the earlier TWIST (Transport Wing Standard), and FALSTAFF (Fighter Aircraft Loading Standard For Fatigue evaluation). After the tradition of these earlier loading sequences, the new loading standards have been given identifying names. For these the origin of the word helicopter (Helix-spiral, pteronwing from the Greek) has provided a convenient basis. The new standards are called: Helix loading standard for hinged or articulated rotors; Felix loading standard for fixed or semi-rigid rotors. This report defines the final form of the two standards, statistical content according to different counting methods and full details of their method of generation. GRA

N86-13323# Army Aviation Engineering Flight Activity, Edwards AFB, Calif.
LIMITED AIRWORTHINESS AND FLIGHT CHARACTERISTICS (A AND FC) TEST OF THE QUICK FIX CONFIGURATION Final Report, 23 May - 27 Jun. 1984
G. L. Skinner, G. M. Bishop, E. J. Tavares, and R. C. Murrell Oct. 1984 67 p
(AD-A157716; USAAEFA-83-20) Avail: NTIS HC A04/MF A01 CSCL 01/3

The US Army Aviation Engineering Flight Activity conducted an evaluation to determine the increase in power required and the change in handling qualities due to the installation of the AN/ALQ-151(V)2 countermeasures system and associated mission equipment on the UH-60A helicopter. Testing conducted between 23 May to 2 June 1984 totaled 12.4 hours. The addition of the Quick Fix System and associated mission equipment created an increase in equivalent flat plate area (F sub e) of 17 sq ft (ft2) for advance ratios (mu) of 0.26 and greater. For mu's less than 0.26, the change in F sub e increased above 17 sq ft as a function of thrust coefficient. Handling qualities of the Quick Fix configured YEH-60A were unchanged from a normal utility configured UH-60A and were determined satisfactory. One deficiency, interference between the main rotor blades and the upper elements of the (no. 3 and no. 4) direction finding dipole antennas during ground taxi and four shortcomings were associated with the Quick Fix configuration. GRA

N86-13324# SRI International Corp., Menlo Park, Calif.
PHYSICAL DISTRIBUTION SYSTEM FOR AIRCRAFT EXTERNAL FUEL TANKS-SURVEY Final Report, 1 Mar. - 31 May 1985
G. B. Andeen, R. D. Kornbluh, T. P. Low, R. H. Monahan, and W. Park Jun. 1985 96 p
(Contract N00600-82-D-8362)
(AD-A158275; DTNSRDC/CMLD-CR-47-85) Avail: NTIS HC A05/MF A01 CSCL 13/4

The general objective of this study was to conduct a survey and analysis of current and planned aircraft external fuel tanks, with emphasis on the disposability and nestability aspects of these fuel tanks. The study focused on design requirements, fabrication and assembly, and physical distribution, with particular attention directed to the use of the robotic equipment for the assembly of nestable fuel tanks aboard the ship. The principal conclusion of this study is that the development of disposable, nestable external aircraft fuel tanks with automated assembly aboard ship, using robotic equipment, is a feasible option for implementation within the next five to ten years. Chapter 1 of the report presents an introduction and summary description of the major results of the survey. Chapter 2 then provides a summary description of the tentative operational requirements established by the Navy for disposable, nestable external aircraft fuel tanks. Chapter 3 presents a discussion of the possible fabrication and assembly techniques and problems for such fuel tanks. Chapter 4 then discusses the physical distribution aspects of external aircraft fuel tanks. Chapter 5 concludes with a listing of the conclusions and recommendations resulting from this analysis. GRA

N86-13325# Hughes Helicopters, Culver City, Calif.
ADVANCED TECHNOLOGY HELICOPTER LANDING GEAR PRELIMINARY DESIGN INVESTIGATION Final Report, Sep. 1983 - Jul. 1984
J. K. Sen, M. W. Votaw, and D. C. Weber Jul. 1985 247 p
(Contract DAAK51-83-C-0039; DA Proj. 1L1-62209-AH-76)
(AD-A158816; HHI-84-284; USAAVSCOM-TR-84-D-20) Avail: NTIS HC A11/MF A01 CSCL 01/3

This report describes the preliminary designs of two configurations of helicopter crashworthy landing gears: (1) with the trailing arms of the main gear coupled with a torque, which forces both shock struts to absorb the kinetic energy of an unsymmetrical crash impact, and (2) with the trailing arms uncoupled; i.e., the torque tube is replaced by a cross tube which is incapable of reacting the high torsional load of an unsymmetrical crash impact. Retractable and fixed landing gears of both configurations have been designed, as well as a standard (noncrashworthy) retractable landing gear. All landing gears are of tailwheel designs. The designs apply the systems approach to crashworthiness where the total

impact energy absorbed is shared by the landing gear, fuselage and seat. The designs of the crashworthy landing gears were completed after a preliminary investigation of crash impact at sink speeds up to 42 fps, roll angles up to + or - 20 degrees and pitch angles up to -10+20 degrees. The crashworthy evaluations were made with program KRASH. A detailed analysis with KRASH was then conducted for all configurations of landing gears. Based on the weight trend curves and cost analysis, a crashworthy design criterion was recommended. This design criterion was the basis for updating the landing gear design. The designs identify the fabrication methods and processes for the landing gear. Estimates of cost and weight of the updated designs are also presented.
GRA

N86-13326# Sikorsky Aircraft, Stratford, Conn.
TRANSMISSION ACOUSTIC VIBRATION TESTING Final Report, Sep. 1982 - Nov. 1983
C. Yoerkie and A. Chory Jul. 1985 85 p
(Contract DAAK51-82-C-0040; DA Proj. 1L2-63201-DB-72)
(AD-A159022; USAAVRADCOM-TR-83-D-34) Avail: NTIS HC A05/MF A01 CSCL 01/3

Laboratory tests were conducted to determine the individual and combined effects of a high contact ratio (HCR) planetary gearset and a stainless steel housing on the acoustic (high frequency) vibration signature of the BLACK HAWK helicopter main transmission. Vibration levels at the planetary mesh frequency increased significantly with the stainless steel housing, but increased unexpectedly with the HCR planetary. The primary reason for the increased response with the HCR was the reduced gear face widths.
GRA

N86-13327# Air Force Inst. of Tech., Wright-Patterson AFB, Ohio. School of Engineering.
AIRCREW DOSE AND ENGINE DUST INGESTION FROM NUCLEAR CLOUD PENETRATION M.S. Thesis
S. P. Conners Mar. 1985 168 p
(AD-A159246; AFIT/GNE/PH/85M-4) Avail: NTIS HC A08/MF A01 CSCL 01/2

This thesis evaluates the threat to aircraft and aircrew from dust and radioactivity in a cloud generated by nuclear surface bursts. A model of the nuclear cloud is generated, using any number and type of weapons and any desire dust size distribution. The cloud is propagated through the atmosphere for a given time, then penetrated by an aircraft. The activity density in the cloud is converted to dose to the crew for a given path through the cloud. Radiation shielding and dust filters are included in the calculations. Alternatively, the cloud dust mass density can be converted to mass trapped in a filter or the cabin, or to the dust mass that has entered the engine. Methods for determining particle size and altitude distributions are presented. The ionizing dose to the crewmember is computed for both sky-shine and the dust trapped in the cabin during cloud passage. A method of computing the shielding power of the crew compartment against sky-shine is presented. Given the air flow rate into a filter or engine, the mass of ingested dust is found. These nuclear cloud and aircraft models are incorporated in a computer code oriented toward operational use. A significant feature of the code includes the ability to easily change the scenario with menu driven options.
GRA

06 AIRCRAFT INSTRUMENTATION

Includes cockpit and cabin display devices; and flight instruments.

For related information see also *19 Spacecraft Instrumentation* and *35 Instrumentation and Photography.*

No abstracts in this category.

07 AIRCRAFT PROPULSION AND POWER

Includes prime propulsion systems and systems components, e.g., gas turbine engines and compressors; and on-board auxiliary power plants for aircraft.

For related information see also *20 Spacecraft Propulsion and Power, 28 Propellants and Fuels,* and *44 Energy Production and Conversion.*

N86-13328*# Teledyne Continental Motors, Muskegon, Mich.
LIGHTWEIGHT TWO-STROKE CYCLE AIRCRAFT DIESEL ENGINE TECHNOLOGY ENABLEMENT PROGRAM, VOLUME 1 Final Report, Dec. 1979 - Aug. 1985
P. D. Freen, S. G. Berenyi, A. P. Brouwers, and M. E. Moynihan Aug. 1985 116 p
(Contract NAS3-22218)
(NASA-CR-174923-Vol-1; NAS 1.26:174923-Vol-1) Avail: NTIS HC A06/MF A01 CSCL 21G

An experimental Single Cylinder Test Engine Program is conducted to confirm the analytically projected performance of a two-stroke cycle diesel engine for aircraft applications. The test engine delivered 78kW indicated power from 1007cc displacement, operating at 3500 RPM on Schnuerle loop scavenged two-stroke cycle. Testing confirms the ability of a proposed 4-cylinder version of such an engine to reach the target power at altitude, in a highly turbocharged configuration. The experimental program defines all necessary parameters to permit design of a multicylinder engine for eventual flight applications; including injection system requirement, turbocharging, heat rejection, breathing, scavenging, and structural requirements. The multicylinder engine concept is configured to operate with an augmented turbocharger, but with no primary scavenge blower. The test program is oriented to provide a balanced turbocharger compressor to turbine power balance without an auxiliary scavenging system. Engine cylinder heat rejection to the ambient air has been significantly reduced and the minimum overall turbocharger efficiency required is within the range of commercially available turbochargers. Analytical studies and finite element modeling is made of insulated configurations of the engines - including both ceramic and metallic versions. A second generation test engine is designed based on current test results.
Author

N86-13329*# Teledyne Continental Motors, Muskegon, Mich.
LIGHTWEIGHT TWO-STROKE CYCLE AIRCRAFT DIESEL ENGINE TECHNOLOGY ENABLEMENT PROGRAM, VOLUME 2 Final Report, Dec. 1979 - Aug. 1985
P. D. Freen, S. G. Berenyi, A. P. Brouwers, and M. E. Moynihan Aug. 1985 150 p refs
(Contract NAS3-22218)
(NASA-CR-174923-Vol-2; NAS 1.26:174923-Vol-2) Avail: NTIS HC A07/MF A01 CSCL 21G

An experimental Single Cylinder Test Engine Program is conducted to confirm the analytically projected performance of a two-stroke cycle diesel engine for aircraft applications. Testing confirms the ability of a proposed 4-cylinder version of such an engine to reach the target power at altitude in a highly turbocharged configuration. The experimental program defines all necessary parameters to permit a design of a multicylinder engine for eventual flight applications.
Author

N86-13330*# Teledyne Continental Motors, Muskegon, Mich.
LIGHTWEIGHT TWO-STROKE CYCLE AIRCRAFT DIESEL ENGINE TECHNOLOGY ENABLEMENT PROGRAM, VOLUME 3 Final Report, Dec. 1979 - Aug. 1985
P. D. Freen, S. G. Berenyi, A. P. Brouwers, and M. E. Moynihan Aug. 1985 282 p
(Contract NAS3-22218)
(NASA-CR-174923-Vol-3; NAS 1.26:174923-Vol-3) Avail: NTIS HC A13/MF A01 CSCL 21G

An experimental Single Cylinder Test Engine Program is conducted to confirm the analytically projected performance of a two-stroke cycle diesel engine for aircraft applications. Testing confirms the ability of a proposed 4-cylinder version of such an engine to reach the target power at altitude in a highly turbocharged configuration. The experimental program defines all necessary parameters to permit design of a multicylinder engine for eventual flight applications. Author

N86-13331# Massachusetts Inst. of Tech., Cambridge. Dept. of Ocean Engineering.
HUB EFFECTS IN PROPELLER DESIGN AND ANALYSIS
M. H. Wang Jul. 1985 183 p
(Contract N00014-82-K-0198)
(AD-A158853; OE-85-14) Avail: NTIS HC A09/MF A01 CSCL 20/4

A numerical model is established for the design of propeller blade shape for a prescribed circulation and a given hub geometry. The vortex lattice approach is adapted for blades and their wakes. The hub is represented by a distribution of dipoles which ends at the hub apex. It is shown that consideration of the hub results in a lower pitch and lower camber at the inner radii. An iterative method is developed for analyzing the interference between the blades and the hub. It is shown that the circulation at the root of a propeller with a hub is larger than the circulation at the root of a propeller without a hub. Two examples show that the increase in thrust due to hub effects has the same order of magnitude as the drag force effects on the hub for propellers which are moderately loaded at the hub. Experiments are carried out for comparison with the numerical results. Excellent agreement is obtained in the circulation distribution for a conventional propeller, and fair agreement for a controllable pitch propeller. Experimental results show what the circulation is, roughly speaking, conserved. A method for estimating the drag force of the hub due to the hub vortex is established by assuming that the circulation is conserved. GRA

08 AIRCRAFT STABILITY AND CONTROL

Includes aircraft handling qualities; piloting; flight controls; and autopilots.

N86-13332*# National Aeronautics and Space Administration. Langley Research Center, Hampton, Va.
A PRELIMINARY EVALUATION OF THE GENERALIZED LIKELIHOOD RATIO FOR DETECTING AND IDENTIFYING CONTROL ELEMENT FAILURES IN A TRANSPORT AIRCRAFT
W. Thomas Bundick Sep. 1985 94 p refs
(NASA-TM-87620; NAS 1.15:87620) Avail: NTIS HC A05/MF A01 CSCL 01C

The application of the Generalized Likelihood Ratio technique to the detection and identification of aircraft control element failures has been evaluated in a linear digital simulation of the longitudinal dynamics of a B-737 aircraft. Simulation results show that the technique has potential but that the effects of wind turbulence and Kalman filter model errors are problems which must be overcome. Author

N86-13333*# National Aeronautics and Space Administration. Langley Research Center, Hampton, Va.
FIT: COMPUTER PROGRAM THAT INTERACTIVELY DETERMINES POLYNOMIAL EQUATIONS FOR DATA WHICH ARE A FUNCTION OF TWO INDEPENDENT VARIABLES
P. Douglas Arbuckle, Steven M. Sliwa, Marie-Louise Roy, and Sherwood H. Tiffany (PRC Kentron, Inc., Hampton, Va.) Oct. 1985 20 p refs
(NASA-TM-86413; L-15983; NAS 1.15:86413) Avail: NTIS HC A02/MF A01 CSCL 01C

A computer program for interactively developing least-squares polynomial equations to fit user-supplied data is described. The program is characterized by the ability to compute the polynomial equations of a surface fit through data that are a function of two independent variables. The program utilizes the Langley Research Center graphics packages to display polynomial equation curves and data points, facilitating a qualitative evaluation of the effectiveness of the fit. An explanation of the fundamental principles and features of the program, as well as sample input and corresponding output, are included. Author

N86-13334# Air Force Academy, Colo.
PITCH RATE VERSUS G COMMAND AS THE LONGITUDINAL FLIGHT CONTROL SYSTEM DESIGN STRATEGY FOR A STATISTICALLY UNSTABLE FIGHTER TYPE AIRCRAFT WITH TWO CONTROL SURFACES
T. P. Webb 2 Jul. 1985 32 p
(AD-A158803; USAFA-TN-85-8) Avail: NTIS HC A03/MF A01 CSCL 01/4

Pitch rate command and normal G command longitudinal flight control systems were designed using linear optimal control theory for a statically unstable, two control surface, fighter-type aircraft at both a power approach and an up-and-away flight condition. The closed-loop systems were then evaluated in man-in-the-loop simulations with pilots attempting random altitude tracking and pitch tracking tasks. The evaluation results indicated that in the power approach flight condition, normal G command was more suitable for altitude tracking and pitch rate command was preferred for pitch tracking. Results for the up-and-away flight condition were inconclusive. GRA

N86-13335# Southwest Research Inst., San Antonio, Tex.
DIGITAL SERVOCONTROLLER SYSTEM. VOLUME 4. RESULTS AND CONCLUSIONS Final Report, Jul. 1983 - Nov. 1984
J. Lopez and K. Miller Feb. 1985 31 p
(AD-A159068; SWRI-14-7676-Vol-4; AFWAL-TR-84-3117-Vol-4) Avail: NTIS HC A03/MF A01 CSCL 09/2

This final report describes an exploratory development effort for the design and fabrication of a digital servocontroller system for load control in full-scale air-frame fatigue tests. Each digital controller replaces four analog controllers. The LSI-11/23 microcomputer in the digital controller executes a PI algorithm to implement direct digital control. It may operate in a stand-alone mode or as a slave processor to a master computer via fiber optic link. Other programmable features specify loop parameters, building load profiles, adjusting control system gains and monitoring alarm and abort conditions. GRA

09 RESEARCH AND SUPPORT FACILITIES (AIR)

Includes airports, hangars and runways; aircraft repair and overhaul facilities; wind tunnels; shock tube facilities; and engine test blocks.

For related information see also *14 Ground Support Systems and Facilities (Space).*

N86-13336# Aeronautical Research Labs., Melbourne (Australia).
A REAL-TIME DATA ACQUISITION SYSTEM FOR A LOW SPEED WIND TUNNEL
B. D. Fairlie Feb. 1985 36 p
(AR-AERO-R-163; AR-003-997; AR-163) Avail: NTIS HC A03/MF A01

A mini-computer based real time data acquisition system designed for use in the Aeronautical Research Laboratories low speed wind tunnel is presented. An overview of the logical arrangement of the software components of the system is provided and their interaction with the mini-computer operating system, data structures, and system hardware is described. Author

N86-13337# Aeronautical Research Labs., Melbourne (Australia).
ALGORITHMS FOR THE REDUCTION OF WIND-TUNNEL DATA DERIVED FROM STRAIN GAUGE FORCE BALANCES
B. D. Fairlie 1985 49 p refs

(ARL/AERO-R-164; AR-004-017) Avail: NTIS HC A03/MF A01

Algorithms and procedures are presented for the reduction of force and moment data derived from wind-tunnel models supported by internal strain-gauge balances. The algorithms are developed in their most general forms, suitable for implementation on the new generation of powerful minicomputers currently being included in wind-tunnel data acquisition systems. Although the emphasis is on the treatment of data derived from sting mounted strain gauge force balances, the analysis is applicable, with only minor modifications, to data derived from modern load-cell based external force balances. Author

N86-13338*# National Aeronautics and Space Administration. Langley Research Center, Hampton, Va.

COMPUTER PROGRAM FOR CALCULATING FLOW PARAMETERS AND POWER REQUIREMENTS FOR CRYOGENIC WIND TUNNELS

David A. Dress Nov. 1985 41 p refs

(NASA-TM-87609; L-16024; NAS 1.15:87609) Avail: NTIS HC A03/MF A01 CSCL 14B

A computer program has been written that performs the flow parameter calculations for cryogenic wind tunnels which use nitrogen as a test gas. The flow parameters calculated include static pressure, static temperature, compressibility factor, ratio of specific heats, dynamic viscosity, total and static density, velocity, dynamic pressure, mass-flow rate, and Reynolds number. Simplifying assumptions have been made so that the calculations of Reynolds number, as well as the other flow parameters can be made on relatively small desktop digital computers. The program, which also includes various power calculations, has been developed to the point where it has become a very useful tool for the users and possible future designers of fan-driven continuous-flow cryogenic wind tunnels. Author

N86-13339# Air Force Engineering and Services Center, Tyndall AFB, Fla. Engineering and Services Lab.

A DURABLE AIRFIELD MARKING SYSTEM Final Report, 23 Jun. 1980 - 30 Sep. 1984

T. Novinson Jun. 1985 52 p

(AF Proj. 2054)

(AD-A157953; AFESC/ESL-TR-84-59) Avail: NTIS HC A04/MF A01 CSCL 01/5

This report describes a 4-year work unit on the selection, development, and testing of a novel airfield marking system on ceramic-coated aluminized steel (CAS) tiles. The CAS tiles were developed to replace painted center marking lines that are obliterated by rubber streaks from jet tires from landing aircraft. The tiles are recessed or set into the pavement by grinding out 50- by 30-foot sections (1/8 inch deep) and bonding the tiles with epoxy/polyamide adhesive (2,000- to 5,000-psi tensile strength). The tiles can be easily cleaned by spraying with aqueous detergent and wiping off the rubber residue. The tiles are flexible, weather-resistant, chemically resistant, and highly reflective in day or evening, without retroreflective glass spheres. At $2.00 to $5.00 sq. ft., the CAS tiles are much more expensive than Federal Specification TT-P-1952 latex paint (about $0.10 sq. ft.), but the high initial cost can be offset in 1 year by lower maintenance costs. Although these CAS tiles are still being tested for Air Force use, the life cycle might be 5 to 10 years before replacement. GRA

N86-13340# Industrieanlagen-Betriebsgesellschaft m.b.H., Ottobrunn (West Germany).

INVESTIGATION FOR THE DEFINITION OF A HYDRAULIC MULTIDEGREE OF FREEDOM VIBRATION FACILITY Final Report

Hahn Reisch Paris ESA 28 Feb. 1985 108 p refs

(Contract ESTEC-5179/82/NL-PL(SC); IABG-342-7027-01/02)

(B-TF-1627; ESA-CR(P)-1950) Avail: NTIS HC A06/MF A01

A six degree-of-freedom vibration test facility for spacecraft structures is proposed. Upper frequency limit is 100 Hz. The main design criteria are: welded steel table with flat surface; mondifferential hydraulic actuators with hydrostatic piston rod bearing, 4 in vertical direction, 4 in horizontal direction; 3 three-stage servovalves in parallel; hydraulic power supply with additional oil accumulators; seismic foundation; automatic control based on analog circuits and coordinated control of the multiple actuator system with respect to the test table; multiaxial safety system; and a control and measurement system based on a 32-bit computer with array-processor. Author (ESA)

N86-13341# Office National d'Etudes et de Recherches Aerospatiales, Paris (France).

TEST OF THE ONERA CRYOGENIC BALANCE IN THE T2 WIND TUNNEL Final Report [ESSAI DE LA BALANCE CRYOGENIC ONERA DANS LA SOUFFLERIE T2 DU CFRT]

M. Bazin Feb. 1985 26 p refs In FRENCH

(Contract DRET-83-34-135)

(ONERA-BT-8/0791-GY) Avail: NTIS HC A03/MF A01

Balance qualification tests in the T2 wind tunnel are described. The feasibility of force measurement in cryogenic conditions was studied. The tests confirm accurate functioning in the temperature range 100 to 300K, showing a good compensation of electrical and mechanical temperature effects. The observed thermal gradients do not influence the required precision of one per thousand of the balance capacity. Author (ESA)

12 ASTRONAUTICS (GENERAL)

For extraterrestrial exploration see *91 Lunar and Planetary Exploration.*

N86-13342*# Eagle Engineering, Inc., Houston, Tex.

PLANETARY SAMPLE RAPID RECOVERY AND HANDLING Final Report

20 Sep. 1985 98 p

(Contract NAS9-17176)

(NASA-CR-171906; NAS 1.26:171906; Rept-85-105) Avail: NTIS HC A05/MF A01 CSCL 22A

Methods for recovering and cost effectively handling planetary samples following return to the vicinity of Earth were designed for planetary mission planners. Three topics are addressed: (1) a rough cost estimate was produced for each of a series of options for the handling of planetary samples following their return to the vicinity of Earth; (2) the difficulty of quickly retrieving planetary samples from low circular and high elliptical Earth orbit is assessed; and (3) a conceptual design for a biological isolation and thermal control system for the returned sample and spacecraft is developed. E.A.K.

N86-13343*# National Aeronautics and Space Administration. Goddard Space Flight Center, Greenbelt, Md.

REPORT ON ACTIVE AND PLANNED SPACECRAFT AND EXPERIMENTS

Norman J. Schofield, Jr., Ronald G. Littlefield, and Mary F. Elsen Feb. 1985 337 p

(NASA-TM-87499; NSSDC/WDC-A-R/S-85-01; NAS 1.15:87499) Avail: NTIS HC A15/MF A01 CSCL 22A

This report provides the professional community with information on current and planned spacecraft activity (including both free-flying spacecraft and Shuttle-attached payloads) for a broad range of scientific disciplines. By providing a brief description of each spacecraft and experiment as well as its current status, it is hoped that this document will be useful to many people interested in the scientific, applied, and operational uses of the data collected. Furthermore, for those investigators who are planning or coordinating future observational programs employing a number of different techniques such as rockets, balloons, aircraft, ships, and buoys, this document can provide some insight into the contributions that may be provided by orbiting instruments. The document includes information concerning active and planned spacecraft and experiments. The information covers a wide range of scientific disciplines: astronomy, earth sciences, meteorology, planetary sciences, aeronomy, particles and fields, solar physics, life sciences, and material sciences. These spacecraft projects represent the efforts and funding of individual countries, as well as cooperative arrangements among different countries. Author

N86-13344# European Space Agency, Paris (France).
REPORT ON THE SCIENTIFIC SATELLITES OF THE EUROPEAN SPACE AGENCY
K. Bennett, V. Domingo, U. O. Frisk, R. Grard, P. Jakobsen, M. Kessler, K. Knott, J.-P. Lebreton, R. G. Marsden, D. E. Page et al May 1985 105 p
(ESA-SP-1072) Avail: NTIS HC A06/MF A01

The activities of the Cos-B, GEOS, ISEE, IUE, and Exosat satellites, and the First Spacelab Payload are summarized. The status of the Giotto, Ulysses (International Solar Polar Mission), Space Telescope, Hipparcos, and EURECA projects is outlined. The SOHO, cluster (cosmic plasma), Kepler (Mars orbiter), Cassini (Saturn orbiter and Titan probe), AGORA (asteroid rendezvous and flyby), X-ray Multimirror Astronomy Mission, Far Infrared and Submillimeter Space Telescope, Lyman (UV astronomy), and QUASAT (VLBI) studies are introduced. Author (ESA)

N86-14197# Joint Publications Research Service, Arlington, Va.
COMMENTS ON ANNIVERSARY OF APOLLO-SOYUZ FLIGHT
Ya. Golovanov *In its* USSR Rept.: Space (JPRS-USP-85-005) 30 Sep. 1985 p 133-130 Transl. into ENGLISH from Komsomolskaya Pravda (Moscow), 14 Jul. 1985 p 3-4 (For primary document see N86-14111 04-88)
Avail: NTIS HC A08

N86-14198# Joint Publications Research Service, Arlington, Va.
SOVIET-FRENCH COMMISSION DISCUSSES JOINT SPACE PROJECTS Abstract Only
In its USSR Rept.: Space (JPRS-USP-85-005) 30 Sep. 1985 p 140 Transl. into ENGLISH from NTR: Probl. i Resheniya (Moscow), no. 1, 28 May - 10 Jun. 1985 p 3 (For primary document see N86-14111 04-88)
Avail: NTIS HC A08

13 ASTRODYNAMICS

Includes powered and free-flight trajectories; and orbit and launching dynamics.

N86-13345*# Smithsonian Institution, Cambridge, Mass.
ANALYTICAL INVESTIGATION OF THE DYNAMICS OF TETHERED CONSTELLATIONS IN EARTH ORBIT, PHASE 2 Quarterly Report, 22 Feb. - 21 Jun. 1985
Enrico Lorenzini Jul. 1985 31 p
(Contract NAS8-36606)
(NASA-CR-171611; NAS 1.26:171611; QR-1) Avail: NTIS HC A03/MF A01 CSCL 22C

This Quarterly Report deals with the deployment maneuver of a single-axis, vertical constellation with three masses. A new, easy to handle, computer code that simulates the two-dimensional dynamics of the constellation has been implemented. This computer code is used for designing control laws for the deployment maneuver that minimizes the acceleration level of the low-g platform during the maneuver. Author

N86-13346# Ricerche e Progetti s.r.l., Turin (Italy).
CROWDING OF THE GEOSTATIONARY ORBIT Final Report
Giorgio Fusco and Alessandro Buratti Paris ESA Oct. 1984 162 p refs
(Contract ESA-5705/83/NL-PP(SC))
(ESA-CR(P)-2050) Avail: NTIS HC A08/MF A01

The number of likely collisions and disturbances suffered by an active geostationary satellite involving abandoned geosynchronous satellites and other active satellites in the same longitudinal slot is evaluated. While the risk of a collision with (and even of disturbances from) abandoned satellites is very remote, the risk of a collision and the number of likely disturbances during the lifetime of a satellite with other satellites operating in the same longitudinal slot could be unacceptably high, its value depending on stationkeeping strategies which, in turn, depend on mission constraints and satellite design. Provisions involving spacecraft and ground station equipment to reduce collision and disturbance risks are discussed. Algorithms to build a detailed model of the population of abandoned objects around the geostationary orbit are presented. Author (ESA)

N86-14130# Joint Publications Research Service, Arlington, Va.
A PRIORI GUARANTEED ACCURACY EVALUATION IN DETERMINING SPACECRAFT ORBIT BY LEAST SQUARES METHOD Abstract Only
P. Ye. Elyasberg *In its* USSR Rept.: Space (JPRS-USP-85-005) 30 Sep. 1985 p 38-39 Transl. into ENGLISH from Kosmich. Issled. (Moscow), v. 22, no. 5, Sep. - Oct. 1984 p 643-650 Previously announced in IAA as A85-15251 (For primary document see N86-14111 04-88)
Avail: NTIS HC A08

14 GROUND SUPPORT SYSTEMS AND FACILITIES (SPACE)

Includes launch complexes, research and production facilities; ground support equipment, e.g., mobile transporters; and simulators.

For related information see also *09 Research Support Facilities (Air).*

N86-13347# Von Karman Inst. for Fluid Dynamics, Rhode-Saint-Genese (Belgium).
AEROTHERMODYNAMICS FOR FUTURE LAUNCHERS. REVIEW OF THE STATE OF THE ART IN EUROPE Final Report
J. F. Wendt and J. A. Essers Paris ESA Mar. 1984 131 p refs
(Contract ESA-5477/83/F-FC(SC))
(VKI-CR-1984-16/AR; ESA-CR(P)-2037) Avail: NTIS HC A07/MF A01

The status of wind tunnel and computational expertise in hypersonic aerothermodynamics, and areas of concern for a reuseable first stage vehicle and a reuseable second stage vehicle were reviewed. Many potentially useful facilities exist but require modernization. Insufficient large-scale facilities are available at M > 5 to permit development tests. Considerable basic computational expertise exists, but techniques for complex geometries and access to very large computers remain problems. The reactivation of 3 existing facilities and the modernization of up to 10 existing facilities is suggested, as well as the examination of 3 new special purpose research facilities. Contact should be with the U.S. authorities for final tests in very large tunnels. A European computer center should be established to efficiently provide essential services to users, in the research and in the design phases. A research program should be initiated to provide the necessary base. Author (ESA)

N86-14095*# National Aeronautics and Space Administration. Johnson (Lyndon B.) Space Center,
FLUORINE DISPOSAL
Allen Rakow *In its* The 1983 NASA/ASEE Summer Faculty Fellowship Research Program Research Reports Sep. 1983 23 p (For primary document see N86-14078 04-85)
Avail: NTIS HC A18/MF A01 CSCL 14B

15 LAUNCH VEHICLES AND SPACE VEHICLES

Includes boosters; manned orbital laboratories; reusable vehicles; and space stations.

N86-13348# RAND Corp., Santa Monica, Calif.
IMPROVING MILSATCOM (MILITARY SATELLITE COMMUNICA-

TION) ACQUISITION OUTCOMES: LEASE VERSUS BUY
P. M. Dinneen and T. H. Quinn Jan. 1985 46 p
(Contract F49620-82-C-0018)
(AD-A158842; RAND/N-2209-AF) Avail: NTIS HC A03/MF A01 CSCL 15/5

This study was requested by the Director of Space Systems and Command, Control, and Communications, Office of the Deputy Chief of Staff (Research, Development, and Acquisition), Headquarters United States Air Force, to assist in improving the outcomes of military satellite communication (MILSATCOM) programs. In view of rapidly rising costs of military space systems, leasing has been suggested as one way of controlling these costs. The purpose of this study, therefore, was to identify and analyze the central considerations relevant to determining whether to lease or by MILSATCOM services. The results of this report should be of interest to members of MILSATCOM acquisition community and others concerned with making lease versus buy decisions in the public sector. The work was conducted under the MILSATCOM Acquisition Policy project of the Project Air Force Resource Management Program. GRA

16 SPACE TRANSPORTATION

Includes passenger and cargo space transportation, e.g., shuttle operations; and rescue techniques.

For related information see also *03 Air Transportation and Safety* and *85 Urban Technology and Transportation.*

N86-13349*# National Aeronautics and Space Administration. Langley Research Center, Hampton, Va.
STRUCTURES AND MATERIALS TECHNOLOGY ISSUES FOR REUSABLE LAUNCH VEHICLES
S. C. Dixon, Darrel R. Tenney, Donald R. Rummler, Allan R. Wieting, and R. M. Bader (AFWAL, Dayton, Ohio) Oct. 1985 30 p refs
Presented at the EASCON 85 18th Ann. Electron. and Aerospace Systems Conf., Washington, D.C., 28-30 Oct. 1985
(NASA-TM-87626; NAS 1.15:87626) Avail: NTIS HC A03/MF A01 CSCL 22B

Projected space missions for both civil and defense needs require significant improvements in structures and materials technology for reusable launch vehicles: reductions in structural weight compared to the Space Shuttle Orbiter of up to 25% or more, a possible factor of 5 or more increase in mission life, increases in maximum use temperature of the external surface, reusable containment of cryogenic hydrogen and oxygen, significant reductions in operational costs, and possibly less lead time between technology readiness and initial operational capability. In addition, there is increasing interest in hypersonic airbreathing propulsion for launch and transmospheric vehicles, and such systems require regeneratively cooled structure. The technology issues are addressed, giving brief assessments of the state-of-the-art and proposed activities to meet the technology requirements in a timely manner. Author

N86-13350# MATRA Espace, Toulouse (France).
REVIEW OF IMPLICATIONS AND USEFULNESS OF SPACECRAFT SERVICING IN LOW EARTH ORBIT (LEO) Final Report
C. Cougnet, G. Berger, Ph. LeBouar, L. Kerstein (MBB, Ottobrunn, West Germany), H. Wartenberg (MBB, Ottobrunn, West Germany), M. Spies (MBB, Ottobrunn, West Germany), Widjaja (SENER), and J. DelToro Paris ESA 22 Oct. 1984 709 p refs
(Contract ESA-5610/83/NL)
(MATRA-092/CC/AB/225-84; ESA-CR(P)-2013) Avail: NTIS HC A99/MF A01

The usefulness, technical and operational implications, and cost effectiveness of the orbital servicing of a spacecraft performed on-board the Space Station, with a direct involvement of man, and automatically in spacecraft orbit with a servicer vehicle were investigated. Mission analysis; and identification and analysis of servicing functions and operations, and of the impacts of servicing requirements on spacecraft design are outlined. Design evolution of a EURECA type platform is discussed. A philosophy and definition of elements required by the servicing functions on board the space station are established. Servicing elements for automatic orbital servicing are defined. Orbital servicing supporting technologies are reviewed. Economic aspects of a platform mission performed with and without orbital servicing are compared. Author (ESA)

N86-13351# Messerschmitt-Boelkow-Blohm G.m.b.H., Ottobrunn (West Germany). Space Systems Studies and Applications.
IN-ORBIT TECHNOLOGY DEMONSTRATION PROGRAM (TDP). ACCOMMODATION STUDY: SPAS
Paris ESA Aug. 1984 507 p
(Contract ESTEC-5711/83/NL-PR)
(MBB-URV-147/84; ESA-CR(P)-2036) Avail: NTIS HC A22/MF A01

An accommodation study for an in-orbit technology demonstration program (TDP) was conducted for a Shuttle Pallet Satellite (SPAS) emphasizing reuse of the existing SPAS-01, which could be employed in an attached Shuttle sortie mode (SPAS-B1) and a short detached mode (SPAS-B1/F). Modifications of SPAS-01 as a short-time free-flying Shuttle subsatellite (SPAS-B2) or as short-time free-flying reusable TDP-experiment carrier (SPAS-B3) were studied. Eight Core Model Payloads (CMP) were identified and the feasibility of accomodation on the SPAS-candidates assessed. For SPAS-B1, 3 CMP with 13 to 16 experiments each were derived for TDP-missions starting in 1986/87. The critical procurement path is the availability of the TDP-experiments in time. The study suggests that from the existing SPAS-01, very promising SPAS-candidate carriers (attached or free-flying type) can be implemented in the TDP-program. The features of SPAS are its flexible program mission application, its versatile adaptions of different payloads and payload types, and its cost beneficial and economic procurement approach options. Author (ESA)

N86-13352# European Space Agency, Paris (France).
EURECA: AN INTRODUCTION TO EUROPE'S FREE-FLYING RETRIEVABLE CARRIER
N. Longdon, comp. May 1985 21 p refs Original contains color illustrations
(ESA-BR-30; ISSN-0250-1589) Avail: NTIS HC A02/MF A01

The European Retrievable Carrier (EURECA) is a reusable platform launched by the Shuttle, released in a free flying mode for 6 months or more, and then retrieved by the Shuttle Orbiter and returned to Earth. Payload capacity is up to 1000 kg. The first EURECA payload is primarily dedicated to material and life sciences which benefit from the microgravity environment. The versatility of the system is demonstrated by the fact that a quarter of the payload weight is taken up by space science and technological experiments. The EURECA provides an excellent test bed to demonstrate in-flight technologies such as direct data relay from low Earth orbits via geostationary satellites to a central operations center, rendezvous and docking, and in-orbit servicing. Earth observation possibilities, and commercial applications (new materials, crystal growth, proteins, and pharmaceutical products) are numerous. Author (ESA)

17 SPACECRAFT COMMUNICATIONS, COMMAND AND TRACKING

Includes telemetry; space communications networks; astronavigation; and radio blackout.

For related information see also *04 Aircraft Communications and Navigation* and *32 Communications.*

N86-13353*# GMD Systems, Lancaster, Calif.
MATHEMATICAL ANALYSIS STUDY FOR RADAR DATA PROCESSING AND ENHANCEMENT. PART 1: RADAR DATA ANALYSIS Final Report
Robert James and James D. Brownlow Aug. 1985 384 p refs

2 Vol.
(Contract NAS2-11491)
(NASA-CR-166616-Pt-1; H-1287-Pt-1; NAS 1.26:166616-Pt-1)
Avail: NTIS HC A17/MF A01 CSCL 17B

A study is performed under NASA contract to evaluate data from an AN/FPS-16 radar installed for support of flight programs at Dryden Flight Research Facility of NASA Ames Research Center. The purpose of this study is to provide information necessary for improving post-flight data reduction and knowledge of accuracy of derived radar quantities. Tracking data from six flights are analyzed. Noise and bias errors in raw tracking data are determined for each of the flights. A discussion of an altiude bias error during all of the tracking missions is included. This bias error is defined by utilizing pressure altitude measurements made during survey flights. Four separate filtering methods, representative of the most widely used optimal estimation techniques for enhancement of radar tracking data, are analyzed for suitability in processing both real-time and post-mission data. Additional information regarding the radar and its measurements, including typical noise and bias errors in the range and angle measurements, is also presented. This is in two parts. This is part 1, an analysis of radar data. Author

N86-13354*# GMD Systems, Lancaster, Calif.
MATHEMATICAL ANALYSIS STUDY FOR RADAR DATA PROCESSING AND ENCHANCEMENT. PART 2: MODELING OF PROPAGATION PATH ERRORS Final Report
Robert James and James D. Brownlow Aug. 1985 124 p refs
2 Vol.
(Contract NAS2-11491)
(NASA-CR-166616-Pt-2; H-1287-Pt-2; NAS 1.26:166616-Pt-2)
Avail: NTIS HC A06/MF A01 CSCL 17B

A study is performed under NASA contract to evaluate data from an AN/FPS-16 radar installed for support of flight programs at Dryden Flight Research Facility of NASA Ames Research Center. The purpose of this study is to provide information necessary for improving post-flight data reduction and knowledge of accuracy of derived radar quantities. Tracking data from six flights are analyzed. Noise and bias errors in raw tracking data are determined for each of the flights. A discussion of an altitude bias error during all of the tracking missions is included. This bias error is defined by utilizing pressure altitude measurements made during survey flights. Four separate filtering methods, representative of the most widely used optimal estimation techniques for enhancement of radar tracking data, are analyzed for suitability in processing both real-time and post-mission data. Additional information regarding the radar and its measurements, including typical noise and bias errors in the range and angle measurements, is also presented. This report is in two parts. This is part 2, a discussion of the modeling of propagation path errors. Author

N86-13355# Messerschmitt-Boelkow-Blohm G.m.b.H., Ottobrunn (West Germany). Space Div.
COMPARATIVE STUDY OF SPACE SEGMENTS FOR THE PROVISION OF FUTURE OPERATIONAL DATA RELAY SATELLITE SERVICES Final Report
Paris ESA Aug. 1984 387 p refs Prepared in cooperation with Erno Raumfahrttechnik GmbH and Thomson-CSF
(Contract ESA-5746/83/NL-DG)
(MBB-DSP-TN/DRS/132/84; ESA-CR(P)-2049) Avail: NTIS HC A17/MF A01

Data relay satellite (DRS) user requirements are identified in terms of required data rate, mission time, availability, and location of DRS and ground station(s). Time dependent mission scenarios are presented. The payload design is screened against constraints stemming from the user satellites. User availability requirements are translated into reliability requirements for payload and service module. European systems cost effectiveness is assessed, and alternative implementation and replenishment strategies are developed considering dedicated, combined, and functionally shared configurations for three payload categories. The resulting satellite systems are defined and a satellite/launcher matrix given for the space segment implementation alternatives. Planning and cost estimates are provided for comparison with minimum costs resulting for a system consisting of satellites of the TV-SAT/L-SAT class with combined payloads. Author (ESA)

N86-14144# Joint Publications Research Service, Arlington, Va.
UNIQUENESS CONDITIONS IN EVALUATION OF LEAST SQUARES METHOD IN NONLINEAR SPACE NAVIGATION PROBLEMS Abstract Only
G. A. Mersov *In its* USSR Rept.: Space (JPRS-USP-85-005) 30 Sep. 1985 p 49 Transl. into ENGLISH from Kosmich. Issled. (Moscow), v. 22, no. 5, Sep. - Oct. 1984 p 804-807 Original language document announced in IAA as A85-15267 (For primary document see N86-14111 04-88)
Avail: NTIS HC A08

N86-14164# Joint Publications Research Service, Arlington, Va.
EXPERIMENTAL CHECKING OF MATHEMATICAL MODEL OF EDDY CURRENTS IN ACTUATING COMPONENTS OF SYSTEMS FOR MAGNETIC ORIENTATION OF ARTIFICIAL EARTH SATELLITES AND SPACECRAFT Abstract Only
V. G. Lebedev, B. I. Rabinovich, R. I. Ashkinazi, and S. V. Viktorov *In its* USSR Rept.: Space (JPRS-USP-85-005) 30 Sep. 1985 p 82 Transl. into ENGLISH from Kosmich. Issled. (Moscow), v. 22, no. 6, Nov. - Dec. 1984 p 945-947 Original language document announced in IAA as A85-19914 (For primary document see N86-14111 04-88)
Avail: NTIS HC A08

N86-14166# Joint Publications Research Service, Arlington, Va.
ORGANIZATION OF SPACE NAVIGATION SYSTEM BASED ON USE OF GEOSTATIONARY SATELLITES
V. E. Abdullayev *In its* USSR Rept.: Space (JPRS-USP-85-005) 30 Sep. 1985 p 90-96 Transl. into ENGLISH from Izv. Akad. Nauk Azerb. SSR: Ser. Fiz.-Tekhn. i Mat. Nauk (Baku), v. 5, no. 2, Mar. - Apr. 1984 p 144-149 (For primary document see N86-14111 04-88)
Avail: NTIS HC A08

18 SPACECRAFT DESIGN, TESTING AND PERFORMANCE

Includes spacecraft thermal and environmental control; and attitude control.

For life support systems see *54 Man/System Technology and Life Support*. For related information see also *05 Aircraft Design, Testing and Performance* and *39 Structural Mechanics*.

N86-13356*# National Aeronautics and Space Administration, Washington, D. C.
REPORT ON THE FINDINGS OF THE JAPANESE INVESTIGATIVE TEAM ON US SPACE STATION DESIGN (KEIDANREN)
Sep. 1985 127 p Transl. into ENGLISH of "Homi Uchu Kichi Keika Chosatan Hokokusho, Ucho (Space)" Rept-23 Space Development Promotion Council (Keidanren), Tokyo, Japan, 1985 p 1-113 Transl. by Scientific Translation Service, Inc., Santa Barbara, Calif.
(Contract NASw-4004)
(NASA-TM-77659; NAS 1.15:77659) Avail: NTIS HC A07/MF A01 CSCL 22B

The objectives, itinerary and results of the Japanese Investigative Team on U.S. Space Station Design (Keidanren), consisting of members of the Space Development Promotion Council and representatives of Japanese industries involved in Japan's space station development effort are presented. This team visited NASA facilities in February, 1985. The objectives of the study team are to gather information on preliminary design efforts toward space station planning in Japan and the promotion of Japanese space related industries, as well as the evaluation of the present status of space environment exploitation in the U.S. This report is intended to be a basic reference for government agencies and industry in addressing the course of action to be taken in the future development of Japan's space station participation. Author

N86-13357*# National Aeronautics and Space Administration. Johnson (Lyndon B.) Space Center,
SPACE STATION PRELIMINARY DESIGN REPORT
Sep. 1982 252 p refs
(NASA-TM-87521; NAS 1.15:87521) Avail: NTIS HC A12/MF A01 CSCL 22B

The results of a 3 month preliminary design and analysis effort is presented. The configuration that emerged consists of a very stiff deployable truss structure with an overall triangular cross section having universal modules attached at the apexes. Sufficient analysis was performed to show feasibility of the configuration. An evaluation of the structure shows that desirable attributes of the configuration are: (1) the solar cells, radiators, and antennas will be mounted to stiff structure to minimize control problems during orbit maintenance and correction, docking, and attitude control; (2) large flat areas are available for mounting and servicing of equipment; (3) Large mass items can be mounted near the center of gravity of the system to minimize gravity gradient torques; (4) the trusses are lightweight structures and can be transported into orbit in one Shuttle flight; (5) the trusses are expandable and will require a minimum of EVA; and (6) the modules are anticipated to be structurally identical except for internal equipment to minimize cost. Author

N86-13358*# Old Dominion Univ., Norfolk, Va. Dept. of Mechanical Engineering and Mechanics.
ADAPTIVE CONTROL OF LARGE SPACE STRUCTURES USING RECURSIVE LATTICE FILTERS Final Report, period ending 31 Dec. 1985
Gene L. Goglia Dec. 1985 80 p refs
(Grant NAG1-429)
(NASA-CR-176402; NAS 1.26:176402) Avail: NTIS HC A05/MF A01 CSCL 22B

The use of recursive lattice filters for identification and adaptive control of large space structures was studied. Lattice filters are used widely in the areas of speech and signal processing. Herein, they are used to identify the structural dynamics model of the flexible structures. This identified model is then used for adaptive control. Before the identified model and control laws are integrated, the identified model is passed through a series of validation procedures and only when the model passes these validation procedures control is engaged. This type of validation scheme prevents instability when the overall loop is closed. The results obtained from simulation were compared to those obtained from experiments. In this regard, the flexible beam and grid apparatus at the Aerospace Control Research Lab (ACRL) of NASA Langley Research Center were used as the principal candidates for carrying out the above tasks. Another important area of research, namely that of robust controller synthesis, was investigated using frequency domain multivariable controller synthesis methods. G.L.C.

N86-13359*# Allied Bendix Aerospace, Teterboro, N.J. Guidance Systems Div.
ASTROPHYSICAL PAYLOAD ACCOMMODATION ON THE SPACE STATION Final Report, 10 Dec. 1984 - 15 Oct. 1985
Bernard P. Woods 15 Oct. 1985 164 p refs
(Contract NAS8-36124)
(NASA-CR-178556; NAS 1.26:178556) Avail: NTIS HC A08/MF A01 CSCL 22B

Surveys of potential space station astrophysics payload requirements and existing point mount design concepts were performed to identify potential design approaches for accommodating astrophysics instruments from space station. Most existing instrument pointing systems were designed for operation from the space shuttle and it is unlikely that they will sustain their performance requirements when exposed to the space station disturbance environment. The technology exists or is becoming available so that precision pointing can be provided from the space station manned core. Development of a disturbance insensitive pointing mount is the key to providing a generic system for space station. It is recommended that the MSFC Suspended Experiment Mount concept be investigated for use as part of a generic pointing mount for space station. Availability of a shirtsleeve module for instrument change out, maintenance and repair is desirable from the user's point of view. Addition of a shirtsleeve module on space station would require a major program commitment. Author

N86-13360# European Space Tribology Lab., Risley (England).
THERMAL VACUUM TESTS ON A HINGE ACTUATOR MECHANISM
J. C. Anderson Paris ESA Jan. 1984 18 p ref
(Contract ESA-5199/NL-PP)
(ESA-ESTL-067; ESA-CR(P)-1921) Avail: NTIS HC A02/MF A01

A Hinge Actuator Mechanism (HAM) which provides a controlled rotary motion for deployment underwent tests in vacuum, over an isothermal range of temperatures from +82 to -68 C. The HAM always operates over this temperature range but the time taken for deployment (rotation through 90 deg) varies from 23.28 sec at +82C to 70.16 sec at -68C. The variation is due to the change in resistivity of the aluminum disk rotor in the eddy current brake used to control deployment speed. Also, at temperatures < -40 C, the torque of the main bearings increases due to the different thermal contractions of the aluminum alloy housings and steel shafts which results in the elimination of radial clearance in the bearings. Author (ESA)

N86-13361# Messerschmitt-Boelkow-Blohm G.m.b.H., Ottobrunn (West Germany).
ASSEMBLY INTEGRATION VERIFICATION (AIV) TEST EFFECTIVENESS STUDY. APPLICABILITY OF SPACELAB APPROACH FOR EQUIPMENT AND SYSTEM TEST FOR ARIANE-4 CLASS SATELLITES. VOLUME 1: EXECUTIVE SUMMARY Final Report
L. Kerstein, W. Farr, H. Maager, J. Weydandt, and Chr. Milan Paris ESA 1985 108 p Prepared in cooperation with Erno Raumfahrttechnik GmbH
(Contract ESTEC-5516/83/NL-PP(SC))
(ERNO-671/AIV-Vol-1; ESA-CR(P)-2035) Avail: NTIS HC A06/MF A01

The overall Spacelab test program on ground, in orbit verification of the Spacelab system during Spacelab mission one, including flight measurement results, test management and organization, test documentation, and test program control procedures are reviewed. Failures observed during ground testing at all levels of testing, integration stages, and flight were classified according to cause. Temperature, thermal vacuum, and random vibration tests are identified as the most effective screening test and are recommended as mandatory tests for the standard environmental test specification on equipment level. The environmental test program on equipment level and the system level assembly test procedures and methods yielded high quality flight hardware. Only two anomalies were noticed during Spacelab mission one. After the first failure investigation on ground including extensive and extreme functional and environmental test programs, the failure with the RAU 21 could not be repeated even by an additional thermal vacuum test on system level. Flight measurements on hardware suggest that the test requirements for Spacelab equipment qualification are adequate, (no requalification was necessary). Author (ESA)

N86-13362# General Electric Co., Whetstone (England). Mechanical Engineering Lab.
STUDY OF THERMAL ANALYSIS METHODS Final Report
J. J. Rebis and P. S. White Paris ESA Dec. 1984 133 p refs
(Contract ESA-5653/83/NL-PB)
(GEC-MEL12.0539; ESA-CR(P)-2045) Avail: NTIS HC A07/MF A01

Lumped parameter and finite element methods were found to be suited to spacecraft thermal analysis after a study of and spatial discretization, temporal discretization, and solution of the equations resulting from these discretizations. Advantages of finite element methods over lumped parameter are: all quantities used in the analysis are systematically derived from the geometric model and material properties (this eliminates the preliminary calculation of conduction links and capacitance values necessary for lumped parameters); the nature of the approximation is well defined and convergence to the true solution can be demonstrated under certain conditions; explicit estimates of accuracy are possible; greater accuracy for a given number of nodes; interpolation of the results can be carried out systematically; and compatibility with mainstream stress analysis programs. Disadvantages linked to its inferior robustness, greater computer resource requirement for the same number of nodes; greater software effort required to obtain the same degree of flexibility, and lack of consistent radiation modeling can be overcome. Author (ESA)

N86-13363# Dornier-Werke G.m.b.H., Friedrichshafen (West Germany).
TWO-PHASE HEAT TRANSPORT SYSTEMS: SYSTEM DEFINITION, VOLUME 1 Final Report
H. Kreeb, P. Moeller, N. H. Pennings (Royal Netherlands Aircraft Factories Fokker), R. S. Bhatti (Societe Anonyme Belge de Constructions Aeronautiques), J. P. Mathieu (Societe Anonyme Belge de Constructions Aeronautiques), and S. vanOost (Societe Anonyme Belge de Constructions Aeronautiques) Paris ESA 28 Jan. 1985 132 p refs
(Contract ESA-5669/83/NL-PB(SC))
(ESA-CR(P)-2052) Avail: NTIS HC A07/MF A01

A heat transport system for space stations (including Columbus) and platforms, with heat rejection capacity in the range 10 to 15 kW per module/platform for a 10 yr mission is defined. A two-phase flow loop driven by an electrically powered liquid pump and with capillary assisted evaporators is selected. To fulfil the requirements of narrow temperature control limits, each two-phase flow concept requires a complex control device. A modular design solution dictates the parallel configuration of all evaporators and heat pipe based radiator panels. A program culminating in integration and test of a demonstration model of the complete system is proposed. Author (ESA)

N86-13364# Erno Raumfahrttechnik G.m.b.H., Bremen (West Germany). Structures Dept.
STANDARDIZATION PROGRAM ON DESIGN ANALYSIS AND TESTING OF INSERTS IN NONMETALLIC SANDWICH COMPONENTS Final Report
W. H. Paul, D. Wagner, and J. Bischoff Paris ESA 1984 397 p refs
(Contract ESA-440/80/NL-AK(SC))
(TR-TS-RP-2-09-84; ESA-CR(P)-2056) Avail: NTIS HC A17/MF A01

The state of the art of insert design technology was reviewed with respect to gains, and problems when applying this technique to nonmetallic sandwich elements. For loading normal to the panel facing it is shown that a design and analysis procedure provided previously may be used for nonmetallic insert/panel design. Material data were generated for the most interesting materials. The failure criteria include static tension, compression, and fatigue life under alternating loads. Residual strength was assessed. Failure modes for in-plane loads of a CFRP facing were investigated. Tests to identify the acceptability of thermal loading with respect to the degradation of strength of potting under thermal loading, were performed. To determine the tolerable torsion of an insert, experience shows that the form locking effect between the surfaces of the potting and the inner side of the upper facing is important to achieve realistic tolerances. Author (ESA)

N86-14090*# Houston Univ., Tex. Dept. of Electrical Engineering.
CONTROL OF SPACE STATIONS Final Report
Kwang Y. Lee *In* NASA. Johnson (Lyndon B.) Space Center The 1983 NASA/ASEE Summer Faculty Fellowship Research Program Research Reports Sep. 1983 8 p refs (For primary document see N86-14078 04-85)
Avail: NTIS HC A18/MF A01 CSCL 22B

N86-14114# Joint Publications Research Service, Arlington, Va.
METHOD FOR SOLVING TWO-POINT BOUNDARY VALUE PROBLEM FOR OPTIMIZATION OF FLIGHTS WITH LOW THRUST Abstract Only
A. I. Glazkov *In its* USSR Rept.: Space (JPRS-USP-85-005) 30 Sep. 1985 p 26 Transl. into ENGLISH from Kosmich. Issled. (Moscow), v. 22, no. 6, Nov. - Dec. 1984 p 842-847 Original language document announced in IAA as A85-19903 (For primary document see N86-14111 04-88)
Avail: NTIS HC A08

N86-14115# Joint Publications Research Service, Arlington, Va.
CHOICE OF OPTIMUM BOUNDARY CONDITIONS IN SPEED OPTIMIZATION PROBLEM Abstract Only
S. A. Voyevodin *In its* USSR Rept.: Space (JPRS-USP-85-005) 30 Sep. 1985 p 26-27 Transl. into ENGLISH from Kosmich. Issled. (Moscow), v. 22, no. 6, Nov. - Dec. 1984 p 848-857 Original language document announced in IAA as A85-19904 (For primary document see N86-14111 04-88)
Avail: NTIS HC A08

N86-14116# Joint Publications Research Service, Arlington, Va.
MATHEMATICAL MODELS OF NONSTATIONARY EDDY CURRENTS AND EDDY MOVEMENTS OF FLUID IN PROBLEMS OF ORIENTATION AND STABILIZATION OF ARTIFICIAL EARTH SATELLITES AND SPACECRAFT 2 Abstract Only
B. I. Rabinovich and V. M. Rogovoy *In its* USSR Rept.: Space (JPRS-USP-85-005) 30 Sep. 1985 p 27 Transl. into ENGLISH from Kosmich. Issled. (Moscow), v. 22, no. 6, Nov. - Dec. 1984 p 867-874 Original language document announced in IAA as A85-19906 (For primary document see N86-14111 04-88)
Avail: NTIS HC A08

N86-14133# Joint Publications Research Service, Arlington, Va.
MATHEMATICAL MODELS OF NONSTATIONARY EDDY CURRENTS AND EDDY MOTIONS OF FLUID IN SPACECRAFT ORIENTATION AND STABILIZATION PROBLEMS 1 Abstract Only
B. I. Rabinovich and V. M. Rogovoy *In its* USSR Rept.: Space (JPRS-USP-85-005) 30 Sep. 1985 p 41 Transl. into ENGLISH from Kosmich. Issled. (Moscow), v. 22, no. 5, Sep. - Oct. 1984 p 678-692 Original language document announced in IAA as A85-15255 (For primary document see N86-14111 04-88)
Avail: NTIS HC A08

N86-14134# Joint Publications Research Service, Arlington, Va.
COMPARISON OF ENERGETICS OF OPTIMUM MANEUVERS AND TWO-IMPULSE MANEUVERS IN SOME PROBLEMS OF MOTION FROM A POINT INTO ORBIT Abstract Only
A. P. Skorokhodov *In its* USSR Rept.: Space (JPRS-USP-85-005) 30 Sep. 1985 p 41-42 Transl. into ENGLISH from Kosmich. Issled. (Moscow), v. 22, no. 5, Sep. - Oct. 1984 p 693-701 Original language document announced in IAA as A85-15256 (For primary document see N86-14111 04-88)
Avail: NTIS HC A08

N86-14135# Joint Publications Research Service, Arlington, Va.
OPTIMUM CONTROL PROGRAMS IN PROBLEM OF INTERORBITAL FLIGHT WITH CONTINUOUS THRUST Abstract Only
S. A. Ishkov and V. V. Salmin *In its* USSR Rept.: Space (JPRS-USP-85-005) 30 Sep. 1985 p 42 Transl. into ENGLISH from Kosmich. Issled. (Moscow), v. 22, no. 5, Sep. - Oct. 1984 p 702-711 Original language document announced in IAA as A85-15257 (For primary document see N86-14111 04-88)
Avail: NTIS HC A08

N86-14163# Joint Publications Research Service, Arlington, Va.
STABILITY OF STATIONARY MOTIONS OF TWO TETHERED BODIES IN ORBIT UNDER INFLUENCE OF GRAVITATIONAL AND AERODYNAMIC FORCES Abstract Only
Ye. M. Levin *In its* USSR Rept.: Space (JPRS-USP-85-005) 30 Sep. 1985 p 81 Transl. into ENGLISH from Kosmich. Issled. (Moscow), v. 22, no. 5, Sep. - Oct. 1984 p 675-682 Original language document announced in IAA as A85-15254 (For primary

document see N86-14111 04-88)
Avail: NTIS HC A08

N86-14199# Joint Publications Research Service, Arlington, Va.
LIST OF RECENT SOVIET SPACE LAUNCHES
In its USSR Rept.: Space (JPRS-USP-85-005) 30 Sep. 1985 p 141-143 Transl. into ENGLISH from various Russian articles (For primary document see N86-14111 04-88)
Avail: NTIS HC A08

19 SPACECRAFT INSTRUMENTATION

For related information see also *06 Aircraft Instrumentation* and *35 Instrumentation and Photography.*

N86-13365*# National Aeronautics and Space Administration. Marshall Space Flight Center, Huntsville, Ala.
DE 1 RIMS OPERATIONAL CHARACTERISTICS
R. C. Olsen (Alabama Univ., Huntsville), R. H. Comfort (Alabama Univ., Huntsville), M. O. Chandler (Alabama Univ., Huntsville), T. E. Moore, J. H. Waite, Jr., D. L. Reasoner, and A. P. Biddle Oct. 1985 45 p refs
(NASA-TM-86527; NAS 1.15:86527) Avail: NTIS HC A03/MF A01 CSCL 14B

The Retarding Ion Mass Spectrometer (RIMS) on the Dynamics Explorer 1 spacecraft observes both the thermal and superthermal (<50 eV) ions of the ionosphere and inner magnetosphere. It is capable of measuring the detailed species distribution function of these ions in many cases. It was equipped with an integral electrometer to permit in-flight calibration of the detector sensitivities and variations thereof. A guide to understanding the RIMS data set is given. The reduction process from count rates to physical quantities is discussed in some detail. The procedure used to establish in-flight calibration is described, and results of a comparison with densities from plasma wave measurements are provided. Finally, a discussion is provided of various anomalies in the data set, including changes of channeltron efficiency with time, spin modulation of the axial sensor heads, apparent potential differences between the sensor heads, and failures of the radial head retarding potential sweep and of the -Z axial head aperture plane bias. Studies of the RIMS data set should be conducted only with a thorough awareness of the material presented here, or in collaboration with one of the scientists actively involved with RIMS data analysis. Author

N86-13366# Centronic Ltd., Croydon (England).
SUN ACQUISITION SENSOR FOR EUROPEAN COMMUNICATIONS SATELLITE
1985 11 p
Avail: NTIS HC A02/MF A01

A development program for a Sun acquisition sensor with 7yr in-orbit life and 5yr storage in a clean room is outlined. The design proposes P-type silicon (10 ohm/cm), nongold solder contacts, glass epoxy boards, and silicones for attaching windows to chip and chip to board. Radiation damage, raw materials, qualification tests, and packing are discussed. Author (ESA)

N86-13367# British Aerospace Dynamics Group, Bristol (England). Space and Communications Div.
DEVELOPMENT OF THE NIMBUS-7 SMMR RETRIEVAL ALGORITHM Final Report
J. E. Charlton, comp. Paris ESA Mar. 1985 113 p refs
(Contract ESA-5545/83/NL-GM(SC))
(BAe-RPT/NIM-7/021; ESA-CR(P)-2053) Avail: NTIS HC A06/MF A01

An iterative algorithm for the extraction of geophysical parameters from the sea surface and intervening atmosphere from the Nimbus 7 microwave radiometer was developed. Surface and atmospheric truth data for the North Atlantic were used to assess the algorithm. Results show that satellite data from the most northerly positioned ship appears to be contaminated by sidelobe pick-up. The derived sea surface temperature exceeds ground truth data for all ships. Insertion of biases for the satellite data considerably reduces the residuals and improves the correlations. The required biases suggest that the calibrated channel at 37 GHz for horizontal polarization, in particular, yields outputs which are too high. Changes from the windspeed model of the original program reduce the correlation of derived parameters with the ground truth. Sea surface humidity predictions are particularly good. Author (ESA)

N86-13368# Norges Tekniske Hoegskole, Trondheim. Electronics Research Lab.
FEASIBILITY STUDY OF CHIRP GENERATOR FOR ERS-1 RADAR ALTIMETER, OPTION A Final Report
J. Dybedal, A. Ronnekleiv, L. P. Solie, and E. Soerlie Paris ESA Jan. 1983 150 p refs
(Contract ESTEC-4845/81/NL-PP(SC))
(ELAB-STF44-F83103; ESA-CR(P)-2058) Avail: NTIS HC A07/MF A01

The design of the surface acoustic wave (SAW) chirp line and accessory electronics, which form the chirp generator of the ERS-1 radar altimeter is reviewed. Tests on the complete generator and submodules are summarized. The expander satisfies specifications at room temperature, producing a chirp with an rms phase deviation from quadratic of 3.7 deg and a signal to noise ratio > 20 dB. The expander gates an LO signal at 300 MHz and expands it in a SAW chirp line using arrays of reflecting holes in YZ-LiNbO3. Amplitude uniformity and stability are provided by a limiter. Extension of the operational temperature range to between minus 25 and plus 55 C is possible with small modifications. Author (ESA)

N86-14154# Joint Publications Research Service, Arlington, Va.
DEVELOPMENT OF INSTRUMENTS FOR VEGA PROBES Abstract Only
A. Barshay *In its* USSR Rept.: Space (JPRS-USP-85-005) 30 Sep. 1985 p 61 Transl. into ENGLISH from Sov. Kirgiziya (Frunze), 22 Jun. 1985 p 4 (For primary document see N86-14111 04-88)
Avail: NTIS HC A08

20 SPACECRAFT PROPULSION AND POWER

Includes main propulsion systems and components, e.g., rocket engines; and spacecraft auxiliary power sources.

For related information see also *07 Aircraft Propulsion, 28 Propellants and Fuels,* and *44 Energy Production and Conversion.*

N86-13369*# Mechanical Technology, Inc., Latham, N. Y.
HPOTP LOW-SPEED FLEXIBLE ROTOR BALANCING, PHASE 1 Final Report
J. Giordano and E. Zorzi 23 Jul. 1985 96 p
(Contract NAS8-35598)
(NASA-CR-171610; NAS 1.26:171610; MTI-85TR28) Avail: NTIS HC A05/MF A01 CSCL 21H

A method was developed that shows promise in overcoming many balancing limitations. This method establishes one or more windows for low speed, out-of-housing balancing of flexible rotors. These windows are regions of speed and support flexibility where two conditions are simultaneously fulfilled. First, the rotor system behaves flexibly; therefore, there is separation among balance planes. Second, the response due to balance weights is large enough to reliably measure. The analytic formulation of the low-speed flexible rotor balancing method is described. The results of proof-of-principle tests conducted under the program are presented. Based on this effort, it is concluded that low speed flexible rotor balancing is a viable technology. In particular, the method can be used to balance a rotor bearing system at low speed which results in smooth operation above more than one bending critical speed. Furthermore, this balancing methodology is applicable to SSME turbopump rotors. Author

N86-14085*# American Univ., Beirut (Lebanon).
A STUDY OF SOME FEATURES OF ac AND dc ELECTRIC POWER SYSTEMS FOR A SPACE STATION Final Report
Jack I. Hanania *In* NASA. Johnson (Lyndon B.) Space Center The 1983 NASA/ASEE Summer Faculty Fellowship Research Program Research Reports Sep. 1983 15 p refs (For primary document see N86-14078 04-85)
Avail: NTIS HC A18/MF A01 CSCL 22B

23 CHEMISTRY AND MATERIALS (GENERAL)

Includes biochemistry and organic chemistry.

N86-13370*# National Aeronautics and Space Administration. Lewis Research Center, Cleveland, Ohio.
MODIFICATIONS OF SYSTEM FOR ELEVATED TEMPERATURE TENSILE TESTING AND STRESS-STRAIN MEASUREMENT OF METAL MATRIX COMPOSITES
Juan O. Diaz 1985 21 p refs Presented at the 1st Symposium on Testing Technology of Metal Matrix Composites, Nashville, 18-20 Nov. 1985; sponsored by the American Society for Testing and Materials
(NASA-TM-87172; E-2813; NAS 1.15:87172) Avail: NTIS HC A02/MF A01 CSCL 11D

Composites consisting of tungsten alloy wires in superalloy matrices are being studied because they offer the potential for increased strength compared to current materials used at temperatures up to at least 1093 C (2000F). Previous research at the NASA Lewis Research Center and at other laboratories in the U.S., Europe, and Japan has demonstrated laboratory feasibility for fiber reinforced superalloys (FRS). The data for the mechanical and physical properties used to evaluate candidate materials is limited and a need exists for a more detailed and complete data base. The focus of this work is to develop a test procedure to provide a more complete FRS data base to quantitatively evaluate the composite's potential for component applications. This paper will describe and discuss the equipment and procedures under development to obtain elevated temperature tensile stress-strain, strength and modulus data for the first generation of tungsten fiber reinforced superalloy composite (TFRS) materials. Tensile stress-strain tests are conducted using a constant crosshead speed tensile testing machine and a modified load-strain measuring apparatus. Elevated temperature tensile tests are performed using a resistance wound commercial furnace capable of heating test specimens up to 1093 C (2000 F). Tensile stress-strain data are obtained for hollow tubular stainless steel specimens serving as a prototype for future composite specimens. Author

N86-13371# Air Force Inst. of Tech., Wright-Patterson AFB, Ohio.
THE DYNAMICS OF THE PHOTOFRAGMENTATION OF KETENE 3-CYCLOPENTENONE, 3,5-CYCLOHEPTADIENONE, AND TROPONE Ph.D. Thesis
B. I. Sonobe 1985 170 p
(AD-A158045; AFIT/CI/NR-85-90D) Avail: NTIS HC A08/MF A01 CSCL 07/3

Photofragment infrared fluorescence methods were used to study energy disposal to the carbon monoxide product of ketone photodissociation. Vibrationally excited CO is formed upon photolysis at 193 nm, but not at 249 and 308 nm. The nascent CO vibrational energy distribution can be characterized by a temperature, T subscript V = 3750 K. The nascent CO rotational energy distribution can be characterized by a temperature, T subscript r = 6700 K. This suggests that ketone undergoes dissociation by a non-linear path following photoexcitation at 193 nm. Time-resolved laser absorption spectroscopy was used to study the energy partitioning in the photoactivated fragmentation of 3-cyclopentenone, 3,5-cycloheptadienone, and tropone. The CO product vibrational energy distribution was measured at photolysis wavelengths of 193, 249, and 308 nm. The experimental distributions are analyzed by comparing them with distributions calculated by using a statistical model. For 3-cyclopentenone and tropone, only the non-fixed energy of the transition state is available for partitioning among the products' vibrational degrees of freedom, whereas, for 3,5-cycloheptadienone, the full reaction exoergicity is available to be randomly distributed among all the developing products' degrees of freedom. This suggests that the products of the dissociation of 3-cyclopentenone and tropone are vibrationally decoupled from one another in the exit channel. Author (GRA)

N86-13372# Rutgers - The State Univ., New Brunswick, N. J. Dept. of Chemistry.
FUNCTIONALIZED VESICLES AS ORGANIC REAGENTS Final Report, 1 May 1982 - 30 Jun. 1985
R. A. Moss 2 Jul. 1985 6 p
(Contract DAAG29-82-K-0122)
(AD-A158381; ARO-19175.18-CH) Avail: NTIS HC A02/MF A01 CSCL 06/1

Our scientific objective is the construction of specific organic reagents based upon functionalized surfactant vesicles. In this proposal, fully-functionalized thiol, imidazole, and hydroxyl vesicles are presented as reagents of special properties. Methods are suggested to chemically differentiate the inner and outer functionalities of multilamellar functional vesicles. Selective deactivation of exterior interior functionalities, as well as reactions which are rate-limited by permeation of substrates through the exterior bilayer of the vesicle. Liposomal systems which should esterify cholesterol are designed in analogy to the lecithin: cholesterol acyl transferase enzyme system. Vesicular systems designed to efficiently cleave toxic phosphates are to be investigated for the possible development of decontamination agents. The proposed research should have implications for synthetic organic, bioorganic, biomimetic and membrane chemistry. In fact, major progress has been made in the areas of functional vesicles, phosphate cleavage, and stereochemical selectivity in micellar systems. GRA

N86-13373# Washington State Univ., Pullman. Dept. of Chemistry.
TEMPERATURE AND PRESSURE COMPONENTS OF SHOCK-INDUCED CHANGES IN THE ELECTRONIC SPECTRUM OF CARBON DISULFIDE M.S. Thesis
R. H. Granholm Aug. 1985 60 p
(Contract N00014-77-C-0232)
(AD-A158627) Avail: NTIS HC A04/MF A01 CSCL 07/4

Liquid carbon disulfide has its first electronic transition centered at 3200 A. Shock-compression of CS2 up to about 80 kilobars has been shown to shift the red edge of this absorption band more than 1600 A towards longer wavelengths. In this work the conditions of temperature and pressure behind the shock wave are controlled to allow their separate effects on the CS2 spectrum to be determined. The shift of the band edge appears to be a function only of temperature and pressure. GRA

N86-13374# Naval Research Lab., Washington, D. C.
ELUTION OF BENZENE AND METHYL ETHYL KETONE FROM CHARCOAL BEDS BY CONTINUED AIR SWEEPING Interim Report, Mar. 1983 - Nov. 1984
J. K. Thompson, L. A. Jonas, and B. E. Walker 4 Sep. 1985 26 p
(DA Proj. F64-651)
(AD-A158804; NRL-MR-5643) Avail: NTIS HC A03/MF A01 CSCL 07/4

Activated carbon, or charcoal, is commonly used in adsorption beds to remove unwanted vapors from air in ventilating systems and in personal protective respirators. The vapor molecules become trapped by adsorption on the extensive surface of the charcoal and hence are removed for the air stream. However, this trapping is not permanent. These adsorbed molecules can desorb again into the passing air stream and be carried along to another adsorption site, where the cycle is repeated. Thus, a dose of vapor fed into a charcoal bed under a continuous flow of air will migrate as wave through the bed and subsequently will appear as a concentration peak in the effluent air stream. The questions arise, then--especially if the vapor is a hazardous material: how long will it take for the eluted vapor dose to appear in the effluent, and what will answer these questions to some extent, and (2) to characterize the kinetics of the process in terms of the Wheeler desorption equation. Test tube-sized beds of Whetlerite were challenged with benzene or methyl ethyl ketone (MEK) in doses less that required for break-through. Then, as air sweeping continued, time and concentration of the benzene or MEK elution peaks were observed and found to be predictable functions of the dosage. The results were also analyzed by adsorption/desorption which were derived monotonci functions of the degree of carbon loading. GRA

N86-13375# Cornell Univ., Ithaca, N.Y. Dept. of Civil Engineering.
MASS TRANSFER COEFFICIENTS AND HENRY'S CONSTANTS FOR PACKED-TOWER AIR STRIPPING OF VOLATILE ORGANICS: MEASUREMENTS AND CORRELATION Final Report, Dec. 1981 - May 1984
J. M. Gosset, C. E. Cameron, B. P. Eckstrom, C. Goodman, and A. H. Lincoff Jun. 1985 302 p
(Contract F08635-82-K-0159)
(AD-A158811; ESL-TR-85-18) Avail: NTIS HC A14/MF A01 CSCL 07/4

Design of packed-tower air-stripping systems for the removal of volatile contaminants from groundwaters requires knowledge of the equilibrium constant relating air and water concentrations (Henry's constant, H), and the applicable mass transfer coefficient (K sub 1a). The objectives of this research were: to evaluate the effects of temperature, ionic strength, and the mutual presence of other organics on the H-values of five volatile compounds of concern to the USAP; and to investigate the effects of temperature, packing size and type, liquid and air loadings, and the mutual presence of other organics on the K sub 1a values of these five compounds--tetrachloroethylene, trichloroethylene, 1,1,1-trichloroethane, chloroform, and methylene chloride. An innovative method for measuring Henry's constants was proposed and evaluated, termed Equilibrium Partitioning In Closed Systems (EPICS). This method relies upon measurement of the ratio of headspace concentrations from two equilibrated bottles containing equal solute masses, but possessing differing liquid volumes. H-values for the five compounds were measured over temperatures ranging from 10 to 30 C using both EPICS and batch, diffused-bubble stripping techniques. Temperature regressions for H were derived. Comparison between methods suggests that EPICS is as precise as the batch-stripping technique, and is probably more accurate, being free of mass transfer limitations. Liquid-phase diffusivity values were measured for the five study compounds at 20 C using a diaphragm diffusion cell. GRA

24 COMPOSITE MATERIALS

Includes laminates.

N86-13376 Illinois Univ., Urbana-Champaign.
PROCESS-INDUCED VISCOELASTIC STRESS IN COMPOSITE LAMINATES Ph.D. Thesis
Robert James Stango 1985 95 p
Avail: Univ. Microfilms Order No. DA8511676

In recent years, considerable interest has developed in evaluating the stress response of composite laminates which is associated with cooling the material system from the cure temperature to room temperature. The present research examine the fundamental nature of time-dependent residual-thermal stresses in composite laminates which are caused by the extreme temperature reduction encountered during the fabrication process. Viscoelastic stress in finite-width, symmetric composite laminates is examined on the basis of a formulation which employs an incremental hereditary integral approach in conjunction with a quasi-three dimensional finite element analysis. A consistent methodology is developed and employed for the characterization of lamina material properties. Special attention is given to the time-dependent stress response at ply-interface locations near the free-edge. In addition, the influence of cooling path on stress history is examined. Recently published material property data for graphite-epoxy lamina is employed in the analysis. Dissert. Abstr.

N86-13377# Royal Aircraft Establishment, Farnborough (England).
EFFECT OF CARBON FIBRE SURFACE TREATMENT ON MOISTURE ABSORPTION AND INTERLAMINAR SHEAR STRENGTH OF CARBON FIBRE/EPOXY RESIN COMPOSITES
O. K. Joshi May 1984 34 p
(AD-A157705; RAE-TR-84047; DRIC-BR-94905) Avail: NTIS HC A03/MF A01 CSCL 11/4

Carbon fibers surface treated to eight different levels of the standard treatment were moulded into unidirectional composites in an epoxy resin. The composites were immersed in boiling water or exposed to a hot humid environment (70C, 95% RH), and the water absorption, swelling and interlaminar shear strength were measured. The reversibility of these effects was studied initially by drying the composite at 70 C in a vacuum oven and further by repeated hygrothermal cycling. In general, more moisture was absorbed for the lower levels of surface treatment where the bond between the fiber and matrix was weaker. Studies of reversibility showed that there was a greater probability of permanent damage for low fiber matrix bond strengths and for specimens immersed in boiling water. GRA

N86-13378# Air Force Wright Aeronautical Labs., Wright-Patterson AFB, Ohio.
COMPOSITES DESIGN Final Report, Jun. - Nov. 1984
S. W. Tsai and T. N. Massard Dec. 1984 144 p
(AF Proj. 2307)
(AD-A157710; AFWAL-TR-84-4183) Avail: NTIS HC A07/MF A01 CSCL 11/4

This report includes the fundamental equations for the stiffness and strength of laminated composites and two approaches to determine the optimum strength of laminates. Formulas for micromechanics and for unsymmetric laminates are simplified so that material and geometric factors can be more easily optimized than the unabridge theory. This report is intended as a source of information for designers, fabricators and researchers of composites. GRA

N86-13379# Puerto Rico Univ., Rio Piedras.
MULTIPLE SCATTERING THEORIES FOR OPTICAL PROPERTIES OF COMPOSITE MATERIALS Final Report, 15 Jun. 1981 - 15 May 1985
M. Gomez-Rodriquez 15 May 1985 101 p
(Grant DAAG29-81-G-0010)
(AD-A158270; ARO-18574-PH) Avail: NTIS HC A06/MF A01 CSCL 11/6

A theoretical model is formulated that predicts the optical properties of nonhomogeneous materials (cermets). It has been found that correlation effects due to the formation process of cermets, quantum size corrections, and renormalized corrections are essential ingredients of a realistic theory for the optical properties of cermets. This is particularly true in the high concentration regime of the metallic minority constituent (when concentration of the metal exceeds 10% volume fraction). The first smoothing approximation was used in the multiple scattering calculation in the context of the random continuum and distinct metallic island models for cermets. The T-Matrix renormalize calculation applied to the; distinct metallic island model for cermets was found to give the best predictive theory. This model predicted the frequency and height of the observed resonance in the imaginary part of the index of refraction with a high degree of precision for a wide regime of concentration and materials. GRA

N86-13380# New York Univ., New York. Inst. of Mathematical Sciences.
EFFECTIVE BEHAVIOR OF COMPOSITE MATERIALS Final

Report, 1 Sep. 1983 - 30 Nov. 1984
G. C. Papanicolaou 23 Apr. 1985 6 p
(Grant AF-AFOSR-0228-80)
(AD-A158941; Rept-5274192; AFOSR-85-0671TR) Avail: NTIS HC A02/MF A01 CSCL 11/4

The main results of our work fall into three categories which we list in order of significance to our present and future work: (1) Focusing a singularity of the nonlinear Schrodinger equation. We have solved by a careful analytical-numerical method the basic question of what the local rate of blow-up is for solutions of the nonlinear Schrodinger equation with cubic nonlinearity in 2 space dimensions. This problem is a basic one that arises in many aspects of nonlinear wave propagation. (2) Selfdiffusion of interacting Brownian motions. Using methods of wave propagation in random media that we had developed earlier, we were able to study the effective behavior of a tagged Brownian particle in interaction with an infinite system of other such particles. (3) Bounds for effective properties of composites by analytic continuation. The analytic continuation method was known to work only for two component materials. In our work we extend it to multicomponent materials by using the theory of several complex variables. GRA

N86-13381# Naval Surface Weapons Center, Silver Spring, Md.
A METHOD TO DETERMINE DYNAMIC ELASTIC CONSTANTS OF THIN SHELL COMPOSITES BY GUIDED ULTRASONIC WAVES
J. V. Foltz, A. L. Bertram, and C. W. Anderson 15 Jun. 1985 32 p
(AD-A159025; NSWC/TR-85-186) Avail: NTIS HC A03/MF A01 CSCL 11/4

Ultrasonic techniques are used to determine the velocities of guided waves in unidirectional metal matrix composite places. Both extensional (fundamental Lamb symmetric) and in-plane shear (SH) plate wave speeds are measured via through-transmission procedures utilizing one-half megahertz broadband transducers. The values recorded for the wave speeds and the plate density are used to calculate the four reduced stiffness coefficients of the plane stress Hooke's Law relationship of the plate. This approach allows the full set of elastic constants required by designers for the analysis of a thin orthotropic plate or shell loaded in its plane to be obtained from only four ultrasonic measurements. The accuracy of the elastic constant determinations may be increased by measuring more than four wave speeds and employing the statistical data reduction method described. GRA

N86-13382# Sandia National Labs., Albuquerque, N. Mex.
ULTRASONIC LONGITUDINAL WAVE VELOCITY IN CARBON-CARBON PITCH AND PITCH/M2 SHAPE STABLE NOSETIP MATERIAL FROM 70 DEG F TO 5400 DEG F
J. H. Gieske Jun. 1985 54 p
(Contract DE-AC04-76DP-00789)
(DE85-017330; SAND-85-0853) Avail: NTIS HC A04/MF A01

A pulse echo method was used in two notched rods of carbon-carbon Pitch materials and one rod of Pitch/M2 shape stable nosetip material to measure the temperature dependence of the longitudinal wave velocity from room temperature to 5400 F. The velocity was constant to within 2% of the room temperature value for the Pitch parent material throughout the temperature range. For the Pitch/M2 material, the velocity increased to a maximum of 10% at 4000 F and then decreased rapidly. Room temperature velocities in the principal directions of the composite are also given for the two Pitch rods, which showed a 15% decrease in velocity near the ends of both rods and near the side of one rod. DOE

N86-13383# Centre d'Essais Aeronautique Toulouse (France). Lab. d'Etudes Materiaux non Metalliques.
TEST OF A MOISTURE CONDITIONING PROCEDURE USING 70 C DISTILLED WATER, INSTEAD OF A GAS ATMOSPHERE AT 70 C, 95% RELATIVE HUMIDITY Test Report [ETALONNAGE D'UN CONDITIONNEMENT HUMIDE DANS L'EAU DISTILLEE A 70 DEG C PAR RAPPORT A UNE ATMOSPHERE GAZEUSE A 70 DEG C, 95% D'HUMIDITE RELATIVE]
15 Mar. 1985 35 p In FRENCH
(M3-431000) Avail: NTIS HC A03/MF A01

The water procedure was tried in order to simplify the water conditioning of organic matrix composites. The tests were made using T-300-N5208 and Fibredux 914 composite materials. Water absorption after 750 hr is larger, but modification of the peeling resistance is very slight. Author (ESA)

N86-13384# Centre d'Essais Aeronautique Toulouse (France). Lab. M4C.
STUDY OF THE MECHANICAL PROPERTIES DISPERSION OF CARBON-EPOXY COMPOSITE MATERIALS Test Report [ETUDE DE LA DISPERSION DES PROPRIETES MECANIQUES DES MATERIAUX COMPOSITES CARBONE-EPOXY]
M. Laparliere 3 Jul. 1984 86 p In FRENCH 2 Vol.
(M2-695600-Pt-1) Avail: NTIS HC A05/MF A01

Mechanical properties of T300/N5208 and the Fibredux 914 primpregnated materials were studied. Results show a low dispersion of tensile properties, 6%CY for Fibredux 914 at 20C. The sampling zones show a small influence on the average measurements on the order of 2%. Delamination resistance is much more variable in both materials, with a higher average for the Fibredux 914. Author (ESA)

N86-13385# Centre d'Essais Aeronautique Toulouse (France). Lab. d'Etudes de Materiaux non Metalliques.
STUDY OF THE DISPERSION OF THE MECHANICAL PROPERTIES OF CARBON-EPOXY COMPOSITE MATERIALS Test Report [ETUDE DE LA DISPERSION DES PROPRIETES MECANIQUES DES MATERIAUX COMPOSITES CARBONE-EPOXY]
6 Feb. 1985 45 p In FRENCH 2 Vol.
(M2-695600-Pt-2) Avail: NTIS HC A03/MF A01

The mechanical testing of carbon epoxy composites was studied, determining the conditions of load transfer from machine to sample. The results show that the hydraulic head of the Instron 100 KN and the mechanical head of the CEAT machines do not introduce a significant flexion load on the sample. Other types of head and samples introduce up to 5,5% flexion load at 50% breaking load. Author (ESA)

N86-13443# Joint Publications Research Service, Arlington, Va.
EFFECT OF GEOMETRY OF FIBER PACKING ON CONSOLIDATION OF FIBROUS COMPOSITION MATERIALS WITH POROUS MATRIX Abstract Only
B. A. Arefyev, L. A. Bondarchuk, T. I. Pavlova, I. I. Renne, V. L. Tikhmyanov, and V. K. Ushakov *In its* USSR Rept.: Mater. Sci. and Met. (JPRS-UMS-85-006) 29 Jul. 1985 p 15 Transl. into ENGLISH from Fiz. i Khim. Obrabotki Mater. (Moscow), no. 2, Mar. - Apr. 1985 p 127-130 (For primary document see N86-13422 04-26)
Avail: NTIS HC A05

N86-13444# Joint Publications Research Service, Arlington, Va.
CONDUCTIVITY OF METAL-CERAMIC MULTILAYER ZrO2-Mo AND Mo-BASED COMPOSITE MATERIALS Abstract Only
S. M. Kats, Z. I. Bylkova, V. N. Bogin, A. P. Filichkin, and N. G. Chubenko *In its* USSR Rept.: Mater. Sci. and Met. (JPRS-UMS-85-006) 29 Jul. 1985 p 16 Transl. into ENGLISH from Poroshkovaya Met. (Kiev), no. 2, Feb. 1984 p 61-64 (For primary document see N86-13422 04-26)
Avail: NTIS HC A05

N86-13445# Joint Publications Research Service, Arlington, Va.
PRODUCTION OF MULTILAYER MAGNETIC SURFACE OF MAGNETICALLY SOFT COMPOSITE MATERIALS Abstract Only
A. E. Ritso, O. A. Katrus, A. A. Laansoo, and R. A. Siymar *In its* USSR Rept.: Mater. Sci. and Met. (JPRS-UMS-85-006) 29 Jul. 1985 p 17 Transl. into ENGLISH from Poroshkovaya Met. (Kiev), no. 2, Feb. 1985 p 70-73 (For primary document see N86-13422 04-26)
Avail: NTIS HC A05

N86-13446# Joint Publications Research Service, Arlington, Va.
CALCULATION OF DAMPING PROPERTIES OF COMPOSITE MATERIALS Abstract Only
V. N. Brinza, B. S. Vekshin, and Ye. V. Kolyadina *In its* USSR Rept.: Mater. Sci. and Met. (JPRS-UMS-85-006) 29 Jul. 1985 p 17 Transl. into ENGLISH from Izv. Vyssh. Ucheb. Zaved.: Chernaya Met. (Moscow), no. 1, Jan. 1985 p 79-81 (For primary document see N86-13422 04-26)
Avail: NTIS HC A05

N86-13447# Joint Publications Research Service, Arlington, Va.
THEORY OF PYROLYSIS OF COMPOSITE POLYMER MATERIAL Abstract Only
A. M. Grishin and S. P. Sinitsyn *In its* USSR Rept.: Mater. Sci. and Met. (JPRS-UMS-85-006) 29 Jul. 1985 p 18 Transl. into ENGLISH from Fiz. Goreniya i Vzryva (Novosibirsk), v. 20, no. 6, Nov. - Dec. 1984 p 67-69 (For primary document see N86-13422 04-26)
Avail: NTIS HC A05

N86-13448# Joint Publications Research Service, Arlington, Va.
CRITICAL BEHAVIOR OF THERMOELECTRIC POWER IN BINARY COMPOSITE MATERIALS Abstract Only
A. S. Skal *In its* USSR Rept.: Mater. Sci. and Met. (JPRS-UMS-85-006) 29 Jul. 1985 p 18 Transl. into ENGLISH from Zh. Eksperim. i Teor. Fiz. (Moscow), v. 88, no. 2, Feb. 1985 p 516-521 (For primary document see N86-13422 04-26)
Avail: NTIS HC A05

N86-13459# Joint Publications Research Service, Arlington, Va.
DETERMINATION OF POROSITY OF THIN SHEETS OF FIBER MATERIALS BASED ON OPTICAL TRANSMISSION COEFFICIENT Abstract Only
A. G. Kostornov, O. V. Kirichenko, S. P. Sakhno, and G. S. Tymchik *In its* USSR Rept.: Mater. Sci. and Met. (JPRS-UMS-85-006) 29 Jul. 1985 p 35 Transl. into ENGLISH from Poroshkovaya Met. (Kiev), no. 10, Oct. 1984 p 86-90 (For primary document see N86-13422 04-26)
Avail: NTIS HC A05

N86-13623# Joint Publications Research Service, Arlington, Va.
RECENT ADVANCES IN COMPOSITE MATERIALS REVIEWED
Laurent Schwartz *In its* West Europe Rept.: Sci. and Technol. (JPRS-WST-85-029) 30 Sep. 1985 p 1-2 Transl. into ENGLISH from Ind. et Tech. (Paris), 10 Apr. 1985 p 18 (For primary document see N86-13622 04-31)
Avail: NTIS HC A04/MF A01

25 INORGANIC AND PHYSICAL CHEMISTRY

Includes chemical analysis, e.g., chromatography; combustion theory; electrochemistry; and photochemistry.

For related information see also *77 Thermodynamics and Statistical Physics.*

N86-13386 Connecticut Univ., Storrs.
AN INVESTIGATION OF PLASMA JET IGNITION AND FLAME JET IGNITION OF LEAN FUEL-AIR MIXTURES Ph.D. Thesis
Durga Nageswara Mittinti 1985 241 p
Avail: Univ. Microfilms Order No. DA8512152

Plasma jet ignition (PJI) is investigated in a cylindrical combustion bomb using methane-air at an equivalence ratio of 0.7. The effects of plasma chamber size and its aspect ratio (depth to diameter of the cavity), spark energy and its duration, plasma medium such as (CH4), (CH4+7O2),(CH4+6O2) and (H2), and the effect of initial pressure are explored. The results are assessed in terms of a combustion index which is a function of the peak pressure and the time the peak is reached. It is found that besides the plasma cavity and orifice size, the aspect ratio and the spark duration have significant influence on the combustion index and there exist optimum values for each plasma chamber. Improved performance is observed with the plasma media of (CH4), (H2) and more significantly with (CH4+6O2+NO2). As the initial pressure is increased, the combustion index is found to decrease. Flame jet ignition (FJI) is developed using (H2+1/2O2) for the initiating flame and methane-air or propane-air mixture in the main chamber. FJI is found to be more effective than PJI.
Dissert. Abstr.

N86-13387 California Univ., Berkeley.
THERMAL RADIATION EFFECTS ON COMBUSTION OF CONDENSED FUELS Ph.D. Thesis
Kwi Young Lee 1984 110 p
Avail: Univ. Microfilms Order No. DA8512898

The effect of thermal radiation on combustion of condensed fuels is studied through simple but realistic mathematical models. Specific subjects investigated in the present study are the determination of radiation blockage, its effects on solid fuel ignition, and the combined radiation and conduction effect on cold-wall flame-quenching. Dissert. Abstr.

N86-13388# Army Fuels and Lubricants Research Lab., San Antonio, Tex.
REPORT ON INVESTIGATION OF ALCOHOL COMBUSTION ASSOCIATED WEAR IN SPARK IGNITION ENGINES, MECHANISMS AND LUBRICANT EFFECTS Interim Report, Sep. 1976 - Dec. 1984
D. W. Naegeli and E. C. Owens Dec. 1984 93 p
(Contracts DAAK70-85-C-0007; DAAK70-78-C-0001; DAAK70-79-C-0175; DE-AI01-79CS-50030)
(AD-A157714; AFLRL-176) Avail: NTIS HC A05/MF A01 CSCL 21/2

An investigation of the effects of alcohol fuels on spark ignition engine wear and deposition was jointly sponsored by the U.S. Department of Energy and the U.S. Army Belvoir Research and Development Center. This research has investigated four alcohol-containing fuels: pure methanol, pure ethanol, methanol in unleaded gasoline, and ethanol in unleaded gasoline (gasohol). Tests were conducted using a variety of single-cylinder research engines and production multicylinder engines, mounted in dynamometer test stands. This testing indicated that pure alcohol fuels reduced the buildup of engine deposits. Also, neat methanol greatly increased engine wear rates at engine temperatures below 75 C, while anhydrous ethanol and the alcohol-gasoline blends did not increase wear rates over that of unleaded gasoline. Engine-based tests were conducted to investigate the effects of variations in lubricant base stocks and additive formulations on the wear observed with methanol. To determine interaction between fuel alcohols and engine metals, two approaches were developed. The role of nitrogen in the wear process was studied by operating a 2.3-liter engine fueled with methanol in a nitrogen-free atmosphere. Bench experiments indicated that formic-acid and peroxides are formed as methanol combustion intermediates. GRA

N86-13389# York Univ., Toronto (Ontario). Dept. of Chemistry.
RELATIONSHIPS BETWEEN ELECTRONIC SPECTROSCOPY AND ELECTROCHEMISTRY. A PROBE OF REORGANISATION ENERGIES
E. S. Dodsworth and A. B. P. Lever May 1985 18 p
(Contract N00014-78-C-0592)
(AD-A157940; TR-2) Avail: NTIS HC A02/MF A01 CSCL 07/4

The electronic spectra and electrochemical potentials of the species Ru(bipy)x(NN)3-x(2+)(bipy = 2,2'-bipyridine, NN = unsaturated diimine, x = 1,2) are correlated via fundamental relationships involving reorganization and solvation energies. It is argued that the presence of two distinct Ru yields ligand charge transfer transitions allows comparison of the reorganization energies therefore. GRA

N86-13390# Catholic Univ. of America, Washington, D.C. Dept. of Chemistry.
REACTION INTERMEDIATES IN AROMATIC FUEL COMBUSTION Final Report, 18 Jul. 1983 - 17 Jul. 1984

W. A. Sanders 17 Jul. 1984 25 p
(Contract N00014-83-K-0586)
(AD-A158029) Avail: NTIS HC A02/MF A01 CSCL 21/4

The oxidation of benzene under fuel-lean conditions has been studied from 1600 to 2300 K in a shock tube using a stabilized CW CO laser to monitor CO production. The result of the kinetic modeling of the CO formation according to the global mechanism of Fujii and Asaba indicates that the rate of CO formation in the early stage of oxidation depends very sensitively on the rate-limiting unimolecular decomposition of benzene. The rate constant obtained for the initiation reaction using a scheme consisting of a set of 25 reactions is given for the pressure range of 1.9 - 2.7 atm. GRA

N86-13391# Air Force Inst. of Tech., Wright-Patterson AFB, Ohio.
DIFFERENTIAL SCATTERING CROSS SECTION AND TOTAL EXTINCTION MEASUREMENTS ON (CH)n SPHERES IN 632.8 nM LASER LIGHT M.S. Thesis
J. M. Dorman 1985 108 p
(AD-A158044; AFIT/CI/NR-85-69T) Avail: NTIS HC A06/MF A01 CSCL 07/4

A new laboratory system for aerosol research is discussed from the aspects of design, construction and preliminary testing. The system is subdivided into two cooperating subsystems known as the Optical System (OS) and the Aerosol Circulation/Sampling System (ACSS). Measurement of the extinction, scattering and absorption cross sections of an aerosol is the object of the Optical System. Aerosol production, containment, and sampling are the tasks of the ACSS. Mie scattering theory for monodisperse aerosols is discussed as it applies to the cross section measurements. Preliminary measurements on Polystyrene microspheres (1.0 micron in diameter) are presented. These measurements strongly indicate that the spheres are actually 0.85 micron in diameter. Problem areas in both the hardware and experimental procedure are presented as a precursor to full scale testing and calibration. GRA

N86-13392# Air Force Inst. of Tech., Wright-Patterson AFB, Ohio.
ELECTRONIC DETECTION OF LOW CONCENTRATIONS OF ORGANOPHOSPHORUS COMPOUNDS WITH A SOLID STATE DEVICE UTILIZING SUPPORTED COPPER + CUPROUS OXIDE ISLAND FILMS Ph.D. Thesis
E. S. Kolesar, Jr. May 1985 565 p
(AD-A158181; AFIT/CI/NR-85-56D) Avail: NTIS HC A24/MF A01 CSCL 07/3

This research is concerned with investigating the electronic properties modified by the exposure of a supported island film of copper + cuprous oxide to low concentrations (1-650 ppm) of diisoprophyl methylphosphonate (DIMP), and the merit of integrating these films with the distributed RC notch network detection device. Electron microscopy and associated diffraction measurements confirmed the film's structure and composition; Auger spectroscopy verified the adsorption of DIMP. DIMP exposure sensitivity is maximized for films with thicknesses less that 80A operated at 90C which have an applied bias greater than 10 volts (direct current). The adsorption of DIMP is quasi-reversible; that is, after a conditioning exposure and purge, the effect of successive challenges and expiations was monitored via corresponding changes in the film's conductivity. Exposure experiments for changes in resistance versus time were fitted to a two-dimensional nucleation and growth model. GRA

N86-13393# Research Triangle Inst., Research Triangle Park, N.C.
STUDY OF MEAN FREE PATH EFFECTS ON GROWTH OF ULTRAFINE METALLIC AEROSOLS Annual Report, 1 Feb. 1984 - 1 Feb. 1985
P. A. Lawless Apr. 1985 20 p
(Contract F49620-84-C-0017)
(AD-A158206; AFOSR-85-0525TR) Avail: NTIS HC A02/MF A01 CSCL 07/4

In the first year of this study on the dynamics of aerosol formation in gaseous atmospheres, the experimental facility was set up, using an exploding wire generator for the production of high concentrations of metallic aerosols. The initial experiments have been devoted to development of sampling methods for the reduced atmosphere environment and, then, to the observation of the types of behavior exhibited by single component aerosols. GRA

N86-13394# California Univ., Santa Barbara. Dept. of Chemistry.
SYNTHESIS, STRUCTURE AND REACTIVITY OF MOLECULES ATTACHED TO ELECTRODE SURFACES Final Report, 15 Apr. 1981 - 15 Apr. 1985
A. T. Hubbard 10 Jul. 1985 43 p
(Grant AF-AFOSR-0149-81)
(AD-A158621; AFOSR-85-0627TR) Avail: NTIS HC A03/MF A01 CSCL 07/4

This project was to determine the structure, orientation, composition and reactivity of the surface molecular species which form spontaneously when metals come into contact with fluids, as in batteries, fuels cells, electronic circuits, marine environments and the atmosphere. These include: determination of the spatial orientations and mode of attachment of typical organic molecules chemically bonded to electrode surfaces; discovery that each orientation of an adsorbed molecule reacts differently; identification and exploration of variables which influence adsorbate orientation (concentration, temperature, potential, electrolyte, solvent, substrate, surface structure, pH and hydrogen bonding); exploration of the influence of oriented adsorbates on electrode rates; preparation of well-defined surfaces under atmospheric conditions; electrodeposition of highly ordered layers of Ag and Cu onto well-defined substrates; discovery of the orderedness of adsorbed ionic layers at well-defined surfaces; direct experimental exploration of the cation-selectivity of metal-solution surfaces. These findings were made possible by a unique combination of surface research techniques in ultra-high vacuum and electrochemistry in solution, employed in a long-term systematic series of investigations. GRA

N86-13395# Allied Corp., Morristown, N.J.
ROLE OF ADDITIVES IN MINIMIZING ZINC ELECTRODE SHAPE CHANGE: THE EFFECT OF LEAD ON THE KINETICS OF Zn(2) REDUCTION IN CONCENTRATED ALKALINE MEDIA Final Technical Report, 20 Sep. 1982 - 20 Sep. 1984
L. S. Melnicki, I. Lazic, and D. Cipris Jul. 1985 88 p
(Contract N00014-82-C-0701)
(AD-A158806) Avail: NTIS HC A05/MF A01 CSCL 07/4

The kinetics of zinc deposition in various media is among the most widely studied systems, along with hydrogen and oxygen reactions. The importance of the zinc electrode originates from the use of zinc as an anode material in commerically important primary and secondary batteries. The Ag-Zn battery, commerically available for a long time, has the highest practical energy and power densities among conventional secondary batteries. The Ni-Zn secondary battery is still under development. Both zinc electrodes operate in concentrated alkaline electrolytes. In spite of the extensive number of studies, the mechanism of zinc reduction in alkaline media is not fully understood. The situation is further complicated in the presence of various metallic additives, which are commonly used in secondary alkaline batteries utilizing zinc anodes to suppress dendrite formation and/or facilitate uniform zinc deposition. Non-uniform zinc deposition leads to the phenomenon known as zinc electrode shape change in secondary batteries. The zinc electrode shape change is considered a leading factor in the premature loss of capacity of zinc batteries and to a generally unacceptably short cycle life. Of all the additives employed, lead appears to be the most commonly used in commercial practice, alone or in combination with other additives. While further work is in order (especially on the dissolution process of zinc, which is also affected by lead) our results point to the possibility of employing electrolyte additives, as opposed to additives to the ZnO paste in practical cells. GRA

N86-13396# Naval Postgraduate School, Monterey, Calif.
EXPERIMENTAL INVESTIGATION OF MAGNESIUM COMBUSTION IN STEAM Contractor Report, Dec. 1984 - May 1985
Y. Chozev and J. Kol Jul. 1985 53 p

(AD-A159109; NPS67-85-004CR) Avail: NTIS HC A04/MF A01 CSCL 21/2

This paper presents a summary of the experimental results and studies of magnesium combustion in steam. The major subject of these studies was to measure the temperature of magnesium particles after the particles had been ejected from an exploding wire. The distribution of particle temperature along the track was measured by the two-color photo-pyrometry method (TC-PPM). A scanning microdensitometer served as a major data reduction tool in analyzing the film density due to the particle tracks as recorded on calibrated film. The initial temperature of the particle ejection from the plasma and at the beginning of combustion is 3430 K + or - 9.1%. At the initial phase of combustion, the particle consists of pure magnesium with spectral emissivity of about 0.25. During the combustion process, magnesium oxide is formed locally on the particle surface. The oxide is in liquid state with emissivity of 0.9. In the second stage of combustion there are changes on the particle surface in correlation with optical density variation and explained by emissivity variations due to peeling of the oxide film and exposure of the pure magnesium surface. Solidification of the particle, which is magnesium oxide, is observed at the measured temperature of 3125 K + or - 5.7%. The spearpoint effect, which is known in the literature as the Blick Effect, was observed at the end of the particle track. The particle supercools below the normal freezing point and then suddenly crystallizes. GRA

N86-13397# Cornell Univ., Ithaca, N.Y. Dept. of Chemistry.
NO CHEMISORPTION ON NI(111): COVERAGE EFFECTS, SITE PREFERENCES AND ADSORPTION GEOMETRY Interim Technical Report
S. S. Sung, R. Hoffman, and P. A. Thiel 3 Sep. 1985 44 p
(Contract N00014-82-K-0576)
(AD-A159110; TR-14) Avail: NTIS HC A03/MF A01 CSCL 07/4

Several possible rationales for the different NO adsorption states observed on a Ni(111) surface are discussed, based on the tight binding calculations of the extended Huckel type. In the two-fold bridge site, as the coverage of NO increases, for perpendicularly adsorbed NO the N-O bonding increases and N-Ni bonding decreases. For slightly bent NO at low coverage and perpendicular NO at high coverage the same trends are obtained. These trends are consistent with the observed N-O, N-Ni stretching frequency change. At coverage 1/3, and in the perpendicular geometry, both N-O bonding and N-Ni bonding increase when NO changes adsorption sites form three-fold to two-fold or from two-fold to on-top. In the on-top site we calculate that both N-O bonding and N-Ni bonding increase when NO changes geometry from bent to perpendicular. In the two-fold bridge site the effect of bending is to produce similar but smaller trends. Author (GRA)

N86-13398# Colorado Univ., Boulder.
STUDIES OF METAL/CARBON SURFACE CHEMISTRY Report, 1 Mar. - 31 May 1985
B. E. Koel 30 Jun. 1985 6 p
(Contract DE-FG22-84PC-70779)
(DE85-015548; DOE/PC-70779/T1) Avail: NTIS HC A02/MF A01

The purpose of this research is to identify stable surface species formed from molecular adsorption and reaction on metal/carbon surfaces. This research has practical application in improving the fundamental understanding of catalytic coal gasification. Well-defined model catalysts for carbon gasification will be studied by vapor depositing alkali and transition metal atoms on carbon surfaces. Vibrational spectroscopy using HREELS and photoelectron spectroscopy of these surfaces will be used to develop an atomic-level understanding of the chemical bonding, structure, and reactivity of the metal carbon surface and of the adsorbed molecular species. DOE

N86-13399# Lawrence Livermore National Lab., Calif.
CONDENSED MATTER AT HIGH SHOCK PRESSURES
W. J. Nellis, N. C. Holmes, A. C. Mitchell, H. B. Radousky, and D. Hamilton 12 Jul. 1985 14 p refs Presented at the 15th Intern. Symp. on Shock Waves and Shock Tubes, Berkeley, Calif., 29 Jul. 1985
(Contract W-7405-eng-48)
(DE85-016443; UCRL-92974; CONF-850767-3) Avail: NTIS HC A02/MF A01

Experimental techniques are described for shock waves in liquids: Hugoniot equation-of-state, shock temperature and emission spectroscopy, electrical conductivity, and Raman spectroscopy. Experimental data are reviewed and presented in terms of phenomena that occur at high densities and temperatures in shocked He, Ar, N2, CO, SiO2-aerogel, H2O, and C6H6. The superconducting properties of Nb metal shocked to 100 GPa (1 Mbar) and recovered intact are discussed in terms of prospects for synthesizing novel, metastable materials. Ultrahigh pressure data for Cu is reviewed in the range 0.3 to 6TPa (3 to 60 Mbar). DOE

N86-13400# Lawrence Livermore National Lab., Calif.
SORPTION DETECTOR SYSTEM FOR CHEMICAL AGENTS DETECTION AND RECOGNITION
D. Olness and T. Hirschfeld 22 Mar. 1985 54 p
(Contract W-7405-eng-48)
(DE85-012775; UCID-20047) Avail: NTIS HC A04/MF A01

The use of the piezoelectric sorption sensor, in which an analyte's absorption in a thin surface layer on a piezoelectric vibrator changes its resonant frequency, has been extensively described. In every instance, the chemical selectivity of the devices hinges on that of the absorbing layer. In a complex environment, a few analytes are so distinctive as to permit this. An alternative approach uses an array of crystals (or of vibrational nodes in a microlithographically cut multivibrator) covered with a number of different absorbing layers. These are so thin that they operate in the saturation mode, with different partition coefficients against air resulting in different frequency shifts for each layer. The behavior in Fourier space of these frequency shifts is then used for pattern recognition of individual chemicals. Mixture overlap can then be handed via time derivative measurements, factor analysis, or correlation spectroscopy. Experimental results from this combination of chemometrics and their Fourier transform mechanical spectroscopy are given. Experimental results of the demonstrated feasibility of a procedure for providing complete selectivity to quartz piezobalance sensors, by using an array of different sensor layers and pattern recognition, are presented. A laboratory test system, based on this technology, is described. DOE

N86-13401# National Bureau of Standards, Boulder, Colo. Center for Chemical Engineering.
SUPERCRITICAL FLUID PROPERTIES Final Report, 1 Oct. 1983 - 31 Oct. 1984
J. F. Ely 1984 68 p refs
(Contract DE-AI05-83OR-21374)
(DE85-011203; DOE/OR-21374/T1) Avail: NTIS HC A04/MF A01

During the past decade there has been intense interest in chemical processing with supercritical fluids as solvents. In this report some preliminary results which bear upon the use of supercritical fluids, carbon dioxide in particular, in chemical processing. Two distinct sets of results are presented in the report: (1) a preliminary wide range equation of state for pure C02, and (2) some preliminary results obtained with a predictive model for mixture thermodynamic properties based on the hard sphere expansion theory. DOE

N86-13402# Lawrence Livermore National Lab., Calif.
INTERACTIONS BETWEEN A LAMINAR FLAME AND END GAS AUTOIGNITION
W. J. Pitz and C. K. Westbrook 15 Jan. 1985 18 p refs Presented at 10th Intern. Colloq. on Dyn. of Explosions and Reactive Systems, Berkeley, Calif., 4 Aug. 1985
(Contract W-7405-eng-48)
(DE85-008957; UCRL-92295-1; CONF-850830-1) Avail: NTIS HC A02/MF A01

A numerical model combining one dimensional fluid mechanics and detailed chemical kinetics is used to examine the interactions between laminar flame propagation and end gas autoignition at high temperatures and pressures of approximately 30 atmospheres. The flame is found to have very little influence on the computed rates of fuel-air autoignition in the end gas, but the subsequent high rate of heat release during autoignition is shown to produce strong acoustic waves in the burned gases. The effects of temperature fluctuations in the end gas on the locations at which autoignition is initiated is also investigated numerically. DOE

N86-13576# United Technologies Research Center, East Hartford, Conn.
RESONANT CARS DETECTION OF OH RADICALS Abstract Only
James F. Verdieck *In* AFOSR The 1985 AFOSR/AFRPL Chem. Rocket Res. Meeting Feb. 1985 3 p (For primary document see N86-13507 04-28)
Avail: NTIS HC A11/MF A01

N86-13607# Joint Publications Research Service, Arlington, Va.
APPLICATION OF COMPUTERS IN ANALYTICAL CHEMISTRY: CALCULATION OF OPTIMUM ACIDITY OF REACTION BETWEEN METAL IONS AND ORGANIC REAGENTS IN SOLUTION
Zhang Sunwei, Pan Fuyou, Yan Jian, and Kong Fangming *In its* China Rept.: Sci. and Technol. (JPRS-CST-85-020) 24 Jun. 1985 p 100-104 refs Transl. into ENGLISH from Hangzhou Daxue Xuebao (Hangzhou), v. 12, no. 1, Jan. 1985 p 98-102 (For primary document see N86-13600 04-31)
Avail: NTIS HC A09/MF A01

N86-14081*# Houston Univ., Clear Lake, Tex. Programs in Science.
ELECTRON MICROSCOPIC OBSERVATIONS OF HYDROGEN IMPLANTATION IN ILMENITES Final Report
Goerge E. Blanford *In* NASA. Johnson (Lyndon B.) Space Center The 1983 NASA/ASEE Summer Faculty Fellowship Research Program Research Reports Sep. 1983 9 p refs (For primary document see N86-14078 04-85)
Avail: NTIS HC A18/MF A01 CSCL 07D

N86-14082*# Arkansas Coll., Batesville.
A PYROLOYSIS TECHNIQUE FOR DETERMINING MICROAMOUNTS OF HYDROGEN IN LUNAR SOIL USING THE HELIUM IONIZATION DETECTOR Final Report
Roberta Bustin *In* NASA. Johnson (Lyndon B.) Space Center The 1983 NASA/ASEE Summer Faculty Fellowship Research Program Research Reports Sep. 1983 p 13 p refs (For primary document see N86-14078 04-85)
Avail: NTIS HC A18/MF A01 CSCL 07D

26 METALLIC MATERIALS

Includes physical, chemical, and mechanical properties of metals, e.g., corrosion; and metallurgy.

N86-13403 Illinois Univ., Urbana-Champaign.
HYDROGEN TRANSPORT AND HYDROGEN EMBRITTLEMENT IN STAINLESS STEELS Ph.D. Thesis
Tsong-Pyng Perng 1985 200 p
Avail: Univ. Microfilms Order No. DA8511659

In order to understand the kinetics of gaseous hydrogen-induced slow crack growth (SCG) in metastable austenitic stainless steels, hydrogen permeation and/or cracking velocity were measured and compared for three types of stainless steels. These included austenitic, ferritic, and duplex alloys. Deformation in AISI 301 resulted in various amounts of martensite, which enhanced the effective hydrogen diffusivity and permeability. No phase transformation was observed in deformed AISI 310. The effective hydrogen diffusivity in this alloy was slightly reduced after plastic deformation, presumably by dislocation trapping. In either the dynamic or static tensile test, AISI 301 exhibited the greatest hydrogen embrittlement and therefore the highest SCG velocity among all the alloys tested. The SCG velocity was believed to be controlled by the rate of accumulation of hydrogen in the embrittlement region ahead of the crack tip and therefore could be explained with the hydrogen transport parameters measured from the permeation experiments. Dissert. Abstr.

N86-13404 Illinois Univ., Urbana.
CORROSION FATIGUE INITIATION AND SHORT CRACK GROWTH IN AN ALUMINUM ALLOY Ph.D. Thesis
Yen-How Huang 1985 174 p
Avail: Univ. Microfilms Order No. DA8511619

A prepitted specimen with a single pit provided a favorable condition for observing crack initiation. Initiation and early growth of corrosion fatigue cracks was followed optically in pre-pitted Al-5454-H32 specimens. Supplementary fractographic, electrochemical and microstructural observations were made. The role of the microstructure with pancake-like grains (approx. 45 micrometers thick) was investigated. Testing was run under load control with R = 0.1,f = 20Hz and various stress ranges in dry air, in 0.5M NaCl at external potentials lower than E sub p (= 735 mV sub sec) or in 0.5M Na2SO2 at several potentials. Dissert. Abstr.

N86-13405 Stanford Univ., Calif.
THE INFLUENCE OF MICROSTRUCTURE ON TEMPER EMBRITTLEMENT OF LOW ALLOY STEEL Ph.D. Thesis
James Edward Wittig 1985 309 p
Avail: Univ. Microfilms Order No. DA89511368

Temper enbrittlement in steels can occur from exposure to temperatures of 300 to 600 C. Segregation of impurities, such as phosphorus, to prior austenite grain boundaries promotes intergranular fracture. In the present investigation, the influence of the steel microstructure on the segregation of phosphorus and the resulting fracture behavior is considered. This project uses analytical electron microscopy of thin foils and extraction replicas of precipitates to study temper embrittlement in two types of steel. One contains 3.5 wt% nickel, 1.7% chromium, 0.6% molybdenum, and 0.1% vanadium, and the other has the same nickel and chromium composition but without molybdenum and vanadium. Both have a bainitic microstructure and identical amounts of carbon, 0.25%, and phosphorous, 0.02%. Comparison of these two alloys reveals the effect of molybdenum on the temper embrittlment phenomenon. Dissert. Abstr.

N86-13406*# National Aeronautics and Space Administration. Langley Research Center, Hampton, Va.
FABRICATION AND EVALUATION OF SUPERPLASTICALLY FORMED/WELD-BRAZED CORRUGATED COMPRESSION PANELS WITH BEADED WEBS
Dick M. Royster, Randall C. Davis, Joseph M. Shinn, Jr., Thomas T. Bales, and H. Ross Wiant Nov. 1985 31 p refs
(NASA-TP-2512; L-15988; NAS 1.60:2512) Avail: NTIS HC A03/MF A01 CSCL 11F

A study was made to investigate the feasibility of superplastically forming corrugated panels with beaded webs and to demonstrate the structural integrity of these panels by testing. The test panels in the study consist of superplastically formed titanium alloy Ti-6Al-4V half-hat elements that are joined by weld-brazing to titanium alloy Ti-6Al-4V caps to form either single-corrugation compression panels or multiple-corrugation compression panels. Stretching and subsequent thinning of the titanium sheet during superplastic forming is reduced by approximately 35 percent with a shallow half-hat die concept instead of a deep die concept and results in a more uniform thickness across the beaded webs. The complete panels are tested in end compression at room temperature and the results compared with analysis. The heavily loaded panels failed at loads approaching the yield strength of the titanium material. At maximum load, the caps wrinkled locally accompanied with separation of the weld-braze joint in the wrinkle. None of the panels tested, however, failed catastrophically in the weld-braze joint. Experimental test results are in good agreement with structural analysis of the panels. Author

N86-13407*# National Aeronautics and Space Administration. Lewis Research Center, Cleveland, Ohio.
POLYMER, METAL AND CERAMIC MATRIX COMPOSITES FOR ADVANCED AIRCRAFT ENGINE APPLICATIONS
D. L. McDanels, T. T. Serafini, and J. A. DiCarlo 1985 26 p refs Presented at the Advanced Composites Conference, Detroit, 3-4 Dec. 1985; sponsored by ASME
(NASA-TM-87132; E-2746; NAS 1.15:87132) Avail: NTIS HC A03/MF A01 CSCL 11F

Advanced aircraft engine research within NASA Lewis is being focused on propulsion systems for subsonic, supersonic, and hypersonic aircraft. Each of these flight regimes requires different types of engines, but all require advanced materials to meet their goals of performance, thrust-to-weight ratio, and fuel efficiency. The high strength/weight and stiffness/weight properties of resin, metal, and ceramic matrix composites will play an increasingly key role in meeting these performance requirements. At NASA Lewis, research is ongoing to apply graphite/polyimide composites to engine components and to develop polymer matrices with higher operating temperature capabilities. Metal matrix composites, using magnesium, aluminum, titanium, and superalloy matrices, are being developed for application to static and rotating engine components, as well as for space applications, over a broad temperature range. Ceramic matrix composites are also being examined to increase the toughness and reliability of ceramics for application to high-temperature engine structures and components. Author

N86-13408*# National Aeronautics and Space Administration. Lewis Research Center, Cleveland, Ohio.
THE EFFECT OF COBALT CONTENT IN U-700 TYPE ALLOYS ON DEGRADATION OF ALUMINIDE COATINGS
I. Zaplatynsky Nov. 1985 15 p refs
(NASA-TM-87173; E-2798; NAS 1.15:87173) Avail: NTIS HC A02/MF A01 CSCL 11F

The influence of cobalt content in U-700 type alloys on the behavior of aluminide coatings is studied in burner rig cyclic oxidation tests at 1100C. It is determined that aluminide coatings on alloys with higher cobalt offer better oxidation protection than the same coatings on alloys containing less cobalt. Author

N86-13409*# National Aeronautics and Space Administration. Lewis Research Center, Cleveland, Ohio.
CURRENT VIEWPOINTS ON OXIDE ADHERENCE MECHANISMS
J. L. Smialek and R. Browning 1985 17 p refs Presented at the 168th Meeting of the Electrochemical Society, Las Vegas, Nev., 15-18 Oct. 1985
(NASA-TM-87168; E-2806; NAS 1.15:87168) Avail: NTIS HC A02/MF A01 CSCL 11F

Additional hot stage Auger experiments have provided surface segregation data for NiCrAl + or - Y or Zr alloys in agreement with other investigations. This data, combined with experimental and theoretical evidence of the Al2O3-metal bond strength, is presented in support of a chemical mechanism of Al2O3 scale adhesion. Both the detrimental effects of sulfur segregation and the beneficial effects of dopant segregation may be important. Chemical features of the dopants are compared in light of these proposed mechanisms, namely delta H sub f (sulfide), delta H sub f (oxide), electron orbital configuration, and insolubility in Ni. Author

N86-13410# Department of the Air Force, Washington, D.C.
TECHNIQUE OF ASSEMBLING STRUCTURES USING VAPOR PHASE SOLDERING Patent Application
N. C. Peterson, inventor (to Air Force) Filed 19 Oct. 1984 15 p
(AD-D011805; US-Patent-Appl-SN-663015) Avail: NTIS HC A02/MF A01 CSCL 13/8

This patent application pertains to a vapor phase process for assembling parts of a lightweight structure of aluminum having a multitude of joints. The process includes the following steps: (1) cleaning surfaces of all the parts; (2) selectively depositing on the surfaces a layer of nickel and then tin; (3) selectively plating on the tin layer where joints occur a lead/tin eutectic alloy solder; (4) add flux; (5) fixturing the parts together to form the structure; (6) heating the structure in a vapor phase apparatus; (7) removing the structure from the fixture; and (8) cleaning the structure. By using the above process an antenna faceplate having over 3000 joints was soldered. Author (GRA)

N86-13411# Naval Surface Weapons Center, Silver Spring, Md.
ZIRCONIUM AS A STRUCTURAL MATERIAL FOR NAVAL SYSTEMS
W. A. Ferrando 29 Mar. 1985 57 p
(NR Proj. F61-545)
(AD-A158201; NSWC/TR-85-48) Avail: NTIS HC A04/MF A01 CSCL 11/6

The important basic physical properties and steps in the manufacture of elemental zirconium and several of its important alloys are discussed. Once considered prohibitively expensive for structural uses, its current cost is becoming competitive with other special alloys for various industrial applications. Its actual life cycle cost in many cases has been considerably lower than that experienced with alternative materials. Some of the physical properties of zirconium which make it particularly attractive for naval use include: high strength (particularly when alloyed), outstanding resistance to all forms of corrosion in seawater (and most other) environments, superior fatigue resistance, and good metallurgical workability. Its oxide compound zirconia has recently become a base material for a new generation of tough ceramics of potential structural use. These ceramics are also candidates for fiber reinforcement. Several modern ceramic fabrication techniques are discussed. Although its moderately high density probably will preclude widespread aerospace usage, zirconium and zirconium-based materials could find extensive application in naval surface systems. Finally, there is a ready availability of the raw ore from friendly nations and a very abundant domestic supply, should other sources fail. This assurance certainly increases the attractiveness of these materials for future Navy needs. GRA

N86-13412# Martin Marietta Labs., Baltimore, Md.
THE DELAYED FRACTURE OF ALUMINUM ALLOYS Final Report
J. R. Pickens, T. J. Langan, and J. A. S. Green Jun. 1985 38 p
(Contract N00014-84-C-0380)
(AD-A158944; MML-TR85-39(C)) Avail: NTIS HC A03/MF A01 CSCL 11/6

The major developments in understanding the mechanisms of stress-corrosion cracking (SCC) in Al-Zn-Mg and Al-Mg alloys are briefly reviewed. In particular, evidence for the involvement of hydrogen embrittlement in the SCC mechanisms is addressed. Specifically, the effect of the loading mode on SCC, the role of grain boundary segregation in cracking, and our overall view of the mechanisms of SCC are discussed. GRA

N86-13413# Naval Postgraduate School, Monterey, Calif.
EFFECT OF TEMPERATURE AND STRAIN RATE ON MICROSTRUCTURE OF A DEFORMED, SUPERPLASTIC Al-10%Mg-0.1%Zr ALLOY M.S. Thesis
D. B. Berthold Jun. 1985 91 p
(AD-A159015; AD-F620001) Avail: NTIS HC A05/MF A01 CSCL 11/6

Development of microstructure during thermomechanical processing of an Al-10%Mg-0.1%Zr alloy was examined in the initial portion of this research. The thermomechanical processing involved solution treating; not working by upset forging at 440 C followed by warm rolling material were deformed at three strain rates at temperatures of 200 C, 300 C, and 400 C and were microstructurally examined. It is found that this alloy statically recrystallizes prior to commencing a test at 400 C, the resultant grains deform by boundary sliding and there is extensive cavitation. During lower temperature deformation it was found that either continuous recrystallization or just with no recrystallization occurs and little or no cavitation takes place. GRA

N86-13414# Naval Postgraduate School, Monterey, Calif.
EFFECT OF STRAIN AND STRAIN RATE ON THE MICRO-

STRUCTURE OF A SUPERPLASTICALLY DEFORMED Al-10%Mg-0.1%Zr ALLOY M.S. Thesis
M. E. Alcamo Jun. 1985 123 p
(AD-A159062) Avail: NTIS HC A06/MF A01 CSCL 11/6

The deformation characteristics of two thermomechanically processed, high-magnesium, aluminum-magnesium-zirconium alloys were investigated. The processing included warm rolling at 300 C to 90 to 95% reduction. Tension testing was done at various temperatures and strain rates and superplastic elongations were observed for both alloys. Subsequently, samples of Al-10%Mg-0 .1% Zr were tested at 300 C to strains ranging from 8% to 267% as well as to fracture. Strain rates of .00667/s and .000667/s were used. These were examined via TEM to observe microstructural changes which occur during deformation. Quantitative analysis of the functional relationship between stress, strain, strain rate, and grain size for this alloy is done in an attempt to fit its deformation response to current models for superplastic deformation. GRA

N86-13415# Semicon Associates, Inc., Lexington, Ky.
A STUDY OF RHENIUM AS AN ALTERNATE SUBSTRATE MATERIAL FOR IMPREGNATED DISPENSER CATHODES Final Report, Oct. 1982 - Sep. 1983
W. L. Ohlinger and C. V. French Jul. 1985 48 p
(Contract F33615-82-C-5041)
(AD-A159113; AFWAL-TR-84-4141) Avail: NTIS HC A03/MF A01 CSCL 11/6

Rhenium powder with an average particle size of 6.8 microns was used to develop the fabrication techniques of rhenium cathodes. Pressing pressures, sintering temperatures, and sintering times were the parameters of concern. The possibility of machining unlubricated, impregnated cathodes was also tested. Electron microscopy, nitrogen permeability, and metallography methods were used to characterize the various matrices and compare them to tungsten matrices. Cathodes impregnated with 5:3:2 or 4:1:1 barium-calcium-aluminate were tested for emission performance and compared to tungsten cathodes. A guard ring structure was installed around the cathode to suppress edge effects. Results indicated that rhenium can be fabricated into a working cathode. Fabrication techniques are not completed, and optimization methods need to be studied. Results from emission testing showed 4:1:1 to be the impregnant of choice for a rhenium matrix due to little or no emission from a 5:3:2 impregnated cathode. Testing also proved that activation procedures must be altered according to the metal used. Recommendations for methods of emission enhancement and future studies were made. GRA

N86-13416# Oak Ridge National Lab., Tenn.
COMBINED SMALL ANGLE X-RAY SCATTERING AND TRANSMISSION ELECTRON MICROSCOPY STUDIES OF Al-Li ALLOYS
S. Spooner, D. B. Williams, and C. M. Sung 1985 15 p Presented at the 3rd Intern. Aluminum-Lithium Conf., Oxfordshire, England, 9 Jul. 1985 Prepared in cooperation with Lehigh Univ., Bethlehem, Pa.
(DE85-016356; CONF-850777-2) Avail: NTIS HC A02/MF A01

Combined small angle X-ray scattering (SAXS) and transmission electron microscopy (TEM) studies have been performed on two binary Al-Li alloys subjected to different pre-aging treatments. Both the SAXS and TEM data indicate that delta (Al3Li) in samples of the two alloys directly quenched to the aging temperature is larger in size than in samples quenched to below room temperature prior to aging. SAXS data indicate an initial rise in scattering center size in Al-9.4 at. % Li, or in the TEM stsudies of delta' in both alloys. It is considered that these observations are evidence that the initial rise in the SAXS data in Al-9.4 at. % Li alloys is due to a phenomenon other than delta' precipitation. The possibility of matrix spinodal decomposiiton in this alloy is one explanation. DOE

N86-13417# Los Alamos National Lab., N. Mex.
HIGH STRAIN RATE DEFORMATION IN FCC METALS AND ALLOYS
P. S. Follansbee 1985 34 p Presented at EXPLOMET '85 - Intern. Conf. on Met. Appl. of Shock Wave and High Strain-Rate Phenomena, Portland, Oreg., 28 Jul. 1985
(Contract W-7405-eng-36)
(DE85-017533; LA-UR-85-3026; CONF-850770-8) Avail: NTIS HC A03/MF A01

The effort of strain rate, and particularly of high strain rates, on deformation mechanisms in materials is of fundamental interest to those who model and analyze dynamic loading. In many materials the strain rate sensitivity is known to increase dramatically when the strain rate is raised above approx. 1000 s(-1). This increase has been interpreted previously as a transmission in deformation mechanism from thermal activation control at low strain rate to dislocation drag control at high strain rate. In copper, copper-aluminum alloys and stainless steel, recent measurements have shown that the increased rate sensitivity found at high strain rates is not due to a transition in deformation mechanism but rather can be explained with standard thermal activation theory. These findings and their implications regarding the formulation of constitutive behavior are presented. DOE

N86-13418# Los Alamos National Lab., N. Mex.
THRESHOLD STRESS MEASUREMENTS IN SHOCK-DEFORMED COPPER
P. S. Follansbee and G. T. Gray 1985 19 p Presented at the Am. Phys. Soc. Topical Conf. on Shock Waves in Condensed Matter., Spokane, 22 Jul. 1985
(Contract W-7405-eng-36)
(DE85-014076; LA-UR-85-2251; CONF-850736-11) Avail: NTIS HC A02/MF A01

The height and shape of the obstacle profile for the dominant obstacle provide information on the nature of the deformed microstructure. These quantities can be measured on recovered shock-deformed material. Purpose of this paper is to investigate shock wave deformation mechanisms by measuring the mechanical threshold, or threshold stress, on shock deformed material. Oxygen-free-electronic (OFE) copper was selected for this study since its shock-deformation behavior has been extensively studied and since these shock-deformation results complement extensive measurements at strain rates up to 10 to the 4th power/sec. Measurements of the mechanical threshold, their implications regarding deformation mechanisms and correlations with the microstructure characterized with TEM are described in this paper. DOE

N86-13419# Los Alamos National Lab., N. Mex.
MUON SPIN RELAXATION STUDY OF EXCHANGE COUPLING IN DILUTE AgMn ALLOYS
R. H. Heffner, D. W. Cooke, R. L. Hutson, M. E. Schillaci, S. A. Dodds, G. A. Gist, and D. E. MacLaughlin 1985 9 p refs Presented at the Intern. Conf. on Magnetism, San Francisco, 26 Aug. 1985 Prepared in cooperation with California Univ., Riverside and Rice Univ., Houston, Tex.
(Contract W-7405-eng-36)
(DE85-014104; LA-UR-85-2106; CONF-850890-1) Avail: NTIS HC A02/MF A01

We have observed for the first time conduction-electron mediated muon-impurity coupling, and deduced the strength of the conduction electron-Mn exchange coupling. Our results are marginally consistent with a wave-vector dependent exchange model. DOE

N86-13420# Societe Nationale Industrielle Aerospatiale, Suresnes (France). Section Materiaux.
CHARACTERIZATION OF 7017 ALUMINUM ALLOYS IN THICK PROFILES, IN THE METALLURGICAL VERSIONS T6510, T76510 AND T736510, TEST REPORT NO. PV-44-607/F [ALLIAGES D'ALUMINIUM 7010: GROS PROFILES, ETATS METALLURGIQUES T6510 - T76510 - T736510, PROCES VERBAL NO. 44-607/F]
Y. Barbaux 30 Jan. 1985 85 p In FRENCH
(Contract STPA-82-96-025)
(PV-44-607/F) Avail: NTIS HC A05/MF A01

Tests to study the feasibility of the substitution of 7X75 alloy molded pieces for aeronautical use by 7010 alloy extruded thick profiles were performed. The results confirm a gain in static characteristics, a good level of toughness and an acceptable performance in crack growth and fatigue. The two first versions are equivalent to the T736510 alloy except for higher static characteristics. Author (ESA)

N86-13421# Centre d'Essais Aeronautique Toulouse (France). Lab. d'Etudes de Materiaux Metalliques.
EVALUATION OF THE TITANIUM IMI 829 ALLOY PRODUCED BY POWDER METALLURGY Test Report [EVALUATION DE L'ALLIAGE DE TITANE IMI 829 ELABORE PAR METALLURGIE DES POUDRES (PROCEDE PSV DU CENG)]
1985 105 p In FRENCH
(M1-610200) Avail: NTIS HC A06/MF A01

A high temperature titanium alloy, (550C) was tested using two grain sizes and two hot isostatic pressures. The static and fatigue properties were measured. The results show elongation, and tensile strength 35% lower than forged material. The fatigue results are also clearly poorer than those of forged material. Author (ESA)

N86-13422# Joint Publications Research Service, Arlington, Va.
USSR REPORT: MATERIALS SCIENCE AND METALLURGY
29 Jul. 1985 80 p refs Transl. into ENGLISH from various Russian articles
(JPRS-UMS-85-006) Avail: NTIS HC A05

Progress is reported in U.S.S.R. Materials Science and Metallurgy. Topics discussed include: aluminum and its alloys; amorphous alloys; beryllium; protective coatings; composite materials; corrosion; energy effects; ferrous metallurgy; glass and ceramics; magnesium; powder metallurgy; steels; thin films; superhard materials; titanium and welding. For individual titles, see N86-13423 through N86-13494.

N86-13423# Joint Publications Research Service, Arlington, Va.
HEREDITARY EFFECT OF DENDRITE LIQUATION OF TITANIUM AND ZIRCONIUM ON STRUCTURE AND PROPERTIES OF ALUMINUM ALLOYS Abstract Only
I. N. Fridlyander, O. A. Setyukov, and N. V. Ruchyeva *In its* USSR Rept.: Mater. Sci. and Met. (JPRS-UMS-85-006) 29 Jul. 1985 p 1 Transl. into ENGLISH from Metalloved. i Term. Obrabotka Metal. (Moscow), no. 5, May 1985 p 43-45 (For primary document see N86-13422 04-26)
Avail: NTIS HC A05

Increasing the amount of titanium in an aluminum alloy is known to produce a finer structure and eliminate fan like structure, but as titanium content nears the limit permitted by standards, some coarseness may also result. The present article discusses chemical and structural features of dendrite formations in the alloy DI6ch and V95pch. Content of copper, manganese and titanium, as determined by micro-X-ray spectral analysis, showed DI6ch to have 1.3 to 2.0% Co and about 1% Ti in central zones, and in dark cells from 2 to 3.6% Co. Other tests with alloys containing 5.0% zinc, 2.5% manganese and 1.8% copper, and varying amounts of titanium and zirconium showed that in zones with coarse structure, Ti content exceeded the normal amounts by 6 to 8 times, while zirconium was found in 1.5 to 2 times the normal amount for the alloy. Increasing smelting temperature of the alloy had little effect. Interdendrite liquation was not eliminated by any of the procedures tested. Author

N86-13424# Joint Publications Research Service, Arlington, Va.
FIBER COMPOSITION MATERIALS FOR STRENGTHENING COMPONENTS OF ALUMINUM AND ITS ALLOYS Abstract Only
V. K. Gribovskiy, I. Kh. Chutayev, A. G. Bakayev, and A. Ye. Azarenko *In its* USSR Rept.: Mater. Sci. and Met. (JPRS-UM-85-006) 29 Jul. 1985 p 1-2 Transl. into ENGLISH from Tekhnol. i Organ. Proizv. (Kiev), no. 3, Jul. - Sep. 1984 p 53-54 (For primary document see N86-13422 04-26)
Avail: NTIS HC A05

Local strengthening is a promising method for increasing the useful life of portions of machinery that are subjected to particularly severe wear conditions. The present article summarizes attempts to improve the wear characteristics of diesel engine compression rings and ring seats. Work at the Central Institute for Diesel Research in Leningrad has focused on plasma resmelting with simultaneous addition of new alloying materials in the compression ring seat area in order to harden and strengthen it. Attempts to add powders or monolithic fibers of stainless steel or nickel were unsuccessful, but better results were achieved with composition materials based on aluminum and containing nickel, nichrome or steel. The continuous feed system for producing such improved pistons is diagrammed and described. The fibers were improved and forging made more stable by an intermittent stretching procedure. Operational tests have indicated that piston life is increased by 1.5 to 1.7 times by this method. Author

N86-13425# Joint Publications Research Service, Arlington, Va.
STRUCTURE AND PROPERTIES OF Al-Mg-Zn CASTING ALLOYS Abstract Only
N. A. Parkhomenko, N. S. Gerchikova, V. V. Cherkasov, and P. P. Pobezhimov *In its* USSR Rept.: Mater. Sci. and Met. (JPRS-UMS-85-006) 29 Jul. 1985 p 2 Transl. into ENGLISH from Metalloved. i Term. Obrabotka Metal. (Moscow), no. 3, Mar. 1985 p 56-57 (For primary document see N86-13422 04-26)
Avail: NTIS HC A05

Diffraction electron microscopy was used to study the fine structure of casting alloys in the system Al-Mg-Zn as a function of alloying and heat treatment conditions. Analysis of mechanical test data for the alloys established certain regularities: as magnesium content increases, strength increases but ductility decreases. The optimal combination of properties is found at Al-5.5% Mg-2.5% Zn. The major hardening phase of the alloys is the T phase (Al2Mg3Zn3) liberated at 160 to 170 C. Upon heating to 190 C or higher, the beta phase (Al3Mg2) begins to form, first at subgrain boundaries, then throughout the entire body of the grain at temperatures over 200 C. Coagulation of T phase particles and beta phase growth lead to a decrease in strength. The best combination of properties of the alloy with optimal composition corresponds to the beginning of the T yields beta phase transition, observed after aging at 80 C for 8 hours plus 190 C for two hours. Author

N86-13426# Joint Publications Research Service, Arlington, Va.
DISCONTINUOUS PRECIPITATION IN ALUMINUM-MAGNESIUM ALLOYS WITH HIGH MAGNESIUM CONTENT Abstract Only
N. N. Buynov and L. I. Kaygorodova *In its* USSR Rept.: Mater. Sci. and Met. (JPRS-UMS-85-006) 29 Jul. 1985 p 3 Transl. into ENGLISH from Fiz. Metal. i Metalloved. (Sverdlovsk), v. 59, no. 1, Jan. 1985 p 91-95 (For primary document see N86-13422 04-26)
Avail: NTIS HC A05

A study was made of the possibility of reducing the grain size in cast Al-Mg alloys by breakdown of a supersaturated solid solution by a discontinuous mechanism. This analysis of the literature indicates that Al-Mg alloys have a number of peculiarities which distinguish them from aluminum alloys of other systems, including slight natural aging with a recovery at low temperatures, easy breaking of bonds between magnesium atoms and vacancies, forming accumulations of vacancies; rapid development of grain boundary segregations; presence of Bardin-Haring dislocation sources; and initial coherent matrix development of metastable beta phase particles. Stresses developing in the alloy upon single phase decomposition do not reach the critical state necessary for decomposition of the supersaturated solid solution by the discontinuous mechanism. This plus the high density of phase particles segrated along grain boundaries prevent decomposition of the supersaturated solid solution during aging. Author

N86-13427# Joint Publications Research Service, Arlington, Va.
STRUCTURE FORMATION IN SILUMINS UPON RAPID CRYSTALLIZATION Abstract Only
V. I. Mazur, V. Z. Kutsova, and K. I. Uzlov *In its* USSR Rept.:

Mater. Sci. and Met. (JPRS-UMS-85-006) 29 Jul. 1985 p 3 Transl. into ENGLISH from Metalloved. i Term. Obrabotka Metal. (Moscow), no. 3, Mar. 1985 p 50-55 (For primary document see N86-13422 04-26)
Avail: NTIS HC A05

Thin films of Al-Si alloys cooled from the liquid state at 10 to the 5th power-10 to the 6th power deg c/s were stored at -196 to +20 C and their structure and phase composition subsequently studied. Droplets of melt were catapulted to a copper drum rotating at 2000 rpm, melt temperature 1100 C. The structure of the alloys was studied by light and electron transmission microscopy. The phase composition was determined at -196 to +20 C by diffractometry. Where the silicon content is 12.7 to 23% with significant heating of the melt beyond the melting point, preferential interaction of dissimilar Al-Si atoms occurs. Metastable phases may be formed: cubic, orthorhombic and hexagonal phases, which break down upon cooling to stable phases, the a-solid solution and silicon. Author

N86-13428# Joint Publications Research Service, Arlington, Va.
INFLUENCE OF ALLOYING ELEMENTS AND IMPURITIES ON MECHANICAL PROPERTIES OF COMPLEX SILUMINS Abstract Only
Yu. B. Bychkov, N. A. Balanayeva, A. A. Ofengenden, and Yu. Ye. Kupershtok *In its* USSR Rept.: Mater. Sci. and Met. (JPRS-UMS-85-006) 29 Jul. 1985 p 4 Transl. into ENGLISH from Metalloved. i Term. Obrabotka Metal. (Moscow), no. 3, Mar. 1985 p 57-59 (For primary document see N86-13422 04-26)
Avail: NTIS HC A05

A study is made of the influence of alloying elements (Si, Cu, Mn, Mg) and impurities (Fe and Zn) over a broad range of concentrations on mechanical properties of Al-Si-Cu alloys in the cast state. The work was performed by passive experimentation with alloys containing 4 to 10% Si, 0.5 to 5% Cu, 0.5 to 0.9% Fe, 0.2 to 0.8% Mn, 0 to 3% Mg and 0.5 to 2.4% Zn. Mechanical properties of the alloys were determined using the individually cast specimens, with five parallel measurements of all properties for each melt. The equations are derived to describe the variation of yield point and ultimate tensile strength as a function of content of the various elements. It is found that as zinc concentration increases, short term tensile strength of the alloys increases slightly, yield point still more. Increasing copper concentration significantly increases tensile strength, yield point and hardness, while elongation decreases. At lower concentrations, silicon decreases tensile strength, increasing it at higher concentrations. Iron decreases the positive influence of silicon on tensile strength. Zinc partially compensates the influence of copper on short term strength. Magnesium increases tensile strength at contents of less than 1.6%. Author

N86-13429# Joint Publications Research Service, Arlington, Va.
STUDY OF FRACTURES IN CAST PARTS OF HIGH-STRENGTH ALUMINUM ALLOY Abstract Only
E. A. Lalayan, R. M. Brodskaya, and V. S. Zolotarev *In its* USSR Rept.: Mater. Sci. and Met. (JPRS-UMS-85-006) 29 Jul. 1985 p 4-5 Transl. into ENGLISH from Metalloved. i Term. Obrabotka Metal. (Moscow), no. 3, Mar. 1985 p 60-62 (For primary document see N86-13422 04-26)
Avail: NTIS HC A05

Results are presented from studies on the quality of cast parts made by counterpressure casting of high strength aluminum alloy AMKh-605, and Al-Cu-Mn-Cr alloys (5.6 to 6.4% Cu, 0.25 to 0.55% Mn, 0.20 to 0.55% Cr, 0.20 to 0.45% Ti, 0.08 to 0.25% Zr, < or = 0.25% Fe, < or = 0.25% Si, < or = 0.05% Mg). Chill castings were heat treated by quenching from 450 C (20 hours) in water, aging at 160 C for five hours with cooling in air. Fractograms of tensile specimens are presented. Scanning electron microscopy allows an ambiguous determination of the cause of failure of a part, be it at initial crystallization crack defects or burns, and also allows a relationship to be established between structure and mechanical properties. Author

N86-13430# Joint Publications Research Service, Arlington, Va.
STUDY OF PERMEABILITY OF TWO-PHASE ZONE IN ALUMINUM AND COPPER ALLOYS Abstract Only
N. Yu. Kolyadina, Yu. Ye. Matveyev, and V. T. Borisov *In its* USSR Rept.: Mater. Sci. and Met. (JPRS-UMS-85-006) 29 Jul. 1985 p 5 Transl. into ENGLISH from Izv. Vyssh. Ucheb. Zaved.: Chernaya Met. (Moscow), no. 1, Jan. 1985 p 4-6 (For primary document see N86-13422 04-26)
Avail: NTIS HC A05

A study is made of permeability in alloys such as silumin (Al-6% Si-0.3% Mg; Al-4% Cu) and tin bronze (Cu-10% Sn; Cu-15% Sn). The method for determining permeability coefficient was based on measurement and analysis of attenuation of twisting oscillations of a terroidal specimen of the alloy in the solid-liquid state. The alloy was crystallized or melted at a predetermined rate, which varied between 0.5 and 4.5 C/min. At a fixed temperature determining the cross section of the liquid phase and dendritic structure of the two phase zone, the specimen was twisted with an elastic filament along the axis of the torus and allowed to oscillate, the amplitude of the oscillations being measured at fixed time intervals. The change in coefficient of permeability and cross section of two phase zone is shown to be similar over the solidification temperature interval. The more rapidly the alloy was crystallized or melted, the less the coefficient of permeability. Author

N86-13431# Joint Publications Research Service, Arlington, Va.
INFLUENCE OF DEGREE OF DEFORMATION ON STRUCTURE AND PROPERTIES OF NATURALLY AGED ALLOY 1163 Abstract Only
L. N. Leshchiner, S. I. Kishkina, and N. S. Gerchikova *In its* USSR Rept.: Mater. Sci. and Met. (JPRS-UMS-85-006) 29 Jul. 1985 p 6 Transl. into ENGLISH from Metalloved. i Term. Obrabotka Metal. (Moscow), no. 2, Feb. 1985 p 61-62 (For primary document see N86-13422 04-26)
Avail: NTIS HC A05

A study was made of the influence of deformation of rolled products on the properties of naturally aged aluminum alloy 1163 (type D16ch) with reduced content of iron and silicon (4.3% Cu, 1.4% Mg, 0.43% Mn, 0.12% Fe, 0.05% Si). Plates 6 to 8 mm thick were cut from hardened, straightened and naturally aged slabs and rolled at normal temperature with 7, 11, 15, 20 and 25% deformation. The plates were straightened by stretching after rolling with residual deformation of about 1% to produce a flat surface. The properties of the specimens were determined in extension, the work of fracture of a specimen with a crack and low cycle fatigue properties were determined, and the dislocation structure was studied by diffraction electron microscopy. Rolling deformation over 7% was found to lead to a decrease in fracture toughness. After 11 to 15% deformation, the increase in strength properties is greater than after 7% deformation, with the same ductility and fracture toughness, homogeneous distribution of dislocations and low cycle fatigue properties no less than in the initial, naturally aged state. Author

N86-13432# Joint Publications Research Service, Arlington, Va.
APPEARANCE OF SUPERPLASTICITY EFFECT IN ALUMINUM ALLOYS WITH LITHIUM Abstract Only
I. N. Fridlyander, Ye. V. Ekhina, T. M. Kunyavskaya, and V. L. Likin *In its* USSR Rept.: Mater. Sci. and Met. (JPRS-UMS-85-006) 29 Jul. 1985 p 6-7 Transl. into ENGLISH from Metalloved. i Term. Obrabotka Metal. (Moscow), no. 2, Feb. 1985 p 62-63 (For primary document see N86-13422 04-26)
Avail: NTIS HC A05

A study was made of the influence of lithium content on the superplasticity characteristics of aluminum alloys containing 5.8 to 6.2% Mg, 1.7 to 2.55% Li, 0.1% Cr, and 0.1% Fe. Ingots 70 mm in diameter were cast in a water-cooled mold, then bars 18 mm in diameter were produced by direct pressing at 400 to 420 C. Temperature-speed tests of specimens of the alloys studied in extension were performed on a test device with a tubular electric furnace. The favorable influence of lithium on the characteristics of superplasticity of the aluminum alloys was found to result from a decrease in grain size and an increase in diffusion processes along grain boundaries. The superplasticity effect appears in alloys containing over 2% Li. Author

N86-13433# Joint Publications Research Service, Arlington, Va.
PRELIMINARY ANNEALING ON CRYSTALLIZATION OF AMORPHOUS Fe80Si6B14 ALLOY Abstract Only
Yu. A. Skakov, V. L. Kozhevnikova, and P. Reykh *In its* USSR Rept.: Mater. Sci. and Met. (JPRS-UMS-85-006) 29 Jul. 1985 p 8 Transl. into ENGLISH from Izv. Vyssh. Ucehb.: Chernaya Met. (Moscow), no. 1, Jan. 1985 p 152 (For primary document see N86-13422 04-26)
Avail: NTIS HC A05

The purpose of this work was to study the influence of preliminary low temperature treatment on crystallization of the amorphous alloy Fe80Si6B14 by X-ray methods. The alloy was produced in the amorphous state by cooling in the liquid state as a strip 10 mm wide and about 50 micrometer thick. Cooled specimens were subjected to isothermal annealing at 250, 300 and 350 C, holding one hour. The specimens were then held from 30 minutes to 2.5 hours at the crystallization point of the alloy (430 C). A 2 micrometer thick layer was removed by electrolytic polishing from either side of the specimens after heat treatment. Analysis of the specimens showed no significant differences from results obtained in the initial specimens. This indicates that stabilization of the amorphous matrix has a volumetric nature, i.e., is not related to changes in the state of the surface or redistribution of zonal stresses. Author

N86-13434# Joint Publications Research Service, Arlington, Va.
INFLUENCE OF CHROMIUM ON CRYSTALLIZATION OF AMORPHOUS Fe-B ALLOYS Abstract Only
S. D. Kaloshkin, A. K. Zaytsev, T. Yu. Mochalova, B. V. Molotilov, V. P. Ovcharov, and I. A. Timilin *In its* USSR Rept.: Mater. Sci. and Met. (JPRS-UMS-85-006) 29 Jul. 1985 p 8-9 Transl. into ENGLISH from Fiz. Metal. i Metalloved. (Sverdlovsk), v. 59, no. 1, Jan. 1985 p 165-170 (For primary document see N86-13422 04-26)
Avail: NTIS HC A05

The purpose of this work was to determine the parameters of crystallization (temperature, heats and effective energies of activation) of amorphous iron-boron alloys containing chromium. Compositions studied included: Fe85(-x)Cr(x)B15 (where x-0, 2, 5, 10, 15 and 18 at.%) and Fe90(-y)Cr10B(y) (where y-12, 14, 15 and 18 at.%). Specimens were obtained by cooling a melt on a spinning drum as a strip 1 to 2 mm wide and about 20 micrometer thick. Studies were performed with a scanning microcalorimeter with continuous heating at 2, 4, 8, 16 and 32 per minute. The increase in thermal stability of amorphous iron-boron alloys observed upon addition of chromium is related to the following factors: chromium prevents diffusion flow of boron away from locations of future iron-based solid solution crystals; the addition of chromium decreases the heat of crystallization; chromium may influence the initial structure of the amorphous alloys. Author

N86-13435# Joint Publications Research Service, Arlington, Va.
RELATIONSHIP OF THERMAL EXPANSION OF AMORPHOUS METAL ALLOYS WITH THEIR HIGH TEMPERATURE PLASTIC PROPERTIES Abstract Only
V. A. Khonik, A. N. Konopkin, and V. A. Zelenskiy *In its* USSR Rept.: Mater. Sci. and Met. (JPRS-UMS-85-006) 29 Jul. 1985 p 9 Transl. into ENGLISH from Fiz. Metal. i Metalloved. (Sverdlovsk), v. 59, no. 1, Jan. 1985 p 204-205 (For primary document see N86-13422 04-26)
Avail: NTIS HC A05

The amorphous metal alloys Pd77.5Cu6Si16.5 and Co70Fe5Si15B10 studied were obtained by quenching from the liquid state. The specimens were 30 to 50 micrometer thick and 0.7 to 1.5 mm wide. Data on thermoexpansion and differential scanning calorimetry are presented. The specimens were heated at 0.07 K/s to an assigned temperature, then deformation was immediately begun at 3.5 x 10 to the minus 2 power mm/s. Study of thermal expansion can reveal amorphous metal alloys which may be superplastic. Manifestation of the superplasticity effect in these alloys requires a crystallization of the material not begun before the glass point is reached. Maximum plasticity is found in amorphous metal alloys in which the interval between the crystallization point and the glass point is broadest. Author

N86-13436# Joint Publications Research Service, Arlington, Va.
ON ANISOTROPY OF MEAN ELECTRICAL RESISTANCE OF BERYLLIUM Abstract Only
G. Ye. Pletenetskiy and G. S. Koshkarev *In its* USSR Rept.: Mater. Sci. and Met. (JPRS-UMS-85-006) 29 Jul. 1985 p 10 Transl. into ENGLISH from Izv. Akad. Nauk SSSR: Metal. (Moscow), no. 2, Mar. - Apr. 1985 p 60-61 (For primary document see N86-13422 04-26)
Avail: NTIS HC A05

Data on mean electrical resistance (MER) of beryllium monocrystals and its temperature dependency in previous research have been contradictory. The present article reports on study of MER anisotropy in monocrystals of 99.99 and 99.6% purity in a broad temperature range from 4.2 to 1535 K. Results showed that in a cryogenic range, anisotropy grew rapidly as temperature increased and was not related to impurity content. In a medium range of 273 to 1023 K, a more complex pattern emerged, where impurities brought some increase in anisotropy, while at higher temperatures it declined as the state of impurities changed. Author

N86-13437# Joint Publications Research Service, Arlington, Va.
COMPLEX NICKEL-ALUMINIDE COATINGS ON NICKEL-CHROMIUM ALLOY EP648-VI Abstract Only
L. A. Monakhova, E. M. Lazarev, V. N. Novilov, B. M. Zakharov, A. B. Varigin, L. A. Lapidovskaya, and K. I. Dikaya *In its* USSR Rept.: Mater. Sci. and Met. (JPRS-UMS-85-006) 29 Jul. 1985 p 11 Transl. into ENGLISH from Izv. Akad. Nauk SSSR: Metal. (Moscow), no. 2, Mar. - Apr. 1985 p 157-160 (For primary document see N86-13422 04-26)
Avail: NTIS HC A05

Studies have shown that oxidation of high chromium content Ni-Cr alloys at temperatures above 1000 C is governed by gas acquisition and evaporation of alloying elements from the metal, leading to improvement of the chromium and resultant intercrystalline corrosion and loss of temper. The present article reports on study of the structure of the alloy EP648-VI with various coatings after oxidation at 1150 C for 24 hours. Coatings were applied by gasothermal spraying and vacuum diffusion calorization. After the thermal treatment, samples were examined metallographically to show that oxygen acquisition and chromium loss were in balance. X-ray phase and electronographic analyses showed that the coatings applied by plasma spraying contained the intermetallide Ni3Al as the basic phase, with a spinel cinder, while coatings applied by diffusion calorization had both NiAl and Ni3Al intermetallides in the coating, and cinders of alpha-Al2O3 and spinel. The sub-zone of spinel that formed prevented oxygen penetration and protected the alloy from loss of chromium and subsequent deterioration. Thus, processes that provide such an impenetrable zone are an important part of such coated alloys. Author

N86-13438# Joint Publications Research Service, Arlington, Va.
INFLUENCE OF Co-Cr-Al-Y COATINGS ON PHYSICAL AND MECHANICAL PROPERTIES OF EI-893 STEEL IN GT-100 TURBINE DRIVE VANES Abstract Only
B. A. Movchan, I. S. Malashenko, V. I. Nikitin, A. I. Runikov, Yu. P. Belolipetskiy, A. M. Klytsina, A. Ye. Levin, Yu. D. Sklyarov, N. P. Vashchilo, K. Yu. Yakovchuk et al *In its* USSR Rept.: Mater. Sci. and Met. (JPRS-UMS-85-006) 29 Jul. 1985 p 12 Transl. into ENGLISH from Probl. Spets. Elektrometal. (Kiev), no. 1, Jan. - Mar. 1985 p 34-41 (For primary document see N86-13422 04-26)
Avail: NTIS HC A05

Coatings of Co-Cr-Al-Y produced by vacuum precipitation were used to protect the drive vanes of a high-pressured peak load gas turbine. Coatings containing 21 to 23% Cr, 11 to 12% Al and up to 0.1% Y were obtained by precipitation in a vacuum in an electron beam evaporator. The vanes were made of deformed heat resistant EI-893VD nickel alloy. After application of the protective layer the parts were subjected to standard heat treatment and shot peening, followed by 2-stage aging under standard conditions. The diffusion layer consisted mainly of (Ni, Co)Al intermetallides and of carbide particles, microhardness 4200 to 4600 MPa, 900 to 1000 MPa higher than the base metal. Optical and electron microscopy revealed that there were no significant changes in the structure or phase composition of the base metal. Laboratory testing revealed that the coatings reliably protected the nickel alloys under static stress conditions at 800 and 850 C in gas turbine fuel ash and air. Additional aging increased the corrosion durability of the coatings. Fatigue strength was satisfactory under normal operating conditions. Author

N86-13439# Joint Publications Research Service, Arlington, Va.
ELECTRIFICATION OF FILLED POLYETHYLENE COATINGS IN FRICTION WITH METAL Abstract Only **c27**
V. S. Mironov *In its* USSR Rept.: Mater. Sci. and Met. (JPRS-UMS-85-006) 29 Jul. 1985 p 12-13 Transl. into ENGLISH from Vestsi Akad. Nauk BSSR (Minsk), no. 1, Jan. - Mar. 1985 p 38-42 (For primary document see N86-13422 04-26)
Avail: NTIS HC A05

A study is presented of the influence of the electrophysical nature and concentration of dispersed filler in polyethylene coatings on the degree and kinetics of relaxation of the charge arising upon friction of the coatings with metal. Repeated experiments established that polyethylene coatings in friction with metal are charged negatively. When a filler is included in high density polyethylene the polarity of the charge of the material remains negative. Electron microscope studies of the surface of filled high density polyethylene coatings showed that friction, as a result of deformation and wear, slightly changes the shape of particles of nickel and teflon and teflon in thin surface layers, the particles remaining separated by intermediate layers of the polymer while graphite particles are spread over the polymer surface, increasing the surface electric conductivity of composite coatings containing graphite. This causes charge dissipation to dominate over charge growth in graphite-filled coatings. Other fillers may increase the electric charge and residual charge. Author

N86-13440# Joint Publications Research Service, Arlington, Va.
INFLUENCE OF TEXTURE OF TITANIUM NITRIDE COATINGS ON WEAR RESISTANCE OF CUTTING TOOLS Abstract Only
G. L. Platonov and V. N. Anikin *In its* USSR Rept.: Mater. Sci. and Met. (JPRS-UMS-85-006) 29 Jul. 1985 p 13 Transl. into ENGLISH from Poroshkovaya Met. (Kiev), no. 2, Feb. 1985 p 40-43 (For primary document see N86-13422 04-26)
Avail: NTIS HC A05

The type of texture obtained or the influence on the operational properties of hard alloy tools with textured coatings are discussed. Flat plates of VK6, T5K10 and TT10K8B hard alloys, onto which coatings of titanium nitride were applied from a gas phase consisting of a mixture of titanium tetrachloride and nitrogen in a current of hydrogen at 900 to 1150 C were studied. Textures appeared regardless of metal substrate at 1050 C and continued through 1150 C. The type of texture in all cases was axial, varying with base alloy and precipitation temperatures. It is indicated that in titanium nitride coatings precipitated under the experimental conditions, axial growth textures, both monaxial and biaxial, are formed on the plates. DOE

N86-13441# Joint Publications Research Service, Arlington, Va.
INFLUENCE OF ANNEALING ON HARDNESS OF VACUUM-DIFFUSION CHROMIUM COATING ON LOW-CARBON STEEL Abstract Only
N. Ye. Yanenskiy, P. I. Melnik, A. V. Galyko, B. N. Nadvornyy, A. S. Stetsenko, and V. N. Yanenskiy *In its* USSR Rept.: Mater. Sci. and Met. (JPRS-UMS-85-006) 29 Jul. 1985 p 14 Transl. into ENGLISH from Tekhnol. i Organ. Proizv. (Kiev), no. 4, Oct. - Dec. 1984 p 35-36 (For primary document see N86-13422 04-26)
Avail: NTIS HC A05

The possibility to increase hardness and wear resistance of vacuum-diffusion chromium coatings on type VSt3ps steel was studied. Specimens 25 mm in diameter and 30 mm high were vacuum chrome plated to a layer thickness of 1.2 to 1.4 mm, with an alpha solid solution of chromium in iron with a transition layer 40 to 50 micron thick at the substrate consisting of a chrome eutectoid. The microhardness of the alpha solution was 180 to 220 kgf/sq mm, of the eutectoid - 240 kgf/sq mm. Specimens were then annealed at 950 and 1050 C for 3 to 5 hours. Sections were cut from the annealed specimens to study the structure, distribution of carbide-forming elements and microhardness. Analysis of the data showed that increasing time and temperature of annealing increased microhardness of the vacuum chrome-plated layer by a factor of 1.5 to 2 while simultaneously increasing the thickness of the hardened layer. The eutectoid sublayer completely disappears in this process. E.A.K.

N86-13442# Joint Publications Research Service, Arlington, Va.
STUDY OF PROPERTIES OF GAS-THERMAL COATINGS OF COMPOSITE NICHROME-ALUMINUM ALLOY POWDERS Abstract Only
Yu. S. Borisov, M. G. Zolotogorov, I. N. Gorbatov, V. R. Kalinovskiy, V. A. Paschchenko, Z. A. Zaytseva, and N. N. Kokorina *In its* USSR Rept.: Mater. Sci. and Met. (JPRS-UMS-85-006) 29 Jul. 1985 p 15 Transl. into ENGLISH from Poroshkovaya Met. (Kiev), no. 10, Oct. 1984 p 50-52 (For primary document see N86-13422 04-26)
Avail: NTIS HC A05

The heat resistance, thermal stability and bond strength of atomized coatings of composite powders containing nichrome and an aluminum alloy with yttrium or lanthanum was studied. It was found that introduction of 0.1% Y leads to formation upon oxidation at 1000 to 1200 C of a finely dispersed scale resistant to thermal shock and having good adhesion to the base. The optimal content of binder and drying conditions were established. The optimal binder content was found to be 1.5 to 3%. Testing of thermal stability showed that the coatings containing rare earth metals began to break down significantly after 200 cycles, whereas coatings made of composite powders containing aluminum E.A.K.

N86-13443# Joint Publications Research Service, Arlington, Va.
EFFECT OF GEOMETRY OF FIBER PACKING ON CONSOLIDATION OF FIBROUS COMPOSITION MATERIALS WITH POROUS MATRIX Abstract Only **c24**
B. A. Arefyev, L. A. Bondarchuk, T. I. Pavlova, I. I. Renne, V. L. Tikhmyanov, and V. K. Ushakov *In its* USSR Rept.: Mater. Sci. and Met. (JPRS-UMS-85-006) 29 Jul. 1985 p 16 Transl. into ENGLISH from Fiz. i Khim. Obrabotki Mater. (Moscow), no. 2, Mar. - Apr. 1985 p 127-130 (For primary document see N86-13422 04-26)
Avail: NTIS HC A05

Production of fibrous composition materials (FCM) by solid phase consolidation of a porous matrix is hampered by unevenness. Analysis of the nature of such consolidation with a hexagonal packing with varying vertical and horizontal spacing is reported. A mathematical model of a porous matrix and absolutely stiff fibers is presented. It is indicated that a hexagonal packing form with alpha = square root of 3 is the best parameter for horizontal spacing of fibers. Reducing the initial porosity of the matrix made it possible to reduce irregularities in the density of the FMC material, especially where relative fiber content is very high. E.A.K.

N86-13444# Joint Publications Research Service, Arlington, Va.
CONDUCTIVITY OF METAL-CERAMIC MULTILAYER ZrO2-Mo AND Mo-BASED COMPOSITE MATERIALS Abstract Only **c24**
S. M. Kats, Z. I. Bylkova, V. N. Bogin, A. P. Filichkin, and N. G. Chubenko *In its* USSR Rept.: Mater. Sci. and Met. (JPRS-UMS-85-006) 29 Jul. 1985 p 16 Transl. into ENGLISH from Poroshkovaya Met. (Kiev), no. 2, Feb. 1984 p 61-64 (For primary document see N86-13422 04-26)
Avail: NTIS HC A05

The possibility to increase heat conductivity of multilayer composites through the layers by replacing the purely oxide layers with cermets consisting of a homogeneous mixture of ZrO2 and

Mo was studied. The specimens were disks 50 mm in diameter and 2 to 3 mm thick, sintered of stacks of plasticized sheet films produced from CaO-stabilized finely milled ZrO2 powder and Mo powder. It is shown that varying the content of the metal-ceramic phase can significantly alter heat conductivity from 20 to 100 W/m.k while retaining the strength and thermal stability of oxide materials. E.A.K.

N86-13445# Joint Publications Research Service, Arlington, Va.
PRODUCTION OF MULTILAYER MAGNETIC SURFACE OF MAGNETICALLY SOFT COMPOSITE MATERIALS Abstract Only **c24**
A. E. Ritso, O. A. Katrus, A. A. Laansoo, and R. A. Siymar *In its* USSR Rept.: Mater. Sci. and Met. (JPRS-UMS-85-006) 29 Jul. 1985 p 17 Transl. into ENGLISH from Poroshkovaya Met. (Kiev), no. 2, Feb. 1985 p 70-73 (For primary document see N86-13422 04-26)
Avail: NTIS HC A05

The direct rolling of powders is used to produce a substrate at least 0.4 mm thick capable of operating at high frequencies and providing a magnetic induction of at least 0.9 T1 with reduced remagnetization losses with a field intensity of 5000 A/m. The ferromagnetic component used was iron powder, obtained by a chemical-metallurgical method. After rolling, the plates were heat-treated in air. The magnetically soft composite material with epoxy resin was treated at 160 C, the material with ethyl silicate at 550 C. Plates of minimum thickness and maximum density were obtained from the composite material with epoxy resin. The method of rolling produces substrates 0.35 to 0.4 mm thick with magnetic induction 1.02 and 1.35 T1 at 5000 and 10,000 A/m. It is found that magnetic circuits of composite materials with silica differ little from circuits made of substrates with epoxy resin for magnetic characteristics. E.A.K.

N86-13446# Joint Publications Research Service, Arlington, Va.
CALCULATION OF DAMPING PROPERTIES OF COMPOSITE MATERIALS Abstract Only **c24**
V. N. Brinza, B. S. Vekshin, and Ye. V. Kolyadina *In its* USSR Rept.: Mater. Sci. and Met. (JPRS-UMS-85-006) 29 Jul. 1985 p 17 Transl. into ENGLISH from Izv. Vyssh. Ucheb. Zaved.: Chernaya Met. (Moscow), no. 1, Jan. 1985 p 79-81 (For primary document see N86-13422 04-26)
Avail: NTIS HC A05

The damping capability of a material consisting of a mixture of strengthening and plate-like granules exposed to a periodic load on its upper surface was studied. It is assumed that granules do not slip relative to each other, that the deformation of the material by the periodic load is elastic and homogeneous, and that the periodic load acts on the specimen at a frequency significantly different from its resonant frequency. It is demonstrated that the method developed for calculation of damping properties of fiber composite materials can be applied to estimation of the damping properties of composite materials consisting of metallic granules. The variation in damping properties of the composite material as a function of relationship of elasticity modulus oscillation decrements, mass and density of the granule materials is obtained and experimentally confirmed. The method of calculation can be used to estimate the damping properties of other composite materials as well. E.A.K.

N86-13447# Joint Publications Research Service, Arlington, Va.
THEORY OF PYROLYSIS OF COMPOSITE POLYMER MATERIALS Abstract Only **c24**
A. M. Grishin and S. P. Sinitsyn *In its* USSR Rept.: Mater. Sci. and Met. (JPRS-UMS-85-006) 29 Jul. 1985 p 18 Transl. into ENGLISH from Fiz. Goreniya i Vzryva (Novosibirsk), v. 20, no. 6, Nov. - Dec. 1984 p 67-69 (For primary document see N86-13422 04-26)
Avail: NTIS HC A05

The pyrolysis of composite polymers was studied by analyzing the decomposition of the corresponding polymers. A mathematical theory of the pyrolysis of composite polymers on the basis of simplified kinetic diagrams and representations of the mechanics of the reacting media was constructed. The direct and reverse problems of pyrolysis are formulated and the direct and reverse problems are analyzed under isothermal or homothermal conditions for one and two-staged kinetics of decomposition of the binder. A method is suggested for solving the reverse problems which was tested on model examples. The influence of the error in experimental data on the solution of the reverse problem is demonstrated. The possibility is demonstrated on model to determine the thermokinetic constants of pyrolysis based on the results of experimental studies. E.A.K.

N86-13448# Joint Publications Research Service, Arlington, Va.
CRITICAL BEHAVIOR OF THERMOELECTRIC POWER IN BINARY COMPOSITE MATERIALS Abstract Only **c24**
A. S. Skal *In its* USSR Rept.: Mater. Sci. and Met. (JPRS-UMS-85-006) 29 Jul. 1985 p 18 Transl. into ENGLISH from Zh. Eksperim. i Teor. Fiz. (Moscow), v. 88, no. 2, Feb. 1985 p 516-521 (For primary document see N86-13422 04-26)
Avail: NTIS HC A05

Thermoelectric power in binary random metal-metal or metal-insulator composites is considered, and its behavior as the hole concentration P1 in the conducting component approaches the threshold of an infinite cluster is analyzed on the basis of site-problem and bond-problem models for phase transitions of the second kind. For calculation of the effective Seeback coefficient in terms of the Peltier heat, its dependence on the properties of the two materials is evaluated for the two extreme cases of almost equal thermal conductivities and very different thermal conductivities. In the first case there are no active seats of thermal emf and the conducting component acts only as a shunt, while the second component in effect vanishes. In the second case electric charges and heat are conducted simultaneously when the carrier concentration is above the threshold level, with isothermal clusters breaking up fast within the critical range and the temperature of the infinite cluster tending to become a linear function of the carrier concentration. E.A.K.

N86-13449# Joint Publications Research Service, Arlington, Va.
TEMPERATURE-FREQUENCY VARIATION OF MECHANICAL LOSSES IN PERIODIC DEFORMATION OF MULTILAYER GLASS-REINFORCED PLASTICS Abstract Only **c27**
L. S. Yelistratova, V. V. Kolokolshikov, and A. S. Podkolayev *In its* USSR Rept.: Mater. Sci. and Met. (JPRS-UMS-85-006) 29 Jul. 1985 p 19 Transl. into ENGLISH from Zh. Prikl. Mekhan. i Tekhn. Fiz. (Novosibirsk), no. 6, Nov. - Dec. 1984 p 139-144 (For primary document see N86-13422 04-26)
Avail: NTIS HC A05

Regularities in the temperature-frequency position and magnitude of the maximum of loss angle tangent and real portion of Young's modulus in multilayer composites were studied. The equations are illustrated with numerical computations of frequency-dependent elastic and damping characteristics of multilayer glass and carbon fiber-reinforced composites in the area of transition of the matrix from vitreous to highly elastic states. E.A.K.

N86-13450# Joint Publications Research Service, Arlington, Va.
CORROSION RESISTANCE OF DIFFUSION AND GALVANIC COATINGS ON STEEL FASTENERS Abstract Only
B. F. Soldatov, Ye. N. Shavlovskiy, N. I. Kaporik, M. Ye. Belitskiy, and A. P. Epik *In its* USSR Rept.: Mater. Sci. and Met. (JPRS-UMS-85-006) 29 Jul. 1985 p 20 Transl. into ENGLISH from Tekhnol. i Organ. Proizv. (Kiev), no. 4, Oct. - Dec. 1984 p 43 (For primary document see N86-13422 04-26)
Avail: NTIS HC A05

The possibility and economic expediency of replacing galvanic coatings on steel fasteners with diffusion coatings which have similar corrosion resistance were studied. Fasteners of type St. 3 steel with M4 thread 13 mm long were tested following diffusion chrome plating, chromo-aluminizing, aluminizing and zinc coating in powder mixtures consisting of the saturating element, an activator and a neutral diluting agent. Thickness of the diffusion layers produced was 20 to 40 micrometers. In corrosion testing, corrosion occurred with all coatings in all corrosive media, diffusion coatings produced after chrome plating chromo-aluminizing being most corrosion resistant. Nickel and chrome galvanic coatings can be replaced with diffusion chromo-aluminized coatings on products that must meet certain esthetic requirements, or chromium diffusion coatings if esthetics are not as important. E.A.K.

N86-13451# Joint Publications Research Service, Arlington, Va.
ANTICORROSION POLYMER PACKING FILM WITH IMPROVED PROTECTIVE PROPERTIES Abstract Only **c27**
N. I. Domantsevich, O. N. Kopyl, and A. N. Tynnyy *In its* USSR Rept.: Mater. Sci. and Met. (JPRS-UMS-85-006) 29 Jul. 1985 p 20 Transl. into ENGLISH from Tekhnol. i Organ. Proizv. (Kiev), no. 4, Oct. - Dec. 1984 p 37-39 (For primary document see N86-13422 04-26)
Avail: NTIS HC A05

A conservation and packaging material was created, type IPP inhibited polymer film, which combines the processes of conservation and packaging of metal products while it significantly improves labor conditions. The IPP is a transparent polymer film based on low-intensity polyethylene modified during extrusion by the addition of a finely dispersed powder of dicyclohexylamine nitrite (DAN) corrosion inhibitor. Vacuum shrink wrapping of motor vehicle metal parts in the film is recommended. High-density polyethylene was used with hexamethyleneimine metanitrobenzoate as the corrosion inhibitor. The new film is superior to IPP in its protective properties, broad temperature interval at which it can be processed and relative cheapness. E.A.K.

N86-13452# Joint Publications Research Service, Arlington, Va.
EXTREMELY HIGH REFLECTIVE CAPABILITY OF ZIRCONIUM BURNING IN AIR UNDER EFFECTS OF CONSTANT CO2 LASER RADIATION Abstract Only **c36**
O. G. Buzykin, A. V. Burmistrov, M. N. Kogan, V. I. Konov, A. M. Prokhorov, and V. G. Ralchenko *In its* USSR Rept.: Mater. Sci. and Met. (JPRS-UMS-85-006) 29 Jul. 1985 p 22 Transl. into ENGLISH from Izv. Akad. Nauk SSSR: Ser. Fiz. (Moscow), v. 49, no. 4, Apr. 1983 p 779-782 Original language document was announced in IAA as A85-35470 (For primary document see N86-13422 04-26)
Avail: NTIS HC A05

It is shown experimentally that in the case of nonisothermal laser ignition of Zr in air, the oxinitride is located in the outer scale layer and determines the reflectivity. The possible mechanisms of formation of the nitride phase on the specimen surface as a result of rapid combustion and transition to a gas-phase-limited reaction are examined. Some previously proposed models describing changes in the reflectivity of Zr and Ti during ignition without allowance for the formation of nitrides are discussed. V.L. (IAA)

N86-13453# Joint Publications Research Service, Arlington, Va.
MECHANICAL LASER CUTTING OF METALS Abstract Only
B. S. Gavryushenko, L. V. Okorokov, N. N. Rykalin, I. Yu. Smurov, A. A. Uglov, and A. P. Khalboshin *In its* USSR Rept.: Mater. Sci. and Met. (JPRS-UMS-85-006) 29 Jul. 1985 p 23 Transl. into ENGLISH from Fiz. i Khim. Obrabotki Mater. (Moscow), no. 2, Mar. - Apr. 1985 p 4-7 (For primary document see N86-13422 04-26)
Avail: NTIS HC A05

The advantages of laser heating which are precise focus and localization, simplicity, maneuverability and stability are outlined. Mechanical laser cutting procedures which use a laser device are diagrammed and described. Cutting with laser heating is compared to cold cutting with analogous conditions. Instrument wear, power features of the cutting process and the quality of the final product are compared. It is indicated that at 1.0 KWT of power, the useful life of the cutting edge quadruples, to 8 minutes. E.A.K.

N86-13454# Joint Publications Research Service, Arlington, Va.
CERTAIN FEATURES OF LASER DESTRUCTION AND DISLOCATIONAL STRUCTURE OF SILICON DURING HEATING AND EFFECTS OF ELECTRICAL FIELD Abstract Only **c36**
M. S. Bakharev, A. A. Gorbachev, L. I. Mirkin, a. S. Mokh, and R. R. Sheverdova *In its* USSR Rept.: Mater. Sci. and Met. (JPRS-UMS-85-006) 29 Jul. 1985 p 23-24 Transl. into ENGLISH from Fiz. i Khim. Obrabotki Mater. (Moscow), no. 2, Mar. - Apr. 1985 p 37-40 (For primary document see N86-13422 04-26)
Avail: NTIS HC A05

The effects of laser processing on silicon monocrystals, comparing properties before irradiation and after gamma-ray laser processing, polishing and annealing for 1.5 hours at 950 C in a vacuum oven are reported. The GOR-100 laser's intensity was varied by focus adjustments. A nearly circular dense zone was found at the site of laser treatment. The dislocational changes in structure were the only variations noted before the melting point, despite the brittleness of pure silicon. After melting, an electrical current transmitted through the silicon resulted in arc-like cracks. Most damage was to the surface. Structural distortions have a semispherical form with 1 to 2 mm diameter and 30-50 mcm depth. Temperature effects are noted in the dislocational structure of the silicon samples. E.A.K.

N86-13455# Joint Publications Research Service, Arlington, Va.
STRUCTURE OF FLOW OF EROSION PLASMA FORMED UPON LASER TREATMENT OF METALS Abstract Only **c75**
L. Ya. Minko, B. T. Fedyushin, Yu. A. Chivel, and A. N. Chumakov *In its* USSR Rept.: Mater. Sci. and Met. (JPRS-UMS-85-006) 29 Jul. 1985 p 24 Transl. into ENGLISH from Kvatovaya Elektron. (Moscow), v. 12, no. 3, Mar. 1985 p 639-640 (For primary document see N86-13422 04-26)
Avail: NTIS HC A05

In metals which are exposed to a laser beam the erosion plasma of the target material has a structured nature like the flow of gas behind the subsonic radiation wave in air. The structure of the flow is observed before and after development of shielding of the laser radiation. Flat specimens of aluminum, zinc and bismuth were exposed to a microsecond Nd laser beam with an energy of almost 40 J. A ruby laser beam with a pulse duration of about 30 ms and regulated delay was used to record shadow photographs of the flame produced. The structure of the erosion plasma is thought to be purely kinetic in origin. The structure of the erosion plasma has dynamic rigidity and can be significant in the formation of the structured subsonic radiation wave in the stage of acceleration of the flame, when the heavy air plasma or air compressed by the shock wave breaks through into the lighter erosion plasma. E.A.K.

N86-13456# Joint Publications Research Service, Arlington, Va.
CERAMICS BASED ON ALUMINUM NITRIDE AND METALS Abstract Only **c27**
Ye. N. Bukharin, A. S. Vlasov, and A. A. Alekseyev *In its* USSR Rept.: Mater. Sci. and Met. (JPRS-UMS-85-006) 29 Jul. 1985 p 28 Transl. into ENGLISH from Steklo i Keram. (Moscow), no. 2 Feb. 1985 p 23-25 (For primary document see N86-13422 04-26)
Avail: NTIS HC A05

The possibility of producing metal-ceramics with service temperatures up to 1000 C was investigated. The cermets were obtained by sintering of binary mixtures of aluminum nitride powder with iron, nickel, chromium, molybdenum and tungsten. The gas medium used was a mixture of nitrogen with hydrogen. Aluminum nitride-metal compositions with 20 to 75% metal were studied. Components were prepared and mixed in a planetary mill. Specimens were shaped by semidry pressing at 20-25 kPa, then sintered in a periodic furnace in the nitrogen-hydrogen mixture. Near theoretical density was obtained in mixtures containing up to 50% iron and chromium, up to 42% nickel and up to 75% molybdenum and tungsten. Hardness of the composites decreases with increasing metal content and varies with hardness of the metal used. Composites containing iron, molybdenum and tungsten have good oxidation resistance of 800 C. Composites with nickel and chromium have significantly higher oxidation resistance at up to 1200 C. Maximum oxidation of specimens containing iron, nickel and chromium at 1000 C occurs in the first 4 hours, while further holding at this temperature causes practically no additional mass change. E.A.K.

N86-13457# Joint Publications Research Service, Arlington, Va.
INFLUENCE OF SODIUM ON MECHANICAL AND CASTING PROPERTIES OF MAGNESIUM-LITHIUM ALLOYS Abstract Only
L. V. Nikulin, A. Ye. Gayevskiy, and L. K. Dodrova *In its* USSR Rept.: Mater. Sci. and Met. (JPRS-UMS-85-006) 29 Jul. 1985 p 29 Transl. into ENGLISH from Izv. Vyssh. Ucheb. Zaved.: Tsvetnaya Met. (USSR), no. 6, Nov. - Dec. 1984 p 79-83 (For primary document see N86-13422 04-26)
Avail: NTIS HC A05

The influence of sodium on the mechanical properties yielded upon crystallization under pressure and the hot shortness of binary and more complex magnesium-lithium alloys was studied. The alloying elements were selected for their influence on strength and ductility of the binary magnesium-lithium base. Mechanical properties were tested on standard specimens cut from ingots 40 mm in diameter and 80 mm high-crystallized under piston pressure 200 MPa to eliminate shrinkage porosity. An increase in content of impurity sodium was found to decrease strength and particularly ductility equally whether specimens were crystallized under high pressure or solidified in a chill mold. The presence of sodium significantly increases hot shortness. E.A.K.

N86-13458# Joint Publications Research Service, Arlington, Va.
THERMOPHYSICAL PROPERTIES OF TUNGSTEN AT HIGH TEMPERATURES Abstract Only
I. V. Seminko, A. D. Krivorotenko, and Ye. N. Fomichev *In its* USSR Rept.: Mater. Sci. and Met. (JPRS-UMS-85-006) 29 Jul. 1985 p 35 Transl. into ENGLISH from Poroshkovaya Met. (Kiev), no. 10, Oct. 1984 p 72-75 (For primary document see N86-13422 04-26)
Avail: NTIS HC A05

The production of reliable values of the enthalpy and heat capacity of tungsten, was studied in the 1200 to 2800 K temperature interval. Standard specimen of the thermodynamic properties of tungsten were formulated, which are now a part of the State Register of Measures and Measurement Instruments of the USSR, number 2458-82. E.A.K.

N86-13459# Joint Publications Research Service, Arlington, Va.
DETERMINATION OF POROSITY OF THIN SHEETS OF FIBER MATERIALS BASED ON OPTICAL TRANSMISSION COEFFICIENT Abstract Only c24
A. G. Kostornov, O. V. Kirichenko, S. P. Sakhno, and G. S. Tymchik *In its* USSR Rept.: Mater. Sci. and Met. (JPRS-UMS-85-006) 29 Jul. 1985 p 35 Transl. into ENGLISH from Poroshkovaya Met. (Kiev), no. 10, Oct. 1984 p 86-90 (For primary document see N86-13422 04-26)
Avail: NTIS HC A05

An analysis is presented of the structure of porous fiber materials by methods of mathematical statistics and the theory of random processes. The interrelationship of porosity with the optical transmission factor of fiber materials is studied within the framework of a single probabilistic-statistical approach. The fiber material models suggested allows structural parameters to be defined as statistical characteristics. Porosity and optical transmission factor of a sheet fiber material are defined with an error of not over 6% where porosity is over 70% as functions of the geometric dimensions of fibers, diameter d and length, sheet thickness h and mean density of geometric fiber centers lambda. A function is established which allows porosity of thin sheets of fiber material to be determined by measuring the optical transmission factor. Author

N86-13460# Joint Publications Research Service, Arlington, Va.
EFFECT OF HEATING CONDITIONS ON AGGLOMERATION OF POWDERED ALUMINUM IN AIR ATMOSPHERE Abstract Only
A. K. Likenbakh, N. A. Zaporina, A. Z. Knipele, V. V. Strod, and L. K. Lepin *In its* USSR Rept.: Mater. Sci. and Met. (JPRS-UMS-85-006) 29 Jul. 1985 p 36 Transl. into ENGLISH from Fiz. Goreniya i Vzryva (Novosibirsk), v. 21, no. 1, Jan. - Feb. 1985 p 73-82 (For primary document see N86-13422 04-26)
Avail: NTIS HC A05

Much recent research has attempted to define the mechanism and quantity agglomeration and fusion of metals in precombustion and combustion. Factors such as the rate of temperature increase have been considered. The present article presents the results of an electron microscope study of the effect of the heating rate on oxide layer breakdown of aluminum particles as related to structure and composition of the gaseous environment. A poly-dispersed aluminum powder with particle diameters averaging 10 mcm is deposited as a coating on corundum or nichrome, then subjected to temperatures of 1173-1473K in a flow of air. The electron microscope images of the powder particles are described at temperatures in that range and heating rates of 2000 to 15,500K/min agglomeration occur without oxide layer breakdown. Thermomechanical reaction of the metal nuclei and the oxide layer and physicochemical oxidation of metals compete in the processes described. The initial state of the oxide layer and other important factors require further study. Author

N86-13461# Joint Publications Research Service, Arlington, Va.
SUPERELASTIC BEHAVIOR OF POWDERED TITANIUM NICKELIDE DURING PRESSING Abstract Only
I. F. Martynova, V. V. Skorokhod, S. M. Solonin, and G. R. Fridman *In its* USSR Rept.: Mater. Sci. and Met. (JPRS-UMS-85-006) 29 Jul. 1985 p 36 Transl. into ENGLISH from Poroshkovaya Met. (Kiev), no. 2, Feb. 1985 p 13-17 Original language document was announced in IAA as A85-28751 (For primary document see N86-13422 04-26)
Avail: NTIS HC A05

The dilatation of TiNi powder during compaction due to superelasticity has been investigated experimentally using X-ray diffraction analysis. It is shown that dilatation occurs in several stages including a significant increase in volume directly after compaction, a slight increase in volume during subsequent heating. It is also shown that the maximum volume recovery does not reach 100 percent and that the extent of volume recovery decreases as the degree of compaction increases. The dilatation effect becomes more pronounced with increasing temperature and porosity. Author

N86-13462# Joint Publications Research Service, Arlington, Va.
GRAIN GROWTH IN HEAT-RESISTANT AUSTENITIC STEEL Abstract Only
I. K. Denisova, V. N. Zakharov, N. M. Karpova, and V. M. Farber *In its* USSR Rept.: Mater. Sci. and Met. (JPRS-UMS-85-006) 29 Jul. 1985 p 38 Transl. into ENGLISH from Metalloved. i Term. Obrabotka Metal. (Moscow), no. 2, Feb. 1985 p 54-56 (For primary document see N86-13422 04-26)
Avail: NTIS HC A05

A study is made of the kinetics of grain grown in type 37Kh12N8G8 steel alloyed with V, Nb, Ti, and Mo and W. The steel is produced in an arc furnace, ingots vacuum molded, subjected to homogenization annealing at 1050C for 8 hr, and forged into 15 x 15 mm bars at 900-1180C. Specimens cut from the bars are heated in a salt bath to 1150, 1200, or 1250C, held 1.5 hours and quenched in water. It is found that the nature of the carbide phase and kinetics of its dissolution in heat-resistant austenitic steels define the tendency of the steel toward grain growth. A decrease in diffusion mobility at atoms in the steel matrix caused by alloying with titanium and tungsten leads to significant decreases in the tendency toward grain growth and grain size variation. Author

N86-13463# Joint Publications Research Service, Arlington, Va.
EFFECT OF ELASTOPLASTIC CYCLIC DEFORMATION ON MECHANICAL CHARACTERISTICS OF STEEL O3Kh13AG19 AT TEMPERATURES OF 293 AND 77 DEG K Abstract Only
V. A. Strizhalo, I. I. Medved, V. V. Suptelya, and L. N. Demidenko *In its* USSR Rept.: Mater. Sci. and Met. (JPRS-UMS-85-006) 29 Jul. 1985 p 39 Transl. into ENGLISH from Probl. Prochnosti (Kiev), no. 4, Apr. 1985 p 36-39 (For primary document see N86-13422 04-26)
Avail: NTIS HC A05

Unstable mechanical loads may occur as short-term overloads that reach or exceed the yield point of given construction materials. The present article reports on a study of the effects of deformation under such overloads on durability and plasticity of alloys made by cryogenic technology. Cyclic loading and subsequent failure are determined for cylindrical samples of O3Kh13ag19 steel with an electromechanical device adapted to place controlled loads and maintain the temperatures of 273 and 77 K. Since low-temperature tensoresistors are impractical under the given parameters, special extensometers and clock-type indicators are substituted. Results indicate that significant changes occur in the deformation diagram, particularly in the zone of elastic-to-plastic transition. Preliminary elastoplastic deformation reduces the material's ability to endure deformation strengthening and increases the likelihood of brittle failure. Temperature reduction has no qualitative effect. Author

N86-13464# Joint Publications Research Service, Arlington, Va.
SPECIFICS OF THE PROCESS OF FAILURE OF STRUCTURAL STEELS STRENGTHENED BY THERMO-MECHANICAL WORKING WITH DEFORMATION IN THE INTERCRITICAL TEMPERATURE INTERVAL Abstract Only
M. L. Bernshteyn, P. D. Odeskiy, and T. M. Gryunvald *In its* USSR Rept.: Mater. Sci. and Met. (JPRS-UMS-85-006) 29 Jul. 1985 p 39-40 Transl. into ENGLISH from Izv. Vyssh. Ucheb. Zaved.: Chernaya Met. (Moscow), no. 1, Jan. 1985 p 85-90 (For primary document see N86-13422 04-26)
Avail: NTIS HC A05

A study is made of the specifics of failure of rolled materials after hardening working by thermomechanical treatment with deformation in the intercritical temperature interval and subsequent high tempering, achieving a tensile strength of at least 500 MPa with exceptional cold shortness. The study is performed on type 15G2SF steel, composition: 0.16% C, 1.45% Mn, 0.60% Si, 0.09% V, 0.006% S, 0.016% P. Treatment consists of austenitization at 930C for 20 minutes with subsequent cooling to the temperature of the middle of the intercrystalline interval and holding at this temperature for one hour with subsequent deformation by rolling with 50% compression in one pass. Studies are performed on nontempered specimens and also after low- and high-temperature tempering at 250 and 650C for one hour. The excellent cold shortness is found to be provided by creation of a specific substructure consisting of large subgrains within which there are much smaller subgrains and by the presence of splits. The specific substructures result from dynamic recrystallization in place, the split from the strong texture formed in thermomechanical treatment. Author

N86-13465# Joint Publications Research Service, Arlington, Va.
MECHANICAL PROPERTIES OF EP794 STEEL + 12Kh18N10T STEEL BIMETAL Abstract Only
V. A. Borisenko and M. G. Parfenov *In its* USSR Rept.: Mater. Sci. and Met. (JPRS-UMS-85-006) 29 Jul. 1985 p 40 Transl. into ENGLISH from Svarochnoye Proizv. (Moscow), no. 4, Apr. 1985 p 18-19 (For primary document see N86-13422 04-26)
Avail: NTIS HC A05

The mechanical properties and structure of a bimetal obtained by explosive welding of a cladding layer of EP794 steel 11 mm thick to a base layer of 12Kh18N10T steel 20 mm thick are studied. Specimens are tested in the initial state and after various types of heat treatment including tempering, annealing, and hardening. The joint is a wavy boundary with deformed, smaller grains on both sides. Melted areas have a characteristic column structure with shrinkage cracks in some inclusions. Annealing at 850C causes recrystallization and coagulation of the carbide phase. Hardening from 1050 C results in the formation of carbides along the deformation texture at the grain boundaries. The bimetal has optimal mechanical properties in its initial state and after hardening. Heat treatment may be required after welding, forging, etc. Author

N86-13466# Joint Publications Research Service, Arlington, Va.
MACRO- AND MICROFRACTOGRAPHIC SPECIFICS OF DISSIPATED IMPACT RUPTURE OF TYPE 45 STEEL IN THE VISCOUS-BRITTLE TRANSITION INTERVAL Abstract Only
L. R. Botvina and G. V. Klevtsov *In its* USSR Rept.: Mater. Sci. and Met. (JPRS-UMS-85-006) 29 Jul. 1985 p 41 Transl. into ENGLISH from Metalloved. i Term. Obrabotka Metal. (Moscow), no. 2, Feb. 1985 p 27-29 (For primary document see N86-13422 04-26)
Avail: NTIS HC A05

The specifics of dissipated rupture at the viscous-brittle transition temperature interval of type 45 steel with a microstructure are studied after annealing at 900C consisting of alternating areas of ferrite and perlite, the apparent cause of its dissipated failure. Impact testing of prismatic specimens with V-shaped stress concentrator is conducted on a swinging hammer at temperatures from 180C to -196C with quantitative macrofractographic analysis performed on an optical microscope and comparator, and microfractographic analysis performed on a type JSM-U3 scanning microscope. X-ray structural analysis of the state of the materials near the fracture surfaces in their central portion is performed on an X-ray diffractometer in cobalt K sub alpha radiation. The studies allowed tracing of the regularities of dissipated fracture in the viscous-brittle transition interval of temperatures. At temperatures of 130C the entire fracture has a fibrous structure. At 90-130C dissipated failure occurs with areas of viscous and brittle fracture in the center of the fracture. At 90 to -196C the fracture is entirely brittle, with a zone of stable crack growth seen in microfractographic analysis at the tip of the notch, indicating that the fracture is concentrated. Author

N86-13467# Joint Publications Research Service, Arlington, Va.
DURABILITY OF STEEL 45 WITH BORIDE COATING IN CORROSIVE-ABRASIVE MEDIA Abstract Only
V. V. Kozub, V. M. Golubets, and M. I. Pashechko *In its* USSR Rept.: Mater. Sci. and Met. (JPRS-UMS-85-006) 29 Jul. 1985 p 41-42 Transl. into ENGLISH from Fiz.-Khim. Mekhan. Mater. (Kiev), v. 21, no. 2, Mar. - Apr. 1985 p 118-120 (For primary document see N86-13422 04-26)
Avail: NTIS HC A05

The effect of a corrosive-abrasive medium on the durability of steel 45 with a boride coating is reported. Samples are tested under roller-bushing conditions at relative creep rates of 0.4, 0.6 and 0.8 m/sec, pressure of 1-5 MPa and 30 minutes duration. Introduction of KOH or HCl gives pH ranging from 12 to 1. Results show that with 2-3 MPa load durability increases, while with higher pressure it decreases. The friction surfaces show microscratches and bright worn spots after creep. In further testing the pores of the boride coating are additionally plated with nickel to prevent corrosion. Wear increases thereafter in correlation to pressure. Corrosive-abrasive media are judged to reduce surface hardness and thus cause accelerated wear in steel 45. Values of 7.4 and 12 pH are not accompanied by changes in the boride coating's properties. Author

N86-13468# Joint Publications Research Service, Arlington, Va.
DISPERSION HARDENING OF HIGH-STRENGTH NiCo-Mo STEELS Abstract Only
A. g. Rakhshtadt, A. V. Kan, O. M. Khovova, M. D. Perkas, and a. F. Yedneral *In its* USSR Rept.: Mater. Sci. and Met. (JPRS-UMS-85-006) 29 Jul. 1985 p 42 Transl. itno ENGLISH from Metalloved. i Term. Obrabotka Metal. (Moscow), no. 5, May 1985 p 33-37 (For primary document see N86-13422 04-26)
Avail: NTIS HC A05

Secondary hardening with emission of special carbides and formation of alloyed martensite is accompanied by a sharp brittle change, which can be partially avoided by careful choice of alloying components. The system Fe-Ni-Mo, in which the Fe-Ni martensite matrix undergoes less embrittlement and less carbon content is found . Molybdenum is the agent causing the secondary hardening. The carbide formed dissolves in austenite starting at 1000C, the alloy retaining plasticity and viscosity. The test steel, which contains 0.3% carbon, is alloyed with 6% molybdenum and, in various samples, 5, 10 and 15% Co. Results show that at 1100-1150C, there is sufficient dissolution of excess phases with preservation of the fine-grain structure. After tempering at 1150 C up to 25% residual austenite remains; processing in liquid nitrogen reduces that percentage. Mechanical tests show that the Fe-Ni martensite retains high plasticity with increased durability. The alloy contains a high degree of saturated alpha-solid solution, thus facilitating its use as a matrix phase for supplemental tempering. Optimum cobalt content is 10%. Author

N86-13469# Joint Publications Research Service, Arlington, Va.
MODELING OF THERMAL FATIGUE AND EROSION OF COMPLEX ALLOYED STEELS IN METAL MELTS Abstract Only
Yu. A. Glukhov and A. D. Abramov *In its* USSR Rept.: Mater. Sci. and Met. (JPRS-UMS-85-006) 29 Jul. 1985 p 43 Transl. into ENGLISH from Fiz.-Khim. Mekhan. Mater. (Kiev), v. 20, no. 6, Nov. - Dec. 1984 p 12-15 (For primary document see N86-13422 04-26)
Avail: NTIS HC A05

Several programs are presented for structural elements cyclically interacting with metal melts for experimental estimation of the corrosion durability of structural elements used in liquid metals. A schematic plan of erosion is studied, including fatigue damage to the element cyclically interacting with the melt, the accumulation of fatigue damage in the surface layers of the structural element being determined by the entire complex of adsorption-diffusion effects, chemical and hydrodynamic desorption in the process of repeated cyclical loading of the cross section by contact with the liquid metal. As an example, conditions of testing of hollow circular and smooth continuous specimens in torsion in a melt are analyzed. The durability of steels under the test condition reaches a maximum at quite different hardening temperatures. Erosion on a base of 15,000 cycles is minimal in the interval of very high hardening temperatures, 1370-1420K. Nitriding and cyaniding of type 4Kh5MFS steel are studied for their influence on erosion resistance in liquid metals. It is found that at less than 2000 cycles the rate of erosion of treated specimens is less than for structurally homogeneous specimens. It then increases rapidly, so that at 3000 cycles due to the development of a system of fatigue cracks erosion of the metal from the surface is much more rapid than for untreated metals. Author

N86-13470# Joint Publications Research Service, Arlington, Va.
STUDY OF EFFECT OF NORMAL REACTOR WATER ON GROWTH RATE OF FATIGUE CRACKS IN 15Kh2NMFA STEEL Abstract Only
V. I. Pokhmurskiy, A. S. Zubehcnko, A. A. Popov, I. P. Gnyp, v. M. Timonin, I. Z. Dutsiak, and I. N. Antoshchak *In its* USSR Rept.: Mater. Sci. and Met. (JPRS-UMS-85-006) 29 Jul. 1985 p 43-44 Transl. into ENGLISH from Fiz.-Khim. Mekhan. Mater. (Kiev), v. 21, no. 2, Mar. - Apr. 1985 p 32-34 (For primary document see N86-13422 04-26)
Avail: NTIS HC A05

High temperature water reduces steel's durability; this factor has recently received more attention by engineers working with pressure systems. To test the steel under conditions approaching normal use, a laboratory autoclave is designed to test pressures up to 18 MPa at water temperature of 350C. The growth of fatigue cracks is measured in compact samples of 25 mm thickness during thermal processing. The device makes it possible to replicate a symmetrical triangular loading pattern; loads are applied in a range of 6.8-11 mHz, with constant temperature control in a sealed chamber. The relationship between the kinetic diagram of fatigue failure and the rate of fatigue crack growth is discussed. Results show less fatigue cracking at lower coefficients of stress intensity, and a correlation as that coefficient and the rate of cracking increases. Further refinement of the methods used is recommended. Author

N86-13471# Joint Publications Research Service, Arlington, Va.
SUPERHARD MATERIALS DEVELOPED Abstract Only
V. Bibikov *In its* USSR Rept.: Mater. Sci. and Met. (JPRS-UMS-85-006) 29 Jul. 1985 p 45-46 Transl. into ENGLISH from Sov. Belorussiya (Minsk), 14 Jun. 1985 p 2 (For primary document see N86-13422 04-26)
Avail: NTIS HC A05

Scientists of the Belorussian Academy of Sciences' Institute of Solid-State and Semiconductor Physics have developed two new superhard materials. Their properties surpass those of their previous counterparts by a substantial measure. The first innovation comes in the form of round black tablets for making cutters, reamers and other metalworking tools. The new tools can operate continuously for 4-6 hours. This is 4-6 times as long as tools made of superhard cubic boron nitride, which was developed at the same institute. The second superhard material developed equals natural diamond in hardness at only a fraction of its cost. It will be used in bits for drilling deep and superdeep boreholes as well as in tools for machining nonferrous metals. In the latter case, the surface of the part becomes almost as smooth as a surface that has been polished. Author

N86-13472# Joint Publications Research Service, Arlington, Va.
MICROMECHANISMS OF ELECTRODIFFUSION FAILURES IN THIN FILM METALLIZATION Abstract Only
V. N. Solovyev, V. F. Sinkevich, and G. A. Dyadyna *In its* USSR Rept.: Mater. Sci. and Met. (JPRS-UMS-85-006) 29 Jul. 1985 p 47 Transl. into ENGLISH from Zh. Tekhn. Fiz. (Leningrad), v. 55, no. 2, Feb. 1985 p 348-353 (For primary document see N86-13422 04-26)
Avail: NTIS HC A05

A microscopic approach is suggested for the construction of models explaining the kinetic properties resulting from the influence of grain boundaries in which without concrete specification of the model of the polycrystal it is possible to produce activation characteristics of a film. The reasons for non-zero divergence of the ion stream are investigated. Processes of particle transfer in disordered media are studied and the influence of dimensional effects of the electric transfer of ions in thin films is discussed. This literature analysis indicates that the activation energy of migration of Al in polycrystalline films varies between 0.3 and 1.2 eV as a function of the structure of the grain and method of production of the film. E sub alpha varies greatly as a function of the structural irregularities in the films. In textured films as well as films with bamboo structure, transfer processes are essentially blocked. Introduction of impurities such as Cu, O2, Mg and Si to films slows the processes of electrodiffusion. Diffusion of amorphous films, particularly at high temperatures, leads to slowing of electrotransfer processes. Author

N86-13473# Joint Publications Research Service, Arlington, Va.
ION NITRIDING OF TITANIUM
D. A. Prokoshkin, T. A. Panayoti, and G. V. Solovyev *In its* USSR Rept.: Mater. Sci. and Met. (JPRS-UMS-85-006) 29 Jul. 1985 p 48-52 refs Transl. into ENGLISH from Izv. Vyssh. Ucheb. Zaved. MV I SSO SSR: Mashinostr. (Moscow), no. 5, May 1985 p 107-110 (For primary document see N86-13422 04-26)
Avail: NTIS HC A05

The effect of various ion nitriding process factors (temperature, duration, pressure, composition of the gaseous medium) on the structure, phase composition, and properties of diffusion layers is studied. It is shown that nitrogen pressure in the chamber has a significant effect on diffusion zone thickness, a relationship which has an extreme nature, and that a nitrided titanium layer of greatest thickness can be achieved in a mixture of nitrogen diluted with argon. It is established that an adequate diffusion layer depth can be attained in titanium VT1-0 with short holding periods and relatively low temperatures. Ion nitriding increases the wear resistance of titanium VT1-0. The effectiveness of using a glow discharge to accelerate the process of gas nitriding titanium is established. Author

N86-13474# Joint Publications Research Service, Arlington, Va.
CALCULATION OF FAILURE CONSTANT FOR TITANIUM ALLOYS Abstract Only
A. G. Bochvar *In its* USSR Rept.: Mater. Sci. and Met. (JPRS-UMS-85-006) 29 Jul. 1985 p 53 Transl. into ENGLISH from Poroshkovaya Met. (Kiev), no. 2, Mar. - Apr. 1985 p 154-156 Original language document was announced in IAA as A85-31523 (For primary document see N86-13422 04-26)

Avail: NTIS HC A05

In an earlier study, a fracture constant, Delta, equal to the squared ratio the theoretical shear and rupture strengths, has been proposed. Here, an attempt is made to determine the value of Delta for pure titanium, commercially pure titanium, and commercial titanium alloys. It is found that for alpha, alpha+beta, and beta titanium alloys, the fracture constant Delta depends only slightly on the chemical composition and structure of the alloy. Thus, at room temperature, Delta varies from 0.10 (for VT9 alloy) to 0.13-0.14 (for pure and commercially pure titanium). For engineering calculations, Delta can be assumed to equal 0.12. Author

N86-13475# Joint Publications Research Service, Arlington, Va.
SUBCRITICAL CRACK DEVELOPMENT UNDER CONSTANT LOAD IN VT6 ALLOY Abstract Only
A. V. Fishgoyt, B. A. Kolachev, and V. A. Grinberg *In its* USSR Rept.: Mater. Sci. and Met. (JPRS-UMS-85-006) 29 Jul. 1985 p 53 Transl. into ENGLISH from Poroshkovaya Met. (Kiev), no. 4, Apr. 1985 p 74-79 (For primary document see N86-13422 04-26)
Avail: NTIS HC A05

Cracking of titanium alloys under constant loads limits their use in construction. The nature of this cracking using VT6 alloy with 6.0% Al and 4.5% V forged in the beta zone with minor deformation in the alpha + beta zone and retaining a platelet structure is described. Samples 125 x 120 x 50 mm are cut, and either immediately annealed at 1023 K or hydrogenated before annealing. Part of the hydrogenated samples are placed under load by insertion of a wedge in a slit for 3 months. The coefficient of stress intensity is measured at the beginning and end of the tests, and the development of the slit is determined microscopically and by ultrasound methods. Results indicate that subcritical cracking is found only in materials subjected to plane deformation. A model relating elements sensitive to deformation to the coefficiency of stress intensity (CSI) is formulated to show the correlation between cracking sites and growth in the CSI. The linear nature of this phenomenon and its connection with hydrogen damage is shown mathematically. As hydrogen diffuses in the crack surface, where great expansion tension is present, a continuing cracking process takes place. A catastrophic decline in impact resistance occurs in the VT6 alloy when hydrogen concentration reaches 0.12% of weight. Author

N86-13476# Joint Publications Research Service, Arlington, Va.
SILICIDE COATINGS FOR PROTECTING TITANIUM-NIOBIUM ALLOYS FROM HIGH-TEMPERATURE OXIDATION Abstract Only
E. M. Lazarev and Z. I. Kornilova *In its* USSR Rept.: Mater. Sci. and Met. (JPRS-UMS-85-006) 29 Jul. 1985 p 54 Transl. into ENGLISH from Fiz. i Khim. Obrabotki Mater. (Moscow), no. 2, Mar. - Apr. 1985 p 96-98 (For primary document see N86-13422 04-26)
Avail: NTIS HC A05

Titanium-niobium alloys have high durability, corrosion resistance, and heat durability, but low wear values and a tendency to stick. A study of silicide coatings with a surface film of nearly pure SiO2 is described. Heat resistance of the test material is studied at 1100C in alloys with 30-50% niobium, showing severe oxidation and formation of slag after 15 hours. The alloys are then coated with silicide by solid-phase diffusion. Electronographic and X-ray study shows the diffusion layer to consist of TiSi2, NbSi2, Ti5Si3 or Nb5Si3. Oxidation and defects in the coating are studied further. Results show that the silicide coatings reduce the rate of oxidation markedly. Increasing the length of oxidation to 25 hours leads to some resorption of the coating. Micro-X-ray spectral analysis shows that near the alloy-slag boundary the titanium alloy undergoes enrichment due to thermodiffusion mobility and high negative free energy of the oxide. Deep oxygen penetration leads to precipitation of fine needles, probably composed of titanium oxides. Author

N86-13477# Joint Publications Research Service, Arlington, Va.
EFFECT OF COMPOSITION OF RAREFIED MEDIUM ON GAS-SATURATED TITANIUM ALLOYS Abstract Only
V. N. Fedirko and M. N. Zima *In its* USSR Rept.: Mater. Sci. and Met. (JPRS-UMS-85-006) 29 Jul. 1985 p 55 Transl. into ENGLISH from Fiz.-Khim. Mekhan. Mater. (Kiev), v. 21, no. 2, Mar. - Apr. 1985 p 124-126 Original language document was announced in IAA as A85-35865 (For primary document see N86-13422 04-26)
Avail: NTIS HC A05

High-temperature treatment of titanium alloys in a rarefied medium can lead to the saturation of the surface of the alloys by interstitial impurities, such as hydrogen, nitrogen, carbon, and oxygen. In order to estimate the effect of various components of the rarefied medium on the gas saturation and the state of the surface of titanium alloys, experiments were conducted on VT1-0 titanium, VT5-1 and PT-7M alpha alloys, 0T4-1 and VT20 pseudo-alpha alloys, VT3-1, VT23, and VT22 alpha+beta alloys, and VT32 pseudo-beta alloy. It is shown that during the treatment of titanium alloys in a vacuum of 0.0133 Pa at 1023 K residual air and carbon dioxide (the inevitable components of a rarefied atmosphere) affect the intensity of gas saturation to a much greater extent than do oil vapors. IAA

N86-13478# Joint Publications Research Service, Arlington, Va.
HOMOGENIZATION OF BETA-SOLID SOLUTION UPON RAPID HEATING OF TWO-PHASE TITANIUM ALLOYS Abstract Only
V. N. Grudnev, A. F. Zhuravlav, B. F. Zhuravlev, O. M. Ivasishin, and P. Ye. Markovskiy *In its* USSR Rept.: Mater. Sci. and Met. (JPRS-UMS-85-006) 29 Jul. 1985 p 55-56 Transl. into ENGLISH from Fiz. Metal. i Metalloved. (Sverdlovsk), v. 59, no. 1, Jan. 1985 p 152-159 (For primary document see N86-13422 04-26)
Avail: NTIS HC A05

High temperature beta phase homogenization during rapid heating is studied in a Ti-Mo alloy by mathematical simulation and experimental observation. The method used allows quantitative estimation of the influence of the two major factors determining development of the process of homogenization of the beta solid solution: heating rate and initial structure dispersion. Successive quenching of specimens from increasing temperatures in the beta area provides a simple and reliable method of observing the process of homogenization. This method allows experimental development of equations similar to those calculated for the beta solid solution area with minimum alloying element content. The experimental and calculated results are similar for a heating rate of 300 K per second. Heating rate and initial structure dispersion are found to be quite significant in the Ti-10% Mo alloy studied. A method was suggested for estimating the concentration state of improverished sectors of the beta solid solution in commercial alloys during rapid heating and used to analyze the influence of heating rates and initial structure dispersion on the process of homogenization. Author

N86-13479# Joint Publications Research Service, Arlington, Va.
CHANGES IN STRUCTURE AND MECHANICAL PROPERTIES OF NIOBIUM-TITANIUM ALLOY DURING OXYGEN SATURATION Abstract Only
Ye. M. Lyutyy, L. I. Gomozov, and O. I. Yeliseyeva *In its* USSR Rept.: Mater. Sci. and Met. (JPRS-UMS-85-006) 29 Jul. 1985 p 56-57 Transl. into ENGLISH from Fiz.-Khim. Mekhan. Mater. (Kiev), v. 21, no. 2, Mar. - Apr. 1985 p 122-124 (For primary document see N86-13422 04-26)
Avail: NTIS HC A05

Factors of internal and external oxidation remain present in alloys of niobium and titanium despite the improvements brought by this combination. The effect of absorption of oxygen from the atmosphere on durability and plasticity of such an alloy with additional aluminum, zirconium, chromium and molybdenum are discussed. Plasticity of flat samples, measured by the angle of deviation, showed that as temperature increased from 700 to 1200 C the short-term tension strength of the alloy dropped sharply, from 550 to 20 MPa. Oxygen was also introduced internally with a slag oxygen source. An oxide phase formed after rapid cooling with needle-like structure. Granule boundaries were judged to be the location of most precipitate formation. With slow cooling (at 5 K/min instead of 50 K/min), spherical precipitates formed instead of the needle-shaped particles. All the mineral components of the alloy except chromium and molybdenum were found in the oxides that formed. Author

N86-13480# Joint Publications Research Service, Arlington, Va.
INTERNAL FRICTION IN TINiCu ALLOY Abstract Only
Yu. N. Vyunenko and V. A. Likhachev *In its* USSR Rept.: Mater. Sci. and Met. (JPRS-UMS-85-006) 29 Jul. 1985 p 57 Transl. into ENGLISH from Izv. Vyssh. Ucheb. Zaved.: Isvetnaya MEt. (USSR), no. 6, Nov. - Dec. 1984 p 83-86 (For primary document see N86-13422 04-26)
Avail: NTIS HC A05

Results are described from measurments of the logarithmic oscillation decrement in an alloy with 50 At.% Ti + 45 At.% Ni + 5 At.% Cu, annealed for one hour at 800 C. The oscillation decrement was determined by the method of freely attenuating oscillations of a torsional pendulum at 45 Hz using cylindrical specimens with a gauge section 15 mm high, 10 mm in diameter. In some tests the metal was held at constant temperature, in others continuously heated or cooled at 2-3 C/min. It was found that TiNiCu was close in its dissipative properties to a TiNi intermetallide in terms of internal friction. No detailed study of the nature of attenuation of oscillations in TiNiCu was performed, but it is noted that apparently the change in delta in TiNiCu differs somewhat from that for TiNi. Author

N86-13481# Joint Publications Research Service, Arlington, Va.
INFLUENCE OF ELECTRON-BEAM HEATING ON STRUCTURE AND PHASE COMPOSITION OF VT9 ALLOY Abstract Only
A. A. Shipko, I. L. Pobol, G. Ye. Gorelik, and A. Ye. Korolev *In its* USSR Rept.: Mater. Sci. and Met. (JPRS-UMS-85-006) 29 Jul. 1985 p 58 Transl. into ENGLISH from Vestsi Akad. Nauk BSSR (Minsk), no. 1, Jan. - Mar. 1985 p 24-28 (For primary document see N86-13422 04-26)
Avail: NTIS HC A05

A study was made of the structure and phase transformations occurring in the surface layer of titanium alloy VT9 when it is heated by an electron beam. The specimens were worked on an electron-beam welding machine modernized for electron beam surface hardening. The temperature field of the specimen was determined by calculation considering the parameters characteristic for the specific heating conditions. It was found that hot-formed state results in the formation of a beta-transformed structure with controlled grain size varying through the thickness of the part. This allows the level of the mechanical characteristics to be changed during heat treatment. The phase composition of the hardened layer is characterized by the presence of small needle martensite and a residual alpha phase, the relative content of which is redistributed with a change in heating temperature. Author

N86-13482# Joint Publications Research Service, Arlington, Va.
STRUCTURE AND INTERNAL FRICTION OF NEAR-EUTECTIC ALLOY SYSTEM Ti-W TEMPERED FROM A LIQUID STATE Abstract Only
F. N. Tavadze, O. Sh. Okrostsvaridze, G. Sh. Darsavelidze, and G. F. Tavadze *In its* USSR Rept.: Mater. Sci. and Met. (JPRS-UMS-85-006) 29 Jul. 1985 p 58-59 Transl. into ENGLISH from Metallov. i Term. Obrabotka Metal. (Moscow), no. 5, May 1985 p 45-48 (For primary document see N86-13422 04-26)
Avail: NTIS HC A05

Results of study of the structure and temperature dependence of internal friction (TDIF) of a near-eutectic Ti-W alloy system obtained from a liquid state at a cooling rate of about 10 degrees/second are presented. The internal friction of the needle-like structure, with thickness of 50-100 mcm and length of 5-10 mm, was measured in a vacuum relaxator with a direct torsion registration at 1 Hz in a temperature range of 20-750 C. Electronographic analysis of the resulting structure showed several highly deformed phases, resulting from the high density of structural defects and high concentrations of additive atoms. There were many voids, microdoubles and defects of formation as well as traces of gases and other impurities. The unstable phase maxima are attributed to processes taking place within or at the boundaries of the phases included in the alloy during rapid cooling. Thus in the range of 380-500 C, the saturated boron solid solution disintegrated in the alpha-titanium. Further study of these phenomena is recommended. Author

N86-13483# Joint Publications Research Service, Arlington, Va.
POSSIBLE MECHANISM OF WAVE FORMATION DURING DETONATION WELDING Abstract Only c37
S. V. Bazdenko, V. F. Demichev, D. Kh. Morozov, and O. P. Pogutse *In its* USSR Rept.: Mater. Sci. and Met. (JPRS-UMS-85-006-) 29 Jul. 1985 p 60 Transl. into ENGLISH from Fiz. Goreniya i Vzryva (Novosibirsk), v. 21, no. 1, Jan. - Feb. 1985 p 130-137 (For primary document see N86-13422 04-26)
Avail: NTIS HC A05

In detonation and magnetic impulse welding, the most durable products result when wave formation occurs on the surface. Various studies have disagreed on theoretical models for this phenomenon. A hypothesis that states that a certain distance behind the contact point, there is a very narrow zone where viscosity drops sharply is discussed. Theoretical and experimental data are compared that show differences between magnetic impulse and detonation welding. A suppressed flow in the viscous parallel current behind the contact point is attributed to diffusion processes. The effect of thermal conductivity was discounted in considering results, which indicated that liquid viscosity was related to the suppressed flow during contact between two currents of liquid, and cumulative factors were the key to the effectiveness of penetration of the speed rotor through the liquid flow. The long submerged flow was unstable in terms of symmetrical and asymmetrical modes of oscillation. The gradual increase in wavelength was attributed to the transition from weak initial heating to rapid heating, with an accompanying change in the flow speed. Author

N86-13484# Joint Publications Research Service, Arlington, Va.
OPTIMIZATION OF TECHNOLOGICAL PARAMETERS OF COLD PRESSURE WELDING OF AD1M THIN ALUMINUM SHEETS Abstract Only c37
V. F. Kuzin, Yu. V. Savinkin, M. N. Tsypona, Ye. A. Kozelo, and M. A. Arkhangelskiy *In its* USSR Rept.: Mater. Sci. and Met. (JPRS-UMS-85-006) 29 Jul. 1985 p 61 Transl. into ENGLISH from Svarochnoye Proizv. (Moscow), no. 4, Apr. 1985 p 9-11 (For primary document see N86-13422 04-26)
Avail: NTIS HC A05

In order to study the influence of tool geometry, tool surface condition, welded material thickness and degree of deformation on the quality of joints produced by cold pressure welding with minimum deformation of the material, a regression analysis was performed on data from an experiment involving cold pressure welding of thin AD1M aluminum sheets (0.3, 0.5 and 0.8 mm thick). It was found that under the experimental conditions used, the length of the welded zone was most greatly influenced by the angle of the tip of the tool used. The optimal angle is 7 degrees. Increasing friction on the contact surface causes an increase in the size of the welded zone, particularly where the tool angle is low or the material is thick. The quality of welding is influenced by the thickness of the welded material. With minimum friction on the contact surface, as thickness of the material increases, 1/S decreases. Maximum friction of the compact surface increases 1/S as the material increases, particularly where the tool angle is low. Author

N86-13485# Joint Publications Research Service, Arlington, Va.
STUDY OF PROCESS OF PORE FORMATION DURING ARGON-ARC WELDING OF ALUMINUM ALLOY 1420 Abstract Only
M. A. Abralov, R. U. Abdurakhmanov, and A. A. Abdurakhimov *In its* USSR Rept.: Mater. Sci. and Met. (JPRS-UMS-85-006) 29 Jul. 1985 p 62 Transl. into ENGLISH from Avtomat. Svarka (Kiev), no. 4, Apr. 1985 p 21-26 (For primary document see N86-13422 04-26)
Avail: NTIS HC A05

The lack of a commonly accepted opinion concerning the source and mechanism of formation of pores during welding of 1420 aluminum alloy hinders control of this defect. A study was therefore made to determine the specifics of pore formation and refine the source of porosity in argon-arc welding of the alloy. Experiments were performed on rectangular specimens 90 x 22 x 1.6 mm which were melted clear through. Butt joints were produced using two specimens of the same size. The major reason for the significant porosity of the alloy was found to be the presence of methane which is formed primarily in the surface layer of the metal. Rapid evolution of the methane mixed with hydrogen begins from the base metal in advance of the melting front and continues in the liquid metal bath. The constricted conditions for floating of gas bubbles generated near the melting zone at the root of the seam as well as continuous delivery of methane and hydrogen from the solid metal lead to the formation of a chain of large pores. Author

N86-13486# Joint Publications Research Service, Arlington, Va.
INFLUENCE OF THERMAL CYCLE ON CHARACTERISTICS OF CYCLICAL CRACK RESISTANCE OF TITANIUM ALLOYS AND THEIR JOINTS PRODUCED BY DIFFUSION WELDING Abstract Only
E. S. Karakozov, S. S. Vasilyeva, and S. V. Ivanov *In its* USSR Rept.: Mater. Sci. and Met. (JPRS-UMS-85-006) 29 Jul. 1985 p 62-63 Transl. into ENGLISH from Svarochnoye Proizv. (Moscow), no. 1, Jan. 1985 p 34-36 (For primary document see N86-13422 04-26)
Avail: NTIS HC A05

Linear fracture mechanics was used to analyze the behavior of titanium alloys VT6Ch and VT16 and welded joints with defects. Specimens of VT16 were annealed to imitate the thermal cycling of diffusion welding at 860 and 960 C, while specimens of VT6Ch were heated to 800, 940 and 1050 C. The crack resistance of the material with a welded seam and imitation thermal cycle of diffusion welding was determined. The cyclical strength of welded joints in VT6Ch was found to be higher than in the base material with stress amplitudes below the yield point, probably resulting from the hardening effect of the martensitic alpha prime phase formed as a result of the beta-alpha prime transformation in the zone of plastic deformation in advance of a propagating crack during cyclical loading. Author

N86-13487# Joint Publications Research Service, Arlington, Va.
KINETICS OF DISSOLUTION OF OXIDE FILMS IN TITANIUM UPON DIFFUSION WELDING Abstract Only
V. V. Peshkov, V. P. Kholodov, and Ye. S. Vorontsov *In its* USSR Rept.: Mater. Sci. and Met. (JPRS-UMS-85-006) 29 Jul. 1985 p 63 Transl. into ENGLISH from Svarochnoye Proizv. (Moscow), no. 4, Apr. 1985 p 35-37 (For primary document see N86-13422 04-26)
Avail: NTIS HC A05

A study was made of the process of dissolution of oxide films in titanium and its alloys. Experiments were performed on specimens 16 mm in diameter and 2 mm thick of technically pure VT1-0 titanium and the alloys OT4 and VT6. The surface was polished, degreased and oxidized in air for 1.8-2.4 x 1000 at 773 (VT1-0), 873 (OT4) and 898 (VT6) K until a bluish oxide 6 x .01 pa air pressure simultaneously, separated by a titanium foil washer 0.1 mm thick to prevent contact between the surfaces. The thickness of the oxide film was measured after heating to determine the amount of dissolved oxide layer. A basic difference was established in the kinetic curves for technically pure titanium and titanium alloyed with aluminum. In technically pure titanium, the curve indicates decrease in the rate of the process as time passes, while in the alloys with aluminum there is a clear bend in the curve, which appears to be combination of two parabolas. Author

N86-13488# Joint Publications Research Service, Arlington, Va.
INFLUENCE OF PRELIMINARY ANNEALING ON STRUCTURE AND PROPERTIES OF VT23 ALLOY WELDED JOINTS AFTER HARDENING Abstract Only
V. S. Lyasotskaya, F. R. Kulikov, N. Yu. Ravdonikas, and Ye. K. Feoktistova *In its* USSR Rept.: Mater. Sci. and Met. (JPRS-UMS-85-006) 29 Jul. 1985 p 63-64 Transl. into ENGLISH from Svarochnoye Proizv. (Moscow), no. 4, Apr. 1985 p 16-18 (For primary document see N86-13422 04-26)
Avail: NTIS HC A05

Results are presented from a study of the influence of preliminary annealing before hardening on the structure and properties of welded joints in VT23 alloy made by argon-arc welding with type SPT-2 welding wire. Hot-rolled plates 30 mm thick were welded, then heated at 800 C for one hour, cooled in air and aged at 500 C for ten hours. Preliminary annealing was performed at 775 to 875 C for one hour with cooling with the furnace before hardening heat treatment, farming larger alpha plates and a smaller number of crystalline structure effects than when a lower heating temperature was used. The combination of preliminary annealing at 850 C plus standard hardening increases ductility, impact toughness and homogeneity of mechanical properties of welded joints in the alloy in comparison to similar heat treatment but without annealing. Author

N86-13489# Joint Publications Research Service, Arlington, Va.
CORROSION RESISTANCE OF WELDED JOINTS IN CERTAIN TITANIUM ALLOYS Abstract Only
G. M. Shelenkov, V. E. Troyanovskiy, V. Ye. Blashchuk, and L. M. Onopriyenko *In its* USSR Rept.: Mater. Sci. and Met. (JPRS-UMS-85-006) 29 Jul. 1985 p 64 Transl. into ENGLISH from AVtomat. Svarka (Kiev), no. 4, Apr. 1985 p 19-20 (For primary document see N86-13422 04-26)
Avail: NTIS HC A05

A study of the corrosion resistance of welded joints in technical titanium VT1-0 and low alloy titanium alloys OT4-1, PT-3 V, AT3 and AT6 was conducted. Disk-shaped specimens 30 mm in diameter and 4-6 mm thick with a circular bilateral seam 40 mm in diameter were studied. Specimens were prepared by manual argon-arc welding with a tungsten electrode, wire diameter 2 mm. Tests were performed in concentrated 99% nitric acid at the boiling point or 3030 hours. The studies showed that welded joints in titanium alloys are subjected to corrosion cracking at minimal corrosion rates. This must be considered in selecting titanium alloys as materials for the manufacture of welded structures and in corrosion testing under stress not only of alloys but also of welded joints. Author

N86-13490# Joint Publications Research Service, Arlington, Va.
DEFORMATION AND STRESSES UPON WELDING OF VT23 TITANIUM ALLOY Abstract Only
I. M. Chertov, A. S. Karpenko, A. P. Ostrovoy, V. N. Zamkov, N. A. Kushnirenko, and V. F. Topolskiy *In its* USSR Rept.: Mater. Sci. and Met. (JPRS-UMS-85-006) 29 Jul. 1985 p 65 Transl. into ENGLISH from Avtomat. Svarka (Kiev), no. 2, Feb. 1985 p 41-43 (For primary document see N86-13422 04-26)
Avail: NTIS HC A05

Results are presented from experiments studying full longitudinal deformations and residual stresses in welded joints in VT23 alloy. But joints in plates measuring 250 x 200 x 6 mm made by argon arc welding with a tungsten electrode and FAn-1 flux were studied. Welding was performed in two passes without finishing of the edges from one side. No welding wire was used. Two methods of heat treatment were used: annealing at 750 C, 1-2 hours with cooling in air and subsequent two-stage aging at 380 C, eight hours plus 550 C, two hours; annealing of individual parts before welding, then aging of the welded joint. Residual longitudinal elongation deformations were produced by welding rather than shortening, resulting from phase transformations upon cooling in the 750-550 C temperature interval. Heat treatment of welded joints consisting of annealing and aging or aging alone leads to complete relief of residual stresses, which may amount to 30% of the tensile strength of the base metal. Author

N86-13491# Joint Publications Research Service, Arlington, Va.
DETERMINING LOCAL HEATING PARAMETERS FOR INCREASING FATIGUE RESISTANCE OF WELDED JOINTS Abstract Only
c39
V. N. Maksimovich, A. A. Chabanenko, P. P. Mikheyev, O. I.

Gushoha, and Yu. F. Kudryavtsev *In its* USSR Rept.: Mater. Sci. and Met. (JPRS-UMS-85-006) 29 Jul. 1985 p 65-66 Transl. into ENGLISH from Probl. Prochnosti (Kiev), no. 4, Apr. 1985 p 32-36 (For primary document see N86-13422 04-26)
Avail: NTIS HC A05

Artificial means of imposing beneficial residual compression tension in concentration zones have been used to increase the bearing strength of metal designs that are subject to varying load conditions. Gas heating has been used effectively to counteract stretching under load. A theoretical determination based on thermoplasticity of optimum parameters for strengthening laminates when the heat is applied to a relatively small section of the test metal and heating is by convection at a temperature that can be described by a Hauss distribution is discussed. The temperature field and the tension generated are regarded as constants. The most common methods of final differences and final elements were rejected in favor of integral-differential equations to show thermoplasticity. Various forms of statistical treatment are presented. They indicate that the effect of external load leads to changes in the fields of applied residual tension. An inverse relationship was noted; it was more pronounced with biaxial stretch. Maximum residual tension was obtained at 400-500 C. Within usual limits for fatigue of welded joints, reduction of residual compression tension did not exceed 30% of initial values. Author

N86-13492# Joint Publications Research Service, Arlington, Va.
INFLUENCE OF STRUCTURE OF HEAT-RESISTANT NICKEL ALLOY ZhS6U ON ITS WELDABILITY IN THE SOLID STATE Abstract Only
V. N. Golubev, F. Sh. Sharifyanov, and A. V. Vlasova *In its* USSR Rept.: Mater. Sci. and Met. (JPRS-UMS-85-006) p 66 Transl. into ENGLISH from Avtomat. Svarka (Kiev), no. 2, Feb. 1985 p 13-16 (For primary document see N86-13422 04-26)
Avail: NTIS HC A05

A study was made of the influence of various structural characteristics of heat-resistant alloys and the phenomenon of superplasticity on the formation of a welded joint by diffusion welding. Studies were performed on heat resistant alloy ZhS6U in the cast state and the same alloy obtained from granules by powder metallurgy. Tests were performed in the 960-1200 C temperature interval at deformation rates .0001 to .1 1/s and showed significant differences in mechanical properties of the alloys obtained by different methods, related to the structural state of the alloy. The cast alloy has low ductility and high resistance to plastic deformation, whereas the powder metallurgy product shows all the signs of superplasticity at 1050-1150 C. The structure formed upon heating to the welding point has decisive influence on the weldability of heat-resistant nickel alloys. The best-quality welded joint is obtained under temperature and speed conditions corresponding to the range of superplastic deformation of the alloy. Author

N86-13493# Joint Publications Research Service, Arlington, Va.
DIFFUSION WELDING OF COPPER-CHROMIUM PSEUDOALLOY WITH COPPER Abstract Only
A. P. Sysoyev, A. V. Sergeyev, and N. F. Kazakov *In its* USSR Rept.: Mater. Sci. and Met. (JPRS-UMS-85-006) 29 Jul. 1985 p 68 Transl. into ENGLISH from Poroshkovaya Met. (Kiev), no. 10, Oct. 1984 p 45-47 (For primary document see N86-13422 04-26)
Avail: NTIS HC A05

A study is made of the possibility of diffusion welding of a Cu-Cr pseudoalloy with copper. Welding was performed on an SDVU-26 machine. Before the parts were placed in the chamber, the surfaces of the copper and alloy were cleansed of oxide film, degreased with acetone and dried with ethyl alcohol. Strength of the joints was studied as a function of temperature and time of isothermal holding. It was found that during vacuum annealing, chromium oxides appeared on the free surface of the alloy. The degree of oxidation during heating of the materials in contact was less, but the lower oxide of chromium was still formed. When welded under conditions producing the maximum joint strength, the hardness of the alloy dropped from 140 to 97 HRB, primarily as a result of annealing of the copper matrix. The hardness of the alloy can be improved by deforming the diffusion welded plates, with a degree of relative deformation of the copper component of the bimetal of 10-13% yielding best results. Author

N86-13494# Joint Publications Research Service, Arlington, Va.
INFLUENCE OF HYDROGEN ON FORMATION OF COLD CRACKS IN SEAMS DURING WELDING OF PIPE STEEL Abstract Only
S. L. Mandelberg, S. V. Buslinskiy, and Yu. L. Bogachek *In its* USSR Rept.: Mater. Sci. and Met. (JPRS-UMS-85-006) 29 Jul. 1985 p 68-69 Transl. into ENGLISH from Avtomat. Svarka (Kiev), no. 2, Feb. 1985 p 1-5 (For primary document see N86-13422 04-26)
Avail: NTIS HC A05

A study was made of the cold crack resistance in seams of low-alloy steels welded using conditions and materials similar to those used for the production of large-diameter pipe. Double-sided, two-layered welded joints were studied in materials of three types: steels of test rolls microalloyed with vanadium and niobium, normalized steel microalloyed with vanadium, and normalized steel containing normal microalloy elements. Rolled sheets of various thicknesses characteristic for the production of pipes were used. It was found that when welded joints of these steels are allowed to cool naturally, cracks do not form, the level of concentration of diffusion hydrogen being comparatively low. Author

27 NONMETALLIC MATERIALS

Includes physical, chemical, and mechanical properties of plastics, elastomers, lubricants, polymers, textiles, adhesives, and ceramic materials.

N86-13495*# National Aeronautics and Space Administration. Lewis Research Center, Cleveland, Ohio.
FRACTURED TOUGHNESS OF SI3N4 MEASURED WITH SHORT BAR CHEVRON-NOTCHED SPECIMENS
Jonathan A. Salem and John L. Shannon, Jr. 1985 19 p refs
Presented at Basic Sci. Meeting of the Am. Ceram. Soc., Baltimore, 17-19 Nov. 1985
(NASA-TM-87153; E-2749; NAS 1.15:87153) Avail: NTIS HC A02/MF A01 CSCL 11G

The short bar chevron-notched specimen is used to measure the plane strain fracture toughness of hot pressed Si3N4. Specimen proportions and chevron-notch angle are varied, thereby varying the amount of crack extension to maximum load (upon which K sub IC is based). The measured toughness (4.68 + or - 0.19 MNm to the 3/2 power) is independent of these variations, inferring that the material has a flat crack growth resistance curve. Author

N86-13496*# Virginia Polytechnic Inst. and State Univ., Blacksburg. Dept. of Engineering Science and Mechanics.
ELASTIC-PLASTIC DEFORMATION OF A METAL-MATRIX COMPOSITE COUPON WITH A CENTER SLOT
Daniel Post, Robert Czarnek, Duksung Joh, Jinmyun Jo, and Yifan Guo Nov. 1985 49 p ref
(Grant NAG1-343)
(NASA-CR-178013; NAS 1.26:178013) Avail. NTIS HC A03/MF A01 CSCL 11D

A comprehensive experimental analysis of deformations of the surface of a metal-matrix specimen is reported. The specimen is a 6-ply [0 + or - 45] sub s boron-aluminum tensile coupon with a central slot. Moire interferometry is used for high-sensitivity whole-field measurements of in-plane displacements. Normal and shear strains are calculated from displacement gradients. Displacement fields are analyzed at various load levels from 15% to 95% of the failure load. Deformations of the boron fibers could be distinguished from those of the matrix. Highly localized plastic slip zones occur tangent to the ends of the slot. Shear strains and concurrent transverse compressive strains in the slip zones reach approximately 10% and 1%, respectively. Upon unloading, elastic recovery in surrounding regions causes a reverse plastic shear strain in the slip zone of about 4%. Longitudinal normal strains on the unslotted ligament peak at the slot boundary at about 1% strain. The strain concentration factor at the end of the slot decreases with load level and the advance of plasticity. Author

N86-13497# Air Force Systems Command, Wright-Patterson AFB, Ohio. Foreign Technology Div.
STUDY OF CROSS-LINKING DENSITY AND THE TYPE OF CROSS LINKAGE IN POLYURETHANE ELASTOMERS
L. M. Sergeyeva, Y. S. Lipatov, and N. I. Binkevich 2 Aug. 1985 12 p Transl. into ENGLISH from mono. "Akademiya Nauk Ukrainskoy" SSR, Kiev, 1967 p 131-137
(AD-A158199; FTD-ID(RS)T-1267-84) Avail: NTIS HC A02/MF A01 CSCL 11/10

From the standpoint of synthesizing cross-linked polymers with the potentially smallest degree of defectiveness of the network, polyurethane polymers are of special interest. The purpose of this work is to study the validity of theories that make it possible to evaluate the cross-linking density based on different physical methods for polyurethane elastomers. One of the main parameters that characterize the structure of cross-linked polymer is the value of the effective cross-linking density or the mean molecular weight of the chain segment between units. The kinetic theory of elasticity and the Flory-Renner theory of swelling are the basis for determining this value. In our study, we used the methods of evaluating the cross-linking density from data about the equilibrium modulus of high elasticity and about the compression of swollen specimens in order to determine the parameter Psi of the Flory equation, which would also make it possible to make these measurements based on data about swelling. GRA

N86-13498# Air Force Wright Aeronautical Labs., Wright-Patterson AFB, Ohio.
FRACTOGRAPHY OF MIXED MODE 1 - 2 FAILURE IN GRAPHITE/EPOXY AND GRAPHITE/THERMOPLASTIC UNIDIRECTIONAL COMPOSITES Final Report, Feb. - Aug. 1984
S. L. Donaldson Jun. 1985 42 p
(AF Proj. 2307)
(AD-A158852; AFWAL-TR-84-4186) Avail: NTIS HC A03/MF A01 CSCL 11/4

The notched off-axis tensile test and the notched three rail shear test were used to produce states of in-plane loading varying from pure Mode I (crack opening) to Mode II (forward shearing). The two material systems tested were Fiberite T300/1034C graphite/epoxy and Imperial Chemical Industries graphite reinforced polyetheretherketone thermoplastic composite (APC-1 PEEK). Using a scanning electron microscope, a detailed examination of the resulting fracture surfaces was conducted. Results at magnification levels of 100X and 800X are presented. Very distinct changes can be observed in each material as the load ratio changes. In addition, for a fixed mode load ratio, large differences can be seen in the matrix deformation patterns between the two material systems. Of particular interest are ductile spike formations seen in the highly shear loaded PEEK specimens. These observations provide some insight as to the increased toughness seen at higher Mode II ratios, and the increased toughness seen in the thermoplastic system. Author (GRA)

N86-13499# Oak Ridge National Lab., Tenn.
ANALYTICAL ELECTRON MICROSCOPY OF SURFACE MODIFIED CERAMICS
P. S. Sklad 1985 5 p Presented at the Joint Meeting of the Electron Microscopy Soc. of Am. and Microbeam Anal. Soc., Louisville, Ky., 5 Aug. 1985
(Contract DE-AC05-84OR-21400)
(DE85-016309; CONF-850840-10) Avail: NTIS HC A02/MF A01

While the effects of implantation on surface sensitive properties may be measured independently, it is important to understand the microstructural evolution leading to these changes. Analytical electron microscopy provides a useful tool for characterizing the microstructures produced in terms of solute concentration profiles, second phase formation, lattice damage, crystallinity of the implanted layer, and annealing behavior. Such analyses allow correlations to be made with theoretical models, property measurements, and results of complimentary techniques. DOE

N86-13500# Oak Ridge National Lab., Tenn.
PREPARATION OF CERAMIC FIBER-CERAMIC MATRIX COMPOSITES BY A FASTER CHEMICAL VAPOR INFILTRATION PROCESS
A. J. Caputo, W. J. Lackey, and D. P. Stinton 1985 15 p refs Presented at the 5th European Conf. on CVD, Uppsala, Sweden, 17 Jun. 1985
(Contract DE-AC05-84OR-21400)
(DE85-016402; CONF-8506171-1) Avail: NTIS HC A02/MF A01

A new, faster process was developed for the fabrication of ceramic fiber-reinforced, ceramic-matrix composites by chemical vapor infiltration. Process and equipment improvements led to the fabrication of preforms with a higher fiber content, and infiltration improvements led to reduced infiltration run times and increased infiltrated densities. These improvements have produced composites with not only higher flexural strengths but also high strain values. The high strain values have been a goal of this work. DOE

N86-13501# Midwest Research Inst., Golden, Colo.
PHOTOGRADATION STUDIES OF SILVER-BACKED POLYACRYLONITRILE (PAN) FILMS
D. M. Smith, A. R. Chugtai, C. A. Sergides, and P. Schissel Jul. 1985 12 p Presented at the SPIE Intern. Tech. Symp. on Optical and Electro-Optical Eng., San Diego, Calif., 18 Aug. 1985 Prepared in cooperation with Denver Univ., Colo.
(Contract DE-AC02-83CH-10093)
(DE85-012154; SERI/TP-255-2751; CONF-850887-11) Avail: NTIS HC A02/MF A01

Fourier transform infrared (FT-IR) reflection-absorbance (RA) measurements have been used to characterize Ag-backed polyacrylonitrile (PAN) films and to study their photodegradation. The optical constants n and k for the polymers are determined in the mid-IR region, and the dependence of RA values on polymer functionality concentration as a function of film thickness calculated. The IR-RA values are nearly linear with the concentration of functionalities for PAN films of thicknesses up to 0.1 (MU)m. Some oxidative photodegradation pathways have been proposed; with radiation of lambda greater than or equal to 250 nm, a polyimine structure is generated. A combination of 1.0% wt of Irganox 1010 and 0.5% wt of Irgastab 2002 in PAN films was found to significantly retard the photodegradation of the polymer without affecting the specularity of the PAN/Ag surface. DOE

N86-13502# Rockwell International Corp., Golden, Colo.
SOLVENT EXTRACTION OF PLUTONIUM (IV) POLYMER BY ORGANOPHOSPHOROUS COMPOUNDS
A. C. Muscatello, J. D. Navratil, and M. E. Killion 23 Mar. 1985 17 p ref Presented at the 189th Natl. Meeting of the Am. Chem. Soc., Miami, 28 Apr. 1985
(Contract DE-AC04-76DP-03533)
(DE85-013229; RFP-3802; CONF-850417-27) Avail: NTIS HC A02/MF A01

We have recently discovered bifunctional organophosphorus reagents and TOPO (trioctylphosphine oxide) extract hydrolytic plutonium (IV) polymer from 0.1 to 7.0 M nitric acid. Other extractants are not effective in the extraction of the polymer. The extraction behavior of the polymer with octylphenyl-N,N-diisobutyl carbamoylmethylphosphine oxide(OOD(IB)CMPO), both alone and mixed with TBP(tri-n-butylphosphate) and with TOPO will be discussed. In addition, the extraction behavior with DHDECMP (Dihexyl-N,N-diethyl carbamoylmethylphosphonate) will be reviewed for comparison. In general, the extraction of the polymer increases with nitric acid concentration and is second-to-third power dependent on extractant concentration. The most efficient stripping agent is 1.0 M sodium carbonate. DOE

N86-13503# Acurex Corp., Mountain View, Calif. Energy and Environmental Div.

CERAMIC FABRIC MATERIAL TESTING
R. Chang and H. Lips Jun. 1985 226 p
(Contract DE-AC21-83MC-20110)
(DE85-013664; DOE/MC-20110/1985) Avail: NTIS HC A11/MF A01

Filter media suitable for use at tempertures greater than 550 F, employing ceramic fibers in their construction, have been under development for several years. These filter media are intended for application in advanced energy processes such as pressurized fluidized bed combustion and gasification as well as many diverse industrial processes with temperatures ranging from 600 to 1,600 F. Present techniques for evaluating ceramic filter performance involve testing in subpilot and pilot-scale facilities which are both time-consuming and expensive. In addition, no standards yet exist for ensuring that the ceramic fabrics supplied for filter use conform to specifications for uniform quality. The objective of this program was to establish rapid test methods that can be used to quantitatively assess ceramic fabrics to be used as hot gas cleaning filters. DOE

N86-13504# Department of Energy, Washington, D. C.
METHOD OF SYNTHESIZING POLYMERS FROM A SOLID ELECTROLYTE Patent Application
T. A. Skotheim, inventor (to DOE) (Brookhaven National Lab.) Filed 19 Oct. 1984 18 p
(Contract DE-AC02-76CH-00016)
(DE85-011623; US-Patent-Appl-SN-662657) Avail: NTIS HC A02/MF A01

A method of synthesizing electrically conductive polymers from a solvent-free solid polymer electrolyte is disclosed. An assembly of a substrate having an electrode thereon, a thin coating of solid electrolyte including a solution of PEO complexed with an alkali salt, and a thin transparent noble metal electrode are disposed in an evacuated chamber into which a selected monomer vapor is introduced while an electric potential is applied across the solid electrolyte to hold the thin transparent electrode at a positive potential relative to the electrode on the substrate, whereby a highly conductive polymer film is grown on the transparent electrode between it and the solid electrolyte. DOE

N86-13505# Centre Technique des Industries Mecaniques, St. Etienne (France).
EVALUATION OF THE EROSION PROTECTION OF LOW INFLAMMABILITY LIQUIDS OF THE HFC TYPE (POLYGLYCOL SOLUTIONS) Final Report [EVALUATION DU POUVOIR DE PROTECTION CONTRE L'USURE DES FLUIDES DIFFICILEMENT INFLAMMABLES DU TYPE HFC (SOLUTIONS DE POLYGLYCOL)]
A. Ridard Mar. 1985 49 p refs In FRENCH
(CETIM-12-E-13-3) Avail: NTIS HC A03/MF A01

Wear tests were peformed using nine commercial low inflammability hydraulic fluids on a Tribolub machine following the procedure normally used with mineral hydraulic oils. The results show that aqueous fluids performance is close to that of mineral oils. The temperature and viscosity effects on the protection properties are also detailed. Author (ESA)

N86-13506# Pennsylvania Univ., Philadelphia. Dept. of Materials Science and Engineering.
MICROSCOPIC OBSERVATIONS AND MECHANICS ANALYSES OF LONG TERM FRACTURE IN POLYETHYLENE PIPING MATERIALS Annual Report, 1 Jan. - 31 Dec. 1984
N. Brown 1 Feb. 1985 68 p Sponsored by Gas Research Inst.
(PB85-219608; GRI-85/0037; AR-1) Avail: NTIS HC A04/MF A01 CSCL 11I

The development of short time quantitative methods for predicting the long time-low stress filure in polyethylene piping materials is discussed. The experimental approach is based on observations of the kinetics and microstructural changes associated with the initiation stage for slow crack growth under plane strain conditions. Several microscopic techniques were used to observe the microstructure of the damage zone that emanates from a notch. The kinetics of growth of the initial damage zone were measured as a function of stress, notch depth, and temperature. Author (GRA)

N86-13439# Joint Publications Research Service, Arlington, Va.
ELECTRIFICATION OF FILLED POLYETHYLENE COATINGS IN FRICTION WITH METAL Abstract Only
V. S. Mironov *In its* USSR Rept.: Mater. Sci. and Met. (JPRS-UMS-85-006) 29 Jul. 1985 p 12-13 Transl. into ENGLISH from Vestsi Akad. Nauk BSSR (Minsk), no. 1, Jan. - Mar. 1985 p 38-42 (For primary document see N86-13422 04-26)
Avail: NTIS HC A05

N86-13449# Joint Publications Research Service, Arlington, Va.
TEMPERATURE-FREQUENCY VARIATION OF MECHANICAL LOSSES IN PERIODIC DEFORMATION OF MULTILAYER GLASS-REINFORCED PLASTICS Abstract Only
L. S. Yelistratova, V. V. Kolokolshikov, and A. S. Podkolayev *In its* USSR Rept.: Mater. Sci. and Met. (JPRS-UMS-85-006) 29 Jul. 1985 p 19 Transl. into ENGLISH from Zh. Prikl. Mekhan. i Tekhn. Fiz. (Novosibirsk), no. 6, Nov. - Dec. 1984 p 139-144 (For primary document see N86-13422 04-26)
Avail: NTIS HC A05

N86-13451# Joint Publications Research Service, Arlington, Va.
ANTICORROSION POLYMER PACKING FILM WITH IMPROVED PROTECTIVE PROPERTIES Abstract Only
N. I. Domantsevich, O. N. Kopyl, and A. N. Tynnyy *In its* USSR Rept.: Mater. Sci. and Met. (JPRS-UMS-85-006) 29 Jul. 1985 p 20 Transl. into ENGLISH from Tekhnol. i Organ. Proizv. (Kiev), no. 4, Oct. - Dec. 1984 p 37-39 (For primary document see N86-13422 04-26)
Avail: NTIS HC A05

N86-13456# Joint Publications Research Service, Arlington, Va.
CERAMICS BASED ON ALUMINUM NITRIDE AND METALS Abstract Only
Ye. N. Bukharin, A. S. Vlasov, and A. A. Alekseyev *In its* USSR Rept.: Mater. Sci. and Met. (JPRS-UMS-85-006) 29 Jul. 1985 p 28 Transl. into ENGLISH from Steklo i Keram. (Moscow), no. 2, Feb. 1985 p 23-25 (For primary document see N86-13422 04-26)
Avail: NTIS HC A05

28 PROPELLANTS AND FUELS

Includes rocket propellants, igniters, and oxidizers; storage and handling; and aircraft fuels.

For related information see also *07 Aircraft Propulsion and Power, 20 Spacecraft Propulsion and Power,* and *44 Energy Production and Conversion.*

N86-13507# Air Force Office of Scientific Research, Bolling AFB, Washington, D.C.
THE 1985 AFOSR/AFRPL CHEMICAL ROCKET RESEARCH MEETING, ABSTRACTS AND AGENDA Interim Report, Mar. 1984 - Feb. 1985
Leonard H. Caveny, ed., Anthony Matuszko, ed., and Wayne E. Roe, ed. Feb. 1985 247 p Meeting held in Lancaster, Calif., 18-21 Mar. 1985
(AF Proj. 2308; AF Proj. 2307; AF Proj. 2303)
(AD-A158291; AFOSR-85-0560TR) Avail: NTIS HC A11/MF A01

Various advances in rocket propulsion technology are presented. Major topics include: energetic material combustion; thermal properties synthesis of new ingredients; combustion stability; acoustic interaction plumes; beamed energy; solar propulsion; and electrical propulsion. For individual titles, see N86-13508 through N86-13584.

N86-13508# Rockwell International Corp., Canoga Park, Calif.
ELECTROLYTIC PREPARATION OF NOVEL AZIDODINITRO COMPOUNDS Abstract Only

Milton B. Frankel and James F. Weber *In* AFOSR THE 1985 AFOSR/AFRPL Chem. Rocket Res. Meeting Feb. 1985 10 p (For primary document see N86-13507 04-28)
Avail: NTIS HC A11/MF A01

Future higher performance propellants will require new classes of more energetic ingredients. Polynitro- and azido-alkyl compounds either have been or are being evaluated for this purpose. Highly substituted geminal dinitro compounds (e.g., R-C(NO2)2X, where X-NO2,CH3,.F) are of particular interest, and substitution of an azido group (X-N3) will further enhance the energetics of such compounds. This results from the fact that the azide group contributes approx. 80 Kcal/mole to the compound without decreasing the O/C ratio. G.L.C.

N86-13509# Idaho Univ., Moscow.
SYNTHESIS OF DIFLUORAMINOXY-, DIFLUORAMINO- OR FLUORODIAZONIUM-CONTAINING MATERIALS Abstract Only
Jeanne M. Shreeve *In* AFOSR The 1985 AFOSR/AFRPL Chem. Rocket Res. Meeting Feb. 1985 3 p (For primary document see N86-13507 04-28)
Avail: NTIS HC A11/MF A01

Future rocket propulsion advances require new stable high energy materials. The research is concerned with the synthesis of stable, highly oxidizing compounds which may contain, but are not limited to nitrogenfluorine bonds and the subsequent investigation of their physical and chemical properties. G.L.C.

N86-13510# North Texas State Univ., Denton. Dept. of Chemistry.
SYNTHESIS OF NEW POLYNITROPOLYHEDRANES Abstract Only
Alan P. Marchand, Suresh C. Suri, and D. Sivakumar Reddy *In* AFOSR The 1985 AFOSR/AFRPL Chem. Rocket Res. Meeting Feb. 1985 3 p (For primary document see N86-13507 04-28)
Avail: NTIS HC A11/MF A01

The current research program centers on the synthesis of polynitropolycyclic compounds. These compounds belong to a new class of explosives and propellants. However, relatively few polynitropolycyclic compounds have thus far been reported. G.L.C.

N86-13511# Morton Thiokol, Elkton, Md.
SYNTHESIS OF HIGH NITROGEN CONTENT HETEROCYCLIC NITRAMINES AND ENERGETIC INTERNAL PLASTICIZERS Abstract Only
Rodney L. Willer and James A. Hartwell *In* AFOSR The 1985 AFOSR/AFRPL Chem. Rocket Res. Meeting Feb. 1985 3 p (For primary document see N86-13507 04-28)
Avail: NTIS HC A11/MF A01

A considerable need exists for energetic materials which are denser and more energetic than 1,3,5,7-tetranitro-1,3,5,7-tetrazocine (HMX) and are thermally and hydrolytically stable. These dense, energetic materials are needed as ingredients for advanced explosives and propellant formulations that would exceed the performance of current formulations and allow future weapons systems to meet projected performance requirements. Most of the effort in this areas has focused on two classes of compounds, the polynitro caged hydrocarbons, typified by octanitrocubane, and the caged nitramine compounds, typified by compounds such as hexanitrohexaazaadamantane and hexanitrohexauzawurtzitane. Some progress has been made with both types of compounds. Author

N86-13512# California Univ., San Diego, La Jolla. Dept. of Chemistry.
SYNTHESIS AND REACTIVITY OF UNSATURATED METAL NITROGEN COMPLEXES Abstract Only
William C. Trogler, Joseph H. Osborne, and Mary Maciejewski *In* AFOSR The 1985 AFOSR/AFRPL Chem. Rocket Res. Meeting Feb. 1985 3 p (For primary document see N86-13507 04-28)
Avail: NTIS HC A11/MF A01

Reactions between organic azides, N3R (R = CH3,C3H5,2,6-CH3)2C6H3, o-biphenyl, SiMe3, SiPh3,CPh3, and neopentyl) and (n-C5Me5)2V lead to (Figure 1) either (n-C5Me5)2VNR or (n-C5Me5)2VN3. Mechanisms for the mode of reactivity will be presented. The nitrene complexes exhibit one unpaired electron according to bulk magnetic susceptibility measurements. At room temperature EPR spectra are observed that reveal both vanadium and nitrogen hyperfine splitting. The three dimensional structure of (n-C5Me5)2VN(2,6(CH3)2(C6H3) was established, in collaboration with Dr. A. Rheingold of the University of Delaware, by X-ray crystallography (Figure 2) and the complex exhibits a linear V-N-R group. The unsymmetrical energetic tetrazene, Ph(PhC(O)N-N-(PhC (0)Ph, was prepared in 4 steps from phenylhydrazine and its reactivity with metal reagents was examined. Group I or II metal alkyls fragment the tetrazene to PhN3 and NH2(C(0)ph) while complexes form with transition metal carbonyls. Recent chemistry obtained with unsaturated nitrogen complexes, that are derived from monosubstituted hydrazines will be discussed. Author

N86-13513# SRI International Corp., Menlo Park, Calif. Energetic Materials Program.
SYNTHESIS AND CHEMISTRY OF POLYNITROALKANES AND POLYNITROOLEFINS Abstract Only
Clifford Bedford and Robert J. Schmitt *In* AFOSR The 1985 AFOSR/AFRPL Chem. Rocket Res. Meeting Feb. 1985 3 p (For primary document see N86-13507 04-28)
Avail: NTIS HC A11/MF A01

Research programs in energetic materials synthesis and mechanisms were hampered by the lack of general methods for synthesizing geminal dinitroslkenes and non-acidic methods for nitramine synthesis. Effort to identify and overcome these research barriers have thus far been directed toward special situations and have met with only limited success. Author

N86-13514# Air Force Rocket Propulsion Lab., Edwards AFB, Calif.
NEW SYNTHETIC TECHNIQUES FOR ADVANCED PROPELLANT INGREDIENTS: SELECTIVE TRANSFORMATIONS AND NEW STRUCTURES Abstract Only
Robert D. Chapman, Scott A. Shackelford, and John L. Andreshak *In* AFOSR The 1985 AFOSR/AFRPL Chem. Rocket Res. Meeting Feb. 1985 3 p (For primary document see N86-13507 04-28)
Avail: NTIS HC A11/MF A01

New chemical transformations and methods are being investigated which potentially lead to energetic target compounds with new and noval molecular structures, or which improve synthetic routes to known compounds that are currently expensive propellant luxuries. Three of four scheduled research tasks are in progress. Author

N86-13515# Illinois Univ., Chicago. Dept. of Chemistry.
FLUOROPOLYAZIDO-ESTERS AS ENERGETIC POLYMERS Abstract Only
Robert M. Moriarty *In* AFOSR The 1985 AFOSR/AFRPL Chem. Rocket Res. Meeting Feb. 1985 2 p (For primary document see N86-13507 04-28)
Avail: NTIS HC A11/MF A01

A method by which the energy rich azido group can be introduced into a fluorine containing polymer was studied. G.L.C.

N86-13516# Air Force Rocket Propulsion Lab., Edwards AFB, Calif.
NEW ENERGETIC POLYMERS AS BINDERS FOR PROPELLANTS Abstract Only
Mostafa A. H. Talukder and Stanley D. Morse *In* AFOSR The 1985 AFOSR/AFRPL Chem. Rocket Res. Meeting Feb. 1985 3 p Prepared in cooperation with Dayton Univ. Research Inst., Edwards AFB, Calif. (For primary document see N86-13507 04-28)
Avail: NTIS HC A11/MF A01

New polymeric syntheses and chain modification techniques are being investigated to obtain improved mechanical properties of known energetic binders, new energetic prepolymer and binder systems, and correlations of polymeric chemical structure to physical/mechanical properties. Its approach centers on new energetic polymer syntheses via cationic polymerization or by synthetic modifications of known polymer. Author

N86-13517# Rockwell International Corp., Canoga Park, Calif.
ENERGETIC FLUORCARBONS Abstract Only
Carl J. Schack and Karl O. Christe *In* AFOSR The 1985 AFOSR/AFRPL Chem. Rocket Res. Meeting Feb. 1985 3 p (For primary document see N86-13507 04-28)
Avail: NTIS HC A11/MF A01

The development of general methods for the synthesis of energetic fluorcarbons and their conversion to olefins and epoxides suitable for the preparation of polyethertype energetic binders is discussed. Fluorocarbons with energetic substituents offer the potential advantages of high energy, high thermal stability high density, and also low sensitivity. Author

N86-13518# Morton Thiokol, Huntsville, Ala.
CONTROL OF THE URETHANE CURE REACTION WITH SOLID, BLOCKED ISOCYANATES Abstract Only
William H. Graham, J. B. Canterberry, Inella G. Shepard, and Jerrell W. Blanks *In* AFOSR The 1985 AFOSR/AFRPL Chem. Rocket Res. Meeting Feb. 1985 3 p (For primary document see N86-13507 04-28)
Avail: NTIS HC A11/MF A01

The problem of controlling the cure kinetics of the isocyanate/hydroxyl reaction and the formation of polyurethanes is discussed. Successful completion of the program would provide unprecidented control of the reaction; the goal would be to demonstrate an infinite potlife below a trigger temperature and a rapid, but controllable, cure above that temperature. More generally, the approach addresses the question of differences in reactivities of molecules in solution and in the solid state. Although the system selected for study involves polyurethane cure chemistry, successful demonstration of the concept would imply that other solid state compounds could be used in triggering desired reactions only above their melt temperature, thus providing temperature sensitive on-off control chemical reactions. Author

N86-13519# State Univ. of New York, Binghamton. Dept. of Chemistry.
PHYSICAL AND CHEMICAL CONSEQUENCES OF ANTIAROMATICITY IN THE BORACYCLOPENTADIENE SYSTEM Abstract Only
John J. Eisch, Sinpei Kozima, and James E. Calle *In* AFOSR The 1985 AFOSR/AFRPL Chem. Rocket Res. Meeting Feb. 1985 3 p (For primary document see N86-13507 04-28)
Avail: NTIS HC A11/MF A01

The mode of chemical bonding between boron atoms and clusters of carbon atoms should have a fundamental importance in determining the macroscopic physical and chemical properties of the resulting organoboron compounds. The stability of the boron-carbon bond is the basis for the use of organoboranes as a route to superior refractory materials, such as the boron carbides. By contrast, the liability or chemical reactivity of the boron-carbon bond in other organoboranes is the basis for the use of these compounds as rocket propellants. Because of the intimate connection between chemical bonding in organoboranes and their macroscopic chemical properties, it is possible to learn how pi-bonding between boron and carbon centers influences the reactivity of the boron center towards oxidants, protolyzing agents and Lewis bases. Author

N86-13520# United Technologies Corp., San Jose, Calif. Chemical Systems Div.
HIGH ENERGY MOLECULES OF HIGH SYMMETRY Abstract Only
William S. Anderson *In* AFOSR The 1985 AFOSR/AFRPL Chem. Rocket Res. Meeting Feb. 1985 2 p (For primary document see N86-13507 04-28)
Avail: NTIS HC A11/MF A01

A series of symmetrical, fully hydroxyl-substituted organic materials is to be prepared and then converted to new, oxygen-rich, high-energy derivatives. The densities, crystal structures and heats of formation of these derivatives will be determined and observed values will be compared with predictions. The expected outcome is a better understanding of the relationship between chemical structure, density, oxidizing power and heat of formation in high-energy molecules. Author

N86-13521# Delaware Univ., Newark. Dept. of Chemistry.
STRUCTURE-DECOMPOSITION RELATIONSHIPS IN NEWER ENERGETIC MATERIALS Abstract Only
Thomas B. Brill and Yoshio Oyumi *In* AFOSR The 1985 AFOSR/AFRPL Chem. Rocket Res. Meeting Feb. 1985 3 p (For primary document see N86-13507 04-28)
Avail: NTIS HC A11/MF A01

Insufficient information exists to discuss the relationship between the molecular structure and the chemical reactivity of energetic materials. Toward remedying this deficiency, determining the molecular structures and decomposition mechanisms of a wide range of new research-type nitramines and other energetic materials prepared by synthesis program and from efforts at Rocketdyne, Morton-Thiokol, UT/CSC, SRI, and NSWC was undertaken. X-ray crystallography is being used for quantitative structure determination, FT-IR spectroscopy at high pressure and with high heating rates and thermal methods are employed for the decomposition studies, and solid-state NMR and NQR spectroscopy is used for analyzing the molecular motion as a function of temperature. The advantage of bringing many techniques to bear on the problem is that a multifaceted understanding of the thermal behavior of an energetic material can be achieved. The results should benefit synthetic chemists and propellant researchers by showing the effects on the physical properties and product formation resulting from specific molecular modifications. Author

N86-13522# Air Force Rocket Propulsion Lab., Edwards AFB, Calif.
DEUTERIUM ISOTOPE EFFECTS IN RDX DECOMPOSITION AND COMBUSTION PROCESSES Abstract Only
Scott A. Shackelford, Stephen L. Rodgers, Michael B. Coolidge, and Robert E. Askins (Morton Thiokol, Inc., Huntsville, Ala.) *In* AFOSR The 1985 AFOSR/AFRPL Chem. Rocket Res. Meeting Feb. 1985 3 p (For primary document see N86-13507 04-28)
Avail: NTIS HC A11/MF A01

The thermal decomposition of RDX was examined using isothermal differential scanning calorimetery (DSC) at a temperature range of 505K to 510K. At this temperature range RDX obeys first order kinetics and shows a primary deuterium isotope effect (2.1 at 505K and 1.7 at 510K). This isotope effect would suggest that the rate limiting step in the decomposition of RDX is C-H bond rupture. Under the experimental conditions employed, the thermal decomposition occurs solely in the liquid phase with RDX. By the time the DSC has equilibrated, the decomposition has already started and the DSC trace is seen as a slow decay. No induction phase can be seen with RDX. The combustion experiments were performed in a window bomb with the burn rates measured by high speed photography. If the assumption is made that the burn rate data is directly proportional to the kinetic rate constants and that all the other factors influencing burn rate remain the same for both the deuterated and hydrogenated materials, then an isotope effect can be derived from a ratio of the RDX burn rate to RDX-d6 burn rate. The isotope effects thus obtained are 1.46 at 1000 psi and 1.37 at 500 psi. At the high temperature limit an isotope effect of 1.35 or greater can be considered to be a primary effect. R.J.F.

N86-13523# Dayton Univ. Research Inst., Edwards AFB, Calif.
FLAME MECHANISMS AND FLAME INHIBITION Abstract Only
J. D. Eversole and D. P. Weaver (AFRPL, Edwards AFB, Calif.) *In* AFOSR The 1985 AFOSR/AFRPL Chem. Rocket Res. Meeting Feb. 1985 3 p (For primary document see N86-13507 04-28)
Avail: NTIS HC A11/MF A01

The definition and understanding of detailed chemical mechanisms in flames are sought. Of special interest are gas-phase mechanisms responsible for, or contributing to, the suppression of afterburning in rocket plumes. An effort was made to approach the problem of determining flame chemistry with a balance between experimental data collection and theoretical flame modelling. Data from a laminar, premixed flat-flame burner is modelled using a detailed reaction, one-dimensional laminar flame computer program. Experimental data is obtained primarily by non-intrusive, optical diagnostic techniques. Most of the uniqueness of this approach lies in the integration of many separate aspects of the general problem. R.J.F.

N86-13524# Nevada Univ., Reno. Dept. of Chemistry and Metallurgical Engineering.
THE SUPPRESSION OF AFTERBURNING IN SOLID ROCKET PLUMES BY POTASSIUM SALTS Abstract Only
Eugene Miller *In* AFOSR The 1985 AFOSR/AFRPL Chem. Rocket Res. Meeting Feb. 1985 3 p (For primary document see N86-13507 04-28)
Avail: NTIS HC A11/MF A01

The effects of K, KOH and KO2 on the afterburning reactions are being studied by introducing them individually into an opposed jet flat diffusion flame of H2-CO-O2-N2 and scanning the flame in small increments by infrared spectroscopy. A vaporizer-burner was built permitting the vaporization of potassium and its salts prior to entering the flame. The emission spectra from the flame is detected by means of a modified absorption spectrophotometer and an optical scanning system. It was found that elemental potassium reduces the infrared radiation for rich and lean hydrogen flames but has a smaller effect on stoichiometric mixtures. KOH in a hydrogen flame inhibits the preflame reactions but actually increases the infrared radiation at levels below that required to prevent combustion totally. K therefore appears to be a more effective inhibitor than KOH as used in these experiments, settling perhaps the disagreement that has arisen in the literature concerning the efficacy of inhibition by potassium in hydrogen flames. CO was not used in these experiments because reaction between H2 and CO produced carbon in the salt vaporizer. The formation of carbon probably also occurs in the rocket plume increasing the infrared signature. Author

N86-13525# Colorado Univ., Boulder. Dept. of Mechanical Engineering.
CHEMICAL KINETICS OF NITRAMINE PROPELLANT COMBUSTION Abstract Only
Melvyn C. Branch *In* AFOSR The 1985 AFOSR/AFRPL Chem. Rocket Res. Meeting Feb. 1985 3 p (For primary document see N86-13507 04-28)
Avail: NTIS HC A11/MF A01

The objective of the studies reported is to provide insight into the chemistry of reactions of gas phase species of importance in the combustion of nitramine propellants. Flame studies and associated chemical kinetic modeling of the gas reactions are being used to evaluate critical reaction paths and energetics and their influence on burn rate. The calculations thus far have identified a mechanism for the rapid reaction between CH2O and NO2 in the fizz zone at the propellant surface. A slower reaction was suggested for the preparation and flame zones standing off the surface which was supported by the exothermic reduction of NO. Both of these results provide a chemical kinetic mechanism to explain previous qualitative suggestions about the nature of the gas reactions of nitramines. The calculations also indicate that gas reactions may affect the reported product distributions in studies of nitramines. Finally, a mechanism for the modification of the reaction rate by NH3 donors was outlined. There are currently very limited experimental data available for detailed comparison to the results of the chemical kinetic modeling. Researchers began low pressure flame studies of CH2O/NO2/N2O mixtures in order to identify reactant, intermediate and product species profiles for comparison to a kinetic model of the flame. Addition of NH3 to the flame gases will also indicate the feasibility of burn rate control by NH2 donors. Author

N86-13526# Emory Univ., Atlanta, Ga. Dept. of Chemistry.
COMBUSION OF HYDROGEN AND HYDROCARBONS IN FLUORINE Abstract Only
Myron Kaufman *In* AFOSR The 1985 AFOSR/AFRPL Chem. Rocket Res. Meeting Feb. 1985 3 p (For primary document see N86-13507 04-28)
Avail: NTIS HC A11/MF A01

In this program both atomic and molecular flames are studied. Low-pressure premixed F2 flames are studied in a stainless-steel burner assembly equipped with CaF2 windows to spectroscopically monitor luminescence and movable Langmuir probes to measure the spacial variation of ionization. For most of the studies, the premixed flames will be diluted with He or Ar. When undiluted flames are burned in this apparatus, interesting behavior was seen in the F2-CH4 flame. Over a range of relative concentrations, including stoiciometric mixtures, this flame burns as short pulses of duration Ca. 1 msec and frequencies of 1 to 10 Hz. This behavior is explained as due to flashback resulting from the high burning velocity of these flames, followed by spontaneous reignition when the hypergolic mixture is replenished to its ignition limit. Author

N86-13527# Georgia Inst. of Tech., Atlanta. School of Aerospace Engineering.
ANALYSIS OF HETEROGENEOUS DIFFUSION FLAME STABILIZATION Abstract Only
Warren C. Strahle and Jechiel I. Jagoda *In* AFOSR The 1985 AFOSR/AFRPL Chem. Rocket Res. Meeting Feb. 1985 3 p (For primary document see N86-13507 04-28)
Avail: NTIS HC A11/MF A01

The ability to calculate complex turbulent reacting flows is in a state of development. The flow investigated here presents a unique challenge to the state-of-the-art. The flow is a fully turbulent two dimensional flow over a backward facing step with wall-blowing of a combustible from the floor behind the step. It is a model for the flowfield in the flame stabilization region of a solid fueled ramjet. The analytical approach has been with a k-e method gradually being improved and modified as one progresses through various stages of complexity - from no-blowing cold flow to foreign gas injection in cold flow and then to the full combustion case. A parallel experimental program either validates the analysis or suggests modifications. Author

N86-13528# Georgia Inst. of Tech., Atlanta. School of Aerospace Engineering.
EXPERIMENTAL INVESTIGATION OF HETEROGENEOUS FLAME STABILIZATION Abstract Only
Jechiel I. Jagoda and Warren C. Strahle *In* AFOSR The 1985 AFOSR/AFRPL Chem. Rocket Res. Meeting Feb. 1985 3 p (For primary document see N86-13507 04-28)
Avail: NTIS HC A11/MF A01

In this project the solid fueled ramjet (SFRJ) is simulated by a flow over a backward facing step with a secondary flow entering the recirculation region through a porous floor. The flow properties are determined using a 2-component Laser Doppler Velocimeter (LDV) system. Bleed gas concentrations are measured, simultaneously, using Rayleigh scattering for the cold flow and spontaneous Raman for concentration and temperature measurements in flows with combustion. Although simultaneous LDV-Rayleigh or Raman measurements are currently being carried out for the simpler configuration of jet like flames, this is the first time the combined techniques are applied to the more complex and practical problems of flame stabilization behind a backward facing step. Author

N86-13529# Dayton Univ. Research Inst., Edwards AFB, Calif.
HIGH PRESSURE SOLID PROPELLANT COMBUSTION ZONE STRUCTURE FROM ANALYSIS OF HYDROXYL RADICAL CHEMILUMINESCENCE Abstract Only
David H. Campbell, Susan Hulsizer, Tim Edwards, and David P. Weaver *In* AFOSR The 1985 AFOSR/AFRPL Chem. Rocket Res. Meeting Feb. 1985 3 p Prepared in cooperation with AFRPL, Edwards AFB, Calif. (For primary document see N86-13507 04-28)
Avail: NTIS HC A11/MF A01

The results presented concern the analysis of the natural chemiluminescence originating from the hydroxyl (OH) radical in the flame above burning ammonium perchlorate (AP) composite propellant. An attempt was made to analyze quantitatively the semi-resolved (approx. 13 nm) OH emission spectra in the 304.0 to 316.0 nm spectral range to obtain a measure of the rotational temperature and vibrational population distribution of this molecule. At present, the chemical kinetic data base is insufficient to relate the final internal energy state distribution of OH to the specific reaction pathways which produce this molecule in specific rotational-vibrational- states. Nonetheless, information about the overall flame zone structure and reaction processes can be deduced from the results. Author

N86-13530# Air Force Rocket Propulsion Lab., Edwards AFB, Calif.
EVALUATION OF HMX PROPELLANT CHEMISTRY FROM RAMAN AND LASER INDUCED FLUORESCENCE SPECIES AND TEMPERATURE MEASUREMENTS Abstract Only
David P. Weaver, Tim Edwards, Susan Hulsizer, and David Campbell *In* AFOSR The 1985 AFOSR/AFRPL Chem. Rocket Res. Meeting Feb. 1985 3 p Prepared in cooperation with Dayton Univ. Research Inst., Edwards AFB, Calif. (For primary document see N86-13507 04-28)
Avail: NTIS HC A11/MF A01

The ability to accurately anticipate the behavior of burning solid rocket motor propellants is highly dependent on specific knowledge of the kinetic mechanisms and heat transfer properties of the reacting species near the surface of the burning propellant. With the development of modern laser diagnostic techniques, the possibility of determining spatially specific species concentrations and temperatures related to the distance (e.g., the reaction time) from the burning propellant surface has emerged. The goal is to gather such experimental information and to construct from it kinetic pathways in a laboratory propellant flame and to correlate their dependence on propellant composition. Such specific chemical information could then be related to known macroscopic properties of the solid propellant such as burning rate. Author

N86-13531# Dayton Univ. Research Inst., Edwards AFB, Calif.
APPLICATION OF MOLECULAR KINETICS MODELS TO THE PREDICTION OF BACKFLOW CONTAMINATION Abstract Only
David H. Campbell and David P. Weaver *In* AFOSR The 1985 AFOSR/AFRPL Chem. Rocket Res. Meeting Feb. 1985 3 p Prepared in cooperation with AFRPL, Edwards AFB, Calif. (For primary document see N86-13507 04-28)
Avail: NTIS HC A11/MF A01

The goal is to obtain a fundamental understanding of the basic physical mechanisms producing the unanticipated high level of backflow contamination observed upstream of the nozzle exit plane of spacecraft rocket nozzles and control thrusters. Information on the internal energy state population distributions, gas species number densities, flow velocities, and degree of condensation near the exit plane of a nozzle will provide the basis for more accurate modeling of the expansion flow inside the nozzle and around the nozzle lip. Such information is critical to the accurate prediction of contamination levels of sensitive spacecraft surfaces. Vibrational and rotational internal energy state populations, translational mode temperature, gas species number densities, and condensed species densities are being acquired in laboratory scale vacuum expansion flows for diatomic and triatomic gas species using non-intrusive laser spectroscopic techniques. A map of these parameters near the nozzle lip will be used to correlate the degree of non-equilibrium and the degree of condensation with the velocity field and gas number density. Author

N86-13532# Dow Chemical Co., Midland, Mich. Thermal Lab.
EVALUATION AND COMPILATION OF THE THERMODYNAMIC PROPERTIES OF HIGH TEMPERATURE SPECIES Abstract Only
Malcolm W. Chase *In* AFOSR The 1985 AFOSR/AFRPL Chem. Rocket Res. Meeting Feb. 1985 5 p (For primary document see N86-13507 04-28)
Avail: NTIS HC A11/MF A01

The re-examination of the five alkaline earth metals, their dimers, oxides, hydroxides, halides, carbonates, sulfides, and sulfates was accomplished. Bibliographies, data graphs, and data summaries were generated for 60 species; this will result in approximately 200 single- and multi-phase thermochemical tables. The examination of experimental/theoretical data for a given species by itself may not be sufficient to indicate potential problems, whereas the examination of families of species often reveals interesting problems and discrepancies. For example, three of the five alkaline earth metals are not well characterized thermodynamically. This study revealed problems with the calcium data. To resolve this problem, two laboratories in the U.S. are currently measuring the low temperature heat capacities and high temperature enthalpy of calcium. In addition, the simultaneous study of the 20 alkaline earth dihalides yields a large framework in which more reliable decisions can be made as to the validity of the available data as well as guide better estimates for missing data. Author

N86-13533# Aerospace Corp., Los Angeles, Calif.
CRITICAL EVALUATION OF HIGH TEMPERATURE CHEMICAL KINETIC DATA Abstract Only
Norman Cohen and Karl Westberg *In* AFOSR The 1985 AFOSR/AFRPL Chem. Rocket Res. Meeting Feb. 1985 3 p (For primary document see N86-13507 04-28)
Avail: NTIS HC A11/MF A01

The rapid growth in chemical kinetic data and in the number of nonspecialist users of such data in DOD-related work has created a need for a reliable, easy-to-use compilation of evaluated rate data and recommended rate coefficients. To answer this need, a program for the evaluation of kinetic data and preparation of consistently formatted data sheets patterned after JANAF Thermochemical Tables was undertaken with the joint support of the Air Force Office of Scientific Research and National Bureau of Standards. The experimental data for the reactions of O storms with methane, ethane, and neopontane at temperatures below Ca. 600 K were reexamined. In the case of methane and ethane, a set of elementary reactions was assembled that describes the complex chemistry occurring in the original studies. With the aid of previously written computer codes, the original data were reanalyzed. It was found in both cases that the measurements were especially sensitive to errors caused by secondary reactions not taken into account originally and to impurities in the reagent alkane. It appears, qualitatively, that the values for the O + CH4 and O + C2H6 rate coefficients were overestimated by approximately factors of 2 to 3 in the 250 to 600 K temperature range. Author

N86-13534# Rockwell International Corp., Canoga Park, Calif.
FUNDAMENTAL STUDIES OF AZIDE DECOMPOSITION AND COMBUSTION Abstract Only
Joseph E. Flanagan, Dean O. Woolery, and Wallace W. Thompson *In* AFOSR The 1985 AFOSR/AFRPL Chem. Rocket Res. Meeting Feb. 1985 3 p (For primary document see N86-13507 04-28)
Avail: NTIS HC A11/MF A01

The utilization of azide (-N3) ingredients is rapidly increasing in a wide spectrum of Air Force applications. Azide materials are primarily characterized by their high positive heats of formation in addition to unique combustion features such as inherent high-burning rates and self-extinguishment at pressure above ambient. The decomposition and combustion characteristics of various aside ingredients via high temperature, high heating rate pyrolysis-gas chromatography-mass spectrometry is discussed. The approach is threefold: (1) azide decomposition chemistry with structure is defined; (2) the effect of amide decomposition chemistry upon selected propellant ingredients is investigated; and (3) the decomposition phenomena is correlated with propellant burn rates. The effort during the first year resulted in a determination of azide decomposition chemistry via high pressure (30 to 500 psig), high heating rate pyrolysis of various azide ingredients consisting of: (1) aliphatic azides; (2) asidonitramines; (3) asidoalcohols; (4) multi-substituted azides; (5) cyclic azide monomers; and (6) azide polymers. Author

N86-13535# AeroChem Research Labs., Inc., Princeton, N. J.
STABILITY OF RDX, AP AND BTTN NEAR ROOM TEMPERATURE Abstract Only
Douglas B. Olson and Robert J. Gill *In* AFOSR The 1985 AFOSR/AFRPL Chem. Rocket Res. Meeting Feb. 1985 3 p (For primary document see N86-13507 04-28)
Avail: NTIS HC A11/MF A01

The overall objective is to gain a more fundamental understanding of chemical reaction mechanism and kinetics responsible for aging of solid rocket propellants at near ambient temperature. The chemical aging process is envisioned to result from the slow decomposition of some ingredients producing highly reactive species which then chemically attack other ingredients, especially the polymer binders. The present studies include the decomposition kinetics of selected pure ingredients as well as the degradation reactions of two binders. Mechanisms will be postulated, using the measured kinetic parameters, and the predictions of his chemical aging model will be compared with available data. A noteworthy aspect of this program is the use of highly specific and ultrasensitive analytical probes which allow studies to be performed at realistic storage temperatures, over a short time spans, and with little degradation, compared to the more usual accelerated testing at high temperatures, which then requires extrapolation of rate coefficients over many decades. Progress to date included measurements of the low temperature decomposition rate coefficients of RDX, AP, and BTTN using gas evolution analysis. Author

N86-13536# Atlantic Research Corp., Alexandria, Va.
FUEL-RICH SOLID PROPELLANT BORON COMBUSTION Abstract Only
Merrill K. King and James J. Komar *In* AFOSR The 1985 AFOSR/AFRPL Chem. Rocket Res. Meeting Feb. 1985 3 p (For primary document see N86-13507 04-28)
Avail: NTIS HC A11/MF A01

Boron particle combustion is retarded by initial presence of an oxide coating. In current boron ignition models, oxygen is assumed to dissolve in the oxide and diffuse to the b/B2O3 interface for reaction. Measurements of exotherms for oxide-coated particles in hot O2/N2 mixtures have quantified oxidation rates, but have not unequivocally established whether oxygen or boron (suggested by theoretical solubility considerations) moves across the oxide. Possible non-equilibrium condensation of boron oxide/hydroxide products during rapid cooling (e.g., nozzle expansion) is also important. Significant performance is lost without such condensation. Past condensation studies have been conducted under unrealistic conditions or involved limited diagnostics, inadequate for mechanism definitions. Regarding the first problem, a unique experiment utilizing two sealed vessels (one containing argon, the other an argon/oxygen mixture) Separated by a controlled thickness/temperature liquid B2O3 film on a porous platinum disk, will be performed. In the second task, a unique combination of large diagnostids and a 2-D windowed expansion section (with pressure taps) attached to a gaseous combustor will be used to quantify oxide/hydroxide condensation pressure at realistic conditions. Author

N86-13537# Air Force Rocket Propulsion Lab., Edwards AFB, Calif.
CRACK GROWTH BEHAVIOR IN A COMPOSITE PROPELLANT WITH STRAIN GRADIENTS Abstract Only
C. T. Liu *In* AFOSR The 1985 AFOSR/AFRPL Chem. Rocket Res. Meeting Feb. 1985 3 p (For primary document see N86-13507 04-28)
Avail: NTIS HC A11/MF A01

The main objective of the Structural Mechanics Research Program is to advance the current understanding of the crack growth behavior in solid propellants. The specific objective of this present research program is to investigate the crack growth behavior in solid propellant in the presence of nonuniform, gross applied strain fields. In this study, the crack growth behavior in a highly filled composite propellant with strain gradients was studied through the use of precracked biaxial specimens. Two different shapes of biaxial specimens were considered; namely, the rectangular shape and the wedge shape. Through cracks with different crack lengths and eccentricities, with respect to the vertical centerline of the specimen, were cut along the horizontal centerline of the specimen. Crack propagation tests were conducted under a constant strain rate condition at room temperature. The measured crack length, load, and time served as input to a computer program that calculated the crack growth rate and the stress intensity factor, and then determined the functional relationship between these two parameters. B.W.

N86-13538# Air Force Rocket Propulsion Lab., Edwards AFB, Calif.
NONLINEAR MODELING AND METHOD OF PREDICTING CRACK GROWTH Abstract Only
C. T. Liu *In* AFOSR The 1985 AFOSR/AFRPL Chem. Rocket Res. Meeting Feb. 1985 3 p (For primary document see N86-13507 04-28)
Avail: NTIS HC A11/MF A01

In the past decade, many experimental studies were directed primarily toward the characterization of fracture behavior in solid propellants under various loading conditions. The experimental results revealed that despite the nonlinear nature of these types of materials, linear viscoelastic fracture mechanics theory or slightly modified nonlinear versions had been successfully used in characterizing the crack growth behavior in same propellants. In order to characterize the fracture behavior in solid propellant, under realistic and general loading conditions, the effect of material nonlinearity on the crack initiation and the subsequent crack growth is required. The objective of this study is to develop a nonlinear crack growth model which can be used to characterize crack growth under large deformation conditions and to determine the range of applicability of the linear theory in predicting crack growth. The approach will involve a combination of analytical and experimental studies. Experiments (destructive and nondestructive) will be conducted to determine the failure process, the damage zone, the failure property, and the strain field ahead of the crack tip. This information will be used to determine the damage parameters associated with the nonlinear viscoelastic constitutive equation and to determine, together with the criteria developed from the theoretical analysis, the failure process zone. B.W.

N86-13539# Dayton Univ., Ohio.
HIGH-RESOLUTION MOVIES OF PROPELLANT DEFLAGRATION Abstract Only
Roger J. Becker, Paul F. Luehrmann, and Janet L. Laird *In* AFOSR The 1985 AFOSR/AFRPL Chem. Rocket Res. Meeting Feb. 1985 3 p (For primary document see N86-13507 04-28)
Avail: NTIS HC A11/MF A01

This program has been designed to enhance the understanding of the behavior of the particles at the surface of a grain during deflagration. A special emphasis has been placed on qualitative knowledge of particles and agglomerates ranging in size from 20 to 70 micrometers. Cooperative behavior and the nature of the immediate particle environment are of particular concern. The ultimate goal of this initative is experiments correlating particle behavior with external parameters, such as the flow field and pressure oscillations. The unique capability of the newly developed copper-vapor laser has been exploited as a light source for front-lit cinephotography. The 30 ns pulse width, 1.2 mj pulse energy, and 5 kHz repetition rate of this laser are ideal for front-lit cinephotography. The short pulse width freezes the motion, the high-energy, monochromatic pulse penetrates the flame, and the 5 kHz repetition rate captures dynamic phenomena. A diode-array detector has also been developed for the servo positioner, due to severe depth-of-field restrictions. B.W.

N86-13540# Purdue Univ., West Lafayette, Ind. School of Aeronautics and Astronautics.
WIDE DISTRIBUTION PROPELLANTS Abstract Only
Robert A. Frederick, Jr. and John R. Osborn *In* AFOSR The 1985 AFOSR/AFRPL Chem. Rocket Res. Meeting Feb. 1985 3 p (For primary document see N86-13507 04-28)

Avail: NTIS HC A11/MF A01

The goal of this research program is to identify conditions which produce local stepwise burning of solid propellants and to identify the physical processes that control the duration of the burn periods and rest periods. Perfecting a technique to continuously measure the local burning rate is a major task in achieving this goal. Measurements are first completed using high-speed photography as a preliminary screening tool. The desired technique, however, is a direct measurement using a laser position detector (LPD). This LPD is being designed and developed to continously record spatially local (40 micron diameter circle), high resolution (20 micron) distance measurements. With an adequate technique perfected, systematic composition are examined to determine the role of AP ignition and combustion properties, and the energetic nature of the binder on the local and average burning rate. Specifically, the binder curative, oxidizer modal size ratio, and pressure are investigated as independent variables. B.W.

N86-13541# United Technologies Corp., San Jose, Calif. Chemical Systems Div.

COUPLING BETWEEN VELOCITY OSCILLATIONS AND SOLID PROPELLANT COMBUSTION Abstract Only

R. S. Brown, A. M. Blackner, P. G. Willoughby, and R. Dunlap *In* AFOSR The 1985 AFOSR/AFRPL Chem. Rocket Res. Meeting Feb. 1985 3 p (For primary document see N86-13507 04-28)

Avail: NTIS HC A11/MF A01

Cold-flow studies are being conducted to define and characterize the basic flowfield and heat transfer mechanisms controlling the coupling between the acoustic velocity and the solid combustion zone. This coupling produces a substantial effect on the overall stability of the combustion pressure, yet substantial deficiencies exist in the current basic knowledge. Previously reported measurements of the oscillatory heat transfer demonstrate that this coupling is extremely nonlinear at relatively low acoustic pressures ($< 0.4\%$). The data also show that the current heuristic model for velocity coupling (which is incorporated into the Standard Stability Prediction Program) is largely wrong; the differences in the head-end and aft-end coupling are reversed from those predicted by the conceptual model. Radial profiles of the acoustic velocity have been measured at several axial stations for two surface Mach numbers, frequencies, and acoustic pressure levels. B.W.

N86-13542# Georgia Inst. of Tech., Atlanta. Dept. of Aerospace Engineering.

FLAME-ACOUSTIC WAVE INTERACTION DURING AXIAL SOLID ROCKET INSTABILITIES Abstract Only

Ben T. Zinn, Brady R. Daniel, Jechiel Jagoda, Uday Hedge, and Subra V. Sankar *In* AFOSR The 1985 AFOSR/AFRPL Chem. Rocket Res. Meeting Feb. 1985 3 p (For primary document see N86-13507 04-28)

Avail: NTIS HC A11/MF A01

This theoretical and experimental research program is concerned with the determination of: (1) the processes which control the driving of axial instabilities by solid propellant flames, and (2) whether existing models can indeed determine the interactions between solid propellant flames and oscillatory flow fields. Since experimental investigation of actual solid propellant flames is currently not possible because of the extremely small dimensions of their combustion zones, the present study investigates the characteristics of a premixed, flat flame stabilized within an acoustic boundary layer next to a porous side wall in a specially developed experimental setup. In this setup, a combustible mixture enters the duct through the porous side wall and it burns in a flat flame stabilized at some distance downstream of the wall which permits performing the indicated diagnostics. Simultaneously, the response of this flame to acoustic excitation is modeled using an approach similar to those utilized to model the responses of solid propellant flames. B.W.

N86-13543# Brigham Young Univ., Provo, Utah.

MECHANISMS FOR ACOUSTIC SUPPRESSION Abstract Only

Merrill W. Beckstead and R. L. Raun *In* AFOSR The 1985 AFOSR/AFRPL Chem. Rocket Res. Meeting Feb. 1985 3 p (For primary document see N86-13507 04-28)

Avail: NTIS HC A11/MF A01

Acoustic suppressants are commonly added to low smoke and smokeless propellants to avoid the problem of combustion instability. Suppressants apparently work by one or more of three mechanisms: (1) energy loss due to viscous dissipation due to drag forces, (2) modification of the propellant combustion response function, or (3) energy interchange due to distributed combustion. Viscous dissipation of acoustic energy by drag forces on a suspended particle is the most commonly recognized mechanism, being a direct analogy to suspended moisture in a fog. A second mechanism can occur with solid additives within the propellant that has a catalytic influence on the combustion response. The third mechanism considered is due to the effect of a particle burning as it traverses a relatively large portion of the system. As it does go, the interchange of energy between the burning particle and the acoustic environment can result in either a driving or damping contribution to the acoustics of the system. This third mechanism is the primary area of study of the current contract. The principle objective of this work is to identify and develop an understanding of the mechanisms whereby acoustic suppressants modify an acoustic wave. B.W.

N86-13544# Alabama Univ., Huntsville. Dept. of Mechanical Engineering.

FLOW FIELD EFFECTS OF COMBUSTION INSTABILITY Abstract Only

T. J. Chung *In* AFOSR The 1985 AFOSR/AFRPL Chem. Rocket Res. Meeting Feb. 1985 3 p (For primary document see N86-13507 04-28)

Avail: NTIS HC A11/MF A01

The main topic of research during the past two years has been the theoretical and numerical studies of the coupling mechanism of acoustic and hydrodynamic wave oscillations and its effects on combustion instability. A question arises: What happens if acoustic oscillations are coupled with the hydrodynamically oscillating system? To see this phenomenon, a rocket motor simulator is considered. An expression is derived for the growth constant in the form, alpha = alpha sub A + alpha sub H, where alpha sub A and alpha sub H refer to the growth constants corresponding to acoustic and hydrodynamic oscillations, respectively. Alpha sub A is a function of the mean flow velocity, acoustic pressure and frequencies, whereas alpha sub H is a function of additional variables such as the vortical component of velocity and hydrodynamic (vortical) frequencies as well as those for alpha sub A. Finite elements are utilized for calculations of mean flow fields, eigenvalue analyses, and the evaluation of the growth constant integrals. Based on this research, it is concluded that an acoustic coupling with hydrodynamic oscillations causes the hydrodynamic stability boundaries to expand into higher as well as lower frequency regions. B.W.

N86-13545# Hersh Acoustical Engineering, Chatsworth, Calif.

ROCKET MOTOR FLOW-TURNING LOSSES Abstract Only

Alan S. Hersh *In* AFOSR The 1985 AFOSR/AFRPL Chem. Rocket Res. Meeting Feb. 1985 3 p (For primary document see N86-13507 04-28)

Avail: NTIS HC A11/MF A01

Flow-turning losses represent one of the least understood mechanisms in the acoustic gain and loss estimates used in rocket motor stability calculations. According to theoretical models proposed by Culick, acoustic energy is absorbed during the energy exchange process governing the interaction between mean flow and longitudinal waves within the interior of rocket motors. A series of experimental investigations were undertaken to provide fundamental understanding of the flow-turning acoustic loss mechanisms. The experimental investigation was unique in four important ways. First, meaningful test data was collected using injection volume flow rates on the order of 100 times the values used in Culick's tests. Second, the detailed two-dimensional surveys of the mean and acoustic profiles across the injection test section were conducted. Third, the effects of mean flow turbulence were removed by signal processing. And fourth, acoustic energy flux losses across the injection test section were directly measured. B.W.

N86-13546# Air Force Office of Scientific Research, Bolling AFB, Washington, D.C.
OVERVIEW: AFOSR INTERESTS IN ROCKET PROPULSION Abstract Only
Leonard H. Caveny *In its* AFOSR/AFRPL Chem. Rocket Res. Meeting Feb. 1985 2 p (For primary document see N86-13507 04-28)
Avail: NTIS HC A11/MF A01

Rocket propulsion requirements, both present and planned, present important challenges that are not addressed adequately by present technologies. Future propulsion systems must be improved to assure that the winning edge is maintained. Because of the recent emphasis on space and the reusable launch vehicle capability to low Earth orbit new considerations for advanced propulsion for orbit transfer are investigated. Transferring the projected large payloads using conventional propulsion imposes severe limitations on the missions. For example, 70% of the mass delivered to low Earth orbit may be the chemical propulsion system required to raise the other 30% (i.e., the active payload) to geosynchronous Earth orbit; nonconventional propulsion offers the promise of reversing this ratio of propulsion and payload masses. Fundamental processes are discussed related to beamed energy and solar propulsion, i.e., radiation transmission and absorption in flowing media, plasma initiation, and chamber configurations. Electric propulsion concepts are also reviewed. B.W.

N86-13547# Air Force Rocket Propulsion Lab., Edwards AFB, Calif.
INTERACTION OF MULTI-DIMENSIONAL MEAN AND ACOUSTIC FIELDS IN SOLID ROCKET COMBUSTION CHAMBERS Abstract Only
Joseph D. Baum and Jay N. Levine *In its* AFOSR/AFRPL Chem. Rocket Res. Meeting Feb. 1985 3 p (For primary document see N86-13507 04-28)
Avail: NTIS HC A11/MF A01

The objective of the present research project is to seek an understanding of the physical mechanisms by which energy is exchanged between the mean and acoustic flow fields in resonance combustion chambers (in particular, solid rocket motors). These processes which have the potential of contributing significantly to the growth or decay of pressure oscillations in solid rocket chambers, have been the subject of much speculation in the past, but have never been thoroughly investigated. Specifically, the phenomena to be investigated are the interaction between the acoustic field in a chamber and a free shear layer (i.e., vortex shedding) and the so called flow turning effect (i.e., energy transfer between the acoustic field in the combustor and the mean flow of combustion products entering the chamber parallel to its axis). A computer program was developed to solve the time dependent, turbulent, compressible Navier-Stokes equations that describe the flow in a combustion chamber and a hard wall tube (utilized to study the phenomenon of sound wave propagation in a coexisting sheared mean flow). Studies were conducted to evaluate explicit versus implicit codes (implicit was chosen as more computationally efficient) and proper definition of the boundary conditions. B.W.

N86-13548# Tennessee Univ., Tullahoma. Center for Laser Applications.
LASER THERMAL PROPULSION Abstract Only c36
Dennis Keefer, Carroll Peters, Herbert Crowder, and Richard Wells *In* AFOSR The 1985 AFOSR/AFRPL Chem. Rocket Res. Meeting Feb. 1985 3 p (For primary document see N86-13507 04-28)
Avail: NTIS HC A11/MF A01

Laser sustained plasmas (LSP) have been proposed as a means of converting beamed energy from a remotely located laser to provide efficient propulsion for orbital transfer. Successful implementation of this concept requires that the detailed energy conversion processes that control plasma stability and fractional energy absorption within the LSP be thoroughly understood. An experimental study of these mechanisms is being conducted using argon plasmas sustained by a continuous wave carbon dioxide laser in a controlled, forced convection flow. Detailed measurements of the plasma temperature field are obtained using digital images of the plasma continuum radiation within a narrow spectral wavelength band. Using the measured temperature field, the interaction among the absorbed laser power, thermal conduction, and thermal radiative transfer can be calculated at each point within the plasma. Author

N86-13549# Pennsylvania State Univ., University Park.
ANALYTICAL MODELING OF STRONG RADIATION GAS-DYNAMIC INTERACTION Abstract Only c36
Charles L. Herkle *In* AFOSR The 1985 AFOSR/AFRPL Chem. Rocket Res. Meeting Feb. 1985 3 p (For primary document see N86-13507 04-28)
Avail: NTIS HC A11/MF A01

The principal objective of this research program is to determine the dominant characteristics of the interaction between a higher power laser beam and a flowing gas. The method of investigation is by numerical analysis with primary emphasis on the steady two-dimensional problem. The one-dimensional problem and the stability characteristics of the interactions are also being considered. The geometry of interest is the convergent portion of a converging-diverging nozzle. In particular, the analysis includes the effects of a converging laser beam with an arbitrary intensity profile. (Present calculations are using a Gaussian beam.) The mass flow through the nozzle is fixed by the back pressure when the nozzle is unchoked, and by the choking condition when the nozzle is operated supercritically. Real gas properties, including viscosity and thermal conductivity, corresponding to those of equilibrium hydrogen are used for all thermodynamic variables. The location of the heat absorption zone and the fraction of power absorbed are found by satisfying the complete conservation laws. B.W.

N86-13550# Illinois Univ., Urbana-Champaign.
EXPERIMENTAL STUDIES OF LASER-SUSTAINED ARGON PLASMAS FOR CW LASER PROPULSION APPLICATIONS Abstract Only c36
Herman KRier and Jyoti Mazumder *In* AFOSR The 1985 AFOSR/AFRPL Chem. Rocket Res. Meeting Feb. 1985 3 p (For primary document see N86-13507 04-28)
Avail: NTIS HC A11/MF A01

Experimental studies of laser-sustained plasmas in pressurized flowing argon are presented. The data shows strong laser energy absorption by argon, approaching 80% at higher powers. The absorption coefficient of air is degraded by the presence of extraneous species with larger electron collisional cross sections. These tend to deexcite free electrons and lower electron temperature, reducing inverse Brehemsstrahlung absorption, the dominant absorption mechanism. The data also indicates a tendency for global absorption to rise with laser power. Plasma size is an eigenvalue solution of the steady state energy balance equations, producing a finite plasma size for a given laser power and flow conditions. The data also suggests asymptotic behavior at high power. As laser power increases, the plasma grows until it reaches a point where radiative losses from the enlarged surface area offsets the increase in power, preventing further growth in absorption length. B.W.

N86-13551# Physical Sciences, Inc., Andover, Mass.
LINEAR AND SATURATED ABSORPTION OF LASER RADIATION IN HEATED CASES Abstract Only c36
Robert H. Krech, Lawren M. Cowles, George E. Caledonia, and David I. Rosen *In* AFOSR The 1985 AFOSR/AFRPL Chem. Rocket Res. Meeting Feb. 1985 3 p (For primary document see N86-13507 04-28)
Avail: NTIS HC A11/MF A01

The physical processes involved in heating the working fluid of a rocket engine with a high power CW laser beam can be simply described. The gas is injected into the stagnation/absorption zone at a temperature most probably determined by regenerative cooling requirements. As the gas flows toward the throat it is heated by absorption of laser radiation. With hydrogen as the primary propellant constituent, the equivalent of nine 10.5 micrometer photons per molecule must be absorbed to reach a stagnation condition that yields a specific impulse of approx. 1000 s. The present program has been directed towards studying the absorption properties of potential high temperature molecular absorbers over the temperature range of 1000 to 3500 K and at CO2 (approx. 10.6 micrometers) and DF (3.8 micrometers) laser wavelengths. These measurements have been performed behind incident and reflected shockwaves. Species studied to date include H2O, CO2, NH3, SF6 and NF3. Small signal (linear) absorption coefficients have been measured for these species (including effects due to dissociation fragments). These measurements have been performed under pressure and temperature conditions, and within non-equilibrium chemical kinetic regimes, appropriate to the propulsion application. B.W.

N86-13552# Physical Sciences, Inc., Andover, Mass.
ENERGY DEPOSITION OF PULSED ONE MICRON LASER RADIATION IN H2 AND AR Abstract Only c36
David I. Rosen and Nelson H. Kemp *In* AFOSR The 1985 AFOSR/AFRPL Chem. Rocket Res. Meeting Feb. 1985 3 p (For primary document see N86-13507 04-28)
Avail: NTIS HC A11/MF A01

In RP (repetitively-pulsed) laser propulsion the propellant energy is supplied by the absorption of short, repetitive laser pulses beamed to the thruster from a remote laser power station. The four principal stages in the operation of the pulsed laser-heated thruster are as follows: (1) ignition/breakdown, (2) post-breakdown plasma absorption and growth under the influence of the laser radiation field, (3) blast wave propagation into the surrounding gas, and (4) late-time expansion and cooling of the laser-heated gas. In a previous study at PSI experimental and theoretical investigations of laser-induced gas breakdown at short laser wavelengths (< 1 micrometer) were carried out for a variety of propellant gas candidates. The results of those studies have helped to establish the threshold irradiances required to initiate an optically absorbing plasma. Experiments were performed to investigate the degree of laser optical absorption and the resulting plasmadynamics which occurs when high energy pulses of 1.05 micrometer laser radiation are focused into various gases at focal intensities above the breakdown threshold (10 to the 10th power 10 to the 13th power w/sq cm). B.W.

N86-13553# Rensselaer Polytechnic Inst., Troy, N.Y. Dept. of Mechanical Engineering, Acoustical Engineering and Mechanics.
ADVANCED ENERGY CONVERSION CONCEPT FOR MICROWAVE BEAMED-ENERGY PROPULSIONS Abstract Only c75
Leik N. Myrabo *In* AFOSR The 1985 AFOSR/AFRPL Chem. Rocket Res. Meeting Feb. 1985 3 p (For primary document see N86-13507 04-28)
Avail: NTIS HC A11/MF A01

An innovative electrostatic force generation principle was investigated. Microwave energy is beamed directly to remote RF linear accelerators (LINAC) enclosed by a specially-shaped body within a planetary atmosphere. A number of low current 5 MeV LINACs eject free-electron charge to a distance of 5 to 10 m from the body, thereby establishing a charge cloud and resultant high electric field between the cloud and body. The free electrons attach to previously neutral oxygen and water molecules, and drag the largely neutral air-mass cloud back to the body which is now positively charged. Repetitively-pulsed operation of the LINACs could give rise to quasisteady electrostatic forces, which accelerate the air-mass working fluid within a stream tube of a given capture area -- as established by the radius of the E-beam at the point of maximum range from the accelerator. Examination of the physics of global body electrostatic charging and artificial atmospheric charging, formulate a model for electrostatic force generation and to analyze the cloud/body interaction physics is proposed. The results of a first-order calculation of anticipated surface-field thrust, free charge, and stored energy are presented. E.A.K.

N86-13554# Stuttgart Univ. (West Germany).
BASIC PROCESSES OF PLASMA PROPULSION Abstract Only c75
Herbert O. Schrade *In* AFOSR The 1985 AFOSR/AFRPL Chem. Rocket Res. Meeting Feb. 1985 3 p (For primary document see N86-13507 04-28)
Avail: NTIS HC A11/MF A01

The acceleration mechanisms and the electrode effects in self magnetic pulsed and continuous MPD-arc thrusters were investigated. The magnetic thrust of a MPD-arc propulsion device increases with the square of current. An explanation is put foreward which also accounts for the electrode and insulator erosion. A plasma instability leads to a deviation off the axisymmetrical current distribution and hence to a current concentration on the anode surface. A simplified rotationally symmetric, two dimensional numerical methods to calculate the flow pressure and current density field for different thruster geometries was set up. The current contour and constant pressure lines of such a numerical calculation for the MPD-Thruster assuring isothermal conditions for the electrons and an isotropic behavior of the heavy particles are shown. To gain a better understanding of the cathode phenomenon and to minimize the erosion rate in MPD-arcs an experiment was initiated. The experimental set up is shown and is placed in a vacuum test vessel which allow pressure variations between 10 to the minus 3rd power and 10,000 Pa for different gases. The electrode system is energized by a pulse forming network of electrolytic capacitors delivering a rectangular current pulse lasting about 2 ns with currents which can be varied between several hundred amperes up to 101A. The test apparatus will determine the cathode attachment behavior, the mass loss, erosion rate and surface damage for different cathode materials under various aperating conditions. E.A.K.

N86-13555# Massachusetts Inst. of Tech., Cambridge. Dept. of Aeronautics and Astronautics.
PERFORMANCE-LIMITING FACTORS IN MPD THRUSTERS Abstract Only c75
Manuel Martinez-Sanchez, Daniel Heimerdinger, Mark Chanty, and David Melanson *In* AFOSR The 1985 AFOSR/AFRPL Chem. Rocket Res. Meeting Feb. 1985 3 p (For primary document see N86-13507 04-28)
Avail: NTIS HC A11/MF A01

Three primary questions in the physics and design of MPD thrusters are addressed: (1) based on a simplified model of the plasma physics (but still retaining the Hall effect), how should an MPD channel be lofted to insure a smooth current distribution; (2) developing a numerical simulation code for off-design or off-shape channels; (3) development of experimental tests and diagnostics to verify the above. This approach differs from the more traditional route, in which the channel shape is arrived at in a purely empirical manner, and also from earlier plasma flow analyses, where the crucial role of the Hall parameter is not accounted for. E.A.K.

N86-13556# Carnegie-Mellon Univ., Pittsburgh, Pa.
EROSION AND ONSET MECHANISMS IN MAGNETOPLASMADYNAMIC THRUSTERS Abstract Only c75
John L. Lawless *In* AFOSR The 1985 AFOSR/AFRPL Chem. Rocket Res. Meeting Feb. 1985 3 p (For primary document see N86-13507 04-28)
Avail: NTIS HC A11/MF A01

Erosion is a major concern in MPD thruster design. To minimize erosion, it is desirable to operate in the diffuse as opposed to spot mode of current conduction. The following efforts are made: (1) to determine the limits of diffuse mode operation; and (2) to quantify erosion rates. At present, there are no theories to answer either question. The relationship between erosion and the experimental phenomenon of onset is clarified. E.A.K.

N86-13557*# Jet Propulsion Lab., California Inst. of Tech., Pasadena.
MAGNETOPLASMADYNAMIC THRUSTER EROSION RESEARCH Abstract Only c75

David Q. King *In* AFOSR The 1985 AFOSR/AFRPL Chem. Rocket Res. Meeting Feb. 1985 3 p (For primary document see N86-13507 04-28)

Avail: NTIS HC A11/MF A01

Magnetoplasmadynamic thruster (MPdT) lifetime at sustained multimagawatt power levels is unknown but will be governed by plasma erosion of thruster surfaces. Before the thruster can be developed for an orbital propulsion application the physics of the erosion mechanisms must be studied. The following key questions that must be resolved to understand erosion are addressed: (1) what are the erosion mechanisms on the anode, cathode, and insulator and what are the quantitative rates for each; (2) what governs the cathode heat balance at high current density and magawatt power levels; (3) what governs the anode heat balance; and (4) how does the cathode work function change with time, and what effect does this have on erosion. The approach aims at developing an understanding of the erosion of the electrode and insulator surfaces by conducting experiments on a steady-state scaled-down MPD device, and by analysis of key processes. B.W.

N86-13558# SeiTec, Cleveland, Ohio.

COMPLETELY MAGNETICALLY CONTAINED ELECTROTHERMAL THRUSTER Abstract Only

George R. Seikel *In* AFOSR The 1985 AFOSR/AFRPL Chem. Rocket Res. Meeting Feb. 1985 3 p (For primary document see N86-13507 04-28)

Avail: NTIS HC A11/MF A01

The highest performance on electrothermal thrusters were measured. It was shown that for both in the 25kW thruster and a MW quasisteady thruster efficiency significantly increases with the applied magnetic field strength up to the experimental limits. At these field strengths the cyclotron radius of the propellant ions becomes smaller than the anode diameter, and heating, containment, and acceleration of the plasma ions can be directly accomplished by the applied radial electric field and expanding axial magnetic nozzle field. E.A.K.

N86-13559*# National Aeronautics and Space Administration. Johnson (Lyndon B.) Space Center,

PLASMA-GAS INTERACTIONS STUDIES IN A HYBRID PLUME PLASMA ROCKET Abstract Only c75

F. R. Chang, W. A. Krueger, T. F. Yang, and J. L. Fisher (Southwest Research Inst., San Antonio, Tex.) *In* AFOSR The 1985 AFOSR/AFRPL Chem. Rocket Res. Meeting Feb. 1985 2 p Prepared in cooperation with MIT, Cambridge (For primary document see N86-13507 04-28)

Avail: NTIS HC A11/MF A01

Plasma-gas interaction was investigated and the basic mechanisms for energy and particle transport. The solution approach assumes cylindrical geometry and includes a multiplicity of atomic reactions, and the presence of a strong magnetic field is described. The principal reactions are electron and ion impact ionization, and charge exchange between hot ions and cold neutrals. Radial particle and energy transport is mainly by diffusion. A modified Bohm diffusion model for plasma in the core of the plume, and classical neutral particle diffusion in the cooler regions of the flow are presented. Neutrals are allowed to free stream in the low density regions, where the collision mean-free-path becomes comparable, or even larger than the characteristic dimensions of the system. E.A.K.

N86-13560*# National Aeronautics and Space Administration. Johnson (Lyndon B.) Space Center,

A TANDEM MIRROR PLASMA SOURCE FOR HYBRID PLUME PLASMA STUDIES Abstract Only c75

T. F. Yang, F. R. Chang, R. H. Miller, K. W. Wenzel, and W. A. Krueger *In* AFOSR The 1985 AFOSR/AFRPL Chem. Rocket Res. Meeting Feb. 1985 3 p Prepared in cooperation with MIT, Cambridge (For primary document see N86-13507 04-28)

Avail: NTIS HC A11/MF A01

A tandem mirror device to be considered as a hot plasma source for the hybrid plume rocket concept is discussed. The hot plamsa from this device is injected into an exhaust duct, which will interact with an annular hypersonic layer of neutral gas. The device can be used to study the dynamics of the hybrid plume, and to verify the numerical predictions obtained with computer codes. The basic system design is also geared towards low weight and compactness, and high power density at the exhaust. The basic structure of the device consists of four major subsystems: (1) an electric power supply; (2) a low temperature, high density plasma gun, such as a stream gun, an MPD source or gas cell; (3) a power booster in the form of a tandem mirror machine; and (4) an exhaust nozzle arrangement. The configuration of the tandem mirror section is shown. E.A.K.

N86-13561# Pennsylvania State Univ., University Park.

COUPLING BETWEEN GAS DYNAMICS AND MICROWAVE ENERGY ABSORPTION Abstract Only c75

Michael M. Micci *In* AFOSR The 1985 AFOSR/AFRPL Chem. Rocket Res. Meeting Feb. 1985 3 p (For primary document see N86-13507 04-28)

Avail: NTIS HC A11/MF A01

Models of the microwave absorption regions with and without gas flows and experimental measurement of key physical parameters such as gas temperature and heat fluxes are exained. Heat losses from the absorption region and the amount of cooling gas required and its effects on final exhaust velocity and efficiency are investigated. Questions to be resolved include the relative roles of conduction, convection and radiation in transferring the absorbed microwave power to thrust power, the stability of such flows and the mixing processes of cold gas with the microwave sustained plasma. The anticipated scientific accomplishment of this program is illustrated. The research provides insight into the entire field of high temperature gas flows driven by radiation absorption. E.A.K.

N86-13562# Electromagnetic Launch Research, Inc., Cambridge, Mass.

PULSED INDUCTIVE ENERGY TRANSFER Abstract Only c75

Peter P. Mongeau and Douglas P. Hart *In* AFOSR The 1985 AFOSR/AFRPL Chem. Rocket Res. Meeting Feb. 1985 3 p (For primary document see N86-13507 04-28)

Avail: NTIS HC A11/MF A01

The pulsed inductive acceleration process was investigated. The basic energy transfer mechanisms and the performance limitations of this device were established. It is indicated that the performance of the metallic induction reaction engine is more dependent on the density of the reaction mass material than on the conductivity of the material and that the existence of a back EMF saturation effect which can inhibit energy transfer to the pulsed inductive system. This saturation effect can be greatly reduced by using a compound pulse coil rather then a face coil to accelerate the reaction mass. E.A.K.

N86-13563# Dayton Univ., Ohio. Research Inst.

LASER DIAGNOSTICS FOR ELECTRIC FIELD MEASUREMENTS Abstract Only c75

Roger J. Becker, Blair A. Barbour, and Alan T. Buswell *In* AFOSR The 1985 AFOSR/AFRPL Chem. Rocket Res. Meeting Feb. 1985 3 p (For primary document see N86-13507 04-28)

Avail: NTIS HC A11/MF A01

The development of accurate means to measure the electric field strength in transient plasmas with good spatial resolution is described. A nonintrusive (optical) measurement that provides reliable data in a conducting medium is described. Selection rule breakdown in a laser scattering measurement was used. The Rayleigh depolarization scattering (RDS) is directed at gas atoms and ions and highly symmetric molecules. The second method uses CARS to measure selection rule breakdown in Raman scattering, and is applied to a wide class of molecules. E.A.K.

N86-13564# Spectron Development Labs., Inc., Costa Mesa, Calif.

OPTICAL TECHNIQUE TO MEASURE ELECTRODE EROSION Abstract Only c74

James D. Trolinger and David F. Schaack *In* AFOSR The 1985 AFOSR/AFRPL Chem. Rocket Res. Meeting Feb. 1985 3 p (For

primary document see N86-13507 04-28)
Avail: NTIS HC A11/MF A01

The failure mechanism in a number of important components and systems is electrical erosion, for example, in electrical propulsion systems or other components exposed to plasmas and arcs. The ability and required technology for high sensitive optical methods to serve as a diagnostic for miniscule amounts of surface erosion are determined. E.A.K.

N86-13565# Rensselaer Polytechnic Inst., Troy, N.Y.
VARIABLE FIELD EFFECTS FOR THE ROTATING FLUIDIZED BED REACTOR Abstract Only **c73**
Owen C. Jones *In* AFOSR The 1985 AFOSR/AFRPL Chem. Rocket Res. Meeting Feb. 1985 3 p (For primary document see N86-13507 04-28)
Avail: NTIS HC A11/MF A01

The rotating fluidized bed nuclear reactor is a concept which has the potential for very large power densities. Large turn-down ratios and very high specific impulses of approx. 25 to 50% higher than those associated with chemical rockets. The technical feasibility of this concept includes material studies of nuclear fuels and thermal-hydraulic studies of the behavior of rotating fluidized beds of various shapes and under centrifugal g-fields. Results of the scoping effort include: (1) evaluation of fluid-bed expansion and development of new predictive techniques; (2) evaluation of the quasi-1-dimensional coupled thermonuclear stability of reactor operation; (3) examination of the hydrodynamic stability of fluidized beds, development of some initial predictive methods, and initiation of a simple experiment to evaluate the results; and (4) evaluation of the potentially concept-killing problems associated with thermal stress in the blind end plate of the reactor. E.A.K.

N86-13566# Rensselaer Polytechnic Inst., Troy, N.Y. Dept. of Chemical Engineering and Environment Engineering.
EFFECT OF INTERFACIAL PHENOMENA ON CONTACT LINE HEAT TRANSFER Abstract Only **c34**
Peter C. Wayner, Jr. *In* AFOSR The 1985 AFOSR/AFRPL Chem. Rocket Res. Meeting Feb. 1985 3 p (For primary document see N86-13507 04-28)
Avail: NTIS HC A11/MF A01

The stability and heat transfer characteristics of the contact line region of an evaporating thin liquid film was examined. The processes of heat, mass and momentum transfer in the film thickness region delta < 10 to the -5th power m was measured. A miniaturized heat transfer cell on the stage of a microscope equipped with a scanning microphotometer was used. The interfacial concepts of disjoining pressure, spreading pressure, fluid microstructure and surface tension are used to analyze the transport processes and to develop a macroscopic suction potential model for the integral heat sink. E.A.K.

N86-13567# R and D Associates, Alexandria, Va.
UNIFIED STUDY OF PLASMA-SURFACE INTERACTIONS FOR SPACE POWER AND PROPULSION Abstract Only **c75**
Peter J. Turchi, John F. Davis, III, Joseph Norwood, Jr., and Craig N. Boyer *In* AFOSR The 1985 AFOSR/AFRPL Chem. Rocket Res. Meeting Feb. 1985 3 p (For primary document see N86-13507 04-28)
Avail: NTIS HC A11/MF A01

The efficiency and lifetime of high specific power/high specific impulse space power and propulsion devices often depend on particle and energy transport at electrodes and insulators in low temperature plasma flows. Actual measurements of particle and field distributions near solid surfaces in controlled plasma flows were studied and used to develop models for particle and energy transport. A unique advantage in such model development is the ability to vary flow conditions, surface orientation, and material properties and to compare data within a unified experimental framework, thereby allowing complicated interactions to be delineated. DOE

N86-13568# Rasor Associates, Inc., Sunnyvale, Calif.
CLOSE-SPACE, HIGH TEMPERATURE KNUDSEN FLOW Abstract Only **c33**
John B. McVey *In* AFOSR The 1985 AFOSR/AFRPL Chem. Rocket Res. Meeting Feb. 1985 3 p (For primary document see N86-13507 04-28)
Avail: NTIS HC A11/MF A01

The discharge processes and performance characteristics of thermionic energy conversion systems operating in the collisionless (Knudsen) mode were investigated. The interelectrode space charge can be reduced by close interelectrode spacings, contact ionization of cesium at the emitter surface or introduction of ions produced in an externally generated arc. It is suggested that structured emitters can increase the current and power densities in the unignited mode by a factor of four. Small diode structures, SAVTECs, with spacing set by thermal expansion, to measure converter performance at interelectrode spacings below 20 micron were used. Measurements covered both the vacuum and unignited regimes. Two variable-spacing planar converters containing mixed cesium and barium vapor are planned to investigate the structured emitter effect. Theoretical studies and computer models of the collisionless thermionic converter and its interaction with an external arc supplement the experimental work. E.A.K.

N86-13569# SRI International Corp., Menlo Park, Calif. Chemical Physics Lab.
TWO-PROTON DETECTION TECHNIQUES FOR ATOMIC FLUORINE Abstract Only **c74**
William K. Bischel *In* AFOSR The 1985 AFOSR/AFRPL Chem. Rocket Res. Meeting Feb. 1985 3 p (For primary document see N86-13507 04-28)
Avail: NTIS HC A11/MF A01

The electronic states of primary interest are shown. The two states that are the focus of the experiments are the sup 2 p sub 1/2 state at 404 cm(-1) and the sup 2 D sub 5/2 state at 117,624 cm(-1), both of which have two photon allowed transitions from the ground state. Two different types of experiments are utilized to detect and study the properties of these excited states. The experiment conducted first is the Raman excitation of the sup 2 P sub 1/2 state. The apparatus for this experiment is illustrated. This experiment will use two visible lasers. The second experiment is the direct two photon excitation of the sup 2 D sub 5/2 state. Fluorescence emission at 775 nm forms the observed signal. This experiment requires laser radiation at 170 nm. The results of both experiments are two fold: (1) new remote detection techniques for atomic fluorine is demonstrated; and (2) a wealth of new data concerning its excited states is generated. Author

N86-13570# California Univ., Berkeley. Dept. of Mechanical Engineering.
COHERENT OPTICAL TRANSIENT SPECTROSCOPY IN FLAMES Abstract Only **c74**
John W. Daily *In* AFOSR The 1985 AFOSR/AFRPL Chem. Rocket Res. Meeting Feb. 1985 3 p (For primary document see N86-13507 04-28)
Avail: NTIS HC A11/MF A01

An actively stabilized CW dye laser is used as a source. By passing the beam through a traveling wave modulator to which a high voltage pulse has been applied, the frequency may be shifted up to 15 GHz within 150 psec for periods of several nanoseconds. Thus, one may shift into or out of resonance with an absorption line of interest and observe the transient behavior that results. The type of transient observed is Free Induction Decay in which the laser beam is suddenly shifted out of resonance with an absorption line and the transient absorption signal observed. The decay rate of the transient signal is the collisional dephasizing rate for that transition. Also illustrated are several other types of excitation, the transient they produce and the quantities one can obtain. The focus of study was on CH in the low pressure flame facility. A complete layout of the equipment in two configurations, one for COTS and another for making high resolution absorption measurements, is shown. Author

N86-13571# Sheffield Univ. (England). Dept. of Chemical Engineering and Fuel Technology.

DEVELOPMENT OF VELOCITY MEASUREMENT TECHNIQUE BY PULSED LASER DOPPLER ANEMOMETRY Abstract Only c36

B. C. R. Ewan and J. Swithenbank *In* AFOSR The 1985 AFOSR/AFRPL Chem. Rocket Res. Meeting Feb. 1985 3 p (For primary document see N86-13507 04-28)
Avail: NTIS HC A11/MF A01

The conventional point measuring ability of laser Doppler anemometry is extended to a line measurement. Two immediate requirements follow from this modification. The first is that of monitoring several points along the line measuring volume simultaneously, leading to a multichannel data collection and analysis system. The second stems from the diminished beam intensity in the measuring volume due to its extension and the need to restore scattered light intensity by increasing laser power or scattering particle diameters. Two parallel lines of study are used. The first aims at developing the optics and signal processing necessary to produce and analyze the Doppler signals. A CW argon ion laser is used operating in a conventional laser Doppler configuration, with the exception of the output lens, which is cylindrical and produces a line intersection within the measurement field. Progress with the argon ion system consists of the completion of the optical arrangement in conjunction with an air jet and suitable particle seeding, capable of producing sonic jets. The second parallel element aims at overcoming the low light level in the measuring volume using the high powers available with pulsed lasers. Author

N86-13572# Stanford Univ., Calif. Dept. of Mechanical Engineering.
QUANTITATIVE FLOW VISUALIZATION Abstract Only c36
Ronald K. Hanson *In* AFOSR The 1985 AFOSR/AFRPL Chem. Rocket Res. Meeting Feb. 1985 5 p (For primary document see N86-13507 04-28)
Avail: NTIS HC A11/MF A01

A method for visualizing a range of flowfield parameters including temperature, velocity, species concentrations, pressure, and, in the case of two-phase flows, droplet or particle distributions is established. Ideally these techniques should be applicable to nonreacting and reacting flows, including plasmas. Most of the work has utilized planar laser induced fluorescence (PLIF), except for particle visualization which uses planar Mie scattering (PMS). The approach and some representative results for temperature and velocity are given. An overview of the fluorescence based temperature sensing strategy, and representative results for instanteous temperature contours in a vertical plane in a rod stabilized, premixed CH4-air flame are provided. A schematic diagram of the two frequency strategy for monitoring velocity, also based on fluorescence, is shown and as are sample results for the axial velocity component in a subsonic, room temperature nitrogen roundjet. For temperature measurements, the light source is a pulsed dye laser system, yielding tunable output near 226 nm. For velocity visualization a tunable CW Art laser is used operating on a single axial mode near 515 nm. Author

N86-13573# Stanford Univ., Calif.
OPTICAL PROCESSING AND PHASE CONJUGATION Abstract Only c74
Lambertus Hesselink *In* AFOSR The 1985 AFOSR/AFRPL Chem. Rocket Res. Meeting Feb. 1985 3 p (For primary document see N86-13507 04-28)
Avail: NTIS HC A11/MF A01

Approaches for making quantitative measurements in combusting flows are investigated. Techniques investigated include optical and digital processing, holography and phase conjugation. Two new diagnostic techniques are investigated. The first technique is a method for obtaining species concentration in a flame using phase conjugation (DFWM). The second technique is a method for making real time velocity measurements in a plane using speckle interferometry. DFWM is superior to the alternative in that the signal strength is substantially higher, which allows for better partial resolution and S/N for a given amount of laser power. The use of a photorefractive recording material for speckle metrology allows real time measurement of velocity in a plane. The first demonstration of DFWM was achieved. The concentration of sodium in a small laboratory flame was measured using the new DFWM technique. The technique shows excellent promise as a diagnostic tool for combustion research. The real time speckle velocimetry work was started. It was demonstrated that photorefractive materials can be used as a recording medium for speckle patterns. Author

N86-13574# Carnegie-Mellon Univ., Pittsburgh, Pa. Dept. of Mechanical Engineering.
STRATEGY FOR ADVANCED SENSING AND CONTROL OF COMBUSTION Abstract Only
Mark L. Nagurka, Juan I. Ramos, and W. A. Sirignano *In* AFOSR The 1985 AFOSR/AFRPL Chem. Rocket Res. Meeting Feb. 1985 3 p (For primary document see N86-13507 04-28)
Avail: NTIS HC A11/MF A01

Approaches to the sensing and control of combustion processes are investigated. A model equation describing the temperature distribution through a propagating flame was studied. The sensing and control problem is formulated such that a suitably defined flame front is driven to or maintained at a desired location. Various definitions for the flame front location have been used to generate control problems for distributed parameter systems (DPS) in a classical format. Using such a definition is possible to state an ordinary differential equation governing the flow velocity and/or mixture ratio. The flow velocity and thermochemical properties of the mixture are collapsed in one parameter V here referred to as velocity. Solution of the partial differential equation governing the temperature distribution together with the ordinary differential equation for V yields the results for the controlled problem. Two sensors at neighboring locations and the temperatures measured by them are employed to determine the velocity V. The gain of the control system is reflected through a characteristic time. Author

N86-13575# Carnegie-Mellon Univ., Pittsburgh, Pa. Dept. of Mechanical Engineering.
THE 1-D LASER DOPPLER INSTRUMENTATION Abstract Only c36
Holger T. Sommer *In* AFOSR The 1985 AFOSR/AFRPL Chem. Rocket Res. Meeting Feb. 1985 3 p (For primary document see N86-13507 04-28)
Avail: NTIS HC A11/MF A01

The development of reliable measurement of instantaneous velocity gradients by obtaining profiles of one component of the velocity vector instantly is presented. The instrument consists of the standard transmitting optics of a LDV system modified with cylindrical lenses to form laser sheets. The laser sheets cross and form a cylindrical LDV measurement volume. The fringes of the volume are oriented perpendicular to the velocity component of interest and scattered light from particles moving through the volume transmits the velocity information to the photodiode array. The signal from the photodiodes is processed in two different ways. The analog LDV-burst is stored on tape. Later on it is digitized and numerically analyzed to obtain the relevant velocity information. The second method of reducing the data involves optical frequency analysis. The laser Doppler signal detected by the photodiodes is high-pass filtered and amplified. This signal drives a Bragg-cell which acts as an optical frequency analyzer. The displacement of the first order of deflection of a laser beam passed through the Bragg-cell is proportional to the signal frequency. By feeding the laser Doppler bursts observed by different photodiodes to the Bragg-cell, and correlating the frequency proportional displacement of the analyzing laser beam with the location along the LDV-volume, a velocity profile is obtained. In order to obtain instantaneous velocity profiles, a time window is opened which is sufficiently short to time resolve the turbulence of the flow. Author

N86-13576# United Technologies Research Center, East Hartford, Conn.
RESONANT CARS DETECTION OF OH RADICALS Abstract Only c25

James F. Verdieck *In* AFOSR The 1985 AFOSR/AFRPL Chem. Rocket Res. Meeting Feb. 1985 3 p (For primary document see N86-13507 04-28)
Avail: NTIS HC A11/MF A01

CARS diagnostics was extended to minority species, in particular radicals, through the techniques of resonant CARS. The essentials of resonance CARS are illustrated. The hydroxy radical was chosen as a candidate molecule because of its seminal importance in both combustion and atmospheric chemistry. The approach taken was to achieve an understanding of the basic physics of electronic resonant CARS in OH, including effects of tuning, laser linewidth dependence, choice of electronic transition, and saturation considerations. The first observation of resonant CARS in OH was made under several conditions, including several different choices of the electronic resonant frequency. The amplitude and shape of a particular CARS spectrum are very sensitive to the precise tuning to the electronic resonance. The OH resonant CARS spectrum has a much greater amplitude than the adjacent water CARS spectrum. In addition to the experiments, the theory of resonant CARS in OH was treated. Agreement between theory and experiment is generally good, except for the experimental observation of satellite structure about the central line. Author

N86-13577# Aerometrics, Inc., Mountain View, Calif.
SPRAY CHARACTERIZATION USING PHASE ANGLE DETECTION Abstract Only **c34**
William D. Bachaio *In* AFOSR The 1985 AFOSR/AFRPL Chem. Rocket Res. Meeting Feb. 1985 3 p (For primary document see N86-13507 04-28)
Avail: NTIS HC A11/MF A01

A method with the potential for obtaining spray drop size and velocity measurements in sprays, two-phase flows, and eventually, in spray combustion is under investigation. The Phase/Doppler method is a unique method for obtaining drop size information wherein the measurements are obtained from the phase of the scattered light. The exact Mie theory was used to verify these results and to investigate the possible effects of light scattered by the combined mechanisms of refraction and reflection. The Mie theory allowed the identification and avoidance of these regions. Calculations based on the simple geometrical optics approach were in excellent agreement with the experimental data for particles greater than 5 micrometers in diameter. Mie theory calculations demonstrated that particles as small as 1 micrometer can be measured. The method consists of an optical system which is the same as a LDV except that three detectors are located at selected spacings behind the receiver aperture. Experiments were conducted to disclose any practical limitations of the method. Monodisperse drop streams were used in conjunction with sprays in the optical path to assess the impact, if any, of random beam attenuations and distortion. Sprays typical of those found in gas turbine combustors were measured. The size distributions, size-velocity correlations, mean and rms velocities for each size class, and the time of arrival were obtained. Author

N86-13578# Yale Univ., New Haven, Conn. Center for Laser Diagnostics.
LASER EMISSION AND COHERENT RAMAN SCATTERING FROM INDIVIDUAL FLOWING DROPLETS Abstract Only **c36**
Richard K. Chang, Marshall B. Long, and Roman Kuc *In* AFOSR The 1985 AFOSR/AFRPL Chem. Rocket Res. Meeting Feb. 1985 3 p (For primary document see N86-13507 04-28)
Avail: NTIS HC A11/MF A01

It may be possible to use the coherent but nondirectional laser emission from individual particles as active markers for flow field visualization and remote illumination. In particular, new applications may be viable with coherent emission droplets as velocimetry markers in otherwise optically dense two phase flows and in overhwelmingly high elastic scattering environments such as near a solid boundary. Furthermore, determination of the chemical species of individual droplets appears to be possible with coherent Raman emission. New research was initiated on the nonlinear optical emission from water droplets and ethanol droplets with and without Rhodamine 6G or Courmarin dyes. Laser emission from individual liquid ethanol droplets containing Rhodamine 6G at wavelengths commensurate with morphology dependent resonances (MDRs) was observed. For a conventional dye laser, optical feedback at selected wavelengths is provided by an external wavelength dispersive element. For a droplet dye laser, higher Q at selected wavelengths is provided by the MDRs associated with the liquid-air interface of the droplet. At these resonances, standing waves result from the total internal reflection at the liquid-air boundary of counterpropagating waves close to the circumference of the droplet. Stimulated Raman scattering (SRS) from individual H2O or ethanol droplets at wavelengths commensurate with MDRs and the spontaneous Raman-Stokes radiation was observed. Author

N86-13579# Yale Univ., New Haven, Conn. Center for Laser Diagnostics.
SIZE AND SHAPE CHARACTERIZATION OF INDIVIDUAL FLOWING DROPLETS BY LASER LIGHT SCATTERING Abstract Only **c36**
Richard E. Chang, Boa-Teh Chu, and Marshall B. Long *In* AFOSR The 1985 AFOSR/AFRPL Chem. Rocket Res. Meeting Feb. 1985 3 p (For primary document see N86-13507 04-28)
Avail: NTIS HC A11/MF A01

A new technique for determining both the size changes and the shape distortions of individual droplets flowing in a linear stream is presented. This technique is based on the whispering gallery modes or more accurately morphology dependent resonances (MDRs) associated with microparicles having a rotational axis symmetry. For size and shape determination, the MDRs in the fluorescence spectra from ethanol droplets tagged with Rhodamine 6G dye were measured. Highly monodisperse tagged ethanol droplets are generated by a modified Berglund-Liu vibrating orifice generator. The droplets have a radius in the 10 to 50 micrometer range with a monodispersity of one part in 10,000 to 100,000 and spacing within a linear stream of approx. 100 micrometer. The evaporation of droplets within a linear stream can be readily determined by measuring the wavelength shift of specific MDRs from successive droplets further downstream from the orifice, since the droplet decreases in size monotonically with time after exiting the orifice. The results demonstrate that the wake of preceding droplets significantly decreases the evaporation rate of a droplet within the linear stream. Author

N86-13580# Spectron Development Labs., Inc., Costa Mesa, Calif.
SPRAY CHARACTERIZATION WITH A NONINTRUSIVE OPTICAL SINGLE PARTICLE COUNTER Abstract Only **c34**
Cecil F. Hess *In* AFOSR The 1985 AFOSR/AFRPL Chem. Rocket Res. Meeting Feb. 1985 3 p (For primary document see N86-13507 04-28)
Avail: NTIS HC A11/MF A01

The understanding of droplet sizing technology in combustion environments using light scattering is studied. The emphasis is on establishing what information of the scattered light is better suited to provide the size and velocity of droplets, which can then yield local mass flux measurements. The studies conducted indicate that the absolute intensity of the scattered light combined with the standard LDV will produce excellent results. This technique was combined with auto calibrating algorithms to compensate for the loss of energy experienced when the laser beams or the scattered light travel through windows and other particles along the path. This is the basis of the IMAX techniques. An alternative and unique approach, referred to as P/MAX, is also under investigation. The P/MAX technique uses beams with polarizations normal to each other. This allows the use of low power single color lasers. In order to perform mass flux measurements in addition to the size and velocity distributions, the active probe volume must be known. This probe volume is a function of particle size and several optical parameters. Author

N86-13581# Arizona State Univ., Tempe.
INTELLIGENT LASER DIFFRACTION INSTRUMENTATION FOR

PARTICLE SIZE ANALYSIS Abstract Only c36
E. Dan Hirleman and Joseph I. Koo *In* AFOSR The 1985 AFOSR/AFRPL Chem. Rocket Res. Meeting Feb. 1985 3 p (For primary document see N86-13507 04-28)
Avail: NTIS HC A11/MF A01

Particle and droplet size distributions, being parameters of fundamental importance, should be priority measurement objectives for intelligent sensors in next generation propulsion systems. Unfortunately there are a number of problematic scientific issues limiting the development of laser light scattering particle sizing instruments capable of autonomous, self-diagnosing operation in hostile environments. Beam steering due to thermal gradients, multiple scattering from high number density aerosols, and contamination of windows and electro-optical components have been and will continue to be potentially catastrophic problems. The research is concentrated in three areas: development of rapid and robust computational algorithms for the laser diffraction inverse scattering problem; synergism of electro-optical detection strategies with the inverse scattering algorithms; and techniques for on-line calibration and performance evaluation particularly with respect to the potential detection and correction for multiple scattering effects. Author

N86-13582# Systems Research Labs., Inc., Dayton, Ohio.
APPLICATION OF ATOMIC FLUORESCENCE TO MEASUREMENT OF COMBUSTION TEMPERATURES IN SOLID PROPELLANTS Abstract Only
Larry P. Goss and Arthur A. Smith *In* AFOSR The 1985 AFOSR/AFRPL Chem. Rocket Res. Meeting Feb. 1985 3 p (For primary document see N86-13507 04-28)
Avail: NTIS HC A11/MF A01

Temperature data on the surface of a solid rocket propellant which can be related to the kinetics of the combustion process is obtained. Laser-induce-fluorescence (LIF) techniques are being used to measure the fluorescence spectrum and lifetime of an impurity introduced into the reacting material. Since spectra and lifetimes of selected impurities have shown by this research to be highly temperature sensitive over the range of interest, it should be possible to obtain a temperature profile of the reacting surface of the propellant. When two rare-earth-ion energy levels are separated by $<$ 100 cm(-1), the upper level typically will not fluoresce at low temperatures, the reason being that multi-phonon relaxation rates are extremely high with small energy gaps since fewer phonons are required for quenching. At low temperatures no population build-up occurs in the upper energy level; therefore, no fluorescence is observed. As temperature increases, population buildup in the upper level increases and fluorescence increases relative to the lower energy level. The temperature dependence of the lifetime is solely determined by the temperature dependence of the nonradiative relaxation rate. Author

N86-13583# Texas Univ. at Dallas, Richardson.
REAL-TIME, TWO-DIMENSIONAL FUEL SPRAY VISUALIZATION Abstract Only c34
Lynn A. Melton and James F. Verdieck (United Technologies Research Center, East Hartford, Conn.) *In* AFOSR The 1985 AFOSR/AFRPL Chem. Rocket Res. Meeting Feb. 1985 3 p (For primary document see N86-13507 04-28)
Avail: NTIS HC A11/MF A01

The development of specific fluorescent additives which reveal directly the desired property from the fluorescence spectrum is studied. Previous work has verified the use of such additives to provide simultaneous visualization of both liquid and vapor phases. The development of fluorescent sensors for droplet temperature measurement is described. Temperature sensor systems follow naturally from the vapor-liquid visualization studies, because both methods exploit the properties of organic exciplexes to interrogate properties of the spray. The essentials of exciplex formation and the subsequent two color fluorescence is illustrated. Because the equilibrium between the monomer and exciplex is temperature dependent, the ratio of the intensities of the emission from E^* and M^* in the liquid phase provide a measure of temperature in the droplet. Thus, laboratory measurements of liquid phase fluorescence spectra as a function of temperature can provide a calibration curve for the intensity ratio, at specific wavelengths, versus temperature. Author

N86-13584# Aerodyne Research, Inc., Billerica, Mass.
SINGLE PARTICLE SIZING BY MEASUREMENT OF BROWNIAN MOTION Abstract Only c70
Alan C. Stanton and Wai K. Cheng *In* AFOSR The 1985 AFOSR/AFRPL Chem. Rocket Res. Meeting Feb. 1985 3 p (For primary document see N86-13507 04-28)
Avail: NTIS HC A11/MF A01

A new optical technique for the measurement of submicron particles, using a laser interferometric system to measure the Brownian motion of isolated particles in a gas stream is investigated. By measurement of the motion of many such particles, the size distribution may be obtained. This technique is unique in that it requires no a priori assumption on the particle size distribution, nor knowledge of the particle optical properties. The experimental approach utilizes a laser interferometer system for measurement of a time dependent signal sensitive to particle displacement. To understand this approach, an appreciation of the characteristic aspects of the Brownian motion of an isolated particle is required. A representation of the motion of a 0.1 micrometer particle is shown. Random changes in particle velocity occur in characteristic times of 10 to the minus 14th power seconds due to collisions with gas molecules. With sufficient time resolution to measure instantaneous particle velocities, one would observe a Maxwellian velocity distribution. The characteristic time for the Maxwellian distribution to evolve is the relaxation time, which is a function of particle size and fluid properties. To understand the properties of the signal, the Brownian motion sensor was simulated using a Monte Carlo technique. Author

N86-13585# Princeton Univ., N. J. Dept. of Mechanical and Aerospace Engineering.
COMBUSTION BEHAVIOR OF FREE BORON SLURRY DROPLETS
F. Takahashi, F. L. Dryer, and F. A. Williams 1 May 1985 27 p
(Contract F49620-82-K-0011)
(AD-A158620; MAE-1702; AFOSR-85-0559TR) Avail: NTIS HC A03/MF A01 CSCL 21/2

This paper reports first observations of the combustion properties of isolated boron/JP-10 slurry droplets in high temperature, atmospheric pressure oxidizing streams under low Reynolds number conditions. Slurry droplets of initial diameter between 400 and 500 micrometers and initial solid mass fraction of 0.3 were studied using single-lens reflex and high speed cine photography under both self illuminated and backlighted conditions. Boron slurry droplets burned for short periods of time with an envelope diffusion flame structure, but then experienced violent disruption for all cases studied. The intensity of the disruption progress was found to be strongly influenced by the temperature of the envelope diffusion flame. The ignition of the boron particles emitted from the initial fuel droplet was also affected by this flame temperature. As this flame temperature was increased by increasing the environmental oxygen content, the disruption occurred at earlier times in the vapor phase burning period. Ignition of the boron particles at high flame temperatures ($>$ 2500K) was accompanied by a popping sound and a bright greenish flash of luminosity. GRA

N86-13586# Institut Franco-Allemand de Recherches, St. Louis (France).
SHORT PRESENTATION AND EVALUATION OF STUDIES ON THE PENETRATION OF JETS FROM HOLLOW SHAPED CHARGES IN COMPRESSIBLE MATERIALS [PRESENTATION SUCCINCTE ET EVALUATION DES ETUDES TRAITANT DE LA PENETRATION DES JETS DE CHARGES CREUSES DANS LES MATERIAUX COMPRESSIBLES]
C.-P. Woidneck 10 Sep. 1984 17 p refs In FRENCH
(ISL-NB-402/84) Avail: NTIS HC A02/MF A01

Experiments and model studies of jet penetration of hollow charges are summarized. A comparison with the experimental results shows the low reliability of the models. Author (ESA)

31 ENGINEERING (GENERAL)

Includes vacuum technology; control engineering; display engineering; and cryogenics.

N86-13587*# Old Dominion Univ., Norfolk, Va. Dept. of Mechanical Engineering and Mechanics.
DYNAMIC IDENTIFICATION FOR CONTROL OF LARGE SPACE STRUCTURES Final Report, period ending 1 May 1983
Samir R. Ibrahim Nov. 1985 64 p refs
(Grant NsG-1649)
(NASA-CR-176380; NAS 1.26:176380) Avail: NTIS HC A04/MF A01 CSCL 13B

This is a compilation of reports by the one author on one subject. It consists of the following five journal articles: (1) A Parametric Study of the Ibrahim Time Domain Modal Identification Algorithm; (2) Large Modal Survey Testing Using the Ibrahim Time Domain Identification Technique; (3) Computation of Normal Modes from Identified Complex Modes; (4) Dynamic Modeling of Structural from Measured Complex Modes; and (5) Time Domain Quasi-Linear Identification of Nonlinear Dynamic Systems. For individual titles, see N86-13588 through N86-13592.

N86-13588*# National Aeronautics and Space Administration. Langley Research Center, Hampton, Va.
A PARAMETRIC STUDY OF THE IBRAHIM TIME DOMAIN MODAL IDENTIFICATION ALGORITHM Final Report c64
Richard S. Pappa and Samir R. Ibrahim (Old Dominion Univ.) *In* Old Dominion Univ. Dyn. Identification for Control of Large Space Struct. Nov. 1985 p 43-72 refs Previously announced as N83-10258 (For primary document see N86-13587 04-31)
Avail: NTIS HC A04/MF A01 CSCL 13B

The accuracy of the Ibrahim time Domain (ITD) identification algorithm in extracting structural model parameters from free response functions was studied using computer simulated data for 65 positions on an isotropic, uniform thickness plate with mode shapes obtained by NASTRAN analysis. Natural frequencies were used to study identification results over ranges of modal parameter values and user selectable algorithm constants. Effects of superimposing various levels of noise onto the functions were investigated. No detrimental effects were observed when the number of computational degrees of freedom allowed in the algorithm was made many times larger than the minimum necessary for adequate identification. The use of a high number of degrees of freedom when analyzing experimental data, for the simultaneous identification of many modes in one computer run are suggested. E.A.K.

N86-13589*# National Aeronautics and Space Administration. Langley Research Center, Hampton, Va.
LARGE MODAL SURVEY TESTING USING THE IBRAHIM TIME DOMAIN IDENTIFICATION TECHNIQUE Final Report c39
Samir R. Ibrahim (Old Dominion Univ.) and Richard S. Pappa *In* Old Dominion Univ. Dyn. Identification for Control of Large Space Struct. Nov. 1985 p 459-465 refs Presented at the AIAA/ASME/ASCE/AHS 22nd Struct., Struct. Dyn. and Mater. Conf., Atlanta, 6-8-1981 Previously announced in IAA as A81-29449 (For primary document see N86-13587 04-31)
(AIAA-81-0528R) Avail: NTIS HC A04/MF A01 CSCL 13B

The ability of the ITD identification algorithm in identifying a complete set of structural modal parameters using a large number of free-response time histories simultaneously in one analysis, assuming a math model with a high number of degrees-of-freedom, has been studied. Identification results using simulated free responses of a uniform rectangular plate, with 225 measurement stations, and experimental responses from a ground vibration test of the Long Duration Exposure Facility (LDEF) Space Shuttle payload, with 142 measurement stations, are presented. As many as 300 degrees-of-freedom were allowed in analyzing these data. In general, the use of a significantly oversized math model in the identification process was found to maintain or increase identification accuracy and to identify modes of low response level that are not identified with smaller math model sizes. The concept of a Mode Shape Correlation Constant is introduced for use when more than one identification analysis of the same structure are conducted. This constant quantifies the degree of correlation between any two sets of complex mode shapes identified using different excitation conditions, different user-selectable algorithm constants, or overlapping sets of measurements. Author

N86-13590*# Old Dominion Univ., Norfolk, Va.
COMPUTATION OF NORMAL MODES FROM IDENTIFIED COMPLEX MODES Final Report c64
Samir R. Ibrahim *In its* Dyn. Identification for Control of Large Space Struct. Nov. 1985 p 446-451 refs Previously announced as N82-75431 and in IAA as A83-22143 (For primary document see N86-13587 04-31)
Avail: NTIS HC 04/MF A01 CSCL 13B

A technique is presented to compute a set of normal modes from a set of measured (damped) complex modes. The number of elements in the modal vectors, which is equal to the number of measurements, can be larger than the number of modes under consideration. It is also shown in this paper that the practice of normal mode approximation to complex modes can lead to considerably large errors when the modes are too complex. A numerical example and a simulated experiment are presented to illustrate the concepts discussed and to support the theory presented. Author

N86-13591*# Old Dominion Univ., Norfolk, Va.
DYNAMIC MODELING OF STRUCTURES FROM MEASURED COMPLEX MODES Final Report c39
Samir R. Ibrahim *In its* Dyn. Identification for Control of Large Space Struct. Nov. 1985 p 898-901 refs Previously announced in IAA as A82-30186 and A83-32988 (For primary document see N86-13587 04-31)
Avail: NTIS HC A04/MF A01 CSCL 13B

A technique is presented to use a set of identified complex modes together with an analytical mathematical model of a structure under test to compute improved mass, stiffness and damping matrices. A set of identified normal modes, computed from the measured complex modes, is used in the mass orthogonality equation to compute an improved mass matrix. This eliminates possible errors that may result from using approximated complex modes as normal modes. The improved mass matrix, the measured complex modes and the higher analytical modes are then used to compute the improved stiffness and damping matrices. The number of degrees-of-freedom of the improved model is limited to equal the number of elements in the measured modal vectors. A simulated experiment shows considerable improvements, in the system's analytical dynamic model, over the frequency range of the given measured modal information. Author

N86-13592*# Old Dominion Univ., Norfolk, Va.
TIME-DOMAIN QUASI-LINEAR IDENTIFICATION OF NONLINEAR DYNAMIC SYSTEMS Final Report c66
Samir R. Ibrahim *In its* Dyn. Identification for Control of Large Space Struct. Nov. 1985 p 35-43 refs Presented at the AIAA/ASME/ASCE/AHS 24th Struct., Struct. Dyn. and Mater. Conf., Lake Tahoe, Nev., 2-4 May 1983 Previously announced in IAA as A83-29811 and A84-36495 (For primary document see N86-13587 04-31)
(AIAA-83-0811-CP) Avail: NTIS HC A04/MF A01

A time-domain linear modal identification technique is applied to identify some highly nonlinear dynamic systems. The modal concept is used to identify such nonlinear systems with the understanding that the resulting modes are only a mathematical representation of the series solution of the nonlinear system under consideration. Naturally, these identified modal parameters are not unique, for nonlinear systems, since they are functions of the systems' amplitudes and hence referred to as quasi-linear. The

approach presented in this paper can be useful in predicting signs of nonlinearities when linearity is assumed. It can also be used to analyze and understand types of nonlinearities of nonlinear systems through successive identifications at different levels of responses.
Author

N86-13593# Grumman Aerospace Corp., Bethpage, N.Y. Corporate Research Center.
TIRE-SOIL INTERACTION MODEL FOR TURNING (STEERED) TIRES Final Report, Aug. 1984 - Mar. 1985
L. L. Karafiath Jul. 1985 34 p
(Contract DAAE07-81-C-4028)
(AD-A157737; RE-700; TACOM-TR-13107) Avail: NTIS HC A03/MF A01 CSCL 13/6

A review of the experimental information on the development of lateral forces on tires traveling at an angle to their center plane is presented and the usefulness of the consideration of the lateral forces for the development of an analytical model is evaluated. Major components of the lateral force have been identified as the forces required to balance the tractive force and the drawbar pull vectorially. These are the shear stresses developing in the contact area and the horizontal component of the normal stresses acting on the in-ground portion or the curved side walls of the tire. The tire-soil interaction model for steady state straight travel has been expanded to include the necessary algorithms for the calculation of these lateral forces. The pattern of tractive force-slip and longitudinal-lateral force relationships is in general agreement with experiments. Author (GRA)

N86-13594# Kerr (Arnold D.), Wilmington, Del.
APPLICATION OF PASTERNAK MODEL TO SOME SOIL-STRUCTURE INTERACTION PROBLEMS. VOLUME 1: SOLUTIONS FOR PLATES CONTINUOUSLY SUPPORTED ON A PASTERNAK BASE Final Report
A. D. Kerr May 1985 31 p 2 Vol.
(Contract DACW39-85-M-1533)
(AD-A157776; WES/TR/K-85-1-Vol-1) Avail: NTIS HC A03/MF A01 CSCL 13/13

This study is reported in two volumes concerning the analyses of continuously supported structures and their foundation responses. Volume I presents the research for the Pasternak Base support and utilizes it for solutions in situations arising with structures. Solutions are offered for a variety of plates subjected to the different loading conditions occurring in the design of such structures. Volume II similarly gives methods of parameter determination of foundation models for use in supported-structure analyses. Four methods for determining the parameter are discussed in detail. GRA

N86-13595# Kerr (Arnold D.), Wilmington, Del.
APPLICATION OF PASTERNAK MODEL TO SOME SOIL-STRUCTURE INTERACTION PROBLEMS. VOLUME 2: DETERMINATION OF FOUNDATION PARAMETERS AND THE CHOICE OF MODELS Final Report
A. D. Kerr May 1985 25 p 2 Vol.
(Contract DACW39-83-M-1533)
(AD-A157777; WES/TR/K-85-1-Vol-2) Avail: NTIS HC A02/MF A01 CSCL 13/13

This study is reported in two volumes concerning the analyses of continuously supported structures and their foundation responses. Volume 2 gives methods of parameter determination of foundation models for use in supported-structure analysis. Four methods for determining these parameters are discussed in detail. Though the last of these, Method 4, has gained reputable comments concerning its calculation of model parameters, the author exposes this method as conceptually invalid, contrary to its acceptance and recognition. The proper methods for determining suitable foundation models and their corresponding parameters are offered. Volume 1 documents research for the Pasternak Base model and its implementation for design of hydrotechnical structures. Solutions are offered for a variety of plates subjected to the different loading conditions common to Corps of Engineers structures. Author (GRA)

N86-13596# Department of the Navy, Washington, D. C.
A METHOD FOR MELT-COATING A SURFACE Patent Application
D. L. Miller, inventor (to Navy) Filed 1 Jul. 1985 12 p
(AD-D011866; US-Patent-Appl-SN-750218) Avail: NTIS HC A02/MF A01 CSCL 13/8

A method for coating a surface comprises providing an electrostatically charged powder, irradiating the powder with energy until the powder or the surface melts, and allowing the surface to solidify. Electrostatically charging a powder causes a charge to be placed on the surface of each particle. It is sometimes referred to as ionizing the powder. If sufficient charge is placed on the powder, the effect is to decrease the bulk density of the powder by increasing the separation between some or all the particles. It is the increased separation that improves the absorption of energy by a powder. GRA

N86-13597# Department of the Navy, Washington, D. C.
NOZZLE FOR SELF-CONTAINED CUTTING TORCHES Patent Application
P. W. Proctor and R. L. Dow, inventors (to Navy) Filed 17 Jun. 1985 16 p
(AD-D011875; US-Patent-Appl-SN-745738) Avail: NTIS HC A02/MF A01 CSCL 13/9

A self contained jet perforator torch for defining large holes in a workpiece such as a large bomb, includes a plurality of ports fluidically connecting a combustion chamber with a slot-like chamber. The ports and the slot-like chamber extend at and angle with respect to the longitudinal centerline of the torch whereby fluid exiting the torch contacts a workpiece at an angle with a normal extending from the workpiece. GRA

N86-13598# Lawrence Livermore National Lab., Calif.
EFFECTIVE MEDIUM THEORY FOR PARTIALLY SATURATED POROUS SOLIDS
J. G. Berryman and L. Thigpen Jul. 1985 16 p refs Presented at the Multiple Scattering of Waves in Random Media and Random Rough Surfaces, University Park, Pa., 29 Jul. 1985
(Contract W-7405-eng-48)
(DE85-016608; UCRL-92358; CONF-850787-1) Avail: NTIS HC A02/MF A01

In the theory of elastic composites, one may construct an effective medium theory by choosing the effective moduli so the forward scattering from isolated elastic inclusions vanishes on average. In the theory of partially saturated porous media, the analogous problem requires knowledge of the multipole scattering coefficients for elastic scattering from isolated inhomogeneities in a fluid-saturated porous medium. Using Biot's equations of poroelasticity, these coefficients for single-scattering from spherical inhomogeneities have been calculated. When these coefficients are used to construct an effective medium theory, the resulting formulas for the effective density and bulk modulus of the composite (liquid/gas) fluid recover Wood's well-known results. Equations for wave propagation through partially saturated porous media with the coefficients deterimined by the effective medium results predict wave speeds agreeing with experiment in the seismological frequency range. DOE

N86-13599# Sandia National Labs., Albuquerque, N. Mex.
DISCUSSION ON THE VIBRATION PROCESS STANDARDS 9958002 AND 9958004
F. Cericola 1985 6 p Presented at the 41st Meeting of the IMOG Subgroup on Environ. Testing, Miamisburg, Ohio, 18 Jun. 1985
(Contract DE-AC04-76DP-00789)
(DE85-017116; SAND-85-1807C; CONF-8506117-3) Avail: NTIS HC A02/MF A01

The Vibration Process Standards 9958002 and 9958004 are Sandia documents that cover the requirements of sinusoidal and random vibration testing with respect to instrumentation, calibration equipment capability and test methods. A six-month calibration procedure for random vibration digital signal analyzers has been developed, and changes are proposed to the six-month waveform distortion survey required by the standards. DOE

N86-13600# Joint Publications Research Service, Arlington, Va.
CHINA REPORT: SCIENCE AND TECHNOLOGY
24 Jun. 1985 198 p refs Transl. into ENGLISH from various Chinese articles
(JPRS-CST-85-020) Avail: NTIS HC A09/MF A01

Numerous topics related to China's science and technology efforts are discussed. Topics include plasma control in tokamak devices, high energy physics, integrated optics, the application of computers to analytical chemistry, and optically pumped gas mixture far infrared radiation lasers. For individual titles, see N86-13601 through N86-13609.

N86-13601# Joint Publications Research Service, Arlington, Va.
PRELIMINARY EXPERIMENTAL RESULTS OF CT-6B TOKAMAK HEATING FIELD VOLTAGE FEEDBACK CONTROL c75
Zheng Shaobai and Shen Zhongqing *In its* China Rept.: Sci. and Technol. (JPRS-CST-85-020) 24 Jun. 1985 p 59-64 Transl. into ENGLISH from Kexue Tongbao (Beijing), no. 12, 1984 p 728-731 (For primary document see N86-13600 04-31)
Avail: NTIS HC A09/MF A01

In order to maintain the constant stability of a tokamak plasma, it is necessary to control the displacement and electric current of the plasma. Generally, the control of displacement is accomplished by applying a vertical field with negative feedback. A similar approach is used in the CT-6B setup where preliminary results have been obtained. The control of plasma current is often accomplished using the method of multiple power sources which are connected sequentially. In recent years, the method of feedback control has been developed in ASDEX to ontrol plasma current. But the two controls are carried out independently. In the CT-6B setup, researchers experiemented with the idea of applying negative feedback control to the voltage of the heating field to control the plasma current and displacement simultaneously. The basic principle of this control technique and some preliminary experimental results are discussed. Author

N86-13602# Joint Publications Research Service, Arlington, Va.
SCHEME FOR HIGH-SPEED REAL-TIME DFT OPERATION FOR RADAR SIGNAL PROCESSING c32
Su Yanguang and Shi Xingrong *In its* China Rept.: Sci. and Technol. (JPRS-CST-85-020) 24 Jun. 1985 p 65-69 ref Transl. into ENGLISH from Dianzi Xuebao (Beijing), v. 12, no. 1, Jan. 1984 p 113-115 (For primary document see N86-13600 04-31)
Avail: NTIS HC A09/MF A01

A scheme of high-speed real-time discrete Fourier transform (DFT) operation is presented for processing radar signals. It may be used to calculate the 8, 16, or 32-point DFT. When 10 MHz clock frequency is used, the operation time per point is about 4 mu s for the complex signal input sequence of 16 bits of wordlength. Under the fixed time-domain weighting adopted, it does not require more equipment or additional operation time. The control circuit is very simple. The shorter the word length of the input sequence, the faster the operation speed. Author

N86-13603# Joint Publications Research Service, Arlington, Va.
ON H PLANE DIELECTRIC LOADING THEORY FOR H PLANE FERRITE PHASE SHIFTER c33
Wen Junding *In its* China Rept.: Sci. and Technol. (JPRS-CST-85-020) 24 Jun. 1985 p 70-75 refs Transl. into ENGLISH from Dianzi Xuebao (Beijing), v. 12, no. 1, Jan. 1984 p 116-119 (For primary document see N86-13600 04-31)
Avail: NTIS HC A09/MF A01

The theoretical and experimental results of a nonreciprocal H plane dielectric-loaded H plane ferrite phase shifter are presented, including the approximate formula of differential phase shift and the transcendental equation of differential phase shift frequency response with zero slope. The results show that this kind of dielectric-loaded technique makes it possible to increase the differential phase shift and the figure of merit, and fabricate devices with wide band and higher average power. Author

N86-13604# Joint Publications Research Service, Arlington, Va.
NATION'S ACHIEVEMENTS IN HIGH ENERGY PHYSICS REVIEWED c73
Zhang Wenyu *In its* China Rept.: Sci. and Technol. (JPRS-CST-85-020) 24 Jun. 1985 p 76-89 Transl. into ENGLISH from Gaoneng Wuli (Beijing), no. 3, Sep. 1984 p 1-6 (For primary document see N86-13600 04-31)
Avail: NTIS HC A09/MF A01

A brief survey of China's achievements in high energy physics research is given. Particle interactions; particle accelerators; proportional, Cerenkov, and scintillation counters; and cosmic rays are among the topics discussed. R.J.F.

N86-13605# Joint Publications Research Service, Arlington, Va.
INTEGRATED OPTICS DEVELOPMENTS OVER PAST DECADE, FUTURE PROSPECTS c74
Yu Rongjin *In its* China Rept.: Sci. and Technol. (JPRS-CST-85-020) 24 Jun. 1985 p 90-95 refs Transl. into ENGLISH from Zhongguo Jiguang (Shanghai), v. 12, no. 4, 20 Apr. 1985 p 193-196 (For primary document see N86-13600 04-31)
Avail: NTIS HC A09/MF A01

Some of the progress on guided-wave optics, fabrication and measurement of waveguides, devices, monolithic integration and microfabrication techniques in China over the past 10 years is surveyed. A brief comment on anticipated trends and needs in the field of integrated optics is given. Author

N86-13606# Joint Publications Research Service, Arlington, Va.
HIGH-PRESSURE, HIGH-TEMPERATURE OPPOSED ANVIL DEVICE DESCRIBED c76
He Yi, Wang Songtao, Qin Zhicheng, Wang Yaoji, and Wang Wenkui *In its* China Rept.: Sci. and Technol. (JPRS-CST-85-020) 24 Jun. 1985 p 96-99 Transl. into ENGLISH from Wuli (Beijing), v. 14, no. 1, Jan. 1985 p 38-39 (For primary document see N86-13600 04-31)
Avail: NTIS HC A09/MF A01

Static high-temperature, high-pressure technology is an important technique for researching solid state phase changes and synthesis of materials. At present, many kinds of devices are used for conducting different high-temperature, high-pressure experiments. The structure of the Bridgman type hard alloy opposed anvil is simple but it can withstand high pressure above 100kbar, and using internal heating method, the temperature can be increased to approximately 1,000 deg. The volume of the high pressure cavity is also large. For this reason, many laboratories abroad are equipped with this kind of device. To conduct research on modification of noncrystalline alloy structures, high pressures of approximately 100kbar are frequently required to obtain greater pressure effects. For this reason, researchers set up this high-temperature, high-pressure device. The design of the container, selection of the pressure device, structure of the high-pressure cavity, and pressure adjustment are described. R.J.F.

N86-13607# Joint Publications Research Service, Arlington, Va.
APPLICATION OF COMPUTERS IN ANALYTICAL CHEMISTRY: CALCULATION OF OPTIMUM ACIDITY OF REACTION BETWEEN METAL IONS AND ORGANIC REAGENTS IN SOLUTION c25
Zhang Sunwei, Pan Fuyou, Yan Jian, and Kong Fangming *In its* China Rept.: Sci. and Technol. (JPRS-CST-85-020) 24 Jun. 1985 p 100-104 refs Transl. into ENGLISH from Hangzhou Daxue Xuebao (Hangzhou), v. 12, no. 1, Jan. 1985 p 98-102 (For primary document see N86-13600 04-31)
Avail: NTIS HC A09/MF A01

The reactions between metal ions and organic reagents which form chelating compounds are widely used in analytical chemistry. The efficiency of chelation is related to the acidity of the reaction medium because of the competition of protons with metal ion and the tendency for the cations to become hydrolysed. The optimum acidity is generally determined experimentally. Adamovich and Salikhov and others have presented the theoretical possibility of calculating the optimum acidity in such reactions and reported that the optimum pH value obtained by calculation tallies well with experimental value. It is relatively easy to establish a functional equation for treatment of the question, but it is difficult to find a solution after the values of all the parameters are substituted, because high degree equations are involved in most cases. The application of a computer can solve a number of complicated problems like the aforesaid. Author

N86-13608# Joint Publications Research Service, Arlington, Va.
IMPROVED ALGORITHM FOR RADAR REAL-TIME DATA PROCESSING c32
Zhang Zhiben *In its* China Rept.: Sci. and Technol. (JPRS-CST-85-020) 24 Jun. 1985 p 105-108 Transl. into ENGLISH from Dianzi Xuebao (Beijing), v. 13, no. 1, Jan. 1985 p 127-128 (For primary document see N86-13600 04-31)
Avail: NTIS HC A09/MF A01

An improved algorithm of arctangent function which needs only two multiplication-division operations for radar real-time data processing is presented. In radar real-time data processing, more often than not, operations of arctangent functions are involved in order to provide an angle accuracy of half the magnitude of the smallest angle measurable with radar. A basic requirement in radar real-time data processing is speed, consequently, the number of operations of multiplication and division employed should be reduced to a minimum. Author

N86-13609# Joint Publications Research Service, Arlington, Va.
PULSED, OPTICALLY PUMPED GAS-MIXTURE FIR LASERS c35
Pan Chengzhi, Han Shaoping, Qin Yi, Hou Qiguo, and Liu Xiuyun *In its* China Rept.: Sci. and Technol. (JPRS-CST-85-020) 24 Jun. 1985 p 122-125 refs Transl. into ENGLISH from Dianzi Chengzhi (Beijing), v. 13, no. 1, Jan. 1985 p 117-119 (For primary document see N86-13600 04-31)
Avail: NTIS HC A09/MF A01

With D2O-CH3I, D2O-CH3F, CH3I-CH3F and D2O-CH3I-CH3F gas mixtures as the active media of far infrared radiation (FIR) lasers, individual FIR laser lines emitted from component gases can be obtained from the same laser simply by tuning the pumping lines of a TEA-CO2 laser. The gas-mixture FIR laser is considered as a new and feasible scheme for producing multiwavelength output in FIR band from the same FIR laser. The results of using gas mixtures as lasing materials are discussed. Binary and tertiary gaseous mixtures of D2O-CH3I, D2O-CH3F, Ch3I-CH3F and D2O-CH2I-CH3F were studied. Author

N86-13610# Joint Publications Research Service, Arlington, Va.
WEST EUROPE REPORT: SCIENCE AND TECHNOLOGY
28 Oct. 1985 73 p Transl. into ENGLISH from various West European articles
(JPRS-WST-85-030) Avail: NTIS HC A04/MF A01

The report is divided into sections on aerospace, biotechnology, computers, factory automation, and microelectronics. Some featured articles are: (1) Dornier develops high resolution display system; (2) Silicon on insulator research; and (3) Development of MBS process for laser, chip manufacture. For individual titles, see N86-13611 through N86-13615.

N86-13611# Joint Publications Research Service, Arlington, Va.
FRG'S DORNIER DEVELOPS HIGH-RESOLUTION DISPLAY SYSTEM c36
Hans-Peter Engelhardt *In its* West Europe Rept.: Sci. and Technol. (JPRS-WST-85-030) 28 Oct. 1985 p 17-20 Transl. into ENGLISH from Dornier Post (West Germany), no. 4, 1984 p 21-23 (For primary document see N86-13610 04-31)
Avail: NTIS HC A04/MF A01

Geographic representations, especially maps, increasingly have to be annotated with rapidly changing supplementary information, e.g., military positions. For this purpose, Dornier has developed the GEOGRID system, the main components of which are mass memory (laser disks), a high resolution display controller (HADIC) and a high resolution color raster display. This system is briefly discussed. Author

N86-13612# Joint Publications Research Service, Arlington, Va.
THOMSON, CNET OF FRANCE IN SILICON-ON-INSULATOR RESEARCH c33
J. P. DellaMussia *In its* West Europe Rept.: Sci. and Technol. (JPRS-WST-85-030) 28 Oct. 1985 p 34-36 Transl. into ENGLISH from Electron. Actualites (Paris), 8 Mar. 1985 p 1 (For primary document see N86-13610 04-31)
Avail: NTIS HC A04/MF A01

A cooperation agreement involving research on a silicon-on-insulator technology designed to make circuits with a low sensitivity to radiations was just signed. This technology should eventually replace the SOS (silicon-on-sapphire) technology still used by Thomson Semiconductors to make military and space circuits, but whose progress is hamperd by problems of cost and defects in the epitaxial layer. The implications of research in this direction are discussed. Author

N86-13613# Joint Publications Research Service, Arlington, Va.
EXCIMER LASER PRODUCES .2 MICRON SEMICONDUCTOR STRUCTURES c76
In its West Europe Rept.: Sci. and Technol. (JPRS-WST-85-030) 28 Oct. 1985 p 37 Transl. into ENGLISH from Chem. Rundschau (West Germany), 31 May 1985 p 5 (For primary document see N86-13610 04-31)
Avail: NTIS HC A04/MF A01

Semiconductor structures 0.2 micrometers in size were manufactured by using the light of an excimer laser in the contact printing method. To increase the storage capacity of a chip, microstructures must become more and more fine and with that their manufacturing methods become more and more expensive. Optical methods for producing such highly resolved structures have the advantage that the light can be basically focused on a point which is about the size of the wavelength used. Excimer lasers which emit between 193 nm and 351 nm, because of very short wavelengths and high UV output are predestined for making highly resolved structures by using photolithography. Microstructures 0.2 micrometers in size can be produced by using the light of an excimer laser. Structural fineness of 0.7 micrometer in size needed to manufacture 4M-bit memories and hyperfrequency GaAs semiconductors can be implemented with the UV light from this laser. Author

N86-13614# Joint Publications Research Service, Arlington, Va.
PHILIPS DEVELOPS MBE PROCESS FOR LASER, CHIP MANUFACTURE c33
In its West Europe Rept.: Sci. and Technol. (JPRS-CST-85-030) 28 Oct. 1985 p 38-39 Transl. into ENGLISH from Frankfurter Zeitung/Blick Durch die Wirtsch. (Frankfurt/Main), 6 Aug. 1985 p 5 (For primary document see N86-13610 04-31)
Avail: NTIS HC A04/MF A01

Molecular beam epitaxy was used in manufacturing a special laser from gallium arsenide and aluminum gallium arsenide which operates at very short wavelengths of 707 nanometers. This has made it possible to achieve high electron mobility in a two dimensional electron gas. Precisely in the semiconductor industry, it is extremely important to control dimensions, makeup and purity of the materials used to achieve the required electrical properties. Epitaxial methods allow more precise operations in which the crystal layer intended for the electronic circuit is not subsequently bombarded with impurity atoms, but in which the operative crystal layer is built up to the desired structure slowly on a substrate. Molecular beam epitaxy with which layers can be grown by positioning of atoms is used. Using this method, molecular beams of the compound elements gallium, arsenic, aluminum, phosphorus and indium strike a heated substrate and are adsorbed there in layers. The growth rate and structure of the layer depend on the beam intensities. In this process, the molecular beams can also be switched on and off by using screens. Author

N86-13615# Joint Publications Research Service, Arlington, Va.
THOMSON SEMICONDUCTORS INTRODUCES PRODUCTS, BALANCES BOOKS c33
Roger Carrasco *In its* West Europe Rept.: Sci. and Technol.

(JPRS-CST-85-030) 28 Oct. 1985 p 40-42 Transl. into ENGLISH from Minis et Micros (Paris), 23 Sep. 1985 p 25 (For primary document see N86-13610 04-31)
Avail: NTIS HC A04/MF A01

Product development at Thomson is discussed. Tono lines are featured. The VME line which consists of about 20 broads, plus software and systems. And the G64 line. Economic analysis and marketing strategy is also briefly discussed. E.R.

N86-13616# Joint Publications Research Service, Arlington, Va.
WEST EUROPE REPORT: SCIENCE AND TECHNOLOGY
8 Nov. 1985 49 p Repr. from various West European articles Transl. into ENGLISH from various West European articles
(JPRS-WST-85-031) Avail: NTIS HC A03/MF A01

The FBIS West Europe Report (Science and Technology) of 8 November 1985 includes items in the following categories: Advanced Materials, the European Automobile Industry, Biotechnology, Civil Aviation, Computers, Microelectronics, and Scientific and Industrial Policy. Of special interest in this issue are articles on the Franco-Italian ATR-42 aircraft, new CMOS gate arrays produced at Thomson Semiconductors in France, the use of organo-metallic epitaxy to produce chips, and custom chips produced by European Silicon Structures. For individual titles, see N86-13617 through N86-13621.

N86-13617# Joint Publications Research Service, Arlington, Va.
CERTIFICATION GRANTED TO FRANCO-ITALIAN ATR 42 c03
In its West Europe Rept.: Sci. and Technol. (JPRS-WST-85-031) 8 Nov. 1985 p 10-13 Repr. from Rev. Aerospatiale (France), Oct. 1985 p 10; 12 (For primary document see N86-13616 04-31)
Avail: NTIS HC A03/MF A01

The Franco-Italian (Aerospatiale/Aeritalia) ATR-42 commercial aircraft has been granted certification. The first production model was to be delivered in November 1985. The joint European venture expects to capture a generous share of the expected market (into the year 2000) of 2200 thirty-fifty and over 100 fifty-seventy passenger aircraft. F.M.R.

N86-13618# Joint Publications Research Service, Arlington, Va.
ATR 42 PRODUCTION WORK IN FRENCH, ITALIAN PLANTS DETAILED c01
In its West Europe Rept.: Sci. and Technol. (JPRS-WST-85-031) 8 Nov. 1985 p 14-19 Repr. from Rev. Aerospatiale (France), Oct. 1985 p 16; 18; 20; 22; 27 (For primary document see N86-13616 04-31)
Avail: NTIS HC A03/MF A01

The ATR-42 passenger aircraft is to be a product of real international cooperation. The Franco-Italian aircraft is to be produced and assembled at three plants in France and one in Italy, with engines supplied by Pratt and Whitney of Canada. The composite wing tips, control surfaces and fairings will be manufactured at Aerospatiale in Nantes. Assembly, integration, and testing of the wing are to be subsequently carried out at the Aerospatiale plant in Sainte Nazaire. The engine nacelles are to be produced by Aerospatiale Meaulte. Manufacturing the fuselage and tail assembly will be the responsibility of Aeritalia in Naples, and final assembly will take place at Aerospatiale's Toulouse plant. Production of the larger version, the ATR-72, will be similarly apportioned. F.M.R.

N86-13619# Joint Publications Research Service, Arlington, Va.
NEW DIGITAL CIRCUITS AT THOMSON SEMICONDUCTOR IN FRANCE c33
J. P. DellaMussia *In its* West Europe Rept.: Sci. and Technol. (JPRS-WST-85-031) 8 Nov. 1985 p 27-29 Transl. into ENGLISH from Electron. Actualites (Paris), 15 Mar. 1985 p 1; 22 (For primary document see N86-13616 04-31)
Avail: NTIS HC A03/MF A01

DCS, Thomson Semiconductors' Semi-Standard Circuits Department, has just announced a CMOS gate array with up to 4,200 gates, standard cells, and a unique 900-component, 3 GHz linear gate array. All of Thomson's gate arrays are supported by Daisy, Valid and Mentor workstations. These are the first fruits of a reorganization begun several months ago to distance the department from the actual design and manufacture of integrated circuits, making it more of an archestrator among customers, workstation manufacturers, independent designers and the various Thomson Semiconductors division. Thomson Semiconductors' silicon sales based on DCS contracts totaled 25,000,000 Frances in 1984. This figure should be double in 1985. Thomson Semiconductors plans to offer 120 new integrated circuits this year, twice the number available in 1984. At the same time, the Munich design center and the American subsidiary, VSI, should open new markets in 1985, bringing exports to an estimated 30 percent of sales. Author

N86-13620# Joint Publications Research Service, Arlington, Va.
CNET OF FRANCE USES ORGANO-METALLIC EPITAXY FOR LASER c36
In its West Europe Rept.: Sci. and Technol. (JPRS-WST-85-030) 8 Nov. 1985 p 30-31 Transl. into ENGLISH from Electron. Actualites (Paris), 22 Mar. 1985 p 26 (For primary document see N86-13616 04-31)
Avail: NTIS HC A03/MF A01

CNET's Bagneux laboratory has just determine the characteristics of the first 1.3 microns GaInAsP laser chips produced by means of organo-metallic epitaxy on InP at atmospheric pressure. The results of the first complete after test (pulsed threshold current density of 1,200 A/sq cm at room temperature for laser 100 microns wide and 500 microns long; low feature dispersion, high quantity yield) are encouraging. They seem to indicate that with appropriate structures (for example, embedded ribbon lasers), it may be possible to construct direct current lasers that function at room temperature with threshold currents of 30 to 100 mA. The results are among the best in the world (CNET's threshold current is only 40% greater than the Thomson record achieved with a reduced-pressure organo-metallic epitaxial method) and are comparable to those recently publilshed by Bell Labs (3,600 A/sq cm at 1.36 microns, the first to have determined the characteristics of lasers made using the same method. Author

N86-13621# Joint Publications Research Service, Arlington, Va.
EUROPEAN SILICON STRUCTURES PLANS CUSTOM CHIPS IN 15 DAYS c33
J. P. DellaMussia *In its* West Europe Rept.: Sci. and Technol. (JPRS-WST-85-031) 8 Nov. 1985 p 35-41 Transl. into ENGLISH from Electron. Actualites (Paris), 6 Sep. 1985 p 1; 16 (For primary document see N86-13616 04-31)
Avail: NTIS HC A03/MF A01

The European Silicon Structures group (called ES20 is about to enter into competition with the American and Japanese giants in the microelectronics field. ES2's goal is to supply or operate all the data-processing resources, in particular silicon compilers, required to design quickly full-custom circuits (exclusive of gate arrays and standard cells) from Paris, London and Munich by 1 Jan. 1986, to test the corresponding circuits in two weeks, using tooling tape, and then to produce them internally in series of up to a few ten thousand parts at competitive prices. F.M.R.

N86-13622# Joint Publications Research Service, Arlington, Va.
WEST EUROPE REPORT: SCIENCE AND TECHNOLOGY
30 Sep. 1985 74 p Transl. into ENGLISH from various West European articles
(JPRS-WST-85-029) Avail: NTIS HC A04/MF A01

Articles from western European publications on science and technology are briefly presented. Some broad areas covered are advanced materials, automobile industry, biotechnology, computers, factory automation, microelectronics, and technology transfer For individual titles, see N86-13623 through N86-13626.

N86-13623# Joint Publications Research Service, Arlington, Va.
RECENT ADVANCES IN COMPOSITE MATERIALS REVIEWED c24
Laurent Schwartz *In its* West Europe Rept.: Sci. and Technol. (JPRS-WST-85-029) 30 Sep. 1985 p 1-2 Transl. into ENGLISH

from Ind. et Tech. (Paris), 10 Apr. 1985 p 18 (For primary document see N86-13622 04-31)
Avail: NTIS HC A04/MF A01

Promises of increased productivity through the use of thermoplastic composites, continuous production, workshops with automatic monitoring are some ways the composites sector is looking for profitability, both at materials and at process level. Speakers at the European Symposium on Composites presented technical solutions likely to reduce production costs. Also included are shorter cycles with thermoplastic dies and stabilized thickening for polyester compounds. Author

N86-13624# Joint Publications Research Service, Arlington, Va.
NEW MATERIALS TO LIGHTEN VEHICLES
M. Castagna *In its* West Europe Rept.: Sci. and Technol. (JPRS-WST-85-029) 30 Sep. 1985 p 6-11 Transl. into ENGLISH from Ing. Automotoristica (Turin), Mar. 1985 p 137-141 Presented at the 1st Inform. Seminar on Subproj. Roarl Transportation, Turin, 15-16 Nov. 1984 (For primary document see N86-13622 04-31)
Avail: NTIS HC A04/MF A01

To evaluate the importance of proceeding with weight reduction work on the various components and subsystems of a vehicle, in terms of the economic balance between expected economies in fuel consumption and possible incremental production costs, a critical analysis was made of the data available in the technical literature, and criteria were identified for substitution of the materials. This study took into consideration, in addition to economic type parameters, also those parameters connected with manufacturing technologies and with design requirements provided indications as to the potential advantages and limits of weight reduction to be achieved through the use of high tensile steels, aluminum alloys, plastic materials including fiber reinforced ones, and plastic and metal laminates, with steel as well as with aluminum skins. Author

N86-13625# Joint Publications Research Service, Arlington, Va.
DIRECT INJECTION DIESEL MOTOR c37
R. Margary *In its* West Europe Rept.: Sci. and Technol. (JPRS-WST-85-029) 30 Sep. 1985 p 18-31 Transl. into ENGLISH from Ing. Automotoristica (Turin), Mar. 1985 p 197-201 Presented at the 1st Inform. Seminar on Subproj. Road Transportation, Turin, 15-16 Nov. 1984 (For primary document see N86-13622 04-31)
Avail: NTIS HC A04/MF A01

A single cylinder combustion concept for a direct injection automotive vehicle Diesel motor, yielding a substantial gain in fuel economy over the precombustion chamber solution with analogous performance ratings was studied. This was followed by the building of a definitive single cylinder prototype. An evaluation was also made of the advantages to be derived from the application of insulation techniques to the combustion chamber in the piston. Author

N86-13626# Joint Publications Research Service, Arlington, Va.
ITALIAN ROBOT MANUFACTURER ENTERS SPANISH MARKET c37
In its West Europe Rept.: Sci. and Technol. (JPRS-WST-85-029) 30 Sep. 1985 p 38-41 Transl. into ENGLISH from Rev. Robotica (Barcelona), May - Jun. 1985 p 27-30 (For primary document see N86-13622 04-31)
Avail: NTIS HC A04/MF A01

Further developments in the utilization of robotics are discussed, especially as concerned with factory automation. The new robots include applications for assembly, loading and unloading, and palletization. The importance of applications engineering is briefly discussed, as are the plans for expansion in Spain. E.R.

32 COMMUNICATIONS

Includes land and global communications; communications theory; and optical communications.

For related information see also *04 Aircraft Communications and Navigation* and *17 Spacecraft Communications, Command and Tracking.*

N86-13627*# National Aeronautics and Space Administration. Lewis Research Center, Cleveland, Ohio.
TESTING OF 30-GHz LOW NOISE RECEIVERS
Martin J. Conroy and Robert J. Kerczewski (Analex Corp.) [1985] 24 p refs Proposed for presentation at the 11th Annual Communication Satellite Systems Conference, San Diego, Calif., 16-20 Mar. 1986; sponsored by AIAA
(NASA-TM-87171; E-2809; NAS 1.15:87171) Avail: NTIS HC A02/MF A01 CSCL 20N

NASA-sponsored studies of the growth in communications traffic have indicated that the frequency spectrum allocated to fix-service satellites at the C and Ku bands will reach saturation by the early 1990's. The next higher frequency bands allocated for communications satellties are 27.5 to 30 GHz for the uplink and 17.7 to 20.2 GHz for the downlink. Current plans for developing satellite systems that use these bands include a NASA demonstration satellite (ACTS). One of the components identified as critical to the success of that mission is a 27.5 to 30 GHz satellite receiver. In response to that identification, NASA has sponsored the development of such a receiver to the proof-of-concept (POC) level. Design and fabrication of such POC model receivers was carried out under parallel contracts awarded to LNR Communications, Inc. of Hauppauge, New York and to ITT Defense Communications Division of Nutley, New Jersey. The most significant of the performance goals were a 5 db maximum noise figure, a 2.5 GHz passband, and e0 dB Rf to If gain. Following delivery of hardware from each of the contractors, an in-house test program was undertaken at NASA's Lewis Research Center in order to verify the contractor-reported performance and to provide a comparison of the two receivers under identical test conditions. The present paper reports the results of those tests. Author

N86-13628# Massachusetts Inst. of Tech., Lexington.
DISTRIBUTED SENSOR NETWORKS Semiannual Technical Summary Report, 1 Apr. - 30 Sep. 1984
R. T. Lacoss 30 Sep. 1984 32 p
(Contract F19628-85-C-0002; ARPA Order 3345; AF Proj. 5D30; AF Proj. 5T10)
(AD-A158033; ESD-TR-84-326) Avail: NTIS HC A03/MF A01 CSCL 17/2

This report describes the work performed on the DARPA Distributed Sensor Networks Program at Lincoln Laboratory during the period 1 April through 30 September 1984. GRA

N86-13629# Massachusetts Inst. of Tech., Cambridge. Lab. of Electronics.
SPEECH RECOGNITION: ACOUSTIC, PHONETIC AND LEXICAL KNOWLEDGE Annual Progress Report, 1 Jul. 1984 - 30 Jun. 1985
V. W. Zue 5 Aug. 1985 310 p
(Contract N00014-82-K-0727; ARPA Order 4585)
(AD-A158264) Avail: NTIS HC A14/MF A01 CSCL 05/7

During this reporting period we continued to make progress on the acquisition of acoustic-phonetic and lexical knowledge. We completed development of a continuous digit recognition system. The system was constructed to investigate the use of acoustic-phonetic knowledge in a speech recognition system. The significant achievements of this study include the development of a soft-failure procedure for lexical access and the discovery of a set of acoustic-phonetic features for verification. We completed a study of the constraints that lexical stress imposes on word recognition. We found that lexical stress information alone can, on the average, reduce the number of word candidates from a large dictionary by more than 80 percent. In conjunction with this study, we successfully developed a system that automatically determines the stress pattern of a word from the acoustic signal. We performed an acoustic study on the characteristics of nasal consonants and nasalized vowels. We have also developed recognition algorithms for nasal murmurs and nasalized vowels in continuous speech. We finished the preliminary development of a system that aligns a speech waveform with the corresponding phonetic transcription. GRA

N86-13630# Georgia Inst. of Tech., Atlanta.
AGILE ELECTROMAGNETICS EXPLOITING HIGH SPEED LOGIC (AEEHSL) Final Report, 1 Jul. 1982 - 30 May 1985
R. B. Efurd and J. M. Baden 1 Jul. 1985 39 p
(Contract N00014-82-K-0441)
(AD-A158380; GIT-A-3305-FTR) Avail: NTIS HC A03/MF A01 CSCL 17/9

This report summarizes the research information that resulted from the program titled Agile Electromagnetic Exploiting High Speed Logic. The key points from this research are: (1) A polarization coded radar was built which performs pulse compression using a polarization code. (2) A Doppler insensitive pulse compression technique was demonstrated. (3) One hundred megahertz digital logic was implemented using conventional construction techniques. (4) Mismatched pulse compression codes were implemented which reduce both the peak and the average range-time sidelobes. and (5) Golay code paris were implemented which yielded zero range-time sidelobes for stationary target radar returns. GRA

N86-13631# Aerospace Corp., El Segundo, Calif. Electronics Research Lab.
CASSEGRAIN REFLECTOR SIDELOBE REDUCTION STUDY
H. E. King, S. Lazar, G. G. Berry, H. B. Dyson, and W. S. Wales 15 Jul. 1985 117 p
(Contract F04701-83-C-0084)
(AD-A158625; TR-0084A(5409-73)-1; SD-TR-85-39) Avail: NTIS HC A06/MF A01 CSCL 17/9

This report presents the results of a 4-month study to reduce the sidelobe levels of a 38 GHz, 2 ft diameter Cassegrain reflector. Both partial and full circumferential shrouds were added to the main reflector. Various shielding techniques to reduce the horn and subreflector radiation characteristics were evaluated. Measured primary patterns for the various horn-subreflector combinations were used to compute the secondary reflector patterns to evaluate the sidelobe improvement. The computed patterns were compared with measured results. GRA

N86-13632# La Jolla Inst., Calif. Center for the Study of Nonlinear Dynamics.
THEORETICAL STUDIES AND DATA ANALYSIS OF WAVE PROPAGATION IN RANDOM MEDIA Semiannual Technical Report, 1 Dec. 1984 - 31 May 1985
S. M. Flatte 15 Jun. 1985 152 p
(Contract MDA903-83-C-0515; ARPA Order 4852)
(AD-A158775; LJI-R-84-329) Avail: NTIS HC A08/MF A01 CSCL 17/2

The objective of this work is to develop a general theoretical framework for calculating fluctuations of signals on waves propagated through random media (WPRM) and to apply this framework to sound through the ocean; light through the atmosphere; radio waves through the ionosphere, solar wind, or interstellar plasma; and any other similar case of waves propagating through continuous media. Comparison with real data is an important aspect of the effort. The two most common signals sent on a carrier are the phase and amplitude of a nearly monochromatic wave. If enough bandwidth is available, one can send a pulse, and one can speak of the intensity and arrival time of that pulse. The technical problem is then to explain the statistical behavior of the intensity and arrival time in terms of medium fluctuations, where the medium is described statistically, usually by a power spectrum covering a large dynamic range of scales. Papers include: Equivalence of path Integral and Moment Equations in WPRM; Intensity Correlations--Solution for the fourth moment of WPRM; Unequal-Frequency Correlations--Two frequency intensity cross spectrum; The Scintillation Theory of Eclipse Shadow Bands. GRA

N86-13633# Random Applications, Inc., Montrose, Colo.
APPLICATIONS OF DIFFERENTIAL PHASE STATISTICS TO STUDIES OF C3 AND SPREAD SPECTRUM COMMUNICATIONS Final Report
R. F. Pawula 1985 4 p
(Contract F49620-83-C-0085)
(AD-A158815; AFOSR-85-0555TR) Avail: NTIS HC A02/MF A01 CSCL 17/2

Three reports have been written under this second year of the contract and are listed in the next section as Papers No. 6, 7, and 8. Paper No. 6 addresses the classical and very complicated problem of finding the probability density function at the output of an RC filter when the input is a binary random telegraph signal whose intervals are described by a renewal process. Paper No. 7 focuses on a particular case in which the desired probability density is the solution of a rather formidable third-order differential equation with non-constant coefficients. A closed form solution is found for one special value of a system characteristics parameter, and a series solution is obtained for general values of the this parameter. Paper No. 8 is concerned with developing methods for calculating the solution to a fourth order differential equation. Although the theory of such equations is well known, a prohibitive amount of algebra is required to determine the coefficients in series solutions, and a computer method is developed in which the algebra is circumvented. The method is quite general, and in an appendix is applied to Bessel's differential equation and, quite surprisingly, a new second solution to Bessel's equation is obtained which does not appear to have been previously noticed. GRA

N86-13634# Air Force Office of Scientific Research, Bolling AFB, Washington, D.C.
SPECIALISTS MEETING ON ATOMIZATION AND NONDILUTE SPRAYS
D. M. Mann and J. M. Tishkoff 17 Jul. 1985 173 p Meeting held in Livermore, Calif., 20-21 Mar. 1985
(AD-A159006; AFOSR-85-0640TR) Avail: NTIS HC A08/MF A01 CSCL 21/4

A specialists meeting on atomization and nondilute spray behavior with 36 participants was held at Sandia National Laboratories, Livermore, California on 20-21 March 1985. Dilute sprays, nondilute sprays, atomization and measurement techniques each were discussed in two-hour topical sessions. Two subsequent discussion periods were used for general discussions and recommendations for future research. Twenty four recommendations were made. GRA

N86-13635# Naval Postgraduate School, Monterey, Calif.
CERENKOV RADIATION FROM PERIODIC BUNCHES FOR A FINITE PATH IN AIR M.S. Thesis
R. G. Bruce Jun. 1985 81 p
(AD-A159027) Avail: NTIS HC A05/MF A01 CSCL 20/7

The equation as derived by F.R. Buskirk and J.R. Neighbours for the power in the diffraction pattern of Cerenkov radiation from periodic bunches in air is experimentally tested at the Naval Postgraduate School Accelerator Laboratory (NPSAL). Previous experiments done at NPSAL are briefly reviewed. The experiment focuses on reducing RF noise and introduces a method for recording experimental data. RF noise is divided into two categories: (1) Noise received directly at the antenna; and (2) noise picked up by the cabling. Category 1 is divided into two subcategories: (a) Cerenkov radiation received by the antenna after being reflected off secondary objects; and (b) residual klystron radiation. Experimental data curves from the third harmonic are compared to theoretical patterns for various finite emission lengths and angle shifts. The data demonstrates tha noise-generated fine structure which appeared in a previous experiment at NPSAL can be eliminated with increased shielding. GRA

N86-13636# Naval Research Lab., Washington, D. C.
BABINET'S PRINCIPLE FOR AN ANISOTROPIC RESISTIVE SURFACE USING DIFFERENT APPROACHES
S. N. Samaddar 10 Sep. 1985 32 p
(AD-A159117; NRL-MR-5648) Avail: NTIS HC A03/MF A01

CSCL 20/3

Extension of Babinet's principle in electromagnetic theory to an inhomogeneous anisotropic (with non-zero off-diagonal terms) resistive sheet is made. Different methods are employed for this purpose so that a better understanding can be gained. Some basic properties of electromagnetic waves, such as odd and even symmetry, are also reviewed for clarity of presentation. GRA

N86-13637# Pacific Northwest Lab., Richland, Wash.
RADAR LOCATION EQUIPMENT DEVELOPMENT PROGRAM, PHASE 1
G. A. Sandness and K. C. Davis Jun. 1985 59 p refs
(Contract DE-AC06-76RL-01830)
(DE85-014523; PNL-5465) Avail: NTIS HC A04/MF A01

The first phase of a planned three-phase project designed to develop a radar system for monitoring waste canisters stored in a thick layer of bedded salt at the Waste Isolation Pilot Plant near Carlsbad, New Mexico is described. The canisters will be contained in holes drilled into the floor of the underground waste storage facility. The initial phase of this project was primarily a feasibility study. Its principal objective was to evaluate the potential effectiveness of the radar method in the planned canister monitoring application. Its scope included an investigation of the characteristics of radar signals backscattered from waste canisters, a test of preliminary data analysis methods, an assessment of the effects of salt and bentonite on the propagation of the radar signals, and a review of current ground-penetrating radar technology. Measurements were made to determine the signal propagation velocities in salt and bentonite (actually a bentonite/sand mixture) and to estimate the signal attenuation rate in the bentonite. A product survey and a literature search were made to identify available ground-penetrating radar systems and alternative antenna designs that may be particularly suitable for this unique application. DOE

N86-13638# Thomson-CSF, Velizy (France). Div. Tubes Electroniques.
THE DEVELOPMENT OF A SUBMILLIMETER WAVE CARCINOTRON OPERATING IN THE FREQUENCY RANGE FROM 850 TO 1000 GHz Final Report [DEVELOPPEMENT D'UN OSCILLATEUR LOCAL LEGER A CARCINOTRON FONCTIONNANT DANS LA BANDE 850-1000 GHZ]
L. Teyssier Paris ESA Dec. 1984 92 p refs In FRENCH; ENGLISH summary
(Contract ESTEC-4768/81/NL-HP)
(TDH-RT-2963-T; ESA-CR(P)-2041) Avail: NTIS HC A05/MF A01

An operating carcinotron device was assembled. It generates a minimal output power of 1 mW between 880 to 990 GHz. The maximum output power of 2.3 mW is reached at several points between 910 and 940 GHz. A mix-matrix tungsten-osmium cathode of 0.5 mm diameter was used. The high voltage range is between 4.9 kV and 8.8 kV, and the total power consumption is 192 W. Total weight 8.2 kg. The cooling is obtained by a 1.5 l/min water flow. For such a frequency range, the limiting factors of the output are the geometrical regularity and the quality of the slow wave structure manufacturing. Author (ESA)

N86-13639# National Telecommunications and Information Administration, Boulder, Colo. Inst. for Telecommunication Sciences.
ATMOSPHERIC RADIO NOISE: WORLDWIDE LEVELS AND OTHER CHARACTERISTICS
A. D. Spaulding and J. S. Washburn Apr. 1985 192 p
(PB85-212942; NTIA-85-173) Avail: NTIS HC A09/MF A01 CSCL 20N

There is a need for an overall, comprehensive usable noise model for application to telecommunication problems. One needed task that was accomplished toward the goal of obtaining such an overall model is the development of an improved atmospheric model The existing worldwide atmospheric noise model was developed from approximately 4 years of measurements from a worldwide network of 16 measurement stations. This network made measurements for 5 years (longer in a few cases) past the completion of CCIR Report 322 in 1963. Also, additional data are now available from other locations, primarily many years of data from 10 Soviet measurement stations. All these additional data was analyzed and an updated worldwide atmospheric noise model has been prepared in both graphical and numerical forms. Results of this analysis show substantial 'corrections; (on the order of 20 dB for some locations) to the 1MHz noise level values given by CCIR Report 322. This new model for atmospheric noise levels and other characteristics is presented and discussed. Author (GRA)

N86-13640# Joint Publications Research Service, Arlington, Va.
WORLDWIDE REPORT: TELECOMMUNICATIONS POLICY, RESEARCH, AND DEVELOPMENT
25 Oct. 1985 50 p refs Transl. into ENGLISH from various worldwide articles
(JPRS-TTP-85-026) Avail: NTIS HC A03/MF A01

A general overview of a variety of policies and research and development efforts by various countries is presented. Most of the contents pertain to policy decisions of a general nature. For individual titles, see N86-13641 through N86-13641.

N86-13641# Joint Publications Research Service, Arlington, Va.
OPTIMAL TRANSFER FUNCTION FOR FIBER OPTIC COMMUNICATIONS
Zhou Shunqin *In its* Worldwide Rept.: Telecommun. Policy, Res. and Develop. (JPRS-TTP-85-026) 25 Oct. 1985 p 4-24 refs Transl. into ENGLISH from Dianzi Xuebao (Beijing), v. 13, no. 2, Mar. 1985 p 11-12 (For primary document see N86-13640 04-32)
Avail: NTIS HC A03/MF A01

An approximation and realization method for an optimal transfer function for a full response digital optic fiber communications receiver is presented. It provides circuit types that approximate realization of an optimal transfer function for an optical receiver in an optic fiber communications system of low and high dispersion. A variable equalization circuit that allows an optical receiver to approximate an optimal transfer function for fiber optic lines of different bandwidth was constructed. A design example of a 1.3 micrometer, 34 Mb/s optical receiver designed with this method and the results of actual tests is presented. This receiver has already been put into operation with good results in an experimental optic fiber communications system with relays at 26.4 km and in the 13.6 km functional 34 Mb/s optic cable communications section built by the Wuhan Municipal Department of Telecommunications. Author

N86-13602# Joint Publications Research Service, Arlington, Va.
SCHEME FOR HIGH-SPEED REAL-TIME DFT OPERATION FOR RADAR SIGNAL PROCESSING
Su Yanguang and Shi Xingrong *In its* China Rept.: Sci. and Technol. (JPRS-CST-85-020) 24 Jun. 1985 p 65-69 ref Transl. into ENGLISH from Dianzi Xuebao (Beijing), v. 12, no. 1, Jan. 1984 p 113-115 (For primary document see N86-13600 04-31)
Avail: NTIS HC A09/MF A01

N86-13608# Joint Publications Research Service, Arlington, Va.
IMPROVED ALGORITHM FOR RADAR REAL-TIME DATA PROCESSING
Zhang Zhiben *In its* China Rept.: Sci. and Technol. (JPRS-CST-85-020) 24 Jun. 1985 p 105-108 Transl. into ENGLISH from Dianzi Xuebao (Beijing), v. 13, no. 1, Jan. 1985 p 127-128 (For primary document see N86-13600 04-31)
Avail: NTIS HC A09/MF A01

N86-13790# Joint Publications Research Service, Arlington, Va.
OBSERVATION OF OPTICAL-RADIO FREQUENCY RESONANCE IN H2O USING WIDE-BAND RUBY LASER SPECTROSCOPY Abstract Only
V. P. Kochanov, V. P. Lopasov, and S. F. Lukyanenko *In its* USSR Rept.: Earth Sci. (JPRS-UES-85-009) 13 Nov. 1985 p 37 Transl. into ENGLISH from Izv. Akad. Nauk SSSR: Ser. Fiz. (Moscow), v. 49, no. 3, Mar. 1985 p 516-520 Original language document was announced in IAA as A85-31864 (For primary

document see N86-13765 04-42)
Avail: NTIS HC A04/MF A01

N86-14105*# East Texas State Univ., Commerce. Dept. of Computer Science.
SIGNAL PROCESSING OF ANTHROPOMETRIC DATA Final Report
Wayne J. Zimmermann *In* NASA. Johnson (Lyndon B.) Space Center The 1983 NASA/ASEE Summer Faculty Fellowship Research Program Research Reports Sep. 1983 9 p refs (For primary document see N86-14078 04-85)
Avail: NTIS HC A18/MF A01 CSCL 17B

33 ELECTRONICS AND ELECTRICAL ENGINEERING

Includes test equipment and maintainability; components, e.g., tunnel diodes and transistors; microminiaturization; and integrated circuitry.

For related information see also *60 Computer Operations and Hardware* and *76 Solid-State Physics.*

N86-13642 Massachusetts Univ., Amherst.
NUMERICAL MODELING OF CARRIER TRANSPORT IN SUBMICRON BIPOLAR TRANSISTORS Ph.D. Thesis
Phung Thien Nguyen 1985 110 p
Avail: Univ. Microfilms Order No. DA8509583

The transport of electrons in submicron bipolar junction transistor (BJT) structures was investigated using the Monte Carlo (MC) method coupled with the conventional drift diffusion equations (DDE). The nonstatic velocity overshoot in the base region of different BJT structures was studied. Specification of the boundary conditions for the MC regional calculations is described. The transit time through the base and collector spacecharge regions is computed using alternately the DDE and MC techniques. The DDE and MC results were compared to demonstrate the effect of velocity overshoot. The switching behavior to different BJT designs was analyzed to illustrate factors that control the switching speed in BJT's. The effects of electron-electron (e-e) scattering in a single particle MC approach and the effects of e-e scattering on the average electron velocity and the velocity distribution are studied. Dissert. Abstr.

N86-13643*# National Aeronautics and Space Administration. Lewis Research Center, Cleveland, Ohio.
VERIFICATION OF COMPUTER-AIDED DESIGNS OF TRAVELING-WAVE TUBES UTILIZING NOVEL DYNAMIC REFOCUSERS AND GRAPHITE ELECTRODES FOR THE MULTISTAGE DEPRESSED COLLECTOR
Peter Ramins, Henry G. Kosmahl, Dale A. Force, Raymond W. Palmer, and James A. Dayton, Jr. Oct. 1985 26 p refs
(NASA-TP-2524; E-2566; NAS 1.60:2524) Avail: NTIS HC A03/MF A01 CSCL 09A

A computational procedure for the design of TWT-refocuser-MDC systems was used to design a short dynamic refocusing system and highly efficient four-stage depressed collector for a 200-W, 8- to 18-GHz TWT. The computations were carried out with advanced, multidimensional computer programs which model the electron beam as a series of disks of charge and follow their trajectories from the RF input of the TWT, through the slow-wave structure and refocusing section, to their points of impact in the depressed collector. Secondary emission losses in the MDC were treated semi-quantitatively by injecting a representative beam of secondary electrons into the MDC analysis at the point of impact of each primary beam. A comparison of computed and measured TWT and MDC performance showed very good agreement. The electrodes of the MDC were fabricated from a particular form of isotropic graphite that was selected for its low secondary electron yield, ease of machinability, and vacuum properties. This MDC was tested (at CW) for more than 1000 hr with negligible degradation in TWT and MDC performances. Author

N86-13644*# National Aeronautics and Space Administration. Langley Research Center, Hampton, Va.
LINEARITY OPTIMIZATION IN A CLASS OF ANALOG PHASE MODULATORS
Chase P. Hearn Nov. 1985 24 p refs
(NASA-TM-86420; L-15982; NAS 1.15:86420) Avail: NTIS HC A02/MF A01 CSCL 04A

This paper examines the ultimate modulating linearity attainable with a phase modulation technique based on the linear addition of quadrature phase carrier signals which have been multiplied by precisely defined nonlinear transformations of the modulating signal. Optimum gain coefficients are derived and plotted to permit implementation of analog phase modulators capable of exceptionally good linearity of phase deviations as large as 5 radians. Author

N86-13645*# National Aeronautics and Space Administration. Lewis Research Center, Cleveland, Ohio.
POTENTIAL FOR USE OF INDIUM PHOSPHIDE SOLAR CELLS IN THE SPACE RADIATION ENVIRONMENT
I. Weinberg, C. K. Swartz, and R. E. Hart, Jr. 1985 9 p refs Presented at the 18th Photovoltaic Specialists Conference, Las Vegas, Nev., 21-25 Oct. 1985; sponsored by IEEE
(NASA-TM-87157; E-2785; NAS 1.15:87157) Avail: NTIS HC A02/MF A01 CSCL 09C

Indium phosphide solar cells were observed to have significantly higher radiation resistance than either GaAs or Si after exposure to 10 MeV proton irradiation data and previous 1 MeV electron data together with projected efficiencies for InP, it was found that these latter cells produced more output power than either GaAs or Si after specified fluences of 10 MeV protons and 1 MeV electrons. Estimates of expected performance in a proton dominated space orbit yielded much less degradation for InP when compared to the remaining two cell types. It was concluded that, with additional development to increase efficiency, InP solar cells would perform significantly better than either GaAs or Si in the space radiation environment. Author

N86-13646# Department of the Air Force, Washington, D.C.
PHASE LOCK ACQUISITION SYSTEM Patent Application
S. P. Caldwell, inventor (to Air Force) Filed 6 Jun. 1984 19 p
(AD-D011804; US-Patent-Appl-SN-617668) Avail: NTIS HC A02/MF A01 CSCL 09/5

The acquisition of phase lock to a reference frequency by a signal acquisition system is accomplished using a voltage controlled oscillator, a wideband frequency discriminator, a prepositioning circuit, and a phase lock loop. The voltage controlled oscillator is prepositioned within a loop bandwidth of the reference frequency by the preposition circuit and the wide band frequency discriminator which provide coarse turning. The voltage controlled oscillator achieves phase lock with the reference frequency when it receives the fine tune signal from the phase lock loop. Using total the discriminator and the phase look loop allows fast acquisition without the need to calibrater the voltage controlled oscillator. Since the discriminator pull-in range is much larger than the phase-lock loop bandwidth, the number of bits can be much smaller than in an acquisition circuit using a digital prepositioning circuit alone. GRA

N86-13647# Department of the Army, Washington, D. C.
CATHODE INCLUDING A NON FLUORINATED LINEAR CHAIN POLYMER AS THE BINDER, METHOD OF MAKING THE CATHODE, AND LITHIUM ELECTROCHEMICAL CELL CONTAINING THE CATHODE Patent Application
E. J. Plichta and M. Salomon, inventors (to Army) Filed 27 Jun. 1985 11 p
(AD-D011807; US-Patent-Appl-SN-749597) Avail: NTIS HC A02/MF A01 CSCL 10/3

Existing technology for the fabrication of cathodes for use in lithium primary and secondary cells utilizes Teflon as the binding material. Teflon or polytetrafluoroethylene is expensive though inert, and its use results in cathode structures of poor mechanical stability. These problems do not easily lend themselves to the large scale production of cathodes in manufacturing. This patent application pertains to a cathode suitable for use in a lithium electrochemical cell. It is made from a mixture of active cathode material, carbon, and non fluorinated linear chain polymer by a method including the steps of: (1) dissolving the non fluorinated linear chain polymer in a non polar solvent at a temperature near the melting point of the polymer; (2) adding the active cathode material and carbon and evaporating the solvent; and (3) grinding the dried mixture into a fine powder and making it into a cathode by pressing the powdered mixture onto both sides of an expanded metal screen and then cutting to the desired dimensions. The cathode can be combined with lithium as the anode and a solution of 0.8 mol 3/dm LiAlCl4 in a mixed organic solvent of 24 mass percent 4-butyrolactone in 1, 2 dimethoxyethane as the electrolyte to provide a mechnically stable, relatively inexpensive lithium electrochemical cell having good cell performance. GRA

N86-13648# Technische Hogeschool, Eindhoven (Netherlands). Dept. of Electrical Engineering.
TRANSIENT SIMULATION OF SUBMICRON DEVICES Interim Report
Th. G. VandeRoer and S. C. Van Someren Greve 2 Jul. 1985 6 p
(Contract DAJA45-84-C-0054)
(AD-A157748; R/D-4663-EE-01; IR-2) Avail: NTIS HC A02/MF A01 CSCL 09/1

Previously the Legendre-Hermite polynomial expansion of Boltzmann's equation (1) has been used to calculate the velocity-field characteristic of InP at room temperature (2). In this report application of the method to a millimetre wave InP Gunn diode is described. Author (GRA)

N86-13649# Air Force Inst. of Tech., Wright-Patterson AFB, Ohio.
USING SOFTWARE TECHNOLOGY TO SPECIFY ABSTRACT INTERFACES IN VLSI DESIGN Ph.D. Thesis
R. R. Gross 1985 156 p
(AD-A158034; AFIT/CI/NR-85-92D) Avail: NTIS HC A08/MF A01 CSCL 09/5

Good techniques for VLSI design change management do not now exist. A principal reason is the absence of effective methods for the specifications of abstract interfaces for VLSI designs. This dissertation presents a new approach to such specification, an approach that extends to the VLSI domain D.L. Parnas's techniques for precise specification of abstract software design interfaces to the VLSI domain. The proposed approach provides important new features, including scalability to VLSI design levels, integration into the design life-cycle, and a uniform treatment of functional, electrical, and geometric design information. A technique is also introduced for attaching a value to the degree of specification adherence of a candidate module. To illustrate and evaluate the proposed approach, an example specification method using it is described and evaluated experimentally. Author (GRA)

N86-13650# Mississippi State Univ., Mississippi State. Dept. of Electrical Engineering.
BULK CMOS VLSI TECHNOLOGY STUDIES. PART 4: DESIGN OF A CMOS MICROSEQUENCER Final Report, Aug. 1982 - Feb. 1985
J. D. Trotter and G. S. Prasad 17 Jun. 1985 216 p
(Contract DAAG29-82-K-0167)
(AD-A158369; ARO-19839.1-EL-A-Pt-4) Avail: NTIS HC A10/MF A01 CSCL 09/5

This thesis discusses the design of a CMOS microsequencer used in a microprogrammed control organization. A preconceived data path performs most of the data manipulation functions for an LSI computer system. The operations are performed as directed by sequences of control microinstructions, which are fetched from a microcode memory using addresses generated by the microsequencer chip. A Programmable Logic Array (PLA) is selected in lieu of random logic to control the circuits within the microsequencer. Extensive use has been made of clocked CMOS over classic CMOS to achieve higher layout density and better performance. The chip has been designed using scalable design rules which means it can be fabricated in 1.2 micron or 3 micron technology. The design used double-layer metal, eliminating the need for extensive poly-interconnect lines. Author (GRA)

N86-13651# Mississippi State Univ., Mississippi State. Dept. of Electrical Engineering.
BULK CMOS VLSI TECHNOLOGY STUDIES. PART 5: THE DESIGN AND IMPLEMENTATION OF A HIGH SPEED INTEGRATED CIRCUIT FUNCTIONAL TESTER Final Report, Aug. 1982 - Feb. 1985
J. D. Trotter and H. D. Robbins 17 Jun. 1985 185 p
(Contract DAAG29-82-K-0167)
(AD-A158370; ARO-19839.1-EL-A-Pt-5) Avail: NTIS HC A09/MF A01 CSCL 14/2

This thesis project discusses the design and implementation of a functional tester to be used in a university laboratory facility for integrated circuit development. The following tester capabilities were desired: (1) 100KHz - 10 MHz Test Frequency, (2) 2K x 64Bit Test Vector Size, (3) Four User Programmable Clocks, (4) Test Vector Input using High-Level Language, and (5) Test Data Manipulation Using a High-Level Language. The functional tester receives test vector data from a Hewlett Packard HP9920A computer and loads this data into functional tester buffer memory. After the data is down-loaded, including certain operational information such as a test clock frequency, programmable clock waveform information, data direction control, etc., the tester initiates the test using random-logic control circuitry to achieve the desired high speeds. The random-logic control circuitry indicates the completion of the test, at which time the resultant data, stored in buffer memory, is up-loaded to the HP9920A for processing. This design approach to a functional tester for laboratory use differs from and improves upon previous methods, in that random-logic control circuitry is used during the test phase to provide greater operating speeds than systems which use microprocessor-control for the complete test. GRA

N86-13652# California Univ., Berkeley. Electronics Research Lab.
JOINT SERVICES ELECTRONICS PROGRAM Annual Report, 1 May 1984 - 28 Feb. 1985
W. G. Oldham 30 Apr. 1985 11 p
(Contract F49620-84-C-0057)
(AD-A158731; UCB/ERL-85-1; AFOSR-85-0669TR) Avail: NTIS HC A02/MF A01 CSCL 09/5

An annual report of the JSEP (Joint Services Electronics Program) in Electromagnetics, Solid State Electronics, Materials and Devices, Quantum Electronics and Information Sciences is presented. In addition, results of the research to date are summarized and significant accomplishments are indicated. GRA

N86-13653# Naval Postgraduate School, Monterey, Calif.
MeV ELECTRON BEAM IRRADIATION EFFECTS ON GaAs (1-x) P (x) LEDS (LIGHT EMITTING DIODES) M.S. Thesis
J. K. Foley Jun. 1985 98 p
(AD-A158832) Avail: NTIS HC A05/MF A01 CSCL 09/1

LEDs of the ternary alloy GaAs(.7)P(.3), were irradiated with a 30 MeV electron beam. The effects this exposure had on peak wavelength, absolute and relative light output intensities, and current-forward bias characteristics were studied. A simple model of LED current controlling mechanisms is described and a mathematical approach for deriving a descriptive damage-constant is provided. Observed irradiation effects consisted of increased current and decreased light output intensity for a given forward bias voltage and indicate that the devices tested are an order of magnitude softer to electron radiation than results previously reported. Damage constants were calculated: group 9 (290 to the -14h power sq cm/e), group A5 (260 to the -14th power sq cm/e), and group 3 (140 to the -14th power sq cm/e). Shielded and un-shielded devices were compared to determine if the secondary electron production for Bremsstrahlung losses would reduce the total fluence required for degradation. The results of this experiment were inconclusive. A procedure was developed to determine the electron beam current density for use in dose estimations. Electron doses were a factor of three higher when compared to the previous method of calculation. GRA

N86-13654# Stanford Univ., Calif. Lab. of Physics.
JOINT SERVICES ELECTRONICS PROGRAM Annual Progress Report, 1 Apr. 1984 - 31 Mar. 1985
S. E. Harris, D. M. Bloom, R. L. Byer, G. S. Kino, and C. F. Quate 15 Jul. 1985 62 p
(Contract N00014-84-K-0327)
(AD-A158840; GL-3891; APR-1) Avail: NTIS HC A04/MF A01 CSCL 09/5

This report is the Annual Progress Report for Joint Services Electronics Program Contract N00014-84-K-0327 for the Faculty of the Edward L. Ginzton Laboratory of Stanford University (S.E. Harris, Director). The report includes contributions on four units: (1) (Unit 85-1: Processor D.M. Bloom) Picosecond Optical Measurements; (2) Unit 85-2: Processor R.L. Byer) Optical and Nonlinear Optical Studies of Single Crystal Fibers; (3) (Unit 85-3: Professor G.S. Kino) Very High Frequency Signal Processing Techniques; (4) Unit 85-4: Professor C.F. Quate) Metal-Vacuum-Metal Tunneling or scanned Tunneling Microscopy. Author (GRA)

N86-13655# Wisconsin Univ., Madison. Dept. of Chemistry.
LUMINESCENT PROPERTIES OF SEMICONDUCTOR ELECTRODES
A. B. Ellis 15 Aug. 1985 134 p
(Contract N00014-78-C-0633)
(AD-A158841; UWIS/DC/TR-85/2) Avail: NTIS HC A07/MF A01 CSCL 09/1

The literature regarding photoluminescence and electroluminescence from semiconductor electrodes is reviewed. GRA

N86-13656# Battelle Pacific Northwest Labs., Richland, Wash.
ELECTRICAL AND THERMAL TRANSPORT PROPERTY STUDIES OF HIGH-TEMPERATURE THERMOELECTRIC MATERIALS Interim Technical Report, 15 May 1984 - 15 May 1985
J. L. Bates, C. W. Griffin, W. J. Weber, and L. C. Olsen Jun. 1985 73 p
(Contract F49620-83-C-0109)
(AD-A158883; AFOSR-85-0723TR) Avail: NTIS HC A04/MF A01 CSCL 20/12

The research effort during this reporting period has continued to emphasize the study of electronically conducting oxides, which was initiated in the previous reporting period. The high-temperature transport property data base has been expanded by continued measurements in several systems under study, and a theoretical model for thermoelectric properties based on a small polaron transport has been developed. The study of the transport properties of the In2O3-SnO2 system, which was initiated during the previous reporting period, has been completed. Low values for the figure of merit were obtained, as expected, for these degenerate-type semiconductors. Some high-temperature materials that exhibit high figures of merit were seen. The theoretical model developed under this program predicts that narrow-band semiconductors with small polaron hopping along inequivalent sites of distorted sublattices can result in increases in both electrical conductivity and Seebeck coefficient with temperature without significant increases in thermal conductivity. High figures of merit, greater than 1.0 at 1000 K, that increases with temperature are predicted by the model. The model is being applied to the divalent metal-doped (Y, La)CrO3 systems with the ABO3 perovskite structure. Transport property data obtained during this reporting period for different divalent metal dopants at different concentrations are being used to evaluate the model. GRA

N86-13657# California Univ., Berkeley. Lawrence Radiation Lab. Electronics Research Lab.
DEVELOPMENT OF HIGH SENSITIVITY X-RAY AND ELECTRON BEAM RESIST PROCESSES Final Technical Report, 15 Dec. 1979 - 29 Jan. 1985
D. W. Hess May 1985 27 p
(Grant AF-AFOSR-80-0078)
(AD-A158968; AFOSR-85-0738TR) Avail: NTIS HC A03/MF A01 CSCL 09/5

The lithographic performance of a polymer resist material is determined by several processes. First, uniform and controllable films of the resist must be reproducibly applied to the surface of substrates. Second, the radiation/polymer interaction is important since it affects the sensitivity of the resist. Third, the development or dissolution process is crucial because this step determines the ability to create useable patterns in the resist film. Finally, for Very Large Scale Integration (VLSI), dry etching processes are replacing liquid techniques; thus, the interaction of resists with glow discharges can often determine the utility of specific materials. Under AFOSR Grant 80-0078, various aspects of the above criteria were studied in order to gain fundamental understanding of these important process steps. GRA

N86-13658# Department of the Navy, Washington, D. C.
GAS RECIRCULATOR FOR ACYCLIC MACHINES Patent Application
T. F. Balsa, inventor (to Navy) Filed 28 May 1985 9 p
(AD-D011873; US-Patent-Appl-SN-737753) Avail: NTIS HC A02/MF A01 CSCL 10/2

The present invention relates to acyclic machines of the type using liquid metal collectors, and more particularly to an improvement for retaining the liquid metal in such machines. Radial type acyclic motors and generators generally include a metallic disk rotor rotating on a shaft between electromagnetic stator poles excited by field coils wound concentric with the shaft. Instead of solid brush, current collectors at the rotor periphery, liquid metal collectors are sometimes used to close the electrical current loop between the shaft and the rotor, and an inert pressurized cover gas fills the gaps between the rotating components and the stationary housing. A cover has recirculator in an acyclic generator having liquid metal collectors for reducing entrainment of the liquid metal in the gas. Radial passages in the stator housing provide natural recirculating paths for the cover gas to flow radially outward along the sides of the rotor and return inwardly through the passages. Scoops or lips located inward of the liquid metal collector divert the outward gas flow into the passages to minimize contact of the gas with the liquid metal. GRA

N86-13659# Department of the Navy, Washington, D. C.
ATOMICALLY MIXED ALLOY COATED CATHODES SPECIFICATION Patent Application
G. A. Haas, A. Shih, and C. R. K. Marrian, inventors (to Navy) Filed 4 Apr. 1985 20 p
(AD-D011877; US-Patent-Appl-SN-719403) Avail: NTIS HC A02/MF A01 CSCL 09/1

The present invention pertains generally to cathodes used in thermionic electron tubes, often used in ultra high frequency and microwave radio transmitters. It is an object of this invention to produce thermionic tube cathodes which consistntly exhibit current densities higher than heretofore achieved. Another object of the present invention is to manufacture cathodes using a method that consistently results in cathodes with a large, defined, level of current density. Another object of the present invention is to produce cathodes with reduced surface work functions by means of atomic scale mixing of two selected metals in a cathode surface coating. A tungsten or tungsten-based matrix cathode impregnated with BaO is simultaneously coated with vapors of two metallic elements, in particular, tungsten and iridium, such that a binary alloy forms on the surface. A layer of BaO then spontaneously dispenses onto the surface of the binary alloy. One of the metallic elements associates with the oxygen of BaO and other with the barium. The molecular dipole of BaO thus becomes more pronounced, and the surface work function results in a greater rate of electron emission from the cathode. GRA

N86-13660# Department of the Army, Washington, D. C.
ANALOG-TO-DIGITAL CONVERTER Patent Application
C. E. Konig and W. J. Skudera, Jr., inventors (to Army) Filed 16 Aug. 1985 21 p
(AD-D011878; US-Patent-Appl-SN-766371) Avail: NTIS

HC A02/MF A01 CSCL 09/5

An apparatus is disclosed which permits a high speed waveform, for example in the form of a series of analog data pulses, to be sampled and converted into a series of digital values. Each analog data pulse is applied in parallel to a multiplicity of A/D converters and to one or more level detectors. Each level detector provides a strobe when the voltage of the analog data pulse crosses a reference threshold. The strobes are applied to delay means whose outputs are a multiplying of delayed strobe pulses which have been delayed by predetermined amounts. Each of the multiplicity of A/D converters samples the analog data pulse in response to the particular delayed strobe applied thereto and provides a digital value of that sample. The largest of the digital values from each of the A/D converters is provided as the output of the apparatus for each analog data pulse. GRA

N86-13661# Department of the Army, Washington, D. C.
SLOT LINE TUNABLE BANDPASS FILTER Patent Application
E. A. Mariani and R. A. Stern, inventors (to Army) Filed 7 Aug. 1985 36 p
(AD-D011881; US-Patent-Appl-SN-763161) Avail: NTIS HC A03/MF A01 CSCL 09/5

A tunable bandpass filter comprising a pair of slot line resonant cavities formed in a metallic film covering the planar surface of a ferrite substrate is studied. A magnetic biasing field of variable magnitude is generated and applied through the ferrite substrate transversely across the slot line resonant cavities. The magnetic field operates to change the electrical length of the resonant cavities due to the fact that the magnetic permeability of the ferrite material changes with the applied field. Author (GRA)

N86-13662# Department of the Army, Washington, D. C.
CATHODE FOR USE IN HIGH ENERGY PRIMARY THIONYL CHLORIDE CELL SYSTEMS AND HIGH ENERGY PRIMARY THIONYL CHLORIDE CELL SYSTEMS INCLUDING THE CATHODE Patent Application
C. W. Walker, Jr., W. L. Wade, Jr., M. Binder, and S. Gilman, inventors (to Army) Filed 22 Aug. 1985 9 p
(AD-D011882; US-Patent-Appl-SN-768271) Avail: NTIS HC A02/MF A01 CSCL 09/1

A cathode is provided for use in high energy primary lithium-thionyl chloride cell systems or calcium-thionyl chloride cell systems. The cathode comprises an expanded metallic current collector screen into which has been pasted a mixture of a low surface area conductive carbon black and a high surface area conductive carbon black previously mixed with a binder. GRA

N86-13663# Los Alamos National Lab., N. Mex.
A 10-MHz HIGH-VOLTAGE MODULATOR WITH PULSE-WIDTH AND REPETITION-RATE AGILITY
G. J. Krausse 1985 7 p Presented at the 5th IEEE Pulsed Power Conf., Washington, D.C., 10 Jun. 1985
(Contract W-7405-eng-36)
(DE85-014117; LA-UR-85-2057; CONF-850616-58) Avail: NTIS HC A02/MF A01

Requirements for control and rapid switching of the proton beam at the Los Alamos Meson Physics Facility (LAMPF) are continually revised to support accelerator upgrades and modifications. A recent upgrade required the development of a 10-MHz high-voltage modulator for an electrostatic kicker with real-time control of pulse width and repetition rate over a range of four decades. The modulator must be capable of producing a voltage pulse across a capacitive load with a rise time of less than or equal to 20 ns (10% to 90%). In addition the falling edge undershoot must be controlled to less than one part in 10(3). The paper describes in detail the circuit design philosophy, layout, and critical areas in system design. DOE

N86-13664# Oak Ridge National Lab., Tenn.
COMPARISON OF ION MILLING TECHNIQUES FOR CROSS-SECTIONAL TEM OF SEMICONDUCTORS
J. T. Luck, C. W. Boggs, and S. J. Pennycook Mar. 1985 3 p Presented at the Joint Meeting of the Electron Microscopy Soc. of Am. and the Microbeam Anal. Soc., Louisville, Ky., 5 Aug. 1985
(Contract DE-AC05-84OR-21400)
(DE85-016596; CONF-850840-16) Avail: NTIS HC A02/MF A01

The use of cross-sectional Transmission Electron Microscopy (TEM) has become invaluable for the characterization of the near-surface regions of semiconductors following ion-implantation and/or transient thermal processing. A fast and reliable technique is required which produces a large thin region while preserving with the original sample surface. New analytical techniques, particularly the direct imaging of dopant distributions, also require good thickness uniformity. Two methods of ion milling are commonly used, and are compared. The older method involves milling with a single gun from each side in turn, whereas a newer method uses two guns to mill from both sides simultaneously. DOE

N86-13665# Argonne National Lab., Ill.
MICROCOMPUTER CONTROLLED CURRENT SHARING EXPERIMENTS WITH PARALLEL CONVERTERS
R. L. Kustom and J. J. Skiles 1985 5 p Presented at the IEEE-Ind. Appl. Soc. Ann. Meeting, Toronto, 6 Oct. 1985 Prepared in cooperation with Wisconsin Univ., Madison
(Contract W-31-109-eng-38)
(DE85-013854; ANL-HEP-CP-85-61; CONF-851071-2) Avail: NTIS HC A02/MF A01

Power conditioning circuits for a Superconductive Magnetic Energy Storage (SMES) coil will require many parallel SCR devices because the operating current is planned to be as high as a few hundred thousand amperes. In order to maintain current balance in the parallel units, a microcomputer controlled system that adjusts the delay angle of individual units is envisioned. Studies and tests on an 8-H model with two parallel 9 kVA bridge circuits are described. DOE

N86-13666# Oak Ridge National Lab., Tenn.
ELECTRICAL SLIDING JOINT LITERATURE REVIEW (VIEWGRAPH PRESENTATION)
G. E. Gorker and S. S. Kalsi 14 Mar. 1985 12 p Presented at the Workshop on High Current Elec. Joints for Tokamaks, Princeton, N.J., 14 Mar. 1985
(Contract DE-AC05-87OR-21400)
(DE85-011571; CONF-8503144-1) Avail: NTIS HC A02/MF A01

This survey covers the following sliding joint options: (1) multilam joints, (2) finger joints, (3) wire brushes, (4) composite copper/graphite brushes, and (5) joint performance at low temperatures. DOE

N86-13667# Illinois Univ., Urbana. Dept. of Ceramic Engineering.
OXIDE ELECTRODES AT HIGH TEMPERATURES
G. P. Wirtz and H. S. Isaacs 1984 5 p Prepared in cooperation with BNL, Upton, N.Y.
(Contract DE-AC02-76CH-00016)
(DE85-006564; BNL-35567) Avail: NTIS HC A02/MF A01

Models and conclusions which aid in the design of high temperature electrodes are presented. DOE

N86-13668# Societe Europeenne de Propulsion, Vernon (France). Space Dept.
ELECTRICAL MOTOR WITH SUPERCONDUCTING WINDING Final Report
J. P. Bugeat and R. Petit Paris ESA 15 Jan. 1985 116 p
(Contract ESTEC-5609/83)
(SEP-TS/SE/BT/10026/85; ESA-CR(P)-2042) Avail: NTIS HC A06/MF A01

The winding of an electrical motor tested under vaccum and at cryogenic temperature (10K) was modified. The niobium-titanium copper wire used allows the motor to run from room temperature to liquid helium temperature. Under the transition temperature (9.5K) heat dissipation in the coil is 0 whereas in a copper wound motor this dissipation is 30 mW. The motor sustained a complete test program including: functional test including torque measurement at cryogenic temperature; endurance test: 750,000 turns performed; environment test: vibration test at qualification level at cryogenic temperature. The tests reveal no degradation of mechanical (plays, friction torque) or electrical (transition temperature) performances. Author (ESA)

N86-13566# Rasor Associates, Inc., Sunnyvale, Calif.
CLOSE-SPACE, HIGH TEMPERATURE KNUDSEN FLOW Abstract Only
John B. McVey *In* AFOSR The 1985 AFOSR/AFRPL Chem. Rocket Res. Meeting Feb. 1985 3 p (For primary document see N86-13507 04-28)
Avail: NTIS HC A11/MF A01

N86-13603# Joint Publications Research Service, Arlington, Va.
ON H PLANE DIELECTRIC LOADING THEORY FOR H PLANE FERRITE PHASE SHIFTER
Wen Junding *In its* China Rept.: Sci. and Technol. (JPRS-CST-85-020) 24 Jun. 1985 p 70-75 refs Transl. into ENGLISH from Dianzi Xuebao (Beijing), v. 12, no. 1, Jan. 1984 p 116-119 (For primary document see N86-13600 04-31)
Avail: NTIS HC A09/MF A01

N86-13612# Joint Publications Research Service, Arlington, Va.
THOMSON, CNET OF FRANCE IN SILICON-ON-INSULATOR RESEARCH
J. P. DellaMussia *In its* West Europe Rept.: Sci. and Technol. (JPRS-WST-85-030) 28 Oct. 1985 p 34-36 Transl. into ENGLISH from Electron. Actualites (Paris), 8 Mar. 1985 p 1 (For primary document see N86-13610 04-31)
Avail: NTIS HC A04/MF A01

N86-13614# Joint Publications Research Service, Arlington, Va.
PHILIPS DEVELOPS MBE PROCESS FOR LASER, CHIP MANUFACTURE
In its West Europe Rept.: Sci. and Technol. (JPRS-CST-85-030) 28 Oct. 1985 p 38-39 Transl. into ENGLISH from Frankfurter Zeitung/Blick Durch die Wirtsch. (Frankfurt/Main), 6 Aug. 1985 p 5 (For primary document see N86-13610 04-31)
Avail: NTIS HC A04/MF A01

N86-13615# Joint Publications Research Service, Arlington, Va.
THOMSON SEMICONDUCTORS INTRODUCES PRODUCTS, BALANCES BOOKS
Roger Carrasco *In its* West Europe Rept.: Sci. and Technol. (JPRS-CST-85-030) 28 Oct. 1985 p 40-42 Transl. into ENGLISH from Minis et Micros (Paris), 23 Sep. 1985 p 25 (For primary document see N86-13610 04-31)
Avail: NTIS HC A04/MF A01

N86-13619# Joint Publications Research Service, Arlington, Va.
NEW DIGITAL CIRCUITS AT THOMSON SEMICONDUCTOR IN FRANCE
J. P. DellaMussia *In its* West Europe Rept.: Sci. and Technol. (JPRS-WST-85-031) 8 Nov. 1985 p 27-29 Transl. into ENGLISH from Electron. Actualites (Paris), 15 Mar. 1985 p 1; 22 (For primary document see N86-13616 04-31)
Avail: NTIS HC A03/MF A01

N86-13621# Joint Publications Research Service, Arlington, Va.
EUROPEAN SILICON STRUCTURES PLANS CUSTOM CHIPS IN 15 DAYS
J. P. DellaMussia *In its* West Europe Rept.: Sci. and Technol. (JPRS-WST-85-031) 8 Nov. 1985 p 35-41 Transl. into ENGLISH from Electron. Actualites (Paris), 6 Sep. 1985 p 1; 16 (For primary document see N86-13616 04-31)
Avail: NTIS HC A03/MF A01

34 FLUID MECHANICS AND HEAT TRANSFER

Includes boundary layers; hydrodynamics; fluidics; mass transfer; and ablation cooling.

For related information see also *02 Aerodynamics* and *77 Thermodynamics and Statistical Physics.*

N86-13669 California Univ., Berkeley.
A STUDY OF TRANSPORT PHENOMENA AND INTERFACE STABILITY DURING SOLIDIFICATION OF BINARY SOLUTIONS USING FRONT TRACKING FINITE ELEMENTS
Hai-Lung Tsai 1984 191 p
Avail: Univ. Microfilms Order No. DA8513017

A new numerical method using front tracking finite elements is developed to solve the multidimensional transient heat and mass transfer equations associated with the solidification of binary solutions. The energy balance equation at the interface is not treated as a boundary condition, but rather as an independent equation whose solution gives the new position of the interface. A special new method is developed to which the interface is tracked in time by two steps: first the magnitude of displacement and the normal direction are independently obtained for each node on the interface, then they are superimposed to determine the new interface position. The numerical method can incorporate realistic thermodynamic conditions on the interface (including the effects of interfacial tension) and can accommodate the nonisothermal as well as the irregular but smooth interface. A novel meshing system based on a systematic exponential gridding concept is developed to yield accurate temperatures in the solid and liquid phases and concentration distribution in the liquid. This numerical method is then employed to study the transport phenomena as well as the morphological stability of a planar interface during a solidification process in a saline solution. Author

N86-13670 Northwestern Univ., Evanston, Ill.
PROBLEMS IN THERMAL CONVECTIVE INSTABILITY Ph.D. Thesis
Michael Roppo 1985 216 p
Avail: Univ. Microfilms Order No. DA8511852

Three problems related to convective instabilities in which buoyancy is a fluid driving force are considered. This buoyancy is produced by imposed temperature gradients across the fluid and is measured by a Rayleigh number. The first problem considers a convection layer heated from below in a time-periodic manner with fluctuations of small amplitude delta. The nonlinear theory is studied by perturbation theory in the neighborhood of the onset of convection. It is shown that the critical Rayleigh number for the onset of convection is increased by an amount sq delta. The second problem is the flow of a fluid in thermosyphons, thin closed loops. The effects of coupling on the steady and unsteady dynamics of the loops was investigated. It is found that the coupling can delay instabilities and the onset of chaos but can give rise to new states that alter the symmetries of the flow. A two-dimensional problem which exhibits free surface driving forces in addition to buoyancy was studied. Amplitude equations for the nonlinear problem are generated by series truncation methods generalizing to free surface problems. Dissert. Abstr.

N86-13671 Wisconsin Univ., Madison.
NON-NEWTONIAN FLOW PAST CURVED EXTERNAL SURFACES Ph.D. Thesis
Nancy Joy D. E. Lambert 1984 143 p
Avail: Univ. Microfilms Order No. DA8511980

The principle motivation of this research is the creation of a foundation for predicting resistance to motion of bodies in nonNewtonian fluids. A theoretical methodology is developed for the solution of two dimensional Navier-Stokes equations for incompressible nonNewtonian fluid flows past a range of elliptical surfaces. For the investigated flow conditions, methods of analysis involving asymptotic matching techniques of boundary layer equations are not appropriate. Such methods usually assume that the surface curvature effects and pressure difference across the boundary layer are negligible. Results of the presented research show that these two effects are significant for the flow conditions at hand. The variational formulation of the governing equations of motion and continuity and their discretization by the finite element method are developed. Solutions are implemented in a form suitable for efficient numerical computation. The effect of the nonNewtonian fluid on the pressure distribution along the external surface is analyzed. The presented results include velocity profiles and shear stresses along the external surfaces. Author

N86-13672 California Univ., Berkeley.
A THREE-DIMENSIONAL ANALYSIS OF NATURAL CONVECTION IN A TOROIDAL LOOP Ph.D. Thesis
Adrienne Gail Lavine 1984 171 p
Avail: Univ. Microfilms Order No. DA8512897

Flow through a toroidal loop oriented in a vertical plane is studied. This system is a simple example of a class of devices known as thermosyphons or natural circulation loops, which have many applications. When the toroidal loop is heated from below and cooled from above, an unstable density gradient is created in the fluid. Under the influence of gravity, the lighter fluid rises and the heavier fluid falls. Thus, the fluid flows due only to natural convection. Experiments on the toroidal thermosyphon have shown that under steady state flow conditions, the axial velocity and the temperature are nonaxisymmetric, the cross stream velocities are nonzero and regions of streamwise flow reversal exist. The simplified one and two dimensional analyses performed to date have not been able to predict these phenomena. The development of a finite difference computer program for performing a three dimensional analysis of the steady state fluid flow and heat transfer in the toroidal thermosyphon is described. Regions of streamwise flow reversal are predicted in some cases. Simplified analyses which do not take the flow reversals into account are shown to be substantially in error. Hence, the current analysis yields insight into the three dimensional aspects of the flow, which could not be predicted by earlier more simplified analyses. Author

N86-13673 Pittsburgh Univ., Pa.
A COMPUTATIONAL ANALYSIS OF PULSATING FLOW IN RIGID AND DEFORMABLE TUBES Ph.D. Thesis
Timothy Mou-Chang Tsai 1984 159 p
Avail: Univ. Microfilms Order No. DA8512556

A computational analysis was made to study pulsating flow in rigid and deformable, uniform and nonuniform tubes. Two dimensionless forms of the Navier-Stokes equations were used, and a forcing function was introduced in the equations as a dynamic input. Numerical results of pulsating flow in rigid and deformable, uniform and nonuniform vessels were compared. For pulsating flow in deformable tubes, effects of the distensibility of the vessel wall on the flow pattern, pressure field, variation of shear stress, boundary layer development, and energy dissipation were studied. With a same temporal Karman number, radial dilation and contraction of the wall motion were found to have significant effects on the dynamic characteristics of the nonlinear flow process. The influence of nonuniformity of a vessel is studied for rigid and deformation cases. Dissert. Abstr.

N86-13674 State Univ. of New York, Stony Brook.
MODELLING A TRANSPORT EQUATION OF TURBULENT REACTIVE MIXING FLOW Ph.D. Thesis
Tong-Ho Johnsom Hsieh 1984 149 p
Avail: Univ. Microfilms Order No. DA8512704

The evolution of the single-point joint scalar probability density function(pdf) of two reactive scalars in idealized turbulent flows was examined by analytical conditioning and the introduction of appropriate scalar intermittency factors. Closure approximations are proposed for turbulent convection, molecular mixing and entrainment. For non-reactive flows, the closed pdf equation for a two-species turbulent mixing flow is investigated by applying it to the thermal mixing layer of a half-heated grid and to the two-scalar mixing layers behind a two-species grid, where each layer is equivalent to the thermal mixing layer of a half-heated grid. The closures used in the nonreactive case are used to predict the evolution of B chemical species statistics in a reacting flow system for which no experimental data is yet available. The closed scalar pdf equation is also applied to a homogeneous reactive grid flow, for which limited measured data exist; namely, the mean and root mean square concentration of the reactants. The predicted statistics of reactants is moderately close to the measured data. Dissert. Abstr.

N86-13675 Johns Hopkins Univ., Baltimore, Md.
TWO UNSTEADY HEAT TRANSFER EXPERIMENTS. PART 1: IN GRID-GENERATED ISOTROPIC TURBULENCE. PART 2: IN LAMINAR OSCILLATORY FLOW IN STRAIGHT AND CONICAL TUBES Ph.D. Thesis
Ralph Sanders Budwig 1985 116 p
Avail: Univ. Microfilms Order No. DA8510405

A screen of closely spaced, parallel, thin wires was placed downstream of a grid generating nearly isotropic turbulence. The screen was normal to the flow and was heated in one of two modes: (1) periodically in time, to generate a train of transversely uniform streamwise thermal ramps, each with a uniform streamwise gradient; and (2) steadily, with transverse nonuniformity, to generate a uniform transverse thermal ramp. The simple temperature and temperature gradient fluctuation statistical properties in both cases were comparable to those encountered with a steadily heated grid producing a uniform transverse thermal ramp. In both modes of heating the temperature fluctuations decreased initially behind the screen and then increased monotonically. The skewness of the temperature fluctuation derivative in the direction of the main gradient was found to be nonzero despite the absence of mean shear. Experiments on the flow field and the dispersion of heat in laminar oscillatory flow in straight and conical around tubes obtained the fluid point displacements by hydrogen bubble visualization in water and the velocity field by hot-wire anemometry in air. The heat lost through the heating frame and the insulated walls of the tube is estimated from wall temperatures extrapolated from radial profiles in the flow. The terms in the energy equation roughly balance. A plug oscillatory flow model theoretical model generates temperature fluctuations which resemble those in the core of the experimental flow. Dissert. Abstr.

N86-13676*# National Aeronautics and Space Administration. Ames Research Center, Moffett Field, Calif.
TRANSONIC SEPARATED FLOW PREDICTIONS BASED ON A MATHEMATICALLY SIMPLE, NONEQUILIBRIUM TURBULENCE CLOSURE MODEL
D. A. Johnson and L. S. King Oct. 1985 14 p refs
(NASA-TM-86826; NAS 1.15:86826) Avail: NTIS HC A02/MF A01 CSCL 20D

A mathematically simple, turbulence closure model designed to treat transonic airfoil flows even with massive separation is described. Numerical solutions of the Reynolds-averaged, Navier-Stokes equations obtained with this closure model are shown to agree well with experiments over a broad range of test conditions. Author

N86-13677*# National Aeronautics and Space Administration. Lewis Research Center, Cleveland, Ohio.
HEAT TRANSFER AND PRESSURE DROP PERFORMANCE OF A FINNED-TUBE HEAT EXCHANGER PROPOSED FOR USE IN THE NASA LEWIS ALTITUDE WIND TUNNEL
G. James VanFossen Nov. 1985 27 p refs
(NASA-TM-87151; E-2623; NAS 1.15:87151) Avail: NTIS HC A03/MF A01 CSCL 20D

A segment of the heat exchanger proposed for use in the NASA Lewis Altitude Wind Tunnel (AWT) facility has been tested under dry and icing conditions. The heat exchanger has the largest pressure drop of any component in the AWT loop. It is therefore critical that its performance be known at all conditions before the final design of the AWT is complete. The heat exchanger segment is tested in the NASA Lewis Icing Research Tunnel (IRT) in order to provide an icing cloud environment similar to what will be encountered in the AWT. Dry heat transfer and pressure drop data are obtained and compared to correlations available in the literature. The effects of icing sprays on heat transfer and pressure drop are also investigated. Author

N86-13678*# National Aeronautics and Space Administration. Lewis Research Center, Cleveland, Ohio.
DETERMINATION OF CONVECTIVE DIFFUSION HEAT/MASS TRANSFER RATES TO BURNER RIG TEST TARGETS COMPARABLE IN SIZE TO CROSS-STREAM JET DIAMETER
Sueleyman A. Goekoglu (Case Western Reserve Univ.) and Gilbert J. Santoro [1985] 15 p refs Proposed for presentation at the 31st International Gas Turbine Conference, Dusseldorf, 8-12 Jun. 1986; sponsored by ASME
(NASA-TM-87176; E-2722; NAS 1.15:87176) Avail: NTIS HC A02/MF A01 CSCL 20D

Two sets of experiments have been performed to be able to predict the convective diffusion heat/mass transfer rates to a cylindrical target whose height and diameter are comparable to, but less than, the diameter of the circular cross-stream jet, thereby simulating the same geometric configuration as a typical burner rig test specimen located in the cross-stream of the combustor exit nozzle. The first set exploits the naphthalene sublimation technique to determine the heat/mass transfer coefficient under isothermal conditions for various flow rates (Reynolds numbers). The second set, conducted at various combustion temperatures and Reynolds numbers, utilized the temperature variation along the surface of the above-mentioned target under steady-state conditions to estimate the effect of cooling (dilution) due to the entrainment of stagnant room temperature air. The experimental information obtained is used to predict high temperature, high velocity corrosive salt vapor deposition rates in burner rigs on collectors that are geometrically the same. The agreement with preliminary data obtained from Na2SO4 vapor deposition experiments is found to be excellent. Author

N86-13679*# National Aeronautics and Space Administration. Lewis Research Center, Cleveland, Ohio.
LUBRICATION OF NONCONFORMAL CONTACTS Ph.D. Thesis
Yeau-Ren Jeng Sep. 1985 154 p refs
(Contract NCC3-30)
(NASA-TM-87120; E-2728; NAS 1.15:87120) Avail: NTIS HC A08/MF A01 CSCL 20D

Minimum film thickness results for piezoviscous-rigid regime of lubrication are developed for a compressible Newtonian fluid with Roelands viscosity. The results provide a basis for the analysis and design of a wide range of machine elements operating in the piezoviscous-rigid regime of lubrication. A new numerical method of calculating elastic deformation in contact stresses is developed using a biquadratic polynomial to approximate the pressure distribution on the whole domain analyzed. The deformation of every node is expressed as a linear combination of the nodal pressures whose coefficients can be combined into an influence coefficient matrix. This approach has the advantages of improved numerical accuracy, less computing time and smaller storage size required for influence matrix. The ideal elastohydrodynamic lubrication is extended to real bearing systems in order to gain an understanding of failure mechanisms in machine elements. The improved elastic deformation calculation is successfully incorporated into the EHL numerical scheme. Using this revised numerical technique and the flow factor model developed by Patir and Cheng (1978) the surface roughness effects on the elastohydrodynamic lubrication of point contact is considered. Conditions typical of an EHL contact in the piezoviscous-elastic regime entrained in pure rolling are investigated. Results are compared with the smooth surface solutions. Experiments are conducted to study the transient EHL effects in instrument ball bearings. Author

N86-13680# Oregon State Univ., Corvallis. Dept. of Civil Engineering.
WAVE FORCE-PHASE METHOD FOR VERTICAL CYLINDERS Final Report, May 1984 - Feb. 1985
J. H. Nath May 1985 76 p
(Contract N62474-82-C-0295)
(AD-A157709; NCEL-CR-85.008) Avail: NTIS HC A05/MF A01 CSCL 20/4

The maximum force and its phase is determined for laboratory wave forces on smooth vertical cylinders. The maximum force coefficient and the normalized phase angle of the force with respect to the wave particle velocity, can be related to the force transfer coefficients, C subscript d and c subscript m, for the Morison equation. This method enables the data to be plotted in a way that immediately shows the drag or inertia dependency for the wave/cylinder conditions. In addition, the C subscript d and C subscript m so derived are more likely to properly predict the maximum value of the force, although they may also increase the rms error between the measured force and the predicted force in the time domain. GRA

N86-13681# Oregon State Univ., Corvallis. Dept. of Civil Engineering.
HIGH REYNOLDS NUMBER WAVE FORCE INVESTIGATION IN A WAVE FLUME Final Report, Sep. 1982 - Feb. 1985
R. T. Hudspeth and J. H. Nath Mar. 1985 225 p
(Contract N62474-82-C-08295)
(AD-A157722; NCEL-CR-85.004) Avail: NTIS HC A10/MF A01 CSCL 20/4

A 12.75 inch diameter vertical cylinder was subjected to large laboratory waves with Keulegan-Carpenter number up to 17 at the local force transducer (20 at the still water surface) and Reynolds number up to 270,000 (320,000 at the still water surface). Local force, local pressures, total force, and the elements for determining the overturning moments were measured. The purpose was to produce a high quality data set in the wave regime where both the velocity and the acceleration-dependent components of the wave forces are important. It was found that the forces were more acceleration-dependent than originally anticipated. The local forces were predicted quite well with the two-term Morison equation using the kinematics from the measurements, the linear, and the stream function wave theories. The best predictions used the measured kinematics. GRA

N86-13682# Illinois Univ., Urbana. Dept. of Mechanical and Industrial Engineering.
A FULLY VISCOUS TWO-DIMENSIONAL UNSTEADY FLOW ANALYSIS APPLIED TO DETONATION TRANSITION IN POROUS EXPLOSIVES Final Technical Report, May 1982 - Mar. 1985
H. Krier, M. R. Dahm, and L. S. Samuelson Jun. 1985 117 p
(Contract F08635-82-K-0321)
(AD-A157794; AD-E801156; UILU-ENG-84-4009;
AFATL-TR-85-12) Avail: NTIS HC A06/MF A01 CSCL 19/4

This report describes significant new progress towards solving the two-dimensional fully viscous unsteady flow in a reactive solid/gas mixture. The results demonstrate that it may be possible to predict whether a warhead with case failure (and filled with fragmented high explosive) will produce a low order detonation which is weaker than the one required to damage a structure. The loss of mass, momentum, and energy through a warhead case opening is a multi-dimensional problem even though the reaction front may progress axially through the damaged explosive. Mass is ejected in a basically radial direction and necessitates a multi-dimensional problem formulation in order to model the deflagration to detonation transition event accurately enough to make meaningful predictions. The appropriate equations of state and continuity equations are formulated and are solved by a finite differencing scheme. Run-up length to detonation in the fragmented explosive bed from a case opening through which mass is ejected should be married with a model of probabilistic case failure on impact to predict warhead lethality. GRA

N86-13683# Coastal Engineering Research Center, Vicksburg, Miss.
ITERATIVE AND PADE SOLUTIONS FOR THE WATER-WAVE DISPERSION RELATION Final Report
H. S. Chen and E. F. Thompson Apr. 1985 24 p

(AD-A157796; CERC-85-4) Avail: NTIS HC A02/MF A01 CSCL 20/4

This report gives the iterative and Pade solutions of the propagating and evanescent wave modes of the dispersion relation for the linear water-wave theory. Their corresponding FORTRAN subroutines are also provided. The Pade solution is generally more efficient than the iterative one in most engineering applications. GRA

N86-13684# United Research Corp., Santa Monica, Calif.
WAVES WHICH TRAVEL UPSTREAM IN BOUNDARY LAYERS Final Report, Mar. 1982 - Aug. 1984
H. L. Rogler Jul. 1985 57 p
(Contract F40600-79-C-0002)
(AD-A157949; AEDC-TR-83-7) Avail: NTIS HC A04/MF A01 CSCL 20/4

Upstream propagation and diffusion of vorticity in a boundary layer is described by a numerical solution of the Orr-Sommerfeld equation. This traveling wave grows very rapidly in the downstream direction. The growth rate is approximately exp(+ R (sub delta)x) where R sub delta is the Reynolds number based on the characteristic boundary layer thickness, and x is the streamwise coordinate nondimensionalized against delta. Far from the boundary layer, the solution oscillates neutrally in the Y-direction. Analyses reveal high frequency wave which oscillates and decays in the y-direction approximately as exp(-i R(sub delta) y - omega Y) where omega is the frequency. This high frequency wave can survive into the freestream. Numerical solutions of the Orr-Sommerfeld equation with a Blasius layer are obtained by a series expansion of Chebyshev polynomials. Since the y-wavenumber of the oscillations increases with increasing Reynolds number, the calculations have been restricted to low Reynolds numbers. In the boundary-value problem, this solution appears as a branch line in Laplace space. It is one of the possible solutions in a mathematically complete description of the spatial evolution of fluctuations. This traveling wave represents one of the upstream influences of a boundary in a calculational domain. Another mechanism of upstream influence is the growing standing wave. GRA

N86-13685# Arnold Engineering Development Center, Arnold Air Force Station, Tenn.
BOUNDARY-VALUE PROBLEM FOR TWO-DIMENSIONAL FLUCTUATIONS IN BOUNDARY LAYERS Final Report, Mar. 1979 - May 1985
S. Tsuge and H. L. Rogler Jul. 1985 51 p Prepared in cooperation with United Research Corp., Santa Monica, Ca
(AD-A157952; AEDC-TR-83-9) Avail: NTIS HC A04/MF A01 CSCL 20/4

The streamwise evolution of disturbances in a boundary layer is described as an asymptotic solution of the forced Orr-Sommerfeld equation. The velocity fluctuations and their derivations are specified along the y-axis. With these boundary conditions, the effects are included of vortical and irrotational free stream disturbances, fluctuations originating from leading edges, and discrete eigenmodes. A Fourier transform in time and a Laplace transform in the streamwise direction are used. Complementary and particular integrals are found and the inverse transforms are taken. Five families of 2-D fluctuations can exist in a parallel-flow, incompressible boundary layer. Three families have exponentially growing fluctuations, one of which is the Tollmien stability wave. Another is an exponentially-growth standing wave that oscillates in time and does not travel. This fluctuation appears as a mathematical pole in transform space, like the stability waves, but does not vanish far away from the boundary layer. A third growing fluctuation appears in Laplace space as a branch line. This continuous spectrum diffuses and travels upstream. The last two of these three growing fluctuations are excluded in our quarter-plane problem that extends forever downstream. Besides the Tollmien wave that can grow or decay in the streamwise direction, the other discrete modes appearing as mathematical poles are damped. Two other decaying fluctuations appear. GRA

N86-13686# Virginia Research Associates, Blacksburg.
NEW FLOW VISUALIZATION TECHNIQUE FOR WATER TUNNEL TESTING OF COMBUSTORS Final Report, Sep. 1984 - Apr. 1985
J. A. Schetz, F. Sebba, and R. L. Simpson Apr. 1985 52 p
(Contract F33615-84-C-2468)
(AD-A158015; AFWAL-TR-85-2042) Avail: NTIS HC A04/MF A01 CSCL 20/4

A new technique for water tunnel flow visualization is based upon the use of a newly developed type of material--neutral-density, bi-liquid foams or polyaphrons. These materials are small, spherical globules of one liquid encapsulated in a thin film of another liquid. It is now possible to make bi-liquid foams when the units are of micron or submircon size, and may be spherical or polyhedral depending upon the relative concentration of oil to water. They are easy to see and photograph in water and they can also be dyed to a variety of intense colors. In this two part study, polyaphrons were used for flow visualization in water tunnel tests of combustors. First, various formulations of the polyaphrons were made to optimize aphron size and density for water tunnel testing. Second, the best polyaphrons were used for flow visualization of real, prototype combustor model. Tests were conducted at 22.5 gpm. This corresponds to Re sub D=23,900, when D is the swirler diameter. Tests showed that polyaphron material proved easy to handle when injected through small tubes and the amount and ratio of injection was easy to control. No clogging of any kind was ever encountered. The pure material broke-up into clumps upon injection. A 50/50 mixture of water polyaphron eliminated clumping. Injection of polyaphrons was also directly compared with the more usual dye injection. Polyaphrons are ideal seeding material for Laser Doppler Velocimetry in water tunnels. GRA

N86-13687# Naval Research Lab., Washington, D. C.
NUMERICAL SIMULATIONS OF ASYMMETRIC MIXING IN PLANAR SHEAR FLOWS Interim Report
F. F. Grinstein, E. S. Oran, and J. P. Boris 23 Aug. 1985 50 p
Original contains color illustrations
(AD-A158024; NRL-MR-5621) Avail: NTIS HC A03/MF A01 CSCL 20/4

Numerical simulations were performed of the evolution of the Kelvin-Helmholtz instability in planar, free shear layers, resulting from coflow past a splitter plate. The calculations solved the time-dependent compressible conservation equations for which new algorithms were developed and tested for inflow and outflow boundary conditions. The transition from laminar flow was triggered by transverse pressure gradients and subsequent vorticity fluctuations at the shear layer, near the tip of the splitter plate. The calculations were performed for a range of free-stream velocity ratios and sizes of the chamber enclosing the system. The simulations showed that the resulting mixing layers have more of the faster fluid than the slower fluid entrained in the roll-ups. This effect is in general agreement with the results of recent splitter-plate experiments of Koochesfahani, Dimotakis and Broadwell (1983). The calculated mixing asymmetry is more apparent when the velocity ratio of the two streams is larger, and does not depend significantly on the separation between the walls of the chamber. GRA

N86-13688# Cambridge Acoustical Associates, Inc., Mass.
SENSITIVITY TO MEAN FLOW PARAMETERS OF THE LOW WAVENUMBER CONTENT OF THE WALL PRESSURE UNDER A TURBULENT BOUNDARY LAYER Final Report, 1 Dec. 1983 - 31 May 1985
J. E. Cole, III 26 Apr. 1985 45 p
(Contract N00014-84-C-0141)
(AD-A158037; CAA-U-1205-333; DTNSRDC-2280) Avail: NTIS HC A03/MF A01 CSCL 20/4

The objective of this study is to examine the sensitivity of the low wavenumber portion of the wall pressure field under a turbulent boundary layer to both flow and wall conditions. The analytical procedure makes use of a method for calculating the broadband correlation function of the wall pressure field in which the specific flow characteristics enter through profiles of the mean velocity shear and turbulence intensity across the boundary layer. The basic assumption used to extend the results of this procedure to narrowband frequency characteristics is that there is a range of large spatial separations in which Strouhal scaling is not important. Several specific boundary layers are considered including flows on smooth and rough walls and in zero, favorable, and adverse pressure gradients. Results are presented for the point pressure, the spatial correlation function, and the low wavenumber spectral level. GRA

N86-13689# Naval Ocean Research and Development Activity, Bay St. Louis, Miss.
PORE PRESSURE RESPONSE TO PROBE INSERTION AND THERMAL GRADIENT: ISIMU-2. (IN SITU HEAT TRANSFER EXPERIMENT) Final Report
M. Riggins, P. J. Valent, H. Li, J. T. Burns, and C. E. Hickox Jul. 1985 81 p
(AD-A158592; NORDA-TN-259) Avail: NTIS HC A05/MF A01 CSCL 08/10

The described experiment and the evaluation of its results were designed to assess the significance of the sediment cracking occurring during piezometer and heater probe insertion, and the influence of the cracking on the subsequent excess pore pressure and thermal fields to be measured in the In Situ Heat Transfer Experiment (ISHTE). The ISHTE is part of the Subseabed Disposal Program (SDP). Observed sediment radial cracking was estimated to penetrate to about one-half penetrator diameter. Measured penetrator insertion pore pressures and excess pore pressure dissipation indicate that sediment cracking has no identifiable influence at the penetration depth of the sensors. Proper prediction of the dissipation of insertion pore pressures was found to require incorporation of a smear factor, accounting for sediment remolding at the piezometer wall. An analytical model to concurrently describe the rise in excess pore pressure due to sediment heating and the pore pressure dissipation radially away from the heat source is described and the results of its application to the experiment data evaluated. GRA

N86-13690# Florida Univ., Gainesville.
FAR-FIELD BOUNDARY CONDITIONS IN NUMERICAL SOLUTIONS OF THE NAVIER-STOKES EQUATIONS Final Report, 24 Oct. 1984 - 1 Apr. 1985
P. J. McKenna 10 May 1985 61 p
(Grant AF-AFOSR-0330-83)
(AD-A158776; AFOSR-85-0625TR) Avail: NTIS HC A04/MF A01 CSCL 20/4

The purpose of this project was to investigate the artificial boundary conditions which must be imposed at the boundary of a numerical grid. Numerical experiments were performed which evaluated various boundary conditions of this type. Of particular interest was the question of whether linearization around the flow at infinity provides an adequate choice of boundary condition for the fully nonlinear equations. Inflow-outflow conditions as well as several choices of periodic boundary conditions were considered. The inflow-outflow conditions worked reasonably well for two dimensional problems. For the periodic conditions, results were mixed. Concerns about over specification when using pure periodic conditions proved to be groundless. However, the method failed when attempting to use periodicity in the two sideways traveling periodic waves. GRA

N86-13691# California Univ., Berkeley. Mathematical Sciences Research Inst.
TURBULENCE AND DYNAMICAL SYSTEMS Final Report, 1 Jul. 1983 - 31 Dec. 1984
A. Chorin, J. Feldman, and C. C. Moore 31 Dec. 1984 21 p
(Grant AF-AFOSR-0265-83)
(AD-A159026; AFOSR-85-0646TR) Avail: NTIS HC A02/MF A01 CSCL 20/4

The emphasis in this program was on the bringing together, in connection with the overall effort on dynamical systems, researchers from physics, mathematics, engineering; working in the various aspects of liquid helium theory, crystal growth, etc. This report summarizes the results of a workshop and contains 8 abstracts on related topics. GRA

N86-13692# Army Engineer Waterways Experiment Station, Vicksburg, Miss. Hydraulics Lab.
USER'S MANUAL FOR THE GENERALIZED COMPUTER PROGRAM SYSTEM. OPEN-CHANNEL FLOW AND SEDIMENTATION, TABS-2. MAIN TEXT Final Report
W. A. Thomas and W. H. McAnally, Jr. Jul. 1985 39 p
(AD-A159249; WES/TR/HL-85-1) Avail: NTIS HC A03/MF A01 CSCL 08/8

TABS-2 is a generalized numerical modeling system for open-channel flows, sedimentation, and constituent transport. It consists of more than 40 computer programs to perform modeling and related tasks. The major modeling components--RMA-2V, STUDH, and RMA-4--calculate two-dimensional, depth-averaged flows, sedimentation, and dispersive transport, respectively. The other programs in the system perform digitizing, mesh generation, data management, graphical display, output analysis, and model interfacing tasks. Utilities include file management and automatic generation of computer job control instructions. TABS-2 has been applied to a variety of waterways, including rivers, estuaries, bays, and marshes. It is designed for use by engineers and scientists who may not have a rigorous computer background. Use of the various components is described in Appendices A-O. The bound version of the report does not include the appendices. A looseleaf form with Appendices A-O is distributed to system users. Author (GRA)

N86-13693# Los Alamos National Lab., N. Mex.
TURBULENCE IN TWO-FIELD INCOMPRESSIBLE FLOW
D. Besnard and F. H. Harlow May 1985 113 p
(Contract W-7405-eng-36)
(DE85-015361; LA-10187-MS) Avail: NTIS HC A06/MF A01

We derive in this report a model for two-field turbulence. This model gives most of the required features, such as mass diffusion, damping of the turbulence in the second fluid due to the presence of the first one, and decay of the turbulent kinetic energy. We also derive from it a k-epsilon model, which could be used for many applications. DOE

N86-13694# California Univ., Berkeley. Lawrence Berkeley Lab.
INVESTIGATION OF THE VERTICAL-FLOW AQUIFER THERMAL ENERGY STORAGE CONCEPT AND NUMERICAL SIMULATION OF THE DORIGNY FIELD EXPERIMENT
C. Doughty and C. F. Tsang May 1985 10 p Presented at the ENERSTOCK ' 85 - Intern. Conf. on Energy Storage for Bldg. Heating and Cooling, Toronto, 22 Sep. 1985
(Contract DE-AC03-76SF-00098)
(DE85-014524; LBL-19645; CONF-850905-3) Avail: NTIS HC A02/MF A01

A mathematical modeling study of the vertical-flow aquifer thermal energy storage concept is made. A history match calculation of the Dorigny field experiment, part of the SPEOS project, is carried out using two simplified models. Then the main heat-loss mechanisms are isolated to study their relative importance. Finally, variations on the Dorigny experimental configuration are studied to examine the behavior of the vertical-flow storage system in general. DOE

N86-13695# Los Alamos National Lab., N. Mex.
EXPERIMENTS WITH NON-DARCY FLOW IN JOINTS WITH LARGE SCALE ROUGHNESS
D. K. Cornwell and H. D. Murphy 1985 11 p refs Presented at the Intern. Symp. on Fundamentals of Rock Joints, Bjorkliden, Sweden, 15 Sep. 1985
(Contract W-7405-eng-36)
(DE85-015714; LA-UR-85-2454; CONF-8509129-2) Avail: NTIS HC A02/MF A01

Joints are normally in contact at roughness asperities. Consequently, the relative roughness, the ratio of the asperity protrusion to the mean flow aperture, is approximately one, which is orders of magnitude greater than that encountered in more usual situations such as pipe and channel flows. In these experiments the joint roughness is idealized with sawtooth corrugations. It is found that Darcy's Law becomes invalid for Reynolds numbers greater than about 100. Hence, for most of these studies the flow is non-Darcian, and so the usual convention of representing pressure losses in terms of an apparent friction factor is adopted. When the roughness peaks are aligned, resulting in maximum flow disturbance, the friction factor increases when the relative roughness is increased, simulating the closure of a joint due to normal-direction loading. However, when the roughness peaks are 180 deg out of phase, so that peaks are opposite valleys, the friction factor initially increases with greater relative roughness, but then decreases. DOE

N86-13696# Sandia National Labs., Albuquerque, N. Mex.
CRITICAL CHARGE FOR THE DIRECT INITIATION OF DETONATION IN GASEOUS FUEL-AIR MIXTURES
W. B. Benedick, C. M. Guirao, R. Knystautas, and J. H. Lee 4 Aug. 1985 30 p refs Presented at the 10th Intern. Colloq. on Dyn. of Explosions and Reactive Systems Berkeley, Calif., 4 Aug. 1985 Prepared in cooperation with McGill Univ., Montreal
(Contract DE-AC04-76DP-00789)
(DE85-016130; SAND-85-1716C; CONF-850830-6) Avail: NTIS HC A03/MF A01

The results of measurements of the critical initiation energy for hydrogen air mixtures performed in a large scale facility are described. These results for hydrogen air mixtures, in conjunction with earlier measurements are used to assess the accuracy of existing phenomenological models. A comprehensive review of the theoretical models used to predict the critical initiation energy of unconfined detonation in reactive mixtures is presented. Three initiation energy models, the surface energy model of Lee, the cell energy model of Vasiliev and Grigoriev, and the detonation kernel model of Ramanurthi and Lee are found to correlate well with the experimental critical charge data for hydrogen air, ethane air, propane air and butane air mixtures. For ethylene air mixtures, none of the existing models predict the whole range of initiation energy data. From examination of the hydrogen air data, the calculated explosion length R0, for critical conditions is of the order of R0 approx. =1.5 d sub c, where d sub c is the critical tube diameter. This is compatible with the reinitiation distance of approx. 2 d sub c for the critical tube situation observed by Ungut, et al. The correlation R0 approx. =1.5 d sub c provides a better estimate of the critical initiation energy than can be obtained from direct measurements which are influenced by the characteristics of the initiation source. DOE

N86-13697# Lawrence Livermore National Lab., Calif.
GRANULAR FLOW: ADVANCED RESEARCH AND TECHNOLOGY DEVELOPMENT (AR AND TD) CONTRACT REVIEW
O. R. Walton 19 Jul. 1985 13 p Presented at the AR and TD Direct Utilization Contractors' Meeting, Morgantown, W. Va., 13 Aug. 1985
(Contract W-7405-eng-48)
(DE85-017267; UCRL-92992; CONF-850878-5) Avail: NTIS HC A02/MF A01

The objective of the granular flow project is to develop an understanding for and an ability to predict the flow behavior of granular solids. New reseach tools are developed as part of this task in the form of new two and three-dimensional discrete particle computer models that can provide detailed information on both the microscopic and macroscopic deformations occurring in flowing granular solids. These computer models calculate the motion of each individual particle in an assembly of many inelastic, frictional particles responding to applied loads, boundaries and/or gravity. New interparticulate force models were developed that realistically simulate collision behavior between spheres and disks under rapid shearing conditions. A new two-dimensional steady-state shearing model, using periodic boundaries on all sides of a primary calculational cell was used to determine the rheologic properties of assemblies of disks and the dependence of these rheologic properties on the shear rate, and on the inelasticity and surface friction properties of the disks. Real boundaries and gravity were added to this two-dimensional model. Three-dimensional steady-state shearing and real boundary models with spherical particles are under development. When these are completed direct comparisons can be made between various existing laboratory studies and the three-dimensional computer simulations. DOE

N86-13698# Argonne National Lab., Ill.
DEVELOPMENT OF CONTACT/IMPACT CAPABILITY FOR THE THREE-DIMENSIONAL FLUID-STRUCTURE INTERACTION CODE: NEPTUNE
R. F. Kulak and C. Fiala 1985 14 p refs Presented at the 8th Intern. Conf. on Struct. Mech. in Reactor Technol., Brussels, 19 Aug. 1985
(Contract W-31-109-eng-38)
(DE85-010264; CONF-850809-52) Avail: NTIS HC A02/MF A01

A method, which uses a family of adaptive contact elements, is developed for treating the mechanics of contact/impact between two deformable bodies. The contact element's nodal connectivity is allowed to change during the computations in order to accommodate finite sliding. The methodology has been implemented into the NEPTUNE finite element program. Results are presented for an illustrative problem. DOE

N86-13699# Massachusetts Inst. of Tech., Cambridge.
STUDY OF DEPOSITION CONTROL USING TRANSPIRATION Technical Progress Report
J. F. Louis and H. Kozlu May 1985 5 p
(Contract DE-AC21-83MC-20334)
(DE85-012799; DOE/MC-20334/T19) Avail: NTIS HC A02/MF A01

Modeling of particle transport across the transpired turbulent boundary layer by introducing the Schmidt number as a function of the normal distance to the wall is performed. A major problem is to determine how the Schmidt number varies within the boundary layer. Schmidt number is affected by the flow structure as well as the mechanics of aerosols. The validated model for transpired turbulent boundary layer has shown that eddy sizes are constant across the boundary layer. Therefore, it is expected that the Schmidt number should be constant for every particle size in the boundary layer operating with strong blowing except for the region very close to the wall. Based on the above analysis, it is expected that these structure differences in the flow will cause a drastic change (i.e., like a step function) of Schmidt number very near the wall. The region close to the wall has to be carefully characterized. For large injection rates, the flow close to the wall is dominated by the injected flow emerging from the porous wall. According to the manufacturer, the porous wall is made of very small beads with a diameter of 6 (MU). Therefore the emerging flow has nonuniformity characterized by a maximum length of 6 (MU) which is appreciably smaller than the particle diameter, i.e., 16 (MU). In the region very close to the wall, the Schmidt number associated with the particles is large. DOE

N86-13700# Sandia National Labs., Albuquerque, N. Mex.
EXPERIMENTAL INVESTIGATION OF HEAT TRANSFER BEHAVIOR OF AQUEOUS FOAMS IN THERMAL ENTRY REGION OF PIPE FLOW
B. F. Blackwell and K. A. Butler 1985 9 p Presented at the Natl. Heat Transfer Conf., Denver, 4 Aug. 1985
(Contract DE-AC04-76DP-00789)
(DE85-012836; SAND-85-1089C; CONF-850810-20) Avail: NTIS HC A02/MF A01

An experimental facility for studying the heat transfer behavior of aqueous foams flowing in the thermal entry region of a pipe has been designed and fabricated. Temperature profiles have been measured at the exit of a 3 m (9.83 ft) long x 2.58 cm (1.015 in.) diameter tube using a chromel/alumel thermocouple probe and a micrometer adjusted traversing mechanism. Two foam consistencies were studied; nominal liquid volume fractions of 0.10 and 0.15. Analytical predictions of temperature profile, boundary layer thickness, and local Nusselt No. are compared with experimental data. It appears that the thermal conductivity variation with liquid volume fraction is more complex than the linear model proposed by other foam experimenters. DOE

N86-13701# New York Univ., New York. Mathematics and Computing Lab.
SHOCK WAVES, INCREASE OF ENTROPY AND LOSS OF INFORMATION
P. D. Lax Oct. 1984 46 p
(Contract DE-AC02-76ER-03077)
(DE85-013645; DOE/ER-03077/240) Avail: NTIS HC A03/MF A01

For the simplified model of a single conservation law, the concepts of genuine nonlinearity, breakdown of classical solutions, solutions in the distribution sense and their nonuniqueness, the viscosity method, finite difference methods, and the shock condition are discussed. For the scalar model, the compactness of solutions constructed by the viscosity and difference methods are also discussed, and the entropy inequality for such solutions is derived. Glimm's estimate for the total variation of solutions of scalar equations that satisfy the shock condition is also derived, and it is shown that a discontinuous solution that satisfies the shock condition also satisfies the entropy condition. Scattered remarks are given about the equations of compressible flow: the increase of entropy, some consequences of Carnot's theorem, and the equipartition of energy in the wake of strong shocks. DOE

N86-13702*# Los Alamos National Lab., N. Mex.
HYBRID SIMULATION CODES WITH APPLICATION TO SHOCKS AND UPSTREAM WAVES
D. Winske 3 Feb. 1985 15 p refs Presented at the 2nd Intern. School of Space Simulation, Kapaa, Hawaii, 3-15 Feb. 1985 Sponsored by NASA
(Contract W-7405-eng-36)
(NASA-CR-176365; NAS 1.26:176365; DE85-007702; LA-UR-85-452; CONF-850266-4) Avail: NTIS HC A02/MF A01 CSCL 20D

Hybrid codes in which part of the plasma is represented as particles and the rest as a fluid are discussed. In the past few years such codes with particle ions and massless, fluid electrons have been applied to space plasmas, especially to collisionless shocks. All of these simulation codes are one dimensional and similar in structure, except for how the field equations are solved. The various approaches that are used (resistive Ohm's law, predictor corrector, Hamiltonian) are described and results from the various codes with examples taken from collisionless shocks and low frequency wave phenomena upstream of shock compared. Author

N86-13703# Lawrence Livermore National Lab., Calif.
CONTRIBUTIONS TO VON KARMAN INSTITUTE LECTURE SERIES ON COMPUTATIONAL FLUID DYNAMICS: ADVECTION-DIFFUSION AND NAVIER-STOKES EQUATIONS
P. M. Gresho Mar. 1985 174 p Presented at Von Karman Inst. Lecture Ser. on Computational Fluid Dyn., Brussels, 25 Mar. 1985
(Contract W-7405-eng-48)
(DE85-010942; UCRL-92275; CONF-8503148-1) Avail: NTIS HC A08/MF A01

An appropriate starting point for the numerical simulation of fluid flow is the study of the simpler, yet important equation of advection-diffusion (AD), in which the velocity field is presumed to be known. Many fluid flow simulations are primarily concerned with the transport and diffusion of scalar quantitites such as heat (temperature) or concentration (e.g., air pollution). Unfortunately, even in these cases, the more difficult to obtain velocity field must (usually) be computed first. We assume that the velocity is known; later we return to the problem of computing the velocity field itself. Two papers are also included on the finite method for solving the time-dependent, incompressible Navier-Stokes equations. DOE

N86-13704# Argonne National Lab., Ill.
FLUID FORCES ON TWO CIRCULAR CYLINDERS IN CROSSFLOW
J. A. Jendrzejczyk and S. S. Chen Jun. 1985 60 p
(Contract W-31-109-eng-38)
(DE85-014294; ANL-85-35) Avail: NTIS HC A04/MF A01

Fluid excitation forces are measured in a water loop for two circular cylinders arranged in tandem and normal to flow. The Strouhal number and fluctuating drag and lift coefficients for both cylinders are presented for various spacings and incoming flow conditions. Results show the effects of Reynolds number, pitch ratio, and upstream turbulence on the fluid excitation forces. DOE

N86-13705# Dornier-Werke G.m.b.H., Friedrichshafen (West Germany).
STUDY OF EARTH OBSERVATION BY FREQUENCY SCANNING. VOLUME 1: EXECUTIVE SUMMARY
D. Miller, H. Schuessler, P. Stuerzenhofaecker, M. Westphal, J. E. Charlton (British Aerospace Dynamics Group, Bristol, UK), T. T. Joyce (British Aerospace Dynamics Group, Bristol, UK), A. Thomson, D. C. Hawkins, and P. R. Foster Paris ESA Nov. 1984 18 p 2 Vol.
(Contract ESTEC-5717/83/NL-MS)
(ESA-CR(P)-2028-Vol-1) Avail: NTIS HC A02/MF A01

Microwave remote sensing from space necessitates instruments to operate under severe constraints. One method of reducing the demands of power and mechanical complexity is to improve the antenna directivity and steer the beam electrically. Frequency scanning provides a simple and elegant means of using frequency to control the antenna beam direction. It enables the beam to be steered rapidly in space without moving large mechanical masses and more efficiently utilises the available r.f. power directing it more precisely to the region of interest. In comparison with active inertiales scanning techniques, frequency scanning is simple and reliable and hence particularly attractive for spaceborne sensors. This study is aimed at exploring the potential of frequency scanning as a technique for reducing the demand of microwave remote sensing instruments on the resources of the spacecraft. The applications for investigation are Scatterometry and imaging Radiometry. Author (ESA)

N86-13706# Dornier-Werke G.m.b.H., Friedrichshafen (West Germany).
STUDY OF EARTH OBSERVATION BY FREQUENCY SCANNING. VOLUME 2 Final Report
D. Miller, H. Schuessler, P. Stuerzenhofaecker, M. Westphal, J. E. Charlton (British Aerospace Dynamics Group, Bristol, UK), T. T. Joyce (British Aerospace Dymanics Group, Bristol, UK), A. Thomson, D. C. Hawkins, and P. R. Foster Paris ESA Nov. 1984 381 p refs 2 Vol.
(Contract ESTEC-5717/83/NL-MS)
(ESA-CR(P)-2028-Vol-2) Avail: NTIS HC A17/MF A01

The potential of frequency scanning for reducing the demand of microwave remote sensing instruments on the resources of the spacecraft in scatterometry and imaging radiometry was investigated. Applied to a single channel passive microwave radiometer, frequency scanning offers saving in mass and avoids a single point failure mode by eliminating the scanning mechanism. However, the wide swath requirement precludes higher microwave frequencies due to the high wrap-up factors that result in high losses. A multifrequency capability can only be achieved by using an antenna structure dedicated to each channel. A frequency sensitive pushbroom system with the potential to offer a better radiometric sensitivity may be superior for applications which require a single frequency and long integration time. Author (ESA)

N86-13707# Universite de Valenciennes et du Hainaut-Cambresis (France).
BEHAVIOR OF SLENDER CONES AT LARGE INCIDENCES Final Report [COMPORTEMENT DES CONES ELANCES A GRANDE INCIDENCE]
A. Morteveille and C. Tournier Jan. 1985 86 p refs In FRENCH
(Contract DRET-83-1095)
Avail: NTIS HC A05/MF A01

Wall velocity gradients in magnitude and direction around slender cones were studied for incidences from 30 to 90 deg. A polarographic method is used to measure the wall instantaneous values without perturbation of the fluid flow. The nonsteady characteristics of each component of the gradient are given. A hydraulic channel with a redox polarographic solution at 20 C was used. The results show an increase of flow instability with incidence, with a maximum at 60 deg for the ideal cone and 75 deg for the blunted cone. Author (ESA)

N86-13566# Rensselaer Polytechnic Inst., Troy, N.Y. Dept. of Chemical Engineering and Environment Engineering.
EFFECT OF INTERFACIAL PHENOMENA ON CONTACT LINE HEAT TRANSFER Abstract Only
Peter C. Wayner, Jr. *In* AFOSR The 1985 AFOSR/AFRPL Chem. Rocket Res. Meeting Feb. 1985 3 p (For primary document see N86-13507 04-28)
Avail: NTIS HC A11/MF A01

N86-13577# Aerometrics, Inc., Mountain View, Calif.
SPRAY CHARACTERIZATION USING PHASE ANGLE DETECTION Abstract Only
William D. Bachalo *In* AFOSR The 1985 AFOSR/AFRPL Chem. Rocket Res. Meeting Feb. 1985 3 p (For primary document see N86-13507 04-28)
Avail: NTIS HC A11/MF A01

N86-13580# Spectron Development Labs., Inc., Costa Mesa, Calif.
SPRAY CHARACTERIZATION WITH A NONINTRUSIVE OPTICAL SINGLE PARTICLE COUNTER Abstract Only
Cecil F. Hess *In* AFOSR The 1985 AFOSR/AFRPL Chem. Rocket Res. Meeting Feb. 1985 3 p (For primary document see N86-13507 04-28)
Avail: NTIS HC A11/MF A01

N86-13583# Texas Univ. at Dallas, Richardson.
REAL-TIME, TWO-DIMENSIONAL FUEL SPRAY VISUALIZATION Abstract Only
Lynn A. Melton and James F. Verdieck (United Technologies Research Center, East Hartford, Conn.) *In* AFOSR The 1985 AFOSR/AFRPL Chem. Rocket Res. Meeting Feb. 1985 3 p (For primary document see N86-13507 04-28)
Avail: NTIS HC A11/MF A01

N86-13768# Joint Publications Research Service, Arlington, Va.
FORMATION OF STRUCTURE OF MIXED REGION UNDER INFLUENCE OF SHEAR FLOW IN STRATIFIED FLUID Abstract Only
L. A. Dykhno *In its* USSR Rept.: Earth Sci. (JPRS-UES-85-009) 13 Nov. 1985 p 9 Transl. into ENGLISH from Izv. Akad. Nauk SSSR: Fiz. Atmosfery i Okeana (Moscow), v. 21, no. 5, May 1985 p 528-536 (For primary document see N86-13765 04-42)
Avail: NTIS HC A04/MF A01

N86-14094*# National Aeronautics and Space Administration. Johnson (Lyndon B.) Space Center,
AN ANALYSIS OF CRYOTRAP HEAT EXCHANGER PERFORMANCE TEST DATA (400 AREA) AND RECOMMENDATIONS FOR A SYSTEM TO HANDLE APOLLO RCS ENGINES Final Report
Allen Rakow *In its* The 1983 NASA/ASEE Summer Faculty Fellowship Research Program Research Report Sep. 1983 15 p (For primary document see N86-14078 04-85)
Avail: NTIS HC A18/MF A01 CSCL 20D

N86-14095*# National Aeronautics and Space Administration. Johnson (Lyndon B.) Space Center,
SPARGER SYSTEM FOR MMH-HELIUM VENTS Final Report
Allen Rakow *In its* The 1983 NASA/ASEE Summer Faculty Fellowship Research Program Research Reports Sep. 1983 17 p (For primary document see N86-14078 04-85)
Avail: NTIS HC A18/MF A01 CSCL 20D

N86-14158# Joint Publications Research Service, Arlington, Va.
ROSSBY AUTOSOLITON Abstract Only
S. V. Antipov, M. V. Nezlin, and A. S. Trubnikov *In its* USSR Rept.: Space (JPRS-USP-85-005) 30 Sep. 1985 p 68 Transl. into ENGLISH from Pisma v Zh. Eksperim. i Teor. Fiz. (Moscow), v. 41, no. 1, Jan. 1985 p 25-28 (For primary document see N86-14111 04-88)
Avail: NTIS HC A08

35 INSTRUMENTATION AND PHOTOGRAPHY

Includes remote sensors; measuring instruments and gages; detectors; cameras and photographic supplies; and holography.

For aerial photography see *43 Earth Resources.* For related information see also *06 Aircraft Instrumentation,* and *19 Spacecraft Instrumentation.*

N86-13708*# Aerojet Techsystems Co., Sacramento, Calif.
ROCKET ENGINE HOT-SPOT DETECTOR Final Report
F. N. Collamore Apr. 1985 185 p refs
(Contract NAS9-16282)
(NASA-CR-171902; NAS 1.26:171902; Rept-16282-T-1646-MA-129T-002F) Avail: NTIS HC A09/MF A01 CSCL 14B

On high performance devices such as rocket engines it is desirable to know if local hot spots or areas of reduced cooling margin exist. The objective of this program is to design, fabricate and test an electronic hot spot detector capable of sensing local hot spot on the exterior circumference of a regeneratively cooled combustion chamber in order to avoid hardware damage. The electronic hot spot sensor consists of an array of 120 thermocouple elements which are bonded in a flexible belt of polyimide film. The design temperature range is from +30 F to +400 F continuously with an intermittent temperature of 500 F maximum. The thermocouple belt consists of 120 equally spaced copper-Constantan thermocouple junctions which is wrapped around the OMS liquid rocket engine combustion chamber, to monitor temperatures of individual cooling channels. Each thermocouple is located over a cooling channel near the injector end of the combustion chamber. The thermocouple array sensor is held in place by a spring loaded clamp band. Analyses show that in the event of a blocked cooling channel the surface temperature of the chamber over the blocked channel will rise from a normal operating temperature of approx. 300 F to approx. 600 F. The hot spot detector will respond quickly to this change with a response time constant less than 0.05 seconds. The hot spot sensor assembly is fabricated with a laminated construction of layers of Kapton film and an outer protective layer of fiberglass reinforced silicone rubber. Author

N86-13709# California Univ., Santa Barbara. Dept. of Physics.
CHARGE-DENSITY WAVES OBSERVED WITH A TUNNELING MICROSCOPE Technical Report, 1 Feb. 1984 - 31 Jan. 1985
R. V. Coleman, B. Drake, P. K. Hansma, and S. Slough 1 Jul. 1985 9 p
(Contract N00014-76-C-0011)
(AD-A158779) Avail: NTIS HC A02/MF A01 CSCL 20/12

Charge-density waves on cleaved surfaces of 1T-TaS2 appeared at 77 K as hexagonal arrays of mounds with spacings of 3.5 + or - 0.3a(o) where a(o)=3.346A is the lattice spacing of the 1T-TaS2. In contrast, cleaved surfaces of 2H-TaSe2 at 77 K showed only atoms. The tunneling microscope was operated under liquid atoms. The tunneling microscope was operated under liquid nitrogen with a Pt(0.8)Ir(0.2) tip for both types of samples. Author (GRA)

N86-13710# Fame Associates, Inc., Fort Collins, Colo.
OPTICAL/INFRARED PROPERTIES OF ATMOSPHERIC AEROSOLS WITH AN IN SITU, MULTI-WAVELENGTH, MULTICHANNEL NEPHELOMETER SYSTEM Final Report, 15 Sep. 1984 - 14 Mar. 1985 on Phase 1

J. B. Wedding, Y. J. Kim, and M. A. Weigand Apr. 1985 63 p
(Contract F49620-84-C-0101)
(AD-A158825; FA-AF-14385; AFOSR-85-0506TR) Avail: NTIS HC A04/MF A01 CSCL 17/8

There exists a need to develop new instrumentation which can provide an in situ, real time measurement of the total differential scattering patterns from individual airborne particles of different composition and shape under natural and man-made atmospheric conditions. During the Phase 1 study, a literature survey was conducted, system requirements developed for an in situ, multiwavelength, multichannel nephelometer system, and technical feasibilities were investigated. Finally, design parameters of the nephelometer system including the particle sampling inlet, the optical system, and the data acquisition system were optimized. The proposed nephelometer system will measure the differential scattering patterns of individual aerosol particles at three laser wavelengths, in three scattering planes. Successful development of such an instrument during the Phase 2 efforts will assist in filling the void of knowledge of the optical/infrared properties of atmospheric aerosols and their interactions with electromagnetic radiation fields. Author (GRA)

N86-13711# Aerospace Corp., El Segundo, Calif. Electronics and Optics Div.

RECTIFICATION AND REGISTRATION OF REMOTELY SENSED DATA Final Report

B. G. Kashef and A. A. Sawchuk 25 Jun. 1985 92 p Prepared in cooperation with University of Southern California, Los Angeles
(Contract F04701-83-C-0084)
(AD-A158827; TR-0084A(9975)-1; SD-TR-85-40) Avail: NTIS HC A05/MF A01 CSCL 17/9

An important problem in any onboard imaging system is the rectification and registration of images generated by onboard sensors. Accurate registration is a key requirement for detecting changes (in position, brightness, texture, boundary, etc.), from one sensed image to the next, as well as classification of data for intelligence gathering and vehicle guidance. This report discusses techniques of finding match points in pairs of images and performing geometric corrections and unwarping to compensate for systematic and random variations in the flight path, ephemeris, and sensor response. Techniques of resampling and interpolation of image data are reviewed, and the particular characteristics of sensors operating over a wide spectrum from visible through infrared and microwave are discussed. Particular attention is given to the rectification and registration of synthetic aperture radar (SAR) imagery, and several future study tasks on this specialized area are outlined. GRA

N86-13712# Northwestern Univ., Evanston, Ill. Dept. of Materials Science.

NEUTRON STRESS MEASUREMENTS WITH A POSITION SENSITIVE DETECTOR

A. D. Krawitz, P. J. Rudnik, B. D. Butler, and J. B. Cohen Aug. 1985 18 p
(Contract N00014-80-C-0116)
(AD-A158882; TR-20) Avail: NTIS HC A02/MF A01 CSCL 18/4

The feasibility of measuring residual and applied stresses with neutrons employing a position sensitive detector (PSD) is demonstrated. Measurements with both a small beam, to probe internal regions, and a large beam, for bulk sampling have been made. With such a detector collection of data is rapid compared to ordinary neutron collection methods. This detector allows more detailed sampling, smaller probe regions and possibly even study of time-dependent processes. The spectrometer geometry is shown. The detector consists of a three-counter array of linear PSD's spanning a usable angular range of 25 degrees 2 theta at a distance of 1220 mm from the sample position. The detectors are stacked in a vertical plane which is normal to the horizontal diffraction plane. The front of the detector housing has an oscillating radial collimator which greatly reduces background and off-axis scattering. The data is rebinned into 0.1 degrees 2 theta increments from the basic channel width of approximately 0.03 degrees and the intensity of the three detectors is added. From these experiments we have shown that the PSD in use at the University of Missouri Research Reactor Facility is an important tool for the application of neutron scattering to engineering materials, in addition to its use in more traditional neutron scattering experiments. This is because of the significant savings in data collection time and the increased range of feasible experiments. The resolution and behavior of this instrument has been demonstrated to be on a par with standard detectors. GRA

N86-13713# North Carolina Univ., Chapel Hill. Inst. of Statistics.

A NOTE ON THE EFFECT OF IGNORING SMALL MEASUREMENT ERRORS IN PRECISION INSTRUMENT CALIBRATION Technical Report, Sep. 1984 - Sep. 1985

R. J. Carroll and C. H. Spiegelman Jun. 1985 17 p
(Contract F49620-82-C-0009)
(AD-A159104; MIMEO-SER-1580; AFOSR-85-0701TR) Avail: NTIS HC A02/MF A01 CSCL 12/1

The authors' focus is the simple linear regression model with measurement errors in both variables. It is often stated that if the measurement error in x is small, then we can ignore this error and fit the model to data using ordinary least squares. There is some ambiguity in the statistical literature concerning the exact meaning of a small error. For example Draper and Smith (1981) state that if the measurement error variance in x is small relative to the variability of the true x's, then errors in the x's can be effectively ignored, see Montgomery and Peck (1983) for a similar statement. Scheffe (1983) and Mandel (1984) argue for a second criterion, which may be informally summarized that the error in x should be small relative to (the standard deviation of the observed Y about the line)/(slope of the line). We argue that for calibration experiments both criteria are useful and important, the former for estimation of x given Y and the latter for confidence intervals for x given Y. Author (GRA)

N86-13714# Department of the Navy, Washington, D. C.

AN OIL/WATER DISPERSER DEVICE FOR USE IN AN OIL CONTENT MONITOR/CONTROL SYSTEM Patent Application

F. D. Kempel, inventor (to Navy) Filed 2 Jul. 1985 17 p
(AD-D011868; US-Patent-Appl-SN-751347) Avail: NTIS HC A02/MF A01 CSCL 13/2

This patent application discloses an oil content monitor/control unit system, including an oil/water disperser device, which is configured to automatically monitor and control processed effluent from an associated oil/water separator so that if the processed effluent exceeds predetermine in-port or at-sea oil concentration lmits, it is either recirculated to an associated oil/water separator via a ship's bilge for additional processing, or diverted to a holding tank for storage. On the other hand, if the oil concentration of the processed effluent is less than predetermine in-port or at-sea limits, it is discharged overboard. The oil/water disperser device is configured to break up any oil present in the processed effluent into uniform droplets for more accurate sensing of the oil present in the processed effluent into uniform droplets for more accurate sensing of the oil-in-water concentration level thereof. The oil/water disperser device has a flow-actuated variable orifice configured into a spring-loaded polyethylene plunger which provides the uniform distribution of oil droplets. GRA

N86-13715# Department of the Navy, Washington, D. C.

TIME RESOLVED EXTENDED X-RAY ABSORPTION FINE STRUCTURE SPECTROMETER Patent Application

H. W. Huang, inventor (to Navy) Filed 17 May 1985 19 p
(AD-D011869; US-Patent-Appl-SN-734986) Avail: NTIS HC A02/MF A01 CSCL 20/6

The present invention relates to an X-ray spectrometer for obtaining EXAFS data from a target material. The target material is exposed to incident pulsed synchrotron/X-ray radiation having a selected range of continuous spectrum and intensity suitable for obtaining EXAFS data from the material. The transmitted or fluorescence X-rays is detected and integrated over a period of time. The integrator is controlled by a rate synchronous with the pulsed radiation. The integration time of the integrator can be varied. A xenon flash is provided for exciting appropriate materials and is controlled by a gating device which is also synchronized with the radiation pulses. Author (GRA)

N86-13716# Department of the Navy, Washington, D. C.
EXPENDABLE BATHYTHERMOGRAPH FOR MEASURING LIGHT ATTENUATION AND TEMPERATURE BELOW THE OCEAN SURFACE Patent Application
C. H. Sinex and B. E. Raff, inventors (to Navy) Filed 12 Jun. 1985 13 p
(AD-D011870; US-Patent-Appl-SN-744084) Avail: NTIS HC A02/MF A01 CSCL 08/10

An expendable bathythermograph sensor is modified to include a fiber optic light pipe mounted thereon to carry incident light to a photodiode unit located inside the sensor. A thermistor is mounted on the sensor, and the photodiode unit includes multiplexed electronics for transmitting both optical and temperature data to measure temperature and light as a function of ocean depth. GRA

N86-13717# Department of the Navy, Washington, D. C.
OIL CONTENT MONITOR/CONTROL SYSTEM AND METHOD Patent Application
R. F. Schmitt, J. A. Gavin, F. D. Kempel, and C. N. Waltrick, inventors (to Navy) Filed 2 Jul. 1985 17 p
(AD-D011871; US-Patent-Appl-SN-751346) Avail: NTIS HC A02/MF A01 CSCL 13/2

This patent application discloses an oil content monitor/control unit system which is configured to automatically monitor and control processed effluent from an associated oil/water separator so that if the processed effluent exceeds predetermined in-port or at-sea oil concentration limits, it is either recirculated to an associated oil/water separator via a ship's bilge for additional processing, or diverted to a holding tank for storage. On the other hand, if the oil concentration of the processed effluent is less than determined in-port or at-sea limits, it is discharged overboard. GRA

N86-13718# Department of the Navy, Washington, D. C.
REMOTE OPTICAL CRACK SENSING SYSTEM Patent Application
S. L. Huang, A. Scotese, and M. Libeskind, inventors (to Navy) Filed 12 Oct. 1984 12 p
(AD-D011872; US-Patent-Appl-SN-660349) Avail: NTIS HC A02/MF A01 CSCL 14/2

An apparatus is disclosed for remotely detecting cracks of sub-critical length which originate from stress raisers in structural material, wherein the apparatus typically comprises a source of light, a continuous length of optical fiber to conduct the light, strain responsive devices coupled to the fiber and bonded to the structural member in close proximity to the stress raisers, and a light responsive detector which is optically coupled to the fiber in order to detect breaks in the fiber induced by either tensile or shear forces eminating from cracks around the stress raisers. Author (GRA)

N86-13719# Department of the Navy, Washington, D. C.
VARIABLE TEMPERATURE TRAP Patent Application
C. Clavell, Jr., inventor (to Navy) Filed 21 Jun. 1985 10 p
(AD-D011874; US-Patent-Appl-SN-747220) Avail: NTIS HC A02/MF A01 CSCL 08/10

Heretofore, arriving at reliable figures for determination of organotin compound concentrations has been hampered due to the lack of a suitable device for trapping the compounds and making an analysis or detection of their presence and concentration. This has been particularly true in the case of seawater analysis where some of the organotin compounds have been leached into seawater from various anti-fouling coatings. The present invention is directed to providing an apparatus responsive to an external control for enabling a precise analysis of organotins in a gas sample by a detector. An elongate glass tube containing a small amount of granular absorbent material held between quartz fiber plugs is coupled to receive the gas sample and concentrate the organotins, as well as being coupled to the detector for subsequent elution. An elongated temperature probe coaxially extends through the longitudinal chamber and into the absorbent material to provide an indication of temperature to the external control. A liquid nitrogen container is shaped to contain the portion of the elongated tube having the longitudinal chamber to lower the chamber's temperature below the temperature required for concentrating the organotins. A helically wound coil about the outside of the elongated tube heats the longitudinal chamber so that at discrete temperature levels a separation is effected and the organotins of interest are eluted from the chamber to the detector thereby allowing a precise analysis of the organotins of interest. GRA

N86-13720# Mason and Hanger-Silas Mason Co., Inc., Amarillo, Tex.
SPECIALIZED INSTRUMENT FOR RADIATION ASSISTANCE TEAMS
J. A. Applegate Aug. 1985 9 p
(Contract DE-AC04-76DP-00487)
(DE85-017390; MHSMP-85-39) Avail: NTIS HC A02/MF A01

A specialized multiradiation instrument for radiation assistance teams (RAT's) has been designed; a working prototype has been constructed and field tested. The instrument detects alpha, beta, and gamma radiation simultaneously with simple red, yellow, and green meter indications and audio outputs. It is basically intended for DOE radiation assistance teams but would have application to any government, military, or industrial radiation accident team. DOE

N86-13721# Sandia National Labs., Albuquerque, N. Mex.
HIGH SPEED MULTI-CHANNEL DATA RECORDER TO REPLACE OSCILLOSCOPE DATA ACQUISITION SYSTEMS
W. F. Filter, J. Chang, C. O. Landron, G. J. Lockwood, D. J. Muron, B. T. Neyer, and L. E. Ruggles 1985 17 p Presented at the 5th IEEE Pulsed Power Conf., Washington, D.C., 10 Jun. 1985
(Contract DE-AC04-76DP-00789)
(DE85-015155; SAND-84-2545C; CONF-850616-70) Avail: NTIS HC A02/MF A01

A photonic high speed analog data recording system previously developed in our laboratory was used for the first time in the operational environment of a large pulsed power accelerator. A retrofit capability of this system is demonstrated by recording waveforms from analog electrical sensors using laser diode transmitters. A key component of the system, a prototype High Speed Multi-Channel Data Recorder, and its application on the Sandia HydraMITE II accelerator are described. DOE

N86-13722# Department of Energy, Washington, D. C.
APPARATUS FOR REMOVABLY HOLDING A PLURALITY OF MICROBALLOONS Patent Application
E. S. Jorgensen, inventor (to DOE) Filed 5 Jun. 1984 9 p
(Contract W-7405-eng-36)
(DE85-006517; US-Patent-Appl-SN-617657) Avail: NTIS HC A02/MF A01

The present invention relates generally to the manipulation of microballoons and more particularly to an apparatus for removably holding a plurality of microballoons in order to more efficiently carry out the filling of the microballoons with a known quantity of gas. DOE

N86-13723# Lawrence Livermore National Lab., Calif.
PHOTOELECTRONIC TRAJECTORY ANATOMY OF RCA-C-73435 IMAGE CONVERTER AND ITS PERFORMANCE
C. C. Lai, L. B. Olk, and R. D. Lear 7 Jun. 1985 6 p refs Presented at the IEEE Conf. on Photoelectron. Imaging, London, 10 Sep. 1985
(Contract W-7405-eng-48)
(DE85-013973; UCRL-91699; CONF-8509104-1) Avail: NTIS HC A02/MF A01

A two dimensional electron optics code, which fully incorporates space charge and self magnetic effects, was used to compute the photoelectronic trajectories in a RCA-C-73435 image converter streak tube. The code reveals the beam trace formations in graphic detail, as well as provides numerical data on static and dynamic imaging parameters, including focused field profile, spatial resolution, linear distortion, transit time dispersion and chromatic aberration. These computational results correlate qualitatively with the experimental ones obtained under corresponding conditions. The study thus establishes a set of computer simulation estimates on tube performance as a function of the electron emitting characteristics at the photocathode and as a function of the electrode voltages. DOE

N86-13724# Institut Franco-Allemand de Recherches, St. Louis (France).
HOLOGRAPHIC STUDY OF THE PARTICLES PRODUCED BY THE INJECTOR IN A VIKING MOTOR [ETUDE HOLOGRAPHIQUE DE LA PULVERISATION PRODUITE PAR UN INJECTEUR DE MOTEUR VIKING]
H. Royer 29 May 1984 40 p refs In FRENCH
(ISL-R-111/84) Avail: NTIS HC A03/MF A01

A microholographic study of the jet of particles produced by the injector on the Ariane launcher is discussed. The experimental set-up included the utilization of a single beam laser. The study was made in order to investigate combustion instabilities in the Ariane motors. The results from 4 holograms show a Rosin Rammler distribution law with modes at 60 and 200 microns. Author (ESA)

N86-13725# Royal Netherlands Aircraft Factories Fokker, Schiphol-Oost.
DEVELOPMENT OF A BREADBOARD COOLER FOR INFRARED REMOTE SENSING PAYLOADS, PHASE 2 Final Report
N. P. Enderberg and E. G. Overbosch Paris ESA May 1984 86 p refs
(Contract ESTEC-4620/81/NL-PP)
(FOK-RV-R-82-072; ESA-CR(P)-1934) Avail: NTIS HC A05/MF A01

The major components of an IR sensor cooler were studied. First and second-stage straps manufactured from glass fiber reinforced plastic pass static and dynamic tests, although the second-stage straps were more critical. Pretensioning problems during assembly of second-stage straps in the cooler were solved. The integrated second-stage suspension passes static, sine-vibration and random vibration tests. The parabolic mirror was made by electroforming on a precision-turned parabolic mandril. Representative flat samples were prepared and optically tested to develop the most appropriate electroforming technique. A full size mandril (die) and mirror were manufactured. Samples of open faced honeycomb were prepared to represent the second-stage radiator. An increased number of sprayed layers with black paint gives the best result. Emittance tests confirm the expected epsilon increase of the emitting area. Author (ESA)

N86-13726# Office of Radiation Programs, Las Vegas, Nev.
REPORT ON AN AUTOMATED CALIBRATION RANGE FOR BROADBAND ISOTROPIC PROBES
J. Johnson Jun. 1985 143 p
(PB85-231470; EPA-520/6-85-021) Avail: NTIS HC A07/MF A01 CSCL 14B

The construction of an automated absolute field generation system using standard gain horns and an anechoic range is discussed. The system operates in the frequency range of 1.12 to 26.5 GHz. The primary purpose of the range is automated evaluation of the frequency response and isotropy of various commercially available microwave hazard survey meters. GRA

N86-13727# Rockwell International Corp., Thousand Oaks, Calif.
DEVELOPMENT AND EVALUATION OF AN INSTANTANEOUS ATMOSPHERIC CORROSION RATE MONITOR Final Report
F. Mansfeld, S. L. Jeanjaquet, M. W. Kendig, and D. K. Roe Jun. 1985 84 p Prepared in cooperation with Portland State Univ., Oreg.
(Contract EPA-68-02-3741)
(PB85-214336; EPA-600/3-85-048) Avail: NTIS HC A05/MF A01 CSCL 14B

A research program was carried out in which a new instantaneous atmospheric corrosion rate monitor (ACRM) was developed and evaluated, and equipment was constructed which will allow the use of many sensors in an economical way in outdoor exposures. In the first task, the ACRM was developed and tested in flow chambers in which relative humidity and gaseous and particulate pollutant levels can be controlled. Diurnal cycles and periods of rain were simulated. The effects of aerosols were studied. A computerized system was used for collection, storage, and analysis of the electrochemical data. In the second task, a relatively inexpensive electronics system for control of the ACRM and measurement of atmospheric corrosion rates was designed and built. In the third task, calibration of deterioration rates of various metallic and nonmetallic materials with the response of the ACRMs attached to these materials was carried out under controlled environmental conditions using the system developed in the second task. A Quality Assurance project plan was prepared with inputs from the Rockwell International Environmental Monitoring and Service Center and Quality Assurance System audits were performed. GRA

N86-14169# Joint Publications Research Service, Arlington, Va.
DETERMINING FLEXURE OF AERIAL CAMERA SMOOTHING GLASS Abstract Only
V. N. Lavrov *In its* USSR Rept.: Space (JPRS-USP-85-005) 30 Sep. 1985 p 107 Transl. into ENGLISH from Geod. i Kartografiya (Moscow), no. 11, Nov. 1984 p 30-33 (For primary document see N86-14111 04-88)
Avail: NTIS HC A08

36 LASERS AND MASERS

Includes parametric amplifiers.

N86-13728# Army Missile Command, Redstone Arsenal, Ala. Advanced Sensors Directorate.
CONCEPT OF LASER LOCATOR SYSTEMS (BASED ON THE GEOMETRY OF THE TRIANGULAR CORNER CUBE REFLECTOR)
H. B. Holl May 1985 95 p
(AD-A157795; AD-E950723; AMSMI/RE-85-12-TR) Avail: NTIS HC A05/MF A01 CSCL 17/3

This report provides a brief discussion of a concept for Laser Locator Systems, and for measuring the horizontal and vertical aspect angles of radiation received from a remote laser transmitter. The systems are grouped in retroreflecting systems and non-retroreflecting systems. The non-reflecting systems are subdivided in three-mirror systems and two-mirror systems, of which the last systems have either two parallel located detector arrays, or orthogonally located linear detector arrays. The radiation receiving components are a triangular corner cube reflector, or sets of dihedral mirrors, or flat-strip mirrors. The concept is useful for radiation from the visible to the millimeter wavelength region for a single pulse or continuous radiation, and is insensitive to hot spots in the radiation. Author (GRA)

N86-13729# Physical Sciences, Inc., Andover, Mass.
EXPERIMENTAL AND THEORETICAL STUDIES OF LASER PROPULSION PHENOMENOLOGY Final Technical Report, 15 Jan. 1984 - 28 Feb. 1985
D. Rosen, G. Caledonia, N. Kemp, R. Krech, and L. Cowles Mar. 1985 37 p
(Contract F49620-83-C-0039)
(AD-A158273; PSI-039; TR-505; AFOSR-85-0577TR) Avail: NTIS HC A03/MF A01 CSCL 20/5

The work performed in this 2-year effort involved two tasks: one dealing with issues related to laser energy absorption in a pulsed thruster and the other dealing with issues related to laser energy absorption in a CW thruster. For the pulsed studies, the first year's effort involved theoretical and experimental investigations of the threshold requirements for achieving laser-induced gas breakdown at short wavelengths (< 1 micrometer). With these breakdown studies completed, the next step, initiated in the second year, was to determine the degree of pulsed laser energy absorption that can be achieved in the laser-initiated plasma. Toward this end pulsed laser energy deposition studies were performed using a pulsed Nd:glass laser as the energy source (wavelength = 1.05 micrometers, pulse duration = 20 ns) and high pressure hydrogen and argon gases as the absorption media. The percentage of laser energy absorbed in the laser-produced plasma was determined from measurements of the fraction of laser energy transmitted through the breakdown region, as well as from optical interferometric measurements to determine the strength of the laser-produced blast wave. The initially deposited energy was inferred from the measured blast wave trajectories by comparing them with predicted trajectories calculated by a detailed hydrodynamic model. Results are presented for the energy deposition efficiency achieved in argon and hydrogen as a function of initial gas pressure (0.3 atm < P < 10 atm). GRA

N86-13730# Battelle Columbus Labs., Ohio.
LASER PRODUCED X-RAY FOR HIGH RESOLUTION LITHOGRAPHY Annual Report, 15 Dec. 1983 - 14 Dec. 1984
H. M. Epstein 17 Apr. 1985 42 p
(Grant AF-AFOSR-0066-82)
(AD-A158734; AFOSR-85-0501TR) Avail: NTIS HC A03/MF A01 CSCL 14/5

During the past year the research effort was concentrated on the rapidly pulsed laser-plasma X-ray source. The effort was divided into three areas: developing the source and system, studying improved diagnostic, and making accurate X-ray measurements over a parameter matrix. GRA

N86-13731# Saint John Fisher Coll., Rochester, N.Y. Dept. of Physics.
MULTILEVEL RELAXATION PHENOMENA AND POPULATION TRAPPING Report, 1 Jul. 1984 - 30 Jun. 1985
F. T. Hioe Apr. 1985 4 p refs
(Contract DE-FG02-84ER-13243)
(DE85-011527; DOE/ER-13243/1) Avail: NTIS HC A02/MF A01

New analytic results have been found for a wide variety of atomic excitation processes which involve the use of amplitude and frequency modulated laser pulses. Our analytic solutions apply equally to mathematically analogous atomic collision problems. DOE

N86-13732# Rochester Univ., N. Y. Lab. for Laser Energetics.
ACTIVE MIRROR BOOSTED 351 nm LASER IRRADIATION FACILITY
T. Kessler, R. Bahr, W. Seka, J. M. Soures, and J. Kelly 1985 6 p Presented at the Conf. on Lasers and Electro-Optics, Baltimore, 21 May 1985
(Contract DE-FC08-85DP-40200)
(DE85-014412; DOE/DP-40124/71(1); CONF-850558-4) Avail: NTIS HC A02/MF A01

The Glass Development Laser, a single beam, frequency tripled Nd:phosphate glass laser, has been upgraded with 25 cm active mirror amplifiers to generate in excess of 300 joules in 1 nsec at 1054 nm and 200 joules at 351 nm. The system design and performance is discussed. DOE

N86-13733# Rochester Univ., N. Y. Lab. for Laser Energetics.
RETROFIT OF A HIGH POWER Nd:GLASS LASER SYSTEM WITH LIQUID CRYSTAL POLARIZERS
S. D. Jacobs, K. A. Ceruga, T. J. Kessler, W. Seka, and R. Bahr Mar. 1985 9 p Presented at the Boulder Damage Symp., Boulder, Colo., 15 Oct. 1984
(Contract DE-FC08-85DP-40200)
(DE85-014415; DOE/DP-40200/07; CONF-8410276-3; Rept-163) Avail: NTIS HC A02/MF A01

The glass development laser (GDL), has been operating at the Laboratory for Laser Energetics since 1978. This Nd:phosphate glass system produces high peak power optical radiation at lambda = 1054 nm or lambda = 351 nm for use in studying the interaction physics of intense laser beams with matter. The amplifier staging incoprates the propagation of linearly and circularly polarized light in rod amplifiers which vary in diameter from 16 nm to 90 mm. Numerous quartz or mica quarter waveplates and Brewster angle dielectric thin film polarizers are required to limit accumulated phase retardation between amplification stages and to accommodate interstage Pockels' cell isolation switches. We have recently replaced most of the waveplate dielectric polarizer combinations in GDL with liquid crystal polarizers. Comprised of 11 (MU)m thick cholesteric fluids sandwiched between optical quality glass plates, liquid crystal polarizers provide excellent polarization properties, low insertion loss, angular insensitivity, and laser damage resistance at lambda = 1054 nm. The design, fabrication, and performance of left handed and right handed circular polarizers will be discussed. DOE

N86-13452# Joint Publications Research Service, Arlington, Va.
EXTREMELY HIGH REFLECTIVE CAPABILITY OF ZIRCONIUM BURNING IN AIR UNDER EFFECTS OF CONSTANT CO2 LASER RADIATION Abstract Only
O. G. Buzykin, A. V. Burmistrov, M. N. Kogan, V. I. Konov, A. M. Prokhorov, and V. G. Ralchenko *In its* USSR Rept.: Mater. Sci. and Met. (JPRS-UMS-85-006) 29 Jul. 1985 p 22 Transl. into ENGLISH from Izv. Akad. Nauk SSSR: Ser. Fiz. (Moscow), v. 49, no. 4, Apr. 1983 p 779-782 Original language document was announced in IAA as A85-35470 (For primary document see N86-13422 04-26)
Avail: NTIS HC A05

N86-13454# Joint Publications Research Service, Arlington, Va.
CERTAIN FEATURES OF LASER DESTRUCTION AND DISLOCATIONAL STRUCTURE OF SILICON DURING HEATING AND EFFECTS OF ELECTRICAL FIELD Abstract Only
M. S. Bakharev, A. A. Gorbachev, L. I. Mirkin, a. S. Mokh, and R. R. Sheverdova *In its* USSR Rept.: Mater. Sci. and Met. (JPRS-UMS-85-006) 29 Jul. 1985 p 23-24 Transl. into ENGLISH from Fiz. i Khim. Obrabotki Mater. (Moscow), no. 2, Mar. - Apr. 1985 p 37-40 (For primary document see N86-13422 04-26)
Avail: NTIS HC A05

N86-13548# Tennessee Univ., Tullahoma. Center for Laser Applications.
LASER THERMAL PROPULSION Abstract Only
Dennis Keefer, Carroll Peters, Herbert Crowder, and Richard Wells *In* AFOSR The 1985 AFOSR/AFRPL Chem. Rocket Res. Meeting Feb. 1985 3 p (For primary document see N86-13507 04-28)
Avail: NTIS HC A11/MF A01

N86-13549# Pennsylvania State Univ., University Park.
ANALYTICAL MODELING OF STRONG RADIATION GAS-DYNAMIC INTERACTION Abstract Only
Charles L. Herkle *In* AFOSR The 1985 AFOSR/AFRPL Chem. Rocket Res. Meeting Feb. 1985 3 p (For primary document see N86-13507 04-28)
Avail: NTIS HC A11/MF A01

N86-13550# Illinois Univ., Urbana-Champaign.
EXPERIMENTAL STUDIES OF LASER-SUSTAINED ARGON PLASMAS FOR CW LASER PROPULSION APPLICATIONS Abstract Only
Herman KRier and Jyoti Mazumder *In* AFOSR The 1985 AFOSR/AFRPL Chem. Rocket Res. Meeting Feb. 1985 3 p (For primary document see N86-13507 04-28)
Avail: NTIS HC A11/MF A01

N86-13551# Physical Sciences, Inc., Andover, Mass.
LINEAR AND SATURATED ABSORPTION OF LASER RADIATION IN HEATED CASES Abstract Only
Robert H. Krech, Lawren M. Cowles, George E. Caledonia, and David I. Rosen *In* AFOSR The 1985 AFOSR/AFRPL Chem. Rocket Res. Meeting Feb. 1985 3 p (For primary document see N86-13507 04-28)
Avail: NTIS HC A11/MF A01

N86-13552# Physical Sciences, Inc., Andover, Mass.
ENERGY DEPOSITION OF PULSED ONE MICRON LASER RADIATION IN H2 AND AR Abstract Only
David I. Rosen and Nelson H. Kemp *In* AFOSR The 1985 AFOSR/AFRPL Chem. Rocket Res. Meeting Feb. 1985 3 p (For primary document see N86-13507 04-28)
Avail: NTIS HC A11/MF A01

N86-13571# Sheffield Univ. (England). Dept. of Chemical Engineering and Fuel Technology.
DEVELOPMENT OF VELOCITY MEASUREMENT TECHNIQUE BY PULSED LASER DOPPLER ANEMOMETRY Abstract Only
B. C. R. Ewan and J. Swithenbank *In* AFOSR The 1985 AFOSR/AFRPL Chem. Rocket Res. Meeting Feb. 1985 3 p (For primary document see N86-13507 04-28)
Avail: NTIS HC A11/MF A01

N86-13572# Stanford Univ., Calif. Dept. of Mechanical Engineering.
QUANTITATIVE FLOW VISUALIZATION Abstract Only
Ronald K. Hanson *In* AFOSR The 1985 AFOSR/AFRPL Chem. Rocket Res. Meeting Feb. 1985 5 p (For primary document see N86-13507 04-28)
Avail: NTIS HC A11/MF A01

N86-13575# Carnegie-Mellon Univ., Pittsburgh, Pa. Dept. of Mechanical Engineering.
THE 1-D LASER DOPPLER INSTRUMENTATION Abstract Only
Holger T. Sommer *In* AFOSR The 1985 AFOSR/AFRPL Chem. Rocket Res. Meeting Feb. 1985 3 p (For primary document see N86-13507 04-28)
Avail: NTIS HC A11/MF A01

N86-13578# Yale Univ., New Haven, Conn. Center for Laser Diagnostics.
LASER EMISSION AND COHERENT RAMAN SCATTERING FROM INDIVIDUAL FLOWING DROPLETS Abstract Only
Richard K. Chang, Marshall B. Long, and Roman Kuc *In* AFOSR The 1985 AFOSR/AFRPL Chem. Rocket Res. Meeting Feb. 1985 3 p (For primary document see N86-13507 04-28)
Avail: NTIS HC A11/MF A01

N86-13579# Yale Univ., New Haven, Conn. Center for Laser Diagnostics.
SIZE AND SHAPE CHARACTERIZATION OF INDIVIDUAL FLOWING DROPLETS BY LASER LIGHT SCATTERING Abstract Only
Richard E. Chang, Boa-Teh Chu, and Marshall B. Long *In* AFOSR The 1985 AFOSR/AFRPL Chem. Rocket Res. Meeting Feb. 1985 3 p (For primary document see N86-13507 04-28)
Avail: NTIS HC A11/MF A01

N86-13581# Arizona State Univ., Tempe.
INTELLIGENT LASER DIFFRACTION INSTRUMENTATION FOR PARTICLE SIZE ANALYSIS Abstract Only
E. Dan Hirleman and Joseph I. Koo *In* AFOSR The 1985 AFOSR/AFRPL Chem. Rocket Res. Meeting Feb. 1985 3 p (For primary document see N86-13507 04-28)
Avail: NTIS HC A11/MF A01

N86-13609# Joint Publications Research Service, Arlington, Va.
PULSED, OPTICALLY PUMPED GAS-MIXTURE FIR LASERS
Pan Chengzhi, Han Shaoping, Qin Yi, Hou Qiguo, and Liu Xiuyun *In its* China Rept.: Sci. and Technol. (JPRS-CST-85-020) 24 Jun. 1985 p 122-125 refs Transl. into ENGLISH from Dianzi Chengzhi (Beijing), v. 13, no. 1, Jan. 1985 p 117-119 (For primary document see N86-13600 04-31)
Avail: NTIS HC A09/MF A01

N86-13611# Joint Publications Research Service, Arlington, Va.
FRG'S DORNIER DEVELOPS HIGH-RESOLUTION DISPLAY SYSTEM
Hans-Peter Engelhardt *In its* West Europe Rept.: Sci. and Technol. (JPRS-WST-85-030) 28 Oct. 1985 p 17-20 Transl. into ENGLISH from Dornier Post (West Germany), no. 4, 1984 p 21-23 (For primary document see N86-13610 04-31)
Avail: NTIS HC A04/MF A01

N86-13620# Joint Publications Research Service, Arlington, Va.
CNET OF FRANCE USES ORGANO-METALLIC EPITAXY FOR LASER
In its West Europe Rept.: Sci. and Technol. (JPRS-WST-85-030) 8 Nov. 1985 p 30-31 Transl. into ENGLISH from Electron. Actualites (Paris), 22 Mar. 1985 p 26 (For primary document see N86-13616 04-31)
Avail: NTIS HC A03/MF A01

N86-13774# Joint Publications Research Service, Arlington, Va.
STUDY OF OPTICAL-ACOUSTICAL PHENOMENA AT SURFACE OF STRONGLY ABSORBING CLEARING FLUIDS Abstract Only
F. V. Bunkin, K. L. Vodopyanov, L. A. Kulevskiy, G. A. Lyakhov, V. G. Mikhalevich, and A. M. Rodin *In its* USSR Rept.: Earth Sci. (JPRS-UES-85-009) 13 Nov. 1985 p 18 Transl. into ENGLISH from Izv. Akad. Nauk SSSR: Ser. Fiz. (Moscow), v. 49, no. 3, Mar. 1985 p 558-563 (For primary document see N86-13765 04-42)
Avail: NTIS HC A04/MF A01

37 MECHANICAL ENGINEERING

Includes auxiliary systems (non-power); machine elements and processes; and mechanical equipment.

N86-13734*# National Aeronautics and Space Administration. Lewis Research Center, Cleveland, Ohio.
DESIGN OF TRACTION DRIVES
Stuart H. Loewenthal and Erwin V. Zaretsky Oct. 1985 49 p refs Submitted for publication
(NASA-RP-1154; E-2143; NAS 1.61:1154) Avail: NTIS HC A03/MF A01 CSCL 13I

Traction drives are among the simplest of all speed-changing mechanisms. Because of their simplicity and their ability to smoothly and continuously adjust speed, they are excellent choices for many drive system applications. They have been used in industrial service for more than 100 years. Today's traction drives have power capacities which rival the best gear and belt drives due to modern traction fluids and highly fatigue-resistant bearing steels. This report summarizes methods to analyze and size traction drives. Lubrication principles, contact kinematics, stress, fatigue life, and performance prediction methods are presented. The effects of the lubricant's traction characteristics on life and power loss are discussed. An example problem is given which illustrates the effects of spin on power loss. Loading mechanism design and the design of nonlubricated friction wheels and rings are also treated. Author

N86-13735*# Cincinnati Univ., Ohio. Dept. of Aerospace Engineering and Engineering Mechanics.
KINEMATICS OF FOLDABLE DISCRETE SPACE CRANES Final Report
Adnan H. Nayfeh 26 Nov. 1985 26 p
(Grant NsG-1185)
(NASA-CR-176360; NAS 1.26:176360) Avail: NTIS HC A03/MF A01 CSCL 13I

Exact kinematic description of a NASA proposed prototype foldable-deployable discrete space crane are presented. A computer program is developed which maps the geometry of the crane once controlling parameters are specified. The program uses a building block type approach in which it calculates the local coordinates of each repeating cell and then combines them with respect to a global coordinates system. Author

N86-13736# Massachusetts Inst. of Tech., Cambridge. Dept. of Materials Science and Engineering.
FUSION WELDING RESEARCH Annual Technical Report
T. W. Eagar, G. B. Hunter, C. D. Allemand, A. Block-Bolten, and G. J. Dunn 30 Apr. 1985 43 p

(Contract N00014-80-C-0384)
(AD-A158253; ATR-5) Avail: NTIS HC A03/MF A01 CSCL 13/8

This report summarizes progress in fundamental research on welding processes. Studies include: metal vapors in the arc; development of a high speed infrared temperature monitor; digital signal analysis as a weld process monitor; convection in arc weld pools; droplet transfer and contact tip wear in gas metal arc welding of titanium; and fracture toughness of HY-80 weldments. GRA

N86-13737# Department of the Navy, Washington, D. C.
LATCH FOR DETACHABLY SECURING ELECTRONIC CARDS ALONG ORTHOGONAL LOADING AXES Patent Application
S. J. Kreta and J. J. Honn, inventors (to Navy) Filed 24 Jun. 1985 9 p
(AD-D011885; US-Patent-Appl-SN-748094) Avail: NTIS HC A02/MF A01 CSCL 13/5

The present invention relates to a latch for detachably securing electronics cards along orthogonal loading axes. A planar fixed gate is rigidly securable to an external supporting structure and is provided with at least one elongated protrusion extending above one of the planar surfaces. A planar movable gate is rigidly securable to an external electronics mountable structure wherein said movable gate is provided with at least one elongated groove on a planar surface. The planar fixed gate and the planar movable gate are abuttingly engagable to each other with the protrusion matingly fitted within the corresponding groove. The orientation of the protrusion and groove are orthogonal to an axis of a first loading force applicable to the moving gate. A fastener such as a threaded bolt rigidly maintains the planar surfaces of the fixed gate in engagement with the movable gate for rigid support along a second loading axis orthogonal to the first loading axis. Author (GRA)

N86-13738# European Space Tribology Lab., Risley (England).
[ACTIVITIES REPORT IN SPACE TRIBOLOGY] Progress Report, 1984
M. J. Todd Paris ESA Jan. 1985 16 p refs
(Contract ESTEC-5615/83/NL-PP)
(ESA-ESTL-72; ESA-CR(P)-2043) Avail: NTIS HC A02/MF A01

Spacecraft mechanism and lubrication tests are summarized. Solar array mechanisms; the Giotto despin mechanism; lead film lubrication; slip ring technology; oils and greases; MOS2 films; gears; lead ion-plated bearings; and fluid lubrication are studied. Author (ESA)

N86-13739# Consulenze Generali Roma (Italy).
CYCLOSYMMETRIC APPROACH TO THE DYNAMICS OF REPETITIVE MODULAR STRUCTURES Final Report
Carlo Arduini and Silvano Sgubini Paris ESA Nov. 1984 403 p refs
(Contract ESTEC-5260/82/NL-PB(SC))
(ESA-CR(P)-2062) Avail: NTIS HC A18/MF A01

The basic theory of cyclosymmetric analysis of modular repetitive structures is introduced. The approach consists of transforming the problem of an N bays structure, with n degrees of freedom each, from an (N.n) degrees of freedom problem to N problems of smaller dimension (e.g., of order n). This is possible for ring type boundary conditions by discrete Fourier transformation. Extension to dynamic response problems and to quasi modular structures is outlined. Author (ESA)

N86-13740# Centre de Recherches Scientifiques et Techniques de l'Industrie des Fabrications Metalliques, Brussels (Belgium).
[ACTIVITIES REPORT OF THE TECHNICAL AND SCIENTIFIC RESEARCH CENTER FOR THE METAL MANUFACTURING INDUSTRY] Annual Report, 1984 [RAPPORT ANNUEL DU COMITE PERMANENT AU CONSEIL GENERAL]
5 Jun. 1985 56 p refs In FRENCH
Avail: NTIS HC A04/MF A01

The research subjects include computerized simulation, metal casting, computer aided design and manufacturing, metallic structures, vessel manufacturing, steel welding, numerical control, flexible manufacturing systems, robotics, automation, and plastics manufacturing. Author (ESA)

N86-13741# Centre Technique des Industries Mecaniques, St. Etienne (France).
COMPUTERIZED SIMULATION AND DISPLAY OF EXTRUDING BY COLD FORGING Final Report [OPTIMIZATION DES PROGRAMMES DE FILAGE MIXTE]
Jean Francois Renaudin and Henri Jean Braudel (Ecole des Mines de Paris, Sophia Antipolis, France) Dec. 1983 117 p refs In FRENCH
(Contracts CETIM-4-79-6122; CETIM-4-77-5310)
(CETIM-1-3L-11-1) Avail: NTIS HC A06/MF A01

Computer programs in FORTRAN 4 were developed to study metal flow in combined cold extrusion of metals. The experimental determination of rheological material properties is required. The programs are named Filmix, Fildr and Filtub. They refer to three procedures to obtain axisymetric bodies. Experimental tests on XC10 steel validate the Filmix program. The tests show the influence of the rheological and tribological parameters. Author (ESA)

N86-13742# Joint Publications Research Service, Arlington, Va.
USSR REPORT: MACHINE TOOLS AND METALWORKING EQUIPMENT
29 Oct. 1985 88 p Transl. into ENGLISH from various Russian articles
(JPRS-UMM-85-014) Avail: NTIS HC A05/MF A01

Articles from journals and other publications of the U.S.S.R. on machine tools and metalworking equipment are presented. They are divided into areas on industry planning and economics, metal cutting and metal forming machine tools, automated lines and aggregated machining systems, and robotics. For individual titles, see N86-13743 through N86-13744.

N86-13743# Joint Publications Research Service, Arlington, Va.
NEW APPLICATIONS OF INDUSTRIAL ROBOTS NOTED
L. Volchkevich *In its* USSR Rept.: Machine Tools and Metalworking Equipment (JPRS-UMM-85-014) 29 Oct. 1985 p 76-79 Transl. into ENGLISH from Izv. (Moscow), 3 Jun. 1985 p 2 (For primary document see N86-13742 04-37)
Avail: NTIS HC A05/MF A01

In recent years new trends in robotics have appeared. The first of these is the switch from loading/transport to industrial robots. These do not merely imitate human actions, but enable both a faster and better performance of industrial operations. The assortment of such operations is rather large: spot and seam welding, cutting, soldering, cleaning of surfaces, removal of burr, painting, and application of galvanic coatings. The foremost achievement here is the improved quality of production through more precise adherence to operating conditions than is possible with manual labor. Productivity is also boosted. The second trend is the switch from hydraulic drive to electromechanical and the development of designs with a great variety of movements. Author

N86-13744# Joint Publications Research Service, Arlington, Va.
PROBLEMS WITH INTEGRATING ROBOTS IN CONVENTIONAL PRODUCTION
Ivan Vasilyevich Vorotyntsev *In its* USSR Rept.: Machine Tools and Metalworking Equipment (JPRS-UMM-85-014) 29 Oct. 1985 p 80-83 Transl. into ENGLISH from Moskov. Pravda (Moscow), 15 Nov. 1984 p 2 (For primary document see N86-13742 04-37)
Avail: NTIS HC A05/MF A01

An interview with a director of a grid and boring machine plant is presented. In the last three years, production at his plant has increased by 27 percent and labor productivity by 20 percent. There are a number of reasons for these increases, in particular the high technical level of production and the development of robotics. The integration of these robots with human workers is discussed, as well as the economic impact and the psychological factors. E.R.

N86-13745# Joint Publications Research Service, Arlington, Va.
USSR REPORT: MACHINE TOOLS AND METALWORKING EQUIPMENT
16 Oct. 1985 95 p Transl. into ENGLISH from various Russian articles
(JPRS-UMM-85-013) Avail: NTIS HC A05

Industry planning and economics, metal cutting and metal forming machine tools, robots, process controls and automation electronics, and technology planning and management automation are some areas into which the articles from Soviet journals and other publications are divided. Some titles of articles presented are: New Efforts to Intensify Machine Tool Production; Machine Tools Made In-House to Modernize Production; Determination of Effective Placement of Equipment in Flexible Automated Production Systems; Robot Control System Modified for Precision Movement; and Active Monitoring of Tool Wear by Acoustical Emissions. For individual titles, see N86-13746 through N86-13748.

N86-13746# Joint Publications Research Service, Arlington, Va.
PROBLEMS WITH ROBOTIZATION OF CONVENTIONAL SHOPS
V. Chernomorskiy *In its* USSR Rept.: Machine Tools and Metalworking Equipment (JPRS-UMM-85-013) 16 Oct. 1984 p 69-73 Transl. into ENGLISH from Pravda Vostoka (Tashkent, USSR), 14 Jul. 1985 p 2 (For primary document see N86-13745 04-37)
Avail: NTIS HC A05

The experiences of robotizing an industrial reactor plant in the U.S.S.R. is presented. The physical environment is discussed: how to accommodate their size. How to gain more use from them is briefly discussed. And how to integrate them with people is also discussed. E.R.

N86-13747# Joint Publications Research Service, Arlington, Va.
ROBOT CONTROL SYSTEM MODIFIED FOR PRECISION MOVEMENT
P. M. Kuznetsov and M. L. Popov *In its* USSR Rept.: Machine Tools and Metalworking Equipment (JPRS-UMM-85-013) 16 Oct. 1985 p 74-77 Transl. into ENGLISH from Izv. Vyssh. Ucheb. Zaved.: Mash. (Moscow), no. 7, Jun. 1985 p 140-143 (For primary document see N86-13745 04-37)
Avail: NTIS HC A05

Questions of automating the robotized assembly of precision cylindrical joints under flexible automated production (GAP) are examined. As indicated by research that was performed, precision in the positioning of existing robot designs does not enable the indicated operation to be performed under GAP conditions. The potential of using additional devices with a view to resolving this task is examined. A specific route is proposed. An arrangement that provides for precision in the motion of mated surfaces is examined. Author

N86-13748# Joint Publications Research Service, Arlington, Va.
NEW ROBOTS BY SOVIET, CEMA MANUFACTURERS DESCRIBED
L. Eygel *In its* USSR Rept.: Machine Tools and Metalworking Equipment (JPRS-UMM-85-013) 16 Oct. 1985 p 78-83 Transl. into ENGLISH from Mater.-Tekhnicheskiye Snabzheniye (Moscow), no. 6, Jun. 1985 p 64-67 (For primary document see N86-13745 04-37)
Avail: NTIS HC A05

Right now integrated mechanization and automation of production processes are being introduced widely and worker manpower engaged in manual labor is being reduced steadily, especially in auxiliary operations. Means for programmed positional control, which are called industrial robots, are being applied to loading, unloading and warehouse transporting operations. These industrial robots and their manufacture are described. Author

N86-13483# Joint Publications Research Service, Arlington, Va.
POSSIBLE MECHANISM OF WAVE FORMATION DURING DETONATION WELDING Abstract Only
S. V. Bazdenko, V. F. Demichev, D. Kh. Morozov, and O. P. Pogutse *In its* USSR Rept.: Mater. Sci. and Met. (JPRS-UMS-85-006) 29 Jul. 1985 p 60 Transl. into ENGLISH from Fiz. Goreniya i Vzryva (Novosibirsk), v. 21, no. 1, Jan. - Feb. 1985 p 130-137 (For primary document see N86-13422 04-26)
Avail: NTIS HC A05

N86-13484# Joint Publications Research Service, Arlington, Va.
OPTIMIZATION OF TECHNOLOGICAL PARAMETERS OF COLD PRESSURE WELDING OF AD1M THIN ALUMINUM SHEETS Abstract Only
V. F. Kuzin, Yu. V. Savinkin, M. N. Tsypona, Ye. A. Kozelo, and M. A. Arkhangelskiy *In its* USSR Rept.: Mater. Sci. and Met. (JPRS-UMS-85-006) 29 Jul. 1985 p 61 Transl. into ENGLISH from Svarochnoye Proizv. (Moscow), no. 4, Apr. 1985 p 9-11 (For primary document see N86-13422 04-26)
Avail: NTIS HC A05

N86-13625# Joint Publications Research Service, Arlington, Va.
DIRECT INJECTION DIESEL MOTOR
R. Margary *In its* West Europe Rept.: Sci. and Technol. (JPRS-WST-85-029) 30 Sep. 1985 p 18-31 Transl. into ENGLISH from Ing. Automotoristica (Turin), Mar. 1985 p 197-201 Presented at the 1st Inform. Seminar on Subproj. Road Transportation, Turin, 15-16 Nov. 1984 (For primary document see N86-13622 04-31)
Avail: NTIS HC A04/MF A01

N86-13626# Joint Publications Research Service, Arlington, Va.
ITALIAN ROBOT MANUFACTURER ENTERS SPANISH MARKET
In its West Europe Rept.: Sci. and Technol. (JPRS-WST-85-029) 30 Sep. 1985 p 38-41 Transl. into ENGLISH from Rev. Robotica (Barcelona), May - Jun. 1985 p 27-30 (For primary document see N86-13622 04-31)
Avail: NTIS HC A04/MF A01

38 QUALITY ASSURANCE AND RELIABILITY

Includes product sampling procedures and techniques; and quality control.

N86-13749*# National Aeronautics and Space Administration. Lewis Research Center, Cleveland, Ohio.
PROBABILITY OF DETECTION OF INTERNAL VOIDS IN STRUCTURAL CERAMICS USING MICROFOCUS RADIOGRAPHY
George Y. Baaklini and Don J. Roth Nov. 1985 23 p refs
(NASA-TM-87164; E-2800; NAS 1.15:87164) Avail: NTIS HC A02/MF A01 CSCL 14D

The reliability of microfocus x-radiography for detecting subsurface voids in structural ceramic test specimens was statistically evaluated. The microfocus system was operated in the projection mode using low X-ray photon energies (<20 keV) and a 10 micro m focal spot. The statistics were developed for implanted subsurface voids in green and sintered silicon carbide and silicon nitride test specimens. These statistics were compared with previously-obtained statistics for implanted surface voids in similar specimens. Problems associated with void implantation are discussed. Statistical results are given as probability-of-detection curves at a 95 percent confidence level for voids ranging in size from 20 to 528 micro m in diameter. Author

N86-13750# California Univ., Los Angeles. Dept. of Materials Science and Engineering.
HIGH FREQUENCY QUANTITATIVE ANALYSIS OF MAGNETOMECHANICAL ACOUSTIC EMISSION Final Report, 15 Jun. 1981 - 14 Mar. 1985
K. Ono Jun. 1985 5 p
(Contract DAAG29-81-K-0116)
(AD-A158222; ARO-18220.8-MS) Avail: NTIS HC A02/MF A01 CSCL 14/2

This report summarizes the results of a research project for development of nondestructive evaluation methods for residual stresses. A method using computerized pattern recognition analysis can successfully estimate the level of residual stress, as well as microstructural changes of ferrous materials and components. GRA

N86-13751# Naval Ocean Systems Center, San Diego, Calif.
ENVIRONMENTAL STRESS SCREENING (ESS) Final Report, Oct. 1983 - Oct. 1984
C. C. Reader Jan. 1985 315 p
(AD-A158262; NOSC/TD-804) Avail: NTIS HC A14/MF A01 CSCL 13/8

The ESS is a technique of testing used for minimizing/eliminating hardware production-line workmanship errors. The application of vibration and temperature environments to items requiring screening can minimize/eliminate such errors as loose wires or parts, cold solder joints, loose screws or nuts, plus other assembly or fabrication type deficiencies. The ESS is applied at all stages of fabrication or assembly. The Naval Sea Systems requested that the commercial equipment used on the Precise Integrated Navigation System (PINS) be surveyed for compliance with NAVSEANOTE 3900 and NAVMAT P-9492. This investigation sought to determine the extent to which the PINS commercial equipment manufacturers apply ESS to their equipment during the manufacturing process and to compare commercial practices with Navy requirements in order to discover and document the differences. This report concludes that the limited investigation conducted does not provide a definitive basis for decision. Several alternatives for screening programs are discussed. GRA

N86-13752# Southwest Research Inst., San Antonio, Tex.
EXPLORATORY DEVELOPMENT ON ADVANCED EDDY CURRENT COIL EXCITATION AND SIGNAL PROCESSING Final Report, 9 Jan. 1981 - 9 Jan. 1984
J. L. Fisher, R. E. Beissner, and J. E. Doherty Apr. 1985 106 p
(Contract F33615-81-C-5036)
(AD-A159228; AFWAL-TR-85-4025) Avail: NTIS HC A06/MF A01 CSCL 14/2

The purpose of this program was to achieve improvements in eddy current performance by analytical and experimental exploratory development of the pulse mode of coil excitation as a means of evaluating surface and near-surface defects in low-conductivity materials used in gas turbine engine components. The program successfully demonstrated that the pulsed eddy current approach is capable of detecting flaws as small as 0.010 inch by 0.005 inch in a Ti-6-4 surface. In addition results indicate that this approach offers a promising way to estimate the depth of surface-breaking flaws. GRA

N86-13753# Sandia National Labs., Albuquerque, N. Mex.
TAPE JOINT DESIGN FOR A VIBRATION TABLE
R. P. Rechard and R. L. Mayes Jul. 1985 51 p
(Contract DE-AC04-76DP-00789)
(DE85-012617; SAND-84-1159) Avail: NTIS HC A04/MF A01

A proposal is made to connect the vibration shaker to its companion horizontal slip table with a large tape joint. An improved connection is needed to reduce the tie taken to switch the shaker from the vertical to the horizontal position and to transmit greater vibration to components bolted to the slip table. The distinct advantages of the tape joint are: self alignment, low mass, and joint stiffness; are important for the connection. For this tape joint design, the joint upset was eliminated; thus the standard design procedure was modified somewhat. To check the feasibility of reaching a 100 kip (445-kN) preload in a 15 in. (38-cm) section, a prototype joint is built. The static and dynamic tests verify the possibility of reaching the high preload. Furthermore, the tests indicate a small hydraulic jack is the best way to insert and remove the tapes. DOE

39 STRUCTURAL MECHANICS

Includes structural element design and weight analysis; fatigue; and thermal stress.

For applications see *05 Aircraft Design, Testing and Performance* and *18 Spacecraft Design, Testing and Performance.*

N86-13754# Aeronautical Research Labs., Melbourne (Australia).
A NUMERICAL INVESTIGATION INTO THE PLASTIC STRESS AND STRAIN FIELDS AROUND A SURFACE CRACK
R. Jones, M. Heller, and J. T. Barnby (Aston Univ.) 1985 17 p refs
(ARL/Struc-R-414; AR-003-990) Avail: NTIS HC A02/MF A01

In recent years a great deal of work has been undertaken in order to characterize the elastic and plastic stress strain fields around a crack which is either in plane strain or plane stress. A number of criteria for assessing severity has been proposed; of these the J integral approach and the strain energy density factor (i.e., S) approach are widely used and it has been shown that S and J are linearly proportional. A methodology for three dimensional elastic-plastic finite element is developed, and the validity of the functional form of the two dimension solution for a three dimensional crack is investigated. Author

N86-13755*# Case Western Reserve Univ., Cleveland, Ohio.
TIME DEPENDENCY OF STRAINRANGE PARTITIONING LIFE RELATIONSHIPS Final Report
Sreeramesh Kalluri and S. S. Manson Aug. 1984 64 p refs
(Grant NAG3-337)
(NASA-CR-174946; NAS 1.26:174946) Avail: NTIS HC A04/MF A01 CSCL 20K

The effect of exposure time (or creep rate) on the CP life relationship is established by conducting isothermal CP tests at varying exposure times on 316 Ss at 1300 and 1500 F. A reduction in the CP cycle life is observed with an increase in the exposure time of the CP test at a given inelastic strain-range. This phenomenon is characterized by modifying the Manson-Coffin type of CP relationship. Two new life relationships: (1) the Steady State Creep Rate (SSRC) Modified CP life relationship, and (2) the Failure Time (FT) Modified CP life relationship, are developed in this report. They account for the effect of creep rate and exposure time within the CP type of waveform. The reduction in CP cyclic life in the long exposure time tests is attributed to oxidation and the precipitation of carbides along the grain boundaries. Author

N86-13756# Arnold Engineering Development Center, Arnold Air Force Station, Tenn.
CRUSHING STRENGTH OF ALUMINUM OXIDE AGGLOMERATES Final Report, Apr. 1983 - Sep. 1984
R. A. Gamble Jul. 1985 40 p Prepared in cooperation with Sverdrup Technology, Inc., Arnold AFS, TN
(AD-A158051; AEDC-TR-85-16) Avail: NTIS HC A03/MF A01 CSCL 20/11

Aluminum oxide, which is formed during combustion of aluminum-based solid propellants, condenses and solidifies in the exhaust flow to form sub-micron-size particles, which may then adhere together to form agglomerates. Particle sampling, which is required for motor performance or environmental impact investigations, is usually done using a probe placed in the supersonic exhaust flow field. The bow shock at the sample probe inlet will decelerate the gas flow which introduces a large velocity differential between the gas and particulate. This differential will result in a sudden increase on the aerodynamic drag on the agglomerates which may cause them to shear apart, thus altering the sample size distribution. In this effort, aluminum oxide agglomerates were formed and then crushed in order to estimate the magnitude of the interparticle forces binding the agglomerate together. The agglomerates were formed by tumbling commercially available aluminum oxide powder in a container, and strength was determined by measuring the load required to crush the agglomerate between two flat plates. Analysis indicated that through, uniformly-shaped particles formed the strongest agglomerates. The experimentally-derived particle bonding forces were in agreement with values predicted by the van der Waal force equation for closely-spaced spheres. Rocket exhaust particulates collected from a test facility exhaust processing system proved to be unstable because of impurities. GRA

N86-13757# Wisconsin Univ., Madison. Mathematics Research Center.

A FUNCTIONAL EQUATION GOVERNING MOVING PHASE BOUNDARIES IN AN ELASTIC BAR Technical Summary Report

T. J. Pence Jun. 1985 40 p
(Contract DAAG29-80-C-0041; Grant NSF MCS-82-10950)
(AD-A158178; MRC-TSR-2827) Avail: NTIS HC A03/MF A01 CSCL 20/11

Certain elastic solids when subjected to sufficiently high loads abruptly change their mechanical properties and yet continue to respond elastically to further loading. In one dimension such mechanically induced elastic phase transitions may be due to a non-monotonic stress-strain curve. This document investigates the cumulative reflection of acoustic waves between the external boundary of the solid and the internal moving boundary separating distinct elastic phases. This latter phase boundary is similar to a gas dynamical shock wave. For the material introduced in this work, a functional equation governing the trajectory of a phase boundary is derived and shown to have a unique solution. This equation is treated asymptotically to determine the large time behavior of the phase boundary. Author (GRA)

N86-13758# Wisconsin Univ., Madison. Mathematics Research Center.

DEVELOPMENT OF SINGULARITIES IN NONLINEAR VISCOELASTICITY Technical Summary Report

J. A. Nohel and M. Renardy May 1985 17 p
(Contract DAAG29-80-C-0041; Grant NSF MCS-82-15064)
(AD-A158190; MRC-TSR-2821) Avail: NTIS HC A02/MF A01 CSCL 20/11

This paper discusses the motion of nonlinear viscoelastic materials with fading memory in one space dimension. It concentrates on viscoelastic solids and briefly remarks on similar results for fluids. After formulating the mathematical problems, the authors survey results for global existence of classical solutions to the initial value problem, provided the initial data are sufficiently small. They then discuss in some detail the development of singularities in initially smooth solutions for large data. GRA

N86-13759# Northwestern Univ., Evanston, Ill. Dept. of Materials Science.

ERRORS DUE TO COUNTING STATISTICS IN THE TRIAXIAL STRAIN (STRESS) TENSOR DETERMINED BY DIFFRACTION Technical Report

P. J. Rudnik and J. B. Cohen 1 Jul. 1985 13 p
(Contract N00014-80-C-0116)
(AD-A158219; TR-18) Avail: NTIS HC A02/MF A01 CSCL 20/11

Knowledge of the errors in a diffraction measurement of residual strains and stresses is useful information, not only in its own right, but also because it permits automation of a measurement to an operator specified precision. There are three sources of these errors: (1) instrumental effects; (2) uncertainties in X-ray elastic constants; and (3) errors in the diffraction peak position related to counting statistics. In this paper the errors are derived for the diffraction measurement of the three dimensional stress and strain tensor due to counting statistics. GRA

N86-13760# Army Materials and Mechanics Research Center, Watertown, Mass.

STATIC FATIGUE OF A SINTERED SILICON NITRIDE Final Report

G. D. Quinn Oct. 1984 16 p
(Contract DE-AI01-77CS51017)
(AD-A158813; AMMRC-TR-84-40) Avail: NTIS HC A02/MF A01 CSCL 11/2

The static fatigue resistance of a sintered silicon nitride was assessed at elevated temperature in air. The material was developed for heat engine applications. No difference in ambient or elevated temperature behavior was noted for the injection-molded or slip-cast versions. The material can maintain 150 MPa flexural stress for up to 1000 hours at 1200 C but is susceptible to slow crack growth and creep phenomena at higher stresses. Author (GRA)

N86-13761# Argonne National Lab., Ill.

SIMULATING DISTRIBUTED REINFORCEMENT EFFECTS IN CONCRETE ANALYSIS

A. H. Marchertas 1985 9 p refs Presented at the 8th Intern. Conf. on Struct. Mech. in Reactor Technol., Brussels, 19 Aug. 1985
(Contract W-31-109-eng-38)
(DE85-009745; CONF-850809-51) Avail: NTIS HC A02/MF A01

The effect of the bond slip is brought into the TEMP-STRESS finite element code by relaxing the equal strain condition between concrete and reinforcement. This is done for the elements adjacent to the element which is cracked. A parabolic differential strain variation is assumed along the reinforcement from the crack, which is taken to be at the centroid of the cracked element, to the point where perfect bonding exists. This strain relationship is used to increase the strain of the reinforcement in the as yet uncracked elements located adjacent to a crack. By the same token the corresponding concrete strain is decreased. This estimate is made assuming preservation of strain energy in the element. The effectiveness of the model is shown by examples. Comparison of analytical results is made with structural test data. The influence of the bonding model on cracking is portrayed pictorially. DOE

N86-13762# Argonne National Lab., Ill.

LONG-TERM ANALYSIS OF SLENDER CONCRETE STRUCTURES WITH CRACKING

J. C. Chern and A. H. Marchertas 1985 13 p Presented at the 8th Intern. Conf. on Struct. Mech. in Reactor Technol., Brussels, 19 Aug. 1985
(Contract W-31-109-eng-38)
(DE85-010275; CONF-850809-46) Avail: NTIS HC A02/MF A01

A special form of the finite element program, which is based on the equilibrium of forces in various cross sections of the beam together with the principle of virtual work, is presented for solving concrete beam problems. This analytical method uses the newly developed rheological element and exponential algorithm for computing time dependent deformation and stress distribution in cracked concrete members subjected to sustained loads, temperature, or drying. Temperature and moisture effects on hydration (aging) and creep rate are included. The rate effects of temperature and moisture on the deformation of concrete are also taken into account in the formulation. Numerical examples are used to illustrate the validity of the analysis on concrete beams. Plain and reinforced concrete beams subjected to bending, heating or drying are analyzed and checked against experimental data. DOE

N86-13763# Engineering System International, Rungis (France).

EMPLOYMENT OF PAM-FISS-BI-PHASE COMPUTER PROGRAM FOR THE STRENGTH ANALYSIS AND FRACTURE/DELAMINATION BEHAVIOR OF COMPONENTS Final Report

E. Haug, P. Dowlatyari, and A. deRouvray Paris ESA Jan. 1985 97 p
(Contract ESTEC-5489/83/NL-PB(SC))
(ESI-ED/83-383/RD/MS-Vol-7; ESA-CR(P)-2057) Avail: NTIS HC A05/MF A01

Numerical static tensile strength analysis and fracture behavior evaluation of a T300/914C carbon-epoxy (CE) composite material are summarized. Matrix (epoxy) macrocrack phenomena such as matrix splitting, matrix delamination and sublaminate matrix crack growth in process zones around notch roots were investigated using two and three-dimensional finite element models (with the PAM-FISS/BI-phase code), and compared to experimental results. For numerical analyses of unidirectional and multilayered notched/unnotched CE tensile specimens, a universal toughness criterion for matrix cracking under tensile static loading is proposed : GI = mode I strain energy release, calibrated at GIc = 0.15 N/mm for the T300 epoxy matrix used. Author (ESA)

N86-13491# Joint Publications Research Service, Arlington, Va.
DETERMINING LOCAL HEATING PARAMETERS FOR INCREASING FATIGUE RESISTANCE OF WELDED JOINTS Abstract Only
V. N. Maksimovich, A. A. Chabanenko, P. P. Mikheyev, O. I. Gushcha, and Yu. F. Kudryavtsev *In its* USSR Rept.: Mater. Sci. and Met. (JPRS-UMS-85-006) 29 Jul. 1985 p 65-66 Transl. into ENGLISH from Probl. Prochnosti (Kiev), no. 4, Apr. 1985 p 32-36 (For primary document see N86-13422 04-26)
Avail: NTIS HC A05

N86-13589*# National Aeronautics and Space Administration. Langley Research Center, Hampton, Va.
LARGE MODAL SURVEY TESTING USING THE IBRAHIM TIME DOMAIN IDENTIFICATION TECHNIQUE Final Report
Samir R. Ibrahim (Old Dominion Univ.) and Richard S. Pappa *In* Old Dominion Univ. Dyn. Identification for Control of Large Space Struct. Nov. 1985 p 459-465 refs Presented at the AIAA/ASME/ASCE/AHS 22nd Struct., Struct. Dyn. and Mater. Conf., Atlanta, 6-8-1981 Previously announced in IAA as A81-29449 (For primary document see N86-13587 04-31)
(AIAA-81-0528R) Avail: NTIS HC A04/MF A01 CSCL 13B

N86-13591*# Old Dominion Univ., Norfolk, Va.
DYNAMIC MODELING OF STRUCTURES FROM MEASURED COMPLEX MODES Final Report
Samir R. Ibrahim *In its* Dyn. Identification for Control of Large Space Struct. Nov. 1985 p 898-901 refs Previously announced in IAA as A82-30186 and A83-32988 (For primary document see N86-13587 04-31)
Avail: NTIS HC A04/MF A01 CSCL 13B

42 GEOSCIENCES (GENERAL)

N86-13764# International Geophysical Year World Data Center A, Boulder, Colo.
MARGINAL ICE ZONE BIBLIOGRAPHY
A. M. Brennan Jun. 1985 101 p
(AD-A159060; GD-17) Avail: NTIS HC A06/MF A01 CSCL 08/12

The issue provides a major bibliography on sea ice, meteorology and oceanography in the marginal ice zone. The topics discussed are: sea ice morphology and characteristics - W. J. Stringer; marginal ice zone bibliography: introduction, subject listing, author listing; note. GRA

N86-13765# Joint Publications Research Service, Arlington, Va.
USSR REPORT: EARTH SCIENCES Abstracts Only
13 Nov. 1985 53 p Transl. into ENGLISH from various Russian articles
(JPRS-UES-85-009) Avail: NTIS HC A04/MF A01

Various topics relating to meteorology, oceanography, terrestrial geophysics, atmospheric physics, and arctic and antarctic research are discussed. Cloud seeding, air-water interactions, the ocean bottom, rotating spheres, acousto-optics, and laser applications are explored. For individual titles, see N86-13766 through N86-13793.

N86-13766# Joint Publications Research Service, Arlington, Va.
GOSKOMGIDROMET PLANS AUTOMATION OF AERIAL CLOUD-SEEDING WORK Abstract Only c47
Vera Dorofeyeva and Vil Dorofeyev *In its* USSR Rept.: Earth Sci. (JPRS-UES-85-009) 13 Nov. 1985 p 2 Transl. into ENGLISH from Literaturnaya Gazeta (Moscow), 26 Jun. 1985 p 11 (For primary document see N86-13765 04-42)
Avail: NTIS HC A04/MF A01

The development and testing of an original computerized complex for cloud-seeding work aimed at inducing rainfall are discussed. During flights on airplanes equipped with this complex, cloud zones that are optimal for seeding are detected with the aid of suitable apparatus and a computer, which issues the necessary recommendations for the crew. The testing of the complex is scheduled for completion this year. Work is to begin this year on inducing additional rainfall over 500,000 hectares of steppe lands in the Ukraine and over areas of 300,000 hectares in Georgia and 100,000 hectares in Uzbekistan. The protection of agricultural crops against hail is called the main direction of the administration's weather-modification work. An account is given of a flight in which hail-bearing clouds were seeded by means of rockets fired from a radar-equipped airplane. The equipping of such airplanes with computerized units for processing multiple-contour radar representations (BOMO) reportedly is planned at an early date. In a radar-computer-BOMO-rocket system of the future, the operation of the radar set will be automated, and rockets will be fired from the airplane on a command from the computer. R.J.F.

N86-13767# Joint Publications Research Service, Arlington, Va.
MODEL INTERPRETATION OF ANNUAL VARIATION OF TEMPERATURE FIELDS OF AIR AND WATER BOUNDARY LAYERS OF WORLD OCEAN Abstract Only c46
A. Ye. Rozhdestvenskiy and M. V. Semenov *In its* USSR Rept.: Earth Sci. (JPRS-UES-85-009) 13 Nov. 1985 p 8 Transl. into ENGLISH from Izv. Akad. Nauk SSSR: Fiz. Atmosfery i Okeana (Moscow), v. 21, no. 5, May 1985 p 537-543 (For primary document see N86-13765 04-42)
Avail: NTIS HC A04/MF A01

Heat exchange between the ocean and atmosphere is largely determined by the temperatures of the boundary layers of these media, especially the annual variation of temperature of the ocean T sub w and atmosphere T sub a. A study was made of the behavior of the phase difference delta phi over the entire area of the world ocean, other than the polar regions, from 60 N to 60 S. The delta phi value was obtained for each 10 deg grid square using the mean T sub w and T sub a climatic values. Over almost the entire world ocean, the temperature of the near-water atmospheric layer in its annual variation outruns ocean surface temperature (delta phi >). The average shift for the entire ocean is 7 days (Atlantic - 8, Indian - 9 and Pacific - 5 days). A table gives the delta phi values in days averaged for 10 deg latitude zones for each of the oceans and the world ocean in a while and the standard deviations from the mean values. The temperature latitudes of the Northern Hemisphere are most uniform with respect to delta phi; the maximum phase shifts are observed there, but there are individual regions in both the tropical zone and in the Antarctic Ocean with extreme delta phi values. In comparison with the Northern Hemisphere temperate latitudes the tropical latitudes and the Antarctic Ocean have a more complex structure of delta phi distribution. The annual variation of temperatures can be explained in a model of thermal interaction between the boundary layers of the ocean and atmosphere. R.J.F.

N86-13768# Joint Publications Research Service, Arlington, Va.
FORMATION OF STRUCTURE OF MIXED REGION UNDER INFLUENCE OF SHEAR FLOW IN STRATIFIED FLUID Abstract Only c34
L. A. Dykhno *In its* USSR Rept.: Earth Sci. (JPRS-UES-85-009) 13 Nov. 1985 p 9 Transl. into ENGLISH from Izv. Akad. Nauk SSSR: Fiz. Atmosfery i Okeana (Moscow), v. 21, no. 5, May 1985 p 528-536 (For primary document see N86-13765 04-42)
Avail: NTIS HC A04/MF A01

The forms of shear instability accompanying the formation of the mixed region are discussed. A number of processes transpiring in the ocean under the influence of the developing and stationary wind are explained. The rectangular flume measured 80 x 16 x 20 cm. Air was fed for creating a velocity shear in the water in a wind channel formed by the flume cover and the free surface of the water. The initial stratification was formed as a result of heat exchange between the cold water and warm air. A stable temperature profile was established in the water with a gradient increasing toward the surface. The initial stratification was evaluated using the temperature gradient in the layer, which was varied from 0.12 to 0.3 C/cm. The following measurements were made: air flow velocity, water low velocity and vertical temperature profile. A laser knife was used in visual observations. A study was made of the main stages in formation of the mixed region. The mechanism of entrainment of fluid by large-scale eddies was explored in depth. This research made it possible to find the dependence of the entrainment rate on the Richardson number. R.J.F.

N86-13769# Joint Publications Research Service, Arlington, Va.
COMPUTATION OF OCEAN UPPER LAYER THERMAL STRUCTURE Abstract Only **c48**
A. Yu. Benilov, N. G. Kozhelupova, and B. N. Filyushkin *In its* USSR Rept.: Earth Sci. (JPRS-UES-85-009) 13 Nov. 1985 p 10 Transl. into ENGLISH from Okeanol. (Moscow), v. 25, no. 3, May - Jun. 1985 p 378-385 (For primary document see N86-13765 04-42)
Avail: NTIS HC A04/MF A01

Specialists at the Oceanology Institute developed a mathematical model which on the basis of meteorological data makes it possible to predict the temperature of the upper quasihomogeneous layer (UQL), its thickness, drift current velocity characteristics of vertical structure of the temperature field in the upper layer of the ocean governed by heating of the ocean from the surface and the convection arising during cooling. This integral model is intended for prediction of UQL short-period changes occurring against the background of seasonal changes. Storm effects during which there can be considerable increases in UQL thickness and formation of a stepped structure of temperature change with depth are superposed on these mean seasonal changes. The work was done in the North Atlantic during the period of spring to summer heating and summer. A value obtained in the case of well-developed wind waves was used as the sea surface resistance coefficient. It was found that the integral model makes it possible to compute change in thickness of the UQL and its temperature for 3 to 4 days in advance with an accuracy acceptable for practical using initial data and current wind velocity and heat flow values at a point. R.J.F.

N86-13770# Joint Publications Research Service, Arlington, Va.
INVESTIGATION OF CHARACTERISTICS OF SYNOPTIC MOVEMENTS ON SPHERE Abstract Only **c47**
A. D. Marushkevich *In its* USSR Rept.: Earth Sci. (JPRS-UES-85-009) 13 Nov. 1985 p 11 Transl. into ENGLISH from Okeanol. (Moscow), v. 25, no. 3, May - Jun. 1985 p 386-394 (For primary document see N86-13765 04-42)
Avail: NTIS HC A04/MF A01

Several numerical experiments were carried out for simulation of movements of a synoptic scale on a sphere. The main objective was clarification of the characteristics of movements of a synotpic scale associated with the Earth's sphericity (in comparison with the beta-plane). The computation region was in the form of a segment of a spherical surface bounded on the north and south by arcs of latitude and on the west and east by meridians. In modeling synoptic eddies consideration was given only the barotropic mode of movements (a vertical uniformity of currents was assumed). The initial equations used were the equations of motion in spherical coordinates in the Boussinesq approximation and in the traditional approximation. Two variants of the model were tested: in spherical coordinates and Cartesian (beta-plane approximation) coordinates. It was concluded that in studies of synoptic movements in the open ocean in regions with a great longitudinal extent (some ten degrees) it is necessary that the Earth's sphericity be taken into account since the use of the beta-plane approximation in this case gives results differing somewhat in qualitative and quantitative respects. R.J.F.

N86-13771# Joint Publications Research Service, Arlington, Va.
VERTICAL STRUCTURE OF TURBULENCE AND TURBULENT EXCHANGE IN EQUATORIAL ZONE OF PACIFIC OCEAN Abstract Only **c48**
A. N. Gezentsvey *In its* USSR Rept.: Earth Sci (JPRS-UES-85-009) 13 Nov. 1985 p 12-13 Transl. into ENGLISH from Okeanol. (Moscow), v. 25, no. 3, May - Jun. 1985 p 414-419 (For primary document see N86-13765 04-42)
Avail: NTIS HC A04/MF A01

The experimental study of intermittence, the determination of the laws of distribution of the sizes of turbulent zones and the coefficients of vertical turbulent exchange in intermittent turbulent fields are extremely timely because without a knowledge of the laws of these phenomena it is impossible to give an adequate description of the vertical redistribution of heat, salt and momentum in the ocean. On the 24th cruise of the Dmitrity Mendeleyev complex hydrophysical measurements were made in the equatorial system of currents in a broad range of spatial-temporal scales. Fluctuations of the current velocity field were measured by the Baklan freely falling probe. Fluctuation measurements were accompanied by registry of depth and mean water temperature. Measurements of velocity fluctuations were made using a sensor of the magnetohydrodynamic type, insensitive to the influence of medium stratification, with a linear characteristic and an instrument noise level approx. 0.07 cm/sec. Measurements were made in the frequency range 4 to 64 Hz with a mean rate of submergence of the probe of 1 m/sec, making it possible to register turbulence in the range of vertical scales from 2 to 25 cm. Author

N86-13772# Joint Publications Research Service, Arlington, Va.
SOME CHARACTERISTICS OF BOTTOM DENSITY CURRENTS Abstract Only **c48**
V. N. Anuchin, V. M. Belokopytov, and V. A. Gritsenko *In its* USSR Rept.: Earth Sci. (JPRS-UES-85-009) 13 Nov. 1985 p 13-14 Transl. into ENGLISH from Okeanol. (Moscow), v. 25, no. 3, May - Jun. 1985 p 420-424 (For primary document see N86-13765 04-42)
Avail: NTIS HC A04/MF A01

Bottom density currents have a number of interesting properties, the most important of which is the propagation of these flows over very great distances without a significant change in their thickness. The authors investigated the plane flow of a denser fluid in a less dense fluid along a sloping bottom, thereby modeling the shelf zone and the continental slope. Salinity stratification is assumed. On the basis of a general system of equations of thermohydrodynamics a system of equations is derived for describing movement of the bottom flow. An analysis of the corresponding laminar flow gave distributions functionally similar to those observed experimentally and a complete inadequate lifetime of the bottom flow, indicating a turbulent nature of the flow of a bottom density current, with a clearly expressed anisotropy of turbulence. Vertical profiles of current velocity and density were obtained for different moments in time, as well as the distributions of turbulent stress obtained as a result of numerical solution. Experimental and computed data are compared. The negative value of turbulent stress at the upper boundary of the flow is apparently one of the main reasons for the great lifetime of bottom density flows. The analysis of the existence and dynamics of bottom density currents indicates that the described model, within the framework of the initial assumptions, makes it possible to describe the internal structure of bottom flows. Author

N86-13773# Joint Publications Research Service, Arlington, Va.
HIGHLY DISPERSE MINERALS IN SEDIMENTS IN NEIGHBORHOOD OF EAST PACIFIC OCEAN RISE DETERMINED FROM DRILLING DATA Abstract Only **c48**
Z. N. Gorbunova *In its* USSR Rept.: Earth Sci. (JPRS-UES-85-009) 13 Nov. 1985 p 14-15 Transl. into ENGLISH from Okeanol. (Moscow), v. 25, no. 3, May - Jun. 1985 p 465-470 (For primary document see N86-13765 04-42)
Avail: NTIS HC A04/MF A01

Extensive materials were collected on the 8th and 14th cruises of the Dmitriy Mendeleyev and the 24th cruise of the Akademik Kurchatov which make it possible to carry out a detailed study of the composition of highly disperse minerals in the region of the East Pacific Ocean Rise. Three boreholes were studied in the neighborhood of the rise. All penetrated through the sedimentary stratum down to the basalt. These materials can be used in studying the lateral change in the composition of highly disperse minerals and also vertically over the extent of formation of the entire sedimentary stratum lying on the basalts of the oceanic crust. The principal research methods were X-ray - diffractometric and electron microscopic. The distribution of highly disperse minerals in boreholes reflects the tectonic history of the ocean. In the samples of metal-bearing sediments above the basalt there is a predominance of minerals formed under the influence of endogenous sources. With increasing distance from the spreading axis their role decreased, with the endogenous minerals being replaced by a terrigenous-volcanic complex. R.J.F.

N86-13774# Joint Publications Research Service, Arlington, Va.
STUDY OF OPTICAL-ACOUSTICAL PHENOMENA AT SURFACE OF STRONGLY ABSORBING CLEARING FLUIDS Abstract Only c36
F. V. Bunkin, K. L. Vodopyanov, L. A. Kulevskiy, G. A. Lyakhov, V. G. Mikhalevich, and A. M. Rodin *In its* USSR Rept.: Earth Sci. (JPRS-UES-85-009) 13 Nov. 1985 p 18 Transl. into ENGLISH from Izv. Akad. Nauk SSSR: Ser. Fiz. (Moscow), v. 49, no. 3, Mar. 1985 p 558-563 (For primary document see N86-13765 04-42)
Avail: NTIS HC A04/MF A01

The clearing of water by laser radiation with a wavelength lambda = 2.94 microns was reported by K. L. Vodop'aynov, et al., (ZhETF, Vol. 82, p 1820, 1982). For further clarification of this problem, the authors studied optical-acoustic phenomena at the surface of a fluid under conditions of strong absorption and optical clearing with emphasis on detection of the characteristics of the thermal and evaporation regimes of generation of acoustic fields by laser radiation. Studies were made of different fluids containing hydroxyl groups (water, ethanol, glycerin, ethylene glycol) with different boundary conditions (free and fixed boundaries). In the case of a free boundary, the laser radiation was directed downward along the normal to the fluid surface, but in the case of a rigid boundary the fluid surface was covered by a backing of transparent material. Experimental results are presented. At the present time there is no certain interpretation of the observed effects. However, it is known that the presence of hydrogen bonds in fluids containing the OH group leads to a strong shift into the region of lesser frequencies of the absorption band. Partial breaking of the hydrogen bonds under the influence of laser radiation can result in a change in the absorption spectrum of the fluid and accordingly a clearing at the laser wavelength. Author

N86-13775*# Joint Publications Research Service, Arlington, Va.
AERIAL LASER SENSING OF OCEAN UPPER LAYER Abstract Only
D. V. Vlasov *In its* USSR Rept.: Earth Sci. (JPRS-UES-85-009) 13 Nov. 1985 p 19 Transl. into ENGLISH from Izv. Akad. Nauk SSSR: Ser. Fiz. (Moscow), v. 49, no. 3, Mar. 1985 p 433-441 (For primary document see N86-13765 04-43)
Avail: NTIS HC A04/MF A01

Applications of laser sensing of the ocean, such as deep bathymetry; determination of the luminescence spectrum of phytoplankton as a sensitive indicator of changes in the external physical parameters of the studied region; monitoring the state of underwater pipelines; conducting search and rescue missions; monitoring pollution; biological observations of the state of algae; searching for schools of fish, etc., are discussed. The Chayka apparatus for laser sensing is discussed. A block diagram is given which is used in describing functioning of this unit. Particular attention is given to the time structure of an echo signal appearing when sensing the upper ocean layer by a short laser pulse propagating through the wave-covered surface. R.J.F.

N86-13776# Joint Publications Research Service, Arlington, Va.
FORMATION OF UNDERWATER OCEANIC VOLCANOES AND ISLANDS IN RELATION TO LITHOSPHERIC THICKNESS AND MOVEMENTS Abstract Only c46
A. M. Gorodnitskiy *In its* USSR Rept.: Earth Sci. (JPRS-UES-85-009) 13 Nov. 1985 p 20 Transl. into ENGLISH from Byul. Mosk. Obshchestva Ispytateley Prirody: Otd. Geol. (Moscow), v. 60, no. 4, Jul. - Aug. 1985 p 24-37 (For primary document see N86-13765 04-42)
Avail: NTIS HC A04/MF A01

A brief review of geological and geophysical data on oceanic volcanoes, relating their formation to the thickness and nature of movements of the lithosphere, is presented. Analysis of the height and composition of such paleovolcanoes and various island chains demonstrated that such characteristics are predicated on the pT factors of magma formation under the lithosphere. The origins of such mountains are determined by plate stresses due to tectonic forces acting at plate boundaries, membrane effects and changes in the thermal regimes of the lithosphere leading to a system of rifts. Author

N86-13777# Joint Publications Research Service, Arlington, Va.
VOLCANOES DISCOVERED WITH RADIO BEAM Abstract Only
In its USSR Rept.: Earth Sci. (JPRS-UES-85-009) 13 Nov. 1985 p 21 Transl. into ENGLISH from Tass (Moscow), 16 May 1985 (For primary document see N86-13765 04-43)
Avail: NTIS HC A04/MF A01

Two giant volcanoes were discovered by Soviety scientists. One of them lies beneath the hot sands of West Sahara and the other under the Antarctic ice in the area of James Ellsworth Land. The craters were spotted with the help of a radio location system installed abroad the Soviet satellites Cosmos-1500 and Cosmos-1602. The system was developed at the Kharkov Institute of Radio Physics and Electronics, the Academy of Science of the Ukraine. The radioeye, with its scanning range of about five hundred kilometers, is able to spot objects less than a kilometer in size. The system, operating automatically, collects, selects and codes data and transmits it back to Earth in ready-to-use form. In the opinion of specialists, the use of Kharkov-made radio locators in orbit has started a new line in the exploration of the Earth's surface and the world ocean. This system has no analogues anywhere in the world for the breadth of scanning and possibilities it offers for immediately sending information, through stationary communications channels, directly to users. R.J.F.

N86-13778# Joint Publications Research Service, Arlington, Va.
COMPUTER-AIDED AERIAL RADIOMETRIC SURVEYING OF SOIL MOISTURE Abstract Only
N. Armand *In its* USSR Rept.: Earth Sci. (JPRS-UES-85-009) 13 Nov. 1985 p 24 Transl. into ENGLISH from Krasnaya Zvezda (Moscow), 30 Jun. 1985 p 2 (For primary document see N86-13765 04-43)
Avail: NTIS HC A04/MF A01

A new method and an apparatus which were developed for aerial radiometric surveying to determine soil moisture content are discussed. The method employs an airborne radiometer operating in tandem with an onboard computer, which converts signals into moisture-content figures. Magnetic recordings of the data are fed into a ground computer which contains information on features of the locality where the survey was made. It is reported that the new apparatus passed field tests in a number of areas. It can be used for other environmental monitoring purposes, such as determining the content of minerals, acids, salts and alkalis in surface water and detecting changes in electrophysical properties of water. Author

N86-13779# Joint Publications Research Service, Arlington, Va.
DISTRIBUTION OF BRIGHTNESS FROM POINT SOURCE OF SCATTERED LIGHT ALONG INCLINED PATH Abstract Only c74
A. S. Drofa and A. L. Usachev *In its* USSR Rept.: Earth Sci. (JPRS-UES-85-009) 13 Nov. 1985 p 28 Transl. into ENGLISH from Izv. Akad. Nauk SSSR: Fiz. Atmosfery i Okeana (Moscow), v. 21, no. 6, Jun. 1985 p 603-608 Original language document was announced in IAA as A85-44481 (For primary document see N86-13765 04-42)
Avail: NTIS HC A04/MF A01

The angular distribution of light scattered from a point source by a cloud layer along an inclined line of sight has been calculated using the Monte Carlo method. The relation of the brightness and asymmetry of the light to cloud layer parameters along the line of sight is examined. It is shown that the asymmetry of the light may be both positive and negative in value depending on cloud layer parameters. In the case of an inclination angle of less than about 80 degrees, displacement of the brightness distribution above and below the line of sight was found. The intensity of scattered light was different in the case of a vertical line of sight when cloud layer parameters were the same as in the inclined case. I.H. (IAA)

N86-13780# Joint Publications Research Service, Arlington, Va.
STATISTICAL CORRELATION BETWEEN OZONE LEVELS OVER ATLANTIC OCEAN AND METEOROLOGICAL VALUES Abstract Only c46
V. M. Bazhanov *In its* USSR Rept.: Earth Sci. (JPRS-UES-85-009) 13 Nov. 1985 p 29 Transl. into ENGLISH from Izv. Akad. Nauk SSSR: Fiz. Atmosfery i Okeana (Moscow), v. 21, no. 6, Jun. 1985 p 609-613 Original language document was announced in IAA as A85-44482 (For primary document see N86-13765 04-42)
Avail: NTIS HC A04/MF A01

The latitudinal distribution of the total amount of ozone in various atmospheric layers was derived from data obtained on board a scientific vessel in the Atlantic Ocean in the period Feburary to June, 1980. The total amount of ozone is given in relation to variations in tropopause height and temperature. The distinctive features of ozone distribution in the Tropical Convergence Zone are discussed. The spectrum of variations in aerosol particle size was correlated with the meteorological parameters of the surface boundary layer. Empirical regression equations are formulated to describe the statistical connection between the total amount of ozone the surface boundary-ration of radioactive tracers in layer. I.H. (IAA)

N86-13781# Joint Publications Research Service, Arlington, Va.
INFLUENCE OF FOG MICROSTRUCTURE ON QUALITY OF OPTICAL IMAGE TRANSMITTED THROUGH IT Abstract Only c74
L. P. Volnistova, A. S. Drofa, and V. P. Snykov *In its* USSR Rept.: Earth Sci. (JPRS-UES-85-009) 13 Nov. 1985 p 29-30 Transl. into ENGLISH from Izv. Akad. Nauk SSSR: Fiz. Atmosfery i Okeana (Moscow), v. 21, no. 6, Jun. 1985 p 507-511 (For primary document see N86-13765 04-42)
Avail: NTIS HC A04/MF A01

Data on the optical transfer function (OTF) of fogs with different microstructures are presented. The OTF of a fog artificially formed in the chamber was determined experimentally by measurement of the brightness profile of the image of a narrow self-luminescent line observable through a fog. The brightness of the line image was measured with a photomultiplier situated behind the focus of a receiving objective. Fog transparency and its microstructure were measured during the experiments. It is found that after fog formation the microstructure is transformed, caused by droplet evaporation due to heat release from the chamber walls and due to droplet precipitation onto the floor and walls. The time required for total disappearance of the fog was 40 to 60 minutes. The experimental data agreed well with the computations. Author

N86-13782# Joint Publications Research Service, Arlington, Va.
EXPERIENCE IN MEASURING MEAN WIND VELOCITY PROFILE IN LOWER TROPOSPHERE BY SODAR ANEMOMETER UNDER INVERSION AND CONVECTIVE CONDITIONS Abstract Only c47
M. A. Kallistratova, Y. Keder, I. V. Petenko, and N. S. Time *In its* USSR Rept.: Earth Sci. (JPRS-UES-85-009) 13 Nov. 1985 p 30-31 Transl. into ENGLISH from Izv. Akad. Nauk SSSR: Fiz. Atmosfery i Okeana (Moscow), v. 21, no. 5, May 1985 p 492-497 Original language document was announced in IAA as A85-40641 (For primary document see N86-13765 04-42)
Avail: NTIS HC A04/MF A01

Specialists at the Atmospheric Physics Institute have developed a solar anemometers for measuring the horizontal component of wind velocity. It is a slant monostatic sodar for measuring the Doppler shift of the frequency of sound reflected from moving air density inhomogeneities. The wind velocity profile was measured on a mast to a height of 32 m with cup anemometers; the mast was at a distance of 40 m from the sodar anemometer. Also employed was a vertical sonar which registered echo signal intensity on a facsimile apparatus which provides data on the spatial-temporal distribution of temperature fluctuations C sub t sq. The type of atmospheric stratification is determined from the form of the facismile records. The combined measurements provided data on the behavior of the wind velocity profile under convective and inversion conditions. E.A.K.

N86-13783# Joint Publications Research Service, Arlington, Va.
STRUCTURAL CHARACTERISTIC OF TEMPERATURE FIELD OVER SEA Abstract Only c47
B. M. Koprov *In its* USSR Rept.: Earth Sci. (JPRS-UES-85-009) 13 Nov. 1985 p 31-32 Transl. into ENGLISH from Izv. Akad. Nauk SSSR: Fiz. Atmosfery i Okeana (Moscow), v. 21, no. 5, May 1985 p 485-491 (For primary document see N86-13765 04-42)
Avail: NTIS HC A04/MF A01

The structural function of the temperature field is described. Measurements in the surface atmospheric layer yielded universal expressions relating C sub t sq and atmospheric surface characteristics. In the surface layer the fields of wind velocity, temperature and humidity have specific characteristics not typical of wind the near-ground layer. Density stratification and the generation of kinetic energy by buoyancy forces are determined to an equal degree by the distribution of temperature and humidity. Temperature, wind velocity and humidity were measured aboard ship at a height of about 10 m and water temperature near the surface. Regular measurements of the structural characteristic and meteorological parameters were made in the Baltic Sea, North Sea, Mediterranean Sea, Red Sea and Indian Ocean. Sensors were 14 m above water level. Among the instruments used was a special difference-type resistance microthermometer (described in some detail, with a block diagram). The correlation between the structural characteristic of temperature and parameters determined from standard meteorological observations is examined. E.A.K.

N86-13784# Joint Publications Research Service, Arlington, Va.
ATMOSPHERIC SYNOPTIC EDDIES OVER OCEAN (DETERMINED FROM EXPERIMENTAL DATA) Abstract Only c46
V. Ye. Lagun and V. F. Romanov *In its* USSR Rept.: Earth Sci. (JPRS-UES-85-009) 13 Nov. 1985 p 32 Transl. into ENGLISH from Izv. Akad. Nauk SSSR: Fiz. Atmosfery i Okeana (Moscow), v. 21, no. 5, May 1985 p 474-484 Original language document was announced in IAA as A85-40640 (For primary document see N86-13765 04-42)
Avail: NTIS HC A04/MF A01

Field data obtained during the POLEX North-79 experiment were used to study synoptic eddies (SEs) over the Norwegian Sea. Numerical calculations of the physical parameters of SEs show that rotation and movement of air masses in the surface layer, and wave-like perturbations in the upper layers. Partial mass transfer between layers was also found. The energy structure of SEs was studied in relation to their energy budget properties. It is concluded that atmospheric circulation over ocean regions is driven by two basic forces: the mean main flow and atmospheric synoptic eddies. The possible contribution of atmospheric eddies to the formation and localization of zones of active sea/air energy exchange is also discussed. I.H. (IAA)

N86-13785# Joint Publications Research Service, Arlington, Va.
INFLUENCE OF PETROLEUM POLLUTION ON OCEAN-ATMOSPHERE GAS EXCHANGE INTENSITY (IN EXAMPLE OF NORTH ATLANTIC) Abstract Only c45
V. V. Alekseyev, P. A. Baranov, A. O. Kokorin, and V. M. Sheremetyev *In its* USSR Rept.: Earth Sci. (JPRS-UES-85-009) 13 Nov. 1985 p 33 Transl. into ENGLISH from Vestn. Mosk. Univ., Ser. 3: Fiz., Astron. (Moscow), v. 26, no. 3, May - Jun. 1985 p 71-74 (For primary document see N86-13765 04-42)

Avail: NTIS HC A04/MF A01

The influence of petroleum pollution on gas exchange intensity was evaluated. Laboratory experiments determined gas transfer through the water-air interface with the presence of a hydrocarbon film on the surface under conditions of wind-wave mixing and during thermal convection. The CO_2 concentration in water and in the air, CO_2 fluxes at the water-air interface and values of the gas exchange rate coefficient were measured. Convection results in an intensification of gas exchange comparable to the influence of wind-wave mixing; a hydrocarbon film reduces the gas exchange rate caused by convection by approximately half. The experimental data were used to estimate the influence of petroleum pollutants on the intensity of gas exchange in the North Atlantic. A map of the probability of North Atlantic pollution is given. As a result of petroleum films there is an average decrease in the rate of gas exchange by 2 to 3%. E.A.K.

N86-13786# Joint Publications Research Service, Arlington, Va.
STATISTICS OF INTENSIVE LIGHT BEAMS IN TURBULENT ATMOSPHERE Abstract Only c74
V. P. Kandidov *In its* USSR Rept.: Earth Sci. (JPRS-UES-85-009) 13 Nov. 1985 p 34 Transl. into ENGLISH from Izv. Akad. Nauk SSSR: Ser. Fiz. (Moscow), v. 49, no. 3, Mar. 1985 p 442-449 Original language document was announced in IAA as A85-31855 (For primary document see N86-13765 04-42)
Avail: NTIS HC A04/MF A01

The propagation of high-intensity laser beams in a turbulent atmosphere is investigated statistically for various radiation conditions. In particular, attention is given to the adaptive focusing of light beams under conditions of the combined effect of nonlinear refraction and inhomogeneities of the medium parameters. The analysis employs numerical methods in the approximation of the parabolic theory of diffraction. V.L. (IAA)

N86-13787# Joint Publications Research Service, Arlington, Va.
NEW METHODS FOR LASER SOUNDING OF ATMOSPHERE ON BASIS OF NONLINEAR EFFECTS Abstract Only c46
V. Ye. Zuyev and Yu. D. Kopytin *In its* USSR Rept.: Earth Sci. (JPRS-UES-85-009) 13 Nov. 1985 p 34-35 Transl. into ENGLISH from Izv. Akad. Nauk SSSR: Ser. Fiz. (Moscow), v. 49, no. 3, Mar. 1985 p 418-427 Original language document was announced in IAA as A85-31852 (For primary document see N86-13765 04-42)
Avail: NTIS HC A04/MF A01

Atmospheric sounding techniques based on nonlinear and coherent optical effects associated with the use of high-power lasers are reviewed with reference to three groups of methods. The first group includes lidar methods relying on optical, acoustic, and radio emissions during remote laser breakdown of the atmosphere as sources of information. The second group comprises methods of nonlinear and coherent Raman spectroscopy at vibrational-rotational transitions of gas molecules and resonant fluctuations of the shape of aerosol particles. The third group includes highly sensitive atmospheric sounding methods based on nonlinear intracavity effects during laser reception of echo signals. The discussion also covers problems related to the nonlinearity of lidar signals and applicability limits of linear equations of optical location in traditional sounding schemes employing high-power laser sources. V.L. (IAA)

N86-13788# Joint Publications Research Service, Arlington, Va.
INTERACTION BETWEEN POWERFUL LASER RADIATION AND ATMOSPHERIC AEROSOLS Abstract Only c46
M. P. Gordin, Yu. N. Grachev, V. S. Loskutov, V. P. Sadovnikov, A. V. Sokolov, and G. M. Strelkov *In its* USSR Rept.: Earth Sci. (JPRS-UES-85-009) 13 Nov. 1985 p 35-36 Transl. into ENGLISH from Izv. Akad. Nauk SSSR: Ser. Fiz. (Moscow), v. 49, no. 3, Mar. 1985 p 450-458 Original language document was announced in IAA as A85-31856 (For primary document see N86-13765 04-42)
Avail: NTIS HC A04/MF A01

Results of theoretical and experimental studies of the propagation of high-power laser beams in aqueous and soot aerosols under conditions of thermally induced beam distortions and aerosol brightening are reviewed. Topics discussed include the interaction of an individual particle and a polydisperse system of particles with a radiation field; changes in the transparency of aerosol layers due to radiation; and the propagation of laser beams through a turbid atmosphere. Most of the results presented here refer to the wavelength 10.6 microns. V.L. (IAA)

N86-13789# Joint Publications Research Service, Arlington, Va.
INVESTIGATION OF NONLINEAR SPECTROSCOPIC EFFECTS IN INTERACTION BETWEEN CO_2-LASER RADIATION AND ATMOSPHERIC GASES Abstract Only c46
B. G. Ageyev, Ye. P. Gordov, Yu. N. Ponomarev, and S. D. Tvorogov *In its* USSR Rept.: Earth Sci. (JPRS-UES-85-009) 13 Nov. 1985 p 36 Transl. into ENGLISH from Izv. Akad. Nauk SSSR: Ser. Fiz. (Moscow), v. 49, no. 3, Mar. 1985 p 459-465 Original language document was announced in IAA as A85-31857 (For primary document see N86-13765 04-42)
Avail: NTIS HC A04/MF A01

The paper is concerned with nonlinear nonresonance light absorption in the case where the frequency field corresponds to a relatively distant wing of the spectral band. The origin of this effect and its qualitative characteristics are investigated by extrapolating the accompanying physical conditions to the case of a strong field. Results of experiments are reported in which the absorptivity of H_2O and D_2O vapors has been studied as a function of pulsed CO_2 laser emission at a wavelength of 10.6 microns. V.L. (IAA)

N86-13790# Joint Publications Research Service, Arlington, Va.
OBSERVATION OF OPTICAL-RADIO FREQUENCY RESONANCE IN H_2O USING WIDE-BAND RUBY LASER SPECTROSCOPY Abstract Only c32
V. P. Kochanov, V. P. Lopasov, and S. F. Lukyanenko *In its* USSR Rept.: Earth Sci. (JPRS-UES-85-009) 13 Nov. 1985 p 37 Transl. into ENGLISH from Izv. Akad. Nauk SSSR: Ser. Fiz. (Moscow), v. 49, no. 3, Mar. 1985 p 516-520 Original language document was announced in IAA as A85-31864 (For primary document see N86-13765 04-42)
Avail: NTIS HC A04/MF A01

An attempt is made to detect the effect of intra-Doppler Stark splitting produced by an intense radio frequency field on the absorption spectrum of probing optical emission under conditions of a complex resonance of the optical and radio frequency fields and the corresponding transitions. In the experiment described here, absorption in H_2O at 694.38 nm is recorded by a wideband intracavity laser spectrometer based on a ruby laser. An analysis of experimental data indicates that the observed narrowing and widening of the trough in the generation spectrum characteristic are caused by a complex optical-radio resonance involving a resonant summation of the amplitudes of the probabilities of weak optical and resolved radio frequency transmition between the M-sublevels of Stark splitting. V.L. (IAA)

N86-13791# Joint Publications Research Service, Arlington, Va.
EFFECTIVENESS OF USE OF ADAPTIVE OPTICAL SYSTEMS UNDER CONDITIONS OF SELF-EFFECT IN ATMOSPHERE Abstract Only c74
P. A. Konyayev, V. P. Lukin, and V. L. Mironov *In its* USSR Rept.: Earth Sci. (JPRS-UES-85-009) 13 Nov. 1985 p 38 Transl. into ENGLISH from Izv. Akad. Nauk SSSR: Ser. Fiz. (Moscow), v. 49, no. 3, Mar. 1985 p 536-540 Original language document was announced in IAA as A85-31867 (For primary document see N86-13765 04-42)
Avail: NTIS HC A04/MF A01

A numerical simulation study of fast phase-conjugated adaptive system is carried out with the aim of evaluating their maximum efficiency with regard to the suppression of the thermal self-defocusing of laser beams. The system is fast in the sense that its response time is significantly less than the characteristic variation time of the temperature of the medium. It is shown that the system can increase the maximum intensity of radiation transmitted through the atmosphere by an order of magnitude. The presence of turbulent fluctuations of refractive index on the path enhances the correction efficiency of thermal distortions in the beam;

however, the phase-correlation scale at the emitting aperture decreases, which makes it necessary to increase the number of control elements of the adaptive mirror. B.J. (IAA)

N86-13792# Joint Publications Research Service, Arlington, Va.
LATITUDE MEASUREMENTS OF COSMIC RADIATION INTENSITY IN STRATOSPHERE AND AT SEA LEVEL ON MARINE ANTARCTIC EXPEDITIONS Abstract Only **c93**
Nikolay Savvich Svirzhevskiy *In its* USSR Rept.: Earth Sci. (JPRS-UES-85-009) 13 Nov. 1985 p 39 Transl. into ENGLISH from "Shirotnyye Izmereniya Intensivnosti Kosmicheskogo Izlucheniya v Stratosfere i na Urovne Morya v Morskikh Antarkticheskikh Ekspeditsiyakh" Moscow, 1983 p 1-16 (For primary document see N86-13765 04-42)
Avail: NTIS HC A04/MF A01

The correlation coefficients (W9R,x, t) for the activity minimum 1975 to 1976 were determined on the basis of: stratospheric latitude measurement; measurement of the flux of soft charged radiation and gamma radiation at sea level as a function of cutoff rigidity Rc and determination of the latitude effect for the charged and gamma radiations; checking of the geomagnetic cutoff thresholds Rc, computed using the IGRF magnetic field model; clarification of the role of the radioactive background for determining the latitude effect for low-energy particles. The design of the instrument used in cosmic ray measurements at sea level the processing of measurement data are described the results of latitude measurements of ionizing and gamma radiations at sea level are presented, latitude stratospheric measurements at the solar activity minimum 1975 to 1976 are outlined. The sea-level latitude measurements gave the flux of charged cosmic radiation and the distribution of cosmic ray intensity as a function of Rc. Comparison of the measurements made in the Northern and Southern Hemispheres in the Atlantic reveals a systematic difference in the Rc values which requires introduction of a correction. E.A.K.

N86-13793# Joint Publications Research Service, Arlington, Va.
HADRON COMPONENT OF COSMIC RADIATION AT ATMOSPHERIC DEPTH 800 g/cm(2) IN ENERGY RANGE 70 TO 700 GeV Abstract Only **c93**
Petr Sergeyevich Vasilyev *In its* USSR Rept.: Earth Sci. (JPRS-UES-85-009) 13 Nov. 1985 p 40 Transl. into ENGLISH from "Adronnaya Komponenta Kosmicheskogo Izlucheniya na Glubine Atmosfery 800 g/cm(2) v Oblasti Energiy (70-700GeV)" Moscow, 1984 p 1-20 (For primary document see N86-13765 04-42)
Avail: NTIS HC A04/MF A01

A spark spectrometer was developed for registry of cosmic radiation hardons. The study of this instrument in the particle beams of the Serpukhovo accelerator made it possible to reduce the systematic errors in the measurement of cosmic radiation hardons to a minimum. Existing methods for studying the hadron component; the characteristics of interaction between pions and protons and spark spectrometer matter obtained using the Serpukhovo accelerator; the parameters of hadron showers in the spark spectrometer, used in studying hadron fluxes in cosmic rays; the ratios of fluxes of pions and protons, the absolute intensities of the flux of neutrons and the total hadron flux at an elevation of 2,000 m above sea level; and the measurement data are discussed. The integral intensities of fluxes of neutrons and hadrons in the energy range >240 GeV were determined. It is found that there is a systematic increase in the eta/P ratio of fluxes in the energy range 120 to 330 GeV. E.A.K.

43 EARTH RESOURCES

Includes remote sensing of earth resources by aircraft and spacecraft; photogrammetry; and aerial photography.

For instrumentation see *35 Instrumentation and Photography.*

N86-13794*# National Aeronautics and Space Administration. Goddard Space Flight Center, Greenbelt, Md.
FUNDAMENTAL REMOTE SENSING SCIENCE RESEARCH PROGRAM: THE SCENE RADIATION AND ATMOSPHERIC EFFECTS CHARACTERIZATION PROJECT Summary Report, 1985
Donald W. Deering Sep. 1985 195 p refs Proc. of the 3rd Ann. SRAEC Principal Investigators Meeting, Cambridge, Mass., 29-31 Jan. 1985 Original contains imagery. Original photography may be purchased from the EROS Data Center, Sioux Falls, S.D. 57198 ERTS
(E86-10011; NASA-TM-86234; NAS 1.15:86234) Avail: NTIS HC A09/MF A01 CSCL 05B

The Scene Radiation and Atmospheric Effects Characterization (SRAEC) Project was established within the NASA Fundamental Remote Sensing Science Research Program to improve our understanding of the fundamental relationships of energy interactions between the sensor and the surface target, including the effect of the atmosphere. The current studies are generalized into the following five subject areas: optical scene modeling, Earth-space radiative transfer, electromagnetic properties of surface materials, microwave scene modeling, and scatterometry studies. This report has been prepared to provide a brief overview of the SRAEC Project history and objectives and to report on the scientific findings and project accomplishments made by the nineteen principal investigators since the project's initiation just over three years ago. This annual summary report derives from the most recent annual principal investigators meeting held January 29 to 31, 1985. For individual titles, see N86-13795 through N86-13812.

N86-13795*# Colorado State Univ., Fort Collins. Coll. of Forestry and Natural Resources.
REFLECTANCE MODELING
James A. Smith, Principal Investigator *In* NASA. Goddard Space Flight Center Fundamental Remote Sensing Sci. Res. Program Sep. 1985 p 38-45 ERTS (For primary document see N86-13794 04-43)
Avail: NTIS HC A09/MF A01 CSCL 05B

The overall goal of this work has been to develop a set of computational tools and media abstractions for the terrain bidirectional reflectance problem. The modeling of soil and vegetation surfaces has been emphasized with a gradual increase in the complexity of the media geometries treated. Pragmatic problems involved in the combined modeling of soil, vegetation, and atmospheric effects have been of interest and one of the objectives has been to describe the canopy reflectance problem in a classical radiative transfer sense permitting easier inclusion of our work by other workers in the radiative transfer field. Author

N86-13796*# Nebraska Univ., Lincoln.
BIDIRECTIONAL REFLECTANCE MODELING OF NON-HOMOGENEOUS PLANT CANOPIES
John M. Norman, Principal Investigator *In* NASA. Goddard Space Flight Center Fundamental Remote Sensing Sci. Res. Program Sep. 1985 p 46-53 ERTS (For primary document see N86-13794 04-43)
Avail: NTIS HC A09/MF A01 CSCL 05B

The objective of this research is to develop a 3-dimensional radiative transfer model for predicting the bidirectional reflectance distribution function (BRDF) for heterogeneous vegetation canopies. The model (named BIGAR) considers the angular distribution of leaves, leaf area index, the location and size of individual subcanopies such as widely spaced rows or trees, spectral and directional properties of leaves, multiple scattering, solar position and sky condition, and characteristics of the soil. The model relates canopy biophysical attributes to down-looking radiation measurements for nadir and off-nadir viewing angles. Therefore, inversion of this model, which is difficult but practical should provide surface biophysical pattern; a fundamental goal of remote sensing. Such a model also will help to evaluate atmospheric limitations to satellite remote sensing by providing a good surface boundary condition for many different kinds of canopies.

Furthermore, this model can relate estimates of nadir reflectance, which is approximated by most satellites, to hemispherical reflectance, which is necessary in the energy budget of vegetated surfaces. Author

N86-13797*# National Aeronautics and Space Administration. Goddard Space Flight Center, Greenbelt, Md.

UNDERSTANDING THE RADIANT SCATTERING BEHAVIOR OF VEGETATED SCENES

Daniel S. Kimes, Principal Investigator *In its* Fundamental Remote Sensing Sci. Res. Program Sep. 1985 p 54-59 ERTS (For primary document see N86-13794 04-43)

Avail: NTIS HC A09/MF A01 CSCL 05B

Knowledge of the physics of the scattering behavior of vegetation will ultimately serve the remote sensing and earth science community in many ways. For example, it will provide: (1) insight and guidance in developing new extraction techniques of canopy characteristics, (2) a basis for better interpretation of off-nadir satellite and aircraft data, (3) a basis for defining specifications of future earth observing sensor systems, and (4) a basis for defining important aspects of physical and biological processes of the plant system. The overall objective of the three-year study is to improve our fundamental understanding of the dynamics of directional scattering properties of vegetation canopies through analysis of field data and model simulation data. The specific objectives are to: (1) collect directional reflectance data covering the entire exitance hemisphere for several common vegetation canopies with various geometric structure (both homogeneous and row crop structures), (2) develop a scene radiation model with a general mathematical framework which will treat 3-D variability in heterogeneous scenes and account for 3-D radiant interactions within the scene, (3) conduct validations of the model on collected data sets, and (4) test and expand proposed physical scattering mechanisms involved in reflectance distribution dynamics by analyzing both field and modeling data. Author

N86-13798*# Purdue Univ., West Lafayette, Ind. Lab. for Applications of Remote Sensing.

MEASUREMENT AND MODELING OF THE OPTICAL SCATTERING PROPERTIES OF CROP CANOPIES

V. C. Vanderbilt, Principal Investigator *In* NASA. Goddard Space Flight Center Fundamental Remote Sensing Sci. Res. Program Sep. 1985 p 60-66 ERTS (For primary document see N86-13794 04-43)

Avail: NTIS HC A09/MF A01 CSCL 20F

The specular reflection process is shown to be a key aspect of radiation transfer by plant canopies. Polarization measurements are demonstrated as the tool for determining the specular and diffuse portions of the canopy radiance. The magnitude of the specular fraction of the reflectance is significant compared to the magnitude of the diffuse fraction. Therefore, it is necessary to consider specularly reflected light in developing and evaluating light-canopy interaction models for wheat canopies. Models which assume leaves are diffuse reflectors correctly predict only the diffuse fraction of the canopy reflectance factor. The specular reflectance model, when coupled with a diffuse leaf model, would predict both the specular and diffuse portions of the reflectance factor. The specular model predicts and the data analysis confirms that the single variable, angle of incidence of specularly reflected sunlight on the leaf, explains much of variation in the polarization data as a function of view-illumination directions. Author

N86-13799*# Hunter Coll., New York.

GEOMETRIC-OPTICAL MODELING OF A CONIFER FOREST CANOPY

Alan H. Strahler, Principal Investigator *In* NASA. Goddard Space Flight Center. Fundamental Remote Sensing Sci. Res. Program Sep. 1985 p 67-71 ERTS (For primary document see N86-13794 04-43)

Avail: NTIS HC A09/MF A01 CSCL 20F

The objective of this research is to explore how the geometry of trees in forest stands influences the reflectance of the forest as imaged from space. Most plant canopy modeling has viewed the canopy as an assemblage of plane-parallel layers on top of a soil surface. For these models, leaf angle distribution, leaf area index, and the angular transmittance and reflectance of leaves are the primary optical and geometric parameters. Such models are now sufficiently well developed to explain most of the variance in angular reflectance measurements observed from homogeneous plant canopies. However, forest canopies as imaged by airborne and spaceborne scanners exhibit considerable variance at quite a different scale. Brightness values vary strongly from one pixel to the next primarily as a function of the number of trees they contain. At this scale, the forest canopy is nonuniform and discontinuous. This research focuses on a discrete-element, geometric-optical view of the forest canopy. Author

N86-13800*# National Aeronautics and Space Administration. Johnson (Lyndon B.) Space Center,

CROP CHARACTERISTICS RESEARCH: GROWTH AND REFLECTANCE ANALYSIS

G. D. Badhwar, Principal Investigator *In* NASA. Goddard Space Flight Center Fundamental Remote Sensing Sci. Res. Program Sep. 1985 p 72-78 ERTS (For primary document see N86-13794 04-43)

Avail: NTIS HC A09/MF A01 CSCL 02C

Much of the early research in remote sensing follows along developing spectral signatures of cover types. It was found, however, that a signature from an unknown cover class could not always be matched to a catalog value of known cover class. This approach was abandoned and supervised classification schemes followed. These were not efficient and required extensive training. It was obvious that data acquired at a single time could not separate cover types. A large portion of the proposed research has concentrated on modeling the temporal behavior of agricultural crops and on removing the need for any training data in remote sensing surveys; the key to which is the solution of the so-called 'signature extension' problem. A clear need to develop spectral estimaters of crop ontogenic stages and yield has existed even though various correlations have been developed. Considerable effort in developing techniques to estimate these variables was devoted to this work. The need to accurately evaluate existing canopy reflectance model(s), improve these models, use them to understand the crop signatures, and estimate leaf area index was the third objective of the proposed work. A synopsis of this research effort is discussed. Author

N86-13801*# Jet Propulsion Lab., California Inst. of Tech., Pasadena.

GROUND REFLECTANCE MEASUREMENTS FROM THEMATIC MAPPER DATA

James E. Conel, Principal Investigator *In* NASA. Goddard Space Flight Center Fundamental Remote Sensing Sci. Res. Program Sep. 1985 p 79-85 refs ERTS (For primary document see N86-13794 04-43)

Avail: NTIS HC A09/MF A01 CSCL 08B

Satellite radiance data are measures of solar radiation that has been reflected by the Earth's surface and scattered and absorbed by atmospheric gases and aerosols. Of concern to geologists are the surface reflectance and the degrading effects on surface resolution and albedo contrast introduced by atmospheric phenomena. The objects of this research have been to: (1) provide an empirical relationship between scanner radiance and ground reflectance allowing interpretation of the satellite data in terms of the surface parameter, and (2) assess the precision with which surface spectral reflectance may be recovered from LANDSAT-4 TM data in the presence of perturbing atmospheric and instrumental factors. The approach is field-oriented, and utilizes ground observations of surface spectral reflectance with portable spectrometers and radiometers to develop the required empirical relationships. Author

N86-13802*# Jet Propulsion Lab., California Inst. of Tech., Pasadena.

THERMAL INFRARED GEOLOGIC REMOTE SENSING

RESEARCH AT THE JET PROPULSION LABORATORY

Mary Jane Bartholomew and Anne B. Kahle, Principle Investigators *In* NASA. Goddard Space Flight Center Fundamental Remote Sensing Sci. Res. Program Sep. 1985 p 86-92 refs Original contains imagery. Original photography may be purchased from the EROS Data Center, Sious Falls, S.D. 57198 ERTS (For primary document see N86-13794 04-43)
Avail. NTIS HC A09/MF A01 CSCL 08G

Remotely sensed thermal infrared spectral data have great potential to improve rock type discrimination if the factors that control thermal infrared spectral reflection and emission can be better understood. Improved rock type discrimination in turn leads to better and more efficient geologic mapping which is carried out in the exploration, assessment and documentation of mineral resources and geologic hazards. Geologic maps also contribute significantly to the understanding of the natural history of the Earth and neighboring planetary bodies. Author

N86-13803*# Jet Propulsion Lab., California Inst. of Tech., Pasadena.

ATMOSPHERIC AND SCIENCE COMPLEXITY EFFECTS ON SURFACE BIDIRECTIONAL REFLECTANCE

David J. Diner, Principal Investigator, John V. Martonchik, William D. Sythe, and Charles Hessom (California Univ., Los Angeles) *In* NASA. Goddard Space Flight Center Fundamental Remote Sensing Sci. Res. Program Sep. 1985 p 93-99 ERTS (For primary document see N86-13794 04-43)
Avail: NTIS HC A09/MF A01 CSCL 20F

Among the tools used in passive remote sensing of Earth resources in the visible and near-infrared spectral regions are measurements of spectral signature and bidirectional reflectance functions (BDRFs). Determination of surface properties using these observables is complicated by a number of factors, including: (1) mixing of surface components, such as soil and vegetation, (2) multiple reflections of radiation due to complex geometry, such as in crop canopies, and (3) atmospheric effects. In order to bridge the diversity in these different approaches, there is a need for a fundamental physical understanding of the influence of the various effects and a quantiative measure of their relative importance. In particular, we consider scene complexity effects using the example of reflection by vegetative surfaces. The interaction of sunlight with a crop canopy and interpretation of the spectral and angular dependence of the emergent radiation is basically a multidimensional radiative transfer problem. The complex canopy geometry, underlying soil cover, and presence of diffuse as well as collimated illumination will modify the reflectance characteristics of the canopy relative to those of the individual elements. Author

N86-13804*# National Aeronautics and Space Administration. Goddard Space Flight Center, Greenbelt, Md.

ATMOSPHERIC EFFECT ON REMOTE SENSING OF THE EARTH'S SURFACE

Robert S. Fraser and Yoram J. Kaufman, Principal Investigators (Maryland Univ., College Park) *In its* Fundamental Remote Sensing Sci. Res. Program Sep. 1985 p 100-106 ERTS (For primary document see N86-13794 04-43)
Avail: NTIS HC A09/MF A01 CSCL 08G

Radiative transfer theory (RT) for an atmosphere with a nonuniform surface is the basis for understanding and correcting for the atmospheric effect on remote sensing of surface properties. In the present work the theory is generalized and tested successfully against laboratory and field measurements. There is still a need to generalize the RT approximation for off-nadir directions and to take into account anisotropic reflectance at the surface. The reflectance at the surface. The adjacency effect results in a significant modification of spectral signatures of the surface, and therefore results in modification of classifications, of separability of field classes, and of spatial resolution. For example, the 30 m resolution of the Thematic Mapper is reduced to 100 m by a hazy atmosphere. The adjacency effect depends on several optical parameters of aerosols: optical thickness, depth of aerosol layer, scattering phase function, and absorption. Remote sensing in general depends on these parameter, not just adjacency effects, but they are not known well enough for making accurate atmospheric corrections. It is important to establish methods for estimating these parameters in order to develop correction methods for atmospheric effects. Such estimations can be based on climatological data, which are not available yet, correlations between the optical parameters and meteorological data, and the same satellite measurements of radiances that are used for estimating surface properties. Knowledge about the atmospheric parameters important for remote sensing is being enlarged with current measurements of them. Author

N86-13805*# EG and G Washington Analytic Services Center, Inc., Lanham, Md.

THE CHARACTERIZATION OF SURFACE VARIGATION EFFECTS ON REMOTE SENSING

William A. Pearce, Principal Investigator *In* NASA. Goddard Space Flight Center Fundamental Remote Sensing Sci. Res. Program Sep. 1985 p 107-113 ERTS (For primary document see N86-13794 04-43)
Avail: NTIS HC A09/MF A01 CSCL 20F

Improvements in remote sensing capabilities hinge very directly upon attaining an understanding of the physical processes contributing to the measurements. In order to devise new measurement strategies and to learn better techniques for processing remotely gathered data, it is necessary to understand and to characterize the complex radiative interactions of the atmosphere-surface system. In particular, it is important to understand the role of atmospheric structure, ground reflectance inhomogeneity and ground bidirectional reflectance type. The goals, then, are to model, analyze, and parameterize the observable effects of three dimensional atmospheric structure and composition and two dimensional variations in ground albedo and bidirectional reflectance. To achieve these goals, a Monte Carlo radiative transfer code is employed to model and analyze the effects of many of the complications which are present in nature. Author

N86-13806*# Los Alamos National Lab., N. Mex. Theoretical Div.

MULTIDIMENSIONAL MODELING OF ATMOSPHERIC EFFECTS AND SURFACE HETEROGENEITIES ON REMOTE SENSING

S. A. W. Gerstl, C. Simmer, and A. Zardecki, Principal Investigators *In* NASA. Goddard Space Flight Center Fundamental Remote Sensing Sci. Res. Program Sep. 1985 p 114-119 ERTS (For primary document see N86-13794 04-43)
Avail: NTIS HC A09/MF A01 CSCL 04A

The overall goal of this project is to establish a modeling capability that allows a quantitative determination of atmospheric effects on remote sensing including the effects of surface heterogeneities. This includes an improved understanding of aerosol and haze effects in connection with structural, angular, and spatial surface heterogeneities. One important objective of the research is the possible identification of intrinsic surface or canopy characteristics that might be invariant to atmospheric perturbations so that they could be used for scene identification. Conversely, an equally important objective is to find a correction algorithm for atmospheric effects in satellite-sensed surface reflectances. The technical approach is centered around a systematic model and code development effort based on existing, highly advanced computer codes that were originally developed for nuclear radiation shielding applications. Computational techniques for the numerical solution of the radiative transfer equation are adapted on the basis of the discrete-ordinates finite-element method which proved highly successful for one and two-dimensional radiative transfer problems with fully resolved angular representation of the radiation field. Author

N86-13807*# Texas Univ., Arlington. Dept. of Electrical Engineering.

SCATTERING MODELS AND BASIC EXPERIMENTS IN THE MICROWAVE REGIME

A. K. Fung and A. J. Blanchard, Principal Investigators *In* NASA. Goddard Space Flight Center Fundamental Remote Sensing Sci.

Res. Program Sep. 1985 p 120-125 ERTS (For primary document see N86-13794 04-43)
Avail: NTIS HC A09/MF A01 CSCL 20N

The objectives of research over the next three years are: (1) to develop a randomly rough surface scattering model which is applicable over the entire frequency band; (2) to develop a computer simulation method and algorithm to simulate scattering from known randomly rough surfaces, Z(x,y); (3) to design and perform laboratory experiments to study geometric and physical target parameters of an inhomogeneous layer; (4) to develop scattering models for an inhomogeneous layer which accounts for near field interaction and multiple scattering in both the coherent and the incoherent scattering components; and (5) a comparison between theoretical models and measurements or numerical simulation. Author

N86-13808*# Massachusetts Inst. of Tech., Cambridge.
REMOTE SENSING OF EARTH TERRAIN
Jin Au Kong, Principal Investigator *In* NASA. Goddard Space Flight Center Fundamental Remote Sensing Sci. Res. Program Sep. 1985 p 126-129 ERTS (For primary document see N86-13794 04-43)
Avail: NTIS HC A09/MF A01 CSCL 08B

The objective of this research is to develop theoretical models that are useful and practical in the remote sensing of the Earth environment including the Earth terrain, the lower and the upper atmospheres. Various models applicable to the microwave remote sensing of vegetation, snow-ice, and atmospheric precipitation have been developed. Such studies shall be extended to the higher frequency range to unify the optical band and the microwave theoretical foundations. The study, which had an emphasis on vegetation canopy to include all terrain media, and the whole Earth environment will be extended. A data base will be developed to generate scene radiation characteristics which will benefit the studies of global inhabitability, meteorological applications, and crop yield. Author

N86-13809*# George Washington Univ., Washington, D.C. Dept. of Electrical Engineering.
DISCRETE RANDOM MEDIA TECHNIQUES FOR MICROWAVE MODELING OF VEGETATED TERRAIN
Roger H. Lang, Principal Investigator *In* NASA. Goddard Space Flight Center Fundamental Remote Sensing Sci. Res. Program Sep. 1985 p 130-135 ERTS (For primary document see N86-13794 04-43)
Avail: NTIS HC A09/MF A01 CSCL 08B

Microwave remote sensing of vegetated terrain has been studied. Vegetation is modeled so that backscattered radar signals can be used to infer parameters which characterize the vegetation and underlying ground. The vegetation is modeled by discrete lossy dielectric scatterers with prescribed characteristics. The goal of the modeling effort is to remotely sense vegetation type (classification), growth stage, and plant/ground moisture. This information can then be used as input into agricultural, forestry and global circulation models. The microwave frequency spectrum, particularly L and C bands, are especially appropriate for this purpose since the wavelength is comparable to plant leaf and stem size. The resulting resonant interaction leads to backscattered data highly depend on plant shape and orientation. In addition, the transparent nature of the atmosphere in this frequency regime allows for algorithm development which requires no atmospheric correction. Author

N86-13810*# Michigan Univ., Ann Arbor. Radiation Lab.
MICROWAVE DIELECTRIC AND PROPAGATION PROPERTIES OF VEGETATION CANOPIES
Fawwaz T. Ulaby, Principal Investigator *In* NASA. Goddard Space Flight Center Fundamental Remote Sensing Sci. Res. Program Sep. 1985 p 136-141 ERTS (For primary document see N86-13794 04-43)
Avail: NTIS HC A09/MF A01 CSCL 20N

A vegetation canopy is a highly inhomogeneous medium at microwave frequencies, and because the scattering elements (leaves, stalks, fruits, and branches) have a nonuniform distribution in orientation, the canopy is likely to exhibit nonisotropic attenuation properties. In some canopies, the stalk may contain the overwhelming majority of the plant's biomass, which suggests that an incident radar wave would be differentially attenuated by the canopy depending on the direction of the incident electric field relative to the stalks' orientation. The propagation properties of a vegetation canopy play a central role in modeling both the backscattering behavior observed by an imaging radar and the emission observed by a radiometer. These propagation properties are in turn governed by the dielectric properties and the size, shape, and slope distributions of the scatteres. In spite of the critical need for canopy propagation models and experimental data, very few investigations had been conducted (prior to this study) to determine the extinction properties of vegetation canopies, either by constituent type (leaves, stalks, etc.) or as a whole. Author

N86-13811*# Kansas Univ. Center for Research, Inc., Lawrence. Remote Sensing Lab.
DETERMINATION OF BACKSCATTERING SOURCES IN VARIOUS TARGETS
R. K. Moore, R. Zoughi, and L. K. Wu, Principal Investigators *In* NASA. Goddard Space Flight Center Fundamental Remote Sensing Sci. Res. Program Sep. 1985 p 142-147 refs ERTS (For primary document see N86-13794 04-43)
Avail: NTIS HC A09/MF A01 CSCL 20N

The objectives of this research are to identify the primary contributors to 10 GHz radar backscatter from various natural and man-made surfaces and objects, and to use this information in developing new and better models for the scatter. When the true sources are known for the scattering that leads to variation in intensity on radar images, the images (and sets of them) may be interpreted more meaningfully in terms of the variation of parameters of interest for science or application. For example, better interpretation of vegetation images may be possible for yield forecasting and stress detection. Author

N86-13812*# Jet Propulsion Lab., California Inst. of Tech., Pasadena.
ACTIVE MICROWAVE PROPERTIES OF VEGETATION CANOPIES
Jack F. Paris, Principal Investigator *In* NASA. Goddard Space Flight Center Fundamental Remote Sensing Sci. Res. Program Sep. 1985 p 148-153 ERTS (For primary document see N86-13794 04-43)
Avail: NTIS HC A09/MF A01 CSCL 20N

Potential users of radar imagery need a better fundamental understanding of the capabilities of radar systems for vegetation studies than past studies provide. One approach is the use of theoretical models to predict observable active microwave properties of vegetation. This in turn requires accurate observations of backscattering coefficients and other active microwave properties in field research studies. The background document for the SRAEC program emphasizes the need to relate electromagnetic parameters to classical biophysical descriptors and to understand the role of polarization, especially cross-polarization. The broad goal of this study is to increase the understanding of the effects of canopy structure on the active microwave properties of vegetation canopies, with particular attention to polarization. Author

N86-13813*# Raytheon Co., Sudbury, Mass. Electro-Optics Systems Lab.
PRECISION POINTING USING A DUAL-WEDGE SCANNER Final Report
Christopher T. Amirault and Charles A. DiMarzio Washington NASA Nov. 1985 35 p refs
(Contract NAS8-33120)
(NASA-CR-3946; NAS 1.26:3946) Avail: NTIS HC A03/MF A01 CSCL 20E

A system was developed for calibrating and precisely pointing a germanium dual-wedge scanner for a CO2 Doppler lidar from an airborne platform. The equations implemented in pointing the scanner and those in the iterative calibration program, which combines available data with estimated parameters of the scanner orientation relative to the axes of the aircraft's inertial navigation system to arrive at corrected scanner parameters are described. The effect of specific error conditions on program performance and the results of the program when used on 1981 test data are investigated. E.A.K.

N86-13814*# Southern Methodist Univ., Dallas, Tex. Dept. of Statistics.
CROP AREA ESTIMATION BASED ON REMOTELY-SENSED DATA WITH AN ACCURATE BUT COSTLY SUBSAMPLE Final Report, 1 Jan. 1984 - 31 Aug. 1985
Richard F. Gunst 31 Aug. 1985 33 p refs
(Contract NCC9-9)
(NASA-CR-176017; NAS 1.26:176017) Avail: NTIS HC A03/MF A01 CSCL 02C

Research activities conducted under the auspices of National Aeronautics and Space Administration Cooperative Agreement NCC 9-9 are discussed. During this contract period research efforts are concentrated in two primary areas. The first are is an investigation of the use of measurement error models as alternatives to least squares regression estimators of crop production or timber biomass. The secondary primary area of investigation is on the estimation of the mixing proportion of two-component mixture models. This report lists publications, technical reports, submitted manuscripts, and oral presentation generated by these research efforts. Possible areas of future research are mentioned. Author

N86-13815# Battelle Inst., Frankfurt am Main (West Germany).
GENERICALLY BASED MOBILITY-TERRAIN DATA BASES Interim Report, Dec. 1984 - Apr. 1985
W. Koeppel and P. Jessl Apr. 1985 4 p
(Contract DAJA45-84-C-0039)
(AD-A157738; R/D-4739-EN-01; IR-2) Avail: NTIS HC A02/MF A01 CSCL 05/2

This document describes three tasks: (1) Concerning task 1-development of a method of assembling generically-based mobility terrain data bases; areas were identified within the generic terrain regions where the classification system output was compared with available CCM-mapping products and recently assembled terrain information on german water-folio products; (2) Task 2 concerns initiation of the development of a procedure for quantitatively estimating the reliability of generically-based mobility terrain data bases; (3) Concerning Task 3 initiation of the development of a procedure for determining the relations among soil dynamic parameters and conventional mobility index numbers (or descriptors) repetitively testing of shear load-displacement behavior was performed within transitional weather period conditions of December 1984 and April 1985 at six sites within the vicinity of Frankfurt. GRA

N86-13816# Wyoming Univ., Laramie. Dept. of Geology and Geophysics.
GEOTHERMAL RESOURCES OF THE WIND RIVER BASIN, WYOMING
B. S. Hickley and H. P. Heasler 1985 58 p refs
(Contract DE-FC07-79ID-12026)
(DE85-016969; DOE/ID-12026/T14) Avail: NTIS HC A04/MF A01

The geothermal resources of the Wind River Basin were investigated. Oil-well bottom-hole temperatures, thermal logs of wells, and heat flow data were interpreted within a framework of geologic and hydrologic constraints basic thermal data, which includes the background thermal gradient and the highest recorded temperature and corresponding depth for each basin, is tabulated. Background heat flow in the Wind River Basin is generally insufficient to produce high conductive gradients. Only where hydrologic systems re-distribute heat through mass movement of water will high temperatures occur at shallow depths. Aquifers which may be have the confinement and structural characteristics necessary to create such geothermal systems are the Lance/Fort Union, Mesa Verde, Frontier, Muddy, Cloverly, Sundance, Nugget, Park City, Tensleep, Amsden, Madison, Bighorn, and Flathead Formations. Of these the Tensleep Sandstone and Madison Limestone are the most attractive in terms of both productivity and water quality. Most of the identified geothermal anomalies in the Wind River Basin occur along complex structures in the southwest and south. The most attractive geothermal prospects identified are anomalous Areas 2 and 3 north of Lander, Sweetwater Station Springs west of Jeffrey City, and the thermal springs southwest of Dubois. Even in these areas, it is unlikely temperatures in excess of 130 to 150(0)F can be developed. DOE

N86-13817# Oak Ridge National Lab., Tenn.
UNUSUAL OCCURRENCE OF MAGHEMITE IN SOILS DEVELOPED ON KNOX GROUP DOLOSTONES
O. C. Kopp and S. Y. Lee 1985 26 p refs Presented at Intern. Clay Mater. Conf., Denver, 28 Jul. 1985
(Contract DE-AC05-84OR-21400)
(DE85-017158; CONF-850775-1) Avail: NTIS HC A03/MF A01

Maghemite, (GAMMA)-Fe2O3, occurred in soils developed from residuum of Knox group dolostones (Cambro-Ordovician age) along Chestnut Ridge on the US Department of Energy Oak Ridge Reservation in Oak Ridge, Tennessee. The parent dolostones in the area, although exposed to weathering, were free of maghemite and magnetite. Scanning electron micrographs and electron probe analyses indicated that the maghemite occurred in several textural types, including replaced oolites, cemented siltstones, and massive to botryoidal material. The most complex replacement by maghemite was revealed by the oolitic texture variety. Oolitic limestone was dolomitized, as revealed by the presence of numerous rhombs, during early diagenesis. During a period of silicification dolomite rhombs were replaced, and much of the remaining oolites and carbonate cements may have been partially replaced. More recently, after uplift and erosion brought these oolitic cherts into the upper weathering zone, the cherts were replaced by iron oxides. Massive chert and siltstone grains in all stages of replacement have been observed. The replacing iron in the soil solution may have originated from ferrous-ferric hydroxide, carbonate, or organic complexes. The replaced iron was converted to maghemite and hematite through dehydration and slow oxidation during pedogenesis. DOE

N86-13818# California Univ., Davis.
CALIFORNIA WATER RESOURCES INSTITUTE PROGRAM FOR 1983 Final Report
J. H. Snyder, J. DeVries, and R. J. Woods Sep. 1984 22 p
(PB85-225837; USGS/G-830-01) Avail: NTIS HC A02/MF A01 CSCL 08H

A synopsis is given of the results of research projects sponsored under Grant Program g-830, the 1083 Water Research Institute Program (WRIP) for the University of California's Water Resources Center. The California WRIP package is a subset of the Center's overall research program effort and contains six one year projects investigating the following areas: clarification of surface waters for recharge through wells, temperature requirements of pacific coastal stream fishes, the implications of total water demand from the adoption of drip irrigation in western agriculture, an economic approach to the estimation of dynamic production function for an irrigated crop, channel and flow relationships in tidal salt marsh wetlands, and chaparral management effects on water and the environment. GRA

N86-13819# Technicolor Government Services, Inc., Fort Collins, Colo.
MAP PROJECTIONS FOR USE WITH THE GEOGRAPHIC INFORMATION SYSTEM
J. E. Lee and J. M. Walsh Jul. 1984 73 p refs
(Contract DE-14-16-0009-83-001)
(PB85-198992; FWS/OBS-84/17) Avail: NTIS HC A04/MF A01 CSCL 08B

This document has been prepared to assist users of the Geographic Information System (GIS), originally developed at the Western Energy and Land Use Team (WELUT), in understanding and using the various map projections which are available. Currently, 20 map projections may be used in the GIS. Users who have been trained in the component software systems of the GIS MOSS (Map Overlay and Statistical System), COS (Cartographic Output System), and AMS (Analytical Mapping System), and who have some introduction to principles of cartography, will find this document most helpful. Author (GRA)

N86-13775*# Joint Publications Research Service, Arlington, Va.
AERIAL LASER SENSING OF OCEAN UPPER LAYER Abstract Only
D. V. Vlasov *In its* USSR Rept.: Earth Sci. (JPRS-UES-85-009) 13 Nov. 1985 p 19 Transl. into ENGLISH from Izv. Akad. Nauk SSSR: Ser. Fiz. (Moscow), v. 49, no. 3, Mar. 1985 p 433-441 (For primary document see N86-13765 04-43)
Avail: NTIS HC A04/MF A01

N86-13777# Joint Publications Research Service, Arlington, Va.
VOLCANOES DISCOVERED WITH RADIO BEAM Abstract Only
In its USSR Rept.: Earth Sci. (JPRS-UES-85-009) 13 Nov. 1985 p 21 Transl. into ENGLISH from Tass (Moscow), 16 May 1985 (For primary document see N86-13765 04-43)
Avail: NTIS HC A04/MF A01

N86-13778# Joint Publications Research Service, Arlington, Va.
COMPUTER-AIDED AERIAL RADIOMETRIC SURVEYING OF SOIL MOISTURE Abstract Only
N. Armand *In its* USSR Rept.: Earth Sci. (JPRS-UES-85-009) 13 Nov. 1985 p 24 Transl. into ENGLISH from Krasnaya Zvezda (Moscow), 30 Jun. 1985 p 2 (For primary document see N86-13765 04-43)
Avail: NTIS HC A04/MF A01

N86-14168# Joint Publications Research Service, Arlington, Va.
PRESSURE FIELD RETRIEVAL BY REMOTE REFRACTOMETRY FROM SPACE Abstract Only
A. S. Gurvich and S. V. Sokolovskiy *In its* USSR Rept.: Space (JPRS-USP-85-005) 30 Sep. 1985 p 106 Transl. into ENGLISH from Izv. Akad. Nauk SSSR: Fiz. Atm. i Okeana (Moscow), v. 21, no. 1, Jan. 1985 p 12-21 Original language document announced in IAA as A85-26291 (For primary document see N86-14111 04-88)
Avail: NTIS HC A08

N86-14170# Joint Publications Research Service, Arlington, Va.
STEREOPHOTOGRAMMETRIC SURVEY OF WAVE-COVERED WATER SURFACE Abstract Only
M. V. Shulmin, Yu. I. Kuchinskiy, and M. P. Shulmina *In its* USSR Rept.: Space (JPRS-USP-85-005) 30 Sep. 1985 p 107-108 Transl. into ENGLISH from Geod. i Kartografiya (Moscow), no. 11, Nov. 1984 p 33-35 (For primary document see N86-14111 04-88)
Avail: NTIS HC A08

N86-14172# Joint Publications Research Service, Arlington, Va.
USE OF REMOTE OPTICAL MEASUREMENTS IN AGRICULTURE Abstract Only
G. I. Belchanskiy, K. Ya. Kondratyev, V. V Kozoderov, N. V. Sazonov, A. G. Topchiyev, and P. P. Fedchenko *In its* USSR Rept.: Space (JPRS-USP-85-005) 30 Sep. 1985 p 109-110 Transl. into ENGLISH from Issled. Zemli iz Kosmosa (Moscow), no. 5, Sep. - Oct. 1984 p 8-24 (For primary document see N86-14111 04-88)
Avail: NTIS HC A08

N86-14173# Joint Publications Research Service, Arlington, Va.
CLASSIFICATION OF TREES BY GROWTH CLASSES ON THE BASIS OF MULTIZONAL PHOTOGRAPHS Abstract Only
A. N. Borisov, V. A. Ivanov, G. A. Ivanchenko, V. S. Kirichuk, and V. V. Kuzmichev *In its* USSR Rept.: Space (JPRS-USP-85-005) 30 Sep. 1985 p 110 Transl. into ENGLISH from Issled. Zemli iz Kosmosa (Moscow), no. 5, Sep. - Oct. 1984 p 25-30 (For primary document see N86-14111 04-88)
Avail: NTIS HC A08

N86-14174# Joint Publications Research Service, Arlington, Va.
EXPERIENCE IN COMPLEX MAPPING OF NATURAL RESOURCES IN AGRARIAN-INDUSTRIAL REGIONS OF NON-CHERNOZEM RSFSR USING SPACE PHOTOMATERIALS Abstract Only
V. A. Sushchenya, L. A. Shevchenko, and V. I. Somova *In its* USSR Rept.: Space (JPRS-USP-85-005) 30 Sep. 1985 p 111 Transl. into ENGLISH from Issled. Zemli iz Kosmosa (Moscow), no. 5, Sep. - Oct. 1984 p 31-40 Original language document announced in IAA as A85-16941 (For primary document see N86-14111 04-88)
Avail: NTIS HC A08

N86-14175# Joint Publications Research Service, Arlington, Va.
POSSIBILITIES OF USE OF AEROSPACE MATERIALS IN PREDICTING OCCURRENCE OF PETROLEUM AND GAS Abstract Only
R. A. Bidzhiyev and L. M. Natapov *In its* USSR Rept.: Space (JPRS-USP-85-005) 30 Sep. 1985 p 112 Transl. into ENGLISH from Issled. Zemli iz Kosmosa (Moscow), no. 5, Sep. - Oct. 1984 p 41-50 Original language document announced in IAA as A85-16942 (For primary document see N86-14111 04-88)
Avail: NTIS HC A08

N86-14176# Joint Publications Research Service, Arlington, Va.
PROBLEMS IN STUDY AND EVALUATION OF CONSEQUENCES OF FOREST FIRES USING AEROSPACE PHOTOGRAPHS Abstract Only
V. V. Furyayev *In its* USSR Rept.: Space (JPRS-USP-85-005) 30 Sep. 1985 p 113 Transl. into ENGLISH from Issled. Zemli iz Kosmosa (Moscow), no. 5, Sep. - Oct. 1984 p 51-57 Original language document announced in IAA as A85-16943 (For primary document see N86-14111 04-88)
Avail: NTIS HC A08

N86-14177# Joint Publications Research Service, Arlington, Va.
COMPUTATION OF REFLECTION OF SOLAR RADIATION FROM VEGETATION COVER BY MONTE-CARLO METHOD Abstract Only
Yu. K. Ross and A. L. Marshak *In its* USSR Rept.: Space (JPRS-USP-85-005) 30 Sep. 1985 p 114 Transl. into ENGLISH from Issled. Zemli iz Kosmosa (Moscow), no. 5, Sep. - Oct. 1984 p 58-67 Original language document announced in IAA as A85-16944 (For primary document see N86-14111 04-88)
Avail: NTIS HC A08

N86-14178# Joint Publications Research Service, Arlington, Va.
REFLECTION INDICATRICES OF VEGETATION CANOPIES Abstract Only
A. Kuusk, Ya. Anton, T. Nilson, U. Peterson, K. Ross, Yu. Ross, and A. Savikhin *In its* USSR Rept.: Space (JPRS-USP-85-005) 30 Sep. 1985 p 115 Transl. into ENGLISH from Issled. Zemli iz Kosmosa (Moscow), no. 5, Sep. - Oct. 1984 p 68-75 (For primary document see N86-14111 04-88)
Avail: NTIS HC A08

N86-14179# Joint Publications Research Service, Arlington, Va.
APPROXIMATE ANALYTICAL FORMULAS FOR COMPUTING SPECTRAL BRIGHTNESS COEFFICIENTS FOR AGRICULTURAL VEGETATION Abstract Only
T. Nilson and A. Kuusk *In its* USSR Rept.: Space (JPRS-USP-85-005) 30 Sep. 1985 p 116 Transl. into ENGLISH from Issled. Zemli iz Kosmosa (Moscow), no. 5, Sep. - Oct. 1984 p 76-83 (For primary document see N86-14111 04-88)
Avail: NTIS HC A08

N86-14180# Joint Publications Research Service, Arlington, Va.
METHOD FOR USING CLUSTERS IN EVALUATING LAND USE AREAS FROM MULTIZONAL PHOTOGRAPHS Abstract Only
L. N. Vasilyev and R. Kachinski *In its* USSR Rept.: Space (JPRS-USP-85-005) 30 Sep. 1985 p 117 Transl. into ENGLISH from Issled. Zemli iz Kosmosa (Moscow), no. 5, Sep. - Oct. 1984 p 94-99 (For primary document see N86-14111 04-88)
Avail: NTIS HC A08

N86-14181# Joint Publications Research Service, Arlington, Va.
METHODS FOR COMPLEX SPACE EXPERIMENT IN USSR FOR STUDYING LAND FROM MANNED SPACECRAFT Abstract Only
B. V. Vinogradov *In its* USSR Rept.: Space (JPRS-USP-85-005) 30 Sep. 1985 p 118 Transl. into ENGLISH from Issled. Zemli iz Kosmosa (Moscow), no. 5, Sep. - Oct. 1984 p 100-106 Original language document announced in IAA as A85-16946 (For primary document see N86-14111 04-88)
Avail: NTIS HC A08

N86-14182# Joint Publications Research Service, Arlington, Va.
EXPERIENCE IN CONDUCTING SUBSATELLITE EXPERIMENTS WITH WATER BODIES IN USSR AND HUNGARIAN PEOPLE'S REPUBLIC Abstract Only
I. F. Berestovskiy, A. A. Gitelson, D. Sabo, and F. Siladi *In its* USSR Rept.: Space (JPRS-USP-85-005) 30 Sep. 1985 p 119 Transl. into ENGLISH from Issled. Zemli iz Kosmosa (Moscow), no. 5, Sep. - Oct. 1984 p 107-111 Original language document announced in IAA as A85-16947 (For primary document see N86-14111 04-88)
Avail: NTIS HC A08

N86-14183# Joint Publications Research Service, Arlington, Va.
POSSIBILITIES OF USING SPACE SURVEY FOR STUDYING SEASONAL CHANGES OF LANDSCAPES IN SOME REGIONS OF USSR Abstract Only
I. N. Yelagin *In its* USSR Rept.: Space (JPRS-USP-85-005) 30 Sep. 1985 p 120 Transl. into ENGLISH from Issled. Zemli iz Kosmosa (Moscow), no. 5, Sep. - Oct. 1984 p 112-114 Original language document announced in IAA as A85-16948 (For primary document see N86-14111 04-88)
Avail: NTIS HC A08

N86-14184# Joint Publications Research Service, Arlington, Va.
ROLE OF LANDSCAPE RESEARCH IN DEVELOPMENT OF SPACE METHODS FOR STUDYING EARTH Abstract Only
Ye. V. Glushko *In its* USSR Rept.: Space (JPRS-USP-85-005) 30 Sep. 1985 p 121 Transl. into ENGLISH from Issled. Zemli iz Kosmosa (Moscow), no. 5, Sep. - Oct. 1984 p 115-121 (For primary document see N86-14111 04-88)
Avail: NTIS HC A08

N86-14186# Joint Publications Research Service, Arlington, Va.
APPLICATION OF STATISTICAL MODEL OF LAYERED MEDIUM FOR COMPUTING THERMAL EMISSION OF ICE COVERS Abstract Only
V. L. Brekhovskikh *In its* USSR Rept.: Space (JPRS-USP-85-005) 30 Sep. 1985 p 122-123 Transl. into ENGLISH from Issled. Zemli iz Kosmosa (Moscow), no. 4, Jul. - Aug. 1984 p 33-38 (For primary document see N86-14111 04-88)
Avail: NTIS HC A08

N86-14187# Joint Publications Research Service, Arlington, Va.
COMPILATION OF LANDSCAPE MAPS AT DIFFERENT SCALES WITH USE OF SPACE PHOTOINFORMATION Abstract Only
V. I. Ryabchikova *In its* USSR Rept.: Space (JPRS-USP-85-005) 30 Sep. 1985 p 123 Transl. into ENGLISH from Issled. Zemli iz Kosmosa (Moscow), no. 4, Jul. - Aug. 1984 p 39-45 Original language document announced in IAA as A84-49029 (For primary document see N86-14111 04-88)
Avail: NTIS HC A08

N86-14190# Joint Publications Research Service, Arlington, Va.
USE OF GOUDRIAAN MODEL FOR STUDYING REFLECTION REGULARITIES IN VEGETATION-SOIL SYSTEM IN OPTICAL RANGE. 1: INFLUENCE OF PHYTOMETRIC PARAMETERS ON SPECTRAL BRIGHTNESS COEFFICIENTS Abstract Only
N. N. Vygodskaya and I. I. Gorshkova *In its* USSR Rept.: Space (JPRS-USP-85-005) 30 Sep. 1985 p 126 Transl. into ENGLISH from Issled. Zemli iz Kosmosa (Moscow), no. 4, Jul. - Aug. 1984 p 61-70 (For primary document see N86-14111 04-88)
Avail: NTIS HC A08

N86-14191# Joint Publications Research Service, Arlington, Va.
ANALYSIS OF SURVEY CONDITIONS AND EFFECT OF NOISE ON QUALITY OF SENSING OF SOIL FORMATIONS Abstract Only
A. B. Karasev and S. V. Pantyukhov *In its* USSR Rept.: Space (JPRS-USP-85-005) 30 Sep. 1985 p 127 Transl. into ENGLISH from Issled. Zemli iz Kosmosa (Moscow), no. 4, Jul. - Aug. 1984 p 71-80 (For primary document see N86-14111 04-88)
Avail: NTIS HC A08

N86-14192# Joint Publications Research Service, Arlington, Va.
NORMALIZATION OF RESPONSE OF RADIOMETRIC INSTRUMENTATION FOR STUDYING EARTH'S NATURAL RESOURCES Abstract Only
G. K. Kholopov, R. Sh. Khisamov, and F. G. Khuzin *In its* USSR Rept.: Space (JPRS-USP-85-005) 30 Sep. 1985 p 128 Transl. into ENGLISH from Issled. Zemli iz Kosmosa (Moscow), no. 4, Jul. - Aug. 1984 p 81-88 Original language document announced in IAA as A84-49032 (For primary document see N86-14111 04-88)
Avail: NTIS HC A08

N86-14193# Joint Publications Research Service, Arlington, Va.
RADIOMETRIC CORRECTION OF MATERIALS OF AEROSPACE SURVEY OF EARTH WITH MKF-6 CAMERA: METHODOLOGY AND USE OF RESULTS Abstract Only
Kh. A. LopesFalkon *In its* USSR Rept.: Space (JPRS-USP-85-005) 30 Sep. 1985 p 129 Transl. into ENGLISH from Issled. Zemli iz Kosmosa (Moscow), no. 4, Jul. - Aug. 1984 p 89-94 Original language document announced in IAA as A84-49033 (For primary document see N86-14111 04-88)
Avail: NTIS HC A08

N86-14194# Joint Publications Research Service, Arlington, Va.
SOME APPROACHES TO ORGANIZATION OF DATA BANK IN SYSTEM FOR STUDYING EARTH'S NATURAL RESOURCES FROM SPACE (USING EXAMPLE OF AGRICULTURE) Abstract Only
Yu. G. Simonov, N. F. Derevyanko, and G. I. Barvyn *In its* USSR Rept.: Space (JPRS-USP-85-005) 30 Sep. 1985 p 130 Transl. into ENGLISH from Issled. Zemli iz Kosmosa (Moscow), no. 4, Jul. - Aug. 1984 p 103-109 Original language document announced in IAA as A84-49035 (For primary document see N86-14111 04-88)
Avail: NTIS HC A08

N86-14195# Joint Publications Research Service, Arlington, Va.
EXPERIMENT FOR EVALUATING ACCURACY IN DETERMINING LAND CATEGORIES ON SPACE SCANNER PHOTOGRAPHS Abstract Only
R. I. Elman, Ye. V. Bakhtinova, A. N. Potapov, R. V. Sviridova, and L. A. Bersneva *In its* USSR Rept.: Space (JPRS-USP-85-005) 30 Sep. 1985 p 131 Transl. into ENGLISH from Issled. Zemli iz Kosmosa (Moscow), no. 4, Jul. - Aug. 1984 p 110-119 Original language document announced in IAA as A84-49036 (For primary document see N86-14111 04-88)
Avail: NTIS HC A08

N86-14196# Joint Publications Research Service, Arlington, Va.
REMOTE TEMPERATURE DETERMINATION OF TERRESTRIAL COVERS FROM POLARIZATION INVARIANT OF MICROWAVE-RADIOTHERMAL EMISSION Abstract Only
G. A. Andreyev, L. F. Borodin, L. V. Zayentsev, and S. N. Rubtsov *In its* USSR Rept.: Space (JPRS-USP-85-005) 30 Sep. 1985 p 132 Transl. into ENGLISH from Issled. Zemli iz Kosmosa (Moscow), no. 4, Jul. - Aug. 1984 p 120-123 (For primary document see N86-14111 04-88)
Avail: NTIS HC A08

44 ENERGY PRODUCTION AND CONVERSION

Includes specific energy conversion systems, e.g., fuel cells and batteries; global sources of energy; fossil fuels; geophysical conversion; hydroelectric power; and wind power.

For related information see also *07 Aircraft Propulsion and Power, 20 Spacecraft Propulsion and Power, 28 Propellants and Fuels*, and *85 Urban Technology and Transportation.*

N86-13820# Kernforschungsanlage, Juelich (West Germany). Projektleitung Energieforschung.
IMPLEMENTING AGREEMENT FOR COOPERATION IN THE DEVELOPMENT OF LARGE SCALE WIND ENERGY CONVERSION SYSTEMS
Mar. 1985 182 p refs Partly in ENGLISH and GERMAN Proc. of 12th Meeting of Experts on Aerodyn. Calculational Methods for WECS; sponsored by Bundesministerium fuer Forschung und Technologie and Technical Univ. of Denmark
(Juel-Spez-304; ISSN-0343-7639) Avail: NTIS HC A09/MF A01

Wind energy converter aerodynamics and turbulence; rotor tip vane performance; performance prediction; airfoil characteristics; rotor performance; and simulation models were discussed. For individual titles, see N86-13821 through N86-13830.

N86-13821# Stuttgart Univ. (West Germany). Inst. fuer Aerodynamik und Gasdynamik.
POLAR MEASUREMENTS ON THE PROFILES: FX 84-w-097, FX 84-w-127, FX 84-w-140, FX 84-w-175, FX 84-w-218 [POLARENMESSUNGEN AN DEN PROFILEN: FX 84-W-097, FX 84-W-127, FX 84-W-140, FX 84-W-175, FX 84-W-218]
D. Althaus *In* Kernforschungsanlage Aerodyn. Calculation Methods for Wind Energy Converters (WECS) Mar. 1985 p 3-28 In GERMAN (For primary document see N86-13820 04-44)
Avail: NTIS HC A09/MF A01

Wind tunnel data on wind turbine blade models in a laminar tunnel at Reynolds numbers between 700,000 and 1.5 million are presented. Flow distribution and velocity data are shown.
Author (ESA)

N86-13822# McAlpine (Sir Robert) and Sons, London (England).
DEVELOPMENT IN AERODYNAMIC CALCULATIONS
Mike B. Anderson *In* Kernforschungsanlage Aerodyn. Calculation Methods for Wind Energy Converters (WECS) Mar. 1985 p 29-39 (For primary document see N86-13820 04-44)
Avail: NTIS HC A09/MF A01

An unsteady aerodynamics models for simulating large wind energy converters is described. For the attached flow region the loads are calculated via a generalized indicial lift function based on the Wagner function. The angle of attack is defined at the 3/4 chord location and thus pitching velocity and virtual mass terms are included. Leading edge stall is incorporated by a simple time delay based on distance travelled in semichord. Trailing edge stall is incorporated via Kirchhoff's law and two first order lags. Time domain simulation of single point power spectra of velocity fluctuations, and coherence function estimates are compared with measurements. Author (ESA)

N86-13823# Technische Hogeschool, Delft (Netherlands). Dept. of Aerospace Engineering.
AN ANALYTICAL THEORY FOR ROTOR TIP VANE PERFORMANCE AND COMPARISON WITH EXPERIMENTAL RESULTS
Theo vanHolten *In* Kernforschungsanlage Aerodyn. Calculation Methods for Wind Energy Converters (WECS) Mar. 1985 p 41-57 refs (For primary document see N86-13820 04-44)
Avail: NTIS HC A09/MF A01

A theoretical method for the performance estimation of tip vane wind turbines was developed to analyze overall forces, total power, and average velocities. It assumes an infinite number of turbines blades and tip vanes. The flow model is equivalent to a time averaged analysis. The model assumes small disturbances, which means that free vorticity convects along trajectories parallel to the undisturbed velocity. Agreement with experiment is satisfactory. Author (ESA)

N86-13824# Central Electricity Generating Board, London (England).
AEROFOIL CHARACTERISTICS OF ROTATING BLADES
David T. Milborrow and J. N. Ross *In* Kernforschungsanlage Aerodyn. Calculation Methods for Wind Energy Converters (WECS) Mar. 1985 p 59-68 refs (For primary document see N86-13820 04-44)
Avail: NTIS HC A09/MF A01

To assess the possibilities of using wind turbine models of modest size for studies of aerodynamic performance and wakes, a study to measure, as directly as possible from rotating blades, angles of attack and the corresponding lift coefficients, using, respectively, the nonintrusive properties of laser anemometery, and small total pressure probes with a wide angle of acceptance was initiated. Measurements at radial stations on a rotating model wind turbine blade yield lift coefficients higher than two dimensional values in the post-stall region, less than fan test results. The study yields drag coefficients higher than two dimensional values, but this may be a function of the small scale of the experiment.
Author (ESA)

N86-13825# Aeronautical Research Inst. of Sweden, Bromma.
UNSTEADY AERODYNAMICS APPLIED TO THE HORIZONTAL AXIS WIND TURBINE DISK
Bjoern Montgomerie *In* Kernforschungsanlage Aerodyn. Calculation Methods for Wind Energy Converters (WECS) Mar. 1985 p 69-82 (For primary document see N86-13820 04-44)
Avail: NTIS HC A09/MF A01

A calculation method to yield external forces in the equations of motion for a complete elastic structure horizontal axis wind turbine elastic model, which includes unsteady effects for improved time history (simulation) and force calculation, and limits the volume of the unsteady method to reduce computer runs was developed. Standard aerodynamic methods are implemented as a part of the complete method. The unsteady effects are applied to the aerodynamic induction factor, to allow easy addition and inclusion of the unsteady effects in an existing method for aerodynamic force calculation. Author (ESA)

N86-13826# Maschinenfabrik Augsburg-Nuernberg A.G., Munich (West Germany).
AERODYNAMIC THEORY IN THE CALCULATION OF THE GROWIAN ROTOR COMPARED WITH SOME EXPERIMENTAL DATA
Reinhold Pernpeintner, G. Huss, and E. Hau *In* Kernforschungsanlage Aerodyn. Calculation Methods for Wind Energy Converters (WECS) Mar. 1985 p 83-96 refs (For primary document see N86-13820 04-44)
Avail: NTIS HC A09/MF A01

The strip (or blade element) theory for predicting wind turbine rotor performance is compared with wind tunnel data, performance measurements on a large unit, and other prediction methods. Comparison of measured and calculated power curves shows that the blade element theory is sufficient in stationnary operation. When comparing the aerodynamic loads on the rotor blades for different load cases, the blade element theory is an excellent, and quick, tool for calculations. Only for cases with fast instationary operation conditions are there differences between theoretical modeling and measurement which cannot be neglected. The limits of the validity of the stationary theory are reached under these conditions. Author (ESA)

N86-13827# Riso National Lab., Roskilde (Denmark).
AERODYNAMIC PERFORMANCE OF A NEW LM 17.2 M ROTOR
Flemming Rasmussen *In* Kernforschungsanlage Aerodyn. Calculation Methods for Wind Energy Converters (WECS) Mar. 1985 p 97-102 refs (For primary document see N86-13820 04-44)

Avail: NTIS HC A09/MF A01

The aerodynamic properties of a 17.2 m diameter rotor mounted on a 55 kW windmill were measured. Power curves were measured for a range of blade tip angles to find the best angle in relation to energy production and stalling characteristics. With this optimum blade setting the flapwise blade root bending moment was measured as a function of wind speed. The drag coefficient at 90 deg angle of attack was calculated from measurements of the integrated value, i.e., the flapwise blade root bending moment as a function of wind speed during stand still. Profile properties are estimated from aerodynamic calculations, and the results compared to profile data from three dimensional wind tunnel measurements. The flapwise blade root bending moment versus blade angular position during one revolution was measured in skew wind and compared with calculations. The influence of surface roughnes introduced at a certain percentage of the section chord and the dependency on the Reynolds number is investigated, and discussed from observed discrepancies in the measured power curves. Author (ESA)

N86-13828# National Aerospace Lab., Amsterdam (Netherlands).
AERODYNAMIC RESEARCH ON WIND TURBINES AT NLR
Otto deVries *In* Kernforschungsanlage Aerodyn. Calculation Methods for Wind Energy Converters (WECS) Mar. 1985 p 103-151 refs (For primary document see N86-13820 04-44)
Avail: NTIS HC A09/MF A01

The aerodynamic calculation of a horizontal axis wind turbine in a steady and homogeneous flow is described. An empirical extension of a blade element calculation method into the turbulent wake state is outlined. Calculations with a vortex method, based on a lifting-line approximation, with a relaxed vortex wake are compared with results from blade element theory and with experiment. Yaw stability at small yaw angles is considered. Author (ESA)

N86-13829# Midwest Research Inst., Golden, Colo. Wind Energy Research Center.
AERODYNAMIC RESEARCH EFFORTS AT SERI WIND ENERGY RESEARCH CENTER AT ROCKY FLATS
James L. Tangler *In* Kernforschungsanlage Aerodyn. Calculation Methods for Wind Energy Converters (WECS) Mar. 1985 p 153-159 refs Sponsored by US Department of Energy (For primary document see N86-13820 04-44)
Avail: NTIS HC A09/MF A01

Performance prediction and enhancement of horizontal axis wind turbines (HAWT) are discussed. A general purpose blade-element/momentum code was developed for rapid parametric studies and for use in annual energy calculations. A post-stall airfoil data synthesization routine accounts for blade aspect ratio effects. A version of the performance code provides better determination of dynamic stall effects on blade loads and performance as influenced by machine yaw angle, unsteady winds, tower shadow, and wind shear. For detailed wind turbine blade optimization, a more sophisticated lifting-surface/prescribed-wake analysis was developed. This code is a transfer of state-of-the-art helicopter theory into a wind turbine design analysis. Airfoil design effort is directed toward satisfying the need to tailor airfoil characteristics specifically for HAWT's. The design criteria and status of this effort are presented. Author (ESA)

N86-13830# National Research Council of Canada, Ottawa (Ontario).
AERODYNAMIC CALCULATIONAL METHODS FOR CURVED-BLADE DARRIEUS VAWT WECS
R. J. Templin *In* Kernforschungsanlage Aerodyn. Calculation Methods for Wind Energy Converters (WECS) Mar. 1985 p 161-172 refs (For primary document see N86-13820 04-44)
Avail: NTIS HC A09/MF A01

Calculation of aerodynamic performance and load distributions for curved-blade wind turbines is discussed. Double multiple stream tube theory, and the uncertainties that remain in further developing adequate methods are considered. The lack of relevant airfoil data at high Reynolds numbers and high angles of attack, and doubts concerning the accuracy of models of dynamic stall are underlined. Wind tunnel tests of blade airbrake configurations are summarized. Author (ESA)

N86-13831# Rasor Associates, Inc., Sunnyvale, Calif.
CLOSE-SPACED HIGH TEMPERATURE KNUDSEN FLOW Annual Report, 16 May 1984 - 15 May 1985
J. B. McVey 15 Jun. 1985 16 p
(Contract F49620-83-C-0068)
(AD-A158280; NSR-22-3; AFOSR-85-0576TR) Avail: NTIS HC A02/MF A01 CSCL 10/2

This work continued to investigate thermionic energy conversion in the Knudsen (collisionless) operating mode. A SAVTEC-type converter with an interelectrode spacing of 18 to 22 microns was tested over a range of emitter temperatures up to about 1700 K. Maximum performance followed the predictions of vacuum-mode analysis for emitter temperatures below 1580 K. Above that temperature the converter operated in the unignited mode, with partial space-charge neutralization by surface ionization of cesium. It was found that collisionless and diffusion mode theories could be extended into the regime of maximum output power for the unignited mode (spacing and electron mean-free path about equal) to give good agreement with the experimental data. The Knudsen-mode thermionic converter with a structured emitter was also investigated. Analysis has shown that associative ionization between barium and cesium is unlikely to be the cause of the current enhancement observed in previously published work. An analysis which considered the trapping of positive ions in the emitter slots has given good qualitative agreement with published data. Work is continuing on this analysis. Parts for a structured emitter variable spacing converter have been constructed and are being assembled. GRA

N86-13832# Westinghouse Electric Corp., Lima, Ohio. Electrical Systems Div.
TWO-HUNDRED TO 300 KVA CONDITIONED POWER SYSTEM - DEVELOPMENT, PHASE 1 Final Report, Sep. 1982 - Mar. 1984
W. E. Hyvarinen Mar. 1985 409 p
(Contract F33615-82-C-2234)
(AD-A158820; Rept-1383R; AFWAL-TR-84-2065) Avail: NTIS HC A18/MF A01 CSCL 10/2

Future large AF electrical generator channels will be required to operate in parallel to supply single large loads. These channels will be required to use a minimum number of conversion stages to maintain the highest possible efficiency. The EW or other large loads will use power converted directly from the variable speed generator, and only that power required to be 400-Hz will be converted by the V.S.C.F. unit. Redundancy for one generator out condition will be required. The protection and control of the parallel bus will require more sophistication and complexity than the systems presently available. Large rating generators, contactors, and distribution systems will require design effort and test. This report covers a design study to meet the requirements of advanced high power EW systems for aircraft. This report covers the design of a 50 kVA, six-phase generator which is spray oil cooled. The output ratings are 60 kVA at 53% speed, 120 kVA at 60% speed and 410 kVA above 83% speed. The generator maximum design speed is 15,000 rpm. GRA

N86-13833# Midwest Research Inst., Golden, Colo. Solar Energy Research Inst.
WIND LOADING ON SOLAR COLLECTORS
S. Bhaduri and L. M. Murphy Jun. 1985 49 p
(Contract DE-AC02-83CH-10093)
(DE85-012151; SERI/TR-253-2169) Avail: NTIS HC A03/MF A01

The present design methodology for the determination of wind loading on the various solar collectors were reviewed and assessed. The total force coefficients of flat plates of aspect ratios 1.0 and 3.0, respectively, at various angles of attack obtained by using the guidelines of the ANSI A58.1-1982, were compared with those obtained by using the methodology of the ASCE Task Committee, 1961, and the experimental results of the full-scale test of heliostats by Peglow. The turbulent energy spectra, currently employed in the building code, are compared with those of Kaimal et al., Lumley, and Ponofsky for wind velocities of 20.0 m/s and 40.24 m/s at an elevation of 9.15 m. The longitudinal spectra of the building code overestimates the Kaimal spectra in the frequency range of 0.007 Hz to 0.08 Hz and underestimates beyond the frequency of 0.08 Hz. The peak angles of attack, on the heliostat, stowed in horizontal position, due to turbulent vertical and lateral components of wind velocity, were estimated by using Daniel's methodology for three wind velocities and compared with the value suggested by the code. The experimental results of a simple test in the laboratory indicate the feasibility of decreasing the drag forces of the flat plate by reducing the solidity ratio. DOE

N86-13834# Midwest Research Inst., Golden, Colo. Solar Energy Research Inst.
REVIEW OF SERI SOLAR POND WORK
F. Zangrando and D. H. Johnson Jul. 1985 53 p
(Contract DE-AC02-83CH-10093)
(DE85-012162; SERI/TR-252-2322) Avail: NTIS HC A04/MF A01

This report provides documentation of SERI's solar pond research effort, which began in 1979. The SERI staff analyzed solar pond topics from modeling and feasibility studies to laboratory experiments on physical properties and hydrodynamical stability. The SERI's perspective on the maturity of this solar technology is described, including the technical state-of-the-art of salt-gradient solar ponds, state of knowledge of pond design, estimated cost ranges for various locations and applications, and perceived barriers to commercial development. Recommendations for future work are also presented. The SERI research and development on solar ponds is described, emphasizing analytical and experimental tools developed at SERI. All AERI and subcontract reports dealing with solar ponds or related system components are summarized, and a bibliography is provided. DOE

N86-13835# Purdue Univ., West Lafayette, Ind. School of Mechanical Engineering.
PERFORMANCE ASSESSMENT OF OTEC POWER SYSTEMS AND THERMAL POWER PLANTS. VOLUME 2: USERS MANUAL FOR PACC-OTECS Final Report
W. Leidenfrost, P. E. Liley, A. T. McDonald, I. Mudawwar, and J. T. Pearson May 1985 76 p Prepared in cooperation with Argonne National Lab., Idaho Falls, Idaho
(Contracts DE-AC03-76SF-00700; DE-AC01-82CD-30718)
(DE85-016792; DOE/SF-00700/T11-Vol-2) Avail: NTIS HC A05/MF A01

A user's manual for an interactive computer program that can calculate the simulated performance of closed cycle ocean thermal energy conversion (OTEC) power systems is presented. The program was developed for use on the IBM personal computer. The program calculate the thermodynamic properties of the working fluids (ammonia and seawater). This manual specifies the power system flow configuration, the input data requirements, and the results calculated by the program. The geometry of the heat exchangers is also described. A listing of the computer program is included. DOE

N86-13836# Argonne National Lab., Ill.
FAR-FIELD MODEL OF THE REGIONAL INFLUENCE OF AFFLUENT PLUMES FROM OCEAN THERMAL ENERGY CONVERSION (OTEC) PLANTS
D. P. Wang Jul. 1985 39 p
(Contract W-31-109-eng-38)
(DE85-016981; ANL/OTEC-EV-3) Avail: NTIS HC A03/MF A01

Ocean thermal energy conversion (OTEC) plants discharge large volumes of cold water into the upper ocean. A three-dimensional, limited-area model was developed to investigate the regional influence of the far-field effluent plume created by the negatively buoyant discharge. The model was applied to discharges from a 40-MW sub e OTEC plant into coastal waters characterized by various ambient ocean conditions. A typical ambient temperature structure and nutrient distribution, as well as the behavior of the effluent plume itself, were strongly modified by the discharge-induced circulation. Although temperature perturbations in the plume were small, upward entrainment of nutrients from below the thermocline was significant. The regional influence of discharges from an 80-MW sub e OTEC plant, the interactions between the discharges from two adjacent 40-MW sub e OTEC plants, and the effects of coastal boundary and bottom discharge were examined with respect to the regional influence of a 40-MW sub e OTEC plant located in deep water off a coast (base case). DOE

N86-13837# Delaware Univ., Newark. Inst. of Energy Conversion.
DEVELOPMENT OF STABLE HIGH EFFICIENCY POLYCRYSTALLINE THIN-FILM SOLAR CELLS BASED ON CuInSe2 Final Report, 16 Mar. 1983 - 15 Mar. 1984
R. W. Birkmire, R. B. Hall, J. E. Phillips, and J. D. Meakin Mar. 1985 300 p
(Contract DE-AC02-83CH-10098)
(DE85-000517; SERI/STR-211-2516) Avail: NTIS HC A13/MF A01

A two-junction, monolithic, optically and electrically coupled solar cell has been designed and a successful prototype produced. Each junction is a thin-film polycrystalline cell, namely, CuInSe2 (CdZn)S and CdTe (CdZn)S. All active semiconductor layers are produced by physical vapor deposition. During this contract year, a procedure for producing thin-film p-type CdTe by physical vapor deposition and a usable transparent interconnect for the tandem cell were developed. DOE

N86-13838*# Wilkes Coll., Wilkes-Barre, Pa.
ELECTRICAL RESEARCH ON SOLAR CELLS AND PHOTOVOLTAIC MATERIALS Final Report
J. Orehotsky 5 Mar. 1985 208 p
(Contract NAS7-918)
(NASA-CR-176384; DOE/JPL-956766-85/01; NAS 1.26:176384; DE85-016575) Avail: NTIS HC A10/MF A01 CSCL 10A

A systematic study of the properties of various polymer pottant materials and of the electrochemical corrosion mechanisms in solar cell materials is required for advancing the technology of terrestrial photovoltaic modules. The items of specific concern in this sponsored research activity involve: (1) kinetics of plasticizer loss in PVB, (2) kinetics of water absorption and desorption in PVB, (3) kinetics of water absorption and desorption in EVA, (4) the electrical properties at PVB as a function of temperature and humidity, (5) the electrical properties of EVA as a function of temperature and humidity, (6) solar cell corrosion characteristics, (7) water absorption effects in PVB and EVA, and (8) ion implantation and radiation effects in PVB and EVA. DOE

N86-13839# New Mexico Inst. of Mining and Technology, Socorro. Dept. of Metallurgical and Materials Engineering.
MICROSTRUCTURAL AND MECHANICAL PROPERTY EVALUATION OF SOLAR COLLECTORS Final Report
O. T. Inal 1 Jun. 1985 23 p
(Contract DE-AS04-78AL-04266)
(DE85-017038; DOE/AL-04266/T2) Avail: NTIS HC A02/MF A01

The overall contributions of the program can be divided into three major areas: (1) nucleation and growth studies of adatom layers through transmission electron microscopy, reflection electron diffraction, and field-ion microscopy techniques; (2) electrodeposition parameter optimization studies for the production of photothermal collector surfaces made in terms of the as plated as well as thermally degraded microstructures; and (3) the thermal degradation mechanisms that emanate from structural alterations were optically modelled for the coatings produced in (2). These three topics are individually summarized. DOE

N86-13840# Studsvik Energiteknik A.B., Nykoping (Sweden).
SMALL SOLAR POWER SYSTEMS PLANT IN ALMERIA SYSTEM EVALUATION AND COMPARISON ON THERMAL BASIS

Final Report
J. Sandgren and M. Andersson 1985 179 p Prepared in cooperation with Theorells Ingenjoersbyra AB, Solna, Sweden
(Contract DE-AC04-76DR-00789)
(DE85-017185; DOE/DR-00789/T13) Avail: NTIS HC A09/MF A01

The International Energy Agency's Small Solar Power Systems (IEA/SSPS) thermo-electric power plant in Almeria, Spain, consists of a distributed collector system (DCS) with three fields and a central receiver system (CRS). During the period of September 1983 to August 1984, the DCS-ACUREX field produced a daily average of 1.13 kWh/sq m. thermal energy from an average direct irradiation onto a field aperture of 4.48 kWh/sq m, and the DCS-MAN field 1.04 kWh/sq m from 5.91 kWh/sq m irradiated energy. In the Spring of 1984, an improved MAN field was put into operation and showed a considerable improvement compared to the original field. It produced 1.88 kWh/sq m thermal energy from 6.96 kWh/sq m daily mean beam irradiation. The CRS plant was proved to be capable of producing twice as much thermal energy per sq m reflector area as the ACUREX field, and it is pointed out that for further development of high temperature applications it has greater opportunities than DCS fields. For solar thermo-electrical power generation, it is necessary to develop more compact thermo-electrical power conversion systems. Of existing engines, Stirling units show potential for adaptation to CRS plants. DOE

N86-13841# Idaho Dept. of Water Resources, Boise.
GEOTHERMAL INVESTIGATION IN IDAHO. PART 14: GEOCHEMICAL AND ISOTOPIC INVESTIGATIONS OF THERMAL WATER OCCURRENCES OF THE BOISE FRONT AREA, ADA COUNTY, IDAHO, WATER INFORMATION BULLETIN NO. 30
A. L. Mayo, A. B. Muller, and J. C. Mitchell Dec. 1984 60 p refs
(Contract DE-AS07-77ET-28407)
(DE85-012905; DOE/ET-28407/T5-Pt-14) Avail: NTIS HC A04/MF A01

A limited chemical and isotopic investigation was undertaken and geological, geophysical, and hydrological data in the literature were reviewed to evaluate the geothermal potential of the Poise area. DOE

N86-13842# Oak Ridge Gaseous Diffusion Plant, Tenn.
FIRST ORDER ESTIMATES OF THE DYNAMICS AND ENERGETICS OF A RAPIDLY DECELERATING FLYWHEEL
G. T. Gillies Jun. 1985 22 p
(Contract DE-AC05-84CT-21400)
(DE85-013908; K/TS-5867) Avail: NTIS HC A02/MF A01

Martin Marietta Energy Systems, Inc., is developing advanced inertial energy storage devices (flywheels) for use in the University of Texas/DARPA homopolar generator. Several order of magnitude estimates for a variety of calculable quantities pertinent to the design of such a flywheel are presented. These include the mass, moment of inertia, and kinetic energy of the rotor. In addition, the equivalent rotor braking torque, peripheral deceleration, and centripedal accelerations are found, along with the braking force and total rotor angular momentum. Next, the differential equation of the rotor is solved in both the general and a particular case, and the Euler-type rigid body equation of motion is considered. Finally, various thermal and electrical effects are studied and the behavior of unbalance forces are examined. DOE

N86-14102*# Prairie View Agricultural and Mechanical Coll., Tex.
SOLAR CONCENTRATOR DEGRADATION IN LOW EARTH ORBIT (LEO) Final Report
Richard G. Thomas *In* NASA. Johnson (Lyndon B.) Space Center The 1983 NASA/ASEE Summer Faculty Fellowship Research Program Research Reports Sep. 1983 12 p refs (For primary document see N86-14078 04-85)
Avail: NTIS HC A18/MF A01 CSCL 12A

45 ENVIRONMENT POLLUTION

Includes air, noise, thermal and water pollution; environment monitoring; and contamination control.

N86-13843# Wright State Univ., Dayton, Ohio. Dept. of Chemistry.
AQUATIC PLANT CONTROL RESEARCH PROGRAM: EVALUATION OF POLYMERS FOR CONTROLLED DELIVERY OF HERBICIDES FOR AQUATIC PLANT CONTROL Final Report
F. W. Harris Jun. 1985 95 p
(Contract DACW39-76-C-0016)
(AD-A157948; WES/TR/A-85-2) Avail: NTIS HC A05/MF A01 CSCL 06/6

This work was conducted to develop and evaluate new polymer compounds containing pendant herbicide substituents with the ultimate purpose of producing effective, economical, and environmentally safe controlled release aquatic herbicides. The synthesis of one of the most promising controlled-release systems prepared and evaluated in this study, i.e., an hydroxy-terminated, low-molecular-weight 2,4-D/Poly GMA adduct, was successively scaled-up to commercial levels. However, the processing of the adduct solution as obtained from the reaction mixture was difficult. A method must be developed to remove the solvent before the procedure can be used to prepare material for field tests. GRA

N86-13844# Brookhaven National Lab., Upton, N. Y.
OXIDIZING AND SCAVENGING CHARACTERISTICS OF APRIL RAINS: OSCAR DATA REPORT
C. M. Benkovitz, V. A. Evans, J. L. Tichler, J. V. Hayes, and K. J. Norden Oct. 1984 245 p
(Contract DE-AC02-76CH-00016)
(DE85-017014; BNL-51881) Avail: NTIS HC A11/MF A01

The organization of this report is as follows: Chapter 1 presents a description of the OSCAR experiment, including its objectives, design, and field deployment. Chapter 2 presents the OSCAR Central Data Coordination function and summarizes the tasks needed to compile each data set. Chapters 3 through 6 address each of the four OSCAR events. A synoptic description of each event is presented in these chapters, followed by a summary of the data captured during the event. Chapter 3 and Appendices C-G then present detailed tabular and graphical displays of the data captured during this event by the intermediate-density precipitation chemistry network, the BNL aircraft and by state/province agency networks. Data form the high-density precipitation chemistry network are being presented in a separate series of reports by Pacific Northwest Laboratory. Detailed displays of the data for events 2 to 4 have not been included in this report; however, selected portions could be developed for interested parties. DOE

N86-13845# Oak Ridge National Lab., Tenn.
CHANGES IN SOIL ACIDITY DUE TO NATURAL PROCESSES AND ACID DEPOSITION
D. W. Johnson 1985 22 p Presented at the NATO ARW Conf. on Effects of Acidic Deposition on Forests, Wetlands and Agr. Ecosystems, Toronto, 12 May 1985
(Contract DE-AC05-84OR-21400)
(DE85-012103; CONF-8505156-1) Avail: NTIS HC A02/MF A01

It is now generally accepted that, in extremely acid soils, soil solution acidity can change rapidly in response to inputs of sulfate due to the salt effect. There is little evidence of rapid change in bulk soil acidity due to acid deposition, however, except in cases where acid inputs are extremely high. Over periods of many decades, soil acidity can be increased due to tree uptake of base cations, humus formation, and natural as well as acid-deposition-enhanced soil leaching. The role of acid deposition in accelerating soil acidification rates can be estimated from elemental budget approaches, but the actual changes in soil acidity due to acid deposition are difficult to document because so few studies combine the measurement of element and proton fluxes with long-term periodic remeasurements of soil acidity. Most empirical observations to date show little change in forest soil acidity from any cause in less than 20 to 30 years. However, some increases in exchangeable or soluble Al3+ without concomitant reductions in exchangeable base cations have been noted at the Solling site in West Germany. These Al3+ releases may be due to dissolution of interlayer Al3+ in 2:1 clays. All attempts to monitor long-term changes in soil acidity should take into account the possibility of seasonal variations due to annual cycling of base-cations by vegetation. The effects of seasonal uptake and return of base cations by vegetation upon the base cation status of surface soils can be considerable and might be confused with long-term trends if not properly accounted for. DOE

N86-13846# California Dept. of Health Services, Berkeley. Industrial Hygiene Lab. Section.

PARTICULATE MATTER ANALYSIS BY ELECTRON MICROSCOPY Final Report

S. B. Hayward, W. John, L. Webber, and J. J. Wesolowski Dec. 1984 71 p
(Contract ARB-A2-058-32)
(PB85-227817; CA/DOH/AIHL/SP-33; ARB-R-85/250) Avail: NTIS HC A04/MF A01 CSCL 06F

The AIHL/CARB Center for Automated Particle Analysis (CAPA) has been established for the development of airborne particle source apportionment techniques. An automated scanning electron microscope with energy-dispersive X-ray analysis is used to characterize individual particles based on their morphological and chemical characteristics. During the initial phase of development at CAPA, sampling and analytical hardware was optimized. Preliminary steps in software development centered around data transfer and spectral processing, coupled with conceptual development of Distribution Analysis, which will ultimately be used for source apportionment. Sampling and analysis techniques were tested on a simple system: bulk source and upwind and downwind ambient air samples from a cement plant on the California coast. Author (GRA)

N86-13847# Southern Research Inst., Birmingham, Ala.

PROTOCOL FOR SIZE-SPECIFIC EMISSION MEASUREMENTS (SIM-5) APPLIED TO PM(10) Final Report

W. E. Farthing, J. D. McCain, A. D. Williamson, and T. E. Ward 1985 21 p refs
(Contract EPA-68-02-3696)
(PB85-200194; EPA-600/D-85-109) Avail: NTIS HC A02/MF A01 CSCL 14B

Aerosol particles can be with drawn from industrial process streams and separated into two or more aerodynamic size fractions with a commercially available inertial impactor or cyclone. However, with this currently-available equipment, the process gas must be sampled at a constant flow rate to provide constant size cut(s). Thus, traversing of a duct in one sampling run while maintaining isokinetic flow rate as in EPA Reference Methods 5 or 17, cannot be performed, because the flow rate cannot be adjusted from point to point to mach stream and sampling nozzle velocities. Sampling theory was analyzed to develop a protocol for existing hardware which limits anisokinetic sampling error to acceptable levels, requires traversing, and is practical enough for source sampling. Anisokinetic sampling error was characterized for aerosol size distributions measured at sources and for hypothetical distributions. A protocol was developed and tested in which net sampling error is always less than 13% even, if anisokinetic error is 20%. GRA

N86-13848# Georgia Inst. of Tech., Atlanta. Environmental Resources Center.

CHARACTERIZATION OF ACID RAIN PHENOMENA, ATLANTA, GEORGIA

K. C. Beck Aug. 1984 51 p refs
(PB85-216943; ERC-04-84; USGS/G-836(03)) Avail: NTIS HC A04/MF A01 CSCL 08H

Rain collection and chemical analysis for pH, Na, K, Mg, Ca, NH4, Cl, NO3 and SO4 was initiated at an urban Atlanta site in August 1983 and is continuing on an event and subevent basis. Additional collecting began at Suburban Stone Mountain in June 1984. Current data do not indicate significant urban-suburban-rural differences in composition for the species studied. Subepisode sampling indicates minor and irregular changes in composition during frontal system rains, but during local rains, particularly intense events following extended dry periods during late spring and summer, there are marked decreases with time in the concentrations of all species except H(+). Stream observations at Stone Mountain provide no evidence for major early regolith modification of rain, other than SO4 removal, but evaporation in a complex path from rock outcrop to stream and possible stream pollution complicate interpretation. Author (GRA)

N86-13849# California Dept. of Health Services, Berkeley. Air and Industrial Hygiene Lab. Section.

DETERMINATION OF ACIDITY IN AMBIENT AIR Final Report

B. R. Appel, Y. Tokiwa, V. Povard, and E. L. Kothny Dec. 1984 87 p
(Contract Arb-A1-159-32)
(PB85-218196; ARB-R-85/243) Avail: NTIS HC A05/MF A01 CSCL 14B

A laboratory and field study was performed to construct and evaluate an automated, semi-continuous monitor for ambient air concentrations of nitric acid (HNO3) and ammonia (NH3) utilizing tungstic acid-coated denuder tubes. In addition, atmospheric concentrations of hydrochloric acid (HCl) were determined. Manual techniques for atmospheric NH3 measurement were also compared. Atmospheric sampling for HNO3 was done in Riverside, CA during September 1984 with the automated tungstic and technique (TAT), and by the denuder difference method (DDM). Author

N86-13785# Joint Publications Research Service, Arlington, Va.

INFLUENCE OF PETROLEUM POLLUTION ON OCEAN-ATMOSPHERE GAS EXCHANGE INTENSITY (IN EXAMPLE OF NORTH ATLANTIC) Abstract Only

V. V. Alekseyev, P. A. Baranov, A. O. Kokorin, and V. M. Sheremetyev *In its* USSR Rept.: Earth Sci. (JPRS-UES-85-009) 13 Nov. 1985 p 33 Transl. into ENGLISH from Vestn. Mosk. Univ., Ser. 3: Fiz., Astron. (Moscow), v. 26, no. 3, May - Jun. 1985 p 71-74 (For primary document see N86-13765 04-42) Avail: NTIS HC A04/MF A01

46 GEOPHYSICS

Includes aeronomy; upper and lower atmosphere studies; ionospheric and magnetospheric physics; and geomagnetism.

For space radiation see *93 Space Radiation.*

N86-13850*# National Aeronautics and Space Administration. Langley Research Center, Hampton, Va.

AIRBORNE LIDAR MEASUREMENTS OF EL CHICHON STRATOSPHERIC AEROSOLS

M. Patrick McCormick and M. T. Osborn (SASC Technologies, Inc., Hampton, Va.) Oct. 1985 89 p refs
(NASA-RP-1148; L-16007; NAS 1.61:1148) Avail: NTIS HC A05/MF A01 CSCL 04A

A NASA Electra airplane, outfitted with a lidar system, was flown in January to February 1983 between the latitudes of 27 deg N and 76 deg N. One of the primary purposes of this mission was to determine the spatial distribution and aerosol characteristics of the El Chichon-produced stratospheric material. This report presents the lidar data from that flight mission. Representative profiles of lidar backscatter ratio, plots of the integrated backscattering function versus latitude, and contours of backscatter mixing ratio versus altitude and latitude are given. It addition, tables containing numerical values of the backscatter ratio and backscattering function versus altitude are supplied for each profile. The largest amount of material produced by the El Chichon eruptions of late March to early April 1982, which was measured by this flight, resided between 35 deg N and 52 deg N. Peak backscatter ratios at a wavelength of 0.6943 micro m decreased from 8 to 10 at the lower latitudes to 3 at the higher latitudes. Backscatter ratio profiles taken while crossing the polar vortex show that the high-altitude material from El Chichon arrived at the north polar region sometime after the winter polar vortex was established. This report presents the results of this mission in a ready-to-use format for atmospheric and climatic studies. Author

N86-13851*# Augsburg Coll., Minneapolis, Minn.
ANALYSIS OF ATOMIC THERMOSPHERIC NITROGEN DENSITY Final Technical Report, 1 Jul. 1983 - 15 Sep. 1985
Mark J. Engebretson [1985] 14 p
(Grant NAG5-349)
(NASA-CR-176354; NAS 1.26:176354) Avail: NTIS HC A02/MF A01 CSCL 04A

A NASA grant provided support for a research project at Augsbury College, Minneapolis, Minnesota for the analysis of atomic nitrogen density data obtained by the Neutral Atmospheric Composition Spectrometer (NACS) on board the Dynamics Explorer-2 satellite. Initial funding was for an exploratory study of the feasibility of obtaining ambient densities of N from source densities of NO. Funding was continued under the Dynamics Explorer Guest Investigator Program when initial studies indicated probable success in obtaining such ambient densities. The major scientific focus of the later work was to be to characterize the behavior of N densities at high latitudes. Author

N86-13852*# Lockheed Missiles and Space Co., Sunnyvale, Calif.
STUDY OF STORM TIME FLUXES OF HEAVY IONS Final Report, 20 May 1980 - 19 Nov. 1985
R. D. Sharp and J. M. Quinn Nov. 1985 26 p
(Contract NASw-3395)
(NASA-CR-176368; NAS 1.26:176368) Avail: NTIS HC A03/MF A01 CSCL 04A

Ion composition data sets from Lockheed instruments on a variety of spacecraft were used in combination with each other and with data from other instruments to address a variety of problems regarding plasma sources, energization and transport within the magnetosphere. The availability of data from several differing orbits has given a highly flexible approach to attacking the continually evolving questions of magnetospheric physics. This approach is very successful and should be continued in the future. E.A.K.

N86-13853# Bedford Research Associates, Mass.
IE DATA PROCESSING
P. Meehan Oct. 1984 65 p
(Contract F19628-82-C-0139)
(AD-A158027; AFGL-TR-85-0007; SR-1) Avail: NTIS HC A04/MF A01 CSCL 04/1

Two satellites are generating and have been generating SSIE (Topside ionosphere plasma monitor) data for several years. Because of the large volume of information (approx. 180 bits/second per satellite) and noise contained in it, a computer software system has been developed at AFGL to handle the data and make it available for in-house use. The intent is to allow AFGL personnel various desired window looks at the data through graphics, listings or data downloading. The building of the SSIE database is an on-going process and new application packages are added as needed. GRA

N86-13854# Army Engineer Waterways Experiment Station, Vicksburg, Miss. Geotechnical Lab.
THE VAIONT SLIDE. A GEOTECHNICAL ANALYSIS BASED ON NEW GEOLOGIC OBSERVATIONS OF THE FAILURE SURFACE. VOLUME 1: MAIN TEXT Final Report
A. J. Hendron, Jr. and F. D. Patton Jun. 1985 257 p
(AD-A158192; WES/TR/GL-85-5-Vol-1) Avail: NTIS HC A12/MF A01 CSCL 08/7

The study confirmed that the Vaiont Slide was a reactivation of an old slide. The slide moved upon one or more clay layers which were continuous over large areas of the surface of sliding. Three-dimensional stability analyses were required due to the magnitude of the upstream inclination of the clay layers forming the base of the slide. The angle of shearing resistance of the clay layers was determined to be about 12 degrees. The fluid pressure distributions used were consistent with the only piezometric data available before the 1963 slide and with an interpretation of the local groundwater flow system including the presence of karstic terrain above the slide. Results of the analyses completed for key periods in the history of the slide agree with the known slide behavior during these periods. The results also indicate that the reduction in the factor of safety caused by reservoir filling alone was approximately 12 percent, while the reduction caused by rainfall or snowmelt ranged from 10 to 18 percent. Correlations made between cumulative precipitation, reservoir levels, and slide movement records provide a well-defined failure envelope. These results explain why the slide was unstable at a given reservoir level and later stable at the same level. Conclusions from these correlations are consistent with the results of the stability analyses. The results of the study also suggest that the slide could have been stabilized by drainage. GRA

N86-13855# Army Engineer Waterways Experiment Station, Vicksburg, Miss. Geotechnical Lab.
THE VAIONT SLIDE. A GEOTECHNICAL ANALYSIS BASED ON NEW GEOLOGIC OBSERVATIONS OF THE FAILURE SURFACE. VOLUME 2: APPENDICES A THROUGH G Final Report
A. J. Hendron, Jr. and F. D. Patton Jun. 1985 117 p
(AD-A158193; WES/TR/GL-85-5-Vol-2) Avail: NTIS HC A06/MF A01 CSCL 08/7

A geotechnical analysis of the failure surface of the Vaiont Slide is given. Precipitation records from 1960 to 1963; the static slope analysis method used for the vaiont slide analyses; sections used in stability analyses; three-dimensional slope stability calculations; calculation of slide velocities; heat generated pore pressure mechanisms; and a summary of geological studies on the slide at vaiont, 1959 to 1964 are discussed. GRA

N86-13856# National Bureau of Standards, Gaithersburg, Md. Quantum Chemistry Group.
APPLICATION OF QUANTUM CHEMISTRY TO ATMOSPHERIC CHEMISTRY Final Report, 1 Oct. 1983 - 30 Sep. 1984
M. Krauss and W. J. Stevens 30 Sep. 1984 118 p
(Grant AF-AFOSR-ISSA-84-0000)
(AD-A158282; AFOSR-85-0563TR) Avail: NTIS HC A06/MF A01 CSCL 07/4

Analysis of the accuracy of the experimentally deduced dissociation energies of refractory metal salts requires a knowledge of the electronic structure of the molecules. Relativistic effective potentials (REP) have now made such calculations for metal containing molecules possible. The present report will describe our tests and applications of the effective potential method. We have just completed a review of the use of effective potentials in molecular quantum chemistry. The review is given in Section 2. In Section 3 the abstract is given for the paper on Relativistic Effective Potential SCF Calculations of AgH and AuH, which has been accepted by the Journal of Computational Chemistry. The preprint for the analysis of the Electronic Structure of FeO and RuO is given in Section 4. Analysis of the orbital structure establishes the basis for an aufbau for the ground state of all the transition metal oxides in the first two rows. Preliminary results were reported for NdO+, NdO, and UO in last years report but a new set of CEP are now being developed for the lanthanides and actinides. This is a preliminary to a study of other lanthanide oxides and to polyatomic systems using the CEP. The abstract for the paper Compact Effective Potentials and Efficient Shared-Exponent Basis Sets for the First- and Second-Row Atoms is given in Section 5. Application to the analysis of the spectra of Al2 is described in the abstract for the paper Electronic State of Al2. GRA

N86-13857# Pittsburgh Univ., Pa. Dept. of Chemistry.
MEASUREMENT OF RATE CONSTANTS OF ELEMENTARY GAS REACTIONS OF IMPORTANCE TO UPPER ATMOSPHERE AND

COMBUSTION SYSTEMS Final Technical Report, 1 Sep. 1980 - 28 Feb. 1985
F. Kaufman 10 May 1985 11 p
(Grant AF-AFOSR-0207-80)
(AD-A158824; SQ08671-84-00661; AFOSR-85-0503TR) Avail: NTIS HC A02/MF A01 CSCL 07/4

The vibrational energy transfer of highly excited HCl and HF was studied by the infrared chemiluminescence method in a series of five papers. HCl(v < or = 7) and HF(v < or = 7) were produced by fast generating reations, e.g., H + IC1 yields (v < or = 7) + I or H +F2 yields (< or = 7) + F in large excess He which relaxes the rotational but not the vibrational excitation. With various added quencher gases, about 200 rate constants for stepwise vibrational energy transfer were measured. They tend to increase rapidly with increasing v, often independent of the vibrational energy defect. For HF (v) + HF (O), self-relaxation, the V-V channel decreases from 55% at v=2 to zero at v > 5 even though the relaxation rate constant rises as v to the 2.7 power. A versatile flow reactor system was built that features three detection methods (laser-induced fluorescence, vacuum u.v. resonance fluorescence, and modulated molecular beam mass spectrometry) plus upstream radical production by IR laser multiphoton decomposition. The NH2 + NO and CH3O + NO2 reactions were studied successfully. The latter was found to have a recombination (CH3ONO2) and disproportionation (CH2O + HNO2) channel and both were measured indirectly. The 18O + NO or O2 isotope exchange reactions were measured, and the results compared with measured and calculated high-pressure limits of the respective recombinations and with NO vibrational relaxation. GRA

N86-13858# Woodard-Clyde Consultants, San Francisco, Calif.
GEOLOGIC CHARACTERIZATION REPORT FOR THE PARADOX BASIN STUDY REGION, UTAH STUDY AREAS. VOLUME 6: SALT VALLEY
Dec. 1984 221 p refs
(Contract DE-AC02-83CH-10140)
(DE85-011699; ONWI-290-Vol-6) Avail: NTIS HC A10/MF A01

Surface landforms in the Salt Valley Area are generally a function of the Salt Valley anticline and are characterized by parallel and subparallel cuestaform ridges and hogbacks and flat valley floors. The most prominent structure in the Area is the Salt Valley anticline. Erosion resulting from the Tertiary uplift of the Colorado Plateau led to salt dissolution and subsequent collapse along the crest of the anticline. Continued erosion removed the collapse material, forming an axial valley along the crest of the anticline. Paleozoic rocks beneath the salt bearing Paradox Formation consist of limestone, dolomite, sandstone, siltstone and shale. The salt beds of the Paradox formation occur in distinct cycles separated by an interbed sequence of anhydrite, carbonate, and clastic rocks. The Paradox Formation is overlain by Pennsylvanian limestone; Permian sandstone; and Mesozoic sandstone, mudstone, conglomerate and shale. No earthquakes have been reported in the area during the period of the historic record and contemporary seismicity appears to be diffusely distributed, of low level and small magnitude. The upper unit includes the Permian strata and upper Honaker trail formation. DOE

N86-13859# Lawrence Livermore National Lab., Calif.
INVERSION OF RAYLEIGH WAVE PHASE VELOCITIES BETWEEN RSNT AND RSON
G. E. Randall and S. R. Yaylor 29 Nov. 1985 19 p refs
(Contract W-7405-eng-48)
(DE85-013242; UCID-20504) Avail: NTIS HC A02/MF A01

Rayleigh wave phase velocities in the Canadian Shield are estimated for the path between RSNT and RSON in the period range of 10 to 100 sec. Frequency dependent stacking techniques are employed to form an estimate of phase velocity from a limited data set of marginal quality. Inversion of the phase velocities for shear velocity structure indicates an average crustal thickness of 40 km which is consistent with results from previous studies. The lower crustal velocities from our study appear to be slightly greater than those from other studies and Sn velocities along the path are about 4.7 km/s. The effectiveness of the frequency dependent stacking techniques confirms the assumption of signal-independent background noise dominating the records for periods less than about 30 sec and signal-dependent multipathing noise dominating for periods longer than about 40 sec. DOE

N86-13860# Los Alamos National Lab., N. Mex.
CHARACTERISTICS OF MICROEARTHQUAKES ACCOMPANYING HYDRAULIC FRACTURING AS DETERMINED FROM STUDIES OF SPECTRA OF SEISMIC WAVEFORMS
M. Fehler and D. Bame Mar. 1985 7 p refs Presented at the Intern. Symp. on Geothermal Energy, Kailua Kona, Hawaii, 26 aug. 1985
(Contract W-7405-eng-36)
(DE85-009556; LA-UR-85-930; CONF-850801-12) Avail: NTIS HC A02/MF A01

A study of the spectral properties of the waveforms recorded during hydraulic fracturing earthquakes has been carried out to obtain information about the physical dimensions of the earthquakes. We find two types of events. The first type has waveforms with clear P and S arrivals and spectra that are very similar to earthquakes occurring in tectonic regions. These events are interpreted as being due to shear slip along fault planes. The second type of event has waveforms that are similar in many ways to long period earthquakes observed at volcanoes and is called long period. Many waveforms of these events are identical, which implies that these events represent repeated activation of a given source. We propose that the source of these long period events is the sudden opening of a channel that connects two cracks filled with fluid at different pressures. The sizes of the two cracks differ, which causes two or more peaks to appear in the spectra, each peak being associated with one physical dimension of the crack. From the frequencies at which spectral peaks occur, we estimate crack dimensions of between 3 and 22m. DOE

N86-13861# Joint Publications Research Service, Arlington, Va.
USSR REPORT: ENERGY
14 Jan. 1985 156 p refs Transl. into ENGLISH from various Russian articles
(JPRS-UEN-85-001) Avail: NTIS HC A08

Progress in energy technology and exploration is reported. Topics discussed include: oil, gas, and coal resources, and energy conservation. For individual titles, see N86-13862 through N86-13864.

N86-13862# Joint Publications Research Service, Arlington, Va.
AZERBAIJAN GEOLOGICAL, GEOPHYSICAL WORK ON LAND DESCRIBED
A. N. Guseynov, A. M. Akhmedov, S. G. Nadirov, and Sh. S. Kocharli *In its* USSR Rept.: Energy (JPRS-UEN-85-001) 14 Jan. 1985 p 1-11 Transl. into ENGLISH of Zerbaydzhanskoye Neftyanoye Khozyaysto (Baku, USSR), no. 6, Jun. 1984 p 1-6
(For primary document see N86-13861 04-46)
Avail: NTIS HC A08

In 1981 to 1983 two oilfields were discovered--The Zardob with three deposits and the Tarsdallyar, with a deposit in the Middle Eocene. The Zardob and Tarsdallyar were prepared for deep drilling by geophysical methods. The Zardob area is located to the northwest of the Muradkhanly field and has a geological structure similar to it. The Tarsdallyar field, a firstling in the interriverine area, is in the southeastern part of the Dzheyranchel synclinorium. It is found that the 16th horizon of the PT [productive series] at the Kyurovdag field is oil-bearing, and the presence of oil is confirmed for the PT's 4th horizon in the axial portion of the northwestern submergence and for the PT's 8th horizon to the southeast of the fold's pericline. E.A.K.

N86-13863# Joint Publications Research Service, Arlington, Va.
POSSIBLE PETROLIFEROUSNESS OF SOUTH CASPIAN UPLIFTS ANALYZED
M. N. Asadov, Sh. A. Azizova, and A. A. Narimanov *In its* USSR Rept.: Energy (JPRS-UEN-85-001) 14 Jan. 1985 p 12-17 refs Transl. into ENGLISH from Azerbaydzhanskoye Neftyanoye

Khozyaystvo (Baku, USSR), no. 6, Jun. 1984 p 7-10 (For primary document see N86-13861 04-46)
Avail: NTIS HC A08

In the Apsheron-Balkhan uplift zone, the Middle Pliocene is represented by Apsheron and Turkmen types of lithofacies, each of which has its own characteristic features. They are distinguished by different compositions and associations of their rock components, which are caused primarily by the presence of different sources that feed the province; the suppliers of terrigenic material to the sedimentation basin. The lithofacies factor is one of the basic criteria in the search for oil and gas, and plays an important role in determining the degree of promise of various areas and of various complexes of sediments. The study of the material content of the types of lithofacies and making comparisons between them is of interest when choosing areas for prospecting and exploration of oil and gas. The structures of the Middle Pliocene were studied. The redbed series (KT) of the Middle Pliocene is divided into separate horizons. Below lie sediments are called the underlying series (PKT). The description of the lithological and petrographic characteristics is not considered correct for the individual horizons but for the KT and PKT cross-sections as a whole it is accurate.
E.A.K.

N86-13864# Joint Publications Research Service, Arlington, Va.
TECTONIC STRESS ON STRUCTURES ALTERS FORMATION PARAMETERS
N. Ter-Karapetyants *In its* USSR Rept.: Energy (JPRS-UEN-85-001) 14 Jan. 1985 p 18-22 Trans. into ENGLISH from Zerbaydzhanskoye Neftyanoye Khozyaystvo (Baku, USSR), no. 6, p 10-14 (For primary document see N86-13861 04-46)
Avail: NTIS HC A08

Changes in values of open porosity, permeability and temperature on the regional scale that are connected with stress on the structure that is caused by tectonic forces was studied. It was established that under overthrusting conditions, azimuthal change in direction of a formation's strike and increase in the formation's dip angle. Parameters were compared by area and by adjacent field.
E.A.K.

N86-13767# Joint Publications Research Service, Arlington, Va.
MODEL INTERPRETATION OF ANNUAL VARIATION OF TEMPERATURE FIELDS OF AIR AND WATER BOUNDARY LAYERS OF WORLD OCEAN Abstract Only
A. Ye. Rozhdestvenskiy and M. V. Semenov *In its* USSR Rept.: Earth Sci. (JPRS-UES-85-009) 13 Nov. 1985 p 8 Transl. into ENGLISH from Izv. Akad. Nauk SSSR: Fiz. Atmosfery i Okeana (Moscow), v. 21, no. 5, May 1985 p 537-543 (For primary document see N86-13765 04-42)
Avail: NTIS HC A04/MF A01

N86-13776# Joint Publications Research Service, Arlington, Va.
FORMATION OF UNDERWATER OCEANIC VOLCANOES AND ISLANDS IN RELATION TO LITHOSPHERIC THICKNESS AND MOVEMENTS Abstract Only
A. M. Gorodnitskiy *In its* USSR Rept.: Earth Sci. (JPRS-UES-85-009) 13 Nov. 1985 p 20 Transl. into ENGLISH from Byul. Mosk. Obshchestva Ispytateley Prirody: Otd. Geol. (Moscow), v. 60, no. 4, Jul. - Aug. 1985 p 24-37 (For primary document see N86-13765 04-42)
Avail: NTIS HC A04/MF A01

N86-13780# Joint Publications Research Service, Arlington, Va.
STATISTICAL CORRELATION BETWEEN OZONE LEVELS OVER ATLANTIC OCEAN AND METEOROLOGICAL VALUES Abstract Only
V. M. Bazhanov *In its* USSR Rept.: Earth Sci. (JPRS-UES-85-009) 13 Nov. 1985 p 29 Transl. into ENGLISH from Izv. Akad. Nauk SSSR: Fiz. Atmosfery i Okeana (Moscow), v. 21, no. 6, Jun. 1985 p 609-613 Original language document was announced in IAA as A85-44482 (For primary document see N86-13765 04-42)
Avail: NTIS HC A04/MF A01

N86-13784# Joint Publications Research Service, Arlington, Va.
ATMOSPHERIC SYNOPTIC EDDIES OVER OCEAN (DETERMINED FROM EXPERIMENTAL DATA) Abstract Only
V. Ye. Lagun and V. F. Romanov *In its* USSR Rept.: Earth Sci. (JPRS-UES-85-009) 13 Nov. 1985 p 32 Transl. into ENGLISH from Izv. Akad. Nauk SSSR: Fiz. Atmosfery i Okeana (Moscow), v. 21, no. 5, May 1985 p 474-484 Original language document was announced in IAA as A85-40640 (For primary document see N86-13765 04-42)
Avail: NTIS HC A04/MF A01

N86-13787# Joint Publications Research Service, Arlington, Va.
NEW METHODS FOR LASER SOUNDING OF ATMOSPHERE ON BASIS OF NONLINEAR EFFECTS Abstract Only
V. Ye. Zuyev and Yu. D. Kopytin *In its* USSR Rept.: Earth Sci. (JPRS-UES-85-009) 13 Nov. 1985 p 34-35 Transl. into ENGLISH from Izv. Akad. Nauk SSSR: Ser. Fiz. (Moscow), v. 49, no. 3, Mar. 1985 p 418-427 Original language document was announced in IAA as A85-31852 (For primary document see N86-13765 04-42)
Avail: NTIS HC A04/MF A01

N86-13788# Joint Publications Research Service, Arlington, Va.
INTERACTION BETWEEN POWERFUL LASER RADIATION AND ATMOSPHERIC AEROSOLS Abstract Only
M. P. Gordin, Yu. N. Grachev, V. S. Loskutov, V. P. Sadovnikov, A. V. Sokolov, and G. M. Strelkov *In its* USSR Rept.: Earth Sci. (JPRS-UES-85-009) 13 Nov. 1985 p 35-36 Transl. into ENGLISH from Izv. Akad. Nauk SSSR: Ser. Fiz. (Moscow), v. 49, no. 3, Mar. 1985 p 450-458 Original language document was announced in IAA as A85-31856 (For primary document see N86-13765 04-42)
Avail: NTIS HC A04/MF A01

N86-13789# Joint Publications Research Service, Arlington, Va.
INVESTIGATION OF NONLINEAR SPECTROSCOPIC EFFECTS IN INTERACTION BETWEEN CO2-LASER RADIATION AND ATMOSPHERIC GASES Abstract Only
B. G. Ageyev, Ye. P. Gordov, Yu. N. Ponomarev, and S. D. Tvorogov *In its* USSR Rept.: Earth Sci. (JPRS-UES-85-009) 13 Nov. 1985 p 36 Transl. into ENGLISH from Izv. Akad. Nauk SSSR: Ser. Fiz. (Moscow), v. 49, no. 3, Mar. 1985 p 459-465 Original language document was announced in IAA as A85-31857 (For primary document see N86-13765 04-42)
Avail: NTIS HC A04/MF A01

N86-14117# Joint Publications Research Service, Arlington, Va.
OBSERVATIONS OF FLUXES OF COLD IONS FROM PLASMASPHERE INTO IONOSPHERE DURING NIGHTTIME IN MIDDLE LATITUDES Abstract Only
V. V. Afonin, P. Bentse, V. V. Bezrukikh, K. I. Gringauz, I. Semerei, and N. F. Smirnova *In its* USSR Rept.: Space (JPRS-USP-85-005) 30 Sep. 1985 p 28 Transl. into ENGLISH from Kosmich. Issled. (Moscow), v. 22, no. 6, Nov. - Dec. 1984 p 884-888 Original language document announced in IAA as A85-19908 (For primary document see N86-14111 04-88)
Avail: NTIS HC A08

N86-14127# Joint Publications Research Service, Arlington, Va.
MECHANISM OF CORPUSCULAR-ATMOSPHERIC RELATIONSHIPS Abstract Only
E. R. Mustel *In its* USSR Rept.: Space (JPRS-USP-85-005) 30 Sep. 1985 p 36-37 Transl. into ENGLISH from Astron. Zh. (Moscow), v. 61, no. 6, Nov. - Dec. 1984 p 1179-1183 Previously announced in IAA as A85-42341 (For primary document see N86-14111 04-88)
Avail: NTIS HC A08

N86-14136# Joint Publications Research Service, Arlington, Va.
DISTURBANCES IN STRATOSPHERE AND MESOSPHERE FROM SOURCE OF ULTRAVIOLET RADIATION Abstract Only
S. I. Kozlov *In its* USSR Rept.: Space (JPRS-USP-85-005) 30 Sep. 1985 p 43 Transl. into ENGLISH from Kosmich. Issled. (Moscow), v. 22, no. 5, Sep. - Oct. 1984 p 712-719 Original language document announced in IAA as A85-15258 (For primary

document see N86-14111 04-88)
Avail: NTIS HC A08

N86-14137# Joint Publications Research Service, Arlington, Va.
COORDINATED INVESTIGATIONS OF PROCESSES IN SUBAURORAL UPPER IONOSPHERE AND THROUGH IN CONCENTRATION OF LIGHT IONS Abstract Only
L. D. Sivtseva, V. M. Filippov, V. L. Khalipov, Yu. I. Galperin, V. A. Yershova, L. M. Nikolayenko, Yu. N. Ponomarev, and V. M. Sinitsyn *In its* USSR Rept.: Space (JPRS-USP-85-005) 30 Sep. 1985 p 43-44 Transl. into ENGLISH from Kosmich. Issled. (Moscow), v. 22, no. 5, Sep. - Oct. 1984 p 720-741 Original language document announced in IAA as A85-15259 (For primary document see N86-14111 04-88)
Avail: NTIS HC A08

N86-14138# Joint Publications Research Service, Arlington, Va.
REGISTRY OF HEAVY IONS IN AURORAL REGION DURING MAGNETIC STORMS Abstract Only
Yu. V. Gotselyuk, S. N. Kuznetsov, and K. Kudela *In its* USSR Rept.: Space (JPRS-USP-85-005) 30 Sep. 1985 p 44-45 Transl. into ENGLISH from Kosmich. Issled. (Moscow), v. 22, no. 5, Sep. - Oct. 1984 p 742-748 Original language document announced in IAA as A85-15260 (For primary document see N86-14111 04-88)
Avail: NTIS HC A08

N86-14139# Joint Publications Research Service, Arlington, Va.
SMALL-SCALE STRUCTURE OF INTENSIVE LONGITUDINAL CURRENTS IN HIGH LATITUDES Abstract Only
A. S. Volokitin, V. V. Krasnoselskikh, Ye. V. Mishin, L. O. Tyurmina, V. A. Sharova, and S. I. Shkolnikova *In its* USSR Rept.: Space (JPRS-USP-85-005) 30 Sep. 1985 p 45 Transl. into ENGLISH from Kosmich. Issled. (Moscow), v. 22, no. 5, Sep. - Oct. 1984 p 749-755 Original language document announced in IAA as A85-15261 (For primary document see N86-14111 04-88)
Avail: NTIS HC A08

N86-14140# Joint Publications Research Service, Arlington, Va.
FORMATION OF PROTON RADIATION BELTS IN REGION OF ENERGIES OF SEVERAL MeV Abstract Only
M. I. Panasyuk and E. N. Sosnovets *In its* USSR Rept.: Space (JPRS-USP-85-005) 30 Sep. 1985 p 46 Transl. into ENGLISH from Kosmich. Issled. (Moscow), v. 22, no. 5, Sep. - Oct. 1984 p 756-762 Original language document announced in IAA as A85-15262 (For primary document see N86-14111 04-88)
Avail: NTIS HC A08

N86-14146# Joint Publications Research Service, Arlington, Va.
CHARGE COMPOSITION OF ELECTRONS IN EARTH'S RADIATION BELT Abstract Only
B. I. Luchkov *In its* USSR Rept.: Space (JPRS-USP-85-005) 30 Sep. 1985 p 50-51 Transl. into ENGLISH from Kosmich. Issled. (Moscow), v. 22, no. 5, Sep. - Oct. 1984 p 809-812 Original language document announced in IAA as A85-15269 (For primary document see N86-14111 04-88)
Avail: NTIS HC A08

N86-14167# Joint Publications Research Service, Arlington, Va.
SPACE APPLICATIONS IN GEOLOGY Abstract Only
N. Lesnaya *In its* USSR Rept.: Space (JPRS-USP-85-005) 30 Sep. 1985 p 102-103 Transl. into ENGLISH from Leninskoye Znamya (Moscow), no. 81, 7 Apr. 1985 p 2-3 (For primary document see N86-14111 04-88)
Avail: NTIS HC A08

N86-14185# Joint Publications Research Service, Arlington, Va.
METHODS FOR CONSTRUCTING ATMOSPHERIC OPTICAL TRANSFER OPERATOR Abstract Only
V. G. Zolotukhin, I. V. Mishin, D. A. Usikov, M. N. Fomenkova, and V. A. Grushin *In its* USSR Rept.: Space (JPRS-USP-85-005) 30 Sep. 1985 p 121-122 Transl. into ENGLISH from Issled. Zemli iz Kosmosa (Moscow), no. 4, Jul. - Aug. 1984 p 14-22 (For primary document see N86-14111 04-88)
Avail: NTIS HC A08

N86-14188# Joint Publications Research Service, Arlington, Va.
USE OF SPACE GEOLOGICAL METHODS IN SEISMOTECTONIC RESEARCH Abstract Only
T. P. Ivanova *In its* USSR Rept.: Space (JPRS-USP-85-005) 30 Sep. 1985 p 124 Transl. into ENGLISH from Issled. Zemli iz Kosmosa (Moscow), no. 4, Jul. - Aug. 1984 p 46-52 Original language document announced in IAA as A84-49030 (For primary document see N86-14111 04-88)
Avail: NTIS HC A08

N86-14189# Joint Publications Research Service, Arlington, Va.
ENGINEERING EVALUATION OF CRUSTAL FAULTS USING SPACE SURVEY DATA Abstract Only
A. L. Revzon *In its* USSR Rept.: Space (JPRS-USP-85-005) 30 Sep. 1985 p 125 Transl. into ENGLISH from Issled. Zemli iz Kosmosa (Moscow), no. 4, Jul. - Aug. 1984 p 53-60 Original language document announced in IAA as A84-49031 (For primary document see N86-14111 04-88)
Avail: NTIS HC A08

47 METEOROLOGY AND CLIMATOLOGY

Includes weather forecasting and modification.

N86-13865 Harvard Univ., Cambridge, Mass.
THE INFLUENCE OF OCEANIC CHEMISTRY, PHYSICS AND BIOLOGY ON ATMOSPHERIC CARBON DIOXIDE Ph.D. Thesis
Fanny Knox Enever 1985 211 p
Avail: Univ. Microfilms Order No. DA8510201

A series of models was developed to predict the level of atmospheric CO2, resulting from given chemical, physical, and biological conditions in the ocean. The surface ocean is divided in these models into average warm surface water and cold, high-latitude region where water sinks out of contact with the atmosphere. The cold surface region is important in determining pCO2 and the extent of this influence depends upon the proportion of the return flow from the surface to the deep ocean which passes through the cold surface region, and also upon the relative magnitudes of the rates of exchange of carbon by gas transfer and on water flux. The chemical composition of the water in the cold surface region is determined by physical mixing of low-nutrient water from the warm surface ocean with high-nutrient water from below, and also by the degree of biological activity in the region. Changes in either physical or biological conditions have the potential to alter pCO2 in the cold surface water and thus in the atmosphere over a total range of several hundred parts per million. A model which includes separate consideration of the high-latitude ocean is used to explore possible conditions during the last glacial period which are in accord with the geological record and which can also account for a low value of atmospheric PCO2 during glacial time. A possible mechanism is presented by which alterations in the distribution of sunlight due to variations in the orbital parameters of the Earth can cause climate change, based on the direct response of biological activity to changing levels of light in high-latitude regions of the ocean. Dissert. Abstr.

N86-13866*# National Aeronautics and Space Administration. Goddard Space Flight Center, Greenbelt, Md.
UNDERSTANDING CLIMATE: A STRATEGY FOR CLIMATE MODELING AND PREDICTABILITY RESEARCH, 1985-1995
O. Thiele, ed. and R. A. Schiffer, ed. Oct. 1985 38 p refs (NASA-RP-1158; Rept-85B0489; NAS 1.61:1158) Avail: NTIS HC A03/MF A01 CSCL 04B

The emphasis of the NASA strategy for climate modeling and predictability research is on the utilization of space technology to understand the processes which control the Earth's climate system and it's sensitivity to natural and man-induced changes and to assess the possibilities for climate prediction on time scales of from about two weeks to several decades. Because the climate is a complex multi-phenomena system, which interacts on a wide range of space and time scales, the diversity of scientific problems addressed requires a hierarchy of models along with the application of modern empirical and statistical techniques which exploit the extensive current and potential future global data sets afforded by space observations. Observing system simulation experiments, exploiting these models and data, will also provide the foundation for the future climate space observing system, e.g., Earth observing system (EOS), 1985; Tropical Rainfall Measuring Mission (TRMM) North, et al. NASA, 1984. Author

N86-13867*# National Aeronautics and Space Administration. Goddard Space Flight Center, Greenbelt, Md.
VAS DEMONSTRATION: (VISSR ATMOSPHERIC SOUNDER) DESCRIPTION Final Report
H. E. Montgomery and L. W. Uccellini Oct. 1985 193 p refs
(NASA-RP-1151; Rept-85F0274; NAS 1.61:1151) Avail: NTIS HC A09/MF A01 CSCL 04B

The VAS Demonstration (VISSR Atmospheric Sounder) is a project designed to evaluate the VAS instrument as a remote sensor of the Earth's atmosphere and surface. This report describes the instrument and ground processing system, the instrument performance, the valiation as a temperature and moisture profiler compared with ground truth and other satellites, and assesses its performance as a valuable meteorological tool. The report also addresses the availability of data for scientific research. Author

N86-13868*# National Aeronautics and Space Administration. Marshall Space Flight Center, Huntsville, Ala.
ATMOSPHERIC ENVIRONMENT FOR SPACE SHUTTLE (STS-51D)
G. L. Jasper, D. L. Johnson, C. K. Hill, and G. W. Batts (Computer Sciences Corp., Huntsville, Ala.) Jun. 1985 43 p refs
(NASA-TM-86524; NAS 1.15:86524) Avail: NTIS HC A03/MF A01 CSCL 04B

A summary of selected atmospheric conditions observed near the space shuttle STS-51D launch time on April 12, 1985, at Kennedy Space Center Florida is presented. Values of ambient pressure, temperature, moisture, ground winds, visual observations (cloud), and winds aloft are included. The sequence of prelaunch Jimsphere measured vertical wind profiles is given in this report. The final atmospheric tape, which consists of wind and thermodynamic parameters versus altitude, for STS-51D vehicle ascent is constructed. The STS-51D ascent atmospheric data tape is compiled by Marshall Space Flight Center's Atmospheric Sciences Division to provide an internally consistent data set for use in post-flight performance assessments. Author

N86-13869*# National Aeronautics and Space Administration. Goddard Space Flight Center, Greenbelt, Md.
DATA CATALOG SERIES FOR SPACE SCIENCE AND APPLICATIONS FLIGHT MISSIONS. VOLUME 4A: DESCRIPTIONS OF METEOROLOGICAL AND TERRESTRIAL APPLICATIONS SPACECRAFT AND INVESTIGATIONS
Carolyn Y. Ng, ed. and Yi-Tsuei P. Sheu, ed. Jul. 1985 126 p 11 Vol.
(NASA-TM-87501; NSSDC/WDC-A-R/S-85-03-Vol-4A; NAS 1.15:87501) Avail: NTIS HC A07/MF A01 CSCL 04B

The National Space Science Data Center (NSSDC) provides data from and information about space science and applications flight investigations in support of additional studies beyond those performed as the principal part of any flight mission. The Earth-orbiting spacecraft for investigations of the earth and its atmosphere is discussed. Geodetic tracking data are included in this category. The principal subject areas presented are meteorology and earth resources survey, and the spacecraft selection is made according to those subjects. All experiments on board the spacecraft are described. No attempt is made to reference investigations that are related to the above disciplines, but that are described in other volumes of this series. E.A.K.

N86-13870# Air Force Inst. of Tech., Wright-Patterson AFB, Ohio.
SAMPLING-RATE EFFECTS ON RADAR-DERIVED RAINFALL ESTIMATES M.S. Thesis
J. L. Fornear Aug. 1985 75 p
(AD-A158203; AFIT/CI/NR-85-87T) Avail: NTIS HC A04/MF A01 CSCL 04/2

This study investigates the errors due solely to sampling intervals that occur with radar-derived total rainfall estimates. The study was limited to nine cold-front passages over eastern Texas, in the Fall of 1984. Digitized, 10.3 cm wavelength radar observations were recorded using a one minute sampling-rate. Total rainfall estimates, for 10 km by 10 km areas, based on these data were considered ground truth totals. Sample-rates, ranging from 5 to 60 minutes, were applied to the recorded data to calculate total rain estimates for each sample rate. These derived rain totals were compared to the ground truth totals, with the differences referred to as errors. These errors were plotted against the sampling-rate. They ranged from over 100% for sample intervals greater than 50 minutes, to less than 25% for intervals less than 15 minutes. The errors were also plotted against the number of samples taken. There was no significant increase in estimate accuracy when greater than seven samples were taken per 80 minute period. Other variables, the mean rain rate, total rain, sequential variability, storm width, and storm speed of movement, were found to have very low correlations with the errors. GRA

N86-13871# Technische Univ., Hanover (West Germany).
METEOROLOGICAL AND CLIMATOLOGICAL CONDITIONS AFFECTING THE VERTICAL STRUCTURE OF VISIBILITY IN NORTHERN GERMANY Final Technical Report, 18 Jan. - 31 Aug. 1985
R. Roth Jun. 1985 162 p
(Contract DAJA37-82-C-0189; DA Proj. 1L1-61102-BH-57)
(AD-A158254; R/D-4033-EN-01) Avail: NTIS HC A08/MF A01 CSCL 04/2

The objective of the program was to establish a climatology of the visibility profile within the height range of 2 to 300m for northern Germany. To achieve this objective continuous measurements of the visual range, temperature and dewpoint temperature at six different height levels on a 300m-radiomast, as well as the registration of the cloud ceiling up to 1500m were performed for about 2.5 years. For selected weather situations additional high resolution vertical soundings by means of a tethersonde in accordance with sodar measurements supplied more detailed data. It turned out that the visibility profile is strongly correlated to the weather situation (low, high etc.) depending on the time of the day and on the season. GRA

N86-13872# Lawrence Livermore National Lab., Calif.
STATISTICAL COMPARISON OF TWO MAJOR GRIDDED TEMPERATURE RECORDS OF THE NORTHERN HEMISPHERE
S. L. Grotch Jul. 1985 5 p refs Presented at the 9th Conf. on Probability and Statist. in Atmospheric Sci., Virginia Beach, Va., 9 Oct. 1985
(Contract W-7405-eng-48)
(DE85-016076; UCRL-92933; CONF-851028-48) Avail: NTIS HC A02/MF A01

The global surface temperature records of the Climate Research Unit (CRU) of the university of East Anglia and that of the Russians were compared to examine their accuracy and any possible discrepancies. The CRU and the Russian gridded temperature curves are in excellent agreement when average Northern Hemisphere behavior is compared. There are, however, several grid points where differences between the two data sets warrant further study. DOE

N86-13873# Emertron, Inc., Silver Spring, Md. Dept. of Electrical Engineering.
HORIZONTAL ELECTRIC FIELDS FROM LIGHTNING RETURN STROKES
E. M. Thomson, M. A. Uman, J. Johnson, J. W. Stone, P. Medelius, and M. Rubenstein 1985 8 p Presented at the Intern. Conf. on Lightning and Static Elec., Paris, 10 Jun. 1985
(Contract DE-AC05-840R-21400)
(DE85-016367; CONF-8506121-2) Avail: NTIS HC A02/MF A01

Measurements are presented of simultaneous horizontal and vertical electric fields from both close and distant lightning return strokes. The data were obtained during summer 1984 at the Kennedy Space Center, Florida, using an electrically isolated spherical antenna with a system bandwidth of 3 Hz to 5 MHz. Lightning signals were obtained from flashes at distances from a few to 100 kilometers. Since the horizontal electric field is in part determined by the local ground conductivity, that parameter was measured as a function of depth. The horizontal fields from lightning return strokes had typically 1/50 the peak amplitude of the vertical fields and waveshapes which were consistant with available theory, as expressed by the wavetilt formula. DOE

N86-13766# Joint Publications Research Service, Arlington, Va.
GOSKOMGIDROMET PLANS AUTOMATION OF AERIAL CLOUD-SEEDING WORK Abstract Only
Vera Dorofeyeva and Vil Dorofeyev *In its* USSR Rept.: Earth Sci. (JPRS-UES-85-009) 13 Nov. 1985 p 2 Transl. into ENGLISH from Literaturnaya Gazeta (Moscow), 26 Jun. 1985 p 11 (For primary document see N86-13765 04-42)
Avail: NTIS HC A04/MF A01

N86-13770# Joint Publications Research Service, Arlington, Va.
INVESTIGATION OF CHARACTERISTICS OF SYNOPTIC MOVEMENTS ON SPHERE Abstract Only
A. D. Marushkevich *In its* USSR Rept.: Earth Sci. (JPRS-UES-85-009) 13 Nov. 1985 p 11 Transl. into ENGLISH from Okeanol. (Moscow), v. 25, no. 3, May - Jun. 1985 p 386-394 (For primary document see N86-13765 04-42)
Avail: NTIS HC A04/MF A01

N86-13782# Joint Publications Research Service, Arlington, Va.
EXPERIENCE IN MEASURING MEAN WIND VELOCITY PROFILE IN LOWER TROPOSPHERE BY SODAR ANEMOMETER UNDER INVERSION AND CONVECTIVE CONDITIONS Abstract Only
M. A. Kallistratova, Y. Keder, I. V. Petenko, and N. S. Time *In its* USSR Rept.: Earth Sci. (JPRS-UES-85-009) 13 Nov. 1985 p 30-31 Transl. into ENGLISH from Izv. Akad. Nauk SSSR: Fiz. Atmosfery i Okeana (Moscow), v. 21, no 5, May 1985 p 492-497 Original language document was announced in IAA as A85-40641 (For primary document see N86-13765 04-42)
Avail: NTIS HC A04/MF A01

N86-13783# Joint Publications Research Service, Arlington, Va.
STRUCTURAL CHARACTERISTIC OF TEMPERATURE FIELD OVER SEA Abstract Only
B. M. Koprov *In its* USSR Rept.: Earth Sci. (JPRS-UES-85-009) 13 Nov. 1985 p 31-32 Transl. into ENGLISH from Izv. Akad. Nauk SSSR: Fiz. Atmosfery i Okeana (Moscow), v. 21, no. 5, May 1985 p 485-491 (For primary document see N86-13765 04-42)
Avail: NTIS HC A04/MF A01

N86-14098*# Texas A&M Univ., College Station. Dept. of Meteorology.
VARIABILITY OF RAINFALL OVER SMALL AREAS Final Report
Robert C. Runnels *In* NASA. Johnson (Lyndon B.) Space Center The 1983 NASA/ASEE Summer Faculty Fellowship Research Program Research Reports Sep. 1983 7 p refs (For primary document see N86-14078 04-85)
Avail: NTIS HC A18/MF A01 CSCL 04B

48 OCEANOGRAPHY

Includes biological, dynamic and physical oceanography; and marine resources.

N86-13874# VMI Research Labs., Lexington, Va.
THE DESIGN OF A BEACH PROFILER Final Report, 22 Feb. 1985 - 21 Feb. 1986
R. A. Erchul Jun. 1985 77 p
(Contract N00014-85-K-0303)
(AD-A157715) Avail: NTIS HC A05/MF A01 CSCL 13/2

Three designs of a beach profiler system were designed by VMI cadets as a part of requirements in the VMI's course Coastal Engineering. All the systems were designed to measure the water depth in the surf zone to within + or - one foot accuracy under all weather conditions. All systems designs used a pressure sensor to measure depth, however, each varied in method of employing this sensor. Two of the designs propelled the sensing unit sub-system while the third design used a push-pull method of employment. The distance of employment into the surf zone varied from 300 to 3,000 feet. The designed systems were fairly economical in cost ranging from $2,020.00 to $4,348.00. Projected scenarios of operations varied in the systems used requiring from one to six personnel for employment. Author (GRA)

N86-13875# Naval Research Lab., Washington, D. C.
LABORATORY STUDIES OF STEEP AND BREAKING DEEP WATER WAVES IN A CONVERGENT CHANNEL Memorandum Report, Aug. 1983 - May 1985
S. E. Ramberg, M. E. Barber, and O. M. Griffin 21 Aug. 1985 45 p
(NR Proj. RR0-2301)
(AD-A158187; NRL-MR-5610) Avail: NTIS HC A03/MF A01 CSCL 08/3

In the present experiments, waves were made to steepen by a convergent section which was installed in NRL's 30m long wave channel. These and other recent experiments have demonstrated that a criterion for the onset of breaking for deep water waves can be simply stated in terms of the wave steepness at breaking. This criterion states that the wave steepness at the onset of breaking is given by H/L* = approx. 0.11, where H is the wave height and L* is the Stokes limiting wavelength. On the evidence available thus far the simple steepness criterion applies equally well to spilling and plunging breakers. Criteria such as this can be readily used to predict the frequency of occurrence of breaking for deep water waves. There are more complex questions relating to energy losses in breaking and related topics which cannot be addressed so simply. From the results of the present experiments it appears that the potential energy loss rates of plunging breakers are twice those of spilling breakers in deep water. Moreover, the potential energy losses in breaking did not significantly alter the total mean drift and return flows in the channel. Most of the energy lost goes into the production of turbulence and into air entrainment in the breaking region. GRA

N86-13876# Naval Research Lab., Washington, D. C.
A FAMILY OF CURVES FOR THE ROUGH SURFACE REFLECTION COEFFICIENT Final Report, 1983 - 1984
A. R. Miller and E. Vegh 31 Jul. 1985 21 p
(NR Proj. W12-53)
(AD-A158195; NRL-8898) Avail: NTIS HC A02/MF A01 CSCL 08/3

This report puts forward statistical models for the sea surface which are used to derive a family of theoretical curves for the rough surface reflection coefficient. One of these curves fits the experimental data curve. Other experimental data points lie within the envelope of the derived curves. There is, therefore, a theoretical basis for the experimental data when the surface roughness exceeds 0.1 rad. GRA

N86-13877# Los Alamos National Lab., N. Mex.
THREE-DIMENSIONAL MODELING OF TSUNAMI WAVES
C. L. Mader 1985 7 p refs Presented at the Tsunami Symp., Victoria, British Columbia, 6 Aug. 1985
(Contract W-7405-eng-36)
(DE85-015724; LA-UR-85-2412; CONF-8508112-1) Avail: NTIS HC A02/MF A01

Two and three-dimensional, time-dependent, nonlinear, incompressible, viscous flow calculations of realistic models of tsunami wave formation and run up have been performed using the Los Alamos-developed SOLA-3D code. The results of the SOLA calculations are compared with shallow-water, long-wave calculations for the same problems using the SWAN code. Tsunami wave formation by a continental slope subsidence has been examined using the two numerical models. The SOLA waves were slower than the SWAN waves and the interaction with the shoreline was more complicated for the SOLA waves. In the SOLA calculation, the first wave was generated by the cavity being filled along the shoreline close to the source of motion. The second wave was generated by the cavity being filled from the deep water end. The two waves interacted along the shoreline resulting in the second wave being the largest wave with a velocity greater than the first wave. The second wave overtook the first wave at later times and greater distances from the source. In the SWAN calculation, the second wave was smaller than the first wave. DOE

N86-13769# Joint Publications Research Service, Arlington, Va.
COMPUTATION OF OCEAN UPPER LAYER THERMAL STRUCTURE Abstract Only
A. Yu. Benilov, N. G. Kozhelupova, and B. N. Filyushkin *In its* USSR Rept.: Earth Sci. (JPRS-UES-85-009) 13 Nov. 1985 p 10 Transl. into ENGLISH from Okeanol. (Moscow), v. 25, no. 3, May - Jun. 1985 p 378-385 (For primary document see N86-13765 04-42)
Avail: NTIS HC A04/MF A01

N86-13771# Joint Publications Research Service, Arlington, Va.
VERTICAL STRUCTURE OF TURBULENCE AND TURBULENT EXCHANGE IN EQUATORIAL ZONE OF PACIFIC OCEAN Abstract Only
A. N. Gezentsvey *In its* USSR Rept.: Earth Sci. (JPRS-UES-85-009) 13 Nov. 1985 p 12-13 Transl. into ENGLISH from Okeanol. (Moscow), v. 25, no. 3, May - Jun. 1985 p 414-419 (For primary document see N86-13765 04-42)
Avail: NTIS HC A04/MF A01

N86-13772# Joint Publications Research Service, Arlington, Va.
SOME CHARACTERISTICS OF BOTTOM DENSITY CURRENTS Abstract Only
V. N. Anuchin, V. M. Belokopytov, and V. A. Gritsenko *In its* USSR Rept.: Earth Sci. (JPRS-UES-85-009) 13 Nov. 1985 p 13-14 Transl. into ENGLISH from Okeanol. (Moscow), v. 25, no. 3, May - Jun. 1985 p 420-424 (For primary document see N86-13765 04-42)
Avail: NTIS HC A04/MF A01

N86-13773# Joint Publications Research Service, Arlington, Va.
HIGHLY DISPERSE MINERALS IN SEDIMENTS IN NEIGHBORHOOD OF EAST PACIFIC OCEAN RISE DETERMINED FROM DRILLING DATA Abstract Only
Z. N. Gorbunova *In its* USSR Rept.: Earth Sci. (JPRS-UES-85-009) 13 Nov. 1985 p 14-15 Transl. into ENGLISH from Okeanol. (Moscow), v. 25, no. 3, May - Jun. 1985 p 465-470 (For primary document see N86-13765 04-42)
Avail: NTIS HC A04/MF A01

N86-14171# Joint Publications Research Service, Arlington, Va.
EQUATORIAL WAVES IN OCEAN SURFACE TEMPERATURE FIELD ACCORDING TO DATA FROM SHIPBOARD AND SATELLITE MEASUREMENTS Abstract Only
A. S. Kazmin, R. Legeckis, and K. N. Fedorov *In its* USSR Rept.: Space (JPRS-USP-85-005) 30 Sep. 1985 p 108-109 Transl. into ENGLISH from Issled. Zemli iz Kosmosa (Moscow), no. 5, Sep. - Oct. 1984 p 3-7 Original language document announced in IAA as A85-16940 (For primary document see N86-14111 04-88)
Avail: NTIS HC A08

51 LIFE SCIENCES (GENERAL)

Includes genetics.

N86-13878*# Louisville Univ., Ky. Dept. of Microbiology and Immunology.
DEVELOPMENT AND TESTING OF A MOUSE SIMULATED SPACE FLIGHT MODEL Semiannual Progress Report, May - Oct. 1985
Gerald Sonnenfeld 1985 6 p refs
(Contract NCC2-213)
(NASA-CR-176359; NAS 1.26:176359; SAPR-6) Avail: NTIS HC A02/MF A01 CSCL 06C

The development and testing of a mouse model for simulating some aspects of weightlessness that occur during space flight, and the carrying out of immunological flight experiments on animals was discussed. The mouse model is an antiorthostatic, hypokinetic, hypodynamic suspension model similar to the one used with rats. It is shown that this murine model yield similar results to the rat model of antiorthostatic suspension for simulating some aspects of weightlessness. It is also shown that mice suspended in this model have decreased interferon-alpha/beta production as compared to control, nonsuspended mice or to orthostatically suspended mice. It is suggested that the conditions occuring during space flight could possibly affect interferon production. The regulatory role of interferon in nonviral diseases is demonstrated including several bacterial and protozoan infections indicating the great significance of interferon in resistance to many types of infectious diseases. E.A.K.

N86-13879*# National Aeronautics and Space Administration, Washington, D. C.
LIFE SCIENCES ACCOMPLISHMENTS
Sep. 1985 95 p refs Original contains color illustrations
(NASA-TM-88177; NAS 1.15:88177) Avail: NTIS HC A05/MF A01 CSCL 06C

From its inception, the main charter of Life Sciences has been to define biomedical requirements for the design and development of spacecraft systems and to participate in NASA's scientific exploration of the universe. The role of the Life Sciences Division is to: (1) assure the health, well being and productivity of all individuals who fly in space; (2) study the origin, evolution, and distribution of life in the universe; and (3) to utilize the space environment as a tool for research in biology and medicine. The activities, programs, and accomplishments to date in the efforts to achieve these goals are detailed and the future challenges that face the division as it moves forward from the shuttle era to a permanent manned presence in space space station's are examined. E.A.K.

N86-13880# Wisconsin Univ., Madison.
STUDY OF TOXIC AND ANTIGENIC STRUCTURES OF BOTULINUM NEUROTOXINS Annual and Final Report, 1 Aug. 1980 - 31 Aug. 1984
B. R. DasGupta Feb. 1985 14 p
(Contract DAMD17-80-C-0100; DA Proj. 3M1-62770-A-871)
(AD-A156642) Avail: NTIS HC A02/MF A01 CSCL 06/5

Amino acid compositions of botulinum neurotoxin (NT) types A, B, E and F were determined. The heavy and light chains of types A, B and E NT were separated, purified, and analyzed for amino acid compositions and partial N-terminal sequence. Selective modification of tyr, his and arg residues and also carboxyl and amino groups of types A and E NT demonstrated the role of these amino acid residues in toxicity and antiquenicity. Type E NT completely detoxified following modification of his, tyr or amino groups has potential as a toxoid. Effects of types A and B NT on rat neuromuscular junctions appear non-identical. Author (GRA)

N86-13881# Systems and Applied Sciences Corp., Anaheim, Calif.
NEW PHYSICAL METHODS FOR BIOLOGICAL AEROSOL DETECTION Contractor Report, Aug. 1982 - Sep. 1984
C. C. Chou and M. Lu May 1985 99 p
(Contract DAAK11-82-C-0113)
(AD-A158218; CRDC-CR-84131) Avail: NTIS HC A05/MF A01 CSCL 15/2

For biological aerosol detection, Fourier transform secondary negative ion mass spectrometry appears to be on the forefront among various new analytical methods evaluated. Various gases liberated upon pyrolyzing bacterial cells lead to several possible techniques. Preliminary experimental results indicated an integrated detection system incorporating non-dispersive IR spectroscopy, piezoelectric sensing, and optical density change measurement would render a fast, accurate detection for pyrolysis gaseous products. GRA

N86-13882# Stanford Univ., Calif.
SMALL X-RAY DIFFRACTION OF IMMUNOGLOBULIN-MEMBRANE COMPLEXES Final Technical Report, 15 Apr. 1981 - 14 Oct. 1984
S. Doniach and K. Hodgson 15 Aug. 1985 8 p
(Contract N00014-81-K-0496)
(AD-A158252) Avail: NTIS HC A02/MF A01 CSCL 06/1

In the first part of this research, specially designed hapten-phospholipid molecules were synthesized to enable the binding of immunoglobulins to artificial phospholipid membranes. In subsequent work, using these immunoglobulin-membrane complexes, electron microscopy was used to reveal the detailed crystalline structure of a two dimensional (2D) immunoglobulin crystal attached to an electron microscope grid. These studies enabled the discovery of a new conformational arrangement of crystals formed from intact immunoglobulin molecules. In a third part of the study, monolayers of protein-membrane complex (in this case the purple membrane from halobacterium halobium) were deposited on a single crystal silicon substrate. Using the technique of grazing incidence X-ray diffraction, diffraction patterns from a single monolayer of protein-lipid complex were obtained for the first time. GRA

N86-13883# Battelle Northwest Labs., Richland, Wash.
DESIGN, CONSTRUCTION AND TESTING OF A dc BIOEFFECTS ENCLOSURE FOR SMALL ANIMALS Final Report
Jul. 1985 180 p refs Sponsored by EPRI
(Contract DE-AC06-76RL-01830; EPRI Proj. 1774-1)
(DE05-016798; EPRI-EA-4189) Avail: NTIS HC A09/MF A01

Large air-ion concentrations moving in high-strength static electric fields are unique to the environment near high-voltage dc (HVdc) transmisison lines. To assess the possible biological effects of this environment, a small-animal exposure system was designed to produce well-characterized levels of the major components of the HVdc environment. Initial steps in the development of this exposure system included studies of various housing geometries and housing materials. Dielectric materials, such as plexiglass and lexan, unacceptably perturbed electric-field and air-ion environments in their vicinity these perturbations depended on the cleanliness of the housing materials and were spatially and temporally variable. Semiconducting materials were also investigated, with satisfactory results. The final cage design employs semiconducting glass walls which span the entire space between the grounded metal-screen cage floors the overhead high-voltage electrodes used to generate the exposure electric fields. The surface conductivity of the glass walls is controlled by a system of energized guard strips located on the outer surfaces of the walls. Electric-field strengths up to 100 kV/m and air-ion concentrations up to 1,000,000 cu b c, are attainable. Initial dosimetric measurements were also performed as part of this project. The ion current collected by the body of a grounded animal was measured as a function of ion concentration and electric-field strength. The ion current collected by a live animal was observed to be significantly less than that collected by a conducting animal model of similar size and shape. This deviation appears to be due to accumulation of electric charge on the fur of exposed animals. DOE

N86-13884# Washington Univ., Seattle. Social Management of Technology Program.
MOLECULAR MECHANISMS OF MUTAGENESIS DETERMINED BY THE RECOMBINANT DNA TECHNOLOGY
W. R. Lee 1985 10 p refs Presented at the 4th Intern. Conf. on Environ. Mutagens, Stockholm, 24 Jun. 1985
(Contract DE-AS05-76EV-03728)
(DE85-016353; CONF-8506137-11) Avail: NTIS HC A02/MF A01

A study of the alteration of the DNA in the mutant gene can determine mechanisms of mutation by distinguishing between mutations induced by transition, transversion, frameshifts of a single base and deletions involving many base pairs. The association of a specific pattern of response with a mutagen will permit detecting mutants induced by the mutagen with a reduced background by removing mutations induced by other mechanisms from the pool of potential mutants. From analyses of studies that have been conducted, it is quite apparent that there are substantial differences among mutagens in their modes of action. Of 31 X-ray induced mutants, 20 were large deletions while only 3 showed normal southern blots. Only one mutant produced a sub-unit polypeptide of normal molecular weight and charge in the in vivo test whereas in vitro synthesis produced a second one. In contrast, nine of thirteen EMS induced mutants produced cross-reacting proteins with sub-unit polypeptide molecular weights equivalent to wild type. DOE

N86-13885# Southwest Research Inst., San Antonio, Tex.
EFFECTS OF 60 Hz ELECTRIC FIELDS ON OPERANT AND SOCIAL STRESS BEHAVIORS OF NONHUMAN PRIMATES Project Technical Status Report, 16 Feb. - 12 Apr. 1985
W. R. Rogers 19 Apr. 1985 33 p
(Contract DE-AC02-80RA-50219)
(DE85-011992; DOE/RA-50219/T4) Avail: NTIS HC A03/MF A01

The objective was to investigate possible behavioral effects of exposure to high-intensity 60 Hz electric fields. Four projects are conducted: (1) aversive sensory character of exposure to fields, (2) threshold intensity for detection of fields, (3) chronic exposure effects on performance of two operant tasks, and (4) observation of behavior of social groups under chronic exposure. Electric field testing with animals has begun. Behavioral testing was suspended for repair of cages and to suppress corona, and to conduct engineering tests. DOE

N86-14080*# Fayetteville State Univ., N.C. Dept. of Biology.
THE SCANNING ELECTRON MICROSCOPE AS A TOOL IN SPACE BIOLOGY Final Report
Roy A. Barrett *In* NASA. Johnson (Lyndon B.) Space Center The 1983 NASA/ASEE Summer Faculty Fellowship Research Program Research Reports Sep. 1983 9 p refs (For primary document see N86-14078 04-85)
Avail: NTIS HC A18/MF A01 CSCL 06B

N86-14088*# North Texas State Univ., Denton. Dept. of Biological Sciences.
INTERACTION BETWEEN ESCHERICHIA COLI AND LUNAR FINES Final Report
Karl R. Johansson *In* NASA. Johnson (Lyndon B.) Space Center The 1983 NASA/ASEE Summer Faculty Fellowship Research Program Research Reports Sep. 1983 21 p refs (For primary document see N86-14078 04-85)
Avail: NTIS HC A18/MF A01 CSCL 06B

N86-14097*# Morgan State Univ., Baltimore, Md.
COMPARATIVE EFFECT OF LUNAR FINES AND TERRESTRIAL ASH ON THE GROWTH OF A BLUE-GREEN ALGA AND GERMINATING RADISH SEEDS Final Report
Esther J. Ridley *In* NASA. Johnson (Lydon B.) Space Center The 1983 NASA/ASEE Summer Faculty Fellowship Research Program Research Reports Sep. 1983 15 p refs (For primary document see N86-14078 04-85)
Avail: NTIS HC A18/MF A01 CSCL 06B

N86-14162# Joint Publications Research Service, Arlington, Va.
ENERGY EXCHANGE OF PLANTS UNDER WEIGHTLESSNESS CONDITIONS Abstract Only
M. G. Tairbekov and A. V. Devyatko *In its* USSR Rept.: Space (JPRS-USP-85-005) 30 Sep. 1985 p 80 Transl. into ENGLISH from Dokl. Akad. Nauk SSSR (Moscow), v. 280, no. 2, Jan. 1985 p 509-512 Original language document announced in IAA as A85-24193 (For primary document see N86-14111 04-88)
Avail: NTIS HC A08

52 AEROSPACE MEDICINE

Includes physiological factors; biological effects of radiation; and weightlessness.

N86-13886*# National Aeronautics and Space Administration. Johnson (Lyndon B.) Space Center,
ENDOCRINE AND FLUID METABOLISM IN MALES AND FEMALES OF DIFFERENT AGES AFTER BEDREST, ACCELERATION AND LOWER BODY NEGATIVE PRESSURE
Carolyn S. Leach, Joan Vernikos-Danellis (NASA. Ames Research Center), Jane M. Krauhs (Northrop Services, Inc., Houston, Tex.), and Harold Sandler (NASA. Ames Research Center) Nov. 1985 52 p refs
(NASA-TM-58270; S-550; NAS 1.15:58270) Avail: NTIS HC A04/MF A01 CSCL 06S

Space shuttle flight simulations were conducted to determine the effects of weightlessness, lower body negative pressure (LBNP), and acceleration of fluid and electrolyte excretion and the hormones that control it. Measurements were made on male and female subjects of different ages before and after bedrest. After admission to a controlled environment, groups of 6 to 14 subjects in the age ranges 25 to 35, 35 to 45, 45 to 55 to 65 years were exposed to +3 G sub z for 15 minutes (G1) and to LBNP (LBNP1) on different days. On 3 days during this prebedrest period, no tests were conducted. Six days of bedrest followed, and the G sub z (G2) and LBNP (LBNP2) tests were run again. Hormones, electrolytes, and other parameters were measured in 24-hour urine pools throughout the experiment. During bedrest, cortisol and aldosterone excretion increased. Urine volume decreased, and specific gravity and osmolality increased. Urinary electrolytes were statistically unchanged from levels during the non-stress control period. During G2, cortisol increased significantly over its control and bedrest levels. Urine volume, sodium, and chloride were significantly lower; specific gravity and osmolality were higher during the control period or bedrest. The retention of fluids and electrolytes after +G sub z may at least partially explain decreased urine volume and increased osmolality observed during bedrest in this study. There were some who indicated that space flight would not affect the fluid and electrolyte metabolism of females or older males any more severely than it has affected that of male astronauts. Author

N86-13887# Army Research Inst. of Environmental Medicine, Natick, Mass.
THE EFFECT OF SPIRONOLACTONE ON THE CARDIOCIRCULATORY RESPONSES TO UPRIGHT TILT AT SEA LEVEL AND AT SIMULATED HIGH ALTITUDE
C. S. Fulco, R. Larsen, P. B. Rock, A. J. Young, and A. Cymerman 19 Jun. 1985 18 p
(DA Proj. 3E1-62777-A-879)
(AD-A157734; USARIEM-M33/85) Avail: NTIS HC A02/MF A01 CSCL 06/15

The objective of this study was to determine if spironolactone (S) alters the cardiocirculatory responses to upright tilt at sea level (SL;50m) and during 44 hours of simulated altitude (HA;4600m). In a double-blind, crossover-designed study, 9 male subjects (age range: 18 to 25 years) received 25 mg orally, 4x/day of either S or an identically-appearing placebo (P) 2 days prior to and during HA. The crossover was separated by two weeks. Heart rate, stroke volume, cardiac output, calf blood flow, total peripheral resistance and system blood pressure were obtained during supine rest and after 10 minutes of 60 degree head-up tilt using an impedance monitor and an electro-sphygmomanometer. Twenty-four hour determinations of urinary volume, sodium and potassium, as well as venous plasma values for sodium, potassium and chloride were obtained daily. There were no statistically significant differences between P and S treatment periods for: caloric, electrolytes; of fluid ingestion; urinary volume or electrolytes; plasma electrolytes; or any of the cardiocirculatory parameters measured in the supine or upright position at SL or during HA. It was concluded that S did not induce a significant diuresis or significantly alter vascular responsiveness to negatively effect the normal cardiocirculatory responses to upright tilt at sea level or simulated high altitude. GRA

N86-13888# School of Aerospace Medicine, Brooks AFB, Tex.
INTERACTIVE SCENARIO COMPUTER MODEL FOR DOSE RATES TO AIRCREWS IN FLIGHT THROUGH NUCLEAR DEBRIS CLOUDS Final Report, Dec. 1981 - Oct. 1984
J. Taboada, D. Hegedusich, and E. L. Bell Jul. 1985 18 p
(AD-A158741; USAFSAM-TR-85-49) Avail: NTIS HC A02/MF A01 CSCL 06/18

An interactive computer model is described for the rapid calculation of gamma radiation doses to aircrews in hypothetical flights through nuclear debris clouds. The model is based on CASSANDRA, a U.S. army developed code for dust concentration calculations at loci through such a cloud. The present model computes local radiation dose integrals along a user-specified flight path. It is designed for efficient interactive operation on a Digital Equipment Corporation Model VAX 11/780 computer. GRA

N86-13889# Northwestern Univ., Evanston, Ill.
ENHANCING SENSITIVITY TO VISUAL MOTION AND ENHANCING VISUAL SENSITIVITY Interim Report, 1 Oct. 1981 - 30 Sep. 1983
R. Sekuler 4 Jun. 1985 28 p
(Grant AF-AFOSR-0246-80)
(AD-A158800; AFOSR-85-0668TR) Avail: NTIS HC A03/MF A01 CSCL 06/16

This report describes progress made from October 1, 1981 to September 30, 1983. During this period work proceeded on three main lines of study: (1) various aspects of visual motion perception, (2) collaborative work on contrast sensitivity and pilots' performance in aircraft simulators, and 3) individual differences in responses to temporal transients. The most extensive of the three work-units dealt with motion perception by human observers. The main findings include the following: (1) Perceived speed of a moving target varies with that target's contrast and retinal eccentricity. In particular, many targets undergo illusory slowing when they appear in the periphery in the visual field, (2) detection of a moving target is often dissociated from the ability to identify the direction in which the target moves. In particular, the accuracy with which target direction can be judged, even for highly visible targets, seems to far less good than previously suspected, (3) relatively small amounts of training can significantly improve an observer's ability to discriminate between two highly similar directions of target motion. Moreover, this effect is well-restricted to the training direction and other, similar directions; the training effect is retained without decrement for at least two months. The results suggest that this improvement with training represents a genuine change in visual function. GRA

N86-13890# Air Force Human Resources Lab., Brooks AFB, Tex.
PILOT-ORIENTED PERFORMANCE MEASUREMENT Final Report, Jan. - Dec. 1983
J. DeMaio, H. H. Bell, and J. Brunderman Aug. 1985 15 p
(AF Proj. 2313)
(AD-A158849; AFHRL-TP-85-18) Avail: NTIS HC A02/MF A01 CSCL 14/2

Aircrew performance measurement is a critical problem in evaluating the quality of a visual simulation system and in determining the effectiveness of aircrew training devices. An effective performance measurement system must be able to separate performance into appropriate components and describe the relationship of these components. This paper describes a performance measurement system developed to analyze pilot performance in maintaining altitude in both straight and turning flight as a function of the object density of the simulated visual environment. The analysis indicates that pilot performance can be divided into perceptual and task difficulty factors and that the effect of the visual environment on each of these factors can be determined. A prototype performance measurement system was developed to describe pilot performance in a simulator. The pilot's task was to maintain altitude at 200 feet both in straight and in turning flight. Pilot performance was sensitive to task difficulty and to visual scene quality. The strength of this performance measurement system was that it analyzed performance in terms of overall task performance and also specific pilot control inputs. GRA

N86-13891# Army Environmental Hygiene Agency, Aberdeen Proving Ground, Md.
HEALTH HAZARD EVALUATION OF LIQUID MONOPROPELLANTS. PHASE 5: COMPARATIVE INHALATION TOXICITIES OF LGP 1776, LGP 1845, AND HAN (HYDROXYLAMMONIUM NITRATE) Final Report
H. L. Snodgrass, Jr. Jun. 1985 33 p
(AD-A159090; USAEHA-75-51-0132-85) Avail: NTIS HC A03/MF A01 CSCL 06/20

A comparison of the inhalation toxicities of two liquid gun propellant (LGP) formulations, LGPs 1776 and 1845, was made using rats. Also assessed was the major chemical component of each, hydroxylammonium nitrate (HAN). Rats exposed to saturated vapors of the two LGPs for 8 hours were uneffected. Following single acute aerosol exposures, LGP 1845 was more toxic, with deaths occurring at concentrations of 1350 to 1603 mg/cu m. After 5 or 10 daily aerosol exposures to the three formulations, comparable dose-dependent effects were noted. These included hematological, organ-to-body weight ratio, and pathological changes, generally at the highest exposure level of 600 mg/cu m. It is concluded that acute exposures to LGP vapors should not be hazardous to man. Also inferred is that the effects of repeated, sublethal exposures to LGPs 1776 and 1845 are quantitatively similar to those observed with HAN, the major chemical component. GRA

53 BEHAVIORAL SCIENCES

Includes psychological factors; individual and group behavior; crew training and evaluation; and psychiatric research.

N86-13892*# National Aeronautics and Space Administration. Langley Research Center, Hampton, Va.
EFFECTS OF DIGITAL ALTIMETRY ON PILOT WORKLOAD
Randall L. Harris, Sr. and Bobby J. Glover Nov. 1985 20 p refs
(NASA-TM-86424; L-15989; NAS 1.15:86424) Avail: NTIS HC A02/MF A01 CSCL 05H

A series of VOR-DME instrument landing approaches was flown in the DC-9 full-workload simulator to compare pilot performance, scan behavior, and workload when using a computer-drum-pointer altimeter (CDPA) and a digital altimeter (DA). Six pilots executed two sets of instrument landing approaches, with a CDPA on one set and a DA on the other set. Pilot scanning parameters, flight performance, and subjective opinion data were evaluated. It is found that the processes of gathering information from the CDPA and the DA are different. The DA requires a higher mental workload than the CDPA for a VOR-DME type landing approach. Mental processing of altitude information after transitioning back to the attitude indicator is more evident with the DA than with the CDPA. E.A.K.

N86-13893# Massachusetts Inst. of Tech., Cambridge. Artificial Intelligence Lab.
HYPOTHESIZING AND REFINING CAUSAL MODELS
R. J. Doyle Dec. 1984 109 p
(Contract N00014-80-C-0505; NR Proj. RR0-1408)
(AD-A158165; AI-M-811) Avail: NTIS HC A06/MF A01 CSCL 06/4

An important common sense competence is the ability to hypothesize causal relations. This paper presents a set of constraints which make the problem of formulating causal hypotheses about simple physical systems a tractable one. The constraints include: (1) a temporal and physical proximity requirement; (2) a set of abstract causal explanations for changes in physical systems in terms of dependences between quantities; and (3) a teleological assumption that dependences in designed physical systems are functions. These constraints were embedded in a learning system which was tested in two domains: a sink and a toaster. The learning system successfully generated and refined naive causal models of these simple physical systems. The causal models which emerge from the learning process support causal reasoning explanation, prediction, and planning. Inaccurate predictions and failed plans in turn indicate deficiencies in the causal models and the need to rehypothesize. Thus, learning supports reasoning which leads to further learning. The learning system makes use of standard inductive rules of inference, as well as the constraints of casual hypotheses to generalize its casual models. Finally, a simple example involving an analogy illustrates another way to repair incomplete causal models. GRA

N86-13894# Massachusetts Inst. of Tech., Cambridge. Artificial Intelligence Lab.
GENERATING AND GENERALIZING MODELS OF VISUAL OBJECTS Memorandum Report
J. H. Connell and M. Brady Jul. 1985 26 p
(Contracts N00014-80-C-0505; N00014-77-C-0389)
(AD-A158197; AI-M-823) Avail: NTIS HC A03/MF A01 CSCL 06/4

We report on initial experiments with an implemented learning system whose inputs are images of two-dimensional shapes. The system first builds semantic network descriptions of shapes based on Brady's smoothed local symmetry representation. It learns shape models from them using a substantially modified version of Winston's ANALOGY program. A generalization of Gray coding enables the representation to be extended and also allows a single operation, called ablation, to achieve the effects of many standard induction heuristics. The program can learn disjunctions, and can learn concepts using only positive examples. We discuss learnability and the pervasive importance of representational hierarchies. GRA

N86-13895# Washington Univ., St. Louis, Mo. Behavior Research Lab.
A PSYCHOPHYSIOLOGICAL MAPPING OF COGNITIVE PROCESSES Annual Report, 1 Mar. 1984 - 28 Feb. 1985
R. Goldstein, J. Stern, and L. Bauer 30 Apr. 1985 49 p
(Contract F49620-83-C-0059)
(AD-A158732; Rept-0059-85-1; AFOSR-85-0664TR; AR-2) Avail: NTIS HC A03/MF A01 CSCL 05/10

The experiment was concerned with the effects of varied cognitive and perceptual (i.e., monitoring) demands on patterns of physiological responding. Cognitive demands were varied by manipulating the number of letters (1, 3, or 5) comprising a briefly-presented set which the subject was instructed to encode, rehearse, and, 5 sec later, compare to a single test letter. Perceptual demands were varied by presenting the subject with a cue stimulus 5 sec prior to the set, informing him of the number of letters contained therein. Several physiological measures were recorded, including HR, EOG and probe evoked potentials sampled from the intervals preceding and following the letter set, and task evoked potentials and blinks elicited by the cue, letter set, and test stimuli. Performance data, i.e., RT and error rates, were also recorded. GRA

N86-13896# Smith-Kettlewell Inst. of Visual Sciences, San Francisco, Calif.
THE SPATIAL AND TEMPORAL PARAMETERS OF VELOCITY DISCRIMINATION Annual Report, 1 Apr. - 30 Sep. 1984
S. P. McKee 20 Dec. 1984 8 p
(Grant AF-AFOSR-0345-82)
(AD-A158735; AFOSR-85-0572TR) Avail: NTIS HC A02/MF A01 CSCL 06/16

The target duration required for the precise discrimination of velocity is quite short, amounting to about 100 msec for a single moving dot or line target. While stroboscopic motion is an adequate substitute for continuous motion in velocity discrimination, optimal discrimination depends on the use of a strobe rate greater than 10 Hz. Generally, human observers have difficulty detecting acceleration in moving targets. Over small distances (0.5 to 1 deg), timing signals from adjacent targets presented in a sequence are pooled, so that information about their relative onset time is lost. For example, given three adjacent lines, separated spatially by 0.1 deg and presented in a sequence (apparent motion) observers are unable to discriminate between a sequence in which a 10 msec interval separates the second from the reverse order (30 msec followed by 10 msec). Velocity discrimination is not affected by blur. Sinusoidal grating targets of 3 cycles per degree or lower produce excellent discrimination. Sinusoidal gratings above 3 cycles per degree in spatial frequency are not adequate for fast velocities (> 1 deg/sec). GRA

N86-13897# Illinois Univ., Champaign. Cognitive Psychophysiology Lab.

THE EVENT RELATED BRAIN POTENTIAL AS AN INDEX OF INFORMATION PROCESSING, COGNITIVE ACTIVITY, AND SKILL ACQUISITION: A PROGRAM OF BASIC RESEARCH Final Report, 1 Sep. 1983 - 31 Aug. 1984

E. Donchin, C. Wickens, and M. G. H. Coles 28 Feb. 1985 774 p
(Contract F49620-83-C-0144)
(AD-A159118; CPL-85-1; AFOSR-85-0662TR) Avail: NTIS HC A99/MF A02 CSCL 05/10

We review a program of research designed to understand the event-related brain potential (ERP) so that it can be used as a tool in the study of cognitive function and in the assessment of man-machine systems. We have conducted a series of studies on the functional significance of ERPs and have demonstrated that the P300 component is related to memory processes. We have used measures of the same component to evaluate workload, to time mental processes, to study the reciprocity of processing resources, and to extend theories of human information processing. We have also made technical advances in the analysis of the distribution of electrical potentials across the scalp. GRA

54 MAN/SYSTEM TECHNOLOGY AND LIFE SUPPORT

Includes human engineering; biotechnology; and space suits and protective clothing.

N86-13898*# Hamilton Standard, Windsor Locks, Conn.

DEVELOPMENT OF A CARBON FORMATION REACTOR FOR CARBON DIOXIDE REDUCTION Final Report

Gary Noyes Sep. 1985 92 p refs
(Contract NAS9-16956)
(NASA-CR-171907; NAS 1.26:171907; SVHSER-9811) Avail: NTIS HC A05/MF A01 CSCL 06K

Applied research, engineering development, and performance evaluation were conducted on a process for formation of dense carbon by pyrolysis of methane. Experimental research showed that dense (0.7 to 1.6 g/cc bulk density and 1.6 to 2.2 g/cc solid density) carbon can be produced by methane pyrolysis in quartz-wool-packed quartz tubes at temperatrues of 1100 to 1300 C. This result supports the condensation theory of pyrolytic carbon formation from gaseous hydrocarbons. A full-scale Breadboard Carbon Formation Reactor (CFR) was designed, fabricated, and tested at 1100 to 1200 C with 380 to 2280 sccm input flows of methane. Single-pass conversion of methane to carbon ranged from 60 to 100 percent, with 89 percent average conversion. Performance was projected for an Advanced Carbon Reactor Subsystem (ACRS) which indicated that the ACRS is a viable option for management of metabolic carbon on long-duration space missions. Author

N86-13899*# National Aeronautics and Space Administration. Lewis Research Center, Cleveland, Ohio.

MASS LOSS OF SHUTTLE SPACE SUIT ORTHOFABRIC UNDER SIMULATED IONOSPHERIC ATOMIC OXYGEN BOMBARDMENT

William Lewis Miller Nov. 1985 14 p refs
(NASA-TM-87149; E-2777; NAS 1.15:87149) Avail: NTIS HC A02/MF A01 CSCL 06K

Many polymeric materials used for thermal protection and insulation on spacecraft degrade significantly under prolonged bombardment by ionospheric atomic oxygen. The covering fabric of the multilayered shuttle space suit is composed of a loose weave of GORE-TEX fibers, Nomex and Kevlar-29, which are all polymeric materials. The complete evaluation of suit fabric degradation from ionospheric atomic oxygen is of importance in reevaluating suit lifetime and inspection procedures. The mass loss and visible physical changes of each test sample was determined. Kapton control samples and data from previous asher and flight tests were used to scale the results to reflect ionospheric conditions at about 220 km altitude. It is predicted that the orthofabric loses mass in the ionosphere at a rate of about 66% of the original orthofabric mass/yr. The outer layer of the two-layer orthofabric test samples shows few easily visible signs of degradation, even when observed at 440X. It is concluded that the orthofabric could suffer significant loss of performance after much less than a year of total exposure time, while the degradation might be undetectable in post flight visual examinations of space suits. E.A.K.

N86-13900*# National Aeronautics and Space Administration. Ames Research Center, Moffett Field, Calif.

HUMAN FACTORS IN SPACE STATION ARCHITECTURE 1: SPACE STATION PROGRAM IMPLICATIONS FOR HUMAN FACTORS RESEARCH

Marc M. Cohen Oct. 1985 13 p refs
(NASA-TM-86702; Rept-85167; NAS 1.15:86702) Avail: NTIS HC A02/MF A01 CSCL 05H

The space station program is based on a set of premises on mission requirements and the operational capabilities of the space shuttle. These premises will influence the human behavioral factors and conditions on board the space station. These include: launch in the STS Orbiter payload bay, orbital characteristics, power supply, microgravity environment, autonomy from the ground, crew make-up and organization, distributed command control, safety, and logistics resupply. The most immediate design impacts of these premises will be upon the architectural organization and internal environment of the space station. E.A.K.

N86-13901# Air Force Inst. of Tech., Wright-Patterson AFB, Ohio.

INFORMATION REQUIREMENTS DETERMINATION: AN EMPIRICAL INVESTIGATION OF OBSTACLES WITHIN AN INDIVIDUAL Ph.D. Thesis

J. R. Valusek 1985 201 p
(AD-A158025; AFIT/CI/NR-85-73D) Avail: NTIS HC A10/MF A01 CSCL 05/8

This research has suggested that the requirements process be divided into two phases: IRD and IRA. There appears to be sufficient evidence to warrant additional investigation of the IRD phase using the model of inconsistency portrayed in this effort. Inconsistency appears to be a matter of perspective. From an analyst's point of view, the variation in users' needs constitutes inconsistency. From a user's point of view, the variation may be a fact of life resulting from perceptions of need that arise from a dynamic environment. This research is an initial attempt to document the requirements process from a user's perspective and to provide the user some external assistance to attempt to reduce the variation in perceptions of needs. It may be that the perceptions of needs always constitute a requirement from the individual's perspective and that the sorting of requirements from wishes must remain the responsibility of the referee. Perhaps tools oriented to both those roles: That of the user and that of the referee, are necessary. The requirements formulation scratchpad (RFS), as a prototype tool to help the user in the problem formulation phase of information requirements determination, was too complex for the research environment of this study. Based on suggestions from this initial investigation, the second generation of the RFS will be much simpler in design. GRA

N86-13902# Royal Netherlands Aircraft Factories Fokker, Schiphol-Oost. Space Div.
STUDY ON DESIGN TECHNIQUES FOR ROBOTS (SPACE APPLICATIONS). VOLUME 1, PART A: TECHNICAL RESULTS Final Report
Robbert J. Hamann, comp. and Wim vanLeeuwen, comp. Paris ESA Feb. 1985 138 p 4 Vol.
(Contract ESA-5718/83/NL-AN(SC))
(FOK-TR-R-84-110-Vol-1-Pt-A; ESA-CR(P)-2048-Vol-1) Avail: NTIS HC A07/MF A01

A space manipulator system is defined, and the kinematics and dynamics of the system are outlined. A system with seven degrees of freedom, rotating joints, electrical actuation, a toroidal work area, and planar/rotational maneuvering is advocated. Its basic application is servicing and maintenance of low Earth orbit platforms for materials processing. The fully extended arm must be able to move a 750 kg payload at 0.02 m/sec. A dedicated programming system must be defined for collision and obstacle avoidance. Author (ESA)

N86-13903# Royal Netherlands Aircraft Factories Fokker, Schiphol-Oost. Space Div.
STUDY ON DESIGN TECHNIQUES FOR ROBOTS (SPACE APPLICATIONS). VOLUME 1, PART B: TECHNICAL RESULTS Final Report
Robbert J. Hamann, comp. and Wim vanLeeuwen, comp. Paris ESA Feb. 1985 247 p refs 4 Vol.
(Contract ESA-5718/83/NL-AN(SC))
(FOK-TR-R-84-110-Vol-1-Pt-B; ESA-CR(P)-2048-Vol-2) Avail: NTIS HC A11/MF A01

Control aspects of robots for maintenance and servicing of low Earth orbit materials processing platforms were studied. Electrical architecture and software organization were analyzed. Work required to develop the robot was identified. Active force feedback control is advocated. Author (ESA)

N86-13904# Royal Netherlands Aircraft Factories Fokker, Schiphol-Oost. Space Div.
STUDY ON DESIGN TECHNIQUES FOR ROBOTS (SPACE APPLICATIONS). VOLUME 2: TECHNICAL APPENDICES Final Report
Robbert J. Hamann, comp. and Wim vanLeeuwen, comp. Paris ESA Feb. 1985 121 p 4 Vol.
(Contract ESA-5718/83/NL-AN(SC))
(FOK-TR-R-84-110-Vol-2; ESA-CR(P)-2048-Vol-3) Avail: NTIS HC A06/MF A01

Forward and inverse kinematics of a robot manipulator system for maintenance and servicing of space platforms; software availability; robot languages; control models and plots; coupling and decoupling; and modeling errors are summarized. Author (ESA)

N86-13905# Royal Netherlands Aircraft Factories Fokker, Schiphol-Oost. Space Div.
STUDY ON DESIGN TECHNIQUES FOR ROBOTS (SPACE APPLICATIONS). VOLUME 3: EXECUTIVE SUMMARY Final Report
Robbert J. Hamann, comp. and Wim vanLeeuwen, comp. Paris ESA Feb. 1985 44 p ref 4 Vol.
(Contract ESA-5718/83/NL-AN(SC))
(FOK-TR-R-84-110-Vol-3; ESA-CR(P)-2048-Vol-4) Avail: NTIS HC A03/MF A01

A space manipulator system is defined, and the kinematics and dynamics of the system are outlined. A system with seven degrees of freedom, rotating joints, electrical actuation, a toroidal work area, and planar/rotational maneuvering is advocated. Its basic application is servicing and maintenance of low Earth Orbit platforms for materials processing. The fully extended arm must be able to move a 750 kg payload at 0.02 m/sec. A dedicated programming system must be defined for collision and obstacle avoidance. Control aspects; electrical architecture; and software organization were analyzed. Work required to develop the robot was identified. Active force feedback control is advocated. Author (ESA)

N86-13906# Purdue Univ., West Lafayette, Ind.
ALERTED MONITORS: HUMAN OPERATORS AIDED BY AUTOMATED DETECTORS Final Report
R. D. Sorkin and D. E. Robinson Dec. 1984 55 p
(Contract DTRS56-83-C-00047)
(PB85-222750; DOT/OST/P34-85/021) Avail: NTIS HC A04/MF A01 CSCL 05H

In an alerted monitor system, an automated detector assists a human operator in the detection and diagnosis of problems occurring in some monitored process. Air traffic control centers and the flight decks of commercial aircraft include many examples of such systems. This project developed a general model of the altered-monitor system and evaluated the effects on system performance of interactions between the human operator and automated detector. One of the types of interaction evaluated (contingent criterion strategy) yields optimal performance from the combined person-machine system. Two laboratory experiments were performed to evaluate the assumptions of the model and the interactions between the operator and automated components. GRA

N86-14091*# Missouri Univ., Columbia. Dept. of Chemical Engineering.
SOLID WASTE TREATMENT PROCESSES FOR SPACE STATION Final Report
Thomas R. Marrero *In* NASA. Johnson (Lyndon B.) Space Center The 1983 NASA/ASEE Summer Faculty Fellowship Research Program Research Reports Sep. 1983 55 p refs (For primary document see N86-14078 04-85)
Avail: NTIS HC A18/MF A01 CSCL 06K

N86-14160# Joint Publications Research Service, Arlington, Va.
BIOLOGICAL LIFE-SUPPORT SYSTEMS FOR LONG-DURATION SPACE FLIGHTS
I. Andreyev and Yevgeniy Yakovlevich Shepelev *In its* USSR Rept.: Space (JPRS-USP-85-005) 30 Sep. 1985 p 71-74 Transl. into ENGLISH from Izv. (Moscow), 11 Feb. 1985 p 3 (For primary document see N86-14111 04-88)
Avail: NTIS HC A08

N86-14161# Joint Publications Research Service, Arlington, Va.
ARCHITECT DISCUSSES SPACE HABITAT DESIGNS
S. Zigunenko *In its* USSR Rept.: Space (JPRS-USP-85-005) 30 Sep. 1985 p 75-77 Transl. into ENGLISH from Pravda (Moscow), 4 Dec. 1984 p 3 (For primary document see N86-14111 04-88)
Avail: NTIS HC A08

55 PLANETARY BIOLOGY

Includes exobiology; and extraterrestrial life.

No abstracts in this category.

59 MATHEMATICAL AND COMPUTER SCIENCES (GENERAL)

No abstracts in this category.

60 COMPUTER OPERATIONS AND HARDWARE

Includes computer graphics and data processing.

For components see *33 Electronics and Electrical Engineering.*

N86-13907*# Space Telescope Science Inst., Baltimore, Md.
A REPORT ON THE ST ScI OPTICAL DISK WORKSTATION
6 Nov. 1985 12 p
(Contract NASw-3783)
(NASA-CR-176369; NAS 1.26:176369) Avail: NTIS HC A02/MF A01 CSCL 09B

The STScI optical disk project was designed to explore the options, opportunities and problems presented by the optical disk technology, and to see if optical disks are a viable, and inexpensive, means of storing the large amount of data which are found in astronomical digital imagery. A separate workstation was purchased on which the development can be done and serves as an astronomical image processing computer, incorporating the optical disks into the solution of standard image processing tasks. It is indicated that small workstations can be powerful tools for image processing, and that astronomical image processing may be more conveniently and cost-effectively performed on microcomputers than on the mainframe and super-minicomputers. The optical disks provide unique capabilities in data storage. E.A.K.

N86-13908# Royal Signals and Radar Establishment, Malvern (England).
SAFE CONTROL SYSTEMS AND THE VIPER MICROPROCESSOR
J. Kershaw Mar. 1985 21 p
(AD-A156617; RSRE-MEMO-3805; DRIC-BR-96082) Avail: NTIS HC A02/MF A01 CSCL 09/2

Most accidents are caused by human error. Computer control systems in aircraft, chemical plant, nuclear reactors and so on could in principle prevent many accidents, but in practice they are not reliable enough to be put in charge of human lives. This Memorandum describes some of the developments in computer hardware and software which are needed before this situation can change, and introduces the VIPER microprocessor which has been designed specifically for ultra-reliable systems. Author (GRA)

N86-13909# Michigan Univ., Ann Arbor. Supercomputer Algorithm Research Lab.
SPARSE ELIMINATION ON VECTOR MULTIPROCESSORS Interim Report, 1 Nov. 1984 - 1 Apr. 1985
D. A. Calahan 16 Apr. 1985 7 p
(Grant AF-AFOSR-0096-84)
(AD-A158274; AFOSR-85-0542TR) Avail: NTIS HC A02/MF A01 CSCL 09/2

Studies of microtasking with up to 16 CRAY X-MP processors for LU decomposition of dense systems of equations have given rise to hybrid algorithms. One issue addressed has been the problem of memory bank conflicts, which increases with the number of processors. Conflict resistant algorithms have been developed. It is possible to assembly-code the X-MP so that accesses are pre-fetched into vector registers. Several reports have been prepared recently under this effort, and a paper entitled Task Granularity Studies in a Many-Processor Cray X-MP has been accepted for publication in Parallel Computing. GRA

N86-13910# Maryland Univ., College Park. Center for Automation Research.
TARGET TRACKING BASED SCENE ANALYSIS
N. Kazor Aug. 1984 57 p
(Contract DAAK70-83-K-0018; DARPA Order 3206)
(AD-A158629; CAR-TR-88; CS-TR-1437) Avail: NTIS HC A04/MF A01 CSCL 09/4

Target Tracking and Scene Analysis are two research areas in Computer Vision which, in the past, have been dealt with as separate problems. Most target tracking systems have the relatively modest goal of detecting and identifying moving objects and tracking them, using prediction and correlation techniques, as long as they move unobscured across the field of view. Most of these systems have been developed with a set of stringent real time constraints which, given current hardware technology, constrains them to employ a set of computationally simple algorithms. Most scene analysis/segmentation systems analyze a given scene based on the static properties of objects such as shape/structure and texture, where the class of objects are generally predefined. These systems tend to be slow whenever the scene is complex, containing many objects. There are advantages to combining the two problems into one. This paper is based on such and idea is concerned with the design of an Intelligent Target Tracking System (ITTS). This experimental system tracks targets based not only on models for targets (shape, motion, etc.), but also on models of the environment through which the targets navigate and of the sensing system(s) employed to acquire the time-varying images on which the analysis is based. The ITTS is composed of a number of processes which can be divided into three processing stages: target recognition, segmentation of time-varying images, and scene model generation. GRA

N86-13911# MacDonald, Dettwiler and Associates Ltd., Richmond (British Columbia). Data Handling and Signal Processing Div.
THE CONSTRUCTION AND TESTING OF A REAL-TIME DIGITAL BREADBOARD PROCESSOR FOR THE ESA REMOTE SENSING SATELLITE SYNTHETIC APERATURE RADAR Final Report
R. W. Okkes and J. C. Degrave Paris ESA Dec. 1984 113 p
(Contract ESA-4739/81/NL-HP)
(Rept-00-0778; ESA-CR(P)-2047) Avail: NTIS HC A06/MF A01

A laboratory model, high-speed, Synthetic Aperture Radar (SAR) breadboard processor was developed to prove the feasibility of real-time processing of C-Band satellite SAR data. A Programmable Signal Processing Element (PSPE) was designed, utilizing vector level data driven control. Two PSPEs in parallel achieve a computation rate of > 100 million operations/sec. A parameter control structure was developed using a distributed hierarchical architecture based on a network of commercial microcomputers. The hierarchical structure allows processing parameters to be computed in real time, and passed to the PSPEs in linked lists so that the signal processing operations are not impeded by control calculations. Speed tests demonstrate that the breadboard can process ERS-1 data in real time, and image quality tests show that the fidelity of the processor is very close to that obtained with low-speed, precision, software processors. Author (ESA)

61 COMPUTER PROGRAMMING AND SOFTWARE

Includes computer programs, routines, and algorithms.

N86-13912# Argonne National Lab., Ill. Mathematics and Computer Science Div.
GRAPH THEORETIC APPROACHES TO DIAGNOSTICS: APPLICATIONS OF LOGIC PROGRAMMING AND CUTSET THEORY TO ASPECTS OF REACTOR AND CIRCUIT ANALYSIS
S. M. Ehrlich, J. R. Gabriel, A. Gonen, and L. Kuchnir Jan. 1985 42 p refs
(Contract W-31-109-eng-38)
(ANL-84-74) Avail: NTIS HC A03/MF A01

Logic programming approaches are described to two graph theoretical problems relevant to reactor and logic circuit analysis: those of cutset verification and subsystem detection. In a graph representation of a system involving components and their interconnections, sets of arcs that divide the graph into two disconnected subgraphs are termed cutsets. Two Prolog programs were developed. The first verifies that a given cutset is, indeed, a cutset (i.e., that there are no sneak paths between the two subgraphs maintaining connectivity). The second detects possible subsystems of a device, thus simplifying the task of fault diagnosis. Author

N86-13913*# Informatics General Corp., Palo Alto, Calif.
CROSSREF FOR THE CRAY
Clayton J. Guest Nov. 1985 77 p
(Contract NAS2-11555)
(NASA-CR-177384; NAS 1.26:177384; TN-84-7104-101-12) Avail: NTIS HC A05/MF A01 CSCL 09B

Crossref for the Cray is a tool used to obtain information about the contents of a library generated with a BUILD statement under COS. It produces a list of all modules in the library; a summary table by modules containing module size, ENTRY POINTS, referenced COMMONs, and required EXTERNALs; a list of unsatisfied EXTERNALs; a summary table of ENTRY POINTS and optionally EXTERNALs; a list of COMMONs; a table of statistics and a table of contents. The output can be formatted to 8 1/2 inch vertical paper or CRT display. Author

N86-13914# Toronto Univ. (Ontario). Inst. for Aerospace Studies.
THE SIMULATION OF TRUCK MOTIONS
L. D. Reid and M. A. Nahon Sep. 1985 117 p refs Sponsored in part by Ontario Ministry of Transportation and Communications
(UTIAS-294; ISSN-0082-5255) Avail: NTIS HC A06/MF A01

A study was carried out to evaluate the ability of a simulator facility to represent the motion environment experienced by a truck driver while performing typical driving maneuvers. Software was developed to command simulator motions in response to a truck model computer program. Measurements of translational acceleration and rotational velocity generated by the simulator's motion drive system were obtained. The predicted driver motion sensations in the truck and in the simulator were generated by a vestibular model and were compared with favorable results. Author

N86-13915*# National Aeronautics and Space Administration. Langley Research Center, Hampton, Va. Dept. of Electrical and Computer Engineering.
PARALLEL COMPUTATION WITH THE FORCE Final Report
Harry F. Jordan (Colorado Univ.) Oct. 1985 14 p refs Submitted for publication
(Contract NAS1-17070; Grant AF-AFOSR-1089-85)
(NASA-CR-177999; ICASE-85-45; NAS 1.26:177999) Avail: NTIS HC A02/MF A01 CSCL 09B

A methodology, called the force, supports the construction of programs to be executed in parallel by a force of processes. The number of processes in the force is unspecified, but potentially very large. The force idea is embodied in a set of macros which produce multiproceossor FORTRAN code and has been studied on two shared memory multiprocessors of fairly different character. The method has simplified the writing of highly parallel programs within a limited class of parallel algorithms and is being extended to cover a broader class. The individual parallel constructs which comprise the force methodology are discussed. Of central concern are their semantics, implementation on different architectures and performance implications. Author

N86-13916*# National Aeronautics and Space Administration. Ames Research Center, Moffett Field, Calif.
EXPERIENCES WITH CRAY MULTI-TASKING
E. N. Miya Nov. 1985 25 p refs
(NASA-TM-88200; A-85424; NAS 1.15:88200) Avail: NTIS HC A02/MF A01 CSCL 09B

The issues involved in modifying an existing code for multitasking is explored. They include Cray extensions to FORTRAN, an examination of the application code under study, designing workable modifications, specific code modifications to the VAX and Cray versions, performance, and efficiency results. The finished product is a faster, fully synchronous, parallel version of the original program. A production program is partitioned by hand to run on two CPUs. Loop splitting multitasks three key subroutines. Simply dividing subroutine data and control structure down the middle of a subroutine is not safe. Simple division produces results that are inconsistent with uniprocessor runs. The safest way to partition the code is to transfer one block of loops at a time and check the results of each on a test case. Other issues include debugging and performance. Task startup and maintenance (e.g., synchronization) are potentially expensive. Author

N86-13917*# Vought Corp., Dallas, Tex.
COMPUTER PROGRAM FOR PREDICTION OF FUEL CONSUMPTION STATISTICAL DATA FOR AN UPPER STAGE THREE-AXES STABILIZED ON-OFF CONTROL SYSTEM
Nov. 1982 126 p refs
(Contract NAS1-15000)
(NASA-CR-166031; NAS 1.26:166031) Avail: NTIS HC A07/MF A01 CSCL 09B

A FORTRAN coded computer program and method to predict the reaction control fuel consumption statistics for a three axis stabilized rocket vehicle upper stage is described. A Monte Carlo approach is used which is more efficient by using closed form estimates of impulses. The effects of rocket motor thrust misalignment, static unbalance, aerodynamic disturbances, and deviations in trajectory, mass properties and control system characteristics are included. This routine can be applied to many types of on-off reaction controlled vehicles. The pseudorandom number generation and statistical analyses subroutines including the output histograms can be used for other Monte Carlo analyses problems. E.A.K.

N86-13918*# Vought Corp., Dallas, Tex.
COMPUTER PROGRAM FOR POST-FLIGHT ANALYSIS OF RIGID BODY MOMENTS ACTING ON A LAUNCH VEHICLE FIRST STAGE
R. N. Knauber Nov. 1982 177 p refs
(Contract NAS1-15000)
(NASA-CR-166033; NAS 1.26:166033) Avail: NTIS HC A09/MF A01 CSCL 09B

A FORTRAN coded computer program and method for evaluation of the rigid body disturbing moments for a launch vehicle first stage based on post-flight measurements is described. The technique is a straightforward deterministic approach. Residual moments are computed to satisfy the equations of motion. Residuals are expressed in terms of altered vehicle characteristics; the aerodynamic coefficients, thrust misalignment, and control effectiveness. This method was used on the Scout launch vehicle and uncovered several significant differences between flight data and wind tunnel data. The computer program is written in FORTRAN IV for a CDC CYBER 173 computer system. E.A.K.

N86-13919*# Vought Corp., Dallas, Tex.
SCOUT TRAJECTORY ERROR PROPAGATION COMPUTER PROGRAM
T. R. Myler Nov. 1982 78 p refs
(Contract NAS1-15000)
(NASA-CR-166030; NAS 1.26:166030; Rept-2-53030/1R-52776) Avail: NTIS HC A05/MF A01 CSCL 09B

Since 1969, flight experience has been used as the basis for predicting Scout orbital accuracy. The data used for calculating the accuracy consists of errors in the trajectory parameters (altitude, velocity, etc.) at stage burnout as observed on Scout flights. Approximately 50 sets of errors are used in Monte Carlo analysis to generate error statistics in the trajectory parameters. A covariance matrix is formed which may be propagated in time. The mechanization of this process resulted in computer program Scout Trajectory Error Propagation (STEP) and is described herein. Computer program STEP may be used in conjunction with the Statistical Orbital Analysis Routine to generate accuracy in the orbit parameters (apogee, perigee, inclination, etc.) based upon flight experience. Author

N86-13920*# Vought Corp., Dallas, Tex.
COMPUTER PROGRAM FOR POST-FLIGHT EVALUATION OF THE CONTROL SURFACE RESPONSE FOR AN ATTITUDE CONTROLLED MISSILE
R. N. Knauber Nov. 1982 69 p
(Contract NAS1-15000)

(NASA-CR-166032; NAS 1.26:166032) Avail: NTIS HC A04/MF A01 CSCL 09B

A FORTRAN IV coded computer program is presented for post-flight analysis of a missile's control surface response. It includes preprocessing of digitized telemetry data for time lags, biases, non-linear calibration changes and filtering. Measurements include autopilot attitude rate and displacement gyro output and four control surface deflections. Simple first order lags are assumed for the pitch, yaw and roll axes of control. Each actuator is also assumed to be represented by a first order lag. Mixing of pitch, yaw and roll commands to four control surfaces is assumed. A pseudo-inverse technique is used to obtain the pitch, yaw and roll components from the four measured deflections. This program has been used for over 10 years on the NASA/SCOUT launch vehicle for post-flight analysis and was helpful in detecting incipient actuator stall due to excessive hinge moments. The program is currently set up for a CDC CYBER 175 computer system. It requires 34K words of memory and contains 675 cards. A sample problem presented herein including the optional plotting requires eleven (11) seconds of central processor time. Author

N86-13921*# Vought Corp., Dallas, Tex.

COMPUTER PROGRAM FOR POST-FLIGHT EVALUATION OF A LAUNCH VEHICLE UPPER-STAGE ON-OFF REACTION CONTROL SYSTEM

R. N. Knauber Nov. 1982 78 p
(Contract NAS1-15000)
(NASA-CR-166029; NAS 1.26:166029) Avail: NTIS HC A05/MF A01 CSCL 09B

This report describes a FORTRAN IV coded computer program for post-flight evaluation of a launch vehicle upper stage on-off reaction control system. Aerodynamic and thrust misalignment disturbances are computed as well as the total disturbing moments in pitch, yaw, and roll. Effective thrust misalignment angle time histories of the rocket booster motor are calculated. Disturbing moments are integrated and used to estimate the required control system total impulse. Effective control system specific inpulse is computed for the boost and coast phases using measured control fuel useage. This method has been used for more than fifteen years for analyzing the NASA Scout launch vehicle second and third-stage reaction control system performance. The computer program is set up in FORTRAN IV for a CDC CYBER 175 system. With slight modification it can be used on other machines having a FORTRAN compiler. The program has optional CALCOMP plotting output. With this option the program requires 19K words of memory and has 786 cards. Running time on a CDC CYBER 175 system is less than three (3) seconds for a typical problem. Author

N86-13922*# Stanford Univ., Calif. Computer Systems Lab.

DEVELOPMENT OF A FLIGHT SOFTWARE TESTING METHODOLOGY Final Report

Edward J. McCluskey and Dorothy M. Andrews Sep. 1985 29 p refs
(Grant NAG2-246)
(NASA-CR-176391; NAS 1.26:176391) Avail: NTIS HC A03/MF A01 CSCL 09B

The research to develop a testing methodology for flight software is described. An experiment was conducted in using assertions to dynamically test digital flight control software. The experiment showed that 87% of typical errors introduced into the program would be detected by assertions. Detailed analysis of the test data showed that the number of assertions needed to detect those errors could be reduced to a minimal set. The analysis also revealed that the most effective assertions tested program parameters that provided greater indirect (collateral) testing of other parameters. In addition, a prototype watchdog task system was built to evaluate the effectiveness of executing assertions in parallel by using the multitasking features of Ada. Author

N86-13923*# Lockheed Missiles and Space Co., Huntsville, Ala. Computational Mechanics Section.

HIGH-ALTITUDE PLUME COMPUTER CODE DEVELOPMENT Final Report

Beverly J. Audeh and Jesse E. Murphy 1 Jul. 1965 28 p refs
(Contract NAS8-34970)
(NASA-CR-171600; NAS 1.26:171600; LMSC-HEC-TR-F042501)
Avail: NTIS HC A03/MF A01 CSCL 09B

The flowfield codes that have been developed to predict rocket motor plumes at high altitude were used to predict plume properties for the RCS motor which show reasonable agreement with experimental data. A systematic technique was established for the calculation of high altitude plumes. The communication of data between the computer codes was standardized. It is recommended that these outlined procedures be more completed, documented and updated as the plume methodology is applied to the varied problems of plume flow and plume impingement encountered by space station design and operation. Author

N86-13924# Naval Surface Weapons Center, Silver Spring, Md.

BOSS: A FORTRAN CODE FOR A RELATIONAL DATABASE MANAGER Final Report

E. Winston 1 May 1985 95 p
(AD-A157067; NSWC/TR-85-56) Avail: NTIS HC A05/MF A01 CSCL 09/2

The report contains documentation for a FORTRAN implementation of a relational database manager. Because the code is written in a high-level language, it is basically transportable to any computer with FORTRAN capability (minor modification may be required for compatibility with a host computer's operating system and compiler). The work was required by U31 to support computer studies requiring the extensive use of minefield planning codes. Author

N86-13925# Department of the Army, Washington, D. C.

ROUTING METHOD IN COMPUTER AIDED CUSTOMIZATION OF A TWO LEVEL AUTOMATED UNIVERSAL ARRAY Patent Application

D. C. Smith and R. Noto, inventors (to Army) 2 Jul. 1985 56 p
(AD-D011808; US-Patent-Appl-SN-751339) Avail: NTIS HC A04/MF A01 CSCL 09/5

This patent application pertains to a routing method implemented in the stored programs of a digital computer which is programmably operated to generate the wire interconnect masks for a two level metallization automated universal array having undefined roadbeds between rows of cells comprised of identical semiconductor device basic units which are further interconnected to provide a particular integrated circuit structure. Conductor routing is provided by a computer aided design system that, among other things, carries out a route analysis process which determines in which roadbed each wire should be tentatively routed in conjunction with generating a routing density profile for minimizing congestion for a particular circuit design, when the roadbed density is exceeded, certain wires are removed under a set of criteria for routing by a pathfinder routing process. Following route analysis, detailed routing and rerouting is performed sequentially by a direct routing process, a greedy channel routing process, and a pathfinder routing process with rerouting being performed after each channel router and pathfinding process. Furthermore, the greedy channel routing process makes a single pass from left to right in all wires which cross successive points simultaneously and, if necessary, deleting a wire or wires which are then rerouted by the pathfinding process. GRA

N86-13926# Cornell Univ., Ithaca, N.Y. Dept. of Computer Science.

REPLICATION AND FAULT-TOLERANCE IN THE ISIS SYSTEM

K. P. Birman Mar. 1985 22 p
(Contract MDA903-85-C-0124; ARPA Order 5378)
(AD-A157775; TR-85-668) Avail: NTIS HC A02/MF A01 CSCL 09/2

The ISIS project seeks to automate the transformation of fault-intolerant program specifications into fault-tolerant implementations. The ISIS system transforms abstract type specifications into fault-tolerant implementations, while insulating both programmers and users from the mechanisms used to achieve fault-tolerance. This paper discusses techniques for fault-tolerant implementation of a specification, methods for achieving improved performance using highly concurrent implementations, and constraints that these place on the ISIS architecture. The performance of an initial version of ISIS is then reviewed. GRA

N86-13927# Advanced Engineering Lab., Adelaide (Australia).
METCUT: A COMPUTER AIDED SYSTEM FOR MACHINING TECHNOLOGY
L. H. S. Luong and R. W. Aitchison Apr. 1985 28 p
(AD-A157941; AEL-0244-TR) Avail: NTIS HC A03/MF A01 CSCL 09/2

This report describes a package of computer programs which has been developed for providing appropriate cutting data for a number of machining applications. The whole package was written in BASIC and can be run on PDP 11 computers running under RSTS operating systems. At present the package can provide cutting data for 9 operations, namely turning, face milling, end milling peripheral, end milling slotting, drilling, tapping, boring, part off and form tools and threading. Operations can be added or deleted from the package as desired. This package is also linked to TKDRAW which is an AEL developed CAD/CAM package for turned components. The package has also been implemented on a DATA GENERAL MV4000 computer, running under a AOS/VS operating system, at the Regency Park Community College. The recommended cutting conditions for the various operations, based on the Machining Data Handbook, represent a tool life of approximately one to two hours of cutting time for most of the common alloys when using high speed steel tools. A tool life of 30 to 60 minutes is applicable for indexable-insert carbide tools. GRA

N86-13928# Electronics Research Lab., Adelaide (Australia).
DIESS: A PROLOG IMPLEMENTATION OF A DOMAIN-INDEPENDENT EXPERT SYSTEM SHELL
R. F. Dancer May 1985 40 p
(AD-A158014; ERL-0330-TR) Avail: NTIS HC A03/MF A01 CSCL 09/2

A software environment suitable for the expression of expert knowledge in a variety of domains has been designed and implemented in the Prolog computer language. This shell is intended to be capable of containing expert systems whose object is the proof of goal symbols in domains of categorical single-valued facts. An example is given of a non-trivial expert system to programme in the IBM Job Control Language. Some conclusions are reached and recommendation given for future developments. GRA

N86-13929# Air Force Inst. of Tech., Wright-Patterson AFB, Ohio.
A REACTIVE LEARNING ENVIRONMENT FOR THE EQUIPMENT PROBLEM SOLVING TECHNIQUES (EPST) SYSTEM M.S. Thesis
D. G. McKenney Aug. 1985 73 p
(AD-A158035; AFIT/CI/NR-85-68T) Avail: NTIS HC A04/MF A01 CSCL 05/9

This thesis describes a user-friendly program that allows students to troubleshoot equipment in a reactive learning environment. The system allows students to develop problem solving strategies while troubleshooting faulty equipment through the use of video scenes with graphic overlays. The student interface contains instructional strategies which access information stored in a database consisting of semantic networks and frames. Student troubleshooting involves moving within equipment, changing device settings, setting up test equipment, and obtaining equipment readings. Important features of the student interface include the simulation of devices based on first order effects, the use of production rules to describe device state transitions, and the use of an emulation algorithm to ripple out device state changes. The student interface also allows users to follow wire connections, set up test equipment, record hypotheses, and get on-line help. The student interface is general in nature. The content of the database can be changed to represent any type of equipment, but the student interface does not have to be redeveloped or modified for the new database. GRA

N86-13930# Defence Research Establishment Atlantic, Dartmouth (Nova Scotia).
A NEW LIBRARY OF SUBROUTINES FOR CALCULATING SMOOTHING SPLINES
D. Hally Jun. 1985 74 p
(AD-A158049; DREA-TM-85/205) Avail: NTIS HC A04/MF A01 CSCL 09/2

Defense Research Establishment Atlantic has, at present, two libraries containing subroutines for calculating splines: IMSL and BSPLIN. A new library has been developed to supplement the IMSL and BSPLIN routines in the realm of smoothing splines. It is not self-contained, making frequent use of subroutines from the BSPLIN library. The new subroutines offer several advantages over the smoothing spline subroutines in the IMSL and BSPLIN libraries: (1) the order of the spline may be picked by the user; (2) the second derivative of the spline is not constrainted to be zero at its end-points; (3) the user of the new subroutines has freedom to choose the number and positions of the knots of the spline; and (4) the new subroutines have, as input, an extra set of weights, delta sub i, i= 1,N, which control the stiffness of the spline between each pair of knots. The new subroutines were initially developed for use in ship hull approximation for the calculation of boundary layer growth on the hull. For this calculation one needs splines whose second derivatives are very well behaved. The additional control afforded by the new subroutines makes them far more suitable for this application than any of the subroutines makes them far more for this application than any of the subroutines currently available in either the IMSL or BSPLIN libraries. GRA

N86-13931# Air Force Inst. of Tech., Wright-Patterson AFB, Ohio.
AN ALGORITHM TO TRANSLATE RELATIONAL ALGEBRA QUERIES INTO QUEL M.S. Thesis
D. F. Blumenthal May 1985 82 p
(AD-A158169; AFIT/CI/NR-85-57T) Avail: NTIS HC A05/MF A01 CSCL 09/2

The work presented in this thesis deals with the development of an algorithm required to translate queries from IMDAS' (Integrated Manufacturing Data Administration System) intermediate representation, relational algebra, into QUEL, the query language of the INGRES subsystem. The algorithm for translating relational algebra query trees into QUEL is used to process queries in a distributed, heterogeneous data base management system used to support computer integrated manufacturing. A node-by-node translation algorithm, as well as an optimal algorithm which uses minimization techniques is presented. A general discussion about implementation is also included. GRA

N86-13932# Colorado School of Mines, Golden. Center for Wave Phenomena.
PRE-STACK KIRCHHOFF INVERSION OF COMMON OFFSET DATA
M. F. Sullivan and J. K. Cohen 4 Jun. 1985 58 p
(Contract N00014-84-K-0049)
(AD-A158205; CWP-027) Avail: NTIS HC A04/MF A01 CSCL 09/2

A pre-stack inversion algorithm is developed for acoustic Kirchhoff, high frequency, common offset data. Given the velocity above a reflector, the interface is located and an angularly-dependent reflection coefficient is computed at each reflection point. A quick post-processing step then calculates the velocity of the lower medium. Lateral velocity variations in the second layer are naturally recovered since each reflection point provides an independent measure of the reflection coefficient. The inversion is performed as a mapping where the response to subsurface test points is examined by an integration over the data. If a test point is on the reflector, the reflection coefficient is returned. Inversion and migration operators both utilize an integral over the data, with each trace in the summation weighted by an amplitude and a phase term. The Kirchhoff offset inversion is first formulated for data acquired over a plane, producing a 3-D reflectivity map.

Since data are commonly collected along a single line, a 2.5-D specialization is also developed. A method for determining the velocity of the lower medium from an angularly-dependent reflection coefficient is then detailed for the 2. GRA

N86-13933# Massachusetts Inst. of Tech., Cambridge. Artificial Intelligence Lab.
ON THE COMPLEXITY OF ID/LP PARSING
G. E. Barton, Jr. Dec. 1984 25 p
(Contract N00014-80-C-0505)
(AD-A158211; AI-M-812) Avail: NTIS HC A02/MF A01 CSCL 09/2

Recent linguistic theories cast surface complexity as the result of interacting subsystems of constraints. For instance, the ID/LP grammar formalism separates constraints on immediate dominance from those on linear order, Shieber (1983) has shown how to carry our direct parsing of ID/LP grammars. His algorithm uses ID and LP constraints directly in language processing, without expanding them into a context-free object grammar. This report examines the computational difficulty of ID/LP parsing; the worst-case runtime of his algorithm is exponential in grammar size. A reduction of the vortex-cover problem proves that ID/LP parsing is NP-complete. The growth of internal data structures is the source of difficulty in Shieber's algorithm. The computational and linguistic implications of these results are discussed. Despite the potential for combinatorial explosion, Shieber's algorithm remains better than the alternative of parsing an expanded object grammar. GRA

N86-13934# Stanford Univ., Calif. Systems Optimization Lab.
ON PROJECTED NEWTON BARRIER METHODS FOR LINEAR PROGRAMMING AND AN EQUIVALENCE TO KARMARKAR'S PROJECTIVE METHOD
P. E. Gill, W. Murray, M. A. Saunders, J. A. Tomlin, and M. H. Wright Jul. 1985 27 p
(Contracts N00014-85-K-0343; DAAG29-84-K-0156; DE-AM03-76SF-00326; DE-AT03-76ER-72018; Grants NCF DCR-84-13211; NCF ECS-83-12142)
(AD-A158212; DE85-015096; SU-SOL-85-11; ARO-21592.6-MA) Avail: NTIS HC A03/MF A01 CSCL 12/1

The authors discuss interior-point methods for linear programming derived by applying a logarithmic barrier transformation and performing projected Newton steps for a sequence of barrier parameters. Under certain conditions, one of these projected Newton barrier methods is shown to be equivalent to Karmarkar's (1984) projective method for linear programming. Details are given of a specific barrier algorithm and its practical implementation. Numerical results are given for several nontrivial test problems. Author (GRA)

N86-13935# Carnegie-Mellon Univ., Pittsburgh, Pa. Dept. of Computer Science.
Ada AS A HARDWARE DESCRIPTION LANGUAGE: AN INITIAL REPORT
M. R. Barbacci, S. Grout, G. Lindstrom, M. Maloney, and E. Organick 8 Dec. 1984 36 p
(Contract F33615-81-K-1539; DARPA Order 4305)
(AD-A158217; CMU-CS-85-104) Avail: NTIS HC A03/MF A01 CSCL 09/3

This paper reports on our initial results in using Ada as a Hardware Description Language. Ada provides abstraction mechanisms to support the development of large software systems. Separate compilation as well as nesting of packages, tasks, and subprograms allow the construction of modular systems communicating through well defined interfaces. The complexity of modern chips (e.g., those proposed in the VHSIC program) will require the use of those features that make Ada a good language for programming-in-the-large. The key to our approach is establishing a writing style appropriate to the objective of describing both the behavior and the structure of hardware components. We model a hardware system as an ensemble of typed objects, where each object is an instance of an abstract data type. The type definition and the associated operations are encapsulated by a corresponding package. In this paper we illustrate our approach through a series of examples, building up a hypothetical hierarchy of hardware components. We conclude by discussing ways to describe arbitrarily complex simulation models and synthesis styles. GRA

N86-13936# Air Force Wright Aeronautical Labs., Wright-Patterson AFB, Ohio.
ISSUES TO BE CONSIDERED IN THE EVALUATION OF TECHNICAL PROPOSALS FROM THE Ada (TRADEMARK) LANGUAGE PERSPECTIVE Final Technical Report
V. L. Castor 10 Jun. 1985 26 p
(AD-A158376; AFWAL-TR-85-1100) Avail: NTIS HC A03/MF A01 CSCL 09/2

This report identifies issues for consideration in the assessment of technical proposals that are submitted in response to a Request For Proposal (RFP) which specifies the use of Ada. Detailed questions are provided on the following five main technical proposal elements; (1) methodology; (2) program design language; (3) implementation language; (4) environment; and (5) personnel. Methodology identifies issues associated with the assessment of the methodology which is proposed for accomplishing the software life cycle tasks specified within the RFP Statement of Work. Program design language identifies issues associated with the assessment of the Ada-based PDL which is proposed for accomplishing the software design tasks specified within the RFP Statement of Work. Implementation language identifies issues associated with the assessment of Ada as the implementation language, as well as the associated Ada compiler and run time support environment which are proposed for accomplishing the software development tasks specified within the RFP Statement of Work. Environment identifies issues associated with the assessment of the programming support environment which is proposed for accomplishing all of the tasks specified within the RFP Statement of Work. Personnel identifies issues associated with the assessment of the qualification of personnel proposed for accomplishing all of the tasks specified within the RFP Statement of Work. Primary emphasis is given to the level of expertise and training associated with each individual with regard to methodologies, Ada-based PDLs, Ada programming, and programming support environments. GRA

N86-13937# Massachusetts Inst. of Tech., Cambridge. Artificial Intelligence Lab.
DESCRIBING SURFACES
M. Brady, J. Ponce, A. Yuille, and H. Asada Jan. 1985 35 p
(Contracts N00014-80-C-0505; N00014-77-C-0389)
(AD-A158940; AI-M-822) Avail: NTIS HC A03/MF A01 CSCL 09/4

This paper continues our work on visual representations of three-dimensional surfaces. The theoretical component is a study of classes of surface curves as a source of constraint on the surface on which they lie, and as a basis for describing it. We analyze bounding contours, surface intersections, lines of curvature, and asymptotes. Our experimental work investigates whether the information suggested by our theoretical study can be computed reliably and efficiently. We demonstrate algorithms that compute lines of curvature of a (Gaussian smoothed) surface; determine planar patches and umbilic regions; extract axes of surfaces of revolution and tube surfaces. We report preliminary results on adapting the curvature primal sketch algorithms of Asada and Brady (1984) to detect and describe surface intersections. GRA

N86-13938# Naval Postgraduate School, Monterey, Calif.
DEVELOPMENT AND ENHANCEMENT OF COMPUTER PERFORMANCE MODELING TOOL (CPMT) M.S. Thesis
J. G. Duarte Jun. 1985 118 p
(AD-A159003) Avail: NTIS HC A06/MF A01 CSCL 09/2

The Computer Performance Modeling Tool (CPMT) is a queueing network simulator to be used in support of Computer Performance and Evaluation courses like CS4400. This thesis is a continuation of the CPMT development project and consists of adaptive and perfective maintenance work to modify the existing simulator to add extended modeling capability and to improve the simulator performance. The thesis effort also included rewriting the CPMT user's manual to reflect new features, establishing a change log for the program and continuing validation of the simulator. GRA

N86-13939# Department of the Navy, Washington, D. C.
COMPUTER-AIDED PROCESS FOR GENERATING CAMERA-READY GRAPHICAL ARTWORK Patent Application
M. J. Caddy, inventor (to Navy) Filed 1 Sep. 1983 47 p
(AD-D011884; US-Patent-Appl-SN-528710) Avail: NTIS HC A03/MF A01 CSCL 09/2

A computer-aided process is disclosed for automatically generating a camera-ready hardcopy of a graphical plot upon command instructions imputted via a conventional storage tube graphics display terminal having an addressable cross-hair cursor and a keyboard. In accordance with an interactive graphics code or program, tabular data coordinates stored in computer file form are retrieved and plotted on appropriately titled and scaled axes with the plotted coordinates being interconnected along curves formed of a smooth or linear nature by interpolation. The graphical plot viewed on the display terminal is further enhanced by inclusion of labels, shaded areas, and reference symbols and characters prior to printing out the hardcopy of an associated hardcopy unit coupled to the display terminal. GRA

N86-13940# Lawrence Livermore National Lab., Calif.
INNER/OUTER ITERATIVE METHODS AND NUMERICAL SCHWARZ ALGORITHMS - 2
G. Rodrique and P. Saylor May 1985 41 p Presented at the IBM Conf. on Vector and Parallel Computations for Sci. Computing, Rome, 28 May 1985 Prepared in cooperation with Illinois Univ., Chicago
(Contract W-7405-eng-48)
(DE85-013197; UCRL-92077-2; CONF-8505157-1) Avail: NTIS HC A03/MF A01

Variants of the numerical Schwarz algorithms for solving elliptic partial differential equations on multiprocessing systems are described and analyzed. The methods are described in terms of domain decomposition techniques and mathematically cast into an inner/outer matrix iteration form. It is shown that under certain matrix nonnegativity conditions that the convergence rate of the global iteration is invariant to the amount of overlap of the subdomains when one inner iteration is taken. DOE

N86-13941# Lawrence Livermore National Lab., Calif.
LTSSCLI: AN ITSS SHELL FOR NLTSS, VERSION 2.0, REVISION 1
D. S. Fisher 10 May 1985 74 p
(Contract W-7405-eng-48)
(DE85-013234; UCID-19896-Rev-1) Avail: NTIS HC A04/MF A01

The LTSS Shell provides an environment within the NLTSS system for the execution of ITSS programs. LTSS programs that make system requests through BASELIB can be reloaded with the Shell compatible library. NBASELIB, to make equivalent requests to the LTSS Shell. The Shell provides a terminal view of NLTSS that closely resembles LTSS, and maps the structure of the LTSS filing system onto the NLTSS directory system. DOE

N86-13942# General Electric Co., Whetstone (England). Mechanical Engineering Lab.
INVESTIGATION OF TECHNIQUES FOR IMPROVING SPACECRAFT THERMAL CONTROL SOFTWARE Final Report
P. E. Newley and N. J. Stock Paris ESA Feb. 1985 188 p refs
(Contract ESA-5670/83/NL-PB)
(GEC-MEL42.0552; ESA-CR(P)-2044) Avail: NTIS HC A09/MF A01

Techniques for improving thermal analysis software in the automatic calculation of conductances and the interpolation of node temperatures were investigated. An approach that links conductance calculation and the interpolation scheme was developed. It involves the creation of a fine mesh of nodes for use in calculating conductance, capacitance and radiative exchange. The number of nodes to be analyzed is then reduced by Gaussian elimination. The reduction process defines an interpolation scheme which enables temperatures at nodes on the fine mesh to be calculated, linear interpolation being used at points in between. Author (ESA)

N86-13943# Ressult, Research and Consulting, Soechtenau (West Germany).
AN ALGORITHM FOR SIMULTANEOUS DETERMINATION OF MODAL FREQUENCIES AND MODAL VECTORS OF A DYNAMIC IMPEDANCE MATRIX
Paris ESA 1985 12 p
(Contract ESA-5619/83/NL-PP)
(ESA-CR(P)-2055) Avail: NTIS HC A02/MF A01

An iteration routine was installed in a distributed element package for dynamic analysis of spacecraft structures. The iteration routine determines simultaneously the eigenvalues and related eigenvectors of a dynamic stiffness matrix given in implicit form, i.e., containing poles. Unlike other routines with the same objective, the routine does not need an a priori knowledge of the poles of the matrix and it works also for gyroscopic and/or nonconservative systems. The installed version, however, is specialized to conservative and nongyroscopic systems. The main intention of this installation is to test the routine in a real world environment in order to decide on its use for nonconservative systems. Test runs are satisfactory, except if poles and zeros of the system are very close, when the scaling of the eigenvectors is poor. Author (ESA)

N86-14103*# Mississippi Valley State Univ., Itta Bena.
FORTRAN PLOTTING SUBROUTINES FOR THE SPACE PLASMA LABORATORY Final Report
Raymond Williams *In* NASA. Johnson (Lyndon B.) Space Center The 1983 NASA/ASEE Summer Faculty Fellowship Research Program Research Reports Sep. 1983 8 p (For primary document see N86-14078 04-85)
Avail: NTIS HC A18/MF A01 CSCL 09B

N86-14104*# Bradley Univ., Peoria, Ill. Dept. of Mathematics.
COMPUTER GRAPHICS APPLICATIONS TO CREW DISPLAYS Final Report
Joan Wyzkoski *In* NASA. Johnson (Lyndon B.) Space Center The 1983 NASA/ASEE Summer Faculty Fellowship Research Program Research Reports Sep. 1983 10 p refs (For primary document see N86-14078 04-85)
Avail: NTIS HC A18/MF A01 CSCL 09B

62 COMPUTER SYSTEMS

Includes computer networks.

N86-13944*# National Aeronautics and Space Administration. Langley Research Center, Hampton, Va.
THE MISSION ORIENTED TERMINAL AREA SIMULATION FACILITY
Jack T. Kaylor, Harold I. Simmons, Patricia B. Naftel (Research Triangle Inst.), Jacob A. Houck, and Randall D. Grove Oct. 1985 63 p refs
(NASA-TM-87621; NAS 1.15:87621) Avail: NTIS HC A04/MF A01 CSCL 09B

The Mission Oriented Terminal Area Simulation (MOTAS) was developed to provide an ATC environment in which flight management and flight operations research studies can be conducted with a high degree of realism. This facility provides a flexible and comprehensive simulation of the airborne, ground-based and communication aspects of the airport terminal area environment. Major elements of the simulation are: an airport terminal area environment model, two air traffic controller stations, several aircraft models and simulator cockpits, four pseudo pilot stations, and a realistic air-ground communications network. MOTAS has been used for one study with the DC-9 simulator and a series of data link studies are planned in the near future. Author

N86-13945# Stanford Univ., Calif.
TECHNIQUES FOR THE DESIGN AND IMPLEMENTATION OF HIGHLY RELIABLE MULTI-PROCESSING SYSTEMS Annual Report, 30 Sep. 1984 - 1 Aug. 1985
D. C. Luckham 10 May 1985 7 p
(Grant AF-AFOSR-0355-83)
(AD-A159236; AFOSR-85-0693TR) Avail: NTIS HC A02/MF A01 CSCL 09/2

During this research period several significant accomplishments were obtained. The completion of implementation of a prototype runtime monitor for detecting deadness errors in Ada tasking was accomplished. The work on runtime monitoring for deadness errors was presented at the IEEE Ada Conference in October 1984, and an invited publication appeared in IEEE Software in March 1985. A new language, called TSL (for Task Sequencing Language) to be used for specifying Ada tasking behavior, was designed and presented at the International Ada Conference in May 1985. Author (GRA)

63 CYBERNETICS

Includes feedback and control theory.

For related information see also *54 Man/System Technology and Life Support.*

N86-13946*# National Aeronautics and Space Administration. Langley Research Center, Hampton, Va.
A METHOD TO STABILIZE LINEAR SYSTEMS USING EIGENVALUE GRADIENT INFORMATION
Carol D. Wieseman Nov. 1985 40 p refs
(NASA-TP-2479; L-15964; NAS 1.60:2479) Avail: NTIS HC A03/MF A01 CSCL 09B

Formal optimization methods and eigenvalue gradient information are used to develop a stabilizing control law for a closed loop linear system that is initially unstable. The method was originally formulated by using direct, constrained optimization methods with the constraints being the real parts of the eigenvalues. However, because of problems in trying to achieve stabilizing control laws, the problem was reformulated to be solved differently. The method described uses the Davidon-Fletcher-Powell minimization technique to solve an indirect, constrained minimization problem in which the performance index is the Kreisselmeier-Steinhauser function of the real parts of all the eigenvalues. The method is applied successfully to solve two different problems: the determination of a fourth-order control law stabilizes a single-input single-output active flutter suppression system and the determination of a second-order control law for a multi-input multi-output lateral-directional flight control system. Various sets of design variables and initial starting points were chosen to show the robustness of the method. Author

N86-13947*# National Aeronautics and Space Administration. Goddard Space Flight Center, Greenbelt, Md.
DESIGN AND IMPLEMENTATION OF A COMPLIANT ROBOT WITH FORCE FEEDBACK AND STRATEGY PLANNING SOFTWARE
Timothy Premack, Franklin M. Strempek, Leonard A. Solis, Steven S. Brodd, Edwin P. Cutler, and Lloyd R. Purves 29 May 1984 99 p refs
(Contract NAS5-28200)
(NASA-TM-86111; NAS 1.15:86111) Avail: NTIS HC A05/MF A01 CSCL 09B

Force-feedback robotics techniques are being developed for automated precision assembly and servicing of NASA space flight equipment. Design and implementation of a prototype robot which provides compliance and monitors forces is in progress. Computer software to specify assembly steps and makes force feedback adjustments during assembly are coded and tested for three generically different precision mating problems. A model program demonstrates that a suitably autonomous robot can plan its own strategy. Author

N86-13948# Maryland Univ., College Park. Center for Automation Research.
MULTIRESOLUTION PATH PLANNING FOR MOBILE ROBOTS
S. Kambhampati and L. S. Davis May 1985 46 p
(Contract DAAK70-83-K-0018)
(AD-A158630; CAR-TR-127; CS-TR-1507) Avail: NTIS HC A03/MF A01 CSCL 09/2

The problem of automatic collision-free path planning is central to mobile robot applications. This report presents an approach to automatic two dimensional path planning based on a quadtree representation. (A quadtree is a recursive decomposition of a 2-D picture into uniformly colored sub i X 2 sub i blocks). The authors introduce hierarchical path searching methods, which make use of this multiresolution representation, to speed up the path planning process considerably. Finally, we discuss the applicability of this approach to mobile robot path planning. GRA

N86-13949# Massachusetts Inst. of Tech., Cambridge. Artificial Intelligence Lab.
MOBILE ROBOT LOCALIZATION USING SONAR
M. Drumheller Jan. 1985 27 p
(Contracts N00014-80-C-0505; N00014-82-K-0334)
(AD-A158819; AI-M-826) Avail: NTIS HC A03/MF A01 CSCL 17/7

This paper describes a method by which range data from a sonar or other type of rangefinder can be used to determine the 2-dimensional position and orientation of a mobile robot inside a room. The plan of the room is modeled as a list of segments indicating the positions of walls. The method works by extracting straight segments from the range data and examining all hypotheses about pairings between the segments and walls in the model of the room. Inconsistent pairings are discarded efficiently by using local constraints based on distances between walls, angles between walls, and ranges between walls along their normal vectors. These constraints are used to obtain a small set of possible positions, which is further pruned using a test for physical consistency. The approach is extremely tolerant of noise and clutter. Transient objects such as furniture and people need not be included in the room model, and very noisy, low-resolution sensors can be used. The algorithm's performance is demonstrated using a Polaroid Ultrasonic Rangefinder, which is a low-resolution, high-noise sensor. GRA

N86-13950# Massachusetts Inst. of Tech., Cambridge. Artificial Intelligence Lab.
DETERMINISTIC PARSING AND LINGUISTIC EXPLANATION: REVISION
R. C. Berwick and A. S. Weinberg Jun. 1985 36 p
(Contract N00014-80-C-0505)
(AD-A159233; AI-M-836Rev) Avail: NTIS HC A03/MF A01 CSCL 05/7

This article summarizes and extends recent results linking deterministic parsing to observed locality principles in syntax. It also argues that grammatical theories based on explicit phrase structure rules are unlikely to provide comparable explanations of why natural languages are built the way they are. GRA

N86-13951# Carnegie-Mellon Univ., Pittsburgh, Pa. Dept. of Psychology.
DISCOVERING QUALITATIVE EMPIRICAL LAWS Interim Report, Jan. - Jun. 1985
P. Langley, H. A. Simon, J. M. Zytkow, and D. H. Fisher 15 Jul. 1985 23 p Prepared in cooperation with California Univ., Irvine and Wichita State Univ., Kans.
(Contract N00014-84-K-0345)
(AD-A159235; TR-85-18; TR-2) Avail: NTIS HC A02/MF A01 CSCL 06/4

The process of scientific discovery is a complex interplay of many activities, ranging from the discovery of empirical laws through the construction of structural models to explain those laws. This paper focuses on the discovery of qualitative empirical laws and concepts. The authors primary examples come from the history of chemistry, and their model of the qualitative discovery process is an AI system named GLAUBER. After describing the system and providing some examples of its operation in the domain of chemistry, they consider GLAUBER's relation to some other AI discovery systems that operate on the tasks of conceptual clustering and language acquisition. Given a set of observations, GLAUBER defines abstract classes and formulates laws stated in terms of these classes. The authors approach was driven by examples from the history of early chemistry specifically by the development of the theory of acids and bases. Although the existing version of GLAUBER covers many of these discoveries, it has numerous limitations that should be remedied in future versions of the system. These include the need for improved evaluation methods, the ability to distinguish between unobserved and unsuccessful reactions, and the ability to run simple experiments in order to test predictions. These improvements suggest the need for two additional revisions - methods for the incremental discovery of classes and laws, and a search organization more robust than the current hill-climbing scheme. GRA

64 NUMERICAL ANALYSIS

Includes iteration, difference equations, and numerical approximation.

N86-13952# Oak Ridge National Lab., Tenn. Mathematics and Statistics Research Section.
THE FORMULATION OF A HYPERBOLIC STEFAN PROBLEM
A. D. Solomon, V. Alexiades, D. G. Wilson, and J. Drake Oct. 1984 26 p refs
(Contract DE-AC05-84OR-21400)
(ORNL-6065) Avail: NTIS HC A03/MF A01

The study of phase change processes governed by hyperbolic heat transfer is at an embryonic stage. Some of the relevant questions are raised and some remarks are made on the formulation and qualitative behavior of a hyperbolic Stefan problem. In particular, an error is corrected in the interface condition appearing in the literature, an explicit solution is presented to a simple one phase problem and its behavior studied. An enthalpy (weak) formulation for a two phase problem is described and a number of numerical experiments based on it are reported. Author

N86-13953*# National Aeronautics and Space Administration. Langley Research Center, Hampton, Va.
SPECTRAL METHODS FOR DISCONTINUOUS PROBLEMS Final Report
Saul Abarbanel (Tel-Aviv Univ.), David Gottlieb (Tel-Aviv Univ.), and Eitan Tadmor (Tel-Aviv Univ.) Aug. 1985 32 p refs Submitted for publication
(Contract NAS1-17070; Grants AF-AFOSR-0089-83; NSF DMS-85-03294; DAAG29-85-K-0190)
(NASA-CR-177974; ICASE-85-38; NAS 1.26:177974) Avail: NTIS HC A03/MF A01 CSCL 12A

Spectral methods yield high-order accuracy even when applied to problems with discontinuities, though not in the sense of pointwise accuracy. Two different procedures are presented which recover pointwise accurate approximations from the spectral calculations. Author

N86-13954*# National Aeronautics and Space Administration. Langley Research Center, Hampton, Va.
ACCURACY OF SCHEMES WITH NONUNIFORM MESHES FOR COMPRESSIBLE FLUID FLOWS Final Report
Eli Turkel (Tel-Aviv Univ.) Sep. 1985 50 p refs Submitted for publication
(Contract NAS1-17070)
(NASA-CR-177988; ICASE-85-43; NAS 1.26:177988) Avail: NTIS HC A03/MF A01 CSCL 12A

The accuracy of the space discretization for time-dependent problems when a nonuniform mesh is used is considered. Many schemes reduce to first-order accuracy while a popular finite volume scheme is even inconsistent for general grids. This accuracy is based on physical variables. However, when accuracy is measured in computational variables then second-order accuracy can be obtained. This is meaningful only if the mesh accurately reflects the properties of the solution. In addition, the stability properties of some improved accurate schemes are analyzed and it can be shown that they also allow for larger time steps when Runge-Kutta type methods are used to advance in time. Author

N86-13955*# National Aeronautics and Space Administration. Langley Research Center, Hampton, Va.
MULTIGRID SOLUTIONS TO QUASI-ELLIPTIC SCHEMES Final Report
Achi Brandt (Weizmann Inst. of Science, Rehovot, Israel) and Shlomo Taasan May 1985 23 p refs
(Contract NAS1-17070; Grant AF-AFOSR-0070-84)
(NASA-CR-177973; ICASE-85-26; NAS 1:26:177973) Avail: NTIS HC A02/MF A01 CSCL 12A

Quasi-elliptic schemes arise from central differencing or finite element discretization of elliptic systems with odd order derivatives on non-staggered grids. They are somewhat unstable and less accurate then corresponding staggered-grid schemes. When usual multigrid solvers are applied to them, the asymptotic algebraic convergence is necessarily slow. Nevertheless, it is shown by mode analyses and numerical experiments that the usual FMG algorithm is very efficient in solving quasi-elliptic equations to the level of truncation errors. Also, a new type of multigrid algorithm is presented, mode analyzed and tested, for which even the asymptotic algebraic convergence is fast. The essence of that algorithm is applicable to other kinds of problems, including highly indefinite ones. Author

N86-13956*# Old Dominion Univ., Norfolk, Va.
MINIMAL NORM CONSTRAINED INTERPOLATION Ph.D. Thesis
Larry Dean Irvine Sep. 1985 107 p refs
(Grant NAG1-363)
(NASA-CR-178001; NAS 1.26:178001) Avail: NTIS HC A06/MF A01 CSCL 12A

In computational fluid dynamics and in CAD/CAM, a physical boundary is usually known only discreetly and most often must be approximated. An acceptable approximation preserves the salient features of the data such as convexity and concavity. In this dissertation, a smooth interpolant which is locally concave where the data are concave and is locally convex where the data are convex is described. The interpolant is found by posing and solving a minimization problem whose solution is a piecewise cubic polynomial. The problem is solved indirectly by using the Peano Kernal theorem to recast it into an equivalent minimization problem having the second derivative of the interpolant as the solution. This approach leads to the solution of a nonlinear system of equations. It is shown that Newton's method is an exceptionally attractive and efficient method for solving the nonlinear system of equations. Examples of shape-preserving interpolants, as well as convergence results obtained by using Newton's method are also shown. A FORTRAN program to compute these interpolants is listed. The problem of computing the interpolant of minimal norm from a convex cone in a normal dual space is also discussed. An extension of de Boor's work on minimal norm unconstrained interpolation is presented. Author

N86-13957*# National Aeronautics and Space Administration. Langley Research Center, Hampton, Va.
STABLE BOUNDARY CONDITIONS AND DIFFERENCE SCHEMES FOR NAVIER-STOKES EQUATIONS Final Report
Pravir Dutt Aug. 1985 90 p refs
(Contract NAS1-17070; Grant NAG1-506)
(NASA-CR-177984; ICASE-85-37; NAS 1.26:177984) Avail: NTIS HC A05/MF A01 CSCL 12A

The Navier-Stokes equations can be viewed as an incompletely elliptic perturbation of the Euler equations. By using the entropy function for the Euler equations as a measure of energy for the Navier-Stokes equations, it was possible to obtain nonlinear energy estimates for the mixed initial boundary value problem. These estimates are used to derive boundary conditions which guarantee L2 boundedness even when the Reynolds number tends to infinity. Finally, a new difference scheme for modelling the Navier-Stokes equations in multidimensions for which it is possible to obtain discrete energy estimates exactly analogous to those we obtained for the differential equation was proposed. Author

N86-13958*# Mills Coll., Oakland, Calif. Math/Science Network.
EXPANDING YOUR HORIZONS IN SCIENCE AND MATHEMATICS Final Report
1985 11 p
(Grant NAG2-335)
(NASA-CR-176372; NAS 1.26:176372) Avail: NTIS HC A02/MF A01 CSCL 12A

Through the presentation of its Expanding Your Horizons in Science and Mathematics career education conferences for secondary school young women, the Math/Science Network continues its efforts to remove the educational, psychological, and cultural barriers which prevent women from entering math-and science-based careers. The Expanding Your Horizons conferences were presented on 77 college, university and high school campuses across the United States. This year, these unique one day conferences reached 15,500 students, 3,000 parents and educators, and involved 3,000 career women who volunteered their services as conference planners, workshop leaders, speakers, and role models. Author

N86-13959*# National Aeronautics and Space Administration. Langley Research Center, Hampton, Va.
PARAMETER IDENTIFICATION FOR A ROBOTIC MANIPULATOR ARM Final Report
D. W. Brewer and J. S. Gibson Sep. 1985 26 p refs
(Contract NAS1-17070)
(NASA-CR-178002; ICASE-85-42; NAS 1.26:178002) Avail: NTIS HC A03/MF A01 CSCL 12A

The development is described of a nonlinear dynamic model for large oscillations of a robotic manipulator arm about a single joint. Optimization routines are formulated and implemented for the identification of electrical and physical parameters from dynamic data taken from an industrial robot arm. Special attention is given to the role of sensitivity in the formulation of robust models of this motion. The importance of actuator effects in the reduction of sensitivity is established and used to develop an electromechanical model of the manipulator system. Author

N86-13960# Stanford Univ., Calif. Dept. of Statistics.
A BEHAVIORAL SUMMARY FOR COMPLETELY RANDOM NETS
A. E. Gelfand 20 Jun. 1985 22 p
(Contract N00014-76-C-0475)
(AD-A157755; TR-359) Avail: NTIS HC A02/MF A01 CSCL 12/1

This paper characterizes the cycle structure of a completely random net. Variables such as number of cycles of a specified length, number of cycles, number of cyclic states and length of cycle are studied. A square array of indicator variables enables convenient study of moment structure. Additionally, exact and asymptotic distributional results are presented. Author (GRA)

N86-13961# Army Missile Command, Redstone Arsenal, Ala. Guidance and Control Directorate.
FURTHER RESULTS FOR APPLICATION OF DISTURBANCE MINIMIZATION CONTROL TECHNIQUES TO A LINEAR, TIME-INVARIANT, SECOND-ORDER STATE SET-POINT REGULATOR PROBLEM
W. L. McCowan 10 Oct. 1984 58 p
(AD-A157793, AD-E950711; AMSMI/RG-85-5-TR) Avail: NTIS HC A04/MF A01 CSCL 12/1

Further results on The Application of Disturbance Minimizing Control Design Techniques to a linear, time-invariant state set-point regulator are presented using a second-order system as an example. A comparison is presented of performance obtained from a controller designed to minimize steady-state error versus one designed to minimize disturbance effects on error dynamics. Two examples are presented to illustrate regions of positive and negative disturbance utility. It is also shown that control energy expenditure can be reduced if use is made of external disturbances. Author (GRA)

N86-13962# Wisconsin Univ., Madison. Mathematics Research Center.
DECAY WITH A RATE FOR NONCOMPACTLY SUPPORTED SOLUTIONS OF CONSERVATION LAWS Technical Summary Report
B. Temple Jun. 1985 66 p
(Contract DAAG29-80-C-0041; Grant NSF DMS-82-10950)
(AD-A158163; MRC-TSR-2831) Avail: NTIS HC A04/MF A01 CSCL 12/1

This document shows that solutions of the Cauchy problem for systems of two conservation laws decay in the supnorm at a rate that depends only on the L sub 1 norm of the initial data. This implies that the dissipation due to the entropy dominates the nonlinearities in the problem at a rate depending only on the L sub 1 norm of the initial data. The main estimate requires an analysis of approximate characteristics for its proof. A general framework is developed for the study of approximate characteristics, and the main estimate is obtained for an arbitrary number of equations. GRA

N86-13963# Wisconsin Univ., Madison. Mathematics Research Center.
ADAPTIVE, SELF-VALIDATING NUMERICAL QUADRATURE Technical Summary Report
G. F. Corliss and L. B. Rall May 1985 42 p
(Contract DAAG29-80-C-0041)
(AD-A158164; MRC-TSR-2815) Avail: NTIS HC A03/MF A01 CSCL 12/1

Integrals of a function of a single variable can be expressed as the sum of a numerical quadrature rule and a remainder term. The quadrature rule is a linear combination of function values and weights, or the integral of a Taylor polynomial, while the remainder term depends on some derivative of the integrand evaluated at an unknown point in the interval of integration. Numerical quadrature is made self-validating by using interval computation to capture both the roundoff and truncation errors made when using a given rule. Necessary derivatives can be generated automatically by using well-known recurrence relations for Taylor coefficients. In order for quadrature methods of this type to be accurate and efficient an accurate scalar product and an adaptive strategy are required. The necessary scalar product and support for interval arithmetic are provided in PASCAL-SC (for microcomputers) and ACRITH (for IBM 370 computers). The adaptive strategy chooses the subintervals of integration and the order of the quadrature formula used in each subinterval on the basis of guaranteed, rather than estimated, information about the error of the numerical integration in each subinterval. The program described implements standard Newton-Cotes, Gaussian, and Taylor series methods for numerical intergration. Ways to handle singularities are discussed, and comparisons are given with a standard numerical integration method. Author (GRA)

N86-13964# Wisconsin Univ., Madison. Mathematics Research Center.
CONVERGENCE OF CARDINAL SERIES Technical Summary Report
C. DEBoor, K. Hoellig, and S. Riemenschneider Jun. 1985 9 p
(Contract DAAG29-80-C-0041; Grant NSF DMS-83-51187)
(AD-A158166; MRC-TSR-2834) Avail: NTIS HC A02/MF A01 CSCL 12/1

The result of this paper is a generalization of an characterization of the limits of multivariate cardinal splines. GRA

N86-13965# Wisconsin Univ., Madison. Mathematics Research Center.
BOUNDARY INTEGRAL TECHNIQUES FOR MULTI-

CONNECTED DOMAINS Technical Summary Report
G. R. Baker and M. J. Shelley Jun. 1985 40 p
(Contract DAAG29-80-C-0041; Grant NSF MCS-83-02549)
(AD-A158171; MRC-TSR-2830) Avail: NTIS HC A03/MF A01
CSCL 12/1

Several boundary integral techniques are available for the computation of the solution to Lapace's equation in multi-connected domains. However, for cases where the domain is changing, such as in incompressible, inviscid fluid flow with free surfaces, iterative methods are highly attractive. The paper describes one such formulation and tests it on circular and elliptic annuli. It is necessary to use interpolated numerical quadrature points to maintain accuracy when regions on the annuli are thin. Author (GRA)

N86-13966# Wisconsin Univ., Madison. Mathematics Research Center.
UNIFORMLY HIGH-ORDER ACCURATE NON-OSCILLATORY SCHEMES 1 Technical Summary Report
A. Harten and S. Osher May 1985 60 p
(Contract DAAG29-80-C-0041)
(AD-A158177; MRC-TSR-2823) Avail: NTIS HC A04/MF A01
CSCL 12/1

The authors begin the construction and the analysis of nonoscillatory shock capturing methods for the approximation of hyperbolic conservation laws. These schemes share many desirable properties with total variation diminishing schemes, but TVD schemes have at most first order accuracy, in the sense of truncation error, at extrema of the solution. This paper constructs a uniformly second order approximation, which is nonoscillatory in the sense that the number of extrema of the discrete solution is not increasing in time. This is achieved via a nonoscillatory piecewise linear reconstruction of the solution form its cell averages, time evolution through an approximate solution of the resulting initial value problem, and averaging of this approximate solution over each cell. Author (GRA)

N86-13967# Wisconsin Univ., Madison. Mathematics Research Center.
A LINEAR COMBINATION TEST FOR DETECTING SERIAL CORRELATION IN MULTIVARIATE SAMPLES Technical Summary Report
R. A. Johnson and T. Langeland Jun. 1985 23 p
(Contract DAAG29-80-C-0041; Grant NSF MCS-82-02205)
(AD-A158179; MRC-TSR-2825) Avail: NTIS HC A02/MF A01
CSCL 12/1

This document proposes a test for detecting serial dependence among multivariate observations. The test statistic is the maximum absolute value of the lag 1 correlation obtainable from a linear combination of the observations. The authors express the statistic in terms of two eigenvalues and then obtain the asymptotic null distribution. Asymptotic power is examined for sequences of local alternatives in a multivariate normal autoregressive process. An explicit expression is obtained for the density of the limit distribution in the bivariate case. They then compare power with the likelihood ratio statistic. Author (GRA)

N86-13968# Liverpool Univ. (England). Dept. of Statistics and Computational Mathematics.
PRACTICAL ASPECTS OF FUNCTIONAL TESTING TECHNIQUES Final Technical Report, 17 Sep. 1981 - 16 Jan. 1985
M. A. Hennell, M. U. Shaikh, S. Presland, and P. Fairfield 31 Jan. 1985 141 p
(Contract DAJA37-81-C-0736; DA Proj. 1T1-61102-BH-57)
(AD-A158184) Avail: NTIS HC A07/MF A01 CSCL 09/2

This document reports an investigation into the processes involved in functional testing. The objective was to determine criteria by means of which the process can be quantified and hence controlled. The report demonstrates that insufficient knowledge about functionality exists for general metrics to be constructed. Indeed it clearly indicates that any method dependent on a knowledge of functionality is unlikely, except in special application areas, to be successful. GRA

N86-13969# Maryland Univ., College Park. Inst. for Physical Science and Technology.
BASIC PRINCIPLES OF FEEDBACK AND ADAPTIVE APPROACHES IN THE FINITE ELEMENT METHOD Final Report
I. Babuska and W. Gui Jul. 1985 30 p
(Contract N00014-85-K-0169; Grant NSF DMS-83-15216)
(AD-A158188; BN-1042) Avail: NTIS HC A03/MF A01 CSCL 12/1

The notion of feedback and adaptivity in numerical computations has attracted great attention in recent years. All the modern ODE's solvers for initial value problems and quadratures are feedback methods. The feedback methods are increasingly in the focus of interest in the area of numerical solution of PDE and computational mechanics. Many reports, preprints and papers dealing with the adaptivity appeared recently. It seems to be that successful computation of today's large complex problems cannot be made without some kind of feedback or adaptive approach. This paper addresses the basic notions of the theory of feedback and adaptive finite element methods. An illustrative example of the finite element method for solving nonlinear differential equation of the elliptic type is presented. Numerical example of regridding process is given. GRA

N86-13970# Wisconsin Univ., Madison. Mathematics Research Center.
COMPUTABLE BOUNDS FOR SOLUTIONS OF INTEGRAL EQUATIONS Technical Summary Report
L. B. Rall May 1985 17 p
(Contract DAAG29-80-C-0041)
(AD-A158189; MRC-TSR-2816) Avail: NTIS HC A02/MF A01
CSCL 12/1

Interval integration is used to obtain inclusions of integral operators of the form g(u)(s) = integral of T(g(s,t,u(s),u(t))dt) which can be carried out on a computer. The resulting inclusions, combined with interval iteration, are used to compute guaranteed upper and lower bounds for solutions of integral equations of the form u = g(u) for s is an element of S. It is also possible to establish existence or nonexistence of solutions of integral equations in given regions on the basis of results of the computation. Examples of applications of this technique to linear and nonlinear integral equations are eigenvalue problems for linear integral operators are given. GRA

N86-13971# Maryland Univ., College Park. Lab. for Numerical Analysis.
THE h-p VERSION OF THE FINITE ELEMENT METHOD Final Report
I. Babuska and B. Guo Jul. 1985 89 p
(Contract N00014-85-K-0169; Grant NSF DMS-83-15216)
(AD-A158194; BN-1043) Avail: NTIS HC A05/MF A01 CSCL 12/1

The paper analyzes the h-p version of the finite element method in two dimensions. It proves that the error of the method measured in the energy norm decreases exponentially. Extensive computational analysis with the code PROBE, shows the practical effectivity of the h-p version, and the applicability of the theoretical asymptotic error estimates in the range of engineering computations and accuracy. GRA

N86-13972# Pittsburgh Univ., Pa. Center for Multivariate Analysis.
ON ASYMPTOTIC DISTRIBUTION OF THE TEST STATISTIC FOR THE MEAN OF THE NONISOTROPIC PRINCIPAL COMPONENT
C. Fang and P. R. Krishnaiah May 1985 16 p
(Contract F49620-85-C-0008)
(AD-A158255; TR-85-20; AFOSR-85-0551TR) Avail: NTIS HC A02/MF A01 CSCL 12/1

Data analysts are often confronted with the problem of large dimensional data. In some of these situations, it is customary to reduce the dimensionality of the problem by using principal component analysis and to perform statistical analysis of the data using the new variables (principal components). For example, the

new variables are used in the area of classification. Chestnut and Floyd (1981) used the principal components as variables in identification of underwater targets. However, the statistical data analysis using the principal components is adhoc since the distributions of the test statistics based upon the principal components are complicated when the covariance matrix is unknown. Very little work was done in the literature on deriving the distributions of these test statistics even in the asymptotic case. In this paper, we derive the asymptotic distribution of the t statistic based upon the new variable (the most important principal component) instead of using any of the original variables. The above asymptotic distribution is shown to be Student's t distribution. The accuracy of the above approximation is studied by comparing the simulated values using the asymptotic expression with the standard Student's t table. It is found that the accuracy of the above approximation is sufficient for many practical situations.
GRA

N86-13973# Pittsburgh Univ., Pa. Center for Multivariate Analysis.
SPECTRA FOR LARGE DIMENSIONAL RANDOM MATRICES
Y. Q. Yin and Z. D. Bai May 1985 14 p
(Contract F49620-85-C-0008)
(AD-A158256; TR-85-17; AFOSR-85-0547TR) Avail: NTIS HC A02/MF A01 CSCL 12/1

In this paper, the authors reviewed some recent developments in the area of large dimensional random matrices. GRA

N86-13974# Pittsburgh Univ., Pa. Center for Multivariate Analysis.
AN ALTERNATE DERIVATION OF THE DISTRIBUTION OF THE CONDITIONED SIGNAL-TO-NOISE RATIO
R. C. Hanumara May 1985 12 p
(Contract F49620-85-C-0008)
(AD-A158257; TR-85-18; AFOSR-85-0548TR) Avail: NTIS HC A02/MF A01 CSCL 09/4

A result in multiple regression analysis is used to derive the probability distribution of the conditioned signal-to-noise ratio.
Author (GRA)

N86-13975# Massachusetts Inst. of Tech., Cambridge. Lab. for Information and Decision.
INTRINSIC NILPOTENT APPROXIMATION
C. Rockland Jun. 1985 121 p
(Contract DAAG29-84-K-0005)
(AD-A158265; ARO-20980.28-MA) Avail: NTIS HC A06/MF A01 CSCL 12/1

This report is a preliminary version of work on an intrinsic approximation process arising in the context of a nonisotropic perturbation theory for certain classes of linear differential and pseudodifferential operators P on a minifold M. A basic issue is that the structure of P itself determines the minimal information that the initial approximation must contain. This may vary from point to point, and requires corresponding approximate state spaces or phase spaces. This approximation process is most naturally viewed from a seemingly abstract algebraic context, namely the approximation of certain infinite dimensional filtered Lie algebras L by (finite-dimensional) graded nilpotent Lie algebras. GRA

N86-13976# Pittsburgh Univ., Pa. Center for Multivariate Analysis.
INFERENCE ON THE RANKS OF THE CANONICAL CORRELATION MATRICES FOR ELLIPTICALLY SYMMETRIC POPULATIONS
P. R. Krishnaiah, J. Lin, and L. Wang May 1985 31 p
(Contract F49620-85-C-0008)
(AD-A158268; TR-85-14; AFOSR-85-0550TR) Avail: NTIS HC A03/MF A01 CSCL 12/1

In this paper, the authors considered the likelihood ratio tests and some other tests for the ranks of the canonical correlation matrices when the underlying distributions are real and complex elliptically symmetric distributions. Also, asymptotic joint distributions of the eigenvalues of the sample canonical correlation matrices are derived under the assumptions mentioned above regarding the underlying distributions. Finally, applications of tests for the rank of the complex canonical correlation matrix in the area of time series in the frequency domain are discussed. GRA

N86-13977# Pittsburgh Univ., Pa. Center for Multivariate Analysis.
A NOTE ON THE INTEGRATED CAUCHY FUNCTIONAL EQUATION
A. A. Alzaid, C. R. Rao, and D. N. Shanbhag May 1985 11 p
(Contract F49620-85-C-0008)
(AD-A158269; TR-85-19; AFOSR-85-0549TR) Avail: NTIS HC A02/MF A01 CSCL 12/1

A new proof is given using de Finneti's theorem on infinite sequence of exchangeable random variables for the solution of the integrated Cauchy functional equation studied by Lau and Rao (1982) in the continuous case and by Shanbhag (1977) in the discrete case. Author (GRA)

N86-13978# Georgia Inst. of Tech., Atlanta.
PARTITIONS OF POINT PROCESSES: MULTIVARIATE POISSON APPROXIMATIONS
R. F. Serfozo May 1985 25 p
(Grant AF-AFOSR-0367-84)
(AD-A158739; AFOSR-85-0626TR) Avail: NTIS HC A02/MF A01 CSCL 12/1

This study shows that when a point process is partitioned into certain uniformly sparse subprocesses, then the subprocesses are asymptotically multivariate Poisson or compound Poisson. Bounds are given for the total-variation distance between the subprocesses and their limits. Several partitioning rules are considered including independent, Markovian, and batch assignments of points.
Author (GRA)

N86-13979# Massachusetts Inst. of Tech., Cambridge. Artificial Intelligence Lab.
CODON CONSTRAINTS ON CLOSED 2D SHAPES
W. A. Richards and D. D. Hoffman 1 May 1984 25 p
(Contract F49620-83-C-0135)
(AD-A158744; AI-M-769; AFOSR-85-0588TR) Avail: NTIS HC A02/MF A01 CSCL 12/1

Codons are simple primitives for describing plane curves. They thus are primarily image-based descriptors. Yet they have the power to capture important information about the 3D world, such as making part boundaries explicit. The codon description is highly redundant (useful for error-correction). This redundancy can be viewed as a constraint on the number of possible codon strings. For smooth closed strings that represent the bounding contour (silhouette) of many smooth 3D objects, the constraints are so strong that sequences containing 6 elements yield only 33 generic shapes as compared with a possible number of 15,625 combinations. An important task for object recognition is the description of the shape of a bounding contour such as a sihouette that outlines as object. Although recognition need require only partial segments of such contours, the internal canoncial description, against which the image contour is compared, is very likely a closed ring. Our concept of most objects should lead us to expect such a closed contour. The description of closed, 2D contours thus is an important ingredient of a system for object recognition. First the author present such a scheme, described in more detail elsewhere and then show how the scheme leads to a hierarchical taxonomy of closed, 2D shapes. GRA

N86-13980# Maryland Univ., College Park. Center for Automation Research.
COMPUTATION OF GEOMETRIC PROPERTIES FROM THE MEDIAL AXIS TRANSFORM IN 0 (n LOG n) TIME
A. Y. Wu, S. K. Bhaskar, and A. Rosenfeld Jun. 1985 40 p
(Contract F49620-83-C-0082)
(AD-A158934; CAR-TR-122; CS-TR-1497; AFOSR-85-0616TR) Avail: NTIS HC A03/MF A01 CSCL 12/1

The digital medial axis transfer (MAT) represents and image subset S as the union of maximal upright squares contained in S.

Brute-force algorithms for computing geometric properties of S from its MAT require time O (sq n), where n is the number of squares. Over the past few years, however, algorithms have been developed that compute properties for a union of upright rectangles in time O (n log n), which makes the use of the MAT much more attractive. This document reviews these algorithms and also present efficient algorithms for computing union-of-rectangle representations of derived sets (union, intersection, complement) and for conversion between the union of rectangles and other representations of a subset. Author (GRA)

N86-13981# Connecticut Univ., Storrs. Dept. of Electrical Engineering and Computer Science.
UNIFIED METHOD FOR DELAY ANALYSIS OF RANDOM MULTIPLE ACCESS ALGORITHMS Interim Report
L. Georgiadis, L. Merakos, and P. Papantoni-Kazakos Aug. 1985 63 p
(Grant AF-AFOSR-0229-83)
(AD-A159108; UCT/DEECS/TR-85-8; AFOSR-85-0712TR) Avail: NTIS HC A04/MF A01 CSCL 12/1

This paper presents a unified method for the delay analysis of a large class of random multiple - access algorithms. This method is based on a powerful theorem referring to regenerative processes, in conjunction with results from the theory of infinite dimensionality linear systems. The method is applied to analyze and compute the per packet expected delays induced by three algorithms, in the presence of the Poisson user model. The considered algorithms are: The controlled ALOHA algorithm, the 0.487 algorithm, and the n-ary stack algorithm. GRA

N86-13982# Air Force Inst. of Tech., Wright-Patterson AFB, Ohio. School of Engineering.
A FINITE ELEMENT SOLUTION OF THE TRANSPORT EQUATION M.S. Thesis
F. A. Tarantino Mar. 1985 196 p
(AD-A159245; AFIT/GNE/PH/85M-19) Avail: NTIS HC A09/MF A01 CSCL 12/1

Using a self adjoint form of the transport equation expressed as a variational integral, finite element equations for the one dimensional, one speed, homogeneous, time independent transport equation in slab geometry were derived and envoded in FORTRAN 77. The accuracy of C sub 0 and C sub 1 continuous fits was compared against an analytical solution for the case of noscatter. It was found that the C fits require an excessive amount of mesh refinement. The C sub 1 fit is very accurate, and does not appear to be computationally excessive. The finite element results were then compared, for the case of isotropic scatter, to a Legendre polynomial solution, and the results of a recently developed code known as Ln. The methods accuracy was sufficiently verified with inexact scattering term evaluation. A technique of exact scattering integral evaluation is proposed that should reduce the amount of refinement required for convergence, and improve computational efficiency. Author (GRA)

N86-13983# Lawrence Livermore National Lab., Calif.
CURRENT METHODS FOR LARGE STIFF ODE SYSTEMS
A. C. Hindmarsh May 1985 5 p refs Presented at the 11th Intern. Assoc. of Math. and Computers Simulation World Congr., Oslo, 5 Aug. 1985
(Contract W-7405-eng-48)
(DE85-012914; UCRL-92641; CONF-850861-3) Avail: NTIS HC A02/MF A01

Initial value problems for ODE systems are especially challenging when they are both large and stiff. Current methods range from explicit to fully implicit. Quasi-steady state, split operator, and hybrid methods are often effective, but require much problem specific setup and rarely allow for error control. General implicit methods with error control have the widest applicability. They involve an algebraic system problem, usually solved with Newton like iterations, combined with direct or iterative linear system methods, sometimes using partitioning. Research is in progress on matrix free iterations. DOE

N86-13588*# National Aeronautics and Space Administration. Langley Research Center, Hampton, Va.
A PARAMETRIC STUDY OF THE IBRAHIM TIME DOMAIN MODAL IDENTIFICATION ALGORITHM Final Report
Richard S. Pappa and Samir R. Ibrahim (Old Dominion Univ.) *In* Old Dominion Univ. Dyn. Identification for Control of Large Space Struct. Nov. 1985 p 43-72 refs Previously announced as N83-10258 (For primary document see N86-13587 04-31)
Avail: NTIS HC A04/MF A01 CSCL 13B

N86-13590*# Old Dominion Univ., Norfolk, Va.
COMPUTATION OF NORMAL MODES FROM IDENTIFIED COMPLEX MODES Final Report
Samir R. Ibrahim *In its* Dyn. Identification for Control of Large Space Struct. Nov. 1985 p 446-451 refs Previously announced as N82-75431 and in IAA as A83-22143 (For primary document see N86-13587 04-31)
Avail: NTIS HC 04/MF A01 CSCL 13B

N86-14079*# University of Southwestern Louisiana, Lafayette. Dept. of Mathematics and Statistics.
ESTIMATION OF FINITE MIXTURES USING THE EMPIRICAL CHARACTERISTIC FUNCTION Final Report
Charles Anderson and Thomas Boullion *In* NASA. Johnson Lyndon B.) Space Center The 1983 NASA/ASEE Summer Faculty Fellowship Research Program Research Reports Sep. 1985 7 p refs (For primary document see N86-14078 04-85)
Avail: NTIS HC A18/MF A01 CSCL 12A

N86-14083*# Arkansas Univ., Little Rock.
FINITE ELEMENT OR GALERKIN TYPE SEMIDISCRETE SCHEMES Final Report
Kanat Durgun *In* NASA. Johnson (Lyndon B.) Space Center The 1983 NASA/ASEE Summer Faculty Fellowship Research Program Research Reports Sep. 1983 14 p refs (For primary document see N86-14078 04-85)
Avail: NTIS HC A18/MF A01 CSCL 12A

N86-14099*# Houston Baptist Univ., Tex. Dept. of Mathematics and Physics.
TRANSFORMATION MATRICES BETWEEN NON-LINEAR AND LINEAR DIFFERENTIAL EQUATIONS Final Report
Robert L. Sartain *In* NASA. Johnson (Lyndon B.) Space Center The 1983 NASA/ASEE Summer Faculty Fellowship Research Program Research Reports Sep. 1983 15 p refs (For primary document see N86-14078 04-85)
Avail: NTIS HC A18/MF A01 CSCL 12A

N86-14101*# Texas Univ., Austin. Dept. of Aerospace and Engineering.
ADVANCED ALGORITHM FOR ORBIT COMPUTATION Final Report
Victor Szenbehely *In* NASA. Johnson (Lyndon B.) Space Center The 1983 NASA/ASEE Summer Faculty Fellowship Research Program Research Reports Sep. 1983 17 p (For primary document see N86-14078 04-85)
Avail: NTIS HC A18/MF A01 CSCL 12A

N86-14129# Joint Publications Research Service, Arlington, Va.
STRUCTURE OF COEFFICIENTS OF SERIES REPRESENTING SOLUTION OF PLANE CIRCULAR RESTRICTED THREE-BODY PROBLEM Abstract Only
Ye. I. Timoshkova and V. B. Titov *In its* USSR Rept.: Space (JPRS-USP-85-005) 30 Sep. 1985 p 38 Transl. into ENGLISH from Astron. Zh. (Moscow), v. 61, no. 6, Nov. - Dec. 1984 p 1211-1217 Previously announced in IAA as A85-42346 (For primary document see N86-14111 04-88)
Avail: NTIS HC A08

65 STATISTICS AND PROBABILITY

Includes data sampling and smoothing; Monte Carlo method; and stochastic processes.

N86-13984# Naval Research Lab., Washington, D. C.
DIFFERENTIAL ENTROPY AND THE STATISTICS OF INSTANTANEOUS FAILURE Memorandum Report, Mar. - Apr. 1985
A. K. Rajagopal, K. L. Ngai, and S. Teitler 23 Aug. 1985 13 p
(AD-A158047; NRL-MR-5627) Avail: NTIS HC A02/MF A01 CSCL 12/1

The dimensionless differential entropy for failure statistics is shown to be equal to unity plus the negative of the expectation of the logarithm of the hazard function. The effect of transformation of the ordering parameter on the latter due to changes in physical conditions is discussed. Author (GRA)

N86-13985# Purdue Univ., West Lafayette, Ind. School of Industrial Engineering.
DECOMPOSITION OF SOME WELL-KNOWN VARIANCE REDUCTION TECHNIQUES: REVISION
B. L. Nelson and B. W. Schmeiser May 1985 39 p Prepared in cooperation with Ohio State Univ., Columbus
(Contract N00014-79-C-0832-Rev)
(AD-A158048; RM-84-6) Avail: NTIS HC A03/MF A01 CSCL 12/1

Proliferation of techniques and lack of unifying structure has hindered both study and application of variance reduction. The author's recently developed unifying structure, presented in detail elsewhere, is a taxonomy that views each variance reduction technique (VRT) as a transformation from one experiment to another. The taxonomy is exhaustive in that any VRT can be expressed as a composition of elemental transformations from six classes. This paper illustrates this taxonomy by using the notation, terminology, and concepts of the taxonomy to discuss seven VRTs. The objective is to use the reader's knowledge of these well-known techniques to provide an introduction and overview of the taxonomy. Author (GRA)

N86-13986# Wisconsin Univ., Madison. Mathematics Research Center.
B-SPLINES AND LINEAR COMBINATIONS OF UNIFORM ORDER STATISTICS Technical Summary Report
A. G. Ignatov and V. K. Kaishev May 1985 28 p
(Contract DAAG29-80-C-0041)
(AD-A158151; MRC-TSR-2817) Avail: NTIS HC A03/MF A01 CSCL 12/1

It is shown in this document that the density of the sum of n independent random variables uniformly distributed on unequal intervals is given by a linear combination of n! B-splines with constant coefficients. Another useful representation of the same density is given using de Boor's definition of the discrete B-spline. It is also shown that the B-spline is the density of a linear combination of order statistics from the uniform distribution on (0,1). This interpretation of the B-spline allows one to establish easily validity of recurrence relations for densities and moments of linear combinations of order statistics as well as to state limit theorems both for B-splines and linear combinations. Examples given illustrate how asymptotic results for B-splines may be applied to linear combinations of order statistics. Using limit theorems of probability theory, two examples of Curry and Schoenberg (1966) for B-splines are derived even in somewhat greater generality. GRA

N86-13987# Wisconsin Univ., Madison. Mathematics Research Center.
APPROXIMATION OF THE INITIAL RESERVE FOR KNOWN RUIN PROBABILITIES Technical Summary Report
E. W. Frees May 1985 26 p
(Contract DAAG29-80-C-0041)
(AD-A158167; MRC-TSR-2822) Avail: NTIS HC A03/MF A01 CSCL 12/1

An important problem in the study of actual risk theory is approximating the probability of ruin within finite time based on a specified initial reserve. This paper addresses the similar, but mathematically different, problem of how to approximate a desired initial reserve given a pre-specified probability of ruin. Although the procedures have desirable asymptotic properties such as consistency and asymptotic normality, these are computer-intensive and would not have been practicable before the wide spread availability of high-speed computers. The procedures rely on simulated realizations of a general risk process. Thus, these can be used in many of the mathematical models of risk processes that appear in the literature such as the Compound Poisson, ARMA and Stochastic Discounting models. Examples of several models are given to demonstrate the versatility of the procedure and to demonstrate that the procedures are computationally feasible. Author (GRA)

N86-13988# Wisconsin Univ., Madison. Mathematics Research Center.
CONDITIONING IN A MISSING DATA PROBLEM Technical Summary Report
C. J. Skinner Jul. 1985 18 p
(Contract DAAG29-80-C-0041; Grant NSF DMS-82-10950)
(AD-A158202; MRC-TSR-2836) Avail: NTIS HC A02/MF A01 CSCL 12/1

Observations are recorded on variables x and y but a mechanism, which may depend on the observed x values, causes some of the y values to be missing. For three parametric examples, exact or approximate ancillary statistics are constructed. Conditioning on these ancillaries enables the missing data mechanism to be ignored under certain conditions. A correspondence is shown between these conditional procedures and the use of the observed information matrix in measuring the dispersion of the maximum likelihood estimator. GRA

N86-13989# Stanford Univ., Calif. Dept. of Operations Research.
THE THEORY OF STANDARDIZED TIME SERIES
P. W. Glynn and D. L. Iglehart Apr. 1985 38 p
(Contract DAAG29-84-K-0030; Grant NSF MCS-82-3483)
(AD-A158383; TR-8; ARO-20927.8-MA) Avail: NTIS HC A03/MF A01 CSCL 12/1

Building on Schruben's work, this document has developed a general framework for the analysis of standardized time series. Under mild assumptions on the output process, the method of standardized time series produces asymptotically valid confidence intervals for steady-state parameters. However, these intervals are asymptotically larger and more variable then those steady-state intervals obtained by a method which consistently estimates the appropriate steady-state variance constant (such as the regenerative method). In this sense, standardized time series confidence intervals are asymptotically less desirable then those constructed by consistent estimation. These results do not, however, preclude the possibility that standardized times series may be superior in certain small sample context; this remains an area for future work. GRA

N86-13990# Purdue Univ., West Lafayette, Ind. School of Industrial Engineering.
MONTE CARLO ANALYSIS OF NONLINEAR STATISTICAL MODELS. 1. THEORY: REVISION
J. J. Swain and B. R. Schmeiser Aug. 1985 18 p Prepared in cooperation with Georgia Inst. of Tech., Atlanta
(Contract N00014-79-C-0832; Grant NSF ECS-82-06498)
(AD-A158613; AD-F630681; RM-85-10) Avail: NTIS HC A02/MF A01 CSCL 12/1

Parameter values of nonlinear statistical models are typically estimated from data using iterative numerical procedures. The resulting joint sampling distribution of the parameter estimators is often intractable, resulting in the use of approximators or Monte Carlo simulation to determine properties of the sampling distribution. This paper develops methods, using linear and quadratic approximators as control variates, that reduce the variance of the Monte Carlo estimator by orders of magnitude. Estimation of means, higher order raw moments, variances, covariances, and percentiles is considered. Author (GRA)

N86-13991# Georgia Inst. of Tech., Atlanta.
EXTREME VALUES OF QUEUES, POINT PROCESSES AND STOCHASTIC NETWORKS Research Progress Report, 30 Sep. 1984 - 15 Jun. 1985
R. F. Serfozo 25 Jun. 1985 5 p
(Grant AF-AFOSR-0367-84)
(AD-A158619; AFOSR-85-0620TR) Avail: NTIS HC A02/MF A01 CSCL 12/1

This document reports on research progress in the following topics: (1) Extreme Values of Queues - Several subtle technical problems remain to present the results in as general and natural setting as possible; (2) Extreme Values of Stochastic Networks - Work should be completed by fall. After that the emphasis will change on this topic to the following one; (3) Optimal Control of Networks of queues - This topic was not in the original proposal, but the investigators have made a breakthrough in this area that they intend to pursue; (4) Point Processes Related to Extreme Values - Several results in the convergence of certain point processes to Poisson processes have been obtained. These are documented in two papers written under this grant; and (5) Extreme Values of Point Processes - This is an area which will be developed later in the research effort. Author (GRA)

N86-13992# North Carolina Univ., Chapel Hill. Center for Stochastic Processes.
BASIC PROPERTIES OF STRONG MIXING CONDITIONS Technical Report, Sep. 1984 - Aug. 1985
R. C. Bradley Jun. 1985 41 p Prepared in cooperation with Indiana Univ., Bloomington
(Contract F49620-82-C-0009; Grant NSF DMS-84-01021)
(AD-A158740; TR-102; AFOSR-85-0619TR) Avail: NTIS HC A03/MF A01 CSCL 12/1

This is a survey of te basic properties of strong mixing conditions for sequences of random variables. The focus will be on the structural properties of these conditions, and not at all on limit theory. For a discussion of central limit theorems and related results under these conditions, the reader is referred to Peligrad or Iosifescu. This survey will be divided into eight sections as follows: (1) Measures of dependence; (2) Five strong mixing conditions; (3) Mixing conditions for two or more sequences; (4) Mixing conditions for Markov chains; (5) Mixing conditions for Gaussian sequences; (6) Some other special examples; (7) The behavior of the dependence coefficients; and (8) Approximation of mixing sequences by other random sequences. Author (GRA)

N86-13993# Massachusetts Inst. of Tech., Lexington.
ADAPTIVE DETECTION IN NONSTATIONARY INTERFERENCE: PART 1 AND PART 2
E. J. Kelly 25 Jun. 1985 139 p
(Contract F19628-85-C-0002)
(AD-A158810; TR-724; ESD-TR-85-197) Avail: NTIS HC A07/MF A01 CSCL 17/9

In this report, which consists of two parts, the problem of radar target detection in a background of nonstationary external interference is considered. The object of the analysis is to treat this problem from the point of view of statistical decision theory, and to derive a signal processing algorithm which accepts the totality of inputs on which final decision is to be based, and performs both interference suppression and target detection. It is assumed that the radar is provided with multiple RF input channels and that target-free samples, from range gates other than one in which a target is being sought, can be used for the estimation of the interference statistics. In Part I a general formulation is given and a likelihood ratio detection rule is derived. GRA

N86-13994# Army Materiel Systems Analysis Activity, Aberdeen Proving Ground, Md.
METHODOLOGY FOR STOCHASTIC MODELING
H. E. Cohen Jan. 1985 43 p Supersedes GWD Interim note, G-144
(AD-A158851; AMSAA-TR-410) Avail: NTIS HC A03/MF A01 CSCL 12/1

The requirement to develop stochastic mathematical models arises across the whole range of engineering and applied research where observations are made of a physical process, corrupted by noise, and it is desired to determine the underlying nature, either in time or frequency, of the observed phenomenon. This paper presents some of the current approaches in stochastic modeling, including adaptive autoregressive models, which have been found to be useful in this area. Author (GRA)

N86-13995# North Carolina Univ., Chapel Hill. Center for Stochastic Processes.
CONTINUITY OF CERTAIN RANDOM INTEGRAL MAPPINGS AND THE UNIFORM INTEGRABILITY OF INFINITELY DIVISIBLE MEASURES
Z. J. Jurek and J. Rosinski Mar. 1985 27 p
(Contract F49620-82-C-0009)
(AD-A159105; TR-95; AFOSR-85-0684TR) Avail: NTIS HC A03/MF A01 CSCL 12/1

In this paper it is shown that the class of probability measures L(Q), which generalizes the classical Levy class L, is homeomorphic with the class ID sub log of all infinitely divisible probability measures having finite logarithmic moment. As an application of this result a set of generators of the entire class L(Q) is described. As a necessary tool, the relationship between the uniform integrability of infinitely divisible measures and of their corresponding Levy measures is studied and this may be of independent interest. Author (GRA)

66 SYSTEMS ANALYSIS

Includes mathematical modeling; network analysis; and operations research.

N86-13996# Stanford Univ., Calif. Systems Optimization Lab.
EXISTENCE OF EQUILIBRIUM PRICES FOR A SIMPLE PLANNING MODEL
H. Hu Jun. 1985 13 p
(Contracts N00014-85-K-0343; DE-AM03-76SF00326)
(AD-A158263; DE85-015095; SU-SOL-85-10) Avail: NTIS HC A02/MF A01 CSCL 12/2

This is a study on linear programming with intensive use of generations. The economic interpretation of the model is given at the end of the paper. GRA

N86-13592*# Old Dominion Univ., Norfolk, Va.
TIME-DOMAIN QUASI-LINEAR IDENTIFICATION OF NON-LINEAR DYNAMIC SYSTEMS Final Report
Samir R. Ibrahim *In its* Dyn. Identification for Control of Large Space Struct. Nov. 1985 p 35-43 refs Presented at the AIAA/ASME/ASCE/AHS 24th Struct., Struct. Dyn. and Mater. Conf., Lake Tahoe, Hev., 2-4 May 1983 Previously announced in IAA as A83-29811 and A84-36495 (For primary document see N86-13587 04-31)
(AIAA-83-0811-CP) Avail: NTIS HC A04/MF A01

67 THEORETICAL MATHEMATICS

Includes topology and number theory.

N86-13997# Wisconsin Univ., Madison. Mathematics Research Center.
REALIZATION THEORY IN HILBERT SPACE Technical Summary Report
D. Salamon Jul. 1985 37 p
(Contract DAAG29-80-C-0041; Grant NSF DMS-82-10950)
(AD-A158172; MRC-TSR-2835) Avail: NTIS HC A03/MF A01 CSCL 12/1

This paper studies the state space representation of time invariant causal, linear input-output operators in continuous time. A realization theorem in the Hilbert space context is established in full generality using unbounded input and output operators. The first step is to construct an abstract state space representation with a prescribed input-output behavior. The second step is to transform this abstract system into a differential equation. The uniqueness problem is discussed in some detail as well as the relation to existing results in realization theory. Author (GRA)

N86-13998# Pittsburgh Univ., Pa. Center for Multivariate Analysis.
A VARIANT OF SHANBHAG'S LEMMA ARISING OUT OF A MODIFIED RAO-RUBBIN CONDITION
A. A. Alzaid, C. R. Rao, and D. N. Shanbhag May 1985 15 p
(Contract F49620-85-C-0008)
(AD-A158608; TR-85-22; AFOSR-85-0558TR) Avail: NTIS HC A02/MF A01 CSCL 12/1

A modified Rao-Rubbin condition for damage models gives rise to a recurrence relation which is somewhat different from that considered by Shanbhag (1977). A complete solution to the new recurrence relation is obtained and its applications are indicated. Author (GRA)

N86-13999# Florida State Univ., Tallahassee. Dept. of Statistics.
INFORMATION IN CENSORED MODELS
M. Hollander, F. Proschan, and J. Sconing Jun. 1985 25 p
(Contract F49620-85-C-0007; AF Proj. 2304)
(AD-A158644; FSU-Statistics-M701; AFOSR-85-177TR; AFOSR-85-01617TR) Avail: NTIS HC A02/MF A01 CSCL 12/1

Criteria are developed for measuring information in the randomly right-censored model. Measures which are appropriate include an extension of Shannon's entropy. The measures are seen to satisfy some fundamental theorems including: (1) the uncensored case is always at least as informative as any censored model, (2) information decreases as censoring increases stochastically, and (3) the information gain is marginally decreasing. GRA

70 PHYSICS (GENERAL)

For geophysics see *46 Geophysics*. For astrophysics see *90 Astrophysics*. For solar physics see *92 Solar physics*.

N86-14000# Air Force Systems Command, Wright-Patterson AFB, Ohio. Foreign Technology Div.
THE PHYSICS AND TECHNOLOGY OF STRONG MAGNETIC FIELDS (CHAPTER 10)
V. R. Karasik 24 Jul. 1985 13 p Transl. into ENGLISH from the book "Fizika i Tekhnika Silnykh Magnitnykh Poley" Moscow, 1964 p 157-166
(AD-A158174; FTD-ID(RS)T-1097-84) Avail: NTIS HC A02/MF A01 CSCL 20/3

The gaseous nitrogen under high pressure enters from the cylinders into the central tube from below and squeezes the liquid (sodium-potassium alloy) from the lower tank along the ring peripheral channel upward. The liquid passes through holes in the external wall of the hydromagnet, enters into the working chamber, and through holes in the internal wall emerges into the central tube; then it is guided into the upper tank. After the basic mass of liquid is found upward, the nitrogen cylinders are disconnected, and both chambers, the upper and lower, are connected with the atmosphere. The pressure is equalized, and the liquid overflows through the special small hole back into the lower chamber. Then the cycle is repeated. GRA

N86-14001# California Univ., Berkeley. Lawrence Berkeley Lab.
MAGNETIC FIELD APPLICATIONS IN MODERN TECHNOLOGY AND MEDICINE
T. S. Tenforde May 1985 37 p refs Presented at the Symp. on Biol. Effects of Static and Extremely-Low-Frequency Magnetic Fields, Neuherberg, West Germany, 13 May 1985
(Contract DE-AC03-76SF-00098)
(DE85-015197; LBL-19711; CONF-8505183-1) Avail: NTIS HC A03/MF A01

A brief summary is given of several major applications of magnetism. A description of the range of magnetic field intensities to which humans are exposed in technologies that utilize large stationary magnetic fields is given. DOE

N86-14002# California Univ., Berkeley. Lawrence Berkeley Lab.
LATTICE AND BYPASS DESIGN FOR A COHERENT XUV FACILITY
A. Jackson, A. A. Garren, and G. Vignola May 1985 6 p refs Presented at the Particle Accelerator Conf., Vancouver, British Columbia, 13 May 1985 Prepared in cooperation with Brookhaven National Lab., Upton, N.Y.
(Contracts DE-AC02-76CH-00016; DE-AC03-76SF-00098)
(DE85-016556; LBL-19486; CONF-850504-242) Avail: NTIS HC A02/MF A01

The design of a magnet lattice and bypass for a coherent radiation facility is discussed. The lattice is the missing magnet FODO structure first proposed by Vignola for a 6 GeV light source. This has been adapted for a 750 to 1300 MeV electron storage ring for use with both conventional insertion devices and a high gain FEL optimized for output at 400 A. The latter device requires that the electron bunch be deflected into a small aperture bypass, then reinjected into the ring where the perturbing effects of the FEL are damped out. DOE

N86-14003# Stanford Linear Accelerator Center, Calif.
IRON DOMINATED MAGNETS
G. E. Fischer Jul. 1985 71 p Presented at the SLAC Summer School on the Phys. of High Energy Particle Accelerators, Stanford, Calif., 15 Jul. 1985
(Contract DE-AC03-76SF-00515)
(DE85-014955; SU-SLAC-PUB-3726; CONF-850771-1) Avail: NTIS HC A04/MF A01

These two lectures on iron dominated magnets are meant for the student of accelerator science and contain general treatments of the subjects design and construction. The material is arranged in the categories: General Concepts and Cost Considerations, Profile Configuration and Harmonics, Magnetic Measurements, a few examples of special magnets and Materials and Practices. Extensive literature is provided. DOE

N86-14004# Brookhaven National Lab., Upton, N. Y.
RANDOM ERRORS IN THE MAGNETIC FIELD COEFFICIENTS OF SUPERCONDUCTING MAGNETS
J. Herrera, R. Hogue, A. Prodell, P. Wanderer, and E. Willen 1985 7 p refs Presented at the Particle Accelerator Conf., Vancouver, British Columbia, 13 May 1985
(Contract DE-AC02-76CH-00016)
(DE85-012261; BNL-36629; CONF-850504-168) Avail: NTIS HC A02/MF A01

Random errors in the multipole magnetic coefficients of superconducting magnet have been of continuing interest in accelerator research. The Superconducting Super Collider (SSC) with its small magnetic aperture only emphasizes this aspect of magnet design, construction, and measurement. With this in mind, we present a magnet model which mirrors the structure of a typical superconducting magnet. By taking advantage of the basic symmetries of a dipole magnet, we use this model to fit the measured multipole rms widths. The fit parameters allow us then to predict the values of the rms multipole errors expected for the SSC dipole reference design D SSC-C5. With the aid of first-order perturbation theory, we then give an estimate of the effect of these random errors on the emittance growth of a proton beam stored in an SSC. DOE

N86-14005# Lawrence Livermore National Lab., Calif.
JASON ELECTROSTATIC BOUNDARY CONDITIONS: A SURVEY
J. M. Zentler Jun. 1985 51 p
(Contract W-7405-eng-48)
(DE85-014521; UCID-20457) Avail: NTIS HC A04/MF A01

The following is a survey of boundary conditions available to the JASON user for solving 2-D electrostatics problems. Simple examples are included for illumination. It is assumed that the reader has some familiarity with JASON terminology, such as PC and cc, and has access to the JASON user's manual. DOE

N86-13584# Aerodyne Research, Inc., Billerica, Mass.
SINGLE PARTICLE SIZING BY MEASUREMENT OF BROWNIAN MOTION Abstract Only
Alan C. Stanton and Wai K. Cheng *In* AFOSR The 1985 AFOSR/AFRPL Chem. Rocket Res. Meeting Feb. 1985 3 p (For primary document see N86-13507 04-28)
Avail: NTIS HC A11/MF A01

71 ACOUSTICS

Includes sound generation, transmission and attenuation.
For noise pollution see *45 Environment Pollution.*

N86-14006*# National Aeronautics and Space Administration. Lewis Research Center, Cleveland, Ohio.
PRELIMINARY MEASUREMENT OF THE NOISE FROM THE 2/9 SCALE MODEL OF THE LARGE-SCALE ADVANCED PROPFAN (LAP) PROPELLER, SR-7A
James H. Dittmar Sep. 1985 22 p refs
(NASA-TM-87116; E-2718; NAS 1.15:87116) Avail: NTIS HC A02/MF A01 CSCL 02A

Noise data on the Large-scale Advanced Propfan (LAP) propeller model SR-7A were taken into the NASA Lewis 8- by 6-Foot Wind Tunnel. The maximum blade passing tone decreases from the peak level when going to higher helical tip Mach numbers. This noise reduction points to the use of higher propeller speeds as a possible method to reduce airplane cabin noise while maintaining high flight speed and efficiency. Comparison of the SR-7A blade passing noise with the noise of the similarly designed SR-3 propeller shows good agreement as expected. The SR-7A propeller is slightly noisier than the SR-3 model in the plane of rotation at the cruise condition. Projections of the tunnel model data are made to the full-scale LAP propeller mounted on the test bed aircraft and compared with design predictions. The prediction method is conservative in the sense that it overpredicts the projected model data. Author

N86-14007*# National Aeronautics and Space Administration. Lewis Research Center, Cleveland, Ohio.
SOME DESIGN PHILOSOPHY FOR REDUCING THE COMMUNITY NOISE OF ADVANCED COUNTER-ROTATION PROPELLERS
James H. Dittmar Aug. 1985 29 p refs
(NASA-TM-87099; E-2692; NAS 1.15:87099) Avail: NTIS HC A03/MF A01 CSCL 20A

Advanced counter-rotation propellers have been indicated as possibly generating an unacceptable amount of noise for the people living near an airport. This report has explored ways to reduce this noise level, which is treated as being caused by the interaction of the upstream propeller wakes and vortices with the downstream propeller. The noise reduction techniques fall into two categories: (1) reducing the strength of the wakes and vortices, and (2) reducing the response of the downstream blades to them. The noise from the wake interaction was indicated as being reduced by increased propeller spacing and decreased blade drag coefficient. The vortex-interaction noise could be eliminated by having the vortex pass over the tips of the downstream blade, and it could be reduced by increased spacing or decreased initial circulation. The downstream blade response could be lessened by increasing the reduced frequency parameter omega or by phasing of the response from different sections to have a mutual cancellation effect. Uneven blade to blade spacing for the downstream blading was indicated as having a possible effect on the annoyance of counter-rotation propeller noise. Although there are undoubtedly additional methods of noise reduction not covered in this report, the inclusion of the design methods discussed would potentially result in a counter-rotation propeller that is acceptably quiet. Author

N86-14008# Rensselaer Polytechnic Inst., Troy, N.Y.
RAY TRANSMISSIONS OVER A SLOPING BOTTOM IN SHALLOW WATER
M. J. Jacobson, W. L. Siegmann, and T. H. Rousseau 1 Aug. 1985 52 p
(Contract N00014-76-C-0288)
(AD-A158017; RPI-152) Avail: NTIS HC A04/MF A01 CSCL 20/1

The effects of a sloping bottom on acoustic transmissions, between a source and receiver at arbitrary but fixed locations, are investigated using ray theory. An isospeed channel is assumed, and bottom angles up to about 3 degrees are considered. Sloping bottom influence on per-ray quantities, including travel time and transmission loss, are examined for cw transmissions. Significant variations are shown to occur, such as travel time changes of more than 200 ms over ranges of about six km. Per-ray transmission loss is found to be influenced strongly by bottom slope, the amount of influence depending upon source-receiver bearing and the bottom loss model used. Variations of more than 20 dB are demonstrated. Effects of a sloping bottom on the total acoustic field are examined also, and the results compared with those for a horizontal bottom. Finally, a simple model of a shallow water front is superposed over the sloping bottom, and travel time is investigated. The sloping bottom effect can induce travel time changes more than 300% larger than the frontal effect for different source-receiver geometries and bottom inclinations. GRA

N86-14009# Tennessee Univ., Knoxville. Ultrasonics Lab.
THEORY OF THE PROPAGATION OF FINITE AMPLITUDE ULTRASONIC WAVES IN PURE MODE DIRECTIONS IN HEXAGONAL AND TRIGONAL CRYSTALS Interim Report
G. Du and M. A. Breazeale Jun. 1985 73 p
(Contract N00014-81-K-0229; NR Proj. RR0-1108)
(AD-A158154; TR-24) Avail: NTIS HC A04/MF A01 CSCL 02/2

The nonlinear theory describing the propagation of finite amplitude ultrasonic waves in pure mode directions in hexagonal and trigonal crystals is developed. By evaluating the coefficient of the term which couples the longitudinal wave of finite amplitude to the transverse modes, one finds the pure mode directions by requiring this coefficient to vanish. The result is that for hexagonal crystals the directions along the symmetry axis and in the basal plane are pure longitudinal mode directions. Pure mode directions are also found for longitudinal waves propagating tangential to a cone whose apex is centered about the symmetry axis and whose apex angle is a function of the second-order elastic constants of the sample under consideration. The third-order elastic constants which determine the magnitude of the second harmonic of an initially sinusoidal ultrasonic wave are evaluated for these additional directions. For finite amplitude longitudinal ultrasonic waves in trigonal crystals, we have specialized to nonpiezoelectric crystals and have evaluated the third-order elastic constants which determine the magnitude of the second harmonic of an initially sinusoidal wave propagating in the following pure mode directions: (1) along the symmetry axis (the c-direction); (2) along the a-direction in the basal plane; (3) along the direction in the basal plane that makes an angle of 60 deg with the a-direction; and (4) along a direction in the b-c plane whose angle with respect to the b-axis is a function of the second-order elastic constants of the crystal under consideration. GRA

N86-14010# Washington State Univ., Pullman. Dept. of Physics.
ACOUSTICAL SCATTERING FROM AN ELASTIC SPHERE IN WATER: SURFACE WAVE GLORY, RESONANCES, AND THE SOMMERFELD-WATSON TRANSFORMATION FOR AMPLITUDES
K. L. Williams Aug. 1985 74 p
(Contracts N00014-85-C-0141; N00014-80-C-0638; RR0-1108)

(AD-A158884) Avail: NTIS HC A04/MF A01 CSCL 20/1

Scattering of acoustic waves from fluid-load elastic spheres with 10 < ka < 100 (where k is the wavenumber of the acoustic wave in the liquid and a the radius of the sphere) is studied, The main emphasis is on understanding the scattered pressure near backscattering. By carrying out a Sommerfeld-Watson Transformation (SWT) it is shown that this pressure includes contributions from specular reflection, transmitted bulk waves, and surface waves. It is shown experimentally that surface wave contributions to near backscattering display a J sub o Bessel function angular dependence characteristic of weak axial focusing along the backscattered direction; i.e., glory scattering. This focusing is modeled by alternate methods which agree and complement each other. One method allows a simple picture of the glory phenomena while the others (which includes the SWT) are more mathematically rigorous. The absolute value of individual Rayleigh and whispering gallery surface wave contributions is found by this modeling. The theoretical results for are tested experimentally using the Rayleigh surface contribution to scattering from a tungsten carbide sphere. The SWT results are also used to find the far field backscattering pressure as a function of ka. These results are used to better understand and interpret the recently developed Resonance Scattering Theory (RST) as applied to acoustic scattering. It is shown that surface wave contributions to backscattering may be summed in a way analogous to the frequency response of a Fabry-Perot resonator. GRA

72 ATOMIC AND MOLECULAR PHYSICS

Includes atomic structure and molecular spectra.

N86-14011# Wisconsin Univ., Madison. Mathematics Research Center.
THE MATHEMATICAL STRUCTURE OF ELEMENTARY PARTICLES: 2 Technical Summary Report
P. Nowosad May 1985 102 p
(Contract DAAG29-80-C-0041)
(AD-A158191; MRC-TSR-2818) Avail: NTIS HC A06/MF A01 CSCL 20/8

This report is the second part of a general theory purporting to describe the mathematical structure of the elementary particles, deriving it from first principles. It consists of Chapters 6 and 7, continuing the MRC Technical Summary Report 2581, October 1983. These chapters study the implications of the SL sub 2 (R) transformation group of the particles geometry. Chapter 6 shows how the discrete series of representations implies the quantization of the geometries and in particular why the electron does not interact strongly. Chapter 7 obtains the resonances as states corresponding to the principal series of representations. Author (GRA)

N86-14012# Washington State Water Research Center, Pullman.
DETERMINATION OF THE ACTIVATION BARRIER TO ENERGY TRANSFER FROM 3 pi pi* TO CHARGE TRANSFER LEVELS VIA STEADY STATE AND TRANSIENT LUMINESCENCE MEASUREMENTS ON BIS(4-CHLOROTHIOPHENOL) (1,10-PHENANTHROLINE) ZINC (II) Interim Technical Report
R. G. Highland and G. A. Crosby 1 Aug. 1985 14 p
(Contract N00014-83-K-0609)
(AD-A158239; TR-3-ONR) Avail: NTIS HC A02/MF A01 CSCL 20/6

Recent studies on mixed ligand chelates of M(II)(BS)2(N-N) M(II) = Zn(II), Cd(II); BS = anion of a substituted benzenethiol; N-N = dinitrogen-heterocycle reveal the existence of multiple level emissions originating from different electronic configurations. The 6.5 K thermally modulated emission of Zn(4-Cl-PhS)2(phen) showed that the population of the emitting levels could be redistributed via heat pulses, a result that suggested an energy barrier between two accessible excited configurations. We report here an initial investigation of the temperature-dependence of both luminescence lifetimes and intensities of Zn(4-Cl-PhS)2(phen) in an attempt to measure the activation barrier between electronic configurations of dissimilar orbital parentages. The effect of temperature on the luminescence intensity and excited state lifetimes of the title compound is interpreted in terms of a barrier to the transfer of energy from the lowest 3 Pi level to lower-lying charge-transfer levels. Fits of an Arrhenius expression to both lifetimes and relative intensities yield an activation energy and preexponential factor of approx. 140/cm and approx. 100,000/s, respectively. GRA

N86-14013# Missouri Univ., Rolla. Dept. of Physics.
METASTABLE INTERACTIONS: DISSOCIATIVE EXCITATION Final Report, Aug. 1981 - Jan. 1985
L. D. Schearer May 1985 81 p
(Contract F33615-81-K-2081)
(AD-A158733; AFWAL-TR-85-2022) Avail: NTIS HC A05/MF A01 CSCL 07/5

The work reported here is concerned with the interaction between thermal energy metastable atoms and molecules and other atoms and molecules in a beam or in a flowing afterglow. The importance of reactions involving metastable species can be traced to the relative ease with which energy can be stored in ensembles of metastable atoms and molecules and the wide variety of reactions in which they can participate. Of particular interest are those processes which involves energy transfer from the metastable system to a second species which results in excited states which fluoresce. Two principal experimental methods have been used: (1) Metastable beams crossed with a target species, (2) Fast flowing rare gas and nitrogen afterglows. A wide variety of metal halogen, Group 2 metastable beams crossed with a target species, (2) Fast flowing rare gas and nitrogen afterglows. A wide variety of metal halogen, Group 2 metals, methane and silane have been reacted with helium, argon and nitrogen metastables. Author (GRA)

N86-14014# Air Force Inst. of Tech., Wright-Patterson AFB, Ohio. School of Engineering.
IDENTIFICATION OF NUCLEAR MATERIALS FROM REMOTE DETECTION OF CHARACTERISTIC GAMMA RAYS M.S. Thesis
L. W. Brasure Mar. 1985 149 p
(AD-A159244; AFIT/GNE/PH/85M-2) Avail: NTIS HC A07/MF A01 CSCL 18/4

This research effort studies the application of Bayes' decision theorem to extending the range of remote identification of nuclear materials. The finite element method was used to develop a radiation transport code which was used to reconstruct a group of three sample sources at distances of 50, 100, 200, 300, 400, and 500 meters. Both the Poisson and multinomial distributions were then used to simulate measured sources in a low count environment at these six ranges. Bayes' theorem was applied to the resulting measured sources to test for positive identification. The results show that a low resolution detector can increase the range of remote detection an average of 100 meters when compared with the method of photopeak identification. Bayes' theorem is unable, however, to identify sources not contained in the library of known sources. GRA

N86-14015# Air Force Inst. of Tech., Wright-Patterson AFB, Ohio. School of Engineering.
ANALYSIS OF THE DYNAMIC BEHAVIOR OF AN INTENSE CHARGED PARTICLE BEAM USING THE SEMIGROUP APPROACH Ph.D. Thesis
M. A. Stafford May 1985 137 p
(AD-A159247; AFIT/DS/ENC/85-1) Avail: NTIS HC A07/MF A01 CSCL 20/7

Dynamic models of a charged particle beam subject to external electromagnetic fields are cast into the abstract Cauchy problem form. Various applications of intense charged particle beams, i.e., beams whose self electromagnetic fields are significant, might require, or be enhanced by, the use of dynamic control constructed from suitably processed measurements of the state of the beam. This research provides a mathematical foundation for future engineering development of estimation and control designs for such beams. Beginning with the Vlasov equation, successively simpler models of intense beams are presented, along with their corresponding assumptions. Expression of a model in abstract Cauchy problem form is useful in determining whether the model is well posed. Solutions of well-posed problems can be expressed in terms of a one-parameter semigroup of linear operators. (The state transition matrix for a system of linear, ordinary, first-order, constant coefficient differential equations is a special case of such a semigroup.) The semigroup point of view allows the application of the rapidly maturing modern control theory of infinite-dimensional systems. An appropriate underlying Banach space is identified for a simple, but non-trivial, single degree of freedom model (the electrostatic approximation model), and the associated one-parameter semigroup of linear operators is characterized. Author (GRA)

N86-14016# Los Alamos National Lab., N. Mex.
SCHEME TO FUNNEL ION BEAMS WITH A RADIO-FREQUENCY QUADRUPOLE
R. H. Stokes and G. N. Minerbo 1985 17 p Presented at the Workshop on High Brightness, High Current, High Duty Factor Ion Injectors, San Diego, Calif., 21 May 1985
(Contract W-7405-eng-36)
(DE85-015689; LA-UR-85-1627; CONF-8505164-3) Avail: NTIS HC A02/MF A01

We describe a proposed method to funnel ion beams using a new form of the radio-frequency quadrupole (RFQ) structure. This RFQ accepts two bunched ion beams and combines them into a single final beam with interlaced microstructure pulses. It also provides uninterrupted periodic transverse focusing to facilitate the funneling of beams with high current and low emittance. DOE

N86-14017# Stanford Linear Accelerator Center, Calif.
LINEAR ACCELERATORS FOR TeV COLLIDERS
P. B. Wilson May 1985 20 p Presented at the 2nd Intern. Workshop on Laser Acceleration of Particles, Los Angeles, 7 Jan. 1985
(Contract DE-AC03-76SF-00515)
(DE85-014958; SU-SLAC-PUB-3674; CONF-850128-17) Avail: NTIS HC A02/MF A01

This paper summarizes four tutorial lectures on linear electron accelerators: Electron Linacs for TeV Colliders, Emittance and Damping Rings, Wake Fields: Basic Concepts, and Wake Field Effects in Linacs. DOE

N86-14018# Los Alamos National Lab., N. Mex.
REACTIVE SCATTERING IN THE BENDING-CORRECTED ROTATING LINEAR MODEL
R. B. Walker and E. F. Hayes 1985 30 p refs Presented at the NATO Workshop on Chem. Reactions in Organic Constrained Systems, Orleans, France, 23 Jun. 1985 Prepared in cooperation with National Science Foundation, Washington, D.C.
(Contract W-7405-eng-36)
(DE85-017539; LA-UR-85-2994; CONF-8506109-2) Avail: NTIS HC A03/MF A01

We review the theory and applications of the Bending-Corrected Rotating Linear Model (BCRLM) to problems in the quantum description of reactions between atoms and diatomic molecules. DOE

N86-14019# Los Alamos National Lab., N. Mex.
COLLECTIVE ION ACCELERATION BY MEANS OF VIRTUAL CATHODES
W. Peter, R. J. Faehl, C. Snell, and M. E. Jones 1985 14 p refs Presented at the Particle Accelerator Conf., Vancouver, British Columbia, 13 May 1985
(Contract W-7405-eng-36)
(DE85-012707; LA-UR-85-1653; CONF-850504-89) Avail: NTIS HC A02/MF A01

Experiments on collective ion acceleration by means of the formation of a virtual cathode have been carried out for a number of years in the Soviet Union and in the United States. Recently, there has been renewed interest in the subject as a possible means of accelerating ions to very high energies. By understanding the physics underlying the acceleration process it may be possible to determine the feasibility of virtual cathode staging for very high energy ion production. For this reason, a theoretical and computational effort is underway at Los Alamos in order to clarify the basic issues of collective ion acceleration by means of virtual cathodes. To support the theoretical effort, simulations were done with the fully electromagnetic and relativistic particle-in-cell code ISIS (in a one-dimensional mode) and the electrostatic one-dimensional code BIGONE. In the simulations, an electron beam of density 6 x 10 to the 11/cc is injected into a one-dimensional box of lenght L. To supply the necessary ions for collective acceleration, a plasma source containing both ions and electrons was initialized near the emitting boundary. Of prime interest in this study was to understand the dynamics of virtual cathode formation and the dynamics of the acceleration process for the ions. In particular, the question of whether the ions are accelerated by a moving potential well or hydrodynamic pressure due to ambipolar expansion is of primary interest. DOE

N86-14020# Lawrence Livermore National Lab., Calif.
ASPECTS OF THREE FIELD APPROXIMATIONS: DARWIN, FROZEN, EMPULSE
25 May 1985 15 p
(Contract W-7405-eng-48)
(DE85-014204; UCID-20453) Avail: NTIS HC A02/MF A01

The traditional approach used to study high energy beam propagation relies on the frozen field approxiamtion. A minor modification of the frozen field approximation yields the set of equations applied to the analysis of the hose instability. These models are contrasted with the Darwin field approximation. A statement is made of the Darwin model equations relevant to the analysis of the hose instability. DOE

N86-14021# Los Alamos Scientific Lab., N. Mex.
POLARIZATION TRANSFER IN ENELASTIC SCATTERING AND PIONIC MODELS OF THE EMC EFFECT
T. A. Carey, K. W. Jones, J. B. McClelland, J. M. Moss, L. B. Rees, N. Tanaka, and A. D. Bacher 1985 3 p refs Presented at the Intern. Symp. on Polarization Phenomena in Nucl. Phys., Osaka, 26 Aug. 1985 Prepared in cooperation with Indiana Univ., Bloomington
(Contract W-7405-eng-36)
(DE85-014119; LA-UR-85-2047; CONF-850807-3) Avail: NTIS HC A02/MF A01

The aim of the experiment reported was to make a precise test of the enhanced pion field model in a medium-energy scattering experiment. the quantity probed is the spin-longitudinal response function, a measure of the nuclear pion density which is used explicitly in the pion-excess models of the EMC effect. The point of reference used is deuterium. The spin-dependent response functions for heavy targets and (2)H are compared using identical experimental techniques. The technique of complete polarization transfer is used to separate the spin-longitudinal and spin-transverse response in the continuum. The experiment consisted of precise determinations of the polarization transfer coefficients for 500 MeV protons inelastically scattered from Pb, Ca, and (2)H. The experiment utilized longitudinal, sideways, and normal polarized beams in conjunction with final polarization analysis from the focal-plane polarimeter of the high-resolution spectrometer. Quantities constructed from these data are the longitudinal and transverse spin-flip probabilities. Calculations were performed of the ratio of longitudinal to transverse response functions and of the EMC effect with the same model. No evidence was found for collectivity in the isovector spin-longitudinal response function. DOE

N86-14084*# Alabama State Univ., Montgomery.
DETERMINATION OF NEUTRON FLUX DISTRIBUTION BY USING ANISN, A ONE-DIMENSIONAL DISCRETE S SUB n ORDINATES TRANSPORT CODE WITH ANISOTROPIC SCATTERING Final Report

Susanta K. Ghorai *In* NASA. Johnson (Lyndon B.) Space Center The 1983 NASA/ASEE Summer Faculty Fellowship Research Program Research Reports Sep. 1983 18 p refs (For primary document see N86-14078 04-85)
Avail: NTIS HC A18/MF A01 CSCL 20H

N86-14100*# Abilene Christian Coll., Tex.
ION BOMBARDMENT AND ADSORPTION STUDIES ON ILMENITE (FeTiO3) BY X-RAY PHOTOELECTRON SPECTROSCOPY Final Report
Paul D. Schulze *In* NASA. Johnson (Lyndon B.) Space Center The 1983 NASA/ASEE Summer Faculty Research Program Research Reports Sep. 1983 10 p refs (For primary document see N86-14078 04-85)
Avail: NTIS HC A18/MF A01 CSCL 08H

73 NUCLEAR AND HIGH-ENERGY PHYSICS

Includes elementary and nuclear particles; and reactor theory.

For space radiation see *93 Space Radiation.*

N86-14022# Air Force Inst. of Tech., Wright-Patterson AFB, Ohio.
COUPLED RADIATION TRANSPORT/THERMAL ANALYSIS OF THE RADIATION SHIELD FOR A SPACE NUCLEAR REACTOR Ph.D. Thesis
W. J. Barattino Jul. 1985 362 p
(AD-A158180; AFIT/CI/NR-85-53D) Avail: NTIS HC A16/MF A01 CSCL 18/6

A coupled radiation transport-heat transfer-stress analysis of the radiation shield for an SP-100 reactor was performed using a numerical code developed at the University of New Mexico and Sandia National Laboratory. For a fast reactor operating at 1.66 MW sub th, the energy deposited and resulting temperature distribution was determined for a shield consisting of tungsten and lithium hydride pressed into a stainless steel honeycomb matrix. While temperature feedback was shown to have a minor effect on energy deposition, the shielding configuration was found to have a major influence in meeting thermal requirements of the lithium hydride. It was shown that a shield optimized for radiation protection will fail because of melting. However, with minor modifications in the shield layering and material selection, the thermal integrity of the shield can be preserved. A shield design of graphite, depleted lithium hydride, tungsten, and natural lithium hydride was shown to satisfy neutron and gamma fluence requirements, maximum temperature limits, and minimize cracking in the LiH portion of the shield. GRA

N86-14023# California Univ., Berkeley. Lawrence Berkeley Lab.
NEW CONTROL TECHNIQUES FOR EXTRACTION OF BEVALAC BEAMS
M. Nyman, W. Chu, B. Mehlman, W. Mirer, H. Oakley, T. Renner, G. Stover, and M. Tekawa May 1985 5 p Presented at the Particle Accelerator Conf., Vancouver, British Columbia, 13-16 May 1985
(Contract DE-AC03-76SF-00098)
(DE85-017640; LBL-18946; CONF-850504-274) Avail: NTIS HC A02/MF A01

Beams of accelerated heavy ions can now be delivered as one second long dc pulses with minimal fluctuations in instantaneous flux. Pulse duration can be held constant to within 1% while keeping a high nonvarying extraction efficiency which minimizes pulse to pulse position shift in the extracted beam. In addition, differing beam intensities over several orders of magnitude can be delivered. Computer adjustment of all measurement and control devices results in linear operation over three orders of magnitude of beam intensity. Control of beam structure is accomplished by a unique combination of dual slope integrators and phase forward predictive circuits in the feedback loop. DOE

N86-14024# Rockwell International Corp., Golden, Colo.
HIGH COUNT RATE GAMMA-RAY SPECTROMETER SYSTEM FOR PLUTONIUM ISOTOPIC MEASUREMENTS
J. G. Fleissner, C. P. Oertel, and A. G. Garrett 1985 20 p Presented at the 26th Ann. Meeting of the Inst. of Nucl. Mater. Management, Abluquerque, N. Mex., 21 Jul. 1985
(Contract DE-AC04-76DP-03533)
(DE85-013212; RFP-3792; CONF-850765-29) Avail: NTIS HC A02/MF A01

The High Count Rate Gamma Ray Spectrometer (HCRS) for plutonium isotopic measurement produces many benefits for both production and safeguards applications. It shortens the count times to approximately ten minutes. Its production rate is about 400% greater. It is easy to use. It requires reduced human exposure, and there is more timely reporting of results. In addition, it is comprised of off the shelf commercial components. F.M.R.

N86-14025# Fermi National Accelerator Lab., Batavia, Ill.
OPERATION OF LARGE CRYOGENIC SYSTEMS
C. H. Rode, B. Ferry, W. B. Fowler, J. Makara, T. Peterson, J. Theilacker, and R. Walker Jun. 1985 6 p refs Presented at the Particle Accelerator Conf., Vancouver, British Columbia, 13 May 1985
(Contract DE-AC02-76CH-03000)
(DE85-017439; FNAL-TM-1314; CONF-850504-267) Avail: NTIS HC A02/MF A01

This report is based on the past 12 years of experiments on R and D and operation of the 27 kW Fermilab Tevatron Cryogenic System. In general the comments are applicable for all helium plants larger than 1000W (400 1/hr) and non mass-produced nitrogen plants larger than 50 tons per day. DOE

N86-14026# Oak Ridge National Lab., Tenn.
THE (58)Ni + n TRANSMISSION, CAPTURE AND DIFFERENTIAL ELASTIC SCATTERING DATA ANALYSIS IN THE RESONANCE REGION
C. M. Perey, F. G. Perey, J. A. Harvey, N. W. Hill, and R. L. Macklin 1985 5 p Presented at the Intern. Conf. on Nucl. Data for Basic and Appl. Sci., SantaFe, N. Mex., 13 May 1985
(Contract DE-AC05-84OR-21400)
(DE85-016157; CONF-850507-52) Avail: NTIS HC A02/MF A01

High-resolution neutron transmission, capture and differential elastic scattering measurements have been made for (58)Ni-enriched targets at the Oak Ridge Electron Linear Accelerator (ORELA) from the eV to the MeV region. The three sets of data were analyzed simultaneously from 10 to 450 keV, and the transmission analysis was extended to 650 keV. For the 52 s-wave resonances observed between 10 and 650 keV, the average level spacing, D0, and the strength function, s0, are 12.2 + - 1.0 keV and (3.1 + - 0.6) x 10(-4), respectively. DOE

N86-14027# Oak Ridge National Lab., Tenn.
STRUCTURE AND HYDRODYNAMICS OF COLLOIDAL SYSTEMS
J. B. Hayter Jul. 1985 17 p Presented at the Intern. Conf. on Neutron Scattering, Santa Fe, N. Mex., 19 Aug. 1985
(Contract DE-AC05-84OR-21400)
(DE85-016294; CONF-850871-6) Avail: NTIS HC A02/MF A01

Colloidal phases (for example, micellar solutions, latex suspensions, ferrofluids and microemulsions) provide excellent model systems with which to test structural and hydrodynamic theories of the liquid state. Interparticle potentials may be attractive or repulsive, and the experimentalist is often free to control the strength, range and symmetry of the interactions. Small-angle neutron scattering (SANS) and small-angle neutron spin-echo (SANSE) provide excellent complementary tools for studying the structure and time-dependence of these systems, where correlation lengths typically vary from about one to several tens of nm. Correlation times are usually in the nsec to (MU) sec range, but may be of order minutes in certain systems. This paper will review some of the current theories and their recent experimental tests, using colloidal systems in which the direct interaction potentials may have spherical, dipolar or cylindrical symmetry and the hydrodynamic interactions may be weak or strong. DOE

N86-14028# Fermi National Accelerator Lab., Batavia, Ill.
VARIABLE CURVATURE PHANTOM
I. Rosenberg, M. Awschalom, and R. K. TenHaken Apr. 1985 4 p
(Contract DE-AC02-76CH-03000)
(DE85-014260; FNAL-TM-1310) Avail: NTIS HC A02/MF A01

The design of a variable curvature dosimetry phantom is briefly described. The phantom was developed to test the accuracy of the dose modification algorithms used to estimate dose distributions inside patient contours. DOE

N86-14029# Stanford Linear Accelerator Center, Calif.
HARDWARE UPGRADE FOR KLYSTRONS IN THE SLC
R. K. Jobe, M. J. Browne, and K. P. Slattery May 1985 3 p Presented at the Particle Accelerator Conf., Vancouver, British Columbia, 13 May 1985
(Contract DE-AC03-76SF-00515)
(DE85-014357; SU-SLAC-PUB-3666; CONF-850504-184) Avail: NTIS HC A02/MF A01

The control and monitoring of the klystrons in the first third of the SLAC linear accelerator has been commissioned, and a program to complete installation by summer 1985 is in progress. A general overview of the new control system for SLAC klystrons is presented along with a detailed description of the Modulator Klystron Support Unit. The MKSU contains all the devices necessary to interface klystron monitoring and control to the SLC control system through a dedicated intelligent CAMAC module. Controlled devices include RF phase and drive controls, the high power modulator status, associated RF signals, waterflow and magnet controls. DOE

N86-14030# Mound Lab., Miamisburg, Ohio.
MOUND ACTIVITIES IN CHEMICAL AND PHYSICAL RESEARCH: JULY DECEMBER 1984
17 Jun. 1985 27 p refs
(Contract DE-AC04-76DP-00053)
(DE85-014402; MIM-3258) Avail: NTIS HC A03/MF A01

Progress reports are presented in the following areas: (1) low-temperature research (deuterium triple point temperature standard, helium second virial as applied to gas thermometry); and (2) separation research (liquid phase thermal diffusion, calcium isotope separation, low temperature trenschaukel, calcium chemical exchange). DOE

N86-14031# GA Technologies, Inc., San Diego, Calif.
DOUBLET 3 Annual Report, 1 Oct. 1983 - 30 Sep. 1984
May 1985 116 p
(Contract DE-AC03-84ER-51044)
(DE85-014369; GA-A-18024) Avail: NTIS HC A06/MF A01

The operating space accessible to Doublet III, together with maximum values of some of the plasma parameters which were achieved during the course of energy confinement and high beta experiments are investigated. For those parameters correlated with good energy confinement, such as elected and ion temperatures, stored energy, and neutron rate, the maximum values were obtained in high current, high toroidal field, divertor discharged with deuterium beam heating. Doublet III was the first tokamak to produce beta values of factor interest. High toriodal beta and low q values were obtained in lower toroidal field, limiter discharges. The most recent experiments were performed with up to 8 MW of neutral beam heating power and up to 1 MW of 60 GHz ECH power. Operations and maintenance are detailed, as is progress in vessel modification MOF, electron cylotron heating MOF, and the Doublet III US/Japan cooperation upgrade. E.R.

N86-14032# Los Alamos Scientific Lab., N. Mex.
LOW POWER REACTOR FOR REMOTE APPLICATIONS
K. L. Meier, R. G. Palmer, and W. L. Kirchner 1985 7 p refs Presented at the 20th Intersoc. Energy Conversion Eng. Conf., Miami Beach, Fla., 18 Aug. 1985
(Contract W-7405-eng-36)
(DE85-012763; LA-UR-85-1870; CONF-850808-6) Avail: NTIS HC A02/MF A01

A compact, low power reactor is being designed to provide electric power for remote, unattended applications. Because of the high fuel and maintenance costs for conventional power sources such as diesel generators, a reactor power supply appears especially attractive for remote and inaccessible locations. Operating at a thermal power level of 135 kWt, the power supply achieves a gross electrical output of 25 kWe from an organic Rankine cycle (ORC) engine. By intentional selection of design features stressing inherent safety, operation in an unattended mode is possible with minimal risk to the environment. Reliability is achieved through the use of components representing existing, proven technology. Low enrichment uranium particle fuel, in graphite core blocks, cooled by heat pipes coupled to an ORC converter insures long term, virtually maintenance free, operation of this reactor for remote applications. DOE

N86-13565# Rensselaer Polytechnic Inst., Troy, N.Y.
VARIABLE FIELD EFFECTS FOR THE ROTATING FLUIDIZED BED REACTOR Abstract Only
Owen C. Jones *In* AFOSR The 1985 AFOSR/AFRPL Chem. Rocket Res. Meeting Feb. 1985 3 p (For primary document see N86-13507 04-28)
Avail: NTIS HC A11/MF A01

N86-13604# Joint Publications Research Service, Arlington, Va.
NATION'S ACHIEVEMENTS IN HIGH ENERGY PHYSICS REVIEWED
Zhang Wenyu *In its* China Rept.: Sci. and Technol. (JPRS-CST-85-020) 24 Jun. 1985 p 76-89 Transl. into ENGLISH from Gaoneng Wuli (Beijing), no. 3, Sep. 1984 p 1-6 (For primary document see N86-13600 04-31)
Avail: NTIS HC A09/MF A01

74 OPTICS

Includes light phenomena.

N86-14033*# National Aeronautics and Space Administration. Marshall Space Flight Center, Huntsville, Ala.
TEST METHOD FOR TELESCOPES USING A POINT SOURCE AT A FINITE DISTANCE Center Director's Discretionary Fund Final Report
Donald B. Griner, David E. Zissa, and Dietrich Korsch (Korsch Optics, Inc.) Sep. 1985 23 p refs
(Proj. H20)
(NASA-TM-86523; NAS 1.15:86523) Avail: NTIS HC A02/MF A01 CSCL 20F

A test method for telescopes that makes use of a focused ring formed by an annular aperture when using a point source at a finite distance is evaluated theoretically and experimentally. The results show that the concept can be applied to near-normal, as well as grazing incidence. It is particularly suited for X-ray telescopes because of their intrinsically narrow annular apertures, and because of the largely reduced diffraction effects. Author

N86-14034# Army Missile Command, Redstone Arsenal, Ala.
REAL TIME LARGE MEMORY OPTICAL PATTERN RECOGNITION
D. A. Gregory Jun. 1984 124 p
(AD-A158023; AD-E950731; AMSMI/RR-84-9-TR) Avail: NTIS HC A06/MF A01 CSCL 14/5

A large memory optical recognition system has been developed and tested. The memory consists of an array of stored holographic Fourier transform matched filters in a VanderLugt type correlator. The filters are stored (on high resolution Kodak plates) and addressed using a novel holographic multi-focus lens. This element acts as a diffraction grating, splitting the input beam into 25 elements and as a lens, producing the Fourier transform of each of the 25 elements. The filters are created and addressed using a HeNe laser and a Hughes liquid crystal light valve (LCLV) to produce a coherent image from a television monitor. The LCLV also allows the filters to be addressed in real time thereby making the use of a transparency as an input scene unnecessary. This provides for real time recognition. Thus far, more than 70 matched filters have been stored on a single holographic plate and addressed in parallel and in real time with good correlations resulting. This research and the results obtained should contribute to allowing serious consideration to be given to the use of optical recognition systems for a wide variety of civilian and military applications. Author (GRA)

N86-14035# Naval Postgraduate School, Monterey, Calif.
HIERARCHICAL IMAGE TO SEGMENTATION TO INFRARED IMAGES M.S. Thesis
J. D. Bloomquist Jun. 1985 71 p
(AD-A158030) Avail: NTIS HC A04/MF A01 CSCL 17/5

Recursive image segmentation with hierarchical scope views is a new technique in image processing which systematically divides an image into smaller and smaller quadrants with each region within the quadrants having a structured descriptor. The regions are then processed to remove noise and to check for connected regions across the quadrant boundaries. The quadrants are then brought back together with the obsecured target enhanced and distinguishable from the background. Infrared image data of five different ship targets with the associated noise and interference was processed by this technique with the target information being greatly enhanced. The procedures developed to evaluate the data were found to be inadequate for the task, neccessitating hand evaluation to extract the target. The technique was proven to be a viable solution for extracting target information from infrared data, but very slow processing times and inadequate evaluation procedures limit the usefulness of the program in its present form. GRA

N86-14036# Massachusetts Inst. of Tech., Cambridge. Artificial Intelligence Lab.
MULTIGRID RELAXATION METHODS AND THE ANALYSIS OF LIGHTNESS, SHADING, AND FLOW
D. Terzopoulos Oct. 1984 25 p
(Contract N00014-80-C-0505)
(AD-A158173; AI-M-803) Avail: NTIS HC A02/MF A01 CSCL 20/6

Image analysis problems, posed mathematically as variational principles or as partial differential equations, are amenable to numerical solution by relaxation algorithms that are local, iterative, and often parallel. Although they are well suited structurally for implementation on massively parallel, locally-interconnected computational architectures, such distributed algorithms are seriously handicapped by an inherent inefficiency at propagating constraints between widely separated processing elements. Hence, they converge slowly when confronted by the large representations necessary for low-level vision. Application of multigrid methods can overcome this drawback, as we established in previous work on 3-D surface reconstruction. In this paper, we develop efficient multiresolution iterative algorithms fo computing lightness, shape-from-shading, and optical flow, and we evaluate the performance of these algorithms on synthetic images. This multigrid methodology is broadly applicable in low-level vision. Notably, it is an appealing strategy to use in conjunction with regularization analysis for the efficient solution of a wide range of ill-posed visual reconstruction problems. GRA

N86-14037# Mississippi State Univ., Mississippi State.
RESULTS OF RESEARCH IN FOUR TOPIC AREAS: THE SINGULARITY EXPANSION METHOD, TRANSIENT SCATTERING MEASUREMENTS, HIGH-FREQUENCY DIFFRACTION AT EDGES RESIDING ON INTERFACES AND CYLINDRICAL COORDINATE REPRESENTATION OF DYADIC GREEN'S FUNCTIONS Final Report, 1 Jan. 1981 - 1 Aug. 1985
L. W. Pearson and A. W. Glisson, Jr. 1 Aug. 1985 7 p
(Contract N00014-81-K-0256)
(AD-A158382) Avail: NTIS HC A02/MF A01 CSCL 12/1

This report briefly presents the results of research in four topic areas investigated during the grant period. These four topic areas are; the Singularity Expansion Method, transient scattering measurements, high frequency diffraction at edges residing on interfaces, and cylindrical coordinate representation of dyadic Green's functions. GRA

N86-14038# Missouri Univ., Kansas City.
OPTICAL CONSTANTS Contractor Report, Sep. 1982 - May 1984
M. R. Querry Jun. 1985 415 p
(Contract DAAK11-82-C-0069)
(AD-A158623; CRDC-CR-85034) Avail: NTIS HC A18/MF A01 CSCL 20/6

Reflectance spectra of 23 materials were acquired at near normal incidence in the ultraviolet, visible and infrared spectral regions. The optical constants of the materials were determined by use of Kramers-Kronig methods. The 23 materials were: (1) Sapphire (Al2O3)E//C, (2) Sapphire (Al2O3)E+C, Oxidized aluminum mirror, (4) Iron, (5) Hematite (Fe2O3)E//C, (6) Hematite (Fe2O3)E+C, (7) Magnetite (Fe3O4), (8) Cuprous oxide (Cu2O) pellet, (9) Zinc oxide (Zno) pellet, (10) Copper Ingot, (11) Brass Ingot (90 Cu/10 Zn), (12) Brass Ingot (85 Cu/15 Zn), (13) Brass Ingot(70 Cu/30 Zn), (14) Dixon KS-2 Graphite pellet, (15) Dixon HPN-2 Graphite pellet, (16) Dixon 200-10 Graphite pellet, (17) Asbury Micro 260 Graphite pellet, (18) Dixon 1102 Intercalated Graphite pellet, (19) Asbury 3222 Intercalated Graphite pellet, (20) Pyrolytic Graphite (on planar face), (21) Pyrolytic Graphite (on planar face), (21) TTF/TCNQ pellet, (22) Cu/TCNQ pellet, and Li/TCNQ pellet. Final data were supplied on punched cards, and in graphical and tabular. GRA

N86-14039# Washington State Univ., Pullman. Dept. of Physics.
LIGHT SCATTERING FROM BUBBLES IN LIQUIDS
D. S. Langley Dec. 1984 131 p
(Contract N00014-80-C-0838)
(AD-A158736; TR-4) Avail: NTIS HC A07/MF A01 CSCL 20/6

The scattering of laser light from bubbles in liquids was photographed, and angular features in the far-zone intensity are compared with models. Diffraction effects are prominent in three regions of the scattering: near the critical angle, and in the forward and backward directions. The forward and backward scattered light exhibits the intensity enhancement known as the glory. Simple geometrical optics is unable to approximate the scattering pattern in the diffraction regions. Physical-optics models are presented for each case and shown to be in agreement with the observations. These models give insight into the optical properties of scatterers whose refractive index is less than that of their surroundings. Comparisons also include the results of Mie theory computations for the critical-angle and forward regions. Some applications of the results to the sizing and detection of bubbles are discussed. GRA

N86-14040# Defence Research Establishment Valcartier (Quebec).
INVESTIGATION OF COLD COLORED SMOKE PRODUCTION
T. Liberman Aug. 1985 43 p
(AD-A158783; DREV-R-4372/85) Avail: NTIS HC A03/MF A01 CSCL 19/1

The main objective of this project is to develop a nonfading colored cold smoke composition for use in a signal cartridge for practice bombs. The primary constraint is that the substance must not require any form of heat to produce the smoke; hence the term cold smoke. The principal use of the colored cold smoke charge is to mark the point of impact of practice bombs used by the Canadian Forces (CF). In summertime, white smoke produced by titanium tetrachloride (TiCl4) is satisfactory; however, colored smoke is required during winter because of the white snow background. Different methods for producing large colored smoke clouds for use as spotting charges are evaluated. The problem of the disappearance, or bleaching, of the orange color from vanadium oxytrichloride (VOCl3) clouds during times of high relative humidity is considered. It is postulated that this is caused by the absorption of large quantities of atmospheric moisture by the smoke. A model has been developed to study the process. This model makes the key predictions concerning the absorption of very large amounts of atmospheric moisture by VOCl3 type smokes above a relative humidity of 80% and the very small importance of temperature as a parameter. These predictions are, in general, corroborated very well by experiment. Possible solutions to this color bleaching problem are discussed, including one that calls for the synthesis of hydrolyzable vanadium compounds with nonhygroscopic leaving groups. GRA

N86-14041# Department of the Navy, Washington, D. C.
AN INTEGRATED WAVELENGTH DEMULTIPLEXER Patent Application
R. E. Reedy, inventor (to Navy) Filed 1 Jul. 1985 28 p
(AD-D011867; US-Patent-Appl-SN-750630) Avail: NTIS HC A03/MF A01 CSCL 20/6

An optical wavelength demultiplexer is fabricated as an integral part of an integrated circuit chip. A waveguide in a common substrate having a chirped diffraction grating receives a number of wavelengths of optically modulated data from a single mode fiber. The wavelengths are diffracted from the plane of the lines of the grating into discrete beams at discrete angles through the substrate and impinge on appropriately located photodetectors. Signals provided by the detectors are fed to an processed by other integrated circuitry also contained on the chip. The common transparent substrate such as fused silica, glass, sapphire, lithium niobate or lithium tantalate mount semiconductor films of Si, Ge GaAs or quaternary alloys that have the detectors and other integrated circuitry that are created by conventional CVD techniques. The waveguide and appropriate chirp grating are formed by established deposition and photolithographic procedures to assure the separation of as many as fifty discrete beams of as many different wavelengths and their projection onto a like number of photodetectors to provide for a heretofore unattainable degree of optical wavelength demultiplexing. Author (GRA)

N86-14042# Department of the Army, Washington, D. C.
OPTICAL RADAR TRANSCEIVER CONTROL APPARATUS Patent Application
R. J. Mongeon, R. J. Wayne, and R. W. Henschke, inventors (to Army) Filed 1 Aug. 1985 21 p
(AD-D011880; US-Patent-Appl-SN-761257) Avail: NTIS HC A02/MF A01 CSCL 17/9

The apparatus is part of an optical radar set and comprises a high powered CO2 pulsed transmitter laser which is injection controlled to operate at a fixed frequency offset from a lower powered CO2 local oscillator laser. A portion of the output of the local oscillator laser is applied to an acousto-optic Bragg cell, together with an RF signal equal to the desired intermediate frequency of the radar set. The upshifted first order output of the Bragg cell is injected into the transmitter laser for stabilization purposes. This results in a stable intermediate frequency for the optical radar set. Author (GRA)

N86-14043# Department of the Navy, Washington, D. C.
OPTOELECTRONIC INTEGRATED CIRCUIT MULTIPLIER Patent Application
R. E. Reedy, J. H. Harris, and D. J. Albares, inventors (to Navy) Filed 20 Jun. 1985 26 p
(AD-D011883; US-Patent-Appl-SN-746704) Avail: NTIS HC A03/MF A01 CSCL 20/6

An apparatus and method for improving VLSI and VHSIC system data transmission relies on a plurality of optoelectronic switches actuated by pulses from at least one light source, a laser. Differing lengths of optical fibers couple the pulsed light from the laser at different times to create a sequence of actuation light pulses for the plurality of optoelectronic switches each time the light source is pulsed. Thus, the information appearing at a plurality of parallel data nodes is converted to serial form at an output bonding pad on the chip. Optionally, a similar pulsing of electroptic switches coupled to an input bonding pad converts serial data to parallel form. Faster input and output switching times are provided, reliability and complexity are reduced, particularly as compared to off-chip arrangements, and power consumption and dissipation are reduced. Author (GRA)

N86-14044# Department of the Navy, Washington, D. C.
FIBER OPTICS AS AN ANGULAR SENSOR Patent Application
H. Rieger, inventor (to Navy) Filed 27 Jun. 1985 12 p
(AD-D011886; US-Patent-Appl-SN-749340) Avail: NTIS HC A02/MF A01 CSCL 17/8

This patent application discloses an uncomplicated, compact and environmentally-immune sensor for the degree of articulation of finger joints in a remote underwater vehicle which uses a length of an optical fiber connected to each finger joint. As the joint is rotated, the bending of the optical fiber changes the attenuation of light through the fibers and a detector monitoring this change provides a signal that is correlated to the degree of articulation. GRA

N86-13564# Spectron Development Labs., Inc., Costa Mesa, Calif.
OPTICAL TECHNIQUE TO MEASURE ELECTRODE EROSION Abstract Only
James D. Trolinger and David F. Schaack *In* AFOSR The 1985 AFOSR/AFRPL Chem. Rocket Res. Meeting Feb. 1985 3 p (For primary document see N86-13507 04-28)
Avail: NTIS HC A11/MF A01

N86-13569# SRI International Corp., Menlo Park, Calif. Chemical Physics Lab.
TWO-PROTON DETECTION TECHNIQUES FOR ATOMIC FLUORINE Abstract Only
William K. Bischel *In* AFOSR The 1985 AFOSR/AFRPL Chem. Rocket Res. Meeting Feb. 1985 3 p (For primary document see N86-13507 04-28)
Avail: NTIS HC A11/MF A01

N86-13570# California Univ., Berkeley. Dept. of Mechanical Engineering.
COHERENT OPTICAL TRANSIENT SPECTROSCOPY IN FLAMES Abstract Only
John W. Daily *In* AFOSR The 1985 AFOSR/AFRPL Chem. Rocket Res. Meeting Feb. 1985 3 p (For primary document see N86-13507 04-28)
Avail: NTIS HC A11/MF A01

N86-13573# Stanford Univ., Calif.
OPTICAL PROCESSING AND PHASE CONJUGATION Abstract Only
Lambertus Hesselink *In* AFOSR The 1985 AFOSR/AFRPL Chem. Rocket Res. Meeting Feb. 1985 3 p (For primary document see N86-13507 04-28)
Avail: NTIS HC A11/MF A01

N86-13605# Joint Publications Research Service, Arlington, Va.
INTEGRATED OPTICS DEVELOPMENTS OVER PAST DECADE, FUTURE PROSPECTS
Yu Rongjin *In its* China Rept.: Sci. and Technol. (JPRS-CST-85-020) 24 Jun. 1985 p 90-95 refs Transl. into ENGLISH from Zhongguo Jiguang (Shanghai), v. 12, no. 4, 20 Apr. 1985 p 193-196 (For primary document see N86-13600 04-31)
Avail: NTIS HC A09/MF A01

N86-13779# Joint Publications Research Service, Arlington, Va.
DISTRIBUTION OF BRIGHTNESS FROM POINT SOURCE OF SCATTERED LIGHT ALONG INCLINED PATH Abstract Only
A. S. Drofa and A. L. Usachev *In its* USSR Rept.: Earth Sci. (JPRS-UES-85-009) 13 Nov. 1985 p 28 Transl. into ENGLISH from Izv. Akad. Nauk SSSR: Fiz. Atmosfery i Okeana (Moscow), v. 21, no. 6, Jun. 1985 p 603-608 Original language document was announced in IAA as A85-44481 (For primary document see N86-13765 04-42)
Avail: NTIS HC A04/MF A01

N86-13781# Joint Publications Research Service, Arlington, Va.
INFLUENCE OF FOG MICROSTRUCTURE ON QUALITY OF OPTICAL IMAGE TRANSMITTED THROUGH IT Abstract Only
L. P. Volnistova, A. S. Drofa, and V. P. Snykov *In its* USSR Rept.: Earth Sci. (JPRS-UES-85-009) 13 Nov. 1985 p 29-30 Transl. into ENGLISH from Izv. Akad. Nauk SSSR: Fiz. Atmosfery i Okeana (Moscow), v. 21, no. 6, Jun. 1985 p 507-511 (For primary document see N86-13765 04-42)
Avail: NTIS HC A04/MF A01

N86-13786# Joint Publications Research Service, Arlington, Va.
STATISTICS OF INTENSIVE LIGHT BEAMS IN TURBULENT ATMOSPHERE Abstract Only
V. P. Kandidov *In its* USSR Rept.: Earth Sci. (JPRS-UES-85-009) 13 Nov. 1985 p 34 Transl. into ENGLISH from Izv. Akad. Nauk SSSR: Ser. Fiz. (Moscow), v. 49, no. 3, Mar. 1985 p 442-449 Original language document was announced in IAA as A85-31855 (For primary document see N86-13765 04-42)
Avail: NTIS HC A04/MF A01

N86-13791# Joint Publications Research Service, Arlington, Va.
EFFECTIVENESS OF USE OF ADAPTIVE OPTICAL SYSTEMS UNDER CONDITIONS OF SELF-EFFECT IN ATMOSPHERE Abstract Only
P. A. Konyayev, V. P. Lukin, and V. L. Mironov *In its* USSR Rept.: Earth Sci. (JPRS-UES-85-009) 13 Nov. 1985 p 38 Transl. into ENGLISH from Izv. Akad. Nauk SSSR: Ser. Fiz. (Moscow), v. 49, no. 3, Mar. 1985 p 536-540 Original language document was announced in IAA as A85-31867 (For primary document see N86-13765 04-42)
Avail: NTIS HC A04/MF A01

N86-14089*# Middlesex County Coll., N.J. Dept. of Mech./Civil Technology.
SPECTRAL REFLECTANCE OF SURFACE SOILS: RELATIONSHIPS WITH SOME SOIL PROPERTIES Final Report
Carl H. Kiesewetter *In* NASA. Johnson (Lyndon B.) Space Center The 1983 NASA/ASEE Summer Faculty Fellowship Research Program Research Reports Sep. 1983 27 p refs (For primary document see N86-14078 04-85)
Avail: NTIS HC A18/MF A01 CSCL 20F

75 PLASMA PHYSICS

Includes magnetohydrodynamics and plasma fusion.
For ionospheric plasmas see *46 Geophysics*. For space plasmas see *90 Astrophysics*.

N86-14045# Hiroshima Univ. (Japan).
POPULATION INVERSION IN A RECOMBINING HYDROGEN PLASMA INTERACTING WITH A HELIUM GAS
Toshiatsu Oda (Hiroshima Univ.) and Utaro Furukane (Ehime Univ., Japan) Nagoya, Japan Nagoya Univ. Aug. 1984 17 p refs
(IPPJ-692) Avail: NTIS HC A02/MF A01

A numerical investigation has shown that the population inverstion between the levels with the principal quantum number i=2 and 3 takes place in a recombining hydrogen plasma which is interacting with a cool and dense helium gas on the basis of a collision-radiative (CR) model. Overpopulation density, which is defined as the difference between the population densities per unit statistical weight of the upper and lower excited levels 3 and 2, is found to be much higher than a threshold level for the laser oscillation in the quasi-steady state when the hydrogen plasma interacts with the helium gas with pressure of approx. 50 Torr. Author

N86-14046# Kyoto Univ. (Japan). Dept. of Electronics.
HIGH ORDER SPLINE INTERPOLATION IN THE PARTICLE SIMULATION
Hirotada Abe, Natsuhiko Sakairi, Ryohei Itatani, and Hideo Okuda (Princeton Univ.) Nagoya, Japan Nagoya Univ. Jun. 1985 37 p refs
Avail: NTIS HC A03/MF A01

In the conventional plasma simulation models using particles, in which the total momentum is conserved, the total energy is not conserved due to nonuniformity of space caused by the spatial grids. The grid spacing was severely limited of order of the Debye length. It is found that the use of the high order spline spatial interpolation removes this limit without a significant increase of the computation and complexity of the algorithm in the system that only the long-wavelength, collective phenomena are important. The theoretical analysis of the total energy is improved compared with the previous work and its scaling law is related to so-called the aliasing error explicitly. The coefficient eta introduced previously is referred as the model index and is used again as a measure of the accuracy of the models for the energy conservation. Author

N86-14047# Yamanashi Univ., Kofu (Japan). Faculty of Engineering.
PARAMETRIC EXCITATION OF ION BERNSTEIN WAVES BY MAGNETOSONIC WAVE
M. Matsumoto, K. Sakai, and S. Takeuchi Nagoya, Japan Nagoya Univ. Jul. 1985 16 p refs
(IPPJ-738) Avail: NTIS HC A02/MF A01

In a uniformly magnetized plasma ion Bernstein waves are parametrically excited by a magnetosonic (pump) wave which propagates perpendicularly to the static magnetic field B sub 0. The pump wave is assumed with K sub 0 not equal to 0 and omega sub 0 approx. equals 2 OMEGA sub 0, OMEGA sub 0 being the ion cyclotron frequency. The growth rate of the excited wave which also propagates perpendicularly to B sub 0 is obtained in the first order of magnitude K sub 0. the analysis is based on a method of intergration along the dynamical trajectory of particle in the static and electromagnetic pump fields. Author

N86-14048# Nagoya Univ. (Japan). Inst. of Plasma Physics.
PRELIMINARY EXPERIMENT ON ELECTRON BEAM INJECTION FOR TOKAMAK CURRENT DRIVE
A. Mohri, S. Kubo, M. Hasegawa, K. Narihara, H. Tanaka (Kyoto Univ.), A. Ando (Kyoto Univ.), K. Ogura (Kyoto Univ.), T. Makewa (Kyoto Univ.), Y. Terumichi (Kyoto Univ.), and S. Tanaka (Kyoto Univ.) Jul. 1985 14 p refs
(IPPJ-739) Avail: NTIS HC A02/MF A01

Electron beams with moderate energies, 0.4 to 2 keV, were injected for 5 ms into a small tokamak WT-2 by using the plasma anode method. The injection into a currentless plasma of a density 2.5 x 10 to the 18th power m(-3) at a toroidal field 1.1 T formed a toroidal current 4 kA, which was nine times the injected beam current. Also, an inductively produced toroidal current was sustained during the injection. Author

N86-14049# Yamanashi Univ., Kofu (Japan). Inst. of Plasma Physics.
UNLIMITED ACCELERATION OF CHARGED PARTICLES BY AN ELECTROMAGNETIC WAVE WITH A PURELY TRANSVERSE ELECTRIC FIELD PROPAGATING PERPENDICULARLY TO A STATIC MAGNETIC FIELD
S. Takeuchi (Yamanashi Univ.), K. Sakai (Yamanashi Univ.), M. Matsumoto (Yamanashi Univ.), and R. Sugihara Jul. 1984 20 p refs
(IPPJ-740) Avail: NTIS HC A02/MF A01

It is found that a charged particle can be trapped by a magnetic neutral sheet which is produced by a static magnetic field B sub 0 and a magnetic field of an electromagnetic wave propagating perpendicularly to B sub 0. Once the particle is trapped, it never detraps and moves with the neutral sheet with the phase velocity. The trapped particle feels a constant force along the sheet and thus gains energy continuously from the wave. A brief discussion is given on how to realize such a slow wave which can interact with the particle. Author

N86-14050# Nagoya Univ. (Japan). Inst. of Plasma Physics.
PHYSICAL MECHANISMS FOR HOT ELECTRON STABILIZATION OF LOW FREQUENCY INTERCHANGE MODES

Heiji Sanuki and Francis F. Chen (California Univ., Los Angeles) Aug. 1985 24 p refs
(IPPJ-741) Avail: NTIS HC A02/MF A01

The stabilization of low frequency background and hot electron interchange modes is studied by using a relatively simple multi-fluid model. Physical pictures for the stabilization mechanisms such as the charge uncovering effect are given and compared with the stabilization of interchange modes by the finite Larmor radius (FLR) effect. Author

N86-14051# Nagoya Univ. (Japan). Inst. of Plasma Physics.
EFFECTS OF NEUTRALS ON INTERNAL FORCES AND THERMAL CONDUCTION OF A PLASMA IN A MAGNETIC FIELD
K. Hirano Aug. 1984 21 p refs
(IPPJ-691) Avail: NTIS HC A02/MF A01

Using the Chapman-Enskog approximation the Boltzmann equation was solved to obtain friction and thermal forces appearing between ions and their parent atoms remaining in a plasma. The heat fluxes due to thermal conduction through ions and atoms were also evaluated. Charge transfer and the elastic scattering assuming the Sutherland potential were adopted as the basic collision process between ions and atoms. It was demonstrated that thermal force on neutrals always pushes them toward higher temperature region across a strong magnetic field but colder place along the field lines if the temperature is higher than 25 eV. A very small amount of neutrals, e.g., 1 ppm to the ion density, is found to be enough for neutrals transfering even much larger heat flux than the one by ion thermal conduction loss at a fusion temperature. Author

N86-14052# GT-Devices, Alexandria, Va.
NUMERICAL MODELS FOR PLASMA-SOLID INTERACTIONS IN ELECTROTHERMAL MASS ACCELERATORS Final Report, 22 Jun. 1982 - 21 Jun. 1985
N. K. Winsor, D. A. Tidman, and S. A. Goldstein Jun. 1985 50 p
(Contract DAAG29-82-C-0013)
(AD-A158637; ARO-19060.2-EG-S) Avail: NTIS HC A03/MF A01 CSCL 20/7

This report describes the physics contents of codes and the results applying them to simulations of electrothermal mass accelerators. The overall objective was to investigate the dynamics of these accelerators including 2D effects. This has involved the development of computer models for the interactions of multi-species plasma with solid surfaces in single and multiple module plasma mass accelerators. The models are being used to make choices between materials and discharge cavity designs most suitable for achieving long lifetime and high rep-rate performance for these accelerators. GRA

N86-14053# Oak Ridge National Lab., Tenn.
THEORY OF RESISTIVITY-GRADIENT-DRIVEN TURBULENCE
L. Garcia, P. H. Diamond, B. A. Carreras, and J. D. Callen Jul. 1985 63 p
(Contract DE-AC05-84OR-21400)
(DE85-015068; ORNL/TM-9363) Avail: NTIS HC A04/MF A01

A theory of the nonlinear evolution and saturation of resistivity driven turbulence, which evolves from linear rippling instabilities, is presented. The nonlinear saturation mechanism is identified both analytically and numerically. Saturation occurs when the turbulent diffusion of the resistivity is large enough so that dissipation due to parallel electron thermal conduction balances the nonlinearly modified resistivity gradient driving term. The levels of potential, resistivity, and density fluctuations at saturation are calculated. A combination of computational modeling and analytic treatment is used in this investigation. DOE

N86-14054# Lawrence Livermore National Lab., Calif.
ELECTROMAGNETIC PARTICLE-IN-CELL PLASMA SIMULATION
A. B. Langdon 22 Apr. 1985 5 p refs Presented at Orbital Dyn. and Appl. To Accelerators Workshop, Berkeley, Calif., 7 Mar. 1985
(Contract W-7405-eng-48)
(DE85-031223; UCRL-92531; CONF-8503105-9) Avail: NTIS HC A02/MF A01

PIC simulation tracks particles through electromagnetic fields calculated self consistently from the charge and current densities of the particles themselves, external sources, and boundaries. Already used extensively in plasma physics, such simulations have become useful in the design of accelerators and their RF sources. DOE

N86-14055# Lawrence Livermore National Lab., Calif.
IMPLICIT PLASMA SIMULATION
A. B. Langdon 3 Mar. 1985 22 p Presented at the 2nd Intern. School for Space Simulation, Honolulu, 3 Feb. 1985
(Contract W-7405-eng-48)
(DE85-016088; UCRL-92259; CONF-850266-8) Avail: NTIS HC A02/MF A01

Implicit time integration methods have been used extensively in numerical modeling of slowly varying phenomena in systems that also support rapid variation. Examples include diffusion, hydrodynamics and reaction kinetics. This article discussed implementation of implicit time integration in plasma codes of the particle in cell family, and the benefits to be gained. DOE

N86-14056# National Electrostatic Corp., Middleton, Wis.
TESTS OF COMPRESSED GEOMETRY NEC ACCELERATION TUBES
J. E. Raatz, R. D. Rathmell, P. H. Stelson, and N. F. Ziegler 1985 12 p refs Presented at the 4th Intern. Conf. on Electrostatic Accelerator Technol. and Assoc. Boosters, Buenos Aires, 15 Apr. 1985 Prepared in cooperation with ORNL
(Contract DE-AC05-84OR-21400)
(DE85-016392; CONF-850470-9) Avail: NTIS HC A02/MF A01

Tests have been performed in the 3 MV Pelletron test machine at NEC on a compressed geometry tube which increases the insulating length of the tube by eliminating the heated electrode assemblies (approx. 2.5 cm thick) at the end of each tube section. Some insert electrodes are changed to provide some trapping of secondary ions. The geometry tested provided an 18% increase in live ceramic in the tube. The compressed geometry tube allowed a terminal voltage of 3.55 MV on the 3 MV column at normal gradients of 30.3 kv/tube gap. The tube was also conditioned to more than 4 MV and remained stable in voltage with few sparks and with low X-ray levels for days at about 4 MV. This same performance could be achieved with or without arc discharge cleaning. DOE

N86-14057# Lawrence Livermore National Lab., Calif.
SLAC DIVERTOR CHANNEL ENTRANCE THERMAL STRESS ANALYSIS
G. L. Johnson, W. Stein, S. C. Lu, and R. A. Riddle 10 Jul. 1985 69 p
(Contract W-7405-eng-48)
(DE85-017877; UCID-20498) Avail: NTIS HC A04/MF A01

X-ray beams emerging from the new SLAC electron-position storage ring (PEP) impinge on the entrance to tangential divertor channels causing highly localized heating in the channel structure. Analyses were completed to determine the temperatures and thermally-induced stresses due to this heating. These parts are cooled with water flowing axially over them at 30(0)C. The current design and operating conditions should result in the entrance to the new divertor channel operating at a peak temperatue of 123(0)C with a peak thermal stress at 91% of yield. Any micro-cracks that form due to thermally-induced stresses should not propagate to the coolant wall nor form a path for the coolant to leak into the storage ring vacuum. DOE

N86-14058# California Univ., Berkeley. Lawrence Berkeley Lab.
EFFECT OF FOCUSING FIELD NONLINEARITIES IN MBE-4 ON TRANSVERSE BEAM DYNAMICS
C. M. Celata, V. O. Brady, L. J. Laslett, L. Smith, and I. Haber May 1985 6 p Presented at the Particle Accelerator Conf., Vancouver, British Columbia, 13 May 1985
(Contract DE-AC03-76SF-00098)

(DE85-016561; LBL-19527; CONF-850504-255) Avail: NTIS HC A02/MF A01

A particle simulation code was used to study the effect on transverse beam dynamics of nonlinearities of the focusing field in a linear accelerator transporting a multiple beam array. Nonlinear field strengths for various multiple-beam design geometries were calculated by relaxation codes for use in the simulation calculation. Nonlinearities due to asymmetry of the electrode array with respect to a single beam were found to be negligible. Electrode end effect nonlinearities led to emittance growth for off-axis beams, though for the geometry of MBE-4, this was negligible. For misaligned beams, a dodecapole field caused significant emittance growth. This was not seen in single particle tracking calculations. Fields due to induced charge on the electrodes can reduce this effect, or the dodecapole field can be eliminated by proper choice of the electrode radius. DOE

N86-14059# Los Alamos National Lab., N. Mex.
DENSE Z-PINCH PLASMAS
J. S. Shlachter, J. E. Hammel, and D. W. Scudder 12 Jul. 1985 4 p Presented at the 17th Intern. Conf. on Phenomena in Ionized Gases, Budapest, 8 Jul. 1985
(Contract W-7405-eng-36)
(DE85-005818; LA-UR-85-179; CONF-850718-1) Avail: NTIS HC A02/MF A01

Early researchers recognized the desirable features of the linear Z-pinch configuration as a magnetic fusion scheme. In particular, a Z-pinch reactor might not require auxiliary heating or external field coils, and could constitute an uncomplicated, high plasma (BETA) geometry. The simple Z pinch, however, exhibited gross MHD instabilities that disrupted the plasma, and the linear Z pinch was abandoned in favor of more stable configurations. Recent advances in pulsed-power technology and an appreciation of the dynamic behavior of an ohmically heated Z pinch have led to a reexamination of the Z pinch as a workable fusion concept. DOE

N86-14060# Sandia National Labs., Albuquerque, N. Mex.
ENGINEERING DESIGN FOR THE PBFA-2 PULSE FORMING SECTION
J. D. Boyes and J. S. Cap 1985 5 p Presented at the 5th IEEE Pulsed Power Conf., Washington, D.C., 10 Jun. 1985
(Contract DE-AC04-76DP-00789)
(DE85-012810; SAND-84-2516C; CONF-850616-17) Avail: NTIS HC A02/MF A01

This paper presents an overview of the conceptual and detailed mechanical design of the PBFA-II Pulse Forming Section. The design goals were configuration specification, modularity for ease of installation and maintenance, durability and low cost. The design process began by determining the basic configuration. As was true throughout the design, access for ease of maintenance is a major driving factor. initial assembly requirements dictated a design of separate, modular units for the intermediate store, line one, and line two/three. Integration with the laser system used to trigger the main gas switch put location, stability and adjustment requirements on both the intermediate store and line one. Cost forced the hardware to be fabricated of aluminum. Design for ease of fabrication further held these costs down. Survival in the water shock environment was addressed through specific design and weld techniques. Critical surfaces on all components had to be capable of carrying the high voltages and currents of the machine. The design was developed through prototype testing in the one module machine, Demon. DOE

N86-14061# Oak Ridge National Lab., Tenn.
IMPACT OF A POLOIDAL DIVERTOR IN IGNITION TOKAMAK DESIGN
D. J. Strickler, Y. K. M. Peng, T. G. Brown, A. E. Dabiri, V. D. Lee, and J. B. Miller 1985 6 p Presented at the 6th Topical Meeting on the Technol. of Fusion Energy, San Francisco, 3 Mar. 1985 Prepared in cooperation with Grumman Aerospace Corp., Bethpage, N.Y., Science Applications International Corp., Oak Ridge, Tenn., McDonnel Douglas Corp., St. Louis, Mo. and Tennessee Univ., Knoxville
(Contract DE-AC05-84OR-21400)
(DE85-012892; CONF-850310-106) Avail: NTIS HC A02/MF A01

System design studies were performed to assess the effect of assuming a poloidal divertor instead of a limiter as a means of impurity control for ignition tokamak configurations. Results show that for the nominal Tokamak Fusion Core Experiment (TFCX) device with superconducting TF coils, a feasible poloidal divertor configuration can be obtained without increasing the major radius. In the TFCX nominal copper TF coil device, however, field limits at the PF coils are exceeded when the effects of asymmetry associated with a poloidal divertor are included. It is found that a 12% increase in the major radius of this device is necessary to simultaneously satisfy the plasma-shaping requirements of a poloidal divertor and the magnetics constraints at the superconducting PF coils. DOE

N86-14062# GA Technologies, Inc., San Diego, Calif.
FUSION PROGRAMS IN APPLIED PLASMA PHYSICS AND DEVELOPMENT AND TECHNOLOGY, FISCAL 1984 Annual Report
T. Ohkawa Apr. 1985 63 p
(Contract DE-AT03-84ER-53158)
(DE85-014551; GA-A-17952) Avail: NTIS HC A04/MF A01

The GA programs in Applied Plasma Physics and Development and Technology have registered substantial accomplishments during fiscal 1984. Theoretical work in the MHD area has contributed to further understanding of the physics governing low-g, high-(BETA) tokamak discharges, including the effects of a cold plasma mantle and an edge-temperature pedestal. The unviersal scaling law for the maximum (BETA) stable to ideal-MHD modes has been verified for Doublet III and has also been validated for JET, DIII-D, and a Double Dee configuration. Experimental work in Applied Plasma Physics included the development of two new high-energy diagnostics, one for gamma rays and one for tritons (or, in a reactor, alpha particles), both of which can yield essential physics information that is not readily obtainable from the panoply of existing diagnostic instruments. The development of current-density profile diagnostic continued, and it was found that the instrument could also be used to obtain relative density profiles throughout a tokamak discharge. And tests of an ergodic magnetic limiter scheme indicated that the configuration has the potential to create a stable, radiating boundary layer while reducing the heat load to the walls in future high-power devices. The work carried out in the area of Development and Technology included a group of reactor systems design studies that bring into focus some of the challenges that will be faced by the engineers of fusion power equipment. Closer to realization are advanced rf equipment and superconducting magnet developments, both under design in the area of plasma technologies. Technological developments that apply directly to current experiments as well as to future devices comprise the rest of the GA D and T program.DOE

N86-14063# Wisconsin Univ., Madison.
EXPERIMENTAL STUDY OF NEOCLASSICAL CURRENTS
M. C. Zarnstorff and S. C. Prager May 1985 46 p
(Contract DE-AC02-83ER-53154)
(DE85-014866; DOE/ER-53154/82) Avail: NTIS HC A03/MF A01

A detailed experimental study is presented of the bootstrap and Pfirsch-Schlueter currents that are predicted by neoclassical transport theory. In a toroidal octupole, on magnetic surfaces within the separatrix, the observed parallel plasma currents are in excellent quantitative agreement with neoclassical theory with regard to the spatial structure (along a magnetic surface), collisionality dependence and toroidal magnetic field dependence. On magnetic surfaces outside the separatrix, the ion portion of the parallel current is in agreement with neoclassical theory but the electron parallel current is observed to obtain a unidirectional component which deviates from and exceeds the theoretical prediction. DOE

N86-14064# Brookhaven National Lab., Upton, N. Y.
EFFICIENT IONIZER FOR POLARIZED H(-) FORMATION
J. G. Alessi 1985 4 p Presented at the Particle Accelerator Conf., Vancouver, British Columbia, 13 May 1985
(Contract DE-AC02-76CH-00016)
(DE85-013294; BNL-36482; CONF-850504-161) Avail: NTIS HC A02/MF A01

An ionizer is under development for a polarized H(-) source based on the resonant charge exchange reaction polarized H(0) + D(-) (YIELDS) polarized H(-) + D(0). The polarized H(0) beam passes throughout the center of a magnetron surface-plasma soruce having an annular geometry, where it crosses a high current (approx.0.5 A), 200 eV D(-) beam. Calculations predict an H(0) (YIELDS) H(-) ionization efficiency of approx.7%, more than an order of magnitude higher than that obtained on present ground state atomic beam sources. In initial experiments using an unpolarized H(0) beam, H(-) currents in excess of 100 (MU)A have been measured. While the ionization efficiency is now only about the same as other methods (Cs beam, for example), the results are encouraging since it appears that by injecting positive ions to improve the space-charge neutralization, and by improving the extraction optics, considerable gains in intensity will be made. We will then use this ionizer with a polarized H(0) beam, and measure the polarization of the resulting H(-) beam. If no depolarization is observed this ionizer will be combined with an atomic beam, cooled to 5 to 6 K, to give a polarized H(-) beam expected to be in the milliampere range for use in the AGS. DOE

N86-14065# Sandia National Labs., Albuquerque, N. Mex.
LASER-TRIGGER SYSTEM DESIGN FOR PBFA 2
R. A. Hamil, L. C. Seamons, R. A. Gerber, R. G. Adams, J. R. Woodworth, R. S. Blackburn, and W. C. Sweatt 1985 5 p Presented at the 5th IEEE Pulsed Power Conf., Washington, D.C., 10 Jun. 1985
(Contract DE-AC04-76DP-00789)
(DE85-013144; SAND-84-2445C; CONF-850616-39) Avail: NTIS HC A02/MF A01

A revolutionary design for triggering a multitude of high voltage gas switches is in the process of being implemented and tested at Sandia National Laboratories. This new laser triggering system for PBFA II consists of five major sybsystems. The first subsystem is a KrF laser which injects as much as 4 J of uv radiation into the optical train. The second subsystem is the optical train consisting of over 300 optical components that split the laser beam into 36 equal uv beamlets which are respectively directed into the trigger section of the PBFA-II gas switches. The third, the alignment system, provides a convenient, reliable, low cost method of sensing the degree of alignment of the KrF laser with respect to the high voltage switches. The fourth subsystem is the mechanical assembly supporting and containing the optical components in a low vibration, environmentally controlled manner. The fifth subsystem is control and diagnostics. These five subsystems act in concert to provide a low maintenance triggering system which is reliable, repeatable, repeatable in performance, and will fire the 36, 5.5-MW, PBFA-11 switches with a total firing spread first to last of 4 ns. DOE

N86-14066# Stanford Linear Accelerator Center, Calif.
GENERATION AND ACCELERATION OF HIGH INTENSITY BEAMS IN THE SLC INJECTOR
M. C. Ross, M. J. Browne, J. E. Clendenin, R. K. Jobe, J. T. Seeman, J. C. Sheppard, and R. F. Stiening Apr. 1985 3 p Presented at the Particle Accelerator Conf., Vancouver, British Columbia, 13 May 1985
(Contract DE-AC03-76SF-00515)
(DE85-013056; SU-SLAC-PUB-3639; CONF-850504-76) Avail: NTIS HC A02/MF A01

A new gun pulser and substantially increased focusing have been added to the first 100 m of the SLAC linac in order to provide a pair of intense electron bunches to the SLC damping ring. Each bunch from this injector must have 5 x 10(10) electrons, an invariant emittance (GAMMA)(epsilon) less than or equal to 1.8 x 10(-3) m-rad and the pair must have an energy spread of less than 2%. Wakefield instabilities present in earlier versions of this injector have been controlled by reducing the transverse beam dimension by a factor of 3. DOE

N86-14067# Edgerton, Germeshausen and Grier, Inc., Idaho Falls, Idaho.
RECENT RESULTS ON IMPLANTATION AND PERMEATION INTO FUSION REACTOR MATERIALS
R. A. Anderl, D. F. Holland, G. R. Longhurst, and D. A. Struttman 1985 25 p Presented at the 2nd Natl. Topical Meeting on Tritium Technol. in Fission, Fusion and Isotopic Appl., Dayton, Ohio, 30 Apr. 1985
(Contract DE-AC07-76ID-01570)
(DE85-014620; EGG-M-20784; CONF-850405-15) Avail: NTIS HC A02/MF A01

This paper reports on implantation-driven permeation experiments that have been made for primary candidate alloy (PCA) and the ferritic steel HT-9 using deuterium ion beams from an accelerator. The results include measurements of the implantation flux and fluence dependence of the deuterium reemission and permeation for specimens heated to approximately 430(0)C. Simultaneous measurements of the ions sputtered from the specimen front surface with a secondary ion mass spectrometer provided some characterization of the surface condition throughout an experiment. For both materials, the permeation rate was lowered by the implantation process. However, the steady state permeation rate for HT-9 was found to be at least a factor of 5 greater than that for PCA. DOE

N86-14068# Rochester Univ., N. Y. Lab. for Laser Energetics.
SCALING OF uv (351 nm) FUSION IMPLOSIONS DRIVEN BY MULTIPLE BEAMS
M. C. Richardson, J. Delettrez, R. L. McCrory, J. M. Soures, C. Verdon, and B. Yaakovi 1984 18 p Presented at the Meeting of the Plasma Phys. Div. of the Am. Phys. Soc., Boston, 27 Oct. 1984
(Contract DE-AC08-80DP-40124)
(DE85-014406; DOE/DP-40124/55; CONF-841010-19) Avail: NTIS HC A02/MF A01

The upconversion of the 24-beam OMEGA laser facility to 351 nm has permitted the study of directly driven, ablative implosions of simple spherical shell targets. Symmetric arrays of six and twelve, approx. 650 ps duration uv (351 nm) beams having total energies in excess of 600 J have been used to study the implosions of 250-350 (MU)m diameter DT-filled glass microballoon targets. Target performance is evaluated by a number of X-ray and neutronics diagnostics and compared to one- and two-dimensional hydrocode calculations. The effect of the improvement in irradiation uniformity provided by 12 beam irradiation will be described, and the expectations for 24-beam irradiated targets discussed. DOE

N86-14069# Los Alamos Scientific Lab., N. Mex.
POSSIBILITY FOR A SELF-CONSISTENT TREATMENT OF TRANSPORT PROCESSES IN A TURBULENT PLASMA
J. P. Mondt Jun. 1985 7 p
(Contract W-7405-eng-36)
(DE85-016214; LA-10464-MS) Avail: NTIS HC A02/MF A01

All commonly used models of plasma dynamics share a common flaw in their a priori validity. In particular, a solid foundation of plasma modelling on microscopic dynamics, as exists for moderately dilute gases, is obscured because of the difficulties inherent in the treatment of the potentially very important interplay between plasma waves and collisional processes. The present report briefly discusses the nature of these difficulties and presents a possible approach towards the establishment of a plasma theory founded on the microscopic particle dynamics. The essence of this approach is the realization that only discrete particle interactions can create correlations. These therefore come into being on different spatial scales depending on their cluster number, after which collective effects magnify them analogous to the growth of initial perturbations in an unstable system. Truncation of the Born-Bogolyubov-Green-Kirkwood-Yvon (BBGKY) hierarchy thereby becomes a possibility through the introduction of a small parameter in initial conditions although the dynamical system in itself does not contain a uniformly small parameter. DOE

N86-14070# GA Technologies, Inc., San Diego, Calif.
HEATING AND CONFINEMENT IN THE DOUBLET 3 TOKAMAK WITH ELECTRON CYCLOTRON HEATING
S. Ejima, G. Jahns, S. H. Lin, C. Moeller, R. Prater, and R. Snider May 1985 6 p Presented at the 12th European Conf. on Controlled Fusion and Plasma Phys., Budapest, 2 Sep. 1985
(Contract DE-AC03-84ER-51044)
(DE85-014323; GA-4-18045; CONF-850927-5) Avail: NTIS HC A02/MF A01

Electron Cyclotron Heating (ECH) experiments on the Doublet III tokamak using inside launch of the extraordinary mode have shown effective bulk electron heating, with plasma stored energy increases of up to 30 kJ and central electron temperature increases up to 2.5 keV. The confinement time for discharges dominated by ECH was found to be similar in magnitude and scaling to that for discharges dominated by neutral beam injection, even though the power deposition profile for ECH discharges appears to be much narrower than for neutral beam heated discharges. Even above the calculated extraordinary mode cutoff density, for which the observed power density profile appears to be broad, perhaps as broad as in the beam heating case, the energy confinement time does not deteriorate. DOE

N86-13455# Joint Publications Research Service, Arlington, Va.
STRUCTURE OF FLOW OF EROSION PLASMA FORMED UPON LASER TREATMENT OF METALS Abstract Only
L. Ya. Minko, B. T. Fedyushin, Yu. A. Chivel, and A. N. Chumakov *In its* USSR Rept.: Mater. Sci. and Met. (JPRS-UMS-85-006) 29 Jul. 1985 p 24 Transl. into ENGLISH from Kvatovaya Elektron. (Moscow), v. 12, no. 3, Mar. 1985 p 639-640 (For primary document see N86-13422 04-26)
Avail: NTIS HC A05

N86-13553# Rensselaer Polytechnic Inst., Troy, N.Y. Dept. of Mechanical Engineering, Acoustical Engineering and Mechanics.
ADVANCED ENERGY CONVERSION CONCEPT FOR MICROWAVE BEAMED-ENERGY PROPULSIONS Abstract Only
Leik N. Myrabo *In* AFOSR The 1985 AFOSR/AFRPL Chem. Rocket Res. Meeting Feb. 1985 3 p (For primary document see N86-13507 04-28)
Avail: NTIS HC A11/MF A01

N86-13554# Stuttgart Univ. (West Germany).
BASIC PROCESSES OF PLASMA PROPULSION Abstract Only
Herbert O. Schrade *In* AFOSR The 1985 AFOSR/AFRPL Chem. Rocket Res. Meeting Feb. 1985 3 p (For primary document see N86-13507 04-28)
Avail: NTIS HC A11/MF A01

N86-13555# Massachusetts Inst. of Tech., Cambridge. Dept. of Aeronautics and Astronautics.
PERFORMANCE-LIMITING FACTORS IN MPD THRUSTERS Abstract Only
Manuel Martinez-Sanchez, Daniel Heimerdinger, Mark Chanty, and David Melanson *In* AFOSR The 1985 AFOSR/AFRPL Chem. Rocket Res. Meeting Feb. 1985 3 p (For primary document see N86-13507 04-28)
Avail: NTIS HC A11/MF A01

N86-13556# Carnegie-Mellon Univ., Pittsburgh, Pa.
EROSION AND ONSET MECHANISMS IN MAGNETOPLASMADYNAMIC THRUSTERS Abstract Only
John L. Lawless *In* AFOSR The 1985 AFOSR/AFRPL Chem. Rocket Res. Meeting Feb. 1985 3 p (For primary document see N86-13507 04-28)
Avail: NTIS HC A11/MF A01

N86-13557*# Jet Propulsion Lab., California Inst. of Tech., Pasadena.
MAGNETOPLASMADYNAMIC THRUSTER EROSION RESEARCH Abstract Only
David Q. King *In* AFOSR The 1985 AFOSR/AFRPL Chem. Rocket Res. Meeting Feb. 1985 3 p (For primary document see N86-13507 04-28)
Avail: NTIS HC A11/MF A01

N86-13558# SciTec, Cleveland, Ohio.
COMPLETELY MAGNETICALLY CONTAINED ELECTROTHERMAL THRUSTER Abstract Only
George R. Seikel *In* AFOSR The 1985 AFOSR/AFRPL Chem. Rocket Res.Meeting Feb. 1985 3 p (For primary document see N86-13507 04-28)
Avail: NTIS HC A11/MF A01

N86-13559*# National Aeronautics and Space Administration. Johnson (Lyndon B.) Space Center,
PLASMA-GAS INTERACTIONS STUDIES IN A HYBRID PLUME PLASMA ROCKET Abstract Only
F. R. Chang, W. A. Krueger, T. F. Yang, and J. L. Fisher (Southwest Research Inst., San Antonio, Tex.) *In* AFOSR The 1985 AFOSR/AFRPL Chem. Rocket Res. Meeting Feb. 1985 2 p Prepared in cooperation with MIT, Cambridge (For primary document see N86-13507 04-28)
Avail: NTIS HC A11/MF A01

N86-13560*# National Aeronautics and Space Administration. Johnson (Lyndon B.) Space Center,
A TANDEM MIRROR PLASMA SOURCE FOR HYBRID PLUME PLASMA STUDIES Abstract Only
T. F. Yang, F. R. Chang, R. H. Miller, K. W. Wenzel, and W. A. Krueger *In* AFOSR The 1985 AFOSR/AFRPL Chem. Rocket Res. Meeting Feb. 1985 3 p Prepared in cooperation with MIT, Cambridge (For primary document see N86-13507 04-28)
Avail: NTIS HC A11/MF A01

N86-13561# Pennsylvania State Univ., University Park.
COUPLING BETWEEN GAS DYNAMICS AND MICROWAVE ENERGY ABSORPTION Abstract Only
Michael M. Micci *In* AFOSR The 1985 AFOSR/AFRPL Chem. Rocket Res. Meeting Feb. 1985 3 p (For primary document see N86-13507 04-28)
Avail: NTIS HC A11/MF A01

N86-13562# Electromagnetic Launch Research, Inc., Cambridge, Mass.
PULSED INDUCTIVE ENERGY TRANSFER Abstract Only
Peter P. Mongeau and Douglas P. Hart *In* AFOSR The 1985 AFOSR/AFRPL Chem. Rocket Res. Meeting Feb. 1985 3 p (For primary document see N86-13507 04-28)
Avail: NTIS HC A11/MF A01

N86-13563# Dayton Univ., Ohio. Research Inst.
LASER DIAGNOSTICS FOR ELECTRIC FIELD MEASUREMENTS Abstract Only
Roger J. Becker, Blair A. Barbour, and Alan T. Buswell *In* AFOSR The 1985 AFOSR/AFRPL Chem. Rocket Res. Meeting Feb. 1985 3 p (For primary document see N86-13507 04-28)
Avail: NTIS HC A11/MF A01

N86-13567# R and D Associates, Alexandria, Va.
UNIFIED STUDY OF PLASMA-SURFACE INTERACTIONS FOR SPACE POWER AND PROPULSION Abstract Only
Peter J. Turchi, John F. Davis, III, Joseph Norwood, Jr., and Craig N. Boyer *In* AFOSR The 1985 AFOSR/AFRPL Chem. Rocket Res. Meeting Feb. 1985 3 p (For primary document see N86-13507 04-28)
Avail: NTIS HC A11/MF A01

N86-13601# Joint Publications Research Service, Arlington, Va.
PRELIMINARY EXPERIMENTAL RESULTS OF CT-6B TOKAMAK HEATING FIELD VOLTAGE FEEDBACK CONTROL
Zheng Shaobai and Shen Zhongqing *In its* China Rept.: Sci. and Technol. (JPRS-CST-85-020) 24 Jun. 1985 p 59-64 Transl.

into ENGLISH from Kexue Tongbao (Beijing), no. 12, 1984 p 728-731 (For primary document see N86-13600 04-31)
Avail: NTIS HC A09/MF A01

N86-14145# Joint Publications Research Service, Arlington, Va.
RADIO EMISSION OF INJECTED ELECTRON BEAM WITH RESPECT TO DIAGNOSIS OF IONOSPHERIC PLASMA Abstract Only
S. A. Pulinets *In its* USSR Rept.: Space (JPRS-USP-85-005) 30 Sep. 1985 p 49-50 Transl. into ENGLISH from Kosmich. Issled. (Moscow), v. 22, no. 5, Sep. - Oct. 1984 p 807-809 Original language document announced in IAA as A85-15268 (For primary document see N86-14111 04-88)
Avail: NTIS HC A08

76 SOLID-STATE PHYSICS

Includes superconductivity.

For related information, see also *33 Electronics and Electrical Engineering* and *36 Lasers and Masers.*

N86-14071# California Univ., Los Angeles. Dept. of Chemistry and Biochemistry.
AuGa2 ON GaSb(001): AN EPITAXIAL, THERMODYNAMICALLY STABILIZED METAL/3-5 COMPOUND SEMICONDUCTOR INTERFACE
J. R. Lince and R. S. Williams Aug. 1985 60 p
(Contract N00014-83-K-0612)
(AD-A157937; TR-7) Avail: NTIS HC A04/MF A01 CSCL 20/12

A new type of metal/semiconductor junction has been developed. Crystalline thin films of the intermetallic compound AuGa2 have been grown by molecular beam epitaxy on GaSb(001) substrates with the orientation AuGa2 is parallel to (0010)Ga2 is parallel to 100GaSb. The resulting films have been characterized by Auger electron spectroscopy, low energy electron diffraction, electron energy loss spectroscopy, scanning electron microscopy, X-ray microprobe analysis, and Rutherford backscattering. The growth procedure is reported, and is discussed in terms of the Au-Ga binary phase diagram. This system is of special interest for contacting technology because the compounds terminate a pseudobinary cut through the Au-Ga-Sb bulk ternary phase diagram, which minimizes the amount of chemical interaction across the metal/semiconductor interface. GRA

N86-14072# Innsbruck Univ. (Austria).
HOT ELECTRON EMISSION IN SEMICONDUCTORS Interim Report, 15 Nov. 1984 - 15 Jan. 1985
E. Gornik, R. Hoepfel, and M. Helm 15 Jan. 1985 6 p
(Contract DAJA45-84-C-0052)
(AD-A158042; R/D-4410-EE-01; IR-1) Avail: NTIS HC A02/MF A01 CSCL 20/12

The hot electron emission from low and high mobility GaAs/GaAlAs heterostructures was investigated in the FIR range at two frequencies. From the analysis a linear dependence of the electron temperature on input power per electron is found, nearly independent of the sample properties. The interaction of drifting carriers with periodic gratings in high mobility GaAs/GaAlAs systems is a promising scheme to obtain microwatt tunable FIR radiation. GRA

N86-14073# Westinghouse Research Labs., Pittsburgh, Pa.
MBE GROWTH OF CdTe AND Hg (1-x) Cd (x) Te FILMS AND MULTILAYER STRUCTURES Final Report, 1 Jan. 1983 - 31 Dec. 1984
R. F. C. Farrow, A. J. Noreika, W. J. Takei, S. Wood, and J. Greggi 16 Apr. 1985 85 p
(Contract DAAG29-83-C-0008)
(AD-A158267; Rept-85-9F3-EPCAD-R2; ARO-20202.4-EL) Avail: NTIS HC A05/MF A01 CSCL 20/2

The MBE growth of CdTe and Hg1-xCdxTe films on InSb and CdTe substrates has been investigated. Growth conditions for high-perfection CdTe films, exactly lattice-matched to InSb substrates, have been identified. These films are ideal for substrates for Hg1-xCdxTe film growth since they are free from low-angle grain boundaries and also provide electrical isolation of the Hg1-xCdxTe film from the InSb substrate. Magnetophotoconductivity studies of abrupt n-CdTe/p-InSb heterojunctions indicate the presence of an n-type inversion layer in the InSb. This could be the basis for a new type of FET device. Conditions for growth of Hg1-xCdxTe films have been explored and films of suitable quality for LWIR device fabrication have been prepared. GRA

N86-14074# Lawrence Livermore National Lab., Calif.
EQUATION OF STATE OF DENSE ARGON: A COMPARISON OF SHOCK AND STATIC STUDIES
M. Ross, H. K. Mao, P. M. Bell, and J. A. Xu Jul. 1985 7 p refs
Presented at the Am. Phys. Soc. Topical Conf. on Shock Waves in Condensed Matter, Spokane, 22 Jul. 1985 Prepared in cooperation with Carnegie Inst. of Washington, D.C.
(Contract W-7405-eng-48)
(DE85-015543; UCRL-93030; CONF-850736-45) Avail: NTIS HC A02/MF A01

In the present paper we report new diamond anvil cell (DAC) measurements for room temperature solid argon to 800 kbars. This isotherm is in excellent agreement with one predicted from a theoretical analysis of shockwave data. These results are important for several reasons. First they demonstrate agreement between shock and static techniques even in cases where shock temperatures are extremely high and a large thermal correction is required to reduce the Hugoniot to an isotherm. Secondly the results suggest that solid argon may provide a useful pressure standard up to 3 Mbar. DOE

N86-14075# California Univ., Berkeley. Lawrence Berkeley Lab.
APPLICATION OF CROSS-SECTIONAL TRANSMISSION ELECTRON MICROSCOPY TO THE CHARACTERIZATION OF ION-IMPLANTED SEMICONDUCTORS
T. Sands Mar. 1985 14 p Presented at the Joint Meeting of the Electron Microscopy Soc. of Am. and the Microbeam Anal. Soc., Louisville, Ky., 5 Aug. 1985 Prepared in cooperation with Bell Telephone Labs., Murray Hill, N.J.
(Contract DE-AC03-76SF-00098)
(DE85-010990; LBL-19162; CONF-850840-7) Avail: NTIS HC A02/MF A01

Direct implantation of dopant ions is the most precise method for obtaining a desired dopant profile in a semiconductor substrate. The most efficient approach is to understand the mechanisms of defect formation and annealing so that guidelines for choosing a set of implantation/annealing conditions can be determined. Since implantation depths are usually much less than one micron, suitable defect characterization techniques must demonstrate high spatial resolution. In this paper, the application of XTEM to understanding the origins and annealing behavior of implantation-related defects is discussed. These applications are illustrated with examples which come primarily from work done at Lawrence Berkeley Laboratory. DOE

N86-14076# Brookhaven National Lab., Upton, N. Y.
POSITRON DIFFUSION IN SI
B. Nielsen, K. G. Lynn, A. Vehanen, and P. J. Schultz Jun. 1985 4 p Presented at the 7th Intern. Conf. on Positron Annihilation, New Delhi, 6 Jan. 1985 Prepared in cooperation with Helsinki Univ. of Tech., Otaniemi, Finland and University of Western Ontario, London
(Contract DE-AC02-76CH-00016)
(DE85-014831; BNL-36700; CONF-850169-16) Avail: NTIS HC A02/MF A01

Positron diffusion in Si(100) and Si(111) has been studied using a variable energy positron beam. The positron diffusion coefficient is found to be D/sub +/ = 2.7 + or - 0.3 cm(2)/sec using a Makhov-type positron implantation profile, which is demonstrated to fit the data more reliably than the more commonly applied exponential profile. The diffusion related parameter, E0, which results from the exponential profile, is found to be 4.2 + or -

0.2 keV, significantly longer than previously reported values. A drastic reduction in E0 is found after annealing the sample at 1300 K, showing that previously reported low values of E0 are probably associated with the thermal history of the sample. DOE

N86-13606# Joint Publications Research Service, Arlington, Va.
HIGH-PRESSURE, HIGH-TEMPERATURE OPPOSED ANVIL DEVICE DESCRIBED
He Yi, Wang Songtao, Qin Zhicheng, Wang Yaoji, and Wang Wenkui *In its* China Rept.: Sci. and Technol. (JPRS-CST-85-020) 24 Jun. 1985 p 96-99 Transl. into ENGLISH from Wuli (Beijing), v. 14, no. 1, Jan. 1985 p 38-39 (For primary document see N86-13600 04-31)
Avail: NTIS HC A09/MF A01

N86-13613# Joint Publications Research Service, Arlington, Va.
EXCIMER LASER PRODUCES .2 MICRON SEMICONDUCTOR STRUCTURES
In its West Europe Rept.: Sci. and Technol. (JPRS-WST-85-030) 28 Oct. 1985 p 37 Transl. into ENGLISH from Chem. Rundschau (West Germany), 31 May 1985 p 5 (For primary document see N86-13610 04-31)
Avail: NTIS HC A04/MF A01

77 THERMODYNAMICS AND STATISTICAL PHYSICS

Includes quantum mechanics; and Bose and Fermi statistics.

For related information see also *25 Inorganic and Physical Chemistry* and *34 Fluid Mechanics and Heat Transfer.*

No abstracts in this category.

80 SOCIAL SCIENCES (GENERAL)

Includes educational matters.

No abstracts in this category.

81 ADMINISTRATION AND MANAGEMENT

Includes management planning and research.

No abstracts in this category.

82 DOCUMENTATION AND INFORMATION SCIENCE

Includes information storage and retrieval technology; micrography; and library science.

For computer documentation see *61 Computer Programming and Software.*

N86-14077# Massachusetts Inst. of Tech., Cambridge. Artificial Intelligence Lab.
CREF: AN EDITING FACILITY FOR MANAGING STRUCTURED TEXT
K. M. Pitman Feb. 1985 26 p
(Contract N00014-80-C-0505; Grant NSF MCS-79-12179)
(AD-A158155; AI-M-829) Avail: NTIS HC A03/MF A01 CSCL 05/8

This paper reports work in progress on an experimental text editor called CREF, the Cross Referenced Editing Facility. CREF deals with chunks of text, called segments, which may have associated features such as keywords or various kinds of links to other segments. Text in CREF is organized into linear collections for normal browsing. The use of summary and cross-reference links in CREF allows the imposition of an auxiliary network structure upon the text which can be useful for zooming in and out or non-local transitions. Although it was designed as a tool for use in complex protocol analysis by a Knowledge Engineer's Assitant, CREF has many interesting features which should make it suitable for a wide variety of applications, including browsing, program editing, document preparation, and mail reading. GRA

83 ECONOMICS AND COST ANALYSIS

Includes cost effectiveness studies.

No abstracts in this category.

84 LAW AND POLITICAL SCIENCE

Includes space law; international law; international cooperation; and patent policy.

No abstracts in this category.

85 URBAN TECHNOLOGY AND TRANSPORTATION

Includes applications of space technology to urban problems; technology transfer; technology assessment; and surface and mass transportation.

For related information see *03 Air Transportation and Safety, 16 Space Transportation,* and *44 Energy Production and Conversion.*

N86-14078*# National Aeronautics and Space Administration. Johnson (Lyndon B.) Space Center,
THE 1983 NASA/ASEE SUMMER FACULTY FELLOWSHIP RESEARCH PROGRAM RESEARCH REPORTS Final Reports
Walter J. Horn, ed. (Texas A&M Univ., College Station) and Michael B. Duke, ed. Sep. 1983 409 p refs Program held in College Station, Tex., 1983
(Grant NGT-44-001-800)
(NASA-CR-171904; NAS 1.26:171904) Avail: NTIS HC A18/MF A01 CSCL 05I

The 1983 NASA/ASEE Summary Faculty Fellowship Research Program was conducted by Texas A&M University and the Lyndon B. Johnson Space Center (JSC). The 10-week program was operated under the auspices of the American Society for Engineering Education (ASEE). The basic objectives of the programs, which began in 1965 at JSC and in 1964 nationally, are (1) to further the professional knowledge of qualified engineering and science faculty members, (2) to stimulate an exchange of ideas between participants and NASA, (3) to enrich and refresh the research and teaching activities of participants' institutions, and (4) to contribute to the research objectives of the NASA Centers. The faculty fellows spent 10 weeks at JSC engaged in a research project commensurate with their interests and background. They worked in collaboration with a NASA/JSC colleague. This document is a compilation of final reports on their research during the summer of 1983. For individual titles, see N86-14079 through N86-14105.

N86-14079*# University of Southwestern Louisiana, Lafayette. Dept. of Mathematics and Statistics.
ESTIMATION OF FINITE MIXTURES USING THE EMPIRICAL CHARACTERISTIC FUNCTION Final Report c64
Charles Anderson and Thomas Boullion *In* NASA. Johnson (Lyndon B.) Space Center The 1983 NASA/ASEE Summer Faculty Fellowship Research Program Research Reports Sep. 1985 7 p refs (For primary document see N86-14078 04-85)
Avail: NTIS HC A18/MF A01 CSCL 12A

A problem which occurs in analyzing LANDSAT scenes is the problem of separating the components of a finite mixture of several distinct probability distributions. A review of the literature indicates this is a problem which occurs in many disciplines, such as engineering, biology, physiology and economics. Many approaches to this problem have appeared in the literature; however, most are very restrictive in their assumptions or have met with only a limited degree of success when applied to realistic situations. A proceudre is investigated with combines the k-L procedure of (Feurverger and McDunnough, 1981) with the MAICE procedure of (Akaike, 1974). The feasibility of this approach is being investigated numerically via the development of a computer software package enabling a simulation study and comparison with other procedures. Author

N86-14080*# Fayetteville State Univ., N.C. Dept. of Biology.
THE SCANNING ELECTRON MICROSCOPE AS A TOOL IN SPACE BIOLOGY Final Report c51
Roy A. Barrett *In* NASA. Johnson (Lyndon B.) Space Center The 1983 NASA/ASEE Summer Faculty Fellowship Research Program Research Reports Sep. 1983 9 p refs (For primary document see N86-14078 04-85)
Avail: NTIS HC A18/MF A01 CSCL 06B

Normal erythrocytes are disc-shaped and are referred to here descriptively as discocytes. Several morphologically variant forms occur normally but in rather small amounts, usually less than one percent of total. It has been shown though, that spiculed variant forms referred to as echinocytes are generated in significant amounts at zero g. Normal red cells have been stressed in vitro in an effort to duplicate the observed discocyte-echinocyte transformation at zero g. The significance of this transformation to extended stay in space and some of the plausible reasons for this transformation are discussed. Author

N86-14081*# Houston Univ., Clear Lake, Tex. Programs in Science.
ELECTRON MICROSCOPIC OBSERVATIONS OF HYDROGEN IMPLANTATION IN ILMENITES Final Report c25
Goerge E. Blanford *In* NASA. Johnson (Lyndon B.) Space Center The 1983 NASA/ASEE Summer Faculty Fellowship Research Program Research Reports Sep. 1983 9 p refs (For primary document see N86-14078 04-85)
Avail: NTIS HC A18/MF A01 CSCL 07D

Hydrogen ion beams were found to form submicrometer, bumpy textures on the surface of ilmenite grains. From this effect, it is believed that similar bumpy textures seen on lunar ilmenite, pyroxene, and olivine grains are likely to be caused by solar wind irradiation. As a consequence, the concentration of bumpy textured grains may be a useful index of surface maturity for lunar soils. An attempt was made to search for grains with these bumpy textures in interplanetary dust and lunar and meteoritic regolith breccias in order to obtain information about the duration of their exposure to the solar wind. Solar wind irradiation was simulated on natural, terrestrial ilmenite. Hydrogen ion beams were directed at small grains and polished sections which were then examined by electron microscopy. B.W.

N86-14082*# Arkansas Coll., Batesville.
A PYROLOYSIS TECHNIQUE FOR DETERMINING MICROAMOUNTS OF HYDROGEN IN LUNAR SOIL USING THE HELIUM IONIZATION DETECTOR Final Report c25
Roberta Bustin *In* NASA. Johnson (Lyndon B.) Space Center The 1983 NASA/ASEE Summer Faculty Fellowship Research Program Research Reports Sep. 1983 13 p refs (For primary document see N86-14078 04-85)
Avail: NTIS HC A18/MF A01 CSCL 07D

A method has been developed which will determine hydrogen in sub-milligram samples of lunar soil. It consists of heating the sample in a pyroprobe followed by the gas chromatographic determination of hydrogen using the helium ionization detector. Using a 7 foot, 1/8 OD stainless steel column packed with Carbosieve S, 120/140 mesh, hydrogen was well-separated from the other gases released from lunar soil. Standards of hydrogen in helium were used for calibration. The limit to detection under the conditions used was about 2 ng. The method was linear from 2 ng to 270 ng. The method was checked using some actual lunar samples. Results were typical of those obtained for lunar soils using other methods. Author

N86-14083*# Arkansas Univ., Little Rock.
FINITE ELEMENT OR GALERKIN TYPE SEMIDISCRETE SCHEMES Final Report c64
Kanat Durgun *In* NASA. Johnson (Lyndon B.) Space Center The 1983 NASA/ASEE Summer Faculty Fellowship Research Program Research Reports Sep. 1983 14 p refs (For primary document see N86-14078 04-85)
Avail: NTIS HC A18/MF A01 CSCL 12A

A finite element of Galerkin type semidiscrete method is proposed for numerical solution of a linear hyperbolic partial differential equation. The question of stability is reduced to the stability of a system of ordinary differential equations for which Dahlquist theory applied. Results of separating the part of numerical solution which causes the spurious oscillation near shock-like response of semidiscrete scheme to a step function initial condition are presented. In general all methods produce such oscillatory overshoots on either side of shocks. This overshoot pathology, which displays a behavior similar to Gibb's phenomena of Fourier series, is explained on the basis of dispersion of separated Fourier components which relies on linearized theory to be satisfactory. Expository results represented. B.W.

N86-14084*# Alabama State Univ., Montgomery.
DETERMINATION OF NEUTRON FLUX DISTRIBUTION BY USING ANISN, A ONE-DIMENSIONAL DISCRETE S SUB n ORDINATES TRANSPORT CODE WITH ANISOTROPIC SCATTERING Final Report c72
Susanta K. Ghorai *In* NASA. Johnson (Lyndon B.) Space Center The 1983 NASA/ASEE Summer Faculty Fellowship Research Program Research Reports Sep. 1983 18 p refs (For primary document see N86-14078 04-85)
Avail: NTIS HC A18/MF A01 CSCL 20H

The purpose of this project was to use a one-dimensional discrete coordinates transport code called ANISN in order to determine the energy-angle-spatial distribution of neutrons in a 6-feet cube rock box which houses a D-T neutron generator at its center. The project was two-fold. The first phase of the project involved adaptation of the ANISN code written for an IBM 360/75/91 computer to the UNIVAC system at JSC. The second phase of the project was to use the code with proper geometry, source function and rock material composition in order to determine the neutron flux distribution around the rock box when a 14.1 MeV neutron generator placed at its center is activated. Author

N86-14085*# American Univ., Beirut (Lebanon).
A STUDY OF SOME FEATURES OF ac AND dc ELECTRIC POWER SYSTEMS FOR A SPACE STATION Final Report c20
Jack I. Hanania *In* NASA. Johnson (Lyndon B.) Space Center The 1983 NASA/ASEE Summer Faculty Fellowship Research Program Research Reports Sep. 1983 15 p refs (For primary document see N86-14078 04-85)
Avail: NTIS HC A18/MF A01 CSCL 22B

This study analyzes certain selected topics in rival dc and high frequency ac electric power systems for a Space Station. The interaction between the Space Station and the plasma environment is analyzed, leading to a limit on the voltage for the solar array and a potential problem with resonance coupling at high frequencies. Certain problems are pointed out in the concept of a rotary transformer, and further development work is indicated in connection with dc circuit switching, special design of a transmission conductor for the ac system, and electric motors. The question of electric shock hazards, particularly at high frequency, is also explored, and a problem with reduced skin resistance and therefore increased hazard with high frequency ac is pointed out. The study concludes with a comparison of the main advantages and disadvantages of the two rival systems, and it is suggested that the choice between the two should be made after further studies and development work are completed. Author

N86-14086*# East Carolina Univ., Greenville, N.C.
NUTRITIONAL CHARACTERISTICS OF MOON DUST FOR SOIL MICROORGANISMS Final Report c91
Takeru Ito *In* NASA. Johnson (Lyndon B.) Space Center The 1983 NASA/ASEE Summer Faculty Fellowship Research Program Research Reports Sep. 1983 17 p refs (For primary document see N86-14078 04-85)
Avail: NTIS HC A18/MF A01 CSCL 03B

Approximately 46% of the lunar sample (10084,151), 125.42 mg, was solubilized in 680 ml 0.01 M salicylic acid. Atomic absorption spectroscopic analysis of the solubilized lunar sample showed the following amount of metal ions: Ca, 3.1; Mg, 4.0; K, 0.09; Na, 0.67; Fe, 7.3; Mn, 1.6; Cu, Ni, Cr, less than 0.1 each. All are in ppm. Salicylic acid used to solubilize the lunar sample was highly inhibitory to the growth of mixed soil microbes. However, the mineral part of the lunar extract stimulated the growth. For optimal growth of the soil microbes the following nutrients must be added to the moon extract; sources of carbon, nitrogen, sulfur, phosphorus, and magnesium in addition to water. Author

N86-14087*# Saint Thomas Univ., Houston, Tex. Dept. of Physics.
SOME APPLICATIONS OF LIE GROUPS IN ASTRODYNAMICS Final Report c90
A. A. Jackson *In* NASA. Johnson (Lyndon B.) Space Center The 1983 NASA/ASEE Summer Faculty Fellowship Research Program Research Reports Sep. 1983 10 p refs (For primary document see N86-14078 04-85)
Avail: NTIS HC A18/MF A01 CSCL 03B

Differential equations that arise in astrodynamics are examined from the standpoint of Lie group theory. A summary of the Lie method is given for first degree differential equations. The Kepler problem in Hamiltonian form is treated by this method. Extension of the Lie method to optimal trajectories is outlined. Author

N86-14088*# North Texas State Univ., Denton. Dept. of Biological Sciences.
INTERACTION BETWEEN ESCHERICHIA COLI AND LUNAR FINES Final Report c51
Karl R. Johansson *In* NASA. Johnson (Lyndon B.) Space Center The 1983 NASA/ASEE Summer Faculty Fellowship Research Program Research Reports Sep. 1983 21 p refs (For primary document see N86-14078 04-85)
Avail: NTIS HC A18/MF A01 CSCL 06B

A sample of mature lunar fines (10084.151) was solubilized to a high degree (about 17 percent) by the chelating agent salicylic acid (0.01. M). The neutralized (pH adjusted to 7.0) leachate was found to inhibit the growth of Escherichia coli (ATCC 259922) in a minimial mineral salts glucose medium; however, the inhibition was somewhat less than that caused by neutralized salicylic acid alone. The presence of lunar fines in the minimal medium was highly stimulatory to growth of E. coli following an early inhibitory response. The bacterium survived less well in the lunar leachate than in distilled water, no doubt because of the salicylate. It was concluded that the sample of lunar soil tested has nutritional value to E. coli and that certain products of fermentation helped to solubilize the lunar soil. Author

N86-14089*# Middlesex County Coll., N.J. Dept. of Mech./Civi Technology.
SPECTRAL REFLECTANCE OF SURFACE SOILS: RELATIONSHIPS WITH SOME SOIL PROPERTIES Final Report c74
Carl H. Kiesewetter *In* NASA. Johnson (Lyndon B.) Space Center The 1983 NASA/ASEE Summer Faculty Fellowship Research Program Research Reports Sep. 1983 27 p refs (For primary document see N86-14078 04-85)
Avail: NTIS HC A18/MF A01 CSCL 20F

Using a published atlas of reflectance curves and physicochemical properties of soils, a statistical analysis was carried out. Reflectance bands which correspond to five of the wavebands used by NASA's Thematic Mapper were examined for relationships to specific soil properties. The properties considered in this study include: Sand Content, Silt Content, Clay Content, Organic Matter Content, Cation Exchange Capacity, Iron Oxide Content and Moisture Content. Regression of these seven properties on the mean values of five TM bands produced results that indicate that the predictability of the properties can be increased by stratifying the data. The data was stratified by parent material, taxonomic order, temperature zone, moisture zone and climate (combined temperature and moisture). The best results were obtained when the sample was examined by climatic classes. The middle Infra-red bands, 5 and 7, as well as the visible bands, 2 and 3, are significant in the model. The near Infra-red band, band 4, is almost as useful and should be included in any studies. General linear modeling procedures examined relationships of the seven properties with certain wavebands in the stratified samples. B.W.

N86-14090*# Houston Univ., Tex. Dept. of Electrical Engineering.
CONTROL OF SPACE STATIONS Final Report c18
Kwang Y. Lee *In* NASA. Johnson (Lyndon B.) Space Center The 1983 NASA/ASEE Summer Faculty Fellowship Research Program Research Reports Sep. 1983 8 p refs (For primary document see N86-14078 04-85)
Avail: NTIS HC A18/MF A01 CSCL 22B

A study is made to develop controllers for the NASA-JSC Triangular Space Station and evaluate their performances to make recommendations for structural design and/or control alternatives. The control system design assumes the rigid body of the Space Station and developes the lumped parameter control system by using the Inverse Optimal Control Theory. In order to evaluate the performance of the control system, a Parameter Estimation algorithm is being developed which will be used in modeling an equivalent but simpler Space Station model. Finally, a scaled version of the Space Station is being built for the purpose of physical experiments to evaluate the control system performance. Author

N86-14091*# Missouri Univ., Columbia. Dept. of Chemical Engineering.
SOLID WASTE TREATMENT PROCESSES FOR SPACE STATION Final Report c54
Thomas R. Marrero *In* NASA. Johnson (Lyndon B.) Space Center The 1983 NASA/ASEE Summer Faculty Fellowship Research Program Research Reports Sep. 1983 55 p refs (For primary document see N86-14078 04-85)
Avail: NTIS HC A18/MF A01 CSCL 06K

The purpose of this study was to evaluate the state-of-the-art of solid waste(s) treatment processes applicable to a Space Station. From the review of available information a source term model for solid wastes was determined. An overall system is proposed to treat solid wastes under constraints of zero-gravity and zero-leakage. This study contains discussion of more promising potential treatment processes, including supercritical water oxidation, wet air (oxygen) oxidation, and chemical oxidation. A low pressure, batch-type treament process is recommended. Processes needed for pretreatment and post-treatment are hardware already developed for space operations. The overall solid waste management system should minimize transfer of wastes from their collection point to treatment vessel. Author

N86-14092*# Southwestern Univ., Georgetown, Tex.
LUNAR LUMINESCENCE MEASUREMENTS Final Report c89
Thomas H. Morgan *In* NASA. Johnson (Lyndon B.) Space Center The 1983 NASA/ASEE Summer Faculty Fellowship Research Program Research Reports Sep. 1983 11 p (For primary document see N86-14078 04-85)
Avail: NTIS HC A18/MF A01 CSCL 03A

Spectra of lunar sites obtained in June 1983 have been analyzed for residual luminescence using the spectral line depth technique. The results or three sites each at three wavelengths are presented. The sites observed were Mare Crisium, Kepler, and Aristarchus. In each case, the value quoted was based not only on the strong Fraunhofer line in the spectral range covered but also on from 11 to 21 weaker lines within 80 A of the strongest feature. These data do not support previous observations. The values given do not indicate a greatly reddened spectrum, and the luminescence spectrum of the mare site is not significantly different from the two young crater sites. These observations cannot be adequately explained by thermal luminescence, theories of direct excitation are also unable to explain the strength of the flux. Author

N86-14093*# Sam Houston State Univ., Huntsville, Tex. Dept. of Physics.
DEVELOPMENT OF A MASS SPECTROMETER SYSTEM FOR THE MEASUREMENT OF INERT GASES IN METEORITES Final Report c90
Russell L. Palma *In* NASA. Johnson (Lyndon B.) Space Center The 1983 NASA/ASEE Summer Faculty Fellowship Research Program Research Reports Sep. 1983 9 p (For primary document see N86-14078 04-85)
Avail: NTIS HC A18/MF A01 CSCL 03B

The study of the inert gases in meteorites has provided many clues as to the origin and evolution of the solar system. Particularly crucial and complex are the gases krypton and xenon. To accurately measure the isotopic compositions of these gases requires a mass spectrometer of high sensitivity and resolution. A previously unused and largely untested mass spectrometer system was brought to the point where it was ready for routine sample analyses. This involved, among other things, focusing the ion beam for optimal peak shape and sensitivity, documenting the instrument's response to a series of characteristic tests such as multplier gain checks, and interfacing the instrument to a computer to run the sample analyses. Following this testing and setting up, three iron meteorite samples were to be analyzed for argon, krypton, and xenon. The three samples were shown in prior work to possibly contain primordial heavy inert gases. Although these analyses have not yet been carried out, it is anticipated that they will be completed in the near future. Author

N86-14094*# National Aeronautics and Space Administration. Johnson (Lyndon B.) Space Center,
AN ANALYSIS OF CRYOTRAP HEAT EXCHANGER PERFORMANCE TEST DATA (400 AREA) AND RECOMMENDATIONS FOR A SYSTEM TO HANDLE APOLLO RCS ENGINES Final Report c34
Allen Rakow *In its* The 1983 NASA/ASEE Summer Faculty Fellowship Research Program Research Reports Sep. 1983 15 p (For primary document see N86-14078 04-85)
Avail: NTIS HC A18/MF A01 CSCL 20D

The current arrangement of a Platecoil heat exchanger which uses LN2 on the inside of parallel tubes, in counter flow to the test cell engine exhaust gases which are drawn through a box surrounding the plates by the existing vacuum blowers is examined. As a result of inadequate performance and special test data it was decided to redesign the system to accommodate an Apollo RCS engine. G.L.C.

N86-14095*# National Aeronautics and Space Administration. Johnson (Lyndon B.) Space Center,
FLUORINE DISPOSAL c14
Allen Rakow *In its* The 1983 NASA/ASEE Summer Faculty Fellowship Research Program Research Reports Sep. 1983 23 p (For primary document see N86-14078 04-85)
Avail: NTIS HC A18/MF A01 CSCL 14B

A preliminary design of an F2 dispoal system for HELSTF is presented along with recommendations on operational policy and identification of potential operational problems. The analysis is based on sizing a system to handle two different modes of the HELSTF Fluorine Flow System (one operational and one catastrophic). This information should serve both as a guide to a final detailed design for HELSTF as well as a reference for subsequent monitoring and/or modification of the system which consists of a charcoal reactor followed by a dry soda lime scrubber. Author

N86-14096*# National Aeronautics and Space Administration. Johnson (Lyndon B.) Space Center,
SPARGER SYSTEM FOR MMH-HELIUM VENTS Final Report c34
Allen Rakow *In its* The 1983 NASA/ASEE Summer Faculty Fellowship Research Program Research Reports Sep. 1983 17 p (For primary document see N86-14078 04-85)
Avail: NTIS HC A18/MF A01 CSCL 20D

Based on a calculated vent flow rate and MMH concentration, a TI-59 program was run to determine total sparger hole area for a given sparger inlet pressure. Hole diameter is determined from a mass transfer analysis in the holding tank to achieve complete capture of MMH. In addition, based on oxidation kinetics and vapor pressure data, MMh atmospheric concentrations are determined 2 ft above the holding tank. Author

N86-14097*# Morgan State Univ., Baltimore, Md.
COMPARATIVE EFFECT OF LUNAR FINES AND TERRESTRIAL ASH ON THE GROWTH OF A BLUE-GREEN ALGA AND GERMINATING RADISH SEED Final Report c51
Esther J. Ridley *In* NASA. Johnson (Lydon B.) Space Center The 1983 NASA/ASEE Summer Faculty Fellowship Research Program Research Reports Sep. 1983 15 p refs (For primary document see N86-14078 04-85)
Avail: NTIS HC A18/MF A01 CSCL 06B

Although it is understood that photosynthetic organisms will be required as components of a closed ecological life support system (CELSS) for a manned lunar based, a basic problem is to identify organisms best capable of utilizing lunar regolith materials. Also, there is need to determine what nutrient supplements have to be added to lunar soils, and at what levels in order to promote high bio-mass production. Author

N86-14098*# Texas A&M Univ., College Station. Dept. of Meteorology.
VARIABILITY OF RAINFALL OVER SMALL AREAS Final Report c47
Robert C. Runnels *In* NASA. Johnson (Lyndon B.) Space Center The 1983 NASA/ASEE Summer Faculty Fellowship Research Program Research Reports Sep. 1983 7 p refs (For primary document see N86-14078 04-85)
Avail: NTIS HC A18/MF A01 CSCL 04B

A preliminary investigation was made to determine estimates of the number of raingauges needed in order to measure the variability of rainfall in time and space over small areas (approximately 40 sq miles). The literature on rainfall variability was examined and the types of empirical relationships used to relate rainfall variations to meteorological and catchment-area characteristics were considered. Relations between the coefficient of variation and areal-mean rainfall and area have been used by several investigators. These parameters seemed reasonable ones to use in any future study of rainfall variations. From a knowledge of an appropriate coefficient of variation (determined by the above-mentioned relations) the number rain gauges needed for the precise determination of areal-mean rainfall may be calculated by statistical estimation theory. The number gauges needed to measure the coefficient of variation over a 40 sq miles area, with varying degrees of error, was found to range from 264 (10% error, mean precipitation = 0.1 in) to about 2 (100% error, mean precipitation = 0.1 in). Author

N86-14099*# Houston Baptist Univ., Tex. Dept. of Mathematics and Physics.
TRANSFORMATION MATRICES BETWEEN NON-LINEAR AND LINEAR DIFFERENTIAL EQUATIONS Final Report c64
Robert L. Sartain *In* NASA. Johnson (Lyndon B.) Space Center The 1983 NASA/ASEE Summer Faculty Fellowship Research Program Research Reports Sep. 1983 15 p refs (For primary document see N86-14078 04-85)
Avail: NTIS HC A18/MF A01 CSCL 12A

In the linearization of systems of non-linear differential equations, those systems which can be exactly transformed into the second order linear differential equation Y'-AY'-BY=0 where Y, Y', and Y' are n x 1 vectors and A and B are constant n x n matrices of real numbers were considered. The 2n x 2n matrix was used to transform the above matrix equation into the first order matrix equation X' = MX. Specially the matrix M and the conditions which will diagonalize or triangularize M were studied. Transformation matrices P and P sub -1 were used to accomplish this diagonalization or triangularization to return to the solution of the second order matrix differential equation system from the first order system. Author

N86-14100*# Abilene Christian Coll., Tex.
ION BOMBARDMENT AND ADSORPTION STUDIES ON ILMENITE (FeTiO3) BY X-RAY PHOTOELECTRON SPECTROSCOPY Final Report c72
Paul D. Schulze *In* NASA. Johnson (Lyndon B.) Space Center The 1983 NASA/ASEE Summer Faculty Research Program Research Reports Sep. 1983 10 p refs (For primary document see N86-14078 04-85)
Avail: NTIS HC A18/MF A01 CSCL 08H

The effects of 5 KeV argon and oxygen ion bombardment on FeTiO3 (ilmenite) at low temperatures have been studied using X-ray photoelectron spectroscopy (XPS). Also, using this same technique, the adsorption of O2, NO, N2O, and CO at 300 K and the adsorption of O2 and D2O at 150K have been studied. Argon and oxygen ion bombardment of ilmenite have confirmed earlier studies on metal oxides that argon ions generally reduce the anion species while oxygen ions generally oxidize the anion species. The two iron states involved were Fe sup +2 and Fe sup O. The reduction of Ti sup +4 was not verified although a significant shift in the Ti(2p1,3) binding energies toward the metallic state was observed after oxygen ion bombardment at low temperatures. At temperatures above 150K, O2 adsorbs dissociatively on ilmenite while D2O adsorbs molecularly below 170K. Above 300 K No, N2O, and CO do not appear to adsorb dissociatively. Low temperature adsorption of D2O was found to be inhibited by predosing the ilmenite with O2. Author

N86-14101*# Texas Univ., Austin. Dept. of Aerospace and Engineering.
ADVANCED ALGORITHM FOR ORBIT COMPUTATION Final Report c64
Victor Szenbehely *In* NASA. Johnson (Lyndon B.) Space Center The 1983 NASA/ASEE Summer Faculty Fellowship Research Program Research Reports Sep. 1983 17 p (For primary document see N86-14078 04-85)
Avail: NTIS HC A18/MF A01 CSCL 12A

Computational and analytical techniques which simplify the solution of complex problems in orbit mechanics, Astrodynamics and Celestial Mechanics were developed. The major tool of the simplification is the substitution of transformations in place of numerical or analytical integrations. In this way the rather complicated equations of orbit mechanics might sometimes be reduced to linear equations representing harmonic oscillators with constant coefficients. Author

N86-14102*# Prairie View Agricultural and Mechanical Coll., Tex.
SOLAR CONCENTRATOR DEGRADATION IN LOW EARTH ORBIT (LEO) Final Report c44
Richard G. Thomas *In* NASA. Johnson (Lyndon B.) Space Center The 1983 NASA/ASEE Summer Faculty Fellowship Research Program Research Reports Sep. 1983 12 p refs (For primary document see N86-14078 04-85)
Avail: NTIS HC A18/MF A01 CSCL 12A

The use of parabolically or spherically-shaped mirrors is being considered in order to increase the solar energy intensity on solar cells. Their use will significantly decrease the size and number of the cells needed for a particular application, hence the total array cost. Questions arise, however, regarding the long-term (five to ten years) efficiency of these devices. Performance degradation of the mirror surfaces might result from known hostile elements in the low earth orbit (LEO) environment (150-350 nautical miles). The degradation issue is addressed in light of present knowledge of this environment. The following characteristics of the LEO environment are identified for study: (1) the vacuum of space; (2) sputtering by the residual atoms and particles in space; (3) solar electromagnetic radiation; (4) contamination of the mirror surface; (5) atomic oxygen interactions with the surface; (6) bombardment of the surface by meteoroids; and (7) irradiation of the surface by ionizing particles (protons). Using the best available information for the magnitudes of the necessary quantities, a mathematical analysis was carried out, where possible, to determine the degradation in reflectance or other loss caused by each characteristic. Otherwise, reasonable estimates are made of corresponding losses, based on already published data. Author

N86-14103*# Mississippi Valley State Univ., Itta Bena.
FORTRAN PLOTTING SUBROUTINES FOR THE SPACE PLASMA LABORATORY Final Report c61
Raymond Williams *In* NASA. Johnson (Lyndon B.) Space Center The 1983 NASA/ASEE Summer Faculty Fellowship Research Program Research Reports Sep. 1983 8 p (For primary document see N86-14078 04-85)
Avail: NTIS HC A18/MF A01 CSCL 09B

The computer program known as PLOTRW was custom made to satisfy some of the graphics requirements for the data collected in the Space Plasma Laboratory at the Johnson Space Center (JSC). The general requirements for the program were as follows: (1) all subroutines shall be callable through a FORTRAN source program; (2) all graphs shall fill one page and be properly labeled; (3) there shall be options for linear axes and logarithmic axes; (4) each axis shall have tick marks equally spaced with numeric values printed at the beginning tick mark and at the last tick mark; and (5) there shall be three options for plotting. These are: (1) point plot, (2) line plot and (3) point-line plot. The subroutines were written in FORTRAN IV for the LSI 11 Digital equipment Corporation (DEC) Computer. The program is now operational and can be run on any TEKTRONICX graphics terminal that uses a DEC Real-Time-11 (RT-11) operating system. Author

N86-14104*# Bradley Univ., Peoria, Ill. Dept. of Mathematics.
COMPUTER GRAPHICS APPLICATIONS TO CREW DISPLAYS Final Report c61
Joan Wyzkoski *In* NASA. Johnson (Lyndon B.) Space Center The 1983 NASA/ASEE Summer Faculty Fellowship Research Program Research Reports Sep. 1983 10 p refs (For primary document see N86-14078 04-85)
Avail: NTIS HC A18/MF A01 CSCL 09B

Astronauts are provided much data and information via the monochrome CRT displays on the orbiter. For this project two areas were investigated for the possible introduction of computer graphics to enhance and extend the utility of these displays. One involved reviewing the current orbiter displays and identifying those which could be improved via computer graphics. As an example, the tabular data on electrical power distribution and control was enhanced by the addition of color and bar charts. The other dealt with the development of an aid to berthing a payload with the Remote Manipulator System (RMS). This aid consists of a graphics display of the top, front and side views of the payload and cargo bay and point of resolution (POR) position and attitude data for the current location of the payload. The initial implementation was on an IBM PC clone. The demonstration software installed in the Johnson Space Center Manipulator Development Facility (MD) was reviewed. Due to current hardware limitations, the MDF verision is slow, i.e., about a 40+ seond update rate and, hence, not real-time. Despite this fact, the evaluation of this additional visual cue as an

RMS operator aid indicates that this display, with modifications for speed, etc., can assist the crew. Further development is appropriate. Author

N86-14105*# East Texas State Univ., Commerce. Dept. of Computer Science.
SIGNAL PROCESSING OF ANTHROPOMETRIC DATA Final Report c32
Wayne J. Zimmermann *In* NASA. Johnson (Lyndon B.) Space Center The 1983 NASA/ASEE Summer Faculty Fellowship Research Program Research Reports Sep. 1983 9 p refs (For primary document see N86-14078 04-85)
Avail: NTIS HC A18/MF A01 CSCL 17B

The Anthropometric Measurements Laboratory has accumulated a large body of data from a number of previous experiments. The data is very noisy, therefore it requires the application of some signal processing schemes. Moreover, it was not regarded as time series measurements but as positional information; hence, the data is stored as coordinate points as defined by the motion of the human body. The accumulated data defines two groups or classes. Some of the data was collected from an experiment designed to measure the flexibility of the limbs, referred to as radial movement. The remaining data was collected from experiments designed to determine the surface of the reach envelope. An interactive signal processing package was designed and implemented. Since the data does not include time this package does not include a time series element. Presently the results is restricted to processing data obtained from those experiments designed to measure flexibility. Author

N86-14106*# National Aeronautics and Space Administration. Lewis Research Center, Cleveland, Ohio.
STIRLING ENGINE SUPPORTING RESEARCH AND TECHNOLOGY Final Report
William A. Tomazic 1985 19 p Presented at the 23rd Automotive Technology Development Contractors' Coordination Meeting, Dearborn, Mich., 21-24 Oct. 1985; sponsored by DOE
(Contract DE-AI01-85CE-50112)
(NASA-TM-87175; DOE/NASA/50112-60; E-2821; NAS 1.15:87175) Avail: NTIS HC A02/MF A01 CSCL 10B

The supporting research and technology effort is intended to provide technical support to the current engine program and also to investigate advanced concepts for the next generation of Stirling engines. Technical areas represented are: seals, materials, engine experiments, combustion, system analysis, cseramics, and tribology. A collage of more recent work in each area is presented. Under seals, analysis and some experimental data on the effect of wear on rod seal performance is presented. The material work described concerns the effect of water content on hydrogen permeation. Results of experiments with the Philips' Advenco engine are presented. A comparison is made of two combustor nozzles, an air atomizing and an ultrasonic atomizing nozzle. A new venture in systems analysis to provide more rigorous Stirling engine simulation is discussed. The results of hydrogen corrosion tests on silicon carbide are presented. Friction and wear tests on candidate materials for engine hot ring tests are discussed. Author

N86-14107 Polish Academy of Sciences, Warsaw.
SCIENTIFIC ACTIVITIES OF THE POLISH ACADEMY OF SCIENCES: INSTITUTE OF FUNDAMENTAL TECHNOLOGICAL RESEARCH IN 1983
Zenon Mroz, ed., Julian Duputat, ed., Aleksandra Krolikowska, ed., and Kasimierz Sobczyk, ed. 1985 249 p
(ISBN-83-01-06288-6; ISSN-0079-523X) Copyright. Avail: Issuing Activity

The Institute of Fundamental Technological Research of the Polish Academy of Sciences (IFTR, PASc) conducts fundamental research and its practical applications in many fields of science and technology. Its principal research areas are: mathematical and physical foundations of the theory of continuous media; mechanics of material behavior in elastic and plastic ranges taking into account plasticity effects, degradation and fracture (metals, soils, rocks, concretes, polymers, composites etc.); mechanics of machinery and civil engineering structures in both linear and non-linear ranges; generation, propagation and properties of acoustic and electromagnetic waves; ultrasonic medical diagnostics; atomic frequency standards; and non-destructive testing of materials and structures. F.M.R.

N86-14108# Office of Naval Research, London (England).
EUROPEAN SCIENCE NOTES, VOLUME 39, NUMBER 7 Monthly Report
L. E. Shaffer Jul. 1985 72 p
(AD-A157708; ESN-39-7) Avail: NTIS HC A04/MF A01 CSCL 05/2

European Science Notes is a monthly publication with brief articles on recent developments in European scientific research. Topics include: Recent European Contributions to Measurement Theory in the Behavioral Sciences; Biology at ETH-Zurich--Inst. for Biotechnology; Molecular biology and biophysics; Inst. for Molecular Biology; and Biological ultrastructure research; at Electromagnetic Wave Interaction with Biological Systems; Chemistry in Europe--An overview; Research in chemistry at the Univ. Louis Pasteur, Strasbourg, France; Expert Systems; Swedish Institute for Metals Research; The Technion--Israel's premier materials research facility; Numerical Analysis at Pavia; Research on Coherent Structures in Turbulent Shear Flows at Tel Aviv Univ.; Spanish University Research in Physics; Modern Optics, Microelectronics, and Thin Films Research at Madrid. GRA

N86-14109# Office of Naval Research, London (England).
EUROPEAN SCIENCE NOTES. VOLUME 39, NUMBER 9
L. E. Shaffer Sep. 1985 55 p
(AD-A158278; ESN-39-9) Avail: NTIS HC A04/MF A01 CSCL 05/2

European Science Notes is a monthly publication with brief articles on recent developments in European Scientific research. Topics include: The Cognitive Structure of Verbal Ability in Israel; Greek Studies into the Psychology of Torturers; Research in Genetics, Molecular Biology, Immunology, and Virology at Swedish Universities; Workshop on Destruction of Bacterial Spores in Food Supplies; Organic Metals Program at Ben Gurion Univ., Integrated Optics Research at Tel Aviv Univ.; Highlights of the 2nd European Conference on Atomic and Molecular Physics. GRA

88 SPACE SCIENCES (GENERAL)

N86-14110*# National Aeronautics and Space Administration. Lewis Research Center, Cleveland, Ohio.
DEVELOPMENT OF THE VOLT-A SHUTTLE EXPERIMENT
William J. Bifano, John M. Bozek, and Dale C. Ferguson 1985 13 p Presented at the 18th Photovoltaic Specialists Conference, Las Vegas, Nev., 21-25 Oct. 1985; sponsored by IEEE
(NASA-TM-87169; E-2807; NAS 1.15:87169) Avail: NTIS HC A02/MF A01 CSCL 12A

The NASA Lewis Research Center (LeRC) is investigating potential problems associated with the operation of high voltage solar cell arrays in the space plasma environment. At high voltages, interactions between the solar array and the space plasma could result in unacceptable levels of electrical discharge (arcing) and/or parasitic losses (current drains from the array to the plasma). The objective of the Voltage Operating Limit Tests (VOLT-A) Shuttle bay experiment is to characterize space plasma/solar cell panel interactions in low earth orbit. VOLT-A consists of an experiment plate subassembly which contains four solar panels, an electronics subassembly and a Langmuir probe subassembly mounted on an MPESS carrier. During a given 8.25 hour data taking period (5-1/2 continuous orbits), the solar panels, which represent state-of-the-art solar cell technologies, will be sequentially subjected to bias voltages in steps ranging from minus 626 V to plus 313 V. Appropriate measurements will be made at each voltage to characterize arcing and parasitic losses. Corresponding measurements of the plasma environment (plasma density, electron temperature and neutral density) will also be made. Data will be recorded on an on-board tape recorder for subsequent data reduction and analysis. Author

N86-14111# Joint Publications Research Service, Arlington, Va.
USSR REPORT: SPACE
30 Sep. 1985 156 p refs Transl. into ENGLISH from various Russian articles
(JPRS-USP-85-005) Avail: NTIS HC A08

Progress in USSR aerospace science and technology is reported. Topics discussed include: aerospace engineering, interplanetary sciences, life sciences, space applications, space policy and administration, and launch tables. For individual titles, see N86-14112 through N86-14199.

N86-14112# Joint Publications Research Service, Arlington, Va.
FORMING TRANSFORMATION MATRICES FOR DIFFERENT PARAMETERS OF MOTION OF CELESTIAL BODIES Abstract Only **c90**
A. A. Sukhanov *In its* USSR Rept.: Space (JPRS-USP-85-005) 30 Sep. 1985 p 24 Transl. into ENGLISH from Kosmich. Issled. (Moscow), v. 22, no. 6, Nov. - Dec. 1984 p 819-827 (For primary document see N86-14111 04-88)
Avail: NTIS HC A08

The computation of matrices for transformation of certain parameters of motion to others is discussed. These matrices are needed to evaluate the influence of small perturbations of different kinds, to study relative motion and to determine and correcting motion. The transformation matrices are not found in explicit form, but are determined by using elementary matrix operations. These expressions make it possible to compute transformation matrices for rectangular phase coordinates and 216 different systems of elements formed from the 20 most frequently used orbital osculating elements. An intermediate system of orbital elements is introduced. The simple formulas make it possible to find the values of 47,089 different transformation matrices of the desired form for the two-body problem. These matrices can be computed for orbits of any type other than linear. E.A.K.

N86-14113# Joint Publications Research Service, Arlington, Va.
FORMING ATTAINABILITY SETS IN CONTROL OF KINETIC MOMENT OF ROTATING ASYMMETRIC SOLID BODY (SPECIAL CASES) Abstract Only **c90**
A. V. Sarychev *In its* USSR Rept.: Space (JPRS-USP-85-005) 30 Sep. 1985 p 25 Transl. into ENGLISH from Kosmich. Issled. (Moscow), v. 22, no. 6, Nov. - Dec. 1984 p 828-841 Original language document announced in IAA as A85-19902 (For primary document see N86-14111 04-88)
Avail: NTIS HC A08

The controlled motion of the vector of the kinetic moment (KMV) of an asymmetric rigid body rotating about the center of mass is examined in the case where the control moment is directed along an axis fixed in the body. Attention is given to the case when this axis and the initial value of the KMV lie in a special plane-P, containing nonperiodic trajectories of the Euler equations of the free rotation of the body. In this case the controlled motion of the KMV occurs in the P-plane and is described by a two-dimensional nonlinear autonomus controlled system. Attainability manifolds for this system are constructed. B.J. (IAA)

N86-14114# Joint Publications Research Service, Arlington, Va.
METHOD FOR SOLVING TWO-POINT BOUNDARY VALUE PROBLEM FOR OPTIMIZATION OF FLIGHTS WITH LOW THRUST Abstract Only **c18**
A. I. Glazkov *In its* USSR Rept.: Space (JPRS-USP-85-005) 30 Sep. 1985 p 26 Transl. into ENGLISH from Kosmich. Issled. (Moscow), v. 22, no. 6, Nov. - Dec. 1984 p 842-847 Original language document announced in IAA as A85-19903 (For primary document see N86-14111 04-88)
Avail: NTIS HC A08

A pulse-spreading (PS) method is proposed for obtaining the initial approximation for optimal jet-powered acceleration in calculations of the low-thrust transfer trajectories of spacecraft in a central gravitational field. The PS method is shown to be superior to existing methods (particularly the transporting-trajectory method) for angular transfer distances of the order of 360 deg and large eccentricities of the initial and/or final orbits. B.J. (IAA)

N86-14115# Joint Publications Research Service, Arlington, Va.
CHOICE OF OPTIMUM BOUNDARY CONDITIONS IN SPEED OPTIMIZATION PROBLEM Abstract Only **c18**
S. A. Voyevodin *In its* USSR Rept.: Space (JPRS-USP-85-005) 30 Sep. 1985 p 26-27 Transl. into ENGLISH from Kosmich. Issled. (Moscow), v. 22, no. 6, Nov. - Dec. 1984 p 848-857 Original language document announced in IAA as A85-19904 (For primary document see N86-14111 04-88)
Avail: NTIS HC A08

Attention is given to a plane problem of time-optimal control involving the setting of a spacecraft into a specified position. The distinctive character of the approach consists in the nonuniqueness of the boundary conditions with respect to the angular coordinates, and its novelty consists in the performance for constraints on the angular velocity of the spacecraft. The optimal control is synthesized, and an analytical solution is obtained. B.J. (IAA)

N86-14116# Joint Publications Research Service, Arlington, Va.
MATHEMATICAL MODELS OF NONSTATIONARY EDDY CURRENTS AND EDDY MOVEMENTS OF FLUID IN PROBLEMS OF ORIENTATION AND STABILIZATION OF ARTIFICIAL EARTH SATELLITES AND SPACECRAFT 2 Abstract Only **c18**
B. I. Rabinovich and V. M. Rogovoy *In its* USSR Rept.: Space (JPRS-USP-85-005) 30 Sep. 1985 p 27 Transl. into ENGLISH from Kosmich. Issled. (Moscow), v. 22, no. 6, Nov. - Dec. 1984 p 867-874 Original language document announced in IAA as A85-19906 (For primary document see N86-14111 04-88)
Avail: NTIS HC A08

A mathematical model for unsteady eddy fluid motions in the tanks of a spacecraft with a liquid propellant rocket engine is considered, assuming the tanks to be equipped with dampers in the form of sharp-edged ribs, and considering the acceleration, deceleration, and correction segments of the orbit. Allowance is made for the kinetic energy of the eddy motions. The model is shown to be identical to the model of unsteady eddy currents in a conducting ferromagnetic at a high Reynolds number, a high magnetic Reynolds number, and a low Strouhal number. The harmonic-balance method is used to reduce the models to a form convenient for solving dynamic problems of a colosed control volume regulator system. B.J. (IAA)

N86-14117# Joint Publications Research Service, Arlington, Va.
OBSERVATIONS OF FLUXES OF COLD IONS FROM PLASMASPHERE INTO IONOSPHERE DURING NIGHTTIME IN MIDDLE LATITUDES Abstract Only **c46**
V. V. Afonin, P. Bentse, V. V. Bezrukikh, K. I. Gringauz, I. Semerei, and N. F. Smirnova *In its* USSR Rept.: Space (JPRS-USP-85-005) 30 Sep. 1985 p 28 Transl. into ENGLISH from Kosmich. Issled. (Moscow), v. 22, no. 6, Nov. - Dec. 1984 p 884-888 Original language document announced in IAA as A85-19908 (For primary document see N86-14111 04-88)
Avail: NTIS HC A08

Electrostatic analyzers aboard the Vertikal'-10 rocket (launched on December 25, 1981 at 22.35 MLT) detected fluxes of cold ions moving from the midlatitude plasmasphere to the ionosphere at night at L = 2. The flux velocity was observed to be approximately 1000 m/s, and the flux density was (0.8-4.0) x 10 to the 8th/sq cm s. Discrepancies between theoretical predictions and experimental observations of the flux values are discussed, and it is noted that the measured fluxes from the plasmasphere are sufficient for sustaining the nighttime ionosphere. B.J. (IAA)

N86-14118# Joint Publications Research Service, Arlington, Va.
SPECTRUM OF PHOTOELECTRONS IN EARTH'S UPPER ATMOSPHERE DURING SOLAR FLARES Abstract Only **c93**
S. V. Avakyan and G. S. Kudryashev *In its* USSR Rept.: Space (JPRS-USP-85-005) 30 Sep. 1985 p 29 Transl. into ENGLISH

from Kosmich. Issled. (Moscow), v. 22, no. 6, Nov. - Dec. 1984 p 889-894 Original language document announced in IAA as A85-19909 (For primary document see N86-14111 04-88)
Avail: NTIS HC A08

A theoretical study of variations of the energy distribution of photoelectrons in the ionosphere during solar flares is performed for the example of the flares of February 25, 1969 and December 27, 1968. The role of Auger electrons in the formation of photoelectrons with energies exceeding 150 to 200 eV is shown to be dominant. The calculation model is confirmed by experimental data on variations of photoelectron intensity and upper-atmospheric emission. It is concluded that the proposed model is suitable for determining the degree of ionospheric disturbances during flares, especially above 100 km, where the role of photoelectrons becomes drastically more significant. B.J. (IAA)

N86-14119# Joint Publications Research Service, Arlington, Va.
SOLAR FLARE X-RADIATION AND HIGH-ENERGY PARTICLES ACCORDING TO OBSERVATIONAL DATA FROM VENERA-13 AND VENERA-14 AUTOMATIC INTERPLANETARY STATIONS Abstract Only c92
S. A. Belyakov, Ye. I. Daybog, A. P. Dyachkov, V. M. Zenchenko, Viktoriya G. Kurt, Yu. I. Logachev, A. I. Rutkovskiy, S. P. Ryumin, V. G. Stolpovskiy, V. G. Yurovitskaya et al *In its* USSR Rept.: Space (JPRS-USP-85-005) 30 Sep. 1985 p 30 Transl. into ENGLISH from Kosmich. Issled. (Moscow), v. 22, no. 6, Nov. - Dec. 1984 p 906-921 Original language document announced in IAA as A85-19911 (For primary document see N86-14111 04-88)
Avail: NTIS HC A08

Venera-13, 14 data obtained from November 1981 to April 1982 are used to examine the correlation between bursts of hard solar X-rays (energy exceeding 0.055 MeV) and solar-cosmic-ray (SCR) flares. Data on solar flares in H-alpha, thermal X-rays, and Type 3 radio bursts were used in the analysis. It is shown that the amplitude of flare-electron intensity (energies exceeding 1.0 MeV) is best correlated with flare importance in the thermal X-ray range (r = 0.8 + or - 0.03). The use of this importance makes it possible to construct solar-longitude dependences of flare electrons and to assess the solar-longitudinal interval of flares in which coronal-propagation effects can be neglected. A practically linear correlation is found between SCR electrons with energies of tens of keV and thermal X-rays. B.J. (IAA)

N86-14120# Joint Publications Research Service, Arlington, Va.
ROLE OF INTRINSIC ENERGY SOURCE IN PHYSICAL BEHAVIOR OF SPLIT COMETARY NUCLEUS Abstract Only c90
V. D. Davydov *In its* USSR Rept.: Space (JPRS-USP-85-005) 30 Sep. 1985 p 31 Transl. into ENGLISH from Kosmich. Issled. (Moscow), v. 22, no. 6, Nov. - Dec. 1984 p 922-941 Original language document announced in IAA as A85-19912 (For primary document see N86-14111 04-88)
Avail: NTIS HC A08

It is hypothesized that the intrinsic energy of a multiple cometary nucleus (MCN) plays the dominant role in the physical behavior of especially active comets. This results from the fact that the relatively low energy of the impact mechanism is capable of sustaining the extremely high level of consumption of solar energy toward the sublilmation of cometary matter from the icy-dust cloud into the nuclear region. The intrinsic activity of the MCN gradually decays in the course of its evolution into a system with a collisionless sturcture. The sudden switch-on of the shock mechanism is associated with the removal of a tail of large clumps around the main mass of the MCN; the most simple reason for this is a powerful tidal effect on the tail. The more complex process of the switch-off of the impact mechanism follows the nontidal division of the main mass of the nucleus. B.J. (IAA)

N86-14121# Joint Publications Research Service, Arlington, Va.
APPROXIMATE SOLUTIONS OF EULER-LAMBERT EQUATION FOR CASE OF SEVERAL REVOLUTIONS ABOUT CENTRAL BODY Abstract Only c90
L. B. Livanov *In its* USSR Rept.: Space (JPRS-USP-85-005) 30 Sep. 1985 p 32 Transl. into ENGLISH from Kosmich. Issled. (Moscow), v. 22, no. 6, Nov. - Dec. 1984 p 942-944 Original language document announced in IAA as A85-19913 (For primary document see N86-14111 04-88)
Avail: NTIS HC A08

Approximate solutions are obtained for the Euler-Lambert equation with the aim of economizing machine time in the framework of designing fuel-optimal spacecraft trajectories. The results, obtained for several revolutions about a central body, are applicable to the Earth-Venus-Earth and Earth-Mars-Earth trajectories. B.J. (IAA)

N86-14122# Joint Publications Research Service, Arlington, Va.
FORMATION OF HIGH-ENERGY SECONDARY ELECTRONS IN LOW-DENSITY MEDIUM AT GREAT ALTITUDES Abstract Only c93
L. V. Kurnosova, L. A. Razorenov, and M. I. Fradkin *In its* USSR Rept.: Space (JPRS-USP-85-005) 30 Sep. 1985 p 32-33 Transl. into ENGLISH from Kosmich. Issled. (Moscow), v. 22, no. 6, Nov. - Dec. 1984 p 947-949 Original language document announced in IAA as A85-19915 (For primary document see N86-14111 04-88)
Avail: NTIS HC A08

The formation of a high-energy secondary electron halo at high altitudes (approximately 500 km) in the upper atmosphere is examined on the basis of Cosmos-225 scintillation-counter data for electron energies of 70 to 1000 and 100 to 1000 MeV. This secondary-electron flux is shown to be roughly equal to the flux of albedo electrons, which serves as a confirmation of Grigorov's (1977) model concerning the existence of a radiation belt formed of electrons with energies exceeding 100 MeV. B.J. (IAA)

N86-14123# Joint Publications Research Service, Arlington, Va.
HARD GAMMA RADIATION BACKGROUND FROM CODING COLLIMATOR OF GAMMA TELESCOPE UNDER SPACE EXPERIMENT CONDITIONS Abstract Only c93
A. P. Aleksandrov, A. N. Berezovoy, A. M. Galper, V. M. Grachev, V. V. Dmitrenko, V. G. Kirillov-Ugryumov, V. V. Lebedev, V. A. Lyakhov, A. A. Moiseyev, S. Ye. Ulin et al *In its* USSR Rept.: Space (JPRS-USP-85-005) 30 Sep. 1985 p 33-34 Transl. into ENGLISH from Kosmich. Issled. (Moscow), v. 22, no. 6, Nov. - Dec. 1984 p 950-951 (For primary document see N86-14111 04-88)
Avail: NTIS HC A08

Coding collimators are used to improve the angular resolution of gamma-ray telescopes at energies above 50 MeV. However, the interaction of cosmic rays with the collimation material can lead to the appearance of a gamma-ray background flux which can have a deleterious effect on measurement efficiency. An experiment was performed on the Salyut-6-Soyuz spacecraft system with the Elena-F small-scale gamma-ray telescope in order to measure the magnitude of this background. It is shown that, even at a zenith angle of approximately zero degrees (the angle at which the gamma-ray observations are made), the coding collimator has only an insignificant effect on the background conditions. B.J. (IAA)

N86-14124# Joint Publications Research Service, Arlington, Va.
SUDDEN DISAPPEARANCE OF QUIESCENT PROMINENCES Abstract Only c92
G. P. Apushkinskiy and N. A. Topchilo *In its* USSR Rept.: Space (JPRS-USP-85-005) 30 Sep. 1985 p 34 Transl. into ENGLISH from Astron. Zh. (Moscow), v. 61, no. 6, Nov. - Dec. 1984 p 1150-1157 Original language document announced in IAA as A85-42338 (For primary document see N86-14111 04-88)
Avail: NTIS HC A08

Cases of the breakup of quiescent prominences on July 2, 1976, and July 30, 1980, are discussed. Radio and optical data at wavelengths 1.35 and 0.8 cm and in the H-alpha line, respectively, confirmed the arch structure of the prominences. The breakup took place both through expansion of the arch and as a consequence of plasma outflow through its bases, in which heat conduction played an insignificant role. Author (IAA)

N86-14125# Joint Publications Research Service, Arlington, Va.
MAGNETIC FIELD DETERMINATION IN QUIESCENT SOLAR PROMINENCES FROM POLARIZATION CHARACTERISTICS OF RADIATED LIGHT Abstract Only c92
M. G. Gornyy, D. V. Kupriyanov, and B. G. Matisov *In its* USSR Rept.: Space (JPRS-USP-85-005) 30 Sep. 1985 p 35 Transl. into ENGLISH from Astron. Zh. (Moscow), v. 61, no. 6, Nov. - Dec. 1984 p 1158-1167 Previously announced in IAA as A85-42339 (For primary document see N86-14111 04-88)
Avail: NTIS HC A08

A method is proposed for the approximate solution of the equations of optical pumping describing the Hanle effect, based on the property of weak anisotropy of the exiting light, in quiescent solar prominences. The polarization characteristics of the emission of a prominence as a function of the magnitude and direction of the magnetic field are calculated on He triplet transitions. The influence of the trapping of resonance radiation on the polarization of the ensemble of emitting atoms is analyzed. Author (IAA)

N86-14126# Joint Publications Research Service, Arlington, Va.
SPATIAL PATTERNS OF MANIFESTATION OF SOLAR ACTIVITY IN TROPOSPHERE Abstract Only c92
R. V. Smirnov *In its* USSR Rept.: Space (JPRS-USP-85-005) 30 Sep. 1985 p 35-36 Transl. into ENGLISH from Astron. Zh. (Moscow), v. 61, no. 6, Nov. - Dec. 1984 p 1168-1178 Previously announced in IAA as A85-42340 (For primary document see N86-14111 04-88)
Avail: NTIS HC A08

A joint analysis of maps of pressure variation in the troposphere (or of pressure dispersions) following geomagnetic disturbances and of maps of advection, wind-speed divergence, etc. makes it possible to advance the concept of solar dependent centers of action (SDCA), of the atmosphere, by means of SDCA, where baroclinic instability is high, a solar disturbance is transmitted and planetary waves develop in the atmosphere. Infrasonic waves are considered as an agent connecting the lower thermosphere and the troposphere. Author (IAA)

N86-14127# Joint Publications Research Service, Arlington, Va.
MECHANISM OF CORPUSCULAR-ATMOSPHERIC RELATIONSHIPS Abstract Only c46
E. R. Mustel *In its* USSR Rept.: Space (JPRS-USP-85-005) 30 Sep. 1985 p 36-37 Transl. into ENGLISH from Astron. Zh. (Moscow), v. 61, no. 6, Nov. - Dec. 1984 p 1179-1183 Previously announced in IAA as A85-42341 (For primary document see N86-14111 04-88)
Avail: NTIS HC A08

In this paper attention is drawn to the results of Brazilian investigators (Martin, et al., 1972; Trivedi, et al., 1973) who concluded that dumping of high-energy particles from the Earths radiation belts down toward the stratosphere occurs in the region of the south magnetic anomaly at times of geomagnetic storms. Assuming that analogous processes occur in the Northern Hemisphere and using the numerical data of the Brazilian investigators and others, it is shown that the total energy flux contained in the dumpings can reach 10 to the 24th erg. Attention is drawn to the very important fact that all four of the main climatic lows of the Northern Hemisphere (North American, Icelandic, Asiatic, and Aleutian) coincide with the main magnetic anomalies, and hence, be above-indicated dumpings of energetic particles play the main role just in the regions of magnetic anomalies and thereby in the regions of climatic lows. Author (IAA)

N86-14128# Joint Publications Research Service, Arlington, Va.
APPROXIMATE CLUSTER ANALYSIS METHOD AND THREE-DIMENSIONAL DIAGRAM OF OPTICAL CHARACTERISTICS OF LUNAR SURFACE Abstract Only c91
N. N. Yevsyukov *In its* USSR Rept.: Space (JPRS-USP-85-005) 30 Sep. 1985 p 37 Transl. into ENGLISH from Astron. Zh. (Moscow), v. 61, no. 6, Nov. - Dec. 1984 p 1184-1191 Previously announced in IAA as A85-42342 (For primary document see N86-14111 04-88)
Avail: NTIS HC A08

An approximate isolation algorithm for the isolation of multidimensional clusters is developed and applied in the construction of a three-dimensional diagram of the optical characteristics of the lunar surface. The method is somewhat analogous to that of Koontz and Fukunaga (1972) and involves isolating two-dimensional clusters, adding a new characteristic, and linearizing, a cycle which is repeated a limited number of times. The lunar-surface parameters analyzed are the 620-nm albedo, the 620/380-nm color index, and the 950/620-nm index. The results are presented graphically; the reliability of the cluster-isolation process is discussed; and some correspondences between known lunar morphology and the cluster maps are indicated. T.K. (IAA)

N86-14129# Joint Publications Research Service, Arlington, Va.
STRUCTURE OF COEFFICIENTS OF SERIES REPRESENTING SOLUTION OF PLANE CIRCULAR RESTRICTED THREE-BODY PROBLEM Abstract Only c84
Ye. I. Timoshkova and V. B. Titov *In its* USSR Rept.: Space (JPRS-USP-85-005) 30 Sep. 1985 p 38 Transl. into ENGLISH from Astron. Zh. (Moscow), v. 61, no. 6, Nov. - Dec. 1984 p 1211-1217 Previously announced in IAA as A85-42346 (For primary document see N86-14111 04-88)
Avail: NTIS HC A08

The properties of the trigonometric polynomials which serves as the coefficients of power series constructed by Timoshkova (1979 and 1980) to represent the first integrals of the plane circular restricted three-body problem of celestial mechanics are investigated analytically. The convergence of the power series is discussed, and it is demonstrated in numerical computations for the earth-moon system that the Jacobi constant C for collinear libration points can be determined from the formally constructed integrals. T.K. (IAA)

N86-14130# Joint Publications Research Service, Arlington, Va.
A PRIORI GUARANTEED ACCURACY EVALUATION IN DETERMINING SPACECRAFT ORBIT BY LEAST SQUARES METHOD Abstract Only c13
P. Ye. Elyasberg *In its* USSR Rept.: Space (JPRS-USP-85-005) 30 Sep. 1985 p 38-39 Transl. into ENGLISH from Kosmich. Issled. (Moscow), v. 22, no. 5, Sep. - Oct. 1984 p 643-650 Previously announced in IAA as A85-15251 (For primary document see N86-14111 04-88)
Avail: NTIS HC A08

In an a priori estimation of the expected accuracy of orbit determination, it is assumed that all the initial data (measurements and a priori information concerning the parameters of the mathematical model) can be divided into groups between which and within which are specified different constraints on the correlation coefficients between errors. Formulas are derived for calculating the guaranteed value of the error of the estimate variance of any estimated parameter when performing single or repeated measurements. B.J. (IAA)

N86-14131# Joint Publications Research Service, Arlington, Va.
INTEGRATION OF EQUATIONS OF MOTION FOR MATERIAL POINT IN GRAVITATIONAL FIELD OF AXIALLY SYMMETRIC PLANET Abstract Only c90
A. R. Golikov *In its* USSR Rept.: Space (JPRS-USP-85-005) 30 Sep. 1985 p 39 Transl. into ENGLISH from Kosmich. Issled. (Moscow), v. 22, no. 5, Sep. - Oct. 1984 p 651-662 Original language document announced in IAA as A85-15252 (For primary document see N86-14111 04-88)
Avail: NTIS HC A08

The paper formulates a general method of searching for an anharmonic approximation expression for the gravitational potential of an axisymmetric planet, allowing integration of the equations of motion of its satellite in quadratures. Though the analysis is performed for oblate spheroidal coordinates, the possibility of using the proposed method for other systems of curved coordinates is demonstrated. B.J.(IAA)

N86-14132# Joint Publications Research Service, Arlington, Va.
PERIODIC REGIMES OF ROTATIONAL MOTION OF SOLID

BODY ABOUT LIBERATION POINT L SUB 4 IN RESTRICTED ELLIPTICAL THREE-BODY PROBLEM Abstract Only c90
Yu. V. Barkin and S. N. Lelyavin *In its* USSR Rept.: Space (JPRS-USP-85-005) 30 Sep. 1985 p 40 Transl. into ENGLISH from Kosmich. Issled. (Moscow), v. 22, no. 5, Sep. - Oct. 1984 p 663-674 Original language document announced in IAA as A85-15253 (For primary document see N86-14111 04-88)
Avail: NTIS HC A08

Several families of periodic solutions are obtained and analyzed for the rotational motion of a rigid body whose center of mass is situated at the L4 libration point of the restricted elliptical three-body problem. It is assumed that the ellipsoid of inertia is nearly a sphere. The investigation is based on the theory of periodic Poincaresolutions for degenerate Hamiltonian systems. B.J.(IAA)

N86-14133# Joint Publications Research Service, Arlington, Va.
MATHEMATICAL MODELS OF NONSTATIONARY EDDY CURRENTS AND EDDY MOTIONS OF FLUID IN SPACECRAFT ORIENTATION AND STABILIZATION PROBLEMS 1 Abstract Only c18
B. I. Rabinovich and V. M. Rogovoy *In its* USSR Rept.: Space (JPRS-USP-85-005) 30 Sep. 1985 p 41 Transl. into ENGLISH from Kosmich. Issled. (Moscow), v. 22, no. 5, Sep. - Oct. 1984 p 678-692 Original language document announced in IAA as A85-15255 (For primary document see N86-14111 04-88)
Avail: NTIS HC A08

The paper examines the development of an adequate mathematical model for eddy currents in a conducting ferromagnetic, valid for the frequency band which characterizes spacecraft attitude and stabilization problems. The model is synthesized on the basis of the asymptotic solution of the appropriate boundary layer equations. This approach is illustrated by the model of an electromagnetic actuator for spacecraft attitude and stabilization systems. B.J.(IAA)

N86-14134# Joint Publications Research Service, Arlington, Va.
COMPARISON OF ENERGETICS OF OPTIMUM MANEUVERS AND TWO-IMPULSE MANEUVERS IN SOME PROBLEMS OF MOTION FROM A POINT INTO ORBIT Abstract Only c18
A. P. Skorokhodov *In its* USSR Rept.: Space (JPRS-USP-85-005) 30 Sep. 1985 p 41-42 Transl. into ENGLISH from Kosmich. Issled. (Moscow), v. 22, no. 5, Sep. - Oct. 1984 p 693-701 Original language document announced in IAA as A85-15256 (For primary document see N86-14111 04-88)
Avail: NTIS HC A08

Optimal multiple-impulse maneuvers are compared with the simplest one- and two-impulse maneuvers in terms of fuel consumption for certain problems involving the transfer of a spacecraft from a point specified by the radius vector and velocity vector into a circular orbit. It is shown that, in general, the optimal transfers are close from the standpoint of energy consumption to the simple impulse maneuvers, the gain achieved through the multiple-impulse transfers amounts to less than 1 percent. However, there are cases when the gain achieved through optimal transfers is significant. B.J.(IAA)

N86-14135# Joint Publications Research Service, Arlington, Va.
OPTIMUM CONTROL PROGRAMS IN PROBLEM OF INTERORBITAL FLIGHT WITH CONTINUOUS THRUST Abstract Only c18
S. A. Ishkov and V. V. Salmin *In its* USSR Rept.: Space (JPRS-USP-85-005) 30 Sep. 1985 p 42 Transl. into ENGLISH from Kosmich. Issled. (Moscow), v. 22, no. 5, Sep. - Oct. 1984 p 702-711 Original language document announced in IAA as A85-15257 (For primary document see N86-14111 04-88)
Avail: NTIS HC A08

Various thrust-vector-control programs are examined for the transfer of a spacecraft with a low-thrust engine between noncoplanar circular Keplerian orbits. The averaging method is used to obtain the model of spacecraft motion; and the optimal control program is determined which minimizes fuel consumption with allowance for constraints connected with spacecraft rotation. Calculations are made of the energy characteristics of interorbit transfers from a low geocentric orbit to a stationary satellite orbit. B.J.(IAA)

N86-14136# Joint Publications Research Service, Arlington, Va.
DISTURBANCES IN STRATOSPHERE AND MESOSPHERE FROM SOURCE OF ULTRAVIOLET RADIATION Abstract Only c46
S. I. Kozlov *In its* USSR Rept.: Space (JPRS-USP-85-005) 30 Sep. 1985 p 43 Transl. into ENGLISH from Kosmich. Issled. (Moscow), v. 22, no. 5, Sep. - Oct. 1984 p 712-719 Original language document announced in IAA as A85-15258 (For primary document see N86-14111 04-88)
Avail: NTIS HC A08

A theoretical investigation is made of disturbances in the stratosphere and mesosphere caused by UV radiation in the 1350 to 4000 A range. It is shown that the effect of this radiation, accompanied by the photodissociation of O2 and minor neutral constituents, can produce a significant reduction in the density of negative ions and, hence, a significant increase in electron density. The effect quantitatively depends on wavelength, height, and especially the type of the principal negative ion. B.J.(IAA)

N86-14137# Joint Publications Research Service, Arlington, Va.
COORDINATED INVESTIGATIONS OF PROCESSES IN SUBAURORAL UPPER IONOSPHERE AND THROUGH IN CONCENTRATION OF LIGHT IONS Abstract Only c46
L. D. Sivtseva, V. M. Filippov, V. L. Khalipov, Yu. I. Galperin, V. A. Yershova, L. M. Nikolayenko, Yu. N. Ponomarev, and V. M. Sinitsyn *In its* USSR Rept.: Space (JPRS-USP-85-005) 30 Sep. 1985 p 43-44 Transl. into ENGLISH from Kosmich. Issled. (Moscow), v. 22, no. 5, Sep. - Oct. 1984 p 720-741 Original language document announced in IAA as A85-15259 (For primary document see N86-14111 04-88)
Avail: NTIS HC A08

An analysis is made of Aureole 1 and 2 satellite data concerning latitude profiles of H(+) and He(+) ion density in the midlatitude and subauroral upper ionosphere. A description is given of measurements of subtroughs, i.e., sharp local decreases of H(+) ion density at midlatitude heights of 800 to 1500 km. Data on the location of the light-ion trough in the nightime sector are compared with measurements of the main trough and the L-shell of its polar wall in the lower F-region. L-shells of the plasmapause are shown to coincide with the diffuse-precipitation boundary during moderate disturbances. A scheme of ion convection and density at various heights in the nighttime subauroral F-region is proposed. B.J.

N86-14138# Joint Publications Research Service, Arlington, Va.
REGISTRY OF HEAVY IONS IN AURORAL REGION DURING MAGNETIC STORMS Abstract Only c46
Yu. V. Gotselyuk, S. N. Kuznetsov, and K. Kudela *In its* USSR Rept.: Space (JPRS-USP-85-005) 30 Sep. 1985 p 44-45 Transl. into ENGLISH from Kosmich. Issled. (Moscow), v. 22, no. 5, Sep. - Oct. 1984 p 742-748 Original language document announced in IAA as A85-15260 (For primary document see N86-14111 04-88)
Avail: NTIS HC A08

An analysis is made of Intercosmos-17 data concerning the distribution and dynamics of fluxes of protons, alpha particles, and C, N, and O nuclei during the intense magnetic storms of October 27, and December 2, 1977. Data on the heavy ions are compared with data obtained with the Explorer-45 and S3-3 satellites. A scattering mechanism is proposed which can explain the detection of heavy ions at low altitudes. B.J. (IAA)

N86-14139# Joint Publications Research Service, Arlington, Va.
SMALL-SCALE STRUCTURE OF INTENSIVE LONGITUDINAL CURRENTS IN HIGH LATITUDES Abstract Only c46
A. S. Volokitin, V. V. Krasnoselskikh, Ye. V. Mishin, L. O. Tyurmina, V. A. Sharova, and S. I. Shkolnikova *In its* USSR Rept.: Space (JPRS-USP-85-005) 30 Sep. 1985 p 45 Transl. into ENGLISH from Kosmich. Issled. (Moscow), v. 22, no. 5, Sep. - Oct. 1984 p 749-755 Original language document announced in IAA as A85-15261 (For primary document see N86-14111 04-88)
Avail: NTIS HC A08

An investigation is made of the small-scale structure of field-aligned currents, detected in the auroral oval using magnetic measurements from the Intercosmos-Bulgaria 1300 satellite. The characteristic transverse size of the currents ranges from 2 to 8 km and the density ranges from 0.00003 to 0.0001 A/sq m. It is shown that some of the current structures correspond to a system of standing Alfven waves, evidently excited by the magnetospheric-convection instability. The size of the structure along the geomagnetic field and the magnitude of anomalous resistance are determined. B.J.(IAA)

N86-14140# Joint Publications Research Service, Arlington, Va.
FORMATION OF PROTON RADIATION BELTS IN REGION OF ENERGIES OF SEVERAL MeV Abstract Only c46
M. I. Panasyuk and E. N. Sosnovets *In its* USSR Rept.: Space (JPRS-USP-85-005) 30 Sep. 1985 p 46 Transl. into ENGLISH from Kosmich. Issled. (Moscow), v. 22, no. 5, Sep. - Oct. 1984 p 756-762 Original language document announced in IAA as A85-15262 (For primary document see N86-14111 04-88)
Avail: NTIS HC A08

Satellite data on the spatial location of intensity peaks of radial profiles (Ljm) of protons in the energy range from 500 keV to 100 MeV near the geomagnetic equator are examined. These data are compared with calculations of Ljm(E), taking into account particle transport under the effect of geomagnetic-field fluctuations (GFF). Calculations and experimental data are shown to agree well for a GFF power spectrum having, along with the principal spectrum component Pm(nu) proportional to nu exp-p (where p is about 2), a dominant spectral component at the frequency nu in the MHz range. B.J. (IAA)

N86-14141# Joint Publications Research Service, Arlington, Va.
DEPENDENCE OF LENGTH OF FREE PATH OF FLARE PARTICLES ON ENERGY Abstract Only c90
Ye. I. Daybog, Viktoriya G. Kurt, and V. G. Stolpovskiy *In its* USSR Rept.: Space (JPRS-USP-85-005) 30 Sep. 1985 p 46-47 Transl. into ENGLISH from Kosmich. Issled. (Moscow), v. 22, no. 5, Sep. - Oct. 1984 p 763-773 Original language document announced in IAA as A85-15263 (For primary document see N86-14111 04-88)
Avail: NTIS HC A08

An analysis is made of the time profiles of fluxes of protons and alpha particles in the 0.1 to 100 MeV/nucleaon range, detected by Prognoz-6 in the solar-flare events of September 24, October 9 and 12, November 22, December 27, 1977. It is shown that a harmonic expansion of the measured field cannot be used to calculate the transport characteristics of solar cosmic rays (SCR). This is evidently due to the fact that the usual procedure for determining the power spectrum of IMF fluctuations does not make it possible to identify the type of inhomogeneity (wave, oscillation, or discontinuity) on which SCR-scattering occurs. B.J.(IAA)

N86-14142# Joint Publications Research Service, Arlington, Va.
OBSERVATION OF SMALL-SCALE SOLAR WIND STRUCTURE ON FRONT OF SHARP INCREASE IN PLASMA FLOW VELOCITY Abstract Only c92
L. A. Avanov, G. N. Zastenker, O. L. Vaysberg, and Yu. I. Yermolayev *In its* USSR Rept.: Space (JPRS-USP-85-005) 30 Sep. 1985 p 47-48 Transl. into ENGLISH from Kosmich. Issled. (Moscow), v. 22, no. 5, Sep. - Oct. 1984 p 774-780 Original language document announced in IAA as A85-15264 (For primary document see N86-14111 04-88)
Avail: NTIS HC A08

The Prognoz-8 Monitor device comprising two electrostatic analyzers was used to measure the energy spectra (in the 0.140 to 4.08 keV./charge range) of the ion component of the solar wind with a time resolution of 1.36 sec and, hence, to investigate the small-scale structure of the solar wind at the front of a sharp increase of plasma-stream velocity. It is shown that, in this region, there exist two plasma streams of different velocity (the velocity gradient being 50 to 70 km/s) having different flow directions. Discontinuities of the kinetic parameters of the ion component are observed over a period of 1.5 to 10 sec. B.J. (IAA)

N86-14143# Joint Publications Research Service, Arlington, Va.
ELECTRICAL AND ELECTROTHERMAL CONDUCTIVITY OF PLANETARY IONOSPHERES, 1: REFINEMENT OF THEORY Abstract Only c91
A. V. Pavlov *In its* USSR Rept.: Space (JPRS-USP-85-005) 30 Sep. 1985 p 48-49 Transl. into ENGLISH from Kosmich. Issled. (Moscow), v. 22, no. 5, Sep. - Oct. 1984 p 781-791 Original language document announced in IAA as A85-15265 (For primary document see N86-14111 04-88)
Avail: NTIS HC A08

The explicit form of the coefficients of the electrical and electrothermal conductivity of electrons in a magnetic field in a multicomponent ionosphere with allowance for the temperature difference between electrons and heavy constituents is determined in the first, second, and third approximations of the Sonin polynomial expansion of the Chapman-Enskog method. General expressions for the electron transport coefficients are obtained, which are reduced to a form convenient for practical application. In the first approximation, equations are derived for determining the ion diffusion velocities in a magnetic field in a multicomponent gas mixture. Approximating expressions are refined for the collision frequencies of electrons with the principal neutral constituents of the upper planetary atmospheres. Equations for determining the ambipolar-diffusion velocities of ions in a multicomponent ionosphere in the absence of a magnetic field (or parallel to it) are obtained in the first, second, and third approximations. B.J. (IAA)

N86-14144# Joint Publications Research Service, Arlington, Va.
UNIQUENESS CONDITIONS IN EVALUATION OF LEAST SQUARES METHOD IN NONLINEAR SPACE NAVIGATION PROBLEMS Abstract Only c17
G. A. Mersov *In its* USSR Rept.: Space (JPRS-USP-85-005) 30 Sep. 1985 p 49 Transl. into ENGLISH from Kosmich. Issled. (Moscow), v. 22, no. 5, Sep. - Oct. 1984 p 804-807 Original language document announced in IAA as A85-15267 (For primary document see N86-14111 04-88)
Avail: NTIS HC A08

A major difficulty in nonlinear problems of space navigation is the multiplicity of minima of the functional used in the least squares method. The present paper establishes conditions under which the global-minimum estimate is justified. The necessity of accounting for nonlinearity is connected with the magnitude of measurement errors and with the size of the region of a priori values of the estimated parameters. B.J. (IAA)

N86-14145# Joint Publications Research Service, Arlington, Va.
RADIO EMISSION OF INJECTED ELECTRON BEAM WITH RESPECT TO DIAGNOSIS OF IONOSPHERIC PLASMA Abstract Only c75
S. A. Pulinets *In its* USSR Rept.: Space (JPRS-USP-85-005) 30 Sep. 1985 p 49-50 Transl. into ENGLISH from Kosmich. Issled. (Moscow), v. 22, no. 5, Sep. - Oct. 1984 p 807-809 Original language document announced in IAA as A85-15268 (For primary document see N86-14111 04-88)
Avail: NTIS HC A08

Data from the ARAKS electron-beam-injection experiment are reviewed. It is shown that conditions under which the beam-particle density is approximately equal to the density of the background plasma are experimentally attainable, while conditions under which the beam-particle density is much less than the density of the background plasma are unattainable. This indicates that ionospheric-plasma diagnostics using adio emission from an injected electron beam is entirely possible, but only along the rocket trajectory. B.J. (IAA)

N86-14146# Joint Publications Research Service, Arlington, Va.
CHARGE COMPOSITION OF ELECTRONS IN EARTH'S RADIATION BELT Abstract Only c46
B. I. Luchkov *In its* USSR Rept.: Space (JPRS-USP-85-005) 30 Sep. 1985 p 50-51 Transl. into ENGLISH from Kosmich. Issled. (Moscow), v. 22, no. 5, Sep. - Oct. 1984 p 809-812 Original language document announced in IAA as A85-15269 (For primary document see N86-14111 04-88)

Avail: NTIS HC A08

Synchrotron-radiation data are used to investigate the charge composition of the electrons (i.e., the content of electrons and positrons) in the radiation belts of Earth and Jupiter. Possible experimental techniques for measuring the sign of high-energy electrons in the radiation belts are examined, with particular attention given to measurements of the circular polarization of synchrotron radiation. B.J. (IAA)

N86-14147# Joint Publications Research Service, Arlington, Va.
WAVE INTERPRETATION OF MEASUREMENTS ON MARS-7 AND VENERA-9 PROBES FOR DETERMINING VELOCITY OF MOTION OF INTERSTELLAR GAS Abstract Only c90
Ye. M. Grivnev *In its* USSR Rept.: Space (JPRS-USP-85-005) 30 Sep. 1985 p 51 Transl. into ENGLISH from Pisma v Astron. Zh. (Moscow), v. 10, no. 12, Dec. 1984 p 908-911 Previously announced in IAA as A85-39191 (For primary document see N86-14111 04-88)
Avail: NTIS HC A08

The measurements of the velocity of interstellar gas in the solar system obtained by the Mars 7 and Venera 9 probes (Bertaux et al., 1976 and 1978) are analyzed in the framework of the density-wave theory of spiral galaxies (Lin et al., 1969), assuming that the gas motion comprises a basic circular motion, a random component arising from a nearby disturbance such as a supernova outburst, and a systematic noncircular motion induced by the gravity field of a spiral density wave. T.K. (IAA)

N86-14148# Joint Publications Research Service, Arlington, Va.
VEGA-1 RELEASES AEROSTAT AND LANDER AT VENUS c91
In its USSR Rept.: Space (JPRS-USP-85-005) 30 Sep. 1985 p 52-53 Transl. into ENGLISH from Komsomolskaya Pravda (Moscow), 12 Jun. 1985 p 1 (For primary document see N86-14111 04-88)
Avail: NTIS HC A08

An important stage of the international project Venus-Halley's Comet has been accomplished. A fundamentally new experiment for the study of the circulation of Venus' atmosphere and of its meteorological parameters was begun on 11 June 1985. Flying a distance of approximately 500 million kilometers in six months, the Vega-1 station reached the vicinity of Venus and on 9 June released a descent module which entered the atmosphere on 11 June. This module separated into a landing module and an aerostatic probe. The aerostatic probe, whose gas bag filled with helium following the separation, is drifting in the atmosphere at an altitude of 54 kilometers. Installed on the probe are a radio-transmitting complex and scientific apparatus for measurements of parameters of Venus' atmosphere and cloud cover. B.W.

N86-14149# Joint Publications Research Service, Arlington, Va.
OBJECTIVES OF VEGA PROJECT RESEARCH Abstract Only c91
T. Breus *In its* USSR Rept.: Space (JPRS-USP-85-005) 30 Sep. 1985 p 54 Transl. into ENGLISH from Kommunist (Moscow), 13 Jun. 1985 p 4 (For primary document see N86-14111 04-88)
Avail: NTIS HC A08

The objectives and methods of meteorological and geochemical studies of the planet Venus are discussed. These studies were done by probes from the automatic interplanetary stations Vega-1 and Vega-2. These experiments called for using aerostatic probes for the first time to obtain information on the dynamics of Venus' atmosphere; determining the atmosphere's sulfuric acid content by direct methods for the first time; obtaining new data on the chemical composition and structure of clouds of Venus and on trace elements in the planet's atmosphere; and determining the element composition of the planet's soil in new locations, with the aid of the stations' landing modules. B.W.

N86-14150# Joint Publications Research Service, Arlington, Va.
VEGA-2 RELEASES AEROSTAT AND LANDER AT VENUS c91
In its USSR Rept.: Space (JPRS-USP-85-005) 30 Sep. 1985 p 55-56 Transl. into ENGLISH from Komsomolskaya Pravda (Moscow), 16 Jun. 1985 p 1 (For primary document see N86-14111 04-88)
Avail: NTIS HC A08

On 15 June 1985, the automatic interplanetary station Vega-2 released landing module and an independent aerostatic probe into the planet's atmosphere. The station has passed beyond Venus to a distance of 24,500 kilometers from its surface and is continuing its flight toward Halley's Comet. On 13 June a descent module separated from the station as it was approaching Venus. This module separated into an aerostatic probe and a landing module on 15 June. Soviet and international networks of ground radio telescopes are receiving information from the probe, which is equipped with a unique radio system, and they are fixing its coordinates and rate of movement. The landing module made a soft landing on the dark side of Venus. The composition and physical characteristics of the atmosphere were studied as the module descended through it. B.W.

N86-14151# Joint Publications Research Service, Arlington, Va.
RESULTS FROM VEGA ATMOSPHERE AND SOIL STUDIES Abstract Only c91
V. Golovachev *In its* USSR Rept.: Space (JPRS-USP-85-005) 30 Sep. 1985 p 57 Transl. into ENGLISH from Trud (Moscow), 16 Jun. 1985 p 3 (For primary document see N86-14111 04-88)
Avail: NTIS HC A08

Data on the atmosphere and soil of the planet Venus received from the aerostatic probe and landing module delivered by the Vega-2 space station are discussed. It is noted that earlier studies of surface rocks on Venus showed that they are intermediate between basalts and granites with respect to content of natural radio-active elements; their feature differ depending on location, however. Quick analysis of the sample taken in the Rusalki plain area indicated that it was soft soil with a compressive strength similar to that of loose andesite-basalt soils on Earth. B.W.

N86-14152# Joint Publications Research Service, Arlington, Va.
PRESS CONFERENCE ON FIRST STAGE OF VEGA PROJECT c91
V. P. Ovcharov *In its* USSR Rept.: Space (JPRS-USP-85-005) 30 Sep. 1985 p 58-59 Transl. into ENGLISH from Sov. Latviya (Riga), 18 Jun. 1985 p 3 (For primary document see N86-14111 04-88)
Avail: NTIS HC A08

An unusual phenomenon--the rapid rotation of Venus' cloud layer around the planet--has received reliable experimental confirmation. The second station flew by Venus on its way to Halley's Comet. Unique scientific information has been transmitted to Earth with the aid of instruments delivered by Vega-1 and Vega-2. The first of these aerostatic probes, which was in flight for 46 hours and traveled more than 10,000 kilometers in the planet's atmosphere, transmitted information which indicates that the clouds carried it around Venus at a rate of 60 to 70 meters a second. The significance of this data to the understanding of the Venusian atmosphere is discussed. B.W.

N86-14153# Joint Publications Research Service, Arlington, Va.
FURTHER COMMENTS ON RESULTS OF VEGA STUDIES OF VENUS Abstract Only c91
A. Pokrovskiy *In its* USSR Rept.: Space (JPRS-USP-85-005) 30 Sep. 1985 p 60 Transl. into ENGLISH from Pravda (Moscow), 1 Jul. 1985 p 3 (For primary document see N86-14111 04-88)
Avail: NTIS HC A08

This article records comments of specialists involved in the Venus probe segment of the Vega project. Results of measurements with the landers and aerostats that were dropped on Venus from the space stations are discussed. B.W.

N86-14154# Joint Publications Research Service, Arlington, Va.
DEVELOPMENT OF INSTRUMENTS FOR VEGA PROBES Abstract Only c19
A. Barshay *In its* USSR Rept.: Space (JPRS-USP-85-005) 30 Sep. 1985 p 61 Transl. into ENGLISH from Sov. Kirgiziya

(Frunze), 22 Jun. 1985 p 4 (For primary document see N86-14111 04-88)
Avail: NTIS HC A08

The development of instruments for the Vega-1 and Vega-2 interplanetary stations is discussed. These instruments were designed for use on landing modules intended for studies of Venus. One of these instruments, the VPD-AV, is intended for controlling all operations for placing aerostatic probes into Venus' atmosphere following their separation from the stations' landing modules. Commands issued by this high-precision, preprogrammed timing device were formulated in accordance with its program and data from pressure and temperature sensors. Two other instruments were installed on the stations' landing modules. Aerosols in Venus' cloud cover were analyzed with the aid of the first of these instrumetns, the ISAV-A. It was equipped for this purpose with a highly sophisticated and precise optical system with its own light source. The second instrument, the ISAV-S, was intended for analyzing the gas composition of Venus' atmosphere by the method of active spectrophotometry. Data was gathered by these instruments during the modules' descent to the surface of Venus. All of this information was electronically processed and transmitted to a Vega station, which relayed it to Earth. G.L.C.

N86-14155# Joint Publications Research Service, Arlington, Va.
BROCHURE ON PHOBOS AND DEIMOS c91
Vladimir Naumovich Zharkov and Aleksandr Vasilyevich Kozenko *In its* USSR Rept.: Space (JPRS-USP-85-005) 30 Sep. 1985 p 62-65 Transl. into ENGLISH from Novoye v Zhizni, Nauke, Tekhn.: Ser. Kosmonavtika, Astron. (Moscow), no. 1, Jan. 1985 p 2-6, 53-54 (For primary document see N86-14111 04-88)
Copyright. Avail: NTIS HC A08

The rotation of Phobos and Deimos is synchronous with the planet, i.e., they always face Mars with the same side. The orbits of the Martian satellites are almost circular; the eccentricity being .015 + or - .001 for Phobos and .0005 + or - .0003 for Deimos. They are also practically in the same plane as Mars' equator, that of Phobos being tilted at 1.02 deg and Deimos 1.82 deg. Semi-major axes of the orbits are 9378.5 and 23,459 km and orbital periods 7h 39 min and 30h 21 min, respectively. Thus, Phobos, while revolving around Mars, moves faster than the daily rotation of the planet, and for a Martian observer it would rise in the west and set in the east. G.L.C.

N86-14156# Joint Publications Research Service, Arlington, Va.
RESULTS OF STUDY OF SURFACE OF FIVE REGIONS ON VENUS BY BISTATIC RADAR METHOD Abstract Only c91
A. I. Kucheryavenkov, O. Ye. Milekhin, A. G. Pavelyev, and O. I. Yakovlev *In its* USSR Rept.: Space (JPRS-USP-85-005) 30 Sep. 1985 p 66-67 Transl. into ENGLISH from Kosmich. Issled. (Moscow), v. 22, no. 6, Nov. - Dec. 1984 p 895-905 (For primary document see N86-14111 04-88)
Avail: NTIS HC A08

A method for processing data from a bistatic radar was improved in order to obtain information on the surface of individual regions on Venus with a resolution substantially better than in the Pioneer-Venus experiment. The improved method made it possible to achieve a surface resolution of 5 to 20 km. In the bistatic radar observations made from Venera-10 the planetary surface was irradiated by monochromatic radio waves with a wavelength 32 cm. The transmitter was aboard the vehicle and registry of the direct signal and the signal reflected from the surface was performed at a ground station. Movement of the mirror reflection point on the Venusian surface caused by satellite motion relative to the planet made it possible to study regions adjacent to the trajectories of motion of a mirror reflection point. Five regions were explored. The first four were in the Southern Hemisphere and the fifth was in the Northern Hemisphere. Author

N86-14157# Joint Publications Research Service, Arlington, Va.
POSSIBILITY OF SPECTROSCOPIC DETECTION OF OXYGEN IN LOWER VENUSIAN ATMOSPHERE Abstract Only c91
V. A. Krasnopolskiy *In its* USSR Rept.: Space (JPRS-USP-85-005) 30 Sep. 1985 p 67-68 Transl. into ENGLISH from Kosmich. Issled. (Moscow), v. 22, no. 5, Sep. - Oct. 1984 p 812-815 (For primary document see N86-14111 04-88)
Avail: NTIS HC A08

The parameters of the Martian magnetic dipole on the basis of measurements from the Mars-2 satellite on 23 to 24 February 1972 were discussed. Although the experimental data have deficiencies (the satellite was without triaxial orientation and the interrogation of the vehicle was infrequent) the magnetograms contain important information. This is because during the 35 hours of measurements the satellite twice reached pericenter on the daytime side and twice reached the region of the magnetic tail on the nighttime side. Simultaneously with the measurements from the Mars-2 the magnetic field was measured from the high-apogee satellite Mars-3 (with triaxial orientation) in the free solar wind. Changes in the dynamic pressure of the solar wind during the time of the measurements were simple. The combined data made it possible to determine field topology, which is compared with the field topology near Venus and a model of a draped magnetosphere corresponding to the observed interplanetary magnetic field. Proof is given that Mars has its own magnetic field with a magnetic moment M sub M>1.5 x 10 to the 22 gauss. cubic cm, this constituting an effective obstacle to the solar wind. The strike of the magnetic tail was traced to 8 R sub M. The problems involved in determining orientation of the dipole on the basis of observations in the tail at distances 6 to 8 R sub M are discussed. On the assumption that a width of the Martian polar cap is approx. 45 deg it is estimated that the magnetic tail of the Martian magnetosphere can extend to 90 R sub M. The real obstacle to the solar wind near Mars is its magnetosphere, not its ionosphere. Near Mars there is an Earth-type, not a Venusian type of interaction with the solar wind. Author

N86-14158# Joint Publications Research Service, Arlington, Va.
ROSSBY AUTOSOLITON Abstract Only c34
S. V. Antipov, M. V. Nezlin, and A. S. Trubnikov *In its* USSR Rept.: Space (JPRS-USP-85-005) 30 Sep. 1985 p 68 Transl. into ENGLISH from Pisma v Zh. Eksperim. i Teor. Fiz. (Moscow), v. 41, no. 1, Jan. 1985 p 25-28 (For primary document see N86-14111 04-88)
Avail: NTIS HC A08

A new nonlinear physical entity, a Rossby autosoliton, has been produced experimentally. It is an undamped, solitary, drifting, anticyclonic vortex which self-organizes in oppositely directed streams in rotating shallow water. It may be thought of as a steady-state soliton model of the Great Red Spot of Jupiter, developed experimentally for the first time. IAA

N86-14159# Joint Publications Research Service, Arlington, Va.
NATURE OF MEGACYCLES IN EVOLUTION OF EARTH, MARS, AND MOON Abstract Only c91
Ye. Ye. Milanovskiy and A. M. Nikishin *In its* USSR Rept.: Space (JPRS-USP-85-005) 30 Sep. 1985 p 69-70 Transl. into ENGLISH from Dokl. Akadem. Nauk SSSR (Moscow), v. 280, no. 5, Feb. 1985 p 1204-1209 Original language document announced in IAA as A85-28924 (For primary document see N86-14111 04-88)
Avail: NTIS HC A08

It is hypothesized that the evolution megacycles of the Earth, Mars, and the Moon began with bursts of tectonic-magmatic activity at both hemispheres, which was then focused in one of them. The specific character of newly formed structures in middle stages of the megacycle in the more active hemisphere depends on the intensity of endogenous processes, the horizontal displacement of asthenosphere matter, and the viscosity and thickness of the lithosphere. The final stage of a megacycle is total cooling of the planet (e.g., the Moon or Mars after the second megacycle), or a pause in its activity (e.g., Mars between the first and second megacycles), or an epoch of crustal cratonization (e.g., the Earth). IAA

N86-14160# Joint Publications Research Service, Arlington, Va.
BIOLOGICAL LIFE-SUPPORT SYSTEMS FOR LONG-DURATION SPACE FLIGHTS c54
I. Andreyev and Yevgeniy Yakovlevich Shepelev *In its* USSR

Rept.: Space (JPRS-USP-85-005) 30 Sep. 1985 p 71-74 Transl. into ENGLISH from Izv. (Moscow), 11 Feb. 1985 p 3 (For primary document see N86-14111 04-88)
Avail: NTIS HC A08

A brief overview of the necessary life support equipment requirements for long term space flights is presented. Self contained, closed, ecological systems for the generation of oxygen are presented as possibilities. G.L.C.

N86-14161# Joint Publications Research Service, Arlington, Va.
ARCHITECT DISCUSSES SPACE HABITAT DESIGNS c54
S. Zigunenko *In its* USSR Rept.: Space (JPRS-USP-85-005) 30 Sep. 1985 p 75-77 Transl. into ENGLISH from Pravda (Moscow), 4 Dec. 1984 p 3 (For primary document see N86-14111 04-88)
Avail: NTIS HC A08

General considerations for the interior design of spacecraft intended for long duration space flight were reviewed from a human factors engineering standpoint. It is important that those responsible for spacecraft design not allow their work to be overshadowed by their sense of gravity and the general restrictions of a terrestrial environment. G.L.C.

N86-14162# Joint Publications Research Service, Arlington, Va.
ENERGY EXCHANGE OF PLANTS UNDER WEIGHTLESSNESS CONDITIONS Abstract Only c51
M. G. Tairbekov and A. V. Devyatko *In its* USSR Rept.: Space (JPRS-USP-85-005) 30 Sep. 1985 p 80 Transl. into ENGLISH from Dokl. Akad. Nauk SSSR (Moscow), v. 280, no. 2, Jan. 1985 p 509-512 Original language document announced in IAA as A85-24193 (For primary document see N86-14111 04-88)
Avail: NTIS HC A08

The plant energy-transfer experiment aboard the Cosmos-1514 biosatellite in December 1983 is considered. Heat release from corn sprouts was measured by a biocalorimeter operating in the 0 to 100 mW range. Results indicate that weightlessness has no effect on the intensity of energy transfer in sprouting seeds. The design of the biocalorimeter is described in some detail. IAA

N86-14163# Joint Publications Research Service, Arlington, Va.
STABILITY OF STATIONARY MOTIONS OF TWO TETHERED BODIES IN ORBIT UNDER INFLUENCE OF GRAVITATIONAL AND AERODYNAMIC FORCES Abstract Only c18
Ye. M. Levin *In its* USSR Rept.: Space (JPRS-USP-85-005) 30 Sep. 1985 p 81 Transl. into ENGLISH from Kosmich. Issled. (Moscow), v. 22, no. 5, Sep. - Oct. 1984 p 675-682 Original language document announced in IAA as A85-15254 (For primary document see N86-14111 04-88)
Avail: NTIS HC A08

The motion of a tethered system of two satellites in geometric orbit is examined. The main satellite is assumed to move in circular orbit at a height of 200 to 250 km above the Earth's surface, while the subsatellite-probe, attached to the main satellite by a thin tether, is assumed to orbit the Earth at a height of 100 to 150 km. In the dynamic analysis the subsatellite is considered as a material point, while the tether is considered as an extensible and ponderable flexible filament. Aerodynamic forces acting on the probe and tether are considered, and it is noted that the stationary motions of the system consist in its uniform revolution as a rigid body about the Earth. The stability of these stationary motions is analyzed, and it is shown that constraints imposed on the tether parameters by the stability requirement are more rigorous than constraints on tether strength. IAA

N86-14164# Joint Publications Research Service, Arlington, Va.
EXPERIMENTAL CHECKING OF MATHEMATICAL MODEL OF EDDY CURRENTS IN ACTUATING COMPONENTS OF SYSTEMS FOR MAGNETIC ORIENTATION OF ARTIFICIAL EARTH SATELLITES AND SPACECRAFT Abstract Only c17
V. G. Lebedev, B. I. Rabinovich, R. I. Ashkinazi, and S. V. Viktorov *In its* USSR Rept.: Space (JPRS-USP-85-005) 30 Sep. 1985 p 82 Transl. into ENGLISH from Kosmich. Issled. (Moscow), v. 22, no. 6, Nov. - Dec. 1984 p 945-947 Original language document announced in IAA as A85-19914 (For primary document see N86-14111 04-88)
Avail: NTIS HC A08

Rabinovich and Rogovoi (1984) developed a mathematical model with Volterra integrodifferential equations describing the dynamics of the electromagnet as the actuation element of a spacecraft stabilization system, taking into account the conductivity of the ferromagnetic core. The present paper describes an experimental verification of the adequacy of this model. The experiment involved the determination of the self-induction coefficient of the coil and the coefficient characterizing energy dissipation in the core. IAA

N86-14165# Joint Publications Research Service, Arlington, Va.
DETERMINING QUASI-REAL-TIME LOCATION OF SHIPS USING GEOSTATIONARY NAVIGATIONAL SATELLITES c04
V. E. Abdullayev, K. Kh. Ismailov, V. N. Vintayev, and G. A. Sosunov *In its* USSR Rept.: Space (JPRS-USP-85-005) 30 Sep. 1985 p 83-89 refs Transl. into ENGLISH from Izv. Akad. Nauk Azerb. SSR: Ser. Fiz.-Tekhn. i Mat. Nauk (Baku), v. 6, no. 1, Jan. - Feb. 1985 p 96-101 (For primary document see N86-14111 04-88)
Avail: NTIS HC A08

Extensive work is being carried out and enormous funds are being expended on development of special space systems, which are based on the Doppler method of determining the location of ships from satellites moving along mid-altitude circular orbits, and which have good precision characteristics, to meet modern navigational requirements in precision, global coverage and speed, regardless of the time and climatic conditions of navigation. However, they all have a common deficiency, considerable time between observations. Based on the common trend in development of satellite systems of the last few years, one can assume the feasibility of developing a navigational system, consisting of satellites in a geostationary orbit, the constancy of coordinates and simplicity of observation of which make it possible to achieve a high saving due to use of the undoubtedly promising passive long-range method of determining the location of an object on the Earth's surface. The systems, the basis of which is the method of determining navigational data, are founded on the noninterrogation principle in which the navigational parameters are determined on a mobile object by comparing the signals received from the satellite to the signals of onboard oscillators. G.L.C.

N86-14166# Joint Publications Research Service, Arlington, Va.
ORGANIZATION OF SPACE NAVIGATION SYSTEM BASED ON USE OF GEOSTATIONARY SATELLITES c17
V. E. Abdullayev *In its* USSR Rept.: Space (JPRS-USP-85-005) 30 Sep. 1985 p 90-96 Transl. into ENGLISH from Izv. Akad. Nauk Azerb. SSR: Ser. Fiz.-Tekhn. i Mat. Nauk (Baku), v. 5, no. 2, Mar. - Apr. 1984 p 144-149 (For primary document see N86-14111 04-88)
Avail: NTIS HC A08

The modern navigation problem is inseparably related to the need for constant and operational support of the navigational personnel with meteorological, navigational and other types of information which could not possibly be provided without use of radio communications. The determination of a ship's position by such fundamental methods as observation of celestial bodies, the use of every possible radioelectronic and radar apparatus, is well known and has been developed in the form of an independent science called marine astronomy. However, with the appearance of present-day requirements, taking into account the high speeds of modern ships when there is a need at all times for reliable information on their position with an accuracy to a meter, all known marine astronomy methods are becoming greatly outmoded. Space navigation systems based on the Doppler method for determining the position of a ship by satellites moving in different circular orbits have good accuracy characteristics. However, a shortcoming of such systems is that the navigationl devices of a ship provide a correction of its position only in the period of presence of the transiting satellite in the zone of radiovisibility. For example, for the American Transit navigational system the mean time between observations at the equator is approximately 1.2 hours. G.L.C.

N86-14167# Joint Publications Research Service, Arlington, Va.
SPACE APPLICATIONS IN GEOLOGY Abstract Only c46
N. Lesnaya *In its* USSR Rept.: Space (JPRS-USP-85-005) 30 Sep. 1985 p 102-103 Transl. into ENGLISH from Leninskoye Znamya (Moscow), no. 81, 7 Apr. 1985 p 2-3 (For primary document see N86-14111 04-88)
Avail: NTIS HC A08

Directions, methods and prospects of spacecraft-aided studies of the Earth in support of geology and mineral prospecting are reported. Author

N86-14168# Joint Publications Research Service, Arlington, Va.
PRESSURE FIELD RETRIEVAL BY REMOTE REFRACTOMETRY FROM SPACE Abstract Only c43
A. S. Gurvich and S. V. Sokolovskiy *In its* USSR Rept.: Space (JPRS-USP-85-005) 30 Sep. 1985 p 106 Transl. into ENGLISH from Izv. Akad. Nauk SSSR: Fiz. Atm. i Okeana (Moscow), v. 21, no. 1, Jan. 1985 p 12-21 Original language document announced in IAA as A85-26291 (For primary document see N86-14111 04-88)
Avail: NTIS HC A08

A preliminary evaluation of pressure-field reconstruction errors in remote refractometry from space is performed on the basis of a numerical experiment. The study isolates the effects of averaging along the refracted beam and the errors caused by the deviation of the real atmosphere from the spherically symmetric shape on the resulting meteorological parameters. It is demonstrated that with disturbances of horizontal dimensions of 300 to 600 km, vertical dimensions of 3 to 8 km, and pressure gradients characteristic of the Earth atmosphere on this scale the pressure-field reconstruction errors are under 0.3 percent. IAA

N86-14169# Joint Publications Research Service, Arlington, Va.
DETERMINING FLEXURE OF AERIAL CAMERA SMOOTHING GLASS Abstract Only c35
V. N. Lavrov *In its* USSR Rept.: Space (JPRS-USP-85-005) 30 Sep. 1985 p 107 Transl. into ENGLISH from Geod. i Kartografiya (Moscow), no. 11, Nov. 1984 p 30-33 (For primary document see N86-14111 04-88)
Avail: NTIS HC A08

Topographic aerial cameras are now in use in which the film is smoothed by being pressed against a smoothing glass on which a grid of fiducial marks is plotted. A significant pressure must be applied for good smoothing. Tests have shown that a pressure of 1.0 to 1.2 x 10 to the 4 Pa is adequate for ensuring a minimum gap between the film and the smoothing glass. The pressure required for smoothing the film causes elastic deformations (flexure) of the smoothing glass and connected parts of the aerial camera. Glass flexure must be taken into account during camera calibration in order to ascertain what photograph distortions could be a result of this bending. Author

N86-14170# Joint Publications Research Service, Arlington, Va.
STEREOPHOTOGRAMMETRIC SURVEY OF WAVE-COVERED WATER SURFACE Abstract Only c43
M. V. Shulmin, Yu. I. Kuchinskiy, and M. P. Shulmina *In its* USSR Rept.: Space (JPRS-USP-85-005) 30 Sep. 1985 p 107-108 Transl. into ENGLISH from Geod. i Kartografiya (Moscow), no. 11, Nov. 1984 p 33-35 (For primary document see N86-14111 04-88)
Avail: NTIS HC A08

A methodology and some devices was developed for a stereophotogrammetric survey of a wave-covered water surface. This makes it possible to obtain and measure quite precisely a model of the investigated sector of a water body, the form, type and characteristics of the waves. A stereophotogrammetric survey of the wave-covered surface must be made simultaneously by two cameras. Enterprise No. 7, in collaboration with the Moscow Institute of Geodetic, Aerial Mapping and Cartographic Engineers, synchronized two 41/7.5 aerial cameras for this purpose. The methodology was worked out in water bodies in Kalinin Oblast where two test areas were established. Geodetic beacons of a special design were developed and fabricated for placement on the bottom of the water body for ensuring synchronization of the cameras at the time of the survey. The plane coordinates of the beacons were determined by trilateration. The adequate number of measurements ensured an accuracy in determining coordinates up to 1 mm. Elevations were determined by geometric leveling with errors up to 1 mm. Author

N86-14171# Joint Publications Research Service, Arlington, Va.
EQUATORIAL WAVES IN OCEAN SURFACE TEMPERATURE FIELD ACCORDING TO DATA FROM SHIPBOARD AND SATELLITE MEASUREMENTS Abstract Only c48
A. S. Kazmin, R. Legeckis, and K. N. Fedorov *In its* USSR Rept.: Space (JPRS-USP-85-005) 30 Sep. 1985 p 108-109 Transl. into ENGLISH from Issled. Zemli iz Kosmosa (Moscow), no. 5, Sep. - Oct. 1984 p 3-7 Original language document announced in IAA as A85-16940 (For primary document see N86-14111 04-88)
Avail: NTIS HC A08

Legeckis (1977) has reported an existence of long waves in the eastern equatorial Pacific Ocean on the basis of data obtained with the aid of a geostationary satellite. The present investigation is concerned with data which confirm these observations. These data are the results of direct measurements of the sea surface temperatures conducted during a voyage of a Soviet research vessel in January 1982. A thermistor, representing a temperature-sensitive resistor device, kept at a depth in the range from 0.15 to 0.20 m was employed for the determination of the sea temperatures. The accuracy of the measurements was 0.05 C. The measured sea surface temperatures were shown in a graph as a function of the position of the ship at the time of measurement. Temperature data obtained on the basis of satellite data (NOAA/NESS) are also represented in the graph. The obtained data provide information regarding the hydrophysical characteristics of the equatorial front for the Northern Hemisphere in winter. There is satisfactory agreement between the two differently derived types of temperature data. IAA

N86-14172# Joint Publications Research Service, Arlington, Va.
USE OF REMOTE OPTICAL MEASUREMENTS IN AGRICULTURE Abstract Only c43
G. I. Belchanskiy, K. Ya. Kondratyev, V. V. Kozoderov, N. V. Sazonov, A. G. Topchiyev, and P. P. Fedchenko *In its* USSR Rept.: Space (JPRS-USP-85-005) 30 Sep. 1985 p 109-110 Transl. into ENGLISH from Issled. Zemli iz Kosmosa (Moscow), no. 5, Sep. - Oct. 1984 p 8-24 (For primary document see N86-14111 04-88)
Avail: NTIS HC A08

In 1983 a number of organizations and institutes began joint work on use of remote measurement data obtained from aircraft and helicopters and ground data in the interests of agriculture. The program includes analysis of the factors influencing spectral reflectivity of soils and vegetation, development of methods for interaction between optical radiation and the soil-vegetation system, use of airborne spectrometric instrumentation for evaluating the chlorophyll content in plant leaves and determining the contamination of vegetation, surface studies of selected standard sectors of agricultural fields, regression analysis of data from surface photometric measurements and the parameters of the phytobiometric state of vegetation, organization of a data bank of spectral standards or keys and analysis of the possibilities of allowance for the distorting influence of the atmosphere. The fundamental theoretical premises for solution of these problems and some of the work done on solution of these problems are examined. Author

N86-14173# Joint Publications Research Service, Arlington, Va.
CLASSIFICATION OF TREES BY GROWTH CLASSES ON THE BASIS OF MULTIZONAL PHOTOGRAPHS Abstract Only c43
A. N. Borisov, V. A. Ivanov, G. A. Ivanchenko, V. S. Kirichuk, and V. V. Kuzmichev *In its* USSR Rept.: Space (JPRS-USP-85-005) 30 Sep. 1985 p 110 Transl. into ENGLISH from Issled. Zemli iz Kosmosa (Moscow), no. 5, Sep. - Oct. 1984 p 25-30 (For primary document see N86-14111 04-88)
Avail: NTIS HC A08

The classification of tree stands has the purpose of evaluating their current status and future potential. The traditional, time-consuming subjective surface methods used for this purpose can be replaced by remote multizonal surveys. A method for automating such work is presented. The method is illustrated using aerial photographs at 1:30,000 for sectors of pine stands taken in August using an MKF-6 camera, as well as surface land inventory data for the same test areas. The procedures for orientation and referencing of the photographs are described in detail. The use of the surface inventory data (coordinates of trees in test area, trunk diameter at height of 1.3 m (d), crown diameter (D), tree height (h), and height to maximum crown diameter (h sub D max)) are also used in the automated procedure. A correlation analysis of the two types of data is given. The information yield from the six spectral zones was studied. Since in ground surveys only the d and h parameters are usually used, it was concluded that three spectral zones would be adequate for obtaining comparable data. These three zones are sufficient for classifying the stand on the basis of degrees of depression. The results are correct for photographs of the scale used and the particular phenological phase of forest vegetation prevailing in August. Author

N86-14174# Joint Publications Research Service, Arlington, Va.
EXPERIENCE IN COMPLEX MAPPING OF NATURAL RESOURCES IN AGRARIAN-INDUSTRIAL REGIONS OF NONCHERNOZEM RSFSR USING SPACE PHOTOMATERIALS Abstract Only **c43**
V. A. Sushchenya, L. A. Shevchenko, and V. I. Somova *In its* USSR Rept.: Space (JPRS-USP-85-005) 30 Sep. 1985 p 111 Transl. into ENGLISH from Issled. Zemli iz Kosmosa (Moscow), no. 5, Sep. - Oct. 1984 p 31-40 Original language document announced in IAA as A85-16941 (For primary document see N86-14111 04-88)
Avail: NTIS HC A08

The following specialized maps must be prepared in the mapping of the natural resources of the Nonchernozem Zone using space photomaterials: natural conditions, present status of environment and resources, conservation of environment and predictions of possible changes in environment. In this zone the makeup of each series can be varied in dependence on the nature of the natural conditions in a specific region. Each series must be supported by a minimum of key maps whose compilation is obligatory for all regions in the Nonchernozem Zone for the purpose of ensuring rational planning of the use of natural resources and their possible restoration. One of the first experiments in compiling a set of maps on the basis of space photographs in two regions differing in natural conditions in Smolensk Oblast and Minsk Oblast (in which agricultural-forestry and agrarian-industrial economies predominate) is described. The compilation of such maps is described in detail. Author

N86-14175# Joint Publications Research Service, Arlington, Va.
POSSIBILITIES OF USE OF AEROSPACE MATERIALS IN PREDICTING OCCURRENCE OF PETROLEUM AND GAS Abstract Only **c43**
R. A. Bidzhiyev and L. M. Natapov *In its* USSR Rept.: Space (JPRS-USP-85-005) 30 Sep. 1985 p 112 Transl. into ENGLISH from Issled. Zemli iz Kosmosa (Moscow), no. 5, Sep. - Oct. 1984 p 41-50 Original language document announced in IAA as A85-16942 (For primary document see N86-14111 04-88)
Avail: NTIS HC A08

In the last few years, aerospace methods have been increasingly employed in applications related to the search for petroleum and gas deposits. The present investigation is concerned with the utilization of aerospace data in a study of the northern part of Western Siberia. The consideration of such data can lead to a substantial reduction in expenses arising in connection with requirements for a use of seismic surveying procedures. Attention is given to the employed method of investigation, the utilized data material, information concerning the basic structure and the sedimentary mantle in the north of West Siberia, an analysis of details regarding aerospace data, and an evaluation of the obtained results. IAA

N86-14176# Joint Publications Research Service, Arlington, Va.
PROBLEMS IN STUDY AND EVALUATION OF CONSEQUENCES OF FOREST FIRES USING AEROSPACE PHOTOGRAPHS Abstract Only **c43**
V. V. Furyayev *In its* USSR Rept.: Space (JPRS-USP-85-005) 30 Sep. 1985 p 113 Transl. into ENGLISH from Issled. Zemli iz Kosmosa (Moscow), no. 5, Sep. - Oct. 1984 p 51-57 Original language document announced in IAA as A85-16943 (For primary document see N86-14111 04-88)
Avail: NTIS HC A08

The problems involved in the evaluation of forest fires on the basis of aerospace photographs are discussed. The principal problems include developing principles and methods for studying the post-fire forest restoration process; formulation of principles and methods for the regionalization of taiga areas on the basis of the degree of damage by fires; working out of methods for the routine inventorying of areas of recently burned-over areas and determination of the post-fire state of forested areas; defining of principles and methods for evaluating potential damage to forested areas and their resistance to fires. The best time for such a survey is from June to August, during the period between total development of the canopy and prior to its autumn coloring. Solar altitude should be 25 deg or more and the cloud cover should not be greater than 10%. The periodicity of receipt of photo-information for the compilation of maps of post-fire dynamics, maps of forest damage and maps of resistance to fires should be 10 to 12 years. This study requires the use of black-and-white, spectrozonal and multizonal photographs at scales 1:15,000, 1:100,000 and 1:1,000,000. Author

N86-14177# Joint Publications Research Service, Arlington, Va.
COMPUTATION OF REFLECTION OF SOLAR RADIATION FROM VEGETATION COVER BY MONTE-CARLO METHOD Abstract Only **c43**
Yu. K. Ross and A. L. Marshak *In its* USSR Rept.: Space (JPRS-USP-85-005) 30 Sep. 1985 p 114 Transl. into ENGLISH from Issled. Zemli iz Kosmosa (Moscow), no. 5, Sep. - Oct. 1984 p 58-67 Original language document announced in IAA as A85-16944 (For primary document see N86-14111 04-88)
Avail: NTIS HC A08

The establishment of the theoretical principles concerning the probing of the plant cover requires a rather detailed examination of biogeophysical problems regarding the reflection of solar radiation from soil and vegetation. Details with respect to the reflection of solar radiation from the plant cover are determined by illumination conditions, the optical properties of soil and plant cover, and structural aspects of the plant cover. Attention is given to a model of the plant structure, the mathematical formulation of the problem, details regarding the employed Monte Carlo method, an appraisal of the accuracy of the Monte Carlo method, and considerations of optimality and probability. Author

N86-14178# Joint Publications Research Service, Arlington, Va.
REFLECTION INDICATRICES OF VEGETATION CANOPIES Abstract Only **c43**
A. Kuusk, Ya. Anton, T. Nilson, U. Peterson, K. Ross, Yu. Ross, and A. Savikhin *In its* USSR Rept.: Space (JPRS-USP-85-005) 30 Sep. 1985 p 115 Transl. into ENGLISH from Issled. Zemli iz Kosmosa (Moscow), no. 5, Sep. - Oct. 1984 p 68-75 (For primary document see N86-14111 04-88)
Avail: NTIS HC A08

A program is prepared for making in situ measurements to ascertain the extent to which the reflection indicatrices (reflectance factors) of different plant canopies differ from one another. Specialists at the Astrophysics and Atmospheric Physics Institute, Estonian Academy of Sciences, carry out measurements of the angular dependence of reflection of solar radiation from natural vegetation canopies and crops in several parts of the spectrum with high angular resolution. The angular dependence of the spectral brightness of vegetation canopies is determined using a narrow-angle aircraft telespectrophotometer mounted on a KA-26 helicopter. Measurements are made at the reflection maximum of the vegetation cover in the green part of the spectrum at lambda = 0.555 microns, at the absorption maximum of chlorophyll at lambda = 0.675 microns and at the maximum reflection plateau lambda = 0.796 microns. The spectral ranges were discriminated by interference light filters with transmission half-widths of 13, 10 and 10 nm respectively. Measurements of the angular characteristics of reflection of fields and natural vegetation were made from a height of 50 microns in a stable illumination regime. Author

N86-14179# Joint Publications Research Service, Arlington, Va.
APPROXIMATE ANALYTICAL FORMULAS FOR COMPUTING SPECTRAL BRIGHTNESS COEFFICIENTS FOR AGRICULTURAL VEGETATION Abstract Only c43
T. Nilson and A. Kuusk *In its* USSR Rept.: Space (JPRS-USP-85-005) 30 Sep. 1985 p 116 Transl. into ENGLISH from Issled. Zemli iz Kosmosa (Moscow), no. 5, Sep. - Oct. 1984 p 76-83 (For primary document see N86-14111 04-88)
Avail: NTIS HC A08

Due to the recent vigorous development of aerospace optical sensing of vegetation a great need has arisen for effective theoretical models of the spectral brightness coefficients of vegetation canopies, especially agricultural vegetation. A model is proposed for formation of spectral brightness coefficients of agricultural crops in the form of approximate analytical formulas. The latter have an acceptable accuracy for all the principal regularities exerting an influence on the value of the spectral brightness coefficient. In the model it is assumed that the vegetation consists of randomly (in conformity to Poisson's law) distributed phytoelements with spherical orientation. The phytoelements reflect and transmit radiation in conformity to Lambert's law and it is assumed that the mirror component of radiation reflected directly from the surface waxy layer of the leaves, whose brightness is described by Fresnel's law, can be added to the reflection from the phytoelements. In this simplified model it is impossible to give a quantitatively correct description of absolutely all the effects associated with the temporal variation and angular dependence of the spectral brightness coefficient of agricultural vegetation. Author

N86-14180# Joint Publications Research Service, Arlington, Va.
METHOD FOR USING CLUSTERS IN EVALUATING LAND USE AREAS FROM MULTIZONAL PHOTOGRAPHS Abstract Only c43
L. N. Vasilyev and R. Kachinski *In its* USSR Rept.: Space (JPRS-USP-85-005) 30 Sep. 1985 p 117 Transl. into ENGLISH from Issled. Zemli iz Kosmosa (Moscow), no. 5, Sep. - Oct. 1984 p 94-99 (For primary document see N86-14111 04-88)
Avail: NTIS HC A08

In the study of agricultural landscapes the problem arises of clustering the results of measurement of multizonal images. In such surveys the spectral brightnesses of vegetation are continuously distributed in some interval and there is no natural cluster. The method developed and the results obtained in the classification of land use areas with cultivated vegetation on multizonal photographs based on an increase in the criterial space of spectral measurements with data on the spatial (geographical) distribution are described. Within the limits of a homogeneous landscape adjacent fields are occupied by different crops. The problem is solved under the condition that two adjacent fields occupied by crops belong to different classes, and this is used as a proximity test in the formalization of a cluster analysis model. The clustering method is applied in inventorying agricultural fields from multizonal space and aerial photographs. A statistical sampling with field clustering is used in the Telefoto-82 experiment executed under the Intercosmos program in the Polish People's Republic in the neighborhood of Wroclaw in July 1982. The results of clustering of 213 fields are presented. Author

N86-14181# Joint Publications Research Service, Arlington, Va.
METHODS FOR COMPLEX SPACE EXPERIMENT IN USSR FOR STUDYING LAND FROM MANNED SPACECRAFT Abstract Only c43
B. V. Vinogradov *In its* USSR Rept.: Space (JPRS-USP-85-005) 30 Sep. 1985 p 118 Transl. into ENGLISH from Issled. Zemli iz Kosmosa (Moscow), no. 5, Sep. - Oct. 1984 p 100-106 Original language document announced in IAA as A85-16946 (For primary document see N86-14111 04-88)
Avail: NTIS HC A08

A combined space experiment involves use of surface, aerial and space vehicles and instrumentation. The implementation of such an experiment requires adherence to a number of rules relating to the comparability of data: temporal, spectral and spatial. In the USSR such experiments have become increasingly complex and have proceeded through the following states: (1) study of space survey transfer function (geophysical experiment in 1969-Ustyurt Plateau); (2) study of reliability and detail of recognition of natural features from space photographs (informational experiment in 1970-Salsk steppes); (3) study of effectiveness of special mapping, revision of existing maps and compilation of new types of maps (mapping experiment in 1971-Altay and Balkhash key sectors); (4) study of dynamics of natural and anthropogenic systems by successive surveys for registry and prediction of changes (dynamic experiment in 1978-Salsk key sector); and (5) study of rhythmic change in natural systems for registry of short-period changes, their prediction and choice of optimum survey conditions (phenological experiment in 1981-Kyzylkum key sector). Author

N86-14182# Joint Publications Research Service, Arlington, Va.
EXPERIENCE IN CONDUCTING SUBSATELLITE EXPERIMENTS WITH WATER BODIES IN USSR AND HUNGARIAN PEOPLE'S REPUBLIC Abstract Only c43
I. F. Berestovskiy, A. A. Gitelson, D. Sabo, and F. Siladi *In its* USSR Rept.: Space (JPRS-USP-85-005) 30 Sep. 1985 p 119 Transl. into ENGLISH from Issled. Zemli iz Kosmosa (Moscow), no. 5, Sep. - Oct. 1984 p 107-111 Original language document announced in IAA as A85-16947 (For primary document see N86-14111 04-88)
Avail: NTIS HC A08

Subsatellite experiments were carried out in June 1983 at Lake Balaton in Hungary and in September 1983 in the Sea of Azov-Don River areas. The objectives included testing and perfecting of methods for interpretation of space information developed in joint research by USSR and Hungarian specialist; obtaining synchronous and quasisynchronous shipboard, aerial and satellite data needed in study of radiation-hydrophysical relationships and the formulation of systematic recommendations on remote determination of hydrochemical and hydrobiological indices of water bodies. Perfecting the methods and technological elements for speedy collection and primary processing of control information in test ranges were of the project. At Lake Balaton there is a test of the so-called direct algorithm for the interpretation of multizonal video-information. Spectral brightness in different channels are compared with the values of hydrochemical, hydrobiological and hydrooptical parameters measured synchronously in a space survey. Author

N86-14183# Joint Publications Research Service, Arlington, Va.
POSSIBILITIES OF USING SPACE SURVEY FOR STUDYING SEASONAL CHANGES OF LANDSCAPES IN SOME REGIONS OF USSR Abstract Only c43
I. N. Yelagin *In its* USSR Rept.: Space (JPRS-USP-85-005) 30 Sep. 1985 p 120 Transl. into ENGLISH from Issled. Zemli iz Kosmosa (Moscow), no. 5, Sep. - Oct. 1984 p 112-114 Original language document announced in IAA as A85-16948 (For primary document see N86-14111 04-88)
Avail: NTIS HC A08

Of the northern regions of the European USSR, almost all of Siberia and the Far East are phenologically very poorly studied. It is virtually impossible to obtain necessary information rapidly in these regions by traditional surface methods. This dictates the use of aviation and artificial Earth satellites with the application of already developed remote phenology methods. The possibilities for the collection of such information in a space survey are examined. In the wooded steppe and taiga regions of Siberia the greatest number of days with a cloudless sky is in January to

March. However, space photographs taken at that time contain the minimum phenological information. In comparison with the winter months, a cloudless sky is very rare in spring, summer and autumn. In the months most suitable for remote phenology (May to August) only 10% of the days are reasonbly clear. In the more southerly, dry regions, such as central Asia, there are considerably more days with few clouds. In winter (November to February) the number of clear days varies in the range 20 to 35%; in summer (June to September) it is 50 to 70%. Accordingly, a phenological survey from space in these regions would have a high probability of success due to the great number of clear days. Author

N86-14184# Joint Publications Research Service, Arlington, Va.
ROLE OF LANDSCAPE RESEARCH IN DEVELOPMENT OF SPACE METHODS FOR STUDYING EARTH Abstract Only **c43**
Ye. V. Glushko *In its* USSR Rept.: Space (JPRS-USP-85-005) 30 Sep. 1985 p 121 Transl. into ENGLISH from Issled. Zemli iz Kosmosa (Moscow), no. 5, Sep. - Oct. 1984 p 115-121 (For primary document see N86-14111 04-88)
Avail: NTIS HC A08

This is an overview of the contributions which space surveys are making to the development of the Earth sciences, with emphasis on landscape (geographical-environmental) research. Space methods are sweeping traditional methods away or are reducing them to a secondary role. Attention is given to 23 branches of the earth sciences with 82 key problems considered which can be investigated by remote sensing methods. The advantages of remote sensing in study of the atmosphere, hydrosphere, biosphere, sociosphere and in landscape geography are discussed. A table gives a detailed listing of the scientific, practical and economic problems which can be solved by space methods. References are made to the monographs, brochures, transactions, collections of articles and individual articles which give the best information concerning different aspects of these problems. Space methods have already served as a basis for a number of fundamental landscape investigations at a regional level. The landscape research method is now also being used in study of the geographical zonality of the world ocean. Author

N86-14185# Joint Publications Research Service, Arlington, Va.
METHODS FOR CONSTRUCTING ATMOSPHERIC OPTICAL TRANSFER OPERATOR Abstract Only **c46**
V. G. Zolotukhin, I. V. Mishin, D. A. Usikov, M. N. Fomenkova, and V. A. Grushin *In its* USSR Rept.: Space (JPRS-USP-85-005) 30 Sep. 1985 p 121-122 Transl. into ENGLISH from Issled. Zemli iz Kosmosa (Moscow), no. 4, Jul. - Aug. 1984 p 14-22 (For primary document see N86-14111 04-88)
Avail: NTIS HC A08

Two methods for the construction of the optical transfer operator of the atmosphere are compared: the method of multiple reflections and the method of spatial-frequency characteristics. Calculation results are presented on the amplitude-frequency characteristics of the atmosphere with a real indicatrix and optical-thickness stratification with respect to altitude. B.J.

N86-14186# Joint Publications Research Service, Arlington, Va.
APPLICATION OF STATISTICAL MODEL OF LAYERED MEDIUM FOR COMPUTING THERMAL EMISSION OF ICE COVERS Abstract Only **c43**
V. L. Brekhovskikh *In its* USSR Rept.: Space (JPRS-USP-85-005) 30 Sep. 1985 p 122-123 Transl. into ENGLISH from Issled. Zemli iz Kosmosa (Moscow), no. 4, Jul. - Aug. 1984 p 33-38 (For primary document see N86-14111 04-88)
Avail: NTIS HC A08

In computing the thermal emission of a medium with the temperature T = const it is customary to use a formula based on the reciprocity theorem in which the brightness temperature T sub br is expressed through the coefficient of reflection (or absorption) of a plane wave incident on the particular medium: T sub br = T(1 -/R/2) or T sub br = TQ. Here /R/2 and Q are the energy coefficients for reflection and absorption, respectively. Such a theoretical approach, in the case of sufficiently smooth temperature changes is also applicable to nonuniformly heated bodies. A one-dimensional randomly inhomogeneous medium occupying the half-space - infinity < z < or = 0 is examined. It is assumed that its dielectric constant is not dependent on temperature. It is shown that there are few difficulties in making analytical computations of the thermal emission of a semi-infinite layer whose dielectric constant changes randomly for interpretation of data from remote sensing of ice covers. The most suitable natural media to which the results can be applied are extensive ice formations such as the Antarctic continental glacier which have a layered structure and a relatively smooth surface. Author

N86-14187# Joint Publications Research Service, Arlington, Va.
COMPILATION OF LANDSCAPE MAPS AT DIFFERENT SCALES WITH USE OF SPACE PHOTOINFORMATION Abstract Only **c43**
V. I. Ryabchikova *In its* USSR Rept.: Space (JPRS-USP-85-005) 30 Sep. 1985 p 123 Transl. into ENGLISH from Issled. Zemli iz Kosmosa (Moscow), no. 4, Jul. - Aug. 1984 p 39-45 Original language document announced in IAA as A84-49029 (For primary document see N86-14111 04-88)
Avail: NTIS HC A08

A methodology is being developed for the detailed mapping of natural resources and conditions on the basis of a series of special-purpose maps with the use of space photoinformation. A fundamental role is played by landscape maps which can serve as base maps. Their content is used in compiling a number of specialized maps, which include maps of vegetation, soils, ground water, geochemical characteristics and others. A detailed description of the preparation of a map compilation in all its aspects, including generalization, editing, legends, etc., is given. This is illustrated for a number of types of terrain in the Soviet subarctic: tundra accumulative plains, tundra mountain folded regions and mountains of intermediate elevation. These examples, prepared at different scales, illustrate the enormous amount of information which can be extracted from space photographs of areas which previously were so remote that their mapping was generally sketchy and unreliable. In addition, the use of space surveys reduces the time required for the preparation of landscape maps by a factor of 3 to 5. Author

N86-14188# Joint Publications Research Service, Arlington, Va.
USE OF SPACE GEOLOGICAL METHODS IN SEISMOTECTONIC RESEARCH Abstract Only **c46**
T. P. Ivanova *In its* USSR Rept.: Space (JPRS-USP-85-005) 30 Sep. 1985 p 124 Transl. into ENGLISH from Issled. Zemli iz Kosmosa (Moscow), no. 4, Jul. - Aug. 1984 p 46-52 Original language document announced in IAA as A84-49030 (For primary document see N86-14111 04-88)
Avail: NTIS HC A08

The role of the geological analysis of space remote sensing images in a complex of geological-geophysical and seismotectonic observations in seismically dangerous areas is evaluated on the example of Fayzabad test region in Tadzhikistan. The interpreted lineaments are shown to correspond to gradient zones of deep-seated geophysical boundaries of the lithosphere; this helps to assess the morphology, kinematics, and seismic features of blocks of the Earth's crust. B.J.

N86-14189# Joint Publications Research Service, Arlington, Va.
ENGINEERING EVALUATION OF CRUSTAL FAULTS USING SPACE SURVEY DATA Abstract Only **c46**
A. L. Revzon *In its* USSR Rept.: Space (JPRS-USP-85-005) 30 Sep. 1985 p 125 Transl. into ENGLISH from Issled. Zemli iz Kosmosa (Moscow), no. 4, Jul. - Aug. 1984 p 53-60 Original language document announced in IAA as A84-49031 (For primary document see N86-14111 04-88)
Avail: NTIS HC A08

The interpretation of space photographs, on the basis of a geomorphological analysis of the images, makes it possible to give an engineering evaluation of faults whose reliability and completeness is considerably greater than the information obtained by engineering field work on the ground for selecting an optimum

variant of the layout of linear structures such as railroads, highways, tunnels, canals and pipelines. The interpretation of space photographs in combination with traditional methods results in the optimizing of such work and a decrease in work input and increase in the completeness of pertinent geological and engineering data, a choice of effective planning solutions in contending with fault zones, and warning of emergency situations when carrying out construction work. All this is illustrated in specific experience gained in such regions as along the Baykal-Amur Railroad and in the Caucasus in the latter case, for example, the completeness and accuracy of interpretation could be considered 100%. On-site geological and engineering work lacked the necessary volume of information on the presence of faults dangerous for construction.
Author

N86-14190# Joint Publications Research Service, Arlington, Va.
USE OF GOUDRIAAN MODEL FOR STUDYING REFLECTION REGULARITIES IN VEGETATION-SOIL SYSTEM IN OPTICAL RANGE. 1: INFLUENCE OF PHYTOMETRIC PARAMETERS ON SPECTRAL BRIGHTNESS COEFFICIENTS Abstract Only
c43
N. N. Vygodskaya and I. I. Gorshkova *In its* USSR Rept.: Space (JPRS-USP-85-005) 30 Sep. 1985 p 126 Transl. into ENGLISH from Issled. Zemli iz Kosmosa (Moscow), no. 4, Jul. - Aug. 1984 p 61-70 (For primary document see N86-14111 04-88)
Avail: NTIS HC A08

In a study of the reflectivity of the vegetation cover in the optical range it is best to use theoretical models of reflection of the vegetation-soil system based on the theory of radiation transfer in a turbid medium. The characteristics of some theoretical models of the radiation regime of the vegetation cover are discussed. One model discussed belongs to a class of models based on the theory of radiation transfer in a turbid homogeneous medium. The vegetation cover is simulated by a layer infinite in the horizontal direction with a random spatial distribution of phytoelements conforming to the Poisson law and consisting of m thin layers of a given thickness. Numerical experiments with this model make it possible to determine the type of dependence between the spectral brightness coefficient and the relative surface of the phytoelements for conditions of sighting to the nadir and a solar altitude greater than 55 deg. The practical application of the results requires the availability of catalogues of coefficients of spectral reflection of soils and individual phytoelements of plants prepared for different regions with allowance for possible changes in the states of soils and plants.
Author

N86-14191# Joint Publications Research Service, Arlington, Va.
ANALYSIS OF SURVEY CONDITIONS AND EFFECT OF NOISE ON QUALITY OF SENSING OF SOIL FORMATIONS Abstract Only
c43
A. B. Karasev and S. V. Pantyukhov *In its* USSR Rept.: Space (JPRS-USP-85-005) 30 Sep. 1985 p 127 Transl. into ENGLISH from Issled. Zemli iz Kosmosa (Moscow), no. 4, Jul. - Aug. 1984 p 71-80 (For primary document see N86-14111 04-88)
Avail: NTIS HC A08

Numerical modeling of remote sensing of the soil cover in the visible spectral range is presented as a contribution to development of an improved remote aerospace method for studying soils. The authors use this model in examining the principal factors exerting an influence on quality of an image obtained by a survey system and characterized by the signal-to-noise (S/N) ratio and contrast. It is found, for example, that many types of soil formations which have experienced degradation, erosion or salinization are characterized by high S/N ratios relative to undergraded sectors. There is a wide range of optimum observation angles for which the S/N ratio and contrast are optimal. The magnitude and range of these angles are slightly dependent on solar zenith angle and change in optical thickness of the atmosphere; the observation angle at which the S/N ratio and contrast reach their maximum is not equal to the angle of the maximum spectral brightness value for the studied formation. Measurements of the coefficients of spectal brightness of natural formations must be accompanied by determinations of solar zenith angle and optical thickness of the atmosphere, as well as the reflection characteristics of the surrounding background.
Author

N86-14192# Joint Publications Research Service, Arlington, Va.
NORMALIZATION OF RESPONSE OF RADIOMETRIC INSTRUMENTATION FOR STUDYING EARTH'S NATURAL RESOURCES Abstract Only
c43
G. K. Kholopov, R. Sh. Khisamov, and F. G. Khuzin *In its* USSR Rept.: Space (JPRS-USP-85-005) 30 Sep. 1985 p 128 Transl. into ENGLISH from Issled. Zemli iz Kosmosa (Moscow), no. 4, Jul. - Aug. 1984 p 81-88 Original language document announced in IAA as A84-49032 (For primary document see N86-14111 04-88)
Avail: NTIS HC A08

A method for the normalization of the response of radiometers both on the basis of spectrozonal photometric parameters and on the basis of their spectral density at some mean wavelength is described. The practical use of this method reveals that it usually ensures a sufficient accuracy in measuring spectrozonal photometric parameters, such as the energy brightness of natural features illuminated by direct and scattered solar radiation. In a refinement of the method a fundamental change is a replacement of the real characteristic of absolute spectral response of each radiometer spectral zone, which is determined as a result of radiometer calibration and thereafter is considered known, by an idealized characteristic. An algorithm is outlined which takes into account the test of the minimum of the standard deviation of the idealized resultant spectral characteristic of the radiometer-measured source system from the real characteristic. In the normalization of the response of a multizonal radiometer intended for remote sensing of the Earth it is not the continuous spectrum which should be used, but some typical spectrum of the Earth's surface with allowance for the absorption lines of atmospheric gases.
Author

N86-14193# Joint Publications Research Service, Arlington, Va.
RADIOMETRIC CORRECTION OF MATERIALS OF AEROSPACE SURVEY OF EARTH WITH MKF-6 CAMERA: METHODOLOGY AND USE OF RESULTS Abstract Only
c43
Kh. A. LopesFalkon *In its* USSR Rept.: Space (JPRS-USP-85-005) 30 Sep. 1985 p 129 Transl. into ENGLISH from Issled. Zemli iz Kosmosa (Moscow), no. 4, Jul. - Aug. 1984 p 89-94 Original language document announced in IAA as A84-49033 (For primary document see N86-14111 04-88)
Avail: NTIS HC A08

The transfer characteristics of the entire multizonal system of an aerospace survey (atmosphere - zonal - filter - objective - photographic film) have a distinct angular dependence relative to its main optical axis. This can result in a nonuniformity in light distribution over the frame field, the appearance of a central spot on photomaterials whose presence greatly lessens the possibilities for their quantitative digital processing and correct interpretation. This effect has been observed in countless cases, as in the joint USSR-Cuba TROPICO-3 space experiment on multizonal photographs of sugarcane fields, with serious resultant distortions. It is found that the nonuniformity of brightness distribution over the frame is essentially dependent on the number of the camera channels, varying from + or - 10 to + or - 25 from the mean brightness and sometimes is asymmetric relative to the center of the frame. This effect is the result of multiplicative noise attributable to the angular dependence of the parameters of the survey system and the scattering properties of the atmosphere. This can cause additional errors or even make image digital processing virtually impossible.
Author

N86-14194# Joint Publications Research Service, Arlington, Va.
SOME APPROACHES TO ORGANIZATION OF DATA BANK IN SYSTEM FOR STUDYING EARTH'S NATURAL RESOURCES FROM SPACE (USING EXAMPLE OF AGRICULTURE) Abstract Only
c43
Yu. G. Simonov, N. F. Derevyanko, and G. I. Barvyn *In its* USSR Rept.: Space (JPRS-USP-85-005) 30 Sep. 1985 p 130 Transl. into ENGLISH from Issled. Zemli iz Kosmosa (Moscow), no. 4, Jul. - Aug. 1984 p 103-109 Original language document announced

in IAA as A84-49035 (For primary document see N86-14111 04-88)
Avail: NTIS HC A08

The problems involved in the logical and physical organization of data in a data bank of space information using the example of solution of problems in the processing of images in the interests of agriculture are discussed. Such a data bank oriented on the monitoring of agricultural production must ensure the possibility of accumulation and comparison of different kinds of data corresponding to administrative-economic units. Data must be organized in such a way as to ensure simple access to the information. The needs of two types of users must be satisfied: users seeking information from the bank directly from a terminal for the purpose of obtaining reference or statistical information relating to some administrative-economic units; programmers involved in processing images or working on automated mapping, using information from the data bank as a reference in the interpretation of current aerospace information, in an analysis of the dynamics of observed objects or phenomena and also for the purpose of compiling special maps. Author

N86-14195# Joint Publications Research Service, Arlington, Va.
EXPERIMENT FOR EVALUATING ACCURACY IN DETERMINING LAND CATEGORIES ON SPACE SCANNER PHOTOGRAPHS Abstract Only c43
R. I. Elman, Ye. V. Bakhtinova, A. N. Potapov, R. V. Sviridova, and L. A. Bersneva *In its* USSR Rept.: Space (JPRS-USP-85-005) 30 Sep. 1985 p 131 Transl. into ENGLISH from Issled. Zemli iz Kosmosa (Moscow), no. 4, Jul. - Aug. 1984 p 110-119 Original language document announced in IAA as A84-49036 (For primary document see N86-14111 04-88)
Avail: NTIS HC A08

Consideration is given to the method and results of a computer experiment concerning the estimation of the accuracy with which land-use categories can be determined on space scanner images. The data examined were obtained with the Fragment multispectra scanner, and the experiment uses the SKANER program employing ASSEMBLER. The percentage of the correct recognition of test plots is taken as the accuracy estimation criterion of their selection. The experiment contains three series of tests: a comparison of two plot-recognition algorithms, estimation of the influence of the number of test plots, and estimation of the influence of fragment shift. The land-use category scheme obtained as the result of the experiment is presented. Author

N86-14196# Joint Publications Research Service, Arlington, Va.
REMOTE TEMPERATURE DETERMINATION OF TERRESTRIAL COVERS FROM POLARIZATION INVARIANT OF MICROWAVE-RADIOTHERMAL EMISSION Abstract Only c43
G. A. Andreyev, L. F. Borodin, L. V. Zayentsev, and S. N. Rubtsov *In its* USSR Rept.: Space (JPRS-USP-85-005) 30 Sep. 1985 p 132 Transl. into ENGLISH from Issled. Zemli iz Kosmosa (Moscow), no. 4, Jul. - Aug. 1984 p 120-123 (For primary document see N86-14111 04-88)
Avail: NTIS HC A08

It is proposed that the polarization invariant be used in determining the thermodynamic temperature of terrestrial covers T sub cov from aboard flight vehicles on the basis of the measured radiobrightness temperatures in vertical T sub ver and horizontal T sub hor polarizations at a sighting angle 45 deg using the expression T sub cov = T sub hor squared/squared T sub hor - T sub ver). Under real conditions the accuracy in determining temperature of surface features can be influenced by the width of the polar diagram of the receiving antenna, random surface irregularities, radiothermal emission of the atmosphere and possible variations of the sighting angle (pitching angle) during spaceflight. For example, the width of the receiving antenna polar diagram exerts no influence on the accuracy in determining the temperature of surface covers. On the other hand, the presence of random surface irregularities necessitates a correction of the polarization invariant. In order to reduce the error in determining T sub cov it is best to use the wavelength range in which there is little thermal emission; i.e., centimeter waves. It was found that the T sub cov error is minimum with an angle of about 43 deg. With this angle the error in determining temperature of pastures, concrete pavements and a lake surface does not exceed 3K in absolute value. Author

N86-14197# Joint Publications Research Service, Arlington, Va.
COMMENTS ON ANNIVERSARY OF APOLLO-SOYUZ FLIGHT c12
Ya. Golovanov *In its* USSR Rept.: Space (JPRS-USP-85-005) 30 Sep. 1985 p 133-139 Transl. into ENGLISH from Komsomolskaya Pravda (Moscow), 14 Jul. 1985 p 3-4 (For primary document see N86-14111 04-88)
Avail: NTIS HC A08

This year, 1985, marks the tenth anniversary of the joint United States - USSR space flight, the Apollo-Soyuz Test Project (ASTP). This high point in international cooperation is celebrated in the USSR with fond memories and hopes for a resumption of similar efforts in the future. A review of the apparent decline of NASA's fortunes over that decade makes it apparent to the writer that a revival of ASTP is all the more timely. He decries the advent of the Star Wars mentality and calls for a return to the more reasonable days of Apollo-Soyuz. F.M.R.

N86-14198# Joint Publications Research Service, Arlington, Va.
SOVIET-FRENCH COMMISSION DISCUSSES JOINT SPACE PROJECTS Abstract Only c12
In its USSR Rept.: Space (JPRS-USP-85-005) 30 Sep. 1985 p 140 Transl. into ENGLISH from NTR: Probl. i Resheniya (Moscow), no. 1, 28 May - 10 Jun. 1985 p 3 (For primary document see N86-14111 04-88)
Avail: NTIS HC A08

The 19th session of the permanent Mixed Soviet-French Commission, which was held in Paris, examined results and prospects of cooperation in basic and applied research, technology, economics, industry and agriculture, in line with the Long-term Program of Intensifying Economic, Industrial and Technical Cooperation for the Period 1980 to 1990. In particular, the commission noted with satisfaction that two projects in the field of gamma-astronomy -- Gamma-1 and Granat -- are in the process of being carried out. Spacecraft are to be launched in line with these projects in coming years. The French side also confirmed its participation in the Soviet project called Fobos, which is planned for the study of Mars and its moon Phobos. This mission is scheduled for 1988. Question of joint experiments during the mission of the next Soviet biological satellite were also discussed. In space meteorology and aeronomy, joint work is being done on the development and perfecting of scientific apparatus for studies of the lower ionosphere, and the possibility of conducting joint experiments on Soviet meteorological satellites is being examined. Author

N86-14199# Joint Publications Research Service, Arlington, Va.
LIST OF RECENT SOVIET SPACE LAUNCHES c18
In its USSR Rept.: Space (JPRS-USP-85-005) 30 Sep. 1985 p 141-143 Transl. into ENGLISH from various Russian articles (For primary document see N86-14111 04-88)
Avail: NTIS HC A08

A list of recent Soviet space launches (21 March 1985 to 19 July 1985) with orbital parameters is given. The majority is in the Cosmos series (26 launches, two of which are multiple, Cosmos 1635 through 1642 (8), and Cosmos 1650 through 1652 (3); the list also includes an Ekran (TV broadcast satellite), Prognoz-10 (to study interplanetary and near-Earth shock waves caused by the interaction of the solar wind and Earth's magnetosphere -- a joint operation with Czechoslovakia), 2 Molniya-3's (communications satellites), the Soyuz T-13 (manned - docked with Salyut-7), and Progress-24 (made joint docking with Soyuz T-13 and Salyut-7). F.M.R.

89 ASTRONOMY

Includes radio and gamma-ray astronomy; celestial mechanics; and astrometry.

N86-14200 Royal Observatory, Edinburgh (Scotland).
OCCASIONAL REPORTS OF THE ROYAL OBSERVATORY, EDINBURGH, NO. 16
1985 20 p refs
(ISSN-0309-099-X) Copyright. Avail: Issuing Activity

Observations and programs made by the Edinburg Royal Observatory are reported. Topics discussed include: (1) a multi-object fiber-optics coupler for the 1.2 m Schmidt telescope; (2) the plate scale of the Schmidt telescope; and (3) a large altazimuth Schmidt telescope design. For individual titles, see N86-14201 through N86-14203.

N86-14201 Royal Observatory, Edinburgh (Scotland).
A MULTIPLE-OBJECT FIBRE-OPTICS COUPLER FOR THE 1.2-m UK SCHMIDT TELESCOPE
F. G. Watson and J. A. Dawe (Australian National Univ., Coonabarabran, Australia) *In its* Occasional Repts. of the Royal Observatory, Edinburgh, No. 16 1985 p 1-7 refs (For primary document see N86-14200 04-89)
Copyright. Avail: Issuing Activity

The rationale for, and design of a spectrograph coupler for a wide-field astronomical telescope are presented, and then system performance was estimated. The coupler is fabricated at the UK Schmidt telescope. E.A.K.

N86-14202 Royal Greenwich Observatory, Hailsham (England).
THE PLATE SCALE OF THE U.K. SCHMIDT TELESCOPE
R. W. Argyle and P. R. Standen *In its* Occasional Repts. of the Royal Observatory, Edinburgh, No. 16 1985 p 9-13 refs (For primary document see N86-14200 04-89)
Copyright. Avail: Issuing Activity

Between 1973 November and 1981 January, 137 plates of the South Galactic Pole centered at RA = OOH 53m.0. Dec. = -28 deg 03' were taken with the U.K. Schmidt Telescope to derive positions, proper motions, parallaxes and photographic photometry for as many stars as possible. The plates were measured on the GALAXY measuring machine. Results for 800 stars with $B - V > 1.2$ and $B < 17.5$ are announced. A by-product of this work is the derivation of accurate plate scales for each plate. Standard coordinates from GALAXY x,y measurements are obtained by using a program GLASTR written for the Vax 11/75. The conversion is effected using the positions of 40 SAO stars well distributed over the 4.5 x 4.5 degree field available to GALAXY. E.A.K.

N86-14203 Australian National Univ., Coonabarabran.
DESIGN FOR A LARGE ALTAZIMUTH SCHMIDT TELESCOPE
J. A. Dawe and F. G. Watson (Royal Observatory, Edinburgh) *In* Royal Observatory Occasional Repts. of the Royal Observatory, Edinburgh, No. 16 1985 p 15-18 refs (For primary document see N86-14200 04-89)
Copyright. Avail: Issuing Activity

The construction of a large altazimuth Schimdt telescope (LAST), incorporating recent advances in telescope design and detector technology is discussed. The telescope represents a most cost-effective method of undertaking ground-based optical astronomy. A preliminary design for such an instrument is described. E.A.K.

N86-14204*# Chicago Univ., Ill.
FOCAL PLANE OPTICS IN FAR-INFRARED AND SUBMILLIMETER ASTRONOMY Preprint Series 40
Roger H. Hildebrand Oct. 1985 33 p refs
(Grant NsG-2057)
(NASA-TM-88186; Rept-86010; NAS 1.15:88186) Avail: NTIS HC A03/MF A01 CSCL 03A

The construction of airborne observatories, high mountain-top observatories, and space observatories designed especially for infrared and submillimeter astronomy has opened fields of research requiring new optical techniques. A typical far-IR photometric study involves measurement of a continuum spectrum in several passbands between approx 30 microns and 1000 microns and diffraction-limited mapping of the source. At these wavelengths, diffraction effects strongly influence the design of the field optics systems which couple the incoming flux to the radiation sensors (cold bolometers). The Airy diffraction disk for a typical telescope at submillimeter wavelengths approx 100 microns-1000 microns is many millimeters in diameter; the size of the field stop must be comparable. The dilute radiation at the stop is fed through a Winston nonimaging concentrator to a small cavity containing the bolometer. The purpose of this paper is to review the principles and techniques of infrared field optics systems, including spectral filters, concentrators, cavities, and bolometers (as optical elements), with emphasis on photometric systems for wavelengths longer than 60 microns. Author

N86-14205*# Columbia Univ., New York. Astrophysics Lab.
DETECTION OF [NI2] LAMBDA 7378 IN SIX SEYFERT GALAXIES
J. P. Halpern and J. B. Oke (California Inst. of Tech.) [1985]
p refs
ant NGL-05-002-134)
ASA-CR-176358; NAS 1.26:176358) Avail: NTIS HC A02/MF A01 CSCL 03A

A line due to [Ni 2] 7378 in the Seyfert galaxies NGC 1068, 2110, 3227, 4151, 5506, and Arp 102 B was detected. The average Ni abundance is about 2 times solar, which is 5 times less than in the filaments of the Crab Nebula. This argues for nucleosynthetic processing in the latter. The [Ni 2] line is spatially revolved in NGC 1068, and shows at least a factor of 4 enhancement in the Ni abundance away from the nucleus. The off-nuclear abundance of Ni in NGC 1068 approaches that of the Crab, which strongly suggests that type supernovae enriched the off-nuclear gas clouds. Author

N86-14206*# Lockheed Missiles and Space Co., Palo Alto, Calif.
AN UNBIASED X-RAY SAMPLING OF STARS WITHIN 25 PARSECS OF THE SUN Final Report
Hugh M. Johnson 15 Aug. 1985 32 p refs
(Contract NAS8-36134)
(NASA-CR-178544; NAS 1.26:178544) Avail: NTIS HC A03/MF A01 CSCL 03A

A search of all of the Einstein Observatory IPC and HRI fields for untargeted stars in the Woolley, et al., Catalogue of the nearby stars is reported. Optical data and IPC coordinates, flux density F sub x, and luminosity L sub x, or upper limits, are tabulated for 126 single or blended systems, and HRI results for a few of them. IPC luminosity functions are derived for the systems, for 193 individual stars in the systems (with L sub x shared equally among blended components), and for 63 individual M dwarfs. These stars have relatively large X-ray flux densities that are free of interstellar extinction, because they are nearby, but they are otherwise unbiased with respect to the X-ray properties that are found in a defined small space around the Sun. Author

N86-14207# Arizona Univ., Tucson.
SPECKLE IMAGE RECONSTRUCTION. APPENDIX 1 Final Report
P. A. Strittmatter and E. K. Hege 1 Apr. 1985 56 p
(Contract F19628-82-K-0025; Grants NSF AST-81-13212; NSF AST-82-01092)
(AD-A158271; AFOSR-85-0635TR-App-1) Avail: NTIS HC A04/MF A01 CSCL 03/2

By adjusting the optical pathlengths of the MMT (Multiple Mirror Telescopes) telescopes, it is possible to make the MMT into a phased array with a 6.86 m baseline. A coherent, phased focus can be achieved with tilted focal planes if the tilt angle is chosen so that the internal phase differences exactly compensate the external phase differences. This amounts to a slight change in configuration such that the beams are brought together at f/8.39 rather than the originally designed f/9. We summarize experiments which have used the MMT subapertures as a phased array and as a coherent, phased telescope, and present a simple analysis of the tilted focal plane geometry for coherent observation. The phased operation of the MMT is important not only for obtaining high angular resolution, but also for obtaining the higher detection sensitivity which results from the better discrimination against the sky emission background for infrared diffraction limited images. Full-aperture (six-beams), diffraction-limited results for the unresolved source Gamma Orinois, the well-known close binary Capella and the resolved red supergiant Betelgeuse, (including a diffraction limited differential speckle image of the latter) are presented. GRA

N86-14208# Arizona Univ., Tucson.
SPECKLE IMAGE RECONSTRUCTION. APPENDIX 2 Final Report
P. A. Strittmatter and E. K. Hege 1 Apr. 1985 322 p
(Contract F19628-82-K-0025; Grants NSF AST-81-13212; NSF AST-82-01092)
(AD-A158272; AFOSR-85-0635TR-App-2) Avail: NTIS HC A14/MF A01 CSCL 03/1

Partial contents include: Size Measurement of a Geosynchronous Satellite Using the MMT (Multiple Mirror Telescope); Speckle Interferometry of Asteroids; High-Speed Digital Signal Processing for Speckle Interferometry; Seeing Calibration of Optical Astronomical Speckle Interferometric Data; Seeing Studies for Speckle Holographic Imaging; A Self Calibrating Shift-and-Add Technique for Speckle Imaging; Physical Diameter and Images of Alpha Orionis; Image Reconstruction from Astronomical Speckle Interferometry; Recovery of Binary Star Orientation and Relative Intensity-A comparison of Techniques; Maximum Magnitude Estimation of Object's Power Spectrum in Stellar Speckle Interferometry; The Differential Speckle Interferometer; Statistical Analysis of the Self-Calibrating Shift-and-Add Image Reconstruction Technique; Adaptive Optics. GRA

N86-14092*# Southwestern Univ., Georgetown, Tex.
LUNAR LUMINESCENCE MEASUREMENTS Final Report
Thomas H. Morgan *In* NASA. Johnson (Lyndon B.) Space Center The 1983 NASA/ASEE Summer Faculty Fellowship Research Program Research Reports Sep. 1983 11 p (For primary document see N86-14078 04-85)
Avail: NTIS HC A18/MF A01 CSCL 03A

90 ASTROPHYSICS

Includes cosmology; and interstellar and interplanetary gases and dust.

N86-14209*# Atmospheric and Environmental Research, Inc., Cambridge, Mass.
EXTENDED ATMOSPHERES OF OUTER PLANET SATELLITES AND COMETS Interim Report, Aug. - Oct. 1985
William H. Smyth and Michael R. Combi Nov. 1985 10 p refs
(Contract NASw-3966)
(NASA-CR-176398; NAS 1.26:176398) Avail: NTIS HC A02/MF A01 CSCL 03B

The new cometary hydrogen particle-trajectory model, completed last year, has been used successfully to analyze observations of Comet P/Giacobini-Zinner. The Pioneer Venus Orbiter Ultraviolet Spectrometer observed the comet at 1216 A (hydrogen Lyman-a) on 11 September 1985 when the comet was 1.03 AU from the Sun and 1.09 AU from Venus. The analysis implies a production rate at 1.03 AU 2.3 x 10 to the 28th power/sec of the water molecules which photodissociate to produce the observed hydrogen. An upper limit for the H2O production rate of Comet P/Halley of 5 x 10 to the 28th power/sec at 2.60 AU was also obtained from the Pioneer Venus instrument. Author

N86-14210# Naval Academy, Annapolis, Md.
INVESTIGATION OF DUST ASSOCIATED WITH SHELL STARS Final Report, 1984 - 1985
M. S. Boehle 9 May 1985 124 p
(AD-A158945; USNA-TSPR-131) Avail: NTIS HC A06/MF A01 CSCL 03/2

This project investigated the association of dust with shell stars. Shell stars are identified by emission lines in their spectra, which have been produced in a shell of hot gas surrounding the star. Additional observed properties have indicated the presence of dust, but the direct association of dust with individual shell stars has not been demonstrated conclusively. The first phase of this project was designed to show the presence of dust around the two shell stars, and the second phase investigated their variability. The technique used for both phases was photoelectric photometry. Two sets of filters, broad band and narrow band, were used, in two photometers. The color index obtained from the broad band filters can detect the effects of dust on the star's light and, when compared to neighboring stars, can show whether the dust is directly associated with the star. Variability was searched for, using both sets of filters. AB Aurigal was not found to have a significant amount of circumsteller dust, but FS Canis Major has a strong indication of circumsteller dust and its observed variability has been shown to be a result of its circumsteller dust shell and not any variation of its actual physical properties. GRA

N86-14211# Los Alamos National Lab., N. Mex.
PREPARATION, ANALYSIS AND RELEASE OF SIMULATED INTERPLANETARY GRAINS INTO LOW GRAIN ORBIT
J. R. Stephens, I. E. Strong, and T. D. Kunkle 1985 7 p Presented at the Workshop on the Inter-Relationship Among Interstellar, Circumstellar and Interplanetary Grains, Wye, Md., 27 Feb. 1985
(Contract W-7405-eng-36)
(DE85-014133; LA-UR-85-1979; CONF-850287-1) Avail: NTIS HC A02/MF A01

Astronomical observations which reflect the optical and dynamical properties of interstellar and interplanetary grains are the primary means of identifying the shape, size, and the chemistry of extraterrestrial grain materials. The formation and optical characterization of simulated interstellar and interplanetary dust with particular emphasis on studying the properties on irregularly shaped particles are studied, as well as efforts to develop the techniques to allow dust experiments to be carried out in low-Earth orbit, thus extending the conditions under which dust experiments may be performed. The objectives are threefold: (1) to elucidate the optical properties, including scattering and absorption, of simulated interstellar grains including SiC, silicates, and carbon grains produced in the laboratory; (2) to develop the capabilities to release grains and volatile materials into the near-Earth environment and study their dynamics and optical properties; and (3) to study the interaction of released materials with the near-Earth environment to elucidate grain behavior in astrophysical environments. Interaction of grains with their environment may, for example, lead to grain alignment or coagulation, which results in observable phenomena such as polarization of light or a change of the scattering properties of the grains. DOE

N86-14087*# Saint Thomas Univ., Houston, Tex. Dept. of Physics.
SOME APPLICATIONS OF LIE GROUPS IN ASTRODYNAMICS Final Report
A. A. Jackson *In* NASA. Johnson (Lyndon B.) Space Center The 1983 NASA/ASEE Summer Faculty Fellowship Research Program Research Reports Sep. 1983 10 p refs (For primary document see N86-14078 04-85)
Avail: NTIS HC A18/MF A01 CSCL 03B

N86-14093*# Sam Houston State Univ., Huntsville, Tex. Dept. of Physics.
DEVELOPMENT OF A MASS SPECTROMETER SYSTEM FOR THE MEASUREMENT OF INERT GASES IN METEORITES Final Report
Russell L. Palma *In* NASA. Johnson (Lyndon B.) Space Center The 1983 NASA/ASEE Summer Faculty Fellowship Research Program Research Reports Sep. 1983 9 p (For primary document see N86-14078 04-85)
Avail: NTIS HC A18/MF A01 CSCL 03B

N86-14112# Joint Publications Research Service, Arlington, Va.
FORMING TRANSFORMATION MATRICES FOR DIFFERENT PARAMETERS OF MOTION OF CELESTIAL BODIES Abstract Only
A. A. Sukhanov *In its* USSR Rept.: Space (JPRS-USP-85-005) 30 Sep. 1985 p 24 Transl. into ENGLISH from Kosmich. Issled. (Moscow), v. 22, no. 6, Nov. - Dec. 1984 p 819-827 (For primary document see N86-14111 04-88)
Avail: NTIS HC A08

N86-14113# Joint Publications Research Service, Arlington, Va.
FORMING ATTAINABILITY SETS IN CONTROL OF KINETIC MOMENT OF ROTATING ASYMMETRIC SOLID BODY (SPECIAL CASES) Abstract Only
A. V. Sarychev *In its* USSR Rept.: Space (JPRS-USP-85-005) 30 Sep. 1985 p 25 Transl. into ENGLISH from Kosmich. Issled. (Moscow), v. 22, no. 6, Nov. - Dec. 1984 p 828-841 Original language document announced in IAA as A85-19902 (For primary document see N86-14111 04-88)
Avail: NTIS HC A08

N86-14120# Joint Publications Research Service, Arlington, Va.
ROLE OF INTRINSIC ENERGY SOURCE IN PHYSICAL BEHAVIOR OF SPLIT COMETARY NUCLEUS Abstract Only
V. D. Davydov *In its* USSR Rept.: Space (JPRS-USP-85-005) 30 Sep. 1985 p 31 Transl. into ENGLISH from Kosmich. Issled. (Moscow), v. 22, no. 6, Nov. - Dec. 1984 p 922-941 Original language document announced in IAA as A85-19912 (For primary document see N86-14111 04-88)
Avail: NTIS HC A08

N86-14121# Joint Publications Research Service, Arlington, Va.
APPROXIMATE SOLUTIONS OF EULER-LAMBERT EQUATION FOR CASE OF SEVERAL REVOLUTIONS ABOUT CENTRAL BODY Abstract Only
L. B. Livanov *In its* USSR Rept.: Space (JPRS-USP-85-005) 30 Sep. 1985 p 32 Transl. into ENGLISH from Kosmich. Issled. (Moscow), v. 22, no. 6, Nov. - Dec. 1984 p 942-944 Original language document announced in IAA as A85-19913 (For primary document see N86-14111 04-88)
Avail: NTIS HC A08

N86-14131# Joint Publications Research Service, Arlington, Va.
INTEGRATION OF EQUATIONS OF MOTION FOR MATERIAL POINT IN GRAVITATIONAL FIELD OF AXIALLY SYMMETRIC PLANET Abstract Only
A. R. Golikov *In its* USSR Rept.: Space (JPRS-USP-85-005) 30 Sep. 1985 p 39 Transl. into ENGLISH from Kosmich. Issled. (Moscow), v. 22, no. 5, Sep. - Oct. 1984 p 651-662 Original language document announced in IAA as A85-15252 (For primary document see N86-14111 04-88)
Avail: NTIS HC A08

N86-14132# Joint Publications Research Service, Arlington, Va.
PERIODIC REGIMES OF ROTATIONAL MOTION OF SOLID BODY ABOUT LIBERATION POINT L SUB 4 IN RESTRICTED ELLIPTICAL THREE-BODY PROBLEM Abstract Only
Yu. V. Barkin and S. N. Lelyavin *In its* USSR Rept.: Space (JPRS-USP-85-005) 30 Sep. 1985 p 40 Transl. into ENGLISH from Kosmich. Issled. (Moscow), v. 22, no. 5, Sep. - Oct. 1984 p 663-674 Original language document announced in IAA as A85-15253 (For primary document see N86-14111 04-88)
Avail: NTIS HC A08

N86-14141# Joint Publications Research Service, Arlington, Va.
DEPENDENCE OF LENGTH OF FREE PATH OF FLARE PARTICLES ON ENERGY Abstract Only
Ye. I. Daybog, Viktoriya G. Kurt, and V. G. Stolpovskiy *In its* USSR Rept.: Space (JPRS-USP-85-005) 30 Sep. 1985 p 46-47 Transl. into ENGLISH from Kosmich. Issled. (Moscow), v. 22, no. 5, Sep. - Oct. 1984 p 763-773 Original language document announced in IAA as A85-15263 (For primary document see N86-14111 04-88)
Avail: NTIS HC A08

N86-14147# Joint Publications Research Service, Arlington, Va.
WAVE INTERPRETATION OF MEASUREMENTS ON MARS-7 AND VENERA-9 PROBES FOR DETERMINING VELOCITY OF MOTION OF INTERSTELLAR GAS Abstract Only
Ye. M. Grivnev *In its* USSR Rept.: Space (JPRS-USP-85-005) 30 Sep. 1985 p 51 Transl. into ENGLISH from Pisma v Astron. Zh. (Moscow), v. 10, no. 12, Dec. 1984 p 908-911 Previously announced in IAA as A85-39191 (For primary document see N86-14111 04-88)
Avail: NTIS HC A08

91 LUNAR AND PLANETARY EXPLORATION

Includes planetology; and manned and unmanned flights. For spacecraft design see *18 Spacecraft Design Testing, and Performance*. For space stations see *15 Launch Vehicles and Space Vehicles*.

N86-14212*# Boeing Aerospace Co., Seattle, Wash.
EXPERIMENTAL INVESTIGATION OF CRATER GROWTH DYNAMICS
Robert M. Schmidt, Kevin R. Housen, Michael D. Bjorkman, and Keith A. Holsapple 1985 5 p refs
(Contract NASw-3291)
(NASA-CR-176392; NAS 1.26:176392) Avail: NTIS HC A02/MF A01 CSCL 03B

This work is a continuation of an ongoing program whose objective is to perform experiments and to develop scaling relationships for large-body impacts onto planetary surfaces. The centrifuge technique is used to provide experimental data for actual target materials of interest. With both power and gas guns mounted on the rotor arm, it is possible to match various dimensionless similarity parameters, which have been shown to govern the behavior of large-scale impacts. The development of the centrifuge technique has been poineered by the present investigators and is documented by numerous publications, the most recent of which are listed below. Understanding the dependence of crater size upon gravity has been shown to be key to the complete determination of the dynamic and kinematic behavior of crater formation as well as ejecta phenomena. Three unique time regimes in the formation of an impact crater have been identified. B.W.

N86-14086*# East Carolina Univ., Greenville, N.C.
NUTRITIONAL CHARACTERISTICS OF MOON DUST FOR SOIL MICROORGANISMS Final Report
Takeru Ito *In* NASA. Johnson (Lyndon B.) Space Center The 1983 NASA/ASEE Summer Faculty Fellowship Research Program Research Reports Sep. 1983 17 p refs (For primary document see N86-14078 04-85)
Avail: NTIS HC A18/MF A01 CSCL 03B

N86-14128# Joint Publications Research Service, Arlington, Va.
APPROXIMATE CLUSTER ANALYSIS METHOD AND THREE-DIMENSIONAL DIAGRAM OF OPTICAL CHARACTERISTICS OF LUNAR SURFACE Abstract Only
N. N. Yevsyukov *In its* USSR Rept.: Space (JPRS-USP-85-005) 30 Sep. 1985 p 37 Transl. into ENGLISH from Astron. Zh. (Moscow), v. 61, no. 6, Nov. - Dec. 1984 p 1184-1191 Previously announced in IAA as A85-42342 (For primary document see N86-14111 04-88)
Avail: NTIS HC A08

N86-14143# Joint Publications Research Service, Arlington, Va.
ELECTRICAL AND ELECTROTHERMAL CONDUCTIVITY OF PLANETARY IONOSPHERES. 1: REFINEMENT OF THEORY Abstract Only
A. V. Pavlov *In its* USSR Rept.: Space (JPRS-USP-85-005) 30 Sep. 1985 p 48-49 Transl. into ENGLISH from Kosmich. Issled. (Moscow), v. 22, no. 5, Sep. - Oct. 1984 p 781-791 Original language document announced in IAA as A85-15265 (For primary

document see N86-14111 04-88)
Avail: NTIS HC A08

N86-14148# Joint Publications Research Service, Arlington, Va.
VEGA-1 RELEASES AEROSTAT AND LANDER AT VENUS
In its USSR Rept.: Space (JPRS-USP-85-005) 30 Sep. 1985 p 52-53 Transl. into ENGLISH from Komsomolskaya Pravda (Moscow), 12 Jun. 1985 p 1 (For primary document see N86-14111 04-88)
Avail: NTIS HC A08

N86-14149# Joint Publications Research Service, Arlington, Va.
OBJECTIVES OF VEGA PROJECT RESEARCH Abstract Only
T. Breus *In its* USSR Rept.: Space (JPRS-USP-85-005) 30 Sep. 1985 p 54 Transl. into ENGLISH from Kommunist (Moscow), 13 Jun. 1985 p 4 (For primary document see N86-14111 04-88)
Avail: NTIS HC A08

N86-14150# Joint Publications Research Service, Arlington, Va.
VEGA-2 RELEASES AEROSTAT AND LANDER AT VENUS
In its USSR Rept.: Space (JPRS-USP-85-005) 30 Sep. 1985 p 55-56 Transl. into ENGLISH from Komsomolskaya Pravda (Moscow), 16 Jun. 1985 p 1 (For primary document see N86-14111 04-88)
Avail: NTIS HC A08

N86-14151# Joint Publications Research Service, Arlington, Va.
RESULTS FROM VEGA ATMOSPHERE AND SOIL STUDIES Abstract Only
V. Golovachev *In its* USSR Rept.: Space (JPRS-USP-85-005) 30 Sep. 1985 p 57 Transl. into ENGLISH from Trud (Moscow), 16 Jun. 1985 p 3 (For primary document see N86-14111 04-88)
Avail: NTIS HC A08

N86-14152# Joint Publications Research Service, Arlington, Va.
PRESS CONFERENCE ON FIRST STAGE OF VEGA PROJECT
V. P. Ovcharov *In its* USSR Rept.: Space (JPRS-USP-85-005) 30 Sep. 1985 p 58-59 Transl. into ENGLISH from Sov. Latviya (Riga), 18 Jun. 1985 p 3 (For primary document see N86-14111 04-88)
Avail: NTIS HC A08

N86-14153# Joint Publications Research Service, Arlington, Va.
FURTHER COMMENTS ON RESULTS OF VEGA STUDIES OF VENUS Abstract Only
A. Pokrovskiy *In its* USSR Rept.: Space (JPRS-USP-85-005) 30 Sep. 1985 p 60 Transl. into ENGLISH from Pravda (Moscow), 1 Jul. 1985 p 3 (For primary document see N86-14111 04-88)
Avail: NTIS HC A08

N86-14155# Joint Publications Research Service, Arlington, Va.
BROCHURE ON PHOBOS AND DEIMOS
Vladimir Naumovich Zharkov and Aleksandr Vasilyevich Kozenko *In its* USSR Rept.: Space (JPRS-USP-85-005) 30 Sep. 1985 p 62-65 Transl. into ENGLISH from Novoye v Zhizni, Nauke, Tekhn.: Ser. Kosmonavtika, Astron. (Moscow), no. 1, Jan. 1985 p 2-6, 53-54 (For primary document see N86-14111 04-88)
Copyright. Avail: NTIS HC A08

N86-14156# Joint Publications Research Service, Arlington, Va.
RESULTS OF STUDY OF SURFACE OF FIVE REGIONS ON VENUS BY BISTATIC RADAR METHOD Abstract Only
A. I. Kucheryavenkov, O. Ye. Milekhin, A. G. Pavelyev, and O. I. Yakovlev *In its* USSR Rept.: Space (JPRS-USP-85-005) 30 Sep. 1985 p 66-67 Transl. into ENGLISH from Kosmich. Issled. (Moscow), v. 22, no. 6, Nov. - Dec. 1984 p 895-905 (For primary document see N86-14111 04-88)
Avail: NTIS HC A08

N86-14157# Joint Publications Research Service, Arlington, Va.
POSSIBILITY OF SPECTROSCOPIC DETECTION OF OXYGEN IN LOWER VENUSIAN ATMOSPHERE Abstract Only
V. A. Krasnopolskiy *In its* USSR Rept.: Space (JPRS-USP-85-005) 30 Sep. 1985 p 67-68 Transl. into ENGLISH from Kosmich. Issled. (Moscow), v. 22, no. 5, Sep. - Oct. 1984 p 812-815 (For primary document see N86-14111 04-88)
Avail: NTIS HC A08

N86-14159# Joint Publications Research Service, Arlington, Va.
NATURE OF MEGACYCLES IN EVOLUTION OF EARTH, MARS, AND MOON Abstract Only
Ye. Ye. Milanovskiy and A. M. Nikishin *In its* USSR Rept.: Space (JPRS-USP-85-005) 30 Sep. 1985 p 69-70 Transl. into ENGLISH from Dokl. Akadem. Nauk SSSR (Moscow), v. 280, no. 5, Feb. 1985 p 1204-1209 Original language document announced in IAA as A85-28924 (For primary document see N86-14111 04-88)
Avail: NTIS HC A08

92 SOLAR PHYSICS

Includes solar activity, solar flares, solar radiation and sunspots.

N86-14119# Joint Publications Research Service, Arlington, Va.
SOLAR FLARE X-RADIATION AND HIGH-ENERGY PARTICLES ACCORDING TO OBSERVATIONAL DATA FROM VENERA-13 AND VENERA-14 AUTOMATIC INTERPLANETARY STATIONS Abstract Only
S. A. Belyakov, Ye. I. Daybog, A. P. Dyachkov, V. M. Zenchenko, Viktoriya G. Kurt, Yu. I. Logachev, A. I. Rutkovskiy, S. P. Ryumin, V. G. Stolpovskiy, V. G. Yurovitskaya et al *In its* USSR Rept.: Space (JPRS-USP-85-005) 30 Sep. 1985 p 30 Transl. into ENGLISH from Kosmich. Issled. (Moscow), v. 22, no. 6, Nov. - Dec. 1984 p 906-921 Original language document announced in IAA as A85-19911 (For primary document see N86-14111 04-88)
Avail: NTIS HC A08

N86-14124# Joint Publications Research Service, Arlington, Va.
SUDDEN DISAPPEARANCE OF QUIESCENT PROMINENCES Abstract Only
G. P. Apushkinskiy and N. A. Topchilo *In its* USSR Rept.: Space (JPRS-USP-85-005) 30 Sep. 1985 p 34 Transl. into ENGLISH from Astron. Zh. (Moscow), v. 61, no. 6, Nov. - Dec. 1984 p 1150-1157 Original language document announced in IAA as A85-42338 (For primary document see N86-14111 04-88)
Avail: NTIS HC A08

N86-14125# Joint Publications Research Service, Arlington, Va.
MAGNETIC FIELD DETERMINATION IN QUIESCENT SOLAR PROMINENCES FROM POLARIZATION CHARACTERISTICS OF RADIATED LIGHT Abstract Only
M. G. Gornyy, D. V. Kupriyanov, and B. G. Matisov *In its* USSR Rept.: Space (JPRS-USP-85-005) 30 Sep. 1985 p 35 Transl. into ENGLISH from Astron. Zh. (Moscow), v. 61, no. 6, Nov. - Dec. 1984 p 1158-1167 Previously announced in IAA as A85-42339 (For primary document see N86-14111 04-88)
Avail: NTIS HC A08

N86-14126# Joint Publications Research Service, Arlington, Va.
SPATIAL PATTERNS OF MANIFESTATION OF SOLAR ACTIVITY IN TROPOSPHERE Abstract Only
R. V. Smirnov *In its* USSR Rept.: Space (JPRS-USP-85-005) 30 Sep. 1985 p 35-36 Transl. into ENGLISH from Astron. Zh. (Moscow), v. 61, no. 6, Nov. - Dec. 1984 p 1168-1178 Previously announced in IAA as A85-42340 (For primary document see N86-14111 04-88)
Avail: NTIS HC A08

N86-14142# Joint Publications Research Service, Arlington, Va.
OBSERVATION OF SMALL-SCALE SOLAR WIND STRUCTURE ON FRONT OF SHARP INCREASE IN PLASMA FLOW VELOCITY Abstract Only
L. A. Avanov, G. N. Zastenker, O. L. Vaysberg, and Yu. I. Yermolayev *In its* USSR Rept.: Space (JPRS-USP-85-005) 30 Sep. 1985 p 47-48 Transl. into ENGLISH from Kosmich. Issled. (Moscow), v. 22, no. 5, Sep. - Oct. 1984 p 774-780 Original

language document announced in IAA as A85-15264 (For primary document see N86-14111 04-88)
Avail: NTIS HC A08

93 SPACE RADIATION

Includes cosmic radiation; and inner and outer Earth's radiation belts.

For biological effects of radiation see *52 Aerospace Medicine*. For theory see *73 Nuclear and High-Energy Physics*.

N86-13792# Joint Publications Research Service, Arlington, Va.
LATITUDE MEASUREMENTS OF COSMIC RADIATION INTENSITY IN STRATOSPHERE AND AT SEA LEVEL ON MARINE ANTARCTIC EXPEDITIONS Abstract Only
Nikolay Savvich Svirzhevskiy *In its* USSR Rept.: Earth Sci. (JPRS-UES-85-009) 13 Nov. 1985 p 39 Transl. into ENGLISH from "Shirotnyye Izmereniya Intensivnosti Kosmicheskogo Izlucheniya v Stratosfere i na Urovne Morya v Morskikh Antarkticheskikh Ekspeditsiyakh" Moscow, 1983 p 1-16 (For primary document see N86-13765 04-42)
Avail: NTIS HC A04/MF A01

N86-13793# Joint Publications Research Service, Arlington, Va.
HADRON COMPONENT OF COSMIC RADIATION AT ATMOSPHERIC DEPTH 800 g/cm(2) IN ENERGY RANGE 70 TO 700 GeV Abstract Only
Petr Sergeyevich Vasilyev *In its* USSR Rept.: Earth Sci. (JPRS-UES-85-009) 13 Nov. 1985 p 40 Transl. into ENGLISH from "Adronnaya Komponenta Kosmicheskogo Izlucheniya na Glubine Atmosfery 800 g/cm(2) v Oblasti Energiy (70-700GeV)" Moscow, 1984 p 1-20 (For primary document see N86-13765 04-42)
Avail: NTIS HC A04/MF A01

N86-14118# Joint Publications Research Service, Arlington, Va.
SPECTRUM OF PHOTOELECTRONS IN EARTH'S UPPER ATMOSPHERE DURING SOLAR FLARES Abstract Only
S. V. Avakyan and G. S. Kudryashev *In its* USSR Rept.: Space (JPRS-USP-85-005) 30 Sep. 1985 p 29 Transl. into ENGLISH from Kosmich. Issled. (Moscow), v. 22, no. 6, Nov. - Dec. 1984 p 889-894 Original language document announced in IAA as A85-19909 (For primary document see N86-14111 04-88)
Avail: NTIS HC A08

N86-14122# Joint Publications Research Service, Arlington, Va.
FORMATION OF HIGH-ENERGY SECONDARY ELECTRONS IN LOW-DENSITY MEDIUM AT GREAT ALTITUDES Abstract Only
L. V. Kurnosova, L. A. Razorenov, and M. I. Fradkin *In its* USSR Rept.: Space (JPRS-USP-85-005) 30 Sep. 1985 p 32-33 Transl. into ENGLISH from Kosmich. Issled. (Moscow), v. 22, no. 6, Nov. - Dec. 1984 p 947-949 Original language document announced in IAA as A85-19915 (For primary document see N86-14111 04-88)
Avail: NTIS HC A08

N86-14123# Joint Publications Research Service, Arlington, Va.
HARD GAMMA RADIATION BACKGROUND FROM CODING COLLIMATOR OF GAMMA TELESCOPE UNDER SPACE EXPERIMENT CONDITIONS Abstract Only
A. P. Aleksandrov, A. N. Berezovoy, A. M. Galper, V. M. Grachev, V. V. Dmitrenko, V. G. Kirillov-Ugryumov, V. V. Lebedev, V. A. Lyakhov, A. A. Moiseyev, S. Ye. Ulin et al *In its* USSR Rept.: Space (JPRS-USP-85-005) 30 Sep. 1985 p 33-34 Transl. into ENGLISH from Kosmich. Issled. (Moscow), v. 22, no. 6, Nov. - Dec. 1984 p 950-951 (For primary document see N86-14111 04-88)
Avail: NTIS HC A08

99 GENERAL

N86-14213*# National Aeronautics and Space Administration. Ames Research Center, Moffett Field, Calif.
EMERGING AEROSPACE TECHNOLOGIES
William F. Ballhaus, Jr. and Laurance A. Milov Sep. 1985 16 p refs
(NASA-TM-86837; Rept-85409; NAS 1.15:86837) Avail: NTIS HC A02/MF A01 CSCL 05D

The United States Government has a long history of promoting the advancement of technology to strengthen the economy and national defense. An example is NASA, which was formed in 1958 to establish and maintain U.S. space technology leadership. This leadership has resulted in technological benefits to many fields and the establishment of new commercial industries, such as satellite communications. Currently, NASA's leading technology development at Ames Research Center includes the Tilt Rotor XV-15, which provides the versatility of a helicopter with the speed of a turboprop aircraft; the Numerical Aerodynamic Simulator, which is pushing the state of the art in advanced computational mathematics and computer simulation; and the Advanced Automation and Robotics programs, which will improve all areas of space development as well as life on Earth. Private industry is involved in maintaining technological leadership through NASA's Commercial Use of Space Program, which provides for synergistic relationships among government, industry, and academia. The plan for a space station by 1992 has framed much of NASA's future goals and has provided new areas of opportunity for both domestic space technology and leadership improvement of life on Earth. Author

SUBJECT INDEX

SCIENTIFIC AND TECHNICAL AEROSPACE REPORTS VOLUME 24 NUMBER 4

Typical Subject Index Listing

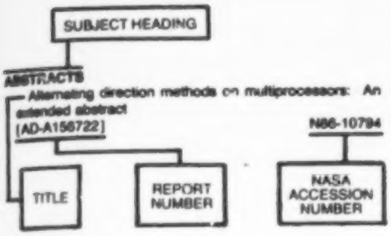

The subject heading is the key to the subject content of the document. Titles, report numbers, and accession numbers of pertinent documents are provided under each subject heading. When the title is insufficiently descriptive of the document content, a title extension has been added, separated from the title by three hyphens. The report number helps to indicate the type of document cited (e.g., NASA report, NASA translation, NASA contractor report). The NASA accession number is the number by which the document abstracts are arranged in this journal and by which the document is sold or requested. The titles, with title extensions if present, are arranged under each subject heading in ascending accession number order. The subject headings have been selected from the latest revision of the *NASA Thesaurus* (NASA SP-7051).

A

ABILITIES
The event related brain potential as an index of information processing, cognitive activity, and skill acquisition: A program of basic research
[AD-A159118] N86-13897

ABLATIVE MATERIALS
Numerical models for plasma-solid interactions in electrothermal mass accelerators
[AD-A158637] N86-14052

ABRASION
Abrasion behavior of aluminum and composite skin coupons, stiffened skins and stiffened panels representative of transport airplane structures
[NASA-TP-2520] N86-13316

ABRASIVES
Durability of steel 45 with boride coating in corrosive-abrasive media N86-13467

ABSORPTANCE
Electrical research on solar cells and photovoltaic materials
[NASA-CR-176384] N86-13638

ABSORPTION CROSS SECTIONS
Differential scattering cross section and total extinction measurements on (CH)n spheres in 632.8 nm laser light
[AD-A158044] N86-13391

ABSORPTION SPECTRA
Temperature and pressure components of shock-induced changes in the electronic spectrum of carbon disulfide
[AD-A158627] N86-13373

ABSORPTIVITY
Linear and saturated absorption of laser radiation in heated cases N86-13551
Time resolved extended X-ray absorption fine structure spectrometer
[AD-D011869] N86-13715

ABUNDANCE
Detection of Ni 2 lambda 7378 in six Seyfert galaxies
[NASA-CR-176358] N86-14205

ACCELERATION STRESSES (PHYSIOLOGY)
Endocrine and fluid metabolism in males and females of different ages after bedrest, acceleration and lower body negative pressure
[NASA-TM-58270] N86-13886

ACCIDENTS
Safe control systems and the VIPER microprocessor
[AD-A156617] N86-13908

ACCURACY
Enhancing sensitivity to visual motion and enhancing visual sensitivity
[AD-A158600] N86-13889
Scout trajectory error propagation computer program
[NASA-CR-166030] N86-13919
Spectral methods for discontinuous problems
[NASA-CR-177974] N86-13953
Accuracy of schemes with nonuniform meshes for compressible fluid flows
[NASA-CR-177988] N86-13954

ACID RAIN
Oxidizing and scavenging characteristics of April rains: OSCAR data report
[DE85-017014] N86-13844
Characterization of acid rain phenomena, Atlanta, Georgia
[PB85-216943] N86-13848

ACIDITY
Application of computers in analytical chemistry: Calculation of optimum acidity of reaction between metal ions and organic reagents in solution N86-13607
Changes in soil acidity due to natural processes and acid deposition
[DE85-012103] N86-13845
Determination of acidity in ambient air
[PB85-218196] N86-13849

ACOUSTIC EMISSION
High frequency quantitative analysis of magnetomechanical acoustic emission
[AD-A158222] N86-13750

ACOUSTIC PROPAGATION
Ray transmissions over a sloping bottom in shallow water
[AD-A158017] N86-14008

ACOUSTIC PROPERTIES
Speech recognition: Acoustic, phonetic and lexical knowledge
[AD-A158264] N86-13629
Study of optical-acoustical phenomena at surface of strongly absorbing clearing fluids N86-13774
Scientific activities of the Polish Academy of Sciences: Institute of Fundamental Technological Research in 1983
[ISBN-83-01-06288-6] N86-14107

ACOUSTIC SCATTERING
Acoustical scattering from an elastic sphere in water: Surface wave glory, resonances, and the Sommerfeld-Watson transformation for amplitudes
[AD-A158884] N86-14010

ACOUSTIC VELOCITY
A method to determine dynamic elastic constants of thin shell composites by guided ultrasonic waves
[AD-A159025] N86-13381

ACOUSTICS
Ray transmissions over a sloping bottom in shallow water
[AD-A158017] N86-14008

ACOUSTO-OPTICS
Study of optical-acoustical phenomena at surface of strongly absorbing clearing fluids N86-13774
Optical radar transceiver control apparatus
[AD-D011880] N86-14042

ACQUISITION
Phase lock acquisition system
[AD-D011804] N86-13646
The event related brain potential as an index of information processing, cognitive activity, and skill acquisition: A program of basic research
[AD-A159118] N86-13897

ACRYLIC RESINS
Photodegradation studies of silver-backed polyacrylonitrile (PAN) films
[DE85-012154] N86-13501
Gas recirculator for acyclic machines
[AD-D011873] N86-13658

ACTINIDE SERIES
Application of quantum chemistry to atmospheric chemistry
[AD-A158282] N86-13856

ACTIVATION ENERGY
Micromechanisms of electrodiffusion failures in thin film metallization N86-13472
Determination of the activation barrier to energy transfer from 3 pi pi* to charge transfer levels via steady state and transient luminescence measurements on Bis(4-Chlorothiophenol) (1,10-Phenanthroline) Zinc (II)
[AD-A158239] N86-14012

ACTIVE SATELLITES
Crowding of the geostationary orbit
[ESA-CR(P)-2050] N86-13346

ACTUATORS
Thermal vacuum tests on a hinge actuator mechanism --- spacecraft component
[ESA-ESTL-067] N86-13360

ADA (PROGRAMMING LANGUAGE)
Ada as a hardware description language: An initial report
[AD-A158217] N86-13935
Issues to be considered in the evaluation of technical proposals from the Ada (trademark) language perspective
[AD-A158376] N86-13936
Techniques for the design and implementation of highly reliable multi-processing systems
[AD-A159236] N86-13945

ADAPTATION
Basic principles of feedback and adaptive approaches in the finite element method
[AD-A158168] N86-13969

ADAPTIVE CONTROL
Adaptive control of large space structures using recursive lattice filters
[NASA-CR-176402] N86-13358

ADAPTIVE OPTICS
Effectiveness of use of adaptive optical systems under conditions of self-effect in atmosphere N86-13791
Speckle image reconstruction: Appendix 2
[AD-A158272] N86-14208

ADDITIVES
Role of additives in minimizing zinc electrode shape change: The effect of lead on the kinetics of Zn(2) reduction in concentrated alkaline media
[AD-A158806] N86-13395
The effect of cobalt content in U-700 type alloys on degradation of aluminide coatings
[NASA-TM-87173] N86-13408

ADHESION
Current viewpoints on oxide adherence mechanisms
[NASA-TM-87168] N86-13409

ADHESIVE BONDING
A durable airfield marking system
[AD-A157953] N86-13339

ADSORPTION
Electronic detection of low concentrations of organophosphorus compounds with a solid state device utilizing supported copper + cuprous oxide island films
[AD-A158181] N86-13392
No chemisorption on Ni(111): Coverage effects, site preferences and adsorption geometry
[AD-A159110] N86-13397
Studies of metal/carbon surface chemistry
[DE85-015548] N86-13398
Oxide electrodes at high temperatures
[DE85-006564] N86-13667
Ion bombardment and adsorption studies on ilmenite (FeTiO3) by X-ray photoelectron spectroscopy
N86-14100

AERIAL PHOTOGRAPHY
Crop area estimation based on remotely-sensed data with an accurate but costly subsample
[NASA-CR-176017] N86-13814

Stereophotogrammetric survey of wave-covered water surface N86-14170
Classification of trees by growth classes on the basis of multizonal photographs N86-14173
Possibilities of use of aerospace materials in predicting occurrence of petroleum and gas N86-14175
Problems in study and evaluation of consequences of forest fires using aerospace photographs N86-14176
Radiometric correction of materials of aerospace survey of Earth with MKF-6 camera: Methodology and use of results N86-14193

AERIAL RECONNAISSANCE
Computer-aided aerial radiometric surveying of soil moisture N86-13778
Use of remote optical measurements in agriculture N86-14172

AERODYNAMIC CHARACTERISTICS
Assessment of aerodynamic and dynamic models in a comprehensive analysis [NASA-TM-86835] N86-13286

AERODYNAMIC CONFIGURATIONS
Double-branched vortex generator [NASA-TM-88201] N86-13298

AERODYNAMIC DRAG
Preliminary report on in-flight measurement of rotor hub drag and lift using the RSRA [NASA-TM-86764] N86-13319
Fluid forces on two circular cylinders in crossflow [DE85-014294] N86-13704
Crushing strength of aluminum oxide agglomerates [AD-A158051] N86-13756

AERODYNAMIC FORCES
Implementing agreement for cooperation in the development of large scale wind energy conversion systems --- conferences [JUEL-SPEZ-304] N86-13820
Development in aerodynamic calculations --- wind energy converters N86-13822
Unsteady aerodynamics applied to the horizontal axis wind turbine disk N86-13825

AERODYNAMIC LOADS
Aerodynamic theory in the calculation of the GROWIAN rotor compared with some experimental data --- wind energy converter N86-13826
Aerodynamic calculational methods for curved-blade Darrieus VAWT WECS --- vertical axis wind turbine wind energy converters (VAWT WECS) N86-13830

AERODYNAMIC STABILITY
Pitch rate versus G command as the longitudinal flight control system design strategy for a statistically unstable fighter type aircraft with two control surfaces [AD-A158803] N86-13334

AERODYNAMICS
PLTTER user's guide [NASA-CR-177385] N86-13291
A tomographic technique for aerodynamics at transonic speeds [NASA-TM-86766] N86-13297

AEROSOLS
Differential scattering cross section and total extinction measurements on (CH)n spheres in 632.8 nm laser light [AD-A158044] N86-13391
Study of mean free path effects on growth of ultrafine metallic aerosols [AD-A158206] N86-13393
Optical/infrared properties of atmospheric aerosols with an in situ, multi-wavelength, multichannel nephelometer system [AD-A158825] N86-13710
Influence of fog microstructure on quality of optical image transmitted through it N86-13781
Interaction between powerful laser radiation and atmospheric aerosols N86-13788
Atmospheric effect on remote sensing of the Earth's surface N86-13804
Multidimensional modeling of atmospheric effects and surface heterogeneities on remote sensing N86-13806
Protocol for size-specific emission measurements (SIM-5) applied to PM(10) [PB85-200194] N86-13847
Airborne lidar measurements of El Chichon stratospheric aerosols [NASA-RP-1148] N86-13850
New physical methods for biological aerosol detection [AD-A158218] N86-13881
Health hazard evaluation of liquid monopropellants. Phase 5: Comparative inhalation toxicities of LGP 1776, LGP 1845, and HAN (hydroxylammonium nitrate) [AD-A159090] N86-13891

AEROSPACE ENGINEERING
USSR report: Space [JPRS-USP-85-005] N86-14111

AEROSPACE ENVIRONMENTS
Mass loss of shuttle space suit orthofabric under simulated ionospheric atomic oxygen bombardment [NASA-TM-87149] N86-13899
Biological life-support systems for long-duration space flights N86-14160

AEROSPACE INDUSTRY
Certification granted to Franco-Italian ATR 42 N86-13617

AEROSPACE MEDICINE
Life sciences accomplishments [NASA-TM-88177] N86-13879

AEROSPACE SAFETY
NASA flight operations review [NASA-CR-176393] N86-13306

AEROSPACE SYSTEMS
Discovery of the Kalman filter as a practical tool for aerospace and industry [NASA-TM-86847] N86-13311
West Europe report: Science and technology [JPRS-WST-85-030] N86-13610

AEROSPACE TECHNOLOGY TRANSFER
USSR report: Space [JPRS-USP-85-005] N86-14111

AEROSTATICS
Vega-2 releases aerostat and lander at Venus N86-14150
Press conference on first stage of Vega project N86-14152
Further comments on results of Vega studies of Venus N86-14153

AEROTHERMODYNAMICS
Aerothermodynamics for future launchers. Review of the state of the art in Europe [VKI-CR-1984-16/AR] N86-13347

AFTERBURNING
Flame mechanisms and flame inhibition N86-13523
The suppression of afterburning in solid rocket plumes by potassium salts N86-13524

AGGLOMERATION
Effect of heating conditions on agglomeration of powdered aluminum in air atmosphere N86-13460
Crushing strength of aluminum oxide agglomerates [AD-A158051] N86-13756

AGING
Influence of degree of deformation on structure and properties of naturally aged alloy 1163 N86-13431

AGING (MATERIALS)
Combined small angle X-ray scattering and transmission electron microscopy studies of Al-Li alloys [DE85-016356] N86-13416
Stability of RDX, AP and BTTN near room temperature N86-13535
Long-term analysis of slender concrete structures with cracking [DE85-010275] N86-13762

AGRICULTURE
Method for using clusters in evaluating land use areas from multizonal photographs N86-14180
Some approaches to organization of data bank in system for studying Earth's natural resources from space (using example of agriculture) N86-14194

AIR
Effect of heating conditions on agglomeration of powdered aluminum in air atmosphere N86-13460

AIR CURRENTS
Investigation of characteristics of synoptic movements on sphere N86-13770
Structural characteristic of temperature field over sea N86-13783

AIR DEFENSE
National airspace system, system requirements specification [AD-A157944] N86-13312

AIR FILTERS
Aircrew dose and engine dust ingestion from nuclear cloud penetration [AD-A159246] N86-13327

AIR POLLUTION
Development and evaluation of an instantaneous atmospheric corrosion rate monitor [PB85-214336] N86-13727
Oxidizing and scavenging characteristics of April rains: OSCAR data report [DE85-017014] N86-13844
Protocol for size-specific emission measurements (SIM-5) applied to PM(10) [PB85-200194] N86-13847

AIR PURIFICATION
Elution of benzene and methyl ethyl ketone from charcoal beds by continued air sweeping [AD-A158804] N86-13374

AIR QUALITY
Particulate matter analysis by electron microscopy [PB85-227817] N86-13846
Characterization of acid rain phenomena, Atlanta, Georgia [PB85-216943] N86-13848
Determination of acidity in ambient air [PB85-218196] N86-13849

AIR TRAFFIC CONTROL
National airspace system, system requirements specification [AD-A157944] N86-13312
Alerted monitors: Human operators aided by automated detectors [PB85-222750] N86-13906
The mission oriented terminal area simulation facility [NASA-TM-87621] N86-13944

AIR WATER INTERACTIONS
Model interpretation of annual variation of temperature fields of air and water boundary layers of world ocean N86-13767
Structural characteristic of temperature field over sea N86-13783
Atmospheric synoptic eddies over ocean (determined from experimental data) N86-13784
Influence of petroleum pollution on ocean-atmosphere gas exchange intensity (in example of North Atlantic) N86-13785
The influence of oceanic chemistry, physics and biology on atmospheric carbon dioxide N86-13865
Understanding climate: A strategy for climate modeling and predictability research, 1985-1995 [NASA-RP-1158] N86-13866

AIRBORNE EQUIPMENT
Determining flexure of aerial camera smoothing glass N86-14169

AIRBORNE/SPACEBORNE COMPUTERS
Computer-aided aerial radiometric surveying of soil moisture N86-13778

AIRCRAFT ACCIDENTS
Aircraft crashing. Analysis and identification methods. Presentation of a solution method [IMFL-4116] N86-13308

AIRCRAFT ANTENNAS
Limited Airworthiness and Flight Characteristics (A and FC) test of the quick fix configuration [AD-A157716] N86-13323

AIRCRAFT COMPARTMENTS
Aircrew dose and engine dust ingestion from nuclear cloud penetration [AD-A159246] N86-13327

AIRCRAFT CONFIGURATIONS
Aircraft of the future [NASA-TM-77952] N86-13318

AIRCRAFT CONTROL
A preliminary evaluation of the generalized likelihood ratio for detecting and identifying control element failures in a transport aircraft [NASA-TM-87620] N86-13332
Pitch rate versus G command as the longitudinal flight control system design strategy for a statistically unstable fighter type aircraft with two control surfaces [AD-A158803] N86-13334

AIRCRAFT DESIGN
Aircraft of the future [NASA-TM-77952] N86-13318

AIRCRAFT ENGINES
Lightweight two-stroke cycle aircraft diesel engine technology enablement program, volume 1 [NASA-CR-174923-VOL-1] N86-13328
Lightweight two-stroke cycle aircraft diesel engine technology enablement program, volume 2 [NASA-CR-174923-VOL-2] N86-13329
Lightweight two-stroke cycle aircraft diesel engine technology enablement program, volume 3 [NASA-CR-174923-VOL-3] N86-13330
Polymer, metal and ceramic matrix composites for advanced aircraft engine applications [NASA-TM-87132] N86-13407

AIRCRAFT EQUIPMENT
Physical distribution system for aircraft external fuel tanks-survey [AD-A158275] N86-13324

AIRCRAFT FUELS
Physical distribution system for aircraft external fuel tanks-survey [AD-A158275] N86-13324

AIRCRAFT LANDING
An investigation into the vertical axis control power requirements for landing VTOL type aircraft onboard nonaviation ships in various sea states [NASA-CR-176355] N86-13294
A durable airfield marking system [AD-A157953] N86-13339

AIRCRAFT NOISE
Transmission acoustic vibration testing [AD-A159022] N86-13326

AIRCRAFT POWER SUPPLIES
Two-hundred to 300 KVA conditioned power system - development, phase 1 [AD-A158820] N86-13832

AIRCRAFT PRODUCTION
Certification granted to Franco-Italian ATR 42 N86-13617

ATR 42 production work in French, Italian plants detailed N86-13618

AIRCRAFT RELIABILITY

Limited Airworthiness and Flight Characteristics (A and FC) test of the quick fix configuration
[AD-A157716] N86-13323

AIRCRAFT SAFETY

Advanced emergency openings for commercial aircraft
[NASA-TM-87580] N86-13305

AIRCRAFT STRUCTURES

ATR 42 production work in French, Italian plants detailed N86-13618

AIRFOILS

A direct-inverse method for transonic and separated flows about airfoils
[NASA-CR-176403] N86-13300

Studies of the flow field near a NACA 4412 aerofoil at nearly maximum lift
[AD-A157750] N86-13301

Aerofoil characteristics of rotating blades --- wind turbine models N86-13824

AIRFRAMES

Digital servocontroller system. Volume 4. Results and conclusions
[AD-A159068] N86-13335

Structures and materials technology issues for reusable launch vehicles
[NASA-TM-87626] N86-13349

AIRPORT TOWERS

Design criteria upgrade for US Army Type 2 air traffic control towers
[AD-A159115] N86-13314

AIRPORTS

A durable airfield marking system
[AD-A157953] N86-13339

ALCOHOLS

Report on investigation of alcohol combustion associated wear in spark ignition engines, mechanisms and lubricant effects
[AD-A157714] N86-13388

ALGEBRA

An algorithm to translate relational algebra queries into QUEL
[AD-A158169] N86-13931

ALGORITHMS

Computational aspects of zonal algorithms for solving the compressible Navier-Stokes equations in three dimensions
[NASA-TM-86774] N86-13296

The evaluation of failure detection and isolation algorithms for restructurable control
[NASA-CR-177983] N86-13310

Algorithms for the reduction of wind-tunnel data derived from strain gauge force balances
[ARL/AERO-R-164] N86-13337

Development of the NIMBUS-7 SMMR retrieval algorithm — Scanning Multichannel Microwave Radiometer (SMMR)
[BAE-RPT/NIM-7/021] N86-13367

A parametric study of the Ibrahim time domain modal identification algorithm N86-13588

Tire-soil interaction model for turning (steered) tires
[AD-A157737] N86-13593

Improved algorithm for radar real-time data processing N86-13608

Multidimensional modeling of atmospheric effects and surface heterogeneities on remote sensing N86-13806

Scattering models and basic experiments in the microwave regime N86-13807

Sparse elimination on vector multiprocessors
[AD-A158274] N86-13909

Target tracking based scene analysis
[AD-A158629] N86-13910

An algorithm to translate relational algebra queries into QUEL
[AD-A158169] N86-13931

Pre-stack Kirchhoff inversion of common offset data
[AD-A158205] N86-13932

On projected Newton barrier methods for linear programming and an equivalence to Karmarkar's projective method
[AD-A158212] N86-13934

Describing surfaces
[AD-A158940] N86-13937

Inner/outer iterative methods and numerical Schwarz algorithms - 2
[DE85-013197] N86-13940

Investigation of techniques for improving spacecraft thermal control software
[GEC-MEL42.0552] N86-13942

An algorithm for simultaneous determination of modal frequencies and modal vectors of a dynamic impedance matrix
[ESA-CR(P)-2055] N86-13943

Multiresolution path planning for mobile robots
[AD-A158630] N86-13948

Multigrid solutions to quasi-elliptic schemes
[NASA-CR-177973] N86-13955

Minimal norm constrained interpolation
[NASA-CR-178001] N86-13956

Computation of geometric properties from the medial axis transform in 0 (n log n) time
[AD-A158934] N86-13980

Unified method for delay analysis of random multiple access algorithms
[AD-A159108] N86-13981

Variable curvature phantom
[DE85-014260] N86-14028

Multigrid relaxation methods and the analysis of lightness, shading, and flow
[AD-A158173] N86-14036

Advanced algorithm for orbit computation N86-14101

ALKALI METALS

Studies of metal/carbon surface chemistry
[DE85-015548] N86-13398

ALKALINE BATTERIES

Role of additives in minimizing zinc electrode shape change: The effect of lead on the kinetics of Zn(2) reduction in concentrated alkaline media
[AD-A158806] N86-13395

ALKALINE EARTH METALS

Evaluation and compilation of the thermodynamic properties of high temperature species N86-13532

ALKENES

Energetic fluorcarbons N86-13517

ALLOYS

High strain rate deformation in FCC metals and alloys
[DE85-017533] N86-13417

Influence of texture of titanium nitride coatings on wear resistance of cutting tools N86-13440

Modeling of thermal fatigue and erosion of complex alloyed steels in metal melts N86-13469

Superhard materials developed N86-13471

Internal friction in TiNiCu alloy N86-13480

Diffusion welding of copper-chromium pseudoalloy with copper N86-13493

Recent results on implantation and permeation into fusion reactor materials
[DE85-014620] N86-14067

ALTERNATING CURRENT

A study of some features of ac and dc electric power systems for a space station N86-14085

ALTIMETERS

Effects of digital altimetry on pilot workload
[NASA-TM-86424] N86-13892

ALTITUDE CONTROL

Pilot-oriented performance measurement
[AD-A158849] N86-13890

ALUMINUM

Abrasion behavior of aluminum and composite skin coupons, stiffened skins and stiffened panels representative of transport airplane structures
[NASA-TP-2520] N86-13316

High strain rate deformation in FCC metals and alloys
[DE85-017533] N86-13417

Influence of Co-Cr-Al-Y coatings on physical and mechanical properties of EI-893 steel in GT-100 turbine drive vanes N86-13438

Micromechanisms of electrodiffusion failures in thin film metallization N86-13472

Optimization of technological parameters of cold pressure welding of AD1M thin aluminum sheets N86-13484

Kinetics of dissolution of oxide films in titanium upon diffusion welding N86-13487

Elastic-plastic deformation of a metal-matrix composite coupon with a center slot
[NASA-CR-178013] N86-13496

Application of quantum chemistry to atmospheric chemistry
[AD-A158282] N86-13856

Optical constants
[AD-A158623] N86-14038

ALUMINUM ALLOYS

Corrosion fatigue initiation and short crack growth in an aluminum alloy N86-13404

Current viewpoints on oxide adherence mechanisms
[NASA-TM-87168] N86-13409

The delayed fracture of aluminum alloys
[AD-A158944] N86-13412

Effect of temperature and strain rate on microstructure of a deformed, superplastic Al-10%Mg-0.1%Zr alloy
[AD-A159015] N86-13413

Effect of strain and strain rate on the microstructure of a superplastically deformed Al-10%Mg-0.1%Zr alloy
[AD-A159062] N86-13414

Characterization of 7017 aluminum alloys in thick profiles, in the metallurgical versions T6510, T76510 and T736510, test report no. PV-44-607/F
[PV-44-607/F] N86-13420

USSR report: Materials science and metallurgy
[JPRS-UMS-85-006] N86-13422

Hereditary effect of dendrite liquation of titanium and zirconium on structure and properties of aluminum alloys N86-13423

Fiber composition materials for strengthening components of aluminum and its alloys N86-13424

Structure and properties of Al-Mg-Zn casting alloys N86-13425

Discontinuous precipitation in aluminum-magnesium alloys with high magnesium content N86-13426

Structure formation in silumins upon rapid crystallization N86-13427

Influence of alloying elements and impurities on mechanical properties of complex silumins N86-13428

Study of fractures in cast parts of high-strength aluminum alloy N86-13429

Study of permeability of two-phase zone in aluminum and copper alloys N86-13430

Influence of degree of deformation on structure and properties of naturally aged alloy 1163 N86-13431

Appearance of superplasticity effect in aluminum alloys with lithium N86-13432

Study of properties of gas-thermal coatings of composite nichrome-aluminum alloy powders N86-13442

Study of process of pore formation during argon-arc welding of aluminum alloy 1420 N86-13485

New materials to lighten vehicles N86-13624

ALUMINUM COATINGS

A durable airfield marking system
[AD-A157953] N86-13339

Effect of heating conditions on agglomeration of powdered aluminum in air atmosphere N86-13460

ALUMINUM COMPOUNDS

Changes in soil acidity due to natural processes and acid deposition
[DE85-012103] N86-13845

ALUMINUM NITRIDES

Ceramics based on aluminum nitride and metals N86-13456

ALUMINUM OXIDES

The effect of cobalt content in U-700 type alloys on degradation of aluminide coatings
[NASA-TM-87173] N86-13408

Current viewpoints on oxide adherence mechanisms
[NASA-TM-87168] N86-13409

Crushing strength of aluminum oxide agglomerates
[AD-A158051] N86-13756

AMBIENCE

Analysis of atomic thermospheric nitrogen density
[NASA-CR-176354] N86-13851

AMBIENT TEMPERATURE

Atmospheric environment for Space Shuttle (STS-51D)
[NASA-TM-86524] N86-13868

Statistical comparison of two major gridded temperature records of the Northern Hemisphere
[DE85-016076] N86-13872

AMINO ACIDS

Study of toxic and antigenic structures of botulinum neurotoxins
[AD-A156642] N86-13880

AMMONIA

Determination of acidity in ambient air
[PB85-218196] N86-13849

AMORPHOUS MATERIALS

USSR report: Materials science and metallurgy
[JPRS-UMS-85-006] N86-13422

Preliminary annealing on crystallization of amorphous Fe80Si6B14 alloy N86-13433

Influence of chromium on crystallization of amorphous Fe-B alloys N86-13434

Relationship of thermal expansion of amorphous metal alloys with their high temperature plastic properties N86-13435

AMPLIFICATION

Active mirror boosted 351 nm laser irradiation facility
[DE85-014412] N86-13732

ANALOG CIRCUITS

Linearity optimization in a class of analog phase modulators
[NASA-TM-86420] N86-13644

ANALOG TO DIGITAL CONVERTERS

Analog-to-Digital converter
[AD-D011878] N86-13660

ANALYSIS (MATHEMATICS)

Discovery of the Kalman filter as a practical tool for aerospace and industry
[NASA-TM-86847] N86-13311

Analytical investigation of the dynamics of tethered constellations in Earth orbit, phase 2
[NASA-CR-171611] N86-13345

Understanding the radiant scattering behavior of vegetated scenes N86-13797

Approximate analytical formulas for computing spectral brightness coefficients for agricultural vegetation N86-14179

ANALYSIS OF VARIANCE
Decomposition of some well-known variance reduction techniques: Revision
[AD-A158048] N86-13985

ANALYTIC FUNCTIONS
Convergence of cardinal series
[AD-A158166] N86-13964

ANALYTICAL CHEMISTRY
Application of computers in analytical chemistry: Calculation of optimum acidity of reaction between metal ions and organic reagents in solution N86-13607

ANALYZERS
Variable temperature trap
[AD-D011874] N86-13719

ANEMOMETERS
Experience in measuring mean wind velocity profile in lower troposphere by sodar anemometer under inversion and convective conditions N86-13782

ANGULAR DISTRIBUTION
Bidirectional reflectance modeling of non-homogeneous plant canopies N86-13796
Geometric-optical modeling of a conifer forest canopy N86-13799
Atmospheric and science complexity effects on surface bidirectional reflectance N86-13803

ANGULAR RESOLUTION
Measurement and modeling of the optical scattering properties of crop canopies N86-13798
Reflection indicatrices of vegetation canopies N86-14178
Analysis of survey conditions and effect of noise on quality of sensing of soil formations N86-14191

ANGULAR VELOCITY
Fiber optics as an angular sensor
[AD-D011886] N86-14044

ANISOTROPY
On anisotropy of mean electrical resistance of beryllium N86-13436
Babinet's principle for an anisotropic resistive surface using different approaches
[AD-A159117] N86-13636
Atmospheric effect on remote sensing of the Earth's surface N86-13804
Microwave dielectric and propagation properties of vegetation canopies N86-13810
Determination of neutron flux distribution by using ANISN, a one-dimensional discrete S sub n ordinates transport code with anisotropic scattering N86-14084

ANNEALING
Preliminary annealing on crystallization of amorphous Fe80Si6B14 alloy N86-13433
Influence of annealing on hardness of vacuum-diffusion chromium coating on low-carbon steel N86-13441
Mechanical properties of EP794 steel + 12Kh18N10T steel bimetal N86-13465
Macro- and microfractographic specifics of dissipated impact rupture of type 45 steel in the viscous-brittle transition interval N86-13466
Subcritical crack development under constant load in VT6 alloy N86-13475
Influence of preliminary annealing on structure and properties of VT23 alloy welded joints after hardening N86-13488

ANNUAL VARIATIONS
Characterization of acid rain phenomena, Atlanta, Georgia
[PB85-216943] N86-13848
Possibilities of using space survey for studying seasonal changes of landscapes in some regions of USSR N86-14183

ANNULI
Test method for telescopes using a point source at a finite distance
[NASA-TM-86523] N86-14033

ANODES
Role of additives in minimizing zinc electrode shape change: The effect of lead on the kinetics of Zn(2) reduction in concentrated alkaline media
[AD-A158806] N86-13395

ANTARCTIC REGIONS
USSR report: Earth sciences
[JPRS-UES-85-009] N86-13765
Volcanoes discovered with radio beam N86-13777
Latitude measurements of cosmic radiation intensity in stratosphere and at sea level on marine antarctic expeditions N86-13792

ANTENNA FEEDS
Cassegrain reflector sidelobe reduction study
[AD-A158625] N86-13631

ANTENNAS
Technique of assembling structures using vapor phase soldering
[AD-D011805] N86-13410
Remote temperature determination of terrestrial covers from polarization invariant of microwave-radiothermal emission N86-14196

ANTHROPOMETRY
Signal processing of anthropometric data N86-14105

ANTIMONY
MBE growth of CdTe and Hg (1-x) Cd (x) Te films and multilayer structures
[AD-A158267] N86-14073

ANVILS
High-pressure, high-temperature opposed anvil device described N86-13606

APERTURES
Experiments with non-Darcy flow in joints with large scale roughness
[DE85-015714] N86-13695
Test method for telescopes using a point source at a finite distance
[NASA-TM-86523] N86-14033

APOLLO SOYUZ TEST PROJECT
Comments on anniversary of Apollo-Soyuz flight N86-14197

APPLICATIONS PROGRAMS (COMPUTERS)
Experiences with Cray multi-tasking
[NASA-TM-88200] N86-13916

APPROACH INDICATORS
An analytical comparison of three visual approach slope indicators: VASIS, T-VASIS and PAPI
[ARL/SYS-R-33] N86-13309

APPROXIMATION
Multiple scattering theories for optical properties of composite materials
[AD-A158270] N86-13379
Spectral methods for discontinuous problems
[NASA-CR-177974] N86-13953
Minimal norm constrained interpolation
[NASA-CR-178001] N86-13956
Uniformly high-order accurate non-oscillatory schemes 1
[AD-A158177] N86-13966
Intrinsic nilpotent approximation
[AD-A158265] N86-13975
Approximation of the initial reserve for known ruin probabilities
[AD-A158167] N86-13987
Aspects of three field approximations: Darwin, frozen, EMPULSE
[DE85-014204] N86-14020
Approximate analytical formulas for computing spectral brightness coefficients for agricultural vegetation N86-14179

AQUATIC PLANTS
Aquatic plant control research program: Evaluation of polymers for controlled delivery of herbicides for aquatic plant control
[AD-A157948] N86-13843

AQUEOUS SOLUTIONS
Evaluation of the erosion protection of low inflammability liquids of the HFC type (polyglycol solutions) --- hydraulic fluids
[CETIM-12-E-13-3] N86-13505
Experimental investigation of heat transfer behavior of aqueous foams in thermal entry region of pipe flow
[DE85-012836] N86-13700

AQUIFERS
Investigation of the vertical-flow aquifer thermal energy storage concept and numerical simulation of the Dorigny field experiment
[DE85-014524] N86-13694

ARC JET ENGINES
Basic processes of plasma propulsion N86-13554

ARC MELTING
Grain growth in heat-resistant austenitic steel N86-13462

ARC WELDING
Study of process of pore formation during argon-arc welding of aluminum alloy 1420 N86-13485
Fusion welding research
[AD-A158253] N86-13736

ARCHITECTURE
Design criteria upgrade for US Army Type 2 air traffic control towers
[AD-A159115] N86-13314

ARCTIC REGIONS
USSR report: Earth sciences
[JPRS-UES-85-009] N86-13765

ARGON
Ion nitriding of titanium N86-13473
Experimental studies of laser-sustained argon plasmas for CW laser propulsion applications N86-13550
Energy deposition of pulsed one micron laser radiation in H2 and AR N86-13552
Equation of state of dense argon: A comparison of shock and static studies
[DE85-015543] N86-14074
Ion bombardment and adsorption studies on ilmenite (FeTiO3) by X-ray photoelectron spectroscopy N86-14100

ARGON PLASMA
Experimental and theoretical studies of laser propulsion phenomenology
[AD-A158273] N86-13729

ARM (ANATOMY)
Passive arm retention curtain
[AD-D011876] N86-13307

ARMED FORCES (FOREIGN)
Investigation of cold colored smoke production
[AD-A158783] N86-14040

ARMED FORCES (UNITED STATES)
Design criteria upgrade for US Army Type 2 air traffic control towers
[AD-A159115] N86-13314

ARRAYS
European silicon structures plans custom chips in 15 days N86-13621
Routing method in computer aided customization of a two level automated universal array
[AD-D011808] N86-13925

ARTIFICIAL INTELLIGENCE
Rectification and registration of remotely sensed data
[AD-A158827] N86-13711
Generating and generalizing models of visual objects
[AD-A158197] N86-13894
Design and implementation of a compliant robot with force feedback and strategy planning software
[NASA-TM-86111] N86-13947
Discovering qualitative empirical laws
[AD-A159235] N86-13951
Codon constraints on closed 2D shapes
[AD-A158744] N86-13979

ASSEMBLING
Technique of assembling structures using vapor phase soldering
[AD-D011805] N86-13410
ATR 42 production work in French, Italian plants detailed N86-13618
Italian robot manufacturer enters Spanish market N86-13625

ASSESSMENTS
Assessment of aerodynamic and dynamic models in a comprehensive analysis
[NASA-TM-86835] N86-13286

ASTEROIDS
Speckle image reconstruction. Appendix 2
[AD-A158272] N86-14208

ASTRODYNAMICS
Some applications of Lie groups in astrodynamics N86-14087
Advanced algorithm for orbit computation N86-14101
Stability of stationary motions of two tethered bodies in orbit under influence of gravitational and aerodynamic forces N86-14163

ASTRONOMICAL COORDINATES
Design for a large altazimuth Schmidt telescope N86-14203

ASTRONOMICAL TELESCOPES
Speckle image reconstruction. Appendix 2
[AD-A158272] N86-14208

ASTRONOMY
A report on the ST ScI optical disk workstation
[NASA-CR-176369] N86-13907
USSR report: Space
[JPRS-USP-85-005] N86-14111

ASTROPHYSICS
Astrophysical payload accommodation on the space station
[NASA-CR-178556] N86-13359

ASYMPTOTIC SERIES
Boundary-value problem for two-dimensional fluctuations in boundary layers
[AD-A157952] N86-13685
A linear combination test for detecting serial correlation in multivariate samples
[AD-A158179] N86-13967
On asymptotic distribution of the test statistic for the mean of the nonisotropic principal component
[AD-A158255] N86-13972

ATLANTA (GA)
Characterization of acid rain phenomena, Atlanta, Georgia
[PB85-216943] N86-13848

ATMOSPHERIC BOUNDARY LAYER
Model interpretation of annual variation of temperature fields of air and water boundary layers of world ocean N86-13767

ATMOSPHERIC CHEMISTRY
Application of quantum chemistry to atmospheric chemistry
[AD-A158282] N86-13856

ATMOSPHERIC CIRCULATION
Wind tunnel simulations of aeolian processes
[NASA-CR-176382] N86-13289
Atmospheric synoptic eddies over ocean (determined from experimental data) N86-13784

Spatial patterns of manifestation of solar activity in troposphere N86-14126
Vega-1 releases aerostat and lander at Venus N86-14148
Further comments on results of Vega studies of Venus N86-14153

ATMOSPHERIC COMPOSITION
Optical/infrared properties of atmospheric aerosols with an in situ, multi-wavelength, multichannel nephelometer system
[AD-A158825] N86-13710
Investigation of nonlinear spectroscopic effects in interaction between CO2-laser radiation and atmospheric gases N86-13789
The characterization of surface varigation effects on remote sensing N86-13805
The influence of oceanic chemistry, physics and biology on atmospheric carbon dioxide N86-13865

ATMOSPHERIC CORRECTION
Discrete random media techniques for microwave modeling of vegetated terrain N86-13809

ATMOSPHERIC DENSITY
A tomographic technique for aerodynamics at transonic speeds
[NASA-TM-86766] N86-13297

ATMOSPHERIC EFFECTS
Erosion and onset mechanisms in magnetoplasmadynamic thrusters N86-13556
Fundamental remote sensing science research program: The Scene Radiation and Atmospheric Effects Characterization Project
[E86-10011] N86-13794
Reflectance modeling N86-13795
Bidirectional reflectance modeling of non-homogeneous plant canopies N86-13796
Ground reflectance measurements from thematic mapper data N86-13801
Atmospheric and science complexity effects on surface bidirectional reflectance N86-13803
Atmospheric effect on remote sensing of the Earth's surface N86-13804
The characterization of surface varigation effects on remote sensing N86-13805
Multidimensional modeling of atmospheric effects and surface heterogeneities on remote sensing N86-13806

ATMOSPHERIC IONIZATION
Disturbances in stratosphere and mesosphere from source of ultraviolet radiation N86-14136

ATMOSPHERIC LASERS
Effectiveness of use of adaptive optical systems under conditions of self-effect in atmosphere N86-13791

ATMOSPHERIC MODELS
Atmospheric radio noise: Worldwide levels and other characteristics
[PB85-212942] N86-13639
Understanding climate: A strategy for climate modeling and predictability research, 1985-1995
[NASA-RP-1158] N86-13866

ATMOSPHERIC OPTICS
Distribution of brightness from point source of scattered light along inclined path N86-13779
Statistics of intensive light beams in turbulent atmosphere N86-13786
Interaction between powerful laser radiation and atmospheric aerosols N86-13788
Effectiveness of use of adaptive optical systems under conditions of self-effect in atmosphere N86-13791
Methods for constructing atmospheric optical transfer operator N86-14185
Analysis of survey conditions and effect of noise on quality of sensing of soil formations N86-14191

ATMOSPHERIC PHYSICS
USSR report: Earth sciences
[JPRS-UES-85-009] N86-13765

ATMOSPHERIC PRESSURE
Combustion behavior of free boron slurry droplets
[AD-A158620] N86-13585
The influence of oceanic chemistry, physics and biology on atmospheric carbon dioxide N86-13865
Pressure field retrieval by remote refractometry from space N86-14168

ATMOSPHERIC REFRACTION
Mathematical analysis study for radar data processing and enhancement. Part 1: Radar data analysis
[NASA-CR-166616-PT-1] N86-13353
Mathematical analysis study for radar data processing and enchancement. Part 2: Modeling of propagation path errors
[NASA-CR-166616-PT-2] N86-13354
Pressure field retrieval by remote refractometry from space N86-14168

ATMOSPHERIC SOUNDING
Experience in measuring mean wind velocity profile in lower troposphere by sodar anemometer under inversion and convective conditions N86-13782
New methods for laser sounding of atmosphere on basis of nonlinear effects N86-13787
VAS demonstration: (VISSR Atmospheric Sounder) description
[NASA-RP-1151] N86-13867

ATMOSPHERIC TEMPERATURE
Model interpretation of annual variation of temperature fields of air and water boundary layers of world ocean N86-13767

ATMOSPHERICS
Atmospheric radio noise: Worldwide levels and other characteristics
[PB85-212942] N86-13639

ATOMIC COLLISIONS
Reactive scattering in the bending-corrected rotating linear model
[DE85-017539] N86-14018

ATOMIC ENERGY LEVELS
Two-proton detection techniques for atomic fluorine N86-13569

ATOMIC EXCITATIONS
Two-proton detection techniques for atomic fluorine N86-13569
Application of atomic fluorescence to measurement of combustion temperatures in solid propellants N86-13582
Magnetic field determination in quiescent solar prominences from polarization characteristics of radiated light N86-14125

ATOMIC RECOMBINATION
Mass loss of shuttle space suit orthofabric under simulated ionospheric atomic oxygen bombardment
[NASA-TM-87149] N86-13899

ATOMIC SPECTRA
Nutritional characteristics of moon dust for soil microorganisms N86-14086
Scientific activities of the Polish Academy of Sciences: Institute of Fundamental Technological Research in 1983
[ISBN-83-01-06288-6] N86-14107

ATOMIZING
Specialists Meeting on Atomization and Nondilute Sprays
[AD-A159006] N86-13634

ATTENUATION
Expendable bathythermograph for measuring light attenuation and temperature below the ocean surface
[AD-D011870] N86-13716

ATTENUATION COEFFICIENTS
Microwave dielectric and propagation properties of vegetation canopies N86-13810

ATTITUDE CONTROL
Pitch rate versus G command as the longitudinal flight control system design strategy for a statistically unstable fighter type aircraft with two control surfaces
[AD-A158803] N86-13334
Computer program for post-flight evaluation of the control surface response for an attitude controlled missile
[NASA-CR-166032] N86-13920

AUGER SPECTROSCOPY
Electronic detection of low concentrations of organophosphorus compounds with a solid state device utilizing supported copper + cuprous oxide island films
[AD-A158181] N86-13392
AuGa2 on GaSb(001): An epitaxial, thermodynamically stabilized Metal/3-5 compound semiconductor interface
[AD-A157937] N86-14071

AURORAL ZONES
Registry of heavy ions in auroral region during magnetic storms N86-14138
Small-scale structure of intensive longitudinal currents in high latitudes N86-14139

AUSTENITE
Specifics of the process of failure of structural steels strengthened by thermo-mechanical working with deformation in the intercritical temperature interval N86-13464

AUSTENITIC STAINLESS STEELS
Grain growth in heat-resistant austenitic steel N86-13462

AUTOMATIC CONTROL
Robot control system modified for precision movement N86-13747
New robots by Soviet, CEMA manufacturers described N86-13748
Goskomgidromet plans automation of aerial cloud-seeding work N86-13766

AUTOMATION
Alerted monitors: Human operators aided by automated detectors
[PB85-222750] N86-13906

AUTOMOBILES
West Europe report: Science and technology
[JPRS-WST-85-030] N86-13610
West Europe report: Science and technology
[JPRS-WST-85-031] N86-13616
West Europe report: Science and technology
[JPRS-WST-85-029] N86-13622
New materials to lighten vehicles N86-13624

AUTOREGRESSIVE PROCESSES
A linear combination test for detecting serial correlation in multivariate samples
[AD-A158179] N86-13967
Methodology for stochastic modeling
[AD-A158851] N86-13984

AXISYMMETRIC BODIES
Computerized simulation and display of extruding by cold forging
[CETIM-1-3L-11-1] N86-13741
Integration of equations of motion for material point in gravitational field of axially symmetric planet N86-14131

AZIDES (ORGANIC)
Electrolytic preparation of novel azidodinitro compounds N86-13508
Synthesis and reactivity of unsaturated metal nitrogen complexes N86-13512
Fluoropolyazido-esters as energetic polymers N86-13515
Fundamental studies of azide decomposition and combustion N86-13534

AZIMUTH
Occasional reports of the Royal Observatory, Edinburgh, no. 16
[ISSN-0309-099-X] N86-14200
Design for a large altazimuth Schmidt telescope N86-14203

B

BACKGROUND RADIATION
Hard gamma radiation background from coding collimator of gamma telescope under space experiment conditions N86-14123

BACKSCATTERING
Radar location equipment development program, phase 1
[DE85-014523] N86-13637
Fundamental remote sensing science research program: The Scene Radiation and Atmospheric Effects Characterization Project
[E86-10011] N86-13794
Bidirectional reflectance modeling of non-homogeneous plant canopies N86-13796
Understanding the radiant scattering behavior of vegetated scenes N86-13797
Discrete random media techniques for microwave modeling of vegetated terrain N86-13809
Microwave dielectric and propagation properties of vegetation canopies N86-13810
Determination of backscattering sources in various targets N86-13811
Active microwave properties of vegetation canopies N86-13812
Acoustical scattering from an elastic sphere in water: Surface wave glory, resonances, and the Sommerfeld-Watson transformation for amplitudes
[AD-A158884] N86-14010
AuGa2 on GaSb(001): An epitaxial, thermodynamically stabilized Metal/3-5 compound semiconductor interface
[AD-A157937] N86-14071

BACTERIA
New physical methods for biological aerosol detection
[AD-A158218] N86-13881

BALANCE
HPOTP low-speed flexible rotor balancing, phase 1
[NASA-CR-171610] N86-13369

BANACH SPACE
Continuity of certain random integral mappings and the uniform integrability of infinitely divisible measures
[AD-A159105] N86-13995
Analysis of the dynamic behavior of an intense charged particle beam using the semigroup approach
[AD-A159247] N86-14015

BANDPASS FILTERS
Slot line tunable bandpass filter
[AD-D011881] N86-13661

BAROCLINIC INSTABILITY
Spatial patterns of manifestation of solar activity in troposphere N86-14126

BARRIERS
Determination of the activation barrier to energy transfer from 3 pi pi* to charge transfer levels via steady state and transient luminescence measurements on Bis(4-Chlorothiophenol) (1,10-Phenanthroline) Zinc (II)
[AD-A158239] N86-14012

BATHYMETERS
Aerial laser sensing of ocean upper layer N86-13775

BATHYTHERMOGRAPHS
Expendable bathythermograph for measuring light attenuation and temperature below the ocean surface [AD-D011870] N86-13716

BAYES THEOREM
Identification of nuclear materials from remote detection of characteristic gamma rays [AD-A159244] N86-14014

BEACHES
The design of a beach profiler [AD-A157715] N86-13874

BEADS
Fabrication and evaluation of superplastically formed/weld-brazed corrugated compression panels with beaded webs [NASA-TP-2512] N86-13406

BEAM CURRENTS
Scheme to funnel ion beams with a radio-frequency quadrupole [DE85-015689] N86-14016

BEAM INJECTION
Collective ion acceleration by means of virtual cathodes [DE85-012707] N86-14019
Preliminary experiment on electron beam injection for tokamak current drive [IPPJ-739] N86-14048
Generation and acceleration of high intensity beams in the SLC injector [DE85-013056] N86-14066
Radio emission of injected electron beam with respect to diagnosis of ionospheric plasma N86-14145

BEAMS (RADIATION)
Metastable interactions: Dissociative excitation [AD-A158733] N86-14013

BEAMS (SUPPORTS)
Long-term analysis of slender concrete structures with cracking [DE85-010275] N86-13762

BEARING (DIRECTION)
Enhancing sensitivity to visual motion and enhancing visual sensitivity [AD-A158800] N86-13889

BEDS
Elution of benzene and methyl ethyl ketone from charcoal beds by continued air sweeping [AD-A158804] N86-13374

BEHAVIOR
Effects of 60 Hz electric fields on operant and social stress behaviors of nonhuman primates [DE85-011982] N86-13885

BENDING
Long-term analysis of slender concrete structures with cracking [DE85-010275] N86-13762

BENZENE
Elution of benzene and methyl ethyl ketone from charcoal beds by continued air sweeping [AD-A158804] N86-13374
Reaction intermediates in aromatic fuel combustion [AD-A158029] N86-13390

BERYLLIUM
USSR report: Materials science and metallurgy [JPRS-UMS-85-006] N86-13422
On anisotropy of mean electrical resistance of beryllium N86-13436

BESS (SATELLITE)
Life sciences accomplishments [NASA-TM-88177] N86-13879

BETA FACTOR
Doublet 3 [DE85-014369] N86-14031

BIAS
Mathematical analysis study for radar data processing and enchancement. Part 2: Modeling of propagation path errors [NASA-CR-166616-PT-2] N86-13354
Electronic detection of low concentrations of organophosphorus compounds with a solid state device utilizing supported copper + cuprous oxide island films [AD-A158181] N86-13392

BIMETALS
Mechanical properties of EP794 steel + 12Kh18N10T steel bimetal N86-13465
Diffusion welding of copper-chromium pseudoalloy with copper N86-13493

BINARY ALLOYS
Muon spin relaxation study of exchange coupling in dilute AgMn alloys [DE85-014104] N86-13419
Influence of sodium on mechanical and casting properties of magnesium-lithium alloys N86-13457
Atomically mixed alloy coated cathodes specification [AD-D011877] N86-13659

BINARY MIXTURES
A study of transport phenomena and interface stability during solidification of binary solutions using front tracking finite elements N86-13669

BINARY STARS
Speckle image reconstruction. Appendix 2 [AD-A158272] N86-14208

BINARY SYSTEMS (MATERIALS)
Critical behavior of thermoelectric power in binary composite materials N86-13448
Ceramics based on aluminum nitride and metals N86-13456

BINDERS (MATERIALS)
Theory of pyrolysis of composite polymer materials N86-13447

BIOCHEMISTRY
Functionalized vesicles as organic reagents [AD-A158381] N86-13372
Design, construction and testing of a dc bioeffects enclosure for small animals [DE05-016798] N86-13883

BIOINSTRUMENTATION
New physical methods for biological aerosol detection [AD-A158218] N86-13881

BIOLOGICAL EFFECTS
Design, construction and testing of a dc bioeffects enclosure for small animals [DE05-016798] N86-13883
Effects of 60 Hz electric fields on operant and social stress behaviors of nonhuman primates [DE85-011982] N86-13885

BIOLOGICAL EVOLUTION
Life sciences accomplishments [NASA-TM-88177] N86-13879

BIOMASS
Microwave dielectric and propagation properties of vegetation canopies N86-13810
Crop area estimation based on remotely-sensed data with an accurate but costly subsample [NASA-CR-176017] N86-13814

BIOMEDICAL DATA
Life sciences accomplishments [NASA-TM-88177] N86-13879

BIOPHYSICS
Active microwave properties of vegetation canopies N86-13812
European Science Notes, Volume 39, Number 7 [AD-A157708] N86-14108

BIOSPHERE
Life sciences accomplishments [NASA-TM-88177] N86-13879

BIOTECHNOLOGY
West Europe report: Science and technology [JPRS-WST-85-030] N86-13610
West Europe report: Science and technology [JPRS-WST-85-031] N86-13616
West Europe report: Science and technology [JPPS-WST-85-029] N86-13622

BIPOLAR TRANSISTORS
Numerical modeling of carrier transport in submicron bipolar transistors N86-13642

BLADE TIPS
An analytical theory for rotor tip vane performance and comparison with experimental results — wind energy converters N86-13823

BLOOD CIRCULATION
The effect of spironolactone on the cardiocirculatory responses to upright tilt at sea level and at simulated high altitude [AD-A157734] N86-13887

BODY FLUIDS
Endocrine and fluid metabolism in males and females of different ages after bedrest, acceleration and lower body negative pressure [NASA-TM-58270] N86-13886

BODY WEIGHT
Health hazard evaluation of liquid monopropellants. Phase 5: Comparative inhalation toxicities of LGP 1776, LGP 1845, and HAN (hydroxylammonium nitrate) [AD-A159090] N86-13891

BOEING 737 AIRCRAFT
A preliminary evaluation of the generalized likelihood ratio for detecting and identifying control element failures in a transport aircraft [NASA-TM-87620] N86-13332

BOLOMETERS
Focal plane optics in far-infrared and submillimeter astronomy [NASA-TM-88166] N86-14204

BOLTZMANN TRANSPORT EQUATION
Transient simulation of submicron devices [AD-A157748] N86-13648
Effects of neutrals on internal forces and thermal conduction of a plasma in a magnetic field [IPPJ-691] N86-14051
Determination of neutron flux distribution by using ANISN, a one-dimensional discrete S sub n ordinates transport code with anisotropic scattering N86-14084

BOMBS (ORDNANCE)
Investigation of cold colored smoke production [AD-A158783] N86-14040

BONDING
Study of properties of gas-thermal coatings of composite nichrome-aluminum alloy powders N86-13442

BOOLEAN ALGEBRA
A behavioral summary for completely random nets [AD-A157755] N86-13960

BORIDES
Durability of steel 45 with boride coating in corrosive-abrasive media N86-13467

BORON
Physical and chemical consequences of antiaromaticity in the boracyclopentadiene system N86-13519
Fuel-rich solid propellant boron combustion N86-13536
Combustion behavior of free boron slurry droplets [AD-A158620] N86-13585

BORON ALLOYS
Preliminary annealing on crystallization of amorphous Fe80Si6B14 alloy N86-13433
Influence of chromium on crystallization of amorphous Fe-B alloys N86-13434

BORON FIBERS
Elastic-plastic deformation of a metal-matrix composite coupon with a center slot [NASA-CR-178013] N86-13496

BORON NITRIDES
Superhard materials developed N86-13471

BOUNDARIES
A functional equation governing moving phase boundaries in an elastic bar [AD-A158178] N86-13757
Minimal norm constrained interpolation [NASA-CR-178001] N86-13956
Boundary integral techniques for multi-connected domains [AD-A158171] N86-13965

BOUNDARY LAYER CONTROL
Ground vibration test of the laminar flow control JStar airplane [NASA-TM-86396] N86-13321

BOUNDARY LAYER FLOW
Studies of the flow field near a NACA 4412 aerofoil at nearly maximum lift [AD-A157750] N86-13301

BOUNDARY LAYER SEPARATION
Studies of the flow field near a NACA 4412 aerofoil at nearly maximum lift [AD-A157750] N86-13301

BOUNDARY LAYER STABILITY
Waves which travel upstream in boundary layers [AD-A157949] N86-13684
Boundary-value problem for two-dimensional fluctuations in boundary layers [AD-A157952] N86-13685

BOUNDARY LAYER TRANSITION
Recent experience in the RAE (Royal Aircraft Establishment) 5-metre wind tunnel of a china clay method for indicating boundary layer transition [AD-A157943] N86-13302
Numerical simulations of asymmetric mixing in planar shear flows [AD-A158024] N86-13687

BOUNDARY LAYERS
Study of deposition control using transpiration [DE85-012790] N86-13699

BOUNDARY VALUE PROBLEMS
Waves which travel upstream in boundary layers [AD-A157949] N86-13684
Boundary-value problem for two-dimensional fluctuations in boundary layers [AD-A157952] N86-13685
Far-field boundary conditions in numerical solutions of the Navier-Stokes equations [AD-A158776] N86-13690
Stable boundary conditions and difference schemes for Navier-Stokes equations [NASA-CR-177984] N86-13957
Uniformly high-order accurate non-oscillatory schemes 1 [AD-A158177] N86-13966
Current methods for large stiff ODE systems [DE85-012914] N86-13963
Choice of optimum boundary conditions in speed optimization problem N86-14115

BRAIN
The event related brain potential as an index of information processing, cognitive activity, and skill acquisition: A program of basic research [AD-A159118] N86-13897

BRAZING
Fabrication and evaluation of superplastically formed/weld-brazed corrugated compression panels with beaded webs
[NASA-TP-2512] N86-13496

BREADBOARD MODELS
Development of a breadboard cooler for infrared remote sensing payloads, phase 2 — spacecraft payloads
[FOK-RV-R-82-072] N86-13725
The construction and testing of a real-time digital breadboard processor for the ESA remote sensing satellite synthetic aperature radar
[REPT-00-0778] N86-13911

BREAKING
Laboratory studies of steep and breaking deep water waves in a convergent channel
[AD-A158167] N86-13875

BREMSSTRAHLUNG
MeV electron beam irradiation effects on GaAs (1-x) P (x) LEDs (Light emitting diodes)
[AD-A158832] N86-13863

BRIGHTNESS
Approximate analytical formulas for computing spectral brightness coefficients for agricultural vegetation
N86-14179
Method for using clusters in evaluating land use areas from multizonal photographs N86-14180
Analysis of survey conditions and effect of noise on quality of sensing of soil formations N86-14191

BRIGHTNESS DISTRIBUTION
Distribution of brightness from point source of scattered light along inclined path N86-13779
Influence of fog microstructure on quality of optical image transmitted through it N86-13781
Geometric-optical modeling of a conifer forest canopy
N86-13799
Use of Goudriaan model for studying reflection regularities in vegetation-soil system in optical range. 1: Influence of phytometric parameters on spectral brightness coefficients N86-14190
Radiometric correction of materials of aerospace survey of Earth with MKF-6 camera: Methodology and use of results N86-14193
Remote temperature determination of terrestrial covers from polarization invariant of microwave-radiothermal emission N86-14196

BRIGHTNESS TEMPERATURE
Application of statistical model of layered medium for computing thermal emission of ice covers N86-14186

BRITTLENESS
Effect of elastoplastic cyclic deformation on mechanical characteristics of steel O3Kh13AG19 at temperatures of 293 and 77 deg K N86-13463
Macro- and microfractographic specifics of dissipated impact rupture of type 45 steel in the viscous-brittle transition interval N86-13466
Dispersion hardening of high-strength NiOCo-Mo steels N86-13468

BROADBAND
Report on an automated calibration range for broadband isotropic probes
[PB85-231470] N86-13726

BROWNIAN MOVEMENTS
Effective behavior of composite materials
[AD-A158941] N86-13380
Single particle sizing by measurement of Brownian motion N86-13584

BRUSHES
Electrical sliding joint literature review (viewgraph presentation)
[DE85-011571] N86-13666

BUBBLES
Light scattering from bubbles in liquids
[AD-A158736] N86-14039

BUNCHING
Scheme to funnel ion beams with a radio-frequency quadrupole
[DE85-015669] N86-14016

BURNERS
Determination of convective diffusion heat/mass transfer rates to burner rig test targets comparable in size to cross-stream jet diameter
[NASA-TM-87176] N86-13678

BURNING RATE
Wide distribution propellants N86-13540

BUTANES
Critical charge for the direct initiation of detonation in gaseous fuel-air mixtures
[DE85-016130] N86-13896

C

C-140 AIRCRAFT
Ground vibration test of the laminar flow control JStar airplane
[NASA-TM-86398] N86-13321

CADMIUM SULFIDES
Development of stable high efficiency polycrystalline thin-film solar cells based on CuInSe2
[DE85-000517] N86-13837

CADMIUM TELLURIDES
Development of stable high efficiency polycrystalline thin-film solar cells based on CuInSe2
[DE85-000517] N86-13837

CALCIUM
Cathode for use in high energy primary thionyl chloride cell systems and high energy primary thionyl chloride cell systems including the cathode
[AD-D011862] N86-13562

CALIBRATING
Experimental investigation of magnesium combustion in steam
[AD-A159109] N86-13396
Discussion on the Vibration Process Standards 9958002 and 9958004
[DE85-017116] N86-13599
A note on the effect of ignoring small measurement errors in precision instrument calibration
[AD-A159104] N86-13713
Report on an automated calibration range for broadband isotropic probes
[PB85-231470] N86-13726
Determining flexure of aerial camera smoothing glass
N86-14169
Speckle image reconstruction. Appendix 2
[AD-A158272] N86-14208

CALIFORNIA
California Water Resources Institute program for 1983
[PB85-225837] N86-13818

CAMERAS
Determining flexure of aerial camera smoothing glass
N86-14169

CAMS
Radar location equipment development program, phase 1
[DE85-014523] N86-13637

CANOPIES (VEGETATION)
Reflectance modeling N86-13795
Bidirectional reflectance modeling of non-homogeneous plant canopies N86-13796
Understanding the radiant scattering behavior of vegetated scenes N86-13797
Measurement and modeling of the optical scattering properties of crop canopies N86-13798
Geometric-optical modeling of a conifer forest canopy
N86-13799
Crop characteristics research: Growth and reflectance analysis N86-13800
Atmospheric and science complexity effects on surface bidirectional reflectance N86-13803
Multidimensional modeling of atmospheric effects and surface heterogeneities on remote sensing N86-13806
Remote sensing of Earth terrain N86-13808
Discrete random media techniques for microwave modeling of vegetated terrain N86-13809
Microwave dielectric and propagation properties of vegetation canopies N86-13810
Determination of backscattering sources in various targets N86-13811
Active microwave properties of vegetation canopies
N86-13812
Computation of reflection of solar radiation from vegetation cover by Monte-Carlo method N86-14177
Reflection indicatrices of vegetation canopies
N86-14178
Approximate analytical formulas for computing spectral brightness coefficients for agricultural vegetation
N86-14179

CARBIDES
Mechanical properties of EP794 steel + 12Kh18N10T steel bimetal N86-13465
Dispersion hardening of high-strength NiOCo-Mo steels N86-13468

CARBON
Physical and chemical consequences of antiaromaticity in the boracyclopentadiene system N86-13519
Development of a carbon formation reactor for carbon dioxide reduction
[NASA-CR-171907] N86-13898

CARBON DIOXIDE
Precision pointing using a dual-wedge scanner
[NASA-CR-3946] N86-13813
Development of a carbon formation reactor for carbon dioxide reduction
[NASA-CR-171907] N86-13898

CARBON DIOXIDE CONCENTRATION
Influence of petroleum pollution on ocean-atmosphere gas exchange intensity (in example of North Atlantic)
N86-13785
The influence of oceanic chemistry, physics and biology on atmospheric carbon dioxide N86-13865

CARBON DIOXIDE LASERS
Extremely high reflective capability of zirconium burning in air under effects of constant CO2 laser radiation
N86-13452
Investigation of nonlinear spectroscopic effects in interaction between CO2-laser radiation and atmospheric gases N86-13789

CARBON DISULFIDE
Temperature and pressure components of shock-induced changes in the electronic spectrum of carbon disulfide
[AD-A158627] N86-13373

CARBON FIBER REINFORCED PLASTICS
Standardization program on design analysis and testing of inserts in nonmetallic sandwich components — spacecraft components
[TR-TS-RP-2-09-84] N86-13364
Study of the mechanical properties dispersion of carbon-epoxy composite materials
[M2-695600-PT-1] N86-13384
Study of the dispersion of the mechanical properties of carbon-epoxy composite materials
[M2-695600-PT-2] N86-13385
Employment of PAM-FISS-BI-phase computer program for the strength analysis and fracture/delamination behavior of components
[ESI-ED/83-383/RD/MS-VOL-7] N86-13763

CARBON FIBERS
Effect of carbon fibre surface treatment on moisture absorption and interlaminar shear strength of carbon Fibre/Epoxy resin composites
[AD-A157705] N86-13377

CARBON MONOXIDE
The dynamics of the photofragmentation of ketene 3-cyclopentenone, 3,5-cycloheptadienone, and tropone
[AD-A158045] N86-13371
Studies of metal/carbon surface chemistry
[DE85-015548] N86-13398
Condensed matter at high shock pressures
[DE85-016443] N86-13399

CARBON MONOXIDE LASERS
Reaction intermediates in aromatic fuel combustion
[AD-A158029] N86-13390

CARBON-CARBON COMPOSITES
Effect of carbon fibre surface treatment on moisture absorption and interlaminar shear strength of carbon Fibre/Epoxy resin composites
[AD-A157705] N86-13377

CARCINOTRONS
The development of a submillimeter wave carcinotron operating in the frequency range from 850 to 1000 GHz
[TDH-RT-2963-T] N86-13638

CARDIOVASCULAR SYSTEM
The effect of spironolactone on the cardiocirculatory responses to upright tilt at sea level and at simulated high altitude
[AD-A157734] N86-13887

CARDS
Latch for detachably securing electronic cards along orthogonal loading axes
[AD-D011885] N86-13737

CARRIER MOBILITY
Positron diffusion in Si
[DE85-014831] N86-14076

CARTESIAN COORDINATES
Italian robot manufacturer enters Spanish market
N86-13626

CARTRIDGES
Investigation of cold colored smoke production
[AD-A158783] N86-14040

CASCADE FLOW
A FORTRAN computer code for calculating flows in multiple-blade-element cascades
[NASA-TM-87104] N86-13295

CASSEGRAIN ANTENNAS
Cassegrain reflector sidelobe reduction study
[AD-A158625] N86-13631

CAST ALLOYS
Study of fractures in cast parts of high-strength aluminum alloy N86-13429

CASTING
Structure and properties of Al-Mg-Zn casting alloys
N86-13425

CATHODE RAY TUBES
Computer graphics applications to crew displays
N86-14104

CATHODES
A study of rhenium as an alternate substrate material for impregnated dispenser cathodes
[AD-A159113] N86-13415

Oxide electrodes at high temperatures
[DE85-006564] N86-13667
Collective ion acceleration by means of virtual cathodes
[DE85-012707] N86-14019

CAUCHY PROBLEM
Decay with a rate for noncompactly supported solutions of conservation laws
[AD-A158163] N86-13962
A note on the integrated Cauchy functional equation
[AD-A158269] N86-13977
Analysis of the dynamic behavior of an intense charged particle beam using the semigroup approach
[AD-A159247] N86-14015

CAVITY RESONATORS
Slot line tunable bandpass filter
[AD-D011881] N86-13661

CEILINGS (METEOROLOGY)
Meteorological and climatological conditions affecting the vertical structure of visibility in northern Germany
[AD-A158254] N86-13871

CELESTIAL MECHANICS
Forming transformation matrices for different parameters of motion of celestial bodies N86-14112
Structure of coefficients of series representing solution of plane circular restricted three-body problem
N86-14129
Integration of equations of motion for material point in gravitational field of axially symmetric planet
N86-14131

CELESTIAL REFERENCE SYSTEMS
Design for a large altazimuth Schmidt telescope
N86-14203

CELL CATHODES
Cathode including a non fluorinated linear chain polymer as the binder, method of making the cathode, and lithium electrochemical cell containing the cathode
[AD-D011807] N86-13647
Cathode for use in high energy primary thionyl chloride cell systems and high energy primary thionyl chloride cell systems including the cathode
[AD-D011882] N86-13662

CELLS
Temperature and pressure components of shock-induced changes in the electronic spectrum of carbon disulfide
[AD-A158627] N86-13373

CELLS (BIOLOGY)
New physical methods for biological aerosol detection
[AD-A158218] N86-13881

CERAMIC COATINGS
A durable airfield marking system
[AD-A157953] N86-13339

CERAMIC MATRIX COMPOSITES
Polymer, metal and ceramic matrix composites for advanced aircraft engine applications
[NASA-TM-87132] N86-13407
Preparation of ceramic fiber-ceramic matrix composites by a faster chemical vapor infiltration process
[DE85-016402] N86-13500

CERAMICS
Zirconium as a structural material for naval systems
[AD-A158201] N86-13411
USSR report: Materials science and metallurgy
[JPRS-UMS-85-006] N86-13422
Conductivity of metal-ceramic multilayer ZrO2-Mo and Mo-based composite materials N86-13444
Ceramics based on aluminum nitride and metals
N86-13456
Analytical electron microscopy of surface modified ceramics
[DE85-016309] N86-13499
Preparation of ceramic fiber-ceramic matrix composites by a faster chemical vapor infiltration process
[DE85-016402] N86-13500
Ceramic fabric material testing
[DE85-013684] N86-13503
West Europe report: Science and technology
[JPRS-WST-85-031] N86-13616
Probability of detection of internal voids in structural ceramics using microfocus radiography
[NASA-TM-87164] N86-13749

CERENKOV RADIATION
Cerenkov radiation from periodic bunches for a finite path in air
[AD-A159027] N86-13635

CERMETS
Multiple scattering theories for optical properties of composite materials
[AD-A158270] N86-13379
Ceramics based on aluminum nitride and metals
N86-13456

CESIUM
Close-space, high temperature Knudsen flow
N86-13568

CHANNEL FLOW
User's manual for the generalized computer program system. Open-channel flow and sedimentation, TABS-2. Main text
[AD-A159249] N86-13692

CHAPMAN-ENSKOG THEORY
Electrical and electrothermal conductivity of planetary ionospheres, 1: Refinement of theory N86-14143

CHARACTERIZATION
Characterization of 7017 aluminum alloys in thick profiles, in the metallurgical versions T6510, T76510 and T736510, test report no. PV-44-607/F
[PV-44-607/F] N86-13420

CHARCOAL
Elution of benzene and methyl ethyl ketone from charcoal beds by continued air sweeping
[AD-A158804] N86-13374

CHARGE TRANSFER
Relationships between electronic spectroscopy and electrochemistry. A probe of reorganisation energies
[AD-A157940] N86-13389
Micromechanisms of electrodiffusion failures in thin film metallization N86-13472
Determination of the activation barrier to energy transfer from 3 pi pi* to charge transfer levels via steady state and transient luminescence measurements on Bis(4-Chlorothiophenol) (1,10-Phenanthroline) Zinc (II)
[AD-A158239] N86-14012
Effects of neutrals on internal forces and thermal conduction of a plasma in a magnetic field
[IPPJ-691] N86-14051

CHARGED PARTICLES
Analysis of the dynamic behavior of an intense charged particle beam using the semigroup approach
[AD-A159247] N86-14015
Unlimited acceleration of charged particles by an electromagnetic wave with a purely transverse electric field propagating perpendicularly to a static magnetic field
[IPPJ-740] N86-14049

CHARTS
Uniformly high-order accurate non-oscillatory schemes 1
[AD-A158177] N86-13966

CHELATES
Application of computers in analytical chemistry: Calculation of optimum acidity of reaction between metal ions and organic reagents in solution N86-13607
Determination of the activation barrier to energy transfer from 3 pi pi* to charge transfer levels via steady state and transient luminescence measurements on Bis(4-Chlorothiophenol) (1,10-Phenanthroline) Zinc (II)
[AD-A158239] N86-14012

CHEMICAL ANALYSIS
Particulate matter analysis by electron microscopy
[PB85-227817] N86-13846
Characterization of acid rain phenomena, Atlanta, Georgia
[PB85-216943] N86-13848
Design, construction and testing of a dc bioeffects enclosure for small animals
[DE05-016798] N86-13883

CHEMICAL BONDS
No chemisorption on Ni(111): Coverage effects, site preferences and adsorption geometry
[AD-A159110] N86-13397
Physical and chemical consequences of antiaromaticity in the boracyclopentadiene system N86-13519

CHEMICAL COMPOSITION
Highly disperse minerals in sediments in neighborhood of East Pacific Ocean rise determined from drilling data
N86-13773
Molecular mechanisms of mutagenesis determined by the recombinant DNA technology
[DE85-016353] N86-13884
Nutritional characteristics of moon dust for soil microorganisms N86-14086

CHEMICAL PROPERTIES
Sorption detector system for chemical agents detection and recognition
[DE85-012775] N86-13400
Synthesis and reactivity of unsaturated metal nitrogen complexes N86-13512

CHEMICAL PROPULSION
Performance-limiting factors in MPD thrusters
N86-13555

CHEMICAL REACTION CONTROL
Control of the urethane cure reaction with solid, blocked isocyanates N86-13518

CHEMICAL REACTIONS
Synthesis and reactivity of unsaturated metal nitrogen complexes N86-13512
Application of computers in analytical chemistry: Calculation of optimum acidity of reaction between metal ions and organic reagents in solution N86-13607

CHEMILUMINESCENCE
High pressure solid propellant combustion zone structure from analysis of hydroxyl radical chemiluminescence N86-13529

CHEMISORPTION
No chemisorption on Ni(111): Coverage effects, site preferences and adsorption geometry
[AD-A159110] N86-13397

CHINA
Recent experience in the RAE (Royal Aircraft Establishment) 5-metre wind tunnel of a china clay method for indicating boundary layer transition
[AD-A157943] N86-13302
China report: Science and technology
[JPRS-CST-85-020] N86-13600

CHIPS (ELECTRONICS)
On H plane dielectric loading theory for H plane ferrite phase shifter N86-13603
CNET of France uses organo-metallic epitaxy for laser
N86-13620
European silicon structures plans custom chips in 15 days N86-13621
An integrated wavelength demultiplexer
[AD-D011867] N86-14041

CHIRP SIGNALS
Feasibility study of chirp generator for ERS-1 radar altimeter, option A
[ELAB-STF44-F83103] N86-13368

CHROMIUM
Influence of chromium on crystallization of amorphous Fe-B alloys N86-13434
Influence of Co-Cr-Al-Y coatings on physical and mechanical properties of EI-893 steel in GT-100 turbine drive vanes N86-13438
Influence of annealing on hardness of vacuum-diffusion chromium coating on low-carbon steel N86-13441
Diffusion welding of copper-chromium pseudoalloy with copper N86-13493

CHROMIUM ALLOYS
Current viewpoints on oxide adherence mechanisms
[NASA-TM-87168] N86-13409
Complex nickel-aluminide coatings on nickel-chromium alloy EP648-VI N86-13437

CIRCUIT BOARDS
Thomson semiconductors introduces products, balances books N86-13615

CIRCUITS
Thomson, CNET of France in silicon-on-insulator research N86-13612
Two-hundred to 300 KVA conditioned power system - development, phase 1
[AD-A158820] N86-13832

CIRCULAR ORBITS
Structure of coefficients of series representing solution of plane circular restricted three-body problem
N86-14129

CIRCULATION
Gas recirculator for acyclic machines
[AD-D011873] N86-13658

CITIES
Characterization of acid rain phenomena, Atlanta, Georgia
[PB85-216943] N86-13848

CIVIL AVIATION
West Europe report: Science and technology
[JPRS-WST-85-030] N86-13610
West Europe report: Science and technology
[JPRS-WST-85-031] N86-13616
Certification granted to Franco-Italian ATR 42
N86-13617
ATR 42 production work in French, Italian plants detailed N86-13618

CLADDING
Mechanical properties of EP754 steel + 12Kh18N10T steel bimetal N86-13465

CLAYS
Recent experience in the RAE (Royal Aircraft Establishment) 5-metre wind tunnel of a china clay method for indicating boundary layer transition
[AD-A157943] N86-13302
The Vaiont Slide. A geotechnical analysis based on new geologic observations of the failure surface. Volume 1: Main text
[AD-A158192] N86-13854

CLIMATE
Meteorological and climatological conditions affecting the vertical structure of visibility in northern Germany
[AD-A158254] N86-13871

CLIMATOLOGY
Understanding climate: A strategy for climate modeling and predictability research, 1985-1995
[NASA-RP-1158] N86-13866
Statistical comparison of two major gridded temperature records of the Northern Hemisphere
[DE85-016076] N86-13872

CLINICAL MEDICINE

Magnetic field applications in modern technology and medicine
[DE85-015197] N86-14001

CLOSED CYCLES

A three-dimensional analysis of natural convection in a toroidal loop N86-13672

Performance assessment of OTEC power systems and thermal power plants. Volume 2: Users manual for PACC-OTECs
[DE85-016792] N86-13835

CLOSED ECOLOGICAL SYSTEMS

Comparative effect of lunar fines and terrestrtrial ash on the growth of a blue-green alga and germinating radish seeds N86-14097

Biological life-support systems for long-duration space flights N86-14160

CLOUD GLACIATION

Heat transfer and pressure drop performance of a finned-tube heat exchanger proposed for use in the NASA Lewis Altitude Wind Tunnel
[NASA-TM-87151] N86-13677

CLOUD SEEDING

Goskomgidromet plans automation of aerial cloud-seeding work N86-13766

CLOUDS

Aircrew dose and engine dust ingestion from nuclear cloud penetration
[AD-A159246] N86-13327

Investigation of cold colored smoke production
[AD-A158783] N86-14040

CLOUDS (METEOROLOGY)

Atmospheric environment for Space Shuttle (STS-51D)
[NASA-TM-86524] N86-13868

CLUSTER ANALYSIS

Approximate cluster analysis method and three-dimensional diagram of optical characteristics of lunar surface N86-14128

Method for using clusters in evaluating land use areas from multizonal photographs N86-14180

CMOS

New digital circuits at Thomson semiconductor in France N86-13619

Bulk CMOS VLSI technology studies. Part 4: Design of a CMOS microsequencer
[AD-A158369] N86-13650

Bulk CMOS VLSI technology studies. Part 5: The design and implementation of a high speed integrated circuit functional tester
[AD-A158370] N86-13651

COAL GASIFICATION

Studies of metal/carbon surface chemistry
[DE85-015548] N86-13398

COATING

A method for melt-coating a surface
[AD-D011866] N86-13596

COATINGS

Sorption detector system for chemical agents detection and recognition
[DE85-012775] N86-13400

The effect of cobalt content in U-700 type alloys on degradation of aluminide coatings
[NASA-TM-87173] N86-13408

Influence of texture of titanium nitride coatings on wear resistance of cutting tools N86-13440

Influence of annealing on hardness of vacuum-diffusion chromium coating on low-carbon steel N86-13441

Study of properties of gas-thermal coatings of composite nichrome-aluminum alloy powders N86-13442

Durability of steel 45 with boride coating in corrosive-abrasive media N86-13467

Silicide coatings for protecting titanium-niobium alloys from high-temperature oxidation N86-13476

COBALT

The effect of cobalt content in U-700 type alloys on degradation of aluminide coatings
[NASA-TM-87173] N86-13408

Influence of Co-Cr-Al-Y coatings on physical and mechanical properties of EI-893 steel in GT-100 turbine drive vanes N86-13438

COBALT ISOTOPES

Macro- and microfractographic specifics of dissipated impact rupture of type 45 steel in the viscous-brittle transition interval N86-13466

CODING

Hybrid simulation codes with application to shocks and upstream waves
[NASA-CR-176365] N86-13702

Coupled radiation transport/thermal analysis of the radiation shield for a space nuclear reactor
[AD-A158180] N86-14022

COEFFICIENTS

Mass transfer coefficients and Henry's constants for packed-tower air stripping of volatile organics: Measurements and correlation
[AD-A158811] N86-13375

A family of curves for the rough surface reflection coefficient
[AD-A158195] N86-13876

COGNITION

A psychophysiological mapping of cognitive processes
[AD-A158732] N86-13895

The event related brain potential as an index of information processing, cognitive activity, and skill acquisition: A program of basic research
[AD-A159118] N86-13897

Information requirements determination: An empirical investigation of obstacles within an individual
[AD-A158025] N86-13901

Deterministic parsing and linguistic explanation: Revision
[AD-A159233] N86-13950

European Science Notes. Volume 39, number 9
[AD-A158278] N86-14109

COHERENT RADIATION

Coherent optical transient spectroscopy in flames N86-13570

COHERENT SCATTERING

Laser emission and coherent Raman scattering from individual flowing droplets N86-13578

COLD PLASMAS

Observations of fluxes of cold ions from plasmasphere into ionosphere during nighttime in middle latitudes N86-14117

COLD WORKING

Computerized simulation and display of extruding by cold forging
[CETIM-1-3L-11-1] N86-13741

COLLIMATORS

Hard gamma radiation background from coding collimator of gamma telescope under space experiment conditions N86-14123

COLLISION AVOIDANCE

Crowding of the geostationary orbit
[ESA-CR(P)-2050] N86-13346

Multiresolution path planning for mobile robots
[AD-A158630] N86-13948

COLLISION PARAMETERS

Possibility for a self-consistent treatment of transport processes in a turbulent plasma
[DE85-016214] N86-14069

COLLISIONLESS PLASMAS

Hybrid simulation codes with application to shocks and upstream waves
[NASA-CR-176365] N86-13702

COLLOIDS

Structure and hydrodynamics of colloidal systems
[DE85-016294] N86-14027

COMBINATORIAL ANALYSIS

On the complexity of ID/LP parsing
[AD-A158211] N86-13933

COMBUSTIBLE FLOW

Optical processing and phase conjugation N86-13573

COMBUSTION

Effect of heating conditions on agglomeration of powdered aluminum in air atmosphere N86-13460

Fundamental studies of azide decomposition and combustion N86-13534

Coupling between velocity oscillations and solid propellant combustion N86-13541

Flame-acoustic wave interaction during axial solid rocket instabilities N86-13542

Mechanisms for acoustic suppression N86-13543

Spray characterization using phase angle detection N86-13577

Size and shape characterization of individual flowing droplets by laser light scattering N86-13579

Spray characterization with a nonintrusive optical single particle counter N86-13580

Single particle sizing by measurement of Brownian motion N86-13584

Direct injection diesel motor N86-13625

Measurement of rate constants of elementary gas reactions of importance to upper atmosphere and combustion systems
[AD-A158824] N86-13857

COMBUSTION CHAMBERS

Interaction of multi-dimensional mean and acoustic fields in solid rocket combustion chambers N86-13547

New flow visualization technique for water tunnel testing of combustors
[AD-A158015] N86-13686

Rocket engine hot-spot detector
[NASA-CR-171902] N86-13708

COMBUSTION CONTROL

Strategy for advanced sensing and control of combustion N86-13574

Computer program for prediction of fuel consumption statistical data for an upper stage three-axes stabilized on-off control system
[NASA-CR-166031] N86-13917

COMBUSTION PHYSICS

The 1985 AFOSR/AFRPL Chemical Rocket Research Meeting, abstracts and agenda
[AD-A158291] N86-13507

Flame mechanisms and flame inhibition N86-13523

COMBUSTION PRODUCTS

Rocket engine hot-spot detector
[NASA-CR-171902] N86-13708

Crushing strength of aluminum oxide agglomerates
[AD-A158051] N86-13756

COMBUSTION STABILITY

The 1985 AFOSR/AFRPL Chemical Rocket Research Meeting, abstracts and agenda
[AD-A158291] N86-13507

Flow field effects on combustion instability N86-13544

Rocket motor flow-turning losses N86-13545

Holographic study of the particles produced by the injector in a Viking motor
[ISL-R-111/84] N86-13724

COMBUSTION TEMPERATURE

Experimental investigation of magnesium combustion in steam
[AD-A159109] N86-13396

Application of atomic fluorescence to measurement of combustion temperatures in solid propellants N86-13582

COMET NUCLEI

Role of intrinsic energy source in physical behavior of split cometary nucleus N86-14120

COMETARY ATMOSPHERES

Extended atmospheres of outer planet satellites and comets
[NASA-CR-176398] N86-14209

COMETS

Method for solving two-point boundary value problem for optimization of flights with low thrust N86-14114

COMMAND AND CONTROL

Improving MILSATCOM (Military Satellite Communication) acquisition outcomes: Lease versus buy
[AD-A158842] N86-13348

COMMERCIAL AIRCRAFT

Certification granted to Franco-Italian ATR 42 N86-13617

ATR 42 production work in French, Italian plants detailed N86-13618

COMMUNICATION NETWORKS

Distributed sensor networks
[AD-A158033] N86-13628

Worldwide report: Telecommunications policy, research, and development
[JPRS-TTP-85-026] N86-13640

Unified method for delay analysis of random multiple access algorithms
[AD-A159108] N86-13981

COMMUNICATION SATELLITES

Improving MILSATCOM (Military Satellite Communication) acquisition outcomes: Lease versus buy
[AD-A158842] N86-13348

Testing of 30-GHz low noise receivers
[NASA-TM-87171] N86-13627

COMMUNITIES

Some design philosophy for reducing the community noise of advanced counter-rotation propellers
[NASA-TM-87099] N86-14007

COMPARISON

Comparison of ion milling techniques for cross-sectional TEM of semiconductors
[DE85-016596] N86-13664

Statistical comparison of two major gridded temperature records of the Northern Hemisphere
[DE85-016076] N86-13872

COMPILERS

European silicon structures plans custom chips in 15 days N86-13621

COMPLETENESS

Waves which travel upstream in boundary layers
[AD-A157949] N86-13684

COMPLEX SYSTEMS

Dynamic modeling of structures from measured complex modes N86-13591

COMPLEXITY

Atmospheric and science complexity effects on surface bidirectional reflectance N86-13803

COMPOSITE MATERIALS

Structures and materials technology issues for reusable launch vehicles
[NASA-TM-87626] N86-13349

Process-induced viscoelastic stress in composite laminates N86-13376

Effective behavior of composite materials
[AD-A158941] N86-13380

Ultrasonic longitudinal wave velocity in carbon-carbon Pitch and Pitch/M2 shape stable nosetip material from 70 deg F to 5400 deg F
[DE85-017330] N86-13382

Polymer, metal and ceramic matrix composites for advanced aircraft engine applications
[NASA-TM-87132] N86-13407

USSR report: Materials science and metallurgy
[JPRS-UMS-85-006] N86-13422

Fiber composition materials for strengthening components of aluminum and its alloys N86-13424

Preparation of ceramic fiber-ceramic matrix composites by a faster chemical vapor infiltration process
[DE85-016402] N86-13500

West Europe report: Science and technology
[JPRS-WST-85-029] N86-13622

Recent advances in composite materials reviewed N86-13623

Electrical sliding joint literature review (viewgraph presentation)
[DE85-011571] N86-13666

COMPOSITION (PROPERTY)

Analysis of atomic thermospheric nitrogen density
[NASA-CR-176354] N86-13851

COMPRESSIBILITY

Short presentation and evaluation of studies on the penetration of jets from hollow shaped charges in compressible materials
[ISL-NB-402/84] N86-13586

COMPRESSIBLE FLOW

Numerical solutions of Navier-Stokes equations for a Butler wing
[NASA-CR-174202] N86-13293

Shock waves, increase of entropy and loss of information
[DE85-013645] N86-13701

COMPRESSION LOADS

Fabrication and evaluation of superplastically formed/weld-brazed corrugated compression panels with beaded webs
[NASA-TP-2512] N86-13406

COMPUTATION

Reflectance modeling N86-13795

Multidimensional modeling of atmospheric effects and surface heterogeneities on remote sensing N86-13806

A new library of subroutines for calculating smoothing splines
[AD-A158049] N86-13930

Pre-stack Kirchhoff inversion of common offset data
[AD-A158205] N86-13932

Boundary integral techniques for multi-connected domains
[AD-A158171] N86-13965

Uniformly high-order accurate non-oscillatory schemes 1
[AD-A158177] N86-13966

Unified method for delay analysis of random multiple access algorithms
[AD-A159108] N86-13981

Approximate analytical formulas for computing spectral brightness coefficients for agricultural vegetation N86-14179

COMPUTATIONAL FLUID DYNAMICS

PLTTER user's guide
[NASA-CR-177385] N86-13291

On applications of chimera grid schemes to store separation
[NASA-TM-88193] N86-13292

Computational aspects of zonal algorithms for solving the compressible Navier-Stokes equations in three dimensions
[NASA-TM-86774] N86-13296

Aerothermodynamics for future launchers. Review of the state of the art in Europe
[VKI-CR-1984-16/AR] N86-13347

Far-field boundary conditions in numerical solutions of the Navier-Stokes equations
[AD-A158776] N86-13690

Contributions to Von Karman Institute lecture series on Computational Fluid dynamics: Advection-diffusion and Navier-Stokes equations
[DE85-010942] N86-13703

Unsteady aerodynamics applied to the horizontal axis wind turbine disk N86-13825

Aerodynamic research on wind turbines at NLR N86-13828

Aerodynamic calculational methods for curved-blade Darrieus VAWT WECS --- vertical axis wind turbine wind energy converters (VAWT WECS) N86-13830

Accuracy of schemes with nonuniform meshes for compressible fluid flows
[NASA-CR-177988] N86-13954

COMPUTATIONAL GRIDS

On applications of chimera grid schemes to store separation
[NASA-TM-88193] N86-13292

Investigation of techniques for improving spacecraft thermal control software
[GEC-MEL42.0552] N86-13942

Accuracy of schemes with nonuniform meshes for compressible fluid flows
[NASA-CR-177988] N86-13954

Multigrid solutions to quasi-elliptic schemes
[NASA-CR-177973] N86-13955

COMPUTER AIDED DESIGN

Hub effects in propeller design and analysis
[AD-A158853] N86-13331

Verification of computer-aided designs of traveling-wave tubes utilizing novel dynamic refocusers and graphite electrodes for the multistage depressed collector
[NASA-TP-2524] N86-13643

Activities report of the Technical and Scientific Research Center for the Metal Manufacturing Industry N86-13740

Computerized simulation and display of extruding by cold forging
[CETIM-1-3L-11-1] N86-13741

Routing method in computer aided customization of a two level automated universal array
[AD-D011806] N86-13925

METCUT: A computer aided system for machining technology
[AD-A157941] N86-13927

Ada as a hardware description language: An initial report
[AD-A158217] N86-13935

Practical aspects of functional testing techniques
[AD-A158184] N86-13968

COMPUTER AIDED MANUFACTURING

METCUT: A computer aided system for machining technology
[AD-A157941] N86-13927

An algorithm to translate relational algebra queries into QUEL
[AD-A158169] N86-13931

COMPUTER AIDED MAPPING

Experiment for evaluating accuracy in determining land categories on space scanner photographs N86-14195

COMPUTER AIDED TOMOGRAPHY

A tomographic technique for aerodynamics at transonic speeds
[NASA-TM-86766] N86-13297

COMPUTER ASSISTED INSTRUCTION

A reactive learning environment for the Equipment Problem Solving Techniques (EPST) system
[AD-A158035] N86-13929

COMPUTER DESIGN

LTSSCLI: An ITSS shell for NLTSS, version 2.0, revision 1
[DE85-013234] N86-13941

COMPUTER GRAPHICS

DAB user's guide
[NASA-CR-177393] N86-13290

Target tracking based scene analysis
[AD-A158629] N86-13910

A reactive learning environment for the Equipment Problem Solving Techniques (EPST) system
[AD-A158035] N86-13929

Computer-aided process for generating camera-ready graphical artwork
[AD-D011884] N86-13939

FORTRAN plotting subroutines for the space plasma laboratory N86-14103

Computer graphics applications to crew displays N86-14104

COMPUTER NETWORKS

Development and enhancement of Computer Performance Modeling Tool (CPMT)
[AD-A159003] N86-13938

LTSSCLI: An ITSS shell for NLTSS, version 2.0, revision 1
[DE85-013234] N86-13941

COMPUTER PROGRAMMING

Simulating distributed reinforcement effects in concrete analysis
[DE85-009745] N86-13761

IE data processing
[AD-A158027] N86-13853

BOSS: A FORTRAN code for a relational database manager
[AD-A157067] N86-13924

Issues to be considered in the evaluation of technical proposals from the Ada (trademark) language perspective
[AD-A158376] N86-13936

COMPUTER PROGRAMS

DAB user's guide
[NASA-CR-177393] N86-13290

A FORTRAN computer code for calculating flows in multiple-blade-element cascades
[NASA-TM-87104] N86-13295

A direct-inverse method for transonic and separated flows about airfoils
[NASA-CR-176403] N86-13300

A real-time data acquisition system for a low speed wind tunnel
[AR-AERO-R-163] N86-13336

Computer program for calculating flow parameters and power requirements for cryogenic wind tunnels
[NASA-TM-87609] N86-13338

Thomson semiconductors introduces products, balances books N86-13615

Distributed sensor networks
[AD-A158033] N86-13628

User's manual for the generalized computer program system. Open-channel flow and sedimentation, TABS-2. Main text
[AD-A158249] N86-13692

Kinematics of foldable discrete space cranes
[NASA-CR-176360] N86-13735

Multidimensional modeling of atmospheric effects and surface heterogeneities on remote sensing N86-13806

Map projections for use with the Geographic Information System
[PB85-196992] N86-13819

IE data processing
[AD-A158027] N86-13853

Crossref for the Cray
[NASA-CR-177384] N86-13913

Experiences with Cray multi-tasking
[NASA-TM-88200] N86-13916

Computer program for prediction of fuel consumption statistical data for an upper stage three-axes stabilized on-off control system
[NASA-CR-166031] N86-13917

Computer program for post-flight analysis of rigid body moments acting on a launch vehicle first stage
[NASA-CR-166033] N86-13918

Computer program for post-flight evaluation of the control surface response for an attitude controlled missile
[NASA-CR-166032] N86-13920

Computer program for post-flight evaluation of a launch vehicle upper-stage on-off reaction control system
[NASA-CR-166029] N86-13921

Development of a flight software testing methodology
[NASA-CR-176391] N86-13922

High-altitude plume computer code development
[NASA-CR-171600] N86-13923

BOSS: A FORTRAN code for a relational database manager
[AD-A157067] N86-13924

DIESS: A prolog implementation of a domain-independent expert system shell
[AD-A158014] N86-13928

Ada as a hardware description language: An initial report
[AD-A158217] N86-13935

Issues to be considered in the evaluation of technical proposals from the Ada (trademark) language perspective
[AD-A158376] N86-13936

Computer-aided process for generating camera-ready graphical artwork
[AD-D011884] N86-13939

LTSSCLI: An ITSS shell for NLTSS, version 2.0, revision 1
[DE85-013234] N86-13941

Multiresolution path planning for mobile robots
[AD-A158630] N86-13948

Minimal norm constrained interpolation
[NASA-CR-176001] N86-13956

Practical aspects of functional testing techniques
[AD-A158184] N86-13968

A finite element solution of the transport equation
[AD-A159245] N86-13982

JASON electrostatic boundary conditions: A survey
[DE85-014521] N86-14005

Determination of neutron flux distribution by using ANISN, a one-dimensional discrete S sub n ordinates transport code with anisotropic scattering N86-14084

FORTRAN plotting subroutines for the space plasma laboratory N86-14103

COMPUTER STORAGE DEVICES

FRG's Domier develops high-resolution display system N86-13611

A report on the ST Sci optical disk workstation
[NASA-CR-176389] N86-13907

COMPUTER SYSTEMS DESIGN

A real-time data acquisition system for a low speed wind tunnel
[AR-AERO-R-163] N86-13336

IE data processing
[AD-A158027] N86-13853

The construction and testing of a real-time digital breadboard processor for the ESA remote sensing satellite synthetic aperature radar
[REPT-00-0778] N86-13911

COMPUTER SYSTEMS PERFORMANCE

Experiences with Cray multi-tasking
[NASA-TM-88200] N86-13916

Development and enhancement of Computer Performance Modeling Tool (CPMT)
[AD-A159003] N86-13938

COMPUTER SYSTEMS PROGRAMS

Development of velocity measurement technique by pulsed laser Doppler anemometry N86-13571

Using software technology to specify abstract interfaces in VLSI design
[AD-A158034] N86-13649

Employment of PAM-FISS-BI-phase computer program for the strength analysis and fracture/delamination behavior of components
[ESI-ED/83-383/RD/MS-VOL-7] N86-13763

Parallel computation with the force
[NASA-CR-177999] N86-13915

Investigation of techniques for improving spacecraft thermal control software
[GEC-MEL42.0552] N86-13942

COMPUTER TECHNIQUES

High frequency quantitative analysis of magnetomechanical acoustic emission
[AD-A158222] N86-13750

Safe control systems and the VIPER microprocessor
[AD-A156617] N86-13908

Replication and fault-tolerance in the ISIS system
[AD-A157775] N86-13926

Computer-aided process for generating camera-ready graphical artwork
[AD-D011884] N86-13939

New control techniques for extraction of Bevalac beams
[DE85-017640] N86-14023

COMPUTER VISION

Target tracking based scene analysis
[AD-A158629] N86-13910

Multiresolution path planning for mobile robots
[AD-A158630] N86-13948

Multigrid relaxation methods and the analysis of lightness, shading, and flow
[AD-A158173] N86-14036

COMPUTERIZED SIMULATION

Aircraft crashing. Analysis and identification methods. Presentation of a solution method
[IMFL-4116] N86-13308

Granular flow: Advanced Research and Technology Development (AR and TD) contract review
[DE85-017267] N86-13697

Development of contact/impact capability for the three-dimensional fluid-structure interaction code: NEPTUNE
[DE85-010264] N86-13698

Contributions to Von Karman Institute lecture series on Computational Fluid dynamics: Advection-diffusion and Navier-Stokes equations
[DE85-010942] N86-13703

Photoelectronic trajectory anatomy of RCA-C-73435 image converter and its performance
[DE85-013973] N86-13723

Computerized simulation and display of extruding by cold forging
[CETIM-1-3L-11-1] N86-13741

Scattering models and basic experiments in the microwave regime N86-13807

Performance assessment of OTEC power systems and thermal power plants. Volume 2: Users manual for PACC-OTECs
[DE85-016792] N86-13835

Small solar power systems plant in Almeria system evaluation and comparison on thermal basis
[DE85-017185] N86-13840

Interactive scenario computer model for dose rates to aircrews in flight through nuclear debris clouds
[AD-A156741] N86-13888

The simulation of truck motions
[UTIAS-294] N86-13914

Development and enhancement of Computer Performance Modeling Tool (CPMT)
[AD-A159003] N86-13938

Design and implementation of a compliant robot with force feedback and strategy planning software
[NASA-TM-86111] N86-13947

Approximation of the initial reserve for known ruin probabilities
[AD-A158167] N86-13967

Collective ion acceleration by means of virtual cathodes
[DE85-012707] N86-14019

High order spline interpolation in the particle simulation N86-14046

Effect of focusing field nonlinearities in MBE-4 on transverse beam dynamics
[DE85-016561] N86-14058

Estimation of finite mixtures using the empirical characteristic function N86-14079

COMPUTERS

West Europe report: Science and technology
[JPRS-WST-85-030] N86-13610

West Europe report: Science and technology
[JPRS-WST-85-031] N86-13616

West Europe report: Science and technology
[JPRS-WST-85-029] N86-13622

CONCENTRATION (COMPOSITION)

Mass transfer coefficients and Henry's constants for packed-tower air stripping of volatile organics: Measurements and correlation
[AD-A158811] N86-13375

Study of mean free path effects on growth of ultrafine metallic aerosols
[AD-A158206] N86-13393

Role of additives in minimizing zinc electrode shape change: The effect of lead on the kinetics of Zn(2) reduction in concentrated alkaline media
[AD-A158806] N86-13395

Pulsed inductive energy transfer N86-13562

An Oil/Water disperser device for use in an oil content Monitor/Control system
[AD-D011868] N86-13714

Oil content Monitor/Control system and method
[AD-D011871] N86-13717

CONCRETE STRUCTURES

Long-term analysis of slender concrete structures with cracking
[DE85-010275] N86-13762

CONCRETES

Simulating distributed reinforcement effects in concrete analysis
[DE85-009745] N86-13761

CONDUCTIVE HEAT TRANSFER

Conductivity of metal-ceramic multilayer ZrO2-Mo and Mo-based composite materials N86-13444

CONFERENCES

Implementing agreement for cooperation in the development of large scale wind energy conversion systems --- conferences
[JUEL-SPEZ-304] N86-13820

CONFIDENCE LIMITS

A note on the effect of ignoring small measurement errors in precision instrument calibration
[AD-A159104] N86-13713

CONFIGURATION INTERACTION

Some design philosophy for reducing the community noise of advanced counter-rotation propellers
[NASA-TM-87099] N86-14007

CONFORMAL MAPPING

On applications of chimera grid schemes to store separation
[NASA-TM-88193] N86-13292

CONIFERS

Geometric-optical modeling of a conifer forest canopy
N86-13799

CONSERVATION

Uniformly high-order accurate non-oscillatory schemes. 1
[AD-A158177] N86-13966

CONSERVATION EQUATIONS

Numerical simulations of asymmetric mixing in planar shear flows
[AD-A158024] N86-13687

Decay with a rate for noncompactly supported solutions of conservation laws
[AD-A158163] N86-13962

CONSERVATION LAWS

Shock waves, increase of entropy and loss of information
[DE85-013645] N86-13701

Decay with a rate for noncompactly supported solutions of conservation laws
[AD-A158163] N86-13962

CONSTANTS

Measurement of rate constants of elementary gas reactions of importance to upper atmosphere and combustion systems
[AD-A158824] N86-13857

Optical constants
[AD-A158623] N86-14038

CONSTRAINTS

Codon constraints on closed 2D shapes
[AD-A158744] N86-13979

CONSTRUCTION

Design criteria upgrade for US Army Type 2 air traffic control towers
[AD-A159115] N86-13314

Composites design
[AD-A157710] N86-13378

CONTACT RESISTANCE

Lubrication of nonconformal contacts
[NASA-TM-87120] N86-13679

CONTAINMENT

Simulating distributed reinforcement effects in concrete analysis
[DE85-009745] N86-13761

CONTAMINANTS

Mass transfer coefficients and Henry's constants for packed-tower air stripping of volatile organics: Measurements and correlation
[AD-A158811] N86-13375

CONTAMINATION

Application of molecular kinetics models to the prediction of backflow contamination N86-13531

CONTINUITY EQUATION

A fully viscous two-dimensional unsteady flow analysis applied to detonation transition in porous explosives
[AD-A157794] N86-13682

CONTINUOUS RADIATION

Linear and saturated absorption of laser radiation in heated cases N86-13551

Ray transmissions over a sloping bottom in shallow water
[AD-A158017] N86-14008

CONTINUOUS SPECTRA

Focal plane optics in far-infrared and submillimeter astronomy
[NASA-TM-88186] N86-14204

CONTINUOUS WAVE LASERS

Reaction intermediates in aromatic fuel combustion
[AD-A158029] N86-13390

Extremely high reflective capability of zirconium burning in air under effects of constant CO2 laser radiation
N86-13452

Experimental studies of laser-sustained argon plasmas for CW laser propulsion applications N86-13550

CONTINUUM MECHANICS

Scientific activities of the Polish Academy of Sciences: Institute of Fundamental Technological Research in 1983
[ISBN-83-01-06288-6] N86-14107

CONTOURS

Codon constraints on closed 2D shapes
[AD-A158744] N86-13979

CONTRAROTATING PROPELLERS

Some design philosophy for reducing the community noise of advanced counter-rotation propellers
[NASA-TM-87099] N86-14007

CONTRAST

Enhancing sensitivity to visual motion and enhancing visual sensitivity
[AD-A158600] N86-13889

CONTROL

Joint services electronics program
[AD-A158731] N86-13652

CONTROL EQUIPMENT

Mass transfer coefficients and Henry's constants for packed-tower air stripping of volatile organics: Measurements and correlation
[AD-A158811] N86-13375

A 10-MHz high-voltage modulator with pulse-width and repetition-rate agility
[DE85-014117] N86-13663

Microcomputer controlled current sharing experiments with parallel converters
[DE85-013854] N86-13665

An Oil/Water disperser device for use in an oil content Monitor/Control system
[AD-D011868] N86-13714

Oil content Monitor/Control system and method
[AD-D011871] N86-13717

New control techniques for extraction of Bevalac beams
[DE85-017640] N86-14023

Optical radar transceiver control apparatus
[AD-D011880] N86-14042

Laser-trigger system design for PBFA 2
[DE85-013144] N86-14065

CONTROL SIMULATION

The simulation of truck motions
[UTIAS-294] N86-13914

CONTROL STABILITY

A method to stabilize linear systems using eigenvalue gradient information
[NASA-TP-2479] N86-13946

CONTROL SURFACES
Pitch rate versus G command as the longitudinal flight control system design strategy for a statistically unstable fighter type aircraft with two control surfaces [AD-A156803] N86-13334
Computer program for post-flight evaluation of the control surface response for an attitude controlled missile [NASA-CR-166032] N86-13920

CONTROL SYSTEMS DESIGN
Digital servocontroller system. Volume 4. Results and conclusions [AD-A159068] N86-13335
Robot control system modified for precision movement N86-13747
Computer program for post-flight evaluation of a launch vehicle upper-stage on-off reaction control system [NASA-CR-166029] N86-13921
Hardware upgrade for klystrons in the SLC [DE85-014357] N86-14029
Control of space stations N86-14090

CONTROL THEORY
Further results for application of disturbance minimization control techniques to a linear, time-invariant, second-order state set-point regulator problem [AD-A157793] N86-13961
Analysis of the dynamic behavior of an intense charged particle beam using the semigroup approach [AD-A159247] N86-14015
Forming attainability sets in control of kinetic moment of rotating asymmetric solid body (special cases) N86-14113

CONTROLLERS
Digital servocontroller system. Volume 4. Results and conclusions [AD-A159068] N86-13335
Safe control systems and the VIPER microprocessor [AD-A156617] N86-13908
Control of space stations N86-14090

CONVECTION
Determination of convective diffusion heat/mass transfer rates to burner rig test targets comparable in size to cross-stream jet diameter [NASA-TM-87176] N86-13678

CONVECTIVE FLOW
A three-dimensional analysis of natural convection in a toroidal loop N86-13672

CONVECTIVE HEAT TRANSFER
Problems in thermal convective instability N86-13670
A three-dimensional analysis of natural convection in a toroidal loop N86-13672
Computation of ocean upper layer thermal structure N86-13769

CONVERGENCE
Multigrid solutions to quasi-elliptic schemes [NASA-CR-177973] N86-13955
Partitions of point processes: Multivariate poisson approximations [AD-A158739] N86-13978
The theory of standardized time series [AD-A158383] N86-13989

COOLANTS
Rocket engine hot-spot detector [NASA-CR-171902] N86-13708

COOLING
Temperature and pressure components of shock-induced changes in the electronic spectrum of carbon disulfide [AD-A158627] N86-13373
Structure and internal friction of near-eutectic alloy system Ti-W tempered from a liquid state N86-13482
Influence of preliminary annealing on structure and properties of VT23 alloy welded joints after hardening N86-13488
Coupling between gas dynamics and microwave energy absorption N86-13561

COOLING FINS
Heat transfer and pressure drop performance of a finned-tube heat exchanger proposed for use in the NASA Lewis Altitude Wind Tunnel [NASA-TM-87151] N86-13677

COOLING SYSTEMS
Development of a breadboard cooler for infrared remote sensing payloads, phase 2 --- spacecraft payloads [FOK-RV-R-82-072] N86-13725
Operation of large cryogenic systems [DE85-017439] N86-14025
SLAC divertor channel entrance thermal stress analysis [DE85-017877] N86-14057

COPPER
High strain rate deformation in FCC metals and alloys [DE85-017533] N86-13417
Threshold stress measurements in shock-deformed copper [DE85-014076] N86-13418
Internal friction in TiNiCu alloy N86-13480
Diffusion welding of copper-chromium pseudoalloy with copper N86-13493
Electrical sliding joint literature review (viewgraph presentation) [DE85-011571] N86-13666

COPPER ALLOYS
Influence of alloying elements and impurities on mechanical properties of complex silumins N86-13428
Study of permeability of two-phase zone in aluminum and copper alloys N86-13430

COPPER OXIDES
Electronic detection of low concentrations of organophosphorus compounds with a solid state device utilizing supported copper + cuprous oxide island films [AD-A158181] N86-13392

COPPER SELENIDES
Development of stable high efficiency polycrystalline thin-film solar cells based on CuInSe2 [DE85-000517] N86-13837

CORRELATION
Inference on the ranks of the canonical correlation matrices for elliptically symmetric populations [AD-A158268] N86-13976

CORRELATION DETECTION
An alternate derivation of the distribution of the conditioned signal-to-noise ratio [AD-A158257] N86-13974

CORROSION
USSR report: Materials science and metallurgy [JPRS-UMS-85-006] N86-13422
Complex nickel-aluminide coatings on nickel-chromium alloy EP648-VI N86-13437
Development and evaluation of an instantaneous atmospheric corrosion rate monitor [PB85-214336] N86-13727
Electrical research on solar cells and photovoltaic materials [NASA-CR-176384] N86-13838

CORROSION PREVENTION
Anticorrosion polymer packing film with improved protective properties N86-13451
Silicide coatings for protecting titanium-niobium alloys from high-temperature oxidation N86-13476

CORROSION RESISTANCE
A durable airfield marking system [AD-A157953] N86-13339
Corrosion fatigue initiation and short crack growth in an aluminum alloy N86-13404
Corrosion resistance of diffusion and galvanic coatings on steel fasteners N86-13450
Anticorrosion polymer packing film with improved protective properties N86-13451
Modeling of thermal fatigue and erosion of complex alloyed steels in metal melts N86-13469
Silicide coatings for protecting titanium-niobium alloys from high-temperature oxidation N86-13476
Corrosion resistance of welded joints in certain titanium alloys N86-13489

CORROSION TESTS
Corrosion fatigue initiation and short crack growth in an aluminum alloy N86-13404
Durability of steel 45 with boride coating in corrosive-abrasive media N86-13467

CORRUGATED PLATES
Fabrication and evaluation of superplastically formed/weld-brazed corrugated compression panels with beaded webs [NASA-TP-2512] N86-13406

CORTICOSTEROIDS
Design, construction and testing of a dc bioeffects enclosure for small animals [DE05-016798] N86-13883

COSMIC DUST
Investigation of dust associated with shell stars [AD-A158945] N86-14210
Preparation, analysis and release of simulated interplanetary grains into low grain orbit [DE85-014133] N86-14211

COSMIC RAYS
Latitude measurements of cosmic radiation intensity in stratosphere and at sea level on marine antarctic expeditions N86-13792
Hadron component of cosmic radiation at atmospheric depth 800 g/cm(2) in Energy Range 70 to 700 GeV N86-13793

COSMOS SATELLITES
List of recent Soviet space launches N86-14199

COST ANALYSIS
New materials to lighten vehicles N86-13624
Engineering design for the PBFA-2 pulse forming section [DE85-012810] N86-14060

COST REDUCTION
Recent advances in composite materials reviewed N86-13623

COUNTER ROTATION
Some design philosophy for reducing the community noise of advanced counter-rotation propellers [NASA-TM-87099] N86-14007

COUNTING
Errors due to counting statistics in the triaxial strain (stress) tensor determined by diffraction [AD-A158219] N86-13759

COUPLERS
Occasional reports of the Royal Observatory, Edinburgh, no. 16 [ISSN-0309-099-X] N86-14200
A multiple-object fibre-optics coupler for the 1.2-m UK Schmidt Telescope N86-14201

COUPLING
Coupled radiation transport/thermal analysis of the radiation shield for a space nuclear reactor [AD-A158180] N86-14022

COVARIANCE
Methodology for stochastic modeling [AD-A158851] N86-13994

CRAB NEBULA
Detection of Ni 2 lambda 7378 in six Seyfert galaxies [NASA-CR-176358] N86-14205

CRACK GEOMETRY
A numerical investigation into the plastic stress and strain fields around a surface crack [ARL/STRUC-R-414] N86-13754

CRACK INITIATION
Corrosion fatigue initiation and short crack growth in an aluminum alloy N86-13404
Crack growth behavior in a composite propellant with strain gradients N86-13537
Nonlinear modeling and method of predicting crack growth N86-13538

CRACK PROPAGATION
Hydrogen transport and hydrogen embrittlement in stainless steels N86-13403
Study of effect of normal reactor water on growth rate of fatigue cracks in 15Kh2NMFA steel N86-13470
Subcritical crack development under constant load in VT6 alloy N86-13475
Fractured toughness of Si3N4 measured with short bar chevron-notched specimens [NASA-TM-87153] N86-13495
Crack growth behavior in a composite propellant with strain gradients N86-13537
Nonlinear modeling and method of predicting crack growth N86-13538
Static fatigue of a sintered silicon nitride [AD-A158813] N86-13760
Long-term analysis of slender concrete structures with cracking [DE85-010275] N86-13762
Characteristics of microearthquakes accompanying hydraulic fracturing as determined from studies of spectra of seismic waveforms [DE85-009558] N86-13860

CRACKING (FRACTURING)
Macro- and microfractographic specifics of dissipated impact rupture of type 45 steel in the viscous-brittle transition interval N86-13466
Influence of hydrogen on formation of cold cracks in seams during welding of pipe steel N86-13494
Pore pressure response to probe insertion and thermal gradient: ISIMU-2. (In situ heat transfer experiment) [AD-A158592] N86-13689
SLAC divertor channel entrance thermal stress analysis [DE85-017877] N86-14057

CRACKS
Remote optical crack sensing system [AD-D011872] N86-13718
Coupled radiation transport/thermal analysis of the radiation shield for a space nuclear reactor [AD-A158180] N86-14022

CRANES
Kinematics of foldable discrete space cranes [NASA-CR-176360] N86-13735

CRASH LANDING
Aircraft crashing. Analysis and identification methods. Presentation of a solution method [IMFL-4116] N86-13308
Abrasion behavior of aluminum and composite skin coupons, stiffened skins and stiffened panels representative of transport airplane structures [NASA-TP-2520] N86-13316

CRASHWORTHINESS
Advanced technology helicopter landing gear preliminary design investigation [AD-A158816] N86-13325

CRATERS
Experimental investigation of crater growth dynamics [NASA-CR-176392] N86-14212

CRAY COMPUTERS
Crossref for the Cray
[NASA-CR-177384] N86-13913

CREEP PROPERTIES
Durability of steel 45 with boride coating in corrosive-abrasive media N86-13467
Time dependency of strainrange partitioning life relationships
[NASA-CR-174946] N86-13755
Static fatigue of a sintered silicon nitride
[AD-A158813] N86-13760
Long-term analysis of slender concrete structures with cracking
[DE85-010275] N86-13762

CRITERIA
Design criteria upgrade for US Army Type 2 air traffic control towers
[AD-A159115] N86-13314

CROP GROWTH
Crop characteristics research: Growth and reflectance analysis N86-13800
Discrete random media techniques for microwave modeling of vegetated terrain N86-13809

CROP IDENTIFICATION
Crop characteristics research: Growth and reflectance analysis N86-13800

CROP INVENTORIES
Determination of backscattering sources in various targets N86-13811
Crop area estimation based on remotely-sensed data with an accurate but costly subsample
[NASA-CR-176017] N86-13814

CROP VIGOR
Determination of backscattering sources in various targets N86-13811

CROSS CORRELATION
Crossref for the Cray
[NASA-CR-177384] N86-13913

CROSS FLOW
Effects of velocity profile and inclination on dual-jet-induced pressures on a flat plate in a crosswind
[NASA-CR-177361] N86-13287

CROSSLINKING
Study of cross-linking density and the type of cross linkage in polyurethane elastomers
[AD-A158199] N86-13497

CRUDE OIL
Influence of petroleum pollution on ocean-atmosphere gas exchange intensity (in example of North Atlantic) N86-13785
Possible petroliferousness of South Caspian uplifts analyzed N86-13863

CRYOGENIC COOLING
Operation of large cryogenic systems
[DE85-017439] N86-14025

CRYOGENIC FLUIDS
Operation of large cryogenic systems
[DE85-017439] N86-14025

CRYOGENIC WIND TUNNELS
Computer program for calculating flow parameters and power requirements for cryogenic wind tunnels
[NASA-TM-87609] N86-13338
Test of the ONERA cryogenic balance in the T2 wind tunnel
[ONERA-BT-8/0791-GY] N86-13341

CRYOGENICS
Charge-density waves observed with a tunneling microscope
[AD-A158779] N86-13709

CRYSTAL DEFECTS
Study of fractures in cast parts of high-strength aluminum alloy N86-13429

CRYSTAL GROWTH
CNET of France uses organo-metallic epitaxy for laser N86-13620
Turbulence and dynamical systems
[AD-A159026] N86-13691
MBE growth of CdTe and Hg (1-x) Cd (x) Te films and multilayer structures
[AD-A158267] N86-14073

CRYSTAL STRUCTURE
No chemisorption on Ni(111): Coverage effects, site preferences and adsorption geometry
[AD-A159110] N86-13397
High energy molecules of high symmetry N86-13520
AuGa2 on GaSb(001): An epitaxial, thermodynamically stabilized Metal/3-5 compound semiconductor interface
[AD-A157937] N86-14071

CRYSTALLIZATION
Experimental investigation of magnesium combustion in steam
[AD-A159109] N86-13396
USSR report: Materials science and metallurgy
[JPRS-UMS-85-006] N86-13422
Structure formation in silumins upon rapid crystallization N86-13427
Preliminary annealing on crystallization of amorphous Fe80Si6B14 alloy N86-13433
Influence of sodium on mechanical and casting properties of magnesium-lithium alloys N86-13457

CRYSTALS
Theory of the propagation of finite amplitude ultrasonic waves in pure mode directions in hexagonal and trigonal crystals
[AD-A158154] N86-14009

CUBIC LATTICES
Superhard materials developed N86-13471

CURING
Control of the urethane cure reaction with solid, blocked isocyanates N86-13518

CURRENT DENSITY
Magnetoplasmadynamic thruster erosion research N86-13557
CNET of France uses organo-metallic epitaxy for laser N86-13620
Atomically mixed alloy coated cathodes specification
[AD-D011877] N86-13659
Electrical sliding joint literature review (viewgraph presentation)
[DE85-011571] N86-13666

CURRENT DISTRIBUTION
Two-hundred to 300 KVA conditioned power system - development, phase 1
[AD-A158820] N86-13832

CURRENT SHEETS
Babinet's principle for an anisotropic resistive surface using different approaches
[AD-A159117] N86-13636

CURTAINS
Passive arm retention curtain
[AD-D011876] N86-13307

CURVATURE
Describing surfaces
[AD-A158940] N86-13937

CURVE FITTING
FIT: Computer program that interactively determines polynomial equations for data which are a function of two independent variables
[NASA-TM-86413] N86-13333

CUTTERS
Influence of texture of titanium nitride coatings on wear resistance of cutting tools N86-13440

CUTTING
Nozzle for self-contained cutting torches
[AD-D011875] N86-13597

CYCLES
Nature of megacycles in evolution of Earth, Mars, and Moon N86-14159

CYCLIC LOADS
Effect of elastoplastic cyclic deformation on mechanical characteristics of steel O3Kh13AG19 at temperatures of 293 and 77 deg K N86-13463
Modeling of thermal fatigue and erosion of complex alloyed steels in metal melts N86-13469

CYLINDRICAL BODIES
A method for calculating flow fields around moving bodies
[NAL-TR-859T] N86-13288
Effect of elastoplastic cyclic deformation on mechanical characteristics of steel O3Kh13AG19 at temperatures of 293 and 77 deg K N86-13463
Wave force-phase method for vertical cylinders
[AD-A157709] N86-13680
High Reynolds number wave force investigation in a wave flume
[AD-A157722] N86-13681

CYLINDRICAL CHAMBERS
The physics and technology of strong magnetic fields (chapter 10)
[AD-A158174] N86-14000

D

DAMAGE
Rocket engine hot-spot detector
[NASA-CR-171902] N86-13708

DAMPING
Calculation of damping properties of composite materials N86-13446
Temperature-frequency variation of mechanical losses in periodic deformation of multilayer glass-reinforced plastics N86-13449
Turbulence in two-field incompressible flow
[DE85-015361] N86-13693

DATA ACQUISITION
A real-time data acquisition system for a low speed wind tunnel
[AR-AERO-R-163] N86-13336
Experiments with non-Darcy flow in joints with large scale roughness
[DE85-015714] N86-13695
High speed multi-channel data recorder to replace oscilloscope data acquisition systems
[DE85-015155] N86-13721

DATA BASE MANAGEMENT SYSTEMS
BOSS: A FORTRAN code for a relational database manager
[AD-A157067] N86-13924
METCUT: A computer aided system for machining technology
[AD-A157941] N86-13927

DATA BASES
PLTTER user's guide
[NASA-CR-177385] N86-13291
Generically based mobility-terrain data bases
[AD-A157738] N86-13815
IE data processing
[AD-A158027] N86-13853
Data catalog series for space science and applications flight missions. Volume 4A: Descriptions of meteorological and terrestrial applications spacecraft and investigations
[NASA-TM-87501] N86-13869
Some approaches to organization of data bank in system for studying Earth's natural resources from space (using example of agriculture) N86-14194

DATA CONVERSION ROUTINES
A parametric study of the Ibrahim time domain modal identification algorithm N86-13588

DATA LINKS
Comparative study of space segments for the provision of future operational data relay satellite services
[MBB-DSP-TN/DRS/132/84] N86-13355

DATA MANAGEMENT
Generically based mobility-terrain data bases
[AD-A157738] N86-13815
Sparse elimination on vector multiprocessors
[AD-A158274] N86-13909

DATA PROCESSING
Mathematical analysis study for radar data processing and enhancement. Part 1: Radar data analysis
[NASA-CR-166616-PT-1] N86-13353
DE 1 RIMS operational characteristics
[NASA-TM-86527] N86-13365
China report: Science and technology
[JPRS-CST-85-020] N86-13600
Improved algorithm for radar real-time data processing N86-13608
Theoretical studies and data analysis of wave propagation in random media
[AD-A158775] N86-13632
IE data processing
[AD-A158027] N86-13853
The event related brain potential as an index of information processing, cognitive activity, and skill acquisition: A program of basic research
[AD-A159118] N86-13897
Pre-stack Kirchhoff inversion of common offset data
[AD-A158205] N86-13932
Computer-aided process for generating camera-ready graphical artwork
[AD-D011884] N86-13939
LTSSCLI: An ITSS shell for NLTSS, version 2.0, revision 1
[DE85-013234] N86-13941
CREF: An editing facility for managing structured text
[AD-A158155] N86-14077

DATA PROCESSING EQUIPMENT
European silicon structures plans custom chips in 15 days N86-13621

DATA RECORDING
High speed multi-channel data recorder to replace oscilloscope data acquisition systems
[DE85-015155] N86-13721

DATA REDUCTION
Algorithms for the reduction of wind-tunnel data derived from strain gauge force balances
[ARL/AERO-R-164] N86-13337
Mathematical analysis study for radar data processing and enhancement. Part 1: Radar data analysis
[NASA-CR-166616-PT-1] N86-13353
Mathematical analysis study for radar data processing and enchancement. Part 2: Modeling of propagation path errors
[NASA-CR-166616-PT-2] N86-13354
Experimental investigation of magnesium combustion in steam
[AD-A159109] N86-13396
The 1-D laser Doppler instrumentation N86-13575
Theoretical studies and data analysis of wave propagation in random media
[AD-A158775] N86-13632
Bulk CMOS VLSI technology studies. Part 4: Design of a CMOS microsequencer
[AD-A158369] N86-13650
Simulating distributed reinforcement effects in concrete analysis
[DE85-009745] N86-13761

Conditioning in a missing data problem
[AD-A158202] N86-13988
FORTRAN plotting subroutines for the space plasma laboratory N86-14103
Signal processing of anthropometric data N86-14105

DATA RETRIEVAL
Development of the NIMBUS-7 SMMR retrieval algorithm --- Scanning Multichannel Microwave Radiometer (SMMR)
[BAE-RPT/NIM-7/021] N86-13367

DATA SAMPLING
Conditioning in a missing data problem
[AD-A158202] N86-13988

DATA STORAGE
PLTTER user's guide
[NASA-CR-177365] N86-13291
A new library of subroutines for calculating smoothing splines
[AD-A158049] N86-13930

DATA STRUCTURES
A real-time data acquisition system for a low speed wind tunnel
[AR-AERO-R-163] N86-13336

DATA TRANSMISSION
Optoelectronic integrated circuit multiplier
[AD-D011883] N86-14043

DECISION MAKING
Alerted monitors: Human operators aided by automated detectors
[PB85-222750] N86-13906

DECOMPOSITION
Structure-decomposition relationships in newer energetic materials N86-13521
Stability of RDX, AP and BTTN near room temperature N86-13535

DEFENSE INDUSTRY
Emerging aerospace technologies
[NASA-TM-86837] N86-14213

DEFLAGRATION
High-resolution movies of propellant deflagration N86-13539
Wide distribution propellants N86-13540

DEFOCUSING
Effectiveness of use of adaptive optical systems under conditions of self-effect in atmosphere N86-13791

DEFORMATION
Effect of temperature and strain rate on microstructure of a deformed, superplastic Al-10%Mg-0.1%Zr alloy
[AD-A159015] N86-13413
High strain rate deformation in FCC metals and alloys
[DE85-017533] N86-13417
Threshold stress measurements in shock-deformed copper
[DE85-014076] N86-13418
Influence of degree of deformation on structure and properties of naturally aged alloy 1163 N86-13431
Specifics of the process of failure of structural steels strengthened by thermo-mechanical working with deformation in the intercritical temperature interval N86-13464
Mechanical properties of EP794 steel + 12Kh18N10T steel bimetal N86-13465
Subcritical crack development under constant load in VT6 alloy N86-13475
Optimization of technological parameters of cold pressure welding of AD1M thin aluminum sheets N86-13484
Deformation and stresses upon welding of VT23 titanium alloy N86-13490
Elastic-plastic deformation of a metal-matrix composite coupon with a center slot
[NASA-CR-178013] N86-13496
Long-term analysis of slender concrete structures with cracking
[DE85-010275] N86-13762

DEGRADATION
The effect of cobalt content in U-700 type alloys on degradation of aluminide coatings
[NASA-TM-87173] N86-13408
Photodegradation studies of silver-backed polyacrylonitrile (PAN) films
[DE85-012154] N86-13501
Mass loss of shuttle space suit orthofabric under simulated ionospheric atomic oxygen bombardment
[NASA-TM-87149] N86-13899
Scientific activities of the Polish Academy of Sciences: Institute of Fundamental Technological Research in 1983
[ISBN-83-01-06288-6] N86-14107

DEIMOS
Brochure on Phobos and Deimos N86-14155

DELAMINATING
Employment of PAM-FISS-BI-phase computer program for the strength analysis and fracture/delamination behavior of components
[ESI-ED/33-383/RD/MS-VOL-7] N86-13763

DELAY
Unified method for delay analysis of random multiple access algorithms
[AD-A159106] N86-13991

DELTA WINGS
Numerical solutions of Navier-Stokes equations for a Butler wing
[NASA-CR-174202] N86-13293

DEMULTIPLEXING
An integrated wavelength demultiplexer
[AD-D011867] N86-14041

DENDRITIC CRYSTALS
Hereditary effect of dendrite liquation of titanium and zirconium on structure and properties of aluminum alloys N86-13423
Study of permeability of two-phase zone in aluminum and copper alloys N86-13430

DENSITY (MASS/VOLUME)
Supercritical fluid properties
[DE85-011203] N86-13401
Study of cross-linking density and the type of cross linkage in polyurethane elastomers
[AD-A158199] N86-13497
High energy molecules of high symmetry N86-13520

DENSITY (NUMBER/VOLUME)
Charge-density waves observed with a tunneling microscope
[AD-A158779] N86-13709

DENSITY DISTRIBUTION
A tomographic technique for aerodynamics at transonic speeds
[NASA-TM-86766] N86-13297
Experimental investigation of magnesium combustion in steam
[AD-A159100] N86-13396
A three-dimensional analysis of natural convection in a toroidal loop N86-13672
Analysis of atomic thermospheric nitrogen density
[NASA-CR-176354] N86-13851

DENSITY WAVE MODEL
Wave interpretation of measurements on Mars-7 and Venera-9 probes for determining velocity of motion of interstellar gas N86-14147

DEOXYRIBONUCLEIC ACID
Molecular mechanisms of mutagenesis determined by the recombinant DNA technology
[DE85-016353] N86-13884

DEPOLARIZATION
Laser diagnostics for electric field measurements N86-13563

DEPOSITION
Role of additives in minimizing zinc electrode shape change: The effect of lead on the kinetics of Zn(2) reduction in concentrated alkaline media
[AD-A158806] N86-13395
Study of deposition control using transpiration
[DE85-012799] N86-13699
Changes in soil acidity due to natural processes and acid deposition
[DE85-012103] N86-13845

DESIGN ANALYSIS
Design criteria upgrade for US Army Type 2 air traffic control towers
[AD-A159115] N86-13314
Hub effects in propeller design and analysis
[AD-A158853] N86-13331
Report on the findings of the Japanese Investigative Team on US Space Station Design (Keidanren)
[NASA-TM-77659] N86-13356
Space station preliminary design report
[NASA-TM-87521] N86-13357
Standardization program on design analysis and testing of inserts in nonmetallic sandwich components --- spacecraft components
[TR-TS-RP-2-09-84] N86-13364
Composites design
[AD-A157710] N86-13378
Tape joint design for a vibration table
[DE85-012617] N86-13753
Aerodynamic research efforts at SERI wind energy research center at Rocky Flats --- Solar Energy Research Institute (SERI) N86-13829
Practical aspects of functional testing techniques
[AD-A158184] N86-13968
Random errors in the magnetic field coefficients of superconducting magnets
[DE85-012261] N86-14004
Preliminary measurement of the noise from the 2/9 scale model of the Large-scale Advanced Propfan (LAP) propeller, SR-7A
[NASA-TM-87116] N86-14006
An analysis of cryotrap heat exchanger performance test data (400 area) and recommendations for a system to handle Apollo RCS engines N86-14094
Fluorine disposal N86-14095
Sparger system for MMH-helium vents N86-14096
Design for a large altazimuth Schmidt telescope N86-14203

DESORPTION
Modeling of thermal fatigue and erosion of complex alloyed steels in metal melts N86-13469
Electrical research on solar cells and photovoltaic materials
[NASA-CR-176384] N86-13836

DETECTION
Time delay of arrival location assessment using four satellites
[AD-A159243] N86-13315
Electronic detection of low concentrations of organophosphorus compounds with a solid state device utilizing supported copper + cuprous oxide island films
[AD-A158181] N86-13392
Sorption detector system for chemical agents detection and recognition
[DE85-012775] N86-13400
Rocket engine hot-spot detector
[NASA-CR-171902] N86-13708
Remote optical crack sensing system
[AD-D011672] N86-13718
Specialized instrument for radiation assistance teams
[DE85-017390] N86-13720
Concept of laser locator systems (based on the geometry of the triangular corner cube reflector)
[AD-A157795] N86-13728
Enhancing sensitivity to visual motion and enhancing visual sensitivity
[AD-A158800] N86-13889
Adaptive detection in nonstationary interference: Part 1 and part 2
[AD-A158810] N86-13993
Identification of nuclear materials from remote detection of characteristic gamma rays
[AD-A159244] N86-14014
Detection of Ni 2 lambda 7378 in six Seyfert galaxies
[NASA-CR-176358] N86-14205
Speckle image reconstruction. Appendix 1
[AD-A158271] N86-14207

DETONATION
A fully viscous two-dimensional unsteady flow analysis applied to detonation transition in porous explosives
[AD-A157794] N86-13682
Critical charge for the direct initiation of detonation in gaseous fuel-air mixtures
[DE85-016130] N86-13696

DETONATION WAVES
Possible mechanism of wave formation during detonation welding N86-13483

DEUTERIUM
Deuterium isotope effects in RDX decomposition and combustion processes N86-13522

DIAPHRAGMS (MECHANICS)
Mass transfer coefficients and Henry's constants for packed-tower air stripping of volatile organics: Measurements and correlation
[AD-A158811] N86-13375

DIATOMIC GASES
Measurement of rate constants of elementary gas reactions of importance to upper atmosphere and combustion systems
[AD-A158824] N86-13857

DIELECTRIC POLARIZATION
Retrofit of a high power Nd:glass laser system with liquid crystal polarizers
[DE85-014415] N86-13733

DIELECTRIC PROPERTIES
Microwave dielectric and propagation properties of vegetation canopies N86-13810

DIELECTRICS
China report: Science and technology
[JPRS-CST-85-020] N86-13600
On H plane dielectric loading theory for H plane ferrite phase shifter N86-13603

DIESEL ENGINES
Lightweight two-stroke cycle aircraft diesel engine technology enablement program, volume 1
[NASA-CR-174923-VOL-1] N86-13328
Lightweight two-stroke cycle aircraft diesel engine technology enablement program, volume 2
[NASA-CR-174923-VOL-2] N86-13329
Lightweight two-stroke cycle aircraft diesel engine technology enablement program, volume 3
[NASA-CR-174923-VOL-3] N86-13330
Direct injection diesel motor N86-13625

DIFFERENTIAL EQUATIONS
Applications of differential phase statistics to studies of C3 and spread spectrum communications
[AD-A158815] N86-13833
Contributions to Von Karman Institute lecture series on Computational Fluid dynamics: Advection-diffusion and Navier-Stokes equations
[DE85-010942] N86-13703

A functional equation governing moving phase boundaries in an elastic bar
[AD-A158176] N86-13757

Further results for application of disturbance minimization control techniques to a linear, time-invariant, second-order state set-point regulator problem
[AD-A157793] N86-13961

Current methods for large stiff ODE systems
[DE85-012914] N86-13983

Some applications of Lie groups in astrodynamics
N86-14087

Transformation matrices between non-linear and linear differential equations N86-14099

DIFFRACTION

Errors due to counting statistics in the triaxial strain (stress) tensor determined by diffraction
[AD-A158219] N86-13759

Test method for telescopes using a point source at a finite distance
[NASA-TM-86523] N86-14033

Results of research in four topic areas: The singularity expansion method, transient scattering measurements, high-frequency diffraction at edges residing on interfaces and cylindrical coordinate representation of dyadic Green's functions
[AD-A158382] N86-14037

DIFFRACTION PATTERNS

Intelligent laser diffraction instrumentation for particle size analysis N86-13581

Cerenkov radiation from periodic bunches for a finite path in air
[AD-A159027] N86-13635

Small X-ray diffraction of immunoglobulin-membrane complexes
[AD-A158252] N86-13882

DIFFUSE RADIATION

Measurement and modeling of the optical scattering properties of crop canopies N86-13798

DIFFUSION

Appearance of superplasticity effect in aluminum alloys with lithium N86-13432

Complex nickel-aluminide coatings on nickel-chromium alloy EP648-VI N86-13437

Influence of annealing on hardness of vacuum-diffusion chromium coating on low-carbon steel N86-13441

Micromechanisms of electrodiffusion failures in thin film metallization N86-13472

Silicide coatings for protecting titanium-niobium alloys from high-temperature oxidation N86-13476

Determination of convective diffusion heat/mass transfer rates to burner rig test targets comparable in size to cross-stream jet diameter
[NASA-TM-87176] N86-13678

Positron diffusion in Si
[DE85-014831] N86-14076

DIFFUSION COEFFICIENT

Mass transfer coefficients and Henry's constants for packed-tower air stripping of volatile organics: Measurements and correlation
[AD-A158811] N86-13375

Numerical modeling of carrier transport in submicron bipolar transistors N86-13642

DIFFUSION FLAMES

Analysis of heterogeneous diffusion flame stabilization
N86-13527

DIFFUSION THEORY

Close-spaced high temperature Knudsen flow
[AD-A158280] N86-13831

DIFFUSION WAVES

Waves which travel upstream in boundary layors
[AD-A157949] N86-13684

DIFFUSION WELDING

Ion nitriding of titanium N86-13473

Influence of thermal cycle on characteristics of cyclical crack resistance of titanium alloys and their joints produced by diffusion welding N86-13486

Kinetics of dissolution of oxide films in titanium upon diffusion welding N86-13487

Influence of structure of heat-resistant nickel alloy ZhS6U on its weldability in the solid state N86-13492

Diffusion welding of copper-chromium pseudoalloy with copper N86-13493

DIFLUORO COMPOUNDS

Syntheis of difluoraminoxy-, difluoramino- or fluorodiazonium-containing materials N86-13509

DIGITAL COMMAND SYSTEMS

Development of a flight software testing methodology
[NASA-CR-176391] N86-13922

DIGITAL COMPUTERS

Application of computers in analytical chemistry: Calculation of optimum acidity of reaction between metal ions and organic reagents in solution N86-13607

DIGITAL NAVIGATION

Effects of digital altimetry on pilot workload
[NASA-TM-86424] N86-13892

DIGITAL SYSTEMS

Digital servocontroller system. Volume 4. Results and conclusions
[AD-A159068] N86-13335

Discussion on the Vibration Process Standards 9958002 and 9958004
[DE85-017116] N86-13599

Distributed sensor networks
[AD-A158033] N86-13628

Agile Electromagnetics Exploiting High Speed Logic (AEEHSL)
[AD-A158380] N86-13630

Analog-to-Digital converter
[AD-D011878] N86-13660

High frequency quantitative analysis of magnetomechanical acoustic emission
[AD-A158222] N86-13750

DIGITAL TECHNIQUES

Optical processing and phase conjugation
N86-13573

DIGITALIS

Effects of digital altimetry on pilot workload
[NASA-TM-86424] N86-13892

DILUTION

Specialists Meeting on Atomization and Nondilute Sprays
[AD-A159006] N86-13634

DIMENSIONAL ANALYSIS

Unified method for delay analysis of random multiple access algorithms
[AD-A159108] N86-13981

DIMENSIONS

On asymptotic distribution of the test statistic for the mean of the nonisotropic principal component
[AD-A158255] N86-13972

Spectra for large dimensional random matrices
[AD-A158256] N86-13973

DINITRATES

Electrolytic preparation of novel azidodinitro compounds N86-13508

DIRECT CURRENT

Design, construction and testing of a dc bioeffects enclosure for small animals
[DE05-016798] N86-13883

DIRECTIVITY

Reflectance modeling N86-13795

Bidirectional reflectance modeling of non-homogeneous plant canopies N86-13796

Understanding the radiant scattering behavior of vegetated scenes N86-13797

Atmospheric and science complexity effects on surface bidirectional reflectance N86-13803

The characterization of surface varigation effects on remote sensing N86-13805

DISPENSERS

A study of rhenium as an alternate substrate material for impregnated dispenser cathodes
[AD-A159113] N86-13415

DISPERSING

Effect of heating conditions on agglomeration of powdered aluminum in air atmosphere N86-13460

DISPLACEMENT MEASUREMENT

Elastic-plastic deformation of a metal-matrix composite coupon with a center slot
[NASA-CR-178013] N86-13496

DISPLAY DEVICES

FRG's Dornier develops high-resolution display system
N86-13611

DISSIPATION

Macro- and microfractographic specifics of dissipated impact rupture of type 45 steel in the viscous-brittle transition interval N86-13466

DISSOCIATION

Application of quantum chemistry to atmospheric chemistry
[AD-A158282] N86-13856

Extended atmospheres of outer planet satellites and comets
[NASA-CR-176398] N86-14209

DISTRIBUTING

Simulating distributed reinforcement effects in concrete analysis
[DE85-009745] N86-13761

DISTRIBUTION

Physical distribution system for aircraft external fuel tanks-survey
[AD-A158275] N86-13324

DISTRIBUTION MOMENTS

Monte Carlo analysis of nonlinear statistical models. 1: Theory: Revision
[AD-A158613] N86-13990

DISTURBING FUNCTIONS

Computer program for post-flight analysis of rigid body moments acting on a launch vehicle first stage
[NASA-CR-166033] N86-13918

DIURETICS

The effect of spironolactone on the cardiocirculatory responses to upright tilt at sea level and at simulated high altitude
[AD-A157734] N86-13887

DIVERTERS

Impact of a poloidal divertor in ignition tokamak design
[DE85-012892] N86-14061

DOCUMENTS

CREF: An editing facility for managing structured text
[AD-A158155] N86-14077

DOPES

Application of cross-sectional transmission electron microscopy to the characterization of ion-implanted semiconductors
[DE85-010990] N86-14075

DOPPLER EFFECT

Experience in measuring mean wind velocity profile in lower troposphere by sodar anemometer under inversion and convective conditions N86-13782

Determining quasi-real-time location of ships using geostationary navigational satellites N86-14165

Organization of space navigation system based on use of geostationary satellites N86-14166

DOPPLER RADAR

Precision pointing using a dual-wedge scanner
[NASA-CR-3946] N86-13813

DOSAGE

Aircrew dose and engine dust ingestion from nuclear cloud penetration
[AD-A159246] N86-13327

DOWNWASH

Some design philosophy for reducing the community noise of advanced counter-rotation propellers
[NASA-TM-87099] N86-14007

DRAINAGE

The Vaiont Slide. A geotechnical analysis based on new geologic observations of the failure surface. Volume 1: Main text
[AD-A158192] N86-13854

DRIFT RATE

Numerical modeling of carrier transport in submicron bipolar transistors N86-13642

DROPS (LIQUIDS)

Laser emission and coherent Raman scattering from individual flowing droplets N86-13578

Size and shape characterization of individual flowing droplets by laser light scattering N86-13579

Spray characterization with a nonintrusive optical single particle counter N86-13580

Intelligent laser diffraction instrumentation for particle size analysis N86-13581

Real-time, two-dimensional fuel spray visualization
N86-13583

Combustion behavior of free boron slurry droplets
[AD-A158620] N86-13585

DUCTS

Laboratory studies of steep and breaking deep water waves in a convergent channel
[AD-A158187] N86-13875

The physics and technology of strong magnetic fields (chapter 10)
[AD-A158174] N86-14000

DURABILITY

A durable airfield marking system
[AD-A157953] N86-13339

Effect of elastoplastic cyclic deformation on mechanical characteristics of steel O3Kh13AG19 at temperatures of 293 and 77 deg K N86-13463

Durability of steel 45 with boride coating in corrosive-abrasive media N86-13467

Dispersion hardening of high-strength NiOCo-Mo steels N86-13468

Modeling of thermal fatigue and erosion of complex alloyed steels in metal melts N86-13469

Study of effect of normal reactor water on growth rate of fatigue cracks in 15Kh2NMFA steel N86-13470

Ion nitriding of titanium N86-13473

Silicide coatings for protecting titanium-niobium alloys from high-temperature oxidation N86-13476

Changes in structure and mechanical properties of niobium-titanium alloy during oxygen saturation
N86-13479

DUST

Aircrew dose and engine dust ingestion from nuclear cloud penetration
[AD-A159246] N86-13327

DYNAMIC CHARACTERISTICS

Study of mean free path effects on growth of ultrafine metallic aerosols
[AD-A158206] N86-13393

Calculation of damping properties of composite materials N86-13446

Structural characteristic of temperature field over sea
N86-13783

Analysis of the dynamic behavior of an intense charged particle beam using the semigroup approach
[AD-A159247] N86-14015

DYNAMIC CONTROL
Further results for application of disturbance minimization control techniques to a linear, time-invariant, second-order state set-point regulator problem
[AD-A157793] N86-13961

DYNAMIC LOADS
Structures and materials technology issues for reusable launch vehicles
[NASA-TM-87626] N86-13349
Wind loading on solar collectors
[DE85-012151] N86-13833

DYNAMIC MODELS
Assessment of aerodynamic and dynamic models in a comprehensive analysis
[NASA-TM-86835] N86-13286
Dynamic identification for control of large space structures
[NASA-CR-176380] N86-13587
Dynamic modeling of structures from measured complex modes N86-13591
Time-domain quasi-linear identification of nonlinear dynamic systems
[AIAA-83-0811-CP] N86-13592
Granular flow: Advanced Research and Technology Development (AR and TD) contract review
[DE85-017267] N86-13697

DYNAMIC RESPONSE
Application of Pasternak model to some soil-structure interaction problems. Volume 1: Solutions for plates continuously supported on a Pasternak base
[AD-A157776] N86-13594
Application of Pasternak model to some soil-structure interaction problems. Volume 2: Determination of foundation parameters and the choice of models
[AD-A157777] N86-13595

DYNAMIC STRUCTURAL ANALYSIS
Ground vibration test of the laminar flow control JStar airplane
[NASA-TM-86398] N86-13321
Dynamic identification for control of large space structures
[NASA-CR-176380] N86-13587
Large modal survey testing using the Ibrahim time domain identification technique
[AIAA-81-0528R] N86-13589
Time-domain quasi-linear identification of nonlinear dynamic systems
[AIAA-83-0811-CP] N86-13592
Cyclosymmetric approach to the dynamics of repetitive modular structures
[ESA-CR(P)-2062] N86-13739
An algorithm for simultaneous determination of modal frequencies and modal vectors of a dynamic impedance matrix
[ESA-CR(P)-2055] N86-13943
Control of space stations N86-14090

DYNAMICAL SYSTEMS
Turbulence and dynamical systems
[AD-A159026] N86-13691
Further results for application of disturbance minimization control techniques to a linear, time-invariant, second-order state set-point regulator problem
[AD-A157793] N86-13961

DYNAMICS EXPLORER 1 SATELLITE
DE 1 RIMS operational characteristics
[NASA-TM-86527] N86-13365

E

EARTH (PLANET)
Nature of megacycles in evolution of Earth, Mars, and Moon N86-14159

EARTH CRUST
Inversion of Rayleigh wave phase velocities between RSNT and RSON
[DE85-013242] N86-13859
Engineering evaluation of crustal faults using space survey data N86-14189

EARTH ENVIRONMENT
Remote sensing of Earth terrain N86-13808

EARTH HYDROSPHERE
Experience in conducting subsatellite experiments with water bodies in USSR and Hungarian People's Republic N86-14182

EARTH MOVEMENTS
Formation of underwater oceanic volcanoes and islands in relation to lithospheric thickness and movements N86-13776

EARTH OBSERVATIONS (FROM SPACE)
Study of Earth observation by frequency scanning. Volume 1: Executive summary
[ESA-CR(P)-2028-VOL-1] N86-13705
Study of Earth observation by frequency scanning. Volume 2
[ESA-CR(P)-2028-VOL-2] N86-13706
Space applications in geology N86-14167
Methods for complex space experiment in USSR for studying land from manned spacecraft N86-14181
Possibilities of using space survey for studying seasonal changes of landscapes in some regions of USSR N86-14183
Role of landscape research in development of space methods for studying Earth N86-14184
Compilation of landscape maps at different scales with use of space photoinformation N86-14187
Some approaches to organization of data bank in system for studying Earth's natural resources from space (using example of agriculture) N86-14194

EARTH ORBITS
Analytical investigation of the dynamics of tethered constellations in Earth orbit, phase 2
[NASA-CR-171611] N86-13345
Review of implications and usefulness of spacecraft servicing in Low Earth Orbit (LEO)
[MATRA-092/CC/AB/225-84] N86-13350
Solar concentrator degradation in Low Earth Orbit (LEO) N86-14102
Development of the VOLT-A shuttle experiment
[NASA-TM-87169] N86-14110
Preparation, analysis and release of simulated interplanetary grains into low grain orbit
[DE85-014133] N86-14211

EARTH RESOURCES
Data catalog series for space science and applications flight missions. Volume 4A: Descriptions of meteorological and terrestrial applications spacecraft and investigations
[NASA-TM-87501] N86-13869
Experience in complex mapping of natural resources in agrarian-industrial regions of Nonchernozem RSFSR using space photomaterials N86-14174
Possibilities of use of aerospace materials in predicting occurrence of petroleum and gas N86-14175
Role of landscape research in development of space methods for studying Earth N86-14184
Normalization of response of radiometric instrumentation for studying Earth's natural resources N86-14192

EARTH RESOURCES INFORMATION SYSTEM
Some approaches to organization of data bank in system for studying Earth's natural resources from space (using example of agriculture) N86-14194

EARTH ROTATION
Investigation of characteristics of synoptic movements on sphere N86-13770

EARTH SURFACE
Volcanoes discovered with radio beam N86-13777
Ground reflectance measurements from thematic mapper data N86-13801
Atmospheric and science complexity effects on surface bidirectional reflectance N86-13803
Atmospheric effect on remote sensing of the Earth's surface N86-13804
The characterization of surface varigation effects on remote sensing N86-13805
Multidimensional modeling of atmospheric effects and surface heterogeneities on remote sensing N86-13806
Scattering models and basic experiments in the microwave regime N86-13807
Discrete random media techniques for microwave modeling of vegetated terrain N86-13809
Determination of backscattering sources in various targets N86-13811

EARTHQUAKES
Inversion of Rayleigh wave phase velocities between RSNT and RSON
[DE85-013242] N86-13859
Characteristics of microearthquakes accompanying hydraulic fracturing as determined from studies of spectra of seismic waveforms
[DE85-009558] N86-13860

ECONOMIC ANALYSIS
Existence of equilibrium prices for a simple planning model
[AD-A158263] N86-13996

ECONOMIC IMPACT
USSR report: Machine tools and metalworking equipment
[JPRS-UMM-85-013] N86-13745

ECONOMICS
USSR report: Machine tools and metalworking equipment
[JPRS-UMM-85-014] N86-13742
Review of SERI solar pond work
[DE85-012162] N86-13834

ECOSYSTEMS
Interaction between Escherichia coli and lunar fines N86-14088

EDDY CURRENTS
Exploratory development on advanced eddy current coil excitation and signal processing
[AD-A159226] N86-13752
Mathematical models of nonstationary eddy currents and eddy movements of fluid in problems of orientation and stabilization of artificial Earth satellites and spacecraft 2 N86-14116
Mathematical models of nonstationary eddy currents and eddy motions of fluid in spacecraft orientation and stabilization problems 1 N86-14133
Experimental checking of mathematical model of eddy currents in actuating components of systems for magnetic orientation of artificial Earth satellites and spacecraft N86-14164

EDGES
Results of research in four topic areas: The singularity expansion method, transient scattering measurements, high-frequency diffraction at edges residing on interfaces and cylindrical coordinate representation of dyadic Green's functions
[AD-A158382] N86-14037

EDITING
CREF: An editing facility for managing structured text
[AD-A158155] N86-14077

EDITING ROUTINES (COMPUTERS)
METCUT: A computer aided system for machining technology
[AD-A157941] N86-13927

EDUCATION
Expanding your horizons in science and mathematics
[NASA-CR-176372] N86-13958
The 1983 NASA/ASEE Summer Faculty Fellowship Research Program research reports
[NASA-CR-171904] N86-14078

EFFICIENCY
Small solar power systems plant in Almeria system evaluation and comparison on thermal basis
[DE85-017185] N86-13840
Solar concentrator degradation in Low Earth Orbit (LEO) N86-14102

EFFLUENTS
Far-field model of the regional influence of affluent plumes from Ocean Thermal Energy Conversion (OTEC) plants
[DE85-016981] N86-13836

EIGENVALUES
A method to stabilize linear systems using eigenvalue gradient information
[NASA-TP-2479] N86-13946
A linear combination test for detecting serial correlation in multivariate samples
[AD-A158179] N86-13967
Computable bounds for solutions of integral equations
[AD-A158189] N86-13970
Spectra for large dimensional random matrices
[AD-A158256] N86-13973
Inference on the ranks of the canonical correlation matrices for elliptically symmetric populations
[AD-A158268] N86-13976

EIGENVECTORS
Boundary-value problem for two-dimensional fluctuations in boundary layers
[AD-A157952] N86-13685

EJECTA
Experimental investigation of crater growth dynamics
[NASA-CR-176392] N86-14212

EJECTION SEATS
Passive arm retention curtain
[AD-D011876] N86-13307

ELASTIC BARS
A functional equation governing moving phase boundaries in an elastic bar
[AD-A158178] N86-13757

ELASTIC DEFORMATION
Effect of elastoplastic cyclic deformation on mechanical characteristics of steel O3Kh13AG19 at temperatures of 293 and 77 deg K N86-13463
Lubrication of nonconformal contacts
[NASA-TM-87120] N86-13679

ELASTIC PROPERTIES
A method to determine dynamic elastic constants of thin shell composites by guided ultrasonic waves
[AD-A159025] N86-13381
Temperature-frequency variation of mechanical losses in periodic deformation of multilayer glass-reinforced plastics N86-13449
Superelastic behavior of powdered titanium nickelide during pressing N86-13461
Errors due to counting statistics in the triaxial strain (stress) tensor determined by diffraction
[AD-A158219] N86-13759
Acoustical scattering from an elastic sphere in water: Surface wave glory, resonances, and the Sommerfeld-Watson transformation for amplitudes
[AD-A158884] N86-14010

ELASTIC SCATTERING
Effective medium theory for partially saturated porous solids
[DE85-016608] N86-13598
The (58)Ni + n transmission, capture and differential elastic scattering data analysis in the resonance region
[DE85-016157] N86-14026
Effects of neutrals on internal forces and thermal conduction of a plasma in a magnetic field
[IPPJ-691] N86-14051
ELASTOMERS
Study of cross-linking density and the type of cross linkage in polyurethane elastomers
[AD-A158199] N86-13497
ELASTOPLASTICITY
Effect of elastoplastic cyclic deformation on mechanical characteristics of steel O3Kh13AG19 at temperatures of 293 and 77 deg K N86-13463
Elastic-plastic deformation of a metal-matrix composite coupon with a center slot
[NASA-CR-178013] N86-13496
A numerical investigation into the plastic stress and strain fields around a surface crack
[ARL/STRUC-R-414] N86-13754
ELECTRIC CHARGE
Charge-density waves observed with a tunneling microscope
[AD-A158779] N86-13709
Determination of the activation barrier to energy transfer from 3 pi pi* to charge transfer levels via steady state and transient luminescence measurements on Bis(4-Chlorothiophenol) (1,10-Phenanthroline) Zinc (II)
[AD-A158239] N86-14012
ELECTRIC CONDUCTORS
Critical behavior of thermoelectric power in binary composite materials N86-13448
Method of synthesizing polymers from a solid electrolyte
[DE85-011623] N86-13504
Cathode for use in high energy primary thionyl chloride cell systems and high energy primary thionyl chloride cell systems including the cathode
[AD-D011882] N86-13662
ELECTRIC CONTACTS
Electrical sliding joint literature review (viewgraph presentation)
[DE85-011571] N86-13666
ELECTRIC EQUIPMENT TESTS
Electrical motor with superconducting winding --- actuators
[SEP-TS/SE/BT/10026/85] N86-13668
ELECTRIC FIELDS
Interpretation of F-106B in-flight lightning signatures
[NASA-CR-176387] N86-13320
Certain features of laser destruction and dislocational structure of silicon during heating and effects of electrical field N86-13454
Laser diagnostics for electric field measurements
N86-13563
Variable field effects for the rotating fluidized bed reactor N86-13565
Horizontal electric fields from lightning return strokes
[DE85-016367] N86-13873
Effects of 60 Hz electric fields on operant and social stress behaviors of nonhuman primates
[DE85-011992] N86-13885
Unlimited acceleration of charged particles by an electromagnetic wave with a purely transverse electric field propagating perpendicularly to a static magnetic field
[IPPJ-740] N86-14049
Effect of focusing field nonlinearities in MBE-4 on transverse beam dynamics
[DE85-016561] N86-14058
ELECTRIC GENERATORS
Two-hundred to 300 KVA conditioned power system - development, phase 1
[AD-A158820] N86-13832
ELECTRIC NETWORKS
Ada as a hardware description language: An initial report
[AD-A158217] N86-13935
ELECTRIC POTENTIAL
Verification of computer-aided designs of traveling-wave tubes utilizing novel dynamic refocusers and graphite electrodes for the multistage depressed collector
[NASA-TP-2524] N86-13643
Tests of compressed geometry NEC acceleration tubes
[DE85-016392] N86-14056
ELECTRIC POWER SUPPLIES
Low power reactor for remote applications
[DE85-012763] N86-14032
A study of some features of ac and dc electric power systems for a space station N86-14085
ELECTRIC PROPULSION
Basic processes of plasma propulsion N86-13554
Optical technique to measure electrode erosion
N86-13564
ELECTRIC ROCKET ENGINES
Completely magnetically contained electrothermal thruster N86-13558
ELECTRICAL ENGINEERING
Joint services electronics program
[AD-A158840] N86-13654
ELECTRICAL FAULTS
Experimental and theoretical studies of laser propulsion phenomenology
[AD-A158273] N86-13729
A study of some features of ac and dc electric power systems for a space station N86-14085
ELECTRICAL MEASUREMENT
Electrical research on solar cells and photovoltaic materials
[NASA-CR-176384] N86-13838
ELECTRICAL PROPERTIES
Electronic detection of low concentrations of organophosphorus compounds with a solid state device utilizing supported copper + cuprous oxide island films
[AD-A158181] N86-13392
A functional equation governing moving phase boundaries in an elastic bar
[AD-A158178] N86-13757
ELECTRICAL RESISTANCE
On anisotropy of mean electrical resistance of beryllium N86-13436
ELECTRICAL RESISTIVITY
Babinet's principle for an anisotropic resistive surface using different approaches
[AD-A159117] N86-13636
Electrical and thermal transport property studies of high-temperature thermoelectric materials
[AD-A158883] N86-13656
ELECTRO-OPTICAL PHOTOGRAPHY
Photoelectronic trajectory anatomy of RCA-C-73435 image converter and its performance
[DE85-013973] N86-13723
ELECTROCHEMICAL CELLS
Cathode including a non fluorinated linear chain polymer as the binder, method of making the cathode, and lithium electrochemical cell containing the cathode
[AD-D011807] N86-13647
ELECTROCHEMISTRY
Relationships between electronic spectroscopy and electrochemistry. A probe of reorganisation energies
[AD-A157940] N86-13389
ELECTRODE MATERIALS
Optical technique to measure electrode erosion
N86-13564
ELECTRODEPOSITION
Synthesis, structure and reactivity of molecules attached to electrode surfaces
[AD-A158621] N86-13394
ELECTRODES
Synthesis, structure and reactivity of molecules attached to electrode surfaces
[AD-A158621] N86-13394
Role of additives in minimizing zinc electrode shape change: The effect of lead on the kinetics of Zn(2) reduction in concentrated alkaline media
[AD-A158806] N86-13395
Verification of computer-aided designs of traveling-wave tubes utilizing novel dynamic refocusers and graphite electrodes for the multistage depressed collector
[NASA-TP-2524] N86-13643
Oxide electrodes at high temperatures
[DE85-006564] N86-13667
Tests of compressed geometry NEC acceleration tubes
[DE85-016392] N86-14056
ELECTROENCEPHALOGRAPHY
The event related brain potential as an index of information processing, cognitive activity, and skill acquisition: A program of basic research
[AD-A159118] N86-13897
ELECTROLUMINESCENCE
MeV electron beam irradiation effects on GaAs (1-x) P (x) LEDs (Light emitting diodes)
[AD-A158832] N86-13653
Luminescent properties of semiconductor electrodes
[AD-A158841] N86-13655
ELECTROLYTES
Role of additives in minimizing zinc electrode shape change: The effect of lead on the kinetics of Zn(2) reduction in concentrated alkaline media
[AD-A158806] N86-13395
Endocrine and fluid metabolism in males and females of different ages after bedrest, acceleration and lower body negative pressure
[NASA-TM-58270] N86-13886
ELECTROMAGNETIC INTERACTIONS
Interaction between powerful laser radiation and atmospheric aerosols N86-13788
The characterization of surface varigation effects on remote sensing N86-13805
ELECTROMAGNETIC MEASUREMENT
Interpretation of F-106B in-flight lightning signatures
[NASA-CR-176387] N86-13320
Measurement and modeling of the optical scattering properties of crop canopies N86-13798
ELECTROMAGNETIC PROPERTIES
Babinet's principle for an anisotropic resistive surface using different approaches
[AD-A159117] N86-13636
Active microwave properties of vegetation canopies
N86-13812
ELECTROMAGNETIC RADIATION
Babinet's principle for an anisotropic resistive surface using different approaches
[AD-A159117] N86-13636
Unlimited acceleration of charged particles by an electromagnetic wave with a purely transverse electric field propagating perpendicularly to a static magnetic field
[IPPJ-740] N86-14049
Electromagnetic particle-in-cell plasma simulation
[DE85-031223] N86-14054
Scientific activities of the Polish Academy of Sciences: Institute of Fundamental Technological Research in 1983
[ISBN-83-01-06288-6] N86-14107
European Science Notes, Volume 39, Number 7
[AD-A157708] N86-14108
ELECTROMAGNETIC SCATTERING
Optical/infrared properties of atmospheric aerosols with an in situ, multi-wavelength, multichannel nephelometer system
[AD-A158825] N86-13710
Fundamental remote sensing science research program: The Scene Radiation and Atmospheric Effects Characterization Project
[E86-10011] N86-13794
ELECTROMAGNETISM
Pulsed inductive energy transfer N86-13562
Agile Electromagnetics Exploiting High Speed Logic (AEEHSL)
[AD-A158380] N86-13630
Joint services electronics program
[AD-A158731] N86-13652
ELECTROMAGNETS
Iron dominated magnets
[DE85-014955] N86-14003
ELECTROMECHANICS
New applications of industrial robots noted
N86-13743
ELECTRON BEAMS
Influence of electron-beam heating on structure and phase composition of VT9 alloy N86-13481
MeV electron beam irradiation effects on GaAs (1-x) P (x) LEDs (Light emitting diodes)
[AD-A158832] N86-13653
Development of high sensitivity X-ray and electron beam resist processes
[AD-A158968] N86-13657
Linear accelerators for TeV colliders
[DE85-014958] N86-14017
Aspects of three field approximations: Darwin, frozen, EMPULSE
[DE85-014204] N86-14020
Preliminary experiment on electron beam injection for tokamak current drive
[IPPJ-739] N86-14048
Radio emission of injected electron beam with respect to diagnosis of ionospheric plasma N86-14145
ELECTRON CYCLOTRON HEATING
Doublet 3
[DE85-014369] N86-14031
Heating and confinement in the Doublet 3 tokamak with electron cyclotron heating
[DE85-014323] N86-14070
ELECTRON DENSITY (CONCENTRATION)
Charge composition of electrons in Earth's radiation belt N86-14146
ELECTRON EMISSION
Verification of computer-aided designs of traveling-wave tubes utilizing novel dynamic refocusers and graphite electrodes for the multistage depressed collector
[NASA-TP-2524] N86-13643
Atomically mixed alloy coated cathodes specification
[AD-D011877] N86-13659
Hot electron emission in semiconductors
[AD-A158042] N86-14072
ELECTRON ENERGY
Heating and confinement in the Doublet 3 tokamak with electron cyclotron heating
[DE85-014323] N86-14070
ELECTRON IRRADIATION
MeV electron beam irradiation effects on GaAs (1-x) P (x) LEDs (Light emitting diodes)
[AD-A158832] N86-13653

ELECTRON MASS
Hybrid simulation codes with application to shocks and upstream waves
[NASA-CR-176365] N86-13702
ELECTRON MICROSCOPES
Charge-density waves observed with a tunneling microscope
[AD-A158779] N86-13709
ELECTRON MICROSCOPY
Electronic detection of low concentrations of organophosphorus compounds with a solid state device utilizing supported copper + cuprous oxide island films
[AD-A158181] N86-13392
Structure and properties of Al-Mg-Zn casting alloys N86-13425
Structure formation in silumins upon rapid crystallization N86-13427
Analytical electron microscopy of surface modified ceramics
[DE85-016309] N86-13499
Comparison of ion milling techniques for cross-sectional TEM of semiconductors
[DE85-016596] N66-13664
Unusual occurrence of maghemite in soils developed on Knox group dolostones
[DE85-017158] N86-13817
Particulate matter analysis by electron microscopy
[PB85-227817] N86-13846
AuGa2 on GaSb(001): An epitaxial, thermodynamically stabilized Metal/3-5 compound semiconductor interface
[AD-A157937] N86-14071
The scanning electron microscope as a tool in space biology N86-14080
Electron microscopic observations of hydrogen implantation in ilmenites N86-14081
ELECTRON MOBILITY
Philips develops MBE process for laser, chip manufacture N86-13614
Numerical modeling of carrier transport in submicron bipoler transistors N86-13642
ELECTRON SPECTROSCOPY
Combined small angle X-ray scattering and transmission electron microscopy studies of Al-Li alloys
[DE85-016356] N86-13416
AuGa2 on GaSb(001): An epitaxial, thermodynamically stabilized Metal/3-5 compound semiconductor interface
[AD-A157937] N86-14071
ELECTRON STATES
Application of quantum chemistry to atmospheric chemistry
[AD-A158282] N86-13856
ELECTRON TRANSITIONS
Temperature and pressure components of shock-induced changes in the electronic spectrum of carbon disulfide
[AD-A158627] N86-13373
Resonant cars detection of OH radicals N86-13576
ELECTRON TUBES
Atomically mixed alloy coated cathodes specification
[AD-D011877] N86-13659
ELECTRON TUNNELING
Charge-density waves observed with a tunneling microscope
[AD-A158779] N86-13709
ELECTRONIC EQUIPMENT
Electronic detection of low concentrations of organophosphorus compounds with a solid state device utilizing supported copper + cuprous oxide island films
[AD-A158181] N86-13392
Joint services electronics program
[AD-A158840] N86-13654
Rocket engine hot-spot detector
[NASA-CR-171902] N86-13708
USSR report: Machine tools and metalworking equipment
[JPRS-UMM-85-013] N86-13745
ELECTRONIC SPECTRA
Relationships between electronic spectroscopy and electrochemistry. A probe of reorganisation energies
[AD-A157940] N86-13389
ELECTRONS
The mathematical structure of elementary particles: 2
[AD-A158191] N86-14011
Theory of resistivity-gradient-driven turbulence
[DE85-015068] N86-14053
ELECTROPHORESIS
Molecular mechanisms of mutagenesis determined by the recombinant DNA technology
[DE85-016353] N86-13884
ELECTROSTATIC CHARGE
A method for melt-coating a surface
[AD-D011866] N86-13596
ELECTROSTATICS
JASON electrostatic boundary conditions: A survey
[DE85-014521] N86-14005
Analysis of the dynamic behavior of an intense charged particle beam using the semigroup approach
[AD-A159247] N86-14015
ELECTROTHERMAL ENGINES
Completely magnetically contained electrothermal thruster N86-13558
ELEMENTARY PARTICLES
The mathematical structure of elementary particles: 2
[AD-A158191] N86-14011
ELLIPTIC DIFFERENTIAL EQUATIONS
Multigrid solutions to quasi-elliptic schemes
[NASA-CR-177973] N86-13955
ELLIPTICAL ORBITS
Periodic regimes of rotational motion of solid body about liberation point L sub 4 in restricted elliptical three-body problem N86-14132
ELLIPTICITY
Non-Newtonian flow past curved external surfaces N86-13671
ELUTION
Elution of benzene and methyl ethyl ketone from charcoal beds by continued air sweeping
[AD-A158804] N86-13374
EMBRITTLEMENT
The influence of microstructure on temper embrittlement of low alloy steel N86-13405
EMERGENCIES
Advanced emergency openings for commercial aircraft
[NASA-TM-87580] N86-13305
EMISSION
Protocol for size-specific emission measurements (SIM-5) applied to PM(10)
[PB85-200194] N86-13847
EMISSION SPECTRA
Condensed matter at high shock pressures
[DE85-016443] N86-13399
High pressure solid propellant combustion zone structure from analysis of hydroxyl radical chemiluminescence N86-13529
Real-time, two-dimensional fuel spray visualization N86-13583
Investigation of dust associated with shell stars
[AD-A158945] N86-14210
EMITTANCE
Scheme to funnel ion beams with a radio-frequency quadrupole
[DE85-015689] N86-14016
ENCLOSURE
Design, construction and testing of a dc bioeffects enclosure for small animals
[DE05-016798] N86-13883
ENDOCRINE GLANDS
Endocrine and fluid metabolism in males and females of different ages after bedrest, acceleration and lower body negative pressure
[NASA-TM-58270] N86-13886
ENERGETIC PARTICLES
Solar flare X-radiation and high-energy particles according to observational data from Venera-13 and Venera-14 automatic interplanetary stations N86-14119
ENERGY ABSORPTION
Coupling between gas dynamics and microwave energy absorption N86-13561
A method for melt-coating a surface
[AD-D011866] N86-13596
Experimental and theoretical studies of laser propulsion phenomenology
[AD-A158273] N86-13729
Small solar power systems plant in Almeria system evaluation and comparison on thermal basis
[DE85-017185] N86-13840
ENERGY CONSERVATION
Polymer, metal and ceramic matrix composites for advanced aircraft engine applications
[NASA-TM-87132] N86-13407
USSR report: Energy
[JPRS-UEN-85-001] N86-13861
ENERGY CONVERSION
Laser thermal propulsion N86-13548
Advanced energy conversion concept for microwave beamed-energy propulsions N86-13553
Close-space, high temperature Knudsen flow N86-13568
ENERGY CONVERSION EFFICIENCY
Aerodynamic performance of a new LM 17.2 m rotor --- wind energy converter N86-13827
Development of stable high efficiency polycrystalline thin-film solar cells based on CuInSe2
[DE85-000517] N86-13837
ENERGY DISSIPATION
Laboratory studies of steep and breaking deep water waves in a convergent channel
[AD-A158187] N86-13875
ENERGY POLICY
Implementing agreement for cooperation in the development of large scale wind energy conversion systems --- conferences
[JUEL-SPEZ-304] N86-13820
ENERGY SOURCES
Role of intrinsic energy source in physical behavior of split cometary nucleus N86-14120
ENERGY SPECTRA
Hadron component of cosmic radiation at atmospheric depth 800 g/cm(2) in Energy Range 70 to 700 GeV N86-13793
Dependence of length of free path of flare particles on energy N86-14141
Observation of small-scale solar wind structure on front of sharp increase in plasma flow velocity N86-14142
ENERGY STORAGE
Microcomputer controlled current sharing experiments with parallel converters
[DE85-013854] N86-13665
First order estimates of the dynamics and energetics of a rapidly decelerating flywheel
[DE85-013908] N86-13842
ENERGY TECHNOLOGY
USSR report: Energy
[JPRS-UEN-85-001] N86-13861
ENERGY TRANSFER
Pulsed inductive energy transfer N86-13562
Measurement of rate constants of elementary gas reactions of importance to upper atmosphere and combustion systems
[AD-A158824] N86-13857
Understanding climate: A strategy for climate modeling and predictability research, 1985-1995
[NASA-RP-1158] N86-13866
Determination of the activation barrier to energy transfer from 3 pi pi* to charge transfer levels via steady state and transient luminescence measurements on Bis(4-Chlorothiophenol) (1,10-Phenanthroline) Zinc (II)
[AD-A158239] N86-14012
Metastable interactions: Dissociative excitation
[AD-A158733] N86-14013
Energy exchange of plants under weightlessness conditions N86-14162
ENGINE DESIGN
Erosion and onset mechanisms in magnetoplasmadynamic thrusters N86-13556
Stirling engine supporting research and technology
[NASA-TM-87175] N86-14106
ENGINE PARTS
Stirling engine supporting research and technology
[NASA-TM-87175] N86-14106
ENGINE TESTS
Report on investigation of alcohol combustion associated wear in spark ignition engines, mechanisms and lubricant effects
[AD-A157714] N86-13388
Stirling engine supporting research and technology
[NASA-TM-87175] N86-14106
ENTHALPY
Thermophysical properties of tungsten at high temperatures N86-13458
The formulation of a hyperbolic Stefan problem
[ORNL-6065] N86-13952
ENTRAINMENT
Formation of structure of mixed region under influence of shear flow in stratified fluid N86-13768
ENTROPY
Shock waves, increase of entropy and loss of information
[DE85-013645] N86-13701
Decay with a rate for noncompactly supported solutions of conservation laws
[AD-A158163] N86-13962
Information in censored models
[AD-A158644] N86-13999
ENTROPY (STATISTICS)
Differential entropy and the statistics of instantaneous failure
[AD-A158047] N86-13984
ENVIRONMENT EFFECTS
Environmental Stress Screening (ESS)
[AD-A158262] N86-13751
ENVIRONMENT MODELS
Understanding climate: A strategy for climate modeling and predictability research, 1985-1995
[NASA-RP-1158] N86-13866
Target tracking based scene analysis
[AD-A158629] N86-13910
ENVIRONMENT SIMULATION
Wind tunnel simulations of aeolian processes
[NASA-CR-176382] N86-13269
ENVIRONMENTAL MONITORING
Development and evaluation of an instantaneous atmospheric corrosion rate monitor
[PB85-214336] N86-13727

ENVIRONMENTAL TESTS
Assembly Integration Verification (AIV) test effectiveness study. Applicability of Spacelab approach for equipment and system test for Ariane-4 class satellites. Volume 1: Executive summary
[ERNO-671/AIV-VOL-1] N86-13361
ENVIRONMENTS
Design criteria upgrade for US Army Type 2 air traffic control towers
[AD-A159115] N86-13314
EPITAXY
CNET of France uses organo-metallic epitaxy for laser N86-13620
EPOXY COMPOUNDS
Energetic fluorcarbons N86-13517
EPOXY MATRIX COMPOSITES
Effect of carbon fibre surface treatment on moisture absorption and interlaminar shear strength of carbon Fibre/Epoxy resin composites
[AD-A157705] N86-13377
Study of the mechanical properties dispersion of carbon-epoxy composite materials
[M2-695600-PT-1] N86-13384
Study of the dispersion of the mechanical properties of carbon-epoxy composite materials
[M2-695600-PT-2] N86-13385
Employment of PAM-FISS-BI-phase computer program for the strength analysis and fracture/delamination behavior of components
[ESI-ED/83-383/RD/MS-VOL-7] N86-13763
EQUATIONS
Supercritical fluid properties
[DE85-011203] N86-13401
EQUATIONS OF MOTION
Non-Newtonian flow past curved external surfaces N86-13671
Modelling a transport equation of turbulent reactive mixing flow N86-13674
Implicit plasma simulation
[DE85-016088] N86-14055
Forming transformation matrices for different parameters of motion of celestial bodies N86-14112
EQUATIONS OF STATE
Condensed matter at high shock pressures
[DE85-016443] N86-13399
A fully viscous two-dimensional unsteady flow analysis applied to detonation transition in porous explosives
[AD-A157794] N86-13682
EQUATORIAL ORBITS
Analytical investigation of the dynamics of tethered constellations in Earth orbit, phase 2
[NASA-CR-171611] N86-13345
EQUATORIAL REGIONS
Vertical structure of turbulence and turbulent exchange in equatorial zone of Pacific Ocean N86-13771
Equatorial waves in ocean surface temperature field according to data from shipboard and satellite measurements N86-14171
EQUILIBRIUM FLOW
A three-dimensional analysis of natural convection in a toroidal loop N86-13672
EROSION
Structure of flow of erosion plasma formed upon laser treatment of metals N86-13455
Modeling of thermal fatigue and erosion of complex alloyed steels in metal melts N86-13469
Erosion and onset mechanisms in magnetoplasmadynamic thrusters N86-13556
Magnetoplasmadynamic thruster erosion research N86-13557
Optical technique to measure electrode erosion N86-13564
ERROR ANALYSIS
Study of the dispersion of the mechanical properties of carbon-epoxy composite materials
[M2-695600-PT-2] N86-13385
Crop area estimation based on remotely-sensed data with an accurate but costly subsample
[NASA-CR-176017] N86-13814
Sampling-rate effects on radar-derived rainfall estimates
[AD-A158203] N86-13870
Scout trajectory error propagation computer program
[NASA-CR-166030] N86-13919
A priori guaranteed accuracy evaluation in determining spacecraft orbit by least squares method N86-14130
Pressure field retrieval by remote refractometry from space N86-14168
ERROR DETECTION CODES
Development of a flight software testing methodology
[NASA-CR-176391] N86-13922
Techniques for the design and implementation of highly reliable multi-processing systems
[AD-A159236] N86-13945
ERRORS
Errors due to counting statistics in the triaxial strain (stress) tensor determined by diffraction
[AD-A158219] N86-13759
Sampling-rate effects on radar-derived rainfall estimates
[AD-A158203] N86-13870
The h-p version of the finite element method
[AD-A158194] N86-13971
ERS-1 (ESA SATELLITE)
Feasibility study of chirp generator for ERS-1 radar altimeter, option A
[ELAB-STF44-F83103] N86-13368
The construction and testing of a real-time digital breadboard processor for the ESA remote sensing satellite synthetic aperature radar
[REPT-00-0778] N86-13911
ERYTHROCYTES
The scanning electron microscope as a tool in space biology N86-14080
ESCHERICHIA
Interaction between Escherichia coli and lunar fines N86-14088
ESTERS
Fluoropolyazido-esters as energetic polymers N86-13515
ESTIMATES
Potential for use of indium phosphide solar cells in the space radiation environment
[NASA-TM-87157] N86-13645
Accuracy of schemes with nonuniform meshes for compressible fluid flows
[NASA-CR-177988] N86-13954
The theory of standardized time series
[AD-A158383] N86-13989
Monte Carlo analysis of nonlinear statistical models. 1. Theory: Revision
[AD-A158613] N86-1399
Variability of rainfall over small areas N86-140
ESTIMATING
Discovery of the Kalman filter as a practical tool for aerospace and industry
[NASA-TM-86847] N86-13311
Microscopic observations and mechanics analyses of long term fracture in polyethylene piping materials
[PB85-219608] N86-13506
Crop area estimation based on remotely-sensed data with an accurate but costly subsample
[NASA-CR-176017] N86-13814
Spectral methods for discontinuous problems
[NASA-CR-177974] N86-13953
ETHANE
Critical charge for the direct initiation of detonation in gaseous fuel-air mixtures
[DE85-016130] N86-13696
ETHYL ALCOHOL
Study of optical-acoustical phenomena at surface of strongly absorbing clearing fluids N86-13774
ETHYLENE COMPOUNDS
Study of optical-acoustical phenomena at surface of strongly absorbing clearing fluids N86-13774
EULER EQUATIONS OF MOTION
Stable boundary conditions and difference schemes for Navier-Stokes equations
[NASA-CR-177984] N86-13957
EULER-LAMBERT EQUATION
Approximate solutions of Euler-Lambert equation for case of several revolutions about central body N86-14121
EURECA (ESA)
EURECA: An introduction to Europe's free-flying retrievable carrier
[ESA-BR-30] N86-13352
EUROPEAN COMMUNICATIONS SATELLITE
Sun acquisition sensor for European Communications Satellite N86-13366
EUROPEAN SPACE AGENCY
Report on the scientific satellites of the European Space Agency
[ESA-SP-1072] N86-13344
EUROPEAN SPACE PROGRAMS
Report on the scientific satellites of the European Space Agency
[ESA-SP-1072] N86-13344
Aerothermodynamics for future launchers. Review of the state of the art in Europe
[VKI-CR-1984-16/AR] N86-13347
EURECA: An introduction to Europe's free-flying retrievable carrier
[ESA-BR-30] N86-13352
EVACUATING (TRANSPORTATION)
Advanced emergency openings for commercial aircraft
[NASA-TM-87580] N86-13305
EVALUATION
Fabrication and evaluation of superplastically formed/weld-brazed corrugated compression panels with beaded webs
[NASA-TP-2512] N86-13406
The effect of cobalt content in U-700 type alloys on degradation of aluminide coatings
[NASA-TM-87173] N86-13408
Discussion on the Vibration Process Standards 9958002 and 9958004
[DE85-017116] N86-13599
Issues to be considered in the evaluation of technical proposals from the Ada (trademark) language perspective
[AD-A158376] N86-13936
Preliminary measurement of the noise from the 2/9 scale model of the Large-scale Advanced Propfan (LAP) propeller, SR-7A
[NASA-TM-87116] N86-14006
Test method for telescopes using a point source at a finite distance
[NASA-TM-86523] N86-14033
Computer graphics applications to crew displays N86-14104
Method for using clusters in evaluating land use areas from multizonal photographs N86-14180
EVENTS
The event related brain potential as an index of information processing, cognitive activity, and skill acquisition: A program of basic research
[AD-A159118] N86-13897
EVOLUTION (DEVELOPMENT)
Role of intrinsic energy source in physical behavior of split cometary nucleus N86-14120
EXCIMER LASERS
Excimer laser produces .2 micron semiconductor structures N86-13613
EXCITATION
Multilevel relaxation phenomena and population trapping
[DE85-011527] N86-13731
Exploratory development on advanced eddy current coil excitation and signal processing
[AD-A159228] N86-13752
EXCRETION
Endocrine and fluid metabolism in males and females of different ages after bedrest, acceleration and lower body negative pressure
[NASA-TM-58270] N86-13886
EXHAUST FLOW SIMULATION
High-altitude plume computer code development
[NASA-CR-171600] N86-13923
EXHAUST GASES
High-altitude plume computer code development
[NASA-CR-171600] N86-13923
EXOBIOLOGY
The scanning electron microscope as a tool in space biology N86-14080
EXPERIENCE
Recent experience in the RAE (Royal Aircraft Establishment) 5-metre wind tunnel of a china clay method for indicating boundary layer transition
[AD-A157943] N86-13302
EXPERIMENT DESIGN
Study of the dispersion of the mechanical properties of carbon-epoxy composite materials
[M2-695600-PT-2] N86-13385
EXPERIMENTATION
Experimental investigation of magnesium combustion in steam
[AD-A159109] N86-13396
Experiments with non-Darcy flow in joints with large scale roughness
[DE85-015714] N86-13695
Experimental investigation of heat transfer behavior of aqueous foams in thermal entry region of pipe flow
[DE85-012836] N86-13700
Test method for telescopes using a point source at a finite distance
[NASA-TM-86523] N86-14033
EXPERT SYSTEMS
DIESS: A prolog implementation of a domain-independent expert system shell
[AD-A158014] N86-13928
EXPLODING WIRES
Experimental investigation of magnesium combustion in steam
[AD-A159109] N86-13396
EXPLOSIVE DEVICES
Advanced emergency openings for commercial aircraft
[NASA-TM-87580] N86-13305
EXPLOSIVES
Synthesis of new polynitropolyhedranes N86-13510
A fully viscous two-dimensional unsteady flow analysis applied to detonation transition in porous explosives
[AD-A157794] N86-13682

EXPOSURE
Time dependency of strainrange partitioning life relationships
[NASA-CR-174946] N86-13755
EXTERNAL STORE SEPARATION
On applications of chimera grid schemes to store separation
[NASA-TM-88193] N86-13292
EXTRACTION
Hierarchical image segmentation to infrared images
[AD-A158030] N86-14035
EXTREME ULTRAVIOLET RADIATION
Lattice and bypass design for a coherent XUV facility
[DE85-016556] N86-14002
EXTRUDING
Characterization of 7017 aluminum alloys in thick profiles, in the metallurgical versions T6510, T76510 and T736510, test report no. PV-44-607/F
[PV-44-607/F] N86-13420
Computerized simulation and display of extruding by cold forging
[CETIM-1-3L-11-1] N86-13741

F

F-106 AIRCRAFT
Interpretation of F-106B in-flight lightning signatures
[NASA-CR-176387] N86-13320
FABRICATION
Composites design
[AD-A157710] N86-13378
Fabrication and evaluation of superplastically formed/weld-brazed corrugated compression panels with beaded webs
[NASA-TP-2512] N86-13406
A study of rhenium as an alternate substrate material for impregnated dispenser cathodes
[AD-A159113] N86-13415
Preparation of ceramic fiber-ceramic matrix composites by a faster chemical vapor infiltration process
[DE85-016402] N86-13500
ATR 42 production work in French, Italian plants detailed N86-13618
Apparatus for removably holding a plurality of microballoons
[DE85-006517] N86-13722
FABRICS
Determination of porosity of thin sheets of fiber materials based on optical transmission coefficient N86-13459
FACE CENTERED CUBIC LATTICES
High strain rate deformation in FCC metals and alloys
[DE85-017533] N86-13417
FAILURE
Macro- and microfractographic specifics of dissipated impact rupture of type 45 steel in the viscous-brittle transition interval N86-13466
The Vaiont Slide. A geotechnical analysis based on new geologic observations of the failure surface. Volume 1: Main text
[AD-A158192] N86-13854
The Vaiont Slide. A geotechnical analysis based on new geologic observations of the failure surface. Volume 2: Appendices A through G
[AD-A158193] N86-13855
Differential entropy and the statistics of instantaneous failure
[AD-A158047] N86-13984
Approximation of the initial reserve for known ruin probabilities
[AD-A158167] N86-13987
FAILURE ANALYSIS
A preliminary evaluation of the generalized likelihood ratio for detecting and identifying control element failures in a transport aircraft
[NASA-TM-87620] N86-13332
Specifics of the process of failure of structural steels strengthened by thermo-mechanical working with deformation in the intercritical temperature interval
N86-13464
Micromechanisms of electrodiffusion failures in thin film metalization N86-13472
Microscopic observations and mechanics analyses of long term fracture in polyethylene piping materials
[PB85-219608] N86-13506
FALLOUT
Aircrew dose and engine dust ingestion from nuclear cloud penetration
[AD-A159246] N86-13327
Interactive scenario computer model for dose rates to aircrews in flight through nuclear debris clouds
[AD-A158741] N86-13888
FAR FIELDS
Far-field boundary conditions in numerical solutions of the Navier-Stokes equations
[AD-A158776] N86-13690
FAR INFRARED RADIATION
Pulsed, optically pumped gas-mixture FIR lasers
N86-13609
Hot electron emission in semiconductors
[AD-A158042] N86-14072
Focal plane optics in far-infrared and submillimeter astronomy
[NASA-TM-88186] N86-14204
FARM CROPS
Reflection indicatrices of vegetation canopies
N86-14178
Approximate analytical formulas for computing spectral brightness coefficients for agricultural vegetation
N86-14179
FAST NUCLEAR REACTORS
Coupled radiation transport/thermal analysis of the radiation shield for a space nuclear reactor
[AD-A158180] N86-14022
FASTENERS
Latch for detachably securing electronic cards along orthogonal loading axes
[AD-D011865] N86-13737
FATIGUE (MATERIALS)
Standardised fatigue loading sequences for helicopter rotors (Helix and Felix). Part 2: Final definition of Helix and Felix
[AD-A156622] N86-13322
Study of effect of normal reactor water on growth rate of fatigue cracks in 15Kh2NMFA steel N86-13470
Design of traction drives
[NASA-RP-1154] N86-13734
Time dependency of strainrange partitioning life relationships
[NASA-CR-174946] N86-13755
Static fatigue of a sintered silicon nitride
[AD-A158813] N86-13760
FATIGUE LIFE
Evaluation of the titanium IMI 829 alloy produced by powder metallurgy
[M1-610200] N86-13421
Determining local heating parameters for increasing fatigue resistance of welded joints N86-13491
FATIGUE TESTS
Digital servocontroller system. Volume 4. Results and conclusions
[AD-A159068] N86-13335
FAULT TOLERANCE
Graph theoretic approaches to diagnostics: Applications of logic programming and cutset theory to aspects of reactor and circuit analysis
[ANL-84-74] N86-13912
Replication and fault-tolerance in the ISIS system
[AD-A157775] N86-13926
FEASIBILITY ANALYSIS
Characterization of 7017 aluminum alloys in thick profiles, in the metallurgical versions T6510, T76510 and T736510, test report no. PV-44-607/F
[PV-44-607/F] N86-13420
FEEDBACK
Basic principles of feedback and adaptive approaches in the finite element method
[AD-A158188] N86-13969
FEEDBACK CONTROL
Pitch rate versus G command as the longitudinal flight control system design strategy for a statistically unstable fighter type aircraft with two control surfaces
[AD-A158803] N86-13334
Preliminary experimental results of CT-6B tokamak heating field voltage feedback control N86-13601
Design and implementation of a compliant robot with force feedback and strategy planning software
[NASA-TM-86111] N86-13947
FEMALES
Expanding your horizons in science and mathematics
[NASA-CR-176372] N86-13958
FERRITES
On H plane dielectric loading theory for H plane ferrite phase shifter N86-13603
Slot line tunable bandpass filter
[AD-D011881] N86-13661
Recent results on implantation and permeation into fusion reactor materials
[DE85-014620] N86-14067
FIBER COMPOSITES
Effect of geometry of fiber packing on consolidation of fibrous composition materials with porous matrix
N86-13443
Calculation of damping properties of composite materials N86-13446
FIBER OPTICS
Optimal transfer function for fiber optic communications N86-13641
Expendable bathythermograph for measuring light attenuation and temperature below the ocean surface
[AD-D011870] N86-13716
Remote optical crack sensing system
[AD-D011872] N86-13718
Fiber optics as an angular sensor
[AD-D011886] N86-14044
Occasional reports of the Royal Observatory, Edinburgh, no. 16
[ISSN-0309-099-X] N86-14200
A multiple-object fibre-optics coupler for the 1.2-m UK Schmidt Telescope N86-14201
FIBER REINFORCED COMPOSITES
Effect of carbon fibre surface treatment on moisture absorption and interlaminar shear strength of carbon Fibre/Epoxy resin composites
[AD-A157705] N86-13377
FIBERS
Fiber composition materials for strengthening components of aluminum and its alloys N86-13424
Determination of porosity of thin sheets of fiber materials based on optical transmission coefficient N86-13459
FIELD EMISSION
Variable field effects for the rotating fluidized bed reactor N86-13565
FIELD THEORY (ALGEBRA)
A method for calculating flow fields around moving bodies
[NAL-TR-859T] N86-13288
FIELD THEORY (PHYSICS)
Structure and hydrodynamics of colloidal systems
[DE85-016294] N86-14027
FIGHTER AIRCRAFT
Pitch rate versus G command as the longitudinal flight control system design strategy for a statistically unstable fighter type aircraft with two control surfaces
[AD-A158803] N86-13334
FILTRATION
Ceramic fabric material testing
[DE85-013684] N86-13503
FINE STRUCTURE
Time resolved extended X-ray absorption fine structure spectrometer
[AD-D011869] N86-13715
FINGERS
Fiber optics as an angular sensor
[AD-D011886] N86-14044
FINITE DIFFERENCE THEORY
On applications of chimera grid schemes to store separation
[NASA-TM-88193] N86-13292
FINITE ELEMENT METHOD
A method for calculating flow fields around moving bodies
[NAL-TR-859T] N86-13288
Study of thermal analysis methods --- spacecraft
[GEC-MEL12.0539] N86-13362
A study of transport phenomena and interface stability during solidification of binary solutions using front tracking finite elements N86-13669
Non-Newtonian flow past curved external surfaces
N86-13671
Development of contact/impact capability for the three-dimensional fluid-structure interaction code: NEPTUNE
[DE85-010264] N86-13698
A numerical investigation into the plastic stress and strain fields around a surface crack
[ARL/STRUC-R-414] N86-13754
Basic principles of feedback and adaptive approaches in the finite element method
[AD-A158188] N86-13969
The h-p version of the finite element method
[AD-A158194] N86-13971
A finite element solution of the transport equation
[AD-A159245] N86-13982
Identification of nuclear materials from remote detection of characteristic gamma rays
[AD-A159244] N86-14014
Finite element or Galerkin type semidiscrete schemes
N86-14083
FLAME PROPAGATION
Interactions between a laminar flame and end gas autoignition
[DE85-008957] N86-13402
Strategy for advanced sensing and control of combustion N86-13574
FLAME SPECTROSCOPY
Coherent optical transient spectroscopy in flames
N86-13570
FLAME TEMPERATURE
Combustion behavior of free boron slurry droplets
[AD-A158620] N86-13585
FLAMES
Flame mechanisms and flame inhibition N86-13523
Combustion of hydrogen and hydrocarbons in fluorine
N86-13526
Experimental investigation of heterogeneous flame stabilization N86-13528

High pressure solid propellant combustion zone structure from analysis of hydroxyl radical chemiluminescence N86-13529

Evaluation of HMX propellant chemistry from Raman and laser induced fluorescence species and temperature measurements N86-13530

Flame-acoustic wave interaction during axial solid rocket instabilities N86-13542

FLEXIBILITY

A computational analysis of pulsating flow in rigid and deformable tubes N86-13673

FLEXIBLE SPACECRAFT

Adaptive control of large space structures using recursive lattice filters [NASA-CR-176402] N86-13358

Stability of stationary motions of two tethered bodies in orbit under influence of gravitational and aerodynamic forces N86-14163

FLIGHT ALTITUDE

Pitch rate versus G command as the longitudinal flight control system design strategy for a statistically unstable fighter type aircraft with two control surfaces [AD-A158803] N86-13334

FLIGHT CHARACTERISTICS

Limited Airworthiness and Flight Characteristics (A and FC) test of the quick fix configuration [AD-A157716] N86-13323

Polymer, metal and ceramic matrix composites for advanced aircraft engine applications [NASA-TM-87132] N86-13407

FLIGHT CONTROL

The evaluation of failure detection and isolation algorithms for restructurable control [NASA-CR-177983] N86-13310

Pitch rate versus G command as the longitudinal flight control system design strategy for a statistically unstable fighter type aircraft with two control surfaces [AD-A158803] N86-13334

Development of a flight software testing methodology [NASA-CR-176391] N86-13922

FLIGHT CREWS

Aircrew dose and engine dust ingestion from nuclear cloud penetration [AD-A159246] N86-13327

Enhancing sensitivity to visual motion and enhancing visual sensitivity [AD-A158800] N86-13889

FLIGHT PATHS

An analytical comparison of three visual approach slope indicators: VASIS, T-VASIS and PAPI [ARL/SYS-R-33] N86-13309

Interactive scenario computer model for dose rates to aircrews in flight through nuclear debris clouds [AD-A158741] N86-13888

FLIGHT TESTS

An analytical comparison of three visual approach slope indicators: VASIS, T-VASIS and PAPI [ARL/SYS-R-33] N86-13309

Limited Airworthiness and Flight Characteristics (A and FC) test of the quick fix configuration [AD-A157716] N86-13323

In-orbit technology demonstration program (TDP). Accommodation study: SPAS [MBB-URV-147/84] N86-13351

Assembly Integration Verification (AIV) test effectiveness study. Applicability of Spacelab approach for equipment and system test for Ariane-4 class satellites. Volume 1: Executive summary [ERNO-671/AIV-VOL-1] N86-13361

Development of a flight software testing methodology [NASA-CR-176391] N86-13922

FLOW CHARACTERISTICS

Computer program for calculating flow parameters and power requirements for cryogenic wind tunnels [NASA-TM-87609] N86-13338

Quantitative flow visualization N86-13572

A computational analysis of pulsating flow in rigid and deformable tubes N86-13673

Sensitivity to mean flow parameters of the low wavenumber content of the wall pressure under a turbulent boundary layer [AD-A158037] N86-13688

FLOW DISTRIBUTION

A method for calculating flow fields around moving bodies [NAL-TR-859T] N86-13288

Numerical solutions of Navier-Stokes equations for a Butler wing [NASA-CR-174202] N86-13293

A FORTRAN computer code for calculating flows in multiple-blade-element cascades [NASA-TM-87104] N86-13295

Computational aspects of zonal algorithms for solving the compressible Navier-Stokes equations in three dimensions [NASA-TM-86774] N86-13296

Ground effects on V/STOL and STOL aircraft: A survey [NASA-TM-86825] N86-13299

Studies of the flow field near a NACA 4412 aerofoil at nearly maximum lift [AD-A157750] N86-13301

Pressure-distribution measurements on a transonic low-aspect ratio wing [NASA-TM-86683] N86-13304

Analysis of heterogeneous diffusion flame stabilization N86-13527

Coupling between velocity oscillations and solid propellant combustion N86-13541

Flow field effects on combustion instability N86-13544

Rocket motor flow-turning losses N86-13545

The 1-D laser Doppler instrumentation N86-13575

Laser emission and coherent Raman scattering from individual flowing droplets N86-13578

Granular flow: Advanced Research and Technology Development (AR and TD) contract review [DE85-017267] N86-13697

Crushing strength of aluminum oxide agglomerates [AD-A158051] N86-13756

High-altitude plume computer code development [NASA-CR-171600] N86-13923

Experimental investigation of crater growth dynamics [NASA-CR-176392] N86-14212

FLOW VELOCITY

Strategy for advanced sensing and control of combustion N86-13574

Sparger system for MMH-helium vents N86-14096

FLOW VISUALIZATION

Recent experience in the RAE (Royal Aircraft Establishment) 5-metre wind tunnel of a china clay method for indicating boundary layer transition [AD-A157943] N86-13302

Pressure-distribution measurements on a transonic low-aspect ratio wing [NASA-TM-86683] N86-13304

Quantitative flow visualization N86-13572

Laser emission and coherent Raman scattering from individual flowing droplets N86-13578

Real-time, two-dimensional fuel spray visualization N86-13583

New flow visualization technique for water tunnel testing of combustors [AD-A158015] N86-13686

FLUID FILTERS

Ceramic fabric material testing [DE85-013684] N86-13503

FLUID FLOW

Experimental investigation of heterogeneous flame stabilization N86-13528

Problems in thermal convective instability N86-13670

Far-field boundary conditions in numerical solutions of the Navier-Stokes equations [AD-A158776] N86-13690

Experiments with non-Darcy flow in joints with large scale roughness [DE85-015714] N86-13695

Experimental investigation of heat transfer behavior of aqueous foams in thermal entry region of pipe flow [DE85-012836] N86-13700

Fluid forces on two circular cylinders in crossflow [DE85-014294] N86-13704

FLUID MECHANICS

Interactions between a laminar flame and end gas autoignition [DE85-008957] N86-13402

FLUID-SOLID INTERACTIONS

Development of contact/impact capability for the three-dimensional fluid-structure interaction code: NEPTUNE [DE85-010264] N86-13698

FLUIDIZED BED PROCESSORS

Variable field effects for the rotating fluidized bed reactor N86-13565

FLUORESCENCE

Quantitative flow visualization N86-13572

Application of atomic fluorescence to measurement of combustion temperatures in solid propellants N86-13582

Real-time, two-dimensional fuel spray visualization N86-13583

FLUORIDES

Fluoropolyazido-esters as energetic polymers N86-13515

FLUORINE

Combusion of hydrogen and hydrocarbons in fluorine N86-13526

Two-proton detection techniques for atomic fluorine N86-13569

Fluorine disposal N86-14095

FLUOROCARBONS

Energetic fluorcarbons N86-13517

FLUOROPOLYMERS

Cathode including a non fluorinated linear chain polymer as the binder, method of making the cathode, and lithium electrochemical cell containing the cathode [AD-D011807] N86-13647

FLUX (RATE)

Determination of neutron flux distribution by using ANISN, a one-dimensional discrete S sub n ordinates transport code with anisotropic scattering N86-14084

An unbiased X-ray sampling of stars within 25 parsecs of the Sun [NASA-CR-178544] N86-14206

FLUX DENSITY

An unbiased X-ray sampling of stars within 25 parsecs of the Sun [NASA-CR-178544] N86-14206

FLYWHEELS

First order estimates of the dynamics and energetics of a rapidly decelerating flywheel [DE85-013908] N86-13842

FOAMS

New flow visualization technique for water tunnel testing of combustors [AD-A158015] N86-13686

Experimental investigation of heat transfer behavior of aqueous foams in thermal entry region of pipe flow [DE85-012836] N86-13700

FOCUSING

Lattice and bypass design for a coherent XUV facility [DE85-016556] N86-14002

Scheme to funnel ion beams with a radio-frequency quadrupole [DE85-015689] N86-14016

Test method for telescopes using a point source at a finite distance [NASA-TM-86523] N86-14033

Effect of focusing field nonlinearities in MBE-4 on transverse beam dynamics [DE85-016561] N86-14058

Focal plane optics in far-infrared and submillimeter astronomy [NASA-TM-88186] N86-14204

FOG

Influence of fog microstructure on quality of optical image transmitted through it N86-13781

FOREST FIRE DETECTION

Problems in study and evaluation of consequences of forest fires using aerospace photographs N86-14176

FORESTS

Geometric-optical modeling of a conifer forest canopy N86-13799

Crop area estimation based on remotely-sensed data with an accurate but costly subsample [NASA-CR-176017] N86-13814

FORMING TECHNIQUES

Fabrication and evaluation of superplastically formed/weld-brazed corrugated compression panels with beaded webs [NASA-TP-2512] N86-13406

Activities report of the Technical and Scientific Research Center for the Metal Manufacturing Industry N86-13740

USSR report: Machine tools and metalworking equipment [JPRS-UMM-85-014] N86-13742

USSR report: Machine tools and metalworking equipment [JPRS-UMM-85-013] N86-13745

FORTRAN

A FORTRAN computer code for calculating flows in multiple-blade-element cascades [NASA-TM-87104] N86-13295

Computer program for post-flight evaluation of a launch vehicle upper-stage on-off reaction control system [NASA-CR-166029] N86-13921

BOSS: A FORTRAN code for a relational database manager [AD-A157067] N86-13924

FORWARD SCATTERING

Light scattering from bubbles in liquids [AD-A158736] N86-14039

FOUNDATIONS

Application of Pasternak model to some soil-structure interaction problems. Volume 1: Solutions for plates continuously supported on a Pasternak base [AD-A157776] N86-13594

FOURIER TRANSFORMATION

Scheme for high-speed real-time DFT operation for radar signal processing N86-13602

Boundary-value problem for two-dimensional fluctuations in boundary layers [AD-A157952] N86-13685

Convergence of cardinal series [AD-A158166] N86-13964

Real time large memory optical pattern recognition [AD-A158023] N86-14034

FRACTOGRAPHY
Macro- and microfractographic specifics of dissipated impact rupture of type 45 steel in the viscous-brittle transition interval N86-13466
Fractography of mixed mode 1 - 2 failure in Graphite/Epoxy and Graphite/Thermoplastic unidirectional composites [AD-A158852] N86-13498

FRACTURE MECHANICS
Study of fractures in cast parts of high-strength aluminum alloy N86-13429
Fractography of mixed mode 1 - 2 failure in Graphite/Epoxy and Graphite/Thermoplastic unidirectional composites [AD-A158852] N86-13498
Employment of PAM-FISS-BI-phase computer program for the strength analysis and fracture/delamination behavior of components [ESI-ED/83-383/RD/MS-VOL-7] N86-13763
Characteristics of microearthquakes accompanying hydraulic fracturing as determined from studies of spectra of seismic waveforms [DE85-009558] N86-13860
Scientific activities of the Polish Academy of Sciences: Institute of Fundamental Technological Research in 1983 [ISBN-83-01-06288-6] N86-14107

FRACTURE STRENGTH
Calculation of failure constant for titanium alloys N86-13474
Fractured toughness of Si3N4 measured with short bar chevron-notched specimens [NASA-TM-87153] N86-13495

FRANCE
Certification granted to Franco-Italian ATR 42 N86-13617
ATR 42 production work in French, Italian plants detailed N86-13618

FRAUNHOFER LINES
Lunar luminescence measurements N86-14092

FRENCH SPACE PROGRAMS
Soviet-French commission discusses joint space projects N86-14198

FREQUENCY DISCRIMINATORS
Phase lock acquisition system [AD-D011804] N86-13646

FREQUENCY SCANNING
Study of Earth observation by frequency scanning. Volume 1: Executive summary [ESA-CR(P)-2028-VOL-1] N86-13705
Study of Earth observation by frequency scanning. Volume 2 [ESA-CR(P)-2028-VOL-2] N86-13706

FREQUENCY SHIFT
Temperature-frequency variation of mechanical losses in periodic deformation of multilayer glass-reinforced plastics N86-13449
Optical radar transceiver control apparatus [AD-D011880] N86-14042

FRICTION
Electrification of filled polyethylene coatings in friction with metal N86-13439

FRICTION FACTOR
A three-dimensional analysis of natural convection in a toroidal loop N86-13672

FUEL COMBUSTION
Thermal radiation effects on combustion of condensed fuels N86-13387
Report on investigation of alcohol combustion associated wear in spark ignition engines, mechanisms and lubricant effects [AD-A157714] N86-13388
Reaction intermediates in aromatic fuel combustion [AD-A158029] N86-13390
Analysis of heterogeneous diffusion flame stabilization N86-13527
Experimental investigation of heterogeneous flame stabilization N86-13528
Combustion behavior of free boron slurry droplets [AD-A158620] N86-13585
Specialists Meeting on Atomization and Nondilute Sprays [AD-A159006] N86-13634

FUEL CONSUMPTION
Direct injection diesel motor N86-13625
Computer program for prediction of fuel consumption statistical data for an upper stage three-axes stabilized on-off control system [NASA-CR-166031] N86-13917
Comparison of energetics of optimum maneuvers and two-impulse maneuvers in some problems of motion from a point into orbit N86-14134

FUEL CONTROL
Polymer, metal and ceramic matrix composites for advanced aircraft engine applications [NASA-TM-87132] N86-13407

FUEL INJECTION
Lightweight two-stroke cycle aircraft diesel engine technology enablement program, volume 1 [NASA-CR-174923-VOL-1] N86-13328
Lightweight two-stroke cycle aircraft diesel engine technology enablement program, volume 2 [NASA-CR-174923-VOL-2] N86-13329
Lightweight two-stroke cycle aircraft diesel engine technology enablement program, volume 3 [NASA-CR-174923-VOL-3] N86-13330
Direct injection diesel motor N86-13625
Specialists Meeting on Atomization and Nondilute Sprays [AD-A159006] N86-13634

FUEL SPRAYS
Size and shape characterization of individual flowing droplets by laser light scattering N86-13579
Real-time, two-dimensional fuel spray visualization N86-13583
Specialists Meeting on Atomization and Nondilute Sprays [AD-A159006] N86-13634

FUEL TANKS
Physical distribution system for aircraft external fuel tanks-survey [AD-A158275] N86-13324

FUEL-AIR RATIO
An investigation of plasma jet ignition and flame jet ignition of lean fuel-air mixtures N86-13386

FUNCTIONAL ANALYSIS
A functional equation governing moving phase boundaries in an elastic bar [AD-A158178] N86-13757
Practical aspects of functional testing techniques [AD-A158184] N86-13968
A note on the integrated Cauchy functional equation [AD-A158269] N86-13977
A variant of Shanbhag's lemma arising out of a modified Rao-Rubbin condition [AD-A158608] N86-13998

FUNCTIONAL DESIGN SPECIFICATIONS
Engineering design for the PBFA-2 pulse forming section [DE85-012810] N86-14060

FURNACES
Appearance of superplasticity effect in aluminum alloys with lithium N86-13432

FUSION (MELTING)
Effect of heating conditions on agglomeration of powdered aluminum in air atmosphere N86-13460

FUSION REACTORS
Recent results on implantation and permeation into fusion reactor materials [DE85-014620] N86-14067

FUSION WELDING
Fusion welding research [AD-A158253] N86-13736

G

GALACTIC RADIATION
Latitude measurements of cosmic radiation intensity in stratosphere and at sea level on marine antarctic expeditions N86-13792

GALERKIN METHOD
Finite element or Galerkin type semidiscrete schemes N86-14083

GALLIUM ANTIMONIDES
AuGa2 on GaSb(001): An epitaxial, thermodynamically stabilized Metal/3-5 compound semiconductor interface [AD-A157937] N86-14071

GALLIUM ARSENIDE LASERS
Philips develops MBE process for laser, chip manufacture N86-13614
CNET of France uses organo-metallic epitaxy for laser N86-13620

GALLIUM ARSENIDES
MeV electron beam irradiation effects on GaAs (1-x) P (x) LEDs (Light emitting diodes) [AD-A158832] N86-13653
Hot electron emission in semiconductors [AD-A158042] N86-14072

GAMMA RAY SPECTRA
Identification of nuclear materials from remote detection of characteristic gamma rays [AD-A159244] N86-14014

GAMMA RAY SPECTROMETERS
High count rate gamma-ray spectrometer system for plutonium isotopic measurements [DE85-013212] N86-14024

GAMMA RAY TELESCOPES
Hard gamma radiation background from coding collimator of gamma telescope under space experiment conditions N86-14123

GAMMA RAYS
Interactive scenario computer model for dose rates to aircrews in flight through nuclear debris clouds [AD-A158741] N86-13888
Identification of nuclear materials from remote detection of characteristic gamma rays [AD-A159244] N86-14014
Coupled radiation transport/thermal analysis of the radiation shield for a space nuclear reactor [AD-A158180] N86-14022

GAS ANALYSIS
Development of a mass spectrometer system for the measurement of inert gases in meteorites N86-14093

GAS CHROMATOGRAPHY
A pyroloysis technique for determining microamounts of hydrogen in lunar soil using the helium ionization detector N86-14082

GAS DYNAMICS
Analytical modeling of strong radiation gas-dynamic interaction N86-13549
Coupling between gas dynamics and microwave energy absorption N86-13561

GAS FLOW
Wave interpretation of measurements on Mars-7 and Venera-9 probes for determining velocity of motion of interstellar gas N86-14147

GAS JETS
Plasma-gas interactions studies in a hybrid plume plasma rocket N86-13559

GAS MIXTURES
Pulsed, optically pumped gas-mixture FIR lasers N86-13609

GAS SPECTROSCOPY
Investigation of nonlinear spectroscopic effects in interaction between CO2-laser radiation and atmospheric gases N86-13789
New physical methods for biological aerosol detection [AD-A158218] N86-13881

GAS TURBINE ENGINES
Exploratory development on advanced eddy current coil excitation and signal processing [AD-A159228] N86-13752

GAS TURBINES
Influence of Co-Cr-Al-Y coatings on physical and mechanical properties of EI-893 steel in GT-100 turbine drive vanes N86-13438

GAS-METAL INTERACTIONS
Effect of composition of rarefied medium on gas-saturated titanium alloys N86-13477

GASEOUS DIFFUSION
Subcritical crack development under constant load in VT6 alloy N86-13475

GASES
Gas recirculator for acyclic machines [AD-D011873] N86-13658

GASOLINE
Report on investigation of alcohol combustion associated wear in spark ignition engines, mechanisms and lubricant effects [AD-A157714] N86-13388

GATES (CIRCUITS)
New digital circuits at Thomson semiconductor in France N86-13619
European silicon structures plans custom chips in 15 days N86-13621

GEARS
Transmission acoustic vibration testing [AD-A159022] N86-13326

GEOCHEMISTRY
Objectives of Vega project research N86-14149

GEODETIC SURVEYS
Data catalog series for space science and applications flight missions. Volume 4A: Descriptions of meteorological and terrestrial applications spacecraft and investigations [NASA-TM-87501] N86-13869

GEOGRAPHIC INFORMATION SYSTEMS
FRG's Dornier develops high-resolution display system N86-13611

GEOGRAPHY
Map projections for use with the Geographic Information System [PB85-198992] N86-13819

GEOLOGICAL FAULTS
Thermal infrared geologic remote sensing research at the Jet Propulsion Laboratory N86-13802
Engineering evaluation of crustal faults using space survey data N86-14189

GEOLOGICAL SURVEYS
Thermal infrared geologic remote sensing research at the Jet Propulsion Laboratory N86-13802
USSR report: Energy [JPRS-UEN-85-001] N86-13861
Space applications in geology N86-14167
Use of space geological methods in seismotectonic research N86-14188

GEOLOGY
The Vaiont Slide. A geotechnical analysis based on new geologic observations of the failure surface. Volume 1: Main text [AD-A158192] N86-13854
The Vaiont Slide. A geotechnical analysis based on new geologic observations of the failure surface. Volume 2: Appendices A through G [AD-A158193] N86-13855
Space applications in geology N86-14167
GEOMAGNETIC PULSATIONS
Formation of proton radiation belts in region of energies of several MeV N86-14140
GEOMETRIC RECTIFICATION (IMAGERY)
Rectification and registration of remotely sensed data [AD-A158827] N86-13711
GEOMETRICAL OPTICS
Geometric-optical modeling of a conifer forest canopy N86-13799
GEOMETRY
DAB user's guide [NASA-CR-177393] N86-13290
No chemisorption on Ni(111): Coverage effects, site preferences and adsorption geometry [AD-A159110] N86-13397
Computation of geometric properties from the medial axis transform in 0 (n log n) time [AD-A158934] N86-13980
A finite element solution of the transport equation [AD-A159245] N86-13982
GEOMORPHOLOGY
Geologic characterization report for the Paradox Basin Study Region, Utah Study Areas. Volume 6: Salt Valley [DE85-011699] N86-13858
GEOPHYSICS
USSR report: Earth sciences [JPRS-UES-85-009] N86-13765
Formation of underwater oceanic volcanoes and islands in relation to lithospheric thickness and movements N86-13776
Azerbaijan geological, geophysical work on land described N86-13862
Formation of high-energy secondary electrons in low-density medium at great altitudes N86-14122
GEOTHERMAL ENERGY EXTRACTION
Review of SERI solar pond work [DE85-012162] N86-13834
GEOTHERMAL RESOURCES
Geothermal resources of the Wind River Basin, Wyoming [DE85-016969] N86-13816
Geothermal investigation in Idaho. Part 14: Geochemical and isotopic investigations of thermal water occurrences of the Boise Front Area, Ada County, Idaho, Water Information Bulletin no. 30 [DE85-012905] N86-13841
GLASS FIBER REINFORCED PLASTICS
Temperature-frequency variation of mechanical losses in periodic deformation of multilayer glass-reinforced plastics N86-13449
GLASS LASERS
Active mirror boosted 351 nm laser irradiation facility [DE85-014412] N86-13732
Retrofit of a high power Nd:glass laser system with liquid crystal polarizers [DE85-014415] N86-13733
GLOBAL POSITIONING SYSTEM
Time delay of arrival location assessment using four satellites [AD-A159243] N86-13315
GLOBULINS
Small X-ray diffraction of immunoglobulin-membrane complexes [AD-A158252] N86-13882
GLOW DISCHARGES
Ion nitriding of titanium N86-13473
GLYCEROLS
Study of optical-acoustical phenomena at surface of strongly absorbing clearing fluids N86-13774
GOLD
AuGa2 on GaSb(001): An epitaxial, thermodynamically stabilized Metal/3-5 compound semiconductor interface [AD-A157937] N86-14071
GRADIENTS
A three-dimensional analysis of natural convection in a toroidal loop N86-13672
Microwave dielectric and propagation properties of vegetation canopies N86-13810
GRAIN BOUNDARIES
Mechanical properties of EP794 steel + 12Kh18N10T steel bimetal N86-13465
Micromechanisms of electrodiffusion failures in thin film metallization N86-13472
GRAIN SIZE
Grain growth in heat-resistant austenitic steel N86-13462
Specifics of the process of failure of structural steels strengthened by thermo-mechanical working with deformation in the intercritical temperature interval N86-13464
Mechanical properties of EP794 steel + 12Kh18N10T steel bimetal N86-13465
Dispersion hardening of high-strength NiOCo-Mo steels N86-13468
GRAMMARS
Deterministic parsing and linguistic explanation: Revision [AD-A159233] N86-13950
GRANULAR MATERIALS
Granular flow: Advanced Research and Technology Development (AR and TD) contract review [DE85-017267] N86-13697
GRAPH THEORY
Graph theoretic approaches to diagnostics: Applications of logic programming and cutset theory to aspects of reactor and circuit analysis [ANL-84-74] N86-13912
GRAPHIC ARTS
Computer-aided process for generating camera-ready graphical artwork [AD-D011884] N86-13939
GRAPHITE
Verification of computer-aided designs of traveling-wave tubes utilizing novel dynamic refocusers and graphite electrodes for the multistage depressed collector [NASA-TP-2524] N86-13643
Electrical sliding joint literature review (viewgraph presentation) [DE85-011571] N86-13666
Coupled radiation transport/thermal analysis of the radiation shield for a space nuclear reactor [AD-A158180] N86-14022
GRAPHITE-EPOXY COMPOSITES
Abrasion behavior of aluminum and composite skin coupons, stiffened skins and stiffened panels representative of transport airplane structures [NASA-TP-2520] N86-13316
Fractography of mixed mode 1 - 2 failure in Graphite/Epoxy and Graphite/Thermoplastic unidirectional composites [AD-A158852] N86-13498
GRAPHITIZATION
Fractography of mixed mode 1 - 2 failure in Graphite/Epoxy and Graphite/Thermoplastic unidirectional composites [AD-A158852] N86-13498
GRATINGS (SPECTRA)
An integrated wavelength demultiplexer [AD-D011867] N86-14041
GRAVITATIONAL FIELDS
Analytical investigation of the dynamics of tethered constellations in Earth orbit, phase 2 [NASA-CR-171611] N86-13345
GRAZING INCIDENCE
Test method for telescopes using a point source at a finite distance [NASA-TM-86523] N86-14033
GREEN'S FUNCTIONS
Results of research in four topic areas: The singularity expansion method, transient scattering measurements, high-frequency diffraction at edges residing on interfaces and cylindrical coordinate representation of dyadic Green's functions [AD-A158382] N86-14037
GROUND EFFECT (AERODYNAMICS)
Ground effects on V/STOL and STOL aircraft: A survey [NASA-TM-86825] N86-13299
GROUND TRUTH
Crop characteristics research: Growth and reflectance analysis N86-13800
Ground reflectance measurements from thematic mapper data N86-13801
Crop area estimation based on remotely-sensed data with an accurate but costly subsample [NASA-CR-176017] N86-13814
VAS demonstration: (VISSR Atmospheric Sounder) description [NASA-RP-1151] N86-13867
Methods for complex space experiment in USSR for studying land from manned spacecraft N86-14181
GROUND WATER
Mass transfer coefficients and Henry's constants for packed-tower air stripping of volatile organics: Measurements and correlation [AD-A158811] N86-13375
Geothermal resources of the Wind River Basin, Wyoming [DE85-016969] N86-13816
GROUP DYNAMICS
Human factors in space station architecture 1: Space station program implications for human factors research [NASA-TM-86702] N86-13900
GROUP THEORY
Some applications of Lie groups in astrodynamics N86-14087
GROWTH
Electronic detection of low concentrations of organophosphorus compounds with a solid state device utilizing supported copper + cuprous oxide island films [AD-A158181] N86-13392
Grain growth in heat-resistant austenitic steel N86-13462
Experimental investigation of crater growth dynamics [NASA-CR-176392] N86-14212
GUNN DIODES
Transient simulation of submicron devices [AD-A157748] N86-13648

H

H ALPHA LINE
Sudden disappearance of quiescent prominences N86-14124
HADRONS
Hadron component of cosmic radiation at atmospheric depth 800 g/cm(2) in Energy Range 70 to 700 GeV N86-13793
HAIL
Goskomgidromet plans automation of aerial cloud-seeding work N86-13766
HANDBOOKS
METCUT: A computer aided system for machining technology [AD-A157941] N86-13927
HARDENERS
Influence of texture of titanium nitride coatings on wear resistance of cutting tools N86-13440
Superhard materials developed N86-13471
HARDENING (MATERIALS)
Influence of annealing on hardness of vacuum-diffusion chromium coating on low-carbon steel N86-13441
Specifics of the process of failure of structural steels strengthened by thermo-mechanical working with deformation in the intercritical temperature interval N86-13464
Mechanical properties of EP794 steel + 12Kh18N10T steel bimetal N86-13465
Modeling of thermal fatigue and erosion of complex alloyed steels in metal melts N86-13469
Superhard materials developed N86-13471
Ion nitriding of titanium N86-13473
Influence of electron-beam heating on structure and phase composition of VT9 alloy N86-13481
HARDNESS
Influence of sodium on mechanical and casting properties of magnesium-lithium alloys N86-13457
Durability of steel 45 with boride coating in corrosive-abrasive media N86-13467
Superhard materials developed N86-13471
HARDWARE
Ada as a hardware description language: An initial report [AD-A158217] N86-13935
HARMONIC OSCILLATION
Study of the influence of an oscillating spoiler on the surrounding aerodynamic field [IMFL-3119] N86-13303
HAZARDS
Health hazard evaluation of liquid monopropellants. Phase 5: Comparative inhalation toxicities of LGP 1776, LGP 1845, and HAN (hydroxylammonium nitrate) [AD-A159090] N86-13891
HAZE
Multidimensional modeling of atmospheric effects and surface heterogeneities on remote sensing N86-13806
HEAD (ANATOMY)
The event related brain potential as an index of information processing, cognitive activity, and skill acquisition: A program of basic research [AD-A159118] N86-13897
HEALTH
Health hazard evaluation of liquid monopropellants. Phase 5: Comparative inhalation toxicities of LGP 1776, LGP 1845, and HAN (hydroxylammonium nitrate) [AD-A159090] N86-13891
HEAT EXCHANGERS
Heat transfer and pressure drop performance of a finned-tube heat exchanger proposed for use in the NASA Lewis Altitude Wind Tunnel [NASA-TM-87151] N86-13677
Review of SERI solar pond work [DE85-012162] N86-13834

Performance assessment of OTEC power systems and thermal power plants. Volume 2: Users manual for PACC-OTECs
[DE85-016792] N86-13835
An analysis of cryotrap heat exchanger performance test data (400 area) and recommendations for a system to handle Apollo RCS engines N86-14094

HEAT FLUX
Coupling between gas dynamics and microwave energy absorption N86-13561
Rocket engine hot-spot detector
[NASA-CR-171902] N86-13708

HEAT OF FORMATION
High energy molecules of high symmetry N86-13520
Tectonic stress on structures alters formation parameters N86-13864

HEAT RESISTANT ALLOYS
The effect of cobalt content in U-700 type alloys on degradation of aluminide coatings
[NASA-TM-87173] N86-13408
Grain growth in heat-resistant austenitic steel
N86-13462
Influence of structure of heat-resistant nickel alloy ZhS6U on its weldability in the solid state N86-13492

HEAT SHIELDING
Coupled radiation transport/thermal analysis of the radiation shield for a space nuclear reactor
[AD-A158180] N86-14022

HEAT STORAGE
Investigation of the vertical-flow aquifer thermal energy storage concept and numerical simulation of the Dorigny field experiment
[DE85-014524] N86-13694

HEAT TRANSFER
Coupling between velocity oscillations and solid propellant combustion N86-13541
Effect of interfacial phenomena on contact line heat transfer N86-13566
A study of transport phenomena and interface stability during solidification of binary solutions using front tracking finite elements N86-13669
Two unsteady heat transfer experiments. Part 1: In grid-generated isotropic turbulence. Part 2: In laminar oscillatory flow in straight and conical tubes N86-13675
Heat transfer and pressure drop performance of a finned-tube heat exchanger proposed for use in the NASA Lewis Altitude Wind Tunnel
[NASA-TM-87151] N86-13677
Determination of convective diffusion heat/mass transfer rates to burner rig test targets comparable in size to cross-stream jet diameter
[NASA-TM-87176] N86-13678
Pore pressure response to probe insertion and thermal gradient: ISIMU-2. (In situ heat transfer experiment)
[AD-A158592] N86-13689
Experimental investigation of heat transfer behavior of aqueous foams in thermal entry region of pipe flow
[DE85-012836] N86-13700
Model interpretation of annual variation of temperature fields of air and water boundary layers of world ocean
N86-13767
Vertical structure of turbulence and turbulent exchange in equatorial zone of Pacific Ocean N86-13771

HEAT TRANSMISSION
Numerical solutions of Navier-Stokes equations for a Butler wing
[NASA-CR-174202] N86-13293

HEAT TREATMENT
Mechanical properties of EP794 steel + 12Kh18N10T steel bimetal N86-13465
Effect of composition of rarefied medium on gas-saturated titanium alloys N86-13477

HEATING
Influence of electron-beam heating on structure and phase composition of VT9 alloy N86-13481
Possible mechanism of wave formation during detonation welding N86-13483
Determining local heating parameters for increasing fatigue resistance of welded joints N86-13491

HEAVY IONS
New control techniques for extraction of Bevalac beams
[DE85-017640] N86-14023
Registry of heavy ions in auroral region during magnetic storms N86-14138

HEIGHT
Laboratory studies of steep and breaking deep water waves in a convergent channel
[AD-A158187] N86-13875

HELICAL FLOW
Preliminary measurement of the noise from the 2/9 scale model of the Large-scale Advanced Propfan (LAP) propeller, SR-7A
[NASA-TM-87116] N86-14006

HELICOPTER DESIGN
Advanced technology helicopter landing gear preliminary design investigation
[AD-A158816] N86-13325

HELICOPTERS
Assessment of aerodynamic and dynamic models in a comprehensive analysis
[NASA-TM-86835] N86-13286
Tradeoff analysis of technology needs for public service helicopters
[NASA-CR-3927] N86-13317
Advanced technology helicopter landing gear preliminary design investigation
[AD-A158816] N86-13325
Transmission acoustic vibration testing
[AD-A159022] N86-13326

HELIOSTATS
Wind loading on solar collectors
[DE85-012151] N86-13833
Small solar power systems plant in Almeria system evaluation and comparison on thermal basis
[DE85-017185] N86-13840

HELIUM
Sparger system for MMH-helium vents N86-14096

HELIUM PLASMA
Population inversion in a recombining hydrogen plasma interacting with a helium gas
[IPPJ-692] N86-14045

HEMATOLOGY
Design, construction and testing of a dc bioeffects enclosure for small animals
[DE05-016798] N86-13883
Health hazard evaluation of liquid monopropellants. Phase 5: Comparative inhalation toxicities of LGP 1776, LGP 1845, and HAN (hydroxylammonium nitrate)
[AD-A159090] N86-13891

HERBICIDES
Aquatic plant control research program: Evaluation of polymers for controlled delivery of herbicides for aquatic plant control
[AD-A157948] N86-13843

HETEROGENEITY
Bidirectional reflectance modeling of non-homogeneous plant canopies N86-13796
Multidimensional modeling of atmospheric effects and surface heterogeneities on remote sensing N86-13806

HETEROJUNCTIONS
Luminescent properties of semiconductor electrodes
[AD-A158841] N86-13655
Development of stable high efficiency polycrystalline thin-film solar cells based on CuInSe2
[DE85-000517] N86-13837

HEURISTIC METHODS
Generating and generalizing models of visual objects
[AD-A158197] N86-13894

HIERARCHIES
Hierarchical image segmentation to infrared images
[AD-A158030] N86-14035

HIGH ALTITUDE
Heat transfer and pressure drop performance of a finned-tube heat exchanger proposed for use in the NASA Lewis Altitude Wind Tunnel
[NASA-TM-87151] N86-13677

HIGH ALTITUDE ENVIRONMENTS
High-altitude plume computer code development
[NASA-CR-171600] N86-13923

HIGH ENERGY ELECTRONS
Hot electron emission in semiconductors
[AD-A158042] N86-14072
Formation of high-energy secondary electrons in low-density medium at great altitudes N86-14122
Charge composition of electrons in Earth's radiation belt N86-14146

HIGH ENERGY INTERACTIONS
Nation's achievements in high energy physics reviewed N86-13604

HIGH FREQUENCIES
High frequency quantitative analysis of magnetomechanical acoustic emission
[AD-A158222] N86-13750
A study of some features of ac and dc electric power systems for a space station N86-14085

HIGH POWER LASERS
Analytical modeling of strong radiation gas-dynamic interaction N86-13549
Retrofit of a high power Nd:glass laser system with liquid crystal polarizers
[DE85-014415] N86-13733
New methods for laser sounding of atmosphere on basis of nonlinear effects N86-13787
Interaction between powerful laser radiation and atmospheric aerosols N86-13788

HIGH PRESSURE
Lightweight two-stroke cycle aircraft diesel engine technology enablement program, volume 1
[NASA-CR-174923-VOL-1] N86-13328
Lightweight two-stroke cycle aircraft diesel engine technology enablement program, volume 2
[NASA-CR-174923-VOL-2] N86-13329
Lightweight two-stroke cycle aircraft diesel engine technology enablement program, volume 3
[NASA-CR-174923-VOL-3] N86-13330
High pressure solid propellant combustion zone structure from analysis of hydroxyl radical chemiluminescence N86-13529
High-pressure, high-temperature opposed anvil device described N86-13606
The physics and technology of strong magnetic fields (chapter 10)
[AD-A158174] N86-14000
Equation of state of dense argon: A comparison of shock and static studies
[DE85-015543] N86-14074

HIGH RESOLUTION
High-resolution movies of propellant deflagration
N86-13539
FRG's Dornier develops high-resolution display system
N86-13611
Speckle image reconstruction. Appendix 1
[AD-A158271] N86-14207

HIGH REYNOLDS NUMBER
Recent experience in the RAE (Royal Aircraft Establishment) 5-metre wind tunnel of a china clay method for indicating boundary layer transition
[AD-A157943] N86-13302
High Reynolds number wave force investigation in a wave flume
[AD-A157722] N86-13681

HIGH SPEED
High speed multi-channel data recorder to replace oscilloscope data acquisition systems
[DE85-015155] N86-13721

HIGH STRENGTH ALLOYS
Dispersion hardening of high-strength NiOCo-Mo steels N86-13468

HIGH STRENGTH STEELS
Dispersion hardening of high-strength NiOCo-Mo steels N86-13468
New materials to lighten vehicles N86-13624

HIGH TEMPERATURE
Modifications of system for elevated temperature tensile testing and stress-strain measurement of metal matrix composites
[NASA-TM-87172] N86-13370
Relationship of thermal expansion of amorphous metal alloys with their high temperature plastic properties
N86-13435
Micromechanisms of electrodiffusion failures in thin film metalization N86-13472
Silicide coatings for protecting titanium-niobium alloys from high-temperature oxidation N86-13476
Homogenization of beta-solid solution upon rapid heating of two-phase titanium alloys N86-13478
Ceramic fabric material testing
[DE85-013684] N86-13503
Critical evaluation of high temperature chemical kinetic data N86-13533
High-pressure, high-temperature opposed anvil device described N86-13606
Oxide electrodes at high temperatures
[DE85-006564] N86-13667
Close-spaced high temperature Knudsen flow
[AD-A158280] N86-13831

HIGH TEMPERATURE ENVIRONMENTS
Study of effect of normal reactor water on growth rate of fatigue cracks in 15Kh2NMFA steel N86-13470

HIGH TEMPERATURE GASES
Determination of convective diffusion heat/mass transfer rates to burner rig test targets comparable in size to cross-stream jet diameter
[NASA-TM-87176] N86-13678
Investigation of dust associated with shell stars
[AD-A158945] N86-14210

HIGH TEMPERATURE PLASMAS
Plasma-gas interactions studies in a hybrid plume plasma rocket N86-13559
A tandem mirror plasma source for hybrid plume plasma studies N86-13560
Effects of neutrals on internal forces and thermal conduction of a plasma in a magnetic field
[IPPJ-691] N86-14051

HIGH TEMPERATURE PROPELLANTS
Completely magnetically contained electrothermal thruster N86-13556

HIGH VOLTAGES
A 10-MHz high-voltage modulator with pulse-width and repetition-rate agility
[DE85-014117] N86-13663
Development of the VOLT-A shuttle experiment
[NASA-TM-87169] N86-14110

HILBERT SPACE
- Realization theory in Hilbert space [AD-A158172] N86-13997

HINGES
- Thermal vacuum tests on a hinge actuator mechanism --- spacecraft component [ESA-ESTL-067] N86-13360

HMX
- Evaluation of HMX propellant chemistry from Raman and laser induced fluorescence species and temperature measurements N86-13530

HOLOGRAPHY
- Optical processing and phase conjugation N86-13573
- Holographic study of the particles produced by the injector in a Viking motor [ISL-R-111/84] N86-13724

HOMOGENEOUS TURBULENCE
- Use of Goudriaan model for studying reflection regularities in vegetation-soil system in optical range. 1: Influence of phytometric parameters on spectral brightness coefficients N86-14190

HOMOGENIZING
- Homogenization of beta-solid solution upon rapid heating of two-phase titanium alloys N86-13478

HOMOPOLAR GENERATORS
- First order estimates of the dynamics and energetics of a rapidly decelerating flywheel [DE85-013908] N86-13842

HONEYCOMB STRUCTURES
- Coupled radiation transport/thermal analysis of the radiation shield for a space nuclear reactor [AD-A158180] N86-14022

HOOKES LAW
- A method to determine dynamic elastic constants of thin shell composites by guided ultrasonic waves [AD-A159025] N86-13381

HORIZONTAL ORIENTATION
- Tire-soil interaction model for turning (steered) tires [AD-A157737] N86-13593

HOT CORROSION
- Rocket engine hot-spot detector [NASA-CR-171902] N86-13708

HOT ELECTRONS
- Physical mechanisms for hot electron stabilization of low frequency interchange modes [IPPJ-741] N86-14050

HOT PRESSING
- Fractured toughness of Si3N4 measured with short bar chevron-notched specimens [NASA-TM-87153] N86-13495

HOT SURFACES
- Rocket engine hot-spot detector [NASA-CR-171902] N86-13708

HUBS
- Preliminary report on in-flight measurement of rotor hub drag and lift using the RSRA [NASA-TM-86764] N86-13319
- Hub effects in propeller design and analysis [AD-A158853] N86-13331

HUMAN BEHAVIOR
- Human factors in space station architecture 1: Space station program implications for human factors research [NASA-TM-86702] N86-13900
- European Science Notes, Volume 39, Number 7 [AD-A157708] N86-14108

HUMAN FACTORS ENGINEERING
- Human factors in space station architecture 1: Space station program implications for human factors research [NASA-TM-86702] N86-13900
- Alerted monitors: Human operators aided by automated detectors [PB85-222750] N86-13906
- Architect discusses space habitat designs N86-14161

HUMAN PERFORMANCE
- The spatial and temporal parameters of velocity discrimination [AD-A158735] N86-13896
- Signal processing of anthropometric data N86-14105

HUMAN REACTIONS
- Enhancing sensitivity to visual motion and enhancing visual sensitivity [AD-A158800] N86-13889

HUMAN WASTES
- Solid waste treatment processes for space station N86-14091

HUMIDITY
- Electrical research on solar cells and photovoltaic materials [NASA-CR-176384] N86-13838
- Investigation of cold colored smoke production [AD-A158783] N86-14040

HYBRID PROPELLANT ROCKET ENGINES
- Plasma-gas interactions studies in a hybrid plume plasma rocket N86-13559

HYBRID PROPELLANTS
- A tandem mirror plasma source for hybrid plume plasma studies N86-13560

HYDRAULIC EQUIPMENT
- Investigation for the definition of a hydraulic multidegree of freedom vibration facility [B-TF-1627] N86-13340

HYDRAULIC FLUIDS
- Evaluation of the erosion protection of low inflammability liquids of the HFC type (polyglycol solutions) --- hydraulic fluids [CETIM-12-E-13-3] N86-13505

HYDRAULIC TEST TUNNELS
- Behavior of slender cones at large incidences N86-13707

HYDROCARBONS
- Synthesis of high nitrogen content heterocyclic nitramines and energetic internal plasticizers N86-13511
- Combusion of hydrogen and hydrocarbons in fluorine N86-13526

HYDRODYNAMICS
- Flow field effects on combustion instability N86-13544
- Wave force-phase method for vertical cylinders [AD-A157709] N86-13680
- High Reynolds number wave force investigation in a wave flume [AD-A157722] N86-13681
- Structure and hydrodynamics of colloidal systems [DE85-016294] N86-14027
- Implicit plasma simulation [DE85-016088] N86-14055

HYDROGEN
- Synthesis, structure and reactivity of molecules attached to electrode surfaces [AD-A158621] N86-13394
- Subcritical crack development under constant load in VT6 alloy N86-13475
- influence of hydrogen on formation of cold cracks in seams during welding of pipe steel N86-13494
- Combusion of hydrogen and hydrocarbons in fluorine N86-13526
- Energy deposition of pulsed one micron laser radiation in H2 and AR N86-13552
- Critical charge for the direct initiation of detonation in gaseous fuel-air mixtures [DE85-016130] N86-13696
- A pyroloysis technique for determining microamounts of hydrogen in lunar soil using the helium ionization detector N86-14082
- Extended atmospheres of outer planet satellites and comets [NASA-CR-176398] N86-14209

HYDROGEN EMBRITTLEMENT
- Hydrogen transport and hydrogen embrittlement in stainless steels N86-13403
- The delayed fracture of aluminum alloys [AD-A158944] N86-13412

HYDROGEN IONS
- Efficient ionizer for polarized H(-) formation [DE85-013294] N86-14064
- Electron microscopic observations of hydrogen implantation in ilmenites N86-14081

HYDROGEN RECOMBINATIONS
- Population inversion in a recombining hydrogen plasma interacting with a helium gas [IPPJ-692] N86-14045

HYDROGENATION
- Subcritical crack development under constant load in VT6 alloy N86-13475

HYDROLOGY
- Geothermal investigation in Idaho. Part 14: Geochemical and isotopic investigations of thermal water occurrences of the Boise Front Area, Ada County, Idaho, Water Information Bulletin no. 30 [DE85-012905] N86-13841

HYDROLYSIS
- Aquatic plant control research program: Evaluation of polymers for controlled delivery of herbicides for aquatic plant control [AD-A157948] N86-13843

HYDROXYL COMPOUNDS
- High energy molecules of high symmetry N86-13520

HYDROXYL RADICALS
- High pressure solid propellant combustion zone structure from analysis of hydroxyl radical chemiluminescence N86-13529
- Resonant cars detection of OH radicals N86-13576

HYPERBOLIC FUNCTIONS
- The formulation of a hyperbolic Stefan problem [ORNL-6065] N86-13952

HYPERSONIC VEHICLES
- Structures and materials technology issues for reusable launch vehicles [NASA-TM-87626] N86-13349

HYPERSONICS
- Aerothermodynamics for future launchers. Review of the state of the art in Europe [VKI-CR-1984-16/AR] N86-13347

HYPOTHESES
- Hypothesizing and refining causal models [AD-A158165] N86-13893

I

ICE FORMATION
- Heat transfer and pressure drop performance of a finned-tube heat exchanger proposed for use in the NASA Lewis Altitude Wind Tunnel [NASA-TM-87151] N86-13677

IDAHO
- Geothermal investigation in Idaho. Part 14: Geochemical and isotopic investigations of thermal water occurrences of the Boise Front Area, Ada County, Idaho, Water Information Bulletin no. 30 [DE85-012905] N86-13841

IDEAL GAS
- Numerical solutions of Navier-Stokes equations for a Butler wing [NASA-CR-174202] N86-13293

IDENTIFYING
- A parametric study of the Ibrahim time domain modal identification algorithm N86-13588
- Identification of nuclear materials from remote detection of characteristic gamma rays [AD-A159244] N86-14014

IGNITION
- An investigation of plasma jet ignition and flame jet ignition of lean fuel-air mixtures N86-13386
- Critical charge for the direct initiation of detonation in gaseous fuel-air mixtures [DE85-016130] N86-13696
- Impact of a poloidal divertor in ignition tokamak design [DE85-012892] N86-14061

IGNITION TEMPERATURE
- Combustion behavior of free boron slurry droplets [AD-A158620] N86-13585

ILLUMINANCE
- Atmospheric and science complexity effects on surface bidirectional reflectance N86-13803

ILMENITE
- Electron microscopic observations of hydrogen implantation in ilmenites N86-14081
- Ion bombardment and adsorption studies on ilmenite (FeTiO3) by X-ray photoelectron spectroscopy N86-14100

IMAGE CONVERTERS
- Photoelectronic trajectory anatomy of RCA-C-73435 image converter and its performance [DE85-013973] N86-13723

IMAGE ENHANCEMENT
- Mathematical analysis study for radar data processing and enhancement. Part 1: Radar data analysis [NASA-CR-166616-PT-1] N86-13353

IMAGE PROCESSING
- Laser thermal propulsion N86-13548
- Optical processing and phase conjugation N86-13573
- Generating and generalizing models of visual objects [AD-A158197] N86-13894
- A report on the ST ScI optical disk workstation [NASA-CR-176369] N86-13907
- Target tracking based scene analysis [AD-A158629] N86-13910
- The construction and testing of a real-time digital breadboard processor for the ESA remote sensing satellite synthetic aperature radar [REPT-00-0778] N86-13911
- Multiresolution path planning for mobile robots [AD-A158630] N86-13948
- Hierarchical image segmentation to infrared images [AD-A158030] N86-14035
- Multigrid relaxation methods and the analysis of lightness, shading, and flow [AD-A158173] N86-14036
- Speckle image reconstruction. Appendix 2 [AD-A158272] N86-14208

IMAGE RECONSTRUCTION
- Speckle image reconstruction. Appendix 1 [AD-A158271] N86-14207
- Speckle image reconstruction. Appendix 2 [AD-A158272] N86-14208

IMAGES
- Generating and generalizing models of visual objects [AD-A158197] N86-13894

IMAGING RADAR
- Microwave dielectric and propagation properties of vegetation canopies N86-13810

IMAGING TECHNIQUES
Hierarchical image segmentation to infrared images
[AD-A158030] N86-14035

IMMUNOLOGY
Development and testing of a mouse simulated space flight model
[NASA-CR-176359] N86-13878
Study of toxic and antigenic structures of botulinum neurotoxins
[AD-A156642] N86-13880
European Science Notes. Volume 39, number 9
[AD-A158278] N86-14109

IMPACT
Impact of a poloidal divertor in ignition tokamak design
[DE85-012892] N86-14061

IMPACT DAMAGE
Macro- and microfractographic specifics of dissipated impact rupture of type 45 steel in the viscous-brittle transition interval N86-13466

IMPACT LOADS
Development of contact/impact capability for the three-dimensional fluid-structure interaction code: NEPTUNE
[DE85-010264] N86-13698

IMPACT RESISTANCE
Subcritical crack development under constant load in VT6 alloy N86-13475

IMPACT TESTS
Macro- and microfractographic specifics of dissipated impact rupture of type 45 steel in the viscous-brittle transition interval N86-13466

IMPREGNATING
A study of rhenium as an alternate substrate material for impregnated dispenser cathodes
[AD-A159113] N86-13415

IMPROVEMENT
Determination of backscattering sources in various targets N86-13811

IMPURITIES
Influence of alloying elements and impurities on mechanical properties of complex silumins N86-13428

IN-FLIGHT MONITORING
Preliminary report on in-flight measurement of rotor hub drag and lift using the RSRA
[NASA-TM-86764] N86-13319

INCIDENCE
Behavior of slender cones at large incidences
N86-13707

INCOMPRESSIBLE FLOW
Boundary-value problem for two-dimensional fluctuations in boundary layers
[AD-A157952] N86-13685
Turbulence in two-field incompressible flow
[DE85-015361] N86-13693

INCREASING
Shock waves, increase of entropy and loss of information
[DE85-013645] N86-13701

INDEPENDENT VARIABLES
Generically based mobility-terrain data bases
[AD-A157738] N86-13815
Monte Carlo analysis of nonlinear statistical models. 1. Theory: Revision
[AD-A158613] N86-13990

INDEXES (DOCUMENTATION)
Crossref for the Cray
[NASA-CR-177384] N86-13913

INDEXES (RATIOS)
The event related brain potential as an index of information processing, cognitive activity, and skill acquisition: A program of basic research
[AD-A159118] N86-13897
Reflection indicatrices of vegetation canopies
N86-14178

INDIUM
MBE growth of CdTe and Hg (1-x) Cd (x) Te films and multilayer structures
[AD-A158267] N86-14073

INDIUM PHOSPHIDES
Potential for use of indium phosphide solar cells in the space radiation environment
[NASA-TM-87157] N86-13645

INDUSTRIAL MANAGEMENT
USSR report: Machine tools and metalworking equipment
[JPRS-UMM-85-014] N86-13742

INDUSTRIAL PLANTS
Safe control systems and the VIPER microprocessor
[AD-A156617] N86-13908

INDUSTRIAL SAFETY
New applications of industrial robots noted
N86-13743

INDUSTRIES
West Europe report: Science and technology
[JPRS-WST-85-031] N86-13616

INELASTIC SCATTERING
Polarization transfer in enelastic scattering and pionic models of the EMC effect
[DE85-014119] N86-14021

INERTIAL CONFINEMENT FUSION
Engineering design for the PBFA-2 pulse forming section
[DE85-012810] N86-14060

INFERENCE
Conditioning in a missing data problem
[AD-A158202] N86-13988

INFINITY
Unified method for delay analysis of random multiple access algorithms
[AD-A159108] N86-13981

INFORMATION
Shock waves, increase of entropy and loss of information
[DE85-013645] N86-13701

INFORMATION DISSEMINATION
Report on the findings of the Japanese Investigative Team on US Space Station Design (Keidanren)
[NASA-TM-77659] N86-13356

INFORMATION SYSTEMS
METCUT: A computer aided system for machining technology
[AD-A157941] N86-13927

INFORMATION THEORY
Joint services electronics program
[AD-A158731] N86-13652
Information in censored models
[AD-A158644] N86-13999
Forming attainability sets in control of kinetic moment of rotating asymmetric solid body (special cases)
N86-14113

INFRARED ASTRONOMY
Focal plane optics in far-infrared and submillimeter astronomy
[NASA-TM-88186] N86-14204

INFRARED IMAGERY
Hierarchical image segmentation to infrared images
[AD-A158030] N86-14035

INFRARED INSTRUMENTS
Development of a breadboard cooler for infrared remote sensing payloads, phase 2 --- spacecraft payloads
[FOK-RV-R-82-072] N86-13725

INFRARED LASERS
China report: Science and technology
[JPRS-CST-85-020] N86-13600
Pulsed, optically pumped gas-mixture FIR lasers
N86-13609

INFRARED PHOTOGRAPHY
Thermal infrared geologic remote sensing research at the Jet Propulsion Laboratory N86-13802

INFRARED RADIATION
Photodegradation studies of silver-backed polyacrylonitrile (PAN) films
[DE85-012154] N86-13501

INFRARED REFLECTION
Concept of laser locator systems (based on the geometry of the triangular corner cube reflector)
[AD-A157795] N86-13728

INFRARED SPECTRA
Optical constants
[AD-A158623] N86-14038

INFRARED SPECTROSCOPY
The dynamics of the photofragmentation of ketene 3-cyclopentenone, 3,5-cycloheptadienone, and tropone
[AD-A158045] N86-13371
New physical methods for biological aerosol detection
[AD-A158218] N86-13881

INHOMOGENEITY
Babinet's principle for an anisotropic resistive surface using different approaches
[AD-A159117] N86-13636
The characterization of surface varigation effects on remote sensing N86-13805
Scattering models and basic experiments in the microwave regime N86-13807

INITIATION
Critical charge for the direct initiation of detonation in gaseous fuel-air mixtures
[DE85-016130] N86-13696

INJECTORS
Generation and acceleration of high intensity beams in the SLC injector
[DE85-013056] N86-14066

INLET FLOW
Sparger system for MMH-helium vents N86-14096

INLET PRESSURE
Sparger system for MMH-helium vents N86-14096

INSERTS
Standardization program on design analysis and testing of inserts in nonmetallic sandwich components --- spacecraft components
[TR-TS-RP-2-09-84] N86-13364

INSTRUMENT APPROACH
An analytical comparison of three visual approach slope indicators: VASIS, T-VASIS and PAPI
[ARL/SYS-R-33] N86-13309

INSTRUMENT ERRORS
A note on the effect of ignoring small measurement errors in precision instrument calibration
[AD-A159104] N86-13713

INSULATORS
Magnetoplasmadynamic thruster erosion research
N86-13557
Thomson, CNET of France in silicon-on-insulator research N86-13612

INTEGRAL EQUATIONS
Numerical solutions of Navier-Stokes equations for a Butler wing
[NASA-CR-174202] N86-13293
Scattering models and basic experiments in the microwave regime N86-13807
Boundary integral techniques for multi-connected domains
[AD-A158171] N86-13965
Computable bounds for solutions of integral equations
[AD-A158189] N86-13970
A finite element solution of the transport equation
[AD-A159245] N86-13982

INTEGRALS
Boundary-value problem for two-dimensional fluctuations in boundary layers
[AD-A157952] N86-13685
Continuity of certain random integral mappings and the uniform integrability of infinitely divisible measures
[AD-A159105] N86-13995

INTEGRATED CIRCUITS
New digital circuits at Thomson semiconductor in France N86-13619
Using software technology to specify abstract interfaces in VLSI design
[AD-A158034] N86-13649
Bulk CMOS VLSI technology studies. Part 5: The design and implementation of a high speed integrated circuit functional tester
[AD-A158370] N86-13651
Routing method in computer aided customization of a two level automated universal array
[AD-D011808] N86-13925
Ada as a hardware description language: An initial report
[AD-A158217] N86-13935
An integrated wavelength demultiplexer
[AD-D011867] N86-14041
Optoelectronic integrated circuit multiplier
[AD-D011883] N86-14043

INTEGRATED OPTICS
China report: Science and technology
[JPRS-CST-85-020] N86-13600
Integrated optics developments over past decade, future prospects N86-13605
European Science Notes. Volume 39, number 9
[AD-A158278] N86-14109

INTERCOSMOS SATELLITES
Small-scale structure of intensive longitudinal currents in high latitudes N86-14139

INTERFACE STABILITY
A study of transport phenomena and interface stability during solidification of binary solutions using front tracking finite elements N86-13669

INTERFACES
Using software technology to specify abstract interfaces in VLSI design
[AD-A158034] N86-13649
Development of contact/impact capability for the three-dimensional fluid-structure interaction code: NEPTUNE
[DE85-010264] N86-13698
AuGa2 on GaSb(001): An epitaxial, thermodynamically stabilized Metal/3-5 compound semiconductor interface
[AD-A157937] N86-14071

INTERFACIAL TENSION
A study of transport phenomena and interface stability during solidification of binary solutions using front tracking finite elements N86-13669

INTERFEROMETRY
Elastic-plastic deformation of a metal-matrix composite coupon with a center slot
[NASA-CR-178013] N86-13496

INTERFERON
Development and testing of a mouse simulated space flight model
[NASA-CR-176359] N86-13878

INTERIOR BALLISTICS
Numerical models for plasma-solid interactions in electrothermal mass accelerators
[AD-A158637] N86-14052

INTERMEDIATE FREQUENCIES

Optical radar transceiver control apparatus
[AD-D011880] N86-14042

INTERMETALLICS

Superelastic behavior of powdered titanium nickelide during pressing N86-13461

INTERNAL FRICTION

Internal friction in TiNiCu alloy N86-13480

Structure and internal friction of near-eutectic alloy system Ti-W tempered from a liquid state N86-13482

INTERNATIONAL COOPERATION

Report on active and planned spacecraft and experiments
[NASA-TM-87499] N86-13343

Report on the findings of the Japanese Investigative Team on US Space Station Design (Keidanren)
[NASA-TM-77659] N86-13356

Soviet-French commission discusses joint space projects N86-14198

INTERPLANETARY MAGNETIC FIELDS

Dependence of length of free path of flare particles on energy N86-14141

INTERPLANETARY MEDIUM

Observation of small-scale solar wind structure on front of sharp increase in plasma flow velocity N86-14142

INTERPLANETARY SPACE

USSR report: Space
[JPRS-USP-85-005] N86-14111

Preparation, analysis and release of simulated interplanetary grains into low grain orbit
[DE85-014133] N86-14211

INTERPLANETARY SPACECRAFT

Planetary sample rapid recovery and handling
[NASA-CR-171906] N86-13342

INTERPLANETARY TRAJECTORIES

Approximate solutions of Euler-Lambert equation for case of several revolutions about central body
N86-14121

INTERPOLATION

A finite element solution of the transport equation
[AD-A159245] N86-13982

High order spline interpolation in the particle simulation N86-14046

INTERSTELLAR GAS

Wave interpretation of measurements on Mars-7 and Venera-9 probes for determining velocity of motion of interstellar gas N86-14147

INTERVALS

Specifics of the process of failure of structural steels strengthened by thermo-mechanical working with deformation in the intercritical temperature interval
N86-13464

Macro- and microfractographic specifics of dissipated impact rupture of type 45 steel in the viscous-brittle transition interval N86-13466

A note on the effect of ignoring small measurement errors in precision instrument calibration
[AD-A159104] N86-13713

INVARIANCE

Multidimensional modeling of atmospheric effects and surface heterogeneities on remote sensing N86-13806

Remote temperature determination of terrestrial covers from polarization invariant of microwave-radiothermal emission N86-14196

INVERSIONS

Boundary-value problem for two-dimensional fluctuations in boundary layers
[AD-A157952] N86-13685

Inversion of Rayleigh wave phase velocities between RSNT and RSON
[DE85-013242] N86-13859

INVERTED CONVERTERS (DC TO AC)

Two-hundred to 300 KVA conditioned power system - development, phase 1
[AD-A158820] N86-13832

INVESTIGATION

Report on the findings of the Japanese Investigative Team on US Space Station Design (Keidanren)
[NASA-TM-77659] N86-13356

Experimental investigation of magnesium combustion in steam
[AD-A159109] N86-13396

Experimental investigation of heat transfer behavior of aqueous foams in thermal entry region of pipe flow
[DE85-012836] N86-13700

INVISCID FLOW

Studies of the flow field near a NACA 4412 aerofoil at nearly maximum lift
[AD-A157750] N86-13301

Boundary integral techniques for multi-connected domains
[AD-A158171] N86-13965

ION ACCELERATORS

Collective ion acceleration by means of virtual cathodes
[DE85-012707] N86-14019

ION BEAMS

Comparison of ion milling techniques for cross-sectional TEM of semiconductors
[DE85-016596] N86-13664

Scheme to funnel ion beams with a radio-frequency quadrupole
[DE85-015689] N86-14016

New control techniques for extraction of Bevalac beams
[DE85-017640] N86-14023

Efficient ionizer for polarized H(-) formation
[DE85-013294] N86-14064

ION DENSITY (CONCENTRATION)

Observation of small-scale solar wind structure on front of sharp increase in plasma flow velocity N86-14142

ION EMISSION

Micromechanisms of electrodiffusion failures in thin film metallization N86-13472

ION IMPLANTATION

Analytical electron microscopy of surface modified ceramics
[DE85-016309] N86-13499

Electrical research on solar cells and photovoltaic materials
[NASA-CR-176384] N86-13838

Recent results on implantation and permeation into fusion reactor materials
[DE85-014620] N86-14067

Application of cross-sectional transmission electron microscopy to the characterization of ion-implanted semiconductors
[DE85-010990] N86-14075

ION IRRADIATION

Ion bombardment and adsorption studies on ilmenite (FeTiO3) by X-ray photoelectron spectroscopy
N86-14100

ION PROBES

Observations of fluxes of cold ions from plasmasphere into ionosphere during nighttime in middle latitudes
N86-14117

ION SOURCES

Comparison of ion milling techniques for cross-sectional TEM of semiconductors
[DE85-016596] N86-13664

Study of storm time fluxes of heavy ions
[NASA-CR-176368] N86-13852

Efficient ionizer for polarized H(-) formation
[DE85-013294] N86-14064

IONIC WAVES

Parametric excitation of ion Bernstein waves by magnetosonic wave
[IPPJ-738] N86-14047

IONIZATION

Combusion of hydrogen and hydrocarbons in fluorine
N86-13526

Close-space, high temperature Knudsen flow
N86-13568

Close-spaced high temperature Knudsen flow
[AD-A158280] N86-13831

IONIZATION CHAMBERS

A pyrolysis technique for determining microamounts of hydrogen in lunar soil using the helium ionization detector N86-14082

IONIZATION COEFFICIENTS

Mass transfer coefficients and Henry's constants for packed-tower air stripping of volatile organics: Measurements and correlation
[AD-A158811] N86-13375

IONOSPHERE

DE 1 RIMS operational characteristics
[NASA-TM-86527] N86-13365

Theoretical studies and data analysis of wave propagation in random media
[AD-A158775] N86-13632

Mass loss of shuttle space suit orthofabric under simulated ionospheric atomic oxygen bombardment
[NASA-TM-87149] N86-13899

IONOSPHERIC CONDUCTIVITY

Electrical and electrothermal conductivity of planetary ionospheres, 1: Refinement of theory N86-14143

IONOSPHERIC CURRENTS

Small-scale structure of intensive longitudinal currents in high latitudes N86-14139

IONOSPHERIC DRIFT

Coordinated investigations of processes in subauroral upper ionosphere and through in concentration of light ions N86-14137

IONOSPHERIC ELECTRON DENSITY

Radio emission of injected electron beam with respect to diagnosis of ionospheric plasma N86-14145

IONOSPHERIC ION DENSITY

Observations of fluxes of cold ions from plasmasphere into ionosphere during nighttime in middle latitudes
N86-14117

Coordinated investigations of processes in subauroral upper ionosphere and through in concentration of light ions N86-14137

IONOSPHERIC SOUNDING

Coordinated investigations of processes in subauroral upper ionosphere and through in concentration of light ions N86-14137

IONS

DE 1 RIMS operational characteristics
[NASA-TM-86527] N86-13365

IRON

Influence of degree of deformation on structure and properties of naturally aged alloy 1163 N86-13431

Dispersion hardening of high-strength NiCoMo steels N86-13468

Iron dominated magnets
[DE85-014955] N86-14003

IRON ALLOYS

Preliminary annealing on crystallization of amorphous Fe80Si6B14 alloy N86-13433

Influence of chromium on crystallization of amorphous Fe-B alloys N86-13434

IRRADIATION

A method for melt-coating a surface
[AD-D011866] N86-13596

Active mirror boosted 351 nm laser irradiation facility
[DE85-014412] N86-13732

Variable curvature phantom
[DE85-014260] N86-14028

Scaling of uv (351 nm) fusion implosions driven by multiple beams
[DE85-014406] N86-14068

ISIS SATELLITES

Replication and fault-tolerance in the ISIS system
[AD-A157775] N86-13926

ISLANDS

Electronic detection of low concentrations of organophosphorus compounds with a solid state device utilizing supported copper + cuprous oxide island films
[AD-A158181] N86-13392

Formation of underwater oceanic volcanoes and islands in relation to lithospheric thickness and movements
N86-13776

ISOLATION

The evaluation of failure detection and isolation algorithms for restructurable control
[NASA-CR-177983] N86-13310

Planetary sample rapid recovery and handling
[NASA-CR-171906] N86-13342

ISOTHERMAL PROCESSES

Equation of state of dense argon: A comparison of shock and static studies
[DE85-015543] N86-14074

ISOTOPE SEPARATION

High count rate gamma-ray spectrometer system for plutonium isotopic measurements
[DE85-013212] N86-14024

ISOTOPES

Deuterium isotope effects in RDX decomposition and combustion processes N86-13522

High count rate gamma-ray spectrometer system for plutonium isotopic measurements
[DE85-013212] N86-14024

ISOTOPIC LABELING

Geothermal investigation in Idaho. Part 14: Geochemical and isotopic investigations of thermal water occurrences of the Boise Front Area, Ada County, Idaho. Water Information Bulletin no. 30
[DE85-012905] N86-13841

ISOTROPIC TURBULENCE

Two unsteady heat transfer experiments. Part 1: In grid-generated isotropic turbulence. Part 2: In laminar oscillatory flow in straight and conical tubes N86-13675

ISRAEL

European Science Notes. Volume 39, number 9
[AD-A158278] N86-14109

ITALY

Certification granted to Franco-Italian ATR 42
N86-13617

ATR 42 production work in French, Italian plants detailed N86-13618

ITERATION

An algorithm for simultaneous determination of modal frequencies and modal vectors of a dynamic impedance matrix
[ESA-CR(P)-2055] N86-13943

Current methods for large stiff ODE systems
[DE85-012914] N86-13983

Monte Carlo analysis of nonlinear statistical models. 1: Theory: Revision
[AD-A158613] N86-13990

ITERATIVE SOLUTION

Development of the NIMBUS-7 SMMR retrieval algorithm --- Scanning Multichannel Microwave Radiometer (SMMR)
[BAE-RPT/NIM-7/021] N86-13367

Iterative and Pade solutions for the water-wave dispersion relation
[AD-A157796] N86-13683

Precision pointing using a dual-wedge scanner
[NASA-CR-3946] N86-13813

Inner/outer iterative methods and numerical Schwarz algorithms - 2
[DE85-013197] N86-13940

Boundary integral techniques for multi-connected domains
[AD-A158171] N86-13965

Computable bounds for solutions of integral equations
[AD-A158169] N86-13970

Multigrid relaxation methods and the analysis of lightness, shading, and flow
[AD-A158173] N86-14036

J

JAPANESE SPACE PROGRAM

Report on the findings of the Japanese Investigative Team on US Space Station Design (Keidanren)
[NASA-TM-77659] N86-13356

JET MIXING FLOW

Nozzle for self-contained cutting torches
[AD-D011875] N86-13597

JET PROPULSION

Numerical models for plasma-solid interactions in electrothermal mass accelerators
[AD-A158637] N86-14052

JOINTS (ANATOMY)

Fiber optics as an angular sensor
[AD-D011886] N86-14044

JOINTS (JUNCTIONS)

Mechanical properties of EP794 steel + 12Kh18N10T steel bimetal N86-13465

Experiments with non-Darcy flow in joints with large scale roughness
[DE85-015714] N86-13695

Tape joint design for a vibration table
[DE85-012617] N86-13753

Parameter identification for a robotic manipulator arm
[NASA-CR-176002] N86-13959

JUPITER RED SPOT

Rossby autosoliton N86-14158

K

KALMAN FILTERS

Discovery of the Kalman filter as a practical tool for aerospace and industry
[NASA-TM-86847] N86-13311

KELVIN-HELMHOLTZ INSTABILITY

Numerical simulations of asymmetric mixing in planar shear flows
[AD-A158024] N86-13687

KEPLER LAWS

Some applications of Lie groups in astrodynamics
N86-14087

KETONES

The dynamics of the photofragmentation of ketene 3-cyclopentenone, 3,5-cycloheptadienone, and tropone
[AD-A158045] N86-13371

Elution of benzene and methyl ethyl ketone from charcoal beds by continued air sweeping
[AD-A158804] N86-13374

KINEMATICS

Kinematics of foldable discrete space cranes
[NASA-CR-176360] N86-13735

Experimental investigation of crater growth dynamics
[NASA-CR-176392] N86-14212

KINETIC THEORY

Interactions between a laminar flame and end gas autoignition
[DE85-008957] N86-13402

KINETICS

Theory of pyrolysis of composite polymer materials
N86-13447

KLYSTRONS

Cerenkov radiation from periodic bunches for a finite path in air
[AD-A159027] N86-13635

Linear accelerators for TeV colliders
[DE85-014958] N86-14017

Hardware upgrade for klystrons in the SLC
[DE85-014357] N86-14029

KNUDSEN FLOW

Close-space, high temperature Knudsen flow
N86-13568

Close-spaced high temperature Knudsen flow
[AD-A158280] N86-13831

L

LAMINAR BOUNDARY LAYER

Recent experience in the RAE (Royal Aircraft Establishment) 5-metre wind tunnel of a china clay method for indicating boundary layer transition
[AD-A157943] N86-13302

LAMINAR FLOW

Ground vibration test of the laminar flow control JStar airplane
[NASA-TM-86398] N86-13321

Interactions between a laminar flame and end gas autoignition
[DE85-008957] N86-13402

Two unsteady heat transfer experiments. Part 1: In grid-generated isotropic turbulence. Part 2: In laminar oscillatory flow in straight and conical tubes N86-13675

LAMINAR MIXING

Numerical simulations of asymmetric mixing in planar shear flows
[AD-A158024] N86-13687

LAMINATES

Process-induced viscoelastic stress in composite laminates N86-13376

Composites design
[AD-A157710] N86-13378

Production of multilayer magnetic surface of magnetically soft composite materials N86-13445

Employment of PAM-FISS-BI-phase computer program for the strength analysis and fracture/delamination behavior of components
[ESI-ED/83-383/RD/MS-VOL-7] N86-13763

LAND ICE

Application of statistical model of layered medium for computing thermal emission of ice covers N86-14186

LAND USE

Method for using clusters in evaluating land use areas from multizonal photographs N86-14180

Experiment for evaluating accuracy in determining land categories on space scanner photographs N86-14195

LANDING GEAR

Advanced technology helicopter landing gear preliminary design investigation
[AD-A158816] N86-13325

LANDING MODULES

Development of instruments for Vega probes
N86-14154

LANDING SITES

A durable airfield marking system
[AD-A157953] N86-13339

LANDSAT SATELLITES

Estimation of finite mixtures using the empirical characteristic function N86-14079

LANDSLIDES

The Vaiont Slide. A geotechnical analysis based on new geologic observations of the failure surface. Volume 1: Main text
[AD-A158192] N86-13854

The Vaiont Slide. A geotechnical analysis based on new geologic observations of the failure surface. Volume 2: Appendices A through G
[AD-A158193] N86-13855

LAPLACE TRANSFORMATION

Boundary-value problem for two-dimensional fluctuations in boundary layers
[AD-A157952] N86-13685

LARGE SPACE STRUCTURES

Adaptive control of large space structures using recursive lattice filters
[NASA-CR-176402] N86-13358

Kinematics of foldable discrete space cranes
[NASA-CR-176360] N86-13735

LARMOR RADIUS

Physical mechanisms for hot electron stabilization of low frequency interchange modes
[IPPJ-741] N86-14050

LASER ANEMOMETERS

Studies of the flow field near a NACA 4412 aerofoil at nearly maximum lift
[AD-A157750] N86-13301

Development of velocity measurement technique by pulsed laser Doppler anemometry N86-13571

LASER APPLICATIONS

Certain features of laser destruction and dislocational structure of silicon during heating and effects of electrical field N86-13454

Structure of flow of erosion plasma formed upon laser treatment of metals N86-13455

High-resolution movies of propellant deflagration
N86-13539

Analytical modeling of strong radiation gas-dynamic interaction N86-13549

Experimental studies of laser-sustained argon plasmas for CW laser propulsion applications N86-13550

Energy deposition of pulsed one micron laser radiation in H2 and AR N86-13552

Laser diagnostics for electric field measurements
N86-13563

Aerial laser sensing of ocean upper layer N86-13775

New methods for laser sounding of atmosphere on basis of nonlinear effects N86-13787

LASER CUTTING

Mechanical laser cutting of metals N86-13453

LASER DOPPLER VELOCIMETERS

Development of velocity measurement technique by pulsed laser Doppler anemometry N86-13571

The 1-D laser Doppler instrumentation N86-13575

LASER FUSION

Laser-trigger system design for PBFA 2
[DE85-013144] N86-14065

LASER HEATING

Mechanical laser cutting of metals N86-13453

LASER INTERFEROMETRY

Single particle sizing by measurement of Brownian motion N86-13584

Experimental and theoretical studies of laser propulsion phenomenology
[AD-A158273] N86-13729

LASER OUTPUTS

Differential scattering cross section and total extinction measurements on (CH)n spheres in 632.8 nm laser light
[AD-A158044] N86-13391

Mechanical laser cutting of metals N86-13453

Structure of flow of erosion plasma formed upon laser treatment of metals N86-13455

Coherent optical transient spectroscopy in flames
N86-13570

Development of velocity measurement technique by pulsed laser Doppler anemometry N86-13571

Quantitative flow visualization N86-13572

Laser emission and coherent Raman scattering from individual flowing droplets N86-13578

Intelligent laser diffraction instrumentation for particle size analysis N86-13581

Application of atomic fluorescence to measurement of combustion temperatures in solid propellants
N86-13582

Concept of laser locator systems (based on the geometry of the triangular corner cube reflector)
[AD-A157795] N86-13728

Multilevel relaxation phenomena and population trapping
[DE85-011527] N86-13731

Active mirror boosted 351 nm laser irradiation facility
[DE85-014412] N86-13732

Study of optical-acoustical phenomena at surface of strongly absorbing clearing fluids N86-13774

Statistics of intensive light beams in turbulent atmosphere N86-13786

Light scattering from bubbles in liquids
[AD-A158736] N86-14039

Optoelectronic integrated circuit multiplier
[AD-D011663] N86-14043

LASER PLASMAS

Laser thermal propulsion N86-13548

Experimental studies of laser-sustained argon plasmas for CW laser propulsion applications N86-13550

Experimental and theoretical studies of laser propulsion phenomenology
[AD-A158273] N86-13729

LASER PROPULSION

Laser thermal propulsion N86-13548

Experimental studies of laser-sustained argon plasmas for CW laser propulsion applications N86-13550

Energy deposition of pulsed one micron laser radiation in H2 and AR N86-13552

Experimental and theoretical studies of laser propulsion phenomenology
[AD-A158273] N86-13729

LASER SPECTROSCOPY

Investigation of nonlinear spectroscopic effects in interaction between CO2-laser radiation and atmospheric gases N86-13789

Observation of optical-radio frequency resonance in H2O using wide-band ruby laser spectroscopy
N86-13790

LASER TARGET INTERACTIONS

Retrofit of a high power Nd:glass laser system with liquid crystal polarizers
[DE85-014415] N86-13733

LASER TARGETS

Apparatus for removably holding a plurality of microballoons
[DE85-006517] N86-13722

Scaling of uv (351 nm) fusion implosions driven by multiple beams
[DE85-014406] N86-14068

LASERS

High-resolution movies of propellant deflagration
N86-13539

Laser produced X-ray for high resolution lithography
[AD-A158734] N86-13730
Fluorine disposal N86-14095

LATCHES
Latch for detachably securing electronic cards along orthogonal loading axes
[AD-D011885] N86-13737

LATITUDE
Statistical correlation between ozone levels over Atlantic Ocean and meteorological values N86-13780

LATITUDE MEASUREMENT
Latitude measurements of cosmic radiation intensity in stratosphere and at sea level on marine antarctic expeditions N86-13792

LATTICES
Lattice and bypass design for a coherent XUV facility
[DE85-016556] N86-14002

LAUNCH VEHICLES
Computer program for post-flight analysis of rigid body moments acting on a launch vehicle first stage
[NASA-CR-166033] N86-13918
Computer program for post-flight evaluation of the control surface response for an attitude controlled missile
[NASA-CR-166032] N86-13920

LAW (JURISPRUDENCE)
National airspace system, system requirements specification
[AD-A157944] N86-13312

LAWS
Discovering qualitative empirical laws
[AD-A159235] N86-13951

LEAD (METAL)
Role of additives in minimizing zinc electrode shape change: The effect of lead on the kinetics of Zn(2) reduction in concentrated alkaline media
[AD-A158806] N86-13395
Development of contact/impact capability for the three-dimensional fluid-structure interaction code: NEPTUNE
[DE85-010264] N86-13698

LEADING EDGES
Boundary-value problem for two-dimensional fluctuations in boundary layers
[AD-A157952] N86-13685

LEARNING
Hypothesizing and refining causal models
[AD-A158165] N86-13893

LEARNING MACHINES
Generating and generalizing models of visual objects
[AD-A158197] N86-13894

LEAST SQUARES METHOD
FIT: Computer program that interactively determines polynomial equations for data which are a function of two independent variables
[NASA-TM-86413] N86-13333
A note on the effect of ignoring small measurement errors in precision instrument calibration
[AD-A159104] N86-13713
Crop area estimation based on remotely-sensed data with an accurate but costly subsample
[NASA-CR-176017] N86-13814
On projected Newton barrier methods for linear programming and an equivalence to Karmarkar's projective method
[AD-A158212] N86-13934
A priori guaranteed accuracy evaluation in determining spacecraft orbit by least squares method N86-14130
Uniqueness conditions in evaluation of least squares method in nonlinear space navigation problems
N86-14144

LEAVES
Bidirectional reflectance modeling of non-homogeneous plant canopies N86-13796
Geometric-optical modeling of a conifer forest canopy
N86-13799
Crop characteristics research: Growth and reflectance analysis N86-13800

LECTURES
Iron dominated magnets
[DE85-014955] N86-14003
Linear accelerators for TeV colliders
[DE85-014958] N86-14017

LEGENDRE FUNCTIONS
Transient simulation of submicron devices
[AD-A157748] N86-13648

LEVITATION
Problems in thermal convective instability N86-13670

LIBRARIES
Crossref for the Cray
[NASA-CR-177384] N86-13913

LIBRATION
Structure of coefficients of series representing solution of plane circular restricted three-body problem
N86-14129
Periodic regimes of rotational motion of solid body about liberation point L sub 4 in restricted elliptical three-body problem N86-14132

LIE GROUPS
A method for calculating flow fields around moving bodies
[NAL-TR-859T] N86-13288
Some applications of Lie groups in astrodynamics
N86-14087

LIFE (DURABILITY)
A durable airfield marking system
[AD-A157953] N86-13339
Role of additives in minimizing zinc electrode shape change: The effect of lead on the kinetics of Zn(2) reduction in concentrated alkaline media
[AD-A158806] N86-13395
Magnetoplasmadynamic thruster erosion research
N86-13557
Time dependency of strainrange partitioning life relationships
[NASA-CR-174946] N86-13755
Long-term analysis of slender concrete structures with cracking
[DE85-010275] N86-13762

LIFE CYCLE COSTS
Zirconium as a structural material for naval systems
[AD-A158201] N86-13411

LIFE SCIENCES
Life sciences accomplishments
[NASA-TM-88177] N86-13879
Effects of 60 Hz electric fields on operant and social stress behaviors of nonhuman primates
[DE85-011992] N86-13885
USSR report: Space
[JPRS-USP-85-005] N86-14111

LIFT
Fluid forces on two circular cylinders in crossflow
[DE85-014294] N86-13704
Aerodynamic research efforts at SERI wind energy research center at Rocky Flats --- Solar Energy Research Institute (SERI) N86-13829

LIGANDS
Determination of the activation barrier to energy transfer from 3 pi pi* to charge transfer levels via steady state and transient luminescence measurements on Bis(4-Chlorothiophenol) (1,10-Phenanthroline) Zinc (II)
[AD-A158239] N86-14012

LIGHT BEAMS
Statistics of intensive light beams in turbulent atmosphere N86-13786

LIGHT EMITTING DIODES
MeV electron beam irradiation effects on GaAs (1-x) P (x) LEDs (Light emitting diodes)
[AD-A158832] N86-13653

LIGHT IONS
Coordinated investigations of processes in subauroral upper ionosphere and through in concentration of light ions N86-14137

LIGHT SCATTERING
Quantitative flow visualization N86-13572
Spray characterization with a nonintrusive optical single particle counter N86-13580
Intelligent laser diffraction instrumentation for particle size analysis N86-13581
Distribution of brightness from point source of scattered light along inclined path N86-13779
Meteorological and climatological conditions affecting the vertical structure of visibility in northern Germany
[AD-A158254] N86-13871
New physical methods for biological aerosol detection
[AD-A158218] N86-13881
Light scattering from bubbles in liquids
[AD-A158736] N86-14039

LIGHT SOURCES
Optoelectronic integrated circuit multiplier
[AD-D011883] N86-14043

LIGHT TRANSMISSION
Expendable bathythermograph for measuring light attenuation and temperature below the ocean surface
[AD-D011870] N86-13716

LIGHT VALVES
Real time large memory optical pattern recognition
[AD-A158023] N86-14034

LIGHTNING
Interpretation of F-106B in-flight lightning signatures
[NASA-CR-176387] N86-13320
Horizontal electric fields from lightning return strokes
[DE85-016367] N86-13873

LIKELIHOOD RATIO
The evaluation of failure detection and isolation algorithms for restructurable control
[NASA-CR-177983] N86-13310

LIMITER CIRCUITS
Preliminary experiment on electron beam injection for tokamak current drive
[IPPJ-739] N86-14048

LIMNOLOGY
Experience in conducting subsatellite experiments with water bodies in USSR and Hungarian People's Republic
N86-14182

LINE SPECTRA
Resonant cars detection of OH radicals N86-13576

LINEAR ACCELERATORS
Advanced energy conversion concept for microwave beamed-energy propulsions N86-13553
Linear accelerators for TeV colliders
[DE85-014958] N86-14017
Hardware upgrade for klystrons in the SLC
[DE85-014357] N86-14029
Effect of focusing field nonlinearities in MBE-4 on transverse beam dynamics
[DE85-016561] N86-14058
Generation and acceleration of high intensity beams in the SLC injector
[DE85-013056] N86-14066

LINEAR ARRAYS
New digital circuits at Thomson semiconductor in France N86-13619

LINEAR PROGRAMMING
On projected Newton barrier methods for linear programming and an equivalence to Karmarkar's projective method
[AD-A158212] N86-13934
Existence of equilibrium prices for a simple planning model
[AD-A158263] N86-13996

LINEAR RECEIVERS
Testing of 30-GHz low noise receivers
[NASA-TM-87171] N86-13627

LINEAR SYSTEMS
A method to stabilize linear systems using eigenvalue gradient information
[NASA-TP-2479] N86-13946
Further results for application of disturbance minimization control techniques to a linear, time-invariant, second-order state set-point regulator problem
[AD-A157793] N86-13961
Realization theory in Hilbert space
[AD-A158172] N86-13997

LINEARITY
Effect of interfacial phenomena on contact line heat transfer N86-13566
Linearity optimization in a class of analog phase modulators
[NASA-TM-86420] N86-13644
A note on the effect of ignoring small measurement errors in precision instrument calibration
[AD-A159104] N86-13713

LINEARIZATION
Transformation matrices between non-linear and linear differential equations N86-14099

LINGUISTICS
Deterministic parsing and linguistic explanation: Revision
[AD-A159233] N86-13950

LIQUID CRYSTALS
Retrofit of a high power Nd:glass laser system with liquid crystal polarizers
[DE85-014415] N86-13733

LIQUID FUELS
Health hazard evaluation of liquid monopropellants. Phase 5: Comparative inhalation toxicities of LGP 1776, LGP 1845, and HAN (hydroxylammonium nitrate)
[AD-A159090] N86-13891

LIQUID HELIUM
Turbulence and dynamical systems
[AD-A159026] N86-13691

LIQUID INJECTION
Holographic study of the particles produced by the injector in a Viking motor
[ISL-R-111/84] N86-13724

LIQUID METALS
Modeling of thermal fatigue and erosion of complex alloyed steels in metal melts N86-13469
Gas recirculator for acyclic machines
[AD-D011873] N86-13658
The physics and technology of strong magnetic fields (chapter 10)
[AD-A158174] N86-14000

LIQUID NITROGEN
Charge-density waves observed with a tunneling microscope
[AD-A158779] N86-13709
An analysis of cryotrap heat exchanger performance test data (400 area) and recommendations for a system to handle Apollo RCS engines N86-14034

LIQUID PHASES
Mass transfer coefficients and Henry's constants for packed-tower air stripping of volatile organics: Measurements and correlation
[AD-A158811] N86-13375

LIQUID PROPELLANT ROCKET ENGINES
Rocket engine hot-spot detector
[NASA-CR-171902] N86-13708

LIQUID ROCKET PROPELLANTS
Mathematical models of nonstationary eddy currents and eddy movements of fluid in problems of orientation and stabilization of artificial Earth satellites and spacecraft 2 N86-14116

LIQUID SURFACES
Experimental investigation of magnesium combustion in steam
[AD-A159109] N86-13396

LIQUID-SOLID INTERFACES
A study of transport phenomena and interface stability during solidification of binary solutions using front tracking finite elements N86-13669

LIQUID-VAPOR INTERFACES
Effect of interfacial phenomena on contact line heat transfer N86-13566

LIQUIDS
Effect of interfacial phenomena on contact line heat transfer N86-13566
Formation of structure of mixed region under influence of shear flow in stratified fluid N86-13768
Light scattering from bubbles in liquids
[AD-A158736] N86-14039

LITHIUM
Appearance of superplasticity effect in aluminum alloys with lithium N86-13432
Cathode including a non fluorinated linear chain polymer as the binder, method of making the cathode, and lithium electrochemical cell containing the cathode
[AD-D011807] N86-13647

LITHIUM ALLOYS
Combined small angle X-ray scattering and transmission electron microscopy studies of Al-Li alloys
[DE85-016356] N86-13416
Influence of sodium on mechanical and casting properties of magnesium-lithium alloys N86-13457

LITHIUM HYDRIDES
Coupled radiation transport/thermal analysis of the radiation shield for a space nuclear reactor
[AD-A158180] N86-14022

LITHIUM SULFUR BATTERIES
Cathode for use in high energy primary thionyl chloride cell systems and high energy primary thionyl chloride cell systems including the cathode
[AD-D011882] N86-13662

LITHOGRAPHY
Development of high sensitivity X-ray and electron beam resist processes
[AD-A158968] N86-13657
Laser produced X-ray for high resolution lithography
[AD-A158734] N86-13730

LITHOLOGY
Possible petroliferousness of South Caspian uplifts analyzed N86-13863

LITHOSPHERE
Formation of underwater oceanic volcanoes and islands in relation to lithospheric thickness and movements N86-13776

LOAD DISTRIBUTION (FORCES)
Tire-soil interaction model for turning (steered) tires
[AD-A157737] N86-13593

LOADING MOMENTS
Algorithms for the reduction of wind-tunnel data derived from strain gauge force balances
[ARL/AERO-R-164] N86-13337

LOADING OPERATIONS
Italian robot manufacturer enters Spanish market N86-13626
Latch for detachably securing electronic cards along orthogonal loading axes
[AD-D011885] N86-13737

LOADS (FORCES)
Standardised fatigue loading sequences for helicopter rotors (Helix and Felix). Part 2: Final definition of Helix and Felix
[AD-A156622] N86-13322
Digital servocontroller system. Volume 4: Results and conclusions
[AD-A159068] N86-13335
Modifications of system for elevated temperature tensile testing and stress-strain measurement of metal matrix composites
[NASA-TM-87172] N86-13370
Calculation of damping properties of composite materials N86-13446
Effect of elastoplastic cyclic deformation on mechanical characteristics of steel O3Kh13AG19 at temperatures of 293 and 77 deg K N86-13463
Subcritical crack development under constant load in VT6 alloy N86-13475
Fractured toughness of Si3N4 measured with short bar chevron-notched specimens
[NASA-TM-87153] N86-13495
Application of Pasternak model to some soil-structure interaction problems. Volume 1: Solutions for plates continuously supported on a Pasternak base
[AD-A157776] N86-13594

LOGARITHMS
On projected Newton barrier methods for linear programming and an equivalence to Karmarkar's projective method
[AD-A158212] N86-13934
Differential entropy and the statistics of instantaneous failure
[AD-A158047] N86-13984

LOGIC CIRCUITS
Bulk CMOS VLSI technology studies. Part 4: Design of a CMOS microsequencer
[AD-A158[illegible]] N86-13650

LOGIC PROGRAMMING
Graph theoretic approaches to diagnostics: Applications of logic programming and cutset theory to aspects of reactor and circuit analysis
[ANL-84-74] N86-13912

LOGISTICS
Low power reactor for remote applications
[DE85-012763] N86-14032

LONG DURATION SPACE FLIGHT
USSR report: Space
[JPRS-USP-85-005] N86-14111
Biological life-support systems for long-duration space flights N86-14160
Architect discusses space habitat designs N86-14161

LONGITUDINAL CONTROL
A preliminary evaluation of the generalized likelihood ratio for detecting and identifying control element failures in a transport aircraft
[NASA-TM-87620] N86-13332
Pitch rate versus G command as the longitudinal flight control system design strategy for a statistically unstable fighter type aircraft with two control surfaces
[AD-A158803] N86-13334

LOOK ANGLES (TRACKING)
Occasional reports of the Royal Observatory, Edinburgh, no. 16
[ISSN-0309-099-X] N86-14200

LOOPS
A three-dimensional analysis of natural convection in a toroidal loop N86-13672

LOSS OF COOLANT
Rocket engine hot-spot detector
[NASA-CR-171902] N86-13708

LOSSES
Shock waves, increase of entropy and loss of information
[DE85-013645] N86-13701
Development of the VOLT-A shuttle experiment
[NASA-TM-87169] N86-14110

LOW ASPECT RATIO WINGS
Pressure-distribution measurements on a transonic low-aspect ratio wing
[NASA-TM-86683] N86-13304

LOW CARBON STEELS
Influence of annealing on hardness of vacuum-diffusion chromium coating on low-carbon steel N86-13441

LOW CONCENTRATIONS
Electronic detection of low concentrations of organophosphorus compounds with a solid state device utilizing supported copper + cuprous oxide island films
[AD-A158181] N86-13392

LOW FREQUENCIES
Hybrid simulation codes with application to shocks and upstream waves
[NASA-CR-176365] N86-13702

LOW NOISE
Testing of 30-GHz low noise receivers
[NASA-TM-87171] N86-13627

LOW SPEED STABILITY
HPOTP low-speed flexible rotor balancing, phase 1
[NASA-CR-171610] N86-13369

LOW SPEED WIND TUNNELS
A real-time data acquisition system for a low speed wind tunnel
[AR-AERO-R-163] N86-13336

LOW TEMPERATURE
Effect of elastoplastic cyclic deformation on mechanical characteristics of steel O3Kh13AG19 at temperatures of 293 and 77 deg K N86-13463
Mound activities in chemical and physical research: July - December 1984
[DE85-014402] N86-14030
Investigation of cold colored smoke production
[AD-A158783] N86-14040
Ion bombardment and adsorption studies on ilmenite (FeTiO3) by X-ray photoelectron spectroscopy N86-14100

LOW THRUST
Optimum control programs in problem of interorbital flight with continuous thrust N86-14135

LOWER ATMOSPHERE
Remote sensing of Earth terrain N86-13808

LOWER BODY NEGATIVE PRESSURE
Endocrine and fluid metabolism in males and females of different ages after bedrest, acceleration and lower body negative pressure
[NASA-TM-58270] N86-13886

LUBRICANT TESTS
Activities report in space tribology
[ESA-ESTL-72] N86-13738

LUBRICANTS
Activities report in space tribology
[ESA-ESTL-72] N86-13738

LUBRICATION
Lubrication of nonconformal contacts
[NASA-TM-87120] N86-13679
Design of traction drives
[NASA-RP-1154] N86-13734

LUMINESCENCE
Combusion of hydrogen and hydrocarbons in fluorine N86-13526
Aerial laser sensing of ocean upper layer N86-13775
Influence of fog microstructure on quality of optical image transmitted through it N86-13781
Determination of the activation barrier to energy transfer from 3 pi pi* to charge transfer levels via steady state and transient luminescence measurements on Bis(4-Chlorothiophenol) (1,10-Phenanthroline) Zinc (II)
[AD-A158239] N86-14012

LUMINOUS INTENSITY
Combustion behavior of free boron slurry droplets
[AD-A158620] N86-13585
Determination of the activation barrier to energy transfer from 3 pi pi* to charge transfer levels via steady state and transient luminescence measurements on Bis(4-Chlorothiophenol) (1,10-Phenanthroline) Zinc (II)
[AD-A158239] N86-14012
Multigrid relaxation methods and the analysis of lightness, shading, and flow
[AD-A158173] N86-14036

LUMPED PARAMETER SYSTEMS
Study of thermal analysis methods --- spacecraft
[GEC-MEL12.0539] N86-13362

LUNAR ALBEDO
Approximate cluster analysis method and three-dimensional diagram of optical characteristics of lunar surface N86-14128

LUNAR ATMOSPHERE
Interaction between Escherichia coli and lunar fines N86-14088

LUNAR BASES
Comparative effect of lunar fines and terrestrtial ash on the growth of a blue-green alga and germinating radish seeds N86-14097

LUNAR CRATERS
Lunar luminescence measurements N86-14092

LUNAR DUST
Electron microscopic observations of hydrogen implantation in ilmenites N86-14081
Nutritional characteristics of moon dust for soil microorganisms N86-14086

LUNAR ENVIRONMENT
Comparative effect of lunar fines and terrestrtial ash on the growth of a blue-green alga and germinating radish seeds N86-14097

LUNAR EVOLUTION
Nature of megacycles in evolution of Earth, Mars, and Moon N86-14159

LUNAR LOGISTICS
Comparative effect of lunar fines and terrestrtial ash on the growth of a blue-green alga and germinating radish seeds N86-14097

LUNAR LUMINESCENCE
Lunar luminescence measurements N86-14092

LUNAR MAPS
Approximate cluster analysis method and three-dimensional diagram of optical characteristics of lunar surface N86-14128

LUNAR SOIL
Electron microscopic observations of hydrogen implantation in ilmenites N86-14081
A pyroloysis technique for determining microamounts of hydrogen in lunar soil using the helium ionization detector N86-14082
Nutritional characteristics of moon dust for soil microorganisms N86-14086
Interaction between Escherichia coli and lunar fines N86-14088

LUNAR SURFACE
Approximate cluster analysis method and three-dimensional diagram of optical characteristics of lunar surface N86-14128

M

MACH NUMBER
Preliminary measurement of the noise from the 2/9 scale model of the Large-scale Advanced Propfan (LAP) propeller, SR-7A
[NASA-TM-87116] N86-14006

MACHINE TOOLS
Influence of texture of titanium nitride coatings on wear resistance of cutting tools N86-13440
Lubrication of nonconformal contacts
[NASA-TM-87120] N86-13679
USSR report: Machine tools and metalworking equipment
[JPRS-UMM-85-014] N86-13742
Problems with integrating robots in conventional production N86-13744
USSR report: Machine tools and metalworking equipment
[JPRS-UMM-85-013] N86-13745
Problems with robotization of conventional shops N86-13746

MACHINE TRANSLATION
An algorithm to translate relational algebra queries into QUEL
[AD-A158169] N86-13931

MACHINERY
Fiber composition materials for strengthening components of aluminum and its alloys N86-13424

MACHINING
A study of rhenium as an alternate substrate material for impregnated dispenser cathodes
[AD-A159113] N86-13415

MAGNESIUM
Experimental investigation of magnesium combustion in steam
[AD-A159109] N86-13396
The delayed fracture of aluminum alloys
[AD-A158944] N86-13412

MAGNESIUM ALLOYS
Effect of strain and strain rate on the microstructure of a superplastically deformed Al-10%Mg-0.1%Zr alloy
[AD-A159062] N86-13414
Structure and properties of Al-Mg-Zn casting alloys N86-13425
Discontinuous precipitation in aluminum-magnesium alloys with high magnesium content N86-13426
Influence of sodium on mechanical and casting properties of magnesium-lithium alloys N86-13457

MAGNESIUM OXIDES
Experimental investigation of magnesium combustion in steam
[AD-A159109] N86-13396

MAGNETIC ANOMALIES
Mechanism of corpuscular-atmospheric relationships N86-14127

MAGNETIC COILS
Iron dominated magnets
[DE85-014955] N86-14003
Impact of a poloidal divertor in ignition tokamak design
[DE85-012892] N86-14061

MAGNETIC CONTROL
Experimental checking of mathematical model of eddy currents in actuating components of systems for magnetic orientation of artificial Earth satellites and spacecraft N86-14164

MAGNETIC DIPOLES
Possibility of spectroscopic detection of oxygen in lower Venusian atmosphere N86-14157

MAGNETIC DISTURBANCES
Spatial patterns of manifestation of solar activity in troposphere N86-14126

MAGNETIC EQUATOR
Formation of proton radiation belts in region of energies of several MeV N86-14140

MAGNETIC FIELD CONFIGURATIONS
Experimental study of neoclassical currents
[DE85-014866] N86-14063
Possibility of spectroscopic detection of oxygen in lower Venusian atmosphere N86-14157

MAGNETIC FIELDS
Slot line tunable bandpass filter
[AD-D011881] N86-13661
The physics and technology of strong magnetic fields (chapter 10)
[AD-A158174] N86-14000
Magnetic field applications in modern technology and medicine
[DE85-015197] N86-14001
Parametric excitation of ion Bernstein waves by magnetosonic wave
[IPPJ-738] N86-14047
Unlimited acceleration of charged particles by an electromagnetic wave with a purely transverse electric field propagating perpendicularly to a static magnetic field
[IPPJ-740] N86-14049
Physical mechanisms for hot electron stabilization of low frequency interchange modes
[IPPJ-741] N86-14050
Effects of neutrals on internal forces and thermal conduction of a plasma in a magnetic field
[IPPJ-691] N86-14051

MAGNETIC INDUCTION
Production of multilayer magnetic surface of magnetically soft composite materials N86-13445

MAGNETIC MATERIALS
Production of multilayer magnetic surface of magnetically soft composite materials N86-13445
Unusual occurrence of maghemite in soils developed on Knox group dolostones
[DE85-017158] N86-13817

MAGNETIC PUMPING
Parametric excitation of ion Bernstein waves by magnetosonic wave
[IPPJ-738] N86-14047

MAGNETIC STORMS
Mechanism of corpuscular-atmospheric relationships N86-14127
Registry of heavy ions in auroral region during magnetic storms N86-14138

MAGNETOHYDRODYNAMIC FLOW
Performance-limiting factors in MPD thrusters N86-13555
Unified study of plasma-surface interactions for space power and propulsion N86-13567

MAGNETOHYDRODYNAMIC STABILITY
Dense Z-pinch plasmas
[DE85-005818] N86-14059

MAGNETOHYDRODYNAMICS
Fusion programs in applied plasma physics and development and technology, fiscal 1984
[DE85-014551] N86-14062
Possibility for a self-consistent treatment of transport processes in a turbulent plasma
[DE85-016214] N86-14069

MAGNETOPLASMADYNAMICS
Basic processes of plasma propulsion N86-13554
Performance-limiting factors in MPD thrusters N86-13555
Erosion and onset mechanisms in magnetoplasmadynamic thrusters N86-13556
Magnetoplasmadynamic thruster erosion research N86-13557
Completely magnetically contained electrothermal thruster N86-13558
Unified study of plasma-surface interactions for space power and propulsion N86-13567

MAGNETOSPHERE
DE 1 RIMS operational characteristics
[NASA-TM-86527] N86-13365
Study of storm time fluxes of heavy ions
[NASA-CR-176368] N86-13852
Possibility of spectroscopic detection of oxygen in lower Venusian atmosphere N86-14157

MAGNETOSPHERIC INSTABILITY
Small-scale structure of intensive longitudinal currents in high latitudes N86-14139

MAGNETOSPHERIC ION DENSITY
Registry of heavy ions in auroral region during magnetic storms N86-14138

MAGNETS
Lattice and bypass design for a coherent XUV facility
[DE85-016556] N86-14002

MAINTAINABILITY
Low power reactor for remote applications
[DE85-012763] N86-14032

MAN MACHINE SYSTEMS
Pitch rate versus G command as the longitudinal flight control system design strategy for a statistically unstable fighter type aircraft with two control surfaces
[AD-A158803] N86-13334
Problems with integrating robots in conventional production N86-13744
Problems with robotization of conventional shops N86-13746
The event related brain potential as an index of information processing, cognitive activity, and skill acquisition: A program of basic research
[AD-A159118] N86-13897
Information requirements determination: An empirical investigation of obstacles within an individual
[AD-A158025] N86-13901

MANAGEMENT
National airspace system, system requirements specification
[AD-A157944] N86-13312

MANAGEMENT METHODS
NASA flight operations review
[NASA-CR-176393] N86-13306
BOSS: A FORTRAN code for a relational database manager
[AD-A157067] N86-13924

MANGANESE
Muon spin relaxation study of exchange coupling in dilute AgMn alloys
[DE85-014104] N86-13419

MANIPULATORS
Study on design techniques for robots (space applications). Volume 1, part A: Technical results
[FOK-TR-R-84-110-VOL-1-PT-A] N86-13902
Study on design techniques for robots (space applications). Volume 1, part B: Technical results
[FOK-TR-R-84-110-VOL-1-PT-B] N86-13903
Study on design techniques for robots (space applications). Volume 2: Technical appendices
[FOK-TR-R-84-110-VOL-2] N86-13904
Study on design techniques for robots (space applications). Volume 3: Executive summary
[FOK-TR-R-84-110-VOL-3] N86-13905
Parameter identification for a robotic manipulator arm
[NASA-CR-178002] N86-13959

MANUFACTURING
Activities report of the Technical and Scientific Research Center for the Metal Manufacturing Industry N86-13740
Environmental Stress Screening (ESS)
[AD-A158262] N86-13751

MAPPING
Map projections for use with the Geographic Information System
[PB85-198992] N86-13819

MAPS
Compilation of landscape maps at different scales with use of space photoinformation N86-14187

MARINE ENVIRONMENTS
Short range aids to navigation systems. Design manual for restricted waterways
[AD-A158213] N86-13313

MARINE METEOROLOGY
Vertical structure of turbulence and turbulent exchange in equatorial zone of Pacific Ocean N86-13771
Statistical correlation between ozone levels over Atlantic Ocean and meteorological values N86-13780
Atmospheric synoptic eddies over ocean (determined from experimental data) N86-13784

MARINE TECHNOLOGY
Zirconium as a structural material for naval systems
[AD-A158201] N86-13411

MARKERS
A durable airfield marking system
[AD-A157953] N86-13339

MARKOV PROCESSES
Partitions of point processes: Multivariate poisson approximations
[AD-A158739] N86-13978
Unified method for delay analysis of random multiple access algorithms
[AD-A159108] N86-13981
Basic properties of strong mixing conditions
[AD-A158740] N86-13992

MARS (PLANET)
Brochure on Phobos and Deimos N86-14155
Possibility of spectroscopic detection of oxygen in lower Venusian atmosphere N86-14157
Nature of megacycles in evolution of Earth, Mars, and Moon N86-14159

MARTENSITE
Dispersion hardening of high-strength NiCoCo-Mo steels N86-13468

MASKING
European silicon structures plans custom chips in 15 days N86-13621

MASS FLOW
Analytical modeling of strong radiation gas-dynamic interaction N86-13549

MASS SPECTROMETERS
DE 1 RIMS operational characteristics
[NASA-TM-86527] N86-13365
Study of storm time fluxes of heavy ions
[NASA-CR-176368] N86-13852
Development of a mass spectrometer system for the measurement of inert gases in meteorites N86-14093

MASS SPECTROSCOPY
New physical methods for biological aerosol detection
[AD-A158218] N86-13881

MASS TRANSFER
Mass transfer coefficients and Henry's constants for packed-tower air stripping of volatile organics: Measurements and correlation
[AD-A158811] N86-13375
A study of transport phenomena and interface stability during solidification of binary solutions using front tracking finite elements N86-13669

Determination of convective diffusion heat/mass transfer rates to burner rig test targets comparable in size to cross-stream jet diameter
[NASA-TM-87176] N86-13678

MATCHED FILTERS
Real time large memory optical pattern recognition
[AD-A158023] N86-14034

MATERIAL ABSORPTION
Neutron stress measurements with a position sensitive detector
[AD-A158882] N86-13712

MATERIALS HANDLING
Planetary sample rapid recovery and handling
[NASA-CR-171906] N86-13342

MATERIALS RECOVERY
Planetary sample rapid recovery and handling
[NASA-CR-171906] N86-13342

MATERIALS SCIENCE
USSR report: Materials science and metallurgy
[JPRS-UMS-85-006] N86-13422

MATHEMATICAL MODELS
A direct-inverse method for transonic and separated flows about airfoils
[NASA-CR-176403] N86-13300
Effective behavior of composite materials
[AD-A158941] N86-13380
Thermal radiation effects on combustion of condensed fuels N86-13387
Interactions between a laminar flame and end gas autoignition
[DE85-008957] N86-13402
Homogenization of beta-solid solution upon rapid heating of two-phase titanium alloys N86-13478
Strategy for advanced sensing and control of combustion N86-13574
Tire-soil interaction model for turning (steered) tires
[AD-A157737] N86-13593
Transonic separated flow predictions based on a mathematically simple, nonequilibrium turbulence closure model
[NASA-TM-86826] N86-13676
Turbulence in two-field incompressible flow
[DE85-015361] N86-13693
Investigation of the vertical-flow aquifer thermal energy storage concept and numerical simulation of the Dorigny field experiment
[DE85-014524] N86-13694
Development of contact/impact capability for the three-dimensional fluid-structure interaction code: NEPTUNE
[DE85-010264] N86-13698
Experimental investigation of heat transfer behavior of aqueous foams in thermal entry region of pipe flow
[DE85-012836] N86-13700
Simulating distributed reinforcement effects in concrete analysis
[DE85-009745] N86-13761
Multidimensional modeling of atmospheric effects and surface heterogeneities on remote sensing N86-13806
Scattering models and basic experiments in the microwave regime N86-13807
Remote sensing of Earth terrain N86-13808
Three-dimensional modeling of Tsunami waves
[DE85-015724] N86-13877
Development and enhancement of Computer Performance Modeling Tool (CPMT)
[AD-A159003] N86-13938
Parameter identification for a robotic manipulator arm
[NASA-CR-178002] N86-13959
A behavioral summary for completely random nets
[AD-A157755] N86-13960
Approximation of the initial reserve for known ruin probabilities
[AD-A158167] N86-13987
Monte Carlo analysis of nonlinear statistical models. 1. Theory: Revision
[AD-A158613] N86-13990
Realization theory in Hilbert space
[AD-A158172] N86-13997
A variant of Shanbhag's lemma arising out of a modified Rao-Rubbin condition
[AD-A158608] N86-13998
Information in censored models
[AD A158644] N86-13999
JASON electrostatic boundary conditions: A survey
[DE85-014521] N86-14005
The mathematical structure of elementary particles: 2
[AD-A158191] N86-14011
Reactive scattering in the bending-corrected rotating linear model
[DE85-017539] N86-14018
Aspects of three field approximations: Darwin, frozen, EMPULSE
[DE85-014204] N86-14020
Polarization transfer in enelastic scattering and pionic models of the EMC effect
[DE85-014119] N86-14021
Theory of resistivity-gradient-driven turbulence
[DE85-015068] N86-14053
Possibility for a self-consistent treatment of transport processes in a turbulent plasma
[DE85-016214] N86-14069
Application of statistical model of layered medium for computing thermal emission of ice covers N86-14186
Use of Goudriaan model for studying reflection regularities in vegetation-soil system in optical range. 1: Influence of phytometric parameters on spectral brightness coefficients N86-14190

MATHEMATICS
Expanding your horizons in science and mathematics
[NASA-CR-176372] N86-13958

MATRICES (MATHEMATICS)
Spectra for large dimensional random matrices
[AD-A158256] N86-13973
Inference on the ranks of the canonical correlation matrices for elliptically symmetric populations
[AD-A158268] N86-13976
Transformation matrices between non-linear and linear differential equations N86-14099

MATRIX MATERIALS
Test of a moisture conditioning procedure using 70 C distilled water, instead of a gas atmosphere at 70 C, 95% relative humidity --- plastic composites
[M3-431000] N86-13383
Effect of geometry of fiber packing on consolidation of fibrous composition materials with porous matrix
N86-13443
Conductivity of metal-ceramic multilayer ZrO2-Mo and Mo-based composite materials N86-13444

MATRIX METHODS
An algorithm for simultaneous determination of modal frequencies and modal vectors of a dynamic impedance matrix
[ESA-CR(P)-2055] N86-13943

MAXIMA
Minimal norm constrained interpolation
[NASA-CR-178001] N86-13956

MAXIMUM LIKELIHOOD ESTIMATES
Inference on the ranks of the canonical correlation matrices for elliptically symmetric populations
[AD-A158268] N86-13976
Conditioning in a missing data problem
[AD-A158202] N86-13988
Estimation of finite mixtures using the empirical characteristic function N86-14079

MEAN FREE PATH
Study of mean free path effects on growth of ultrafine metallic aerosols
[AD-A158206] N86-13393

MEASURE AND INTEGRATION
European Science Notes, Volume 39, Number 7
[AD-A157708] N86-14108

MEASURING INSTRUMENTS
Discussion on the Vibration Process Standards 9958002 and 9958004
[DE85-017116] N86-13599
A note on the effect of ignoring small measurement errors in precision instrument calibration
[AD-A159104] N86-13713

MECHANICAL DEVICES
Design criteria upgrade for US Army Type 2 air traffic control towers
[AD-A159115] N86-13314

MECHANICAL DRIVES
Design of traction drives
[NASA-RP-1154] N86-13734
Two-hundred to 300 KVA conditioned power system - development, phase 1
[AD-A158820] N86-13832

MECHANICAL MEASUREMENT
Study of the dispersion of the mechanical properties of carbon-epoxy composite materials
[M2-695600-PT-2] N86-13385

MECHANICAL PROPERTIES
Study of the mechanical properties dispersion of carbon-epoxy composite materials
[M2-695600-PT-1] N86-13384
Characterization of 7017 aluminum alloys in thick profiles, in the metallurgical versions T6510, T76510 and T736510, test report no. PV-44-607/F
[PV-44-607/F] N86-13420
Influence of alloying elements and impurities on mechanical properties of complex silumins N86-13428
Influence of Co-Cr-Al-Y coatings on physical and mechanical properties of EI-893 steel in GT-100 turbine drive vanes N86-13438
Effect of elastoplastic cyclic deformation on mechanical characteristics of steel O3Kh13AG19 at temperatures of 293 and 77 deg K N86-13463
Mechanical properties of EP794 steel + 12Kh18N10T steel bimetal N86-13465

MECHANIZATION
New robots by Soviet, CEMA manufacturers described
N86-13748

MEDIA
Reflectance modeling N86-13795

MEDICAL SERVICES
Tradeoff analysis of technology needs for public service helicopters
[NASA-CR-3927] N86-13317

MELTING
A method for melt-coating a surface
[AD-D011866] N86-13596

MEMORY
The event related brain potential as an index of information processing, cognitive activity, and skill acquisition: A program of basic research
[AD-A159118] N86-13897

MENTAL PERFORMANCE
Hypothesizing and refining causal models
[AD-A158165] N86-13893
The event related brain potential as an index of information processing, cognitive activity, and skill acquisition: A program of basic research
[AD-A159118] N86-13897

MERCURY CADMIUM TELLURIDES
MBE growth of CdTe and Hg (1-x) Cd (x) Te films and multilayer structures
[AD-A158267] N86-14073

MESOSPHERE
Disturbances in stratosphere and mesosphere from source of ultraviolet radiation N86-14136

MESSAGE PROCESSING
LTSSCLI: An ITSS shell for NLTSS, version 2.0, revision 1
[DE85-013234] N86-13941

METABOLISM
Endocrine and fluid metabolism in males and females of different ages after bedrest, acceleration and lower body negative pressure
[NASA-TM-58270] N86-13886

METAL COATINGS
Fuel-rich solid propellant boron combusion
N86-13536
Atomically mixed alloy coated cathodes specification
[AD-D011877] N86-13659

METAL COMBUSTION
Extremely high reflective capability of zirconium burning in air under effects of constant CO2 laser radiation
N86-13452

METAL CUTTING
Mechanical laser cutting of metals N86-13453
USSR report: Machine tools and metalworking equipment
[JPRS-UMM-85-014] N86-13742
USSR report: Machine tools and metalworking equipment
[JPRS-UMM-85-013] N86-13745

METAL FATIGUE
Modeling of thermal fatigue and erosion of complex alloyed steels in metal melts N86-13469

METAL IONS
Application of computers in analytical chemistry: Calculation of optimum acidity of reaction between metal ions and organic reagents in solution N86-13607

METAL MATRIX COMPOSITES
Modifications of system for elevated temperature tensile testing and stress-strain measurement of metal matrix composites
[NASA-TM-87172] N86-13370
A method to determine dynamic elastic constants of thin shell composites by guided ultrasonic waves
[AD-A159025] N86-13381
Polymer, metal and ceramic matrix composites for advanced aircraft engine applications
[NASA-TM-87132] N86-13407
Elastic-plastic deformation of a metal-matrix composite coupon with a center slot
[NASA-CR-178013] N86-13496

METAL POWDER
A study of rhenium as an alternate substrate material for impregnated dispenser cathodes
[AD-A159113] N86-13415
Production of multilayer magnetic surface of magnetically soft composite materials N86-13445
Superelastic behavior of powdered titanium nickelide during pressing N86-13461

METAL SURFACES
Synthesis, structure and reactivity of molecules attached to electrode surfaces
[AD-A158621] N86-13394

METAL VAPORS
Fusion welding research
[AD-A158253] N86-13736

METAL WORKING
Specifics of the process of failure of structural steels strengthened by thermo-mechanical working with deformation in the intercritical temperature interval N86-13464
Activities report of the Technical and Scientific Research Center for the Metal Manufacturing Industry N86-13740
Computerized simulation and display of extruding by cold forging
[CETIM-1-3L-11-1] N86-13741
USSR report: Machine tools and metalworking equipment
[JPRS-UMM-85-014] N86-13742
USSR report: Machine tools and metalworking equipment
[JPRS-UMM-85-013] N86-13745

METAL-METAL BONDING
Current viewpoints on oxide adherence mechanisms
[NASA-TM-87168] N86-13409

METALLIC PLASMAS
Pulsed inductive energy transfer N86-13562

METALLIZING
Micromechanisms of electrodiffusion failures in thin film metallization N86-13472

METALLURGY
Influence of degree of deformation on structure and properties of naturally aged alloy 1163 N86-13431

METALS
High strain rate deformation in FCC metals and alloys
[DE85-017533] N86-13417
Electrification of filled polyethylene coatings in friction with metal N86-13439
Conductivity of metal-ceramic multilayer ZrO2-Mo and Mo-based composite materials N86-13444
Ceramics based on aluminum nitride and metals N86-13456
European Science Notes, Volume 39, Number 7
[AD-A157708] N86-14108

METASTABLE STATE
Metastable interactions: Dissociative excitation
[AD-A158733] N86-14013

METEORITES
Development of a mass spectrometer system for the measurement of inert gases in meteorites N86-14093

METEORITIC COMPOSITION
Development of a mass spectrometer system for the measurement of inert gases in meteorites N86-14093

METEOROLOGICAL INSTRUMENTS
VAS demonstration: (VISSR Atmospheric Sounder) description
[NASA-RP-1151] N86-13867

METEOROLOGICAL PARAMETERS
Statistical correlation between ozone levels over Atlantic Ocean and meteorological values N86-13780
Meteorological and climatological conditions affecting the vertical structure of visibility in northern Germany
[AD-A158254] N86-13871
Spatial patterns of manifestation of solar activity in troposphere N86-14126
Vega-1 releases aerostat and lander at Venus N86-14148
Objectives of Vega project research N86-14149
Vega-2 releases aerostat and lander at Venus N86-14150

METEOROLOGICAL RADAR
Sampling-rate effects on radar-derived rainfall estimates
[AD-A158203] N86-13870

METEOROLOGICAL SATELLITES
Data catalog series for space science and applications flight missions. Volume 4A: Descriptions of meteorological and terrestrial applications spacecraft and investigations
[NASA-TM-87501] N86-13869

METEOROLOGY
Marginal ice zone bibliography
[AD-A159060] N86-13764
USSR report: Earth sciences
[JPRS-UES-85-009] N86-13765
VAS demonstration: (VISSR Atmospheric Sounder) description
[NASA-RP-1151] N86-13867

METHANE
An investigation of plasma jet ignition and flame jet ignition of lean fuel-air mixtures N86-13386
Development of a carbon formation reactor for carbon dioxide reduction
[NASA-CR-171907] N86-13898

METHYL COMPOUNDS
Elution of benzene and methyl ethyl ketone from charcoal beds by continued air sweeping
[AD-A158804] N86-13374
Electronic detection of low concentrations of organophosphorus compounds with a solid state device utilizing supported copper + cuprous oxide island films
[AD-A158181] N86-13392

METHYLHYDRAZINE
Sparger system for MMH-helium vents N86-14096

MICE
Development and testing of a mouse simulated space flight model
[NASA-CR-176359] N86-13878

MICROBALLOONS
Apparatus for removably holding a plurality of microballoons
[DE85-006517] N86-13722

MICROCOMPUTERS
Microcomputer controlled current sharing experiments with parallel converters
[DE85-013854] N86-13665
Computer graphics applications to crew displays N86-14104

MICROELECTRONICS
West Europe report: Science and technology
[JPRS-WST-85-030] N86-13610
West Europe report: Science and technology
[JPRS-WST-85-031] N86-13616
West Europe report: Science and technology
[JPRS-WST-85-029] N86-13622
European Science Notes, Volume 39, Number 7
[AD-A157708] N86-14108

MICROHARDNESS
Effect of composition of rarefied medium on gas-saturated titanium alloys N86-13477

MICROMECHANICS
Micromechanisms of electrodiffusion failures in thin film metallization N86-13472

MICROORGANISMS
The scanning electron microscope as a tool in space biology N86-14080
Nutritional characteristics of moon dust for soil microorganisms N86-14086

MICROPROCESSORS
Thomson semiconductors introduces products, balances books N86-13615
Safe control systems and the VIPER microprocessor
[AD-A156617] N86-13908

MICROSTRUCTURE
The influence of microstructure on temper embrittlement of low alloy steel N86-13405
Effect of temperature and strain rate on microstructure of a deformed, superplastic Al-10%Mg-0.1%Zr alloy
[AD-A159015] N86-13413
Effect of strain and strain rate on the microstructure of a superplastically deformed Al-10%Mg-0.1%Zr alloy
[AD-A159062] N86-13414
Threshold stress measurements in shock-deformed copper
[DE85-014076] N86-13418
Macro- and microfractographic specifics of dissipated impact rupture of type 45 steel in the viscous-brittle transition interval N86-13466
Analytical electron microscopy of surface modified ceramics
[DE85-016309] N86-13499
Influence of fog microstructure on quality of optical image transmitted through it N86-13781
Microstructural and mechanical property evaluation of solar collectors
[DE85-017038] N86-13839

MICROWAVE EMISSION
Advanced energy conversion concept for microwave beamed-energy propulsions N86-13553

MICROWAVE EQUIPMENT
A family of curves for the rough surface reflection coefficient
[AD-A158195] N86-13876

MICROWAVE FREQUENCIES
Study of Earth observation by frequency scanning. Volume 1: Executive summary
[ESA-CR(P)-2028-VOL-1] N86-13705
Study of Earth observation by frequency scanning. Volume 2
[ESA-CR(P)-2028-VOL-2] N86-13706

MICROWAVE IMAGERY
Discrete random media techniques for microwave modeling of vegetated terrain N86-13809

MICROWAVE RADIOMETERS
Development of the NIMBUS-7 SMMR retrieval algorithm --- Scanning Multichannel Microwave Radiometer (SMMR)
[BAE-RPT/NIM-7/021] N86-13367

MICROWAVE RESONANCE
Observation of optical-radio frequency resonance in H2O using wide-band ruby laser spectroscopy N86-13790

MICROWAVE SCATTERING
Microwave dielectric and propagation properties of vegetation canopies N86-13810

MICROWAVE SENSORS
Active microwave properties of vegetation canopies N86-13812

MICROWAVE SPECTRA
Discrete random media techniques for microwave modeling of vegetated terrain N86-13809

MICROWAVE TRANSMISSION
The development of a submillimeter wave carcinotron operating in the frequency range from 850 to 1000 GHz
[TDH-RT-2963-T] N86-13638

MICROWAVES
Coupling between gas dynamics and microwave energy absorption N86-13561
Report on an automated calibration range for broadband isotropic probes
[PB85-231470] N86-13726
Fundamental remote sensing science research program: The Scene Radiation and Atmospheric Effects Characterization Project
[E86-10011] N86-13794
Scattering models and basic experiments in the microwave regime N86-13807
Remote sensing of Earth terrain N86-13808
Remote temperature determination of terrestrial covers from polarization invariant of microwave-radiothermal emission N86-14196

MIE SCATTERING
Differential scattering cross section and total extinction measurements on (CH)n spheres in 632.8 nm laser light
[AD-A158044] N86-13391
Quantitative flow visualization N86-13572
Light scattering from bubbles in liquids
[AD-A158736] N86-14039

MILITARY AIRCRAFT
Physical distribution system for aircraft external fuel tanks-survey
[AD-A158275] N86-13324

MILITARY SPACECRAFT
Improving MILSATCOM (Military Satellite Communication) acquisition outcomes: Lease versus buy
[AD-A158842] N86-13348

MILKY WAY GALAXY
Wave interpretation of measurements on Mars-7 and Venera-9 probes for determining velocity of motion of interstellar gas N86-14147

MILLING (MACHINING)
Comparison of ion milling techniques for cross-sectional TEM of semiconductors
[DE85-016596] N86-13664

MINERAL DEPOSITS
Thermal infrared geologic remote sensing research at the Jet Propulsion Laboratory N86-13802
Space applications in geology N86-14167

MINERAL OILS
Evaluation of the erosion protection of low inflammability liquids of the HFC type (polyglycol solutions) --- hydraulic fluids
[CETIM-12-E-13-3] N86-13505

MINERALS
Highly disperse minerals in sediments in neighborhood of East Pacific Ocean rise determined from drilling data N86-13773

MINIMAX TECHNIQUE
Minimal norm constrained interpolation
[NASA-CR-178001] N86-13956

MINIMUM VARIANCE ORBIT DETERMINATION
A prion guaranteed accuracy evaluation in determining spacecraft orbit by least squares method N86-14130

MIRRORS
Active mirror boosted 351 nm laser irradiation facility
[DE85-014412] N86-13732
Solar concentrator degradation in Low Earth Orbit (LEO) N86-14102

MISSILES
Computer program for post-flight evaluation of the control surface response for an attitude controlled missile
[NASA-CR-166032] N86-13920

MIXING
Peport on investigation of alcohol combustion associated wear in spark ignition engines, mechanisms and lubricant effects
[AD-A157714] N86-13388

MIXTURES
Recent experience in the RAE (Royal Aircraft Establishment) 5-metre wind tunnel of a china clay method for indicating boundary layer transition
[AD-A157943] N86-13302
An investigation of plasma jet ignition and flame jet ignition of lean fuel-air mixtures N86-13386
Critical charge for the direct initiation of detonation in gaseous fuel-air mixtures
[DE85-016130] N86-13696

MOBILITY
Generically based mobility-terrain data bases
[AD-A157738] N86-13815

MODAL RESPONSE

Dynamic identification for control of large space structures
[NASA-CR-176380] N86-13587

A parametric study of the Ibrahim time domain modal identification algorithm N86-13588

Dynamic modeling of structures from measured complex modes N86-13591

MODE (STATISTICS)

Computation of normal modes from identified complex modes N86-13590

MODELS

Multiple scattering theories for optical properties of composite materials
[AD-A158270] N86-13379

Electronic detection of low concentrations of organophosphorus compounds with a solid state device utilizing supported copper + cuprous oxide island films
[AD-A158181] N86-13392

Determination of porosity of thin sheets of fiber materials based on optical transmission coefficient N86-13459

Modeling of thermal fatigue and erosion of complex alloyed steels in metal melts N86-13469

Subcritical crack development under constant load in VT6 alloy N86-13475

Possible mechanism of wave formation during detonation welding N86-13483

Application of Pasternak model to some soil-structure interaction problems. Volume 1: Solutions for plates continuously supported on a Pasternak base
[AD-A157776] N86-13594

Application of Pasternak model to some soil-structure interaction problems. Volume 2: Determination of foundation parameters and the choice of models
[AD-A157777] N86-13595

Experimental investigation of heat transfer behavior of aqueous foams in thermal entry region of pipe flow
[DE85-012836] N86-13700

Reflectance modeling N86-13795

Understanding the radiant scattering behavior of vegetated scenes N86-13797

Measurement and modeling of the optical scattering properties of crop canopies N86-13798

Geometric-optical modeling of a conifer forest canopy N86-13799

Crop characteristics research: Growth and reflectance analysis N86-13800

Determination of backscattering sources in various targets N86-13811

Active microwave properties of vegetation canopies N86-13812

The design of a beach profiler
[AD-A157715] N86-13874

Hypothesizing and refining causal models
[AD-A158165] N86-13893

The mission oriented terminal area simulation facility
[NASA-TM-87621] N86-13944

Method for using clusters in evaluating land use areas from multizonal photographs N86-14180

MODULARITY

Cyclosymmetric approach to the dynamics of repetitive modular structures
[ESA-CR(P)-2062] N86-13739

MODULATORS

Hardware upgrade for klystrons in the SLC
[DE85-014357] N86-14029

MODULUS OF ELASTICITY

Modifications of system for elevated temperature tensile testing and stress-strain measurement of metal matrix composites
[NASA-TM-87172] N86-13370

MOIRE EFFECTS

Elastic-plastic deformation of a metal-matrix composite coupon with a center slot
[NASA CR-178013] N86-13496

MOISTURE CONTENT

Test of a moisture conditioning procedure using 70 C distilled water, instead of a gas atmosphere at 70 C, 95% relative humidity --- plastic composites
[M3-431000] N86-13383

Computer-aided aerial radiometric surveying of soil moisture N86-13778

MOLECULAR BEAM EPITAXY

Philips develops MBE process for laser, chip manufacture N86-13614

AuGa2 on GaSb(001): An epitaxial, thermodynamically stabilized Metal/3-5 compound semiconductor interface
[AD-A157937] N86-14071

MOLECULAR BIOLOGY

European Science Notes, Volume 39, Number 7
[AD-A157708] N86-14108

European Science Notes. Volume 39, number 9
[AD-A158278] N86-14109

MOLECULAR COLLISIONS

Metastable interactions: Dissociative excitation
[AD-A158733] N86-14013

Reactive scattering in the bending-corrected rotating linear model
[DE85-017539] N86-14018

MOLECULAR ENERGY LEVELS

Determination of the activation barrier to energy transfer from 3 pi pi* to charge transfer levels via steady state and transient luminescence measurements on Bis(4-Chlorothiophenol) (1,10-Phenanthroline) Zinc (II)
[AD-A158239] N86-14012

MOLECULAR EXCITATION

Coherent optical transient spectroscopy in flames N86-13570

MOLECULAR ORBITALS

Application of quantum chemistry to atmospheric chemistry
[AD-A158282] N86-13856

MOLECULAR STRUCTURE

High energy molecules of high symmetry N86-13520

Structure-decomposition relationships in newer energetic materials N86-13521

Close-spaced high temperature Knudsen flow
[AD-A158280] N86-13831

Application of quantum chemistry to atmospheric chemistry
[AD-A158282] N86-13856

European Science Notes. Volume 39, number 9
[AD-A158278] N86-14109

MOLECULES

Synthesis, structure and reactivity of molecules attached to electrode surfaces
[AD-A158621] N86-13394

Small X-ray diffraction of immunoglobulin-membrane complexes
[AD-A158252] N86-13882

Extended atmospheres of outer planet satellites and comets
[NASA-CR-176398] N86-14209

MOLNIYA SATELLITES

List of recent Soviet space launches N86-14199

MOLYBDENUM

Conductivity of metal-ceramic multilayer ZrO2-Mo and Mo-based composite materials N86-13444

Grain growth in heat-resistant austenitic steel N86-13462

Dispersion hardening of high-strength NiOCo-Mo steels N86-13468

MONITORS

An Oil/Water disperser device for use in an oil content Monitor/Control system
[AD-D011868] N86-13714

Alerted monitors: Human operators aided by automated detectors
[PB85-222750] N86-13906

MONOPROPELLANTS

Health hazard evaluation of liquid monopropellants. Phase 5: Comparative inhalation toxicities of LGP 1776, LGP 1845, and HAN (hydroxylammonium nitrate)
[AD-A159090] N86-13891

MONTE CARLO METHOD

Determination of porosity of thin sheets of fiber materials based on optical transmission coefficient N86-13459

Numerical modeling of carrier transport in submicron bipolar transistors N86-13642

The characterization of surface variation effects on remote sensing N86-13805

Computer program for prediction of fuel consumption statistical data for an upper stage three-axes stabilized on-off control system
[NASA-CR-166031] N86-13917

Decomposition of some well-known variance reduction techniques: Revision
[AD-A158048] N86-13985

Monte Carlo analysis of nonlinear statistical models. 1. Theory: Revision
[AD-A158613] N86-13990

Computation of reflection of solar radiation from vegetation cover by Monte-Carlo method N86-14177

MOTION PERCEPTION

Enhancing sensitivity to visual motion and enhancing visual sensitivity
[AD-A158800] N86-13889

MOTION SIMULATION

The simulation of truck motions
[UTIAS-294] N86-13914

MOTORS

Gas recirculator for acyclic machines
[AD-D011873] N86-13658

MOUNTAINS

Formation of underwater oceanic volcanoes and islands in relation to lithospheric thickness and movements N86-13776

MOUNTING

Astrophysical payload accommodation on the space station
[NASA-CR-178556] N86-13359

MOVING TARGET INDICATORS

Enhancing sensitivity to visual motion and enhancing visual sensitivity
[AD-A158800] N86-13889

MULTIPLIERS

Optoelectronic integrated circuit multiplier
[AD-D011883] N86-14043

MULTIPROCESSING (COMPUTERS)

Sparse elimination on vector multiprocessors
[AD-A158274] N86-13909

Parallel computation with the force
[NASA-CR-177999] N86-13915

Inner/outer iterative methods and numerical Schwarz algorithms - 2
[DE85-013197] N86-13940

Techniques for the design and implementation of highly reliable multi-processing systems
[AD-A159236] N86-13945

MULTIPROGRAMMING

Parallel computation with the force
[NASA-CR-177999] N86-13915

MULTISPECTRAL PHOTOGRAPHY

Method for using clusters in evaluating land use areas from multizonal photographs N86-14180

MULTISTATIC RADAR

Results of study of surface of five regions on Venus by bistatic radar method N86-14156

MULTIVARIATE STATISTICAL ANALYSIS

A linear combination test for detecting serial correlation in multivariate samples
[AD-A158179] N86-13967

MUONS

Muon spin relaxation study of exchange coupling in dilute AgMn alloys
[DE85-014104] N86-13419

MUTATIONS

Molecular mechanisms of mutagenesis determined by the recombinant DNA technology
[DE85-016353] N86-13884

N

N-P-N JUNCTIONS

Numerical modeling of carrier transport in submicron bipolar transistors N86-13642

NATIONAL AIRSPACE SYSTEM

National airspace system, system requirements specification
[AD-A157944] N86-13312

NATURAL LANGUAGE (COMPUTERS)

Deterministic parsing and linguistic explanation: Revision
[AD-A159233] N86-13950

NAVIER-STOKES EQUATION

A method for calculating flow fields around moving bodies
[NAL-TR-859T] N86-13288

Numerical solutions of Navier-Stokes equations for a Butler wing
[NASA-CR-174202] N86-13293

Computational aspects of zonal algorithms for solving the compressible Navier-Stokes equations in three dimensions
[NASA-TM-86774] N86-13296

Interaction of multi-dimensional mean and acoustic fields in solid rocket combustion chambers N86-13547

Non-Newtonian flow past curved external surfaces N86-13671

A computational analysis of pulsating flow in rigid and deformable tubes N86-13673

Transonic separated flow predictions based on a mathematically simple, nonequilibrium turbulence closure model
[NASA-TM-86826] N86-13676

Far-field boundary conditions in numerical solutions of the Navier-Stokes equations
[AD-A158776] N86-13690

Contributions to Von Karman Institute lecture series on Computational Fluid dynamics: Advection-diffusion and Navier-Stokes equations
[DE85-010942] N86-13703

Stable boundary conditions and difference schemes for Navier-Stokes equations
[NASA-CR-177964] N86-13957

NAVIGATION AIDS

Short range aids to navigation systems. Design manual for restricted waterways
[AD-A158213] N86-13313

Uniqueness conditions in evaluation of least squares method in nonlinear space navigation problems N86-14144

NAVIGATION SATELLITES

Determining quasi-real-time location of ships using geostationary navigational satellites N86-14165

Organization of space navigation system based on use of geostationary satellites N86-14166

NAVSTAR SATELLITES
Time delay of arrival location assessment using four satellites
[AD-A159243] N86-13315

NEAR INFRARED RADIATION
A multiple-object fibre-optics coupler for the 1.2-m UK Schmidt Telescope N86-14201

NEODYMIUM LASERS
Structure of flow of erosion plasma formed upon laser treatment of metals N86-13455
Active mirror boosted 351 nm laser irradiation facility
[DE85-014412] N86-13732
Retrofit of a high power Nd:glass laser system with liquid crystal polarizers
[DE85-014415] N86-13733

NEPHELOMETERS
Optical/infrared properties of atmospheric aerosols with an in situ, multi-wavelength, multichannel nephelometer system
[AD-A158825] N86-13710

NETS
Passive arm retention curtain
[AD-D011876] N86-13307

NETWORK CONTROL
Extreme values of queues, point processes and Stochastic Networks
[AD-A158619] N86-13991

NEUROMUSCULAR TRANSMISSION
Study of toxic and antigenic structures of botulinum neurotoxins
[AD-A156642] N86-13880

NEUTRAL ATMOSPHERES
Analysis of atomic thermospheric nitrogen density
[NASA-CR-176354] N86-13851

NEUTRAL PARTICLES
Effects of neutrals on internal forces and thermal conduction of a plasma in a magnetic field
[IPPJ-691] N86-14051

NEUTRON COUNTERS
Neutron stress measurements with a position sensitive detector
[AD-A158882] N86-13712

NEUTRON SCATTERING
Neutron stress measurements with a position sensitive detector
[AD-A158882] N86-13712
Structure and hydrodynamics of colloidal systems
[DE85-016294] N86-14027

NICHROME (TRADEMARK)
Effect of heating conditions on agglomeration of powdered aluminum in air atmosphere N86-13460

NICKEL
No chemisorption on Ni(111): Coverage effects, site preferences and adsorption geometry
[AD-A159110] N86-13397
Dispersion hardening of high-strength NiOCo-Mo steels N86-13468
The [illegible])Ni + n transmission, capture and differential elastic scattering data analysis in the resonance region
[DE85-016157] N86-14026
Detection of Ni 2 lambda 7378 in six Seyfert galaxies
[NASA-CR-176358] N86-14205

NICKEL ALLOYS
Current viewpoints on oxide adherence mechanisms
[NASA-TM-87166] N86-13409
Complex nickel-aluminide coatings on nickel-chromium alloy EP648-VI N86-13437
Study of properties of gas-thermal coatings of composite nichrome-aluminum alloy powders N86-13442
Superelastic behavior of powdered titanium nickelide during pressing N86-13461

NIMBUS 7 SATELLITE
Development of the NIMBUS-7 SMMR retrieval algorithm — Scanning Multichannel Microwave Radiometer (SMMR)
[BAE-RPT/NIM-7/021] N86-13367

NIOBIUM
Grain growth in heat-resistant austenitic steel N86-13462
Internal friction in TiNiCu alloy N86-13480

NIOBIUM ALLOYS
Silicide coatings for protecting titanium-niobium alloys from high-temperature oxidation N86-13476
Changes in structure and mechanical properties of niobium-titanium alloy during oxygen saturation N86-13479
Influence of hydrogen on formation of cold cracks in seams during welding of pipe steel N86-13494

NITRAMINE PROPELLANTS
Synthesis of high nitrogen content heterocyclic nitramines and energetic internal plasticizers N86-13511
Synthesis and chemistry of polynitroalkanes and polynitroolefins N86-13513
Structure-decomposition relationships in newer energetic materials N86-13521
Chemical kinetics of nitramine propellant combustion N86-13525

NITRIC ACID
Solvent extraction of plutonium (IV) polymer by organophosphorous compounds
[DE85-013229] N86-13502
Determination of acidity in ambient air
[PB85-218196] N86-13849

NITRIDING
Ion nitriding of titanium N86-13473

NITRO COMPOUNDS
Synthesis of new polynitropolyhedranes N86-13510
Synthesis of high nitrogen content heterocyclic nitramines and energetic internal plasticizers N86-13511
Synthesis and chemistry of polynitroalkanes and polynitroolefins N86-13513

NITROGEN
Computer program for calculating flow parameters and power requirements for cryogenic wind tunnels
[NASA-TM-87609] N86-13338
Ion nitriding of titanium N86-13473
The physics and technology of strong magnetic fields (chapter 10)
[AD-A158174] N86-14000

NITROGEN ATOMS
Analysis of atomic thermospheric nitrogen density
[NASA-CR-176354] N86-13851

NOISE
Mathematical analysis study for radar data processing and enchancement. Part 2: Modeling of propagation path errors
[NASA-CR-166616-PT-2] N86-13354

NOISE (SOUND)
Preliminary measurement of the noise from the 2/9 scale model of the Large-scale Advanced Propfan (LAP) propeller, SR-7A
[NASA-TM-87116] N86-14006

NOISE REDUCTION
Preliminary measurement of the noise from the 2/9 scale model of the Large-scale Advanced Propfan (LAP) propeller, SR-7A
[NASA-TM-87116] N86-14006
Some design philosophy for reducing the community noise of advanced counter-rotation propellers
[NASA-TM-87099] N86-14007

NOISE SPECTRA
Atmospheric radio noise: Worldwide levels and other characteristics
[PB85-212942] N86-13639

NOMENCLATURES
Active microwave properties of vegetation canopies N86-13812

NONDESTRUCTIVE TESTS
High frequency quantitative analysis of magnetomechanical acoustic emission
[AD-A158222] N86-13750
Scientific activities of the Polish Academy of Sciences: Institute of Fundamental Technological Research in 1983
[ISBN-83-01-06288-6] N86-14107

NONEQUILIBRIUM FLOW
Transonic separated flow predictions based on a mathematically simple, nonequilibrium turbulence closure model
[NASA-TM-86826] N86-13676

NONLINEAR EQUATIONS
Transformation matrices between non-linear and linear differential equations N86-14099

NONLINEAR OPTICS
Joint services electronics program
[AD-A158840] N86-13654
New methods for laser sounding of atmosphere on basis of nonlinear effects N86-13787
Investigation of nonlinear spectroscopic effects in interaction between CO2-laser radiation and atmospheric gases N86-13789

NONLINEAR SYSTEMS
Time-domain quasi-linear identification of nonlinear dynamic systems
[AIAA-83-0811-CP] N86-13592
Parameter identification for a robotic manipulator arm
[NASA-CR-178002] N86-13959

NONLINEARITY
Nonlinear modeling and method of predicting crack growth N86-13538
Shock waves, increase of entropy and loss of information
[DE85-013645] N86-13701
Development of singularities in nonlinear viscoelasticity
[AD-A158190] N86-13758
Three-dimensional modeling of Tsunami waves
[DE85-015724] N86-13877
Monte Carlo analysis of nonlinear statistical models. 1. Theory: Revision
[AD-A158613] N86-13990

NONNEWTONIAN FLOW
Non-Newtonian flow past curved external surfaces N86-13671

NONNEWTONIAN FLUIDS
Specialists Meeting on Atomization and Nondilute Sprays
[AD-A159006] N86-13634
Non-Newtonian flow past curved external surfaces N86-13671

NORTHERN HEMISPHERE
Statistical comparison of two major gridded temperature records of the Northern Hemisphere
[DE85-016076] N86-13872

NOSE TIPS
Ultrasonic longitudinal wave velocity in carbon-carbon Pitch and Pitch/M2 shape stable nosetip material from 70 deg F to 5400 deg F
[DE85-017330] N86-13382

NOTCH SENSITIVITY
Fractured toughness of Si3N4 measured with short bar chevron-notched specimens
[NASA-TM-87153] N86-13495

NOTCH TESTS
Macro- and microfractographic specifics of dissipated impact rupture of type 45 steel in the viscous-brittle transition interval N86-13466
Fractured toughness of Si3N4 measured with short bar chevron-notched specimens
[NASA-TM-87153] N86-13495

NOZZLE DESIGN
Nozzle for self-contained cutting torches
[AD-D011875] N86-13597

NOZZLE FLOW
Application of molecular kinetics models to the prediction of backflow contamination N86-13531

NUCLEAR AUXILIARY POWER UNITS
Coupled radiation transport/thermal analysis of the radiation shield for a space nuclear reactor
[AD-A158180] N86-14022

NUCLEAR EXPLOSION EFFECT
Aircrew dose and engine dust ingestion from nuclear cloud penetration
[AD-A159246] N86-13327
Interactive scenario computer model for dose rates to aircrews in flight through nuclear debris clouds
[AD-A158741] N86-13888

NUCLEAR EXPLOSIONS
Time delay of arrival location assessment using four satellites
[AD-A159243] N86-13315
Aircrew dose and engine dust ingestion from nuclear cloud penetration
[AD-A159246] N86-13327

NUCLEAR METEOROLOGY
Aircrew dose and engine dust ingestion from nuclear cloud penetration
[AD-A159246] N86-13327

NUCLEAR PHYSICS
European Science Notes. Volume 39, number 9
[AD-A158278] N86-14109

NUCLEAR RADIATION
Multidimensional modeling of atmospheric effects and surface heterogeneities on remote sensing N86-13806

NUCLEAR REACTORS
Variable field effects for the rotating fluidized bed reactor N86-13565
Safe control systems and the VIPER microprocessor
[AD-A156617] N86-13908

NUCLEAR RESEARCH
Nation's achievements in high energy physics reviewed N86-13604

NUCLEATION
Electronic detection of low concentrations of organophosphorus compounds with a solid state device utilizing supported copper + cuprous oxide island films
[AD-A158181] N86-13392
Microstructural and mechanical property evaluation of solar collectors
[DE85-017038] N86-13839

NULL ZONES
A linear combination test for detecting serial correlation in multivariate samples
[AD-A158179] N86-13967

NUMERICAL ANALYSIS
Numerical solutions of Navier-Stokes equations for a Butler wing
[NASA-CR-174202] N86-13293
Non-Newtonian flow past curved external surfaces N86-13671
Transonic separated flow predictions based on a mathematically simple, nonequilibrium turbulence closure model
[NASA-TM-86826] N86-13676

Numerical simulations of asymmetric mixing in planar shear flows
[AD-A158024] N86-13687
Far-field boundary conditions in numerical solutions of the Navier-Stokes equations
[AD-A158776] N86-13690
A numerical investigation into the plastic stress and strain fields around a surface crack
[ARL/STRUC-R-414] N86-13754
Coupled radiation transport/thermal analysis of the radiation shield for a space nuclear reactor
[AD-A158180] N86-14022
Multigrid relaxation methods and the analysis of lightness, shading, and flow
[AD-A158173] N86-14036
European Science Notes, Volume 39, Number 7
[AD-A157708] N86-14108
Use of Goudriaan model for studying reflection regularities in vegetation-soil system in optical range. 1: Influence of phytometric parameters on spectral brightness coefficients N86-14190

NUMERICAL CONTROL
Computer program for prediction of fuel consumption statistical data for an upper stage three-axes stabilized on-off control system
[NASA-CR-166031] N86-13917

NUMERICAL FLOW VISUALIZATION
Waves which travel upstream in boundary layers
[AD-A157949] N86-13684

NUMERICAL INTEGRATION
Adaptive, self-validating numerical quadrature
[AD-A158164] N86-13963
Computable bounds for solutions of integral equations
[AD-A158189] N86-13970

NUMERICAL STABILITY
Waves which travel upstream in boundary layers
[AD-A157949] N86-13684

O

OCEAN BOTTOM
Pore pressure response to probe insertion and thermal gradient: ISIMU-2. (In situ heat transfer experiment)
[AD-A158592] N86-13689
Some characteristics of bottom density currents
N86-13772
Highly disperse minerals in sediments in neighborhood of East Pacific Ocean rise determined from drilling data
N86-13773
Formation of underwater oceanic volcanoes and islands in relation to lithospheric thickness and movements
N86-13776

OCEAN CURRENTS
Vertical structure of turbulence and turbulent exchange in equatorial zone of Pacific Ocean N86-13771
Some characteristics of bottom density currents
N86-13772

OCEAN DATA ACQUISITIONS SYSTEMS
Development of the NIMBUS-7 SMMR retrieval algorithm --- Scanning Multichannel Microwave Radiometer (SMMR)
[BAE-RPT/NIM-7/021] N86-13367
The design of a beach profiler
[AD-A157715] N86-13874
Role of landscape research in development of space methods for studying Earth N86-14184

OCEAN DYNAMICS
The influence of oceanic chemistry, physics and biology on atmospheric carbon dioxide N86-13865

OCEAN SURFACE
Expendable bathythermograph for measuring light attenuation and temperature below the ocean surface
[AD-D011870] N86-13716
Aerial laser sensing of ocean upper layer N86-13775
Atmospheric synoptic eddies over ocean (determined from experimental data) N86-13784
Influence of petroleum pollution on ocean-atmosphere gas exchange intensity (in example of North Atlantic)
N86-13785
Laboratory studies of steep and breaking deep water waves in a convergent channel
[AD-A158187] N86-13875
A family of curves for the rough surface reflection coefficient
[AD-A158195] N86-13876
Stereophotogrammetric survey of wave-covered water surface N86-14170

OCEAN TEMPERATURE
Model interpretation of annual variation of temperature fields of air and water boundary layers of world ocean
N86-13767
Computation of ocean upper layer thermal structure
N86-13769
The influence of oceanic chemistry, physics and biology on atmospheric carbon dioxide N86-13865
Equatorial waves in ocean surface temperature field according to data from shipboard and satellite measurements N86-14171

OCEAN THERMAL ENERGY CONVERSION
Far-field model of the regional influence of affluent plumes from Ocean Thermal Energy Conversion (OTEC) plants
[DE85-016981] N86-13836

OCEANOGRAPHIC PARAMETERS
Structural characteristic of temperature field over sea
N86-13783
The influence of oceanic chemistry, physics and biology on atmospheric carbon dioxide N86-13865

OCEANOGRAPHY
Marginal ice zone bibliography
[AD-A159060] N86-13764
USSR report: Earth sciences
[JPRS-UES-85-009] N86-13765
Understanding climate: A strategy for climate modeling and predictability research, 1985-1995
[NASA-RP-1158] N86-13866

OCEANS
Model interpretation of annual variation of temperature fields of air and water boundary layers of world ocean
N86-13767

OIL EXPLORATION
Azerbaijan geological, geophysical work on land described N86-13862
Possible petroliferousness of South Caspian uplifts analyzed N86-13863
Possibilities of use of aerospace materials in predicting occurrence of petroleum and gas N86-14175

OIL FIELDS
Geothermal resources of the Wind River Basin, Wyoming
[DE85-016969] N86-13816

OIL RECOVERY
Azerbaijan geological, geophysical work on land described N86-13862
Possible petroliferousness of South Caspian uplifts analyzed N86-13863

OILS
Pressure-distribution measurements on a transonic low-aspect ratio wing
[NASA-TM-86683] N86-13304
An Oil/Water disperser device for use in an oil content Monitor/Control system
[AD-D011868] N86-13714
Oil content Monitor/Control system and method
[AD-D011871] N86-13717

ON-LINE SYSTEMS
A reactive learning environment for the Equipment Problem Solving Techniques (EPST) system
[AD-A158035] N86-13929

ONE DIMENSIONAL FLOW
Hybrid simulation codes with application to shocks and upstream waves
[NASA-CR-176365] N86-13702

ONTOGENY
Crop characteristics research: Growth and reflectance analysis N86-13800

OPENINGS
Nozzle for self-contained cutting torches
[AD-D011875] N86-13597

OPERATOR PERFORMANCE
The simulation of truck motions
[UTIAS-294] N86-13914

OPERATORS
Uniformly high-order accurate non-oscillatory schemes 1
[AD-A158177] N86-13966

OPERATORS (MATHEMATICS)
Computable bounds for solutions of integral equations
[AD-A158189] N86-13970
Intrinsic nilpotent approximation
[AD-A158265] N86-13975
Continuity of certain random integral mappings and the uniform integrability of infinitely divisible measures
[AD-A159105] N86-13995
Realization theory in Hilbert space
[AD-A158172] N86-13997
Methods for constructing atmospheric optical transfer operator N86-14185

OPERATORS (PERSONNEL)
Pre-stack Kirchhoff inversion of common offset data
[AD-A158205] N86-13932

OPTICAL COMMUNICATION
Optimal transfer function for fiber optic communications N86-13641

OPTICAL DATA PROCESSING
Optical processing and phase conjugation
N86-13573
A report on the ST Scl optical disk workstation
[NASA-CR-176369] N86-13907
Real time large memory optical pattern recognition
[AD-A158023] N86-14034
Design for a large altazimuth Schmidt telescope
N86-14203

OPTICAL DATA STORAGE MATERIALS
Excimer laser produces .2 micron semiconductor structures N86-13613

OPTICAL DISKS
A report on the ST Scl optical disk workstation
[NASA-CR-176369] N86-13907

OPTICAL EMISSION SPECTROSCOPY
Coherent optical transient spectroscopy in flames
N86-13570

OPTICAL EQUIPMENT
Remote optical crack sensing system
[AD-D011872] N86-13718
An integrated wavelength demultiplexer
[AD-D011867] N86-14041

OPTICAL MEASUREMENT
Optical technique to measure electrode erosion
N86-13564
Joint services electronics program
[AD-A158840] N86-13654
European Science Notes, Volume 39, Number 7
[AD-A157708] N86-14108

OPTICAL MEMORY (DATA STORAGE)
Real time large memory optical pattern recognition
[AD-A158023] N86-14034

OPTICAL MICROSCOPES
Macro- and microfractographic specifics of dissipated impact rupture of type 45 steel in the viscous-brittle transition interval N86-13466

OPTICAL PROPERTIES
Multiple scattering theories for optical properties of composite materials
[AD-A158270] N86-13379
Determination of porosity of thin sheets of fiber materials based on optical transmission coefficient N86-13459
Photodegradation studies of silver-backed polyacrylonitrile (PAN) films
[DE85-012154] N86-13501
Active mirror boosted 351 nm laser irradiation facility
[DE85-014412] N86-13732
Retrofit of a high power Nd:glass laser system with liquid crystal polarizers
[DE85-014415] N86-13733
Fundamental remote sensing science research program: The Scene Radiation and Atmospheric Effects Characterization Project
[E86-10011] N86-13794
Measurement and modeling of the optical scattering properties of crop canopies N86-13798
Atmospheric effect on remote sensing of the Earth's surface N86-13804
Microstructural and mechanical property evaluation of solar collectors
[DE85-017038] N86-13839
Test method for telescopes using a point source at a finite distance
[NASA-TM-86523] N86-14033
Multigrid relaxation methods and the analysis of lightness, shading, and flow
[AD-A158173] N86-14036
Investigation of cold colored smoke production
[AD-A158783] N86-14040
Approximate cluster analysis method and three-dimensional diagram of optical characteristics of lunar surface N86-14128

OPTICAL PUMPING
China report: Science and technology
[JPRS-CST-85-020] N86-13600
Pulsed, optically pumped gas-mixture FIR lasers
N86-13609

OPTICAL RADAR
Precision pointing using a dual-wedge scanner
[NASA-CR-3946] N86-13813
Airborne lidar measurements of El Chichon stratospheric aerosols
[NASA-RP-1148] N86-13850
Optical radar transceiver control apparatus
[AD-D011880] N86-14042

OPTICAL RESONANCE
Observation of optical-radio frequency resonance in H2O using wide-band ruby laser spectroscopy
N86-13790

OPTICAL THICKNESS
Analysis of survey conditions and effect of noise on quality of sensing of soil formations N86-14191

OPTICAL TRACKING
Target tracking based scene analysis
[AD-A158629] N86-13910

OPTICAL TRANSFER FUNCTION
Influence of fog microstructure on quality of optical image transmitted through it N86-13781
Methods for constructing atmospheric optical transfer operator N86-14185

OPTICAL TRANSITION
Two-proton detection techniques for atomic fluorine N86-13569

OPTICAL WAVEGUIDES
Integrated optics developments over past decade, future prospects N86-13605

OPTICS
Focal plane optics in far-infrared and submillimeter astronomy [NASA-TM-88186] N86-14204

OPTIMAL CONTROL
Comparison of energetics of optimum maneuvers and two-impulse maneuvers in some problems of motion from a point into orbit N86-14134
Optimum control programs in problem of interorbital flight with continuous thrust N86-14135

OPTIMIZATION
Composites design [AD-A157710] N86-13378
Optimal transfer function for fiber optic communications N86-13641
Linearity optimization in a class of analog phase modulators [NASA-TM-86420] N86-13644
A method to stabilize linear systems using eigenvalue gradient information [NASA-TP-2479] N86-13946
Further results for application of disturbance minimization control techniques to a linear, time-invariant, second-order state set-point regulator problem [AD-A157793] N86-13961

ORBIT CALCULATION
Approximate solutions of Euler-Lambert equation for case of several revolutions about central body N86-14121
Integration of equations of motion for material point in gravitational field of axially symmetric planet N86-14131

ORBITAL ELEMENTS
Report on active and planned spacecraft and experiments [NASA-TM-87499] N86-13343

ORBITAL MANEUVERS
Comparison of energetics of optimum maneuvers and two-impulse maneuvers in some problems of motion from a point into orbit N86-14134
Optimum control programs in problem of interorbital flight with continuous thrust N86-14135

ORBITAL MECHANICS
Scout trajectory error propagation computer program [NASA-CR-166030] N86-13919
Advanced algorithm for orbit computation N86-14101

ORBITAL POSITION ESTIMATION
Report on active and planned spacecraft and experiments [NASA-TM-87499] N86-13343
Scout trajectory error propagation computer program [NASA-CR-166030] N86-13919

ORGANIC MATERIALS
Mass transfer coefficients and Henry's constants for packed-tower air stripping of volatile organics: Measurements and correlation [AD-A158811] N86-13375

ORGANIC PHOSPHORUS COMPOUNDS
Electronic detection of low concentrations of organophosphorus compounds with a solid state device utilizing supported copper + cuprous oxide island films [AD-A158181] N86-13392
Solvent extraction of plutonium (IV) polymer by organophosphorous compounds [DE85-013229] N86-13502

ORGANISMS
Comparative effect of lunar fines and terrestrtrial ash on the growth of a blue-green alga and germinating radish seeds N86-14097

ORGANOMETALLIC COMPOUNDS
CNET of France uses organo-metallic epitaxy for laser N86-13620
Variable temperature trap [AD-D011874] N86-13719
Determination of the activation barrier to energy transfer from 3 pi pi* to charge transfer levels via steady state and transient luminescence measurements on Bis(4-Chlorothiophenol) (1,10-Phenanthroline) Zinc (II) [AD-A158239] N86-14012

ORR-SOMMERFELD EQUATIONS
Boundary-value problem for two-dimensional fluctuations in boundary layers [AD-A157952] N86-13685

OSCILLATING FLOW
Two unsteady heat transfer experiments. Part 1: In grid-generated isotropic turbulence. Part 2: In laminar oscillatory flow in straight and conical tubes N86-13675

OSCILLATIONS
Coupling between velocity oscillations and solid propellant combustion N86-13541
Parameter identification for a robotic manipulator arm [NASA-CR-178002] N86-13959

OUTPUT
Two-hundred to 300 KVA conditioned power system - development, phase 1 [AD-A158820] N86-13832
Operation of large cryogenic systems [DE85-017439] N86-14025

OXIDATION
Current viewpoints on oxide adherence mechanisms [NASA-TM-87168] N86-13409
Silicide coatings for protecting titanium-niobium alloys from high-temperature oxidation N86-13476
Changes in structure and mechanical properties of niobium-titanium alloy during oxygen saturation N86-13479
Kinetics of dissolution of oxide films in titanium upon diffusion welding N86-13487
Oxidizing and scavenging characteristics of April rains: OSCAR data report [DE85-017014] N86-13844
Optical constants [AD-A158623] N86-14038

OXIDE FILMS
Electronic detection of low concentrations of organophosphorus compounds with a solid state device utilizing supported copper + cuprous oxide island films [AD-A158181] N86-13392
Experimental investigation of magnesium combustion in steam [AD-A159109] N86-13396
Current viewpoints on oxide adherence mechanisms [NASA-TM-87168] N86-13409
Effect of heating conditions on agglomeration of powdered aluminum in air atmosphere N86-13460
Kinetics of dissolution of oxide films in titanium upon diffusion welding N86-13487

OXIDES
Fuel-rich solid propellant boron combusion N86-13536
Electrical and thermal transport property studies of high-temperature thermoelectric materials [AD-A158883] N86-13656
Oxide electrodes at high temperatures [DE85-006564] N86-13667

OXIDIZERS
Combusion of hydrogen and hydrocarbons in fluorine N86-13526

OXYGEN
Mass loss of shuttle space suit orthofabric under simulated ionospheric atomic oxygen bombardment [NASA-TM-87149] N86-13899
Ion bombardment and adsorption studies on ilmenite (FeTiO3) by X-ray photoelectron spectroscopy N86-14100

OXYNITRIDES
Extremely high reflective capability of zirconium burning in air under effects of constant CO2 laser radiation N86-13452

OZONE
Oxidizing and scavenging characteristics of April rains: OSCAR data report [DE85-017014] N86-13844

OZONOMETRY
Statistical correlation between ozone levels over Atlantic Ocean and meteorological values N86-13780

P

PACIFIC OCEAN
Vertical structure of turbulence and turbulent exchange in equatorial zone of Pacific Ocean N86-13771
Highly disperse minerals in sediments in neighborhood of East Pacific Ocean rise determined from drilling data N86-13773

PADE APPROXIMATION
Iterative and Pade solutions for the water-wave dispersion relation [AD-A157796] N86-13683

PANELS
Abrasion behavior of aluminum and composite skin coupons, stiffened skins and stiffened panels representative of transport airplane structures [NASA-TP-2520] N86-13316
Fabrication and evaluation of superplastically formed/weld-brazed corrugated compression panels with beaded webs [NASA-TP-2512] N86-13406

PARABOLOID MIRRORS
Development of a breadboard cooler for infrared remote sensing payloads, phase 2 --- spacecraft payloads [FOK-RV-R-82-072] N86-13725

PARALLEL PROCESSING (COMPUTERS)
Experiences with Cray multi-tasking [NASA-TM-88200] N86-13916
Multigrid relaxation methods and the analysis of lightness, shading, and flow [AD-A158173] N86-14036

PARALLEL PROGRAMMING
Parallel computation with the force [NASA-CR-177999] N86-13915
Multigrid relaxation methods and the analysis of lightness, shading, and flow [AD-A158173] N86-14036

PARAMETER IDENTIFICATION
Dynamic identification for control of large space structures [NASA-CR-176380] N86-13587
Large modal survey testing using the Ibrahim time domain identification technique [AIAA-81-0528R] N86-13589
Application of Pasternak model to some soil-structure interaction problems. Volume 2: Determination of foundation parameters and the choice of models [AD-A157777] N86-13595
Parameter identification for a robotic manipulator arm [NASA-CR-178002] N86-13959
A priori guaranteed accuracy evaluation in determining spacecraft orbit by least squares method N86-14130
Uniqueness conditions in evaluation of least squares method in nonlinear space navigation problems N86-14144

PARAMETERIZATION
A parametric study of the Ibrahim time domain modal identification algorithm N86-13588

PARSING ALGORITHMS
On the complexity of ID/LP parsing [AD-A158211] N86-13933
Deterministic parsing and linguistic explanation: Revision [AD-A159233] N86-13950

PARTIAL DIFFERENTIAL EQUATIONS
Inner/outer iterative methods and numerical Schwarz algorithms - 2 [DE85-013197] N86-13940
Multigrid relaxation methods and the analysis of lightness, shading, and flow [AD-A158173] N86-14036
Finite element or Galerkin type semidiscrete schemes N86-14083

PARTICLE ACCELERATION
Unlimited acceleration of charged particles by an electromagnetic wave with a purely transverse electric field propagating perpendicularly to a static magnetic field [IPPJ-740] N86-14049

PARTICLE ACCELERATOR TARGETS
The (58)Ni + n transmission, capture and differential elastic scattering data analysis in the resonance region [DE85-016157] N86-14026

PARTICLE ACCELERATORS
Nation's achievements in high energy physics reviewed N86-13604
A 10-MHz high-voltage modulator with pulse-width and repetition-rate agility [DE85-014117] N86-13663
Iron dominated magnets [DE85-014955] N86-14003
Tests of compressed geometry NEC acceleration tubes [DE85-016392] N86-14056
Engineering design for the PBFA-2 pulse forming section [DE85-012810] N86-14060
Laser-trigger system design for PBFA 2 [DE85-013144] N86-14065

PARTICLE BEAMS
Analysis of the dynamic behavior of an intense charged particle beam using the semigroup approach [AD-A159247] N86-14015
Engineering design for the PBFA-2 pulse forming section [DE85-012810] N86-14060
Laser-trigger system design for PBFA 2 [DE85-013144] N86-14065
Generation and acceleration of high intensity beams in the SLC injector [DE85-013056] N86-14066

PARTICLE DIFFUSION
Electrical and electrothermal conductivity of planetary ionospheres, 1: Refinement of theory N86-14143

PARTICLE FLUX DENSITY
Dependence of length of free path of flare particles on energy N86-14141

PARTICLE IN CELL TECHNIQUE
Electromagnetic particle-in-cell plasma simulation [DE85-031223] N86-14054

PARTICLE INTERACTIONS
Nation's achievements in high energy physics reviewed N86-13604

PARTICLE MOTION
First order estimates of the dynamics and energetics of a rapidly decelerating flywheel
[DE85-013908] N86-13842
PARTICLE PRECIPITATION
Mechanism of corpuscular-atmospheric relationships
N86-14127
Registry of heavy ions in auroral region during magnetic storms N86-14138
PARTICLE SIZE DISTRIBUTION
A study of rhenium as an alternate substrate material for impregnated dispenser cathodes
[AD-A159113] N86-13415
Discontinuous precipitation in aluminum-magnesium alloys with high magnesium content N86-13426
Effect of heating conditions on agglomeration of powdered aluminum in air atmosphere N86-13460
Wide distribution propellants N86-13540
Mechanisms for acoustic suppression N86-13543
Spray characterization using phase angle detection
N86-13577
Intelligent laser diffraction instrumentation for particle size analysis N86-13581
Single particle sizing by measurement of Brownian motion N86-13584
Holographic study of the particles produced by the injector in a Viking motor
[ISL-R-111/84] N86-13724
Protocol for size-specific emission measurements (SIM-5) applied to PM(10)
[PB85-200194] N86-13847
PARTICLE THEORY
The mathematical structure of elementary particles: 2
[AD-A158191] N86-14011
PARTICLE TRAJECTORIES
Extended atmospheres of outer planet satellites and comets
[NASA-CR-176398] N86-14209
PARTICLES
Experimental investigation of magnesium combustion in steam
[AD-A159109] N86-13396
PARTICULATE SAMPLING
Study of deposition control using transpiration
[DE85-012799] N86-13699
Particulate matter analysis by electron microscopy
[PB85-227817] N86-13846
Protocol for size-specific emission measurements (SIM-5) applied to PM(10)
[PB85-200194] N86-13847
Characterization of acid rain phenomena, Atlanta, Georgia
[PB85-216943] N86-13848
PASSENGER AIRCRAFT
Certification granted to Franco-Italian ATR 42
N86-13617
ATR 42 production work in French, Italian plants detailed N86-13618
PATTERN RECOGNITION
Speech recognition: Acoustic, phonetic and lexical knowledge
[AD-A158264] N86-13629
High frequency quantitative analysis of magnetomechanical acoustic emission
[AD-A158222] N86-13750
Generating and generalizing models of visual objects
[AD-A158197] N86-13894
Multiresolution path planning for mobile robots
[AD-A158630] N86-13948
Real time large memory optical pattern recognition
[AD-A158023] N86-14034
Experiment for evaluating accuracy in determining land categories on space scanner photographs N86-14195
PATTERN REGISTRATION
Rectification and registration of remotely sensed data
[AD-A158827] N86-13711
PAVEMENTS
A durable airfield marking system
[AD-A157953] N86-13339
PAYLOAD RETRIEVAL (STS)
Planetary sample rapid recovery and handling
[NASA-CR-171906] N86-13342
EURECA: An introduction to Europe's free-flying retrievable carrier
[ESA BR-30] N86-13352
PENETRATION
Short presentation and evaluation of studies on the penetration of jets from hollow shaped charges in compressible materials
[ISL-NB-402/84] N86-13586
PERCEPTION
Determination of backscattering sources in various targets N86-13811
Information requirements determination: An empirical investigation of obstacles within an individual
[AD-A158025] N86-13901
PERFORMANCE
Solar concentrator degradation in Low Earth Orbit (LEO) N86-14102
PERFORMANCE PREDICTION
Microscopic observations and mechanics analyses of long term fracture in polyethylene piping materials
[PB85-219608] N86-13506
Photoelectronic trajectory anatomy of RCA-C-73435 image converter and its performance
[DE85-013973] N86-13723
Aerodynamic research efforts at SERI wind energy research center at Rocky Flats --- Solar Energy Research Institute (SERI) N86-13829
PERFORMANCE TESTS
Assembly Integration Verification (AIV) test effectiveness study. Applicability of Spacelab approach for equipment and system test for Ariane-4 class satellites. Volume 1: Executive summary
[ERNO-671/AIV-VOL-1] N86-13361
Bulk CMOS VLSI technology studies. Part 5: The design and implementation of a high speed integrated circuit functional tester
[AD-A158370] N86-13651
Aerodynamic performance of a new LM 17.2 m rotor --- wind energy converter N86-13827
Practical aspects of functional testing techniques
[AD-A158184] N86-13968
Tests of compressed geometry NEC acceleration tubes
[DE85-016392] N86-14056
An analysis of cryotrap heat exchanger performance test data (400 area) and recommendations for a system to handle Apollo RCS engines N86-14094
PERIODIC FUNCTIONS
Periodic regimes of rotational motion of solid body about liberation point L sub 4 in restricted elliptical three-body problem N86-14132
PERIODIC VARIATIONS
Far-field boundary conditions in numerical solutions of the Navier-Stokes equations
[AD-A158776] N86-13690
PERIPHERAL VISION
Enhancing sensitivity to visual motion and enhancing visual sensitivity
[AD-A158800] N86-13889
PERMEABILITY
A study of rhenium as an alternate substrate material for impregnated dispenser cathodes
[AD-A159113] N86-13415
Study of permeability of two-phase zone in aluminum and copper alloys N86-13430
Experiments with non-Darcy flow in joints with large scale roughness
[DE85-015714] N86-13695
Tectonic stress on structures alters formation parameters N86-13864
PERMEATING
Hydrogen transport and hydrogen embrittlement in stainless steels N86-13403
PERMITTIVITY
Application of statistical model of layered medium for computing thermal emission of ice covers N86-14186
PERSONNEL
Magnetic field applications in modern technology and medicine
[DE85-015197] N86-14001
PERTURBATION
Ground reflectance measurements from thematic mapper data N86-13801
Multidimensional modeling of atmospheric effects and surface heterogeneities on remote sensing N86-13806
Stable boundary conditions and difference schemes for Navier-Stokes equations
[NASA-CR-177984] N86-13957
Forming transformation matrices for different parameters of motion of celestial bodies N86-14112
PERTURBATION THEORY
Intrinsic nilpotent approximation
[AD-A158265] N86-13975
PETROLOGY
Possible petroliferousness of South Caspian uplifts analyzed N86-13863
Tectonic stress on structures alters formation parameters N86-13864
PH FACTOR
Durability of steel 45 with boride coating in corrosive-abrasive media N86-13467
Oxidizing and scavenging characteristics of April rains: OSCAR data report
[DE85-017014] N86-13844
PHASE COHERENCE
Speckle image reconstruction. Appendix 1
[AD-A158271] N86-14207
PHASE CONJUGATION
Optical processing and phase conjugation
N86-13573
PHASE CONTROL
Hardware upgrade for klystrons in the SLC
[DE85-014357] N86-14029
PHASE DIAGRAMS
Mechanical properties of EP794 steel + 12Kh18N10T steel bimetal N86-13465
AuGa2 on GaSb(001): An epitaxial, thermodynamically stabilized Metal/3-5 compound semiconductor interface
[AD-A157937] N86-14071
PHASE LOCKED SYSTEMS
Phase lock acquisition system
[AD-D011804] N86-13646
PHASE MODULATION
Linearity optimization in a class of analog phase modulators
[NASA-TM-86420] N86-13644
PHASE SHIFT
Spray characterization using phase angle detection
N86-13577
China report: Science and technology
[JPRS-CST-85-020] N86-13600
On H plane dielectric loading theory for H plane ferrite phase shifter N86-13603
Speckle image reconstruction. Appendix 1
[AD-A158271] N86-14207
PHASE TRANSFORMATIONS
Critical behavior of thermoelectric power in binary composite materials N86-13448
Ceramics based on aluminum nitride and metals
N86-13456
Structure and internal friction of near-eutectic alloy system Ti-W tempered from a liquid state N86-13482
The formulation of a hyperbolic Stefan problem
[ORNL-6065] N86-13952
PHASE VELOCITY
Inversion of Rayleigh wave phase velocities between RSNT and RSON
[DE85-013242] N86-13859
PHENOLOGY
Possibilities of using space survey for studying seasonal changes of landscapes in some regions of USSR
N86-14183
PHOBOS
Brochure on Phobos and Deimos N86-14155
PHOSPHATES
Functionalized vesicles as organic reagents
[AD-A158381] N86-13372
PHOTOCHEMICAL REACTIONS
Disturbances in stratosphere and mesosphere from source of ultraviolet radiation N86-14136
PHOTODECOMPOSITION
Photodegradation studies of silver-backed polyacrylonitrile (PAN) films
[DE85-012154] N86-13501
PHOTODISSOCIATION
The dynamics of the photofragmentation of ketene 3-cyclopentenone, 3,5-cycloheptadienone, and tropone
[AD-A158045] N86-13371
Disturbances in stratosphere and mesosphere from source of ultraviolet radiation N86-14136
PHOTOELECTRON SPECTROSCOPY
Spectrum of photoelectrons in Earth's upper atmosphere during solar flares N86-14118
PHOTOGEOLOGY
Possibilities of use of aerospace materials in predicting occurrence of petroleum and gas N86-14175
Use of space geological methods in seismotectonic research N86-14188
Engineering evaluation of crustal faults using space survey data N86-14189
PHOTOGRAMMETRY
Experiment for evaluating accuracy in determining land categories on space scanner photographs N86-14195
PHOTOGRAPHIC FILM
Photodegradation studies of silver-backed polyacrylonitrile (PAN) films
[DE85-012154] N86-13501
Determining flexure of aerial camera smoothing glass
N86-14169
PHOTOINTERPRETATION
Possibilities of use of aerospace materials in predicting occurrence of petroleum and gas N86-14175
PHOTOLITHOGRAPHY
Excimer laser produces .2 micron semiconductor structures N86-13613
PHOTOLUMINESCENCE
Luminescent properties of semiconductor electrodes
[AD-A158841] N86-13655
PHOTOMAPPING
Space applications in geology N86-14167
Experience in complex mapping of natural resources in agrarian-industrial regions of Nonchernozem RSFSR using space photomaterials N86-14174
Problems in study and evaluation of consequences of forest fires using aerospace photographs N86-14176

Compilation of landscape maps at different scales with use of space photoinformation N86-14187

PHOTOMETERS

An integrated wavelength demultiplexer [AD-D011867] N86-14041

PHOTOMETRY

Use of remote optical measurements in agriculture N86-14172

The plate scale of the U.K. Schmidt Telescope N86-14202

Focal plane optics in far-infrared and submillimeter astronomy [NASA-TM-88186] N86-14204

PHOTONS

Two-proton detection techniques for atomic fluorine N86-13569

PHOTONUCLEAR REACTIONS

Multilevel relaxation phenomena and population trapping [DE85-011527] N86-13731

PHOTORECONNAISSANCE

Determining flexure of aerial camera smoothing glass N86-14169

PHOTOVOLTAIC EFFECT

Electrical research on solar cells and photovoltaic materials [NASA-CR-176384] N86-13838

PHYSICAL CHEMISTRY

Discovering qualitative empirical laws [AD-A159235] N86-13951

PHYSIOCHEMISTRY

Spectral reflectance of surface soils: Relationships with some soil properties N86-14089

PHYSIOLOGICAL EFFECTS

The effect of spironolactone on the cardiocirculatory responses to upright tilt at sea level and at simulated high altitude [AD-A157734] N86-13887

PHYSIOLOGICAL RESPONSES

A psychophysiological mapping of cognitive processes [AD-A158732] N86-13895

PILOT PERFORMANCE

Pilot-oriented performance measurement [AD-A158849] N86-13890

Effects of digital altimetry on pilot workload [NASA-TM-86424] N86-13892

PILOTS (PERSONNEL)

Passive arm retention curtain [AD-D011876] N86-13307

Pitch rate versus G command as the longitudinal flight control system design strategy for a statistically unstable fighter type aircraft with two control surfaces [AD-A158803] N86-13334

PIONS

Polarization transfer in enelastic scattering and pionic models of the EMC effect [DE85-014119] N86-14021

PIPE FLOW

Experimental investigation of heat transfer behavior of aqueous foams in thermal entry region of pipe flow [DE85-012836] N86-13700

PIPES (TUBES)

A computational analysis of pulsating flow in rigid and deformable tubes N86-13673

Two unsteady heat transfer experiments. Part 1: In grid-generated isotropic turbulence. Part 2: In laminar oscillatory flow in straight and conical tubes N86-13675

Development of a carbon formation reactor for carbon dioxide reduction [NASA-CR-171907] N86-13898

The physics and technology of strong magnetic fields (chapter 10) [AD-A158174] N86-14000

PISTON ENGINES

Lightweight two-stroke cycle aircraft diesel engine technology enablement program, volume 1 [NASA-CR-174923-VOL-1] N86-13328

Lightweight two-stroke cycle aircraft diesel engine technology enablement program, volume 2 [NASA-CR-174923-VOL-2] N86-13329

Lightweight two-stroke cycle aircraft diesel engine technology enablement program, volume 3 [NASA-CR-174923-VOL-3] N86-13330

PITTING

Corrosion fatigue initiation and short crack growth in an aluminum alloy N86-13404

PLANAR STRUCTURES

Latch for detachably securing electronic cards along orthogonal loading axes [AD-D011885] N86-13737

PLANE STRAIN

Fractured toughness of Si3N4 measured with short bar chevron-notched specimens [NASA-TM-87153] N86-13495

A numerical investigation into the plastic stress and strain fields around a surface crack [ARL/STRUC-R-414] N86-13754

PLANETARY ATMOSPHERES

Electrical and electrothermal conductivity of planetary ionospheres, 1: Refinement of theory N86-14143

Extended atmospheres of outer planet satellites and comets [NASA-CR-176398] N86-14209

PLANETARY ENVIRONMENTS

Results of study of surface of five regions on Venus by bistatic radar method N86-14156

PLANETARY EVOLUTION

Formation of underwater oceanic volcanoes and islands in relation to lithospheric thickness and movements N86-13776

Nature of megacycles in evolution of Earth, Mars, and Moon N86-14159

PLANETARY GRAVITATION

Integration of equations of motion for material point in gravitational field of axially symmetric planet N86-14131

PLANETARY MAGNETIC FIELDS

Possibility of spectroscopic detection of oxygen in lower Venusian atmosphere N86-14157

PLANETARY ORBITS

integration of equations of motion for material point in gravitational field of axially symmetric planet N86-14131

PLANETARY RADIATION

Charge composition of electrons in Earth's radiation belt N86-14146

PLANETARY SURFACES

Wind tunnel simulations of aeolian processes [NASA-CR-176382] N86-13289

PLANETARY WAVES

Rossby autosoliton N86-14158

PLANNING

Existence of equilibrium prices for a simple planning model [AD-A158263] N86-13996

PLANTS (BOTANY)

Microwave dielectric and propagation properties of vegetation canopies N86-13810

Energy exchange of plants under weightlessness conditions N86-14162

PLASMA ACCELERATORS

Numerical models for plasma-solid interactions in electrothermal mass accelerators [AD-A158637] N86-14052

PLASMA CONTROL

China report: Science and technology [JPRS-CST-85-020] N86-13600

Preliminary experimental results of CT-6B tokamak heating field voltage feedback control N86-13601

Doublet 3 [DE85-014369] N86-14031

Dense Z-pinch plasmas [DE85-005818] N86-14059

Heating and confinement in the Doublet 3 tokamak with electron cyclotron heating [DE85-014323] N86-14070

PLASMA CURRENTS

Preliminary experimental results of CT-6B tokamak heating field voltage feedback control N86-13601

Experimental study of neoclassical currents [DE85-014866] N86-14063

PLASMA DENSITY

Dense Z-pinch plasmas [DE85-005818] N86-14059

PLASMA DIAGNOSTICS

Fusion programs in applied plasma physics and development and technology, fiscal 1984 [DE85-014551] N86-14062

Radio emission of injected electron beam with respect to diagnosis of ionospheric plasma N86-14145

PLASMA ENGINES

Plasma-gas interactions studies in a hybrid plume plasma rocket N86-13559

Optical technique to measure electrode erosion N86-13564

PLASMA FOCUS

Dense Z-pinch plasmas [DE85-005818] N86-14059

PLASMA GENERATORS

Performance-limiting factors in MPD thrusters N86-13555

Study of storm time fluxes of heavy ions [NASA-CR-176368] N86-13852

PLASMA HEATING

Preliminary experimental results of CT-6B tokamak heating field voltage feedback control N86-13601

PLASMA INTERACTIONS

Plasma-gas interactions studies in a hybrid plume plasma rocket N86-13559

Unified study of plasma-surface interactions for space power and propulsion N86-13567

Population inversion in a recombining hydrogen plasma interacting with a helium gas [IPPJ-692] N86-14045

Numerical models for plasma-solid interactions in electrothermal mass accelerators [AD-A158637] N86-14052

PLASMA JETS

An investigation of plasma jet ignition and flame jet ignition of lean fuel-air mixtures N86-13386

PLASMA PHYSICS

High order spline interpolation in the particle simulation N86-14046

Fusion programs in applied plasma physics and development and technology, fiscal 1984 [DE85-014551] N86-14062

PLASMA PROPULSION

Basic processes of plasma propulsion N86-13554

Performance-limiting factors in MPD thrusters N86-13555

Plasma-gas interactions studies in a hybrid plume plasma rocket N86-13559

A tandem mirror plasma source for hybrid plume plasma studies N86-13560

Unified study of plasma-surface interactions for space power and propulsion N86-13567

PLASMA SHEATHS

Study of storm time fluxes of heavy ions [NASA-CR-176368] N86-13852

PLASMA WAVES

Parametric excitation of ion Bernstein waves by magnetosonic wave [IPPJ-738] N86-14047

Possibility for a self-consistent treatment of transport processes in a turbulent plasma [DE85-016214] N86-14069

PLASMAPAUSE

Coordinated investigations of processes in subauroral upper ionosphere and through in concentration of light ions N86-14137

PLASMAS (PHYSICS)

Structure of flow of erosion plasma formed upon laser treatment of metals N86-13455

Laser diagnostics for electric field measurements N86-13563

Hybrid simulation codes with application to shocks and upstream waves [NASA-CR-176365] N86-13702

Physical mechanisms for hot electron stabilization of low frequency interchange modes [IPPJ-741] N86-14050

Electromagnetic particle-in-cell plasma simulation [DE85-031223] N86-14054

Implicit plasma simulation [DE85-016088] N86-14055

PLASMASPHERE

Observations of fluxes of cold ions from plasmasphere into ionosphere during nighttime in middle latitudes N86-14117

PLASTIC DEFORMATION

Temperature-frequency variation of mechanical losses in periodic deformation of multilayer glass-reinforced plastics N86-13449

Elastic-plastic deformation of a metal-matrix composite coupon with a center slot [NASA-CR-178013] N86-13496

PLASTIC PROPERTIES

Relationship of thermal expansion of amorphous metal alloys with their high temperature plastic properties N86-13435

Effect of elastoplastic cyclic deformation on mechanical characteristics of steel O3Kh13AG19 at temperatures of 293 and 77 deg K N86-13463

Changes in structure and mechanical properties of niobium-titanium alloy during oxygen saturation N86-13479

Scientific activities of the Polish Academy of Sciences: Institute of Fundamental Technological Research in 1983 [ISBN-83-01-06288-6] N86-14107

PLASTICIZERS

Synthesis of high nitrogen content heterocyclic nitramines and energetic internal plasticizers N86-13511

PLASTICS

Temperature-frequency variation of mechanical losses in periodic deformation of multilayer glass-reinforced plastics N86-13449

PLATELETS

Subcritical crack development under constant load in VT6 alloy N86-13475

PLATES (STRUCTURAL MEMBERS)

Technique of assembling structures using vapor phase soldering [AD-D011805] N86-13410

Large modal survey testing using the Ibrahim time domain identification technique [AIAA-81-0528R] N86-13589
Application of Pasternak model to some soil-structure interaction problems. Volume 1: Solutions for plates continuously supported on a Pasternak base [AD-A157776] N86-13594
Application of Pasternak model to some soil-structure interaction problems. Volume 2: Determination of foundation parameters and the choice of models [AD-A157777] N86-13595

PLOTTING
DAB user's guide [NASA-CR-177393] N86-13290
FORTRAN plotting subroutines for the space plasma laboratory N86-14103

PLUMES
Plasma-gas interactions studies in a hybrid plume plasma rocket N86-13559
A tandem mirror plasma source for hybrid plume plasma studies N86-13560
Far-field model of the regional influence of affluent plumes from Ocean Thermal Energy Conversion (OTEC) plants [DE85-016981] N86-13836

PLUTONIUM
Solvent extraction of plutonium (IV) polymer by organophosphorous compounds [DE85-013229] N86-13502
High count rate gamma-ray spectrometer system for plutonium isotopic measurements [DE85-013212] N86-14024

POINT SOURCES
Test method for telescopes using a point source at a finite distance [NASA-TM-86523] N86-14033

POINTS (MATHEMATICS)
Extreme values of queues, point processes and Stochastic Networks [AD-A158619] N86-13991

POISSON DENSITY FUNCTIONS
Unified method for delay analysis of random multiple access algorithms [AD-A159108] N86-13981

POISSON EQUATION
Partitions of point processes: Multivariate poisson approximations [AD-A158739] N86-13978
Use of Goudriaan model for studying reflection regularities in vegetation-soil system in optical range. 1: Influence of phytometric parameters on spectral brightness coefficients N86-14190

POLAND
Scientific activities of the Polish Academy of Sciences: Institute of Fundamental Technological Research in 1983 [ISBN-83-01-06288-6] N86-14107

POLAR COORDINATES
Polar measurements on the profiles: FX 84-w-097, FX 84-w-127, FX 84-w-140, FX 84-w-175, FX 84-w-218 --- wind energy converters N86-13821

POLARIZATION (CHARGE SEPARATION)
Physical mechanisms for hot electron stabilization of low frequency interchange modes [IPPJ-741] N86-14050
Efficient ionizer for polarized H(-) formation [DE85-013294] N86-14064

POLARIZATION (SPIN ALIGNMENT)
Polarization transfer in enelastic scattering and pionic models of the EMC effect [DE85-014119] N86-14021

POLARIZATION CHARACTERISTICS
Measurement and modeling of the optical scattering properties of crop canopies N86-13798
Active microwave properties of vegetation canopies N86-13812
Magnetic field determination in quiescent solar prominences from polarization characteristics of radiated light N86-14125
Remote temperature determination of terrestrial covers from polarization invariant of microwave-radiothermal emission N86-14196

POLARIZED LIGHT
Magnetic field determination in quiescent solar prominences from polarization characteristics of radiated light N86-14125

POLARIZERS
Retrofit of a high power Nd:glass laser system with liquid crystal polarizers [DE85-014415] N86-13733

POLICIES
Tradeoff analysis of technology needs for public service helicopters [NASA-CR-3927] N86-13317
West Europe report: Science and technology [JPRS-WST-85-031] N86-13616

POLLUTION CONTROL
Mass transfer coefficients and Henry's constants for packed-tower air stripping of volatile organics: Measurements and correlation [AD-A158811] N86-13375
An Oil/Water disperser device for use in an oil content Monitor/Control system [AD-D011868] N86-13714
Oil content Monitor/Control system and method [AD-D011871] N86-13717

POLLUTION MONITORING
Development and evaluation of an instantaneous atmospheric corrosion rate monitor [PB85-214336] N86-13727
Protocol for size-specific emission measurements (SIM-5) applied to PM(10) [PB85-200194] N86-13847

POLOIDAL FLUX
Impact of a poloidal divertor in ignition tokamak design [DE85-012892] N86-14061

POLYCRYSTALS
Superhard materials developed N86-13471
Micromechanisms of electrodiffusion failures in thin film metallization N86-13472
Development of stable high efficiency polycrystalline thin-film solar cells based on CuInSe2 [DE85-000517] N86-13837

POLYESTERS
Recent advances in composite materials reviewed N86-13623

POLYETHYLENES
Electrification of filled polyethylene coatings in friction with metal N86-13439
Microscopic observations and mechanics analyses of long term fracture in polyethylene piping materials [PB85-219608] N86-13506

POLYMER CHEMISTRY
Method of synthesizing polymers from a solid electrolyte [DE85-011623] N86-13504
Fluoropolyazido-esters as energetic polymers N86-13515
New energetic polymers as binders for propellants N86-13516
Control of the urethane cure reaction with solid, blocked isocyanates N86-13518

POLYMER MATRIX COMPOSITES
Theory of pyrolysis of composite polymer materials N86-13447
Mass loss of shuttle space suit orthofabric under simulated ionospheric atomic oxygen bombardment [NASA-TM-87149] N86-13899

POLYMER PHYSICS
Method of synthesizing polymers from a solid electrolyte [DE85-011623] N86-13504

POLYMERIC FILMS
Anticorrosion polymer packing film with improved protective properties N86-13451
Development of high sensitivity X-ray and electron beam resist processes [AD-A158968] N86-13657

POLYMERIZATION
Aquatic plant control research program: Evaluation of polymers for controlled delivery of herbicides for aquatic plant control [AD-A157948] N86-13843

POLYNOMIALS
FIT: Computer program that interactively determines polynomial equations for data which are a function of two independent variables [NASA-TM-86413] N86-13333
Transient simulation of submicron devices [AD-A157748] N86-13648
Lubrication of nonconformal contacts [NASA-TM-87120] N86-13679

POLYURETHANE RESINS
Study of cross-linking density and the type of cross linkage in polyurethane elastomers [AD-A158199] N86-13497
Control of the urethane cure reaction with solid, blocked isocyanates N86-13518

POPULATION INVERSION
Population inversion in a recombining hydrogen plasma interacting with a helium gas [IPPJ-692] N86-14045

POPULATIONS
Multilevel relaxation phenomena and population trapping [DE85-011527] N86-13731

POROSITY
Determination of porosity of thin sheets of fiber materials based on optical transmission coefficient N86-13459
Study of process of pore formation during argon-arc welding of aluminum alloy 1420 N86-13485

POROUS MATERIALS
Effect of geometry of fiber packing on consolidation of fibrous composition materials with porous matrix N86-13443
Effective medium theory for partially saturated porous solids [DE85-016608] N86-13598

POSITION (LOCATION)
Time delay of arrival location assessment using four satellites [AD-A159243] N86-13315
Mobile robot localization using sonar [AD-A158819] N86-13949
Determining quasi-real-time location of ships using geostationary navigational satellites N86-14165
Organization of space navigation system based on use of geostationary satellites N86-14166

POSITION INDICATORS
Concept of laser locator systems (based on the geometry of the triangular corner cube reflector) [AD-A157795] N86-13728

POSITIONING
New robots by Soviet, CEMA manufacturers described N86-13748

POSITIVE IONS
Changes in soil acidity due to natural processes and acid deposition [DE85-012103] N86-13845

POSITRONS
Positron diffusion in Si [DE85-014831] N86-14076

POSTFLIGHT ANALYSIS
Mathematical analysis study for radar data processing and enhancement. Part 1: Radar data analysis [NASA-CR-166616-PT-1] N86-13353
Computer program for post-flight analysis of rigid body moments acting on a launch vehicle first stage [NASA-CR-166033] N86-13918

POTASSIUM
The suppression of afterburning in solid rocket plumes by potassium salts N86-13524

POTENTIAL ENERGY
Laboratory studies of steep and breaking deep water waves in a convergent channel [AD-A158187] N86-13875

POTTING COMPOUNDS
Electrical research on solar cells and photovoltaic materials [NASA-CR-176384] N86-13838

POWDER (PARTICLES)
Recent experience in the RAE (Royal Aircraft Establishment) 5-metre wind tunnel of a china clay method for indicating boundary layer transition [AD-A157943] N86-13302
A method for melt-coating a surface [AD-D011866] N86-13596

POWDER METALLURGY
A study of rhenium as an alternate substrate material for impregnated dispenser cathodes [AD-A159113] N86-13415
Evaluation of the titanium IMI 829 alloy produced by powder metallurgy [M1-610200] N86-13421
USSR report: Materials science and metallurgy [JPRS-UMS-85-006] N86-13422

POWDERED ALUMINUM
Study of properties of gas-thermal coatings of composite nichrome-aluminum alloy powders N86-13442
Effect of heating conditions on agglomeration of powdered aluminum in air atmosphere N86-13460

POWER CONDITIONING
Microcomputer controlled current sharing experiments with parallel converters [DE85-013854] N86-13665
Two-hundred to 300 KVA conditioned power system - development, phase 1 [AD-A158820] N86-13832

POWER REACTORS
Low power reactor for remote applications [DE85-012763] N86-14032

POWER SERIES
Structure of coefficients of series representing solution of plane circular restricted three-body problem N86-14129

POWER SPECTRA
Theoretical studies and data analysis of wave propagation in random media [AD-A158775] N86-13632
Speckle image reconstruction. Appendix 2 [AD-A158272] N86-14208

POWER SUPPLY CIRCUITS
Electrical sliding joint literature review (viewgraph presentation) [DE85-011571] N86-13666

POWER TRANSMISSION (LASERS)
Optical radar transceiver control apparatus [AD-D011880] N86-14042
PRECIPITATION
Solar concentrator degradation in Low Earth Orbit (LEO) N86-14102
PRECIPITATION (METEOROLOGY)
Remote sensing of Earth terrain N86-13808
Oxidizing and scavenging characteristics of April rains: OSCAR data report [DE85-017014] N86-13844
PRECIPITATION HARDENING
Dispersion hardening of high-strength NiOCo-Mo steels N86-13468
PRECISION
A note on the effect of ignoring small measurement errors in precision instrument calibration [AD-A159104] N86-13713
Robot control system modified for precision movement N86-13747
PRECONDITIONING
Test of a moisture conditioning procedure using 70 C distilled water, instead of a gas atmosphere at 70 C, 95% relative humidity --- plastic composites [M3-431000] N86-13383
PREDICTION ANALYSIS TECHNIQUES
Nonlinear modeling and method of predicting crack growth N86-13538
High Reynolds number wave force investigation in a wave flume [AD-A157722] N86-13681
An analytical theory for rotor tip vane performance and comparison with experimental results --- wind energy converters N86-13823
Aerodynamic theory in the calculation of the GROWIAN rotor compared with some experimental data --- wind energy converter N86-13826
Understanding climate: A strategy for climate modeling and predictability research, 1985-1995 [NASA-RP-1158] N86-13866
Spectral reflectance of surface soils: Relationships with some soil properties N86-14089
PREDICTIONS
Application of molecular kinetics models to the prediction of backflow contamination N86-13531
Non-Newtonian flow past curved external surfaces N86-13671
Preliminary measurement of the noise from the 2/9 scale model of the Large-scale Advanced Propfan (LAP) propeller, SR-7A [NASA-TM-87116] N86-14006
PREPARATION
Preparation of ceramic fiber-ceramic matrix composites by a faster chemical vapor infiltration process [DE85-016402] N86-13500
PRESSING (FORMING)
A study of rhenium as an alternate substrate material for impregnated dispenser cathodes [AD-A159113] N86-13415
PRESSURE
Effects of velocity profile and inclination on dual-jet-induced pressures on a flat plate in a crosswind [NASA-CR-177361] N86-13287
Temperature and pressure components of shock-induced changes in the electronic spectrum of carbon disulfide [AD-A158627] N86-13373
Atmospheric environment for Space Shuttle (STS-51D) [NASA-TM-86524] N86-13868
PRESSURE CHAMBERS
High-pressure, high-temperature opposed anvil device described N86-13606
PRESSURE DEPENDENCE
Ion nitriding of titanium N86-13473
PRESSURE DISTRIBUTION
Effects of velocity profile and inclination on dual-jet-induced pressures on a flat plate in a crosswind [NASA-CR-177361] N86-13287
Studies of the flow field near a NACA 4412 aerofoil at nearly maximum lift [AD-A157750] N86-13301
Pressure-distribution measurements on a transonic low-aspect ratio wing [NASA-TM-86683] N86-13304
Non-Newtonian flow past curved external surfaces N86-13671
Sensitivity to mean flow parameters of the low wavenumber content of the wall pressure under a turbulent boundary layer [AD-A158037] N86-13688
Pressure field retrieval by remote refractometry from space N86-14168
PRESSURE GRADIENTS
Heat transfer and pressure drop performance of a finned-tube heat exchanger proposed for use in the NASA Lewis Altitude Wind Tunnel [NASA-TM-87151] N86-13677
Experiments with non-Darcy flow in joints with large scale roughness [DE85-015714] N86-13695
PRESSURE MEASUREMENT
Studies of the flow field near a NACA 4412 aerofoil at nearly maximum lift [AD-A157750] N86-13301
Pressure-distribution measurements on a transonic low-aspect ratio wing [NASA-TM-86683] N86-13304
PRESSURE SENSORS
Pore pressure response to probe insertion and thermal gradient: ISIMU-2. (In situ heat transfer experiment) [AD-A158592] N86-13689
The design of a beach profiler [AD-A157715] N86-13874
PRESSURE VESSELS
Study of effect of normal reactor water on growth rate of fatigue cracks in 15Kh2NMFA steel N86-13470
PRIMARY BATTERIES
Role of additives in minimizing zinc electrode shape change: The effect of lead on the kinetics of Zn(2) reduction in concentrated alkaline media [AD-A158806] N86-13395
Cathode for use in high energy primary thionyl chloride cell systems and high energy primary thionyl chloride cell systems including the cathode [AD-D011882] N86-13662
PRIMATES
Effects of 60 Hz electric fields on operant and social stress behaviors of nonhuman primates [DE85-011992] N86-13885
PRINCIPLES
Basic principles of feedback and adaptive approaches in the finite element method [AD-A158188] N86-13969
PRINTED CIRCUITS
Latch for detachably securing electronic cards along orthogonal loading axes [AD-D011885] N86-13737
PROBABILITY DENSITY FUNCTIONS
Applications of differential phase statistics to studies of C3 and spread spectrum communications [AD-A158815] N86-13633
Modelling a transport equation of turbulent reactive mixing flow N86-13674
PROBABILITY DISTRIBUTION FUNCTIONS
An alternate derivation of the distribution of the conditioned signal-to-noise ratio [AD-A158257] N86-13974
Estimation of finite mixtures using the empirical characteristic function N86-14079
PROBABILITY THEORY
B-splines and linear combinations of uniform order statistics [AD-A158151] N86-13986
Approximation of the initial reserve for known ruin probabilities [AD-A158167] N86-13987
Adaptive detection in nonstationary interference: Part 1 and part 2 [AD-A158810] N86-13993
PROBLEM SOLVING
Discovery of the Kalman filter as a practical tool for aerospace and industry [NASA-TM-86847] N86-13311
Information requirements determination: An empirical investigation of obstacles within an individual [AD-A158025] N86-13901
A reactive learning environment for the Equipment Problem Solving Techniques (EPST) system [AD-A158035] N86-13929
Spectral methods for discontinuous problems [NASA-CR-177974] N86-13953
JASON electrostatic boundary conditions: A survey [DE85-014521] N86-14005
PROCESS CONTROL (INDUSTRY)
USSR report: Machine tools and metalworking equipment [JPRS-UMM-85-013] N86-13745
PROCESS HEAT
Review of SERI solar pond work [DE85-012162] N86-13834
PRODUCT DEVELOPMENT
Sun acquisition sensor for European Communications Satellite N86-13366
Thomson semiconductors introduces products, balances books N86-13615
New materials to lighten vehicles N86-13624
New robots by Soviet, CEMA manufacturers described N86-13748
PRODUCTION ENGINEERING
Study of mean free path effects on growth of ultrafine metallic aerosols [AD-A158206] N86-13393
New applications of industrial robots noted N86-13743
Problems with integrating robots in conventional production N86-13744
Problems with robotization of conventional shops N86-13746
Robot control system modified for precision movement N86-13747
Operation of large cryogenic systems [DE85-017439] N86-14025
PRODUCTION MANAGEMENT
ATR 42 production work in French, Italian plants detailed N86-13618
PRODUCTIVITY
New applications of industrial robots noted N86-13743
Problems with integrating robots in conventional production N86-13744
PROGNOZ SATELLITES
Observation of small-scale solar wind structure on front of sharp increase in plasma flow velocity N86-14142
List of recent Soviet space launches N86-14199
PROGRAM VERIFICATION (COMPUTERS)
Experiences with Cray multi-tasking [NASA-TM-88200] N86-13916
Development of a flight software testing methodology [NASA-CR-176391] N86-13922
Techniques for the design and implementation of highly reliable multi-processing systems [AD-A159236] N86-13945
PROGRAMMING LANGUAGES
DIESS: A prolog implementation of a domain-independent expert system shell [AD-A158014] N86-13928
An algorithm to translate relational algebra queries into QUEL [AD-A158169] N86-13931
PROJECT MANAGEMENT
NASA flight operations review [NASA-CR-176393] N86-13306
PROJECTION
Map projections for use with the Geographic Information System [PB85-198992] N86-13819
PROP-FAN TECHNOLOGY
Preliminary measurement of the noise from the 2/9 scale model of the Large-scale Advanced Propfan (LAP) propeller, SR-7A [NASA-TM-87116] N86-14006
PROPANE
Interactions between a laminar flame and end gas autoignition [DE85-008957] N86-13402
Critical charge for the direct initiation of detonation in gaseous fuel-air mixtures [DE85-016130] N86-13696
PROPELLANT BINDERS
New energetic polymers as binders for propellants N86-13516
Energetic fluorcarbons N86-13517
PROPELLANT CHEMISTRY
The 1985 AFOSR/AFRPL Chemical Rocket Research Meeting, abstracts and agenda [AD-A158291] N86-13507
Electrolytic preparation of novel azidodinitro compounds N86-13508
Syntheis of difluoroaminoxy-, difluoramino- or fluorodiazonium-containing materials N86-13509
Synthesis of new polynitropolyhedranes N86-13510
Synthesis and chemistry of polynitroalkanes and polynitroolefins N86-13513
New synthetic techniques for advanced propellant ingredients: Selective transformations and new structures N86-13514
Fluoropolyazido-esters as energetic polymers N86-13515
New energetic polymers as binders for propellants N86-13516
Energetic fluorcarbons N86-13517
Physical and chemical consequences of antiaromaticity in the boracyclopentadiene system N86-13519
Evaluation of HMX propellant chemistry from Raman and laser induced fluorescence species and temperature measurements N86-13530
PROPELLANT COMBUSTION
The 1985 AFOSR/AFRPL Chemical Rocket Research Meeting, abstracts and agenda [AD-A158291] N86-13507
Chemical kinetics of nitramine propellant combustion N86-13525
Combusion of hydrogen and hydrocarbons in fluorine N86-13526

Application of molecular kinetics models to the prediction of backflow contamination N86-13531

PROPELLANT PROPERTIES

The 1985 AFOSR/AFRPL Chemical Rocket Research Meeting, abstracts and agenda
[AD-A158291] N86-13507

New synthetic techniques for advanced propellant ingredients: Selective transformations and new structures N86-13514

PROPELLANT TANKS

Mathematical models of nonstationary eddy currents and eddy movements of fluid in problems of orientation and stabilization of artificial Earth satellites and spacecraft 2 N86-14116

PROPELLANTS

Synthesis of new polynitropolyhedranes N86-13510

Fundamental studies of azide decomposition and combustion N86-13534

PROPELLER BLADES

Hub effects in propeller design and analysis
[AD-A158853] N86-13331

Preliminary measurement of the noise from the 2/9 scale model of the Large-scale Advanced Propfan (LAP) propeller, SR-7A
[NASA-TM-87116] N86-14006

PROPELLERS

Some design philosophy for reducing the community noise of advanced counter-rotation propellers
[NASA-TM-87099] N86-14007

PROPULSION SYSTEM PERFORMANCE

Overview: AFOSR interests in rocket propulsion N86-13546

PROPYL COMPOUNDS

Electronic detection of low concentrations of organophosphorus compounds with a solid state device utilizing supported copper + cuprous oxide island films
[AD-A158181] N86-13392

PROTECTIVE COATINGS

USSR report: Materials science and metallurgy
[JPRS-UMS-85-006] N86-13422

Corrosion resistance of diffusion and galvanic coatings on steel fasteners N86-13450

Development of high sensitivity X-ray and electron beam resist processes
[AD-A158968] N86-13657

PROTON BEAMS

Aspects of three field approximations: Darwin, frozen, EMPULSE
[DE85-014204] N86-14020

PROTON BELTS

Formation of proton radiation belts in region of energies of several MeV N86-14140

PROTON DENSITY (CONCENTRATION)

Formation of proton radiation belts in region of energies of several MeV N86-14140

PROTON ENERGY

Formation of proton radiation belts in region of energies of several MeV N86-14140

PROTON IRRADIATION

Potential for use of indium phosphide solar cells in the space radiation environment
[NASA-TM-87157] N86-13645

PROTOTYPES

New flow visualization technique for water tunnel testing of combustors
[AD-A158015] N86-13686

Specialized instrument for radiation assistance teams
[DE85-017390] N86-13720

PROXIMITY

Method for using clusters in evaluating land use areas from multizonal photographs N86-14180

PSYCHOPHYSIOLOGY

A psychophysiological mapping of cognitive processes
[AD-A158732] N86-13895

The event related brain potential as an index of information processing, cognitive activity, and skill acquisition: A program of basic research
[AD-A159118] N86-13897

PUBLIC HEALTH

Tradeoff analysis of technology needs for public service helicopters
[NASA-CR-3927] N86-13317

PUBLIC RELATIONS

Some design philosophy for reducing the community noise of advanced counter-rotation propellers
[NASA-TM-87099] N86-14007

PULSE DURATION

New control techniques for extraction of Bevalac beams
[DE85-017640] N86-14023

PULSE GENERATORS

Pulsed inductive energy transfer N86-13562

A 10-MHz high-voltage modulator with pulse-width and repetition-rate agility
[DE85-014117] N86-13663

High speed multi-channel data recorder to replace oscilloscope data acquisition systems
[DE85-015155] N86-13721

Engineering design for the PBFA-2 pulse forming section
[DE85-012810] N86-14060

Generation and acceleration of high intensity beams in the SLC injector
[DE85-013056] N86-14066

PULSED LASERS

Energy deposition of pulsed one micron laser radiation in H2 and AR N86-13552

Development of velocity measurement technique by pulsed laser Doppler anemometry N86-13571

Experimental and theoretical studies of laser propulsion phenomenology
[AD-A158273] N86-13729

Multilevel relaxation phenomena and population trapping
[DE85-011527] N86-13731

PULSED RADIATION

Interpretation of F-106B in-flight lightning signatures
[NASA-CR-176387] N86-13320

CNET of France uses organo-metallic epitaxy for laser N86-13620

PULSES

Analog-to-Digital converter
[AD-D011878] N86-13660

PYROLYSIS

Theory of pyrolysis of composite polymer materials N86-13447

Fundamental studies of azide decomposition and combustion N86-13534

New physical methods for biological aerosol detection
[AD-A158218] N86-13881

Development of a carbon formation reactor for carbon dioxide reduction
[NASA-CR-171907] N86-13898

A pyroloysis technique for determining microamounts of hydrogen in lunar soil using the helium ionization detector N86-14082

PYROLYTIC GRAPHITE

Optical constants
[AD-A158623] N86-14038

Q

QUADRATURES

Adaptive, self-validating numerical quadrature
[AD-A158164] N86-13963

QUALITY CONTROL

Analysis of survey conditions and effect of noise on quality of sensing of soil formations N86-14191

QUANTITATIVE ANALYSIS

High pressure solid propellant combustion zone structure from analysis of hydroxyl radical chemiluminescence N86-13529

High frequency quantitative analysis of magnetomechanical acoustic emission
[AD-A158222] N86-13750

QUANTUM CHEMISTRY

Application of quantum chemistry to atmospheric chemistry
[AD-A158282] N86-13856

QUARTZ

Development of a carbon formation reactor for carbon dioxide reduction
[NASA-CR-171907] N86-13898

QUENCHING (COOLING)

Relationship of thermal expansion of amorphous metal alloys with their high temperature plastic properties N86-13435

QUEUEING THEORY

Development and enhancement of Computer Performance Modeling Tool (CPMT)
[AD-A159003] N86-13938

Extreme values of queues, point processes and Stochastic Networks
[AD-A158619] N86-13991

R

RADAR

China report: Science and technology
[JPRS-CST-85-020] N86-13600

Scheme for high-speed real-time DFT operation for radar signal processing N86-13602

Improved algorithm for radar real-time data processing N86-13608

Agile Electromagnetics Exploiting High Speed Logic (AEEHSL)
[AD-A158380] N86-13630

RADAR ATTENUATION

Mathematical analysis study for radar data processing and enchancement. Part 2: Modeling of propagation path errors
[NASA-CR-166616-PT-2] N86-13354

RADAR CORNER REFLECTORS

Concept of laser locator systems (based on the geometry of the triangular corner cube reflector)
[AD-A157795] N86-13728

RADAR ECHOES

Discrete random media techniques for microwave modeling of vegetated terrain N86-13809

RADAR EQUIPMENT

Radar location equipment development program, phase 1
[DE85-014523] N86-13637

RADAR FILTERS

Mathematical analysis study for radar data processing and enhancement. Part 1: Radar data analysis
[NASA-CR-166616-PT-1] N86-13353

Mathematical analysis study for radar data processing and enchancement. Part 2: Modeling of propagation path errors
[NASA-CR-166616-PT-2] N86-13354

RADAR IMAGERY

Mathematical analysis study for radar data processing and enhancement. Part 1: Radar data analysis
[NASA-CR-166616-PT-1] N86-13353

Rectification and registration of remotely sensed data
[AD-A158827] N86-13711

Determination of backscattering sources in various targets N86-13811

Active microwave properties of vegetation canopies N86-13812

RADAR NETWORKS

Mathematical analysis study for radar data processing and enhancement. Part 1: Radar data analysis
[NASA-CR-166616-PT-1] N86-13353

RADAR REFLECTORS

Cassegrain reflector sidelobe reduction study
[AD-A158625] N86-13631

RADAR RESOLUTION

Mathematical analysis study for radar data processing and enhancement. Part 1: Radar data analysis
[NASA-CR-166616-PT-1] N86-13353

Mathematical analysis study for radar data processing and enchancement. Part 2: Modeling of propagation path errors
[NASA-CR-166616-PT-2] N86-13354

RADAR SCATTERING

Determination of backscattering sources in various targets N86-13811

RADAR TARGETS

Adaptive detection in nonstationary interference: Part 1 and part 2
[AD-A158810] N86-13993

RADAR TRACKING

Concept of laser locator systems (based on the geometry of the triangular corner cube reflector)
[AD-A157795] N86-13728

RADIANT FLUX DENSITY

Latitude measurements of cosmic radiation intensity in stratosphere and at sea level on marine antarctic expeditions N86-13792

RADIATION ABSORPTION

Coupling between gas dynamics and microwave energy absorption N86-13561

Time resolved extended X-ray absorption fine structure spectrometer
[AD-D011869] N86-13715

RADIATION BELTS

Mechanism of corpuscular-atmospheric relationships N86-14127

Charge composition of electrons in Earth's radiation belt N86-14146

RADIATION COUNTERS

Spray characterization with a nonintrusive optical single particle counter N86-13580

High count rate gamma-ray spectrometer system for plutonium isotopic measurements
[DE85-013212] N86-14024

RADIATION DAMAGE

MeV electron beam irradiation effects on GaAs (1-x) P (x) LEDs (Light emitting diodes)
[AD-A158832] N86-13653

RADIATION DETECTORS

Specialized instrument for radiation assistance teams
[DE85-017390] N86-13720

RADIATION DOSAGE

Variable curvature phantom
[DE85-014260] N86-14028

RADIATION EFFECTS

Potential for use of indium phosphide solar cells in the space radiation environment
[NASA-TM-87157] N86-13645

Study of optical-acoustical phenomena at surface of strongly absorbing clearing fluids N86-13774
Electrical research on solar cells and photovoltaic materials
[NASA-CR-176384] N86-13838

RADIATION HAZARDS
Specialized instrument for radiation assistance teams
[DE85-017390] N86-13720

RADIATION MEASUREMENT
Time resolved extended X-ray absorption fine structure spectrometer
[AD-D011869] N86-13715

RADIATION SHIELDING
Aircrew dose and engine dust ingestion from nuclear cloud penetration
[AD-A159246] N86-13327
Multidimensional modeling of atmospheric effects and surface heterogeneities on remote sensing N86-13806

RADIATIVE HEAT TRANSFER
Fundamental remote sensing science research program: The Scene Radiation and Atmospheric Effects Characterization Project
[E86-10011] N86-13794
Reflectance modeling N86-13795
Understanding the radiant scattering behavior of vegetated scenes N86-13797
Measurement and modeling of the optical scattering properties of crop canopies N86-13798
Atmospheric and scence complexity effects on surface bidirectional reflectance N86-13803
The formulation of a hyperbolic Stefan problem
[ORNL-6065] N86-13952
Use of Goudriaan model for studying reflection regularities in vegetation-soil system in optical range. 1: Influence of phytometric parameters on spectral brightness coefficients N86-14190

RADIATIVE TRANSFER
Atmospheric effect on remote sensing of the Earth's surface N86-13804
The characterization of surface varigation effects on remote sensing N86-13805
Multidimensional modeling of atmospheric effects and surface heterogeneities on remote sensing N86-13806
Coupled radiation transport/thermal analysis of the radiation shield for a space nuclear reactor
[AD-A158180] N86-14022

RADIO ALTIMETERS
Feasibility study of chirp generator for ERS-1 radar altimeter, option A
[ELAB-STF44-F83103] N86-13368

RADIO EMISSION
Radio emission of injected electron beam with respect to diagnosis of ionospheric plasma N86-14145

RADIO FREQUENCIES
Advanced energy conversion concept for microwave beamed-energy propulsions N86-13553

RADIO FREQUENCY INTERFERENCE
Cerenkov radiation from periodic bunches for a finite path in air
[AD-A159027] N86-13635

RADIO FREQUENCY SHIELDING
Cerenkov radiation from periodic bunches for a finite path in air
[AD-A159027] N86-13635

RADIO WAVES
Theoretical studies and data analysis of wave propagation in random media
[AD-A158775] N86-13632
Volcanoes discovered with radio beam N86-13777

RADIOACTIVE MATERIALS
Specialized instrument for radiation assistance teams
[DE85-017390] N86-13720
Identification of nuclear materials from remote detection of characteristic gamma rays
[AD-A159244] N86-14014

RADIOACTIVE WASTES
Radar location equipment development program, phase 1
[DE85-014523] N86-13637

RADIOACTIVITY
Specialized instrument for radiation assistance teams
[DE85-017390] N86-13720
Interactive scenario computer model for dose rates to aircrews in flight through nuclear debris clouds
[AD-A158741] N86-13888

RADIOCHEMISTRY
Geothermal investigation in Idaho. Part 14: Geochemical and isotopic investigations of thermal water occurrences of the Boise Front Area, Ada County, Idaho. Water Information Bulletin no. 30
[DE85-012905] N86-13841

RADIOGRAPHY
Probability of detection of internal voids in structural ceramics using microfocus radiography
[NASA-TM-87164] N86-13749

RADIOMETERS
Computer-aided aerial radiometric surveying of soil moisture N86-13778
Normalization of response of radiometric instrumentation for studying Earth's natural resources N86-14192
Remote temperature determination of terrestrial covers from polarization invariant of microwave-radiothermal emission N86-14196

RADIOMETRIC CORRECTION
Radiometric correction of materials of aerospace survey of Earth with MKF-6 camera: Methodology and use of results N86-14193

RADOMES
Cassegrain reflector sidelobe reduction study
[AD-A158625] N86-13631

RAIN
Goskomgidromet plans automation of aerial cloud-seeding work N86-13766
Sampling-rate effects on radar-derived rainfall estimates
[AD-A158203] N86-13870
Variability of rainfall over small areas N86-14098

RAIN GAGES
Variability of rainfall over small areas N86-14098

RAMAN SPECTRA
Two-proton detection techniques for atomic fluorine N86-13569
Laser emission and coherent Raman scattering from individual flowing droplets N86-13578

RAMAN SPECTROSCOPY
Resonant cars detection of OH radicals N86-13576
New physical methods for biological aerosol detection
[AD-A158218] N86-13881

RAMJET ENGINES
Experimental investigation of heterogeneous flame stabilization N86-13528

RANDOM ACCESS
Unified method for delay analysis of random multiple access algorithms
[AD-A159108] N86-13981

RANDOM ERRORS
Random errors in the magnetic field coefficients of superconducting magnets
[DE85-012261] N86-14004

RANDOM NUMBERS
Decomposition of some well-known variance reduction techniques: Revision
[AD-A158048] N86-13985

RANDOM SIGNALS
Theoretical studies and data analysis of wave propagation in random media
[AD-A158775] N86-13632

RANDOM VARIABLES
A note on the integrated Cauchy functional equation
[AD-A158269] N86-13977
B-splines and linear combinations of uniform order statistics
[AD-A158151] N86-13986
Basic properties of strong mixing conditions
[AD-A158740] N86-13992
Continuity of certain random integral mappings and the uniform integrability of infinitely divisible measures
[AD-A159105] N86-13995
A variant of Shanbhag's lemma arising out of a modified Rao-Rubbin condition
[AD-A158608] N86-13998

RANGEFINDING
Mobile robot localization using sonar
[AD-A158819] N86-13949

RANKINE CYCLE
Low power reactor for remote applications
[DE85-012763] N86-14032

RAREFIED GASES
Effect of composition of rarefied medium on gas-saturated titanium alloys N86-13477

RATES (PER TIME)
Waves which travel upstream in boundary layers
[AD-A157949] N86-13684
Sampling-rate effects on radar-derived rainfall estimates
[AD-A158203] N86-13870

RAYLEIGH WAVES
Inversion of Rayleigh wave phase velocities between RSNT and RSON
[DE85-013242] N86-13859

RDX
Deuterium isotope effects in RDX decomposition and combustion processes N86-13522
Stability of RDX, AP and BTTN near room temperature N86-13535

REACTION CONTROL
Computer program for post-flight evaluation of a launch vehicle upper-stage on-off reaction control system
[NASA-CR-166029] N86-13921

REACTION KINETICS
Reaction intermediates in aromatic fuel combustion
[AD-A158029] N86-13390
Role of additives in minimizing zinc electrode shape change: The effect of lead on the kinetics of Zn(2) reduction in concentrated alkaline media
[AD-A158806] N86-13395
The influence of microstructure on temper embrittlement of low alloy steel N86-13405
Electrification of filled polyethylene coatings in friction with metal N86-13439
The 1985 AFOSR/AFRPL Chemical Rocket Research Meeting, abstracts and agenda
[AD-A158291] N86-13507
Control of the urethane cure reaction with solid, blocked isocyanates N86-13518
Chemical kinetics of nitramine propellant combustion N86-13525
Evaluation of HMX propellant chemistry from Raman and laser induced fluorescence species and temperature measurements N86-13530
Application of molecular kinetics models to the prediction of backflow contamination N86-13531
Critical evaluation of high temperature chemical kinetic data N86-13533
Stability of RDX, AP and BTTN near room temperature N86-13535
Fuel-rich solid propellant boron combusion N86-13536
Application of atomic fluorescence to measurement of combustion temperatures in solid propellants N86-13582
Modelling a transport equation of turbulent reactive mixing flow N86-13674
Measurement of rate constants of elementary gas reactions of importance to upper atmosphere and combustion systems
[AD-A158824] N86-13857
The event related brain potential as an index of information processing, cognitive activity, and skill acquisition: A program of basic research
[AD-A159118] N86-13897
Reactive scattering in the bending-corrected rotating linear model
[DE85-017539] N86-14018

REACTIVITY
Synthesis, structure and reactivity of molecules attached to electrode surfaces
[AD-A158621] N86-13394

REACTOR MATERIALS
Recent results on implantation and permeation into fusion reactor materials
[DE85-014620] N86-14067

REACTOR SAFETY
Simulating distributed reinforcement effects in concrete analysis
[DE85-009745] N86-13761

REACTOR TECHNOLOGY
Graph theoretic approaches to diagnostics: Applications of logic programming and cutset theory to aspects of reactor and circuit analysis
[ANL-84-74] N86-13912

REAGENTS
Functionalized vesicles as organic reagents
[AD-A158381] N86-13372
Application of computers in analytical chemistry: Calculation of optimum acidity of reaction between metal ions and organic reagents in solution N86-13607

REAL TIME OPERATION
A real-time data acquisition system for a low speed wind tunnel
[AR-AERO-R-163] N86-13336
Improved algorithm for radar real-time data processing N86-13608
The construction and testing of a real-time digital breadboard processor for the ESA remote sensing satellite synthetic aperature radar
[REPT-00-0778] N86-13911
Real time large memory optical pattern recognition
[AD-A158023] N86-14034

RECOGNITION
Sorption detector system for chemical agents detection and recognition
[DE85-012775] N86-13400

REDUCED GRAVITY
The scanning electron microscope as a tool in space biology N86-14080
Solid waste treatment processes for space station N86-14091

REDUCTION (CHEMISTRY)
Role of additives in minimizing zinc electrode shape change: The effect of lead on the kinetics of Zn(2) reduction in concentrated alkaline media
[AD-A158806] N86-13395

REENTRY VEHICLES
Ultrasonic longitudinal wave velocity in carbon-carbon Pitch and Pitch/M2 shape stable nosetip material from 70 deg'F to 5400 deg F
[DE85-017330] N86-13382

REFLECTANCE
A durable airfield marking system
[AD-A157953] N86-13339
Extremely high reflective capability of zirconium burning in air under effects of constant CO2 laser radiation
N86-13452
Fundamental remote sensing science research program: The Scene Radiation and Atmospheric Effects Characterization Project
[E86-10011] N86-13794
Reflectance modeling N86-13795
Bidirectional reflectance modeling of non-homogeneous plant canopies N86-13796
Understanding the radiant scattering behavior of vegetated scenes N86-13797
Geometric-optical modeling of a conifer forest canopy
N86-13799
Crop characteristics research: Growth and reflectance analysis N86-13800
Ground reflectance measurements from thematic mapper data N86-13801
Thermal infrared geologic remote sensing research at the Jet Propulsion Laboratory N86-13802
Atmospheric and science complexity effects on surface bidirectional reflectance N86-13803
Atmospheric effect on remote sensing of the Earth's surface N86-13804
The characterization of surface varigation effects on remote sensing N86-13805
Discrete random media techniques for microwave modeling of vegetated terrain N86-13809
Pre-stack Kirchhoff inversion of common offset data
[AD-A158205] N86-13932
Spectral reflectance of surface soils: Relationships with some soil properties N86-14089
Computation of reflection of solar radiation from vegetation cover by Monte-Carlo method N86-14177
Reflection indicatrices of vegetation canopies
N86-14178
Application of statistical model of layered medium for computing thermal emission of ice covers N86-14186
Use of Goudriaan model for studying reflection regularities in vegetation-soil system in optical range. 1: Influence of phytometric parameters on spectral brightness coefficients N86-14190

REFLECTION
A family of curves for the rough surface reflection coefficient
[AD-A158195] N86-13876

REFRACTIVITY
Recent experience in the RAE (Royal Aircraft Establishment) 5-metre wind tunnel of a china clay method for indicating boundary layer transition
[AD-A157943] N86-13302
Spray characterization using phase angle detection
N86-13577

REFRACTORY MATERIALS
Static fatigue of a sintered silicon nitride
[AD-A158813] N86-13760

REGENERATIVE COOLING
Rocket engine hot-spot detector
[NASA-CR-171902] N86-13708

REGIONS
Marginal ice zone bibliography
[AD-A159060] N86-13764

REGISTERS (COMPUTERS)
Sparse elimination on vector multiprocessors
[AD-A158274] N86-13909

REGRESSION ANALYSIS
A note on the effect of ignoring small measurement errors in precision instrument calibration
[AD-A159104] N86-13713

REGULATORS
Further results for application of disturbance minimization control techniques to a linear, time-invariant, second-order state set-point regulator problem
[AD-A157793] N86-13961

REINFORCEMENT (STRUCTURES)
Simulating distributed reinforcement effects in concrete analysis
[DE85-009745] N86-13761

REINFORCING FIBERS
Zirconium as a structural material for naval systems
[AD-A158201] N86-13411

REINFORCING MATERIALS
Effect of geometry of fiber packing on consolidation of fibrous composition materials with porous matrix
N86-13443

RELATIVITY
Theory of resistivity-gradient-driven turbulence
[DE85-015068] N86-14053

RELAXATION (MECHANICS)
Multilevel relaxation phenomena and population trapping
[DE85-011527] N86-13731

RELIABILITY
Low power reactor for remote applications
[DE85-012763] N86-14032

REMOTE SENSING
Two-proton detection techniques for atomic fluorine
N86-13569
Remote optical crack sensing system
[AD-D011872] N86-13718
Aerial laser sensing of ocean upper layer N86-13775
Fundamental remote sensing science research program: The Scene Radiation and Atmospheric Effects Characterization Project
[E86-10011] N86-13794
Understanding the radiant scattering behavior of vegetated scenes N86-13797
Geometric-optical modeling of a conifer forest canopy
N86-13799
Crop characteristics research: Growth and reflectance analysis N86-13800
Thermal infrared geologic remote sensing research at the Jet Propulsion Laboratory N86-13802
Atmospheric and science complexity effects on surface bidirectional reflectance N86-13803
Atmospheric effect on remote sensing of the Earth's surface N86-13804
The characterization of surface varigation effects on remote sensing N86-13805
Multidimensional modeling of atmospheric effects and surface heterogeneities on remote sensing N86-13806
Remote sensing of Earth terrain N86-13808
Discrete random media techniques for microwave modeling of vegetated terrain N86-13809
Crop area estimation based on remotely-sensed data with an accurate but costly subsample
[NASA-CR-176017] N86-13814
VAS demonstration: (VISSR Atmospheric Sounder) description
[NASA-RP-1151] N86-13867
Identification of nuclear materials from remote detection of characteristic gamma rays
[AD-A159244] N86-14014
Pressure field retrieval by remote refractometry from space N86-14168
Computation of reflection of solar radiation from vegetation cover by Monte-Carlo method N86-14177
Reflection indicatrices of vegetation canopies
N86-14178
Methods for complex space experiment in USSR for studying land from manned spacecraft N86-14181
Role of landscape research in development of space methods for studying Earth N86-14184
Analysis of survey conditions and effect of noise on quality of sensing of soil formations N86-14191
Normalization of response of radiometric instrumentation for studying Earth's natural resources
N86-14192
Remote temperature determination of terrestrial covers from polarization invariant of microwave-radiothermal emission N86-14196

REMOTE SENSORS
Development of a breadboard cooler for infrared remote sensing payloads, phase 2 --- spacecraft payloads
[FOK-RV-R-82-072] N86-13725

REMOVAL
Mass transfer coefficients and Henry's constants for packed-tower air stripping of volatile organics: Measurements and correlation
[AD-A158811] N86-13375

RENDEZVOUS SPACECRAFT
Comments on anniversary of Apollo-Soyuz flight
N86-14197

REPORTS
Report on the findings of the Japanese Investigative Team on US Space Station Design (Keidanren)
[NASA-TM-77659] N86-13356
Results of research in four topic areas: The singularity expansion method, transient scattering measurements, high-frequency diffraction at edges residing on interfaces and cylindrical coordinate representation of dyadic Green's functions
[AD-A158382] N86-14037
The 1983 NASA/ASEE Summer Faculty Fellowship Research Program research reports
[NASA-CR-171904] N86-14078

REQUIREMENTS
Information requirements determination: An empirical investigation of obstacles within an individual
[AD-A158025] N86-13901

RESCUE OPERATIONS
Tradeoff analysis of technology needs for public service helicopters
[NASA-CR-3927] N86-13317

RESEARCH
Agile Electromagnetics Exploiting High Speed Logic (AEEHSL)
[AD-A158380] N86-13630
Results of research in four topic areas: The singularity expansion method, transient scattering measurements, high-frequency diffraction at edges residing on interfaces and cylindrical coordinate representation of dyadic Green's functions
[AD-A158382] N86-14037
Scientific activities of the Polish Academy of Sciences: Institute of Fundamental Technological Research in 1983
[ISBN-83-01-06288-6] N86-14107

RESEARCH AND DEVELOPMENT
Report on the findings of the Japanese Investigative Team on US Space Station Design (Keidanren)
[NASA-TM-77659] N86-13356
The 1985 AFOSR/AFRPL Chemical Rocket Research Meeting, abstracts and agenda
[AD-A158291] N86-13507
Worldwide report: Telecommunications policy, research, and development
[JPRS-TTP-85-026] N86-13640
Bulk CMOS VLSI technology studies. Part 5: The design and implementation of a high speed integrated circuit functional tester
[AD-A158370] N86-13651
Activities report of the Technical and Scientific Research Center for the Metal Manufacturing Industry N86-13740
Aquatic plant control research program: Evaluation of polymers for controlled delivery of herbicides for aquatic plant control
[AD-A157948] N86-13843
Operation of large cryogenic systems
[DE85-017439] N86-14025
Fusion programs in applied plasma physics and development and technology, fiscal 1984
[DE85-014551] N86-14062
The 1983 NASA/ASEE Summer Faculty Fellowship Research Program research reports
[NASA-CR-171904] N86-14078
European Science Notes. Volume 39, number 9
[AD-A158278] N86-14109

RESERVOIRS
The Vaiont Slide. A geotechnical analysis based on new geologic observations of the failure surface. Volume 1: Main text
[AD-A158192] N86-13854
The Vaiont Slide. A geotechnical analysis based on new geologic observations of the failure surface. Volume 2: Appendices A through G
[AD-A158193] N86-13855

RESIDUAL STRESS
Neutron stress measurements with a position sensitive detector
[AD-A158882] N86-13712
High frequency quantitative analysis of magnetomechanical acoustic emission
[AD-A158222] N86-13750

RESIN MATRIX COMPOSITES
Polymer, metal and ceramic matrix composites for advanced aircraft engine applications
[NASA-TM-87132] N86-13407

RESONANCE
Size and shape characterization of individual flowing droplets by laser light scattering N86-13579
The (58)Ni + n transmission, capture and differential elastic scattering data analysis in the resonance region
[DE85-016157] N86-14026

RESONANT FREQUENCIES
Resonant cars detection of OH radicals N86-13576

RESONANT VIBRATION
Transmission acoustic vibration testing
[AD-A159022] N86-13326

RESOURCES
USSR report: Energy
[JPRS-UEN-85-001] N86-13861

RESOURCES MANAGEMENT
Improving MILSATCOM (Military Satellite Communication) acquisition outcomes: Lease versus buy
[AD-A158842] N86-13348

RESPIRATION
Health hazard evaluation of liquid monopropellants. Phase 5: Comparative inhalation toxicities of LGP 1776, LGP 1845, and HAN (hydroxylammonium nitrate)
[AD-A159090] N86-13891

RETARDING
The suppression of afterburning in solid rocket plumes by potassium salts N86-13524

RETINA
Enhancing sensitivity to visual motion and enhancing visual sensitivity
[AD-A158800] N86-13889

RETROFITTING
Retrofit of a high power Nd:glass laser system with liquid crystal polarizers [DE85-014415] N86-13733

RETROREFLECTORS
Concept of laser locator systems (based on the geometry of the triangular corner cube reflector) [AD-A157795] N86-13728

REUSABLE LAUNCH VEHICLES
Aerothermodynamics for future launchers. Review of the state of the art in Europe [VKI-CR-1984-16/AR] N86-13347
Structures and materials technology issues for reusable launch vehicles [NASA-TM-87626] N86-13349

REVERSED FLOW
A three-dimensional analysis of natural convection in a toroidal loop N86-13672

REVISIONS
A variant of Shanbhag's lemma arising out of a modified Rao-Rubbin condition [AD-A158608] N86-13993

REYNOLDS NUMBER
Computer program for calculating flow parameters and power requirements for cryogenic wind tunnels [NASA-TM-87609] N86-13338
Transonic separated flow predictions based on a mathematically simple, nonequilibrium turbulence closure model [NASA-TM-86826] N86-13676
Waves which travel upstream in boundary layers [AD-A157949] N86-13684
Experiments with non-Darcy flow in joints with large scale roughness [DE85-015714] N86-13695

RHENIUM
A study of rhenium as an alternate substrate material for impregnated dispenser cathodes [AD-A159113] N86-13415

RIBBONS
European silicon structures plans custom chips in 15 days N86-13621

RIGID STRUCTURES
A computational analysis of pulsating flow in rigid and deformable tubes N86-13673
Computer program for post-flight analysis of rigid body moments acting on a launch vehicle first stage [NASA-CR-166033] N86-13918

RISK
Short range aids to navigation systems. Design manual for restricted waterways [AD-A158213] N86-13313
Approximation of the initial reserve for known ruin probabilities [AD-A158167] N86-13987

RIVERS
Experience in conducting subsatellite experiments with water bodies in USSR and Hungarian People's Republic N86-14182

ROBOTICS
Physical distribution system for aircraft external fuel tanks-survey [AD-A158275] N86-13324
USSR report: Machine tools and metalworking equipment [JPRS-UMM-85-014] N86-13742
Problems with integrating robots in conventional production N86-13744
USSR report: Machine tools and metalworking equipment [JPRS-UMM-85-013] N86-13745
Problems with robotization of conventional shops N86-13746
Study on design techniques for robots (space applications). Volume 1, part A: Technical results [FOK-TR-R-84-110-VOL-1-PT-A] N86-13902
Study on design techniques for robots (space applications). Volume 1, part B: Technical results [FOK-TR-R-84-110-VOL-1-PT-B] N86-13903
Study on design techniques for robots (space applications). Volume 2: Technical appendices [FOK-TR-R-84-110-VOL-2] N86-13904
Study on design techniques for robots (space applications). Volume 3: Executive summary [FOK-TR-R-84-110-VOL-3] N86-13905
Design and implementation of a compliant robot with force feedback and strategy planning software [NASA-TM-86111] N86-13947
Parameter identification for a robotic manipulator arm [NASA-CR-178002] N86-13959

ROBOTS
Italian robot manufacturer enters Spanish market N86-13626
New applications of industrial robots noted N86-13743
Robot control system modified for precision movement N86-13747
New robots by Soviet, CEMA manufacturers described N86-13748
Study on design techniques for robots (space applications). Volume 1, part A: Technical results [FOK-TR-R-84-110-VOL-1-PT-A] N86-13902
Study on design techniques for robots (space applications). Volume 1, part B: Technical results [FOK-TR-R-84-110-VOL-1-PT-B] N86-13903
Study on design techniques for robots (space applications). Volume 2: Technical appendices [FOK-TR-R-84-110-VOL-2] N86-13904
Study on design techniques for robots (space applications). Volume 3: Executive summary [FOK-TR-R-84-110-VOL-3] N86-13905
Design and implementation of a compliant robot with force feedback and strategy planning software [NASA-TM-86111] N86-13947
Multiresolution path planning for mobile robots [AD-A158630] N86-13948
Mobile robot localization using sonar [AD-A158819] N86-13949

ROCKET ENGINES
Erosion and onset mechanisms in magnetoplasmadynamic thrusters N86-13556
Magnetoplasmadynamic thruster erosion research N86-13557
Holographic study of the particles produced by the injector in a Viking motor [ISL-R-111/84] N86-13724
Experimental and theoretical studies of laser propulsion phenomenology [AD-A158273] N86-13729

ROCKET EXHAUST
Flame mechanisms and flame inhibition N86-13523
The suppression of afterburning in solid rocket plumes by potassium salts N86-13524

ROCKET NOZZLES
Application of molecular kinetics models to the prediction of backflow contamination N86-13531

ROCKET PROPELLANTS
The 1985 AFOSR/AFRPL Chemical Rocket Research Meeting, abstracts and agenda [AD-A158291] N86-13507
Electrolytic preparation of novel azidodinitro compounds N86-13508
Syntheis of difluoraminoxy-, difluoramino- or fluorodiazonium-containing materials N86-13509
Synthesis and reactivity of unsaturated metal nitrogen complexes N86-13512
New synthetic techniques for advanced propellant ingredients: Selective transformations and new structures N86-13514
Fluoropolyazido-esters as energetic polymers N86-13515
New energetic polymers as binders for propellants N86-13516
Physical and chemical consequences of antiaromaticity in the boracyclopentadiene system N86-13519

ROCKET SOUNDING
Observations of fluxes of cold ions from plasmasphere into ionosphere during nighttime in middle latitudes N86-14117

ROLL FORMING
Specifics of the process of failure of structural steels strengthened by thermo-mechanical working with deformation in the intercritical temperature interval N86-13464

ROOM TEMPERATURE
Equation of state of dense argon: A comparison of shock and static studies [DE85-015543] N86-14074

ROTARY STABILITY
HPOTP low-speed flexible rotor balancing, phase 1 [NASA-CR-171610] N86-13369

ROTARY WING AIRCRAFT
Assessment of aerodynamic and dynamic models in a comprehensive analysis [NASA-TM-86835] N86-13286
Tradeoff analysis of technology needs for public service helicopters [NASA-CR-3927] N86-13317

ROTARY WINGS
Standardised fatigue loading sequences for helicopter rotors (Helix and Felix). Part 2: Final definition of Helix and Felix [AD-A156622] N86-13322

ROTATING BODIES
Variable field effects for the rotating fluidized bed reactor N86-13565
Forming attainability sets in control of kinetic moment of rotating asymmetric solid body (special cases) N86-14113

ROTATING DISKS
Unsteady aerodynamics applied to the horizontal axis wind turbine disk N86-13825

ROTATING SPHERES
Investigation of characteristics of synoptic movements on sphere N86-13770

ROTATION
Aerofoil characteristics of rotating blades --- wind turbine models N86-13824
Fiber optics as an angular sensor [AD-D011886] N86-14044
Press conference on first stage of Vega project N86-14152

ROTOR AERODYNAMICS
Development in aerodynamic calculations --- wind energy converters N86-13822
Unsteady aerodynamics applied to the horizontal axis wind turbine disk N86-13825
Aerodynamic theory in the calculation of the GROWIAN rotor compared with some experimental data --- wind energy converter N86-13826
Aerodynamic performance of a new LM 17.2 m rotor --- wind energy converter N86-13827
Aerodynamic research on wind turbines at NLR N86-13828
Aerodynamic research efforts at SERI wind energy research center at Rocky Flats --- Solar Energy Research Institute (SERI) N86-13829

ROTOR LIFT
Preliminary report on in-flight measurement of rotor hub drag and lift using the RSRA [NASA-TM-86764] N86-13319

ROTOR SYSTEMS RESEARCH AIRCRAFT
Preliminary report on in-flight measurement of rotor hub drag and lift using the RSRA [NASA-TM-86764] N86-13319

ROTORCRAFT AIRCRAFT
Tradeoff analysis of technology needs for public service helicopters [NASA-CR-3927] N86-13317

ROTORS
Preliminary report on in-flight measurement of rotor hub drag and lift using the RSRA [NASA-TM-86764] N86-13319
HPOTP low-speed flexible rotor balancing, phase 1 [NASA-CR-171610] N86-13369
Aerodynamic theory in the calculation of the GROWIAN rotor compared with some experimental data --- wind energy converter N86-13826
First order estimates of the dynamics and energetics of a rapidly decelerating flywheel [DE85-013908] N86-13842

ROUGHNESS
Experiments with non-Darcy flow in joints with large scale roughness [DE85-015714] N86-13695
Scattering models and basic experiments in the microwave regime N86-13807

ROUTES
Routing method in computer aided customization of a two level automated universal array [AD-D011808] N86-13925

RUNWAYS
Abrasion behavior of aluminum and composite skin coupons, stiffened skins and stiffened panels representative of transport airplane structures [NASA-TP-2520] N86-13316
A durable airfield marking system [AD-A157953] N86-13339

RUPTURING
Macro- and microfractographic specifics of dissipated impact rupture of type 45 steel in the viscous-brittle transition interval N86-13466

RUTHENIUM
Relationships between electronic spectroscopy and electrochemistry. A probe of reorganisation energies [AD-A157940] N86-13389

S

S WAVES
The (58)Ni + n transmission, capture and differential elastic scattering data analysis in the resonance region [DE85-016157] N86-14026

SAFETY
Safe control systems and the VIPER microprocessor [AD-A156617] N86-13908

SAFETY DEVICES
Advanced emergency openings for commercial aircraft [NASA-TM-87580] N86-13305

SAFETY MANAGEMENT
NASA flight operations review [NASA-CR-176393] N86-13306

SAHARA DESERT (AFRICA)
Volcanoes discovered with radio beam N86-13777

SALICYLATES
Interaction between Escherichia coli and lunar fines N86-14088

SALINITY
Review of SERI solar pond work [DE85-012162] N86-13834

SALYUT SPACE STATION
List of recent Soviet space launches N86-14199

SAMPLES
Planetary sample rapid recovery and handling [NASA-CR-171906] N86-13342
Elastic-plastic deformation of a metal-matrix composite coupon with a center slot [NASA-CR-178013] N86-13496
A linear combination test for detecting serial correlation in multivariate samples [AD-A158179] N86-13967

SAMPLING
Decomposition of some well-known variance reduction techniques: Revision [AD-A158048] N86-13985
Monte Carlo analysis of nonlinear statistical models. 1. Theory: Revision [AD-A158613] N86-13990

SANDWICH STRUCTURES
Standardization program on design analysis and testing of inserts in nonmetallic sandwich components --- spacecraft components [TR-TS-RP-2-09-84] N86-13364
Production of multilayer magnetic surface of magnetically soft composite materials N86-13445

SATELLITE ATTITUDE CONTROL
Mathematical models of nonstationary eddy currents and eddy motions of fluid in spacecraft orientation and stabilization problems 1 N86-14133
Experimental checking of mathematical model of eddy currents in actuating components of systems for magnetic orientation of artificial Earth satellites and spacecraft N86-14164

SATELLITE CONTROL
Optimum control programs in problem of interorbital flight with continuous thrust N86-14135

SATELLITE IMAGERY
Methods for complex space experiment in USSR for studying land from manned spacecraft N86-14181
Experience in conducting subsatellite experiments with water bodies in USSR and Hungarian People's Republic N86-14182
Compilation of landscape maps at different scales with use of space photoinformation N86-14187
Use of space geological methods in seismotectonic research N86-14188
Engineering evaluation of crustal faults using space survey data N86-14189
Experiment for evaluating accuracy in determining land categories on space scanner photographs N86-14195

SATELLITE NETWORKS
Comparative study of space segments for the provision of future operational data relay satellite services [MBB-DSP-TN/DRS/132/84] N86-13355

SATELLITE OBSERVATION
Volcanoes discovered with radio beam N86-13777
Solar flare X-radiation and high-energy particles according to observational data from Venera-13 and Venera-14 automatic interplanetary stations N86-14119
Results of study of surface of five regions on Venus by bistatic radar method N86-14156
Pressure field retrieval by remote refractometry from space N86-14168

SATELLITE ORBITS
Report on active and planned spacecraft and experiments [NASA-TM-87499] N86-13343
List of recent Soviet space launches N86-14199

SATELLITE ORIENTATION
Mathematical models of nonstationary eddy currents and eddy motions of fluid in spacecraft orientation and stabilization problems 1 N86-14133
Experimental checking of mathematical model of eddy currents in actuating components of systems for magnetic orientation of artificial Earth satellites and spacecraft N86-14164

SATELLITE PERTURBATION
Integration of equations of motion for material point in gravitational field of axially symmetric planet N86-14131

SATELLITE ROTATION
Periodic regimes of rotational motion of solid body about liberation point L sub 4 in restricted elliptical three-body problem N86-14132

SATELLITE SOUNDING
Registry of heavy ions in auroral region during magnetic storms N86-14138

SATELLITE-BORNE INSTRUMENTS
Development of a breadboard cooler for infrared remote sensing payloads, phase 2 --- spacecraft payloads [FOK-RV-R-82-072] N86-13725

SATELLITE-BORNE PHOTOGRAPHY
Experience in complex mapping of natural resources in agrarian-industrial regions of Nonchernozem RSFSR using space photomaterials N86-14174
Possibilities of use of aerospace materials in predicting occurrence of petroleum and gas N86-14175
Problems in study and evaluation of consequences of forest fires using aerospace photographs N86-14176
Possibilities of using space survey for studying seasonal changes of landscapes in some regions of USSR N86-14183
Radiometric correction of materials of aerospace survey of Earth with MKF-6 camera: Methodology and use of results N86-14193

SCALARS
Modelling a transport equation of turbulent reactive mixing flow N86-13674

SCALE (CORROSION)
Current viewpoints on oxide adherence mechanisms [NASA-TM-87168] N86-13409

SCALE MODELS
Preliminary measurement of the noise from the 2/9 scale model of the Large-scale Advanced Propfan (LAP) propeller, SR-7A [NASA-TM-87116] N86-14006

SCALING LAWS
Scaling of uv (351 nm) fusion implosions driven by multiple beams [DE85-014406] N86-14068

SCANNERS
Precision pointing using a dual-wedge scanner [NASA-CR-3946] N86-13813

SCANNING
Macro- and microfractographic specifics of dissipated impact rupture of type 45 steel in the viscous-brittle transition interval N86-13466
Effects of digital altimetry on pilot workload [NASA-TM-86424] N86-13892

SCATTER PLATES (OPTICS)
Occasional reports of the Royal Observatory, Edinburgh, no. 16 [ISSN-0309-099-X] N86-14200
The plate scale of the U.K. Schmidt Telescope N86-14202

SCATTERING
Scattering models and basic experiments in the microwave regime N86-13807
A finite element solution of the transport equation [AD-A159245] N86-13982
Results of research in four topic areas: The singularity expansion method, transient scattering measurements, high-frequency diffraction at edges residing on interfaces and cylindrical coordinate representation of dyadic Green's functions [AD-A158382] N86-14037

SCATTERING COEFFICIENTS
Understanding the radiant scattering behavior of vegetated scenes N86-13797
Measurement and modeling of the optical scattering properties of crop canopies N86-13798
Active microwave properties of vegetation canopies N86-13812

SCATTERING CROSS SECTIONS
Differential scattering cross section and total extinction measurements on (CH)n spheres in 632.8 nm laser light [AD-A158044] N86-13391
Comparison of ion milling techniques for cross-sectional TEM of semiconductors [DE85-016596] N86-13664
Optical/infrared properties of atmospheric aerosols with an in situ, multi-wavelength, multichannel nephelometer system [AD-A158825] N86-13710
Fundamental remote sensing science research program: The Scene Radiation and Atmospheric Effects Characterization Project [E86-10011] N86-13794

SCAVENGING
Lightweight two-stroke cycle aircraft diesel engine technology enablement program, volume 1 [NASA-CR-174923-VOL-1] N86-13328
Lightweight two-stroke cycle aircraft diesel engine technology enablement program, volume 2 [NASA-CR-174923-VOL-2] N86-13329
Lightweight two-stroke cycle aircraft diesel engine technology enablement program, volume 3 [NASA-CR-174923-VOL-3] N86-13330
Oxidizing and scavenging characteristics of April rains: OSCAR data report [DE85-017014] N86-13844

SCENE ANALYSIS
Fundamental remote sensing science research program: The Scene Radiation and Atmospheric Effects Characterization Project [E86-10011] N86-13794
Understanding the radiant scattering behavior of vegetated scenes N86-13797
Atmospheric and science complexity effects on surface bidirectional reflectance N86-13803
Multidimensional modeling of atmospheric effects and surface heterogeneities on remote sensing N86-13806
Target tracking based scene analysis [AD-A158629] N86-13910

SCHMIDT TELESCOPES
Occasional reports of the Royal Observatory, Edinburgh, no. 16 [ISSN-0309-099-X] N86-14200
A multiple-object fibre-optics coupler for the 1.2-m UK Schmidt Telescope N86-14201
The plate scale of the U.K. Schmidt Telescope N86-14202
Design for a large altazimuth Schmidt telescope N86-14203

SCHROEDINGER EQUATION
Effective behavior of composite materials [AD-A158941] N86-13380

SCIENCE
Expanding your horizons in science and mathematics [NASA-CR-176372] N86-13958
European Science Notes. Volume 39, number 9 [AD-A158278] N86-14109

SCIENTIFIC SATELLITES
Report on the scientific satellites of the European Space Agency [ESA-SP-1072] N86-13344

SCOUT LAUNCH VEHICLE
Scout trajectory error propagation computer program [NASA-CR-166030] N86-13919

SEA ICE
Marginal ice zone bibliography [AD-A159060] N86-13764
Application of statistical model of layered medium for computing thermal emission of ice covers N86-14186

SEA LEVEL
Latitude measurements of cosmic radiation intensity in stratosphere and at sea level on marine antarctic expeditions N86-13792

SEA STATES
An investigation into the vertical axis control power requirements for landing VTOL type aircraft onboard nonaviation ships in various sea states [NASA-CR-176355] N86-13294

SEA SURFACE TEMPERATURE
Equatorial waves in ocean surface temperature field according to data from shipboard and satellite measurements N86-14171

SEA TRUTH
Experience in conducting subsatellite experiments with water bodies in USSR and Hungarian People's Republic N86-14182

SEA WATER
Variable temperature trap [AD-D011874] N86-13719
The influence of oceanic chemistry, physics and biology on atmospheric carbon dioxide N86-13865

SEARCHING
Tradeoff analysis of technology needs for public service helicopters [NASA-CR-3927] N86-13317
Multiresolution path planning for mobile robots [AD-A158630] N86-13948

SECONDARY EMISSION
Formation of high-energy secondary electrons in low-density medium at great altitudes N86-14122

SECONDARY FLOW
Double-branched vortex generator [NASA-TM-88201] N86-13298

SEDIMENT TRANSPORT
User's manual for the generalized computer program system. Open-channel flow and sedimentation, TABS-2. Main text [AD-A159249] N86-13692

SEDIMENTS
Pore pressure response to probe insertion and thermal gradient: ISIMU-2. (in situ heat transfer experiment) [AD-A158592] N86-13689
User's manual for the generalized computer program system. Open-channel flow and sedimentation, TABS-2. Main text [AD-A159249] N86-13692
Highly disperse minerals in sediments in neighborhood of East Pacific Ocean rise determined from drilling data N86-13773

SEISMIC WAVES
Characteristics of microearthquakes accompanying hydraulic fracturing as determined from studies of spectra of seismic waveforms
[DE85-009558] N86-13860
SEISMOLOGY
Use of space geological methods in seismotectonic research N86-14188
SELECTIVE DISSEMINATION OF INFORMATION
Data catalog series for space science and applications flight missions. Volume 4A: Descriptions of meteorological and terrestrial applications spacecraft and investigations
[NASA-TM-87501] N86-13869
SELENIDES
Charge-density waves observed with a tunneling microscope
[AD-A158779] N86-13709
SELF DIFFUSION (SOLID STATE)
Effective behavior of composite materials
[AD-A158941] N86-13380
SEMICONDUCTING FILMS
MBE growth of CdTe and Hg (1-x) Cd (x) Te films and multilayer structures
[AD-A158267] N86-14073
SEMICONDUCTOR DEVICES
Thomson, CNET of France in silicon-on-insulator research N86-13612
Philips develops MBE process for laser, chip manufacture N86-13614
New digital circuits at Thomson semiconductor in France N86-13619
SEMICONDUCTOR JUNCTIONS
AuGa2 on GaSb(001): An epitaxial, thermodynamically stabilized Metal/3-5 compound semiconductor interface
[AD-A157937] N86-14071
SEMICONDUCTORS (MATERIALS)
Certain features of laser destruction and dislocational structure of silicon during heating and effects of electrical field N86-13454
Excimer laser produces .2 micron semiconductor structures N86-13613
Luminescent properties of semiconductor electrodes
[AD-A158841] N86-13655
Comparison of ion milling techniques for cross-sectional TEM of semiconductors
[DE85-016596] N86-13664
Electrical research on solar cells and photovoltaic materials
[NASA-CR-176384] N86-13838
Application of cross-sectional transmission electron microscopy to the characterization of ion-implanted semiconductors
[DE85-010990] N86-14075
SENSITIVITY
Development of high sensitivity X-ray and electron beam resist processes
[AD-A158968] N86-13657
Enhancing sensitivity to visual motion and enhancing visual sensitivity
[AD-A158800] N86-13889
Speckle image reconstruction. Appendix 1
[AD-A158271] N86-14207
SEPARATED FLOW
Transonic separated flow predictions based on a mathematically simple, nonequilibrium turbulence closure model
[NASA-TM-86826] N86-13676
SEPARATION
Current viewpoints on oxide adherence mechanisms
[NASA-TM-87168] N86-13409
SEPARATORS
An Oil/Water disperser device for use in an oil content Monitor/Control system
[AD-D011868] N86-13714
Oil content Monitor/Control system and method
[AD-D011871] N86-13717
SERIES (MATHEMATICS)
Applications of differential phase statistics to studies of C3 and spread spectrum communications
[AD-A158815] N86-13633
A linear combination test for detecting serial correlation in multivariate samples
[AD-A158179] N86-13967
A note on the integrated Cauchy functional equation
[AD-A158269] N86-13977
SERVICE MODULES
Review of implications and usefulness of spacecraft servicing in Low Earth Orbit (LEO)
[MATRA-092/CC/AB/225-84] N86-13350
SERVOMECHANISMS
Digital servocontroller system. Volume 4. Results and conclusions
[AD-A159068] N86-13335
SET THEORY
Computation of geometric properties from the medial axis transform in 0 (n log n) time
[AD-A158934] N86-13980
Forming attainability sets in control of kinetic moment of rotating asymmetric solid body (special cases)
N86-14113
SEYFERT GALAXIES
Detection of Ni 2 lambda 7378 in six Seyfert galaxies
[NASA-CR-176358] N86-14205
SHADOWS
Multigrid relaxation methods and the analysis of lightness, shading, and flow
[AD-A158173] N86-14036
SHALLOW WATER
Ray transmissions over a sloping bottom in shallow water
[AD-A158017] N86-14008
SHAPED CHARGES
Short presentation and evaluation of studies on the penetration of jets from hollow shaped charges in compressible materials
[ISL-NB-402/84] N86-13586
SHAPES
Size and shape characterization of individual flowing droplets by laser light scattering N86-13579
Generating and generalizing models of visual objects
[AD-A158197] N86-13894
Codon constraints on closed 2D shapes
[AD-A158744] N86-13979
Multigrid relaxation methods and the analysis of lightness, shading, and flow
[AD-A158173] N86-14036
SHEAR FLOW
Studies of the flow field near a NACA 4412 aerofoil at nearly maximum lift
[AD-A157750] N86-13301
Numerical simulations of asymmetric mixing in planar shear flows
[AD-A158024] N86-13687
Formation of structure of mixed region under influence of shear flow in stratified fluid N86-13768
SHEAR LAYERS
Numerical simulations of asymmetric mixing in planar shear flows
[AD-A158024] N86-13687
SHEAR STRAIN
Elastic-plastic deformation of a metal-matrix composite coupon with a center slot
[NASA-CR-178013] N86-13496
SHEAR STRENGTH
Calculation of failure constant for titanium alloys
N86-13474
SHEAR STRESS
Non-Newtonian flow past curved external surfaces
N86-13671
SHIELDING
Cassegrain reflector sidelobe reduction study
[AD-A158625] N86-13631
SHIPS
An investigation into the vertical axis control power requirements for landing VTOL type aircraft onboard nonaviation ships in various sea states
[NASA-CR-176355] N86-13294
Short range aids to navigation systems. Design manual for restricted waterways
[AD-A158213] N86-13313
Determining quasi-real-time location of ships using geostationary navigational satellites N86-14165
Organization of space navigation system based on use of geostationary satellites N86-14166
SHOCK LOADS
Superhard materials developed N86-13471
SHOCK SPECTRA
Hybrid simulation codes with application to shocks and upstream waves
[NASA-CR-176365] N86-13702
SHOCK TESTS
A parametric study of the Ibrahim time domain modal identification algorithm N86-13588
SHOCK TUBES
Reaction intermediates in aromatic fuel combustion
[AD-A158029] N86-13390
SHOCK WAVES
Temperature and pressure components of shock-induced changes in the electronic spectrum of carbon disulfide
[AD-A158627] N86-13373
Condensed matter at high shock pressures
[DE85-016443] N86-13399
Shock waves, increase of entropy and loss of information
[DE85-013645] N86-13701
Experimental and theoretical studies of laser propulsion phenomenology
[AD-A158273] N86-13729
A functional equation governing moving phase boundaries in an elastic bar
[AD-A158178] N86-13757
Uniformly high-order accurate non-oscillatory schemes 1
[AD-A158177] N86-13966
SHORAN
Short range aids to navigation systems. Design manual for restricted waterways
[AD-A158213] N86-13313
SHUTTLE PALLET SATELLITES
In-orbit technology demonstration program (TDP). Accommodation study: SPAS
[MBB-URV-147/84] N86-13351
SIDELOBES
Cassegrain reflector sidelobe reduction study
[AD-A158625] N86-13631
SIGNAL ANALYSIS
Discussion on the Vibration Process Standards 9958002 and 9958004
[DE85-017116] N86-13599
SIGNAL DETECTION
The evaluation of failure detection and isolation algorithms for restructurable control
[NASA-CR-177983] N86-13310
Intelligent laser diffraction instrumentation for particle size analysis N86-13581
SIGNAL DETECTORS
Phase lock acquisition system
[AD-D011804] N86-13646
SIGNAL DISTORTION
Signal processing of anthropometric data N86-14105
SIGNAL GENERATORS
Feasibility study of chirp generator for ERS-1 radar altimeter, option A
[ELAB-STF44-F83103] N86-13368
SIGNAL PROCESSING
China report: Science and technology
[JPRS-CST-85-020] N86-13600
Scheme for high-speed real-time DFT operation for radar signal processing N86-13602
Rectification and registration of remotely sensed data
[AD-A158827] N86-13711
Exploratory development on advanced eddy current coil excitation and signal processing
[AD-A159228] N86-13752
DIESS: A prolog implementation of a domain-independent expert system shell
[AD-A158014] N86-13928
Adaptive detection in nonstationary interference: Part 1 and part 2
[AD-A158810] N86-13993
Hardware upgrade for klystrons in the SLC
[DE85-014357] N86-14029
Signal processing of anthropometric data N86-14105
SIGNAL TO NOISE RATIOS
An alternate derivation of the distribution of the conditioned signal-to-noise ratio
[AD-A158257] N86-13971
Analysis of survey conditions and effect of noise on quality of sensing of soil formations N86-14191
SILICIDES
Silicide coatings for protecting titanium-niobium alloys from high-temperature oxidation N86-13476
SILICON
Influence of degree of deformation on structure and properties of naturally aged alloy 1163 N86-13431
Certain features of laser destruction and dislocational structure of silicon during heating and effects of electrical field N86-13454
European silicon structures plans custom chips in 15 days N86-13621
Potential for use of indium phosphide solar cells in the space radiation environment
[NASA-TM-87157] N86-13645
Positron diffusion in Si
[DE85-014831] N86-14076
SILICON ALLOYS
Structure formation in silumins upon rapid crystallization N86-13427
Influence of alloying elements and impurities on mechanical properties of complex silumins N86-13428
Preliminary annealing on crystallization of amorphous Fe80Si6B14 alloy N86-13433
SILICON CARBIDES
Analytical electron microscopy of surface modified ceramics
[DE85-016309] N86-13499
Preparation of ceramic fiber-ceramic matrix composites by a faster chemical vapor infiltration process
[DE85-016402] N86-13500
SILICON FILMS
Thomson, CNET of France in silicon-on-insulator research N86-13612

SILICON JUNCTIONS
New digital circuits at Thomson semiconductor in France N86-13519
SILICON NITRIDES
Fractured toughness of Si3N4 measured with short bar chevron-notched specimens [NASA-TM-87153] N86-13495
Static fatigue of a sintered silicon nitride [AD-A158813] N86-13760
SILVER
Muon spin relaxation study of exchange coupling in dilute AgMn alloys [DE85-014104] N86-13419
Photodegradation studies of silver-backed polyacrylonitrile (PAN) films [DE85-012154] N86-13501
SILVER ZINC BATTERIES
Role of additives in minimizing zinc electrode shape change: The effect of lead on the kinetics of Zn(2) reduction in concentrated alkaline media [AD-A158806] N86-13395
SIMULATION
An investigation into the vertical axis control power requirements for landing VTOL type aircraft onboard nonaviation ships in various sea states [NASA-CR-176355] N86-13294
A preliminary evaluation of the generalized likelihood ratio for detecting and identifying control element failures in a transport aircraft [NASA-TM-87620] N86-13332
Pitch rate versus G command as the longitudinal flight control system design strategy for a statistically unstable fighter type aircraft with two control surfaces [AD-A158803] N86-13334
Investigation of the vertical-flow aquifer thermal energy storage concept and numerical simulation of the Dorigny field experiment [DE85-014524] N86-13694
Hybrid simulation codes with application to shocks and upstream waves [NASA-CR-176365] N86-13702
Simulating distributed reinforcement effects in concrete analysis [DE85-009745] N86-13761
The mission oriented terminal area simulation facility [NASA-TM-87621] N86-13944
Random errors in the magnetic field coefficients of superconducting magnets [DE85-012261] N86-14004
Aspects of three field approximations: Darwin, frozen, EMPULSE [DE85-014204] N86-14020
Variable curvature phantom [DE85-014260] N86-14028
Electromagnetic particle-in-cell plasma simulation [DE85-031223] N86-14054
Implicit plasma simulation [DE85-016088] N86-14055
Use of Goudriaan model for studying reflection regularities in vegetation-soil system in optical range. 1: Influence of phytometric parameters on spectral brightness coefficients N86-14190
SINGLE CRYSTALS
On anisotropy of mean electrical resistance of beryllium N86-13436
Certain features of laser destruction and dislocational structure of silicon during heating and effects of electrical field N86-13454
SINGULARITY (MATHEMATICS)
Development of singularities in nonlinear viscoelasticity [AD-A158190] N86-13758
SINTERING
Ceramics based on aluminum nitride and metals N86-13456
Probability of detection of internal voids in structural ceramics using microfocus radiography [NASA-TM-87164] N86-13749
Static fatigue of a sintered silicon nitride [AD-A158813] N86-13760
SITES
Design criteria upgrade for US Army Type 2 air traffic control towers [AD-A159115] N86-13314
SIZE DETERMINATION
Single particle sizing by measurement of Brownian motion N86-13584
SIZE DISTRIBUTION
Size and shape characterization of individual flowing droplets by laser light scattering N86-13579
Spray characterization with a nonintrusive optical single particle counter N86-13580
SKID LANDINGS
Abrasion behavior of aluminum and composite skin coupons, stiffened skins and stiffened panels representative of transport airplane structures [NASA-TP-2520] N86-13316
SKIN (STRUCTURAL MEMBER)
Abrasion behavior of aluminum and composite skin coupons, stiffened skins and stiffened panels representative of transport airplane structures [NASA-TP-2520] N86-13316
SKY BRIGHTNESS
Bidirectional reflectance modeling of non-homogeneous plant canopies N86-13796
SLEEP
Endocrine and fluid metabolism in males and females of different ages after bedrest, acceleration and lower body negative pressure [NASA-TM-58270] N86-13886
SLENDER CONES
Behavior of slender cones at large incidences N86-13707
SLITS
Subcritical crack development under constant load in VT6 alloy N86-13475
SLOPES
An analytical comparison of three visual approach slope indicators: VASIS, T-VASIS and PAPI [ARL/SYS-R-33] N86-13309
Ray transmissions over a sloping bottom in shallow water [AD-A158017] N86-14008
SLOTS
Elastic-plastic deformation of a metal-matrix composite coupon with a center slot [NASA-CR-178013] N86-13496
Slot line tunable bandpass filter [AD-D011881] N86-13661
SLURRIES
Combustion behavior of free boron slurry droplets [AD-A158620] N86-13585
SMOKE
Investigation of cold colored smoke production [AD-A158783] N86-14040
SNEAK CIRCUIT ANALYSIS
Graph theoretic approaches to diagnostics: Applications of logic programming and cutset theory to aspects of reactor and circuit analysis [ANL-84-74] N86-13912
SNOW COVER
Remote sensing of Earth terrain N86-13808
SODAR
Experience in measuring mean wind velocity profile in lower troposphere by sodar anemometer under inversion and convective conditions N86-13782
SODIUM
Influence of sodium on mechanical and casting properties of magnesium-lithium alloys N86-13457
SODIUM CARBONATES
Solvent extraction of plutonium (IV) polymer by organophosphorous compounds [DE85-013229] N86-13502
SOFTWARE ENGINEERING
Experiences with Cray multi-tasking [NASA-TM-88200] N86-13916
SOIL MAPPING
Use of Goudriaan model for studying reflection regularities in vegetation-soil system in optical range. 1: Influence of phytometric parameters on spectral brightness coefficients N86-14190
Analysis of survey conditions and effect of noise on quality of sensing of soil formations N86-14191
SOIL MOISTURE
Computer-aided aerial radiometric surveying of soil moisture N86-13778
Discrete random media techniques for microwave modeling of vegetated terrain N86-13809
SOILS
Reflectance modeling N86-13795
Bidirectional reflectance modeling of non-homogeneous plant canopies N86-13796
Discrete random media techniques for microwave modeling of vegetated terrain N86-13809
Unusual occurrence of maghemite in soils developed on Knox group dolostones [DE85-017158] N86-13817
Changes in soil acidity due to natural processes and acid deposition [DE85-012103] N86-13845
Spectral reflectance of surface soils: Relationships with some soil properties N86-14089
Results from Vega atmosphere and soil studies N86-14151
Use of remote optical measurements in agriculture N86-14172
SOLAR ARRAYS
Solar concentrator degradation in Low Earth Orbit (LEO) N86-14102
SOLAR CELLS
Potential for use of indium phosphide solar cells in the space radiation environment [NASA-TM-87157] N86-13645
Development of stable high efficiency polycrystalline thin-film solar cells based on CuInSe2 [DE85-000517] N86-13837
Electrical research on solar cells and photovoltaic materials [NASA-CR-176384] N86-13838
Solar concentrator degradation in Low Earth Orbit (LEO) N86-14102
Development of the VOLT-A shuttle experiment [NASA-TM-87169] N86-14110
SOLAR COLLECTORS
Wind loading on solar collectors [DE85-012151] N86-13833
Microstructural and mechanical property evaluation of solar collectors [DE85-017038] N86-13839
Small solar power systems plant in Almeria system evaluation and comparison on thermal basis [DE85-017185] N86-13840
SOLAR COSMIC RAYS
Dependence of length of free path of flare particles on energy N86-14141
SOLAR ENERGY
Review of SERI solar pond work [DE85-012162] N86-13834
SOLAR FLARES
Spectrum of photoelectrons in Earth's upper atmosphere during solar flares N86-14118
Solar flare X-radiation and high-energy particles according to observational data from Venera-13 and Venera-14 automatic interplanetary stations N86-14119
Dependence of length of free path of flare particles on energy N86-14141
SOLAR MAGNETIC FIELD
Magnetic field determination in quiescent solar prominences from polarization characteristics of radiated light N86-14125
SOLAR PONDS (HEAT STORAGE)
Review of SERI solar pond work [DE85-012162] N86-13834
SOLAR POSITION
Bidirectional reflectance modeling of non-homogeneous plant canopies N86-13796
SOLAR PROMINENCES
Sudden disappearance of quiescent prominences N86-14124
Magnetic field determination in quiescent solar prominences from polarization characteristics of radiated light N86-14125
SOLAR PROTONS
Dependence of length of free path of flare particles on energy N86-14141
SOLAR RADIATION
Ground reflectance measurements from thematic mapper data N86-13801
Computation of reflection of solar radiation from vegetation cover by Monte-Carlo method N86-14177
Analysis of survey conditions and effect of noise on quality of sensing of soil formations N86-14191
SOLAR RADIO EMISSION
Sudden disappearance of quiescent prominences N86-14124
SOLAR REFLECTORS
Photodegradation studies of silver-backed polyacrylonitrile (PAN) films [DE85-012154] N86-13501
SOLAR SEA POWER PLANTS
Performance assessment of OTEC power systems and thermal power plants. Volume 2: Users manual for PACC-OTECs [DE85-016792] N86-13835
Far-field model of the regional influence of affluent plumes from Ocean Thermal Energy Conversion (OTEC) plants [DE85-016981] N86-13836
SOLAR SENSORS
Sun acquisition sensor for European Communications Satellite N86-13366
SOLAR SIMULATORS
Photodegradation studies of silver-backed polyacrylonitrile (PAN) films [DE85-012154] N86-13501
SOLAR SPECTRA
Magnetic field determination in quiescent solar prominences from polarization characteristics of radiated light N86-14125
SOLAR TERRESTRIAL INTERACTIONS
Spectrum of photoelectrons in Earth's upper atmosphere during solar flares N86-14118

Spatial patterns of manifestation of solar activity in troposphere N86-14126
Mechanism of corpuscular-atmospheric relationships N86-14127

SOLAR WIND
Theoretical studies and data analysis of wave propagation in random media [AD-A158775] N86-13632
Electron microscopic observations of hydrogen implantation in ilmenites N86-14081

SOLAR WIND VELOCITY
Observation of small-scale solar wind structure on front of sharp increase in plasma flow velocity N86-14142

SOLAR X-RAYS
Solar flare X-radiation and high-energy particles according to observational data from Venera-13 and Venera-14 automatic interplanetary stations N86-14119

SOLDERED JOINTS
Technique of assembling structures using vapor phase soldering [AD-D011805] N86-13410

SOLDERING
Technique of assembling structures using vapor phase soldering [AD-D011805] N86-13410

SOLID ELECTROLYTES
Method of synthesizing polymers from a solid electrolyte [DE85-011623] N86-13504

SOLID PHASES
Effect of geometry of fiber packing on consolidation of fibrous composition materials with porous matrix N86-13443
Silicide coatings for protecting titanium-niobium alloys from high-temperature oxidation N86-13476

SOLID PROPELLANT COMBUSTION
Deuterium isotope effects in RDX decomposition and combustion processes N86-13522
High pressure solid propellant combustion zone structure from analysis of hydroxyl radical chemiluminescence N86-13529
Evaluation of HMX propellant chemistry from Raman and laser induced fluorescence species and temperature measurements N86-13530
Fuel-rich solid propellant boron combustion N86-13536

SOLID PROPELLANT ROCKET ENGINES
The suppression of afterburning in solid rocket plumes by potassium salts N86-13524
Rocket motor flow-turning losses N86-13545
Overview: AFOSR interests in rocket propulsion N86-13546
Interaction of multi-dimensional mean and acoustic fields in solid rocket combustion chambers N86-13547
Linear and saturated absorption of laser radiation in heated cases N86-13551

SOLID PROPELLANTS
Crushing strength of aluminum oxide agglomerates [AD-A158051] N86-13756

SOLID ROCKET BINDERS
Stability of RDX, AP and BTTN near room temperature N86-13535

SOLID ROCKET PROPELLANTS
Evaluation of HMX propellant chemistry from Raman and laser induced fluorescence species and temperature measurements N86-13530
Stability of RDX, AP and BTTN near room temperature N86-13535
Crack growth behavior in a composite propellant with strain gradients N86-13537
Nonlinear modeling and method of predicting crack growth N86-13538
High-resolution movies of propellant deflagration N86-13539
Wide distribution propellants N86-13540
Coupling between velocity oscillations and solid propellant combustion N86-13541
Flame-acoustic wave interaction during axial solid rocket instabilities N86-13542
Mechanisms for acoustic suppression N86-13543
Flow field effects on combustion instability N86-13544
Overview: AFOSR interests in rocket propulsion N86-13546
Application of atomic fluorescence to measurement of combustion temperatures in solid propellants N86-13582

SOLID STATE DEVICES
Electronic detection of low concentrations of organophosphorus compounds with a solid state device utilizing supported copper + cuprous oxide island films [AD-A158181] N86-13392
Joint services electronics program [AD-A158731] N86-13652

SOLID WASTES
Solid waste treatment processes for space station N86-14091

SOLIDIFICATION
Experimental investigation of magnesium combustion in steam [AD-A159109] N86-13396
A study of transport phenomena and interface stability during solidification of binary solutions using front tracking finite elements N86-13669

SOLIDS
Effective medium theory for partially saturated porous solids [DE85-016608] N86-13598
A functional equation governing moving phase boundaries in an elastic bar [AD-A158178] N86-13757
Development of singularities in nonlinear viscoelasticity [AD-A158190] N86-13758
Numerical models for plasma-solid interactions in electrothermal mass accelerators [AD-A158637] N86-14052

SOLITARY WAVES
Rossby autosoliton N86-14158

SOLUBILITY
Mass transfer coefficients and Henry's constants for packed-tower air stripping of volatile organics: Measurements and correlation [AD-A158811] N86-13375

SOLUTIONS
Application of computers in analytical chemistry: Calculation of optimum acidity of reaction between metal ions and organic reagents in solution N86-13607

SOLVATION
Relationships between electronic spectroscopy and electrochemistry. A probe of reorganisation energies [AD-A157940] N86-13389

SOLVENT EXTRACTION
Solvent extraction of plutonium (IV) polymer by organophosphorous compounds [DE85-013229] N86-13502

SONAR
Mobile robot localization using sonar [AD-A158819] N86-13949

SOOT
Thermal radiation effects on combustion of condensed fuels N86-13387

SORPTION
Sorption detector system for chemical agents detection and recognition [DE85-012775] N86-13400

SOUND TRANSMISSION
Transmission acoustic vibration testing [AD-A159022] N86-13326
Ray transmissions over a sloping bottom in shallow water [AD-A158017] N86-14008

SOUND WAVES
Transmission acoustic vibration testing [AD-A159022] N86-13326
Flame-acoustic wave interaction during axial solid rocket instabilities N86-13542
Mechanisms for acoustic suppression N86-13543
Flow field effects on combustion instability N86-13544
Rocket motor flow-turning losses N86-13545
A functional equation governing moving phase boundaries in an elastic bar [AD-A158178] N86-13757

SOYUZ SPACECRAFT
List of recent Soviet space launches N86-14199

SPACE CHARGE
Close-spaced high temperature Knudsen flow [AD-A158280] N86-13831

SPACE COMMERCIALIZATION
Emerging aerospace technologies [NASA-TM-86837] N86-14213

SPACE DEBRIS
Crowding of the geostationary orbit [ESA-CR(P)-2050] N86-13346

SPACE FLIGHT
Comments on anniversary of Apollo-Soyuz flight N86-14197

SPACE MAINTENANCE
Review of implications and usefulness of spacecraft servicing in Low Earth Orbit (LEO) [MATRA-092/CC/AB/225-84] N86-13350
Space station preliminary design report [NASA-TM-87521] N86-13357
Study on design techniques for robots (space applications). Volume 1, part A: Technical results [FOK-TR-R-84-110-VOL-1-PT-A] N86-13902
Study on design techniques for robots (space applications). Volume 1, part B: Technical results [FOK-TR-R-84-110-VOL-1-PT-B] N86-13903
Study on design techniques for robots (space applications). Volume 2: Technical appendices [FOK-TR-R-84-110-VOL-2] N86-13904
Study on design techniques for robots (space applications). Volume 3: Executive summary [FOK-TR-R-84-110-VOL-3] N86-13905

SPACE NAVIGATION
Uniqueness conditions in evaluation of least squares method in nonlinear space navigation problems N86-14144

SPACE PERCEPTION
Describing surfaces [AD-A158940] N86-13937

SPACE PLASMAS
Hybrid simulation codes with application to shocks and upstream waves [NASA-CR-176365] N86-13702
FORTRAN plotting subroutines for the space plasma laboratory N86-14103
Development of the VOLT-A shuttle experiment [NASA-TM-87169] N86-14110
Observation of small-scale solar wind structure on front of sharp increase in plasma flow velocity N86-14142

SPACE PROBES
Vega-2 releases aerostat and lander at Venus N86-14150
Press conference on first stage of Vega project N86-14152

SPACE PROCESSING
Energy exchange of plants under weightlessness conditions N86-14162

SPACE SHUTTLE PAYLOADS
Report on active and planned spacecraft and experiments [NASA-TM-87499] N86-13343

SPACE SHUTTLES
Endocrine and fluid metabolism in males and females of different ages after bedrest, acceleration and lower body negative pressure [NASA-TM-58270] N86-13886
Computer graphics applications to crew displays N86-14104

SPACE SIMULATORS
Development and testing of a mouse simulated space flight model [NASA-CR-176359] N86-13878

SPACE STATIONS
Report on the findings of the Japanese Investigative Team on US Space Station Design (Keidanren) [NASA-TM-77659] N86-13356
Space station preliminary design report [NASA-TM-87521] N86-13357
Astrophysical payload accommodation on the space station [NASA-CR-178556] N86-13359
Two-phase heat transport systems: System definition, volume 1 --- space stations [ESA-CR(P)-2052] N86-13363
Human factors in space station architecture 1: Space station program implications for human factors research [NASA-TM-86702] N86-13900
Study on design techniques for robots (space applications). Volume 1, part A: Technical results [FOK-TR-R-84-110-VOL-1-PT-A] N86-13902
Study on design techniques for robots (space applications). Volume 1, part B: Technical results [FOK-TR-R-84-110-VOL-1-PT-B] N86-13903
Study on design techniques for robots (space applications). Volume 2: Technical appendices [FOK-TR-R-84-110-VOL-2] N86-13904
Study on design techniques for robots (space applications). Volume 3: Executive summary [FOK-TR-R-84-110-VOL-3] N86-13905
A study of some features of ac and dc electric power systems for a space station N86-14085
Control of space stations N86-14090
Solid waste treatment processes for space station N86-14091
Emerging aerospace technologies [NASA-TM-86837] N86-14213

SPACE SUITS
Mass loss of shuttle space suit orthofabric under simulated ionospheric atomic oxygen bombardment [NASA-TM-87149] N86-13899

SPACE TRANSPORTATION SYSTEM FLIGHTS
Atmospheric environment for Space Shuttle (STS-51D) [NASA-TM-86524] N86-13868

SPACE VEHICLE CHECKOUT PROGRAM
Assembly Integration Verification (AIV) test effectiveness study. Applicability of Spacelab approach for equipment and system test for Ariane-4 class satellites. Volume 1: Executive summary [ERNO-671/AIV-VOL-1] N86-13361

SPACEBORNE ASTRONOMY
Astrophysical payload accommodation on the space station
[NASA-CR-178556] N86-13359

SPACEBORNE EXPERIMENTS
Report on the scientific satellites of the European Space Agency
[ESA-SP-1072] N86-13344
EURECA: An introduction to Europe's free-flying retrievable carrier
[ESA-BR-30] N86-13352
Fluorine disposal N86-14095
Energy exchange of plants under weightlessness conditions N86-14162
Methods for complex space experiment in USSR for studying land from manned spacecraft N86-14181

SPACEBORNE PHOTOGRAPHY
Space applications in geology N86-14167

SPACECRAFT CABINS
Architect discusses space habitat designs N86-14161

SPACECRAFT CHARGING
Mathematical models of nonstationary eddy currents and eddy motions of fluid in spacecraft orientation and stabilization problems 1 N86-14133

SPACECRAFT COMMUNICATION
Improving MILSATCOM (Military Satellite Communication) acquisition outcomes: Lease versus buy
[AD-A158842] N86-13348

SPACECRAFT COMPONENTS
Thermal vacuum tests on a hinge actuator mechanism --- spacecraft component
[ESA-ESTL-067] N86-13360
Standardization program on design analysis and testing of inserts in nonmetallic sandwich components --- spacecraft components
[TR-TS-RP-2-09-84] N86-13364

SPACECRAFT CONFIGURATIONS
Space station preliminary design report
[NASA-TM-87521] N86-13357

SPACECRAFT CONTROL
Adaptive control of large space structures using recursive lattice filters
[NASA-CR-176402] N86-13358
Choice of optimum boundary conditions in speed optimization problem N86-14115
Comparison of energetics of optimum maneuvers and two-impulse maneuvers in some problems of motion from a point into orbit N86-14134

SPACECRAFT DESIGN
EURECA: An introduction to Europe's free-flying retrievable carrier
[ESA-BR-30] N86-13352
Space station preliminary design report
[NASA-TM-87521] N86-13357
Study of thermal analysis methods --- spacecraft
[GEC-MEL12.0539] N86-13362
Human factors in space station architecture 1: Space station program implications for human factors research
[NASA-TM-86702] N86-13900
Investigation of techniques for improving spacecraft thermal control software
[GEC-MEL42.0552] N86-13942
Architect discusses space habitat designs N86-14161

SPACECRAFT ENVIRONMENTS
Development and testing of a mouse simulated space flight model
[NASA-CR-176359] N86-13878
Endocrine and fluid metabolism in males and females of different ages after bedrest, acceleration and lower body negative pressure
[NASA-TM-58270] N86-13886
Human factors in space station architecture 1: Space station program implications for human factors research
[NASA-TM-86702] N86-13900
Biological life-support systems for long-duration space flights N86-14160

SPACECRAFT INSTRUMENTS
Development of instruments for Vega probes N86-14154

SPACECRAFT LUBRICATION
Activities report in space tribology
[ESA-ESTL-72] N86-13738

SPACECRAFT MANEUVERS
Choice of optimum boundary conditions in speed optimization problem N86-14115

SPACECRAFT MOTION
Stability of stationary motions of two tethered bodies in orbit under influence of gravitational and aerodynamic forces N86-14163

SPACECRAFT ORBITS
A priori guaranteed accuracy evaluation in determining spacecraft orbit by least squares method N86-14130

SPACECRAFT POWER SUPPLIES
Coupled radiation transport/thermal analysis of the radiation shield for a space nuclear reactor
[AD-A158180] N86-14022

SPACECRAFT RADIATORS
Two-phase heat transport systems: System definition, volume 1 --- space stations
[ESA-CR(P)-2052] N86-13363
Development of a breadboard cooler for infrared remote sensing payloads, phase 2 --- spacecraft payloads
[FOK-RV-R-82-072] N86-13725

SPACECRAFT STABILITY
Space station preliminary design report
[NASA-TM-87521] N86-13357
Mathematical models of nonstationary eddy currents and eddy movements of fluid in problems of orientation and stabilization of artificial Earth satellites and spacecraft 2 N86-14116
Mathematical models of nonstationary eddy currents and eddy motions of fluid in spacecraft orientation and stabilization problems 1 N86-14133
Stability of stationary motions of two tethered bodies in orbit under influence of gravitational and aerodynamic forces N86-14163
Experimental checking of mathematical model of eddy currents in actuating components of systems for magnetic orientation of artificial Earth satellites and spacecraft N86-14164

SPACECRAFT STRUCTURES
Investigation for the definition of a hydraulic multidegree of freedom vibration facility
[B-TF-1627] N86-13340
Polymer, metal and ceramic matrix composites for advanced aircraft engine applications
[NASA-TM-87132] N86-13407
An algorithm for simultaneous determination of modal frequencies and modal vectors of a dynamic impedance matrix
[ESA-CR(P)-2055] N86-13943

SPACECRAFT TRACKING
Report on active and planned spacecraft and experiments
[NASA-TM-87499] N86-13343

SPACECREW TRANSFER
Comments on anniversary of Apollo-Soyuz flight N86-14197

SPACELAB
Assembly Integration Verification (AIV) test effectiveness study. Applicability of Spacelab approach for equipment and system test for Ariane-4 class satellites. Volume 1: Executive summary
[ERNO-671/AIV-VOL-1] N86-13361

SPARK CHAMBERS
Hadron component of cosmic radiation at atmospheric depth 800 g/cm(2) in Energy Range 70 to 700 GeV N86-13793

SPARK IGNITION
Report on investigation of alcohol combustion associated wear in spark ignition engines, mechanisms and lubricant effects
[AD-A157714] N86-13388

SPATIAL DISTRIBUTION
Airborne lidar measurements of El Chichon stratospheric aerosols
[NASA-RP-1148] N86-13850
Determination of neutron flux distribution by using ANISN, a one-dimensional discrete S sub n ordinates transport code with anisotropic scattering N86-14084

SPECIFIC HEAT
Supercritical fluid properties
[DE85-011203] N86-13401
Thermophysical properties of tungsten at high temperatures N86-13458

SPECIFICATIONS
National airspace system, system requirements specification
[AD-A157944] N86-13312

SPECTRA
Study of the influence of an oscillating spoiler on the surrounding aerodynamic field
[IMFL-3119] N86-13303

SPECTRAL EMISSION
Experimental investigation of magnesium combustion in steam
[AD-A159109] N86-13396
Bidirectional reflectance modeling of non-homogeneous plant canopies N86-13796
Use of Goudriaan model for studying reflection regularities in vegetation-soil system in optical range. 1: Influence of phytometric parameters on spectral brightness coefficients N86-14190

SPECTRAL ENERGY DISTRIBUTION
Spectra for large dimensional random matrices
[AD-A158256] N86-13973

SPECTRAL REFLECTANCE
Ground reflectance measurements from thematic mapper data N86-13801
Optical constants
[AD-A158623] N86-14038

SPECTRAL RESOLUTION
Focal plane optics in far-infrared and submillimeter astronomy
[NASA-TM-88186] N86-14204

SPECTRAL SENSITIVITY
Normalization of response of radiometric instrumentation for studying Earth's natural resources N86-14192

SPECTRAL SIGNATURES
Crop characteristics research: Growth and reflectance analysis N86-13800
Atmospheric and science complexity effects on surface bidirectional reflectance N86-13803
Atmospheric effect on remote sensing of the Earth's surface N86-13804

SPECTROGRAPHS
Lunar luminescence measurements N86-14092
A multiple-object fibre-optics coupler for the 1.2-m UK Schmidt Telescope N86-14201

SPECTROMETERS
Time resolved extended X-ray absorption fine structure spectrometer
[AD-D011869] N86-13715
Analysis of atomic thermospheric nitrogen density
[NASA-CR-176354] N86-13851

SPECTROPHOTOMETERS
Reflection indicatrices of vegetation canopies N86-14178

SPECTROSCOPIC ANALYSIS
Hadron component of cosmic radiation at atmospheric depth 800 g/cm(2) in Energy Range 70 to 700 GeV N86-13793

SPECTROSCOPIC TELESCOPES
Speckle image reconstruction. Appendix 1
[AD-A158271] N86-14207

SPECTROSCOPY
Relationships between electronic spectroscopy and electrochemistry. A probe of reorganisation energies
[AD-A157940] N86-13389

SPECTRUM ANALYSIS
Thermal infrared geologic remote sensing research at the Jet Propulsion Laboratory N86-13802
Reflection indicatrices of vegetation canopies N86-14178
Approximate analytical formulas for computing spectral brightness coefficients for agricultural vegetation N86-14179

SPECULAR REFLECTION
Measurement and modeling of the optical scattering properties of crop canopies N86-13798
Speckle image reconstruction. Appendix 1
[AD-A158271] N86-14207
Speckle image reconstruction. Appendix 2
[AD-A158272] N86-14208

SPEECH RECOGNITION
Speech recognition: Acoustic, phonetic and lexical knowledge
[AD-A158264] N86-13629

SPEED CONTROL
Two-hundred to 300 KVA conditioned power system - development, phase 1
[AD-A158820] N86-13832

SPHERES
Apparatus for removably holding a plurality of microballoons
[DE85-006517] N86-13722
Acoustical scattering from an elastic sphere in water: Surface wave glory, resonances, and the Sommerfeld-Watson transformation for amplitudes
[AD-A158884] N86-14010
Solar concentrator degradation in Low Earth Orbit (LEO) N86-14102

SPHERICAL ANTENNAS
Horizontal electric fields from lightning return strokes
[DE85-016367] N86-13873

SPHERICAL COORDINATES
Numerical solutions of Navier-Stokes equations for a Butler wing
[NASA-CR-174202] N86-13293
Investigation of characteristics of synoptic movements on sphere N86-13770

SPILLING
Laboratory studies of steep and breaking deep water waves in a convergent channel
[AD-A158187] N86-13875

SPIN EXCHANGE
Muon spin relaxation study of exchange coupling in dilute AgMn alloys
[DE85-014104] N86-13419

SPLINE FUNCTIONS

A new library of subroutines for calculating smoothing splines
[AD-A158049] N86-13930

Convergence of cardinal series
[AD-A158166] N86-13964

B-splines and linear combinations of uniform order statistics
[AD-A158151] N86-13986

High order spline interpolation in the particle simulation N86-14046

SPOILERS

Study of the influence of an oscillating spoiler on the surrounding aerodynamic field
[IMFL-3119] N86-13303

SPRAY CHARACTERISTICS

Spray characterization using phase angle detection N86-13577

Spray characterization with a nonintrusive optical single particle counter N86-13580

Real-time, two-dimensional fuel spray visualization N86-13583

SPRAYERS

Heat transfer and pressure drop performance of a finned-tube heat exchanger proposed for use in the NASA Lewis Altitude Wind Tunnel
[NASA-TM-87151] N86-13677

SPREAD SPECTRUM TRANSMISSION

Applications of differential phase statistics to studies of C3 and spread spectrum communications
[AD-A158815] N86-13633

STABILITY

Astrophysical payload accommodation on the space station
[NASA-CR-178556] N86-13359

Experimental investigation of heterogeneous flame stabilization N86-13528

Flame-acoustic wave interaction during axial solid rocket instabilities N86-13542

STABILIZATION

Physical mechanisms for hot electron stabilization of low frequency interchange modes
[IPPJ-741] N86-14050

STABLE OSCILLATIONS

Waves which travel upstream in boundary layers
[AD-A157949] N86-13684

STAINLESS STEELS

Hydrogen transport and hydrogen embrittlement in stainless steels N86-13403

High strain rate deformation in FCC metals and alloys
[DE85-017533] N86-13417

Development of contact/impact capability for the three-dimensional fluid-structure interaction code: NEPTUNE
[DE85-010264] N86-13698

Coupled radiation transport/thermal analysis of the radiation shield for a space nuclear reactor
[AD-A158180] N86-14022

STANDARD DEVIATION

A note on the effect of ignoring small measurement errors in precision instrument calibration
[AD-A159104] N86-13713

STANDARDIZATION

Standardization program on design analysis and testing of inserts in nonmetallic sandwich components --- spacecraft components
[TR-TS-RP-2-09-84] N86-13364

STANDARDS

Discussion on the Vibration Process Standards 9958002 and 9958004
[DE85-017116] N86-13599

Scientific activities of the Polish Academy of Sciences: Institute of Fundamental Technological Research in 1983
[ISBN-83-01-06288-6] N86-14107

STANDING WAVES

Waves which travel upstream in boundary layers
[AD-A157949] N86-13684

Boundary-value problem for two-dimensional fluctuations in boundary layers
[AD-A157952] N86-13685

STARS

An unbiased X-ray sampling of stars within 25 parsecs of the Sun
[NASA-CR-178544] N86-14206

Investigation of dust associated with shell stars
[AD-A158945] N86-14210

STATIC LOADS

Static fatigue of a sintered silicon nitride
[AD-A158813] N86-13760

STATIONARY ORBITS

Crowding of the geostationary orbit
[ESA-CR(P)-2050] N86-13346

STATIONKEEPING

Analytical investigation of the dynamics of tethered constellations in Earth orbit, phase 2
[NASA-CR-171611] N86-13345

STATISTICAL ANALYSIS

Theoretical studies and data analysis of wave propagation in random media
[AD-A158775] N86-13632

Probability of detection of internal voids in structural ceramics using microfocus radiography
[NASA-TM-87164] N86-13749

A family of curves for the rough surface reflection coefficient
[AD-A15[illegible]95] N86-13876

Scout trajectory error propagation computer program
[NASA-CR-166030] N86-13919

Development and enhancement of Computer Performance Modeling Tool (CPMT)
[AD-A159003] N86-13938

B-splines and linear combinations of uniform order statistics
[AD-A158151] N86-13986

Conditioning in a missing data problem
[AD-A158202] N86-13988

Spectral reflectance of surface soils: Relationships with some soil properties N86-14089

Application of statistical model of layered medium for computing thermal emission of ice covers N86-14186

Speckle image reconstruction. Appendix 2
[AD-A158272] N86-14208

STATISTICAL DECISION THEORY

Adaptive detection in nonstationary interference: Part 1 and part 2
[AD-A158810] N86-13993

STATISTICAL DISTRIBUTIONS

On asymptotic distribution of the test statistic for the mean of the nonisotropic principal component
[AD-A158255] N86-13972

Identification of nuclear materials from remote detection of characteristic gamma rays
[AD-A159244] N86-14014

STATISTICAL TESTS

Inference on the ranks of the canonical correlation matrices for elliptically symmetric populations
[AD-A158268] N86-13976

STEADY STATE

A three-dimensional analysis of natural convection in a toroidal loop N86-13672

Determination of the activation barrier to energy transfer from 3 pi pi* to charge transfer levels via steady state and transient luminescence measurements on Bis(4-Chlorothiophenol) (1,10-Phenanthroline) Zinc (II)
[AD-A158239] N86-14012

STEAM

Experimental investigation of magnesium combustion in steam
[AD-A159109] N86-13396

STEELS

A durable airfield marking system
[AD-A157953] N86-13339

The influence of microstructure on temper embrittlement of low alloy steel N86-13405

USSR report: Materials science and metallurgy
[JPRS-UMS-85-006] N86-13422

Influence of Co-Cr-Al-Y coatings on physical and mechanical properties of EI-893 steel in GT-100 turbine drive vanes N86-13438

Effect of elastoplastic cyclic deformation on mechanical characteristics of steel O3Kh13AG19 at temperatures of 293 and 77 deg K N86-13463

Specifics of the process of failure of structural steels strengthened by thermo-mechanical working with deformation in the intercritical temperature interval N86-13464

Mechanical properties of EP794 steel + 12Kh18N10T steel bimetal N86-13465

Macro- and microfractographic specifics of dissipated impact rupture of type 45 steel in the viscous-brittle transition interval N86-13466

Durability of steel 45 with boride coating in corrosive-abrasive media N86-13467

Modeling of thermal fatigue and erosion of complex alloyed steels in metal melts N86-13469

Study of effect of normal reactor water on growth rate of fatigue cracks in 15Kh2NMFA steel N86-13470

Influence of hydrogen on formation of cold cracks in seams during welding of pipe steel N86-13494

STEFAN-BOLTZMANN LAW

The formulation of a hyperbolic Stefan problem
[ORNL-6065] N86-13952

STELLAR LUMINOSITY

An unbiased X-ray sampling of stars within 25 parsecs of the Sun
[NASA-CR-178544] N86-14206

STELLAR SPECTRA

The plate scale of the U.K. Schmidt Telescope N86-14202

An unbiased X-ray sampling of stars within 25 parsecs of the Sun
[NASA-CR-178544] N86-14206

Investigation of dust associated with shell stars
[AD-A158945] N86-14210

STELLAR STRUCTURE

The plate scale of the U.K. Schmidt Telescope N86-14202

STEPPING MOTORS

Electrical motor with superconducting winding --- actuators
[SEP-TS/SE/BT/10026/85] N86-13668

STEREOPHOTOGRAPHY

Stereophotogrammetric survey of wave-covered water surface N86-14170

STIFFNESS

A computational analysis of pulsating flow in rigid and deformable tubes N86-13673

STIFFNESS MATRIX

Dynamic modeling of structures from measured complex modes N86-13591

STIRLING CYCLE

Stirling engine supporting research and technology
[NASA-TM-87175] N86-14106

STOCHASTIC PROCESSES

Determination of porosity of thin sheets of fiber materials based on optical transmission coefficient N86-13459

The theory of standardized time series
[AD-A158383] N86-13989

Extreme values of queues, point processes and Stochastic Networks
[AD-A158619] N86-13991

Methodology for stochastic modeling
[AD-A158851] N86-13994

Information in censored models
[AD-A158644] N86-13999

STORAGE RINGS (PARTICLE ACCELERATORS)

SLAC divertor channel entrance thermal stress analysis
[DE85-017877] N86-14057

STORMS

Oxidizing and scavenging characteristics of April rains: OSCAR data report
[DE85-017014] N86-13844

STRAIN ENERGY METHODS

A numerical investigation into the plastic stress and strain fields around a surface crack
[ARL/STRUC-R-414] N86-13754

STRAIN GAGE BALANCES

Algorithms for the reduction of wind-tunnel data derived from strain gauge force balances
[ARL/AERO-R-164] N86-13337

STRAIN MEASUREMENT

Simulating distributed reinforcement effects in concrete analysis
[DE85-009745] N86-13761

STRAIN RATE

Effect of temperature and strain rate on microstructure of a deformed, superplastic Al-10%Mg-0.1%Zr alloy
[AD-A159015] N86-13413

Effect of strain and strain rate on the microstructure of a superplastically deformed Al-10%Mg-0.1%Zr alloy
[AD-A159062] N86-13414

High strain rate deformation in FCC metals and alloys
[DE85-017533] N86-13417

Crack growth behavior in a composite propellant with strain gradients N86-13537

Time dependency of strainrange partitioning life relationships
[NASA-CR-174946] N86-13755

STRAPS

Passive arm retention curtain
[AD-D011876] N86-13307

Development of a breadboard cooler for infrared remote sensing payloads, phase 2 --- spacecraft payloads
[FOK-RV-R-82-072] N86-13725

STRATIFICATION

Formation of structure of mixed region under influence of shear flow in stratified fluid N86-13768

Decomposition of some well-known variance reduction techniques: Revision
[AD-A158048] N86-13985

STRATIGRAPHY

Geothermal resources of the Wind River Basin, Wyoming
[DE85-016969] N86-13816

Geologic characterization report for the Paradox Basin Study Region, Utah Study Areas. Volume 6. Salt Valley
[DE85-011699] N86-13858

STRATOSPHERE

Airborne lidar measurements of El Chichon stratospheric aerosols
[NASA-RP-1148] N86-13850

Disturbances in stratosphere and mesosphere from source of ultraviolet radiation N86-14136

STRATOSPHERE RADIATION

Latitude measurements of cosmic radiation intensity in stratosphere and at sea level on marine antarctic expeditions N86-13792

STREAK CAMERAS

Photoelectronic trajectory anatomy of RCA-C-73435 image converter and its performance
[DE85-013973] N86-13723

STRENGTH

Laser diagnostics for electric field measurements
N86-13563

STRESS ANALYSIS

Process-induced viscoelastic stress in composite laminates N86-13376

Microscopic observations and mechanics analyses of long term fracture in polyethylene piping materials
[PB85-219608] N86-13506

Simulating distributed reinforcement effects in concrete analysis
[DE85-009745] N86-13761

Coupled radiation transport/thermal analysis of the radiation shield for a space nuclear reactor
[AD-A158180] N86-14022

SLAC divertor channel entrance thermal stress analysis
[DE85-017877] N86-14057

STRESS CONCENTRATION

Macro- and microfractographic specifics of dissipated impact rupture of type 45 steel in the viscous-brittle transition interval N86-13466

Elastic-plastic deformation of a metal-matrix composite coupon with a center slot
[NASA-CR-178013] N86-13496

STRESS CORROSION CRACKING

The delayed fracture of aluminum alloys
[AD-A158944] N86-13412

Study of effect of normal reactor water on growth rate of fatigue cracks in 15Kh2NMFA steel N86-13470

STRESS INTENSITY FACTORS

Study of effect of normal reactor water on growth rate of fatigue cracks in 15Kh2NMFA steel N86-13470

Subcritical crack development under constant load in VT6 alloy N86-13475

A numerical investigation into the plastic stress and strain fields around a surface crack
[ARL/STRUC-R-414] N86-13754

STRESS MEASUREMENT

Threshold stress measurements in shock-deformed copper
[DE85-014076] N86-13418

Neutron stress measurements with a position sensitive detector
[AD-A158882] N86-13712

STRESS TENSORS

Errors due to counting statistics in the triaxial strain (stress) tensor determined by diffraction
[AD-A158219] N86-13759

STRESS-STRAIN RELATIONSHIPS

Modifications of system for elevated temperature tensile testing and stress-strain measurement of metal matrix composites
[NASA-TM-87172] N86-13370

A numerical investigation into the plastic stress and strain fields around a surface crack
[ARL/STRUC-R-414] N86-13754

STRESS-STRAIN-TIME RELATIONS

A functional equation governing moving phase boundaries in an elastic bar
[AD-A158178] N86-13757

STRESSES

Environmental Stress Screening (ESS)
[AD-A158262] N86-13751

STRIPPING (DISTILLATION)

Mass transfer coefficients and Henry's constants for packed-tower air stripping of volatile organics: Measurements and correlation
[AD-A158811] N86-13375

STROUHAL NUMBER

Sensitivity to mean flow parameters of the low wavenumber content of the wall pressure under a turbulent boundary layer
[AD-A158037] N86-13688

STRUCTURAL ANALYSIS

Combustion behavior of free boron slurry droplets
[AD-A158620] N86-13585

Computation of normal modes from identified complex modes N86-13590

Dynamic modeling of structures from measured complex modes N86-13591

Application of Pasternak model to some soil-structure interaction problems. Volume 1: Solutions for plates continuously supported on a Pasternak base
[AD-A157776] N86-13594

Application of Pasternak model to some soil-structure interaction problems. Volume 2: Determination of foundation parameters and the choice of models
[AD-A157777] N86-13595

Basic properties of strong mixing conditions
[AD-A158740] N86-13992

STRUCTURAL ENGINEERING

Application of Pasternak model to some soil-structure interaction problems. Volume 2: Determination of foundation parameters and the choice of models
[AD-A157777] N86-13595

STRUCTURAL MEMBERS

Modifications of system for elevated temperature tensile testing and stress-strain measurement of metal matrix composites
[NASA-TM-87172] N86-13370

Specifics of the process of failure of structural steels strengthened by thermo-mechanical working with deformation in the intercritical temperature interval
N86-13464

Modeling of thermal fatigue and erosion of complex alloyed steels in metal melts N86-13469

STRUCTURAL PROPERTIES (GEOLOGY)

Geothermal resources of the Wind River Basin, Wyoming
[DE85-016969] N86-13816

Azerbaijan geological, geophysical work on land described N86-13862

Tectonic stress on structures alters formation parameters N86-13864

STRUCTURAL RELIABILITY

Aircraft crashing. Analysis and identification methods. Presentation of a solution method
[IMFL-4116] N86-13308

STRUCTURAL VIBRATION

Dynamic identification for control of large space structures
[NASA-CR-176380] N86-13587

Time-domain quasi-linear identification of nonlinear dynamic systems
[AIAA-83-0811-CP] N86-13592

SUBMILLIMETER WAVES

The development of a submillimeter wave carcinotron operating in the frequency range from 850 to 1000 GHz
[TDH-RT-2963-T] N86-13638

SUBROUTINES

Computer program for prediction of fuel consumption statistical data for an upper stage three-axes stabilized on-off control system
[NASA-CR-166031] N86-13917

A new library of subroutines for calculating smoothing splines
[AD-A158049] N86-13930

SUBSONIC FLOW

A direct-inverse method for transonic and separated flows about airfoils
[NASA-CR-176403] N86-13300

SUBSTITUTES

Characterization of 7017 aluminum alloys in thick profiles, in the metallurgical versions T6510, T76510 and T736510, test report no. PV-44-607/F
[PV-44-607/F] N86-13420

SUBSTRATES

A study of rhenium as an alternate substrate material for impregnated dispenser cathodes
[AD-A159113] N86-13415

Effect of heating conditions on agglomeration of powdered aluminum in air atmosphere N86-13460

Mechanical properties of EP794 steel + 12Kh18N10T steel bimetal N86-13465

Photodegradation studies of silver-backed polyacrylonitrile (PAN) films
[DE85-012154] N86-13501

Application of cross-sectional transmission electron microscopy to the characterization of ion-implanted semiconductors
[DE85-010990] N86-14075

SULFATES

Oxidizing and scavenging characteristics of April rains: OSCAR data report
[DE85-017014] N86-13844

SULFIDES

Charge-density waves observed with a tunneling microscope
[AD-A158779] N86-13709

SUPERCHARGERS

Lightweight two-stroke cycle aircraft diesel engine technology enablement program, volume 1
[NASA-CR-174923-VOL-1] N86-13328

Lightweight two-stroke cycle aircraft diesel engine technology enablement program, volume 2
[NASA-CR-174923-VOL-2] N86-13329

Lightweight two-stroke cycle aircraft diesel engine technology enablement program, volume 3
[NASA-CR-174923-VOL-3] N86-13330

SUPERCONDUCTING MAGNETS

Microcomputer controlled current sharing experiments with parallel converters
[DE85-013654] N86-13665

Random errors in the magnetic field coefficients of superconducting magnets
[DE85-012261] N86-14004

Impact of a poloidal divertor in ignition tokamak design
[DE85-012892] N86-14061

SUPERCONDUCTING POWER TRANSMISSION

Electrical motor with superconducting winding --- actuators
[SEP-TS/SE/BT/10026/85] N86-13668

SUPERCRITICAL FLUIDS

Supercritical fluid properties
[DE85-011203] N86-13401

SUPERPLASTICITY

Fabrication and evaluation of superplastically formed/weld-brazed corrugated compression panels with beaded webs
[NASA-TP-2512] N86-13406

Effect of temperature and strain rate on microstructure of a deformed, superplastic Al-10%Mg-0.1%Zr alloy
[AD-A159015] N86-13413

Effect of strain and strain rate on the microstructure of a superplastically deformed Al-10%Mg-0.1%Zr alloy
[AD-A159062] N86-13414

Appearance of superplasticity effect in aluminum alloys with lithium N86-13432

Influence of structure of heat-resistant nickel alloy ZhS6U on its weldability in the solid state N86-13492

SUPERSONIC SPEEDS

Preliminary measurement of the noise from the 2/9 scale model of the Large-scale Advanced Propfan (LAP) propeller, SR-7A
[NASA-TM-87116] N86-14006

SUPPRESSORS

Mechanisms for acoustic suppression N86-13543

SURFACE ACOUSTIC WAVE DEVICES

Feasibility study of chirp generator for ERS-1 radar altimeter, option A
[ELAB-STF44-F83103] N86-13368

SURFACE CRACKS

Mechanical properties of EP794 steel + 12Kh18N10T steel bimetal N86-13465

A numerical investigation into the plastic stress and strain fields around a surface crack
[ARL/STRUC-R-414] N86-13754

SURFACE DEFECTS

Exploratory development on advanced eddy current coil excitation and signal processing
[AD-A159228] N86-13752

SURFACE DIFFUSION

Corrosion resistance of diffusion and galvanic coatings on steel fasteners N86-13450

SURFACE FINISHING

Influence of texture of titanium nitride coatings on wear resistance of cutting tools N86-13440

Production of multilayer magnetic surface of magnetically soft composite materials N86-13445

A method for melt-coating a surface
[AD-D011866] N86-13596

SURFACE LAYERS

Modeling of thermal fatigue and erosion of complex alloyed steels in metal melts N86-13469

Structural characteristic of temperature field over sea
N86-13783

Scattering models and basic experiments in the microwave regime N86-13807

SURFACE NAVIGATION

Short range aids to navigation systems. Design manual for restricted waterways
[AD-A158213] N86-13313

SURFACE PROPERTIES

Current viewpoints on oxide adherence mechanisms
[NASA-TM-87168] N86-13409

Durability of steel 45 with boride coating in corrosive-abrasive media N86-13467

Ion nitriding of titanium N86-13473

Unified study of plasma-surface interactions for space power and propulsion N86-13567

Describing surfaces
[AD-A158940] N86-13937

SURFACE REACTIONS

No chemisorption on Ni(111): Coverage effects, site preferences and adsorption geometry
[AD-A159110] N86-13397

Erosion and onset mechanisms in magnetoplasmadynamic thrusters N86-13556

Magnetoplasmadynamic thruster erosion research
N86-13557

Optical technique to measure electrode erosion
N86-13564

SURFACE ROUGHNESS

Lubrication of nonconformal contacts
[NASA-TM-87120] N86-13679

SURFACE STABILITY

Calculation of damping properties of composite materials N86-13446

SURFACE TEMPERATURE

Remote temperature determination of terrestrial covers from polarization invariant of microwave-radiothermal emission N86-14196

SURFACE WAVES

Acoustical scattering from an elastic sphere in water: Surface wave glory, resonances, and the Sommerfeld-Watson transformation for amplitudes [AD-A158884] N86-14010

SURVEILLANCE

Distributed sensor networks [AD-A158033] N86-13628

SURVEYS

Conditioning in a missing data problem [AD-A158202] N86-13988

SUSPENSION SYSTEMS (VEHICLES)

Development of a breadboard cooler for infrared remote sensing payloads, phase 2 --- spacecraft payloads [FOK-RV-R-82-072] N86-13725

SWITCHES

Laser-trigger system design for PBFA 2 [DE85-013144] N86-14065

SWITCHING

Numerical modeling of carrier transport in submicron bipolar transistors N86-13642

SWITCHING CIRCUITS

Optoelectronic integrated circuit multiplier [AD-D011883] N86-14043

SWITCHING THEORY

A behavioral summary for completely random nets [AD-A157755] N86-13960

SYMMETRICAL BODIES

Cyclosymmetric approach to the dynamics of repetitive modular structures [ESA-CR(P)-2062] N86-13739

SYMMETRY

Babinet's principle for an anisotropic resistive surface using different approaches [AD-A159117] N86-13636

Scaling of uv (351 nm) fusion implosions driven by multiple beams [DE85-014406] N86-14068

SYNCHROTRON RADIATION

Charge composition of electrons in Earth's radiation belt N86-14146

SYNOPTIC METEOROLOGY

Investigation of characteristics of synoptic movements on sphere N86-13770

Atmospheric synoptic eddies over ocean (determined from experimental data) N86-13784

SYNTHESIS (CHEMISTRY)

Synthesis, structure and reactivity of molecules attached to electrode surfaces [AD-A158621] N86-13394

Syntheis of difluoraminoxy-, difluoramino- or fluorodiazonium-containing materials N86-13509

Synthesis of new polynitropolyhedranes N86-13510

Synthesis of high nitrogen content heterocyclic nitramines and energetic internal plasticizers N86-13511

Synthesis and reactivity of unsaturated metal nitrogen complexes N86-13512

Synthesis and chemistry of polynitroalkanes and polynitroolefins N86-13513

New synthetic techniques for advanced propellant ingredients: Selective transformations and new structures N86-13514

Structure-decomposition relationships in newer energetic materials N86-13521

Aquatic plant control research program: Evaluation of polymers for controlled delivery of herbicides for aquatic plant control [AD-A157948] N86-13843

Investigation of cold colored smoke production [AD-A158783] N86-14040

SYNTHETIC APERTURE RADAR

Rectification and registration of remotely sensed data [AD-A158827] N86-13711

The construction and testing of a real-time digital breadboard processor for the ESA remote sensing satellite synthetic aperature radar [REPT-00-0778] N86-13911

SYSTEM EFFECTIVENESS

National airspace system, system requirements specification [AD-A157944] N86-13312

SYSTEM FAILURES

The evaluation of failure detection and isolation algorithms for restructurable control [NASA-CR-177983] N86-13310

SYSTEM IDENTIFICATION

Time-domain quasi-linear identification of nonlinear dynamic systems [AIAA-83-0811-CP] N86-13592

SYSTEMS ANALYSIS

Structures and materials technology issues for reusable launch vehicles [NASA-TM-87626] N86-13349

SYSTEMS ENGINEERING

Two-phase heat transport systems: System definition, volume 1 --- space stations [ESA-CR(P)-2052] N86-13363

Study on design techniques for robots (space applications). Volume 1, part A: Technical results [FOK-TR-R-84-110-VOL-1-PT-A] N86-13902

Study on design techniques for robots (space applications). Volume 1, part B: Technical results [FOK-TR-R-84-110-VOL-1-PT-B] N86-13903

Study on design techniques for robots (space applications). Volume 2: Technical appendices [FOK-TR-R-84-110-VOL-2] N86-13904

Study on design techniques for robots (space applications). Volume 3: Executive summary [FOK-TR-R-84-110-VOL-3] N86-13905

METCUT: A computer aided system for machining technology [AD-A157941] N86-13927

Laser-trigger system design for PBFA 2 [DE85-013144] N86-14065

SYSTEMS INTEGRATION

New robots by Soviet, CEMA manufacturers described N86-13748

Laser-trigger system design for PBFA 2 [DE85-013144] N86-14065

SYSTEMS STABILITY

A method to stabilize linear systems using eigenvalue gradient information [NASA-TP-2479] N86-13946

T

TABLES (DATA)

Evaluation and compilation of the thermodynamic properties of high temperature species N86-13532

Critical evaluation of high temperature chemical kinetic data N86-13533

TAILLESS AIRCRAFT

Aircraft of the future [NASA-TM-77952] N86-13318

TARGET RECOGNITION

Enhancing sensitivity to visual motion and enhancing visual sensitivity [AD-A158800] N86-13889

Target tracking based scene analysis [AD-A158629] N86-13910

Adaptive detection in nonstationary interference: Part 1 and part 2 [AD-A158810] N86-13993

TARGETS

Distributed sensor networks [AD-A158033] N86-13628

TAYLOR SERIES

Adaptive, self-validating numerical quadrature [AD-A158164] N86-13963

TECHNOLOGICAL FORECASTING

Aircraft of the future [NASA-TM-77952] N86-13318

TECHNOLOGY ASSESSMENT

In-orbit technology demonstration program (TDP). Accommodation study: SPAS [MBB-URV-147/84] N86-13351

Assembly Integration Verification (AIV) test effectiveness study. Applicability of Spacelab approach for equipment and system test for Ariane-4 class satellites. Volume 1: Executive summary [ERNO-671/AIV-VOL-1] N86-13361

Study of Earth observation by frequency scanning. Volume 1: Executive summary [ESA-CR(P)-2028-VOL-1] N86-13705

Study of Earth observation by frequency scanning. Volume 2 [ESA-CR(P)-2028-VOL-2] N86-13706

TECHNOLOGY TRANSFER

Report on the findings of the Japanese Investigative Team on US Space Station Design (Keidanren) [NASA-TM-77659] N86-13356

West Europe report: Science and technology [JPRS-WST-85-029] N86-13622

Emerging aerospace technologies [NASA-TM-86837] N86-14213

TECHNOLOGY UTILIZATION

Magnetic field applications in modern technology and medicine [DE85-015197] N86-14001

TECTONICS

Geologic characterization report for the Paradox Basin Study Region, Utah Study Areas. Volume 6: Salt Valley [DE85-011699] N86-13858

Tectonic stress on structures alters formation parameters N86-13864

Use of space geological methods in seismotectonic research N86-14188

TELECOMMUNICATION

Applications of differential phase statistics to studies of C3 and spread spectrum communications [AD-A158815] N86-13633

Atmospheric radio noise: Worldwide levels and other characteristics [PB85-212942] N86-13639

Worldwide report: Telecommunications policy, research, and development [JPRS-TTP-85-026] N86-13640

TELEPHOTOMETRY

Reflection indicatrices of vegetation canopies N86-14178

TELESCOPES

Test method for telescopes using a point source at a finite distance [NASA-TM-86523] N86-14033

TELEVISION SYSTEMS

Worldwide report: Telecommunications policy, research, and development [JPRS-TTP-85-026] N86-13640

TEMPER (METALLURGY)

Specifics of the process of failure of structural steels strengthened by thermo-mechanical working with deformation in the intercritical temperature interval N86-13464

Mechanical properties of EP794 steel + 12Kh18N10T steel bimetal N86-13465

Dispersion hardening of high-strength NiOCo-Mo steels N86-13468

TEMPERATURE

Variable temperature trap [AD-D011874] N86-13719

TEMPERATURE CONTROL

Planetary sample rapid recovery and handling [NASA-CR-171906] N86-13342

Two-phase heat transport systems: System definition, volume 1 --- space stations [ESA-CR(P)-2052] N86-13363

Investigation of techniques for improving spacecraft thermal control software [GEC-MEL42.0552] N86-13942

TEMPERATURE DEPENDENCE

Ultrasonic longitudinal wave velocity in carbon-carbon Pitch and Pitch/M2 shape stable nosetip material from 70 deg F to 5400 deg F [DE85-017330] N86-13382

Effect of elastoplastic cyclic deformation on mechanical characteristics of steel O3Kh13AG19 at temperatures of 293 and 77 deg K N86-13463

Specifics of the process of failure of structural steels strengthened by thermo-mechanical working with deformation in the intercritical temperature interval N86-13464

Ion nitriding of titanium N86-13473

Structure and internal friction of near-eutectic alloy system Ti-W tempered from a liquid state N86-13482

Mound activities in chemical and physical research: July December 1984 [DE85-014402] N86-14030

TEMPERATURE DISTRIBUTION

Experimental investigation of magnesium combustion in steam [AD-A159109] N86-13396

Strategy for advanced sensing and control of combustion N86-13574

Computation of ocean upper layer thermal structure N86-13769

Structural characteristic of temperature field over sea N86-13783

Far-field model of the regional influence of affluent plumes from Ocean Thermal Energy Conversion (OTEC) plants [DE85-016981] N86-13836

TEMPERATURE EFFECTS

Thermal vacuum tests on a hinge actuator mechanism --- spacecraft component [ESA-ESTL-067] N86-13360

Effect of temperature and strain rate on microstructure of a deformed, superplastic Al-10%Mg-0.1%Zr alloy [AD-A159015] N86-13413

Certain features of laser destruction and dislocational structure of silicon during heating and effects of electrical field N86-13454

Effect of heating conditions on agglomeration of powdered aluminum in air atmosphere N86-13460

Determining local heating parameters for increasing fatigue resistance of welded joints N86-13491

Tectonic stress on structures alters formation parameters N86-13864

TEMPERATURE GRADIENTS

Temperature-frequency variation of mechanical losses in periodic deformation of multilayer glass-reinforced plastics N86-13449

Effect of heating conditions on agglomeration of powdered aluminum in air atmosphere N86-13460

Computation of ocean upper layer thermal structure N86-13769

TEMPERATURE MEASUREMENT

Strategy for advanced sensing and control of combustion N86-13574

Real-time, two-dimensional fuel spray visualization N86-13583

Expendable bathythermograph for measuring light attenuation and temperature below the ocean surface [AD-D011870] N86-13716

Mound activities in chemical and physical research: July December 1984 [DE85-014402] N86-14030

Remote temperature determination of terrestrial covers from polarization invariant of microwave-radiothermal emission N86-14196

TEMPERATURE PROFILES

Experimental investigation of heat transfer behavior of aqueous foams in thermal entry region of pipe flow [DE85-012836] N86-13700

TEMPERING

The influence of microstructure on temper embrittlement of low alloy steel N86-13405

TENSILE PROPERTIES

Evaluation of the titanium IMI 829 alloy produced by powder metallurgy [M1-610200] N86-13421

Remote optical crack sensing system [AD-D011872] N86-13718

TENSILE STRENGTH

A durable airfield marking system [AD-A157953] N86-13339

Modifications of system for elevated temperature tensile testing and stress-strain measurement of metal matrix composites [NASA-TM-87172] N86-13370

Specifics of the process of failure of structural steels strengthened by thermo-mechanical working with deformation in the intercritical temperature interval N86-13464

Employment of PAM-FISS-BI-phase computer program for the strength analysis and fracture/delamination behavior of components [ESI-ED/83-383/RD/MS-VOL-7] N86-13763

TERMINAL BALLISTICS

Short presentation and evaluation of studies on the penetration of jets from hollow shaped charges in compressible materials [ISL-NB-402/84] N86-13586

TERRAIN

Generically based mobility-terrain data bases [AD-A157738] N86-13815

Possibilities of using space survey for studying seasonal changes of landscapes in some regions of USSR N86-14183

TERRAIN ANALYSIS

Fundamental remote sensing science research program: The Scene Radiation and Atmospheric Effects Characterization Project [E86-10011] N86-13794

Reflectance modeling N86-13795

Ground reflectance measurements from thematic mapper data N86-13801

Remote sensing of Earth terrain N86-13808

Discrete random media techniques for microwave modeling of vegetated terrain N86-13809

Method for using clusters in evaluating land use areas from multizonal photographs N86-14180

Role of landscape research in development of space methods for studying Earth N86-14184

Compilation of landscape maps at different scales with use of space photoinformation N86-14187

Analysis of survey conditions and effect of noise on quality of sensing of soil formations N86-14191

Remote temperature determination of terrestrial covers from polarization invariant of microwave-radiothermal emission N86-14196

TERRESTRIAL RADIATION

Fundamental remote sensing science research program: The Scene Radiation and Atmospheric Effects Characterization Project [E86-10011] N86-13794

Charge composition of electrons in Earth's radiation belt N86-14146

TEST FACILITIES

Investigation for the definition of a hydraulic multidegree of freedom vibration facility [B-TF-1627] N86-13340

Laboratory studies of steep and breaking deep water waves in a convergent channel [AD-A158187] N86-13875

TETHERED SATELLITES

Analytical investigation of the dynamics of tethered constellations in Earth orbit, phase 2 [NASA-CR-171611] N86-13345

Stability of stationary motions of two tethered bodies in orbit under influence of gravitational and aerodynamic forces N86-14163

TEXTURES

Influence of texture of titanium nitride coatings on wear resistance of cutting tools N86-13440

THEMATIC MAPPING

Ground reflectance measurements from thematic mapper data N86-13801

Atmospheric effect on remote sensing of the Earth's surface N86-13804

THERMAL ANALYSIS

Study of thermal analysis methods --- spacecraft [GEC-MEL12.0539] N86-13362

Investigation of techniques for improving spacecraft thermal control software [GEC-MEL42.0552] N86-13942

Coupled radiation transport/thermal analysis of the radiation shield for a space nuclear reactor [AD-A158180] N86-14022

THERMAL BLOOMING

Effectiveness of use of adaptive optical systems under conditions of self-effect in atmosphere N86-13791

THERMAL CONDUCTIVITY

Critical behavior of thermoelectric power in binary composite materials N86-13448

Electrical and thermal transport property studies of high-temperature thermoelectric materials [AD-A158883] N86-13656

Experimental investigation of heat transfer behavior of aqueous foams in thermal entry region of pipe flow [DE85-012836] N86-13700

Effects of neutrals on internal forces and thermal conduction of a plasma in a magnetic field [IPPJ-691] N86-14051

Electrical and electrothermal conductivity of planetary ionospheres, 1: Refinement of theory N86-14143

THERMAL DECOMPOSITION

Theory of pyrolysis of composite polymer materials N86-13447

Deuterium isotope effects in RDX decomposition and combustion processes N86-13522

THERMAL DIFFUSION

Silicide coatings for protecting titanium-niobium alloys from high-temperature oxidation N86-13476

Mound activities in chemical and physical research: July December 1984 [DE85-014402] N86-14030

THERMAL EMISSION

Application of statistical model of layered medium for computing thermal emission of ice covers N86-14186

Remote temperature determination of terrestrial covers from polarization invariant of microwave-radiothermal emission N86-14196

THERMAL EXPANSION

Relationship of thermal expansion of amorphous metal alloys with their high temperature plastic properties N86-13435

THERMAL FATIGUE

Modeling of thermal fatigue and erosion of complex alloyed steels in metal melts N86-13469

THERMAL INSTABILITY

Problems in thermal convective instability N86-13670

THERMAL MAPPING

Thermal infrared geologic remote sensing research at the Jet Propulsion Laboratory N86-13802

Experience in complex mapping of natural resources in agrarian-industrial regions of Nonchernozem RSFSR using space photomaterials N86-14174

THERMAL RADIATION

Thermal radiation effects on combustion of condensed fuels N86-13387

Metastable interactions: Dissociative excitation [AD-A158733] N86-14013

THERMAL RESISTANCE

Study of properties of gas-thermal coatings of composite nichrome-aluminum alloy powders N86-13442

Silicide coatings for protecting titanium-niobium alloys from high-temperature oxidation N86-13476

THERMAL STABILITY

Study of properties of gas-thermal coatings of composite nichrome-aluminum alloy powders N86-13442

Conductivity of metal-ceramic multilayer ZrO2-Mo and Mo-based composite materials N86-13444

THERMAL STRESSES

Variable field effects for the rotating fluidized bed reactor N86-13565

SLAC divertor channel entrance thermal stress analysis [DE85-017877] N86-14057

THERMAL VACUUM TESTS

Thermal vacuum tests on a hinge actuator mechanism --- spacecraft component [ESA-ESTL-067] N86-13360

THERMIONIC CATHODES

Atomically mixed alloy coated cathodes specification [AD-D011877] N86-13659

THERMIONIC DIODES

Close-spaced high temperature Knudsen flow [AD-A158280] N86-13831

THERMIONIC EMITTERS

Close-spaced high temperature Knudsen flow [AD-A158280] N86-13831

THERMIONIC POWER GENERATION

Close-space, high temperature Knudsen flow N86-13568

Close-spaced high temperature Knudsen flow [AD-A158280] N86-13831

THERMOCHEMISTRY

Evaluation and compilation of the thermodynamic properties of high temperature species N86-13532

THERMOCOUPLES

Rocket engine hot-spot detector [NASA-CR-171902] N86-13708

THERMODYNAMIC EQUILIBRIUM

A study of transport phenomena and interface stability during solidification of binary solutions using front tracking finite elements N86-13669

THERMODYNAMIC PROPERTIES

Theory of pyrolysis of composite polymer materials N86-13447

The 1985 AFOSR/AFRPL Chemical Rocket Research Meeting, abstracts and agenda [AD-A158291] N86-13507

THERMODYNAMICS

Evaluation and compilation of the thermodynamic properties of high temperature species N86-13532

The formulation of a hyperbolic Stefan problem [ORNL-6065] N86-13952

Coupled radiation transport/thermal analysis of the radiation shield for a space nuclear reactor [AD-A158180] N86-14022

THERMOELECTRIC MATERIALS

Electrical and thermal transport property studies of high-temperature thermoelectric materials [AD-A158883] N86-13656

THERMOELECTRICITY

Critical behavior of thermoelectric power in binary composite materials N86-13448

Electrical and thermal transport property studies of high-temperature thermoelectric materials [AD-A158883] N86-13656

THERMOPHYSICAL PROPERTIES

Thermophysical properties of tungsten at high temperatures N86-13458

THERMOPLASTIC RESINS

Fractography of mixed mode 1 - 2 failure in Graphite/Epoxy and Graphite/Thermoplastic unidirectional composites [AD-A158852] N86-13498

Recent advances in composite materials reviewed N86-13623

THERMOSIPHONS

A three-dimensional analysis of natural convection in a toroidal loop N86-13672

THICKNESS

Electronic detection of low concentrations of organophosphorus compounds with a solid state device utilizing supported copper + cuprous oxide island films [AD-A158181] N86-13392

THIN FILMS

Multiple scattering theories for optical properties of composite materials [AD-A158270] N86-13379

USSR report: Materials science and metallurgy [JPRS-UMS-85-006] N86-13422

Structure formation in silumins upon rapid crystallization N86-13427

Micromechanisms of electrodiffusion failures in thin film metallization N86-13472

Effect of interfacial phenomena on contact line heat transfer N86-13566

Excimer laser produces .2 micron semiconductor structures N86-13613

Development of stable high efficiency polycrystalline thin-film solar cells based on CuInSe2 [DE85-000517] N86-13837

AuGa2 on GaSb(001): An epitaxial, thermodynamically stabilized Metal/3-5 compound semiconductor interface [AD-A157937] N86-14071

MBE growth of CdTe and Hg (1-x) Cd (x) Te films and multilayer structures [AD-A158267] N86-14073

THIN WALLED SHELLS
A method to determine dynamic elastic constants of thin shell composites by guided ultrasonic waves
[AD-A159025] N86-13381
THREE BODY PROBLEM
Analytical investigation of the dynamics of tethered constellations in Earth orbit, phase 2
[NASA-CR-171611] N86-13345
Structure of coefficients of series representing solution of plane circular restricted three-body problem
N86-14129
Periodic regimes of rotational motion of solid body about liberation point L sub 4 in restricted elliptical three-body problem N86-14132
THREE DIMENSIONAL BODIES
A numerical investigation into the plastic stress and strain fields around a surface crack
[ARL/STRUC-R-414] N86-13754
Understanding the radiant scattering behavior of vegetated scenes N86-13797
THREE DIMENSIONAL FLOW
Numerical solutions of Navier-Stokes equations for a Butler wing
[NASA-CR-174202] N86-13293
A three-dimensional analysis of natural convection in a toroidal loop N86-13672
Development of contact/impact capability for the three-dimensional fluid-structure interaction code: NEPTUNE
[DE85-010264] N86-13698
THREE DIMENSIONAL MOTION
Fiber optics as an angular sensor
[AD-D011886] N86-14044
THRESHOLD CURRENTS
CNET of France uses organo-metallic epitaxy for laser
N86-13620
THRUST VECTOR CONTROL
Comparison of energetics of optimum maneuvers and two-impulse maneuvers in some problems of motion from a point into orbit N86-14134
Optimum control programs in problem of interorbital flight with continuous thrust N86-14135
THRUST-WEIGHT RATIO
Polymer, metal and ceramic matrix composites for advanced aircraft engine applications
[NASA-TM-87132] N86-13407
TILES
A durable airfield marking system
[AD-A157953] N86-13339
TIMBER INVENTORY
Crop area estimation based on remotely-sensed data with an accurate but costly subsample
[NASA-CR-176017] N86-13814
Classification of trees by growth classes on the basis of multizonal photographs N86-14173
TIME
Ion nitriding of titanium N86-13473
TIME DEPENDENCE
Ion nitriding of titanium N86-13473
A study of transport phenomena and interface stability during solidification of binary solutions using front tracking finite elements N86-13669
Time dependency of strainrange partitioning life relationships
[NASA-CR-174946] N86-13755
Aquatic plant control research program: Evaluation of polymers for controlled delivery of herbicides for aquatic plant control
[AD-A157948] N86-13843
Three-dimensional modeling of Tsunami waves
[DE85-015724] N86-13877
Application of statistical model of layered medium for computing thermal emission of ice covers N86-14186
TIME LAG
Time delay of arrival location assessment using four satellites
[AD-A159243] N86-13315
TIME MEASUREMENT
A parametric study of the Ibrahim time domain modal identification algorithm N86-13588
TIME RESPONSE
Dynamic identification for control of large space structures
[NASA-CR-176380] N86-13587
Time-domain quasi-linear identification of nonlinear dynamic systems
[AIAA-83-0811-CP] N86-13592
TIME SERIES ANALYSIS
Inference on the ranks of the canonical correlation matrices for elliptically symmetric populations
[AD-A158268] N86-13976
The theory of standardized time series
[AD-A158383] N86-13989
TIN COMPOUNDS
Variable temperature trap
[AD-D011874] N86-13719
TIP SPEED
Preliminary measurement of the noise from the 2/9 scale model of the Large-scale Advanced Propfan (LAP) propeller, SR-7A
[NASA-TM-87116] N86-14006
TIRES
Tire-soil interaction model for turning (steered) tires
[AD-A157737] N86-13593
TITANIUM
Hereditary effect of dendrite liquation of titanium and zirconium on structure and properties of aluminum alloys
N86-13423
Grain growth in heat-resistant austenitic steel
N86-13462
Ion nitriding of titanium N86-13473
Internal friction in TiNiCu alloy N86-13480
Fusion welding research
[AD-A158253] N86-13736
TITANIUM ALLOYS
Fabrication and evaluation of superplastically formed/weld-brazed corrugated compression panels with beaded webs
[NASA-TP-2512] N86-13406
Evaluation of the titanium IMI 829 alloy produced by powder metallurgy
[M1-610200] N86-13421
Superelastic behavior of powdered titanium nickelide during pressing N86-13461
Calculation of failure constant for titanium alloys
N86-13474
Subcritical crack development under constant load in VT6 alloy N86-13475
Silicide coatings for protecting titanium-niobium alloys from high-temperature oxidation N86-13476
Effect of composition of rarefied medium on gas-saturated titanium alloys N86-13477
Homogenization of beta-solid solution upon rapid heating of two-phase titanium alloys N86-13478
Changes in structure and mechanical properties of niobium-titanium alloy during oxygen saturation
N86-13479
Influence of electron-beam heating on structure and phase composition of VT9 alloy N86-13481
Structure and internal friction of near-eutectic alloy system Ti-W tampered from a liquid state N86-13482
Influence of thermal cycle on characteristics of cyclical crack resistance of titanium alloys and their joints produced by diffusion welding N86-13486
Kinetics of dissolution of oxide films in titanium upon diffusion welding N86-13487
Influence of preliminary annealing on structure and properties of VT23 alloy welded joints after hardening
N86-13488
Corrosion resistance of welded joints in certain titanium alloys N86-13489
Deformation and stresses upon welding of VT23 titanium alloy N86-13490
Determining local heating parameters for increasing fatigue resistance of welded joints N86-13491
TITANIUM CHLORIDES
Investigation of cold colored smoke production
[AD-A158783] N86-14040
TITANIUM NITRIDES
Influence of texture of titanium nitride coatings on wear resistance of cutting tools N86-13440
TOKAMAK DEVICES
China report: Science and technology
[JPRS-CST-85-020] N86-13600
Preliminary experimental results of CT-6B tokamak heating field voltage feedback control N86-13601
Doublet 3
[DE85-014369] N86-14031
Preliminary experiment on electron beam injection for tokamak current drive
[IPPJ-739] N86-14048
Theory of resistivity-gradient-driven turbulence
[DE85-015068] N86-14053
Impact of a poloidal divertor in ignition tokamak design
[DE85-012892] N86-14061
Heating and confinement in the Doublet 3 tokamak with electron cyclotron heating
[DE85-014323] N86-14070
TOLERANCES (PHYSIOLOGY)
Development and testing of a mouse simulated space flight model
[NASA-CR-176359] N86-13878
TOLLMEIN-SCHLICHTING WAVES
Boundary-value problem for two-dimensional fluctuations in boundary layers
[AD-A157952] N86-13685
TOOLING
European silicon structures plans custom chips in 15 days N86-13621
TOPOGRAPHY
Geologic characterization report for the Paradox Basin Study Region, Utah Study Areas. Volume 6: Salt Valley
[DE85-011699] N86-13858
TORCHES
Nozzle for self-contained cutting torches
[AD-D011875] N86-13597
TOROIDAL PLASMAS
Doublet 3
[DE85-014369] N86-14031
Preliminary experiment on electron beam injection for tokamak current drive
[IPPJ-739] N86-14048
Experimental study of neoclassical currents
[DE85-014866] N86-14063
TOROIDS
A three-dimensional analysis of natural convection in a toroidal loop N86-13672
TOUGHNESS
Zirconium as a structural material for naval systems
[AD-A158201] N86-13411
Fractography of mixed mode 1 - 2 failure in Graphite/Epoxy and Graphite/Thermoplastic unidirectional composites
[AD-A158852] N86-13498
TOXICITY
Functionalized vesicles as organic reagents
[AD-A158381] N86-13372
Health hazard evaluation of liquid monopropellants. Phase 5: Comparative inhalation toxicities of LGP 1776, LGP 1845, and HAN (hydroxylammonium nitrate)
[AD-A159090] N86-13891
TOXINS AND ANTITOXINS
Study of toxic and antigenic structures of botulinum neurotoxins
[AD-A156642] N86-13880
TRACKING NETWORKS
Distributed sensor networks
[AD-A158033] N86-13628
TRACKING RADAR
Mathematical analysis study for radar data processing and enhancement. Part 1: Radar data analysis
[NASA-CR-166616-PT-1] N86-13353
TRACTION
Tire-soil interaction model for turning (steered) tires
[AD-A157737] N86-13593
Design of traction drives
[NASA-RP-1154] N86-13734
TRAINING DEVICES
A reactive learning environment for the Equipment Problem Solving Techniques (EPST) system
[AD-A158035] N86-13929
The mission oriented terminal area simulation facility
[NASA-TM-87621] N86-13944
TRAJECTORIES
Photoelectronic trajectory anatomy of RCA-C-73435 image converter and its performance
[DE85-013973] N86-13723
TRAJECTORY ANALYSIS
Forming transformation matrices for different parameters of motion of celestial bodies N86-14112
TRAJECTORY OPTIMIZATION
Method for solving two-point boundary value problem for optimization of flights with low thrust N86-14114
Choice of optimum boundary conditions in speed optimization problem N86-14115
Approximate solutions of Euler-Lambert equation for case of several revolutions about central body
N86-14121
TRANSFER FUNCTIONS
Optimal transfer function for fiber optic communications N86-13641
TRANSFER ORBITS
Laser thermal propulsion N86-13548
Method for solving two-point boundary value problem for optimization of flights with low thrust N86-14114
Comparison of energetics of optimum maneuvers and two-impulse maneuvers in some problems of motion from a point into orbit N86-14134
Optimum control programs in problem of interorbital flight with continuous thrust N86-14135
TRANSFORMATIONS (MATHEMATICS)
A behavioral summary for completely random nets
[AD-A157755] N86-13960
Computation of geometric properties from the medial axis transform in 0 (n log n) time
[AD-A158934] N86-13980
Advanced algorithm for orbit computation N86-14101
Forming transformation matrices for different parameters of motion of celestial bodies N86-14112
TRANSIENT RESPONSE
Laser diagnostics for electric field measurements
N86-13563
TRANSLATIONAL MOTION
The simulation of truck motions
[UTIAS-294] N86-13914

TRANSMISSION
Comparison of ion milling techniques for cross-sectional TEM of semiconductors
[DE85-016596] N86-13664
TRANSMISSION EFFICIENCY
Determination of porosity of thin sheets of fiber materials based on optical transmission coefficient N86-13459
TRANSMISSION LINES
Slot line tunable bandpass filter
[AD-D011881] N86-13661
TRANSMISSIONS (MACHINE ELEMENTS)
Transmission acoustic vibration testing
[AD-A159022] N86-13326
TRANSMITTER RECEIVERS
Optical radar transceiver control apparatus
[AD-D011880] N86-14042
TRANSMITTERS
Worldwide report: Telecommunications policy, research, and development
[JPRS-TTP-85-026] N86-13640
TRANSONIC FLOW
A direct-inverse method for transonic and separated flows about airfoils
[NASA-CR-176403] N86-13300
Transonic separated flow predictions based on a mathematically simple, nonequilibrium turbulence closure model
[NASA-TM-86826] N86-13676
TRANSONIC SPEED
A tomographic technique for aerodynamics at transonic speeds
[NASA-TM-86766] N86-13297
TRANSPARENCE
Recent experience in the RAE (Royal Aircraft Establishment) 5-metre wind tunnel of a china clay method for indicating boundary layer transition
[AD-A157943] N86-13302
Influence of fog microstructure on quality of optical image transmitted through it N86-13781
TRANSPIRATION
Study of deposition control using transpiration
[DE85-012799] N86-13699
TRANSPORT AIRCRAFT
Abrasion behavior of aluminum and composite skin coupons, stiffened skins and stiffened panels representative of transport airplane structures
[NASA-TP-2520] N86-13316
Aircraft of the future
[NASA-TM-77952] N86-13318
Alerted monitors: Human operators aided by automated detectors
[PB85-222750] N86-13906
TRANSPORT PROPERTIES
Wind tunnel simulations of aeolian processes
[NASA-CR-176382] N86-13289
Performance-limiting factors in MPD thrusters
N86-13555
Electrical and thermal transport property studies of high-temperature thermoelectric materials
[AD-A158883] N86-13656
A study of transport phenomena and interface stability during solidification of binary solutions using front tracking finite elements N86-13669
A finite element solution of the transport equation
[AD-A159245] N86-13982
Coupled radiation transport/thermal analysis of the radiation shield for a space nuclear reactor
[AD-A158180] N86-14022
Electrical and electrothermal conductivity of planetary ionospheres, 1: Refinement of theory N86-14143
TRANSPORT THEORY
Experimental study of neoclassical currents
[DE85-014866] N86-14063
TRANSVERSE WAVES
Unlimited acceleration of charged particles by an electromagnetic wave with a purely transverse electric field propagating perpendicularly to a static magnetic field
[IPPJ-740] N86-14049
TRAPPING
Multilevel relaxation phenomena and population trapping
[DE85-011527] N86-13731
TRAPS
Variable temperature trap
[AD-D011874] N86-13719
TRAVELING WAVE TUBES
Verification of computer-aided designs of traveling-wave tubes utilizing novel dynamic refocusers and graphite electrodes for the multistage depressed collector
[NASA-TP-2524] N86-13643
TRAVELING WAVES
Waves which travel upstream in boundary layers
[AD-A157949] N86-13684
Far-field boundary conditions in numerical solutions of the Navier-Stokes equations
[AD-A158776] N86-13690
TREES (MATHEMATICS)
An algorithm to translate relational algebra queries into QUEL
[AD-A158169] N86-13931
TREES (PLANTS)
Classification of trees by growth classes on the basis of multizonal photographs N86-14173
TRIAXIAL STRESSES
Errors due to counting statistics in the triaxial strain (stress) tensor determined by diffraction
[AD-A158219] N86-13759
TRIBOLOGY
Activities report in space tribology
[ESA-ESTL-72] N86-13738
TRIGONOMETRIC FUNCTIONS
Structure of coefficients of series representing solution of plane circular restricted three-body problem
N86-14129
TROPOSPHERE
Experience in measuring mean wind velocity profile in lower troposphere by sodar anemometer under inversion and convective conditions N86-13782
TROPOSPHERIC WAVES
Spatial patterns of manifestation of solar activity in troposphere N86-14126
TRUCKS
The simulation of truck motions
[UTIAS-294] N86-13914
TSUNAMI WAVES
Three-dimensional modeling of Tsunami waves
[DE85-015724] N86-13877
TUNGSTEN
Thermophysical properties of tungsten at high temperatures N86-13458
Grain growth in heat-resistant austenitic steel
N86-13462
Coupled radiation transport/thermal analysis of the radiation shield for a space nuclear reactor
[AD-A158180] N86-14022
TUNING
Slot line tunable bandpass filter
[AD-D011881] N86-13661
Hot electron emission in semiconductors
[AD-A158042] N86-14072
TURBIDITY
Use of Goudriaan model for studying reflection regularities in vegetation-soil system in optical range. 1: Influence of phytometric parameters on spectral brightness coefficients N86-14190
TURBINE BLADES
Polar measurements on the profiles: FX 84-w-097, FX 84-w-127, FX 84-w-140, FX 84-w-175, FX 84-w-218 --- wind energy converters N86-13821
An analytical theory for rotor tip vane performance and comparison with experimental results --- wind energy converters N86-13823
Aerofoil characteristics of rotating blades --- wind turbine models N86-13824
Aerodynamic theory in the calculation of the GROWIAN rotor compared with some experimental data --- wind energy converter N86-13826
TURBINE PUMPS
HPOTP low-speed flexible rotor balancing, phase 1
[NASA-CR-171610] N86-13369
TURBOFAN ENGINES
Effects of velocity profile and inclination on dual-jet-induced pressures on a flat plate in a crosswind
[NASA-CR-177361] N86-13287
TURBOMACHINERY
A FORTRAN computer code for calculating flows in multiple-blade-element cascades
[NASA-TM-87104] N86-13295
TURBULENCE
An investigation into the vertical axis control power requirements for landing VTOL type aircraft onboard nonaviation ships in various sea states
[NASA-CR-176355] N86-13294
Coupling between velocity oscillations and solid propellant combustion N86-13541
Turbulence and dynamical systems
[AD-A159026] N86-13691
Turbulence in two-field incompressible flow
[DE85-015361] N86-13693
Fluid forces on two circular cylinders in crossflow
[DE85-014294] N86-13704
Vertical structure of turbulence and turbulent exchange in equatorial zone of Pacific Ocean N86-13771
Laboratory studies of steep and breaking deep water waves in a convergent channel
[AD-A158187] N86-13875
Theory of resistivity-gradient-driven turbulence
[DE85-015068] N86-14053
TURBULENCE EFFECTS
Statistics of intensive light beams in turbulent atmosphere N86-13786
TURBULENT BOUNDARY LAYER
Studies of the flow field near a NACA 4412 aerofoil at nearly maximum lift
[AD-A157750] N86-13301
Recent experience in the RAE (Royal Aircraft Establishment) 5-metre wind tunnel of a china clay method for indicating boundary layer transition
[AD-A157943] N86-13302
Sensitivity to mean flow parameters of the low wavenumber content of the wall pressure under a turbulent boundary layer
[AD-A158037] N86-13686
TURBULENT FLOW
Analysis of heterogeneous diffusion flame stabilization
N86-13527
The 1-D laser Doppler instrumentation N86-13575
Modelling a transport equation of turbulent reactive mixing flow N86-13674
Study of deposition control using transpiration
[DE85-012799] N86-13699
Formation of structure of mixed region under influence of shear flow in stratified fluid N86-13768
Vertical structure of turbulence and turbulent exchange in equatorial zone of Pacific Ocean N86-13771
Development in aerodynamic calculations --- wind energy converters N86-13822
TURNING FLIGHT
Pilot-oriented performance measurement
[AD-A158849] N86-13890
TWO DIMENSIONAL BODIES
Electronic detection of low concentrations of organophosphorus compounds with a solid state device utilizing supported copper + cuprous oxide island films
[AD-A158181] N86-13392
A numerical investigation into the plastic stress and strain fields around a surface crack
[ARL/STRUC-R-414] N86-13754
TWO DIMENSIONAL FLOW
Analysis of heterogeneous diffusion flame stabilization
N86-13527
Non-Newtonian flow past curved external surfaces
N86-13671
A fully viscous two-dimensional unsteady flow analysis applied to detonation transition in porous explosives
[AD-A157794] N86-13682
Boundary-value problem for two-dimensional fluctuations in boundary layers
[AD-A157952] N86-13685
Far-field boundary conditions in numerical solutions of the Navier-Stokes equations
[AD-A158776] N86-13690
TWO PHASE FLOW
Two-phase heat transport systems: System definition, volume 1 --- space stations
[ESA-CR(P)-2052] N86-13363
Spray characterization using phase angle detection
N86-13577
Size and shape characterization of individual flowing droplets by laser light scattering N86-13579
Specialists Meeting on Atomization and Nondilute Sprays
[AD-A159006] N86-13634
Turbulence in two-field incompressible flow
[DE85-015361] N86-13693

U

U.S.S.R.
USSR report: Earth sciences
[JPRS-UES-85-009] N86-13765
U.S.S.R. SPACE PROGRAM
Methods for complex space experiment in USSR for studying land from manned spacecraft N86-14181
Comments on anniversary of Apollo-Soyuz flight
N86-14197
Soviet-French commission discusses joint space projects N86-14198
List of recent Soviet space launches N86-14199
ULTRAPURE METALS
Calculation of failure constant for titanium alloys
N86-13474
ULTRASONIC RADIATION
A method to determine dynamic elastic constants of thin shell composites by guided ultrasonic waves
[AD-A159025] N86-13381
Ultrasonic longitudinal wave velocity in carbon-carbon Pitch and Pitch/M2 shape stable nosetip material from 70 deg F to 5400 deg F
[DE85-017330] N86-13382
Theory of the propagation of finite amplitude ultrasonic waves in pure mode directions in hexagonal and trigonal crystals
[AD-A158154] N86-14009

ULTRASONICS
Scientific activities of the Polish Academy of Sciences: Institute of Fundamental Technological Research in 1983
[ISBN-83-01-06288-6] N86-14107
ULTRAVIOLET RADIATION
Scaling of uv (351 nm) fusion implosions driven by multiple beams
[DE85-014406] N86-14068
Disturbances in stratosphere and mesosphere from source of ultraviolet radiation N86-14136
ULTRAVIOLET SPECTRA
Optical constants
[AD-A158623] N86-14038
ULTRAVIOLET SPECTROMETERS
Extended atmospheres of outer planet satellites and comets
[NASA-CR-176398] N86-14209
UNIFORM FLOW
Numerical solutions of Navier-Stokes equations for a Butler wing
[NASA-CR-174202] N86-13293
UNITED STATES
Emerging aerospace technologies
[NASA-TM-86837] N86-14213
UNIVERSITIES
The 1983 NASA/ASEE Summer Faculty Fellowship Research Program research reports
[NASA-CR-171904] N86-14078
UNLOADING
Italian robot manufacturer enters Spanish market N86-13626
UNSTEADY FLOW
Numerical solutions of Navier-Stokes equations for a Butler wing
[NASA-CR-174202] N86-13293
A computational analysis of pulsating flow in rigid and deformable tubes N86-13673
A fully viscous two-dimensional unsteady flow analysis applied to detonation transition in porous explosives
[AD-A157794] N86-13682
Waves which travel upstream in boundary layers
[AD-A157949] N86-13684
Development in aerodynamic calculations --- wind energy converters N86-13822
Unsteady aerodynamics applied to the horizontal axis wind turbine disk N86-13825
UNSTEADY STATE
Two unsteady heat transfer experiments. Part 1: In grid-generated isotropic turbulence. Part 2: In laminar oscillatory flow in straight and conical tubes N86-13675
UPGRADING
Design criteria upgrade for US Army Type 2 air traffic control towers
[AD-A159115] N86-13314
UPPER ATMOSPHERE
Remote sensing of Earth terrain N86-13808
Measurement of rate constants of elementary gas reactions of importance to upper atmosphere and combustion systems
[AD-A158824] N86-13857
Spectrum of photoelectrons in Earth's upper atmosphere during solar flares N86-14118
Formation of high-energy secondary electrons in low-density medium at great altitudes N86-14122
UPPER IONOSPHERE
Coordinated investigations of processes in subauroral upper ionosphere and through in concentration of light ions N86-14137
UPPER STAGE ROCKET ENGINES
Computer program for post-flight evaluation of a launch vehicle upper-stage on-off reaction control system
[NASA-CR-166029] N86-13921
UPSTREAM
Waves which travel upstream in boundary layers
[AD-A157949] N86-13684
Hybrid simulation codes with application to shocks and upstream waves
[NASA-CR-176365] N86-13702
UPWASH
Some design philosophy for reducing the community noise of advanced counter-rotation propellers
[NASA-TM-87099] N86-14007
USER MANUALS (COMPUTER PROGRAMS)
DAB user's guide
[NASA-CR-177393] N86-13290
PLTTER user's guide
[NASA-CR-177385] N86-13291
User's manual for the generalized computer program system. Open-channel flow and sedimentation, TABS-2. Main text
[AD-A159249] N86-13692
Performance assessment of OTEC power systems and thermal power plants. Volume 2: Users manual for PACC-OTECs
[DE85-016792] N86-13835
USER REQUIREMENTS
Comparative study of space segments for the provision of future operational data relay satellite services
[MBB-DSP-TN/DRS/132/84] N86-13355
Bulk CMOS VLSI technology studies. Part 5: The design and implementation of a high speed integrated circuit functional tester
[AD-A158370] N86-13651
Information requirements determination: An empirical investigation of obstacles within an individual
[AD-A158025] N86-13901
Unified method for delay analysis of random multiple access algorithms
[AD-A159108] N86-13981
UTAH
Geologic characterization report for the Paradox Basin Study Region, Utah Study Areas. Volume 6: Salt Valley
[DE85-011699] N86-13858
UTILIZATION
Application of statistical model of layered medium for computing thermal emission of ice covers N86-14186

V

V/STOL AIRCRAFT
Ground effects on V/STOL and STOL aircraft: A survey
[NASA-TM-86825] N86-13299
VACUUM
Influence of Co-Cr-Al-Y coatings on physical and mechanical properties of EI-893 steel in GT-100 turbine drive vanes N86-13438
VACUUM DEPOSITION
Influence of annealing on hardness of vacuum-diffusion chromium coating on low-carbon steel N86-13441
VACUUM MELTING
Grain growth in heat-resistant austenitic steel N86-13462
VALLEYS
Geologic characterization report for the Paradox Basin Study Region, Utah Study Areas. Volume 6: Salt Valley
[DE85-011699] N86-13858
VALUE
On asymptotic distribution of the test statistic for the mean of the anisotropic principal component
[AD-A158255] N86-13972
Conditioning in a missing data problem
[AD-A158202] N86-13988
Extreme values of queues, point processes and Stochastic Networks
[AD-A158619] N86-13991
VAN DER WAAL FORCES
Crushing strength of aluminum oxide agglomerates
[AD-A158051] N86-13756
VANADIUM
Grain growth in heat-resistant austenitic steel N86-13462
VANADIUM ALLOYS
Influence of hydrogen on formation of cold cracks in seams during welding of pipe steel N86-13494
VANES
Influence of Co-Cr-Al-Y coatings on physical and mechanical properties of EI-893 steel in GT-100 turbine drive vanes N86-13438
VAPOR PHASES
Technique of assembling structures using vapor phase soldering
[AD-D011805] N86-13410
VAPORS
Health hazard evaluation of liquid monopropellants. Phase 5: Comparative inhalation toxicities of LGP 1776, LGP 1845, and HAN (hydroxylammonium nitrate)
[AD-A159090] N86-13891
VARIABILITY
Study of the mechanical properties dispersion of carbon-epoxy composite materials
[M2-695600-PT-1] N86-13384
Variability of rainfall over small areas N86-14098
VARIABLE PITCH PROPELLERS
Hub effects in propeller design and analysis
[AD-A158853] N86-13331
VARIANCE (STATISTICS)
A note on the effect of ignoring small measurement errors in precision instrument calibration
[AD-A159104] N86-13713
VARIATIONAL PRINCIPLES
Multigrid relaxation methods and the analysis of lightness, shading, and flow
[AD-A158173] N86-14036
VARIATIONS
Variability of rainfall over small areas N86-14098
VECTOR ANALYSIS
Sparse elimination on vector multiprocessors
[AD-A158274] N86-13909
VECTORS (MATHEMATICS)
Sparse elimination on vector multiprocessors
[AD-A158274] N86-13909
VEGA PROJECT
Vega-1 releases aerostat and lander at Venus N86-14148
Objectives of Vega project research N86-14149
Vega-2 releases aerostat and lander at Venus N86-14150
Results from Vega atmosphere and soil studies N86-14151
Press conference on first stage of Vega project N86-14152
Further comments on results of Vega studies of Venus N86-14153
VEGETATION
Use of remote optical measurements in agriculture N86-14172
Compilation of landscape maps at different scales with use of space photoinformation N86-14187
VEGETATION GROWTH
Classification of trees by growth classes on the basis of multizonal photographs N86-14173
VEGETATIVE INDEX
Reflectance modeling N86-13795
Geometric-optical modeling of a conifer forest canopy N86-13799
Crop characteristics research: Growth and reflectance analysis N86-13800
Remote sensing of Earth terrain N86-13808
Discrete random media techniques for microwave modeling of vegetated terrain N86-13809
Active microwave properties of vegetation canopies N86-13812
Use of Goudriaan model for studying reflection regularities in vegetation-soil system in optical range. 1: Influence of phytometric parameters on spectral brightness coefficients N86-14190
VELOCITY
Spray characterization using phase angle detection N86-13577
Boundary-value problem for two-dimensional fluctuations in boundary layers
[AD-A157952] N86-13685
Sensitivity to mean flow parameters of the low wavenumber content of the wall pressure under a turbulent boundary layer
[AD-A158037] N86-13688
The spatial and temporal parameters of velocity discrimination
[AD-A158735] N86-13896
VELOCITY DISTRIBUTION
The 1-D laser Doppler instrumentation N86-13575
Non-Newtonian flow past curved external surfaces N86-13671
Behavior of slender cones at large incidences N86-13707
VELOCITY MEASUREMENT
New flow visualization technique for water tunnel testing of combustors
[AD-A158015] N86-13686
Wave interpretation of measurements on Mars-7 and Venera-9 probes for determining velocity of motion of interstellar gas N86-14147
VENTING
Sparger system for MMH-helium vents N86-14096
VENUS (PLANET)
Vega-2 releases aerostat and lander at Venus N86-14150
Results from Vega atmosphere and soil studies N86-14151
VENUS ATMOSPHERE
Vega-1 releases aerostat and lander at Venus N86-14148
Objectives of Vega project research N86-14149
Vega-2 releases aerostat and lander at Venus N86-14150
Results from Vega atmosphere and soil studies N86-14151
Further comments on results of Vega studies of Venus N86-14153
Development of instruments for Vega probes N86-14154
VENUS CLOUDS
Objectives of Vega project research N86-14149
Vega-2 releases aerostat and lander at Venus N86-14150
Press conference on first stage of Vega project N86-14152
Further comments on results of Vega studies of Venus N86-14153
VENUS PROBES
Development of instruments for Vega probes N86-14154

VENUS SURFACE

Results from Vega atmosphere and soil studies N86-14151

Results of study of surface of five regions on Venus by bistatic radar method N86-14156

VERTICAL DISTRIBUTION

Vertical structure of turbulence and turbulent exchange in equatorial zone of Pacific Ocean N86-13771

Structural characteristic of temperature field over sea N86-13783

Meteorological and climatological conditions affecting the vertical structure of visibility in northern Germany [AD-A158254] N86-13871

VERTICAL ORIENTATION

Wave force-phase method for vertical cylinders [AD-A157709] N86-13680

High Reynolds number wave force investigation in a wave flume [AD-A157722] N86-13681

Atmospheric environment for Space Shuttle (STS-51D) [NASA-TM-86524] N86-13868

VERTICAL TAKEOFF AIRCRAFT

An investigation into the vertical axis control power requirements for landing VTOL type aircraft onboard nonaviation ships in various sea states [NASA-CR-176355] N86-13294

VERY LARGE SCALE INTEGRATION

Using software technology to specify abstract interfaces in VLSI design [AD-A158034] N86-13649

Bulk CMOS VLSI technology studies. Part 4: Design of a CMOS microsequencer [AD-A158369] N86-13650

Bulk CMOS VLSI technology studies. Part 5: The design and implementation of a high speed integrated circuit functional tester [AD-A158370] N86-13651

VIBRATION

HPOTP low-speed flexible rotor balancing, phase 1 [NASA-CR-171610] N86-13369

Sorption detector system for chemical agents detection and recognition [DE85-012775] N86-13400

VIBRATION DAMPING

Computation of normal modes from identified complex modes N86-13590

Dynamic modeling of structures from measured complex modes N86-13591

VIBRATION MEASUREMENT

Discussion on the Vibration Process Standards 9958002 and 9958004 [DE85-017116] N86-13599

VIBRATION MODE

Large modal survey testing using the Ibrahim time domain identification technique [AIAA-81-0528R] N86-13589

VIBRATION SIMULATORS

Tape joint design for a vibration table [DE85-012617] N86-13753

VIBRATION TESTS

Ground vibration test of the laminar flow control JStar airplane [NASA-TM-86398] N86-13321

Investigation for the definition of a hydraulic multidegree of freedom vibration facility [B-TF-1627] N86-13340

Dynamic identification for control of large space structures [NASA-CR-176380] N86-13587

A parametric study of the Ibrahim time domain modal identification algorithm N86-13588

Large modal survey testing using the Ibrahim time domain identification technique [AIAA-81-0528R] N86-13589

Tape joint design for a vibration table [DE85-012617] N86-13753

VISCOELASTICITY

Process-induced viscoelastic stress in composite laminates N86-13376

Development of singularities in nonlinear viscoelasticity [AD-A158190] N86-13758

VISCOSITY

Experiments with non-Darcy flow in joints with large scale roughness [DE85-015714] N86-13695

VISCOUS FLOW

Numerical solutions of Navier-Stokes equations for a Butler wing [NASA-CR-174202] N86-13293

A fully viscous two-dimensional unsteady flow analysis applied to detonation transition in porous explosives [AD-A157794] N86-13682

VISIBILITY

Meteorological and climatological conditions affecting the vertical structure of visibility in northern Germany [AD-A158254] N86-13871

VISIBLE INFRARED SPIN SCAN RADIOMETER

VAS demonstration: (VISSR Atmospheric Sounder) description [NASA-RP-1151] N86-13867

VISIBLE SPECTRUM

Optical constants [AD-A158623] N86-14038

VISUAL DISCRIMINATION

Enhancing sensitivity to visual motion and enhancing visual sensitivity [AD-A158800] N86-13889

VISUAL PERCEPTION

An analytical comparison of three visual approach slope indicators: VASIS, T-VASIS and PAPI [ARL/SYS-R-33] N86-13309

Enhancing sensitivity to visual motion and enhancing visual sensitivity [AD-A158800] N86-13889

Pilot-oriented performance measurement [AD-A158849] N86-13890

A psychophysiological mapping of cognitive processes [AD-A158732] N86-13895

The spatial and temporal parameters of velocity discrimination [AD-A158735] N86-13896

VOIDS

Probability of detection of internal voids in structural ceramics using microfocus radiography [NASA-TM-87164] N86-13749

VOLATILITY

Mass transfer coefficients and Henry's constants for packed-tower air stripping of volatile organics: Measurements and correlation [AD-A158811] N86-13375

VOLCANOES

Formation of underwater oceanic volcanoes and islands in relation to lithospheric thickness and movements N86-13776

Volcanoes discovered with radio beam N86-13777

Airborne lidar measurements of El Chichon stratospheric aerosols [NASA-RP-1148] N86-13850

VOLTAGE CONTROLLED OSCILLATORS

Phase lock acquisition system [AD-D011804] N86-13646

VORTEX GENERATORS

Double-branched vortex generator [NASA-TM-88201] N86-13298

VORTICES

Double-branched vortex generator [NASA-TM-88201] N86-13298

Waves which travel upstream in boundary layers [AD-A157949] N86-13684

Some design philosophy for reducing the community noise of advanced counter-rotation propellers [NASA-TM-87099] N86-14007

Rossby autosoliton N86-14158

W

WAFERS

CNET of France uses organo-metallic epitaxy for laser N86-13620

European silicon structures plans custom chips in 15 days N86-13621

WAKES

Some design philosophy for reducing the community noise of advanced counter-rotation propellers [NASA-TM-87099] N86-14007

WALL PRESSURE

Sensitivity to mean flow parameters of the low wavenumber content of the wall pressure under a turbulent boundary layer [AD-A158037] N86-13688

WARNING SYSTEMS

Report on an automated calibration range for broadband isotropic probes [PB85-231470] N86-13726

WASTE DISPOSAL

Radar location equipment development program, phase 1 [DE85-014523] N86-13637

WASTE TREATMENT

Solid waste treatment processes for space station N86-14091

WATER

Study of optical-acoustical phenomena at surface of strongly absorbing clearing fluids N86-13774

Observation of optical-radio frequency resonance in H2O using wide-band ruby laser spectroscopy N86-13790

Acoustical scattering from an elastic sphere in water: Surface wave glory, resonances, and the Sommerfeld-Watson transformation for amplitudes [AD-A158884] N86-14010

Extended atmospheres of outer planet satellites and comets [NASA-CR-176398] N86-14209

WATER COOLED REACTORS

Study of effect of normal reactor water on growth rate of fatigue cracks in 15Kh2NMFA steel N86-13470

WATER DEPTH

The design of a beach profiler [AD-A157715] N86-13874

Laboratory studies of steep and breaking deep water waves in a convergent channel [AD-A158187] N86-13875

WATER FLOW

Some characteristics of bottom density currents N86-13772

WATER POLLUTION

Mass transfer coefficients and Henry's constants for packed-tower air stripping of volatile organics: Measurements and correlation [AD-A158811] N86-13375

An Oil/Water disperser device for use in an oil content Monitor/Control system [AD-D011868] N86-13714

Oil content Monitor/Control system and method [AD-D011871] N86-13717

Influence of petroleum pollution on ocean-atmosphere gas exchange intensity (in example of North Atlantic) N86-13785

WATER RESOURCES

California Water Resources Institute program for 1983 [PB85-225837] N86-13818

Experience in conducting subsatellite experiments with water bodies in USSR and Hungarian People's Republic N86-14182

WATER TREATMENT

Mass transfer coefficients and Henry's constants for packed-tower air stripping of volatile organics: Measurements and correlation [AD-A158811] N86-13375

WATER TUNNEL TESTS

New flow visualization technique for water tunnel testing of combustors [AD-A158015] N86-13686

WATER WAVES

High Reynolds number wave force investigation in a wave flume [AD-A157722] N86-13681

Atmospheric synoptic eddies over ocean (determined from experimental data) N86-13784

Laboratory studies of steep and breaking deep water waves in a convergent channel [AD-A158187] N86-13875

Stereophotogrammetric survey of wave-covered water surface N86-14170

Equatorial waves in ocean surface temperature field according to data from shipboard and satellite measurements N86-14171

WATERWAYS

User's manual for the generalized computer program system. Open-channel flow and sedimentation, TABS-2. Main text [AD-A159249] N86-13692

WAVE DISPERSION

Iterative and Pade solutions for the water-wave dispersion relation [AD-A157796] N86-13683

WAVE DRAG

Wave force-phase method for vertical cylinders [AD-A157709] N86-13680

WAVE EXCITATION

Parametric excitation of ion Bernstein waves by magnetosonic wave [IPPJ-738] N86-14047

WAVE INTERACTION

Hybrid simulation codes with application to shocks and upstream waves [NASA-CR-176365] N86-13702

WAVE PROPAGATION

Mathematical analysis study for radar data processing and enchancement. Part 2: Modeling of propagation path errors [NASA-CR-166616-PT-2] N86-13354

A method to determine dynamic elastic constants of thin shell composites by guided ultrasonic waves [AD-A159025] N86-13381

Effective medium theory for partially saturated porous solids [DE85-016608] N86-13598

Theoretical studies and data analysis of wave propagation in random media [AD-A158775] N86-13632

Iterative and Pade solutions for the water-wave dispersion relation
[AD-A157796] N86-13683
Waves which travel upstream in boundary layers
[AD-A157949] N86-13684
Microwave dielectric and propagation properties of vegetation canopies N86-13810
Theory of the propagation of finite amplitude ultrasonic waves in pure mode directions in hexagonal and trigonal crystals
[AD-A158154] N86-14009
Parametric excitation of ion Bernstein waves by magnetosonic wave
[IPPJ-738] N86-14047
Unlimited acceleration of charged particles by an electromagnetic wave with a purely transverse electric field propagating perpendicularly to a static magnetic field
[IPPJ-740] N86-14049
Scientific activities of the Polish Academy of Sciences: Institute of Fundamental Technological Research in 1983
[ISBN-83-01-06288-6] N86-14107

WAVEFORMS
Analog-to-Digital converter
[AD-D011878] N86-13660

WAVEGUIDES
China report: Science and technology
[JPRS-CST-85-020] N86-13600
On H plane dielectric loading theory for H plane ferrite phase shifter N86-13603

WEAR
Report on investigation of alcohol combustion associated wear in spark ignition engines, mechanisms and lubricant effects
[AD-A157714] N86-13388
Fiber composition materials for strengthening components of aluminum and its alloys N86-13424

WEAR INHIBITORS
Silicide coatings for protecting titanium-niobium alloys from high-temperature oxidation N86-13476
Evaluation of the erosion protection of low inflammability liquids of the HFC type (polyglycol solutions) --- hydraulic fluids
[CETIM-12-E-13-3] N86-13505

WEAR TESTS
Superhard materials developed N86-13471
Evaluation of the erosion protection of low inflammability liquids of the HFC type (polyglycol solutions) --- hydraulic fluids
[CETIM-12-E-13-3] N86-13505

WEATHER
Meteorological and climatological conditions affecting the vertical structure of visibility in northern Germany
[AD-A158254] N86-13871

WEATHER FORECASTING
Goskomgidromet plans automation of aerial cloud-seeding work N86-13766

WEATHERING
Unusual occurrence of maghemite in soils developed on Knox group dolostones
[DE85-017158] N86-13817

WEBS (SUPPORTS)
Fabrication and evaluation of superplastically formed/weld-brazed corrugated compression panels with beaded webs
[NASA-TP-2512] N86-13406

WEDGES
Subcritical crack development under constant load in VT6 alloy N86-13475

WEIGHT INDICATORS
Test of the ONERA cryogenic balance in the T2 wind tunnel
[ONERA-BT-8/0791-GY] N86-13341

WEIGHT REDUCTION
Structures and materials technology issues for reusable launch vehicles
[NASA-TM-87626] N86-13349
New materials to lighten vehicles N86-13624

WEIGHTLESSNESS
Development and testing of a mouse simulated space flight model
[NASA-CR-176359] N86-13878
Energy exchange of plants under weightlessness conditions N86-14162

WEIGHTLESSNESS SIMULATION
Endocrine and fluid metabolism in males and females of different ages after bedrest, acceleration and lower body negative pressure
[NASA-TM-58270] N86-13886

WELD STRENGTH
Study of properties of gas-thermal coatings of composite nichrome-aluminum alloy powders N86-13442
Influence of thermal cycle on characteristics of cyclical crack resistance of titanium alloys and their joints produced by diffusion welding N86-13486
Determining local heating parameters for increasing fatigue resistance of welded joints N86-13491

WELD TESTS
Influence of thermal cycle on characteristics of cyclical crack resistance of titanium alloys and their joints produced by diffusion welding N86-13486
Corrosion resistance of welded joints in certain titanium alloys N86-13489

WELDABILITY
Optimization of technological parameters of cold pressure welding of AD1M thin aluminum sheets
N86-13484
Study of process of pore formation during argon-arc welding of aluminum alloy 1420 N86-13485
Corrosion resistance of welded joints in certain titanium alloys N86-13489
Deformation and stresses upon welding of VT23 titanium alloy N86-13490
Influence of structure of heat-resistant nickel alloy ZhS6U on its weldability in the solid state N86-13492
Diffusion welding of copper-chromium pseudoalloy with copper N86-13493

WELDED JOINTS
Fabrication and evaluation of superplastically formed/weld-brazed corrugated compression panels with beaded webs
[NASA-TP-2512] N86-13406
Influence of thermal cycle on characteristics of cyclical crack resistance of titanium alloys and their joints produced by diffusion welding N86-13486
Influence of preliminary annealing on structure and properties of VT23 alloy welded joints after hardening
N86-13488
Deformation and stresses upon welding of VT23 titanium alloy N86-13490
Determining local heating parameters for increasing fatigue resistance of welded joints N86-13491
Influence of structure of heat-resistant nickel alloy ZhS6U on its weldability in the solid state N86-13492
Influence of hydrogen on formation of cold cracks in seams during welding of pipe steel N86-13494

WELDING
USSR report: Materials science and metallurgy
[JPRS-UMS-85-006] N86-13422
Possible mechanism of wave formation during detonation welding N86-13483
Optimization of technological parameters of cold pressure welding of AD1M thin aluminum sheets
N86-13484

WELLS
Geothermal resources of the Wind River Basin, Wyoming
[DE85-016969] N86-13816

WEST GERMANY
Meteorological and climatological conditions affecting the vertical structure of visibility in northern Germany
[AD-A158254] N86-13871

WETLANDS
User's manual for the generalized computer program system. Open-channel flow and sedimentation, TABS-2. Main text
[AD-A159249] N86-13692

WIDE ANGLE LENSES
A multiple-object fibre-optics coupler for the 1.2-m UK Schmidt Telescope N86-14201

WIND (METEOROLOGY)
Atmospheric environment for Space Shuttle (STS-51D)
[NASA-TM-86524] N86-13868

WIND EFFECTS
Wind tunnel simulations of aeolian processes
[NASA-CR-176382] N86-13289

WIND PROFILES
Experience in measuring mean wind velocity profile in lower troposphere by sodar anemometer under inversion and convective conditions N86-13782
Atmospheric environment for Space Shuttle (STS-51D)
[NASA-TM-86524] N86-13868

WIND TUNNEL APPARATUS
Test of the ONERA cryogenic balance in the T2 wind tunnel
[ONERA-BT-8/0791-GY] N86-13341

WIND TUNNEL MODELS
Recent experience in the RAE (Royal Aircraft Establishment) 5-metre wind tunnel of a china clay method for indicating boundary layer transition
[AD-A157943] N86-13302
Aerofoil characteristics of rotating blades --- wind turbine models N86-13824

WIND TUNNEL TESTS
Wind tunnel simulations of aeolian processes
[NASA-CR-176382] N86-13289
Double-branched vortex generator
[NASA-TM-83201] N86-13298
Study of the influence of an oscillating spoiler on the surrounding aerodynamic field
[IMFL-3119] N86-13303
Algorithms for the reduction of wind-tunnel data derived from strain gauge force balances
[ARL/AERO-R-164] N86-13337
Test of the ONERA cryogenic balance in the T2 wind tunnel
[ONERA-BT-8/0791-GY] N86-13341
Polar measurements on the profiles: FX 84-w-097, FX 84-w-127, FX 84-w-140, FX 84-w-175, FX 84-w-218 --- wind energy converters N86-13821
Preliminary measurement of the noise from the 2/9 scale model of the Large-scale Advanced Propfan (LAP) propeller, SR-7A
[NASA-TM-87116] N86-14006

WIND TUNNEL WALLS
Study of the influence of an oscillating spoiler on the surrounding aerodynamic field
[IMFL-3119] N86-13303

WIND TUNNELS
Recent experience in the RAE (Royal Aircraft Establishment) 5-metre wind tunnel of a china clay method for indicating boundary layer transition
[AD-A157943] N86-13302
Heat transfer and pressure drop performance of a finned-tube heat exchanger proposed for use in the NASA Lewis Altitude Wind Tunnel
[NASA-TM-87151] N86-13677

WIND TURBINES
Implementing agreement for cooperation in the development of large scale wind energy conversion systems --- conferences
[JUEL-SPEZ-304] N86-13820
Polar measurements on the profiles: FX 84-w-097, FX 84-w-127, FX 84-w-140, FX 84-w-175, FX 84-w-218 --- wind energy converters N86-13821
Development in aerodynamic calculations --- wind energy converters N86-13822
An analytical theory for rotor tip vane performance and comparison with experimental results --- wind energy converters N86-13823
Aerofoil characteristics of rotating blades --- wind turbine models N86-13824
Unsteady aerodynamics applied to the horizontal axis wind turbine disk N86-13825
Aerodynamic theory in the calculation of the GROWIAN rotor compared with some experimental data --- wind energy converter N86-13826
Aerodynamic research on wind turbines at NLR
N86-13828
Aerodynamic calculational methods for curved-blade Darrieus VAWT WECS --- vertical axis wind turbine wind energy converters (VAWT WECS) N86-13830

WIND VELOCITY
Influence of petroleum pollution on ocean-atmosphere gas exchange intensity (in example of North Atlantic)
N86-13785
Wind loading on solar collectors
[DE85-012151] N86-13833

WIND VELOCITY MEASUREMENT
Experience in measuring mean wind velocity profile in lower troposphere by sodar anemometer under inversion and convective conditions N86-13782

WINDPOWER UTILIZATION
Implementing agreement for cooperation in the development of large scale wind energy conversion systems --- conferences
[JUEL-SPEZ-304] N86-13820
Aerodynamic research efforts at SERI wind energy research center at Rocky Flats --- Solar Energy Research Institute (SERI) N86-13829

WINDPOWERED GENERATORS
Implementing agreement for cooperation in the development of large scale wind energy conversion systems --- conferences
[JUEL-SPEZ-304] N86-13820
An analytical theory for rotor tip vane performance and comparison with experimental results --- wind energy converters N86-13823
Aerodynamic theory in the calculation of the GROWIAN rotor compared with some experimental data --- wind energy converter N86-13826
Aerodynamic performance of a new LM 17.2 m rotor --- wind energy converter N86-13827
Aerodynamic research efforts at SERI wind energy research center at Rocky Flats --- Solar Energy Research Institute (SERI) N86-13829
Aerodynamic calculational methods for curved-blade Darrieus VAWT WECS --- vertical axis wind turbine wind energy converters (VAWT WECS) N86-13830

WINDS ALOFT
Atmospheric environment for Space Shuttle (STS-51D)
[NASA-TM-86524] N86-13868

WINTER
Investigation of cold colored smoke production
[AD-A158783] N86-14040
WIRE
Routing method in computer aided customization of a two level automated universal array
[AD-D011808] N86-13925
WIRE WINDING
Electrical motor with superconducting winding --- actuators
[SEP-TS/SE/BT/10026/85] N86-13668
WORDS (LANGUAGE)
Speech recognition: Acoustic, phonetic and lexical knowledge
[AD-A158264] N86-13629
WORKLOADS (PSYCHOPHYSIOLOGY)
Pilot-oriented performance measurement
[AD-A158849] N86-13890
Effects of digital altimetry on pilot workload
[NASA-TM-86424] N86-13892
WYOMING
Geothermal resources of the Wind River Basin, Wyoming
[DE85-016969] N86-13816

X

X RAY ABSORPTION
Time resolved extended X-ray absorption fine structure spectrometer
[AD-D011869] N86-13715
X RAY ANALYSIS
Complex nickel-aluminide coatings on nickel-chromium alloy EP648 VI N86-13437
Particulate matter analysis by electron microscopy
[PB85-227817] N86-13846
X RAY DIFFRACTION
Small X-ray diffraction of immunoglobulin-membrane complexes
[AD-A158252] N86-13882
X RAY FLUORESCENCE
Time resolved extended X-ray absorption fine structure spectrometer
[AD-D011869] N86-13715
X RAY SCATTERING
Combined small angle X-ray scattering and transmission electron microscopy studies of Al-Li alloys
[DE85-016356] N86-13416
X RAY SOURCES
Laser produced X-ray for high resolution lithography
[AD-A158734] N86-13730
X RAY STRESS MEASUREMENT
Errors due to counting statistics in the triaxial strain (stress) tensor determined by diffraction
[AD-A158219] N86-13759
X RAY TELESCOPES
Test method for telescopes using a point source at a finite distance
[NASA-TM-86523] N86-14033
X RAYS
Development of high sensitivity X-ray and electron beam resist processes
[AD-A158968] N86-13657
Laser produced X-ray for high resolution lithography
[AD-A158734] N86-13730

Y

YIELD POINT
Effect of elastoplastic cyclic deformation on mechanical characteristics of steel O3Kh13AG19 at temperatures of 293 and 77 deg K N86-13463
YIELD STRENGTH
Modifications of system for elevated temperature tensile testing and stress-strain measurement of metal matrix composites
[NASA-TM-87172] N86-13370

Z

ZENITH
Analysis of survey conditions and effect of noise on quality of sensing of soil formations N86-14191
ZETA PINCH
Dense Z-pinch plasmas
[DE85-005818] N86-14059
ZINC
The delayed fracture of aluminum alloys
[AD-A158944] N86-13412
ZINC ALLOYS
Structure and properties of Al-Mg-Zn casting alloys
N86-13425
ZINC COATINGS
Corrosion resistance of diffusion and galvanic coatings on steel fasteners N86-13450
ZINC COMPOUNDS
Determination of the activation barrier to energy transfer from 3 pi pi* to charge transfer levels via steady state and transient luminescence measurements on Bis(4-Chlorothiophenol) (1,10-Phenanthroline) Zinc (II)
[AD-A158239] N86-14012
ZIRCONIUM
Hereditary effect of dendrite liquation of titanium and zirconium on structure and properties of aluminum alloys
N86-13423
Extremely high reflective capability of zirconium burning in air under effects of constant CO2 laser radiation
N86-13452
ZIRCONIUM ALLOYS
Zirconium as a structural material for naval systems
[AD-A158201] N86-13411
Effect of strain and strain rate on the microstructure of a superplastically deformed Al-10%Mg-0.1%Zr alloy
[AD-A159062] N86-13414
ZIRCONIUM OXIDES
Conductivity of metal-ceramic multilayer ZrO2-Mo and Mo-based composite materials N86-13444

PERSONAL AUTHOR INDEX

SCIENTIFIC AND TECHNICAL AEROSPACE REPORTS VOLUME 24 NUMBER 4

Typical Personal Author Index Listing

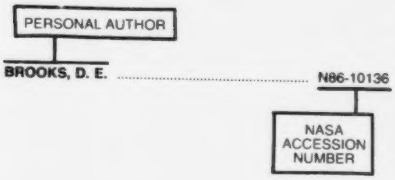

Listings in this index are arranged alphabetically by personal author. The NASA accession number denotes the number by which the citation is identified.

A

ABARBANEL, S. N86-13953
ABDULLAYEV, V. E. N86-14165
N86-14166
ABDURAKHIMOV, A. A. N86-13485
ABDURAKHMANOV, R. U. N86-13485
ABE, H. N86-14046
ABOLHASSANI, J. S. N86-13293
ABRALOV, M. A. N86-13485
ABRAMOV, A. D. N86-13469
ACREE, C. W., JR. N86-13319
ADAMS, R. G. N86-14065
AFONIN, V. V. N86-14117
AGEYEV, B. G. N86-13789
AITCHISON, R. W. N86-13927
AKHMEDOV, A. M. N86-13862
ALBARES, D. J. N86-14043
ALCAMO, M. E. N86-13414
ALEKSANDROV, A. P. N86-14123
ALEKSEYEV, A. A. N86-13456
ALEKSEYEV, V. V. N86-13785
ALESSI, J. G. N86-14064
ALEXIADES, V. N86-13952
ALLEMAND, C. D. N86-13736
ALTHAUS, D. N86-13821
ALZAID, A. A. N86-13977
N86-13998
AMIRAULT, C. T. N86-13813
ANDEEN, G. B. N86-13324
ANDERL, R. A. N86-14067
ANDERSON, C. N86-14079
ANDERSON, C. W. N86-13381
ANDERSON, J. C. N86-13360
ANDERSON, M. B. N86-13822
ANDERSON, W. S. N86-13520
ANDERSSON, M. N86-13840
ANDO, A. N86-14048
ANDRESHAK, J. L. N86-13514
ANDREWS, D. M. N86-13922
ANDREYEV, G. A. N86-14196
ANDREYEV, I. N86-14160
ANIKIN, V. N. N86-13440
ANTIPOV, S. V. N86-14158
ANTON, Y. N86-14178
ANTOSHCHAK, I. N. N86-13470
ANUCHIN, V. N. N86-13772
APPEL, B. R. N86-13849
APPLEGATE, J. A. N86-13720
APUSHKINSKIY, G. P. N86-14124
ARBUCKLE, P. D. N86-13333
ARDUINI, C. N86-13739
AREFYEV, B. A. N86-13443
ARGYLE, R. W. N86-14202
ARKHANGELSKIY, M. A. N86-13484
ARMAND, N. N86-13778
ASADA, H. N86-13937
ASADOV, M. N. N86-13863
ASHKINAZI, R. I. N86-14164
ASKINS, R. E. N86-13522
AUDEH, B. J. N86-13923
AVAKYAN, S. V. N86-14118
AVANOV, L. A. N86-14142
AWSCHALOM, M. N86-14028
AZARENKO, A. Y. N86-13424
AZIZOVA, S. A. N86-13863

B

BAAKLINI, G. Y. N86-13749
BABUSKA, I. N86-13969
N86-13971
BACHAIO, W. D. N86-13577
BACHER, A. D. N86-14021
BACK, W. E. N86-13314
BADEN, J. M. N86-13630
BADER, R. M. N86-13349
BADHWAR, G. D. N86-13800
BAHR, R. N86-13732
N86-13733
BAI, Z. D. N86-13973
BAKAYEV, A. G. N86-13424
BAKER, G. R. N86-13965
BAKHAREV, M. S. N86-13454
BAKHTINOVA, Y. V. N86-14195
BALANAYEVA, N. A. N86-13428
BALES, T. T. N86-13406
BALLHAUS, W. F., JR. N86-14213
BALSA, T. F. N86-13658
BAME, D. N86-13860
BARANOV, P. A. N86-13785
BARATTINO, W. J. N86-14022
BARBACCI, M. R. N86-13935
BARBAUX, Y. N86-13420
BARBER, M. E. N86-13875
BARBOUR, B. A. N86-13563
BARKIN, Y. V. N86-14132
BARLOW, A. N86-13291
BARNBY, J. T. N86-13754
BARRETT, R. A. N86-14080
BARSHAY, A. N86-14154
BARTHOLOMEW, M. J. N86-13802
BARTON, G. E., JR. N86-13933
BARVYN, G. I. N86 14194
BATES, J. L. N86-13656
BATTS, G. W. N86-13868
BAUCHSPIES, J. S. N86-13317
BAUER, L. N86-13895
BAUM, J. D. N86-13547
BAZDENKO, S. V. N86-13483
BAZHANOV, V. M. N86-13780
BAZIN, M. N86-13341
BECK, K. C. N86-13848
BECKER, R. J. N86-13539
N86-13563
BECKSTEAD, M. W. N86-13543
BEDFORD, C. N86-13513
BEISSNER, R. E. N86-13752
BELCHANSKIY, G. I. N86-14172
BELITSKIY, M. Y. N86-13450
BELL, E. L. N86-13888
BELL, H. H. N86-13890
BELL, P. M. N86-14074
BELOKOPYTOV, V. M. N86-13772
BELOLIPETSKIY, Y. P. N86-13438
BELYAKOV, S. A. N86-14119
BEMENT, L. J. N86-13305
BENEDICK, W. B. N86-13696
BENEK, J. A. N86-13292
BENILOV, A. Y. N86-13769
BENKOVITZ, C. M. N86-13844
BENNETT, K. N86-13344
BENTSE, P. N86-14117
BERENYI, S. G. N86-13328
N86-13329
N86-13330
BERESTOVSKIY, I. F. N86-14182
BEREZOVOY, A. N. N86-14123
BERGER, G. N86-13350
BERNSHTEYN, M. L. N86-13464
BERRY, G. G. N86-13631
BERRYMAN, J. G. N86-13598
BERSNEVA, L. A. N86-14195
BERTHOLD, D. B. N86-13413
BERTRAM, A. L. N86-13381
BERWICK, R. C. N86-13950
BESNARD, D. N86-13693
BEZRUKIKH, V. V. N86-14117
BHADURI, S. N86-13833
BHASKAR, S. K. N86-13980
BHATTI, R. S. N86-13363
BIBIKOV, V. N86-13471
BIDDLE, A. P. N86-13365
BIDZHIYEV, R. A. N86-14175
BIFANO, W. J. N86-14110
BINDER, M. N86-13662
BINKEVICH, N. I. N86-13497
BIRKMIRE, R. W. N86-13837
BIRMAN, K. P. N86-13926
BISCHEL, W. K. N86-13569
BISCHOFF, J. N86-13364
BISHOP, G. M. N86-13323
BJORKMAN, M. D. N86-14212
BLACKBURN, R. S. N86-14065
BLACKNER, A. M. N86-13541
BLACKWELL, B. F. N86-13700
BLANCHARD, A. J. N86-13807
BLANFORD, G. E. N86-14081
BLANKS, J. W. N86-13518
BLASHCHUK, V. Y. N86-13489
BLOCK-BOLTEN, A. N86-13736
BLOOM, D. M. N86-13654
BLOOMQUIST, J. D. N86-14035
BLUMENTHAL, D. F. N86-13931
BOCHVAR, A. G. N86-13474
BOEHLE, M. S. N86-14210
BOGACHEK, Y. L. N86-13494
BOGGS, C. W. N86-13664
BOGIN, V. N. N86-13444
BONDARCHUK, L. A. N86-13443
BONNICE, W. N86-13310
BORIS, J. P. N86-13687
BORISENKO, V. A. N86-13465
BORISOV, A. N. N86-14173
BORISOV, V. T. N86-13430
BORISOV, Y. S. N86-13442
BORODIN, L. F. N86-14196
BOTVINA, L. R. N86-13466
BOULLION, T. N86-14079
BOYER, C. N N86-13567
BOYES, J. D. N86-14060
BOZEK, J. M. N86-14110
BRADLEY, R. C. N86-13992
BRADY, M. N86-13894
N86-13937
BRADY, V. O. N86-14058
BRANCH, M. C. N86-13525
BRANDT, A. N86-13955
BRASURE, L. W. N86 14014
BRAUDEL, H. J. N86-13741
BREAZEALE, M. A. N86-14009
BREKHOVSKIKH, V. L. N86-14186
BRENNAN, A. M. N86-13764
BREUS, T. N86-14149
BREWER, D. W. N86-13959
BRILL, T. B. N86-13521
BRINZA, V. N. N86-13446
BRODD, S. S. N86-13947
BRODSKAYA, R. M. N86-13429
BROUWERS, A. P. N86-13328
N86-13329
N86-13330
BROWN, N. N86-13506
BROWN, R. S. N86-13541
BROWN, T. G. N86-14061
BROWNE, M. J. N86-14029
N86-14066
BROWNING, R. N86-13409
BROWNLOW, J. D. N86-13353
N86-13354
BRUCE, R. G. N86-13635
BRUNDERMAN, J. N86-13890
BRYANT, W. R., JR. N86-13317
BUDWIG, R. S. N86-13675
BUGEAT, J. P. N86-13668
BUKHARIN, Y. N. N86-13456
BUNDICK, W. T. N86-13332

BUNKIN, F. V. N86-13774
BURATTI, A. N86-13346
BURMISTROV, A. V. N86-13452
BURNS, J. T. N86-13689
BUSLINSKIY, S. V. N86-13494
BUSTIN, R. N86-14082
BUSWELL, A. T. N86-13563
BUTLER, B. D. N86-13712
BUTLER, K. A. N86-13700
BUYNOV, N. N. N86-13426
BUZYKIN, O. G. N86-13452
BYCHKOV, Y. B. N86-13428
BYER, R. L. N86-13654
BYLKOVA, Z. I. N86-13444

C

CADDY, M. J. N86-13939
CALAHAN, D. A. N86-13909
CALDWELL, S. P. N86-13646
CALEDONIA, G. N86-13729
CALEDONIA, G. E. N86-13551
CALLE, J. E. N86-13519
CALLEN, J. D. N86-14053
CAMERON, C. E. N86-13375
CAMPBELL, D. N86-13530
CAMPBELL, D. H. N86-13529
N86-13531
CANTERBERRY, J. B. N86-13518
CANTWELL, E. R. N86-13298
CAP, J. S. N86-14060
CAPUTO, A. J. N86-13500
CAREY, T. A. N86-14021
CARLSON, L. A. N86-13300
CARRASCO, R. N86-13615
CARRERAS, B. A. N86-14053
CARROLL, R. J. N86-13713
CASTAGNA, M. N86-13624
CASTOR, V. L. N86-13936
CAVENY, L. H. N86-13507
N86-13546
CAZIER, F. W., JR. N86-13321
CELATA, C. M. N86-14058
CERICOLA, F. N86-13599
CERUGA, K. A. N86-13733
CHABANENKO, A. A. N86-13491
CHADERJIAN, N. M. N86-13296
CHANDLER, M. O. N86-13365
CHANG, F. R. N86-13559
N86-13560
CHANG, J. N86-13721
CHANG, R. N86-13503
CHANG, R. E. N86-13579
CHANG, R. K. N86-13578
CHANTY, M. N86-13555
CHAPMAN, R. D. N86-13514
CHARLTON, J. E. N86-13367
N86-13705
N86-13706
CHASE, M. W. N86-13532
CHEN, F. F. N86-14050
CHEN, H. S. N86-13683
CHEN, S. S. N86-13704
CHENG, W. K. N86-13584
CHENGZHI, P. N86-13609
CHERKASOV, V. V. N86-13425
CHERN, J. C. N86-13762
CHERNOMORSKIY, V. N86-13746
CHERTOV, I. M. N86-13490
CHIVEL, Y. A. N86-13455
CHORIN, A. N86-13691
CHORY, A. N86-13326
CHOU, C. C. N86-13881
CHOZEV, Y. N86-13396
CHRISTE, K. O. N86-13517
CHU, B. T. N86-13579
CHU, W. N86-14023
CHUBENKO, N. G. N86-13444
CHUGTAI, A. R. N86-13501
CHUMAKOV, A. N. N86-13455
CHUNG, T. J. N86-13544
CHUTAYEV, I. K. N86-13424
CIPRIS, D. N86-13395
CLAVELL, C., JR. N86-13719
CLENDENIN, J. E. N86-14066
COHEN, H. E. N86-13994
COHEN, J. B. N86-13712
N86-13759
COHEN, J. K. N86-13932
COHEN, M. M. N86-13900
COHEN, N. N86-13533
COLE, J. E., III N86-13688
COLEMAN, R. V. N86-13709
COLES, M. G. H. N86-13897
COLLAMORE, F. N. N86-13708
COMBI, M. R. N86-14209
COMFORT, R. H. N86-13365
CONEL, J. E. N86-13801
CONNELL, J. H. N86-13894
CONNERS, S. P. N86-13327
CONROY, M. J. N86-13627
COOKE, D. W. N86-13419
COOLIDGE, M. B. N86-13522
CORLISS, G. F. N86-13963
CORNWELL, D. K. N86-13695
COUGHERTY, F. C. N86-13292
COUGNET, C. N86-13350
COWLES, L. N86-13729
COWLES, L. M. N86-13551
CROSBY, G. A. N86-14012
CROWDER, H. N86-13548
CUTLER, E. P. N86-13947
CYMERMAN, A. N86-13887
CZARNEK, R. N86-13496

D

DABIRI, A. E. N86-14061
DAHM, M. R. N86-13682
DAILY, J. W. N86-13570
DANCER, R. F. N86-13928
DANIEL, B. R. N86-13542
DARSAVELIDZE, G. S. N86-13482
DARTS, J. N86-13322
DASGUPTA, B. R. N86-13880
DAVIS, J. F., III N86-13567
DAVIS, K. C. N86-13637
DAVIS, L. S. N86-13948
DAVIS, R. C. N86-13406
DAVYDOV, V. D. N86-14120
DAWE, J. A. N86-14201
N86-14203
DAYBOG, Y. I. N86-14119
N86-14141
DAYTON, J. A., JR. N86-13643
DEBOOR, C. N86-13964
DEERING, D. W. N86-13794
DEGRAVE, J. C. N86-13911
DELETTREZ, J. N86-14069
DELLAMUSSIA, J. P. N86-13612
N86-13619
N86-13621
DELTORO, J. N86-13350
DEMAIO, J. N86-13890
DEMICHEV, V. F. N86-13483
DEMIDENKO, L. N. N86-13463
DENISOVA, I. K. N86-13462
DEREVYANKO, N. F. N86-14194
DEROUVRAY, A. N86-13763
DESSE, J. M. N86-13303
DEVRIES, J. N86-13818
DEVRIES, O. N86-13828
DEVYATKO, A. V. N86-14162
DIAMOND, P. H. N86-14053
DIAZ, J. O. N86-13370
DICARLO, J. A. N86-13407
DIKAYA, K. I. N86-13437
DIMARZIO, C. A. N86-13813
DINER, D. J. N86-13803
DINNEEN, P. M. N86-13348
DITTMAR, J. H. N86-14006
N86-14007
DIXON, S. C. N86-13349
DMITRENKO, V. V. N86-14123
DODDS, S. A. N86-13419
DODROVA, L. K. N86-13457
DODSWORTH, E. S. N86-13389
DOHERTY, J. E. N86-13752
DOMANTSEVICH, N. I. N86-13451
DOMINGO, V. N86-13344
DONALDSON, S. L. N86-13498
DONCHIN, E. N86-13897
DONIACH, S. N86-13882
DORMAN, J. M. N86-13391
DOROFEYEV, V. N86-13766
DOROFEYEVA, V. N86-13766
DOUGHTY, C. N86-13694
DOW, R. L. N86-13597
DOWLATYARI, P. N86-13763
DOYLE, R. J. N86-13893
DRAKE, B. N86-13709
DRAKE, J. N86-13952
DRESS, D. A. N86-13338
DROFA, A. S. N86-13779
N86-13781
DRUMHELLER, M. N86-13949
DRYER, F. L. N86-13585
DU, G. N86-14009
DUARTE, J. G. N86-13938
DUKE, M. B. N86-14078
DUNLAP, R. N86-13541
DUNN, G. J. N86-13736
DUPUTAT, J. N86-14107
DURGUN, K. N86-14083
DUTSIAK, I. Z. N86-13470
DUTT, P. N86-13957
DYACHKOV, A. P. N86-14119
DYADYNA, G. A. N86-13472
DYBEDAL, J. N86-13368
DYKHNO, L. A. N86-13768
DYSON, H. B. N86-13631

E

EAGAR, T. W. N86-13736
ECKSTROM, B. P. N86-13375
EDWARDS, P. R. N86-13322
EDWARDS, T. N86-13529
N86-13530
EFURD, R. B. N86-13630
EHRLICH, S. M. N86-13912
EISCH, J. J. N86-13519
EJIMA, S. N86-14070
EKHINA, Y. V. N86-13432
ELLIS, A. B. N86-13655
ELLISON, J. F. N86-13321
ELMAN, R. I. N86-14195
ELSEN, M. F. N86-13343
ELY, J. F. N86-13401
ELYASBERG, P. Y. N86-14130
ENDERBERG, N. P. N86-13725
ENEVER, F. K. N86-13865
ENGEBRETSON, M. J. N86-13851
ENGELHARDT, H. P. N86-13611
EPIK, A. P. N86-13450
EPSTEIN, H. M. N86-13730
ERCHUL, R. A. N86-13874
ESHLEMAN, J. N86-13299
ESSERS, J. A. N86-13347
EVANS, V. A. N86-13844
EVERSOLE, J. D. N86-13523
EWAN, B. C. R. N86-13571
EYGEL, L. N86-13748

F

FAEHL, R. J. N86-14019
FAIRFIELD, P. N86-13968
FAIRLIE, B. D. N86-13336
N86-13337
FANG, C. N86-13972
FANGMING, K. N86-13607
FARBER, V. M. N86-13462
FARR, W. N86-13361
FARROW, R. F. C. N86-14073
FARTHING, W. E. N86-13847
FEDCHENKO, P. P. N86-14172
FEDIRKO, V. N. N86-13477
FEDOROV, K. N. N86-14171
FEDYUSHIN, B. T. N86-13455
FEHLER, M. N86-13860
FELDMAN, J. N86-13891
FEOKTISTOVA, Y. K. N86-13488
FERGUSON, D. C. N86-14110
FERRANDO, W. A. N86-13411
FERRY, B. N86-14025
FIALA, C. N86-13898
FILICHKIN, A. P. N86-13444
FILIPPOV, V. M. N86-14137
FILTER, W. F. N86-13721
FILYUSHKIN, B. N. N86-13769
FISCHER, G. E. N86-14003
FISHER, D. H. N86-13951
FISHER, D. S. N86-13941
FISHER, J. L. N86-13559
N86-13752
FISHGOYT, A. V. N86-13475
FLANAGAN, J. E. N86-13534
FLATTE, S. M. N86-13832
FLEISSNER, J. G. N86-14024
FLORES, J. N86-13296
FOLEY, J. K. N86-13653
FOLLANSBEE, P. S. N86-13417
N86-13418
FOLTZ, J. V. N86-13381
FOMENKOVA, M. N. N86-14185
FOMICHEV, Y. N. N86-13458
FORCE, D. A. N86-13643
FORNEAR, J. L. N86-13870
FOSTER, P. R. N86-13705
N86-13706
FOWLER, W. B. N86-14025
FRADKIN, M. I. N86-14122
FRANKEL, M. B. N86-13508

FRASER, R. S. N86-13804
FREDERICK, R. A., JR. N86-13540
FREEN, P. D. N86-13328
N86-13329
N86-13330
FREES, E. W. N86-13987
FRENCH, C. V. N86-13415
FRIDLYANDER, I. N. N86-13423
N86-13432
FRIDMAN, G. R. N86-13461
FRISK, U. O. N86-13344
FULCO, C. S. N86-13887
FUNG, A. K. N86-13807
FURUKANE, U. N86-14045
FURYAYEV, V. V. N86-14176
FUSCO, G. N86-13346
FUYOU, P. N86-13607

G

GABRIEL, J. R. N86-13912
GALPER, A. M. N86-14123
GALPERIN, Y. I. N86-14137
GALYKO, A. V. N86-13441
GAMBLE, R. A. N86-13756
GARCIA, L. N86-14053
GARREN, A. A. N86-14002
GARRETT, A. G. N86-14024
GAVIN, J. A. N86-13717
GAVRYUSHENKO, B. S. N86-13453
GAYEVSKIY, A. Y. N86-13457
GELFAND, A. E. N86-13960
GEOFFROY, P. N86-13308
GEORGIADIS, L. N86-13981
GERBER, R. A. N86-14065
GERCHIKOVA, N. S. N86-13425
N86-13431
GERSTL, S. A. W. N86-13806
GEZENTSVEY, A. N. N86-13771
GHORAI, S. K. N86-14084
GIBSON, J. S. N86-13959
GIESKE, J. H. N86-13382
GILL, P. E. N86-13934
GILL, R. J. N86-13535
GILLIES, G. T. N86-13842
GILMAN, S. N86-13662
GIORDANO, J. N86-13369
GIST, G. A. N86-13419
GITELSON, A. A. N86-14182
GLAZKOV, A. I. N86-14114
GLISSON, A. W., JR. N86-14037
GLOVER, B. J. N86-13892
GLUKHOV, Y. A. N86-13469
GLUSHKO, Y. V. N86-14184
GLYNN, P. W. N86-13989
GNYP, I. P. N86-13470
GOEKOGLU, S. A. N86-13678
GOGLIA, G. L. N86-13358
GOLDSTEIN, R. N86-13895
GOLDSTEIN, S. A. N86-14052
GOLIKOV, A. R. N86-14131
GOLOVACHEV, V. N86-14151
GOLOVANOV, Y. N86-14197
GOLUBETS, V. M. N86-13467
GOLUBEV, V. N. N86-13492
GOMEZ-RODRIQUEZ, M. N86-13379
GOMOZOV, L. I. N86-13479
GONEN, A. N86-13912
GOODMAN, C. N86-13375
GORBACHEV, A. A. N86-13454
GORBATOV, I. N. N86-13442
GORBUNOVA, Z. N. N86-13773
GORDIN, M. P. N86-13788
GORDOV, Y. P. N86-13789
GORELIK, G. Y. N86-13481
GORKER, G. E. N86-13666
GORNIK, E. N86-14072
GORNYY, M. G. N86-14125
GORODNITSKIY, A. M. N86-13776
GORSHKOVA, I. I. N86-14190
GOSS, L. P. N86-13582
GOSSET, J. M. N86-13375
GOTSELYUK, Y. V. N86-14138
GOTTLIEB, D. N86-13953
GRACHEV, V. M. N86-14123
GRACHEV, Y. N. N86-13788
GRAHAM, W. H. N86-13518
GRANHOLM, R. H. N86-13373
GRARD, R. N86-13344
GRAY, G. T. N86-13418
GREELEY, R. N86-13289
GREEN, J. A. S. N86-13412
GREGGI, J. N86-14073
GREGORY, D. A. N86-14034
GRESHO, P. M. N86-13703
GREVE, S. C. V. S. N86-13648
GRIBOVSKIY, V. K. N86-13424
GRIFFIN, C. W. N86-13656
GRIFFIN, O. M. N86-13875
GRINBERG, V. A. N86-13475
GRINER, D. B. N86-14033
GRINGAUZ, K. I. N86-14117
GRINSTEIN, F. F. N86-13687
GRISHIN, A. M. N86-13447
GRITSENKO, V. A. N86-13772
GRIVNEV, Y. M. N86-14147
GROSS, R. R. N86-13649
GROTCH, S. L. N86-13872
GROTHAUS, M. G. N86-13320
GROUT, S. N86-13935
GROVE, R. D. N86-13944
GRUDNEV, V. N. N86-13478
GRUSHIN, V. A. N86-14185
GRYUNVALD, T. M. N86-13464
GUEST, C. J. N86-13913
GUI, W. N86-13969
GUIRAO, C. M. N86-13696
GUNDY, K. L. N86-13296
GUNST, R. F. N86-13814
GUO, B. N86-13971
GUO, Y. N86-13496
GURVICH, A. S. N86-14168
GUSEYNOV, A. N. N86-13862
GUSHCHA, O. I. N86-13491

H

HAAS, G. A. N86-13659
HABER, I. N86-14058
HALL, R. B. N86-13837
HALL, S. N86-13310
HALLY, D. N86-13930
HALPERN, J. P. N86-14205
HAMANN, R. J. N86-13902
N86-13903
N86-13904
N86-13905
HAMIL, R. A. N86-14065
HAMILTON, D. N86-13399
HAMMEL, J. E. N86-14059
HANANIA, J. I. N86-14085
HANSMA, P. K. N86-13709
HANSON, R. K. N86-13572
HANUMARA, R. C. N86-13974
HARLOW, F. H. N86-13693
HARRIS, F. W. N86-13843
HARRIS, J. H. N86-14043
HARRIS, R. L., SR. N86-13892
HARRIS, S. E. N86-13654
HART, D. P. N86-13562
HART, R. E., JR. N86-13645
HARTEN, A. N86-13966
HARTWELL, J. A. N86-13511
HARVEY, J. A. N86-14026
HASEGAWA, M. N86-14048
HASTINGS, R. C. N86-13301
HAU, E. N86-13826
HAUG, E. N86-13308
N86-13763
HAWKINS, D. C. N86-13705
N86-13706
HAYES, E. F. N86-14018
HAYES, J. V. N86-13844
HAYTER, J. B. N86-14027
HAYWARD, S. B. N86-13846
HEARN, C. P. N86-13644
HEASLER, H. P. N86-13816
HEDGE, U. N86-13542
HEFFNER, R. H. N86-13419
HEGE, E. K. N86-14207
N86-14208
HEGEDUSICH, D. N86-13888
HEIMERDINGER, D. N86-13555
HELLER, M. N86-13754
HELM, M. N86-14072
HENDRON, A. J., JR. N86-13854
N86-13855
HENNELL, M. A. N86-13968
HENSCHKE, R. W. N86-14042
HERKLE, C. L. N86-13549
HERMSTAD, D. N86-13291
HERRERA, J. N86-14004
HERSH, A. S. N86-13545
HESS, C. F. N86-13580
HESS, D. W. N86-13657
HESSELINK, L. N86-13573
HESSOM, C. N86-13803
HICKLEY, B. S. N86-13816
HICKOX, C. E. N86-13689
HIGHLAND, R. G. N86-14012
HILDEBRAND, R. H. N86-14204
HILL, C. K. N86-13868
HILL, N. W. N86-14026
HINDMARSH, A. C. N86-13983
HIOE, F. T. N86-13731
HIRANO, K. N86-14051
HIRLEMAN, E. D. N86-13581
HIRSCHFELD, T. N86-13400
HODGSON, K. N86-13862
HOELLIG, K. N86-13964
HOEPFEL, R. N86-14072
HOFFMAN, D. D. N86-13979
HOFFMAN, R. N86-13397
HOGUE, R. N86-14004
HOLL, H. B. N86-13728
HOLLAND, D. F. N86-14067
HOLLANDER, M. N86-13999
HOLMES, N. C. N86-13399
HOLSAPPLE, K. A. N86-14212
HOLST, T. L. N86-13296
HONN, J. J. N86-13737
HORN, W. J. N86-14078
HOUCK, J. A. N86-13944
HOUSEN, K. R. N86-14212
HSIEH, T. H. J. N86-13674
HU, H. N86-13996
HUANG, H. W. N86-13715
HUANG, S. L. N86-13718
HUANG, Y. H. N86-13404
HUBBARD, A. T. N86-13394
HUDSPETH, R. T. N86-13681
HULSIZER, S. N86-13529
N86-13530
HUNTER, G. B. N86-13736
HUSS, G. N86-13826
HUTSON, R. L. N86-13419
HYVARINEN, W. E. N86-13832

I

IBRAHIM, S. R. N86-13587
N86-13588
N86-13589
N86-13590
N86-13591
N86-13592
IGLEHART, D. L. N86-13989
IGNATOV, A. G. N86-13986
INAL, O. T. N86-13839
IRVINE, L. D. N86-13956
ISAACS, H. S. N86-13667
ISHIGURO, T. N86-13288
ISHKOV, S. A. N86-14135
ISMALILOV, K. K. N86-14165
ITATANI, R. N86-14046
ITO, T. N86-14086
IVANCHENKO, G. A. N86-14173
IVANOV, S. V. N86-13486
IVANOV, V. A. N86-14173
IVANOVA, T. P. N86-14188
IVASISHIN, O. M. N86-13478

J

JACKSON, A. N86-14002
JACKSON, A. A. N86-14087
JACKSON, K. E. N86-13316
JACOBS, S. D. N86-13733
JACOBSON, M. J. N86-14008
JAGODA, J. N86-13542
JAGODA, J. I. N86-13527
N86-13528
JAHNS, G. N86-14070
JAKOBSEN, P. N86-13344
JAKUBOWSKI, A. L. N86-13287
JAMES, R. N86-13353
N86-13354
JASPER, G. L. N86-13868
JEANJAQUET, S. L. N86-13727
JENDRZEJCZYK, J. A. N86-13704
JENG, Y. R. N86-13679
JESSL, P. N86-13815
JIAN, Y. N86-13607
JO, J. N86-13496
JOAG, R. N86-13287
JOBE, R. K. N86-14029
N86-14066
JOH, D. N86-13496
JOHANSSON, K. R. N86-14088
JOHN, W. N86-13846
JOHNSON, D. A. N86-13676
JOHNSON, D. H. N86-13834
JOHNSON, D. L. N86-13868
JOHNSON, D. W. N86-13845

JOHNSON, G. L. N86-14057
JOHNSON, H. M. N86-14206
JOHNSON, J. N86-13726
N86-13873
JOHNSON, R. A. N86-13967
JOHNSON, W. N86-13286
JONAS, L. A. N86-13374
JONES, K. W. N86-14021
JONES, M. E. N86-14019
JONES, O. C. N86-13565
JONES, R. N86-13754
JORDAN, H. F. N86-13915
JORGENSEN, E. S. N86-13722
JOSHI, O. K. N86-13377
JOYCE, T. T. N86-13705
N86-13706
JUNDING, W. N86-13603
JUREK, Z. J. N86-13995

K

KACHINSKI, R. N86-14180
KAHLE, A. B. N86-13802
KAISHEV, V. K. N86-13986
KALINOVSKIY, V. R. N86-13442
KALLISTRATOVA, M. A. N86-13782
KALLURI, S. N86-13755
KALOSHKIN, S. D. N86-13434
KALSI, S. S. N86-13666
KAMBHAMPATI, S. N86-13948
KAN, A. V. N86-13468
KANDIDOV, V. P. N86-13786
KAPORIK, N. I. N86-13450
KARAFIATH, L. L. N86-13593
KARAKOZOV, E. S. N86-13486
KARASEV, A. B. N86-14191
KARASIK, V. R. N86-14000
KARPENKO, A. S. N86-13490
KARPOVA, N. M. N86-13462
KASHEF, B. G. N86-13711
KATRUS, O. A. N86-13445
KATS, S. M. N86-13444
KAUFMAN, F. N86-13857
KAUFMAN, M. N86-13526
KAUFMAN, Y. J. N86-13804
KAYGORODOVA, L. I. N86-13426
KAYLOR, J. T. N86-13944
KAYNAK, U. N86-13296
KAZAKOV, N. F. N86-13493
KAZMIN, A. S. N86-14171
KAZOR, N. N86-13910
KEDER, Y. N86-13782
KEEFER, D. N86-13548
KEENER, E. R. N86-13304
KEHOE, M. W. N86-13321
KELLY, E. J. N86-13993
KELLY, J. N86-13732
KEMP, N. N86-13729
KEMP, N. H. N86-13552
KEMPEL, F. D. N86-13714
N86-13717
KENDIG, M. W. N86-13727
KERCZEWSKI, R. J. N86-13627
KERR, A. D. N86-13594
N86-13595
KERSHAW, J. N86-13908
KERSTEIN, L. N86-13350
N86-13361
KESSLER, M. N86-13344
KESSLER, T. N86-13732
KESSLER, T. J. N86-13733
KHALBOSHIN, A. P. N86-13453
KHALIPOV, V. L. N86-14137
KHISAMOV, R. S. N86-14192
KHOLODOV, V. P. N86-13487
KHOLOPOV, G. K. N86-14192
KHONIK, V. A. N86-13435
KHOVOVA, O. M. N86-13468
KHUZIN, F. G. N86-14192
KIESEWETTER, C. H. N86-14089
KILLION, M. E. N86-13502
KIM, Y. J. N86-13710
KIMES, D. S. N86-13797
KING, D. Q. N86-13557
KING, H. E. N86-13631
KING, L. S. N86-13676
KING, M. K. N86-13536
KINO, G. S. N86-13654
KIRCHNER, W. L. N86-14032
KIRICHENKO, O. V. N86-13459
KIRICHUK, V. S. N86-14173
KIRILLOV-UGRYUMOV, V. G. N86-14123
KISHKINA, S. I. N86-13431
KLEVTSOV, G. V. N86-13466
KLYTSINA, A. M. N86-13438
KNAUBER, R. N. N86-13913
N86-13920
N86-13921
KNIPELE, A. Z. N86-13460
KNOTT, K. N86-13344
KNYSTAUTAS, R. N86-13696
KOCHANOV, V. P. N86-13790
KOCHARLI, S. S. N86-13862
KOEL, B. E. N86-13398
KOEPPEL, W. N86-13815
KOGAN, M. N. N86-13452
KOKORIN, A. O. N86-13785
KOKORINA, N. N. N86-13442
KOL, J. N86-13396
KOLACHEV, B. A. N86-13475
KOLESAR, E. S., JR. N86-13392
KOLOKOLSHIKOV, V. V. N86-13449
KOLYADINA, N. Y. N86-13430
KOLYADINA, Y. V. N86-13446
KOMAR, J. J. N86-13536
KONDRATYEV, K. Y. N86-14172
KONG, J. A. N86-13808
KONIG, C. E. N86-13660
KONOPKIN, A. N. N86-13435
KONOV, V. I. N86-13452
KONYAYEV, P. A. N86-13791
KOO, J. I. N86-13581
KOPP, O. C. N86-13817
KOPROV, B. M. N86-13783
KOPYL, O. N. N86-13451
KOPYTIN, Y. D. N86-13787
KORNBLUH, R. D. N86-13324
KORNILOVA, Z. I. N86-13476
KOROLEV, A. Y. N86-13481
KORSCH, D. N86-14033
KOSHKAREV, G. S. N86-13436
KOSMAHL, H. G. N86-13643
KOSTORNOV, A. G. N86-13459
KOTHNY, E. L. N86-13849
KOZELO, Y. A. N86-13484
KOZENKO, A. V. N86-14155
KOZHELUPOVA, N. G. N86-13769
KOZHEVNIKOVA, V. L. N86-13433
KOZIMA, S. N86-13519
KOZLOV, S. I. N86-14136
KOZLU, H. N86-13699
KOZODEROV, V. V. N86-14172
KOZUB, V. V. N86-13467
KRASNOPOLSKIY, V. A. N86-14157
KRASNOSELSKIKH, V. V. N86-14139
KRAUHS, J. M. N86-13886
KRAUSS, M. N86-13856
KRAUSSE, G. J. N86-13663
KRAWITZ, A. D. N86-13712
KRECH, R. N86-13729
KRECH, R. H. N86-13551
KREEB, H. N86-13363
KRETA, S. J. N86-13737
KRIER, H. N86-13550
N86-13682
KRISHNAIAH, P. R. N86-13972
N86-13976
KRIVOROTENKO, A. D. N86-13458
KROLIKOWSKA, A. N86-14107
KRUEGER, W. A. N86-13559
N86-13560
KUBO, S. N86-14048
KUC, R. N86-13578
KUCHERYAVENKOV, A. I. N86-14156
KUCHINSKIY, Y. I. N86-14170
KUCHNIR, L. N86-13912
KUDELA, K. N86-14138
KUDRYASHEV, G. S. N86-14118
KUDRYAVTSEV, Y. F. N86-13491
KUHN, R. E. N86-13299
KULAK, R. F. N86-13698
KULEVSKIY, L. A. N86-13774
KULIKOV, F. R. N86-13488
KUNKLE, T. D. N86-14211
KUNYAVSKAYA, T. M. N86-13432
KUPERSHTOK, Y. Y. N86-13428
KUPRIYANOV, D. V. N86-14125
KURNOSOVA, L. V. N86-14122
KURT, V. G. N86-14119
N86-14141
KUSHNIRENKO, N. A. N86-13490
KUSTOM, R. L. N86-13665
KUTSOVA, V. Z. N86-13427
KUUSK, A. N86-14178
N86-14179
KUZIN, V. F. N86-13484
KUZMICHEV, V. V. N86-14173
KUZNETSOV, P. M. N86-13747
KUZNETSOV, S. N. N86-14138

L

LAANSOO, A. A. N86-13445
LACKEY, W. J. N86-13500
LACOSS, R. T. N86-13628
LAGUN, V. Y. N86-13784
LAI, C. C. N86-13723
LAIRD, J. L. N86-13539
LALAYAN, E. A. N86-13429
LAMBERT, N. J. D. E. N86-13671
LANDRON, C. O. N86-13721
LANG, R. H. N86-13809
LANGAN, T. J. N86-13412
LANGDON, A. B. N86-14054
N86-14055
LANGELAND, T. N86-13967
LANGLEY, D. S. N86-14039
LANGLEY, P. N86-13951
LAPARLIERE, M. N86-13384
LAPIDOVSKAYA, L. A. N86-13437
LARSEN, R. N86-13887
LASLETT, L. J. N86-14058
LAVINE, A. G. N86-13672
LAVROV, V. N. N86-14169
LAWLESS, J. L. N86-13556
LAWLESS, P. A. N86-13393
LAX, P. D. N86-13701
LAZAR, S. N86-13631
LAZAREV, E. M. N86-13437
N86-13476
LAZIC, I. N86-13395
LEACH, C. S. N86-13886
LEAR, R. D. N86-13723
LEBEDEV, V. G. N86-14164
LEBEDEV, V. V. N86-14123
LEBOUAR, P. N86-13350
LEBRETON, J. P. N86-13344
LEE, G. N86-13297
LEE, J. E. N86-13819
LEE, J. H. N86-13696
LEE, K. Y. N86-13387
N86-14090
LEE, S. Y. N86-13817
LEE, V. D. N86-14061
LEE, W. R. N86-13884
LEGECKIS, R. N86-14171
LEIDENFROST, W. N86-13835
LELYAVIN, S. N. N86-14132
LEPIN, L. K. N86-13460
LESHCHINER, L. N. N86-13431
LESNAYA, N. N86-14167
LEVER, A. B. P. N86-13389
LEVIN, A. Y. N86-13438
LEVIN, Y. M. N86-14163
LEVINE, J. N. N86-13547
LI, H. N86-13689
LIBERMAN, T. N86-14040
LIBESKIND, M. N86-13718
LIKENBAKH, A. K. N86-13460
LIKHACHEV, V. A. N86-13480
LIKIN, V. L. N86-13432
LILEY, P. E. N86-13835
LIN, J. N86-13976
LIN, S. H. N86-14070
LINCE, J. R. N86-14071
LINCOFF, A. H. N86-13375
LINDSTROM, G. N86-13935
LIPATOV, Y. S. N86-13497
LIPS, H. N86-13503
LITTLEFIELD, R. G. N86-13343
LIU, C. T. N86-13537
N86-13538
LIVANOV, L. B. N86-14121
LOCKWOOD, G. J. N86-13721
LOEWENTHAL, S. H. N86-13734
LOGACHEV, Y. I. N86-14119
LONG, M. B. N86-13578
N86-13579
LONGDON, N. N86-13352
LONGHURST, G. R. N86-14067
LOPASOV, V. P. N86-13790
LOPESFALKON, K. A. N86-14193
LOPEZ, J. N86-13335
LORENZINI, E. N86-13345
LOSKUTOV, V. S. N86-13788
LOUIS, J. F. N86-13699
LOW, T. P. N86-13324
LU, M. N86-13881
LU, S. C. N86-14057
LUCHKOV, B. I. N86-14146
LUCK, J. T. N86-13664
LUCKHAM, D. C. N86-13945
LUEHRMANN, P. F. N86-13539
LUKIN, V. P. N86-13791
LUKYANENKO, S. F. N86-13790

LUONG, L. H. S. N86-13927
LYAKHOV, G. A. N86-13774
LYAKHOV, V. A. N86-14123
LYASOTSKAYA, V. S. N86-13488
LYNN, K. G. N86-14076
LYUTYY, Y. M. N86-13479

M

MAAGER, H. N86-13361
MACIEJEWSKI, M. N86-13512
MACKLIN, R. L. N86-14026
MACLAUGHLIN, D. E. N86-13419
MADER, C. L. N86-13877
MAKARA, J. N86-14025
MAKEWA, T. N86-14048
MAKSIMOVICH, V. N. N86-13491
MALASHENKO, I. S. N86-13438
MALONEY, M. N86-13935
MANDELBERG, S. L. N86-13494
MANN, D. M. N86-13634
MANSFELD, F. N86-13727
MANSON, S. S. N86-13755
MAO, H. K. N86-14074
MARCHAND, A. P. N86-13510
MARCHERTAS, A. H. N86-13761
N86-13762
MARGARY, R. N86-13625
MARIANI, E. A. N86-13661
MARINO, K. L. N86-13313
MARKOVSKIY, P. Y. N86-13478
MARRERO, T. R. N86-14091
MARRIAN, C. R. K. N86-13659
MARSDEN, R. G. N86-13344
MARSHAK, A. L. N86-14177
MARTINEZ-SANCHEZ, M. N86-13555
MARTONCHIK, J. V. N86-13803
MARTYNOVA, I. F. N86-13461
MARUSHKEVICH, A. D. N86-13770
MASSARD, T. N. N86-13378
MATHIEU, J. P. N86-13363
MATISOV, B. G. N86-14125
MATSUMOTO, M. N86-14047
N86-14049
MATUSZKO, A. N86-13507
MATVEYEV, Y. Y. N86-13430
MAYES, R. L. N86-13753
MAYO, A. L. N86-13841
MAZUMDER, J. N86-13550
MAZUR, V. I. N86-13427
MCANALLY, W. H., JR. N86-13692
MCCAIN, J. D. N86-13847
MCCLELLAND, J. B. N86-14021
MCCLUSKEY, E. J. N86-13922
MCCORMICK, M. P. N86-13850
MCCOWAN, W. L. N86-13961
MCCRORY, R. L. N86-14068
MCCULLEY, M. N86-13314
MCDANELS, D. L. N86-13407
MCDONALD, A. T. N86-13835
MCFARLAND, E. R. N86-13295
MCGEE, L. A. N86-13311
MCKEE, S. P. N86-13896
MCKENNA, P. J. N86-13690
MCKENNEY, D. G. N86-13929
MCVEY, J. B. N86-13568
N86-13831
MEAKIN, J. D. N86-13837
MEDELIUS, P. N86-13873
MEDVED, I. I. N86-13463
MEEHAN, P. N86-13853
MEHLMAN, B. N86-14023
MEHTA, R. D. N86-13298
MEIER, K. L. N86-14032
MELANSON, D. N86-13555
MELNICKI, L. S. N86-13395
MELNIK, P. I. N86-13441
MELTON, L. A. N86-13583
MERAKOS, L. N86-13981
MERSOV, G. A. N86-14144
MICCI, M. M. N86-13561
MIKHALEVICH, V. G. N86-13774
MIKHEYEV, P. P. N86-13491
MILAN, C. N86-13361
MILANOVSKIY, Y. Y. N86-14159
MILBORROW, D. T. N86-13824
MILEKHIN, O. Y. N86-14156
MILLAR, J. N86-13309
MILLER, A. R. N86-13876
MILLER, D. N86-13705
N86-13706
MILLER, D. L. N86-13596
MILLER, E. N86-13524
MILLER, J. B. N86-14061
MILLER, K. N86-13335
MILLER, R. H. N86-13560
MILLER, W. L. N86-13899
MILOV, L. A. N86-14213
MINERBO, G. N. N86-14016
MINKO, L. Y. N86-13455
MIRER, W. N86-14023
MIRKIN, L. I. N86-13454
MIRONOV, V. L. N86-13791
MIRONOV, V. S. N86-13439
MISHIN, I. V. N86-14185
MISHIN, Y. V. N86-14139
MITCHELL, A. C. N86-13399
MITCHELL, J. C. N86-13841
MITTINTI, D. N. N86-13386
MIYA, E. N. N86-13916
MOCHALOVA, T. Y. N86-13434
MOELLER, C. N86-14070
MOELLER, P. N86-13363
MOHRI, A. N86-14048
MOIR, I. R. M. N86-13302
MOISEYEV, A. A. N86-14123
MOKH, A. S. N86-13454
MOLOTILOV, B. V. N86-13434
MONAHAN, R. H. N86-13324
MONAKHOVA, L. A. N86-13437
MONDT, J. P. N86-14069
MONGEAU, P. P. N86-13562
MONGEON, R. J. N86-14042
MONTGOMERIE, B. N86-13825
MONTGOMERY, H. E. N86-13867
MOORE, C. C. N86-13691
MOORE, C. L. N86-13287
MOORE, R. K. N86-13811
MOORE, T. E. N86-13365
MORGAN, T. H. N86-14092
MORIARTY, R. M. N86-13515
MOROZOV, D. K. N86-13483
MORSE, S. D. N86-13516
MORTEVEILLE, A. N86-13707
MOSS, J. M. N86-14021
MOSS, R. A. N86-13372
MOTYKA, P. N86-13310
MOVCHAN, B. A. N86-13438
MOYNIHAN, M. E. N86-13328
N86-13329
N86-13330
MROZ, Z. N86-14107
MUDAWWAR, I. N86-13835
MULLER, A. B. N86-13841
MULTER, J. N86-13313
MURON, D. J. N86-13721
MURPHY, H. D. N86-13695
MURPHY, J. E. N86-13923
MURPHY, L. M. N86-13833
MURRAY, W. N86-13934
MURRELL, R. C. N86-13323
MUSCATELLO, A. C. N86-13502
MUSTEL, E. R. N86-14127
MYLER, T. R. N86-13919
MYRABO, L. N. N86-13553

N

NADIROV, S. G. N86-13862
NADVORNYY, B. N. N86-13441
NAEGELI, D. W. N86-13338
NAFTEL, P. B. N86-13944
NAGURKA, M. L. N86-13574
NAHON, M. A. N86-13914
NAPIER, T. R. N86-13314
NARIHARA, K. N86-14048
NARIMANOV, A. A. N86-13863
NATAPOV, L. M. N86-14175
NATH, J. H. N86-13680
N86-13681
NAVRATIL, J. D. N86-13502
NAYFEH, A. H. N86-13735
NELLIS, W. J. N86-13399
NELSON, B. L. N86-13985
NEWLEY, P. E. N86-13942
NEYER, B. T. N86-13721
NEZLIN, M. V. N86-14158
NG, C. Y. N86-13869
NGAI, K. L. N86-13984
NGUYEN, P. T. N86-13642
NIELSEN, B. N86-14076
NIKISHIN, A. M. N86-14159
NIKITIN, V. I. N86-13438
NIKOLAYENKO, L. M. N86-14137
NIKULIN, L. V. N86-13457
NILSON, T. N86-14178
N86-14179
NOHEL, J. A. N86-13758
NORDEN, K. J. N86-13844
NOREIKA, A. J. N86-14073
NORMAN, J. M. N86-13796
NORWOOD, J., JR. N86-13567
NOTO, R. N86-13925
NOVILOV, V. N. N86-13437
NOVINSON, T. N86-13339
NOWOSAD, P. N86-14011
NOYES, G. N86-13898
NYMAN, M. N86-14023

O

OAKLEY, H. N86-14023
ODA, T. N86-14045
ODESKIY, P. D. N86-13464
OERTEL, C. P. N86-14024
OFENGENDEN, A. A. N86-13428
OGAWA, S. N86-13288
OGURA, K. N86-14048
OHKAWA, T. N86-14062
OHLINGER, W. L. N86-13415
OKE, J. B. N86-14205
OKKES, R. W. N86-13911
OKOROKOV, L. V. N86-13453
OKROSTSVARIDZE, O. S. N86-13482
OKUDA, H. N86-14046
OLDHAM, W. G. N86-13652
OLK, L. B. N86-13723
OLNESS, D. N86-13400
OLSEN, L. C. N86-13656
OLSEN, R. C. N86-13365
OLSON, D. B. N86-13535
ONO, K. N86-13750
ONOPRIYENKO, L. M. N86-13489
ORAN, E. S. N86-13687
OREHOTSKY, J. N86-13838
ORGANICK, E. N86-13935
OSBORN, J. R. N86-13540
OSBORN, M. T. N86-13850
OSBORNE, J. H. N86-13512
OSHER, S. N86-13966
OSTROVOY, A. P. N86-13490
OVCHAROV, V. P. N86-13434
N86-14152
OVERBOSCH, E. G. N86-13725
OWENS, E. C. N86-13388
OYUMI, Y. N86-13521

P

PAGE, D. E. N86-13344
PALMA, R. L. N86-14093
PALMER, R. G. N86-14032
PALMER, R. W. N86-13643
PANASYUK, M. I. N86-14140
PANAYOTI, T. A. N86-13473
PANTYUKHOV, S. V. N86-14191
PAPANICOLAOU, G. C. N86-13380
PAPANTONI-KAZAKOS, P. N86-13981
PAPPA, R. S. N86-13588
N86-13589
PARFENOV, M. G. N86-13465
PARIS, J. F. N86-13812
PARK, W. N86-13324
PARKHOMENKO, N. A. N86-13425
PASCHCHENKO, V. A. N86-13442
PASHECHKO, M. I. N86-13467
PATTON, F. D. N86-13854
N86-13855
PAUL, W. H. N86-13364
PAVELYEV, A. G. N86-14156
PAVLOV, A. V. N86-14143
PAVLOVA, T. I. N86-13443
PAWULA, R. F. N86-13633
PEARCE, W. A. N86-13805
PEARSON, J. T. N86-13835
PEARSON, L. W. N86-14037
PENCE, T. J. N86-13757
PENG, Y. K. M. N86-14061
PENNINGS, N. H. N86-13363
PENNYCOOK, S. J. N86-13664
PEREY, C. M. N86-14026
PEREY, F. G. N86-14026
PERKAS, M. D. N86-13468
PERNG, T. P. N86-13403
PERNPEINTNER, R. N86-13826
PESHKOV, V. V. N86-13487
PETENKO, I. V. N86-13782
PETER, W. N86-14019
PETERS, C. N86-13548
PETERSON, N. C. N86-13410
PETERSON, T. N86-14025
PETERSON, U. N86-14178
PETIT, R. N86-13668
PHILLIPS, J. E. N86-13837

PICKENS, J. R. N86-13412
PITMAN, K. M. N86-14077
PITZ, W. J. N86-13402
PLATONOV, G. L. N86-13440
PLETENETSKIY, G. Y. N86-13436
PLICHTA, E. J. N86-13647
POBEZHIMOV, P. P. N86-13425
POBOL, I. L. N86-13481
PODKOLAYEV, A. S. N86-13449
POGUTSE, O. P. N86-13483
POKHMURSKIY, V. I. N86-13470
POKROVSKIY, A. N86-14153
PONCE, J. N86-13937
PONOMAREV, Y. N. N86-13789
N86-14137
POPOV, A. A. N86-13470
POPOV, M. L. N86-13747
POST, D. N86-13496
POTAPOV, A. N. N86-14195
POVARD, V. N86-13849
PRAGER, S. C. N86-14063
PRASAD, G. S. N86-13650
PRATER, R. N86-14070
PREMACK, T. N86-13947
PRESLAND, S. N86-13968
PROCTOR, P. W. N86-13597
PRODELL, A. N86-14004
PROKHOROV, A. M. N86-13452
PROKOSHKIN, D. A. N86-13473
PROSCHAN, F. N86-13999
PULINETS, S. A. N86-14145
PURVES, L. R. N86-13947

Q

QIGUO, H. N86-13609
QUATE, C. F. N86-13654
QUERRY, M. R. N86-14038
QUINN, G. D. N86-13760
QUINN, J. M. N86-13852
QUINN, T. H. N86-13348

R

RAATZ, J. E. N86-14056
RABINOVICH, B. I. N86-14116
N86-14133
N86-14164
RADOUSKY, H. B. N86-13399
RAFF, B. E. N86-13716
RAJAGOPAL, A. K. N86-13984
RAKHSHTADT, A. G. N86-13468
RAKOW, A. N86-14094
N86-14095
N86-14096
RALCHENKO, V. G. N86-13452
RALL, L. B. N86-13963
N86-13970
RAMBERG, S. E. N86-13875
RAMINS, P. N86-13643
RAMOS, J. I. N86-13574
RANDALL, G. E. N86-13859
RAO, C. R. N86-13977
N86-13998
RASMUSSEN, F. N86-13827
RATHMELL, R. D. N86-14056
RAUN, R. L. N86-13543
RAVDONIKAS, N. Y. N86-13488
RAZORENOV, L. A. N86-14122
READER, C. C. N86-13751
REASONER, D. L. N86-13365
REBIS, J. J. N86-13362
RECHARD, R. P. N86-13753
REDDY, D. S. N86-13510
REEDY, R. E. N86-14041
N86-14043
REES, L. B. N86-14021
REID, L. D. N86-13914
REISCH, H. N86-13340
RENARDY, M. N86-13758
RENAUDIN, J. F. N86-13741
RENNE, I. I. N86-13443
RENNER, T. N86-14023
REVZON, A. L. N86-14189
REYKH, P. N86-13433
RICHARDS, W. A. N86-13979
RICHARDSON, M. C. N86-14068
RIDARD, A. N86-13505
RIDDLE, R. A. N86-14057
RIDLEY, E. J. N86-14097
RIEGER, H. N86-14044
RIEMENSCHNEIDER, S. N86-13964
RIGGINS, M. N86-13689
RITSO, A. E. N86-13445
ROBBINS, H. D. N86-13651
ROBINSON, D. E. N86-13906
ROCK, P. B. N86-13887
ROCKLAND, C. N86-13975
RODE, C. H. N86-14025
RODGERS, S. L. N86-13522
RODIN, A. M. N86-13774
RODRIGUEZ, O. N86-13303
RODRIQUE, G. N86-13940
ROE, D. K. N86-13727
ROE, W. E. N86-13507
ROGERS, W. R. N86-13885
ROGLER, H. L. N86-13684
N86-13685
ROGOVOY, V. M. N86-14116
N86-14133
ROMANOV, V. F. N86-13784
RONGJIN, Y. N86-13605
RONNEKLEIV, A. N86-13368
ROPPO, M. N86-13670
ROSEN, D. N86-13729
ROSEN, D. I. N86-13551
N86-13552
ROSENBERG, I. N86-14028
ROSENFELD, A. N86-13980
ROSINSKI, J. N86-13995
ROSKAM, J. N86-13294
ROSS, J. N. N86-13824
ROSS, K. N86-14178
ROSS, M. N86-14074
ROSS, M. C. N86-14066
ROSS, Y. N86-14178
ROSS, Y. K. N86-14177
ROTH, D. J. N86-13749
ROTH, R. N86-13871
ROUSSEAU, T. H. N86-14008
ROY, M. L. N86-13333
ROYER, H. N86-13724
ROYSTER, D. M. N86-13406
ROZHDESTVENSKIY, A. Y. N86-13767
RUBENSTEIN, M. N86-13873
RUBTSOV, S. N. N86-14196
RUCHYEVA, N. V. N86-13423
RUDNIK, P. J. N86-13712
N86-13759
RUGGLES, L. E. N86-13721
RUMMLER, D. R. N86-13349
RUNIKOV, A. I. N86-13438
RUNNELS, R. C. N86-14098
RUTKOVSKIY, A. I. N86-14119
RYABCHIKOVA, V. I. N86-14187
RYKALIN, N. N. N86-13453
RYUMIN, S. P. N86-14119

S

SABO, D. N86-14182
SADOVNIKOV, V. P. N86-13788
SAKAI, K. N86-14047
N86-14049
SAKAIRI, N. N86-14046
SAKHNO, S. P. N86-13459
SALAMON, D. N86-13997
SALEM, J. A. N86-13495
SALMIN, V. V. N86-14135
SALOMON, M. N86-13647
SAMADDAR, S. N. N86-13636
SAMUELSON, L. S. N86-13682
SANDERS, W. A. N86-13390
SANDGREN, J. N86-13840
SANDLER, H. N86-13886
SANDNESS, G. A. N86-13637
SANDS, T. N86-14075
SANKAR, S. V. N86-13542
SANTORO, G. J. N86-13678
SANUKI, H. N86-14050
SARTAIN, R. L. N86-14099
SARYCHEV, A. V. N86-14113
SAUNDERS, M. A. N86-13934
SAVIKHIN, A. N86-14178
SAVINKIN, Y. V. N86-13484
SAWCHUK, A. A. N86-13711
SAYLOR, P. N86-13940
SAZONOV, N. V. N86-14172
SCHAACK, D. F. N86-13564
SCHACK, C. J. N86-13517
SCHEARER, L. D. N86-14013
SCHETZ, J. A. N86-13287
N86-13686
SCHIFFER, R. A. N86-13866
SCHILLACI, M. E. N86-13419
SCHIMMEL, M. L. N86-13305
SCHISSEL, P. N86-13501
SCHMEISER, B. R. N86-13990
SCHMEISER, B. W. N86-13985
SCHMIDT, R. M. N86-14212
SCHMIDT, S. F. N86-13311
SCHMITT, R. F. N86-13717
SCHMITT, R. J. N86-13513
SCHOFIELD, N. J., JR. N86-13343
SCHRADE, H. O. N86-13554
SCHUESSLER, H. N86-13705
N86-13706
SCHULTZ, P. J. N86-14076
SCHULZE, P. D. N86-14100
SCHWARTZ, L. N86-13623
SCONING, J. N86-13999
SCOTESE, A. N86-13718
SCUDDER, D. W. N86-14059
SEAMONS, L. C. N86-14065
SEBBA, F. N86-13686
SEEMAN, J. T. N86-14066
SEIKEL, G. R. N86-13558
SEKA, W. N86-13732
N86-13733
SEKULER, R. N86-13889
SEMENOV, M. V. N86-13767
SEMEREI, I. N86-14117
SEMINKO, I. V. N86-13458
SEN, J. K. N86-13325
SERAFINI, T. T. N86-13407
SERFOZO, R. F. N86-13978
N86-13991
SERGEYEV, A. V. N86-13493
SERGEYEVA, L. M. N86-13497
SERGIDES, C. A. N86-13501
SETYUKOV, O. A. N86-13423
SGUBINI, S. N86-13739
SHACKELFORD, S. A. N86-13514
N86-13522
SHAFFER, L. E. N86-14108
N86-14109
SHAIKH, M. U. N86-13968
SHANBHAG, D. N. N86-13977
N86-13998
SHANNON, J. L., JR. N86-13495
SHAOBAI, Z. N86-13601
SHAOPING, H. N86-13609
SHARIFYANOV, F. S. N86-13492
SHAROVA, V. A. N86-14139
SHARP, R. D. N86-13852
SHAVLOVSKIY, Y. N. N86-13450
SHELENKOV, G. M. N86-13489
SHELLEY, M. J. N86-13965
SHEPARD, I. G. N86-13518
SHEPELEV, Y. Y. N86-14160
SHEPPARD, J. C. N86-14066
SHEREMETYEV, V. M. N86-13785
SHEU, Y. T. P. N86-13869
SHEVCHENKO, L. A. N86-14174
SHEVERDOVA, R. R. N86-13454
SHIH, A. N86-13659
SHINN, J. M., JR. N86-13406
SHIPKO, A. A. N86-13481
SHKOLNIKOVA, S. I. N86-14139
SHLACHTER, J. S. N86-14059
SHREEVE, J. M. N86-13509
SHULMIN, M. V. N86-14170
SHULMINA, M. P. N86-14170
SHUNQIN, Z. N86-13641
SIEGMANN, W. L. N86-14008
SILADI, F. N86-14182
SIMMER, C. N86-13806
SIMMONS, H. I. N86-13944
SIMON, H. A. N86-13951
SIMONOV, Y. G. N86-14194
SIMPSON, R. L. N86-13686
SIMPSON, W. E. N86-13317
SINEX, C. H. N86-13716
SINITSYN, S. P. N86-13447
SINITSYN, V. M. N86-14137
SINKEVICH, V. F. N86-13472
SIRIGNANO, W. A. N86-13574
SIVTSEVA, L. D. N86-14137
SIYMAR, R. A. N86-13445
SKAKOV, Y. A. N86-13433
SKAL, A. S. N86-13448
SKILES, J. J. N86-13665
SKINNER, C. J. N86-13988
SKINNER, G. L. N86-13323
SKLAD, P. S. N86-13499
SKLYAROV, Y. D. N86-13438
SKOROKHOD, V. V. N86-13461
SKOROKHODOV, A. P. N86-14134
SKOTHEIM, T. A. N86-13504
SKUDERA, W. J., JR. N86-13660
SLATTERY, K. P. N86-14029
SLIWA, S. M. N86-13333
SLOUGH, S. N86-13709
SMIALEK, J. L. N86-13409
SMIRNOV, R. V. N86-14126

SMIRNOVA, N. F.	N86-14117
SMITH, A. A.	N86-13582
SMITH, D. C.	N86-13925
SMITH, D. M.	N86-13501
SMITH, J. A.	N86-13795
SMITH, L.	N86-14058
SMITH, M. W.	N86-13313
SMUROV, I. Y.	N86-13453
SMYTH, W. H.	N86-14209
SNELL, C.	N86-14019
SNIDER, R.	N86-14070
SNODGRASS, H. L., JR.	N86-13891
SNYDER, J. H.	N86-13818
SNYKOV, V. P.	N86-13781
SOBCZYK, K.	N86-14107
SOERLIE, E.	N86-13368
SOKOLOV, A. V.	N86-13788
SOKOLOVSKIY, S. V.	N86-14168
SOLDATOV, B. F.	N86-13450
SOLIE, L. P.	N86-13368
SOLIS, L. A.	N86-13947
SOLOMON, A. D.	N86-13952
SOLONIN, S. M.	N86-13461
SOLOVYEV, G. V.	N86-13473
SOLOVYEV, V. N.	N86-13472
SOMMER, H. T.	N86-13575
SOMOVA, V. I.	N86-14174
SONGTAO, W.	N86-13606
SONNENFELD, G.	N86-13878
SONOBE, B. I.	N86-13371
SORKIN, R. D.	N86-13906
SOSNOVETS, E. N.	N86-14140
SOSUNOV, G. A.	N86-14165
SOURES, J. M.	N86-13732
	N86-14068
SPAULDING, A. D.	N86-13639
SPIEGELMAN, C. H.	N86-13713
SPIES, M.	N86-13350
SPOONER, S.	N86-13416
STAFFORD, M. A.	N86-14015
STANDEN, P. R.	N86-14202
STANGO, R. J.	N86-13376
STANTON, A. C.	N86-13584
STEGER, J. L.	N86-13292
STEIN, W.	N86-14057
STELSON, P. H.	N86-14056
STEPHENS, J. R.	N86-14211
STERN, J.	N86-13895
STERN, R. A.	N86-13661
STETSENKO, A. S.	N86-13441
STEVENS, M. E.	N86-13294
STEVENS, W. J.	N86-13856
STIENING, R. F.	N86-14066
STINTON, D. P.	N86-13500
STOCK, N. J.	N86-13942
STOKES, R. H.	N86-14016
STOLPOVSKIY, V. G.	N86-14119
	N86-14141
STONE, J. W.	N86-13873
STOVER, G.	N86-14023
STRAHLE, W. C.	N86-13527
	N86-13528
STRAHLER, A. H.	N86-13799
STRELKOV, G. M.	N86-13788
STREMPEK, F. M.	N86-13947
STRICKLER, D. J.	N86-14061
STRITTMATTER, P. A.	N86-14207
	N86-14208
STRIZHALO, V. A.	N86-13463
STROD, V. V.	N86-13460
STRONG, I. E.	N86-14211
STRUTTMAN, D. A.	N86-14067
STUERZENHOFAECKER, P.	N86-13705
	N86-13706
SUGIHARA, R.	N86-14049
SUKHANOV, A. A.	N86-14112
SULLIVAN, M. F.	N86-13932
SUNG, C. M.	N86-13416
SUNG, S. S.	N86-13397
SUNWEI, Z.	N86-13607
SUPTELYA, V. V.	N86-13463
SURI, S. C.	N86-13510
SUSHCHENYA, V. A.	N86-14174
SVIRIDOVA, R. V.	N86-14195
SVIRZHEVSKIY, N. S.	N86-13792
SWAIN, J. J.	N86-13990
SWARTZ, C. K.	N86-13645
SWEATT, W. C.	N86-14065
SWITHENBANK, J.	N86-13571
SYSOYEV, A. P.	N86-13493
SYTHE, W. D.	N86-13803
SZENBEHELY, V.	N86-14101

T

TAASAN, S.	N86-13955
TABOADA, J.	N86-13888
TADMOR, E.	N86-13953
TAIRBEKOV, M. G.	N86-14162
TAKAHASHI, F.	N86-13585
TAKEI, W. J.	N86-14073
TAKEUCHI, S.	N86-14047
	N86-14049
TALUKDER, M. A. H.	N86-13516
TANAKA, H.	N86-14048
TANAKA, N.	N86-14021
TANAKA, S.	N86-14048
TANGLER, J. L.	N86-13829
TARANTINO, F. A.	N86-13982
TAVADZE, F. N.	N86-13482
TAVADZE, G. F.	N86-13482
TAVARES, E. J.	N86-13323
TEITLER, S.	N86-13984
TEKAWA, M.	N86-14023
TEMPLE, B.	N86-13962
TEMPLIN, R. J.	N86-13830
TENFORDE, T. S.	N86-14001
TENHAKEN, R. K.	N86-14028
TENNEY, D. R.	N86-13349
TER-KARAPETYANTS, N.	N86-13864
TERUMICHI, Y.	N86-14048
TERZOPOULOS, D.	N86-14036
TEYSSIER, L.	N86-13638
THEILACKER, J.	N86-14025
THIEL, P. A.	N86-13397
THIELE, O.	N86-13866
THIGPEN, L.	N86-13598
THOMAS, R. G.	N86-14102
THOMAS, S. D.	N86-13296
THOMAS, W. A.	N86-13692
THOMPSON, E. F.	N86-13683
THOMPSON, J. K.	N86-13374
THOMPSON, W. W.	N86-13534
THOMSON, A.	N86-13705
	N86-13706
THOMSON, E. M.	N86-13873
TICHLER, J. L.	N86-13844
TIDMAN, D. A.	N86-14052
TIFFANY, S. H.	N86-13333
TIKHMYANOV, V. [illegible]	N86-13443
TIME, N. S.	N86-13782
TIMILIN, I. A.	N86-13434
TIMONIN, V. M.	N86-13470
TIMOSHKOVA, Y. I.	N86-14129
TISHKOFF, J. M.	N86-13634
TITOV, V. B.	N86-14129
TIWARI, S. N.	N86-13293
TODD, M. J.	N86-13738
TOKIWA, Y.	N86-13849
TOMAZIC, W. A.	N86-14106
TOMLIN, J. A.	N86-13934
TOPCHILO, N. A.	N86-14124
TOPCHIYEV, A. G.	N86-14172
TOPOLSKIY, V. F.	N86-13490
TOURNIER, C.	N86-13707
TROGLER, W. C.	N86-13512
TROLINGER, J. D.	N86-13564
TROSIN, J.	N86-13290
	N86-13291
TROST, T. F.	N86-13320
TROTTER, J. D.	N86-13650
	N86-13651
TROYANOVSKIY, V. E.	N86-13489
TRUBNIKOV, A. S.	N86-14158
TSAI, H. L.	N86-13669
TSAI, S. W.	N86-13378
TSAI, T. M. C.	N86-13673
TSANG, C. F.	N86-13694
TSUGE, S.	N86-13685
TSYPONA, M. N.	N86-13484
TURCHI, P. J.	N86-13567
TURKEL, E.	N86-13954
TVOROGOV, S. D.	N86-13789
TYMCHIK, G. S.	N86-13459
TYNNYY, A. N.	N86-13451
TYURMINA, L. O.	N86-14139

U

UCCELLINI, L. W.	N86-13867
UGLOV, A. A.	N86-13453
ULABY, F. T.	N86-13810
ULIN, S. Y.	N86-14123
UMAN, M. A.	N86-13873
USACHEV, A. L.	N86-13779
USHAKOV, V. K.	N86-13443
USIKOV, D. A.	N86-14185
UZLOV, K. I.	N86-13427

V

VALENT, P. J.	N86-13689
VALUSEK, J. R.	N86-13901
VANDERBILT, V. C.	N86-13798
VANDEROER, T. G.	N86-13648
VANFOSSEN, G. J.	N86-13677
VANHOLTEN, T.	N86-13823
VANLEEUWEN, W.	N86-13902
	N86-13903
	N86-13904
	N86-13905
VANOOST, S.	N86-13363
VARIGIN, A. B.	N86-13437
VASHCHILO, N. P.	N86-13438
VASILYEV, L. N.	N86-14180
VASILYEV, P. S.	N86-13793
VASILYEVA, S. S.	N86-13486
VAYSBERG, O. L.	N86-14142
VEGH, E.	N86-13876
VEHANEN, A.	N86-14076
VEKSHIN, B. S.	N86-13446
VERDIECK, J. F.	N86-13576
	N86-13583
VERDON, C.	N86-14068
VERNIKOS-DANELLIS, J.	N86-13886
VIGNOLA, G.	N86-14002
VIKTOROV, S. V.	N86-14164
VINOGRADOV, B. V.	N86-14181
VINTAYEV, V. N.	N86-14165
VLASOV, A. S.	N86-13456
VLASOV, D. V.	N86-13775
VLASOVA, A. V.	N86-13492
VODOPYANOV, K. L.	N86-13774
VOLCHKEVICH, L.	N86-13743
VOLNISTOVA, L. P.	N86-13781
VOLOKITIN, A. S.	N86-14139
VORONTSOV, Y. S.	N86-13487
VOROTYNTSEV, I. V.	N86-13744
VOTAW, M. W.	N86-13325
VOYEVODIN, S. A.	N86-14115
VYGODSKAYA, N. N.	N86-14190
VYUNENKO, Y. N.	N86-13480

W

WADE, W. L., JR.	N86-13662
WAGNER, D.	N86-13364
WAGNER, E.	N86-13310
WAITE, J. H., JR.	N86-13365
WALES, W. S.	N86-13631
WALKER, B. E.	N86-13374
WALKER, C. W., JR.	N86-13662
WALKER, R.	N86-14025
WALKER, R. B.	N86-14018
WALSH, J. M.	N86-13819
WALTON, O. R.	N86-13697
WALTRICK, C. N.	N86-13717
WANDERER, P.	N86-14004
WANG, D. P.	N86-13836
WANG, L.	N86-13976
WANG, M. H.	N86-13331
WARD, T. E.	N86-13847
WARTENBERG, H.	N86-13350
WASHBURN, J. S.	N86-13639
WATSON, F. G.	N86-14201
	N86-14203
WAYNE, R. J.	N86-14042
WAYNER, P. C., JR.	N86-13566
WEAVER, D. P.	N86-13523
	N86-13529
	N86-13530
	N86-13531
WEBB, T. P.	N86-13334
WEBBER, L.	N86-13846
WEBER, D. C.	N86-13325
WEBER, J. F.	N86-13508
WEBER, W. J.	N86-13656
WEDDING, J. B.	N86-13710
WEIGAND, M. A.	N86-13710
WEINBERG, A. S.	N86-13950
WEINBERG, I.	N86-13645
WELLS, R.	N86-13548
WEN, C. T.	N86-13320
WENDT, J. F.	N86-13347
WENKUI, W.	N86-13606
WENYU, Z.	N86-13604
WENZEL, K. W.	N86-13560
WESOLOWSKI, J. J.	N86-13846
WESTBERG, K.	N86-13533
WESTBROOK, C. K.	N86-13402
WESTPHAL, M.	N86-13705
	N86-13706

WESTPHAL, R. V.	N86-13298
WEYDANDT, J.	N86-13361
WHITE, P. S.	N86-13362
WIANT, H. R.	N86-13406
WICKENS, C.	N86-13897
WIDJAJA	N86-13350
WIESEMAN, C. D.	N86-13946
WIETING, A. R.	N86-13349
WILLEN, E.	N86-14004
WILLER, R. L.	N86-13511
WILLIAMS, B. R.	N86-13301
WILLIAMS, D. B.	N86-13416
WILLIAMS, F. A.	N86-13585
WILLIAMS, K. L.	N86-14010
WILLIAMS, R.	N86-14103
WILLIAMS, R. S.	N86-14071
WILLIAMSON, A. D.	N86-13847
WILLOUGHBY, P. G.	N86-13541
WILSON, D. G.	N86-13952
WILSON, P. B.	N86-14017
WINSKE, D.	N86-13702
WINSOR, N. K.	N86-14052
WINSTON, E.	N86-13924
WIRTZ, G. P.	N86-13667
WITTIG, J. E.	N86-13405
WOIDNECK, C. P.	N86-13586
WOOD, S.	N86-14073
WOODS, B. P.	N86-13359
WOODS, R. J.	N86-13818
WOODWORTH, J. R.	N86-14065
WOOLERY, D. O.	N86-13534
WOZNIAKOWSKI, C. M.	N86-13315
WRIGHT, M. H.	N86-13934
WU, A. Y.	N86-13980
WU, L. K.	N86-13811
WYZKOSKI, J.	N86-14104

X

XINGRONG, S.	N86-13602
XIUYUN, L.	N86-13609
XU, J. A.	N86-14074

Y

YAAKOVI, B.	N86-14068
YAKOVCHUK, K. Y.	N86-13438
YAKOVLEV, O. I.	N86-14156
YANENSKIY, N. Y.	N86-13441
YANENSKIY, V. N.	N86-13441
YANG, T. F.	N86-13559 N86-13560
YANGUANG, S.	N86-13602
YAOJI, W.	N86-13606
YAYLOR, S. R.	N86-13859
YEDNERAL, A. F.	N86-13468
YEGER, S.	N86-13318
YELAGIN, I. N.	N86-14183
YELISEYEVA, O. I.	N86-13479
YELISTRATOVA, L. S.	N86-13449
YERMOLAYEV, Y. I.	N86-14142
YERSHOVA, V. A.	N86-14137
YEVSYUKOV, N. N.	N86-14128
YI, H.	N86-13606
YI, Q.	N86-13609
YIN, Y. Q.	N86-13973
YOERKIE, C.	N86-13326
YOUNG, A. J.	N86-13887
YUILLE, A.	N86-13937
YUROVITSKAYA, V. G.	N86-14119

Z

ZAKHAROV, B. M.	N86-13437
ZAKHAROV, V. N.	N86-13462
ZAMKOV, V. N.	N86-13490
ZANGRANDO, F.	N86-13834
ZAPLATYNSKY, I.	N86-13408
ZAPORINA, N. A.	N86-13460
ZARDECKI, A.	N86-13806
ZARETSKY, E. V.	N86-13734
ZARNSTORFF, M. C.	N86-14063
ZASTENKER, G. N.	N86-14142
ZAYENTSEV, L. V.	N86-14196
ZAYTSEV, A. K.	N86-13434
ZAYTSEVA, Z. A.	N86-13442
ZELENSKIY, V. A.	N86-13435
ZENCHENKO, V. M.	N86-14119
ZENOBI, T. J.	N86-13307
ZENTLER, J. M.	N86-14005
ZHARKOV, V. N.	N86-14155
ZHIBEN, Z.	N86-13608
ZHICHENG, Q.	N86-13606
ZHONGQING, S.	N86-13601
ZHURAVLAV, A. F.	N86-13478
ZHURAVLEV, B. F.	N86-13478
ZIEGLER, N. F.	N86-14056
ZIGUNENKO, S.	N86-14161
ZIMA, M. N.	N86-13477
ZIMMERMANN, W. J.	N86-14105
ZINN, B. T.	N86-13542
ZISSA, D. E.	N86-14033
ZOLOTAREV, V. S.	N86-13429
ZOLOTOGOROV, M. G.	N86-13442
ZOLOTUKHIN, V. G.	N86-14185
ZORZI, E.	N86-13369
ZOUGHI, R.	N86-13811
ZUBEHCNKO, A. S.	N86-13470
ZUE, V. W.	N86-13629
ZUYEV, V. Y.	N86-13787
ZYTKOW, J. M.	N86-13951

CORPORATE SOURCE INDEX

SCIENTIFIC AND TECHNICAL AEROSPACE REPORTS VOLUME 24 NUMBER 4

Typical Corporate Source Index Listing

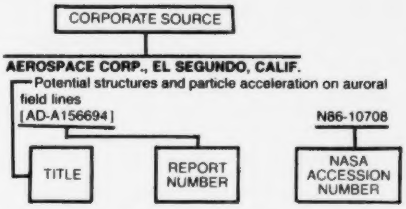
CORPORATE SOURCE
AEROSPACE CORP., EL SEGUNDO, CALIF.
Potential structures and particle acceleration on auroral field lines
[AD-A156694]
N86-10708
TITLE
REPORT NUMBER
NASA ACCESSION NUMBER

Listings in this index are arranged alphabetically by corporate source. The title of the document provides the user with a brief description of the subject matter. The report number helps to indicate the type of document cited (e.g., NASA report, translation, NASA contractor report). The NASA accession number denotes the number by which the citation is identified. The titles are arranged under each corporate source in ascending accession number order.

A

ABILENE CHRISTIAN COLL., TEX.
Ion bombardment and adsorption studies on ilmenite (FeTiO3) by X-ray photoelectron spectroscopy N86-14100

ACUREX CORP., MOUNTAIN VIEW, CALIF.
Ceramic fabric material testing [DE85-013684] N86-13503

ADVANCED ENGINEERING LAB., ADELAIDE (AUSTRALIA).
METCUT: A computer aided system for machining technology [AD-A157941] N86-13927

AEROCHEM RESEARCH LABS., INC., PRINCETON, N. J.
Stability of RDX, AP and BTTN near room temperature N86-13535

AERODYNE RESEARCH, INC., BILLERICA, MASS.
Single particle sizing by measurement of Brownian motion N86-13584

AEROJET TECHSYSTEMS CO., SACRAMENTO, CALIF.
Rocket engine hot-spot detector [NASA-CR-171902] N86-13708

AEROMETRICS, INC., MOUNTAIN VIEW, CALIF.
Spray characterization using phase angle detection N86-13577

AERONAUTICAL RESEARCH INST. OF SWEDEN, BROMMA.
Unsteady aerodynamics applied to the horizontal axis wind turbine disk N86-13825

AERONAUTICAL RESEARCH LABS., MELBOURNE (AUSTRALIA).
An analytical comparison of three visual approach slope indicators: VASIS, T-VASIS and PAPI [ARL/SYS-R-33] N86-13309
A real-time data acquisition system for a low speed wind tunnel [AR-AERO-R-163] N86-13336
Algorithms for the reduction of wind-tunnel data derived from strain gauge force balances [ARL/AERO-R-164] N86-13337
A numerical investigation into the plastic stress and strain fields around a surface crack [ARL/STRUC-R-414] N86-13754

AEROSPACE CORP., EL SEGUNDO, CALIF.
Cassegrain reflector sidelobe reduction study [AD-A158625] N86-13631
Rectification and registration of remotely sensed data [AD-A158827] N86-13711

AEROSPACE CORP., LOS ANGELES, CALIF.
Critical evaluation of high temperature chemical kinetic data N86-13533

AIR FORCE ACADEMY, COLO.
Pitch rate versus G command as the longitudinal flight control system design strategy for a statistically unstable fighter type aircraft with two control surfaces [AD-A158803] N86-13334

AIR FORCE ENGINEERING AND SERVICES CENTER, TYNDALL AFB, FLA.
A durable airfield marking system [AD-A157953] N86-13339

AIR FORCE HUMAN RESOURCES LAB., BROOKS AFB, TEX.
Pilot-oriented performance measurement [AD-A158849] N86-13890

AIR FORCE INST. OF TECH., WRIGHT-PATTERSON AFB, OHIO.
Time delay of arrival location assessment using four satellites [AD-A159243] N86-13315
Aircrew dose and engine dust ingestion from nuclear cloud penetration [AD-A159246] N86-13327
The dynamics of the photofragmentation of ketene 3-cyclopentenone, 3,5-cycloheptadienone, and tropone [AD-A158045] N86-13371
Differential scattering cross section and total extinction measurements on (CH)n spheres in 632.8 nm laser light [AD-A158044] N86-13391
Electronic detection of low concentrations of organophosphorus compounds with a solid state device utilizing supported copper + cuprous oxide island films [AD-A158181] N86-13392
Using software technology to specify abstract interfaces in VLSI design [AD-A158034] N86-13649
Sampling-rate effects on radar-derived rainfall estimates [AD-A158203] N86-13870
Information requirements determination: An empirical investigation of obstacles within an individual [AD-A158025] N86-13901
A reactive learning environment for the Equipment Problem Solving Techniques (EPST) system [AD-A158035] N86-13929
An algorithm to translate relational algebra queries into QUEL [AD-A158169] N86-13931
A finite element solution of the transport equation [AD-A159245] N86-13982
Identification of nuclear materials from remote detection of characteristic gamma rays [AD-A159244] N86-14014
Analysis of the dynamic behavior of an intense charged particle beam using the semigroup approach [AD-A159247] N86-14015
Coupled radiation transport/thermal analysis of the radiation shield for a space nuclear reactor [AD-A158180] N86-14022

AIR FORCE OFFICE OF SCIENTIFIC RESEARCH, BOLLING AFB, WASHINGTON, D.C.
The 1985 AFOSR/AFRPL Chemical Rocket Research Meeting, abstracts and agenda [AD-A158291] N86-13507
Overview: AFOSR interests in rocket propulsion N86-13546
Specialists Meeting on Atomization and Nondilute Sprays [AD-A159006] N86-13634

AIR FORCE ROCKET PROPULSION LAB., EDWARDS AFB, CALIF.
New synthetic techniques for advanced propellant ingredients: Selective transformations and new structures N86-13514
New energetic polymers as binders for propellants N86-13516
Deuterium isotope effects in RDX decomposition and combustion processes N86-13522
High pressure solid propellant combustion zone structure from analysis of hydroxyl radical chemiluminescence N86-13529
Evaluation of HMX propellant chemistry from Raman and laser induced fluorescence species and temperature measurements N86-13530
Application of molecular kinetics models to the prediction of backflow contamination N86-13531
Crack growth behavior in a composite propellant with strain gradients N86-13537
Nonlinear modeling and method of predicting crack growth N86-13538
Interaction of multi-dimensional mean and acoustic fields in solid rocket combustion chambers N86-13547

AIR FORCE SYSTEMS COMMAND, WRIGHT-PATTERSON AFB, OHIO.
Study of cross-linking density and the type of cross linkage in polyurethane elastomers [AD-A158199] N86-13497
The physics and technology of strong magnetic fields (chapter 10) [AD-A158174] N86-14000

AIR FORCE WRIGHT AERONAUTICAL LABS., WRIGHT-PATTERSON AFB, OHIO.
Composites design [AD-A157710] N86-13378
Fractography of mixed mode 1 - 2 failure in Graphite/Epoxy and Graphite/Thermoplastic unidirectional composites [AD-A158852] N86-13496
Issues to be considered in the evaluation of technical proposals from the Ada (trademark) language perspective [AD-A158376] N86-13936

ALABAMA STATE UNIV., MONTGOMERY.
Determination of neutron flux distribution by using ANISN, a one-dimensional discrete S sub n ordinates transport code with anisotropic scattering N86-14084

ALABAMA UNIV., HUNTSVILLE.
Flow field effects on combustion instability N86-13544

ALLIED BENDIX AEROSPACE, TETERBORO, N.J.
Astrophysical payload accommodation on the space station [NASA-CR-178556] N86-13359

ALLIED CORP., MORRISTOWN, N.J.
Role of additives in minimizing zinc electrode shape change: The effect of lead on the kinetics of Zn(2) reduction in concentrated alkaline media [AD-A158806] N86-13395

AMERICAN UNIV., BEIRUT (LEBANON).
A study of some features of ac and dc electric power systems for a space station N86-14085

ARGONNE NATIONAL LAB., IDAHO FALLS, IDAHO.
Performance assessment of OTEC power systems and thermal power plants. Volume 2: Users manual for PACC-OTECs [DE85-016792] N86-13835

ARGONNE NATIONAL LAB., ILL.
Microcomputer controlled current sharing experiments with parallel converters [DE85-013854] N86-13665
Development of contact/impact capability for the three-dimensional fluid-structure interaction code: NEPTUNE [DE85-010264] N86-13698
Fluid forces on two circular cylinders in crossflow [DE85-014294] N86-13704
Simulating distributed reinforcement effects in concrete analysis [DE85-009745] N86-13761
Long-term analysis of slender concrete structures with cracking [DE85-010275] N86-13762
Far-field model of the regional influence of affluent plumes from Ocean Thermal Energy Conversion (OTEC) plants [DE85-016981] N86-13836
Graph theoretic approaches to diagnostics: Applications of logic programming and cutset theory to aspects of reactor and circuit analysis [ANL-84-74] N86-13912

ARIZONA STATE UNIV., TEMPE.
Intelligent laser diffraction instrumentation for particle size analysis N86-13581

ARIZONA UNIV., TUCSON.
Speckle image reconstruction. Appendix 1 [AD-A158271] N86-14207

Speckle image reconstruction. Appendix 2
[AD-A158272] N86-14208

ARKANSAS COLL., BATESVILLE.
A pyroloysis technique for determining microamounts of hydrogen in lunar soil using the helium ionization detector N86-14082

ARKANSAS UNIV., LITTLE ROCK.
Finite element or Galerkin type semidiscrete schemes N86-14083

ARMY AVIATION ENGINEERING FLIGHT ACTIVITY, EDWARDS AFB, CALIF.
Limited Airworthiness and Flight Characteristics (A and FC) test of the quick fix configuration
[AD-A157716] N86-13323

ARMY CONSTRUCTION ENGINEERING RESEARCH LAB., CHAMPAIGN, ILL.
Design criteria upgrade for US Army Type 2 air traffic control towers
[AD-A159115] N86-13314

ARMY ENGINEER WATERWAYS EXPERIMENT STATION, VICKSBURG, MISS.
User's manual for the generalized computer program system. Open-channel flow and sedimentation, TABS-2. Main text
[AD-A159249] N86-13692
The Vaiont Slide. A geotechnical analysis based on new geologic observations of the failure surface. Volume 1: Main text
[AD-A158192] N86-13854
The Vaiont Slide. A geotechnical analysis based on new geologic observations of the failure surface. Volume 2: Appendices A through G
[AD-A158193] N86-13855

ARMY ENVIRONMENTAL HYGIENE AGENCY, ABERDEEN PROVING GROUND, MD.
Health hazard evaluation of liquid monopropellants. Phase 5: Comparative inhalation toxicities of LGP 1776, LGP 1845, and HAN (hydroxylammonium nitrate)
[AD-A159090] N86-13891

ARMY FUELS AND LUBRICANTS RESEARCH LAB., SAN ANTONIO, TEX.
Report on investigation of alcohol combustion associated wear in spark ignition engines, mechanisms and lubricant effects
[AD-A157714] N86-13388

ARMY MATERIALS AND MECHANICS RESEARCH CENTER, WATERTOWN, MASS.
Static fatigue of a sintered silicon nitride
[AD-A158813] N86-13760

ARMY MATERIEL SYSTEMS ANALYSIS ACTIVITY, ABERDEEN PROVING GROUND, MD.
Methodology for stochastic modeling
[AD-A158851] N86-13994

ARMY MISSILE COMMAND, REDSTONE ARSENAL, ALA.
Concept of laser locator systems (based on the geometry of the triangular corner cube reflector)
[AD-A157795] N86-13728
Further results for application of disturbance minimization control techniques to a linear, time-invariant, second-order state set-point regulator problem
[AD-A157793] N86-13961
Real time large memory optical pattern recognition
[AD-A158023] N86-14034

ARMY RESEARCH INST. OF ENVIRONMENTAL MEDICINE, NATICK, MASS.
The effect of spironolactone on the cardiocirculatory responses to upright tilt at sea level and at simulated high altitude
[AD-A157734] N86-13887

ARNOLD ENGINEERING DEVELOPMENT CENTER, ARNOLD AIR FORCE STATION, TENN.
Boundary-value problem for two-dimensional fluctuations in boundary layers
[AD-A157952] N86-13685
Crushing strength of aluminum oxide agglomerates
[AD-A158051] N86-13756

ATLANTIC RESEARCH CORP., ALEXANDRIA, VA.
Fuel-rich solid propellant boron combusion N86-13536

ATMOSPHERIC AND ENVIRONMENTAL RESEARCH, INC., CAMBRIDGE, MASS.
Extended atmospheres of outer planet satellites and comets
[NASA-CR 176398] N86-14209

AUGSBURG COLL., MINNEAPOLIS, MINN.
Analysis of atomic thermospheric nitrogen density
[NASA-CR-176354] N86-13851

AUSTRALIAN NATIONAL UNIV., COONABARABRAN.
Design for a large altazimuth Schmidt telescope N86-14203

B

BATTELLE COLUMBUS LABS., OHIO.
Laser produced X-ray for high resolution lithography
[AD-A158734] N86-13730

BATTELLE INST., FRANKFURT AM MAIN (WEST GERMANY).
Generically based mobility-terrain data bases
[AD-A157738] N86-13815

BATTELLE NORTHWEST LABS., RICHLAND, WASH.
Design, construction and testing of a dc bioeffects enclosure for small animals
[DE05-016798] N86-13883

BATTELLE PACIFIC NORTHWEST LABS., RICHLAND, WASH.
Electrical and thermal transport property studies of high-temperature thermoelectric materials
[AD-A158883] N86-13656

BEDFORD RESEARCH ASSOCIATES, MASS.
IE data processing
[AD-A158027] N86-13853

BELL TELEPHONE LABS., INC., MURRAY HILL, N. J.
Application of cross-sectional transmission electron microscopy to the characterization of ion-implanted semiconductors
[DE85-010990] N86-14075

BOEING AEROSPACE CO., SEATTLE, WASH.
Experimental investigation of crater growth dynamics
[NASA-CR-176392] N86-14212

BRADLEY UNIV., PEORIA, ILL.
Computer graphics applications to crew displays N86-14104

BRIGHAM YOUNG UNIV., PROVO, UTAH.
Mechanisms for acoustic suppression N86-13543

BRITISH AEROSPACE DYNAMICS GROUP, BRISTOL (ENGLAND).
Development of the NIMBUS-7 SMMR retrieval algorithm
[BAE-RPT/NIM-7/021] N86-13367

BROOKHAVEN NATIONAL LAB., UPTON, N. Y.
Oxide electrodes at high temperatures
[DE85-006564] N86-13667
Oxidizing and scavenging characteristics of April rains: OSCAR data report
[DE85-017014] N86-13844
Lattice and bypass design for a coherent XUV facility
[DE85-016556] N86-14002
Random errors in the magnetic field coefficients of superconducting magnets
[DE85-012261] N86-14004
Efficient ionizer for polarized H(-) formation
[DE85-013294] N86-14064
Positron diffusion in Si
[DE85-014831] N86-14076

C

CALIFORNIA DEPT. OF HEALTH SERVICES, BERKELEY.
Particulate matter analysis by electron microscopy
[PB85-227817] N86-13846
Determination of acidity in ambient air
[PB85-218196] N86-13849

CALIFORNIA UNIV., BERKELEY.
Thermal radiation effects on combustion of condensed fuels N86-13387
Coherent optical transient spectroscopy in flames N86-13570
Joint services electronics program
[AD-A158731] N86-13652
A study of transport phenomena and interface stability during solidification of binary solutions using front tracking finite elements N86-13669
A three-dimensional analysis of natural convection in a toroidal loop N86-13672
Turbulence and dynamical systems
[AD-A159026] N86-13691

CALIFORNIA UNIV., BERKELEY. LAWRENCE BERKELEY LAB.
Investigation of the vertical-flow aquifer thermal energy storage concept and numerical simulation of the Dorigny field experiment
[DE85-014524] N86-13694
Magnetic field applications in modern technology and medicine
[DE85-015197] N86-14001
Lattice and bypass design for a coherent XUV facility
[DE85-016556] N86-14002
New control techniques for extraction of Bevalac beams
[DE85-017640] N86-14023
Effect of focusing field nonlinearities in MBE-4 on transverse beam dynamics
[DE85-016561] N86-14058

Application of cross-sectional transmission electron microscopy to the characterization of ion-implanted semiconductors
[DE85-010990] N86-14075

CALIFORNIA UNIV., BERKELEY. LAWRENCE RADIATION LAB.
Development of high sensitivity X-ray and electron beam resist processes
[AD-A158968] N86-13657

CALIFORNIA UNIV., DAVIS.
California Water Resources Institute program for 1983
[PB85-225837] N86-13818

CALIFORNIA UNIV., IRVINE.
Discovering qualitative empirical laws
[AD-A159235] N86-13951

CALIFORNIA UNIV., LOS ANGELES.
High frequency quantitative analysis of magnetomechanical acoustic emission
[AD-A158222] N86-13750
AuGa2 on GaSb(001): An epitaxial, thermodynamically stabilized Metal/3-5 compound semiconductor interface
[AD-A157937] N86-14071

CALIFORNIA UNIV., RIVERSIDE.
Muon spin relaxation study of exchange coupling in dilute AgMn alloys
[DE85-014104] N86-13419

CALIFORNIA UNIV., SAN DIEGO, LA JOLLA.
Synthesis and reactivity of unsaturated metal nitrogen complexes N86-13512

CALIFORNIA UNIV., SANTA BARBARA.
Synthesis, structure and reactivity of molecules attached to electrode surfaces
[AD-A158621] N86-13394
Charge-density waves observed with a tunneling microscope
[AD-A158779] N86-13709

CAMBRIDGE ACOUSTICAL ASSOCIATES, INC., MASS.
Sensitivity to mean flow parameters of the low wavenumber content of the wall pressure under a turbulent boundary layer
[AD-A158037] N86-13688

CARNEGIE INSTITUTION OF WASHINGTON, D. C.
Equation of state of dense argon: A comparison of shock and static studies
[DE85-015543] N86-14074

CARNEGIE-MELLON UNIV., PITTSBURGH, PA.
Erosion and onset mechanisms in magnetoplasmadynamic thrusters N86-13556
Strategy for advanced sensing and control of combustion N86-13574
The 1-D laser Doppler instrumentation N86-13575
Ada as a hardware description language: An initial report
[AD-A158217] N86-13935
Discovering qualitative empirical laws
[AD-A159235] N86-13951

CASE WESTERN RESERVE UNIV., CLEVELAND, OHIO.
Time dependency of strainrange partitioning life relationships
[NASA-CR-174946] N86-13755

CATHOLIC UNIV. OF AMERICA, WASHINGTON, D.C.
Reaction intermediates in aromatic fuel combustion
[AD-A158029] N86-13390

CENTRAL ELECTRICITY GENERATING BOARD, LONDON (ENGLAND).
Aerofoil characteristics of rotating blades N86-13824

CENTRE D'ESSAIS AERONAUTIQUE TOULOUSE (FRANCE).
Test of a moisture conditioning procedure using 70 C distilled water, instead of a gas atmosphere at 70 C, 95% relative humidity
[M3-431000] N86-13383
Study of the mechanical properties dispersion of carbon-epoxy composite materials
[M2-695600-PT-1] N86-13384
Study of the dispersion of the mechanical properties of carbon-epoxy composite materials
[M2-695600-PT-2] N86-13385
Evaluation of the titanium IMI 829 alloy produced by powder metallurgy
[M1-610200] N86-13421

CENTRE DE RECHERCHES SCIENTIFIQUES ET TECHNIQUES DE L'INDUSTRIE DES FABRICATIONS METALLIQUES, BRUSSELS (BELGIUM).
Activities report of the Technical and Scientific Research Center for the Metal Manufacturing Industry N86-13740

CENTRE TECHNIQUE DES INDUSTRIES MECANIQUES, ST. ETIENNE (FRANCE).
Evaluation of the erosion protection of low inflammability liquids of the HFC type (polyglycol solutions)
[CETIM-12-E-13-3] N86-13505
Computerized simulation and display of extruding by cold forging
[CETIM-1-3L-11-1] N86-13741

CENTRONIC LTD., CROYDON (ENGLAND).
Sun acquisition sensor for European Communications Satellite N86-13366

CHICAGO UNIV., ILL.
Inner/outer iterative methods and numerical Schwarz algorithms - 2
[DE85-013197] N86-13940
Focal plane optics in far-infrared and submillimeter astronomy
[NASA-TM-88186] N86-14204

CINCINNATI UNIV., OHIO.
Kinematics of foldable discrete space cranes
[NASA-CR-176360] N86-13735

COASTAL ENGINEERING RESEARCH CENTER, VICKSBURG, MISS.
Iterative and Pade solutions for the water-wave dispersion relation
[AD-A157796] N86-13683

COLORADO SCHOOL OF MINES, GOLDEN.
Pre-stack Kirchhoff inversion of common offset data
[AD-A158205] N86-13932

COLORADO STATE UNIV., FORT COLLINS.
Reflectance modeling N86-13795

COLORADO UNIV., BOULDER.
Studies of metal/carbon surface chemistry
[DE85-015548] N86-13398
Chemical kinetics of nitramine propellant combustion N86-13525

COLUMBIA UNIV., NEW YORK.
Detection of Ni 2 lambda 7378 in six Seyfert galaxies
[NASA-CR-176358] N86-14205

CONNECTICUT UNIV., STORRS.
An investigation of plasma jet ignition and flame jet ignition of lean fuel-air mixtures N86-13386
Unified method for delay analysis of random multiple access algorithms
[AD-A159108] N86-13981

CONSULENZE GENERALI ROMA (ITALY).
Cyclosymmetric approach to the dynamics of repetitive modular structures
[ESA-CR(P)-2062] N86-13739

CORNELL UNIV., ITHACA, N.Y.
Mass transfer coefficients and Henry's constants for packed-tower air stripping of volatile organics: Measurements and correlation
[AD-A158811] N86-13375
No chemisorption on Ni(111): Coverage effects, site preferences and adsorption geometry
[AD-A159110] N86-13397
Replication and fault-tolerance in the ISIS system
[AD-A157775] N86-13926

D

DAYTON UNIV., OHIO.
High-resolution movies of propellant deflagration N86-13539
Laser diagnostics for electric field measurements N86-13563

DAYTON UNIV. RESEARCH INST., EDWARDS AFB, CALIF.
New energetic polymers as binders for propellants N86-13516
Flame mechanisms and flame inhibition N86-13523
High pressure solid propellant combustion zone structure from analysis of hydroxyl radical chemiluminescence N86-13529
Evaluation of HMX propellant chemistry from Raman and laser induced fluorescence species and temperature measurements N86-13530
Application of molecular kinetics models to the prediction of backflow contamination N86-13531

DEFENCE RESEARCH ESTABLISHMENT ATLANTIC, DARTMOUTH (NOVA SCOTIA).
A new library of subroutines for calculating smoothing splines
[AD-A158049] N86-13930

DEFENCE RESEARCH ESTABLISHMENT VALCARTIER (QUEBEC).
Investigation of cold colored smoke production
[AD-A158783] N86-14040

DELAWARE UNIV., NEWARK.
Structure-decomposition relationships in newer energetic materials N86-13521
Development of stable high efficiency polycrystalline thin-film solar cells based on CuInSe2
[DE85-000517] N86-13837

DENVER UNIV., COLO.
Photodegradation studies of silver-backed polyacrylonitrile (PAN) films
[DE85-012154] N86-13501

DEPARTMENT OF ENERGY, WASHINGTON, D. C.
Method of synthesizing polymers from a solid electrolyte
[DE85-011623] N86-13504
Apparatus for removably holding a plurality of microballoons
[DE85-006517] N86-13722

DEPARTMENT OF THE AIR FORCE, WASHINGTON, D.C.
Technique of assembling structures using vapor phase soldering
[AD-D011805] N86-13410
Phase lock acquisition system
[AD-D011804] N86-13646

DEPARTMENT OF THE ARMY, WASHINGTON, D. C.
Cathode including a non fluorinated linear chain polymer as the binder, method of making the cathode, and lithium electrochemical cell containing the cathode
[AD-D011807] N86-13647
Analog-to-Digital converter
[AD-D011878] N86-13660
Slot line tunable bandpass filter
[AD-D011881] N86-13661
Cathode for use in high energy primary thionyl chloride cell systems and high energy primary thionyl chloride cell systems including the cathode
[AD-D011882] N86-13662
Routing method in computer aided customization of a two level automated universal array
[AD-D011808] N86-13925
Optical radar transceiver control apparatus
[AD-D011880] N86-14042

DEPARTMENT OF THE NAVY, WASHINGTON, D. C.
Passive arm retention curtain
[AD-D011876] N86-13307
A method for melt-coating a surface
[AD-D011866] N86-13596
Nozzle for self-contained cutting torches
[AD-D011875] N86-13597
Gas recirculator for acyclic machines
[AD-D011873] N86-13658
Atomically mixed alloy coated cathodes specification
[AD-D011877] N86-13659
An Oil/Water disperser device for use in an oil content Monitor/Control system
[AD-D011868] N86-13714
Time resolved extended X-ray absorption fine structure spectrometer
[AD-D011869] N86-13715
Expendable bathythermograph for measuring light attenuation and temperature below the ocean surface
[AD-D011870] N86-13716
Oil content Monitor/Control system and method
[AD-D011871] N86-13717
Remote optical crack sensing system
[AD-D011872] N86-13718
Variable temperature trap
[AD-D011874] N86-13719
Latch for detachably securing electronic cards along orthogonal loading axes
[AD-D011885] N86-13737
Computer-aided process for generating camera-ready graphical artwork
[AD-D011884] N86-13939
An integrated wavelength demultiplexer
[AD-D011867] N86-14041
Optoelectronic integrated circuit multiplier
[AD-D011883] N86-14043
Fiber optics as an angular sensor
[AD-D011886] N86-14044

DORNIER-WERKE G.M.B.H., FRIEDRICHSHAFEN (WEST GERMANY).
Two-phase heat transport systems: System definition, volume 1
[ESA-CR(P)-2052] N86-13363
Study of Earth observation by frequency scanning. Volume 1: Executive summary
[ESA-CR(P)-2028-VOL-1] N86-13705
Study of Earth observation by frequency scanning. Volume 2
[ESA-CR(P)-2028-VOL-2] N86-13706

DOW CHEMICAL CO., MIDLAND, MICH.
Evaluation and compilation of the thermodynamic properties of high temperature species N86-13532

DRAPER (CHARLES STARK) LAB., INC., CAMBRIDGE, MASS.
The evaluation of failure detection and isolation algorithms for restructurable control
[NASA-CR-177983] N86-13310

E

EAGLE ENGINEERING, INC., HOUSTON, TEX.
Planetary sample rapid recovery and handling
[NASA-CR-171906] N86-13342

EAST CAROLINA UNIV., GREENVILLE, N.C.
Nutritional characteristics of moon dust for soil microorganisms N86-14086

EAST TEXAS STATE UNIV., COMMERCE.
Signal processing of anthropometric data N86-14105

ECLECTECH ASSOCIATES, INC., NORTH STONINGTON, CONN.
Short range aids to navigation systems. Design manual for restricted waterways
[AD-A158213] N86-13313

ECOSYSTEMS INTERNATIONAL, INC., CROFTON, MD.
NASA flight operations review
[NASA-CR-176393] N86-13306

EDGERTON, GERMESHAUSEN AND GRIER, INC., IDAHO FALLS, IDAHO.
Recent results on implantation and permeation into fusion reactor materials
[DE85-014620] N86-14067

EG AND G WASHINGTON ANALYTIC SERVICES CENTER, INC., LANHAM, MD.
The characterization of surface vargation effects on remote sensing N86-13805

ELECTROMAGNETIC LAUNCH RESEARCH, INC., CAMBRIDGE, MASS.
Pulsed inductive energy transfer N86-13562

ELECTRONICS RESEARCH LAB., ADELAIDE (AUSTRALIA).
DIESS: A prolog implementation of a domain-independent expert system shell
[AD-A158014] N86-13928

EMERTRON, INC., SILVER SPRING, MD.
Horizontal electric fields from lightning return strokes
[DE85-016367] N86-13873

EMORY UNIV., ATLANTA, GA.
Combusion of hydrogen and hydrocarbons in fluorine N86-13526

ENGINEERING SYSTEM INTERNATIONAL, RUNGIS (FRANCE).
Employment of PAM-FISS-BI-phase computer program for the strength analysis and fracture/delamination behavior of components
[ESI-ED/83-383/RD/MS-VOL-7] N86-13763

ERNO RAUMFAHRTTECHNIK G.M.B.H., BREMEN (WEST GERMANY).
Comparative study of space segments for the provision of future operational data relay satellite services
[MBB-DSP-TN/DRS/132/84] N86-13355
Assembly Integration Verification (AIV) test effectiveness study. Applicability of Spacelab approach for equipment and system test for Ariane-4 class satellites. Volume 1: Executive summary
[ERNO-671/AIV-VOL-1] N86-13361
Standardization program on design analysis and testing of inserts in nonmetallic sandwich components
[TR-TS-RP-2-09-84] N86-13364

EUROPEAN SPACE AGENCY, PARIS (FRANCE).
Report on the scientific satellites of the European Space Agency
[ESA-SP-1072] N86-13344
EURECA: An introduction to Europe's free-flying retrievable carrier
[ESA-BR-30] N86-13352

EUROPEAN SPACE TRIBOLOGY LAB., RISLEY (ENGLAND).
Thermal vacuum tests on a hinge actuator mechanism
[ESA-ESTL-067] N86-13360
Activities report in space tribology
[ESA-ESTL-72] N86-13738

F

FAME ASSOCIATES, INC., FORT COLLINS, COLO.
Optical/infrared properties of atmospheric aerosols with an in situ, multi-wavelength, multichannel nephelometer system
[AD-A158825] N86-13710

FAYETTEVILLE STATE UNIV., N.C.
The scanning electron microscope as a tool in space biology N86-14080

FERMI NATIONAL ACCELERATOR LAB., BATAVIA, ILL.
Operation of large cryogenic systems
[DE85-017439] N86-14025
Variable curvature phantom
[DE85-014260] N86-14028

FLORIDA STATE UNIV., TALLAHASSEE.
Information in censored models
[AD-A158644] N86-13999

FLORIDA UNIV., GAINESVILLE.
Far-field boundary conditions in numerical solutions of the Navier-Stokes equations
[AD-A158776] N86-13690

G

GA TECHNOLOGIES, INC., SAN DIEGO, CALIF.
Doublet 3
[DE85-014369] N86-14031

Fusion programs in applied plasma physics and development and technology, fiscal 1984
[DE85-014551] N86-14062
Heating and confinement in the Doublet 3 tokamak with electron cyclotron heating
[DE85-014323] N86-14070

GENERAL ELECTRIC CO., WHETSTONE (ENGLAND).
Study of thermal analysis methods
[GEC-MEL12.0539] N86-13362
Investigation of techniques for improving spacecraft thermal control software
[GEC-MEL42.0552] N86-13942

GEORGE WASHINGTON UNIV., WASHINGTON, D.C.
Discrete random media techniques for microwave modeling of vegetated terrain N86-13809

GEORGIA INST. OF TECH., ATLANTA.
Analysis of heterogeneous diffusion flame stabilization N86-13527
Experimental investigation of heterogeneous flame stabilization N86-13528
Flame-acoustic wave interaction during axial solid rocket instabilities N86-13542
Agile Electromagnetics Exploiting High Speed Logic (AEEHSL)
[AD-A158380] N86-13630
Characterization of acid rain phenomena, Atlanta, Georgia
[PB85-216943] N86-13848
Partitions of point processes: Multivariate poisson approximations
[AD-A158739] N86-13978
Monte Carlo analysis of nonlinear statistical models. 1. Theory: Revision
[AD-A158613] N86-13990
Extreme values of queues, point processes and Stochastic Networks
[AD-A158619] N86-13991

GMD SYSTEMS, LANCASTER, CALIF.
Mathematical analysis study for radar data processing and enhancement. Part 1: Radar data analysis
[NASA-CR-166616-PT-1] N86-13353
Mathematical analysis study for radar data processing and enchancement. Part 2: Modeling of propagation path errors
[NASA-CR-166616-PT-2] N86-13354

GRUMMAN AEROSPACE CORP., BETHPAGE, N.Y.
Tire-soil interaction model for turning (steered) tires
[AD-A157737] N86-13593
Impact of a poloidal divertor in ignition tokamak design
[DE85-012892] N86-14061

GT-DEVICES, ALEXANDRIA, VA.
Numerical models for plasma-solid interactions in electrothermal mass accelerators
[AD-A158637] N86-14052

H

HAMILTON STANDARD, WINDSOR LOCKS, CONN.
Development of a carbon formation reactor for carbon dioxide reduction
[NASA-CR-171907] N86-13898

HARVARD UNIV., CAMBRIDGE, MASS.
The influence of oceanic chemistry, physics and biology on atmospheric carbon dioxide N86-13865

HELSINKI UNIV. TECHNOLOGY, OTANIEMI (FINLAND).
Positron diffusion in Si
[DE85-014831] N86-14076

HERSH ACOUSTICAL ENGINEERING, CHATSWORTH, CALIF.
Rocket motor flow-turning losses N86-13545

HIROSHIMA UNIV. (JAPAN).
Population inversion in a recombining hydrogen plasma interacting with a helium gas
[IPPJ-692] N86-14045

HOUSTON BAPTIST UNIV., TEX.
Transformation matrices between non-linear and linear differential equations N86-14099

HOUSTON UNIV., CLEAR LAKE, TEX.
Electron microscopic observations of hydrogen implantation in ilmenites N86-14081

HOUSTON UNIV., TEX.
Control of space stations N86-14090

HUGHES HELICOPTERS, CULVER CITY, CALIF.
Advanced technology helicopter landing gear preliminary design investigation
[AD-A158816] N86-13325

HUNTER COLL., NEW YORK.
Geometric-optical modeling of a conifer forest canopy N86-13799

I

IDAHO DEPT. OF WATER RESOURCES, BOISE.
Geothermal investigation in Idaho. Part 14: Geochemical and isotopic investigations of thermal water occurrences of the Boise Front Area, Ada County, Idaho, Water Information Bulletin no. 30
[DE85-012905] N86-13841

IDAHO UNIV., MOSCOW.
Synthesis of difluoraminoxy-, difluoramino- or fluorodiazonium-containing materials N86-13509

ILLINOIS UNIV., CHAMPAIGN.
The event related brain potential as an index of information processing, cognitive activity, and skill acquisition: A program of basic research
[AD-A159118] N86-13897

ILLINOIS UNIV., CHICAGO.
Fluoropolyazido-esters as energetic polymers N86-13515

ILLINOIS UNIV., URBANA.
Corrosion fatigue initiation and short crack growth in an aluminum alloy N86-13404
Oxide electrodes at high temperatures
[DE85-006564] N86-13667
A fully viscous two-dimensional unsteady flow analysis applied to detonation transition in porous explosives
[AD-A157794] N86-13682

ILLINOIS UNIV., URBANA-CHAMPAIGN.
Process-induced viscoelastic stress in composite laminates N86-13376
Hydrogen transport and hydrogen embrittlement in stainless steels N86-13403
Experimental studies of laser-sustained argon plasmas for CW laser propulsion applications N86-13550

INDIANA UNIV., BLOOMINGTON.
Basic properties of strong mixing conditions
[AD-A158740] N86-13992
Polarization transfer in enelastic scattering and pionic models of the EMC effect
[DE85-014119] N86-14021

INDUSTRIEANLAGEN-BETRIEBSGESELLSCHAFT M.B.H., OTTOBRUNN (WEST GERMANY).
Investigation for the definition of a hydraulic multidegree of freedom vibration facility
[B-TF-1627] N86-13340

INFORMATICS GENERAL CORP., PALO ALTO, CALIF.
DAB user's guide
[NASA-CR-177393] N86-13290
PLTTER user's guide
[NASA-CR-177385] N86-13291
Crossref for the Cray
[NASA-CR-177384] N86-13913

INNSBRUCK UNIV. (AUSTRIA).
Hot electron emission in semiconductors
[AD-A158042] N86-14072

INSTITUT DE MECANIQUE DES FLUIDES DE LILLE (FRANCE).
Study of the influence of an oscillating spoiler on the surrounding aerodynamic field
[IMFL-3119] N86-13303
Aircraft crashing. Analysis and identification methods. Presentation of a solution method
[IMFL-4116] N86-13308

INSTITUT FRANCO-ALLEMAND DE RECHERCHES, ST. LOUIS (FRANCE).
Short presentation and evaluation of studies on the penetration of jets from hollow shaped charges in compressible materials
[ISL-NB-402/84] N86-13586
Holographic study of the particles produced by the injector in a Viking motor
[ISL-R-111/84] N86-13724

INTERNATIONAL GEOPHYSICAL YEAR WORLD DATA CENTER A, BOULDER, COLO.
Marginal ice zone bibliography
[AD-A159060] N86-13764

J

JET PROPULSION LAB., CALIFORNIA INST. OF TECH., PASADENA.
Magnetoplasmadynamic thruster erosion research N86-13557
Ground reflectance measurements from thematic mapper data N86-13801
Thermal infrared geologic remote sensing research at the Jet Propulsion Laboratory N86-13802
Atmospheric and science complexity effects on surface bidirectional reflectance N86-13803
Active microwave properties of vegetation canopies N86-13812

JOHNS HOPKINS UNIV., BALTIMORE, MD.
Two unsteady heat transfer experiments. Part 1: In grid-generated isotropic turbulence. Part 2: In laminar oscillatory flow in straight and conical tubes N86-13675

JOINT PUBLICATIONS RESEARCH SERVICE, ARLINGTON, VA.
USSR report: Materials science and metallurgy
[JPRS-UMS-85-006] N86-13422
Hereditary effect of dendrite liquation of titanium and zirconium on structure and properties of aluminum alloys N86-13423
Fiber composition materials for strengthening components of aluminum and its alloys N86-13424
Structure and properties of Al-Mg-Zn casting alloys N86-13425
Discontinuous precipitation in aluminum-magnesium alloys with high magnesium content N86-13426
Structure formation in silumins upon rapid crystallization N86-13427
Influence of alloying elements and impurities on mechanical properties of complex silumins N86-13428
Study of fractures in cast parts of high-strength aluminum alloy N86-13429
Study of permeability of two-phase zone in aluminum and copper alloys N86-13430
Influence of degree of deformation on structure and properties of naturally aged alloy 1163 N86-13431
Appearance of superplasticity effect in aluminum alloys with lithium N86-13432
Preliminary annealing on crystallization of amorphous Fe80Si6B14 alloy N86-13433
Influence of chromium on crystallization of amorphous Fe-B alloys N86-13434
Relationship of thermal expansion of amorphous metal alloys with their high temperature plastic properties N86-13435
On anisotropy of mean electrical resistance of beryllium N86-13436
Complex nickel-aluminide coatings on nickel-chromium alloy EP648-VI N86-13437
Influence of Co-Cr-Al-Y coatings on physical and mechanical properties of EI-893 steel in GT-100 turbine drive vanes N86-13438
Electrification of filled polyethylene coatings in friction with metal N86-13439
Influence of texture of titanium nitride coatings on wear resistance of cutting tools N86-13440
Influence of annealing on hardness of vacuum-diffusion chromium coating on low-carbon steel N86-13441
Study of properties of gas-thermal coatings of composite nichrome-aluminum alloy powders N86-13442
Effect of geometry of fiber packing on consolidation of fibrous composition materials with porous matrix N86-13443
Conductivity of metal-ceramic multilayer ZrO2-Mo and Mo-based composite materials N86-13444
Production of multilayer magnetic surface of magnetically soft composite materials N86-13445
Calculation of damping properties of composite materials N86-13446
Theory of pyrolysis of composite polymer materials N86-13447
Critical behavior of thermoelectric power in binary composite materials N86-13448
Temperature-frequency variation of mechanical losses in periodic deformation of multilayer glass-reinforced plastics N86-13449
Corrosion resistance of diffusion and galvanic coatings on steel fasteners N86-13450
Anticorrosion polymer packing film with improved protective properties N86-13451
Extremely high reflective capability of zirconium burning in air under effects of constant CO2 laser radiation N86-13452
Mechanical laser cutting of metals N86-13453
Certain features of laser destruction and dislocational structure of silicon during heating and effects of electrical field N86-13454
Structure of flow of erosion plasma formed upon laser treatment of metals N86-13455
Ceramics based on aluminum nitride and metals N86-13456
Influence of sodium on mechanical and casting properties of magnesium-lithium alloys N86-13457
Thermophysical properties of tungsten at high temperatures N86-13458
Determination of porosity of thin sheets of fiber materials based on optical transmission coefficient N86-13459
Effect of heating conditions on agglomeration of powdered aluminum in air atmosphere N86-13460
Superelastic behavior of powdered titanium nickelide during pressing N86-13461
Grain growth in heat-resistant austenitic steel N86-13462

Effect of elastoplastic cyclic deformation on mechanical characteristics of steel O3Kh13AG19 at temperatures of 293 and 77 deg K N86-13463
Specifics of the process of failure of structural steels strengthened by thermo-mechanical working with deformation in the intercritical temperature interval N86-13464
Mechanical properties of EP794 steel + 12Kh18N10T steel bimetal N86-13465
Macro- and microfractographic specifics of dissipated impact rupture of type 45 steel in the viscous-brittle transition interval N86-13466
Durability of steel 45 with boride coating in corrosive-abrasive media N86-13467
Dispersion hardening of high-strength NiOCo-Mo steels N86-13468
Modeling of thermal fatigue and erosion of complex alloyed steels in metal melts N86-13469
Study of effect of normal reactor water on growth rate of fatigue cracks in 15Kh2NMFA steel N86-13470
Superhard materials developed N86-13471
Micromechanisms of electrodiffusion failures in thin film metallization N86-13472
Ion nitriding of titanium N86-13473
Calculation of failure constant for titanium alloys N86-13474
Subcritical crack development under constant load in VT6 alloy N86-13475
Silicide coatings for protecting titanium-niobium alloys from high-temperature oxidation N86-13476
Effect of composition of rarefied medium on gas-saturated titanium alloys N86-13477
Homogenization of beta-solid solution upon rapid heating of two-phase titanium alloys N86-13478
Changes in structure and mechanical properties of niobium-titanium alloy during oxygen saturation N86-13479
Internal friction in TiNiCu alloy N86-13480
Influence of electron-beam heating on structure and phase composition of VT9 alloy N86-13481
Structure and internal friction of near-eutectic alloy system Ti-W tempered from a liquid state N86-13482
Possible mechanism of wave formation during detonation welding N86-13483
Optimization of technological parameters of cold pressure welding of AD1M thin aluminum sheets N86-13484
Study of process of pore formation during argon-arc welding of aluminum alloy 1420 N86-13485
Influence of thermal cycle on characteristics of cyclical crack resistance of titanium alloys and their joints produced by diffusion welding N86-13486
Kinetics of dissolution of oxide films in titanium upon diffusion welding N86-13487
Influence of preliminary annealing on structure and properties of VT23 alloy welded joints after hardening N86-13488
Corrosion resistance of welded joints in certain titanium alloys N86-13489
Deformation and stresses upon welding of VT23 titanium alloy N86-13490
Determining local heating parameters for increasing fatigue resistance of welded joints N86-13491
Influence of structure of heat-resistant nickel alloy ZhS6U on its weldability in the solid state N86-13492
Diffusion welding of copper-chromium pseudoalloy with copper N86-13493
Influence of hydrogen on formation of cold cracks in seams during welding of pipe steel N86-13494
China report: Science and technology
[JPRS-CST-85-020] N86-13600
Preliminary experimental results of CT-6B tokamak heating field voltage feedback control N86-13601
Scheme for high-speed real-time DFT operation for radar signal processing N86-13602
On H plane dielectric loading theory for H plane ferrite phase shifter N86-13603
Nation's achievements in high energy physics reviewed N86-13604
Integrated optics developments over past decade, future prospects N86-13605
High-pressure, high-temperature opposed anvil device described N86-13606
Application of computers in analytical chemistry: Calculation of optimum acidity of reaction between metal ions and organic reagents in solution N86-13607
Improved algorithm for radar real-time data processing N86-13608
Pulsed, optically pumped gas-mixture FIR lasers N86-13609
West Europe report: Science and technology
[JPRS-WST-85-030] N86-13610
FRG's Dornier develops high-resolution display system N86-13611
Thomson, CNET of France in silicon-on-insulator research N86-13612
Excimer laser produces .2 micron semiconductor structures N86-13613
Philips develops MBE process for laser, chip manufacture N86-13614
Thomson semiconductors introduces products, balances books N86-13615
West Europe report: Science and technology
[JPRS-WST-85-031] N86-13616
Certification granted to Franco-Italian ATR 42 N86-13617
ATR 42 production work in French, Italian plants detailed N86-13618
New digital circuits at Thomson semiconductor in France N86-13619
CNET of France uses organo-metallic epitaxy for laser N86-13620
European silicon structures plans custom chips in 15 days N86-13621
West Europe report: Science and technology
[JPRS-WST-85-029] N86-13622
Recent advances in composite materials reviewed N86-13623
New materials to lighten vehicles N86-13624
Direct injection diesel motor N86-13625
Italian robot manufacturer enters Spanish market N86-13626
Worldwide report: Telecommunications policy, research, and development
[JPRS-TTP-85-026] N86-13640
Optimal transfer function for fiber optic communications N86-13641
USSR report: Machine tools and metalworking equipment
[JPRS-UMM-85-014] N86-13742
New applications of industrial robots noted N86-13743
Problems with integrating robots in conventional production N86-13744
USSR report: Machine tools and metalworking equipment
[JPRS-UMM-85-013] N86-13745
Problems with robotization of conventional shops N86-13746
Robot control system modified for precision movement N86-13747
New robots by Soviet, CEMA manufacturers described N86-13748
USSR report: Earth sciences
[JPRS-UES-85-009] N86-13765
Goskomgidromet plans automation of aerial cloud-seeding work N86-13766
Model interpretation of annual variation of temperature fields of air and water boundary layers of world ocean N86-13767
Formation of structure of mixed region under influence of shear flow in stratified fluid N86-13768
Computation of ocean upper layer thermal structure N86-13769
Investigation of characteristics of synoptic movements on sphere N86-13770
Vertical structure of turbulence and turbulent exchange in equatorial zone of Pacific Ocean N86-13771
Some characteristics of bottom density currents N86-13772
Highly disperse minerals in sediments in neighborhood of East Pacific Ocean rise determined from drilling data N86-13773
Study of optical-acoustical phenomena at surface of strongly absorbing clearing fluids N86-13774
Aerial laser sensing of ocean upper layer N86-13775
Formation of underwater oceanic volcanoes and islands in relation to lithospheric thickness and movements N86-13776
Volcanoes discovered with radio beam N86-13777
Computer-aided aerial radiometric surveying of soil moisture N86-13778
Distribution of brightness from point source of scattered light along inclined path N86-13779
Statistical correlation between ozone levels over Atlantic Ocean and meteorological values N86-13780
Influence of fog microstructure on quality of optical image transmitted through it N86-13781
Experience in measuring mean wind velocity profile in lower troposphere by sodar anemometer under inversion and convective conditions N86-13782
Structural characteristic of temperature field over sea N86-13783
Atmospheric synoptic eddies over ocean (determined from experimental data) N86-13784
Influence of petroleum pollution on ocean-atmosphere gas exchange intensity (in example of North Atlantic) N86-13785
Statistics of intensive light beams in turbulent atmosphere N86-13786
New methods for laser sounding of atmosphere on basis of nonlinear effects N86-13787
Interaction between powerful laser radiation and atmospheric aerosols N86-13788
Investigation of nonlinear spectroscopic effects in interaction between CO2-laser radiation and atmospheric gases N86-13789
Observation of optical-radio frequency resonance in H2O using wide-band ruby laser spectroscopy N86-13790
Effectiveness of use of adaptive optical systems under conditions of self-effect in atmosphere N86-13791
Latitude measurements of cosmic radiation intensity in stratosphere and at sea level on marine antarctic expeditions N86-13792
Hadron component of cosmic radiation at atmospheric depth 800 g/cm(2) in Energy Range 70 to 700 GeV N86-13793
USSR report: Energy
[JPRS-UEN-85-001] N86-13861
Azerbaijan geological, geophysical work on land described N86-13862
Possible petroliferousness of South Caspian uplifts analyzed N86-13863
Tectonic stress on structures alters formation parameters N86-13864
USSR report: Space
[JPRS-USP-85-005] N86-14111
Forming transformation matrices for different parameters of motion of celestial bodies N86-14112
Forming attainability sets in control of kinetic moment of rotating asymmetric solid body (special cases) N86-14113
Method for solving two-point boundary value problem for optimization of flights with low thrust N86-14114
Choice of optimum boundary conditions in speed optimization problem N86-14115
Mathematical models of nonstationary eddy currents and eddy movements of fluid in problems of orientation and stabilization of artificial Earth satellites and spacecraft 2 N86-14116
Observations of fluxes of cold ions from plasmasphere into ionosphere during nighttime in middle latitudes N86-14117
Spectrum of photoelectrons in Earth's upper atmosphere during solar flares N86-14118
Solar flare X-radiation and high-energy particles according to observational data from Venera-13 and Venera-14 automatic interplanetary stations N86-14119
Role of intrinsic energy source in physical behavior of split cometary nucleus N86-14120
Approximate solutions of Euler-Lambert equation for case of several revolutions about central body N86-14121
Formation of high-energy secondary electrons in low-density medium at great altitudes N86-14122
Hard gamma radiation background from coding collimator of gamma telescope under space experiment conditions N86-14123
Sudden disappearance of quiescent prominences N86-14124
Magnetic field determination in quiescent solar prominences from polarization characteristics of radiated light N86-14125
Spatial patterns of manifestation of solar activity in troposphere N86-14126
Mechanism of corpuscular-atmospheric relationships N86-14127
Approximate cluster analysis method and three-dimensional diagram of optical characteristics of lunar surface N86-14128
Structure of coefficients of series representing solution of plane circular restricted three-body problem N86-14129
A priori guaranteed accuracy evaluation in determining spacecraft orbit by least squares method N86-14130
Integration of equations of motion for material point in gravitational field of axially symmetric planet N86-14131
Periodic regimes of rotational motion of solid body about liberation point L sub 4 in restricted elliptical three-body problem N86-14132
Mathematical models of nonstationary eddy currents and eddy motions of fluid in spacecraft orientation and stabilization problems 1 N86-14133
Comparison of energetics of optimum maneuvers and two-impulse maneuvers in some problems of motion from a point into orbit N86-14134
Optimum control programs in problem of interorbital flight with continuous thrust N86-14135
Disturbances in stratosphere and mesosphere from source of ultraviolet radiation N86-14136
Coordinated investigations of processes in subauroral upper ionosphere and through in concentration of light ions N86-14137
Registry of heavy ions in auroral region during magnetic storms N86-14138

Small-scale structure of intensive longitudinal currents in high latitudes N86-14139
Formation of proton radiation belts in region of energies of several MeV N86-14140
Dependence of length of free path of flare particles on energy N86-14141
Observation of small-scale solar wind structure on front of sharp increase in plasma flow velocity N86-14142
Electrical and electrothermal conductivity of planetary ionospheres, 1: Refinement of theory N86-14143
Uniqueness conditions in evaluation of least squares method in nonlinear space navigation problems N86-14144
Radio emission of injected electron beam with respect to diagnosis of ionospheric plasma N86-14145
Charge composition of electrons in Earth's radiation belt N86-14146
Wave interpretation of measurements on Mars-7 and Venera-9 probes for determining velocity of motion of interstellar gas N86-14147
Vega-1 releases aerostat and lander at Venus N86-14148
Objectives of Vega project research N86-14149
Vega-2 releases aerostat and lander at Venus N86-14150
Results from Vega atmosphere and soil studies N86-14151
Press conference on first stage of Vega project N86-14152
Further comments on results of Vega studies of Venus N86-14153
Development of instruments for Vega probes N86-14154
Brochure on Phobos and Deimos N86-14155
Results of study of surface of five regions on Venus by bistatic radar method N86-14156
Possibility of spectroscopic detection of oxygen in lower Venusian atmosphere N86-14157
Rossby autosoliton N86-14158
Nature of megacycles in evolution of Earth, Mars, and Moon N86-14159
Biological life-support systems for long-duration space flights N86-14160
Architect discusses space habitat designs N86-14161
Energy exchange of plants under weightlessness conditions N86-14162
Stability of stationary motions of two tethered bodies in orbit under influence of gravitational and aerodynamic forces N86-14163
Experimental checking of mathematical model of eddy currents in actuating components of systems for magnetic orientation of artificial Earth satellites and spacecraft N86-14164
Determining quasi-real-time location of ships using geostationary navigational satellites N86-14165
Organization of space navigation system based on use of geostationary satellites N86-14166
Space applications in geology N86-14167
Pressure field retrieval by remote refractometry from space N86-14168
Determining flexure of aerial camera smoothing glass N86-14169
Stereophotogrammetric survey of wave-covered water surface N86-14170
Equatorial waves in ocean surface temperature field according to data from shipboard and satellite measurements N86-14171
Use of remote optical measurements in agriculture N86-14172
Classification of trees by growth classes on the basis of multizonal photographs N86-14173
Experience in complex mapping of natural resources in agrarian-industrial regions of Nonchernozem RSFSR using space photomaterials N86-14174
Possibilities of use of aerospace materials in predicting occurrence of petroleum and gas N86-14175
Problems in study and evaluation of consequences of forest fires using aerospace photographs N86-14176
Computation of reflection of solar radiation from vegetation cover by Monte-Carlo method N86-14177
Reflection indicatrices of vegetation canopies N86-14178
Approximate analytical formulas for computing spectral brightness coefficients for agricultural vegetation N86-14179
Method for using clusters in evaluating land use areas from multizonal photographs N86-14180
Methods for complex space experiment in USSR for studying land from manned spacecraft N86-14181
Experience in conducting subsatellite experiments with water bodies in USSR and Hungarian People's Republic N86-14182
Possibilities of using space survey for studying seasonal changes of landscapes in some regions of USSR N86-14183
Role of landscape research in development of space methods for studying Earth N86-14184
Methods for constructing atmospheric optical transfer operator N86-14185
Application of statistical model of layered medium for computing thermal emission of ice covers N86-14186
Compilation of landscape maps at different scales with use of space photoinformation N86-14187
Use of space geological methods in seismotectonic research N86-14188
Engineering evaluation of crustal faults using space survey data N86-14189
Use of Goudriaan model for studying reflection regularities in vegetation-soil system in optical range. 1: Influence of phytometric parameters on spectral brightness coefficients N86-14190
Analysis of survey conditions and effect of noise on quality of sensing of soil formations N86-14191
Normalization of response of radiometric instrumentation for studying Earth's natural resources N86-14192
Radiometric correction of materials of aerospace survey of Earth with MKF-6 camera: Methodology and use of results N86-14193
Some approaches to organization of data bank in system for studying Earth's natural resources from space (using example of agriculture) N86-14194
Experiment for evaluating accuracy in determining land categories on space scanner photographs N86-14195
Remote temperature determination of terrestrial covers from polarization invariant of microwave-radiothermal emission N86-14196
Comments on anniversary of Apollo-Soyuz flight N86-14197
Soviet-French commission discusses joint space projects N86-14198
List of recent Soviet space launches N86-14199

K

KANSAS UNIV. CENTER FOR RESEARCH, INC., LAWRENCE.
An investigation into the vertical axis control power requirements for landing VTOL type aircraft onboard nonaviation ships in various sea states
[NASA-CR-176355] N86-13294
Determination of backscattering sources in various targets N86-13811
KERNFORSCHUNGSANLAGE, JUELICH (WEST GERMANY).
Implementing agreement for cooperation in the development of large scale wind energy conversion systems
[JUEL-SPEZ-304] N86-13820
KERR (ARNOLD D.), WILMINGTON, DEL.
Application of Pasternak model to some soil-structure interaction problems. Volume 1: Solutions for plates continuously supported on a Pasternak base
[AD-A157776] N86-13594
Application of Pasternak model to some soil-structure interaction problems. Volume 2: Determination of foundation parameters and the choice of models
[AD-A157777] N86-13595
KYOTO UNIV. (JAPAN).
High order spline interpolation in the particle simulation N86-14046

L

LA JOLLA INST., CALIF.
Theoretical studies and data analysis of wave propagation in random media
[AD-A158775] N86-13632
LAWRENCE LIVERMORE NATIONAL LAB., CALIF.
Condensed matter at high shock pressures
[DE85-016443] N86-13399
Sorption detector system for chemical agents detection and recognition
[DE85-012775] N86-13400
Interactions between a laminar flame and end gas autoignition
[DE85-008957] N86-13402
Effective medium theory for partially saturated porous solids
[DE85-016608] N86-13598
Granular flow: Advanced Research and Technology Development (AR and TD) contract review
[DE85-017267] N86-13697
Contributions to Von Karman Institute lecture series on Computational Fluid dynamics: Advection-diffusion and Navier-Stokes equations
[DE85-010942] N86-13703
Photoelectronic trajectory anatomy of RCA-C-73435 image converter and its performance
[DE85-013973] N86-13723
Inversion of Rayleigh wave phase velocities between RSNT and RSON
[DE85-013242] N86-13859
Statistical comparison of two major gridded temperature records of the Northern Hemisphere
[DE85-016076] N86-13872
Inner/outer iterative methods and numerical Schwarz algorithms - 2
[DE85-013197] N86-13940
LTSSCLI: An ITSS shell for NLTSS, version 2.0, revision 1
[DE85-013234] N86-13941
Current methods for large stiff ODE systems
[DE85-012914] N86-13983
JASON electrostatic boundary conditions: A survey
[DE85-014521] N86-14005
Aspects of three field approximations: Darwin, frozen, EMPULSE
[DE85-014204] N86-14020
Electromagnetic particle-in-cell plasma simulation
[DE85-031223] N86-14054
Implicit plasma simulation
[DE85-016088] N86-14055
SLAC divertor channel entrance thermal stress analysis
[DE85-017877] N86-14057
Equation of state of dense argon: A comparison of shock and static studies
[DE85-015543] N86-14074
LEHIGH UNIV., BETHLEHEM, PA.
Combined small angle X-ray scattering and transmission electron microscopy studies of Al-Li alloys
[DE85-016356] N86-13416
LIVERPOOL UNIV. (ENGLAND).
Practical aspects of functional testing techniques
[AD-A158184] N86-13968
LOCKHEED MISSILES AND SPACE CO., HUNTSVILLE, ALA.
High-altitude plume computer code development
[NASA-CR-171600] N86-13923
LOCKHEED MISSILES AND SPACE CO., PALO ALTO, CALIF.
An unbiased X-ray sampling of stars within 25 parsecs of the Sun
[NASA-CR-178544] N86-14206
LOCKHEED MISSILES AND SPACE CO., SUNNYVALE, CALIF.
Study of storm time fluxes of heavy ions
[NASA-CR-176368] N86-13852
LOS ALAMOS NATIONAL LAB., N. MEX.
High strain rate deformation in FCC metals and alloys
[DE85-017533] N86-13417
Threshold stress measurements in shock-deformed copper
[DE85-014076] N86-13418
Muon spin relaxation study of exchange coupling in dilute AgMn alloys
[DE85-014104] N86-13419
A 10-MHz high-voltage modulator with pulse-width and repetition-rate agility
[DE85-014117] N86-13663
Turbulence in two-field incompressible flow
[DE85-015361] N86-13693
Experiments with non-Darcy flow in joints with large scale roughness
[DE85-015714] N86-13695
Hybrid simulation codes with application to shocks and upstream waves
[NASA-CR-176365] N86-13702
Multidimensional modeling of atmospheric effects and surface heterogeneities on remote sensing N86-13806
Characteristics of microearthquakes accompanying hydraulic fracturing as determined from studies of spectra of seismic waveforms
[DE85-009558] N86-13860
Three-dimensional modeling of Tsunami waves
[DE85-015724] N86-13877
Scheme to funnel ion beams with a radio-frequency quadrupole
[DE85-015689] N86-14016
Reactive scattering in the bending-corrected rotating linear model
[DE85-017539] N86-14018
Collective ion acceleration by means of virtual cathodes
[DE85-012707] N86-14019
Dense Z-pinch plasmas
[DE85-005818] N86-14059
Preparation, analysis and release of simulated interplanetary grains into low grain orbit
[DE85-014133] N86-14211

LOS ALAMOS SCIENTIFIC LAB., N. MEX.

Polarization transfer in enelastic scattering and pionic models of the EMC effect [DE85-014119] N86-14021

Low power reactor for remote applications [DE85-012763] N86-14032

Possibility for a self-consistent treatment of transport processes in a turbulent plasma [DE85-016214] N86-14069

LOUISVILLE UNIV., KY.

Development and testing of a mouse simulated space flight model [NASA-CR-176359] N86-13878

M

MACDONALD, DETTWILER AND ASSOCIATES LTD., RICHMOND (BRITISH COLUMBIA).

The construction and testing of a real-time digital breadboard processor for the ESA remote sensing satellite synthetic aperature radar [REPT-00-0778] N86-13911

MARTIN MARIETTA LABS., BALTIMORE, MD.

The delayed fracture of aluminum alloys [AD-A158944] N86-13412

MARYLAND UNIV., COLLEGE PARK.

Target tracking based scene analysis [AD-A158629] N86-13910

Multiresolution path planning for mobile robots [AD-A158630] N86-13948

Basic principles of feedback and adaptive approaches in the finite element method [AD-A158188] N86-13969

The h-p version of the finite element method [AD-A158194] N86-13971

Computation of geometric properties from the medial axis transform in 0 (n log n) time [AD-A158934] N86-13980

MASCHINENFABRIK AUGSBURG-NUERNBERG A.G., MUNICH (WEST GERMANY).

Aerodynamic theory in the calculation of the GROWIAN rotor compared with some experimental data N86-13826

MASON AND HANGER-SILAS MASON CO., INC., AMARILLO, TEX.

Specialized instrument for radiation assistance teams [DE85-017390] N86-13720

MASSACHUSETTS INST. OF TECH., CAMBRIDGE.

Hub effects in propeller design and analysis [AD-A158853] N86-13331

Performance-limiting factors in MPD thrusters N86-13555

Plasma-gas interactions studies in a hybrid plume plasma rocket N86-13559

A tandem mirror plasma source for hybrid plume plasma studies N86-13560

Speech recognition: Acoustic, phonetic and lexical knowledge [AD-A158264] N86-13629

Study of deposition control using transpiration [DE85-012799] N86-13699

Fusion welding research [AD-A158253] N86-13736

Remote sensing of Earth terrain N86-13808

Hypothesizing and refining causal models [AD-A158165] N86-13893

Generating and generalizing models of visual objects [AD-A158197] N86-13894

On the complexity of ID/LP parsing [AD-A158211] N86-13933

Describing surfaces [AD-A158940] N86-13937

Mobile robot localization using sonar [AD-A158819] N86-13949

Deterministic parsing and linguistic explanation: Revision [AD-A159233] N86-13950

Intrinsic nilpotent approximation [AD-A158265] N86-13975

Codon constraints on closed 2D shapes [AD-A158744] N86-13979

Multigrid relaxation methods and the analysis of lightness, shading, and flow [AD-A158173] N86-14036

CREF: An editing facility for managing structured text [AD-A158155] N86-14077

MASSACHUSETTS INST. OF TECH., LEXINGTON.

Distributed sensor networks [AD-A158033] N86-13628

Adaptive detection in nonstationary interference: Part 1 and part 2 [AD-A158810] N86-13993

MASSACHUSETTS UNIV., AMHERST.

Numerical modeling of carrier transport in submicron bipolar transistors N86-13642

MATRA ESPACE, TOULOUSE (FRANCE).

Review of implications and usefulness of spacecraft servicing in Low Earth Orbit (LEO) [MATRA-092/CC/AB/225-84] N86-13350

MCALPINE (SIR ROBERT) AND SONS, LONDON (ENGLAND).

Development in aerodynamic calculations N86-13822

MCDONNELL-DOUGLAS ELECTRONICS CO., ST. LOUIS, MO.

Impact of a poloidal divertor in ignition tokamak design [DE85-012892] N86-14061

MCGILL UNIV., MONTREAL (QUEBEC).

Critical charge for the direct initiation of detonation in gaseous fuel-air mixtures [DE85-016130] N86-13696

MECHANICAL TECHNOLOGY, INC., LATHAM, N. Y.

HPOTP low-speed flexible rotor balancing, phase 1 [NASA-CR-171610] N86-13369

MESSERSCHMITT-BOELKOW-BLOHM G.M.B.H., OTTOBRUNN (WEST GERMANY).

In-orbit technology demonstration program (TDP). Accommodation study: SPAS [MBB-URV-147/84] N86-13351

Comparative study of space segments for the provision of future operational data relay satellite services [MBB-DSP-TN/DRS/132/84] N86-13355

Assembly Integration Verification (AIV) test effectiveness study. Applicability of Spacelab approach for equipment and system test for Ariane-4 class satellites. Volume 1: Executive summary [ERNO-671/AIV-VOL-1] N86-13361

MICHIGAN UNIV., ANN ARBOR.

Microwave dielectric and propagation properties of vegetation canopies N86-13810

Sparse elimination on vector multiprocessors [AD-A158274] N86-13909

MIDDLESEX COUNTY COLL., N.J.

Spectral reflectance of surface soils: Relationships with some soil properties N86-14089

MIDWEST RESEARCH INST., GOLDEN, COLO.

Photodegradation studies of silver-backed polyacrylonitrile (PAN) films [DE85-012154] N86-13501

Aerodynamic research efforts at SERI wind energy research center at Rocky Flats N86-13829

Wind loading on solar collectors [DE85-012151] N86-13833

Review of SERI solar pond work [DE85-012162] N86-13834

MILLS COLL., OAKLAND, CALIF.

Expanding your horizons in science and mathematics [NASA-CR-176372] N86-13958

MISSISSIPPI STATE UNIV., MISSISSIPPI STATE.

Bulk CMOS VLSI technology studies. Part 4: Design of a CMOS microsequencer [AD-A158369] N86-13650

Bulk CMOS VLSI technology studies. Part 5: The design and implementation of a high speed integrated circuit functional tester [AD-A158370] N86-13651

Results of research in four topic areas: The singularity expansion method, transient scattering measurements, high-frequency diffraction at edges residing on interfaces and cylindrical coordinate representation of dyadic Green's functions [AD-A158382] N86-14037

MISSISSIPPI VALLEY STATE UNIV., ITTA BENA.

FORTRAN plotting subroutines for the space plasma laboratory N86-14103

MISSOURI UNIV., COLUMBIA.

Solid waste treatment processes for space station N86-14091

MISSOURI UNIV., KANSAS CITY.

Optical constants [AD-A158623] N86-14038

MISSOURI UNIV., ROLLA.

Metastable interactions: Dissociative excitation [AD-A158733] N86-14013

MORGAN STATE UNIV., BALTIMORE, MD.

Comparative effect of lunar fines and terrestrtrial ash on the growth of a blue-green alga and germinating radish seeds N86-14097

MORTON THIOKOL, ELKTON, MD.

Synthesis of high nitrogen content heterocyclic nitramines and energetic internal plasticizers N86-13511

MORTON THIOKOL, HUNTSVILLE, ALA.

Control of the urethane cure reaction with solid, blocked isocyanates N86-13518

MOUND LAB., MIAMISBURG, OHIO.

Mound activities in chemical and physical research: July December 1984 [DE85-014402] N86-14030

N

NAGOYA UNIV. (JAPAN).

Preliminary experiment on electron beam injection for tokamak current drive [IPPJ-739] N86-14048

Physical mechanisms for hot electron stabilization of low frequency interchange modes [IPPJ-741] N86-14050

Effects of neutrals on internal forces and thermal conduction of a plasma in a magnetic field [IPPJ-691] N86-14051

NATIONAL AERONAUTICS AND SPACE ADMINISTRATION, WASHINGTON, D. C.

Aircraft of the future [NASA-TM-77952] N86-13318

Report on the findings of the Japanese Investigative Team on US Space Station Design (Keidanren) [NASA-TM-77659] N86-13356

Life sciences accomplishments [NASA-TM-88177] N86-13879

NATIONAL AERONAUTICS AND SPACE ADMINISTRATION. AMES RESEARCH CENTER, MOFFETT FIELD, CALIF.

Assessment of aerodynamic and dynamic models in a comprehensive analysis [NASA-TM-86835] N86-13286

On applications of chimera grid schemes to store separation [NASA-TM-88193] N86-13292

Computational aspects of zonal algorithms for solving the compressible Navier-Stokes equations in three dimensions [NASA-TM-86774] N86-13296

A tomographic technique for aerodynamics at transonic speeds [NASA-TM-86766] N86-13297

Double-branched vortex generator [NASA-TM-88201] N86-13298

Ground effects on V/STOL and STOL aircraft. A survey [NASA-TM-86825] N86-13299

Pressure-distribution measurements on a transonic low-aspect ratio wing [NASA-TM-86683] N86-13304

Discovery of the Kalman filter as a practical tool for aerospace and industry [NASA-TM-86847] N86-13311

Preliminary report on in-flight measurement of rotor hub drag and lift using the RSRA [NASA-TM-86764] N86-13319

Transonic separated flow predictions based on a mathematically simple, nonequilibrium turbulence closure model [NASA-TM-86826] N86-13676

Human factors in space station architecture 1: Space station program implications for human factors research [NASA-TM-86702] N86-13900

Experiences with Cray multi-tasking [NASA-TM-88200] N86-13916

Emerging aerospace technologies [NASA-TM-86837] N86-14213

NATIONAL AERONAUTICS AND SPACE ADMINISTRATION. GODDARD SPACE FLIGHT CENTER, GREENBELT, MD.

Report on active and planned spacecraft and experiments [NASA-TM-87499] N86-13343

Fundamental remote sensing science research program: The Scene Radiation and Atmospheric Effects Characterization Project [E86-10011] N86-13794

Understanding the radiant scattering behavior of vegetated scenes N86-13797

Atmospheric effect on remote sensing of the Earth's surface N86-13804

Understanding climate: A strategy for climate modeling and predictability research, 1985-1995 [NASA-RP-1158] N86-13866

VAS demonstration: (VISSR Atmospheric Sounder) description [NASA-RP-1151] N86-13867

Data catalog series for space science and applications flight missions. Volume 4A: Descriptions of meteorological and terrestrial applications spacecraft and investigations [NASA-TM-87501] N86-13869

Design and implementation of a compliant robot with force feedback and strategy planning software [NASA-TM-86111] N86-13947

NATIONAL AERONAUTICS AND SPACE ADMINISTRATION. JOHNSON (LYNDON B.) SPACE CENTER,

Space station preliminary design report [NASA-TM-87521] N86-13357

Plasma-gas interactions studies in a hybrid plume plasma rocket N86-13559

A tandem mirror plasma source for hybrid plume plasma studies N86-13560

Crop characteristics research: Growth and reflectance analysis N86-13800

Endocrine and fluid metabolism in males and females of different ages after bedrest, acceleration and lower body negative pressure
[NASA-TM-58270] N86-13886

The 1983 NASA/ASEE Summer Faculty Fellowship Research Program research reports
[NASA-CR-171904] N86-14078

An analysis of cryotrap heat exchanger performance test data (400 area) and recommendations for a system to handle Apollo RCS engines N86-14094

Fluorine disposal N86-14095

Sparger system for MMH-helium vents N86-14096

NATIONAL AERONAUTICS AND SPACE ADMINISTRATION. LANGLEY RESEARCH CENTER, HAMPTON, VA.

Advanced emergency openings for commercial aircraft
[NASA-TM-87580] N86-13305

Abrasion behavior of aluminum and composite skin coupons, stiffened skins and stiffened panels representative of transport airplane structures
[NASA-TP-2520] N86-13316

Ground vibration test of the laminar flow control JStar airplane
[NASA-TM-86398] N86-13321

A preliminary evaluation of the generalized likelihood ratio for detecting and identifying control element failures in a transport aircraft
[NASA-TM-87620] N86-13332

FIT: Computer program that interactively determines polynomial equations for data which are a function of two independent variables
[NASA-TM-86413] N86-13333

Computer program for calculating flow parameters and power requirements for cryogenic wind tunnels
[NASA-TM-87609] N86-13338

Structures and materials technology issues for reusable launch vehicles
[NASA-TM-87626] N86-13349

Fabrication and evaluation of superplastically formed/weld-brazed corrugated compression panels with beaded webs
[NASA-TP-2512] N86-13406

A parametric study of the Ibrahim time domain modal identification algorithm N86-13588

Large modal survey testing using the Ibrahim time domain identification technique
[AIAA-81-0528R] N86-13589

Linearity optimization in a class of analog phase modulators
[NASA-TM-86420] N86-13644

Airborne lidar measurements of El Chichon stratospheric aerosols
[NASA-RP-1148] N86-13850

Effects of digital altimetry on pilot workload
[NASA-TM-86424] N86-13892

Parallel computation with the force
[NASA-CR-177999] N86-13915

The mission oriented terminal area simulation facility
[NASA-TM-87621] N86-13944

A method to stabilize linear systems using eigenvalue gradient information
[NASA-TP-2479] N86-13946

Spectral methods for discontinuous problems
[NASA-CR-177974] N86-13953

Accuracy of schemes with nonuniform meshes for compressible fluid flows
[NASA-CR-177988] N86-13954

Multigrid solutions to quasi-elliptic schemes
[NASA-CR-177973] N86-13955

Stable boundary conditions and difference schemes for Navier-Stokes equations
[NASA-CR-177984] N86-13957

Parameter identification for a robotic manipulator arm
[NASA-CR-178002] N86-13959

NATIONAL AERONAUTICS AND SPACE ADMINISTRATION. LEWIS RESEARCH CENTER, CLEVELAND, OHIO.

A FORTRAN computer code for calculating flows in multiple-blade-element cascades
[NASA-TM-87104] N86-13295

Modifications of system for elevated temperature tensile testing and stress-strain measurement of metal matrix composites
[NASA-TM-87172] N86-13370

Polymer, metal and ceramic matrix composites for advanced aircraft engine applications
[NASA-TM-87132] N86-13407

The effect of cobalt content in U-700 type alloys on degradation of aluminide coatings
[NASA-TM-87173] N86-13408

Current viewpoints on oxide adherence mechanisms
[NASA-TM-87168] N86-13409

Fractured toughness of Si3N4 measured with short bar chevron-notched specimens
[NASA-TM-87153] N86-13495

Testing of 30-GHz low noise receivers
[NASA-TM-87171] N86-13627

Verification of computer-aided designs of traveling-wave tubes utilizing novel dynamic refocusers and graphite electrodes for the multistage depressed collector
[NASA-TP-2524] N86-13643

Potential for use of indium phosphide solar cells in the space radiation environment
[NASA-TM-87157] N86-13645

Heat transfer and pressure drop performance of a finned-tube heat exchanger proposed for use in the NASA Lewis Altitude Wind Tunnel
[NASA-TM-87151] N86-13677

Determination of convective diffusion heat/mass transfer rates to burner rig test targets comparable in size to cross-stream jet diameter
[NASA-TM-87176] N86-13678

Lubrication of nonconformal contacts
[NASA-TM-87120] N86-13679

Design of traction drives
[NASA-RP-1154] N86-13734

Probability of detection of internal voids in structural ceramics using microfocus radiography
[NASA-TM-87164] N86-13749

Mass loss of shuttle space suit orthofabric under simulated ionospheric atomic oxygen bombardment
[NASA-TM-87149] N86-13899

Preliminary measurement of the noise from the 2/9 scale model of the Large-scale Advanced Propfan (LAP) propeller, SR-7A
[NASA-TM-87116] N86-14006

Some design philosophy for reducing the community noise of advanced counter-rotation propellers
[NASA-TM-87099] N86-14007

Stirling engine supporting research and technology
[NASA-TM-87175] N86-14106

Development of the VOLT-A shuttle experiment
[NASA-TM-87169] N86-14110

NATIONAL AERONAUTICS AND SPACE ADMINISTRATION. MARSHALL SPACE FLIGHT CENTER, HUNTSVILLE, ALA.

DE 1 RIMS operational characteristics
[NASA-TM-86527] N86-13365

Atmospheric environment for Space Shuttle (STS-51D)
[NASA-TM-86524] N86-13868

Test method for telescopes using a point source at a finite distance
[NASA-TM-86523] N86-14033

NATIONAL AEROSPACE LAB., AMSTERDAM (NETHERLANDS).

Aerodynamic research on wind turbines at NLR
N86-13828

NATIONAL AEROSPACE LAB., TOKYO (JAPAN).

A method for calculating flow fields around moving bodies
[NAL-TR-859T] N86-13288

NATIONAL AIRSPACE SYSTEM PROGRAM OFFICE, WASHINGTON, D.C.

National airspace system, system requirements specification
[AD-A157944] N86-13312

NATIONAL BUREAU OF STANDARDS, BOULDER, COLO.

Supercritical fluid properties
[DE85-011203] N86-13401

NATIONAL BUREAU OF STANDARDS, GAITHERSBURG, MD.

Application of quantum chemistry to atmospheric chemistry
[AD-A158282] N86-13856

NATIONAL ELECTROSTATIC CORP., MIDDLETON, WIS.

Tests of compressed geometry NEC acceleration tubes
[DE85-016392] N86-14056

NATIONAL RESEARCH COUNCIL OF CANADA, OTTAWA (ONTARIO).

Aerodynamic calculational methods for curved-blade Darrieus VAWT WECS N86-13830

NATIONAL SCIENCE FOUNDATION, WASHINGTON, D.C.

Reactive scattering in the bending-corrected rotating linear model
[DE85-017539] N86-14018

NATIONAL TELECOMMUNICATIONS AND INFORMATION ADMINISTRATION, BOULDER, COLO.

Atmospheric radio noise: Worldwide levels and other characteristics
[PB85-212942] N86-13839

NAVAL ACADEMY, ANNAPOLIS, MD.

Investigation of dust associated with shell stars
[AD-A158945] N86-14210

NAVAL OCEAN RESEARCH AND DEVELOPMENT ACTIVITY, BAY ST. LOUIS, MISS.

Pore pressure response to probe insertion and thermal gradient: ISIMU-2. (In situ heat transfer experiment)
[AD-A158592] N86-13689

NAVAL OCEAN SYSTEMS CENTER, SAN DIEGO, CALIF.

Environmental Stress Screening (ESS)
[AD-A158262] N86-13751

NAVAL POSTGRADUATE SCHOOL, MONTEREY, CALIF.

Experimental investigation of magnesium combustion in steam
[AD-A159109] N86-13396

Effect of temperature and strain rate on microstructure of a deformed, superplastic Al-10%Mg-0.1%Zr alloy
[AD-A159015] N86-13413

Effect of strain and strain rate on the microstructure of a superplastically deformed Al-10%Mg-0.1%Zr alloy
[AD-A159062] N86-13414

Cerenkov radiation from periodic bunches for a finite path in air
[AD-A159027] N86-13635

MeV electron beam irradiation effects on GaAs (1-x) P (x) LEDs (Light emitting diodes)
[AD-A158832] N86-13653

Development and enhancement of Computer Performance Modeling Tool (CPMT)
[AD-A159003] N86-13938

Hierarchical image segmentation to infrared images
[AD-A158030] N86-14035

NAVAL RESEARCH LAB., WASHINGTON, D. C.

Elution of benzene and methyl ethyl ketone from charcoal beds by continued air sweeping
[AD-A158804] N86-13374

Babinet's principle for an anisotropic resistive surface using different approaches
[AD-A159117] N86-13636

Numerical simulations of asymmetric mixing in planar shear flows
[AD-A158024] N86-13687

Laboratory studies of steep and breaking deep water waves in a convergent channel
[AD-A158187] N86-13875

A family of curves for the rough surface reflection coefficient
[AD-A158195] N86-13876

Differential entropy and the statistics of instantaneous failure
[AD-A158047] N86-13984

NAVAL SURFACE WEAPONS CENTER, SILVER SPRING, MD.

A method to determine dynamic elastic constants of thin shell composites by guided ultrasonic waves
[AD-A159025] N86-13381

Zirconium as a structural material for naval systems
[AD-A158201] N86-13411

BOSS: A FORTRAN code for a relational database manager
[AD-A157067] N86-13924

NEBRASKA UNIV., LINCOLN.

Bidirectional reflectance modeling of non-homogeneous plant canopies N86-13796

NEVADA UNIV., RENO.

The suppression of afterburning in solid rocket plumes by potassium salts N86-13524

NEW MEXICO INST. OF MINING AND TECHNOLOGY, SOCORRO.

Microstructural and mechanical property evaluation of solar collectors
[DE85-017038] N86-13839

NEW YORK UNIV., NEW YORK.

Effective behavior of composite materials
[AD-A158941] N86-13380

Shock waves, increase of entropy and loss of information
[DE85-013645] N86-13701

NORGES TEKNISKE HOEGSKOLE, TRONDHEIM.

Feasibility study of chirp generator for ERS-1 radar altimeter, option A
[ELAB-STF44-F83103] N86-13368

NORTH CAROLINA UNIV., CHAPEL HILL.

A note on the effect of ignoring small measurement errors in precision instrument calibration
[AD-A159104] N86-13713

Basic properties of strong mixing conditions
[AD-A158740] N86-13992

Continuity of certain random integral mappings and the uniform integrability of infinitely divisible measures
[AD-A159105] N86-13995

NORTH TEXAS STATE UNIV., DENTON.

Synthesis of new polynitropolyhedranes N86-13510

Interaction between Escherichia coli and lunar fines N86-14088

NORTHWESTERN UNIV., EVANSTON, ILL.
Problems in thermal convective instability N86-13870
Neutron stress measurements with a position sensitive detector
[AD-A158882] N86-13712
Errors due to counting statistics in the triaxial strain (stress) tensor determined by diffraction
[AD-A158219] N86-13759
Enhancing sensitivity to visual motion and enhancing visual sensitivity
[AD-A158800] N86-13889

O

OAK RIDGE GASEOUS DIFFUSION PLANT, TENN.
First order estimates of the dynamics and energetics of a rapidly decelerating flywheel
[DE85-013908] N86-13842

OAK RIDGE NATIONAL LAB., TENN.
Combined small angle X-ray scattering and transmission electron microscopy studies of Al-Li alloys
[DE85-016356] N86-13416
Analytical electron microscopy of surface modified ceramics
[DE85-016309] N86-13499
Preparation of ceramic fiber-ceramic matrix composites by a faster chemical vapor infiltration process
[DE85-016402] N86-13500
Comparison of ion milling techniques for cross-sectional TEM of semiconductors
[DE85-016596] N86-13664
Electrical sliding joint literature review (viewgraph presentation)
[DE85-011571] N86-13666
Unusual occurrence of maghemite in soils developed on Knox group dolostones
[DE85-017158] N86-13817
Changes in soil acidity due to natural processes and acid deposition
[DE85-012103] N86-13845
The formulation of a hyperbolic Stefan problem
[ORNL-6065] N86-13952
The (58)Ni + n transmission, capture and differential elastic scattering data analysis in the resonance region
[DE85-016157] N86-14026
Structure and hydrodynamics of colloidal systems
[DE85-016294] N86-14027
Theory of resistivity-gradient driven turbulence
[DE85-015068] N86-14053
Tests of compressed geometry NEC acceleration tubes
[DE85-016382] N86-14056
Impact of a poloidal divertor in ignition tokamak design
[DE85-012892] N86-14061

OFFICE NATIONAL D'ETUDES ET DE RECHERCHES AEROSPATIALES, PARIS (FRANCE).
Test of the ONERA cryogenic balance in the T2 wind tunnel
[ONERA-BT-8/0791-GY] N86-13341

OFFICE OF NAVAL RESEARCH, LONDON (ENGLAND).
European Science Notes, Volume 39, Number 7
[AD-A157708] N86-14108
European Science Notes. Volume 39, number 9
[AD-A158278] N86-14109

OFFICE OF RADIATION PROGRAMS, LAS VEGAS, NEV.
Report on an automated calibration range for broadband isotropic probes
[PB85-231470] N86-13726

OHIO STATE UNIV., COLUMBUS.
Decomposition of some well-known variance reduction techniques: Revision
[AD-A158048] N86-13985

OLD DOMINION UNIV., NORFOLK, VA.
Numerical solutions of Navier-Stokes equations for a Butler wing
[NASA-CR-174202] N86-13293
Adaptive control of large space structures using recursive lattice filters
[NASA-CR-176402] N86-13358
Dynamic identification for control of large space structures
[NASA-CR-176380] N86-13587
Computation of normal modes from identified complex modes N86-13590
Dynamic modeling of structures from measured complex modes N86-13591
Time-domain quasi-linear identification of nonlinear dynamic systems
[AIAA-83-0811-CP] N86-13592
Minimal norm constrained interpolation
[NASA-CR-178001] N86-13956

OPERATIONS RESEARCH, INC., ROCKVILLE, MD.
Tradeoff analysis of technology needs for public service helicopters
[NASA-CR-3927] N86-13317

OREGON STATE UNIV., CORVALLIS.
Wave force-phase method for vertical cylinders
[AD-A157709] N86-13680
High Reynolds number wave force investigation in a wave flume
[AD-A157722] N86-13681

P

PACIFIC NORTHWEST LAB., RICHLAND, WASH.
Radar location equipment development program, phase 1
[DE85-014523] N86-13637

PENNSYLVANIA STATE UNIV., UNIVERSITY PARK.
Analytical modeling of strong radiation gas-dynamic interaction N86-13549
Coupling between gas dynamics and microwave energy absorption N86-13561

PENNSYLVANIA UNIV., PHILADELPHIA.
Microscopic observations and mechanics analyses of long term fracture in polyethylene piping materials
[PB85-219608] N86-13506

PHYSICAL SCIENCES, INC., ANDOVER, MASS.
Linear and saturated absorption of laser radiation in heated cases N86-13551
Energy deposition of pulsed one micron laser radiation in H2 and AR N86-13552
Experimental and theoretical studies of laser propulsion phenomenology
[AD-A158273] N86-13729

PITTSBURGH UNIV., PA.
A computational analysis of pulsating flow in rigid and deformable tubes N86-13673
Measurement of rate constants of elementary gas reactions of importance to upper atmosphere and combustion systems
[AD-A158624] N86-13857
On asymptotic distribution of the test statistic for the mean of the nonisotropic principal component
[AD-A158255] N86-13972
Spectra for large dimensional random matrices
[AD-A158256] N86-13973
An alternate derivation of the distribution of the conditioned signal-to-noise ratio
[AD-A158257] N86-13974
Inference on the ranks of the canonical correlation matrices for elliptically symmetric populations
[AD-A158268] N86-13976
A note on the integrated Cauchy functional equation
[AD-A158269] N86-13977
A variant of Shanbhag's lemma arising out of a modified Rao-Rubbin condition
[AD-A158608] N86-13998

POLISH ACADEMY OF SCIENCES, WARSAW.
Scientific activities of the Polish Academy of Sciences: Institute of Fundamental Technological Research in 1983
[ISBN-83-01-06288-6] N86-14107

PORTLAND STATE UNIV., OREG.
Development and evaluation of an instantaneous atmospheric corrosion rate monitor
[PB85-214336] N86-13727

PRAIRIE VIEW AGRICULTURAL AND MECHANICAL COLL., TEX.
Solar concentrator degradation in Low Earth Orbit (LEO) N86-14102

PRINCETON UNIV., N. J.
Combustion behavior of free boron slurry droplets
[AD-A158620] N86-13585

PUERTO RICO UNIV., RIO PIEDRAS.
Multiple scattering theories for optical properties of composite materials
[AD-A158270] N86-13379

PURDUE UNIV., WEST LAFAYETTE, IND.
Wide distribution propellants N86-13540
Measurement and modeling of the optical scattering properties of crop canopies N86-13798
Performance assessment of OTEC power systems and thermal power plants. Volume 2: Users manual for PACC-OTECs
[DE85-016792] N86-13835
Alerted monitors: Human operators aided by automated detectors
[PB85-222750] N86-13906
Decomposition of some well-known variance reduction techniques: Revision
[AD-A158048] N86-13985
Monte Carlo analysis of nonlinear statistical models. 1: Theory: Revision
[AD-A158613] N86-13990

R

R AND D ASSOCIATES, ALEXANDRIA, VA.
Unified study of plasma-surface interactions for space power and propulsion N86-13567

RAND CORP., SANTA MONICA, CALIF.
Improving MILSATCOM (Military Satellite Communication) acquisition outcomes: Lease versus buy
[AD-A158842] N86-13348

RANDOM APPLICATIONS, INC., MONTROSE, COLO.
Applications of differential phase statistics to studies of C3 and spread spectrum communications
[AD-A158815] N86-13633

RASOR ASSOCIATES, INC., SUNNYVALE, CALIF.
Close-space, high temperature Knudsen flow N86-13568
Close-spaced high temperature Knudsen flow
[AD-A158280] N86-13831

RAYTHEON CO., SUDBURY, MASS.
Precision pointing using a dual-wedge scanner
[NASA-CR-3946] N86-13813

RENSSELAER POLYTECHNIC INST., TROY, N.Y.
Advanced energy conversion concept for microwave beamed-energy propulsions N86-13553
Variable field effects for the rotating fluidized bed reactor N86-13565
Effect of interfacial phenomena on contact line heat transfer N86-13566
Ray transmissions over a sloping bottom in shallow water
[AD-A158017] N86-14008

RESEARCH TRIANGLE INST., RESEARCH TRIANGLE PARK, N.C.
Study of mean free path effects on growth of ultrafine metallic aerosols
[AD-A158206] N86-13393

RESSULT. RESEARCH AND CONSULTING, SOECHTENAU (WEST GERMANY).
An algorithm for simultaneous determination of modal frequencies and modal vectors of a dynamic impedance matrix
[ESA-CR(P)-2055] N86-13943

RICE UNIV., HOUSTON, TEX.
Muon spin relaxation study of exchange coupling in dilute AgMn alloys
[DE85-014104] N86-13419

RICERCHE E PROGETTI S.R.L., TURIN (ITALY).
Crowding of the geostationary orbit
[ESA-CR(P)-2050] N86-13346

RISO NATIONAL LAB., ROSKILDE (DENMARK).
Aerodynamic performance of a new LM 17.2 m rotor N86-13827

ROCHESTER UNIV., N. Y.
Active mirror boosted 351 nm laser irradiation facility
[DE85-014412] N86-13732
Retrofit of a high power Nd:glass laser system with liquid crystal polarizers
[DE85-014415] N86-13733
Scaling of uv (351 nm) fusion implosions driven by multiple beams
[DE85-014406] N86-14068

ROCKWELL INTERNATIONAL CORP., CANOGA PARK, CALIF.
Electrolytic preparation of novel azidodinitro compounds N86-13508
Energetic fluorcarbons N86-13517
Fundamental studies of azide decomposition and combustion N86-13534

ROCKWELL INTERNATIONAL CORP., GOLDEN, COLO.
Solvent extraction of plutonium (IV) polymer by organophosphorous compounds
[DE85-013229] N86-13502
High count rate gamma-ray spectrometer system for plutonium isotopic measurements
[DE85-013212] N86-14024

ROCKWELL INTERNATIONAL CORP., THOUSAND OAKS, CALIF.
Development and evaluation of an instantaneous atmospheric corrosion rate monitor
[PB85-214336] N86-13727

ROYAL AIRCRAFT ESTABLISHMENT, BEDFORD (ENGLAND).
Recent experience in the RAE (Royal Aircraft Establishment) 5-metre wind tunnel of a china clay method for indicating boundary layer transition
[AD-A157943] N86-13302

ROYAL AIRCRAFT ESTABLISHMENT, FARNBOROUGH (ENGLAND).
Studies of the flow field near a NACA 4412 aerofoil at nearly maximum lift
[AD-A157750] N86-13301

Standardised fatigue loading sequences for helicopter rotors (Helix and Felix). Part 2: Final definition of Helix and Felix
[AD-A156622] N86-13322
Effect of carbon fibre surface treatment on moisture absorption and interlaminar shear strength of carbon Fibre/Epoxy resin composites
[AD-A157705] N86-13377

ROYAL GREENWICH OBSERVATORY, HAILSHAM (ENGLAND).
The plate scale of the U.K. Schmidt Telescope
N86-14202

ROYAL NETHERLANDS AIRCRAFT FACTORIES FOKKER, SCHIPHOL-OOST.
Development of a breadboard cooler for infrared remote sensing payloads, phase 2
[FOK-RV-R-82-072] N86-13725
Study on design techniques for robots (space applications). Volume 1, part A: Technical results
[FOK-TR-R-84-110-VOL-1-PT-A] N86-13902
Study on design techniques for robots (space applications). Volume 1, part B: Technical results
[FOK-TR-R-84-110-VOL-1-PT-B] N86-13903
Study on design techniques for robots (space applications). Volume 2: Technical appendices
[FOK-TR-R-84-110-VOL-2] N86-13904
Study on design techniques for robots (space applications). Volume 3: Executive summary
[FOK-TR-R-84-110-VOL-3] N86-13905

ROYAL OBSERVATORY, EDINBURGH (SCOTLAND).
Occasional reports of the Royal Observatory, Edinburgh, no. 16
[ISSN-0309-099-X] N86-14200
A multiple-object fibre-optics coupler for the 1.2-m UK Schmidt Telescope N86-14201

ROYAL SIGNALS AND RADAR ESTABLISHMENT, MALVERN (ENGLAND).
Safe control systems and the VIPER microprocessor
[AD-A156617] N86-13908

RUTGERS - THE STATE UNIV., NEW BRUNSWICK, N. J.
Functionalized vesicles as organic reagents
[AD-A158381] N86-13372

S

SAINT JOHN FISHER COLL., ROCHESTER, N.Y.
Multilevel relaxation phenomena and population trapping
[DE85-011527] N86-13731

SAINT THOMAS UNIV., HOUSTON, TEX.
Some applications of Lie groups in astrodynamics
N86-14087

SAM HOUSTON STATE UNIV., HUNTSVILLE, TEX.
Development of a mass spectrometer system for the measurement of inert gases in meteorites N86-14093

SANDIA NATIONAL LABS., ALBUQUERQUE, N. MEX.
Ultrasonic longitudinal wave velocity in carbon-carbon Pitch and Pitch/M2 shape stable nosetip material from 70 deg F to 5400 deg F
[DE85-017330] N86-13382
Discussion on the Vibration Process Standards 9958002 and 9958004
[DE85-017116] N86-13599
Critical charge for the direct initiation of detonation in gaseous fuel-air mixtures
[DE85-016130] N86-13696
Experimental investigation of heat transfer behavior of aqueous foams in thermal entry region of pipe flow
[DE85-012836] N86-13700
High speed multi-channel data recorder to replace oscilloscope data acquisition systems
[DE85-015155] N86-13721
Tape joint design for a vibration table
[DE85-012617] N86-13753
Engineering design for the PBFA-2 pulse forming section
[DE85-012810] N86-14060
Laser-trigger system design for PBFA 2
[DE85-013144] N86-14065

SANTA CLARA UNIV., CALIF.
Wind tunnel simulations of aeolian processes
[NASA-CR-176382] N86-13289

SCHOOL OF AEROSPACE MEDICINE, BROOKS AFB, TEX.
Interactive scenario computer model for dose rates to aircrews in flight through nuclear debris clouds
[AD-A158741] N86-13888

SCIENCE APPLICATIONS INTERNATIONAL CORP., OAK RIDGE, TENN.
Impact of a poloidal divertor in ignition tokamak design
[DE85-012892] N86-14061

SEITEC, CLEVELAND, OHIO.
Completely magnetically contained electrothermal thruster N86-13558

SEMICON ASSOCIATES, INC., LEXINGTON, KY.
A study of rhenium as an alternate substrate material for impregnated dispenser cathodes
[AD-A159113] N86-13415

SHEFFIELD UNIV. (ENGLAND).
Development of velocity measurement technique by pulsed laser Doppler anemometry N86-13571

SIKORSKY AIRCRAFT, STRATFORD, CONN.
Transmission acoustic vibration testing
[AD-A159022] N86-13326

SMITH-KETTLEWELL INST. OF VISUAL SCIENCES, SAN FRANCISCO, CALIF.
The spatial and temporal parameters of velocity discrimination
[AD-A158735] N86-13896

SMITHSONIAN INSTITUTION, CAMBRIDGE, MASS.
Analytical investigation of the dynamics of tethered constellations in Earth orbit, phase 2
[NASA-CR-171611] N86-13345

SOCIETE EUROPEENNE DE PROPULSION, VERNON (FRANCE).
Electrical motor with superconducting winding
[SEP-TS/SE/BT/10026/85] N86-13668

SOCIETE NATIONALE INDUSTRIELLE AEROSPATIALE, SURESNES (FRANCE).
Characterization of 7017 aluminum alloys in thick profiles, in the metallurgical versions T6510, T76510 and T736510, test report no. PV-44-607/F
[PV-44-607/F] N86-13420

SOUTHERN METHODIST UNIV., DALLAS, TEX.
Crop area estimation based on remotely-sensed data with an accurate but costly subsample
[NASA-CR-176017] N86-13814

SOUTHERN RESEARCH INST., BIRMINGHAM, ALA.
Protocol for size-specific emission measurements (SIM-5) applied to PM(10)
[PB85-200194] N86-13847

SOUTHWEST RESEARCH INST., SAN ANTONIO, TEX.
Digital servocontroller system. Volume 4. Results and conclusions
[AD-A159068] N86-13335
Exploratory development on advanced eddy current coil excitation and signal processing
[AD-A159228] N86-13752
Effects of 60 Hz electric fields on operant and social stress behaviors of nonhuman primates
[DE85-011992] N86-13885

SOUTHWESTERN UNIV., GEORGETOWN, TEX.
Lunar luminescence measurements N86-14092

SPACE TELESCOPE SCIENCE INST., BALTIMORE, MD.
A report on the ST ScI optical disk workstation
[NASA-CR-176369] N86-13907

SPECTRON DEVELOPMENT LABS., INC., COSTA MESA, CALIF.
Optical technique to measure electrode erosion
N86-13564
Spray characterization with a nonintrusive optical single particle counter N86-13580

SRI INTERNATIONAL CORP., MENLO PARK, CALIF.
Physical distribution system for aircraft external fuel tanks-survey
[AD-A158275] N86-13324
Synthesis and chemistry of polynitroalkanes and polynitroolefins N86-13513
Two-proton detection techniques for atomic fluorine
N86-13569

STANFORD LINEAR ACCELERATOR CENTER, CALIF.
Iron dominated magnets
[DE85-014955] N86-14003
Linear accelerators for TeV colliders
[DE85-014958] N86-14017
Hardware upgrade for klystrons in the SLC
[DE85-014357] N86-14029
Generation and acceleration of high intensity beams in the SLC injector
[DE85-013056] N86-14066

STANFORD UNIV., CALIF.
The influence of microstructure on temper embrittlement of low alloy steel N86-13405
Quantitative flow visualization N86-13572
Optical processing and phase conjugation
N86-13573
Joint services electronics program
[AD-A158840] N86-13654
Small X-ray diffraction of immunoglobulin-membrane complexes
[AD-A158252] N86-13882
Development of a flight software testing methodology
[NASA-CR-176391] N86-13922
On projected Newton barrier methods for linear programming and an equivalence to Karmarkar's projective method
[AD-A158212] N86-13934
Techniques for the design and implementation of highly reliable multi-processing systems
[AD-A159236] N86-13945
A behavioral summary for completely random nets
[AD-A157755] N86-13960
The theory of standardized time series
[AD-A158383] N86-13989
Existence of equilibrium prices for a simple planning model
[AD-A158263] N86-13996

STATE UNIV. OF NEW YORK, BINGHAMTON.
Physical and chemical consequences of antiaromaticity in the boracyclopentadiene system N86-13519

STATE UNIV. OF NEW YORK, STONY BROOK.
Modelling a transport equation of turbulent reactive mixing flow N86-13674

STUDSVIK ENERGITEKNIK A.B., NYKOPING (SWEDEN).
Small solar power systems plant in Almeria system evaluation and comparison on thermal basis
[DE85-017185] N86-13840

STUTTGART UNIV. (WEST GERMANY).
Basic processes of plasma propulsion N86-13554
Polar measurements on the profiles: FX 84-w-097, FX 84-w-127, FX 84-w-140, FX 84-w-175, FX 84-w-218
N86-13821

SVERDRUP TECHNOLOGY, INC., ARNOLD AIR FORCE STATION, TENN.
Crushing strength of aluminum oxide agglomerates
[AD-A158051] N86-13756

SYSTEMS AND APPLIED SCIENCES CORP., ANAHEIM, CALIF.
New physical methods for biological aerosol detection
[AD-A158218] N86-13881

SYSTEMS RESEARCH LABS., INC., DAYTON, OHIO.
Application of atomic fluorescence to measurement of combustion temperatures in solid propellants
N86-13582

T

TECHNICOLOR GOVERNMENT SERVICES, INC., FORT COLLINS, COLO.
Map projections for use with the Geographic Information System
[PB85-198992] N86-13819

TECHNISCHE HOGESCHOOL, DELFT (NETHERLANDS).
An analytical theory for rotor tip vane performance and comparison with experimental results N86-13823

TECHNISCHE HOGESCHOOL, EINDHOVEN (NETHERLANDS).
Transient simulation of submicron devices
[AD-A157748] N86-13648

TECHNISCHE UNIV., HANOVER (WEST GERMANY).
Meteorological and climatological conditions affecting the vertical structure of visibility in northern Germany
[AD-A158254] N86-13871

TELEDYNE CONTINENTAL MOTORS, MUSKEGON, MICH.
Lightweight two-stroke cycle aircraft diesel engine technology enablement program, volume 1
[NASA-CR-174923-VOL-1] N86-13328
Lightweight two-stroke cycle aircraft diesel engine technology enablement program, volume 2
[NASA-CR-174923-VOL-2] N86-13329
Lightweight two-stroke cycle aircraft diesel engine technology enablement program, volume 3
[NASA-CR-174923-VOL-3] N86-13330

TENNESSEE UNIV., KNOXVILLE.
Theory of the propagation of finite amplitude ultrasonic waves in pure mode directions in hexagonal and trigonal crystals
[AD-A158154] N86-14009
Impact of a poloidal divertor in ignition tokamak design
[DE85-012892] N86-14061

TENNESSEE UNIV., TULLAHOMA.
Laser thermal propulsion N86-13548

TEXAS A&M UNIV., COLLEGE STATION.
A direct-inverse method for transonic and separated flows about airfoils
[NASA-CR-176403] N86-13300
Variability of rainfall over small areas N86-14098

TEXAS TECHNOLOGICAL UNIV., LUBBOCK.
Interpretation of F-106B in-flight lightning signatures
[NASA-CR-176387] N86-13320

TEXAS UNIV., ARLINGTON.
Scattering models and basic experiments in the microwave regime N86-13807

TEXAS UNIV., AUSTIN.
Advanced algorithm for orbit computation N86-14101

TEXAS UNIV. AT DALLAS, RICHARDSON.
Real-time, two-dimensional fuel spray visualization
N86-13583

THEORELLS INGENJOERSBYRA A.B., SOLNA (SWEDEN).
Small solar power systems plant in Almeria system evaluation and comparison on thermal basis
[DE85-017185] N86-13840

THOMSON-CSF, VELIZY (FRANCE).
The development of a submillimeter wave carcinotron operating in the frequency range from 850 to 1000 GHz
[TDH-RT-2963-T] N86-13638

TORONTO UNIV. (ONTARIO).
The simulation of truck motions
[UTIAS-294] N86-13914

U

UNITED RESEARCH CORP., SANTA MONICA, CALIF.
Waves which travel upstream in boundary layers
[AD-A157949] N86-13684

UNITED TECHNOLOGIES CORP., SAN JOSE, CALIF.
High energy molecules of high symmetry N86-13520
Coupling between velocity oscillations and solid propellant combustion N86-13541

UNITED TECHNOLOGIES RESEARCH CENTER, EAST HARTFORD, CONN.
Resonant cars detection of OH radicals N86-13576

UNIVERSITE DE VALENCIENNES ET DU HAINAUT-CAMBRESIS (FRANCE).
Behavior of slender cones at large incidences
N86-13707

UNIVERSITY OF SOUTHERN CALIFORNIA, LOS ANGELES.
Rectification and registration of remotely sensed data
[AD-A158827] N86-13711

UNIVERSITY OF SOUTHWESTERN LOUISIANA, LAFAYETTE.
Estimation of finite mixtures using the empirical characteristic function N86-14079

UNIVERSITY OF WESTERN ONTARIO, LONDON.
Positron diffusion in Si
[DE85-014831] N86-14076

V

VIRGINIA POLYTECHNIC INST. AND STATE UNIV., BLACKSBURG.
Effects of velocity profile and inclination on dual-jet-induced pressures on a flat plate in a crosswind
[NASA-CR-177361] N86-13287
Elastic-plastic deformation of a metal-matrix composite coupon with a center slot
[NASA-CR-178013] N86-13496

VIRGINIA RESEARCH ASSOCIATES, BLACKSBURG.
New flow visualization technique for water tunnel testing of combustors
[AD-A158015] N86-13686

VMI RESEARCH LABS., LEXINGTON, VA.
The design of a beach profiler
[AD-A157715] N86-13874

VON KARMAN INST. FOR FLUID DYNAMICS, RHODE-SAINT-GENESE (BELGIUM).
Aerothermodynamics for future launchers. Review of the state of the art in Europe
[VKI-CR-1984-16/AR] N86-13347

VOUGHT CORP., DALLAS, TEX.
Computer program for prediction of fuel consumption statistical data for an upper stage three-axes stabilized on-off control system
[NASA-CR-166031] N86-13917
Computer program for post-flight analysis of rigid body moments acting on a launch vehicle first stage
[NASA-CR-166033] N86-13918
Scout trajectory error propagation computer program
[NASA-CR-166030] N86-13919
Computer program for post-flight evaluation of the control surface response for an attitude controlled missile
[NASA-CR-166032] N86-13920
Computer program for post-flight evaluation of a launch vehicle upper-stage on-off reaction control system
[NASA-CR-166029] N86-13921

W

WASHINGTON STATE UNIV., PULLMAN.
Temperature and pressure components of shock-induced changes in the electronic spectrum of carbon disulfide
[AD-A158627] N86-13373
Acoustical scattering from an elastic sphere in water: Surface wave glory, resonances, and the Sommerfeld-Watson transformation for amplitudes
[AD-A158884] N86-14010
Light scattering from bubbles in liquids
[AD-A158736] N86-14039

WASHINGTON STATE WATER RESEARCH CENTER, PULLMAN.
Determination of the activation barrier to energy transfer from 3 pi pi* to charge transfer levels via steady state and transient luminescence measurements on Bis(4-Chlorothiophenol) (1,10-Phenanthroline) Zinc (II)
[AD-A158239] N86-14012

WASHINGTON UNIV., SEATTLE.
Molecular mechanisms of mutagenesis determined by the recombinant DNA technology
[DE85-016353] N86-13884

WASHINGTON UNIV., ST. LOUIS, MO.
A psychophysiological mapping of cognitive processes
[AD-A158732] N86-13695

WESTINGHOUSE ELECTRIC CORP., LIMA, OHIO.
Two-hundred to 300 KVA conditioned power system - development, phase 1
[AD-A158820] N86-13832

WESTINGHOUSE RESEARCH LABS., PITTSBURGH, PA.
MBE growth of CdTe and Hg (1-x) Cd (x) Te films and multilayer structures
[AD-A158267] N86-14073

WICHITA STATE UNIV., KANS.
Discovering qualitative empirical laws
[AD-A159235] N86-13951

WILKES COLL., WILKES-BARRE, PA.
Electrical research on solar cells and photovoltaic materials
[NASA-CR-176384] N86-13838

WISCONSIN UNIV., MADISON.
Luminescent properties of semiconductor electrodes
[AD-A158841] N86-13655
Microcomputer controlled current sharing experiments with parallel converters
[DE85-013854] N86-13665
Non-Newtonian flow past curved external surfaces
N86-13671
A functional equation governing moving phase boundaries in an elastic bar
[AD-A158178] N86-13757
Development of singularities in nonlinear viscoelasticity
[AD-A158190] N86-13758
Study of toxic and antigenic structures of botulinum neurotoxins
[AD-A156642] N86-13880
Decay with a rate for noncompactly supported solutions of conservation laws
[AD-A158163] N86-13962
Adaptive, self-validating numerical quadrature
[AD-A158164] N86-13963
Convergence of cardinal series
[AD-A158166] N86-13964
Boundary integral techniques for multi-connected domains
[AD-A158171] N86-13965
Uniformly high-order accurate non-oscillatory schemes 1
[AD-A158177] N86-13966
A linear combination test for detecting serial correlation in multivariate samples
[AD-A158179] N86-13967
Computable bounds for solutions of integral equations
[AD-A158189] N86-13970
B-splines and linear combinations of uniform order statistics
[AD-A158151] N86-13986
Approximation of the initial reserve for known ruin probabilities
[AD-A158167] N86-13987
Conditioning in a missing data problem
[AD-A158202] N86-13988
Realization theory in Hilbert space
[AD-A158172] N86-13997
The mathematical structure of elementary particles: 2
[AD-A158191] N86-14011
Experimental study of neoclassical currents
[DE85-014866] N86-14063

WOODARD-CLYDE CONSULTANTS, SAN FRANCISCO, CALIF.
Geologic characterization report for the Paradox Basin Study Region, Utah Study Areas. Volume 6: Salt Valley
[DE85-011699] N86-13858

WRIGHT STATE UNIV., DAYTON, OHIO.
Aquatic plant control research program: Evaluation of polymers for controlled delivery of herbicides for aquatic plant control
[AD-A157948] N86-13843

WYOMING UNIV., LARAMIE.
Geothermal resources of the Wind River Basin, Wyoming
[DE85-016969] N86-13816

Y

YALE UNIV., NEW HAVEN, CONN.
Laser emission and coherent Raman scattering from individual flowing droplets N86-13578
Size and shape characterization of individual flowing droplets by laser light scattering N86-13579

YAMANASHI UNIV., KOFU (JAPAN).
Parametric excitation of ion Bernstein waves by magnetosonic wave
[IPPJ-738] N86-14047
Unlimited acceleration of charged particles by an electromagnetic wave with a purely transverse electric field propagating perpendicularly to a static magnetic field
[IPPJ-740] N86-14049

YORK UNIV., TORONTO (ONTARIO).
Relationships between electronic spectroscopy and electrochemistry. A probe of reorganisation energies
[AD-A157940] N86-13389

CONTRACT NUMBER INDEX

SCIENTIFIC AND TECHNICAL AEROSPACE REPORTS VOLUME 24 NUMBER 4

Typical Contract Number Index Listing

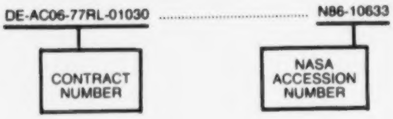

Listings in this index are arranged alphanumerically by contract number. Under each contract number the NASA accession numbers denoting documents that have been produced as a result of research done under that contract are arranged in ascending order. The NASA accession number denotes the number by which the citation is identified.

AF PROJ. 5D30 .... N86-13628
AF PROJ. 5T10 .... N86-13628
AF PROJ. 2054 .... N86-13339
AF PROJ. 2303 .... N86-13507
AF PROJ. 2304 .... N86-13999
AF PROJ. 2307 .... N86-13378
N86-13498
N86-13507

AF PROJ. 2308 .... N86-13507
AF PROJ. 2313 .... N86-13890
AF-AFOSR-ISSA-84-0000 .... N86-13856
AF-AFOSR-80-0078 .... N86-13657
AF-AFOSR-0066-82 .... N86-13730
AF-AFOSR-0070-84 .... N86-13955
AF-AFOSR-0089-83 .... N86-13953
AF-AFOSR-0096-84 .... N86-13909
AF-AFOSR-0149-81 .... N86-13394
AF-AFOSR-0207-80 .... N86-13857
AF-AFOSR-0228-80 .... N86-13380
AF-AFOSR-0229-83 .... N86-13981
AF-AFOSR-0246-80 .... N86-13889
AF-AFOSR-0265-83 .... N86-13691
AF-AFOSR-0330-83 .... N86-13690
AF-AFOSR-0345-82 .... N86-13896
AF-AFOSR-0355-83 .... N86-13945
AF-AFOSR-0367-84 .... N86-13978
N86-13991

AF-AFOSR-1089-85 .... N86-13915
ARB-A1-159-32 .... N86-13849
ARB-A2-058-32 .... N86-13846
ARPA ORDER 3345 .... N86-13628
ARPA ORDER 4585 .... N86-13629
ARPA ORDER 4852 .... N86-13632
ARPA ORDER 5378 .... N86-13926
CETIM-4-77-5310 .... N86-13741
CETIM-4-79-6122 .... N86-13741
DA PROJ. F64-651 .... N86-13374
DA PROJ. 1L1-61102-AH-45 .... N86-13316
DA PROJ. 1L1-61102-BH-57 .... N86-13871
DA PROJ. 1L1-62209-AH-76 .... N86-13325
DA PROJ. 1L2-63201-DB-72 .... N86-13326
DA PROJ. 1T1-61102-BH-57 .... N86-13968
DA PROJ. 3E1-62777-A-879 .... N86-13887
DA PROJ. 3M1-62770-A-871 .... N86-13880
DAAE07-81-C-4028 .... N86-13593
DAAG29-80-C-0041 .... N86-13757
N86-13758
N86-13962
N86-13963
N86-13964
N86-13965
N86-13966
N86-13967
N86-13970
N86-13986
N86-13987
N86-13988
N86-13997
N86-14011
DAAG29-81-G-0010 .... N86-13379
DAAG29-81-K-0116 .... N86-13750
DAAG29-82-C-0013 .... N86-14052
DAAG29-82-K-0122 .... N86-13372
DAAG29-82-K-0167 .... N86-13650
N86-13651

DAAG29-83-C-0008 .... N86-14073
DAAG29-84-K-0005 .... N86-13975
DAAG29-84-K-0030 .... N86-13989
DAAG29-84-K-0156 .... N86-13934
DAAG29-85-K-0190 .... N86-13953
DAAK11-82-C-0069 .... N86-14038
DAAK11-82-C-0113 .... N86-13881
DAAK51-82-C-0040 .... N86-13326
DAAK51-83-C-0039 .... N86-13325
DAAK70-78-C-0001 .... N86-13388
DAAK70-79-C-0175 .... N86-13388
DAAK70-83-K-0018 .... N86-13910
N86-13948

DAAK70-85-C-0007 .... N86-13388
DACW39-76-C-0016 .... N86-13843
DACW39-83-M-1533 .... N86-13595
DACW39-85-M-1533 .... N86-13594
DAJA37-81-C-0736 .... N86-13968
DAJA37-82-C-0189 .... N86-13871
DAJA45-84-C-0039 .... N86-13815
DAJA45-84-C-0052 .... N86-14072
DAJA45-84-C-0054 .... N86-13648
DAMD17-80-C-0100 .... N86-13880
DARPA ORDER 3206 .... N86-13910
DARPA ORDER 4305 .... N86-13935
DE-AC01-82CD-30718 .... N86-13835
DE-AC02-76CH-00016 .... N86-13504
N86-13667
N86-13844
N86-14002
N86-14004
N86-14064
N86-14076
DE-AC02-76CH-03000 .... N86-14025
N86-14028
DE-AC02-76ER-03077 .... N86-13701
DE-AC02-80RA-50219 .... N86-13885
DE-AC02-83CH-10093 .... N86-13501
N86-13833
N86-13834
DE-AC02-83CH-10098 .... N86-13837
DE-AC02-83CH-10140 .... N86-13858
DE-AC02-83ER-53154 .... N86-14063
DE-AC03-76SF-00098 .... N86-13694
N86-14001
N86-14002
N86-14023
N86-14058
N86-14075
DE-AC03-76SF-00515 .... N86-14003
N86-14017
N86-14029
DE-AC03-76SF-00700 .... N86-13835
DE-AC03-84ER-51044 .... N86-14031
N86-14070
DE-AC04-76DP-00053 .... N86-14030
DE-AC04-76DP-00487 .... N86-13720
DE-AC04-76DP-00789 .... N86-13382
N86-13599
N86-13696
N86-13700
N86-13721
N86-13753
N86-14060
N86-14065
DE-AC04-76DP-03533 .... N86-13502
N86-14024
DE-AC04-76DR-00789 .... N86-13840
DE-AC05-84CT-21400 .... N86-13842
DE-AC05-84OR-21400 .... N86-13499
N86-13500
N86-13664
N86-13817
N86-13845
N86-13952
N86-14026
N86-14027
N86-14053
N86 14056
N86-14061
DE-AC05-87OR-21400 .... N86-13666
DE-AC05-840R-21400 .... N86-13873
DE-AC06-76RL-01830 .... N86-13637
N86-13883

DE-AC07-76ID-01570 .... N86-14067
DE-AC08-76SF-00515 .... N86-14066
DE-AC08-80DP-40124 .... N86-14068
DE-AC21-83MC-20110 .... N86-13503
DE-AC21-83MC-20334 .... N86-13699
DE-AI01-77CS51017 .... N86-13760
DE-AI01-79CS-50030 .... N86-13388
DE-AI01-85CE-50112 .... N86-14106
DE-AI05-83OR-21374 .... N86-13401
DE-AM03-76SF-00326 .... N86-13934
DE-AM03-76SF00326 .... N86-13996
DE-AS04-78AL-04266 .... N86-13839
DE-AS05-76EV-03728 .... N86-13884
DE-AS07-77ET-28407 .... N86-13841
DE-AT03-76ER-72018 .... N86-13934
DE-AT03-84ER-53158 .... N86-14062
DE-FC07-79ID-12026 .... N86-13816
DE-FC08-85DP-40200 .... N86-13732
N86-13733

DE-FG02-84ER-13243 .... N86-13731
DE-FG22-84PC-70779 .... N86-13398
DE-14-16-0009-83-001 .... N86-13819
DOT-CG-835285-A N86-13313
DRET-83-34-135 .... N86-13341
DRET-83-250 .... N86-13303
DRET-83-452 .... N86-13308
DRET-83-1095 .... N86-13707
DTRS56-83-C-00047 .... N86-13906
EPA-68-02-3696 .... N86-13847
EPA-68-02-3741 .... N86-13727
EPRI PROJ. 1774-1 .... N86-13883
ESA-440/80/NL-AK(SC) N86-13364
ESA-4739/81/NL-HP N86-13911
ESA-5199/NL-PP N86-13360
ESA-5477/83/F-FC(SC) N86-13347
ESA-5545/83/NL-GM(SC) N86-13367
ESA-5610/83/NL N86-13350
ESA-5619/83/NL-PP N86-13943
ESA-5653/83/NL-PB N86-13362
ESA-5669/83/NL-PB(SC) N86-13363
ESA-5670/83/NL-PB N86-13942
ESA-5705/83/NL-PP(SC) N86-13346
ESA-5718/83/NL-AN(SC) N86-13902
N86-13903
N86-13904
N86-13905
ESA-5746/83/NL-DG N86-13355
ESTEC-4620/81/NL-PP N86-13725
ESTEC-4768/81/NL-HP N86-13638
ESTEC-4845/81/NL-PP(SC) N86-13368
ESTEC-5179/82/NL-PL(SC) N86-13340
ESTEC-5260/82/NL-PB(SC) N86-13739
ESTEC-5489/83/NL-PB(SC) N86-13763
ESTEC-5516/83/NL-PP(SC) N86-13361
ESTEC-5609/83 .... N86-13668
ESTEC-5615/83/NL-PP N86-13738
ESTEC-5711/83/NL-PR N86-13351
ESTEC-5717/83/NL-MS N86-13705
N86-13706

F04701-83-C-0064 .... N86-13631
N86-13711

F08635-82-K-0159 .... N86-13375
F08635-82-K-0321 .... N86-13682
F19628-82-C-0139 .... N86-13853
F19628-82-K-0025 .... N86-14207
N86-14208

F19628-85-C-0002 .... N86-13628
N86-13993

F33615-81-C-5036 .... N86-13752
F33615-81-K-1539 .... N86-13935
F33615-81-K-2081 .... N86-14013
F33615-82-C-2234 .... N86-13832
F33615-82-C-5041 .... N86-13415
F33615-84-C-2468 .... N86-13686
F40600-79-C-0002 .... N86-13684
F49620-82-C-0009 .... N86-13713
N86-13992
N86-13995

F49620-82-C-0018 N86-13348
F49620-82-K-0011 N86-13585
F49620-83-C-0039 N86-13729
F49620-83-C-0059 N86-13895
F49620-83-C-0068 N86-13831
F49620-83-C-0082 N86-13980
F49620-83-C-0085 N86-13633
F49620-83-C-0109 N86-13656
F49620-83-C-0135 N86-13979
F49620-83-C-0144 N86-13897
F49620-84-C-0017 N86-13393
F49620-84-C-0057 N86-13652
F49620-84-C-0101 N86-13710
F49620-85-C-0007 N86-13999
F49620-85-C-0008 N86-13972
N86-13973
N86-13974
N86-13976
N86-13977
N86-13998
IABG-342-7027-01/02 N86-13340
MDA903-83-C-0515 N86-13632
MDA903-85-C-0124 N86-13926
NAG1-28 N86-13320
NAG1-343 N86-13496
NAG1-363 N86-13956
NAG1-429 N86-13358
NAG1-506 N86-13957
NAG2-246 N86-13922
NAG2-256 N86-13287
NAG2-335 N86-13958
NAG3-337 N86-13755
NAG5-349 N86-13851
NASW-3291 N86-14212
NASW-3395 N86-13852
NASW-3554 N86-13317
NASW-3783 N86-13907
NASW-3966 N86-14209
NASW-4004 N86-13356
NASW-4006 N86-13318
NAS1-15000 N86-13917
N86-13918
N86-13919
N86-13920
N86-13921
NAS1-17070 N86-13915
N86-13953
N86-13954
N86-13955
N86-13957
N86-13959
NAS1-17556 N86-13310
NAS2-11491 N86-13353
N86-13354
NAS2-11555 N86-13290
N86-13291
N86-13913
NAS3-22218 N86-13328
N86-13329
N86-13330
NAS5-28200 N86-13947
NAS7-918 N86-13838
NAS8-33120 N86-13813
NAS8-34970 N86-13923
NAS8-35598 N86-13369
NAS8-36124 N86-13359
NAS8-36134 N86-14206
NAS8-36606 N86-13345
NAS9-16282 N86-13708
NAS9-16956 N86-13898
NAS9-17176 N86-13342
NCC1-68 N86-13293
NCC2-60 N86-13289
NCC2-213 N86-13878
NCC2-242 N86-13294
NCC3-30 N86-13679
NCC9-9 N86-13814
NCF DCR-84-13211 N86-13934
NCF ECS-83-12142 N86-13934
NGL-05-002-134 N86-14205
NGT-44-001-800 N86-14078
NR PROJ. F61-545 N86-13411
NR PROJ. RR0-1108 N86-14009
NR PROJ. RR0-1408 N86-13893
NR PROJ. RR0-2301 N86-13875
NR PROJ. W12-53 N86-13876
NSF AST-81-13212 N86-14207
N86-14208
NSF AST-82-01092 N86-14207
N86-14208
NSF DMS-82-10950 N86-13962
N86-13988
N86-13997
NSF DMS-83-15216 N86-13969
N86-13971
NSF DMS-83-51187 N86-13964
NSF DMS-84-01021 N86-13992
NSF DMS-85-03294 N86-13953
NSF ECS-82-06498 N86-13990
NSF MCS-79-12179 N86-14077
NSF MCS-82-3483 N86-13989
NSF MCS-82-02205 N86-13967
NSF MCS-82-10950 N86-13757
NSF MCS-82-15064 N86-13758
NSF MCS-83-02549 N86-13965
NSG-1174 N86-13300
NSG-1185 N86-13735
NSG-1649 N86-13587
NSG-2057 N86-14204
N00014-76-C-0288 N86-14008
N00014-76-C-0475 N86-13960
N00014-77-C-0232 N86-13373
N00014-77-C-0389 N86-13894
N86-13937
N00014-78-C-0011 N86-13709
N00014-78-C-0592 N86-13389
N00014-78-C-0633 N86-13655
N00014-79-C-0832 N86-13990
N00014-79-C-0832-REV N86-13985
N00014-80-C-0116 N86-13712
N86-13759
N00014-80-C-0384 N86-13736
N00014-80-C-0505 N86-13893
N86-13894
N86-13933
N86-13937
N86-13949
N86-13950
N86-14036
N86-14077
N00014-80-C-0838 N86-14010
N86-14039
N00014-81-K-0229 N86-14009
N00014-81-K-0256 N86-14037
N00014-81-K-0496 N86-13882
N00014-82-C-0701 N86-13395
N00014-82-K-0198 N86-13331
N00014-82-K-0334 N86-13949
N00014-82-K-0441 N86-13630
N00014-82-K-0576 N86-13397
N00014-82-K-0727 N86-13629
N00014-83-K-0586 N86-13390
N00014-83-K-0609 N86-14012
N00014-83-K-0612 N86-14071
N00014-84-C-0141 N86-13688
N00014-84-C-0380 N86-13412
N00014-84-K-0049 N86-13932
N00014-84-K-0327 N86-13654
N00014-84-K-0345 N86-13951
N00014-85-C-0141 N86-14010
N00014-85-K-0169 N86-13969
N86-13971
N00014-85-K-0303 N86-13874
N00014-85-K-0343 N86-13934
N86-13996
N00600-82-D-8362 N86-13324
N62474-82-C-0295 N86-13680
N62474-82-C-08295 N86-13681
PROJ. H20 N86-14033
RR0-1108 N86-14010
STPA-82-96-025 N86-13420
W-31-109-ENG-38 N86-13665
N86-13698
N86-13704
N86-13761
N86-13762
N86-13836
N86-13912
W-7405-ENG-36 N86-13417
N86-13418
N86-13419
N86-13663
N86-13693
N86-13695
N86-13702
N86-13722
N86-13860
N86-13877
N86-14016
N86-14018
N86-14019
N86-14021
N86-14032
N86 14059
N86-14069
N86-14211
W-7405-ENG-48 N86-13399
N86-13400
N86-13402
N86-13598
N86-13697
N86-13703
N86-13723
N86-13859
N86-13872
N86-13940
N86-13941
N86-13983
N86-14005
N86-14020
N86-14054
N86-14055
N86-14057
N86-14074
199-99-00 N86-13886
327-05-02 N86-14213
352-02-03 N86-14204
482-52-22 N86-13900
490-02-02-77 N86-13917
N86-13918
N86-13919
N86-13920
N86-13921
500-33-05 N86-13749
505-31-01 N86-13292
N86-13296
505-31-04 N86-13295
505-31-21 N86-13304
505-31-53 N86-13297
505-31-53-10 N86-13338
505-31-83-01 N86-13954
N86-13955
N86-13957
N86-13959
505-31-83-92 N86-13956
505-33-7A N86-13734
505-33-43-07 N86-13321
505-33-43-13 N86-13946
505-33-53-09 N86-13316
505-33-62 N86-13407
N86-13679
505-34-03-05 N86-13333
505-34-03-07 N86-13310
N86-13332
505-35-13-06 N86 13892
505-37-01 N86-13916
505-40-7A N86-13677
505-40-62 N86-13328
N86-13329
N86-13330
505-42-23-56 N86-13305
505-42-51 N86-13319
505-43-01 N86-13287
N86-13299
505-43-43-04 N86-13406
505-45-33-11 N86-13944
505-45-58 N86-14006
N86-14007
505-51-11 N86-13676
505-60-31 N86-13298
505-63-01 N86-13409
505-63-11 N86-13408
505-63-81 N86-13370
506-41-4C N86-13899
506-41-11 N86-13645
N86-14110
506-43-11-04 N86-13496
506-51-11 N86-13353
N86-13354
506-53-33-07 N86-13349
506-58-22 N86-13643
506-58-23-04 N86-13644
532-06-11 N86-13311
533-04-12 N86-13678
533-13-01 N86-13755
535-05-121 N86-13495
627-21-14-70 N86-13850
650-60-23 N86-13627
677-24-01 N86-13794
778-35-13 N86-14106
999-53-02 N86-13290
N86-13291
N86-13913

REPORT/ACCESSION NUMBER INDEX

SCIENTIFIC AND TECHNICAL AEROSPACE REPORTS VOLUME 24 NUMBER 4

Typical Report Number Index Listing

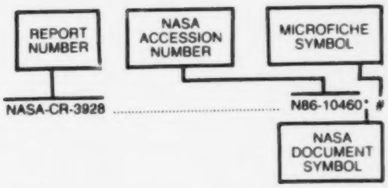

Listings in this index are arranged alphanumerically by report number. The NASA accession number denotes the number by which the citation is identified. An asterisk (*) indicates that the item is a NASA report. A pound sign (#) indicates that the item is available on microfiche.

A-85356 .... N86-13299* #
A-85424 .... N86-13916* #

AD-A156617 .... N86-13908 #
AD-A156622 .... N86-13322 #
AD-A156642 .... N86-13880 #
AD-A157067 .... N86-13924 #
AD-A157705 .... N86-13377 #
AD-A157708 .... N86-14108 #
AD-A157709 .... N86-13680 #
AD-A157710 .... N86-13378 #
AD-A157714 .... N86-13388 #
AD-A157715 .... N86-13874 #
AD-A157716 .... N86-13323 #
AD-A157722 .... N86-13681 #
AD-A157734 .... N86-13887 #
AD-A157737 .... N86-13593 #
AD-A157738 .... N86-13815 #
AD-A157748 .... N86-13648 #
AD-A157750 .... N86-13301 #
AD-A157755 .... N86-13960 #
AD-A157775 .... N86-13926 #
AD-A157776 .... N86-13594 #
AD-A157777 .... N86-13595 #
AD-A157793 .... N86-13961 #
AD-A157794 .... N86-13682 #
AD-A157795 .... N86-13728 #
AD-A157796 .... N86-13683 #
AD-A157937 .... N86-14071 #
AD-A157940 .... N86-13389 #
AD-A157941 .... N86-13927 #
AD-A157943 .... N86-13302 #
AD-A157944 .... N86-13312 #
AD-A157948 .... N86-13843 #
AD-A157949 .... N86-13684 #
AD-A157952 .... N86-13685 #
AD-A157953 .... N86-13339 #
AD-A158014 .... N86-13928 #
AD-A158015 .... N86-13686 #
AD-A158017 .... N86-14008 #
AD-A158023 .... N86-14034 #
AD-A158024 .... N86-13687 #
AD-A158025 .... N86-13901 #
AD-A158027 .... N86-13853 #
AD-A158029 .... N86-13390 #
AD-A158030 .... N86-14035 #
AD-A158033 .... N86-13628 #
AD-A158034 .... N86-13649 #
AD-A158035 .... N86-13929 #
AD-A158037 .... N86-13688 #
AD-A158042 .... N86-14072 #
AD-A158044 .... N86-13391 #
AD-A158045 .... N86-13371 #
AD-A158047 .... N86-13984 #
AD-A158048 .... N86-13985 #
AD-A158049 .... N86-13930 #
AD-A158051 .... N86-13756 #
AD-A158151 .... N86-13986 #
AD-A158154 .... N86-14009 #
AD-A158155 .... N86-14077 #
AD-A158163 .... N86-13962 #
AD-A158164 .... N86-13963 #
AD-A158165 .... N86-13893 #
AD-A158166 .... N86-13964 #
AD-A158167 .... N86-13987 #
AD-A158169 .... N86-13931 #
AD-A158171 .... N86-13965 #
AD-A158172 .... N86-13997 #
AD-A158173 .... N86-14036 #
AD-A158174 .... N86-14000 #
AD-A158177 .... N86-13966 #
AD-A158178 .... N86-13757 #
AD-A158179 .... N86-13967 #
AD-A158180 .... N86-14022 #
AD-A158181 .... N86-13392 #
AD-A158184 .... N86-13968 #
AD-A158187 .... N86-13875 #
AD-A158188 .... N86-13969 #
AD-A158189 .... N86-13970 #
AD-A158190 .... N86-13758 #
AD-A158191 .... N86-14011 #
AD-A158192 .... N86-13854 #
AD-A158193 .... N86-13855 #
AD-A158194 .... N86-13971 #
AD-A158195 .... N86-13876 #
AD-A158197 .... N86-13894 #
AD-A158199 .... N86-13497 #
AD-A158201 .... N86-13411 #
AD-A158202 .... N86-13988 #
AD-A158203 .... N86-13870 #
AD-A158205 .... N86-13932 #
AD-A158206 .... N86-13393 #
AD-A158211 .... N86-13933 #
AD-A158212 .... N86-13934 #
AD-A158213 .... N86-13313 #
AD-A158217 .... N86-13935 #
AD-A158218 .... N86-13881 #
AD-A158219 .... N86-13759 #
AD-A158222 .... N86-13750 #
AD-A158239 .... N86-14012 #
AD-A158252 .... N86-13882 #
AD-A158253 .... N86-13736 #
AD-A158254 .... N86-13871 #
AD-A158255 .... N86-13972 #
AD-A158256 .... N86-13973 #
AD-A158257 .... N86-13974 #
AD-A158262 .... N86-13751 #
AD-A158263 .... N86-13996 #
AD-A158264 .... N86-13629 #
AD-A158265 .... N86-13975 #
AD-A158267 .... N86-14073 #
AD-A158268 .... N86-13976 #
AD-A158269 .... N86-13977 #
AD-A158270 .... N86-13379 #
AD-A158271 .... N86-14207 #
AD-A158272 .... N86-14208 #
AD-A158273 .... N86-13729 #
AD-A158274 .... N86-13909 #
AD-A158275 .... N86-13324 #
AD-A158278 .... N86-14109 #
AD-A158280 .... N86-13831 #
AD-A158282 .... N86-13856 #
AD-A158291 .... N86-13507 #
AD-A158369 .... N86-13650 #
AD-A158370 .... N86-13651 #
AD-A158376 .... N86-13936 #
AD-A158380 .... N86-13630 #
AD-A158381 .... N86-13372 #
AD-A158382 .... N86-14037 #
AD-A158383 .... N86-13989 #
AD-A158592 .... N86-13689 #
AD-A158608 .... N86-13998 #
AD-A158613 .... N86-13990 #
AD-A158619 .... N86-13991 #
AD-A158620 .... N86-13585 #
AD-A158621 .... N86-13394 #
AD-A158623 .... N86-14038 #
AD-A158625 .... N86-13631 #
AD-A158627 .... N86-13373 #
AD-A158629 .... N86-13910 #
AD-A158630 .... N86-13948 #
AD-A158637 .... N86-14052 #
AD-A158644 .... N86-13999 #
AD-A158731 .... N86-13652 #
AD-A158732 .... N86-13895 #
AD-A158733 .... N86-14013 #
AD-A158734 .... N86-13730 #
AD-A158735 .... N86-13896 #
AD-A158736 .... N86-14039 #
AD-A158739 .... N86-13978 #
AD-A158740 .... N86-13992 #
AD-A158741 .... N86-13888 #
AD-A158744 .... N86-13979 #
AD-A158775 .... N86-13632 #
AD-A158776 .... N86-13690 #
AD-A158779 .... N86-13709 #
AD-A158783 .... N86-14040 #
AD-A158800 .... N86-13889 #
AD-A158803 .... N86-13334 #
AD-A158804 .... N86-13374 #
AD-A158806 .... N86-13395 #
AD-A158810 .... N86-13993 #
AD-A158811 .... N86-13375 #
AD-A158813 .... N86-13760 #
AD-A158815 .... N86-13633 #
AD-A158816 .... N86-13325 #
AD-A158819 .... N86-13949 #
AD-A158820 .... N86-13832 #
AD-A158824 .... N86-13857 #
AD-A158825 .... N86-13710 #
AD-A158827 .... N86-13711 #
AD-A158832 .... N86-13653 #
AD-A158840 .... N86-13654 #
AD-A158841 .... N86-13655 #
AD-A158842 .... N86-13348 #
AD-A158849 .... N86-13890 #
AD-A158851 .... N86-13994 #
AD-A158852 .... N86-13498 #
AD-A158853 .... N86-13331 #
AD-A158882 .... N86-13712 #
AD-A158883 .... N86-13656 #
AD-A158884 .... N86-14010 #
AD-A158934 .... N86-13980 #
AD-A158940 .... N86-13937 #
AD-A158941 .... N86-13380 #
AD-A158944 .... N86-13412 #
AD-A158945 .... N86-14210 #
AD-A158968 .... N86-13657 #
AD-A159003 .... N86-13938 #
AD-A159006 .... N86-13634 #
AD-A159015 .... N86-13413 #
AD-A159022 .... N86-13326 #
AD-A159025 .... N86-13381 #
AD-A159026 .... N86-13691 #
AD-A159027 .... N86-13635 #
AD-A159060 .... N86-13764 #
AD-A159062 .... N86-13414 #
AD-A159068 .... N86-13335 #
AD-A159090 .... N86-13891 #
AD-A159104 .... N86-13713 #
AD-A159105 .... N86-13995 #
AD-A159108 .... N86-13981 #
AD-A159109 .... N86-13396 #
AD-A159110 .... N86-13397 #
AD-A159113 .... N86-13415 #
AD-A159115 .... N86-13314 #
AD-A159117 .... N86-13636 #
AD-A159118 .... N86-13897 #
AD-A159228 .... N86-13752 #
AD-A159233 .... N86-13950 #
AD-A159235 .... N86-13951 #
AD-A159236 .... N86-13945 #
AD-A159243 .... N86-13315 #
AD-A159244 .... N86-14014 #
AD-A159245 .... N86-13982 #
AD-A159246 .... N86-13327 #
AD-A159247 .... N86-14015 #
AD-A159249 .... N86-13692 #

AD-D011804 .... N86-13646 #
AD-D011805 .... N86-13410 #
AD-D011807 .... N86-13647 #
AD-D011808 .... N86-13925 #
AD-D011866 .... N86-13596 #
AD-D011867 .... N86-14041 #
AD-D011868 .... N86-13714 #
AD-D011869 .... N86-13715 #

AD-D011870 .... N86-13716 #
AD-D011871 .... N86-13717 #
AD-D011872 .... N86-13718 #
AD-D011873 .... N86-13658 #
AD-D011874 .... N86-13719 #
AD-D011875 .... N86-13597 #
AD-D011876 .... N86-13307 #
AD-D011877 .... N86-13659 #
AD-D011878 .... N86-13660 #
AD-D011880 .... N86-14042 #
AD-D011881 .... N86-13661 #
AD-D011882 .... N86-13662 #
AD-D011883 .... N86-14043 #
AD-D011884 .... N86-13939 #
AD-D011885 .... N86-13737 #
AD-D011886 .... N86-14044 #

AD-E801156 .... N86-13682 #
AD-E950711 .... N86-13961 #
AD-E950723 .... N86-13728 #
AD-E950731 .... N86-14034 #

AD-F620001 .... N86-13413 #
AD-F630681 .... N86-13990 #

AEDC-TR-83-7 .... N86-13684 #
AEDC-TR-83-9 .... N86-13685 #
AEDC-TR-85-16 .... N86-13756 #

AEL-0244-TR .... N86-13927 #

AFATL-TR-85-12 .... N86-13682 #

AFESC/ESL-TR-84-59 .... N86-13339 #

AFGL-TR-85-0007 .... N86-13853 #

AFHRL-TP-85-18 .... N86-13890 #

AFIT/CI/NR-85-53D .... N86-14022 #
AFIT/CI/NP-85-56D .... N86-13392 #
AFIT/CI/NR-85-57T .... N86-13931 #
AFIT/CI/NR-85-67T .... N86-13870 #
AFIT/CI/NR-85-68T .... N86-13929 #
AFIT/CI/NR-85-69T .... N86-13391 #
AFIT/CI/NR-85-73D .... N86-13901 #
AFIT/CI/NR-85-90D .... N86-13371 #
AFIT/CI/NR-85-92D .... N86-13649 #

AFIT/DS/ENC/85-1 .... N86-14015 #

AFIT/GNE/PH/85M-2 .... N86-14014 #
AFIT/GNE/PH/85M-4 .... N86-13327 #
AFIT/GNE/PH/85M-19 .... N86-13982 #

AFIT/GSO/PH/84D-5 .... N86-13315 #

AFLRL-176 .... N86-13386 #

AFOSR-85-177TR .... N86-13999 #
AFOSR-85-0501TR .... N86-13730 #
AFOSR-85-0503TR .... N86-13857 #
AFOSR-85-0506TR .... N86-13710 #
AFOSR-85-0525TR .... N86-13393 #
AFOSR-85-0542TR .... N86-13909 #
AFOSR-85-0547TR .... N86-13973 #
AFOSR-85-0548TR .... N86-13974 #
AFOSR-85-0549TR .... N86-13977 #
AFOSR-85-0550TR .... N86-13976 #
AFOSR-85-0551TR .... N86-13972 #
AFOSR-85-0555TR .... N86-13633 #
AFOSR-85-0558TR .... N86-13998 #
AFOSR-85-0559TR .... N86-13585 #
AFOSR-85-0560TR .... N86-13507 #
AFOSR-85-0563TR .... N86-13856 #
AFOSR-85-0572TR .... N86-13896 #
AFOSR-85-0576TR .... N86-13831 #
AFOSR-85-0577TR .... N86-13729 #
AFOSR-85-0588TR .... N86-13979 #
AFOSR-85-0616TR .... N86-13980 #
AFOSR-85-0619TR .... N86-13992 #
AFOSR-85-0620TR .... N86-13991 #
AFOSR-85-0625TR .... N86-13630 #
AFOSR-85-0626TR .... N86-13978 #
AFOSR-85-0627TR .... N86-13394 #
AFOSR-85-0635TR-APP-1 .... N86-14207 #
AFOSR-85-0635TR-APP-2 .... N86-14208 #
AFOSR-85-0640TR .... N86-13634 #
AFOSR-85-0646TR .... N86-13691 #
AFOSR-85-0662TR .... N86-13897 #
AFOSR-85-0664TR .... N86-13895 #
AFOSR-85-0668TR .... N86-13889 #
AFOSR-85-0669TR .... N86-13652 #
AFOSR-85-0671TR .... N86-13380 #
AFOSR-85-0684TP .... N86-13995 #
AFOSR-85-0693TR .... N86-13945 #

AFOSR-85-0701TR .... N86-13713 #
AFOSR-85-0712TR .... N86-13981 #
AFOSR-85-0723TR .... N86-13656 #
AFOSR-85-0738TR .... N86-13657 #
AFOSR-85-01617TR .... N86-13999 #

AFWAL-TR-84-2065 .... N86-13832 #
AFWAL-TR-84-3117-VOL-4 .... N86-13335 #
AFWAL-TR-84-4141 .... N86-13415 #
AFWAL-TR-84-4183 .... N86-13378 #
AFWAL-TR-84-4186 .... N86-13496 #
AFWAL-TR-85-1100 .... N86-13936 #
AFWAL-TR-85-2022 .... N86-14013 #
AFWAL-TR-85-2042 .... N86-13686 #
AFWAL-TR-85-4025 .... N86-13752 #

AI-M-769 .... N86-13979 #
AI-M-803 .... N86-14036 #
AI-M-811 .... N86-13893 #
AI-M-812 .... N86-13933 #
AI-M-822 .... N86-13937 #
AI-M-823 .... N86-13894 #
AI-M-826 .... N86-13949 #
AI-M-829 .... N86-14077 #
AI-M-836REV .... N86-13950 #

AIAA-81-0528R .... N86-13589* #
AIAA-83-0811-CP .... N86-13592* #

AMMRC-TR-84-40 .... N86-13760 #

AMSAA-TR-410 .... N86-13994 #

AMSMI/RE-85-12-TR .... N86-13728 #

AMSMI/RG-85-5-TR .... N86-13961 #

AMSMI/RR-84-9-TR .... N86-14034 #

ANL-HEP-CP-85-61 .... N86-13665 #

ANL-84-74 .... N86-13912 #
ANL-85-35 .... N86-13704 #

ANL/OTEC-EV-3 .... N86-13836 #

APR-1 .... N86-13654 #

AR-AERO-R-163 .... N86-13336 #

AR-1 .... N86-13506 #
AR-2 .... N86-13895 #
AR-003-963 .... N86-13309 #
AR-003-990 .... N86-13754 #
AR-003-997 .... N86-13336 #
AR-004-017 .... N86-13337 #
AR-163 .... N86-13336 #

ARB-R-85/243 .... N86-13849 #
ARB-R-85/250 .... N86-13846 #

ARL/AERO-R-164 .... N86-13337 #

ARL/STRUC-R-414 .... N86-13754 #

ARL/SYS-R-33 .... N86-13309 #

ARO-18220.8-MS .... N86-13750 #
ARO-18574-PH .... N86-13379 #
ARO-19060.2-EG-S .... N86-14052 #
ARO-19175.18-CH .... N86-13372 #
ARO-19839.1-EL-A-PT-4 .... N86-13650 #
ARO-19839.1-EL-A-PT-5 .... N86-13651 #
ARO-20202.4-EL .... N86-14073 #
ARO-20927.8-MA .... N86-13989 #
ARO-20990.28-MA .... N86-13975 #
ARO-21592.6-MA .... N86-13934 #

ATR-5 .... N86-13736 #

AVSCOM-TR-85-B-7 .... N86-13316* #

B-TF-1627 .... N86-13340 #

BAE-RPT/NIM-7/021 .... N86-13367 #

BN-1042 .... N86-13969 #
BN-1043 .... N86-13971 #

BNL-35567 .... N86-13667 #
BNL-36482 .... N86-14064 #
BNL-36629 .... N86-14004 #
BNL-36700 .... N86-14076 #
BNL-51881 .... N86-13844 #

CA/DOH/AIHL/SP-33 .... N86-13846 #

CAA-U-1205-333 .... N86-13688 #

CAR-TR-88 .... N86-13910 #
CAR-TR-122 .... N86-13980 #
CAR-TR-127 .... N86-13948 #

CERC-85-4 .... N86-13683 #

CERL-TR-P-85/13 .... N86-13314 #

CETIM-1-3L-11-1 .... N86-13741 #
CETIM-12-E-13-3 .... N86-13505 #

CMU-CS-85-104 .... N86-13935 #

CONF-841010-19 .... N86-14068 #
CONF-850128-17 .... N86-14017 #
CONF-850169-16 .... N86-14076 #
CONF-850266-4 .... N86-13702* #
CONF-850266-8 .... N86-14055 #
CONF-850287-1 .... N86-14211 #
CONF-850310-106 .... N86-14061 #
CONF-850405-15 .... N86-14067 #
CONF-850417-27 .... N86-13502 #
CONF-850470-9 .... N86-14056 #
CONF-850504-76 .... N86-14066 #
CONF-850504-89 .... N86-14019 #
CONF-850504-161 .... N86-14064 #
CONF-850504-168 .... N86-14004 #
CONF-850504-184 .... N86-14029 #
CONF-850504-242 .... N86-14002 #
CONF-850504-255 .... N86-14058 #
CONF-850504-267 .... N86-14025 #
CONF-850504-274 .... N86-14023 #
CONF-850507-52 .... N86-14026 #
CONF-850558-4 .... N86-13732 #
CONF-850616-17 .... N86-14060 #
CONF-850616-39 .... N86-14065 #
CONF-850616-58 .... N86-13663 #
CONF-850616-70 .... N86-13721 #
CONF-850718-1 .... N86-14059 #
CONF-850736-11 .... N86-13418 #
CONF-850736-45 .... N86-14074 #
CONF-850765-29 .... N86-14024 #
CONF-850767-3 .... N86-13399 #
CONF-850770-8 .... N86-13417 #
CONF-850771-1 .... N86-14003 #
CONF-850775-1 .... N86-13817 #
CONF-850777-2 .... N86-13416 #
CONF-850787-1 .... N86-13596 #
CONF-850801-12 .... N86-13860 #
CONF-850807-3 .... N86-14021 #
CONF-850808-6 .... N86-14032 #
CONF-850809-46 .... N86-13762 #
CONF-850809-51 .... N86-13761 #
CONF-850809-52 .... N86-13698 #
CONF-850810-20 .... N86-13700 #
CONF-850830-1 .... N86-13402 #
CONF-850830-6 .... N86-13696 #
CONF-850840-7 .... N86-14075 #
CONF-850840-10 .... N86-13499 #
CONF-850840-16 .... N86-13664 #
CONF-850861-3 .... N86-13983 #
CONF-850871-6 .... N86-14027 #
CONF-850878-5 .... N86-13697 #
CONF-850887-11 .... N86-13501 #
CONF-850890-1 .... N86-13419 #
CONF-850905-3 .... N86-13694 #
CONF-850927-5 .... N86-14070 #
CONF-851028-48 .... N86-13872 #
CONF-851071-2 .... N86-13665 #
CONF-8410276-3 .... N86-13733 #
CONF-8503105-9 .... N86-14054 #
CONF-8503144-1 .... N86-13666 #
CONF-8503148-1 .... N86-13703 #
CONF-8505156-1 .... N86-13845 #
CONF-8505157-1 .... N86-13940 #
CONF-8505164-3 .... N86-14016 #
CONF-8505183-1 .... N86-14001 #
CONF-8506109-2 .... N86-14018 #
CONF-8506117-3 .... N86-13599 #
CONF-8506121-2 .... N86-13873 #
CONF-8506137-11 .... N86-13864 #
CONF-8506171-1 .... N86-13500 #
CONF-8508112-1 .... N86-13877 #
CONF-8509104-1 .... N86-13723 #
CONF-8509129-2 .... N86-13695 #

CPL-85-1 .... N86-13897 #

CRDC-CR-84131 .... N86-13881 #
CRDC-CR-85034 .... N86-14038 #

CS-TR-1437 .... N86-13910 #
CS-TR-1497 .... N86-13980 #
CS-TR-1507 .... N86-13948 #

CSDL-R-1799	N86-13310* #
CWP-027	N86-13932 #
DE05-016796	N86-13883 #
DE85-000517	N86-13837 #
DE85-005818	N86-14059 #
DE85-006517	N86-13722 #
DE85-006564	N86-13667 #
DE85-007702	N86-13702* #
DE85-008957	N86-13402 #
DE85-009558	N86-13860 #
DE85-009745	N86-13761 #
DE85-010264	N86-13698 #
DE85-010275	N86-13762 #
DE85-010942	N86-13703 #
DE85-010990	N86-14075 #
DE85-011203	N86-13401 #
DE85-011527	N86-13731 #
DE85-011571	N86-13666 #
DE85-011623	N86-13504 #
DE85-011699	N86-13858 #
DE85-011992	N86-13885 #
DE85-012103	N86-13845 #
DE85-012151	N86-13833 #
DE85-012154	N86-13501 #
DE85-012162	N86-13834 #
DE85-012261	N86-14004 #
DE85-012617	N86-13753 #
DE85-012707	N86-14019 #
DE85-012763	N86-14032 #
DE85-012775	N86-13400 #
DE85-012799	N86-13699 #
DE85-012810	N86-14060 #
DE85-012836	N86-13700 #
DE85-012892	N86-14061 #
DE85-012905	N86-13841 #
DE85-012914	N86-13983 #
DE85-013056	N86-14066 #
DE85-013144	N86-14065 #
DE85-013197	N86-13940 #
DE85-013212	N86-14024 #
DE85-013229	N86-13502 #
DE85-013234	N86-13941 #
DE85-013242	N86-13859 #
DE85-013294	N86-14064 #
DE85-013645	N86-13701 #
DE85-013684	N86-13503 #
DE85-013854	N86-13665 #
DE85-013908	N86-13842 #
DE85-013973	N86-13723 #
DE85-014076	N86-13418 #
DE85-014104	N86-13419 #
DE85-014117	N86-13663 #
DE85-014119	N86-14021 #
DE85-014133	N86-14211 #
DE85-014204	N86-14020 #
DE85-014260	N86-14028 #
DE85-014294	N86-13704 #
DE85-014323	N86-14070 #
DE85-014357	N86-14029 #
DE85-014369	N86-14031 #
DE85-014402	N86-14030 #
DE85-014406	N86-14068 #
DE85-014412	N86-13732 #
DE85-014415	N86-13733 #
DE85-014521	N86-14005 #
DE85-014523	N86-13637 #
DE85-014524	N86-13694 #
DE85-014551	N86-14062 #
DE85-014620	N86-14067 #
DE85-014631	N86-14076 #
DE85-014866	N86-14063 #
DE85-014955	N86-14003 #
DE85-014958	N86-14017 #
DE85-015068	N86-14053 #
DE85-015095	N86-13996 #
DE85-015096	N86-13934 #
DE85-015155	N86-13721 #
DE85-015197	N86-14001 #
DE85-015361	N86-13693 #
DE85-015543	N86-14074 #
DE85-015548	N86-13398 #
DE85-015689	N86-14016 #
DE85-015714	N86-13695 #
DE85-015724	N86-13877 #
DE85-016076	N86-13872 #
DE85-016088	N86-14055 #
DE85-016130	N86-13696 #
DE85-016157	N86-14026 #
DE85-016214	N86-14069 #
DE85-016294	N86-14027 #
DE85-016309	N86-13499 #
DE85-016353	N86-13884 #
DE85-016356	N86-13416 #
DE85-016367	N86-13873 #
DE85-016392	N86-14056 #
DE85-016402	N86-13500 #
DE85-016443	N86-13399 #
DE85-016556	N86-14002 #
DE85-016561	N86-14058 #
DE85-016575	N86-13838* #
DE85-016596	N86-13664 #
DE85-016608	N86-13598 #
DE85-016792	N86-13835 #
DE85-016969	N86-13816 #
DE85-016981	N86-13836 #
DE85-017014	N86-13844 #
DE85-017038	N86-13839 #
DE85-017116	N86-13599 #
DE85-017158	N86-13817 #
DE85-017185	N86-13840 #
DE85-017267	N86-13697 #
DE85-017330	N86-13382 #
DE85-017390	N86-13720 #
DE85-017439	N86-14025 #
DE85-017533	N86-13417 #
DE85-017539	N86-14018 #
DE85-017640	N86-14023 #
DE85-017877	N86-14057 #
DE85-031223	N86-14054 #
DOE/AL-04266/T2	N86-13839 #
DOE/DP-40124/55	N86-14068 #
DOE/DP-40124/71(1)	N86-13732 #
DOE/DP-40200/07	N86-13733 #
DOE/DR-00789/T13	N86-13840 #
DOE/ER-03077/240	N86-13701 #
DOE/ER-13243/1	N86-13731 #
DOE/ER-53154/82	N86-14063 #
DOE/ET-28407/T5-PT-14	N86-13841 #
DOE/ID-12026/T14	N86-13816 #
DOE/JPL-956766-85/01	N86-13838* #
DOE/MC-20110/1985	N86-13503 #
DOE/MC-20334/T19	N86-13699 #
DOE/NASA/50112-60	N86-14106* #
DOE/OR-21374/T1	N86-13401 #
DOE/PC-70779/T1	N86-13398 #
DOE/RA-50219/T4	N86-13885 #
DOE/SF-00700/T11-VOL-2	N86-13835 #
DOT/OST/P34-85/021	N86-13906 #
DREA-TM-85/205	N86-13930 #
DREV-R-4372/85	N86-14040 #
DRIC-BR-94478	N86-13302 #
DRIC-BR-94905	N86-13377 #
DRIC-BR-95846	N86-13322 #
DRIC-BR-96009	N86-13301 #
DRIC-BR-96082	N86-13908 #
DTNSRDC-2280	N86-13688 #
DTNSRDC/CMLD-CR-47-85	N86-13324 #
E-2143	N86-13734* #
E-2566	N86-13643* #
E-2623	N86-13677* #
E-2692	N86-14007* #
E-2701	N86-13295* #
E-2718	N86-14006* #
E-2722	N86-13678* #
E-2728	N86-13679* #
E-2746	N86-13407* #
E-2749	N86-13495* #
E-2777	N86-13899* #
E-2785	N86-13645* #
E-2798	N86-13408* #
E-2800	N86-13749* #
E-2806	N86-13409* #
E-2807	N86-14110* #
E-2809	N86-13627* #
E-2813	N86-13370* #
E-2821	N86-14106* #
EA-85-U-305	N86-13313 #
EGG-M-20784	N86-14067 #
ELAB-STF44-F83103	N86-13368 #
EPA-520/6-85-021	N86-13726 #
EPA-600/D-85-109	N86-13847 #
EPA-600/3-85-048	N86-13727 #
EPRI-EA-4189	N86-13883 #
ERC-04-84	N86-13848 #
ERL-0330-TR	N86-13928 #
ERNO-671/AIV-VOL-1	N86-13361 #
ESA-BR-30	N86-13352 #
ESA-CR(P)-1921	N86-13360 #
ESA-CR(P)-1934	N86-13725 #
ESA-CR(P)-1950	N86-13340 #
ESA-CR(P)-2013	N86-13350 #
ESA-CR(P)-2028-VOL-1	N86-13705 #
ESA-CR(P)-2028-VOL-2	N86-13706 #
ESA-CR(P)-2035	N86-13361 #
ESA-CR(P)-2036	N86-13351 #
ESA-CR(P)-2037	N86-13347 #
ESA-CR(P)-2041	N86-13636 #
ESA-CR(P)-2042	N86-13668 #
ESA-CR(P)-2043	N86-13738 #
ESA-CR(P)-2044	N86-13942 #
ESA-CR(P)-2045	N86-13362 #
ESA-CR(P)-2047	N86-13911 #
ESA-CR(P)-2048-VOL-1	N86-13902 #
ESA-CR(P)-2048-VOL-2	N86-13903 #
ESA-CR(P)-2048-VOL-3	N86-13904 #
ESA-CR(P)-2048-VOL-4	N86-13905 #
ESA-CR(P)-2049	N86-13355 #
ESA-CR(P)-2050	N86-13346 #
ESA-CR(P)-2052	N86-13363 #
ESA-CR(P)-2053	N86-13367 #
ESA-CR(P)-2055	N86-13943 #
ESA-CR(P)-2056	N86-13364 #
ESA-CR(P)-2057	N86-13763 #
ESA-CR(P)-2058	N86-13368 #
ESA-CR(P)-2062	N86-13739 #
ESA-ESTL-72	N86-13738 #
ESA-ESTL-067	N86-13360 #
ESA-SP-1072	N86-13344 #
ESD-TR-84-326	N86-13628 #
ESD-TR-85-197	N86-13993 #
ESI-ED/83-383/RD/MS-VOL-7	N86-13763 #
ESL-TR-85-18	N86-13375 #
ESN-39-7	N86-14108 #
ESN-39-9	N86-14109 #
E86-10011	N86-13794* #
FA-AF-14385	N86-13710 #
FNAL-TM-1310	N86-14028 #
FNAL-TM-1314	N86-14025 #
FOK-RV-R-82-072	N86-13725 #
FOK-TR-R-84-110-VOL-1-PT-A	N86-13902 #
FOK-TR-R-84-110-VOL-1-PT-B	N86-13903 #
FOK-TR-R-84-110-VOL-2	N86-13904 #
FOK-TR-R-84-110-VOL-3	N86-13905 #
FSU-STATISTICS-M701	N86-13999 #
FTD-ID(RS)T-1097-84	N86-14000 #
FTD-ID(RS)T-1267-84	N86-13497 #
FWS/OBS-84/17	N86-13619 #
GA-A-17952	N86-14062 #
GA-A-18024	N86-14031 #
GA-4-18045	N86-14070 #
GD-17	N86-13764 #
GEC-MEL12 0539	N86-13362 #
GEC-MEL42 0552	N86-13942 #
GIT-A-3305-FTR	N86-13631 #
GL-3891	N86-13654 #
GRI-85/0037	N86-13506 #

H-1287-PT-1 N86-13353* #
H-1287-PT-2 N86-13354* #

HHI-84-284 N86-13325 #

ICASE-85-26 N86-13955* #
ICASE-85-37 N86-13957* #
ICASE-85-38 N86-13953* #
ICASE-85-42 N86-13959* #
ICASE-85-43 N86-13954* #
ICASE-85-45 N86-13915* #

IMFL-3119 N86-13303 #
IMFL-4116 N86-13306 #

IPPJ-691 N86-14051 #
IPPJ-692 N86-14045 #
IPPJ-738 N86-14047 #
IPPJ-739 N86-14048 #
IPPJ-740 N86-14049 #
IPPJ-741 N86-14050 #

IR-1 N86-14072 #
IR-2 N86-13648 #
IR-2 N86-13815 #

ISBN-83-01-06288-6 N86-14107

ISL-NB-402/84 N86-13586 #

ISL-R-111/84 N86-13724 #

ISSN-0079-523X N86-14107
ISSN-0082-5255 N86-13914 #
ISSN-0250-1589 N86-13352 #
ISSN-0309-099-X N86-14200
ISSN-0343-7639 N86-13820 #
ISSN-0389-4010 N86-13288 #

JPRS-CST-85-020 N86-13600 #

JPRS-TTP-85-026 N86-13640 #

JPRS-UEN-85-001 N86-13861 #

JPRS-UES-85-009 N86-13765 #

JPRS-UMM-85-013 N86-13745 #
JPRS-UMM-85-014 N86-13742 #

JPRS-UMS-85-006 N86-13422 #

JPRS-USP-85-005 N86-14111 #

JPRS-WST-85-029 N86-13622 #
JPRS-WST-85-030 N86-13610 #
JPRS-WST-85-031 N86-13616 #

JUEL-SPEZ-304 N86-13820 #

K/TS-5867 N86-13842 #

KU-FRL-623-1 N86-13294* #

L-15949 N86-13321* #
L-15964 N86-13945* #
L-15982 N86-13644* #
L-15983 N86-13333* #
L-15988 N86-13406* #
L-15989 N86-13892* #
L-16007 N86-13850* #
L-16012 N86-13305* #
L-16018 N86-13316* #
L-16024 N86-13338* #

LA-UR-85-179 N86-14059 #
LA-UR-85-452 N86-13702* #
LA-UR-85-930 N86-13660 #
LA-UR-85-1627 N86-14016 #
LA-UR-85-1653 N86-14019 #
LA-UR-85-1870 N86-14032 #
LA-UR-85-1979 N86-14211 #
LA-UR-85-2047 N86-14021 #
LA-UR-85-2057 N86-13663 #
LA-UR-85-2106 N86-13419 #
LA-UR-85-2251 N86-13418 #
LA-UR-85-2412 N86-13877 #
LA-UR-85-2454 N86-13695 #
LA-UR-85-2994 N86-14018 #
LA-UR-85-3026 N86-13417 #

LA-10187-MS N86-13693 #
LA-10464-MS N86-14069 #

LBL-18946 N86-14023 #
LBL-19162 N86-14075 #
LBL-19486 N86-14002 #
LBL-19527 N86-14058 #
LBL-19645 N86-13694 #
LBL-19711 N86-14001 #

LJI-R-84-329 N86-13632 #

LMSC-HEC-TR-F042501 N86-13923* #

MAE-1702 N86-13585 #

MATRA-092/CC/AB/225-84 N86-13350 #

MBB-DSP-TN/DRS/132/84 N86-13355 #

MBB-URV-147/84 N86-13351 #

MHSMP-85-39 N86-13720 #

MIM-3258 N86-14030 #

MIMEO-SER-1580 N86-13713 #

MML-TR85-39(C) N86-13412 #

MRC-TSR-2815 N86-13963 #
MRC-TSR-2816 N86-13970 #
MRC-TSR-2817 N86-13986 #
MRC-TSR-2818 N86-14011 #
MRC-TSR-2821 N86-13758 #
MRC-TSR-2822 N86-13987 #
MRC-TSR-2823 N86-13966 #
MRC-TSR-2825 N86-13967 #
MRC-TSR-2827 N86-13757 #
MRC-TSR-2830 N86-13965 #
MRC-TSR-2831 N86-13962 #
MRC-TSR-2834 N86-13964 #
MRC-TSR-2835 N86-13997 #
MRC-TSR-2836 N86-13988 #

MTI-85TR28 N86-13369* #

M1-610200 N86-13421 #
M2-695600-PT-1 N86-13384 #
M2-695600-PT-2 N86-13385 #
M3-431000 N86-13383 #

NAL-TR-859T N86-13288 #

NAS 1.15:58270 N86-13886* #
NAS 1.15:77659 N86-13356* #
NAS 1.15:77952 N86-13318* #
NAS 1.15:86111 N86-13947* #
NAS 1.15:86234 N86-13794* #
NAS 1.15:86398 N86-13321* #
NAS 1.15:86413 N86-13333* #
NAS 1.15:86420 N86-13644* #
NAS 1.15:86424 N86-13892* #
NAS 1.15:86523 N86-14033* #
NAS 1.15:86524 N86-13868* #
NAS 1.15:86527 N86-13365* #
NAS 1.15:86683 N86-13304* #
NAS 1.15:86702 N86-13900* #
NAS 1.15:86764 N86-13319* #
NAS 1.15:86766 N86-13297* #
NAS 1.15:86774 N86-13296* #
NAS 1.15:86825 N86-13299* #
NAS 1.15:86826 N86-13676* #
NAS 1.15:86835 N86-13286* #
NAS 1.15:86837 N86-14213* #
NAS 1.15:86847 N86-13311* #
NAS 1.15:87099 N86-14007* #
NAS 1.15:87104 N86-13295* #
NAS 1.15:87116 N86-14006* #
NAS 1.15:87120 N86-13679* #
NAS 1.15:87132 N86-13407* #
NAS 1.15:87149 N86-13899* #
NAS 1.15:87151 N86-13677* #
NAS 1.15:87153 N86-13495* #
NAS 1.15:87157 N86-13645* #
NAS 1.15:87164 N86-13749* #
NAS 1.15:87168 N86-13409* #
NAS 1.15:87169 N86-14110* #
NAS 1.15:87171 N86-13627* #
NAS 1.15:87172 N86-13370* #
NAS 1.15:87173 N86-13408* #
NAS 1.15:87175 N86-14106* #
NAS 1.15:87176 N86-13678* #
NAS 1.15:87499 N86-13343* #
NAS 1.15:87501 N86-13869* #
NAS 1.15:87521 N86-13357* #
NAS 1.15:87580 N86-13305* #
NAS 1.15:87609 N86-13338* #
NAS 1.15:87620 N86-13332* #
NAS 1.15:87621 N86-13944* #
NAS 1.15:87626 N86-13349* #
NAS 1.15:88177 N86-13879* #
NAS 1.15:88186 N86-14204* #
NAS 1.15:88193 N86-13292* #
NAS 1.15:88200 N86-13916* #
NAS 1.15:88201 N86-13298* #
NAS 1.26:3927 N86-13317* #
NAS 1.26:3946 N86-13813* #
NAS 1.26:166029 N86-13921* #
NAS 1.26:166030 N86-13919* #
NAS 1.26:166031 N86-13917* #
NAS 1.26:166032 N86-13920* #
NAS 1.26:166033 N86-13918* #
NAS 1.26:166616-PT-1 N86-13353* #
NAS 1.26:166616-PT-2 N86-13354* #
NAS 1.26:171600 N86-13923* #
NAS 1.26:171610 N86-13369* #
NAS 1.26:171611 N86-13345* #
NAS 1.26:171902 N86-13708* #
NAS 1.26:171904 N86-14078* #
NAS 1.26:171906 N86-13342* #
NAS 1.26:171907 N86-13898* #
NAS 1.26:174202 N86-13293* #
NAS 1.26:174923-VOL-1 N86-13328* #
NAS 1.26:174923-VOL-2 N86-13329* #
NAS 1.26:174923-VOL-3 N86-13330* #
NAS 1.26:174946 N86-13755* #
NAS 1.26:176017 N86-13814* #
NAS 1.26:176354 N86-13851* #
NAS 1.26:176355 N86-13294* #
NAS 1.26:176358 N86-14205* #
NAS 1.26:176359 N86-13878* #
NAS 1.26:176360 N86-13735* #
NAS 1.26:176365 N86-13702* #
NAS 1.26:176368 N86-13852* #
NAS 1.26:176369 N86-13907* #
NAS 1.26:176372 N86-13958* #
NAS 1.26:176380 N86-13587* #
NAS 1.26:176382 N86-13289* #
NAS 1.26:176384 N86-13838* #
NAS 1.26:176387 N86-13320* #
NAS 1.26:176391 N86-13922* #
NAS 1.26:176392 N86-14212* #
NAS 1.26:176393 N86-13306*
NAS 1.26:176398 N86-14209* #
NAS 1.26:176402 N86-13358* #
NAS 1.26:176403 N86-13300* #
NAS 1.26:177361 N86-13287* #
NAS 1.26:177384 N86-13913* #
NAS 1.26:177385 N86-13291* #
NAS 1.26:177393 N86-13290* #
NAS 1.26:177973 N86-13955* #
NAS 1.26:177974 N86-13953* #
NAS 1.26:177983 N86-13310* #
NAS 1.26:177984 N86-13957* #
NAS 1.26:177988 N86-13954* #
NAS 1.26:177999 N86-13915* #
NAS 1.26:178001 N86-13956* #
NAS 1.26:178002 N86-13959* #
NAS 1.26:178013 N86-13496* #
NAS 1.26:178544 N86-14206* #
NAS 1.26:178556 N86-13359* #
NAS 1.60:2479 N86-13946* #
NAS 1.60:2512 N86-13406* #
NAS 1.60:2520 N86-13316* #
NAS 1.60:2524 N86-13643* #
NAS 1.61:1148 N86-13850* #
NAS 1.61:1151 N86-13867* #
NAS 1.61:1154 N86-13734* #
NAS 1.61:1158 N86-13866* #

NAS-SR-1000 N86-13312 #

NASA-CR-3927 N86-13317* #
NASA-CR-3946 N86-13813* #
NASA-CR-166029 N86-13921* #
NASA-CR-166030 N86-13919* #
NASA-CR-166031 N86-13917* #
NASA-CR-166032 N86-13920* #
NASA-CR-166033 N86-13918* #
NASA-CR-166616-PT-1 N86-13353* #
NASA-CR-166616-PT-2 N86-13354* #
NASA-CR-171600 N86-13923* #
NASA-CR-171610 N86-13369* #
NASA-CR-171611 N86-13345* #
NASA-CR-171902 N86-13708* #
NASA-CR-171904 N86-14078* #
NASA-CR-171906 N86-13342* #
NASA-CR-171907 N86-13898* #
NASA-CR-174202 N86-13293* #
NASA-CR-174923-VOL-1 N86-13328* #
NASA-CR-174923-VOL-2 N86-13329* #
NASA-CR-174923-VOL-3 N86-13330* #
NASA-CR-174946 N86-13755* #
NASA-CR-176017 N86-13814* #
NASA-CR-176354 N86-13851* #
NASA-CR-176355 N86-13294* #

NASA-CR-176358 N86-14205* #
NASA-CR-176359 N86-13878* #
NASA-CR-176360 N86-13735* #
NASA-CR-176365 N86-13702* #
NASA-CR-176368 N86-13852* #
NASA-CR-176369 N86-13907* #
NASA-CR-176372 N86-13958* #
NASA-CR-176380 N86-13587* #
NASA-CR-176382 N86-13289* #
NASA-CR-176384 N86-13838* #
NASA-CR-176387 N86-13320* #
NASA-CR-176391 N86-13922* #
NASA-CR-176392 N86-14212* #
NASA-CR-176393 N86-13306*
NASA-CR-176398 N86-14209* #
NASA-CR-176402 N86-13358* #
NASA-CR-176403 N86-13300* #
NASA-CR-177361 N86-13287* #
NASA-CR-177384 N86-13913* #
NASA-CR-177385 N86-13291* #
NASA-CR-177393 N86-13290* #
NASA-CR-177973 N86-13955* #
NASA-CR-177974 N86-13953* #
NASA-CR-177983 N86-13310* #
NASA-CR-177984 N86-13957* #
NASA-CR-177988 N86-13954* #
NASA-CR-177999 N86-13915* #
NASA-CR-178001 N86-13956* #
NASA-CR-178002 N86-13959* #
NASA-CR-178013 N86-13496* #
NASA-CR-178544 N86-14206* #
NASA-CR-178556 N86-13359* #

NASA-RP-1148 N86-13850* #
NASA-RP-1151 N86-13867* #
NASA-RP-1154 N86-13734* #
NASA-RP-1158 N86-13866* #

NASA-TM-58270 N86-13886* #
NASA-TM-77659 N86-13356* #
NASA-TM-77952 N86-13318* #
NASA-TM-86111 N86-13947* #
NASA-TM-86234 N86-13794* #
NASA-TM-86398 N86-13321* #
NASA-TM-86413 N86-13333* #
NASA-TM-86420 N86-13644* #
NASA-TM-86424 N86-13892* #
NASA-TM-86523 N86-14033* #
NASA-TM-86524 N86-13868* #
NASA-TM-86527 N86-13365* #
NASA-TM-86683 N86-13304* #
NASA-TM-86702 N86-13900* #
NASA-TM-86764 N86-13319* #
NASA-TM-86766 N86-13297* #
NASA-TM-86774 N86-13296* #
NASA-TM-86825 N86-13299* #
NASA-TM-86826 N86-13676* #
NASA-TM-86835 N86-13286* #
NASA-TM-86837 N86-14213* #
NASA-TM-86847 N86-13311* #
NASA-TM-87099 N86-14007* #
NASA-TM-87104 N86-13295* #
NASA-TM-87116 N86-14006* #
NASA-TM-87120 N86-13679* #
NASA-TM-87132 N86-13407* #
NASA-TM-87149 N86-13899* #
NASA-TM-87151 N86-13677* #
NASA-TM-87153 N86-13495* #
NASA-TM-87157 N86-13645* #
NASA-TM-87164 N86-13749* #
NASA-TM-87168 N86-13409* #
NASA-TM-87169 N86-14110* #
NASA-TM-87171 N86-13627* #
NASA-TM-87172 N86-13370* #
NASA-TM-87173 N86-13408* #
NASA-TM-87175 N86-14106* #
NASA-TM-87176 N86-13678* #
NASA-TM-87499 N86-13343* #
NASA-TM-87501 N86-13869* #
NASA-TM-87521 N86-13357* #
NASA-TM-87580 N86-13305* #
NASA-TM-87609 N86-13338* #
NASA-TM-87620 N86-13332* #
NASA-TM-87621 N86-13944* #
NASA-TM-87626 N86-13349* #
NASA-TM-88177 N86-13879* #
NASA-TM-88186 N86-14204* #
NASA-TM-88193 N86-13292* #
NASA-TM-88200 N86-13916* #
NASA-TM-88201 N86-13298* #

NASA-TP-2479 N86-13946* #
NASA-TP-2512 N86-13406* #
NASA-TP-2520 N86-13316* #
NASA-TP-2524 N86-13643* #

NCEL-CR-85.004 N86-13681 #
NCEL-CR-85.008 N86-13680 #

NORDA-TN-259 N86-13689 #

NOSC/TD-804 N86-13751 #

NPS67-85-004CR N86-13396 #

NRL-MR-5610 N86-13875 #
NRL-MR-5621 N86-13687 #
NRL-MR-5627 N86-13984 #
NRL-MR-5643 N86-13374 #
NRL-MR-5648 N86-13636 #

NRL-8898 N86-13876 #

NSR-22-3 N86-13831 #

NSSDC/WDC-A-R/S-85-01 N86-13343* #
NSSDC/WDC-A-R/S-85-03-VOL-4A N86-13869* #

NSWC/TR-85-48 N86-13411 #
NSWC/TR-85-56 N86-13924 #
NSWC/TR-85-186 N86-13381 #

NTIA-85-173 N86-13639 #

OE-85-14 N86-13331 #

ONERA-BT-8/0791-GY N86-13341 #

ONWI-290-VOL-6 N86-13858 #

ORI-TR-2459 N86-13317* #

ORNL-6065 N86-13952 #

ORNL/TM-9363 N86-14053 #

PB85-198992 N86-13819 #
PB85-200194 N86-13847 #
PB85-212942 N86-13639 #
PB85-214336 N86-13727 #
PB85-216943 N86-13848 #
PB85-218196 N86-13849 #
PB85-219608 N86-13506 #
PB85-222750 N86-13906 #
PB85-225837 N86-13818 #
PB85-227817 N86-13846 #
PB85-231470 N86-13726 #

PNL-5465 N86-13637 #

PSI-039 N86-13729 #

PV-44-607/F N86-13420 #

QR-1 N86-13345* #

R/D-4033-EN-01 N86-13871 #
R/D-4410-EE-01 N86-14072 #
R/D-4663-EE-01 N86-13648 #
R/D-4739-EN-01 N86-13815 #

RAE-TM-AERO-2007 N86-13302 #
RAE-TM-AERO-2026 N86-13301 #

RAE-TR-84047 N86-13377 #
RAE-TR-84085 N86-13322 #

RAND/N-2209-AF N86-13348 #

RE-700 N86-13593 #

REPT-2-53030/1R-52776 N86-13919* #
REPT-00-0778 N86-13911 #
REPT-85-9F3-EPCAD-R2 N86-14073 #
REPT-85-105 N86-13342* #
REPT-85B0489 N86-13866* #
REPT-85F0274 N86-13867* #
REPT-163 N86-13733 #
REPT-0059-85-1 N86-13895 #
REPT-1383R N86-13832 #
REPT-16282-T-1646-MA-129T-002F N86-13708* #
REPT-85047 N86-13286* #
REPT-85131 N86-13304* #
REPT-85167 N86-13900* #
REPT-85288 N86-13319* #
REPT-85318 N86-13297* #
REPT-85340 N86-13296* #
REPT-85409 N86-14213* #
REPT-85424 N86-13311* #
REPT-86010 N86-14204* #
REPT-86045 N86-13292* #
REPT-86064 N86-13298* #

REPT-5274192 N86-13380 #

RFP-3792 N86-14024 #
RFP-3802 N86-13502 #

RM-84-6 N86-13985 #
RM-85-10 N86-13990 #

RPI-152 N86-14008 #

RSRE-MEMO-3805 N86-13908 #

S-550 N86-13886* #

SAND-84-1159 N86-13753 #
SAND-84-2445C N86-14065 #
SAND-84-2516C N86-14060 #
SAND-84-2545C N86-13721 #
SAND-85-0853 N86-13382 #
SAND-85-1089C N86-13700 #
SAND-85-1716C N86-13696 #
SAND-85-1807C N86-13599 #

SAPR-6 N86-13878* #

SD-TR-85-39 N86-13631 #
SD-TR-85-40 N86-13711 #

SEP-TS/SE/BT/10026/85 N86-13668 #

SERI/STR-211-2516 N86-13837 #

SERI/TP-255-2751 N86-13501 #

SERI/TR-252-2322 N86-13834 #
SERI/TR-253-2169 N86-13833 #

SQ08671-84-00661 N86-13857 #

SR-1 N86-13853 #
SR-33 N86-13309 #

SU-SLAC-PUB-3639 N86-14066 #
SU-SLAC-PUB-3666 N86-14029 #
SU-SLAC-PUB-3674 N86-14017 #
SU-SLAC-PUB-3726 N86-14003 #

SU-SOL-85-10 N86-13996 #
SU-SOL-85-11 N86-13934 #

SVHSER-9811 N86-13898* #

SWRI-14-7676-VOL-4 N86-13335 #

TACOM-TR-13107 N86-13593 #

TAMRF-3224-85-12 N86-13300* #

TDH-RT-2963-T N86-13638 #

TN-84-7104-101-12 N86-13913* #
TN-85-7104-306-23 N86-13291* #
TN-85-7104-306-26 N86-13290* #

TR-TS-RP-2-09-84 N86-13364 #

TR-2 N86-13389 #
TR-2 N86-13951 #
TR-3-ONR N86-14012 #
TR-4 N86-14039 #
TR-7 N86-14071 #
TR-8 N86-13989 #
TR-14 N86-13397 #
TR-18 N86-13759 #
TR-20 N86-13712 #
TR-24 N86-14009 #
TR-85-14 N86-13976 #
TR-85-17 N86-13973 #
TR-85-18 N86-13951 #
TR-85-18 N86-13974 #
TR-85-19 N86-13977 #
TR-85-20 N86-13972 #
TR-85-22 N86-13998 #
TR-85-668 N86-13926 #
TR-95 N86-13995 #
TR-102 N86-13992 #
TR-359 N86-13960 #
TR-505 N86-13729 #
TR-724 N86-13993 #
TR-0084A(5409-73)-1 N86-13631 #
TR-0084A(9975)-1 N86-13711 #

UCB/ERL-85-1 N86-13652 #

UCID-19896-REV-1 N86-13941 #
UCID-20047 N86-13400 #

UCID-20453 .... N86-14020 #
UCID-20457 .... N86-14005 #
UCID-20498 .... N86-14057 #
UCID-20504 .... N86-13859 #

UCRL-91699 .... N86-13723 #
UCRL-92077-2 .... N86-13940 #
UCRL-92259 .... N86-14055 #
UCRL-92275 .... N86-13703 #
UCRL-92295-1 .... N86-13402 #
UCRL-92358 .... N86-13598 #
UCRL-92531 .... N86-14054 #
UCRL-92641 .... N86-13983 #
UCRL-92933 .... N86-13872 #
UCRL-92974 .... N86-13399 #
UCRL-92992 .... N86-13697 #
UCRL-93030 .... N86-14074 #

UCT/DEECS/TR-85-8 .... N86-13981 #

UILU-ENG-84-4009 .... N86-13682 #

US-PATENT-APPL-SN-528710 .... N86-13939 #
US-PATENT-APPL-SN-617657 .... N86-13722 #
US-PATENT-APPL-SN-617668 .... N86-13646 #
US-PATENT-APPL-SN-660349 .... N86-13718 #
US-PATENT-APPL-SN-662657 .... N86-13504 #
US-PATENT-APPL-SN-663015 .... N86-13410 #
US-PATENT-APPL-SN-667685 .... N86-13307 #
US-PATENT-APPL-SN-719403 .... N86-13659 #
US-PATENT-APPL-SN-734986 .... N86-13715 #
US-PATENT-APPL-SN-737753 .... N86-13658 #
US-PATENT-APPL-SN-744084 .... N86-13716 #
US-PATENT-APPL-SN-745738 .... N86-13597 #
US-PATENT-APPL-SN-746704 .... N86-14043 #
US-PATENT-APPL-SN-747220 .... N86-13719 #
US-PATENT-APPL-SN-748094 .... N86-13737 #
US-PATENT-APPL-SN-749340 .... N86-14044 #
US-PATENT-APPL-SN-749597 .... N86-13647 #
US-PATENT-APPL-SN-750218 .... N86-13596 #
US-PATENT-APPL-SN-750630 .... N86-14041 #
US-PATENT-APPL-SN-751339 .... N86-13925 #
US-PATENT-APPL-SN-751346 .... N86-13717 #
US-PATENT-APPL-SN-751347 .... N86-13714 #
US-PATENT-APPL-SN-761257 .... N86-14042 #
US-PATENT-APPL-SN-763161 .... N86-13661 #
US-PATENT-APPL-SN-766371 .... N86-13660 #
US-PATENT-APPL-SN-768271 .... N86-13662 #

USAAEFA-83-20 .... N86-13323 #

USAAVRADCOM-TR-83-D-34 .... N86-13326 #

USAAVSCOM-TR-84-D-20 .... N86-13325 #

USAEHA-75-51-0132-85 .... N86-13891 #

USAFA-TN-85-8 .... N86-13334 #

USAFSAM-TR-85-49 .... N86-13888 #

USARIEM-M33/85 .... N86-13887 #

USCG-D-18-85 .... N86-13313 #

USGS/G-830-01 .... N86-13818 #
USGS/G-836(03) .... N86-13848 #

USNA-TSPR-131 .... N86-14210 #

UTIAS-294 .... N86-13914 #

UWIS/DC/TR-85/2 .... N86-13655 #

VKI-CR-1984-16/AR .... N86-13347 #

WES/TR/A-85-2 .... N86-13843 #

WES/TR/GL-85-5-VOL-1 .... N86-13854 #
WES/TR/GL-85-5-VOL-2 .... N86-13855 #

WES/TR/HL-85-1 .... N86-13692 #

WES/TR/K-85-1-VOL-1 .... N86-13594 #
WES/TR/K-85-1-VOL-2 .... N86-13595 #

☆U.S. GOVERNMENT PRINTING OFFICE: 1986-431-573/40002

FEDERAL DEPOSITORY LIBRARY PROGRAM

The Federal Depository Library Program provides Government publications to designated libraries throughout the United States. The Regional Depository Libraries listed below receive and retain at least one copy of nearly every Federal Government publication, either in printed or microfilm form, for use by the general public. These libraries provide reference services and inter-library loans; however, they are *not* sales outlets. You may wish to ask your local library to contact a Regional Depository to help you locate specific publications, or you may contact the Regional Depository yourself.

ARKANSAS STATE LIBRARY
One Capitol Mall
Little Rock, AR 72201
(501) 371-2326

AUBURN UNIV. AT MONTGOMERY LIBRARY
Documents Department
Montgomery, AL 36193
(205) 279-9110, ext. 253

UNIV. OF ALABAMA LIBRARY
Documents Dept.—Box S
University, AL 35486
(205) 348-7369

DEPT. OF LIBRARY, ARCHIVES AND PUBLIC RECORDS
Third Floor—State Cap.
1700 West Washington
Phoenix, AZ 85007
(602) 255-4121

UNIVERSITY OF ARIZONA LIB.
Government Documents Dept.
Tucson, AZ 85721
(602) 626-5233

CALIFORNIA STATE LIBRARY
Govt. Publications Section
P.O. Box 2037
Sacramento, CA 95809
(916) 322-4572

UNIV. OF COLORADO LIB.
Government Pub. Division
Campus Box 184
Boulder, CO 80309
(303) 492-8834

DENVER PUBLIC LIBRARY
Govt. Pub. Department
1357 Broadway
Denver, CO 80203
(303) 571-2131

CONNECTICUT STATE LIBRARY
Government Documents Unit
231 Capitol Avenue
Hartford, CT 06106
(203) 566-4971

UNIV. OF FLORIDA LIBRARIES
Library West
Documents Department
Gainesville, FL 32611
(904) 392-0367

UNIV. OF GEORGIA LIBRARIES
Government Reference Dept.
Athens, GA 30602
(404) 542-8951

UNIV. OF HAWAII LIBRARY
Govt. Documents Collection
2550 The Mall
Honolulu, HI 96822
(808) 948-8230

UNIV. OF IDAHO LIBRARY
Documents Section
Moscow, ID 83843
(208) 885-6344

ILLINOIS STATE LIBRARY
Information Services Branch
Centennial Building
Springfield, IL 62706
(217) 782-5185

INDIANA STATE LIBRARY
Serials Documents Section
140 North Senate Avenue
Indianapolis, IN 46204
(317) 232-3686

UNIV. OF IOWA LIBRARIES
Govt. Documents Department
Iowa City, IA 52242
(319) 353-3318

UNIVERSITY OF KANSAS
Doc. Collect.—Spencer Lib.
Lawrence, KS 66045
(913) 864-4662

UNIV. OF KENTUCKY LIBRARIES
Govt. Pub. Department
Lexington, KY 40506
(606) 257-3139

LOUISIANA STATE UNIVERSITY
Middleton Library
Govt. Docs. Dept.
Baton Rouge, LA 70803
(504) 388-2570

LOUISIANA TECHNICAL UNIV. LIBRARY
Documents Department
Ruston, LA 71272
(318) 257-4962

UNIVERSITY OF MAINE
Raymond H. Fogler Library
Tri-State Regional Documents Depository
Orono, ME 04469
(207) 581-1680

UNIVERSITY OF MARYLAND
McKeldin Lib.—Doc. Div.
College Park, MD 20742
(301) 454-3034

BOSTON PUBLIC LIBRARY
Government Docs. Dept.
Boston, MA 02117
(617) 536-5400 ext. 226

DETROIT PUBLIC LIBRARY
Sociology Department
5201 Woodward Avenue
Detroit, MI 48202
(313) 833-1409

MICHIGAN STATE LIBRARY
P.O. Box 30007
Lansing, MI 48909
(517) 373-0640

UNIVERSITY OF MINNESOTA
Government Pubs. Division
409 Wilson Library
309 19th Avenue South
Minneapolis, MN 55455
(612) 373-7813

UNIV. OF MISSISSIPPI LIB.
Documents Department
University, MS 38677
(601) 232-5857

UNIV. OF MONTANA
Mansfield Library
Documents Division
Missoula, MT 59812
(406) 243-6700

NEBRASKA LIBRARY COMM.
Federal Documents
1420 P Street
Lincoln, NE 68508
(402) 471-2045
In cooperation with University of Nebraska-Lincoln

UNIVERSITY OF NEVADA LIB.
Govt. Pub. Department
Reno, NV 89557
(702) 784-6579

NEWARK PUBLIC LIBRARY
5 Washington Street
Newark, NJ 07101
(201) 733-7812

UNIVERSITY OF NEW MEXICO
Zimmerman Library
Government Pub. Dept.
Albuquerque, NM 87131
(505) 277-5441

NEW MEXICO STATE LIBRARY
Reference Department
325 Don Gaspar Avenue
Santa Fe, NM 87501
(505) 827-2033, ext. 22

NEW YORK STATE LIBRARY
Empire State Plaza
Albany, NY 12230
(518) 474-5563

UNIVERSITY OF NORTH CAROLINA AT CHAPEL HILL
Wilson Library
BA/SS Documents Division
Chapel Hill, NC 27515
(919) 962-1321

UNIVERSITY OF NORTH DAKOTA
Chester Fritz Library
Documents Department
Grand Forks, ND 58202
(701) 777-2617, ext. 27
(In cooperation with North Dakota State Univ. Library)

STATE LIBRARY OF OHIO
Documents Department
65 South Front Street
Columbus, OH 43215
(614) 462-7051

OKLAHOMA DEPT. OF LIB.
Government Documents
200 NE 18th Street
Oklahoma City, OK 73105
(405) 521-2502

OKLAHOMA STATE UNIV. LIB.
Documents Department
Stillwater, OK 74078
(405) 624-6546

PORTLAND STATE UNIV. LIB.
Documents Department
P.O. Box 1151
Portland, OR 97207
(503) 229-3673

STATE LIBRARY OF PENN.
Government Pub. Section
P.O. Box 1601
Harrisburg, PA 17105
(717) 787-3752

TEXAS STATE LIBRARY
Public Services Department
P.O. Box 12927—Cap. Sta.
Austin, TX 78711
(512) 471-2996

TEXAS TECH UNIV. LIBRARY
Govt. Documents Department
Lubbock, TX 79409
(806) 742-2268

UTAH STATE UNIVERSITY
Merrill Library, U.M.C. 30
Logan, UT 84322
(801) 750-2682

UNIVERSITY OF VIRGINIA
Alderman Lib.—Public Doc.
Charlottesville, VA 22901
(804) 924-3133

WASHINGTON STATE LIBRARY
Documents Section
Olympia, WA 98504
(206) 753-4027

WEST VIRGINIA UNIV. LIB.
Documents Department
Morgantown, WV 26506
(304) 293-3640

MILWAUKEE PUBLIC LIBRARY
814 West Wisconsin Avenue
Milwaukee, WI 53233
(414) 278-3000

ST. HIST LIB. OF WISCONSIN
Government Pub. Section
816 State Street
Madison, WI 53706
(608) 262-4347

WYOMING STATE LIBRARY
Supreme Ct. & Library Bld.
Cheyenne, WY 82002
(307) 777-6344

National Aeronautics and
Space Administration
Code NIT-4
Washington, D.C.
20546

Official Business
Penalty for Private Use, $300

SPECIAL FOURTH-CLASS RATE
POSTAGE & FEES PAID
NASA
WASHINGTON, D.C.
PERMIT No. G 27

NASA

POSTMASTER: If Undeliverable (Section 158
Postal Manual) Do Not Return